

Q
1
S3
V.81
1978
N/C

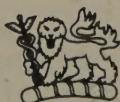
SCI

PAMPHLET BOX

Physics Abstracts

Science Abstracts Series A
July-December 1978

Subject Index (A – L)



inspec

The Institution of

Electrical Engineers

CONTENTS

Title page	i	Subject index	S1503
Abbreviations and acronyms	iii		

SIX-MONTHLY INDEXES TO SCIENCE ABSTRACTS

Cumulative indexes to Science Abstracts are published twice a year covering the period January-June and July-December. They comprise author and subject indexes and some specialised or 'small' indexes. For Physics Abstracts and Electrical & Electronics Abstracts the Author Index and Subject Index are published as separate volumes. In this case the Small Indexes are included in the Author Index volume.

Subject Index

The Subject index provides an alphabetical subject key to the articles included in the abstracts journal. Some general guidance on its use is given below:

1. Look in the index for the name of the specific subject in which you are interested. In most cases this name will be a heading in the index and you will find relevant articles listed under it. The majority of the subject headings fall into the following categories: property, phenomena, substance or named objects, instrument, device, theory, method, process, application, event.
2. Occasionally you will be directed from the subject heading chosen to a different heading under which the relevant or additional articles are listed.
3. If you do not find the subject heading you first chose, try a more general heading.
4. Each entry under the heading relates to an article appearing in the abstracts journal and gives the serial number of that article in the journal preceded by the last digit of the current year, e.g. 8-12345; ie. Abstract number 12345 in the abstracts journal for 1978.

The language of the article, if it is not in English, is also indicated. e.g. digital frequency meter jamming, distribution function determ. (Russian) 8-41575.

Each entry starts with a Keyword or Keyphrase considered to be most relevant to the heading. On sorting these Keywords, the qualifying prefixes are usually ignored. (e.g. α -brass, 5-sulphosalicylic, 31 Cygni, n-Ge are sorted under brass, sulphosalicylic, Cygni, Ge respectively).

There are three main Keyword lists; alphabetical A-Z, elementary particles, and chemical symbols (organic substances are written and not given as chemical formula). More than one Keyword list may be present under each subject heading.

For document on, say, 'photoemission of germanium' at least two access points 'photoemission' and 'Germanium' are provided. Under the heading 'photoemission' the Keyword will be 'Ge' and under 'germanium' the Keyword will be 'photoemission'.

In a case like this, it is advisable and quicker to use the heading 'photoemission' and go straight to the chemical symbol list for 'Ge'.

Intermetallic compounds are indexed under the appropriate alloy headings. The chemical formula is used as Keyword. However, it is important to realise in searching the chemical symbol list that, at present, alloys and intermetallic compounds are sorted separately. For example FeCo is sorted at the end of the Fe- list e.g. Fe-Al, ... Fe-Co, ... Fe-Si, ... Fe-Si-B, ... FeCo, ... FeSi and so on in this order.

Physics Abstracts

Science Abstracts Series A

July-December 1978

Subject Index (A – L)




inspec
The Institution of
Electrical Engineers

Physics Abstracts is published twice monthly by the Institution of Electrical Engineers. Twice-yearly subject and author indexes covering the period January-June and July-December are included in the subscription. Printed by G. A. Pindar & Son Ltd., Scarborough, N. Yorkshire, England. Second class postage paid at Piscataway, NJ 08854 USA.

© 1979: THE INSTITUTION OF ELECTRICAL ENGINEERS

July-December 1978

1 - A) xobal teidu?



IEE
The Institution of
Electrical Engineers

Abbreviations and Acronyms

Abbreviations and acronyms are used in the modifiers in all INSPEC Cumulative Subject Indexes. Individual terms should be readily understood in the context of the subject headings. However, for users' guidance, two lists of these abbreviations and acronyms together with their meanings are published below. The main list contains mixed terms, and the special list contains terms more appropriate to some specific subject areas.

Main list of Keyword Abbreviations

AC	alternating current	E1, E2	electric dipole, quadrupole
ACV	air cushion vehicle	EAS	extensive air shower
A/D	analogue-to-digital	ECG	electrocardiography (-gram)
ADP	administrative data processing	EDP	electronic data processing
AES	Auger electron spectra (-oscopy)	EEG	electroencephalography (-gram)
AF	audio frequency	EHD	electrohydrodynamics
AFC	automatic frequency control	EHF	extremely high frequency
AFL	abstract family of languages	EHV	extra high voltage
AGC	automatic gain control	ELDOR	electron electron double resonance
AM	amplitude modulation	ELF	extremely low frequency
ANS	Astronomical Netherlands Satellite	EM	electromagnetic
APR	acoustic paramagnetic resonance	EMC	electromagnetic compatibility
APS	appearance potential spectra (-oscopy)	EMF	electromotive force
APW	augmented plane wave	EMG	electromyography (-gram)
ATR	attenuated total reflection	ENDOR	electron nuclear double resonance
ATS	applications technology satellite	EOS	earth observatory satellite
AVC	automatic volume control	EPMA	electron probe microanalysis
		EPR	electron paramagnetic resonance
		ERPS	extramolecular relaxation polarisation shift
		ERTS	earth resources technology satellite
		ESCA	electron spectroscopy for chemical analysis
		ESF1	epitaxial silicon film on insulator
		EUV	extreme ultraviolet
		EXAFS	extended X-ray absorption fine structure
		FCC	face centred cubic
		FDM	frequency division multiplex(ing)
		FEM	field emission microscopy
		FET	field effect transistor
		FFT	fast Fourier transform
		FIM	field ion microscopy
		FM	frequency modulation
		FP	freezing point
		FSK	frequency-shift keying
		GAMBIT	gate modulated bipolar transistor
		GARP	global atmospheric research programme
		GATE	GARP Atlantic tropical experiment
		HCP	hexagonal close packed
		HEED	high energy electron diffraction
		HF	high frequency or Hartree-Fock
		HFB	Hartree-Fock-Bogoliubov
		HFS	hyperfine structure
		HV	high voltage
		IC	integrated circuit
		IF	intermediate frequency
		IGFET	insulated gate field effect transistor
		I ² L	integrated injection logic
		I ² L	isoplanar I ² L
		ILS	instrument landing system
CAD	computer aided design		
CAI	computer assisted instruction		
CATV	community antenna TV		
CCD	charge-coupled device		
CDI	collector diffusion isolation		
CDM	code division multiplexing		
CDW	charge-density wave		
CEM	channel electron multiplier		
COM	computer output to microfilm		
CP	charge, parity		
CPT	charge, parity, time		
CRO	cathode ray oscilloscope		
CRT	cathode ray tube		
CVD	chemical vapour deposition		
CW	continuous wave		
D/A	digital-to-analogue		
DC	direct current		
DDC	direct digital control		
DDL	diode-diode logic		
DFB	distributed feedback		
DH	double heterostructure		
DIL	dual-in-line		
DM	delta modulation		
DMSS	Defence Meteorological Satellite System		
DOVETT	double velocity transit time		
DPCM	differential pulse code modulation		
DPSK	differential phase shift keying		
DTA	differential thermal analysis		

IMPATT	impact avalanche transit time	PC	printed circuit
INDOR	internuclear double resonance	PCB	printed circuit board
INTELSAT	international telecommunications satellite consortium	PCAC	partially conserved axial currents
I/O	input/output	PCB	printed circuit board
IR	infrared	PF	power factor
ISR	intersecting storage ring	PFM	pulse frequency modulation
		PID (PI, PD)	proportional+integral+differential (derivative)
		PLA	phase locked arrays
		PLC	programmable logic control
		PLL	phase locked loops
LC	inductance-capacitance	PM	pulse modulation
LEC	liquid encapsulated Czochralski	PMR	proton magnetic resonance
LED	light emitting diode	POS	point of scale
LEED	low energy electron diffraction	PPI	plan position indicator
LF	low frequency	PPM	pulse position or pulse phase modulation or parts per million
LMC	Large Magellanic Cloud		
LPE	liquid phase epitaxy	PRF	pulse recurrence (repetition) frequency
LSA	limited space charge accumulation	PROM	programmable read-only memory
LSI	large-scale integration	PSK	phase shift keying
LTE	local thermodynamic equilibrium	PTM	pulse time modulation
LV	low voltage	PWM	pulse width modulation
M1, M2	magnetic dipole, quadrupole		
MBE	molecular beam epitaxy		
MBPF	many-body perturbation theory		
MCD	magnetic circular dichroism	QED	quantum electrodynamics
MESFET	metal semiconductor field effect transistor		
MF	medium frequency		
MFP	mean free path		
MHD	magnetohydrodynamics	RAM	random access memory
MIC	microwave integrated circuit	RC	resistance-capacitance
MIM	metal-insulator-metal	R & D	research and development
MIS	metal-insulator-semiconductor, management information system	RF	radio frequency
		RFI	radio frequency interference
MMF	magnetomotive force	RHEED	reflection high energy electron diffraction
MNOS	metal-nitride-oxide-semiconductor	RLC	resistance-inductance-capacitance
MOS	metal-oxide-semiconductor	RMS	root-mean-square
MOSFET	metal-oxide-semiconductor field effect transistor	ROM	read-only memory
		RPA	random phase approximation
MOST	metal-oxide-semiconductor transistor		
MP	melting point		
MSI	medium scale integration		
MTBF	mean-time between failures		
MTF	modulation transfer function	SAS	small astronomy satellite
MUF	maximum usable function	SAW	surface acoustic waves
		SCF	self consistent field
		SCL	space charge limited
NAND	not-and (logic)	SCPT	self consistent perturbation theory
NC	numerical control	SCR	silicon controlled rectifier
NDT	nondestructive testing	SDM	space division multiplexing
NEMO	non-empirical molecular orbitals	SEM	scanning electron microscope
NMR	nuclear magnetic resonance	SFE	solar-flare effect
NOR	not-or (logic)	SHF	superhigh frequency
NQR	nuclear quadrupole resonance	SHG	second harmonic generation
NRM	nuclear remanent magnetisation	SIMS	secondary ion mass spectrometer
		SISAM	spectrometer with interference selective amplitude modulation
SMC	Small Magellanic Cloud		
SMS	synchronous meteorological satellite		
S/N	signal-to-noise		
SOS	silicon on sapphire		
SQUID	superconducting quantum interference device		
SSB	single sideband		
SSC	sudden storm commencement		
SST	supersonic transport		
STD	salinity-temperature-depth		
STD	subscriber trunk dialling		
STEM	scanning transmission electron microscopy		
STOL	short take-off and landing		
SWR	standing wave ratio		
SXAPS	soft X-ray appearance potential spectrum		
DAO	orbital astronomical observatory		
OCR	optical character recognition		
ODMR	optical detection of magnetic resonance		
OER	oxygen enhancement ratio		
OGO	orbiting geophysical observatory		
OR	operations research		
OSO	orbiting solar observatory		
OTF	optical transfer function		
PABX	private automatic branch exchange		
PAC	perturbed angular correlation		
PXB	private branch exchange		

TCR	temperature coefficient of resistance
TDM	time division multiplex(ing)
TDMA	time division multiple access
TE	transverse electric
TEA	transversely excited atmospheric
TEM	transverse electromagnetic, transmission electron microscopy
TLD	thermoluminescent dosimeter(-ry)
TM	transverse magnetic
TRAPATT	trapped plasma avalanche triggered transit
TRM	thermoremanent magnetisation
TSC	thermally stimulated currents
TSEE	thermally stimulated exo-electron emission
TTL	transistor transistor logic
TV	television
TW	travelling wave
TWT	travelling wave tube
UHF	ultra high frequency
UHV	ultra high voltage
ULF	ultra low frequency
UMD	unitised microwave devices
UPS	ultraviolet photoelectron spectra
US	ultrasonic
UV	ultraviolet
VDM	vector dominance model
VDU	visual display unit
VLBI	very long base line interferometry
VOR	VHF omnidirectional range
VPE	vapour phase epitaxy
VRC	visual record computer
VSF	vestigial sideband
VSWR	voltage standing wave ratio
VTOL	vertical take-off and landing
VTR	voltage transformation ratio
XPS	X-ray photoelectron spectra

Special List

a. Liquid Crystals

BBEA	4-butoxybenzal-4 ethylaniline
COC	cholesteryl oleyl carbonate
HBAB	hexyloxybenzylidene-p' aminobenzonitrile
HOBHA	p-n-heptyloxy-benzylidene-p-n heptylaniline
MBBA	methoxy-benzylidene-butyl-aniline
PAA	paraazoxyanisole
PAP	paraazoxyphenetole
TBBA	terephthal-bis-butylaniline

b. Orbital Calculation

APSG	Antisymmetric product of separated geminals
CEPA	coupled electron pair approximation
CGTO	contracted Gaussian-type orbital
CHF	coupled Hartree-Fock
CI	configuration interaction
CIEH	charge iterated extended Huckel
CI-HY	configuration interaction Hylleras
CNDO	complete neglect of differential overlap

CPA	coherent potential approximation
CS	coupled states
DECENT	distribution of exact classical energy transfer
DODS	different orbitals for different spins
DV-X α	discrete variational X α method
EB	exponential Born
ECP	effective core potential
EFM	extended Flygare method
EHP	electron-hole potential method
EHT	extended Huckel theory
EPEN	empirical potential energy function based on interactions of electrons and nuclei
ESE	essential structural elements
FPT	finite perturbation theory
FSGO	floating spherical Gaussian orbitals
GCM	generator coordinate method
GHF-NO-CI	generalised Hartree-Fock/natural orbital/configuration interactions
GIAO	gauge-invariant atomic orbitals
GO	Gaussian orbitals
GOO	generalised Overhauser orbitals
GPM	ground potential model
GSO	general spin orbitals
GTO	Gaussian-type orbitals
GVB	generalised valence bond
HAM	hydrogenic atoms in molecules
HFO	Hartree-Fock-Overhauser
HFSL	Hartree-Fock-Slater-Latter
HMO	Huckel molecular orbitals
HOMO	highest occupied molecular orbitals
HORM	hybrid orbital rehybridisation method
ICDF	intermediate coupling Dirac-Fock
IEPA	independent electron pair approximation
INDO	intermediate neglect of differential overlap
INO	iterative natural orbital
IOC- ω	inclusion of the overlap charges in the omega
IRDO	intermediate retention of differential overlap
IVO	improved virtual orbitals
KKR	Korringa-Kohn-Rostoker
LCAO	linear combination of atomic orbitals
LCBO	linear combinations of (semi-localised) band orbitals
LCGO	linear combination of Gaussian orbitals
LCRO	linear combination of Rydberg orbitals
LMTO	linear combination of muffin tin orbitals
LSD	local spin density
LUMO	lowest unoccupied molecular orbitals
MADO	Mulliken approximation for differential overlap
MC PE SCF	multiconfiguration paired excitation SCF
MCZDO	multi-centre zero differential overlap
MEDO	multipole expansion of diatomic overlap
MIEHM	modified iterative extended Huckel method
MO	molecular orbitals
MOCIC	molecular orbital constraint of interaction coordinates

MODPOT	model potential
MRD	multi-reference double excitation
MRINDO	modified Rydberg INDO
MS-MA	Murrell-Shaw-Musher-Amos perturbation theory
MT X α	muffin-tin X α
MWH	Mulliken-Wolfsberg-Helmholz semi-empirical method
NCMET	non-closed shell many electron theory
NDDO	neglect of diatomic differential overlap
NEMO	non-empirical molecular orbitals
NEVE	non-empirical valence electron
NNNDO	neglect of non-neighbour differential overlap
NPOST	non-perturbative open-shell theory
NPSO	non-paired spatial orbitals
NTO	natural transition orbitals
OPHF	orbital polarised Hartree-Fock
OPW	orthogonal plane wave
PCG VB	pairwise correlated generalised valence bond
PCILOCC	perturbative configuration interaction using localised orbitals for crystal calculation
PERTCI	perturbation configuration interaction calculation
PERICI	perturbation configuration interaction
PNO-CI	pair natural orbital configuration interaction
POL	pair orthogonalised Lowdin
PPDP/S	Pariser-Parr-Del Bene-Pople/Segal calculations
PPP	Pariser-Parr-Pople
PRDDO	partial retention of diatomic differential overlap
QDMBPT	quasi-degenerate many-body perturbation theory
RCNDO	Rydberg CNDO
RINDO	Rydberg INDO
RKKY	Rudermann-Kittel-Kasuya-Yosida
RORTE	relaxed orbital relativistic transition energies
RPM	relaxation potential model
SALC	symmetry adapted linear combinations of atomic orbitals
SAMO	simulated ab initio molecular orbitals
SCRF	self-consistent reaction field
SDO	shielded diatomic orbitals
SEHF	spin extended Hartree-Fock
SINDO	scaled INDO
SOG	strongly orthogonal geminal
SOS	sum over states
SOT	sum over triplets
SPA	separated pair approximation
SPHF	spin polarised Hartree-Fock
SPIN-CIPS	spin symmetry adapted generalisation of CIPS
SPPA	self-consistent polarisation propagator approximation
SRAS	symmetry restricted multi-configuration annihilation of single excitations
SRMCASE	symmetry restricted multi-configuration annihilation of single excitations
STO	Slater-type orbitals

STP	Slater transfer Preuss
SUHF	spin unrestricted Hartree-Fock with local approximation for correlations
TDHF	time dependent Hartree-Fock
UCHF	uncoupled Hartree-Fock
UHF	unrestricted Hartree-Fock
VB	valence bond
VGAO	variable gauge atomic orbitals
VRDDO	variable retention of diatomic differential overlap
VSEPR	valence shell electron pair repulsion
c. Organic Substances	
ABS resin	acrylonitrile-butadiene-styrene
DMSO	dimethyl sulphoxide
DPPH	diphenylpicrylhydrazyl
EDA	ethylene diamine
EDTA	ethylene diamine tetra-acetic acid
PMMA	polymethylmethacrylate
PTFE	polytetrafluoroethylene
PVC	polyvinyl chloride
TCNE	tetracyanoethylene
TCNQ	tetracyanoquinodimethane
TGS	triglycine sulphate
TGSe	triglycine selenate
TMMC	tetramethylammonium manganese chloride
TTF	tetrathiofulvalinium
TTT	tetrathiotetracene
d. Reactor Technology	
AGR	advanced gas-cooled reactor
ATWS	anticipated transients without scram
BWR	boiling water reactor
CSM	continuous slowing down models
CTR	controlled thermonuclear reactor
EBR	experimental breeder reactor
ECC	emergency core cooling
ECELR	epithermal critical experiment laboratory reactor
FBR	fast breeder reactor
FFHR	fusion-fission hybrid reactor
FFTF	fast flux test facilities
FTR	fast test reactor
GCFR	gas-cooled fast breeder reactor
HCDA	hypothetical core disruptive accident
HFER	hot fuel examination facility
HFIR	high flux isotope reactor
HTGR	high temperature gas-controlled reactor
HWR	heavy water reactor
LMFBR	liquid metal fast breeder reactor
LOCA	loss of coolant accident
LOFT	loss of fluid test
LWR	light water reactor
MSR	molten salt reactor
PBF	power bursts facility
PBR	pebble bed reactor
PWR	pressurised water reactor
SGHWR	steam generating heavy water reactor
ZPPR	zero power plutonium reactor

Subject Index

Subject

Index

ab initio calculations continued
 CO₂, X-ray K-absorp. spectra, ab initio restricted HF calc. 8-86883
 CO₂, anomalous energy minimum surfaces 8-86791
 CO₂, H⁺, geom. struct., ab initio mol. orbital study 8-86791
 CO₂, effective core potentials calcs. rel. to bond lengths and angles 8-86464
 C₂, cubic, ab initio band struct. calcs. within local density functional formalism 8-87310
 C, II, isotope shift and screening, pseudo-relativistic HF calc. 8-90099
 Cl⁻, pair polarizability, ab initio SCF MO energies 8-70741
 CHCl₃, dispersion quadrupole coupling const., nuclear mag. shielding, geometry depend. 8-82882
 methylene anion, electron affinity, A₁, B₂ T₂ value, ab initio MRD-CI method calcs. 8-50478
 methylene anion, vibronic energy levels, ab initio CI, pot. curves calcs. 8-50479
 methylene ion, pot. energy surfaces of excited states, ab initio GTO SCF CI calcs. 8-58602
 methylenimine, n → π* transition, ab initio SCF MO CI calc. 8-58584
 molecular electron scatt., ab initio theory including polarisation 8-50640
 molecular quadrupole potential functional calc., MO constraint of interaction coordinates 8-74631
 molecules of rows 1-3, equilib. geometries, orbital energies, ab initio rel. to pseudopot. calcs. 8-82613
 monofluoromethane, force constants and IR intensities, ab initio SCF finite difference method 8-86783
 monofluoromethane, X-ray photoelectron spectral line width of F core, ab initio HF calc. 8-62841
 organic molts., IR intensities, analytical orbital hybridisation model, mol. charge distrib. 8-74630
 oxirene, ab initio calc., energy levels and geom. struct. of C₂H₂ isomers 8-62716
 partial atomic charges, calc. from ab initio mol. electrostatic pot. appls. 8-70739
 peptide architectural units, ab initio SCF MO calcs. 8-96004
 photochemical reaction, avoided crossings in excited states, potential energy surfaces 8-76881
 polycetylene type infinite chain cryst., energy bands, ab initio Hartree-Fock orbital calc. 8-60066
 polyatomic closed-shell systems, ab initio Hartree-Fock instabilities 8-78628
 polydiacetylene backbone sequence, electronic structure, unrestricted HF approach 8-63975
 porphine, ab initio CI calcs., electronic absorpt. spectra 8-78639
 propane, vertical electronic spectrum, ab initio MRD-CI calcs. 8-70810
 protein architectural units, ab initio SCF MO calcs. 8-96004
 pyridine, π-electronic structure, ab initio VB calcs. 8-70749
 pyrrole, excited state electronic struct., ab initio SCF and CI calcs. 8-78644
 rare earth ternary borides, R₂R₃B₂ superconduct., re-entrant magnetism, energy band calcs. 8-52140
 silaethylene, triplet carbeneoid isomers, thermodynamic stability 8-90076
 silanes, ab initio calcs. using FSGO, internal rot. 8-82639
 small, medium and large systems, ab initio and approx. rigorous calcs. 8-62714
 surface states, three-dim. crystal ab initio SCF-LCAO calc. of impurity clustering 8-5620
 tetrafluoromethane, X-ray photoelectron spectral line width of F core, ab initio HF calc. 8-62841
 three-atom ab initio energy surface calc. 8-82663
 transition metal complexes, counterintuitive orbital mixing in Geminal-pirical, ab initio MO calcs. 8-90078
 transition metal nitrosyls, ab initio HF calcs. 8-90082
 trifluoroacetic acid, ab initio MO calcs. of geometry, torsional barriers 8-90313
 van der Waals forces between mols., 8-62868
 water, proton affinity, many-body Rayleigh-Schrodinger perturbation theory 8-92497
 Ziegler-Natta type catalysis, reaction pathways, ab initio SCF-LCAO-MO calcs. 8-5689
 Al-H₂O, mol. complex, electronic struct. calcs. 8-66465
 Ar, KCl and KBr, Auger electron spectra, obs. and relativistic multi-configurational Dirac-Fock calc. 8-50524
 Ar, excited state pot. curves, ab initio CI calc. 8-78643
 ArF₃ laser emission, ab initio configuration interaction calcs. on electronic states 8-63083
 ArF₃ electronic states, ab initio RHF CI calcs. 8-66474
 ArHCl, ab initio FGO calc. 8-50467
 ArKr⁺, absorpt. spectra, ab initio calc. of potential energy curves 8-74568
 ArO₂ laser, long-range electronic states, ab initio configuration interaction calcs. 8-63084
 AuH, AuCl, ZZ, 8-86766
 BH, electron density, basis set, electron correlation effects 8-74580
 BH₃, spin-extended Hartree-Fock ab initio calculations for small radicals 8-70746
 BN, cubic, ab initio SCF calcs., band structure ground state props. 8-51891
 B₂N₂H₂ electronic spin, magnetic susceptibilities, ab initio calcs. 8-74571
 B(OH)₃, hydrogen bond, ab initio MO calcs. 8-58588
 BeH, spin-extended Hartree-Fock ab initio calculations for smaller radicals 8-70746
 BeH₂, pot. energy curve, minimal basis ab initio VB calcs. 8-50477
 C⁺, effective valence shell Hamiltonian, ab initio calcs. 8-82610
 C⁺, effective valence shell Hamiltonian, ab initio calcs. 8-82611
 C⁺, (n=1,2,3) effective valence shell Hamiltonian, ab initio calcs. 8-82611
 C₂, electron spectrum, ab initio MRD CI calcs. 8-90089
 C₂H₂, vibrational SCF, CI, CEPA-RNO structure and energy calcs. 8-94197
 CH₃SiH₃, ab initio GTO calc. 8-94187
 CN⁻, ab initio full CI calcs. 8-50480

ab initio calculations continued

- CO, X-ray K-absorpt. spectra, vibr. fine struct., ab initio restricted HF calc. 8-86883
- CO₂, anomalous energy minima surfaces 8-86791
- CO₂, H⁺, geom. struct., ab initio mol. orbital study 8-62939
- Cd, effective core potentials calcs. rel. to bond lengths and energies 8-66464
- CdS, cubic, ab initio band struct. calcs. within local density functional formalism 8-87910
- Ce II, isotope shift and screening, pseudo-relativistic HF calc. 8-90096
- Cl⁻, pair polarisability, ab initio SCF MO energies 8-70741
- CHCl₃, deuteron quadrupole coupling const., nuclear mag. shielding, geometry depend. 8-58586
- CoCl₂, electronic energy levels, calc. by conventional and X α Hartree-Fock methods 8-66470
- CoO₂, ionisation, electron density relax. effects, ab initio calcs. 8-50466
- CoO₂, ionisation, electron density relax. effects, ab initio calcs. 8-50466
- CS, discrete level raising into far continuum, oscillator strength to shape reson. transfer 8-78624
- CuCl₂, electronic energy levels calc. by conventional and X α Hartree-Fock methods 8-66470
- F+H₂→HF+H energy profile, minimal basis, ab initio VB calcs. 8-50477
- F₂CS, pot. surfaces, X¹A₁, a³A₂ and a³A₂(b₁) states, ab initio SCF calcs. 8-86795
- FH, reactive processes, ab initio MCSCF-CI and dimeric in mols. calc. 8-56881
- FHCl₃, deuteron quadrupole coupling const., nuclear mag. shielding, geometry depend. 8-58586
- FHFH, deuteron quadrupole coupling const., nuclear mag. shielding, geometry depend. 8-58586
- FeF₂, electronic states, ab initio calcs., UV spectrum, elucidation 8-74570
- H+Br₂→HBr+Br, pot. energy surface, ab initio generalised valence bond calc. 8-73026
- H+methane→methane+H, nucleophilic substitution, ab initio pot. energy classical trajectory anal. 8-68886
- H₂, photoionisation, body-frame Hund's case ab initio description 8-94295
- H₂⁺, nonadiabatic vibrational energies, ab initio calcs. 8-90142
- H₂+Ar, vibro energy transfer rate, ab initio calcs. 8-82821
- H₂, CI calc. of three dimens. pot. energy surface 8-56882
- H₂, three atom ab initio energy surface calcs. 8-82663
- H₂⁺, ground and excited state pot. energy surfaces and geom. struct., SCF and CI calcs. 8-78769
- H₂⁺, (n=3,7,9,11), stability, structure, ab initio MO calcs. 8-74810
- HC, radical, electron affinity, ab initio SCF and CI calcs. 8-50468
- HCN and HNC, analytic functions from pot. energy surfaces 8-62743
- HCN, dipole moment derivative sign anomaly, CGTO, ab initio calc. 8-74795
- HCN, HNC, electronic reorganisation, with core ionisation 8-94196
- HCN, SCF, ab initio ground state pot. energy surface, geometry, rel. to HCN⁻ 8-78646
- HCN⁻, SCF, ab initio ground state pot. energy surface, geometry, rel. to HCN 8-78646
- HCN⁺, photoelectron spectra of third electronic state, ab initio calc. of pot. energy surface 8-70871
- HCO₂⁺, geom. struct., ab initio mol. orbital study 8-62939
- HCl, bond dependence of dipole polarisabilities 8-74573
- HD⁺, nonadiabatic vibrational energies, ab initio calcs. 8-90142
- HF, bond dependence of dipole polarisabilities 8-74573
- HF, force consts., ab initio CI calcs. (French) 8-90093
- HF, pot. energy curve, minimal basis, ab initio VB calcs. 8-50477
- HNO₂, HON, electronic reorganisation, with core ionisation 8-94196
- H₂⁺, ab initio calc. of three lowest states 8-62711
- H₂O, electron density, basis set, electron correl. effects 8-74581
- H₂O, force constants, ab initio CI calcs. (French) 8-90093
- H₂O, free energy of liq. water, ab initio Monte Carlo calc. 8-83975
- H₂O+Li⁺, ab initio GTO calc. of vibro intensity changes of spectroscopic parameters 8-58583
- H₂O₂, geometry, internal rot. barriers, electron correl. calcs. 8-70751
- HOCl, photodissoc., ab initio SCF CI calcs. 8-50604
- HPO, mol. struct. and props., ab initio, calc. Gaussian lobe orbital 8-62713
- HS₂, ground and first excited states, geometry, ab initio SCF calcs. 8-50657
- HS₂, rotamers, electronic and geometrical structures, ab initio floating GO basis calcs. 8-74572
- H₂S, electron density, basis set, electron correl. effects 8-74581
- H₂S, gas-phase, states in valence photoelectron spectrum 8-94284
- H₂S, KLL Auger spectrum, obs. and ab initio SCF CI calcs. 8-50654
- H₂O, ground and first excited states, geometry, ab initio SCF calcs. 8-50657
- H₂S and HNSI, analytic functions from pot. energy surfaces 8-62743
- H₂S and HNSI isomers, MRD-CI calcs. of struct. and stability 8-82635
- He+H₂, collision-induced dipole, ab initio VB calc. 8-94202
- He+H₂, Van der Waals pot., ab initio SCF model 8-74728
- HeNO₂, molecular geometry and stability 8-90075
- HeH, effective core potentials calcs. rel. to bond lengths and energies 8-66464
- HgH₂, HgCl₂, ZZ, 8-86767
- KrF, electronic states, ab initio POL CI calcs. 8-66474
- KrF, fluorescence spectrum, theoretical modelling using electronic potential curves 8-63086
- KrF, laser emission, ab initio config. interaction calcs., on electronic states 8-63083
- KrO, laser, low-lying electronic states, ab initio config. interaction calcs. 8-63084
- Li (100), O₂ adsorption, cluster models, ab initio HF LCAO theory 8-71978
- Li⁺, pair polarisability, ab initio SCF MO energies 8-70741
- Li-H₂O (ethylene) 8-66465
- Li-like ions, fine struct. in 2s² 1P and 1s2s² 1P states 8-66471
- Li₂, BO hypersurface and vibronic states, coupled electron pair approx. 8-94203
- LiBH₄, pot. surface and geometry, ab initio calcs. 8-86771
- LiH, positron affinity, ab initio LCAO MO SCF calc. 8-82870

ab initio calculations continued

- LiH⁺, spin-extended Hartree-Fock ab initio calculations for small radicals 8-70746
- MnCl₂, electronic energy levels calc. by conventional and X α Hartree-Fock methods 8-66470
- N+H₂⁺, triplet state ab initio CI pot. energy surfaces 8-74729
- N⁺+H₂, triplet state ab initio CI pot. energy surfaces 8-74729
- N₂, X-ray K-absorpt. spectra, vibr. fine struct., ab initio restricted HF calc. 8-86883
- NH₃⁺, triplet state ab initio CI pot. energy surfaces 8-74729
- NH₃+SO₂, donor-acceptor adduct form., ab initio calcs. 8-82612
- N₂H₂(N₂D₂), ground and first excited state small vibr. coupling, ab initio CI calc. 8-62791
- NH₂INH₃, β decay effect on H-bond, ab initio LCAO SCF MO calc. 8-76894
- NO₂, vertical electronic spectra, ab initio calcs. 8-66538
- NO₂⁺, ab initio VB wave functions, π -electrons 8-70748
- NO₂⁺, vertical electronic spectra, ab initio calcs. 8-66538
- NO₂⁺, vertical electronic spectra, ab initio calcs. 8-66538
- N₂O⁺, pot. energy hypersurface characts. calc. in O⁺+N₂→N+NO⁺ react. 8-60996
- NH⁺(¹⁵NH⁺)(¹⁴ND⁺), ab initio CI calc. A₁ type doubling in X² Π states 8-82714
- Na₃, electronic struct., pot. energy surface, ab initio CI study 8-70996
- NaF, ab-initio calc. of cohesion energy, compressibility and density 8-71782
- NaK, ab initio and pseudopot. energy curves 8-90068
- Na(1s), X-ray photoelectron spectrum, binding energy, at. compared with metal 8-70800
- Ne+H₂, Van der Waals pot., ab initio SCF model 8-74728
- Ne, H₂ clusters, ab initio LCAO MO SCF calc., struct. and energy 8-66704
- Ne, H₂ clusters, ab initio LCAO MO SCF calc., struct. and energy 8-66704
- NiF₂+CO, Ar matrix isolated, ab initio MO calcs. 8-92458
- Ni(Ni)-ethylene cluster complex 8-82641
- O₂⁺, ab initio pot. curves of X² Π , A² Π , a² Σ , Σ , states 8-66483
- O₂⁺, ab initio CI STO calc. 8-74585
- O₃, ab initio projected unrestricted Hartree-Fock calcs. 8-58582
- O₃, ab initio VB wave functions, π -electrons 8-70748
- O₃, approximate spin extended HF calcs., singlet and triplet states 8-78621
- OCS photolytic laser, for fusion research 8-59002
- OH, spin-extended Hartree-Fock ab initio calculations for small radicals 8-70746
- OH+CO₂→HCO₃ react., MO-LCAO-SCF calcs., energy barrier 8-76846
- PN, valence state interactions, ab initio and semiempirical estimates 8-74567
- Re₂Cl₂, Re₂Cl₃, ab initio calcs. of metal-metal bond 8-82633
- SF₆, KLL Auger spectrum, obs. and ab initio SCF CI calcs. 8-50654
- SN⁺, struct. vibr. spectra, ab initio calcs. 8-66475
- SN⁺, struct. vibr. spectra, ab initio calcs. 8-66475
- SO₂, ground state, ab initio and MOD POT calcs. 8-66466
- SO₂, KLL Auger spectrum, obs. and ab initio SCF CI calcs. 8-50654
- SOH, ground and first excited states, geometry, ab initio SCF calcs. 8-50657
- SbH₃, inversion barrier, ab initio SCF calcs. 8-78615
- Si (111), surface relax., mol. SCF calcs. 8-91522
- SiH₄, ab initio Hartree-Fock SCF-LCAO-MO method 8-94195
- SiH₄, Si-Si double bond, ab initio GO calc. 8-94187
- SiH₄, barrier to internal rotation 8-66680
- SiH₃F₂, ab initio Hartree-Fock SCF-LCAO-MO method 8-94195
- SiH₃F₂, ab initio Hartree-Fock SCF-LCAO-MO method 8-94195
- SiO₂, mol., ab initio SCF calcs., ground state stability, struct., vibr. freqs. 8-86781
- TiSe₂ (IT), structurally induced semimetal-to-semicond. transition, ab initio LCAO calc. 8-51896
- U, ab initio effective core pots., relativistic corrections 8-50483
- Xe+Ag, quasimolecular L and Ag L X-ray excitation thresholds, electron correl. calc. and expt. 8-78793
- XeF₂, laser emission, ab initio config. interaction calcs. on electronic states 8-63083
- XeF(Cl)(Br)(I) covalent and ionic states, spectroscopic props., ab initio CI calcs. 8-90092
- XeO, laser, low-lying electronic states, ab initio config. interaction calcs. 8-63084
- Xe₂⁺, Xe₂⁺, Xe₂⁺, pot. energy curves, relativistic ab initio effective core pots. 8-86800

abacs see nomograms

aberrations

- aberrations in optics and particle optics only
- see also lenses; optical instrument testing; particle optics
- achromatic imaging, of distant objects, with plane, concave holographic gratings 8-94372
- acoustic-optic frequency shifter, beam quality, heterodyne interferometry meas. 8-79127
- annular pupil system, use of orthogonal polynomials, app. to Fraunhofer diff. 8-50714
- aspheric surface primary characts., analysis using Delano diagram (German) 8-90381
- aspherical deformations, rotationally symmetrical, representative model (German) 8-90375
- astigmatic coherent processor analysis 8-78927
- astigmatism, due to surface cylindricity, vectorial representation (Russian) 8-87121
- astigmatism of central and peripheral cornea, asymm. meas. by photokeratometry 8-64981
- birefringence elements in optical systems, generalisation of pupil function 8-55310
- chromatic, CF chromatic aberration-free projection system, optical microscopes appl. 8-89534
- chromatic aberration first-order theory, secondary spectrum correction with common glasses 8-90382
- coma, optimally balanced, influence on refractive images of annular object (Czech) 8-50710
- condenser synthesis, astigmatism-free, using spherical mirrors 8-50887
- curved crystal spectrometer geometrical aberrations: analytical and numerical study 8-78002

aberrations continued

Deflection distortion in scanning electron-beam systems 8-74835
 design techniques, for desk and pocket calculators 8-71181
 diffracted wave field aberrations 8-94376
 diffraction images of bar and edge objects, influence of optimum balanced coma 8-74850
 diffraction patterns of off-axis gaussian beams in optical system with astigmatism and coma 8-55309
 diffuse system design, optimum conditions, appl. to optical system 8-50886
 electron beams, aberration averaging, image and deflection component design 8-74830
 electron microscopy, HV, accurate stigmating using optical diff. pattern of micrograph 8-49941
 electron optics, spherical aberration, for teaching 8-54135
 electrostatic mirror, axisymmetric, two-electrode paraxial props., aberrations 8-71025
 electrostatic round lenses, asymptotic aberration coeffs., systematic transformations 8-74828
 elliptical square-law medium, astigmatic Gaussian beams 8-94427
 eye, chromatic stereopsis, opposition of photometric and dioptric factors (*Italian*) 8-56986
 eye, fish, chromatic aberration and effect on refr. state 8-64985
 eye, longit. chromatic aberration meas. by chromoretinoscopy 8-56967
 eye chromatic aberration, effects on accommodation response 8-69042
 Fabry-Perot etalon, optical thickness error compensation 8-49889
 first surface simplified aspherising procedure (*Russian*) 8-63013
 Gaussian beam, free-space propagation, wave eqn. solns. 8-87008
 Gaussian beams, off-axis, aberrated Fraunhofer diff. patterns 8-66753
 glass sampling, of simplex variants and of multiplets (*German*) 8-90484
 grating mounting with large aberrations, aberration balancing 8-66906
 grille spectrometer efficiency, effect of aberrations 8-70195
 half-symmetric image geometry 8-66773
 holographic binary information image reconstruction, aberrations, shrinkage effects 8-78967
 holographic gratings formed on aspheric substrates for aberration correction 8-63187
 holographic microscopy, aberrations, due to wavelength shift, elimination technique 8-74861
 holographic optical element design and construction 8-55315
 holographic screens production with third order spheric aberration compensation (*Russian*) 8-90404
 Hunt aberration generator 8-59119
 interferometry, multiwavelength testing using modified Twyman-Green interferometer 8-59169
 ion microscope aberrations and image form., study by magnetic anal. of beam from HF source 8-55293
 laser beam, intensity mapping aberrations 8-66855
 laser beam, phase compensated, propag. through atm. turbulence 8-83012
 laser beam thermal lensing in SiO₂ plate 8-63148
 laser self-focusing suppression through low-pass spatial filtering and relay imaging 8-74938
 laser system, high energy, optical distortion, active control 8-83019
 laser system, high energy, optical distortion sources 8-83018
 lens, multi-element, defective surfaces, tilt meas. 8-66886
 lens model of high-energy atm. laser propag. 8-69454
 lens optimisation using Walsh functions, FEE-based criterion 8-79097
 lens system design with extended depth of focus, Version 14 optimisation program 8-90489
 lenses, crossed, electron optical image position, ang. magnification aberration 8-50691
 lenses, calc., thin, modified relations using Caddington variables (*Czech*) 8-50885
 magnetic deflection systs., aberration correction 8-66740
 magnetic spectrometer design with corrected second-order aberrations, theory 8-89604
 Marechal evaluation of Strehl definition, Dini expansion of wave aberration function 8-71043
 mass spectrometer uncoupled, sector charged particle analyser, image props. 8-70218
 maximum Strehl intensity ratio intensity ratio image plane determ., remarks (*German*) 8-71038
 metallic film apodising and attenuating filters, phase shifts and aberrations 8-90514
 monochromatic aberrations, third order, correction of four lens objective 8-87123
 monochromators with off-axis mirrors, distortion and split-image curvature 8-59141
 objective, 3-mirror design, optical scheme 8-55431
 objective, concentric, longitudinal spherical aberrations calc. method (*Russian*) 8-71184
 optical collimating system alignment by shearing plate 8-79126
 optical relay, system design, secondary colour reduction 8-83067
 optical systems, refractive index nonlinearity influence (*Russian*) 8-58921
 photographic objective axial ray bundles achromatisation and Staebli-Ligotsky isoplanasic condition (*Russian*) 8-65988
 precision objectives, high resolution, image-forming quality (*German*) 8-87120
 prism, cone-shaped, combined elec./mag. fields, relativistic particle optics 8-50690
 prism, wedge-shaped, combined elec./mag. fields, relativistic particle optics 8-50689
 radiation pyrometer temp. meas., effect on metrological characts. 8-77920
 refractive index gradient tolerance in optical elements 8-71179
 Schmidt telescopes, achromatic condition (*Japanese*) 8-89062
 space charge ion optics, influence of chromatic aberrations 8-55294
 spherical mirror folded cavities, astigmatism elimination and regulation (*Chinese*) 8-90431
 third order formulae for optical systems with Fresnel surfaces (*Russian*) 8-63014
 transmission grating, facet-type, aberrations for cosmic X-ray and XUV spectroscopy 8-85851
 uncentred surface system, field aberrations of object meridional points 8-82923
 unstable optical resonators with tilted spherical mirrors, design eqns. 8-74930

abrasion

see also *hardness*; *wear*

brittle abrasive material, rating capability for elastic deformation 8-56680
 diamond, polycrystalline tool, wear in rock removal processes 8-64724
 ductile metals, velocity depend. of erosion by solid particles, at low incidence angles 8-87311
 friction machine, residual stresses meas., appl. to wear resist., surface wear 8-60906
 Haynes Stellite 6B, Al₂O₃ particle erosion of surface, SEM obs. 8-88545
 Haynes Stellite 6B, particle erosion damage, TEM obs. 8-88546
 impact, abrasion, wear, review (*German*) 8-88536
 metal wear energy balance under abrasive and boundary friction, expt. 8-85006
 metals, effects of microstruct. on wear resistance 8-92367
 optical glass surfacing, using loose abrasives, impregnated diamonds and electro-plated diamonds 8-50956
 phenolic resin, linen impregnated, abrasion, SEM obs. 8-64742
 PMMA, abrasion, SEM obs. 8-64742
 polyethylene-Fe, wear resistance on steel counterbody, exam. 8-68826
 powder, ultra fine, surface roughness effect on formation by rotating friction mill (*Japanese*) 8-95709
 PTFE, abrasion, SEM obs. 8-64742
 Relite-base alloy compositions wear caused by sliding abrasive material stream 8-95813
 rocks hardness and abrasiveness determ., suggested methods 8-96313
 solid lubrications dynamics, obs. using Micro Contact Imager 8-85002
 steel, abrasive wear resistance, effects of microstruct. 8-92367
 steel, stainless, austenitic, CC Ni-Al, γ -phase, fracture mechanical aspects of abrasive friction, wear, chip formation 8-72865
 transparent materials, defective surface layer formation during abrasion, laser-induced breakdown (*Russian*) 8-53007
 wear mechanism review 8-72891
 wear resistance, hardfacing, review 8-72937
 wear resistance, surface treatments, selection procedure, review 8-72892
 Al, polycrystalline, abrasion, deform., fatigue, study by exoelectron microscope (*Japanese*) 8-74108
 Al-Al₂O₃ eutectic, abrasive fragmentation (*Czech*) 8-64715
 Al₂O₃, abrasive, wear in simulated hot grinding 8-56784
 Fe, cast, abrasive wear rel. to lamellar or spheroidal graphite content (*German*) 8-85000
 Fe, cast, white Cr alloyed, wear resistance, effect on abrasive hardness 8-64722
 Fe, degree of charging of surfaces polished by TiC and synthetic diamond micropowders 8-60880
 Fe-based materials, wear resistance, surface hardening processes, review 8-72894
 Fe-C-Cr-Mo(Ni)(V), white cast, effect of abrasion on carbide microstructure (*German*) 8-88540
 SiC, abrasive, wear in simulated hot grinding 8-56784
 Ti, degree of charging of surfaces polished by TiC and synthetic diamond micropowders 8-60880
 Ti-Cr, sintered, friction and wear, structural factors 8-60843
 Ti-Cr-TiC, sintered, friction and wear, structural factors 8-60843
 Ti-TiC system, sintered, friction and wear, structural factors 8-60843

abrasive wear see *abrasion*

absolute gravity see *gravity*

absolute pressure measurement see *pressure measurement*

absolute temperature see *temperature*

absorbers (surge) see *surge protection*

absorption
 for absorption of substances see *sorption*
 see also *acoustic wave absorption*; *electromagnetic wave absorption*
 No entries

absorption spectra see *spectra*

absorption wavemeters see *wavemeters*

abundance ratio see *element relative abundance*; *isotope relative abundance*

a.c. generators
 fusion reactor, ohmic heating energy storage for power reactor, costing 8-58495

a.c. network analysers see *network analysers*

acceleration
 see also *acceleration measurement*; *accelerometers*
 ball, radius of gyration determ., using air track, undergrad. demonstration 8-49606
 charged body free fall motion in gravit. field, field energies and equivalence principles 8-49740
 explosion-induced accel. of cylindrical metal liners, form stability anal. 8-83425
 flow, separated, supersonic, caused by throttling in round duct 8-63446
 humans exposed to centrifugation, optoelectronic ear oximeter calibration 8-92734
 ion collective acceleration, by intense relativistic electron beam, localised pinch model 8-87460
 Phobos secular acceleration, value and origin 8-89100
 plasma sheet, adiabatic accel. of ions induced by convection 8-88997
 pulmonary blood flow, spatial distribution in dogs in increased force environments 8-92664
 quasar absorption line clouds, radiative accel. 8-57683
 relativistic negative acceleration components 8-86058
 solar flare particles pulsed accel., plasma turbulence, ion-acoustic and Langmuir waves 8-96450
 solar wind heating and acceleration, implications of coronal fast waves evanescence 8-89147
 statistical particle acceleration models for Cassiopeia A supernova remnant 8-57606
 steady plane isochoric flows, acceleration and pressures 8-81845
 teaching of accelerated motion, by 'racetrack' game 8-62022
 water drops accel. to terminal vel., drag coeff. 8-61506

acceleration measurement
 doubly integrating vibration accelerometer random input anal. (*Russian*) 8-77873
 gas gravimeter use for variable linear acceleration meas. 8-77875
 hand-arm energy dissipation in using vibratory tools and accel. levels 8-96116

accelerators (particle) *see particle accelerators*

accelerometers *see also acceleration measurement*

- Cactus, on Castor satellite, Earth's radiative balance meas. (French) 8-81530
Cactus accelerometer, in-orbit performance on D5B satellite 8-61698
doubly integrating vibration accelerometer random input anal. (Russian) 8-77873
finger tremor amplitude and freq. artefact reduced routine meas., portable equipment (German) 8-85407
pendulum vibration errors (Russian) 8-77874
seismic sensors, mechanical frequency charact., influencing factors (Japanese) 8-85722

accidents

- see also electric shocks; explosions; safety*
accident handling in Federal Republic of Germany 8-53530
aircraft crashes in thunderstorm downbursts, analysis 8-53693
CEGB nuclear power station emergency arrangements 8-55050
CEGB nuclear power station emergency monitoring procedures 8-55053
criticality accidents at facilities processing fissile material, charact., detect. and action procedures (French) 8-55054
fast reactor whole core accidents, fission products role 8-54854
fusion reactors, air detritiation operation, computer model and scale expt. 8-66413
gamma radiation dosimetry, Al_2O_3 TLD 8-57076
GCFR core support structural assembly, seismic response via modal synthesis 8-89942
HTGR, consequence anal. of hypothetical accidents, core heatup and afterheat removal 8-58381
HTGR hypothetical accidents, consequences following breach of primary circuit and safeguard failure (German) 8-58390
HTR, expt. JAERI, safety anal. of fission product behaviour and hypothetical accident (Japanese) 8-66330
HWR, explosive rupture of power channel pressure tube 8-70605
investigation, advance prep. 8-57083
ionising radiation, conclusions from unusual events in German Democratic Republic 8-53520
ionising radiation exposure, dose estimation using TSC in human nail 8-73253
LMFBR head closures, dynamic struct. response to HCDA 8-70617
Lucens reactor accident, alarm and surveillance 8-50283
LWR 1300 MWe system, design of containment to withstand core melt 8-66335
LWR core meltdown, activity release and aerosol charact. 8-82469
LWR hydrogen formation during core melt accident 8-50267
LWRs, accident prevention study 8-66356
molten fuel-coolant interaction studies, simulated reactor accident, wind-scale shock tube rig 8-58363
National Arrangements for Incidents Involving Radioactivity, NAIR 8-65136
neutron dosimetry methods for accidental exposures, Czechoslovak intercomparison 8-57075
nuclear, HCDA, REXCO code, comparison with flexible vessel expts. 8-70618
nuclear accident features affecting emergency measures 8-55055
nuclear accident phenomena, human elements (French) 8-57084
nuclear accidents, use of mobile remote-handling equipment (French) 8-53525
nuclear accidents in power stations of Electricité de France, protection organisation (French) 8-55049
nuclear emergency conditions, monitoring and handling 8-57082
Nuclear Energy Research Centre, Mol. Belgium, emergency plan organisation in event of major accident (French) 8-53527
nuclear fuel transportation in Canada, emergency planning 8-50411
nuclear plant equipment response to aircraft impact 8-50416
nuclear plant risks assessment 8-50281
nuclear power plant, aircraft impact, simplified derivation of reaction-time history 8-89958
nuclear power plant, fast alarm system to optimise protection of public 8-55048
nuclear power plant, fire hazard 8-50269
nuclear power plant emergencies, prevention of excessive irradiation of staff and population (Russian) 8-50286
nuclear power reactor emergency medical assistance programmes 8-53532
nuclear power station, due to loss of coolant, multiple-element model and computer solution 8-66358
nuclear power station, hot water leakage from first loop, 22.8 MPa initial pressure, flow charact. 8-66357
nuclear power stations in Italy, district emergency exercises 8-55052
nuclear reactor accidents, meas. of crit. environmental exposure by I radioisotopes 8-57081
nuclear reactors, molten fuel-coolant interaction modelling, INTER and CEFRA (Czech) 8-66352
nuclear safety exercises carried out in French industrial facilities (French) 8-55051
PWR, determ. of typical accidents and consequences, rel. to emergency planning (French) 8-50285
PWR, peak cladding temp. sensitivity to LOCA reflood parameters 8-86639
radiation accident casualties, organisation and planning of medical aid (French) 8-53528
radiation accident casualty, organisational forms of medical care in German Democratic Republic 8-53529
radiation accident caused by ^{192}Ir radiography source 8-53514
radiation accident handling, conf., Vienna, Austria (Feb.-Mar., 1977) 8-53518
radiation accidents, effects on public, casualty management 8-53519
radiation accidents, follow-up study programme for irradiated persons 8-53522
radioactive glove box accident, surgical treatment of wound contaminated by ^{239}Pu and Am (French) 8-53521
radiological accidents, operational organisation (French) 8-53531
Radiological Emergency Response Planning and Preparedness Training Programmes, USA 8-57079
radiological emergency response training programme 8-57080
radiological major accidents, USA planning guides 8-53526
radionuclide users in Israel, surveillance and accident prevention 8-57077

accidents continued

- reactor containment liner seismic reliability under statistical uncertainty, cracking 8-89948
Reactor Safety Study (Wash-1400) and implications for radiological emergency response planning 8-50284
risk evaluation of high level waste solidification plant 8-50273
steam generator, modular, liquid Na heated, pressure and temp. loading in breakdown situation (Czech) 8-50264
Swiss emergency organisation for nuclear and chemical accidents 8-57078
Swiss Federal Institute for Reactor Research emergency organisation 8-55047
thermal explosions, fragmentation requirements for detonation 8-71368
 ^{60}Co 20 Ci source, site radiography incident 8-53523
 ^{60}Co 3000 Ci source, accidental fall and retrieval in teletherapy room 8-53524
I radioisotopes, high efficiency mixed species air sampling, readout and dose assessment system 8-57074
 $^{106}RuO_4$ in lung, in vivo meas. and dosimetry 8-53515

accommodation coefficient *see sorption*

accumulators *see secondary cells*

acidity *see pH*

acids, organic *see organic compounds*

acoustic analysis

- atmospheric infrasound waves recording method and computer anal. (Russian) 8-65407
finite element, automobile exhaust system design appl. 8-51003
layer potentials for two dimensional mechanical vibrations (French) 8-59337
source location on spherical or plane surface 8-92421

acoustic applications

- see also ultrasonic applications*
atmosphere acoustic sounding technique, appls. to siting studies 8-81467
beam forming with vibrator arrays, seismic field tests near Tulsa and Handy 8-61338
diagnosis using nonlinear effects, asymptotic feasibility anal., props. of layer on halfspace object 8-63248
Doppler sounder for wind profile meas. in boundary layer 8-65413
extrusion, benefit of vibrations 8-51135
free gas concentration in liquids, rapid anal. by acoustic method 8-91041
gas-liquid mixtures, flowing, gas conc. meas., acoustic method 8-59448
microscopy, recent developments (Japanese) 8-79177
microscopy, scanning acoustic, Gray scale 8-94494
nuclear power plant diagnostic system using noise anal. 8-50279
reflection acoustic microscopy, contrast 8-55533

acoustic arrays

- atmospheric echo sounder, design from loudspeaker elements 8-87226
beam forming with vibrator arrays, seismic field tests near Tulsa and Handy 8-61338
beamforming a towed line array of unknown shape 8-63230
conformal array beam patterns and directivity indices 8-55523
dynamically focused US diagnostic phased array 8-61232
high resolution cross sensor beamforming for uniform line array 8-50988
hydrophone array response calc. errors due to two dimensional beam pattern assumption 8-66972
irregular, amplitude shading coeffs., steering, beam pattern generation 8-83178
marine seismic refl. data acquisition using extended arrays 8-77340
mutual interaction of nearest neighbours in compact planar array 8-50979
parametric acoustic array max. conversion efficiency anal. 8-71242
parametric acoustic receiving array vibration sensitivity anal. 8-66971
parametric array, selected mode excitation in shallow-water sound propagation 8-59182
parametric radiator, influence of dispersive medium on charact. 8-94470
passive ranging of acoustic source 8-71241
penetration into a sand sediment of difference-frequency sound generated by a parametric array 8-63227
performance sensitivity of array detectors to a priori spatial knowledge 8-55524
scattering of sound by sound, relation to the parametric receiving array 8-90563
sparse array technique, min. output variance, S/N ratio 8-83177
steered planar nearfield transducer calibration array 8-59214
towed-line array, iterative technique for, ambient-noise, horizontal-directionality est. 8-55525
transmit/receive 2D ceramic piezoelectric arrays, construction and performance, medical, NDT appls. 8-87223
undersea acoustic holographic transducer array development 8-59209
underwater C-mode US imaging by electronically scanned coaxial circular spherical receiving array 8-59222

acoustic delay lines

- see also ultrasonic delay lines*
chalcogenide glasses, photoelastic props. 8-55420
SAW delay line, variable, using magnetostrictive metallic glass film overlays 8-63240
 $LiNbO_3$, ion implanted, acoustic model of SAW delay lines (French) 8-55540

acoustic detectors *see acoustic transducers*

acoustic devices

- see also acoustic delay lines; acoustic generators; acoustic microwave devices; acoustic parametric devices; acoustic radiators; acoustic receivers; acoustic resonators; acoustic transducers; bells; surface acoustic wave devices; ultrasonic devices*
amplitude-frequency charact., temp. instability effect of matching layer 8-59220
conical acoustic lens, fabrication and test results 8-51019
conical acoustic lens, opto-acoustic feasibility design 8-51020
filter components for ANSI standard psychoacoustic testing 8-83198
multichamber sound reflector, design parameters 8-94500

acoustic dispersion

- see also ultrasonic dispersion*
multimode waveguide with uneven walls, sound attenuation 8-83147
plasma, acoustic wave interaction, diagnostics appl. 8-83541

acoustic dispersion continued

- polymers, highly oriented, elastic wave dispersion relations 8-51618
 quasi-Lorentz gas, Temkin-Dobbins formula 8-55502
 solid, phase and group vels., determ. for dispersive waves 8-81848
 US materials testing, three layered medium, dispersion relation for interference waves 8-72980

acoustic echoes *see echo***acoustic emission**

- see also ultrasonic materials testing*
 B-Al₂O₃-Na₂O, AE during breakdown under Na⁺ transport 8-67860
 aviation and astronautics, conference, Tel Aviv (1977) 8-81517
 defect coordinates in anisotropic shells, plates, determination, using acoustic emission 8-80707
 detection, calibrated capacitance transducer 8-71256
 detection system sensitivity, direct comparison method 8-56848
 elastic stress monitoring 8-53176
 electroacoustic, analytic and diagnostic equipment 8-63249
 fatigue crack growth in aircraft wing test, AE detection 8-60925
 fibre reinforced composite failure analysis 8-80691
 fracture toughness testing, inspection technique 8-68860
 gas flow in duct, self-excited oscillations 8-55670
 glass, Gaussian size distrib. of rigid particles, AE anal. 8-62181
 glass sphere mixture, polydisperse system, AE anal. 8-62180
 granodiorite, fracture under uniaxial compression, mech. and AE meas. (Japanese) 8-56748
 industrial appl. 8-68850
 intensity, calc. using fracture kinetic concept and phenomenological model 8-85110
 Langmuir soliton formation with ion-acoustic density emission 8-75328
 liquid crystals, defect dynamics study 8-91232
 monitoring difficulties overcome by optical detectors 8-60968
 NDT of aircraft struct. 8-53177
 particle size distrib. charact. by AE 8-62179
 plastically deformed crystal, bubble formation mechanism in liq. He (Russian) 8-85066
 porcelain enamel layers on steel, H₂ induced fracture of layers 8-76752
 pressure vessels, thin-walled, containing surface flaws, fracture mechanics and acoustic emission exam. of failure 8-84981
 rock mechanics, appl. of AE (Japanese) 8-56845
 rocks, failure processes and AE under compression (Japanese) 8-56749
 signal recovery technique appl. to AE anal. of martensitic transformation 8-60965
 simulation by SiC grain brittle fracture and elastic sphere impact, freq. anal. 8-55504
 sound production in moving stream, Lighthill's acoustic analogy, jet noise 8-79313
 source localisation, application of correlation techniques 8-87220
 source location on spherical or plane surface 8-92421
 steel, high strength, alloy, initiation of cracks at delayed fracture, AE study 8-72868
 steel, low, effect of pressurisation on acoustic emission charact. during tensile testing 8-92304
 steel, Si-Mn-Ni-Cr-Mo, acoustic emission during stress corrosion cracking appl. to materials testing 8-53042
 technological strength and nondestructive methods of testing during heat treatment 8-85090
 temperature dependence 8-53136
 transducer construction principles evaluated 8-59239
 US cavitation emission from insulated plant tissues 8-59185
 Al, acoustic emission under plastic deform., spectral anal., dislocation mean free path 8-84934
 Al alloy, fracture toughness testing, acoustic emission, inspection technique 8-68860
 Al alloy D16T, acoustic emission temp. depend. 8-53136
 Al-Cu (4 wt.%) AE during deform., effect of aging at 170°C 8-64597
 Al-Mg solid soln., AE during plastic deform. 8-64592
 Cd, grain size effect on acoustic emission generated during plastic deformation 8-80609
 Cu, grain size effect on acoustic emission generated during plastic deformation 8-80609
 GaP:N LED, acoustic emission, NDT of dislocation motion 8-91759
 H₂O, acoustic rad. from ionising particles 8-71793
 He gas jet noise source, absolute calibr. for acoustic emission appls. 8-59228
 He gas jet use in AE anal. 8-80701
 NaCl(I), acoustic radiation generated by ionising particles 8-87726
 Na₂O-CaO-SiO₂, origins of acoustic emission in fracture 8-72889
 NbTi, dynamic stress effects, supercond. magnet training problems 8-49870
 Ti, grain size effect on acoustic emission generated during plastic deformation 8-80609
 Zn single cryst., in metal melt, plastic deform. and fracture obs. by acoustic emission (Russian) 8-56737
 Zn-Al (0.4 wt.%) grain size effect on acoustic emission generated during plastic deformation 8-80609
- acoustic equipment**
see also acoustic arrays; acoustic wave interferometers; ultrasonic equipment
 atmospheric sounder, balloonborne, design and construction 8-57353
 audible warning devices, effectiveness on emergency vehicles 8-87200
 audiometer, screening, and real-time computer techniques 8-81009
 digital sound spectrograph for speech signal anal. 8-63251
 directive acoustic spectrum analyzer using moving microphones 8-66992
 kit of instruments for statistical research 8-87215
 noise meas. systems and equipment 8-83189
 portable digital spectrum analyser by GenRad, Model 2512 8-57933
 radio-acoustic sounder for tropospheric temp. meas. 8-53726
 sound level meter and microphones for intensity meas. 8-83194
 sound level meters, modern standards and features 8-83191
- acoustic field**
 accelerated sphere in arbitrary fluid medium 8-50966
 Atlantic bottlenose dolphin, echolocation signal propag. 8-88721
 correction of near-field acoustic meas. using arbitrary meas. transducers 8-66996

acoustic field continued

- directivity of loudspeaker, and subjective hearing event (German) 8-79174
 echo sounder transducer, field plotter 8-59238
 far field sound wave generation in liquids by laser pulse 8-83882
 jet of gas, axisymmetric, free, steady state, sound emitted, review (French) 8-67244
 liquid layer, floating on liquid half-space, acoustic field generated by laser beam 8-51615
 machine panels, insertion loss, meas. and evaluation 8-87193
 membrane, infinite, acoustic radiation due to fluid loading discontinuity 8-90579
 multimode waveguide, with periodic boundaries, acoustic field of volume-velocity sources 8-94463
 noise environments, use of coherence and phase data between two receivers 8-59194
 nonrectangular reverberation chamber, design and construction 8-83196
 oscillating body of revolution, sound field anal. 8-90583
 paper membrane sound generation by impulsive tension 8-90581
 parametric acoustic source, numerical method for nearfield calc. 8-63221
 penetration into a sand sediment of difference-frequency sound generated by a parametric array 8-63227
 plate with line impedance discontinuities, acoustic transmission and scatt. 8-90553
 radiation field computation for sound channels using coherence theory 8-79152
 radiation press. on an absorbing sphere 8-79153
 radiator directivity pattern calc. from near-field sound meas. 8-83149
 rectangular room, instantaneous excitation of one dim. sound waves (German) 8-87201
 room impression, index, definition on basis of subjective examination (German) 8-87202
 sound generation and transmission in flow ducts with axial temperature gradients 8-90551
 submerged elastic shell, acoustic radiation 8-90572
 time transformation of acoustic eqn., flow effects on sound field, wind tunnel noise meas. appl. 8-87198
 US fields radiated into liquid by normal modes of plate driven by pulsed beam 8-50995
 US visualisation in air (French) 8-87212
 vibrating sphere near rigid or compliant wall, near field and impedance 8-94476
 visualisation by optical holography 8-59216
 wave incident on moving plate 8-63218
 waveguides, excitation of sound pressure field by spherical pulse 8-50971
 waveguides, sound pressure field variation as function of refractive index 8-94464
- acoustic generators**
see also earphones; loudspeakers; photoacoustic effect
 digital generation of acoustic excitation impulses 8-90618
 electroacoustic and aerodynamic calibrated sound sources, compared 8-55543
 gas-jet sound generator, Hartmann type, influence of jet temp. on charact. 8-51025
 stepped pressure concentrator, anal. of reson. freq. gain and press. distrib. under reson. and nonreson. conditions 8-90619
 underwater parametric acoustic source beamwidth control 8-75011
 vortex sound generators 8-50975
- acoustic holography**
 applications and theory review, background and current status 8-74866
 Fourier holograms, long-wavelength, recording and reconstructing themes 8-87029
 lens theory and construction 8-55536
 liquid surface imaging 8-53175
 materials testing, defects reconstruction by signal locus curves (German) 8-92435
 moving acoustic source image reconstruction by temporal reference holography 8-79171
 numerical image reconstruct., applicability conditions for Fourier transform (Japanese) 8-59208
 passive imaging systems, effective utilisation of spectral spread 8-71250
 raster choice 8-74867
 scanned, motion effects on image quality 8-71249
 undersea acoustic holographic transducer array development 8-59209
 underwater acoustic holographic image reconstruction for moving objects 8-75019
 weld flaw study using ultrasonic holography (Dutch) 8-68855
 wideband signals, ang. resolution, image intensity 8-83182
 B₂GeO₂₀, cryst. powder, phonon electroacoustic echo signal storage 8-68055
 H₂O, cavitation nuclei conc., holographic and hydrodynamic obs. 8-83440
 acoustic imaging
see also acoustic holography
 biliary tree gas appearance in US B-scan 8-80930
 bispectral passive imaging system for machine-system diagnosis 8-63239
 Bragg diffraction imaging for medical use 8-53463
 brass/water interface, Rayleigh wave reflectivity, meas. 8-59187
 conical acoustic lens, fabrication and test results 8-81019
 conical acoustic lens, opto-acoustic feasibility design 8-81020
 display system using computer-generated integral photograph appl. to US images 8-87021
 dynamically focused US diagnostic phased arrays 8-61232
 echocardiogram computer-assisted interactive interpretation 8-80938
 echocardiography, two-dimens., wall motion and thickening quantification by computer-aided contouring 8-80937
 fluid velocity vector and temp. fields reconstruction, three-dimens., from acoustic transmission meas. 8-51261
 hepatic metastases detect. by grey-scale US scanning 8-73179
 holograms of acoustic field, moire processing 8-55539
 instant photographic technique 8-68079
 jet noise meas., source location, appl. to acoustic mirror, telescope and polar correl. techniques 8-83169

acoustic imaging continued

- PCB, nematic liq. cryst., US imaging, convertor, acousto-optical effect 8-59218
- radiotherapy treatment planning, appl. of US imaging (*German*) 8-53463
- reflective acoustic microscope, signal processing, image enhancement 8-75022
- scanning microscope, characteristic material signatures 8-63259
- scanning microscopes with partially coherent source and detector 8-58923
- scanning microscopy, Gray scale 8-94494
- schlieren method sensitivity for LF US wave visualisation 8-55501
- spatial sampling effect on image reconstruction 8-51021
- three-dimensional display improvement 8-59225
- tissue refractive index spatial distrib. meas. by US computer assisted tomography 8-69161
- transmission microscope optimisation 8-51022
- transmit/receive 2D ceramic piezoelectric arrays, construction and performance, medical, NDT appls. 8-87223
- underwater C-mode US imaging by electronically scanned coaxial circular spherical receiving array 8-59222
- underwater US video system (*German*) 8-94471
- US applications, conference, Brighton (1977) 8-59223
- US B-scan recording on video tape-recorder 8-77095
- US grey scale scanner dynamic range testing 8-69169
- US imaging equipment, quality control problems 8-69171
- US imaging system, high resolution for defect detect. 8-53169
- US imaging system using moving random phase mask and third order correlation function anal. 8-63244
- US imaging systems, high-resolution, real-time 8-69160
- US in medical diagnostics, for teaching 8-49620
- US liver sector scans, echoes across diaphragm 8-69165
- US multiple section tomogram simultaneous display equipment 8-61227
- US ophthalmological signal acquisition and image enhancement 8-57045
- US real-time B-scan machine attachment for three-dimensional display 8-61229
- US transmission image reconstruction, inverse scatt. and tomography 8-61231
- zero-order Raman-Nath method for acoustic beam longitudinal character visualisation 8-71252

acoustic impedance

- see also acoustic wave velocity*
- cylindrical duct with impedance walls, attenuation calc. 8-83146
- electret US transducer performances and prospects 8-59244
- fibre masses, closed front, amplitude depend. damping 8-83144
- Highland bagpipe, acoustics of the chanter and reed 8-94491
- lung, distributed response of complex branching duct networks 8-57027
- mastoid, human, model of mech. system imitating acoustic props. 8-80886
- ocean bottom input impedance meas., particle vel. hydrophone appls. 8-94475
- orifice in infinite thin plate, linear acoustic resistance, theory (*Chinese*) 8-90546
- plate with line impedance discontinuities, acoustic transmission and scatt. 8-90553
- reverberation time, absorption and impedance, theoretical model used for calcs. of a room 8-90601
- shear-wave transducers for laboratory sediments 8-51033
- single-transducer coupler for diagnostic pulsed Doppler or pulse-echo US instrumentation 8-61236
- speech, vocal tract losses, influence on damping of reson. freqs. 8-85325
- stiffening ring, longitudinal-mode and flexural-mode impedances 8-83320
- surface waves on complex impedance ground 8-55491
- US velocity meas., fixed-path interferometer, phase error elimination 8-83197
- vibrating sphere near rigid or compliant wall, near field and impedance 8-94476
- waveguides at cutoff freqs. 8-59215
- ³He, liq., transverse acoustic impedance, Landau theory 8-51778

acoustic insulating materials *see noise abatement***acoustic intensity**

- see also acoustic noise; loudness*
- binaural summation of the loudness of pure tones 8-92638
- fibre masses, closed front, influence on acoustic damping 8-83144
- machine, meas. technique of acoustic power with an intensity meter 8-83188
- ocean acoustic propag., long range, statistical anal. of signal intensity 8-90569
- sound channel intensity distrib. using coherence theory 8-79152

acoustic intensity measurement

- club noise control by electronic power reduction 8-51004
- cochlear excitation, electric circuit model and overpressure meas. in guinea pigs (*French*) 8-85316
- loudspeakers efficiency determ. method 8-51028
- machine, meas. technique of acoustic power with an intensity meter 8-83188
- machine panels, insertion loss, meas. and evaluation 8-87193
- microphones for sound-level meas. 8-83190
- noise meas. systems and equipment 8-83189
- precision acoustic meter (*French*) 8-71254
- sound level meter meas. accuracy 8-59211
- sound level meter with octave band filters and two microphones 8-83194
- sound level meters, modern standards and features 8-83191

acoustic magnetic resonance

- see also acoustic nuclear magnetic resonance; acoustic paramagnetic resonance*
- No entries

acoustic measurements *see acoustic variables measurement***acoustic microwave devices**

- see also acoustic transducers; surface acoustic wave devices*
- 1.2 GHz temperature stable SAW oscillator 8-59226
- SAW oscillator, status and designs review 8-55542

acoustic microwave devices continued

- surface-skimming bulk wave controlled quartz crystal oscillator 8-59250
- GaAs n-h⁺ epitaxial structure for CW electroacoustic amplifier 8-59235

acoustic mode of crystals *see lattice dynamics***acoustic noise**

- additive masking effects of noise bands of different levels 8-57021
- aerodynamically generated sound, extension to relaxing media 8-90567
- air conditioning system, subjective responses and meas. 8-83168
- aircraft, fuselage, light, interior noise, laboratory studies 8-90596
- aircraft, general aviation types, interior noise, acoustic field studies 8-90595
- aircraft flyover noise, modelled by acoustic scatt. by moving prolate spheroid 8-94458
- aircraft noise index, psychological assessment 8-55507
- aircraft noise meas., cause of structural vibrations 8-87187
- AM noise, rate and modulation thresholds detect. by mass 8-85320
- anaesthesia during tooth hard tissue operations, BN-1 apparatus 8-85350
- audiometric testing, A-weighted equivalents of permissible ambient noise 8-69107
- auditory masking effects on lip movements during speech 8-65061
- bearings, rolling, varying compliance vibrations 8-90582
- bispectral passive imaging system for machine-system diagnosis 8-63239
- blast propagation, statistics of amplitude and spectrum 8-63224
- burning vortex ring, turbulent, acoustic emission 8-94676
- channel flow, convective vel. to wall press. fluctuations, numerical simulation 8-94829
- circular flow ducts, broadband noise atten. spectra, measured and predicted 8-63237
- collinear interaction of noise with finite amplitude tone 8-55490
- community annoyance, effect of emergency vehicle audible warning devices 8-87200
- control equipment noise reduction, steam power, chemical, petrochemical industries appl. 8-51002
- dental drill with noise, vibr. radiointerference reduction 8-85450
- diffraction by screen above locally reacting, infinitely large plane 8-79158
- distant shipping noise statistics, Edgeworth series 8-55496
- earplugs, real-ear noise attenuation and effectiveness 8-87199
- fans noise generation, various types comparison 8-63238
- flow noise past rod, wind tunnel expts. 8-50978
- free shear layer tone phenomenon, probe interface 8-71324
- gas flow in duct, self-excited oscillations 8-55670
- hearing temporary threshold shift from noise exposure in squirrel monkey 8-88715
- hearing threshold shifts following 3 days noise exposure in chinchilla 8-88712
- helicopter rotor noise, simplified Mach number scaling law 8-83167
- Hong Kong, reverberation time in high-rise areas 8-59197
- impulsive discharge noise, balloon burst and engine exhaust systems, acoustic pulse parameters determ. 8-90588
- impulsive sounds, large amplitude, human response to house vibr. caused by sonic booms or air blasts 8-90589
- industrial process control valve systems, noise analysis 8-79163
- infrasound, exptl. study of levels in transportation 8-88726
- jet, of gas, axisymmetric, free, steady-state, sound emitted, review (*French*) 8-67244
- jet, sound power output, turbulent jet into gas with different sp. ht. 8-94789
- jet, subsonic sound propagation due to a source near the duct exit 8-83446
- jet engine exhaust noise, orderly struct. as a source 8-94786
- jet engine exhaust noise, source coherence 8-94787
- jet exhaust noise, large-scale struct. importance 8-94792
- jet exhaust noise, prediction of in-flight levels 8-87178
- jet exhaust noise, shear layer instability effect 8-94791
- jet noise source modification due to forward flight 8-63466
- jet noise suppressors, lab. comparison 8-59193
- jet turbulence, interaction with pure tone sound 8-94790
- laboratory air blowers 8-61975
- LF noise, effect on people, review 8-92673
- loudness perception, for short-duration tones in masking noise 8-65047
- low pressure axial flow fans, effects of rot. freq., blade thickness and profile 8-59195
- machine, meas. technique of acoustic power with an intensity meter 8-83188
- motor vehicle racing and shooting noise 8-55510
- moving point source above finite impedance reflecting plane 8-59179
- New York City, environmental noise codes 8-59202
- occupational exposure, permanent threshold shift, from an A-weighted Leq of 89 dB 8-92644
- paper membrane sound generation by impulsive tension 8-90581
- PL/1 computer program for calculating subjective noise characts. 8-59192
- resonators, concentric tube, with unpartitioned cavities, anal. 8-90587
- resource letter on environmental noise control 8-61949
- rivers, acoustic noise from breaking ice 8-53671
- road traffic, noise propag., scale model anal. 8-59196
- road traffic, noise propag. in streets, multiple-reflection diffuse-scatt. model 8-87190
- road traffic, statistical treatment in arbitrary sound propag. environment (*Japanese*) 8-59199
- road traffic acoustic behaviour near traffic lights, computer simulation 8-90597
- road vehicles, noise at roundabouts 8-90594
- road-traffic noise rating using continuous judgement by category (*Japanese*) 8-83170
- signal processing, sparse array technique, min. output variance, S/N ratio 8-83177
- sleep, disturbance by noise 8-92645
- small air jet and quiet valve noise obs. 8-83165
- social surveys, on noise annoyance 8-87189
- sound production in moving stream, Lighthill's acoustic analogy, jet noise 8-79313

acoustic noise continued

- sound recording and reproduction quality eval. in motion picture studio recording room (*Russian*) 8-55518
- sound scattering in an urban street 8-51000
- Space Shuttle, environmental effects during launch and reentry 8-85681
- speech comprehension ability of hard-of-hearing, calc. model (*Dutch*) 8-73165
- statistical estimation of percentage of overexposed noise-impacted workers 8-92671
- steam hammer noise, noise prediction using a small scale model 8-90598
- supersonic jet noise suppression by coaxial cold/heated jet flows 8-63468
- tapered unconstrained beams, vibration damping 8-51106
- threshold shift and cochlear pathology in the Mongolian gerbil 8-65035
- time transformation of acoustic eqn., flow effects on sound field, wind tunnel noise meas. appl. 8-87198
- towed-line array, iterative technique for ambient-noise horizontal-directionality est. 8-55525
- traffic, reverberant meas. rel. to noise level prediction 8-75013
- traffic noise in a high-rise city 8-94482
- trailing-edge turbulent flow noise, incident surface pressure field effect 8-90865
- transonic wind tunnel, noise level effect on model characts. (*French*) 8-71411
- turbulence generated noise, coherent struct. model 8-94675
- turbulence-generated noise in pipe flow, book contrib. 8-59385
- turbulent jet, acoustic power distrib. 8-67238
- turbulent jet, noise spectrum calc. 8-67236
- turbulent jet noise, press. depend. for choked and subsonic jets (*Chinese*) 8-67235
- turbulent shear flow, large-scale coherent structure 8-94671
- urban, relative importance of different sources 8-51001
- urban noise, math. model for noise level prediction 8-90599
- USA, 1977 state noise restrictions 8-59203
- USA, environmental noise control programs 8-59201
- USA urban noise survey, community response 8-90586
- CdS, photoconducting, surface acoustic noise amplification by carrier drift 8-72208
- Fe-Cr-Al, attenuation and vel. of acoustic shock waves, amplitude depend. 8-63810
- He gas jet noise source, absolute calibr. 8-59228

acoustic noise measurement

- 500 MW power station, methods (*German*) 8-55517
- air conditioning system, subjective responses and meas. 8-83168
- automobiles, acoustic noise measuring techniques in automobile development (*German*) 8-79178
- coherence and phase data between two receivers, use in eval. of noise environments 8-59194
- data anal. using digital techniques 8-83193
- digital instruments, Bruel & Kjaer products review 8-94493
- digital voltmeter for noise and vibration meas. 8-55538
- duct noise active attenuation meas. 8-90592
- electroacoustic, analytic and diagnostic equipment 8-63249
- emission detection system sensitivity, direct comparison method 8-56848
- equivalent continuous noise level meter requirements 8-83195
- generalised system and equipment 8-83189
- jet noise, source location, appl. of acoustic mirror, telescope and polar correl. techniques 8-83169
- machine, meas. technique of acoustic power with an intensity meter 8-83188
- machinery acoustic noise meas. standards and reference sources (*French*) 8-83185
- mean energy density, noise level determ. 8-51018
- microphones for sound-level meas. 8-83190
- motorway free-flow traffic noise obs. 8-90591
- nuclear power plant diagnostic system using noise anal. 8-50279
- plasterboard sound reduction indices and meas. 8-87196
- real-time frequency analysers for acoustic noise control 8-83192
- signature analysis systems with Fourier analyzer 8-87195
- sound level meters, modern standards and features 8-83191
- structure-borne sound levels, effects of walls and floors in multistorey buildings (*German*) 8-94483
- test acoustic chambers 8-87218
- traffic noise measurement method and results (*Spanish*) 8-59219
- turbojet noise suppression investigations using hydrodynamic press. meas. and cross-correlation techniques 8-79157
- wind noise, expts. on human beings 8-92648

acoustic nuclear magnetic resonance

- CsI, acoustic NMR, role of incoherent phonons (*Russian*) 8-80230
- InSb, acoustic NMR, role of incoherent phonons (*Russian*) 8-80230

acoustic paramagnetic resonance

- liquid, APR line form. induced by anisotropic spin-lattice interactions (*Russian*) 8-52338
- molecular cryst., phonon scatt. times below 10K, optically-detected APR 8-88228

acoustic parametric amplifiers

- GaAs n-n⁺ epitaxial structure for CW microwave electroacoustic amplifier 8-59235

acoustic parametric devices

- see also acoustic parametric amplifiers; acoustic parametric oscillators*
- arrays, max. conversion efficiency anal. 8-71242
- curved face parametric projector for marine sediment penetration 8-51032
- dispersive acoustic systems, nonlinear and parametric phenomena 8-55489
- nearfield calc. for parametric acoustic source 8-63221
- rectangular aperture sources, source level and beam pattern prediction 8-63219
- selected mode excitation in shallow-water sound propagation 8-59182
- US radiator, influence of dispersive medium on characts. 8-94470

acoustic parametric oscillators

- azimuthal angle of T-D mode induced scatt. from parametric ion-acoustic wave 8-75322

acoustic radiators

- see also acoustic generators; Doppler effect*
- cylindrical shell, coupled vibrations giving high intensity US radiators 8-59236
- cylindrical shell driven by line force, sound radiation 8-94480
- directivity pattern calc. from near-field sound meas. 8-83149
- flame acoustic radiation rel. to flame loudspeakers 8-59227
- infinite thin plate driven by longitudinal force 8-50998
- membrane, infinite, acoustic radiation due to fluid loading discontinuity 8-90579
- parametric acoustic radiators, high-power, operating characts. 8-94469
- parametric acoustic sources of rectangular aperture, source level and beam pattern prediction 8-63219
- parametric US radiator, saturation-limited operation 8-94467
- rectangular plate complex mode vibration and sound radiation 8-83163
- short column vibrator, apparent elasticity analysis and applications 8-59242
- US exponential solid horn, finite element analysis 8-94496

acoustic reactance *see acoustic impedance***acoustic receivers**

- see also microphones*
- parametric acoustic receiving array vibration sensitivity anal. 8-66971

acoustic resistance *see acoustic impedance***acoustic resonators**

- 220 MHz acoustic bulk wave resonator and filter realisation 8-59245
- 300 MHz oscillators using SAW resonators and delay lines 8-59255
- application in gas phase conc. meas. in flowing gas-liq. mixture 8-59448
- concentric tube, with unpartitioned cavities, anal. 8-90587
- eccentric spherical cavity, calc. of acoustic resonant frequencies 8-90548
- flexural piezoelectric bimorph vibrator, spurious response suppression (*Japanese*) 8-59233
- heat exchanger tube bank duct acoustic resonances 8-90550
- helical, technique for broadband tuning, MHz to GHz range 8-94502
- horizontal-shear surface wave grating resonators 8-59249
- nonlinear oscillation theory 8-50974
- open and closed end pipes, for teachers 8-81774
- quartz, electron irradiated, optical and anelastic absorptions and resonator freq. 8-64385
- quartz SAW resonator deep etching 8-59248
- quartz SAW resonator tuning by shorted reflector opening 8-59246
- resonant oscills. in tube with jet inlet 8-59440
- SAW delay line and resonator oscillators for phase locking 8-59254
- SAW interdigital transducer, inverse phase, suppression of direct transmission in resonator filters (*Chinese*) 8-79181
- SAW resonator filters using tapered gratings 8-87224
- SAW resonators, comparison of metal strip and waffle iron arrays 8-51030
- steam means, Gentilly-I generating station, acoustic phenomena 8-89944
- stepped pressure concentrator, anal. of reson. freq., gain, and press. distrib. under reson. and nonreson. conditions 8-90619
- tunable variable bandwidth/frequency SAW resonator 8-59247
- US cell, new design for millilitre liquid samples 8-87213
- US spectrum, RF field in multidomain struct. 8-68056
- ZnO, film, SAW resonators 8-83199

acoustic streaming

- drop evaporation rate in forced convective flow with transverse sound fields 8-51224
- dynamic characts. in field of acoustic dipole 8-50973
- gas bubbles, influence of microstreaming on growth due to rectified diffusion 8-51232
- US perturbation obs. at cellular level 8-61214

acoustic superradiance

- acoustors, superadiationless phase transition, theory and expt. detect. (*Russian*) 8-71805
- crystals with paraelectric impurities, superradiative transitions, acoustic and EM excitation 8-66872
- KCl:Li⁺, coherent excitation by EM and acoustic waves, induction and echo signal study 8-67773
- KCl:OH⁻ type dipole-phonon system, superradiative phase transition (*Russian*) 8-71806

acoustic surface wave devices *see surface acoustic wave devices***acoustic surface waves** *see surface acoustic waves***acoustic transducers**

- see also acoustoelectric transducers; ultrasonic transducers*
- array directional response anal., model 8-66973
- broadband constant beamwidth, theoretical new approach 8-90616
- broadband piezoelectric transducer design 8-51029
- capacitance transducer, calibrated, for detection of acoustic emission 8-71256
- condenser electret transducer design principle 8-59231
- curved face parametric projector for marine sediment penetration 8-51032
- emission detection system sensitivity, direct comparison method 8-56848
- emission transducer construction principles evaluated 8-59239
- mutual interaction of nearest neighbours in compact planar array 8-50979
- reciprocity calibration in unconventional acoustic geometries 8-83200
- SAW, frequency band broadening of phase shifters 8-55532
- SAW generation in crystals with high dielec. const. 8-83203
- SAW interdigital transducer, inverse phase, suppression of direct transmission in resonator filters (*Chinese*) 8-79181
- sonar, towed type, portable, for ocean acoustic meas., features 8-69550
- US impulse thickness gauges, comparison of three element and single element transducers 8-72988
- KTaO₃, light-sensitive surface-barrier generation of acoustic vol. waves 8-63252
- LiNbO₃ X-cut plate shear transducer, direction of displacement 8-51031

acoustic variables measurement

- see also acoustic intensity measurement; acoustic noise measurement; acoustic wave velocity measurement; Q-factor measurement; ultrasonic measurement*
- automobile development appl. (*German*) 8-87219

acoustic variables measurement continued

- concert halls acoustics, spatial impression, lateral refls., musical level (*German*) 8-79164
 correction of near-field acoustic meas. using arbitrary meas. transducers 8-66996
 directivity of loudspeaker and subjective hearing event (*German*) 8-79174
 holograms of acoustic field, moire processing 8-55539
 interior acoustics CAD (*Polish*) 8-59205
 laser interferometer, acoustic vibration meas. 8-71253
 loudspeaker signal displacement meas., optical method 8-51023
 muffler characts., acoustic impulse technique 8-59217
 noise generation by control equipment, steam power, chemical, petrochemical industries appl. 8-51002
 n-paraffins, generalised eqn. of state from acoustical meas. 8-51642
 reflection from obstructions in pipes with flow, meas. method 8-63246
 regenerative sound system investigation using time-delay spectrometry 8-51006
 reverberation house construction, acoustic power meas. appl. (*German*) 8-51024
 reverberation room sound absorpt. meas. precision assessment 8-59210
 signal mean frequency meas. (*Russian*) 8-81441
 small-chamber method applied to investigations of sound-absorbing systems at high sound pressure levels 8-94497
 sound pressure in insert earphone couplers and real ears 8-65152
 underwater sound arrival angle estimation by multiple cross-correlation meas. 8-66978
 US transducer power output meas. using modulated radiation pressure 8-59230

acoustic velocity see acoustic wave velocity**acoustic wave absorption**

- see also noise abatement; ultrasonic absorption*
 anisotropic sound energy flow effects in reverberation room plane absorber meas. precision 8-55482
 attenuation by absorptive barriers (*Japanese*) 8-59198
 binary mixture, high-frequency sound absorpt. near crit. separation point 8-83881
 building insulation meas. dependence on type of loudspeaker (*German*) 8-75021
 circular ducts, effect of expansion chamber 8-55485
 circular flow ducts, broadband noise atten. spectra, measured and predicted 8-63237
 cylindrical duct with impedance walls, attenuation calc. 8-83146
 damping, fluid induced, in refrigeration machinery manifolds 8-83164
 degenerate semiconductor, nonparabolic, acoustic wave absorption/amplification coefficient 8-64069
 double walls, sound transmission loss and cavity absorbent materials (*Japanese*) 8-79167
 duct, air conditioning, active sound absorpt. 8-90555
 enclosure, thermoviscous dissipation at walls, normal mode theory 8-83171
 flass, phonon avalanches, exptl. conditions for obs. 8-71822
 gas mixture, modified rough sphere model, rel. to sound absorpt. 8-93597
 gas-vapour droplets, nonuniform mixture, acoustic wave attenuation 8-83154
 insulating material losses and performance factors (*Spanish*) 8-55516
 landscaped office, effect of screens on sound attenuation 8-94486
 laser light diffraction, appl. to meas. of acoustic and acousto-optic props. of crystals (*Polish*) 8-76425
 metal, phonon spectra, singularities caused by local geometry of Fermi surface 8-91401
 metal surface, resonant absorpt. of sound (*Russian*) 8-95216
 N-wave propagating in circular tube, nonlinear attenuation and wall effects 8-50972
 oblique incidence sound absorpt. characts. of materials using cross-correlation methods (*Japanese*) 8-83172
 partition airborne-sound transmission loss, effect of sound-absorptive facings 8-79166
 porous material, estimation of reverberant sound absorpt. coeff. (*Japanese*) 8-83145
 radiation press. on an absorbing sphere 8-79154
 reverberant sound absorpt. coeff. of plane porous material, theory (*Japanese*) 8-79168
 reverberation room sound absorpt. meas. precision assessment 8-59210
 reverberation time, absorption and impedance, theoretical model used for calcs. of a room 8-90601
 shock pulses in Al rods, amplitude-dependent attenuation 8-55503
 small-chamber method applied to investigations of sound-absorbing systems at high sound pressure levels 8-94497
 space absorber composed of porous materials, reverberant sound absorption coeff. 8-55519
 stratosphere and ionosphere, LF waves, relax. absorpt. (*Russian*) 8-65356
 surface ducts, attenuation 8-63231
 turbulence, acoustic energy conversion to turbulent kinetic energy 8-63420
 two-phase medium, sound wave absorpt. and dispersion 8-94466
 underwater absorption of sound by sound 8-59180
 Fe-Cr-Al, attenuation and vel. of acoustic shock waves, amplitude depend. 8-63810
 Ge:Sb, acoustic attenuation, uniaxial stress effects 8-59863
 KCl:OH⁻, paraelec. system, acoustic susceptibility in strong phonon-coupling approx. 8-71801
 LiNbO₃, LF sound attenuation, internal friction 8-63804
 NH₄Br(Cl), anomalous sound attenuation above λ point 8-51617

acoustic wave amplification

- see also acoustoelectric effects*
 degenerate semiconductor, nonparabolic, acoustic wave absorption/amplification coefficient 8-64069
 non-linear ultrasound absorption in an electromagnetic wave field under quantum size effect conditions 8-87745
 nonuniform flow, sound amplification 8-83158
 piezoelectric semiconductor, amplification and vel. change of acoustic waves due to external temp. gradient 8-84260
 semiconductor, validity criteria of phenomenological theory of electron obs. and amp. of sound 8-91733

acoustic wave amplification continued

- thermal fluctuations during amplification of magnetoacoustic surface waves 8-88158
 thermopiezosemiconductor, critical drift velocity for US amplification 8-60169
 thermopiezosemiconductors 8-76114
 GaAs n-n⁺ epitaxial structure for CW microwave electroacoustic amplifier 8-59235
 LiTaSi₃ piezoelec. semicond., acoustic wave generation, amplification material appl. (*Russian*) 8-72464
acoustic wave attenuation *see acoustic dispersion; acoustic wave absorption; acoustic wave scattering; acoustic wave transmission; ultrasonic absorption*
acoustic wave diffraction
see also ultrasonic diffraction
 baffles, symmetrical planar, sound diffraction (*Czech*) 8-90558
 cracks, diff. of elastic waves 8-79161
 cylindrical shell, fluid filled, plane acoustic press. pulse diff. 8-90559
 double-layer waveguides, normal mode diffraction 8-94482
 farfield scatt. from prolate spheroid, meas. and anal. 8-94459
 ocean, diff., refl. and interf. during near grazing and near normal ocean surface backscatt. 8-90570
 pencil conical beam diffraction on acoustically soft sphere (*Ukrainian*) 8-90547
 plane wave diff. by semicircular infinite strip, comment 8-83134
 rigid planar screens, diff. of arbitrarily oriented directional sources 8-83137
 screen above locally reacting, infinitely large plane 8-79158
 shock wave diffraction, nonlinear problem soln. (*Russian*) 8-75171
 statistically stationary traffic noise shielding by simple obstacles 8-90590
 surface ducts, attenuation 8-63231
 thin phase grating diff. eqn. solns. 8-54198
 thin screen, study of shielding efficiency (*French*) 8-87188
 transducer array directional response anal. model 8-66972
 variable density cylinder, plane wave diff. 8-50977
acoustic wave diffusion see acoustic wave scattering
acoustic wave effects
see also acoustic magnetic resonance; acousto-optical effects; acoustoelectric effects; biological effects of acoustic radiation; sonoluminescence; ultrasonic effects
 critical sound pressure level in mass transfer processes, analytic expressions 8-90633
 drop evaporation rate in forced convective flow with transverse sound fields 8-51224
 gas bubbles, influence of microstreaming on growth due to rectified diffusion 8-51232
 heat transfer in turbulent flow 8-59394
 liquid crystals acoustic storage effect 8-94992
 sieving of fine powders by sonic oscillating air column (*Japanese*) 8-95712
 solar chromosphere models, short period acoustic heating theory appl. (*Italian*) 8-85926
 steam, film condensation in tube, heat transfer, vibr. effect 8-51044
 turbulent boundary layer, compressible, extended mixing length appls. 8-94655
 water jets, two-dimensional, effects of applied sound (*Japanese*) 8-79353
 H₂O, contact angle measurement, effect of acoustic energy 8-95207
acoustic wave interference
see also acoustic wave interferometers; acoustic wave interferometry
 frequency band broadening of phase shifters of SAW 8-55532
 ocean, diff., refl. and interf. during near grazing and near normal ocean surface backscatt. 8-90570
 US materials testing, three layered medium, dispersion relation for interference waves 8-72980
acoustic wave interferometers
see also acoustic wave interferometry
 correlation interferometers rel. to binaural perception and resolving power of bats (*French*) 8-80883
 echosonde interferometer for atmospheric research 8-57347
acoustic wave interferometry
see also acoustic wave interferometers
 US velocity meas., fixed-path interferometer, phase error elimination 8-83197
acoustic wave propagation
see also acoustic dispersion; atmospheric acoustics; Doppler effect; liquid helium sound propagation; seismic waves; shock waves; surface acoustic waves; ultrasonic propagation; underwater sound
 absorbing boundary conditions for wave equation 8-59320
 accelerated sphere in arbitrary fluid medium 8-50966
 anisotropic layered medium, plane wave transmission 8-83150
 array processing using freq.-wavenumber approach 8-66974
 bone, wave propag. in piezoelectric two-layered cylindrical shell with hexagonal symmetry 8-55487
 circular ducts, effect of expansion chamber 8-55485
 classical Lamb problem, time-harmonic soln. for elastic head waves 8-63215
 composite, fibre-reinforced, layered harmonic elastic waves, dispersion 8-63223
 correlation coeff. meas. for signals with stationary additive noise 8-94489
 crystal classification by acoustic props. 8-79344
 curved ducts with central partition 8-55486
 cylindrical duct with impedance walls, attenuation calc. 8-83146
 cylindrical surfaces with nonuniform vel. distrib. radiated power and radiation loading 8-50969
 directivity pattern calc. from near-field sound meas. 8-83149
 ducted propag. asymptotic theory based on local evanescent wave fields 8-55484
 ducts, nearly annular, acoustic propagation 8-83141
 energy-absorbent media, wave theory generalisation (*Russian*) 8-77725
 explosive signals in shallow water computer simulation 8-79960
 fibrous networks in viscous media, acoustic theory of wave motion 8-59177
 fluid velocity vector and temp. fields, reconstruction, three-dimens., with aid of computer 8-51261
 generalized beam pattern assoc. with approx. solns. of source extraction integral eqn. 8-51009

acoustic wave propagation continued
granular solid, one-dimens.; small amplitude wave behaviour 8-59339
high thermal conductivity media, model equations for the nonlinear acoustics 8-90565
hydrophone array response calc. errors due to two-dimensional beam pattern assumption 8-66972
infinite plate with losses, flexural vibr. in fluid 8-83319
inhomogeneous anisotropic media, ray approx. 8-83153
inhomogeneous granular solid, one dimens. accel. waves, speed, amplitude 8-87288
inhomogeneous medium, Poincaré-Lighthill-Kuo method 8-83133
intensity distrib. in sound channels; coherence theory 8-79152
laminated composite, nonlinear transient pulse propag., interface reflection effect 8-63222
layered acoustic waveguide, group delay time, temp. coeff. var. 8-83152
LF multipath fluctuations in the ocean, statistical anal. 8-90571
linear, perfect fluid at rest with piecewise indefinitely differentiable characteristics appl. (French) 8-55488
liquid, nonviscous, laser-induced acoustic waves 8-63808
liquid crystals, acoustical activity 8-83880
liquid-vapour mixture, acoustic wave propag. 8-90972
metal, nonlinear interaction of strong and weak sound waves 8-59865
multimode waveguide with uneven walls, sound attenuation 8-83147
multipath signal, individual pulse resolution, signal processing techniques 8-83176
nonhomogeneous elastic rods, similarity soln. of wave propagation 8-59323
nonlinear wave propagation, analytic solns. for accel. waves, non-equilib. effects 8-94890
normal mode amplitudes in random ocean, statistical theory 8-50981
ocean, long range acoustic propag., statistical anal. of signal intensity 8-90569
ocean, sound propagation in an ocean shelf zone of arbitrary profile 8-90576
ocean surface ducts with rough boundaries 8-55493
piezoelectric rods, hexagonal crystal symmetry, wave propagation 8-56429
polymers, highly oriented, elastic wave dispersion relations 8-51618
quasilinear hyperbolic systems, propag. of weak discontinuities when charact. shock occurs 8-79153
radiation from a submerged elastic shell subjected to a time harmonic internal press., calc. 8-90572
Rayleigh wave, propag., isotropic elastic material with homog. strain 8-94460
rods, elastic, linear, nonhomogeneous, propag. and decay of shock and accel. waves 8-83278
signal processing, sparse array technique, min. output variance, S/N ratio 8-83177
solar atmosphere, efficiency of one-dimens. hydrodynamic codes 8-57520
solar atmosphere upper layers, convective noise waves dissipation in mag. struct. 8-65600
solid superconductors, Ginzburg-Landau and linear elasticity eqns. 8-95395
sonar range prediction, inherent errors 8-66977
surface waves on complex impedance ground 8-55491
thermosphere, wave-induced diffusion effects on acoustic-gravity waves 8-61637
underwater duct problems, variational anal. techniques 8-90574
underwater parametric acoustic source beamwidth control 8-75011
underwater propagation prediction measuring system at sea, WPA prototype 8-69552
underwater sound propagation in presence of randomly perturbed parabolic profile 8-94477
underwater US pulse propag. and reflection by small targets 8-50986
vapour-droplet mixtures, small perturbation propagation 8-95111
wave propagation and underwater acoustics, book 8-90577
waveguide, limited frequency sound suppression 8-83148
waveguide, rough boundary, spatial and temporal correl. functions for stochastic part of sound field 8-90560

acoustic wave reflection

see also echo; reverberation; ultrasonic reflection
cylindrical cavity in absorptive medium, elastic wave reflection 8-55582
enclosure, thermoviscous dissipation at walls, normal mode theory 8-83171
forward reflection from rough sea surface statistical anal. 8-50983
interface of two highly stressed elastic half-spaces 8-63213
moving and rotating barriers, math. anal. 8-93539
multichamber sound reflector, design parameters 8-94500
obstructions in pipes with flow, meas. method 8-63246
ocean, diff., refl. and interf. during near grazing and near normal ocean surface backscatt. 8-90570
ocean, Stoneley wave effects on plane wave reflection coeffs., bottom reflection characts. 8-87180
ocean bottom layering influence on reflected FM signal characts. 8-50991
plane hyperdetonation shock wave reflection from rigid wall 8-75167
plane wave reflection from a plate immersed in and floating on a liquid 8-83132
road traffic, noise propag. in streets, multiple-reflection diffuse-scatt. model 8-87190
rough sea surface reflected signal and sea wave spectrum 8-94474
SAW reflection by strips, grooves and arrays of strips and grooves 8-63214
spatial impression of concert halls, lateral refls., musical level (German) 8-79164
spherical sound wave reflection from rigid sphere 8-66969
statistically stationary traffic noise shielding by simple obstacles 8-90590
underwater sound, reflection from a variable-index half space 8-94472
underwater US pulse propag. and reflection by small targets 8-50986
KTaO₃, light-sensitive surface-barrier generation of acoustic vol. waves 8-63252

acoustic wave refraction

see also acoustic dispersion; ultrasonic refraction
Helmholtz eqn., test of Born and Rytov approx. using Epstein problem 8-63212
shear layer refraction theories, comparison, parameters for open jet wind tunnel shear layer correction 8-90556
acoustic wave scattering
see also ultrasonic scattering
atmosphere, scattering from locally homogeneous turbulence 8-87177
buried inhomogeneities, general 3-D formalism 8-94461
cylindrical shells, resonance scatt. 8-83138
elliptical cylinders, scatt. matrix for elastic waves 8-59324
farfield scatt. from prolate spheroid, meas. and anal. 8-94459
flaws, reciprocity theory appl. 8-72941
inhomogeneous medium, spherically stratified, direct and inverse scatt. problems 8-71239
inverse scalar wave scatt., statistical estimation (Russian) 8-54200
matrix theory of elastic wave scatt., conservation law 8-63217
membranes and plates, with line constants, acoustic scattering 8-90554
metal, Raman scatt. of sound in quantising mag. field 8-60171
mode conversion rates, due to scatt. from ocean bottom roughness 8-63228
multimode waveguide with uneven walls, sound attenuation 8-83147
ocean, diff., refl. and interf. during near grazing and near normal ocean surface backscatt. 8-90570
plane harmonic elastic P and S wave scatt. by spherical inclusions and cavities 8-89353
plate with line impedance discontinuities, acoustic transmission and scatt. 8-90553
point sources scatt. by moving prolate spheroid, aircraft noise appl. 8-94458
quadratic sound channel, first order scatt. resulting for temp. fluctuations 8-83136
resonant acoustic scattering by swimbladder-bearing fish 8-87183
resonant scatt. from spherical cavities in elastic and viscoelastic media 8-79150
rigid body with thin liquid coating 8-50968
road traffic, noise propag. in streets, multiple-reflection diffuse-scatt. model 8-87190
rows of cylindrical obstacles in shallow water 8-87182
SAW reflective-array-compression filters, nonsynchronous scatt. loss 8-71246
scattering of sound by sound, relation to the parametric receiving array 8-90563
sea surface backscatter under shadowing conditions 8-94473
semimetal, Raman scatt. of sound in quantising mag. field 8-60171
SH waves, multiple scatt. by arbitrary cross section cylinders 8-63216
silicone rubber cylinders and spheres 8-79149
spherically stratified medium, construction of solns. 8-90557
submerged elastic bodies, resonance excitation by sound scatt., linear approx. theory 8-55495
surface wave scatt. from elastic cylinders, Regge poles 8-50967
thin plate, effect of line-discontinuity admittance on sound scattered by plate vibration 8-55494
thin stiffened Al plate, underwater acoustic backscattering and echo struct. characts. 8-55492
transient scatt. by arbitrary axisymm. surfaces 8-79151
underwater, multiple bounce channels, scatt. function 8-83162
underwater Fermat paths, phase and amplitude 8-79159
vol. reverberation from scatt. layers and biological meas. 8-81194
waveguide, rough boundary, spatial and temporal correl. functions for stochastic part of sound field 8-90560
LiNbO₃, Y-Z, SAW scatt. from groove 8-60019

acoustic wave transmission

see also ultrasonic transmission
circular ducts, method of weighted residuals with trigonometric basis functions 8-59174
circular plate, sound pulse transmission characts. 8-59170
duct, nonuniform, finite element method for acoustic transmission 8-83140
heavily-damped cylindrical fuselage 8-83166
homomorphic deconvolution, reverberant and distortional channels 8-90606
interdigital transducers, quasioacoustic wave propagation, field theory anal. 8-66998
laminated plate, reinforced by beams of different mech. impedances 8-90584
landscape office, effect of screens on sound attenuation 8-94486
maisonettes, flanking transmission of sound, effect of woodwool shuttering in party floors 8-94487
plate, orthotropic multilayered, acoustic transmission loss 8-83143
plate, orthotropic multilayered, vibr. modes, acoustic transmission 8-83142
plate with line impedance discontinuities, acoustic transmission and scatt. 8-90553
sound generation and transmission in flow ducts with axial temperature gradients 8-90551

acoustic wave velocity

see also acoustic dispersion; liquid helium sound propagation; shock waves; ultrasonic velocity
acoustic wave interaction, diagnostics appl. 8-83541
aqueous salt solns., as function of conc., temp., and press. 8-79668
Bose gas, imperfect, quasiparticle sound velocity, temp. depend. 8-51761
collisionless regime, amplitude dependent sound velocity (Russian) 8-52037
contained spherically symmetric fluid, sound speed from natural freq. spectra 8-61344
heat exchanger tube bank duct acoustic resonances 8-90550
n-heptane, self-excited thermoacoustic oscils. in heat transfer 8-79186
human skull, acoustic losses and vel. meas., rel. to diagnostic imaging 8-69159
inhomogeneous granular solid, one dimens. accel. waves, speed, amplitude 8-87288
Kaprolon, compressibility, elec. cond., sound vel. behind shock front 8-95105
liquid, calc. method 8-67834
liquid, thermophysical properties rel. to compressibility 8-83964
long range propag. in oceans, signal speed variations 8-50984

acoustic wave velocity continued

- mantle rocks, thermally activated point defects interpretation of low vel. zone 8-88806
- marine sediments and rocks, sound vel.-density relations 8-50982
- metal, light scatt. from surface acoustic phonons 8-76484
- metal, phonon spectra, singularities caused by local geometry of Fermi surface 8-91401
- metal, theory of electronic transport of sound packets in parallel mag. field (*Russian*) 8-84261
- mixed metal chloride acousto-optical props. (*Russian*) 8-60419
- nonideal gaseous mixtures, prediction of acoustic vels. 8-67306
- n-paraffins, generalised eqn. of state from acoustical meas. 8-51642
- piezoelectric semiconductor, amplification and vel. change of acoustic waves due to external temp. gradient 8-84260
- rare earth orthochromites, mag. interactions and weak ferromagnetism 8-52220
- seawater sound speed eqns. for varying salinity and temp. 8-81193
- semiconductor, opaque, light scatt. from surface acoustic phonons 8-76484
- shock-compressed porous solids (*Russian*) 8-71788
- shock-compressed uniform solid, lateral discharge ang. semiempirical formula (*Russian*) 8-55910
- underwater ray theory for sound speed profiles with two dim. variation 8-50987
- water, subcooled, choked expansion and the isentropic homogeneous equilb. model for 2-phase flow 8-91034
- AgI, sound vels. near phase transitions with negative dP/dT 8-83885
- Fe-Cr-Al, attenuation and vel. of acoustic shock waves, amplitude depend. 8-63810
- Pb₂KNb₂O₅, SAW props., rel. to device appl. 8-71923
- Si film, hydrogenated amorphous, Brillouin scatt. 8-72538
- V₂Si, neutron irradi., sound velocity, magnetic susceptibility and upper critical field 8-88074

acoustic wave velocity measurement

see also *ultrasonic velocity measurement*

- phase velocity meas. using CW feedback technique 8-83187
- rocks sound velocity determination, suggested methods 8-81433
- solid, phase and group vels. determ. for dispersive waves 8-81848

acoustic waveguides

- dispersive acoustic systems, nonlinear and parametric phenomena 8-55489
- double-layer waveguides, normal mode diffraction 8-94462
- excitation of sound pressure field in ideal waveguide by spherical pulse 8-50971
- grating waveguide modes 8-59172
- impedance of acoustic and structural waveguides at their cutoff frequencies 8-59215
- layered acoustic waveguide, group delay time, temp. coeff. var. 8-83152
- limited frequency sound suppression 8-83148
- multimode waveguide with periodic boundaries, acoustic field of volume-velocity sources 8-94463
- multimode waveguide with uneven walls, sound attenuation 8-83147
- rods and clad rods, elastic waves anal., tutorial review 8-94608
- rough boundary, spatial and temporal correl. functions for stochastic part of sound field 8-90560
- rough walled, acoustic propagation in material of fluctuating refr. index 8-90549
- sound pressure field variation as function of refractive index 8-94464

acoustic waves

see also *acoustic emission; magnetoacoustic effects; shock waves; surface acoustic waves; ultrasonic waves*

- gas dynamics with relaxation effects, acoustic waves, nonequilibrium atmosphere effects, review 8-79390
- quartz substrate, surface and bulk acoustic waves excited by interdigital transducers, optical diffr. study (*Chinese*) 8-50965
- solar chromosphere, acoustic shock waves dissipation and H⁺ radiation 8-96454
- spectral theory for acoustic wave eqns., generalised Neumann boundary conditions 8-59173
- terrestrial atmosphere acoustic-gravity waves, generation mechanisms (*Russian*) 8-85621
- time transformation of acoustic eqn., flow effects on sound field, wind tunnel noise meas. appl. 8-87198
- variational expressions systematic derivation 8-93536

acoustical laboratories

see also *anechoic chambers*

- nonrectangular reverberation chamber design and construction 8-83196

acoustics

- see also *acoustic applications; acoustic devices; acoustic equipment; acoustic noise; anechoic chambers; architectural acoustics; atmospheric acoustics; audio acoustics; hearing; musical acoustics; photoacoustic effect; sound reproduction; ultrasonics; underwater sound; vibrations*
- Acoustical Soc. Amer. 96th meeting, Hawaii, 1978 Nov. 8-90545
- acoustics, speech and signal processing, conf., Tulsa, USA, 1978, April 8-63242
- cross-spectral anal., statistical parameters of estimators 8-83180
- history, Kircher's 'Phonurgia nova' (*German*) 8-81788
- jet turbulence, interaction with pure tone sound 8-94790
- resonance, open and closed end pipes, for teachers 8-81774
- system identification, from multiple input/output data, comment and reply 8-83179

acousto-optical devices

see also *acousto-optical effects*

- acoustic emission monitoring difficulties overcome by optical detectors 8-60968
- anisotropic acoustooptic deflector, using optically active uniaxial crystals. 8-66928
- astronomical radio spectrograph for spectral integration 8-69694
- beam quality, of acousto-optic frequency shifters 8-79127
- chalcogenide glasses, optimum glasses for acoustic delay lines and deflectors 8-55420
- deflector, planar optoacoustic, expt. 8-74995
- holocinematography, high speed, acousto-optic beam deflection for spatial freq. multiplexing 8-74860
- laser beam deflector quality factor N/r, comparison of holographic and acousto-optical deflectors (*French*) 8-55318
- laser Doppler velocimeter with variable frequency shift for combustion flow meas. (*Japanese*) 8-67294

acousto-optical devices continued

- laser interferometer, acoustic vibration meas. 8-71253
- lensless convolver using SAW device with polarisation discrimination detect. 8-79170
- memory correlator, long duration, using acousto-photorefractive effect 8-79124
- memory correlator using acousto-photorefractive effect 8-71248
- modulator, appl. to laser Doppler anemometers 8-83082
- modulator, intracavity, 212.8 nm pulse burst generation of Nd:YAG laser 8-74934
- modulator, standing wave, thermal detuning effects 8-71197
- modulator temporal response, physical optics model in low scatt. efficiency limit 8-66897
- modulators, for laser freq. changes 8-74932
- optical signal and image processing, conference, San Diego (1977) 8-74853
- PCB, nematic liq. cryst., US imaging, converter, acousto-optical effect 8-59218
- planar, SAW loss meas. using light beam diffraction 8-74996
- Pockels readout optical modulator, acoustooptic snapshot, optical, signal spectrum analyser 8-90494
- processors for wideband electronic signals 8-79137
- pulsed acousto-optical modulator RF driver for laser mode locking 8-90438
- SAW device for optical image processing 8-71051
- semiconductor acoustic DFB laser, high speed repetitive Q-switching 8-83007
- signal processor, multichannel 8-66990
- solar radio spectrograph 8-73631
- spectrum analyser for radar signal processing 8-78942
- surface acousto-optic lens, Fourier and Mellin transform props. 8-78926
- TE=TM mode converter utilizing doubly confined optical and acoustic waveguide struct. 8-83087
- tunable switched directional couplers of two thin film waveguides using SAW 8-75003
- US transducer, liq. cryst. cell for US visualisation (*German*) 8-79179
- wideband acousto-optic radiometry 8-77983
- wideband thin film modulators and switches, for optical communication 8-63206
- As₂S₃, thin film optical waveguide 8-83051
- GaAs, optically pumped laser with acoustic distributed feedback 8-82977
- α-LiIO₃, piezoelec. mat. for acoustooptic cells, piezoelectric transducers 8-95575
- LiNbO₃, high freq. plane acousto-optical light modulators (*Russian*) 8-79106
- TeO₂ broad bandwidth devices bonded with Sn 8-50910
- TeO₂, paratellurite deflectors, bandwidth, scanning linearity (*Chinese*) 8-90501

acousto-optical effects

see also *acousto-optical devices*

- chalcogenides, prod. and acoustooptic props. (*Russian*) 8-63158
- cylindrical light beam diffr. on wideband US signal 8-50698
- dielectric waveguides, optoacoustic interaction, Raman-Nath type diffr. 8-87153
- ferroelectric mats., conf., Novosibirsk, USSR (Sep. 1976) 8-76393
- glass, magneto-optical properties of US light diffr. 8-76437
- gyrotropic media, diffr. of light by acoustic waves 8-72485
- holograms of acoustic field, moire processing 8-55539
- intense laser beam diffraction by long US wave in liquid column 8-60421
- laser light diffraction, appl. to meas. of acoustic and acousto-optic props. of crystals (*Polish*) 8-76425
- light diffraction, elastic surface wave parallel to light beam, expt. investigation 8-82904
- light diffraction by two adjacent parallel US waves, soln. of boundary value problems 8-90358
- light diffraction by US beam in homogeneous isotropic dielectric plate, anal. 8-82905
- light modulation assoc. with periodic deform. with liquid crystal layer 8-52471
- liquid containing gas bubbles, thermal generation of sound 8-50994
- liquid crystals, instabilities generated by US field, review 8-91235
- MBBA, nematic liq. cryst., ultrasound produced rolls, spatial coherence props. of scatt. light 8-75534
- metal, isotropic, Brillouin scatt. 8-80367
- methylammonium aluminium sulphate, third order elastic const. from stress shifted reson. freqs. 8-55905
- mixed metal chloride acousto-optical props. (*Russian*) 8-60419
- NDT by acousto-optical imaging, resolution 8-53165
- optical fibres, phase modulation of coherent light using HF sound 8-87142
- pentacene, in p-terphenyl, electronic excitation transport, acousto-optical effects 8-72079
- SAW, light scattering on internal refl. 8-64345
- SAW holographic visualisation, improved S/N ratio (*French*) 8-75023
- semiconductor, sound-induced anomalous transmission of light below plasma edge 8-68475
- surface acoustic wave diffr. of light beam propag. parallel to surface 8-66752
- time-resolved, opto-acoustic spectroscopy, nonradiative yields and rate const. 8-58052
- uniaxial ferroelectric, US vel. and absorpt. anisotropy and crit. anomalies, acousto-opt. obs. 8-95574
- US wave 3D meas. in transparent solids, Doppler-shifted light scatt. technique 8-90613
- AgCl, single cryst., optical, acoustic and acousto-optical props. (*Czech*) 8-76417
- α-Al₂O₃, trigonal crystal, optical heterodyne detection using collinear acousto-optic interaction 8-66927
- CsAl(SO₄)₂·12H₂O, third order elastic const. from stress shifted reson. freqs. 8-55905
- Ge, photoelastic const. determ. 8-68474
- Hg-As-S modulating glasses, optical parameters and struct. (*Russian*) 8-63159
- Hg-As-S-I system, glasses, optical and acousto-optical props. 8-83053
- KAl(SO₄)₂·12H₂O, third order elastic const. from stress shifted reson. freqs. 8-55905

acousto-optical effects continued

- LiNbO₃, leaky SAW and guided light Bragg interaction, theoretical anal. 8-72484
 LiNbO₃, partial waves of SAW, direct meas. by light scatt. 8-66994
 LiNbO₃, trigonal crystal, optical heterodyne detection using collinear acousto-optic interaction 8-66927
 NH₄Al(SO₄)₂·12H₂O, third order elastic const. from stress shifted reson. freqs. 8-55905
 NaBi(MoO₄)₂, photoelastic props., acousto-optical figure of merit meas. 8-60420
 PbMoO₄, SAW props. 8-63920
 α-SiO₂, trigonal crystal, optical heterodyne detection using collinear acousto-optic interaction 8-66927
 TlBr-TlI KRS-5 single crystals, acousto-optical characts. 8-71165

acoustoelasticity *see elasticity***acoustoelectric devices**

- see also acoustoelectric transducers*
 measuring equipment for noise anal. and machine diagnosis 8-63249
 memory correlator using GaAs Schottky diodes 8-66989
 LiNbO₃-InSb amplifier production, role of protective films 8-95220

acoustoelectric effects

- acoustic wave resonant transmission across piezoelectric gap 8-87855
 anisotropic semiconductor, US amplification, kinetic theory, chain fraction method (*Russian*) 8-68054
 degenerate semiconductor, nonparabolic, acoustic wave absorption/amplification coefficient 8-64069
 elastic nonlinearities in dielec., piezoelec., and pyroelec. crystals. 8-79155
 electrostrictive solid, acoustic to EM wave conversion 8-91734
 ferroelectric material, r.f. echo 8-95549
 interdigital transducers, quasiacoustic wave propagation, field theory anal. 8-66998
 metal, acoustoelectric effects, anisotropy (*Russian*) 8-91732
 metal, strong and weak sound waves propag., nonlinear effects (*Russian*) 8-60168
 non-linear ultrasound absorption in an electromagnetic wave field under quantum size effect conditions 8-87745
 parametric interaction of EM and acoustic waves in solids, theory 8-60166
 piezoelectric ceramic, excitation of acoustoelectric oscils. by ionising radiation 8-56191
 piezoelectric material, r.f. echo 8-95549
 piezoelectric semiconductor, amplification and vel. change of acoustic waves due to external temp. gradient 8-84260
 piezoelectric semiconductors, nonlinear noise amplification 8-60167
 semiconductor, validity criteria of phenomenological theory of electron obs. and amp. of sound 8-91733
 semiconductor in mag. and US wave fields, electronic density of states (*Russian*) 8-72056
 slow shift SAW in attenuating piezo-electric and piezosemicond. surface structs. 8-79872
 sound velocity, amplitude dependent, in collisionless regime (*Russian*) 8-52037
 thermopiezosemiconductor critical drift velocity for US amplification 8-60169
 thermopiezosemiconductors, amplification of longitudinal acoustic waves 8-76114
 TsTS polarized ceramic film, Lamb waves near. crit. freq. study (*Russian*) 8-52039
 Ag₃SbS₃, piezoelec. semicond., residual cond., ultrasound photoabsorpt. (*Russian*) 8-72465
 Bi₂GeO₂₀, cryst. powder, phonon electroacoustic echo signal storage 8-68055
 CdS, lattice attenuation meas. by US injection method 8-76480
 CdS, photoconducting, surface acoustic noise amplification by carrier drift 8-72208
 n-GaAs, impact ionisation initiated by acoustoelectric effect 8-52038
 GaAs n-n⁺ epitaxial structure for CW microwave electroacoustic amplifier 8-59235
 n-GaAs, piezoelectric semiconductor, influence of acoustic phonon disturbances on conductivity 8-91697
 InSb, acoustoelectric effect at 77K 8-72209
 n-InSb, acoustoelectric gain coeff., nonlinear elec. field depend. 8-76115
 n-InSb, degenerate, acoustomagnetoelc. effect obs. 8-72207
 n-InSb, threshold field dependence on sample length, 77K 8-76116
 LiNbO₃, electroacoustic correlation memory effect 8-88001
 LiNbO₃, film, Lamb waves near. crit. freq. study (*Russian*) 8-52039
 Pb₃MgNb₂O₉, diffuse phase transition, Brillouin scatt. and acoustic phonons 8-76401
 Pb_{0.975}Sn_{0.025}Se, film, acoustic wave modulation of electron current 8-64067
 SiC, absorption of US waves 8-72210
 SiC, sound absorption 8-88000
 Ti₃Ta₄, piezoelec. semicond., acoustic wave generation, amplification material appl. (*Russian*) 8-72464

acoustoelectric transducers

- see also earphones; headphones; hydrophones; loudspeakers; microphones*
 electret transducer equations by Lagrange's equation 8-83202
 electret-slot-effect-transducer, two-port eqns. (*German*) 8-75024
 phase insensitive, operation and optimisation procedures, comparison with piezoelectric transducer 8-90617
 pulse detector, appl. of current amplification by vibrating membrane of piezoresistive semicond. 8-75025
 transmission matrices 8-51027
 SbSI materials, piezoelectric props. rel. to use as electroacoustic transducers 8-52445

acoustooptics *see acousto-optical effects***actinide alloys**

- see also actinide compounds; plutonium alloys; uranium alloys*
 conference on rare earths and actinides, Durham, England (July 1977) 8-84115
 fission reactor fuel, irradiation effects 8-86606
 magnetic properties, review 8-84383
 thermoelectric power of nearly magnetic systems 8-84197
 Ce_{1-x}Th_x, mixed valence systems, spin dynamics and mag. ordering 8-68162
 NpRe₂, mag. susceptibility 8-68182
 Pt-actinide diatomic mol., calc. dissociation energy 8-78832

actinide alloys continued

- RhTh, mol. vapour above Th-U-Rh-graphite, dissociation energy, mass spect. 8-78832
 Th-U alloy fuel behaviour in organic-cooled reactor 8-86605
 Th-U metallic fuel, irradiation performance 8-86608
 Th-U Na-bonded metal fuel, transient heating test 8-86607
 Th-Zr, supercond. transition temp. depend. on constitution 8-88056
 ThNi₃, methanation catalyst, AES and characteristic energy loss spectra 8-56915
 ThRe₂, mag. susceptibility 8-68182

actinide compounds

- see also compounds of individual actinides, e.g. uranium compounds*
see also actinide alloys
 binding and transition energies, expt. and theoret. comparison, review 8-50497
 ESCA spectra, intense shake-up satellites, model 8-50589
 halides and oxides, stability study, energy difference between trivalent and tetravalent metal states 8-79553
 magnetic properties, review 8-84383

actinide metal compounds *see actinide compounds***actinide metals** *see actinides***actinides**

- see also individual actinides, e.g. uranium*
 band structure Fermi surface, magnetisation density 8-84140
 binding and transition energies, expt. and theoret. comparison, review 8-50497
 chemical separation from PUREX raffinates using organic solvents 8-66676
 conference on rare earths and actinides, Durham, England (July 1977) 8-84115
 EPR, expt. techniques, electronic and nuclear props. 8-52337
 industrial dusts, lung clearance studies at NRPB 8-65137
 magnetic properties, review 8-84383
 preparation and refining 8-84705
 research developments since 1950 8-84116
 self-consistent relativistic muffin-tin calc., atomic vol. and bulk modulus Ac-Am 8-72065
 spin fluctuation theory, for mag. and elec. props., appl. to actinides 8-91869
 structural properties rel. to f electrons 8-83951
 thermoelectric power of nearly magnetic systems 8-84197
 X-ray 3d spectra, 4f and 5f states 8-84681

actinium

- see also nuclei with*
 No entries

actinium compounds

- No entries

actinometers *see radiometers***actinometry** *see radiometry***activation analysis** *see chemical analysis by nuclear reactions and scattering***active circuits** *see active networks***active networks**

- biomembrane electronic cct. model utilising time variant negative res. 8-88696
 thermocouple dynamic error correction cct. 8-77909

active nitrogen *see nitrogen***active oxygen** *see oxygen***actuators**

- see also electric actuators*
 attitude and orbit control systems, conference, Noordwijk (1977) 8-65480
 mechanical actuator, stepper motor, appl. to control of scientific apparatus 8-62683
 nuclear steam system, globe main steam isolation valve unbalanced forces and novel actuator design 8-50288

adaptive control

- see also adaptive optics; adaptive systems*
 digital computer applications to process control, conference, The Hague (1977) 8-49808
 dimensional gauging using scanning laser beam 8-57898
 EEG phasic event detection by microprocessor 8-57091

adaptive optics

- active optical systems, real-time control over optical wave fronts 8-71187
 astronomical image processing digital techniques 8-81555
 laser adaptive resonator expt. config. 8-55386
 laser beam, phase compensated, propag. through atm. turbulence 8-83012
 laser resonator, intracavity deformable mirror adaptive optical system 8-87078
 laser resonator active control techniques 8-71122
 laser system, high energy, optical distortion, active control 8-83019
 nonlinear optical phase conjugation for laser systems 8-79072
 nonlinear optical phase conjugation for pulsed laser systems 8-59092
 phase conjugate optics and real-time holography 8-83034
 phase conjugate reflection, pulsed 10.6 μm, via intracavity degenerate four-wave mixing 8-87097
 phase determination of amplitude modulated complex wavefront 8-55305
 phase estimates from slope-type wave-front sensors 8-66770
 thermal blooming compensation, equivalent thin lens model 8-87108
 thermal-blooming compensation, using closed-loop adaptive single parameter system 8-94407

adaptive systems

- see also adaptive control; adaptive optics; cognitive systems; pattern recognition*

- ripple noise pitch detection by human, adaptive model 8-73166

adding machines *see calculating apparatus***adherence** *see adhesion***adhesion**

- adhesively bonded metallic panels, 2-ply, finite element and integral eqns. anal. of fatigue crack growth 8-92347
 apparatus, for adherence, wear resist. and thermal shock meas. of thin films 8-72943
 axisymmetric butt joints, stress anal. in torsion and tension, response of adhesives 8-63397
 biomembranes, bivalent cations effect 8-64946
 bonded lap joints, elastic stresses theory 8-55563

adhesion continued

- bonded plate or membrane strips, exam. of adhesive fracture 8-59342
 concrete, joints glued with reaction resinous mortar, photoelastic exam. (German) 8-76825
 corrosion protective coatings, organic, performance evaluation of adhesion and permeability 8-64764
 debond dynamics for elastic strip, Timoshenko beam props. and steady motion 8-55604
 diamond surface soldered to metal film, contact strength determ. device 8-60910
 double cantilever beam, adhesive fracture specimen, crack tip stress field anal. 8-55602
 double lapped composite joints, efficiency in bending, of steel/B reinforced Al or epoxy adherends 8-68870
 epoxy Al bonded, adhesive joints under complex loading, development of failure criterion 8-92344
 epoxy resin, glass bead-filled, elastic moduli, interfacial slippage effect anal. 8-76688
 epoxy resin-Al alloy 5086, scarf joint test specimen, mixed mode adhesive fracture, bond angle effect 8-68768
 film, diamond indentation and draw tester for meas. of ultra-adherence 8-72944
 film adhesion testing, simple real-time holographic interferometry method 8-92411
 graphite reinforced epoxy steel scarf joint, adhesively bonded, exam. of failure 8-92350
 ice, single crystal, friction of steel ball load, velocity and temp. depend. (Japanese) 8-88537
 inelastic electron tunnelling spectroscopy studies 8-92440
 joint failure, adhesive/electronically conducting substrate, exam. of electrochemical aspects, 8-60979
 laminates, fracture, effect of adhesive layers 8-90791
 metal adhesion experiment for Spacelab 8-88621
 metal elements, adhesively bonded, cracked or with discontinuities, analysis procedures 8-90793
 metal panels, adhesively bonded, cracked, fracture anal., crack tip stress intensity factors 8-90792
 metal surface, AES anal. in adhesion, friction and wear 8-53179
 metallic interfaces, self-consistent electronic densities and adhesive energies 8-72005
 NDT characterisation of metallic substrate surfaces prior to adhesive bonding 8-53166
 polyamide-Cu(Ni) oxalate, oxalate decomposition kinetics, in polymeric medium, thermogravimetry and DTA 8-52749
 polyethylene films, adhesive props. improvement by corona discharge appl. (French) 8-92438
 polymer, particle-filled, elastic moduli, interfacial slippage effect anal. 8-76688
 polymer adsorption/adhesion, smooth surface, mech. stress effects (Russian) 8-50672
 polymer films, to metals and non-metals, principles and meas. methods (Czech) 8-80709
 polysilicane gel on glass plate, elastic deformation in adhesion of solids 8-60010
 polyurethane, adherence on glass 8-83336
 PTFE-Al, adhesion joints, effect of Cu and CuO 8-53183
 PTFE/graphite bond in H_2PO_4 environment, electrochemical exam. of joint failure 8-60979
 rubber, peeling initiation and propag. 8-76824
 rubbery polymer film, on glass surface, interfacial dislocations spontaneously created by peeling 8-73011
 short-range interactions mediated by a solvent with surface adhesion 8-71973
 steel, joints glued with reaction resinous mortar, photoelastic exam. (German) 8-76825
 steel-aluminium plates, exam. of adhesion strength by impulse loading 8-84943
 strength measurement of electroplates, device 8-56843
 structural bonded joints, fatigue crack growth of adhesive bond line cracks 8-92346
 superconducting magnet, effect of adhesion between turns 8-89507
 thin film growth, surface self-diffusion coeff., adhesion energy of evap. material 8-84080
 US spectroscopic NDT 8-76805
 viscoelastic bodies, adhesion and fracture mechanics, review 8-83336
 Al, adhesively bonded and weld bonded aircraft struct. subjected to acoustic excitation, determ. of sonic fatigue life 8-92351
 Al, joints glued with reaction resinous mortar, photoelastic exam. (German) 8-76825
 Al, thin foil, adhesion and friction, rel. to observed dislocation density 8-64706
 Al-Cu-Mg-Mn (4.5, 1.5, 0.6, wt.%), alloy 2024-T81, plates, adhesively bonded, exam. of fatigue crack growth 8-92349
 Al-epoxy adhesive systems, opening and edge-sliding fracture toughness 8-95805
 Al-graphite adhesion and contact angle, effects of metal additives (Japanese) 8-60008
 Al-Zn-Mg-Cu-Cr, (5.6, 2.5, 1.6, 0.3 wt.%), laminates, 8 and 22 layers, adhesively bonded exam. of fatigue crack propag. 8-92345
 Al-Zn-Mg-Cu-Cr, (5.6, 2.5, 1.6, 0.3 wt.%), alloy 7075, plates, adhesively bonded, exam. of fatigue crack growths 8-92348
 $Al_2O_3/Nb/Al_2O_3$ joint, solid state bonded, exam. of bond fracture strength 8-76826
 Au fine particles, adhesion, role of twinning and surface energy, TEM obs. 8-72009
 Au to Al_2O_3 solid state reaction bond, effect of ambient atmosphere 8-67914
 Ni dendrites on Al, CVD, selective solar photothermal absorber 8-52683
 Si_3N_4/Zr joint, solid state bonded exam. of bond fracture strength 8-76826
 W fibre reinforced epoxy resin, strength of metal-polymer adhesive contact, time-temp. depend. 8-68753

adiabatic compression, plasma see *plasma heating*

adiabatic demagnetisation see *magnetic cooling*

adion see *adsorption*

admittance, electric see *electric admittance*

admittance, electric, measurement see *electric admittance measurement*

ADP (ammonium dihydrogen phosphate) see *ammonium compounds*

adsorbed layers

see also *monolayers*

- adatom, valence shell energy level shift (French) 8-67900
 AES, chem. state effects, for water and simple organic cpds. 8-72687
 AES, chemical-state effects 8-92566
 angle resolved photoemission, multiple scatt. approach 8-72693
 bond geometry, determ. using photoemission 8-71951
 Born-Green-Yvon eqn., two-dimensional, with anisotropic interac. 8-79882
 butane, on graphite, struct. and dynamics, neutron scatt. study 8-87870
 catalytic reaction, high temp. IR obs. 8-88655
 chlorophyll-a on aerosol, absorpt. spectra 8-53327
 core level photoemission from adsorption layers, book contrib. 8-95673
 core level spectra, correlation effects 8-68605
 core level spectra of adsorbates, exactly soluble limits of model 8-80459
 dibenzotetrathiafulvalene, adsorbed on Au, Al, ionisation and polarisation energies of mol., UPS meas. 8-79886
 directional photoemission, book contrib. 8-95674
 electrolytic double layer, light absorpt., electrochromic changes 8-84551
 electron binding energies reference level problem in photoelectron spectra of solids and adsorbates 8-69396
 electron spectroscopy of surfaces, review 8-92169
 electronic state of adatom, depend. on conc. 8-72001
 electronic states, adsorbate induced rel. to photoemission, book contrib. 8-95326
 ethylene, adsorbed on Na zeolite, uniaxial rot., translational dynamics 8-91538
 film, on BCC cryst., modelling of order-disorder transition, Monte-Carlo method 8-60033
 gravimetric measurement of sorption isotherms, errors 8-67905
 heterogeneous systems, self-diffusion, NMR pulsed field gradient (German) 8-60341
 1-hexene-water(D_2O), field-induced surface reactions, field ionis. mass spectra obs. 8-95949
 hydrocarbons, adsorbed on Ru(001), characterisation by electron-stimulated desorp. 8-71958
 indirect long-range oscillatory interaction between adsorbed atoms 8-71997
 inert gas atom adsorbed on graphite surface, excitation spectrum 8-71943
 Kapitza resistance, heat transfer rel. to adsorbed monolayer (Russian) 8-51758
 LEED examination of interaction of adsorbed atoms 8-95237
 LEED from disordered overlayer, model calc. 8-84074
 light metal atoms, raising of superconductor critical temp. (Russian) 8-84337
 macromolecules, energy of interaction between two spherical particles 8-53271
 methane, on graphite, struct. and dynamics, neutron diffr. and inelastic scatt. 8-87869
 methanol on Ag(110) catalyst, oxidation 8-88556
 mobile monolayer adsorption, critical props. of Bergmann's model (German) 8-84073
 molecule above metal surface, damping of mechanism for excited state 8-92160
 monocarboxylic acids, chemisorbed on Al_2O_3 , tunnelling spectroscopy 8-91545
 monolayer of patches covered by mobile and localised adsorbed mols. 8-72004
 monolayers, oriented phase transitions (Russian) 8-75936
 neutral molecules adsorbed on dielectric surface, excitation spectrum 8-71943
 neutron diffraction and inelastic scatt. from adsorbed mols. 8-87869
 nitrilotri (methylenephosphonic acid), adsorption on $BaSO_4$ crystals, effect on crystal growth 8-88417
 nonpolar molecules, adsorbed on metal surface, depolarisation interaction 8-51820
 octane-water interface, water photo-oxidation in presence of adsorbed porphyrins 8-64933
 organic compound, two-dimensional condensation with adsorbed mol. reorient. 8-61051
 organic solvent, on Si surface (Russian) 8-91537
 oriented molecules, inelastic low energy electron scatt. 8-72653
 oscillatory indirect interaction between adsorbed atoms, non-asymptotic behaviour in tight-binding models 8-72000
 photoemission, adsorbate induced, book contrib. 8-95668
 photoemission, ang.-resolved, independent atomic centre approx. 8-84701
 photoemission, angle-resolved, from adsorbates, book contrib. 8-95669
 photoemission from adsorbed molecules, atomic dipole theory 8-84695
 plasmon mediated interaction between physically adsorbed atoms in presence of metallic surface 8-71991
 polymer flexible lattice chain in limited vol., behaviour (Russian) 8-70992
 porous solid with below-freezing pt. adsorbate, isothermal adsorption and dimensional changes obs. 8-75925
 pyridine, on Ag(100), (111) and polycryst. electrode surfaces intense Raman spectra 8-72492
 rhodamine B dye, on PbO powder layers, charge storage and photocond. 8-64056
 rose bengal, adsorbed on ZnO electrode, reson. Raman spectra 8-76446
 structural and electron alterations, electron-phonon interaction effects (Russian) 8-87880
 structural and electronic reconstructions in adsorbed layer on metal surface 8-84280
 superelastic electron scattering (French) 8-56039
 surface EXAFS study of adsorbate Auger electron intensity on single cryst. surfaces 8-66562
 surface structure of solids and adsorbates by LEED 8-94953
 thermal desorption and conversion kinetics, AES study 8-71959

adsorbed layers continued

thermodynamic relations of Pippard's type for dielectric and magnetic properties of adsorbed layers near a λ -transition 8-79881/U, non two-dimensional order-disorder phenomena, Monte Carlo simulation 8-67904

two-dimensional system, monolayers, permeation and evaporation resistance, attractive forces effects 8-67892

valence photoemission from adsorbates, book contrib. 8-95672

water, adsorbed in monolayer hydrate of halloysite, NMR obs. of mol. motion 8-95226

water, on porous glass, proton spin-lattice relax. meas. by pulse NMR 8-84053

XPS, line shapes and multiple lines 8-84702

XPS, plasmon effects on core level spectra 8-60347

Ag, on Si (111), electronic and cryst. struct., Schottky barrier form. obs. 8-84091

Al, on Si (111), theoretical study 8-95366

Al-adsorbed monolayer-Al junction, elec. cond. mech. 8-95386

Ar, monolayer adsorbed on graphite, lattice dynamics 8-75946

BaO, on Si photofield, cathode, work function, and emission props. (Russian) 8-68608

Br₂-graphite systems, adsorbed and intercalated, EXAES 8-72638

C is contaminant buildup on conductors (insulators) in X-ray ESCA 8-95981

C electrode, breakdown voltage dependence on adsorbed gases 8-75465

CO, adsorbed on metal surface, collective vibr. modes, dipole interactions 8-50533

CO, adsorbed on Ni(Pt), intermediate UPS/XPS synchrotron radiation study 8-52633

CO, adsorbed on Pt (111), oxidation process, reflection-absorp. IR study 8-76468

CO, on metals, valence photoemission book contrib. 8-95672

CO, on Ni(100) surface, angle resolved UV photoemission 8-56570

CO, on Pd, photoelectron spectra, 40-180 eV, adsorbate sensitivity enhancement 8-80453

CO, on Pt surface, IR spectrum obs. in presence of free CO 8-74654

CO, oriented molecules, vibrationally inelastic electron scatt. 8-67907

CO, Photoelectron angular distrib. of C and O K-shell ionisation 8-52628

Cl, chemisorbed layer on Si (111), SCF LCAO calcs. of Si band struct. 8-88010

Cl, on Ag(111) props. struct. AES study 8-72024

H chemisorbed on metal surface, electron correl. friction, coeff. 8-60026

H, on Si (100) surface, LEED and AES meas. 8-60016

H, on Si (100)(1x1) surface, LEED study 8-67910

H₂ adsorbed on Pd black, vibr. spectrum assignments, inelastic neutron scatt. obs. 8-71942

H₂, on Cu, adsorbate induced photoemission, book contrib. 8-95668

H₂, on Si and Ge surface, cluster model approach for electronic struct. 8-56205

H₂, on W surface, energy spectra for electron stimulated desorption of H⁺ calc. 8-79892

H₂, oriented molecules, vibrationally inelastic electron scatt. 8-67907

H₂O, adsorbed, surface-induced NMR line splittings and augmented relax. rates 8-64288

H₂O, adsorbed on kaolinite clays, dielec. props. 8-76381

H₂O molecule in pores of zeolites, intermed. state of enhanced mobility 8-60027

H₂O vapour, chemisorbed on Hg, Ag, Pb, Ga, Fe, Pt effect on surface props. 8-60187

H₂O+CO₂, photoassisted reaction on SrTiO₃ (111) face, methane form. 8-76878

H₂ adsorpt. on zeolites with varied Si/Al ratios 8-60029

³He on graphite 8-87842

³He, specific heat, second layer adsorbed on Grafoil 8-87843

⁴He on Nuclepore filter, specific heat (Japanese) 8-79852

I, on Ag (111), geometry and bond length, surface EXAFS 8-71952

InSb, irradi. real and clean surfaces, work function 8-95336

Kr, on graphite, Potts lattice gas, renormalisation-group treatment 8-67908

Kr, on graphite, X-ray diff. from 2-D solid 8-75498

Kr, submonolayer, adsorbed on graphite, melting, X-ray scatt. obs. 8-95234

N₂, dense monolayer on graphite cleavage face, phase transition 8-56034

N₂ monolayer adsorbed on graphite, lattice dynamics 8-75946

N₂, oriented molecules, vibrationally inelastic electron scatt. 8-67907

NH₃ on graphite, structure and dynamics, neutron diff. and inelastic scatt. 8-87869

NO₂ adsorbed on Cu, species identification, struct. disson. chemisorption, desorption, UV photoelectron spectroscopy 8-52635

NO, first adsorbed layer on graphite, BN₂ and lamellar halides, critical and triple point temps. 8-91548

Na, on Ni(001), core-level photoelectron diffraction 8-95691

Ni, on W (111), surface site geometry and diffusion charact. of Ni atoms 8-71953

Ni, quasisatomatic excitation, causing energy loss peak, UPS 8-72691

No, on graphite, melting and polymorphism 8-84063

O₂ chemisorbed on Al (100), photoemission, ang. depend. MO cluster model calc. 8-76576

O₂, chemisorption on W (110), Monte Carlo modelling of phase changes 8-71969

O, on Ni, photoemission intensities from core states 8-95654

O, on Ni (001), electronic struct., KKR calc. 8-56200

O single layer on Au, ferromag. props., thermomag. effect (Russian) 8-64256

O₂ adsorbed on PbSe, XPS (UPS) obs. lattice diffusion and sticking coeff. 8-52637

O₂ chemisorbed on Hg, Ag, Pb, Ga, Fe, Pt effect on surface props. 8-60187

O₂ on Ag, EPR of O₂, rate of angular reorientation 8-72413

O₂ on Cu, ion-bombarded, ejected particle ang. distrib. 8-95643

O₂ on GaAs(Pt), surface electronic struct. (surface chem.) using synchrotron radiation 8-53254

O₂ on SiO₂ supported, W, EPR evidence for surface mobility of O₂ 8-84046

Re₂, on W (211) surface, disson. thermodynamics 8-87863

S, on polycrystalline Ni surface, H₂ ion induced desorption 8-84069

adsorbed layers continued

Se (2x2) overlayer, on Ni (001) surface, angular resolved UPS 8-76584

Se, on Ni, photoemission intensities from core states 8-95654

Se, on Ni (100), electronic orbitals, angle-integrated UPS 8-72224

Ta-containing Ta sheet, radioactive electron emission spectrum (exoelectrons), surface elec. field and Auger effects 8-72705

Ti, on Ni, photoemission intensities from core states 8-95654

Te, on Ni(001), core-level photoelectron diffraction 8-95659

Ti₂ adsorbed on hydrated silica, NMR relax. chem. shift 8-72427

Xe, adsorbed monolayer, THEED intensity meas. 8-84075

Xe, on NiCl₂ phase transition identified as 2D polymorphic transform. 8-56040

Xe physisorbed layer, UPS spectra, lateral interaction 8-92174

adsorption

see also heat of adsorption

albumin, human serum, adsorption studies, feasibility of radiolabelling 8-85359

alkali halides, of gas, stress depend. of chem. pot. 8-91541

alkali halides, of inert gas atoms, pot. energy calcs. 8-67902

alkaline earth oxides, of O₂, electron transfer, EPR obs. 8-76296

Auger matrix element, multicentre, ang. depend. calc. for solids and adsorbate systems 8-92151

batch adsorption for pore diffusion with film resistance and an irreversible isotherm 8-84047

bovine serum, meas. at interfaces by drop volume technique 8-60009

chabazite, of Ar-N₂ mixture, test of eqns. for gas mixture adsorption on heterogeneous surface 8-60030

chemostress coefficient, adatom-solid substrate interaction 8-91540

chrysotile, of organic micropollutants, XPS and gas solid elution chromatography exam. 8-80790

crocidolite, of organic micropollutants, XPS and gas solid elution chromatography exam. 8-80790

cycling zone adsorption, travelling wave, continuous flow equilib. staged model, 8-64874

cylindrical channel walls, adsorption from fluid in Poiseuille flow 8-84048

disperse system adsorption on hydrated solid phase surface exchange cations effect 8-64893

dissociative adsorption, quantum chem. theory, adatom-solid potentials 8-73087

dust, of SO₂, in atmosphere 8-96287

electrode, metal, effect of solvent interaction on elec. double layer struct., adsorpt. 8-61023

equilibrium, anomalies near crit. points of substrate 8-79895

exponential adsorption isotherm, modified form. 8-87864

field emission current fluctuation, power spectral density (Japanese) 8-88407

formaldehyde, on Ru(110), UPS study, 80K 8-73080

gas adsorption data analysis, pore size and size distribution, determ. review 8-63939

gas-solid interface, EPR centres induced by microwave gas plasma 8-80215

glasses, porous, of water, osmotic flow, filtration investig. 8-53248

graphite, of Ar, orientational ordering of incommensurate monolayers, LEED obs. 8-95233

graphite, of O-H₂ (p-D₂), NMR, orientational behaviour, weak crystal field 8-75935

graphitised C black, of inert gases, gas-solid virial coeffs. 8-75928

graphitised carbon black, of Ar, (methane), surface excess isotherms, gravimetric determ. 8-51816

graphon, of Ar, high press. and temp., gas density profile theory 8-67903

halide, of O₂, bidimensional condensation (French) 8-75941

halloysite, Al₂O₃(SiO₂)₂(H₂O)₂, NMR study of adsorbed water, molecular motions 8-95226

hard sphere gas interacting with hard wall, density profile, virial expansion 8-63928

heterogeneous nucleation systems, crit. conditions, characterising formation 8-56023

heterogeneous surface, gas mixture, adsorption, expt. data analysis 8-60030

homogeneous surface, adsorpt. of single gases statistical thermodynamics 8-79877

homogeneous surfaces, statistical mech. of collisions, which lower desorption rate (German) 8-84072

homopolymer chain adsorpt. on uniform surface 8-53316

Inconel 600, fusion reactor vac. vessel, air, N₂ adsorpt., thermal desorpt., heat treatment effects 8-54880

inverse power law potentials about polygonal prisms and in polygonal cavities 8-95232

β -lactoglobulin, meas. at interfaces by drop volume technique 8-60009

lipid bilayer, of cytochrome c 8-69001

liquid mixture, adsorption on solid, equilib. thermodynamic correlations 8-84045

lysozyme absorpt. meas. at interfaces by drop volume technique 8-60009

metal, of H₂ and N₂, permeation through metal barrier, adsorpt. processes 8-63879

metal, of He, interaction energy, quantum mech. density functional formalism calc. comp. with expt. 8-67914

metal, of inert gas, interaction energy, quantum mech. density functional formalism calc. 8-67911

metal, of molecule monolayer, IR spectra exam. by surface EM wave spectroscopy 8-71967

metal film, evaporated, of gases, rel. to surface area 8-79909

metal films, evaporated, with BCl₃, HCl, interaction, adsorpt. 8-75945

metal ion adsorption, nucleation effects (German) 8-68635

metal oxide surfaces, of electron acceptors, strength and distrib. of electron donor sites 8-84055

metal surface, alkali adsorption, finite barrier model, bounded electron gas static semiclassical response 8-72221

metal surface, work function change on simultaneous adsorption of atoms of two different elements 8-60184

metal surface struct. and initial stages of reactivity, review 8-68837

metallic surfaces, adsorption of inorganic and organic molecules, mechanism and effects, exam. (German) 8-51828

metallic surfaces, thin film appls. 8-75943

methyl iodide removal by Ag impregnated Al and zeolite 8-53719

adsorption continued

- mixed gas adsorption, on heterogeneous solid surface, kinetics 8-95231
 mixed gas adsorption, review of theories 8-75942
 modulated molecular beam mass spectrometry, anal., appl. to nonlinear systems 8-56944
 nonplanar geometry, physical adsorption 8-79887
 organic compound, two-dimensional condensation with adsorbed mol. reorient. 8-61051
 organophilic montmorillonites, of methanol-benzene mixtures, effect of surface modification 8-84056
 Percus-Yevick and hypernetted chain theories, second and third virial coeffs. for hard-sphere gas 8-60031
 physical adsorption, high press. and temp., gas density profile theory 8-67903
 polymer adsorption into surface pores, computer simulation, phase transition (*Russian*) 8-51824
 polymer adsorption/adhesion, smooth surface, mech. stress effects (*Russian*) 8-50672
 polymer attached to surface, dynamics, bead and spring model 8-75931
 polymer flexible lattice chain in limited vol., behaviour (*Russian*) 8-70992
 polymers, adsorption transition, excluded vol. effects, Monte Carlo and enumeration calcs. 8-67906
 polymers, of gases, sorption, permeation investigs., review 8-67868
 polystyrene, porous gel, solute elution behaviour in high performance liq. chromatography 8-92524
 polystyrene latex particles, of poly(vinyl alcohol), influence of temp. 8-85206
 proteins, of non-paramag. compounds, spin probe investigation 8-65153
 reconstructed surfaces, effect of adsorbed atoms or mols. 8-95214
 semiconductors, adsorption, boundary layer and electron theories (*German*) 8-95236
 SI units, in adsorption expts., replacement of Langmuirs and exposure proposed 8-62175
 silica (metallised) gels, thermal cond., 10-200K, cryogenic appls. 8-79828
 silica gels, surface treatment, adsorption properties (*Japanese*) 8-95855
 solution adsorption, from liq. chromatography 8-84054
 static AES technique, appls. 8-84685
 statistical mechanics, virial expansion, eqn. of state and isotherms (*German*) 8-95235
 steel, stainless, oxidised, of Cs 8-84061
 superconductor, raising of critical temp. (*Russian*) 8-84337
 surface, solid, of microdrop, stability, dynamics 8-51790
 surface EXAFS study of adsorbate Auger electron intensity on single cryst. surfaces 8-66562
 surface properties of materials, Conf., Missouri, USA (August 1977) 8-87867
 transition and free-electron like metals, of alkali metals, valence electronic struct., wave-function matching calcs. 8-72235
 two-particle correlation function for fluid-solid surface interaction 8-79880
 ultrahigh vacuum chamber for Raman studies of gases adsorbed on metals 8-81991
 volatile chlorides, adsorption isotherms meas. using radionuclides and chromatography 8-76902
 Vycor glass, of ^4He from ^3He - ^4He mixtures 8-84023
 Vycor porous glass, of carbonium ions, reson. Raman spectra 8-84571
 water, press. effects on surface tension, adsorpt. of hydrocarbon-gases and CO_2 , 0-50°C 8-56024
 zeolite (Itaya), of H^+ , NH_4^+ , Cd^{2+} , Cu^{2+} (*Japanese*) 8-95951
 Ag electrode, of metal ions, kinetics, surface struct. 8-79873
 Ag, I_2 adsorption site on Ag(111), X-ray anal. 8-84679
 Ag, of O_2 , catalytic oxidation mechanism 8-61046
 Ag, single crystal, adsorption of metal ions on (111) and (100) surfaces (*German*) 8-68636
 Ag surface, of inert gases, physisorption energies 8-71944
 AgBr, of cyanine, pH depend. 8-62254
 Al, alkali metal adion-surface interaction energy, density formalism calcs. 8-68069
 Al, of alkanes, thermal accommodation coeffs., translational and internal gas-solid energy exchange 8-92506
 Al, of O_2 , relation between energy-band and cluster model 8-52048
 Al_2O_3 , adsorption of H_2O , energetics, effects of adsorption temperature on surface processes 8-60028
 $\alpha\text{-Al}_2\text{O}_3$, of $\text{H}(\text{H}_2)$, microweighing and X-ray obs. (*German*) 8-51825
 $\gamma\text{-Al}_2\text{O}_3$, of methane, γ -radiolysis, reaction kinetics 8-95940
 As_2Se_3 , glassy, with adsorbed $\text{H}_2\text{O}(\text{NH}_3)(\text{NO}_2)(\text{O}_2)(\text{CO}_2)(\text{CO})$, surface cond., photocond. 8-80038
 Au electrode, of metal ions, kinetics, surface struct. 8-79873
 Au electrodes, of Br^- , specular reflect. investig. 8-61047
 Au, of O_2 , Auger spectra 8-87879
 Au, of Pb, formation of AuPb_2 epitaxial layer, LEED, AES study of Au/AuPb₂ interface 8-71988
 BaTiO_3 , of O_2 , mechanism calc. 8-63927
 C activated, of 0.98 mol.% Ar, vol. adsorption capacity 8-75933
 C, activated, vol. adsorption capacity for selected trace contaminants 8-56031
 C, of gas, rate depend. on granule size and gas flow velocity 8-56033
 CdS, surface energy levels, O(C) adsorpt., AES study (*Japanese*) 8-88008
 ^{60}Co removal from waste water, adsorption on activated charcoal with oxine 8-58365
 $\text{Cr}_2\text{O}_3\cdot\text{SH}_2\text{O}$, heat-treated, narrow particle size distrib., surface props. 8-85210
 CsI, of Ar- O_2 mixture, test of eqns. for gas mixture adsorption on heterogeneous surface 8-60030
 Cu (100), of CO, UV and X-ray photoelectron spectra, LEED 8-56037
 Cu (210) surface, of O_2 , LEED and AES meas. 8-71998
 Cu, adsorbed mol. monolayers, UV-visible spectra 8-72619
 Cu, influence of cryst. orientation on work function, with and without adsorbed S (*French*) 8-76134
 Cu, of CO, angle-resolved UPS and adsorbate induced struct. 8-71983
 Cu, of H, potential energy curves, pairwise additive model calcs. 8-73087

adsorption continued

- Cu, of NO , species identification, struct., dissociation, chemisorption, desorption, UV photoelectron spectroscopy 8-52635
 Cu, of O, on (001) surface, deep core level XPS anisotropy 8-72690
 Cu, of Xe, stay time meas. 8-56044
 Cu surface, of Sr^{2+} , ^{90}Sr tracer expt., immersion time conc. and temp. depends. 8-87863
 Cu surfaces, of O_2 adsorbed, exam. of structure by LEED, O_2 pressure-temp. diagram (*Japanese*) 8-79884
 Cu(100), adsorption and incorporation of O_2 8-56042
 Fe (001), of CO, random occupation of adsorption sites, LEED exam. 8-63930
 Fe, of alkanes, thermal accommodation coeffs., translational and internal gas-solid energy exchange 8-92506
 Fe surface, purposeful modification by gas adsorption, charact. by photoemission 8-71955
 GaAs, of Cs(Rb)(Na), LEED, AES, EELS study 8-68068
 GaP (001), of Cs, photoemission meas. 8-87874
 Ge (111) of K and O_2 , rel. to work function, K thermodesorpt. spectra 8-79874
 Ge, of Au, effect on I-V characteristics, field emission study 8-67925
 Ge:Na (111) surface, of O_2 , adsorpt. rate, work function, surface cond. changes investig. 8-79875
 H_2 , permeation through metal barrier, adsorpt. processes 8-63879
 InP surface, of Cl, electron spectroscopic obs. 8-56036
 InSb, of Cs(Rb)(Na), LEED, AES, EELS study 8-68068
 KBr, of Ar and Kr, potential energies calc. 8-71993
 Li, of O_2 (100) surface, cluster models, ab initio HF LCAO theory 8-71978
 LiF, ^4He scatt., selective adsorption induced intensity maxima 8-72667
 LiF (001), of H_2 , molecular orbital calc. 8-87878
 LiF, selective adsorption of ^3He and ^4He , atomic beam scatt. meas., binding energies 8-63935
 $\text{MgCaH}_{1.72}$, synthesis and struct. (*Japanese*) 8-84751
 MgO , of $\text{CO}(\text{N}_2)(\text{NO})(\text{O}_2)$, 77 to 150K, mol. motion anal. 8-84051
 MgO , of $\text{H}(\text{H}_2)$, microweighing and X-ray obs. (*German*) 8-51825
 MgO , of NO , adsorbate dimer form., heat of dissociation, EPR obs. 8-82755
 Mo (011) face, of Sr and La, influence of substrate electronic struct. on props. 8-60032
 Mo, of N_2 , surface coverage 8-60036
 $\text{Mo}_2\text{O}_3\text{-Al}_2\text{O}_3$, reduced catalyst, of O_2 , O^- form. 8-85197
 MoS_2 , of Cs and O_2 , LEED, Auger and work function meas. 8-71994
 Mo(100), of Co, LEED, AES, study 8-87873
 Mo(110) and (100) surface, surface reson. states and adsorption of 4d atoms 8-71982
 N_2 , permeation through metal barrier, adsorpt. processes 8-63879
 Na montmorillonite, of water, adsorption meas. at -5°C 8-65540
 NaBr, of Ar and Kr, potential energies calc. 8-71993
 NaCl, of CO, electrostatic interaction energy 8-74592
 NaCl, of N_2 , electrostatic information energy 8-74592
 NaF, selective adsorption of ^3He and ^4He , atomic beam scatt. meas., binding energies 8-63935
 Nb film, of SO_2 , adsorpt., corrosion 8-79897
 $\text{NbSe}_2(2\text{H})$ -hydrazine, intercalation compd., kinetic studies by transmittance meas. at 1600 nm 8-71981
 Ni (100), of chalcogen, structure, force consts., binding energies and photoemission, importance of final state multiplet splitting 8-71966
 Ni catalyst, Al_2O_3 supported, of CO in H_2 -He, effect of H_2S on IR spectrum 8-71945
 Ni, of CO, mol. orientation, ion scatt. 8-71949
 Ni, of CO on stepped surface, adsorpt.-desorpt. behaviour, LEED, AES, thermal flash desorpt. study 8-71984
 Ni, of H_2 , initial sticking coeff. for polycryst. O_2 and S covered surface 8-63937
 Ni, of Xe, Kr and CO_2 , stay time meas. 8-56044
 NiO, of $\text{CO}+\text{N}_2\text{O}$, catalysed reaction in Neel transition region 8-53258
 Ni(111), of acetylene, benzene form., vibr. spectra 8-95952
 Ni(111) surface, of H_2 , at low temps., LEED meas. 8-56045
 PbTe (111), of O_2 , UPS and XPS exam. 8-71962
 Pd (111), electronic states calc. and adsorbate-induced photoemission struct. interpretation 8-60179
 Pd, of CO, on (111) surface, catalytic oxidation, mol. beam investig. 8-88656
 Pd(001), of CO, LEED, electron energy loss spectra study, surface struct. effect on weak chemisorpt. bonding 8-71987
 Pd(111), of CO and O_2 , mutual interactions, transient product formation 8-87871
 Pt (100), of acetylene or ethylene, intermolecular forces and kinetics of adsorption 8-75930
 Pt (100), of H_2S , intermolecular forces and kinetics of adsorption 8-75930
 Pt (111), surface reaction with acetylene, ethylene, and H_2 , EELS 8-71947
 Pt (111) surface, stepped, of O_2 , CO, C_2N_2 and ethylene 8-71992
 Pt electrodes, of Au, in aq. HCl 8-56914
 Pt, of Cs field-emission microscopy 8-51822
 Pt, of O_2 , AES, LEED and thermal desorption spectroscopy exam. 8-79891
 Pt, surfaces (111) and $6(111)\times(111)$, CO adsorption, EELS and thermal desorption spectroscopy 8-91547
 Pt(111), of NO, anal. of adsorption processes and surface reactions, vibration spectroscopy 8-87868
 Re, coadsorption of ethylene and O_2 , thermal desorption study (*French*) 8-85194
 Ru (001), of NO, inelastic electron scatt. dissociation energies adsorbed state depend. 8-95956
 Ru electrodes, adsorption and surface reactions, cyclic voltammetry and X-ray emission spectrometry 8-61018
 Si, planar and O_2 etched (111) surface, CO adsorption, AES, SEM, ESD, flash desorption mass spectra 8-63934
 Si:H film, amorphous, elec. cond., effect of adsorbed gases and illumination 8-88048
 SiO_2 , adsorption of H_2O , surface treatment and methylation effects 8-84058
 $\alpha\text{-SiO}_2$, of $\text{H}(\text{H}_2)$, microweighing and X-ray obs. (*German*) 8-51825
 $\text{SiO}_2\text{-ZrO}_2$ adsorbents, coprecipitated, porous struct. rel. to form. conditions 8-53263
 Sn, O_2 precursor adsorption, chemisorption activation energy 8-71950

adsorption continued

- SnO₂, of H₂O, isotherms 8-56038
 SnO₂, of O₂(CO)(H₂O vapours), effect on cond. 8-76067
 SnO₂:ThO₂, exposed to CO gas, self-oscill. phenomenon 8-68032
 SrTiO₃, (111) face, photoassisted reaction of adsorbed H₂O+CO₂, producing methane 8-76878
 Ta film, of SO₂, adsorpt., corrosion 8-79897
 Ti film, of SO₂, adsorpt., corrosion 8-79897
 TiO₂, X-irrad., adsorpt. of O₂, EPR meas. 8-80211
 TiCl₄, of water vapour, 273, 283 and 293K 8-56035
 TiI₄, of water vapour, 273, 283 and 293K 8-56035
 U binding, by brown coal, from seawater, IR spectroscopic obs. 8-82855
 U(VI), extraction from sea water using polyacrylamide gel containing metal hydroxides 8-54861
 V, extended fine struct. above L-shell appearance pot. thresholds, CO adsorption effects 8-92148
 W (001) surface, of CO, electron energy loss spectra 8-71999
 W (011) face, of Sr and La, influence of substrate electronic struct. on props. 8-60032
 W (100), of La, depend. of work function, heat of adsorpt. on surface coverage, contact potential study 8-67912
 W (110), of O, adatom interaction energies, Monte Carlo calc. 8-71948
 W, alkali metal adion-surface interaction energy, density formalism calcs. 8-68069
 W, methane dissoc. by adsorption-desorption process 8-92511
 W, of CO, mol. orientation, ion scatt. 8-71949
 W, of CO(H₂)(O₂), surface reflectance spectroscopy on low index planes 8-71965
 W, of C(O), Auger signal comparison using differential and integral Auger spectra 8-76561
 W, of Fe, work function and field emission obs. (Japanese) 8-91536
 W, of O₂, electron stimulated desorpt. study, 300K, kinetics, order-disorder transition 8-71985
 W, of O₂ and H₂, on (100), effect on NVV Auger spectra, comp. to band struct. calcs. 8-72643
 WC, microcrystalline, mol. dynamics, motion of H₂O and H₂ mols. adsorbed on surface, catalytic activity 8-71941
 WO₃, of O₂ (propene), adsorption, struct., rel. to catalysis 8-51826
 W(100), of H, nondipole electron impact vibr. excitations obs. 8-63922
 W(111), of Ni, surface site geometry, diffusion charact. 8-75944
 ZnO 1010 surface, reaction of O₂, AES, LEED, EPR, desorpt., surface cond. and work function expts. 8-95950
 ZnO (0001), of alkali metal, anomalous behaviour of Na 8-79883
 ZnO, of Ba, effect on low energy cathodolum. 8-60522
 ZnO, of ethylene, adsorption rate spectra, freq. response method 8-51817
 ZnO, of H₂O vapour, annealing and grinding effects 8-68656
 ZnO powder, adsorption of O₂, H₂, light effects (Japanese) 8-95230
 Zr(HPO₄)₂, of pyridine, IR spectra, acidity 8-92377

aerials see *antennas***aerodromes** see *airports***aerodynamics**

- see also *hypersonic flow*; *jets*; *shock waves*; *supersonic flow*; *transonic flow*; *turbulence*; *wind tunnels*
 ablating body, solution for stable shape (Russian) 8-75162
 ablating body shape, numerical soln. method (Russian) 8-75134
 aeroelasticity of unsteady aerodynamics, force calc. methods (French) 8-75095
 aerofoil, dynamic forces acting, subsonic instabilities (French) 8-67213
 aerofoil, two-dimens., in incompressible flow, unsteady motion 8-67171
 aerofoil with jet flap, incompressible flow past 8-59414
 air diffuse discharge, gasdynamic effects 8-81294
 aircraft dynamics, unsteady airloads prediction, aeroelastic anal. 8-71346
 airfoil interference in two-dimens. steady flow 8-71356
 asymmetric flow past wings, nonlinear-discrete vortex method 8-71351
 atmospheric turbulence, aircraft response, math. modelling 8-81274
 axisymmetric rigid body in air, stability of unperturbed motion (Russian) 8-86146
 body of revolution, slender, nonlinear normal forces, Reynolds no. influence (German) 8-51191
 body shape for minimal radiative heat inflow, spacecraft atmospheric entry (Russian) 8-77457
 cascade, with large-deflection oscills., unsteady aerofoil theory, numerical soln. (Japanese) 8-67211
 conference on unsteady flow, Ottawa, Canada, (Sept. 1977) 8-71347
 convex body aerodynamics in rarefied mol. flow, kinetic theory 8-59424
 cylinder in cross flow, skin friction and vortex shedding freqs. 8-94758
 disturbance fields of unsteady singularities in uniform motion 8-71355
 drag, supersonic wave, of planar singularity distribts. 8-83430
 electroacoustic and aerodynamic calibrated sound sources compared 8-55543
 elliptic cylinder unsteady aerodynamics and vortex induced oscillations, test results 8-94746
 finite-particle scheme for three-dimens. gas dynamics 8-67218
 flow past airfoils with oscill. jet flaps, quasisteady theory 8-63467
 gas flow in duct, self-excited oscillations 8-55670
 gas flows in gravitational field (Russian) 8-67212
 hydroplaning of a rotating cylinder on water 8-63522
 hydroplaning plate, lift, drag 8-63523
 hypersonic flow, slender vehicle dynamics, viscous interaction or support interference 8-71363
 internal gas flow anal. by large particles method (Russian) 8-79355
 isotope separation by gaseous diffusion, aerodynamic effects 8-59469
 Joukowski airfoil, unsteady viscous flow, bound-vorticity distrib., numerical anal. 8-51169
 laser velocimetry principles and appls. (French) 8-63518
 lifting wing calcs., spanwise integrations, computational economy improvement 8-71344
 Mach number expansion, of Navier-Stokes equations, Lighthill's theory to non-adiabatic cases 8-83372
 metallic tethers in ionospheric plasma, electrodynamics and aerodynamics 8-69652

aerodynamics continued

- Navier-Stokes eqns., bluff body aerodynamics, numerical simulation methods 8-75115
 nonlinear formulation for low-frequency transonic flow 8-94761
 numerical solution of a class of integral equations arising in two-dimensional aerodynamics 8-62086
 ogive cylinder, mag. suspended, subsonic flow, reverse Magnus flow, turbulent boundary layer 8-51153
 oscillating flow over aerofoil, vel. field, surface press. 8-75164
 potential flow over wing with free vortex 8-63444
 re-entry, streaming, of vel. and temp., in oscill. boundary layers 8-83358
 real gas effects in cryogenic wind tunnels 8-94760
 spheroids, harmonically oscillating, unsteady airload prediction, analytical soln. 8-51184
 spinning cone, spin rate effect on side force 8-71349
 subsonic and supersonic aerodynamics, SOUSSA computer code 8-71352
 subsonic flow past pulsating airfoil 8-71348
 supercritical profile with oscill. control surface in subsonic flow (French) 8-71357
 supersonic flow over hemisphere-cylinder at incidence up to 19° 8-59419
 supersonic flutter of heated circular cylindrical shells with temperature-dependent material properties 8-71289
 symmetrical flow past double wedge at subsonic Mach nos. 8-51182
 transonic flow, unsteady, implicit shock-fitting computational scheme 8-94763
 transonic flow around bodies of rotation (Russian) 8-87357
 transonic indicial method, shock motion effect 8-94769
 transonic wind tunnel, noise level effect on model characts. (French) 8-71411
 tubes with ball seatings, basic groups, appl. in flowmeters (Russian) 8-67287
 two-airfoil systems, with aerodynamic interference, flutter anal. 8-51181
 unsteady airloads on oscill. wings and bodies 8-71354
 unsteady airloads on wing-store configs. in subsonic flow 8-71358
 unsteady airstream, two-dimens. viscous flow past aerofoil, numerical predictions 8-75166
 unsteady boundary layers, separated and attached, review 8-71313
 unsteady boundary layers with reversal and separation 8-75163
 unsteady subsonic and supersonic inviscid flow 8-71350
 unsteady viscous flow around aerofoil, numerical soln. procedures 8-75165
 wing, rectangular, with tip clearance in channel, aerodynamic characts. 8-59415
 wing tip-shed vortex, decay, injected air jet modification 8-63434
 wings, lift and pitching moment meas. in oscill. gusts 8-71353

aeronomy see *meteorology*; *terrestrial atmosphere*; *upper atmosphere***aerosols**see also *foams*

- absorption of solar, diffuse and reflected visible radiation (Russian) 8-96291
 actinide industrial dusts, lung clearance studies at NRPB 8-65137
 aerosol particles diffusion and gravitational settling in tube 8-90976
 aerosol precipitatin from laminar gas stream, free convection effect 8-83459
 air pollutants three-dimens. distrib. in Los Angeles basin 8-61542
 air pollution, from combustion, particle size distrib., health hazards 8-81394
 airborne lidar aerosol measurements during the ASSESS II mission 8-73489
 Aitken counter, portable photo-recording, for small atm. aerosols detect. 8-57355
 amosite fibres, collection efficiency of nuclepore filters 8-81341
 Ankara atmosphere, trace elements and size distribts. determ. by thermal neutron activation anal. 8-81377
 atmosphere, aerosol content determ. from photometric obs. of stars 8-92976
 atmosphere, aerosol properties rel. to solar aureole, photogrammetry 8-57315
 atmosphere, aerosol-induced heating effects on convective boundary layer 8-69409
 atmosphere, aircraft studies during GATE radiation subprogram 8-81408
 atmosphere, ambient sulphate aerosols laser-Raman monitoring 8-69532
 atmosphere, ambient sulphate particles size discrimination and chemical comp. by diffusion sampling 8-69528
 atmosphere, anal. of water-soluble S compounds 8-96282
 atmosphere, aureole around UV source at finite distance 8-77320
 atmosphere, chemical characterisation, progress and problems 8-68969
 atmosphere, conc. meas. by lidar 8-85693
 atmosphere, expt. meas. of inhomogeneities 8-77304
 atmosphere, five year record of fall-out in Liege industrial region 8-81375
 atmosphere, formaldehyde conc. and contrib. to rainwater 8-57243
 atmosphere, growth kinetics during SO₂ oxidation 8-96255
 atmosphere, ice splinter production during riming 8-85662
 atmosphere, incoherent optical propag. effects 8-92987
 atmosphere, individual microparticles identification via micro-Raman spectrometer 8-68970
 atmosphere, individual submicron sulphate particles detect. technique 8-69527
 atmosphere, influence on thermal effects of stratosphere O₃ depletion at 85°N latit. 8-81279
 atmosphere, instrumental anal. of light element comp. 8-69516
 atmosphere, interactions with NO_x and O₃ 8-81342
 atmosphere, large condensation nuclei meas. using laser photoelec. spectrometer (Russian) 8-65408
 atmosphere, light beam coherence through optically dense turbid layer 8-55300
 atmosphere, light scattering problem, integral formulation 8-63010
 atmosphere, limitation on electrical measures 8-69431
 atmosphere, mass conc. meas. by Nd:glass lidar, ASSESS II Spacelab mission simulation (German) 8-69649
 atmosphere, particle size distrib. statistical characts. rel. to light attenuation coeffs. (Russian) 8-53702
 atmosphere, particulate S compounds phys. props. 8-96285

aerosols continued

- atmosphere, peak short term dustfall meas. from dust-generating industry 8-81386
- atmosphere, physical characts. 8-69430
- atmosphere, precipitation scavenging rates of background aerosol 8-85648
- atmosphere, propagation calc. use of average complex refr. index 8-57314
- atmosphere, props. rel. to visible and near IR light attenuation up to 30 km (Russian) 8-61558
- atmosphere, radiation, attenuation in absorpt. bands of moistened particles (Russian) 8-65384
- atmosphere, radiation modulation of aerosol state by moving clouds (Russian) 8-88916
- atmosphere, remote sensing of particle size distrib., analytical inversions 8-73508
- atmosphere, remote sensing of particle size distrib., analytical inversions 8-73509
- atmosphere, scatt. meas. of irregular particles versus Mie theory 8-58918
- atmosphere, size distrib. meas. with particle Doppler shift spectrometer 8-69515
- atmosphere, solar radiation absorpt., cloud and aerosol effects on heating rate 8-57319
- atmosphere, stratified aerosol layers, meas. by searchlight probing technique 8-92892
- atmosphere, structure function of conc. fluctuations 8-92980
- atmosphere, sulphate and nitrate assay via ion chromatography anal. 8-68974
- atmosphere, surface layer aerosols variability, spectral transmittance method (Russian) 8-69448
- atmosphere, turbidity meas. across Los Angeles Basin 8-92982
- atmosphere, visibility meas. using long-path laser transmissometer 8-85751
- atmosphere, water uptake and equilib. sizes at high relative humidities 8-61516
- atmosphere aerosol attenuation, influence on atmospheric and oceanic temp. determ. by remote sounding (Russian) 8-81430
- atmosphere aerosol boundary layer effects on brightness oscillations of daytime sky 8-81406
- atmosphere dust, meas. via personal CIP-type sampler 8-81469
- atmosphere of South American continent, S- and trace elements concs. in aerosols 8-57245
- atmosphere particulate pollution, climatological effects 8-85678
- atmosphere particulates measurement, anal. and calibration techniques 8-69531
- atmospheric aerosol, absolute element concs., PIXE and AAS comparison 8-85237
- atmospheric aerosol, turbidity characts. determ. from spectral actinometric obs. 8-92986
- atmospheric particulates, chemical characterisation via light scatt. method 8-69533
- atmospheric transverse velocity single-beam meas. 8-53747
- atmospheric water vapour and aerosol optical depth determ. by remote sensing 8-65389
- atomisation of liquid by impinging jets, expt. and theory 8-87373
- beam broadening in randomly inhomogeneous cloudy aerosol medium (Russian) 8-58911
- benzo(a)pyrene and C black combined aerosol form., rel. to air pollution and health hazards 8-80796
- binary homogeneous nucleation theory, limiting behaviour 8-92517
- charge distribution, meas. via variable freq. electrostatic mobility analyser 8-77945
- charging migration and EHD transport 8-88660
- classification pulse amplitude analyser 8-61587
- collection efficiency of nucleopore filters with asbestos fibres 8-57351
- condensation nuclei counter, with inherent size resolution capability 8-81470
- condensing turbulent annular-mist flow wall and interfacial shear stress 8-94812
- cylindrical particles, diffusophoretic force in binary gas mixture 8-68936
- cylindrical particles, thermophoresis under creep conditions 8-68935
- deposition, diffusion model description (German) 8-59446
- deposition on plate in turbulent flow 8-87380
- detector in cryogenic systems 8-81986
- diffusion, polydispersity, unipolar charging, charging mobility analysis 8-61059
- diffusion, polydispersity unipolar charging, particle dielectric constant and ion mobility effects 8-61058
- diffusion and sedimentation in Poiseuille tube flow 8-59463
- diffusophoresis along curved surface 8-83432
- dry deposition, filtration model rel. to trace metal deposition from atmosphere 8-7344
- dust storms, aerosol and momentum mixing, fast-response meas. 8-65364
- electric arc, plasma stream form., aerosol particles effect 8-51390
- electrolyte aqueous soln. drops, ion emission due to laser heating 8-59063
- electrostatic image force charged particle deposition in rectangular and cylindrical channels with laminar flow 8-83491
- equilibrium surface area rel. to vol. prod. rate 8-61066
- fine particle charging by unipolar ions, review and expt. 8-88658
- flow, disperse drop composition meas. 8-55682
- fluid jet impinging upon void aerosol impactors 8-59202
- ground level meas. of N-Greenland summer tropospheric aerosol 8-85645
- heteromolecular nucleation and condensation, multi-dimensions theory 8-92518
- IR wavelengths extinction by aerosols in coastal fog 8-81400
- Jupiter atmosphere, atmospheric aerosol props. from near IR polarisation studies 8-85899
- layer, depth, remote meas. by microwave-modulated laser (Russian) 8-57338
- lidar obs. at 0.7 and 10.6 μm wavelength 8-69459
- LWR core meltdown, activity release and aerosol characts. 8-82469
- marine atmosphere, lightly polluted, condensation nuclei conc. correl. smokes 8-81376
- microscopic particles, heating by laser beams 8-50838
- monodisperse particles dry deposition on simulated grass surfaces 8-81396

aerosols continued

- nonpherical particles size distrib. from scatt. meas. (Mie theory 8-58909)
- optical depth of Saharan dust, NOAA-3 MERR reflected radiance meas. 8-65390
- optical extinction in 0.5-14 μm wavelength range 8-57318
- optical extinction measurements, forward scattering corrections in aerosol media, monodisperses 8-94367
- organic compounds in aerosol samples 8-73463
- organic constituents, effect on fog and clouds 8-73465
- organic material in atmospheric aerosols 8-73464
- particle charging in continuum regime 8-90349
- particle deposition in channel due to diffusion and electric charge 8-90978
- particle deposition in sampling lines, expts 8-81473
- particle neutralisation to Boltzmann's equilib. by corona discharge 8-61064
- particle response to impulse, at small Knudsen no. 8-90977
- particle separation efficiencies of wire grids 8-87381
- particle size determination by light scattering, unknown refractive index 8-95957
- particles from oil-fired burners, size distrib. characterisation using Beta distrib. 8-81384
- particles sizing, influence of chemical struct. 8-81471
- photochemical aerosol formation, primary pollutants effects (Japanese) 8-57305
- photophoretic motion of nonvolatile particles, thermal diffusion effect 8-79364
- plasma, highly-dispersed aerosol, nonisothermal, thermionic, electron density function determ. 8-91066
- pneumatic nebuliser efficiency enhancement through appl. of elec. field 8-95966
- pollen and spores, long distance transport in troposphere 8-73466
- polystyrene latex particles, particle sizing by forward lobe scatt. intensity ratio 8-71031
- polystyrene monodisperse, ^{51}Cr tagged aerosol, prod. using aerosol centrifuge 8-92519
- power plant plume, induced snowfall prod. 8-81284
- respirable aerosol mass conc. meas. using piezoelec. microbalance 8-69518
- Satura, atmosphere, atmospheric aerosol props. from near IR polarisation studies 8-85899
- size and charge distrib. appl. of four-parameter distrib. model 8-85213
- size distrib. characterisation, modified beta density function 8-69432
- size distrib. determ. from mobility distrib. of charged fraction 8-61065
- size distribution meas. with cascade impactor instrument using quartz crystal microbalance sensing elements 8-65904
- sizing using slotted virtual impactor 8-57350
- sky intensity information, content, polarisation meas. at right angles to solar direction 8-81401
- smokes, atmospheric, gravitational sedimentation velocity (Russian) 8-85619
- smokes, atmospheric, optical probing, homogeneous particle model appl. (Russian) 8-77328
- solid aerosol collection in spouted bed, electric field effect 8-91019
- solid phase motion, large Reynolds no., carrying agent drag 8-79363
- stratosphere, aerosol layer, climatic effects, review 8-81531
- stratosphere, balloon obs. of particle layer injected by aircraft at 23 km 8-81283
- stratosphere, dust meas. (1970-1977) 8-73445
- stratosphere, environment monitoring system, benefit assessment 8-73507
- stratosphere, global content vars. rel. to fluctuations of solar radiation and temp. in troposphere 8-81327
- stratosphere, Mount Agung eruption as test of global climatic perturbation 8-69440
- stratosphere, remote anal. by differential scatter lidar system 8-69524
- stratosphere, S hemisphere meas. by impactor and in situ single-particle detect. 8-73437
- submicron aerosols, collection efficiencies of spheres, rel. to washout in atm. 8-81395
- surface aerosols in Capr Verde, physical and chemical props. 8-85640
- troposphere, effect on atmospheric IR cooling rates 8-88886
- troposphere, particles physico-chemical property models 8-92898
- troposphere, SO_2 aerosols chem. props. 8-96255
- ultrafine particles in gas, information on size, surface, props. from photoelectron emission 8-68598
- urban aerosol, size-fractionated, C, N, and O determ. by particle elastic scatt. anal. 8-81466
- urban plume particulates collected on Anderson 8-stage impactor stages, chemical anal. 8-69433
- Venus atmosphere, H_2SO_4 aerosols characts. from isophotes, spacecraft obs. 8-81575
- Venus clouds, H_2SO_4 aerosol medium IR optical props. and spectrum 8-65526
- Wilson Cloud form. by low altitude nuclear explosion, water aerosol and droplets characts. 8-53704
- X-ray fluoresc. anal. 8-85269
- β -active, emission electrification in external field 8-83497
- AgI, preliminary tests of cumulus cloud seeding technique 8-57352
- C aerosol visibility vs. particle size distrib. 8-88911
- Cd , Pb , Mn in particle, size fractionated aerosols, flameless atomic absorpt. determs. 8-69434
- CuS aerosol prepared by burning pyrotechnic mixture, crystallisation activity 8-96279
- HNO_3 -water, homogeneous nucleation, relative humidity depend. 8-71846
- H_2O droplet, CO_2 laser beam clearing process, transmission function ratio 8-88919
- H_2SO_4 aerosols form. expt. and theory 8-96256
- H_2SO_4 air pollution, new detector, aerosol mobility chromatograph 8-96297
- H_2SO_4 -water, homogeneous nucleation, relative humidity depend. 8-71846
- La_2O_3 aerosol, controlled production technique 8-76929
- $(\text{NH}_4)_2\text{SO}_4$ production, under elevated temp. inversion in Cleveland Country, model 8-81397
- $\text{PuO}_2\text{-UO}_2$ Na aerosol from LMFBR HCDA conditions characterisation 8-94104

aerosols continued

- Rn-Th monitor for earthquake prediction research 8-73532
- S compounds, techniques for chem. comp. determ. 8-95976
- S containing aerosols, continuous meas. and speciation by flame photometry 8-95974
- S containing aerosols, continuous in situ meas. by flame photometry and thermal analysis 8-96296
- S containing aerosols, physical characts. 8-96284
- S, in atmosphere, meas. via compact X-ray fluoresc. analyser 8-68971
- S pollutants in atm. cont., Dubrovnik, Yugoslavia, (Sep. 1977) 8-96281
- S, SO_2 and related species sampling and anal. of atm. aerosols 8-96283
- S, total conc. meas. using pulsed electrostatic precipitator and flame photometer 8-95975
- SO_2 , heterogeneous conversion to SO_4^{2-} , rel. to urban air pollution 8-80789
- SO_2 , photooxidation, aerosol evolution, rel. to air pollution 8-81392
- SO_4^{2-} containing aerosols, dynamics, review 8-96286
- SO_4^{2-} , individual submicron size particles detect. method 8-95973

aerospace

- see also aerospace computing; aerospace control; aerospace instrumentation; aerospace propulsion; aerospace simulation; aerospace test facilities; aircraft; ground support systems; space research; space vehicles; terrestrial atmosphere
- aeronautical meteorology, progress and challenges 8-53692
- European Space Research and Technology Centre (ESTEC) 8-69651

aerospace applications of computing see aerospace computing**aerospace computer control**

- see also aerospace computing
- remote programming, real time computers, space flight on-board expts. (German) 8-53791
- star tracker, microprocessor controlled CCD, STELLAR design 8-53792
- Viking lander remote diagnostic techniques 8-57426

aerospace computing

- see also aerospace computer control
- ablation, multidimens., embedding in inverse heat cond. problem, finite difference method 8-94508
- design, unsteady boundary layers with reversal and separation 8-75163
- large deflection anal. of tail-wheel struct. of light aircraft 8-83272
- lifting wing calcs., spanwise integrations, computational economy improvement 8-71344
- orbital transfer using two fixed-magnitude impulses 8-81518
- rocket propellants, thermodynamic evolution, extension of Huff's method 8-75054
- streaming, of vel. and temp., in oscill. boundary layers 8-83358
- subsonic and supersonic aerodynamics, SOUSSA computer code 8-71352
- supersonic wave drag of planar singularity distributions 8-83430

aerospace control

- see also air traffic control; attitude control
- aeroplane, deformable control systems, numerical anal. of lateral dynamic stability 8-51057
- artificial satellites, conf., Rome, Italy (Mar. 1978) 8-96384
- astronaut transfer in weightlessness, biomechanical model 8-96106
- aviation and astronautics, conference, Tel Aviv (1977) 8-81517
- dynamics problems, gradient method for optimal control 8-69638
- Mars descent trajectories using parachute-rocket system for soft landing 8-69640
- Mars orbit emplacement using atmospheric braking, control algorithm 8-69639
- satellite eccentricity oscills., compensation with stabilizer 8-69643
- soft landing guidance algorithms based on terminal control principles 8-73602
- three-impulse min-time orbital transfer generation, numerical method 8-73607
- transonic flow, unsteady force and moment alleviation by control devices in airflow 8-71362

aerospace engines

- aviation and astronautics, conference, Tel Aviv (1977) 8-81517
- jet exhaust noise, prediction of in-flight levels 8-87178

aerospace instrumentation

- see also Langmuir probes
- cosmic-ray fluxes, expt. determ. 8-85778
- induced background radiation, gamma and X-ray meas. 8-85821
- laser ranging systems, NASA applications 8-81527
- radioactivity induced in scintillator materials 8-85822
- spacecraft instrumentation radioisotope thermoelectric generator 8-85824
- star tracker, microprocessor controlled CCD, STELLAR design 8-53792

aerospace propulsion

- see also aerospace engines
- attitude and orbit control systems, conference, Noordwijk (1977) 8-65480
- EM slingshot system for space propulsion 8-77462
- interstellar ramjets infeasibility 8-81520
- ion-propelled space tug optimisation 8-53798
- series-staged fission powered starship, direct propulsion 8-61706

aerospace simulation

- see also aerospace test facilities
- active noise reduction system for ear defenders 8-92748
- ASSESS II Spacelab mission simulation results (German) 8-69649
- complex structure fatigue life prediction using critical location concept 8-59348
- Earth resource satellite attitude meas. and control requirements 8-65482
- glass particles impacting on metal barriers, piercing, stony meteorite simulation 8-89043
- micrometeoroid impact, laboratory simulation 8-57510
- modal test methods and applications 8-79252
- spacecraft, meteoroid impacts effect on attitude motion, analytical model 8-73608
- star simulator design 8-85814

aerospace test facilities

- see also wind tunnels
- attitude and orbit control systems, conference, Noordwijk (1977) 8-65480
- hypersonic re-entry vehicle, heat transfer meas. in separated laminar base flow 8-61708
- modal test methods and applications 8-79252
- space, qualification of optical instruments, using long duration exposure facility 8-85826
- Viking lander remote diagnostic techniques 8-57426

AFC see automatic frequency control**afterglows**

- Is, level density meas. by fluorescence, effect of dye laser intensity 8-67474
- electron energy distrib., radial variation 8-71570
- electron temp. relax. in afterglow plasma 8-51280
- hollow cathode stationary afterglow apparatus, for at. props. studies 8-63619
- inert gas discharge, electron-atom bremsstrahlung, time decay 8-63620
- pulsed DC discharge afterglow, electron conc. and temp., double-probe technique 8-63632
- Ar, electron-atom bremsstrahlung continuum, afterglow decay (German) 8-83626
- Ar, metastable $^3\text{P}_2$, deactivation in afterglow, plasma characts. 8-55769
- Ar+Ar($^3\text{P}_2$)($^3\text{P}_0$), flowing afterglow metastable decay rates, diffusion, two- and three-body rate consts. 8-73027
- Ar+Kr($^3\text{P}_2$), flowing afterglow metastable decay rates, diffusion, two- and three-body rate consts. 8-73027
- Ar+methane, CH chemiluminesc. in flowing afterglow 8-64839
- Ar+Xe($^3\text{P}_2$), flowing afterglow metastable decay rates, diffusion, two- and three-body rate consts. 8-73027
- BaS:Cu, thermoluminesc. and decay 8-80426
- CaS, phosphor, tunnel luminescence (Russian) 8-72577
- $\text{H}_2\text{S}^+ + \text{HCN} \rightleftharpoons \text{H}_2\text{CN}^+ + \text{H}_2\text{S}$, equilib., rate coeffs. and proton affinity, flowing afterglow 8-56885
- He afterglow plasma, $\text{He}(2^3\text{S}_1) + e \rightarrow \text{He}(1^1\text{S}_0) + e + \text{KE}$, rate const., electron energy distrib. 8-71571
- He, electron energy distrib. and collisions during decay, peculiarities 8-63621
- He pulsed discharge, He, mol. formation in early afterglow, time-resolved spectra 8-63585
- He-Hg pulsed discharge afterglow, metastable He+Hg inelastic collision 8-50627
- $\text{He}(2^3\text{S}) + \text{H}_2\text{O}(\text{H}_2\text{S})$, energy transfer processes, reaction products, UV and visible obs. in flowing afterglow 8-85138
- Kr, afterglow spectra of pulsed discharge, levels populated by dissociative recombination 8-83640
- N_2 , afterglow, short-lived, electron and ion density enhancement obs. 8-63625
- N_2 , catalysis and quenching by SF_6 8-51376
- N_2 , mol. excitation, in glow discharge and afterglow 8-63623
- N_2 , pink afterglow, ionisation and ion conversion mechanisms 8-63624
- N_2 , Rayleigh-Lewis and pink afterglows, mechanisms 8-63622
- N_2 - H_2 mixture, glow discharge, ionisation and excitation obs. 8-67505
- Ne, 1s atom prod. by recombination, press. depend. 8-59716
- Ne afterglow plasma, electron energy distrib. function 8-63587
- Ne, diffusion, collisions, decay freqs., fluoresc. obs., calcs. 8-59715
- Ne, electron-atom bremsstrahlung continuum, afterglow decay (German) 8-83626
- Ne, negative afterglow, pulse excited, at. spectral lines, microwave quenching 8-63591
- Ne-He DC glow discharge electron density decay, microwave cavity obs. 8-91167
- Xe, afterglow, $6s_{1/2}$ metastable atom density decay rate 8-63612
- Xe afterglow, $6s'(1/2)_0$, $6s'(1/2)_1$ at. states, collisional relax., population decay 8-63617
- Xe- N_2 , afterglow, $6s_{1/2}$ metastable atom density decay rate 8-63612

AGC see automatic gain control**age (Earth)** see geochronology**age determination, radioactive** see radioactive dating**age hardening** see precipitation hardening**ageing**

- see also precipitation hardening; strain ageing
- Al alloy, type AK4-1T1, effect of high temp. ageing, on endurance of thin welded joints 8-80570
- austenitic stainless steel, 18 Cr-11 Ni, directly aged, nucleation of M_{23}C_6 carbides (Polish) 8-52806
- α -brass, quenched, secondary defect form. during ageing, TEM obs. 8-88482
- cellulose-PAN copolymer, luminesc., ageing effect 8-64401
- creep theory, thermodynamic pots. (Russian) 8-63318
- creep theory for ageing bodies, with growing slit 8-63329
- E-glass fibre strength, effect of forming and ageing atmos. 8-92283
- ester-imide varnishes, electroinsulating, thermal resist. (Polish) 8-84014
- Hastelloy N, Si additions, comp. of eta carbide after ageing 8-52816
- Inconel alloy 718, exam. of struct., properties and continuum synthesis of ductile fracture 8-76736
- martensite ageing, influence of neutron irradiation (Czech) 8-84859
- MOS structs. formed on stain films on Si wafers, electrophysical props. (Russian) 8-52095
- nylon-6,6, creep meas. at const. temp., humidity 8-95883
- optical fibres, UV curable epoxy acrylate coated, long-term mech. behaviour 8-95802
- Ostwald ripening and its application to precipitates and colloids in ionic crystals and glasses [Review] 8-80548
- plastics, materials testing, application-oriented test standardisation (French) 8-85061
- polyester foil, static polarisation depend. on heat ageing 8-60688
- polyester varnishes, electroinsulating, thermal resist. 8-84014
- polyethylene terephthalate, glass-rubber transition determ., small-angle X-ray scatt., ageing 8-95145
- polystyrene fibre, ageing effects on elongation to fracture (German) 8-76750
- polyurethane foam solar concentrator, thermal and thermohydrolytic ageing 8-92281
- PVC, antiplasticisation rel. to ageing and nonlinear viscoelasticity 8-52929

ageing continued

- radiation concentrators with silazane protective coatings, UV exposure, tests 8-79092
 SAW oscillator frequency stability developments 8-59253
 sputtered metal silicide solar selective absorbing surfaces 8-52671
 steel, alloy, ageing characts., precipitation and coarsening of VC, TiC, and V-Ti-C in ferrite 8-84874
 steel, alloy, cluster formation susceptibility in 40 KhN, influence of isothermal working in H₂ (Russian) 8-56643
 steel, alloy, maraging, 250-grade, ductility and toughness of hot isostatically pressed powder 8-52925
 steel, alloy, type 36NKhTYu, plastic deformation, effect of surface condition on initial stage 8-84929
 steel, alloy maraging, type Kh13N8D2TM, conditions for formation of stable austenite 8-84868
 steel, austenitic, 800H, effect of hardening processes on initial stress-strain curve 8-84846
 steel, austenitic, Kh12N20T3R, ageing, submicroscopic struct. role in dispersion hardening (Russian) 8-64549
 steel, Cr-Mo-V, brittle failure, heat treatment and influence of cold plastic deform. 8-72858
 steel, maraging, 18% Ni content, exam. of age hardening-grain size relationships 8-84833
 steel, maraging, heating of thin samples with brief ageing, N6G4M, ON18K9M5T 8-52866
 steel, maraging, investigation with lower Ni and Co contents (Chinese) 8-84812
 steel, maraging low-Ni, isothermal martensitic transformations (Russian) 8-88465
 steel, martensitic, delayed fractures suppression, by neutron irradiation (Czech) 8-67743
 steel, mild, etching method for revealing plastic deformation 8-72825
 steel, Ni-Cr, (4.1, wt.%), isothermal embrittlement, AES exam. of grain boundary segregation 8-60814
 steel, phase separation, effect of plastic deform. and heat treatment (Polish) 8-92295
 steel, stainless, C-Cr-Ni-Mn-V, non mag., aged, struct. and mech. props. (Russian) 8-56666
 steel, stainless, Cr-Ni, maraging, effect of Mo, Co additions on hardening 8-84835
 steel, stainless, fatigue crack morphology of type 304 cycled at const. stress amplitude at elev. temps. 8-64671
 steel, stainless, ferritic, subjected to 475°C embrittlement, exam. of fracture toughness 8-84982
 steel, stainless, ferritic and duplex, Mossbauer effect study of 475°C embrittlement 8-52933
 steel, stainless, maraging, Cr-Co, effect of ageing on microstruct., TEM and neutron diffraction exam. 8-84867
 steel, stainless, maraging, high strength, exam. of ageing embrittlement (Japanese) 8-84972
 steel, stainless, radiation-thermal treatment, N₂O₄ coolant action, intergranular corrosion (Russian) 8-58357
 Ag film, on mica, microstruct. changes 8-72013
 Al alloy 7001, ageing effect on hardness and tensile props. rel. to delay time till quenching 8-92286
 Al alloy 7075, fracture props., effect of thermomechanical treatment 8-60793
 Al alloys, fracture, grain size effect 8-60781
 Al-Ag, discontinuous decomposition (Polish) 8-52808
 Al-Ag (up to 40 at.%), exam. of anelastic phenomena and structural state 8-76693
 Al-Ag alloy, ageing exam. by X-ray electron spectroscopy and electron diff. exam. (Russian) 8-60685
 Al-Ag alloy, second ageing stage, diffuse electron and X-ray scatt. (Russian) 8-68711
 Al-Cu (3.71 wt.%), stress oriented precipitation of Guinier-Preston zones and θ' 8-52809
 Al-Cu (4 wt.%), AE during deform., effect of ageing at 170°C 8-64597
 Al-Cu (4 wt.%), aged to contain Guinier Preston zones, crystallographic fatigue crack growth 8-60832
 Al-Cu-Mg-Mn-Fe-Si, alloy D16, effect of mechanothermal treatment on mech. props. 8-56674
 Al-Cu-Mg-Si-Mn (2.5, 0.7, 0.7, 0.5 wt.%), alloy AK6, US inspection of heat treatment quality 8-76681
 Al-Cu(Mg), age-hardenable, US cavitation erosion mechanisms, effects of comp. and heat treatment 8-53002
 Al-Ge (2 wt.%), quenched and aged, deform. slip line obs. 8-51544
 Al-Li solid soln., decomposition exam. by secondary ion ion emission (Russian) 8-68696
 Al-Mg-Ag, age effect on age hardening (Japanese) 8-52831
 Al-Si, internal friction and Si precipitate nucleation 8-60690
 Al-Si-Cu-Mg, alloy AL32, ageing of castings produced by pressure die castings 8-56650
 Al-Zn, dil. alloy, ageing and reversion, annealing curves, X-ray obs. 8-88485
 Al-Zn, discontinuous decomposition (Polish) 8-52808
 Al-Zn alloys, room temp. decomp. of metastable phases precipitated at 200°C 8-84814
 Al-Zn-Mg, precipitation of η' phase, heat treatment, electron microscope obs. 8-68699
 Al-Zn-Mg (6.1.5%), influence of ageing and cold work on tensile and fracture props. (Japanese) 8-52842
 Al-Zn-Mg alloy, thermomechanically treated, precip. behaviour 8-84856
 Al-Zn-Mg alloys, decomposition kinetics, resistivity meas., extended jump model 8-84766
 Al-Zn-Mg-Ti, Ti effect on microstructure during ageing 8-64568
 Al-Zn-Mg(Mg-Ti), TEM exam. of early stage ageing behaviour, exam. of precip. kinetics 8-56645
 As₂Se₃, amorphous, electrophotographic props., photodecomp. effect 8-49918
 Au films on Si substrate, solid-solid reactions 8-95369
 Au, pure metal and Au-Sn dil. alloy, vacancy clusters, quenching and ageing 8-76671
 Be bronze, struct. and props. after ageing under load 8-84932
 Bi-Sb interface, film, thermoelectricity, ageing differential efficiency (German) 8-60146
 CdS:Cd(In), Cu- or defect-compensated, optical ageing rel. to storage cond. 8-84247

ageing continued

- Co-Cu-Fe-Ce, mag. characteristics of sintered permanent magnets 8-60312
 Co-Fe-Nb alloy, mag. precipitation-hardening and Bloch wall pinning 8-80173
 Co-Fe-Ti (12.6 wt.%), semihard permanent magnet, magnetic precipitation hardening 8-52830
 Co-Fe-Ti alloy, precipitation hardened, rel. between struct. and mag. props. 8-95470
 Cr₂O₃-Al₂O₃, solid soln., effect of Cr on point of zero charge 8-61021
 Cu-Mn (38 to 58 wt.%), age hardened, exam. of precipitation and strengthening 8-72782
 Cu-Ni-Nb-Al, formation of γ' and γ'' precipitates 8-76655
 Cu-Ni-Sn (15, 9 wt.%), age hardening accompanying phase transition 8-64551
 Cu-Ti (4 wt.%), aged, stress corrosion cracking in Cu-NH₃ solutions, effect of pH, Cu and NH₃ conc. 8-88562
 Fe-Al-C, low C, precip. of carbides and cementite after quenching and ageing 8-52814
 Fe-Be, formation of quasi-periodic distrib. of precipitates during ageing (Russian) 8-56642
 Fe-Co-V(2%) alloy, correl. of resistivity with microstructure 8-72896
 Fe-Cr-Co (31 wt.%, 23 wt.%), microstruct. and mag. props., ageing and thermomag. treatment effects 8-76769
 Fe-Cr-Co-V alloy, microstruct. and mag. props. 8-68221
 Fe-Cr-Ni-Nb-C, austenitic, splat quenching 8-72798
 Fe-Mn-Ni, fracture toughness, thermomechanical treatment effects 8-60794
 Fe-N single crystals, solid soln. stress assisted nucleation of α'' precipitates 8-52810
 Fe-Ni-Al-Ti alloy, N27Yu2T2, aged austenite, diffuse electron scatt. distrib. during martensitic deform. (Russian) 8-60669
 Fe-Ni-C (31.24, 0.21 wt.%) effect of deformation and ageing after deformation, on martensitic transformation temp. 8-76650
 Fe-Pt (24 at.%), colour metallographic technique, for studying microstructural reproducibility, in martensitic transformations 8-72954
 Fe-W-Cr-Mo-Co with austenitic phase, magnetic and mech. props., cold working and ageing effects (Japanese) 8-60678
 (Fe_{0.5}Ni_{0.5})₇₅P₁₆B₆Al₃ glass, struct. relax. as origin of Curie temp. ageing 8-84418
 Fe₂O₃-Al₂O₃, solid solns., effect on Fe on point of zero charge 8-61021
 GaAs-AlGaAs transverse junction stripe laser, single mode behaviour after 12000 hr ageing test 8-66831
 Hf-Nb (30 to 50 at.%) exam. of beta phase decomposition processes 8-76674
 LiO₂-2SiO₂, glass, devitrification with ageing 8-79536
 Na₂O-SiO₂, glass, devitrification with ageing 8-79536
 Nb, blister form. on single crystal under Ne⁺ ion bombardment 8-71772
 Nb-H, behaviour of H in Nb, relation to mech. props. 8-80572
 Nb-Zr-C alloy, creep in vacuum, prolonged high-temp. ageing effects (Russian) 8-56692
 Nb-Zr-C alloy, long term strength rel. to carbide precipitate geometry (Ukrainian) 8-92266
 Ni-Cr-Fe-Mo-Co (21.41, 19.28, 8.64, 2.16 wt.%), Hastelloy alloy X, exam. of thermal stability 8-84865
 Ni-Cr-Ti-Al-Fe-Co (19.65, 2.40, 1.37, 0.78, 0.52 wt.%), strength of γ' hardened alloy, ageing exam. 8-88501
 Ni-Cr-Ti-Al-Mo-Nb-Fe (13-16, 2.35-2.75, 1.3-1.7, 2.8-3.2, 1.8-2.2, 2.0 wt.%), heat resistant props, mech props. struct., stepwise ageing effects (Russian) 8-76666
 Ni-Fe solid soln., precip. hardened, paramag.-ferromag. transition on ageing 8-52255
 Ni-maraging weld metal, increasing fracture toughness by heat treatment 8-72871
 α -Ni-Zn, continuous precipitation kinetics (Russian) 8-76652
 Pb-Ca-Sn, effect of Sn additions on precipitation behaviour, of Pb-Ca alloys (German) 8-52821
 SiO₂-ZrO₂ adsorbents, coprecipitated, porous struct. rel. to form. conditions 8-53263
 Sm-Co, decomp. kinetics when aged, X-ray mag. props. and metallography study (Russian) 8-56644
 Sn-Ni metastable alloy, surface film comp., time depend., XPS 8-60870
 steel, austenitic stainless, 18 Cr-11 Ni, effect of boron on nucleation of M₂₃C₆ carbides (Polish) 8-84808
 Ta-O solid soln., interstitial ordering and precipitation at 100 to 270°C, exam. 8-52813
 Ti alloy, hardening heat treatment, alloying element effects development trends 8-95759
 Ti alloy, VT16, decomposition of metastable β -phase (Russian) 8-68710
 Ti alloy, VT23, ht. treatment effects on fracture (Russian) 8-80623
 α + β Ti alloys, fracture, influence of phase comp. in VT16 and VT9, quenching effects (Russian) 8-56665
 Ti-Al-Cr-Mo-Fe(V)(Zr), effect of structure and heat treatment on tensile strength, ductility, fatigue limit and notch sensitivity 8-56711
 α -Ti-Al-Zr (6.16, 5.23 wt.%), alloy IMI 685, electron microscope observations of strain induced hydrides 8-72828
 α -Ti-Al-(Zr), embrittlement due to ageing 8-56673
 Ti-Cr (15 at.%), aged omega phase, electron microscope exam. 8-72783
 Ti-Cr(Mo), alpha precipitation kinetics 8-68697
 Ti-Cu-Al(Zr)(Sn)(Nb)(Mo), heat treatable alloys, effect of alloying on strength, tensile props. 8-56671
 β -Ti-Fe, (7.1 wt.%) exam. of ω phase formation, by X-ray diff. and Mossbauer spectroscopy 8-52800
 β -Ti-Mo-V-Fe-Al (8.8, 2.3 wt.%), metastable alloy, microstruct. and mech. props. ageing time and temp. effect 8-64569
 Ti-V (19 at.%), aged ω -phase precipitation, incomplete proximity effect 8-60252
 TiO₂, rutile ceramic, in strong electric field (Polish) 8-52869
 Zn film, RF sputtered, ageing processes 8-84322
 ZnS, electroluminescent, ageing rate, voltage effects (Russian) 8-84662

ageing characteristics *see* ageing**agriculture**

- climatic change effects on food production, statistical models limitations 8-57303
- crop discrimination, radiowave backscatter from vegetation, water cloud model 8-57274
- crop response to hail suppression seeding, Nelspruit project, South Africa 8-57257
- crops, Landsat data, pattern recognition, temporal trend analysis 8-65440
- drought effects on agriculture in United Kingdom, 1975-76 period 8-57298
- drought in England and Wales, 1975-6, effect on agriculture 8-88890
- European agriculture rel. to climatic change 8-85679
- expansion in late 19th century rel. to CO₂ levels in atmosphere 8-53717
- hail-prevention operations, cost effectiveness estimation methods anal. 8-93013
- historic climate correl. with wheat prices and wages 8-81346
- Israel, water shortage, and supply, long-run policy for agriculture 8-61454
- microwave probe for subsurface soil moisture profiling 8-65939
- nitrogenous fertilisers and soil as atmospheric N₂O source 8-61419
- perennial grasses potential yield and yield shortfall due to water deficit, agroclimatic estimate 8-61450
- radiation and isotopes appl., development trends 8-55041
- remote sensing, environmental potential survey in Japan 8-57374
- soil warming, simultaneous heat and mass transfer governing eqns., waste heat utilisation 8-94562
- subsurface drainage and irrigation, expt. evaluation of theoretical solns. 8-61465
- tobacco shreds, effect of glycerol and sucrose additions, on props. (Japanese) 8-85113
- UV radiation meas. in agricultural production, instrument (Russian) 8-65969
- wheat, plant canopy light absorption model 8-88913
- winter wheat yield on Great Plains, Landsat data and soil moisture evaluation 8-65351
- world predicament and climatic change, need for interdisciplinary research 8-57300
- N fertilisers, perturbation of stratospheric O₃, independent variables anal. 8-73505
- P loading of lake from non-point agricultural sources, uncertainty analysis 8-81262

air

- see also* terrestrial atmosphere
- air positive corona discharge between coaxial cylinders, critical density estimation 8-67595
- air-propane flame, chem. anal. of reaction zone by Raman spectra 8-64837
- air-steam mixtures, heat transfer to moving droplets 8-90997
- arc discharge high-temp. transport obs. 8-71577
- breakdown, submillimetric laser induced 8-67446
- breakdown in superimposed DC and HF electric fields 8-67571
- breakdown potential, pulse lamp irradiation effects (Russian) 8-83518
- breakdown voltages, from normal to cryogenic temps. 8-59692
- corona discharge ion density and mobility obs. 8-67594
- DC corona Trichel pulse development at atm. pressure, obs. 8-67588
- diffuse discharge, gasdynamic effects 8-81294
- discharge, sputtered cathode metal atoms, time-resolved light emission 8-716018
- discharge, wall stabilised arc, current step changes, conductance transient effects 8-87547
- dry and moist, primary ionisation coeffs., secondary ionisation coeffs. for water surface 8-65376
- EHF clear air refractivity calc. procedure 8-57266
- electric breakdown, positive point-plane gap, critical press. prediction, v./press. characts. 8-87583
- electric breakdown voltage, 300-2100K (Russian) 8-61370
- electric breakdown voltage hysteresis, electrode coating effects 8-87553
- electrostatic forces effect on thermodynamic props. and equilibrium composition 8-55710
- flow in vertical tube, laminar and turbulent heat transfer 8-71332
- fluid dynamic equations, acoustic energy conservation, vibrational relaxation effects 8-90566
- gap discharge zone probabilistic features 8-67582
- glacier structure and flow rel. to elongated air bubbles in ice (Japanese) 8-88861
- HF corona discharge ignition characteristics 8-67589
- high temp. elec. breakdown characts., theory and obs. 8-87581
- high-current discharge cond. zone, HF mag. field probe 8-71589
- high-current pulse discharge, near-electrode process dynamics 8-71602
- isobutane-air, in packed bed, heat and mass transfer, axial mass dispersion 8-75200
- laser-evaporated microplasma radial glow and temp. distrib. 8-67387
- laser-produced spark ionisation channel effect on long discharge 8-67468
- liquid, transport of neutron and secondary rays from 14 MeV source 8-50234
- long air gap minimum breakdown voltage and time estimation 8-67575
- long rod-to-plane air gap voltage/time characteristic for switching impulses 8-67576
- negative point-plane corona, electrical characts. 8-71567
- neutron-stimulated luminescence 8-86567
- non-self-sustained discharge plasma ionisation instability obs. 8-71609
- parallel discharge growth during impulse breakdown, mechanism (German) 8-636078
- plasma, surface treatment of polyester fabric, effect on surface struct., props. 8-95831
- point-to-plane gap corona and breakdown in supersonic airstream 8-67573
- point-to-plane negative corona discharge in supersonic airstream 8-67585
- positive point corona current continuous component 8-67586
- predischARGE current meas. in compressed air 8-87555
- pulsed corona discharge channel fast heating process 8-67560
- radiative cooling behind strong shock waves 8-91030
- rod-to-plane air gap breakdown under negative impulse voltage 8-67563
- air continued
- rod-to-plane air gap impulse-voltage delayed streamer and leader formation 8-67570
- rod-to-plane air gap impulse-voltage primary and secondary streamer obs. 8-67569
- space-time distribution of refractive index of air in Mongolia 8-81335
- temperature measurement, using rot. Raman spectra 8-62200
- thermal conductivity, 400-1200K 8-75249
- He-air, thermal cond. meas., conc. depend., 315K, 330K (Russian) 8-71421
- I partition equilibrium between air and NaOH aq. effect of CO₂ conc. 8-78474
- SF₆-air mixture impulse discharge characteristics of 30 cm gaps 8-67572
- air bases *see* airports
- air blast circuit breakers
- core electron temperature at current zero, 3 kA, spectral meas. 8-87526
- electrical gradient during high current phase, plasma probe methods 8-87527
- energy clogging, current and voltage meas. at different press. 8-87531
- local electrical properties, near current zero, optimisation 8-87516
- very high current arcs, elec. conductance of arc gap 8-87524
- air bubbles *see* bubbles
- air compressors *see* compressors
- air conditioning
- see also* ventilation
- ducts, active sound absorpt. 8-90555
- laboratories, automatic temp. control and meas. (Japanese) 8-86245
- noise, subjective responses and meas. 8-83168
- air permeability *see* permeability
- air pollution
- see also* air pollution detection and control; smoke
- acid rain rel. to S compounds long range transport, chem. aspects 8-81391
- advection equation soln., using second-order moments with and without width correction 8-85655
- aerosol, ambient sulphate particles size discrimination and chemical comp. by diffusion sampling 8-69528
- aerosol, individual microparticles identification via micro-Raman spectrometer 8-68970
- aerosols, anal. of water-soluble S compounds 8-96282
- aerosols, influence on thermal effects of stratosphere, O₃ depletion at 85°N latit. 8-81279
- aerosols, size distrib. characterisation, modified beta density function 8-69432
- aldehydes, formation by photochemical reactions (Japanese) 8-88648
- alkyl Pb and Se compounds, detect. via gas chromatograph-microwave plasma detector 8-68975
- Ankara atmosphere aerosol, trace elements and size distrib. determ. by thermal neutron activation anal. 8-81377
- annual average concentration around single source, rapid estimation technique 8-81382
- atmospheric dispersion, completely Lagrangian random-walk model 8-81380
- atmospheric pollution 1978, conference, Paris, France, (April 1978) 8-81373
- Belgium, meteorological episodes increasing air pollution 8-81374
- benzo(a)pyrene and C black combined aerosol form., rel. to air pollution and health hazards 8-80796
- biosphere, radioactive contamination, influencing factors, 1962-76, Hungary (Hungarian) 8-92711
- boundary layer, pollutant field from multiple sources (Russian) 8-69443
- breakdown voltage of air, effect of sand particle pollution 8-81363
- Chicago Area Program, mesoscale meteorology 8-77294
- chinnok weather effects 8-61534
- chlorofluoromethanes, CCl₂F₂ and CCl₃F in Wuppertal-Dusseldorf region, ground level meas. 8-73478
- chlorofluoromethanes in stratosphere, vertical distrib. 8-73476
- chlorofluoromethanes in upper troposphere and lower stratosphere, vertical distrib. 8-73477
- cloud condensation nuclei from paper mill effluents, induced fog (French) 8-96270
- cloud dose data file fast correction for changes in dispersion parameters 8-80969
- coal smoke particles, atmospheric natural radioactivity (Rumanian) 8-53723
- combustion aerosols, particle size distrib., health hazards 8-81394
- continuous point sources, conc. Gaussian distrib. calc. (Dutch) 8-61546
- continuous point sources, effects prediction (Dutch) 8-61545
- continuous point sources, German calc. models (Dutch) 8-61548
- continuous point sources Gaussian distrib. anal. (Dutch) 8-61611
- cooling tower plumes from energy centres, predicted climatology 8-61541
- diffusion parameters estimation, use of routine meteorological data 8-85649
- dimethyl-N-nitrosamine, assessment is urban air 8-81378
- dispersal, three-dimens. particle-in-cell method, comparison to regional tracer studies 8-92967
- dispersion, modelling by smeared conc. approximation 8-81381
- dispersion, overlay technique, topography problem, long term conc. 8-81389
- dispersion during calm wind situations, analytical modelling 8-81385
- dust generating industry, peak short term dustfall meas. and effect on residential development 8-81386
- effective chimney heights estimation based on rawinsonde obs. 8-85684
- environmental pollution by nuclear fission products 8-85607
- formaldehyde, concs. in rain water and on atmospheric aerosol 8-57243
- Freon-12 absorpt. coeffs. for CO₂ laser radiation, press. and temp. depend. 8-55170
- gamma-rays from extended sources, energy distrib. calc., rel. to remote spectroscopy 8-61586
- Gaussian plume model parameters determ. from diffusion-convection eqn. integration 8-81399
- highway traffic, heavy metals contamination of roadside soils and plants in Alexandria district, Egypt 8-81171

air pollution continued

- hydrocarbon mixtures, photochemical reactivities 8-61533
hydrometeorology, pollutants atmospheric transport to water systems 8-96240
integrated energy systems, environment impacts 8-73506-8
Japan, measurement of electric and small ion mobility, pollution aspects 8-92931
Liege industrial region, five-year record of atmospheric fall-out 8-81375
Livermore Regional Air Quality model, appl. in San Francisco Bay area 8-92966
Livermore Regional Air Quality model, concept and development 8-92965
London, urban plume, early obs. 8-88907
marine atmosphere, lightly polluted, dark smokes, and acid pollution study 8-81376
mass consistent atmospheric flux model (MASCOT) for complex terrain regions 8-92964
mass consistent model for wind fields over complex terrain 8-92906
mass diffusion from point source in turbulent shear layer 8-92968
mesoscale air quality model, appl. in long range pollution problems 8-81388
methane, conc. over ocean, var. with latit. 8-81372
methyl chloroform, impact on stratospheric O_3 8-53722
monodisperse particles dry deposition on simulated grass surfaces 8-81396
nuclear plant airborne effluent variable-trajectory puff advection model modifications 8-94149
ocean data and information services, appl. to air pollution problems 8-69463
oil fired power station SO_2 critical conc. calc. (Dutch) 8-61547
organic micropollutants, adsorpt. on chrysotile and crocidolite, rel. to carcinogenic props. 8-80790
organochlorine residues in rainwater 8-73495
residence times of pollutants, determ. via CO_2 content 8-69445
troposphere, chemical-kinetic criteria of effect of substances of natural and anthropogenic origin (Russian) 8-53699-8
troposphere, CO_2 pollution, effects on temperature and O_3 distrib. 8-57246
particles from oil-fired burners, size distrib. characterisation, using Beta distrib. 8-81384
particulate matter emitted by Mount Etna volcano, heavy metal chem. 8-61491
particulate pollution, climatological effects 8-85678-8
particulates, chemical characterisation via light scatter method 8-69533
particulates and gaseous pollutants measurement, anal. diff. calibration techniques 8-69531
photochemical aerosol formation, primary pollutants effects (Japanese) 8-57305
plume rise at large distances from multiple source region 8-85688
plumes from power stations, ionisation effects 8-88909
point source plumes, optimal diffusivity 8-85667
pollutants vertical diffusion, study using airborne gas chromatography and numerical modelling 8-69435
power plant plume, induced snowfall prod. 8-81284
radiative effects of elevated pollutant layers 8-65382
radioactive effluent gases from nuclear power industry, ambient contamination (Spanish) 8-61540
radioactive fallout on Milan 1976-7, influence of Chinese nuclear expts. (Italian) 8-58501
radioactive waste, risk anal. of high-level waste management systems in Germany 8-50272
radioactivity dispersion, population dose calc. 8-85384
radioactive release assessment, importance of vars. in deposition vel. 8-80979
reactor air borne plume deposition estimation model, evaluation 8-94148
reactor near stack dose calc., diffusion model applicability 8-94147
snow strong acidity on Mt. Blanc ref. to air pollution 8-61259
Space Shuttle, environmental effects during launch and reentry 8-85681
spatial distrib., objective interpolation formulae 8-65412
stratosphere, aerosol content var. rel. to fluctuations of solar radiation and temp. in troposphere 8-81327
stratospheric O_3 reduction estimates, effects of water vapour changes 8-73444
stratosphere, particle layer injected by aircraft at 23 km, balloon obs. 8-81283
submicron aerosols, collection efficiencies of spheres, rel. to washout in clouds 8-81395
synoptic weather maps and typical local conditions (Spanish) 8-88891
thermal pollution (from fuel and energy consumption) effects on weather and climate 8-61539
trace gases vertical conc. from solar radiation absorpt. spectra (Russian) 8-69442
trace metal aerosol, dry deposition meas. and filtration model 8-73444
transport and deposition, puff-on-cell model 8-85682
transport in Upper Silesian Industrial District, deposition and washout 8-92960
troposphere, interhemispheric gradients of CO_2 , CH_4 , CO , and N_2O 8-81289
troposphere, N_2O continuous meas. 8-81318
troposphere, NO_2 vertical column abundance, optical absorpt. meas. 8-85632
troposphere, Saharan dust cont. over Atlantic from air cont. meas. 8-92897
turbidity meas. across Los Angeles Basin 8-92982
turbulent atmosphere, pollution release, exposure freq. distrib. 8-81388
turbulent diffusion in boundary layers with Rossby number similarity 8-92896
urban plume particulates collected on Anderson 8-stage impactor stages, chemical anal. 8-69433
urban-rural, complex air pollution effects, two-dimens. numerical simulation 8-81369
urbanisation and pollutant effects on thermal structure in various climatic regimes 8-61500
Vizcaya, Spain, Na, Mg, Cr, Al, Ti, Cu, Ag, Zn, Co and Ni content in atm. and rainwater (Spanish) 8-57264

air pollution continued

- Vizcaya, Spain, Na, Mg, Cr, Al, Ti, Cu, Ag, Zn, Co and Ni content in sedimentable powders (Spanish) 8-57265
volcano eruption cloud particles, St. Augustine, Alaska 8-57180
wind speed averaging in pollutants conc. equation 8-57307
 CO abundance, geographical, seasonal and secular vars. (Russian) 8-53700
 CO_2 content of atmosphere, role of C storage by forests and oceans 8-53718
 CO_2 future atm. level prediction using atm. and ocean models 8-61549
 CO_2 input from burning wood 8-81368
Cd, Pb, Mn in particle size fractionated aerosols, flameless atomic absorpt. determ. 8-69434
 α -Fe- O_2 analysis of car exhaust by Mossbauer spectroscopy 8-92963
 H^+ in E United States precip., concs. behaviour 8-92962
 HNO_3 vapour and particulate NO_3^- global tropospheric meas. 8-88904
 HNO_3 -water, homogeneous nucleation, relative humidity depend. 8-71846
 H_2SO_4 aerosols form., exp. and theory 8-96258
 H_2SO_4 -water, homogeneous nucleation, relative humidity depend. 8-71846
HT⁺ release in a room, radiation dose 8-74513
Hg fallout in Hawaii 8-61551
 NH_4^+ , NO_3^- in rain water collected at Jülich, Germany N-telope comp. 8-57284
 $(NH_4)_2SO_4$ aerosol production and elevation in Cleveland Country, model 8-81397
 NO_3^- in E United States precip., concs. behaviour 8-92962
 NO_3^- atmospheric fluxes from N_2O supersaturated surface waters 8-57223
 N_2O sources, sinks and vars. meas. 8-85631
 O_3 stratospheric perturbation by N fertilisers, independent variables and 8-73505
 O_3 , tropospheric, long-range transport 8-61514
OH+dimethyl sulphide, flash photolysis reson. fluores. rate consts. determ. pollution aspects 8-93913
OH+OCS(CS_2), flash photolysis reson. fluores. rate consts. determ., global cycle 8-93914
Pb, V, Cd, Zn, Cu, conc. in snow of Mt. Blanc ref. to air pollution 8-81258
Rn, concentration of ^{222}Rn , ^{220}Rn and decay products in room air, exhalation, ventilation and deposition effects 8-73261
 ^{222}Rn in biologically produced gas from reactor cooling pond 8-80976
S aerosols, in atm., phys. props. 8-96285
S and trace elements in aerosols from South American continent, conc. relationships 8-57245
S compounds homogeneous oxidation in atmosphere 8-96258
S-containing aerosols, physical characteristics 8-96284
S isotopic comp. in atm. precip. around Sudbury, Ontario 8-81368
S pollutant, long-range transmission, simulation, two-dimens. pseudospectral dispersion model 8-57306
S pollutants in atm., conc. in Dubrovnik, Yugoslavia, (Sept. 1977) 8-96284
 SO_2 adsorption and oxidation on atmospheric particles 8-96283
 SO_2 conc. determ. using H β laser (Russian) 8-69434
 SO_2 conc. in Milan urban atmosphere in winter (Italian) 8-57302
 SO_2 diffusion-coupled oxidation 8-65371
 SO_2 , heterogeneous oxidation on SiO_2 particles, urban air pollution 8-80789
 SO_2 , homogeneous oxidation mechanism in troposphere 8-96257
 SO_2 mesoscale air quality model, appl. 8-81388
 SO_2 , oxidation in moist atm., aerosol growth kinetics 8-96255
 SO_2 photooxidation, aerosol evolution, rel. to air pollution 8-81392
 SO_2 pollution zones definition and assessment 8-81383
 SO_2 removal from atm. by dew 8-81376
 SO_2 transport over Mediterranean sea 8-81390
 SO_2 -containing aerosols, dynamics, review 8-96286
 SO_2 in E United States precip. (conc.) behaviour 8-92963
 SO_2 -natural sources in tropical humid area (French) 8-81374
 SO_2 , tropospheric aerosols chem. props. 8-96254
spectrophotometric anal. of pollutant gas in Wind scale AGR gas chromatographic and radiochemical anal. 8-73125
UCG inhaled particle distribution, clearance, initial bifurcation and trajectory of rats 8-73267
air pollution detection and control
aerosol classification, pulse amplitude analysis 8-61587
aerosol collection efficiency of nucleopore filters with asbestos fibres 8-57351
aerosol mass conc. meas. by Nd-glass filter, ASSESS H-Space lab mission simulation (German) 8-69642
aerosol measurement, particle deposition, in sampling lines 8-81472
aerosol mobility, chromatography, new detection for H_2SO_4 air pollution 8-96297
aerosol compounds, techniques for chem. comp. determ. 8-95976
aerosol sizing using slotted virtual impactor 8-57350
aerosols, chemical characterisation, progress and problems 8-68969
aerosols, instrumental anal. of light element comp. 8-69516
aerosols, limitation on electrical measures 8-69431
aerosols, remote anal. by differential scattering lidar systems 8-69524
aerosols, size distrib. meas. with particle Doppler shift spectrometer 8-69535
aerosols, sulphate and nitrate assay via ion chromatography anal. 8-68974
air quality evaluation, daily profiles methods (French) 8-92969
air monitoring instruments, review 8-61590
asbestos fibres, collection efficiency of nucleopore filters 8-57351
asbestos, X-ray diff. anal., calibration standards 8-69517
assessment of operating rules (Dutch) 8-57320
cascade impactation instrument using quartz crystal microbalance sensing elements, particle size distribution 8-69504
centralised supervision system, in Fos-Etang de Berre region 8-81410
charcoal tube sampling technique, meas. accuracy 8-69508
 CO dose meter for working places exposed to extreme peaks of CO contamination 8-81096
coherent anti-Stokes Raman scattering for quantitative gas anal. 8-68968
collective dose commitment for estimate of radioactive pollution concept and calcs. (German) 8-74504

- air pollution detection and control continued**
- computerised monitoring system, program system (Japanese) 8-81414
- continuous monitoring instrumentation, selection, maintenance 8-77316
- correlation spectrometry meas. of air pollution and CEC remote sensing campaign report 8-88908
- data interpretation via pollution roses, appl. to data from meas. systems near refineries 8-81379
- density distrib., flow pattern in Tanabe area, Japan, numerical anal. (Japanese) 8-96289
- deposition research using rain gauges (Dutch) 8-81367
- determination by Stark modulated microwave spectroscopy 8-57337
- differential absorption lidar systems for atm. gases remote meas. 8-69525
- differential-absorption lidar technique for remote meas. of atm. gases 8-61603
- dust, airborne, respirable fraction, performance characts. of samplers matched to them 8-53438
- dust, polarisation and interference microscopy appls. 8-61544
- dust cyclone operation, anal. 8-57362
- dust sampler, CIP type, for personal use 8-81469
- dust samples, neutron activation anal. using high-rate loss-free gamma spectroscopy system 8-61129
- Dutch national air pollution monitoring system, local and reference point 8-69465
- electrostatic precipitation technology development, stack gas ionisation by electron beams 8-57346
- elemental analysis at sub-particle level (Russian) 8-81465
- environmental measurement, conf., Gathersburg, Maryland, USA (Sept. 76) 8-69504
- ethane, in air, IR spectra, optical-acoustic investig. (Russian) 8-74663
- ethylene, in air, IR spectra, optical-acoustic investig. (Russian) 8-74663
- ethylene in exhaust gas, optoacoustic detect. using fine-selectable CO₂ laser 8-56947
- exhaust gas radiation treatment, NO_x oxidation and NO₂ reduction 8-80765
- exhaust gas radiation treatment, SO₂ oxidation in moist O₂-N₂ mixture 8-80766
- fallout nuclei determin. 19th Chinese test 8-82520
- Fourier transform IR absorpt. spectroscopy, airborne, for atm. comp. meas. 8-61604
- Fourier transform IR spectroscopy appl., conf., Columbia, USA (June 1977) 8-58067
- Fourier transform spectroscopy appl. far IR 8-58069
- Fourier transform spectroscopy meas. 8-61564
- gas analyser, portable, 1920 to 1978 development 8-61124
- German laws, standards, guidelines and limiting values (Dutch) 8-75312
- global sulphur cycle study, reaction rate determination, atmospheric modelling appl. 8-82902
- and filter collection efficiency, effect of Stokes and Reynolds numbers 8-61592
- halocarbons, gas chromatography detect. 8-85739
- halofluorocarbons, background levels in situ quantification 8-69530
- high acidity measurement, comparative tests near industrial installations in Fos-Etang de Berre region 8-81464
- industrial chimney design for satisfactory emission (Dutch) 8-81364
- industrial flare flames, smoke detection and control by electric fields 8-81360
- intracavity laser Raman spectrometer, appls. 8-65973
- ionisation type smoke detector, model for response 8-88933
- IR laser heterodyne spectroscopy for trace gases remote detect. 8-61606
- IR laser technique for SO₂ conc. determ. (Russian) 8-69434
- IR spectrometer, INFRAMEK-E, operational principles (Hungarian) 8-54474
- laser absorption spectroscopy for point monitoring of gases ambient concs. using tunable lasers 8-61607
- laser high sensitivity point monitoring of atm. gases 8-69532
- laser monitoring techniques for trace gases 8-69521
- laser photoelectric spectrometer for large condensation nuclei meas. (Russian) 8-65408
- laser systems appl. to atm. monitoring 8-69520
- laser velocimetry techniques using CO₂ laser 8-61623
- lidar return signal geometrical compression, atm. remote sensing appl. 8-57329
- lidar system, two-freq. downward looking, for atm. monitoring 8-69523
- lidar systems for atmospheric pollution monitoring 8-53765
- Los Angeles basin, pollutants three-dimens. distrib. 8-61542
- LWR strawaway fuel cycle effluent projections 8-94110
- magnetic particle fallout recorded in recent ombrotrophic peat sections 8-61519
- mapping, provisional, of pollution effects indicators 8-81387
- methane, in air, IR spectra, optical-acoustic investig. (Russian) 8-74663
- methyl iodide, removal by Ag impregnated Al and zeolite 8-53719
- monitoring, computer automation of CO₂ laser long-path absorption system 8-92971
- monitoring, on site automatic analysers, review (French) 8-81451
- monitoring networks, automatic systems 8-93009
- multielement analysis of environmental samples by samples by X-ray fluorescence spectrometry 8-69513
- multiway sorption filters, development and use for radioactive iodine removal from air 8-61543
- national environmental monitoring system 8-77329
- non-methane hydrocarbons, monitoring via photoionisation 8-73549
- nuclear installations, radioactivity release, air monitoring emergency procedures 8-70610
- nuclear pollutant release assessment, FERMIAN computational system environmental transport and dose calc. 8-94150
- optical methods, appl. resonant fluorescence, Raman scattering and LIDAR (Czech) 8-81350
- optical methods of pollution detection (Czech) 8-60444
- organic component analysis using capillary GC/MS computer technique 8-80799
- organic pollutants, determ. via gas chromatography after cryogenic sampling 8-81468
- air pollution detection and control continued**
- ozone analysers, for industrial plant monitoring and control (Japanese) 8-57308
- Paris street, atmospheric pollution survey network 8-81463
- particle sizing, 0.05 to 5.0 μ m, using laser instrument 8-61624
- particulate matter catch from EPA and ASME-ASTM sampling trains 8-73547
- phosgene, spectrophone meas. at selected CO, CO₂ laser wavelengths 8-57310
- piezoelectric microbalance, for respirable aerosol mass conc. meas. 8-69518
- pulp mill stack plume meas., LANDSAT satellite multispectral scanner subsystem data appl. 8-88905
- pulsed electrostatic precipitator and flame photometer for total S aerosol conc. meas. 8-95975
- quantitative analytical spectroscopy using scanning tunable dye laser 8-81362
- radioactive aerosol dispersiveness in main ventilation system 8-70650
- radioactive contaminant unplanned release meas. and countermeasures 8-89994
- radioactive fallout in air and rain, results to end of 1977 8-82535
- radioactivity meas. at Nuclear Research Institute using scintillation probe and GM tube (Czech) 8-88906
- radioactivity standards for environmental monitoring, prep. 8-80816
- radiometer, airborne dual-channel IR heterodyne, for atm. meas. 8-57369
- radionuclide airborne release assessment, determ. of atm. stability categories 8-73504
- radiosonde system, 403 MHz, for boundary layer study 8-85723
- Raman scattering analytical techniques using tunable lasers 8-61134
- reactor containment air contamination, sampling and measurement techniques (French) 8-89997
- remote detection, appl. of LiNbO₃ tunable parametric oscillator 8-59089
- remote monitoring using discretely-tunable IR gas lasers and heterodyne detect. techniques 8-61605
- remote probing, generalised method for environmental surveillance 8-57363
- remote sensing from space 8-61621
- residual carbonaceous material in urban airborne particulates Raman microprobe 8-69449
- selective quantitative measurement of pollutants, appl. of CO and CO₂ lasers 8-69526
- small mass, status (Japanese) 8-92667
- smoke density meter, maximum sensitivity determination, flue gas optical density spectral analysis appl. 8-69500
- smokes, atmospheric, optical probing, homogeneous particle model appl. (Russian) 8-77328
- SO₂ air pollution levels modelling and forecasting, statistical approach 8-81398
- SO₂ molecules in air, remote sensing methods assessment (Japanese) 8-96288
- spectrometer, laser absorpt. for high sensitivity pollution detect. 8-57373
- standards, administrative aspects (Dutch) 8-57311
- stratospheric O₃ and aerosols, economic anal. of environment monitoring system 8-73507
- sulphate aerosol, individual submicron particles detect. technique 8-69527
- survey aircraft for sample collection and anal. (Dutch) 8-81366
- survey vehicle for air pollution monitoring (Dutch) 8-81365
- test gas atmospheres, calibration standards, generated by gas phase titration 8-69507
- toxic gas detection, appl. of MOS devices 8-76908
- trace elements, meas. accuracy using neutron activation anal. 8-69509
- tunable semiconductor diode laser system for long-path monitoring 8-69522
- turbulent atmospheric transport, Monte Carlo simulation, radioactive pollution appl. 8-61550
- urban aerosol, size-fractionated, N₂ and O₂ determ. by particle elastic scatt. anal. 8-81466
- UV double-beam photometer, for atm. O₃ calibration, 8-69505
- venturi-jet scrubber, gas absorpt. with chem. reaction, performance study 8-81393
- water vapour isotopes, spectrophone meas. at selected CO, CO₂ laser wavelengths 8-57310
- West German LWR power plant stack monitoring, legal and technical aspects 8-89988
- West German nuclear plant airborne radioactive effluent monitoring 8-89990
- Ar release from TRIGA reactor, comparison of γ -ray detectors 8-57309
- F determ. in atm. samples by $\text{F}(\text{p},\alpha)\text{O}$ react. using low energy accelerator 8-85239
- HCl gas in ambient air, detection using coated piezoelec. quartz cryst. 8-92532
- H₂S in air, preconc. determ. by flame photometric detection 8-92535
- H₂SO₄ dissociation and absorpt. consts. ultrahigh resolution obs. of 8.2, 11.9 μ m bands 8-70825
- I radioisotopes, high efficiency mixed species air sampling, readout and dose assessment system 8-57074
- NO, absorpt. characts. of ν_2 band, vel. to atm. meas. 8-57316
- NO isotopes, spectrophone meas. at selected CO, CO₂ laser wavelengths 8-57310
- NO/NO₂/O₃ monitors, intercalibration 8-69529
- NO₂ spatial distribution, detectivity estimation of DAS lidar 8-92991
- N₂O emission from soils during nitrification of fertilizer 8-57313
- O₃ atmospheric profile, airborne dual-channel IR heterodyne radiometer meas. 8-57369
- O₃ calibration methods, accuracy 8-69506
- O₃ monitoring apparatus, chemiluminescence reaction with ethylene 8-66310
- ²¹⁰Pb tropospheric residence time 8-85396
- ²¹⁰Po determ. in air, radiochem. separation and α -counting method 8-73113
- Rn barrier to reduce indoor airborne Rn progeny 8-73262
- Rn daughter concentrations in air of dwellings in Great Britain 8-77118
- Rn/Tn daughter air conc. meas. by filter method, general formula 8-70711
- ²²²Rn low conc. meas. in air, scintillation method 8-92970

air pollution detection and control continued

- ²²²Rn, passive environmental monitor based on exoelectron dosimeter 8-82523
 Ru, determ. in automobile exhaust-emission, by chem. ionisation mass spectrometry 8-61079
 S, compact X-ray fluoresc. analyser 8-68971
 S containing aerosols, continuous meas. and speciation by flame photometry 8-95974
 S containing aerosols, continuous in situ meas. by flame photometry and thermal analysis 8-96296
 S, SO₂⁻² and related species, sampling and anal. of atm. aerosols 8-96283
 SO₂, atmospheric, fluoresc. monitoring using NO γ-bands 8-73121
 SO₂, continuous-running, direct-reading recorder 8-53743
 SO₂ emission reduction, from steam generators burning pulverised brown coal (German) 8-53724
 SO₂ remote meas. at 4 μm with continuously tunable source 8-77365
 SO₂ remote sensing by correl. spectrometry and differential lidar 8-96298
 SO₂ small automatic monitoring network, practical experiences 8-81462
 SO₂⁻² aerosols, ambient, laser-Raman monitoring 8-69532
 SO₂⁻², individual submicron size particles detect. method 8-95973
⁹⁰Sr tropospheric residence time 8-85396

air pumps see compressors**air terminals see airports****air traffic**

- nuclear fuel transport by air, feasibility and economics 8-94154

air-traffic control

- see also aircraft
 meteorological conditions forecasting procedures, development and improvement 8-92950

aircraft

- see also aerospace control; aerospace instrumentation; air-traffic control; helicopters
 accidents in thunderstorm downbursts, analysis 8-53693
 aeroautoelasticity, active control and suppression of flutter in aircraft (Russian) 8-67079
 aeroelastic analysis, unsteady airloads prediction 8-71346
 air pollution sample collection and anal. equipment (Dutch) 8-81366
 aircraft noise meas., cause of structural vibrations 8-87187
 angular vibration power spectral density prediction model 8-83323
 flyover noise, modelled by acoustic scatt. by moving prolate spheroid 8-94458
 infrasound, effect on people, exptl. study of levels 8-88726
 jet exhaust noise, prediction of in-flight levels 8-87178
 motion in atm. turbulence, math. modelling 8-81274
 noise, insulation of buildings 8-55508
 noise, interior, general aviation types of aircraft, acoustic field studies 8-90595
 noise, interior, light aircraft fuselage laboratory studies 8-90596
 noise index, psychological assessment 8-55507
 rudder-bars force meas. (French) 8-49825
 skin, lightning damage simulation 8-87575
 sound transmission into heavily-damped cylindrical fuselage 8-83166
 stratospheric aircraft, aerosol particle exhaust layer obs. at 23 km 8-81283
 tail-wheel struct. of light aircraft, large deflection anal. 8-83272

aircraft communication

- optical fibre, cost models for A-7 aircraft ALOFT project 8-59131

airfields see airports**airglow**

- see also atmospheric spectra; aurora; nightglow; sky brightness; twilight
 ionosphere heating by radio waves, effects on airglow emissions 8-77403
 polar airglow, mag. ordering obs. 8-57378
 space sciences, conf., Trivandrum, India (Jan. 1977) 8-69586
 wave component identification, multiple-point method 8-73526
 N₂ dissociation by electron impact and EUV photoabsorpt., rel. to aurora and airglow 8-58847
 N₂⁺(A²Π_g) Meinel band deactivation cross sections 8-66635
 Na I D lines dayglow diurnal var. obs. at Poona 8-69558
 O II 7320-7330 Å emissions meas. at twilight 8-88962
 OH emission, waves and winds, 80-100 km altitude 8-93025
 OH Meinel bands, in airglow, rot. temp., radiative lifetime 8-61643
 OH Meinel bands' intensity distrib., OH⁺ quenching mechanisms 8-65447

airports

- aeronautical meteorology, progress and challenges 8-53692
 weather service, future trends 8-53694
 weather-related aircraft accidents, analysis 8-53693

alarm systems

- nuclear power plant, fast alarm system to optimise protection of public 8-55048
 radio emergency warning system, earthquake prediction appl. (Japanese) 8-85497
 Swiss Federal Institute for Reactor Research, emergency organisation 8-55047

albedo

- absorbing-scattering semitransparent planar layer, flat temp. waves 8-90683
 aurora and nightglow satellite obs., contamination due to scatt. by clouds and snow 8-77385
 auroral albedo profile, over snow-covered ground, rocket obs. 8-77384
 climatic changes due to intensive solar energy production, albedo modification 8-85680
 climatic model experiments, simulated changes, solar energy conversion effects 8-81354
 Galilean satellites, radar obs. during 1976, results 8-61788
 Iapetus, normal reflectance from lunar occultation obs. 8-85897
 Io, surface albedo rel. to laboratory samples 8-53865
 Io spectral albedo, implications of Na and K doped NH₃ frosts, reflectance spectra 8-84561
 local energy exchange dynamics and climatic boundary conditions, solar energy conversion effects, preliminary examination 8-81355
 Mars atmosphere, optical props. during 1971 dust storm (Russian) 8-93138
 Mars surface, global colour vars. obs. 8-65527
 Mercury albedo features, IAU nomenclature 8-53848

albedo continued

- Mercury albedo features, longits. and nomenclature 8-53849
 meteoroids from Periodic Comet d'Arrest, particle size distrib. and albedo 8-53876
 Milne problem and spherical albedo, law of darkening, forward and backward scatt. effects 8-77483
 planetary albedo and long-term climatic change numerical modelling 8-77315
 Rhea, normal reflectance from lunar occultation obs. 8-85897
 Saturn, far UV albedo from rocket obs. of spectrum 8-53867
 Titan, normal reflectance from lunar occultation obs. 8-85897
 Uranus rings, low albedo rel. to ice sputtering by radiation belt protons 8-89116
 Venus clouds, H₂SO₄ aerosol medium IR single scatt. albedo 8-65526

alclad see aluminium alloys**Alfven waves see magnetohydrodynamic waves; solid-state plasma****algebra**

- see also Boolean algebra; linear algebra; matrix algebra
 affine Lie algebra A_n⁽¹⁾, explicit construction 8-89626
 associative Hamiltonian algebras 8-69975
 C* algebra, completely positive maps 8-49716
 complete sets of observables on the sphere in four-dimensional Euclidean space 8-70015
 division rings with evolution 8-89296
 K-flows quasi-free reversible, generalised 8-54297
 modular operator, local observables, in von Neumann algebras, duality in QFT, CPT invariance 8-81793
 net cohomology over Minkowski space 8-93561
 noncommutative algebra, two point function calcs. 8-57734
 operator algebras and Banach spaces, perturbation of flow 8-49630
 quantum theory, dilations of irreversible evolutions 8-65794
 superpositioned exponential processes, resolution and parameter evaluation (German) 8-89294
 two centre problem, linear algebra of integrals (Russian) 8-89368
 von Neumann algebras, complete normal dissipations 8-89358

algorithm theory

- annular plate, algorithm for numerical soln. of critical buckling 8-83275
 education, implications of algorithm theory for instructional design 8-81735
 power series, class of algorithms for obtaining rational approximants 8-54169
 water network anal. using node recording algorithms and admittance matrix 8-85613

algorithms (computer listings) see subroutines**aliphatic compounds see organic compounds****alkali metal alloys**

- see also caesium alloys; lithium alloys; potassium alloys; rubidium alloys; sodium alloys
 alkali metal-Au alloys, elec. props. 8-84187
 dilute binary solutions, heat of formation 8-75840
 nontransition element/alkali metal systems, direct calorimetric exam. 8-84775

alkali metal compounds

- see also alkali metal alloys; alkali metal halides; caesium compounds; francium compounds; lithium compounds; potassium compounds; rubidium compounds; sodium compounds
 alkali borate glass networks, π-electron distrib. SCF INDO LCAO-MO calc., O basicity 8-79924
 alkali hydrides, bulk props. prediction from molecular behaviour 8-51468
 alkali-alkaline earth ceramic solid solutions, with tetragonal tungsten bronze struct., low freq. optical modes 8-76477
 alkali-alkaline earth silicate glasses, IR refl. spectra (Japanese) 8-52505
 antimonide photocathodes, prep. and props. 8-84693
 chalcogenides, van der Waals pots. determ. 8-83767
 chloride-AlCl₃, molten mixture, vap. pres. meas. 8-87779
 cryptand complex, with anion or solvated electron, optical absorpt. spectra 8-52526
 hydroxides, dissoc. energies and bond lengths, ion props. depend. 8-86801
 metaborates, dissoc. energies and bond lengths, ion props. depend. 8-86801
 metaphosphate glasses exam. of temp. dependence of thermo-optical const. 8-88286
 metaphosphate glasses exam. of thermo-optical and photoelastic props. 8-88287
 molybdates M^{III}M^{III}(MoO₄)₂, M^{III}=Al,Sc,Fe,In, struct. transitions, phenomenological approach 8-51674
 multialkali photocathodes, secondary emission characts. 8-84687
 nitrates, lattice energy, standard heat of formation, electron affinity 8-91295
 NMR spectra of alkali metal nuclei, shielding and quadrupole coupling consts. 8-84487
 oxide-Al₂O₃-SiO₂ glass, EPR 8-91930
 oxides in vitreous silica, effects on viscosity. 8-64580
 perchlorates, elec. transport during struct. transforms. 8-59971
 perhenates, UV photoelectron spectra 8-50575
 polyaluminates, synthesis, solar furnace appl. 8-84746
 silicate glass, CuO doped, ESR spectra of Cu⁺, quadrupole effects 8-64265
 tungstates, M^{III}M^{III}(WO₄)₂, M^{III}=Sc,In, struct. transitions, phenomenological approach 8-51674
 M₂O-MnO-B₂O₃ glasses, M=Li, Na, K, glass-forming region and physicochem. props. 8-63678
 M₂O(MF)₂-BeO-P₂O₅ glasses, M=alkali metal, alkaline earth, Cd or Zn, glass-formation 8-67656
- alkali metal halides**
 see also compounds of individual alkali metals, e.g. sodium compounds
 adsorption, of inert gas adatoms, pot. energy calcs. 8-67902
 alkali halide-Hg, EPR and optical props. 8-91933
 alkali halides, F-centre trapping of conduction electrons, photocond. study 8-56179
 binding energies of vacancy pairs 8-51533
 birefringence, annealing effects, photoelasticity 8-72483
 bound polarons, vibronic theory, appl. to F-centre excited states 8-84150

alkali metal halides continued

- bromide-VBr₂ systems, cryst. struct., DTA investig. (German) 8-72766
- chlorides: F⁻(Br⁻)(I⁻), anion impurities substitution, energies of soln., association and migration 8-83831
- chlorides, I⁻ or Br⁻ doped, optical investigation of atomic hydrogen centres 8-88351
- chlorides, modified electronic charge density 8-79554
- defect formation, kinetics 8-67713
- defect formation, model of excitonic mech. 8-91337
- deformation dipole model, rel. to dielectric props. 8-72454
- diamagnetic susceptibility, interatomic charge transfer effect 8-50660
- dibenzo-18-crown-6 complex, ESCA, binding energy 8-50584
- dipolons, graphical method for binding energy determ. 8-59805
- doped angle crystals, latent hardening 8-51607
- elastic moduli determ. 8-91373
- elasto-optic coefficients, signs 8-64346
- electron impact, elastic scatt., model, static and static exchange calcs. 8-94321
- electron spin transfer in alkali chlorides and alkali bromides doped with divalent vanadium 8-87949
- electron-phonon interactions, review 8-63991
- equations of state under high press. 8-55935
- exchange charge polarisation, dielectric const., Dick and Overhauser model 8-55832
- exchange charge shell model analysis of strain derivatives of static polarisability, effective charge parameter 8-91296
- F⁻centres, thermal and photolytic decay processes 8-95053
- F-centre, cluster-Bethe lattice treatment 8-63762
- F-centre lasers, tunable IR emission 8-59030
- F-centres, binding energies of positron to F and F' colour centres 8-87667
- F-centres, influence of purity of crystals on stability of F-centres and interstitials 8-91336
- heat pipe apparatus for coloration of laser-quality alkali halide crystals 8-74917
- high pressure phase transformations, transformed fraction and reaction rate meas. 8-51667
- impurity aggregation kinetics for divalent impurity dipoles 8-79630
- impurity-vacancy complexes, association and orientation energies 8-51578
- impurity-vacancy dipole interaction with relaxed and nonrelaxed holes (Russian) 8-75661
- interatomic forces, Born model anal. on US data 8-55833
- interionic potentials, completely cryst. independent specification of Born-Mayer potentials 8-55828
- interionic potentials, cryst. independent shell parameters and fitted Born-Mayer pots. 8-55827
- IR absorpt. in molecules, clusters and microcrystals 8-80363
- irradiated, annealing 8-92494
- irradiated, chemiluminesc. process during dissolution (Russian) 8-92133
- isomorphous salts in aq. solns., viscosity 8-95173
- lattice energy, binding, indeterminacy principle theory 8-59777
- melting, appl. of microscopic theory 8-79748
- melting, dislocation theory, cooperative effects 8-59934
- molecular clusters, equilib. geom. form, energy and vib. spectrum 8-55269
- molecular orbital theory, relativistic, in Dirac Slater model (Japanese) 8-66480
- molecules, interaction potential 8-58612
- molten, ionic radii and X-ray diff. patterns 8-59732
- molten, struct. determ. by X-ray scatt. 8-87609
- morphology of growth and evaporation surface 8-79544
- Mott-Littleton dielectric theory 8-80274
- nonradiative Auger effect, oppositely charged defect centres, autoionisation-tunnel relax. of electron excitation 8-72112
- optic mode Gruneisen parameters and strain derivatives, Born-Mayer and Szigeti model 8-55929
- optical components, cryst. growth from melt 8-50955
- Ostwald ripening and its application to precipitates and colloids in ionic crystals and glasses [Review] 8-80548
- pelletting technique for solid sampling in IR spectroscopy 8-87171
- photochromic as optical processing elements 8-83056
- photoelectron spectra of ionic mols. using mol. beam technique 8-50576
- piezo-optical properties, temperature dependence 8-92050
- polymorphic transformations, sudden, theoretical considerations 8-51666
- radiolysis, growth of colloidal metal inclusions 8-92493
- resonance Raman scattering, electron-phonon interaction for F-centres 8-68519
- second-neighbour interaction potential 8-91298
- self trapped exciton, optical detection of spin relax. processes 8-60358
- short range interactions, static polarisabilities 8-71702
- solutions, homogeneous nucleation, glass form, press. depend. 8-51649
- solutions, ionic hydration, review 8-92501
- solutions, tetrahedral hydration of ions, Raman obs. 8-55804
- stability and melting 8-71839
- static polarisability, vol. depend. 8-52428
- substrate, gas adsorption, stress depend. of chem. pot. 8-91541
- surfaces, step struct. 8-79866
- surfaces, step structures 8-79865
- three body interaction effects on cohesive props. 8-83770
- transport phenomena, appl. to solid state devices 8-55976
- two-photon absorpt. coeffs. 355 and 266 nm 8-83037
- V⁻centres, vacancy induced splitting of excited states, Na⁺ structure 8-51931
- van der Waals interaction energy eval. 8-71705
- van der Waals pots. determ. 8-83767
- vibrational modes due to three impurity clusters 8-75773
- vibronic spectra of O₂⁻ and NO₂⁻ ions in alkali halides, press. effects 8-52532
- CdCl₂-NaCl, KCl molten salt mixtures, US velocity and adiabatic compressibility obs. 8-75730
- NaCl-type structure, MgO epitaxy, RHEED meas. 8-67920

alkali metals

- see also caesium; francium; lithium; potassium; rubidium; sodium
- adsorption, on free-electron like and transition metals, valence electronic struct., wave-function matching calcs. 8-72235
- adsorption, on metal surface, finite barrier model, bounded electron gas static semiclassical response 8-72221
- adsorption on Ni, depend. of electron state of adatom on conc. 8-72001
- alkali atom+methane derivative, collisional ionisation, nitromethane, perfluoromethyl bromide (iodide) electron affinities 8-66639
- alkali ion+alkali atom, differential scatt. meas. 8-62903
- alkali metal, model potential calculation of binding energy and compressibility 8-91632
- alkali metal atom+inert gas atom, hyperfine transition spectral line shift, quantum corrections 8-82655
- atom, excited hyperfine and Stark parameters, meas. and calc. 8-86814
- atom, fine-struct. of excited nd and nf states, at. core effect 8-58606
- atom, two-photon transitions to Rydberg levels, dye laser reference wavelengths 8-94221
- atom, valence electron ground states, nonlocal Hellmann model potentials 8-50476
- atoms, electron impact excitation, integrated cross-section calc. 8-62921
- atoms, excitation transfer in slow collisions between identical particles (Russian) 8-78799
- colliding atoms, optical excitation to state of quasibound motion (Russian) 8-58784
- elastic constants, temp. depend. 8-51603
- elasticity moduli, third order, temp. depend. (Russian) 8-63798
- electrical resistivity, temp. depend. 8-64022
- electronic magnetic susceptibilities calc. 8-52204
- flash lamp, absolute spectral distrib. and radiant output 8-66510
- inert gas-alkali metal, inhomogeneous mixture, nonequilib. processes under conditions of T-layer form. 8-91079
- lattice vibrations and Gruneisen parameter 8-59917
- liquid, collective excitations and short-range order 8-63665
- liquid, salt solns., phase equilib., and chem. 8-73040
- M+XF₆, X=S, Se, Te, Mo, W, Re, Ir, Pt, collisional ionisation 8-55226
- optical spectra, agreement with theory (French) 8-72558
- paramagnetic gas in radiation field, magnetisation 8-78667
- solutions, cation-electron interactions 8-73037
- susceptibility, paramag. and electronic 8-52205
- thermal properties and Gruneisen parameters, employing model pot. 8-71815
- vapour condensation from gas flow (He, Ar, N₂), heat and mass transfer 8-75192
- vapour O-O transition resonance line obs. (Russian) 8-57999
- D+M→D⁺+M⁺ (M=alkali metal atom), ion-pair form. 8-58779
- GaAs, surface segregation of implanted alkali metals, photoemitter prep. and characts. (French) 8-60544
- H⁺+M⁺ (M=alkali metal atom), ion-ion recombination 8-58779
- He⁺+alkali metal atom, ionisation cross sections, binary encounter approx. with HF electron vel. distrib. 8-55225
- He⁺+Na(K)(Cs), 5-100 keV, electron capture form. of fast metastable He 8-74760
- NH₃-alkali metal solutions, metal-nonmetal transition Hall mobility, electrodeless meas. 8-56194

alkaline earth alloys

- see also beryllium alloys; magnesium alloys
- Sr-Ti, phase diagrams (Russian) 8-80513
- Al-Al₂Ca, eutectic alloy, unidirectionally solidified, exam. of growth and crystallography 8-72771
- Ba-Eu, phase diag. (Russian) 8-80514
- Ba-Nd, phase diagram, microstruct., X-ray, chemical and thermal diffusion anal. (Russian) 8-52761
- Ba-Ti, phase diagrams (Russian) 8-80513
- Ba-Yb, phase diag. (Russian) 8-80514
- BaNiSn₃, cryst. struct. rel. to ThCr₂Si₂ type (German) 8-51470
- BaPd, gaseous, dissociation energies, obs. and calc. values 8-58864
- BaPtSn₃, cryst. struct. rel. to ThCr₂Si₂ type (German) 8-51470
- BaRh, gaseous, dissociation energies, obs. and calc. values 8-58864
- Bi₂Sr_{1-x}Eu_x, supercond. and mag. ordering 8-56252
- Ca-Ag(In), liquid alloy, thermodynamic exam 8-75848
- La_{1-x}Ca_xNi₂, H₂ sorption props. 8-91533
- Sr-Nd, phase diagram, microstruct., X-ray, chemical and thermal diffusion anal. (Russian) 8-52761
- SrNiSn₃, cryst. struct. rel. to ThCr₂Si₂ type (German) 8-51470

alkaline earth compounds

- see also barium compounds; beryllium compounds; calcium compounds; magnesium compounds; radium compounds; strontium compounds
- alkali-alkaline earth ceramic solid solutions, with tetragonal tungsten bronze struct., low freq. optical modes 8-76477
- alkali-alkaline earth silicate glasses, IR refl. spectra (Japanese) 8-52505
- chalcogenides, static dielec. const. 8-84513
- chalcogenides, van der Waals pots. determ. 8-83767
- fluorides, crack propag., cryst. props. effects 8-75720
- fluorides, elasto-optic coefficients, signs 8-64346
- fluorite type crystal, effects of anharmonicity and disorder on Raman scatt. at high temp. 8-80349
- halides, aq. solns., activity and osmotic coeffs. 8-53242
- halides, thermodynamic and structural props., computer simulation 8-75849
- halides, transport phenomena, appl. to solid state devices 8-55976
- halides, van der Waals pots. determ. 8-83767
- hydroxyapatites, elec. cond., charge carrier identification 8-67855
- metaphosphate glasses exam. of temp. dependence of thermo-optical const. 8-88286
- metaphosphate glasses exam. of thermo-optical and photoelastic props. 8-88287
- oxide based compounds, thermodynamic study using CaF₂ electrolyte 8-53241
- oxides, electron transfer between adsorbed O₂⁻ ions, EPR obs. 8-76296
- oxides, occurrence in sunspots and cool stars 8-85933
- oxides, photoelastic consts. 8-71781
- M₂O(MF₂)-BeO-P₂O₅ glasses, M=alkali metal, alkaline earth, Cd or Zn, glass-formation 8-67656

alkaline earth metals

- see also barium; beryllium; calcium; magnesium; radium; strontium
 atom, multiphoton ionisation spectroscopy of even- and odd-parity states 8-86973
 atom, multiphoton ionisation spectroscopy 8-82703
 atoms and ions, regularities within Stark widths of reson. lines 8-78662
 ion, valence electron ground states, nonlocal Hellmann-model potentials 8-50476

alkalinity

see pH

allotropism

see polymorphism

alloy steel

- 1Kh18N9Ti, physico-mech. props. after boring in metallic melts (Russian) 8-56736
 12Kh18N9Ti-TiB₂, eutectic alloy, high temp. props. 8-84931
 30KhGSNA, strength under combined compound stresses and corrosive environment (Russian) 8-56803
 40Kh, surface working effects on crack resist. (Russian) 8-56734
 40Kh, thermally strengthened, influence of loading rate and sea water on K_{IC} value (Russian) 8-56799
 40KhNMA, fretting-corrosion in vacuum-chromized Ti alloy VT-3 couple (Russian) 8-56804
 A533 B, fatigue crack propagation, grain size and temp. effects 8-56727
 A-533 B, J_{IC}-testing, statistical eval. of different techniques 8-56828
 ageing charact., precipitation and coarsening of VC, TiC, and V-Ti-C in ferrite 8-84874
 alternating bending, fracture surface appearance of Ck 45 (German) 8-52995
 austenitic, Ni free, TEM exam. of corrosion 8-85029
 bainitic, morphological characteristics 8-88582
 carbide lattice, kinetics of its destruction in NC6 (Polish) 8-92280
 carbide transitions during post-strain ageing and tempering (Russian) 8-95741
 carburized case parameters, effect on props. of 20Kh3MVFA and 12Kh2N4A 8-52999
 case hardened, MnCr, shot peening effect on bending fatigue strength (German) 8-56777
 case-hardened cast, contact endurance rel. to austenizing (Russian) 8-56805
 cementite decomposition during plastic deform. alloying element effects 8-84768
 cluster formation, susceptibility in 40 KhN, influence of isothermal working in H₂ (Russian) 8-56643
 cold formability (French) 8-60681
 constructional, fatigue cracking in corrosive media 8-85081
 corrosion-impact-cyclic strength of boring bars, effective hardening treatment 8-53034
 Cr-Mo-V, fatigue, failure probability based on residual strength 8-68797
 crack arrest toughness determination 8-72867
 cyclic strength after strain hardening and tempering, precip. hardened 40FT 8-52988
 delayed retardation phenomena of fatigue crack growth, exam. 8-56745
 die steels for cold plastic working, powder metallurgy charact. 8-68649
 ductility, hydrostatic press. effects 8-80615
 electrochemical steel, hysteresis curves, plotting (Russian) 8-76269
 eutectoid pearlitic, exam. of microstructures, dominating ductility (Japanese) 8-849178
 failure charact. of steel 15G2AFDps, effect of loading freq. and temp., SEM exam. of failure surface 8-84995
 fatigue crack closure over stress ratio range, stress intensity threshold, in HT80 8-80619
 fatigue crack growth from a surface flaw 8-68803
 fatigue crack initiation and propagation at notch tip, HY140 steel 8-80647
 fatigue crack initiation and propagation at notch tip, HY180 steel 8-80647
 fatigue crack propagation rate in types 15KP, ST3, 15G and 10G251 with different yield strengths 8-52987
 fatigue resistance when strengthened by nitrides and welded joints, grades 14G2AFD and 15G2AFDps 8-95790
 fracture and high temp. props. of 4940, 5332, 1225K 8-60821
 fracture toughness, type 4340, effect of partially dissolved N₂ 8-80642
 fracture toughness and dynamic strength, surface active agent effects (Russian) 8-56812
 hardened and tempered parts, nondestructive magnetic inspection 8-95889
 heat treated, alloying element distrib. effects, mech. props. 8-84978
 high alloy, ledeburite, wear and corrosion-resistant coating by chemical vapour deposition 8-92403
 high C, amorphous, produced by rapid quenching from melt, hardness and strength 8-59764
 high speed, anode potential determ. of tempering quality 8-53139
 high speed, atomised powder, defects in parts produced by hot isostatic pressing 8-60612
 high speed, powder, cold isostatic compaction effect on morphological props. 8-52747
 high speed, wear resistant coating of TiN, TiO₂, CVD 8-92406
 high speed working curve, sample production for spectrochemical anal. from Fe dilution method (Japanese) 8-53050
 high strength, alloy initiation of cracks at delayed fracture AE study 8-72868
 high strength, low alloy, mech. props. 8-60739
 high strength, low alloy, plate, impaired ductility in sheared edges 8-60727
 high strength, low alloy, rare earth treated, ductile fracture mech. 8-64658
 high strength steels HT80, HY130, quenching and tempering effect on H₂ diffusion (Japanese) 8-64565
 high strength structural materials, microstruct. influences on fatigue and fracture resist. 8-56728
 high-alloy, phases (Chinese) 8-95728
 high-speed, quenched and tempered notch toughness, ultimate and yield strength in tension and compression 8-95782
 high-strength, endurance in air and NaCl soln., loading freq. effects (Russian) 8-56810
 high-strength low-alloy stress corrosion cracking (Ti) in NaCl solution (Japanese) 8-92401

alloy steel continued

- (high-temp. combined ht. treatment) and mech. working, C content effects (Russian) 8-52854
 interaction with Nd:glass laser light 8-92147
 ledeburite, fracture during hot plastic deformation exam. 8-56755
 low alloy, alloying constituents, XES determ. 8-73126
 low alloy, cleavage fracture, fine scale precipitation dispersion effect, TEM obs. 8-60788
 low alloy, exam. of fatigue crack, growth, and Paris Law parameter relationship 8-92343
 low alloy, fatigue fractographs (Japanese) 8-92335
 low alloy, high strength, correlation between fracture toughness, tensile props., fracture morphology 8-60789
 low alloy, high strength, ductile failure criteria for blunting crack 8-64657
 low alloy, naval, stretch zone width meas., COD for ductile crack initiation 8-68813
 low alloy, pearlite block, exam. of crystallographic features, formation processes (Japanese) 8-84799
 low alloy, thermally fatigued, fracture toughness 8-72872
 low alloy, type 3sp, effect of temp. at end of rolling on mech. props., and coercive force 8-72799
 low alloy, type 4340, quenched and tempered, effect of plastic strain followed by ageing, on torsion fatigue resistance 8-92360
 low alloy, type SNCM 8, rotor disc, exam. of fracture, using a integral approach 8-92352
 low alloy ferritic, sub-micron cavity nucleation, SEM obs. 8-95753
 low alloy medium C, sliding interfaces, division of heat and surface temp. rel. to oxidative wear 8-64712
 low alloy weldment cracking causes creep resisting 8-56760
 low alloys, high strength, stress corrosion cracking in saturated Ca(OH)₂ solns. due to Cl⁻ and SO₄²⁻ additions 8-88567
 low C, Cr-Ni (25, 25 wt.%), σ phase form. prestrain effects (Japanese) 8-92260
 low C, effects of pre-treatment on graphitisation behaviour (Japanese) 8-84860
 maraging, 18% Ni, effect of solution and ageing treatments, on microstruct. tensile props., fracture toughness 8-80648
 maraging, 250-grade, ductility and toughness of hot isostatically pressed powder 8-52925
 maraging, (18 wt.% Ni), solution annealed, exam. of cryogenic tensile, fatigue, and fracture props. 8-92311
 maraging, Cr-Co, effect of ageing on microstruct., TEM and neutron diffraction exam. 8-84867
 maraging, fatigue crack growth, during impact tests, exam. of kinetics 8-88525
 maraging, fracture toughness data, comparison with equivalent energy and energy per unit area data 8-92965
 maraging, grain refinement due to cyclic heat treatment 8-52971
 maraging, heating of thin samples with brief ageing N6G4M, ON18K9MST 8-52866
 maraging, investigation with lower Ni and C contents (Chinese) 8-84812
 maraging, SCC, subcritical flow growth, comparison of aircraft alloys in NaCl soln. 8-53028
 maraging, type 200, effect of free on cyclic crack growth in air water environment 8-84680
 maraging, type Kh18N8D21M, conditions for formation of stable austenite 8-84868
 maraging 250-grade, fatigue crack growth model, notch analysis of fracture approach 8-52984
 (maraging low Ni) phase transformations (Russian) 8-88465
 martensitic, fatigue crack form. associated with cyclic slip deform. along prior austenite grain boundaries 8-60831
 martensitic transform. microkinetics, in type N24M 8-56637
 martensitic transform. during deformation of types N28, N29, N30 and N31 8-56639
 microstruct. and fracture of steel 52100, exam. as function of austenitising in temp. range 800 to 1100°C 8-76673
 microstructure characteristics, statistical processes (German/English) 8-95834
 microstructure of cup and cone fracture surface, effect of size of disperse phase particles (Russian) 8-68762
 Ni-C-Mo, TRIP steel, exam. of transformation behaviour 8-76718
 nitride phase hardening, precipitation and solution kinetics after heat treatment 8-95756
 notched beam, fatigue crack emanates from notch root, fracture strength 8-72866
 oriented Si steel, magnetisation hysteresis loops prediction 8-84221
 plastic deformation, type 36Kh17V, effect of surface condition on initial stage 8-84929
 plates, comparison of dynamic tear and Charpy V notch impact props. 8-92357
 potentiostatic control limitations in stress corrosion crack growth meas., in NaOH soln. 8-53031
 potentiostatic development of structures 8-95887
 pressure vessel A508-C12 steel, microcrack formation during stress-relief annealing of a weldment 8-80629
 quenched, types 37KhGSF and 44KhGSF, X-ray diff. testing of heat treatment 8-56834
 rare earth additions review 8-72786
 rectangular beam, stress-strain anal. of cyclic plastic bending and torsion 8-90734
 silver, elastic limit, bending strength, and ductility rel. to tempering temp. after quenching 8-95764
 sintered, Cr-Mo, CaF addition effects on stress heterogeneity 8-60611
 softening process in deformed type 15GyTi metallographs (Russian) 8-52840
 splat cooling of Fe-Mo-C alloy, microstruct. changes 8-84855
 static and fatigue strength tensor and compression test results 8-95810
 steel, high Ni, orientational variations of martensite transform. during deform of metastable austenite 8-84805
 steel, low alloy, sheet, welded hydraulic machine valve chamber strength and toughness 8-68820
 stress corrosion cracking in deionised water, temp. effects 6K300M 8-53039
 structural components, flow assessment based on cleavage fracture hypothesis 8-60804

alloy steel continued

structural transformations during heat treatment, and wear resistance of steel U20Kh6T2D, 8-88484
surface plastic deform., effect of heating conditions, type 45, 8-53033
temper embrittlement control progress, 8-72797
tempered martensite embrittlement, and retained austenite, exam., 8-56754
thermal and electro-physical props. of various heat resisting stampings (Russian) 8-51698
thermodynamic prediction of Ae temp. additions of Mn, Si, Ni, Cr, Mo, Cu 8-64524
transformer, formation of perfect cubic texture in thin sheets (Russian) 8-80557
type 25GS, increasing fatigue resistance by surface plastic deformation 8-88530
wear resistant diffusion coatings of B-Cr (Si) on type U18, 8-56823
weld metal, contrib. to mechanism of Nb(CN) precip. (Slovakian) 8-84816
welds, distrib. of Cr, Ni, Mo, Si, Ti, laser emission, microanal. method 8-61110
C and low-alloy steel inherent austenitic grain size determ., exam. of methods used 8-85071
C-Cr-Mo-V, high speed, exam. of fracture toughness and critical flow anal. 8-72848
Cr (9 wt. %), SiO₂ vapour deposited coating, exam. of corrosion protective props. 8-88563
Cr, austenitic boundary layers form by short laser pulse, reaction 8-88555
Cr, cast, fracture toughness and fatigue crack propagation, structural components of hydro-turbines, in water and air, 8-68822
Cr, quenched and tempered steel, effect on H diffusion coeff. and solubility (Japanese) 8-52857
Cr, thermodynamic anal. of facing process using other metals, 8-60878
Cr-C (2.14, 1.08 at. %) tempered, resistance to small plastic deformation, strain relaxation (Russian) 8-56698
Cr-C (12, 0.2 wt. %) growth of grain, boundary ferrite allotriomorphs, photoemission electron microscope exam. 8-88468
Cr-Cu-Mn-C, HT 80, effect of grain size on sensitivity to shear cracking (German) 8-72856
Cr-Mn, powder forged, fracture processes and fracture toughness 8-72870
Cr-Mn, with increased N content, X-ray spectra, microanalysis (Bulgarian) 8-53304
Cr-Mn-Si steel, heat-treatment quality, higher harmonics of EPR obs. 8-70094
Cr-Mo, alloy SCM3, hydrogen embrittlement, (delayed) fracture, exam. (Japanese) 8-64620
Cr-Mt, low-alloy, material selection for nuclear LMFBR steam generators 8-54834
Cr-Mo, pitting and crevice corrosion, exam. (Japanese) 8-64769
Cr-Mo, quenched and tempered steel, effect on H diffusion coeff. and solubility (Japanese) 8-52855
Cr-Mo (2.25, 1.1 wt. %), relationship between minimum creep rate and time to fracture 8-56759
Cr-Mo-V, creep crack growth temp. depends 525 to 600°C, 8-64634
Cr-Mo-V, creep fatigue interaction, 8-60841
Cr-Mo-V, creep fracture microstruct. effects, 8-64668
Cr-Mo-V, creep/fatigue interaction, 8-64632
Cr-Mo-V, low alloy, creep fatigue interaction 8-64673
Cr-Mo-V, medium strength, correlation between crack initiation, propagation, and microstruct., 8-60787
Cr-Mo-V, normalised and tempered, size and geometry effect on creep cracking behaviour, 8-64630
Cr-Mo-V, press. vessel, fracture, effect of tempering, 8-60799
Cr-Mo-V, rupture strength and thermal fatigue, charact. investigation 8-72857
Cr-Mo-V, steamline bends, restorative heat treatment effects, 8-68716
Cr-Mo-V, stress relief cracking mechanism, 8-64669
Cr-Mo-V (0.5, 0.5, 0.25 wt. %), heat treated, microstructural effect on threshold region fatigue, 8-56757
Cr-Mo-V (0.5, 0.5, 0.25 wt. %), comparison of methods of correlating creep crack growth 8-60826
Cr-Mo-V (0.5, 0.5, 0.25 wt. %), creep crack growth temp. effect 8-64667
Cr-Mo-V, press. vessel, crack growth under creep 8-60827
Cr-Mo-V, P, quenched temper brittleness in relation to V and B concs. 8-52986
Cr-Mo-V (W), for bolts, stress relaxation data, 8-60699
Cr-Ni, maraging effect of Mo, Co additions on hardening, 8-84833
Cr-Ni, soaking at forging temp., effect on struct. and mech. props. (Czech) 8-64628
Cr-Ni-Mo-V-Nb, for bolts, stress relaxation data 8-60699
Cr-Ni-Ti, austenitic stainless, creep deformation effects on intergranular TiC dispersion stability 8-84912
Cr-plated, H₂ distrib., laser-mass spectrometer investig. 8-61113
Cr steel, influence of ultrasound on tempering processes (Russian) 8-52827
Cr-V (1.5, 0.5 wt. %) cavitation effect of temp. and V content 8-64638
Cr-Mo-V compact tension specimen, thickness effect, 8-68764
Cr-Mo-V, failure in post yield regime using single edge notched tension specimen, 8-68765
Cr-Mo-V, low alloy, dispersed phase of VC hardening mechanism (Czech) 8-60676
Fe-C-Mo, dynamics of transform interface, ferrite-austenite interface 8-52795
Fe-C-Mo, dynamics of transform interface, at intermediate temps. 8-52796
Fe-C-Si-S liquid, desulphurisation with CaO exam. of reaction mechanisms 8-80742
Fe-C-Zn (0.45 wt. % C, 1.56 wt. % Zn), pearlite transformation during continuous cooling 8-80538
Fe-Cr-Co-W-Ni-C alloy, KKhVN transforms during annealing and nature of hardening (Russian) 8-56653
Fe-Cr-C steel, carbide formation during chemoising, exam. in terms of ternary phase diagrams 8-56818
Fe-Cr-Mo-C, X-ray investigation after friction and oxidation 8-52897
Fe-Cr-Mo-Si-V, various steels, short rod stress intensity factor tests up to 700K, exam. 8-60815

alloy steel continued

Fe-Cr-Ni-Mo-Al, (13, 8, 2, 1 wt. %), H₂ effects on fracture, exam. 8-60809
Fe-Ni, effect of metallurgy on stress corrosion cracking, and hydrogen embrittlement 8-60885
Fe-Ni-C (9, 0.1 wt. %), effect of intercritical tempering on impact energy, exam. of mech. props. 8-52861
Fe-Ni-Cr-Mo, exam. of tapered tensile specimen for stress corrosion threshold stress testing 8-53055
Fe-Ni-Cr-Mo-V-C, H₂S stress corrosion cracking effects of overload, exam. 8-60886
Fe-Ni-Cr-Mo-V-C, HY130, effect of H₂ and impurities on brittle fracture, review 8-60765
Fe-Ni-Cr-Sb-C effect of Ni, Sb, on temper embrittlement 8-60813
Fe-Ni-Mn-Si-Cr-Ni-Mo, effect of metallurgy on stress corrosion cracking, and hydrogen embrittlement 8-60885
Fe-Si (6.5 wt. %) steel, core mat. development (Korean) 8-60852
Mn (1 to 10 wt. %), Mossbauer, X-ray and electron microscope studies of martensite 8-56621
Mn, as rolled bainitic, tensile, impact and machinability props., transport appl. 8-88503
Mn form of twinned struct. (Russian) 8-64542
Mn, H₂ embrittlement mechanism (Korean) 8-68774
Mn, unmachined samples, impact figure testing 8-56838
Mn-Cr-V, structural changes during solution annealing (Czech) 8-84864
Mn-steel, cryst. geometry in formation of ε and α martensitic phases (Russian) 8-76648
Mn-steel, influence of ultrasound on tempering processes (Russian) 8-52827
Mn-Ti-B rare earth, distrib. of B (Chinese) 8-84811
Mo, quantitative anal. of carbides formed during tempering, 8-64571
Mo-V, creep rupture strength, heat treatment effects (German) 8-72834
Mo-W, high speed, best quenching heat treatment 8-84852
Nb-V cold rolled, HSLA, prod. by precipitation hardening, annealing 8-88471
NbCN precipitation in HSLA steel, exam. by electrical resistivity meas. 8-84822
Ni (1 to 9 wt. %), Mossbauer, X-ray and electron microscope studies of martensite, 8-56621
Ni (5.5 wt. %), fatigue fracture toughness, crack prop., at low temp. 8-68823
Ni, cross grider connections, fatigue strength, design stress, 8-64700
Ni, microstruct. plastic zone size and crack prop., 8-60790
Ni, sintered, relation between microstruct. microchemistry and mech. props. 8-64504
Ni-Al γ phase fracture, mechanical aspects of abrasive friction, wear, chip formation 8-72865
Ni-Cr-Mo, fatigue crack growth during impact tests, exam. of kinetics 8-88525
Ni-Cr (4, 1 wt. %), isothermal embrittlement, AES exam. of grain boundary segregation 8-60814
Ni-Cr, Sb, doped, temper embrittlement, susceptibility intercritical heat treatment effect 8-64570
Ni-Cr-Mn, type 4340, exam. of intergranular brittle fracture, by impact tests, Auger spectroscopy 8-52978
Ni-Cr-Mo, alloy, SNCM8, mech. strength under combined alternating strength 8-64690
Ni-Cr-Mo, alloys, SNCM8, SAE 4161, heat treated, residual stress at fatigue fracture surface (Japanese) 8-64622
Ni-Cr-Mo, SNCM8 exam. of delayed fracture using fracture mechanics (Japanese) 8-52961
Ni-Cr-Mo-V, exam. of temper embrittlement susceptibility, 8-76737
Ni-Cr-Mo-V, turbine rotor shaft, fracture toughness, validity criterion for K_{ISCC}, 8-72861
Ni-Cr-Mo-V, type HY130, temper embrittlement due to intergranular segregation, effect on H₂ induced cracking 8-76735
Ni-Cr-P (0.06 wt. %), influence of intercritical heat treatment on temper embrittlement susceptibility 8-52863
Ni-Cr (Mo), quenched and tempered steel, effect on H diffusion coeff. and solubility (Japanese) 8-52857
Ni-martensite, weld metal, increasing fracture toughness by heat treatment 8-72871
Ni-Mo, powder forged, fracture processes and fracture toughness 8-72870
Ni-Mo-V fracture toughness data, comparison with equivalent energy and energy per unit area data, 8-52965
NiCr, random load fatigue crack prop., 8-64692
Si (3 wt. %), grain oriented, core losses (Japanese) 8-60393
Si (3 wt. %), grain oriented, lowest core loss 8-91887
Si (3 wt. %), high permeability, grain oriented, 8-91886
Si (3 wt. %), loss prediction, from distorted waveforms, 8-76273
Si killed steel, effect of Al addition to Zn on phase composition and morphology of products of Fe-Zn reaction (Polish) 8-85021
Si, upper bainite morphology (Czech) 8-64537
Si-Mn-Ni-Cr-Mo, acoustic emission during stress corrosion cracking appl. to materials testing 8-53042
Si-Mn(Mo-Cr), heat treated, exam. of microfractographic aspects of fatigue cracks (Japanese) 8-52959
SiO₂ inclusion formation on introduction of solid SiO₂ into molten steel (Russian) 8-80530
Ti-Cr-KhV3M steel alloy, reaction during sintering and heat treatment 8-60617
V, quantitative anal. of carbides formed during tempering, 8-64571
W-Mo-V-TiC, powder, TiC effect on milling, pressing and sintering 8-60607
alloying additions
alloy, heat-resistant, alloying and heat treatment effects on strength and fracture, 8-95758
diffusion into Fe, (Russian) 8-79779
metal film, vacuum deposited, grain struct., influence of impurities and alloying elements (Russian) 8-56048
steel, 12Kh18N9Ti-TiB, eutectic alloy, high temp. props. 8-84931
steel, austenitic, corrosion resistant, strengthening by alloying with N₂, 8-95757
steel, austenitic, Ni-Cr high alloy, Ni, P, and Ni effect on stress corrosion cracking and stacking fault energy (Czech) 8-60873
steel, austenitic stainless, Mo-bearing, ellipsometric meas. of passive films, optical constants (Japanese) 8-85041

alloying additions continued

- steel, austenitic stainless stacking fault energy, effect of C, exam. 8-80553
- steel, C, diffusion of H_2 , SCC via martensite form. cooling rate changes on Mn and Ni addition (*Russian*) 8-56813
- steel, cementite decomposition during plastic deform., alloying element effects 8-84768
- steel, creep-resistant pipe steel, influence of chemical comp. on formability (*German*) 8-84900
- steel, ferritic stainless, Cr-Mo, Mo effect on pitting pot., AES anal. 8-95852
- steel, low C, type AISI 1010, effect of Se, Te additions on fatigue props. 8-92359
- steel, rare earth additions review 8-72786
- steel, rare earth metal additions effects on mech. props. 8-52829
- steel, sintered, Cr-Mo, CaF addition effects on struct. heterogeneity 8-60611
- steel, stainless, Cr-Ni, maraging, effect of Mo, Co additions on hardening 8-84835
- steel, stainless, recrystallisation texture, effect of Cu, Ti additions on development (*Japanese*) 8-80558
- surface layer alloying effect on electroerosion working (*Russian*) 8-64760
- Ag-Cu-Sn(Zn)(Au), effect of additions on eutectic and peritectic temp., of binary alloys 8-84801
- Al alloys, Cu interdiffusion with sintered Al powder, struct. effect at high press. 8-60606
- Al-Cu(Zn-Mg), age hardening, conditions leading to localised plastic deform. and fracture in slip bands during fatigue 8-64670
- Al-Fe, cast, influence of Zr on precipitation, solidification and grain size (*Rumanian*) 8-84813
- Al-Mg-Ag, age effect on age hardening (*Japanese*) 8-52831
- Al-Mg-Si-Mn, Mn addition effects on fracture 8-60791
- Al-Mn (0.35 wt.%), quenched exam. of Mn-vacancy interaction 8-76676
- Al-Si eutectic, Na, Sb and Sr alloying addition effects on microstructure (*French*) 8-64548
- Al-Zn-Mg-Ti, Ti effect on microstructure during ageing 8-64568
- Cr, optimum alloying with rare earth metals, Ti, Zr, Hf, Nb, Ta 8-68651
- Cu-Mn(Fe)(Ni)(Zn)(Ge), effect of impurities on Cu recrystallisation 8-52836
- Cu-Ni cast alloy, effect of addition of Ni, Mn, Si, Al, and Fe 8-85033
- Cu-Zn, cyclic stress/strain curves in monocrystalline and polycrystalline samples, cold work and Zn addition effects 8-95786
- Fe base binary alloys, thermoelectric force caused by internal adsorption (*Russian*) 8-95288
- Fe, grey cast, corrosion resist., Cu alloying additions effect (*Russian*) 8-56807
- Fe-Al-Ni-Co-Cu alloys, Ti alloying and deoxidising addition (*Russian*) 8-80181
- Fe-C-Ni-Cr(Cu), dynamically hot pressed, mech. props., additives effect 8-60620
- Fe-Cr (20 wt.%) high temp. oxidation behaviour with small La additions (0 to 1.3 wt.%) (*Japanese*) 8-85039
- Fe-Cr-Al, elec. heating alloy, effect of rare earth additives on quality (*Chinese*) 8-84825
- Fe-Cr-Ni-Cu-Sn, Cu and Sn effect on Cr and Ni segregation (*German*) 8-72777
- Fe-Mn-C-Si alloy G20, effect of Si and Mn additions on phase composition in multiple γ - α transitions (*Russian*) 8-95743
- Fe-Mn(Sb)(Sn), additive effect on eutectoid transformation of Fe 8-52799
- Fe-Ni (3 wt.%), grain boundary segregation of Sn and P embrittling additions, STEM microanal. 8-76654
- Fe-Ni-Cr-Mn-Al-Ti Incoloy 800, exam. of scale morphology, alloying element distrib. after oxidation 8-80677
- Fe-Ni-V-Co, Co influence on age hardening (*Russian*) 8-68703
- Fe-Si (6.5 wt.%), ductility and mag. props., Ni and Mn addition effects 8-76704
- Fe-Si-Al (6.4 wt.%), Sendust alloy, effect of Ni content on mag. props. 8-72897
- Fe-Si-Mn, effect of Mn addition on mag. props. and elec. resist. 8-91890
- Fe-TiB₂, eutectic alloy, high temp. props. 8-84931
- Fe-Zn, coating on low C rimming steel, effect of addition of Al on phase composition and morphology (*Polish*) 8-53014
- Fe₃C, cementite, modified by rare earth metal and alloying additions, thermal stability (*Russian*) 8-56663
- Ga-Al, effect of Al on solidification kinetics, and morphology of Ga 8-56628
- Mo-TiN (3.5 vol.%), failure characts. exam. 8-68788
- Nb₂Sn superconductors, bronze-processed, effect of Ta additions 8-95404
- Ni-B, hydrogen embrittlement, effect of B additions (*Japanese*) 8-84973
- Ni-Co-H system, phase transform. under high H₂ press., Co additive effects (*Russian*) 8-60645
- Pb-Ca-Sn, effect of Sn additions on precipitation behaviour, of Pb-Ca alloys (*German*) 8-52821
- Ti alloy, hardening heat treatment, alloying element effects development trends 8-95759
- Ti-Cu-Al(Zr)(Sn)(Nb)(Mo), heat treatable alloys, effect of alloying on strength, tensile props. 8-56671
- W fibre, KAl, KSi, KSiAl and KSiGa addition effects on workability (*German*) 8-64357
- W-ThO₂ fibre reinforced Ni base alloys, powdered matrices, fibre/matrix interaction above 1300°C, alloying effects (*Russian*) 8-95755

alloys

- alloys such as Au-Cu, Au-Cu-Zn are indexed under components of the named elements i.e. gold alloys, copper alloys, zinc alloys in these examples
- see also actinide alloys; alkali metal alloys; alkaline earth alloys; alloying additions; aluminium alloys; antimony alloys; arsenic alloys; bismuth alloys; boron alloys; cadmium alloys; dilute alloys; eutectic alloys; gallium alloys; germanium alloys; indium alloys; lead alloys; liquid alloys; mercury alloys; rare earth alloys; selenium alloys; silicon alloys; solid solutions; tellurium alloys; thallium alloys; tin alloys; transition metal alloys; zinc alloys
- AB alloy, equilib. props. by Markovian simulation 8-91302

alloys continued

- activity coefficient and short-range order, correl. (*Russian*) 8-56614
- activity coefficient of nonmetallic solutes in liquid metals and binary alloys 8-52766
- AES, quantitative analysis (*Polish*) 8-76967
- alloys, X-ray fluoresc. anal., using matrix correctional procedure 8-80817
- amorphous, electronic struct. 8-72062
- amorphous, mag. props. and appls. 8-95475
- amorphous, struct. relax., compositional SRO 8-79538
- antiferromagnetic, nesting type model, spin fluctuations. 8-84435
- BCC metals and alloys, review of plastic deformation and work hardening (*German*) 8-84946
- binary, atomic misfit effect on coexistence and spinodal transform. boundary 8-60644
- binary, atomic roughness and chemical adsorption at solid-liquid interface (*French*) 8-51787
- binary, electronic density of states in Bethe lattice, using Weaire-Thorpe Hamiltonian 8-51870
- binary, estimation of electron backscattering factor 8-72649
- binary, model substitutionally disordered, electron momentum density 8-56061
- binary, nonequilib. crystn. dynamics, eqns. for supercooling, supersaturation of melt (*Russian*) 8-95736
- binary, oxidation, solid solution scale formation, approx. calc. of O₂ activity profile 8-88577
- binary, selective oxidation with quasiparabolic kinetics, fixed alloy-scale boundary soln. 8-72930
- binary, solid state second phase redistribution in applied field 8-51721
- binary, with mixed ferro- and antiferromag. exchange, magnetisation, phenomenological theory (*German*) 8-56297
- binary alloy, electron localisation, self-consistent theory (*French*) 8-60088
- binary alloy, phenomenological theory of interdiffusion, role of nonequilib. vacancies (*Russian*) 8-59966
- binary alloy, quenched, time evolution of struct. function free energy 8-55937
- binary alloys, preferential sputtering with diffusion, equilib. distrib. 8-68592
- binary alloys, random, dielec. matrix and related props. 8-51916
- binary alloys, simple model to describe isothermic phase transform. 8-75832
- binary random Heisenberg ferromagnet transition temp. crit. conc., RKKY model 8-52266
- binary substitutional, short-range ordering kinetics, vacancy behaviour 8-55867
- binary substitutional alloy, with long range order, electron energy spectrum (*Russian*) 8-84121
- binary substitutional alloy with long range order, electron energy spectra (*Russian*) 8-75974
- cemented carbides, indentation fracture, surface fracture toughness nature 8-60849
- compositional modulation spectra, line shape 8-76491
- concentrated, vacancy formation energies determ. 8-63756
- continuous plastic cracks in ordered alloys, discrete dislocation analysis 8-80625
- corrosion resistance in geothermal brine environments 8-85032
- corrosion resistant surface alloy, form. by ion implantation 8-88569
- creep rupture like improvement mechanism, reheat treatment 8-64666
- crystallisation, apparatus for decanting solid and liquid phases 8-56597
- density of electronic states, dressed-cluster approx. 8-95249
- disordered, orbital mag. susceptibility of conduction electrons CPA calc. 8-76217
- disordered, spectral functions, augmented space formalism 8-84126
- disordered alloys, electronic struct., CPA calc., short-range order 8-63964
- disordered alloys, transport phenomena theory, coherent pot. approx. 8-87958
- disordered binary alloys, X-ray diffuse scatt. effect of correlation 8-71640
- disperse state formation (*Russian*) 8-52757
- dissolution controlled cracking mechanism, repassivation effects 8-64772
- FCC, model for form. of annealing twins 8-59818
- ferromagnet, amorphous, dipolar mechanisms for mag. anisotropy 8-64233
- ferromagnetic, hyperfine field systematics of nonmag. ions 8-60093
- ferromagnetic, temp. depend. of mag. props. and sp. ht. mag. phase transition region 8-64207
- ferromagnetic alloys, conc. spin fluctuations, SCR theory and CPA calc. 8-64290
- ferromagnetic random binary alloys, elastic neutron scatt. cross section 8-91845
- fracture toughness and fatigue crack growth data, of metallic alloys, compendium of sources 8-84963
- grain boundary drag 8-51550
- hard alloy powder mixtures, compressibility in hydrostatic working 8-68645
- heat-resistant, alloying and heat treatment effects on struct. and strength 8-95758
- Heisenberg antiferromagnetic alloy, critical behaviour (*Russian*) 8-88128
- Heisenberg ferromagnetic alloy, critical behaviour (*Russian*) 8-88127
- heterogeneous nucleation activity, and melting point ratio correlation 8-92255
- high temperature, mechanical, thermal and corrosion props. 8-95763
- highly resistive, temp. depend. on elec. resist. 8-91657
- homovalent disordered solid alloy, entropy-vol. correlation 8-63868
- hydride forming phase hardening 8-52833
- intermetallic phases with L1₂ and D0₃ struct., atom incompressibility, lattice parameter approach 8-91294
- irradiated, segregation, inverse Kirkendall effect, effect of constitution on void swelling 8-91472
- irradiated, solute segregation and precipitation effects on void swelling 8-67741
- local composition determ., assessment of TEM direct lattice imaging technique 8-53294
- magnetic, Lifshitz point occurrence, reviews 8-52265
- magnetic binary alloys, phase separation, double Ising system 8-91835
- magnetic properties from Rhodes-Wohlfarth plot 8-52190

alloys continued

- magnetic ternary alloys, statistical theory of electrical resistivity 8-87969
- multicomponent phase diagram calc., NPL alloy data bank 8-92243
- mutual alloying behaviour of the elements straddling the line Li-Mg-Cu-Au in the long periodic table 8-84769
- nitriding methods and programmed control system 8-95857
- ordered, with $L1_2$ structure, dissociation of superdislocations and plastic deform. mech. (Russian) 8-52909
- ordering alloys, effect of press. on phase diagrams and order-disorder transforms. 8-52797
- phase transformations, role of phase boundaries 8-72772
- polycrystalline, LF viscosity meas. 8-80576
- positron localisation in ordered and disordered alloys 8-79962
- quenched binary alloy at low temps., time evolution, phase separation 8-86670
- radiation damage prediction and measurement 8-75693
- random magnetic alloys, mean field effective medium theory, Ising model appl., phases 8-84438
- refractory metal alloy, heat resistance and cold brittleness, achievements and trends 8-95718
- sigma phase structure, ionicity modified pair pot. model anal. 8-51466
- sintered mats., complex diffusion alloying 8-68650
- solidification mechanisms, contribution of microgravity expts. 8-88457
- stress corrosion cracking (Japanese) 8-56820
- structural, fracture at temps. approaching absolute zero 8-72877
- substitutional alloys with large mass disorder, phonon modes 8-95122
- super alloys, cast, phase volume fraction determ. using manual point count practice 8-53052
- super alloys, phase extraction, chemical and X-ray diff. anal. 8-72951
- super alloys, phases (Chinese) 8-95728
- surface layer alloying effect on electroerosion working (Russian) 8-64760
- surface layer anal. with emission spectrochemical anal. (Japanese) 8-92570
- surface layer effects on bulk props. 8-85049
- surface segregation, appl. of quantification of atom-probe FIM data 8-62263
- surface segregation, existence of surface miscibility gaps within regular soln. theory 8-71909
- temper embrittlement kinetics, ternary and binary alloys, computer simulation 8-84953
- ternary alloys, AB-AC quasi-binary sections of order-disorder phase diagram 8-88463
- ternary and multicomponent systems, partial molal props. calc. 8-79784
- thermal cycling fracture 8-60839
- thermal expansion characts. determ. using strain gauges 8-81942
- thermoemission props. determ., meas. instrument based on scanning electron beam 8-74025
- thermophysical charact., peculiarities of temp. depend., dimensional change meas. (Russian) 8-95868
- two-component layered system, with interpenetrating components, thermoelec. and galvanomag. props. 8-79982
- void swelling under irradiation, theory 8-75692
- wear resistant, hardfacing, review 8-72937
- CsCl type, nearest neighbour distance and atomic props. 8-51465

alnico alloys *see iron alloys***Al₂O₃** *see alumina***Al₂O₃-α** *see corundum***α-Al₂O₃** *see corundum***alpha-decay***see also alpha-decay theory; alpha-particle spectra*

- A=215, nuclear data sheets, decay characteristics and level struct. 8-58224
- A=219, nuclear data sheets, decay characts. and level struct. 8-58225
- A=223, nuclear data sheets, decay characts. and level struct. 8-58226
- A=227, nuclear data sheets, decay characts. and level struct. 8-58227
- Conway granite, reinvestigation of 4.4 MeV alpha-activity 8-57210
- explosive r process cooling process 8-69791
- fission-emitted alpha particles, energy spectrum, fission fragment shape and orientation depends. 8-74346
- lifetimes, comparison of calc. methods 8-78325
- phenomenological pot. and folding model results relation for nuclear α-clustering 8-78289
- probabilities of α-, β- and γ-transitions accompanied by changes in nuclear shape (Russian) 8-89820
- radioactive nuclide decay data for reactor calcs., activation products and related isotopes 8-82426
- rocks, Scandinavian, giant and dwarf haloes rel. to unknown radioactivity 8-81157
- ²³²Am, absolute γ yields 8-86516
- ²⁴¹Am, α-decay low-energy γ-radiation (French) 8-74342
- ²¹¹At half life, branching ratio of electron capture and α decay modes 8-58253
- ²¹²Bi, isomeric states from α-activities 8-82282
- ¹²C, positive-parity states, anomalous α-decay props. 8-62511
- ⁴⁰Ca, isoscalar multipole resonances 8-66190
- Cs, A=114-118, neutron deficient isotopes, half lives, β⁺, γ, delayed p and α meas. 8-70489
- ¹⁸Hg, A=181-185, α-decay, Pt rot. states and moments of inertia staggering 8-89779
- ⁸Li(β⁺Be)(α)α, obs. of ⁸Be state at ~6 MeV 8-93938
- Na neutron rich isotopes, β-delayed emission of n, 2n, α, t 8-74343
- ²⁰Ne, α decay from 8p-4h O⁺ state, branching ratios 8-50132
- ²⁰Ne→α₀+¹⁶O, exam. of high spin states in ²⁰Ne 8-50066
- ¹⁶O, α-decay from excited states produced in ¹⁶O(¹²C,¹²C)¹²C 8-50189
- ¹⁶O→α₀+¹²C, exam. of high spin states in ¹⁶O 8-50066
- ¹⁷O α-cluster states, α-decay orbital momenta and parities with ¹³C(⁶Li,d) and α-decay (Russian) 8-86486
- Po light isotopes, α-decay width calcs., Feshbach theory 8-89829
- ²⁰⁸Po, L-shell ionisation in α-decay 8-78324
- ²¹²Po, isomer with spin and parity 8⁺, α- and γ-decay 8-82283
- ²³⁰Th α-decay, search for the K^π=0⁺ excited states in ²³⁰Ra 8-86504
- ⁴⁴Ti, lowest T=2 state decay, branching ratios from ⁴⁶Ti(p,t) 42 MeV 8-78304

alpha-decay theory*see also alpha decay*

- antisymmetrisation in α-decay and α-transfer based on cluster representation 8-86514
- bound α-particle motion in α-decay, comment on various functions 8-86515
- Coulomb repulsive energy, as cause of or barrier to α-decay 8-66253
- decay widths, alpha particle struct. effect 8-62513
- Feshbach theory of nuclear reactions, α-decay width calcs., light Po isotopes appl. 8-89829
- quantum mechanics, α-particle emission as violation of usual interpretation 8-62108
- superheavy region, neutron drip line, energy density mass formula extrapolation 8-93932
- e⁺e⁻ pair production probability determ. 8-50133
- ²⁴¹Am, e⁺e⁻ pair production probability determ. 8-50133
- ¹²C, 3α system, resonating group method, α-decay width 8-50108
- ²⁰Ne, coexistence of shell struct. and cluster struct. 8-78279
- ¹⁶O→¹²C+α, alpha spectroscopic factors, K-harmonics method 8-62512

alpha-particle absorption

No entries

alpha-particle angular distribution*see also alpha-particle spectra*

- ⁹Be(³He,α)⁶Be(O), reaction mechanism and isoscalar giant resonances in C¹³ (French) 8-78341
- ⁹Be(d,α)⁷Li 12.17 to 14.43 MeV, α ang. distrib., excitation functions 8-54770
- ⁷Li(α,α) at 2, 4 and 7 MeV, ang. distrib. calcs., 2α+t system model 8-50110
- ²⁰⁸Pb(³He,α)²⁰⁷Pb, 70 MeV, deephole states, T_{1/2}=45/2 components 8-82362
- ²⁰⁸Pb(α,α'), 96 MeV, ang. distrib., breathing mode states, DWBA calcs. 8-50183
- ¹⁹²Pt(α,α'), 24 MeV, α-angular distrib. for 0⁺, 2⁺, 2⁺, 4⁺, 4⁺ and 3⁻ state excitation 8-70550
- Sb(t,α), A=121, 123, ang. distrib. at 12 MeV, DWBA anal. 8-62546
- ¹⁴⁴Sm(α,α'), 96 MeV, ang. distrib., breathing mode states, DWBA calcs. 8-50183
- ²³⁸U fission, quasistatic scission configurations obtained from long range particle accompanied fission distributions 8-74411
- ²³Ni(α,α'), 18 MeV, A=64,66,68,70, compound and precompound α emission spectra 8-82367
- ²³Ni(p,α), 12.5 MeV, A=64,66,68,70, compound and precompound α emission spectra 8-82367

alpha-particle attenuation *see alpha-particle absorption***alpha-particle detection and measurement***see also alpha-particle spectrometers; radioactivity measurement*

- air pollution control at Nuclear Research Institute (Czech) 8-88906
- alpha spectral line intensity gauge using semiconductor detector (Italian, Spanish) 8-86716
- bidimensional spectra and ang. correlation for the ⁷Li(d,α)α reaction, 7.0 MeV 8-82357
- cellulose nitrate α-particle detector for Rn short lived daughters, results and calibration (Czech) 8-62663
- cerenkov counter for spacecraft application 8-86734
- coral, alpha emitter analysis by solid-state track detect., Bikini lagoon 8-53661
- corona flow counter, multi-filament (Slovak) 8-55094
- emulsion layers, α-irradiated, processing by iron oxalate developer (Russian) 8-50443
- free air ionisation chamber, mean level response for α-rays 8-90024
- IR spectroscopy appl. to charged part. dose meas. in cellulose triacetate 8-94145
- magnetic spectrom. with position- and cutting angle-sensitive detectors, ang. distrib. reconstruction 8-70687
- mean ionising cross-section and charge produced, meas. method 8-78577
- pressure gauge, exptl. accuracy (Japanese) 8-58537
- range, energy and range straggling, stopping power meas. 8-73815
- real-time environmental α-β-γ radiation monitoring system 8-94152
- REM ratemeter for direct reading of dose equivalent rate 8-53502
- Ar gas, high press., recombination luminescence in scintillation induced by alpha particles 8-50441
- Ar, liquid, scintillation decay due to α-particles and electrons 8-55099
- LiF thin layers, effect of LET on thermolum. props. 8-73255
- ²¹⁰Po determ. in air, radiochem. separation and α-counting method 8-73113
- ²²²Rn low conc. meas. in air, α-scintillation method 8-92970
- Si detector, ionisation energy for channelled 160 MeV α-particles 8-62680
- Si surface barrier detectors, direct meas. of plasma delays due to fission fragments and α-particles 8-58546
- Si surface barrier detectors, meas. of plasma delay differences due to ²⁵²Cf fission fragments and α-particles 8-58547
- p-Si surface barrier detectors, charact. meas. (Bulgarian) 8-82592
- TlBr₄, inorganic scintillator, use in nucl. and accelerated particle detection 8-58540
- U ore detection, using trace detection sensitive to ²²²Rn α-particles (Hungarian) 8-77339
- ZnS scintillator, field monitoring of alpha-emitting contaminants in environment 8-70646

alpha-particle effects

- bronchial cancer induction by α-emitting warm particles 8-96078
- chromatographic support materials decomposition by ionising radiation (German) 8-92587
- metals, stopping power for 28 MeV α-particles, re-evaluation 8-79651
- CaTiSiO₃, sphene, α decay radiation damage, effect on track etching characts. 8-65435
- Nb-Zr (1 wt.%), He bubble growth, α-particle effects 8-67749
- Nb₃Ge(Sn), electron irradiation at cryogenic temps., effect on T_c and transport props. 8-52122
- Nb₃Sn, radiation damage effect on superconducting props. 8-52127
- Pt alloy, fission-fragment-induced He blistering 8-86601

alpha-particle interactions see *alpha particle-nucleus reactions*

alpha-particle model see *nuclear cluster model*

alpha particle-nucleus reactions

for *inelastic alpha particle-nucleus scattering*, see "alpha particle-nucleus scattering"

multi-nucleon transfer and direct reactions, nuclear struct., review 8-50060

multiple collision model anal., at high and relativistic energies 8-86542

multiplicity distribution, shape, and low-fold coincidence probabilities 8-54779

primary cosmic ray interactions with photoemulsion nuclei using satellite Intercoms-6 (Russian) 8-93063

target nucleon+ α potential, microscopic model with antisymmetrisation effects 8-62516

(α , ^3He), 55 and 65 MeV, on 1p and 2s1d shell nuclei, A=12 to 40 8-82365

(α , ^4He) reaction in 1p- and 2s1d-shell nuclei, A-depend. of neutron binding energy 8-74379

$^{48}\text{Ca}(\alpha,2n\gamma)^{50}\text{Ti}$, high spin states in ^{50}Ti 8-54675

Ag+ α , 720 MeV, correlated energy spectra of light fragments, fireball and coalescence models 8-62555

AgBr($^4\text{He,X}$), 2.1 GeV, central collisions, Maxwell-Boltzmann distrib. anal. 8-66315

$^{109}\text{Ag}(\alpha,2n\gamma)$, γ studies, ^{111}In level struct., spin, parity 8-58249

Ag(α ,X), 16.5 GeV/c, inelastic cross sections, multiplicity, ang. and momentum distrib. 8-82359

Al+ α , 720 MeV, correlated energy spectra of light fragments, fireball and coalescence models 8-62555

$^{27}\text{Al}(\alpha,p)$, (α ,d), (α ,t), 50 MeV, reaction mechanism determ. (Russian) 8-54778

$^{27}\text{Al}(\alpha,n)$, ^{30}P high spin states, recoil dist. lifetime meas. 8-74386

$^{27}\text{Al}(\alpha,t)$, 25 MeV, DWBA anal. of triton ang. distrib. meas. 8-54776

$^{38}\text{Ar}(\alpha,p\gamma)^{41}\text{K}$, level props. of ^{41}K below 3.3 MeV 8-62588

$^{75}\text{As}(\alpha,4n\gamma)$, 30-55 MeV, obs. of ^{75}Br levels and prolate deform. 8-50088

$^{197}\text{Au}(\alpha,3n)$, simple formula for excitation functions 8-93978

$^{197}\text{Au}(\alpha,p)$, (α ,d), (α ,t), 50 MeV, reaction mechanism determ. (Russian) 8-54778

$^{197}\text{Au}(\alpha,2n)$, simple formula for excitation functions 8-93978

^{11}B , (α , γ), 15.5-19.5 MeV, excitation curve ang. distrib., cross section, ^{15}N resonances 8-94019

$^9\text{Be}(\alpha,n)$, 100 MeV, neutron polarisation meas. 8-70726

$^9\text{Be}(\alpha,n\gamma)$, secondary reaction yield for meas. of Be coating thickness 8-82600

Br(α ,X), 16.5 GeV/c, inelastic cross sections, multiplicity, ang. and momentum distrib. 8-82359

$^{12}\text{C}+\alpha$, 2.5 GeV-nucleon, nuclear fragmentation meas. (Russian) 8-54773

$^{40}\text{Ca}(\alpha,n\gamma)$ 20 MeV, ^{43}Ti , lifetime and γ decay of isomeric 19/2 $^-$ state 8-70486

$^{43}\text{Ca}(\alpha,n\gamma)$, 8-15 MeV, ^{46}Ti deduced levels, spin assignments and γ -decay, band struct. 8-78302

C(α ,X), 16.5 GeV/c, inelastic cross sections, multiplicity, ang. and momentum distrib. 8-82359

Cd($\alpha,2n\gamma$), 17-33 MeV, $^{112,114,116,118}\text{Sn}$ collective bands, spin, parity, γ meas. 8-54719

$^{250}\text{Cf}(\alpha,t)$ 28 MeV, ^{251}Es level struct. and p states, level transitions 8-78268

$^{59}\text{Co}(\alpha,p)$, (α ,d), (α ,t), 50 MeV, reaction mechanism determ. (Russian) 8-54778

$^{59}\text{Co}(\alpha,t)$, 25 MeV, DWBA anal. of triton ang. distrib. meas. 8-54776

$^{52}\text{Cr}(\alpha,2n\gamma)^{54}\text{Fe}$, high spin states in ^{54}Fe 8-54675

Cr(α ,p), 18, 26 MeV, levels in $^{53,55,57}\text{Mn}$, J-depend., spins, parities 8-78397

Dy(α ,xn γ)Er, 90 MeV, preequilibrium and equilibrium de-excitation processes 8-50185

$^{166}\text{Er}(^4\text{He},xn\alpha\gamma)$, angular momentum effects in pre-equilibrium processes 8-50208

$^{166}\text{Er}(^4\text{He},xn\gamma)$, angular momentum effects in pre-equilibrium processes 8-50208

Eu(α ,2n) and (α ,4n), ^{153}Tb excited states, rot. bands, spin, parity 8-62552

$^{19}\text{F}(\alpha,t)$, 25 MeV, DWBA anal. of triton ang. distrib. meas. 8-54776

$^{19}\text{F}(\alpha,n)^{20}\text{Ne}$, 2.6-5.1 MeV, cross sections, excitation function 8-54777

Fe+ α , 7-24 MeV, ^{59}Ni formation cross section, poss. prod. in cosmic dusts 8-78399

$^2\text{H}(\alpha,n)$, 100 MeV, neutron polarisation meas. 8-70726

$^2\text{H}(\alpha,pn)$, 15-42 MeV, three body calc., reaction mech. 8-70546

$^2\text{H}(\alpha,pa)n$, 18 MeV, cross section, ang. depend. meas., semiphenomenological anal. 8-58292

H(α ,X), 16.5 GeV/c, inelastic cross sections, multiplicity, ang. and momentum distrib. 8-82359

($^4\text{He},2nf$), statistical model anal. of fission isomer production Pu, A=235, 237 8-66326

($^4\text{He},xn\gamma$) ^{239}Am , statistical model anal. of fission isomer production 8-66326

$^4\text{He}+\text{ZZ}$ 8-70561

$^4\text{He}+\alpha$, 75.2 MeV, TDHF calcs. using separable three dims. wavefunctions 8-50111

$^{198}\text{Hg}(\alpha,2n)$, 30 MeV, levels of ^{200}Pb and isomers 8-66192

$^{39}\text{K}(\alpha,p)$, 9.5, 16 MeV, ^{42}Ca high spin states, lifetimes, multipole mixing ratios 8-50186

$^{24}\text{Mg}(\alpha,^{12}\text{C})^{16}\text{O}$, 12.7-17.4 MeV, quasimol. resonance in excitation function, $^{12}\text{C}+^{16}\text{O}$ system, spins 8-54775

$^{24}\text{Mg}(\alpha,\gamma)$, 1.5-3.8 MeV, determ. of ^{28}Si levels and resonances 8-66205

$^{55}\text{Mn}(\alpha,\alpha)$, 4.5 to 7 MeV, Coulomb excitation, search for 1.29 MeV 1/2 $^-$ level 8-82360

$^{92}\text{Mo}(\alpha,p2n)$ 43 MeV, ^{93}Tc 17/2 $^-$ isomer, internal conversion coeffs., parity mixing search 8-78255

$^{15}\text{N}(\alpha,\gamma)^{18}\text{F}$, hadronic nuclear-parity violation with change of isospin, γ spectrum search 8-94018

$^{64}\text{N}(\alpha,n\gamma)$, 8.2 MeV, ^{67}Zn , γ spectroscopy of low spin states 8-78303

$^{20}\text{Ne}(^4\text{He},^8\text{He})$, 117 MeV, ^{16}Ne mass excess and diproton decay width 8-78245

$^{58}\text{Ni}(\alpha,p\gamma)$, 17 and 19.5 MeV, ^{61}Cu γ -cascade multiplicities, entry state depend. on excitation energy 8-82311

$^{62}\text{Ni}(\alpha,n\gamma)$, 8-14 MeV, γ ray study of ^{65}Zn odd-parity states, energies, transitions 8-50120

alpha particle-nucleus reactions continued

$^{64}\text{Ni}(\alpha,n)^{67}\text{Zn}$, 6.5 to 17.0 MeV, γ ray studies of levels below 2.0 MeV in ^{67}Zn 8-62483

Ni(α , ^3He), 172.5 MeV, double-differential cross-sections determ. 8-82363

$^{16}\text{O}+^4\text{He}$, 3-D TDHF calcs. 8-54781

$^{16}\text{O}(^4\text{He},^8\text{He})$, 117 MeV, ^{12}O mass excess and diproton decay width 8-78245

$^{16}\text{O}(\alpha,d)^{18}\text{F}$, 28 to 33.6 MeV, forward angle yield, optical potential of incident channel 8-58291

$^{16}\text{O}(\alpha,\gamma)^{20}\text{Ne}$, 6.9-10.2 MeV, level and isospin mixing parameters 8-66292

$^{17}\text{O}(\alpha,d)^{19}\text{F}$, 47.5 MeV, population of positive parity states, DWBA anal. 8-70548

$^{18}\text{O}(\alpha,\gamma)$, 0.6 to 2.3 MeV, props. of ^{22}Ne compound states, astrophys. reaction rate 8-57545

O(α ,X), 16.5 GeV/c, inelastic cross sections, multiplicity, ang. and momentum distrib. 8-82359

$^{182}\text{Os}(\text{He},xn\gamma)$, K-isomer population levels 8-93927

$^{31}\text{P}(\alpha,n)$, 14.4 MeV, obs. of ^{34}Cl high spin states 8-82289

$^{31}\text{P}(\alpha,n)$, high spin negative parity states in ^{34}Cl , lifetime meas. 8-74327

$^{208}\text{Pb}(\alpha,4n)$, 41-51 MeV, yrast states in ^{208}Po anal. 8-78307

$^{208}\text{Pb}(\alpha,d)^{210}\text{Bi}$, 33 and 48 MeV, two-step contrib. in two-nucleon transfer reactions 8-82364

Pb(α ,f), 0.65, 1.74, 4.12 GeV, fission fragment recoil characts. 8-89925

$^{107}\text{Pd}(\alpha,2n\gamma)^{104}\text{Cd}$, high-spin states in $^{104,105}\text{Cd}$ anal. 8-62484

$^{107}\text{Pd}(\alpha,n\gamma)^{105}\text{Cd}$, high-spin states in $^{104,105}\text{Cd}$ anal. 8-62484

$^{107}\text{Pd}(\alpha,3n\gamma)^{105}\text{Cd}$, high-spin states in $^{104,105}\text{Cd}$ anal. 8-62484

Pt(α ,d), A=194, 196, 198, 35.1 MeV, stripping strength, Au excitation energies, high spin states 8-78398

Pt(α ,xn), Hg isotopes, level energies, B(E2) values, rot. aligned bands 8-70483

$^{87}\text{Rb}(\alpha,2n\gamma)$, 30-55 MeV, ^{89}Y high spin states from γ -ang. distrib. 8-93941

$^{36}\text{S}(\alpha,n\gamma)$, 6.0-7.8 MeV, ^{39}Ar , energy level spin and parity assignments, level spectroscopy 8-93943

$^{45}\text{Sc}(\alpha,p\gamma)$, ^{48}T excited states, level struct., lifetimes, from DSA and $\gamma\gamma$ coincidence meas. 8-74326

$^{45}\text{Sc}(\alpha,p\gamma)$, 11 MeV, high spin states in ^{48}Ti 8-74378

$^{84}\text{Sr}(\alpha,n\gamma)$, 16.7 MeV, high spin states in ^{87}Zr 8-74383

Sr($\alpha,2n\gamma$), 28, 35 MeV, high spin states in $^{86,88}\text{Zr}$ 8-74383

Ta+ α , 720 MeV, correlated energy spectra of light fragments, fireball and coalescence models 8-62555

Te(α ,t) 35 MeV, ^1I , A=121, 123, 125, mass excesses, ^{121}I energy levels 8-78246

Th(α ,f), 0.65, 1.74, 4.12 GeV, fission fragment recoil characts. 8-89925

$^{50}\text{Ti}(\alpha,2n\gamma)^{52}\text{Cr}$, high spin states in ^{52}Cr 8-54675

$^{205}\text{Ti}(\alpha,2n)^{207}\text{Bi}$, spin and parity assignment of ^{207}Bi levels 8-89788

$^{205}\text{Ti}(\alpha,3n)$, 35-51 MeV, ^{206}Bi high-spin states anal. 8-82368

$^4\text{U}(^4\text{He},xn)$ A=233-235, x=1-4, cross sections, fission evaporation competition in Pu isotopes 8-66325

$^{236}\text{U}(\alpha,\alpha'f)$, 50 MeV, total KE release 8-78426

$^{238}\text{U}+^4\text{He}$, expt. and relativistic two fluid model energy spectra 8-78298

U(α ,f), 0.65, 1.74, 4.12 GeV, fission fragment recoil characts. 8-89925

$^{50}\text{V}(\alpha,d)$, 14 MeV, ^{52}Cr 4.57 MeV excited state, 8 $^+$ assignment 8-74380

$^{51}\text{V}(\alpha,t)$, 25 MeV, DWBA anal. of triton ang. distrib. meas. 8-54776

$^{64}\text{Zn}(\alpha,n)$, ^{67}Ge , EM transition, gamma ray and internal conversion electron meas. 8-89823

$^{64}\text{Zn}(\alpha,n\gamma)$, ^{67}Ge , mass excess and low lying states, comparison with $^{63,65}\text{Ni}$, $^{65,67}\text{Zn}$ and ^{69}Ge 8-66213

$^{90}\text{Zr}(\alpha,2n\gamma)$, 28 MeV, high spin states above 8 $^+$ isomer in ^{92}Mo 8-89786

alpha particle-nucleus scattering

Brueckner-generator-coord. method, α - α scatt. 8-62487

eikonal approx. and distortions in heavy particle stripping mechanism (Russian) 8-78337

inelastic reactions at 3.6 GeV/nucleon 8-82358

monopole excitations in heavy nuclei, hadron induced 8-86471

Rutherford experiment, computer programs for high-school expts. 8-86094

Rutherford scattering, analogous demonstration by mech. expt. using mag. disc (German) 8-81778

(α , α), antisymmetrisation effects, α pot. form factor, optical model anal. 8-82366

(α , α) scatt. near Coulomb barrier and matter distrib. of medium and heavy nuclei 8-66291

(α , α') spectra of light nuclei, multipole giant resonances 8-86462

α - α scatt., 75.2 MeV, TDHF calcs. in 2 and 3 dimensions 8-78401

α - α scatt. phase shift calc., microscopic wave function of ^8Be 8-62503

α -scattering system, microscopic nucl. cluster model of ^8Be 8-54703

$^{138}\text{Ba}+\alpha$, closed shell 82 neutron nucleus, B(E2)-values 8-66296

$^{12}\text{C}(\alpha,\alpha'c)$, 104 MeV, CC ^{12}C , isoscalar giant quadrupole resonance 8-78238

$^{40}\text{Ca}(\alpha,\alpha)$, 29 MeV, optical pot., double folding model for anomalous large angle scatt. 8-70551

$^{40}\text{Ca}(\alpha,\alpha)$, backward angle anomaly, resonating group method macroscopic study 8-74382

$^{40}\text{Ca}(\alpha,\alpha)$ 140 MeV, modified optical pot., folding pots. and energy depend. 8-70549

Ca(α , α), (α , α'), 1.4 GeV, theoretical anal. 8-66293

$^{140}\text{Ce}+\alpha$, closed shell 82 neutron nucleus, B(E2)-values 8-66296

$^{52}\text{Cr}(\alpha,\alpha)$, 15-19 MeV, inelastic scatt. form factors, Coulomb-nuclear interference region 8-66288

Cu(α , α), A=63 and 65, 48 MeV, I.L. potential depth, optical model anal. 8-50187

$^{56}\text{Fe}(\alpha,\alpha)$, 15-19 MeV, inelastic scatt. form factors, Coulomb-nuclear interference region 8-66288

$^4\text{He}(\alpha,\alpha)$ elastic scatt. 32.6 to 35.4 MeV, ^8Be levels by double resonance formalism 8-62553

$^7\text{Li}(\alpha,\alpha)$ at 2, 4 and 7 MeV, ang. distrib. calcs., $2\alpha+t$ system model 8-50110

$^{24}\text{Mg}(\alpha,\alpha'\gamma)$ 104 MeV, nuclear deformation from ang. correlations, coupled channel anal. 8-78301

alpha particle-nucleus scattering continued

- ²⁶Mg (α, α') 104 MeV, nuclear deformation from ang. correlations, coupled channel anal. 8-78301
- ¹⁴²Nd + α , closed shell 82 neutron nucleus, B(E2)-value 8-66296
- Ne(α, α), A=20,22, large angle elastic scatt., 24.6-31.7 MeV, single Regge pole anal. 8-70547
- ⁵⁸Ni(α, α), elast. and inelast., 29-58 MeV, coupled channels anal. 8-66289
- ⁵⁸Ni(α, α) 140 MeV, modified optical pot., folding pots. and energy depend. 8-70549
- ⁶⁰Ni(α, α), 15-19 MeV, inelastic scatt. form factors, Coulomb-nuclear interference region 8-66288
- ⁶⁰Ni(α, α), elast. and inelast., 29-34 MeV, coupled channels anal. 8-66289
- Ni(α, α), A=62 and 64, 48 MeV, I.L. potential depth, optical model anal. 8-50187
- ¹⁶O(α, α), 28 to 33.6 MeV, optical potential of incident channel 8-58291
- ¹⁶O(α, α)¹⁶O, 6.9-10.2 MeV, level and isospin mixing parameters 8-66292
- ¹⁸Os(α, α') A=188,190,192, 4_3^+ level population, hexadecapole vibrs. 8-89780
- ²⁰⁸Pb(α, α'), 96 MeV, ang. distrib., breathing mode states, DWBA calcs. 8-50183
- ²⁰⁸Pb(α, α'), cross section calc. using microscopic wave functions 8-50142
- ¹⁹²Pt(α, α'), 24 MeV, α -angular distrib. for 0^+ , 2^+ , 2^{++} , 4^+ , 4^{++} and 3^- state excitation 8-70550
- ¹⁹⁴Pt(α, α'), 7-17.5 MeV, Coulomb excitation, low lying collective state reduced matrix elements, triaxiality 8-82269
- ²⁸Si (α, α') 104 MeV, nuclear deformation from ang. correlations, coupled channel anal. 8-78301
- ²⁸Si(α, α'), 104 MeV, ang. correl. meas., sensitivity to quadrupole deform. 8-54774
- ¹⁴⁴Sm + α , closed shell 82 neutron nucleus, B(E2)-value 8-66296
- ¹⁴⁴Sm(α, α'), 96 MeV, ang. distrib., breathing mode states, DWBA calcs. 8-50183
- ¹²²Te, backscatt. of ⁴He, ¹⁴N, ¹⁶O, and ¹⁸O, reorientation effect meas. 8-50209
- ¹²⁸Te backscatt. of ⁴He, ¹⁴N, ¹⁶O, and ¹⁸O, reorientation effect meas. 8-50209
- ⁴⁸Ti(α, α') 5.2-5.8 MeV, B(E2) value meas. for $3/2^-$ to $7/2^-$ transition 8-82308
- ⁹⁰Zn(α, α'), 18 MeV, A=64,66,68,70, compound and precompound α emission spectra 8-82367
- ⁶⁴Zn(α, α), 15-19 MeV, inelastic scatt. form factors, Coulomb-nuclear interference region 8-66288
- Zn(α, α), A=64 and 66, 48 MeV, I.L. potential depth, optical model anal. 8-50187
- ⁹⁰Zr (α, α) 40 to 140 MeV, modified optical pot., folding pots. and energy depend. 8-70549
- ⁹⁰Zr(α, α), E=26.2-166 MeV, antisymmetrisation effects, α pot., form factor, optical model anal. 8-82366

alpha-particle scattering see *alpha particle-nucleus scattering***alpha-particle spectra**

- see also *alpha-particle angular distribution*
- automatic evaluation of isotope anal. of nuclear fuels, isotope dilution, mass and α spectrometry 8-55120
- complex alpha-spectra evaluation using program ALFUN 8-74552
- fission-emitted alpha particles, energy spectrum, fission fragment shape and orientation depends. 8-74346
- massive transfer in heavy ion reactions on rare-earth targets, α - γ coincidence 8-70556
- spectral line intensity gauge using semiconductor detector (*Italian, Spanish*) 8-86716
- (α, α') spectra of light nuclei, multipole giant resonances 8-86462
- Ag + α , 720 MeV, correlated energy spectra of light fragments, fireball and coalescence models 8-62555
- Al + α , 720 MeV, correlated energy spectra of light fragments, fireball and coalescence models 8-62555
- ¹³⁸Ba + α , closed shell 82 neutron nucleus, B(E2)-values 8-66296
- ¹²C(¹⁶O, α)²⁴Mg, population of resonant ¹²C + ¹²C states 8-62563
- ¹⁴⁰Ce + α , closed shell 82 neutron nucleus, B(E2)-values 8-66296
- Cs, A=114-118, neutron deficient isotopes, half lives, β^+ , γ , delayed p and α meas. 8-70489
- ⁶Li(d, α)⁴He*, 13.6 MeV, α spectra, excited state of ⁴He, spin, parity 8-54771
- ¹⁴²Nd + α , closed shell 82 neutron nucleus, B(E2)-value 8-66296
- ⁵⁸Ni + ¹⁶O, deep-inelastic collisions, light particle pre-equilibrium emission 8-54786
- ²⁰⁸Pb(³He, α)²⁰⁷Pb, 70 MeV, deephole states, T₃=45/2 components 8-82362
- ¹⁴⁴Sm + α , closed shell 82 neutron nucleus, B(E2)-value 8-66296
- Ta + α , 720 MeV, correlated energy spectra of light fragments, fireball and coalescence models 8-62555
- ²³⁴U spectrum, surface barrier detectors, charact. meas. (*Bulgarian*) 8-82592
- ²³⁵U(n, α), thermal, α -particle spectra 8-78425
- ²³⁵U(n, f), thermal, α -particle spectra 8-78425
- ²³⁸U(e, α)²³⁴Th, cross section, α -spectra, γ -spectra of ²³⁴Th decay 8-58262

alpha-particle spectrometers

- see also *alpha-particle spectra*
- complex alpha-spectra evaluation using program ALFUN 8-74552
- counting system with Si surface barrier detector 8-82565
- scintillation, liquid, radiometric determ. of U content (*Czech*) 8-69487
- Si semiconductor detect., stopping power and straggling in liqs. 8-82563
- p-Si surface barrier detectors, charact. meas. (*Bulgarian*) 8-82592
- U analysis in phosphate fertilisers and other materials using liq. scintillation spectrometry 8-53280

alpha-particles

- see also *cosmic ray alpha-particles and helium nuclei*
- fusion-generated alpha particles driven plasma transport 8-83533
- Tokamak, fusion reactor, axisymmetric, slowing-down alpha particle loss, Monte-Carlo calc. 8-59653
- Ge, stopping power for fast channelled α -particles 8-79654

alpha-radiation see *alpha-particles***alpha-rays** see *alpha-particles***alpha-rhythm** see *bioelectric potentials***alpha-rhythm measurement** see *electroencephalography***altimeters**see also *radioaltimeters*balloon ascent meter (*Japanese*) 8-61567**altitude measurement** see *height measurement***alumina**see also *corundum*

- abrasive, wear in simulated hot grinding 8-56784
- addition to molten PbO-SiO₂ system, effect on PbO activity 8-60663
- adsorption of electron acceptors, strength and distrib. of electron donor sites, ESR meas. 8-84055
- adsorption of H₂O, energetics, effects of adsorption temperature on surface processes 8-60028
- β -Al₂O₃-Na₂O, AE during breakdown under Na⁺ transport 8-67860
- aluminophosphate glass, multicomponent, 3.2 micron broad absorption band computer anal., residual H₂O vibr. 8-52478
- amorphous, implanted ion detection by X-ray emission anal. in TEM 8-51575
- amorphous film, non-thermal switching in Al-Al₂O₃-Al struct. (*Russian*) 8-80069
- amorphous layers for MIS structs., prep. and props. (*Slovak*) 8-64122
- anodic, on Al alloy, characteristic emission of negatively charged particles during tensile deform. 8-92179
- anodic barrier film characts., ISS/SIMS 8-53021
- anodic film, transient pitting during film growth 8-56817
- anomalous absorpt. in far IR region 8-56464
- atomic disorder, dominant type 8-63757
- biaxially stressed, exam. of localised impact damage 8-72846
- cabal glass:SiO₂(TiO₂), microheterogeneity, and elec. cond. 8-83997
- ceramics, ladder structures, interference phenomena explanation 8-72898
- ceramics, sintering condition effects on props. (*German*) 8-56604
- chemisorption, of formic acid, electron tunnelling spectra study 8-84049
- chemisorption of monocarboxylic acids, tunnelling spectroscopy 8-91545
- chemisorption of propylene by η phase, desorption and D exchange obs. 8-51827
- coating for Al mirrors, highly efficient refl. type polarisers for 10.6 μ m laser radiation 8-71177
- coating protective, on SiC fibres in Ni-Cr alloy based composites, IR investigation 8-60623
- coatings, detonation deposited on steel, prep., wear resist., antifriction props. 8-60877
- composite film, barrier layer, ellipsometric meas. 8-67918
- composite films, elec. instability 8-68452
- crack resistance and crack velocity, evaluation using controlled fracture expts. 8-72881
- cyclic fatigue in direct push-pull, exam. 8-56746
- cylindrical voids, exam. of instability 8-79603
- electrical properties under isentropic compression up to 500 GPa 8-71789
- electron beam deposition, heating of multiple layer structs. (*Russian*) 8-92192
- erosion impact of annealed 310 stainless steel, SEM and TEM study 8-64725
- exoelectron emission, energy and ang. distrib. anal. (*German*) 8-92180
- extraction and prep. for technical ceramics (*German*) 8-53200
- filled epoxy composite, shock wave compression, 0.4-3.7 GPa 8-59856
- film, anodised, in strong elec. field, pulsed V-I characteristics (*Russian*) 8-64156
- film, CVD, props. rel. to deposition parameters 8-92197
- film, dielec. props., AC and DC elec. characts. 8-68445
- film, form., cross-sections, struct. obs. 8-67917
- film, self drifting of ionic charges, detection by surface potential decay method 8-72295
- film, single-layer, 2.8 μ m and 3.8 μ m absorpt. meas. 8-90463
- film on stainless steel in water, Gaussian ultrasonic beam refl. 8-67896
- floating zone melting, forced and free convection, computer simulation 8-88423
- floating zone melting, forced convection, computer simulation 8-88422
- formation of Al-SiO₂ film-substrate interface 8-91571
- fracture, multiaxial, general approach to statistical anal. 8-90785
- fracture resistance, exam. 8-76826
- fracture toughness specimen, appl. of wedge indentation technique for precracking 8-85087
- grain size and fracture toughness, effect of fracture toughness test methods 8-72883
- growth in Ni-Al, morphology and spalling model 8-53030
- Haynes Stellite 6B, Al₂O₃ particle erosion of surface, SEM obs. 8-88545
- heat treatment rel. to texture of γ -Al₂O₃ 8-72789
- hydrated gel synthesis by homogeneous precip. method using NaAlO₂, phase change by heating (*Japanese*) 8-68937
- initial sintering, method for obtaining surface diffusion coeffs., appl. to shrinkage data 8-95713
- IR spectra, comparison to inelastic electron tunnelling spectra (*French*) 8-68489
- IR transparent materials, forward and backward scatt. data 8-59099
- kaolinite to mullite reaction series, reexam. of solid state phase transformations 8-64535
- laminated coatings, for fuel confinement, fusion reactor target appls. 8-60883
- low solubility in Mg₂Si₂O₆, enstatite, rel. to palaeogeotherm uncertainties 8-65283
- MAOS memory element, stored charge volatility 8-52100
- MAOS structure, for memory appl., cond. and charge storage 8-52099
- mullite fibre reinforced mullite, in vitro degradation, bending strength, Young's modulus, density meas. 8-85011
- NMR, multilevel, spin-locking, spin-locked echo and rotary saturation associated with two-quantum transition 8-80245
- photocathode, for windowless XUV photodiode, photoefficiency 20 to 250 eV 8-65963
- plasma-anodised, current efficiency 8-91797

alumina continued

- porous, sintered, delayed failure, static fatigue in distilled water 8-64750
- porous film, elec. cond. charact. 8-76179
- powder, disintegration of powder particle agglomerates under the action of an alternating electric field 8-68642
- powder, injected into induction plasma, particle temp. and trajectory 8-59607
- powder, particle size analysis, using centrifugal sedimentation (*German*) 8-57890
- pressing method, for the telecommunication industry (*Hungarian*) 8-52728
- rapid firing, XPS study of cryst. struct. 8-68663
- reactive hot pressing, exam. of pressing characteristics 8-80499
- RF sputtered film, transient current meas. 8-52113
- rods, quenched, exam. of contact induced strength degradation 8-76731
- Si-Al₂O₃-SiO₂ in MIS struct., charge accumulation and spreading (*Russian*) 8-64116
- silica, vitreous, effects on viscosity of impurity alkali oxide, OH, Al₂O₃ and Ga₂O₃ 8-64580
- single crystal, fracture mirror formation, anisotropy of fracture surface energy and elastic constants 8-68824
- sinterability, NH₄AlO(OH)HCO₃ crystallinity effect (*Japanese*) 8-52711
- sinterability, NH₄AlO(OH)HCO₃ synthesis conditions effect (*Japanese*) 8-52710
- sintered, containing MgAl₂O₄ precipitates, Mg distribution at grain boundaries 8-80498
- sintered, MgO-enhanced densification, test of second phase and impurity segregation models 8-64511
- sintered, residual stress meas., piezospectroscopic technique 8-52704
- sintering of single phase and multiphase components (*German*) 8-80494
- stress value determination by bending tests, comparison with crack tip theory 8-67154
- supported catalysts, X-ray fluoresc. anal. using matrix correctional procedure 8-80817
- supported Ni catalyst, CO adsorpt. in H₂-He, effect of H₂S on IR spectrum 8-71945
- temperature drop parameter when testing with const. thermal flux 8-51049
- thermal etching of α -phase (*German, English*) 8-60934
- thermoluminescence glow curves and emission spectra, 90-500K, for UV dosimetry grade Al₂O₃ 8-72615
- thick vacuum condensates, electron microscopy struct. investig. (*Russian*) 8-95242
- TLD for dosimetry after accidental gamma radiation release 8-57076
- UV visible absorpt. by laser calorimetry, wavelength modulation spectroscopy 8-66876
- vacuum vessel for Petula Tokamak RF hating expts. 8-70634
- void formation by fast neutron irradiation, TEM exam. 8-51591
- waveguide for CW CO₂ laser 8-55376
- wetting by Cu-Sn-Ti alloys 8-71904
- Al, anodic film, formed in H₂SO₄, electron microscopy 8-68843
- Al-Al₂O₃-Al, oxide film prod. by pulsed evap., capacitor prod. and characts. (*Russian*) 8-60584
- Al-Al₂O₃-Al, thin film capacitors, dielec. losses 8-76382
- Al-Al₂O₃-Al, tunnelling junctions (*Russian*) 8-60232
- Al-Al₂O₃-Al junctions, Dy doped at Al₂O₃-Al interface, electron transport mechanisms and barrier height 8-91778
- Al-Al₂O₃-Al structure, elec. cond. 261 to 418K (*Russian*) 8-64144
- Al-Al₂O₃-Al(Au), thin films, elec. props. (*Czech*) 8-76159
- Al-Al₂O₃-M, thin film sandwich, leakage current and dielec. relax., 80-500K 8-76158
- Al-Al₂O₃-electrolyte, electroluminesc., nondestructive electronic avalanche 8-68563
- Al-oxide-electrolyte system, luminesc. spectra (*Russian*) 8-76539
- AlN-Al₂O₃ powders, hot pressing, crystalline phase obs. 8-95720
- α -Al₂O₃, adsorption of H(H₂), microweighing and X-ray obs. (*German*) 8-51825
- γ -Al₂O₃, adsorption of methane, γ -radiolysis, reaction kinetics 8-95940
- Al₂O₃, coating, wear characteristics, comparison of coated and uncoated WC hard metals 8-92365
- Al₂O₃, dense, surface segregation of Ca under exposure to steam and steam-CO 8-85013
- Al₂O₃ film, Al embedded, non-ohmic conduction behaviour 8-64157
- β -Al₂O₃, new slip casting technique for fabrication of ceramics 8-84745
- Al₂O₃ on Al, anodic oxide film, effect of interface roughness on cracking 8-76755
- β -Al₂O₃ phases, synthesized, effect of starting Al₂O₃ composition and halogen ion additions, on structural state 8-76620
- α -Al₂O₃, trigonal crystal, optical heterodyne detection using collinear acousto-optic interaction 8-66927
- Al₂O₃, vitreous-bonded, eval. of proof testing to assure against delayed failure 8-84954
- Al₂O₃:Cr²⁺, Jahn-Teller study, EPR data anal. 8-84172
- Al₂O₃:Eu, surface luminesc. centres excitation characts. 8-52560
- Al₂O₃:Fe²⁺, phonon spectroscopy using superconducting tunnel junctions 8-91389
- Al₂O₃:Fe³⁺, mag. susceptibility, cryst. field calc. 8-76035
- Al₂O₃:Gd³⁺, mag. susceptibility, cryst. field calc. 8-76035
- Al₂O₃:Ni³⁺, heat transfer at low temperatures 8-91493
- Al₂O₃:Si,Ti photostimulated thermolum., and appl. to UV dosimetry 8-53511
- Al₂O₃:V³⁺, frequency crossing signals of V³⁺ ions, conc. depend. study using thermal phonons 8-95115
- Al₂O₃:V³⁺, phonon scattering, comparison between theory and experiment 8-95116
- Al₂O₃:V⁴⁺, dil. solution, stimulated phonon emission 8-63817
- Al₂O₃/CuO, thin film interaction, CuAl₂O₄ form. (*Russian*) 8-52697
- Al₂O₃/Nb/Al₂O₃ joint, solid state bonded, exam. of bond fracture strength 8-76826
- Al₂O₃-Au cermet, optical constants, incl. proximity effects 8-56446
- Al₂O₃-B₂O₃-P₂O₅ glasses, formation and props. 8-83737
- Al₂O₃-Cr₂O₃, microstrain correction 8-59852
- β -Al₂O₃-H₂O, H⁺ and H₃O⁺ conduction, dehydration effect 8-51726
- β -Al₂O₃-H₂O, stability and dehydration 8-51693
- alumina** continued
- β -Al₂O₃-K₂O/K ferrite, interfaces and solid soln., thermal expansion and lattice parameter variations 8-55959
- β -Al₂O₃-M₂O, M=Ag, K, Rb, Na, Eu, X-ray diffuse scatt. 8-71725
- B-Al₂O₃-M₂O, M=Na, Ag, Rb, K, far IR absorption and ionic cond. 8-72512
- Al₂O₃-MgO-H₂O fast proton conductor 8-91480
- β -Al₂O₃-Na₂O, ²³Na NMR spectrum, correl. effects 8-76324
- β -Al₂O₃-Na₂O, EPR and optical absorpt. studies of X-ray produced defects 8-95517
- β -Al₂O₃-Na₂O, microwave absorpt., low-temp. dielectric props. anomalies, ion tunnelling states 8-92013
- β -Al₂O₃-Na₂O, superionic anisotropic ceramic, prod. by microwave sintering (*French*) 8-52742
- β -Al₂O₃-Na₂O, thermal etching (*German, English*) 8-60934
- β -Al₂O₃-Na₂O, vacuum hot pressed, densification kinetics 8-72758
- β -Al₂O₃-Na₂O:Fe, coordination site, oxidation state, Mossbauer, absorpt., emission spectra, mag. susceptibility meas. 8-68431
- β -Al₂O₃-Na₂O:Mg, ionic cond., effect of microstruct. and phase composition 8-67859
- β -Al₂O₃-Na₂O:Ag²⁺, EPR measurements 8-95515
- Al₂O₃-Na₂O-LiO₂ (8.8, 0.75 wt.%) exam. of Na⁺ resistivity as function of temp. grain size model 8-80654
- β -Al₂O₃-Na₂O-MgO, blocking defects observed by high resolution electron microscopy 8-55879
- β -Al₂O₃-Na₂O-SiO₂, solid electrolytes, exam. of microstruct. ionic resistivity 8-80566
- Al₂O₃-Nd₂O₃, phase-diagram at 1100°C (*Japanese*) 8-79747
- Al₂O₃-Pr₂O₃, phase diagram at high temps. (*Japanese*) 8-88449
- Al₂O₃-Si, alternating layers, dielec. facet reflector for semiconductor lasers 8-66841
- Al₂O₃-SiO₂, thermomech. props., dependence on struct. and composition 8-84748
- Al₂O₃-SiO₂ heat insulating refractories, prep., physical, thermal, structural props. 8-68662
- Al₂O₃-Sm₂O₃, phase diagram at high temp. (*Japanese*) 8-92253
- Al₂O₃-TiC, multiphase ceramics, mech. strengthening due to dispersion of non-metallic particles (*German*) 8-60674
- Al₂O₃-TiO₂, coatings, detonation deposited on steel, prep., wear resist., antifriction props. 8-60877
- Al₂O₃-W cermet, phase bonding 8-52745
- Al₂O₃-ZrO₂, microstructure effect on friability 8-64515
- Al₂O₃-ZrO₂-SiO₂, fusion cast refractory, effects of glassy phase on thermal cycling resist. 8-84956
- Al₂O₃(H₂O)₃, gibbsite, synthetic, crystallinity and topotactic reactions, X-ray diff. obs. 8-63851
- (Al₂O₃)_nMgO, n=1.1, high temp. creep, dislocation behaviour 8-80593
- β -Al₂O₃-(K₂Na_{1-x})₂O, anomalous behaviour in ionic cond. obs. 8-87818
- Au to Al₂O₃ solid state reaction bond, effect of ambient atmosphere 8-67914
- CaO-Al₂O₃, molten binary slag, dissolved C study (*Japanese*) 8-60662
- CaO-Al₂O₃ melt, solubility of H₂O at 1600°C 8-51687
- CaO-Al₂O₃-SiO₂ glass, remanent magnetisation, log t low 8-68300
- CaO-SiO₂-Al₂O₃, slag phase, activity of components at 1873K (*Polish*) 8-52775
- Co-Al₂O₃ catalysts, reducing and sulphiding treatments, XPS obs. 8-85196
- Cr₂O₃-Al₂O₃ solid solns., effect of Cr on point of zero charge 8-61021
- Cu-Al₂O₃ powder, electrolytic deposition 8-84743
- D plasma interaction, surface structure, chemistry and resistivity changes 8-53010
- Fe/Al₂O₃ composite film, optical props., rel. to solar collector appls. 8-72622
- Fe₂O₃-Al₂O₃, solid solns., effect on Fe on point of zero charge 8-61021
- K₂O-Al₂O₃ system, high temp. thermodynamics and phase equilibria 8-80521
- Li₂O-Al₂O₃-P₂O₅:V⁴⁺, glass exam. of ESR spectrum of V⁴⁺, optical spectra, and structure 8-88180
- MgO-Al₂O₃-Cr₂O₃, vacuum vaporisation, Langmuir method 8-95149
- MgO-Al₂O₃-SiO₂, exam. of microstructure and crystallisation kinetics 8-80501
- MgO-CaO-SiO₂-Al₂O₃-Na₂O.P₂O₅, effect of NaPO₃ on phase composition rel. to basic refractories 8-80528
- (MgO)_x(Al₂O₃)_{1.8}, spinel, X-ray refl. topography, dislocation substructures during creep form. (*French*) 8-68737
- MnO-Al₂O₃-SiO₂ glass, optical spectra 8-68528
- Mo-Al₂O₃, catalysts, reducing and sulphiding treatments, XPS obs. 8-85196
- Mo-Mn-Fe-Si/Al₂O₃ ceramic seal, interfacial phases 8-72011
- Mo₂O₃-Al₂O₃, reduced catalyst, adsorption of O₂, O⁻ form. 8-85197
- Na₂O-Al₂O₃-B₂O₃-Fe₂O₃ glass, Mossbauer expts., 85-500K 8-80260
- Na₂O-Al₂O₃-B₂O₃-SiO₂, glass, ESR exam. of paramagnetic centres formed during mech. destruction by grinding 8-88188
- β -Na₂O-Al₂O₃, high-field ²³Na NMR 8-64284
- Ni/Al₂O₃ composite film, optical props., rel. to solar collector appls. 8-72622
- Ni/Al₂O₃ methanation catalysts, nonreduced, IR spectra 8-88288
- NiO-NiAl₂O₄-Al₂O₃, heterogeneous solid state reactions, role of phase boundaries, dynamic equil. at interfaces 8-71848
- Pb-Al₂O₃ composites, mech. alloyed, hot hardness meas. (*Japanese*) 8-84830
- PbO-Al₂O₃-B₂O₃ vitreous system with relaxation structure, spinodal decomposition 8-75553
- Pd, catalyst hollow cone dark field microscopy on γ -alumina substrates 8-61049
- Rh/ γ -Al₂O₃ disperse δ -phase, chemisorpt. of CO, IR spectra, site distrib., mol. mobility 8-72496
- Si₃N₄-Al₂O₃, hot-pressed with crystn. grain boundary phases, prep. 8-95715
- Si₃N₄-Al₂O₃-Y₂O₃, sintered, observation of a noncrystalline phase 8-64536
- Si₃N₄-AlN-SiO₂-Al₂O₃ solid-liquid equilibria 8-92247
- SiO₂-Al₂O₃ based minerals, phase equil., struct., comp. (*French*) 8-60659

alumina continued

- SiO₂-Al₂O₃-CaO-MgO, liq. silicic and slag, struct, density, surface tension (*Polish*) 8-83711
 TiB₂-Al₂O₃, thermal stability of composite materials 8-60638
 TiO₂-Al₂O₃-P₂O₅ glass, ESR of Ti³⁺, exam. 8-88181
 V/Al₂O₃ composite film, optical props., rel. to solar collector appls. 8-72622
 W-Al₂O₃ granular film, percolation conductivity 8-84319
 ZrO₂-ZnAl₂O₄ transparent glass-ceramic, microstruct. and props. 8-59960

aluminium

see also nuclei with

- acoustic emission under plastic deform., spectral anal., dislocation mean free path 8-84934
 acoustic velocity, shock-compressed uniform solid, lateral discharge ang. semiempirical formula (*Russian*) 8-55910
 addition to Si killed steel, effect of Al addition to Zn on phase composition and morphology of products of Fe-Zn reaction (*Polish*) 8-85021
 adhesively bonded and weldbonded aircraft struct. subjected to acoustic excitation, determ. of sonic fatigue life 8-92351
 adion-surface interaction energy, density formalism calcs. for alkali metal ions 8-68069
 adsorption, of O₂ (NO), 80 to 290K, 10⁻⁶ to 10⁻² Pa, XPS study 8-95657
 adsorption of O₂, relation between energy-band and cluster model 8-52048
 AES, obtaining density of states information from self-deconvolution of Auger band-type spectra 8-92150
 alternating bending of single crystals, shear strain accumulation and microstrain distrib. (*Russian*) 8-60706
 amorphous, heavy ion ranges, He⁺ backscatt. obs. 8-63796
 annealed, subjected to torsional impact loading strain-rate effects 8-92303
 annihilation spectrum, narrow component, Fermi impulse of electrons, plastic deform. recovery (*Czech*) 8-64591
 anodic barrier film charact., ISS/SIMS 8-53021
 anodic film, formed in H₂SO₄, electron microscopy 8-68843
 anodisation, influence of substrate orientation 8-88581
 anodisation, intensity of luminesc. and film thickness 8-80413
 anodised, photostimulated exoelectron emission, effect of oxide thickness 8-80461
 atom, ion beam bombardment, (1s⁻¹2p⁻¹)¹P₁ state nonstatistical population, X-ray spectrum 8-62894
 atom, Stark broadening of reson. lines, 3961.5 and 3944 Å 8-58622
 atomic electron impact excitation cross sections calc. (*Russian*) 8-55240
 atomistic images of field ion microscopy at high temps. 8-55792
 atoms and ions, regularities within Stark widths and reson. lines 8-78662
 Auger emission target, contrib. of reflected electrons 8-92152
 Auger spectrum, KLL, plasmon gain satellite obs. 8-76562
 bicrystal, fatigue crack initiation, crystal boundary effects (*Japanese*) 8-92328
 Bragg diffraction, anharmonic contributions, Mossbauer study 8-76358
 bremsstrahlung, β generated, spectral shape depend. on target thickness 8-56545
 Bremsstrahlung distrib. from 22 MeV electron irradiation 8-59840
 cast, strength and plasticity under hydrostatic pressure 8-56694
 cast, US and X-ray testing of castings, moulds and die-casting machines 8-53097
 cathodes for glow discharge and hollow cathode spectroscopic light sources 8-82047
 chemisorption, of formic acid, electron tunnelling spectra study 8-84049
 coated C fibre, stress rupture 8-80628
 coated diffraction gratings, UV light polarisation at grazing incidence 8-87129
 coating on Ni alloys, spontaneous form. of diffusion barrier (*German*) 8-71886
 coating on steel, thickness meas. using radioisotope thickness gauge (*Russian*) 8-56582
 cold rolled, X-ray diffr. and optical microscope exam. of fatigue damage (*Japanese*) 8-84976
 cold rolled and annealed, substruct., near fatigue crack tip, X-ray microbeam technique exam. (*Japanese*) 8-64621
 Compton profile from 662 keV γ-ray spectroscopy 8-56539
 concentration in atmospheric sedimentable powder, in Vizcaya, Spain (*Spanish*) 8-57265
 convoy electrons from solids, ion vel. and Z and target material depend. 8-84692
 core electron expansion, kinetic energy in Compton profiles 8-72628
 corrosion resistant surface alloys, form. by ion implantation 8-88569
 creep and dislocation distribution, influence of electron irradiation (*Russian*) 8-95775
 cutting of bicrystal to compare mechanism for large crystals and polycrystals (*Japanese*) 8-60871
 cylindrical metal liners, explosion-accelerated, form stability anal. 8-83425
 cylindrical rod, stress wave propag. from electrical discharge 8-59866
 Debye Waller determ. from modified Cheveau model 8-59918
 defect annealing during plastic deform. 8-88478
 defect annealing study by positron annihilation, and elec. resistivity meas. 8-51584
 deformation, in situ, of [111] single crystal, HVEM obs. 8-52886
 depth profiling of ³He ion implantation 8-59830
 determination by spark-source mass spectroscopic anal., sensitivity calibration 8-68962
 diffusion, of Cu(Zn), isotope effect 8-84006
 diffusion into Si₃N₄ film, AES and depth profiling 8-51744
 diffusion into Si, in open tube, high vacuum system 8-91349
 dislocation loops, mechanical multipole moments determ. 8-55868
 dislocation substructure formation under hydrostatic extrusion 8-56696
 dissolution of amorphous Si into Al at Si-Al interface 8-95188
 dynamic compaction, mixture theory of porous solids 8-63315
 elastic properties (*Russian*) 8-56678
 electrodes, use of soluble corrosion inhibitors to suppress electrode dissolution 8-88565

aluminium continued

- electron beam deposition on SiO₂ in FET, effect on electron trapping 8-80060
 electron beam reflection, high current (*Russian*) 8-84690
 electron diffraction, medium energy 8-83682
 electron liquid, plasmon dispersion 8-56099
 electron MFP determ. by depth and ang. depend. of inelastically scatt. electron spectra 8-92154
 electron spectroscopy, energy loss and photoemission 8-72682
 electron-phonon scattering rates, anisotropic, meas. on Fermi surface 8-87753
 electronic charge density, OPW-based pseudopot. calc. 8-87896
 electronic momentum densities by two-dimensional angular correlation of annihilation radiation 8-91605
 electronic states, model pseudopotential 8-91582
 electrons around vacancies, electron density calc. 8-64003
 EM generation of ultrasound, obs. of anomalies 8-84131
 endochronic theory of viscoplasticity, steady waves in impacted plate, Al numerical calc. 8-83282
 epoxy Al bonded, adhesive joints under complex loading, development of failure criterion 8-92344
 equation of state under very high dynamic load (*German*) 8-59858
 etching technique for revealing plastic zones 8-72955
 explosive compaction of metal powders 8-64501
 failure under hydrostatic press., kinetics 8-52944
 fatigue crack initiation, model using probabilistic technique 8-68800
 fatigue induced dislocation struct. and hardening, exam. (*Japanese*) 8-64624
 FCC, strain hardening and recovery by pure metal mode, high temp. deform. (*Japanese*) 8-52843
 Fermi surface, scattering anisotropy of conduction electrons on dislocations (*Russian*) 8-60051
 film, beam splitter phase coatings, for producing phase quadrature interferometer outputs 8-77974
 film, dispersion curve of surface plasma waves, rel. to refl. power minimum curve (*French*) 8-88372
 film, energy losses of 20-40 keV electrons 8-92153
 film, evaporated, interaction with BCl₃, HCl, adsorpt. 8-75945
 film, mean free path for plasmon excitation, 1.5 to 10.9 keV 8-51915
 film, photoelectron-grain boundary scatt. in MOS struct. 8-64120
 film, polycryst., chemisorpt. of O₂, synchrotron radiation photoemission expts., 70-150 eV 8-95228
 film, reflection coeff., effects of plasma bursts prod. 8-56547
 film, room temp. oxidation, scanning HEED expts. 8-91567
 film, single cryst., elastoresist. effect 8-84321
 film, vacuum deposited, rate and press. depend. of contamination 8-72732
 film, vacuum deposited, structural changes during annealing at temp. near melting point 8-84096
 film deposition, step coverage optimisation by computer simulation and SEM 8-51838
 film deposition on Kapton laminates by electron beam evaporation 8-76603
 films, action of plasma in capacitive electrode HF discharge (*Russian*) 8-95818
 fission product ranges and kinetic energies 8-94037
 foil, elec. explosion, dielec. breakdown 8-67388
 foil, elec. explosion, immersion medium effects 8-67389
 foil, electrostatic spray painting using Van de Graaff generator, teaching demonstration 8-54136
 foil, large M0 K X-ray, anisotropy from Ne on Al foil 8-55254
 foil, modification of texture by fatigue, X-ray diffr. exam. 8-88477
 foil, quenched, anomalous annealing phenomena, quantitative study 8-80565
 foil, sputtering with ²⁵²Cf fission products, desorbed secondary ions 8-68596
 fracture due to shock waves leaving surface, shear stresses 8-51128
 fusion reactor, Al min. activity blanket design for TFTR upgrade 8-58460
 fusion reactor blanket/shield design 8-54899
 gases in metals, detection by vacuum spark technique, appl. to Al wire 8-61094
 glass fibre reinforced plastic/polyurethane foam/Al sandwich, flexural props. (*Japanese*) 8-56707
 grain refinement, effect of Al₃Ti, TiC and B 8-52828
 granular, hopping cond., supercond., magnetoresist., Zeeman splitting 8-60243
 graphite fibre reinforced, temp. and press. effect on interface chemistry mech. prop. meas. 8-64595
 Gruneisen parameter, behaviour at high press. 8-83899
 heat capacity of granular film 0-4.5K, crit. coupling between grains 8-84348
 heat of soln. of H, electron charge distrib. calc. 8-51689
 high β-plasma in spindle-cusp mag. container, laser produced 8-59650
 hyperfine interactions of implanted Fe, conversion electron Mossbauer spectroscopy 8-52391
 impact strength, exam. with pulsed drop impact loading 8-84944
 implantation of Si, Al, Hf, Ta into InP and GaAs, form. of protective oxide 8-79622
 interface, Al (111)-Al (111), self-consistent electronic densities and adhesive energies 8-72005
 ion implanted, ranges of implanted 10-30 keV D⁺ 8-83858
 ion plated coating on steel (*Japanese*) 8-80477
 ion-excited Auger emission from sample trays in Auger-sputter profiling study 8-52607
 irradiated, containing self-interstitials and vacancies, electronic transport props. 8-60105
 isothermal compression curves to 120 kbar, X-ray diffr. study 8-83876
 isotropic, Brillouin scatt. 8-80367
 joints glued with reaction resinous mortar, photoelastic exam. (*German*) 8-76825
 laminate with polyethylene, flexural fatigue props. (*Japanese*) 8-56751
 laminated coatings, for fuel confinement, fusion reactor target appls. 8-60883
 laser driven shock waves vel., risetime, luminosity struct. meas. using shocks own luminosity 8-59857
 laser impact, multiple crater refl., effect on refl. props. 8-52596
 lattice atom displacements near end of implanted μ⁺ tracks 8-55890
 liquid, density fluctuations 8-55806
 liquid, dynamical struct. factor 8-71667

aluminium continued

- liquid, electron correlations, evidence 8-55805
 liquid, electron momentum density, perturbed Green's function method 8-60052
 liquid film, electron diffraction 8-83721
 liquid metal embrittlement by Ga 8-64653
 magnetoresistivity, linear growth, in strong mag. fields (Russian) 8-51972
 mechanical deformation with superimposed insonation, volume effects 8-60723
 melt, exam. of H₂ bubble origin, using first bubble technique 8-85115
 metal, Auger spectra, plasmon satellite intensity 8-64432
 metal-poor stars, spectra and Al/Fe ratios 8-57549
 metallisation on (100)Si, Si epitaxial regrowth and grain struct. 8-79901
 mirror, Al₂O₃ coated, highly efficient refl. type polarisers for 10.6 µm laser radiation 8-71177
 mirror reflectance 8 to 12 µm, normal to high incident angles, Y₂O₃, HfO₂ protective layers 8-79090
 molten, dissolution of Fe and Fe alloys (Japanese) 8-71858
 molten fine wires, migration in thin Si wafer, vertical p-n junction fabrication 8-68077
 molten reactor fuel-coolant interaction simulation, water-molten Al reaction 8-58363
 monovacancy formation parameters, temp. depend. 8-75658
 muonic K-shell X-ray transitions, nuclear charge radius 8-66195
 neutron yield calcs., electron beam incidence 8-95622
 orthogonal cut surface, effect of cutting condition on residual stress (Japanese) 8-85035
 orthogonal cut surface, relations between residual stress and moire strain, exam. (Japanese) 8-85036
 overlayers on Si (111), theoretical study 8-95366
 oxidation by exposure to O₂ and H₂O, soft XPS exam. 8-80683
 oxidation in water, oxide growth rate and struct. 8-76783
 particulate combustion process model (Russian) 8-85164
 phonon dispersion relations and Debye-Waller factor calcs. 8-51630
 PIXE anal., conc. profile determ. using beam energy variation 8-76965
 plasma, hot dense homogeneous, X-ray production rate and ionisation state density, calc. 8-71458
 plasma etching in CCl₄, end point determ. by spectroscopy 8-76786
 plastically deformed, influence of microstruct. on energy stored 8-84894
 polishing in H₃PO₄ and HClO₄+methanol, polarisation curves 8-56851
 polycrystalline, abrasion, deform., fatigue, study by exoelectron microscope (Japanese) 8-74108
 polycrystalline, recrystallisation, synchrotron X-ray topography dynamic expts. 8-67621
 polycrystalline, secondary ion emission angle, energy distrib. depend. 8-76569
 porous anodic films on Al, ion beam thinned, electron microscope exam. 8-92390
 positron annihilation characteristics, effect of temp. 8-64427
 positron-vacancy interactions, equilib. temp. depend. of positron annihilation 8-76547
 powder, disintegration of powder particle agglomerates under the action of an alternating electric field 8-68642
 powder, protective coatings of Ni, Cu, Fe and their alloys (Russian) 8-60881
 powders, grain size determ. by sedimentation, automatic recording system 8-60897
 proton irradiated, muon spin rotation study at low temps. 8-92011
 PTFE-Al, adhesion joints, effect of Cu and CuO 8-53183
 α-quartz:Al, Ag, EPR of A-Ag centres 8-88186
 rapid melting and solidification of surface layer, exam. using computer heat flow model 8-83228
 reactive etching in RF plasma containing halogen species 8-72923
 reactor irradiated, neutron inelastic scattering meas. of phonon dispersion curves 8-75758
 recovery features, TEM and positron lifetime meas. examination, 8-80611
 reverse finish cutting, exam. (Japanese) 8-85034
 screw dislocation core, atomic struct. calc., modified lattice-statics approach 8-75669
 seawater concentration and distrib., control by biological activity 8-61437
 SEM, electron channelling patterns 8-83697
 sheet, in-plane stretching, limit strain meas. 8-80573
 sheet metal, texture heterogeneity, numerical simulation (French) 8-92274
 shock pulse attenuation in rods 8-55503
 single crystals, effect of environment on liquid-metal embrittlement, stress corrosion cracking and corrosion fatigue 8-64676
 sintered powder, interdiffusion with Cu, struct. effect at high press. 8-60606
 sputtering and chem. attack by H ions of 100 eV energy 8-95635
 steel, Al content determ. by fast neutron radiation (Hungarian) 8-92586
 steel, fibre reinforced Al, fracture mechanics under fatigue (Czech) 8-64629
 steel fibre reinforced Al, fatigue strength (Czech) 8-60748
 steel-aluminium plates, exam. of adhesion strength by impulse loading 8-84943
 stopping power for 28 MeV α-particles, re-evaluation 8-79651
 stopping power meas. for 4-5 MeV/N ¹⁶O, ⁴⁰Ar, ⁶⁵Cu, and ⁸⁴Kr 8-70720
 storage ring vacuum chambers, glow discharge processing versus bakeout 8-70658
 strained, anisotropic electron scatt. in elec. resist. 8-91656
 structure changes in single cryst. under influence of static and dynamic stresses (Russian) 8-92300
 subgrain growth during annealing after cold work 8-56656
 substruct. developed during recrystallisation, exam. (Japanese) 8-64566
 supercond. film, resistance, effective medium approach 8-60249
 superconducting, crystalline and granular, tunnelling meas. 8-84355
 superconducting Al heat switch and plated press-contacts 8-54377
 superconducting film, anomalous resistive state due to light pulse 8-52157

aluminium continued

- superconducting film, quasiparticle injection, tunnel junction characts. 8-76193
 superconducting film in presence of Formvar, excess elec. cond. above T_c 8-60250
 superconducting particles, nucl. relax. and supercond. fluctuations 8-60251
 superconducting small particles, Josephson-coupled, local fluctuation effects 8-72308
 superconductivity, stimulation and enhancement by external micropower irradiation (Russian) 8-95394
 superconductor, appl. of non-local extension to Gaspari-Gyorffy theory 8-80093
 superconductor, quasiparticles, nonequilib. distrib. function 8-91810
 surface, (100), chemisorbed O, photoemission ang. depend., MO cluster model calc. 8-76576
 surface, (100), inelastic LEED at beam emergence condition 8-83690
 surface, (100), overlayer covered systems, angle-resolved UPS, substrate effects 8-84694
 surface, chem. anal., low energy ISS compared with SIMS 8-64908
 surface, Cl₂, CO₂, NH₃ and alkanes thermal accommodation coeffs., translational (internal) gas-solid energy exchange 8-92506
 surface, CO₂ laser energy coupling into ionised blowoff material 8-72641
 surface, H⁺(H₂⁺) ion impact, energy refl. coeffs. 8-54969
 surface, ion impact, mol. effects in electron emission 8-80446
 surface, laser supported detonation waves, initiation 8-63568
 surface, nearly-free-electron metal, origin of surface reson. states 8-95322
 surface, O₂ layer thickness, reson. α-scatt. from ¹⁶O 8-64778
 surface, oxidation, synchrotron radiation photoelectron obs. 8-52634
 surface, proton bombarded at 450 keV, X-ray bremsstrahlung, 2.5-8.5 keV 8-80436
 surface, pure, oxidised element determ. by SIMS 8-85247
 surface, slow-positron emission 8-95079
 surface cracks, small, size estimation using SAW 8-76793
 surface layer structure in magnetic field (Russian) 8-56268
 surface plasmon dispersion curves, splitting by Ag surface layers 8-60178
 surface resonances and oxidation 8-72225
 surface sliding damage, no lubrication, materials depend. (Japanese) 8-56780
 thermal conductivity, min. 8-76050
 thermal conductivity maximum, temp. range 4.2 to 70K, plastic deform. influence 8-76049
 thermoelectric power and Nernst-Ettingshausen effect 8-56134
 thin foil, adhesion and friction, rel. to observed dislocation density 8-64706
 ultrafine particle, positron annihilation exam. 8-56542
 unpaired ion-ion interaction, transverse phonon branch, neutron scatt. expt. (Russian) 8-87751
 US velocity, anomalous response to applied stress 8-63811
 UV emission under inert gas ion bombard. 8-84664
 vacancy, mechanical multipole moments determ. 8-55868
 vacancy formation energy calc. within density functional and second order perturbation formalisms 8-67975
 vacancy formation enthalpy, positron annihilation spectroscopy 8-67707
 vacuum deposited, structural singularities and porosity (Russian) 8-75950
 vacuum deposited metal film, elec. field effect on residual struct. 8-51836
 vapour deposition on substrates, splash-free, using modified W helix 8-52689
 volume contraction accompanying solidification 8-52791
 X-ray absorption, shock wave compression meas. (German) 8-95618
 X-ray emission spectra, high energy plasmon satellite intensities 8-64430
 XPS, achromatic X-ray source, spectrum iterative deconvolution 2p spectrum 8-72689
 XPS theory, core level spectra, plasmon creation 8-72701
 XPS theory, valence band spectra band struct. 8-72702
 ZZ 8-91367
 Ag-BN-Si-Al sandwich, humidity sensitive threshold switching 8-88046
 Al, cryst. and polycryst., inhomogeneity effects on galvanomagnetic props. 8-60109
 Al I, relativistic and cancellation effects in line strength ratios 8-82689
 Al IV, V, beam foil spectra, 1100-1900 Å, lifetime meas. 8-70919
 Al sequence, 4s²S-4p²P transition, f-values 8-78651
 Al, US and X-ray testing of castings, moulds and die-casting machines 8-53097
 Al XIII, hot pinched plasma, Lyman series Stark profiles, electron density determ. 8-51348
 Al:¹¹¹In, electron irradi., defect trapping at impurities 8-55892
 Al:¹²B, relax. mechanism for polarised implant 8-87693
 Al:²⁴Na, diffusion of Na, determ. of diffusion coeff. and activation energy 8-51746
 Al:Er(Dy), orbit-lattice coupling, nonuniform strain effects 8-88182
 Al:He, pseudopotential calc. of screening of He atom 8-51917
 Al:WO₃ films, resistive state, effect of UHF rad. on dynamic cond. (Russian) 8-52154
 Al/brass/Al bimetal, three layers, formed by cold rolling, exam. of formation of intermetallic phases at interface 8-56658
 Al-adsorbed monolayer-Al junction, elec. cond. mech. 8-95386
 Al-Al oxide-Bi₂Pr₃ tunnel junction, cryst. field struct. obs. in conductance 8-84358
 Al-Al₂O₃-Al, non-thermal switching in Al₂O₃ amorphous film (Russian) 8-80069
 Al-Al₂O₃-Al, thin film capacitors, dielec. losses 8-76382
 Al-Al₂O₃-Al junctions, Dy doped at Al₂O₃-Al interface, electron transport mechanisms and barrier height 8-91778
 Al-Al₂O₃-Al structure, elec. cond. 261 to 418K (Russian) 8-64144
 Al-Al₂O₃-Al structure, tunnel I-V characts., transmission coeffs. 8-80068
 Al-Al₂O₃-Al(Au), thin films, elec. props. (Czech) 8-76159
 Al-Al₂O₃-M, thin film sandwich, leakage current and dielec. relax., 80-500K 8-76158
 Al-Al₂O₃-electrolyte, electroluminesc., nondestructive electronic avalanche 8-68563

aluminium continued

- Al-Al₂O₃-Al tunnel junction, Fe doped, Kondo-type zero-bias conductance 8-56237
- Al-AlN-Au, voltage controlled negative resist., O₂ press. effect 8-72281
- Al-Au bimetal thin film interdiffusion zone, intermetallic phase form kinetics, 70-160°C 8-75891
- Al-barium stearate-Al struct., intrinsic voltage in insulating film 8-72277
- Al-Be, two-layer foils, mech. props. (Russian) 8-51858
- Al-epoxy adhesive systems, opening and edge-sliding fracture toughness 8-95805
- Al-Fe interface, O₂ content, reson. α -scatt. from ¹⁶O 8-64778
- Al-GaAs Schottky barrier diode, prep. by MBE on GaAs, and characts. 8-72257
- Al-GaAs(110) structure, interface states, photoemission study 8-95359
- Al-graphite adhesion and contact angle, effects of metal additives (Japanese) 8-60008
- Al-KCl composite, far IR absorption 8-56466
- Al-lead stearate-Hg, transient and alternating electric currents 8-84311
- Al-matrix, composites preparation by Na-process, interface reactions 8-84742
- Al-nSi-Al, p⁺np⁺ reach through structs., electronic cond. mechanism 8-64103
- Al-oxide-electrolyte system, luminesc. spectra (Russian) 8-76539
- Al-Plexiglas, double layer barrier, deform. of electron spectra (Russian) 8-84292
- Al-polyferrocene-Al structure, I-V and I-d characts. 8-80064
- Al-Si, ion plated contacts (Rumanian) 8-88029
- Al-Si structure, contact resist. and bulk resist. of Si, pulse method 8-52083
- Al-Si₃N₄-Al thin-film cold cathode, electrical forming, expt. 8-76160
- Al-Si₃N₄-SiO₂-Ge structure, small signal HF photo EMF meas. 8-52097
- Al-SiO₂ film-substrate interface, obs. of Al₂O₃ and free Si 8-91571
- Al-SiO₂ interface, chem. struct., deposition conditions depend. 8-72007
- Al-SiO₂-Au, thin layer struct., electroluminesc. (French) 8-76531
- Al-SiO₂-Si structs., implanted B⁺ ions, high-freq. CV characts. (Russian) 8-80056
- Al-SiO₂-Si structure, small signal HF photo EMF meas. 8-52097
- Al-SiO₂-Si:B ions, annealing effect on energy spectrum of radiation defects (Russian) 8-88488
- Al-SiO₂-Si-Pb, MIS system, photocurrent, effect of supercond. to normal transition in Pb 8-72271
- Al-SiO₂-Au cathode, emitted electron energy distrib. 8-52645
- Al-SiO₂(+SiO₂)-Si structures, I-V and C-V characts., current and capacitance kinetics 8-88043
- Al-SiO-Al structure, tunnel I-V characts., transmission coeffs. 8-80068
- Al-Ta-poly-Si interdiffusion, Ta barrier effect, Auger anal. 8-71888
- Al+Al, (Cl)(F), molecular K X-ray transitions, mol. radiative electron capture effect 8-58802
- Al+H⁺, K-shell ionisation cross sections for 15-65 keV protons 8-90284
- Al+H(D)(He)(Li) ions, K-shell ionis., universal cross sections 8-62895
- Al+He⁺, X-ray spectra, two-electron one-photon transition in solid target, 2 MeV 8-94209
- Al₂O₃-ZrO₂, multiphase ceramics, mech. strengthening due to dispersion of non-metallic particles (German) 8-60674
- ²⁶Al from meteorites, possible 'record' of solar wind action and luminosity variations 8-61830
- ²⁶Al isotopic anomalies in solar system, local proton irradiation model 8-93128
- ²⁷Al in aqueous soln., quadrupolar relax., motions of hydration water mols. 8-64291
- Au-Si-Al structure electrode mass transfer and switching with memory 8-95389
- Au-tetrathiotetracene-Al systems, dark cond., photocond. mechanisms rel. to contact phenomena (Russian) 8-52103
- B fibre reinforced Al, fracture mechanical study, unidirectional composites 8-88520
- B fibre reinforced Al, unidirectional, K-calibration and compliance curves 8-88518
- B fibre reinforced strength determ. procedure in annular specimens (Russian) 8-95864
- B-Al cast braid, crystallisation and structuring of Al matrix (Russian) 8-52725
- B-epoxy-Al sandwich laminate, influence of residual stresses on tensile strength 8-60703
- CaO:Al, X-ray and UV luminesc., electron-hole recombination processes (Russian) 8-76528
- CdS:Al photoelectric props., optical absorption vacuum deposited film 8-60162
- Cu-Al powder mixture, elec. discharge reaction sintering 8-64507
- α -Fe₂O₃:Al, hematite, spin reorientation, Mossbauer spectra obs. 8-72356
- Ge:Al film, amorphous, ion implantation, effect on cond. 8-83839
- KCl-Al composite, optical and IR reflectance 8-56465
- Li, one-electron calcs. of X-ray absorpt. and emission, jellium model 8-56543
- Mo fibre reinforced, SEM study (Slovenian) 8-84923
- ¹⁶O⁺+Al, energy-loss straggling, charge exchange effects 8-58799
- Si:Al, absorpt. line broadening 8-95594
- Si:Al, acceptor levels, IR spectra 8-67972
- Si:Al, bound multiexciton complexes, work function thermodynamic determ. 8-72078
- Si:Al, bound-exciton absorption 8-56507
- Si:Al, edge luminesc. spectra of acceptors, multiexciton complexes 8-56517
- Si:Al film, amorphous, ion implantation, effect on cond. 8-83839
- Si-Al, film, quantitative anal. by DC arc optical emission spectroscopy 8-68940
- Si-Ge:Al, hot-pressed alloy, thermoelec. props. 8-91711
- Si-SiO₂-Al structure, mechanical stress at Si(111) surface 8-63921
- SiO₂:Al, vitreous state, EPR of Al defects 8-91951
- SiO₂:Al film, ion-implanted, electron trapping behaviour 8-67729
- W:K-Al-Si, state of bonding, distribution of impurities 8-92212

aluminium continued

- Zn:Al, ion implantation of Al, defect flow induced outdiffusion 8-63779
- ZnS:Ag,Al, computer calc. of band model for luminesc. and photocond. (Russian) 8-52542
- ZnS:Al, signal enhancement by field modulation, ODMR expts. 8-56406
- ZnSe:Cu, Al, single cryst., low-voltage red cathodolum. 8-80423
- aluminium alloys**
see also **aluminium compounds**
- 1201, preliminary forging effects on struct. and mech. props. of extruded sections (Russian) 8-80564
- 7075-T6, H₂ effects and Cd segregation to grain boundaries 8-84764
- ageing, high temp. effect on endurance of thin walled joints of alloy AK4-1T1 8-80570
- ageing effect on hardness and tensile props. rel. to delay time till quenching, in alloy 7001 8-92286
- AK4-1, preliminary forging effects on struct. and mech. props. of extruded sections (Russian) 8-80564
- Alclad, 2024-T3, dimpled loaded-hole fatigue strength, effect of interf. 8-72948
- Alinco 5, thermal treatment in mag. field, mag. props. 8-91905
- analysis by ion microprobe, quantitative, using matrix ion species ratios 8-61070
- bronze, O free, annealing in photoemission electron microscope, twin density recrystallised grain size relation (German) 8-52850
- buckling under axial compression on circ. integrally stringer-stiffened shell 8-63346
- cast struct form. in continuous casting (German) 8-92256
- chevron fracture in tube reduction by spinning in alloys 7178 and M580 8-64664
- corrosion fatigue strength, tensile prestrain effects (Japanese) 8-56819
- crack closure during fatigue crack growth, for two thicknesses of alloy BS 2L71 8-68792
- crack opening displacement, expt. and FEM study 8-68811
- crack tip studies, stretched zone and COD 8-68812
- cylindrical parts, crack detection by two channel eddy current inspection unit 8-72998
- D16, Fe and Si impurity effects on K_{ic} 8-84990
- D16, preliminary forging effects on struct. and mech. props. of extruded sections (Russian) 8-80564
- deformation processes in sheet materials, application of failure maps 8-56718
- delayed retardation phenomena of fatigue crack growth, exam. 8-56745
- desorption of neutral mols. by electron and ion bombardment of vacuum material 6061 8-95229
- determination by spark-source mass spectroscopic anal., sensitivity calibration 8-68962
- dilute, Hall coeff., calc. by 4-OPW approx. 8-76052
- dilute, size effect of impurity atoms rel. to trapping radii for migrating self-interstitials 8-75690
- disc, quality factor of vibr. rel. to gravit. radiation detector 8-75093
- dislocation dynamic props., investigation by impact loading for alloy D16 (Russian) 8-85069
- Duralumin, contact angs. meas., aq. ethanol (glycerine) solns., 20-70°C 8-56025
- dynamic material behaviour under nearly uniaxial strain conditions, modified Kolsky apparatus 8-85070
- electroforming, study of process variables in the electromagnetic bulging of tubes 8-80582
- embrittlement by cathodic H₂, surface film effect 8-64643
- endurance determ. method over wide range of load asymmetry 8-56836
- epoxy resin-Al alloy 5086, scarf joint test specimen, mixed mode adhesive fracture, bond angle effect 8-68768
- fatigue, alloy 2024, loading sequence, normal and reversed sequence effect 8-68791
- fatigue crack, low growth rate 8-64701
- fatigue crack arrest, corrosive environment, at low stress intensities 8-92415
- fatigue crack closure for 2024-T3 alloy 8-72833
- fatigue crack closure with negative stress ratio, following single tensile overloads in alloy 2024-T3 8-64687
- fatigue crack delay behaviour, alloy 2024-T3, effect of stress level 8-68790
- fatigue crack growth, crack closure 8-80650
- fatigue crack growth, delayed retardation phenomenon, from single overload in A2017, A5083 8-92317
- fatigue crack growth, effect of frequency changes 8-64693
- fatigue crack growth, exam. of some aspects 8-56772
- fatigue crack growth model, notch analysis of fracture approach, Al 2024-T3 and Al 7075-T6 8-52984
- fatigue crack growth testing, A356 T6 and 2219-T851, decreasing stress intensity technique, computer-controlled 8-72949
- fatigue crack propag., mechanism of overload effect 8-56730
- fatigue crack propag. and fractography under periodic oversteering, exam. (Japanese) 8-52958
- fatigue cracked alloy 7075 T6, repair machining and inspection of components 8-80689
- fatigue endurance scatter in transitional region of fatigue curve (Russian) 8-56738
- fatigue life distrib., statistical anal., mixed Weibull distrib. (Japanese) 8-72841
- fatigue testing, exam. of scale relationship of endurance limit 8-60914
- fatigue tests with axial and diametral extensometers 8-85062
- fracture, dynamic, of Al alloy 6061-T6 cylinder, expt. rel. to Mott's theory 8-64651
- fracture, grain size effect 8-60781
- fracture initiation and propagation during strip drawing 8-64663
- fracture micromechanisms, fracture toughness, exam. 8-56766
- fracture props., effect of thermomechanical treatment 8-60793
- fracture toughness testing, acoustic emission, inspection technique 8-68860
- fracture toughness under plane stress 8-92316
- fretting fatigue tests, effects of environmental H₂O, O₂ 8-92407
- grain refinement, effect of Al₃Ti, TiC and B 8-52828
- granules of AK5M2, rolling speed effects 8-60604
- heat treatment of semifinished products of alloy 01420 before cold deformation 8-84873

aluminium alloys continued

- high strength structural mats., microstruct. influences on fatigue and fracture resist. 8-56728
inelastic electron scattering by dislocations (*Russian*) 8-79988
internal fatigue crack growth in vacuum 8-56729
laminates, fracture of bonded 2024-T3/7075-T6 8-56722
limiting plastic props. (*Russian*) 8-88504
loading freq. effect on fatigue growth rate 8-83873
marine atmosphere stress corrosion tests on precracked specimens, corrosion product wedging effect 8-88570
melt, contact reactions with Fe group metals 8-60879
 β_1 -Ni-Al, premartensitic transformation 8-76645
notch sensitivity in fatigue 8-60757
oxide-covered, characteristic emission of negatively charged particles during tensile deform. 8-92179
pipe, creep-resistant, influence of chem. comp. on formability (*German*) 8-84900
pit propagation, influence of anions 8-72917
pitting corrosion rel. to load-carrying capacity of sheets (*Russian*) 8-56806
plastic, anisotropic hardening pot., stress/strain relation under combined axial load/torsion 8-52896
plastic deformation under abruptly changing loading or strain paths 8-56700
plastic zone form. and fatigue crack growth 8-64702
plastically anisotropic, non-associated flow law (*Polish*) 8-80603
plasticity due to superimposed macroscopic and static strains 8-60719
quenching rate rel. to mech. props., residual stresses, optimum quench coolings (*French*) 8-64562
radiography with gamma rays, using Se electroradiographic plates, comparison with X-ray plates 8-72978
rare earth alloys, AlAl_2 , ordered, NMR determ. of hyperfine fields 8-84180
rare earth alloys, RFe_4Al_8 , cryst. struct. mag. props. and hyperfine interactions 8-87648
rare earth trialuminides, long period polytypes, electron diff., high resolution imaging 8-83781
rare earth- Co_2 -Al, dil., nonmag. impurities effect on ordering temp. 8-84427
rare earth-Fe-Al alloys, RFe_4Al_8 , mag. props. 8-52250
reactive etching in RF plasma containing halogen species 8-72923
SCC, subcritical flow growth, comparison of aircraft alloys in NaCl soln. 8-53028
selection using fracture mechanics 8-56725
sheets, type 7004, asymmetrical solidification structures, fluid flow, in W arc welds 8-84794
spectrochemical analysis with glow-discharge lamp (*Japanese*) 8-85262
steel, alloy, Fe-Cr-Ni-Mo-Al, (13, 8, 2, 1, wt.%), H_2 effects on fracture, exam. 8-60809
steel, stainless, austenitic, CC Ni-Al, γ -phase, fracture mechanical aspects of abrasive friction, wear, chip formation 8-72865
stress corrosion cracking, of AA7075 effect of orientation and loading history 8-95835
stress corrosion cracking protection, by γ_1 - Al_2O_3 anodic film 8-95836
thermally activated deformation, exam. of hypothesis 8-72820
type 6061, A356, forging of liquid and partially solid alloys 8-80569
US structure monitoring of parts of AK4-1 and D16 8-53082
yield surface of material subjected to combined cyclic loadings 8-84905
Al alloy D16T, acoustic emission temp. depend. 8-53136
Al bronze, anisotropic bend ductility in single phase alloys 8-60726
Al-2024-T351 alloy, precipitation hardening, thermal cond. 8-91661
Al-Al₃Ni eutectic, effect of some thermal parameters on the directional solidification process 8-88456
Al-Ag, discontinuous decomposition (*Polish*) 8-52808
Al-Ag, nonhomogeneity of deform. 8-84888
Al-Ag, resonance splitting of phonons 8-75759
Al-Ag (up to 40 at.%), exam. of anelastic phenomena and structural state 8-76693
Al-Ag alloy, ageing exam. by X-ray electron spectroscopy and electron diff. exam. (*Russian*) 8-60685
Al-Ag alloy, second ageing stage, diffuse electron and X-ray scatt. (*Russian*) 8-68711
Al-Ag-Al, eutectic alloy, exam. of terminal solid solubility limits 8-76633
Al-Ag-Si alloys, phase equilibria at 500°C (*Russian*) 8-56612
Al-Al₃ eutectic, abrasive fragmentation (*Czech*) 8-64715
Al-Al₃Ca, eutectic alloy, unidirectionally solidified, exam. of growth and crystallography 8-72771
Al-Au bimetal thin film interdiffusion zone, intermetallic phase form kinetics, 70-160°C 8-75891
Al-Cr(V)(Ti), dil., electron irradiated, interaction of self interstitials with undersized solute atoms 8-63789
Al-Cu, electric discharge sintering of powder mixtures 8-60605
Al-Cu, O transport during fatigue crack growth 8-52981
Al-Cu, thermal conductivity, data anal. and synthesis 8-95284
Al-Cu, US wave propag. velocity, exam. 8-72982
Al-Cu (10 wt.%), inverse segregation 8-52819
Al-Cu (1.7 at.%), age-hardening, resistivity change by low temp. deform. (*Japanese*) 8-84831
Al-Cu (2.12 at.%), irradiated by 8J CO_2 laser pulses, metastable precipitate and amorphous phase (*French*) 8-80552
Al-Cu (3.5 wt.%), precipitation on stationary and non-stationary grain boundaries 8-84820
Al-Cu (3.71 wt.%), stress oriented precipitation of Guinier-Preston zones and θ' 8-52809
Al-Cu (4 wt.%), AE during deform., effect of ageing at 170°C 8-64597
Al-Cu (4 wt.%), aged to contain Guinier Preston zones, crystallographic fatigue crack growth 8-60832
Al-Cu (4 wt.%), elastic accommodation of semicoherent θ' 8-64543
Al-Cu (4 wt.%), enhanced precipitation under electron irradiation in HVEM 8-52818
Al-Cu (4 wt.%), single crystals, positron trapping at precipitates 8-76554
Al-Cu (4.5 wt.%), volume contraction accompanying solidification 8-52791
Al-Cu (up to 0.5 at.%), neutron damage rate, interpretation of results 8-63794
Al-Cu alloy prod., Cu interdiffusion with sintered Al powder, struct. effect at high press. 8-60606

aluminium alloys continued

- Al-Cu alloy RR58, high strain fatigue life, prior treatment effect 8-60835
Al-Cu alloys, quenched rapidly, microstruct. 8-56668
Al-Cu film, galvanostatic formation anodic oxide, Rutherford backscattering and depth profiling 8-92395
Al-Cu film bilayers, growth kinetics of θ phase, He^+ backscatt. and X-ray exam. 8-84105
Al-Cu-Fe alloys, solid and liquid, exam. of constitution and mag. props. (*German*) 8-52206
Al-Cu-Mg, alloys A-U4, A-U4G1, A-U2GN, effect of environment on fatigue crack growth 8-64677
Al-Cu-Mg alloy, influence of plastic deformation on fatigue limits, for prestrained components 8-68799
Al-Cu-Mg alloy RR58, comparison of methods of correlating creep crack growth 8-60826
Al-Cu-Mg-Mn (4.5, 1.5, 0.6 wt.%), alloy 2024-T3, exam. of residual strength of plate containing crack, fracture anal. 8-90792
Al-Cu-Mg-Mn (4.5, 1.5, 0.6, wt.%), alloy 2024-T81, plates, adhesively bonded, exam. of fatigue crack growth 8-92349
Al-Cu-Mg-Mn (4.5, 1.5, 0.6 wt.%), thin sheet, exam. of fracture toughness, and fatigue crack growth 8-92353
Al-Cu-Mg-Mn-Fe-Si, alloy D16, effect of mechanisothermal treatment on mech. props. 8-56674
Al-Cu-Mg-Si-Mn (2.5, 0.7, 0.7, 0.5 wt.%), alloy AK6, US inspection of heat treatment quality 8-76681
Al-Cu-Mg-(Si), inclusions, oriented distrib. metallography and effects on anisotropy (*Russian*) 8-80589
Al-Cu-Ni, directionally solidified, exam. of struct. of two phase alloys 8-80537
Al-CuAl, eutectic, thermal instability in temp. gradient 8-52851
Al-Cu(Ag)(Ge), dil., deviation from Matthiessen's rule at high temps. 8-64025
Al-Cu(Mg), age-hardenable, US cavitation erosion mechanisms, effects of comp. and heat treatment 8-53002
Al-Cu(Zn-Mg), age hardening, conditions leading to localised plastic deform. and fracture in slip bands during fatigue 8-64670
Al-Fe, cast, influence of Zr on precipitation, solidification and grain size (*Rumanian*) 8-84813
Al-Fe, electron irradiated, interstitial-solute complexes, internal friction spectra 8-92289
Al-Fe-Si, eutectic alloy growth, by twinning plane propagation (*French*) 8-60667
Al-Ga (10 wt.%), exam. of ^{27}Al diffusion by NMR technique 8-87813
Al-Ga-In, liq. alloys, excess Gibbs functions 633 to 1173K 8-60655
Al-Ge, directionally solidified lamellar eutectics, specimen prep. for TEM (*German, English*) 8-95885
Al-Ge (2 wt.%), quenched and aged, deform. slip line obs. 8-51544
Al-Ge, Al₃Ge, Ge precip., ion irradi., dose rate and temp. depend. 8-79642
Al-In (40, 70 wt.%), liq. phase immiscible system, solidification in microgravity 8-84770
Al-In emulsion, solidification mechanisms at zero gravity, review 8-88458
Al-Li, dil., quenched and irradi., recovery, resist. and internal friction obs. 8-52848
Al-Li solid soln., decomposition exam. by secondary ion ion emission (*Russian*) 8-68696
Al-M, dil. alloy, electronic states of 3d-transition metal (M) impurities 8-64005
Al-Mg, alloy 5083, effect of environmental factors on stress corrosion cracking 8-80684
Al-Mg, dil., long-range solute-host interactions 8-95062
Al-Mg, fracture during superplastic flow 8-60729
Al-Mg, new metastable phase 8-52772
Al-Mg, thermal conductivity, data anal. and synthesis 8-95284
Al-Mg (2 wt.%) subgrain formation at low stresses 8-84928
Al-Mg (5 wt.%) deformed bars, cold rolled, exam. of microstruct. by thin foil TEM 8-88502
Al-Mg (5.5%), creep, absence of instantaneous plastic strain upon stress changes 8-75718
Al-Mg (7 wt.%), corrosion cracking, exam. of slip dissolution and hydrogen embrittlement mechanisms 8-72852
Al-Mg alloy AMg6, mech. props. of welded joints, impurity effects 8-95789
Al-Mg solid soln., AE during plastic deform. 8-64592
Al-Mg-Ag, age effect on age hardening (*Japanese*) 8-52831
Al-Mg-Li alloy, 01420, surface layer props. (*Russian*) 8-80674
Al-Mg-Li-Si system, phase diag. (*Russian*) 8-80515
Al-Mg-Si, dendritic non-homogeneity 8-56641
Al-Mg-Si (Alcan 6351), plastically deformed, influence of microstruct. on energy stored 8-84894
Al-Mg-Si-Mn, Mn addition effects on fracture 8-60791
Al-Mg-Ti(Zr), struct. and factors determining brittle intermediate compound form. 8-52817
Al-Mg-Zn, interdiffusion 8-51751
Al-Mg-(Zn)(-Zn-Cu), exam. of precipitation struct. by neutron scattering 8-92270
Al-Mg(Mg-Cu)(Cu), Al_2O_3 fibre reinforced, exam. of interface interactions during fabrication 8-76616
Al-Mn, anodisation, intensity of luminesc. and film thickness 8-80413
Al-Mn, dil., ^{54}Mn Knight shift meas. using nucl. orientation 8-68396
Al-Mn, dil., coherent propag. and strain-induced localisation of muons 8-95537
Al-Mn (0.35 wt.%), quenched exam. of Mn-vacancy interaction 8-76676
Al-Mn (1 wt.%), subgrain growth during annealing after cold work 8-56656
Al-Mn alloys, study of solidification by rapid cooling (*Japanese*) 8-88459
Al-Mn-Si, recrystallisation and precipitation 8-52824
Al-Mn-Zr (0.9, 0.4%), strain induced continuous recrystn., rel. to superplastic behaviour 8-84915
Al-Mn(Cu)(Ag), solute atom displacement in mixed dumbbell interstitials for FCC lattice 8-79631
Al-Ni-Ti, calc. of phase equilibria using thermodynamic values from different models 8-60646
Al-Pb(Bi)(Cd), containing low melting point inclusions, impact props., temp. depend. 8-60792
Al-Si, hypereutectic silumins, P and Na modification 8-84792

aluminium alloys continued

- Al-Si, internal friction and Si precipitate nucleation 8-60690
 Al-Si (8 wt.%), threshold H_2 for pore form. during solidification 8-52794
 Al-Si eutectic, directionally solidified, tensile props. 8-64531
 Al-Si eutectic, Na, Sb and Sr alloying addition effects on microstructure (*French*) 8-64548
 Al-Si-Cu-Mg, alloy AL32, ageing of castings produced by pressure die castings 8-56650
 Al-Si-Cu-Ni alloy casting, thermal props. 8-95814
 Al-Sn, (<0.28 wt.%) corrosion behaviour in 16% HCl 8-85054
 Al-Sn, dil. alloy, vacancy-impurity interaction, exam. by electrical resistivity meas. at 77K (*German*) 8-83846
 Al-T alloys, relationship between struct. and thermodynamic props. (*German*) 8-91307
 Al-Ti-B alloys, segregation of Ti, electron microscope exam. 8-52820
 Al-Ti-Si phase diagram, calc., interpretation of grain refinement results 8-84781
 Al-Zn, dil., grain boundary diffusion 8-91475
 Al-Zn, dil. alloy, ageing and reversion, annealing curves, X-ray obs. 8-88485
 Al-Zn, discontinuous decomposition (*Polish*) 8-52808
 Al-Zn, formation of Guinier-Preston zones, and their limit temp. (*Japanese*) 8-84861
 Al-Zn, nonhomogeneity of deform. 8-84888
 Al-Zn, precipitation struct. and phys. props. effect of miscibility gap (*German*) 8-92265
 Al-Zn, short range order, many electron effects, pseudopotential method 8-79954
 Al-Zn, solid soln., exam. of evolution by thermo EMF meas. (*French*) 8-52862
 Al-Zn (4.5 at.%), age-hardening, resistivity change by low temp. deform. (*Japanese*) 8-84831
 Al-Zn (7 at.%), liquid quenched, early stage phase separation, exam. 8-68698
 Al-Zn alloys, relation between microhardness and average radius of Guinier-Preston zones 8-95811
 Al-Zn alloys, room temp. decomp. of metastable phases precipitated at 200°C 8-84814
 Al-Zn coated steel sheet, chromate passivation protection against wet-storage stain 8-95854
 Al-Zn-Mg, effect of microstruct. on localised shear failure 8-52996
 Al-Zn-Mg, grain boundary segregation, AES meas. 8-72781
 Al-Zn-Mg, O transport during fatigue crack growth 8-52981
 Al-Zn-Mg, plastic instability rel. to grain boundary failure at low temps. 8-56702
 Al-Zn-Mg, precipitation of η' phase, heat treatment, electron microscope obs. 8-68699
 Al-Zn-Mg, thermomechanically treated, precip. behaviour 8-84856
 Al-Zn-Mg (2.64, 1.40 at.%), age-hardening, resistivity change by low temp. deform. (*Japanese*) 8-84831
 Al-Zn-Mg (5.25 wt.%) observation of stress corrosion cracking 8-60868
 Al-Zn-Mg (6.15%), influence of ageing and cold work on tensile and fracture props. (*Japanese*) 8-52842
 Al-Zn-Mg (6.27, 2.94 wt.%), single crystals, effect of environment on liquid-metal embrittlement, stress corrosion cracking and corrosion fatigue 8-64676
 Al-Zn-Mg alloy, stress corrosion cracking, exam. (*Japanese*) 8-53026
 Al-Zn-Mg alloys, decomp. kinetics from Young's modulus obs., microprocesses (*German*) 8-64522
 Al-Zn-Mg alloys, decomposition kinetics, resistivity meas., extended jump model 8-84766
 Al-Zn-Mg-Cu, alloy 7075, hydrostatic pressure effects on ductile fracture 8-60779
 Al-Zn-Mg-Cu, alloy 7075, fatigue, loading sequence, normal and reversed sequence effect 8-68791
 Al-Zn-Mg-Cu, alloy 7075, effect of purity level, dispersoid type, heat treatment, on fracture toughness 8-80636
 Al-Zn-Mg-Cu, alloy 7075-T6, corrosion in halide solutions, exam. of anion dependency 8-60867
 Al-Zn-Mg-Cu, alloy 7075-T6, fatigue crack closure with negative stress ratio, following single tensile overloads 8-64687
 Al-Zn-Mg-Cu, inclusions, oriented distrib. metallography and effects on anisotropy (*Russian*) 8-80589
 Al-Zn-Mg-Cu alloy, laminated, adhesively bonded alloy 7075-T6, exam. of fracture resistance 8-76754
 Al-Zn-Mg-Cu alloys, effect of alloying elements as stress corrosion failure using regression analysis 8-80669
 Al-Zn-Mg-Cu-Cr, (5.6, 2.5, 1.6, 0.3 wt.%), laminates, 8 and 22 layers, adhesively bonded exam. of fatigue crack propag. 8-92345
 Al-Zn-Mg-Cu-Cr, (5.6, 2.5, 1.6, 0.3 wt.%), alloy 7075, plates, adhesively bonded, exam. of fatigue crack growths 8-92348
 Al-Zn-Mg-Mn, correlation of microscopic features, with macroscopic crack propagation 8-60800
 Al-Zn-Mg-Ti, Ti effect on microstructure during ageing 8-64568
 Al-Zn-Mg-Zr (6.45, 2.08, 0.11 wt.%), exam. of cyclic stress strain response in corrosion fatigue 8-64788
 Al-Zn-Mg(Mg-Ti), TEM exam. of early stage ageing behaviour, exam. of precip. kinetics 8-56645
 AlBi, X-ray fluorescence analysis (*Japanese*) 8-88663
 Al₂Ce, Al₃Ce, nucl. orientation exam. of Ce ground state at very low temp. 8-67999
 Al₂Cu, single cryst. elastic const., 4.2-300K 8-72803
 Al_{10.4}Ga_{0.08}V, low temp. thermal expansion 8-95167
 Al₃Ni dendrite facets, determ. cryst. direction by SEM (*French*) 8-87893
 Al₃Ti, effect on grain refinement in Al 8-52828
 Al₁₀V, low temp. thermal expansion 8-95167
 Au-Al system, influence of current on phase form. in diffusion layer (*Russian*) 8-52826
 Au₂MnAl, Heusler alloy, ferromag., NMR meas. 8-76320
 CeAl₂, anisotropic magnetostriction near antiferromagnetic transition 8-88157
 CeAl₂, conf. Kondo system, sp. ht. meas. 8-52210
 CeAl₂, low temp. mag. behaviour, neutron diffr. 8-84395
 CeAl₂, mag. anisotropy, transition, crystal field splitting 8-52243
 CeAl₂, NMR, cryst. field effects and mag. order in low temp. phase 8-68391
 CeAl₂, sp. ht. in high mag. fields, Kondo effect 8-52284

aluminium alloys continued

- CeAl₃, anomalous resistivity maxima in metallic magnetic system 8-79977
 CeAl₃, singlet ground state at T=0, mag. ordering 2.5-6K 8-84388
 CeAl₃, valence mixed state, Kondo lattice, Anderson localisation models (*Japanese*) 8-51945
 Ce_{1-x}La_xAl₂, extraordinary Hall effects, 4.2-300K, cryst. field interaction 8-79980
 Ce_{1-x}Pr_xAl₂, mixed mag. phase at low temp. 8-68228
 Co-Al, mag. struct. of Co rich intermetallic cpd., neutron scatt., cluster model 8-80130
 Co-Al-Cr(Nb)(Ta), eutectic alloys, charact. by melting, oxidation resistance and composition 8-52768
 Co-Al-Nb, monovariant directionally solidified eutectics, struct. and mech. props. (*Russian*) 8-92254
 Co-Cr-Al, eutectic alloy, unidirectional solidification, oxidation and tensile tests 8-52790
 Co-Cr-Al, exam. of cyclic oxidation resistance at 1100 and 1200°C, comparison with Ni-Cr-Al system 8-88572
 CoAl, bonding, self-consistent energy bands 8-91610
 Co_{49.6}Al_{50.4}, Compton scatt., 59.54 keV γ -rays, charge transfer study 8-68578
 Cr-Al, disordered alloy, effect of high press. on resistivity 8-95286
 CrAl, semicond. solid solns., temp. depend. of elec. resist. at high temp. 8-67941
 α -Cu-Al, binary substitutional, short-range ordering kinetics, vacancy behaviour 8-55867
 Cu-Al, change in force constant due to volume effects 8-75778
 Cu-Al, critical voltage effect (*Japanese*) 8-91206
 Cu-Al, diffusive redistrib. during friction (*Russian*) 8-52999
 Cu-Al, dispersion hardening by internal oxidation 8-56649
 Cu-Al, eutectic composition, exam. of high temp. mechanical behaviour (*French*) 8-72818
 α -Cu-Al, FCC, fractographic obs. of SCC 8-64786
 Cu-Al, faulted dipoles, geometry and form. 8-59809
 Cu-Al, impurity concentration effects 8-75777
 Cu-Al, internally oxidised, structural, elec. and mech. characts. 8-60761
 Cu-Al, intrinsic temp. depend. of stacking-fault energy 8-51564
 Cu-Al, lamellar eutectoids, calorimetric determ. of interfacial enthalpy 8-60668
 Cu-Al, magnetic susceptibility, comp. and temp. depend., melting effects 8-52202
 α -Cu-Al, short range ordered, struct. and new superlattice phase 8-52756
 Cu-Al, sulphurisation solid state phenomena 8-64781
 Cu-Al, surface segregation during adsorption and low pressure oxidation (*French*) 8-75932
 Cu-Al (10 wt.%), water-quenched, tensile fatigue strength at high temp. in vacuo (*Japanese*) 8-72837
 Cu-Al (10.4%), creep, absence of instantaneous plastic strain upon stress changes 8-75718
 Cu-Al (11.6 wt.%), mech. props., tempering temps. effects 8-76669
 Cu-Al (13 at.%), polycryst., effect of grain size, specimen thickness, on mech. props. 8-84945
 Cu-Al (14.8 at.%), vacancy formation energy determ. 8-63756
 Cu-Al (6.4 wt.%), rolled low stacking fault energy alloy, struct. and texture 8-52844
 α -Cu-Al alloy, short range order structure 8-91303
 Cu-Al composite, simulation of tensile behaviour and fracture void initiation (*Japanese*) 8-52948
 Cu-Al film, thermoelec. power, 80-350K 8-68096
 Cu-Al-Ni, habit plane for SIM $\gamma \rightleftharpoons \beta'$ transform. 8-56640
 Cu-Al-Ni-Fe, (10, 5, 5 wt.%), cast microstruct. 8-80535
 Cu-Al-Si-Co (2.8, 1.8, 0.4 wt.%), superplastic phase, exam. of mech. props. 8-52891
 Cu-Ni-Nb-Al, formation of γ' and γ'' precipitates 8-76655
 β -Cu-Zn-Al, electron microscope exam. of premartensitic state 8-72801
 β -Cu-Zn-Al, ordering 8-68687
 Cu-Zn-Al, pseudoelastic alloy, exam. of fatigue props. 8-76744
 Cu-Zn-Al (19.3, 13.0 wt.%), effect of hydrostatic or uniaxial stress on elastic const., near martensitic transformation point 8-76697
 γ -Cu₂Al₃, struct. refining from diffr. meas. 8-55834
 Cu₂MnAl, ferromag. Heusler alloy, polarised neutron study of mag. moment density 8-84391
 Cu₂Mn_{0.98}Al_{1.02}, Heusler alloy, hyperfine fields at sp elements, spin echo NMR meas. 8-84496
 DyAl₂, conduction electron spin and orbital polarisation effects 8-80228
 ErAl₂, conduction electron spin and orbital polarisation effects 8-80228
 (ErCo)₂(ErAl₂)_{1-x}, mag. and struct. investigations of intermetallic systems 8-95440
 (Fe,Co)PbAl, metallic glass, viscous flow, alloying effect 8-79793
 Fe-Al, atom-probe field ion microscopy obs. (*French*) 8-86389
 Fe-Al, hardness after nitriding, metallographic, electron microscopic and microprobe anal. 8-51608
 Fe-Al, local ordering, neutron scatt. study 8-64193
 Fe-Al, paramag. props., T_c to 1500K 8-68153
 Fe-Al (0.069 and 0.158 wt.%), internally oxidised, low temp. deform. (*Japanese*) 8-52876
 Fe-Al (12 wt.%) alloy 23 kHz US transducer piezomagnetic props. 8-59240
 Fe-Al (16 wt.%), improvement of certain props. discussion (*Chinese*) 8-84826
 Fe-Al (40 at.%) B₂ type ordered alloy, C migration, resistivity meas. (*French*) 8-52868
 Fe-Al (up to 7.2%), oxidation process 8-85022
 Fe-Al alloy layers, formed by reaction of Fe alloy with molten Al (*Japanese*) 8-72926
 Fe-Al eutectic alloy, duplex crystals, unit cell parameters, appl. of Weissenberg technique 8-67684
 Fe-Al-C, low C, precip. of carbides and cementite after quenching and ageing 8-52814
 Fe-Al-C, mag. permeability disaccommodation 8-88141
 Fe-Al-Cr (10, 5 to 10, wt.%), corrosion by coal char, SEM and X-ray diffr. exam. 8-88573
 Fe-Al-Ni-Co-Cu alloys, Ti alloying and deoxidising addition (*Russian*) 8-80181

aluminium alloys continued

- Fe-Al-Si, bending test, mech. props. under high press. and temp. (*Japanese*) 8-76711
 Fe-C-Al system, liq.-solid equil. at high press., influence of graphitising elements (*Russian*) 8-56613
 Fe-Cr-Al, attenuation and vel. of acoustic shock waves, amplitude depend. 8-63810
 Fe-Cr-Al, elec. heating alloy, effect of rare earth additives on quality (*Chinese*) 8-84825
 Fe-Cr-Al (14, 0.1 to 2 wt.%), oxidation at high temps. (*Japanese*) 8-60872
 Fe-Cr-Al alloys, low temp. sp. ht., resistivity and coercive force 8-63866
 Fe-Cr-Al-Y ($Y-Al_2O_3$)(Y_2O_3), preparation and exam. of mech. props. 8-52720
 Fe-Cr-Co-Al (27.5, 17.5, 0.5) alloy, magnetic props. and microstructure 8-72367
 Fe-Cr-Co-Al (27.5, 17.5, 0.5 wt.%) alloy, induced anisotropy 8-76239
 Fe-Ni-Al, correlation of microscopic features, with macroscopic crack propagation 8-60800
 Fe-Ni-Al alloys, phase diagram, miscibility gap, DTA meas. 8-92237
 Fe-Ni-Al-Ti, N27Yu2T2, aged austenite, diffuse electron scatt. distrib. during martensitic deform. (*Russian*) 8-60669
 Fe-Ni-Cr-Mn-Al-Ti Incoloy 800, exam. of scale morphology, alloying element distrib. after oxidation 8-80677
 Fe-Si-Al (6.4 wt.%), Sendust alloy, effect of Ni content on mag. props. 8-72897
 FeAl B2 struct., band struct. and density of states, KKR calc. 8-63969
 FeAl, bonding, self-consistent energy bands 8-91610
 FeAl, isomer shift, electronic charge density 8-80264
 FeAl, positron localisation in metallic alloys 8-79962
 Fe₃Al, magnetic form factor 8-76222
 Fe₃Al, ordered alloys, atomic order parameters from topology of electron-microscope diff. contrast from antiphase boundaries, quantitative determ. 8-95016
 Fe₃Al, partly disordered B2 struct., spin wave dispersion relation 8-64201
 Fe₃Al, slip geometry and pseudoelastic behaviour, effect of crystal orientation (*French*) 8-87681
 Fe₄₉Al_{50.3}, Compton scatt., 59.54 keV γ -rays, charge transfer study 8-68578
 (Fe_{0.5}Ni_{0.5})₃P₁₆B₆Al₃ glass, struct. relax. as origin of Curie temp. ageing 8-84418
 (Fe_{1-x}Ni_x)₇₅P₁₆B₆Al₃, amorphous alloy, low temp. elec. resist. saturation 8-68005
 Ga-Al, effect of Al on solidification kinetics, and morphology of Ga 8-56628
 Ga-Al alloys, solubility of GaAs, in multilayer LPE of Ga_xAl_{1-x}As 8-52690
 Gd-Al, amorphous alloy, mag. coupling 8-88108
 Gd-Al, amorphous alloy films, mag. phase diagram, spin glass and ferromag. regions 8-68234
 Gd-Al, amorphous film, microwave mag. reson. 8-91948
 Gd_{0.9}La_{0.1}Al₂, ferromag., NMR of ¹³⁹La 8-52377
 GdMn₂-GdAl₃, intermetallics, mag. props., 80-650K 8-60282
 (GdMn₂)₁(GdAl₃)_{1-x}, mag. and struct. investigations of intermetallic systems 8-95440
 Ge-Al film, amorphous, EPR meas. 8-80212
 Ge-Al film, elec. resist. and IR transmission, comp. and substrate temp. depend. 8-52112
 HoAl₂, heat capacity, 1.5-12K, magnetocryst. anisotropy effects 8-68236
 HoAl₂, magnetoelastic effects on elastic consts., 4.2-280K 8-72385
 (La,Ce)Al₂, conf. Kondo system, sp. ht. meas. 8-52210
 (La,Gd)Al₂, mag. props. 8-52299
 LaAl₂, cryst. field splitting and spin-spin interaction of Eu²⁺ and Gd³⁺, ESR meas. 8-68370
 LaAl₂:Gd³⁺(Eu²⁺), cryst. field parameters, relax. rates 8-84482
 LaAl₃-Ce, dil., linewidth of cryst. field excitations 8-67988
 (La_{1-x}Gd_x)Al₂, dil., reverse resistance anomaly 8-76054
 La_{1-x}Tb_xAl₂, supercond., 0.6 meV cryst. field transitions, neutron spectroscopy 8-67991
 LiAl, semimetallic, B32 struct., electronic props. 8-56062
 Mg-Al-Ti(Pb) systems, phase diag., electrode pots. (*Russian*) 8-80516
 Mn-Al, vacuum codeposited, disorder of MnAl₆ phase in recovery process 8-51854
 Mn-Al alloys, permanent magnet material development 8-91895
 Mn-Al permanent magnets, defect structure, mag. props. TEM obs. 8-91902
 Mn-Cu-Al alloy under torsion, anomalous elasticity and transformation plasticity obs. (*Russian*) 8-75834
 Mn₅₅Al₄₅ alloy, permanent mag. props., depend. on particle size 8-91899
 Mo fibre reinforced, SEM study (*Slovenian*) 8-84923
 Mo fibre reinforced AlMg, SEM study (*Slovenian*) 8-84923
 Nb-Al-Si, supercond. transition temp., Si conc. depend. 8-84339
 Nb₃Al, anomalous resistivity, insight from band theory 8-60106
 Nb₃Al, BCC struct., cold working and converting to A-15 struct. 8-64553
 Nb₃Al, metallic bonding, electronic states calcs. 8-79916
 Nb₃Al, multifilamentary wires, supercond. props. 8-64175
 Nb₃Al, neutron irradiated, A15 compound, recovery of T_c by annealing 8-52132
 Nb₃Al, quantum interference and Josephson effect (*Russian*) 8-56259
 Nb₃Al, quasi-one-dimensional supercond., giant enhancement of nucl. relax. rate near T_c 8-56257
 Nb₃Al, supercond. transition temp., rel. to A15 phase stability 8-52137
 Nb₃Al, ZZ 8-91613
 Nb₃(AlSi), ternary supercond. alloy films, T_c props. (*Russian*) 8-88055
 Nb₃Al_{0.2}Si_{0.8}, A-15 alloy synthesis by on implantation 8-80489
 NdAl₂, conduction electron spin and orbital polarisation effects 8-80228
 Ni superalloy Mar-M200, slow fatigue crack propagation rate meas. using high freq. resonant technique 8-52983
 Ni-Al, CC Ni-Al (42 at.%), Al₂O₃ growth, morphology and spalling model 8-53030

aluminium alloys continued

- Ni-Al, effect of solute misfit and temp. on irradiation induced segregation 8-72779
 Ni-Al (51 to 55 at.%), vacancy defective, TEM exam. of structure 8-76677
 Ni-Al solid solns., N₂⁺ irradi., void ordering 8-79644
 Ni-Al-Cr, precipitation-strengthened, mechanical props. 8-84968
 Ni-Al-Cr-Co-Ti, Waspaloy, exam. of dislocation-precipitate interaction, cyclic stress-strain behaviour 8-84925
 Ni-Al-Ti, eutectic alloy charact. by melting temp., composition and oxidation resistance 8-52771
 Ni-Al-Ti, soln. temp. of hardening intermetallic phase in heat resistant alloys 8-52865
 Ni-Co-Cr-Mo-Ti-Al Nimonic 105, loading frequency and environmental effects on high temp. fatigue crack growth 8-64675
 Ni-Co-Cr-Ta-Al-W-Mo-Ti, cast, phase volume fraction determ. using manual point count practice 8-53052
 Ni-Cr-Al (15, 5 wt.%), oxide dispersion strengthened, effect of dispersoids on oxidation 8-80679
 Ni-Cr-Al-Ti (Ti-Co), exam. of back stress role in creep behaviour of particle strengthened alloys 8-52889
 Ni-Cr-Co-Al-Ti-W-Ta-Mo, IN 738 LC, loading frequency and environmental effects on high temp. fatigue crack growth 8-64675
 Ni-Cr-Co-Mo-Al-Ti alloys, Waspaloy, Astroloy, exam. of microstruct. effect on crack growth 8-52977
 Ni-Cr-Nb-Al eutectic alloys, sulphidation/oxidation at high temps., corrosion mechanism 8-2934
 Ni-Cr-Ti-Al-Fe-Co (19.65, 2.40, 1.37, 0.78, 0.52 wt.%), strength of γ' hardened alloy, ageing exam. 8-88501
 Ni-Cr-Ti-Al-Mo-Nb-Fe (13-16, 2.35-2.75, 1.3-1.7, 2.8-3.2, 1.8-2.2, 2.0 wt.%), heat resistant props, mech props. struct., stepwise ageing effects (*Russian*) 8-76666
 Ni-Fe-Nb-Al, mag. props. and struct. (*Chinese*) 8-84450
 Ni-Ni₃Al-Ni₃Nb, directionally solidified, role of twinning in cyclic stress strain behaviour 8-80605
 Ni₃ (Al,Ti), flow stress and work hardening, exam. of temp. depend. by tensile tests 8-84839
 NiAl, bonding, self-consistent energy bands 8-91610
 NiAl, oxidation, effect of gaseous NaCl 8-95853
 NiAl precipitation hardening of medium C steel, fatigue behaviour 8-84983
 β' -NiAl, self-consistent embedded-cluster model for mag. impurities 8-67973
 NiAl-Cr eutectic alloy, directional solidification singularities (*Russian*) 8-68678
 Ni₃Al, dissociation of superdislocations and plastic deform. mech. (*Russian*) 8-52909
 Ni₃Al, ductility in poly- and single crystals, compressive and tensile tests 8-56715
 Ni₃Al, Mossbauer spectra, exam. of struct., superlattice population anal. 8-88240
 NiCr-AlY sintered fibre metal struct. abradable seal material, friction and wear 8-56785
 NiCr-MoAl-ThO₂ (13.3 wt.%), powder, mech. alloying 8-84744
 NIPBAI, metallic glass, viscous flow, alloying effect 8-79793
 Pd-Al alloys, Fermi level position rel. to mixing behaviour, Al activity, thermodynamic props. (*German*) 8-75835
 Pr-Cu-Al system, X-ray and microscopic anal. (*Ukrainian*) 8-84774
 Si-Al, composite, simulation of tensile behaviour and fracture void initiation (*Japanese*) 8-52948
 Si-Al electrical steel, surface oxidation during annealing 8-68838
 Sm₂(Co_{1-x}Al_x)₁₇ (*Russian*) 8-64202
 TbAl₂, conduction electron spin and orbital polarisation effects 8-80228
 Tb,Gd_{1-x}Al₂, magnetic anisotropy, magnetostriction 8-56364
 Ti alloy VT3-1, large forgings, heat treatment, struct. and mech. props. 8-52864
 α - β Ti alloy VT9, influence of phase comp. on fracture (*Russian*) 8-56665
 Ti-Al, VT5-1, strength variation under influence of shock waves (*Russian*) 8-92299
 Ti-Al (6.1 wt.%), hot rolled sheet, ductile fracture nuclei, SEM obs. 8-64654
 Ti-Al-Cr-Mo-Fe(V)(Zr), effect of structure and heat treatment on tensile strength, ductility, fatigue limit and notch sensitivity 8-56711
 Ti-Al-Mo-Cr (4.5, 5, 1.5 wt.%), CORONA-5, effect of microstructure and heat treatment on fracture 8-60805
 Ti-Al-Mo-Zr (Cr-Fe), effect of heating on thermal stability of phases, lattice constants and chem. comp. 8-56672
 Ti-Al-Sn (5, 2.5 wt.%), ductile fracture at low temps. 8-64659
 Ti-Al-Sn (5, 2.5 wt.%), electron microscope and X-ray diff. exam., of basal and near basal hydrides 8-80550
 Ti-Al-Sn (5, 2.5 wt.%), fracture mechanism at cryogenic temps. 8-64642
 Ti-Al-Sn-Zr-Mo (6.2, 4.5 wt.%), surface cracking under unidirectional loading 8-56753
 Ti-Al-Sn(V)(V-Cr)(Mo-V), electrochemical behaviour under tensile stress in boiling H₂SO₄ and acidic chloride solns. 8-95851
 Ti-Al-V, oxidation by water vapour (*French*) 8-76787
 Ti-Al-V (Mo-Sn)(Zr), environmental effects in alloy fretting, effect on fatigue props. 8-56787
 Ti-Al-V (6, 4, wt.%), delayed retardation phenomena of fatigue crack growth, exam. 8-56745
 Ti-Al-V (6, 4 wt.%), fatigue crack propag. under dwell time conditions 8-80639
 Ti-Al-V (6, 4 wt.%), void formation and growth, tensile fracture, exam. 8-80637
 Ti-Al-V (6, 4 wt.%) effect of high temp. oxidation on eddy current conductivity 8-76770
 Ti-Al-V (6.4 wt.%), fretting fatigue resistant coating, for steel/Ti-Al-V mating surfaces 8-64721
 Ti-Al-V (6.4 wt.%), strongly textured, influence of cryst. orientation on fracture toughness 8-84951
 Ti-Al-V (6.4 wt.%), surface cracking under unidirectional loading 8-56753
 Ti-Al-V (6.4 wt.%), surgical implant ion beam textured, stress/strain relations, fatigue characts. 8-73297
 Ti-Al-V alloy, thermophysical meas. above 1450K, using subsecond transient technique 8-95161
 Ti-Al-V-(Sn), SCC, subcritical flow, growth, comparison of aircraft alloys in NaCl soln. 8-53028

aluminium alloys continued

- Ti-Al-Zr (6.5 wt.%), alloy IMI 685, SEM exam. of crack growth 8-72849
 α -Ti-Al-Zr (6.16, 5.23 wt.%), alloy IMI 685, electron microscope observations of strain induced hydrides 8-72828
 α -Ti-Al-(Zr), embrittlement due to ageing 8-56673
 Ti-Cu-Al, heat treatable alloys, effect of alloying on strength, tensile props. 8-56671
 β -Ti-Mo-V-Fe-Al (8, 8, 2, 3, wt.%), exam. of stress induced H_2 migration 8-87823
 β -Ti-Mo-V-Fe-Al (8,8,2,3 wt.%), metastable alloy, microstruct. and mech. props. ageing time and temp. effect 8-64569
 $Ti_{0.75}Al_{0.25}H_x$, $x \approx 1.5$, metastable hydride form. 8-51682
 U-Cr-Al (0.2, 0.1 at.%) fuel elements with high swelling resistance for KS-ISO reactor 8-78471
 UAl₃-UNi₂, phase relationships, thermal, microscopic and X-ray exam. (German) 8-88447
 UAl₃+2Al→UAl₄, effect on Young's modulus and rupture strength in dispersion reactor fuel (German) 8-62596
 V-Al/Cu-Ge composite tape, transition temp., upper crit. field. 8-68126
 V₃Al, ZZ 8-91613
 YAl₃, de Haas-van Alphen effect 8-91590
 YbAl₃, Mossbauer effect obs. of induced hyperfine field 8-52396
 YbCuAl, mixed valence behaviour, mag. props. 8-68150
 Yb₂Sc_{1-x}Al₃, valence fluctuation system, suscept. meas. 8-68149
 Zn-Al (0.4 wt.%), grain size effect on acoustic emission generated during plastic deformation 8-80609
 Zn-Al (22 wt.%), meas. of plasticity parameters under superplastic flow 8-60710
 Zn-Al (22 wt.%), superplastic deform. rate rel. to flow stress, determ. methods 8-60709
 Zn-Al (22 wt.%), superplastic, eutectoid alloy, ductility and fracture 8-60819
 Zn-Al alloys, dislocations obs. in superplastic deformation 8-51549
 Zr-Al (8.6 wt.%), effect of fast neutron irradiation on irradiation growth of Zr₃Al 8-55896
 Zr-Al getter pumping in beam driven Tokamaks 8-50401
 Zr-Al martensite, DO₁₉ phase formation, selected area diff. obs. 8-84779
 Zr-Al (8.6 wt.%), mech. props., corrosion and fast neutron irradiation influence 8-84948
 β -Zr-Mo-Al-(La), metastable, deform. induced transform. 8-52805
 Zr-Zr₂Al₃, diffusion weldings between 1000 and 1300°C, electron microprobe anal. (German) 8-84011
 Zr₃Al, disordering by 1 MeV electron irradiation 8-51583
 Zr₃Al, ordered, exam. of Young's modulus and thermal expansion coeff. 8-72805
 Zr₃Al, ordered, strengthening by fast neutron irradiation 8-84838
 Zr₃Al, ordered polycrystals, ductile fracture 8-64641
 Zr(Al_{1-x}Co_x)₂, Laves phase, H_2 absorption capacity meas. 8-87866
 Zr(Al_{1-x}Fe_x)₂, Laves phase, H_2 absorption capacity meas. 8-87866

aluminium compounds

see also alumina; aluminium alloys

- anodic films, influence of substrate orientation 8-88581
 chloroaluminium phthalocyanine, sublimed layer, IR absorption, vibr. assignments 8-55174
 GaAs-Ga_{1-x}Al_xAs, ultrathin layer heterostruct., pseudopot. calcs. 8-95343
 gadolinium aluminium sulphate hexahydrate, ESR of V³⁺, 21.5 GHz, 4.2K 8-91942
 methylammonium aluminium sulphate, third order elastic consts. from stress shifted reson. freqs. 8-55905
 oxide film, anodic, colloidal metal, origin of colour, optical props. meas. 8-68571
 rare earth halide-Al halide system, potential R ion laser, spectroscopic props. 8-66812
 (Al,Ga)As DH injection lasers, internal quantum efficiency, algorithm for meas. 8-66822
 (Al,Ga)As long-lived DH injection lasers for fibre optic communication, degradation exam. 8-50778
 (Al,Ga)As/GaAs, LPE grown heterostructures, X-ray diff. exam. of interfacial elastic strains 8-72019
 (Al,Ga)As-GaAs laser, transverse junction stripe, high temp. single mode CW operation 8-74918
 Al-AlN-Au, voltage controlled negative resist., O₂ press. effect 8-72281
 Al-Ga-As heterostruct. with confined current flow, fabrication 8-68081
 Al-H₂O, mol. complex, electronic struct. calcs. 8-66465
 AlAs epilayers, MBE growth on GaAs, self-terminating thermal oxidation 8-92374
 AlAs-GaAs (100) interface, tight binding calc. of electronic struct. 8-95342
 AlAs-GaAs (110) interface, self-consistent calc. of interface states and electronic struct. 8-52066
 AlAs-GaAs abrupt (110) interface, electronic struct. 8-95339
 AlAs-GaAs heterojunctions, on graphite substrate, props., solar cell appls. 8-91760
 AlAs-GaAs monolayer crystal, two-photon absorpt. spectrum 8-52589
 AlCl₃, force and compliance consts., OVFF, UBFF and GVFF models 8-50663
 AlCl₃, soln., IR spectra 8-74649
 AlCl₃-alkali chloride, molten mixture, vap. pres. meas. 8-87779
 AlCl₃-TbCl₃, vap., high-energy laser medium props., for fusion ignition 8-63075
 AlCl₃, distortion from T_d symm. 8-63706
 AlF, hyperfine structure simulated by computer programme 8-50538
 AlF₆³⁻, octahedral complex, ionis. energy, SCF-X α study 8-70967
 AlFeF₃·7H₂O, Mossbauer spectra, thermal decomp. products 8-80258
 AlGaAs CW oxide defined stripe laser, optical feedback effects 8-79045
 AlGaAs constricted DH diodes, stable single filament laser action obs. 8-55358
 (AlGa)As DH laser, insulating C film deposition to prevent facet deterioration 8-87049
 (AlGa)As, transverse junction stripe single mode oscillating laser, gain spectra 8-55356
 AlGaAs-GaAs, double heterostructure, optically induced dislocation glide, cooperative phenomena 8-74911
 AlGaAs-GaAs DH laser, carrier leakage, physical mechanisms 8-66824
 AlGaAs-GaAs DH lasers, accelerated life test 8-66830
 Al_{0.3}Ga_{0.7}As:Te(SN), impurity effects on interface morphology of LPE films on corrugated GaAs substrates 8-88435
 Al_{0.5}Ga_{0.5}As, first order phonon spectrum replicas 8-60467
 Al_{0.5}Ga_{0.5}As:O insulator layers on GaAs, meas. of MIS capacitors 8-95371
 Al_{1-x}Ga_xAs laser, transverse junction stripe, with low threshold current and high efficiency 8-82985
 Al_{1-x}Ga_xAs, transient-mode LPE on GaP 8-72746
 Al_{1-x}Ga_xAs, analytic approx. for Fermi energy 8-63973
 Al_{1-x}Ga_xAs DH p-n junction, surface recomb. effects on current, luminesc. expts. 8-72246
 n-Al_{1-x}Ga_xAs, epitaxial, photolum. emission and excitation spectra 8-76526
 Al_{1-x}Ga_xAs heterojunction LED, fabrication by negative profiling of substrate and characts. 8-56523
 Al_{1-x}Ga_xAs, LPE, cathodoluminesc. obs. 8-68565
 Al_{1-x}Ga_xAs layer, LPE, graded band gap solar cell, composition profile, Rutherford backscatt. 8-76612
 Al_{1-x}Ga_xAs native oxide, low leakage, MOS characterisation 8-91795
 Al_{1-x}Ga_xAs, p-n homojunction, hot carrier recomb., overheating luminesc. 8-92122
 Al_{1-x}Ga_xAs p-n junction, photolum. and current, interface recomb. effects 8-95346
 Al_{1-x}Ga_xAs, Raman spectroscopy, characterisation of thin films and heterostructures 8-76439
 Al_{1-x}Ga_xAs:Cr, high resist. film, photolum. and photocond. meas. 8-72596
 Al_{1-x}Ga_xAs:O, appl. as insulating layer in MIS struct. 8-64115
 Al_{1-x}Ga_xAs-GaAs heterojunction photodiodes, high-efficiency fast-response 8-52073
 Al_{1-x}Ga_xAs-GaAs multilayer heterostructures, optical birefringence 8-64422
 Al_{1-x}Ga_xAs-GaAs n-n heterojunction, LPE, Auger profiling and absence of rectification 8-95349
 Al_{1-x}Ga_xAs-GaAs-Al_{1-x}Ga_{1-x}As photopumped quantum-well laser, room temp. CW operation 8-74908
 AlGaAsP/GaAs heterojunction, X-ray characterisation of defects 8-95239
 Al_{1-x}Ga_{1-x}As_{1-x}Sb_xGa_{1-x}Sb_x buried heterojunction electroabsorption modulation 8-55439
 Al_{1-x}Ga_{1-x}In_xAs, LPE on InP, solid-liq. equilib. calcs. 8-84083
 Al_{1-x}Ga_{1-x}P, IR phonons, lattice reflection spectra 8-51626
 Al_{1-x}Ge_{1-x}Sb, photolum. spectra 8-95602
 AlH, SCF pot. curves, 0.1-10 Bohr, ground and excited states 8-58610
 AlH⁺, SCF pot. curves, 0.1-10 Bohr, ground and excited states 8-58610
 AlH₃, effect of 1 MeV Co⁶⁰ γ -irrad. on isothermal decomp. 8-92472
 AlH₃, photoelectric effect spectra and kinetics, photochem. mechanism colour centres 8-56506
 AlH₃, photographic processes, thermo- and electrochemical transformations 8-89576
 AlH₃, photolytic decomp. using high-intensity UV light 8-92472
 AlI, electronic spectrum, Franck-Condon factors, r-centroids 8-62817
 AlI₃, molten, electrical cond., press. effect, 0-1 kbar 8-55963
 Al_{1-x}In_xSb, DC sputtering and struct. 8-52674
 AlN, VPE by closed space vapour process, and optical absorpt. edge 8-88371
 AlN, wetting by Ni alloys 8-80710
 AlN-Al₂O₃ powders, hot pressing, crystalline phase obs. 8-95720
 AlN-SiC, solid solns. series rel. to new materials in Si-C-Al-O-N system 8-95159
 Al₂N₃, dispersion in transformer steel for cubic texture formation (Russian) 8-80557
 AlNbO₄, diffuse refl. and luminesc. spectra 8-56516
 Al₂Nb₂O₇, new phase of mixed oxide 8-59787
 AlO, A-X transition, Franck-Condon factors computation, iterative method compared with Langer's method 8-86762
 AlO, D² Σ -X² Σ , Franck-Condon factors and V-centroids (Russian) 8-74642
 AlO stellar IR bands rel. to Mira phenomena 8-69801
 Al(OH)₃, unit cell, determinantal eqns. for scale factor, temp. factors, quantitative chem. contents 8-75609
 Al(OH)₃Cl_{3-x} soln., IR spectra 8-74649
 Al₂O₃(H₂O)₃, gibbsite, synthetic, crystallinity and topotactic reactions, X-ray diff. obs. 8-63851
 Al₂(OH)₄(SO₄)₇H₂O, aluminite, cryst. struct. determ. and refined 8-83782
 Al₂O₃N₂, spinel, crystal struct. model 8-91333
 γ -AlOOD, boehmite, hydrogen bond, neutron profile refinement of struct. 8-71701
 AlP(As)(Sb), avalanche breakdown voltage for p-n junction, calc. 8-88020
 α -AlPO₄, berlinite, SAW props. 8-79871
 AlPO₄, berlinite, temperature-compensated cuts for SAW devices 8-60018
 AlPO₄ hydrothermal synthesis 8-60562
 AlPO₄, vibr. normal modes, rel. to α -quartz phonon dispersion curve 8-75750
 Al₂(SO₄)₃ soln., adiabatic and apparent molal compressibility determ. from US vel. meas. 8-63797
 AlSb (110), wave functions and surface struct. 8-91519
 Al₂SiO₅, EPR of Fe³⁺ at V-band and the pair spectra 8-80204
 Al_{0.23}Te_{0.77}, amorphous semicond., radial distrib. anal. by X-ray diff. 8-71678
 Ca₂(Si,Al)₁₂(O,N)₁₆, α' -Sialon ceramics, prep. and characterisation 8-84750
 CsAl(SO₄)₂·12H₂O, third order elastic consts. from stress shifted reson. freqs. 8-55905
 CsAl(SO₄)₂·12H₂O:Cr³⁺, ESR spectra 8-91944
 (Fe_{1-x}³⁺Al_x³⁺)₂O₇²⁻, γ to α transform. elec. cond. study, oxidation initial stage kinetics, lacunar spinel form. 8-92384
 Fe_{2.6-x}Ti_{0.4x}Al_xO₆, Fe_{2.4-x}Ti_{0.6x}Al_xO₄, titanomagnetite, monodomain, mag. props. 8-56346
 Ga_{1-x}Al_xAs, metal-gap channel waveguides, intensity modulation 8-66899
 GaAlAs, DH CW diode laser, picosecond pulse generation 8-83002

aluminium compounds continued

- (GaAl)As DH laser, low-current, proton-bombarded, design and characts. 8-87059
GaAlAs DH laser diode, deep level associated with slow degradation 8-87050
(GaAl)As, DH lasers, degradation mechanisms, temp. depend. 8-66825
(GaAl)As high performance diode laser, high-reflectivity cavity mirrors 8-82994
(GaAl)As injection lasers, self-pulsations, Q-switching and mode-locking effects 8-66827
(GaAl)As lasers, low threshold proton isolated, spectral and transient response 8-87052
GaAlAs novel DH lasers fabrication 8-50803
GaAlAs-GaAs double heterostructure, interfacial recomb. velocity, photolum. meas. 8-68075
GaAlAs-GaAs epitaxial heterostructures for integrated optics functional elements 8-50948
Ga_{0.5}Al_{0.5}As-GaAs, DH, interfacial recomb., photolum. time decay meas. 8-95347
Ga_{1-x}Al_xAs DH injection laser diode, long-term-degraded, TEM obs. 8-71102
Ga_{1-x}Al_xAs-GaAs DH lasers, very low threshold, grown by metalorganic CVD 8-55365
Ga_{1-x}Al_xAs, channelled substrate, planar struct. and DFB lasers 8-79032
Ga_{1-x}Al_xAs LPE layers, diffusion limited growth, thickness comparison with GaAs 8-87892
Ga_{1-x}Al_xAs p-i-n structure photoelectric props. 8-95353
Ga_{1-x}Al_xAs Schottky barrier, oxide free, surface composition and fabrication 8-68084
Ga_{1-x}Al_xAs, VPE, on-time comp. depend. 8-67915
Ga_{1-x}Al_xAs-GaAs injection laser, branching waveguide coupler fabrication by LPE 8-63202
Ga_{1-x}Al_xAs-GaAs laser, distributed Bragg confinement, room temp. operation 8-74907
Ga_xAl_{1-x}As embedded stripe DH laser monolithically integrated with strip waveguide 8-59025
Ga_xAl_{1-x}As, LPE, GaAs solubility in Ga-Al alloys investig. 8-52690
Ga_xAl_{1-x}As-GaAs DH laser, continuous room temp. operation 8-55363
Ga_{1-x}Al_xAs_{1-y}P_y-GaAs quaternary heterojunction, misfit dislocation charact. by synchrotron radiation white beam topography 8-63771
Ga_{1-x}Al_xP, two-phonon optical absorpt. 8-88341
Ga_{1-x}Al_xSb p-n homojunction LPE and photovoltaic effect obs. (French) 8-64108
Ga_{1-x}Al_xSb p-n structure, variable-gap, electroluminescence 8-52582
Ga_{1-x}Al_xSb, small wave vector modes 8-75785
n-Ga_{1-x}Al_xSb, transport phenomena in low and high mag. fields 8-80007
GaAs-(Ga,Al)As heterostructure transmission photocathodes, characts. and epitaxial growth (French, English) 8-52616
GaAs-(Ga,Al)As light modulators and distributed Bragg reflector laser, monolithic integration 8-50944
GaAs-(GaAl)As epitaxial layers and DH lasers, deep centre 1.02 eV luminesc. 8-80387
GaAs-Al_{1-x}Ga_xAs lar, PbO-SiO₂ glass optical coating 8-71113
GaAs-Al_{1-x}Ga_xAs, optically pumped taper coupled laser, second order Bragg reflector 8-50788
GaAs-Al_{1-x}Ga_xAs, DH laser, effect of bulk nonradiative recombination 8-82967
GaAs-Al_{1-x}Ga_xAs DH laser structures, high-resolution composition profiling with photolum. 8-71101
GaAs-Al_{1-x}Ga_xAs DH laser, room temp. threshold current 8-79019
GaAs-Al_{1-x}Ga_xAs stripe geometry DH laser, threshold current density, effect of optical mode losses 8-59008
GaAs-Al_{1-x}Ga_xAs superlattice, mag. field induced dimensionality change 8-64381
GaAs-AlAs, pseudobinary alloy, phase diagram calc. 8-52786
GaAs-AlAs alternating monolayers, zone folding effects on phonons 8-72510
GaAs-AlAs and related monolayer heterostructures, pseudopot. calc. 8-60198
GaAs-AlAs layered superlattices, deposited by MBE, exam. of crystal growth kinetics 8-72739
GaAs-AlGaAs DH laser with buried facet 8-55373
GaAs-AlGaAs transverse junction stripe laser, single mode behaviour after 12000 hr ageing test 8-66831
GaAs-Ga_{1-x}Al_xAs, superlattice umklapp processes in resonant Raman scattering 8-64362
GaAs-Ga_{1-x}Al_xAs n⁺-v-n junction, avalanche carrier multiplication (Russian) 8-76140
GaAs-Ga_{1-x}Al_xAs superlattice, sub-band dimensionality 8-63981
GaAs-GaAlAs, DH laser material, LPE grown, obs. of melt carryover 8-91553
GaAs-GaAlAs DH LED, transient current trap spectroscopy 8-80049
GaAs-GaAlAs DH laser diode, lateral modes 8-59009
GaAs-GaAlAs injection lasers on semi-insulating substrates using laterally diffused junctions 8-55364
GaAs-GaAlAs LEDs, deep levels (French) 8-56218
KAl(SO₄)₂·12H₂O, third order elastic const. from stress shifted reson. freqs. 8-55905
KAlSiO₄ metastable polymorph, prep. by ion exchange with RbAlSiO₄, struct. 8-79585
KPO₃·Al(PO₃)₃·U, vibronic excitation, absorption and emission spectra 8-52524
K₂SO₄·Al₂(SO₄)₃·24H₂O, stirring effect on crystalline quality of soln. grown crystals 8-91281
LiCl-AlCl₃, phase diagram determ. by DTA and X-ray anal. (Japanese) 8-92250
Li_{0.5}Fe_{2.5}Al_{0.33}O₄·Co, single cryst., domain struct., mag. annealing effect depend. on induced anisotropy 8-68290
LiPO₃·Al(PO₃)₃·U, vibronic excitation, absorption and emission spectra 8-52524
Li_x(Si,Al)₁₂(O,N)₁₆, α'-Sialon ceramics, prep. and characterisation 8-84750
MgAl₂Fe_{2-x}O₄, comp. effects on ferrite characts. 8-52305
MgAl₂O₄, IR spectrum exam. 8-76454
NH₄Al(SO₄)₂·12H₂O, third order elastic const. from stress shifted reson. freqs. 8-55905
Na₈Al₆Ge₆O₂₄·CO₃·2H₂, cryst. struct. 8-83805

aluminium compounds continued

- NaCl-AlCl₃, phase diagram determ. by DTA and X-ray anal. (Japanese) 8-92250
NaCl-AlCl₃-CrCl₃, molten, electrochemical exam. of Cr 8-56939
NaPO₃·Al(PO₃)₃·U, vibronic excitation, absorption and emission spectra 8-52524
Nd-Al-Cl complex, Nd³⁺ vapour phase laser expts. 8-66813
Si-Al-O-N system, TEM exam. of X phase structure 8-56606
Si₂-Al-O-N₂, hot pressed, exam. of fracture mechanisms 8-72879
SiAlON system, β', 15 R phases, oxidation resist. (French) 8-72899
Si₃N₄-AlN-SiO₂-Al₂O₃ solid-liquid equilibria 8-92247
SrAl₂Si₂O₈, TEM obs. of feldspar and hexacelsian polymorphs 8-83827
Tb-Al-Cl vapour complex, fusion laser gain medium 8-63073
TbCl₃(AlCl₃)₂ complex, potential Tb³⁺ vapour laser system, fluoresc. obs. 8-66812
Y₂(Si,Al)₁₂(O,N)₁₆, α'-Sialon ceramics, prep. and characterisation 8-84750
- aluminosilicate glasses**
alkali oxide-Al₂O₃-SiO₂ glass, EPR 8-91930
fibres clad with B₂O₃-SiO₂ effect of drawing tension on residual stresses 8-64554
machinable glass ceramic, elastic moduli, press. and temp. derivatives 8-52873
mullite crystallisation from glass powder, during hot pressing 8-60639
nitrides formed by reduction with C (Japanese) 8-68929
Al₂Mn₃Si₃O₁₂, spin correlations and phase transitions, neutron diffr. exam. 8-84390
Al₂O₃-SiO₂-P₂O₅, refractory glasses, exam. of liquid immiscibility and crystallisation 8-55814
Al₂O₃-Y₂O₃-SiO₂ containing TiO₂, La₂O₃, exam. of elastic moduli and refractive indices 8-80502
CaO-Al₂O₃-SiO₂ glass, remanent magnetisation, log t low 8-68300
CaO-Al₂O₃-SiO₂-ZnO, continuous unidirectional crystn. of fibrous metasilicates from melt 8-95739
CaO-Li₂O-Al₂O₃-SiO₂:Nd³⁺, CaO enriched, laser-type glasses, spectroscopic behaviour 8-60497
CaO-MgO-Al₂O₃-SiO₂-ZnO, continuous unidirectional crystn. of fibrous metasilicates from melt 8-95739
CaO-SiO₂-Al₂O₃, effect of Al₂O₃ on viscosity if ternary aluminosilicates (Japanese) 8-83989
K₂(F,O)-Al₂O₃-B₂O₃-SiO₂, props. 8-63677
K₂O-Al₂O₃-B₂O₃-SiO₂, glass, ESR exam. of paramagnetic centres formed during mech. destruction by grinding 8-88188
K₂O-Al₂O₃-SiO₂ system, crystallisation of glasses in primary phase field of leucite 8-67658
LiAlSiO₄ glass-ceramic, fracture phenomena as function of initial flaw size and temp. 8-95797
LiO₂-Al₂O₃-SiO₂, bonding of Si-O exam. by X-ray emission spectra 8-52594
Li₂O-Al₂O₃-SiO₂, glass ceramic, elastic props. at high press., US meas. 8-83863
Li₂O-Al₂O₃-4SiO₂, glass-ceramic, tensile creep and high temp. fracture 8-52914
LiTaO₃-SiO₂-Al₂O₃, transparency in relation to microstruct. 8-53005
MgO-Al₂O₃-SiO₂, exam. of microstructure and crystallisation kinetics 8-80501
MgO-Al₂O₃-SiO₂, metastable liq. phase separation region, electron microscope exam. 8-88451
MgO-Al₂O₃-SiO₂ glass ceramic, nucleation, effect of electric fields 8-83742
MgO-Al₂O₃-SiO₂ glass, features of crystallisation, in the presence of the thermal decomposition of tetrabutoxytitanium 8-87627
MgO-BaO-Al₂O₃-SiO₂, glass, IR absorpt. spectra and solid struct. exam. 8-88314
MnO-Al₂O₃-SiO₂ glass, spin freezing, muon spin depolarisation, superparamag. domain model 8-68272
MnO-SiO₂-Al₂O₃, effect of Al₂O₃ on viscosity if ternary aluminosilicates (Japanese) 8-83989
Na₂O-Al₂O₃-SiO₂, formation from alkoxides phys. and chem. evolution 8-80503
Na₂O-Al₂O₃-SiO₂ glasses, elec. cond. and cation mobility 8-59973
Na₂O-Al₂O₃-SiO₂-TiO₂, effect of Cr₂O₃, NiO, and MgO additions on crystallisation 8-87626
Na₂O-MgO-Al₂O₃-SiO₂, chemical durability at different pH values 8-72902
Na₂O-SiO₂-Al₂O₃, effect of Al₂O₃ on viscosity if ternary aluminosilicates (Japanese) 8-83989
Nd₂O₃-Al₂O₃-SiO₂ glass, exam. of spectroscopic and luminescent props. 8-88364
PbO-SiO₂-Al₂O₃, effect of Al₂O₃ on viscosity if ternary aluminosilicates (Japanese) 8-83989
PbO-SiO₂-Al₂O₃-(K₂O), corrosion in acid, leaching kinetics 8-92378
SiO₂-Al₂O₃-B₂O₃-Li₂O (Li₂O·Na₂O) (Na₂O) glass exam. of optical props. 8-88277
SiO₂-Al₂O₃-B₂O₃-MgO-CaO-Na₂O, strengthened by ion exchange, exam. of internal stresses using polarising microscope 8-88549
SiO₂-NaO-K₂O-CaO-MgO-Al₂O₃ melt, anodic dissolution of Co and Ni in melt 8-88582
TiO₂-containing slag-glasses, phase separation and glass-ceramic formation 8-51424
ZnO-Al₂O₃-SiO₂, transparent glass-ceramics, EPR obs. of glass crystallisation 8-80507
ZnO-Al₂O₃-SiO₂, transparent glass ceramics, heat treatment effect on microstruct. 8-56667
ZnO-Al₂O₃-SiO₂, transparent glass-ceramic, microstruct., physical props., crystallisation ht. treatment depend. 8-80506

a.m. (modulation) see amplitude modulation

ambient temperature see temperature

americium

see also nuclei with

- Debye-Waller factor, temp. depend., Mossbauer effect meas. 8-83902
ions, electronic props., Dirac-Fock studies 8-60094
movement through food chain 8-61264
radioactive waste, low conc. meas. in earth samples, appl. of Si(Li) X-ray detector 8-58505
²⁴¹Am, biological availability, influence of DTPA at soil-plant and plant-animal interfaces 8-73264

americium continued

²⁴¹Am, conc. in thermonuclear test debris, collected near Bikini Atoll 8-96103

²⁴²Am/²³⁹⁺²⁴⁰Pu activity ratio rel. to global fallout 8-57263

americium compounds

No entries

ammeters

picoammeter for atmospheric measurement of elec. cond. and small ion mobility, pollution aspects 8-92931

servo-controlled balance, absolute ampere determ. 8-82003

ammonia

adsorbed, effect on elec. cond. of amorphous Si:H film 8-88048

adsorbed gas, on glassy AsSe, surface cond., photocond. 8-80038

adsorbed on graphite, struct. and dynamics, neutron diff. and inelastic scatt. 8-87869

adsorption, on Al(Fe), thermal accommodation coeffs., translational (internal) gas-solid energy exchange 8-92506

alkali metal-NH₃ solutions, metal-nonmetal transition Hall mobility, electrodeless meas. 8-56194

atmosphere, aircraft meas. of NH₃ budget contribs. 8-73469

atmosphere, NH₃ ν vibr.-rot. band identification in ground level solar spectra 8-81287

atmospheric pollution detection, high sensitivity, using tunable diode laser 8-57373

chemisorption on clean Fe (100) and (111) surfaces, LEED and thermal desorption 8-71996

compressed gas, electron drift vel., density depend. 8-63534

crystal, rotation mol. motion (*Russian*) 8-87762

depletion in atmosphere of Uranus, theory and obs. 8-53870

dimer, (NH₃)₂, intermol. pot. calc. 8-58764

frosts, Na and K doped, reflectance spectra and implications for Io surface 8-84561

gas, sensing probe, potentiometric, micro-size 8-61071

gas, with variable physical props., pipe flow, turbulent momentum and heat transfer calc. 8-90869

interstellar, obs. in southern H II regions 8-69863

laser, high power, 12.08 μm, optically pumped, for appl. to UF₆ isotope separation 8-74923

laser, two-photon-excited, 16 μm emission, wavelength meas. technique 8-71085

laser lines, far IR, optical pumping by CO₂ laser 8-90415

laser submillimetre with optical pumping energy yield, emission pulse delay time depend. on pumping pulse (*Russian*) 8-71088

LCAO-MO-SCF calcs., analysis of Gaussian basis sets rel. to one-electron props. 8-55122

liquid, localised excess electrons, semicontinuum models 8-73129

molecule, 10.6 μm region absorption lines, diode laser meas. 8-58689

molecule, 9.5 μm region diode laser spectra 8-58688

molecule, and ND₃, new electronic state, multiphoton ionis. obs. 8-74717

molecule, computer controlled CARS spectra of Q branches 8-62241

molecule, Doppler free coherent two-photon transients, collision induced relax. time, meas., Stark switching 8-90249

molecule, electron impact, dissociation cross-sections, fragment obs. 8-62936

molecule, field ionis., critical energy deficits, field depend. 8-82852

molecule, heavy nucleus isotope shift calcs. 8-86917

molecule, IR-microwave double reson., rot. and vibr. relax., inversion layers 8-86902

molecule, laser saturation spectroscopy in time delayed mode 8-86976

molecule, linear response function, diagonal ARPA calcs. 8-74594

molecule, localisability in MO calcs., measured by absolute overlap and 2nd moment dispersions 8-74557

molecule, mol. vibr., G-intensity sum rule 8-74632

molecule, on Pt surface, heterogeneous reaction of decomp., stimulation by CO₂ laser 8-61052

molecule, photosensitisation by Hg, fluoresc. spectrum 8-90198

molecule, pseudospectral dipole oscillator strength distribs. 8-50503

molecule, saturated absorpt. at 888 cm⁻¹ using tunable diode laser 8-94239

molecule, self-assoc., matrix isolation vibr. spectroscopy, complex form. studies 8-62952

molecule, spectral parameters, Lamb dip method investig. 8-89560

molecule, time-resolved four-level double-reson. signal, coherent transients effects 8-78732

molecule, two-photon population inversion, adiabatic rapid passage 8-78763

nitrided steel surface wear-related topography 8-60847

non-metastable absorption at 23.1 GHz, first obs. towards compact H II region W3 (OH) 8-65677

plasma, surface treatment of polyester fabric, effect on surface struct., props. 8-95831

resonantly enhanced four-wave parametric generation of 823 cm⁻¹ radiation 8-63151

sensing probe, potentiometric, micro-size 8-61071

solid, lattice dynamics, atom-atom model of intermol. forces 8-75751

special-purpose frequency standard and clock 8-57913

Stark effect modulation at 2.2 μm (*French*) 8-50912

Stark shift, microwave Σ-transitions in presence of strong elec. fields 8-90213

thermodynamic props., anal. of data tables 8-93636

two photon excited 16 μm laser 8-58986

two-photon pumping, of four-level system, to obtain 12.16 μm radiation for isotope separation 8-90414

viscosity measurements using oscillating disc type viscometer 8-51273

Hg+2NH₃→HgNH₃+NH₃, photosensitised, HgNH₃ complex lifetime 8-53193

HgNH₃ complex, fluoresc., lifetime meas. 8-53193

N₂-NH₃ mixture, viscosity measurements using oscillating disc type viscometer 8-51273

NH₃⁺, ionisation pot. of ²E state, Jahn-Teller effect 8-62948

¹⁴NH₃, J=13, K=13 inversion line displacement as function of pressure (*French*) 8-70815

¹⁵NH₃, two-photon spectroscopy, double resonance studies with a new coincidence 8-70888

NH₃-CO₂ gas mixture, thermal diffusion const. 8-67300

NH₃-H₂O, solar absorption refrigeration system, Seoul, Korea (*Korean*) 8-51052

NH₃+He(Ar), ammonia inversion spectrum press. broadening 8-86915

ammonia continued

NH₃+He(H₂), rot. relax. double and triple reson. obs. 8-66570

NH₃+He(H₂), rot. relax., double and triple reson. obs. 8-90196

NH₃+SO₂, donor-acceptor adduct form., ab initio calcs. 8-82612

NH₃+Xⁿ⁺, (X=Ar,Kr,Xe,U), Auger emission line shape after dissociation 8-86838

NH₃D Stark cell noise reduction for CO₂ laser beam 8-59059

NH₃TNH₃, β decay effect on H-bond, ab initio LCAO SCF MO calc. 8-76894

Na-NH₃ film, vapour deposited, elec. resistivity, metal-nonmetal transition 8-84317

Na-NH₃ solid mixture, cond., three component reactive percolation model 8-68003

TaS₂, intercalated with NH₃, charge transfer, PAC meas. 8-76366

Xe(nf)+NH₃, at. Rydberg state further excitation by rot. transfer, field ionis. obs. 8-58795

ammonia clocks see *atomic clocks***ammonium compounds**

ammonium Rochelle salt, incommensurate phases and ferroelectricity 8-52455

halides, anomalous sound attenuation above lambda point 8-51617

lithium ammonium tartrate monohydrate, spontaneous shear strain, X-ray obs. 8-56433

(NH₄)₂SO₄:Mn²⁺, ferroelec. phonon driven phase transform., reduction of spin Hamiltonian consts. 8-92033

NH₄Cl, PMR free induction decay shape and moments 8-68394

proton spin relax. and phonons in ammonium salts 8-84493

proton spins, relaxation time of dipolar energy 8-76333

Rochelle salt-ammonium Rochelle salt mixed cryst., elastic props., piezoelec. reson. method 8-76390

sodium ammonium tartrate, polarisation, improper ferroelec. transition 8-72477

Tutton's salts, (NH₄)₂M(SO₄)₂·6H₂O, IR spectra, correl. of vibr. freq. and N...O distance for NH₃D⁺ 8-92066

[(NH₄)_{0.16}K_{0.84}]SO₄, reorientational relax. times, quasielastic neutron scatt. obs. 8-55821

ADP-type crystals, electrooptic effect in ultraviolet region 8-76431

Cu(NH₃)₄PtCl₆, Cu(NH₃)₄²⁺ cation mol. orbital parameters 8-64011

Mg₂S₂O₃·(NH₄)₂ S₂O₃-H₂O system, 20°C isotherm (*French*) 8-52506

ND₄Cl, order-disorder transformation, elasticity and heat capacity temp. depend., US obs. 8-71851

ND₄D₂PO₄ type ferroelects., distrib. functions and thermodynamic props. 8-76409

ND₄NO₃, low temp. phase, Raman scatt. meas. 8-84568

(NH₄,Cs)Cl, negative isotope effect on II-III phase transition (*German*) 8-95155

(NH₄,Rb)Cl, negative isotope effect on II-III phase transition (*German*) 8-95155

NH₄⁺, in rain water collected at Jülich, Germany, N isotope comp. 8-57284

NH₄⁺ motion in solids, nucl. spin-lattice relax. exam. 8-56388

NH₄⁺, nuclear quadrupole coupling and mol. deformations 8-90191

NH₄⁺, removal of, using Itaya-zeolite (*Japanese*) 8-95951

NH₄⁺, solvation in water, discrete, continuum and discrete-continuum models 8-73130

NH₄⁺+e, dissociative recomb. reaction in interstellar clouds, products, statistical theory 8-57604

NH₄Ag₂I₃, Raman spectra, internal vibrs. of NH₄⁺ ions 8-72497

NH₄Ag₂I₃, thin film solid state battery 8-76876

NH₄AlCl₆, crystal struct., X-ray, Raman, IR and NMR 8-63720

NH₄Al(SO₄)₂·12H₂O, third order elastic consts. from stress shifted reson. freqs. 8-55905

(NH₄)₂BeF₂, paraelec. phase, cryst. struct. 8-95025

(NH₄)₂BeF₄, improper ferroelec., incommensurate-commensurate transitions 8-60404

(NH₄)₂BeF₄, incommensurate-commensurate phase transition 8-87760

(NH₄)₂BeF₄, powder, IR spectra, assignments, mol. libration, in paraelec. and ferroelec. phases 8-88299

(NH₄)₂BeF₄, unmatched phase, second optical harmonic generation (*Russian*) 8-79073

NH₄Br, aq. soln., IR reflectivity spectra, Kramers-Kronig anal. 8-68500

NH₄Br, birefr. and opt. rot. near structural phase transition points 8-75823

NH₄Br, λ-type phase transition, Brillouin scattering 8-79725

NH₄Br, NMR under high press. 8-84485

NH₄Br, partially disordered, librational modes below 235K, Raman scatt. obs. 8-72500

NH₄Br, partially disordered, librational modes below disorder-order phase transition temp. 8-79680

NH₄Br, phase diagrams, from Raman meas. under high press. 8-52776

NH₄Br, self-polarisation at order-disorder transition 8-52432

NH₄Br, ZZ 8-75792

NH₄Br:Cu²⁺, ESR and absorpt. spectra, 300-1500 nm 8-60492

NH₄Cl, aq. soln., IR reflectivity spectra, Kramers-Kronig anal. 8-68500

NH₄Cl, dispersion of vibrational excitations, Raman scatt. 8-84588

NH₄Cl doped ice microcrystals, activation energy of Debye's dipolar relax., influence of salt content (*French*) 8-56424

NH₄Cl, molar heat capacity near order-disorder transform. under high press. 8-51697

NH₄Cl, NMR under high press. 8-84485

NH₄Cl, obs. of Raman scatt. by Cu vapour laser 8-95586

NH₄Cl, order parameter, electro-optic measurement 8-88280

NH₄Cl, order-disorder transition exam. by optical second harmonic generation 8-51671

NH₄Cl, order-disorder phase transition, type of multicritical point, non-linear quadratic susceptibility 8-83947

NH₄Cl, self-polarisation at order-disorder transition 8-52432

NH₄Cl, ZZ 8-75792

NH₄Cl:Cr³⁺, ESR of Cr³⁺ centres, room temp. 8-91943

NH₄Cl·Br, phonon dispersion 8-75760

NH₄ClO₄, proton spin relax. and phonons 8-84493

NH₄ClO₄, single ion props. by lattice energy minimisation 8-83769

(NH₄)₂Co(SO₄)₂·6H₂O, submillimeter ESR meas., SH³ term of effective spin Hamiltonian 8-64264

(NH₄)₂CrO₄, ZZ 8-88326

(NH₄)₂(Cu(H₂O)₆)(CuSO₄)₄, cryst. struct. determ. by X-ray diff. 8-55839

ammonium compounds continued

- NH_4F , electron distribution and charge transfer in NH_4^+ ion 8-91291
 $\text{NH}_4\text{H}_2\text{AsO}_4\text{-NH}_4\text{H}_2\text{PO}_4$, EPR spectra of central peak fluctuations 8-91932
 $\text{NH}_4\text{H}_2\text{AsO}_4\text{:Cr}^{3+}$, fast and slow dynamic reorientation 8-80306
 $\text{NH}_4\text{H}_2\text{AsO}_4\text{:Cr}^{3+}$, ENDOR spectra 8-88224
 $\text{NH}_4\text{H}_2\text{PO}_4$, cryst., cascade UV generation, by harmonic generation, temp. stabilisation calcs. 8-66868
 $\text{NH}_4\text{H}_2\text{PO}_4$, improper antiferroelec. phase transition, elastic props., free energy, thermodynamic theory 8-80299
 $\text{NH}_4\text{H}_2\text{PO}_4$, ruby SHG, comparison with RbH_2AsO_4 8-50856
 $\text{NH}_4\text{H}_2\text{PO}_4$, surface effects on strength of whiskers and microcrysts. (Russian) 8-51864
 $\text{NH}_4\text{H}_2\text{PO}_4$, tunable coherent radiation generation below 250 nm at MW power levels 8-59080
 $(\text{NH}_4)_2\text{H}_2\text{P}_2\text{O}_7\text{:Cr}^{3+}$, EPR exam. above and below T_c 8-68363
 $(\text{NH}_4)_2\text{Hf}(\text{C}_2\text{O}_4)_2\cdot n\text{H}_2\text{O}$, electric field gradient at metal site, γ -ray perturbed ang. correlation meas. 8-52380
 NH_4I , $(\text{NH}_4)_{0.16}\text{K}_{0.84}\text{I}$ and $(\text{NH}_4)_{0.16}\text{K}_{0.84}\text{Br}$, reorientation motion of NH_4^+ 8-79542
 NH_4I , NMR under high press. 8-84485
 NH_4I , phase diagrams, from Raman meas. under high press. 8-52776
 NH_4I , phase transitions, SHG obs. 8-76398
 NH_4LiSO_4 , ferroelec., PMR line shape and spin-lattice relax. 8-88205
 NH_4LiSO_4 , I-II phase transition in improper ferroelec., hydrostatic press. effects 8-84533
 NH_4LiSO_4 , phase transforms., SHG obs. 8-76398
 $(\text{NH}_4)_2\text{Mg}(\text{S}_2\text{O}_3)_2\cdot 6\text{H}_2\text{O}$, isolation, struct., decomposition (French) 8-52506
 $(\text{NH}_4)_2\text{Mo}_2\text{Cl}_9\cdot \text{H}_2\text{O}$, resonance Raman spectra, $\text{MO}_2\text{Cl}_8^{4-}$ vibrs. 8-64350
 NH_4N_3 , cryst. struct. determ. by neutron diff. 8-79574
 NH_4NO_2 , thermal anal. by energy-dispersive X-ray diff. 8-91440
 NH_4NO_3 , intrinsic electroluminescence obs. 8-80420
 NH_4NO_3 , low temp. phase, Raman scatt. meas. 8-84568
 NH_4NO_3 , Raman spectra of low temp. phases 8-92081
 NH_4NO_3 , soln., Raman spectral studies of NO_3^- motion and interaction 8-92067
 NH_4OCN formation, in interaction of CO, NO and H_2 over Pt, Rh, Ru and Os 8-73082
 NH_4OH , aerosols existence in planetary atms., IR reflectivity spectra, Kramers-Kronig anal. 8-68500
 NH_4OH , IR reflectivity spectra, Kramers-Kronig anal. 8-68500
 $(\text{NH}_4)_2\text{PO}_3\text{F}$, H_2O , X-ray diffraction and Raman spectra struct. determ., external mode temp. depend. (French) 8-52507
 $(\text{NH}_4)_2\text{PuS}_3$, synthesis and cryst. struct. (German) 8-79588
 NH_4ReO_4 , ND_4ReO_4 , Raman spectrum, temp. depend. 8-80335
 $(\text{NH}_4)_2\text{SO}_4$ aerosol production under elevated temp. inversion in Cleveland Country, model 8-81397
 $(\text{NH}_4)_2\text{SO}_4$, Brillouin scatt. from room temp. to -70°C 8-52517
 $(\text{NH}_4)_2\text{SO}_4$, ferroelec., dielec. behaviour and nature of phase transition 8-88262
 $(\text{NH}_4)_2\text{SO}_4$ ferroelectric, X-ray anal. of sub-lattice order parameters 8-92035
 $(\text{NH}_4)_2\text{SO}_4$, ferroelec., ion group reorientation temp. and press. depend., PMR obs. 8-72470
 $(\text{NH}_4)_2\text{SO}_4$, intrinsic electroluminescence obs. 8-80420
 $(\text{NH}_4)_2\text{SO}_4$, reorientational relax. times, quasielastic neutron scatt. obs. 8-55821
 $(\text{NH}_4)_2\text{SO}_4$ rounded particles, Mueller scatt. matrices 8-90366
 $(\text{NH}_4)_2\text{SO}_4$, single crystal growth from aq. soln. (Japanese) 8-92182
 $(\text{NH}_4)_2\text{SO}_4\text{:Cd}^{2+}$, ferroelec. transition, soft mode contrib., EPR obs. 8-72469
 $(\text{NH}_4)_2\text{SO}_4\text{:Cr}^{3+}$, EPR study of ferroelec. phase transition 8-64337
 $(\text{NH}_4)_2\text{Sb}_6\text{M}_{0.5}\text{IVCl}_6$, ($\text{M}^{\text{IV}}=\text{Se}, \text{Te}, \text{Sn}$), ^{121}Sb Mossbauer effect 8-84506
 $(\text{NH}_4)_2\text{SeO}_4\cdot 2\text{NH}_4\text{HSeO}_4$, cryst. struct. 8-71715
 $\text{NaNd}_2\text{C}_4\text{H}_2\text{D}_6\cdot 4\text{D}_2\text{O}$, ferroelec. phase, incommensurate satellite refls. 8-84531
 $\text{NaNH}_4\text{SO}_4\cdot 2\text{H}_2\text{O}$, ferroelec. and thermal props. 8-83968
 $\text{NaNH}_4\text{SeO}_4\cdot 2\text{H}_2\text{O}$, ferroelectric crystal, effect of hydrostatic pressure on phase transition 8-52453
 RbNH_4SO_4 , ferroelec., ion group reorientation temp. and press. depend., PMR obs. 8-72470

amorphisation

- Heisenberg model, amorphisation (Russian) 8-80118
GaAs, amorphous layer formation, ion implantation, IR spectra 8-95063
GaAs, optical modulation spectra, proton damage effect 8-76487
In, amorphization by ion implantation 8-52135
Si, ion-implanted, cryst. to amorphous transform., ESR expts. and composite model 8-59825

amorphous magnetic materials see magnetic properties of amorphous substances**amorphous semiconductors**

- see also chalcogenide glasses; electrical conductivity of amorphous semiconductors and insulators; insulators
anthracene-tetracene amorphous films, host-guest energy transfer 8-60505
band structure and forbidden gap in glasses and amorphous semiconductors, review 8-75987
carrier pulse propagation, macroscopic theory 8-72154
covalent, local struct., bonding and electronic props. 8-51882
electrical conductivity and threshold switching by computer simulation 8-88002
electron-hole recombination, mech. 8-72196
enhanced diffusion mechanisms, review 8-67847
galvanomagnetic phenomena, model, transport phenomena in presence of medium range disorder (French) 8-56162
glass, Anderson model, thermoelectric power 8-84241
II-IV-V₂, solid-state inductance, theory and expt. 8-56138
injected charge drift and localisation in amorphous and organic layers (German) 8-91794
lattice dynamics of disordered or unstable lattices 8-75790
light irradiation, nonequib. electron distrib. function in forbidden gap (Russian) 8-75988
lone-pair, effect of electronegativity difference on defect chemistry 8-72063
phosphate glasses: Cu^{2+} , EPR, optical spectra 8-72399
phosphate glasses: V^{4+} , EPR, optical spectra 8-72399

amorphous semiconductors continued

- photostimulated processes in inorganic materials and optical information storage, review 8-82926
solid-state inductance, theory and expt. 8-56138
sputtered amorphous film heterostructure solar cell and laser fabrication 8-64472
superconductivity feasibility model (Russian) 8-80092
tetrahedral glasses, disorder 8-51423
very far IR properties 8-80344
violanthrene-A film, amorphous and crystalline, carrier mobility differences 8-60125
 $\text{Al}_{0.25}\text{Te}_{0.75}$, amorphous semicond., radial distrib. anal. by X-ray diff. 8-71678
As-Se-Ge, amorphous film, relief-type hologram mode, hologram replication (Japanese) 8-78959
As₂Te₃-GaAs, amorphous-monocrystalline heterojunctions, space charge limited conduction 8-64099
As_{0.3}Te_{0.48}Ge_{0.1}Si_{0.12}, amorphous film, transient switching processes 8-84232
CC NiO, amorphous, charge transport in band tails 8-76026
Cd₃Ge₃As₁₁, band gap, DC cond., elastic consts., and glass transition temp., pressure depend. 8-72064
FeO-P₂O₅ glasses, electrical and mechanical losses 8-80283
Fe₂O₃-B₂O₃-PbO glass, semicond., elec. resist. meas. 8-95300
GaAs, amorphous layer formation, ion implantation, IR spectra 8-95063
Ge, amorphous, EPR expts. 8-88167
Ge, amorphous, far IR absorption 8-88306
Ge, amorphous, thermoelec. power in phonon-assisted hopping regime, Coulomb effects 8-76097
Ge amorphous film, effects of ion implantation on structure 8-55881
Ge, amorphous overlayer on ultrathin Pt film, effect on cond. 8-72284
Ge, electron scattering, inelastic, 70-1400 eV, mean free path 8-84696
Ge film, ^{74}Ge ion implanted, defect struct. obs. 8-51848
Ge, interface structural model between amorphous and crystalline phase 8-63941
Ge:Al(Sb) film, amorphous, ion implantation, effect on cond. 8-83839
Ge:inert gas, ion implantation, UV photoemission exam. 8-80457
Ge:Mn, amorphous, cond. increase by Mn doping 8-72155
Ge:Sb(In), film, electronic props. 8-84330
Ge-Pb_{1-x}Sn_xTe, amorphous/crystalline heterojunction, rectification props., IR detector appl. (Japanese) 8-60197
Ge-S film, amorphous, photo-induced ESR and optical absorption edge shift 8-88374
Ge-Se-Fe films, metallic and semicond., amorphous, mag. and elec. props. 8-52319
H₂WO₃ film, effect of struct. on optical and electrical props. 8-84671
(In, Ga)Sb, sputter deposited amorphous film, impulse stimulated explosive crystallisation 8-84098
MoO₃-P₂O₅ glass, thermoelec. power meas. 8-84242
Pb_{1-x}Sn_xTe-PbTe, amorphous/crystalline heterojunction, rectification props., IR detector appl. (Japanese) 8-60197
SSe, ($x=10, 15, 40$), amorphous crystal transition, appl. of Kolmogorov-Avrami equation 8-67649
Sb electrodeposit, explosive crystn., semicond-semimetal transition and IR absorpt. 8-51849
Sb₂S₃:Ag, sensitised photolysis and structure of latent photographic image 8-89574
Se, amorphous, friction and wear under lightly loaded contact 8-64740
Se amorphous layer structure, influence of vacuum deposition conditions (German) 8-63957
Se, carrier lifetime and drift mobilities 8-87985
Se, crystallisation kinetics correlation with molecular structure 8-94998
Se, film, photodeposition by Selor process struct. 8-75962
Se, film, photodeposition by Selor process, kinetics 8-75963
Se, film, photodeposition by Selor process, struct. and kinetics 8-75964
Se, photoinjection of holes onto triphenylamine doped bisphenol-A-polycarbonate polymer 8-72191
Se, red amorphous film, textural change, thermal and photo effects 8-63951
Se, Se:Te, negative magnetoresist., doping depend. 8-56161
Se, vitreous, mech. props. at temps. <300K, uniaxial compression tests (French) 8-55908
Si, amorphous, dissolution with Al 8-95188
Si, amorphous, EPR expts. 8-88167
Si, amorphous, epitaxial regrowth by pulsed laser beam 8-91554
Si, amorphous, hydrogenated, spin depend. photoluminesc. 8-72589
Si, amorphous, hydrogenated, diffusion of D₂, SIMS anal. 8-75877
Si, amorphous, optically detected ESR obs. 8-84500
Si, amorphous, Si implanted, substrate-orientation depend. of epitaxial regrowth rate 8-79900
Si, amorphous, thermoelec. power in phonon-assisted hopping regime, Coulomb effects 8-76097
Si, amorphous and crystalline, hydrogenation and dehydrogenation 8-51677
Si, amorphous film, epitaxial laser crystallisation 8-84078
Si, amorphous layer, ion-implanted, spatially controlled cryst. regrowth by laser irradiation 8-55810
Si, amorphous thin films, appl. in solar cells, recent developments 8-80016
Si, electron-hole recombination, mech. 8-72196
Si film, amorphous and polycrystallised, localised states, elec. and optical props. 8-64008
Si film, effect of gas exposure on EPR signal 8-84475
Si film, hydrogenated amorphous, Brillouin scatt. 8-72538
Si film, plasma preparation 8-72740
Si film, plasma-deposited, H₂ evolution, mass spectrometry and RHEED obs. 8-72050
Si films, crystallisation kinetics and morphology, TEM obs. 8-84093
Si, glow discharge deposited, photolum. decay 8-72590
Si, heavy ion ranges, He⁺ backscatt. obs. 8-63796
Si, hydrogenated, work function and Auger spectroscopy of initial oxidation 8-76132
Si, interface structural model between amorphous and crystalline phase 8-63941

amorphous semiconductors continued

- Si, phonon spectroscopy, amorphous versus crystalline material 8-83898
 Si, photoconductivity, mag. field depend. 8-80023
 Si, photovoltaic characts., rel. to appl. in solar cells 8-84253
 Si sputtered film, solar energy selective absorber, spectral emissivity 8-83045
 Si, thin film, evaporated amorphous, hydrogenation by plasma treatment 8-91555
 Si whisker, amorphous, meas. of Young's modulus 8-83865
 Si, whisker growth in amorphous state, in SiH_4 -Ar atmosphere, visual obs. 8-84112
 Si:Al(Sb) film, amorphous, ion implantation, effect on cond. 8-83839
 Si:As, melting by high power ns laser pulsing, As diffusion 8-79789
 Si:H, rehydrogenation, photoluminesc. recovery 8-72571
 Si:Mn, amorphous, cond. increase by Mn doping 8-72155
 Si:N, amorphous, DC sputtered, enhanced, photocond. 8-56183
 Si:P(B), film, electronic props. 8-84330
 Si-H, amorphous, energy gap negative-U states, Si-H-Si three centre bond model 8-91606
 Si-H(-D), film, IR and Raman spectra, H bonding effects 8-72515
 $\text{Si}_3\text{C}_{1-x}$, photoluminesc., comp. depend. 8-68541
 SiH_4 polymer film, struct. rel. to amorphous solid 8-72048
 Si_3N_4 , amorphous, charge transport in band tails 8-76026
 $\text{Si}_{12}\text{Te}_{48}\text{As}_{30}\text{Ge}_{10}$, amorphous film, elec. cond. mechanisms, temp. depend. (Japanese) 8-80078
 TiO_2 - SiO_2 , semicond. glass, small polaron hopping cond. 8-60126
 TiO_2 - SiO_2 , semicond. glass, optical props. 8-60412
 V_2O_5 - P_2O_5 glass, thermoelec. power meas. 8-84242
 mV_2O_5 -(100-m) P_2O_5 , (m=100-2), V(IV) complexes conc., absorpn. and ESR spectra 8-64266
 WO_3 - P_2O_5 glass, thermoelec. power meas. 8-84242

amorphous state

- see also electrical conductivity of amorphous metals and alloys; electrical conductivity of amorphous semiconductors and insulators; electron energy states of amorphous solids; magnetic properties of amorphous substances; vitreous state
 alloy, struct. relax., compositional SRO 8-79538
 dielectric ribbon-form material, rapid quenching from melt (Japanese) 8-92210
 film, anomalous scatt. of photoinjected electrons (Russian) 8-52642
 hard sphere model of noncrystalline solids, homogeneous and isotropic appl. to metallic glasses 8-83731
 insulators, noncryst., electron density captured at traps, liberated to conduction band 8-87946
 liquids and amorphous solids, similarity and short range order parameters 8-83730
 magnetic powder, prep. by atomisation technique 8-92213
 metal, electronic density of states 8-51868
 Ni-Co-P, electrical and mag. props. 8-95281
 noncrystalline materials, personal review by Sir Nevill Mott 8-55811
 origin of thermal anomalies, struct. model 8-91256
 PMMA, viscoelastic props., γ -irrad. influence (Russian) 8-88492
 polyalkylene terephthalates, amorphous and cryst., durability under stretching (Russian) 8-88511
 polyethylene, melt crystallized, amorphous phase, IR spectrum 8-76463
 polymer, amorphous, segmental distrib., light-, neutron- and X-ray scatt., piezooptical and dielec. meas., review 8-51444
 polymer, oriented, amorphous-crystalline low ang. X-ray diagrams, supermol. struct. models, schematic representation (Russian) 8-87630
 polymer solutions, conc., Adam-Gibbs theory, for viscoelasticity and glass transition 8-83353
 polymethylpentene, viscoelastic props., γ -irrad. influence (Russian) 8-88492
 quartz, amorphous and crystalline, surface polaritons and splitting of optical frequencies 8-72090
 RHEED patterns from amorphous surface, refr. correction 8-71646
 s-p superconductor, Eliashberg function, phonon spectrum 8-88066
 solid, abnormal bonding and electronic states in forbidden energy gap 8-51942
 structure determination by diffraction methods, philosophical aspects 8-50665
 transition metal binary alloy, amorphous and crystalline, superconducting transition temp. correlation with solute conc. 8-52139
 very far IR props. of amorphous solids 8-80344
 Al_2O_3 amorphous layers in MIS structures, prep. and physical props. (Slovak) 8-64122
 As, amorphous, bonding coordination defects, Raman scatt. and IR absorption meas. 8-60498
 As, amorphous, electron and phonon density of states calcs., comp. to XPS 8-56066
 As, amorphous and cryst., phonon density of states calc., comp. to IR absorpt. and neutron scatt. data 8-55924
 $\text{Au}_{1-x}\text{Si}_x$, amorphous film, spectra 0.01-6.2 eV, $0.13 \leq x \leq 0.5$ 8-68574
 B, struct. changes on Zn incorporation 8-79596
 BaTiO_3 , phonon spectroscopy, amorphous versus crystalline material 8-83898
 C film, growth under ion impact in butane plasma, and IR transparency 8-52688
 C, ranges of implanted 10-30 keV D^+ 8-83858
 $\text{Cr}_{11}\text{Ge}_8$, CrGe , and $\text{Cr}_{11}\text{Ge}_{19}$ films, short-range order, electron diff. obs. (Russian) 8-56050
 Fe, amorphous, realistic structural model, search for Bernal holes 8-83734
 Fe-Si amorphous film, conversion electron Mossbauer effect 8-72440
 Fe-Si amorphous film, Hall const. and magnetoresistive effect 8-52105
 $\text{Fe}_{40}\text{Ni}_{40}\text{B}_{20}$, amorphous alloy, ductile-brittle transition temp., relation to composition 8-52972
 $\text{Fe}_{40}\text{Ni}_{40}\text{P}_{20}$, amorphous alloy, ductile-brittle transition temp., relation to composition 8-52972
 $\text{Fe}_{40}\text{Ni}_{40}\text{P}_{10}\text{B}_{10}$, amorphous alloy, ductile-brittle transition temp., relation to composition 8-52972
 Ge-Ga alloys, amorphous, far IR absorption 8-88306
 $\text{La}_{18}\text{Au}_{22}$, amorphous, evidence for short wavelength cutoff in fluctuation spectrum 8-68113
 MoO_3 , film, colour centre studies, optical absorpt. spectra 8-71724
 $\text{Nb}_{50}\text{Ni}_{50-x}\text{Fe}_x$, mag. interactions 8-95432

amorphous state continued

- Ni, amorphous film, getter sputtered at 25K, resistivity, Curie temp. 8-52673
 Ni-B amorphous alloy film, atomic and electronic transport (French) 8-84325
 Pb microclusters, mol. beam electron diff., amorphous struct. 8-66703
 Pd-Si, amorphous, US velocity, freq. and temp. depend. 8-63812
 $\text{Pd}_{70}\text{Fe}_{10}\text{Si}_{20}$ alloy, amorphous to cryst. transition, 350 to 450°C, Mossbauer spectra 8-59758
 Sb electrodeposit, explosive crystn., semicond-semimetal transition and IR absorpt. 8-51849
 SiO_2 , amorphous, fast-time heat capacity, heat pulse propagation 8-51700
 SiO_2 , amorphous, surface phonon theory 8-84044
 SiO_2 , amorphous and crystalline, surface polaritons and splitting of optical frequencies 8-72090
 SiO_2 , amorphous and cryst., Compton profile study 8-88378
 SiO_2 , phonon spectroscopy, amorphous versus crystalline material 8-83898
 SiO_2 , struct. and chem. bonding 8-51422
 TiO_2 , phonon spectroscopy, amorphous versus crystalline material 8-83898
 V, amorphous film, supercond. props., gaseous impurities effect (Russian) 8-72301
 $\text{Zr}_{40}\text{Cu}_{60-x}\text{M}_x$, (M=Gd, Tb, Fe or Mn), mag. interactions 8-95432
 $\text{Zr}_{73}\text{Rh}_{25}$, amorphous, evidence for short wavelength cutoff in fluctuation spectrum 8-88113
 ZrSiO_4 , mechanochemical effect by mechanical grinding (Japanese) 8-84754

amorphous state structure see noncrystalline state structure**amplification**

see also acoustic wave amplification; amplifiers

- laser beam, saturation parameter from gain meas. 8-66797
 magnetic field amplification during radiation era 8-96577
 optical beam, lateral wave amplification through refl. from active medium 8-78987

amplification measurement see gain measurement**amplifiers**

- see also amplification; d.c. amplifiers; differential amplifiers; fluidic amplifiers; microwave amplifiers; operational amplifiers; power amplifiers; preamplifiers; pulse amplifiers; ring lasers; wideband amplifiers
 blood pressure instruments, direct systolic/diastolic meas., review 8-69234
 current, temp. signals in presence of EM disturbances appl. (German) 8-86267
 degenerate, swept-gain, steady-state pulse behaviour 8-87033
 ECG amplifiers, instruments and maintenance, review 8-69232
 electrolyte electrical conductivity meas., voltage amp. for temp. compensation (German) 8-54399
 high sensitivity, LF operation of millivoltmeters appl. (German) 8-74032
 membrane potentials tracing system, using amplifier for voltage clamping (German) 8-61285
 negative feedback for passive value parameter transducer error correction (Russian) 8-49819
 phase sensitive amplifiers, appl. to interference suppression and light detection (Czech) 8-86331
 sample and hold, for stimulus artifact suppression in bioelectric recordings 8-77163
 voltage, temperature signals in presence of EM disturbances appl. (German) 8-86267
 LiNbO_3 - InSb amplifier production, role of protective films 8-95220

amplifying see amplification**amplitude modulation**

see also pulse amplitude modulation

- far IR spectrometer with interference selective AM 8-86362
 microwave backscatter modulation by shoaling ocean waves 8-57212
 multimode optical fibre phase modulators and discriminators, theory 8-55446
 multimode optical fibre phase modulators and discriminators, expts. 8-55449
 total internal reflection modulator, small glancing angles 8-74987

analogue computer applications see analogue simulation**analogue computer circuits**

- see also function generators; operational amplifiers
 plasma diagnostics, Thomson scatt. system, analogue data processing circuits 8-87488

analogue computer methods see analogue simulation**analogue computers**

- see also analogue-digital conversion; digital-analogue conversion
 optical analogue computer performance advantages 8-78949

analogue digital computers see hybrid computers**analogue-digital conversion**

see also digital-analogue conversion

- 12 kHz IC resistance-frequency converter (Russian) 8-81963
 astronomy, photon counting and analogue TV systems with digital real time image processing 8-96402
 CRO storage, Gould Advance OS4000 using A/D and D/A converters 8-93673
 digital plot system developed for nondestructive materials testing exam. 8-53067
 digital storage instrum. and function generator electronic modelling appls. 8-77937
 digitising error from period and freq. counting techniques 8-61570
 electro-optic A/D conversion using channel waveguide modulators 8-66898
 fusion reactor, diagnostics of radial plasma transport rate, data acquisition and handling system 8-54937
 miniature pressure-frequency converter with pulse output 8-57926
 multichannel, without timing skew, for LF biological signals 8-61271
 multichannel complex for hydrophysical data conversion for computer anal. (Russian) 8-65427
 ophthalmological tissue differentiation, digitisation of HF US signals 8-80935
 optical A/D conversion using single halftone photograph 8-78919
 pulse sequence fast A/D conversion 8-55119
 punched register for astronomical elec. photometer (Russian) 8-93117
 selsyn rotor angle-to-digital code convertor, design (Russian) 8-65915

analogue-digital conversion continued

- SQUID magnetometer, broadband- and higher-power, for small signal A-D convertor 8-62211
- two-phase A/D convertor processes small analogue signals (*German*) 8-61572
- US time-coordinate convertors for distance meas., design aspects (*Russian*) 8-77857
- video image digitiser, interactive, appl. to interferogram anal. 8-58021

analogue-digital convertors *see analogue-digital conversion***analogue simulation**

- aortic dynamics in man, analogue simulation model 8-80903
- effective annealing time determ. 8-88475
- heat conduction, inverse nonlinear problems, simulation methods 8-94513
- heat conduction of metallic joints, using electrolytic tank 8-83207
- hot film transmitters, thermal processes, Beuken method appl. (*German*) 8-55546
- nuclear reactor neutron field, one-group diffusion approximation and finite difference methods appl. (*Russian*) 8-74416

analytical chemistry *see chemical analysis***anaphoresis** *see electrophoresis***AND gates** *see logic gates***Anderson model**

- amorphous solid, frozen liquid phonons disorder parameter, Anderson localisation 8-75784
- binary alloy type of disorder, numerical study of localisation 8-64009
- chemisorption on metal, intra-adsorbate Coulomb correl. and surface struct. roles 8-71979
- chemisorption on metal, intra-adsorbate Coulomb correl. and surface struct. roles 8-71980
- demagnetisation through level crossing, effect of charge fluctuations 8-52193
- disordered system, conductivity near mobility edges 8-76038
- electron systems, 2D disorder, transport props. in strong mag. fields 8-95318
- ferromagnetism, basic models, classification of theories (*Rumanian*) 8-91840
- intermediate valence compounds, phonon produced instabilities, periodic Anderson model 8-79964
- local electron interaction, orthogonality catastrophe, overlap integral, Anderson theorem in general case 8-67962
- local moments and localised states, review of early work on Anderson model 8-72327
- localisation and recursion method 8-84167
- magnetic alloys, dil., spin correlation 8-84385
- magnetic alloys, dil., transition metal hosts, props. review 8-84417
- metal surface, electron correl. in chemisorbed H atom, friction coeff. 8-60026
- metals, indirect mag. coupling between local moments 8-52207
- noncrystalline system, continuous and discontinuous metal insulator transitions 8-56076
- one dimensional site disordered lattice, AC conductivity 8-84199
- rare earth compounds, spinless periodic Anderson model with phonons, appl. to mixed valence systems 8-84153
- rare earth compounds, valence mixed state, Kondo lattice, Anderson localisation models (*Japanese*) 8-51945
- soluble local moment problem 8-52194
- superconductivity, magnetic impurity effects, Anderson model 8-52148
- transition metal oxides, sulphides, and selenides, Mott transition electronic and mag. phase diagrams 8-51894
- Al-Mn, dil., coherent propag. and strain-induced localisation of muons 8-95537
- Si, dangling bonds, EPR, localised states and unpaired electrons on microcrack surfaces 8-52351

anechoic chambers

- design principles 8-51007
- National Bureau of Standards, acoustic props. 8-87217

anelastic relaxation

- see also Bordoni effect; creep; elastic aftereffect; internal friction; Snoek effect; stress relaxation; Zener relaxation*
- BCC metals, HF mech. relax. peak 8-91379
- borate glasses, mechanical relax. in transition range 8-80575
- inelastic solids, anelastic relaxation anal., extended to creep at high temp., appl. to internal friction (*French*) 8-63806
- phenolformaldehyde resin moulding compounds, dynamic testing (*German*) 8-76699
- plastic powder compact rheological characteristics (*Japanese*) 8-95770
- polymer blends, viscoelastic props. (*Russian*) 8-72808
- polymers, highly elastic state, mechanical losses and relaxation processes (*Russian*) 8-76698
- polyphenylquinoxaline cyclotriphosphazine hexaithiocyanate networks, dynamic mech. props. (*Russian*) 8-72809
- polypropylene, cold-drawn isotactic bars and thin films, microstruct. and annealing 8-95760
- Fe, US velocity anomalies at elevated temp. 8-75830
- Ni cold worked, annealed, exam. of anelastic relaxation at low temp. 8-84877
- Ni, pure and doped, mech., mag. relax. meas. dumb-bell self-interstitial reorientation (*German*) 8-52879

anelasticity

- see also anelastic relaxation*
- austenitic stainless steel, type 316, anelasticity and creep transients 8-84880
- Earth, surface waves phase vel. and attenuation simultaneous inversion, Love waves appl. 8-85491
- polymeric glasses, non-elastic deformation, thermodynamic and kinetic anal. 8-64604
- quartz, electron irradiated, optical and anelastic absorptions and resonator freq. 8-64385
- string vibrating against rigid wall, partially elastic or anelastic impact, energy calcs. 8-67028
- Al-Ag (up to 40 at.%), exam. of anelastic phenomena and structural state 8-76693
- Fe-Co-V, anelastic phenomena, related to atomic order, exam. of magnetostriction (*French*) 8-80579
- Mn_{0.82}Fe_{2.18}O₄, anelasticity, 280 to 730K, 125 kHz vibr. study 8-87740

anemometers*see also laser velocimeters*

- constant resistance hot wire, flow average temp. variations, reading effects (*Russian*) 8-88925
- cup, rain-induced errors in mean wind speed meas. in surface layer at sea 8-61485
- electrodynamic spectral anemometer 8-87422
- four wire probe for turbulent flow temp. and vel. meas. 8-67290
- hot film and hot wire anemometers, signal-to-noise ratio 8-94861
- hot wire, const. current, response to temp. fluctuations 8-94860
- hot wire, probes, X-configuration dynamic testing device 8-87421
- hot wire and hot film temperature compensating circuits, temp. probe appl. 8-59510
- hot wire anemometer response in a flow with acoustic disturbances 8-63517
- hot wire anemometry of turbulent spot interaction with turbulent boundary layer 8-90858
- hot-film anemometer, calibration of low-vel., flow direction 8-91043
- hot-wire, computerised, for vel.- and temp.-meas. in heat turbulent flow 8-91040
- hot-wire, fluctuation data anal. with end-loss correction for supersonic flow 8-55703
- hot-wire, response to stream temp. perturbations 8-83503
- hot-wire, spatial vorticity distrib. meas. technique 8-67289
- hot-wire, temp. compensation errors estimation (*Russian*) 8-57345
- hot-wire anemometry combined with smoke flow visualisation, technique, appl. to turbulent boundary layer 8-91044
- hot-wire sensor, effect of centrifugal and Coriolis forces on rotating probe 8-94862
- inside-out type, constructional details 8-59516
- laser Doppler, acousto-optical modulator using TeO₂ 8-83082
- laser Doppler system, optics and signal processor for turbulent low speed flows (*French*) 8-59521
- laser fringe anemometers, light scatt. aspects, particle size meas. appl. 8-83020
- low and high turbulence flows, hot wire measurement based analysis 8-59511
- multicomponent frequency shifting self-aligning laser velocimeters 8-87423
- pocket air flow anemometer with built-in calculator, appls. (*German*) 8-75242
- spatial flow field determination, hot wire anemometry based analysis 8-59512
- time-of-flight laser anemometer, for velocity meas. in atm. 8-69469
- turbulent and high frequency fluctuating flow, mean static pressure measurement, hot wire anemometer and Pitot tube combined appl. 8-57889
- turbulent flow measurement by laser Doppler anemometry, concentration and size of tracer particles, theoretical limits 8-59514
- two-wire probe in nonisothermal flow, simultaneous vel. and temp. meas. 8-91042

angle measurement *see angular measurement***angular correlation techniques**

- oriented nuclei, β - γ correl., G-parity nonconservation 8-54723
- three body sequential decay X(a,b)Y(c)Z processes, parity, spin, reaction mechs. info. from ang. correl. method 8-50222
- Pb-Ni-Si, metallic glass, electron irradi., positron annihilation radiation, angular correlation study 8-84678

angular measurement*see also angular velocity measurement*

- angle etalon constr., angular scale, polygon calibration appl. (*German*) 8-77852
- auto-collimating telescope calibration methods (*German*) 8-77848
- interferometers appl., light (*Czech*) 8-49794
- large-scale angle inspection unit 8-77864
- laser interferometer for autocollimating telescope calibration (*German*) 8-77853
- magnetic angle convertor accuracy test method 8-77948
- selsyn rotor angle-to-digital code convertor, design (*Russian*) 8-65915
- sine bar devices application, meas. errors anal. 8-81944
- standards reproduction, autocollimating telescopes appl. (*German*) 8-77851
- telescopes appl., auto-collimating, absolute calibration methods (*German*) 8-86239
- tribometric meas., angle detector (*French*) 8-92434

angular momentum

- free relativistic spin-1/2 particle energy-momentum invariants and kinetic moment (*French*) 8-62287
- galaxies in Local Group 8-93400
- ion+polar molecule collisions, average dipole orientation theory, ang. momentum conservation 8-92466
- minimum uncertainty states of angular momentum system 8-93559
- star formation, angular momentum considerations 8-69781
- stars, ang. momentum transfer during steady disc accretion 8-65609
- I₂, angular momentum transfer, elastic, inelastic collisions, orientation and polarised fluoresc. 8-90271

angular momentum theory*see also quantum theory; Regge poles and trajectories*

- angular structure of unique spherical shells, appl. to ang. momentum quantisation 8-73873
- axisymmetric spacetime, ang. momentum and Dirac charge quantisation 8-70045
- calculation program ANG MOM 8-89359
- Clebsch-Gordan coefficients for meson sector in SO(8) model of elementary particles 8-58135
- dipole sum rules for products of 3-j symbols 8-65803
- DWBA computer program for heavy-ion transfer reactions 8-50145
- electron in magnetic field, induced angular momentum, classical and quantum calcs. 8-86060
- harmonics on 3-sphere, Lie group SU(2) 8-57813
- orthonormalization method, angular momentum coupling of fermions in single j-shell 8-50100
- radiating point charge, energy and ang. momentum splitting 8-69996
- reactance matrices, fine struct. cross sections, JAJOMP RE program 8-90312
- recursion relations for traces of products of angular momentum operators in the spherical basis 8-65805
- Schwinger boson representation for the quantized rotator 8-93602

angular momentum theory continued

- SU(2), eigenstates of complex linear combinations of J_1 , J_2 , J_3 8-58139
 Co²⁺ in crystals, Racah parameter 8-56110

angular velocity measurement

- differential frequency angular rate and displacement sensor, construction (*Russian*) 8-70106
 frequency-voltage converter appl. (*Polish*) 8-70101
 induction motors, piezoelectric pick-up appl. (*Russian*) 8-65911
 precision increase, using structural redundancy (*Russian*) 8-49804

anisotropy, magnetic see *magnetic anisotropy***anisotropy, magnetocrystalline** see *magnetic anisotropy***annealing**

- see also *graphitising; magnetic annealing; recrystallisation annealing; solution annealing; stress relaxation*
 alkali metal halides, irradiated 8-92494
 amorphous alloy, struct. relax., compositional SRO 8-79538
 anthracene, single cryst., X-radiation damage recovery, using triplet state exciton probe 8-75694
 baddeleyite-corundum refractories, creep and annealing 8-84907
 biotite, thermal decomposition, stability of ferromag. products 8-57195
 α -brass, dislocation structure around crack tips in early stage of fatigue 8-60830
 α -brass, drawability correlation with sheet metal texture 8-60683
 α -brass, electron irradiated, defect production and interdiffusion 8-67739
 α - β brass, exam. of creep fracture by tensile tests 8-88531
 α -brass, FCC, fractographic obs. of SCC 8-64786
 α -brass, single crystal, obstacle strength variation during stress relaxation 8-68723
 brass (70/30), interaction of annealing twins in fcc metals and alloys 8-68712
 brass/water interface leaky Rayleigh wave reflectivity loss meas. 8-59187
 ceramics, archaeological, dating by alpha-recoil tracks in mica 8-70237
 defect prod. and annealing, radiation-induced, computer expts. 8-87710
 effective annealing time determ. using analogue computer 8-88475
 ethanol-water system, metastable states, hydrates existence and props., low temp. 8-71835
 fission track annealing characteristics of epidote, appls. to geochronology, geol. 8-94038
 heat treatment, struct. and mech. props. 8-52864
 Ising model, restricted annealing of random models 8-80154
 metal, defect annealing study by positron annihilation, and elec. resistivity meas. 8-51584
 metals, plant deform. and recrystallisation textures 8-68708
 metals and alloys, FCC, model for form. of annealing twins 8-59818
 methane, effects of impurities and annealing on triple point 8-83919
 microcomputer precision regulator, electron field emitters and multiple multichannel analyser 8-86384
 MIS dielectrics, charge centre removal, low press. RF annealing technique 8-56230
 MIS dielectrics, charge centres, removal by RF annealing 8-88035
 Monel, in thermoluminesc. dosimeter, low dose meas. (*Japanese*) 8-86696
 nodular graphite, annealed, fracture behaviour at low temps. 8-72875
 nylon 66, doubly oriented, annealing of drawn and rolled samples, struct. 8-52859
 olivine, naturally deformed, recovery process, rel. to Earth upper mantle mech. state 8-96202
 organic crystals, γ -irrad., positron lifetime rel. to free radical conc. 8-72635
 PET, thermodynamic equilb. melting parameters, effect of annealing 8-71837
 phenolformaldehyde resin, sp. ht. obs. (*German*) 8-75845
 poly-1,6-di-N-carbazolyl-2,4-hexadiyne, synthesis, thermal expansion, photocond., optical transition 8-76858
 polyamide-6, fibrillar struct. and annealing, small-angle X-ray diffr. 8-75565
 polycarbonate, dielec. relax. and ductile brittle transition 8-52438
 polycarbonate, impact behaviour, effects of thermal pre-treatment and mol. wt. 8-95798
 polycarbonate fibre, highly-oriented, drawing behaviour and mech. props. 8-76708
 polyethylene, chain-extended, oriented, microindentation hardness 8-76728
 polyethylene, high-density, dielec. loss, below 4.2K, antioxidant, annealing and drawing effects 8-84518
 polyethylene, oriented, elastic stiffness constants, US meas. 8-76690
 polyethylene, polyethylene-D₄, migration and copolymerisation at high press. with shearing stress 8-51678
 polymer crystallisation, growth rates, nucleation, annealing and random copolymer crystallisation 8-51435
 polypropylene, cold-drawn isotactic bars and thin films, microstruct. and annealing 8-95760
 polystyrene-poly(styrene-*b*-butadiene-*b*-styrene) polyblends, electron micrographs for struct. 8-51442
 post irradiation annealing facility 8-70649
 PVC, amorphous, orientation study by creep thermomechanical method, computer anal. 8-75561
 PVC-Cu composite, annealing effects on elec. resist. 8-68060
 quartz, plant deform. and recrystallisation textures 8-68708
 α -quartz, Raman FTIR spectra, surface layer and vol. spectra comparison 8-52491
 ruby, cryst., optical properties, effect of annealing near melting point 8-90419
 S glass-Ni sphere composite, exam. of crack shape and fracture toughness 8-72886
 semiconductor layer, implanted, effectiveness of annealing by millisecond laser pulses 8-55885
 steel, 40Kh, heat-treated, wear during friction under extreme conditions 8-85007
 steel, alloy, cluster formation susceptibility in 40 KhN, influence of isothermal working in H₂ (*Russian*) 8-56643
 steel, alloy, low C, effects of pre-treatment on graphitisation behaviour (*Japanese*) 8-84860

annealing continued

- steel, alloy, type 25Gs, increasing fatigue resistance by surface plastic deformation 8-88530
 steel, anisotropic rolled plate, fatigue crack growth, rel. to laminated struct. and inclusions 8-92313
 steel, austenitic stainless, FCC, fractographic obs. of SCC 8-64786
 steel, austenitic stainless, interaction of annealing twins in fcc metals and alloys 8-68712
 steel, austenitic stainless, tensile fracture, phase transform. effect, comparison of stable and metastable phases 8-60798
 steel, C, coarsening of dispersed particles, in solid matrices 8-56651
 steel, C, cold rolled St3Kp, annealed, mag. nondestructive inspection of strip and ribbon 8-60913
 steel, CC Cr-Ni, soaking at forging temp., effect on struct. and mech. props. (*Czech*) 8-64628
 steel, cementite coarsening in type 1080 in a temp. gradient 8-88486
 steel, high hardenability carburising, accelerated annealing technique 8-84857
 steel, low C, capped, cold rolled sheet, deep drawability, effect of carbide size, cold reduction annealing 8-64559
 steel, low C, cold swaged, exam. of H₂ attack mechanisms 8-76791
 steel, low C, fatigue crack tip, observation of crack closure phenomena, by electron microscopy 8-68794
 steel, mild, implantation of Cu(Cr), annealing and rolling behaviour of conc. profiles 8-75684
 steel, Nb-V, cold rolled, HSLA, prod. by precipitation hardening, annealing 8-88471
 steel, stainless, electrode material, annealing temp. cycle which improves emission props. 8-95858
 steel, stainless, fatigue crack morphology of type 304 cycled at const. stress amplitude at elev. temps. 8-64671
 steel, stainless, prestrained, heat treatment effect on fatigue strength (*Czech*) 8-60747
 steel, stainless, type 304, exam. of H₂ induced cracking 8-76738
 steel, tool, NC6, carbide lattice, kinetics of its destruction (*Polish*) 8-92280
 steel, TRIP, strengthened by hydrostatic extrusion, struct. and mechanical props. (*Russian*) 8-76647
 steel, type A508, C1 2, microcrack formation during stress-relief annealing of a weldment 8-80629
 steel, X5CrNiTi26.6, ferrite-austenitic struct., optical and electron microscopy 8-84848
 steel fibre reinforced Ag, exam. of recrystallisation behaviour (*German*) 8-84849
 steel nitride phase hardening, precipitation and solution kinetics after heat treatment 8-95756
 steel stainless, solar energy collector optical props. rel. to heat treatment 8-94455
 Teflon, phosphor embedded, fast neutron dosimetry using S activation 8-70648
 TLD, effect of post irradiation annealing on fading characteristics 8-90030
 TLD fading characteristics effect of post irradiation annealing 8-90029
 vibrational spectra crystals with split configuration interstitial (*Russian*) 8-76450
 zircaloy 2, annealed, corrosion fatigue in aqueous soln. at 575K 8-64789
 Zircaloy-2 cladding, creep and creep rupture props., 1000 to 1500°C, effect of annealing 8-78470
 Ag film, annealing study of elec. resist. and defect density 8-76167
 Ag-Cd alloys, internally oxidised, thermal stability of CdO, exam. of particle coarsening 8-76789
 Ag-Fe, implanted, Mossbauer conversion electrons spectroscopy, rel. to dose and annealing temp. 8-52397
 Ag-Ga solid soln., internally oxidised, hardness (*Japanese*) 8-60744
 Ag-Ni, two ductile phase alloy, exam. of softening behaviour after cold rolling 8-72847
 Ag-Sn (0 to 6 wt.%) exam. of bulk diffusion of ¹¹³Sn and ¹¹⁰Ag 8-75864
 Al and Al-Mn (1 wt.%), subgrain growth during annealing after cold work 8-56656
 Al, annealed, subjected to torsional impact loading strain-rate effects 8-92303
 Al bronze, O free, annealing in photoemission electron microscope, twin density recrystallised grain size relation (*German*) 8-52850
 Al, cold rolled and annealed, substruct. near fatigue crack tip, X-ray microbeam technique exam. (*Japanese*) 8-64621
 Al, dynamic defect annealing during plastic deform. 8-88478
 Al, electron-irrad., NQR, EFG around vacancies and interstitials 8-88220
 Al, fatigue induced dislocation struct. and hardening, exam. (*Japanese*) 8-64624
 Al film, vacuum deposited, structural changes during annealing at temp. near melting point 8-84096
 Al foil, quenched, anomalous annealing phenomena, quantitative study 8-80565
 Al, recovery features, TEM and positron lifetime meas. examination 8-80611
 Al, substruct. developed during recrystallisation, exam. (*Japanese*) 8-64566
 Al/brass/Al bimetal, three layers, formed by cold rolling, exam. of formation of intermetallic phases at interface 8-56658
 Al-CuAl₃ eutectic, thermal instability in temp. gradient 8-52851
 Al-Li alloy, dil., quenched and irrad., recovery, resist. and internal friction obs. 8-52848
 Al-Mn (0.35 wt.%), quenched exam. of Mn-vacancy interaction 8-76676
 Al-SiO₂-Si:B ions, annealing effect on energy spectrum of radiation defects (*Russian*) 8-88488
 Al-Sn, dil. alloy, vacancy-impurity interaction, exam. by electrical resistivity meas. at 77K (*German*) 8-83846
 Al-Zn, dil. alloy, ageing and reversion, annealing curves, X-ray obs. 8-88485
 Al-Zn, precipitation struct. and phys. props. effect of miscibility gap (*German*) 8-92265
 Al₂O₃, cylindrical voids, exam. of instability 8-79603
 α -Al₂O₃, ion bombard., vol. expansion, annealing compaction, surface props. 8-67748
 As, film A1-type supercond. vapour-quenched transition temp., A7-type phase transition 8-52145
 As₂S₃ film, effect of light exposure and heat cycling 8-94417

annealing continued

- As₂Se₃ and As₄Se₃Ge glasses, struct. changes, Mn²⁺ EPR expts. 8-79534
- As₂Se₃Ge, glass, light irradi. induced changes in optical and elec. props. (*Japanese*) 8-68031
- AsTeCu_x (0 ≤ x ≤ 0.4) glass, effect of Cu on elec. cond. and thermoelectricity, 100 to 370K 8-87978
- As₂Te₂Ge(Si) glass, struct. changes, Mn²⁺ EPR expts. 8-79534
- Au film bicrystals, exam. of low energy planes for tilt grain boundaries 8-51551
- Au films on Si substrate, solid-solid reactions 8-95369
- Au polycrystalline wire, internal oxidation of impurities 8-83842
- Au-Cd (47.5 at.%), effect of cooling rates on stress-strain behaviour 8-76721
- Au-Cr alloy pressure gauges, annealing effects 8-49854
- Be bronze BrB2, quenched deformed, substruct. and props., effect of prerecrystallisation annealing (*Russian*) 8-60677
- Bi, film A1-type supercond. vapour-quenched transition temp., A7-type phase transition 8-52145
- Bi, quenching and annealing of defects, elec. resist. meas. 8-87973
- Bi:Sb(Te), quenching and annealing of defects, elec. resist. meas. 8-87973
- C fibres, Al coated, effect of annealing on ultimate tensile strength and fracture 8-56744
- CaSO₄:Dy, fast neutron dosimetry using S activation 8-70648
- CaSO₄:Dy, TLD phosphor, gamma-ray induced sensitisation 8-74542
- CaTiSiO₅, sphere, effects of thermal annealing on track etching rate 8-65435
- Cd-Ag, polycryst. quenched foil, the influence of Ag on the recovery spectrum 8-76661
- Cd-Ag, polycryst. wire, cold worked, resistivity changes 8-68827
- Cd-Zn, polycryst. wire, cold worked, resistivity changes 8-68827
- Cd-Zn (Ag), annealed, work softened, exam. of crystallographic texture, hardness 8-80559
- CdTe, single cryst. IR laser window, low absorption at 10.6 μm 8-79081
- (Co, Cu, Fe)₂Ce, sintered permanent magnets, magnetic charact. 8-60608
- (Co,Cu,Fe)₂Ce, sintered, mag. props. 8-68302
- Co-P, amorphous alloy, domain struct., effect of annealing 8-60304
- Co-Pt, struct. and mag. props. rel. to degree of order 8-72368
- Cu, annealed, cyclic plasticity under cyclic nonproportional strain histories, cyclic hardening, memory erasure, strain hardening 8-88510
- Cu annealed and cold rolled, with bamboo structure, exam. of grain boundaries as vacancy sources in diffusional creep 8-88508
- Cu, cold worked, determ., of dislocation pinning and unpinning stages, using internal friction meas. 8-92278
- Cu, electrical conductivity, effect of cyclic strains and work hardening at 4.2K 8-91655
- Cu, electrodeposited coating, annealing effect on struct. and microhardness (*Russian*) 8-76668
- Cu, electron-irrad., stage III recovery kinetics 8-63792
- Cu film, annealing effect on grain size 8-72015
- Cu film, electrodeposited, recrystallisation kinetics, X-ray scatt. (*Russian*) 8-60045
- Cu, interaction of annealing twins in fcc metals and alloys 8-68712
- Cu, isochronal recovery of high energy d-Be neutron damage 8-51592
- Cu, O free, annealing in photoemission electron microscope, twin density recrystallised grain size relation (*German*) 8-52850
- Cu, very low atomic displacement threshold energy obs. 8-95078
- Cu wire, residual elec. resist., size effect and grain boundary contribs., heat treatment effects (*Russian*) 8-56126
- α-Cu-Al, binary substitutional, short-range ordering kinetics, vacancy behaviour 8-55867
- α-Cu-Al, FCC, fractographic obs. of SCC 8-64786
- Cu-Al-Si-Co (2.8, 1.8, 0.4 wt.%), superplastic phase, exam. of mech. props. 8-52891
- Cu-Be-Ni-Zr, anodic behaviour of intermetallic phase 8-72895
- Cu-MgO, dispersion hardened, prep. by milling Cu and Mg oxidising atmos. (*German*) 8-64509
- Cu-SiO₂ single crystals, dispersion hardened, exam. of yield stress between 77 to 1200K 8-76720
- β-Cu-Zn-(Ni)-(Mn), order-disorder transformation temperature effect on quench hardening 8-95745
- CuCr₂Se₄, magnetic properties obs. 8-76227
- CuInTe₂:Zn, donor impurity in diffusion, elec. and optical props. 8-68504
- DySe, formation and crystallographic charact. of thin film phase 8-91574
- Fe, Armco, microstruct., effect of strain rate on change, due to tension-compression 8-80614
- Fe, cast, inoculated with Ce, exam. of phase composition 8-56620
- Fe, cast grey, effect of quenching conditions, on elastic modulus 8-56675
- Fe, fatigue fracture strength and failure, at 77K after cyclic loading at room temp. 8-84996
- Fe film, amorphous and polycrystalline, Hall effect, resistivity and mag. moment 8-91786
- Fe, film mag. structures and stresses, ferromagnetic resonance 8-72375
- Fe, powder, reduction annealing, thermodynamic anal. 8-60597
- Fe waisted cylinders, fatigue, exam. of Miner's rule 8-64689
- Fe:¹³³Xe, heavy ion implantation, recovery, Mossbauer effect meas. 8-52393
- Fe-Al (40 at.%) B₂ type ordered alloy, C migration, resistivity meas. (*French*) 8-52868
- Fe-C-Cu (0.21, 0.2 wt.%), neutron irradiated, torsional props. effect of Cu additions and annealing temp. 8-56699
- Fe-Co, damping capacity of Gentalloy, internal friction meas., mech. and mag. depend. (*Japanese*) 8-52875
- Fe-Co (35 wt.% and 52 wt.%), heat treated, decrease in sensitivity of mag. props. to mech. stresses (*Russian*) 8-56363
- Fe-Co (5 to 25 wt.%), exam. of damping capacity of Gentalloy 8-72800
- Fe-Co-Cr-W-Ni-C, alloy KKhVN, transforms. during annealing and nature of hardening (*Russian*) 8-56653
- Fe-Cr, oxidation, in H₂/H₂O vapour mixtures, epitaxial oxide phase formation, effect on oxidation 8-88568
- Fe-Cr-Co, effect of heat treatment on strain gauge factor 8-72802

annealing continued

- Fe-Cr-Ni, electron irradiated, resistivity during annealing, 4.2-1300K 8-87962
- Fe-Cr-Ni, textured (α+γ) alloy, α' lath martensite formation 8-95749
- Fe-Cu (1.2 wt.%) effect of precipitation on recrystallisation, texture 8-88476
- Fe-Ge (10 to 50 at.%), phase diagram rel. to heat treatment, supercooling diagram (*German*) 8-92240
- Fe-Ni base metallic glass, annealing embrittlement 8-64635
- Fe-Ni-C, thin foil, high voltage TEM exam. of martensitic form. 8-92264
- Fe-Ni-Mo, inhomogeneous solid solns., annealed and work hardened states, X-ray K-absorption spectra (*Russian*) 8-56544
- Fe-Si (6.5 wt.%), ductility and mag. props., Ni and Mn addition effects 8-76704
- Fe-Si-Al (6.4 wt.%), Sendust alloy, effect of Ni content on mag. props. 8-72897
- Fe₈₀B₂₀, crystallisation of amorphous alloys, TEM and X-ray diffr. exam. of struct., growth characts. 8-79539
- Fe₅₀Ni₃₀B₂₀, crystallisation of amorphous alloys, TEM and X-ray diffr. exam. of struct., growth characts. 8-79539
- Fe₃₃Ni₃₃Cr₁₂P₁₂B₆, Metglas 2826A, Hall resistivity, effect of thermal cycling and annealing 8-56125
- GaAs, anodic oxide film, annealing effect on carrier density profile 8-88040
- n-GaAs, electron and gamma ray irradiated, introduction and annealing of defects 8-67736
- GaAs, implantation disorder, flux and fluence depend., electrorefl. expts. 8-83833
- GaAs, reactor-irradiated, anisotropy in diffuse small angle neutron scatt. 8-51598
- GaAs:Be, annealing effect during MBE 8-79898
- GaAs:Se, and undoped sample, annealed, surface cond. change, n-p double layer 8-64095
- GaAs:Se, implanted, annealing with O-free CVD Si₃N₄ encapsulant 8-83834
- GaAs:Te, heavily-doped, annealing-induced prismatic dislocation loops and elec. changes 8-51546
- GaAs_{1-x}P_x, diffusion of implanted Zn ions, ion microbe analysis 8-95190
- GaAs_{0.9}P_{0.1}:P:Be, differential resistivity, Hall effect and secondary ion mass spectrometry meas. 8-84213
- GaP LED degradation, effect of γ-irradiation 8-95610
- GaP:N(Te), ion implanted at 40 keV, refl. spectra, 210-2000 nm, annealing (*Russian*) 8-80386
- GaP:Si, elec. props. following 1.7 MeV electron irradiation 8-80005
- Gd-Co, and Gd-Co-Mo films, amorphous, mag. props., annealing effects 8-64235
- Gd-Fe film, amorphous, mag. props., annealing effects 8-64235
- GdCo film, amorphous, sputtered, in-plane anisotropy induced by rare gas annealing 8-84458
- Ge (111) surface, 500 eV Ar⁺ bombard., high temp. annealing, recovery, RHEED obs. 8-87723
- Ge, deformation, annealing characts., X-ray study 8-75713
- n-Ge:Cu, characts. of radiation defects 8-55893
- n-Ge:Sb, fast neutron irradi. effects on donor conc., and annealing 8-56107
- n-Ge:Sb, γ-irrad. effects on donor conc. and compensation by acceptors 8-56106
- Ge-Cu (0, 23, 40 at.%), amorphous film struct. (*German*) 8-95391
- Ge-S film, amorphous, photo-induced ESR and optical absorption edge shift 8-88374
- Ge_{1-x}Se_x, 0 < x < 0.2, crystallisation in amorphous bulk and thin films 8-55813
- H₂WO₄ film, effect of struct. on optical and electrical props. 8-84671
- Hg_{0.6}Cd_{0.4}Te, annealing temp. effect on carrier conc. 8-72167
- HgTe, vacancy doping by off-stoichiometry, influence on transport props. 8-55862
- HoCo film, amorphous, sputtered, in-plane anisotropy induced by rare gas annealing 8-84458
- In_{0.4}Ga_{0.6}Sb, influence of annealing on microstruct., exam. 8-56669
- InSb, high-purity specimen irradiated at 80K, transport prop. and defect annealing 8-95307
- α-In₂Se₃, far infrared optical study of ordered and disordered forms 8-84572
- Ir-W (0.3 wt.%), P segregation to grain boundaries, effect on high temp. ductility 8-95754
- KBr, X-irradiated, at 80K, interstitial K ions associated with interstitial Br ions (*Russian*) 8-75655
- KBr:Rb, H-centre interaction with Rb⁺ ion 8-75662
- KBr-KCl, birefringence, annealing effects, photoelasticity 8-72483
- KCl birefringence, annealing effects, photoelasticity 8-72483
- KCl, irradiated crystal, determ. of oscillator strength of V₃-centre (*Russian*) 8-92095
- KCl:Ca²⁺(Sr²⁺), impurity precip., flotation density obs. 8-51690
- KCl:Sr, Ca, simultaneous diffusion, coefficients meas. 8-79813
- K(H_{1-x}D_x)₂PO₄, single cryst., 77K, γ-radiation damage centres, and EPR obs. 8-68379
- KH₂PO₄, soft branch Brillouin spectra, quasielastic central peak suppression by annealing 8-95588
- LiF:Mg, thermal annealing effects on sensitivity and fading of dosimeter 8-82522
- Li₂O-Al₂O₃-P₂O₅:V⁴⁺, glass exam. of ESR spectrum of V⁴⁺, optical spectra, and structure 8-88180
- Mg, recrystallisation after cold rolling 8-72790
- MgCd, effect on order, of compression deformation 8-52924
- MgO, plastically deformed, recovery of internal friction at room temp. (*French*) 8-80577
- Mo, hardened sub-structure, high-temp. radiation resist. (*Russian*) 8-56654
- Mo:N, ion implanted proton-irradiated, annealing behaviour 8-91362
- Mo-SiO₂-Si, Mo-Si pellicular structures, struct. transitions during vacuum thermal treatment (*Russian*) 8-95238
- Mo-SiO₂-Si, R/MOS struct., heat treatment effects 8-76683
- MoSi₂, integrated intensities and lattice parameters, X-ray anal. 8-63733
- Na₂O-SiO₂, effect of annealing on absorbed H₂O action on temp. spectra of internal friction 8-88487
- Na₂O-SiO₂ fibre, reactivity to atmospheric moisture below annealing range, internal friction measurement 8-92288

annealing continued

- Nb, blister form. on single crystal under Ne^+ ion bombardment 8-71772
- Nb, effect of O ion irradiation on supercond. 8-52131
- Nb, H_2 loaded, cold worked, plastic deformation, exam. of α internal friction peak 8-92307
- Nb, high purity, faceting of boundaries 8-83826
- Nb, isochronal recovery of high energy d-Be neutron damage 8-51592
- Nb, neutron irradi., microvoid form., ang. correl. and yield strength meas., TEM obs. 8-88381
- Nb, neutron irradiation, low temp., 15 MeV, effect on superconducting props. 8-52179
- Nb, superconductor, neutron irradiation, low temp., effect on critical current 8-52180
- Nb-Ga-Cu, phase diagram, metallographic and X-ray study, annealed and as-cast supercond. crit. temp. (Russian) 8-56617
- Nb-Sn(Ge), A-15 compound formation by ion implantation 8-51572
- Nb-Zr (1 wt.%), He bubble growth, α -particle effects 8-67749
- Nb_3Al , BCC struct., cold working and converting to A-15 struct. 8-64553
- $\text{Nb}_3(\text{AlSi})$, ternary supercond. alloy films, T_c props. (Russian) 8-88055
- $\text{Nb}_3\text{Al}_{0.2}\text{Si}_{0.8}$, A-15 alloy synthesis by ion implantation 8-80489
- Nb_3Ge amorphous films, X-ray diff. analysis of microstruct. 8-72035
- Nb_3Ge , neutron irradiated, A15 compound, recovery of T_c by annealing 8-52132
- Nb_3Sn , critical current enhancement by low temp. fast neutron induced flux pinning centres 8-52177
- Nb_3Sn , effect of O ion irradiation on supercond. 8-52131
- Nb_3Sn , filamentary conductors, type-II, low temp. 30 GeV proton effects on critical props. 8-52178
- Nb_3Sn , radiation damage effect on superconducting props. 8-52127
- Nb_3Sn superconductor, low temp. deuteron irradiation 8-52182
- $\text{Nb}_3\text{Sn}(\text{Al})$, neutron irradiated, A15 compound, recovery of T_c by annealing 8-52132
- $\text{Nb}_3\text{Sn}(\text{Ge})$, resistivity and T_c measurement after low temp. neutron irradiation 8-52123
- NbTi , filamentary conductors, type-II, low temp. 30 GeV proton effects on critical props. 8-52178
- Nd-Co film, amorphous, exam. of domain struct. 8-68336
- Ni based superalloy, interaction of annealing twins in fcc metals and alloys 8-68712
- Ni cold worked, annealed, exam. of anelastic relaxation at low temp. 8-84877
- Ni film, electrodeposited, recrystallisation kinetics, X-ray scatt. (Russian) 8-60045
- Ni film, mag. structures and stresses, ferromag. resonance 8-72375
- Ni film on leucosapphire, island growth as annealing in Ag vapour (Russian) 8-51830
- Ni, O free, annealing in photoemission electron microscope, twin density recrystallised grain size relation (German) 8-52850
- Ni single crystals, cyclically deformed, effect on domain patterns and dislocations 8-71740
- Ni, sputtered, on Si, annealing effects on transmission electron diff. patterns, silicide form. 8-91562
- Ni-Al (51 to 55 at.%), vacancy defective, TEM exam. of structure 8-76677
- Ni-Fe, epitaxial thin film, mag. structures and stresses, ferromag. resonance 8-72375
- Ni-Fe-Nb, Hardperm alloy, sheets, effect of sheet thickness, and annealing, on mag. props. 8-76772
- Ni-ThO₂, irradiated with 5 MeV Ni^{++} , ThO₂ redistrib. 8-71771
- Ni-Zn diffusion couple, annealing and reaction diffusion (Japanese) 8-51749
- Ni_3Al , Mossbauer spectra, exam. of struct., superlattice population anal. 8-88240
- Ni_2Cr , neutron irradi., point defect prod. and annealing 8-87718
- $\text{Ni}_{0.36}\text{Zn}_{0.64}\text{Fe}_2\text{O}_4$, normal grain growth 8-72796
- Pb, effect of O ion irradiation on supercond. 8-52131
- $\text{PbO-Bi}_2\text{O}_3\text{-GeO}_2$, exam. of glass forming and liquid phase separation regions, and optical props. 8-88453
- PbTe, carrier conc. inhomogeneity 8-52019
- Pd, transport props. 40 mK-6K 8-51968
- $\text{Pd}_{77.5}\text{Cu}_6\text{Si}_{16.5}$ metallic glass, diffusion of Au 8-55983
- $\text{Pd}_{80}\text{Si}_{20}$, amorphous alloy crystn., high press. effect 8-95001
- Pt, electron and deuteron irradi., close Frenkel pair recomb. during annealing 8-87716
- Pt foil, quenched, 1.2 MeV electron irradi., subthreshold irradi. effects 8-51585
- Pt, isochronal recovery of high energy d-Be neutron damage 8-51592
- Pt, recovery of thermal-neutron-irradiated samples 8-95081
- Pt-Si contact, annealed in H_2 ambient, elec. props. 8-64110
- Rh, film, annealing effect on struct., TEM, electron diff. study 8-76682
- (Sn), films, influence of annealing on thermopower and conductivity 8-91782
- Sb film A1-type supercond. vapour-quenched transition temp., A7-type phase transition 8-52145
- Si (111) surface, 500 eV Ar^+ bombard., high temp. annealing, recovery, RHEED obs. 8-87723
- Si, annealed, electron irradiated, positron annihilation 8-87713
- Si, deformation, annealing characts., X-ray study 8-75713
- Si electron beam deposited film, epitaxy by pulsed laser annealing 8-56055
- Si, electron irradi., effect on positron annihilation 8-76552
- Si film, amorphous, effects of annealing of gap states 8-72115
- Si film, amorphous, plasma-deposited, H_2 evolution, mass spectrometry and RHEED obs. 8-72050
- Si film, amorphous and polycrystallised, localised states, elec. and optical props. 8-64008
- Si, heavily doped implantation layers, laser beam annealing 8-88481
- Si, ion implantation damage, annealing, role of stresses 8-75679
- Si, ion implanted, laser annealing, periodic regrowth phenomena 8-67724
- Si, ion implanted, laser-annealed, theoretical anal. of thermal and mass transport 8-91364
- Si, ion implanted, photovoltaic effect related to annealing 8-76111
- Si, ion-implanted, disorders, nature and annealing behaviour, review 8-83836
- Si, ion-implanted layers, impurity profile meas. after laser annealing 8-87702

annealing continued

- Si, ion-implanted layers, residual defects after high temp. annealing 8-87695
- p-Si, neutron irradiated, elec. props. 8-51939
- Si, oxidation stacking faults and microdefects, growth behaviour during high temp. annealing 8-72901
- Si, P diffused sample, stacking faults and dislocations formation from interstitials 8-95059
- Si, radiation-doped and annealed, carrier density and mobility meas. 8-56145
- Si, single crystal, kinetics of annealing of vacancy complexes 8-87666
- Si, stacking fault formation, elimination by preoxidation annealing in $\text{N}_2/\text{HCl}/\text{O}_2$ mixtures 8-88550
- Si:As, elec. activation of implanted As during low temp. anneal, Hall effect meas. 8-51571
- Si:As, implanted, spatially varied activation during regrowth of amorphous layers, sheet resist. and backscatt. obs. 8-71749
- Si:B, conc. profile of implanted cryst., by $^{11}\text{B}(\text{p},\alpha)$ chem. anal., annealing (German) 8-83843
- p-Si:B, high temp. treatment, effects on ion implanted impurity distrib. profile 8-79625
- Si:B, implemented laser annealed samples, unidirectional contraction 8-71747
- Si:B, ion implanted, laser and thermal annealing compared, TEM obs. 8-75681
- Si:B, TEM study of stacking fault form. and annealing 8-51566
- Si:B(P), diffusion induced imperfections, laser annealing, rel. to junction characts. 8-75678
- Si:Cu, interaction between vacancy emitting absorbing precipitates and dislocations, TEM obs. 8-71755
- Si:O, cryst., annealed, struct. defects 8-75673
- Si:O film, thermally deposited, semi-insulating, crystallographic study 8-75954
- Si:Pb, implanted, laser annealing 8-75685
- Si:Pb, implanted and annealed, impurity redistrib. 8-75689
- Si:Sb, ion implanted, annealing behaviour of stress 8-63778
- Si-SiO₂ interface, stacking fault-free region formation by annealing 8-51561
- SiC fibre reinforced Ni-Cr alumina coated fibres, hot pressed, annealed, IR study 8-60623
- SiC fibres reinforced Ni complex alloy, influence of TiN coating on fibre matrix interaction (Russian) 8-95820
- Si_3N_4 , hot-pressed with crystn. grain boundary phases, prep. 8-95715
- $\text{Si}_3\text{N}_4\text{-Al}_2\text{O}_3$, hot-pressed with crystn. grain boundary phases, prep. 8-95715
- SiO₂ film on Si, negative bias instability 8-91773
- SiO₂:Al film, ion-implanted, electron trapping behaviour 8-67729
- $\text{Sm}(\text{Co}_{1-x}\text{Cu}_x)_{7.8}$ alloys, coercive fields, domain wall energies, mag. and metallographic exam. 8-91897
- SmSe, formation and crystallographic charact. of thin film phase 8-91574
- Sn, effect of O ion irradiation on supercond. 8-52131
- Sn-Ni, equiatomic, metastable, transformation kinetics, Avrami parameters calc. method 8-92239
- TbSe, formation and crystallographic charact. of thin film phase 8-91574
- Th, ion irradi., surface C and O, AES obs. 8-71775
- α -Ti alloy, VT1-1, cold rolled, recrystn. texture and prop. anisotropy 8-52846
- Ti alloys, AT3 and AT6, tensile props. prolonged oxidation effects 8-85050
- Ti alloys, β -annealing and controlled rate quenching effects 8-80568
- Ti, sheets, porous, production and props. 8-60602
- Ti, strip prod. by powder rolling 8-80493
- Ti-Al (6.1 wt.%), hot rolled sheet, ductile fracture nuclei, SEM obs. 8-64654
- Ti-Al-Sn (5, 2.5 wt.%), ductile fracture at low temps. 8-64659
- Ti-Al-Sn (5, 2.5 wt.%), electron microscope and X-ray diff. exam., of basal and near basal hydrides 8-80550
- Ti-Cu-Al(Zr)(Sn)(Nb)(Mo), heat treatable alloys, effect of alloying on strength, tensile props. 8-56671
- Ti-Permalloy thin film diffusion couples, low temp. interdiffusion interdiffusion 8-71889fic
- TiB₂, low-temp. neutron irradi., electrical resistance and stored energy 8-67744
- TiSi₂, crystal atomic struct., X-ray diff. exam., lattice parameters and integrated intensities 8-75647
- U-Nb (14 at.%), exam. of shape memory effects 8-76694
- $\text{US}_2\text{N}_2\text{O}_2$, neutron diffraction exam. of structure 8-79777
- V, annealing after irradiation with 210 keV He at 625°C at high fluences 8-67751
- V, blister form and stress build-up, under the bombardment, surface prep. effects 8-95094
- V, effect of O ion irradiation on supercond. 8-52131
- V, first wall fusion reactor material, anneal-blistering 8-55897
- V, internal friction α -peak origin 8-95773
- V, superconductor, neutron irradiation, low temp., effect on critical current 8-52180
- V_3Ga , filamentary conductors, type-II, low temp. 30 GeV proton effects on critical props. 8-52178
- V_3Ga , neutron irradiation and annealing 8-52130
- V_3Ga , supercond. transition temp., as-cast and annealed (Russian) 8-56618
- V_3Si , neutron irradiated, A15 compound, recovery of T_c by annealing 8-52132
- W, grain boundary migration initiated by high hydrostatic press. 8-51554
- W, thermal neutron irradiated, radiation damage and stage III defect annealing 8-51586
- W-K-Al-Si, state of bonding, distribution of impurities 8-92212
- W-Fe, dil., spin glass props., DC mag. susceptibility meas. 8-68283
- W-Ni liquid alloys, sintered, coarsening of W grains, exam. 8-56598
- W-Zr (2.92, 7.42 and 10.02 wt.%), and W_2Zr , thermal expansion, elec. resistance, 100-900°C, crystallisation 8-91455
- (Y,Eu,Tm,Ca)₃(Fe,Ge)₅O₁₂ garnet film coercivity, new annealing method 8-84459
- (Y,Sm,Lu,Ca)₃(Fe,Ge)₅O₁₂ garnet film coercivity, new annealing method 8-84459
- YCo₅ film, amorphous, sputtered, in-plane anisotropy induced by rare gas annealing 8-84458

annealing continued

- ($\text{Y}_{1-x}\text{Co}_x$) Co_2 , anisotropy fields, coercivities, annealing effects 8-91898
 YbSe, formation and crystallographic charact. of thin film phase 8-91574
 Zn, dislocation struct. stability, effect of deformational and thermal annealing 8-64567
 Zn, hot rolled, grain boundary fine structures, TEM exam. 8-76680
 ZnO, adsorpt. of H_2O vapour, annealing and grinding effects 8-68656
 Zn_3P_2 , photovoltaic material and Schottky diode characteristics 8-64066
 ZnSe:In elec. transport props., effect of Zn-annealing, 300 to 77K 8-76075
 Zr base alloys, irradiation growth, dislocation model 8-51595
 Zr-Ru(Pd), heat treated, mech. props. and struct. 8-80571

annealing, magnetic see *magnetic annealing***anodes**

- arc, vac., anode spot form., threshold current time depend. 8-87515
 cylindrical proportional counter, gas multiplication factor dependence on anode wire attachment 8-78560
 energy balance of anode in low-pressure heavy-current discharge with hollow cathode (*Russian*) 8-51369
 foilless anode electron-beam laser with chopper-wheel gas pulser 8-63122
 high-speed rotating anode disc, spot motion and erosion calc. 8-71498
 low-pressure discharge anode sheath in crossed fields, electron density distrib. 8-75424
 rotating-anode X-ray tube apparatus 8-58100

anodes, electrochemical see *electrochemical electrodes***anodic machining** see *electrolytic machining***anodisation**

- anodic oxidation technique, carbide determ. in annealed high speed steels (*Japanese*) 8-85040
 chalcopyrite oxidation, in acidic chloride medium electrochem. study 8-95817
 layered semiconductor, anodisation as layer counting method 8-76776
 steel, high speed, annealed, carbide determ. by anodic oxidation technique (*Japanese*) 8-85040
 Al, anodisation, intensity of luminesc. and film thickness 8-80413
 Al, influence of substrate orientation and anodising conditions 8-88581
 Al-Cu film, galvanostatic formation anodic oxide, Rutherford backscattering and depth profiling 8-92395
 Al-Mn, anodisation, intensity of luminesc. and film thickness 8-80413
 Al_2O_3 composite films, elec. instability 8-68452
 Co, anodic dissolution into silicate glass melt 8-88582
 Cu, friction under electrolyte immersion condition 8-64738
 Fe, anodic dissolution in acidic chloride solns., exam. 8-92389
 GaAs, anodic oxidation using O plasma, and oxide layer evaluation 8-85015
 GaAs, epitaxial and metallic thin-films, anodic oxidation anal. 8-80673
 GaAs interface with anodic and thermal oxides, comparison of AES and ESCA 8-95980
 GaAs, plasma anodisation in DC discharge, AES and MIS diode expts. 8-95826
 $\text{GaAs}_{1-x}\text{P}_x$, heterogeneous struct. obs. by anodisation-electrorefl. technique 8-84088
 $\text{Ga}_3\text{In}_{1-x}\text{As}_x\text{P}_{1-x}$, anodisation, effect of pH, current density and illumination 8-95823
 InP, anodisation, effect of pH, current density and illumination 8-95823
 InP interface with anodic and thermal oxides, comparison of AES and ESCA 8-95980
 Nb_3Sn , AC losses, surface effects 8-64171
 Ni, anodic dissolution into silicate glass melt 8-88582
 Pb, passivation in H_2SO_4 soln. 8-76871

anodised coatings see *anodised layers***anodised layers**

- ellipsometric observation of anodic film growth, automated interpretation 8-56902
 nucleation, growth rel. to electrode pot. variation 8-68634
 strong elec. field, pulsed V-I characteristics (*Russian*) 8-64156
 Al, 1100, anodic barrier film characts., ISS/SIMS 8-53021
 Al alloys, oxide-covered, characteristic emission of negatively charged particles during tensile deform. 8-92179
 Al, anodic film, formed in H_2SO_4 , electron microscopy 8-68843
 Al, anodised, photostimulated exoelectron emission, effect of oxide thickness 8-80461
 Al, influence of substrate orientation 8-88581
 Al oxide anodic film, colloidal metal, origin of colour, optical props. meas. 8-68571
 Al, porous anodic film, ion beam thinned, electron microscopy 8-92390
 Al-oxide-electrolyte system, luminesc. spectra (*Russian*) 8-76539
 $\gamma_1\text{-Al}_2\text{O}_3$, anodic film, stress corrosion cracking protection of Al alloys 8-95836
 Al_2O_3 , anodic film transient pitting during film growth 8-56817
 Al_2O_3 , composite film, barrier layer, ellipsometric meas. 8-67918
 Al_2O_3 , films, form., cross-sections, struct. obs. 8-67917
 Al_2O_3 , plasma-anodised, current efficiency 8-91797
 GaAs anodic oxide film, self drifting of ionic charges, detection by surface potential decay method 8-72295
 GaAs anodic oxide film, optical props. 8-72626
 GaAs, anodic oxide film, annealing effect on carrier density profile 8-88040
 GaAs oxide, growth-induced damage from photolum. expts. 8-75953
 GaAs oxide, in-depth profiles, XPS expts. 8-84086
 GaAs oxide, passivated layers, quantitative in-depth profile, AES-SIMS thermal, anodic and plasma oxidations 8-84087
 GaAs oxide, refl. and transmission, 0.01-6 eV 8-95613
 GaP, anodically grown insulating layers, prep. and props. (*German*) 8-64158
 GaP, single-crystal, anodically oxidised layers, AES measurements 8-91556
 IrO_x , anodic films, electrochem. characts., electrochromic system 8-80316
 SiC, surface luminesc. in presence of anodisation 8-52579
 Ta, anodic barrier film characts., ISS/SIMS 8-53021

anodised layers continued

- Ta_2O_5 , anodic film with Au counterelectrodes, conduction process 8-84312
 Ta_2O_5 , film, dielec. props. meas., two layer Maxwell-Wagner model 8-76373
 Ti, growth kinetics, determ. (*French*) 8-76788
 TiO_2 , anodically formed layers, film instability obs. 8-72916
 WO_3 , antirefl. coating on textured W surface, for solar absorber appl., props. 8-63157

anodised thin films see *anodised layers***anolytes** see *electrolytes***anomalous skin effect**

- metal, surface roughness effect on light absorptivity 8-80314
 plasma anomalous skin effect conditions 8-67544

antenna accessories

- see also *antenna feeders; directional couplers*
 radome and backstructure design improvements 8-57449

antenna arrays

- see also *antenna phased arrays; directional couplers; microwave antenna arrays*
 acoustic sounder, design from loudspeaker elements for atmospheric appls. 8-87226
 Australian synthesis telescope, design, array config. 8-69690
 biomedical telemetry, transmission and reception with embedded antennae 8-77125
 radiotelescope transmission lines, antenna arrays and impedance transformation 8-96399
 three-ring antenna, radiation characts. when used for electron plasma waves excitation 8-91107
 Very Large Array, phase switching, Walsh function appl. in radioastronomy 8-81539

antenna components see *antenna accessories***antenna feeders**

- radiotelescope, chromatism due to blocking and feed scatt. 8-73630

antenna lobe patterns see *antenna radiation patterns***antenna patterns** see *antenna radiation patterns***antenna phased arrays**

- space antenna, self-deploying large parabolic antenna and array design 8-57450
 UTR-2 radiotelescope, expt. techniques, data processing, for decametric survey of discrete northern sources 8-57461

antenna radiation patterns

- brightness temps. estimates from scanning radiometer data 8-85716
 horizontal electric dipole, quasi-static subsurface-to-subsurface and subsurface-to-air 8-73375
 plasma antenna system: dual-integral-equation method 8-75361
 point source in magnetoplasma, cyclotron harmonic waves and reson. cone 8-91098
 radiotelescope, Effelsberg 100 m, large dynamic range obs. 8-96391
 three-ring antenna, radiation characts. when used for electron plasma waves excitation 8-91107

antenna theory

- circular aperture antenna immersed in plasma, induced HF thermal noise 8-87496
 Fredholm eqn. of the second kind for current distrib. in antenna theory (*Chinese*) 8-66708
 radiation and scatt. from wires and surfaces, free space impedance functions 8-86999
 Sommerfeld integral, numerical approximations for fast convergence 8-66727
 transfer functions, space-variant, for inhomogeneous scatt. media characterisation 8-71012
 wide-angle spherical mirror under oblique illum., EM diffr. in focal region 8-58888
 wire loop laid on ground, radiation resistance calc., antenna for parametric depth sounding (*Chinese*) 8-61565

antennas

- see also *antenna radiation patterns; dipole antennas; directive antennas; microwave antennas; mobile antennas; radar antennas; reflector antennas; scanning antennas*
 circular aperture immersed in plasma, induced HF thermal noise calc. 8-87496
 Debye screening and electron conc. nonuniformity effects on cylindrical antenna on satellite 8-69563
 Doppler sodar antenna configs. for horizontal wind meas. 8-65410
 gravitational wave antennas, with and without piezoelectric ceramics, elec. equivalent circuits 8-73915
 piezoelectric gravitational antenna for use at 3 mK 8-58103
 plasma, whistler wave ducting caused by antenna actions 8-59586
 variable profile for RATAN-600 (Soviet) radiotelescope (*Czech*) 8-53824

antibaryons see *baryons***anticorrosion coatings** see *corrosion protective coatings***antiferromagnetism**

No entries

antiferroelectric materials

- see also *antiferroelectricity; ferroelectric materials*
 noncentrally symmetric phase identification using SHG 8-74947
 perovskite crystals, static and dynamic aspects of PAC meas. 8-88241
 perovskite structure, semiconductor props., review (*Polish*) 8-56437
 SHG determ. of ferroelec. and antiferroelec. props. 8-74947
 squaric acid, ^{13}C chemical shift tensor study of antiferroelec. second order phase transition 8-52462
 TTF-TCNQ crystal, antiferroelec. ordering of electronic polarisation, simple model anal. 8-92028
 BiTaO_4 , X-ray and ESR study of phase changes 8-72476
 DyVO_4 , Jahn-Teller phase transition and improper antiferroelectricity (*Japanese*) 8-80294
 KCN, optical F centres and phase transitions 8-56504
 $\text{NH}_4\text{H}_2\text{AsO}_4\text{-NH}_4\text{H}_2\text{PO}_4$, EPR spectra of central peak fluctuations 8-91932
 $\text{NH}_4\text{H}_2\text{AsO}_4\text{:Cr}^{5+}$, fast and slow dynamic reorientation 8-80306
 $\text{NH}_4\text{H}_2\text{AsO}_4\text{:Cr}^{5+}$, ENDOR spectra 8-88224
 $\text{NH}_4\text{H}_2\text{PO}_4$, improper antiferroelec. phase transition, elastic props., free energy, thermodynamic theory 8-80299
 $(\text{NH}_4)_2\text{SeO}_4\cdot 2\text{NH}_4\text{HSeO}_4$, cryst. struct. 8-71715
 NaCN, optical F centres and phase transitions 8-56504

antiferroelectric materials continued

- NaNO₂, adiabatic and isothermal elastic compliances, critical behaviour 8-92031
 NaNO₂, elastic constants and US attenuation coeffs., anisotropic charact. 8-63809
 Pb(Zr,Ti,Ge)O₃, antiferro-ferroelectric transition 8-95565
 PbZrO₃-monocryst., elec. cond., permittivity, polarisation, para- and ferro- to antiferroelec. phase transistions 8-60402

antiferroelectricity

see also *antiferroelectric materials*

- gamma-rays generation by fast electrons travelling through antiferroelectric or antiferromagnetic crystalline structures 8-76545
 DyVO₄, Jahn-Teller phase transition and improper antiferroelectricity (*Japanese*) 8-80294

antiferromagnetic Curie temperature see *Curie temperature***antiferromagnetic-ferromagnetic**

transitions see *ferromagnetic-*

antiferromagnetic transitions**antiferromagnetic-paramagnetic**

transitions see *paramagnetic-*

antiferromagnetic transitions**antiferromagnetic properties of substances**

see also *antiferromagnetism; magnetic semiconductors*

- alkali bromide-VBr₂ systems, cryst. struct., DTA investig. (*German*) 8-72766
 bis(diethylammonium) copper tetrachloride, mag. susceptibility, EPR spectra 8-68193
 copper formate.4D₂O, field-induced antiferromag. order above T_n 8-84389
 Cr-Au alloys, dil., elec. resist., 77-700K 8-64035
 diammonium layer compound, ND₃-(CH₃)₂-ND₃CuCl₄, antiferromag., magneto-optical meas. birefringence 8-68483
 diethylammonium copper tetrachloride, antiferromag. mode excitation in EPR spectra 8-56373
 dimethyl ammonium manganese chloride, sp. ht., quasi-one dimens. behaviour 8-52293
 DPPH-benzene, organic radical, pressure induced mag. ordering (*Russian*) 8-88120
 Mn_{1.98-2}Cr_{0.02}Sb, Mossbauer effect exam. 8-68432
 perovskites, ordered, mag. props. (*French*) 8-95434
 press. depend. of effective mag. fields on ⁵⁷Fe nuclei 8-52383
 rare earth alloys, amorphous, magnetoresistivity, exchange scatt. model 8-95287
 rare earth alloys, amorphous, random anisotropy antiferromag. model 8-95428
 rare earth alloys, RFe₄Al₈, cryst. struct. mag. props. and hyperfine interactions 8-87648
 rare earth amorphous alloys, antiferromagnetism, mol. field approx. 8-80142
 rare earth cobalt alloy, RCo₂, itinerant system, weak ferromagnetism 8-52191
 rare earth intermetallics, RGa₂, mag. susceptibility, 1.5-300K and Neel temp. 8-68184
 rare earth orthochromites, mag. interactions and weak ferromagnetism 8-52220
 rare earth systems with singlet ground states, low freq. modes 8-68131
 rare earth-Ga₂ intermetallics, mag. structs. 8-84394
 rare earth-Zn₁₂, mag. props. and structs. 8-84393
 TMMC:M, impurity (M) effects on Neel temp. and low temp. mag. susceptibility 8-88113
 TMMC, antiferromag. coupling in linear chains, molecular orbital approach 8-52239
 TMMC, exchange-narrowed EPR linewidth, temp. depend. 8-52292
 TMMC, field-suppression of spin fluctuations, NMR obs. 8-91971
 TMMC, linear Heisenberg antiferromag., effect of mag. field on 3d ordering and spin correlations 8-68229
 TMMC, one-dimens. Heisenberg magnet, EPR sidebands 8-88163
 transition metal alloy, electronic structure, mag. props. 8-95254
 Au-Mn alloys, equiatomic region of phase diagrams crystallographic and mag. exam. 8-52755
 Ba₂Fe₂O₁₁, antiferromagnet, exam. of mag. props. by mag. meas., and Mossbauer spectroscopy 8-52256
 BaVS₃, exam. of ferromagnetic, antiferromagnetic behaviour, depending on stoichiometry 8-52233
 Bi₂Fe₄O₉, mag. struct., neutron diffr. meas. 8-91844
 Ca₂Fe₂(Mn₂)Ge₃O₁₂, single magnetic sublattice antiferromagnetic garnets 8-52652
 Ca₃Mn₂Ge₃O₁₂, highly anisotropic garnet, neutron diffr. obs. of mag. struct. 8-68168
 CdS, model S=1/2 amorphous antiferromagnet, spin polarisation 8-52288
 CeAg(Mg)(Zn), magnetic struct. and cryst. field, neutron diffr. exam. 8-72328
 CeAl₂, anisotropic magnetostriction near antiferromagnetic transition 8-88157
 CeAl₃, conf. Kondo system, sp. ht. meas. 8-52210
 CeAl₂, low temp. mag. behaviour, neutron diffr. 8-84395
 CeAl₃, mag. anisotropy, transition, crystal field splitting 8-52243
 CeCl₃(Br₃), interaction parameters, high freq. meas. of adiabatic differential susceptibility 8-68211
 CeMn₂Si₂, cryst. and mag. struct. determ. 8-52225
 CeS, mag. props., sp. ht. and thermal expansion 8-60292
 CeSe, mag. props., sp. ht. and thermal expansion 8-60292
 CeTe, mag. props., sp. ht. and thermal expansion 8-60292
 CeZn, mag. struct. and cryst. field effects 8-52223
 Cm, antiferromag. state, paramag. suscept. meas., electronic struct. (*Czech*) 8-80133
 CoCO₃, spin wave excitation by uniform precession of magnetisation due to two magnon scatt. 8-68207
 CoCO₃, weak ferromag., antiferromag. reson., phenomenological theory 8-60339
 CoCO₃, weakly ferromag., light scatt. on spin waves (*Russian*) 8-72419
 CoF₂, domain formation in staggered field induced by uniaxial stress, neutron diffr. exam. 8-76289
 Co_{0.9}Ni_{0.1}Cl₂.6H₂O, calorimetry, γ-type transitions of sp. ht. 8-68256
 CoO, collinear antiferromag., equiv. type-II mag. struct. 8-56296
 CoU₂S₅, mag. struct., exchange energy, magnetisation and neutron diffr. expts. 8-68170
 (Cr, Mn)₂As, mag. props. and struct. 8-64190

antiferromagnetic properties of substances continued

- Cr, antiferromagnetic, polarisation domain effects on US velocity 8-52329
 Cr complex, trimeric clusters, low temp. mag. props. 8-76261
 Cr, Fermi surface, stress depend., from quantum oscill. effects, rel. to itinerant antiferromagnetism 8-91597
 Cr, ferromagnetic surface layer on antiferromag. bulk, determ. by surface magnetoplasma wave detect. 8-68356
 Cr, single modulation state, temp. limits of cryomagnetic method 8-72374
 Cr, spin density waves detected by Ta mag. hyperfine field meas. 8-60364
 Cr, surface electronic struct., tight-binding approx. calcs. 8-64090
 Cr-Al, disordered alloy, effect of high press. on resistivity 8-95286
 Cr-Co, dil., Neel temp., impurity conc. depend. calc. 8-68232
 Cr-Fe, antiferromag. phase boundary, neutron diffr. meas. 8-95437
 Cr-Fe, dil., Neel temp., impurity conc. depend. calc. 8-68232
 Cr-Fe, low conc. alloys, coexistence of itinerant antiferromagnetism with paramagnetism 8-84386
 Cr-Mn alloy, strain wave and spin density wave intensities, neutron diffr. 8-60266
 Cr-Pt, dil., effect of Pt on itinerant antiferromagnetism 8-64191
 Cr-Re, dil. alloy, mag. susceptibility temp. depend., thermal expansion coeff. (*Russian*) 8-76225
 Cr-V alloy, strain wave and spin density wave intensities, neutron diffr. 8-60266
 CrAl, semicond. solid solns., depend. of energy gap 8-67941
 CrAs, heat capacity, enthalpy increments, thermodynamic props., 5 to 1280K 8-91450
 CrB₂, NMR of ¹¹B meas. 8-56397
 CrS_{1-x}Se_x, antiferromag. props., struct., variations near Neel temp. 8-64199
 CsCoCl₃, anisotropic antiferromag., inelastic neutron scatt. study 8-60274
 Cs₂FeCl₅H₂O, mag. phase boundaries, susceptibility, 3D Heisenberg antiferromag. behaviour 8-84420
 CsMnF₃, struct. with compensated magnetisation in noncollinear phase (*Russian*) 8-88095
 CsNiCl₃, antiferromag. coupling in linear chains, molecular orbital approach 8-52239
 CsNiCl₃, nuclear spin-lattice relax., temp. depend., anisotropic effects 8-64293
 CsNiCl₃, one-dimens. antiferromag., US attenuation 8-88156
 CsVCl₃, antiferromag. coupling in linear chains, molecular orbital approach 8-52239
 CuCl₂.2H₂O, antiferromag. to paramag. transition, high field magnetisation meas. 8-64204
 γ-Cu(IO₃)₂, cryst. struct. and mag. behaviour 8-79571
 Cu_{1-x}In_xCr₂S₄, light induced magnetisation 8-76275
 Dy, anomalous thermal expansion, interferometric meas. 8-52333
 Dy, helical antiferromagnetic phase, basal plane anisotropy 8-84412
 DyAG, adiabatic magnetisation, optical obs. 8-88283
 DyAG, forced magnetostriction meas. 8-68349
 DyAu_{3.6}, ordering temps. and effective moments 8-60283
 DyFeO₃, spin reorientation near Morin temp., magneto-optical exam. 8-68284
 DyMo₂S₈, supercond. and antiferromag. coexistence, neutron study 8-95401
 DyPO₄, susceptibility near mag. phase boundaries 8-52258
 DyVO₄, basal plane magnetisation anisotropy under Jahn-Teller distortion 8-68222
 Er, paramagnetic and antiferromagnetic states, optical absorption (*Russian*) 8-56497
 ErCu, cubic antiferromag., mag. excitations inelastic neutron scatt. meas. 8-72341
 ErH₃, cryst. fields and mag. props. 8-68181
 EuM₂Ge₂, M=Mn, Fe, Co, Ni, Cu, magnetism and hyperfine interactions 8-76228
 EuMg₂, cryst. and mag. props., ordering 8-68185
 EuSe, mag. struct. and transition temp., indirect exchange 8-91860
 EuTe, field depend. correl. function theory of Raman scatt. near antiferromag.-paramag. transition 8-68490
 EuTe, mag. struct. and transition temp., indirect exchange 8-91860
 Fe, Neel temp. 8-88124
 Fe-Mn, annealed, α-γ phase transformation obs. 8-75831
 Fe-Mn-Co-Ni-Cr, antiferromag. props., Neel temp. determ. 8-88124
 Fe-Pt alloy, ordered, anisotropy of mag. props. (*Russian*) 8-60280
 FeBO₃, photoinduced linear birefringence (*Russian*) 8-52469
 FeBO₃, critical indices splitting of sublattice magnetisation (*Russian*) 8-60299
 Fe₂B₇O₁₃, ferroelec., mag. ordering, neutron diffr. meas. 8-72331
 FeBr₂, dynamic Jahn-Teller system, Raman scatt. from electronic excitations and phonons 8-56474
 FeCl₂, antiferromag. reson., temp. depend. 8-68384
 FeCl₂, dynamic Jahn-Teller system, Raman scatt. from electronic excitations and phonons 8-56474
 Fe_{1-x}Cl_xCd_x, randomly disordered, tricrit. behaviour, light scatt. 8-68255
 Fe_(1-x)Co_xCl₂.2H₂O, random mixture of anisotropic antiferromags., isotropic state obs. 8-84396
 Fe₂Cu_{1-x}Rh_xS₄, mag. tetrahedral intrasublattice interaction, X-ray, magnetisation and Mossbauer expts. 8-52241
 FeF₂, antiferromag. spin flop boundary 8-84419
 FeF₂, magnon-acoustic phonon hybridisation in far IR absorpt. spectra 8-60271
 FeGe₂, mag. struct., Mossbauer method 8-60268
 Fe₂, far IR magnetoabsorption, excitation of two spin deviations 8-80339
 Fe_{1-x}Mg_xCl₂, magnetic excitations 8-91852
 Fe₂Mn_{1-x}Pt_x, ferro-antiferromag. transform. at 4.2K (*Russian*) 8-88117
 FeMo₂S₄, Mossbauer spectra, 79-300K, Neel pt. determ. 8-60360
 Fe_{1-x}O, wustite, phonon and magnon props., inelastic neutron scatt. 8-52236
 α-Fe₂O₃, film, prep. by reactive condensation and mag. props. 8-64241
 α-Fe₂O₃, haematite, birefr. under uniaxial stress in mag. field (*Russian*) 8-88285
 Fe₂O₃, haematite, mag. domain distrib., appl. of mag. Laue neutron diffr. method 8-95455

antiferromagnetic properties of substances continued

- Fe₂O₃, haematite, optical indicatrix deform. and rot. during field induced phase transition 8-68482
- γ-Fe₂O₃, prep. from thermal decomp. of [Fe₃(HCOO)₆(OH)₂][HCOO₄H₂O and characterisation 8-80741
- Fe₂O₃, shocked hematite, Mossbauer exam. 8-64304
- Fe₂O₆, O₂ annealed, optical absorpt., spin struct., polaronic absorpt., cryst. field transitions 8-68493
- FeOOH, high-pressure phase, neutron diffraction study 8-52212
- β-FeOOH, ultrafine particles, mag. struct., Mossbauer spectroscopy 8-72372
- FePt₃, neutron scattering study of spin waves 8-91856
- Fe₄₈Rh₅₂, hyperfine mag. field at ⁵⁷Fe and ¹¹⁹Sn nuclei, press. depend. (Russian) 8-80266
- FeS, zinc blende type, mag. struct. (French) 8-91846
- FeSb₂O₄, defect struct. and mag. transition, elec. transport and Mossbauer expts. 8-59803
- Fe₂TiO₄, ulvöspinel, mag. props. weak ferromag. in 4-200K temp. range 8-56351
- FeU₂S₅, mag. struct., exchange energy, magnetisation and neutron diff. expts. 8-68170
- Gd compounds, NaCl type, exchange striction 8-84409
- Gd-Y alloy, anomalous thermal expansion, interferometric meas. 8-52333
- GdAlO₃, crossover effects near spin-flop multicritical point 8-68245
- GdCl₃, interaction parameters, high freq. meas. of adiabatic differential susceptibility 8-68211
- GdM₂Ge₂, M=Mn, Fe, Co, Ni, Cu, magnetism and hyperfine interactions 8-76228
- GdMg₃, mag. props., Mg conc. depend. 8-84392
- GdP, electronic struct., mag. exchange and elec. transport props. 8-87974
- GdP-GdS systems, mag. exchange interactions, free carrier conc. 8-60278
- GdS, electronic struct., mag. exchange and elec. transport props. 8-87974
- GdS, metallic FCC antiferromag., phonon Raman scatt. 8-60458
- ³He with C particles, pulsed NMR, mag. susceptibility surface induced ferromagnetism, antiferromagnetic exchange interaction 8-79844
- Hg_{0.9}Zn_{0.1}Cr₂Se₄, absorption spectra near the absorption edge 8-80340
- Ho, magnetoelastic interactions 8-64252
- Ho-Sn, dil. alloy, hyperfine interaction of ¹¹⁹Sn, Mossbauer meas. 8-91998
- KCoF₃, antiferromag., ⁵⁹Co NMR exam. 8-76332
- KCoF₃, NMR, magnon-phonon interaction contribution to nuclear spin-lattice relax. 8-88207
- K₂Co₂(SO₄)₃, cubic langbeinite struct., low temp. mag. susceptibility 8-56299
- KCuF₃, chain-like antiferromag., parallel susceptibility 8-80137
- KCuF₃, one-dimensional S=1/2 Heisenberg antiferromag., mag. energy, optical birefringence meas. 8-52467
- K₂FeF₄, two dimensional planar antiferromag., mag. excitations, Raman and far IR spectra obs. 8-72343
- KMnF₃, antiferromag., multi-magnon luminesc. sidebands 8-76525
- KMnF₃, spin density parameters at ¹⁹F nuclei 8-68001
- K₂Mn₂M_{1-x}F₄, (M=Mg,Zn,Cd), 2-dimens. antiferromag., sidebands on EPR lines 8-56370
- K₂Mn₂Mg_{1-x}F₄, EPR spectra 8-76298
- K₂Mn₂(SO₄)₃, cubic langbeinite struct., low temp. mag. susceptibility 8-56299
- KMn_{0.18}Zn_{0.82}F₃, excitation of Mn⁺ clusters, neutron scatt. 8-68200
- KNiF₃, antiferromag. domain wall motion obs. by X-ray synchrotron topography 8-88139
- KNiF₃, electronic UV laser excited Raman, scatt. by mag. excitons 8-68492
- KNiF₃, isotropic antiferromag., phase diagrams, US meas. 8-68350
- KNiF₃, spin density parameters at ¹⁹F nuclei 8-68001
- K₂NiF₄, electronic UV laser excited Raman, scatt. by mag. excitons 8-68492
- K₂Ni₂(SO₄)₃, cubic langbeinite struct., low temp. mag. susceptibility 8-56299
- KVF₃, antiferromag. ordering points, thermal anal. and X-ray diff. meas. (French) 8-84421
- (La,Ce)Al₂, conf. Kondo system, sp. ht. meas. 8-52210
- LiH, nucl. antiferromag. struct., neutron diff. and dynamic polarisation (French) 8-88226
- Mn complex, manganese (II)(1,2,4-triazole)₂(NCS)₂, 2-dimens. Heisenberg antiferromag., mag. props. 8-72336
- Mn-Cu alloy, plastic deform. mechanism and shape-memory effect, mag. struct. obs. (Russian) 8-60705
- γ-Mn-Fe, FCC→FCT transform. temp. and Neel temp., X-ray and neutron diff. expts. (Russian) 8-84797
- γ-Mn-Ni-C, elastic anomalies, martensitic transformation in Mn rich alloys 8-84807
- Mn-Pt (<29 at.%), eutectoid transform., antiferromag. struct. transform. (French) 8-92259
- Mn-ZnF₂, crit. neutron scatt. 8-52249
- MnCl₂·4H₂O, biaxial antiferromag., bicritical region, sp. ht. meas. 8-68246
- MnCo₃, weak ferromag., antiferromag. reson., phenomenological theory 8-60339
- MnCrF₃, antiferromag., mag. struct. (French) 8-52211
- Mn₃Cr₂Ge₃O₁₂ garnet, antiferromag. ordering (Russian) 8-80146
- MnF₂, antiferromag., multi-magnon luminesc. sidebands 8-76525
- MnF₂, antiferromag. domains, obs. using neutron technique 8-64213
- MnF₂, nuclear spin lattice relax. exam. 8-76331
- MnF₂, one-magnon luminesc. sidebands of excitonic transition 8-60517
- MnF₂, reson. NMR near phase transition 8-76265
- MnF₂, surface spin-flop and antiferromag. spin-flop transition 8-52257
- MnF₂, two-exciton many photon absorption, effect of statistical props. of light on intensity (Russian) 8-95589
- MnF₂, uniaxial antiferromag. anisotropy in paramag. susceptibility, cluster variation theory 8-52200
- MnF₂·Ni²⁺, IR fluoresc., field depend., exchange energy 8-68543
- Mn_{2-x}Fe_xSb, Mossbauer effect exam. 8-68432
- MnO, Jahn-Teller effect on optical absorption spectra 8-52484
- MnS, crit. behaviour, neutron diff. exam. 8-80169
- Mn₂Sb_{1-x}Sn_x, mag. transitions, Mossbauer meas. 8-52406
- MnSi, itinerant electron system, neutron scatt. 8-68194
- Mn₂Zn_{1-x}F₂, CPA estimate for Neel temp. 8-76245

antiferromagnetic properties of substances continued

- NaMnCl₃, mag. props., 2-25K, antiferromag.-paramag. transition (Russian) 8-88125
- NaNiF₃, electronic UV laser excited Raman, scatt. by mag. excitons 8-68492
- NdFeTiO₅, mag. susceptibility, 4.2-77K, antiferromag. ordering obs. 8-68186
- NdFeTiO₅, magnetic props. and crystal growth 8-92185
- Ni complex, tris(ethylenediamine)nickel(II) nitrate, mag. props. from susceptibility and sp. ht. meas., 0.3-3.0K 8-91877
- Ni-Fe film, unidirectional anisotropy by exchange coupling, appl. to biasing of magnetoresist. read head 8-91907
- Ni-Mn alloy, disordered, exchange-anisotropy field, magnetisation curves 8-72365
- Ni-Mn alloy, disordered, mag. struct., high field twist deform. 8-68166
- Ni₃B₂O₁₁, cubic, Raman spectrum, 88-295K, vibr. anomalies 8-76479
- NiF₂, electronic UV laser excited Raman, scatt. by mag. excitons 8-68492
- NiF₂, weak ferromag., antiferromag. reson., phenomenological theory 8-60339
- Ni₂Mn(Mn,Mn_{1-x}), Heusler alloy, antiferromagnetic order, X-ray and neutron diff. 8-64189
- NiO, antiferromag. domains, obs. using neutron technique 8-64213
- NiO fine particles, mag. props. rel. to physicochem. props. 8-52315
- NiO, mag. transition, neutron scatt. exam. 8-56313
- NiO:⁶⁷Zn, perturbed ang. correl. 8-95535
- NiS₂, high press. effect on mag. transition temps. 8-91866
- NiS₂, mag. struct. at 5K, polarised neutron study 8-80131
- NiS₂, neutron diff. anomaly at Curie temp., antiferromag. refl. 8-76260
- NiS_{2-x}Se_x, mag. struct., ⁵⁷Fe Mossbauer study 8-56409
- NiSnCl₆·6H₂O, ESR line shift at very low temps. 8-56375
- NpRe₂, mag. susceptibility 8-68182
- α-O₂, elementary excitations, effect of mag. anisotropy (Russian) 8-76317
- Pr, magnetic ordering due uniaxial stress, mag. excitons by neutron scatt. 8-84467
- Rb₂CoF₄, two dims. Ising like antiferromag., spin wave excitations 8-72342
- Rb₂Co₂Mg_{1-x}F₄, neutron scatt. exam., obs. of two dims. mag. long range order 8-56295
- Rb₂FeF₄, two dimensional planar antiferromag., mag. excitations, Raman and far IR spectra obs. 8-72343
- Rb₂FeF₄, 1D antiferromagnetic system, Mossbauer investigation 8-95533
- RbMnCl₃, antiferromag. static mag. props. (Russian) 8-60270
- RbMnF₃, antiferromag., multi-magnon luminesc. sidebands 8-76525
- RbMnF₃, isotropic antiferromag., phase diagrams, US meas. 8-68350
- RbMnF₃, isotropic antiferromag., crossover behaviour of mag. phase boundary, US meas. 8-80145
- RbVF₃, antiferromag. ordering points, thermal anal. and X-ray diff. meas. (French) 8-84421
- SmAu_{2.6}, ordering temps. and effective moments 8-60283
- SmH₂, low temp. sp. ht., antiferromag. ordering and cryst. field splitting effects 8-84439
- SmMg₂, cryst. and mag. props., ordering 8-68185
- SmSb_{1-x}S_x, magnetic ordering and configuration mixing 8-68179
- Sr₂Fe₁₀O₂₂, mag. props. and spin order 8-52232
- SrNd₂Fe₂O₇, mag. struct., neutron diff. determ. (French) 8-52224
- TbAu_{3.6}, ordering temps. and effective moments 8-60283
- TbMg₃, mag. props., Mg conc. depend. 8-84392
- TbPO₄, anomalous magnetostriction at low temp. 8-84470
- TbPO₄, sp. ht., 0.5-10K 8-52298
- (Ti_{1-x}V_x)₂O₃, spin glass to antiferromag. regime 8-52276
- (Ti_{1-x}V_x)₂O₃, spin glass and metallic antiferromagnetism 8-68268
- TiBr-VBr₂ system, cryst. struct., DTA investig. (German) 8-72766
- TmSe, mixed valence systems, spin dynamics and mag. ordering 8-68162
- Tm₂Se, 0.87<x<1.05, mag., thermal and transport props., comp. depend. 8-68239
- U dinitrides, elec. and mag. props. 8-84399
- UGeY, (Y=S, Se, Te), mag. ordering, neutron diff. obs. 8-72329
- UN, phonon dispersion relation near Neel temp., neutron coherent inelastic scatt. 8-59900
- UP-PrP (NdP) systems, mag. phase diagrams 8-84424
- V-Cr, elastic moduli, US pulse echo meas. 8-84881
- V₂O₃, low temp. antiferromag. phase, mag. struct. 8-52213
- V₆O₁₁, sp. ht., 0.4-50K 8-72358
- V₂S₃, single cryst., mag. props. 8-88098
- YFeO₃, mag. domain walls, photomagnetic effects, ⁵⁷Fe NMR obs. 8-95464
- ZnCr₂Se₄, magnetoelastic coupling, mag. suscept. meas. 8-76288
- Zn_{1-x}Fe_{0.85-x}O, prep. and struct., mag. and semicond. props. (French) 8-51506

antiferromagnetic resonance

- NMR, resonant, near mag. transition 8-76265
- relaxation processes, spin-sound wave coupling 8-60340
- spin waves studied by microwave absorpt. 8-91960
- stationary and transition processes in region of identical nucl. and electron mag. reson. freqs. (Russian) 8-80225
- TMMC, one-dimensional, EPR at HF and low temp. 8-80205
- CoCo₃, weak ferromag., antiferromag. reson., phenomenological theory 8-60339
- CoCo₃, weakly ferromag., light scatt. on spin waves (Russian) 8-72419
- FeCl₂, antiferromag. reson., temp. depend. 8-68384
- Fe_{1-x}Mg_xCl₂, magnetic excitations 8-91852
- MnCo₃, weak ferromag., antiferromag. reson., phenomenological theory 8-60339
- MnF₂, reson. NMR near phase transition 8-76265
- NiF₂, weak ferromag., antiferromag. reson., phenomenological theory 8-60339
- α-O₂, elementary excitations, effect of mag. anisotropy (Russian) 8-76317

antiferromagnetism

see also *antiferromagnetic properties of substances; exchange interactions (electron); metamagnetism*
 acoustic wave nonlinear self-interaction in antiferromag. with easy plane anisotropy (*Russian*) 8-80187
 alloy, binary, with mixed ferro- and antiferromag. exchange, magnetisation, phenomenological theory (*German*) 8-56297
 alloys, Lifshitz point occurrence, review 8-52265
 alloys, nesting type model, spin fluctuations 8-84435
 amorphous magnet, Behe-Peierls-Weiss approx. 8-76263
 anisotropic antiferromagnet, correction to scaling in specific heat 8-80168
 anisotropic chain, spin wave spectrum 8-60273
 Blume-Capel model for plane-triangular and FCC lattices 8-80114
 critical dynamics above crit. temp., dipolar coupling 8-52286
 critical resistivity of antiferromagnets below T_c 8-68004
 critical thermodynamics of antiferromagnet with two pairs of mag. sublattices (*Russian*) 8-60300
 cubic antiferromagnet, applied stress effects on equilib. config. 8-56365
 dielectric, crit. behaviour of exciton relaxation consts. 8-84442
 dilute Heisenberg antiferromagnet, mean spin on finite clusters 8-68139
 domains, ferromagnetic and antiferromagnetic, neutron techniques for obs., review 8-64213
 FCC alloys, atomic ordering and antiferromagnetism 8-72330
 ferroelectric antiferromagnets, exchange enhancement of the magnetoelectric coupling 8-88159
 ferroelectric ferro- and antiferromagnet, energy gap in spin wave spectrum 8-91858
 field-theory renormalization and critical dynamics above T_c : helium, antiferromagnets, and liquid-gas systems 8-87767
 gamma-rays generation by fast electrons travelling through antiferroelectric or antiferromagnetic crystalline structures 8-76545
 Heisenberg antiferromagnet, dil. with random first- and second-neighbour exchange bonds, CPA theory 8-52187
 Heisenberg antiferromagnet, disordered, magnetic atom-conc. near percolation threshold, mag. props. (*Russian*) 8-80171
 Heisenberg antiferromagnet, one-dimens., Friedel type oscils. 8-60296
 Heisenberg antiferromagnet, phase transitions in quantum spin systems 8-84434
 Heisenberg antiferromagnetic alloy, critical behaviour (*Russian*) 8-88128
 Heisenberg model, dil. CPA calc. 8-68263
 Heisenberg model, ground state energy, pair correl. 8-72321
 Heisenberg model, phase diagram and multicrit. behaviour 8-56337
 Heisenberg model, quasilow dimensional, small dilution perturbation theory at OK 8-56281
 Heisenberg model, second order self-energy 8-56279
 Hubbard antiferromag. semiconductor, electron correlations, weak coupling 8-67969
 Hubbard model, electron struct. in mag. field (*Russian*) 8-60287
 Hubbard model, FCC lattice, mag. and elec. props. 8-56334
 Hubbard model, itinerant antiferromagnetism 8-91841
 Hubbard model, Mott metal-insulator transition, ten-fold spin-orbital degeneracy 8-52285
 insulating systems, magnetic, review of expts. 8-68240
 insulator, antiferromag., light scatt. in strong mag. field 8-72523
 intermediate valence compounds, phonon produced instabilities, periodic Anderson model 8-79964
 Ising model, antiferromagnet, phase boundary determ. by real space renormalisation group methods 8-88134
 Ising model, ferromag. and antiferromag. in mag. field, new perturbation approach 8-56336
 Ising model, three-dimensional, two-spin correlation function, method for phase diagram 8-56323
 Ising model, two-dimens., interface free energy 8-60261
 Ising $S=1, 1/2$ mixture, one-dimens., random, mag. props., spin distrib. 8-95407
 Ising site model, random mixtures, Monte Carlo simulation 8-73935
 Ising site model, random mixtures, Monte Carlo simulation 8-73936
 isotropic antiferromagnet, magnetic moment and sp. ht. fluctuations near critical temp. 8-91867
 itinerant electron, mag. excitations 8-56305
 itinerant electron antiferromagnet, localised spin coupling 8-68142
 itinerant-electron antiferromagnet, effect of mag. field on crit. temp. 8-60293
 Krieger-James approx. of short range order effects, antiferro- and ferro-mag. 8-56276
 local field at positive muon 8-92010
 magnon damping due to impurity scatt. 8-68206
 metal, antiferromag., magnetoresistance, two band model 8-79979
 metal, antiferromagnetic, nesting type model, spin fluctuations 8-56329
 metal, with paramag. impurities, Neel temp., impurity conc. depend. calc. 8-68232
 moving dislocations, interactions with spin waves in antiferromagnet (*Russian*) 8-56303
 neutron optical activity in helicoidal antiferromagnetic materials 8-74419
 one-dimensional dilute Heisenberg system, mag. props. 8-64179
 one-dimensional disordered spin system with isotropic antiferromag. interaction, susceptibility and Knight shift (*Russian*) 8-88202
 parallel susceptibility of chain-like antiferromagnets 8-80137
 parametric excitation on spin waves in the induced magnetoelastic crystals (*Russian*) 8-60272
 Peierls-Hubbard model, quasione dimens., antiferromagnetism and Peierls distortion 8-67931
 phase transformations in strong mag. fields, mag. moments collapse, strengthened magnetoelastic links (*German*) 8-68227
 quadratic antiferromagnet, with easy-plane anisotropy, spin wave theory 8-91855
 random exchange interactions, and 'frustration effect' 8-68212
 residual stress induced domains in antiferromags., specific heat meas. anal. 8-60286
 resistivity of magnetic systems, critical behaviour 8-87955
 semiconductor, magnon-plasmon interaction and its effect on Raman scatt., theory 8-56302
 semiconductor, sound propagation 8-72211
 spin-one Ising system, phase diagram 8-95441

antiferromagnetism continued

static properties of spin systems with truncated secular dipolar coupling 8-88130
 strongly correlated electrons in narrow bands 8-76218
 superfluid flow states, existence from Ginzburg-Landau theory (*Russian*) 8-72085
 transition metals, conf., Toronto, Canada (Aug. 1977) 8-91577
 transverse dynamical susceptibility within the local exchange approx. 8-76229
 triangular antiferromagnetic lattice, ground state energy, upper bound determ. using renormalisation 8-76212
 triangular Ising lattice with small second neighbour interaction crit. temps. 8-56331
 two-spin light scattering, disordered phase rutile antiferromags., MnF_2 , NiF_2 8-80336
 Wolff model, effective mag. interactions between impurity and conduction electrons 8-68143
 X-Y antiferromagnet, one-dimens., Friedel type oscils. 8-60296

antihyperons see hyperons**antimony**

see also *nuclei with*
 amorphous film, elect. resist. 8-95390
 atom, integral K-shell Compton scattering, cross-section, for 1250 keV photons 8-90128
 carrier energy spectrum, effect of hydrostatic pressure 8-87903
 de Haas-van Alphen effect, effective mass, Fermi levels 8-75982
 determination, in combustible municipal solid waste, by AAS 8-85229
 determination in Cu alloys, inverse voltamperometry method 8-61099
 diamond, zz 8-91367
 diffusion and solid solubility in Fe, 773-873K, ion backscatt. anal., rel. to intergranular embrittlement 8-71880
 diffusion in Si, implantation damage effects 8-55988
 electrodeposit, amorphous, explosive crystn., semicond-semimetal transition and IR absorpt. 8-51849
 electron density at nucleus, press. depend., Hartree SCF calcs., Mossbauer shift press. depend. 8-56411
 epitaxial growth on Bi substrate 8-95246
 Fermi surface, tension effect (*Russian*) 8-75980
 film, X-ray diffr. anal., {001} textured growth 8-72016
 film A1-type supercond. vapour-quenched transition temp., A7-type phase transition 8-52145
 film with epitaxial thin Fe film 8-56572
 foil, traversed by $\text{H}^+(\text{He}^+)$, energy loss and straggling meas. 8-95100
 ion implantation, combined with Si vacuum deposition (*Japanese*) 8-88428
 magnetoresistivity, mutual drag effect, temp. depend 8-52012
 NQR, nucl. spin-lattice relax., 4.2K 8-91984
 spin splitting meas. from de Haas-van Alphen effect, g-factors 8-51881
 thermoelectric figure of merit, 1-12 kbar, 100K 8-80013
 whiskers, quantum oscils. of magnetoresist. (*Russian*) 8-60145
 zone centre phonons and elastic consts., hydrostatic press. depend. 8-59905
 Al, zz 8-91367
 Be, zz 8-91367
 Bi, zz 8-91367
 Bi:Sb, quenching and annealing of defects, elec. resist. meas. 8-87973
 Bi-Sb interface, film, thermoelectricity, ageing differential efficiency (*German*) 8-60146
 C, zz 8-91367
 $\text{Ca}_2\text{P}_2\text{O}_7\text{Sb}$, (Sb,Mn), luminesc., activation, colour centres (*Russian*) 8-92123
 $\text{Ca}_3(\text{PO}_4)_2\text{Sb}$, (Sb,Mn), luminesc., activation, colour centres (*Russian*) 8-92123
 Ge, zz 8-91367
 Ge:S film, amorphous, ion implantation, effect on cond. 8-83839
 Ge:Sb, acoustic attenuation, uniaxial stress effects 8-59863
 n-Ge:Sb, fast neutron irradi. effects on donor conc., and annealing 8-56107
 n-Ge:Sb, γ -irrad. effects on donor conc. and compensation by acceptors 8-56106
 Ge:Sb, neutron irradi., carrier mobility theory and expt. 8-56166
 Ge:Sb, phonon thermal cond. calc. 8-71893
 Ge:Sb,Cu, exactly compensated, impurity absorpt. and photocond. spectra 8-56189
 Ge:Sb film, electronic props. 8-84330
 Ge-Sb, D^+ complexes and band form., photocond. 8-84251
 K, zz 8-91367
 Li/Sb interface, CESR meas. 8-80218
 Mg, zz 8-91367
 Sb, zz 8-91367
 Sb:Te, de Haas-van Alphen effect, effective mass, Fermi levels 8-75982
 Sb₄, gaseous, atomisation enthalpy and enthalpy of form., mass-spectroscopic Knudsen cell method 8-80780
 Si, zz 8-91367
 Si:Sb, ion implanted, annealing behaviour of stress 8-63778
 Si:Sb, multiparticle impurity complexes (*Russian*) 8-72601
 Si:Sb, shallow donor electrons, hyperfine interactions, reply to Onffroy's calcs. 8-51934
 Si:Sb, shallow donor states with strong central cell perturbation theory 8-51933
 Si:Sb device, anal. using SEM-AES-IMA combination with SIM spectrometer (*Japanese*) 8-85249
 Si:Sb film, amorphous, ion implantation, effect on cond. 8-83839
 SnO_2Sb , and pure cryst., microstruct., X-ray diffr., optical and electron microscope studies 8-79619
 Te:Sb, 96 to 500K, cond. Hall const., hole mobility, conc., dislocation effects (*Russian*) 8-64039
 ZnTe:Sb film, elec. props. 8-76172

antimony alloys

see also *antimony compounds*
 $\text{Mn}_{1.98-2}\text{Cr}_x\text{Fe}_{0.02}\text{Sb}$, Mossbauer effect exam. 8-68432
 steel, alloy, Fe-Ni-Cr-Sb-C effect of Ni, Sb, on temper embrittlement 8-60813
 Ag-Sb, Ag-ZZ 8-84730
 Ag-Sb, cold-worked, lattice defects, convolution relations for X-ray line breadth calcs. 8-51394
 Bi:Sb, semimetallic alloy, microwave spectroscopy 8-87908

antimony alloys continued

- Bi-Cd-Sb, calc. of phase equilibria using thermodynamic values from different models 8-60646
 Bi-Sb, crack appearance in diffusion zones (*Russian*) 8-76727
 Bi_{1-x}Sb_x, semicond.-semimetal transition, temp. and press. depend. of transport props. 8-76120
 Bi_{0.8}Sb_{0.2}-Sn, current carrier energy spectrum (*Russian*) 8-60139
 CaSb, resist., susceptibility and thermopower rel. to electronic struct. 8-67935
 Cu-Sb, cold-worked, lattice defects, convolution relations for X-ray line breadth calcs. 8-51394
 Cu-Sb, electron work function, contact pot. difference meas. 8-80041
 Cu₈₂Sb₁₇, X-ray K-absorption discontinuity, extended fine struct. 8-76556
 DySb, quadrupole scatt. anisotropy, magnetically ordered material 8-64034
 Fe, cast, Mg-Sb, despheroidising composition and distribution of phases, X-ray obs. (*Russian*) 8-95732
 Fe-Sb, additive effect on eutectoid transformation of Fe 8-52799
 Fe-Ti-Sb-C alloys, Sb trapping effect on temper embrittlement, ion beam study 8-92312
 FeSb₂, phase structure, X-ray crystallography (*French*) 8-91305
 Fe_{1+x}Sb, phase structure, X-ray crystallography (*French*) 8-91305
 HoSb, quadrupole scatt. anisotropy, magnetically ordered material 8-64034
 Mn_{2-x}Fe_xSb, Mossbauer effect exam. 8-68432
 MnSb, electronic state, neutron diffr. study 8-87906
 MnSb, resist., susceptibility and thermopower rel. to electronic struct. 8-67935
 Mn_{1+x}Sb_{1-x}Sn_x, magnetisation and Curie temp., prep. and comp. depends. 8-64200
 Mn₂Sb_{1-x}Sn_x, mag. transitions, Mossbauer meas. 8-52406
 Nb₂Sb, NQR study, ⁹³Nb nuclear relax. 8-88073
 Nb₂Sb, resist. characts. in normal state 8-51963
 NiSb, resist., susceptibility and thermopower rel. to electronic struct. 8-67935
 Ni₂Sb₂, cryst. struct. (*German*) 8-83775
 Pb-Sb, crystal struct., supercond. after subjection to high press. 8-88064
 PdMnSb, Heusler alloy, hyperfine fields of 5sp shell impurities substituting Sb, Mossbauer spectra 8-80261
 Pd₂MnSb, Heusler alloy, hyperfine fields of 5sp shell impurities substituting Sb, Mossbauer spectra 8-80261
 Pt-Sb, amorphous sputtered film, elec. props. 8-68006
 Sb-Au, amorphous film, elect. resist. 8-95390
 Sb-Ge, unidirectionally solidified, exam. of compressive props. and struct. 8-68730
 Sb-Sn, dil., de Haas-van Alphen effect, effective mass, Fermi levels 8-75982
 Sb-Te-Bi, miscibility limits, computer study 8-79773
 Sn-Sb dil. liq. alloy, electrodiffusion and electroconvection, effective diffusion coeff., apparent effective valence 8-87802
 Te-Sb, liq., elec. cond. 8-84186
 V₃Si-Sb, cryst. struct., supercond. T_c comp. depend. 8-51494

antimony compounds

- see also antimony alloys*
 Mossbauer effect of ¹²¹Sb in mixed valence cpds. M₂¹Sb_{0.5}M_{0.5}^{IV}Cl₆, (M^I=NH₄⁺, Rb or Cs, M^{IV}=Se, Te or Sn) 8-84506
 Ba₃Sb₂NiO₉, 6H, cation ordering, powder neutron diffr. obs. 8-55852
 Bi_{1-x}Sb_xSi, atomic substitution and ferroelec. phase transition 8-68464
 Bi_{0.52}Sb_{0.48}Te₃, thermoelec. solid soln., homogeneity, effects of prep. method 8-52698
 Bi_{2-x}Sb_xTe₃, solid soln. film on mica substrate, effect of stresses on elec. cond. 8-51859
 Bi₂Te₃-Sb₂Te₃ film, residual cond. 8-52110
 Bi₂Te₃-Sb₂Te₃ solid solns., powders, particle shapes determ., device 8-60899
 FeSb₂O_{4-y}, defect struct. and mag. transition, elec. transport and Mossbauer expts. 8-59803
 (GeTe)_x(AgSbTe₂)_{1-x}, thermoelectric props. of monolithic and pressed samples at 300K 8-80009
 In_{1-x}Ga_xAs-GaSb_{1-y}As_y, new heterostruct. characts. 8-72247
 LiBa₃Sb₂Ti₂O₂₁, insertion of Li, X-ray and neutron diffr. study (*French*) 8-91324
 Sb-Te-Bi, computer study of miscibility limits, 273 to 300K 8-52781
 SbCl₃OPCl₃, vibr. amplitude and normal coord. anal. (*German*) 8-66536
 SbF₃ (f⁰⁺, e⁰⁻)-X₂1 transition, rot. anal. 8-74657
 SbF₃, IR spectra of solid and gas, rel. to struct. (*French*) 8-78692
 SbF₃, muon Coulomb capture ratio 8-62959
¹²¹SbF₆²⁻, radical, prep. and EPR comparison with other hexafluoride radicals 8-68381
 SbF₃(NH₂)₂CS and SbF₃[(NH₂)₂CS]₂, X-ray cryst. struct., IR spectrum (*French*) 8-87643
 SbH₃, inversion barrier, ab initio SCF calcs. 8-78615
 SbI₃, intermolecular bonding study using ¹²⁹I Mossbauer effect 8-72438
 SbNbO₄, ferroelec. anomalous photovoltaic effect and photocond. 8-52449
 Sb₂O₃, additive in ZnO sintering 8-80497
 Sb₂O₃ glass, X-ray diffr. anal. of struct. 8-87621
 Sb₂O₆, IR and Raman spectra vibr. spectra, valence force field calc., pot. function (*French*) 8-50549
 Sb₂O₃Cl₂, cryst. struct. refined 8-79572
 2MASb₂O₇I, polytype, crystal structure determination 8-91316
 Sb₂S₃, electronic struct., X-ray emission, XPS, UPS obs. 8-52638
 Sb₂S₃, ferroelectric semiconductor, effect of screening by conduction electrons on phase transitions 8-84537
 Sb₂S₃, influence of temp. on NQR spectra of ^{121,123}Sb 8-60354
 Sb₂S₃ layered biaxial cryst., surface phonon polaritons (*Russian*) 8-60021
 Sb₂S₃:Ag, sensitised photolysis and structure of latent photographic image 8-89574
 SbSBr, optical B_u modes of paraelectric phase, simple model 8-75747
 SbSI, abrupt polarisation changes under influence of external forces 8-68459
 SbSI, birefr. and phase transitions 8-60405
 SbSI, ferroelec., phase transitions, birefringence meas. 8-56440

antimony compounds continued

- SbSI, ferroelec. semicond., laser-modulated reflectance near T_c 8-72552
 SbSI, ferroelectric semiconductor, effect of screening by conduction electrons on phase transitions 8-84537
 SbSI, free energy function, temp. depend. and anisotropy of dielec. const., ferro- and paraelec. phases 8-64330
 SbSI materials, piezoelectric props. rel. to use as electroacoustic transducers 8-52445
 SbSI, max. vel. of domain boundaries in polarisation reversal, Barkhausen effect meas. 8-60411
 SbSI, optical B_u modes of paraelectric phase, simple model 8-75747
 SbSI, paraelectric phase, jump-like switching processes, ferroelec. surface layer 8-92038
 SbSI, tricrit. point at 1.4 kbar and 235K 8-68463
 Sb₂Se₃, liq. struct. anal., neutron diffr. study 8-79519
 Sb₂Se₃-Se-SbSeI, exam. of glass formation, IR transmission spectra 8-88452
 SbSeI, optical B_u modes of paraelectric phase, simple model 8-75747
 SbTaO₄, X-ray and ESR study of phase changes 8-72476
 Te-Sb₂Te₃ oriented eutectic, microhardness, influence of size of phases (*Russian*) 8-92322
 Ti₂Te-Sb₂Te cross section of Ti-Sb-Te system, new TiSbTe₂ and Ti₂SbTe₅ cpds. 8-52778
 ZnO-Sb₂O₃-O₂ system, cpd. forming reactions 8-52699

antineutrinos *see* neutrinos**antineutrons *see* neutrons****antinucleons *see* nucleons****antiphase boundaries**

- ferromagnetic ordered structures, domain structure, effect of defects, electron microscopy 8-64214
 Au₁Mn₄, electron diffraction and microscopy obs. 8-75512
 (Ba₂Nb₂Si₂O₂₆)_n.Ba₃Nb₂Ti₂O₂₁, multiple intergrowth and microdomains obs. by electron diffr. and microscopy (*French*) 8-95160
 Cu₃Sn, one-dimens. long period superstructs. with Zn and Ni additions 8-83777
 Fe₃Al, ordered alloys, atomic order parameters from topology of electron-microscope diffr. contrast from antiphase boundaries, quantitative determ. 8-95016
 Mn-Al permanent magnets, defect structure, mag. props. TEM obs. 8-91902

antiphase domains*see also antiphase boundaries*

- Au-Cu-Ag dental alloy, age-hardened, struct. and morphology 8-92272
 Fe₂Si, etching of slip produced antiphase domain boundaries 8-63769
 SrAl₂Si₂O₈, TEM obs. of feldspar and hexacelsian polymorphs 8-83827

antiprotons *see* protons**antireflection coatings**

- application technology, review of problems 8-83069
 baffle edge design using optical black coating 8-59154
 Bragg reflector statistical analysis 8-66882
 design method for two given wavelength coating 8-59102
 IR optical scanning system, narcissus effect suppression, computer results 8-59151
 multilayer, for camera objectives, practical effectiveness 8-58081
 multilayer optical interference coatings via glow discharge polymerization techniques 8-87170
 noise in optical instruments, stray light reduction, space appls. 8-59153
 rain erosion resistant antireflective coatings for IR windows 8-83050
 single-layer film 2.8 μm, 3.8 μm absorpt. meas. 8-90463
 solar energy photothermal conversion, optical performance of absorber-reflector combinations 8-63168
 stray light problems in optical systems, conf., Reston, VA., USA (Apr. 1977) 8-59112
 stray light reduction from optical components 8-59114
 three-layer equivalent film design 8-66884
 TiO₂ antireflection coatings by a low temperature spray process 8-90537
 CaF₂ trapezoid, ThF₄ and ZnSe coated, IR characterisation by internal-refl. spectra 8-71161
 InSb spin-flip Raman laser external-cavity system, oscill. characts. 8-55383
 PbO-SiO₂ glass, optical coating for GaAs-Al_xGa_{1-x}As laser 8-71113
 SiO₂ antireflection coatings for InP/CdS solar cells 8-50871
 WO₃, on textured W surface, for solar absorber appl., props. 8-63157

aperture cards *see* microforms**API gravity *see* density****apodisation *see* acoustic imaging; optical images****apparatus *see* instrumentation; instruments****apparent porosity *see* porosity****appearance potential *see* ionisation potential****appearance potential spectra**

- Be, anisotropy, theoretical investigation by K-emission, APS, and Compton profiles 8-63970
 V, extended fine struct. above 2s appearance potential edge, AEAPS spectra 8-72647
 V, extended fine struct. above L-shell appearance pot. thresholds 8-92148

appearance potential spectroscopy

- field dispersed ion analysis, comparison with conventional technique for O⁺, CO⁺, and CO₂⁺ 8-85234
 recent developments (*Japanese*) 8-78052
 soft X-ray SXAPS, noise source and sensitivity 8-49949

Appleton layer *see* ionosphere**appliances, domestic *see* domestic appliances****applied mechanics *see* mechanics****approximation theory**

- see also function approximation; interpolation; least squares approximations*
 chemistry, method of successive approx., teaching 8-89281
 linear harmonic oscillator on lattice, wave functions, energy eigenvalues, Pade approximant method 8-57817
 molecular dynamics, L-F approx. method, second order secular eqn. soln. 8-66458

approximation theory continued

- multivariate approximants with branch points, off diagonal approximants 8-54160
- multivariate approximants with branch points, practical evaluation 8-54161
- rectangular matrix pseudoinverse using column approx., inconsistency systems of linear eqns. solns. 8-62061
- smear concentration approximation, appl. to air pollution modelling 8-81381
- steam pressure and temp. in relation to enthalpy and entropy, approximation formulæ in binary polynomial form (*German*) 8-59532

apr see *acoustic paramagnetic resonance*

APT see *problem oriented languages*

APW calculations

- A15 compounds, plasma energies, tight-binding energy-band model 8-84159
- Al (001) surface, nearly-free-electron metal, origin of surface reson. states 8-95322
- crystalline thin films, band struct. calc., appl. to Cu monolayers 8-87899
- transition metal, model potential, generalised APW formulation 8-91579
- transition metals, second series, electronic band Brillouin zone APW calc., electronic config. effects 8-51883
- XPS, angle-resolved, interpretation 8-72696
- CoAl, bonding, self-consistent energy bands 8-91610
- Cs, electronic transition from self consistent APW $X\alpha$ calcs. 8-51884
- FeAl, bonding, self-consistent energy bands 8-91610
- Gd, self consistent relativistic ferromag. band struct. 8-91609
- $\text{Li}_2\text{Ag}_2\text{In}_x$, optical props., struct., energy bands, interband transitions 8-72539
- $\text{Li}_2\text{Cd}_2\text{In}_x$, optical props., struct., energy bands, interband transitions 8-72539
- Nb_3Si , Nb_3Sn , Nb_3Ge , Nb_3Ga , Nb_3Al , electronic struct., electron-phonon interactions, X-ray spectra 8-91613
- Nb_3Sn , electronic struct., APW method 8-72066
- Ni, X-ray absorption and emission K and L spectra, APW calc. 8-68579
- NiAl, bonding, self-consistent energy bands 8-91610
- $\text{Pd}_{1-x}\text{Ag}_x\text{H}_2$, superconducting transition temp., APW band struct. calcs. 8-95393
- PdH, electronic struct. and proton spin-lattice relax. calc. 8-67937
- UGe_3 , de Haas-van Alphen effect, band struct. calc. 8-72068
- V_3Si , V_3Sn , V_3Ge , V_3Al , electronic struct., electron-phonon interactions, X-ray spectra 8-91613

arc discharges see *arcs (electric)*

arc furnaces

- thermal plasma aspects (*German*) 8-75402

arc heaters see *arc furnaces*

arc lamps

- alkali metal vapour flash lamp, absolute spectral distrib. and radiant output 8-66510
- Eimac Xe arc lamp, radiant power rel. to hollow cathode lamp 8-89547
- inert gas flash lamp, absolute spectral distrib. and radiant output 8-66510
- pulsed lamps, parameter changes with different charge conditions (*Russian*) 8-83642
- UV sources for curing 8-88443
- H-He arc lamp, 60-360 nm, calibration 8-87117
- Hg-Sn halide arc, molecular optical absorption obs. 8-75457

arc welding

- temperature meas. and physics of welding arc 8-55771
- Ar plasma welding, compressed arc V-I characteristic obs. (*Russian*) 8-83628

archaeology

- archaeomagnetic data compared with analytical representation of geomag. field for last 2000 years 8-73305
- artifacts as sedimentary particles in fluvialite environment 8-70239
- bristlecone pine and ancient Egypt, rel. to calibration of radiocarbon dates 8-70234
- ceramic dating by alpha-recoil tracks in mica 8-70237
- ceramic sculpture from Oaxaca, Mexico, authentication by thermolum. and style 8-70238
- dating of prehistoric Great Basin petroglyphs by neutron activation anal. 8-70243
- electron probe analysis, sampling stylus 8-70246
- floating tree-ring chronology from NE.Scotland, radiocarbon meas. 8-70236
- glass, crystallisation after 1000 years storage 8-79536
- neutron activation analysis, comparison of results from Lawrence Berkeley Lab. and Hebrew University 8-70245
- obsidian, Mayan, source correl. for S.Belize artifacts 8-70244
- physical methods, review 8-58104
- quartz inclusion morphology for thermolum. dating, effect of HF etching 8-70240
- radiocarbon age determinations, procedures for comparing and combining 8-70235
- soil resistance meter, geological and archaeological applications (*German*) 8-57361
- Stonehenge, new meas. in 1978 April survey 8-85860
- thermoluminescence dating, effect of radioactivity within quartz 8-70241
- thermoluminescence dating of pottery, ^{87}Rb dose-rate contrib. 8-70242
- ^{14}C dating of geological and archaeological samples 8-92993

architectural acoustics

- see also *anechoic chambers; echo; noise abatement; reverberation*
- Acoustical Soc. Amer. 96th meeting, Hawaii, 1978 Nov. 8-90545
- CAD, based on digital meas. techniques (*Polish*) 8-59205
- concert hall acoustics, room impression as an overall concept of spaciousness and liveliness (*German*) 8-94484
- concert halls, hearing impressions of loudspeaker reproductions and orchestras (*German*) 8-94485
- concert halls, primary sound suppression (*German*) 8-75014
- decaying sound fields and spatial variation 8-79165
- domestic sound insulation deficiencies and remedies 8-83175
- double walls, sound transmission loss and cavity absorbent materials (*Japanese*) 8-79167

architectural acoustics continued

- enclosure, thermoviscous dissipation at walls, normal mode theory 8-83171
- history, Kircher's 'Phonurgia nova' (*German*) 8-81788
- horizontal wall acoustic insulation methods (*Spanish*) 8-87207
- insulating material losses and performance factors (*Spanish*) 8-55516
- insulation meas. dependence on type of loudspeaker (*German*) 8-75021
- interoffice speech privacy criteria and suspended ceiling acoustic insulation 8-83173
- landscaped office, effect of screens on sound attenuation 8-94486
- loudspeaker placement, reverberation problems (*German*) 8-87204
- maisonettes, flanking transmission of sound, effect of woodwool shuttering in party floors 8-94487
- multistorey buildings, reduction of structure-borne sound levels by floors and walls (*German*) 8-94483
- noise level definitions and building design criteria 8-83174
- oblique incidence sound absorpt. characts. of materials using cross-correlation methods (*Japanese*) 8-83172
- open-plan offices, acoustical parameters 8-55520
- open-plan spaces, acoustic props. and design for school classroom 8-77653
- partition airborne-sound transmission loss, effect of sound-absorptive facings 8-79166
- plasterboard sound reduction indices and meas. 8-87196
- radio studio acoustics planning for SDR's Stuttgart Broadcasting House (*German*) 8-71243
- rectangular room, instantaneous excitation of one-dim. sound waves (*German*) 8-87201
- regenerative sound system investigation using time-delay spectrometry 8-51006
- reverberant sound absorpt. coeff. of plane porous material, theory (*Japanese*) 8-79168
- reverberation studies, re. telephone loud speaker system 8-94488
- reverberation time, absorption and impedance, theoretical model used for calcs. of a room 8-90601
- room acoustics determination, noise abatement appl. 8-75016
- room impression index, definition on basis of subjective examination (*German*) 8-87202
- room resonance, computer-aided anal. 8-87205
- room resonances, absorption, effect on stereo loudspeakers freq. response (*Italian*) 8-51005
- sound differences in sensory space for sound reproduction engineering (*Russian*) 8-55521
- sound insulation design and transmission field meas. 8-87206
- sound system design aid, HP 97 program 8-75015
- space absorber composed of porous materials, reverberant sound absorption coeff. 8-55519
- spatial impression of concert halls, lateral refls., musical level (*German*) 8-79164
- timber frame constructions, sound insulation of wood joist floors 8-87203
- transmission function in rooms rel. to acoustic amplification systems 8-59204
- TV and motion picture stages, noise and insulation 8-79169

arcing see *arcs (electric)*

arcing, switches see *circuit-breaking arcs*

arcs (electric)

see also *arc furnaces; arc lamps; arc welding; circuit-breaking arcs*

- 8-67472
- ablation-stabilised arc temp. distrib. model 8-71585
- AC arc, axially blown with N_2 , field strength and energy balance eqn. 8-87523
- aerosol particles, effect on fast plasma stream form. in an elec. arc 8-51390
- air, transport coeffs. meas. 8-59709
- air arc discharge high-temp. transport obs. 8-71577
- anode sheath in high pressure high current arc 8-67467
- arc column, helical instability limits 8-71564
- arc quenching system for transient and statistical flashover, fusion reactor systems 8-75455
- arcing and surface damage in DITE Tokamak, SEM obs. 8-59611
- azimuthal conductivity, radial distrib. function 8-51374
- boundary layer cooling of atmospheric arcs, arc interruption by moving rod 8-87545
- cathode damage from 300 ns, 4.5 A arc, material comparisons 8-87579
- cathode region activity during transition to arc (*French*) 8-91172
- cathode spots on Ag, Ni, Cu, and W vac. arc discharge electrodes, model 8-91179
- chemically reactive arc-heated gas flow, ion saturation current fluctuation probe 8-63574
- circuit breaking air blast arc, near current zero, local elec. props., optimisation 8-87516
- column helical instability in axial mag. field, damping and RF-DC discharge 8-71595
- constriction phenomenon due to longit. high vel. flow 8-87546
- controlled generators, spectra, rel. to quantummetric meas. (*Russian*) 8-74072
- cross-flow arc behaviour, theory and expt. 8-75484
- crossed-field arc discharge contraction ion source 8-86382
- current distribution in hollow-cathode arc discharge 8-67537
- DC arc, selective volatilisation of elements, in external mag. field, anal. appls. 8-68938
- DC arc as spectroscopic light source, mag. field effect on line intensities 8-87550
- DC melting plasmatron, low pressure characts. (*Russian*) 8-94945
- DC vacuum arc emitted particle flux 8-75470
- dense plasma, H_β line red shift expt. 8-67473
- double plasma arc, rotation in graphite tube 8-71599
- Duoplasmatron discharge resonance radiation emission model 8-67477
- Elenbaas-Heller eqn. solution by analogy 8-71584
- emission spectrometry, current developments (*Japanese*) 8-86356
- energy balance of anode in low-pressure heavy-current discharge with hollow cathode (*Russian*) 8-51369
- enrichment by plasma centrifuge, rotational velocity meas. 8-74502
- finite length, electrode-stabilised free arc in longit. mag. field, dynamic equilib. model 8-87551
- fireball plasma formation, transmission line model 8-59702

arcs (electric) continued

- flow stability, axial, cathode emission mechanism change effect 8-83638
 free-burning arc continuous radiation rel. to electrode erosion 8-71578
 free-burning arc isothermal-channel theory 8-71587
 Freeman type ion source in low press. arc operation, discharge characteristics and beam quality 8-66006
 gap with displacement by mag. field 8-87513
 heat transfer bibliography 8-63425
 helical arc column, dynamic equilibrium model 8-71593
 high current, burning in channel 8-63614
 high current density arcs in narrow channels, calc. and appl. 8-55762
 high current vacuum arc, with axial mag. field, current distrib. meas. 8-87572
 high-current constricted-arc anode heat balance obs. 8-71499
 high-current free-burning arcs, magnetically-driven plasma flow model 8-71588
 high-speed rotating anode disc, spot motion and erosion calc. 8-71498
 hollow cathode arc, Langmuir probe meas. for discharge model 8-87533
 hollow cathode arc, theory 8-67452
 hollow cathode arc discharge, electron energies, excitation and ionisation speeds (*German*) 8-91170
 hollow-cathode arc discharge, electron energy distrib. and ionisation velocity 8-67534
 hollow-cathode arc discharge impedance/frequency characteristic obs. 8-67536
 hollow-cathode low-pressure discharge critical current determ. 8-67538
 HV heavy-current arc gap 8-87514
 impulse breakdown in air gaps obs., using schlieren studies 8-87518
 inert gas rotating arc meas. in plasma centrifuge 8-75438
 intense ion source discharge, delay of arc starvation saturation 8-79457
 laminar and turbulent, longitudinal mag. field effect on characts. 8-71565
 low-current vacuum arcs, cathode mechanism, erosion rate calcs. 8-75448
 LV switching-off process, phenomena (*Slovak*) 8-55761
 magnetically blown flat arc, dynamics of heavy current arcs (*German*) 8-87509
 magnetically deflected arcs, forward and retrograde motion, cathode oxide film effects 8-87576
 metal vapour arc, cathode spot model, energy balance 8-79484
 metal vapour arc, in vacuum, axial mag. field effects 8-87573
 metal vapour lamp, additive partial pressure determ. from self-reversed spectral line maxima 8-67476
 momentum generation in high-current arc 8-71586
 motion of low-press. arc in strong mag. field 8-83637
 neutral beam, pulsed, arc (arc filament) power supplies, for fusion reactor 8-70637
 nozzle flow arcs, high current, scaling characts. 8-59707
 plasma, low-temp. diagnostics by scatt. and resonance fluorescence 8-67482
 plasma, of free jet laminar core, axial flow, strong localised disturbance effect 8-91178
 plasma arc heater, rotating mag. field interaction with gas stabilised discharge 8-71598
 plasma electron density, interferometric meas. 8-67479
 post-arc column temp. variation obs. 8-71591
 pressurised field distortion spark gaps, arc voltage waveforms, electrode material effects 8-87549
 quasistationary plasma, scatt. diagnostics using periodically pulsed UV lasers 8-67481
 rod/plane gap, air arc channel transient characts. under impulse voltage 8-87544
 spectral line intensity, comp. changes effects (*Russian*) 8-75452
 spectrum, correl. rels. (*Russian*) 8-70196
 thermal ion spectrum, meas. by CW CO₂ laser 90° scatt. 8-67480
 thermal shock fracture toughness eval. by arc discharge heating 8-72835
 Tokamak, Diva, metal impurities origin, arcing ion sputtering, evap. 8-59691
 tornado, contrib. of vortex-stabilised arc to energy 8-53711
 vacuum arc anode spot, ion currents and interaction with axial mag. fields 8-75469
 vacuum arc anode spot form., threshold current time depend. 8-87515
 vacuum arc cathode plasma interaction with transverse mag. fields 8-75468
 vacuum arc cathode spot dynamic models 8-75481
 voltage gradient in fully-developed turbulent air flow 8-71597
 wall stabilised arc, current step changes, conductance transient effects 8-87547
 wall-stabilised arc, N atom Stark broadened VUV lines 8-90107
 wall-stabilised arc conductivities with Cu vapour contamination 8-75458
 Ar arc deviation from Saha-Boltzmann equilibrium, heavy-particle effects 8-67596
 Ar atmospheric arc plasma deviation from LTE 8-67604
 Ar cascade arc light emission, effect of pulsed microwave field 8-67599
 Ar high-pressure arc plasma, IR continuum emission obs. 8-71604
 Ar high-pressure helical arc phase velocity in longitudinal mag. field 8-71594
 Ar high-pressure plasma elec. conductivity obs. 8-71448
 Ar I and II transition probability determ. from improved branching ratio obs. 8-66514
 Ar ion system, collisional radiative model 8-71080
 Ar, low voltage arc, ionisation waves, hydrodynamical model including inelastic interaction 8-87563
 Ar low voltage arc, positive column ionisation waves, hydrodynamic model 8-79481
 Ar neutral system collisional radiation model 8-67535
 Ar, plasma, electron-ion recombination in extinguishing arc 8-59687
 Ar plasma diagnostic method for partial LTE 8-67606
 Ar, radial temp. profile calc. 8-67457
 Ar, stabilised electric arc, laminar plasma flow section, length and characts. 8-91177
 Ar wall-stabilised arc electron and heavy-particle temp. variations 8-67602

arcs (electric) continued

- Ar-cascade arc, spectral sensitivity of radiation detectors in VUV range, report (*German*) 8-82037
 C cathode damage and vapour/thermionic arc transition obs. 8-71603
 CO₂ laser discharges, electrode surface field and preionisation effects on spatial distrib. of arcs 8-63054
 CaH₂ in RF-excited heat pipe oven, efficient arc source 8-63162
 Cl⁻ free-bound continuum radiation threshold broadening obs. 8-71579
 Cr, arc, steady, vac., plasma ion mass and energy diagnostics 8-51385
 Cs, dense plasma, elec. and radiative heat cond. evaluation 8-71452
 Cs fully-ionised plasma hollow-cathode arc discharge theory 8-67533
 Cs plasma, ohmic heating, electrical conduction temp. depend. 8-71442
 Cs vapour, oscill. in low voltage arc discharge growth 8-51386
 Cs-Ba triode arc switch, high-current, low-voltage, pulsed control 8-71551
 Cu, arc, steady, vac., plasma ion mass and energy diagnostics 8-51385
 Cu cathodes, erosion, vacuum to atmospheric press. arcs 8-79482
 Cu vacuum arc, erosion products from cathode spot region 8-75447
 Cu, vapour production method, hollow cathode arc., Ar buffer gas 8-86981
 Cu-N₂, effect of Cu vapour on wall stabilised arc extinguishing times 8-87548
 Fe, arc, steady, vac., plasma ion mass and energy diagnostics 8-51385
 Fe oxides, disperse, chemical reduction in discharges (*Russian*) 8-95915
 H, 1.06 μ m laser scatt. 8-51347
 H arc axial ground state population meas. 8-67598
 H⁻ ion yield from duoplasmatron discharge 8-75382
 H₂ arc plasma Balmer spectrum decay and two-fluid model 8-67603
 H₂ stabilised arc as vacuum UV radiation standard for 600 to 900 Å 8-66879
 H_u line Stark profiles in low-density arc, exptl. discrepancies 8-67470
 He continuum radiation emission obs. to near vacuum UV 8-71582
 He flowing discharge, glow/arc transition and cathode-zone wave structure obs. 8-75475
 He high-current pulse discharge plasma partial LTE disturbances 8-67600
 He I plasma arc, spectral line profiles, $\lambda\lambda=4471$ Å and 4922 Å (*French*) 8-83625
 He plasma He I 4471 Å line profile obs. at high electron density 8-67472
 Hg DC vacuum arc anchored cathode spot current density obs. 8-75467
 Hg vapour, optically pumped positive column, collisional processes 8-87499
 Hg, vertical high-press. arcs, convection 8-59701
 MgH₂ in RF-excited heat pipe oven, efficient arc source 8-63162
 Mo, arc, steady, vac., plasma ion mass and energy diagnostics 8-51385
 Mo, arc, vac., stabilised, plasma props. 8-51384
 N arc, radiation transport 8-79486
 N₂, arc jet enthalpy meas. by fast miniature total calorimetric probe 8-67486
 N₂ arc vacuum UV radiation loss calc. 8-71581
 N₂ plasma jet anode root behaviour rel. to hollow-anode thermal insulation 8-71554
 N₂-CO₂ mixture non-self-sustained discharge ionisation instabilities, obs. 8-71610
 Na-Hg-Xe cylindrical high pressure arc discharge, acoustic resonance 8-67454
 Ne II line Stark broadening in pulsed arc, obs. 8-67469
 Ne, wall stabilised arc column in longit. mag. field, screw instability 8-87551
 SF₆, particle densities in decaying plasma 8-75442
 Ta hollow arc cathode, emission current density 8-76574
 Ti, arc, steady, vac., plasma ion mass and energy diagnostics 8-51385
 W exploding wire, peripheral arc initiation 8-87559
 Xe I level deviation from Boltzmann population in steady-state plasma 8-67605

area measurement

- optical planimeter metrological characteristic test results 8-79148
 pendant drops, profile area meas. 8-81943
 powder compacts, intermediate stage sintering, surface area reduction kinetics, anal. 8-76614
 surface balance, monolayer parameters meas. in radiation field 8-82092
 two-phase systems, mean specific surface area, light transmission meas. (*German*) 8-89431
 Fe₂O₃ powder, heat of adsorp. of stearic acid, surface area meas., flow microcalorimetry 8-81974

argon

- see also nuclei with
 adsorbed dense monolayer on graphite cleavage face, phase transition 8-56034
 adsorption, on graphitised carbon black, surface excess isotherms, gravimetric determ. 8-51816
 adsorption, on graphon, high press. and temp., gas density profile theory 8-67903
 adsorption on activated C, vol. adsorption capacity 8-75933
 adsorption on graphite, orientational ordering of incommensurate monolayers, LEED obs. 8-95233
 adsorption potential energies on NaBr and KBr, calc. 8-71993
 afterglow, electron-atom bremsstrahlung continuum, afterglow decay (*German*) 8-83626
 AR+Mg₂, matrix isolated laser photoluminescence spectra, electronic absorpt., emission, vibronic and vibr. relax. 8-82744
 arc, radial temp. profile calc. 8-67457
 arc, stabilised laminar plasma flow section, length and characts. 8-91177
 arc column, helical instability limits 8-71564
 arc deviation from Saha-Boltzmann equilibrium, heavy-particle effects 8-67596
 atmospheric arc plasma deviation from LTE 8-67604
 atom, 8-78671
 atom, 3p⁵5p config. aligned in discharge, interf. signals, lifetimes and collision cross sections 8-70796
 atom, (e,2e) coplanar symmetry reaction, factorised distorted-wave approx., 400-1200 eV 8-55246

argon continued

atom, clustering of atoms around positron and positive ions 8-55270
 atom, collisional depolarisation of selectively excited 2p levels (*French*) 8-86830
 atom, Compton profile, local density approx., Kohn-Sham self consistent scheme 8-94193
 atom, electron and positron scattering, elastic, 100 and 500 eV, second-order eikonal approx. 8-78814
 atom, electron impact excitation, multiple-collision diffraction theory 8-82844
 atom, electron impact ionisation, differential cross sections 8-58839
 atom, electron impact ionisation, L_3 -shell alignment, Auger electrons angular distribution 8-58838
 atom, electron impact ionisation of inner shells, coincidence experiment theory 8-58837
 atom, electron impact ionisation, cross section ratios 8-94326
 atom, electron impact ionisation, energy resolution and angular correlation of scattered and ejected electrons 8-70939
 atom, electron scattering, in laser radiation field, free-free cross sections measured 8-74762
 atom, electron scattering, in laser radiation field, free-free cross sections, resonant structure 8-74763
 atom, electron scattering, elastic, at low-energy, polarised orbital calculation 8-82840
 atom, electron-impact ionisation, low energy, triple-differential cross section 8-74773
 atom, generalised oscillation strengths, with outer shell effects, $2p^6$ subshell 8-50507
 atom, impulse Compton profiles, atomic optimised potential model 8-74618
 atom, KLL and KLM Auger electron spectra, observed and relativistic multi-configurational Dirac-Fock calculation 8-50524
 atom, metastable, electron impact excitation cross-sections calculated 8-94323
 atom, metastable 3P_2 deactivation in afterflow, plasma characteristics 8-55769
 atom, multiphoton ionisation, EM field gradient forces 8-66608
 atom, optical oscillator strengths, 3p-ns and 3p-nd transitions, independent particle model 8-86816
 atom, photoelectron spectrum angular distribution, abnormality in strong magnetic field 8-50666
 atom, population inversion, intershell transitions, photoionisation, from UV irradiation (*Russian*) 8-70803
 atom, trapping of nonresonant radiation, lifetimes of 4p and 5p levels 8-62766
 atom, unpolarised, spin polarisation of ejected electrons 8-78765
 atom, weakly ionised, energy transfer at high pressure 8-58845
 atom, X-ray emission and X-ray photoelectron spectra, satellite peaks 8-66492
 atomic K α X-ray satellite spectra, gas phase measured 8-66496
 atoms, autoionising states excitation by electron impact, threshold effects 8-62923
 autoionising state $3s^{-1}4p^1P$, collision aligned, decay, triple differential cross section 8-86831
 breakdown in superimposed DC and HF electric fields 8-67571
 breakdown voltage and voltage-current characteristics, observed, up to 2400°C 8-87510
 bubbles in PtSi after 20 to 160 keV sputtering, TEM and backscattering spectrometry observed 8-64435
 cascade arc light emission, effect of pulsed microwave field 8-67599
 Clausius-Mossotti function, examination of variation with gas density 8-52418
 cold plasma generator, optical emission spectra and electrical parameters (*Ukrainian*) 8-67374
 collision induced light scattering spectra, pair polarisability 8-55135
 compressed gas, electron drift velocity, density dependent 8-63534
 continuous optical discharge maintenance in applied magnetic field 8-75396
 crystal, exciton examination 8-51898
 discharge, positive column, axial electric field in transverse magnetic field 8-55766
 discharge rotating plasma column LF oscillations 8-71481
 electric breakdown, high pressure, gas discharge form 8-87567
 electric breakdown voltage, 300-2100K (*Russian*) 8-51370
 electrical breakdown, low-pressure, gap with thermionic cathode, upper and lower breakdown voltages 8-79405
 electron back diffusion, electric field influence 8-75251
 flow, alkali metal vapour, condensation, heat and mass transfer 8-75192
 flow in vertical tube, laminar and turbulent heat transfer 8-71332
 free jet, homogeneous nucleation of clusters, noncrystalline structure (*French*) 8-79760
 gas, light depolarisation, pair-pair correlations 8-63536
 glow discharge, cylindrical hollow cathode, ignition and breakdown experiments 8-91169
 glow discharge, imprisonment of resonant radiation in cold cathode region 8-59703
 heat exchange, radiant plate, diametrical gas flow (*Russian*) 8-94565
 high-pressure arc plasma, IR continuum emission observed 8-71604
 high-pressure breakdown by Nd:glass laser radiation 8-75399
 high-pressure helical arc phase velocity in longitudinal magnetic field 8-71594
 high-pressure plasma electrical conductivity observed 8-71448
 impurities in He quantum magnetometer, influence on signal parameters (*Russian*) 8-82010
 induction plasma torch, temperatures and velocities effects of cool central gas feed 8-94942
 inductively-coupled RF plasma torch, computer model 8-71559
 ion, implanted in amorphous and crystalline materials, detection by X-ray emission analysis in TEM 8-51575
 ion beam divergence characteristics of two-grid accelerator systems 8-82074
 ion impact on C foil, energy loss 8-55902
 ion laser, collisional radiative model and experiment 8-55338
 ion system, collisional radiative model 8-71080
 ions, slow, nuclear emulsion track width by photometric measurement 8-94167
 ions for preparation of nuclear filters from polymers 8-86714
 isotope separation by axial flow turbomachine model 8-78500
 laminar plasma jet, H_2 diffusion observed 8-71557
 laser, CW high power, design parameters (*Japanese*) 8-59019
 laser, electron beam excited, absorption characteristics 8-82948

argon continued

laser, high pressure, tunable 8-50755
 laser, radiation spectrum and influence of Fabry-Perot plate (*Polish*) 8-78993
 laser-evaporated microplasma radial glow and temperature distribution 8-67387
 liquid, closed circuit for electron irradiation of LiH at 90K (*French*) 8-62214
 liquid, compressibility, long wavelength limit of liquid structure factor 8-67633
 liquid, drift of ionisation electrons 8-55100
 liquid, magnetic field-induced temperature changes 8-57960
 liquid, new description of random stacks (*French*) 8-79512
 liquid, recombination luminescence 8-60521
 liquid, scintillation decay due to α -particles and electrons 8-55099
 liquid, short range order parameter 8-83712
 liquid, triple point, depolarised Rayleigh scattering from fluids of spherical molecules 8-88319
 liquid, triplet state of self-trapped exciton states, evidence of existence, luminescence measured 8-72608
 loaded K heat pipe performance characteristics 8-89934
 low voltage arc, ionisation waves, hydrodynamical model including inelastic interaction 8-87563
 methane-Ar, liquid mixture, self-diffusion and nuclear magnetic relaxation (*Russian*) 8-87799
 methane-Ar liquid mixture, viscoelastic properties, acoustic relaxation (*Russian*) 8-75736
 monolayer, adsorbed on graphite, lattice dynamics 8-75946
 negative glow fast electron density relation to discharge pressure and current 8-67528
 neutral system collisional radiation model 8-67535
 nucleation, Ar in He carrier gas, supersonic nozzle flow 8-94871
 plasma, constricted discharge, electron density and temperature and gas temperature, iterative method (*German*) 8-83627
 plasma, electron density, microwave reflection measured 8-59674
 plasma, electron-ion recombination, 300 to 500K, in discharge tube 8-59714
 plasma, electron-ion recombination in extinguishing arc 8-59687
 plasma, EM waves, parametric decay near upper hybrid frequency 8-59590
 plasma, Gaunt factor temperature depends, from Ar II and Ca II Stark widths 8-87491
 plasma, H impurity, equilibrium state of highly ionised plasma 8-83597
 plasma, ion energy level populations in crossed electrical and magnetic fields 8-67428
 plasma, operating characteristics, numerical study 8-67309
 plasma, recombination, kinetics of stimulated atomic populations (*Russian*) 8-87436
 plasma bridge neutraliser operation with 10 cm beam diameter etching source 8-74102
 plasma development by laser radiation absorption 8-75392
 plasma diagnostic method for partial LTE 8-67606
 plasma interaction with flat anode 8-71497
 plasma quantummeter, quantitatively coupled, for emission spectrochemistry analysis (*Japanese*) 8-83624
 plasma welding, compressed arc V-I characteristic observed (*Russian*) 8-83628
 POPOP-Ar- N_2 , electron beam pumped, intense laser emission at 381 nm 8-74898
 positive column, local transverse magnetic field, striation frequency spectra, microwave probe 8-87562
 positive column, moving striations in longitudinal homogeneous magnetic field 8-67523
 positron annihilation decay constants, temperature, electrical, and magnetic field dependent, computer analysis 8-78809
 positron annihilation in rare gases, Doppler broadening measured, electron momentum distributions 8-55131
 precursor shock waves, electron density and associated ionisation 8-67217
 pulsed plasma, electrical conductivity observed at 10 atm and 15000K 8-71449
 recombination luminescence in scintillation induced by alpha particles 8-50441
 RF discharge plasma, magnetically stabilised, electron temperature using optical spectroscopy (*German*) 8-63582
 scintillation detectors applied (*Czech*) 8-86727
 shear viscosity determination under high pressure, using capillary viscometer 8-55708
 solid, dead layer effects in UV reflectance of excitons 8-72553
 solid, density at melting and isochoric equations of state 8-83915
 solid, enthalpy of sublimation, internal energy, determined from vapour pressure 8-91435
 solid, heat capacity, possible dimensions effect 8-75844
 solid, improved unsymmetrised SCF approximation for strongly anharmonic crystals 8-75791
 solid, vibrational and thermal properties, effect of polarisability 8-71807
 solid and liquid, Raman spectra 8-84580
 spectroscopic light source carrier gas glow discharge and hollow cathode types 8-82047
 stony meteorites, light noble gases analysis compilation 8-65574
 surface, desorption of He, application of simplified continuum model 8-87860
 thermal conductivity, law of corresponding states (*Russian*) 8-87426
 thermal conductivity, near 300K, density dependent, 0.8-35 MPa 8-67304
 thermosphere, Ar density profiles measured between 90 and 220 km altitude 8-77383
 triple point realisation, reference temperature applied 8-73997
 twin-hollow-cathode interferometer-spectrometer, discharge characteristics (*German*) 8-67461
 US vels. and absorption coefficients, determined of relaxation times 8-63530
 UV photoion density measured using high pressure Langmuir probe 8-51340
 vibrational relaxation of Cl_2 , impurities, stochastic classical trajectory approach 8-79707
 wall-stabilised arc electron and heavy-particle temperature variations 8-67602
 weakly ionised plasma turbulence in longitudinal magnetic field 8-75338
 Ar, dense gas, thermal conduct. and viscosity coeffs., irreversibility and Kirkwood superposition hypothesis (*French*) 8-94881
 Ar I and II transition probability determined from improved branching ratio observed 8-66514
 Ar II, (e,2e), photoelectron and conventional spectroscopies 8-90298
 Ar II, magnetically confined plasma, pulsating ion laser action 8-78994

argon continued

- Ar IX, Ne I like reson., and Na I-like satellite lines, relativistic HF calc., beam-foil spectra 8-94210
 Ar, microwave breakdown of nanosecond duration, calc. of threshold fields 8-94948
 Ar plasma, shock tube data on radiative cooling, IR laser techniques 8-79472
 Ar triple point cells, comparison 8-73996
 Ar⁺, electron impact ionis. cross section 8-50647
 Ar⁺, in Ar, transverse diffusion coeff., reson. charge exchange effects 8-63533
 Ar⁺ laser freq. stabilisation by ¹²⁷I₂ absorption lines at 582 THz 8-90430
 Ar¹⁵⁺, population of ⁴P_{3/2} state meas. by cascading processes 8-94315
 Ar¹⁸⁺ detection, efficiency of ⁷LiF TLD 8-53504
 Ar²⁺, levels of 2p³3p⁵ 8-74574
 Ar:K seeded plasma, temperature diagnostics 8-67427
 Ar:NH₃ solid, crystal impurity librational relax., phonon assisted transitions, direct, Orbach and Raman processes 8-83887
 Ar:NO₂, Raman spectra, high press., low temp. effects 8-52479
 Ar:O₂(N₂), long-wave UV luminesc. (*Russian*) 8-88347
 Ar/O₂ plasma treatment of SiO₂ surface, reactivity modification 8-64890
 Ar-cascade arc, spectral sensitivity of radiation detectors in VUV range, report (*German*) 8-82037
 Ar-Cs⁺, ion mobility and interaction pot., drift tube meas. at 300K 8-59537
 Ar-H₂ plasma, thermodynamic properties 8-63542
 Ar-HCl, Van der Waals mol., far IR spectrum, anisotropic intermol. force effects 8-62869
 Ar-He(Ne), thermal cond., composition dependence 8-51276
 Ar-Kr, liq. mixture, excess thermodynamic props. 8-75836
 Ar-Kr, pair pot. function calcs. 8-74726
 Ar-Kr mixture, thermal cond., 120-273K 8-83514
 Ar-Kr-F₂ mixture, electron beam pumped, spectroscopy and kinetics of 248, 414 nm bands 8-63081
 Ar-methane + Cl ions, energy straggling 8-58785
 Ar-monochlorodifluoromethane mixture, US vels. and absorption coeffs., determ. of relaxation times 8-63530
 Ar-N₂ electron beam pumped laser characs. at 25-350°C 8-58984
 Ar-N₂ gas scintillation MWPC for high-intensity 5-10 keV X-rays 8-82575
 Ar-N₂ interaction, electron gas pot. calc., Gordon-Kim model, ang. orientation depend. 8-70893
 Ar-N₂ laser, intense proton beam pumping 8-78998
 Ar-N₂ mixture, adsorption on chabazite, test of eqns. for gas mixture adsorption on heterogeneous surface 8-60030
 Ar-N₂-H₂ plasma equilibrium compositions and thermodynamic props. 8-71433
 Ar-O₂ mixture, adsorption on CsI, test of eqns. for gas mixture adsorption on heterogeneous surface 8-60030
 Ar-SF₆ mixture, space discharge excited by electron beam (*Russian*) 8-83629
 Ar-SF₆ mixture, space discharge excited by electron beam (*Russian*) 8-83630
 Ar-Xe gaseous mixtures, collision-induced microwave absorpt. 8-78680
 Ar-Xe-NF₃ mixture, fluorescence from e-beam excitation at low temp. and high press. (*French*) 8-58727
 Ar+Ar, K-X-ray excitation, 2.5-8 MeV, impact parameter depend. 8-50628
 Ar+Ar(³P₂)(³P₀), flowing afterglow metastable decay rates, diffusion, two- and three-body rate consts. 8-73027
 Ar+benzene (³B_u(S₁)), rot. relax. to Boltzmann distrib. 8-86936
 Ar+BrCN(HCN), CN quartet state production, fluoresc. anal. 8-68888
 Ar+C⁺, charge transfer cross-sections, 0.7-2.4 keV, C⁺(²P) and C⁺(⁴P) 8-58806
 Ar+CO₂, 301_M-000 band, intensities, press.- and self-broadening coeffs. meas. 8-78695
 Ar+Cs, two-photon ionisation spectra, satellites, absorption line shape 8-82668
 Ar+H, low energy elastic scatt. cross section MCSCF calc., van der Waals forces 8-70897
 Ar+H₂, vibr. energy transfer rate, ab initio calcs. 8-82821
 Ar+H₂⁺, 10 keV dissoci. charge exchange collisions 8-94319
 Ar+H₂O(D₂O), (³P_{0,2}) state quenching cross sections 8-70912
 Ar+H₂O(O₃), collisional energy transfer in unimol. reaction, classical trajectory calcs. 8-62882
 Ar+H₃⁺, dissoci., 400-800 keV, product charge state distrib. model 8-82838
 Ar+H⁺, collisional electron detachment, complete ang. distrib. 8-66650
 Ar+H⁺, electron capture cross sections 8-62912
 Ar+HCl, rotationally inelastic collision, planar trajectory, classical centrifugal decoupling calcs. 8-58788
 Ar+HCl(DCl) potential, asymmetric, isotope substitution effect, Legendre expansion coord. transformation 8-70894
 Ar+He₂(³Σ), press. depend. reactions, rate coeffs. 8-64823
 Ar+He⁺(Li⁺), up to 70 keV, symmetric (antisymmetric) reson. charge transfer cross sections (*Korean*) 8-50636
 Ar+He⁺ Penning ionisation, semiclassical descretisation procedure 8-90275
 Ar+Kr(³P₂), flowing afterglow metastable decay rates, diffusion, two- and three-body rate consts. 8-73027
 Ar+methane, CH chemiluminesc. in flowing afterglow 8-64839
 Ar+methane, low energy collision, close coupling and coupled states, rot. transitions 8-78784
 Ar+N₂, (A³Σ_u⁺, ν=0,1) metastable state quenching rate coeffs. 8-90206
 Ar+N₂, collinear collision, vibr.-translation energy transfer, model calc. 8-66634
 Ar+N₂, rot. inelastic cross-section, IOS calcs., partial wave parameters 8-50616
 Ar+N₂(TIF), scatt., l_z-conserving sudden approx. calcs. 8-66628
 Ar+Na, differential cross-section at thermal energy, Na-Ar ground state pot. 8-58769
 Ar+Na(³P_{1/2})→Na(³P_{3/2})+Ar, angular scatt. distrib., Doppler spectrosc. obs. 8-94309
 Ar+Ne, elastic scatt. absolute total cross section, long range interaction 8-58768

argon continued

- Ar+Ne²⁺(Ar²⁺), electron transfer cross-section, <100 eV 8-66654
 Ar+O⁺(⁴S)(²D), charge transfer reactions, cross-sections meas. 8-92462
 Ar+O(¹D), deactivation rate consts., 110-330K 8-88628
 Ar+Rb(Cs), metal atom spectral line breadth and shift, Van der Waals pot. calc. 8-90126
 Ar+S⁺, molecular K-X-ray production, projectile charge depend. 8-90188
 Ar+TiO, collision cross-section meas. 8-55202
 Ar+TIF collisions, small angle scattering, calc. cross sections 8-70915
 Ar+U³⁶⁺, radiative charge exchange 16, 64, 256 MeV/amu 8-55234
 Ar+Xe, lightly doped, Xe 5d(3/2)₁ photoexcited state radiative decay and energy transfer 8-74605
 Ar+Xe, relaxation processes of Xe*(³P₂) metastable atoms 8-50624
 Ar+Xe(³P₂), flowing afterglow metastable decay rates, diffusion, two- and three-body rate consts. 8-73027
 Ar+Xe(F₂), proton excited mixtures, energy transfer processes 8-66647
 Ar⁺+2Ar→Ar₂⁺+Ar, gas phase reaction rate const. calc. 8-92457
 Ar⁺+Ar, elastic scatt. and charge exchange, differential cross section, 2.7-20 eV 8-66660
 Ar⁺+C, beam-foil spectra, Ar⁺ ion orientation, ang. variation 8-86944
 Ar⁺+H₂, charge transfer reactions, excited products, Ar initially metastable 8-68879
 Ar⁺+H₂O, 50 to 250 keV, OH radical form. 8-56890
 Ar⁺+H₂(v_i=0)→ArH⁺+H, electronic nonadiabatic transitions, two-state model calc. 8-73035
 Ar⁺+He, X²Σ and A²Π states, CI pots. 8-74727
 Ar⁺+Kr(Xe), thermal energy charge transfer reaction rates, mass spectrometric obs. 8-61000
 Ar⁺+N₂, energy transfer, vibronic excitation, emission spectra 8-66578
 Ar⁺+SO₂(H₂S), emission spectra obs. 8-50622
 Ar²⁺+He(Ne)(Ar)(Kr), electron transfer cross-section, <100 eV 8-66654
 Ar²⁺+Kr(Xe), thermal energy charge transfer reaction rates, mass spectrometric obs. 8-61000
 Ar³⁺+He, electron transfer cross-section, <100 eV 8-66654
 Ar₂⁺Σ_u⁺ excimer state, photoionis. cross section 8-70882
 Ar₂, excited state pot. curves, ab initio CI calc. 8-78643
 Ar₂, near IR absorpt. spectra 8-66547
 Ar₂, photoelectron spectra 8-78748
 Ar₂⁺, dissoci. recomb., total rate coeff. depend. on electron temp. 8-58817
 Ar₂⁺, photodissoc. cross sections at 3.0 and 3.5 eV 8-62861
 Ar₂⁺, photodissoc. cross-section, 6200-8600 Å 8-78761
 Ar₂⁺, weakly bound excited states, dissoci. energies 8-78748
³⁶Ar, separation, calc. of thermal diffusion cascade (*Rumanian*) 8-58862
³⁶Ar-⁴⁰Ar, thermal diffusion column transport coefficients (*Rumanian*) 8-51274
³⁹Ar in meteorites, evidence for Maunder minimum in solar activity 8-57529
⁴⁰Ar-³⁹Ar dating, inert gas extraction system incorporating ultra-high vac. furnace 8-77918
⁴¹Ar release from TRIGA reactor, comparison of γ-ray detectors 8-57309
 Ar⁺+I₂, ion-pair form. differential cross-section, 25-133 eV, metastable Ar 8-78787
 Ar⁺(³P)+CO₂(X¹Σ_g⁺), differential elastic and quenching cross-sections 8-58773
 Ar⁺(³P)+Fe(CO)₅, chemiluminesc. 8-61014
 Ar⁺(4p), (5p) states, lifetimes and two-body rate consts. meas. 8-63058
 Br₂+Ar, ergodic deactivation, anharmonic effects on transfer rate 8-82818
 CO-Ar mixture non-self-sustained discharge instability obs. 8-71612
 CO₂-Ar laser, thermally pumped, output power enhancement by Ar gas addition 8-55336
 CO₂+Ar, broadening of 30⁰₁←00⁰₀ band 8-86865
 CS₂+He(Ar)(N₂), perturbed rot. diffusion of CS₂, IR spectra 8-75245
 Cd-Ar low-pressure discharge column, energy balance obs. 8-67504
 Cl, in Ar and He gas, diffusion const. of atom 8-71417
 ClF+Ar, shock wave, vibr. relax., laser schlieren meas. 8-90267
 CsCl(Cs₂Cl₂)+Ar(Kr)(Xe), collision-induced ion-pair form., absolute cross sections 8-73029
 Fe:Ar, mag. hyperfine interaction, temp. depend. 8-68420
 H⁺+He(Ar), electron detachment cross sections 8-58810
 H⁺+He(Ar) electron transfer cross sections 8-58809
 H₂-Ar(Kr)(He) mixtures, intermol. forces 8-62867
 H₂-N₂-Ar, two-phase flow film boiling, in vap. generator, heat transfer 8-75190
 HCl+Ar, rot. linewidth calcs., using different pots. 8-66602
 HCl+Ar(He), rot. excitation, infinite order sudden approx. 8-74740
 HCl+HCl(Ar), pure rot. Raman lines, press. broadening cross sections 8-74702
 He/Ar and N₂/Ar ratio vars. in fault zone groundwater air bubbles for earthquake prediction 8-88803
 He-Ar, collision-induced absorption, exact line shapes 8-66512
 He-Ar gas mixture, velocity slip in free jet expansions 8-90951
 He+Ar(Kr), translation band spectral moments, induced dipole moments 8-55218
 He+H₂(He)(Ar)(N₂), fast metastable at. collisional destruction cross section 8-74760
 He⁺+Ar, charge transfer cross section, kinetic energy dependence in low energy region (*Japanese*) 8-90100
 He⁺+Ar, low energy charge transfer collisions, kinetic energy depend. 8-86947
 He⁺+Ar, Penning ionisation, laser modified collisional effects in electron energy spectrum 8-90278
 Hg-Ar, low press. discharge positive column ionisation processes 8-75445
 K-Ar dating of ore mineralisations in Erma River Area, Bulgaria 8-81115
 Kr⁺+He(Ar), vel. changing collisions studied by saturated absorpt. 8-62892
 Li₂O, Ar⁺ implantation, depth distrib. by proton backscatt. 8-51577
 N₂-Ar, liq. mixture, isotropic Raman line shape theory 8-88298

argon continued

- N_2 -Ar liq. mixtures, coherently excited mol. vibrs., dephasing time 8-62813
 N_2 -Ar mixture non-self-sustained discharge instability obs. 8-71612
 N_2 -Ar mixtures in 300-1050K range, rot. energy relaxation 8-50617
 N_2 +Ar, total differential cross section, diffr. oscils. quenching 8-66625
 NH_3 +He(Ar), ammonia inversion spectrum press. broadening 8-86915
 $N_2(X^1\Sigma_g^+)$ +Ar($^3P_{2,0}$) \rightarrow Ar(1S)+ $N_2(C^3\Pi_u)$, sensitised fluoresc., vel. depend. 8-90204
Ne-Ar, high press. mixture, AC discharges, one-dimensional numerical simulation 8-67451
Ne-Ar mixtures, glazed electrode AC discharge mode transition obs. 8-67558
Ne+Ar(Kr), translation band spectral moments, induced dipole moments 8-55218
 O_2 -Ar system, low temp. liquid-vapour equil. 8-83927
 S^+ +Ar, double K-vacancy prod., X-ray X-ray coincidence and fluoresc. yields obs. 8-55230
 SF_6 - N_2 -Ar mixture high-current multispark discharge switching characteristic 8-67444
Xe-Kr-Ar mixtures, VUV continuous spectrum prod. in low volt. lamp (Russian) 8-75451

argon compounds

- ArCl, neutral and negative ion states SCF pot. energy curves 8-62745
ArF, 50 mJ double discharge excimer laser, spectroscopy and characts. 8-63082
ArF, covalent and ionic states, ab initio CI calcs. 8-78634
ArF, laser emission, ab initio config. interaction calcs. on electronic states 8-63083
ArF, laser expts. on $^2\Sigma$ - $^2\Sigma$ transitions 8-63080
Ar $_2$ F, electronic states, ab initio POL CI calcs. 8-66474
ArF*, in Ar-F $_2$ proton-excited mixtures, production and quenching 8794307
Ar $_2$ F*, in Ar-F $_2$ proton-excited mixtures, production and quenching 8-94307
ArH, neutral and negative ion states SCF pot. energy curves 8-62745
ArHCl, ab initio FGO calc. 8-50467
ArHCl, pot. energy surface of Van der Waals complex 8-94299
ArI $_2$, van der Waals mol., fluoresc. spectrum, predissoc. 8-66584
ArKr, intermol. pots., differential cross-sections inversion calcs. 8-66619
ArKr $^+$, absorpt. spectra, ab initio calc. of potential energy curves 8-74568
ArO, lasing, low-lying electronic states, ab initio config. interaction calcs. 8-63084
ArXeF*, gain meas. at 4416 Å 8-50758

arithmetic (digital) *see digital arithmetic***aromatic compounds** *see organic compounds***arrays (antenna)** *see antenna arrays***arsenic***see also nuclei with*

- 3d binding energy in As, GaAs, As $_2$ O $_3$, and As $_2$ O $_5$, ESCA absolute energy calibr. 8-92171
amorphous, bonding coordination defects, Raman scatt. and IR absorption meas. 8-60498
amorphous, electron and phonon density of states calcs., comp. to XPS 8-56066
amorphous, electron irradi.-induced paramag. centres, 77K 8-88187
amorphous and cryst., phonon density of states calc., comp. to IR absorpt and neutron scatt. data 8-55924
atom, ($4^2S_{3/2}$) state, kinetic obs. using time resolved reson. fluoresc. 8-94211
depth profiles in Si-SiO $_2$ -Si structs., ion microanal. (Japanese) 8-85251
determination, in combustible municipal solid waste, by AAS 8-85229
determination, in Si, by AES (Japanese) 8-91356
determination in ores of reduced heteropoly acids, photometric method 8-61103
determination in Si by ion microanal. (Japanese) 8-85250
diffusion in Si, proton enhanced diffusion and vacancy migration 8-67747
diffusion in Si melted by high power ns laser pulse 8-79789
distribution and speciation in natural waters and marine algae 8-81210
dose depend. in laser annealing 8-91354
film Al-type supercond. vapour-quenched transition temp., A7-type phase transition 8-52145
pseudopotential, self-consistent, band struct. 8-84141
X-ray absorption edge, chem. shift, electron binding energy in compounds 8-62822
zone centre phonons and elastic const., hydrostatic press. depend. 8-59905
As $_4$, gaseous, atomisation enthalpy and enthalpy of form., mass-spectroscopic Knudsen cell method 8-80780
GaN:As, implanted single cryst. film, cathodolum. 8-60523
Ge:As, photoconductivity oscillation with respect to applied mag. field (Russian) 8-80026
In-Ge:As, Schottky barrier tunnel junction, zero bias resistance, temp. depend. 8-72258
Se:As, trigonal, defect and impurity electron levels, surface photovoltage spectra 8-72108
Si:As, elec. activation of implanted As during low temp. anneal, Hall effect meas. 8-51571
Si:As, implanted, spatially varied activation during regrowth of amorphous layers, sheet resist. and backscatt. obs. 8-71749
Si:As, ion implanted, anomaly of elec. activation by additional Ne irradiation 8-84211
Si:As, Orbach spin-lattice relax. rate, uniaxial stress depend. 8-72391
Si:As, shallow donor electrons, hyperfine interactions, reply to Onffroy's calcs. 8-51934
Si:As, shallow donor states with strong central cell perturbation theory 8-51933
Si:As, time-resolved reflectivity during laser annealing 8-92086
Si:As device, anal. using SEM-AES-IMA combination with SIM spectrometer (Japanese) 8-85249
p-ZnSe:As, ion implantation and heat treatment 8-87700

arsenic alloys*see also arsenic compounds*

- Ag-As, α -phase alloy, thermopower at low temps. 8-84196
(Cr, Mn) $_2$ As, mag. props. and struct. 8-64190
Eu $_2$ As $_3$, cryst. struct. of high and low temp. phases 8-75626
Fe-Mn-As, crystal struct. and magnetic props. of intermetallic cmpds. with Cu $_2$ Sb type struct. (Japanese) 8-59785
Mn $_{1-x}$ Fe $_x$ As, high-pressure phase, magnetic properties 8-52247
Mn $_{1-x}$ Fe $_x$ As, mag. props. in ground state (Russian) 8-56294

arsenic compounds*see also arsenic alloys*

- silicones, fungicidal protection of optical components made of chem. unstable glass 8-59107
As-S system, glass forming ability and phase diagram 8-59760
As-Se system glasses, point defects, positron lifetime spectra meas. 8-88380
As-Se-Ge, amorphous film, relief-type hologram mode, hologram replication (Japanese) 8-78959
As-Se(S), glassy and crystalline, point defect exam. by positron annihilation 8-72637
 $^{75}AsF_6^{2-}$, radical, prep. and EPR comparison with other hexafluoride radicals 8-68381
AsGeS, ZZ 8-52639
AsH $_3$, forbidden millimetre-wave transitions 8-55165
AsI $_3$, mol. beam photodissoc. 8-56906
As $_2$ O $_3$, As 3d and O 1s binding energies, ESCA absolute energy calibr. 8-92171
As $_2$ O $_3$, electronic struct., X-ray emission, XPS, UPS obs., CNDO cluster calc. 8-52638
(As $_2$ O $_3$) $_n$, claudetite I, vibr. spectra, force field calc. (French) 8-60447
As $_2$ O $_5$, As 3d and O 1s binding energies, ESCA absolute energy calibr. 8-92171
As $_4$ O $_6$, IR and Raman spectra vibr. spectra, valence force field calc., pot. function (French) 8-50549
AsO $_2$ (OH) $_2^-$ ion, O $_2$ exchange in water, in NaAsO $_2$ aq. solns. 8-92459
As $_2$ (S,Se,Te) $_3$ glasses, Hall mobility composition depend. 8-68042
As $_2$ S $_3$, amorphous, electrodiffusion profile meas. of Ag migration 8-87822
As $_2$ S $_3$, amorphous film, photooxidation, substrate depend. 8-64866
As $_2$ S $_3$, amorphous thin films resonant Raman scattering 8-68505
As $_2$ S $_3$, crystalline struct. X-ray induced paramag. states and luminesc. 8-95520
As $_2$ S $_3$, electronic struct., X-ray emission, XPS, UPS obs. 8-52638
As $_2$ S $_3$, evaporated film, optical props., depend. on light exposure and heat cycling 8-68572
As $_2$ S $_3$ film, effect of light exposure and heat cycling 8-94417
As $_2$ S $_3$ films, use in recording phase relief holograms (Russian) 8-50741
As $_2$ S $_3$ glass, localised paramag. states, As $_4$ S $_6$, As $_4$ S $_4$ units, mol. analogue models 8-60087
As $_2$ S $_3$, IR transparent materials, forward and backward scatt. data 8-59099
As $_2$ S $_3$ single-layer film 2.8 μ m, 3.8 μ m absorpt. meas. 8-90463
As $_2$ S $_3$:Ag, amorphous US props. 8-51616
As $_2$ S $_3$ -AsBr $_3$, glass, exam. of combination scatter spectra in IR 8-88315
As $_2$ S $_3$, thin film optical waveguide, for acoustoptic modulators 8-83051
As $_2$ S $_3$ glass, Raman and IR spectra, struct. model 8-80330
As $_2$ S $_{1-x}$ glass, Raman spectra, chem. struct. (Russian) 8-76469
As $_2$ S $_{100-x}$, structural changes (Russian) 8-51427
(As $_2$ S $_3$)(AsI $_3$) $_{1-x}$ glass, Raman spectra, chem. struct. (Russian) 8-76469
As $_2$ S $_3$ (Se $_3$), thermal expansion at low temperatures 8-83982
As $_2$ Sb, As $_2$ Sb $_2$, AsSb $_3$, and AsSb, gaseous, atomisation enthalpy and enthalpy of form., mass-spectroscopic Knudsen cell method 8-80780
As $_2$ Sb $_2$ O $_6$, AsSb $_2$ O $_6$ and As $_2$ SbO $_6$, gaseous, atomisation enthalpy and enthalpy of form., mass-spectroscopic Knudsen cell method 8-80780
AsSe film, chalcogenide glasses band gap variation 8-90461
As $_2$ Se $_3$, amorphous, electrophotographic props., photodecomp. effect 8-49918
As $_2$ Se $_3$, amorphous, electron irradi.-induced paramag. centres, 77K 8-88187
As $_2$ Se $_3$, amorphous layers, injected charge drift and localisation (German) 8-91794
As $_2$ Se $_3$, contact influence on AC cond. 8-76076
As $_2$ Se $_3$ glass, density of optically induced localised paramagnetic states 8-52354
As $_2$ Se $_3$ glass, struct. changes, Mn $^{2+}$ EPR expts. 8-79534
As $_2$ Se $_3$, glassy, dielectric const. determ. 8-72449
As $_2$ Se $_3$, glassy, with adsorbed H $_2$ O(NH $_3$)(NO $_2$)(O $_2$)(CO $_2$)(CO), surface cond., photocond. 8-80038
As $_2$ Se $_3$, glassy struct. X-ray induced paramag. states and luminesc. 8-95520
As $_2$ Se $_3$, neutrality of luminescence centres 8-88356
As $_2$ Se $_3$ single-layer film 2.8 μ m, 3.8 μ m absorpt. meas. 8-90463
As $_2$ Se $_3$:Ag, amorphous, US props. 8-51616
As $_2$ Se $_3$ -InI $_3$, glass system, IR spectra 8-64365
As $_2$ Se $_3$ -Ti $_2$ Se (Ti $_2$ Se $_2$) (Ti), glass, hot pressed, temp. dependence of optical absorption edge 8-88328
As $_{60}$ Se $_{40}$, amorphous films, spectral characts. of photodarkening 8-76494
As $_4$ Se $_2$ Ge, glass, light irradi. induced changes in optical and elec. props. (Japanese) 8-68031
As $_4$ Se $_2$ Ge glass, struct. changes, Mn $^{2+}$ EPR expts. 8-79534
As $_4$ Se $_{100-x}$ -S $_x$ Ge $_{10}$ film strip-loaded waveguide formed in graded-index LiNbO $_3$ planar waveguide 8-74965
AsSe $_{1.5-x}$ Te $_x$ glasses, physical props. 8-68028
As $_2$ (Se $_{1-x}$ Te $_x$) $_3$, thermal cond. of solid solution and melt 8-67874
As $_2$ Se $_3$ -Te $_{3-x}$ chalcogenide glasses, cond. meas., field strength and temp. depend. 8-84225
As $_2$ Te $_3$, amorphous, AC conductivity, temp. depend. 8-72153
As $_2$ Te $_3$ -GaAs, amorphous-monocrystalline heterojunctions, space charge limited conduction 8-64099
As $_2$ Te $_3$ +Ti $_2$, glassy system, composition depend. of activation energy, thermopower meas. 8-64052
As $_2$ Te $_{100-x}$ glassy system, composition depend. of activation energy, thermopower meas. 8-64052

arsenic compounds continued

- AsTeCu₂ ($0 \leq x \leq 0.4$) glass, effect of Cu on elec. cond. and thermoelectricity, 100 to 370K 8-87978
 As_{0.3}Te_{0.48}Ge_{0.1}Si_{0.12}, amorphous film, transient switching processes 8-84232
 As₂Te₂Ge(Si) glass, struct. changes, Mn²⁺ EPR expts. 8-79534
 As₅₀Te₄₅I₅, glass, semicond., elec. switching, high press. effects 8-72212
 As₂Te₂Se₂, amorphous and cryst. phases, ¹²⁵Te Mossbauer expts. 8-88232
 Au-As₂Se₃ contact, model of charge injection 8-68088
 C₈AsF₃ intercalation compound, NMR and static mag. susceptibility meas. 8-88214
 Cd-As-S chalcogenide glass system, prod. and acoustooptic props. (*Russian*) 8-63158
 Cu-As-Se glasses, recording and erasure by laser beam (*Russian*) 8-71170
 Cu₄(As_{0.4}Se_{0.6})_{1.2}, amorphous, ⁷⁷Se NMR, comp. depend. 8-76329
 Cu₁₀As₃₁Se₃₈O₂₁, chalcogenide glass, exam. of electron mechanism of photo induced changes 8-87998
 Ge-As-Te system, glasses, magnetochemical exam. 8-88092
 H(UO₂AsO₄)₄H₂O, H motion, PMR obs. 8-80239
 Hg-As-S chalcogenide glass system, prod. and acoustooptic props. (*Russian*) 8-63158
 Hg-As-S modulating glasses, optical parameters and struct. (*Russian*) 8-63159
 Hg-As-S-I system, glasses, optical and acousto-optical props. 8-83053
 PbS-As₂S₃ glass, elastic props. temp. depend. 8-71780
 Sb₂O₃, electronic struct., X-ray emission, XPS, UPS obs., CNDO cluster calc. 8-52638
 Si-As-Te glasses, crystallisation kinetics under influence of water vapour 8-59762
 Si₁₂Te₄₈As₃₀Ge₁₀, amorphous film, elec. cond. mechanisms, temp. depend. (*Japanese*) 8-80078
 Ti₇Se₄Te₃, amorphous semicond., nuclear spin-lattice relaxation by localised electronic states, modification by spin diffusion 8-52372
 Zn-As-S chalcogenide glass system, prod. and acoustooptic props. (*Russian*) 8-63158

art

- oil paintings, neutron activation anal., for teachers 8-81761

articulation (speech) *see speech***artificial hearts** *see artificial organs***artificial intelligence**

- see also adaptive systems; biocybernetics; brain models; heuristic programming; neural nets*
 cardiac image description and analysis, interactive knowledge-based systems approach 8-81031
 optical coding method, scene analysis 8-82924

artificial kidneys *see artificial organs***artificial limbs**

- above knee prosthesis, feasibility of active control scheme 8-81081
 above-knee prosthesis, myoelectric control system development 8-53575
 afferent nerve stimulation in below-elbow amputees 8-57125
 control device design for severe motor impairment patients 8-96114
 manipulator, computer controlled, for use as remotely controlled arm 8-81083
 microcomputer-aided arm prosthesis using myoelectric pattern recognition 8-53576
 multifunctional prosthetic hand portable control system 8-57127
 sensory feedback code comparison using electrocutaneous tracking 8-69255
 two-leg, Duckling type, hydraulically powered dummy rider control system 8-57124
 upper-limb prostheses multifunctional control microprocessor system, myoelectric signal identification method 8-88766

artificial organs*see also prosthetics*

- blood circulation assistance and replacement devices (*German*) 8-53564
 bubble oxygenator, O₂ transfer controlling factors 8-53568
 circulation system with gas enrichment using membrane oxygenators, mass spectrometer inlet system study (*German*) 8-73294
 extracorporeal blood oxygenator safety and efficacy, review 8-77153
 extracorporeal circulation, blood filter evaluation 8-69250
 haemodialysis, effect on evoked pots. and EEG freq. 8-61160
 haemodialysis, fracture phenomena, of bovine, swine 8-92746
 heart and mock circulatory system, math. model 8-81080
 implantable electronic pancreas and blood glucose monitor 8-88767
 oxygenator using microchannel membrane, transport and flow phenomena 8-69253
 poly(vinyl alcohol)-based membranes for haemodialysis (*Japanese*) 8-96115
 ventricle, all-pneumatic system, cardiovascular dynamics simulation 8-81082

artificial satellites

- 1967-92A, tidal perturbations 8-61307
 1973-101A orbit, upper atmosphere wind determ. 8-73560
 aircraft satellite data link, for meteorological reconnaissance data transmission 8-96299
 Ariel 4 (1971-109A), definitive orbit 8-73604
 attitude and orbit control systems, conference, Noordwijk (1977) 8-65480
 autonomous navigation problems, shoreline information 8-53732
 Cactus accelerometer, in-orbit performance on D5B satellite 8-61698
 CETI transmitter/receiver in Earth orbit 8-61758
 collision frequency, debris belt creation 8-89035
 communication satellites, orbital perturbation and stationkeeping, literature survey 8-89039
 communications satellite system measurements 8-61712
 COS-B satellite obs., appl. of X- γ synchronisation to non-parametric anal. of NP 0532 pulsar 8-73729
 Cosmos 248 (1968-90A), orbit analysis and gravity odd zonal harmonics 8-81100
 Cosmos 462, orbit. rel. to air density vars. from January 1972 to April 1975 near 200 km 8-57377
 Cosmos 782, American biological expts., results 8-85818
 Cosmos 929, atmospheric re-entry 1978 February 8-85819

artificial satellites continued

- Cosmos 954 debris, airborne gamma-ray spectrometer detection 8-85784
 Cosmos series, applications, review 8-69650
 design for optimal continuous coverage 8-73603
 dual-spin satellite magnetic attitude control system, geomag. field effects 8-65484
 Earth resource satellite attitude meas. and control requirements 8-65482
 Earth resources data, satellite on-board processing 8-61626
 Earth surface obs. satellite remote sensor/attitude control system interface 8-65481
 Earthnet, monitoring Earth's environment 8-88921
 eccentricity oscills., compensation with stabilizer 8-69643
 effective isotropic radiated power meas., error anal. using calibrated radio star 8-93070
 equations of motion, numerical integration methods (*Japanese*) 8-85837
 ETS-II satellite, 1.7 GHz, 11.5 GHz, 34.5 GHz wave propag. rel. to rain precipitation strength (*Japanese*) 8-85669
 Explorer I, United States first satellite, launched in 1958, achievements 8-85817
 fragmentation in orbit 8-53858
 gamma-ray telescope artificial satellite, axis orientation determ. 8-53787
 geodesy, geometrical and dynamic methods, development (*Polish*) 8-88780
 geodetic satellites, appl. to realisation of ocean dynamics four-dimensional reference system 8-77176
 geodetic satellites, role of orbit determ. in altimeter data anal. 8-77177
 GEOS booms and mechanisms 8-85825
 GEOS electron beam experiment S 329 8-93075
 Geos I, natural magnetospheric emissions identification 8-53774
 Geos satellite, first six months' obs. 8-61705
 geostationary, methods for numerical integration of eqns. of motion 8-69659
 geostationary, plasmopause sounding feasibility 8-93043
 geostationary satellite VHF Faraday rotation mea. for ionospheric electron content 8-61599
 geosynchronous, ATS programme progress 8-81515
 gyrodampers in passive attitude control system 8-96379
 gyrostatic satellite in circular orbit, regular precessions 8-93082
 HEAO B, scheduled launch and observing opportunities 8-69647
 HEAO-B satellite, sensitivity rel. to deep X-ray surveys predictions and strategies 8-96567
 HEOS-2 meas. of magnetospheric charged particles 8-61671
 Hermes, geostationary communications satellite, Canadian design 8-93068
 initial orbit determ. using angles and angular rates of movement 8-53795
 INTELSAT IV, in-orbit liquid slosh tests, anal. 8-81516
 Interkosmos-Kopernik 500 in ionosphere plasma, Debye screening and electron conc. nonuniformity 8-69563
 International Sun-Earth Explorer B minimum-model project 8-61702
 International Sun-Earth Explorer mission 8-61701
 International Ultraviolet Explorer (IUE), in-flight performance 8-96383
 International Ultraviolet Explorer (IUE), spacecraft and instrumentation 8-96382
 International Ultraviolet Explorer geosynchronous orbit 8-89060
 ionosphere satellites, waveguide propag. expts. at MF, general results 8-69604
 ionosphere satellites, whistler-mode pulse propag. expts. at medium freqs. 8-69605
 ISEE 1 and 2, electron density expt. 8-85803
 ISEE 1 and 2, medium energy particles expt. 8-85811
 ISEE 1 and 2 fluxgate magnetometers 8-85804
 ISEE spacecraft, experimental investigations and instruments, review 8-85785
 ISEE spacecraft instrumentation for solar and interplanetary electron meas. 8-85786
 ISEE-1, electron spectrometer expt. 8-85809
 ISEE-1, solar wind expt. 8-85800
 ISEE-1 and -2, quadrispherical LEPEDEAS for plasma meas. 8-85801
 ISEE-1 and ISEE-2, fast plasma expt. 8-85800
 ISEE-1 and ISEE-2, plasma wave investigation 8-85802
 ISEE-1 and ISEE-C, nuclear and ionic charge distrib. particle expts. 8-85790
 ISEE-1 spacecraft, quasi-static and low-freq. elec. fields meas. via spherical double probes 8-85808
 ISEE-A, DC and low-freq. elec. field meas. instrumentation 8-85807
 ISEE-A, plasma comp. expt. 8-85810
 ISEE-A and -B, energetic particle fluxes in magnetosphere and interplanetary space, expt. 8-85799
 ISEE-A spacecraft, Stanford University VLF wave injection expt. receiver 8-85806
 ISEE-B project, Sun-Earth Explorer (*German*) 8-81526
 ISEE-B satellite, EGD positive ion expt. 8-85805
 ISEE-C cosmic ray electrons and nuclei expt. 8-85792
 ISEE-C cosmic ray isotope spectrometer 8-85797
 ISEE-C low energy proton expt. 8-85791
 ISEE-C medium energy cosmic ray expt. 8-85798
 ISEE-C multidetector cosmic ray telescope expt. 8-85789
 ISEE-C plasma wave expt. 8-85794
 ISEE-C solar wind ion comp. expt. 8-85793
 ISEE-C solar wind plasma expt. 8-85788
 ISEE-C three-dimens. radio mapping expt. 8-85796
 ISEE-C vector He magnetometer 8-85795
 ISEE-C X-ray spectrometer expt. 8-85787
 isotope-powered satellite design for Shuttle launches 8-61709
 Kosmos 954 descent and radioactivity surveillance in Switzerland (*German*) 8-77119
 Lageos for crustal movement meas. 8-65441
 Lagrange configurations in space system dynamics 8-73606
 LANDSAT imagery photoprints, pulp mill stack plume meas., air pollution appl. 8-88905
 LF radio sounding of plasmopause by geostationary satellite 8-69648
 magnetic damping of rotation, shielding effects 8-69646
 magnetic field effects, exponential damping 8-69645

association
see also association of liquids; associative ionisation
 acetic acid, protonated complexes, IR and Raman spectra (French)
 8-78691
 acetic acid dimer, gas phase, H-bonded complex struct. from elec.
 dipole moment obs. 8-74791
 chloroaluminium phthalocyanine, sublimed layer, IR absorption, vibr.
 assignments 8-55174
 desorption kinetics with precursor intermediates 8-87876
 1,5-dichloroanthracene, photodimerisation, orientational defects, lattice
 energy 8-80724
 dimers, dissociating, in nonisothermal ideal gas phase, stationary state
 anal. 8-76848
 double molecules, with weak reson. bond, quasilinear (Russian)
 8-74640
 ettringite, expansion by H₂O adsorption, exam. 8-64806
 ferrofluids, exptl. obs. of agglomeration in presence of mag.
 field (French) 8-92514
 formic acid dimer, gas phase, H-bonded complex struct. from elec.
 dipole moment obs. 8-74791

acetone-chloroform (i-iodomethane) ($-CS_2$), liq. mixture, excess Gruneisen parameter, intermol. interaction 8-67635
alkaline earth halides, solns. in methanol, conductance data anal., assoc. consts. 8-71875
amide group in soln., interactions, IR, Raman spectral investigs., peptide, protein struct., review 8-90330
benzene, in Br_2 -carbon tetrachloride soln., complex form., IR spectra 8-70828
benzene-ethylene dichloride ($-CCl_4$), liq. mixture, excess Gruneisen parameter, intermol. interaction 8-67635
t-butanol-acetone-cyclohexane, complexation, thermodynamic parameters (Russian) 8-76905
carbon tetrachloride-benzene, liq. mixture, excess Gruneisen parameter, intermol. interaction 8-67635
chloroform-acetone, liq. mixture, excess Gruneisen parameter, intermol. interaction 8-67635
chloroform-hexamethylphosphoramide complex, mol. motion and assoc., PMR obs. (French) 8-72429
cyclodextrins, diffusion in aq. polymer solns., complex form. 8-91460
disperse systems, coagulation, slow, turbulent 8-53259
ethanol, assoc. in dil. soln., dielec. obs., dipole moment meas. 8-83714
ethanol, solns., local struct. equilib., light scatt. and IR spectra obs. 8-84564
ethylene dichloride-benzene, liq. mixture, excess Gruneisen parameter, intermol. interaction 8-67635
ethylenediamine- H_2O mixtures, inhibition of Ps form. by NO_3^- ions 8-95988
phenol-(d_4)-dioxan-(acetonitrile), in carbon tetrachloride ($CDCl_3$) solns., H-bonds vibr. relax. bands anal. 8-84560
PMMA, stereoregular, assoc. in dilute soln., PMR obs. 8-76321
quasilatice theory, complexation, thermodynamic parameters calcs., spectroscopic appls. (Russian) 8-76905
Raman spectra of liq. phase weak H-bonds, short range order and anharmonicity effects 8-64357
solutions, H bonding and anomalous saturation 8-52426
solvation, classical mean space charge model 8-76841
water, and ionic dissoc. products, polarisation model 8-91216
water, IR spectrum, influence of Cu^{2+} ions 8-72501
water-HF(HBr)(HCl) complex, in supersat. soln., Raman spectra assignments 8-70840
H-bonded species, in soln., vibr. relax. model 8-84559
 SCN^- , associated with metallic cations in aq. soln., press. effect, Raman spectra (French) 8-80333

associative ionisation
atom+atom collision, Penning and assoc. ionisation, complex. pot. and electron spectrum 8-94310
atom+metastable atom collisions, ionis. processes 8-62907
Ar, precursor shock waves, electron density and assoc. ionisation 8-67217
 $Cs(nP)+Cs(6S)$, assoc. ionisation, threshold energy, Cs_2^+ dissoc. energy 8-58804
He+He, metastable atoms, collisional ionisation cross-sections 8-70911
 $He^+ + H(H_2)(Ar)$, metastable state, ionis. processes 8-62907
 $Hg(6^3P_0) + Hg(6^3P_1) \rightarrow Hg_2^+ + e$, plasma formation by strong Hg line irradi., mechanism 8-83585
 $^6Li^+ + ^7Li^+$, laser-induced Penning and associative ionis., $^{13}Li_2^+$ enrichment 8-58796
 $O_3 + ^1U(Th)$, assoc. ionis. cross sections, in crossed beams, mass spectra obs. 8-94317

astatine

see also nuclei with
No entries

astatine compounds

No entries

asteroids

1974OT, astrometric obs. 8-89107
1974OU, astrometric obs. 8-89107
1976 AA, ephemeris for 1978 July-1979 May period 8-69733
1976 AA, precise position for 1977 Dec. 16 8-73673
1977 HA, astrometric obs. 8-89107
1977 HB, precise position for 1978 Apr. 10 8-73673
1977 HB, recovery, precise positions for 1978 May 9-10 8-53862
1977 OA, discovery, 1977 July 18-19 positions 8-77518
1977 RA, precise positions, (1977 September 23 to December 8) 8-53860
1977 UB (Chiron), accurate orbit, nature and status 8-53863
1977 UB (Chiron) astrometric obs. 8-89107
1978 (532) 1, discovery of possible satellite of Herculina 8-69734
1978 CA, precise positions, orbital elements, ephemeris 8-73672
1978 CA, precise positions (1978, March 7 to 12) 8-57486
1978 DA, ephemeris continuation for 1978 July-September period 8-61784
1978 DA, precise position for 1978 Apr. 9 8-73673
1978 DA, precise positions (1978, March 4 to 12) 8-57487
1978 PA, discovery positions for probable Amor-type object 8-81579
1978 PA, semiaccurate positions, (1978 August 14 and 15) 8-81580
1978 RA=1975 TB, ephemeris continuation and B magnitude law 8-89106
1978 RA, fast-moving asteroidal object approximate positions and photometry 8-85887
1978 RA (=1975 TB), precise positions, orbital elements and ephemeris 8-93141
1978 SB, fast-moving object, discovery positions and magnitudes 8-93142
1978 SB, positions, orbital elements and ephemeris 8-93143
1978 SB, positions and UBV photometry 8-96422
1978 SB, precise positions for 1978 Oct., orbital elements, ephemeris for 1978 Oct.-Dec. 8-96423
270 Anahita, photoelectric photometry during 1975-77 period 8-61783
Apollo objects, total number and chance rediscoveries 8-89105
astrometry, equatorial coords. for 19 objects in 1972-4 period (*French*) 8-81577
bombardment by planetesimals scattered from Jupiter zone 8-53859
186 Celuta, slowly spinning asteroid, photometry rel. to rot. period and comp. type 8-61782
Ceres, meridian obs. (1974 to 1977) 8-69660
313 Chaldaea, photoelectric photometry during 1975-77 period 8-61783
close approaches to Earth, list of events 8-73621
close-approaches to Earth, Amor and Apollo groups 8-61785
dynamic processes on Earth, extraterrestrial causes, rel. to extinction of life 8-92820
59 Elpis, photoelectric lightcurves and rotation period 8-69729
433 Eros, astrometric obs. during 1975 opposition 8-57485
families, concs. in proper elements space statistics and mapping 8-96420
37 Fides, photoelectric photometry during 1975-77 period 8-61783
fragmentation in orbit 8-53858
6 Hebe, size from 1977 March 5 γ Ceti A occultation obs. 8-53856
108 Hecuba, motion in restricted three-body problem, nonlinear oscils. (*German*) 8-57488
532 Herculina, occultation of SAO 120774, discovery of 1978 (532) 1 possible satellite 8-69734
Juno, meridian obs. (1974 to 1977) 8-69660
22 Kalliope, light curves, phase function, pole and dimensions 8-53857
Kirkwood Gaps and stability of conservative periodic systems 8-65544
216 Kleopatra, photoelectric photometry during 1975-77 period 8-61783
97 Klotho, photoelectric photometry during 1975-77 period 8-61783
lightcurves, simulation by rot. of three-axes ellipsoid model 8-61781
main belt objects, precise posns. in 1975-6 period 8-77515
mean motion resonant with Jupiter, short-periodic perturbations 8-53803
mining prospects 8-61786
Minor Planet Circulars 4391-4424, precise posns., elements, ephemerides, new nos. and names 8-81578
minor planet circulars 4425-4482, precise posns., elements, ephemerides, new nos. and names 8-85886
Minor Planet Circulars 4483-4520, precise posns., elements, new nos. and ephemerides 8-93140
missing planet origin rejected 8-69732
orbits and FK4 equator and equinox corrections 8-69727
orbits identification, ephemerides calc. (*Chinese*) 8-69731
Pallas, meridian obs. (1974 to 1977) 8-69660
Pallas, occultation of SAO 85009, 1978 May 29, corrected prediction, photoelec. obs. 8-57430
Pallas, occultation of SAO 85009 on 1978 May 29, prediction 8-53861
471 Papagena, photoelectric photometry during 1975-77 period 8-61783
photoelectric photometry during 1975-77 period 8-61783
photometry in 0.56-2.2 μ range for 30 objects 8-69725
planetoids in early solar system, ^{26}Al as heat source 8-65511
polarimetry of particulate surfaces 8-58011
population in circumterrestrial space 8-73599
precise positions, obs. at Sydney Observatory during (1976) 8-69735
precise positions for 18 objects meas. at Torino 8-69730
precise positions for nine selected objects in 1976-7 period 8-77514
primordial metamorphism via elec. induction in T Tauri-like solar wind 8-69728
S-type, spin rate 8-77516
80 Sappho, photoelectric photometry during 1975-77 period 8-61783
structure of asteroid belt 8-69737
surface materials mineralogical characts. from reflectance spectra 8-69736
terrestrial cratering, plate tectonics and evolution of life 8-96421

asteroids continued

topographic changes on airless bodies, meteorite impact and ejecta deposition 8-65523
Trojan asteroids and fictitious objects at 1/1 resonance, long-period effects 8-85830
Trojans, elliptic restricted three-body problem, invariant relation 8-69726
UBV photometry of 145 faint objects 8-69724
unidentified objects found during search for short-period comets 8-85907
Vesta, meridian obs. (1974 to 1977) 8-69660
Vesta, possible eucrite parent body, implications of Moore County quench temp. 8-96444

astigmatism see aberrations**astrobiology** see extraterrestrial life**astrometry**

1974OT, astrometric obs. 8-89107
1974OU, astrometric obs. 8-89107
1976 AA, precise position for 1977 Dec. 16 8-73673
1977 HA, astrometric obs. 8-89107
1977 HB, precise position for 1978 Apr. 10 8-73673
1977 HB, recovery, precise positions for 1978 May 9-10 8-53862
1977 OA, discovery, 1977 July 18-19 positions 8-77518
1977 RA, precise positions, (1977 September 23 to December 8) 8-53860
1977 UB (Chiron) astrometric obs. 8-89107
1978 CA, precise positions (1978, March 7 to 12) 8-57486
1978 CA, precise positions for 1978 Mar. 8-73672
1978 DA, precise position for 1978 Apr. 9 8-73673
1978 DA, precise positions (1978, March 4 to 12) 8-57487
1978 RA (=1975 TB), precise positions, (1978 September 10 to 12) 8-93141
1978 SB, precise positions, (1978 October 6 to 11) 8-93143
1978 SB, precise positions for 1978 Oct., orbital elements, ephemeris for 1978 Oct.-Dec. 8-96423
ADS 8887, photographically unresolved visual binary, parallax and orbit 8-57593
Allegheny Observatory parallax program, astrometric constants for 47 stars 8-53923
asteroids, precise positions for 18 objects meas. at Torino 8-69730
asteroids, precise positions for nine selected objects in 1976-7 period 8-77514
asteroids, precise posns. in 1975-6 period for 30 main belt objects 8-77515
astrolabes concurrent obs., 1966-1975 period, Universal Time determ. (*Russian*) 8-73617
astronomical azimuth determ., accuracy, geodetic networks orientation control appl. 8-92774
astronomical refraction, general theory (*Russian*) 8-89045
 ϵ Aurigae, eclipsing binary, astrometric study from Sproul 61-cm refractor plates 8-89219
binary stars, speckle interferometry with 1 m telescope 8-69831
binary* stars orbital solutions, derivation for unseen companions 8-93313
binary stars unresolved by speckle interferometry, epochs of obs., (1975-77) 8-73735
Bordeaux Observatory, equatorial coords. for asteroids, planets and Moon in 1972-4 period (*French*) 8-81577
Comet Bradfield (1978c), precise positions, 1978 (February 15 to March 12) 8-65551
Comet Bradfield (1978o), precise position for 1978 Oct. 18 8-96439
Comet Bradfield (1978o), precise positions for 1978 Oct. 8-96433
comet discovery, 1977 July 18-19 positions 8-77518
Comet Fujikawa (1978n), precise position, (1978, October 10) 8-93166
Comet Fujikawa (1978n), precise position for 1978 Oct. 11 8-96434
Comet Fujikawa (1978n), precise positions, (1978, October 13 to 14) 8-93168
Comet Giclas (1978k), precise positions, (1978 September 10 to 12) 8-89122
Comet Haneda-Campos (1978j), precise positions for 1978 Sept. 8-85913
Comet Kohler (1977m), precise positions, (1977 October 4 to 1978 April 8) 8-73680
Comet Kohler (1977m), precise posns. for 1977 October-1978 March period 8-61806
Comet Machholz (1978l), precise positions, total visual magnitude estimates, 1978 Sept. 8-89130
Comet Machholz (1978l), precise positions 1978 Sept.-Oct., magnitudes 8-93163
Comet Meier (1978f), positions, elements, ephemeris, magnitudes and spectrum 8-53881
Comet Meier (1978f), posns., elements, ephemeris and magnitudes 8-61801
Comet Meier (1978f), precise positions, 1978, April 30 to (May 8) 8-53884
Comet Meier (1978f), precise positions, (1978, May 2 to June 9) 8-69751
comet Meier (1978f), precise positions and magnitude estimates (1978 May-June) 8-69748
Comet Meier (1978f), precise positions for 1978 Apr.-May, total visual magnitude estimates 8-57505
Comet Meier (1978f), precise posns. (1978 May-July) 8-77520
Comet Meier (1978f), precise posns. and total visual mag. estimates (1978 Apr.-May) 8-57504
Comet Seargent (1978m), precise positions, (1978, October 2 to 4) 8-93164
Comet Seargent (1978m), precise positions (1978, October 6) 8-96432
Comet Seargent (1978m), precise positions for 1978 Oct. 8-96436
Comet Seargent (1978m), precise positions for 1978 Oct. 8-96438
Comet Tsuchinshan (1977q), precise posns. (1977 Nov.-1978 Jan.) 8-61804
Comet West (1978a), precise positions for 1978 Jan.-May 8-61799
compact radiosources positions from VLBI obs. 8-81698
31= α^2 Cygni, astrometric studies 8-69779
declination obs. of circumpolar stars with meridian circle (*Japanese*) 8-89044
digital image centring algorithm for astrometric positioning 8-69696

astrometry continued

- double star measures at Lick Observatory, Mount Hamilton, California 8-85979
- double stars, micrometer obs. 8-57582
- double stars, photographic measures 8-57581
- Earth daily free nutation parameters, determ. technique 8-96126
- 433 Eros, astrometric obs. during 1975 opposition 8-57485
- FK4 equator and equinox corrections from asteroid orbits 8-69727
- fundamental star catalogue system, improvement via relative determs. of celestial bodies coordinates 8-53797
- Galilean satellites, photometric eclipses anal. rel. to theory of motion 8-53864
- Greenwich Obs. Time and Latitude Service, Time Report (April-June, 1977) 8-69661
- Greenwich Obs. Time and Latitude Service, Time Report (July-September 1977) 8-73619
- Greenwich Obs. Time and Latitude Service, Time Report (October to December, 1977) 8-89046
- image analysis system, software and astrometric appl. 8-53834
- Jupiter faint satellites (VI-XIII), astrometric obs., (1974 to 1977) 8-89107
- Jupiter inner satellites, mutual phenomena in 1979, ephemerides and astrometric aspects 8-53866
- latitude variation, computation for national ephemeris calc. 8-88776
- Lick proper motions referred to galaxies, precession and galactic rot. determ. 8-65487
- lunar occultations, obs. at Sydney Observatory during (1974-1976) 8-69658
- Mars, obs. with Algiers astrolabe (winter 1973) (*French*) 8-61775
- Mars, obs. with Danjon astrolabe of San Fernando Observatory (*French*) 8-57483
- Mars, photographic position meas. (*Russian*) 8-93137
- Mars, position obs. with Paris astrolabe (1975 to 1976) (*French*) 8-61776
- Martian satellites, history of discovery and positional obs. (1877 to 1977) 8-89101
- meridian circles pivot errors, new determ. method 8-53822
- meridian passages of stars obs. at Dresden Univ., microclimatic effects (*Russian*) 8-73612
- Minor Planet Circulars 4391-4424, precise posns. for asteroids and 15 comets 8-81578
- minor planet circulars 4425-4482, precise posns. for asteroids and eight comets 8-85886
- Minor Planet Circulars 4483-4520, precise posns. for asteroids and 13 comets 8-93140
- minor planets, meridian obs. (1974 to 1977) 8-69660
- minor planets, precise positions obs. at Sydney Observatory during (1976) 8-69735
- NGC 7027, planetary nebula, position meas. with small Schmidt telescope 8-73749
- Nova Cygni 1978, discovery report and precise position 8-85962
- Nova Cygni 1978, spectrum, precise position and photometry 8-89211
- objectivisation of observations with circumzenithal, using photoelec. device (*Russian*) 8-73654
- χ^1 Orionis, new solar-type astrometric binary, parallax and orbital elements 8-73740
- Palmer Schmidt plates, astrometric accuracy 8-57455
- parallaxes of objects at cosmological distances, meas. via radiointerferometric techniques 8-53796
- Periodic Comet Arend-Rigaux (1977k), precise positions for 1977 Oct.-1978 Mar. 8-65548
- Periodic Comet Ashbrook-Jackson (1977g), precise position for 1978 Apr. 5 8-53887
- Periodic Comet Chernykh (1977l), precise positions 1977 Aug.-1978 Mar. 8-53886
- Periodic Comet Chernykh (1977l), precise posns., improved elements and ephemeris 8-69747
- Periodic Comet Gehrels 3 (1975o), precise positions for 1978 Feb.-Mar. 8-73677
- Periodic Comet Giclas (1978k), precise position, (1978, September 14) 8-85916
- Periodic Comet Giclas (1978k), precise positions 1978 Sept., elliptical elements, ephemeris 8-93162
- Periodic Comet Gunn, precise positions for 1977 Oct. and Dec. 8-69750
- Periodic Comet Haneda-Campos, precise positions, (1978 August 11 to September 5) 8-89121
- Periodic Comet Haneda-Campos (1978j), precise position for 1978 Sept. 29 8-93167
- Periodic Comet Haneda-Campos (1978j), precise positions, (1978 September 2 and September 8) 8-89124
- Periodic Comet Haneda-Campos (1978j), precise positions 1978 Aug.-Sept., ephemeris for 1978 Sept.Oct. 8-89131
- Periodic Comet Haneda-Campos (1978j), precise positions (1978, September 6 and 8) 8-85914
- Periodic Comet Haneda-Campos (1978j), precise positions (1978, August 10 to September 12) 8-89127
- Periodic Comet Kojima (1977r), precise positions for 1978 Jan. and Mar. 8-65549
- Periodic Comet Sanguin (1977p), precise posns. (1977 Nov.-1978 Jan.) 8-73685
- Periodic Comet Schuster (1977o), precise positions, 1977 October 16 and (1978 January 2) 8-65550
- Periodic Comet Schwassmann-Wachmann 1, precise posns. (1977 Dec.-1978 March) 8-69746
- Periodic Comet Van Biesbroeck (1977s), precise posns. (1978 April-May) 8-73686
- Periodic Comet Van Biesbroeck (1977s), precise posns. (1978 Jan.-May) 8-61802
- Periodic Comet Wild 2, (1978b), precise positions, (1978 February 8 to April 12) 8-53885
- Periodic Comet Wild 2 (1978b), precise positions (1978 Feb.-Apr.) 8-53880
- Periodic Comet Wild 2 (1978b), precise positions for 1978 Mar.-May 8-73676
- Periodic Comet Wild 2 (1978b), precise posns. (1978 February-April) 8-73681
- Periodic Comet Wild 2 (1978b), precise posns. and magnitudes (1978 Jan.-May) 8-61803
- phase photoelectric device for time service transit instrument (*Russian*) 8-73632

astrometry continued

- phase photoelectric device on Dresden Univ. transit instrument, obs. results (*Russian*) 8-73634
- photoelectric device for stellar transit times recording (*Russian*) 8-73635
- photoelectric device with high time resolution, obs. results (*Russian*) 8-73633
- photoelectric method of recording stellar transit times (*Russian*) 8-73652
- photoelectric transit instrument results (*Russian*) 8-73613
- photographic zenith tube plates, new reduction method 8-73656
- planetary positions calc. using programmable pocket calculator (*Norwegian*) 8-69700
- planets, meridian obs. (1974 to 1977) 8-69660
- planets and natural satellites position meas. 8-81573
- positional astronomy and definition of ephemeris pole 8-93078
- prismatic astrolabe, improved drive and instrumental characts. (*Russian*) 8-89066
- proper motion star catalogues, comparison, systematic errors (*Russian*) 8-93126
- radio sources, precise optical positions in FK 4 system, pilot programme results 8-65709
- S-type stars, secular parallax and mean absolute magnitude 8-81623
- Saturn, astrolabe obs. at Paris (1971-6) (*French*) 8-85896
- Saturn, obs. with Algiers Observatory Danjon astrolabe (1969 to 1974) (*French*) 8-61794
- Saturn, obs. with CERGA Observatory Danjon astrolabe, (1974 to 1976) (*French*) 8-61793
- Saturn, obs. with Paris astrolabe (1975-1976) (*French*) 8-89115
- Saturn satellites mutual phenomena in 1979-1980, ephemerides and astrometric aspects 8-53868
- β Scorpii, multiple star, lunar occultation astrometry 8-57583
- star positions, statistical approach to Brosche's model for catalogue comparisons 8-81559
- stars in vicinity of PSR 1913+16 binary pulsar, astrometry and photometry 8-93219
- stars trigonometric parallaxes, determ. by Yerkes Observatory 40 inch refractor 8-89168
- stellar transit times recording and errors (*Russian*) 8-73653
- Sun, positions in 1976, CERGA astrolabe obs. (*French*) 8-69760
- supernova in MCG -4-32-23, precise position, photographic magnitude 8-57568
- systematic errors elimination in obs. with transit instrument (*Russian*) 8-73615
- systematic errors in astrometric obs., spectral anal. of obs. series (*Russian*) 8-73614
- 45, 97 and 102 μ , Tauri, astrometric studies 8-69779
- time observations, scientific problems and organization (*Russian*) 8-73616
- Tokyo Astronomical Obs., Time and Latitude Bulletins (July-September 1977) 8-73618
- transit instrument automation (*Russian*) 8-73636
- Trapezium type multiple systems, relative proper motions (*Russian*) 8-93314
- trigonometric parallaxes for southern hemisphere stars 8-69780
- Venus, photographic position meas. (*Russian*) 8-93121
- Venus, photographic position meas. (*Russian*) 8-93135
- vertical circle meas. of stars, aberration of light rel. to spectral type (*German*) 8-73702
- visual binary stars, southern, new obs., orbits and masses 8-96502
- visual double stars, astrometric meas. at Nice (*French*) 8-89224
- visual double stars, micrometer obs., (1975 to 1977) 8-89218
- visual double stars measured at Las Campanas Observatory, Chile 8-85978
- ZTL-180 zenith telescope, micrometer screw turn from declination arc. obs. (*Russian*) 8-89067
- ZTL-180 zenith telescope, objective distortion determ. from visual obs. of star pairs (*Russian*) 8-89068
- 20,986, new unresolved astrometric binary 8-57594

astronautics see space research**astronomical catalogues**

- see also *astrometry*
- 2A catalogue of X-ray sources, review 8-73659
- absorption-line objects 8-86036
- Arecibo 2380 MHz survey of bright galaxies 8-57470
- 5C2 survey revised distances of optical objects from radiosources 8-57472
- 4C radiosources clustering 8-96556
- comets, obs. in Greek and Roman sources before 410 AD 8-77658
- compact galaxies on UK Schmidt plates 8-81687
- compact groups of compact galaxies, eighth list, 32 objects (*Russian*) 8-93125
- decametric survey of discrete northern sources, catalogue of 329 objects, 10-20° declinations 8-57471
- decametric survey of discrete northern sources, spectra of 266 sources in 10-1400 MHz range 8-57664
- equatorial IR catalogue (EIC), 2.7 μ high-precision sky survey results 8-81560
- ESO-B and SRC-J sky surveys, limiting magnitude 8-69706
- ESO/Uppsala galaxies, second catalogue 8-77497
- extragalactic emission-line objects, Univ. of Michigan List IV 8-77494
- FK4 equator and equinox corrections from asteroid orbits 8-69727
- fundamental star catalogue system, improvement via relative determs. of celestial bodies coordinates 8-53797
- galaxies and clusters of galaxies in SMC direction 8-96410
- gamma-ray sources, COS B catalogue and identifications 8-73775
- GB2 sky survey at 1400 MHz, differential radiosource counts 8-54063
- HD catalogue and E.C. Pickering, American astrophysics, history 8-86102
- IR astronomical survey data processing techniques 8-81553
- late-type stars, intermediate-band photometry, catalogue 8-81558
- LMC radiosources at 3.4 cm catalogue and spectral indices 8-65695
- LMC supergiant stars, comments on catalogue of Stock et al. (*French*) 8-53941
- meteorite craters on Earth, form., props. and catalogue 8-96411
- parallax stars in Herstmoneux programme, second list 8-77498
- Perth 70 catalogue, determ. of meridian circle pivot errors 8-53822
- planetary nebulae, southern, red-sensitive objective-prism survey list of suspected objects 8-77496

astronomical catalogues continued

- proper motion star catalogues, comparison, systematic errors (*Russian*) 8-93126
 QSO spectra, catalogue of absorpt. line lists for 108 objects 8-53840
 radiosources, S4 5 GHz survey between +35° and +70° declination 8-69893
 radiosources isotropy in B2 catalogue 8-73766
 Royal Astronomical Society, catalogue of archives and manuscripts 8-69705
 S-type stars in Southern Milky Way, objective prism survey and BVI photometry 8-61754
 small-scale radio struct. in Sharpless H II regions at 4.995 GHz, high-resolution catalogue 8-61755
 SMC wing, photoelectric UVB sequence 8-69874
 solar diatomic molecular lines in 7100-7600 Å range, table 8-77495
 solar type IV bursts, catalogue preparation (*Italian*) 8-96459
 star clusters in SMC, identifications and coordinates 8-89086
 star positions, statistical approach to Brosche's model for catalogue comparisons 8-81559
 stellar photometry, catalogue of homogeneous data in UBV photoelectric system 8-96409
 stellar spectral energy distribution for 50 stars, 3200-7550 Å region (*Russian*) 8-65620
 Trapezium-type multiple systems, catalogue of 87 systems with O- and B-type primaries (*Russian*) 8-61753
 H I 21 cm absorption towards extragalactic radiosources, catalogues of 819 sources 8-57638

astronomical ephemerides

- 1975 YA, ephemeris for 1978 July-1979 May period 8-69733
 1978 CA, ephemeris for 1978 Jul.-Oct. 8-73672
 1978 DA, ephemeris continuation for 1978 July-September period 8-61784
 1978 RA=1975 TB, ephemeris continuation and B magnitude law 8-89106
 1978 RA (=1975 TB), ephemeris (1978 September 13 to October 3) 8-93141
 1978 SB, orbital elements and ephemeris, (1978 September 9 to October 29) 8-93143
 1978 SB, precise positions for 1978 Oct., orbital elements, ephemeris for 1978 Oct.-Dec. 8-96423
 Apollo asteroids, chance rediscoveries rel. to reliable ephemerides 8-89105
 asteroid orbits identification, ephemerides calc. (*Chinese*) 8-69731
 British Astronomical Association Handbook 8-85828
 Comet Bradfield, parabolic elements and ephemeris, 1978 July 31 to (1979 January 7) 8-65551
 Comet Bradfield (1978o), parabolic orbital elements, ephemeris for 1978 Oct.-Nov. 8-96433
 Comet Fujikawa (1978n), orbital elements and ephemeris (1978, October 9 to December 8) 8-93168
 Comet Giclas (1978k), elliptical orbit ephemeris, (1978, September 9 to October 19) 8-89122
 Comet Haneda-Campos (1978j), orbital elements, ephemeris for 1978 Sep. 8-85913
 Comet Machholz (1978l), parabolic orbital elements, ephemeris for 1978 Oct.-Nov. 8-93163
 Comet Machholz (1978l), total visual mags. and ephemeris continuation 8-93159
 Comet Macholz (1978l), orbital elements and ephemeris (1978, September 19 to October 9) 8-89126
 Comet Meier (1978f), orbital elements and ephemeris, (1978 May 12 to July 11) 8-53884
 Comet Meier (1978f), positions, elements, ephemeris, magnitudes and spectrum 8-53881
 Comet Meier (1978f), posns., elements, ephemeris and magnitudes 8-61801
 Comet Seargent (1978m), parabolic orbital elements, ephemeris for 1978 Oct.-Nov. 8-96436
 Comet Seargent (1978m), parabolic orbital elements and ephemeris, (1978, September 29 to October 29) 8-93164
 Comet West (1978a), ephemeris, (1978, June 11 to September 9) 8-61807
 P/Daniel, predicted orbital elements 8-53883
 EZ Hydrae, eclipsing binary, photometric obs. and primary min. ephemeris 8-73737
 Jupiter inner satellites, mutual phenomena in 1979, ephemerides 8-53866
 Kepler and ephemerides of the early seventeenth century 8-77659
 Leda (Jupiter XIII), continuation ephemeris (1978 Sept.-1979 May) 8-69739
 Minor Planet Circulars 4391-4424, ephemerides for five asteroids 8-81578
 minor planet circulars 4425-4482, ephemerides for seven asteroids and four comets 8-85886
 Minor Planet Circulars 4483-4520, ephemerides for 45 asteroids 8-93140
 national ephemerides, latit. var. calc. 8-88776
 Neptune II (Nereid), ephemeris, (1978 May 12 to September 19) 8-53873
 Pallas, occultation of SAO 85009 on 1978 May 29, prediction 8-53861
 Periodic Comet Chernykh (1977l), precise posns., improved elements and ephemeris 8-69747
 Periodic Comet Comas Sola (1977n), ephemeris for 1978 July-1979 June period 8-69749
 Periodic Comet Giclas (1978k), elliptical elements, ephemeris for 1978 Oct.-Dec. 8-93162
 Periodic Comet Gunn, ephemeris continuation for 1978 July-1979 April period 8-61805
 Periodic Comet Haneda-Campos, ephemeris (1978, September 19 to November 18) 8-89121
 Periodic Comet Haneda-Campos (1978j), ephemeris for 1978 Oct.-Dec. 8-93167
 Periodic Comet Haneda-Campos (1978j), precise positions 1978 Aug.-Sept., ephemeris for 1978 Sept.-Oct. 8-89131
 Periodic Comet Jackson-Neujmin, ephemeris for 1978 June 21-1979 January 7 period 8-53878
 Periodic Comet Schwassmann-Wachmann 1, 1978-9 ephemeris 8-77521

astronomical ephemerides continued

- Periodic Comet Shajn-Schaldach, ephemeris for 1978 June-1979 March period 8-53879
 Periodic Comet Tuttle-Giacobini-Kresak, 1978-9 ephemeris 8-73684
 Periodic Comet Whipple (1977h), ephemeris, (1978 June 21 to 1979 April 17) 8-53882
 Periodic Comet Wild 2 (1978b), ephemeris for 1978 Jul.-Sept. 8-73676
 Pluto, 1978 P 1, discovery of possible satellite, ephemeris 8-69744
 Pluto, 1978 P 1, possible satellite, orbit and eclipses ephemeris 8-93152
 Saturn satellites mutual phenomena in 1979-1980, ephemerides 8-53868
 solar total eclipse, 1979, February 26, ephemeris 8-85928

astronomical instruments

- see also *astronomical observations; astronomical techniques; astronomical telescopes; radiotelescopes*
 acousto-optical radio spectrograph for spectral integration 8-69694
 acousto-optical solar radio spectrograph 8-73631
 airborne 33 GHz radiometer system for 3K background anisotropy mapping 8-61735
 airborne IR observations, methods and instruments 8-69688
 airbrush, for planetary mapping from photographic obs. 8-53833
 amplitude interferometer, white light, 180 degree rot. shear astronomical appl. 8-77977
 Apollo lunar surface science stations shutdown 8-57425
 aspheric grating for EUV astronomy 8-57451
 aspheric objective for a coronagraph (*Japanese*) 8-89063
 astronomical TV system, appl. to study of meteor bright line spectra 8-61817
 Australian Astronomical Society, conf. Melbourne, Australia (May-June '77) 8-69655
 automated isophotometer for large photographic plates (*Japanese*) 8-89069
 automated system for detect. of cosmic radio bursts at VHF and UHF 8-77489
 balloon borne interference spectrometers operation and appl. to solar UV obs. (*Japanese*) 8-57442
 balloon-borne experiment, for obs. of diffuse cosmic X-radiation above 20 keV 8-54096
 bifilar sundial, theory 8-93119
 blink comparator, semi-automated, for large photographic plates (*Japanese*) 8-89081
 blink microscope, exam. of new microscope at Lyon Observatory (*French*) 8-61742
 bolometer, composite, for submm. wavelengths 8-65964
 capacity type detector for low vel. dust meas. during cometary fly-by mission 8-93113
 Cassegrain echelle spectrograph at Mt. John Observatory, New Zealand 8-69689
 chopper for deep space IR interferometer/spectrometer 8-81545
 chopping photometer, for stellar obs. in northern light zone (*Norwegian*) 8-69699
 digital electronic integrator, for radioastronomical obs. processing (*Russian*) 8-57465
 digital register for elec. photometer (*Russian*) 8-93117
 discrete photoelectric tracking system of variable precision (*Russian*) 8-57458
 echelle spectrograph for high-resolution stellar spectra 8-96396
 European USSR bolide network, photographic determ. of bolides topocentric coordinates 8-61818
 four-channel photon-counting spectrophotometer, for stellar Ca II H and K flux meas. 8-73646
 Fulton's orrery, 19th century instrument to demonstrate planetary system motions 8-69695
 gamma-ray detectors, counters and telescopes (*Polish*) 8-96394
 HEAO 1 scanning modulation collimator, X-ray source positions meas. 8-93459
 HEAO-B satellite, sensitivity rel. to deep X-ray surveys predictions and strategies 8-96567
 History of Sciences Collections, Royal Swedish Academy of Sciences, catalogue 8-81789
 holographic grating, calc., for very wide field camera (*French*) 8-81547
 image tube with fibre optics, cooling effect 8-96401
 image-intensifier spectrograph, description and use 8-73647
 imaging system using intensity triple correlator 8-74846
 impact mass spectrometer for chemical analysis on comet fly-by mission 8-93112
 intensity microphotometer with step-drives, for negatives transparency conversion (*Russian*) 8-57457
 interferometer, long-baseline amplitude, pupil space design 8-53832
 interferometer, Michelson far IR 8-93118
 interferometer-grating spectrograph for high resolution spectroscopy in middle UV 8-77490
 International Sun Earth Explorer 1, electron spectrometer expt. 8-85809
 International Sun-Earth Explorer 1, solar wind expt. 8-85800
 International Sun-Earth Explorer 1 and 2, fast plasma expt. 8-85800
 International Sun-Earth Explorer 1 and 2, plasma wave investigation 8-85802
 International Sun-Earth Explorer A, DC and low-freq. elec. field meas. instrumentation 8-85807
 International Sun-Earth Explorer A, plasma comp. expt. 8-85810
 International Sun-Earth Explorer B, EGD positive ion expt. 8-85805
 International Sun-Earth Explorer spacecraft, expts. and instruments 8-85785
 International Sun-Earth Explorer spacecraft instrumentation for solar and interplanetary electron meas. 8-85786
 International Sun-Earth Explorer-1, quasi-static and low-freq. elec. fields meas. 8-85808
 International Sun-Earth Explorers, electron density expt. 8-85803
 International Sun-Earth Explorers 1 and 2, fluxgate magnetometers 8-85804
 International Sun-Earth Explorers 1 and 2, medium energy particles expt. 8-85811
 International Ultraviolet Explorer (IUE) instrumentation, in-flight performance 8-96383
 International Ultraviolet Explorer (IUE) spacecraft, instrumentation 8-96382

astronomical instruments continued

interplanetary plasma wave expt. on International Sun-Earth Explorer C spacecraft 8-85794
 IR heat trap field optics, compact lens-mirror system 8-55422
 IR photometer for stellar obs. 8-69795
 iris photometer for large photographic plates (*Japanese*) 8-89070
 ITT FW-130 photomultiplier, nonlinearities 8-85852
 lamellar-grating interferometer, balloon-borne, appl. to solar brightness temp. meas. 8-85921
 laser experiments on Spacelab missions, for atmospheric meas. 8-53793
 laser ranging equipment, computer system (*Japanese*) 8-89080
 laser ranging equipment, photoelectric circuit (*Japanese*) 8-89075
 laser ranging equipment, range gate (*Japanese*) 8-89076
 laser ranging equipment, range meas. system (*Japanese*) 8-89074
 laser ranging equipment, system controller (*Japanese*) 8-89079
 laser ranging equipment, telescope drive (*Japanese*) 8-89078
 laser ranging equipment, timing system (*Japanese*) 8-89077
 mass spectrometer, space-borne, in-flight calibration device 8-93115
 McMullan 4 cm electronographic camera, appl. to high-dispersion stellar spectroscopy 8-73644
 meridian circles pivot errors, new determ. method 8-53822
 Michelson Fourier transform spectrophotometer for stellar obs. 8-81550
 Michelson interferometer, sequential analysis of fringes, scanning rate influence 8-77976
 mirrors, large scale lightweight, replication 8-66963
 mirrors for space use, light-weight replicated optics 8-66965
 Mylar beam splitter efficiency in far IR interferometer 8-55434
 optical instrument measuring mark parameters rel. to stellar visibility 8-61736
 optical multi-element detectors, characts. 8-53830
 optical noise reduction, space appls. 8-59153
 optical polarimeter, detector array and polarising optics 8-57453
 Palomar Schmidt plates, astrometric accuracy 8-57455
 phase photoelectric device for time service transit instrument (*Russian*) 8-73632
 phase photoelectric device on Dresden Univ. transit instrument, obs. results (*Russian*) 8-73634
 photoelectric device for objectivisation of obs. with circumzenithal (*Russian*) 8-73654
 photoelectric device for stellar transit times recording (*Russian*) 8-73635
 photoelectric device with high time resolution, obs. results (*Russian*) 8-73633
 photometer for night natural illumination measurement in 0.4 to 1.2 μm spectral region 8-57367
 photometers, thermal stability rel. to Balmer-index photometry 8-96404
 photon counting magnetograph and polarimeter for stellar circular polarisation meas. (*Russian*) 8-65500
 Pioneer Venus Orbiter cloud photopolarimeter 8-57429
 Pioneer-Venus large probe infrared radiometer optical system 8-81543
 Pioneer-Venus large probe IR radiometer optical system 8-61715
 polarimeter, attached to multi-channel spectrophotometer (*Japanese*) 8-89072
 polarimeter, elliptical, for astronomy and atm. sciences 8-61745
 polarimeter, near IR, for solar corona emission line obs. 8-61740
 polarimeter, spectrum scanning Stokes, for solar research 8-61741
 prismatic astrolabe, improved drive and instrumental characts. (*Russian*) 8-89066
 proportional counter, spherical, with isotropic sensitivity, for soft γ -radiation 8-61732
 quasi-microscope concept for planetary missions, stereo pictures 8-81546
 Radcliffe Cassegrain d-camera, vel. system 8-73645
 radio mapping expt. in International Sun-Earth Explorer C spacecraft 8-85796
 resonant electromechanical modulators, appl. as choppers and scanners 8-53831
 Schmidt camera, direct, quasi-telecentric and telecentric combinations of interference filters 8-57441
 secondary electron conduction vidicon digiral TV camera for stellar obs. 8-54457
 solar magnetograph calibration programme (*Russian*) 8-65499
 solar magnetometer at Kodaikanal Observatory, design and performance 8-61743
 solar neutrino spectroscopy at low energies, In loaded liq. scintillator 8-73639
 solar radio bursts, recording instrumentation and data reduction (*Italian*) 8-96458
 solar spectrometer, reson. scatt., apparatus and instrumental errors 8-96393
 spectrometer, mm-wave, intensity calibration error evaluation 8-53821
 spectrometers, secondary spectrum of thin three-lens optical systems (*Russian*) 8-57456
 spectrophotometer, for short term variability obs. in stellar spectra 8-73643
 star magnitude simulator, IC device 8-81742
 star simulator design 8-85814
 stellar sensor assembly, solar simulation for testing off-axis light attenuation 8-61714
 stigmatic EUV spectroheliometer for photometry of dynamic phenomena 8-53825
 sundial, latitude-independent, theory and construction 8-81549
 television systems, photon counting and analogue, with digital real time image processing 8-96402
 toroidal diffraction grating, spectral image at point at spectrometer entrance slit (*Russian*) 8-57452
 transit instrument automation (*Russian*) 8-73636
 two-star photoelectric photometer at Wise Observatory, performance assessment 8-73657
 UVB photoelectric photometer for amateur use 8-65502
 vector He magnetometer on International Sun-Earth Explorer C spacecraft 8-85795
 Viking 1 and 2 expeditions, scientific results (*Hungarian*) 8-73666
 Viking IR thermal mapper, design 8-57440
 Viking Lander camera, optical system and design 8-53794
 Viking Lander camera, stray light control 8-61713
 X-ray, polarimeter, for solar and extrasolar obs. 8-57454

astronomical instruments continued

X-ray detector, large area MWPC, high-background rejection 8-93108
 X-ray detector on Ariel 5 satellite, design and performance 8-53826
 X-ray mirror objectives, testing 8-85850
 X-ray spectrometer expt. on International Sun-Earth Explorer C spacecraft 8-85787
 X-ray spectrometer for rocket-borne, solar obs., biaxial optical guider (*Polish*) 8-61744
 CsI crystals, in scintillation counters, nonstatistical counting rates due to phosphoresc. 8-95597

astronomical observations

see also gamma-ray astronomical observations; infrared astronomical observations; radioastronomical observations; ultraviolet astronomical observations; visible astronomical observations; X-ray astronomical observations
 ξ Andromedae, spectroscopic binary, photometric and spectroscopic obs. (*Russian*) 8-57588
 CD-38°245, metal-deficient halo red giant, spectrum, photometry and Ca/H ratio 8-69797
 UV Ceti, anomalous flare activity obs. 8-89202
 comets in 1973, review of observations, discoveries and recoveries 8-73683
 comets in 1974, review of observations, discoveries and recoveries 8-73682
 cosmic ray nuclei from 3000 MeV to 50 GeV per nucleon, charge comp. and energy spectra 8-93059
 CH Cygni, linear polarisation vars. rel. to circumstellar dust grains form. 8-69808
 V1016 Cygni, photometric and spectroscopic obs. rel. to proto-planetary nebula mass ejection 8-85947
 Cygnus X-1, optical and X-ray evidence for 78/39-day period 8-89274
 Deimos, 100 years since discovery, review of studies 8-73670
 Fourier transforms of data sampled at unequal observational intervals 8-69697
 galactic particle radiation, satellite obs. (*Danish*) 8-69631
 HR 1614 group of metal-overabundant stars, late-type stars intermediate-band photometry 8-53935
 late-type main-sequence stars near Sun, intermediate-band photometry 8-53934
 LTT 2437, most metal-deficient subdwarf, spectrum, photometry and Ca/H ratio 8-69797
 M67, main-sequence stars differential blanketing rel. to Hyades and Coma 8-57597
 M87 halo globular clusters, metallicity meas. 8-89244
 Mars, integral photometry 8-61780
 meteors, observation methods in Poland, review (*Polish*) 8-61750
 Molonglo southern radio sources, optical spectra 8-96555
 Nova Cygni 1978, spectrum, precise position and photometry 8-89211
 Nova Persei 1974 (V400 Persei), light curve and spectral evolution 8-73715
 Nova Scuti 1975 (V373 Scuti), light curve and spectral evolution 8-73715
 PHL 938, quasar, continuum spectrum reddening due to dust 8-96561
 Phobos, 100 years since discovery, review of studies 8-73670
 PKS 2126-15, bright quasi-stellar object with neutral colour and redshift of (3.27) 8-93450
 Pulkovo, short history 8-81538
 quasars, slitless spectroscopy of large redshift objects 8-96562
 V861 Scorpii (HD 152667), eclipsing binary, identification with X-ray source (OAO 1653-40) 8-69838
 Skibotn Observatory, in northern light zone, stellar obs. with chopping photometer (*Norwegian*) 8-69699
 solar flares, studies using optical, X-ray and radio data 8-85156
 solar wind, Helios 1 obs. of latitudinal extent of high-speed stream 8-57419
 Ulugh Beg observatory, meridian instrument axis azimuth rel. to continental blocks rot. 8-53613
 Venus, plasma electron obs. in wake 8-77510

astronomical observatories

Arecibo Observatory, ionospheric props. meas. without rockets 8-81488
 Canadian camera network and Innisfree meteorite recovery and orbit determ. 8-65563
 Canary Islands, site selection by JOSO for solar observatory 8-65497
 Hermonieux parallax programme, second list of meas. stars 8-77498
 Lyon, new blink microscope (*French*) 8-61742
 Mt. Hopkins multiple mirror telescope 8-93109
 Potsdam Observatory, long-term latitude determs. rel. to principal components var. 8-57158
 Skibotn Observatory, in northern light zone, stellar photometric obs. (*Norwegian*) 8-69698
 Smithsonian Astrophysical Observatory, H maser improvements 8-58971
 solar optical observatory testing sites in China, atm. temp. vars. in surface layer (*Chinese*) 8-69680
 South African Astronomical Observatory, user guide to telescope facilities 8-73628
 southern hemisphere observatories, cooperative obs. programmes feasibility 8-69681
 Wise Observatory, photoelectric UVB photometry performance assessment 8-73657

astronomical spectra

see also atmospheric spectra; stellar spectra
 γ -ray sources, possible X-ray counterparts spectra rel. to identifications 8-54092
 2A 1102+384 (Markarian 421) BL Lacertae object, low-energy X-ray spectrum 8-54083
 Abell 1367 galaxy cluster, obs. rel. to galaxies redshift-magnitude bands and evolution 8-54033
 absorption spectra of QSOs and BL Lacertae objects 8-86036
 AO 0235+164, BL Lacertae object, radio study of $z=0.524$ absorpt. system 8-65680
 asteroid surface materials mineralogical characts. from reflectance spectra 8-69736
 B2 1225+31, spectrum of bright quasar 8-93447
 Balmer discontinuity strengths, interstellar absorption effects 8-89238
 Becklin-Neugebauer source in Orion, high resolution 1.5 to 5 micron spectroscopy 8-93368
 blending effects 8-62851

astronomical spectra continued

- bright sporadic meteor, spectrum obtained with Wampler scanner 8-57508
 3C273, spectroscopic obs. and redshift of associated galaxy 8-77606
 4C 25.05, H₂ lines identification in spectrum of quasar (*Russian*) 8-69905
 3C 58, spectra of faint knots in SNR 8-93375
 Canis Major R1 and OB1 associations, Fabry-Perot obs. of assoc. expanding gas shells 8-93336
 Cassiopeia A, supernova remnant, search for X-ray line emission 8-57607
 clusters of galaxies, radio spectrum slope rel. to intracluster gas heating and X-ray emission 8-57655
 Coma galaxy cluster, low energy X-ray absorpt. obs. 8-86025
 Coma/A1367 supercluster of galaxies and environment 8-65700
 Comet Kohoutek (1973XII), Swann band profiles 8-85909
 Comet Meier (1978f), positions, elements, ephemeris, magnitudes and spectrum 8-53881
 Comet Sargent (1978m), UV spectral obs. by IUE 8-96436
 Comet West (1976 VI), IR obs., results 8-81591
 Comet West (1976 VI), spectrophotometry after perihelion passage, emission features vars. 8-57503
 comets, brightness var. in molecular emission bands 8-81590
 comets, possible detect. of newly created CN radicals 8-61798
 compact galaxies, spectroscopic and photometric obs. 8-77603
 compact galaxies on UK Schmidt plates 8-81687
 cosmic microwave background, spectral lines of prestellar origin (*Russian*) 8-77628
 Crab Nebula filaments, shock waves hydrodynamics effects on spectra 8-85997
 Cygnus Loop, 25 MHz struct. and radio spectrum 8-54027
 Cygnus Loop, search for O VII X-ray line emission 8-93379
 decametric survey of discrete northern sources, spectra of 266 sources in 10-1400 MHz range 8-57664
 diffuse X-ray background spectrum, 20 keV spectral index change determ. 8-69916
 double radio sources in directions of rich galaxy clusters, spectral indices and polarisation 8-57662
 elliptical galaxies, late M giants population synthesis rel. to colours and spectra, comp. effects 8-57626
 ESO 103-G35, type I Seyfert, optical counterpart of H 1834-653 X-ray source 8-96547
 ESO 140-G43 (Fairall-51), new southern Seyfert 1 galaxy, spectrum and red shift 8-54044
 ESO/Uppsala galaxies, spectroscopic and photometric obs., second catalogue 8-77497
 EUV spectrum of hot, optically-thin interstellar plasma 8-81665
 extragalactic objects UV spectra, International Ultraviolet Explorer (IUE) obs. 8-96540
 forbidden lines in quasars and active galaxies, theory 8-93408
 Fourcade-Figueroa galaxy near NGC 5128, struct., spectrum and red shift 8-73758
 G333.6-0.2, G298.2-0.3, southern compact H II regions, IR emission lines obs. 8-96522
 G333.6-0.2, powerful H II region, 2 μ m line emission detect. 8-54017
 G45.1+0.1, 8-13 μ m spectrophotometry of compact H II region 8-65672
 G48.6+0.0, galactic H II region, direction, H I, OH and H₂CO absorpt. line meas. 8-85996
 galactic dust globules, microwave spectral lines obs. 8-57609
 galactic interstellar extinction law, effect of varying 2200 Å feature 8-85990
 Galactic IR obs. at 2.4 μ m wavelength by balloon (*Japanese*) 8-61924
 galactic nucleus, H110 α recomb. line emission vels. 8-69885
 galaxies, active nuclei, physical props. from emission-line spectra 8-57650
 galaxies, Doppler shifts distrib. for relativistic gas 8-65492
 galaxies, late-type H I obs. rel. to integral props. derivation 8-86015
 galaxies, radio recombination line studies of nearby objects 8-93397
 galaxies active and normal nuclei, radio spectra compared with quasars 8-57646
 galaxies active nuclei, continuous optical spectra 8-57644
 galaxies active nuclei, H emission-line spectra 8-96557
 galaxy pairs containing one Markarian and one normal galaxy, morphology and spectra 8-96535
 gamma-ray burst source on 1976 August 16, balloon-borne obs., energy spectrum 8-54078
 gamma-ray diffuse radiation, MeV excess in energy spectrum 8-73777
 gaseous nebulae, Fe abundances from forbidden Fe III and Fe VI lines intensities 8-53806
 gravitational waves, cosmological, spectrum rel. to temp. fluctuations in primordial background radiation 8-65728
 H 2155-304, optical counterpart position and spectrum 8-93478
 Haro 15, spectrophotometry and morphology of galaxy with UV excess (*Russian*) 8-93387
 Heiles 2, interstellar dark dust cloud, HC₂N and HC₃N obs. 8-54023
 Helix Nebula, abundance anomalies in planetary nebula 8-86001
 Hercules X-1, high-energy X-ray spectrum 8-93473
 IC 1318, giant H II region, large-scale line splitting discovery 8-96521
 IC 4997, O III 4363 Å forbidden line/H γ intensity ratio vars. 8-86003
 interplanetary magnetic field fluctuations, freq. spectra rel. to mean field direction 8-85905
 interstellar dark globules, IR surface brightness and emergent spectra 8-53999
 interstellar diffuse clouds, OH and HD column densities rel. to temps. determ. 8-93385
 interstellar gas, UV absorption line obs. of vel. distrib. 8-89235
 interstellar H₂, vibrationally excited, search for 8150 Å emission line 8-93346
 interstellar H I survey from Lyman α absorption meas. towards 100 stars 8-93357
 interstellar molecular cloud near RCW 36, H₂CO and OH obs. 8-69862
 interstellar molecular clouds, line profiles rel. to radiation transport and kinematics 8-93347
 interstellar OH, ¹⁶OH/¹⁸OH abundance ratio obs. in three H II regions 8-54024

astronomical spectra continued

- interstellar UV absorption lines in HR 1099 direction, Copernicus obs. 8-93358
 Io Na D-line emission, comparison of observed and theoretical line profiles 8-93145
 IR heterodyne spectroscopy 8-85859
 IR molecular line emission from grain surfaces in dense interstellar clouds 8-61905
 IR source assoc. with Sh 2-149, spectral type and luminosity class 8-73772
 IR sources, 10 μ m silicate absorpt. band equivalent widths and dust temps. 8-57614
 IR sources, galactic, IR fluxes calcs. for polysaccharide grain model 8-54008
 IR sources assoc. with double-lobed refl. nebulae, far IR continua 8-54009
 Jupiter, atmosphere, ¹²CH₄/¹³CH₄ ν_4 band, line parameters, 7.7 micron transmission 8-85894
 Jupiter, far IR spectrum showing NH₃ rotational bands 8-85891
 Jupiter, L-bursts in decametric radio spectra 8-96424
 Jupiter, microwave spectrum of atmosphere 8-85889
 Jupiter, S II forbidden line emission from thermal plasma 8-93146
 Jupiter, spectrophotometry in far IR 8-85890
 Jupiter, whistler mode noise spectrum in inner magnetosphere 8-89112
 Jupiter atmosphere, GeH₄ abundance from IR spectrum anal. 8-61791
 Jupiter atmosphere, trace constituents upper limits from 5 μ m spectrum anal. 8-61790
 Kirchhoff's laws of spectral analysis, computer laboratory exercises 8-73790
 Kobayashi-Berger-Milon (1975IX), Swann band profiles 8-85909
 M101, spectra of H II regions, comp. gradient across spiral galaxy 8-65683
 M31, inner nuclear regions, spectral features and dwarf content 8-86005
 M32-1, planetary nebula in M32, spectroscopic evidence that M32 is in front of (M31) 8-93394
 M82 as exploding radiogalaxy, image tube spectrogram evidence 8-69880
 Markarian 132, spectrum and redshift systems 8-89248
 Markarian 298 (=IC 1182-4) central condensations, spectral energy distributions. (*Russian*) 8-57641
 Markarian 374, Seyfert galaxy, spectra of double nucleus components 8-69882
 Markarian II, 180 and 421, spectra of stellar population 8-54047
 Mars, disc IR spectra compared with terrestrial analogues optical props. 8-85879
 Mars surface, Viking lander sites spectral reflectance and colours 8-85881
 meteor, fast sporadic spectrum 8-93170
 meteor bright line spectra, study via astronomical TV system 8-61817
 methane 6819 Å line interpretation rel. to inhomogeneous scattering models for Uranus and Neptune 8-53871
 microwave background radiation spectrum, statistical anal. of data 8-86039
 Molonglo southern radio sources, optical spectra 8-96555
 N132D, supernova remnant in LMC similar to Cassiopeia A, photographic and spectroscopic study 8-93345
 nebulae, dusty, lines surface brightnesses in non on-the-spot (OTS) models 8-85995
 nebulae, photoelectric spectrophotometry of compact objects 8-89236
 NGC 1052, elliptical galaxy, H I 21 cm spectrum and rot. 8-69873
 NGC 1068, Seyfert galaxy, 2-2.5 μ m spectrum, H₂ detect. 8-57636
 NGC 1068, Seyfert galaxy, silicate emission feature from IR photometry 8-54035
 NGC 2742, spiral galaxy, rot. and mass. (*French*) 8-89255
 NGC 315, NGC 6251, very large radio galaxies, 11.1 cm obs. rel. to spectral index vars. 8-86014
 NGC 3256, peculiar galaxy, kinematics from emission lines meas. 8-96537
 NGC 3620, southern emission-line galaxy at low galactic latitude 8-86022
 NGC 4151, UV photometry and extended spectrum of Seyfert galaxy 8-89249
 NGC 4473, flattened elliptical galaxy, spectroscopic obs., dynamics 8-57631
 NGC 4945, galaxy, water vapour emission obs. 8-93427
 NGC 5236 (M83), Sc galaxy, CO emission distrib. and vels. 8-65689
 NGC 5506, X-ray Seyfert, spectra 8-93411
 NGC 5907, rotation and mass of edge-on galaxy from spectra (*French*) 8-77595
 NGC 6302 chem. composition of planetary nebula 8-96525
 NGC 6720, O III 5007 Å forbidden line obs., vel. structure of planetary nebula 8-61909
 NGC 6946, spiral galaxy, N overabundance in nucleus (*French*) 8-89257
 NGC 7027, 16-38 μ m spectral obs. and dust model of planetary nebula 8-93354
 NGC 7027, planetary nebula, forbidden Mn V transitions identification 8-50496
 NGC 7027, planetary nebula, UV emission line spectrum rel. to interstellar reddening, IUE obs. 8-96524
 NGC 7027, planetary nebula, near IR obs. 8-73748
 NGC 7027 and NGC 7293, spectral obs. of planetary nebulae (*Russian*) 8-61897
 NGC 7213, S0 galaxy with Seyfert nucleus, spectra and direct obs. 8-86024
 NGC 7822 (W1) optical studies of kinematics rel. to supernova remnant struct. 8-54028
 nightglow continuum between 0.8 and 1.1 μ m, Soviet obs. 8-81483
 nonlinear inverse Compton radiation spectrum, deepest descents method 8-85840
 OQ 172, H₂ lines identification in spectrum of quasar (*Russian*) 8-69905
 Orion Molecular Cloud, NH₃ spectrum and new dynamical model 8-93373
 Orion Nebula, C I IR forbidden emission lines obs. 8-85987
 Orion Nebula, S III 9096 Å forbidden line, Fabry-Perot obs., abundance determ. 8-96515

astronomical spectra continued

- Periodic Comet Ashbrook-Jackson (1977g), spectroscopic obs. 8-96437
- Periodic Comet Gielas (1978k), spectroscopic obs. 8-96437
- Perseus galaxy cluster, low energy X-ray absorpt. obs. 8-86025
- Perseus galaxy cluster, obs. rel. to galaxies redshift-magnitude bands and evolution 8-54033
- PHL 938, quasar, continuum spectrum reddening due to dust 8-96561
- PKS 2126-15, bright quasi-stellar object with neutral colour and redshift of (3.27) 8-93450
- planetary corona, collisional model for spectral line profiles 8-77508
- planetary nebulae, molecular abundances and IR spectra 8-53998
- planetary nebulae, photoelectric spectrophotometry of emission lines, abundances 8-81677
- planetary nebulae of overall field and galactic centre, spectra and physical characts. 8-54029
- primordial microwave radiation, recomb. lines calc. 8-54097
- pulsar radio signals spectra and microstruct., relativistic electron beam model 8-65639
- Q 1246-057, absorpt. line spectrum, presence of outflowing material 8-93453
- QSO 0242+622, spectrum and luminosity of low redshift object 8-93451
- QSO absorption line spectra for six high-redshift objects 8-93449
- QSO absorption line systems, radiation-driven outflow models 8-57687
- QSO redshift $(1+z)/(1+z_e)$ distrib. 8-65715
- QSO spectra, catalogue of absorpt. line lists for 108 objects 8-53840
- QSOs, emission-line spectra and redshift distrib. 8-57677
- QSOs, physics of absorpt. line regions 8-57680
- quasar absorption lines, origin 8-57684
- quasars, absorpt. lines statistics and line-locking 8-57681
- quasars, accretion discs thermal emission as source of optical continuum 8-54075
- quasars, Doppler shifts distrib. for relativistic gas 8-65492
- quasars, H emission-line spectra 8-96557
- quasars, IR energy distrib. obs. 8-57645
- quasars, optical surveys, electronographically recorded low-dispersion slitless spectra 8-57467
- quasars, props. of $Z_{abs} > Z_{em}$ systems rel. to origins of QSO absorpt. line systems 8-57682
- quasars, slitless spectroscopy of large redshift objects 8-96562
- quasars, spectra obtained with low-dispersion Fehrenbach prism computer simulation 8-57468
- quasars absorption lines, line-locking hypothesis, intervening galaxies absorpt. and $z=1.95$ peak in redshifts 8-57685
- quasars relative luminosities determ. from emission line strengths 8-61931
- quasi-stellar objects, absorpt. lines in spectra 8-57679
- quasi-stellar radio sources from 4C and Parkes catalogues, spectra and photometry 8-65714
- radiation redistrib., diffuses reflection effects 8-53819
- radio galaxies, narrow-lined, spectrophotometry 8-93391
- radio galaxies, optical emission-line spectra 8-57643
- radio quiet quasistellar objects, obs. at 3.3 mm wavelength 8-81703
- radio sources, galactic, OH radio lines absorpt. obs. 8-54068
- radio sources, spectral index distrib. rel. to source counts freq. depend. 8-96554
- radio sources from Molonglo Deep Survey, radio and optical spectra 8-69900
- radiogalaxies, spectrophotometry of three objects 8-54066
- radiosources, coordinated photometric and spectroscopic observations of strong extragalactic 90 GHz sources 8-93440
- radiosources, spectroscopic obs. in 3200-5700 Å range of 34 program objects 8-86032
- radiosources with flat or inverted spectra, optical and radio props. 8-81697
- S104, 609 MHz aperture synthesis obs. of H II region 8-57618
- S106, H II region, radio obs. of assoc. mol. cloud, CO, HCO⁺ HCN, OH and formaldehyde lines 8-61906
- S140 IR, far IR spectrum 8-93372
- HM Sagittae, planetary nebula excited by Wolf-Rayet star, spectrum 8-54003
- Saturn, echelle spectrogram 8-96426
- Saturn, HD detect. at 6063.88 Å, D/H abundance ratio calc. 8-57495
- Saturn, spectrophotometry in far IR 8-85890
- Saturn far UV spectrum, rocket obs. 8-53867
- Serpens X-1, Ariel 5 obs. and models of spectrum and time var. 8-81707
- Seyfert 2 galaxies, spectrophotometry 8-93391
- Seyfert galaxies, broad H lines prod. by suprathermal protons passing through neutral gas (*Russian*) 8-57642
- Seyfert galaxies, IR energy distrib. obs. 8-57645
- Seyfert galaxies, obs. at 1.3 and 2.8 cm wavelength, spectra 8-69866
- Seyfert galaxies, optical emission-line spectra 8-57643
- SNRs, coronal line emission obs. and shock-heated plasma temp. determ. 8-65676
- solar system objects, International Ultraviolet Explorer (IUE) obs. 8-93133
- Space Telescope, prospects for spectroscopic and direct work 8-57444
- supernova remnants, H abundance rel. to H deficiency in Type I supernovae 8-53969
- supernova remnants, young, thermal X-rays theoretical spectra 8-73751
- Sz 80, southern emission-line galaxy at low galactic latitude 8-86022
- Titan, Kuiper bands detect. in spectrum 8-85898
- TMC2, interstellar dark dust clouds, HC₃N and HC₇N obs. 8-54023
- Tycho's supernova remnant, filaments spectrum 8-73747
- Uranus, H₂ quadrupole lines detect. in spectrum 8-93149
- Uranus, HD detect. at 6063.88 Å, D/H abundance ratio calc. 8-57495
- Uranus, HD line obs. and atmospheric D/H ratio 8-57497
- Uranus, limb brightening within methane 7300 Å band 8-85902
- variable radiosources, spectra, RATAN-600 radiotelescope obs. (*Russian*) 8-61927
- Venus, cloud properties from airborne obs. of near-IR reflectivity spectrum 8-53850
- Venus, CO₂ 7883 Å band, high-dispersion spectroscopic obs. near superior conjunction 8-53851
- Venus, IR bands rel. to H₂SO₄ aerosol medium optical props. 8-65526

astronomical spectra continued

- Virgo cluster X-ray source, power-law spectrum rel. to two-source struct. 8-54090
- Virgo/galaxy cluster, low energy X-ray absorpt. obs. 8-86025
- X-radiation diffuse background above 20 keV, spectrum from balloon obs. 8-54096
- X-ray binary systems, K-fluorescence lines in spectra 8-93456
- X-ray emission from optically thin plasmas, abundance effects on continuum spectrum 8-53814
- X-ray emission spectrum, multiple Compton scatts. effect, Monte Carlo calcs. 8-96389
- X-ray sources in galactic centre and Cygnus region, spectral characts. 8-54079
- Zeeman components with hyperfine structure, line strengths and splittings 8-77482
- zodiacal light IR radiance model and meas. 8-81588
- zodiacal light spectrum, Doppler shifts meas. 8-85904
- I Zw 92, III Zw 77, compact galaxies with broad emission lines, spectra 8-73760
- C II regions assoc. with reflection nebulae, recombination line spectra 8-69857
- CH in diffuse interstellar medium, optical and radio obs. 8-93356
- C₂H (butadiynyl) radical, detect. towards (IRC+10216) 8-93374
- CO emission from late-type galaxies 8-89250
- H I absorption in QSO spectra, search for absorption by clusters of galaxies 8-93448
- H I Ly/He ratio for flares, quasars and prominences 8-61826
- H I regions, 21 cm spectra rel. to galactic shocks 8-54042
- H I regions, galactic, emission absorpt. obs. from Arecibo 8-57610
- H II regions, chemical comp. of galactic and extragalactic regions 8-93359
- H II regions, high-excitation, effects of inhomogeneities on spectra 8-54007
- H II regions, radio recombination line obs. of C and H from 10 areas 8-93360
- H II regions, weak shocks props. rel. to line strengths 8-93348
- H II regions emission line spectra, influence of star, gas density and chemical comp. 8-61911
- H II regions radio emission spectra, consequences of improper analytic methods 8-54000
- HC₃N, detect. in interstellar space 8-93370
- H₂O 22 GHz maser emission from W3(OH), 49N and 51, spatial distrib. 8-93355
- H₂O, interstellar maser lines very-high-velocity satellite features generation by stimulated Raman scatt. 8-73746
- H₂O maser source near NGC 2071, discovery and spectrum 8-73768
- H₂O sources spectra, autocorrel. anal. 8-65713
- H₂O⁺, interstellar, unsuccessful search and abundance upper limit 8-69860
- He II recombination lines, calc. intensities in UV 8-94212
- NH₃, interstellar, spectra in southern radio sources 8-69863
- NH₃, non-metastable absorption at 23.1 GHz, first obs. towards W3(OH) 8-65677
- O III 51.8 μ forbidden emission line obs. of Orion Nebula 8-65510
- OH 1.6 GHz maser emission from W3(OH), 49 N and 51, spatial distrib. 8-93355
- OH maser emission from W3(OH), Zeeman effect 8-93377
- OH radicals, microwave spectra data tables 8-50542
- S II, fine-structure transitions by electron impact 8-65493

astronomical spectroscopy *see astronomical spectra; spectroscopy*

astronomical techniques

- see also astrometry; radioastronomical techniques*
- airborne IR observations, methods and instruments 8-69688
- Ap stars, recognition in Vilnius photometric system 8-65635
- asteroid families, clustering technique for concs. anal. in proper elements space 8-96420
- astrometry using Paloma Schmidt plates, accuracy 8-57455
- astrometry with small Schmidt telescope, NGC 7027 position meas. 8-73749
- Australian Astronomical Society, conf. Melbourne, Australia (May-June '77) 8-69655
- auto-correlation method for superegiant semi-period of variation determ. 8-61854
- averaging method for secular behaviour of dynamical systems 8-77469
- Balmer-index photometry, quantitative anal. of influencing factors 8-96404
- binary stars orbital solutions, derivation for unseen companions 8-93313
- bolides topocentric coordinates determination, use of photography 8-61818
- celestial mechanics, common derivation of averaging method and two-timescale method 8-85835
- celestial mechanics, orbitally stable multistep methods 8-85834
- clusters of galaxies assoc. with QSOs, detection using radio source morphology 8-93434
- comets motion, correction for nongravitational effects, comparison of methods 8-61811
- compact radio sources, mapping from VLBI data 8-89266
- cosmic ray electrons, detect. by synchrotron radiation in geomag. and interstellar mag. fields 8-57412
- dark nebulae, visual extinctions determ. via star counts 8-57612
- digital image centring algorithm for astrometric positioning 8-69696
- digital image processing applications, conference, San Diego (1977) 8-81528
- digital image processing techniques for planetary program and Earth resources information 8-96408
- early-type stars photospheric expansion, meas. via. Fourier anal. technique 8-93224
- Earth daily free nutation parameters, determ. technique 8-96126
- eclipsing binary systems with dislike envelopes, light curve interpretation, appl. to HZ Herculis 8-65658
- eclipsing variable stars, Fourier anal. of light curves 8-93311
- eclipsing variables, Fourier anal. of light curves, photometric perturbs. 8-96507
- eclipsing variables, light curve Fourier analysis, eclipse parameters, geometrical determinacy 8-96503
- electronographic recording of low-dispersion slitless spectra, quasar appl. 8-57467
- elemental abundances, empirical determ. method tested on H II regions 8-61908

astronomical techniques continued

- EM sounding of Moon using surface magnetometer meas. 8-65518
extragalactic object reddening determ. method 8-54039
extrasolar planets, direct imaging with space telescope during stationary occultations 8-85858
extreme subdwarf stars, metal abundances from mol. band strengths, theoretical approach 8-93221
fast transient phenomena, physical mechanisms affecting observations (*Italian*) 8-93105
Fourier analysis of data with closely spaced frequencies, erroneous results 8-89298
Fourier analysis of light curves of eclipsing binaries for transit eclipses 8-96506
Fourier transform IR spectroscopy appl., conf., Columbia, USA (June 1977) 8-58067
Fourier transform spectroscopy, airborne IR obs. 8-61747
Fourier transformation of data sampled at unequal intervals 8-69697
Fourier transforms appl. to contrast profile method of vector mag. field meas. 8-53839
fundamental quasisimonochromatic stellar photoelectric photometry, accuracy (*Russian*) 8-65505
fundamental star catalogue system, improvement via relative determs. of celestial bodies coordinates 8-53797
galactic nuclei, variable, photometric techniques, finding charts and comparison stars 8-81691
Galaxy local structure, determ. from stellar kinematics (*Russian*) 8-77608
Galilean satellites, edge-finding technique for dias. determ. from Pioneer data 8-85893
gamma-ray telescope artificial satellite, axis orientation determ. 8-53787
Geminid meteor stream, orbital period from quantitative simplicity index 8-53889
globular clusters, age and chemical comp. determ., review (*Polish*) 8-61751
gravitational waves detection, proposed search for correl. with neutrino bursts 8-77567
holographic emulsions for stellar spectra recording by interferometric method 8-73651
hypersensitisation of photographic emulsion (*Swedish*) 8-85853
image analysis, general system software and appls. 8-53834
image processing digital techniques 8-81555
image processing techniques 8-87022
image reconstruction, from incomplete and noisy data 8-53837
image reconstruction performance of image-plane sharpness criteria 8-93123
image restoration by regularisation method, appls. (*Italian*) 8-93124
image restoring with maximum entropy, Poisson sources and background 8-66769
infrared heterodyne spectroscopy in astronomy 8-85859
initial orbit determ. using angles and angular rates of movement of artificial satellites 8-53795
interference-phase method of mag. field meas. in solar atm. (*Russian*) 8-65509
interference-phase method of ray vel. meas. in solar atm. (*Russian*) 8-65508
interplanetary magnetic sector structure, mapping via comet plasma tail disconnections 8-93155
interplanetary particle sampling 8-57459
interstellar diffuse clouds temperatures, determ. from HD and OH column densities 8-93385
IR laser heterodyne spectroscopy for trace gases remote detect. in planetary atms. 8-61606
IR observation technique 8-61738
latitude variation, computation for national ephemerids calc. 8-88776
lunar laser ranging, polishing and Foucault test of receiving telescope mirror (*Japanese*) 8-89065
lunar minerals trace element nondestructive anal. using proton microprobe 8-64911
lunar seismograms, use of surface reflections 8-65504
M-type supergiants, photoelectric two-dimensional spectral classification 8-53936
magnetic fields, dual magnetometer method extension for use on dual spinning spacecraft 8-77459
meridian circles pivot errors, new determ. method 8-53822
meteor bright line spectra, study via astronomical TV system 8-61817
meteor observation 8-57509
meteorites, diamond-containing; polished thin section preparation technique 8-65566
meteors, observation methods in Poland, review (*Polish*) 8-61750
meteors, television photographs photometry 8-96441
microparticle studies by space-borne instrumentation 8-57460
neutrino bursts detection, proposed search for correl. with gravit. waves 8-77567
optical lunar occultation meas., statistically rigorous reduction 8-73650
Orwo ZU 2 plate with improved props., astron. appl. (*German*) 8-89571
period computation for δ Scuti stars (*French*) 8-85949
personal equation determ. method 8-89443
photoelectric photometry at Wise Observatory, performance assessment 8-73657
photoelectric scanning of globular clusters (*Italian*) 8-93343
photographic position meas. of Venus (*Russian*) 8-93121
photographic zenith tube plates, new reduction method 8-73656
Photometric Data Systems (PDS) photometry of open cluster NGC 2420, error anal. 8-57600
photometry of atmospheric IR emission, statistical props. of sky noise (*French*) 8-53731
photometry of rich clusters of galaxies 8-89264
photometry of white dwarf stars, calibration 8-85938
planetary atmosphere, remote sensor, high resolution Fourier transform spectropolarimetry 8-57469
planetary atmospheres, eqn. of transfer for optical depths >100 , soln. method 8-96414
planetary mapping by airbrush technique 8-53833
planetary positions calc. using programmable pocket calculator (*Norwegian*) 8-69700
planets, nonsolar, detect. via spinning IR interferometer 8-85977
point summation technique, appl. to faint X-ray sources detect. near COS-B γ -ray positions 8-54093

astronomical techniques continued

- polar axis misalignment determ. for equatorial instruments 8-69685
polarimetry of atmosphereless solar system bodies 8-58011
radiative transfer inversion problems, Backus-Gilbert formalism 8-89054
radical vel. meas. using telluric A-band on objective prism spectra (*Japanese*) 8-89083
radio interferometry, amateur radio telescope design 8-85849
radio sources, ang. struct. investigation via lunar occultations, resolving power 8-65712
reddening determ. method in uvby photometric system 8-73655
rotating body observation using high-resolution spectroscopy, appl. to Sun 8-96403
satellite orbital lifetimes, prediction methods 8-73605
solar corona and comet digital image enhancement 8-81556
solar EUV output measurement, techniques and appl. to aeronomy 8-57535
solar mag. field intensity determ. for nonspot mag. regions 8-96452
solar magnetic field meas. review 8-81607
solar magnetic fields determination, multi-dimensional non-LTE polarised radiation transfer in mag. fluxtubes 8-69673
solar radio emission polarisation in 1.9-3.5 cm wavelength region, obs. method (*Russian*) 8-65587
solar type IV radio events, FFT anal. rel. to pulsating structs. 8-96455
speckle holography measurements of stars ξ Cancri and ADS 3358 8-93120
speckle interferometry, atm. nonisoplanicity meas. using double stars 8-65387
speckle interferometry, binary stars obs. with 1 m telescope 8-69831
speckle interferometry, effects of spectral bandwidths and exposure times 8-69701
speckle interferometry, meas. of binary stars 8-85973
speckle interferometry, online digital autocorrelator 8-81548
speckle interferometry of binary stars, computer simulations in photon-counting mode 8-53836
spectrophotometry of low-luminosity stars with Carnegie image tube 8-57466
spectroscopic binary stars orbits, test of circularity 8-93321
star cluster high resolution imaging by speckle interferometry, simulation 8-77492
stellar absolute magnitude determ. methods 8-96405
stellar absolute spectrophotometry and UVB photometry, comparison of results 8-96476
stellar atmospheres, vel. gradients determ. from spectral lines differential Doppler shifts 8-57538
stellar Ca II H and K emission, flux meas. by four-channel photon-counting spectrophotometer 8-73646
stellar clusters, appls. to cosmic distance measurement 8-57599
stellar high-dispersion spectroscopy, appl. of McMullan 4 cm electronographic camera 8-73644
stellar holographic interferometric technique, mutual coherence function 8-53838
stellar magnetic fields, vector-operator algebra technique for stationary states determ. 8-73698
stellar radial vel. determ. methods 8-96406
stellar radial velocities, Radcliffe Cassegrain d-camera vel. system 8-73645
stellar space density derivation methods, systematic comparison 8-61917
stellar speckle interferometry, wave correlation scale meas. 8-65388
stellar spectra, photographic equivalent widths calibration against solar photoelectric equivalent widths, feasibility 8-73658
stellar spectral classification, rel. to use of H-R diagram as astronomical tool 8-81619
stellar uvby β photometric system, absolute luminosity calibrations check by means of small trigonometric parallaxes 8-57463
stereophotogrammetry of Mars surface 8-77493
strip photometry of diffuse objects, globular clusters multicolor obs. 8-89229
surface photometry of barred spiral galaxies, computerised digital reduction method 8-81690
terrestrial longit. determ., without time, from obs. of lunar altitude 8-85836
turbulent-degraded image reconstruction using nonredundant aperture arrays 8-93122
universal time measurement, results from lunar laser ranging 8-85854
UV and visible astronomy from space 8-61704
vacuum UV Cherenkov source as radiation standard (*Russian*) 8-63164
video stereophotogrammetry, interactive computerised, for Mars Viking 1975 Lander data 8-81557
Viking 1 and 2 expeditions, scientific results (*Hungarian*) 8-73666
Viking Orbiter and Lander stereo image processing 8-81554
visual binary star orbit, computation method for any eccentricity (*French*) 8-85974
Voigt lines, random array, curve-of-growth function 8-89055
X-ray source position determ., parameter estimation method 8-61748
X-ray sources, binarity detect. via Doppler effect (*Russian*) 8-77623
H II regions radio emission analysis, consequences of improper analytic methods 8-54000
H II regions weak shocks, isothermal Mach number determ. from line ratios 8-93348
Hy equivalent width computation method for objective-prism astrophotograph, for SMC stars 8-57462

astronomical telescopes

- see also radiotelescopes
altazimuth-mounted computer-controlled, zenithal blind spot 8-53823
autoguider, photoelectric control component (*German*) 8-73649
British large IR telescope on Mauna Kea, construction 8-69686
comet telescope, timing system (*Japanese*) 8-89071
compound catadioptric telescopes with all spherical surfaces, design 8-69682
direct imaging with space telescope during stationary occultations for extrasolar planet detection 8-85858
double Compton gamma-ray telescope, background sensitivity to atmospheric neutrons 8-53827
drive, controlled 300 Hz freq. supply 8-61746
drive, of laser ranging equipment (*Japanese*) 8-89078

astronomical telescopes continued

- extinction coefficient meas. from distant contrast, using astronomical telephotometer 8-61730
 focusing testers, anal. of optical and construction parameters 8-83070
 four-mirror unobscured anastigmatic telescope, with all-spherical surfaces 8-57439
 gamma-ray, large scale telescopes for high resolution obs. 8-93114
 gamma-ray Compton telescope, high ang. resolution, 0.3-10.0 MeV directivity (*Portuguese*) 8-85847
 gamma-ray telescope artificial satellite, axis orientation determ. 8-53787
 Gregorian reflector, renovation of 18th century instrument 8-61734
 Hadamard transform X-ray telescope 8-53828
 Hadamard X-ray spectrometer with wide field-of-view 8-53829
 HEAO B, scheduled launch and X-ray telescope observing opportunities 8-69647
 HEAO-B X-ray telescope, observing program 8-57443
 IR, current developments review 8-61737
 IR, NASA 3-m telescope on Mauna Kea 8-96398
 IR, UK 3.8-m telescope on Mauna Kea 8-96397
 IR flux collector on Tenerife 8-69684
 large azimuthal telescope, search and guide system 8-57446
 large azimuthal telescope complex, automated control system 8-73641
 large azimuthal telescope major system design 8-73640
 large azimuthal telescope mirror, shop tests using modified Hartmann method 8-87173
 large azimuthal telescope primary mirror, blank grinding and polishing 8-90541
 large precision mirrors, possibilities of mass reduction 8-79100
 long wavelength IR, ang. response meas., off-axis rejection performance 8-61739
 lunar laser ranging telescope, Earth/Moon motion study appl. 8-93106
 mirror of lunar laser ranging receiving telescope, polishing and Foucault test (*Japanese*) 8-89065
 mirror surface testing of 6m LAT mirror, Hartmann method under shop conditions 8-90540
 monochromators of concave grating mounting for space telescopes, VUV region 8-73629
 Mt. Hopkins multiple mirror telescope 8-93109
 multidetector cosmic ray telescope expt. on International Sun-Earth Explorer C spacecraft 8-85789
 multiple mirror telescope, design, review 8-69687
 next generation designs, rotating shoe mounting (*Norwegian*) 8-69683
 objective, 3-mirror design, optical scheme 8-55431
 orbiting, IR detector cryogenic cooling requirements 8-96400
 polar axis misalignment determ. for equatorial instruments 8-69685
 Radcliffe Cassegrain telescope, d-camera vel. system 8-73645
 RGO 30-inch coude, appl. of McMullen 4 cm electronographic camera to high-dispersion spectroscopy 8-73644
 Salyut-4 orbiting solar telescope, design, obs. results 8-53783
 Schmidt 105 cm, Hartmann test (*Japanese*) 8-89073
 Schmidt 105 cm, polar axis setting (*Japanese*) 8-89064
 Schmidt telescope, astrometry appl., NGC 7027 position meas. 8-73749
 Schmidt telescopes, achromatic condition (*Japanese*) 8-89062
 seeing, wavelength depend., atm. inhomogeneity effects 8-92979
 sky noise at focus, photometry of atmospheric IR emission, statistical props. (*French*) 8-53731
 sky noise correl. for IR telescope focal plane (*French*) 8-53725
 South African Astronomical Observatory, user guide to telescope facilities 8-73628
 Space Telescope, prospects for spectroscopic and direct work 8-57444
 star seeker using semidisc light-flux modulator, accuracy anal. 8-73648
 steerable dish of mirror units, next generation telescope (*Norwegian*) 8-85846
 stray radiation, expt. meas. and computer analysis 8-61752
 transmission grating, facet-type, aberrations for cosmic X-ray and XUV spectroscopy 8-85851
 upper atmosphere, background effects in scintillation telescopes 8-85823
 Wyoming Infrared Telescope (Jelm Mountain), IR universe exploration 8-85848
 X-ray, actively shielded 8-81540
 X-ray, large scale telescopes for high resolution obs. 8-93114
 X-ray, mirror, on Salyut-4, gas-filled proportional photon counter 8-86746
 ZTL-180 zenith telescope, micrometer screw turn from declination arc. obs. (*Russian*) 8-89067
 ZTL-180 zenith telescope, objective distortion determ. from visual obs. of star pairs (*Russian*) 8-89068
 SiO₂ lightweight 370 mm mirror fabrication and testing 8-57447

astronomy see astronomy and astrophysics**astronomy and astrophysics**

- see also *astronomical catalogues; astronomical instruments; astronomical observations; astronomical observatories; astronomical spectra; clusters of galaxies; cosmology; extraterrestrial life; galaxies; gamma-ray astronomy; infrared astronomy; intergalactic matter; interplanetary matter; interstellar magnetic fields; occultations; radioastronomy; solar system; stars; ultraviolet astronomy; X-ray astronomy*
 acceleration of particles in astrophysical conditions 8-81537
 American Astronomical Society, 152nd meeting, Madison, Wisconsin (June 1978) 8-96385
 Aryabhata, 5th century Indian astronomer and mathematician, life and works 8-65741
 astrology in undergraduate astronomy courses 8-61991
 atmospheric refraction, general theory (*Russian*) 8-89045
 Australian Astronomical Society, conf. Melbourne, Australia (May-June '77) 8-69655
 Bibliographia Kepleriana. Supplements and continuation 1975-1978 8-77657
 British Astronomical Association Handbook (1978) 8-85828
 British optical astronomy, advances 8-69844
 civilisation and astronomy in time of Aryabhata I, 5th century AD 8-89289
 convection in meteorology, aspects relevant to astrophysics 8-88898
 cosmic plasma properties from magnetospheric research, use in astrophys. 8-93051
 Doppler shift, distrib. for relativistic gas 8-65492

astronomy and astrophysics continued

- education, nonscience majors, innovative course based on mass-radius diagram of states of matter 8-62002
 education, test item file construction and use 8-86054
 education, university courses and career prospects 8-69931
 education, university science course for talented high-school students 8-89282
 electron burst relaxation in fluctuating plasma, formal dynamical model 8-83579
 Evans, Thomas Simpson, 1777-1818, mathematician and astronomer 8-89287
 flicker noises, stochastic prop. 8-57473
 gravitational collapse, finite-particle scheme for three-dimens. gas dynamics 8-67218
 great year in Greek, Persian and Hindu astronomy 8-81790
 H-R diagram, IAU Symposium 80 review 8-96511
 H-R diagram, use as astronomical tool, review of IAU Symposium (No.80) 8-81619
 heavy stable neutral lepton, astrophysical consequences of existence 8-93091
 Henry Norris Russell, and Hertzsprung-Russell (H-R) diagram 8-69957
 historical astronomical events and Gospel records rel. to Christ's birth date 8-93127
 International Astronomical Union 1976 system of constants (*Russian*) 8-73611
 Johann Georg Soldner (1776-1834), forgotten bicentenary 8-81787
 Kepler and Mars, construction and rejection of first oval orbit 8-62027
 Laplace, P.S., chronology and citations of early work, 1770-1773 period 8-93505
 magnetic buoyancy in rotating gas, effect of fine electrical and thermal conductivities 8-57436
 Mesoamerican calendrical systems chronology reconstruction 8-81782
 MHD induction, simplest physical model of generator 8-71548
 Newcomb, Simon, American astronomer, 1835-1909, life and works 8-93504
 planetarium design, model from Mesquite Schools, near Dallas 8-81777
 planetarium run by students in Durham, New Hampshire 8-65503
 plasma nonlinear magnetoacoustic waves, damping, simulation 8-79423
 plasma physics in astronomy (*Russian*) 8-89057
 Quetelet, A.L.J., life and spread of science in Belgium during 19th century (*French*) 8-65742
 Royal Astronomical Society, catalogue of archives and manuscripts 8-69705
 Smiley, Charles Hugh (1903-77), solar eclipse authority, biography 8-62024
 solar and solar-terrestrial physics, illustrated glossary 8-57537
 space astronomy, NASA prospects 8-69654
 Spacelab 2 mission, astrophysical payload summary 8-85816
 steady disc accretion by stars, ang. momentum transfer 8-65609
 Stonehenge, new meas. in 1978 April survey 8-85860
 strong EM waves in collisionless homogeneous plasma, waveform, polarisation and nonlinear effects 8-53809
 sundial, latitude-independent, theory and construction 8-81549
 Universum, Swedish astronomical information project (*Swedish*) 8-86048
 Voigt functions, partial derivatives 8-89052
 B-like ions, highly ionised, up to Fe XXII, Breit-Pauli approximation 8-53810
 H₂, (4,0) S(1) quadrupole line intensity and pressure shift 8-90178
 He-like ions, level populations and line intensities for stationary plasmas 8-53811
 He-like ions, line intensities results 8-89051

astronomy computing

- see also *computerised instrumentation*
 asteroid orbits identification, ephemerides calc. (*Chinese*) 8-69731
 blink comparator, semi-automated, for large photographic plates (*Japanese*) 8-89081
 celestial mechanics, diurnal motion of Sun seen from Mercury, computer aided soln., teaching aspects 8-61969
 digital image centring algorithm for astrometric positioning 8-69696
 galaxy evolution, three-dimens. computer simulation 8-81551
 image analysis, general system software and appls. 8-53834
 image reconstruction, from incomplete and noisy data 8-53837
 IR astronomical survey data processing techniques 8-81553
 Kirchhoff's laws of spectral analysis, computer laboratory exercises 8-73790
 large cosmic ray showers, computer simulation using models of hadronic collisions 8-57415
 laser ranging equipment, computer system (*Japanese*) 8-89080
 LISP programming language appl. (*Polish*) 8-61749
 lunar seismograms, use of surface reflections 8-65504
 photographic zenith tube plates, new reduction method 8-73656
 programs for high-school expts. 8-86094
 radio astronomy, direct transform hardware processing of rot. synthesis data 8-85856
 radio astronomy, direct transform hardware processing of rot. synthesis data 8-85857
 radioastronomical data recording and processing, real-time, multichannel system (*Russian*) 8-65507
 radiometer instability influence on meas. results, reduction by computer (*Russian*) 8-65506
 satellite orbital lifetimes, prediction methods 8-73605
 solar radio bursts, recording instrumentation and data reduction (*Italian*) 8-96458
 spectra obtained with low-dispersion Fehrenbach prism, computer simulation 8-57468
 telescope stray radiation, expt. meas. and computer analysis 8-61752
 universe model, computer simulation of galaxy distrib. in Lick catalogue 8-81718
 X-ray source counts, spectral anal. rel. to binarity detect. via Doppler effect (*Russian*) 8-77623
 X-ray source position determ., parameter estimation method 8-61748
 H₂O sources spectra, autocorrel. anal. 8-65713

astrophysics computing

see also computerised instrumentation

acoustic waves in solar atmosphere, efficiency of one-dimens. hydrodynamic codes 8-57520
 asymmetric rigid body problem, arbitrarily torqued, variation of parameters approach 8-93528
 meteorite impact and ejecta deposition on airless planetary bodies, topographic effects 8-65523
 planetary positions calc. using programmable pocket calculator (*Norwegian*) 8-69700
 plasma diffusion rates, automatic computation, stellar interiors appl. 8-57434
 speckle interferometry of binary stars, computer simulations in photon-counting mode 8-53836
 GeH₄, IR spectra, Jovian atm. absorpt. profile, computer simulation 8-81584

asynchronous motors see induction motors**atmosphere, solar** see solar atmosphere**atmosphere, terrestrial** see terrestrial atmosphere**atmosphere, upper** see upper atmosphere**atmospheric acoustics**

Concorde sonic boom, long distance focusing 8-83160
 diffraction by screen above locally reacting, infinitely large plane 8-79158
 fluid dynamic equations, acoustic energy conservation, vibrational relaxation effects 8-90566
 gas dynamics with relaxation effects, acoustic waves, nonequilibrium atmosphere effects, review 8-79390
 gravity-acoustic waves, dispersive eqns. obtained by kinetic eqn. method (*Russian*) 8-85620
 infrasound waves recording methods and computer anal. (*Russian*) 8-65407
 ionosphere, acoustic waves generation by LF radiowaves 8-69581
 lower atmosphere, acoustic-gravity waves generation by ionosphere press. oscills. 8-77296
 meteorological appl. of acoustic radar (*Spanish*) 8-88944
 monostatic sounding, pattern recognition studies 8-65416
 radioacoustical sounding by continuous radiation method (*Russian*) 8-88927
 review of recent advances 8-73493
 scattering from locally homogeneous turbulence 8-87177
 sodar, sounding technique appl. to siting studies 8-81467
 sodar meas., improved quantitative display techniques 8-77332
 sonic booms during launch and reentry of Space Shuttle, environmental effects 8-85681
 sonic-boom press. signature distortion by high-speed jets 8-79156
 sounding of radiation fog 8-69419
 sounding with balloonborne instrument, scatt. structs. vertical profile 8-57353
 stratosphere and ionosphere, LF waves relax. absorpt. (*Russian*) 8-65356
 turbojet noise suppression investigations using hydrodynamic press. meas. and cross-correlation techniques 8-79157
 turbulence effects on interference near hard boundary 8-83159

atmospheric chemistry

see also atmospheric composition

auroral O, O₂ and N₂ emissions, rocket meas. rel. to chemistry and energy transfer 8-57380
 chlorofluorocarbons, stratospheric photodissoc., residence times 8-53703
 dimethyl-N-nitrosamine in urban air, concs. and chemistry 8-81378
 F-region, polar cap and auroral zone, math. model 8-65458
 gas dynamics with relaxation effects, acoustic waves, nonequilibrium atmosphere effects, review 8-79390
 ionosphere, midlatitude, dynamical model for 100-1000 km altitude range 8-53768
 ionosphere holes and spread-F, ion chemistry and transport 8-88982
 laser spectroscopy relevant to stratospheric photochemistry 8-88951
 Livermore Regional Air Quality model, appl. in San Francisco Bay area 8-92966
 Livermore Regional Air Quality model, concept and development 8-92965
 mesosphere, ion bunching model 8-73424
 mesosphere, Na atoms distrib. and Na I 5893 Å nightglow obs. 8-88961
 methane+O₂⁺, reaction rate const. kinetic energy depend., 300K, 0.125-0.450 torr 8-76850
 multiple scattering effect on photodissociation 8-85692
 negative ions, photodissoc. and photodetachment 8-66609
 ozone, chemical-kinetic criteria of effect of substances of natural and anthropogenic origin (*Russian*) 8-53699
 ozone, radiative-photochemical model for temp. coupling effects on O₃ depletion 8-57246
 particulate matter emitted by Mount Etna volcano, heavy metal chem. 8-61491
 photochemical aerosol formation, primary pollutants effects (*Japanese*) 8-57305
 photochemical reactivities of gaseous hydrocarbon mixtures 8-61533
 pollution long range transport rel. to acid rain, chem. aspects 8-81391
 reaction rates and photochemical data 8-77312
 review 8-81317
 stratosphere, concise chem. model 8-85634
 stratosphere, intense ionisation events, effects on NO₂, O₃ and climate, rel. to life extinction 8-96273
 stratosphere, model, Monte Carlo anal. of imprecisions due to reaction rates 8-85635
 stratosphere, N₂⁺, O₂⁺ and NO⁺ reactions with various mols., reaction rate coeffs. and product distrib. 8-81305
 stratosphere, O₃ reduction by NO_x injection, effects of water vapour changes 8-73444
 stratosphere, positive ion chemistry of formaldehyde and methanol 8-57251
 stratosphere photochemical-radiative damping and instability, numerical results 8-81286
 thermosphere, chemistry rel. to polar airglow mag. ordering 8-57378
 troposphere, NO₂ vertical column abundance, optical absorpt. meas. 8-85632
 troposphere, O₃ distrib. and origin 8-85663
 troposphere, O₃ form. and long-range transport 8-61514
 troposphere, SO₄²⁻ aerosols chem. props. 8-96254

atmospheric chemistry continued

upper atmosphere H chemistry, role of H-implanted interplanetary dust grains 8-65445
 water vapour photolysis in primitive prebiological atmosphere 8-73514
 BrONO₂, stratospheric photolysis, UV and IR spectra 8-53227
 CO₂ in lower atmosphere, chemistry rel. to concs. 8-96336
 CO₂ increase effects on stratospheric O₃, photochem. and radiative transfer model 8-65370
 CO₂-HCO₃⁻-CO₃²⁻ system through geologic time 8-73515
 Cl+HNO(H₂O₂)(HO₂), rate consts., stratospheric appl. 8-85125
 Cl+HO₂, react. rate const. determ. at 298K (*French*) 8-64817
 Cl+NO+N₂→NOCl+N₂, rate const. temp. depend. 8-76828
 ClCO₃NO₂, synthesis by UV irradi. of Cl₂, NO₂, CO in air, decomp. kinetics 8-76880
 ClO⁻+NO(NO₂)(SO₂)(CO₂), rate consts. at 300K 8-76829
 Cl(P)+methane, absolute rate and temp. depend. 8-80731
 H⁺+N₂ collision, binary encounter calcs. of proton energy deposition 8-74746
 HCl+O⁻(O₂⁻)(NO₂⁻)(CO₃⁻)(CO₄⁻), rate consts. at 300K 8-76829
 HNO₃/NO₂ conc. ratio in daytime stratosphere 8-73460
 HO₂+NO reaction rate constant effects on O₃ perturbations, model of stratosphere 8-73474
 HO₂+O₃→OH+2O₂, rate coeff., effects on stratospheric O₃ 8-96275
 HO, NO₂+N₂⇌HO₂+NO₂+N₂ react., kinetics, RRKM theory appl. 8-73032
 H₂SO₄, aerosols form., expt. and theory 8-96256
 N₂ dissociation by electron impact and EUV photoabsorpt., rel. to aurora and airglow 8-58847
 N₂⁺, electron impact dissociative recomb. coeffs. inferred from Atmosphere Explorer meas., objections 8-86957
 N(²D)+O₂, chemically excited NO form., 90-180K IR obs. 8-90163
 NO/NO₂/O₃, photostationary state relationship rel. to monitors intercalibration 8-69529
 NO₂ and airborne particles interactions 8-81342
 N₂O⁺, pot. energy hypersurface characs. calc. in O⁺+N₂→N+NO⁺ react. 8-60996
 O⁺ reactions with N₂, O₂, and NO, nonthermal rate coeffs. in ionosphere 8-57375
 O₂, IR nightglow bands excitation mechanism, reaction rate consts. 8-65448
 O₃ and airborne particles interactions 8-81342
 O₃ destruction, ion cycle importance 8-53697
 O₃ in stratosphere, CO₂ conc. increase effects 8-57250
 O₃ layer, changes in chemical balance 8-92933
 O₃ photolysis, O(¹D) quantum yields as function of temp. (230-320K) and wavelength (295-320 nm) 8-56903
 O(¹D) formation by O₃ photolysis, tropospheric meas. 8-73536
 O(¹D), quantum yields from O₃ photolysis as function of temp. (230-320K) and wavelength (295-320 nm) 8-56903
 O⁺(²D)+N₂, charge exchange rate coefficient, effect of N₂⁺ recomb. on aeronomic determ. 8-88954
 OH Meinel bands, in airglow, rot. temp., radiative lifetime 8-61643
 OH Meinel bands intensity distrib. in airglow, OH^{*} quenching mechanisms 8-65447
 OH+dimethyl sulphide, flash photolysis reson. fluoresc. rate consts. determ., pollution aspects 8-95913
 OH+OCS(CS₂), flash photolysis reson. fluoresc. rate consts. determ., global S cycle 8-95914
 S compounds homogeneous oxidation in atmosphere 8-96258
 S cycle study, atmospheric pollution modelling appl. 8-92902
 SO₂, adsorption and oxidation on atmospheric particles 8-96287
 SO₂ diffusion-coupled oxidation 8-65371
 SO₂, heterogeneous conversion to SO₄²⁻, rel. to urban air pollution 8-80789
 SO₂, homogeneous oxidation mechanism in troposphere 8-96257
 SO₂, oxidation in moist atm., aerosol growth kinetics 8-96255
 SO₂, photooxidation, aerosol evolution, rel. to air pollution 8-81392

atmospheric composition

see also atmospheric chemistry; atmospheric structure

aerosol, absolute element concs., PIXE and AAS, comparison 8-85237
 aerosol, ambient sulphate particles size discrimination and chemical comp. by diffusion sampling 8-69528
 aerosol, individual microparticles identification via micro-Raman spectrometer 8-68970
 aerosol, particle size distrib. statistical characters. rel. to light attenuation coeffs. (*Russian*) 8-53702
 aerosol, stratospheric, in S hemisphere, meas. by impactor and in situ single-particle detect. 8-73437
 aerosol conc. meas. by lidar 8-85693
 aerosol particles water uptake and equilib. sizes at high relative humidities 8-61516
 aerosols, chemical characterisation, progress and problems 8-68969
 aerosols, instrumental anal. of light element comp. 8-69516
 aerosols, physical characts. 8-69430
 aerosols, remote anal. by differential scatter lidar system 8-69524
 aerosols, size distrib. meas. with particle Doppler shift spectrometer 8-69515
 aerosols, sulphate and nitrate assay via ion chromatography anal. 8-68974
 aerosols from Mount Agung eruption as test of global climatic perturbation 8-69440
 air quality evaluation, daily profiles method (*French*) 8-92969
 alkyl Pb and Se compounds, detect. via gas chromatograph-microwave plasma detector 8-68975
 Ankara atmosphere aerosol, trace elements and size distrib. determ. by thermal neutron activation anal. 8-81377
 boundary layer fluxes determ. over natural grassland, aerodynamic method 8-73480
 carbonaceous pollutants, ¹⁴C/¹²C ratios rel. to origins and residence times 8-69445
 chlorofluoromethanes CCl₂F₂ and CCl₃F in Wuppertal-Dusseldorf region, ground level meas. 8-73478
 chlorofluoromethanes in stratosphere, vertical distrib. 8-73476
 chlorofluoromethanes in upper troposphere and lower stratosphere, vertical distrib. 8-73477
 coal smoke particles, atmospheric natural radioactivity (*Rumanian*) 8-53723

atmospheric composition continued

- condensation nuclei, counter with inherent size resolution capability 8-81470
- D-region, positive ion comp. diurnal vars. during storm after-effect 8-65451
- D-region irregularities, comp. effects on partial refls. 8-81495
- differential-absorption lidar technique for remote meas. of atm. gases 8-61603
- dimethyl-N-nitrosamine, assessment is urban air 8-81378
- exosphere, H atoms vel. distrib. from OGO-5 meas. of Lyman α emission 8-61642
- exosphere, H global density distrib. vars., escape fluxes 8-93023
- exosphere, H latitude vars., rel. to polar wind, heating and charge exchange processes 8-93024
- formaldehyde, concs. in rain water and on atmospheric aerosol 8-57243
- Fourier transform IR absorpt. spectroscopy, airborne, for atm. comp. meas. 8-61604
- free radical meas. by matrix isolation and EPR 8-73535
- N.Greenland summer tropospheric aerosol, ground level meas. and elemental anal. 8-85645
- halofluorocarbons, background levels in situ quantification 8-69530
- high aerosol layers, influence on atmospheric and oceanic temp. determ. by remote sounding (*Russian*) 8-81430
- hydrocarbons, concs. over Pacific 8-73468
- ice nuclei from snowfall induced by power plant plume, comp. 8-81284
- ionosphere, analytic partial derivatives for incoherent scatter data least-squares fitting 8-73581
- ionosphere, electron density and recomb. coeff. profiles calc. rel. to absorpt. and rocket meas. 8-69559
- ionosphere, lower NO densities rel. to radiowave absorpt. meas. 8-81492
- ionosphere, midlatitude, dynamical model for 100-1000 km altitude range 8-53768
- ionosphere, total electron content diurnal and seasonal trends, obs. at Waltair 8-69596
- ionosphere, total electron content meas. at Gauhati, using ATS-6 140 MHz transmissions 8-69598
- ionosphere, total electron content numerical model, corrections for satellite tracking systems 8-69587
- ionosphere, total electron content obs. at Kurukshetra, using ATS-6 140 MHz transmissions 8-69597
- ionosphere, two-ion plasma comp. rel. to whistlers group vel. 8-87452
- ionosphere holes and spread-F, ion chemistry and transport 8-88982
- IR laser heterodyne spectroscopy for trace gases remote detect. 8-61606
- laser absorption spectroscopy for point monitoring of gases ambient concs. using tunable lasers 8-61607
- lidar techniques for atm. struct. and comp. obs., proposed Spacelab program 8-61602
- Liege industrial region, five year record of atmospheric fall-out 8-81375
- Limb Infrared Monitor of Stratosphere (LIMS) radiometer, design and performance, expt. goals 8-61601
- Livermore Regional Air Quality model, appl. in San Francisco Bay area 8-92966
- Livermore Regional Air Quality model, concept and development 8-92965
- magnetic particle fallout recorded in recent ombrotrophic peat sections 8-61519
- magnetosphere, plasma comp. expt. on International Sun-Earth Explorer A 8-85810
- marine atmosphere, lightly polluted, dark smokes and acid pollution study 8-81376
- marine atmosphere, SO₂ meas. at concs. lower than ppb 8-81340
- mesopause, lidar meas. of Na conc. and neutral temp. 8-61613
- mesosphere, comp. changes due to Earth encounter with interstellar cloud, climatic effects 8-57292
- mesosphere, H₂O vapour amount rel. to particle sizes in noctilucent clouds 8-57248
- mesosphere, ion bunches form. and concs. 8-73424
- mesosphere, lower, O₃ abundance from backscattered solar radiances 8-69414
- mesosphere, Na atoms distrib. and Na I 5893 Å nightglow obs. 8-88961
- methane, conc. over ocean, var. with latit. 8-81372
- methane atmospheric sources and sinks 8-73472
- nitrogenous trace gases, preliminary ¹⁵N studies 8-73470
- non-methane hydrocarbons, monitoring via photoionisation 8-73549
- organic compounds in aerosol samples 8-73463
- organic pollutants, determ. via gas chromatography after cryogenic sampling 8-81468
- organochlorine residues in rainwater 8-73495
- particulate matter, props. inferred from lidar and solar radiometer obs. and aircraft meas. 8-61501
- particulate matter emitted by Mount Etna volcano, heavy metal chem. 8-61491
- particulates, chemical characterisation via light scatt. method 8-69533
- particulates and gaseous pollutants measurement, anal. and calibration techniques 8-69531
- pollutant annual average concentration around single source, rapid estimation technique 8-81382
- pollutants vertical diffusion, study using airborne gas-chromatography and numerical modelling 8-69435
- radiation belts, energetic O ions charge states theory 8-77427
- remote monitoring using discretely-tunable IR gas lasers and heterodyne detect. techniques 8-61605
- ring current, energetic neutral particles as source of low-latit. E-region ionisation 8-77415
- SO₂ air pollution levels modelling and forecasting, statistical approach 8-81398
- stratosphere, aerosol layer, climatic effects, review 8-81331
- stratosphere, balloon obs. of particle layer injected by aircraft at 23 km 8-81283
- stratosphere, daytime, HNO₃/NO₂ conc. ratio 8-73460
- stratosphere, dichlorodifluoromethane and N₂O conc. meas., mixing ratios 8-81281
- stratosphere, dust meas., (1970-1977) 8-73445
- stratosphere, H₂O vapour meas. using UV fluoresc. hygrometer (*French*) 8-65401

atmospheric composition continued

- stratosphere, intense ionisation events, effects on NO₂, O₃ and climate, rel. to life extinction 8-96273
- stratosphere, lower, NO and O₃ concs. geographical vars. 8-73438
- stratosphere, mass spectrometric meas. of negative ions 8-96274
- stratosphere, N₂O vertical distrib., from balloon meas. of solar spectra 8-61493
- stratosphere, NO and HNO₃ obs. in N.hemisphere for three seasons 8-81288
- stratosphere, thermal struct. and trace constituents, effects of solar UV variability 8-61492
- stratosphere O₃ density perturbations, photochemical-radiative damping rel. to instability 8-81286
- stratosphere O₃ depletion prediction, effect of temp. coupling 8-57246
- stratosphere O₃ depletion thermal effects at 85°N latit., airborne particles influence 8-81279
- stratosphere O₃ reduction estimates, effects of water vapour changes 8-73444
- stratosphere positive ions, comp. meas. 8-88877
- sulphate aerosol, individual submicron particles detect. technique 8-69527
- surface aerosols in Cape Verde Is., physical and chemical props. 8-85640
- surface layer aerosols variability, spectral transmittance method (*Russian*) 8-69448
- thermosphere, electric field momentum coupling characts. 8-88958
- thermosphere, electron temp. and density relationship in daytime at solar minimum, model 8-61638
- thermosphere, lower, CO₂ concs. meas. 8-96336
- thermosphere, lower, O and O₂ density meas. by mass spectrometer technique 8-57348
- thermosphere, midlatit. models seasonal vars. at solar max. and low geomag. activity 8-57376
- thermosphere, model based on satellite drag data 8-69555
- thermosphere, neutral comp. meas. between 90 and 220 km by rocket-borne mass spectrometer 8-77383
- thermosphere, photoelectron daytime energy distrib. meas. by AE-E satellite 8-88953
- thermosphere, tidal vars. 8-96334
- thermosphere, transport processes in diurnal tide, satellite meas. 8-88959
- thermosphere neutral composition, momentum source signatures 8-77380
- trace gases at Sepik River coast, Papua New Guinea 8-85642
- trace gases vertical conc. from solar radiation absorpt. spectra (*Russian*) 8-69442
- trace species, multiple scattering effect on concs. 8-85692
- troposphere, HNO₃ vapour and particulate NO₃⁻ global meas. 8-88904
- troposphere, interhemispheric gradients of CF₂Cl₂, CFCI₃, CCl₄ and N₂O 8-81289
- troposphere, N₂O continuous meas. 8-81318
- troposphere, NO₂ vertical column abundance, optical absorpt. meas. 8-85632
- troposphere, O₃ distrib. and origin 8-85663
- troposphere, Sahara dust cont. over N.Atlantic from air cond. meas. 8-92897
- upper atmosphere, H₂O prod. from H-implanted interplanetary dust grains 8-65445
- upper atmosphere, neutral comp., rel. to F₂-layer hemispherical differences 8-69603
- upper atmosphere He dynamics, use of Jacchia (1977) empirical model 8-77381
- urban plume particulates collected on Anderson 8-stage impactor stages, chemical anal. 8-69433
- Vizcaya, Spain, B, Mg, Cr, Mn, Fe, Co, Ni, Pb, Ga, Ge and Si conc. in atm. and rainwater (*Spanish*) 8-57264
- Vizcaya, Spain, Na, Mg, Cr, Al, Ti, Cu, Ag, Zn, Co and Ni content in sedimentable powders (*Spanish*) 8-57265
- water droplets, sources and effects of surface organic monolayers 8-69412
- water vapour of extraterrestrial origin, possible role in Sun-weather relationships 8-69416
- ¹⁰Be, cosmic-ray-produced, mean tropospheric residence time at north temperate latits. 8-85633
- C, non-methane organic, in global troposphere 8-73462
- CO abundance, geographical, seasonal and secular vars. (*Russian*) 8-53700
- CO abundance determ. by analysing solar spectra 8-85643
- CO, production from oxidation of vegetation hydrocarbon emissions 8-88881
- CO₂ content of atmosphere, role of C storage by forests and oceans 8-53718
- CO₂ effects on long-term global sea surface temp. vars. 8-73398
- CO₂, future atm. level prediction using atm. and ocean models 8-61549
- CO₂ increase effects on stratospheric O₃, photochem. and radiative transfer model 8-65370
- CO₂ input from burning wood 8-81368
- CO₂ record at Mauna Loa Observatory, short-term disturbances 8-88879
- CO₂ rel. to C reservoir changes 8-57278
- Cd, Pb, Mn in particle size fractionated aerosols, flameless atomic absorpt. determs. 8-69434
- CIO radical, IR vibr.-rot. spectra, background data for atm. meas. 8-58679
- H⁺ in E United States precip., concs. behaviour 8-92962
- H⁺, O⁺, conc. in upper atm., Aureole 2 satellite mass spectrometer obs. 8-53766
- H₂, production from oxidation of vegetation hydrocarbon emissions 8-88881
- H₂O, abundance determ. by analysing solar spectra 8-85643
- H₂O, vapour, condensation in presence of H₂SO₄ and HNO₃ pollutants 8-81343
- H₂O vapour conc. meas. by laser absorpt. techniques 8-61595
- H₂S contrib. to atmospheric S cycle 8-73473
- NH₃ budget contribs., aircraft meas. 8-73469
- NH₃, ν_2 vibr.-rot. band identification in ground level solar spectra 8-81287
- NH₄⁺, NO₃⁻, in rain water collected at Julich, Germany, N isotope comp. 8-57284

atmospheric composition continued

- (NH₄)₂SO₄ aerosol production under elevated temp. inversion in Cleveland Country, model 8-81397
 NO density in lower E-region, diurnal and seasonal effects at low latitudes. 8-88976
 NO global morphology in lower E-region 8-88975
 NO/NO₂/O₃ contents measurement, monitors intercalibration 8-69529
 NO₃, stratospheric, obs. 8-88880
 NO₃⁻ in E United States precip., concs. behaviour 8-92962
 N₂O, abundance determ. by analysing solar spectra 8-85643
 N₂O abundance meas. over USSR (*Russian*) 8-96265
 N₂O, atmospheric fluxes from N₂O supersaturated surface waters 8-57223
 N₂O emission from soils during nitrification of fertiliser 8-57313
 N₂O from soil treated with nitrogenous fertilisers 8-61419
 N₂O, global and regional meas. 8-73471
 N₂O measurements, laboratory intercalibration 8-81277
 N₂O, sources, sinks and vars. meas. 8-85631
 O₂ in early Precambrian atmosphere, photodissociation rather than photosynthesis 8-81409
 O₃, calibration reference instrument calibration 8-73524
 O₃, columnar meas. by aircraft-borne UV spectrophotometer 8-73522
 O₃, conc. rel. to visibility reduction in Midwest 8-61507
 O₃, daytime and nighttime distrib., ground-based mm wavelength obs. 8-57256
 O₃, densities in stratosphere and mesosphere rel. to radiative equilib. temps. 8-81280
 O₃, global monthly vars. correl. with solar activity 8-85664
 O₃, global vertical distrib. 8-73475
 O₃, ground level monitoring apparatus, chemiluminescence reaction with ethylene 8-96310
 O₃ in stratosphere, CO₂ conc. increase effects 8-57250
 O₃ layer, changes in chemical balance 8-92933
 O₃ meas. during Aladdin 74 program above Wallops Island 8-57247
 O₃, near surface meas. at Hohenpeissenberg, historical review (*German*) 8-65369
 O₃ profile, determ. from outgoing thermal radiation 8-92945
 O₃ profile, from photodissoc. wave obs. 8-79407
 O₃ profiles rel. to solar mag. activity 8-65373
 O₃, remote meas. in IR absorpt. bands, information content estimation (*Russian*) 8-88883
 O₃, stratospheric, perturbation by N fertilisers, independent variables anal. 8-73505
 O₃ stratospheric 10 μ absorption line obs. with IR heterodyne spectrometer 8-61494
 O₃ total amount at Belsk, Poland, harmonic anal. 8-92883
 O₃ total content, comparison of simultaneous IRIS, BUUV and ground based meas. 8-81291
 O₃ total content determ. using remote spectroscopy 8-65437
 O₃, total content meas. using four-filter photometer 8-61597
 O₃ total content trends, from daily Dobson data 8-92915
 O₃, tropospheric, long-range transport 8-61514
 O₃ vars. correl. with cloudiness vars. rel. to UV radiation protection 8-73456
 O₃, vertical profile calc. from umkehr obs. 8-81328
 O₃, Belgian obs. (1977 Oct.-Dec.) (*French, Flemish*) 8-92903
²²²Rn, automatic counter for continual unattended operation 8-73539
²²²Rn continuous meas. for air-sea gas exchange field determ. 8-73534
 S and trace elements in aerosols from South American continent, conc. relationships 8-57245
 S, compact X-ray fluoresc. analyser 8-68971
 S pollutants in atm., conf., Dubrovnik, Yugoslavia (Sep. 1977) 8-96281
 SO₂ conc. determ. using HBr laser (*Russian*) 8-69484
 SO₂ conc. in Milan urban atmosphere in winter (*Italian*) 8-53721
 SO₂, pollution zones definition and assessment 8-81383
 SO₂ small automatic monitoring network, practical experiences 8-81462
 SO₄²⁻ aerosols, ambient, laser-Raman monitoring 8-69532
 SO₄²⁻ in E United States precip., concs. behaviour 8-92962

atmospheric density see *atmospheric pressure and density*

atmospheric disturbances see *atmospheric movements; thunderstorms*

atmospheric duct see *atmospheric electromagnetic wave propagation*

atmospheric dynamics see *atmospheric movements*

atmospheric electricity

see also *atmospheric electromagnetic wave propagation; atmospheric ionisation; atmospheric; aurora; electrojets; ionosphere; lightning; thunderstorms*

- aerosols, limitation on electrical measures 8-69431
 air diffuse discharge, gasdynamic effects 8-81294
 auroral electrojet region, elec. fields and mag. effects of solar flares 8-69576
 auroral oval, daytime, field-aligned currents rel. to radio aurora and energetic particles 8-88966
 auroral zone, quasiperiodic elec. fields and assoc. electron precip., models 8-88977
 auroral zone electric fields, conductivities and currents, latitudinal distrib. 8-77399
 auroral zone electric fields at 1 R_e altitude 8-57397
 bow shock, current-driven instabilities in laminar perpendicular shock 8-77430
 breakdown voltage of air, effect of sand particle pollution 8-81363
 charged particles precip. by parallel elec. field, model 8-65459
 conduction current, direct meas. 8-85637
 cumulonimbus clouds, elec. field strength and raindrop spectra, study from mobile ground station 8-92943
 daytime magnetopause, electric field topology 8-57398
 DP-2 current system, rel. to pulses in interplanetary mag. field B_z-component 8-73583
 drop electrification by evaporation or vapour condensation (*French*) 8-61511
 dry and moist air, primary ionisation coeffs., secondary ionisation coeffs. for water surface 8-65376
 E-region, cross polar cap horizontal currents rel. to mag. disturbances and elec. fields 8-77405
 F-region, ambient elec. field rel. to gradient drift instability high-altitude limit 8-88984
 F-region, convective elec. field rel. to electron density and ion vel. during isolated substorm 8-65452

atmospheric electricity continued

- F-region, large-amplitude oscillating field appl. to equatorial spread-F control 8-69602
 F-region, polar cap and auroral zone, math. model 8-65458
 F-region, poleward-directed elec. fields at subauroral latitudes. 8-88970
 F-region convective electric field determ. from rocket meas. of thermal ion spectra 8-57386
 F-region horizontal elec. field reversal assoc. with spread-F in equatorial ionograms 8-69560
 fair weather condition concept in atm. elec. 8-61517
 Harang discontinuity electric field, auroral radar and rocket double-probe obs. 8-88971
 interplanetary elec. field penetration of magnetosphere, balloon meas. 8-57408
 ionosphere, 3-dimens. current model rel. to quiet time vertical magnetic field component over India 8-61326
 ionosphere, Chatanika incoherent scatter radar obs. of field-aligned currents 8-57387
 ionosphere, elec. field oscils. meas. near auroral arc, assoc. with MHD wave 8-65457
 ionosphere, elec. fields prod. by polar field-aligned currents 8-65455
 ionosphere, electric currents and fields due to field-aligned auroral currents 8-96339
 ionosphere, equatorial, elec. field and electrojet changes correlated with interplanetary mag. field 8-85766
 ionosphere, equatorial, meridional currents detect. 8-85767
 ionosphere, equatorial convection field rel. to mid-latit. trough location, Ariel 4 obs. 8-85765
 ionosphere, lunar tides contrib. to elec. current system 8-77382
 ionosphere, polar cap elec. fields from Tordo 1 polar cusp Ba plasma injection expt. 8-77402
 ionosphere, polar elec. fields transmission to Equator 8-65456
 ionosphere, quiet nighttime, elec. fields rel. to calculated and measured decay rates 8-81493
 ionosphere, zonal and meridional elec. fields effects in evening sector 8-69571
 ionosphere and magnetosphere, current distribution quantitative modelling 8-88988
 ionosphere current systems, rel. to press. oscils. and atmosphere acoustic-gravity waves 8-77296
 ionosphere electric currents during 23 October 1976 solar eclipse, mag. obs. in Australia 8-81498
 ionosphere high-latitude electrostatic turbulence, polarisation, freq. and wavelengths 8-88981
 ionosphere, polar-equatorial coupling during magnetically active periods 8-93029
 lightning intracloud discharges, elec. dipole axis inclination determ. 8-73440
 magnetosphere, assoc. elec. field, mag. field and electron precip. fluctuations 8-81507
 magnetosphere, Birkeland currents and limits to double-adiabatic approximation for hot collisionless plasma 8-75262
 magnetosphere, energy flow and current systems closure, rel. to upstream solar wind parameters 8-57400
 magnetosphere, field-aligned selfconsistent elec. field 8-69615
 magnetosphere, macroscopic electric fields 8-69609
 magnetosphere, signature of parallel electric fields in collisionless plasma 8-77439
 magnetosphere electric convection field, model 8-89004
 magnetosphere high-latitude electrostatic turbulence, polarisation, freq. and wavelengths 8-88981
 magnetosphere midlatitude convection elec. fields, rel. to ring current development 8-57395
 magnetosphere parallel electric field, signature in ion and electron distributions in vel. space 8-89005
 magnetosphere plasma sheet, plasma flows during substorms rel. to field-aligned elec. field 8-96357
 magnetosphere tail, explosive tearing mode reconnection and cross-tail EMFs 8-88992
 measurement of elec. cond. and small ion mobility, pollution aspects 8-92931
 Pc 5 micropulsation resonance region, elec. fields meas. by dual auroral radar system 8-65454
 plasmasphere, dynamo electric field aligned currents theory 8-81499
 plasmasphere, outer, elec. currents and fields rel. to whistler ducts form. 8-57407
 potential of rocket and electron beam injection expts. (*Russian*) 8-93069
 solar modulation of atmospheric electrification, possible implications for Sun-weather relationship 8-57261
 Sq currents, appl. to equatorial F-region motions deduction 8-96344
 thermosphere, auroral energy input rel. to electrodynamics and neutral and ion drifts 8-65446
 thermosphere, electric field momentum coupling characts. 8-88958
 thundercloud elec. field meas. by balloon-borne coronascope 8-61577
 thunderstorm, electric field and wind profile, balloon meas. 8-85636
 thunderstorm charge build up, charging mechanisms 8-81320
 thunderstorm electric fields, 10-year study of Minneapolis area 8-57253
 thunderstorms, elec. fields, precip. elements charge and size, airborne obs. 8-73485
 tornado, contrib. of vortex-stabilised arc to energy 8-53711
 ULF elec. fields and particle precip. in aurora, rocket meas. 8-96337
 vertical component pulsations correl. with mag. components during Pc 1 event 8-61687
 winter thunderstorms, anomalous, of Hokuriku coast, lightning polarity and charge struct. 8-73443

atmospheric electromagnetic wave propagation

see also *atmospheric light propagation; ionospheric electromagnetic wave propagation; magnetospheric electromagnetic wave propagation; ionospheric electromagnetic wave propagation*

- 35 GHz wave attenuation along slant path by rain (*Japanese*) 8-85671
 atmosphere, radiation modulation of aerosol state by moving clouds (*Russian*) 8-88916
 atmosphere, surface radiative flux, clear and cloudy conditions, parametrisation accuracy 8-77325
 attenuation at 230 GHz, meas. 8-73425
 circumglobal signals in Atlantic equatorial zone (*Russian*) 8-69585
 cloud effects on global middle UV radiation meas. at ground 8-92882

atmospheric electromagnetic wave propagation continued

- decametric radiowaves emitted by dipole, propag. problem 8-69399
- dielectric spheroids, backscatter matrix 8-66716
- Earth-satellite paths, 11.5 GHz, annual and annual-worst-month statistics of fading 8-57238
- Earth-space communication links, path diversity performance 8-69424
- ETS-II satellite, 1.7 GHz, 11.5 GHz, 34.5 GHz wave propag. rel. to rain precipitation strength (*Japanese*) 8-85669
- evaporation ducts, polarisation depend. of transient signals 8-57269
- incoherent energy and coherent time of depolarised microwaves, interferometric analysers 8-96277
- IR attenuation, 8-13 μm , by H_2O vapour (*Russian*) 8-88915
- mm wave attenuation in rain 8-96280
- polar electric fields, transmission to Equator 8-65456
- radar propag. through turbulence, scintillation detection using monopole techniques 8-85717
- radiances in absorpt. bands, calc. methods including multiple scatt. 8-61554
- radio aurora, spatially ordered structure, spaced radar obs. 8-73561
- radiowave backscatter from vegetation, water cloud model 8-57274
- radiowave propag. through turbulent atmosphere, phase difference and derivative fluctuations 8-92951
- radiowave propagation, numerical approximations of Sommerfeld integral for fast convergence 8-66727
- radiowaves, refr. index struct. parameter from refractivity and amplitude scintillation meas. at 36 GHz 8-81316
- rain attenuation and depolarization of Earth-satellite transmissions at freq. greater than 10 GHz (*French*) 8-53689
- random media, wave propag. and weak scatt. 8-66722
- remote sensing of atmosphere, land and sea props. 8-93015
- satellite effective isotropic radio power meas., error anal. using calibrated radio star 8-93070
- solar radiation absorpt. spectra, atm. trace gases vertical conc. (*Russian*) 8-69442
- solar radiation absorption, cloud and aerosol effects on heating rate 8-57319
- solar radiation obs. and predicted values in urban area 8-57317
- surface layer aerosols variability, spectral transmittance method (*Russian*) 8-69448
- transfer functions, space-variant, for inhomogeneous scatt. media characterisation 8-71012
- two-layer model appl. to calibration of astronomical mm. obs. 8-53691
- UHF diffuse radar aurora, rapid scan Doppler vel. maps 8-77388
- URSI Commission F, First Open Symposium (La Baule, France, 1977 April 28-May 6) 8-57321
- UV backscatter expt., airborne, for O_3 distrib. determ., error anal. 8-92985
- VLF hiss emissions, simultaneous obs. at Brorfelde, Chambon-la-Forêt and Moshiri 8-81509
- VLF hiss progrg. characts. obs. at low latit. ground stations 8-69561
- wavy water surface thermal radioemission obs. at 3.5 and 14.5 MHz (*Russian*) 8-61425
- weather radar calibration, correl. with rain gauge data (*Japanese*) 8-85670
- H_2O vapour laser 118.6 μm radiation absorption by H_2O vapour, temp. and press. effects meas. 8-75255
- O_2 induced absorption band effects on transmission in 6 μm region (*Russian*) 8-69446

atmospheric electron precipitation

- see also *aurora; radiation belts*
- aurora, pulsating, electrons charact. energy from optical spectra 8-88969
- aurora, pulsating, precipitating electrons flux modulation 8-73562
- aurora, ULF elec. fields and particle precip., rocket meas. 8-96337
- auroral electron beam, electrostatic noise generation 8-85759
- auroral electron diffuse surge zone, equatorial boundary model 8-69610
- auroral electrons energy distrib., incoherent scatter radar and photometric meas. comparison 8-77390
- auroral zone, quasiperiodic elec. fields and assoc. electron precip., models 8-88977
- daily variations, rocket meas. 8-69575
- energetic electron belt form. and decay during 1974 July 4-6 mag. storm. 8-69617
- harmonic instabilities in electron plasma 8-77424
- inner zone electrons induced precip., obs. 8-88996
- ionosphere, ELF transmission anomalies and energetic particle precip. 8-93040
- ionosphere, high-energy electron flux during 1971 December 16 magnetic storm 8-69564
- ionosphere turbulent polar cusp, temps. and low-energy particles and Kelvin-Helmholtz instability 8-96343
- magnetosphere, assoc. elec. field, mag. field and electron precip. fluctuations 8-81507
- magnetosphere, multi-harmonic electron cyclotron instabilities 8-87442
- magnetosphere energetic electrons, nonlinear pitch angle scatt. by coherent VLF waves 8-89011
- magnetospheric energetic electron environment model revision 8-61681
- parallel electric field effects on precip., model 8-65459
- plasmasphere origin, dimensions and particle precip. 8-69584
- polar cusp, precip. geographical distrib. rel. to airglow mag. ordering 8-57378
- substorm growth phase effects, Scandinavian obs. 8-96352
- sudden commencement absorption events at S. pole, rel. to lower cleft boundary latit. 8-77437
- X-ray aurorae prod. by energetic electrons precip., imaging from Space-lab 8-61608
- X-rays from magnetospheric electrons, rocket-borne, astronomy affected 8-61640

atmospheric energetics see *atmospheric movements***atmospheric humidity**

- see also *hygrometers*
- absolute humidity, correl. with atmospheric absorpt. at 460 μm 8-96295
- aerosol particles water uptake and equilb. sizes at high relative humidities 8-61516
- atmosphere ocean interfacial conditions, influence on bulk evaporation coeffs., isotopic method determ. 8-85576

atmospheric humidity continued

- boundary layer, temp. and humidity correl. above warm wet surface 8-85646
- boundary layer fluxes determ. over natural grassland, aerodynamic method 8-73480
- capacitive dew-point sensor 8-81421
- coastal zone, indicators of long-term var. of hydrometeorologic elements (*Russian*) 8-77258
- convective boundary layer, temperature-humidity covariance budget 8-73430
- W.Europe, IR attenuation meas. of water vapour content 8-53698
- frost, snow, heat transfer, cond., radiation and water vapour diffusion model 8-94563
- frost point meas. systematic error using Meteorological Office Mk3 hygrometer 8-73538
- heat and mass atmospheric transfer from nuclear power station spray cooling 8-94078
- intertropical convergence zone struct. over GATE area 8-57283
- IR continuous absorption by water vapour, calc. (*Russian*) 8-96293
- IR fluctuation hygrometer, design, calibration, field trial results 8-77368
- London storm, August 1975, humidity meas. and urban effects on precip. 8-81339
- microwave refraction coeff. rel. to humidity 8-69398
- objective statistical analysis using remote sounding data 8-61524
- radiation fog, water vapour meas. and relationship to dew 8-73446
- radiowave attenuation at 225 GHz meas., correlation with surface water vapour density 8-85624
- stratosphere, H_2O vapour meas. using UV fluoresc. hygrometer (*French*) 8-65401
- stratosphere, lower, aircraft meas. of humidity, S.England, 1972-76 period 8-73488
- stratosphere, water vapour mixing ratio from solar brightness temp. balloon-borne obs. 8-85921
- stratosphere water vapour changes, effects on O_3 reduction estimates 8-73444
- surface humidity rel. to precipitable water vap., India 8-81273
- surface layer, accuracy of moments of vel., temp. and humidity vars. 8-82891
- thermodynamics of moist air 8-85673
- tree growth rel. to transpirational flow and air humidity (*Russian*) 8-65066
- Typhoon June (1975), water vapour and clouds liq. water meas. by scanning microwave spectrometer 8-73436
- upper atmosphere, H_2O prod. from H-implanted interplanetary dust grains 8-65445
- water metastable states, phase diagram (*Russian*) 8-95129
- water vapour of extraterrestrial origin, possible role in Sun-weather relationships 8-69416
- water vapour profile, meas. from atmosphere brightness temps. in H_2O 1.35 cm resonance region (*Russian*) 8-81403

atmospheric ionisation

- see also *atmospheric radioactivity; ionosphere*
- charge transport, rel. to ion chamber response to particulate matter 8-88933
- cosmic ray ion-pair production rate above 18 km altitude, parametrisation 8-65469
- D-region, water cluster ions, mass spectrometer results analysis 8-61659
- dry and moist air, primary ionisation coeffs., secondary ionisation coeffs. for water surface 8-65376
- E-region, low-latitude, ionisation by energetic ring current particles 8-77415
- F-region, equatorial ionisation density irregularities rel. to HF and VHF spread-F echoes 8-85764
- F-region, polar cap and auroral zone, math. model 8-65458
- F-region electron density max., harmonic analysis and periodicities 8-73383
- HV laboratory ion density due to repetitive impulse generation 8-65913
- ion formation, nonstationary effects of gravity waves in lower ionosphere 8-73567
- ionisation, quiet nighttime, calculated and measured decay rates comparison 8-81493
- ionosphere, electron density and recomb. coeff. profiles calc. rel. to absorpt. and rocket meas. 8-69559
- ionosphere, ion formation at high latits. during mag. quiet periods 8-69582
- ionosphere, lower, effects of solar flares Fe XXV 1.87 Å line emission 8-65588
- ionosphere, midlatitude, dynamical model for 100-1000 km altitude range 8-53768
- ionosphere, total electron density nighttime behaviour 8-69570
- mesosphere, ion bunching model 8-73424
- meteor trails, causes of fluctuations in effective linear electron density 8-73687
- plumes from power stations, ionisation effects 8-88909
- radiation belts, energetic O ions charge states theory 8-77427
- spread-F bubbles, nonlinear Rayleigh-Taylor mode theory in two dimensions 8-88986
- stratosphere, intense ionisation events, effects on NO_2 , O_3 and climate, rel. to life extinction 8-96273
- stratosphere, mass spectrometric meas. of negative ions 8-96274
- stratosphere, positive ion chemistry of formaldehyde and methanol 8-57251
- stratosphere positive ions, comp. meas. 8-88877
- upper atmosphere, ionisation due to X-ray pulse, Auger electrons form. 8-53767
- upper atmosphere, photoelectron spectra allowing for Auger effect 8-69557
- whistler ducts in outer plasmasphere, form. 8-57407
- O , low-energy electrons integral scatt. cross section 8-69556

atmospheric light propagation

- 8 to 12 μm IR emission attenuation obs. (*Russian*) 8-61556
- absorption at 460 μm , determ. 8-96295
- aerosol, H_2O -droplet, CO_2 laser beam clearing process, transmission function ratios 8-88919
- aerosol attenuation, influence on atmospheric and oceanic temp. determ. by remote sounding (*Russian*) 8-81430
- aerosol content determ. from photometric obs. of stars 8-92976

atmospheric light propagation continued

- aerosol inhomogeneity expt. meas. 8-77304
 aerosol layer depth remote meas. by microwave-modulated laser (*Russian*) 8-57338
 aerosol turbidity characteristics, determ. from spectral actinometric obs. 8-92986
 amplitude modulated laser beam prog. in random inhomogeneous medium, phase fluctuation anal. 8-87017
 astronomical refraction, general theory (*Russian*) 8-89045
 atmosphere, turbidity meas. across Los Angeles Basin 8-92982
 attenuation and turbulence simulation in pulsed laser Doppler velocimeter system 8-73513
 attenuation by aerosols in absorpt. bands of moistened particles (*Russian*) 8-65384
 attenuation coefficients, rel. to aerosol particle size distrib. statistical characts. (*Russian*) 8-53702
 attenuation exponents in visible and near IR up to 30 km, experimental profiles (*Russian*) 8-61558
 aureole around UV source at finite distance 8-77320
 aureole radiance field about point source in scatt.-absorbing medium 8-77319
 beam broadening in randomly inhomogeneous cloudy aerosol medium (*Russian*) 8-58911
 boundary layer, birefringence under wind speed gradient shear 8-69453
 boundary layer above ocean waves, scaling laws for optically relevant turbulent parameter C_s^2 8-85677
 cloud reflectance with laser beam illumination, multiple scatt. contrib. 8-85686
 cloud rotational Raman and double scatt., lidar meas. 8-77318
 coherence of light beam through optically dense turbid layer 8-55300
 collimated laser beam propag., corner-cube reflector and plane mirror comparison in folded-path and direct transmission 8-85697
 collimated laser beam propag. in turbulent atm., phase fluctuations spectrum 8-78914
 colour of ocean, Monte Carlo model including atm. and ocean scatt., absorpt. 8-61421
 contrast reduction of broadband optical signals 8-69455
 daylight, spectral distrib., 280-2800 nm, Australia 8-69452
 directional scattering coeffs. in droplet and crystal clouds, meas. (*Russian*) 8-96292
 extinction, rel. to fog and clouds liq. water content 8-81404
 extinction and absorption coeffs. of fog and clouds, organic aerosol effects 8-73465
 extinction coefficient meas. from distant contrast, using astronomical telephotometer 8-61730
 finite optical beam in extremely strong turbulence, variance, covariance of irradiance 8-63008
 image reconstruction performance of image-plane sharpness criteria 8-93123
 image resolution through turbulence over ocean, optical transfer function 8-85695
 image transmission, two-dimens., through randomly inhomogeneous medium, using Jamin interferometer 8-50706
 imaging through turbulent atm., spatial freq. resolution of rot. shearing interferometer 8-69450
 incoherent, absorption and scattering, effects on optical/optronical systems 8-92987
 intensity fluctuations, frozen turbulence hypothesis expt. (*Russian*) 8-61557
 interference pattern fluctuation statistics in turbulent atmospheric layer 8-53727
 inverse greenhouse effect prod. by cometary impact, rel. to ice ages and ecological catastrophes 8-53714
 IR wavelengths extinction by aerosols in coastal fog 8-81400
 irregular particle scattering, meas. results versus Mie theory 8-58918
 isoplanation measurement using speckle interferometry 8-65385
 laser, high-energy, simplified aberrated lens model 8-69454
 laser absorption method for H_2O vapour conc. meas. 8-61595
 laser beam, monochromatic, absorption and scattering problems 8-92988
 laser beam, phase compensated, propag. through atm. turbulence 8-83012
 laser beam broadening and depolarization in dense water-droplet fogs 8-92981
 laser beam intensity fluctuations in medium with Kolmogorov turbulence, distrib. function (*Russian*) 8-71034
 laser beam intensity fluctuations in turbulent atm. over water surface (*Russian*) 8-69449
 laser beam line spread instrumentation for propag. meas. 8-83013
 laser beam line spread instrumentation for propag. meas. 8-83015
 laser beam transmission at 10.6 μm , analytic model of bleaching 8-85688
 laser propagation in turbulent atm., detector nonlinearity effects on statistics of fluctuating signal 8-55301
 laser technology for atm. science, conf., San Diego, USA (Aug. 77) 8-85748
 laser transmission meas. at 10.6 μm 8-92977
 lidar backscatter from horizontal ice crystal plates 8-92984
 lidar observations of smoke and dust clouds at 0.7 and 10.6 μm wavelengths 8-69459
 lidar polarisation meas. for cloud phase discrimination 8-96269
 lidar probing of fogs and clouds, double scatt. approx. 8-73512
 lidar return signal geometrical compression, atm. remote sensing appl. 8-57329
 lidar returns from fog, doubly scatt. radiation contrib. 8-77326
 lidar scattering from clouds at 347, 694 nm, polarisation props. 8-85689
 long-path high-resolution transmission meas., comparison with LOW-TRAN 3B predictions 8-92972
 Lorentzian coefficient approx. for efficient transmittance profile calc. 8-61552
 Mie calculations for different aerosols, use of average complex refr. index 8-57314
 mirages, stratified medium light ray trajectories, educational aspects 8-69940
 molecular absorption, Lowtran 3B model 8-85690
 multiple pulse detection in atmospheric turbulence 8-92974
 multispectral extinction data, analytic inversion in anomalous diff. approx. 8-87016

atmospheric light propagation continued

- nonisoplanatic effects, speckle interferometry meas. using double stars 8-65387
 nonspherical particles size distrib. from scatt. meas., Mie theory 8-58909
 optical extinction by aerosols in 0.5-14 μm wavelength range 8-57318
 outgoing thermal radiation, meas. rel. to O_3 profile determ. 8-92945
 partially coherent radiation, extended Rayleigh-Sommerfeld integral method results 8-65386
 particulates, light scatt. method for chemical characterisation 8-69533
 photon transport problems, modified Monte Carlo procedure 8-61560
 propagation problems, conf., Oslo, Norway (May 1978) 8-93044
 radiative transfer through fog, 2D numerical soln. algorithm 8-71032
 random medium, correl. and struct. functions for arbitrary optical beams 8-66756
 reflection by clouds, path length difference and wavelength correl. (*Russian*) 8-69447
 refractive index structure parameter meas. by optical scintillator 8-65411
 remote sensing of particle size distrib., analytical inversions 8-73508
 remote sensing of particle size distrib., analytical inversions 8-73509
 scattering from large dielec. spheres, lidar signal analysis from rainfall 8-66754
 scattering matrices, Mueller, for nonspherical particles 8-90366
 scattering of partially coherent radiation by surface, atm. turbulence influence 8-58915
 scintillation, conditional fading statistics 8-66757
 scintillation, in optical lunar occultation meas., statistically rigorous reduction 8-73650
 seeing for astronomical telescope, wavelength depend., atm. inhomogeneity effects 8-92979
 signal current probability distrib., optical heterodyne receivers in turbulent atm., theory 8-78916
 signal current probability distrib., optical heterodyne receivers in turbulent atm., expt. 8-78917
 signal discrete reception in turbulent atm. 8-73511
 slant path propag. characts. (*French*) 8-96294
 speckle interferometry, bandwidths, exposure times, effects on MTF 8-69701
 speckle propagation through turbulence 8-66758
 spectral transmittance profiles calc. method 8-85696
 stratosphere, scatt. profiles rel. to dust meas., (1970-1977) 8-73445
 sunset obs. from Apollo-Soyuz, light refr. study from space (*Russian*) 8-65383
 surface layer aerosols variability, spectral transmittance method (*Russian*) 8-69448
 temperature effect on 15 μm region transmission function, thermal remote sounding appl. 8-77327
 temperature fluctuations, modified spectrum rel. to optical propag. 8-92980
 thermal blooming compensation, equivalent thin lens model 8-87108
 transmittance, profile depend., line parameter vars. 8-77322
 turbid atmosphere, transparency characts. calc. 8-81407
 turbidity index, skylight at South Pole station, Antarctica, polarising radiometer meas. 8-57320
 turbulence effect on optical goniometer accuracy 8-55461
 turbulence phase distortion, modal compensation 8-69451
 turbulent atmospheres, optimum processing of light fields, synthesis of algorithms 8-71047
 turbulent-degraded image reconstruction using nonredundant aperture arrays 8-93122
 upper atmosphere, light propag. rel. to solar irradiation flux between 120 and 400 nm 8-57536
 water vapour, IR attenuation meas. in W.Europe 8-53698
 water vapour, IR continuum absorpt. calc. (*Russian*) 8-96293
 water vapour, pressure broadened absorpt. in 10 μm region, O_2 addition effects 8-92975
 water vapour continuum absorption, 3.5 to 4.0 μm region 8-92973
 water vapour continuum IR absorpt. near 1200 cm^{-1} , temp. depend. 8-85687
 wave correlation scale meas. with stellar speckle interferometry 8-65388
 Wise Observatory, extinction coeffs. for photoelectric UVB photometry 8-73657

atmospheric measuring apparatus

- see also air pollution detection and control; ionospheric measuring apparatus; meteorological instruments
 acoustic Doppler sounder for wind profile meas. in boundary layer 8-65413
 acoustic echo sounder, design from loudspeaker elements 8-87226
 acoustic sounder, balloonborne, design and construction 8-57353
 air pollution, Dutch national monitoring system, focal and reference point 8-69465
 Aitken counter, portable photo-recording, for small atm. aerosols detect. 8-57355
 automatic ^{222}Rn counter for continual unattended operation 8-73539
 Balloon Altitude Mosaic Measurements Program 8-81455
 balloon borne mass spectrometer, liquid He cryopump and opening device 8-77370
 balloon-borne ion sampling package 8-69497
 cine camera, time-lapse mechanism design, clouds and lightning photography appl. 8-85747
 condensation nuclei counter with inherent size resolution capability 8-81470
 coronasonde, balloon-borne, for thundercloud elec. field meas. 8-61577
 differential absorption lidar systems for atm. gases remote meas. 8-69525
 digital instrument, for radio refr. index meas. 8-86321
 Doppler light detection and ranging systems for turbulence meas. 8-73554
 double Compton gamma-ray telescope, background sensitivity to atmospheric neutrons 8-53827
 dust, airborne, respirable fraction, performance characts. of samplers matched to them 8-53438
 dust sampler, CIP type, for personal use 8-81469
 echosonde applications, review 8-73493
 echosonde interferometer for atmospheric research 8-57347
 electronic chopper for UV source for cloud extinction meas. 8-79087

atmospheric measuring apparatus continued

electrostatic mobility analyser, variable freq., for aerosol charge distrib. meas. 8-77945
 flash counter and interval recorder 8-88928
 French incoherent scatter facility, gravity waves detect. in lower atmosphere 8-81478
 gas chromatograph-microwave plasma detector, appl. to atmospheric alkyl Pb and Se compounds detect. 8-68975
 high acidity analysers, comparative tests near industrial installations in Fos-Etang de Berre region 8-81464
 interferometer, rot. shearing, for imaging through turbulent atm., spatial freq. resolution 8-69450
 International Sun Earth Explorer 1, electron spectrometer expt. 8-85809
 International Sun-Earth Explorer 1 and 2, fast plasma expt. 8-85800
 International Sun-Earth Explorer 1 and 2, plasma wave investigation 8-85802
 International Sun-Earth Explorer A, DC and low-freq. elec. field meas. instrumentation 8-85807
 International Sun-Earth Explorer A, plasma comp. expt. 8-85810
 International Sun-Earth Explorer A, Stanford University VLF wave injection expt. receiver 8-85806
 International Sun-Earth Explorer B, EGD positive ion expt. 8-85805
 International Sun-Earth Explorer-1, quasi-static and low-freq. elec. fields meas. 8-85808
 International Sun-Earth Explorers, electron density expt. 8-85803
 International Sun-Earth Explorers 1 and 2, fluxgate magnetometers 8-85804
 International Sun-Earth Explorers 1 and 2, medium energy particles expt. 8-85811
 International Sun-Earth Explorers 1 and 2, quadrispherical LEPEDEAS for plasma meas. 8-85801
 IR optical system input diff. effects and use of spatial apodisation 8-79113
 IR radiometer, passbands for clear-air-turbulence detect. 8-96318
 IR system performance in airborne environment 8-82039
 laser absorption spectrometer, for point monitoring of gases ambient concs. 8-61607
 laser anemometer, time-of-flight, for velocity meas. in atm. 8-69469
 laser experiments on Spacelab missions, for atmospheric meas. 8-53793
 laser photoelectric spectrometer for large condensation nuclei meas. (Russian) 8-65408
 laser radar system, steerable 8-53746
 laser transmissometer, long-path, for visibility meas., field testing 8-85751
 lidar system, two-freq. downward looking, for atm. monitoring 8-69523
 Limb Infrared Monitor of Stratosphere (LIMS) radiometer, design and performance, expt. goals 8-61601
 mass spectrometer meas. technique for O and O₂ in lower thermosphere 8-57348
 micro-Raman spectrometer, for individual aerosol microparticles identification 8-68970
 multislit spectrometer for the night airglow observation 8-73542
 narrow beam spectral radiometer for 4-14.5 μm atm. radiance meas. 8-61596
 nucleopore filters, amosite fibres collection efficiency 8-81341
 optical scintillometer, saturation-resistant, for refr. index struct. parameter meas. 8-65411
 particle camera, aircraft-borne, for in situ photography of cloud particles 8-85750
 photoelectric detector for daytime lightning 8-57336
 photoelectric spectrometer giving integrated parameters in real time (French) 8-53730
 photoionisation mass spectrometer, balloon-borne for stratospheric gas meas. 8-85732
 photometer, four-filter, for total atm. O₃ meas. 8-61597
 photometer for night natural illumination measurement in 0.4 to 1.2 μm spectral region 8-57367
 polarimeter, elliptical, for astronomy and atm. sciences 8-61745
 pollution in Paris streets, survey network 8-81463
 pollution monitoring, centralised supervision system in Fos-Etang de Berre region 8-81410
 pollution remote sensing from space 8-61621
 pressure modulator radiometer for atm. gas emission meas. 8-81457
 radiometer, airborne dual-channel IR heterodyne, for atm. meas. 8-57369
 radiometer, directional, for longwave radiation meas. at ground 8-73537
 radiometer, remote sensing, four band mm-wave radiometer design 8-96324
 radiosonde system, 403 MHz, for boundary layer study 8-85723
 remote automatic station on radio link for wind and temp. monitoring 8-85726
 rocketborne IR spectrometer 8-81460
 satellite cloud picture recorder for reception of APT pictures 8-81434
 scanning interferometric multiplex photometer, airglow appls. 8-62216
 sky brightness and polarisation, using photomultiplier, for teachers 8-81768
 smoke detector, ionisation type, model for response 8-88933
 Spacelab passive atm. sounders, attitude control and stabilisation 8-65483
 spectrometer, Fabry-Perot, signal noise limitations in data retrieval, winds, temp. and emission rate 8-93763
 spin scan camera system, on geostationary satellite, for global weather monitoring 8-61600
 temperature sensors, salt spray induced humidity sensitivity 8-69489
 TIROS N microwave sounder unit, blackbody calibration 8-93016
 tracking receiver direction finder for whistler mode signals, initial results 8-77429
 UV fluorescence hygrometer, stratospheric M₂O vapour meas. (French) 8-65401
 UV photometer for atmospheric ozone monitors calibration 8-77960
 UV spectrophotometer, aircraft-borne, for columnar atm. O₃ meas. 8-73522
 visible IR spin-scan radiometer, fibre optics 8-59160
 water vapour meas. in stratosphere by photodissociation with L α 8-77369
 weather radar calibration, correl. with rain gauge data (Japanese) 8-85670

atmospheric measuring apparatus continued

X-ray fluorescence S analyser, for particulate effluent meas. 8-68971
 Zeeman photometer for Na I dayglow meas. 8-69558
 CO, CO₂ lasers, appl. to atmospheric pollutants selective quantitative meas. 8-69526
 NO/NO₂/O₃ monitors, intercalibration 8-69529
 O₃ calibration reference instrument calibration 8-73524
 O₃, ground level monitoring apparatus, chemiluminescence reaction with ethylene 8-96310
 SO₂ small automatic monitoring network, practical experiences 8-81462

atmospheric measuring instruments see *atmospheric measuring apparatus*

atmospheric motion see *atmospheric movements*

atmospheric movements
 see also *atmospheric turbulence*; *wind*
 advection equation soln., using second-order moments with and without width correction 8-85655
 aerosol dry deposition, filtration model rel. to trace metal deposition from atmosphere 8-73441
 African intertropical aerojet, eastern inertial perturbations (French) 8-61512
 E.African low-level jet stream, five-day oscill. 8-53705
 ageostrophic motion forcing, semi-geostrophic eqns., isentropic coord. model 8-69405
 air pollution density distrib., flow pattern in Tanabe area, Japan, numerical anal. (Japanese) 8-96289
 atmosphere, stratified surface layer, turbulence and diffusion, basic Lagrange characts. 8-81270
 atmosphere, surface tides, New Zealand 8-85665
 Baffin Island, circumpolar vortex vars. rel. to Holocene palaeo-winds and palynology 8-57262
 baroclinic instabilities of deep fluid 8-79307
 baroclinic instability development (Russian) 8-65357
 baroclinic ultralong waves stability on midlatit. beta-plane 8-73484
 boundary layer, convective matching layer 8-81310
 boundary layer, diabatic baroclinic, parametrisation for circulation modelling (Russian) 8-88882
 boundary layer, dissipation modelling under forced convection conditions 8-92900
 boundary layer, marginally unstable interfacial gravity waves (French) 8-92888
 boundary layer, Navier-Stokes eqns. soln. 8-92956
 boundary layer, similarity parameters from first-order closure and data 8-92893
 boundary layer, stability, baroclinicity and scale-height ratio effects on drag laws 8-73429
 boundary layer, vertical currents induced by orography and turbulence 8-96278
 boundary layer, wind shears and inversions (German) 8-81336
 boundary layer, with Rossby number similarity, turbulent diffusion 8-92896
 boundary layer flow over hills, stratification effects 8-53707
 boundary layer flow over topography, Cartesian model 8-92904
 California, synoptic circulation rel. to late Quaternary climate and existence of Ice Age refugium 8-57293
 Chandler tides calc. 8-69413
 circulation over oceans in equatorial latits., numerical calc. 8-92949
 circulation type over N.Atlantic, effect on Gulf Stream channel line oscills. 8-92841
 circulation types, correl. with temp. and precip. fluctuations for Europe and N.America 8-92958
 convection, Lorenz system, 14-D generalization 8-75131
 convection in boundary layer, lidar obs. 8-65366
 convection in meteorology, aspects relevant to astrophysics 8-88898
 convection plume over fire in polytropic atmosphere (Russian) 8-96262
 convective planetary boundary layer, eddy diffusivities from numerical model 8-85667
 convective precipitation, mechanical effect of urban area 8-81338
 Coriolis force field, influence on fluid motion within ellipsoidal cavity (Russian) 8-81296
 diffusion from small island and undisturbed ocean site 8-85647
 diffusion parameters estimation, use of routine meteorological data 8-85649
 E-layer, h-type, at Uppsala, downward movements rel. to origin 8-81497
 E-layer, temperate latit., duration and movement from skywave backscatter obs. 8-85761
 Ekman boundary layer pumping and topography interaction in stratified atm. 8-73486
 energetic particle movement and distrib. rel. to Pc 1 generation 8-61680
 equatorial spread-F, high freq. drift waves with wavelengths below ion gyroradius 8-88973
 equatorial waves, zonal boundary effects 8-85586
 exchange stabilities principle (French) 8-88871
 F₂-layer field-aligned and field-perpendicular vels. theory 8-85760
 F-region, artificially-injected gases dispersal in night-time atm. 8-65460
 F-region, equatorial, irregularity patches origin and motion 8-77404
 F-region, equatorial, motions deduction from Sq currents 8-96344
 F-region, incoherent scatter radar meas. of electron density and ion vel. during isolated substorm 8-65452
 F-region, nonstationary nighttime disturbances produced by internal gravity waves 8-73565
 F-region nighttime dynamics from airglow features mapping 8-88980
 flow around hollow, math. model, natural quarry ventilation appl. (Russian) 8-65358
 flow over north Urals assuming stable stratosphere (Russian) 8-53712
 frontal waves development, numerical simulation accounting for mountain ridges effect (Russian) 8-53701
 gas dynamics with relaxation effects, acoustic waves, nonequilibrium atmosphere effects, review 8-79390
 Gaussian plume model parameters determ. from diffusion-convection eqn. integration 8-81399
 general circulation, twelve-component model (Russian) 8-96263
 general circulation above 100 km, empirical model 8-73558
 general circulation at altitudes >100 km, empirical model 8-61664
 general circulation models, stability and extremal props. (Russian) 8-53716

atmospheric movements continued

- geostrophic large-scale drag coefficient estimation 8-61488
 global problems of fluid dynamics 8-96173
 gravity wave-meanflow interaction, indication in upper atmosphere radar obs. 8-81282
 gravity waves, ground level, in SE.Australia, microbarographs obs. 8-73439
 gravity waves, ray tracing, tornadic storms and hurricanes warning system 8-73448
 gravity waves generated during solar eclipse, obs. 8-88887
 gravity waves in thermosphere, source in tropospheric jet stream (*French*) 8-69554
 gravity-acoustic waves, dispersive eqns. obtained by kinetic eqn. method (*Russian*) 8-85620
 ground layer, stratified, under coniferous forest canopy, vertical air motions (*Russian*) 8-96266
 high-latitude ionospheric dynamics, Doppler method studies 8-73569
 horizontal scales of motion in free convective GATE obs. 8-85653
 hydrodynamic-type system, existence of anomalous modes, rel. to weather patterns (*Russian*) 8-65361
 hydrodynamics, vertical eqn. of motion and wind eqns. 8-69428
 hydrostatic mountain waves numerical simulation 8-73432
 Indian summer monsoon rel. to tropospheric flow patterns over southern hemisphere 8-81334
 internal waves excited by travelling forcing effects, compressibility influence 8-61495
 intertropical convergence zone, air circulation 8-92948
 ionosphere, mid-latitude F_2 -layer, ion and neutral gas vel. oscils. rel. to lunar tide 8-61656
 ionosphere, plasma density depletions motion in artificially created equatorial spread-F 8-88972
 ionosphere, polar, motions rel. to airglow mag. ordering 8-57378
 ionosphere, polar cap connection during Tordo 1 polar cusp Ba plasma injection expt. 8-77402
 ionosphere, quiet nighttime thermal plasma fluxes rel. to calculated and measured decay rates 8-81493
 ionosphere, rocket-borne meas. of ion convection in dayside aurora 8-77391
 ionosphere, travelling disturbances, electron density spectra 8-77398
 ionosphere, travelling disturbances, possible correl. with jet stream activity 8-69601
 ionosphere, travelling disturbances characts. over Thumba 8-69590
 ionosphere drift parameters determined by full correl. anal., effect of filtering 8-65450
 ionosphere F-region, gravity waves, obs. during tornado outbreak (1974, April 3) 8-85753
 ionosphere height rises, relationship with polar mag. substorms and spread-F occurrence 8-81494
 ionosphere holes and spread-F, ion chemistry and transport 8-88982
 ionosphere photoelectrons flux, low-altitude plasma line anisotropy theory 8-77414
 ionosphere plasma stream propag., controlled expt. with rocket-borne plasma gun 8-57424
 ionospheric, lower, layer struts. response to gravity waves 8-81290
 jet, horizontal five-layer, instability 8-79348
 jet stream, medium scale gravity waves generation and vertical energy flux into thermosphere 8-81479
 Kelvin-Helmholtz billows, finite amplitude, evolution 8-81293
 large scale flow, two-dimensional turbulent flow anal. 8-69395
 line convection, radar obs., high resolution colour display 8-88894
 Livemore Regional Air Quality model, concept and development 8-92965
 local circulation in Rome area, surface obs. 8-81264
 London storm, August 1975, urban effects on airflow and precip. 8-81339
 low-level jet, struct. investigations (*German*) 8-69422
 magnetic tail, plasma flow pulsations obs. 8-77436
 magnetosphere, Alfvén and compressional waves coupling 8-89001
 magnetosphere, equatorward-moving absorpt. during auroral absorpt. substorm onset 8-96362
 magnetosphere, high-energy electron drift echoes at geostationary orbit 8-61678
 magnetosphere, low-energy plasma sunward flow obs. at synchronous orbit 8-77435
 magnetosphere, pitch angle dispersion of drifting energetic protons at synchronous orbit 8-77428
 magnetosphere, polar cap convection rel. to boundary mag. fields, laboratory simulation 8-57396
 magnetosphere, transport coeffs. for plasma with quasicollisions 8-71440
 magnetosphere, transport of dissipating photoelectrons 8-69611
 magnetosphere convection, one-dimensional gasdynamical model 8-81508
 magnetosphere dynamics rel. to equatorial ionosphere, effects of polar-equatorial elec. coupling 8-93029
 magnetosphere electric convection field, model 8-89004
 magnetosphere frontside boundary layer, plasma flow and reconnection problem 8-89010
 magnetosphere midlatitude convection elec. fields, rel. to ring current development 8-57395
 magnetosphere ring current plasma injection, correl. with solar wind parameters 8-96363
 magnetotail, energetic particle pitch angle data rel. to tail configuration near midnight 8-96354
 mesometeorological stationary problem of flow around obstacle 8-81271
 mesoscale cellular convection rel. to seagull flight behaviour 8-81269
 mesosphere, equatorial circulation indices seasonal vars. at Thumba 8-85630
 moist circulation maintenance and available energy 8-57281
 momentum flux by standing eddies 8-81314
 neutral atmosphere layer structures, density response to gravity waves 8-81290
 northern atmosphere in summer and winter, vertical eddy momentum transport 8-57249
 numerical simulation models, optimal numerical filters fitted for noise damping 8-92997
 ocean-atmosphere interaction parametrisation for storm conditions, atm. circulation models appl. (*Russian*) 8-65359
 Pc 5 micropulsation resonance region, drift vels. meas. by dual auroral radar system 8-65454

atmospheric movements continued

- perturbations, laminar and turbulent, from photodissoc. wave obs. 8-79407
 planetary standing waves in northern hemisphere in July, model 8-61487
 planetary wave forcing, quasigeostrophic theory 8-73482
 planetary waves, rel. to stratosphere zonal winds correl. with 27-day solar rot. 8-88878
 plasma sheet, plasma flows and mag. field vectors during substorms 8-96357
 plasmopause, drift wave analysis 8-61650
 plasmasphere, dynamo electric field aligned currents theory 8-81499
 plume rise at large distances from multiple-source region 8-85683
 point explosion in arbitrary atmosphere with radiative heat transfer 8-53708
 pollutant dispersion during calm wind situations, analytical modelling 8-81385
 pollutant transport and diffusion, puff-on-cell model 8-85682
 pollutants dispersal, three-dimens. particle-in-cell method, comparison to regional tracer studies 8-92967
 pollutants dispersion, completely Lagrangian random-walk model 8-81380
 pollution dispersion, modelling by smeared conc. approximation 8-81381
 pollution transport in Upper Silesian Industrial District, deposition and washout 8-92960
 quasi-geostrophic eqn., bifurcation and nonlinear soln. stability 8-57242
 radiation belts, particles radial diffusion from geomagnetic field fluctuations at synchronous orbit 8-96359
 radioactivity dispersion, population dose calc. 8-85381
 remote sensing by VHF radar expts. 8-88938
 Rossby wave, critical layer evolution 8-79329
 Rossby waves, long period oscils., book contrib. 8-61435
 rotating stratified fluid, internal and inertial waves 8-67245
 rotation rate of upper atmosphere from Cosmos 408 rocket orbit 8-73559
 sea surface temp. response to atm. forcing, N.Atlantic 8-73399
 source disturbances simulating orographic effects, upstream boundary values (*German*) 8-65375
 stratified flow past three-dimens. obstacles 8-71383
 stratosphere, annual and semi-annual waves obs. using Nimbus 5 selective chopper radiometer data 8-81315
 stratosphere, global scale waves with zonal wave number zero 8-61515
 stratosphere, internal waves interaction with mean flow, rel. to quasi-biennial oscill. 8-69404
 stratosphere photochemical-radiative damping and instability, numerical results 8-81286
 Sun-weather relation, energetics study 8-81285
 surface layer, accuracy of moments of vel., temp. and humidity vars. 8-92891
 thermosphere, circulation systems, northern hemisphere, 80-100 km altitude 8-81481
 thermosphere, diurnal tide seasonal-latitudinal struct. 8-77377
 thermosphere, lower, gravity waves detect. by French incoherent scatter facility 8-81478
 thermosphere, macroturbulent scales estimation around 100 km altitude 8-61635
 thermosphere, momentum sources signatures in neutral comp. 8-77380
 thermosphere, transport processes in diurnal tide, satellite meas. 8-88959
 thermosphere, wave-induced diffusion effects on acoustic-gravity waves 8-61637
 thermosphere neutral and ion drifts, effect of auroral energy input 8-65446
 tidal energy distrib. with altitude, wind field influence (*Russian*) 8-69402
 tides, generated by differential heating between land and sea 8-65374
 tornadoes, numerical simulation of lab. vortex expts. 8-69411
 tropical circulation, role of horizontal friction forces (*Russian*) 8-65360
 troposphere, eddy transport of sensible heat and momentum, time spectral anal. 8-92899
 troposphere, jet stream, source of thermospheric gravity waves (*French*) 8-69554
 troposphere, middle, organised vertical vels. and correl. with clouds 8-92939
 troposphere dynamical indices, lack of response to solar mag. sector crossings 8-57244
 typhoons, transform in northern latits. 8-92947
 unstable surface layer, horizontal vel. spectra 8-73427
 upper atmosphere, irregular motions from radiometric meas. (*Russian*) 8-96333
 upper atmosphere, OH emission, waves and winds, 80-100 km altitude 8-93025
 upper atmosphere, travelling quasi 2-day wave in meteor region 8-81480
 upper atmosphere He dynamics, use of Jacchia (1977) empirical model 8-77381
 vertical diffusion, study using airborne gas-chromatography and numerical modelling 8-69435
 vertical sounder radiances rel. to midlatit. 300 mb flow patterns 8-92983
 vorticity and divergence in dynamic meteorology 8-88893
 vorticity area index, correl. with solar plages 8-73459
 water pollutants atmospheric transport, new direction in hydrometeorology 8-96240
 wave amplitude vacillation in baroclinic flow, model 8-69407
 wave effects on brightness oscillations of daytime sky 8-81406
 wave generation and frontal collapse 8-77300
 waves and jet stream growth and decay, linear and nonlinear contribs. 8-57280
 waves in lower stratosphere, radar meas. 8-81292
 waves on axisymm. mean flows in compressible atms., generalised Eliassen-Palm and Charney-Drazin theorems 8-81306
 zonal atmospheric circulation model, numerical expts. (*Russian*) 8-81295
 H^+ , transport behaviour rel. to concs. in E United States precip. 8-92962

atmospheric movements continued

- NO₃⁻, transport behaviour rel. to concs. in E United States precip. 8-92962
 Na layer wave-like structure, lidar obs. 8-88955
 O₃, tropospheric, long-range transport 8-61514
 S pollutants, long-range transmission, simulation, two-dimens. pseudospectral dispersion model 8-57306
 SO₄²⁻, transport behaviour rel. to concs. in E United States precip. 8-92962

atmospheric noise *see* **atmospherics****atmospheric optics**

- see also* **airglow**; **atmospheric light propagation**; **sky brightness**; **sunlight**; **twilight**
 circumhorizontal arc observed over Austin, Texas 8-77324
 light flash excited by γ -quantum pulse without direct visibility of source 8-69457
 mirage occurrence conditions, ray tracing theory 8-77323
 mirages, stratified medium light ray trajectories, educational aspects 8-69940
 multiple scattering effect on photodissociation 8-85692
 optical depth of Saharan dust, NOAA 3 VHR reflected radiance meas. 8-65390
 parhelia, brilliant display 1977 January 22, obs. at Toronto, Ontario, Canada 8-85694
 radiation balance, zonally averaged model, improvements 8-61559
 solar aureole almuantar radiance meas., comparison between photographic and photoelec. methods 8-77321
 transparency channel form. by photodissoc. wave 8-79407
 turbidity from Campbell-Stokes sunshine recorder traces 8-88912
 twinkling of stars 8-53726
 visibility meas. using long-path laser transmissometer 8-85751
 visibility reduction rel. to O₃ conc. in Midwest 8-61507
 C aerosol visibility vs. particle size distrib. 8-88911
 NO, absorpt. characts. of γ -O band, rel. to atm. meas. 8-57316

atmospheric pollution *see* **air pollution****atmospheric precipitation**

- see also* **atmospheric electron precipitation**; **atmospheric proton precipitation**; **ice**; **rain**; **snow**
 American Southwest, evidence for cold, dry full-glacial climate 8-57296
 aurora, daytime, rocket-borne meas. of particle precip. and ion convection 8-77391
 auroral particle instantaneous energy deposition, determ. from optical emissions 8-81491
 Central Europe, large-scale precip. field components extraction for forecasting purposes 8-92940
 charged particles precipitation, parallel elec. field signature in vel. space distrib. 8-89005
 climate fluctuations, relation of moistening to thermal regime 8-92937
 convective precipitation, mechanical effect of urban area 8-81338
 convective shallow cloud model, precip. mechanisms 8-81311
 cumulus congestus clouds, NE Colorado, graupel particles characts. 8-81312
 cyclonic storm, rainbands, precip. cores and generating cells 8-81307
 daily precipitation occurrence process, Markov chain modelling 8-61464
 dew, relationship to radiation fog 8-73446
 Fergana Valley, heavy precip. forecasting 8-92946
 hail, Doppler radar spectra at vertical incidence 8-65368
 hail, during thunderstorm of 1976 June 27 at Heatree, Devon, England 8-57288
 hail suppression seeding, Ag analysis 8-65367
 hail suppression seeding, crop response anal., Nelspruit project, South Africa 8-57257
 hail-prevention operations, cost effectiveness estimation methods anal. 8-93013
 hailfalls kinetic energy, hailstone spectra anal. 8-92924
 hailpads calibration 8-93001
 hailstone samples, Project DUSTORM, microprobe anal., element abundances 8-73453
 hailstone trajectories determ. from crystallography, D content and radar backscatt. 8-61614
 hailstones, foreign material obs. and derivation 8-96260
 hailstorms variability on South African plateau 8-92911
 ice accretions, crystal structure rel. to hailstones 8-85668
 London, urban effects in severe storm in August (1975) 8-81339
 microphysics, book 8-88896
 microwave cross-polarization due to precipitation in atmosphere (French) 8-53674
 Middle Europe, 1708-54 precipitation record for Zurich (German) 8-85661
 non-spherical hydrometeors scattering properties (French) 8-53676
 numerical prediction, methods and results 8-69393
 parameter meas. method using radar reflectivity and optical extinction (French) 8-53729
 pine forest wet canopy evap. meas. 8-61460
 radar derived statistics on precip. patterns struct. 8-57260
 scavenging rates of background aerosol 8-85648
 snow, estimated water equivalents and melting characts. in river drainage basins 8-96249
 storms, principal component anal., hail index (French) 8-96267
 surface humidity rel. to precipitable water vap., India 8-81273
 temporal fluctuations, averaging for continents Europe and N.America 8-92958
 Texas High Plains, precipitation climatology 8-92959
 thunderstorms, elec. fields, precip. elements charge and size, airborne obs. 8-73485
 E United States precipitation, SO₄²⁻, NO₃⁻ and H⁺ concs. behaviour 8-92962
 urban effects on precipitation, metropolitan Detroit-Windsor example 8-92917
 weather modification technology, statistical approach, review 8-53706
 S isotopic comp. in atm. precip. around Sudbury, Ontario 8-81361

atmospheric pressure *see* **atmospheric pressure and density****atmospheric pressure and density**

- 500 mb height evaluation from Nimbus-6 soundings 8-53695
 anomalous local atm. press. correl. with secular gravity vars., USSR (Russian) 8-53612
 N.Atlantic Ocean, sea level press. fields rel. to Gulf Stream channel line oscills. 8-92841

atmospheric pressure and density continued

- atmosphere, surface tides, New Zealand 8-85665
 aurora, O densities rel. to O, O₂ and N₂ emission meas. 8-57380
 Belgium, continental anticyclonic conditions rel. to air pollution increases 8-81374
 boundary layer, press. fluctuations, ground effects 8-61498
 boundary layer near water surface, diurnal characts., equatorial region, GATE meas. 8-61527
 coastal zone, indicators of long-term var. of hydrometeorologic elements (Russian) 8-77258
 cyclogenesis in lee of Alps 8-77305
 F-region, incoherent scatter radar meas. of electron density and ion vel. during isolated substorm 8-65452
 gravity waves, ground level, in SE.Australia, microbarographs obs. 8-73439
 gravity waves generated during solar eclipse, obs. 8-88887
 ionosphere, props. meas. at Arecibo Observatory 8-81488
 ionosphere modification, plasma densities in artificially created equatorial spread-F 8-88972
 ionosphere pressure oscillations, generation of atmospheric acoustic-gravity waves 8-77296
 ionosphere total electron content at Sagamore Hill, solar cycle var. 8-81496
 ionospheric, lower, layer structs. response to gravity waves 8-81290
 magnetosphere low-energy plasma at synchronous orbit, temp. and density 8-77435
 magnetosphere plasma sheet, plasma flows during substorms rel. to field-aligned press. gradient 8-96357
 marine atmosphere, baric disturbances ocean stationary surface and internal waves generation (Russian) 8-77252
 marine equatorial atmosphere, surface press. rel. to general circulation features 8-92949
 mesopause, ion-neutral collision freqs. and mean temps., Arecibo radar meas. 8-88957
 mesosphere, ion bunches form. and concs. 8-73424
 monsoon depressions in Bay of Bengal, freq. of first occurrence, 10-day epochs, 1891-1970 period 8-81303
 neutral atmosphere layer structures, density response to gravity waves 8-81290
 Norway Station/Sanae (Antarctica), surface temp. and sea-level press. 8-81324
 ocean-atmosphere interactions along North American west coast, 1965-69 period, preliminary anal. 8-61508
 plasma sheet, press. anisotropies meas. 8-89009
 plasmopause location and H⁺ density decreases, correl. 8-81500
 pressure, long-period fluctuations, statistical analysis (Russian) 8-81298
 pressure fluctuations, influence on Earth surface tidal tilts (Russian) 8-88790
 protonosphere, plasma densities meas. rel. to quiet night ionosphere decay rates 8-81493
 sea level nonperiodic vars. of synoptic freq. on tidal sea shelf (Russian) 8-65320
 sea level pressure anomalies predictability over N.Pacific Ocean 8-92905
 stratosphere, 200 mb geopotential heights rel. to annual and semi-annual waves 8-81315
 stratosphere O₃ density perturbations, photochemical-radiative damping rel. to instability 8-81286
 subarctic frontal zone position rel. to typhoon trajectories seasonal activity over NW.Pacific 8-61526
 surface layer press. perturbs. due to ocean swell waves (Russian) 8-65362
 synoptic object localisation, long-period tidal fluctuations (Russian) 8-81321
 thermosphere, circulation systems, northern hemisphere, 80-100 km altitude 8-81481
 thermosphere, local time var. of density, altitude depend. 8-61636
 thermosphere, model based on satellite drag data 8-69555
 thermosphere, neutral comp. and density profiles between 90 and 220 km 8-77383
 thunderstorm gust front detection, sensitive pressure-jump sensor design 8-57357
 tropical circulation, role of horizontal friction forces (Russian) 8-65360
 troposphere, upper air pressure field anal. using surface-derived data 8-61523
 United States, synoptic weather situations assoc. with major wildland fires 8-61499
 unusual weather frequency variability over last century 8-73479
 upper atmosphere, background gas press. rel. to He dynamics, use of Jacchia (1977) empirical model 8-77381
 upper atmosphere, density fluctuations rel. to meteor trails linear electron density 8-73687
 upper atmosphere, density vars. from January 1972 to April 1975 near 200 km 8-57377
 western disturbance intensification moving from central Iran to NW India 8-81302
 CO₂, number densities in lower thermosphere 8-96336

atmospheric propagation *see* **atmospheric electromagnetic wave propagation****atmospheric proton precipitation***see also* **aurora**; **radiation belts**

- aurora, ULF elec. fields and particle precip., rocket meas. 8-96337
 auroral oval, daytime, energetic protons rel. to radio aurora and field-aligned currents 8-83966
 auroral protons, as source of atmospheric water vapour, role in Sun-weather relationships 8-69416
 energy deposition in N₂, binary encounter calcs. 8-74746
 ionosphere turbulent polar cusp, temps. and low-energy particles and Kelvin-Helmholtz instability 8-96343
 polar cap aurora, proton-induced, N₂ bands intensities 8-77389
 X-ray K-shell emission at satellite altitude 8-61641

atmospheric radiation*see also* **aurora**

- absorption of solar, diffuse and reflected visible radiation (Russian) 8-96291
 auroral electron beam, electrostatic noise generation 8-85759
 boundary layer, radiation balance over salt marsh 8-61481
 boundary layer, turbulent and radiative transport interaction in development of fog and low-level stratus 8-81313

atmospheric radiation continued

- brightness temperatures in H_2O 1.35 cm reson. region, vars. (*Russian*) 8-81403
- Cherenkov radiation in large cosmic ray showers, computer simulation using hadronic collision models 8-57415
- daylight, spectral distrib., 280-2800 nm, Australia 8-69452
- Earth surface thermal radiation, calc. for randomly inhomogeneous stratified media (*Russian*) 8-96312
- energetic ions and EM radiation in auroral regions 8-81490
- exosphere, H atoms vel. distrib. from OGO-5 meas. of Lyman α emission 8-61642
- GATE radiation subprogram, aircraft studies 8-81408
- hourly solar radiation amounts in Thailand, statistical distrib. 8-96271
- insolation measurements at Las Vegas, in United States 8-69427
- IR emission, Lambertian, of spherical surface, radiation press. on satellite (*French*) 8-81529
- IR emission, sky noise correl. for IR telescope focal plane (*French*) 8-53725
- IR emission, statistical props. of sky noise (*French*) 8-53731
- IR radiance meas., 4-14.5 μm range, by narrow beam spectral radiometer 8-61596
- magnetosphere coherent VLF waves, nonlinear pitch angle scatt. of energetic electrons 8-89011
- magnetosphere natural emissions, Geos I identification 8-53774
- methane, IR radiation flux 8-71268
- near IR solar radiation, direct and scattered fluxes (*Russian*) 8-81299
- outgoing thermal radiation, meas. rel. to O_3 profile determ. 8-92945
- pollutant layers, radiative effects 8-65382
- radiative balance, meas. by Cactus accelerometer on Castor satellite (*French*) 8-81530
- radiometer, directional, for longwave radiation meas. at ground 8-73537
- radiometric sounding data and operational numerical weather prediction 8-53696
- sea ice, energy exchange in central Arctic 8-85584
- solar intensity obs., global insolation on horizontal and tilted surfaces 8-81275
- subauroral red arc event caused by kinetic Alfvén waves 8-93026
- submillimetre outgoing radiation obs. in broad spectral bands (*Russian*) 8-65443
- surface radiative flux, clear and cloudy conditions, parametrisation accuracy 8-77325
- thermal microwave radiances from hydrometeor clouds 8-85638
- thermal radiation, particulate pollution effects rel. to climatology 8-85678
- thermal radiation, rel. to Earth global heat balance annual var. 8-73300
- troposphere, IR radiation, cloud height, thickness and overlap effects 8-57252
- Typhoon June (1975), obs. by scanning microwave spectrometer 8-73436
- X-ray K-shell emission at satellite altitude from proton precipitation 8-61641
- X-rays from magnetospheric electrons, rocket-borne astronomy affected 8-61640
- O I 5577 Å forbidden line and O_2 7620 Å band auroral excitation 8-88964

atmospheric radioactivity

see also fallout

- biosphere, radioactive contamination, influencing factors, 1962-76, Hungary (*Hungarian*) 8-92711
- boundary layer, natural radioactivity continuous meas. method (*Flemish*) 8-61612
- cloud dose data file fast correction for changes in dispersion parameters 8-80969
- cosmogenic radioisotope flux onto Earth's surface and atm., magnitude and time var. 8-61634
- Czechoslovak Rez Nuclear Research Institute airborne radioactive release monitoring 8-89991
- dispersion, population dose calc. 8-85381
- gamma-rays from extended sources, energy distrib. calc., rel. to remote spectroscopy 8-61586
- inner radiation belt, max. radiation dose following 1962 STARFISH explosion 8-69612
- LWR core meltdown, activity release and aerosol characts. 8-82469
- natural, pollution with coal smoke particles (*Rumanian*) 8-53723
- natural radiation exposure, New Zealand, soil survey and air doses for ^{226}Ra and ^{232}Th daughters and ^{40}K 8-88747
- nuclear plant emission, radiation exposure calc. (*German*) 8-82531
- pollution control at Nuclear Research Institute (*Czech*) 8-88906
- radionuclide airborne release assessment, determ. of atm. stability categories 8-73504
- radionuclide release assessment, importance of vars. in deposition vel. 8-80979
- reactor near-stack dose calc., diffusion model applicability 8-94147
- risk anal. of high-level waste management systems in Germany 8-50272
- Switzerland, radioactivity surveillance and descent of Kosmos 954 (*German*) 8-77119
- turbulent atmospheric transport, Monte Carlo simulation, radioactive pollution appl. 8-61550
- West German LWR power plant stack monitoring, legal and technical aspects 8-89988
- West German nuclear plant airborne radioactive effluent monitoring 8-89990
- ^7Be , cosmic-ray-produced, mean tropospheric residence time at north temperate latits. 8-85633
- ^{14}C concentration in Earth's atmosphere, corrections with astrophysical and geophysical phenomena 8-61477
- ^{14}C concentration in Earth's atm. with variations of geomag. field, spectral anal. 8-61478
- ^{14}C formation by solar flare particles 8-92886
- ^{14}C variations rel. to 11-year solar cycle 8-92885
- ^3H formation by solar flare particles 8-92886
- Rn daughter concentrations in air of dwellings in Great Britain 8-77118
- ^{222}Rn low conc. meas. in air, α -scintillation method 8-92970

atmospheric spectra

see also atmospheric optics

- absorption at 460 μm , determ. 8-96295

atmospheric spectra continued

- absorption of solar, diffuse and reflected visible radiation (*Russian*) 8-96291
- aurora, 2150 Å spectral feature, contrib. from N II lines 8-61645
- aurora, artificial, ground-based optical meas. during Excede 2 test 8-89038
- aurora, artificial, time-depend. spectrum in Precede expt. 8-89037
- aurora, pulsating, 5577 Å/4278 Å column emission ratio rel. to particle characts. 8-88969
- aurora, rocket meas. and anal. of O_2 , N_2 and O emissions 8-57380
- aurora, UV spectrum between 2100 Å and 2300 Å 8-88963
- auroral electron beam, electrostatic noise power flux spectra 8-85759
- auroral emissions, photometry rel. to precipitating electrons energy distrib. 8-77390
- dichlorodifluoromethane, diode laser spectra near 10.8 μm , air-broadening effects 8-61555
- F-region convective electric field determ. from rocket meas. of thermal ion spectra 8-57386
- far IR emission spectra calcs. 8-92978
- formaldehyde, Doppler-limited spectra of C-H stretching fundamentals 8-70831
- Freon-12, absorpt. coeffs. for CO_2 laser radiation, press. and temp. depend. 8-55170
- gamma-ray spectra from double Compton gamma-ray telescope, background sensitivity to atmospheric neutrons 8-53827
- geocorona, collisional model for spectral line profiles 8-77508
- hail, Doppler radar spectra at vertical incidence 8-65368
- ionosphere, auroral, field-normal plasma-line scatt. detect. expt. 8-73580
- ionosphere, travelling disturbances, electron density spectra 8-77398
- ionosphere incoherent ion backscatter spectrum, stimulated Brillouin scatt. detect. 8-77412
- ionosphere plasma line, low-altitude anisotropy theory 8-77414
- IR radiance meas., 4-14.5 μm range, by narrow beam spectral radiometer 8-61596
- IR spectral band transmittance, modelling, Prony's method 8-70202
- meteor bright line spectra, study via astronomical TV system 8-61817
- outgoing thermal radiation, O_3 9.6 μm absorpt. band rel. to density profile 8-92945
- polar airglow, N, N_2 emission obs. rel. to mag. ordering 8-57378
- rain drop spectra and fine structure on different time bases (*French*) 8-53681
- Raman scattering analytical techniques using tunable lasers 8-61134
- solar radiation absorpt. spectra, atm. trace gases vertical conc. (*Russian*) 8-69442
- solar radiation at Earth's surface, spectral distribution model 8-69456
- stratosphere, HNO_3 concs. in N.hemisphere from 11.2 μm band radiance 8-81288
- stratosphere, laser spectroscopy relevant to photochem. 8-88951
- stratosphere, solar radiation absorption, in O_2 Herzberg continuum, influence of O_4 and O_2N_2 dimers 8-87429
- sunlight, spectral actinometric obs. for atmospheric aerosol turbidity characts. determ. 8-92986
- thermosphere, O I 63 μm emission spectrometric meas. 8-81474
- thermosphere, photoelectron energy spectra, rocket born meas. in 2-100 eV range 8-77379
- transmittance profiles calc. method 8-85696
- water vapour, 1 to 8 μm absorpt. 8-81402
- water vapour, absorpt. at 7.1 cm^{-1} , temp. depend. 8-82722
- water vapour, absorption near 4250 cm^{-1} 8-82729
- water vapour, IR continuum absorpt. calc. (*Russian*) 8-96293
- water vapour, pressure broadened absorpt. in 10 μm region, O_2 addition effects 8-92975
- water vapour, spectral transmission at wavelengths 0.7 to 1 μm 8-85685
- water vapour band absorption, remote sensing 8-65389
- water vapour continuum absorption, 3.5 to 4.0 μm region 8-92973
- water vapour continuum IR absorpt. near 1200 cm^{-1} , temp. depend. 8-85687
- weak absorption lines, detect. by Nd:glass and dye laser system 8-89561
- whistlers, partly ducted, over Europe, spectrographic traces and morphology 8-65463
- CO , solar radiation absorpt. spectra rel. to atmospheric abundance (*Russian*) 8-53700
- CO_2 , IR energy levels and line intensities 8-85691
- CO_2 line freqs. in 4.3 μ region 8-88910
- ClO radical, IR vibr.-rot. spectra, background data for atm. meas. 8-58679
- H_2O 1.35 cm resonance region, atmospheric brightness temp. vars. (*Russian*) 8-81403
- H_2O , IR continuum absorpt. due to librational mode of dimer 8-66542
- H_2O , residual IR absorption obs. during solar brightness temp. balloon-borne meas. 8-85921
- H_2SO_4 , dissociation and absorpt. const., ultrahigh resolution obs. of 8.2, 11.3 μm bands 8-70825
- N_2 bands in proton-induced polar cap aurora, intensities 8-77389
- N_2^+ 3914 Å, auroral emission rel. to instantaneous particle energy deposition rate 8-81491
- $\text{N}_2^+(\text{A}^3\Pi_u-\text{X}^2\Sigma_g^+)$ system in aurora, vibr. development and quenching effects 8-88967
- $\text{N}_2(\text{B}^3\Pi_g-\text{A}^3\Sigma_u^+)$ system in aurora, vibr. development and quenching effects 8-88967
- NH_3 , ν_2 vibr.-rot. band identification in ground level solar spectra 8-81287
- NO , $v=0,1$ states, spectroscopic data calc. 8-86851
- NO_3 , absorpt. spectrum nighttime obs. 8-88880
- O I 5577 Å forbidden line rel. to O_2 and OH band spectra 8-61639
- O I auroral emissions, ground-based photometric meas. 8-77387
- O I UV nightglow obs. at midlatit. 8-81482
- O II 7320-7330 Å emissions meas. at twilight 8-88962
- O_2 1.27 μ A-band intensity in lower atmosphere (*Japanese*) 8-61486
- O_2 1.27 μ emission, auroral enhancement 8-81485
- O_2 7594 Å A-band on objective prism spectra of stars, radical vel. meas. appl. (*Japanese*) 8-89083
- O_2 , IR nightglow bands excitation mechanism, reaction rate const. 8-65448
- O_2 induced absorption band effects on transmission in 6 μm region (*Russian*) 8-69446
- O_3 , columnar meas. by aircraft-borne UV spectrophotometer 8-73522

atmospheric spectra continued

- O₃, daytime and nighttime distrib., ground-based mm wavelength obs. 8-57256
 O₃, remote meas. in IR absorpt. bands, information content estimation (*Russian*) 8-88883
 O₃ stratospheric 10 μ absorption line obs. with IR heterodyne spectrometer 8-61494
 OH Meinel bands, in airglow, rot. temp., radiative lifetime 8-61643
 OH Meinel bands intensity distrib. in airglow, OH* quenching mechanisms 8-65447
 OH(X² π) nightglow emissions, theory and meas. in (9-3) band 8-88960
 OH(8-3) 7274 Å band rel. to O₂ and forbidden O I spectra 8-61639
 O₂(0-1) 8645 Å band rel. to OH and forbidden O I spectra 8-61639

atmospheric structure

see also *atmospheric composition*

- acoustic remote sensing, review 8-73493
 baroclinic boundary layer structure 8-81326
 boundary layer, surface roughness change effects 8-77306
 cloud field over Transcaucasia, statistical struct. 8-92942
 dayside aurora, particles and ion convection meas. rel. to ionosphere struct. 8-77391
 E_s-layer, temperate zone, maps of $f_oE_s > 7$ MHz 8-73579
 E_s-layer, temperature latit., skywave backscatter studies 8-85761
 E-region height variations, influence of lunar tides 8-77382
 equatorial ionosphere holes and spread-F, ion chemistry and transport 8-88982
 F-region, electron density trough form. during isolated substorm, incoherent scatter radar meas. 8-65452
 F-region, equatorial, irregularity patches localised origin 8-77404
 F-region, equatorial ionisation density irregularities rel. to HF and VHF spread-F echoes 8-85764
 F-region, hmF2 meas. at low. latit. mag. conjugate regions rel. to neutral winds determ. 8-81477
 F-region, travelling ionospheric disturbances by gravity waves due to tornado outbreak 8-85753
 F-region striated Ba clouds, electron density struct. meas. 8-88974
 F-region vars. rel. to thermospheric diurnal tide seasonal-latitudinal struct. 8-77377
 Harang discontinuity, electric field meas. by auroral radar and rocket double-probes 8-88971
 intertropical convergence zone, air circulation 8-92948
 intertropical convergence zone struct. over GATE area 8-57283
 ionosphere, analytic partial derivatives for incoherent scatter data least-squares fitting 8-73581
 ionosphere, equatorial, EM state rel. to interplanetary mag. field vars. 8-77413
 ionosphere, heterogeneous structure of low-latitude region 8-96338
 ionosphere, mid-latitude sporadic-E layer, irregular structure from incoherent scatter radar obs. 8-96342
 ionosphere height rises, relationship with polar mag. substorms and spread-F occurrence 8-81494
 ionosphere mid-latitude trough, low energy plasma obs. during major mag. storm 8-88987
 ionosphere mid-latitude trough, scintillation of extraterrestrial radio noise sources signals 8-73574
 ionosphere mid-latitude trough location, noon and midnight obs. by Ariel 4 8-85765
 ionosphere trough region, detached auroral arcs obs. 8-88965
 ionosphere turbulent polar cusp, temps. and low-energy particles and Kelvin-Helmholtz instability 8-96343
 ionospheric, lower, layer structs. response to gravity waves 8-81290
 layer structures, density response to gravity waves 8-81290
 lidar techniques for atm. struct. and comp. obs., proposed Spacelab program 8-61602
 low-level jet, struct. investigations (*German*) 8-69422
 magnetosphere, field-aligned electron irregularities rel. to partly ducted whistlers propag. 8-65463
 magnetosphere, low-energy plasma obs. at synchronous orbit 8-77435
 magnetosphere, structure and stability properties 8-77440
 magnetotail configuration near midnight during quiet and weakly disturbed periods, mag. field modelling 8-96354
 marine atmosphere, ranked interaction with ocean on sub-semidiurnal scales (*Russian*) 8-77260
 marine boundary layer, microwave radiometric sensing 8-57272
 meteor zone, statistical modelling from Geminid shower radar obs. 8-61816
 multilayer model, electrodynamic state, horiz. mag. field component influence (*Russian*) 8-73556
 nocturnal boundary layer, height determ. 8-73450
 ocean-atmosphere interactions along North American west coast, 1965-69 period, preliminary anal. 8-61508
 palaeomagnetosphere, third type of planetary magnetosphere during polarity reversals and geomag. excursions 8-61683
 radiation belts outer boundary variations, Kosmos 426 data 8-69614
 rain, fine structure meas. (*French*) 8-53680
 rain drop spectra and fine structure on different time bases (*French*) 8-53681
 refractive index structure parameter, determ. from refractivity and amplitude scintillation meas. at 36 GHz 8-81316
 spread-F bubbles, nonlinear Rayleigh-Taylor mode theory in two dimensions 8-88986
 statically stable zones, simultaneous tethered balloon and monostatic acoustic sounder records comparison 8-73451
 stratified aerosol layers meas. by searchlight probing technique 8-92892
 surface layer, structural turbulence coeff. depend. on height (*Russian*) 8-69400
 surface layer above snow (*Russian*) 8-96264
 thermal plumes detect. by acoustic echo sounder 8-57259
 thermosphere, lower, thin shear turbulent layers induced by tides and gravity waves non-linear interaction 8-65444
 thermosphere, polar airglow mag. ordering 8-57378
 thermosphere, tidal struct. at equinox 8-81476
 troposphere, refr. index struct. parameter height distrib. with lower boundary spatial transition 8-73491
 troposphere, stratified layers rel. to VHF radar partial refl. from clear atmosphere 8-81278
 troposphere, vertical structure from ground-based IR radiometry 8-57273

atmospheric structure continued

- troposphere thermal structure, acoustic sounding technique appl. to siting studies 8-81467
 turbulent flow in two and three dimensions, microstructures rel. to numerical weather prediction 8-69395
 turbulent interface layers, theory 8-71323
 typhoons, transform in northern latits. 8-92947
 whistler ducts, formation theory 8-57407
 Na layer wave-like structure, lidar obs. 8-88955

atmospheric techniques

- see also *air pollution detection and control*; *geophysical equipment*; *ionospheric measuring apparatus*; *ionospheric techniques*; *meteorological instruments*
 acoustic remote sensing, review 8-73493
 acoustic sounding of atmosphere, pattern recognition studies 8-65416
 acoustic sounding technique, appls. to siting studies 8-81467
 actinometric method for tropospheric meas. of O(¹D) formation by O₃ photolysis 8-73536
 aerosol, ambient sulphate particles size discrimination and chemical comp. by diffusion sampling 8-69528
 aerosol, individual microparticles identification via micro-Raman spectrometer 8-68970
 aerosol, stratospheric, conc. and sizes, meas. via impactor and in situ single-particle detect. 8-73437
 aerosol charge distribution, determ. via variable freq. electrostatic mobility analyser 8-77945
 aerosol content determ. from photometric obs. of stars 8-92976
 aerosol layer depth remote meas. by microwave-modulated laser (*Russian*) 8-57338
 aerosol mass conc. meas. by Nd:glass lidar, ASSESS II Spacelab mission simulation (*German*) 8-69649
 aerosol measurement, particle deposition in sampling lines 8-81472
 aerosol particles sizing, influence of chemical struct. 8-81471
 aerosol turbidity characteristics, determ. from spectral actinometric obs. 8-92986
 aerosols, chemical characterisation, progress and problems 8-68969
 air pollutant deposition research using rain gauges (*Dutch*) 8-81367
 air quality evaluation, daily profiles method (*French*) 8-92969
 air-truth lidar polarisation studies of orographic clouds 8-73454
 airborne gas-chromatography, appl. to atmosphere vertical diffusion meas. 8-69435
 cloud cover, forecasting from middle troposphere organised vertical vels. 8-92939
 cloud extinction meas. using electronic chopper for UV source 8-79087
 conduction current meas., direct method, new instrumentation 8-85637
 correlation and spectral analysis, appl. to hydrometeorologic elements in coastal zone (*Russian*) 8-77258
 cumulonimbus clouds, elec. field strength and raindrop spectra, study from mobile ground station 8-92943
 cumulus cloud seeding technique, preliminary tests 8-57352
 differential-absorption lidar technique for remote meas. of atm. gases 8-61603
 Doppler radar meas. of wind in extratropical cyclones, colour display system 8-61594
 dry ice appls. to on-top seeding of convective clouds 8-73531
 dustfall, short term, from dust generating industry, meas. and effect on residential development 8-81386
 EHF clear air refractivity calc. procedure 8-57266
 elemental analysis at sub parts per trillion concs., via SONRES 8-81465
 Excede 2 test, artificial auroral expt., ground-based optical meas. 8-89038
 extinction coefficient meas. from distant contrast, using astronomical telephotometer 8-61730
 F-region neutral winds, determ. from ionosonde meas. of hmF2 at low latit. mag. conjugate regions 8-81477
 flameless atomic absorption spectroscopy, appl. to Cd, Pb and Mn determ. in size fractionated aerosols 8-69434
 foil impactor impressions of water and ice particles, interpretation, rel. to hail research 8-57356
 Fourier transform IR absorpt. spectroscopy, airborne, for atm. comp. meas. 8-61604
 Fourier transform spectroscopy, Doppler-limited high-accuracy, 10⁶ samples 8-58068
 Fourier transform spectroscopy appl., far IR 8-58069
 free radical meas. by matrix isolation and EPR 8-73535
 gases abundance determ. by analysing solar spectra 8-85643
 gusts, local forecasting method (*German*) 8-85727
 hail-prevention operations, cost effectiveness estimation methods anal. 8-93013
 hailstone trajectories determ. from crystallography, D content and radar backscatt. 8-61614
 halofluorocarbons background levels, in situ quantification technique 8-69530
 heavy precipitation of Fergana Valley, short-term forecasting 8-92946
 high acidity measurement, comparative tests near industrial installations in Fos-Etang de Berre region 8-81464
 hydrometeor size and shape determ. using radar differential reflectivity and differential phase shift 8-57270
 infrasound waves recording methods and computer anal. (*Russian*) 8-65407
 ion chromatography, new analytical technique for sulphate and nitrate assay in ambient aerosols 8-68974
 IR emission, statistical props. of sky noise at telescope focus (*French*) 8-53731
 IR laser heterodyne spectroscopy for trace gases remote detect. 8-61606
 IR laser technique for SO₂ conc. determ. (*Russian*) 8-69484
 laser absorption method for H₂O vapour conc. meas. 8-61595
 laser absorption spectroscopy for point monitoring of gases ambient concs. using tunable lasers 8-61607
 laser single-beam transverse velocity meas. 8-53747
 laser technology for atm. science, conf., San Diego, USA (Aug. 77) 8-85748
 laser velocimetry techniques using CO₂ laser 8-61623
 LF radio sounding of plasmopause by geostationary satellite 8-69648
 lidar and solar radiometer obs. compared with aircraft meas. of particulate props. 8-61501

atmospheric techniques continued

- lidar measurement of Na conc. and neutral temp. at mesopause level 8-61613
- lidar polarisation meas. for cloud phase discrimination 8-96269
- lidar probing of fogs and clouds, double scatt. approx. 8-73512
- lidar return signal geometrical compression, atm. remote sensing appl. 8-57329
- lidar techniques for atm. struct. and comp. obs., proposed Spacelab program 8-61602
- lightning, intracloud discharges inclination from mag. fields meas. 8-73440
- lightning current wave forms, deduction from radiated EM fields, Maxwell eqns. exact soln. appl. 8-73442
- lightning ground-flash multiple-stroke discriminator cct. 8-81446
- lightning stroke current meas. using optical fibre cable and optoelectronic conversion, rocket launched 8-92930
- magnetopause obs., techniques and results 8-61668
- magnetosphere, high-latit., Echo 4 electron beam expt. and artificial auroral streaks obs. 8-89036
- magnetosphere magnetic fields, dual magnetometer method extension for use on dual spinning spacecraft 8-77459
- magnetosphere VLF wave injection experiment, receiver on International Sun-Earth Explorer A 8-85806
- magnetotail, Alfvén wave generation via proton accelerator 8-73582
- marine atmosphere, microwave radiometry appls. 8-81415
- meteorological conditions forecasting procedures for aviation, development and improvement 8-92950
- natural radioactivity continuous meas. method in surface layer (*Flemish*) 8-61612
- non-methane hydrocarbons, monitoring via photoionisation 8-73549
- northern hemisphere annual temperature approximation, simple method 8-81345
- numerical weather forecasting, determ. of boundary layer orography and turbulence-induced vertical currents 8-96278
- ocean surface wind and waves, radar meas. techniques 8-81418
- optimal sampling and anal. method 8-73530
- optimum difference schemes, synthesis on sphere 8-93011
- organic pollutants, determ. via gas chromatography after cryogenic sampling 8-81468
- organochlorine residues in rainwater, extraction method 8-73495
- parallel electric field, signature in ion and electron distribs. in vel. space, 8-89005
- particle elastic scattering analysis, appl. to C, N and O determ. in size fractionated urban aerosols 8-81466
- particle sizing, 0.05 to 5.0 μm , using laser instrument 8-61624
- particulates, chemical characterisation via light scatt. method 8-69533
- particulates and gaseous pollutants measurement, anal. and calibration techniques 8-69531
- photon transport problems, modified Monte Carlo procedure 8-61560
- plasmaopause sounding from geostationary satellite, feasibility 8-93043
- pollutant annual average concentration around single source, rapid estimation technique 8-81382
- pollutants, selective quantitative meas. using CO and CO₂ lasers 8-69526
- pollutants dispersion, completely Lagrangian random-walk model 8-81380
- pollutants origin and residence times determination, ¹⁴C appl. 8-69445
- pollution, continuous point sources, effects prediction (*Dutch*) 8-61545
- pollution dispersion, modelling by smeared conc. approximation 8-81381
- pollution effects indicators, provisional map 8-81387
- pollution remote sensing from space 8-61621
- pollution spatial distrib., objective interpolation formulae 8-65412
- Precede, artificial auroral expt., summarised results 8-89037
- precipitation collection and chemical anal. 8-57368
- precipitation over Central Europe, large-scale field components extraction for forecasting purposes 8-92940
- precipitation parameter meas. method using radar reflectivity and optical extinction (*French*) 8-53729
- pulse Doppler radar obs. of severe thunderstorms 8-85651
- radar applications in Polish meteorological service 8-92992
- radar appls. in meteorology and atmospheric behaviour research, review 8-77371
- radar obs., high resolution colour display of line convection 8-88894
- radar precipitation maps as lightning indicators 8-85652
- radar propag. through turbulence, scintillation detection using monopulse techniques 8-85717
- radio meteor wind data, anal. using finite element approximation 8-81475
- radio refractive index measurement, digital instrument appl. 8-86321
- radio-acoustic sounding methods for tropospheric temp. meas. 8-53728
- radioacoustical sounding by continuous radiation method (*Russian*) 8-88927
- rain induced attenuation and cross-polarization calcs., two new methods (*French*) 8-53677
- rain intensity distribution, conversion to shorter or longer integration times 8-61520
- rain parameter diagram, methods and appls. 8-57349
- rain-rates, estimates for attenuating radar 8-73540
- rainfall meas. by microwave attenuation in 1-3 cm band 8-65414
- Raman scattering analytical techniques using tunable lasers 8-61134
- remote monitoring using discretely-tunable IR gas lasers and heterodyne detect. techniques 8-61605
- remote sensing by VHF radar expts. 8-88938
- remote sensing of atmosphere, land and sea props. 8-93015
- remote sensing of particle size distribs., analytical inversions 8-73508
- remote sensing of particle size distribs., analytical inversions 8-73509
- remote spectroscopy for total O₃ content determ. 8-65437
- satellite effective isotropic radio power meas., error anal. using calibrated radio star 8-93070
- searchlight probing technique for stratified aerosol layers meas. 8-92892
- simultaneous tethered balloon and monostatic acoustic sounder records of statically stable zones 8-73451
- sodar meas., improved quantitative display techniques 8-77332
- solar aureole alimucantar radiance meas., comparison between photographic and photoelec. methods 8-77321
- solar aureole rel. atm. aerosol props., photogrammetry 8-57315

atmospheric techniques continued

- speckle interferometry, atm. nonisoplanicity meas. using double stars 8-65387
- speckle interferometry for atm. isoplanatism meas. 8-65385
- spectral transmittance method, for surface layer aerosols variability meas. (*Russian*) 8-69448
- stellar speckle interferometry, wave correlation scale meas. 8-65388
- storm motion in three dimensions, detection by conventional weather radar 8-57360
- stratosphere, laser spectroscopy relevant to photochem. 8-88951
- stratosphere trace gases, meas. via positive ions comp. meas. 8-88877
- sulphate aerosol, individual submicron particles detect. technique 8-69527
- temperature, five-day average low and high temp. anomalies forecasting procedure 8-92938
- temperature determination by remote sounding, aerosol attenuation effects on accuracy (*Russian*) 8-81430
- thermal neutron activation analysis, appl. to Ankara aerosol trace elements and size distribs. 8-81377
- thermal remote sounding, temp. effect on 15 μm region transmission function 8-77327
- trace gases vertical conc. from solar radiation absorpt. spectra (*Russian*) 8-69442
- upper atmosphere, statistical modelling from Geminid meteor shower radar obs. 8-61816
- urban plume particulates collected on Anderson 8-stage impactor stages, chemical anal. 8-69433
- VHF technique for space-time mapping of lightning discharge processes 8-85721
- water vapour profile, meas. from atmosphere brightness temps. in H₂O 1.35 cm resonance region (*Russian*) 8-81403
- wave component identification on airglow charts, multiple-point method 8-73526
- weak absorption lines, detect. by Nd:glass and dye laser system 8-89561
- weather modification programmes, meteorological satellites appls. 8-96259
- weather-forecasting, statistical model 8-92941
- whistler mode signals direction finding, initial results from tracking receiver system 8-77429
- whistlers, automatic observation 8-89014
- X-ray aurorae prod. by energetic electrons precip., imaging from Space-lab 8-61608
- zonal atmospheric circulation model, numerical expts. (*Russian*) 8-81295
- HCl gas in ambient air, detection using coated piezoelec. quartz cryst. 8-92532
- H₂O vapour and cloud liquid determ. by dual freq. ground-based microwave radiometry 8-93007
- H₂S in air, preconc., determ. by flame photometric detection 8-92535
- NO, absorpt. characts. of γ -O band, rel. to atm. meas. 8-57316
- NO/NO₂/O₃ contents measurement, monitors intercalibration 8-69529
- O₃ profile, determ. from outgoing thermal radiation 8-92945
- O₃ total content, comparison of simultaneous IRIS, BUUV and ground based meas. 8-81291
- ²²²Rn continuous meas. for air-sea gas exchange field determ. 8-73534
- S pollution, meas. via compact X-ray fluoresc. analyser 8-68971
- SO₂, meas. in marine atmosphere at concs. lower than ppb 8-81340
- SO₄²⁻ aerosols, ambient, laser-Raman monitoring 8-69532
- atmospheric temperature**
see also *atmospheric thermodynamics*
- aerosols from Mount Agung eruption as test of global climatic perturbation 8-69440
- air pollution survey vehicle measurements (*Dutch*) 8-81365
- N America, late Pleistocene palaeoclimates inferred from speleothems stable isotope studies 8-57297
- American Southwest, evidence for cold, dry full-glacial climate 8-57296
- baroclinic boundary layer structure 8-81326
- Belgium, near-ground temps. rel. to air pollution increases 8-81374
- boundary layer, energy characts. of urban-rural surfaces in greater St. Louis area 8-61484
- boundary layer, friction vel. and temp. scale from temp. and wind vel. profiles 8-81268
- boundary layer, stably stratified, temp. vars. rel. to turbulence and internal waves spectra (*Russian*) 8-81297
- boundary layer, steady-state characts. of inversions capping well-mixed layer 8-61483
- boundary layer, temp. and humidity correl. above warm wet surface 8-85646
- boundary layer, wind shears and inversions (*German*) 8-81336
- boundary layer fluxes determ. over natural grassland, aerodynamic method 8-73480
- boundary layer near water surface, diurnal characts., equatorial region, GATE meas. 8-61527
- brightness temperatures in H₂O 1.35 cm reson. region, vars. (*Russian*) 8-81403
- climatic effects of sunspots and volcanic dust, statistical evidence from long-term temp. records 8-69439
- coastal zone, indicators of long-term var. of hydrometeorologic elements (*Russian*) 8-77258
- convective boundary layer, temperature-humidity covariance budget 8-73430
- daily maximum on mountain slope, time series anal. 8-73457
- dew point data, simultaneous eqns. soln. method for noise variance spectra estimation 8-57354
- Drake Passage, temp. changes rel. to Antarctic polar frontal zone variability during summer (1976-1977) 8-85579
- droplet growth and initial dew point temp. accuracy in cloud chamber on space shuttle 8-96268
- dry penetrative convection 8-92889
- equatorial topside ionosphere, ion temp. troughs and interhemispheric plasma transport 8-96340
- European air temperature change patterns 8-92957
- exospheric, models seasonal vars. at solar max. and low geomag. activity 8-57376
- F-region, electron heat cond. importance in energy balance 8-61649
- five-day average low and high temp. anomalies, forecasting procedure 8-92938

atmospheric temperature continued

forecasting, short-term via statistical model, method and accuracy 8-92941
 frost point meas. systematic error using Meteorological Office Mk3 hygrometer 8-73538
 global temperature distribution, rel. to Earth heat balance annual var. 8-73300
 ground layer, stratified, under coniferous forest canopy, temp. distrib. (*Russian*) 8-96266
 heating due to 9.6 μm O_3 band in inhomogeneous atm. 8-88918
 historic climate correl. with wheat prices and wages 8-81346
 hourly temperatures generation, stochastic model 8-61502
 intertropical convergence zone struct. over GATE area 8-57283
 ionosphere, analytic partial derivatives for incoherent scatter data least-squares fitting 8-73581
 ionosphere, props. meas. at Arecibo Observatory 8-81488
 ionosphere, temp. and electron density relaxation rel. to radiowave interaction nonstationary processes (*Russian*) 8-93028
 ionosphere heating by radio waves, predictions for Arecibo and satellite power station 8-77403
 ionosphere plasma, electron densities and temps. during major mag. storm 8-88987
 ionosphere turbulent polar cusp, temps. and low-energy particles and Kelvin-Helmholtz instability 8-96343
 land and sea surface temp. fields, seasonal vars., NOAA 5 satellite IR obs. 8-85676
 latitudinal variations, comparison with minimum entropy exchange models (*Russian*) 8-53716
 Limb Infrared Monitor of Stratosphere (LIMS) radiometer, design and performance, expt. goals 8-61601
 line thermal numerical model, initial conditions influence 8-92932
 local weather prediction, hydrodynamic methods 8-61521
 London storm, August 1975, urban heat island effects on precip. 8-81339
 magnetosphere low-energy plasma at synchronous orbit, temp. and density 8-77435
 mass consistent atmospheric flux model (MASCON) for complex terrain regions 8-92964
 mesopause, ion-neutral collision freqs. and mean temps., Arecibo radar meas. 8-88957
 mesopause, lidar meas. of Na conc. and neutral temp. 8-61613
 microclimatic effects on stellar obs. with photoelec. transit instrument (*Russian*) 8-73612
 monitoring by remote automatic station on radio link 8-85726
 monthly means over central England 8-73497
 northern hemisphere annual temperature approximation, simple method 8-81345
 Norway Station/Sanae (Antarctica), surface temp. and sea-level press. 8-81324
 ozoneosphere, temp. coupling effect on O_3 depletion prediction 8-57246
 power spectrum of temp. fluctuations, rel. to optical propag. 8-92980
 probability forecasts, nonexistence of ordinal relationships between measures of accuracy and value 8-61503
 profiles from Nimbus-6 soundings 8-53695
 radiative equilibrium temperatures in stratosphere and mesosphere, stellar occultation and BUUV O_3 data 8-81280
 remote sounding, temp. effect on 15 μm region transmission function 8-77327
 solar activity-weather relationship, study of temp. and rainfall at Oxford 8-85674
 spectral transfer of turbulent energy and temp. variance 8-61489
 stability category determ. for airborne radionuclide release assessment 8-73504
 stratosphere, annual and semi-annual waves obs. using Nimbus 5 selective chopper radiometer data 8-81315
 stratosphere, temp. profile vars. rel. to effect of water vapour changes on O_3 reduction 8-73444
 stratosphere, thermal struct. and trace constituents, effects of solar UV variability 8-61492
 stratosphere, ultralong temp. waves during 1973 austral winter 8-92901
 stratosphere temperatures, no correl. with seasonal var. of equatorial ionosphere radio waves absorpt. 8-85762
 stratospheric sudden warming, planetary-scale forcing of USA Jan. 77 weather 8-57279
 surface layer, accuracy of moments of vel., temp. and humidity vars. 8-92891
 surface layer temp. vars. at solar optical observatory testing sites in China (*Chinese*) 8-69680
 surface temperature changes nonlinear response in climate model, ice-albedo, lapse-rate and cloud-top feedbacks 8-69438
 temporal fluctuations, averaging for continents Europe and N.America 8-92958
 thermal effects of stratosphere O_3 depletion at 85°N latit., airborne particles influence 8-81279
 thermal plumes detect. by acoustic echo sounder 8-57259
 thermal pollution from fuel and energy consumption, effects on weather and climate 8-61539
 thermosphere, electric field momentum coupling characts. 8-88958
 thermosphere, electron temp. and density relationship in daytime at solar minimum, model 8-61638
 thermosphere, lower, gravity waves detect. by French incoherent scatter facility 8-81478
 thermosphere, model based on satellite drag data 8-69555
 thermosphere, tidal struct. at equinox, temp. and vel. fields predictions 8-81476
 thermosphere, transport processes in diurnal tide, satellite meas. 8-88959
 tropical indescendent cloud occurrence rel. to tropopause temp. 8-85675
 troposphere, solar radiation and temp. fluctuations rel. to stratospheric aerosol vars. 8-81327
 troposphere, temp. lapse rate rel. to refr. effects on satellite range meas. 8-73609
 troposphere, temp. meas. by radio-acoustic sounding methods 8-53728
 troposphere, temp. meas. rel. to climatological effects of particulate pollution 8-85678
 troposphere and lower stratosphere, cirrus clouds influence on IR cooling rate 8-73455

atmospheric temperature continued

troposphere thermal structure, acoustic sounding technique appl. to siting studies 8-81467
 Typhoon June (1975), temp. distrib. meas. by scanning microwave spectrometer 8-73436
 unusual weather frequency variability over last century 8-73479
 variance spectrum in inertial and dissipation range of isotropic turbulence 8-61490
 vertical sounder radiances rel. to midlatit. 300 mb flow patterns 8-92983
 vertical temperature profiles, determ. by remote sounding, influence of aerosol attenuation (*Russian*) 8-81430
 winter heat island formation over Milan city (*Italian*) 8-53709
 winter season temperature outlooks by objective methods 8-85641
 winter temp. in central England, time series, running means appl. 8-65378
 zonally averaged climate model 8-81347
 $(\text{NH}_4)_2\text{SO}_4$ aerosol production under elevated temp. inversion in Cleveland Country, model 8-81397

atmospheric thermodynamics*see also atmospheric temperature*

aerosol-induced heating effects on convective boundary layer 8-69409
 air-water interface, energy transfers at high wind speeds, effect of spray 8-85574
 Arabian Sea, wind stress, sensible and latent heat fluxes, ISMEX-73 data 8-85627
 atmosphere, exchange stabilities principle (*French*) 8-88871
 auroral particle instantaneous energy deposition, determ. from optical emissions 8-81491
 baroclinic boundary layer structure 8-81326
 boundary layer, diabatic baroclinic, parametrisation for circulation modelling (*Russian*) 8-88882
 boundary layer, energy characts. of urban-rural surfaces in greater St. Louis area 8-61484
 boundary layer, heterogeneous surface of large aerodynamic roughness, transfer characts. 8-73487
 boundary layer, steady-state characts. of inversions capping well-mixed layer 8-61483
 boundary layer, three-dimens. model rel. to expt. data 8-73428
 Bowen's ratio determ. in equatorial Atlantic region 8-81330
 climatic models, stability and extremal props. (*Russian*) 8-53716
 convecting columns interaction over linear heat sources, wind effect (*Russian*) 8-55637
 convection parametrisation, conditional instability of second kind hypothesis appl. 8-61530
 convective boundary layer, temperature-humidity covariance budget 8-73430
 cumulus convection initiation mechanisms and development 8-69410
 dry penetrative convection 8-92889
 Earth encounter with interstellar cloud, effects on terrestrial heat budget 8-57292
 evaporating downdraught model comparison with obs. behind squall lines 8-92913
 global heat balance, annual var. 8-73300
 ionosphere, midlatitude, dynamical model for 100-1000 km altitude range 8-53768
 Italy, vorticity generation and energy budget, 1961-65 period 8-81350
 Kelvin-Helmholtz billows, finite amplitude, evolution and energy budget 8-81293
 kinetic energy maintenance in tropical disturbances over E.Atlantic, GATE data 8-77307
 magnetosphere, significance of plasma flow pulsations in mag. tail 8-77436
 W.Mediterranean, energy budget (*Spanish*) 8-88846
 mesoscale downdraughts, assoc. with cool ocean surface waters, GATE results 8-69365
 moist air behaviour 8-85673
 nuclear power station spray cooling, heat and mass atmospheric transfer 8-94078
 ocean-atmosphere interaction parametrisation for storm conditions, atm. circulation models appl. (*Russian*) 8-65359
 ocean/atmosphere ranked interaction on sub-semidiurnal time scales (*Russian*) 8-77260
 planetary standing waves in northern hemisphere in July, model 8-61487
 point explosion in arbitrary atmosphere with radiative heat transfer 8-53708
 river to atmosphere heat and mass transfer data 8-96253
 river/atmosphere time dependent, single dimensional heat exchange, analysis (*Bulgarian*) 8-57221
 sea-atmosphere heat-transfer expts. (*Russian*) 8-81206
 snow cover energy budget, energy flux meas. 8-92859
 spectral transfer of turbulent energy and temp. variance 8-61489
 storms, principal component anal., hail index (*French*) 8-96267
 stratosphere O_3 depletion thermal effects at 85°N latit., radiative-convective model 8-81279
 stratosphere photochemical-radiative damping and instability, numerical results 8-81286
 stratosphere-mesosphere, O_3 densities rel. to radiative equilb. temps. 8-81280
 Sun-weather relation, energetics study 8-81285
 temperature variance spectrum in inertial and dissipation range of isotropic turbulence 8-61490
 temperature wave generator for diurnal temp. wave propag. simulation 8-85735
 thermal mixing layer development over water and heated land, lab. simulation 8-73449
 thermal pollution from fuel and energy consumption, effects on weather and climate 8-61539
 thermosphere, effect of auroral energy input on neutral and ion drifts 8-65446
 thermosphere, lower, gravity waves detect. and vertical energy flux 8-81478
 thermosphere, vertical energy flux from medium scale gravity waves generated by jet stream 8-81479
 tides, generated by differential heating between land and sea 8-65374
 tropical coastal region, lower troposphere features during rainfall 8-81332
 troposphere, eddy transport of sensible heat and momentum, time spectral anal. 8-92899

atmospheric thermodynamics continued

- turbulence, two-layer quasi-geostrophic, baroclinic energy transport and conversion 8-81186
- turbulent boundary layer, penetrative convection regime, entrainment rate (*Russian*) 8-69401
- turbulent exchange coefficients for sensible heat and H₂O vapour under advection conditions 8-92907
- two-level primitive eqn. atm. model for climatic sensitivity expts. 8-81348
- upper atmosphere, field-aligned auroral currents energy input 8-96339
- urbanisation and pollutant effects on thermal struct. in various climatic regimes 8-61500
- vegetation-atmosphere interaction, simplified one-dimens. theory 8-61479
- zonally averaged climate model 8-81347

atmospheric turbulence

- air diffuse discharge, gasdynamic effects 8-81294
- aircraft response, math. modelling 8-81274
- amplitude scintillation meas. on mm. microwave links 8-85623
- attenuation and turbulence simulation in pulsed laser Doppler velocimeter system 8-73513
- baroclinic boundary layer structure 8-81326
- boundary layer, birefringence under wind speed gradient shear 8-69453
- boundary layer, dissipation effects on parallel shear instability near ground 8-69406
- boundary layer, dissipation modelling under forced convection conditions 8-92900
- boundary layer, eddy convection vel. 8-92894
- boundary layer, multi-component linear digital simulation 8-61513
- boundary layer, stably stratified, turbulence and internal waves spectra (*Russian*) 8-81297
- boundary layer, three-dimens. model rel. to expt. data 8-73428
- boundary layer, turbulent and radiative transport interaction in development of fog and low-level stratus 8-81313
- boundary layer, vertical currents induced by orography and turbulence 8-96278
- boundary layer, with Rossby number similarity, turbulent diffusion 8-92896
- boundary layer above ocean waves, scaling laws for optically relevant turbulent parameter C_2^2 8-85677
- boundary layer turbulence and air-sea interactions 8-92953
- boundary layer turbulent fluxes modelling in stable conditions 8-61482
- Bowen's ratio determ. in equatorial Atlantic region 8-81330
- clear-air-turbulence detection, IR radiometer passbands 8-96318
- cloud development in turbulent atm., drop spectrum evolution 8-81325
- clouds, turbulence rel. to drops stochastic coagulation kinetic eqn. 8-92944
- collimated laser beam propag., corner-cube reflector and plane mirror comparison in folded-path and direct transmission 8-85697
- diffusion parameters estimation, use of routine meteorological data 8-85649
- Doppler light detection and ranging systems for turbulence meas. 8-73554
- downslope severe windstorm and aircraft turbulence event induced by mountain wave 8-73431
- eddy diffusion, explicit scale-depend. coeffs. 8-67191
- eddy flux measurements over ocean, related transfer coeffs. 8-81265
- electro-optical system image evaluation, subjective effects of electronic and turbulent noise 8-65023
- electrostatic turbulence, spectral energies 8-77433
- energy dissipation, statistical props. 8-81267
- exchange coefficients for sensible heat and H₂O vapour under advection conditions 8-92907
- F-region, equatorial turbulence spectrum rel. to HF and VHF spread-F echoes 8-85764
- finite optical beam in extremely strong turbulence, variance, covariance of irradiance 8-63008
- image reconstruction, turbulence-degraded, using nonredundant aperture arrays 8-93122
- image resolution through turbulence over ocean, optical transfer function 8-85695
- imaging through turbulent atm., spatial freq. resolution of rot. shearing interferometer 8-69450
- interference pattern fluctuation statistics in turbulent atmospheric layer 8-53727
- ionosphere high-latitude electrostatic turbulence, polarisation, freq. and wavelengths 8-88981
- ionosphere turbulent polar cusp, temps. and low-energy particles and Kelvin-Helmholtz instability 8-96343
- IR airborne astronomy, fluctuating sky emission meas. and interpretation 8-81552
- kinetic energy maintenance in tropical disturbances over E. Atlantic, GATE data 8-77307
- laser beam, phase compensated, propag. through atm. turbulence 8-83012
- laser beam intensity fluctuations in medium with Kolmogorov turbulence, distrib. function (*Russian*) 8-71034
- laser beam intensity fluctuations in turbulent atm. over water surface (*Russian*) 8-69449
- laser beam propag., monochromatic, problems 8-92988
- laser propagation, high-energy, simplified aberrated lens model 8-69454
- laser propagation in turbulent atm., detector nonlinearity effects on statistics of fluctuating signal 8-55301
- light beam coherence through optically dense turbid layer 8-55300
- light fields optimum processing, synthesis of algorithms 8-71047
- macroturbulence rel. to zonal circulation model, numerical expts. (*Russian*) 8-81295
- magnetosphere high-latitude electrostatic turbulence, polarisation, freq. and wavelengths 8-88981
- mass diffusion from point source in turbulent shear layer 8-92968
- mesometeorological stationary problem of flow around obstacle 8-81271
- momentum transfer during abrupt laminar-turbulent transition in boundary layer 8-65365
- multiple pulse detection in atmospheric turbulence 8-92974
- neutral wind profile following surface roughness change, calc. 8-73483

atmospheric turbulence continued

- optical goniometer accuracy effect of atm. turbulence 8-55461
 - optical heterodyne receivers in turbulent atm., signal current probability distrib., theory 8-78916
 - optical heterodyne receivers in turbulent atm., signal current probability distrib., expt. 8-78917
 - optical intensity fluctuations, frozen turbulence hypothesis expt. (*Russian*) 8-61557
 - optical signal discrete reception in turbulent atm. 8-73511
 - partially coherent radiation propag., extended Rayleigh-Sommerfeld integral method results 8-65386
 - phase distortion, modal compensation 8-69451
 - pollutants concentration equation, wind speed averaging 8-57307
 - pollutants dispersion, completely Lagrangian random-walk model 8-81380
 - pollution release into turbulent atm., exposure freq. distrib. from multiple cloud sources 8-57255
 - pollution transport, Monte Carlo simulation, radioactive particles appl. 8-61550
 - radar propag. through turbulence, scintillation detection using monopulse techniques 8-85717
 - radiowave propag. through turbulent atmosphere, phase difference and derivative fluctuations 8-92951
 - scattering of partially coherent radiation by surface, atm. turbulence influence 8-58915
 - scintillation, conditional fading statistics 8-66757
 - seeing for astronomical telescope, wavelength depend., atm. inhomogeneity effects 8-92979
 - shearing layers, growth, limiting thickness, dominant eddy scale 8-92955
 - speckle propagation through turbulence 8-66758
 - spectral inequalities in two-dimens. turbulence (*Russian*) 8-69403
 - spectral transfer of turbulent energy and temp. variance 8-61489
 - stratified surface layer, turbulence and diffusion, basic Lagrange characts. 8-81270
 - surface layer, structural turbulence coeff. depend. on height (*Russian*) 8-69400
 - temperature fluctuations, modified spectrum rel. to optical propag. 8-92980
 - temperature variance spectrum in inertial and dissipation range of isotropic turbulence 8-61490
 - thermosphere, lower, thin shear turbulent layers induced by tides and gravity waves non-linear interaction 8-65444
 - thermosphere, macroturbulent scales estimation around 100 km altitude 8-61635
 - troposphere, momentum flux maintenance by transient eddies 8-73435
 - troposphere, VHF radar signals turbulence scatt. from clear atmosphere 8-81278
 - turbulence, book 8-90839
 - turbulent boundary layer, penetrative convection regime, entrainment rate (*Russian*) 8-69401
 - turbulent interface layers, theory 8-71323
 - twinkling of stars 8-53726
 - two and three dimensional turbulent flow, vorticity anal. rel. to numerical weather prediction 8-69395
 - two-dimensional turbulence on the surface of a sphere 8-73447
 - two-layer quasi-geostrophic turbulence, simple special case 8-81186
 - unstable surface layer, horizontal vel. spectra 8-73427
 - upper atmosphere, irregular motions from radiometric meas. (*Russian*) 8-96333
 - whirlwind, ring-shaped, onset caused by rising air in stratified atmosphere (*Russian*) 8-77298
 - wind obs. in clear air using FM-CW Doppler radar 8-57271
 - wind velocity gust factors, analytical approach 8-88897
- atmospheric wind** *see* **wind**
- atmospherics**
- see also* **atmospheric electromagnetic wave propagation**; **whistlers**
 - chorus generation by energetic electrons during substorms, theory 8-96356
 - discrete VLF line radiation within transmitter-induced amplification bands, satellite obs. 8-96360
 - HF band, statistical characts. of signal and atmospheric noise mixture 8-57276
 - magnetosphere natural emissions, Geos I identification 8-53774
 - UHF emissions from lightning discharge considered as plasma 8-61497
 - VLF hiss emissions, simultaneous obs. at Brorfelde, Chambon-la-Forêt and Moshiri 8-81509
 - VLF hiss propag. characts. obs. at low latit. ground stations 8-69561
 - VLF quasiperiodic emissions interaction with micropulsations, model 8-61682
 - VLF sferics from Union City, Oklahoma tornadic storm 8-85639
- atom-atom collisions**
- alkali metal atom+inert gas atom, hyperfine transition spectral line shift, quantum corrections 8-82655
 - atom+metastable atom collisions, ionis. processes 8-62907
 - atomic to molecular ion conversion, rate constant calc. 8-64835
 - conference, electronic and atomic collisions, Paris (July 1977) 8-58758
 - diatomic molecules, variable screening model 8-74587
 - electronic state transitions, two-level collision system calcs. 8-62893
 - excitation transfer in slow collisions between identical particles (*Russian*) 8-78799
 - gas laser, atomic constants and collision cross sections determ. by level crossing 8-50763
 - inelastic, Penning and assoc. ionisation, complex. pot. and electron spectrum 8-94310
 - inert gas, metastable atoms, scatt. 8-62906
 - inert gas metastable state collisions, intermediate energies 8-62904
 - inert gases, collision induced polarisabilities, perturbation treatment 8-86778
 - ion pair forming collisions, dynamics 8-66661
 - ion-ion collisions, crossed beam expts. 8-58843
 - ionisation collisions, improved impulse approx. 8-74754
 - laser radiation field effects, ang. momentum anal., quantum mech. theory 8-74733
 - long range interaction, polarisation of emitted light 8-62902
 - nonadiabatic collisions, Franck-Condon approach for electronic state quenching 8-66640

atom-atom collisions continued

nuclear motion, quantum-mech. and classical treatment, book contrib. 8-74736
 one-atom detection in individual ionisation tracks, heavy ion stopping in buffer gas 8-70802
 optical excitation to state of quasibound motion (*Russian*) 8-58784
 optically pumped vapour, transverse relaxation (*Polish*) 8-55229
 outershell excitation, diabatic mol. orbitals 8-62901
 radiative collision-induced photoionisation 8-62858
 Rydberg atom+atom collision, depopulation, ionisation 8-62908
 spectral line broadening theory, use of multipole expansions 8-74611
 stimulated collision-induced fluoresc. 8-86811
 stripping cross sections, binary encounter approx. theory 8-50618
 two-photon absorpt., collisionally perturbed, reson. profile and strengths, degeneracy and Doppler shift 8-55156
 Ar, $3p^5 5p$ config. aligned in discharge, interf. signals, lifetimes and collision cross sections 8-70796
 Ar, collisional depolarisation of selectively excited 2p levels (*French*) 8-86830
 Ar+Ar, K-X-ray excitation, 2.5-8 MeV, impact parameter depend. 8-50628
 Ar+Ar(3P_2)(3P_0), flowing afterglow metastable decay rates, diffusion, two- and three-body rate consts. 8-73027
 Ar+He* Penning ionisation, semiclassical descretisation procedure 8-90275
 Ar+Kr(3P_2), flowing afterglow metastable decay rates, diffusion, two- and three-body rate consts. 8-73027
 Ar+Xe, lightly doped, Xe $5d(3/2)_1$ photoexcited state radiative decay and energy transfer 8-74605
 Ar+Xe, relaxation processes of Xe*(3P_2) metastable atoms 8-50624
 Ar+Xe(3P_2), flowing afterglow metastable decay rates, diffusion, two- and three-body rate consts. 8-73027
 Ar+Xe(F_2), proton excited mixtures, energy transfer processes 8-66647
 B+He (methane), B atom K-shell binding energy by Auger spectra 8-50525
 Be+He (methane), Be atom K-shell binding energy by Auger spectra 8-50525
 C+He (methane), C atom K-shell binding energy by Auger spectra 8-50525
 Cd, 6^3P_1 level, relax. of alignment and population 8-70795
 Cs+Ar, two-photon ionisation spectra, satellites, absorption line shape 8-82668
 Cs+Ar(Kr)(Xe), spectral line breadth and shift, Van der Waals pot. calc. 8-90126
 Cs+Xe (neopentane), Cs line shape broadening, satellite data inversion, interaction pot. 8-74608
 Cs(n^2D_1)+Cs($6^3S_{1/2}$) collisions, inelastic cross sections 8-74753
 Cs(nP)+Cs($6S$), assoc. ionisation, threshold energy, Cs_2^+ dissociation energy 8-58804
 D+M→D⁺+M⁺ (M=alkali metal atom), ion-pair form. 8-58779
 Eu*+Sr+h ν →Eu+Sr*, photon assisted collisional energy transfer 8-90285
 F+Xe, enhanced quenching in intense KrF laser light, computer modelling 8-55232
 F+Xe(H⁺)(H₂), ($^2P_{3/2}$) state quenching, Franck-Condon approach 8-66640
 Fe+H in solar atmosphere, Fe I lines press. shifts rel. to limb shift 8-89150
 H(D)+Cs, 40 keV, prod. of polarised H⁺ or D⁺ ions, low emittance 8-55078
 H+H, atom-atom pots., Hilbert Schmidt expansion, transition operators 8-66621
 H+Li(Li₂), superthermal collisions, photon and positive ion prod. 8-78788
 H+N, stripping cross-sections, binary encounter approx. theory 8-50618
 H⁺+He⁺, charge transfer and ionis. cross sections, coincidence meas. 8-50634
 He in transient plasma, excitation transfer between excited states 8-70914
 He+Ar(Kr), translation band spectral moments, induced dipole moments 8-55218
 He+H, stripping cross-section, 0.3 to 3 keV 8-78807
 He+H₂(He)(Ar)(N₂), fast metastable at. collisional destruction cross section 8-74760
 He+He, metastable atoms, collisional ionisation cross-sections 8-70911
 He+Hg, metastable He, collision rate consts. in pulsed discharge after-flow 8-50627
 He+Ne pot., differential cross section, quantum mechanical inversion 8-70896
 He⁺+He(Ne), model pot. for low energy scatt. 8-66642
 He⁺+Pb, at. beam and surface interaction, scatt. ion yield oscills. 8-55221
 He⁺+H(H₂)(Ar), metastable state, ionis. processes 8-62907
 He(2^3S) collisions, elastic scatt., Penning ionisation, polarisations (*Russian*) 8-70922
 Hg+He, laser excitation of Hg $6s6d^3D_1$ level, transition probabilities and collisional excitation transfer 8-55146
 Hg+He(Xe), collisionally induced coherence, orientation and alignment, transfer among $6s6d$ levels 8-74747
 Hg+Hg, depolarising collisions in positive column of discharge 8-83639
 Hg+Ti, Ti sensitised fluorescence 8-70778
 Hg(6^3P_0)+Hg(6^3P_1)→Hg₂⁺+e, plasma formation by strong Hg line irr., mechanism 8-83585
 Hg($6^3P_{2,0}$)+inert gas, diffusion in low-current discharge 8-63618
 K+H, covalent and ionic states interaction, config. mixing 8-50613
 K+He, 93 eV, excitation of K atom, photon-scatt.-atom coincidence study 8-82829
 K+Hg, electronic excitation, integral cross-section, 50-1500 eV 8-62888
 K+K(Na), excitation in slow collisions 8-70918
 K(4^2P)+He(Ne)(Ar)(Kr)(Xe), collisional excitation, differential cross-sections 8-66643
 Kr+Xe, excitation transferred populations, absorpt. profile analysis 8-74748
 Kr*+He(Ar), vel. changing collisions studied by saturated absorpt. 8-62892
 Li+He, direct excitation of Li I (nl) levels in keV collisions 8-90280

atom-atom collisions continued

$^6Li^+ + ^7Li^+$, laser-induced Penning and associative ionis., $^{13}Li_2^+$ enrichment 8-58796
 Na, energy transfer with 3P-excited atoms, fluoresc. spectrum 8-66498
 Na, f-states collisional ang. momentum mixing by inert gas 8-58780
 Na, resonant collisions in laser beam 8-78782
 Na+H, covalent and ionic states interaction, config. mixing 8-50613
 Na+inert gas, $4D_{3/2}$ and $4D_{5/2}$ levels relax. 8-50526
 Na+Kr(Xe), excimer bands, multiperturber interactions 8-66497
 Na+Kr(Xe), reson. line broadening, press. depend. 8-66596
 Na+Ne, Na($3s \rightarrow 3p$) excitation, impact parameter depend. 8-58794
 Na($P_{1/2}$)+Ar→Na($P_{3/2}$)+Ar, angular scatt. distrib., Doppler spectrosc. obs. 8-94309
 Na($^2P_{3/2}$)+Hg, differential scatt. cross sections 8-66644
 Na($^2P_{3/2}$)+Hg, laser excited atoms, differential cross sections 8-62905
 Ne 6328 \AA laser transition, homogeneous saturation due to collisions, weak collision model 8-78995
 Ne, thermalisation of level populations 8-66649
 Ne+Ar(Kr), translation band spectral moments, induced dipole moments 8-55218
 Ne+Ne, excitation transfer, coupling coeffs., temp. depend., fluoresc. meas. 8-58620
 Ne+Ne collisions, simultaneous emission of two photons 8-70917
 Ne+Ne(He), $7d'$ states, isotope shift, press. shift, press. broadening, two-photon spectra obs. 8-55155
 Ne+Ne(Ne*)(Ne $^{2+}$), $2s$ vacancy prod. 8-50623
 Ne*+Ne, close coupling calc. 8-66652
 O (1D), collisional quenching by inert gas atoms 8-66648
 O+O→O₂, chemiluminesc. matrix reaction, diffusion controlled, 8-20K 8-61013
 Rb+Ar(Kr)(Xe), spectral line breadth and shift, Van der Waals pot. calc. 8-90126
 S+inert gas (N₂)(H₂), rare gas sulphide S(1S) emissions 8-82828
 S+S→S₂, chemiluminesc. matrix reaction, diffusion controlled, 8-20K 8-61013
 Se($^2P_{1/2}$)+inert gas, gas phase flash photolytic deexcitation obs., 1000K (*Russian*) 8-50626
 Sr, associative ionisation of laser-excited Rydberg states, mass spectrometry obs. 8-94303
 Te($^2P_{1/2}$)+inert gas, gas phase flash photolytic deexcitation obs., 1000K (*Russian*) 8-50626
 Xe+Bi, Bi K α X-ray lines, Doppler broadening 8-62759
 Xe+F, collision in laser field, ang. momentum anal., quantum mech. theory 8-74733
 Xe+He, saturated absorpt. of $3.51 \mu\text{m}$ line, vel. changing collisions by line width 8-86819

atom-ion collisions

see also charge exchange

alkali ion+alkali atom, differential scatt. meas. 8-62903
 atom+H⁺, innershell ionisation 8-62930
 atom+ion collisions, electron capture, quasi-molecular binding corrections 8-90287
 atom+light ion, dipole transitions in K-shell ionisation 8-90281
 atom+multiply charged ion, charge exchange 8-58813
 atoms and highly charged ions, charge exchange 8-62913
 bare ion+hydrogenic ion, forward electron capture, third Born approx. calcs. 8-58782
 conference, electronic and atomic collisions, Paris (July 1977) 8-58758
 Coulomb ionisation of inner shell electrons, screening effects 8-74749
 Coulombic ionisation of inner shells 8-62898
 diabatic molecular orbitals for inner-shell excitation 8-62897
 diatomic molecules, variable screening model 8-74587
 electron capture processes in ion-atom collisions, review 8-70930
 excitation in energetic ion-atom collisions accompanied by electron emission, book contrib. 8-74756
 F ions recoiling in gases, hyperfine interactions 8-74735
 fast heavy ion+atom, and solid targets, ionis. and excitation states 8-70927
 H⁺+Mg collisions double electron capture 8-58777
 halogens, surface ionisation, on LaB₆, using ion source 8-60538
 heavy ion+atom, $1s\sigma$ MO excitation probability and binding energy, X-ray coincidence 8-94316
 heavy ion+atom, radiative electron capture, target thickness depend. 8-58778
 heavy ion collisions, $3d\sigma$ mol. orbital ionisation 8-94311
 high-Z atom+H(He)(O)(F)(Cl) ions, $1s\sigma$ vacancy prod., relativistic and Coulomb deflection effects 8-58801
 highly charged atom+ion, slow collisions, one-electron capture 8-58776
 highly ionised ion+atom (molecule), many-electron transitions in violent encounter 8-90274
 inert gas, field ionis. and proton capture, critical energy deficits 8-82853
 inert gas ions, X*($^2P_{1/2}$), conversion into dimer ions 8-70903
 inner shell vacancy formation 8-70926
 ion+ion, Coulomb-Born and unitarised Coulomb-Born cross-sections 8-82815
 ion excited state lifetimes meas. using orientation transfer in Penning collisions (*French*) 8-50621
 ion-metal atom processes, charge exchange cross sections, calcs. and computer program 8-55236
 ionisation, post collision interactions in at. excitation processes 8-58803
 K-shell atomic ionisation by heavy particle, electronic relativistic effects, Dirac wavefunctions, semiclassical effects 8-78792
 K-shell ionis., X-ray prod. cross section for incident H⁺, ^4He and ^{14}N ions 8-70923
 K-shell ionisation probability by protons, $E_p=100 \text{ keV}$ -2 MeV, impact parameter depend. (*Japanese*) 8-86945
 K-shell ionization in heavy-ion collisions, book contrib. 8-82834
 M-subshell ionisation cross section, by H⁺ impact, binary encounter approx. 8-62890
 molecular beam or atomic beam as target for ion-atom collision studies 8-70971
 multiply charged collision systems, slightly asymm., curve crossings, constraints. MO theory 8-74734
 nuclear motion, quantum-mech. and classical treatment, book contrib. 8-74736

atom-ion collisions continued

- one electron charge transfer and capture, partial and total cross sections 8-70931
 perturbed stationary state, improved approach 8-90282
 radiative charge exchange, high energy 8-55234
 radiative collision-induced photoionisation 8-62858
 Rydberg atom+ion, collision theory 8-62909
 structure and collisions of ions and atoms, book 8-74554
 superheavy, positron form. 8-62873
 two k-shell vacancy systems, one-electron and two-electron one-photon transitions 8-58775
 x-ray production in heavy ion-atom collisions, book contrib. 8-74757
 $A^+ + 2A \rightarrow A_2^+ + A$, gas phase reaction rate const. calc. 8-92457
 Ag, K-shell ionis., X-ray prod. cross section for incident H^+ , 4He and ^{15}N ions 8-70923
 Ag+Ag symmetric collisions, MO-2p σ radiation anisotropy, quasimolecular nature 8-70924
 Ag+ H^+ , K-shell ionisation, 7-15 MeV, relativistic effects 8-82830
 Ag+ H^+ , L-shell ionisation at large scatt. angles 8-90283
 Ag+ H^+ , X-ray emission, optical transition radn. 8-58618
 Ag+ I^+ , impact parameter depend. of K X-rays 8-94308
 Al, ion beam bombardment, $(1s^{-1}2p^{-1})^1P_1$ state nonstatistical population, X-ray spectrum 8-62894
 Al+Al, (Cl)(F), molecular K X-ray transitions, mol. radiative electron capture effect 8-58802
 Al+H(D)(He)(Li) ions, K-shell ionis., universal cross sections 8-62895
 Al+ He^+ , X-ray spectra, two-electron one-photon transition in solid target, 2 MeV 8-94209
 Ar+ H^+ , collisional electron detachment, complete ang. distrib. 8-66650
 Au+ H^+ , K-shell ionisation, 7-15 MeV, relativistic effects 8-82830
 Au+X, X=H, H₂, He, C, N, O, cross-section, closure-Born approx. 8-66630
 B, K-shell ionis., double and single, cross section meas. by ion bombardment 8-50629
 B, X-ray spectra, chemical bonding and multiple ionis. effects 8-50630
 Be, K-shell ionis., double and single, cross section meas. by ion bombardment 8-50629
 Be, X-ray spectra, chemical bonding and multiple ionis. effects 8-50630
 Br+Br, symmetric collisions, MO-2p σ radiation anisotropy, quasimolecular nature 8-70924
 C+ H^+ (He⁺), K-shell ionisation, impact parameter depend. 8-62891
 C³⁺+Ar, continuum electron capture, projectile vel. and Z depend. 8-55222
 C³⁺+H(H₂), q=1-4, single electron capture cross sections 8-55233
 Ca, X-ray production by protons by 0.5 to 2.0 MeV energy 8-66646
 Cl ions+Ar-methane, (isobutane), energy straggling 8-58785
 Cl Al, molecular K X-ray transitions, mol. radiative electron capture effect 8-58802
 Co, X-ray spectra, chemical bonding and multiple ionis. effects 8-50630
 Cr, X-ray production by protons by 0.5 to 2.0 MeV energy 8-66646
 Cr, X-ray spectra, chemical bonding and multiple ionis. effects 8-50630
 Cs⁺+X, X=H, H₂, He, C, N, O, cross-section, closure-Born approx. 8-66630
 Cu, K-shell ionis., X-ray prod. cross section for incident H^+ , 4He and ^{15}N ions 8-70923
 Cu, large angle K-shell ionisation probabilities, projectile charge and mass depend. 8-74750
 Cu+Cl¹⁸, X-ray cross sections, projectile fluoresc. yields 8-74751
 Cu+ H^+ , X-ray emission, optical transition radn. 8-58618
 D₃⁺+inert gas, ion decay, 1-40 eV (Russian) 8-90286
 F-Al, molecular K X-ray transitions, mol. radiative electron capture effect 8-58802
 F+Xe(H⁺)(H₂), (²P_{3/2}) state quenching, Franck-Condon approach 8-66640
 Fe, X-ray production by protons by 0.5 to 2.0 MeV energy 8-66646
 Fe, X-ray spectra, chemical bonding and multiple ionis. effects 8-50630
 Fe+Fe, symmetric collisions, MO-2p σ radiation anisotropy, quasimolecular nature 8-70924
 Gd+ H^+ , K-shell ionisation, 7-15 MeV, relativistic effects 8-82830
 Ge+Ge, symmetric collisions, MO-2p σ radiation anisotropy, quasimolecular nature 8-70924
 H⁺, calc. of mobility in He, 10 to 700K 8-66629
 H+ H^+ , excitation ang. differential cross section, 25, 50 and 100 keV incident 8-66651
 H+ H^+ , resonant charge exchange in planetary coronas rel. to spectral line profiles 8-77508
 H+heavy charged ion, total electron capture cross section charge depend. oscill. behaviour 8-66656
 H+heavy ion (highly stripped), electron loss, charge state depend. 8-70921
 H⁺+H(He), electron detachment cross sections 8-90265
 H⁺+He(Ar), electron detachment cross sections 8-58810
 H⁺+atom, electron capture, two-state atomic expansion 8-62912
 H⁺+C(N)(O)(Ne)(Ar), electron capture cross sections 8-62912
 H⁺+Cs(6s), elastic scatt., pot. determ. from differential cross-sections meas. 8-78778
 H⁺+H, charge transfer cross section calc., up to 100 keV 8-55235
 H⁺+H(1s), radiative charge exchange, 1-50 MeV 8-55234
 H⁺+He, excitation, ang. differential cross-sections for 25, 50 and 100 keV protons 8-82832
 H⁺+He(Ar) electron transfer cross sections 8-58809
 H⁺+multielectron atom, fast collision, electron capture, differential cross section calcs. 8-94318
 H⁺+Na(K), excited state form. by inelastic processes, energy partitioning 8-82833
 H⁺+Na(Mg)(Al)(Si)(Ti), K-shell ionisation cross sections for 15-65 keV protons 8-90284
 H(1s)+p→p+H(1s), 15-200 keV, ang. distrib., differential cross sections calc. 8-82839
 He+ H^+ , determ. of He excited state populations by two-photon reson. ionisation spectroscopy 8-82707
 He+ H^+ (H₂⁺)(H₃⁺)(He⁺) collisions, polarisation degree of prominent He lines 8-70916
 He+He⁺, excitation cross-section calcs. 8-90273

atom-ion collisions continued

- He+He⁺, resonant charge transfer cross sections, 2 to 100 eV 8-66655
 He+N₂⁺, (A²Π_g) Meinel band deactivation cross sections above thermal energies 8-66635
 He⁺+alkali metal atom, ionisation cross sections, binary encounter approx. with HF electron vel. distrib. 8-55225
 He⁺+H, unpolarised and spin-change collision, low energy 8-86943
 He⁺+He, 2P level, direct and charge-exchange excitation, 150-1000 keV 8-70913
 He⁺+He 35 keV collisions, He I 1s3d levels, cascade-free lifetime meas. 8-58607
 He⁺+Mg(Zn), inelastic collisions, 2-800 eV, excited state form. 8-94312
 He⁺+Na(K), excited state form. by inelastic processes, energy partitioning 8-82833
 He⁺+Na(K)(Cs), 5-100 keV, electron capture form. of fast metastable He 8-74760
 He⁺+Pb, at. beam and surface interaction, scatt. ion yield oscills. 8-55221
 He²⁺+He, He⁺ form. in various electron states (Russian) 8-58815
 He²⁺+He(Ne), electron capture collisions, spin conservation 8-82837
 He₂⁺+Mg(Zn), inelastic collisions, 2-800 eV, excited state form. 8-94312
 Hg+He⁺, autoionisation, 5-20 eV, electron and ion ang. distrib. 8-78795
 Hg(6³P₁)+Li⁺(Na⁺)(K⁺), excitation, optical polarisation fractions and mag. sublevels obs. 8-50619
 Kr²⁴⁺+Ge, K X-ray prod., impact parameter depend. 8-58800
 Li+inert gas collisions, electron loss cross-section meas. (French) 8-86941
 Li⁺+X, X=H, H₂, He, C, N, O, cross-section, closure-Born approx. 8-66630
 Mg+H<sup>+(He⁺), inner-shell ionisation, target atom ionic alignment, Born approx. 8-78789
 Mg+H<sup>+(He⁺) and electron impact ionis., Auger study of collisionally induced alignment 8-90279
 Mn, X-ray spectra, chemical bonding and multiple ionis. effects 8-50630
 N⁸⁺+H(H₂), q=1-5, single electron capture cross sections 8-55233
 N₂⁺+H⁺, fluoresc. efficiency, 3914 Å band of N₂⁺ (1N), 100 eV-10 MeV 8-74697
 Nb+Kr, excitation of 1s σ and 2p σ quasimolecular radiation 8-78801
 Nb+Nb symmetric collisions, MO-2p σ radiation anisotropy, quasimolecular nature 8-70924
 Ne, one-electron and two-electron one-photon transitions 8-58775
 Ne+Ar¹²⁺(Xe²⁴⁺)(Pb⁴⁰⁺), X-ray transitions 8-66641
 Ne+Ne(Ne⁺)(Ne²⁺), 2s vacancy prod. 8-50623
 Ne⁺+Kr, low vel. collision, enhanced K-L vacancy sharing ratios, X-ray prod. cross section 8-78790
 Ni+H(D)(He)(Li)(C)(O)(F) ions, K-shell ionis., universal cross sections 8-62895
 O, K-shell ionis., double and single, cross section meas. by ion bombardment 8-50629
 O³⁺+Ar, continuum electron capture, projectile vel. and Z depend. 8-55222
 O³⁺+H(H₂), q=1-5, single electron capture cross sections 8-55233
¹⁶O³⁺+Al, energy-loss straggling, charge exchange effects 8-58799
 Pb+H⁺, K-shell ionisation, 7-15 MeV, relativistic effects 8-82830
 Pb⁺+Z (42≤Z≤92), 1s σ MO excitation probability and binding energy, X-ray coincidence 8-94316
 S⁺+Ar, double K-vacancy prod., X-ray X-ray coincidence and fluoresc. yields obs. 8-55230
 S³⁺+Ar, molecular K-X-ray production, projectile charge depend. 8-90188
 Se, X-ray production by protons by 0.5 to 2.0 MeV energy 8-66646
 Si, K-shell ionis., X-ray prod. cross section for incident H^+ , 4He and ^{15}N ions 8-70923
 Si+He⁺, X-ray spectra, two-electron one-photon transition in solid target, 2 MeV 8-94209
 Si³⁺+He, q=2-11, K-shell fluoresc. yields, charge-state depend. 8-55231
 Ta+ H^+ , K-shell ionisation, 7-15 MeV, relativistic effects 8-82830
 Th+ H^+ , K-shell ionisation, 7-15 MeV, relativistic effects 8-82830
 Ti, X-ray production by protons by 0.5 to 2.0 MeV energy 8-66646
 Ti+S ion, KLⁿ X-ray satellites, intensity distrib., photoabsorpt. effects 8-78657
 U³⁶⁺+N(Ne)(Ar)(Kr), radiative charge exchange, 16, 64, 256 MeV/amu 8-55234
 V, X-ray production by protons by 0.5 to 2.0 MeV energy 8-66646
 W, N-shell ionisation by proton impact 8-78800
 Xe+ H^+ , M-subshell ionisation cross section, binary encounter approx. 8-62890
 Xe⁺+Ag, quasimolecular L and Ag L X-ray excitation thresholds, electron correl., calc. and expt. 8-78793
 Yb+ H^+ , K-shell ionisation, 7-15 MeV, relativistic effects 8-82830</sup></sup>

atom-molecule collisions

- see also atom-molecule reactions; molecular rotational-vibrational energy transfer
 alkali+molecule, apparatus for energy, angle and mass anal. of products 8-70970
 alkali atom+hexafluoride molecule, collisional ionisation 8-55226
 alkali atom+methane derivative, collisional ionisation, nitromethane, perfluoromethyl bromide (iodide) electron affinities 8-66639
 atom+diatom, body-fixed formulation for close-coupling calc. 8-78768
 atom+diatom, energy transfer, vibronic excitation, emission spectra 8-66578
 atom+diatom, scatt., l-conserving sudden approx. calcs. 8-66628
 atom+diatom collinear collision, refined Born approx. 8-74724
 classical trajectory calcs., empirical testing of nonrandom integration method 8-50607
 cyanoacetylene+He, collisional excitation of interstellar molecule 8-81664
 diatom+atom, rot. transitions, mols. in Π state 8-82825
 highly ionised ion+atom (molecule), many-electron transitions in violent encounter 8-90274
 inert gas ion+oxides, energy loss spectra 8-58798
 ion pair forming collisions, dynamics 8-66661
 methane+X⁺, (X=Ar,Kr,Xe,U), Auger emission line shape after dis-soc. 8-68638

atom-molecule collisions continued

- molecular basis sets as energy approaches excitation threshold 8-78783
- Morse oscillator+atom, collinear collision, T-V energy transfer, de-excitation process 8-90268
- Morse oscillator+atom, collinear collision, T-V energy transfer, excitation and dissociation processes 8-90269
- multiply charged collision systems, slightly asymm., curve crossings, constraints, MO theory 8-74734
- nonadiabatic collisions, Franck-Condon approach for electronic state quenching 8-66640
- one-electron atom+methane, collisional energy transfer by octupole coupling 8-62881
- reactive and charge transfer collisions, between ions and molecules 8-62914
- vibration-rotation transitions, optical potential approach 8-62885
- Ar+H₂O(D₂O), (³P_{0,2}) state quenching cross sections 8-70912
- Ar+HCl, rotationally inelastic collision, planar trajectory, classical centrifugal decoupling calcs. 8-58788
- Ar+methane, low energy collision, close coupling and coupled states, rot. transitions 8-78784
- Ar+N₂, (A³Σ_u⁺, ν=0,1) metastable state quenching rate coeffs. 8-90206
- Ar+N₂, collinear collision, vibr.-translation energy transfer, model calc. 8-66634
- Ar+N₂(TIF), scatt., l_z-conserving sudden approx. calcs. 8-66628
- Ar+TiO, collision cross-section meas. 8-55202
- Ar+TIF collisions, small angle scattering, calc. cross sections 8-70915
- Ar+Xe(F₂), proton excited mixtures, energy transfer processes 8-66647
- Ar⁺+I₂, ion-pair form. differential cross-section, 25-133 eV, metastable Ar 8-78787
- Ar⁺(³P)+CO₂(X¹Σ_g⁺), differential elastic and quenching cross-sections 8-58773
- B+He (methane), B atom K-shell binding energy by Auger spectra 8-50525
- BN, X-ray spectra, chemical bonding and multiple ionis. effects 8-50630
- Be+He (methane), Be atom K-shell binding energy by Auger spectra 8-50525
- BeO, X-ray spectra, chemical bonding and multiple ionis. effects 8-50630
- Br+CO₂(HCl), quenching of 4²P_{1/2} state, vib. excitation, temp. depend. 8-58792
- Br₂+Ar, ergodic deactivation, anharmonic effects on transfer rate 8-82818
- Br(4²P_{1/2})+N₂O, electronic-vibr. energy transfer obs. 8-55220
- C+He (methane), C atom K-shell binding energy by Auger spectra 8-50525
- C³⁺+H(H₂), q=1-4, single electron capture cross sections 8-55233
- CH₄+H⁺(He⁺)(O⁺), 1 MeV dissociation, kinetic energy spectra 8-94302
- CN(B²Σ)+N(C)(O) collisions, in CO-N₂-Ar mixtures, shock wave induced, cross section (*Russian*) 8-74638
- CO+He, collisional excitation of interstellar molecule 8-81664
- CO+Kr(³P₁), (¹P₁) A¹II-X¹Σ⁺ and b³Σ⁺-a³Π sensitised fluorescence, isotope effects 8-82761
- CO+X⁺, X=Ar,Kr,Xe,U, Auger emission line shape after dissociation 8-86838
- CO₂+Ar(N₂), 301_m-000 band, intensities, press.- and self-broadening coeffs. meas. 8-78695
- CO₂+X⁺, (X=Ar,Kr,Xe,U), Auger emission line shape after dissociation 8-86838
- Cl ions+Ar-methane, (isobutane), energy straggling 8-58785
- ClF+Ar, shock wave, vibr. relax., laser schlieren meas. 8-90267
- Cs+D₂O, ion-pair form., energy, angle and mass anal. of products 8-70970
- Cs+Xe (neopentane), Cs line shape broadening, satellite data inversion, interaction pot. 8-74608
- CsCl(Cs₂Cl₂)+Ar(Kr)(Xe), collision-induced ion-pair form., absolute cross sections 8-73029
- D₂+H⁺, differential inelastic and reactive scatt., low energies 8-62911
- D₃⁺+inert gas, ion decay, 1-40 eV (*Russian*) 8-90286
- F+Xe(H⁺)(H₂), (²P_{3/2}) state quenching, Franck-Condon approach 8-66640
- H+Br₂(Cl₂), nonreactive scatt., long range anisotropic pot. determ. 8-66626
- H+H₂, atom-atom pots., Hilbert Schmidt expansion, transition operators 8-66621
- H+H₂, elastic differential cross section high resolution meas. 8-50610
- H+H₂→H+H+H, two path dissociation 8-62875
- H+Li(Li₂), superthermal collisions, photon and positive ion prod. 8-78788
- H⁺+N₂ collision, binary encounter calcs. of proton energy deposition 8-74746
- H₂-⁴¹+He, 200-850 eV, attenuation and fragmentation 8-62968
- H₂+H⁺ differential inelastic and reactive scatt., low energies 8-62911
- H₂+inert gas, cross section meas. with state selected beams 8-62910
- HCl+Ar, rot. linewidth calcs., using different pots. 8-66602
- HCl+HCl(Ar), pure rot. Raman lines, press. broadening cross sections 8-74702
- H₂O+positive ion, inelastic scatt., 4-6 eV energy loss region 8-90277
- He+CO, nuclear mag. shielding coeffs., interaction geometry depend., chemical shift, gauge invariant method 8-62866
- He+H₂, collision dynamics, generalised Langevin eqn. approach 8-70900
- He+H₂, collision-induced dipole, ab initio VB calc. 8-94202
- He+H₂, final quantum state assignment, improved quasiclassical histogram method 8-66617
- He+H₂(D₂)(T₂), vibr.-rot. transitions, optical potential approach 8-62885
- He+H₂(He)(Ar)(N₂), fast metastable at. collisional destruction cross section 8-74760
- He+HCl(CO), energy sudden approx., beam scatt. meas. mol. anisotropy effects 8-78802
- He²⁺+H₂(O₂), electron capture collisions, spin conservation 8-82837
- He⁺+H(H₂)(Ar), metastable state, ionis. processes 8-62907
- Hg+N₂, inelastic collision, 6³D₁ population transfer to other 6s6d Hg levels, fluoresc. obs. 8-78791
- I(⁵2P_{1/2})+benzene-d₆(-d₈), fluoresc. quenching, spin-orbit interaction, isotope effect obs. 8-62763

atom-molecule collisions continued

- I(⁵2P_{1/2})+Br₂, deactivation kinetics, time-resolved spectrosc. obs. 8-95916
- I(⁵2P_{1/2})+HCl(HBr)(NO), electronic-vibrational energy transfer, fluoresc. obs. 8-66579
- K+halogenated methane, negative ion form., electron affinities, bond dissociation energies 8-82827
- Kr+CO₂, collision dynamics, generalised Langevin eqn. approach 8-70900
- Kr+CO₂(001), deactivation pathways, quantal close-coupling calcs. 8-58787
- Kr+H₂O(D₂O), (³P_{0,2}) state quenching cross sections 8-70912
- Li⁺+CO(CO₂)(N₂O), vibr. excitation, 70 to 1500 eV 8-82824
- N⁹⁺+H(H₂), q=1-5, single electron capture cross sections 8-55233
- N₂+Ar, total differential cross section, diff. oscils. quenching 8-66625
- N₂+H, stripping cross-section, 0.3 to 3 keV 8-78807
- N₂+N⁺, molecular-orbital X-rays, recoil effects 8-66645
- N₂+X⁺, (X=Ar,Kr,Xe,U), Auger emission line shape after dissociation 8-86838
- NH₃+He(Ar), ammonia inversion spectrum press. broadening 8-86915
- NH₃+Hg, photosensitisation, NH₃ fluoresc. 8-90198
- NH₃+X⁺, (X=Ar,Kr,Xe,U), Auger emission line shape after dissociation 8-86838
- N₂(X¹Σ_g⁺)+Ar(³P_{2,0})→Ar(¹S)+N₂(C¹Π_u), sensitised fluoresc., vel. depend. 8-90204
- Ne+inert gas, cross section meas. with state selected beams 8-62910
- O¹⁰⁺+H(H₂), q=1-5, single electron capture cross sections 8-55233
- O₂+X⁺, (X=Ar,Kr,Xe,U), Auger emission line shape after dissociation 8-86838
- O₂(¹Δ_g)+I(³P_{3/2}), possible electronic transition chem. laser 8-63116
- S+inert gas (N₂)(H₂), rare gas sulphide S(S) emissions 8-82828
- Xe, high Rydberg state, ionis. by collision with organic mols. 8-50620
- Xe+CO(N₂), ¹²⁹Xe chem. shielding, second virial coeff. 8-66563
- XeF+He(Ne)(Xe), radiative lifetime and collisional quenching kinetics 8-94289
- XeF⁺+He(Xe)(NF₃)(F₂), quenching rates for XeF in (B) state 8-58730
- XeO* production through collisional electronic energy transfer from two-photon excited Xe atoms 8-62775
- Xe(nf)+NH₃, at. Rydberg state further excitation by rot. transfer, field ionis. obs. 8-58795

atom-molecule reactions

- see also atom-molecule collisions
- atom+diatom, A+BC, ZZ 8-80729
- atom+diatom, transition states, trapped trajectories and classical bound states in continuum 8-88630
- electron transfer reactions, semiempirical pot. energy surfaces calcs. 8-73022
- exothermic triatomic exchange reactions, prod. energy distrib., statistical dynamic model 8-92455
- exothermic trihalogen Borne-Bunker reaction, long lived intermediates, comment 8-92464
- exothermic trihalogen Borne-Bunker reaction, long lived intermediates, reply 8-92465
- finite element methods for reactive scattering 8-92453
- fluoromethane+Br, isotope selective photobromination, using c.w. CO₂ laser irradi. in excess inert gas 8-76843
- formaldehyde+Cl, rate const. 8-85136
- impulsive triatomic reaction, vibr. state distrib., impulsive energy release model 8-92456
- methane+H(HO)(O)(O₂), H abstraction, rate const. calcs. 8-95921
- tetrafluoroethylene+O, triplet difluoromethane spectra, phosphoresc. and triplet-triplet annihilation 8-53196
- Ar+BrCN(HCN), CN quartet state production, fluoresc. anal. 8-68888
- Ar+He₂(³Σ), press. depend. reactions, rate coeffs. 8-64823
- Ar+methane, CH chemiluminesc. in flowing afterglow 8-64839
- ArF⁺, in Ar-F₂ proton-excited mixtures, production and quenching 8-94307
- Ar₂F⁺, in Ar-F₂ proton-excited mixtures, production and quenching 8-94307
- Ba+N₂O, reaction, electronic branching, statistical and dynamical influences 8-92451
- Br+Br₂, atom-exchange, rate and activation energy, trajectory model and pot. energy surface 8-64811
- Br+H₂, laser field interacting with collision dynamics, model system 8-62876
- Br+O₂→BrO+O₂, reaction rate constant, 200-360K 8-73024
- BrO+O→Br+O₂, reaction rate constant, 200-360K 8-73024
- C+N₂, reaction, CNN radical prod., matrix isolation study 8-86880
- Ca+HF(DF), beam reaction, vibr. excitation 8-68877
- Ca+O₂(CO₂), CaO form., product states obs. 8-92450
- Ca+O₂(CO₂)(N₂O), reaction, electronic branching, statistical and dynamical influences 8-92451
- Ca(4s4p³P)+N₂O, absolute chemiluminesc. cross-section and photon yield 8-53208
- Cl+D₂→DCl+Cl, LEPS pot. energy surface, rate const., isotope effect, quasiclassical trajectory calc. 8-56887
- Cl+H₂S→HCl+HS, laser-initiated chain reactions, rate const., product energy distrib. 8-85144
- Cl+HBr, ZZ 8-80729
- Cl+HI, chem. laser, energy distrib., spectrosc. obs. 8-71096
- Cl+HNO(H₂O₂)(HO₂), rate const., stratospheric appl. 8-85125
- Cl+H(D)I, exothermic triatomic exchange reactions, prod. energy distrib., statistical dynamic model 8-92455
- Cl+NO+N₂→NOCl+N₂, rate const. temp. depend. 8-76828
- Cl(²P)+methane, absolute rate and temp. depend. 8-80731
- ³⁶Cl+H₂(D₂) reactions, characterisation, effect of ethylene-I₂ scavenger 8-73071
- CsCl(Cs₂Cl₂)+Ar(Kr)(Xe), collision-induced ion-pair form., absolute cross sections 8-73029
- D+F₂(Cl₂), exothermic triatomic exchange reactions, prod. energy distrib., statistical dynamic model 8-92455
- D+HCl(HBr)(HI), abstraction and exchange reactions 8-73025
- F+DX, (X=I, Br, Cl), H abstraction, absolute reaction rate, H/D isotope effect 8-80721
- F+formic acid (formaldehyde), microscopic reaction dynamics, branching ratio, IR chemiluminesc. 8-73021

atom-molecule reactions continued

- F+H₂, collinear quasiclassical trajectory study 8-80718
 F+H₂, transition states, trapped trajectories and classical bound states in continuum 8-88630
 F+H₂, ZZ 8-80729
 F+H₂→FH+H, collinear probability, quantum calc. using pot. energy surface 8-64829
 F+H₂→FH+H, vibr.-rot. energy distrib. of HF, DWBA calc. 8-80722
 F+HD→HF+D(DF+H), branching ratios, information theory test by classical trajectory calcs. 8-64822
 F+HX₂ (X=I, Br, Cl), H abstraction, absolute reaction rate, H/D isotope effect 8-80721
 F₂+H(D)(T)(Mu), impulsive triatomic reaction, vibr. state distrib., impulsive energy release model 8-92456
 Fe(CO)₅+Ar*(P), chemiluminesc. 8-61014
 Ge+O₂(NO)(N₂O), reaction rate consts. at 350K 8-53186
 H+Br₂→HBr+Br, pot. energy surface, ab initio generalised valence bond calc. 8-73026
 H+Cl₂, impulsive triatomic reaction, vibr. state distrib., impulsive energy release model 8-92456
 H+Cl₂(H₂), activation energy and trajectory calcs., temp. and isotope effects 8-76835
 H+Cl₂(SCL₂)(S₂Cl₂)(SOCl₂)(SO₂Cl₂), energy disposal, HCl IR chemiluminesc. obs. 8-92484
 H+F₂, vibr. prod. distrib., Einstein coeffs. 8-92448
 H+F₂(Cl₂), exothermic triatomic exchange reactions, prod. energy distrib., statistical dynamic model 8-92455
 H+H₂, CI calc. of three dims. pot. energy surface 8-56882
 H+H₂, collinear, quantum mech. reactive scatt., exchange kernels calcs. 8-68880
 H+H₂, least squares fit to ab initio pot. energy function 8-56883
 H+H₂, reactive scatt., sudden approx. calcs. 8-68878
 H+H₂, transition states, trapped trajectories and classical bound states in continuum 8-88630
 H+H₂(v=1)→H₂+H, exchange reaction, classical trajectory method, vibr. excitation, partial rate consts. 8-60993
 H+H₂→H₂+H, IR laser induced reaction 8-80761
 H+N₂O→NO+OH, rate const., 2000-2850K, combustion of H₂/N₂O/CO/Ar 8-85162
 H+N₂(O₂), charge prod. cross sections and differential scatt. calcs. 8-94313
 H+NH₂→NH₃ react., force, density anal. 8-60997
 H+O₂, singlet state O₂ form., reaction mechanism, mass spectrometric obs. 8-53204
 H+O₂→OH+O, combustion, quasiclassical trajectory calcs. 8-53201
 H+O₂, absolute reaction rate const., 219-360K 8-80734
 H₂-Ar⁺+He, 200-850 eV, attenuation and fragmentation 8-62968
 H₂+H(I), activation energy and trajectory calcs., temp. and isotope effects 8-76835
 HF+D, vibr. threshold energies, reagent energy effects 8-85145
 HF+H(D), kinetic isotope effect and temp. depend. 8-53202
 HO₂+Cl react. rate const. determ. at 298K (French) 8-64817
 He+H₂⁺, reactive and dissociative scatt., crossed-beam and trajectory obs. 8-64833
 He(2³S)+H₂O(H₂S), energy transfer processes, reaction products, UV and visible obs. in flowing afterglow 8-85138
 Hg+2NH₃→HgNH₃+NH₃, photosensitised, HgNH₃ complex lifetime 8-53193
 Ho+N₂O→HoO*+N₂, chemiluminesc. reaction, cross-section 8-76847
 I⁺+I₂(Br₂)(Cl₂)(IBr)(ICl)(BrCl), collisional deactivation and reaction rate consts., obs. 8-80738
 I(5²P_{1/2})+Br₂, deactivation kinetics, time-resolved spectrosc. obs. 8-95916
 I(5²P_{1/2})+Br₂, deactivation kinetics, Br(4²P_{1/2}) prod., time-resolved spectrosc. obs. 8-95917
 Li+Cl₂(SF₆) (dichlorofluoromethane) (German) 8-92485
 Li+Li₂→Li₃, rovibronic symmetry correlation 8-92461
 Mg-In+H₂→MgH₂, kinetics, catalytic effect of In 8-76851
 Mg+O₃, matrix reaction, IR spectra, isotope shifts and blue matrix shift 8-80736
 Mg*+Cl₂ crossed beams, chemical reaction, metastable Mg as new light source of forbidden lines 8-90112
 N, at. recombination, Smith side tube method obs. 8-68881
 N+BrCu(CH₃)(C₂H₂)(CCl₂)(CHCl₃), CN quartet state production, fluoresc. anal. 8-68888
 N(2³D)+O₂, chemiexcited NO form., 90-180K IR obs. 8-90163
 NO⁺+atmospheric gases, thermal energy reaction rates 8-92443
 Na+HX(J,v)→NaX+H, (X=F,Cl), reaction rate, rot. excitation depend. 8-64818
 Ne+HeH⁺, collinear reaction, pot. energy surface SCF-LCAO-MO and DIM calc. 8-92467
 O+HCl, vibr. excited, laser enhanced reaction rate, OH vibr. distrib. obs. 8-95912
 O+HI, HOI formation, matrix reaction, IR spectra, isotope shifts and band assignments 8-80737
 O+NO binary reaction, crossed beams, NO₂ chemiluminesc. 8-64843
 O₂, IR nightglow bands excitation mechanism, reaction rate consts. 8-65448
 O₂+La(Y)(Sc), crossed beam chemiluminescence reaction, spectral simulation, hyperthermal energy meas. 8-80732
 O₂⁺+atmospheric gases, thermal energy reaction rates 8-92443
 O₂+U(Th), assoc. ionis. cross sections, in crossed beams, mass spectra obs. 8-94317
 O(1D)+CO, deactivation rate consts. temp. depend., 113-333K 8-88629
 O(1D)+Xe(Kr)(Ar), deactivation rate consts., 110-330K 8-88628
 O(3P)+2-methyl-2-butene, reaction rate consts. meas. 8-61001
 O(3P)+C₂O₂→3CO, reaction dynamics and monoxide vibr. distrib., laser reson. absorpt. method 8-68882
 O(3P)+CN(v) react., prod. energy distrib. meas., CO vibr. level population (German) 8-76833
 O(3P)+O₃, bimolecular reaction rate coeff. reactant vibr. excitation depend., reson. fluoresc. obs. 8-76837
 O*+H₂S, chemiluminesc. matrix reaction, diffusion controlled, 8-20K, O(3P) 8-61013
 O*+H₂→OH*+H, rate const. and vibr. energy distrib. in OH*, for O(3P) 8-60998
 RbF+K collision complex, rot. energy effect on branching fraction for reactive decay 8-73023
 S+O₂→SO₂, chemiluminesc. matrix reaction, diffusion controlled, 8-20K 8-61013

atom-molecule reactions continued

- Si+F₂, fast flow reactor, second order rate coeff. determ. 8-80723
 Si+O₂(NO)(N₂O), reaction rate consts. at 350K 8-53186
 Sn+Cl₂(Br₂), reactive scatt., ang. distrib. and time-of-flight spectra 8-64842
 Sn+N₂O, chemiluminesc., high temp. fast flow reactor kinetics obs. 8-88636
 Sn+O₂, crossed mol. beam kinetics, SnO time of flight recoil vel. spectra 8-68883
 Sn(5p²3P₀), kinetic studies of ground state atoms, by resonance line absorpt. 8-85128
 Sr+HF(DF), beam reaction, vibr. excitation 8-68877
 Sr⁺+N₂O→SrO⁺+N₂, visible chemiluminescence, absolute cross section and photon yields 8-92463
 Sr*(P₁)+HCl(HF), laser-excited atom reaction, energy deposition 8-85134
 T+fluoroform, 4.5 to 6.0 eV, substitution reactions 8-85146
 T+HT→TH+T, collinear reactivity bands 8-85143
 Te(P₁)+Te₂, gas phase flash photolytic deexcitation obs., 1000K (Russian) 8-50626

atom probe field ion microscopy

- energy-focused atom probe design and performance 8-85276
 evaporation pulse generator 8-78041
 metal oxide surface layer, TOF atom probe anal. 8-64766
 Fe-Al, atom-probe field ion microscopy obs. (French) 8-86389
 GaAs, time of flight atom-probe mass spectra 8-92584
 Si, chemisorption of H₂, atom-probe FIM obs. 8-71968
 W, atom-probe field ion microscopy obs. (French) 8-86389

atom-surface impact

- see also sputtering
 atomic beam spectrometer using a LiF analyzer crystal, for surface studies in UHV 8-71651
 beam scattering, semiempirical determ. of atom-surface interaction 8-72676
 biological specimen surface struct. determ. 8-53584
 classical scattering, cutoffs and shadows 8-80448
 cooling by metal snow, origin of effect and elimination 8-71494
 Debye-Waller factor from atom-surface scatt. 8-92164
 extinction theorem in atom-surface scatt. 8-88393
 gas-surface potential calc., double rainbow scatt. appl. 8-80443
 graphite, interaction and band struct. effects for He derived from scatt. data 8-92162
 multiple hits in atom-surface diffraction 8-80449
 plasma cooling by metal snow, expt. evidence 8-71495
 response functions for cryst. and surfaces, appl. to surface scatt. 8-72669
 scattering, coupled channel calcs., symmetry appls. 8-92156
 scattering from surface with regular one-dimens. roughness elements 8-92166
 stationary sinusoidal hard wall surface with one-dimens. periodicity 8-92161
 sudden decoupling approximations, for atom-surface scatt. 8-64437
 Ag, Ne scatt. from (111) surface, double rainbow scatt. distrib. 8-80443
 Cu (001) surface, scatt. of He and Ne atoms at 20K 8-80451
 Cu-Be-O surface, O(2S) impact, secondary electron yield 8-58797
 LiF, ⁴He scatt., selective adsorption induced intensity maxima 8-72667
 LiF, 63 meV He atom scatt., single Rayleigh phonon interaction 8-80447
 LiF (001), scatt. of He(Ne), sudden decoupling approxs. 8-64437
 LiF (001), scatt. of Ne, coupled channel calcs., symmetry appls. 8-92156
 LiF, selective adsorption of ³He and ⁴He, atomic beam scatt. meas., binding energies 8-63935
 Mo [110], metastable He impact, secondary electron spectra 8-95642
 NaF, selective adsorption of ³He and ⁴He, atomic beam scatt. meas., binding energies 8-63935
 Si (100) surface, diff. of He atoms obs. 8-52609
 W (110), scatt. of He(Ne), sudden decoupling approxs. 8-64437
 W (110), scatt. of Ne, coupled channel calcs., symmetry appls. 8-92156
 W (112), He atom scatt., theory for stationary sinusoidal hard wall surface wall one-dimens. periodicity 8-92161

atomic absorption spectroscopy

- analysis instrumentation in clinical enzymology 8-88675
 atmospheric aerosol, absolute element concs., PIXE and AAS, comparison 8-85237
 atomic absorption spectrophotometer, two-channel, microcomputer-based, appls. 8-56926
 atomisation, in graphite ballast furnace, reliability improvement (Russian) 8-85279
 automatic sampler, for flame at. absorption 8-65974
 bibliography, (July-Dec. 1977) 8-53276
 bibliography, January-June 1978 8-95969
 capacitor dielectric fluid test and anal., quality assurance 8-80272
 combustible municipal solid waste, Sb and As determ. by AAS 8-85229
 development in USSR, 1965-1975, science metrics investig. 8-61104
 direct atomisation, in graphite furnace AAS, drift compensating digital peak leader appls. 8-68939
 discrete chemistry, new approach to water analysis 8-88674
 electrothermal atomisation, for absolute at. absorpt. anal. methods 8-85260
 flame emission, atomic absorption, and atomic fluorescence spectrometry, review of literature 1975-1977 8-85224
 flameless AAS, anal. response shape and position 8-92545
 flux-grown magnetic garnets, comp. anal. by AAS 8-92585
 glacier regelation ice chem. comp., indication of press. melting 8-61447
 graphite disc atomiser, for flameless atomic absorption spectrophotometer, exam. 8-54463
 graphite tubes, for at. absorpt. spectroscopy, pyrolytic coating method optimisation 8-76940
 matrix effects, in graphite furnace technique, furnace conditions effects 8-85230
 metals and alloys, thermodynamic props., evaporation, optical spectral method appls., review (Russian) 8-75822
 near IR absorption analysis, differential compensation method 8-80819

atomic absorption spectroscopy continued

- noble metals anal. review 8-85264
 nonflame atomiser, programmed unit for at. absorpt. anal. 8-54462
 programmable multielement atomic absorption system 8-80803
 pulsed dye laser double beam spectrometer, instrumental noise sources 8-88662
 pulsed hollow cathode lamp characteristics 8-67530
 rainwater, multielement anal. 8-69512
 selective spectral line modulation AAS 8-89546
 self-scanned photodiode array spectrometer, for flame at. absorpt. meas. 8-70191
 thyristor thermostabiliser for at. absorpt., spectroscopy with non-flame atomisation, power supply (*Russian*) 8-76977
 trace metal analysis in water, accuracy in AAS and AES using graphite furnace 8-69510
 Zeeman-modulated sources, RF-excited hollow-cathode lamps 8-85275
 Ba, determ. in seawater, matrix effects in graphite furnace AAS 8-85230
 Ca, determ. in lake sediments, by atomic absorption spectroscopy 8-95970
 Cd, determ. using modified flameless at. absorpt. spectrophotometer 8-82044
 Cu, in powder rock samples, determ. using graphite capsule flame atomiser (*Russian*) 8-85278
 Ge($3P_0$)+O₂(Cl₂)(COS)(N₂O)(NO₂)(NO+Ar) oxidation reacts., gas phase, kinetics 8-92468
 Hg, determ. in water samples, error anal. 8-69519
 Na, flame absorption and fluorescence, laser saturation broadening 8-88661
 Ni, determ. in serum, matrix effects in graphite furnace AAS 8-85230
 Pb, determ. in steel wire, AAS determ. 8-68939
 Pb, in powder rock samples, determ. using graphite capsule flame atomiser (*Russian*) 8-85278
 Se, determ. matrix effects in graphite furnace AAS 8-85230
 Sn(4^3P_0)+O₂(Cl₂)(COS)(N₂O)(NO₂)(NO+Ar) oxidation reacts., gas phase, kinetics 8-92468
 Ta foil lining of graphite furnace, at. spectrosc. 8-74078
 Ta treated, graphite atomiser tubes, for high temp. AAS 8-73093
 U, in water, determ. by AAS after ion exchange preconcentration 8-85231
 W filaments on electrothermal atomiser, atomic absorption spectrophotometry appl. 8-86346
 Zn, determ. in acetone, by AAS being W filament electrothermal atomiser 8-86346

atomic beams

- see also atom-molecule reactions; atom-surface impact; particle velocity analysis; plasma-beam interactions*
 high resolution spectroscopy of fast beams 8-89557
 neutral particle beam, controlled energy distrib., prod. method 8-78038
 neutral-beam divergence due to imperfect magnetic shielding 8-78489
 number fluctuation effect on intensity correlations in resonance fluorescence, photon antibunching 8-50499
 resonance fluorescence, multiat. and transit-time effects on photon-correlation meas. 8-86812
 target for ion-atom collision studies 8-70971
 tube with laser pump, interaction eqns. (*Russian*) 8-74801
 two frequency separated oscill. fields method for beam interrogation 8-89596
 vapour absorption cells and beam generating ovens for synchrotron radiation spectroscopy 8-66688
 Cs beam clock development for satellites 8-57910
 Cs beam frequency standard design for satellites 8-57911
 Cs beam frequency standard drift and noise performance rel. to velocity distributions 8-57912
 H, beam, $2^2S_{1/2}$ metastable ats., nonadiabatic transition in mag. field 8-55157
 H beam production in maser dissociator, performance characts. 8-87034
 He, high-flux fast neutral beam source 8-54507
 K atom clusters, cluster beam Stern-Gerlach mag. deflection 8-54504
 Li/Li₂ supersonic nozzle beam characts. by spectroscopic techniques 8-55255

atomic clocks

- see also frequency measurement; time measurement*
 31st Annual Frequency Control Symposium, Atlantic City (1977) 8-57905
 beam interrogation in Ramsey cavity, two freq. separated oscillating fields technique 8-89596
 frequency standard prediction error analysis 8-57906
 International Atomic Time, role of primary standards 8-89459
 International time and freq. comparison using Loran-C radio waves (*Japanese*) 8-81951
 quantum mechanically treated atomic clock in curved space time 8-54271
 standard time/freq. service in East Germany (*German*) 8-93658
 time scale realisation models and predictions 8-57907
 US Naval Observatory clock time scale 8-89460
 Ag beam mag. resonance apparatus as freq. standard, features 8-89458
 Cs beam clock development for satellites 8-57910
 Cs beam deflection system for time and freq. primary standard 8-89453
 Cs beam freq. standards, freq. offset due to spectral impurities 8-89455
 Cs beam standard, Ramsey cavity and beam optics design, expt. 8-89456
 Cs clock, laser synchronisation between observatories of Paris and San Fernando (*French*) 8-89461
 Cs controlled digital clocks for high precision time meas. (*German*) 8-77871
 Cs long beam primary clock, accuracy, reliability 8-89454
 H generator, freq. shift due to atomic collisions with storage flask walls 8-77870
 H maser, time-dependent freq. shift obs. 8-89457
 H maser design for NAVSTAR Global Positioning System satellite clock 8-58969
 $^{199}\text{Hg}^+$ trapped ion frequency standard 8-57914

atomic clocks continued

- Rb controlled digital clocks for high precision time meas. (*German*) 8-77871
 Rb, portable clock for transcontinental and intercontinental time comparison 8-57908
 Rb portable clock transcontinental/intercontinental comparison 8-54345
- atomic clusters**
 Born-Green-Yvon eqn., two-dimensional, with anisotropic interac. 8-79882
 formation, by ion bombardment of single cryst. surface 8-92157
 free jet, homogeneous nucleation of clusters, noncryst. struct. (*French*) 8-79760
 homomorphic cluster CPA analyticity 8-82872
 homomorphic cluster CPA for off-diagonal randomness 8-82873
 muffin-tin potential and SW X α SCF calcs. for core levels (*German*) 8-82874
 Ag clusters, charge distrib., density of states, CNDO calcs. 8-70995
 Ar, clustering of atoms around positron and positive ions 8-55270
 Cu, cluster and bulk, struct. and electronic props. 8-95592
 Cu, metal cluster, optical spectroscopy, atom to bulk 8-95591
 Cu_n, cluster formation, by ion bombardment of single cryst. surface 8-92157
 H₂⁺+He, 200-850 eV, attenuation and fragmentation 8-62968
 H_n⁺ (n=3,5,7,9,11), stability, struct., ab initio MO calcs. 8-74810
 He, clustering of atoms around positron and positive ions 8-55270
⁴He trimer and tetramer, binding energy, appl. of ATMS 8-94349
 K atom clusters, cluster beam Stern-Gerlach mag. deflection 8-54504
 Li₃, multibody and stability considerations, small clusters 8-90333
 Na clusters, electronic relaxation energies in KL_{2,3}L_{2,3} Auger transitions, SCF-X α -SW calcs. 8-90334
 Na particle, consisting of ats., metallic Na, model, electronic levels 8-50673
 Na₃, electronic struct., pot. energy surface, ab initio CI study 8-70996
 Ne, clustering of atoms around positron and positive ions 8-55270
 O, chemisorbed on Al (100), photoemission ang. depend., MO cluster model calc. 8-76576
 Pb microclusters, mol. beam electron diffr., amorphous struct. 8-66703
 Re₂, adsorbed on W (211) surface, dissoci., thermodynamics 8-87861
 S_n, properties of small aggregates rel. to metallic character of Te_n 8-86985
 SF₆, pure and H₂ mixture photolysis, S atom nucleation particulate formation 8-76836
 Se_n, properties of small aggregates rel. to metallic character of Te_n 8-86985
 Te_n, small aggregate, metallic character 8-86985
- atomic collision processes** *see atomic inelastic collisions; elastic scattering of atoms and molecules*
- atomic electric moment**
 inert gas mixture, collision-induced absorption, exact line shapes, appl. to He-Ar 8-66512
 spectral line collisional broadening, classical and quantum theories, radiator motion effect 8-86822
 spectroscopy quantum chem. teaching, fluctuating elec. dipoles, light absorpt. 8-73802
⁹¹Zr, hyperfine struct. and nucl. elec. quadrupole moment, at. beam mag. reson. meas. 8-55133
- atomic electron configuration interactions** *see atomic electron correlations*
- atomic electron correlations**
 alkali metal, fine-struct. of excited nd and nf states, at. core effect 8-58606
 closed shells, fast CI method calcs. 8-90090
 configuration interaction, iterative variational method calcs. 8-55127
 correlation energy calculation, from CHF method 8-90087
 electron scatt. and photoionis., correlation effects 8-58842
 first-row atoms, ground states, using CI wavefunctions 8-74583
 inner shell generalised oscill. strengths, with outer shell effects 8-50507
 integral equation numerical soln. in pair approx. 8-90065
 interaction energy, direct calc. with CI wavefunctions 8-66477
 intermediate-coupling eigenfunctions for f^dd and f^dd configs. 8-62732
 MC-SCF theory, orthonormality-constrained orbital optimisations 8-86766
 open shell systems, coupled cluster approach 8-58595
 photoionisation, ion alignment, many electron correl. effect 8-74622
 s-electron binding energy regularities in f³S^m configs. 8-62731
 satellite peaks, relationship between X-ray emission and X-ray photoelectron spectra 8-66492
 SCF basis sets of moderate size, efficient methods 8-58593
 second row atoms, statistical correlation energies 8-78637
 theory, inverse matrix diagonal and off diagonal elements, self energy perturbation theory 8-82607
 transition metal, 3-d, density functional theory 8-58578
 Ar, Compton profile, local density approx., Kohn-Sham self consistent scheme 8-94193
 Ar, KLL and KLM Auger electron spectra, obs. and relativistic multi-configurational Dirac-Fock calc. 8-50524
 Ar, outer shell photoelectron spectrum, correl. satellites 8-78671
 Ar²⁺, levels of 2p³3p⁵ 8-74574
³⁷Ar, M/L capture ratio, multiconfig. Hartree-Fock calc. atomic electron correlations 8-62510
 Ba, Auger spectra, strong correl. in 4d-spectrum 8-50522
 Be sequence, (Z=4 to 10, 14), ³P₁→¹S₀ intercombination line, CI calc., Breit interaction 8-78641
⁷Be, L/K capture ratio, multiconfig. Hartree-Fock calc., atomic electron correlations 8-62510
 Cd, photoionisation cross section, many-body perturbation theory, dipole length and vel. calc. 8-78674
 Cl I, photoionisation cross section, calc. by many-body perturbation theory 8-62771
 Gd³⁺, hyperfine interactions, relativistic CI using many-body calcs. 8-78638
 H⁺-like ions, electron correlation and Coulomb hole in momentum space 8-86793
 H+He(Ne)(Ar)(Kr)(Xe), low energy elastic scatt. cross section MCSCF calc., van der Waals forces 8-70897
 He, CI wavefunctions, ang. correl. of electrons 8-62730
 He, correlation energy of ground state, pair approx. 8-90065

atomic electron correlations continued

- He, electron impact, 3^3P_g and 1^3D_u states excitation, electron correlation influence, Rudge-type approx. 8-74771
 He, electron impact excitation, 3^3P_g and 1^3D_u states, electron correlation influence, Born-Oppenheimer approx. 8-74770
 He excited states, relativistic corrections 8-62734
 He isoelectronic series, electron correlation and Coulomb hole in momentum space 8-86793
 He, photoionisation, frozen-core HF perturbation theory, oscillator strength, dipole length and vel. calc. 8-78672
 He⁺⁺, doubly excited, spatial correl. of at. electrons 8-70760
 Kr, 3p core hole spectrum, many electron description 8-50517
 Kr, Compton profile, local density approx., Kohn-Sham self consistent scheme 8-94193
 Li, quartet states, absolute term values, CI calcs. 8-58596
 Li, quartet states, transition energies, oscill. strengths, CI calcs. 8-58597
 Li⁺, isoelectronic series, electron correlation and Coulomb hole in momentum space 8-86793
 Mg, K Auger transition rates, orbital relax. and interchannel interaction effects 8-50521
 Ne, Compton profile, local density approx., Kohn-Sham self consistent scheme 8-94193
 Ne, converged E⁽²⁾ values 8-66479
 Ne, ground state, configuration interaction, iterative variational method calcs. 8-55127
 Ne⁺, converged E⁽²⁾ values 8-66479
 O, 2-photon excitation, cross-section calcs. 8-58641
 Sr, Auger spectra, strong correl. in 3d-spectrum 8-50522
 Tb I, 4f⁸5d6s² config., hyperfine struct. analysis 8-62732
 Xe, 5s, 5p ESCA spectrum, photoionisation many electron description 8-50516
 Xe II, 5p⁶6s and 5p⁴5d configs., config. interaction effects 8-66478

atomic electron impact excitation

see also electron spectra

- alkali metal atoms, integrated cross-section calc. 8-62921
 Bethe theory, inelastic collisions of fast charged particles 8-58783
 bremsstrahlung, series expan. for intensity components 8-50648
 conference, electronic and atomic collisions, Paris (July 1977) 8-58758
 correlation effects 8-58842
 electron bremsstrahlung energy spectra, 1 to 2000 keV, neutral atoms Z=2 to 92 8-62920
 electron-ion bremsstrahlung with shielding 8-66667
 electron-ion collisions, crossed beam expts. 8-58843
 fast electron and positron scatt. 8-62918
 gases, low energy positron interactions, review 8-50651
 glow discharges, atomic and ionic spectral line excitation in cathodic region (Russian) 8-63611
 high Rydberg atoms, dipole transitions, impact parameter method 8-62922
 inelastic exchange kernels, semiclassical exchange approximation theory 8-50642
 inert gases, electron beam excited, absorpt. characts. 8-82948
 inner shell generalised oscill. strengths, with outer shell effects 8-50507
 neutral atoms, electron interaction, free-free radiative transitions, review 8-90295
 optical model for electron spin polaris. 8-50646
 photoelectric effect and electron diffusion in gases 8-81745
 positive ions, evaluation of radial integrals in Coulomb-Born approx. 8-74768
 R-matrix method, application to atoms and ions 8-58833
 R-matrix method, basic concepts, rel. to other theories electron scatt. 8-58832
 resonance obs. optical excitation functions 8-58841
 variational methods, appl. to at. scatt., review 8-86951
 X-ray spectra of impact excit. highly charged ions, dielectronic satellites 8-62762
 Ag, population mechanism, highly-excited states, hollow cathode discharge (Russian) 8-63610
 Al, electron impact excitation cross sections calc. (Russian) 8-55240
 Ar, autoionising states excitation by electron impact, threshold effects 8-62923
 Ar, electron-atom bremsstrahlung continuum, afterglow decay (German) 8-83626
 Ar, metastable, electron impact excitation cross-sections calcs. 8-94323
 Ar, multiple-collision diff. theory 8-82844
 Ar, weakly ionised, energy transfer at high press. 8-58845
 B⁺, collision strength for 2p state, close-coupling calc. 8-55247
 B³⁺, cross-sections, modified Oppenheimer approx. 8-82843
 Ba, electron scatt., elastic and inelastic (5¹D, 6¹P) cross sections, 20-100 eV 8-74769
 Ba, emission spectra, 50 to 90 nm 8-82846
 Ba, scatt. from excited atoms, 30 and 100 eV, inelastic and superelastic 8-86933
 Be²⁺, cross-sections, modified Oppenheimer approx. 8-82843
 C, electron scatt., at. field bremsstrahlung, photon linear polaris. 8-62927
 C⁴⁺, cross-sections, modified Oppenheimer approx. 8-82843
 Ca, electron impact, 3p⁶ subshell excitation, VUV spectra (Russian) 8-90117
 Cs, optical reson. line electron impact excitation cross sections, polaris. 8-55244
 Cu, electron impact, excitation function (maxima, cross-sections) 8-50650
 Cu, population mechanism, highly-excited states, hollow cathode discharge (Russian) 8-63610
 Eu⁺, resonant line excitation 8-82847
 Fe III, Fe VI, electron impact excitation cross sections and gaseous nebulae Fe abundances 8-53806
 Ga, electron impact excitation cross sections calc. (Russian) 8-55240
 H, 2s state, differential cross section, plane-wave approx. 8-86953
 H, (1s-2s) excitation, dynamic polaris. pot. 8-78818
 H and hydrogenic ions, cross-sections and rates 8-50649
 H, Born and classical cross-sections, comparison (German) 8-86952
 H, electron impact, inelastic scatt. semiclassical exchange approximation theory 8-50642

atomic electron impact excitation continued

- H, electron impact ionisation, electron-photon coincidence meas. 8-55242
 H, electron inelastic scatt., effective exchange potentials 8-90300
 H, electron-photon excitation, high-energy resonant cross sections 8-70938
 H, gas discharge source for electron scatt. expts. 8-94332
 H isoelectronic series, electron impact ionisation, electron ang. momentum exchange 8-78820
 H, n=3 level, coherent excitation by electron impact, density matrix anal. 8-78817
 H, simplified model, low and medium energy 8-86954
 H-like ions, electron impact excitation to S states exchange effects 8-58835
 H-like ions, electron impact excitation to s state 8-58836
 H-like ions, electron impact excitation, Coulomb Born approx. 8-58840
 H-like ions, electron impact excitation, Coulomb modified Glauber approx. calcs. 8-94324
 H-like ions, Glauber exchange amplitudes for electron scatt. 8-74772
 He, 2¹S and 2³S excitation cross sections, partial wave anal. 8-90301
 He 2³S-3³S electron impact excitation, first Born and Glauber cross sections 8-55243
 He, 3³P level, spontaneous decay probability, expt. and theoretical values 8-50501
 He, absolute total scatt. cross sections, 0.5 to 50 eV 8-74765
 He, cross-sections, modified Oppenheimer approx. 8-82843
 He, electron impact, 3^3P_g and 1^3D_u states excitation, electron correlation influence, Rudge-type approx. 8-74771
 He, electron impact excitation, 3^3P_g and 1^3D_u states, electron correlation influence, Born-Oppenheimer approx. 8-74770
 He, electron impact fluorescence, polarisation of 5876 line 8-82848
 He, electron impact spectroscopy for Compton profile meas. 8-90299
 He, excited S, D and F state radiative lifetimes, electron impact method 8-94325
 He, high Rydberg state, dipole transitions, impact parameter method 8-62922
 He I, transfer excitation energy between n=5 levels 8-70942
 He in transient plasma, excitation transfer between excited states 8-70914
 He⁺, electron impact excitation to S states exchange effects 8-58835
 He⁺, electron impact ionisation, electron ang. momentum exchange 8-78820
 He⁺, electron inelastic scatt., effective exchange potentials 8-90300
 He⁺, electron scatt., Glauber exchange amplitudes 8-74772
 He-like ions, electron impact, collision strengths for fine-struct. transitions 8-62925
 Hg, electron impact spectra, intermediate energy 8-82842
 Hg, electron inelastic scatt., spin-polarisation, differential cross-section, DWBA 8-50644
 Hg, slow electron collision effective cross section, quenching probability 8-50627
 In, electron impact excitation cross sections calc. (Russian) 8-55240
 K, optical reson. line electron impact excitation cross sections, polaris. 8-55244
 Kr, electron impact excitation of autoionis. states 8-90302
 Kr, metastable, electron impact excitation cross-sections calcs. 8-94323
 Kr, threshold excitation spectra 8-70936
 Li⁺, cross-sections, modified Oppenheimer approx. 8-82843
 Li²⁺, electron impact ionisation, electron ang. momentum exchange 8-78820
 Mg, cross sections 10, 20, 40 eV 8-70940
 N³⁺, cross-sections, modified Oppenheimer approx. 8-82843
 Ne, autoionising states, scatt. electron spectra, post collision interaction effects 8-58819
 Ne, electron-atom bremsstrahlung continuum, afterglow decay (German) 8-83626
 Ne, metastable level deactivation by electron collision in low press. discharge 8-83520
 Ne, multiple-collision diff. theory 8-82844
 Ne, weakly ionised, energy transfer at high press. 8-58845
²¹Ne, ground state, electronic pumping, alignment transfer with multiple diffusion (French) 8-50643
 O, low-energy electrons integral scatt. cross section 8-69556
 O⁶⁺, cross-sections, modified Oppenheimer approx. 8-82843
 Rb, optical reson. line electron impact excitation cross sections, polaris. 8-55244
 Rb⁺, electron impact excitation, absolute cross-sections 8-82849
 S II, fine-structure transitions by electron impact 8-65493
 Ti, electron impact excitation cross sections calc. (Russian) 8-55240
 Xe, electron impact polaris. and excitation functions 8-66665
 Xe, electron scatt., optical model for electron spin polaris. 8-50646
 Yb, 5p ionisation, 40 to 120 nm 8-82845

atomic electron impact ionisation

see also electron spectra

- Cr, double K-shell ionisation by electron impact, X-ray spectra 8-62928
 electron-ion collisions, crossed beam expts. 8-58843
 highly charged ions, ionis. from 3s sub-level 8-90297
 inert gas, electron impact double ionisation, binary encounter approx. calcs. 8-90294
 inert gases, cross section ratios 8-94326
 inner atomic shells, coincidence expts. theory 8-58837
 inner shell generalised oscill. strengths, with outer shell effects 8-50507
 innershell ionisation, positron impact 8-62930
 innershell ionisation, relativistic electron impact 8-62930
 metal vapour, autoionising and ionising processes 8-58830
 positive ions, electron impact ionisation, cross-sections calc. 8-70943
 post collision interactions in at. excitation processes 8-58803
 R-matrix appls., quantum defect, frame transportation 8-58761
 two-particle-hole Tamm-Dancoff approximation (2ph-TDA) equations for closed-shell atoms and molecules 8-70937
 variational methods, appl. to at. scatt., review 8-86951
 Ar, (e,2e) coplanar symmetry reaction, factorised distorted-wave approx., 400-1200 eV 8-55246
 Ar, electron impact ionis., L₂-shell alignment, Auger electrons ang. distrib. 8-58838
 Ar, electron impact ionis., differential cross sections 8-58839

atomic electron impact ionisation continued

- Ar, electron impact ionis. of inner shells, coincidence expt. theory 8-58837
 Ar, energy resolution and ang. correl. of scatt. and ejected electrons 8-70939
 Ar II, (e,2e), photoelectron and conventional spectroscopies 8-90298
 Ar, low-energy, triple-differential cross section 8-74773
 Ar, weakly ionised, energy transfer at high press. 8-58845
 Ar⁺, electron impact ionis. cross section 8-50647
 C, 7-1000 eV, cross-section 8-86956
 C III, C IV, electron impact ionisation 8-70941
 Cd, Auger electron spectra, electron impact excited, vap. and solid state differences 8-52603
 Cr, double K-shell ionisation by electron impact 8-62929
 Fe, double K-shell ionisation by electron impact, X-ray spectra 8-62928
 Fe, double K-shell ionisation by electron impact 8-62929
 Fe¹⁴⁺, Fe¹⁵⁺, ionis. from 3s sub-level 8-90297
 H, gas discharge source for electron scatt. expts. 8-94332
 H⁺, electron detachment by electron impact, 1s state product, Born approx. 8-78816
 H⁺-positron, charge exchange, excited positronium states form. 8-58873
 He, 7-1000 eV, cross-section 8-86956
 He, (e,2e) coplanar symmetry reaction, factorised distorted-wave approx., 200-1200 eV 8-55246
 He, distorted wave approx., 80-250 eV 8-86955
 He, electron impact ionis., triple differential cross section 8-62924
 He, electron impact ionisation, emitted electron ang. distrib. 8-55241
 He hollow-cathode discharge, Ba⁺ and Sr⁺ formation 8-67527
 He, mechanism of (e,2e) reaction 8-62926
 He⁺ ions, electron impact ionisation 8-66666
 He+e, generalised differential oscillator strengths 8-55239
 K, polarised, ionis. by polarised electrons in crossed beam expt. 8-50645
 Kr, electron impact ionis. of inner shells, coincidence expt. theory 8-58837
 Mg, Auger electron spectra, electron impact excited, vap. and solid state differences 8-52603
 Mg+H⁺(He⁺) and electron impact ionis., Auger study of collisionally induced alignment 8-90279
 Mn, elastic and inelastic electron scatt. 10 to 100 eV 8-70934
 N, 7-1000 eV, cross-section 8-86956
 N IV, N V, electron impact ionisation 8-70941
 Ne, (e,2e) coplanar symmetry reaction, factorised distorted-wave approx., 400-1200 eV 8-55246
 Ne, electron impact ionis., differential cross sections 8-58839
 Ne, electron impact ionisation cross-section 8-58844
 Ne, noncoplanar symmetric (e,2e) reaction, factorised distorted-wave approx., 0.4-2.5 keV 8-55245
 Ne, weakly ionised, energy transfer at high press. 8-58845
 Neⁿ⁺ (n=1-4), electron impact ionisation cross-section 8-58844
 O, 7-1000 eV, cross-section 8-86956
 O, low-energy electrons integral scatt. cross section 8-69556
 Xe, electron impact ionis. of inner shells, coincidence expt. theory 8-58837
 Xe, noncoplanar symmetric (e,2e) reaction, factorised distorted-wave approx., 0.4-2.5 keV 8-55245
 Zn, Auger electron spectra, electron impact excited, vap. and solid state differences 8-52603

atomic electron scattering *see* **atomic electron impact excitation; atomic electron impact ionisation; elastic scattering of electrons by atoms and molecules**

atomic emission spectroscopy

- air, elemental anal. at sub parts per trillion concs. via SONRES 8-81465
 alloy steel welds, distrib. of Cr, Ni, Mn, Si, Ti, laser emission microanal. method 8-61110
 combustion diagnostics, laser Raman and fluoresc. techniques 8-88635
 continuum source atomic fluorescence spectrometer, wavelength modulated, appls. 8-70190
 data processing systems (*Japanese*) 8-88685
 flame emission, atomic absorption, and atomic fluorescence spectrometry, review of literature 1975-1977 8-85224
 hollow cathode lamp, pulsing conditions optimisation 8-65972
 inelastic mean free paths of solids, data tables 8-84686
 instrumentation, review of current developments (*Japanese*) 8-86356
 laser excited at. fluoresc. flame spectrometry, improvement of detection limits 8-61073
 metals and alloys, thermodynamic props., evaporation, optical spectral method appls., review (*Russian*) 8-75822
 metastable transfer emission spectroscopy, for trace materials in gas flows detection 8-85257
 multielement determination, using at. emission echelle spectrometer with image dissector and vidicon tubes 8-61081
 Nimocast, diffusion of Cs, AES, SIMS depth profile study (*German*) 8-84008
 plasma quantometer, quantitatively coupled, for emission spectrochem. anal. (*Japanese*) 8-83624
 plasma wall sputtered metal density meas. by atomic fluorescence spectroscopy 8-67422
 refractory refinement during prep. by self propagating high temp. synthesis 8-60634
 review 1976-1977 8-80797
 review of principles, instrumentation, methodologies, appls., teacher education appl. 8-69927
 saturation of energy levels 8-65980
 sediment leachates, trace element anal., multielement-direct reading method 8-69514
 single atom detection, by 1- and 2-photon SONRES 8-85282
 spectrochemical analysis with glow-discharge lamp (*Japanese*) 8-85262
 steel, austenitic stainless, oxidation of (100)-plane, LEED-AES obs. (*German*) 8-68841
 trace metal analysis in water, accuracy in AAS and AES using graphite furnace 8-69510
 trace metal conc. in waste water, spectrochem. anal. 8-61106
 wavelength modulation, using CW dye laser 8-61083
 Mn, determ. by plasma jet emission spectroscopy, using desolvation system with US nebuliser 8-68960

atomic emission spectroscopy continued

- Mo, diffusion of Cs, AES, SIMS depth profile study (*German*) 8-84008
 Na, flame absorption and fluorescence, laser saturation broadening 8-88661
 Ni, diffusion of Cs, AES, SIMS depth profile study (*German*) 8-84008
 TZM, diffusion of Cs, AES, SIMS depth profile study (*German*) 8-84008

atomic energy *see* **nuclear power**

atomic excited states

- see also* **atomic metastable states; atomic resonant states**
 alkali metal atoms, excited hyperfine and Stark parameters, meas. and calc. 8-86814
 field ionisation mechanisms 8-70761
 field-ionisation of Rydberg states, depend. on $|m_l|$ 8-58856
 gas discharge, photoionis. at low illumination intensity, nonlinearities, effective cross section 8-87517
 Group IVA elements, excited states, quadrupole moments, Sternheimer shielding factors 8-82630
 hadronic atom level shifts, multiple scat. expansion 8-70978
 halogen, negative ion form. in dissoc. attachment by 0-8 eV electrons 8-74776
 inert gases, photoionisation cross sections of excited atoms and dimers 8-66523
 ion excited state lifetimes meas. using orientation transfer in Penning collisions (*French*) 8-50621
 ionisation in EM field by electron diffusion (*Russian*) 8-86798
 lanthanides, Rydberg spectra and ionisation thresholds, time resolved resonant multistep technique 8-82701
 level crossing, using laser excitation (*Rumanian*) 8-50510
 magnetic scattering of neutrons on excited atoms or mols., cross sections, neutron polarisation (*Russian*) 8-55249
 metal vapour laser, upper and lower laser states population densities, simultaneous determ. method 8-87042
 open shell excited states, perturbation effects, restricted Hartree-Fock calcs. 8-86770
 plasma, population distrib., electron-density variation influence 8-87431
 quasi-hydrogenic atoms, Rydberg states 8-90098
 retardation effects on high Rydberg states, retarded R⁻³ polarisation pot. 8-82629
 Rydberg atom+atom collision, expts. 8-62908
 Rydberg atom+ion, collision theory 8-62909
 Rydberg atoms, microwave ionisation and excitation 8-94217
 Rydberg states, fine struct. splitting, quantum beat and double reson. spectroscopy 8-86979
 SCF treatment of higher excited states, method and its appl. to Si II 8-82658
 SCF wavefunctions 8-90099
 transition metal, atom, ion, solid, M_{2,3} excitation spectra 8-91653
 Ag, excitation by FK α and AlK α ESCA sources 8-53301
 Al, electron impact excitation cross sections calc. (*Russian*) 8-55240
 Al, 3p⁵p config. aligned in discharge, interf. signals, lifetimes and collision cross sections 8-70796
 Au, excitation by FK α and AlK α ESCA sources 8-53301
 Ba, multiphoton ionis. spectroscopy of even- and odd-parity states 8-86973
 Ba+N₂O, reaction, electronic branching, statistical and dynamical influences 8-92451
 Br^{*}(4²P_{1/2}) yield, in Br₂(IBr) photodissoc., wavelength depend., collisional release 8-64857
 C, theoretical ionis. energies and oscill. strengths, excited s-, p- and d-levels 8-86823
 Ca, multiphoton ionis. spectroscopy of even- and odd-parity states 8-86973
 Ca+O₂(CO₂)(N₂O), reaction, electronic branching, statistical and dynamical influences 8-92451
 Ca(4s4p³P)+N₂O, absolute chemiluminesc. cross-section and photon yield 8-53208
 Cd I, absorption spectrum, simultaneous excitation of two electrons 8-58614
⁵⁵Cr, ⁷P states HFS, level crossing technique, core polarisation, spin orbit interaction, config. mixing 8-78668
 Cs, discrete level raising into far continuum, oscillator strength to shape reson. transfer 8-78624
 Cs, excited state, two-photon ionisation by ruby laser light 8-74621
 Cs, fine-struct. of excited nd and nf states, at. core effect 8-58606
 Cu, electron impact, excitation function (maxima, cross-sections) 8-50650
 Dy I excited states, lifetime meas. using single photon counting method 8-70793
 Eu⁺+Sr, light-induced collisional energy transfer 8-50614
 Eu⁺+Sr+h ν →Eu⁺+Sr⁺, photon assisted collisional energy transfer 8-90285
 Ga, electron impact excitation cross sections calc. (*Russian*) 8-55240
 H, excited state interaction with photon field, simultaneous eqns. 8-66481
 H, in elec. field, semi-classical approx. (*Russian*) 8-86797
 H, self-interaction of excited at. with radiation field 8-86794
 H, Stark effect, asymptotic expansion for level width 8-70783
 H⁺+Na(K), excited state form. by inelastic processes, energy partitioning 8-82833
 H^{*}, radiative magnetic energy shift, H in 2p state 8-58601
 He, double excited states, lifetime meas. by beam-foil technique 8-74590
 He, electron impact, ³P_s and ^{1,3}D_s states excitation, electron correlation influence, Rudge-type approx. 8-74771
 He, electron impact excitation, ³P_s and ^{1,3}D_s states, electron correlation influence, Born-Oppenheimer approx. 8-74770
 He, excited S, D and F state radiative lifetimes, electron impact method 8-94325
 He excited states, relativistic corrections 8-62734
 He, Galerkin-Petrov method, nonlinear parameters 8-78619
 He I, II excited state population densities in non-LTE plasmas 8-67328
 He isoelectronic sequences, screening constants, ground and excited states 8-62701
 He isoelectronic series, energy level and classifications of doubly-excited states 8-62736

atomic excited states continued

- He, two-electron excited states 8-58605
 He, variational energies for highly excited states 8-62737
 He+H⁺, determ. of He excited state populations by two-photon reson. ionisation spectroscopy 8-82707
 He⁺+He(Ne), model pot. for low energy scatt. 8-66642
 He⁺+Mg(Zn), inelastic collisions, 2-800 eV, excited state form. 8-94312
 He⁺+Na(K), excited state form. by inelastic processes, energy partitioning 8-82833
 He⁺+Mg(Zn), inelastic collisions, 2-800 eV, excited state form. 8-94312
 He⁺⁺, doubly excited, spatial correl. of at. electrons 8-70760
 Hg, 5d spin-orbit X-ray excitation, 21-2700 eV, by ESCA sources 8-53301
 Hg, laser stepwise excitation of 6s6d6³D₁ level, transition probabilities and collisional excitation transfer 8-55146
 Hg+He(Xe), collisionally induced coherence, orientation and alignment, transfer among 6s6d levels 8-74747
 Hg+N₂, inelastic collision, 6³D₁ population transfer to other 6s6d Hg levels, fluoresc. obs. 8-78791
 Hg(6³P)+O₂, photosensitized reaction, excited intermediates, energy transfer detect. 8-73030
 I⁺+I₂(Br₂)(Cl₂)(IBr)(ICl)(BrCl), collisional deactivation and reaction rate consts., obs. 8-80738
 I(5²P_{1/2})+Br₂, deactivation kinetics, time-resolved spectrosc. obs. 8-95916
 I(5²P_{1/2})+Br₂, deactivation kinetics, Br(4²P_{1/2}) prod., time-resolved spectrosc. obs. 8-95917
 I(5²P_{1/2})+HCl(HBr)(NO), electronic-vibrational energy transfer, fluoresc. obs. 8-66579
 In, electron impact excitation cross sections calc. (Russian) 8-55240
 In I, 6²S_{1/2} state lifetime meas. by Hanle effect method 8-90097
 K, two-step photoionisation, triple crossed beam obs. 8-66616
 La I, lifetimes of z²F_{5/2}, z²D_{3/2}, z⁴G_{5/2} and y²D_{3/2} states 8-66489
 Li isoelectronic sequences, screening constants, ground and excited states 8-62701
 Li-like ions, fine struct. in 1s2p² 4P and 1s2s2p 4P^o states 8-66471
 Mn V, forbidden transitions laboratory wavelengths and excitation potentials 8-50496
 Na, energy transfer with 3P-excited atoms, fluoresc. spectrum 8-66498
 Na, fine-struct. of excited nd and nf states, at. core effect 8-58606
 Na isoelectronic sequence, Bethe excitation cross-sections 8-82657
 Na, Rydberg states, diamag. struct. 8-50484
 Na, Rydberg states, millimeter spectra, quantum defect, fine struct., polarisability, field ionis. obs. 8-82672
 Na(2³P_{1/2})+Hg, laser excited atoms, differential cross sections 8-62905
²²Na, Rydberg states, fine struct. splitting, quantum beat and double reson. spectroscopy 8-86979
 Na*(3p)+Na₂, collisional and radiative processes, fluoresc. decay obs. 8-66638
 Ne+Ne(He), 7d' states, isotope shift, press. shift, press. broadening, two-photon spectra obs. 8-55155
 Ne⁺+Kr, low vel. collision, enhanced K-L vacancy sharing ratios, X-ray prod. cross section 8-78790
 O II, III, IV, beam-foil spectra, mean lives, 270-490 angstrom 8-55223
 O(¹D)+CO, deactivation rate consts. temp. depend., 113-333K 8-88629
 O(¹D)+Xe(Kr)(Ar), deactivation rate consts., 110-330K 8-88628
 Pb(3²P_{1/2})+H, spin-orbit relax., fluoresc. intensity meas. 8-82681
 Rb, ²D states, fine struct. 8-90098
 Rb, oscillator strengths of 5s-4d first forbidden lines 8-86824
 RbHe(Ne), spin relax., Rb hyperfine interaction in Van der Waals mol. 8-94201
 S⁺+Ar, double K-vacancy prod., X-ray X-ray coincidence and fluoresc. yields obs. 8-55230
 S(¹S), in OCS laser, collisional electronic energy transfer, for fusion research 8-59003
 Se(3²P₁)+inert gas, gas phase flash photolytic deexcitation obs., 1000K (Russian) 8-50626
 Si II, transition probabilities between excited states, SCF treatment 8-82658
 Sr, associative ionisation of laser-excited Rydberg states, mass spectrometry obs. 8-94303
 Sr, multiphoton ionis. spectroscopy of even- and odd-parity states 8-86973
 Sr*(3²P₁)+HCl(HF), laser-excited atom reaction, energy deposition 8-85134
 Te(3²P₁)+inert gas, gas phase flash photolytic deexcitation obs., 1000K (Russian) 8-50626
 Tl, electron impact excitation cross sections calc. (Russian) 8-55240
 Xe, 5d(3/2), photoexcited state radiative decay 8-74605
 Xe, high Rydberg states, radiative lifetimes and transition probabilities 8-86817
 Xe, three level systems, obs. of isotope shifts 8-82670
 Xe(nf)+NH₃, at. Rydberg state further excitation by rot. transfer, field ionis. obs. 8-58795
 Y I, Y II, lifetimes of excited states, rel. to solar abundance determ. 8-86815
 Yb(6³P₁), Zeeman splitting, high-resolution time-resolved quantum beat spectra 8-8640
 Zr I, lifetimes of excited states, rel. to solar abundance determ. 8-86815

atomic explosions see nuclear explosions**atomic fine structure**

- electron polarisation produced by reson. ionisation by intense EM field (Russian) 8-50518
 nonlinear resonances of accelerated atoms and molecules (Russian) 8-50488
 reactance matrices, fine struct. cross sections, JAJOMPRE program 8-90312
 Rydberg states, fine struct. splitting, quantum beat and double reson. spectroscopy 8-86979
⁴He(3²P), fine struct., level crossing obs. 8-82686
 Be I isoelectronic sequence, radiative props. determ. by model-pot. method 8-70788
 C³⁺, fine struct. and lifetimes, doubly excited quartet system 8-78827
 Cs, fine-struct. of excited nd and nf states, at. core effect 8-58606

atomic fine structure continued

- H I, in solar chromosphere, substates population rel. to H α seven components and 9873 MHz line 8-89151
 H α , Balmer line emission fine struct., Stark effect (German) 8-82673
 H α , line shape, plasma broadened, fine struct. effects at low electron densities 8-62765
 He, electron impact excitation of high Rydberg state, impact parameter method 8-62922
 He, triplet P state splittings, higher order corrections of theoretical calc., book contrib. 8-82632
 He-like ions, electron impact, collision strengths for fine-struct. transitions 8-62925
 Li, A=6,7 two-photon intracavity dye laser spectroscopy 8-82706
 Li-like ions, fine struct. in 1s2p² 4P and 1s2s2p 4P^o states 8-66471
 N⁴⁺, fine struct. and lifetimes, doubly excited quartet system 8-78827
 Na, fine-struct. of excited nd and nf states, at. core effect 8-58606
 Na, Rydberg states, millimeter spectra, quantum defect, fine struct., polarisability, field ionis. obs. 8-82672
 NaI isoelectronic sequence, 3s-3p and 3p-3d transitions, ionisation energy 8-70773
 O⁺, photodetachment, fine struct. transitions, photoelectron spectra 8-55151
 O⁵⁺, fine struct. and lifetimes, doubly excited quartet system 8-78827
 Rb, ²D states, fine struct. 8-90098
 Rb, fine-struct. splittings in visible region, ²D states 8-50656
 S II, fine-structure transitions by electron impact 8-65493
 S⁺, photodetachment, fine struct. transitions, photoelectron spectra 8-55151
 Sr II, ²F states, fine struct. splitting 8-50494

atomic fluorescence

- 1s2p² 4P levels, lifetimes and line fluoresc. yields 8-74612
 asymmetric resonance fluorescence spectra, in partially coherent fields 8-66503
 colliding atoms, optical excitation to state of quasibound motion (Russian) 8-58784
 collision induced, high incident laser intensity effect 8-86811
 cooperative spontaneous emission, short-range Coulomb interactions 8-58619
 dipole transition, transient behaviour in intense laser field (German) 8-66520
 excitation spectroscopy, time-resolved photoluminescence emission and lifetime meas., synchrotron radiation use 8-66687
 gas laser, atomic constants and collision cross sections determ. by level crossing 8-50763
 heavy ion transitions, beam-foil decay curves, theoretical simulation 8-74755
 high Z atoms, L shell fluorescence yields, K to L transfer of vacancies 8-74606
 inner shell bound-bound radiative transitions, analytical description 8-82684
 intensity correlations in resonance fluorescence with atomic number fluctuations, photon antibunching 8-50499
 ion beam ejected particles from metallic targets, continuous emission spectra (Russian) 8-55140
 ion excited state lifetimes meas. using orientation transfer in Penning collisions (French) 8-50621
 level crossing, using laser excitation (Rumanian) 8-50510
 metal atoms sputtered by light and heavy particles, velocity distrib. meas. by fluorescence spectroscopy 8-95626
 neutral atoms, electron interaction, free-free radiative transitions, review 8-90295
 photon time-correlated counting, for fluoresc. decay signal analysis 8-49910
 radiance expressions, steady-state, for continuum excitation 8-82680
 radiation capture in cylindrical volumes of finite dimensions 8-66500
 rare earth ion potential vapour laser systems, spectroscopic props. 8-66812
 resonance atomic beam fluorescence, multiat. and transit-time effects on photon-correlation meas. 8-86812
 resonance fluorescence, intensity and phase fluctuating light 8-82683
 resonance fluorescence in vacuum UV, detection of low gas densities 8-54341
 resonance fluorescence with recoil effects, quantum statistical theory 8-78660
 saturation of energy levels in analytical spectroscopy 8-65980
 sideband prediction in strong-field reson. fluoresc. 8-55139
 spectral density of resonance fluorescence, two level atom in intense radiation fields 8-58961
 spectroscopy of atoms near a wall (Dutch) 8-70972
 stimulated collision-induced fluoresc. and stimulated Raman scatt. 8-87103
 three-level atom reson. fluorescence, statistical props. 8-78661
 three-level atom resonance fluoresc., polaris. depend. 8-50500
 three-level system, cooperative cascade emission 8-78659
 three-level system, reson. interaction of opposite waves, relax. consts. of common level 8-50511
 two-atom system, continuously pumped, radiation props., master eqn. 8-86828
 two-level atom, multiphoton reson. fluoresc. in strong low-freq. field 8-55154
 Weisskopf-Heitler effect, intrinsic laser linewidth contrib. 8-70782
 Ag, matrix isolated, fluoresc. spectra. excimeric bond effects 8-50498
 Ar⁺+C, beam-foil spectra, Ar⁺ ion orientation, ang. variation 8-86944
 Ar*(4p),(5p) states, lifetimes and two-body rate consts. meas. 8-63058
 As, (4³S_{3/2}) state, kinetic obs. using time resolved reson. fluoresc. 8-94211
 Ba, radiative decay of autoionisation states (Ukrainian) 8-82682
 Bi, excited in discharge region, new light source of forbidden lines 8-90112
 Ca, electron impact, 3p⁶ subshell excitation, VUV spectra (Russian) 8-90117
 Ca, radiative decay of autoionisation states (Ukrainian) 8-82682
 Cd, 6³P₁ level, relax. of alignment and population 8-70795
 Cd₂, vapour, excited by photodissociation, fluoresc. yields 8-55138
 Cl, form. from HCl dissociation, excitation in afterflow, light emission 8-90115
 Cs, optical reson. line electron impact excitation cross sections, polaris. 8-55244

atomic fluorescence continued

- Cs, superfluorescence (*Dutch*) 8-70780
 Cs-He, new absorption/emission bands perturbed Cs transitions assignment, pot. energy curves 8-66486
 Er³⁺, luminesc. sensitisation by Yb³⁺, in liq., efficiency (*Russian*) 8-90116
 Eu²⁺ in aqueous solution, multiphoton excitation and emission 8-94222
 H⁺, fluoresc. in γ - and UV-irrad. solvent matrices at 77K 8-70779
 H⁺, ion-surface collision with Mo, optical radiation emission 8-95644
 H-like ions, fluoresc. polarisation of Stark quenched spin-polarised beam 8-66501
 He, 3P level, spontaneous decay probability, expt. and theoretical values 8-50501
 He, electron impact fluorescence, polarisation of 5876 line 8-82848
 He, excited S, D and F state radiative lifetimes, electron impact method 8-94325
 He⁺+C, beam-foil spectra, He atom orientation, ang. variation 8-86944
 He⁺+Mg(Zn), inelastic collisions, 2-800 eV, excited state form. 8-94312
 He₂⁺+Mg(Zn), inelastic collisions, 2-800 eV, excited state form. 8-94312
 Hg, two-photon excitation by photodissoc. of Hg halide 8-90114
 Hg+He, laser excitation of Hg 6s6d³D₁ level, transition probabilities and collisional excitation transfer 8-55146
 Hg+He(Xe), collisionally induced coherence, orientation and alignment, transfer among 6s6d levels 8-74747
 Hg+N₂, inelastic collision, 6³D₁ population transfer to other 6s6d Hg levels, fluoresc. obs. 8-78791
 Hg+Ti, Ti sensitised fluorescence 8-70778
 HgI₂(Br₂), vapour, excited by photodissociation, fluoresc. yields 8-55138
 I(5²P_{1/2})+benzene-d₀(-d₆), fluoresc. quenching, spin-orbit interaction, isotope effect obs. 8-62763
 I(5²P_{1/2})+HCl(HBr)(NO), electronic-vibrational energy transfer, fluoresc. obs. 8-66579
 InI, vapour, excited by photodissociation, fluoresc. yields 8-55138
 K, optical reson. line electron impact excitation cross sections, polaris. 8-55244
 K+He, 93 eV, excitation of K atom, photon-scatt.-atom coincidence study 8-82829
 K+Hg, electronic excitation, integral cross-section, 50-1500 eV 8-62888
 Kr VIII beam-foil decay curves for resonance transitions 8-74755
 Mg, excited in discharge region, new light source of forbidden lines 8-90112
 Mg XI-SV ions, 2131-1s31 and 2121-1s21 radiative transitions and non-radiative decay probabilities 8-70781
 Na atomic beam, Autler-Townes effect in double optical resonance 8-66499
 Na D₂ line, resonance fluorescence, photon antibunching, quantisation of light 8-66791
 Na, energy transfer with 3P-excited atoms, fluoresc. spectrum 8-66498
 Na, flame absorption and fluorescence, laser saturation broadening 8-88661
 Na, spectra, emission and absorpt., inert gas matrix 8-90106
 Na, two-photon excitation in flame, saturation broadening, fluoresc. obs., broad-band excitation 8-74625
 Na vapour, transient optical nutations in D₂ line 8-66507
 Na vapour seeded He hypersonic flow, velocity profile visualisation 8-59530
 Na+Kr(Xe), excimer bands, multiperturber interactions 8-66497
 Na+Kr(Xe), reson. line broadening, press. depend. 8-66596
 Na*(3p)+Na₂, collisional and radiative processes, fluoresc. decay obs. 8-66638
 Ne, reson. interaction of opposite waves, relax. consts. of common level 8-50511
 Ne+Ne, excitation transfer, coupling coeffs., temp. depend., fluoresc. meas. 8-58620
 O(3P)+O₃, bimolecular reaction rate coeff. reactant vibr. excitation depend., reson. fluoresc. obs. 8-76837
 Pb(3P^o)+H, spin-orbit relax., fluoresc. intensity meas. 8-82681
 Rb, optical reson. line electron impact excitation cross sections, polaris. 8-55244
 S⁺+Ar, double K-vacancy prod., X-ray X-ray coincidence and fluoresc. yields obs. 8-55230
 SF₆Cl, multiphoton dissoc., real-time Cl atom fluoresc. detect. 8-86923
 Sr, radiative decay of autoionisation states (*Ukrainian*) 8-82682
 Tb³⁺ in TbCl₃(AlCl₃)_x complex, potential vapour laser system, fluoresc. obs. 8-66812
 Tb³⁺, luminesc. sensitisation by Yb³⁺, in liq., efficiency (*Russian*) 8-90116
 Ti, stimulated Raman scatt. and stimulated collision induced fluoresc. 8-87103
 TII, vapour, excited by photodissociation, fluoresc. yields 8-55138
 Xe, 5d(3/2)₁ photoexcited state radiative decay 8-74605
 Xe, afterglow, 6s₂ metastable atom density decay rate 8-63612
 Xe, electron impact polaris. and excitation functions 8-66665
 Xe, laser light irrad. in mag. field, light modulation expt. 8-82699
 Xe, second continuum fluoresc. excited by synchrotron radn. 8-90113
 ZnI₂, vapour, excited by photodissociation, fluoresc. yields 8-55138

atomic fluorescence spectroscopy *see atomic emission spectroscopy***atomic forces**

- binary gas mixtures, force consts., intermol. pots. calcs. 8-66624
 diatomic bonding energy, changes due to Van der Waals interactions with other atoms 8-95012
 DNA, improved definition of A and B forms, atom-atom potential functions method 8-96000
 inert gas mixture, collision-induced absorption, exact line shapes, appl. to He-Ar 8-66512
 interatomic potential between two equal ions 8-94300
 ions in dipolar solvent, potential of mean force, linearised hypernetted chain approx. calcs. 8-55798
 like atoms in static gravitational field 8-54270
 minimum potential energy per particle configuration, one-dimens. system 8-70084

atomic forces continued

- retardation effects on high Rydberg states, retarded R⁻⁵ polarisation pot. 8-82629
 Yukawa potential function, determ. of phase shifts 8-58237
 Ar-Kr, pair pot. function calcs. 8-74726
 ArKr, intermol. pots., differential cross-sections inversion calcs. 8-66619
 Cl⁻, pair polarisability, ab initio SCF MO energies 8-70741
 Cs-He, new absorption/emission bands perturbed Cs transitions assignment, pot. energy curves 8-66486
 He-Ar(Kr)(Xe), intermol. forces, combining rules 8-66622
 He+H (inert gas atom), long range interactions for (2¹S) and (2³S) states 8-70895
 He+Ne pot., differential cross section, quantum mechanical inversion 8-70896
 Li⁺, pair polarisability, ab initio SCF MO energies 8-70741
 N₂, solid, lattice dynamical calcs., use of anisotropic at.-at. pot. functions, α - γ transition 8-71811
 Ne+Ar(Kr)(Xe), elastic scatt. absolute total cross section, long range interaction 8-58768

atomic hyperfine structure*see also Lamb shift*

- alkali metal atom+inert gas atom, hyperfine transition spectral line shift, quantum corrections 8-82655
 alkali metal atoms, excited hyperfine and Stark parameters, meas. and calc. 8-86814
 electron polarisation produced by reson. ionisation by intense EM field (*Russian*) 8-50518
 EPR, at. parameters calc. using Hermann-Skillman wavefunction, He to Bi 8-91956
 excitation regimes in higher shells 8-70955
 exotic atoms, hyperfine splitting, recoil corrections calcs. 8-50667
 fast atomic beams, high-resolution spectroscopy 8-89557
 first-row atoms, ground states, using CI wavefunctions 8-74583
 laser spectroscopy techniques, review 8-70975
 longitudinal decoupling of free hyperfine interactions, influence of time depend. effects 8-50655
 muonium, hyperfine splitting 8-74806
 muonium, hyperfine splitting correction 8-94336
 muonium, hyperfine splitting of ground-state 8-94337
 positronium, fermion-antifermion eqn., static interaction limit 8-62963
 positronium, hyperfine splitting 8-74806
 positronium hyperfine struct., $m\alpha^6$ contribs. from two photon virtual annihilation 8-89642
 surface wave polarisation in hyperfine dipolar mag. transitions (*French*) 8-50504
 weak field absolute induction meas. HFS magnetometer 8-77949
¹³⁵Ba, ¹³⁷Ba Fourier transform NMR, NQR studies 8-94261
⁴⁰Ca, nucl. mag. moment, hyperfine interaction of electron in L, M and N regimes 8-70448
⁵⁹Co, mag. hyperfine struct. analysis, spectral lines 4000 to 4300 Å 8-62752
⁵⁵Cr, ⁷P states HFS, level crossing technique, core polarisation, spin orbit interaction, config. mixing 8-78668
 Cs, 6²S_{1/2}-6²S_{3/2} transition ($\lambda=8521$ Å) with hyperfine splitting, curves of growth 8-66513
 Cs, HFS, isotope shift related to nucl. charge rad. 8-78826
 Fe, hyperfine interaction parameters, effect of local exchange, X α and HF calcs. 8-78622
 Gd³⁺, hyperfine interactions, relativistic CI using many-body calcs. 8-78638
 H, beam, 2²S_{1/2} metastabld ats., nonadiabatic transition in mag. field 8-55157
 H, hyperfine freq. meas. of ground state 8-78984
 H-He, H hyperfine struct. shift, commutator computational method 8-78608
 H-like ions, excitation regimes, nucl. orientation due to hyperfine interaction 8-70928
 He-F, doublet series laser lines near 700 μ m, hyperfine splitting and broadening meas. 8-63070
 He-like ions, excitation regimes, nucl. orientation due to hyperfine interaction 8-70928
¹⁹⁹Hg⁺, hyperfine separation of ground-state, optical double-reson. 8-78828
¹⁹⁹Hg⁺ trapped ion frequency standard 8-57914
 I, laser 1.315 μ m transition line struct. 8-59000
 In, 451.1 nm transition, HFS and ¹¹³In-¹¹⁵In isotope shift 8-82674
 Ir, hyperfine interaction parameters, effect of local exchange, X α and HF calcs. 8-78622
 Li, A=6,7 two-photon intracavity dye laser spectroscopy 8-82706
⁷Li, level-crossing method for HFS and at. lifetimes 8-66678
²¹Ne, 2p³3p config., hyperfine mag. const. by laser level-crossing technique 8-50509
 Pt group, even atom config., parametric calcs. 8-82631
 Rb 5²P_{1/2} state, Hanle effect intensities 8-66521
 RbHe(Ne), spin relax., Rb hyperfine interaction in Van der Waals mol. 8-94201
⁸⁵Rb, ground state dipole HFS diamagnetic shift, high field optical pumping expt. 8-90129
⁸⁵Rb+(⁸⁷Rb⁺), hyperfine struct., in-flight saturated absorption laser spectrosc. 8-78650
⁸⁷Rb, surface wave polarisation in hyperfine dipolar mag. transitions (*French*) 8-50504
 Ru, hyperfine interaction parameters, effect of local exchange, X α and HF calcs. 8-78622
 Tb I, 4f⁸5d6s² config., hyperfine struct. analysis 8-62732
²³⁸U, hyperfine struct. and isotope shift meas., laser separation by two-step photoionisation 8-78822
 W, isotope shifts in visible region and HFS 8-82694
⁹¹Zr, hyperfine struct. and nucl. elec. quadrupole moment. at. beam mag. reson. meas. 8-55133

atomic inelastic collisions

- see also atom-atom collisions; atom-ion collisions; atom-molecule collisions; atom-molecule reactions; beam-foil spectra; ionisation of atoms*
 asymmetric scattering, spin-1 particle by non-central field 8-55214
 atom+charged particle anisotropic collision, spectral line shift and broadening, polarisation depend. 8-82695
 atom+oscillator, collinear collision, distorted wave perturbation theory 8-74731
 atomic collisions in solids, book contrib. 8-75697

atomic inelastic collisions continued

- Auger process in atomic collisions 8-62899
 Bethe theory, inelastic collisions of fast charged particles 8-58783
 cooling/heating rates for collision in light fields (*Russian*) 8-62874
 dielectronic recombination amplitudes, scaling props. 8-58781
 distorted wave perturbation theory, higher order, accuracy and convergence 8-74731
 Doppler line profile, saturation, influence of atomic collisions 8-70792
 fast heavy ion+atom, and solid targets, ionis. and excitation states 8-70927
 induced moments in at. and mols., polarisability density concept limitations 8-70964
 inner-shell ionisation, semi-classical theory 8-62896
 lineshape analysis for collision induced spectra 8-70787
 magnetic scattering of neutrons on excited atoms or mols., cross sections, neutron polarisation (*Russian*) 8-55249
 near-adiabatic collisions, theory, electron translation factor method 8-81889
 near-adiabatic collisions, theory, scatt. coord. method 8-81890
 pair polarisabilities, continuum electrostatic theory 8-86769
 potential scatt., separable expansion method, off-shell T matrix 8-93564
 rainbow scattering, Regge pole anal. 8-58774
 relaxation coefficients, meas. method (*French*) 8-58771
 relaxed sudden approx., moderate collision energies 8-70902
 scattering amplitudes, Regge representation calcs. 8-58770
 semiclassical scatt. matrix, Massey parameter expansion 8-58759
 spectral line collisional broadening, classical and quantum theories, radiator motion effect 8-86822
 spectral line shapes, linear and nonlinear, atom or mol. cross sections 8-70899
 spectroscopy of atoms near a wall (*Dutch*) 8-70972
 Three-electron Auger transitions in atoms with two inner shell vacancies 8-62900
 μ +atom, e^+e^- pair prod., energy spectrum, screening effects (*Russian*) 8-55250
 Ar, collision induced light scatt. spectra, pair polarisability 8-55135
 Eu*+Sr, light-induced collisional energy transfer 8-50614
 H atoms in cylindrical hydrogenic plasma, transport code 8-51284
 H generator, freq. shift due to atomic collisions with storage flask walls 8-77870
 H-like ions, excitation regimes, nucl. orientation due to hyperfine interaction 8-70928
 H+H, pair polarisabilities, continuum electrostatic theory 8-86769
 He-like ions, excitation regimes, nucl. orientation due to hyperfine interaction 8-70928
 Hg(6^3P)+O₂, photosensitised reaction, excited intermediates, energy transfer detect. 8-73030
 O⁺, electron loss, forward peak oscill. struct. 8-78796
 Si⁺ electron loss, forward peak oscill. struct. 8-78796

atomic magnetic moment

- see also gyromagnetic ratio
 paramagnetic gas in radiation field, magnetisation 8-78667
 Co, atomic magnetic moments comparison to values of ferromagnetic metal 8-52244
 Fe, atomic magnetic moments comparison to values of ferromagnetic metal 8-52244
 Ni, atomic magnetic moments comparison to values of ferromagnetic metal 8-52244

atomic mass

- see also isotopes; mass spectra; nuclear mass
 relative mass evaluation, input values 8-70949
 XY₆-type molecules, Coriolis coupling const., at. mass effect, XCl₆ appls. 8-66684

atomic metastable states

- 1s2p²P levels, lifetimes and line fluoresc. yields 8-74612
 atom+metastable atom collisions, ionis. processes 8-62907
 Doppler-free linear single-photon spectroscopy 8-50487
 inert gas, metastable atoms, scatt. 8-62906
 inert gas collisions, intermediate energies 8-62904
 positive column, metastable atom radial transport, effect of wall boundary conditions 8-67493
 Ar, metastable, electron impact excitation cross-sections calcs. 8-94323
 Ar, metastable ³P₂ deactivation in afterglow, plasma characts. 8-55769
 Ar+Ar(³P₂)(³P₀), flowing afterglow metastable decay rates, diffusion, two- and three-body rate const. 8-73027
 Ar+H₂O(D₂O), (³P_{0,2}) state quenching cross sections 8-70912
 Ar+Kr(³P₂), flowing afterglow metastable decay rates, diffusion, two- and three-body rate const. 8-73027
 Ar+Xe, relaxation processes of Xe*(³P₂) metastable atoms 8-50624
 Ar+Xe(³P₂), flowing afterglow metastable decay rates, diffusion, two- and three-body rate const. 8-73027
 Ar*(³P)+CO₂(X¹ Σ_g^+), differential elastic and quenching cross-sections 8-58773
 Bi beams excited passing discharge region, new light source of forbidden lines 8-90112
 Ca+O₂(CO₂), CaO form., product states obs. 8-92450
 Cu, ground and metastable populations, buffer gas effect 8-82955
 CuCl pulsed laser, time depend. of Cu-atom conc. in ground and metastable states 8-66806
 H (2s) metastable state elastic electron scatt. 8-55238
 H, beam, 2²S_{1/2} metastable at., nonadiabatic transition in mag. field 8-55157
 He 2³S-3³S electron impact excitation, first Born and Glauber cross sections 8-55243
 He (2³P)+Ca(Sr), collisional quenching of metastable states, excitation transfer cross sections 8-66653
 He I 1s3d levels, cascade-free lifetime meas., using He⁺+He 35 keV collisions 8-58607
 He low-current discharge, metastable atoms, radial density distrib. obs. and calc. 8-67495
 He, metastable, deexcitation process on Mo [110] impact 8-95642
 He, metastable 1s2s¹S state, photoionisation, perturbation theory calcs. 8-78759
 He, Voigt profile, line absorpt. calcs. of 388.9 nm triplet, 501.6 nm singlet lines 8-90123
 He+H (inert gas atom), long range interactions for (2¹S) and (2³S) states 8-70895

atomic metastable states continued

- He+H₂(He)(Ar)(N₂), fast metastable at. collisional destruction cross section 8-74760
 He+He, metastable atoms, collisional ionisation cross-sections 8-70911
 He+Hg, metastable He, collision rate const. in pulsed discharge afterglow 8-50627
 He⁺+Na(K)(Cs), 5-100 keV, electron capture form. of fast metastable He 8-74760
 He*+Ar, Penning ionisation, laser modified collisional effects in electron energy spectrum 8-90278
 He*+H(H₂)(Ar), metastable state, ionis. processes 8-62907
 He(2³S) collisions, elastic scatt., Penning ionisation, polarisations (*Russian*) 8-70922
 He(2³S)+H₂O(H₂S), energy transfer processes, reaction products, UV and visible obs. in flowing afterglow 8-85138
 He(2³S₁)+e \rightarrow He(1¹S₀)+e+KE, in afterglow, rate const., electron energy distrib. 8-71571
 Hg(6³P_{2,0})+inert gas, diffusion in low-current discharge 8-63618
 Kr, DC glow discharge excited atoms, radial conc. distrib. obs. 8-67494
 Kr, metastable, electron impact excitation cross-sections calcs. 8-94323
 Kr+H₂O(D₂O), (³P_{0,2}) state quenching cross sections 8-70912
 Kr(³P₁)(³P₁)+CO, A¹ Π -X¹ Σ^+ and b³ Σ^+ -a³ Π sensitised fluorescence, isotope effects 8-82761
 Kr*+He, persistence of velocity following elastic collisions 8-78779
 Kr*+He(Ar), vel. changing collisions studied by saturated absorpt. 8-62892
 Li, quartet states, absolute term values, CI calcs. 8-58596
 Li, quartet states, transition energies, oscill. strengths, CI calcs. 8-58597
 Mg beams excited passing discharge region, new light source of forbidden lines 8-90112
 N(³D)+O₂, chemically excited NO form., 90-180K IR obs. 8-90163
 N₂(X¹ Σ_g^+)+Ar(³P_{2,0}) \rightarrow Ar(³S)+N₂(C³ Π_u), sensitised fluoresc., vel. depend. 8-90204
 Ne discharge positive column in longitudinal mag. field, metastable atom radial density distrib. obs. 8-67496
 Ne, Doppler-free linear single-photon spectroscopy 8-50487
 Ne, metastable level deactivation by electron collision in low press. discharge 8-83520
 Ne+Ne(He), 7d' states, isotope shift, press. shift, press. broadening, two-photon spectra obs. 8-55155
 O⁺+atmospheric gases, thermal energy reaction rates 8-92443
 O(³S) impact on Cu-Be-O surface, secondary electron yield 8-58797
 O(³S) metastable state, radiative lifetime determ. 8-74614
 Sr⁺+N₂O \rightarrow SrO⁺+N₂, visible chemiluminescence, absolute cross section and photon yields 8-92463
 Tl, (6p²P_{3/2}), from selective photodissoc. of TlBr 8-90243
 Xe, afterglow, 6s_{1/2} metastable atom density decay rate 8-63612
 Xe*(³P)+Ca(Sr), collisional quenching of metastable states, excitation transfer cross sections 8-66653

atomic orbitals see atomic structure**atomic orbitals calculations**

- see also GO calculations; GTO calculations; STO calculations
 Auger effect, semi-empirical models for electron energy calcs. 8-50519
 binding and transition energies, expt. and theoret. comparison, review 8-50497
 contour calcs., teaching approach 8-93500
 electron affinity, MNDO semi-empirical SCF-MO calcs. for atoms, mols., negative ions 8-74578
 electron integrals transformation method, program in FORTRAN IV H 8-82603
 electron shakeoff accompanying beta-decay, probability for K- and L-shells 8-94204
 ESCA photoionisation cross section, relative intensities calcs., comparisons 8-50464
 incomplete basis set problem, Hartree-Fock energy, perturbative corrections 8-70744
 inert gases, collision induced polarisabilities, perturbation treatment 8-86778
 inverse matrix diagonal and off diagonal elements, self energy perturbation theory 8-82607
 Koopmans atomic valence electron ionisation energy, 1/Z expansion method, reorganisation corrections 8-78623
 lower bound Hamiltonians for atoms and mols., projection operator method 8-82602
 n-electron atomic wavefunction, Schrodinger inequalities, many-electron densities 8-94191
 negative quantum chemical calcs. 8-62703
 orbital amplitudes of nuclei, extrapolation procedure, gaussian basis set and nucl. cusp eqn. 8-74560
 oxygen-type atoms, subdivision of 2p-shell 8-82609
 p-block at., energy levels, position orbital calcs., electron repulsion integrals, teaching appl. 8-93494
 pseudo-orbital theory, cluster expansion of wavefunction 8-62706
 quasi-energetic spectra of quantum systems in classical monochromatic fields 8-78981
 R-matrix method, atomic continuum processes calc., program 8-74558
 universal atomic basis sets, light atom HF ground state energies 8-78605
 X_n optimised STO exponents 8-62721
 Ag, semiempirical, relativistic oscillator strengths including core polarisation for p-, s-, d-series 8-74609
 Al, electron impact excitation cross sections calc. (*Russian*) 8-55240
 Ar, electron scattering, elastic, at low-energy, polarised orbital calc. 8-82840
 Ar IX, Ne I like reson. and Na I-like satellite lines, relativistic HF calc., beam-foil spectra 8-94210
 Ar, KLL and KLM Auger electron spectra, obs. and relativistic multi-configurational Dirac-Fock calc. 8-50524
 Au, semiempirical, relativistic oscillator strengths including core polarisation for p-, s-, d-series 8-74609
 B, ground state wave function, 2s-2p electron promotion effect 8-86779
 B, ground state wavefunction, SCF HF calc. 8-90070
 Be, ground state wavefunction, SCF HF calc. 8-90070

atomic orbitals calculations continued

- Be sequence, ($Z=4$ to 10, 14), $^3P_1 \rightarrow ^1S_0$ intercombination line, CI calc., Breit interaction 8-78641
 C, effective valence shell Hamiltonian, ab initio calcs. 8-82611
 C, ground state wavefunction, SCF HF calc. 8-90070
 C, effective valence shell Hamiltonian, ab initio calcs. 8-82611
 Cn , ($n=1,2,3$) effective valence shell Hamiltonian, ab initio calcs. 8-82611
 Cl VIII, Ne I like reson. and Na I-like satellite lines, relativistic HF calc., beam-foil spectra 8-94210
 Cs, discrete level raising into far continuum, oscillator strength to shape reson. transfer 8-78624
 Cu, semiempirical, relativistic oscillator strengths including core polarisation for p-, s-, d-series 8-74609
 Fe, hyperfine interaction parameters, effect of local exchange, $X\alpha$ and HF calcs. 8-78622
 Ga, electron impact excitation cross sections calc. (Russian) 8-55240
 H, relativistic Dirac eqn., for teachers 8-62019
 H₂-like at. orbitals, shape, teaching appl. 8-93496
 He, electron scattering, elastic, at low-energy, polarised orbital calc. 8-82840
 He, excited states, Galerkin-Petrov method, nonlinear parameters 8-78619
 He, ground state wavefunction, SCF HF calc. 8-90070
 He, Hartree-Fock energy, perturbative corrections, incomplete basis set problem 8-70744
 He, photoionisation, frozen-core HF perturbation theory, oscillator strength, dipole length and vel. calc. 8-78672
 He⁺, wave function structure, complex coord. method 8-94190
 He⁺+alkali metal atom, ionisation cross sections, binary encounter approx. with HF electron vel. distrib. 8-55225
 In, electron impact excitation cross sections calc. (Russian) 8-55240
 Ir, hyperfine interaction parameters, effect of local exchange, $X\alpha$ and HF calcs. 8-78622
 K²⁺, photoionisation cross-section, R-matrix theory 8-82702
 Kr, 3p core hole spectrum, many electron description 8-50517
 Li, ground state wavefunction, SCF HF calc. 8-90070
 Li, s²S and 2²P states, spin-optimised SCF general spin orbitals 8-82617
 Ne, electron scattering, elastic, at low-energy, polarised orbital calc. 8-82840
 Ne, ground state wavefunction, SCF HF calc. 8-90070
 Ne, photoionisation, complex amplitudes at low energy singly and doubly excited resons. 8-78673
 Ru, hyperfine interaction parameters, effect of local exchange, $X\alpha$ and HF calcs. 8-78622
 Ti, electron impact excitation cross sections calc. (Russian) 8-55240
 U, ab initio effective core pots., relativistic corrections 8-50483
 Xe, 5s, 5p ESCA spectrum, photoionisation many electron description 8-50516

atomic polarisability

- dynamic multipole polarisability, functional calcs. 8-74595
 inert gases, collision induced polarisabilities, perturbation treatment 8-6778
 nonuniform arbitrary elec. field-induced moments polarisability density concept limitations 8-70964
 pair of atoms, long range effects, intrinsic polarisability rel. to hyperpolarisability 8-78824
 pair polarisabilities, continuum electrostatic theory 8-86769
 polarisation propagator calculations of frequency-dependent polarisabilities, Verdet constants, and energy weighted sum rules 8-58647
 quantum static multipole polarisabilities 8-82859
 R-matrix method, appl. to atoms and mols. 8-58833
 R-matrix method, atomic continuum processes calc., program 8-74558
 retardation effects on high Rydberg states, retarded R^{-5} polarisation pot. 8-82629
 Ag, semiempirical, relativistic oscillator strengths including core polarisation for p-, s-, d-series 8-74609
 Ar, collision induced light scatt. spectra, pair polarisability 8-55135
 Au, semiempirical, relativistic oscillator strengths including core polarisation for p-, s-, d-series 8-74609
 B⁺, dynamic multipole polarisability, coupled Hartree-Fock 8-82858
 Be, dynamic multipole polarisability, coupled Hartree-Fock 8-82858
 Be, freq.-depend. polarisabilities and Verdet consts., calcs. 8-62781
 Be I isoelectronic sequence, radiative props. determ. by model-pot. method 8-70788
 C²⁺, dynamic multipole polarisability, coupled Hartree-Fock 8-82858
 Cl⁺, pair polarisability, ab initio SCF MO energies 8-70741
⁵⁵Cr, ⁷P states HFS, level crossing technique, core polarisation, spin orbit interaction, config. mixing 8-78668
 Cu, semiempirical, relativistic oscillator strengths including core polarisation for p-, s-, d-series 8-74609
 H, dynamic multipole polarisability, functional calcs. 8-74595
 H, imaginary frequency multipole polarisability and long-range dispersion consts, functional calcs. 8-74596
 H, multipole polarisability and shielding factors, hydrodynamic analogy to quantum mech. 8-66677
 H-like atoms, multipole polarisability, dynamic, for S state, closed-form expression 8-82857
 H+H, pair polarisabilities, continuum electrostatic theory 8-86769
 He, dynamic multipole polarisability, functional calcs. 8-74595
 He, dynamic polarisability, CHF method 8-50472
 He, freq.-depend. polarisabilities and Verdet consts., calcs. 8-62781
 He, imaginary frequency multipole polarisability and long-range dispersion consts, functional calcs. 8-74596
 He⁺, dynamic multipole polarisability, functional calcs. 8-74595
 He⁺, imaginary frequency multipole polarisability and long-range dispersion consts, functional calcs. 8-74596
 He₂, pair polarisability correl. effects, SCF-CI-GTO-SO calc. 8-82651
 In²⁺, emission spectrum, 340 to 6500 Å, ionisation pot. and dipole polarisability 8-78654
 Li⁺, dynamic multipole polarisability, functional calcs. 8-74595
 Li⁺, imaginary frequency multipole polarisability and long-range dispersion consts, functional calcs. 8-74596
 Li⁺, pair polarisability, ab initio SCF MO energies 8-70741
 Na, Rydberg states, millimeter spectra, quantum defect, fine struct., polarisability, field ionis. obs. 8-82672
 atomic power *see nuclear power*
 atomic reactors *see fission reactors*
 atomic resonant states
 AC Stark splitting in doubly reson, three-photon ionisation, nonmonochromatic field 8-94220
 alkali metal atoms, excited hyperfine and Stark parameters, meas. and calc. 8-86814
 asymmetric resonance fluorescence spectra, in partially coherent fields 8-66503
 atom, two-photon resonant ionis. 8-58631
 cumulative resonance in atomic ground state induced by modulated light field 8-66518
 dielectronic recombination amplitudes, scaling props. 8-58781
 electron elastic scatt., Feshbach resonances 8-58831
 electron scatt., optical excitation functions 8-58841
 electron scatt. using dilatation transforms., restricted perturbation methods 8-50639
 fluorescence, reson., in at. beam, multiat. and transit-time effects on photon-correlation meas. 8-86812
 fluorescence, resonance, in vacuum UV, detection of low gas densities 8-54341
 fluorescence, resonance, with recoil effects, quantum statistical theory 8-78660
 heavy ion transitions, beam-foil decay curves, theoretical simulation 8-74755
 J-dependence of intensity-dependent polarization change in atomic reson. lines 8-70775
 laser-induced line shifts and double-quantum Lamb dips 8-86825
 light wave resonant interaction with atoms and molecules (Ukrainian) 8-66515
 many-electron systems, complex-coord. method extension 8-74591
 multilevel systems, nonlinear reson. freq. shifts and saturation effects 8-78675
 multiphoton resonant ionis., model calc. 8-62773
 nonlinear resonances of accelerated atoms and molecules (Russian) 8-50488
 quantum motion in reson. field of standing light wave (Russian) 8-50508
 radiation capture in cylindrical volumes of finite dimensions 8-66500
 resonant two-photon ionisation in partially coherent radiation field 8-66525
 Schrodinger equation solution for atom near metallic surface, resonant state, jellium model 8-80033
 soft photon approx. accuracy for resonances in electron scatt. in laser field 8-70935
 stimulated collision-induced fluoresc. and stimulated Raman scatt. 8-87103
 three-level atom reson. fluorescence, statistical props. 8-78661
 three-level atom resonance fluoresc., polaris. depend. 8-50500
 three-level system, reson. interaction of opposite waves, relax. consts. of common level 8-50511
 two-level atom, multiphoton reson. fluoresc. in strong low-freq. field 8-55154
⁴He(3³P), fine struct., level crossing obs. 8-82686
 Ar, electron scatt. in laser radiation field, free-free cross sections, reson. struct. 8-74763
 Ar IX, Ne I like reson. and Na I-like satellite lines, relativistic HF calc., beam-foil spectra 8-94210
 Ba, diamag. quasi-Landau spectrum near ionis. threshold, two-photon ionis. spectra obs. 8-58642
 Be⁺, ²P^o shape resonance, complex-coord. method calc. 8-74591
 Cl VIII, Ne I like reson. and Na I-like satellite lines, relativistic HF calc., beam-foil spectra 8-94210
 Cs, multiphoton ionisation, reson. peak amplitude, temporal effects 8-78760
 Cs, optical reson. line electron impact excitation cross sections, polaris. 8-55244
 Cs, photoplasma, optical excitation in radiation diffusion conditions 8-55227
 Cs, reson. multiphoton ionisation by ultrashort laser pulsed, 1.06 µm 8-58630
 Cs, resonantly excited in cylindrical discharge plasma, effective lifetimes 8-79413
 CsI, four-photon ionisation near 6f resonance 8-70801
 Fe XXIII and XXIV, reson. and intersystem transitions, oscill. strength, lifetime, beam-foil spectra 8-82685
 Fr I, wavelength estimate of first and second resonance lines 8-58617
 H, electron-photon excitation, high-energy resonant cross sections 8-70938
 H, highly excited resonant states, Stark effect, nonperturbative regime 8-70786
 H, two-photon absorpt. of ultrashort pulses, reson. intensities 8-59077
 H⁺, autoionising states, electric field effect 8-50528
 H⁺+H(D), elastic scatt. and charge exchange, resonances 8-78777
 He, metastable, deexcitation process on Mo [110] impact 8-95642
 He+He⁺, resonant charge transfer cross sections, 2 to 100 eV 8-66655
 He⁺+Ar(N₂)(He), up to 70 keV, symmetric (antisymmetric) reson. charge transfer cross sections (Korean) 8-50636
 K, optical reson. line electron impact excitation cross sections, polaris. 8-55244
 K, resonantly excited in cylindrical discharge plasma, effective lifetimes 8-79413
 K, two photon excitation by opposing light beams, reson. lines polarisation studies 8-82705
 Kr, DC glow discharge excited atoms, radial conc. distrib. obs. 8-67494
 Kr VIII beam-foil decay curves for resonance transitions 8-74755
 Li⁺+Ar, up to 70 keV, symmetric (antisymmetric) reson. charge transfer cross sections (Korean) 8-50636
 Na, ²P_{3/2}-²S_{1/2} reson., light scatt. polarisation change 8-55144
 Na, reson. multiphoton ionisation, broadband laser AC Stark splitting 8-70808
 Na, resonant collisions in laser beam 8-78782
 Na, resonant three-photon ionis., saturation effects 8-58632
 Na, Rydberg states, millimeter spectra, quantum defect, fine struct., polarisability, field ionis. obs. 8-82672
 Na-like ions, transition probabilities for reson. transitions 8-66494
 Na+Kr(Xe), reson. line broadening, press. depend. 8-66596

atomic resonant states continued

- Ne, photoionisation, complex amplitudes at low energy singly and doubly excited reson. 8-78673
 Ne, reson. interaction of opposite waves, relax. const. of common level 8-50511
 Rb, optical reson. line electron impact excitation cross sections, polaris. 8-55244
 Rb, resonance lines 7800.23 and 7947.6 Å, Stark broadening obs. 8-66508
 Rb, resonantly excited in cylindrical discharge plasma, effective lifetimes 8-79413
 Sr, diamag. quasi-Landau spectrum near ionis. threshold, two-photon ionis. spectra obs. 8-58642
 Sr⁺, inversion and lasing on optically pumped reson. line 8-70798
 Xe, reson. line excitation, Auger decay 8-70804
 Zn I isoelectronic series transitions, theoretical oscillator strengths 8-74616

atomic scattering factors see crystal atomic structure; crystallography; lattice dynamics**atomic spectra**

- see also atomic fluorescence; atomic hyperfine structure; atomic spectral line breadth; atomic structure; beam-foil spectra; conversion electron spectra; radiative corrections; Russell-Saunders coupling; Stark effect; Zeeman effect
 absorption profile of at. beam nonorthogonal to laser light, optical freq. standard appl. 8-74940
 alkali metal vapour flash lamp, absolute spectral distrib. and radiant output 8-66510
 alkaline earth atoms, multiphoton ionisation spectroscopy 8-82703
 chemistry and spectroscopy 8-89556
 cold atoms, trapping and storage in laser field 8-86826
 dipole transition, transient behaviour in intense laser field (German) 8-66520
 excitation by coherent pumping, induced Raman scatt. 8-66519
 forbidden decay modes of one- and two-electron ions, book contrib. 8-82679
 heavy atom valence shells, transition probability of valence shells, relativistic pseudopot. calc. 8-86803
 heavy atoms, strongly forbidden M₁ transitions, g-factor anomalies (Russian) 8-78648
 heavy elements, 74Z<93, L-subshell vacancy relative radiative decay rates 8-55137
 Heisenberg's work on anomalous Zeeman effect and multiple spectra of atoms 8-70784
 high-Z electronic and muonic atoms, QED, strong and supercritical fields, book contrib. 8-74193
 inert gas, electron beam pumped, visible absorpt. rel. to visible laser development 8-63057
 inert gas atom adsorbed on graphite surface, excitation spectrum 8-71943
 inert gas flash lamp, absolute spectral distrib. and radiant output 8-66510
 inert gases, electron beam excited, absorpt. characts. 8-82948
 ion beam, from saddle-field ion source, gas depend. characts., at. spectroscopy appls. 8-78039
 ions, highly ionised, review 8-62755
 IR spectral lines, 10000-40000 Å 8-50490
 J-dependence of intensity-dependent polarization change in atomic reson. lines 8-70775
 lanthanides, doubly ionised, f-d interaction 8-90102
 lanthanides, Rydberg spectra and ionisation thresholds, time resolved resonant multistep technique 8-82701
 laser-induced line shifts and double-quantum Lamb dips 8-86825
 level-crossing and line-crossing in atomic spectroscopy, appl. of terms 8-70799
 mesonic atom and nuclear E1 transitions, dynamic electron screening 8-55260
 metastable states, Doppler-free linear single-photon spectroscopy 8-50487
 monochromatic laser radiation, excitation of atomic, mol. energy level transitions, inhomogeneous and mixed line broadening 8-55147
 monochromatic laser radiation, excitation of atomic or mol. energy level transitions, strictly homogeneous line broadening 8-58629
 monopole H atom, spectra, energy levels, transition probabilities (Chinese) 8-90322
 muonic atoms, Dirac-Fock method 8-74805
 muonic atoms, nuclear polarisation energy shifts, phenomenologically extended microscopic calcs. 8-94335
 non-Rydberg atomic spectroscopy, review 8-90127
 nonlinear resonances of accelerated atoms and molecules (Russian) 8-50488
 polarisation propagator calculations of frequency-dependent polarisabilities, Verdet constants, and energy weighted sum rules 8-58647
 quantum motion in reson. field of standing light wave (Russian) 8-50508
 radiative portion of electronic transitions, continuum-field description 8-82894
 radiative transitions, classical theory appl. 8-74597
 Raman effect, spontaneous, three-level system in intense laser fields 8-86802
 rare earth elements, atomic energy levels, data tables 8-86805
 rare earth metals, photoionisation thresholds and Rydberg spectra 8-66522
 rare earth metals, spectra analysis, present state and trends 8-62749
 resonant scattering of laser pulses by a system of N atoms 8-74617
 Rydberg constant, using a hand-calculator, for teachers 8-81765
 Rydberg states, simultaneous strong elec. and mag. fields 8-78663
 soft photon approx. accuracy for resonances in electron scatt. in laser field 8-70935
 solar line intensities, OSO-7 obs. of limb brightening in EUV range 8-69759
 spectroscopy quantum chem. teaching, fluctuating elec. dipoles, light absorpt. 8-73802
 surface wave polarisation in hyperfine dipolar mag. transitions (French) 8-50504
 Thomas-Fermi model, atoms in strong mag. field 8-62724
 transition probabilities, bibliography (1914-1977) 8-74598
 two internal-vacancy atoms, Green function calcs. (Russian) 8-50451
 two k-shell vacancy systems, one-electron and two-electron one-photon transitions 8-58775

atomic spectra continued

- two-internal-vacancy atoms, characts., Green's function calcs. (Russian) 8-50450
 two-level atom, interaction with laser pulse 8-86827
 two-level system, strongly coupled, induced transition probabilities and energy 8-66598
 two-photon absorpt., collisionally perturbed, reson. profile and strengths, degeneracy and Doppler shift 8-55156
 two-photon spectroscopy, ultra-high-resolution, Doppler-free 8-49909
 ultra-soft X-ray emission spectroscopy, correl. with electron spectroscopy 8-50558
 ultrahigh resolution spectroscopy using light echo effect (Russian) 8-70774
 Wigner-Weisskopf atom in one-dimens. radiation field, relax. to equilibrium. 8-62769
 Wolf-Rayet stars, calc. of oscillator strengths of transitions for ion spectra C III, N IV, and O V (Russian) 8-57566
 X-ray absorption edge-shifts, empirical relations, effective ionic charge for isoelectronic series 8-55136
 H atoms, two-photon transition matrix elements, group theory calc. 8-62776
 Ag, oscillator strengths, relativistic HF, core-polarisation model pot. 8-86818
 Al I, relativistic and cancellation effects in line strength ratios 8-82689
 Al sequence, 4s²S-4p²P transition, f-values 8-78651
 Al XIII, hot pinched plasma, Lyman series Stark profiles, electron density determ. 8-51348
 Ar I and II transition probability determ. from improved branching ratio obs. 8-66514
 Ar IX, Ne I like reson. and Na I-like satellite lines, relativistic HF calc. and expt. 8-94210
 Au I, absorpt. spectrum obs., 1300 to 1900 Å 8-62751
 Au, oscillator strengths, relativistic HF, core-polarisation model pot. 8-86818
 Au, transition probability of valence shells, relativistic pseudopot. calc. 8-86803
 B-like ions, highly ionised, up to Fe XXII, Breit-Pauli approximation 8-53810
 Ba, emission spectra, 50 to 90 nm, electron impact excitation 8-82846
 Ba I, absorption spectrum, 1560 to 1770 Å 8-66487
 Ba I, hook method, gf values of intercombination line, 7911.38 Å 8-66511
 Ba, transition probability of valence shells, relativistic pseudopot. calc. 8-86803
 Ba⁺, transition probability of valence shells, relativistic pseudopot. calc. 8-86803
 Be, freq.-depend. polarisabilities and Verdet const., calcs. 8-62781
 Be sequence, (Z=4 to 10, 14), ³P₁-¹S₀ intercombination line, CI calc., Breit interaction 8-78641
 Bi, 6p_{3/2}-6p_{1/2}, search for optical rot. induced by weak neutral currents 8-82710
 Bi, UV absorption spectrum, flash photolysis method 8-90105
 Br II levels, NF values meas. in Ne-Br₂ mixtures 8-62753
 C, radiative lifetimes of visible and near IR transitions, solar abundance 8-50506
 Ca II, in fast sporadic meteor spectrum, low-energy electron excitation 8-93170
 Ca⁺, transition probability of valence shells, relativistic pseudopot. calc. 8-86803
 Cd, absolute photoabsorption. cross section, 40-250 eV 8-58613
 Cd I, absorption spectrum, simultaneous excitation of two electrons 8-58614
 Cl, L X-ray emitting levels, lifetimes 8-66493
 Cl VIII, Ne I like reson. and Na I-like satellite lines, relativistic HF calc., beam-foil spectra 8-94210
 Cl⁺, far UV spectra in solns. 8-94208
⁵⁹Co, mag. hyperfine struct. analysis, spectral lines 4000 to 4300 Å 8-62752
 Cr, atomic transition probabilities, oscill. strengths 8-74601
 Cr I in photospheric spectra, solar abundance and oscillator strengths 8-69757
 Cs, 6S-7S, parity violation search in highly forbidden mag. transition 8-82709
 Cs, photoplasma, optical excitation in radiation diffusion conditions 8-55227
 Cs, transition probability of valence shells, relativistic pseudopot. calc. 8-86803
 Cs vapour, coherent anti-Stokes Raman scatt. 8-71146
 Cs-He, new absorption/emission bands perturbed Cs transitions assignment, pot. energy curves 8-66486
 Cu, ground and metastable populations, buffer gas effect 8-82955
 Cu, oscillator strengths, relativistic HF, core-polarisation model pot. 8-86818
 Dy II spark spectrum, isotope shift, config. mixing 8-58628
 Eu³⁺, intracavity enhancement of absorpt. in nanosecond regime 8-78839
 F III, IV, beam-foil spectra, mean lives, 2150-3200 angstrom 8-55224
 Fe I lines limb shift in solar atmosphere, pressure shifts effect 8-89150
 Fe III, Fe VI, electron impact excitation cross sections and gaseous nebulae Fe abundances 8-53806
 Fe IV, spectrum, term anal., rel. to RR Telescopic 8-82677
 Fe IX, Fe X, forbidden transitions, solar coronal spectrum appl. 8-77537
 Fe X and XIV, solar line intensity ratio and coronal temp. determ. 8-73697
 Fe XIX, Fe XX, Fe XXI, forbidden lines obs. in solar flares 8-57519
 Fe XXII, XXIII, Be I and B I like spectra from laser-produced plasma, classification 8-67410
 Fe^{19a}, forbidden line in UV, Tokamak plasma diagnostics 8-83602
 Fr I, wavelength estimate of first and second resonance lines 8-58617
 Ga I, relativistic and cancellation effects in line strength ratios 8-82689
 Ga I, Rydberg series, discrete levels and continua of finite bandwidth 8-74603
 Ge I, transition probabilities, 4p²-4p4d and 4p²-4p5s, 1900-4700 Å (French) 8-74600
 H atom, relativistic, in superstrong mag. fields 8-90095
 H atom energy spectrum in expanding Robertson-Walker universe 8-73869

atomic spectra continued

- H emission spectrum, last observable line, rel. to solar obs. through Earth atm. 8-77536
- H, emission-line spectra in quasars and active galactic nuclei 8-96557
- H, exponential decay law for $2P_{1/2} \rightarrow 1S_{1/2}$ transition 8-78649
- H, $n=3$ level, coherent excitation by electron impact, density matrix anal. 8-78817
- H with quark embedded in nucleus, at. spectral lines 8-62965
- H⁻, grazing incidence collision with surface, Balmer radiation, elliptical polarisation 8-86804
- H⁻ vac. UV spectra, narrow reson. at 1129.5 Å, H-arc spectra 8-66490
- H⁺, grazing incidence collision with surface, Balmer radiation, elliptical polarisation 8-86804
- H-like atoms, dipole transitions, asymptotic expansion of radial-dipole integral 8-82667
- H₂, Balmer line emission fine struct., Stark effect (*German*) 8-82673
- H(D), ground state Lamb shift, isotope shift and relativistic nuclear recoil correction 8-82696
- H α , in solar chromosphere, seven components rel. to 9873 MHz line 8-89151
- He, freq.-depend. polarisabilities and Verdet consts., calcs. 8-62781
- He II recombination lines, calc. intensities in UV 8-94212
- He, optical excitation function of 5876 Å line near threshold 8-70797
- He, radiation from hollow-cathode discharge in weak mag. field 8-70789
- He-like ions, line intensities for stationary plasmas 8-53811
- He-like ions, line intensities for non-stationary plasmas 8-53812
- He-like ions, line intensities results 8-89051
- He-like ions, $P_1^0-1^1S_0$ and $^3P_1^0-1^1S_0$ intercombination-line transitions 8-70771
- He+Ar(Kr), translation band spectral moments, induced dipole moments 8-55218
- Hg, transition probability of valence shells, relativistic pseudopot. calc. 8-86803
- I, spectral transition probabilities, 500-1050 nm 8-82676
- In, 451.1 nm transition, HFS and ^{113}In - ^{115}In isotope shift 8-82674
- In, I, relativistic and cancellation effects in line strength ratios 8-82689
- In I, Rydberg series, discrete levels and continua of finite bandwidth 8-74603
- In V, spectrum, levels in $4d^6s$ and $4d^65d$ configs. 8-62748
- In²⁺, emission spectrum, 340 to 6500 Å, ionisation pot. and dipole polarisability 8-78654
- Kr I, high resolution polarisation spectroscopy of 557 nm transition 8-74602
- La I, lifetimes of $z^2F_{5/2}$, $z^2D_{3/2}$, $z^4G_{5/2}$ and $y^2D_{3/2}$ states 8-66489
- Li, absorpt. spectra, high mag. field, quasi-Landau reson. 8-90109
- Li I, IR emission spectrum, extended anal. 8-62747
- Li, quartet states, transition energies, oscill. strengths, CI calcs. 8-58597
- Mg II solar UV doublet obs. (*Japanese*) 8-61831
- Mg VII, UV lines, theoretical intensity ratios 8-90108
- Mn, atomic transition probabilities, oscill. strengths 8-74601
- Mn, $M_{2,3}$ absorpt. spectra in UV, single-config. Hartree-Fock multiplet theory 8-78656
- Mn V, $3d^3-3d^24p$ transition obs. energy level assignments 8-55134
- Mn V, forbidden transitions laboratory wavelengths 8-50496
- Mo IX, X, XI, 4p-4d transitions obs. 8-82669
- Mo XIII and XVII, spectra, perturbation theory with model pot. 8-58579
- Mo XXX to Mo XXXII, XUV spectra in laser prod. plasma 8-50493
- N II 2144 Å, emission feature obs. in UV aurora 8-88963
- N, radiative lifetimes of visible and near IR transitions, solar abundance 8-50506
- N, Stark broadened VUV lines in wall-stabilised arc, 1100-1800 Å 8-90107
- Na, absorption D-line shape, rel. to single-mode laser intensity 8-66491
- Na, Rydberg states, diamag. struct. 8-50484
- Na, Rydberg states, millimeter spectra, quantum defect, fine struct., polarisability, field ionis. obs. 8-82672
- Na, spectra, emission and absorpt., inert gas matrix 8-90106
- Na, two-photon optical free-induction decay 8-90138
- Na, vap., two-photon echo, quantum beats, superposition relax. 8-83041
- Na-like ions, transition probabilities for reson. transitions 8-66494
- NaI isoelectronic sequence, 3s-3p and 3p-3d transitions, ionisation energy 8-70773
- Nb VIII, IX, X, 4p-4d transitions obs. 8-82669
- Ne, 2p-1s transition, time-resolved spectroscopy 8-90103
- Ne I, at. state densities meas. in Ne-Br₂ mixture 8-62753
- Ne II 12.8 μ fine-struct. line in Nova Cygni 1975, contrib. to 10 micron excess 8-93269
- Ne, one-electron and two-electron one-photon transitions 8-58775
- Ne, radiation from hollow-cathode discharge in weak mag. field 8-70789
- Ne, thermalisation of level populations 8-66649
- Ne-O₂, DC glow discharge, Ne I spectral line intensities 8-74610
- Ne+Ar(Kr), translation band spectral moments, induced dipole moments 8-55218
- ²¹Ne, ground state, electronic pumping, alignment transfer with multiple diffusion (*French*) 8-50643
- Ni XI, Ni XII, forbidden transitions, solar coronal spectrum appl. 8-77537
- Np, UV emission spectra, Fourier transform spectroscopy appl. 8-58060
- O I 5577 Å forbidden line rel. to O₂ and OH band atmospheric spectra 8-61639
- O I auroral emissions, ground-based photometric meas. 8-77387
- O II, III, IV, beam-foil spectra, mean lives, 270-490 angstrom 8-55223
- O III, forbidden lines in quasars and active galaxies, theory 8-93408
- O III 51.8 μ forbidden emission line obs. of Orion Nebula 8-65510
- O IV solar intersystem line obs. in EUV, electron density at 10¹⁰K 8-53903
- O, radiative lifetimes of visible and near IR transitions, solar abundance 8-50506
- O⁵⁺, spectra, 7-32 nm, doubly excited quartet system 8-62757
- Pb muonic isotopes, A=204, 206, 207, 208, nuclear polarisation energy shifts, RPA calcs. 8-94334

atomic spectra continued

- Rb, fine-struct. splittings in visible region, ²D states 8-50656
- Rb+H⁺, single photon emission following double K-shell ionisation, contrib. to superheavy element search data 8-50625
- ⁸⁵Rb+(⁸⁵Rb⁺), hyperfine struct., in-flight saturated absorption laser spectrosc. 8-78650
- ⁸⁷Rb, surface wave polarisation in hyperfine dipolar mag. transitions (*French*) 8-50504
- S I ground configuration, wavelengths of observed transitions between levels 8-50489
- S II forbidden line emission from thermal plasma of Jupiter 8-93146
- S II-VII, spectra, 1050-5500 Å, beam-foil expt. with 100-700 keV ions 8-50495
- S III-IV, beam-foil study, 500 to 1200 Å 8-66488
- S, in CS₂ and SCO, L_{III}-absorption spectra 8-86807
- S, L X-ray emitting levels, lifetimes 8-66493
- S XI, UV lines, theoretical intensity ratios 8-90108
- S⁶⁺, spectra, 500-1200 Å, lifetimes 8-62756
- Se VI, 2400 to 90 Å spectrum anal. 8-58616
- Si IX, UV lines, theoretical intensity ratios 8-90108
- Si, L X-ray emitting levels, lifetimes 8-66493
- ⁵⁰Sn, L_{2,3} X-ray emission spectra, line breadth 8-62760
- Sn[Sp²(P₀)], kinetic studies of ground state atoms, by resonance line absorpt. 8-85128
- Sr II, ²F states, fine struct. splitting 8-50494
- Sr³⁺, spectra, 250-6500 Å 8-62754
- Ta IV, 2900 to 200 Å spectrum anal. 8-58615
- ⁵²Te, L_{2,3} X-ray emission spectra, line breadth 8-62760
- Tl, 6p_{1/2}-6p_{3/2}, search for optical rot. induced by weak neutral currents 8-82710
- Tl I, relativistic and cancellation effects in line strength ratios 8-82689
- Tl I, Rydberg series, discrete levels and continua of finite bandwidth 8-74603
- Tl, self-broadening of 377.6 reson. line 8-82692
- Tl, two-photon laser spectroscopy and ionisation 8-55153
- U III, in hexamethyl phosphoric triamide soln., absorption spectrum, intensities, oscill. strengths 8-74599
- V, atomic transition probabilities, oscill. strengths 8-74601
- V I, IR emission spectrum meas. 8-62746
- V I, photographic emission spectrum remeas. 8-62750
- V III, absolute oscill. strengths determ. 8-82691
- V IV, 3d²-3d4f transitions obs. 190 to 650 Å 8-62758
- V XX, Be I like spectra from laser-produced plasma, classification 8-67410
- W ion emission from PLT Tokamak, W ion soft X-ray emission effects 8-83537
- W, isotope shifts in visible region and HFS 8-82694
- Xe, atom-diatom paradox, phenomenological description of spectroscopic props. 8-78766
- Xe, three level systems, obs. of isotope shifts 8-82670
- Xe, time resolved spectra, UV and near UV continuums 8-78653
- Xe-Kr-Ar mixtures, VUV continuous spectrum prod. in low volt. lamp (*Russian*) 8-75451
- Xe+He, saturated absorpt. of 3.51 μ m line, vel. changing collisions by line width 8-86819
- Y VI, VII, VIII, 4p-4d transitions obs. 8-82669
- Yb, 1060-1700 Å 8-82675
- Yb, electron impact excitation, 40 to 120 nm, 5p ionisation 8-82845
- Zr, absorption spectra, isolated in rare gas matrices 8-78652
- Zr VII, VIII, IX, 4p-4d transitions obs. 8-82669
- Zr XI and XV, spectra, perturbation theory with model pot. 8-58579

atomic spectral line breadth

- AC Stark splitting in doubly reson. three-photon ionisation, nonmonochromatic field 8-94220
- alkali metal atom+inert gas atom, hyperfine transition spectral line shift, quantum corrections 8-82655
- atom+charged particle anisotropic collision, spectral line shift and broadening, polarisation depend. 8-82695
- atom-atom collisions, use of multipole expansions in spectral line broadening theory 8-74611
- collisional line broadening, classical and quantum theories, radiator motion effect 8-86822
- complex spectral bands, separation into components, Alentsev-Fock method (*Russian*) 8-90229
- complex spectral bands, separation into components, Alentsev-Fock method (*Russian*) 8-90230
- cumulative resonance in atomic ground state induced by modulated light field 8-66518
- dispersion-absorption plots, for spectral line shape anal. for RF and microwave spectrometry 8-89511
- Doppler line profile, saturation, influence of atomic collisions 8-70792
- Doppler-free laser-induced dichroism and birefringence 8-82711
- flameless AAS, anal. response shape and position 8-92545
- Fraunhofer lines, progressive sound waves effect on profiles (*Russian*) 8-73689
- inert gas atom adsorbed on graphite surface, excitation spectrum 8-71943
- inert gas mixture, collision-induced absorption, exact line shapes, appl. to He-Ar 8-66512
- laser spectroscopy conf., Jackson Lake Lodge, WY, USA, 1977 July 8-82666
- lineshape analysis for collision induced spectra 8-70787
- monochromatic laser radiation, excitation of atomic, mol. energy level transitions, inhomogeneous and mixed line broadening 8-55147
- monochromatic laser radiation, excitation of atomic or mol. energy level transitions, strictly homogeneous line broadening 8-58629
- monopole H atom, spectra, energy levels, transition probabilities (*Chinese*) 8-90322
- optical Ramsey fringes in two-photon spectroscopy, time delayed pulsed Doppler free technique 8-82708
- plasma, axially symmetric, Doppler broadened optical line emission interpretation model 8-75276
- plasma, Gaunt factor temp. depends., from Ar II and Ca II Stark widths 8-87491
- plasma, line width variation within Stark broadened multiplets 8-91073
- pressure effects on spectral lines 8-82690
- solar C I multiplets at 1560 and 1657 Å, overlapping emission peaks obs. and theory 8-93178

atomic spectral line breadth continued

- spectral line shapes, linear and nonlinear, atom or mol. cross sections 8-70899
- spectroscopy of atoms near a wall (*Dutch*) 8-70972
- two-level atom, EM radiation interaction, elec.- and mag.-dipole contrs., reaction field 8-94215
- two-level atom, phase shifts in weakly amplitude modulated light scatt., linewidth effect 8-50505
- ultrahigh resolution spectroscopy using light echo effect (*Russian*) 8-70774
- Voigt lines, random array, curve-of-growth function 8-89055
- Ar, 3p⁵5p config. aligned in discharge, interf. signals, lifetimes and collision cross sections 8-70796
- Ba II 4554 Å solar resonance line formation, empirical NLTE analysis 8-53907
- Be, Doppler effects in X-ray spectra excited by accelerated ions 8-86808
- Ca and Ca⁺, spectral lines collision broadening and shifts 8-58624
- Ca II H and K line profiles rel. to temperature and electron density of solar chromosphere 8-53908
- Ca II stellar emission line, V/R ratio rel. to mass loss 8-93208
- Cs, 6²S_{1/2}-6²P_{3/2} transition (λ=8521 Å) with hyperfine splitting, curves of growth 8-66513
- Cs-He, new absorption/emission bands perturbed Cs transitions assignment, pot. energy curves 8-66486
- Cs+Ar, two-photon ionisation spectra, satellites, absorption line shape 8-82668
- Cs+Ar(Kr)(Xe), spectral line breadth and shift, Van der Waals pot. calc. 8-90126
- Cs+Xe (neopentane), Cs line shape broadening, satellite data inversion, interaction pot. 8-74608
- Eu, Kα line widths, precise meas. 8-62761
- Fe I line profiles and magnetic field in quiet network regions of solar photosphere 8-69758
- Fe II multiplet anomalous line contours in α Cygni spectrum (*Russian*) 8-93243
- H I, solar Lyman-α and Lyman-β calibrated full disc profiles 8-93185
- H I Lyman α chromospheric emission line profile in UV spectrum of giant star α Bootis 8-81620
- H₂ line profiles in planetary corona, collisional model 8-77508
- H lines in plasma, electron width and shift (*Russian*) 8-67421
- H⁺ vac. UV spectra, narrow reson. at 1129.5 Å, H-arc spectra 8-66490
- H_α line shape, plasma broadened, fine struct. effects at low electron densities 8-62765
- Hα line profile in star T Tauri, obs. of fast var. (*French*) 8-61859
- He I, 4471 Å line profile in various plasmas, ion perturbation effects 8-94214
- He II, Stark broadening of VUV transitions at 304, 1215, 1640 Å 8-66506
- He plasma, Stark shift and line broadening in 3-D stochastic laser field 8-50502
- He, Voigt profile, line absorpt. calcs. of 388.9 nm triplet, 501.6 nm singlet lines 8-90123
- He-F, doublet series laser lines near 700 μm, hyperfine splitting and broadening meas. 8-63070
- He-Ne laser plasma, line profiles meas. by optogalvanic spectroscopy 8-62233
- ¹⁹⁹Hg⁺, hyperfine separation of ground-state, optical double-reson. 8-78828
- I, laser 1.315 μm transition line struct. 8-59000
- Kr, 3p X-ray photoelectron spectrum, many-electron effects 8-50513
- Mg, Doppler effects in X-ray spectra excited by accelerated ions 8-86808
- Mg II k chromospheric emission line profile in UV spectrum of giant star α Bootis 8-81620
- N, Stark broadened VUV lines in wall-stabilised arc, 1100-1800 Å 8-90107
- N₂, dynamically induced electronic transitions of matrix isolated atom 8-63825
- Na, absorption D-line shape, rel. to single-mode laser intensity 8-66491
- Na D-line emission from Io, comparison of observed and theoretical line profiles 8-93145
- Na, flame absorption and fluorescence, laser saturation broadening 8-88661
- Na, reson. multiphoton ionisation, broadband laser AC Stark splitting 8-70808
- Na, two-photon excitation in flame, saturation broadening, fluoresc. obs., broad-band excitation 8-74625
- Na+Kr(Xe), excimer bands, multiperturber interactions 8-66497
- Na+Kr(Xe), reson. line broadening, press. depend. 8-66596
- Ne II lines from pulsed arc plasma, Stark broadening 8-66504
- Ne, photoionisation, complex amplitudes at low energy singly and doubly excited reson. 8-78673
- Ne+Ne(He), 7d¹ states, isotope shift, press. shift, press. broadening, two-photon spectra obs. 8-55155
- Rb+Ar(Kr)(Xe), spectral line breadth and shift, Van der Waals pot. calc. 8-90126
- Se, Doppler effects in X-ray spectra excited by accelerated ions 8-86808
- ⁵⁰Sn, L_{2,3} X-ray emission spectra, line breadth 8-62760
- Ta, Kα line widths, precise meas. 8-62761
- ⁵²Te, L_{2,3} X-ray emission spectra, line breadth 8-62760
- Tl, self-broadening of 377.6 reson. line 8-82692
- Tm, Kα line widths, precise meas. 8-62761
- Xe, 3.51 μm laser transition, phase-changing broadening, inert gas perturbers 8-82949
- Xe+Bi, Bi Kα X-ray lines, Doppler broadening 8-62759
- Xe+He, saturated absorpt. of 3.51 μm line, vel. changing collisions by line width 8-86819
- Xe+Kr, excitation transferred populations, absorpt. profile analysis 8-74748

atomic structure

- see also atomic electron correlations; atomic excited states; atomic fine structure; atomic orbitals calculations; atomic polarisability; atomic spectra; nuclear screening; Russell-Saunders coupling; triplet state
- 3d⁵, 4f⁶ configurations, partial level density, statistical props. of atomic energy levels 8-70732
- adatom, valence shell energy level shift (*French*) 8-67900

atomic structure continued

- alkali metal atom, valence electron ground states, model potentials 8-50476
- alkaline earth positive ions, valence electron ground states, model potentials 8-50476
- asymptotic expansions in motion of two electrons in nuclear field 8-66459
- atomic physics in nuclear experiments, conference, Haifa, Israel, Aug. 1976 8-70947
- Born-Oppenheimer energy, energy states of one electron, two nuclei interaction 8-90052
- bound s-state of electron in screened Coulomb field 8-58581
- cold atoms, trapping and storage in laser field 8-86826
- convex structure of electrons 8-62685
- Coulomb potential with cut-off, exact eigenvalues 8-62692
- diagrammatic many-body perturbation expansion, computer program 8-50454
- diagrammatic many-body perturbation expansion, ladder energies, computer program 8-50455
- diagrammatic many-body perturbation expansion, ring energies, computer program 8-50456
- electron density studies, quantum chem., basic concepts 8-70731
- electronic 4s, 3d energy levels, textbook diagram, teaching 8-73801
- exotic atoms containing monopoles, energy levels and stationary states (*Chinese*) 8-86982
- ground state energy, atomic shell model 8-50460
- HF coreless pseudopot. for atoms K through Zn 8-55121
- high-Z electronic and muonic atoms, QED, strong and supercritical fields, book contrib. 8-74193
- highly ionised atoms, relativistic effects, book contrib. 8-74588
- intermediate states, far off-reson., temporal coherence in multiphoton absorpt. 8-50458
- ions with partly filled L-shells, relativistic Hartree-Fock energy calcs. 8-82656
- isoelectronic changes, energy density eqn. 8-70768
- K-shell vacancy production, by charged particles, relativistic effects calc. 8-58600
- kaonic ¹²C, coupled channel formalism, role of Λ(1405), binding effect, Pauli blocking 8-55261
- kinetic energy, bound on lowest order gradient correction 8-62709
- light atoms, large-q form factors, calcs. for ³Li to ¹⁹K, ²²Ti 8-58589
- light atoms, large-q form factors for momentum transfer 8-70734
- magnetic interactions of electrons (*German*) 8-82610
- molecular internal stresses, stress tensor, one electron system 8-62686
- multi-configuration Hartree-Fock program 8-50471
- muonic atoms, electron screening calculations in O, Al, Fe, In, Ho, Au, Th 8-94339
- muonic atoms, energy-level values, electrodynamic corrections 8-62956
- N-electron atomic Hamiltonian first eigenvalue, Hartree-Fock approx. method 8-90062
- nonrelativistic atomic and ionic binding energies 8-90054
- numerical HF radial function during SCF iteration, convergence 8-58574
- one-electron density at nucleus, expectation values 8-90053
- orbital cross-sections, bonding interactions, spring model, teaching aid 8-93503
- perturbation, periodically time-depend., quasi-states theory (*German*) 8-82601
- positron annihilation in rare gases, Doppler broadening meas., electron mom. distrib. 8-55131
- quantum beats in atomic and nuclear physics 8-70772
- rare earth elements, atomic energy levels, data tables 8-86805
- Rydberg constant, using a hand-calculator, for teachers 8-81765
- spin density of open-shell systems, pseudo-orbital theory 8-62706
- structure and collisions of ions and atoms, book 8-74554
- thermochemical properties of atoms and molecules in specific quantum states 8-68911
- total energies, virial-statistical method 8-62696
- transition metal, 3-d, density functional theory 8-58578
- two internal-vacancy atoms, Green function calcs. (*Russian*) 8-50451
- two-internal-vacancy atoms, characts., Green's function calcs. (*Russian*) 8-50450
- two-parameter statistical model 8-55124
- unitary group generators representation matrices calcs. 8-78610
- universal atomic basis sets, light atom HF ground state energies 8-78605
- Ar²⁺, levels of 2p⁵3p⁵ 8-74574
- As, (4⁵S_{3/2}) state, kinetic obs. using time resolved reson. fluoresc. 8-94211
- Au, relativistic effective core pots., appl. to AuH and AuCl ab initio calcs. 8-86767
- B⁺, Hund's first rule, new interpretation 8-78620
- B-like ions, highly ionised, up to Fe XXII, Breit-Pauli approximation 8-53810
- Be, Hund's first rule, new interpretation 8-78620
- Bi, parity nonconservation, weak electron-electron interaction, light polarisation, vapour optical activity (*Russian*) 8-55132
- C²⁺, Hund's first rule, new interpretation 8-78620
- Ca III, atomic structure determ. by model pot. method 8-86777
- Ca, isotopes 40, 42, 44, 48, charge distrib., Hartree-Fock anal. (*Russian*) 8-70747
- Ce II, isotope shift and screening, pseudo-relativistic HF calc. 8-90096
- F I, and isoelectronic series, Z=10-100, L-shell energy struct. and level classification 8-55129
- H atom, relativistic model of spin 1/2 particles interacting with external EM field 8-70756
- H atom, strongly magnetised, quantum number assignments, semi-classical approach 8-90055
- H, energy levels in strong mag. field 8-90071
- H, relativistic spin 1/2 particle dynamics 8-70001
- H⁺, ground state energy, post-adiabatic approx. calcs. 8-58827
- H⁻, magnetic interactions of electrons (*German*) 8-82610
- H-He, H hyperfine struct. shift, commutator computational method 8-78608
- H-positron bound state, effective one-body pot. to prove absence 8-82871
- H₂, magnetic interactions of electrons (*German*) 8-82610
- He isoelectronic series, energy level and classifications of doubly-excited states 8-62736

atomic structure continued

- He, magnetic interactions of electrons (*German*) 8-82610
 Hf, neutral atom, partial level density, statistical props. of atomic energy levels 8-70732
 Hg(6^3P_1)+Li⁺(Na⁺)(K⁺), excitation, optical polarisation fractions and mag. sublevels obs. 8-50619
 Ho, K X-rays, energy shifts, role of atomic struct. 8-70777
 In V, spectrum, levels in $4d^6s$ and $4d^5d$ configs. 8-62748
 KrI, $4p^25p$ and $4p^26p$ configs., level radiative lifetimes meas. 8-58625
 Li I, and isoelectronic series, $Z=10-100$, L-shell energy struct. and level classification 8-55129
 Li, quartet states, absolute term values, CI calcs. 8-58596
 Mn V, $3d^3-3d^4p$ transition obs. energy level assignments 8-55134
 Mo XIII and XVII, spectra, perturbation theory with model pot. 8-58579
 Na, core polarisation effect on oscillator strengths and energy level locations 8-82688
 Ne, atomic structure determ. by model pot. method 8-86777
 Pb, parity nonconservation, weak electron-electron interaction, light polarisation, vapour optical activity (*Russian*) 8-55132
 Pt group, even atom config., parametric calcs. 8-82631
 S I ground configuration, wavelengths of observed transitions between levels 8-50489
 Sc IV, atomic structure determ. by model pot. method 8-86777
 Ta II, even-parity states, partial level density, statistical props. of atomic energy levels 8-70732
 Tl, parity nonconservation, weak electron-electron interaction, light polarisation, vapour optical activity (*Russian*) 8-55132
 V, energy levels in all stages of ionisation, data anal. 8-94207
 Zr XI and XV, spectra, perturbation theory with model pot. 8-58579

atomic structure, crystals *see crystal atomic structure***atomic weight** *see atomic mass***atoms**

- see also exotic atoms; helium atoms; hydrogen neutral atoms; positronium*
 No entries

attaching *see joining processes***attenuation** *see absorption; dispersion (wave); scattering; transmission***attenuation measurement**

- duct noise active attenuation meas. 8-90592
 microwave path- and area-integrated rainfall meas. 8-65414
 optical fibre attenuation meas. instrument 8-59138
 optical fibre cables for field trials, meas. methods (*German*) 8-50922
 optical fibres, numerical aperture depend. spectral loss meas. 8-66942
 RF instrumentation based on superconducting quantum interference 8-57995
 underground optical cable transmission meas. 8-50942

attitude control

- biaxial optical guider for rocket-borne solar obs. (*Polish*) 8-61744
 dual-spin satellite magnetic attitude control system, geomag. field effects 8-65484
 Earth resource satellite attitude meas. and control requirements 8-65482
 Earth surface obs. satellite remote sensor/attitude control system interface 8-65481
 INTEL SAT IV, in-orbit liquid slosh tests, anal. 8-81516
 and orbit control systems, conference, Noordwijk (1977) 8-65480
 satellite stabilizer system, rate-optimal parameters 8-69641
 satellites, gyrodampers in passive control system 8-96379
 solar radiation pressure induced orbital perturbation analysis 8-89041
 space vehicles, star pattern recognition using CCD star sensors 8-96380
 spacecraft, meteoroid impacts effect on attitude motion, analytical model 8-73608
 Spacelab passive atm. sounders, attitude control and stabilisation 8-65483

audio acoustics

- see also audio recording; audio systems; hearing; speech*
 concert halls, hearing impressions of loudspeaker reproductions and orchestras (*German*) 8-94485
 interior acoustics CAD (*Polish*) 8-59205
 TV and motion picture stages, noise and insulation 8-79169

audio equipment

- see also gramophones; loudspeakers; microphones; pick-ups*
 oscillator, modified transistor radio, for teachers 8-81772

audio recording

- digital photographic sound track recording optimisation (*Russian*) 8-89580
 dual message tape preparation, for dichotic listening research 8-57010
 head-related stereophonic recording techniques, dummy head method 8-61286
 noise eval. in motion picture studio recording room (*Russian*) 8-55518
 photographic, computer simulation 8-78022

audio systems

- see also acoustic devices; acoustic equipment*
 club noise control by electronic power reduction 8-51004
 sound system design aid, HP 97 program 8-75015
 transmission function in rooms rel. to acoustic amplification systems 8-59204

auditory activity *see hearing***auditory perception** *see hearing***Auger effect**

- adsorbates, thermal desorption and conversion kinetics, AES study 8-71959
 AES, microarea anal. system with submicron anal. capacity, performance tests 8-73106
 AES of surfaces 8-85277
 alkali halide, with oppositely charged defect centres, autoionisation-tunnel relax. of electron excitation 8-72112
 atom, inner-shell photoionis., anisotropy of X-rays and Auger electrons 8-58633
 atomic collisions, quasi-molecule Auger decay 8-62899
 backscattering factor, estimation for low atomic number elements and their alloys 8-72649
 beam foil spectroscopy, extensions, lifetime meas., book contrib. 8-74758
 binary metal alloys, quantitative analysis (*Polish*) 8-76967

Auger effect continued

- blanking resistive heating for Auger spectroscopy and LEED using retarding field analyzer 8-54509
 bronze P, friction with steel, boundary lubrication conditions, element conc. anal. of films 8-85001
 ceramics SEM and anal. techniques (*German*) 8-56832
 chemical state effects in AES 8-72687
 chemical state effects in AES 8-92566
 chloromethanes, Auger electron spectra and chem. shift 8-90231
 cobalt phthalocyanine film, sorption of O₂ and water, AES obs. 8-91531
 codedoped with S on (111) surface, AES and photoelectron spectra 8-71957
 core hole relaxation energies 8-80439
 data acquisition of Auger and line optical information 8-63019
 depth profile analysis, influence of impurity gases in UHV systems 8-76958
 elastic and inelastic contribs. to secondary electron yield struct. 8-72642
 electron spectroscopic quantitative surface analysis 8-92552
 elements $10 \leq Z \leq 100$, semiempirical Auger electron energies 8-62774
 epitaxial growth, vapour phase, growth mode characterisation 8-87885
 ESCA studies of Ga, As, GaAs, Ga₂O₃, As₂O₃ and As₂O₅ 8-92171
 ESCA using X-ray photons >1500 eV, Au M_α X-rays (2123 eV) 8-72683
 film sandwich structures Auger anal. 8-72030
 free metal atoms photoelectron and Auger spectra, core level energies 8-50522
 gas-surface interactions, mol. beam apparatus 8-72675
 glass surface anal. by AES 8-60013
 graphite, energetic ion sputtering, appl. of AES-SIMS (IMA)-FDS combined systems to physical and chemical processes 8-95636
 graphite, surface cleaning, air cleavage and UHV cleavage, obs. using Au decoration 8-80665
 n-InP, magneto-impurity resonances, obs. of central cell struct. 8-95303
 insulating film, Auger depth profiling by angle lapping 8-53287
 internal photoemission peaks 8-52621
 ion+atom collisions, Auger spectra, book contrib. 8-74756
 ion-excited Auger emission from sample trays in Auger-sputter profiling study 8-52607
 Kane model, three-band, Auger recombination overlap integrals, kp approx. (*Russian*) 8-87897
 keratin-NaCl, Na Auger electron spectra 8-53339
 L-LM Coster-Kronig processes, role in Auger spectroscopy 8-56548
 laser fusion targets, vapour deposited coatings, surface finish obs. 8-60863
 light elements, $Z > 10$, K-LL Auger process, review 8-50523
 MBE, obs. by LEED-AES (*Japanese*) 8-91564
 mesic and muonic mol. ion formation in liq. He, X-ray intensities, Auger and Stark transitions 8-94338
 metal, narrow band, quasiautomatic Auger spectra 8-60536
 metal oxides, Auger quantitative anal. 8-73104
 metal surface, AES anal. in adhesion, friction and wear 8-53179
 metal surface, chemisorption, vac. UV photoelectron spectrometer for study (*Japanese*) 8-62264
 metal surfaces, clean, AES anal., contamination effects obs. 8-53293
 metal-semiconductor thin film preparation under UHV conditions 8-72733
 metallic film continuity, observations by Auger spectroscopy 8-64433
 methane+X⁺, (X=Ar,Kr,Xe,U), Auger emission line shape after dis-soc. 8-86838
 microscopy, Auger electron, instrumental capabilities 8-70227
 multicentre Auger matrix element, ang. depend. calc. for solids and adsorbate systems 8-92151
 muonic atom cascade program, X-ray calcs. and cataloguing 8-90323
 plasmon effects in electron spectroscopies of valence state 8-56098
 positive ions, photoionisation and Auger effect 8-90135
 quantitative anal. of impurities (*Japanese*) 8-91356
 SEM-AES-IMA combination with SIM spectrometer, Si device anal. appls. (*Japanese*) 8-85249
 semi-empirical models for electron energy calcs. 8-50519
 semiconductor, diamond-like narrow-gap, Auger recomb. calc. 8-63978
 soda-lime glass, depth profiles of Na and Ca by SIMS and AES 8-51805
 solid surface, Auger neutralisation of slow protons 8-72668
 solid surface and thin film analysis 8-80825
 spectral, convolution and deconvolution 8-52601
 static AES, appls. to surface reaction and submonolayer adsorption 8-84685
 steel, alloy, HY130, temper embrittlement due to Si intergranular segregation, effect on H₂ induced cracking 8-76735
 steel, alloy, Ni-Cr-Mn, type 4340 intergranular brittle fracture, exam. by impact testing and Auger spectroscopy 8-52978
 steel, austenitic stainless, temper embrittled, type 304, Auger spectroscopic exam. of grain boundary surface phases 8-76741
 steel, ferritic stainless, Cr-Mo, Mo effect on pitting pot., AES anal. 8-95852
 steel, Ni-Cr, (4.1, wt.%), isothermal embrittlement, AES exam. of grain boundary segregation 8-60814
 steel, Ni-Cr, intergranular segregation of P in austenite, grain boundary coherency depend. 8-84761
 steel, stainless, quantitative AES with computer evaluation 8-76949
 steel, stainless, surface cleaning by H⁺ bombard., AES study 8-53022
 steel, stainless 316, ion sputtered, surface anal. by Auger effect and SEM 8-95632
 surface, density of states, information from self-deconvolution of Auger band-type spectra 8-92150
 surface analysis, review of AES technique and applications 8-68946
 surface analysis, system, modular combined ESCA, UPS, AES, and SIMS 8-73107
 surface analysis by synchrotron radiation and sputter Auger techniques 8-61130
 surface characterisation, multiple technique instrument, ESCA, scanning Auger, UPS and SIMS 8-73108
 surface EXAFS study of adsorbate Auger electron intensity on single cryst. surfaces 8-66562
 surface structure analysis at high press. 8-73103
 tetrachloromethane, Auger emission anomalous spectra and yield, chemical species depend. 8-55152

Auger effect continued

- tetrafluoromethane, Auger emission anomalous spectra and yield, chemical species depend. 8-55152
- thin film structures, chemical anal. by Auger spectroscopy (*Russian*) 8-92581
- Three-electron Auger transitions in atoms with two inner shell vacancies 8-62900
- transition metal, 3d, electron-electron interaction, X-ray excited Auger spectra 8-91631
- upper atmosphere, ionisation due to X-ray pulse, Auger electrons form. 8-53767
- upper atmosphere, photoelectron spectra allowing for Auger effect 8-69557
- wear study, analytical surface tool, review 8-64718
- X-Y recorder for Auger spectrometer using pulse height analyser, computer interfaces 8-49942
- zinc blende structured semiconductor surface analysis by X-ray photoelectron spectroscopy (*Japanese*) 8-88672
- Ag (100) surface, angle-resolved Auger emission 8-72650
- Ag, AES, valence band spectra, solid-state and atomic features 8-72646
- Ag, adsorbed on Si (111), electronic and cryst. struct., Schottky barrier form. obs. 8-84091
- Ag, Auger $M_{4,5}$ -VV spectrum, quasi-atomic final states 8-72688
- Ag, cluster growth and nucleation on Mo (100), UHV-SEM, AES/(RHEED or LEED) obs. comparison 8-63956
- Ag, solid state and atomic features in the valence band Auger spectra 8-76563
- AgCuSe, X-ray photoelectron and Auger spectra 8-56561
- AgGaSe₂ and Ag₂GaSe₆, XPS, Auger and direct electron spectra 8-52620
- Ag₂Se, X-ray photoelectron and Auger spectra 8-56561
- Al alloys, 7075-T6, H₂ effects and Cd segregation to grain boundaries 8-84764
- Al, Auger emission target, contrib. of reflected electrons 8-92152
- Al, Auger spectra, plasmon satellite intensity 8-64432
- Al, Auger spectrum, KLL, plasmon gain satellite obs. 8-76562
- Al, oxidation, in water, oxide growth rate and struct. 8-76783
- Al-SiO₂ film-substrate interface, obs. of Al₂O₃ and free Si 8-91571
- Al-SiO₂ interface, chem. struct., deposition conditions depend. 8-72007
- Al-Ta-poly-Si interdiffusion, Ta barrier effect, Auger anal. 8-71888
- Al-Zn-Mg, grain boundary segregation, AES meas. 8-72781
- Al_{0.9}Ga_{0.1}As-GaAs n-n heterojunction, LPE, Auger profiling and absence of rectification 8-95349
- Ar, electron impact ionis., L₂-shell alignment, Auger electrons ang. distrib. 8-58838
- Ar, KLL and KLM Auger electron spectra, obs. and relativistic multi-configurational Dirac-Fock calc. 8-50524
- Au, AES, valence band spectra, solid-state and atomic features 8-72646
- Au, adsorption of O₂, Auger spectra 8-87879
- Au film, ionic sputtering and AES anal. (*French*) 8-76959
- Au films on Si substrate, solid-solid reactions 8-95369
- Au, high current density plated, Co diffusing out, oxidation kinetics, AES meas. 8-92393
- Au, solid state atomic features in the valence band Auger spectra 8-76563
- Au-Ag bilayers, conc. profile by AES, interdiffusion coefficient determ. (*French*) 8-84077
- Au-Cu alloy, surface comp. as function of temp., AES expts. 8-95212
- AuPb₂, epitaxial layer, formation during Pb absorpt. on Au, LEED, AES study of Au/AuPb₂ interface 8-71988
- B, K-shell binding energy, Auger spectra after collision with He and methane 8-50525
- BN, pyrolytic, in contact with various metals, friction and transfer behaviour 8-88535
- Ba, strong correl. in 4d-Auger spectrum 8-50522
- Be (0001) surface, work function and purity, AES, LEED and photoelectron spectra meas. 8-68606
- Be, Auger emission target, contrib. of reflected electrons 8-92152
- Be, K-shell binding energy, Auger spectra after collision with He and methane 8-50525
- C, K-shell binding energy, Auger spectra after collision with He and methane 8-50525
- CO, adsorbed on stepped Ni, thermal decomposition, LEED, AES, thermal flash desorption study 8-71984
- CO₂+X⁺⁺, (X=Ar,Kr,Xe,U), Auger emission line shape after dissoc. 8-86838
- CU, solid state and atomic features in the valence band Auger spectra 8-76563
- Cd, Auger electron spectra, electron impact excited, vap. and solid state differences 8-52603
- CdS, surface energy levels, O(C) adsorpt., AES study (*Japanese*) 8-88008
- CeO₂-Y₂O₃ film, surface characterisation, XPS, ESCA, and AES expts. 8-72028
- Cl compounds, chemical shifts of X-ray electron and Auger lines 8-86912
- Co, monolayer, oxidation, quasisimultaneous SIMS, AES, XPS 8-72919
- ⁵⁷Co, disintegrating nucleus, energy absorpt. by mol. environment 8-80775
- Cr-O system, initial oxidation, combination anal. using ESCA, AES and SIMS 8-72924
- Cu, (100), oxidation, electron spectroscopic study 8-64782
- Cu (210) surface, adsorption of O₂, LEED and AES meas. 8-71998
- Cu, AES, valence band spectra, solid-state and atomic features 8-72646
- Cu, chemisorpt. of CO, SIMS, AES, desorpt. meas. 8-87875
- Cu compounds, chemical shifts of X-ray electron and Auger lines 8-86912
- Cu, L_{2,3}VV and MVV Auger spectra 8-68583
- Cu, MVV Auger spectra, atomic model and valence band features 8-72644
- Cu molybdates, valence band X-ray induced Auger spectra and XPS 8-80813
- Cu oxides, valence band X-ray induced Auger spectra and XPS 8-80813
- Cu surface, surface cleaning by H⁺ bombard., AES study 8-53022

Auger effect continued

- Cu-Al, surface segregation during adsorption and low pressure oxidation (*French*) 8-75932
- Cu-Ni, chemisorpt. of CO, SIMS, AES, desorpt. meas. 8-87875
- Cu-Ni, film, preferential sputtering due to altered layer struct., AES meas. 8-76573
- CuInS₂(Se₂)(Te₂), thin films and photovoltaic devices, AES evaluation 8-67928
- CuInS₂(Se₂)(Te₂), thin film, bulk polycryst. and single cryst. samples, AES 8-72648
- Cu₂O, Auger quantitative anal. 8-73104
- CuSe, X-ray photoelectron and Auger spectra 8-56561
- Cu₂Se, X-ray photoelectron and Auger spectra 8-56561
- Fe based alloys, solute segregation to grain boundaries, AES 8-72780
- α-Fe, grain boundary segregation of C, N₂ and C Auger spectroscopy 8-72778
- Fe-Mn (8 wt.%), quenched, exam. of intergranular embrittlement 8-76745
- Fe-Ni (3 wt.%), grain boundary segregation microanal. using X-ray (STEM) and AES 8-87685
- Fe-O system, initial oxidation, combination anal. using ESCA, AES and SIMS 8-72924
- Fe-Si (1%), LEED-Auger exam. of (110) surfaces 8-71915
- Fe-Si (2.35 wt.%), misorientation dependence of grain boundary segregation, Auger spectroscopy exam. 8-76629
- Fe₂O₃, film, quantitative sputter rates, AES, ellipsometry determ. 8-72661
- Fe_{1-x}Pd_x film, air-exposed, comp. profiles by AES, ESCA and ion sputtering 8-95245
- Ga, effect of L₁L_{2,3}M Coster-Kronig processes on L_{2,3}MM Auger spectrum 8-72681
- GaAs, (100), comp. and struct. of differently prepared surfaces, LEED and AES 8-91524
- GaAs (110), valence band Auger spectra, from Ga and As CCV transitions 8-92149
- GaAs, electronic surface structure Cs(Rb)(Na) adsorpt. processes, AES, LEED, EELS, study 8-68068
- GaAs interface with anodic and thermal oxides, comparison of AES and ESCA 8-95980
- GaAs, ion bombardment, composition changes, AES 8-72662
- GaAs oxide, passivated layers, quantitative in-depth profile, AES-SIMS thermal, anodic and plasma oxidations 8-84087
- GaAs oxide, plasma grown, semiquantitative chemical depth profiles, Auger spectroscopy and neutron activation anal. 8-53284
- GaAs, plasma anodisation in DC discharge, AES and MIS diode expts. 8-95826
- GaAs, surface (111), (111), (110), XPS, photo-Auger ionisation cross section, electron mean free paths 8-56558
- GaAs, surface segregation of implanted alkali metals, photoemitter prep. and characts. (*French*) 8-60544
- GaAs:Se, implanted, annealing with O-free CVD Si₃N₄ encapsulant 8-83834
- GaAs:Sn, surface segregation of Sn during MBE, SIMS and AES 8-72031
- Ga_{0.9}In_{0.1}As, alloy film surface processes controlling growth by MBE RHEED and AES exam. 8-84084
- p-Ga_{0.9}In_{0.1}As, Auger recomb., theory and luminesc. expts. 8-56518
- Ga_{0.9}In_{0.1}P alloy films, surface processes controlling growth by MBE, RHEED and AES exam. 8-84084
- GaP, single-crystal, anodically oxidised layers, AES measurements 8-91556
- Gd₃(MoO₄)₃, domain structure obs. by GdF₃ decoration, AES meas. 8-84544
- H₂O, double hole states POCl calc., Auger spectrum 8-78630
- H₂S, double hole states POCl calc., Auger spectrum 8-78630
- H₂S, KLL Auger spectrum, obs. and ab initio SCF CI calc. 8-50654
- He, metastable, deexcitation process on Mo [110] impact 8-95642
- p-InAs, Auger recomb., theory and luminesc. expts. 8-56518
- INP interface with anodic and thermal oxides, comparison of AES and ESCA 8-95980
- INP surface, interaction with Cl, electron spectroscopic obs. 8-56036
- InSb, electronic surface struct., Cs(Rb)(Na) absorpt., AES, LEED, EELS study 8-68068
- InSb film, synthesis by 2-source mol. beam technique and AES characterisation 8-72729
- Ir (110), chemisorption of CO, preexponential factor and desorption energy 8-71963
- Ir(111) surface, electron beam induced desorption and dissociation of chemisorbed CO, LEED and AES 8-56043
- LaB₆, clean and oxidised (100) surface, LEED, AES, work function, evaporation meas. 8-71989
- Mg, Auger electron spectra, electron impact excited, vap. and solid state differences 8-52603
- Mg, Auger spectrum, KLL, plasmon gain satellite obs. 8-76562
- Mg, K Auger transition rates, orbital relax. and interchannel interaction effects 8-50521
- Mg, lineshape of KL₂L₃(¹D₂) line 8-60535
- Mg-MgF₂, sputtered films, opt. props. 8-80430
- Mg+H⁺(He⁺) and electron impact ionis., Auger study of collisionally induced alignment 8-90279
- MgO-ZnO, solid soln., surface comp., Auger and XPS investig. 8-51806
- MnZn ferrites, Ti substituted, mag. permeab. meas., grain boundary comp. AES obs. 8-95473
- Mo, monolayer, oxidation, quasisimultaneous SIMS, AES, XPS 8-72919
- Mo, RF sputtered, diffusion barrier props. 8-71887
- Mo, sputtering yield meas. by AES 8-95633
- Mo⁺⁺, photoionisation and Auger effect 8-90135
- Mo-O system, initial oxidation, combination anal. using ESCA, AES and SIMS 8-72924
- MoS₂, adsorption of Cs and O₂, LEED, Auger and work function meas. 8-71994
- Mo(100), adsorpt. of CO, LEED, AES, study 8-87873
- N₂+X⁺⁺, (X=Ar,Kr,Xe,U), Auger emission line shape after dissoc. 8-86838
- NH₃+X⁺⁺, (X=Ar,Kr,Xe,U), Auger emission line shape after dissoc. 8-86838
- Na clusters, electronic relaxation energies in KL_{2,3}L_{2,3} Auger transitions, SCF-Xα-SW calcs. 8-90334
- Na, lineshape of KL₂L₃(¹D₂) line 8-60535

Auger effect continued

- Nb, sputter deposited film, O contamination, Auger anal. 8-52669
 NbN superconducting reactively sputtered film, Auger anal. 8-72297
 Ne ion, energy of metastable K-LL Auger transition (*Russian*) 8-82704
 Ne, orbital relaxation and final-state channel mixing, in Auger effect 8-50520
 Ni, chemisorpt. of CO, SIMS, AES, desorpt. meas. 8-87875
 Ni dissolution of C through (110) surface, LEED and AES meas. 8-63932
 Ni, epitaxial film on NaCl, struct. and purity 8-72047
 Ni, photoelectric effect in paramag. and ferromag. states, Auger spectra 8-95649
 Ni plating, surface props. of Ni after each step of activation process 8-95243
 Ni, sputtered, on Si, annealing effects on transmission electron diffraction patterns, silicide form. 8-91562
 Ni stepped surface, morphology exam. by LEED and ARS 8-71913
 Ni surface, adsorbed S, H₂⁺ ion induced desorption, AES meas. 8-84069
 Ni surface, S and O₂ covered, polycrystalline, initial sticking coeff. of H₂, LEED and AES 8-63937
 Ni-Al(Ti)(Mo)(Si), effect of solute misfit and temp. on irradiation induced segregation 8-72779
 Ni-Au, dil., orientation depend. of surface segregation, AES and SEM obs. 8-71908
 Ni-O system, initial oxidation, combination anal. using ESCA, AES and SIMS 8-72924
 Ni-W (2%), Mg diffusion meas., 970-1330K, appl. of vapour collect and AES method 8-75876
 Ni₃C film, thermal decomposition, AES meas. 8-56056
 NiO (100) surface, sulphurisation by H₂S, AES, LEED, RHEED structural study (*French*) 8-64888
 NiO, Auger quantitative anal. 8-73104
 O₂, electron impact ionis., mean energy expended per ion pair 8-74777
 O₂+Xⁿ⁺, (X=Ar,Kr,Xe,U), Auger emission line shape after dissociation 8-86838
 PZT, ferroelec. film, elec. props., composition anal., AES 8-84530
 Pb, Auger emission target, contrib. of reflected electrons 8-92152
 Pb, epitaxial growth on Ag (111) and Cu (111) LEED, RHEED, AES study 8-84090
 PbO₂, Auger quantitative anal. 8-73104
 Pb_{1-x}Sn_xTe, MBE, O₂ uptake, AES, XPS and UPS expts. 8-95227
 Pd, film, on ZnO, struct., elec. props., AES, UPS study 8-76168
 Pd-Ag, surface segregation, Auger studies 8-87849
 Pt (100), adsorption of acetylene or ethylene, intermolecular forces and kinetics of adsorption 8-75930
 Pt (100), adsorption of H₂S, intermolecular forces and kinetics of adsorption 8-75930
 Pt (111) stepped surface, adsorption of O₂, CO, C₂N₂ and ethylene 8-71992
 Pt, adsorption of O₂, AES, LEED and thermal desorption spectroscopy exam. 8-79891
 Pt-C, C layer formation on (111) surface, temp. depend., LEED, AES study 8-71911
 Pt-Pd alloy, surface composition determ. by AES 8-79869
 SF₆, Auger emission anomalous spectra and yield, chemical species depend. 8-55152
 SF₆, KLL Auger spectrum, obs. and ab initio SCF CI calc. 8-50654
 SO₂, double hole states POCI calc., Auger spectrum 8-78630
 SO₂, KLL Auger spectrum, obs. and ab initio SCF CI calc. 8-50654
 Se compounds, chemical shifts of X-ray electron and Auger lines 8-86912
 Si (100) surface, LEED and AES meas. 8-60016
 Si (110), chemisorption of Cl, LCAO calcs., Auger line shapes, localized density of states 8-56202
 Si (111) surface, anal. by ion-electron spectroscopy 8-72670
 Si, AES examination of Ar⁺ ion retention during Ar sputtering 8-56552
 Si, amorphous, hydrogenated, work function and Auger spectroscopy of initial oxidation 8-76132
 Si, Auger lineshape, one-electron theory for L₂₃VV and L₁L₂₃V 8-72645
 Si, epitaxial regrowth and grain struct. of Al metallisation on (100)Si 8-79901
 Si, spectral, convolution and deconvolution 8-52601
 Si surface, planar and O₂ etched, CO adsorption, SEM, AES, and desorption meas. 8-63934
 Si surface, valence band Auger line shape, corrected numerical results 8-52602
 Si, work function and Auger spectroscopy of initial oxidation 8-76132
 Si-SiO₂ interface, Auger-sputter profiling obs. of P pileup 8-95240
 Si-SiO₂ interface morphology, P pileup effect, Auger sputter profiling 8-72006
 Si-transition metal silicide interface, chemical state, AES expts. 8-91767
 SiC, energetic H and Ar ion sputtering, AES-SIMS-FDS combined obs. 8-80444
 SiC, energetic ion sputtering, appl. of AES-SIMS (IMA)-FDS combined systems to physical and chemical processes 8-95636
 SiC-SiO₂ interface, Auger anal. 8-95375
 Si₃N₄ film, diffusion of Al, AES and depth profiling 8-51744
 Si₃N₄ film, with varying refr. index, AES and XPS 8-72029
 SiO₂, phase comp., electron spectroscopy obs. 8-60042
 Si₂Te₃ surface reaction, AES exam. 8-63931
 Sr, strong correl. in 3d-Auger spectrum 8-50522
 SrTiO₃ (111), surface struct., electronic props., LEED, AES, UPS study, photoelectrochem. cell anode appl. 8-84035
 SrTiO₃, surface defects, electronic struct., LEED, AES, UPS study 8-84273
 Ta film, determ. of thickness and O, N content 8-80824
¹⁸²Ta-containing Ta sheet, radioactive electron emission spectrum (exoelectrons), surface elec. field and Auger effects 8-72705
 Te, film, AES, LEED, XPS, energy loss spectra studies oxidation effects 8-73086
 Te, Te cpds., Auger spectra 8-58638
 TeO₂, film, AES, LEED, XPS, energy loss spectra studies 8-73086
 Th, ion irradiation, surface C and O, AES obs. 8-71775
 ThNi₅, methanation catalyst, AES and characteristic energy loss spectra 8-56915

Auger effect continued

- Ti, chemisorption of N₂, O₂ and CO on polycryst. surfaces, secondary electron yield obs. 8-71971
 Ti film, ultra-thin, AES and XPS anal. 8-91573
 Ti, monolayer, oxidation, quasimultaneous SIMS, AES, XPS 8-72919
 α-Ti, S, C and Cl diffusion, AES meas. 8-51735
 Ti-sapphire interface, solid-state reaction 8-72008
 TiD₂, clean and contaminated films, fabrication and AES 8-52600
 Ti, epitaxial growth on Ag (111) and Cu (111), LEED, RHEED, AES study 8-84090
 UIr₃, (100) surface reconstruction, LEED, AES, electron energy loss spectra study 8-75918
 V, extended fine struct. above 2s appearance potential edge, AEAPS spectra 8-72647
 V, extended fine struct. above L-shell appearance potential thresholds 8-92148
 W (100), CO/H₂ surface complex, flash desorption and AES obs. 8-73083
 W, adsorption of C(O), Auger signal comparison using differential and integral Auger spectra 8-76561
 W, wire, exam. of grain boundary segregation, using Auger spectroscopy, new technique 8-80551
 WC-Co composite, surface anal. by quantitative AES 8-76622
 WC-Co composite chemical characterisation by AES and ISS 8-76621
 WC-Co sputter deposited film, struct. and comp. 8-72023
 W(100), NVV Auger spectra, O₂(H₂) adsorption effects, comp. to band struct. calcs. 8-72643
 Xe, reson. line excitation, Auger decay 8-70804
 Zn, Auger electron spectra, electron impact excited, vap. and solid state differences 8-52603
 ZnO 1010 surface, reaction of O₂, AES, LEED, EPR, desorpt., surface cond. and work function expts. 8-95950
 ZnO (0001), adsorption of alkali metal, anomalous behaviour of Na 8-79883
 ZnO, electron beam induced decomposition and desorption, AES and contact potential difference meas. 8-79893
 ZnS, chemisorption of O₂ after illumination and in presence of CO and O₂ 8-87877
 ZrNi₅, methanation catalyst, AES and characteristic energy loss spectra 8-56915
 ZrO₂-Y₂O₃ film, surface characterisation, XPS, ESCA, and AES expts. 8-72028
- Auger electrons** see *Auger effect*
Auger showers see *cosmic ray showers and bursts*
Auger spectra see *Auger effect*
Auger spectroscopy see *Auger effect*
augmented plane wave calculations see *APW calculations*
aural null direction finders see *radio direction-finding*

aurora

- see also *airglow; atmospheric electron precipitation; atmospheric proton precipitation; atmospheric spectra*
 afternoon sector, obs. of pulsating aurora after twilight 8-81486
 albedo profile over snow-covered ground, rocket obs. 8-77384
 arcs location near substorm onsets 8-88968
 artificial auroral streaks during Echo 4 electron beam expt., beam magnetospheric interactions 8-89036
 curl and shear instability 8-77433
 currents, magnetometer array and radar backscatt. joint obs., N.Scandinavia 8-85768
 dayside arcs and convection 8-81484
 dayside aurora, rocket-borne meas. of particles and ion convection 8-77391
 dayside emissions, obs. from Scandinavia 8-85755
 detached auroral arcs in ionosphere trough region, obs. 8-88965
 displays recorded by low-light sensor, DMSP nighttime images 8-88942
 electric field oscils. meas. near auroral arc, assoc. with MHD wave 8-65457
 electric fields, conductivities and currents in auroral zone, latitudinal distrib. 8-77399
 electric fields in auroral zone at 1 R_s altitude 8-57397
 electrojet region, elec. fields and mag. effects of solar flares 8-69576
 electron beam, electrostatic noise generation 8-85759
 electron diffuse surge zone, equatorial boundary model 8-69610
 electron precipitation, energy distrib. from incoherent scatter radar and photometric meas. 8-77390
 energetic ions and EM radiation in auroral regions 8-81490
 energy dissipation due to ionospheric currents, high-resolution altitude profiles 8-88978
 Excede 2 test, artificial auroral expt., ground-based optical meas. 8-89038
 field-aligned currents, effect on ionosphere currents and elec. fields 8-96339
 Harang discontinuity, electric field meas. by auroral radar and rocket double-probes 8-88971
 historical records, occurrence correl. with solar activity long-period vars. (*French*) 8-73695
 magnetic field line merging and slippage in auroral arcs 8-77393
 magnetosphere auroral absorption substorm, onset obs. 8-96362
 magnetospheric physics, review of selected topics 8-65466
 optical emission features in aurora and nightglow, satellite obs., ground scatt. effect 8-77385
 parallel electric field, signature in ion and electron distrib. in vel. space 8-89005
 particle instantaneous energy deposition, determ. from optical emissions 8-81491
 Pc 5 micropulsation resonance region, examination by dual auroral radar system 8-65454
 Precede, artificial auroral expt., summarised results 8-89037
 pulsating aurora, optical-particle characteristics 8-88969
 pulsating aurora, review 8-73562
 quiet auroral arcs, feedback instability in ionosphere-magnetosphere system 8-57379
 radar echoes drift meas. using radar auroragraph 8-65436
 radiation transport, multidimensional, in plane-parallel atmosphere, appl. to 4.3 μm auroral arc 8-88917
 radio aurora, spatially ordered structure, spaced radar obs. 8-73561
 radio aurora in dayside auroral oval, rel. to field-aligned currents and energetic particles 8-88966

aurora continued

- radio auroral signals, maximum entropy spectral anal. 8-93006
 review 8-77386
 southern oval, spherical harmonic analysis 8-81487
 spectral feature at 2150 Å, contrib. from N II lines 8-61645
 subauroral red arc event caused by kinetic Alfvén waves 8-93026
 substorms, electron flux intensity rel. to form of auroral absorpt. bays 8-69619
 substorms, HF signals statistical characts. 8-69583
 thermosphere, effect of auroral energy input on neutral and ion drifts 8-65446
 UHF diffuse radar aurora, rapid scan Doppler vel. maps 8-77388
 ULF elec. fields and particle precip., rocket meas. 8-96337
 UV aurora, spectrum between 2100 Å and 2300 Å 8-88963
 westward electrojet, rel. to Pc 5 activity in morning sector 8-61685
 X-ray auroral prod. by energetic electrons precip., imaging from Space-lab 8-61608
 X-ray source region determ. by high-altitude balloon obs. over Thompson, Canada (*Japanese*) 8-61644
 N₂ 15300 Å high-resolution electronic emission spectrum, lab. meas. 8-66549
 N₂ bands in proton-induced polar cap aurora, intensities 8-77389
 N₂ dissociation by electron impact and EUV photoabsorpt., rel. to aurora and airglow 8-58847
 N₂⁺(A²Π_g) Meinel band deactivation cross sections 8-66635
 N₂⁺(A²Π_g-X²Σ_g⁺) system, vibr. development and quenching effects 8-88967
 N₂(B³Π_g-A²Σ_u⁺) system, vibr. development and quenching effects 8-88967
 O I 5577 Å forbidden line and O₂ 7620 Å band auroral excitation 8-88964
 O I emissions, ground-based photometric meas. 8-77387
 O₂, O₂ and N₂ emissions, rocket meas. and anal. 8-57380
 O₂ 1.27 μ emission, auroral enhancement 8-81485

auroral ionisation see aurora**austenitic stainless steel**

- 304, intergranular H₂ assisted fracture, exam. of mechanism 8-80644
 316 trapping up to 7 eV D, depth profiles 8-71751
 advanced reactors, materials and design 8-78452
 anelasticity and creep transients in type 316 stainless steel 8-84880
 boiler tubes, use of mag. field intensity meter to detect magnetic oxide 8-76794
 corrosion, in high temp. Na, influence of steel comp. 8-80675
 corrosion and electrochem. behaviour in NaOH soln. containing ClO₃⁻ (*Japanese*) 8-72928
 corrosion resistant welded joints, cold working effects on mech. and corrosion props. (*Hungarian*) 8-52838
 corrosion-resistant, strengthening by alloying with N₂ 8-95757
 crack growth of X6CrNi1811 and X6CrNiMo1713 under Na cooled fast breeder reactor conditions (*German*) 8-56798
 crack propagation 8-60797
 cyclic strain induced creep, relation between modes of stress and strain superposition 8-60733
 deformation and fracture rel. to grain-boundary reaction nodules 8-80591
 equivalent alternating stress from two-level multiple-step wave (*Japanese*) 8-92333
 even elongation and relative hardening, effects of struct., comp. and testing temp. 8-52926
 fast neutron irradi., effect on mech. props. 8-92309
 fatigue behaviour, influence of stressing conditions (*French*) 8-68776
 fatigue crack growth rates in type 316, effects of overloads on growth rate 8-64688
 fatigue cracks, steel 07Kh25N12G2T US monitoring of growth rate 8-60917
 fatigue damage, under sawtooth wave strain cycling at elevated temp. (*Japanese*) 8-84977
 fatigue life of type 316, effect of hold times, explanation in terms of grain boundary sliding damage 8-72851
 FCC, fractographic obs. of SCC 8-64786
 ferrite volume fraction, high-speed determ. by XDXRD 8-76628
 fracture toughness and transition temp., T₅₀, effect of cooling rate and supercooling temp. 8-84987
 fusion reactor materials, material requirements exam., review 8-50257
 grain boundary migration during high temp. creep, TEM exam. 8-88509
 grain growth, time dependence and activation energy 8-72787
 interaction of a mealting twins in fcc metals and alloys 8-68712
 irradiation induced creep, AISI 316, 20% cold worked effect of temp. change 8-72816
 irradiation induced creep by alpha particles, in type 316 steels (*French*) 8-72791
 LMFBR performance, effects of irradiation creep and swelling 8-78482
 mechanical behaviour of type 316 stainless steel from 760 to 1204 C 8-86604
 metastable, fatigue damage, static and dynamic simultaneous obs. (*French*) 8-88516
 neutron irradi., He release kinetics, 600 to 850°C 8-79638
 neutron irradi., swelling due to gamma prime and M₂₃(C₁Si)₆ form. 8-51590
 nucleation, of M₂₃C₆ carbides, from directly aged 18 Cr-11 Ni (*Polish*) 8-52806
 oxidation of (100)-plane, LEED-AES obs. (*German*) 8-68841
 pitting and crevice corrosion, effect of Mo, Si and N (*Japanese*) 8-92399
 pitting corrosion, effect of Cr, Mo and N content on resist. 8-80668
 stacking fault energy, effect of C, exam. 8-80553
 steam generator tubing, stress corrosion cracking in NaOH soln. 8-60866
 strain growth, due to thermal stress ratcheting, exam. 8-92354
 strengthening by modified ausforming 8-76665
 stress corrosion cracking and stacking fault energy, N₂, P and Ni effects (*Czech*) 8-60875
 stress corrosion cracking in boiling MgCl solution (*Japanese*) 8-92400
 stress corrosion cracking in concentrated chloride solution 8-56825
 stress relaxation, model, experiment confirmation of model 8-92293
 stressed state blistering 8-95085
 structural inhomogeneity in rolled steel, electron and optical microscope exam. 8-72827

austenitic stainless steel continued

- surgical implant ion beam textured, stress/strain relations, fatigue characts. 8-73297
 temper embrittled, type 304, Auger spectroscopic exam. of grain boundary surface phases 8-76741
 tensile fracture, phase transform. effect, comparison of stable and metastable phases 8-60798
 transgranular slip obs. 8-80595
 tube carburised layer metallographic determ. 8-85077
 type 304 with He distrib., foil, effect of momentum transfer, damage energy gradient, on He distrib. 8-71773
 X-ray elastic constants, determination by ψ_0 oscillation method (*Japanese*) 8-64575
 Cr-Ni, effect of boron on nucleation of M₂₃C₆ carbides (*Polish*) 8-84808
 Cr-Ni (18,12 wt.%), containing coarse irregular carbide precipitates along grain boundaries, ductility 8-60718
 Cr-Ni (18,8 wt.%), stress-corrosion cracking in conc. MgCl₂ soln. 8-85057
 Cr-Ni-Ti, creep deform. effects on intergranular TiC dispersion stability 8-84912
 Mn-N interaction, internal friction obs. 8-84883
 Mo-bearing, ellipsometric meas. of passive films, optical constants (*Japanese*) 8-85041
 Ni-Al, γ-phase, fracture mechanical aspects of abrasive friction, wear, chip formation 8-72865

austenitic steel

- see also *austenitic stainless steel*
 800H, effect of hardening processes on initial stress-strain curve 8-84846
 AISI 4340, effect of step quenching on microstruct. and fracture toughness 8-84834
 alloy steel, austenitic, Ni free, TEM exam. of corrosion process 8-85029
 bainitic, morphological characteristics 8-68682
 deformed, struct., texture and mech. props. of product of transform. 8-92273
 fracture toughness props. of A533B, prior austenite grain size effect 8-60780
 grain boundary sliding, exam. by tensile creep tests 8-76715
 grain size rating methods, comparison 8-85074
 heat resistant, mag. permeability increase, measurement method 8-53039
 high speed, supercooled, austenite decomposition kinetics 8-92233
 high speed, tempered, etching reagents for austenite grain boundaries 8-80704
 intergranular defectiveness determ. using inductive instruments 8-53075
 martensite lattice struct. obtained by deform. of steel 70Kh5G4 (*Russian*) 8-88464
 martensitic transform. temp., singularities in 50Kh2N22 (*Russian*) 8-68689
 mechanical properties, -196 to +250°C, and kinetics of phase transforms., for steel 0Kh14AG12M (*Russian*) 8-92297
 mechanical props. of DIN X8 CRNIMONB 1616 and DIN X2 CRNI 189, FBR safety anal. 8-60966
 Mn-Cr-Ni-N, N effect on relaxation behaviour, internal friction temp. depend. (*Russian*) 8-52872
 pearlitic, weld, US testing, frequency and beam angle choice 8-60950
 precipitation hardened, ductility of grain boundaries and crack propag. (*German*) 8-52834
 precipitation hardened Kh15N27T3MR, exam. of elasticity props. 8-56687
 precipitation hardening, effect on fatigue strength 8-84829
 pressure vessel, fatigue design criteria 8-60758
 proof stress meas. in N28G1.5, by internal friction 8-56638
 submicroscopic structure of Kh12N20T3R, and role in dispersion hardening (*Russian*) 8-64549
 supercooled, transformation kinetics into spheroidised pearlite (*Russian*) 8-95742
 surface hardening, mechanism 8-85048
 thermodynamic props. of C in austenite, relationship with cryst. lattice anomalies of martensite (*Russian*) 8-59781
 tool, thermal treatment effect on abrasive wear resistance 8-92369
 toughness evaluation inconsistency of AISI 4340 austenitised at increasing temp. 8-52982
 transform. kinetics of supercooled austenite in 12Kh1MF, structural method 8-52801
 weld testing review (*German*) 8-53068
 C and low-alloy steel inherent austenitic grain size determ., exam. of methods used 8-85071
 Cr-Ni, X5CrNiTi26.6, ferrite-austenitic struct., optical and electron microscopy 8-84848
 Cr-Ni-Mo-V, quenched, morphology, structural constitution after austenite form. by heating (*Russian*) 8-68709
 Fe-C alloys, thermodynamics of proeutectoid ferrite transform. re-exam. 8-84763
 Fe-Cr-Ni-Nb-C, austenitic, splat quenching 8-72798
 Fe-Ni, inverted casting process for very rapid growth of large crystals 8-84791
 Fe-Ni-C, inverted casting process for very rapid growth of large crystals 8-84791
 Fe-Ni-Cr austenitic steel, martensitic transform. kinetics, metastability criterion (*French*) 8-68690
 Fe-Ni-Ti, inverted casting process for very rapid growth of large crystals 8-84791
 Ni-Cr, intergranular segregation of P 8-84761

autoionisation

- see also *Auger effect*
 acetylene, ionis. efficiency curves by electron impact, CH₂⁺(C₂H⁺) form., ~10 eV 8-62935
 atomic K- and L-shell shakeoff probability, following β-decay, hydrogenic wave function 8-94204
 lanthanides, Rydberg spectra and ionisation thresholds, time resolved resonant multistep technique 8-82701
 metal vapour, electron impact, ionis. and autoionis. 8-58830
 molecular electron impact, autoionising states 8-58852
 rate coeffs. for quadruply and quintuply ionised atoms, solar corona appl. 8-74619
 three-electron atomic systems, autoionising states decay calcs. 8-78670

autoionisation continued

- Ar, ($3s^{-1}4p^1P$) autoionising state decay, triple differential cross section 8-86831
 Ar, autoionising states excitation by electron impact, threshold effects 8-62923
 Ba I, absorption spectrum, 1560 to 1770 Å 8-66487
 Ba, radiative decay of autoionisation states (*Ukrainian*) 8-82682
 Be⁻, $2p^0$ shape resonance, complex-coord. method calc. 8-74591
 Ca, radiative decay of autoionisation states (*Ukrainian*) 8-82682
 Gd atom, long-lived autoionisation state (*Russian*) 8-94216
 H⁺, autoionising states, electric field effect 8-50528
 H⁺, S autoionising states, time stability theory 8-90130
 HCN⁻, SCF ab initio ground state pot. energy surface, geometry, rel. to HCN 8-78646
 Hg+He²⁺, autoionisation, 5-20 eV, electron and ion ang. distrib. 8-78795
 K²⁺, photoionisation cross-section, R-matrix theory 8-82702
 Kr, electron impact excitation of autoionis. states 8-90302
 NO, autoionisation struct. at first ionisation limit, photoionis. data 8-58748
 NO, UV photoelectron spectrum, autoionisation from Rydberg state, vibr. progressions, Franck-Condon factors 8-50583
 Ne, autoionising states, scatt. electron spectra, post collision interaction effects 8-58819
 Sr, radiative decay of autoionisation states (*Ukrainian*) 8-82682

automatic control

- aviation and astronautics, conference, Tel Aviv (1977) 8-81517
 bipedal walking, linear stabilisation (*Russian*) 8-51055
 C-CD based control system for Si cryst. growth 8-68623
 CANDU secondary coolant circuit chemistry control, automated system development 8-66359
 clinical electrophysiology laboratory automatic control system 8-57110
 crack length automatic recording in sheet samples 8-60907
 crystallizer for growing single crystals from solutions with precision control of supersaturation 8-80465
 Febry-Perot interferometer, with automated data acquisition and stabilisation system 8-70180
 gamma-ray irradiator for dosimeter calibration, automatic irradi. time control (*Japanese*) 8-66452
 gas flow control, automated, transducer 8-59508
 laser absorption calorimeter automation 8-74084
 lathe during metal removing, vibration control systems reviews (*Russian*) 8-70118
 magnetic induction, stabilised source 8-94360
 NMR spectrometer, pulse, controlled by programmable digital unit (*Czech*) 8-77952
 optical adjustment and control subsystem, for OMEGA-10 multibeam laser system 8-50847
 photographic camera films, automatic exposure 8-65992
 rotating-anode X-ray tube apparatus 8-58100
 sedimentation anal., automatic recording system 8-60897
 spectrometer automatic control unit for discrete recording 8-58049
 stopped-flow systems, automated, for fast react. rate anal. methods, review 8-95971
 surgical aspiration automatic control device for cardiac surgery (*French*) 8-61282
 telescope, large azimuthal complex, automated control system 8-73641
 tilt meters, photoelectric, with negative feedback, block diagrams anal. (*Russian*) 8-88948
 Tokamak, automatic TO-1, plasma concentration control (*Russian*) 8-91160
 US thickness gauge, Kwarts-6, design of automatic control block 8-73005
 voltage stabiliser attachment circuit 8-57981

automatic frequency control

- EPR spectrometer, 2 mm band, with re-entrant resonator 8-86311
 reference time interval reproduction device 8-77869

automatic gain control

- optical path electronic simulator GaAlAs laser power control loop (*German*) 8-82987

automatic test equipment

- cineangiocardigrams, automatic anal. using TV system on line with minicomputer 8-92699
 digital automatic thermodynamic enthalpy and specific heat determ. equipment 8-57951
 disc-on-disc apparatus, for adherence, wear resist. and thermal shock meas. of thin films 8-72943
 eddy current inspection of fastener holes, computer automation, exam. 8-53040
 electromagnetic device for loading and measuring wear in vacuum 8-56841
 fatigue crack growth testing, decreasing stress intensity technique, computer-controlled 8-72949
 ferromagnetic probe inspection unit for automatic inspection of welded tubing 8-56860
 ferromagnetic probe unit, MD-10F, automatic 8-56861
 gas turbine blades, exam. using automated vibrating bench 8-64800
 intrinsic semiconductor IR detector array data acquisition system 8-77991
 leak test, automatic, nondestructive, design, evaluation and implementation for IC assemblies 8-53180
 machines, crank driven, electromech. system for stabilisation and programming static load 8-64801
 mechanical oscillation damping characts., apparatus for examining, based on amplitude-frequency relationship resonant trough 8-64803
 optical fibres measurement system 8-50909
 pacemaker testing automation using microcomputer (*German*) 8-81068
 particle size distrib., on-line measurement techniques, instruments (*German*) 8-60895
 programmable semiautomatic instruments for quantitative struct. anal., geometric eval. in materials lab. (*German, English*) 8-64798
 regulation of CO₂ conc. in climatic cabinets for corrosion testing (*German*) 8-53069
 reproducible adjustment of test equipment, procedure utilising computer controlled electronics (*German*) 8-60927
 stamped disc surface inspection by automated eddy current unit 8-92430

automatic test equipment continued

- steel tubes, ferromag., complex of devices for automatic nondestructive testing 8-53092
 steel weld fatigue life estimation, multichannel NDT monitor 8-56846
 thermal meas. using data logger and computer 8-81966
 US, online inspection, steel plate manufacture appl. 8-80702
 US automatic inspection of tubing 8-56865
 US echo pulse flaw detectors, use of auxiliary sensitivity regulation 8-60951
 US equipment for monitoring drill and casing tubes 8-53085
 US units for inspecting thin walled tubing 8-88606
 vibration test rig for wear meas. of granules 8-56840
 X-ray quality control, automatic exposure relay 8-95893

automatic testing

- automatic anomalous noise meas. for ferroelectric capacitor parameters, not in equilb. (*French*) 8-74029
 experimental control system, exam. of mech. props. under complex stress conditions 8-64802
 industrial resistance thermometers testing using incomplete bridge balancing technique 8-73998
 particle size distrib., on-line measurement techniques, instruments (*German*) 8-60895
 polymer cyclic deformation amplitude, automatic meas., apparatus design 8-85082
 US inspection, automatic, thin walled large diameter pipes, flaw size classification 8-60949
 US inspection of heated objects by SGK-2Ts system 8-95894

automation, social aspects *see social aspects of automation***automobile industry**

- acoustic noise measuring techniques, exterior, interior noise in automobile development (*German*) 8-79178
 automatic induction hardening equipment 8-92284

automobiles

- acoustic measurements in automobile development (*German*) 8-87219
 exhaust system design, finite element acoustic analysis 8-51003
 motor vehicle racing and shooting noise 8-55510

avalanche diodes

- see also avalanche photodiodes*
 photodetector, characts. (*Swedish*) 8-89545

avalanche photodiodes

- optical fibre communication, cabling, light source and receiver technology, review 8-59125
 GaAs, electroabsorpt. avalanche photodiode waveguide detectors 8-65965
 GaInAsP-InP avalanche photodiode, fabrication and characts. 8-54454
 Ge, non-repeated 50 km transmission experiment using low-loss optical fibres 8-79108
 Si, stress enhanced diffusion of B, using SiO₂ diffusion masks, photodiode fabrication 8-67865

avalanches, carrier *see impact ionisation***avalanches, electron** *see electron avalanches***avalanches, electron-hole** *see impact ionisation***avogadro's number** *see constants***axicons** *see lenses***axiomatic field theory**

- $\lambda\pi^4$ field theory with internal symm., string representation 8-70266
 $\lambda\phi^4$ theory, dual string theory from Feynman graph expansion 8-54544
 $(\lambda\phi^4)_2$ quantum field model, soliton mass and surface tension 8-58109
 Φ^4 model anal. using perturbation theory anharmonic oscillator strong coupling 8-89622
 ϕ^3 interaction, four-dimensional Green's function model (*Russian*) 8-77775
 ϕ^4 model, Padé approximants, EM form factor, pseudoscalar particles 8-74122
 Bogoljubov axiomatic approach, global axioms and S-functional (*Russian*) 8-54572
 Bogoljubov axiomatic approach, necessary classes of generalised functions (*Russian*) 8-54571
 book, PCT, spin and statistics 8-78102
 complex ϕ^4 theory, Euclidean path integrals and Feynman-Dyson-Wick perturbation expansion 8-49957
 coupling of logics 8-62104
 covariant representations of nuclear *-algebra, C*-algebra comparison, Wightman axioms 8-58120
 degree of freedom, cutoff and space time struct. 8-66031
 derivative analyticity relations, high-energy status 8-66043
 dissipative systems with a Liapounov function, quantum rules 8-89611
 $g\phi^4$ theory, strong coupling limit of Green functions, anharmonic oscillator appl. 8-78071
 Gell-Mann-Loy function in scalar field theory, $g\phi^4/4!$ appl. (*Russian*) 8-82116
 hadron form factors, axiomatic local constraints (*Russian*) 8-58190
 Heisenberg eqns. on C* algebra of quasilocal observables, boson and fermion systems 8-57854
 Klauder augmented theory, Green function formalism, ϕ^4 model 8-78094
 Lie-admissible local powers, incompatibility with Wightman axioms and spin statistics theorem 8-93793
 local props. in field theories without strict locality 8-86401
 massive Thirring model with bosons, asymptotic scale invariance 8-93799
 multiparticle S-matrix in field theory two dims. space-time models, factorisation 8-62324
 $P(\phi)_2$, two-dims. model, existence of three phases 8-49951
 probabilistic techniques in field theory 8-49952
 relativistic, reconstruction of local observable algebras from Euclidean Green's functions 8-54522
 scalar field theories, finite amplitudes in perturbation theory, ϕ^4 models, pass. renormalisation 8-93794
 singularities of Borel transform in renormalisable theories, massive $g\phi^4$ theory 8-62304
 (super- ϕ^4)₄, model, Euclidean formulation 8-93797
 trace anomaly of a conformally invariant quantum field in curved space-time 8-54278
 two-dims. U(1)-Goldstone model, QFT on lattice 8-74158

axiomatic field theory continued

- Ward identity, conformally invariant form, Green's function and two conserved currents 8-86421
 Wightman formulation, nontranslationally covariant currents and symm. of S-matrix 8-58133
 Wightman functions, decomposition in Euclidean framework 8-54566
 $\Lambda\phi^4$ theory, high temp. expansion without lattice, strong coupling expansion 8-58124
 $\lambda\phi^2$, quantum field as limit of sine Gordon field 8-82094

backplane wiring see wiring**backscatter**

- see also *particle backscattering*
 absorbing-scattering layered material, light beam diffusion obs. method 8-62215
 auroral currents, magnetometer array and radar backscatt. joint obs., N.Scandinavia 8-85768
 calorimeter, BB2, for high-power CW laser energy meas. 8-54372
 chemical identification of substances fixed on silica gel, using Raman spectroscopy (French) 8-88664
 dielectric spheroids, backscatter matrix 8-66716
 differential scatter lidar system, for atm. aerosols remote anal. 8-69524
 Doppler US blood velocity meas., phase-locked loop technique 8-61234
 electron beam, surface thickness monitoring, object accessible from one side 8-60944
 F-region, equatorial, backscatter obs. rel. to irregularity patches localised origin 8-77404
 hailstone trajectories determ. from crystallography, D content and radar backscatt. 8-61614
 incoherent backscatter from rough surfaces, two-scale model re-examined 8-71013
 ionosphere, backscatter radar data rel. to O I 6300 Å nightglow intensity 8-77401
 ionosphere, low-altitude plasma line anisotropy theory 8-77414
 ionosphere, stimulated reson. line scatt. with Eiscat radar 8-57389
 ionosphere equatorial spread-F, VHF and UHF backscatter from high freq. drift waves 8-88973
 ionosphere temperature latitude E_s -layer, skywave backscatter studies 8-85761
 lidar backscatter from horizontal ice crystal plates 8-92984
 Loran-A (1.85 MHz) radio wave backscatter from ocean waves, Doppler spectra (Japanese) 8-85737
 mesosphere, lower, O_3 abundance from backscattered solar radiances 8-69414
 microwave backscatter modulation by shoaling ocean waves 8-57212
 Milne problem and spherical albedo, law of darkening, forward and backward scatt. effects 8-77483
 ocean surface, radar backscatter rel. to wind speed and fetch 8-77247
 periodic surface characterisation by US diffraction spectroscopy 8-60974
 radar cross-sections of ocean surface, friction vel. depend. 8-77246
 sea echo radar spectra resolution limitation inferred from ionospheric Doppler broadening 8-81489
 sea waves, low-angle backscatter of microwave radar, long-period feature origin 8-57218
 suspension, particle size and concentration, determ. by light backscatter technique 8-85214
 thin stiffened Al plate, underwater acoustic backscattering and echo struct. characts. 8-55492
 US diffraction scanner for in vivo tissue characterisation 8-61226
 UV backscatter expt., airborne, for O_3 distrib. determ., error anal. 8-92985
 wave propagation in inhomogeneous media, backscatter folding series (Russian) 8-73862

backward wave oscillations see *backward wave tubes; electromagnetic oscillations***backward wave tubes**

- see also *carcinotrons*
 No entries

bagging see *packaging***balanced amplifiers** see *differential amplifiers***balanced input amplifiers** see *differential amplifiers***balances**

- see also *weighing*
 capacitance-torsion balance for measuring small stresses and strains 8-73988
 electronic microbalance and precision balance design (German) 8-57935
 electronic scales and precision instrum. (German) 8-70100
 Faraday balance susceptometer, computer controlled 8-65946
 Faraday magnetic balance for metalloprotein solns. in 6.5-300K range 8-70170
 glass-ceramic beam, for 1 kg balance, props. (German) 8-89472
 inertial, direct reading, for student demonstrations, experiment 8-86081
 mass change meas., automatic recording system, exam. 8-57901
 mechanical, with electronic displacement sensor, precision 8-77866
 microbalance, Cahn-RG, mass artifacts in water vap. 8-65909
 microbalance techniques, conf., Boston, USA (Nov. 1977) 8-65905
 piezoelectric microbalance, for respirable aerosol mass conc. meas. 8-69518
 ponderomatic meas. for fluid detection in chem. anal. 8-68953
 quartz crystal microbalance sensing elements in cascade impaction instrument, particle size meas. 8-65904
 small weight, automation problems (Polish) 8-70099
 surface balance, Langmuir-type, monolayer parameters meas. in radiation field 8-82092
 thermal noise effect on meas. appls. 8-65906
 two-string balance microprocessor operation (German) 8-57936

ball lightning see *lightning***ballistics**

- see also *impact (mechanical); military equipment*
 armour material, selection criterion 8-53063
 shot put, maximum range, for teachers 8-61985
 supersonic aircraft simulation using high speed jets, sonic-boom press. signature 8-79156

balloons

- see also *aircraft*
 ascent meter (Japanese) 8-61567
 Balloon Altitude Mosaic Measurements Program 8-81455
 satellite solar cell calibration using high-altitude balloon (Japanese) 8-61700
 stratosphere, ion sampling package 8-69497

band gap see *energy gap***band model of magnetism**

- see also *Hubbard model*
 alloys, crystalline and amorphous mag. props. from Rhodes-Wohlfarth plot 8-52190
 amorphous ferromagnets, itinerant electron model, Invar anomalies, review 8-95413
 antiferromagnet, itinerant electron, mag. excitations 8-56305
 antiferromagnetism of strongly correlated electrons in narrow bands 8-76218
 disordered system, orbital mag. susceptibility of conduction electrons 8-76217
 ferromagnet, disordered itinerant-electron, spin waves 8-95427
 ferromagnetic metal, itinerant electron model, for US propagation and structural instabilities 8-95508
 ferromagnetic semiconductor, electronic spectrum, influence of finite carrier conc. 8-76220
 ferromagnetic transition metals, electron spin polarisation, review 8-76591
 ferromagnetic transition metals, electron spin polarisation, review 8-76592
 ferromagnetism, basic models, classification of theories (Rumanian) 8-91840
 Hubbard model, itinerant antiferromagnetism 8-91841
 Hubbard model, partly filled narrow band, electron correlation and mag. props. 8-67968
 itinerant electron antiferromagnet, localised spin coupling 8-68142
 itinerant electron ferromagnet, effective Lorentz force and Landau level 8-80120
 itinerant electron ferromagnet with domain struct., spin waves 8-64182
 itinerant electron ferromagnetism, spin fluctuation theory 8-80151
 itinerant electron ferromagnetism at zero temp. 8-56285
 itinerant electron magnetism, neutron scatt. 8-68194
 itinerant ferromagnet in disordered phase, energy band struct. 8-68141
 itinerant magnetism, quasispin model, effect of short-range order 8-68144
 itinerant-electron antiferromagnet, effect of mag. field on crit. temp. 8-60293
 rare earth cobalt alloy, RCO_2 , itinerant system, weak ferromagnetism 8-52191
 rare earth intermetallics, mag. props. 8-84380
 rare earth metals, ferromag. ordering (Russian) 8-60262
 rare earth-Co alloys, spin wave spectra 8-56304
 rare earths, heavy, mag., electronic struct., book 8-60259
 resistivity anomalies of ferromag. metals near Curie temp., itinerant mag. electron theory 8-95292
 s-d electron model, finite temp. diagram technique, perturbation theory 8-67932
 semiconductor, ferromagnetic, electronic quasiparticle spectrum in sf-model 8-52188
 spin-density-functional formalism 8-68140
 Stoner ferromagnetism, criteria in doped semimetals, uncompensated metals, derivation 8-68145
 susceptibility of cryst. with strong s-d exchange (Russian) 8-56283
 transition metal alloy, ferromag., local environment effect on atomic moments, itinerant model 8-68188
 transition metal alloys, spin glass behaviour, simple itinerant model 8-84436
 transition metals, conf., Toronto, Canada (Aug. 1977) 8-91577
 two-dimensional layer, model, electron-correlated density-wave states 8-51919
 Wolff model, effective mag. interactions between impurity and conduction electrons 8-68143
 Cr, Fermi surface, stress depend., from quantum oscill. effects, rel. to itinerant antiferromagnetism 8-91597
 Cr-Fe, low conc. alloys, coexistence of itinerant antiferromagnetism with paramagnetism 8-84386
 Cr-Pt, dil., effect of Pt on itinerant antiferromagnetism 8-64191
 Fe, photoelectron spin polarisation and itinerant magnetism 8-68602
 Fe, spin polarisation in electron field emission, surface magnetism 8-68607
 (FeCoNi) B_{20} , glass, evidence supporting split-band model from magnetostriiction 8-95509
 Fe $_3$ Pt, Invar alloy, theory of elastic-anomalies, rel. to Stoner theory of band magnetism 8-95505
 Gd, self consistent relativistic ferromag. band struct. 8-91609
 Ni (111), band struct. and temp.-depend. mag. exchange splitting, angle resolved photoemission obs. 8-60546
 Ni, anomalous resistivity near Curie temp., band theoretical calc. 8-56127
 Ni, ferro- to paramag. transition, angular resolved photoemission 8-68603
 Ni, spin polarisation in electron field emission, surface magnetism 8-68607
 Ni $_2$ Pt $_{1-x}$, disordered alloy, itinerant system, induced magnetism 8-52191
 Pd-transition metal, dil., itinerant versus localised magnetism 8-64188

band-pass filters

- see also *crystal filters*
 contrast enhancing filter for banded chromosomes 8-92755
 feedback optical system using liquid crystal light valves 8-66924
 microcomputer based digital filter for electroencephalogram processing 8-73278
 peripheral auditory system, anal., noise appls. 8-80888
 ripple noise pitch detection by human, adaptive model 8-73166
 SAW, with -50 dB sidelobes using unweighted interdigital transducers 8-71244
 SAW, withdrawal weighted, CAD 8-66991
 SAW bandpass filters, TV receiver appls. 8-51008

band-pass filters continued

- SAW narrow pass band, frequency stability study (*Japanese*) 8-90603
SAW narrow pass band, transmission systems appl. (*Japanese*) 8-90602

band structure

see also *band structure of crystalline metals; band structure of crystalline semiconductors and insulators; band structure of semimetals; band theory models and calculation methods; Brillouin zones; conduction bands; degenerate semiconductors; electron energy states of amorphous solids; electron energy states of liquid metals; electron energy states of liquid semiconductors; energy gap; Fermi surface; many-valley semiconductors; valence bands*

- Bloch electrons, closure of bands in a mag. field 8-79918
crystals, Schrodinger eqn. calcs. variational cellular method, general formulation 8-94192
cumulative type infinite chain cryst., energy bands, ab initio Hartree-Fock orbital calc. 8-60066
disordered solid, l-depend. pseudopot. in theory of band struct. 8-84124
FCC, BCC and SC crystals, electronic struct. tight binding model 8-84123
film, linear APW method, muffin-tin potential, appl. to Cu monolayers 8-87899
polyacetylene type infinite chain cryst., energy bands, ab initio Hartree-Fock orbital calc. 8-60066
rare earth ternary borides, RRh_4B_4 , supercond., re-entrant magnetism, energy band calcs. 8-52140
TCNQ salt, $(\text{NMP})_x(\text{Phen})_{1-x}(\text{TCNQ})$, band filling and disorder 8-87968
TCNQ salt, NMP-TCNQ, realisation of disordered Hubbard model, dielec. props. 8-79917
transition metal compounds, electronically driven lattice instabilities, role of p-d hybridisation 8-63835
TTF-TCNQ, band struct., Fermi surface and density of states, LCAO calc. 8-60048
unit-cell scheme in solids, kq representation based 8-87898
H linear chain of atoms, electronic struct. calc. 8-79969
n- $\text{Hg}_{1-x}\text{Mn}_x\text{Te}$, quantum transport phenomena, exchange interaction influence 8-76093
 $\text{K}_2\text{Pt}(\text{CN})_4\text{Br}_{0.3}\cdot 3\text{H}_2\text{O}$, Krogmann salt, non-empirical localised orbital cal. of electronic struct. 8-91636
LiAl, semimetallic, B32 struct., electronic props. 8-56062
Mo ternary chalcogenides, supercond., muffin-tin orbitals and atomic-sphere approx. 8-51871
 Na_2WO_3 enhanced T_c , interband coupling 8-91804
 $\text{PdH}_{0.72}$, Compton profiles, comparison with band struct. calcs. 8-84675
 TiCl_3 , electronic band struct., tight-binding approx. 8-51872
 $\text{VD}_{0.77}$, Compton profiles, comparison with band struct. calcs. 8-84675
 $\text{VH}_{0.71}$, Compton profiles, comparison with band struct. calcs. 8-84675
 VO_2 , metallic, magnetisation distribution and band structure 8-76223

band structure of crystalline metals

- A15 compound trends, self consistent band calcs. 8-79925
A15 compounds, struct. transform., comparison of Landau theories 8-67824
actinides, band structure Fermi surface, magnetisation density 8-84140
alloys, density of electronic states, dressed-cluster approx. 8-95249
 $\text{Cu}_2\text{Ni}_{1-x}$, soft X-ray emission spectra 8-95620
electron momentum distributions, effect of symmetry 8-63962
elementary excitations in crystals, dielectric theory 8-60076
rare earth, 5d energy band widths 8-63971
rare earths, band structure Fermi surface, magnetisation density 8-84140
rare earths, heavy, mag., electronic struct., book 8-60259
s-d electron model, finite temp. diagram technique, perturbation theory 8-67932
transition and noble metal dilute alloys, Einstein's temp. and vibrational entropy, rel. to electronic struct. 8-83900
transition metal, 4d, photoabsorption spectra near K-edge 8-92144
transition metal, impurities, as probes of critical points, in host band structure 8-91645
transition metal alloy, electronic structure, mag. props. 8-95254
transition metal alloys, BCC crystal struct. dependence on band struct. 8-83778
transition metal alloys, density of states and complex band struct. for one-dimens. model 8-79919
transition metal alloys, elastic properties, vol. depend. 8-95103
transition metal alloys, ferromag., with atomic short range order, local environment effects on electronic struct., Fe-V appl. 8-67936
transition metal impurities in transition and noble metal hosts, electronic struct. 8-75990
transition metals, second series, electronic band Brillouin zone APW calc., electronic config. effects 8-51883
V-Ru, electronic states calculation 8-95255
Ag, empirical parametrisation of electronic structure 8-91585
Ag, valence band Auger spectra 8-76563
 β -AgMg, de Haas-van Alphen effect, LMTO band struct. and Fermi surface 8-75984
Al, model pseudopotential 8-91582
Al, XPS theory, valence band spectra band struct. 8-72702
Au, valence band Auger spectra 8-76563
Be, anisotropy, theoretical investigation by K-emission, APS, and Compton profiles 8-63970
Be, XPS theory, valence band spectra band struct. 8-72702
Ca, FCC, ground-state props. 8-75989
CaSb, resist., susceptibility and thermopower rel. to electronic struct. 8-67935
Cd, photoelectron spectra 4d spin-orbit splitting, crystal field and band-broadening effects, CNDO calcs. 8-76577
Ce, p core states calc., linear muffin-tin orbitals method 8-91607
Co, tunnelling electron spin polarisation rel. to band struct. 8-68095
Co-Si-Ge system, X-ray diff. exam., band struct. (*Russian*) 8-56623
Cr-Al, disordered alloy, effect of high press. on resistivity 8-95286
Cs, electronic transition from self consistent APW Xa calcs. 8-51884
Cu, angle-resolved photoemission, band struct. 8-95680
Cu, Bloch states, photoelectron spectra, angle resolved 8-92175
Cu, empirical parametrisation of electronic structure 8-91585
Cu film, APW band struct. calc., muffin-tin potential 8-87899

band structure of crystalline metals continued

- Cu, parametrised, separable potential for band structure calculations 8-79912
Cu, valence band Auger spectra 8-76563
 $\text{Cu}_2\text{Ni}_{1-x}$ solutions of KKR-CPA equations for paramagnetic alloys 8-95256
 $\text{Cu}_2\text{Ni}_{1-x}$ Fermi surface of concentrated paramag. alloys 8-95257
 $\text{Cu}_2\text{Ni}_{1-x}$ random alloy, angle-resolved photoemission 8-95683
 $\text{Cu}(110)$, photoemission, bulk versus surface effects 8-52626
Eu intermetallic compounds, valence fluctuations, role of charge screening 8-51944
Eu-transition metal intermetallics, valence fluctuations 8-91649
Fe, tunnelling electron spin polarisation rel. to band struct. 8-68095
 α -Fe-based dil. solid solutions, electronic struct., hyperfine interactions 8-79968
FeAl, B2-cpd., band struct. and density of states, KKR calc. 8-63969
Gd, self consistent relativistic ferromag. band struct. 8-91609
La, FCC, ground-state props. 8-75989
La, p core states calc., linear muffin-tin orbitals method 8-91607
 $\text{Li}_2\text{Ag}_2\text{In}_x$, optical props., struct., energy bands, interband transitions 8-72539
 $\text{Li}_2\text{Cd}_2\text{In}_x$, optical props., struct., energy bands, interband transitions 8-72539
Lu, band structure, influence of relativistic effects 8-75991
Mg, XPS theory, valence band spectra band struct. 8-72702
MnSb, electronic state, neutron diff. study 8-87906
MnSb, resist., susceptibility and thermopower rel. to electronic struct. 8-67935
 $\text{Mo}_2\text{Nb}_{1-x}$, is the rigid-band model valid? 8-95258
Na, XPS theory, valence band spectra band struct. 8-72702
Nb, electronic and optical properties 8-91612
Nb, high-temperature nonlinear electrical resistivity, supposed failure of Boltzmann eqn. 8-91664
Nb, optical spectroscopy, for investigation of electronic struct. 8-91611
 Nb_3Si , Nb_3Sn , Nb_3Ge , Nb_3Ga , Nb_3Al , electronic struct., electron-phonon interactions, X-ray spectra 8-91613
 Nb_3Sn , electronic struct., APW method 8-72066
 Nb_3Sn , electronic struct. from three-dimens. k.p model 8-84139
Ni (100), angle resolved photoemission, final-state effects 8-56565
Ni (111), band struct. and temp.-depend. mag. exchange splitting, angle resolved photoemission obs. 8-60546
Ni and Ni alloys, tunnelling electron spin polarisation rel. to band struct. 8-68095
Ni, angle-resolved photoemission, band struct. 8-95680
Ni, ferromagnetic, electron-magnon interactions 8-68205
Ni, polarisation-dependent angle-resolved photoemission for band structure studies 8-95678
Ni-Re, dil. alloys, two-band Mott conductivity (*Russian*) 8-60118
NiSb, resist., susceptibility and thermopower rel. to electronic struct. 8-67935
Pd, Compton profiles, comparison with band struct. calcs. 8-84675
Pd, hydride and alloys, electronic band struct., comparative study of electric and mag. props. 8-95259
 $\text{Pd}_{1-x}\text{Ag}_x\text{H}_x$, superconducting transition temp., APW band struct. calcs. 8-95393
PdH, electronic struct. and proton spin-lattice relax. calc. 8-67937
PdSb, electronic struct., optical transitions, Fermi surface 8-51885
Pt, 5d band structure effects on line shapes and intensities of core electron excitations 8-92177
Sc, sp. ht. data rel. to electronic props. 8-83971
Ta, optical spectroscopy, for investigation of electronic struct. 8-91611
Th, FCC, ground-state props. 8-75989
Th, p core states, linear muffin-tin orbitals method 8-91607
 UGe_3 , de Haas-van Alphen effect, band struct. calc. 8-72068
V, Compton profiles, comparison with band struct. calcs. 8-84675
 VO_2 , metallic phase, electronic props., plasma freq., Hall coeff. 8-84195
 V_3Si electronic struct. from three-dimens. k.p model 8-84139
 V_3Si , V_3Sn , V_3Ge , V_3Ga , V_3Al , electronic struct., electron-phonon interactions, X-ray spectra 8-91613
W (001), clean and H_2 chemisorbed, angle resolved photoemission, symmetry-related polarisation effects 8-56566
W, polarisation-dependent angle-resolved photoemission for band structure studies 8-95678
W(100), NVV Auger spectra, $\text{O}_2(\text{H}_2)$ adsorption effects, comp. to band struct. calcs. 8-72643
Zr, X-ray K-absorpt. spectra 8-76558
 ZrV_2 , Laves-phase, cubic to rhombohedral transition, lattice electron instability 8-92261

band structure of crystalline semiconductors and insulators

- see also *conduction bands; energy gap; valence bands*
diamond, Compton profiles, X-ray struct. factors, band struct., LCAO calc. 8-51889
diamond, electronic energy bands of diamond-type crystals, appl. of EHT method 8-87907
diamond, pseudopotential method of band struct. anal. 8-51886
dimethyl cadmium, photoelectron spectra, 4d spin-orbit splitting, crystal field and band-broadening effects, CNDO calcs. 8-76577
electronic structure of solids under laser irradiation 8-91614
elemental semiconductor, electric susceptibility from chemical-bond approach 8-51922
ferroelectric semiconductor, vibronic, interband light absorption 8-72555
ferromagnetic semiconductor, electronic spectrum, influence of finite carrier conc. 8-76220
graphite, electronic props., self-consistent LCAO calc. 8-51887
graphite, neutron irradiated, effect on quantum limit Shubnikov-de Haas oscils. 8-95304
Hubbard antiferromag. semiconductor, electron correlations, weak coupling 8-67969
 II_2V_2 semiconductors, spin-orbit and cryst. field splittings of valence band 8-63980
III-V semiconductors, ionic tetrahedral, electrical susceptibility, chemical bond approach 8-87931
inert gas crystals, excitons exam. 8-51898
interband light scattering in semimetals and semiconductors (*Russian*) 8-60485
modulation spectroscopy, two-ray methods, appl. to band struct. determ. (*Russian*) 8-54469

band structure of crystalline semiconductors and insulators continued

- optical orientation of electronic and nuclear spins 8-79928
polydiacetylene, photoconduction in multilayer structs. and single cryst. 8-80024
polydiacetylene backbone sequence, electronic structs., unrestricted HF approach 8-63975
semiconductor neutral point defect electronic struct., self consistent method 8-91641
semiconductor with nonspherical bands, diamag. excitons and Franz-Keldysh effect 8-72554
singularities of the small polaron effective mass 8-63989
tetrathiotetracene, cond. mechanisms and refined energy level spectrum (*Russian*) 8-52103
tetravalent, fundamental absorpt. spectra, direct interband transitions 8-63972
transition metal dioxides, elec. struct. props., two-band model calcs. 8-67934
transition metal hydrides, electronic struct., heat of formation, single particle lifetimes, Dingle temp. meas. 8-51923
 V_2V_3 compounds, electronic struct., X-ray emission, XPS, UPS obs. 8-52638
 As_2Se_3 , polarised light reflectance spectra, band struct. 8-63979
BN, cubic, ab initio SCF calcs., band struct., ground state props. 8-51891
BN, cubic, energy band and piezoelec. calcs. 8-72071
 $BaTiO_3$, XPS, band struct., density of states, photoionisation cross sections 8-52629
 $Bi_{1-x}Sb_x$, semicond.-semimetal transition, temp. and press. depend. of transport props. 8-76120
 $CdCr_2S_4(Se_4)$, spin depend. phonon Raman scatt., band struct. 8-68491
 CdI_2 , UV reflectivity meas., band struct., LCAO calcs. 8-72545
 CdS , cubic, ab initio band struct. calcs. within local density functional formalism 8-87910
 CdS , up-conversion and optical storage, spatially modulated band struct. 8-64397
 $n-CdSnAs_2$, optical absorption rel. to energy spectra (*Russian*) 8-75994
 CrO_2 , band struct., cryst. binding and ESCA spectra, X_α cluster calc. 8-64443
 $CrAl$, semicond. solid solns., temp. depend. of elec. resist. at high temp. 8-67941
 CuH , electronic struct., heat of formation, single particle lifetimes, Dingle temp. meas. 8-51923
 CuF_2 , Cu_2P , electronic struct. of valence bands, X-ray spectra and XPS 8-92176
 EuS , pure and Gd doped, electronic struct., mag. exchange and elec. transport props. 8-87974
 FeO , Fe_3O_4 , Fe_2O_3 , absorption spectra, 0.1-6 eV, one electron energy level diagram 8-52487
 Fe_3O_4 , rel. to photocond., 70-130K, temp. range including metal-semicond. transition (*Russian*) 8-56178
 $GaAs$, deep level trap emission identification by indirect conduction minima technique 8-84163
 $p-GaAs$, electronic props. 8-68040
 $GaAs$, indirect band edge, determ. by quantum-well bandfilling 8-92120
 $GaAs$, k-linear coupling, E_1' transitions 8-91583
 $GaAs$, modulation spectroscopy, two-ray methods (*Russian*) 8-54469
 $n-GaSb:Te(Se)$, forbidden optical band gap, Moss-Burstein effect 8-88335
 $GaSb-InAs$ superlattices, two-dim. electronic structure 8-75995
 GdP , electronic struct., mag. exchange and elec. transport props. 8-87974
 GdS , electronic struct., mag. exchange and elec. transport props. 8-87974
 Ge , electronic energy bands of diamond-type crystals, appl. of EHT method 8-87907
 Ge , electronic struct. from SCF calc. using intersecting spheres model 8-51888
 Ge , interband Faraday ellipticity 8-92052
 Ge , pseudopotential method of band struct. anal. 8-51886
 $Hg_{1-x}Cd_xTe$, quasi-local acceptor levels and electron mobility 8-67974
 $Hg_{1-x}Cd_xTe$, zero-gap semicond. with nonparabolic band struct., hot electron mobility and conc. 8-76080
 $N-InAs$, Moss-Burstein effect, S, Sn, Te dopants 8-64389
 $InAs-GaSb$ superlattices, two-dim. electronic structure 8-75995
 InN film, refl. and transmission spectra, band struct. 8-72625
 $n-In_2O_3$ film, RF sputter grown, substrate bias effect on elec. and optical props. 8-64150
 $n-InSb$, directional temp. of hot electrons under elec. and mag. fields 8-84135
 $KNbO_3$, complex electronic dielectric const. from tight binding energy bands 8-60054
 $KNbO_3$, XPS, band struct., density of states, photoionisation cross sections 8-52629
 $KTaO_3$, complex electronic dielectric const. from tight binding energy bands 8-60054
 $LiNbO_3$, band struct. and spontaneous polarisation calcs. 8-95261
 $NaCl$ (100) face, angle-resolved photoemission 8-56567
 $NaNbO_3$, band struct., polarisation and piezoelec. consts. calc. 8-52448
 PbI_2 , tight binding band structure using scaled parameters 8-79927
 PbI_2 , UV reflectivity meas., band struct., LCAO calcs. 8-72545
 $Pb_{1-x}Sn_xTe$, band struct. and phonon energies, tunnelling spectroscopy 8-72070
 $Pb_{1-x}Sn_xY$ ($Y=Te, Se, S$), interband absorption under linearly polarised light excitation 8-92089
 $p-PbTe$, thermorefl., 1.0-4.6 eV 8-76492
 PdH , electronic struct., heat of formation, single particle lifetimes, Dingle temp. meas. 8-51923
 $PdH_{0.72}$, Compton profile, electronic struct. (*German*) 8-92140
 Si (111), chemisorption of $H_2(Cl)$, conduction-band surface resonance 8-52051
 Si , Auger lineshape, one-electron theory for $L_{23}VV$ and $L_{123}V$ 8-72645
 Si , electronic energy bands of diamond-type crystals, appl. of EHT method 8-87907
 Si , electronic struct. from SCF calc. using intersecting spheres model 8-51888
 Si , exchange and correlation pot., band struct. calc. 8-56068
 Si modulation spectroscopy, two-ray methods (*Russian*) 8-54469

band structure of crystalline semiconductors and insulators continued

- Si , neutral point defect electronic struct., self consistent method 8-91641
 Si , screening of ions, band struct. calcs. with screening variants 8-67938
 Si surface, ideal and 2x1 chain-reconstructed, electronic struct. determ. 8-52050
 Si surface (100), vicinal plane surface band struct. electron inversion layers, minigaps 8-68062
 Si , with non-spherical pots. for two basis atoms, electronic struct. 8-72069
 SiO_2 , electronic structure, theory 8-95260
 SiO_2 , new interpretation of structure 8-84120
 $Si(111)$, conduction-band surface resonance 8-52051
 $\alpha-Sn$, electronic energy bands of diamond-type crystals, appl. of EHT method 8-87907
 Sn , semicond., pseudopotential method of band struct. anal. 8-51886
 $Sn_{0.7}Pb_{0.3}Te$ mixed cryst., cryst. growth and assessment 8-80463
 SnS_2 , UV reflectivity meas., band struct., LCAO calcs. 8-72545
 $SnSe$, electronic band struct. determ. 8-51890
 $SnSe_2$, band struct., angle resolved photoelectron spectra meas. 8-72680
 $SnSe_2$, intercalated with cyclopropylamine, photoelectron spectra study of electronic struct. 8-84698
 $SrTiO_3$, XPS, band struct., density of states, photoionisation cross sections, theoretical determ. 8-52629
 $4Hb-TaS_2$, Fermi surfaces, charge transfer and charge density waves 8-79926
 $Ti-H$, proton spin-lattice relaxation time, band struct. 8-56395
 TiO_{1+x} , conduction band determ. 8-60055
 $(Ti_2O_3)_{1-x}(V_2O_3)_x$, lattice polarisability, electronic contribs. IR refl. obs. 8-59904
 TiP , TiP_2 , electronic struct. of valence bands, X-ray spectra and XPS 8-92176
 TiS_2 , carrier-lattice coupling 8-63822
 $TiSe_2$, UPS, excitonic instability indicated from study of band struct. 8-56069
 US , electronic struct. calc. 8-91615
 $VD_{0.77}$, Compton profile, electronic struct. (*German*) 8-92140
 $VO_{6.71}$, Compton profile, electronic struct. (*German*) 8-92140
 VO , octahedral clusters, electronic struct., X_α discrete variation and SW methods 8-63976
 VO_2 clusters in metallic and semiconductor phases, electronic struct., X_α calcs. 8-63977
 $Zn,Cd_{1-x}Te$, reflection spectra, energy band struct. comp. depend. (*Russian*) 8-56500
 ZnP , Zn_3P_2 , electronic struct. of valence bands, X-ray spectra and XPS 8-92176
 ZnP_2 , absorption edge meas. 8-80380
 $ZnTe$, band parameters from bound exciton, donor-acceptor pair excitation luminescence 8-92111
 Zr compounds, X-ray K-absorpt. spectra 8-76558

band structure of semimetals

- As , pseudopotential, self-consistent, band struct. 8-84141
 Bi , band structure model parameters, deformation theory (*Russian*) 8-56067
 $Bi:Sb$, semimetallic alloy, microwave spectroscopy 8-87908
 $Hg_{1-x}Cd_xTe$, quasi-local acceptor levels and electron mobility 8-67974
 $Hg_{1-x}Cd_xTe$, single-LO-phonon and -plasmon recombination channels narrow-bandgaps 8-91728
 $NbSe_3$, chemical bonding and dimensionality 8-75992
 $TiSe_2$, carrier-lattice coupling 8-63822
 $TiSe_2$, semimetallic behaviour band struct. from local-density functional approach 8-56070
 $TiSe_2$, UPS, excitonic instability indicated from study of band struct. 8-56069

band theory models and calculation methods

- see also APW calculations; band model of magnetism; band structure; cellular method; free-electron approximation; Hubbard model; KKR calculations; k.p. calculations; Kronig-Penney model; muffin-tin potential; nearly-free-electron approximation; OPW calculations; pseudopotential methods; relativistic band structure calculations; tight-binding calculations
Brillouin scattering, resonant, analogy to modulation spectroscopy (*Japanese*) 8-68526
cubic crystal electronic energy band calc. by LCGO method, FORT-RAN IV program 8-75977
Density-functional pseudopotential approach to crystal phase stability and electronic structure 8-72058
empirical parametrisation of electronic structure 8-91585
FCC clusters, size and shape depend., tight binding approximation 8-79920
film, crystalline, band theory of size-quantised electron states 8-75976
integral characteristics of the electron structure of crystalline surfaces 8-64078
ionicity, Pauling's and Phillips' comparison by empirical LCAO band theory 8-51464
Kane model, three-band, Auger recombination overlap integrals, kp approx. (*Russian*) 8-87897
metal, new method for solving Boltzmann equation for electron 8-72127
muffin tin orbital method for surface and films 8-95331
one-electron approximation, effect of correl. and defects 8-63960
parametrised, separable potential for band structure calculations 8-79912
s-d electron model, finite temp. diagram technique, perturbation theory 8-67932
semiconductor, Falicov-Kimball model, intermediate valence states, metal-insulator transition 8-51897
semiconductor, zincblende-type, valence band effective mass strain depend. 8-51880
transition metal, one-electron theory, atomic sphere approx. to KKR and LMTO methods 8-91584
 Bi , band structure model parameters, deformation theory (*Russian*) 8-56067
 Fe , itinerant model of spin polarised field emission 8-95685
 $GaAs$, k-linear coupling, E_1' transitions 8-91583
 Ge , valence band effective mass strain depend. 8-51880
 $HgSe(Te)$, dynamic dielectric function, IR absorpt. meas. 8-68508

band theory models and calculation methods continued

InSb-type semiconductor, spatial dispersion of permittivity 8-67967
 $\text{Mo}_2\text{Nb}_{1-x}\text{O}_6$ is the rigid-band model valid? 8-95258

bands (kink) see *kink bands***bandwidth compression**

optical image anal. and digital simulation 8-94373

Bardeen-Cooper-Schrieffer theory see *BCS theory***barium**

see also *nuclei with*

abundance determ. in stony meteorites 8-65557
 adsorption on ZnO, effect on low-energy cathodolum. 8-60522
 atom, Auger spectra, strong correl. in 4d-spectrum 8-50522
 atom, Ba I, absorption spectrum, 1560 to 1770 Å 8-66487
 atom, diagam. quasi-Landau spectrum near ionis. threshold, two-photon ionis. spectra obs. 8-58642
 atom, electron scatt., elastic and inelastic (5^1D , 6^1P) cross sections, 20-100 eV 8-74769
 atom, electron scatt. from excited atoms, 30 and 100 eV, inelastic and superelastic 8-86933
 atom, multiphoton ionis. spectroscopy of even- and odd-parity states 8-86973
 atom, transition probability of valence shells, relativistic pseudopot. calc. 8-86803
 atomic photoionisation, ion alignment, many electron correl. effect 8-74622
 atoms, emission spectra, 50 to 90 nm, electron impact excitation 8-82846
 coating on W tip, photoemission in electric field (*French*) 8-80458
 determination, in seawater, matrix effects in graphite furnace AAS 8-85230
 elastic properties, Debye temp., 20°C, 20 to 70 kbar, US wave velocity meas. 8-87735
 F-region plasma clouds, high altitude limit of gradient drift instability 8-88984
 F-region striated Ba clouds, electron density struct. meas. 8-88974
 film, work function and struct. 8-80040
 gas laser, pulse repetition frequency scaling law 8-82954
 ionosphere, Tordo 1 polar cusp Ba plasma injection expt. 8-77402
 neutron yield calcs., electron beam incidence 8-95622
 radiative decay of autoionisation states (*Ukrainian*) 8-82682
 solution in liq. ammonia, conductance at -62.37°C 8-91459
 submonolayer film on Mo(011) face, surface diffusion, manifestation of phase states (*Russian*) 8-91539
 superconductivity, pressure dependence, ion core 8-91805
 vapour, efficient Raman conversion of XeCl excimer laser radiation 8-79069
 Ba I, hook method, g° values of intercombination line, 7911.38 Å 8-66511
 Ba I, oscillator strength meas. 8-74607
 Ba II, even isotopes, optical isotope shifts, Lamb-dip spectro. obs. 8-78666
 Ba II, Stark half-widths, line shifts, calcs. (*Russian*) 8-62764
 Ba II 4554 Å solar resonance line formation, empirical NLTE analysis 8-53907
 Ba⁺ ion cloud containment in RF trap, <50 ions, optical sideband cooling 8-75407
 Ba⁺, transition probability of valence shells, relativistic pseudopot. calc. 8-86803
 Ba-N₂O flame, candidate chem. laser reactions, intracavity dye laser absorpt. meas. 8-63108
¹³⁵Ba, ¹³⁷Ba Fourier transform NMR, NQR studies 8-94261
¹³⁵Ba²⁺, ¹³⁷Ba²⁺, aq. ions, nucl. quadrupole relax. 8-64287
¹⁴⁰Ba, diffusion behaviour in SiC, 1650 to 1850°C 8-79814
¹⁴⁰Ba, volatile fission product, diffusion in Mo, 1400-2000K (*Russian*) 8-91485
 Cs-Ba triode arc switch, high-current, low-voltage, pulsed control 8-71551
 Ge:Ba, Ca, recomb. props. 8-56156
 He hollow-cathode discharge, Ba⁺ and Sr⁺ formation 8-67527
 KCl:Ba²⁺, precipitation kinetics, supersaturation effects, geometry of formed heterophase struct. (*Russian*) 8-84824
 KCl:CO₃²⁻, Ba²⁺, shift and broadening of local vibr. bands, temp. depend. 8-87755
 Ni:Ba⁺, ion implantation, effect on inelastic refl. and energy losses of fast primary electrons 8-55900
 Pb₂Ge₃O₁₁:BaO, impurities, static central peak 8-92079

barium compounds

aluminate:Eu, effect of non-stoichiometry on luminesc. 8-68550
 mordenite, dehydrated, position of cations and molecules, electron probe anal. 8-51509
 stearate film, between Al electrodes, intrinsic voltage 8-72277
 tienshanite, cryst. struct. determ. 8-83800
 BH⁺, spin-extended Hartree-Fock ab initio calculations for small radicals 8-70746
 (Ba,Sr)Fe₁₂O₁₉, Ferroxdure, developments and research 8-84455
 Ba-N₂O, reaction, electronic branching, statistical and dynamical influences 8-92451
 BaAl₂Si₂O₈-SiO₂, celsian solid solns., effects on polymorphic transform. kinetics 8-68677
 BaB₆, (La,Ba)B₆, (Ea,Ba)B₆, single crystal growth for thermionic emission 8-92183
 BaBrF, cryst. at. struct. by X-ray diff. 8-75641
 BaCO₃-SrCO₃-CaCO₃, phase inhomogeneity effects on oxide cathode props. 8-52614
 BaCO₃-SrCO₃-TiO₂(ZrO₂), ternary systems, solid-phase synthesis 8-52733
 Ba_{0.92}Ca_{0.08}TiO₃ ceramic, uniaxial stress effects, US dilatometric and dielec. meas. 8-52454
 BaCl₂, conc. solns., vel. correls. calcs., diffusion, cond. and transference props. 8-85166
 BaCl₂, solns. in methanol, conductance data anal., assoc. consts. 8-71875
 BaClF, localised vibr. of U-centres 8-75779
 BaClF, two types of F-centres, identification by ENDOR 8-60355
 BaClF:Sm²⁺, energy levels, optical props. 8-84631
 Ba(ClO₄)₂, anhydrous, phase transition obs. (*French*) 8-83939
 Ba(ClO₄)₂, soln. in liq. ammonia, conductance at -62.37°C 8-91459
 BaClO₃.H₂O→BaClO₃, dehydration process 8-59932
 Ba(ClO₃)₂.H₂O, γ-irrad. defects, ³⁵Cl NQR, 77 and 300K 8-91981
 BaCl₂.2H₂O, cryst. struct. determ. by neutron diff. 8-75639

barium compounds continued

BaCo_{1.5}Fe_{16.5}O₂₇, type W ferrite, spin reorientation 8-60301
 BaCrO₄, ZZ 8-88326
 BaCuO_{2+x} (0≤x≤0.12), study of mag. and elec. props. rel. to the non-stoichiometry (*French*) 8-95051
 Ba₂EuNbO₆, luminescence Raman spectra, means for localisation of binding energy levels (*German*) 8-88304
 Ba₂EuTaO₆, luminescence Raman spectra, means for localisation of binding energy levels (*German*) 8-88304
 BaF₂, anharmonicity vibrs. and correlation effects, neutron diff. 8-55915
 BaF₂, Brillouin scatt. and high temp. disorder 8-80365
 BaF₂, colour centre thermal stability 8-83811
 BaF₂, crack propag., cryst. props. effects 8-75720
 BaF₂, F-centres, muffin-tin approx. inadequacy 8-63761
 BaF₂, muon Coulomb capture ratio 8-62959
 BaF₂, optical breakdown threshold, illuminated spot dimension effects 8-68582
 BaF₂, optical ceramic, hot pressing in vacuum, rel. to spectral transmission 8-52730
 BaF₂, superionic conductor, theoretical investigation of Raman scatt. 8-80351
 BaF₂, vol. depend. of refr. index 8-88275
 BaF₂:Er³⁺, single-site multiphonon and energy transfer relax. 8-52547
 BaF₂:Mn²⁺, far IR absorption spectra 8-76507
 BaF₂:Ti²⁺, electronic struct. and EPR of Ti²⁺ 8-76034
 BaF₂:Tm²⁺, EPR, optical recording in weak mag. field 8-68376
 BaF₂-CaF₂-SrF₂:Gd³⁺, luminescence spectrum of Gd³⁺ ion and solid solution region obs. 8-84638
 BaF₂:NiF₂-CrF₃, X-ray crystallography study, phase identification at 700°C, cryst. symm. (*French*) 8-95733
 BaF₂-UF₄-CrF₃ solid soln., surface degradation, complex admittance analysis 8-55980
 Ba₂Fe₂BO₃ (B=Re, Te, W, Mo), siegnette magnets with hexagonal barium titanate structure 8-76397
 BaFe₂O₄-Fe₂O₃-ZnFe₂O₄ system, phase relations at 1200°C 8-72767
 Ba₂Fe₁₈O₂₇, hexagonal ferrite, W-struct., Mossbauer spectra of Fe³⁺ and Fe²⁺ 8-88242
 Ba₂Fe₂O₁₁, antiferromagnet, exam. of mag. props. by mag. meas., and Mossbauer spectroscopy 8-52256
 β-BaFe₂Si₅, and low temp. α polymorph., cryst. struct. 8-67690
 Ba₂FeSbO₆, siegnette magnets with hexagonal barium titanate structure 8-76397
 BaFe₂Ti₂O₁₁, R-type hexaferrite, spin struct. and mag. props. 8-52216
 BaGeF₆, Group IV hexafluoride anion radical γ-irrad., EPR spectra 8-72411
 Ba(H₂PO₄)₂, triclinic, cryst. struct. (*French*) 8-55848
 BaI, mol. dissoc. energy, high temp. mass spectra 8-58863
 BaKPO₃.H₂O, cryst. struct. (*French*) 8-51480
 Ba(N₃)₂, thermal decomp., role of defects 8-73033
 Ba(NO₃)₂, press. derivatives of elastic-moduli, ultrasonic velocity meas. 8-95102
 Ba(NO₃)₂.H₂O, hexagonal, piezoelec., electro-optic, dielec., elastic, thermoelastic props., space groups 8-76388
 Ba₂Na(Nb,Ti)₅O₁₅, prep. and electro-opt. props. 8-76432
 Ba₂NaNb₂O₁₅, ferroelec., cathodolum. spectral and temp. depend. 8-84665
 Ba₂NaNb₂O₁₅, ferroelec. conversion to single domain, elec. and photoelec. props. 8-88271
 (Ba₃Nb₂Si₄O₂₆)_n.Ba₃Nb₄Ti₄O₁₁, n=3/2 to 29/2, intergrowth series, electron microscope obs. (*French*) 8-83762
 (Ba₃Nb₂Si₄O₂₆)_n.Ba₃Nb₄Ti₄O₂₁, multiple intergrowth and microdomains obs. by electron diff. and microscopy (*French*) 8-95160
 BaO adsorbed on Si photofield cathode, work function and emission props. (*Russian*) 8-68608
 BaO, at. charge densities, X-ray struct. factors 8-79566
 BaO crown and flint glasses, Ag and Cu diffusion for optical waveguide fabrication 8-59166
 BaO, electron energy loss and secondary emission mechanisms, plasmon losses 8-76565
 BaO, microwave-laser double reson. spectra 8-82757
 BaO, optical-optical double reson. of excited states, Parkinson band system 8-70857
 BaO:Mn²⁺, impurity pot. well shape calcs. 8-87950
 BaO-B₂O₃, composition effects on mean dispersion 8-80313
 BaO-B₂O₃-UO₂²⁺, Nd³⁺ glass, radiative and nonradiative energy transfer 8-60508
 BaO-B₂O₃-SiO₂:Ti³⁺, elec. cond., struct. 8-72148
 BaO-B₂O₃-SiO₂:Ti³⁺, optical absorpt. spectra 8-72564
 BaO-BaX₂-P₂O₅ glass, X=F, Cl, Br, conductivity 8-67862
 BaO-Fe₂O₃, splat quenching struct. and crystn. mechanism (*French*) 8-51426
 BaO-Fe₂O₃-Na₂O glass, mag. props. 8-88123
 BaO-La₂O₃-GeO₂, exam. of glass forming region, properties and crystallisation 8-88454
 BaO-M₂O-B₂O₃ glass, UV absorpt., inherent absorpt. wavelength and oscill. strength, cation effects 8-80374
 BaO-P₂O₅ glass, diffusion of Cu⁺, fluoresc. meas. 8-59980
 BaO-SiO₂ glass ceramic, nucleation, effect of electric fields 8-83742
 Ba₃(PO₄)₂ transition metal ion, optical and magnetic props. 8-64196
 BaPO₃F-Al₂O₃-B₂O₃ glasses, phys. props. 8-63676
 Ba₁₀(PO₄)₆(OH)₂, cryst., IR spectra, band assignments 8-60442
 BaPbF₆, Group IV hexafluoride anion radical γ-irrad., EPR spectra 8-72411
 BaS:Cu, thermoluminesc. and decay 8-80426
 BaSO₄, barite, crystal struct. and sulphate force consts. 8-83784
 BaSO₄, barytes, with large magnitude of emitted light, thermolum. curves 8-88368
 BaSO₄, crystal growth, effect of nitrilotri (methylenephosphonic acid) adsorption 8-88417
 BaSO₄, single cryst., neutron bombard. effect on struct. 8-63793
 Ba₃Sb₂NiO₆, 6H, cation ordering, powder neutron diff. obs. 8-55852
 Ba_{0.25}Sr_{0.75}Nb₂O₆, fast-response pyroelec. cryst. detector 8-49904
 Ba_{0.25}Sr_{0.75}Nb₂O₆, quadratic susceptibility dispersion meas., oscillator model including structure 8-59078
 Ba_{0.25}Sr_{0.75}Nb₂O₆, thermal and spectral variations in the photovoltaic current in ferroelectrics 8-91719
 Ba_{0.5}Sr_{0.5}Nb₂O₆, temp. depend. of Raman spectra 8-72524
 Ba_{0.5}Sr_{0.5}Nb₂O₆:Y(La)(Tm), dielectric and electrooptic props. 8-68466

barium compounds continued

- Ba₂Sr_{1-x}Nb₂O₆, anomalous photovoltaic effect and photocond. 8-52449
- Ba₂Sr_{1-x}Nb₂O₆, ferroelec., cathodlum. spectral and temp. depend. 8-84665
- Ba_{1-x}Sr_xNiO_{3-y}, Sr substitution effect, powder X-ray diffr. 8-51498
- BaTbO₃, perovskite struct., Tb⁴⁺ EPR obs., cryst. field parameters determ. (Italian) 8-52350
- Ba₂TiGe₂O₈-Ba₂TiSi₂O₈, pseudobinary system, pyroelectricity and related props. 8-95553
- BaTiO₃, 90° electric domain processes, mech. stress, X-ray diffr. 8-72478
- BaTiO₃, A₁(TO) phonon spectrum, ferroelectric phase transition, Raman scatt. meas. 8-56478
- BaTiO₃, adsorpt. of O₂, mechanism calc. 8-63927
- BaTiO₃, anomalous photovoltaic effect and photocond. 8-52449
- BaTiO₃, automatic anomalous noise meas. for ferroelectric capacitor parameters, not in equilib. (French) 8-74029
- BaTiO₃, c-domain cryst., HF dispersion of permittivity 8-60379
- BaTiO₃, ceramic, positive temp. coeff. resistivity, investigation as function of Ti-Ba ratio 8-72151
- BaTiO₃, ceramics, calcination effects, TiO₂ powder eval. (Japanese) 8-64516
- BaTiO₃, critical hyper-Raman scattering 8-76466
- BaTiO₃, cubic-tetragonal phase transition, birefringence meas., surface distortion effects 8-95564
- BaTiO₃, dielec. and elastic consts., temp. depend. (Russian) 8-64307
- BaTiO₃, donor doped, elec. props., effect of kinetic processes 8-64042
- BaTiO₃, doped, loss mechanism and domain stabilisation 8-84542
- BaTiO₃, Doppler-broadened positron annihilation 8-64428
- BaTiO₃, dynamic Rayleigh light scatt. in region of ferroelectric-paraelectric transition 8-64371
- n-BaTiO₃, elec. transport props., theoretical discussion and expt. 8-84215
- BaTiO₃, ferroelec. ceramic, mech. strength, for single crystals and Ca and Co modified specimens 8-64332
- BaTiO₃, ferroelectric ceramic, dielec., piezoelec. and elastic props., orientational contrib. 8-68468
- BaTiO₃, LF relaxational polarisation 8-68460
- BaTiO₃, logarithmic velocity variations for longitudinal US waves near ferroelec. transition 8-72472
- BaTiO₃, magnetochemical exam. of phase transition, mag. suscept. meas. 8-88265
- BaTiO₃, martensite type phase transition 8-64326
- BaTiO₃, monocrystalline, dielectric loss after superposition of unidirectional electric field time depend. (Slovak) 8-52435
- BaTiO₃, optical wave reflectance (Japanese) 8-87012
- BaTiO₃, para to ferroelec. transition, strong Rayleigh scatt. 8-76486
- BaTiO₃, perovskite structure, semiconductor props. (Polish) 8-56437
- BaTiO₃, phonon spectroscopy, amorphous versus crystalline material 8-83898
- BaTiO₃, photo-ferroelectric noise effect (Russian) 8-52450
- BaTiO₃, polariton freq. meas. by Raman scattering and permittivity 8-76006
- BaTiO₃, Rayleigh wave generation by surface piezoelectricity 8-71925
- BaTiO₃, single cryst., elec. cond., 800-1200°C, nonstoichiometric disorder 8-51989
- BaTiO₃, struct. changes due to cubic-tetragonal phase transition 8-60407
- BaTiO₃ type crystals, determ. of phase transitions using symmetry breaking theory (French) 8-83950
- BaTiO₃ type perovskite ferroelectric, neutron irradiated, amplification of freq. dispersion of permittivity (Russian) 8-52419
- BaTiO₃, vibronic ferroelec., spontaneous birefringence calc. 8-68473
- BaTiO₃, XPS, band struct., density of states, photoionisation cross sections 8-52629
- BaTiO₃:Co, charact. behaviour of spontaneous polarisation and dielec. const. 8-60382
- BaTiO₃:Cu, photoferroelec. props., Jahn-Teller effect, laser irradiation effect on pyroelec. props. 8-60400
- BaTiO₃-Ni(Co, Mn)Fe₂O₄, ceramic, exam. of prep. and physical props. 8-68655
- Ba₂V₂O₇, V-O-V bridge stretching freq. correl. with bond angle 8-74636
- BaV₂S₃, exam. of ferromagnetic, antiferromagnetic behaviour, depending on stoichiometry 8-52233
- BaWO₄, refr. index, single crystals having scheelite struct. 8-79082
- Ba₂X₃, α, intermediate phases, cryst. struct. (X=IIb, IIb, IVb, Vb element) 8-83793
- BaZn_{1.38}Co_{0.62}Fe₁₆O₂₇, W-type hexaferrite cryst., first order magnetisation processes 8-95472
- Ba₂Zn₂Fe₁₂O₂₂, anisotropic magnetisation and susceptibility 8-84411
- α-BaZrF₆ with [Zr₂F₁₂]⁴⁺ complex, cryst. struct. (French) 8-51477
- Ba[Fe(CN)₆]NO₂·2H₂O, NMR, H₂O orient. (French) 8-52366
- γ-DBa(PO₃)₂, polyphosphate, crystal structure determination (French) 8-91314
- dibarium cobalt formate tetrahydrate Cu²⁺ doped, EPR of Cu-Co interactions 8-60334
- Eu_{0.5}Ba_{0.5}TiO₃, ferromag., ferroelec., ceramic, Curie temps. determ. 8-68230
- KCl-BaCl₂ supersaturated solid soln., deformed, BaCl₂ precipitation kinetics, metastable region (Russian) 8-60673
- K₂O-BaO-SiO₂ glass, rare earth ion activated, spectral intensity, effect of number of 4f electrons 8-84602
- LiNbO₃:Fe, calc. of photorefraction (Russian) 8-92032
- MgO-BaO-Al₂O₃-SiO₂, glass, IR absorpt. spectra and solid struct. exam. 8-88314
- NaCl:BaCl₂, oriented growth of BaCl₂ phases, platelet-matrix interface structure and energy 8-87793
- NpBa₄Zr₁₂F₆₄ glass, Mossbauer spectrum, evidence for charge states 3+ and 4+ (French) 8-88231
- Pb_{2-x}Ba_xLi_{0.5}Nb_{1.5}O₆, dielectric const., temp. and Ba conc. 8-64308
- (Pb_{0.715}Ba_{0.285})_{0.991}(Zr_{0.707}Ti_{0.293})_{0.981}Bi_{0.019}O₃, slim loop ferroelec. ceramic, shock wave compressed, elec. response 8-80293
- SiO/BaO complex, new switching effect in MIM thin-film structures 8-80067
- SiO₂-Al₂O₃-B₂O₃-MgO-CaO-Na₂O, strengthened by ion exchange, exam. of internal stresses using polarising microscope 8-88549
- SrAl₂O₄-BaAl₂O₄ system, solid solubility, α-β transition 8-63860
- Sr_{0.5}Ba_{0.5}Nb₂O₆, ferroelec., dielec. behaviour 8-80309

barium compounds continued

- Sr_{0.5}Ba_{0.5}Nb₂O₆ film, pyroelectric effects, origin 8-88258
- WO₃-BaO film, electrochromic coloration and decoloration, BaO additive effects 8-72620
- Barkhausen effect**
- anisotropic materials, magnetisation reversal, 1/H law 8-84454
- ferromagnets, nondestructive inspection by magnetic noise method 8-72997
- film, general behaviour and stationarity along hysteresis loop 8-56357
- magnetic thin films, statistical anal., instrumentation, computer interfacing 8-82008
- magneto inductive pick-up for Barkhausen noise spectra meas. (Russian) 8-65945
- steel, magnetisation transitions, Barkhausen noise 8-91894
- Fe-Si, stress and plastic deform. effect on Barkhausen effect, instrumentation 8-52313
- NiCo ferrite, induced mag. anisotropy, hysteresis loops, Barkhausen effect (Russian) 8-64203
- Barnett effect** see gyromagnetic effect; magnetisation
- barometers**
- No entries
- barometric pressure** see atmospheric pressure and density
- barrages** see dams
- barrel distortion** see aberrations
- barretters** see thermistors
- baryon-baryon interactions**
- see also baryon-baryon scattering; hyperon-nucleon interactions; nucleon-nucleon interactions
- No entries
- baryon-baryon scattering**
- see also baryon-baryon interactions; hyperon-nucleon scattering; nucleon-nucleon scattering
- line reversal symmetry breaking, simple rearrangement and absorption models 8-62326
- p+baryon elastic scattering, polarisation phenomena in hadron collisions at small momentum transfer (Russian) 8-58196
- baryon decay**
- see also baryon hadronic decay; baryon leptonic decay; hyperon decay
- charmed baryon semi-leptonic decay and quark effective masses, SU₄ symmetry 8-58185
- form factors, semi-leptonic weak interactions, book contrib. 8-78162
- neutron half life meas., p registration method (Russian) 8-93879
- strange baryonium, spectrum, decay, production 8-93854
- SU(3) symmetry breaking in baryon resonance decay 8-89712
- baryon hadronic decay**
- charmed baryons, nonleptonic decays 8-66118
- charmed-baryon nonleptonic decays, parity-violating amplitudes 8-62398
- pseudoscalar transition between spin-1/2 and spin 5/2 baryon 8-50032
- weak radiative decay, sum rules, octet/sextet and 20-plet dominance 8-62400
- D₁₃(1510)→P₁₁(940)+γ, Melosh transform, [70.1⁻]→[56.0⁺]+γ (Russian) 8-66116
- Δ, I=3/2 half mass enhancement in 10.3 GeV/c π⁺p interactions 8-66117
- Ω⁻→ΛK⁻, Ω⁻ lifetime, spin from K⁻p→Ω⁻+X, 8.25 GeV/c 8-93877
- Ω⁻→Ξ⁰π⁻, Ξ⁰π⁰, or Λ⁰k⁺, nonleptonic decay rates, ΔI=1/2 contrib. 8-62399
- baryon interactions** see baryon-baryon interactions; lepton-hadron interactions; meson-baryon interactions; photon-hadron interactions
- baryon leptonic decay**
- neutron β-decay, first order radiative corrections to e, ν and e-ν asymmetry coefficients 8-58254
- m, polarised, false effects in decay triple correlation, time-parity violation search (Russian) 8-78180
- baryon photoproduction**
- see also hyperon production; neutron production; proton production
- No entries
- baryon production**
- see also baryon photoproduction; hyperon production; neutron production; proton production
- breakup, exotic final state interaction, intermediate Δ, ΔN threshold parameters 8-50043
- Δ⁺⁺, prod. in νp→μ⁺Δ⁺⁺, 5-100 GeV 8-93873
- Δ⁺⁺, production in pp→pμ⁺n, 800 MeV 8-70385
- Δ⁺⁺(1232) inclusive prod. in π⁺p, π⁺p, K⁺p at 16 GeV/c 8-66169
- eN→eπΔ, low energy, ΔN axial form factors soft-pion theory 8-70380
- π⁺p→p⁰Δ⁺⁺(1236) or ωΔ⁺⁺(1236), 10.3 GeV/c, cross-section meas. 8-82248
- D+hadron, inclusive π, N spectra in high energy hadronic reactions, d fragmentation region (Russian) 8-54809
- baryon resonances**
- see also hyperon resonances
- baryonium, review of QCD, duality, string models and bag models 8-78135
- baryonium, spectrum and prod. mechanisms 8-74295
- baryonium interactions, string model, dual amplitudes (Russian) 8-54620
- baryonium model from qq̄q̄q hadron spectrum, T- and M-diquonium 8-58172
- baryonium Regge trajectories exchange in medium and high energy scatt., expt. evidence 8-50022
- colour model, mass splittings of heavy mesons and baryons (Chinese) 8-78146
- DC K⁺p, 32 GeV/c, resonance inclusive prod. cross sections, quark model comparison 8-93913
- exotic baryon resonance with isospins ≥5/2, existence, sum rule in Reggeon field theory (Russian) 8-93824
- extended Regge trajectories, modified Chew-Frautschi plot for meson and baryon resonances 8-82176
- hadronic resonance props., consideration as compound of bradyons and tachyons 8-58163
- narrow resonance in an open channel 8-66099
- narrow states in pp, qq̄q̄ mesons, BB bound states, duality, expt. 8-62378
- nuclear forces and isobar configs. in nuclei, review 8-50093
- nuclear interactions of strange particles and resonances, conf. Warsaw, Poland (Oct. 1976) 8-70406

baryon resonances continued

- photocoupling anal. in relativistic quark model 8-66086
 quark bag model, spectroscopic appls., baryonium, gluonium, quark phase of matter, review 8-50008
 relativistic hadron couplings, unified framework, symms., quark models (*German*) 8-50012
 strange baryonium, spectrum, decay, production 8-93854
 SU(3) symmetry breaking in baryon resonance decay 8-89712
 SU(4) broken symm., duality, baryon+baryon and baryon+antibaryon exotic mesons prod. 8-89629
 d breakup, exotic final state interaction, intermediate Δ , ΔN threshold parameters 8-50043
 Δ , I=3/2 high mass enhancement in 10.3 GeV/c π^+p interactions 8-66117
 $\Delta(1232)$, nucl. double beta decay and resonances 8-54722
 $\Delta(1232)$, πN scatt., separable interactions for three-body problems 8-78113
 $\Delta(1232)$ isobar in nuclei, one-boson-exchange and straton model anal. (*Chinese*) 8-78275
 $\Delta(1232)$ -N(938) mass difference, determ. of πN coupling const. in MIT bag model 8-78149
 $\Delta(1236)$ effect on imaginary component of NN phase shifts 8-70398
 $\Delta(1236)$ M1 and E2 photoexcitation $N \rightarrow \Delta$ in $\gamma N \rightarrow \pi N$ 8-70377
 $\Delta(1236)$ -resonance effects in nucl. matter 8-82302
 Δ resonance admixtures in NN problem, OBE model, d electrodisintegration 8-70373
 Δ^+ isobar mass and total width, $M^{3/2}_{1+}$ amplitude pole position from $\gamma p \rightarrow N\pi$ (*Russian*) 8-86453
 Δ^{++} , prod. in $\nu p \rightarrow \mu^+ \Delta^{++}$, 5-100 GeV 8-93873
 Δ^{++} , production in $pp \rightarrow p\pi^+n$, 800 MeV 8-70385
 $\Delta^{++}(1232)$ inclusive prod. in π^+p , π^-p , K^-p at 16 GeV/c 8-66169
 Δ^{++} prod. in $\pi^+p \rightarrow \Delta^{++}\pi^0\pi^0$ at 4 GeV/c 8-82232
 $eN \rightarrow e\Delta$, low energy, ΔN axial form factors soft-pion theory 8-70380
 $\gamma N \rightarrow \Delta$ magnetic dipole photoexcitation, singular integral equations 8-50040
 $\gamma p \rightarrow e^+e^-p$, reson. struct. obs. background process (*Russian*) 8-89722
 K^+p , phase shift anal., exotic reson. Z_1^* 8-62456
 $K^+p \rightarrow \Lambda p n\pi^+$, 12 GeV/c, narrow resonant state in $\Lambda\Delta^{++}(1232)$ and $\Sigma^+(1385)p$ combinations 8-89744
 $N^*(1234)$ saturating effect on binding of light nuclei 8-58231
 NN negative-parity reson., six-quark bag 8-74210
 NN resonances 8-62431
 NN systems, resonances due to annihilation, baryonium states, many channel N/D method 8-66143
 NNN system, bound and reson. states using Fadeev eqns. (*Russian*) 8-89804
 $np \rightarrow pX$, 800 MeV, proton spectra, $\pi N(1232)$ resonance 8-62437
 $pd \rightarrow d\pi^+n$, 585 MeV, Glauber theory, NN and $N\Delta$ amplitudes 8-62525
 pp inelastic scatt. in $\Delta(1232)$ prod. region, parity violation 8-62435
 $pp \rightarrow K^+K^+$ missing mass, stable six quark state search, mass range 2.1-2.4 GeV 8-89742
 $pp \rightarrow ppp_{\text{forward}} + \text{anything}$, observation of qq with qq \bar{q} bound states, pseudobaryons and baryonium 8-58219
 $pp \rightarrow ppp\pi^+$, 100 GeV/c diffraction and Δ^{++} prod. in exclusive interactions 8-93909
 pp spin observables, possible dibaryon resonance 8-78224
 pp total cross section, spin dependence, relativistic model of $\Delta(1232)$ prod. 8-62436
 pp total cross-section difference of pure helicity states, 2100 to 2500 MeV, obs. of structs. 8-78206
 $\pi A \rightarrow \pi^+X$ with $\Delta(1240)$ slow isobar intermediate prod. in heavy nuclei, cross section (*Russian*) 8-89917
 πd system, resonances near ΔN threshold, Argand diagrams 8-62582
 $\pi N \rightarrow N\pi\pi$, 1.65-1.97 GeV/c², πN resonance coupling to $\Delta\pi$ and ρN channels 8-66149
 πN partial wave anal. 1.6 to 10 GeV, possible high spin resonances in Argand plots 8-70403
 $\pi^-p \rightarrow \pi^0n$, charge exchange polarisation parameter meas., 617 to 2267 MeV/c 8-82231
 $\pi^+p \rightarrow \text{four prong final states}$, 10.3 GeV/c, resonance prod. cross-sections 8-74276
 $\pi^+p \rightarrow \rho^0\Delta^{++}(1236)$ or $\omega\Delta^{++}(1236)$, 10.3 GeV/c, cross-section meas. 8-82248
 Q^2Q^2 resonances in baryon-antibaryon systems, NN scattering and $NN \rightarrow \pi^+\pi^-$ 8-58171
 $^3\text{He}(\pi,\pi)$, role of spin isospin effects in $\Delta(1236)$ resonance domain (*Russian*) 8-78423
 $^4\text{He}+\pi^+ \rightarrow \pi^+\pi^-\text{ppd}$, 1.7 GeV/c, cross section, $\Delta(1232)$ and $\rho(770)$ resonance prod. 8-89911
 pp , polarised p, resonant like structs. in mass region 2100 to 2800 MeV 8-89745

baryon scattering see *baryon-baryon scattering; lepton-hadron scattering; meson-baryon scattering; photon-hadron scattering*

baryons

see also *baryon resonances; hyperons; nucleons*

- charmed, discoveries during 1974-7, and associated theory (*Czech*) 8-86103
 charmed baryons, dipole mag. moments, new U_3 scheme using u, d, c quarks 8-58165
 charmed baryons, magnetic moments by SU_3 and SU_4 symmetry 8-82209
 cosmology, baryon symmetric big bang 8-61945
 cosmology, baryon-symmetric, cosmic microwave background distortions 8-65727
 multibaryonic systems, 3n-quark systems, MIT bag model 8-70321
 nonrelativistic quark model with one gluon exchange pot., baryon spectroscopy in $SU(6) \otimes O(3)$ 8-78147
 positive parity excited baryons in quark model with hyperfine interactions 8-82161
 spectral function sum rules for quark and baryon fields, using lightlike charges 8-93822
 SU(4) symmetry breaking pattern and baryon masses 8-89690
 topological expansion for baryons and mesons, Veneziano scheme 8-70335

barysphere see *Earth core*

batch processing (industrial)

- Tarapur Atomic Power Station radioactive waste discharge monitoring 8-89989

batteries see *cells (electric); primary cells; secondary cells; solar cells*

Bauschinger effect

- compressible materials, flow behaviour 8-55573
 cyclic plasticity and masing behaviour in metals and alloys 8-64616
 energy based theory 8-63316
 metal, polycryst., Bauschinger effect and mutual restriction between grains 8-52895
 metallic media, varying loads, elevated temp. inelastic anal. using state variable theories 8-83264
 orthotropic compressible plastic yielding, derivation of elementary equation (*German*) 8-84902
 steel, medium C, fatigue behaviour of NiAl precipitation hardening 8-84983
 steel, spheroidized, Bauschinger effect and work hardening 8-64596
 Ti-V, cyclic stress-strain response 8-60700

Bayard-Alpert gauges see *ionisation gauges*

Bayes methods

- Bayesian deconvolution, convergent props. 8-57861
 Bayesian deconvolution, noise props. 8-57862
 cervical cancer automatic cytoscreeing, atypical cells classification 8-73289
 charged particle mass, confidence density method for parameter estimation (*Chinese*) 8-81811
 deconvolution, appl. and algorithm implementation 8-70103
 myocardial-stress perfusion scintigraphy, predictive value in patients without previous infarction 8-73205
 ophthalmology diagnosis, computer assisted 8-92739
 optimum filter for image restoration (*Ukrainian*) 8-55308
 statistic inference, subjective Bayesian approach 8-57729

bays (magnetic) see *geomagnetic variations*

BCS theory

see also *many-body problems*

- Josephson motor, rotational solns. in BCS theory 8-72310
 neutron star matter, 3P_2 pairing near transition temp. 8-57571
 nonequilibrium superconductors, transients, phonon distrib., supercond. gap, Boltzmann-BCS formulation 8-52149
 nuclear matter, thermodynamic model, shear viscosity temp. dependence 8-62499
 self-consistent selection of a superconducting representation for the BCS model 8-88067
 superconductivity, magnetic impurity effects, Anderson model 8-52148
 superconductor in EM field, nonlinear behaviour (*Russian*) 8-68108
 thermal expansion in supercond. state based on weak coupling BCS theory 8-80094
 two-band systems, BCS pairing and Peierls distortion compatibility 8-88068
 Ge, A=64, 66, 68, 70, Lipkin-Nogami method, ground state props. 8-50103
 NbSe₃, non-ohmic transport props. near phase tranistions 8-72213
 Ni, A=58, 60, 62, 64, 66, Lipkin-Nogami method, ground state props. 8-50103
 Zn, A=60, 62, 64, 66, 68, Lipkin-Nogami method, ground state props. 8-50103

beam choppers

No entries

beam-foil spectra

- 16 to 110 MeV beam energy, 20 to 350 nm wavelength 8-78655
 forbidden decay modes of one- and two-electron ions, book contrib. 8-82679
 introduction and review 8-70925
 Al IV, V, beam foil spectra, 1100-1900 Å, lifetime meas. 8-70919
 Ar IX, Ne I like reson. and Na I-like satellite lines, relativistic HF calc. and expt. 8-94210
 Ar¹⁵⁺, population of $^4P_{3/2}$ state meas. by cascading processes 8-94315
 Ar⁺+C, beam-foil spectra, Ar⁺ ion orientation, ang. variation 8-86944
 B IV, V, beam-foil meas. of mean lives below 450 Å 8-90120
 C foil+H₂⁺(H⁺), 0.5-2.5 MeV, forward electron vel. distrib., peak shape 8-78794
 C II, III, IV, radiative mean life meas. by beam-foil technique 8-90121
 C³⁺, fine struct. and lifetimes, doubly excited quartet system 8-78827
 C-foil, secondary electron yield from heavy ion beam-tilted-foil expts. 8-62889
 CO₂⁺, thin foil impact, dissoc. struct. effects in ionic fragment energy spectra 8-50631
 Cl VII, Ne I like reson. and Na I-like satellite lines, relativistic HF calc., and expt. 8-94210
 Cl XIII-XV, $\Delta n=0$ transitions, lifetime meas. beam-foil spectra 8-78798
 F III, IV, beam-foil spectra, mean lives, 2150-3200 angstrom 8-55224
 Fe 16 to 110 MeV beam energy, 20 to 350 nm wavelength 8-78655
 Fe XXIII and XXIV, reson. and intersystem transitions, oscill. strength, lifetime, beam-foil spectra 8-82685
 H-like ions, excitation regimes, nucl. orientation due to hyperfine interaction 8-70928
 H₂⁺ expt. determ. struct., foil-induced dissoc. fast mol-ion beam 8-74752
 He, double excited states, lifetime meas. by beam-foil technique 8-74590
 He-like ions, excitation regimes, nucl. orientation due to hyperfine interaction 8-70928
 He⁺+C, beam-foil spectra, He atom orientation, ang. variation 8-86944
 Kr VIII beam-foil decay curves for resonance transitions 8-74755
 N⁴⁺, fine struct. and lifetimes, doubly excited quartet system 8-78827
 NII, NIII level lifetimes, beam-foil method meas. 8-94314
 N₂O⁺, thin foil impact, dissoc. struct. effects in ionic fragment energy spectra 8-50631
 O II, III, IV, beam-foil spectra, mean lives, 270-490 angstrom 8-55223
 O IV(VI), circular polarisation of light emitted in beam-foil collisions, cascade free lifetimes 8-55228
 O³⁺, fine struct. and lifetimes, doubly excited quartet system 8-78827
 O²⁺, spectra, 7-32 nm, doubly excited quartet system 8-62757
 S II-VII, spectra, 1050-5500 Å, beam-foil expt. with 100-700 keV ions 8-50495
 S III-IV, 500 to 1200 Å 8-66488
 S⁸⁺, spectra, 500-1200 Å, lifetimes 8-62756

beam-foil spectra continued

- Si XI, allowed transitions, radiative lifetimes and oscill. strengths meas. 8-78797
- Si XII, allowed transitions, radiative lifetimes and oscill. strengths meas. 8-78797
- Y I, Y II, lifetimes of excited states, rel. to solar abundance determ. 8-86815
- Zr I, lifetimes of excited states, rel. to solar abundance determ. 8-86815

beam-foil spectroscopy

- heavy ion, decay curves influence of cascades, theoretical simulation 8-74755
- large M0 K X-ray, anisotropy from Ne on Al foil 8-55254
- lifetime meas., extension of techniques, book contrib. 8-74758

beam handling equipment

- accelerator grid assemblies, 120 keV, fabrication and brazing 8-66379
- beam profile low matter secondary emission monitor 8-70665
- betatron, 5 MeV, bremsstrahlung radiation ang. distrib. and penetrating power 8-70657
- betatron bremsstrahlung field shaping apparatus for teletherapy 8-57062
- CTR neutral beam source, SCR series switch and impulse crowbar 8-66395
- cyclotron, emittance measuring instrumentation, program for phase ellipse area (*German*) 8-58512
- Darmstadt linear accelerator electron scatt. facility, beam transport and spectrom. 8-70679
- deflecting septum magnet for cyclic accelerator 8-78525
- deflection system for SEM 8-58096
- deuteron beam production, by localised source in focused discharge 8-58093
- direct current accelerator for 14 MeV neutron prod., thermal-mech. design 8-66383
- double focusing bending magnet, meas. of optical props. with thin alpha source 8-55073
- electron beam charge monitor, single pulse toroidal coil type 8-78036
- electron beam current monitor using secondary emission detection 8-78033
- electron beam production, by localised source in focused discharge 8-58093
- electron storage ring VEPP-3, proposal to install supercond. wiggler magnet, synchrotron radiation prod. 8-62671
- electrostatic inflector and extractor for cyclic accelerators, HV expts. 8-50421
- electrostatic lenses, accelerating, decelerating heavy ion beams focusing 8-89588
- Faraday double transmitting cup, ion optical control device 8-82556
- fast particle beam differential scatt. instrument 8-86381
- floating deck modulators for high voltage protection of ion beam accelerators 8-66392
- fusion reactor, beam-profile fast scan monitor 8-54941
- fusion reactor 120 keV neutral beam, calorimetric and optical beam diagnostics 8-54933
- fusion reactor 150 kV negative ion test stand, electronics system 8-54934
- fusion reactor coil design, cost anal., for neutral beam magnets 8-55005
- fusion reactor neutral beam injector, beam line studies 8-54969
- fusion reactor neutral beam transport system 8-54968
- interferometric chopper for neutrons and X-rays 8-82088
- ion beam scanning device for rapid meas. of emittance and brightness 8-58522
- ion temperatre diagnostic system design and operation at Princeton 8-54942
- iris-loaded waveguide, inhomogeneous ferrite filled, autoacceleration 8-79441
- magnetic analyser for compact cyclotron 8-66439
- magnetic lens, wide-angle focusing device for low energy π collection 8-70664
- magnetically isolated annular relativistic electron beam 8-78037
- Mainz 300 MeV linear accelerator, energy loss system of electron scatt. facility 8-58524
- Mirror Fusion Test Facility, neutral beam injection, optimisation by computer graphics 8-66376
- neutral atomic beam source, power supply system 8-66393
- neutral beam high power injector cryopumps, design and performance, for fusion reactor 8-74494
- neutral beam injection system, for TFTR 8-54971
- neutral beam injection system cryopump, liq. He-cooled, for fusion reactor H₂ pumping 8-74495
- neutral beam injection vac. components, for fusion reactor 8-74493
- neutral beam injector, monoenergetic, power flow and gas flow models 8-66398
- neutral beam injectors, electrostatic energy recovery system 8-66400
- neutral beam injectors, for Princeton Large Torus, component design 8-54966
- neutral beam lines, for Princeton Large Torus, development and testing 8-54967
- neutral beam system, 120 keV, for fusion reactor ignition 8-66377
- neutral beam system, for ignition Tokamak 8-54973
- neutral beam test stand, 120 keV, computer based diagnostic and control system 8-66389
- neutral beams, continuously operating, mech. design criteria 8-66380
- neutral injection beam line, parameter studies, computer programme 8-66390
- neutral injection beam power monitor system for fusion reactor 8-54944
- neutral injection system, for JAERI experimental fusion reactor 8-54972
- neutrons, ultracold, zone mirrors for high resolution image form. 8-87003
- noncylindrical symmetric space-charge flow, Coriolis and centripetal accel. 8-91182
- nuclear filters, prep. from polymers using Ar ions 8-86714
- PLT toroidal field coils, operational deflection meas. 8-62627
- polarimeter designs for high energy p and d beams, polarised beam spin anal. 8-58516
- polarised ion sources and low energy collector rings, H⁺, D⁺ beams 8-58515

beam handling equipment continued

- polarised proton beams, higher energy, conf., Ann Arbor, MI, USA, Oct. 1977 8-58514
- polarising Soler guides for cold neutrons 8-54501
- profile monitor using holed sampling disc 8-54498
- proton radiography beam line establishment at Fermi National Accelerator Laboratory 8-65121
- pulsed electron accelerator current density distrib. multichannel recorder 8-58520
- ring-type state selector and space focuser for mols. with positive induced dipole moment, appl. to mol. beam maser 8-54503
- SIN injector cyclotron, RF system improvements 8-90005
- space charge lens for high current ion beams 8-55075
- superconducting bending magnets, 10.8 T.m, design and construction 8-82559
- superconducting RF particle separator, negative 16 to 37 GeV beam, results 8-89589
- superconducting wiggler magnet, 5T design for dedicated synchrotron radiation source at Daresbury 8-62672
- synchrotron miniature pulse deflector construction 8-82545
- TFTR neutral beam injector, calorimeter and beam dump design 8-66382
- TFTR type neutral beam system, ion accelerator design and fabrication 8-66381
- thermal neutron non adiabatic spin flippers 8-70668
- thyristor modulator with periodically interrupted supply, microtron appl. 8-55061
- Torus accelerator, transport of high current relativistic electron beams in large vols. (*Russian*) 8-82544
- UHV beam line at SSRL for spectral range 4-4000 eV, monochromatised radiation 8-62673
- undulators, quasi monochromatic synchrotron radiation, spectra for strong and weak fields 8-63000
- wiggler magnets, standard, effects on synchrotron radiation spectrum and storage ring operation 8-62670
- wigglers, conference on synchrotron radiation instrumentation, Orsay, France (Sept. 1977) 8-62999
- ZGS beam transport for transverse and longitudinally polarised protons 8-55074
- C stripper foils, lifetime enhancement, heavy ion bombardment 8-94156
- Cu-Ge neutron monochromator 8-71643

beam handling techniques

- see also *mass spectroscopy; particle optics*
- β -ray interference elimination by mag. deflection, for X-ray meas. following neutron activation 8-74101
- atomic/molecular beam interrogation in Ramsey cavity, two freq. separated oscillating fields technique 8-89596
- Berkeley 88 inch cyclotron, systematics in the control settings, beam parameter prediction 8-78526
- colliding beam arrangement using laser linac, feasibility study, laser accelerator problems 8-78521
- crossed-field energy analyser, stigmatic, focusing and dispersing props. 8-74832
- delayed coincidence techniques with accelerator beams, anal., optimisation rules 8-78598
- depolarisation during acceleration and storage of polarised protons and deuterons 8-58519
- duopigatron, preacceleration effects on ion beam transmission effects 8-87005
- electron beam, intense, ns, production in linear accelerator, space charge and radiation field effects 8-70654
- electron image deflection system, crossed elec. and mag. field, intensity modulation 8-89592
- electron polarisation by radiative separation in inhomogeneous mag. field practicality 8-82076
- electronic cooling, developments (*Russian*) 8-86712
- electrostatic lens, for acceleration and deceleration of high intensity ion beams 8-89595
- energy monochromatization of relativistic proton beam using laser 8-90010
- heavy particle beam, electron cooling, magnetisation effects (*Russian*) 8-70219
- heavy particle beam cooling in an electron flux, mag. field effects 8-82557
- heavy-ion intense beam, periodic focusing, mag. channels 8-55079
- high energy deposition from pulsed electron beams 8-54500
- high resolution spectrometer facility at LAMPF, beam line 8-62674
- intense negative ion beams from N₂ cluster ions, size specification 8-87006
- ion beam accelerator, multimegawatt, high-voltage power system, design philosophy, for fusion reactor 8-62613
- ion beam deviation, plasma boundary neutralisation surface depend. (*Russian*) 8-59613
- ion beam energy meas. of Van de Graaff accelerator using generating voltmeter 8-58508
- ion beam image transformation using magnetic quadrupole lenses 8-55071
- ion beam impurity anal. by backscatt. meas. 8-70223
- ion beam profile imaging by Ti tritide collector 8-78032
- ion beam steering by aperture displacement for tetrode accelerating structure 8-82075
- ion beams, divergence, effect of preacceleration voltage 8-66743
- jet target intense neutron source 8-66384
- low energy ion beams, conference, Salford, Sept. 1977 8-66444
- mitigation of residual space charge ion optics effects in gas cell by adjustment of beam permeance 8-74105
- multiple scatt. of particle beams, axial mag. field effect 8-70712
- muon low momentum surface beam for LAMPF 8-70672
- negative ion beam, generation, transport and accel., fusion reactor appl. 8-66378
- neutral particle beam, controlled energy distrib., prod. method 8-78038
- neutron spin echo, matrix anal. 8-86715
- noncylindrical symmetric space-charge flow, momentum eqns. 8-91181
- overneutralised electron beams in metal vapour, ion focusing theory and expt. 8-75366
- particle beam, flux control, charge. exchange method (*Russian*) 8-70662

beam handling techniques continued

- pinched beam diode, geometrical focusing of intense ion beams 8-58898
- PLT, neutral beam test stand, data acquisition system 8-62622
- Polarised beam from the University of Manitoba spiral ridge cyclotron 8-70660
- polarised beams, acceleration and storage 8-58518
- polarised proton beam production in high energy hyperon decay 8-58517
- polarised proton beams, higher energy, conf., Ann Arbor, MI, USA, Oct. 1977 8-58514
- proton beam calib., limits on differential hysteresis in Enge split-pole spectrograph 8-55082
- proton beam energy spread determ. from $^{12}\text{C}(\text{p,p})$ excitation function at 14.232 MeV 8-70669
- pulsed charged beams, phase meas. and control 8-58523
- relativistic electron beam generation, in foil-less diodes 8-89593
- relativistic electron beams, high current, pulse length adjustment 8-65997
- relativistic electron beams, transport in laser prod. plasma channel 8-71568
- RF ion source, 15 cm diameter, stable working conditions calcs. 8-86388
- slow neutron polarisation by polarised proton filter using ethylene glycol 8-90046
- stochastic cooling tests on proton beams, initial cooling expt. 8-90006
- TMX injector system, mech. design 8-66403
- trapping dynamics, in weak cold beam plasma instability, DC elec. field effects 8-83581
- TRIUMF biomedical negative pion beam line, tuning 8-96113
- wedge type ion beam divergence profile calc. 8-82555
- p beams cooling and storage, high energy collisions with protons 8-54654
- Cs beam deflection system for time and freq. primary standard 8-89453
- Cs beam standard, Ramsey cavity and beam optics design, expt. 8-89456
- ^{127}T ions, 20 MeV, emerging from gas stripper, absolute charge state yields 8-55066
- K atom clusters, cluster beam Stern-Gerlach mag. deflection 8-54504
- ^{149}Sm polarising filter for thermal neutrons 8-54502
- U, 50 keV beam prod. by charge exchange in gas and metal vapour targets 8-70675

beam-trapping *see self-trapping***bearings (machine)** *see machine bearings***behavioural sciences** *see social and behavioural sciences***bells***see also musical instruments*

- eccentric, vibr. meas., discussion of warble suppression 8-90612

bending*see also bending strength; buckling; stress analysis; torsion*

- adhesive bonded lap joints, elastic stresses theory 8-55563
- bar (tube), compressible, combined loading, elastic-plastic problem 8-63311
- beam of stepped thickness, Timoshenko theory 8-94600
- beam on nonlinear spring support, random vibr. 8-55585
- beams, effect of secondary terms 8-79237
- bi-material, elastic composite, Southwell's analogues for plane and bending problems 8-87265
- biaxial flexure test, exam. of loading factors 8-80695
- brass, anisotropic bend ductility in single phase alloys 8-60726
- α -brass, dislocation structure around crack tips in early stage of fatigue 8-60830
- bronze, anisotropic bend ductility in single phase alloys 8-60726
- composite, steady creep bending stresses 8-71280
- concrete plates, cracked, and beams existence of critical strain energy release rate 8-76765
- constructional material fatigue resistance test under asymmetric loading 8-85083
- contactless temp. meas. in circular cyclic bending, using thermoelectric radiation sensors 8-57947
- cylinder, thin, deformation due to band press. 8-94595
- cylindrical elastic tubes, collapse and buckling under combined bending and pressure loads 8-83277
- cylindrical shell, heated, large deflection 8-63289
- cylindrical shell, transverse shear effect on axial crack 8-67090
- cylindrical shell with circular cut out, uniform bending, strength and flexural rigidity 8-87282
- dynamic fracture toughness determination, by instrumented impact tests 8-68861
- Earth lithosphere bending at trench, elastic-perfectly plastic anal. 8-81135
- elastic beams, 1-D, stability in torsional extension (*German*) 8-87270
- elastoplastic anal. using ASKA program system, bending, isotropic/kinematic hardening 8-63312
- flagella bend propagation, derivation of eqns. of motion and simulation 8-77074
- frame structs., large deflection anal. by fictitious forces 8-83249
- fusion reactor coil, multilayer structs., laminated beam theory anal. 8-55011
- impact three point bend testing for notched and precracked specimens, testing and data analysis procedures 8-53053
- initial flaw shape, effect on cracks emanating from fastener holes under combined stress 8-64694
- lithosphere, elastic-perfectly plastic bending under generalised loading, appl. to Kuril Trench 8-73341
- LMFBR assembly, fuel pin deformations, analytical method, computational code (SHADOW) 8-54829
- membrane, prestressed, dynamic loading 8-51068
- mesh analysis processes, convergence (*German*) 8-87257
- metal, ductile fracture criterion 8-60817
- piezoelectric thin plates, integer polynomial solns. (*Russian*) 8-52444
- plastic bending and torsion of simple geometries, subjected to cyclic loading, stress-strain analysis 8-90734
- plastics, bending fatigue, exam. of new method of testing 8-53056
- plate, circ., with initial deflection, nonsymmetrical bending under mid-plane forces 8-79238
- plate, thick, containing eccentric spherical cavity, transverse bending stresses 8-63288
- plate, thin circular, bending, parabolic loading over concentric elliptic limaçon 8-59299
- plate bending theory, optimal thickness distrib. (*Russian*) 8-63295
- plate contiguous to fluid, shock loading, bending 8-90765
- plate with aperture, bending moments, exact. soln. 8-94598
- PMMA/PVC, cracking in layered composites 8-95808
- polyethylene, low density, SEM exam. of environmental stress cracking 8-53011
- polyethylene, pyramidal crystals, soln.-grown, collapse mechanics 8-76713
- polymer, soln.-grown cryst., diffr. line-broadening, bending contrib. 8-75574
- polymer cyclic deformation amplitude, automatic meas., apparatus design 8-85082
- prism bending to helical form, formal perturbation scheme 8-55558
- reinforced tube, bending and flexure 8-51076
- sandwich plate, modified Berger method, large thermal bending anal. 8-63297
- screw connections, bend and tension loaded, hysteresis (*German*) 8-87312
- shadow methods, reflected, transmitted, obs. of sharp V-notched plates, under pure bending 8-90777
- shafts, with abrupt changes of section, flexibility of shafts 8-90711
- steatite, ceramic, exam. of thermal damage by strength meas. 8-84997
- steel, alloy, C-Cr-Mo-V, exam. of fracture toughness and critical flow anal. 8-72848
- steel, alloy, rectangular beam, stress-strain anal. of cyclic plastic bending and torsion 8-90734
- steel, alloy, type 36NKhTYu, plastic deformation, effect of surface condition on initial stage 8-84929
- steel, C, prestrain effect on non ductile transition temp. and bending speed relationship (*Japanese*) 8-84919
- steel, Ck 45, alternating bending, fracture surface appearance (*German*) 8-52995
- steel, high strength, low alloy, fatigue crack growth from a surface flaw 8-68803
- steel, low-C, sheet, thin, residual stresses determ. after bending 8-60708
- steel, mild, exam. of fatigue damage, using thermography 8-92356
- steel, mild, fatigue crack growth from a surface flaw 8-68803
- steel, mild cylindrical shells, limit loading under loop bending moment 8-80581
- steel, nuclear pressure vessel, type A533B-1, three point bending, yield stress, exam., Charpy V-notch and precracked specimens 8-92310
- steel, rolled, effect of inclusions on torsional fatigue 8-92314
- steel, stainless, corrosion fatigue cracking in NaCl aqueous solution, fractographic anal. (*Japanese*) 8-53023
- steel, stainless, martensitic SUS 403-B, high temp. rotating bending fatigue 8-60756
- steel, stainless 304, stress crack initiation in chloride soln., role of corrosion pits (*Japanese*) 8-92397
- steel, type 20, fatigue, low cycle, exam. of damage accumulation rule, for loading in air and H impregnating medium 8-64649
- steel reinforced concrete beams, mech. strength determ. under combined bending and tension 8-60749
- structural anal., soln. by orthogonal collocation 8-51063
- structures of discontinuous shape, finite element analysis (*Japanese*) 8-83238
- surface crack shape change in bending fatigue, resonant fatiguing apparatus 8-72950
- tail-wheel struct. of light aircraft, large deflection anal. 8-83272
- thin circular quadrant, singularly loaded, with clamped radial edges and free circular edge 8-63300
- thin plates, optimal loading calc. by duality theory (*Russian*) 8-63409
- three point bend tests, notched or precracked specimens, load displacement measurement and work determ. 8-53054
- three point bending tests, calc. of yield stress, review 8-92310
- toroidal field coils, bending-free, for Tokamak reactor 8-55012
- vibrations in their plates layer potential method of solution (*French*) 8-59336
- Zircaloy 4, stress relaxation in bending 8-68719
- Al, adhesively bonded and weld bonded aircraft struct. subjected to acoustic excitation, determ. of sonic fatigue life 8-92351
- Al alloy 2024, loading sequence, normal and reversed sequence effect 8-68791
- Al, alternating bending of single crystals, shear strain accumulation and microstrain distrib. (*Russian*) 8-60706
- Al bronze, anisotropic bend ductility in single phase alloys 8-60726
- Al, cold rolled, X-ray diffr. and optical microscope exam. of fatigue damage (*Japanese*) 8-84976
- Al-Zn-Mg-Cu, alloy 7075, fatigue, loading sequence, normal and reversed sequence effect 8-68791
- Al_2O_3 , evaluation of crack resistance and crack velocity, using controlled fracture experiments 8-72881
- Al_2O_3 rods, quenched, exam. of contact induced strength degradation 8-76731
- Al_2O_3 , stress value determination by bending tests, comparison with crack tip theory 8-67154
- C fibre reinforced epoxy phenol plastic, resistance to interlayer shear and elec. resistivity 8-68752
- C steel, type 45, inelasticity under cyclic strain in active media 8-80613
- Cu alloys, flat spring, mechanical props. in bending, stress relax. test, 23 to 232°C 8-72806
- Cu, single crystals, effect of stacking fault energy on extrusion and intrusion development 8-72826
- Cu single crystals, positron trapping by edge dislocations, produced by bending 8-80606
- α -Cu-Zn (5.3 to 21.8 wt.%), single crystals, effect of stacking fault energy on extrusion and intrusion development 8-72826
- Fe, Armco, inelasticity when under cyclic strain, in active media 8-80613
- InSb, plastically bent single crystals, dislocation struct. obs. 8-59816
- $\text{Na}_2\text{O-CaO-SiO}_2$, evaluation of crack resistance and crack velocity, using controlled fracture experiments 8-72881
- Si, monocrystalline, effect of notch root radius on fracture behaviour 8-76751
- SiC, hot pressed, brittle fracture and subcritical crack growth 8-72885
- Si_3N_4 , hot pressed, slow crack growth from controlled surface flaws 8-80632

bending continued

bending continued

- Ti, fatigue fracture surface microstruct., electron microscope obs. 8-60834
 β -Ti-Mo-V-Fe-Al (8, 8, 2, 3, wt.%), exam. of stress induced H₂ migration 8-87823
 U-Mo (10 wt.%), commercial alloys, influence of metallurgical factors on fracture processes (*French*) 8-60751
 WC-Co, various combinations, fracture chars. in bending, compression, and toughness tests 8-60808
 Zn, alternating bending of single crystals, shear strain accumulation and microstrain distrib. (*Russian*) 8-60706
 Zn, single crystals, positron trapping by edge dislocations, produced by bending 8-80606

bending of light *see* gravitation; light

bending strength

- beam (plate) pure bending, dynamic fracture, axial force effect 8-63385
 borsic fibre reinforced Ti, unidirectional, K-calibration and compliance curves 8-88518
 combined bend mode specimens, calc. of stress intensity factors 8-79284
 double lapped composite joints, efficiency in bending, of steel/B reinforced Al or epoxy adherends 8-68870
 ductile crack extension, evaluation of resistance in single notch edge specimens 8-68807
 elastic springs, thin, of constants cross section, elastic behaviour calc. and obs. (*German*) 8-87269
 epoxy Al bonded, adhesive joints under complex loading, development of failure criterion 8-92344
 epoxy resin, mech. and thermal props., amine hardeners, added softeners and filter effects (*Polish*) 8-68741
 glass fibre reinforced plastic/polyurethane foam/Al sandwich, flexural props. (*Japanese*) 8-56707
 glass plate, flexure crack propag., expt. and anal. 8-80620
 graphite, oxidation, corrosion resistance, bend strength, assessment for rotary glass fibre making apparatus 8-64753
 ice shelves, floating, tidal flexure cracks, fracture mechanics 8-69368
 mullite fibre reinforced mullite, in vitro degradation, bending strength, Young's modulus, density meas. 8-85011
 notched beam, fatigue crack emanates from notch root, fracture strength 8-72866
 phenol formaldehyde resin, (Novolak) with filler, mech. props. determ. (*German*) 8-84933
 phenol formaldehyde resin (Novolak), with and without feldspar filler, mech. and thermal props. determ. (*German*) 8-84828
 phenol resin (Resol), with and without feldspar filler, mech. and thermal props. determ. (*German*) 8-84828
 plates, rectangular thin, effect of different edge flexibility coeffs. on transverse vibrs. 8-83294
 plates stiffened, large amplitude flexural vibrs. 8-83307
 polymer-TiO₂ composite, dielec. props. (*Japanese*) 8-95540
 polyurethane foam, rigid integral, effect on flexural and compressive strength, due to tall oil oligoether, 8-68743
 steel, austenitic, precipitation hardening, effect on fatigue strength 8-84829
 steel, C and alloy, notched beam, fatigue crack emanates from notch root, fracture strength 8-72866
 steel, case hardened, MnCr, shot peening effect on bending fatigue strength (*German*) 8-56777
 steel, constructional, fracture toughness in cyclic loading 8-72860
 steel, fracture toughness and dynamic strength, surface active agent effects (*Russian*) 8-56812
 steel, MnCr (16, 5 wt.%), bending fatigue behaviour improvement by surface treatment (*German*) 8-84957
 steel, Ni, cross girder connections, fatigue strength, design stress 8-64700
 steel, short-cycle, fatigue, stress concentration effect 8-95859
 steel, silver, elastic limit, bending strength, and ductility rel. to tempering temp. after quenching 8-95764
 steel bar deformation meas. by holographic interferometry using four point bending machine 8-60721
 steel beams, inelastic, mild, flexural behaviour and lateral buckling anal. under cyclic loads (*Japanese*) 8-87283
 test apparatus under high press. and temp. (*Japanese*) 8-76795
 Al/polyethylene/Al sandwich construction, flexural fatigue props. (*Japanese*) 8-56751
 Al-Mg alloy AMg6, mech. props. of welded joints, impurity effects 8-95789
 B fibre reinforced Al, unidirectional, K-calibration and compliance curves 8-88518
 Cr-Mo-V, steamline bends, restorative heat treatment effects 8-68716
 Fe-Al-Si, bending test, mech. props. under high press. and temp. (*Japanese*) 8-76711
 Fe-B alloy reinforced polysulphone exam. of tensile and flexure props. 8-72823
 Fe-Ni-C (9, 0.1 wt.%), effect of intercritical tempering on impact energy, exam. of mech. props. 8-52861
 Fe₃₂Ni₃₆Cr₁₄P₁₂B₆, shear band form. 8-68756
 Ni carbonyl powder, sheet filtration materials with metallic gauze backing layers, bending strength and ductility 8-60613
 Ni-based-Ta(Cu,N) hard metals, isostatic hot pressing influence on mechanical properties 8-92219
 PVC-Cu, particulate composite, mech. props. effect of particle size 8-95799
 TiC-Mo₂C-Ni cermets, influence of anomalous phases on strength 8-92228
 W fibre reinforced Ni-Cr alloys, Ni, Co, Co alloys, and Ni alloys, effect of alloying on structural stability, mech. props. 8-56600

berkelium

see also nuclei with

No entries

berkelium compounds

No entries

beryllium

see also nuclei with

- anisotropy, theoretical investigation by K-emission, APS, and Compton profiles 8-63970
 atom, Doppler effects in X-ray spectra excited by accelerated ions 8-86808
 atom, dynamic multipole polarisability, coupled Hartree-Fock 8-82858

beryllium continued

- atom, freq.-depend. polarisabilities and Verdet consts., calcs. 8-62781
 atom, ground state wavefunction, SCF HF calc. 8-90070
 atom, Hund's first rule, new interpretation 8-78620
 atom, K-shell ionis., double and single, cross section meas. by ion bombardment 8-50629
 atom, X-ray spectra, chemical bonding and multiple ionis. effects 8-50630
 Auger emission target, contrib. of reflected electrons 8-92152
 casting, produced in zero gravity environment, BeO particles uniform distrib. 8-72753
 channelled-ion scatt. yield, oscillatory, for 1.9 MeV ⁴He⁺ 8-52610
 coatings, α -radiation meas. of thickness 8-82600
 core electron expansion, kinetic energy in Compton profiles 8-72628
 film as opt. filter in He discharge lamp, for photoelectron spectroscopy 8-79115
 forest dislocation effect on single twin layer development in single crystals 8-63775
 fusion reactor material, response to He⁺ bombardment determ. 8-86691
 inelastic electron scattering near K-edge 8-52606
 ion bombarded, chemical effects on secondary photon and ion emission 8-95637
 isoelectronic series, inner-shell photoionis. cross sections 8-74623
 magnetoresistance at low angles between current and mag. field (*Russian*) 8-68012
 main-sequence stars, Li, Be and B abundances rel. to envelopes hydrodynamical instabilities 8-93202
 neutron wave propagation across discontinuity, two group calcs. 8-89931
 plasma, laser-produced, recombination effects 8-94935
 polycrystalline, metallographic observation of cleaved grains 8-72824
 stopping power for 28 MeV α -particles, re-evaluation 8-79651
 surface, (0001), work function and purity, AES, LEED and photoelectron spectra meas. 8-68606
 surface, contact ang. meas., aq. ethanol (glycerine) solns., 20-70°C 8-56025
 thermal neutron wave propagation 8-58320
 X-ray emission spectrum, double plasmon high energy satellite 8-72639
 XPS theory, core level spectra, plasmon creation 8-72701
 XPS theory, valence band spectra band struct. 8-72702
 ZZ 8-91367
 Al-Be, two-layer foils, mech. props. (*Russian*) 8-51858
 B⁺, electron impact excitation of 2p state, close-coupling calc. 8-55247
 Be I isoelectronic sequence, radiative props. determ. by model-pot. method 8-70788
 Be sequence, (Z=4 to 10, 14), ³P₁→¹S₀ intercombination line, CI calc., Breit interaction 8-78641
 Be⁻, low-energy ²P^o shape resonance, complex-coord. method calc. 8-74591
 Be²⁺, electron impact excitation, cross-sections, modified Oppenheimer approx. 8-82843
 Be-SiO-p-Si, MIS solar cell, performance figures 8-88030
 Be+He (methane), Be atom K-shell binding energy by Auger spectra 8-50525
 Be₂, polarisability, generalised London formula for dispersion coeff. 8-82662
 Be(¹S), total X-ray scatt., two-electron density functions 8-70889
⁹Be, nuclear mag:spin-lattice relaxation times 8-86889
⁹Be²⁺, aq. ions, nucl. quadrupole relax. 8-64287
 CdTe:Be, impurity modes and IR absorption 8-76506
 Cu-Be-O surface, O(²S) impact, secondary electron yield 8-58797
 GaAs:Be, annealing effect during MBE 8-79898
 GaAs:Be planar p-n junction, Be ion implantation, fabrication and chars. 8-88022
 InP:Be, planar reactive deposition on CdS, heterostruct. formation and elec. evaluation 8-72738
 Ni, blistering model, correlation between blister diameter and skin thickness 8-95067
 Pu-Be neutron source, for activation anal., β -ray meas. 8-73114
 SiC:Be, film donor impurity, diffusion influence on elec. and optical props. 8-87942
 α -SiC:Be, piezoresist. rel. to acceptor levels 8-60129
 ZnS:Be, impurity modes and IR absorption 8-76506

beryllium alloys

see also beryllium compounds

- bronze, struct. and props. after ageing under load 8-84932
 Be bronze, electrolytic polishing using cylindrical stationary electrode 8-64783
 Be bronze, electropolishing using cylindrical electrode moving forwards 8-64784
 Be bronze BrB₂, quenched deformed, substruct. and props., effect of prerecrystallisation annealing (*Russian*) 8-60677
 Be-Co (0-50 at.%) alloys, thermal, metallographic and X-ray anal., phase diagram (*Russian*) 8-56611
 Be-Cu surface, secondary electron yield, for electron multiplier ion detector 8-74094
 Be-Nb-Zr, glassy and partially crystalline, supercond. T_c and struct. props. 8-60239
 Be-Ru, dil., quadrupole interactions at ⁹⁹Ru, TDPAC meas. 8-91996
 Be₄₀Ti₅₀Zr₁₀, metallic glass, thermoelectric power and resist. 8-95289
 Cu-Be, impurity concentration effects 8-75777
 Cu-Be, solute atom displacement in mixed dumbbell interstitials for FCC lattice 8-79631
 Cu-Be (0.99 wt.%), direct obs. of small Guinier-Preston zones 8-72776
 Cu-Be alloy, CA 172, flat spring, mechanical props. in bending, stress relax. test, 23 to 232°C 8-72806
 Cu-Be alloy, X-ray diffr. pattern singularities (*Russian*) 8-67682
 Cu-Be-Ni-Zr, anodic behaviour of intermetallic phase 8-72895
 Fe-Be, formation of quasi-periodic distrib. of precipitates during ageing (*Russian*) 8-56642
 LaBe₁₃-Er(Dy), dil., ESR, crystalline elec. field splitting, exchange parameters 8-52348
 LuBe₁₃-Er, dil., ESR, crystalline elec. field splitting, exchange parameters 8-52348
 NbMo₂Be, predicted A15 struct. and T_c=30K 8-76182

beryllium alloys continued

Ni-Be alloy, precip. sequence 8-80549

Ti-Be-Si glass ribbons, physical and mech. props. 8-95767

beryllium compounds*see also beryllium alloys*BeF₂, aq. glass, 76K, solvated electron spectrum evolution, following ns radiolysis 8-88295BeF₂ glass, nonlinear refr. index, meas. of electronic and nucl. contribs. 8-50866BeF₂, K-emission spectra, optical effects 8-64431BeF₂, vitreous, IR and reduced Raman spectra, weak Raman bands 8-68498

BeH, spin-extended Hartree-Fock ab initio calculations for small radicals 8-70746

BeH₂, localisability in MO calcs., measured by absolute overlap and 2nd moment dispersions 8-74557BeH₂, pot. energy curve, minimal basis ab initio VB calcs. 8-50477BeHHe⁺, from BeHT β -decay potential energy curves 8-56910

BeO, finite assemblies, thermal neutron wave propagation 8-58320

BeO, induced lung carcinogenesis in rats, high-fired oxides 8-96077

BeO, K-emission spectra, optical effects 8-64431

BeO, particles uniform distrib. in Be casting prod. in zero gravity expt. 8-72753

BeO, sputtering by low energy H and D 8-95630

BeO, X-ray spectra, chemical bonding and multiple ionis. effects 8-50630

BeO- UO_2 , ceramic fission reactor fuels, fabrication and performance, review 8-58392BeO- UO_2 fuel testing, annular core pulse reactor 8-86593BeSO₄ soln. in H₂O, methanol-H₂O, US dispersion, 3-60 MHz (*German*) 8-59862BeSO₄.4H₂O, p-p vector orient., PMR obs. 8-52361BeSO₄.4H₂O, SHG at 2660 angstroms 8-90451Be₂SiO₄:P, EPR and ENDOR 8-76295Li₂O-BeO-SiO₂, X-ray diffr. exam. of phase equilibrium 8-80522**Bessel differential equation** *see Bessel functions***Bessel functions**

Einzel-type electrostatic field with rot. symmetry, Fourier-Bessel soln. 8-82878

higher monotonicity properties of certain Sturm-Liouville functions 8-57750

polaron theory, Bessel function integral, asymptotic evaluation 8-56082

recurrence relations for phase shifts of certain classes of potentials 8-89364

spherical Bessel functions j_n and y_n of integer order and real argument 8-89321

squares of positive zeros, nonlinear eqns. and sum rules 8-49639

torsional vibrs. of spherical shell, numerical results 8-59322

wave diffraction by thin phase grating, difference eqn. solns. 8-54198

zeros of Bessel functions, algebraic eqns. 8-49640

beta-decay*see also beta-decay theory; beta-ray spectra; nuclear electron capture*

A=215, nuclear data sheets, decay characteristics and level struct. 8-58224

A=219, nuclear data sheets, decay characts. and level struct. 8-58225

A=223, nuclear data sheets, decay characts. and level struct. 8-58226

A=227, nuclear data sheets, decay characts. and level struct. 8-58227

atomic K- and L-shell shakeoff probability, following β -decay, hydrogenic wave function 8-94204

double beta decay, lepton number conservation 8-58256

explosive r process cooling process 8-69791

LMFBR burnup calc., allowance for ²³⁹Np 8-89936many electron effect on K-shell internal ionisation accompanying β -decay 8-86839nuclear matter, β -stable, electrically neutral, constrained variational calc. 8-58243probabilities of α -, β - and γ -transitions accompanied by changes in nuclear shape (*Russian*) 8-89820

radioactive nuclide decay data for reactor calcs., activation products and related isotopes 8-82426

rotational invariance in beta-ray ang. distrib. 8-66252

stellar hot dense matter, beta transition rates 8-73699

³H labelled compounds, β decay fragmentation potential energy curves 8-56910⁹⁹Tc^m compounds, chemically induced decay constant variation 8-93968²³⁰Ac, prod., decay characts. 8-54724³Ag, A=97, 98 and 99^m decay spectral meas. 8-93976¹¹⁰Ag^m disintegration, scheme of ¹¹⁰Cd (*French*) 8-58248¹²²Ag decay, struct. of neutron rich even-even Cd nuclei 8-66249²⁶Al, as planetoid heat source in early solar system 8-65511⁴⁴Ar β decay into ⁴⁴K, neutron rich isotopes, weak coupling predictions, γ -ray meas. 8-74336⁴⁵Ar, β -decay scheme and half life, K deduced energy levels 8-78319⁴⁶Ar, β -decay scheme and half life, K deduced energy levels 8-78319¹²B, aligned, β ang. distribs., second class currents 8-50126¹²B β -decay, conserved vector current, elementary particle approach 8-66246¹²B, oriented nuclei, β - γ ang. correl., G-parity nonconservation 8-54723¹²B spin polarisation meas. from β -decay, product of ¹⁰⁰Mo(¹⁴N,¹²B)¹⁰²Ru 8-50196

Ba, A=117, 119, 121, delayed proton emitters, positron-proton coincidence meas. 8-78326

¹³⁹Ba β -decay into ¹³⁹La, γ -rays, energy levels 8-70492¹⁴³Ba decay to ¹⁴³La, β -branching and log ft values 8-50129¹⁴⁵Ba, fission product, β -decay anal. 8-78323¹²Be core excited T=2 levels, spin, half life from ¹⁰Be(t,p), 12 MeV 8-66210¹⁹⁹Bi→¹⁹⁹Pb, spectra meas. 8-78316²⁰¹Bi→²⁰¹Pb, spectra meas. 8-78316²⁴⁸Bk, spectroscopic studies 8-78314⁹⁰Br, experimental Q β -values 8-93974⁴⁵Ca, internal bremsstrahlung photon intensity and energy yield 8-86509¹¹⁵Cd^m, decay to ¹¹⁵In, decay scheme, unified model description of odd mass In nuclei 8-66251¹⁴⁵Ce, fission product, β -decay anal. 8-78323**beta-decay** continued⁵⁷Cr mass excess, half life, ground state spin and parity, from ⁴⁸Ca(¹¹B, pn) 8-70436Cs, A=114-118, neutron deficient isotopes, half lives, β^+ , γ , delayed p and α meas. 8-70489⁶Cs, A=139-144, beta endpoint energy measurements 8-93975⁶¹Cu, ⁶¹Ni multiparticle configs., transition probabilities from shell model 8-70496⁶⁷Cu, multiparticle configs. in ⁶⁷Zn 8-70496¹⁶⁹Er, internal bremsstrahlung photon intensity and energy yield 8-86509¹⁴³Eu^m, decay obs., struct. determ. 8-50130¹⁴⁸Eu decay, ¹⁴⁸Sm energy levels, struct. interpretation from boson expansion model (*Russian*) 8-78261¹⁵²Eu, K-forbidden beta transition, spectral shape anal. 8-74335²⁰F β -spectra, cf conserved vector current predictions 8-50131²⁰Fe, β - γ directional correlation, second class current 8-50127⁶²Ga, superallowed Fermi β -transition, half life and β -ray end point energy 8-78320⁶⁷Ga, multiparticle configs. in ⁶⁷Zn 8-70496⁷³Ga, β -decay rate for estimation of ultra-high pressure 8-77927¹⁴³Gd^m, β^+ and EC decay 8-50130¹⁷⁰Ho, 43 s and 2.76 min states, energies and intrinsic structs. 8-78321⁹In, A=104, 106, β -decay half lives and decay schemes 8-74333⁹In, A=120-129, total β -decay energies and masses of strongly neutron rich isotopes 8-86512¹¹³In decay to ¹¹³In, decay scheme, unified model description of odd mass In nuclei 8-66251¹²⁰In, β -decay, half life and decay schemes, ¹²⁰Sn level struct. 8-86510K, A=48, 49, 50, half lives, γ meas. 8-74341³⁸K^m superallowed Fermi β -decay half lives 8-82318⁹³Kr, experimental Q β -values 8-93974¹⁴⁵La, fission product, β -decay anal. 8-78323⁸Li(β)⁸Be*(α), obs. of ⁸Be state at ~6 MeV 8-93938¹⁷⁷Lu decay, beta spectral shapes 8-74337²⁸Mg, isospin forbidden β -decay 8-78315⁵⁷Mn half life 8-82321⁶⁰Mn, mass and β -decay half life, ⁶⁰Fe struct. and mass excess 8-78317¹²N, aligned, β ang. distribs., second class currents 8-50126¹²N, oriented nuclei, β - γ ang. correl., G-parity nonconservation 8-54723¹²N→¹²C(g.s.), second-class axial current, meas. alignment-positron-momentum correl. 8-82317Na neutron rich isotopes, β -delayed emission of n, 2n, α , t 8-74343⁹²Nb⁸, cross-section and half-life from ⁸³Nb(n,2n), 14.8 MeV 8-70491¹⁰³Nb, superallowed Q β -values 8-93974¹⁴⁰Os, superallowed Fermi β -decay half lives 8-82318¹⁶O(0⁺) \rightarrow ¹⁶N(0⁻) β decay and μ capture reactions, mesonic exchange correction 8-58257⁸Pa, A=236, 238, β strength function struct., influence on β -delayed fission 8-89826¹⁴⁷Pm, internal bremsstrahlung photon intensity and energy yield 8-86509¹⁴⁹Pm→¹⁴⁹Sm, beta decay matrix elements 8-70488¹⁴⁶Pr β -decay, ¹⁴⁶Nd level scheme and transitions 8-86476¹⁵⁰Pr decay into ¹⁵⁰Nd vibr. levels 8-89817²³⁰Ra, prod., decay characts. 8-54724⁸Rb, A=88-94, beta endpoint energy measurements 8-93975¹⁸⁶Re→¹⁸⁶Os, absolute log ft values, beta spectra, directional correlation coeff. and WS potential parameters calc. (*Rumanian*) 8-82316³⁵S, internal bremsstrahlung photon intensity and energy yield 8-86509⁴²Sc, ground state β -decay, weak non-analogue Fermi branch, branching ratio upper limit 8-70495⁷⁴Se, A=85, 86, experimental Q β -values 8-93974¹⁰⁶Sn β^+ /EC decay, ¹⁰⁶In level scheme determ. 8-93971¹²¹Sn^m→¹²¹Sn^g→¹²¹Sb, branching fraction, K-shell IC coeff. 8-82319⁹⁷Tc^m, β -decay rate for estimation of ultra-high pressure 8-77927¹⁰²Tc, β -decay, deduced ¹⁰²Ru levels 8-86513¹⁰³Tc, experimental Q β -values 8-93974¹⁰⁴Tc, β -decay, γ -spectra, ¹⁰⁴Ru level scheme determ. 8-82313¹²⁸Te $\beta\beta$ decay ratio of ¹²⁸Te/¹³⁰Te half lives 8-66250²³⁴Th β^- decay into ²³⁴Pa isomers, low energy γ -spectrum 8-70493²⁰⁴Tl, beta-transition, spectral shape, small-order deviation 8-74338⁹⁰Y internal bremsstrahlung, evidence for detour transitions in β -decay processes 8-66247¹⁷⁵Yb, levels of ¹⁶⁵Tm and decay scheme, γ -ray and conversion electron spectra 8-74334⁷¹Zn^m decay, ⁷¹Ga ang. correlations, level spin assignments and multipole mixing ratios 8-78305**beta-decay theory***see also beta-decay; beta-ray spectra*

A=24-28 nuclei, reliability of calculated decay props. 8-93970

atomic rearrangement processes 8-54725

closed shell \pm one nucleon nuclei, axial vector coupling const. quenching 8-89824double-beta decay, electron-neutrino pair emission via $\Delta(1232)$ resonance 8-54722

historical introduction, weak interactions, book 8-78133

neutron, first order radiative corrections to e, ν and e- ν asymmetry coefficients 8-58254one-body Gamow Teller β -decay matrix elements for 1s-0d shell, empirical renormalisation 8-66248proton decay, β -delayed proton radioactivity, book contrib. 8-82322

superheavy region, neutron drip line, energy density mass formula extrapolation 8-93932

V-A theory, neutron beta-decay (*Russian*) 8-58255 β -delayed neutron decay, statistical model, Monte Carlo techniques, fictional pandemonium nucleus calcs. 8-89830⁸B, isospin symmetry breaking in A=8 mirror decays 8-93973⁸Li, isospin symmetry breaking in A=8 mirror decays 8-93973⁸Li→⁸He+ β , β -decay strength calcs., microscopic continuum wave function 8-62503

beta-particles *see* *beta-rays*
beta-radiation *see* *beta-rays*
beta-ray absorption
see also *electron absorption*
 No entries

beta-ray angular distribution
see also *beta-ray spectra*
 $A=12$, decay of $T=1$ isospin triplet, β -ray anisotropy 8-78322
 rotational invariance in beta-ray ang. distrib. 8-66252
 ^{12}B , aligned, β ang. distrib., second class currents 8-50126
 ^{12}B spin polarisation meas. from β -decay, product of $^{100}\text{Mo}(^{14}\text{N}, ^{12}\text{B})^{102}\text{Ru}$ 8-50196
 ^{12}N , aligned, β ang. distrib., second class currents 8-50126

beta-ray detection and measurement
see also *beta-ray spectrometers; radioactivity measurement*
 air pollution control at Nuclear Research Institute (Czech) 8-88906
 automated Rn-Th monitor for earthquake prediction research 8-73532
 Cherenkov counting of plants for β -emitter radioassay, sample prep. 8-81088
 cylindrical proportional counter, gas multiplication factor dependence on anode wire attachment 8-78560
 direct meas. of β absorbed dose rate by discriminator and filter (Japanese) 8-74511
 Ge, hyperpure, β end-point-energy meas. 8-78587
 liquid scintillation instrumentation development 8-86728
 liquid scintillator determ. of dose rates from homogeneously distrib. β , γ - and EC, γ -emitters in phantom organs 8-53501
 low activity beta-ray measurements, us Pu-Be neutron source and beta spectrometer 8-73114
 real-time environmental α - β - γ radiation monitoring system 8-94152
 seawater density determ., possible use of beta-emitting radioisotopes (Russian) 8-65423
 soil and vegetation, surface β -activity caused by nuclear explosion products, depend. on isotope vertical migration 8-86700
 ultra-thin bonded TLD for skin dose meas. complying with ICRP recommendation 8-92709
 ^{14}C meas. in proportional counter, continuous examination of counting efficiency 8-58548
 ^{131}I in milk, extreme low level determ. 8-92703
 Ne flash tube chambers for electron and photon detection 8-58552
 Si(Li) detectors, unfolding procedure for slowly varying pulse height spectra of β -particles 8-50430
 T in water, flow cell type detector for continuous monitoring in high γ -background 8-82524

beta-ray effects
see also *electron beam effects*
 chromatographic support materials decomposition by ionising radiation (German) 8-92587
 α -autoradiography of irradiated nuclear fuel, effect of β radiation (German) 8-78466
 Al bremsstrahlung, β generated, spectral shape depend. on target thickness 8-56545
 Cu, bremsstrahlung, β generated, spectral shape depend. on target thickness 8-56545
 Pb, bremsstrahlung, β generated, spectral shape depend. on target thickness 8-56545
 Sn, bremsstrahlung, β generated, spectral shape depend. on target thickness 8-56545

beta-ray polarisation
 No entries

beta-ray scattering *see* *beta-ray effects; collision processes; energy loss of particles; particle backscattering; potential scattering; transport processes*

beta-ray spectra
see also *beta-decay theory*
 ^{99}Ag , $A=97, 98$ and 99^{m} decay spectral meas. 8-93976
 ^{90}Br , experimental Q_{β} -values 8-93974
 ^{143}Ce , 1404 keV beta transition, spectral shape, ^{143}Pr 57 keV state 8-74339
 ^{132}Cs , $A=139-144$, beta endpoint energy measurements 8-93975
 ^{152}Eu , K-forbidden beta transition, spectral shape anal. 8-74335
 ^{20}F β -spectra, cf conserved vector current predictions 8-50131
 ^{20}Fe , β - γ directional correlation, second class current 8-50127
 $^{72}\text{Ga} \rightarrow ^{72}\text{Ge}$, gamma and beta-ray spectra, intensities, branching ratios, spin and parity assignments (Korean) 8-50128
 ^{119}In , $A=104, 106$, β -decay half lives and decay schemes 8-74333
 ^{93}Kr , experimental Q_{β} -values 8-93974
 ^{177}Lu decay, beta spectral shapes 8-74337
 ^{103}Nb , experimental Q_{β} -values 8-93974
 ^{186}Rb , $A=88-94$, beta endpoint energy measurements 8-93975
 $^{186}\text{Re} \rightarrow ^{186}\text{Os}$ beta decay (Rumanian) 8-82316
 ^{86}Se , $A=85, 86$, experimental Q_{β} -values 8-93974
 ^{103}Tc , experimental Q_{β} -values 8-93974
 ^{204}Tl , beta-transition, spectral shape, small-order deviation 8-74338

beta-ray spectrometers
see also *beta-ray spectra; electron spectrometers*
 double focusing crossed field electron spin polarimeter, theory, construction, and operation 8-86761
 Ge, hyperpure, β end-point-energy meas. 8-78587
 magnetic, response function correction 8-74532
 magnetic lens, adjustable current-supply stabiliser 8-74528
 multistrip β semicond. detectors for magnetic spectrometers 8-78545
 position sensitive proportional counter for a β -ray spectrom. 8-86732
 short lifetime meas., β -spectrometer, plastic scintillator, effects of light guide and mag. field (Japanese) 8-90016
 Si(Li) detectors, unfolding procedure for slowly varying pulse height spectra of β -particles 8-50430
 Si(Li) electron spectrometer on-line with an automatic irradiation apparatus 8-90014

beta-rays
see also *electrons*
 No entries

beta spectrometers *see* *beta-ray spectrometers*

betatrons
 bremsstrahlung field shaping apparatus for teletherapy 8-57062
 bremsstrahlung radiation, ang. distrib. and penetrating power 8-70657
 electromagnet pulsed power supply 8-82546
 neutron dose levels of 8 MeV linear accelerator and 18 MeV betatron used in radiotherapy (German) 8-69221

betatrons continued
 single-particle dynamics, linear theory of perfect machines 8-78879
 synchrotron radiation formation, role of betatron vibrs. (Russian) 8-50684

Bethe-Salpeter equation
 dressed fermions in Abelian gauge theories 8-82093
 exact three dimens. reduction, off mass shell amplitudes 8-70247
 gauge theory, dressed quark-gluon vertices, instantaneous approx. 8-78091
 Lagrangian bound state formalism, dynamical vacuum instability 8-74146
 massless chromodynamics, vacuum rearrangement 8-70327
 meson bound state eqn. and solutions 8-78101
 meson decay; weak, EM, strong, Bethe-Salpeter model, effective quark mass 8-70336
 meson structure wave functions in relativistic straton model, Bethe-Salpeter eqn. (Chinese) 8-50011
 numerical soln. to spinor Bethe-Salpeter eqn. and Goldstein problem 8-86400
 plasma two-particle bound state, lifetimes and level shifts 8-75265
 positronium, Bethe-Salpeter equation, Coulomb like kernel 8-93831
 scattering states arising from Bethe-Salpeter eqn. 8-54553
 two fermion EM bound state systems, axial and covariant gauges 8-78058
 wave function asymptotic behaviour as relative time $\rightarrow \infty$ (Chinese) 8-82113
 wave function divergence at origin 8-74147

Bethe-Uhlenbeck equations *see* *quantum statistical mechanics*

bevatrons *see* *synchrotrons*

bicrystals
 α - β brass, two-phase bicrystals, plastic deform. and fracture mechanism 8-84898
 α - β brass two-phase bicrystals, activated slip systems during yielding 8-84911
 electron diffraction spots, computer indexing (French) 8-75507
 grain boundary sliding and intergranular fracture 8-75717
 metal, mech. behaviour, continuous theory of dislocations appl. 8-67717
 Al, bicrystal, fatigue crack initiation, crystal boundary effects (Japanese) 8-92328
 Al, cutting of bicrystal to compare mechanism for large crystals and polycrystals (Japanese) 8-60871
 Au bicrystals, interaction of lattice dislocations with grain boundaries, electron microscope obs. 8-51579
 Au, dislocation networks in twin boundaries, TEM obs. 8-51556
 Cu bicrystals, effect of grain boundary on tensile deformation (Japanese) 8-88495
 Cu, cutting of bicrystal to compare mechanism for large crystals and polycrystals (Japanese) 8-60871
 Cu, epitaxial, on (111) Au, periodic arrays of misfit dislocations, electron diffr. 8-51857
 Cu-Ni bimetallic films, dislocation wall form. during interdiffusion, TEM obs. 8-51856
 Fe-Si (3.5 wt.%), cutting of bicrystal to compare mechanism for large crystals and polycrystals (Japanese) 8-60871
 Ge bicrystal cleavage plane, Shubnikov-de Haas oscills. (Russian) 8-64094
 MgO bicrystals, formed by welding single crystals with H_3PO_4 , exam. 8-56796
 NiO, oriented bicrystal growth by floating zone and Verneuil's method (French) 8-92186
 Pd, epitaxial, on (111) Au, periodic arrays of misfit dislocations, electron diffr. 8-51857
 Zn, cutting of bicrystal to compare mechanism for large crystals and polycrystals (Japanese) 8-60871

biexcitons *see* *excitonic molecules*

big-bang theory *see* *cosmology*

bimetallic strips *see* *bimetals*

bimetallic wire *see* *bimetals*

bimetals
 bronze-steel, phase composition and struct. of diffusional interlayer in fusion zone, X-ray analysis 8-56821
 explosively welded, dissipation of US oscillations at boundary layers 8-53124
 explosively welded, US oscillation dissipation at boundary layer 8-53157
 Al/brass/Al bimetal, three layers, formed by cold rolling, exam. of formation of intermetallic phases at interface 8-56658
 Al-Au bimetal thin film interdiffusion zone, intermetallic phase form kinetics, 70-160°C 8-75891
 Cu-Ni bicrystal, misfit dislocation config., moire patterns, interdiffusion effects 8-84110
 Cu-Ni bimetallic films, dislocation wall form. during interdiffusion, TEM obs. 8-51856
 Cu-Ni thin film couples, interfacial reactions, contact resistance meas. 8-63882

binaries (stellar) *see* *binary stars*

binary sequences
 peripheral auditory system, anal., noise appls. 8-80888

binary stars
 $16 M_{\odot}$ supergiant with $1 M_{\odot}$ neutron star companion, double core evolution 8-53980
 2A 0042+323 (3U 0042+32), periodic behaviour rel. to binary nature 8-54089
 A-type central stars of planetary nebulae, radial vel. study 8-81629
 accretion disc inner region model (Russian) 8-69843
 accretion disc interaction with stellar mag. field, plasma diffusion across Alfvén surface 8-93461
 accretion discs (Polish) 8-89175
 adiabatic pulsations of tidally perturbed rotating stars 8-89172
 ADS 8887, photographically unresolved visual binary, parallax and orbit 8-57593
 Am stars in spectroscopic binary systems, evolutionary status, statistical anal. 8-93262
 ξ Andromedae, spectroscopic binary, photometric and spectroscopic obs. (Russian) 8-57588
 λ Andromedae, UV spectrum obs. by International Ultraviolet Explorer 8-96475

binary stars continued

- angular momentum loss from star with rapidly rot. core in close binary system (*Russian*) 8-93196
 V535 Arae, A-type evolved contact system 8-65650
 UX Arietis, Copernicus UV obs. of Lyman α and Mg II emission 8-81651
 γ Arietis, visual binary Ap-system, photometry 8-85950
 ϵ Aurigae, eclipsing binary, astrometric study from Sproul 61-cm refractor plates 8-89219
 ϵ Aurigae, fine analysis of atmosphere of primary F-type supergiant 8-85976
 IU Aurigae, light curve study of early-type close binaries in triple systems 8-89222
 α Aurigae, UV spectrum obs. by International Ultraviolet Explorer 8-96475
 α Aurigae (Capella), intense line emission in soft X-ray spectrum 8-93228
 B-type and Be-type stars, search for binaries 8-57551
 ZZ Bootis, double spectrum eclipsing binary, revised spectrographic and photometric elements 8-61885
 44=1 Bootis, eclipsing binary, variable light curve obs. and implications 8-61887
 TZ Bootis, W Ursae Majoris system, spectroscopic and photoelectric obs. 8-69832
 ξ Cancri, speckle holography meas. of double star 8-93120
 UW Canis Majoris, O-type massive evolved contact system 8-65651
 α Canis Majoris (Sirius), possible orbits for third star 8-93312
 α Canis Majoris (Sirius), search for surrounding nebulosity 8-93242
 RS Canum Venaticorum, quiescent X-ray emission obs. 8-81659
 RS Canum Venaticorum binaries, observational selection and evolution 8-89208
 YZ Cassiopeiae, Fourier analysis of light curves for transit eclipses 8-96506
 AO Cassiopeiae, O-type evolved contact system 8-93302
 cataclysmic binaries, connection as source of accretion disc viscosity 8-93307
 cataclysmic variables, theoretical UVB colours of accretion discs 8-61865
 CD-42¹⁴⁴⁶² (V3885 Sagittarii), dwarf nova in permanent outburst 8-53966
 ER Cephei, contact binary in open cluster NGC 188, BV light curves 8-77580
 U Cephei, eclipsing binary, hot/cool spots obs. in UV light curves 8-57577
 EM Cephei, eclipsing binary, spectroscopic obs. of shell (*Russian*) 8-57587
 EE Cephei, obs. of long period eclipsing binary (*Italian*) 8-93319
 UV Ceti, anomalous flare activity obs. 8-89202
 XY Ceti, light vars. of eclipsing binary with Am spectra 8-93310
 α Ceti (Mira), enhanced activity of B-type component at 1976 light minimum 8-81636
 α Ceti (Mira), rapid light vars. of companion star during 1977 light min. 8-96492
 Z Chamaeleontis, monitoring of southern dwarf nova, 1954-76 period 8-93272
 RS Chamaeleontis, uvby photometry of bright double-lined A-type eclipsing binary 8-69833
 close binaries, distortion effects on struct. 8-57584
 close binary systems, problem of components oblique rot. axes 8-96509
 colliding stellar winds, X-ray emission upper limits 8-65607
 common-proper-motion pairs in South Galactic Cap, identifications 8-73734
 CRL 2104, CRL 2179, late WC stars, 2 to 4 μ m spectrophotometry and circumstellar dust 8-96491
 V1073 Cygni, A-type evolved contact system 8-65650
 MR Cygni, eclipsing binary, photometric elements, period changes 8-61884
 V367 Cygni, eclipsing binary, spectroscopic study 8-53984
 V1016 Cygni, IR spectrum and evidence for cool star 8-93266
 CH Cygni, new active period, model, double system with accretion disc (*Russian*) 8-69813
 V729 Cygni, O-type evolved contact system, masses 8-93309
 32 Cygni, opacity wavelength depend. in atm. of K-type supergiant component 8-73741
 V389 Cygni, peculiar (Ap-type) binary, spectroscopic obs. 8-85975
 9 Cygni, radial. vel. and orbital elements of new spectroscopic binary 8-69826
 Cygnus X-1, new period in X-ray binary system (*German*) 8-81712
 Cygnus X-1, optical and X-ray evidence for 78/39-day period 8-89274
 Cygnus X-1, optical polarisation orbital vars. rel. to binary system inclination 8-54077
 Cygnus X-1, short-term time variability 8-93466
 Cygnus X-1, status report 8-77618
 Cygnus X-2, optical variability upper limits 8-96564
 detached double-lined eclipsing binaries, revised photometric elements 8-61886
 disc accretion by mag. neutron stars, model 8-93294
 double star measures at Lick Observatory, Mount Hamilton, California 8-85979
 double stars, micrometer obs. 8-57582
 double stars, photographic measures 8-57581
 double stars, rectilinear trajectory errors (*French*) 8-89223
 AI Draconis, period and spectroscopic orbit of eclipsing binary 8-89221
 dwarf novae, EUV obs. from Apollo-Soyuz Test Project 8-93252
 dwarf novae, hard X-ray emission from 47 objects 8-93275
 early-type contact binaries, uvby beta photometry 8-53981
 eclipsing, Fourier anal. of light curves 8-69830
 eclipsing and spectroscopic binaries, period distrib. 8-69829
 eclipsing binaries, extragalactic distance indicators 8-93396
 eclipsing binaries, with periods <5 days, period-mass ratio relations 8-57585
 eclipsing binaries in ω Centauri, search for new variables 8-61895
 eclipsing double-lined binaries, photometric elements of 14 detached systems 8-69834
 eclipsing variable stars, Fourier anal. of light curves 8-93311
 eclipsing variables, Fourier anal. of light curves, photometric perturbs. 8-96507

binary stars continued

- eclipsing variables, light curve Fourier analysis, eclipse parameters, geometric determinacy 8-96503
 α Equulei, radial vel. vars. from microphotometer scans 8-77581
 evolution of close double stars 8-73733
 Feige 24, spectroscopy of EUV source, binary orbit, mass 8-93218
 fission in damped rotating polytropes 8-93209
 formation, angular momentum considerations 8-69781
 Fourier analysis of light curves of eclipsing binaries for transit eclipses 8-96506
 G24-16, parallax and astrometric orbit from Sproul plate series 8-53983
 galactic bulge X-ray sources, models, binary systems 8-81706
 gamma-ray pulsars without radio emission in binary systems 8-53975
 U Geminorum, magnitude estimates for 1978 Oct. 8-96493
 YY Geminorum, VRI photoelectric photometry and absolute dimensions 8-69827
 globular cluster X-ray source, evolution of 100 M_{\odot} black hole in binary 8-61932
 gravitational collapse of rot. gas cloud, binary systems form. 8-65494
 gravitational waves interaction, tidal reson. 8-93089
 RS Gruis, dwarf Cepheid in binary system 8-77559
 hard binaries in large N-body systems, two-body tidal dissipation effects 8-93329
 HD 135774-5, radial vel. and orbital elements of new spectroscopic binary 8-69826
 HD 147508, spectroscopic binary, orbit from photoelectric radial vels. 8-69839
 HD 153919, HDE 226868, X-ray sources, IUE UV spectrum obs. 8-96569
 HD 153919 (3U 1700-37), binary X-ray source, radial vel. data in blue spectral region 8-61888
 HD 153919 (4U 1700-37), optical oscills. obs. 8-96572
 HD 165052, O-type binary, spectroscopic obs., masses and radii 8-93308
 HD 167771, O-type binary, spectroscopic obs., masses and radii 8-93308
 HD 17576, UV subdwarf companion discovery from uvby β photometry 8-96479
 HD 181330, spectroscopic binary, orbit from photoelectric radial vels. 8-93320
 HD 226868 (Cygnus X-1), periodicity in optical light curve during X-ray flare 8-81652
 HD 47129 (Plaskett's star), massive O-star binary system, variable linear polarisation obs. 8-53989
 HD 47732, double-lined binary, spectroscopic orbit 8-57574
 HD 47732, young close binary in NGC 2264, photometry and struct. 8-57575
 HD 67084, new southern spectroscopic binary, radial vels., orbital elements 8-57592
 HD 67198, new southern spectroscopic binary, radial vels. 8-57592
 HD 698, massive spectroscopic binary, spectral obs., evolutionary state, mass loss 8-57590
 HD 77581 (Vela X-1), X-ray obs. and UVB photometry 8-65722
 HD 9996, Ap star, spectroscopic obs. 8-77558
 HDE 245770 (A0535+26), spectroscopy and orbital periods 8-93306
 Hercules X-1, high-energy X-ray spectrum 8-93473
 HZ Herculis, abnormal N III emission lines in 1978 Aug. spectrum 8-81661
 HZ Herculis, Bowen fluorescence mechanism evidence 8-53985
 HZ Herculis, eclipsing binary, light curve interpretation rel. to disclike envelope struct. 8-65658
 u Herculis, eclipsing binary, photometric elements, period changes 8-61884
 AD Herculis, eclipsing binary, spectroscopic obs. and orbital elements 8-73738
 α Herculis, location of α^2 Herculis along line of sight 8-73739
 AM Herculis, narrow-band photoelectric obs. (*Russian*) 8-77565
 HZ Herculis, nonperiodic optical flickering obs. 8-53988
 AM Herculis, photometric and polarimetric obs. 8-65657
 DQ Herculis, photometric study of light curve 71 s oscill. 8-93259
 HZ Herculis, refl. effect turn-off (*Russian*) 8-69840
 AM Herculis, spectroscopic obs., H lines and He II 4686 Å line intensities 8-57589
 AM Herculis, UVBRI light curves 8-85972
 AM Herculis, X-ray binary, optical variability 8-53952
 AM Herculis (3U 1809+50), single accretion column model 8-57578
 HZ Herculis (Hercules X-1), IUE UV spectrum obs. 8-96569
 HZ Herculis (Hercules X-1), optical pulsation theoretical calcs. 8-57580
 HZ Herculis (Hercules X-1), orbital precession 8-65718
 HR 1099, optical linear polarisation meas. 8-53958
 HR 1099, quiescent X-ray emission obs. from RS Canum Venaticorum star 8-81659
 HR 1099, UV spectrum obs. by International Ultraviolet Explorer 8-96475
 HR 1099, X-ray outburst obs. from RS Canum Venaticorum star 8-81658
 HR 1099 (V711 Tauri), Copernicus UV obs. of Lyman α and Mg II emission 8-81651
 HR 6902, radial vel. and orbital elements of new spectroscopic binary 8-69826
 HR 976, Am-type star, soft X-ray source obs. 8-81634
 χ^2 Hydrae, eclipsing binary, four-colour photometry, orbital elements, dimensions and He abundance 8-65653
 EZ Hydrae, eclipsing binary, photometric obs. and primary min. ephemeris 8-73737
 AI Hydrae, light curves and photometric elements of eclipsing binary 8-65652
 TT Hydrae, UVB photometry, improved light elements 8-69837
 AI Hydrae, uvby photometric obs. of eclipsing F-type binary 8-69835
 5 Lacertae, obs. of second max. for long period spectroscopic binary 8-57591
 late B-type stars, duplicity characts. 8-57547
 LB 3459, short period eclipsing binary system containing two O-type subdwarfs, uvby photometry 8-53987
 libration in close binary systems, effects on light curves 8-57579
 LMC X-4, identification with eclipsing binary system, review (*German*) 8-81713
 LSI+61³⁰³, counterpart of γ -ray source CG 135+1 and highly variable radio source 8-54095

binary stars continued

- β Lyrae, H emission profiles rel. to pattern of gaseous flow in system 8-57576
- MV Lyrae, polarisation and spectrum obs., polar class candidate (*Russian*) 8-93322
- magnetic binaries, charged particle motion 8-69828
- metal-poor binaries, He abundance determ. 8-81660
- VV Monocerotis, eclipsing binary, orbital elements and dimensions (*French*) 8-89225
- nearby stellar systems, ranking method for exploration 8-81522
- neutron star, accreting, magnetopause struct. 8-65647
- NGC 2281, open cluster, UVB photometry, binary star freq., luminosity function 8-81663
- novae, low-temp. photonuclear p-nuclei nucleosynthesis in degenerate H burning zones 8-57540
- O-type binary and stellar wind search 8-89197
- OBN, OBC stars, short period binaries frequency 8-53951
- open clusters, dynamics of close binaries and single stars (*Russian*) 8-61890
- Y Ophiuchi, anomalous Cepheid, evidence for duplicity 8-53990
- orbital elements for 15 visual binaries 8-85969
- orbital solutions with unseen companions, measured coordinates interpretation 8-93313
- χ^1 Orionis, new solar-type astrometric binary, parallax and orbital elements 8-73740
- λ Orionis A, far UV flux, emission line obs. of surrounding H II region 8-93303
- EQ Pegasi (BD+19°5116), flare active binary system 8-61868
- X Persei, distance determ., 3U 0352+30 optical counterpart (*Chinese*) 8-69836
- 12 Persei, masses and luminosities from speckle interferometric obs. 8-93305
- AG Persei, two-colour photometry of eclipsing binary system, apsidal motion 8-96504
- 20 Persei, visual binary, radial vel. obs. 8-73736
- X Persei (2U 0352+30), spectral line variations (*Russian*) 8-65655
- β Persei (Algol), detection of B component, mass determ. 8-65654
- β Persei (Algol), light curve at 10 μ m near secondary min. 8-93315
- β Persei (Algol) type semi-detached binaries, rotational vels. 8-89220
- GK Persei (Nova 1901), visual magnitude estimate for 1978 July 8-69807
- AE Phoenicis, W Ursae Majoris type system, orbit 8-85970
- RZ Piscium, UVB photometry, light minima (*Russian*) 8-93323
- planet formation, Goldreich-Ward planetesimal accretion 8-61883
- polarisation by Thomson scatt. in optically thin envelopes, appl. to binary inclinations determ. 8-81655
- PSR 1913+16, astrometry and photometry of stars in vicinity of binary pulsar 8-93219
- PSR 1913+16, optical candidate discovery, position, magnitude 8-69819
- pulsar binary origin and asymmetric supernova explosions 8-69816
- pulsar/supernova remnant associations, possible origin in close binary systems 8-85965
- pulsars, radio and X-ray, review 8-69820
- pulsars, relation between speed ups and variation of gravitational constant 8-73728
- pulsating binary X-ray sources, periodic timing residual 8-65718
- AU Puppis, A-type evolved contact system 8-65650
- V Puppis, light curve study of early-type close binaries in triple systems 8-89222
- VV Puppis, proper motion meas., distance and luminosity 8-96510
- radiation pressure force influence on critical surfaces 8-96505
- UU Sagittae, eclipsing binary, central star of Abell 63 planetary nebula 8-93304
- HM Sagittae, IR spectrum and evidence for cool star 8-93266
- WZ Sagittae, orbital parameter determ. for recurrent nova 8-93317
- WZ Sagittae, recurrent nova, physical parameters, present state, past and future evolution 8-85948
- U Sagittae, theoretical light curve of contact system 8-77578
- v Sagittarii, absorpt. lines identification as Fe II high level transitions 8-93316
- α Scorpii, location of α^2 Scorpii along line of sight 8-73739
- V861 Scorpii, near IR meas. rel. to orbital phase 8-93324
- V861 Scorpii, X-ray emission from unseen companion 8-89226
- V861 Scorpii (HD 152667), eclipsing binary, identification with X-ray source (OAO 1653-40) 8-69838
- V861 Scorpii (HD 152677), H α emission features vars. 8-77579
- CV Serpentis, BVRI photoelectric obs., but no eclipse 8-85971
- 41 Sextantis A, new metallic line spectroscopic binary 8-53982
- short period, X- and γ -ray bursts from mag. reconnection 8-81654
- SMC X-2, Be-type optical candidate 8-77619
- solar companion star effects on orbits of comets 8-81567
- southern spectroscopic and eclipsing binaries, cooperative obs. feasibility 8-69681
- southern visual binaries, orbits and masses 8-96502
- speckle interferometry at 5200 Å for 30 objects 8-65656
- speckle interferometry meas. 8-85973
- speckle interferometry of binary stars, computer simulations in photon-counting mode 8-53836
- spectroscopic binaries, test of circularity of orbits 8-93321
- static two-body problem and attraction law, post Newtonian approx. 8-93574
- steady disc accretion, ang. momentum transfer 8-65609
- Sun, reality of companion star questioned 8-57475
- V471 Tauri, BV photometry of white dwarf eclipsing binary, light curve vars. 8-96508
- ξ Tauri, near UV spectrum of shell star 8-81653
- tidally distorted stars, Roche coords. appl. to small oscils. 8-77577
- 4U 0115+63, orbital elements and nature of hard X-ray transients 8-93470
- 4U 0115+63, pulsating X-ray transient, optical counterpart identification and orbital period 8-61939
- 4U 0115+63, transient X-ray binary, absorpt. feature discovery at 20 keV 8-69909
- 4U 0115+63, X-ray transient, position and pulse profile 8-93467
- 3U 1223-62, binary X-ray pulsar, Ariel V obs. 8-96566
- 4U 1538-52, binary X-ray pulsar, early B-type supergiant as counterpart 8-93472
- 4U 1538-52, eclipsing binary pulsating system, position meas. by HEAO-1 8-96570
- 4U 1700-37, binary X-ray source, X-ray position 8-54094

binary stars continued

- 3U 1700-37, further Copernicus X-ray obs. 8-96568
- 4U 1735-44 (MXB 1735-44), optical identification and similarity to (Scorpius X-1) 8-93468
- unresolved binary stars, epochs of speckle interferometric obs., (1975-77) 8-73735
- UX Ursae Majoris, anomalous 1977 period change for nova-like eclipsing binary 8-85956
- AN Ursae Majoris, polarisation of AM Herculis-type nova-like binary 8-85958
- AW Ursae Majoris, theoretical light curve of contact system 8-77578
- W Ursae Majoris, vars. of period and light curve of eclipsing binary (*Italian*) 8-93318
- V 78 in ω Centauri, cluster membership determ. 8-73743
- visual binaries, orbital elements for 12 systems (*Russian*) 8-69842
- visual binaries, speckle interferometry with 1 m telescope 8-69831
- visual binary star orbit, computation method for any eccentricity 8-85974
- visual double stars, astrometric meas. at Nice (*French*) 8-89224
- visual double stars, micrometer obs., (1975 to 1977) 8-89218
- visual double stars, orbits determ. (*French*) 8-53986
- visual double stars, relative motion meas. in 17 pairs (*French*) 8-57586
- visual double stars measured at Las Campanas Observatory, Chile 8-85978
- white dwarf with mass accretion, H shell flashes rel. to symbiotic stars vars. 8-57550
- Wolf-Rayet stars in SMC, spectral classification 8-73716
- X-ray binary systems, K-fluorescence lines in spectra 8-93456
- X-ray binary systems, massive, gas streams and accretion discs 8-93464
- X-ray binary systems, models, X-ray transfer, Monte Carlo study 8-93463
- X-ray burst sources, properties, binary systems (*Russian*) 8-93477
- X-ray sources, binarity detect. via Doppler effect (*Russian*) 8-77623
- X-ray sources, review of current knowledge in 0.5 to 10 keV range 8-69915
- 20,986, new unresolved astrometric binary 8-57594
- He white dwarfs rejuvenation by mass accretion 8-73712
- HgMn stars, incidence among late B-type stars rel. to duplicity and rot. 8-89199

binding energy

- see also lattice energy; nuclear binding energy; nuclear forces
- AB $_2$ X $_6$, crystalline compounds, computation of internal energy 8-75623
- actinides, expt. and theoret. binding and transition energies, review 8-50497
- alkali halide, binding energies of positron to F and F' colour centres 8-87667
- alkali halide, dipolons, graphical method for binding energy determ. 8-59805
- alkali halide dibenzo-18-crown-6 complex, ESCA, binding energy 8-50584
- alkali halide molecular clusters, equilib. geom., form. energy and vib. spectrum 8-55269
- alkali halides, binding energies of vacancy pairs 8-51533
- alkali halides, three body interaction effects on cohesive props. 8-83770
- alkali metal, model potential calculation of binding energy and compressibility 8-91632
- atom, s-electron binding energy regularities in 1 s^m configs. 8-62731
- atomic chemisorption, chemical trends, core-hole relax. effects, jellium model 8-76909
- atomic electron binding energies calcs. 8-86768
- core hole relaxation energies 8-80439
- covalent semiconductor, electronic and struct. energies calc. 8-59874
- diatomic bonding energy, changes due to Van der Waals interactions with other atoms 8-95012
- dielectric medium, impurity dispersion self energy calcs. 8-52536
- education, bubble cohesion in foam, binding energy calc. 8-61978
- electron binding energies reference level problem in photoelectron spectra of solids and adsorbates 8-63936
- electrostatic potential predictions, basis set depend. 8-74786
- ESCA studies of Ga, As, GaAs, Ga $_2$ O $_3$, As $_2$ O $_3$ and As $_2$ O $_5$ 8-92171
- exciton to neutral acceptor, calcs. using atomic-like variable wave function 8-79937
- exciton-ionised donor complex, binding energy, effective electron-hole interaction pot. 8-67949
- formaldehyde, orbital contribs. to relax. energies accompanying core ionis., Δ SCF HF calcs. 8-82642
- GaP, reevaluation of bandgap and free exciton binding energy 8-60061
- hydrocarbons, saturated and unsaturated, ionisation spectral intensities, correlation effects 8-90234
- ionic, rel. to nonrelativistic neutral atom 8-90054
- lower bounds to ground state eigenvalues, Pade approximants 8-49722
- metal, inhomogeneous electron system, nonlocal exchange and correlation 8-56097
- metal, van der Waals energy estimation 8-91634
- metal-H system, bond energy calcs. 8-51940
- metals, close packed, relationship between cohesive energy, and allotropic transformation temp., exam. 8-52802
- molecular electron binding energies calcs. 8-86768
- monohalobenzenes, inner shell excitation and ionis., electron energy loss spectra, XPS, assignments 8-62934
- muonic atom, heavy, 1s $_{1/2}$ levels, self-energy corrections 8-55262
- noble metals, pseudopot. exam. of electronic props. 8-51960
- organometallics, group V, XPS spectra interpretation, pot. model 8-50587
- positronium oxidation react. in aq. soln., positron hydration energy 8-61039
- quasimolecules, superheavy, binding energy of inner-shell electrons, monopole approx. 8-62949
- rare earths, excitation energies for 4f electrons, relativistic calc. 8-72117
- semiconductor multiple bound excitons, binding energy calc. 8-51900
- transition metal, 3d and 4d, local density theory, mech. and mag. props. evaluation 8-91630

binding energy continued

- transition metal, BCC, phonon dispersion curves and elastic, calc. using cohesive energy 8-59885
- transition metal, chemisorpt. of H, Hubbard-type surface mol. model binding energy calcs. 8-71990
- transition metal clusters, cohesive energy and level statistics 8-95267
- transition metal hydrides, electronic struct., heat of formation, single particle lifetimes, Dingle temp. meas. 8-51923
- transition metal surface (adsorbate), intermediate UPS/XPS synchrotron radiation study 8-52633
- transition metals, electronic structure and ordering of sp defects 8-91639
- Al, elastic properties (*Russian*) 8-56678
- alkali halides, interatomic forces, Born model anal. on US data 8-55833
- As, X-ray absorption edge, chem. shift, electron binding energy in compounds 8-62822
- Au organometallics, ESCA core binding energies 8-50586
- Au, pseudopotential, fitted to elastic data 8-75705
- BN, cubic, ab initio SCF calcs., band struct., ground state props. 8-51891
- CO, orbital contribs. to relax. energies accompanying core ionis., Δ SCF HF calcs. 8-82642
- COH⁺, orbital contribs. to relax. energies accompanying core ionis., Δ SCF HF calcs. 8-82642
- Co(ethylenediamine)₃(ClO₄)₃, ESCA chem. shift meas., internal standards 8-50585
- Cu, adsorption of CO, angle-resolved UPS and adsorbate induced struct. 8-71983
- Cu molybdates, valence band X-ray induced Auger spectra and XPS 8-80813
- Cu oxides, valence band X-ray induced Auger spectra and XPS 8-80813
- Cu, X-ray absorption edge, chem. shift, electron binding energy in compounds 8-62822
- CuH, electronic struct., heat of formation, single particle lifetimes, Dingle temp. meas. 8-51923
- Fe complexes, Mossbauer isomer shift and core electron binding energies of Fe 8-82620
- Fe, ferromagnetic, cluster method, environmental effects 8-95405
- GaAs, excitons, diamond like semiconductor, variational calculation of binding energies 8-79938
- GaP, shallow impurity states, free exciton binding energy 8-79960
- n-Ge, Mott transition, dielec. enhancement and conduction electron screening, donor binding energy 8-72073
- H atom, proton spreading in strong mag. field 8-70769
- H₂, metallic, cohesive energy determ. 8-91301
- p-H₂, solid, anisotropic contribs. to ground state props. 8-83914
- H₂⁺, in mag. field, LCAO calcs. 8-82628
- H₂⁺, ground and excited state pot. energy surfaces and geom. struct., SCF and CI calcs. 8-78769
- HCN, vibr. fine struct. accompanying core ionis., STO calcs. 8-62844
- HCO⁺, orbital contribs. to relax. energies accompanying core ionis., Δ SCF HF calcs. 8-82642
- ³He, superfluid, response theory calcs., corrections to mag. susceptibility, binding energies, density 8-67883
- ⁴He trimer and tetramer, binding energy, appl. of ATMS 8-94349
- HgXe, fluoresc. spectra, pot. curves and binding energy 8-66581
- K surface, clean and O₂-exposed, X-ray and UV photoelectron spectra 8-52636
- KNa₂, binding energy and lattice const., nonparametric calc. (*Russian*) 8-51462
- Li₃, geom. struct. and binding energy, diatomic-in-molecules 8-74785
- Li₄, geom. struct. and binding energy, diatomic-in-molecules 8-74785
- LiF, selective adsorption of ³He and ⁴He, atomic beam scatt. meas., binding energies 8-63935
- ^{6,7}LiH(D), cryst., cohesive energy, force const., lattice freq., Debye temp., Gruneisen parameters, calc. 8-91293
- MnS(Se)(Te), core level binding energies and valence band spectra, XPS meas. 8-80455
- Mo, X-ray absorption edge, chem. shift, electron binding energy in compounds 8-62822
- Mo-C dilute alloy defect cluster nucleation and growth under 1250 keV electron microscope (*Japanese*) 8-87663
- Mo(110) and (100) surface, surface reson. states and adsorption of 4d atoms 8-71982
- NO, adsorbed on Cu, species identification, struct., dissociation, chemisorption, desorption, UV photoelectron spectroscopy 8-52635
- N₂P₂Cl₆, ionisation energy and electronic struct., UV photoelectron spectra and X α calcs. 8-94281
- Na particle, consisting of ats., metallic Na, model, electronic levels 8-50673
- NaF, ab-initio calc. of cohesion energy, compressibility and density 8-71782
- NaF, selective adsorption of ³He and ⁴He, atomic beam scatt. meas., binding energies 8-63935
- NaI, Xe⁺ ion bombard., sputtering processes, time of flight meas. 8-88392
- Na(1s), X-ray photoelectron spectrum, binding energy, at. compared with metal 8-70800
- Ni (100), adsorbed chalcogen, structure, force consts., binding energies and photoemission, importance of final state multiplet splitting 8-71966
- Pb, elastic properties (*Russian*) 8-56678
- Pb, X-ray absorption edge, chem. shift, electron binding energy in compounds 8-62822
- Pb⁺+Z (42<Z<92), 1s MO excitation probability and binding energy, X-ray coincidence 8-94316
- Pd, metal cluster, calculated structural stability 8-95268
- PdH, electronic struct., heat of formation, single particle lifetimes, Dingle temp. meas. 8-51923
- RbCl(Br)(I), Xe⁺ ion bombard., sputtering processes, time of flight meas. 8-88392
- Rh (111), chemisorbed and condensed CO, energy level shifts 8-87865
- (SN)_x, film, brominated, XPS, electronic struct. 8-72678
- S₂N₄, film, brominated, XPS, electronic struct. 8-72678
- Si (111) surface, clean, ESCA obs., Ni(Au) surface impurities 8-52640
- Si, density functional theory, energy calcs., core effects 8-72106

binding energy continued

- n-Si, Mott transition, dielec. enhancement and conduction electron screening, donor binding energy 8-72073
- Si, van der Waals electron correlation energy 8-95013
- Si⁴⁺+He, q=2-11, K-shell fluoresc. yields, charge-state depend. 8-55231
- ZnO, optical gain and induced absorption from excitonic mols. 8-84609
- ZnSe, single cryst., electron-hole drops, boundary luminesc. (*Russian*) 8-80412

Bingham plastics and solids see *rheology***bioacoustics**

- see also *biological effects of acoustic radiation; biomedical ultrasonics; hearing; sonar*
- Acoustical Soc. Amer. 96th meeting, Hawaii, 1978 Nov. 8-90545
- anaesthesia during tooth hard tissue operations, BN-1 apparatus 8-85350
- Atlantic bottlenose dolphin, echolocation signal propag. 8-88721
- bat, mustache, aural representation in Doppler-shifted-CF-processing area of auditory cortex 8-80892
- bovine blood vessel walls US vel. meas. 8-85333
- echo-locating animal, neurocorrelometer model 8-96059
- echolocation, bat, accuracy of meas. of target angular coords. using equi-signal zone 8-77071
- green tree frog, female discrimination of intermediate sounds in synthetic call continuum 8-69109
- haemoglobin, US attenuation and dispersion, Kramers-Kronig relative 8-83135
- heart vibration quantitative characterisation by multipolar acoustic heart model, minicomputer method 8-85429
- human skull, acoustic losses and vel. meas., rel. to diagnostic imaging 8-69159
- lung, distributed response of complex branching duct networks 8-57027
- lung, modal struct. of asymmetrically branching duct networks 8-57028
- mammalian testes, freq. depend. of US absorpt. coeff. 8-61213
- mammalian tissues, compilation of empirical US props. 8-88727
- L-serine, in aqueous solns., US spectra using automatic recording spectrometer 8-75735
- sound analysis, reversible computer method adapted to bioacoustical expts. 8-57137

biocontrolsee also *biocybernetics*

- adenylate cyclase regulation, depend. on sugar transport system, review 8-69031
- arm movements controlled by peripheral feedback, in humans, simulation 8-80891
- arterial pressure-flow relationships in anaesthetised dog 8-69120
- arterial system least energy regulation 8-53434
- arterial system math. model, press.-flow relationships 8-53435
- biochemical multiple-loop negative feedback control networks, oscills., periodic metabolic systems 8-85285
- body temperature humidification, effect on patient thermal regulation 8-85295
- breathing control hierarchical goal-seeking model description 8-80899
- breathing control hierarchical goal-seeking model performance 8-80900
- cardiac output control mechanism modelling (*Japanese*) 8-69133
- cell growth regulation, effects of cell density and metabolite flux on dynamics 8-85296
- cell growth regulation, effects of cell density and metabolite flux on dynamics 8-88701
- cell permeability polarity and control by phytochrome, red light irradiation 8-77025
- drug-carrying microspheres, intravascular mag. guidance 8-73188
- electromyogram envelope spectral anal., muscular control study 8-92750
- eye, error-correcting mechanisms in large saccades 8-61175
- eye, pursuit movements of disappearing moving target 8-61174
- eye movements while reading, annotated bibliography 8-53394
- eye torsional movements, rapid phase, in humans 8-69045
- heart rate variation during ergometric test, computer interpretation 8-85430
- motor unit recruitment and firing freq. control in elec. stimulated muscles of cat 8-81092
- muscle, myosin regulated, changes in crossbridge attachment 8-53361
- muscle, striated, reversible loss of Ca control of tension assoc. with removal of regulatory light chains, scallop 8-53360
- oculomotor control system, expt. set-up for clinical investigation, visual, acoustic, vestibular stimulations 8-80990
- peripheral polymorphonuclear leucocyte system model, humans 8-56956
- pupil noise amplitude control, interaction of sensory and motor mechanisms 8-64998
- respiratory airflow pattern modelling by optimisation criteria 8-80898
- respiratory control in cats, interactions between central and vagal mechanisms 8-53436
- respiratory control system, time series cluster anal. 8-56959
- respiratory control system simulation, state-of-the-art 8-53441
- rotation of man in weightlessness, biomechanical models 8-96106
- sensorimotor control and learning model 8-69033
- skeletal muscle general myocybernetic control model 8-53385
- trans epithelial ion transport endogenous regulation, implications of ouabain-like activity in toad skin 8-73147

biocybernetics

- see also *artificial intelligence; brain models; man-machine systems; neural nets*
- associative information processing structure 8-85300
- average evoked potentials, a posteriori Wiener filtering theory and practice 8-96038
- bladder smooth muscle impulse propag., math. anal. (*Japanese*) 8-53359
- cardiac output control mechanism modelling (*Japanese*) 8-69133
- cell kinetic parameters estimation from flow microfluorimetry 8-73143
- cell population auto-activation, math. model 8-77017
- comparmental analysis in biology, medicine and ecology, mathematical foundations 8-68978

biocybernetics continued

- compartmental systems, multi-input and multi-output, controllability, observability and structural identifiability 8-76978
- compartments, stochastic theory, general time-depend. reversible systems 8-64916
- diffused substance kinetics in biological systems 8-53312
- dissipative systems, dynamical field theory, hierarchical struct. of field thermodynamics 8-73132
- EEG alpha and non-alpha intervals alternation, queueing theory model 8-96040
- excitable medium diffusion discrete models and spatial patterns 8-93629
- excitable medium model with existence of several stable pulses of different duration 8-77036
- genetic systems, dynamics of neutral mutation 8-86220
- human brain functions rel. to foundations of physics, science and technology 8-73823
- interdisciplinary aspects and problems 8-53553
- mathematical biology meeting, Philadelphia, USA, (Aug. 1976) 8-53311
- monaural intensity processing, nonlinear-algebraic approach 8-57012
- motoneurone cross-correlated firing patterns, recurrent inhibition effects 8-80861
- motoneurones excited by phasic muscle stretches, discharge pattern shaping, recurrent inhibitory feedback effects 8-85303
- muscle, striated, analytical soln. to isometric mechanogram of Hill's model 8-73168
- renal medulla single loop solute cycling model, transient behaviour 8-73167
- robots and manipulators, symposium, Warsaw (Sept., 1976) 8-53574
- sensorimotor control and learning model 8-69033
- skeletal muscle general myocybernetic control model 8-53385
- systems theory (*Japanese*) 8-73134

biodiffusion

- cell division control by tension or diffusion 8-64962
- haemoglobin, human and *Lumbricus terrestris*, conc. depend. of self-diffusion 8-68984
- ionic channels in excitable membranes, current problems and biophysical approaches 8-53369
- leaf CO₂ absorption and diffusion, sun vs. shade leaves 8-80850
- lecithin-cholesterol interaction, effect of lecithin struct. 8-64922
- lipid bilayer diffusion transport modelled by dimeric β -cyclodextrin complexes, cryst. struct. anal. 8-80838
- lipid-water smectic phase, water and thermal diffusivity, light scatt. meas. 8-96031
- membrane and near-membrane transport processes, effect of volumetric charges 8-53366
- neurones of large horse-leech, electrophysiological characts. rel. to intracellular Na⁺ conc. 8-53374
- periodic conversions in biological system solns., optical mixing method obs. 8-96029
- stratum corneum of rat, surfactant diffusion and sorption phenomena, model for human skin 8-77007
- water diffusion meas. by pulsed gradient NMR, cell struct. size determ. 8-77159
- K⁺ ion flux through membrane channels, nerve impulses, random walk anal. 8-77045

bioelectric phenomena

see also *bioelectric potentials*; *biomagnetism*

- amygdaloid kindling phenomenon extended first approx. model 8-53378
- atrial trabecula membrane, frog, accommodation, repeat responses and anode-breaking excitation 8-64956
- auditory cortex of moustache bat, aural representation in Doppler-shifted-CF-processing area 8-80892
- axon Na conductance and Ca transport, squid, mol. model 8-85305
- barbiturate-induced slow outward currents in *Aplysia* neurones 8-80866
- bilayer membrane, galvano-static regime of non-steady process 8-64963
- biomembranes, proton transport, mol. mechanisms 8-96035
- biopolymer negative resistance, rel. to living cell props. 8-64923
- bone, piezoelectric effect on exposure to US, effect of sample rot. 8-80913
- brain impedograph, computerised 8-77139
- cell electric circuit model, alternating signal interaction 8-77011
- cell electric circuit model, alternating signal interaction 8-77012
- cell-cell junction membrane form., quantum jumps of cond. 8-73145
- charge transfer in thin membranes, discrete models, nonsteady state at high polarising voltages 8-69023
- charged disk interactions in various dielectric media, biological cell modelling 8-66706
- chitin, in lobster shell and apodeme, piezoelec. rel. to remodelling 8-64929
- chlorophyll a film, charge injection and storage 8-53317
- chlorophyll-a, microcryst., trapped-electron doping in photovoltaic sandwich cells 8-53334
- chlorophyll-acceptor and chlorophyll+protein-acceptor lamellar systems, steady photocond. 8-53328
- chloroplasts, photoinduced dielectric const. shift (*French*) 8-61147
- chromaffin granule electrophoretic mobility meas. by light scatt., effect of Ca²⁺ and Mg²⁺ 8-53357
- cochlear nucleus neurone response, model of phase struct. of binaural stimulus 8-80887
- conductance fluctuations in cultured spinal neurones induced by γ -aminobutyric acid 8-80867
- cortical periodic complex cells, cat, spatial freq. selectivity 8-69057
- digitalis inotropy rel. to enhanced slow inward Ca current 8-61155
- EEG, nonstationary, anal. by approx. canonical expansion method 8-53555
- EEG alpha and non-alpha intervals alternation, queueing theory model 8-96040
- electrical contact generation by tattooing C into skin tissue 8-77122
- electrocutaneous stimulation, energy threshold meas. and channel capacity estimation (*Japanese*) 8-53573
- electromotor system of Torpedo, as model cholinergic system 8-53388
- embryonic skeletal muscle differentiation, electrophysiological and biochem. membrane props. 8-53363
- excitable cell model, numerical method 8-53376

bioelectric phenomena continued

- excitable fibre, steady speeds of spread of stable and unstable impulses, depend. on membrane ionic currents 8-53382
- excitable medium model with existence of several stable pulses of different duration 8-77036
- excitable medium self-sustained activity, role of inhomogeneity 8-64968
- expansion-contraction behaviour in sea pen, control by conduction systems 8-53387
- file clam mantle edge mechanical and chemical sensitivity 8-53429
- gastrointestinal electrical rhythm freq. estimation using autoregressive modelling 8-80855
- gating charge immobilisation by inactivation-simulating substance 8-61154
- gramicidin A ion channel kinetic behaviour, electrostatic calcs. 8-53368
- ion channel, energy and pot. profiles and interactions between ions 8-53367
- ionic channel formation in living cell membrane, microelectrode obs. 8-53372
- ionic channels in excitable membranes, current problems and biophysical approaches 8-53369
- lateral geniculate nucleus, cat, electrophysiological classification of X- and Y-cells 8-64996
- light response and kinetics in *Aplysia* giant neuron 8-53381
- lipid bilayer, 1 MHz US effects on cond. and capacitance 8-77082
- lipid bilayer electrical strength fall after UV irradiat. 8-69002
- lipid bilayer gramicidin A channel cation flux interaction 8-56957
- lipid bilayer membrane, melting point rel. to electrostatic field 8-92602
- lipid bilayers, Ca²⁺ transport system of rat liver mitochondria 8-64966
- living tissue electrical excitation theory development (*French*) 8-88703
- magnetoencephalogram genesis mechanisms 8-53432
- membrane and near-membrane transport processes, effect of volumetric charges 8-53366
- membrane dynamic equation solving, practical algorithm 8-77038
- motoneurone transmitter output rel. to muscle fibre growth, lobster 8-64974
- motor conduction velocity and H-reflex in infancy and childhood 8-61164
- motor unit recruitment and firing freq. control in elec. stimulated muscles of cat 8-81092
- muscle, cat tibialis posterior, motor units, neuro-mechanical props., speed-force relations 8-80856
- muscle, skeletal, contraction time in normal children 8-61163
- muscle, smooth, intestinal cell, voltage clamp studies of hyperpolarising inactivation 8-80847
- muscles, smooth, of elastic arteries, biophys. props. 8-69011
- myenteric plexus, mediation of slow synaptic excitation by substance P 8-73153
- myocardium contraction amplitude depend. on freq. of elec. stimulation, frog 8-77027
- myotubes, human, cultured, acetylcholine-induced conductance fluctuations 8-61157
- nematode oesophagus pumping mechanism 8-69121
- nerve excitability, interactions between intrinsic membrane protein and elec. field 8-53377
- nerve excitable membrane, EM wave effect on surface charge density 8-85334
- nerve-muscle anisotropic syncytia, spread of flat front of excitation 8-53383
- nerve-muscle anisotropic syncytia elec. props., steady form of excitation front 8-69037
- nervous system microcircuits involving dendrites 8-53390
- neuromuscular blockade monitoring device, twitch box 8-77132
- neuromuscular frequency-depend. block and temp.-induced seizure in ts mutant of *Drosophila* 8-56963
- neuromuscular junction, snake, synaptic channel gating differences at twitch and slow junctions 8-80868
- neuron model, ICs, teaching aid 8-85301
- neuron populations as information processing system, stochastic properties 8-80860
- neurone Ca conduction units, *Helix aspersa* 8-77041
- neurone local hormonal communication, *Aplysia* 8-69040
- neurones A and B of mollusc, effect of acetylcholine chloride and choline chloride on resting pot. and membrane resist. 8-53375
- pain mechanisms, neural network model 8-85307
- ray, Black Sea, electric organ discharge structure 8-64969
- receptive field types in lateral geniculate body and functional model 8-69046
- retardation currents in excitable membranes and models of flicker noise 8-92618
- retina, toad, evidence for passive electrotonic interactions in red rods 8-92627
- retina of *Limulus*, spatially synchronised oscillatory response theory 8-73158
- retinal ganglion cell of cat, refractoriness in maintained discharge 8-64991
- retinal responsivity compression, V-log I functions and increment thresholds 8-61181
- rod outer segment adaptation anal. based on a simple equiv. cct. 8-73157
- saphenous nerve normal sensory cond. in man 8-61162
- skeletal muscle fibre with helicoidal T system, linear elec. props. 8-80852
- skeletal muscle general myocybernetic control model 8-53385
- stimulus artifact suppression, sample and hold amplifier system 8-77163
- synthetic voltage-dependent cation-selective transmembrane channel characterisation 8-77009
- tissue impedance meas. by phase-sensitive voltage and current detection 8-53602
- two-tone suppression in cat auditory nerve, rate-intensity and temporal anal. 8-61194
- ventricular excitation, digital simulation, computer model evaluation 8-85302
- vision with moving eyes, microelectrode studies of single neurons (*German*) 8-53397
- visual cell, proposed role of cyclic GMP 8-64997

bioelectric phenomena continued

- visual prosthesis design, human factors and electrophysiological considerations 8-53583
- visual stimulator, computer-controlled 8-69230
- yeast cells, singular, dielec. props. 8-88699
- Cl⁻ active transport inhibition by piretanide, in teleost intestine cell 8-64967
- K currents induced by acetylcholine in Aplysia neurones, slow relax. 8-80865
- Na channel, fully coupled excited state model, conductance in volt. clamped case 8-85297
- Na permeability inactivation in squid giant nerve fibres, review of exptl. work 8-73154

bioelectric potentials

- see also *contact potential*; *electrocardiography*; *electroencephalography*
- above-knee prosthesis, myoelectric control system development 8-53575
- acoustically evoked potentials in EEG, meas. by adaptive matched filters (*German*) 8-88755
- action potentials from two different sources, distinction using dual channel audio monitor 8-61293
- alpha frequency rel. to head size, implications for brain wave model 8-69035
- amplifier system for voltage clamping, used for tracing membrane potentials (*German*) 8-61285
- articular cartilage, electromechanical props. during compression and stress relaxation 8-92667
- auditory averaged electroencephalic response to tone pips in normal-hearing and hearing-impaired subjects 8-65049
- auditory evoked potential development in early childhood, longit. study 8-77061
- auditory evoked potentials in normal human subjects, age-related vars. 8-77063
- auditory evoked response due to 3 GHz microwave pulses, mammals 8-53444
- auditory evoked responses, computer driven bipolar stimulator 8-57011
- auditory nerve, two-tone suppression, stimulus freq. effect, physiological and psychophysical obs. 8-85317
- average evoked potentials, a posteriori Wiener filtering theory and practice 8-96038
- average visual evoked response estimation, predictor-subtractor-restorer filter 8-65143
- axon, squid giant, dispersive structure (*Japanese*) 8-61158
- bacterial sensory electrophysiology, motility depend. on membrane pot. and chemotaxis 8-53373
- biosignal processing, spurious signal detection method (*German*) 8-92722
- bladder smooth muscle impulse propag., math. anal. (*Japanese*) 8-53559
- body surface potential distribution map recording and processing 8-57116
- brain electrical sources, human, 3D localisation, quantitative evaluation 8-92613
- brain evoked potentials, processing, computer techniques 8-92728
- brain rhythmic activity generation models (*Dutch*) 8-73150
- brain stem evoked responses, acoustically depend. wave V latencies 8-85318
- brain-stem auditory evoked response in young and old adults, normal variability 8-77064
- cardiac biopotential distribution laws rel. to functional state 8-65142
- cardiac inverse generator, dipole crosstalk 8-92615
- chemical synapse, feedback mechanism model through elec. current 8-96043
- click-evoked brainstem potentials in man using high pass noise masking 8-61193
- clinical electrophysiology laboratory automatic control system 8-57110
- colour vision physiological measurement facility, monkey detected responses (*Japanese*) 8-92752
- cone specific c-wave in turtle retina 8-69060
- cortical spreading depression, math. model 8-80857
- crayfish stretch receptor repetitive firing behaviour nonlinear systems anal. 8-80853
- curve crossing problem for Gaussian stochastic processes, neural modelling appl. 8-85299
- demyelinated nerve fibre conduction failure, effect of prolonging action pot. 8-73152
- digestive tract electrical rhythms simulation 8-64970
- dipole sources in conducting tissues 8-64915
- EEG and evoked potentials, intracerebral current contribs. 8-92611
- EEG bispectra computation computer program, in FORTRAN 8-92727
- EEG data during sleep stages, stationarity and normality 8-92610
- electro-oculogram, interocular comparison of eye movements while reading, normal and amblyopic subjects 8-53393
- electro-oculographic response, recording and interpretation review (*Italian*) 8-73156
- electro-oculographic response interocular comparison, unpredictability of residual long-term effects 8-53392
- electromyography, clinical, computer anal. 8-80985
- electrooculogram, eye movements of African chameleons, spontaneous saccade timing 8-69053
- electroretinogram, automatic meas. of b-wave amplitude and peak latency (*German*) 8-80993
- electroretinographic response rel. to vars. of visual performance during day 8-77051
- electroretinography, clinical, use of Mingograph ink-jet recorder 8-92731
- EMG, abdominal, for uterus activity recording (*German*) 8-92712
- EMG, surface, digital simulation, spectral anal. 8-80863
- EMG, surface, model for digital simulation 8-80862
- EMG amplifier, wideband isolated, cct. 8-57089
- EMG and temporal information during gait, clinical telemetry 8-80994
- EMG curves peak detection algorithm 8-96107
- EMG index for localised muscle fatigue 8-57093
- EMG motor command extraction by pulse counting method (*Japanese*) 8-53546
- EMG of biceps brachii muscle, single motor unit action pot. model 8-53386

bioelectric potentials continued

- EMG of temporal muscle in rhesus monkey, spectral anal. 8-69039
- EMG quantitative analysis instrument 8-81041
- EMG recording computer editing 8-80999
- EMG signal processing rel. to human locomotion, optimality criterion 8-92612
- EMG spontaneous activity in paretic skeletal muscle, LF bizarre discharges 8-80864
- EMG/US transducer for biodynamic research, speech appl. 8-77164
- epicardial and body surface pot. meas. in intact dog, transfer coeffs. calc. 8-92614
- epithelial K active transport system of insect midgut, pump-mediated efflux 8-80846
- evoked potential optimal filtering in sequential range (*German*) 8-85401
- evoked potentials, single trial, S/N ratio and response variability 8-61159
- evoked potentials, transient, in man, size and orientation specificity 8-69056
- evoked potentials and EEG freq. in patients undergoing haemodialysis and kidney transplantation 8-61160
- extracellular action potential recording, interference suppression 8-61294
- eye, of horseshoe crab, anal. of adapting bump model 8-73160
- eye slow cell responses in insects, colour adaptation 8-64988
- eyeblink response to startle evoking stimuli in humans, excitatory and inhibitory components 8-77050
- frequency-following potential components in man 8-77062
- functional electrical stimulation control using volitional EMG signal 8-57128
- gastrointestinal electrical activity, Hodgkin-Huxley type electronic modelling 8-61165
- gastrointestinal electrical rhythm frequency estimation by autoregressive modelling 8-56948
- giant axons, time-ordered state, spatially organised struct. obs. in squid 8-53380
- gramicidin A channel cation permeation interactions and anion binding 8-53370
- heart contraction kinetics recording using thorax elec. fields (*Czech*) 8-77138
- heart electrical generator integral characts. in normal humans 8-69244
- hippocampus pyramidal cells, somatostatin as excitatory transmitter 8-64973
- hypothalamic neurone spontaneous firing over narrow temp. interval 8-56961
- intestinal electrical activity, motility, computer anal. of electrophysiological study on dogs 8-80851
- limbic spindle re-appraisal 8-69036
- Limulus ventral nerve photoreceptor response height vs. stimulus intensity curve 8-69058
- lipid bilayer, interaction of cytochrome c 8-69001
- measurement in living tissue, effect on simultaneous O₂ partial press. determ. (*German*) 8-85453
- membrane responsiveness curve automated on-line determ. 8-92761
- microcomputer-aided arm prosthesis using myoelectric pattern recognition 8-53576
- mitochondria and submitochondrial particle membrane pot. generation in anaerobic conditions 8-69015
- mitochondrial membrane pot., respiratory chain study by method of penetrating ions 8-64951
- monosynaptic potentials onset and propagation, discrete-dynamic equations 8-77040
- motoneurone cross-correlated firing patterns, recurrent inhibition effects 8-80861
- motoneurones excited by phasic muscle stretches, discharge pattern shaping, recurrent inhibitory feedback effects 8-85303
- motor unit action potential duration meas. by surface electrode EMG 8-81039
- multi-microelectrode system for simultaneous recording of closely spaced neurons (*Japanese*) 8-61284
- multiunit spike train separation techniques evaluation criteria 8-85422
- muscle, smooth, effect of hyperosmolar soln. on elec. connections between cells 8-69027
- muscle spindle afferent activity and tone meas. in man, apparatus generating controlled ramp movements 8-77121
- myoelectric multistate control systems, operator error 8-81076
- nerve and muscle isolated preps., 2450 MHz radiation effects 8-53443
- nerve biopotential recording by laminated electrodes 8-92760
- nerve cell impulse flows, determ. of quantity of useful information 8-69038
- nerve impulse, physical mechs., ion transport through membranes, review 8-85306
- nerve impulse equation, dynamic responses of impulse 8-64972
- nerve impulse propagation, subthreshold solns. of Hodgkin-Huxley eqns. 8-77044
- nerve impulse radial decline in restricted cylindrical extracellular space 8-53379
- nerve-muscle anisotropic syncytia, electrotonic membrane pot. distrib. 8-64971
- neural spike trains, relationship of post-stimulus time and interval histograms to time characts. 8-69032
- neuromuscular blockade by amantadine by suppression of acetylcholine receptor ionic cond. 8-64975
- neuromuscular system output response, effect of correlated adjacent interspike interval sequences of input, computer simulation 8-80858
- neuronal populations, diffusely-connected, computer simulation 8-53384
- neuronal spike-train statistical anal. methods 8-73149
- neurones of large horse-leech, electrophysiological characts. rel. to intracellular Na⁺ conc. 8-53374
- neurophysiology, computer assisted unit data acquisition/reduction 8-61266
- nonspiking neurones, pharmacological evidence for fast Na channels 8-73151
- optic tectum extracellular recording, reproducible manufacture of metal-filled microelectrodes 8-69263
- perimetry by visual evoked pot. recording limitations 8-69049
- photic one-second stimulation, on/off effects in background EEG activity 8-69047
- photoreceptor visual response rel. to metarhodopsin transitions, barnacle 8-69050

bioelectric potentials continued

- photosensory membrane of Limulus ventral nerve photoreceptor, effect of extracellular Ca/Na ratio 8-69067
 polarised spherical cell, ionic conc. profiles and charge distrib. 8-73144
 recording using surface electrodes, methods of reducing movement interference (*German*) 8-85405
 repetitive firing computer models nonlinear systems anal. 8-80854
 repetitive muscular contraction, localised fatigue evaluation from EMG power spectrum 8-57103
 retina of turtle, horizontal cells influence on bipolar cells' membrane pot. 8-88708
 retinal ganglion cells of cat, response patterns for moving contours 8-69059
 retinal light responses, simultaneous recording by extra- and intracellular electrodes in crayfish 8-69055
 retinal on-centre bipolar cell, ionic mechanisms of rod and cone signals 8-61177
 retinula peripheral cells within Drosophila visual mutants, response to monochromatic white-noise 8-69078
 rod early receptor potential isolation from frog retina 8-69066
 rod ERG, human, rel. to psychophysical responses in light and dark adaptation 8-69063
 rod ERG of mudpuppy, effect of dim red backgrounds 8-69062
 rod network in turtle retina, elec. spread 8-80874
 scalp potentials, dipole layer model 8-77035
 semicircular canal primary afferents, impulse weight functions, frog 8-69116
 sinatorial node of rabbit heart, vagal stimulation, K⁺ permeability and extracellular transients 8-92608
 single unit activity, computer program for generating on-line raster dot displays 8-57087
 skeletal muscle activity pattern in humans rel. to muscle fibre type composition 8-80869
 soma potential of interneurons controls transmitter release on monosynaptic pathway in Aplysia 8-56964
 somatosensory evoked potential measurement and analysis on a small laboratory computer 8-92729
 speech production, recruitment and discharge patterns of single motor units 8-65054
 spinal and sub-cortical evoked pots. following stimulation of posterior tibial nerve in man 8-69034
 squid joint axon membrane potential fluctuations, cross-correlations 8-92616
 subcellular particle membrane pot. diff., proton channels in oxidative phosphorylation 8-64964
 superior colliculus directional selectivity in hamster rel. to strobe-rearing and dark-rearing 8-69052
 transmitter release quanta, evidence against subunits 8-77042
 trigeminal motoneuron activity during sleep, intracellular anal., cct. 8-53389
 unitary synaptic potentials rel. to behavioural sequence timing 8-61161
 vertex short latency acoustic responses in cat, factors affecting amplitudes and latencies 8-61192
 visual acuity assessment by evoked pots., temporal depend. of spatial freq. selectivity 8-64995
 visual cell microvilli membrane fragment protonic and ionic processes, cephalopod 8-73159
 visual cortex, critical period interaction, kitten 8-56972
 visual cortex functional specialisation of rhesus monkey 8-80873
 visual cortex neurones, rabbit, organisation of background activity 8-69044
 visual cortical area 19 of cat, periodic complex cells 8-56974
 visual evoked cortical potentials in men during compression and saturation in He-O₂ 8-61173
 visual evoked potential evidence of adaptation to spatial Fourier components in humans 8-69051
 visual evoked potential on-line evaluation by sliding average form. (*German*) 8-85402
 visual evoked potential recovery, cumulative inhibitory effect of repetitively flashed stimuli 8-69048
 visual evoked potential to search in short-term memory, late components 8-61172
 visual evoked potentials, monocular, recording under binocular conditions 8-81035
 visual evoked potentials and latent chromatic response (*Japanese*) 8-92629
 visual evoked potentials to sine wave modulated light in normals and patients, interhemispheric relationships 8-77049
 visual evoked response in strabismic and anisometropic amblyopia, effects of check size and retinal locus 8-61171
 visual evoked response of humans, nonlinear anal. 8-92622
 visual pigment system kinetics, bistable system measurements appl. 8-92624
 visual pigment system kinetics, mathematical anal. 8-92623
 visual-neural correlate of speechreading ability 8-64992
 visually evoked elec. and mag. response simultaneous recording for diagnosis 8-53558
 Na current in cardiac and nervous tissues, validity of dV_{max}/dt as meas. 8-77037

biographical dictionaries *see* **biographies****biographies**

- Aryabhata, 5th century Indian astronomer and mathematician, life and works 8-65741
 Evans, Thomas Simpson, 1777-1818, mathematician and astronomer 8-89287
 Heisenberg, the birth of quantum mechanics (*Polish*) 8-89291
 Henry Norris Russell, and Hertzsprung-Russell (H-R) diagram 8-69957
 Kepler, Johann (1571-1630), Bibliographia Kepleriana. Supplements and continuation 1975-1978 8-77657
 Kepler, Johann (1571-1630) and ephemerides of the early seventeenth century 8-77659
 Mach, Ernst, autobiographical manuscripts as source material 8-86098
 Max Born, biography, review of contributions to physics 8-86100
 Millikan, Robert A., contribs. to physics teaching 8-69956
 Newcomb, Simon, American astronomer, 1835-1909, life and works 8-93504

biographies continued

- H.C. Oersted, first spark of electrotechnology, biography (*French*) 8-69955
 p.-O. Lowdin's scientific and other activities 8-62023
 Pickering, E.C., Henry Draper Memorial and American astrophysics 8-86102
 Quetelet, A.L.J., life and spread of science in Belgium during 19th century (*French*) 8-65742
 Smiley, Charles Hugh (1903-77) 8-62024
 Taylor, G.I., contrib. to EHD 8-86099
 Ting, personal recollection of ψ meson discovery (*Polish*) 8-73820
 Zubov, Nikolai Nikolaevich (1885-1960), oceanologist (*Russian*) 8-86101

biological cybernetics *see* **biocybernetics****biological effects of acoustic radiation**

- see also* **biomolecular effects of radiation**; **cellular effects of radiation**
 auditory nerve responses and cochlear microphonics in cats using pulsed US 8-61200
 bone, piezoelectric effect on exposure to US, effect of sample rot. 8-80913
 chinchilla, threshold shifts following 3 days noise exposure 8-88712
 genetically deaf animals, differentiation of infrasonic and sonic effects in mice 8-57037
 human response to house vibr. caused by sonic booms or air blasts 8-90589
 human whole-body, vibrations, biodynamic response and variability 8-92672
 infrasound, exptl. study of levels in transportation 8-88726
 LF noise, effect on people, review 8-92673
 lipid bilayer, 1 MHz US effects on cond. and capacitance 8-77082
 noise, air conditioning system, subjective responses and meas. 8-83168
 noise, asymptotic threshold shift in chinchillas exposed to impulse noise 8-57019
 noise, hearing protection, types and limitations 8-55509
 noise, industrial deafness risk, British Government code of practice 8-55513
 noise, statistical estimation of percentage of overexposed noise-impacted workers 8-92671
 noise-induced threshold shift and cochlear pathology in the Mongolian gerbil 8-65035
 sleep, disturbance by noise 8-92645
 squirrel monkey, temporary threshold shift from noise exposure 8-88715
 thyroid substances levels in blood serum of rats exposed to 0.2, 0.6 and 1 W/cm² of US energy 8-69134
 US cavitation emission from insonated plant tissues 8-59185
 US in medical diagnosis, theory and advantages 8-92682
 US irradiation from diagnostic instruments (*Japanese*) 8-80936
 US perturbation obs. at cellular level 8-61214
 US toxicity, effect on adult mortality and litter size of mouse 8-69135
 visual field displacements evoked by intense sound exposure, humans 8-85332

biological effects of gamma-rays

- see also* **biomolecular effects of radiation**; **cellular effects of radiation**
 amino acid, in polycryst., γ -irrad. induced radical pair form., 77K, EPR obs. 8-85292
 amino acid stimutable transport system in rat liver after whole-body γ -irrad. 8-65098
 amino acid transport hormonal control in liver of rats exposed to whole-body γ -irrad. 8-65099
 aneurysmal bone cyst response to low doses of ⁶⁰Co gamma radiation with prolonged treatment 8-73196
 aspartate transcarbamylase, solid, enzyme activity and allosteric characts. after gamma irradi. 8-53341
 aspartate transcarbamylase, solid, sedimentation and subunit interactions, after gamma irradi. 8-53342
 bacteriophage DNA and protein cross-linkage by ⁶⁰Co gamma-rays 8-77002
 blood extracorporeal irradiation with ¹³⁷Cs, expt. research and clinical appl. (*German*) 8-69149
 Bowman-Birk soybean proteinase inhibitor, gamma irradi. 8-53343
 capillary blood flow, long-term effects of ⁶⁰Co gamma and fission spectrum neutrons, mouse 8-80927
 cervical stage III carcinoma treatment, two regimes with same TDF but differing morbidity 8-53474
 Chinese hamster cells, ⁶⁰Co-irrad., computer anal. of survival curve data 8-85344
 chromatin extracted from cultured mammalian cells, gamma radiolysis, DNA alkali-labile strand damage 8-77003
 cockroach, reproductive behaviour, pheromone production and release 8-85341
 cytidine-5'-monophosphate, γ -irrad. aq. soln., spin-trapped radicals, liq. chromatography and EPR spectroscopy 8-53340
 deoxyribonucleoprotein, gamma-ray protein damage 8-53338
 DNA, enzymatic digestion, separation by ion exchange chromatography 8-85290
 DNA, single-stranded, alkali-labile sites and post-irrad. effects induced by H radicals 8-68994
 DNA break rejoining capacity rel. to mouse age 8-69148
 E. coli strains, two with lambda lysogens, induced radioresist. 8-69140
 Ehrlich ascites vital cell UV primary fluoresc. rel. to ⁶⁰Co γ -ray dose 8-69142
 embryonic bone and cartilage, effects of in vitro gamma irradi. 8-65089
 erythropoietin action, identification of two components by irradi. in vitro 8-65094
 glyceraldehyde-3-phosphate dehydrogenase radiolysis, active-site and SH loss 8-77000
 herpesviruses, survival and immunological characts. 8-77089
 low-dose RBE and quality factor for X-rays and gamma-rays 8-73175
 lymphocytes, in vitro ⁶⁰Co gamma-ray response of leucoagglutinin stimulated human cells 8-57041
 mammal gonads, radiation induced morphological and endocrinological changes (*Russian*) 8-77090
 mammalian cell radiosensitivity, effect of NaCl solns. containing radiosensitisers and radioprotectors 8-69146
 mammary carcinoma C3H response to fractionated irradi., rel. to fractionation number and intertreatment interval 8-53453

biological effects of gamma-rays continued

- neutron radiotherapy, nature and significance of radiation outside beam 8-53477
 papain inactivated by OH radicals and H₂O₂, optical density, amino acid composition and fluoresc. 8-53344
 primordial germ cells of fish *Oryzias latipes*, nucl. size changes 8-53451
 radiotherapy with multiple daily sessions with ⁶⁰Co and 250 kV X-rays, clinical experience 8-53475
 testes, glucose 6-phosphate dehydrogenase studies following partial body γ -irrad. 8-80924
 testes, isocitrate dehydrogenase studies after partial-body γ -irrad. 8-80923
 thymidine, frozen aq. solns., final products of gamma radiolysis 8-77001
 thymidine-5-monophosphate, γ -irrad. aq. soln., spin-trapped radicals, liq. chromatography and EPR spectroscopy 8-53340
 thymocyte membrane props. modification by hyperthermia and gamma-rays 8-69017
 tumour curability rel. to vol. in murine carcinoma and sarcoma 8-61215
 tumour recurrences, immunogenic and nonimmunogenic, time distrib. following local irrad. 8-65090
⁶⁶Ga tumour uptake in rats after whole-body ⁶⁰Co irrad. 8-65081
¹⁹²Ir radiographic source, radiation accident 8-53514
 O₂ enhancement effect, photo-reactivation of γ -radiation damage 8-77087

biological effects of ionising particles

- see also biomolecular effects of radiation; cellular effects of radiation*
 amoeba irradiated by thermal neutrons, absorbed dose estimation 8-53449
 bacteriophage T7, radiation inactivation 8-65083
 beta emitters, insoluble, ingested, dose to gastrointestinal tract 8-65134
 beta-emitting radionuclides from reactor accident, ingestion, acute toxicity 8-65082
 beta-rays, high-energy, hazards to eye lens and gonads 8-65131
 bronchial cancer induction by α -emitting warm particles 8-96078
 capillary blood flow, long-term effects of ⁶⁰Co gamma and fission spectrum neutrons, mouse 8-80927
 cell progression, in broad bean roots, monoenergetic neutron effects 8-65086
 Chlamydomonas reinhardi, dividing, X-ray and proton-induced ultrastruct. changes 8-65085
 Chlorella pyrenoidosa synchronised cultures, effect of extremely low doses of secondary radiation from ³²P 8-73176
 chromosome aberrations as dosimetric technique for fission neutrons at 0.2 to 50 rad 8-69145
 E.coli AB2463 recA response to fast neutron beams, 4 to 27 MeV, rel. to dosimetry intercomparison 8-65077
 electron probe microanalysis, charging effect in electron-irrad. ice 8-57141
 fast neutron irradiation of cells cultured in monolayer, dosimetric aspects 8-69218
 heavy particle comparison for therapy, acute and late reactions in mice 8-85338
 heavy particle comparison for therapy, cell survival, OER and RBE 8-85337
 heavy particle comparison for therapy, cell survival vs. depth 8-85336
 lens opacification in mice exposed to 14 MeV neutrons 8-65097
 leukaemia risk from neutrons, rel. to max. permissible dose for occupational exposure 8-53448
 lung carcinogenesis in rats, induced by inhaled high-fired ²³⁹PuO₂, BeO 8-96077
 lung tissue localised irrad. using radioactive microspheres, prod. and props. 8-53445
 lymphocyte death and transform., effects of X-ray and neutrons 8-69144
 mammal gonads, radiation induced morphological and endocrinological changes (Russian) 8-77090
 mammalian cell, survival of normal and hybrid X-ray resist. lines exposed to X-rays and protons 8-80929
 mammalian cells in vitro, 300 keV X-ray, 14 MeV neutron and pion⁻ effects 8-69155
 neutron carcinogenesis, dose and dose-rate effects in BALB/c mice 8-53455
 neutron dose measurements in a dummy for test animal irradiation in a reactor 8-61218
 neutron radiotherapy, nature and significance of radiation outside beam 8-53477
 neutrons generated by 70 MeV protons on Li, OER and RBE meas. 8-65079
 spores of *Bacillus subtilis*, mutagenic effect of water-t 8-80928
 TEM, low-temp., radiation damage, review 8-57147
 thermal neutron beam response of hamster and HeLa cells containing various concs. of ¹⁰B 8-73178
 thorotrast and ²²⁴Ra radiobiological significance 8-96076
 thorotrast biological effects, conf., Alta, USA (July 1974) 8-96068
 thorotrast cases, bone irradiation meas. results 8-96092
 thorotrast patients, α -ray tissue dose 8-96093
 thorotrast patients, Danish, malignancies 8-96074
 thorotrast patients, endosteal α -particle dose 8-96094
 thorotrast patients, German, malignancies and estimated tissue dose 8-96062
 thorotrast patients, Portuguese, malignancies 8-96073
 tissue-equivalent gas, energy loss of H, C, N and O ions for elastic nuclear collisions 8-86759
 yeast cells, alpha-irrad., UV-induced reactivation 8-80920
²³⁸Pu IV citrate chronic exposure effect on embryonic development of fish eggs 8-53447
²³⁹Pu, endosteal cell dose and relative distrib. factors compared to ²²⁶Ra 8-96091
²³⁹PuO₂, alpha-particle freq. in lung cells 8-69151
²²⁶Ra in humans, radiation induced malignancies 8-96075
²²⁶Ra and daughters, radioactive props. and biological behaviour 8-96090
²²⁶Ra biological effects, conf., Alta, USA (July 1974) 8-96068
²²⁶Ra, endosteal cell dose and relative distrib. factors compared to ²²⁶Ra 8-96091
²²⁴Ra injections into humans, soft-tissue effects 8-96070

biological effects of ionising particles continued

- ²²⁴Ra injections into humans, skeletal effects 8-96071
²²⁴Ra preparation, for ankylosing spondylitis therapy 8-96089
²²⁴Ra, short-lived α -emitter, late effects after incorporation in mice 8-96069
²²⁴Ra usage in radiotherapy and radiobiology, brief history 8-96085
²²⁴Ra use in treatment of ankylosing spondylitis and rheumatoid synovitis 8-96086
²²⁷Th, short-lived α -emitter, late effects after incorporation in mice 8-96069

biological effects of microwaves

- see also biomolecular effects of radiation; cellular effects of radiation*
 auditory responses in mammals, using 3 GHz pulses 8-53444
 chronotropic effects in isolated rat heart 8-69137
 energy absorption of animals, effect of Plexiglas animal holders 8-92674
 exposure biological expts., compact light-weight Gaussian-beam launcher 8-96119
 eye lens thermal stresses, humans 8-80914
 hazard assessment methodology for USA Army Radiation Protection Program 8-85389
 heating of tissue, effect of surface cooling and blood flow 8-57038
 murine brain rapid thermal fixation using microwave device 8-92689
 nerve and muscle isolated preps., 2450 MHz radiation effects 8-53443
 neuron response by individual *Aplysia* pacemakers, CW and pulsed radiation 8-92675
 nonionising electromagnetic radiation bioeffects research and related occupational health aspects 8-73172
 porphyrin free base, triplet state electron spin echoes, fluoresc. detection 8-70856
 protection standards, American and European 8-80973
 R. spherulites, triplet state electron spin echoes, fluoresc. detection 8-70856
 sources, potentially hazardous, review 8-73173
 temperature and corticosterone relationships in rats 8-92676
 thermographic observability of tumours with microwave heating 8-73193
 thermographic turnover detect., microwave enhancement with swept-freq. illum. 8-73194

biological effects of radiation

- see also biological effects of acoustic radiation; biological effects of gamma-rays; biological effects of ionising particles; biological effects of microwaves; biological effects of ultraviolet radiation; biological effects of X-rays; biomolecular effects of radiation; cellular effects of radiation; dosimetry; radiation therapy*
 biosphere and active solar processes link, role of Earth's natural electromag. field 8-61211
 breast cancer induction in humans by ionising radiation 8-61217
 cancer deaths in atomic plant employees rel. to low-level exposure 8-85339
 carcinogenesis, link between radiation and chemical effects, time factors 8-53446
 Chalk River Nuclear Laboratories research in radiation biology, environment and radiation protection 8-61222
 civilisations possible self-annihilation through thermonuclear war 8-81562
 coagulation in gastrointestinal haemorrhages, using laser endoscope (German) 8-69178
 EM, in transmission stations, employees protection, Polish and international regulations (Polish) 8-61263
 EM, non-ionising, hazards in the laboratory and effects on skin and eyes 8-96064
 EM, state of research (German) 8-88728
 EM energy deposition in biological tissue at 900 and 450 MHz 8-69222
 EM wave exposure facilities for bioeffects research, survey 8-73174
 energy, environment and health, Failla Memorial Lecture, learning from nucl. experience 8-80982
 fallout effects of Nagasaki atomic bomb 8-85393
 HV transmission line elec. and mag. field exposure effects and hazards 8-77083
 inhaled hot particle toxicity, recommendations of German Commission on Radiation Protection 8-69150
 low-level, current estimates of hazards to human populations, review 8-57043
 meat, biochemical procedure for detect. of radiation treatment 8-65075
 nonionising electromagnetic radiation bioeffects research and related occupational health aspects 8-73172
 optical radiations, effects on men, directives and unit derivation (Hungarian) 8-57040
 photobiological process relative quantum yield determ. using light of different spectral composition 8-65154
 phototherapy, effect of prolonged illum. on luteinising hormone concs. in human infants 8-69138
 pion⁻ beam stopping distrib. determ. by charge collector 8-53513
 retina thermal injury following laser irrad., asymptotic rate process calcs. 8-80916
 rhabdome transmittance decrease due to blue light, rel. to desensitisation of peripheral photoreceptors 8-64993
 spectral luminous efficacy maximum, definition (German) 8-54333
 teeth, human, thermal stress effects and surface cracking assoc. with laser use 8-80915
 thymic region shielding in radiobiology expts., dosimetry in irrad. mouse cadavers 8-61257
 VHF portable transceivers, heating by induction field, expt. using phantoms 8-57039
¹⁴⁴e inhalation effect of influenza virus infection on pulmonary retention and mouse survival 8-85340
¹³¹I therapy for toxic diffuse goitre, incidence of hypothyroidism within 1 year 8-65116
¹³¹I treatment of hyperthyroidism, carcinogenesis, comparison with surgery 8-85374
³²P-diphosphonate dose determ. in patients with bone metastases from prostatic carcinoma 8-61251
²³⁹Pu acute inhalation, early mortality and morbidity estimate 8-96079
²³⁹Pu, lymphoid tumours and leukaemia induced in mice by bone-seeking radionuclides 8-69141

biological effects of radiation continued

- ²²⁶Ra, lymphoid tumours and leukaemia induced in mice by bone-seeking radionuclides 8-69141
²²⁶Ra-burdened dog skeleton, Rn retention rel. to age and dosage 8-65092
⁹⁰Sr, lymphoid tumours and leukaemia induced in mice by bone-seeking radionuclides 8-69141
 U, miners Rn daughter inhalation and pulmonary cancer incidence 8-96080
 UO₂ inhaled particle distrib. and clearance on first bifurcation and trachea of rats 8-73267

biological effects of ultraviolet radiation

- see also biomolecular effects of radiation; cellular effects of radiation*
 N-acetylglucosamide, substrate-inhibitor of lysozyme, localisation of unpaired electrons 8-68992
 acid amide+H₂O₂, aq. solns., photolysis, EPR study of spin-trapped radicals formed during photolysis 8-68996
 cell, surface photoelectron micrographs and quantum yields 8-61148
 cell sterilisation modes, cell killing and early differentiation 8-65093
 cells, Chinese hamster, postreplication repair enhancement 8-92678
 DNA unscheduled synthesis in UV irradiated spleen lymphocytes after X-irradiation, rat 8-69156
 E. coli K-12 cells, inhibition of X-ray induced UV resistance by nitrofurantoin 8-85342
 E. coli strains, two with lambda lysogens, induced radioresist. 8-69140
 Escherichia coli radiation-damage inducible system, rel. to UV light mutagenesis 8-53458
 eye, 300 to 400 nm, literature review 8-57042
 eye, lens pigmentation in humans rel. to UV light exposure 8-65100
 eye, review 8-80917
 eye lens fluorescence due to UV stimulation, appl. to pupillary response meas. 8-64977
 ferricytochrome, photoreduction in presence and absence of electron donor 8-53337
 lipid bilayer electrical strength fall after UV irradiation 8-69002
 liposome proton permeability increase on peroxide photo-oxidation of lipids 8-69024
 mammalian gonads, radiation induced morphological and endocrinological changes (Russian) 8-77090
 photosynthetic reactions of leaf discs and chloroplast preps. of crop species, 298 nm radiation effects 8-61220
 postreplication repair enhancements in UV-irradiated Chinese hamster cells by irradiation in G₂- or S-phase 8-77085
 postreplication repair in mammalian cells, model 8-80918
 pyrimidine dimers, excision repair of UV damage in monkey kidney cells 8-53332
 retinal damage by 325 nm He-Cd laser radiation 8-69136
 RNA, heterogeneous nucl., effects of UV irradiation, and postirradiation on size in murine cells 8-69139
 skin cancer incidence modelling 8-77091
 skin Na entry site irreversible inhibition by photosensitive amiloride analogue, in frog 8-69030
 thymine dimer excision from DNA of UV-irradiated plant seedlings 8-61221
 thymine dimer excision kinetics in UV-irradiated human cells 8-53331
 yeast, inducible enzyme synthesis, UV effects on regulation and activity per cell 8-69157
 yeast cells, alpha-irradiation, UV-induced reactivation 8-80920
 H₂O₂, UV prod. of OH radicals, reactions with peptides in aq. soln., EPR 8-68993

biological effects of X-rays

- see also biomolecular effects of radiation; cellular effects of radiation*
 abdominal epidermis histogenesis and age depend. of X-ray sensitivity in flesh fly metamorphosis 8-65084
 adoptive antibody responses in DBA/2 and BALB/c mice, differential effects of preirradiation 8-80926
 bone, mouse, rel. between ²³⁹Pu deposition in bone and ⁵⁹Fe uptake in marrow 8-85395
 bone marrow erythrocytes of mice, X-ray induced micronuclei 8-77088
 breast dose and cancer risk due to fluoroscopic chest exams. of women with tuberculosis 8-65128
 cell sterilisation modes, cell killing and early differentiation 8-65093
 Chlamydomonas reinhardtii, dividing, X-ray and proton-induced ultrastructural changes 8-65085
 Chlorella pyrenoidosa synchronised cultures, effect of extremely low doses of secondary radiation from ³²P 8-73176
 chromosome aberration specificity, X-irradiated human T-cell line 8-80921
 DNA, transforming, X-ray sensitivity rel. to presence of free radicals 8-68995
 DNA, X-ray induced damage in rat cerebellar neurons and brain tumour cells 8-80922
 DNA unscheduled synthesis in UV irradiated spleen lymphocytes after X-irradiation, rat 8-69156
 E. coli K-12 cells, inhibition of X-ray induced UV resistance by nitrofurantoin 8-85342
 E. coli strains, two with lambda lysogens, induced radioresist. 8-69140
 Ehrlich ascites carcinoma cell fluorescence after X-irradiation 8-69143
 epithelium of hamster cheek pouch, enhancement of DMBA tumour genesis by repeated low-level exposures 8-53456
 erythropoietin action, identification of two components by irradiation in vitro 8-65094
 ferredoxin of adrenal cortex, destruction of chromophore centre on exposure to X-irradiation 8-76993
 fluoroscopy, organ dose per unit exposure, estimation method for artificial pneumothorax 8-96097
 hyperthermia and X-ray combined effects on CHO cells, rel. to temp. and order of appl. 8-65088
 hyperthermia effect on nonhistone proteins isolated with DNA 8-80843
 leukaemic cell line, mouse, radioprotection by procaine 8-65080
 life shortening of mice exposed to fractionated X-irradiation, repair and biochemical protection 8-69153
 liposomal membrane permeability, radioresist. 8-80919
 low-dose RBE and quality factor for X-rays and gamma-rays 8-73175
 lung carcinoma treatment by local irradiation and Corynebacterium parvum, mice 8-65091
 lymph nodes, calf, study of interaction between histone F2b and DNA 8-85346

biological effects of X-rays continued

- lymphocyte death and transformation, effects of X-ray and neutrons 8-69144
 lymphoma cell survival after X-irradiation, effect of vitamin E 8-92677
 mammalian gonads, radiation induced morphological and endocrinological changes (Russian) 8-77090
 mammalian cell, survival of normal and hybrid X-ray resistant lines exposed to X-rays and protons 8-80929
 mammalian cells in vitro, 300 keV X-ray, 14 MeV neutron and pion effects 8-69155
 1-methyl cytosine: 5-fluorouracil X-irradiation at 300K, EPR 8-64941
 mitochondrial protein synthesis in rat liver after whole-body X-irradiation 8-80925
 mitotic crossover increase in Nicotiana tabacum after 150 kVp X-irradiation 8-61219
 mouse ovaries, X-ray effect on population of granulosa cells (Russian) 8-73177
 necrosis of mouse tails, tolerance after repeated X-ray irradiation 8-96067
 ovarian tumour genesis, effect of normal ovarian tissue 8-53452
 parabiont rats, leukaemia and lymphoma 8-53457
 pre-implantation embryos and implantation reaction in mouse, acute X-irradiation effects 8-69154
 radiography, stochastic late effects after partial body irradiation 8-69152
 radiotherapy with multiple daily sessions with ⁶⁰Co and 250 kV X-rays, clinical experience 8-53475
 rice, excised mature embryos, effect of 6.5 to 20 kR X-rays 8-85347
 spinal cord, rat, effect of single and fractionated doses 8-65076
 splenic cells, rat, enhanced cytotoxic reactivity after X-irradiation 8-85343
 thyroid tumours in infant rats 8-65096
 Triturus cristatus carnifex Laur., X-ray irradiated homotransplanted skin survival time (Italian) 8-85335
 L-tryptophan-HCl radical form. 8-64940
 tumour cell survival with fractionated doses, pitfalls in use of in vitro survival curves 8-77084
 tumour X-irradiation in vivo, enhanced lymphocyte-mediated killing of tumour cells 8-77086
 tumour X-ray response rel. to growth characters. 8-53454
 Pt complex potentiation, of X-irradiation lethal effects, rodent cells 8-85345

biological fluid dynamics*see also haemodynamics*

- body temperature humidification, effect on patient thermal regulation 8-85295
 breathing control hierarchical goal-seeking model description 8-80899
 breathing control hierarchical goal-seeking model performance 8-80900
 breathing work, effect of decreasing inspiratory phase time, analogue integrator meas. 8-85331
 bronchial system model, pulsations, meas. by laser photon correlation 8-87420
 cerebrospinal fluid system models, rel. to third intracranial ventricle dynamic displacement detection 8-57035
 cilia, fluid transport between parallel plates 8-69123
 cilia motion, appl. of Stokes flow due to a Stokeslet in a pipe 8-67268
 cochlear fluid mechanics, kinetic theory 8-53440
 diffused substance kinetics in biological systems 8-53312
 eye, hydrodynamic model of aqueous flow in posterior chamber 8-69122
 fish olfactory organ nares, laser velocimeter flow vel. meas. (German) 8-69262
 functional residual capacity meas. in neonates with endotracheal tubes 8-53556
 functional residual capacity meas. instrumentation for neonates and small animals 8-53590
 kidney model transient behaviour 8-65065
 lung airway, human cylindrical laminar channel flow model, electrostatic precipitation 8-83491
 lung emptying patterns, multiple breath N₂ washout data 8-92666
 lung numerical modelling, human 8-80911
 lung perfusion determination by dilution principle with expiration detection of indicator (German) 8-85326
 lung perfusion determination using O isotopes and dilution principle (German) 8-85327
 lung ventilation-perfusion imaging vs. angiography in dogs 8-65113
 lung volume change estimation from torso hemicircumferences using Whitney gauge transducers 8-65141
 nematode oesophagus pumping mechanism 8-69121
 ovum transport in oviduct, mechs. 8-80905
 pulmonary function testing, continuous distribution of specific ventilation from N₂ washout 8-92665
 pulsing elastic alveoles, gas transport, conc. depolarisation (French) 8-85328
 radionuclide mean clearance time transverse section imaging 8-73222
 renal counterflow systems, numerical solution of differential equations 8-92662
 renal medulla single loop solute cycling model, transient behaviour 8-73167
 respirable fraction of airborne dust, performance characters. of samplers 8-53438
 respiration, external, anal. determ. of energy expenditure of man 8-69268
 respiratory airflow pattern modelling by optimisation criteria 8-80898
 respiratory control in cats, interactions between central and vagal mechanisms 8-53436
 respiratory control system, time series cluster anal. 8-56959
 respiratory control system simulation, state-of-the-art 8-53441
 respiratory function telemetering by combined sensor 8-80995
 respiratory monitors, instrumentation and maintenance, review 8-69236
 respiratory rate and ventilation digital recorder 8-81005
 respiratory system, role of the Van der Pol oscillator 8-65073
 respiratory total resistance meas. in pre-school children using modification of forced oscill. technique 8-77129
 semicircular canal primary afferents, impulse weight functions, frog 8-69116
 spatially constricted flow meas. using laser Doppler velocimeter 8-71409
 spermatozoa swimming in cervix, effects of dynamical interaction and peripheral layer viscosity 8-69126

biological fluid dynamics continued

- steady flow in collapsible tubes 8-57033
- synovial fluid, pathological, rheological props. (*German*) 8-57032
- tree growth rel. to transpirational flow and air humidity (*Russian*) 8-65066
- ventilation scintigraphy, comparative analysis of ^{81m}Kr and ^{133}Xe 8-85360
- ventilation-perfusion ratio distrib. determ. from inert gas data with enforced smoothing algorithm 8-61208
- vocal cord vibration, computer model of air vol. displacement 8-69111
- O_2 consumption meas. with flow-through system, accuracy assessment 8-65067

biological macromolecules *see macromolecules; molecular biophysics***biological sciences** *see biology***biological specimen preparation**

- aortic elastin, freeze-dried, SEM 8-65160
- bone, technique for studying collagen fibres and ground substance 8-57150
- cell cultures, equipment used in a modern laboratory 8-85457
- Cherenkov counting of plants for β -emitter radioassay 8-81088
- critical point dryer, low-cost, with continuous flow dehydration attachment, for electron microscopy 8-53595
- cryo-ultramicrotomy and myofibrillar fine struct., review 8-53592
- electron beam X-ray microanal. of frozen hydrated bulk specimens 8-57142
- electron microscopy, light microscope attachment for isolating small specific areas from slide embedded monolayers 8-53596
- embedding with GMA and Quetol 523 for electron microscopic obs. on semi-thin sections for light microscopy 8-53588
- erythrocytes, technique for observing 3D dim. struct. with a cryo-SEM 8-92765
- freeze-drying technique for chem. unfixed tissue for electron microscopy 8-65164
- freeze-fracture electron microscopy freezing method evaluation by low temp. X-ray diff. 8-57145
- freeze-fracture preparation for SEM 8-61290
- freeze-fracture specimen temp. changes during rapid quenching in liq. coolants 8-57140
- GMA-Quetol 523, ultraviolet polymerisation in embedding procedure for semithin sections prod. 8-92767
- grid handling, of semi-thin sections of GMA-Quetol 523 embedded tissue, with reference to O_2O_4 8-92766
- hard tissue matrix internal space study by SEM, dentine appl. 8-77169
- laser microbeam for tissue sampling in biochemistry (*German*) 8-69175
- lymphocyte surface morphology, human, SEM obs., review 8-53599
- melamine resin, as water containing embedding medium for electron microscopy 8-92764
- micromanipulator using microscope focus, appl. to yeast asci single spore isolation 8-61292
- myocardial tissue, shock-frozen, preservation as shown by cryo-ultramicrotomy and freeze-fracture studies 8-53593
- PIXE analysis of thick biological samples, elimination of charging 8-88775
- plasma membrane, unfixed, ultrathin frozen sections, ultrastructure 8-65161
- polymeric cryoprotectants in preservation of biological ultrastruct., aq. soln. low temp. states 8-65157
- polymeric cryoprotectants in preservation of biological ultrastructure, physiological effects 8-65158
- polymeric cryoprotectants in preservation of biological ultrastructure, morphological aspects 8-65159
- postcontamination avoidance using room with controlled microclimate, for electron microscopy 8-54350
- rapid freezing device for use under controlled and reproducible conditions 8-57139
- resin removal solutions for use on 1 μm thick epoxy sections 8-65165
- SEM, metallic deposition in specimens presenting cavities using sputter coater 8-77171
- SEM, non-conductive specimens, determ. of thickness and grain size of deposited films by TEM 8-77170
- SEM chamber attachment for fracturing and coating frozen biological samples 8-69260
- SEM specimen cleaning by puncture perfusion 8-57149
- tissue dispersions, unglycerinated, freeze-etching by appl. of oil emulsion technique 8-53594
- trace metals determination, microwave oven-based wet digestion technique 8-92542
- X-ray microanalysis of diffusible elements, methods of drying ultrathin cryosections 8-77166
- X-ray microanalysis of diffusible elements, rapid freezing and ultrathin section prep. 8-77165

biological techniques and instruments

- see also biological specimen preparation; biomedical equipment; biomedical measurement; microelectrodes; specimen preparation*
- amino acid linear sequence form., cryo-sublimation of frozen aqueous solns. 8-95993
- anaerobic environment integrated system 8-80987
- animal biotelemetry studies, historical perspectives and recent applications 8-69266
- artery length-force and vol.-press. relations, meas. and empirical formulae 8-65072
- atomic beam scattering, for surface struct. determ. 8-53584
- audio dual channel monitor for distinguishing action pots. from two different sources 8-61293
- autoradiography, direct deposition method, radioactivity detect. 8-77167
- bacterial growth meas. using conductivity changes 8-61288
- bacterial movement tracking using one-dimens. fringe system 8-73299
- bacteriochlorophyll, photooxidation, picosecond absorption spectroscopy investig. 8-82053
- bioanalytical systems using mass spectrometry with atmospheric press. ionisation 8-88680
- biopolymer time-resolved reson. Raman spectroscopy 8-76999
- birefringence analysis in biological materials 8-56954
- blood cell profile/direct meas. using SEM beam reference lines 8-81094

biological techniques and instruments continued

- blood gas sampler, for gas chromatography, design, construction and characteristics (*Japanese*) 8-85458
- blood sedimentation rate free from gravity influence, rapid determ. from density meas. (*German*) 8-81085
- bone healing, use of anodised Ta electrode, meas. of electrochem. reactions 8-95931
- cancer, appls. of EPR and NMR, review 8-69173
- cell analysis in flow systems, geometry for orienting flat cells 8-77161
- cell high-speed analysis, laser absorpt. and scatt. meas. (*German*) 8-92687
- cell medically relevant class determ., scatt. light cluster anal., cervical smear tests (*German*) 8-92686
- cell morphological parameters extraction from diff. pattern, Fourier optical approach 8-92749
- cell suspension six-channel aggregometer 8-81001
- cellular identification of free cells by light microscopy and SEM 8-53589
- chemiluminescence of aldehyde-preserved plant tissues on exposure to salts of heavy metals 8-77160
- chromosome band online linear scanning, human, BANDSCAN computer program 8-92758
- cinemicrographs, time lapse, of cultured cells, computer-aided analysis 8-92756
- colour vision physiological measurement facility, monkey detected responses (*Japanese*) 8-92752
- computer control of isolated heart preparation for biomedical research 8-53603
- computerised multiple response parameters meas. 8-57136
- contrast enhancing filter for banded chromosomes 8-92755
- convective heat loss assessment from humans in cold water 8-81093
- culture device for cell growth, quantitative microscopy and autoradiography 8-65163
- cytofluorometer, imaging system for correlating fluoresc. cell meas. in flow 8-61240
- cytometry, hydrodynamic orientation of sperm heads in flow systems 8-77162
- cytophotometric and autoradiographic simultaneous anal. device 8-77172
- cytophotometric histogram, computer aided analysis of cell-cycle phase 8-92759
- deep body temperature measurement using piezoelectric transducer, sampled data system, unrestrained domestic fowl appl. 8-57152
- displays, three dimens., in biostereometrics 8-81010
- DNA distributions automatic processing and interpretation 8-92757
- earthworm locomotor behaviour pattern meas. 8-88772
- electric field exposure of miniature swine, vertical 60 Hz fields 8-53587
- electrochemical cell for determ. of O_2 partial press. in biological fluids 8-85420
- electrodes, laminated, for nerve biopotential recording 8-92760
- electron diffraction, cryst. bending and high resolution protein struct. determ. 8-53325
- electron microscope, fluoro-autoradiography, improvement of efficiency 8-65162
- electron microscope image texture discrimination and automated meas., pituitary tissue appl. 8-57099
- electron microscopy freeze-fracture image enhancement by reversal processing of sheet film 8-62267
- electron photomicrography of marine microorganisms on submerged surfaces 8-85454
- electron probe microanalysis, charging effect in electron-irrad. ice 8-57141
- electrophoresis, deflected-lamina, biological materials fractionation in space 8-85397
- electrophoretic separator, continuous flow, for biological materials on sounding rocket 8-85398
- electrostimulators, new Russian devices 8-85353
- EM wave exposure facilities for bioeffects research, survey 8-73174
- emulsion scintillation counting of ^{222}Rn and ^{226}Ra 8-81089
- endocrine research, continuous blood sampling and time series anal. 8-77130
- endogastric probe for telemetric pH meas. (*German*) 8-85452
- energy loss spectrometry microanal. using field emission STEM 8-53286
- epicardial and body surface pot. meas. in intact dog, transfer coeffs. calc. 8-92614
- EPR, rat liver and hepatoma mitochondrial lipids, stochastic anal. 8-76984
- EPR and saturation transfer EPR, fast computation, master supermatrix eqn. soln. 8-62213
- EPR and saturation transfer EPR, fast computation, perturbation approach 8-62212
- EPR and saturation transfer EPR, fast computation, perturbation approx. extension for overmodulation 8-82754
- EPR studies of metalloproteins 8-64936
- erythrocyte high gradient magnetic separation 8-53585
- erythrocytes of human blood, diameter meas. by specific elec. cond. 8-53353
- extracellular action potential recording, interference suppression 8-61294
- fibre optic heterodyne interferometer for vibr. meas. in biological systems 8-77101
- field-desorption mass spectrometry, principle and technique, appl. to corins and vitamin B_{12} 8-80821
- fingerprints, phys. props. and detect. methods 8-78056
- fingerprints, radiographic and physicochem. techniques, for detect. 8-78055
- flow velocity determination with pulsed NMR, appl. to plants 8-83506
- flow velocity meas. at olfactory organ nares of fishes, laser velocimetry (*German*) 8-69262
- fluid density measurement techniques, biological macromolecules in solution appl. 8-92751
- fluid mixing and bottling unit improvement 8-61291
- fluorescence polarimeter for flow cytometry 8-73191
- Fluorescent EXAFS data using solid state detector, for metals in dilute biological systems 8-66595
- fluorocarbon detection by gas chromatography (*German*) 8-96117
- Fourier transform. IR obs. of complex systems 8-68945
- Fourier transform IR spectroscopy of polymer systems 8-58870

biological techniques and instruments continued

functional residual capacity meas. instrumentation for neonates and small animals 8-53590
 gel permeation chromatography of interacting multicomponent systems, protein isomerisation study 8-68950
 gel permeation chromatography of interacting multicomponent systems, protein isomerisation kinetic consts. determ. 8-68951
 gross surgical specimen photography, centimetre rule/elevator rod technique 8-61287
 heart muscle cells, paraffin-embedded, cryofracture, SEM and TEM obs. 8-57148
 holographic microscopy, image plane holograms of test target, blood cells and hair 8-58944
 image analysis system, 2D TAS Leitz, compact bone substance porosity determ. (*German*) 8-92753
 image intensifier TV X-ray detector, high sensitivity, biological structure diff. study appl. 8-89609
 inelastic electron tunnelling spectroscopy appls. 8-92770
 inelastic electron tunnelling spectroscopy appls. 8-92771
 interference microscopy, for plant cell wall and cytoplasm refr. index determ. 8-57151
 ionic channel formation in living cell membrane, microelectrode obs. 8-53372
 ionisation mass spectrometer, with dedicated minicomputer, biological appls. 8-53586
 iontophoresis, gated HV system with accurate current monitoring 8-69259
 IR photography, principles and appls., book 8-82068
 laser desorpt.- mass spectrometry, polar nonvolatile bio-organic mol. anal. appl. 8-92534
 laser exposure of mammalian cells using evanescent fields created in optical waveguides 8-73298
 laser flash absorption change kinetics spectroscopy at 820 nm, photosynthesis study appl. 8-92769
 laser photo-CIDNP as surface probe for proteins in soln. 8-73138
 light absorption and orientation of absorpt. momenta in biological structs. 8-53326
 light transmission microscope, object diff. evaluation, object and field stop spectrum separation (*German*) 8-92685
 lipid bilayers, solvent-depleted membrane prep. from conc. lipid solns. 8-53347
 lymphocyte carbohydrate metabolism in response to mitogens, liq. scintillation vial for radiometric assay 8-61248
 magnetic relaxation study of micro-struct. of water-protein layer of spin-labelled lysozyme preps. 8-76980
 magnetic susceptibility instrument, supercond., automatic, biological appl. 8-57153
 meat, biochemical procedure for detect. of radiation treatment 8-65075
 mechanostimulator, physiological appl. 8-92762
 membrane potentials tracing system, using amplifier for voltage clamping (*German*) 8-61285
 membrane responsiveness curve automated on-line determ. 8-92761
 metal ions, in complexes and biological systems, preliminary vibr. assignment method 8-62953
 metalloenzymes, ^{113}Cd as NMR active site probe 8-68999
 metalloprotein solns., use of Faraday magnetic balance 8-70170
 method for gaining access to auditory nerve of guinea pig 8-85455
 microanalysis biological tissue using Raman laser microprobe 8-88773
 microbiology applications of pattern recognition 8-81084
 microelectrode, metal-filled, reproducible manufacture 8-69263
 microkymography, flow vel. meas. in microvascular bed after exdotoxin administration (*German*) 8-77173
 microscope, phase-locked interf., design and construction 8-49894
 microspectrophotometer, rapid scanning, rhodopsin photoproduct kinetics in frog retinas 8-92763
 microwave device, for murine brain rapid thermal fixation 8-92689
 microwave exposure source, compact light-weight Gaussian-beam launcher 8-96119
 microwave exposure system for study of effects on isolated nerve and muscle preps. 8-53443
 model sampling/identification, input signal anal. 8-69267
 molecular spectroscopy, conference, Wroclaw, Poland (Sept. 1977) 8-62951
 motion online detection in digital video images, mice identification in labyrinth expts. (*German*) 8-92754
 motion transducer for use in intact in vitro human lumbar spine 8-57155
 motor unit recruitment and firing freq. control in elec. stimulated muscles of cat 8-81092
 multi-microelectrode system for simultaneous recording of closely spaced neurons (*Japanese*) 8-61284
 muscle, mech. pulse propag. vel. meas. using piezoelectric crystals, elastic moduli 8-92668
 muscle, skeletal, deriving viscoelastic modulus from transient pulse propag. 8-77077
 muscle, smooth, intestinal cell, voltage clamp studies of hyperpolarising inactivation 8-80847
 nanosecond flash photolysis, techniques and biological appls. 8-68905
 neurophysiology, computer assisted unit data acquisition/reduction 8-61266
 neutron activation anal., optimal conditions, blood appl. (*Bulgarian*) 8-85280
 neutron activation anal., using standard reference materials as multielement irradi. standards 8-80815
 neutron activation anal. of biological samples, device for opening quartz ampoules 8-61121
 neutron activation analysis, gamma-ray spectra prediction, detection limits, computational procedure 8-85242
 neutron activation analysis in vivo, rats 8-73115
 NMR, noninvasive meas. of biological information, magnetic focus generation (*Japanese*) 8-85355
 NMR, two-dimens., state-of-the-art 8-74044
 NMR determination of phys. and biological struct. (*Rumanian*) 8-49874
 NMR for biological and medical imaging 8-69172
 NMR imaging of living organisms (*Polish*) 8-77098
 NMR spin echo pulsed gradient, cell struct. size determ. from water diffusion 8-77159
 noninvasive beam-wave reflectometer for complex permittivity meas. at microwave freqs. 8-74030

biological techniques and instruments continued

oculomotor control system, expt. set-up for clinical investigation, visual, acoustic, vestibular stimulations 8-80990
 optical microscopy, online difference image method (*German*) 8-92688
 optical mixing method, for periodic conversions obs. in biological system solns. 8-96029
 optical rotating spiral scanner for frog muscle contraction meas. 8-96120
 paramagnetic metal ions as structural probes for NMR investigation of inorganic and bioinorganic compounds 8-62828
 particle counting and vol. determ. in suspensions, optical-electronic device 8-57894
 passive dynamic characteristics of man in lying posture, testing apparatus 8-80893
 pattern recognition of biological specimens via matched spatial filtering 8-69261
 permittivity meas. for lossy high dielec. constant materials, method 8-93732
 photobiological process relative quantum yield determ. using light of different spectral composition 8-65154
 photoelectron spectroscopy, impact on biology 8-65156
 photometric device for arterial thrombosis investigations 8-85456
 photoreceptor spectral sensitivity on-line computation using programmable pocket calculator 8-69264
 photosynthesis, picosec. spectroscopic investig. 8-68964
 photosynthesis, picosecond spectroscopy appls. 8-53601
 photosynthetic systems, computer assisted scanning and kinetic spectrophotometry 8-68963
 picosecond fluorescence spectroscopy, competing events 8-58051
 PIXE, synaptic vesicle ion content determ. 8-61166
 plant photosynthesis, signal II, electron spin-echo method 8-96118
 Plexiglas animal holders, effect on microwave energy absorpt. 8-92674
 PMR, nuclear Overhauser enhancement difference spectroscopy, for macromolecules 8-81091
 position sensitive, X-ray, detectors, linear, circular, two-dimens. 8-62281
 pressure jump method for fast kinetics using optical rotation and circular dichroism 8-77175
 prosthetics, in vivo method for evaluation of effects of materials on arterial thrombosis 8-81071
 protein crystallography, MWPC as area detector 8-65166
 protein NMR spectra, comparison of convolution and pulse methods for line narrowing 8-78729
 protein structure least squares refinement technique based on fast Fourier transform algorithm 8-91197
 proton microprobe for nondestructive trace element analysis 8-64911
 psychophysics as method of meas. of biosystems (*Japanese*) 8-53591
 pulse radiolysis appl. to biomolecule reactions and struct., review 8-61145
 radioactive microsphere prep. and props. for localised irradi. of lung tissue 8-53445
 radioimmunoassay, probe for fine struct. of biological systems, review 8-73217
 radioimmunoassay techniques development 8-88743
 Raman studies of biomembranes, phospholipid-d, as nonperturbing components 8-53330
 random pulse train inputs, use of digital filters (*Japanese*) 8-53547
 relaxation spectrometry, injected white noise as soln. of phase problem 8-76830
 replicon autoradiograms, computer-assisted measurement 8-92692
 resonance Raman effect, appl. to β -carotin, haeme proteins and rhodopsin (*Hungarian*) 8-74666
 retinal light responses, simultaneous recording by extra- and intracellular electrodes in crayfish 8-69055
 room temperature phosphorimetry, anal. technique, review, methodology, instrumentation, appls. 8-95972
 scanning microscope, depth of field rel. to thick biological slice obs. 8-86328
 SEM, image interpretation 8-53597
 SEM, photographic densitometry, appl. to chromosomes 8-77168
 SEM and human lymphocyte surface morphology, review 8-53599
 SEM/STEM cold stage thick specimen heating model 8-61289
 single unit activity, computer program for generating on-line raster dot displays 8-57087
 skeletal muscle bulk specimen, quantitative X-ray microanal. of diffusible ions 8-57143
 slow flash photolysis using conventional spectrophotometer, visual pigment appl. 8-68904
 spatially constricted flow meas. using laser Doppler velocimeter 8-71409
 spectroscopic/electrochemical cell for protein studies 8-76832
 spin labels, appl. to study of assoc. of adenosine, AMP, ADP and ATP 8-81086
 spin labels and biomembranes, review 8-69265
 spin probe investigation of adsorpt. of ion-paramag. compounds on proteins 8-65153
 spiral biological object indexing, use of optical diffractometer 8-96121
 stimulus artifact suppression, sample and hold amplifier system 8-77163
 stimulus generator for evoked response studies 8-57011
 subnanosecond single photon counting fluorescence spectroscopy using tunable dye laser excitation 8-86355
 superconducting susceptometer, automatic, sensitivity calibration, biological appl. 8-57154
 surface dynamic representation by TV moire topography (*German*) 8-89430
 synchrotron radiation low angular scatter in biopolymer solns., use of proportional chambers 8-65155
 TEM, low-temp., radiation damage, review 8-57147
 TEM, low-temp., struct. determ. of frozen, hydrated, cryst. biological specimens 8-57146
 TEM, thin section uniform region quantitative meas. 8-58097
 tissue impedance meas. by phase-sensitive voltage and current detection 8-53602
 trace element characterisation, by instrumental neutron activation anal. 8-73116
 trace element determination, using DC plasma echelle spectrometer, automated 8-53277
 tunnelling spectroscopy, appls., review 8-92588

biological techniques and instruments continued

- uniaxial testing of soft human tissues, in vitro apparatus 8-61295
- US transducer, shear-wave vel. meas., bone elastic moduli determ. 8-83201
- US/EMG transducer for biodynamic research, speech appl. 8-77164
- Ussing miniature chamber for obs. of size and shape of lateral intercellular spaces in living epithelium 8-77032
- vector impedance meter for biological tissue 8-57138
- vertebrate cornea, transparent layered structure thickness monitor 8-92737
- vibro-interference, for 3-dimens. imaging of biospecimens using holography 8-53584
- video-tracking of micro-circulation, appl. of bit-slice processors (*German*) 8-88749
- virus size measurement using optical microscope, Virometer design 8-61296
- visual physiology and psychophysics polar coordinate data 8-56988
- visual stimulator, computer-controlled, for electrophysiology expts. 8-69230
- X-ray absorption spectroscopy using synchrotron radiation, appl. to metalloproteins 8-64938
- X-ray diffraction data acquisition using position-sensitive counter (*Japanese*) 8-88774
- X-ray diffraction study of biological structs. in native form, selection of radiation 8-81087
- X-ray diffraction with synchrotron radiation, absorpt. factor, CsDNA appl. 8-76988
- X-ray kinetic diffr., position sensitive counter 8-62283
- X-ray laser holography, possible appl. to crystal and biological microstructure 8-55322
- X-ray microanalysis, iso-atomic droplets as models 8-53598
- X-ray spectrometry, energy dispersive, ultramicroanalysis of biological fluids 8-92768
- zeugmatography, state of the art 8-74043
- Dy³⁺, free-radical relax. agent in biological tissues 8-81090
- Ga melting-point apparatus for thermometer calibration, enzymologic appl. 8-85460
- K channel blocking agent, 3,4-diaminopyridine 8-69028
- Na⁺ multicompartiment flow model of frog skin epidermis, experimental verification 8-92607
- O₂ partial pressure and bioelectric potential simultaneous meas. in living tissue (*German*) 8-85453
- ³¹P NMR investigation of heart physiology 8-69018
- ³¹P NMR studies of isolated rat liver cells 8-61150
- Pb, determ. in aqueous solns. by Delves Cup technique and flameless atomic absorpt. spectrometry 8-68973
- Pu skeletal level estimation based on DTPA induced excretion in faeces 8-85390

biology

- see also biological fluid dynamics; biological techniques and instruments; biophysics; blood; cardiology; ecology; evolution (biological); medicine; physiology; zoology*
- aquatic life, protocols for evaluating effects of chemical substances 8-53604
- Arrhenius equation and accel. testing 8-53182
- Central Atlantic Ocean, biological characts. rel. to irradiance meas. (*Russian*) 8-77257
- S.Atlantic Ocean, sea water plankton content rel. to hydroptic struct. variability (*Russian*) 8-77262
- biochemical reactions, stratification (*Russian*) 8-57884
- biochemical systems stability anal., practical guide 8-73135
- biochemistry and biophysics horizons, book 8-68977
- biosphere and active solar processes link, role of Earth's natural electromag. field 8-61211
- compartmental models with delays, phys. realisability 8-53313
- coniferous forest canopy, vertical air motion in underlying stratified ground layer (*Russian*) 8-96266
- dissipative systems, dynamical field theory, hierarchical struct. of field thermodynamics 8-73132
- mathematical biology meeting, Philadelphia, USA, (Aug. 1976) 8-53311
- porous solid with below-freezing pt. adsorbate, isothermal adsorption and dimensional changes obs. 8-75925
- roadside soil and plants in Alexandria district, Egypt, contamination with Cd, Ni, Pb and Zn 8-81171
- vegetation, hydrocarbon emissions oxidation as atmospheric CO and H₂ source 8-88881
- vegetation layer, effect on ground surface temp. and moisture content 8-73373
- zero gravity expts. on Cosmos 782 satellite, results 8-85818

biology computing

- see also computerised instrumentation; computerised signal processing*
- aortic dynamics in man, analogue simulation model 8-80903
- articulatory to-acoustic transformation in vocal tract, inversion by computer sorting 8-69110
- BANDSCAN, program for online linear scanning of human banded chromosomes 8-92758
- bladder smooth muscle impulse propag., math. anal. (*Japanese*) 8-53539
- cardiovascular research database system 8-53549
- cytophotometric histogram, computer aided analysis of cell-cycle phase 8-92759
- DNA distributions automatic processing and interpretation 8-92757
- DOTS, program for generating on-line raster dot displays of single unit activity 8-57087
- ergometric test, computer interpretation of heart-rate var., anal. of cardiac control in exercise 8-85430
- flagella bend propagation, derivation of eqns. of motion and simulation 8-77074
- gastrointestinal electrical rhythm frequency estimation by autoregressive modelling 8-56948
- head injury model with viscoelastic brain tissue, mech. response 8-69117
- intestinal electrical activity, motility, computer anal. of electrophysiological study on dogs 8-80851
- leucine aminopeptidase crystalline aggregates, interpretation of electron microscope images 8-68988
- membrane dynamic equation solving, practical algorithm 8-77038
- neuronal populations, diffusely-connected, computer simulation 8-53384

biology computing continued

- pattern recognition in microbiology 8-81084
- photoreceptor spectral sensitivity on-line computation using programmable pocket calculator 8-69264
- protein structure least squares refinement technique based on fast Fourier transform algorithm 8-91197
- psychoacoustical aspects of synthesized vertical local cues, computer synthesis 8-61198
- renal counterflow systems, numerical solution of differential equations 8-92662
- replicon autoradiograms, computer-assisted measurement 8-92692
- sound analysis, reversible computer method adapted to bioacoustical expts. 8-57137
- ventricular function computer simulation, development of model and parameter estimation 8-53439
- vertebral model, computer-aided technique for 3-D finite element model generation 8-92591
- visual cortex neurones, rabbit, organisation of background activity 8-69044
- visual cortical neurone reaction patterns to const. illum. 8-80871
- Na⁺ multicompartiment flow model of frog skin epidermis, experimental verification 8-92607

biomagnetism

- erythrocyte high gradient magnetic separation 8-53585
- field detection by invertebrates Tenebrio and Talitrus, distinct from light detect. 8-77073
- magnetic auditory evoked response using SQUID 8-80889
- magnetic susceptibility applications, review of literature 1975-1977 8-82006
- magnetocardiograms from normal hearts, interpretation (*Japanese*) 8-53433
- magnetoencephalogram genesis mechanisms 8-53432
- magnetoencephalography, correl. with EEG for normals and patients 8-65062
- magnetometry of human heart in small ferromag. enclosure, using SQUID 8-92726
- nerve conduction velocity, biomagnetic response of lobster circumesophageal connective 8-92619
- SQUID detector appl., techniques 8-96061
- static and low frequency magnetic fields, biological effects review (*Slovak*) 8-88722
- susceptibility instrument, supercond., automatic, biological appl. 8-57153
- visually evoked elec. and mag. response simultaneous recording for diagnosis 8-53558

biomechanics

- see also biological fluid dynamics*
- acrylic bone cement spinal fixation, mech. props. 8-81072
- ankle joint, human, compliance 8-57034
- arm movements controlled by peripheral feedback, in humans, simulation 8-80891
- arterial wall axial deform. and anisotropy (*Japanese*) 8-53437
- arteriografr, fracture phenomena, of bovine, swine 8-92746
- artery length-force and vol.-press. relations, meas. and empirical formulae 8-65072
- articular cartilage, electromechanical props. during compression and stress relaxation 8-92667
- articulated total body model, generation of child data sets from anthropometric data, for crashes 8-80912
- biopolymer materials, review of mechanics of tissue 8-69131
- biped locomotion control, digital simulation 8-80904
- body motion computer-aided tracking using CCD image sensor 8-61269
- bone, piezoelectric effect on exposure to US, effect of sample rot. 8-80913
- bone elastic modulus meas., US transducer fabrication 8-83201
- bone mechanical properties determ. in vivo, noncontacting EM device 8-77133
- bone morphology and fracture, exam. 8-57036
- bovine hip bone, compression tests, effect of specimen shape and size on mech. props. and fracture mode 8-69132
- brain injury, pulse loading effect 8-57029
- brain tissue, human, nonlinear constitutive relations 8-80910
- cat eardrum model as thin shell using finite element method 8-65036
- cell membrane nuclear hydrodynamic shear, non-equil. Ising model, master eqn. 8-61146
- chitin, in lobster shell and apodeme, piezoelec. rel. to remodelling 8-64929
- cochlea, 3-dim. model, point-impedance charact. of basilar membrane 8-57009
- cochlea, two dimensional model, method for computing motion 8-65037
- compact bone, empirical strength theory, biaxial stress characts. 8-77081
- corneal wound holographic stress testing in postoperative patients, specular illum. arrangement 8-65102
- coronary arteries, human, mech. prop. changes with age 8-65068
- crutch walking, lower-limb vertical ground-reaction forces 8-77079
- elbow three-dimensional rotation 8-69129
- epithelium of small intestine, mech. props. of intercellular contacts 8-53351
- erythrocyte, sectioned, generalised theory of geometrical shape 8-65071
- erythrocyte osmotic fragility curve, statistical synthesis 8-65070
- eye, elasticity of sclera and choroid in humans, rel. to scleral rigidity and accommodation 8-80907
- eye lens thermoelastic stresses due to microwaves 8-80914
- eyeblink, human, dynamics model 8-61167
- flagella bend propagation, derivation of eqns. of motion and simulation 8-77074
- foot vertical force during walking, continuous meas. device (*Japanese*) 8-73273
- foot/floor contact temporal patterns during walking, automated on-line meas. system 8-77128
- gait, representation by 4 dimens. vectors (*German*) 8-88723
- gait joint torque and energy patterns in normal humans 8-80897
- hand-arm system, distributed-parameter dynamic model 8-92663
- Haversian bone, exam. of mechanical failure at microstructural level 8-77080

biomechanics continued

- head injury model with viscoelastic brain tissue, mech. response 8-69117
- head-neck impact response using realistic human model 8-80909
- heart, elastic props., forces, stresses and press. (*Dutch*) 8-73170
- heart contractility, muscle tissue quality and sliding filament micromechanism (*Dutch*) 8-73171
- heart muscle, behaviour of myosin projections during staircase phenomenon 8-53362
- heart vibration quantitative characterisation by multipolar acoustic heart model, minicomputer method 8-85429
- hip, human, kinematics and kinetics 8-69130
- intervertebral joint, systems identification for material props. 8-69125
- intestinal motor activity, math. model 8-77078
- lateral tibial plateau, axisymm. finite element anal. 8-69127
- lecithin membrane, depend. of Young's modulus in plane of membrane on deform. 8-80894
- left ventricular function, normal and abnormal, vel.-strain relationship 8-69119
- lumbar spine motion transducer for use in intact in vitro preps. 8-57155
- lung, distributed response of complex branching duct networks 8-57027
- medullary implants with porous coating, stress distrib. 8-69256
- muscle, active frog skeletal, isometric tension, slow stretch effect, X-ray diff. study 8-80906
- muscle, glycerol-extracted fibrillar fibres, cross-bridge slippage induced by AMP-PNP and stretch 8-77075
- muscle, mech. pulse propag. vel. meas. using piezoelectric crystals, elastic moduli 8-92668
- muscle, myosin regulated, changes in crossbridge attachment 8-53361
- muscle, skeletal, deriving viscoelastic modulus from transient pulse propag. 8-77077
- muscle, skeletal, tension development, F-actin subunits struct. non-equiv. model 8-64959
- muscle, striated, analytical soln. to isometric mechanogram of Hill's model 8-73168
- muscle, striated, reversible loss of Ca control of tension assoc. with removal of regulatory light chains, scallop 8-53360
- muscle mechanics thermodynamic model 8-80908
- nematode oesophagus pumping mechanism 8-69121
- passive dynamic characteristics of man in lying posture, testing apparatus 8-80893
- postural equilibrium automatic meas. and real-time evaluation in man, instrumentation system 8-77127
- prosthetic, joint function restoration, biomech. operating principles 8-69257
- prosthetic heart valves, rigid leaflet and caged-ball types, diastolic ventricular mechs. 28-81079
- pupil noise amplitude control, interaction of sensory and motor mechanisms 8-64998
- skull-brain system, human, prolate spheroidal viscoelastic shell containing viscoelastic fluid, axisymm. vibrs. 8-80901
- soft tissue nonlinear viscoelastic behaviour 8-69128
- soft tissues, tension field theories 8-65064
- sperm flagella equation of motion 8-80895
- stabilograms, influence of platform geometry 8-81038
- student laboratory expts. using a crane boom 8-81759
- uniaxial testing of soft human tissues, in vitro apparatus 8-61295
- urease shear inactivation, metal ion effect, rel. to shear deform. effects in enzyme catalysis 8-76982
- ventricular function computer simulation, development of model and parameter estimation 8-53439
- ventricular wall dynamics and obs. on blood flow 8-80896
- virus solid, low density, yield stress model 8-88725
- visceral smooth muscles in vertebrates, viscoelastic and plastic props. 8-73169
- vocal cord vibration, computer model of air vol. displacement 8-69111

biomedical applications of computing *see medical computing***biomedical electronics**

- see also electrocardiography; electroencephalography; microelectrodes; patient monitoring; patient treatment; prosthetics; sensory aids*
- ECG-telemetry apparatus, single-channel, PLL demodulator appl. (*German*) 8-57097
- electronic meas. application areas 8-57094
- EM radiation probes, implantable, design factors 8-73258
- EMG amplifier, wideband isolated, cct. 8-57089
- implantable electronic pancreas and blood glucose monitor 8-88767
- intensive care instrumentation 8-53559
- manipulator, computer controlled, for use as remotely controlled arm 8-81083
- measurement of temp., press. and flow, for teaching 8-49621
- microprocessor applications to biomedical systems 8-57095
- nervous system, electrical stimulation, laboratory research (*Norwegian*) 8-77096
- pain relief via pulse generator implantation in human body 8-96112
- particle simulation unit for counter circuitry testing 8-81002
- piezoelectric insulin pump and valves for diabetes patients 8-53565
- radionuclide cardiac motion study, computer-processed, ECG gating device 8-73210
- simulated inductors, large voltage swing, used for oscillator and floating coupling cct. 8-69227
- speech formant extraction, tracking loop filters 8-65051
- teletherapy machine electronic dual timer 8-85358

biomedical engineering

- see also biomedical electronics; biomedical equipment; orthotics; patient treatment; prosthetics; sensory aids*
- blood pulsative flow digital simulation by finite element method 8-92670
- clinical engineering and health care in nonaffluent underdeveloped nations 8-80991
- communications conf., EUROCON, Venice, 1977, May 8-53552
- conference, Stuttgart, Germany, (May-June 1978) 8-80988
- dental materials, uses and props., review 8-53548
- education in France 8-73807
- interdisciplinary aspects and problems 8-53553
- physics aspects (*German*) 8-92735
- picture communication systems 8-57104
- polycarbonate purification for medical use 8-84759

biomedical engineering continued

- polymeric biomaterials for blood-contacting appls., problems and new dimensions 8-85423
- review of nucl. medicine 1977 8-85459
- signal processing and telemetry, digital bandpass analysis 8-57107
- undergraduate degree program, state university approach 8-77646

biomedical equipment

- see also biomedical electronics; biomedical measurement; orthotics; prosthetics; radiography; radioisotope scanning and imaging; sensory aids*
- 60 Hz harmonic eliminator 8-77124
- A/D conversion, multichannel, without timing skew, for LF biological signals 8-61271
- acoustically evoked potentials in EEG, meas. by adaptive matched filters (*German*) 8-88755
- adaptive correlation ratemeter for Doppler foetal heart rate meas. 8-88732
- anaerobic environment integrated system 8-80987
- analysis instrumentation in clinical enzymology 8-88675
- applanation tonometer correlations for intraocular press. meas. 8-77047
- arrhythmia detection using a low-power, CMOS processor 8-73276
- arterial pO₂ intravascular monitoring using catheter-tip polarographic electrode (*German*) 8-85408
- arterial pressure modulator for perfusion circuit of isolated organ (*French*) 8-81004
- audio dual channel monitor for distinguishing action pots. from two different sources 8-61293
- audiometer, screening, and real-time computer techniques 8-81009
- autotransfusion, variable-speed pump head control 8-57121
- betatron bremsstrahlung field shaping apparatus for teletherapy 8-57062
- blood, filter evaluation 8-69250
- blood cell differential counter, ADC 500, pattern recognition based image processing system 8-73282
- blood flow measurement by US Doppler method, computer-aided determ. of angles (*German*) 8-80931
- blood gas analysers, review 8-69238
- blood pressure electric sensor for extracorporeal circulations (*German*) 8-92721
- blood pressure instruments, direct systolic/diastolic meas., review 8-69234
- blood pressure instruments, noninvasive arterial meas. using US Doppler effect 8-69167
- body motion computer-aided tracking using CCD image sensor 8-61269
- body radioactivity measurement, SABRE 3 computer system 8-85425
- bone conduction vibrators, calibration force levels 8-65046
- bone mechanical properties determ. in vivo, noncontacting EM device 8-77133
- brain impedograph, computerised 8-77139
- cardiac arrhythmia monitors, review 8-69233
- cardiac noise, automatic segment anal. (*German*) 8-88759
- cardiac output analysers, equipment, maintenance and ccts., review 8-69239
- cardiac output measurement, in vitro comparison of six commercially available thermofusion systems 8-77135
- cardiotachygram, anal. of recurring beat sequences (*German*) 8-88753
- cathetron for cervical cancer treatment, description for teaching 8-49617
- cell recognition and counting using adaptive coherent optical processor 8-77120
- cell suspension six-channel aggregometer 8-81001
- cephalostat for speech physiology research 8-65140
- cerebral blood flow computer for use in angiogram theatres 8-73227
- cinéangiocardigrams, automatic anal. using TV system on line with minicomputer 8-92699
- clinical chemistry temperature standard, Ga melting-point 8-80997
- clinical laboratory technology, new developments, diagnostic immunology and microbiology 8-81037
- cold urticaria diagnosis and treatment assessment, stable low temp. source 8-61276
- colour TV, single tube SICOLOR, appl. to endoscopy (*German*) 8-88758
- computer-aided intensive care in paediatrics (*German*) 8-88754
- computerised tomography, basic physics, mathematics and data reconstruction 8-73218
- computerised tomography, Shimadzu scanner SCT-100N, development (*Japanese*) 8-61277
- computerised tomography body scanners, comparison of translate-rotate, pure rotary types 8-69211
- computerised tomography scanner resolution, geometrical limitations 8-73237
- constant current supply for percutaneous electrophoresis of amino acids and urea 8-61237
- critical care unit instrumentation care and servicing, book 8-69231
- CW FM sonar with aural displays, improvements 8-87221
- cytofluorometer, imaging system for correlating fluoresc. cell meas. in flow 8-61240
- data evaluation system, for use with gamma cameras in nuclear medicine 8-92732
- dermatological photobiology, fibre optic light guides for phototesting 8-53472
- displays, three dimens., in biostereometrics 8-81010
- drip feed unit microprocessor control development 8-53563
- dynamic motion simulator for testing plastic ligaments and tendons (*German*) 8-81070
- ECG, cordless electrocardiograph and heart rate meter (*Japanese*) 8-80984
- ECG, interactive analysis techniques with Random Access Mass Storage ECG Analysis System 8-81034
- ECG amplifiers, instruments and maintenance, review 8-69232
- ECG arrhythmia simulator for monitor testing 8-61270
- echo distribution evaluation (*German*) 8-80934
- echocardiogram computer-assisted interactive interpretation 8-80938
- EEG frequency analyser, real-time, microprocessor monitored 8-57092
- and electrical safety, for nurses, book 8-57100
- electrically rechargeable hand held device for painful subjective sensation prod. in teeth, pulpa vitality (*German*) 8-80944

biomedical equipment continued

- electro-medical apparatus, guideline for provisional safety standard (*Japanese*) 8-73274
- electro-medical servicing, quality maintenance 8-77126
- electrochemical cell for determ. of O₂ partial press. in biological fluids 8-85420
- electroconvulsive therapy, servo-controlled volt. machine 8-77148
- electroconvulsive therapy pulse instrument 8-53562
- electromechanical system for diagnosis of spinal abnormalities 8-73286
- electrostimulators, new Russian devices 8-85353
- electrosurgery system using HF surgery unit Radiotom 704 8-73292
- EM syringe for injecting energy into deep-lying tissues 8-53545
- EMG quantitative analysis instrument 8-81041
- endoscopic coagulation of mucous membrane lesions using HF elec. current (*German*) 8-80945
- endoscopic laser photocoagulation, use of gas jet appositional pressurisation 8-53468
- endoscopic manometry in gastroenterology 8-92730
- endoscopic system advances 8-57096
- epidural intracranial pressure meas. by piezoresist. transducer (*German*) 8-85404
- extracellular action potential recording, interference suppression 8-61294
- extracorporeal blood oxygenator safety and efficacy, review 8-77153
- eye contrast sensitivity testing instrument 8-73275
- eye refractor, automatic, optical system 8-61274
- eye testing using screen image divider 8-57114
- fibre endoscope, image quality improvement 8-71219
- fibre endoscope one-component objective dimensional design (*Russian*) 8-69228
- fibre optic, catheter transducer, side hole type, for intracardiac press. meas. (*Japanese*) 8-73272
- fibre optic catheter-tip micromanometer as intracardiac press. transducer (*Japanese*) 8-73270
- fibre optic endoscope, incoherent optical power launching limits 8-63193
- finger tremor amplitude and freq. artefact reduced routine meas., portable equipment (*German*) 8-85407
- flowmeters, digital 2D full range Doppler velocity meter for cardiovascular diagnosis 8-88731
- fluorescence polarimeter for flow cytometry 8-73191
- fluorescent X-ray intensifying screen efficiency determ., standard method 8-69198
- fluoroscopic spot film system image quality evaluation and optimisation 8-69205
- fluoroscopy, kVp variable, with automatic brightness stabilisation, X-ray tube pot. var. 8-69202
- foetal breathing monitor for humans in utero, US pulsed Doppler instrument 8-69164
- foot vertical force during walking, continuous meas. device (*Japanese*) 8-73273
- foot/floor contact temporal patterns during walking, automated on-line meas. system 8-77128
- frame recording method for intermittent X-ray TV to reduce exposure dose in fluoroscopy (*Japanese*) 8-89607
- gamma camera, influence of digital representation on image quality (*German*) 8-88738
- gamma-camera image information prob., methods of checking (*German*) 8-88734
- gamma-camera used in nuclear medical examinations, developments in photographic recording (*German*) 8-88733
- gonioscopy, foot-operated camera trip for Nikon photo slit lamp 8-80986
- haematofluorometer, for testing Pb poisoning 8-53554
- haemodynamic and cineangiographic data treatment, computer system SYSCORMORAM 8-81030
- headlight, light-operated remote-control device for handicapped persons 8-53571
- hearing aid measurement system comparison 8-65151
- heart-rate store, PLL circuit, portable (*German*) 8-65139
- heat exchanger for heating/cooling blood, thermal design, equipment and blood props. considerations, appls. 8-92744
- holographic stress testing of corneal wounds in postoperative patients, specular illum. arrangement 8-65102
- Humphrey Vision Analyser, reliability and validity of refr. error meas. 8-61265
- image enhancement using 2-dimens. digital filters (*Italian*) 8-53539
- image quality descriptor relationships using signal detect. theory 8-71050
- impedance camera for spatially specific meas. of thorax 8-53464
- impedance meter, AC, battery-operated, for contact resist. determ. before patient monitoring 8-81006
- incubators, portable, improvements 8-81055
- infusion pump control by labour and foetal heart rate (*German*) 8-85415
- instruction in biomedical instrumentation, modular laboratory equipment development 8-89283
- intensive care instrumentation 8-53559
- intensive care unit, use and acceptance of automated monitoring systems 8-81057
- intensive care unit/coronary care unit safety 8-69252
- intensive monitoring computer system, SOLO, one-patient multiparameter bedside monitor 8-81053
- intracranial pressure telemetric meas. (*German*) 8-85403
- ion-selective disc electrodes with neutral cation-carriers for automated electroanal. of serum (*German*) 8-73269
- iontophoresis, gated HV system with accurate current monitoring 8-69259
- labour meter with tape recorder for ambulatory patients (*German*) 8-85413
- laser endoscope, coagulation in gastrointestinal haemorrhages (*German*) 8-69178
- laser stethoscope, non-contact high sensitivity, using interferometer technique (*German*) 8-69176
- laser surgical unit for clinical rhinology (*German*) 8-69177
- Lexiscope, portable pocket size X-ray imaging system for medical/dental radiography 8-92701
- lung gas analysis using redox gas sensors (*German*) 8-85440
- magnification skeletal radiography, imaging parameters and clinical relevance 8-69185

biomedical equipment continued

- mammographic image quality comparison phantom 8-85357
- mammographic screen-film systems, comparison of laboratory and clinical evaluations 8-69187
- mammography, utility of modelling 8-69188
- mass spectrometer, blood gas anal., silicone rubber catheter operating mechanism (*Japanese*) 8-61273
- mechanostimulator, physiological appl. 8-92762
- medical CRT displays, review 8-69240
- microcirculation semiquantitative demonstration using US noninvasive meas. method (*German*) 8-85348
- microcomputer based digital filter for electroencephalogram processing 8-73278
- microcomputer scanning system for respiratory mass spectrometer 8-88756
- microcomputer system for on-line analysis of electroencephalographic data 8-73277
- microcomputers for bedside monitoring of patients (*German*) 8-88751
- microcomputers in biomedical and clinical applications 8-73283
- microprocessor based instrument, Dinamap, for arterial press. automatic determ. 8-96108
- micturition reflex elec. restoration, sequential stimulator 8-53567
- Mingograph in clinical electroretinography 8-92731
- mobile gamma camera with remote image processing computer system, for nuclear medicine 8-92700
- muscle spindle afferent activity and tone meas. in man, apparatus generating controlled ramp movements 8-77121
- nasal air emission in speech disorders, electrodynamic evaluation 8-77134
- neuromuscular blockade monitoring device, twitch box 8-77132
- neurophysiology, computer assisted unit data acquisition/reduction 8-61266
- neutron activation in vivo total body anal. using 14 MeV neutrons, calibration and evaluation of system 8-53490
- neutron source for radiotherapy, gas target, energy spectra, flux, dose rates 8-92698
- NMR, field-focusing, formation of chemical scans in man 8-85354
- oesophageal motility study in humans, circumferentially-sensitive miniature press. sensor 8-77131
- oesophageal multiprobe for temp., ECG and heart and lung sound meas. 8-77146
- optical fibre applications, review (*Italian*) 8-53540
- optical instrumentation appl. in medicine, conf., Boston, USA (Sept. 1977) 8-69184
- oximeter calibration, humans exposed to centrifugation 8-92734
- passive dynamic characteristics of man in lying posture, testing apparatus 8-80893
- perimeter localising, for visual field study and retinal tear location 8-85442
- phoneme recognition system based on human audition, psychophysical expts. 8-69115
- piezoelectric strain gauge transducer, for clinical recording of ocular microtremor 8-96109
- pilot function and working capacity medical and physiological investigation apparatus 8-85399
- plastic scintillation filament detector system for ¹⁴CO₂ breath anal. tests 8-65122
- plotting instrument for close-range photogrammetry 8-77137
- pneumothorax diagnosis in deep-sea divers, using Sonicaid portable instrument 8-85351
- portable low-dose X-ray imaging system 8-85375
- positron camera, 3-D imaging, noise anal. 8-85445
- positron camera, 3-dimens., for nucl. medicine 8-73225
- positron emission transaxial tomograph, PETT IV and computer system 8-80959
- postural equilibrium automatic meas. and real-time evaluation in man, instrumentation system 8-77127
- pressure regulator for proportional regulation of two gas pressures, anaesthetic appl. 8-53560
- pulsed Doppler blood velocity meter readout 8-69158
- pupillometer, objective device using counter-rot. perspex blocks 8-81000
- radiographic equipment acceptance testing, systems approach 8-69203
- radiographic equipment servicing by hospital-based group 8-69247
- radiographic film/screen combinations and patient exposure, Nationwide Survey of X-ray Trends 8-73233
- radiographic image quality comparison for different screen/film combinations by subjective judgments 8-73229
- radiographic imaging, digital video acquisition system for extraction of subvisual information 8-69208
- radiographic intensifying screen information content and contrast, comparison of rare earth with CaWO₄ 8-73232
- radiographic proximity X-ray image intensifier tube 8-69206
- radiographic tomography, comparative survey of multi-directional units 8-61242
- radiographic X-ray image intensifier video system, design characts. 8-69209
- radiographic X-ray image intensifier video system, psychophys. evaluation rel. to system measures 8-73234
- radiographic X-ray tube current, effect of electron evaporation 8-69204
- radiography, equipment needs for radiology department, math. model 8-65107
- radiography, falling load technique, performance evaluation 8-69201
- radiography, held radiograph technique and radiation protection 8-73199
- radiography, principles of design of assemblies 8-57065
- radiography, systems approach to scale of equipment 8-57064
- radiography, test phantom for meas. of phys. parameters (*German*) 8-57068
- recorders, direct-writing analogue type, biomedical appls., techniques and maintenance, review 8-69241
- respiration calorimetry determination of O₂-calorie equivalence of thyroid patients and normal subjects (*German*) 8-85412
- respiratory monitors, instrumentation and maintenance, review 8-69236
- respiratory rate and ventilation digital recorder 8-81005
- respiratory total resistance meas. in pre-school children using modification of forced oscill. technique 8-77129
- respirometer, flowmeter-polarographic electrode sensor, for respiratory function telemetering 8-80995

biomedical equipment continued

- respirometer, noncommercial respiratory transducer for EEG laboratory 8-65138
 retinoscopic system, theory including aperture stops 8-85308
 roentgenocardiograph with photoelectronic sensors, calibration device 8-57061
 scintigraphic camera systems and their assessment by computer 8-57063
 scintigraphy and angiography, equipment for quant. evaluation and off-line operation (*German*) 8-88736
 scintillation camera single-photon computed tomography, optimised collimator 8-77106
 sonic anaesthesia during tooth hard tissue operations, BN-1 apparatus 8-85350
 spectrophotometric standards, glass filter SRM 930 by NBS, clinical laboratory appl. 8-54331
 SQUID magnetometry, low-level, of human heart in small ferromag. enclosure 8-92726
 stimulus generator for evoked response studies 8-57011
 stomach double-contrast exam. using Orbiskop 8-73200
 surgical aspiration automatic control device for cardiac surgery (*French*) 8-61282
 Synthalizer, three dims. synthesis and analysis by optical dissection 8-81011
 tape recorder three-channel modulation scheme for biological signals 8-61272
 technical servicing, determ. of range of preventive maintenance 8-85421
 telemetry, transmission and reception with embedded antennae 8-77125
 teletherapy machine electronic dual timer 8-85358
 test instruments, scientific and medical instrumentation capability 8-69242
 thermometers, electronic, review 8-69235
 thoracic impedance of humans, meas. using automatic recording device on defibrillator 8-61239
 three dimensional imaging, conf., San Diego, USA (Aug. 1977) 8-78971
 tissue characterisation by computer-aided US method (*German*) 8-80932
 TOMAX autostereoscopic display, three-dimens. viewing of tomographic data 8-85446
 toxic compounds, enzymatic sensor for continuous determ. (*French*) 8-73099
 transmit/receive 2D ceramic piezoelectric arrays, construction and performance, medical, NDT appls. 8-87223
 transthoracic intramyocardial pacing wire for emergencies 8-69254
 TRIUMF biomedical negative pion beam line, tuning 8-96113
 US diagnostic equipment, portable radiation-force balance 8-69163
 US diagnostic equipment, US power and intensities produced 8-69162
 US diagnostic instrument performance evaluation, work of USA AAPM and AIUM 8-69170
 US diagnostic instruments, output meas., irradi. effects (*Japanese*) 8-80936
 US Doppler velocimetry for 3D blood flow meas. 8-88730
 US flowmeter for measuring rapidly changing gas flows, freq. range, excitation and signal processing (*German*) 8-83502
 US grey scale scanner dynamic range testing 8-69169
 US imaging equipment, quality control problems 8-69171
 US imaging systems, high-resolution, real-time 8-69160
 US implantable CW Doppler blood flowmeter, optimal system design 8-53460
 US instrumentation standardisation, physician's need 8-69168
 US pulse-echo equipment, tissue equiv. test objects for routine performance checks 8-73182
 US Pulse-echo transducer standardization 8-73181
 US real-time diagnostic system for dynamic and still images, wireless echovision 8-65101
 vaginal photoplethysmographic transducer, blood vol. change monitoring in menstruation 8-92733
 vascular interface system for automation of haemodynamic monitoring and therapy 8-81054
 ventricle volume characts., nuclear medical determ., appl. of computer system (*German*) 8-88737
 ventricular arrhythmia on-line study, computer system 8-81060
 vertebrate cornea, transparent layered structure thickness monitor 8-92737
 video correlating system for blood flow vel. meas. in microvessels 8-53543
 video processor for computer calc. of press.-vol. indices from left ventriculograms 8-53495
 video-tracking of micro-circulation, appl. of bit-slice processors (*German*) 8-88749
 vision testing instrument, determ. of visual acuity and depth perception threshold 8-81007
 visual stimulator, computer-controlled, for electrophysiology expts. 8-69230
 visual stimulator for flicker fusion expt. 8-96053
 vitreous surgery via pars plana, instrument design 8-81056
 writing aid for motor handicapped, microprocessor-based device, LOGOS 8-81077
 X-ray diagnostic table, computer controlled, multidirectional, CAS-SETTELESS spotfilm device (*Japanese*) 8-61278
 X-ray films sensitive to green light, reciprocity law failure 8-69199
 X-ray machines, pulsating pot., filter method for peak volt. and inherent filtration meas. 8-73201
 X-ray picture digital transmission over voice-grade telephone channels, laser scanning system 8-80953
 X-ray screen-film processing sensitometry standard developed by ANSI 8-69196
 CO₂ partial pressure in blood, meas. by rapid response electrode system (*German*) 8-85409
 O₂ analyser instrumentation and operation 8-69237
 O₂ consumption and CO₂ prod. continuous meas. for men in hyperbaric chambers 8-81008
 O₂ electrode, membrane-covered catheter-tip system, construction and performance 8-81003
 O₂ partial pressure measurement with thin-layer polarographic probe, intracortical appl. (*German*) 8-85410
 Ra storage safe, design, safety, ease of use 8-92736

biomedical equipment continued

- ¹²⁷Xe, handling and dispensing technique 8-85378
¹²⁷Xe, simple device for efficient transfer and unit dose packaging 8-85377
- biomedical measurement**
 see also biological techniques and instruments; biomedical equipment; electrocardiography; electroencephalography; radiography; X-ray apparatus
 arterial pressure automatic determ., using microprocessor based instrument, Dinamap 8-96108
 arterial pulse wave vel. meas. by Doppler shifted US and EM flowmetry 8-69229
 arteriovenous O₂ difference, noninvasive meas. method (*German*) 8-85441
 bacteria counts, light scatt. pattern anal. 8-80946
 bioacoustic tissue property determ. by US pulse echo anal. (*German*) 8-85349
 bioelectric signal recording using surface electrodes, methods of reducing movement interference (*German*) 8-85405
 biotelemetry, literature survey 8-80996
 blood, light back-scattering theory 8-77099
 blood cell neutrophil automated classification, feature selection 8-73281
 blood flow speed and quantity determ. from digital angiograms (*German*) 8-92690
 blood flow vel. meas. in microvessels using video correl. system 8-53543
 blood flows and vols. in patients with transposition of great vessels, indicator-dilution meas. 8-61209
 blood gas analysers, review 8-69238
 blood gas sampler, for gas chromatography, design, construction and characteristics (*Japanese*) 8-85458
 blood pressure, blood gas anal., silicone rubber catheter operating mechanism (*Japanese*) 8-61273
 blood pressure for extracorporeal circulations, elec. sensor (*German*) 8-92721
 blood pressure instruments, direct systolic/diastolic meas., review 8-69234
 blood pressure instruments, noninvasive arterial meas. using US Doppler effect 8-69167
 blood sedimentation rate free from gravity influence, rapid determ. from density meas. (*German*) 8-81085
 blood velocity, catheter meas., cross correl. technique 8-80943
 blood velocity noninvasive meas. in large vessels, broadband pulsed Doppler US system 8-61224
 body movements, using microwave interferometers (*French*) 8-53469
 bone biopsy, automatic image anal., var. in rib architecture 8-61253
 bone mechanical properties determ. in vivo, noncontacting EM device 8-77133
 bone mineral concentration estimation by beta-ray backscatt. (*German*) 8-69179
 bone mineral measurement using polychromatic X-rays, correls. 8-53478
 bone mineral measurement using X-ray (low energy γ -ray) transmission, positioning errors 8-96084
 brain impedance, computerised system 8-77139
 breath anal. by gas chromatography, use of relative time programming 8-61268
 capacitoplethysmography for heart and lung meas. (*Japanese*) 8-53465
 cardiac output analysers, equipment, maintenance and ccts., review 8-69239
 cardiac output and shunt calc. from dye dilution curves using automated catheterisation system 8-81023
 cardiac output automatic determ. by indicator dilution in computerised monitoring system 8-81022
 cardiac output measurement, in vitro comparison of six commercially available thermodilution systems 8-77135
 cardiac output on-line determ. by thermodilution in coronary care unit 8-81021
 cardiocirculatory measurement, noninvasive RF EM transcutaneous meas. technique (*Italian*) 8-85352
 cell medically relevant class determ., scatt. light cluster anal., cervical smear tests (*German*) 8-92686
 cerebral blood flow computer for use in angiogram theatres 8-73227
 cerebral regional blood flow meas. with ¹³³Xe, functional landscapes in brain 8-85356
 chromosome size meas., fast karyotype approach 8-61153
 cineangiocardiograms, automatic anal. using TV system on line with minicomputer 8-92699
 composite signal anal., by cepstral inverse filtering, biomedical appl. 8-69243
 corneal wound holographic stress testing in postoperative patients, specular illum. arrangement 8-65102
 coronary sinus blood flow on-line computerised assessment by thermodilution 8-81024
 cortical bone diameter meas., manual and computer-aided methods comparison 8-85376
 dental enamel, SnF₂ treated, depth profiling by ESCA 8-53298
 dielectrography methods and apparatus, recording capacitance changes due to blood vol. fluctuations 8-57046
 Doppler sonographic flow meas. over small cross-sections in vitro and in vivo (*German*) 8-88729
 electrical resistance of human body (*German*) 8-53541
 electro-oculographic response, recording and interpretation review (*Italian*) 8-73156
 electromyogram envelope spectral anal., muscular control study 8-92750
 electronic meas. application areas 8-57094
 electronics of temp., press. and flow meas., for teaching 8-49621
 electroretinogram, automatic meas. of b-wave amplitude and peak latency (*German*) 8-80993
 EM radiation probes, implantable, design factors 8-73258
 EMG, abdominal, for uterus activity recording (*German*) 8-92712
 EMG and temporal information during gait, clinical telemetry 8-80994
 EMG index for localised muscle fatigue 8-57093
 endocrine research, continuous blood sampling and time series anal. 8-77130

biomedical measurement continued

epidural intracranial pressure meas. by piezoresist. transducer (*German*) 8-85404
 EPR investigation of high-spin Fe III in cancer 8-53466
 essential hypertension statistical analysis 8-89309
 evoked potential optimal filtering in sequential range (*German*) 8-85401
 eye refractive error, simplified anal. of meridional refr. data 8-65149
 eye refractive error measurement using Humphrey Vision Analyser, reliability and validity 8-61265
 ferritin, iron core particle size distrib., Mossbauer determ. 8-92696
 fibre optic, catheter transducer, side hole type, for intracardiac press. meas. (*Japanese*) 8-73272
 fibre optic catheter-tip micromanometer as intracardiac press. transducer (*Japanese*) 8-73270
 finger tremor amplitude and freq. artefact reduced routine meas., portable equipment (*German*) 8-85407
 flowmeters, digital 2D full range Doppler velocity meter for cardiovascular diagnosis 8-88731
 foetal heart rate recording, interference due to infusion pump (*German*) 8-85414
 foetal ventricular ejection time, registration and clinical significance 8-85417
 foot vertical force during walking, continuous meas. device (*Japanese*) 8-73273
 force distribution under human foot, online meas. system 8-96110
 functional residual capacity meas. in neonates with endotracheal tubes 8-53556
 functional residual capacity meas. instrumentation for neonates and small animals 8-53590
 gastric emptying measurement by scintigraphy, techniques and errors 8-73206
 heart contraction kinetics recording using thorax elec. fields (*Czech*) 8-77138
 heart volume determination by angiography, X-ray magnification estimation 8-73197
 herpes simplex virus radiometric detect. 8-65117
 impedance plethysmography, influence of erythrocyte vel. 8-61238
 intensive care, O₂ conc., blood O₂, fluid balance, ocular microtremor, for teaching 8-49622
 intensive care instrumentation 8-53559
 intraocular pressure measurement, applanation tonometer correls. 8-77047
 intravascular O₂ saturation continuous meas. using fibre optic catheter (*German*) 8-85411
 IR photography, principles and appls., book 8-82068
 laser interferometer for detecting biological signals due to displacement (*Italian*) 8-53467
 left ventricular ejection fraction determ. using multicryst. scintillation camera 8-73213
 left ventricular ejection fraction determ. using radionuclides 8-80962
 left ventricular function evaluation using ECG synchronised scintillation camera 8-65110
 left ventricular regional function anal. from cineangiogram, computer system appl. 8-80963
 leg long bone growth meas. in children from radiogram, error reduction using computer processing 8-77103
 lung closing volume meas. using acoustic He analyser 8-61223
 lung emptying patterns, multiple breath N₂ washout data 8-92666
 lung gas analysis using redox gas sensors (*German*) 8-85440
 lung perfusion determination by dilution principle with expiration detection of indicator (*German*) 8-85326
 lung perfusion determination using O isotopes and dilution principle (*German*) 8-85327
 lung tissue stereological parameter computer anal. 8-73280
 lung volume change estimation from torso hemircumferences using Whitney gauge transducers 8-65141
 lymphocyte carbohydrate metabolism in response to mitogens, liq. scintillation vial for radiometric assay 8-61248
 magnetocardiograms from normal hearts, interpretation (*Japanese*) 8-53433
 magnetometry of human heart in small ferromag. enclosure, using SQUID 8-92726
 metabolic substrate regional utilisation rate meas. by emission tomography 8-69183
 microwave complex permittivity meas. using noninvasive beam-wave reflectometric instrumentation 8-74030
 Mossbauer spectroscopy of Fe deposits in thalassaemic heart tissue 8-73202
 motor unit action potential duration meas. by surface electrode EMG 8-81039
 nasal air emission in speech disorders, electrodynamic evaluation 8-77134
 neutron activation in vivo total body anal. using 14 MeV neutrons, calibration and evaluation of system 8-53490
 NMR, noninvasive meas. of biological information, magnetic focus generation (*Japanese*) 8-85355
 NMR images using line scanning method, appl. to tumorous rat leg 8-92683
 NMR spin density imaging using line shaped mag. field 8-73190
 ocular microtremor clinical recording, using piezoelec. strain gauge transducer 8-96109
 oesophageal multiprobe for temp., ECG and heart and lung sound meas. 8-77146
 oximeter calibration, humans exposed to centrifugation 8-92734
 percutaneous electrophoresis of amino acids and urea 8-61237
 pH measurement techniques, equipment 8-77158
 photon absorptiometry of soft tissue and fluid content, method, precision and accuracy 8-73221
 physics aspects in medical engineering (*German*) 8-92735
 pleural liquids in weak fields, PMR relaxation times, medical diagnosis appl. (*French*) 8-73187
 psychophysics as method of meas. of biosystems (*Japanese*) 8-53591
 pulmonary function testing, continuous distribution of specific ventilation from N₂ washout 8-92665
 pupillary response meas., use of black light stimulation 8-64977
 radiochromatograms, thin-layer, anal. by proportional chamber 8-77174
 radioimmunoassay, probe for fine struct. of biological systems, review 8-73217
 radioimmunoassay techniques development 8-88743

biomedical measurement continued

radionuclide mean clearance time transverse section imaging 8-73222
 radionuclide measurement in large samples using liq.-filled Cherenkov counter 8-53491
 random pulse train inputs, use of digital filters (*Japanese*) 8-53547
 reaction timing, digital timer cct., CMOS, LED 8-53600
 renal length, from radiograms, importance of renal inclination as meas. by US 8-77092
 respiration calorimetry determination of O₂-calorie equivalence of thyroid patients and normal subjects (*German*) 8-85412
 respiratory function telemetering by combined sensor 8-80995
 respiratory rate and ventilation digital recorder 8-81005
 respiratory total resistance meas. in pre-school children using modification of forced oscill. technique 8-77129
 reticulocyte production rhythm investigation by spectral analysis 8-73279
 retinal blood flow, laser Doppler meas. 8-69174
 serum automated electroanal. using ion-selective disc electrodes with neutral cation-carriers (*German*) 8-73269
 signal processing, common structure for filters, correlators and Fourier analysers (*German*) 8-88748
 signal processing using microcomputer 8-81012
 skin conductivity measurement, electrode materials (*German*) 8-85406
 somatosensory evoked potential measurement and analysis on a small laboratory computer 8-92729
 SQUID detector appl. in biomagnetism, techniques 8-96061
 structure extraction, search-free technique, appl. to M-mode echocardiogram and chromosome image 8-81025
 telemetry, transmission and reception with embedded antennae 8-77125
 thermal conductivity and thermal diffusivity simultaneous meas. technique 8-57098
 thermography, colour, environmental physiology appl. 8-58043
 thermometers, electronic, review 8-69235
 thermometry considerations in localised hyperthermia, review 8-53561
 thoracic impedance of humans, meas. using automatic recording device on defibrillator 8-61239
 thrombophlebitis diagnosis, reliability of Doppler and impedance techniques 8-77144
 thyroid I measurement by X-ray fluoresc. scanning, effect of background radiation change 8-73216
 thyroid uptake meas., influence of gland depth, mass and lobe separation 8-61245
 tissue refractive index spatial distrib. meas. by US computer assisted tomography 8-69161
 tooth surface moire topography (*German*) 8-80992
 trace element anal. with low power monoenergetic X-ray tube 8-70686
 transcutaneous pO₂ measurement in computer-assisted monitoring of infants 8-85432
 two way scanning method for total body in vivo neutron activation anal. 8-92697
 US attenuation of soft tissues, signal processing of broadband pulsed US 8-77094
 US blood flow spectral anal. using coherent optics 8-53459
 US flowmeter data processing, transfer function modelling of arteries 8-61225
 vectorcardiogram, computer treated, discrimination between normals, LBBB with and LBBB without myocardial infarction 8-85448
 ventilation-perfusion ratio distrib. determ. from inert gas data with enforced smoothing algorithm 8-61208
 ventriculography, algorithm for automatic selection of end diastolic and end systolic cine frames 8-88757
 vertebrate cornea, transparent layered structure thickness monitor 8-92737
 video processor for computer calc. of press.-vol. indices from left ventriculograms 8-53495
 visual acuity of amblyopic eyes, meas. reliability 8-65011
 visual contrast sensitivity function rapid meas. 8-56975
 visual evoked potentials, monocular, recording under binocular conditions 8-81035
 visual field, Bausch and Lomb Autoplot tangent screen standardisation 8-64976
 CO₂ expiratory concentration analysis by computer 8-57106
 CO₂ partial pressure in blood, meas. by rapid response electrode system (*German*) 8-85409
¹⁴CO₂ breath analysis tests, plastic scintillation filament detector system 8-65122
 Ca in vivo measurement by ³⁷Ar method, inert gas elimination in humans 8-61247
 CaO, coherent/incoherent scatt. cross-sections of 136-278 keV γ -rays 8-70881
¹³¹I measurement in human thyroid gland, use of NaI(Tl) scintillation survey meter 8-80970
 O₂ analyser instrumentation and operation 8-69237
 O₂ consumption and CO₂ prod. continuous meas. for men in hyperbaric chambers 8-81008
 O₂ consumption meas. with flow-through system, accuracy assessment 8-65067
 O₂ electrode, membrane-covered catheter-tip system, construction and performance 8-81003
 O₂ partial pressure determ. in biological fluids, electrochem. cell 8-85420
 O₂ partial pressure measurement with thin-layer polarographic probe, intracardial appl. (*German*) 8-85410
 P, in urine, 14 MeV neutron activation method (*French*) 8-61254
 Pb, determ. in aqueous solns. by Delves Cup technique and flameless atomic absorpt. spectrometry 8-68973
 Pu body burden estimation from urine data influenced by DTPA therapy 8-73259
 Pu skeletal level estimation based on DTPA induced excretion in faeces 8-85390
²²⁶Ra body burden determ., postprandial changes in exhalation rate of Rn prod. in vivo 8-69224
¹⁰⁶RuO₄ in lung, in vivo meas. and dosimetry 8-53515

biomedical phenomena

see also biomagnetism

drug-nucleic acid interactions, conformational flexibility at intercalation site 8-96005

biomedical phenomena continued

- erythrocyte membranes, ESR study of abnormalities in Duchenne muscular dystrophy 8-96111
- space motion sickness medication, biomedical parameters interference 8-53536

biomedical ultrasonics

- 4 MHz range-gated US Doppler flowmeter design and application 8-59527
- abdominal and pelvic diagnosis, US and computed tomography evaluation 8-61228
- arterial haemodynamic transfer function calc. from Doppler US flowmeter waveforms 8-61235
- arterial pulse wave vel. meas. by Doppler shifted US and EM flowmetry 8-69229
- aspiration-biopsy transducer development 8-61233
- attenuation measurement of soft tissues, signal processing of broadband pulsed US 8-77094
- B-scan recording on video tape-recorder 8-77095
- B-scanning in medicine, book 8-73180
- beam detector, two-dimensional 8-94495
- biliary tree gas appearance in US B-scan 8-80930
- biodynamic research, US/EMG transducer, speech appl. 8-77164
- blood flow measurement by US Doppler method, computer-aided determ. of angles (*German*) 8-80931
- blood flow spectral anal. using coherent optics 8-53459
- blood pressure instruments, noninvasive arterial meas. using US Doppler effect 8-69167
- blood velocity noninvasive meas. in large vessels, broadband pulsed Doppler US system 8-61224
- Bragg diffraction imaging for medical use 8-53462
- cardiac valve motion obs. CW FM sonar 8-61230
- CW FM sonar with aural displays, improvements 8-87221
- data compression 8-77093
- diagnostic equipment, portable radiation-force balance 8-69163
- diagnostic equipment, US power and intensities produced 8-69162
- diagnostic instrument performance evaluation, work of USA AAPM and AIUM 8-69170
- diagnostic instruments, output meas., irradi. effects (*Japanese*) 8-80936
- diagnostic methods 8-77145
- diagnostic system, real-time, for dynamic and still images, wireless echovision 8-65101
- diagnostic uses of US in medicine and biology, bibliography 8-69166
- diffraction scanner for in vivo tissue characterisation 8-61226
- digital US imaging with microprocessor manipulation 8-96082
- Doppler sonographic flow meas. over small cross-sections in vitro and in vivo (*German*) 8-88729
- Doppler US blood velocity meas., phase-locked loop technique 8-61234
- dynamically focused US diagnostic phased array 8-61232
- echo distribution evaluation (*German*) 8-80934
- echocardiogram, M-mode, computer-assisted anal. 8-80942
- echocardiogram computer-assisted interactive interpretation 8-80938
- echocardiogram on-line computer anal. 8-80941
- echocardiography, 2D, transducer beam profile effects on tissue aperture detection 8-73185
- echocardiography, two-dimens., wall motion and thickening quantification by computer-aided contouring 8-80937
- echographic information related to left ventricle and mitral valve in diastole, anal. by small computer 8-80939
- equivalent circuit anal. of US rod concentrators for US surgery 8-50997
- flowmeter data processing, transfer function modelling of arteries 8-61225
- flowmeter for measuring rapidly changing gas flows, freq. range, excitation and signal processing (*German*) 8-83502
- foetal breathing monitor for humans in utero, US pulsed Doppler instrument 8-69164
- foetal heart rate recording, interference due to infusion pump (*German*) 8-85414
- gas analyser for lung closing vol. meas. 8-61223
- grey scale scanner dynamic range testing 8-69169
- grey tone rapid process films for US imaging 8-96081
- heart rate meas. (foetal), adaptive correlation ratemeter 8-88732
- hepatic metastases detect. by grey-scale US scanning 8-73179
- image feature enhancement via digital processing 8-73183
- image reconstruction processing limitations 8-73184
- imaging systems, high-resolution, real-time 8-69160
- imaging techniques, theory and advantages 8-92682
- imaging techniques and appls., for teaching 8-49620
- implantable CW Doppler blood flowmeter, optimal system design 8-53460
- instrumentation standardisation, physician's need 8-69168
- left ventricular diameter-time curve shape from M-mode echocardiogram, automated anal. 8-80940
- liver sector scans, echoes across diaphragm 8-69165
- local circulatory system characterisation by CW Doppler US flow meas. 8-57109
- mammalian tissues, US vel. and atten. 8-57044
- microcirculation semiquantitative demonstration using US noninvasive meas. method (*German*) 8-85348
- multiple section tomogram simultaneous display equipment 8-61227
- ophthalmological signal acquisition and image enhancement 8-57045
- ophthalmological tissue differentiation, digitisation of HF US signals 8-80935
- optical instrumentation appl. in medicine, conf., Boston, USA (Sept. 1977) 8-69184
- patient diagnosis, experiences in private practice 8-92680
- pneumothorax diagnosis in deep-sea divers, using Sonicaid portable instrument 8-85351
- pulse echo analysis, bioacoustic tissue prop. determ. (*German*) 8-85349
- pulse-echo equipment, US tissue equiv. test objects for routine performance checks 8-73182
- Pulse-echo transducer standardization 8-73181
- pulsed Doppler blood velocity meter readout 8-69158
- quality control problems for diagnostic US imaging equipment 8-69171
- radiotherapy treatment planning, appl. of US imaging (*German*) 8-53463

biomedical ultrasonics continued

- real-time B-scan machine attachment for three-dimensional display 8-61229
- reconstructive US tomography 8-92681
- renal inclination measurement, importance in radiographic meas. of renal length 8-77092
- single-transducer coupler for diagnostic pulsed Doppler or pulse-echo US instrumentation 8-61236
- structure extraction, search-free technique, appl. to M-mode echocardiogram and chromosome image 8-81025
- swept-frequency diffraction by cylinders and arrays for tissue characterisation 8-53461
- third intracranial ventricle dynamic displacement detection 8-57035
- thrombophlebitis diagnosis, reliability of Doppler and impedance techniques 8-77144
- tissue characterisation by computer-aided US method (*German*) 8-80932
- tissue characterisation by computer-aided US method (*German*) 8-80933
- tissue characterisation pattern recognition approach 8-73186
- tissue refractive index spatial distrib. meas. by US computer assisted tomography 8-69161
- TOMAX autostereoscopic display, three-dimens. viewing of tomographic data 8-85446
- transmission image reconstruction, inverse scatt. and tomography 8-61231
- ultrasensitive US system for NDT, medical diagnosis and nonlinear US 8-59224
- US Doppler velocimetry for 3D blood flow meas. 8-88730

biomembrane transport

see also osmosis

- acetylcholine receptor electrophoretic movement in embryonic muscle cell membrane 8-85298
- active transport and energy transformation, quantum mechanism 8-53364
- amino acid permeability of *E. coli* K-12 8-77029
- axon, squid giant, temp. effects on gating currents 8-96037
- axon Na conductance and Ca transport, squid, mol. model 8-85305
- barbiturate-induced slow outward currents in *Aplysia* neurones 8-80866
- bilayer membrane, galvano-static regime of non-steady process 8-64963
- bioenergetics and proton-electron systems of membranes, review 8-96030
- biological membranes, transport props., rel. to synthetic membranes 8-77030
- carbohydrate active transport in membrane vesicles of *Acholeplasma laidlawii* cells 8-64965
- cell permeability polarity and control by phytochrome, red light irradi. of mass 8-77025
- cell-cell junction membrane form., quantum jumps of cond. 8-73145
- charge transfer in thin membranes, discrete models, nonsteady state at high polarising voltages 8-69023
- chemiosmotic theory of ATP synthesis 8-61151
- conductance fluctuations in cultured spinal neurones induced by γ -aminobutyric acid 8-80867
- cortical spreading depression, math. model 8-80857
- crosslinked collagen membranes, transport props., physical props. effects 8-77028
- digitalis inotropy rel. to enhanced slow inward Ca current 8-61155
- electromotor system of *Torpedo*, as model cholinergic system 8-53388
- epithelial K active transport system of insect midgut, pump-mediated efflux 8-80846
- erythrocyte Ca transport in myotonic muscular dystrophy patients 8-80849
- excitable fibre, steady speeds of spread of stable and unstable impulses, depend. on membrane ionic currents 8-53382
- fusion rosettes in *Paramecium*, possible function as Ca^{2+} gates 8-56958
- gastrointestinal electrical activity, Hodgkin-Huxley type electronic modelling 8-61165
- gating charge immobilisation by inactivation-simulating substance 8-61154
- glucose transport in human red cell ghosts, effect of chlorpromazine and temp. 8-77026
- gramicidin A channel cation permeation interactions and anion binding 8-53370
- gramicidin A ion channel kinetic behaviour, electrostatic calcs. 8-53368
- Halobacterium halobium* R_1 cells, photogeneration of two-vector transmembrane gradient of protons 8-80845
- intervesicular lipid transfer, direct fusion of phospholipid vesicles, kinetic basis comparison 8-96034
- ion channel, energy and pot. profiles and interactions between ions 8-53367
- ion transport and chem. reactions in brown adipose tissue, network thermodynamics 8-92606
- ionic channel formation in living cell membrane, microelectrode obs. 8-53372
- ionic channels in excitable membranes, current problems and biophysical approaches 8-53369
- light response and kinetics in *Aplysia* giant neuron 8-53381
- Light-regulated body ion balance in marine slug *Elysia viridis* (Mantag) 8-73146
- lipid bilayer, 1 MHz US effects on cond. and capacitance 8-77082
- lipid bilayer diffusion transport modelled by dimeric β -cyclodextrin complexes, cryst. struct. anal. 8-80838
- lipid bilayer electrical strength fall after UV irradi. 8-69002
- lipid bilayer gramicidin A channel cation flux interaction 8-56957
- lipid bilayer membrane permeability modification by drugs 8-69026
- lipid bilayers, Ca^{2+} transport system of rat liver mitochondria 8-64966
- lipid bilayers containing gangliosides, cholera toxin effect, formation of ion transport channels 8-88702
- lipid phase transition, cluster model, appl. to bilayer mol. passive permeation and struct. relax. 8-53346
- lipid-water smectic phase, water and thermal diffusivity, light scatt. meas. 8-96031
- liposomal membrane permeability, radioresist. 8-80919

biomembrane transport continued

- liposome proton permeability increase on peroxide photo-oxidation of lipids 8-69024
 mitochondria and submitochondrial particle membrane pot. generation in anaerobic conditions 8-69015
 mitochondrial membrane Ca^{2+} interaction, influence of oestrogens 8-53349
 mitochondrial membrane pot., respiratory chain study by method of penetrating ions 8-64951
 monosynaptic potentials onset and propagation, discrete-dynamic equations 8-77040
 muscle, smooth, effect of hyperosmolar soln. on elec. connections between cells 8-69027
 muscle, smooth, intestinal cell, voltage clamp studies of hyperpolarising inactivation 8-80847
 myocardium contraction amplitude depend. on freq. of elec. stimulation, frog 8-77027
 myotubes, human, cultured, acetylcholine-induced conductance fluctuations 8-61157
 nerve excitability, interactions between intrinsic membrane protein and elec. field 8-53377
 nerve impulse, physical mechs., ion transport through membranes, review 8-85306
 nerve impulse equation, dynamic responses of impulse 8-64972
 nerve impulse propagation, subthreshold solns. of Hodgkin-Huxley eqns. 8-77044
 neuromuscular blockade by amantadine by suppression of acetylcholine receptor ionic cond. 8-64975
 neuromuscular junction, snake, synaptic channel gating differences at twitch and slow junctions 8-80868
 neurone Ca conduction units, *Helix aspersa* 8-77041
 neurones of large horse-leech, electrophysiological characts. rel. to intracellular Na^+ conc. 8-53374
 nonspiking neurones, pharmacological evidence for fast Na channels 8-73151
 oxidative phosphorylation mechanism, role of closed condition of mitochondrial membranes 8-77013
 phospholipid artificial membrane phase state and passive permeab. for Ca ions, effect of valinomycin 8-80836
 phospholipid bilayer melting transition, thermodynamic fluctuations, ion permeability, statistical mechanics model 8-73140
 photosensory membrane of *Limulus* ventral nerve photoreceptor, effect of extracellular Ca/Na ratio 8-69067
 plants, transfer cells and their roles in transport of solutes 8-73148
 polarised spherical cell, ionic conc. profiles and charge distrib. 8-73144
 poly-L-lysine, membrane phase, transport processes, helix-coil transition 8-77031
 protein transfer across microsomal membranes reassembled from separated membrane components 8-69029
 proton transport, mol. mechanisms 8-96035
 pulsing elastic alveoles, gas transport, conc. depolarisation (*French*) 8-85328
 responsiveness curve automated on-line determ. 8-92761
 retardation currents in excitable membranes and models of flicker noise 8-92618
 rod outer segment adaptation anal. based on a simple equiv. cct. 8-73157
 sarcoplasmic reticulum Ca^{2+} , Mg^{2+} -ATPase transient kinetics obs. by fluoresc. 8-61156
 sarcoplasmic reticulum membrane rearrangements on peroxide oxidation of lipids 8-69025
 sinatorial node of rabbit heart, vagal stimulation, K^+ permeability and extracellular transients 8-92608
 single-file ionic transport theory, reduced flow diagrams 8-69022
 skin Na entry site irreversible inhibition by photosensitive amiloride analogue, in frog 8-69030
 stratum corneum of rat, surfactant diffusion and sorption phenomena, model for human skin 8-77007
 subcellular particle membrane pot. diff., proton channels in oxidative phosphorylation 8-64964
 sugar transport system dependent regulation of adenylate cyclase, review 8-69031
 synthetic voltage-dependent cation-selective transmembrane channel characterisation 8-77009
 teaching, single-file diffusion 8-54127
 thymocyte membrane props. modification by hyperthermia and gamma-rays 8-69017
 transepithelial ion transport endogenous regulation, implications of ouabain-like activity in toad skin 8-73147
 transmitter kinetics model computer simulation results 8-92617
 viral infection, membrane leakiness, rel. to development of antiviral agents 8-53371
 visual cell, proposed role of cyclic GMP 8-64997
 visual cell microvilli membrane fragment protonic and ionic processes, cephalopod 8-73159
 volumetric charge effects on membrane and near-membrane transport processes 8-53366
 water diffusion meas. by pulsed gradient NMR, cell struct. size determ. 8-77159
 Ca conductance, inactivation without fluorimetry in *Cs*-loaded *Aplysia* neurones 8-56965
 Ca pump driven by ATP in squid giant axons 8-77043
 Cl^- active transport inhibition by piracetamide, in teleost intestine cell 8-64967
 K channel blocking agent, 3,4-diaminopyridine 8-69028
 K^+ ion flux through membrane channels, nerve impulses, random walk anal. 8-77045
 K^+ permeability of mitochondrial and artificial bilayer membranes 8-53365
 Na channel, fully coupled excited state model, conductance in volt. clamped case 8-85297
 Na permeability inactivation in squid giant nerve fibres, review of exptl. work 8-73154
 Na^+ multicompartiment flow model of frog skin epidermis, experimental verification 8-92607
 Zn^{2+} , transport in cation-exchange membranes 8-96033

biomembranes

- see also *biomembrane transport; lipid bilayers*
 adhesion of artificial membranes, bivalent cations effect 8-64946

biomembranes continued

- Na , K -ATPase membrane prep. struct. characts. studied by paramag. probes 8-64930
 ATPase of *A-laidlawii* membrane, Arrhenius plot artifacts due to temp. depend. of substrate-binding affinity 8-64949
 atrial trabecula membrane, frog, accommodation, repeat responses and anode-breaking excitation 8-64956
 bacterial sensory electrophysiology, motility depend. on membrane pot. and chemotaxis 8-53373
 bacteriorhodopsin orientation in *Halobacterium halobium*, selective proteolysis investig. 8-77010
 basilar membrane model using digital filter for voice features extraction 8-77069
 basilar membrane point-impedance charact. in cochlear mechs. 8-57009
 bioenergetics and proton-electron systems of membranes, review 8-96030
 biomembranes, lipid-protein interactions, flexoelectric effects 8-92600
 birefringence analysis in biological materials 8-56954
 brain rhythmic activity generation models (*Dutch*) 8-73150
 cell adhesion models, reaction kinetics and forces 8-80844
 cell electric circuit model, alternating signal interaction 8-77011
 cell electric circuit model, alternating signal interaction 8-77012
 cell membrane nuclear hydrodynamic shear, non-equal. Ising model, master eqn. 8-61146
 chemical reaction kinetics, modelling non-enzymatic influence of membranes 8-64945
 chloroplast millisecond afterglow, activation and suppression 8-96025
 chromaffin granule electrophoretic mobility meas. by light scatt., effect of Ca^{2+} and Mg^{2+} 8-53357
 dynamic aspects, review 8-69005
 embryonic skeletal muscle differentiation, electrophysiological and biochem. membrane props. 8-53363
 epithelium, living, size and shapes of lateral intercellular spaces 8-77032
 epithelium of small intestine, mech. props. of intercellular contacts 8-53351
 erythrocyte electrophoretic mobility, effect of UHF EM radiation 8-53442
 erythrocyte membrane, phys. state of lipids, X-ray diffr. 8-80835
 erythrocyte membrane lattices, partially disordered, X-ray scatt., anal. method applied 8-91196
 erythrocyte membranes, ESR study of abnormalities in Duchenne muscular dystrophy 8-96111
 erythrocytes of human blood, diameter meas. by specific elec. cond. 8-53353
 excitable biomembrane electronic cct. model utilising time variant negative res. 8-88696
 excitable cell model, numerical method 8-53376
 excitable medium model with existence of several stable pulses of different duration 8-77036
 fluorescent probe interaction with surface structs. of *E. coli* 8-69007
 intervesicular lipid transfer, direct fusion of phospholipid vesicles, kinetic basis comparison 8-96034
 kidney membrane conformational changes anal. after renal ischemia 8-73142
 lecithin-cholesterol interaction, effect of lecithin struct. 8-64922
 lecithin membrane, depend. of Young's modulus in plane of membrane on deform. 8-80894
 lecithin membranes, mag. susceptibility anisotropy, phase contrast microscope obs. 8-92601
 lecithin-water system, structural changes 8-96023
 lipid bilayer structure, X-ray refl. phases from oriented model membrane systems 8-96022
 lipid monolayer, statistical mech. theory 8-73141
 liposome phasic transitions, use of hydrophobic fluoresc. probes 8-96021
 mechanoreceptors, energy transform. problem 8-96058
 membrane dynamic equation solving, practical algorithm 8-77038
 mitochondria and submitochondrial particle membrane pot. generation in anaerobic conditions 8-69015
 mitochondria membrane Ca^{2+} interaction, influence of oestrogens 8-53349
 myenteric plexus, mediation of slow synaptic excitation by substance P 8-73153
 myocardium mitochondria lipid composition and phase transitions rel. to depth of hypothermia, rats and dogs 8-53350
 nematode oesophagus pumping mechanism 8-69121
 nerve excitable membrane, EM wave effect on surface charge density 8-85334
 nerve-muscle anisotropic syncytia, electrotonic membrane pot. distrib. 8-64971
 neurones A and B of mollusc, effect of acetylcholine chloride and choline chloride on resting pot. and membrane resist. 8-53375
 phospholipid artificial membrane phase state and passive permeab. for Ca ions, effect of valinomycin 8-80836
 phospholipid vesicles, surface charge equilib. distrib., calc. method 8-96019
 phospholipid vesicles, surface charge equilib. distrib., calc. results 8-96020
 photoreceptor membrane, lipid free radical oxidation kinetics rel. to lipid composition 8-80872
 photosynthesis, interaction of paramag. probe I (12,3) with bean chloroplast membranes 8-77015
 plasma membrane, unfixed, ultrathin frozen sections, ultrastructure 8-65161
 protein, double layer mediated energy conversion using imposed freq. and wavelength 8-88695
 protein-lipid interactions, ^2H NMR investig. 8-80826
 purple membrane, new intermediates in bacteriorhodopsin photochem. conversion 8-96010
 purple membrane of halophil cells, homogeneity based on IR spectra 8-69003
 retina of turtle, horizontal cells influence on bipolar cells' membrane pot. 8-88708
 retinal disc membrane, frog, isorhodopsin chromophore conform. and orientation 8-64980
 rhodomere transmittance decrease due to blue light, rel. to desensitisation of peripheral photoreceptors 8-64993
 rod outer segment shedding, intraocular initiation 8-85309

biomembranes continued

- sarcoplasmic reticulum membrane rearrangements on peroxide oxidation of lipids 8-69025
 spherical three-layer particles as cell models, light scatt. and attenuation, shell effect 8-82913
 spin labels applications, review 8-69265
 squid joint axon membrane potential fluctuations, cross-correlations 8-92616
 thylakoid membranes, pulsed NMR, photosynthesis appl. 8-80839
 thymocyte membrane props. modification by hyperthermia and gamma-rays 8-69017
 unilamellar lipid vesicles, in vivo breakdown, gamma-ray PAC study 8-53348
 US perturbation obs. at cellular level 8-61214
 visual cells, daily rhythms and vision research 8-61176

biomolecular effects of radiation

see also biological effects of ... (type of radiation)

- N-acetylglucosamide, substrate-inhibitor of lysozyme, localisation of unpaired electrons 8-68992
 acid amide+H₂O₂, aq. solns., photolysis, EPR study of spin-trapped radicals formed during photolysis 8-68996
 albumin, human serum, kinetics of eosin-sensitised photochemilum. of solns. 8-68991
 amino acid, in polycryst., γ -irrad. induced radical pair form., 77K, EPR obs. 8-85292
 amino acid sequence threadlike cryst. growth, light irrad., polycondensation 8-96009
 aspartate transcarbamylase, solid, enzyme activity and allosteric characts. after gamma irrad. 8-53341
 aspartate transcarbamylase, solid, sedimentation and subunit interactions, after gamma irrad. 8-53342
 bacteriochlorophyll a, bacterial photosynthesis primary electron transfer processes, psec. dynamics 8-80841
 bacteriophage DNA and protein cross-linkage by ⁶⁰Co gamma-rays 8-77002
 bacteriophage T7, radiation inactivation 8-65083
 bacteriopheophytin, bacterial photosynthesis primary electron transfer processes, psec. dynamics 8-80841
 bacteriorhodopsin, new intermediates in photochem. conversions 8-96010
 bacteriorhodopsin, primary intermediates in photochem. cycle 8-96011
 bacterioviridine photo-oxidation in monomer and aggregated states, free radical form., EPR 8-76994
 Bowman-Birk soybean proteinase inhibitor, gamma irrad. 8-53343
 chlorophyll and analogues, role of O₂ in regeneration of photoreduced pigments in soln. 8-68980
 chlorophyll-a, microcryst., trapped-electron doping in photovoltaic sandwich cells 8-53334
 chlorophyll-acceptor and chlorophyll+protein-acceptor lamellar systems, steady photocond. 8-53328
 chromatin extracted from cultured mammalian cells, gamma radiolysis, DNA alkali-labile strand damage 8-77003
 creatine monohydrate, single cryst., radiation damage, ENDOR obs. 8-96016
 cytidine-5'-monophosphate, γ -irrad. aq. solns., spin-trapped radicals, liq. chromatography and EPR spectroscopy 8-53340
 deoxyribonucleoprotein, gamma-ray protein damage 8-53338
 DNA, double strand breaks, recombination, formation of chromosomal rearrangements 8-85289
 DNA, gamma-irradiated, enzymatic digestion, separation by ion exchange chromatography 8-85290
 DNA, single-stranded, alkali-labile sites and post-irrad. effects induced by H radicals 8-68994
 DNA, transforming, X-ray sensitivity rel. to presence of free radicals 8-68995
 DNA, UV irrad. of mammalian cells, postreplication repair model 8-80918
 DNA, X-ray induced damage in rat cerebellar neurons and brain tumour cells 8-80922
 DNA break rejoining capacity rel. to mouse age 8-69148
 enzyme activity rate reduction by EM fields (Russian) 8-61142
 ferredoxin of adrenal cortex, destruction of chromophore centre on exposure to X-irrad. 8-76993
 ferricytochrome, photoreduction in presence and absence of electron donor 8-53337
 ferricytochrome c photoreduction, transient absorpts. in indole aq. solns., 600 to 800 nm 8-53228
 glyceraldehyde-3-phosphate dehydrogenase radiolysis, active-site and SH loss 8-77000
 indole, aq. solns., flash photolysis, transient absorpts., 600 to 800 nm 8-53228
 lipid, peroxide photo-oxidation, increase in liposome proton permeab. 8-69024
 lysozyme, 0.01% soln., mag. and radiofreq. effects on activity 8-61136
 malignancy analysis based on somatic mutation 8-69147
 metarhodopsin transitions rel. to visual response in barnacle photoreceptor 8-69050
 1-methyl cytosine: 5-fluorouracil X-irrad. at 300K, EPR 8-64941
 nanosecond flash photolysis, techniques and biological appls. 8-68905
 optical asymmetry correl. with parity violating weak interaction 8-69000
 papain inactivated by OH radicals and H₂O₂, optical density, amino acid composition and fluoresc. 8-53344
 peptide aqueous solution, EPR of spin-trapped radicals, OH radical reactions 8-68993
 pheophytin-a, photochem. generation of cation-radical, spectral-kinetic characts. 8-96008
 photosynthesis, in vitro models 8-77023
 photosynthetic systems, temperature dependence of excitation transfer 8-92598
 pulse radiolysis appl. to biomolecule reactions and struct., review 8-61145
 pyrimidine dimers, excision repair of UV damage in monkey kidney cells 8-53332
 rhodopseudomonas sphaeroides, reaction centre triplet state fluoresc. mag. field depend. 8-53358
 rhodopsin, bathorhodopsin and isorhodopsin, mech. of photoconversion 8-53336

biomolecular effects of radiation continued

- rhodopsin, bovine, photochem. cis-trans isomerisation at liq. He temps. 8-64939
 rhodopsin flash photolysis, rabbit retina 8-76996
 RNA, heterogeneous nucl., effects of UV irrad. and postirrad. incubation on size in murine cells 8-69139
 thymidine, frozen aq. solns., final products of gamma radiolysis 8-77001
 thymidine-5-monophosphate, γ -irrad. aq. soln., spin-trapped radicals, liq. chromatography and EPR spectroscopy 8-53340
 thymine dimer excision from DNA of UV-irrad. plant seedlings 8-61221
 thymine dimer excision kinetics in UV-irrad. human cells 8-53331
 L-tryptophan-HCl radical form. after X-irrad. 8-64940
 ubiquinone-Fe complex, bacterial photosynthesis primary electron transfer processes, psec. dynamics 8-80841
 visual pigment reactions, coupling of charge stabilisation, torsion and bond alternation 8-64999
 visual pigments, slow flash photolysis using conventional spectrophotometer 8-68904
 vitamins, B group, γ -irrad. resist. 8-76890
 water photo-oxidation in presence of porphyrins adsorbed on octane-water interface 8-64933

biomolecules *see macromolecules; molecular biophysics*

bionics *see biocybernetics*

biophysics

- see also biological fluid dynamics; biomechanics; cardiology; cellular biophysics; haemodynamics; hearing; molecular biophysics; speech; vision*
 antennular chemosensitivity in spiny lobster, amino acids as feeding stimuli 8-53431
 biochemistry and biophysics horizons, book 8-68977
 book, physics for applied biologists 8-53310
 convective heat loss assessment from humans in cold water 8-81093
 cutaneous pressure sensitivity, effect of skin surface temp. on localisation error and two-point threshold 8-77072
 diffused substance kinetics in biological systems 8-53312
 dissipative systems, dynamical field theory, hierarchical struct. of field thermodynamics 8-73132
 energy expenditure of man, anal. determ. from external respiration parameters 8-69268
 heart tissue, thalassaemic, Mossbauer spectra of Fe deposits 8-73202
 history in USSR 8-93506
 human skin and subcutaneous tissue, unsteady state heat transfer, similarity transformations 8-95990
 hyperthermia in dogs, rel. to post surgical rewarming by thoracic flush 8-80834
 hyperthermia research, importance of good thermal dosimetry 8-64942
 magnetic field detection by invertebrates Tenebrio and Talitrus, distinct from light detect. 8-77073
 mathematical biology meeting, Philadelphia, USA, (Aug. 1976) 8-53311
 muscle contraction, simulation of thermophysical processes 8-96063
 nucleus growth, spatial kinetic systems, multi-stationary state transitions, Langevin stochastic approach 8-73136
 oyster shell, IR and atomic mineral anal. 8-61116
 radioactive contamination in aquatic organisms, evaluation by statistical and information theory 8-53535
 smell meas., status (Japanese) 8-92661
 spaceflight factors combined effects on man 8-53537
 thermal insulation of animal coats and human clothing, review 8-73139
 tissue, perfused, macroscopic temp. distrib. 8-64944
 vibration effects on continuous manual control 8-61169
 vibrations of seated subjects, effect of position of axis of rot. on discomfort 8-85461
 vitalism, nonlinear transforms in Hilbert space 8-73133

Biot-Savart law *see electromagnetism*

biotite *see mica*

biotransport

- see also biotransport; biological fluid dynamics; biomembrane transport; cell motility; cellular transport and dynamics; neurophysiology*
 actinide industrial dusts, lung clearance studies at NRPB 8-65137
 albumin, bovine serum, solutions, fluctuation transport theory 8-70057
 ovum transport in oviduct, mechs. 8-80905
 oxyhaemoglobin dissociation curve direct obs. in man in vivo, computer investigation 8-85433
 transuranics biological availability, influence of DTPA at soil-plant and plant-animal interfaces 8-73264
 water exchange dynamics of body in aormal and pathological conditions 8-64914
²⁵²CfCl₃, metabolism in rat and effect of in vivo DTPA chelation therapy 8-85387
 Pu body burden estimation from urine data influenced by DTPA therapy 8-73259
 Pu IV citrate, monomeric, containing ²³⁷Pu and ²³⁹Pu, early retention in mice 8-80983
 Pu translocation from simulated wound sites in rat 8-77117
²⁰¹Tl distribution in stressed rats, imaging, organ uptake and myocardial kinetics 8-65114

bipolar integrated circuits

- phototransistor static characteristics, effect of insulating p-n junction (Russian) 8-52069

bipolar transistors

see also bipolar integrated circuits

- III-V semiconductor, low temperature, high mobility transistor materials 8-87970
 Si/Si₃N₄ substrate/film system, implantation effects on substrate hardening and film stress reduction 8-71748

bipoles *see network analysis*

birefringence

- see also flow birefringence; Kerr electro-optical effect; light polarisation; magneto-optical effects; mechanical birefringence; optical constants; optical rotation*
 anthracene, birefr. changes due to thermal expansion 8-52468
 atomic degenerate system, Doppler-free laser-induced dichroism and birefringence 8-82711
 biaxial crystal plate, refl. and trans. wave amplitude 8-95573

birefringence continued

- biological material, birefr. analysis 8-56954
cholesteric liq. cryst., helical sense and pitch from birefringence meas. 8-59744
colloids, macromolecules, particle size distribution, reduced electric dipole moments, polarisabilities using electric birefringence 8-95958
compensator with adjustable birefr. dispersion 8-82017
condensed phases, picosec. relax. polarisation spectrosc. meas. 8-68530
copper acetate monohydrate, ESR in resonant cavity, meas. of Cotton-Mouton-Voigt effect (*French*) 8-89514
cyano-biphenyls, nematic liq. crystals, director fluctuation quenching by mag. field (*French*) 8-87613
diammonium layer compound, $\text{ND}_3\cdot(\text{CH}_3)_2\text{ND}_3\text{CuCl}_4$, antiferromag., magneto-optical meas. birefringence 8-68483
DOBAMBC, smectic A to C transform., birefringence and optical rotary power 8-75812
electronic polarizabilities of ions in doubly refracting crystals 8-79551
trans-4'-ethoxy-4'-alkanoyloxyazobenzenes, nematogenic liquid crystals, birefr., order parameters, vol. changes during nematic-isotropic transitions 8-59742
Freon-11, liq., elec. birefringence (*French*) 8-88278
glass narrow sandwich seal, correction factor for thermal expansion mismatch 8-75110
4'-n-heptyloxy-4-cyanobiphenyl, 70CB, anomalous mag. field induced birefr. in isotropic phase 8-56461
interface of uniaxial crystals, EM wave refl. and refr. laws, tensor derivation 8-71029
kaolinite, aq. suspension, mag. and optical props., Fe_2O_3 impure particles 8-76933
large-molecule system, field-induced birefringence theory 8-76421
laser active materials, ruby and garnet, crystal defects influence obs., on energetic effectiveness (*Czech*) 8-79022
macromolecular, solutions, mol. orientation, time-depend. torque, rot. diffusion eqn. 8-68471
MBBA, nematic, birefringence determ. by new simple method 8-79526
microwave at gyrotropic boundary by inclined plane wave (*Slovak*) 8-55281
myosin rod, and subfragments, flexibility, birefringence relax. in soln. 8-53320
nematic liquid cryst., birefringence determ. by new simple method 8-79526
numerical optical data processor, representation and implementation 8-78947
optical systems containing birefringence elements, generalisation of pupil function 8-55310
4-n-pentylphenylthiol-4-n'-octyloxybenzoate, birefringence, crit. suppression 8-76422
phenanthrene birefr. changes due to thermal expansion 8-52468
plastic birefringent filters, design, construction and system appls. 8-50943
polycarbonate fibre, highly-oriented, drawing behaviour and mech. props. 8-76708
polyethylene terephthalate, mech. props., influence of cryst. arrangement and noncryst. region struct. 8-76707
polyethylene terephthalate, uni- and biaxially drawn films, preferred planar orientation 8-80590
polyethylene terephthalate fibres, interdependence between struct. and thermal contraction (*Rumanian*) 8-91259
polymer, uniaxial, fluoresc. polarisation, orientation and mol. dynamics effects 8-76516
polymer films and sheets 8-80590
polymers, birefringence coeff., polarisation-spectral method (*Russian*) 8-52470
polyphenylenesilanesquinoxane, cast film, correlation between optical and mech. anisotropy 8-95000
prism couplers, birefringent, for thin film optical waveguides 8-55468
pulsating X-ray sources, radiation polarisation and beaming, vacuum birefringence effect in mag. field (*Russian*) 8-93476
quartz, birefr. and opt. rot. near structural phase transition points 8-75823
quartz, synthetic, lattice distortions, optical inhomogeneities by X-ray topography and optical birefringence meas. 8-55887
rare earth compounds, paramagnetic, Faraday and Cotton-Mouton effects for acoustic phonons 8-52476
rod outer segment, Rana pipiens, birefringence meas. of struct. inhomogeneities 8-77048
silicate glasses, stabilised, exam. of stress relaxation and deformation 8-92292
stressed state in reactor pressure vessels, model studies by polarised optics 8-78454
tanane, crit. behaviour near ferroelec.-ferroelastic transition 8-52459
twisted anisotropic media, light propag., appl. to photoreceptors 8-63004
 $\text{AlGa}_{1-x}\text{As-GaAs}$ multilayer heterostructures, optical birefringence 8-64422
 $\text{Ba}_2\text{TiGe}_2\text{O}_8\text{-Ba}_2\text{TiSi}_2\text{O}_8$, pseudobinary system, pyroelectricity and related props. 8-95553
 BaTiO_3 , cubic-tetragonal phase transition, birefringence meas., surface distortion effects 8-95564
 BaTiO_3 , vibronic ferroelec., spontaneous birefringence calc. 8-68473
 CdSiP_2 , birefringence meas. 8-56455
 CoCo_3 , birefringence of light (*Russian*) 8-56456
 CsCuCl_3 , birefr. and opt. rot. near structural phase transition points 8-75823
 FeBO_3 , photoinduced linear birefringence (*Russian*) 8-52469
 $\alpha\text{-Fe}_2\text{O}_3$, haematite, birefr. under uniaxial stress in mag. field (*Russian*) 8-88285
 Fe_2O_3 , haematite, optical indicatrix deform. and rot. during field induced phase transition 8-68482
 $\text{Gd}_2(\text{MoO}_4)_3$, electro-optical properties 8-88281
 $\text{Gd}_2(\text{MoO}_4)_3$, spontaneous electrooptic effect, role of induced birefringence 8-68480
KBr-KCl, birefringence, annealing effects, photoelasticity 8-72483
 KCdF_3 , structural phase transitions using linear birefringence studies 8-76424
KCl birefringence, annealing effects, photoelasticity 8-72483
 KCuF_3 , one-dimensional $S=1/2$ Heisenberg antiferromag., mag. energy, optical birefringence meas. 8-52467

birefringence continued

- KMnF_3 , birefr. and opt. rot. near structural phase transition points 8-75823
 $\text{KTa}_{1-x}\text{Nb}_x\text{O}_3$, local polarisability in quantum paraelec. and quantum ferroelec. phases 8-64325
 $\text{LiNbO}_3\text{:Fe}$ crystal conductivity and photoinduced birefringence obs. (*Russian*) 8-60151
 $(\text{NH}_4\text{Cs})\text{Cl}$, negative isotope effect on II-III phase transition (*German*) 8-95155
 NH_4B_6 , birefr. and opt. rot. near structural phase transition points 8-75823
 NH_4Cl , order parameter, electro-optic measurement 8-88280
 $(\text{NH}_4\text{Rb})\text{Cl}$, negative isotope effect on II-III phase transition (*German*) 8-95155
 NaNbO_3 , birefr., temp. depend., behaviour at $P\rightleftharpoons N$ struct. transition 8-64331
 $\text{NdGa}_2\text{O}_{12}$ wafer, dislocations, etch pits and birefr. obs. 8-83818
Ne, two and three level systems, laser induced dichroism and birefr. 8-79065
 O_2 solid film, optical and structural props. 8-56052
PLZT ceramic birefringence props., transverse electro-optical meas. 8-72487
 RbMnCl_3 , structural phase transition 8-91442
 SbSI , birefr. and phase transitions 8-60405
 SbSI , ferroelec., phase transitions, birefringence meas. 8-56440
 $\text{SiO}_2\text{-Al}_2\text{O}_3\text{-B}_2\text{O}_3\text{-MgO-CaO-Na}_2\text{O}$, strengthened by ion exchange, exam. of internal stresses using polarising microscope 8-88549
ZnSe, twinning effect on electro-optical props. 8-68478

bismuth

see also nuclei with

- atom, $6p_{1/2}^3\text{-}6p_{3/2}^3$, search for optical rot. induced by weak neutral currents 8-82710
atom, L-shell X-ray photoelectric cross sections, fluorescence spectra 8-58636
atom, parity nonconservation in heavy atoms, weak electron-electron interaction (*Russian*) 8-55132
atom, UV absorption spectrum, flash photolysis method 8-90105
atomic beam excited passing discharge region, new light source of forbidden lines 8-90112
Azbel-Kaner type cyclotron reson. obs. 8-56379
band structure' model parameters, deformation theory (*Russian*) 8-56067
charge carrier drift velocity (*Russian*) 8-84208
defects, quenching and annealing, resist. meas. 8-87973
deformation theory of the charge carrier spectrum from Shubnikov-de-Haas data (*German*) 8-84235
diffusion in liquid Cu (*Japanese*) 8-59962
diffusion thermoelectric power in mag. field, calcs. 8-56167
electromechanical polishing method 8-53073
electron gas heating at low temp. 8-60133
electron isoenergetic surface, variation of connectivity under press. (*Russian*) 8-60050
electron properties, carrier spectrum, review 8-84137
failure under hydrostatic press., kinetics 8-52944
Faraday effect, in vapour, P-invariance in M1 transitions, calc. 8-82805
Fermi surface, $2^{1/2}$ order electron phase transition under extension (*Russian*) 8-75981
film, carrier conc. and mobility, resist., galvanomag. and thermoelec. meas. 8-52111
film, charge carrier scatt. (*Russian*) 8-80079
film, elec. cond., obs. of epitaxial growth mechanism (*French*) 8-84329
film, optical props. as function of wavelength (*Russian*) 8-52591
film, size effect on electrical cond. 8-84331
film, X-ray diffr. anal., {001} textured growth 8-72016
film Al-type supercond. vapour-quenched transition temp., A7-type phase transition 8-52145
foil, traversed by $\text{H}^+(\text{He}^+)$, energy loss and straggling meas. 8-95100
grain boundary scattering effect on temp. depend. of electroresistivity, galvanomagnetic effect (*Russian*) 8-56148
growth of single cryst. wires with high resistivity ratios 8-68622
HF EM wave propagation in Voigt configuration 8-68045
 k_{for} for 8-80822
lightly doped, superconductivity, resist. obs. 8-64160
liquid, collective motions, cold neutron scatt. obs. 8-67639
liquid, elec. cond. and assoc. optical scattering 8-76040
liquid, electrical resistivity with spin-orbit scatt. 8-64018
metal cluster generator for gas-phase electron diff., variation of microcryst. with size 8-63645
microcontact, resistivity at low temp. (*Russian*) 8-80054
nonequilibrium phonons, negative differential cond., life time oscils. (*Russian*) 8-76117
positron annihilation parameters, temp. depend. 8-76553
positron annihilation rates, electron-electron and electron-positron correl. effects 8-76548
pulsed Ettingshausen cooling 8-91670
recrystallisation, effect of Sb, Sn and Pb 8-52841
static skin effect 8-56177
substrate, epitaxial growth of Sb 8-95246
thermomagnetic waves obs. (*Russian*) 8-80008
thermopower meas., 9K-40 mK 8-91673
US propagation anomalies, under hydrostatic press. (*Russian*) 8-83884
vacuum deposited metal film, elec. field effect on residual struct. 8-51836
vapour deposited on NaCl cleavages, crystallinity depend. on deposition parameters 8-63955
whiskers, hardness, elec. props. (*Russian*) 8-51874
zone centre phonons and elastic consts., hydrostatic press. depend. 8-59905
Bi-Sb interface, film, thermoelectricity, ageing differential efficiency (*German*) 8-60146
Bi-YIG layer struct., Landau electron absorpt. mechanism, spin wave amplification 8-72344
 Bi_2 , vap., optically pumped, laser action 8-71081
 ^{210}Bi , separation from ^{210}Pb , using silica gel ion exchanger 8-86961
 CaS:Bi , Tm, phosphor sensitisation mechanism, energy transfer 8-60507
 CdS:Bi film, implantation and post annealing, superlinearity 8-52028

bismuth continued

- InSb-Bi, thermodynamic props. (*German*) 8-75847
 LiTiZn ferrites, elec. resist., mag. props., effect of Bi addition 8-95474
 Xe+Bi, Bi K α X-ray lines, Doppler broadening 8-62759

bismuth alloys

see also *bismuth compounds*

- Al-Bi, containing low melting point inclusions, impact props., temp. depend. 8-60792
 AlBi, X-ray fluorescence analysis (*Japanese*) 8-88663
 Bi-Sb, semimetallic alloy, microwave spectroscopy 8-87908
 Bi-Cd-Sb, calc. of phase equilibria using thermodynamic values from different models 8-60646
 Bi-Pb-Sn, molten metallic system, contribution to sign inversion of effective charge (*Czech*) 8-60656
 Bi-Sb, crack appearance in diffusion zones (*Russian*) 8-76727
 Bi-Sn, dil., superconductivity, resist. obs. 8-64160
 Bi-Te, dil., superconductivity, resist. obs. 8-64160
 Bi-Te, dil. alloy, elec. cond. depend. on Te conc. (*Russian*) 8-76042
 Bi-Te, electron isoenergetic surface, variation of connectivity under press. (*Russian*) 8-60050
 Bi_{1-x}Pr_x-Al oxide-Al tunnel junction, cryst. field struct. obs. in conductance 8-84358
 Bi_{1-x}Sb_x, semicond.-semimetal transition, temp. and press. depend. of transport props. 8-76120
 Bi₈₈Sb₁₂-Sn, current carrier energy spectrum (*Russian*) 8-60139
 Bi₃Sr_{1-x}Eu_x, supercond. and mag. ordering 8-56252
 Cd-Pb-Bi-Sn system, ternary liq. alloys, thermodynamic props. 8-51701
 Fe, cast, Mg, despheroidising effect of Bi, Sn on graphite in alloy 8-56670
 Hg-Bi, liquid dilute amalgams, elec. cond. and thermoelec. power 8-51976
 In-Bi alloy system at high press. and temp. 8-92238
 In₂Bi, de Haas-van Alphen effect 8-91594
 Mn-Bi, film, ZZ 8-68014
 Mn-Bi eutectic alloy, mag. anisotropy 8-68220
 MnBi film, magnetic reversal mechanism, hysteresis loops for polycryst. and single cryst. specimens (*Russian*) 8-60318
 MnBi film for recording optical information, analogue characts. (*Russian*) 8-50716
 MnBi films, stability of magneto-optical props. on pulse heating (*Russian*) 8-88282
 Pb-Bi, liquid alloy, chemical and intrinsic diffusion coeffs., exam. (*German*) 8-83987
 Pb-Bi, peritectic reaction, microstruct. changes 8-52753
 Pb-Bi (4.1 at.%) solid soln., tetragonal distortion field for substitutional Bi atoms, neutron scatt. 8-51568
 PtPb₃Bi, cryst. struct. (*German*) 8-59783
 Sb-Te-Bi, miscibility limits, computer study 8-79773
 Sn-Bi, supercooled, dendritic growth rates (*Russian*) 8-80533
 Ti-Bi-Pb, phonon anomaly near Fermi surface topological transition, phonon softening at X point 8-95120

bismuth compounds

see also *bismuth alloys*

- halides, X-ray L_{III}-absorption edges 8-82750
 molybdates, on SiO₂, EPR rel. to surface processes (*French*) 8-64271
 Bi₁₂GeO₂₀, cryst. powder, phonon electroacoustic echo signal storage 8-68055
 Bi-Sb narrow gap semiconductor, EM wave propagation in direction parallel to mag. field 8-80014
 Bi₂Al(Ga)₄O₉, fluoresc. and X-ray data 8-80403
 Bi₂B₂O₇, crystal growth from melt, exam. of growth kinetics 8-72717
 Bi₂Bi₂Fe₂Ti₂O₈, dielec. and magnetoelec. props. 8-95562
 BiBi₄Ti₃FeO₁₅, perovskite-like layer-type ferroelec. magnetic cpd., Mossbauer expts., 80-1200K 8-64329
 BiBr₃-HgBr₂(-CdBr₂), molten, elec. cond., 500-870K, composition depend. 8-55965
 BiCl₆³⁻, model force fields and vibr. amplitudes calcs. 8-62780
²⁰⁹BiF₆²⁻, radical, prep. and EPR comparison with other hexafluoride radicals 8-68381
 Bi₂Fe₂O₉, mag. struct., neutron diffr., transition 8-52217
 Bi₂Fe₂O₉, mag. struct., neutron diffr. meas. 8-91844
 Bi₁₂GeO₂₀, electrophys., props. determ. (*Russian*) 8-51987
 Bi₁₂GeO₂₀, pulse photocond., V-I characts., 0.35-0.55 μ m (*Russian*) 8-68048
 Bi₁₂GeO₂₀, single crystals, optical homogeneity depend. on growth conditions 8-95007
 Bi₁₂GeO₂₀ vacuum-deposited film elec. and photoelec. props. (*Russian*) 8-60237
 Bi₁₂GeO₂₀ wide-zone dielectric injection contact characteristics (*Russian*) 8-60236
 Bi₃, molten, electrical cond., press. effect, 0-1 kbar 8-55963
 Bi₃, UV reflectivity meas. 8-72545
 Bi₃-Cr³⁺, ESR, spin-lattice relax., temp. depend. 8-88178
 Bi₃-Mn²⁺, ESR, spin-lattice relax., temp. depend. 8-88178
 Bi₂O₃ and sillenite struct. derivatives, MO_x.6Bi₂O₃, IR and Raman spectra, vibr. anal. 8-76464
 Bi₂O₃, doped, secondary ion emission, at. and mol. processes 8-68588
 Bi₂O₃, electronic struct., X-ray emission, XPS, UPS obs. 8-52638
 Bi₂O₃, molten, reaction with water, reactor fuel-coolant interaction simulation 8-58363
 Bi₂O₃, transmission spectra of thin films 8-76440
 BiOI, synthesis, thermal decomposition in dry O₂ (*French*) 8-53205
 BiOI, UV reflectivity meas. 8-72545
 Bi₂RO₂₀, R=Ge, Si, photoinduced birefringence, dynamic transparency prod. 8-90472
 BiSb, optical B_u modes of paraelectric phase, simple model 8-75747
 BiSb, Azbel-Kaner type cyclotron reson. obs. 8-56379
 BiSb, hybrid resonance in a quantising magnetic field 8-67933
 Bi_{1-x}Sb_x, semiconductor, anomalous conductance in strong electric and longit. quantised mag. field (*Russian*) 8-76084
 Bi_{1-x}Sb_x-Pb (0.08 $\leq x \leq 0.13$) Seebeck, magneto-Seebeck coeff., longitudinal Nernst coeffs. 8-56168
 Bi₄Sb_{1-x}SI_x, atomic substitution and ferroelec. phase transition 8-68464
 Bi_{0.52}Sb_{1.48}Te₃ thermoelec. solid soln., homogeneity, effects of prep. method 8-52698
 Bi_{1-x}Sb_xTe₃, solid soln. film on mica substrate, effect of stresses on elec. cond. 8-51859

bismuth compounds continued

- BiSeBr, optical B_u modes of paraelectric phase, simple model 8-75747
 BiSeI, optical B_u modes of paraelectric phase, simple model 8-75747
 Bi₁₂SiO₂₀ crystals, for real-time coherent object edge reconstruction 8-90372
 Bi₁₂SiO₂₀, volume hologram polarisation props. and appls. 8-74859
 Bi₂Sn₂O₇, prep., stability, and crystallographic exam. (*French*) 8-51510
 BiTaO₄, X-ray and ESR study of phase changes 8-72476
 Bi₂Te₃, chemical bonding models, correctness test using mag. susceptibility, and chemical substitution 8-67680
 Bi₂Te₃-Sb₂Te₃ film, residual cond. 8-52110
 Bi₂Te₃-Sb₂Te₃ solid solns., powders, particle shapes determ., device 8-60899
 BiTeI, influence of lamination effects on mag. suscept. (*Russian*) 8-80125
 Bi₂(Te_{1-x}S_x)₃, thin cryst. two-dimens. system, electronic props. 8-60181
 Bi₂Te_{3-x}Se_x thermoelec. mat., prep. effects on inhomogeneities 8-51576
 BiTiNbO₆, cryst. struct. determ. (*German*) 8-79570
 BiVO₄, linear coupling between soft optical and ferroelastic acoustic modes 8-79716
 Bi₂WO₆ single crystal, growth from flux in Bi₂WO₆-Na₂WO₄, below transformation temperature 8-72713
 BsSI, optical B_u modes of paraelectric phase, simple model 8-75747
 (Gd,Bi)₃(Fe,Ga)₅O₁₂ magneto-optic film, ion irr. effect on storage props. 8-52324
 (GdPrBi)₃(FeGaIn)₅O₁₂, pure and In³⁺ doped, near IR absorpt. and Faraday rot. 8-95580
 KCl:BiCl₃, electrical cond. as a function of temp., charge transport mechanism 8-83996
 NaBi(MoO₄)₂, photoelastic props., acousto-optical figure of merit meas. 8-60420
 Na₂O-B₂O₃-Bi₂O₃-SiO₂, heterophase glass, diffusion and elec. cond. 8-67858
 PbBi₄Ti₄O₁₅ ceramic, dielec. props., temp. depend. 8-95561
 Pb(Mg_{0.5}W_{0.5})O₃-BiFeO₃, dielec. props., cryst. struct. 8-84534
 PbO-Bi₂O₃-GeO₂, exam. of glass forming and liquid phase separation regions, and optical props. 8-88453
 PdBi₂O₆, cryst. struct. (*French*) 8-51516
 Sb-Te-Bi, computer study of miscibility limits, 273 to 300K 8-52781
 Te-Bi₂Te₃ oriented eutectic, microhardness, influence of size of phases (*Russian*) 8-92322
 Y_{3-x}Bi_xFe₂O₁₂, ferrite-garnet formation 8-52737
 (YGdYbBi)₃(FeAl)₅O₁₂, epitaxial garnet film, with mag. compensation point, behaviour of 'compromise' phase boundary 8-60321
 (YLaBi)₃(FeGa)₅O₁₂, pure and In³⁺ doped, near IR absorpt. and Faraday rot. 8-95580

Bitter patterns see *magnetic domains*

bitumen see *materials*

BL Lacertae-type objects

- 1418+54, new violently variable BL Lacertae object, historical light curve 8-93410
 absorption spectra 8-86036
 AO 0235+164, radio study of z=0.524 absorpt. system 8-65680
 B2 1101+38, UV spectrum from International Ultraviolet Explorer (IUE) obs. 8-96540
 extragalactic nature (*Russian*) 8-69888
 linear optical polarisation, obs. (*Russian*) 8-57640
 local space density, of BL Lacertae objects, galaxies active nuclei and quasars 8-57676
 Markarian 180 and 421, spectra of stellar population 8-54047
 Markarian 421 (2A 1102+384), low-energy X-rays detect. 8-54083
 Markarian 421 and 501, polarisation data 8-93406
 Mk 421, optical counterpart of 2A 1102+384, X-ray emission detect. 8-57698
 nebulosity around non-stellar type objects 8-57648
 ON 325, extragalactic nature (*Russian*) 8-69888
 physical problems 8-57649
 PKS 0548-322, possible BL Lacertae object, low-energy X-rays detect. 8-89270
 review, characts. and relation to QSOs and normal galaxies 8-89259
 white holes, appearance rel. to quasars and BL Lacertae objects 8-81650

black holes

see also *gravitational collapse*

- accretion disks around massive black holes: persistent emission spectra 8-93296
 C-metric black hole solution to vac. Einstein field eqns. 8-89216
 Circinus X-1, black hole candidate, position meas. 8-93459
 collapsing relativistic stars, linearised odd-parity radiation 8-93297
 cosmological density 8-77573
 Cygnus A model, radio source powered by M87 type knots 8-57661
 Cygnus X-1, possible black hole, astronomical background to speculations (*French*) 8-77624
 Cygnus X-1, status report 8-77618
 density matrix in quantum electrodynamics, equivalence principle and Hawking effect 8-66060
 domains of stationary communications in space-time 8-62133
 dust, thin spherical shell, around black hole, dynamics, Russner-Nordstrom geometry 8-77481
 early universe, thermal radiation during quantum era rel. to relic radiation origin (*Russian*) 8-81717
 Einstein vacuum field eqns. solns. using local symm., rotating body neutrals 8-54257
 elastic spacetime rel. to black holes and gravitational waves 8-73625
 EM generalisation of Robinson's identity, Kerr uniqueness theorem 8-81649
 EM radiation near black holes and neutron stars 8-53978
 exponential amplification in gravitational field of ultrarelativistic rotating body 8-93594
 five-dimensional theory, conditions of existence of horizons 8-73907
 formation of neutron stars and black holes (*Swedish*) 8-69823
 galactic centre, distrib. of stars and dust, black hole hypothesis 8-86010
 in galactic nucleus, black hole sustenance rel. to quasars power source 8-57632

black holes continued

- globular cluster X-ray source, evolution of 100 M_{\odot} black hole in binary 8-61932
- gravitational cyclotron instability, mechanism for cosmic radio emission 8-65724
- gravitational inertial field and critical systems, free motion 8-93484
- Hawking effect, thermal nature of the density matrix for black hole particle prod. (*Russian*) 8-89644
- Hawking effect and Euclidean QFT 8-73732
- Hawking mini black-holes origin and cold early Universe 8-93298
- hot universe with primordial black holes, neutrino radiation kinetics (*Russian*) 8-93485
- Kerr black holes, energetics, reversible transformations 8-85968
- Kerr naked singularity, classical instability 8-57834
- Kerr-Newman background space, nonstatic nuclear forces, meson field at black hole event horizon 8-61880
- magnetosphere, charge particle trapping 8-57573
- massive vector fields and black holes 8-96499
- massless quantum fields in curved asymptotically flat space-time, particle creation near black hole (*Russian*) 8-57846
- mini black holes fast explosive evaporation in plasma and solar flares, analogy, energy conversion processes 8-96388
- missing mass in galaxies, role of brown dwarfs and black holes 8-61879
- in N-body stellar systems, two-body tidal dissipation rel. to form. 8-93329
- neutron stars mass upper limit for stability against black hole form. 8-96498
- NGC 4151, X-ray flares in Seyfert, thermal model and central black hole 8-93407
- non-linear wave equations in a curved background space 8-65827
- particle emission model, for teachers 8-62018
- perturbation due to a rotating, enclosing spherical shell of matter 8-81648
- primordial, search for high energy gamma ray bursts 8-54084
- primordial, upper bound on number density calc., big bang nucleosynthesis 8-65649
- primordial black hole development 8-93299
- primordial low mass black holes evaporation and H recomb. kinetics (*Russian*) 8-61943
- production of massive objects in active galactic nuclei unlikely 8-89261
- QSOs, black flash model 8-57673
- quantum gravitational fluctuations, energy dissipation mechanism 8-57572
- quantum gravity, unpredictability 8-54277
- quantum mechanical particle prod., black hole radiance 8-81647
- quark confinement, event horizons around a particle surrounded by a static confinement potential 8-66075
- quasars, accreting black holes model 8-57678
- quasars, accretion discs thermal continuum as optical emission source 8-54075
- quasars and galaxy nuclei, black hole gravity power model 8-57667
- radiation hydrodynamics of high-luminosity accretion 8-77571
- radiation pressure effects on spherical accretion 8-61725
- radiation-dominated non-relativistic gas, Bondi accretion problem 8-77575
- radio galaxies, relativistic jets and beams 8-96541
- Reissner-Nordstrom black hole, force free fields 8-77572
- Rosen's bimetric theory of gravity, orbital topography and other astro-physical consequences 8-54274
- rotating black hole, Kerr metric, spontaneous creation of massive spin 1/2 particles 8-89217
- scalar charge, instability under monopole perturbations 8-77576
- Schwarzschild, in ext. mag. field, radiation emitted by relativistic particles 8-96501
- Schwarzschild electrodynamics, rel. to black holes and neutron stars 8-77480
- Seyfert nuclei, black flash model 8-57673
- spherical stellar system, distrib. of stars around massive central black hole 8-65660
- spontaneous particle creation in strong gravitational field, semiclassical theory 8-54281
- stationary, uniqueness theorems 8-96500
- superluminal particles motion in gravit. field of nonrot. black hole (*Russian*) 8-93103
- supermassive objects rel. to radiogalaxies 8-61882
- supermassive stars and black holes, work of Johann Georg Soldner (1776-1834) 8-81787
- supersymmetric, in supergravity, spin 3/2 perturbation of Schwarzschild black hole 8-93300
- symmetry of charged rotating body metrics 8-77776
- theory and observational methods (*Hungarian*) 8-77574
- thermodynamic mechanisms, review 8-93301
- tidal disruption by a massive black hole and collisions in galactic nuclei 8-77597
- trace anomalies in a two-dimensional de Sitter metric and black-body radiation 8-65841
- unified gravit. and electromag. field theory of black-hole evaporation 8-53979
- vacuum black holes, gravit. radiation scatt. 8-65648
- white holes, appearance rel. to quasars and BL Lacertae objects 8-81650
- white holes present appearance 8-61881

blast waves see shock waves**Bloch walls** see magnetic domain walls**blood**

see also haemodynamics

- albumin, human serum, adsorption studies, feasibility of radiolabelling 8-85359
- arterial pO_2 intravascular monitoring using catheter-tip polarographic electrode (*German*) 8-85408
- arterial thrombosis, in vivo method for evaluation of effects of materials 8-81071
- arteriovenous O_2 difference, noninvasive meas. method (*German*) 8-85441
- blood analysis, optimal conditions (*Bulgarian*) 8-85280
- bone marrow ^{32}P effects during postnatal development of Swiss albino mice 8-53450
- bubble oxygenator, O_2 transfer controlling factors 8-53568

blood continued

- cardiac chamber imaging, comparison of red blood cells labelled with $^{99}Tc^m$ in vitro and in vivo 8-65109
- cell differential counter, ADC 500, pattern recognition based image processing system 8-73282
- cell high-speed analysis, laser absorpt. and scatt. meas. (*German*) 8-92687
- cell smear pathology differentiation by optical transform method 8-69248
- clotting of rabbit blood, Fourier transform. IR obs. 8-68945
- coagulation in gastrointestinal haemorrhages, using laser endoscope (*German*) 8-69178
- electrophoretic waveform analysis for blood serum protein composition determ. 8-64928
- endocrine research, continuous blood sampling and time series anal. 8-77130
- erythrocyte, human, steady rate of glycolysis rel. to ATP conc., quantitative model 8-53354
- erythrocyte, sectioned, generalised theory of geometrical shape 8-65071
- erythrocyte Ca transport in myotonic muscular dystrophy patients 8-80849
- erythrocyte electrophoretic mobility, effect of UHF EM radiation 8-53442
- erythrocyte high gradient magnetic separation 8-53585
- erythrocyte membrane, phys. state of lipids, X-ray diffr. 8-80835
- erythrocyte membrane lattices, partially disordered, X-ray scatt., anal. method applied 8-91196
- erythrocyte membranes, ESR study of abnormalities in Duchenne muscular dystrophy 8-96111
- erythrocyte osmotic fragility curve, statistical synthesis 8-65070
- erythrocyte survival after slow freezing in glycerol, temp. depend., human cells 8-77019
- erythrocytes, slowly frozen human cells, phys.-chem. basis of protection by glycerol 8-77020
- erythrocytes, technique for observing 3D dim. struct. with a cryo-SEM 8-92765
- erythrocytes of human blood, diameter meas. by specific elec. cond. 8-53353
- extracorporeal irradiation with ^{137}Cs , expt. research and clinical appl. (*German*) 8-69149
- filter evaluation 8-69250
- frozen red cell structure and function, freezing patterns and post-thaw survival 8-64960
- gas analysers, review 8-69238
- gas sampler, for gas chromatograph, design, construction and characteristics (*Japanese*) 8-85458
- glucose regulation parameter estimation, optimal inputs 8-64920
- haematofluorometer, for testing Pb poisoning 8-53554
- heat exchanger for heating/cooling blood, thermal design, equipment and blood props. considerations, appls. 8-92744
- implantable electronic pancreas and blood glucose monitor 8-88767
- intracerebral spontaneous haematoma diagnosis and prognosis by computed tomography 8-73195
- intravascular O_2 saturation continuous meas. using fibre optic catheter (*German*) 8-85411
- laminar blood flow, gas and heat transport, platelet and protein diffusion 8-92669
- leucocyte, human, fluorochromed with acridine orange, spectral char-acts. 8-96024
- leukocytes automatic anal., nuclear texture parameters appl. 8-77136
- light back-scattering, multipole expansion of integral photon density expressions 8-77099
- liposomal membrane permeability, radioresist. 8-80919
- lung numerical modelling, human 8-80911
- lymphocyte death and transform., effects of X-ray and neutrons 8-69144
- lymphocytes, in vitro ^{60}Co gamma-ray response of leucoagglutinin stimulated human cells 8-57041
- monitoring of blood vol. change in menstruation, vaginal photoplethysmographic transducer 8-92733
- neutrophil automated classification, feature selection 8-73281
- oximeter calibration, humans exposed to centrifugation 8-92734
- oxygenator using microchannel membrane, transport and flow phenomena 8-69253
- oxyhaemoglobin dissociation curve direct obs. in man in vivo, computer investigation 8-85433
- peripheral polymorphonuclear leucocyte system model, humans 8-56956
- polymeric biomaterials for blood-contacting appls., problems and new dimensions 8-85423
- red blood cell profile direct meas. using SEM beam reference lines 8-81094
- red cell suspensions, haemoglobin NMR relax., T_1 and T_2 meas. 8-80832
- reticulocyte production rhythm investigation by spectral analysis 8-73279
- rheological and thermophysical fluid props., physicochem. composition depend. 8-80902
- sedimentation rate free from gravity influence, rapid determ. from density meas. (*German*) 8-81085
- serum automated electroanal. using ion-selective disc electrodes with neutral cation-carriers (*German*) 8-73269
- serum Fe after whole-body ^{60}Co irradi., rel. to ^{67}Ga tumour uptake 8-65081
- surgical aspiration automatic control device for cardiac surgery (*French*) 8-61282
- thyroid substances levels in blood serum of rats exposed to 0.2, 0.6 and 1 W/cm² of US energy 8-69134
- viscosity factors in severe nondiabetic and diabetic retinopathy 8-65069
- viscosity variations associated with hyperlipoproteinaemia (*German*) 8-57031
- CO_2 partial pressure in blood, meas. by rapid response electrode system (*German*) 8-85409
- Fe III, high-spin, in cancer, EPR 8-53466

blood circulation see haemodynamics**blood dynamics** see haemodynamics**blood flow** see haemodynamics

blood platelets *see* **blood**

blue brittleness *see* **brittleness**

boilers

- burner with diffusive control, intermixing of gas streams with transverse swirled air flow 8-87418
- dryout, premature in conventional and nuclear power station evaporators, model 8-94120
- dynamic simulation of the Gentilly-1 reboiler system 8-82439
- heat transfer in vertical steam generating tube, at low pressures and moderate mass velocities of flow, post-dryout coeff. calc. 8-67257
- HTGR steam power plant, nonlinear dynamic model, digital simulation 8-78437
- LMFBR, H burden from steam side corrosion in Na heated steam generators 8-58355
- LMFBR, leak detection by acoustic spectra meas. (Czech) 8-54849
- LMFBR, water leaks in secondary cooling circuit boilers 8-86572
- nuclear LMFBR steam generator, Cr-Mo low alloy steels comparison 8-54834
- pollution detection and control, SO₂ emission reduction by limestone-additive process (German) 8-53724
- PWR natural circulation U-tube steam generator, digital code UTSG 8-50242
- PWR with straight tube steam generator, 1300 MW, characts. (German) 8-50292
- steam generator, modular, liquid Na heated, pressure and temp. loading in breakdown situation (Czech) 8-50264
- steam generator, multiple tube rupture, radiological consequences 8-74452
- steam-generating tube, bubble/plug flow boiling regimes, elevated press., drift vel. and void fraction determs. 8-87379
- TPP 210 A steam generator, radiant heat flux distrib., light model simulation 8-94567
- tube, serpentine geometry at high press., two phase heat transfer 8-94077
- vibration analysis of heat exchanger and steam generator designs 8-66333

boiling

see also **boiling point**

- Alad'ev wall superheat correl., expt. validity test 8-83393
- annuli, concentric (eccentric), with turbulence promoters, boiling crisis 8-55639
- bubble growth in slow formation regime of nucleate pool boiling 8-90687
- bubble population prediction in flow boiling, from gas bubble nucleation 8-90696
- bubbles, active nucleation site spatial distrib., bubble flow density 8-71267
- BWR boiling noise, local and global component obs. and calc. 8-94066
- capillary and porous surfaces, liquid boiling and evap. heat transfer 8-94526
- channel, rectangular, forced flow boiling and burnout 8-94530
- channel flow, thermally induced two-phase flow instabilities, thermal nonequilib. 8-51240
- critical heat flux variation, very nonuniform annular heat release 8-51043
- cryogenic liquids, boiling, crit. heat flux, heating surface props. effects 8-90662
- drop, gradient explosion, under conditions of bulk heat release 8-83226
- ethanol, boiling, crit. heat flux in low press. region 8-90663
- ethanol-water mixture, saturated, min. film boiling temp. on horiz. stainless steel and Cu surfaces 8-90692
- extended liquid masses, film boiling heat transfer, partial evaporation method 8-90668
- falling film rewetting 8-75906
- ferromagnetic layer boiling, mag. characteristics meas. 8-59499
- film boiling, minimum heat flux anal. 8-90665
- film boiling destabilisation, liq. drop falling onto hot liq. surface 8-94588
- film boiling on small wires, prediction of elec. field effects on most unstable wavelength 8-87239
- film boiling under natural convection conditions, heat transfer 8-83231
- flow instabilities in sustained and transient boiling, inlet subcooling effect 8-94809
- forced convection quench data rel. to steady-state nucleate boiling data 8-90995
- Freon-113, pure and mixed with methanol, EHD coupled minimum film boiling, surface wave model 8-87240
- Freon-114, Leidenfrost phenomena, crit. press. obs. 8-90667
- Freon-11, pool-boiling, heat transfer from inclined plate 8-51046
- gas and vapour bubble nucleation on brass surface in water 8-71845
- heat exchange, nonstationary, with phase transformations, delayed boiling influence (Russian) 8-83235
- heat transfer, bubbling and boiling, under conditions of free and forced convection 8-90637
- heat transfer conference, Aug. 78, Toronto, Canada 8-90624
- heat transfer during boiling on circumferential fins 8-59272
- heat transfer in two-phase thermosyphons 8-90686
- horizontal cylinder, local boiling heat flux density, saturated, subcooled conditions 8-90659
- horizontal heated surface, post-nucleate boiling and crit. heat flux models 8-90664
- hot surface quenching rate, countercurrent single- and two-phase flow effects 8-59451
- incipient boiling, transition to film boiling 8-90660
- incipient boiling characteristics at atmospheric and subatmospheric pressures 8-90688
- instability of gradient explosion 8-83917
- isopropanol, nucleate pool boiling, bubble freq. model, surface effects 8-90651
- laminar vapour flow in film boiling, stability limits 8-90832
- law of metastability, appl. to effect of mag. field on boiling liqs. 8-79199
- Leidenfrost effect, demonstrations 8-81744
- liquid film, nucleate boiling suppression 8-75055
- liquid films, boiling, heat transfer peculiarities 8-90656
- liquid jet, burnout in nucleate boiling 8-90991
- liquid thin film rupture, heat-transfer surface state effect 8-55552
- boiling continued
 - liquid-gas bubbles system, phase transition kinetics and kinetic eqns. 8-83933
 - LMFBR, coolant start of boiling detection by acoustic method 8-86646
 - metal-polar fluid boundary, double electric layer effect on boiling 8-59274
 - methanol, boiling, on Cu surface, rel. to H₂O 8-90654
 - mixture, binary, nucleate boiling heat transfer, conc. depend. 8-87249
 - narrow spaces, heat transfer mechanism with boiling, interferometry obs. 8-94527
 - nucleate, subcooled, latent heat transport contrib. 8-75046
 - nucleate, surface topography 8-90653
 - nucleate boiling, heat transfer model 8-75056
 - nucleate boiling, single bubble growth at wall, shape and departure 8-90647
 - nucleate boiling bubble dynamics, calc. 8-90648
 - nucleate boiling of liq. Ar, N₂, in centrifugal accel. field, heat transfer and flux 8-94538
 - nucleate pool boiling, bubble freq. model, surface effects 8-90651
 - organic heat carriers, charact. (German) 8-79198
 - peak heat flux in pool boiling, hydrodynamic and surface effects 8-90661
 - polynary mixtures, natural convection boiling, heat transfer 8-90658
 - pool boiling, heat transfer stability prediction, finite disturbances 8-75044
 - pool boiling heat transfer from horizontal plates (Japanese) 8-67016
 - pool boiling in very low gravity, proposed spacelab expt. 8-63849
 - quenching temperature, 0.03-1.3 MPa, base material thermal props. depend. 8-94587
 - refrigerants, nucleate boiling, oil impurity effects 8-90657
 - Reynolds analogy for boiling, heat transfer 8-59277
 - rod bundles, boiling crisis and press. drop, heat transfer enhancement devices 8-55638
 - saturated liquid, boiling onset, film boiling transition, crit. heat flux densities (Russian) 8-83234
 - spheres in vertical flow, transient transition boiling heat fluxes 8-90994
 - steam generating tubes, burnout mechanism 8-90984
 - steam-generating tube, bubble/plug flow boiling regimes, elevated press., drift vel. and void fraction determs. 8-87379
 - subcooled film boiling heat transfer from spheres 8-51047
 - subcooled forced convection boiling heat transfer at subatmospheric pressure 8-94525
 - subcooled nucleate boiling, mechanistic model 8-90697
 - subcooled two-phase water flow, boiling mechanism during burnout 8-94529
 - superheated droplets, flash boiling, undergraduate student expt. 8-81748
 - surfaces covered with capillary-porous structures, heat transfer with boiling, approximate theory 8-94537
 - transient, bubble nucleation and growth instabilities 8-90649
 - transient effects, leading up to nucleate boiling 8-90650
 - transient flow boiling in duct, dynamics 8-94528
 - tube, vertical, steam generating annular flow, dry-out position prediction, computer model 8-59447
 - two-phase boundary layer, temp. fluctuations 8-51222
 - vaporisation sites, number variation with fluid layer height 8-59273
 - void fraction and phase distrib. meas. in transient flow boiling by neutron scatt. 8-94870
 - water, crit. outflow, compressibility effect on hydrodynamics, resistance coeff. 8-55684
 - water, pool boiling, produced by distrib. internal heat sources, in homogeneous nucl. reactor 8-90685
 - water, transition boiling under forced convective conditions, reactor accident condition 8-89961
 - water boiling in tube, critical heat flux 8-83232
 - water droplet evaporation, heat transfer characts., on heated surfaces 8-59269
 - water droplets react. with molten Na 8-71263
 - water jet impinging on hot surface, boiling heat transfer 8-90993
 - BF₃, boiling/condensation heat transfer props., cryogenic appls. 8-79192
 - CO, boiling/condensation heat transfer props., cryogenic appls. 8-79192
 - Cu, horizontal plate, pool-boiling heat transfer, nucleation centre size, surface roughness 8-90652
 - H₂-N₂-Ar, two-phase flow film boiling, in vap. generator, heat transfer 8-75190
 - H₂O, boiling, crit. heat flux in low press. region 8-90663
 - H₂O, boiling, on Cu surface, rel. to methanol 8-90654
 - H₂O, nucleate pool boiling, bubble freq. model, surface effects 8-90651
 - H₂O, squeezed boiling, internal characts. 8-90655
 - He liquid, transient heat transfer, static coolant 8-75049
 - He, liquid film, transient heat transfer, film boiling regime 8-83219
 - NO, boiling/condensation heat transfer props., cryogenic appls. 8-79192
 - Na, liq., in vert. pipe, hydraulic resistance under boiling conditions 8-90968
 - Na, liquid, local boiling behind local flow blockage, simulated LMFBR fuel subassembly 8-54842
 - Na, pool boiling heat transfer, liq. head effects 8-89951
 - Na transient boiling in single-pin annular channel under loss of flow 8-89933
 - Na- UO_2 interaction, dropping experiments and subassembly test 8-82460
- boiling point
 - see also* **boiling; heat of vaporisation**
 - organic compounds, crit. temps. correl. with boiling pts. 8-91421
 - solutions, dilute, colligative props., kinetic derivation from elastic collision processes 8-91048
 - vapour-liquid equilibrium, T-x meas. by semi-micro method 8-87782
 - Ne, normal boiling point reproducibility, cryostat appl. 8-79757
 - TiNO₃, boiling and melting pts., heats of transformation, solid-solid transformation 8-91441
 - Xe, suitability as temperature fixed point 8-77838
- bolometers**
 - 100 GHz bolometer mount efficiency meas. calorimeter (Japanese) 8-54460

bolometers continued

- autobalancing radiometer, electrical compensation 8-86067
figure of merit for comparison of types of thermal detectors (*German*) 8-57954
film thermal device appl. 8-70189
immersion thermistor bolometer use in radiometer 8-70188
laser power meter, sensitive meas. IR to vacuum UV spectral range 8-82031
molecular beam detector using fast supercond. bolometer 8-86383
mount, effective efficiency meas., computerised calorimeter system 8-86272
submillimetre wavelength composite bolometer 8-65964
surface temperature contactless meas. instrument 8-57946
thin film structures, characts. (*German*) 8-62226
Ge cryogenic bolometer, for 20 to 500 μm spectral region 8-70187

Boltzmann equation

- see also *transport processes*
accommodation coefficients, effects on evaporation and condensation (*Japanese*) 8-81933
BBGKY hierarchy, scaling method of kinetic eqn. derivation 8-54286
electrical resistivity with spin-orbit scatt. 8-64018
electron ensemble, weak turbulence, diffusion and collisions in elec. and mag. fields (*German*) 8-83564
electronic transport coeff., soln. between Mori-Green-Kubo formulae and Boltzmann approx. 8-79971
fast-electron transfer in lamellar materials 8-86230
gas-particle mixtures, effect of thermal radiation on shock wave 8-91032
gaseous mixture, Boltzmann kinetic equations, soln. methods 8-83511
global solutions, bounded convex domain 8-57876
glow discharge cathode region microscopic model 8-67524
kinetic theory of one-dimensional evaporation and condensation problem (*Japanese*) 8-81932
Kubo formula derivation of Boltzmann equation, resolvent method 8-95277
Landau-Lifshitz hydrodynamic fluctuations in nonequilib. systems, Boltzmann eqn. reduction 8-81929
linear Boltzmann eqn. with external EM forces 8-93630
linear Boltzmann equation, transport and scatt. props. and solns. 8-93628
low-pressure discharge electron kinetics 8-75483
metal, new method for solving Boltzmann equation for electron 8-72127
metal-liquid He interface, electron-phonon interaction, thermal boundary resistance 8-67899
metallic film, oscill. kinetic effects, boundary electron scatt. (*Russian*) 8-52104
mixtures of reacting gases, extension of Chapman Enskog method (*Russian*) 8-57878
nonlinear, classes of exact solns. 8-49779
nonlinear Boltzmann eqn., rarefied gas, fluid dynamical limit 8-79336
nonlinear Boltzmann-Enskog equation and asymptotic behaviour of the time autocorrelation functions 8-70079
nonlinear electrical conductivity theory based on integral Boltzmann eqn. 8-72125
one group, integral transport eqn. for homogeneous sphere, neutron scatt., classical diffusion, anal. 8-62589
quantum Boltzmann eqn., Hartree Fock configuration-space analogue 8-49780
randomly-packed spherical particle bed, coord.-no. distrib., effective thermal cond., stat. thermodynamic theory 8-75028
reactor shielding materials, Pb, and steel, γ leakage spectra, numerical integration of Boltzmann eqn. 8-58350
relaxation time approximation 8-65888
resolution of transport equation, by linearisation (*French*) 8-79989
Saturn's rings, vel. dispersion calc. 8-61795
semiconductor, rel. to nonlinear current density 8-56149
teaching, transport processes in gases, relax. approx. to Boltzmann eqn. approach 8-73804
velocity distrib. function of light ions in heavy gas in elec. field 8-83526
 H_2 -H mixture positive column, static electric charact. 8-67500
HF+HF, momentum exchange rate, Boltzmann eqn. predictions 8-78781
 ^4He , superfluid, Boltzmann transport equation, search for exponentially damped surface solns. 8-67878
 N_2 , electron energy distrib. and transport coeffs. in $\text{E} \times \text{B}$ fields 8-51277
 N_2 , electron swarm develop., Boltzmann eqn. anal. 8-79487
Nb, high-temperature nonlinear electrical resistivity, supposed failure of Boltzmann eqn. 8-91664
Ne-Cu pulsed discharge, electron energy distrib., ionis. rate 8-51387

Boltzmann-Vlasov equation see *Vlasov equation*

bond angles

- bridging bond angle variations in siloxanes, silicates, Si nitrides and sulphides, mol. orbital calc. on model systems 8-55125
t-butylphosphine, microwave spectrum, meas., determ. 8-58675
chloroethane diradical, MINDO/3 for optimised geometry and heat of form. 8-78830
chloromethylene radical, MINDO/3 for optimised geometry and heat of form. 8-78830
dichloromethylene radical, MINDO/3 for optimised geometry and heat of form. 8-78830
ethylene, mol. geometry, ab initio calcs., basis set depend. 8-82636
cis-formic acid ($-\text{d}_2, \text{d}_2$), and isotopic forms, bond lengths and angs., microwave spectrum obs. 8-55169
methyl meristotrope, mol. and cryst. struct. 8-95047
peptide, NMR spectroscopy study 8-88694
protein, NMR spectroscopy study 8-88694
selenoacetaldehyde, microwave spectrum, struct. internal rot. barrier, CCSe bond 8-74645
thermal-motion correction for bond angles, harmonic approx. 8-55777
tris(dimethylamino)phosphorus, ^{15}N and ^{31}P NMR aligned in liq. cryst., geom. struct. 8-82751
 CdX_2 , (X=Br, Cl), spectroscopic parameters of mols. from vibr. isotopic effects 8-74798
 CdXY , (X, Y=Cl, Br, I), spectroscopic parameters of mols. from vibr. isotopic effects 8-74798
 $\text{Co}(\text{CO})_3$, bond angles, hybrid bond orbital calcs. 8-94188
 $\text{Cr}(\text{CO})_3$, bond angles, hybrid bond orbital calcs. 8-94188

bond angles continued

- $\text{Fe}(\text{CO})_3$, bond angles, hybrid bond orbital calcs. 8-94188
 GaAs , (110) surface, bond angle and lengths of rearranged As and Ga atoms 8-71918
 HCN , SCF ab initio ground state pot. energy surface, geometry, rel. to HCN^- 8-78646
 HCN^- , SCF ab initio ground state pot. energy surface, geometry, rel. to HCN 8-78646
 HeNO_2 , molecular geometry and stability, ab initio calcs. 8-90075
 HgX_2 , (X=Cl, Br), spectroscopic parameters of mols. from vibr. isotopic effects 8-74798
 HgXY , (X, Y=Cl, Br, I), spectroscopic parameters of mols. from vibr. isotopic effects 8-74798
 $\text{Mn}(\text{CO})_3$, bond angles, hybrid bond orbital calcs. 8-94188
 $\text{NiF}_2 + \text{CO}$, Ar matrix isolated, ab initio MO calcs. 8-92458
 O_3 , MC SCF and MC CI calc., open and closed form mols. 8-78831
 $\text{P}_2\text{O}_4(\text{OH})_4^{2-}$ group, electronic struct. calcs. 8-67971
 $^{32}\text{SF}_2$, $^{34}\text{SF}_2$, matrix IR spectra, vibr. and force fields, bond angle (*German*) 8-74662
 $\text{Si}_2\text{O}_6(\text{OH})_6^{6-}$ group, electronic struct. calcs. 8-67971
 ThV_2O_7 , V-O-V bridge stretching freq. correl. with bond angle 8-74636
 $(\text{UO})_2\text{V}_2\text{O}_7$, V-O-V bridge stretching freq. correl. with bond angle 8-74636
 ZnX_2 , (X=Cl, Br, I), spectroscopic parameters of mols. from vibr. isotopic effects 8-74798
 ZnXY , (X, Y=Cl, Br, I), spectroscopic parameters of mols. from vibr. isotopic effects 8-74798

bond lengths

- acetylene, chemisorption on Pt (111), ethylidyne group form., LEED and ELS obs. 8-73075
acetylene, vibr. fine struct. accompanying core ionis., STO calcs. 8-62844
alkali hydroxides, dissoc. energies and bond lengths, ion props. depend. 8-86801
alkali metaborates, dissoc. energies and bond lengths, ion props. depend. 8-86801
asymmetric top molecules, R_g -struct., bond length mass depend. 8-94230
basis set effect, and approx. natural orbitals, SCF CI GTO calcs. 8-76904
bis(fluoroxy)difluoromethane, ab initio MO calcs. of geometry, torsional barriers 8-90313
carbonyl groups, intermol. interactions in $\text{H}_2\text{CO}-\text{H}_2\text{CO}$ system, quantum chem., classical calcs. 8-86932
chlorobenzene- d_5 , and isotopic forms, microwave spectrum, rot. consts. 8-58667
chloroethane diradical, MINDO/3 for optimised geometry and heat of form. 8-78830
chloromethylene radical, MINDO/3 for optimised geometry and heat of form. 8-78830
dichlorodinitromethane, mol. struct., electron diffr. investig. 8-86950
dichloromethylene radical, MINDO/3 for optimised geometry and heat of form. 8-78830
dimethyl phosphine- d_4 , ZZ 8-90167
dimethyl sulphide- d_4 , ZZ 8-90167
ethylidifluoroborane, microwave, Raman, IR spectra, conform., dipole moments, vibr. assignment 8-90155
ethylene, chemisorption on Pt (111), ethylidyne group form., LEED and ELS obs. 8-73075
ethylene, mol. geometry, ab initio calcs., basis set depend. 8-82636
fluoroxypoxytrifluoromethane, ab initio MO calcs. of geometry, torsional barriers 8-90313
cis-formic acid ($-\text{d}_2, \text{d}_2$), and isotopic forms, bond lengths and angs., microwave spectrum obs. 8-55169
group IV elements, ^{57}Fe isomer shift, quadrupole coupling and interat. distance correl. 8-52408
ice, press. effects on Raman spectrum 8-95582
methyl meristotrope, mol. and cryst. struct. 8-95047
methyl phosphine- d_2 , ZZ 8-90167
molecules of rows 1-3, equilib. geometries, orbital energies, ab initio rel. to pseudopot. calcs. 8-82613
selenoacetaldehyde, microwave spectrum, struct. internal rot. barrier, C=Se bond 8-74645
trifluoroacetic acid, ab initio MO calcs. of geometry, torsional barriers 8-90313
trimethyl phosphine- d_6 , ZZ 8-90167
 AuF_3 , ^{19}F NMR chemical shift, crystal chemistry 8-87645
 AuH , AuCl , ZZ 8-86767
 BaSO_4 , barite, crystal struct. and sulphate force consts. 8-83784
 $\text{Ca}_3\text{HPO}_4\text{SO}_4 \cdot 4\text{H}_2\text{O}$, synthetic, cryst. struct. and relation to brushite and gypsum 8-83785
Cd, effective core potentials calcs. rel. to bond lengths and energies 8-66464
ClO, rot. spectrum, mol. parameters in $\nu=0$, $\nu=1$ states 8-70821
 ^{37}Cl , pure rot. Raman spectrum 8-94252
Cu-Br, EXAFS study, in CuBr_2 8-52593
Cu-N, EXAFS study, in $[\text{Cu}(\text{NH}_3)_4]^{2+}$ 8-52593
Cu-O, EXAFS study, in CuO , Cu_2O , $\text{CuSO}_4 \cdot 5\text{H}_2\text{O}$, $\text{Cu}(\text{OH})_2$ and $\text{Cu}(\text{NO}_3)_2 \cdot 3\text{H}_2\text{O}$ 8-52593
 GaAs , (110) surface, bond angle and lengths of rearranged As and Ga atoms 8-71918
 HCN , SCF ab initio ground state pot. energy surface, geometry, rel. to HCN^- 8-78646
 HCN , vibr. fine struct. accompanying core ionis., STO calcs. 8-62844
 HCN^- , SCF ab initio ground state pot. energy surface, geometry, rel. to HCN 8-78646
HCl, bond dependence of dipole polarisabilities 8-74573
HF, bond dependence of dipole polarisabilities 8-74573
HNC (DNC), anharmonic force field, equilib. struct., rot. consts. and bond lengths 8-90147
HSiN-HNSi isomers, MRD-CI calcs. of struct. and stability 8-82635
 HeNO_2 , molecular geometry and stability, ab initio calcs. 8-90075
Hg, effective core potentials calcs. rel. to bond lengths and energies 8-66464
 HgH , HgCl_2 , ZZ 8-86767
 I_2 , adsorption on $\text{Ag}(111)$, adsorbate-substrate bond length X-ray anal. 8-84679
KOH, MHD plasma mol., pot. energy curves and dipole moment, bond lengths 8-71462

bond lengths continued

- (NH₄)₂M(SO₄)₆·6H₂O, Tutton's salts, IR spectra, correl. of vibr. freq. and N...O distance for NH₄D⁺ 8-92066
 O₃, MC SCF and MC CI calc., open and closed form mols. 8-78831
 OH⁻+CO₂→HCO₃⁻ react., MO-LCAO-SCF calcs., energy barrier 8-76846
 OHO bonds, O-H vs. O...O distance correlation and geometric isotope effect 8-75615
 PbSO₄, anglesite, crystal struct. and sulphate force consts. 8-83784
 SiO₄ tetrahedra, mean Si-O bond lengths var. 8-63699
 SrSO₄, celestite, crystal struct. and sulphate force consts. 8-83784
³T₂, pure rot. and rot.-vibr. Raman spectrum 8-94253
 XeF₂, pure rot. Raman spectrum 8-94254

bonds (adhesive) *see* **adhesion****bonds (chemical)**

- see also* **binding energy**; **bond angles**; **bond lengths**; **crystal binding**; **hydrogen bonds**; **intermolecular forces**; **lattice energy**
 A₂B_{2n} mols. and ions, strengths of A-A single bonds symmetries 8-74790
 acetylene, and -d₂, integrated IR intensity, meas. and interpretation 8-66551
 acetylene chemisorbed on Pd (100) and Ru (0001) surfaces, substrate effects on bonding, electronic spectrum 8-63933
 actinide cpds., ESCA spectra, intense shake-up satellites, model 8-50589
 AES, chemical-state effects 8-92566
 alkali halides, diamagnetic susceptibility, interatomic charge transfer effect 8-50660
 alkanes, electron density, bond order, hydrogen suppressed graphs, extended Huckel theory 8-90088
 atomic and molecular negative ions, quantum chemical calcs. 8-62703
 atomic orbital cross-sections, bonding interactions, spring model, teaching aid 8-93503
 benzenes, substituted, optical bond anisotropies, by depolarised Rayleigh scatt. 8-90171
 benzyl chloride, mol. polarisability, bond polarisability derivatives 8-74793
 bromobenzene, mol. polarisability, bond polarisability derivatives 8-74793
 cis-3,5-dibromo-4-oxo-2,2,6,6-tetramethylpiperidin-1-yloxy, cryst. struct., secondary and multi-centre bonding 8-63751
 conjugated molecule, H₃C-NC₅H₄-CH-CH-C₆H₄-O, large second-order polarisability, resonance struct. 8-66683
 coordination compounds, ligands studied by XPS 8-62842
 coreless pseudopot. for atoms K through Zn 8-55121
 covalent amorphous semiconductors, local struct., bonding and electronic props. 8-51882
 covalent elements, cohesion in condensed phases, corrections to simple Huckel approx. 8-59779
 covalent elements, cohesion of σ and π bonds in condensed phases, simple Huckel approx. 8-59778
 crystal symmetry, implications in charge density studies 8-71694
 diatomic bonding energy, changes due to Van der Waals interactions with other atoms 8-95012
 2,4-dibromo-1,5-diphenylpenta-3-one, cryst. struct., secondary and multi-centre bonding 8-63751
 diethyl tin dihalides, cryst. struct., secondary and multi-centre bonding 8-63751
 dimethyl phosphine-d₄, ZZ 8-90167
 dimethyl sulphide-d₄, ZZ 8-90167
 DNA calf thymus binding to cis- and trans-dichlorodiammineplatinum(II) extended X-ray absorpt. spectra 8-85291
 DNA pyrimidines, cryst., lattice dynamics 8-75766
 double molecules, with weak reson. bond, quasilinear (*Russian*) 8-74640
 education, H₂⁺ bonding and virial theorem 8-49599
 electrode surface, covalently bound molecules, redox reactions, steric effects 8-73077
 electron pair mechanism, non-specialist teaching appl. 8-89279
 fluorophosphate glasses, rare-earth activated, luminesc., bonding 8-64415
 furane, crystalline, lattice vibr. 8-79694
 [2,2](2,5)furanophane, through bond and through space interactions, UPS obs. 8-82786
 graphite, adsorbed butane, struct. and dynamics, neutron scatt. study 8-87870
 graphite ribbon, interlayer interaction effects on diamagnetism London theory 8-52201
 halogen molecular crystal, bond charge model, for lattice dynamics 8-79692
 hexagonal layers, lattice distortions, chem. bond model 8-79560
 homopolymers, ESCA methods, core levels of simple homopolymers 8-88673
 iodobenzene bis(dichloroacetate), cryst. struct., secondary and multi-centre bonding 8-63751
 iodobenzene diacetate 8-63751
 metal-H system, bond energy calcs. 8-51940
 metal-ligand, complex anion electronic struct., outer sphere cation effects, X-ray fluoresc. spectra 8-86884
 metal-rich compounds, struct. and props. 8-95045
 methyl phosphine-d₂, ZZ 8-90167
 molecular electric field gradient, overlap and ligand contr. 8-58575
 molecule, electronic struct. and physicochem. props., modified partial neglect of differential overlap 8-82645
 myoglobin, Fe-O₂ bonding and oxyhaeme struct. 8-96006
 nylon-6 fibre, chain rupture and tensile deform. viscosity-av. mol. wt. obs. 8-76714
 optical harmonic generation in ferroelec. materials 8-76395
 orbital interaction and chemical bonds. Exchange repulsion and rehybridization in chemical reactions 8-85142
 organometallics, group V, XPS spectra interpretation, pot. model 8-50587
 pentacoordinated ferrous porphyrins, ¹H and ¹⁹F NMR, hyperfine shift, π electron binding 8-78719
 phenol (-d₁, -d₃, -d₆), excited A state, normal vibr. freqs, force consts., compliance coeffs. 8-50534
 PMMA, amorphous, structural cause of orientation modification, exam. 8-67664

bonds (chemical) continued

- polyethylene film, chain rupture and tensile deform., viscosity-av. mol. wt. obs. 8-76714
 polyethylene terephthalate, chain rupture and tensile deform., viscosity-av. mol. wt. obs. 8-76714
 polymer film, supermolecular structure and mech. stress distrib. among chem. bonds 8-75562
 polymers, crosslinked, specific characts. (*German*) 8-75585
 polymers, struct., bonding, reactivity by ESCA 8-53299
 polypropylene, film and fibre, chain rupture and tensile deform., viscosity-av. mol. wt. obs. 8-76714
 polystyrene, amorphous, structural cause of orientation modification, exam. 8-67664
 pyridine, π -electronic structs., ab initio VB calcs. 8-70749
 p-quaterphenyl, mol., charge density and bond orders, polynomial matrix method 8-74808
 rare earth cpds., ESCA spectra, intense shake-up satellites, model 8-50589
 rare earth intermetallics, RGa₃, AlB₂-type struct., electron transfer, bonding, heat of form. theory 8-92499
 rare earth monobismuthides, thermal expansion, thermal cond., 300-900K 8-91453
 sandwich compounds, orbitally degenerate, EPR 8-86893
 semiconductor-electrolyte contact, electrolytic decomposition and photodecomposition 8-95357
 semiconductor-metal Schottky barrier interfaces in pairing model, covalent-ionic trend 8-95367
 shock waves, starvation kinetics 8-64841
 surfaces, electron spectroscopy, review 8-92169
 [2,2](2,5)thiophenophane, through bond and through space interactions, UPS obs. 8-82786
 thiophosphoryl compounds, bond ionisation energies, mol. struct. from UV photoelectron spectra 8-82782
 transition metal cpds., ESCA spectra, intense shake-up satellites, model 8-50589
 transition metal dichalcogenides, optical phonon modes and localised effective charges, reflection spectra 8-76453
 triatomic mol. bond-bond interaction force consts., simple MO theory 8-50452
 triatomic systems, compliance const., L matrix approx. method 8-74797
 trimethyl phosphine-d₆, ZZ 8-90167
 urea, bond electron density distrib., 123K, simple refinement 8-55857
 SnTe-PbTe-GeTe, alloy semiconductor, phase transition (*Japanese*) 8-91443
 [Mo₂Br₈]⁴⁻, electronic and reson. Raman spectra, Mo-Mo band 8-82745
 Ag (111) surface, adsorbed I, geometry and bond length, surface EXAFS 8-71952
 Ag, matrix isolated, fluoresc. spectra, excimeric bond effects 8-50498
 AgClO₃, ClO₂ spin Hamiltonian 8-60326
 AgGaSe₂, and Ag₂GaSe₆, XPS, Auger and direct electron spectra 8-52620
 Al₂O₃-W cermet, phase bonding 8-52745
 AuH, AuCl, ZZ 8-86767
 BH₃F, B-F bond, interference density and kinetic energy 8-74566
 BN, cubic, ab initio SCF calcs., band struct., ground state props. 8-51891
 Bi₂Te₃, chemical bonding models, correctness test using mag. susceptibility, and chemical substitution 8-67680
 Cd, effective core potentials calcs. rel. to bond lengths and energies 8-66464
 CeO₂:Yb³⁺, ENDOR, evidence for covalency 8-80247
 CoAl, bonding, self-consistent energy bands 8-91610
 Cu, cluster and bulk, struct. and electronic props. 8-95592
 Cu complex, with acetylene, Ar matrix-isolated EPR obs., bonding 8-50564
 Cu(I) olfactory binding site 8-96060
 D₅O₂⁺, isotope effects, easily polarisable H and D bonds 8-94231
 (Fe,Cr)₃C, reln. between bond energy and X-ray emission line shifts 8-50555
 FeAl, bonding, self-consistent energy bands 8-91610
 H₂-like molecules, change of binding type and dissoci. in strong mag. field 8-62744
 HNO₂, and protonated forms, electrostatic pot. predictions, basis set depend. 8-74786
 Hg, effective core potentials calcs. rel. to bond lengths and energies 8-66464
 HgH, HgCl₂, ZZ 8-86767
 KAl₂Br₇, NQR double-reson., Al₂Br₇⁻ ion in cryst. 8-91993
 LiNC, mols. with polytypical bond, spatial distrib. and motion of Li 8-66533
 LiO₂-Al₂O₃-SiO₂, bonding of Si-O exam. by X-ray emission spectra 8-52594
 N compounds, influence of chemical bond on relative muonic capture rates in elements 8-58874
 NH₄F, electron distribution and charge transfer in NH₄⁺ ion 8-91291
 Na_{4-x}(Si_{1-x}P_x)O₄, (0≤x≤0.25), exam. of Na ion conductivity by impedance meas. (*French*) 8-51731
 NbSe₃, chemical bonding and dimensionality 8-75992
 Ni (100) surface, model, bonding of S 8-56027
 Ni-Pd-P, Ni-Pt-P, amorphous and electronic structs., NMR Knight shifts and linewidths meas. 8-68400
 NiAl, bonding, self-consistent energy bands 8-91610
 NiO:Fe, estimation of 4s covalent bonding of Fe²⁺ and Fe³⁺ ions, Mossbauer spectra 8-72441
 O₂F(Cl)(Br) radicals, matrix IR spectra, bonding 8-90160
 PdH_{0.72}, Compton profile, electronic struct. (*German*) 8-92140
 Pt(O)-Pt(O) dimers, bounding in a d¹⁰-d¹⁰ system 8-74579
 Re₂Cl₈²⁻, Re₂Cl₈³⁻, ab initio calcs. of metal-metal bond 8-82633
 Rh₄(CO)₁₂, bond energy terms from thermochem. data 8-62967
 Rh₆(CO)₁₆, bond energy terms from thermochem. data 8-62967
 Ru complex, HF calc., electron densities and Mossbauer isomer shift, chemical binding 8-50470
 S compounds, influence of chemical bond on relative muonic capture rates in elements 8-58874
 SbF₃(NH₃)₂CS and SbF₃[(NH₃)₂CS]₂, X-ray cryst. struct., IR spectrum (*French*) 8-87643
 SbI₃, intermolecular bonding study using ¹²⁹I Mossbauer effect 8-72438

bonds (chemical) continued

- Se compounds, influence of chemical bond on relative muonic capture rates in elements 8-58874
 SeMoOCl₇, prep., cryst. struct., characterisation (*French*) 8-63722
 Si (111) surface, Al overlayers, theoretical study 8-95366
 Si (111) surface, surface energy bands and atomic position of chemisorbed Cl 8-56041
 Si, chemically etched, model of structural transforms. during thermal oxidation 8-79557
 Si, van der Waals electron correlation energy 8-95013
 Si-H, amorphous, energy gap negative-U states, Si-H-Si three centre bond model 8-91606
 Si₂H₄, Si-Si double bond, ab initio GO calc. 8-94187
 SiO₂, amorphous, struct. and chem. bonding 8-51422
 SiO₂, pseudopotential study of bonding and structure 8-75622
 SiO₂-Na₂O(Li₂O) glasses, bonding of Si-O exam. by X-ray emission spectra 8-52594
 TaS₂/pyridine intercalated, struct. and bonding 8-91323
 TiC, Shockley surface states and bonding 8-91739
 TiC, TiN and VC, charge distrib. and bond ionicity 8-63961
 U compounds, equatorial bonds, MO calcs. 8-82621
 VC, TiC and TiN, charge distrib. and bond ionicity 8-63961
 VD_{0.77}, Compton profile, electronic struct. (*German*) 8-92140
 VH_{0.71}, Compton profile, electronic struct. (*German*) 8-92140
 V₂Si, electron charge distrib., martensitically transforming single cryst., X-ray diffr. meas. 8-75631
 W-K-Al-Si, state of bonding, distribution of impurities 8-92212
 ZnIn₂S₄, valence band photoemission spectroscopy 8-56569
 ZnO, chemisorpt. of pyridine, acetone, dimethyl sulphoxide, UPS, mol. orbitals effect on bonding 8-72699

bone

- aneurysmal cyst response to low doses of ⁶⁰Co gamma radiation with prolonged treatment 8-73196
 biocompatible implants, developed for bone fracture prevention, development research criteria 8-77155
 biopsy, automatic image anal., var. in rib architecture 8-61253
 bovine hip bone, compression tests, effect of specimen shape and size on mech. props. and fracture mode 8-69132
 compact, empirical strength theory, biaxial stress characts. 8-77081
 cortical bone diameter meas., manual and computer-aided methods comparison 8-85376
 dose factors for radiosensitive tissues in bone irradiated by surface-deposited radionuclides 8-53512
 dosimetry of beta-emitting volume-seeking radionuclides in human bone, mean skeletal dose factors 8-77115
 elastic moduli determ., US transducer, shear-wave vel. meas. 8-83201
 embryonic bone and cartilage, effects of in vitro gamma irradiation 8-65089
 Haversian bone, exam. of mechanical failure at microstructural level 8-77080
 healing, use of anodised Ta electrode, meas. of electrochem. reactions 8-95931
 lateral tibial plateau, axisymm. finite element anal. 8-69127
 leg long bone growth meas. in children from radiogram, error reduction using computer processing 8-77103
 mechanical model with appl. to human upper tibia, porous material, deform. (*Japanese*) 8-88724
 mechanical properties determ. in vivo, noncontacting EM device 8-77133
 medullary implants with porous coating, stress distrib. 8-69256
 metabolic bone disease diagnosis using whole-body retention of ⁹⁹Tc^m-diphosphonate 8-73208
 mineral concentration estimation by beta-ray backscatt. (*German*) 8-69179
 mineral measurement using polychromatic X-rays, correls. 8-53478
 morphology and fracture, exam. 8-57036
 piezoelectric effect on exposure to US, effect of sample rot. 8-80913
 porosity of compact bone substance, TAS Leitz 2D image analysis system (*German*) 8-92753
 radioisotope uptake, rel. between ²³⁹Pu deposition in bone and ⁵⁹Fe uptake in marrow 8-85395
 radionuclide imaging in infants and children, review 8-77107
 scintigraphy clinical comparison of ⁹⁹Tc^m-diphosphonate and -pyrophosphate 8-65112
 scintigraphy in osteomalacia 8-73204
 SEM, technique for studying collagen fibres and ground substance 8-57150
 skeletal system computerised tomography examination 8-88740
 spinal fixation using acrylic bone cement, mech. props. 8-81072
 ulna, mineral meas. using X-ray (low energy γ -ray) transmission, positioning errors 8-96084
²²⁸Ra-burdened dog skeleton, Rn retention rel. to age and dosage 8-65092

Boolean algebra

- see also *Boolean functions; formal logic*
 axiomatisation of set of formulae of intuitionistic logic 8-57730

Boolean functions

- No entries

Boolean lattices see *Boolean algebra***bootstrap models** see *bootstrapping***bootstrap theory** see *bootstrapping***bootstrapping**

- 1/N dual unitarisation, triple bare pomeron parameters of Gribov's Lagrangian 8-74232
 conformal invariant field theory solns. (*Russian*) 8-58142
 dual topological unitarisation, review of S-matrix developments for hadron bootstrap theory 8-62381
 gamma-ray multiplicity meas., fast converging bootstrap method for data anal. 8-70730
 Hagedorn's bootstrap model of early Universe, dense matter eqn. of state, external mag. field 8-86044
 J-dependence of statistical bootstrap mass spectrum, S-matrix and semi-classical formalism comparison 8-86448
 nucleon-nucleon collisions, cumulative pion prod., inelastic rescatt. contrib., statistical bootstrap model (*Russian*) 8-54766
 planar bootstrap, Regge cuts cancellation, asymptotic terms 8-54619
 planar bootstrap model calcs., QQ and QQQ mass spectra 8-89685
 S-matrix, planar, building of cylinder correction in topological expansion or dual unitarisation 8-62321

bootstrapping continued

- statistical bootstrap model, hadronic mass spectrum, pion condensation, boson gas 8-70345
 uncorrelated jet model with Bose-Einstein statistics, statistical bootstrap model 8-86445
 π^+p , 2-9 GeV/c, large angle elastic scatt. cross sections, parton and bootstrap model test 8-78209
 π^+p elastic scatt., 1.9-9.5 GeV, test of parton and statistical bootstrap models 8-89728

bootstraps see *bootstrapping***borate glasses**

- alkali borate, Mossbauer expts. 85-500K 8-80260
 alkali borate glass networks, π -electron distrib. SCF INDO LCAO-MO calc., O basicity 8-79924
 biased spectral decomposition in glass, ¹¹B NMR spectroscopy 8-88198
 calibo glass:Eu³⁺, Ho³⁺, energy transfer 8-76510
 mechanical relaxation in transition range 8-80575
 Al₂O₃-B₂O₃-P₂O₅ glasses, formation and props. 8-83737
 B₂O₃-Fe₂O₃, Fe₂O₃ crystallite formation, Mossbauer obs. 8-68429
 B₂O₃-Li₂O-LiCl glass system, exam. of ionic conductivity of Li (*French*) 8-51730
 BaO-B₂O₃, composition effects on mean dispersion 8-80313
 BaO-B₂O₃:UO₂²⁺, Nd³⁺ glass, radiative and nonradiative energy transfer 8-60508
 BaO-M₂O₇-B₂O₃, UV absorpt., inherent absorpt. wavelength and oscill. strength, cation effects 8-80374
 BaPO₃F-Al₂O₃-B₂O₃ glasses, phys. props. 8-63676
 Fe₂O₃-B₂O₃-PbO glass, semicond., elec. resist. meas. 8-95300
 K₂O-B₂O₃:Cu II, glass, O basicity, ESR study 8-80199
 K₂O-CaO-B₂O₃:CuII, immiscibility, ESR detect. 8-80200
 Li⁺-rich, high elec. cond. 8-84000
 Li₂O-B₂O₃ glass, conductivity, permittivity, and dielectric loss obs., mixed isotope effect 8-95182
 Li₂O-B₂O₃ glass system, 4-coordinated B atomic fraction determ. 8-94999
 M₂O-MnO-B₂O₃ glasses, M=Li, Na, K, glass-forming region and physicochem. props. 8-63678
 Na borate glass, nonradiative energy transfer from Sm³⁺→Nd³⁺ 8-80394
 Na₂-B₂O₃ glass, pulsed EPR study of Cu 8-84479
 Na₂O-B₂O₃, covered with PbO film, deep penetration of Pb²⁺ ions 8-79535
 Na₂O-B₂O₃ glass, struct. interpretation of ¹⁰B and ¹¹B NMR spectra 8-80241
 Na₂O-B₂O₃ melt, crystallisation of Na₂B₆O₁₃ 8-59763
 Na₂O-B₂O₃-Na₂SO₄ glass, exam. of chemical differentiation, using Cu ion segregation 8-87625
 Na₂O-NaF-B₂O₃ glass, nature of conductivity 8-63876
 Na₂O.2B₂O₃-Fe₂O₃, Fe₂O₃ crystallite formation, Mossbauer obs. 8-68429
 Na₂S.9H₂O-NaOH-H₃BO₃, glass, IR and Raman spectra of boroultamarine, exam. of S₃ presence 8-68502
 PbO-2B₂O₃-Fe₂O₃ glass, Mossbauer study, struct., crystallite formation, broadened quadrupole doublet 8-59761
 PbO-Al₂O₃-B₂O₃ vitreous system with relaxation structure, spinodal decomposition 8-75553
 PbO-ZnO-B₂O₃, Corning 7575 seal glass, devitrification 8-79532
 PbO.3B₂O₃:Fe₂O₃, EPR of Fe³⁺ ions 8-72400
 Sn borate glasses, IR and ¹¹⁹Sn Mossbauer spectra 8-60438
 ZnO-B₂O₃, glass, ESR exam. of paramagnetic centres formed during mech. destruction by grinding 8-88188

Bordoni effect

- thermally activated double kink form. model without approximations 8-63805

boron

- see also *nuclei with*

- abundance determ. in rocks, soils, plants, waters and fertilisers 8-85559
 addition to C fibres, effect on struct. and physical props. 8-68715
 atom, electron affinity, modified variational approx. 8-66679
 atom, ground state energy, HF calc., second-order correction 8-86784
 atom, ground state wave function, 2s-2p electron promotion effect 8-86779
 atom, ground state wavefunction, SCF HF calc. 8-90070
 atom, K-shell ionis., double and single, cross section meas. by ion bombardment 8-50629
 atom, X-ray spectra, chemical bonding and multiple ionis. effects 8-50630
 atoms and ions, regularities within Stark widths of reson. lines 8-78662
 chemical transport with I₂, BI₃ synthesis 8-52682
 concentration determ. in atm. and rainwater in Vizcaya, Spain (*Spanish*) 8-57264
 determination, in Si, by AES (*Japanese*) 8-91356
 diamond:B, thermoluminesc., TSC, correlation meas. 8-88369
 diamond:B hopping conductivity in range 12 to 1300K 8-51994
 diffusion, stress-enhanced, in Si, using SiO₂ diffusion masks, photodiode fabrication 8-67865
 diffusion in Si, implantation damage effects 8-55988
 diffusion in Si, proton enhanced diffusion and vacancy migration 8-67747
 diffusion in SiC, polytype struct. effect 8-59983
 effect on grain refinement in Al 8-52828
 fibre addition to graphite reinforced epoxy, radiographic inspection aid 8-95880
 fibre reinforced Al, fracture mechanical study, unidirectional composites 8-88520
 fibre reinforced Al, unidirectional, K-calibration and compliance curves 8-88518
 fibre reinforced Al strength determ. procedure in annular specimens (*Russian*) 8-95864
 fibre reinforced epoxy, fracture mechanical study, unidirectional composites 8-88520
 filled elastomer mould, surface coating for wear prevention in mould 8-64728
 inorganic B, in St. Lawrence Estuary, determ. (*French*) 8-77274
 main-sequence stars, Li, Be and B abundances rel. to envelopes hydrodynamical instabilities 8-93202

boron continued

- neutron irradiated, quantitative anal. using cellulose nitrate solid state track detectors 8-56937
 polymorphic modifications, struct. changes on Zn incorporation 8-79596
 purity evaluation by elec. meas. 8-59822
 semiconductor properties and use for making devices, review 8-60131
 Al:¹⁰B, relax. mechanism for polarised implant 8-87693
 Al-SiO₂-Si structs., implanted B⁺ ions, high-freq. CV characts. (*Russian*) 8-80056
 Al-SiO₂-Si:B ions, annealing effect on energy spectrum of radiation defects (*Russian*) 8-88488
 B IV, V, beam-foil meas. of mean lives below 450 Å 8-90120
 B⁺, dynamic multipole polarisability, coupled Hartree-Fock 8-82858
 B⁺ fraction from Freeman type high current source for implantation appl. 8-66005
 B⁺, Hund's first rule, new interpretation 8-78620
 B⁺, electron impact excitation, cross-sections, modified Oppenheimer approx. 8-82843
 B-Al cast braid, crystallisation and structuring of Al matrix (*Russian*) 8-52725
 B-epoxy-Al sandwich laminate, influence of residual stresses on tensile strength 8-60703
 B-like ions, highly ionised, up to Fe XXII, Breit-Pauli approximation 8-53810
 B+He (methane), B atom K-shell binding energy by Auger spectra 8-50525
 B₂+inert gas atom, pot. interactions 8-55219
 B₂, ground state, multiconfig. SCF CI calcs. 8-58590
¹⁰B enriched coatings, neutron collimators, comparison with Gd₂O₃ coatings 8-82564
¹⁰B enrichment by low-temp. exchange in BF₃.SO₂ system (*Japanese*) 8-55251
¹⁰B separation using anion exchange resin, isotopic plateau holding displacement chromatography (*Japanese*) 8-56886
 GaAs:B, electron or neutron irradiated, low symmetry interstitial B centre 8-79605
 Si:B, bound multiexciton complexes, work function thermodynamic determ. 8-72078
 Si:B, conc. profile of implanted cryst., by ¹¹B(p,α) chem. anal., annealing (*German*) 8-83843
 Si:B, diffusion induced imperfections, laser annealing, rel. to junction characts. 8-75678
 Si:B, diffusion with BN, expt. (*Bulgarian*) 8-59824
 Si:B, dopant density determ. by nucl. track technique 8-55886
 Si:B, doping, pyrolytic BN wafer as diffusion source characterisation 8-91352
 Si:B, Ge(P), impurity-pair diffusion, influence of elastic stresses 8-87824
 Si:B, heavily diffusion-doped layers, Co diffusion 8-59982
 p-Si:B, high temp. treatment, effects on ion implanted impurity distrib. profile 8-79625
 Si:B, implemented laser annealed samples, unidirectional contraction 8-71747
 Si:B, impurity conc. from photoluminesc. anal. 8-63785
 Si:B, impurity excited state lifetimes 8-60083
 Si:B, ion implanted, laser and thermal annealing compared, TEM obs. 8-75681
 Si:B, ion implanted, localised defects, TEM study 8-87699
 Si:B, ion implanted, struct. of rod defects, TEM obs. 8-71744
 Si:B, multiparticle impurity complexes (*Russian*) 8-72601
 Si:B, near intrinsic (100) and (111) samples, inert and oxidising ambients, diffusion, segregation 8-75882
 Si:B, p-n junction form. by B deposition and laser-induced diffusion 8-87690
 Si:B, piezothermoelec. power 8-56173
 Si:B, polycrystalline, depth profiles of implanted B atoms, meas. by secondary ion mass spec. (*Japanese*) 8-67734
 Si:B, predeposition of B using BBr₃ 8-55882
 Si:B, SEM obs. of dislocations using Schottky barrier EBIC technique 8-79614
 Si:B, TEM study of stacking fault form. and annealing 8-51566
 Si:B device, anal. using SEM-AES-IMA combination with SIM spectrometer (*Japanese*) 8-85249
 Si:B film, electronic props. 8-84330
 Si-B, diffusion-free annealing, use of scanning CW Kr laser 8-91345
 Si-B, P diffusion and activity after Ar ion bombardment 8-95192
 Si-Ge:B, hot-pressed alloy, thermoelec. props. 8-91711
 α-SiC:B, piezoresist. rel. to acceptor levels 8-60129
 p-SiC:B (4H), absorption spectra of bound excitons 8-88338

boron alloys*see also boron compounds*

- low-temp. resistivity in mag. field 8-91667
 steel, Mn-Ti-B-rare earth, distrib. of B (*Chinese*) 8-84811
 Al-Ti-B alloys, segregation of Ti, electron microscope exam. 8-52820
 B-Cr(Si), diffusion coatings on alloy steel U8, wear resistance 8-56823
 Co-Ga-B, phase diagram, metallographic, X-ray and electron probe anal. 8-92241
 Co₄₀Ni₄₀B₂₀, magnetostriction, temp. depend. 8-91921
 Co₇₄Si₁₀B₁₆, amorphous toroidal core, switching characts. and domain structs. 8-95477
 (Fe,Co)_{0.8}B_{0.2} alloy amorphous thin films, anisotropic mag. and microstruct. props. 8-95487
 (Fe,Co)PBAI, metallic glass, viscous flow, alloying effect 8-79793
 (Fe,Mo)₈₀B₂₀, glassy alloy, Curie temp. and crystn. temp., Mo additions effect, Mossbauer spectra 8-68428
 Fe-B, amorphous metallic glasses, high-temp. mag. anal. 8-91258
 Fe-B, binary alloys, giant ΔE effect and Elinvar characts. 8-76291
 Fe-B, metallic glass, Mossbauer investigation of electronic struct. 8-92009
 Fe-B, rapidly quenched metastable solid solns., prop. and mag. props. 8-92218
 Fe-B amorphous alloy, crystallisation kinetics 8-83736
 Fe-B glass, crystallisation kinetics, elec. resist. meas. 8-83741
 Fe-B metallic glass, hardness, elastic moduli, density, cryst. temp., mech. props., for flywheel appl. (*Dutch*) 8-52878
 Fe-B metallic glass, role of Fe₃B in crystn., mag. and Mossbauer expts. 8-94997

boron alloys continued

- Fe-B metallic glasses, crystn. kinetics by differential scanning calorimetry 8-91257
 Fe-C-B, amorphous, room-temp. saturation induction 8-95476
 Fe-C-B, splat cooled, formation of metastable crystalline phases and glasses 8-88461
 Fe-Co-B, metallic glass, Mossbauer investigation of electronic struct. 8-92009
 Fe-Co-C-B, amorphous, room-temp. saturation induction 8-95476
 Fe-Ni-B, metallic glass, Mossbauer investigation of electronic struct. 8-92009
 Fe-Ni-B-(P) amorphous alloys, mag. annealing mechanism, induced anisotropy 8-95484
 Fe-Ni-C-B, and Fe-Ni-Co-B-C-Si, amorphous, room-temp. saturation induction 8-95476
 Fe-Ni-Cr-P-B, Metglas 2826A, hardness, elastic moduli, density, cryst. temp., mech. props., for flywheel appl. (*Dutch*) 8-52878
 Fe-Si-B magnetic powder, amorphous, prep. by atomisation technique 8-92213
 Fe_{100-x}B_x (11.5≤x≤22), magneto-volume effect 8-91922
 Fe_{100-x}B_x, mag. and struct. props., comp. depend. 8-60314
 Fe_{100-x}B_x, metallic glass, magnetisation meas. 8-80134
 Fe₈₀B₂₀, crystallisation of amorphous alloys, TEM and X-ray diffr. exam. of struct., growth characts. 8-79539
 Fe₈₀B₂₀, evaluation of complex Mossbauer spectra 8-60370
 Fe₈₀B₂₀, ferromagnetic metallic glasses, Brillouin scattering 8-92085
 Fe₈₀B₂₀, magnetostriction, temp. depend. 8-91921
 Fe₈₀B₂₀, metallic glass, Mossbauer spectroscopy 8-60365
 Fe₈₀B₂₀ Metglas, Mossbauer spectra line broadening 8-52400
 Fe₆₅Co₃₅B, crystalline disordered, evaluation of complex Mossbauer spectra 8-60370
 (FeCoNi)₈B₂₀, glass, evidence supporting split-band model from magnetostriction 8-95509
 (Fe_{0.5}Co_{0.1})₇₈Si₁₂B₁₀, (Fe_{1-x}Co_x)₇₈Si₁₂B₁₀ amorphous ribbons, magnetomech. coupling and saturation magnetostriction 8-68353
 Fe₃Co₇₀Si₁₅B₁₀, amorphous toroidal core, switching characts. and domain structs. 8-95477
 (Fe_{1-x}Co_{100-x})_{100-(y+z)}Si_yB_z amorphous ribbon, mag. moment and Curie temp., comp. depend. 8-95421
 Fe₇₈Mo₂B₂₀, exam. of mag. props. between 300 and 900K 8-85010
 Fe₄₀Ni₄₀B₂₀, metallic glass, embrittlement kinetics and crystn., quenching influence 8-68766
 Fe₅₀Ni₃₀B₂₀, crystallisation of amorphous alloys, TEM and X-ray diffr. exam. of struct., growth characts. 8-79539
 Fe₃₂Ni₃₆Cr₁₄P₁₂B₆, Metglas 2826A, Hall resistivity, effect of thermal cycling and annealing 8-56125
 Fe₃₂Ni₃₆Cr₁₄P₁₂B₆, shear band form. 8-68756
 Fe₄₀Ni₃₈Mo₄B₁₈ glassy alloy, high permeability, low field mag. characts. 8-68301
 Fe₄₀Ni₄₀P₁₄B₆ amorphous ribbon, mag. anisotropy distrib. near surface 8-95430
 Fe₄₀Ni₄₀P₁₄B₆, amorphous toroidal core, switching characts. and domain structs. 8-95477
 Fe₄₀Ni₄₀P₁₄B₆, ferromagnetic metallic glasses, Brillouin scattering 8-92085
 Fe₄₀Ni₄₀P₁₄B₆, Metglas 2826, amorphous ribbon core, appl. in force transducer 8-93669
 Fe_xNi_{80-x}P₁₄B₆, amorphous, sp. ht. and susceptibility meas., spin glass and micromag. props. 8-68274
 Fe_xNi_{80-x}P₁₄B₆ metallic glasses, low temp. resistivities 8-91659
 (Fe_{0.5}Ni_{0.5})₇₅P₁₅B₆Al₃ glass, struct. relax. as origin of Curie temp. ageing 8-84418
 (Fe_{1-x}Ni_x)₇₅P₁₅B₆Al₃, amorphous alloy, low temp. elec. resist. saturation 8-68005
 Fe₂₉Ni₄₉P₁₄B₆Si₂, Metglas 2826B, Hall, elec. resist., magnetisation and heat capacity meas. 8-68019
 Fe₃SiB₂, Mossbauer spectra, 140-784K, spin rotation 8-52409
 Fe₇₅(Si_{0.5}B_{0.5})₂₅ film, amorphous, sputtered, ferromag., thermal stability 8-76280
 Fe₇₈Si₁₀B₁₂, amorphous toroidal core, switching characts. and domain structs. 8-95477
 La-B, phase and thermodynamic props., vaporisation 8-51660
 Ni-B, hydrogen embrittlement, effect of B additions (*Japanese*) 8-84973
 Ni-B alloy film, magnetisation-temp. characts., order-disorder trans-form. (*Japanese*) 8-76279
 Ni-B alloys, amorphous, thermal anal. and X-ray diffr., solidification struct. development (*French*) 8-91253
 Ni-B amorphous alloy film, atomic and electronic transport (*French*) 8-84325
 Ni₄₀Fe₃₀B₂₀, magnetostriction, temp. depend. 8-91921
 Ni₇₈P₁₄B₈, Ni₈₀P₁₂B₈, amorphous mag. clusters, sp. ht. meas. 8-68274
 NiPBAI, metallic glass, viscous flow, alloying effect 8-79793
 Ti-B, binary inclusions, interaction with diamond in polycryst. diamond sintering (*Chinese*) 8-80484
 WCuB prep. by infiltration of W skeleton by CuB, hardness meas. (*German*) 8-64508

boron compounds*see also boron alloys*

- acetylacetonatobutyl halides, equilib. reacts. redistribution of -F, -Cl monofunctional groups (*French*) 8-64816
 boranes, B₉H₁₂OCH₃Si(CH₃)₂, C₂B₁₀H₁₀Br₂, B₁₈C₄H₂₂, cryst. struct. (*Czech*) 8-87649
 boranes, OCH₃(B₉C₂H₁₀)₂Co and (C₂H₅)₂Co₂CB₉H₁₀⁻, cryst. struct. (*Czech*) 8-87649
 borophosphate glasses, effect of F on props. 8-67657
 borsic fibre reinforced Ti, unidirectional, K-calibration and compliance curves 8-88518
 cabal glass:SiO₂(TiO₂), microheterogeneity, and elec. cond. 8-83997
 carborane anion, ¹¹B NMR 8-90190
 core electron expansion, kinetic energy in Compton profiles 8-72628
 hydrides, doubly isotopic, in 2-step nucl. fusion dissipative confinement, using inert gas hydride laser 8-82506
 hydrides and related cpds., cryst. struct., secondary and multi-centre bonding 8-63751
 organoarsinoboranes, ¹¹B NMR 8-90190
 trimethylamino borane, ¹¹B NMR 8-90190
 B-C system, region of existence of B₂C phase 8-76636
 B-Zn solid soln., struct. changes on Zn incorporation into α- and β-rhombohedral B 8-79596

boron compounds continued

- BC boronising sintering of porous stainless steel 8-60594
 BC, ion bombarded, chemical effects on secondary photon and ion emission 8-95637
 BC, sintered and hot pressed, friction and wear, 20 to 1500°C 8-60844
 B₂C, gas suspended, coolant for catalysed D fusion reactor blanket 8-58400
 B₂C, metallography and Knoop microhardness (*French*) 8-76730
 B₂C, quantitative electron microanalysis (*French*) 8-76948
 B₂C rings, Al bonded, exam. of fabrication techniques 8-72748
 B₂C, sputtering yield, use as first wall material 8-95629
 B₂C, thermal cond., nonstoichiometry effect 8-63887
 B₂C, used as control rods in FBR, irradiation effects 8-67742
 BCl₃ gaseous phototropic shutter control of CO₂ laser PRF 8-50833
 BCl₃, interaction with evaporated metal films, adsorpt. 8-75945
 BCl₃, isotope enrichment, heterogeneous condensation in presence of CO₂ laser irradiat. 8-70953
 BCl₃, vibr. excited states distrib. in reson. radiation, photodissoc. rate 8-50603
 BCl₃-H₂, photochem. with Ti, Pb catalysts, isotopic excitation by laser 8-64882
 BCl₃+H₂ laser induced chemistry, theory 8-76884
 BF₃, ¹¹B NMR chem. shift, temp. depend., virial coeffs. 8-58722
 BF₃, boiling/condensation heat transfer props., cryogenic appls. 8-79192
 BF₃ proportional counter, high press. (*Japanese*) 8-66453
 BF₃, X-ray fluorescence, electronic struct. determ. 8-86887
 BF₂H₄⁺, AB₆, non-transition element complexes, shapes and other props. 8-82647
 BFHOH, transient mol. form., microwave spectroscopic obs. 8-74643
 BF₃SO₃, ¹⁰B enrichment by low-temp. exchange (*Japanese*) 8-55251
 BH, electron density, basis set, electron correl. effects 8-74581
 BH, localisability in MO calcs., measured by absolute overlap and 2nd moment dispersions 8-74557
 BH, pot. curve, one-config. Hartree-Fock-Roothaan calc. for force const. 8-82627
 BH, variation-perturbation minimal Gaussian geminal basis sets correl. energy calc. 8-78629
 BH₃, localisability in MO calcs., measured by absolute overlap and 2nd moment dispersions 8-74557
 BH₄⁻ motion in solids, nucl. spin-lattice relax. exam. 8-56388
 BH₄⁻, reduction of IrCl₆ by hydrolysis products 8-76854
 B₁₀H₁₄, cryst. struct. (*Czech*) 8-87649
 B₂H₆, mol., static electron densities 8-79552
 B₂H₁₀, ¹¹B NMR line broadening, B-B coupling 8-62826
 B₂H₉, ¹¹B NMR line broadening, B-B coupling 8-62826
 B₂H₇ compounds, doubly-isotopic, laser driven nuclear fusion, energy release 8-78499
 B₁₀H₁₂As⁻, ¹¹B NMR 8-90190
 BHDBr₂, and isotopic forms, mol. pot. const., amplitudes, Coriolis coupling, centrifugal distortion 8-50662
 BHCl₂, and isotopic forms, mol. pot. const., amplitudes, Coriolis coupling, centrifugal distortion 8-50662
 BHF₂, and isotopic forms, mol. pot. const., amplitudes, Coriolis coupling, centrifugal distortion 8-50662
 BH₃F⁻, B-F bond, interference density and kinetic energy 8-74566
 BH(OH)₂, transient mol. form., microwave spectroscopic obs. 8-74643
 B₁₀H₁₂S, ¹¹B NMR 8-90190
 B₁₀H₁₂Se, ¹¹B NMR 8-90190
 B₁₀H₁₂Te, ¹¹B NMR 8-90190
 B₁₃, direct synthesis, chem. transport of B with I₂ 8-52682
 BN, adsorption of NO, crit. and triple point temps. of first adsorbed layer 8-91548
 BN, crystal structure stability, P-T diagrams 8-51886
 BN, cubic, ab initio SCF calcs., band struct., ground state props. 8-51891
 BN, cubic, energy band and piezoelec. calcs. 8-72071
 BN, cubic, water catalysed form. 8-53199
 BN diffusion semiconductor technology appl. (*Bulgarian*) 8-59824
 BN, hardness rel. to temp., phase compositions 8-60752
 BN, hexagonal, long optical vibrs., elastic const. from valence force const. 8-51621
 BN, in Ag-BN-Si-Al sandwich, humidity sensitive threshold switching 8-88046
 BN particle, microanal. by energy loss spectrometry using field emission STEM 8-53286
 BN, powder-cushion gripping to promote good alignment in tensile testing 8-92418
 BN, production kinetics of gasification of organosilicon binders 8-60635
 BN, pyrolytic, diffusion source for Si 8-91352
 BN, pyrolytic, in contact with various metals, friction and transfer behaviour 8-88535
 BN, toughening by stress-induced phase transforms. 8-80635
 BN, wurtzite type, effect of TiB₂ and B additions, on transformation to zinc blende type 8-80542
 BN, X-ray spectra, chemical bonding and multiple ionis. effects 8-50630
 B₃N₂H₆, allowed character of 1900 Å band, two-photon spectra 8-74719
 B₃N₂H₆, electronic struct., mag. susceptibilities, ab initio calcs. 8-74571
 BO, radiative lifetime, first excited state 8-62848
 BO₂, gas, optically detected mag. reson. spectrum, X²Π rovibronic sublevels 8-82756
 BO₂, radiative lifetime, first excited state 8-62848
 BO₃³⁻, X-ray fluorescence, electronic struct. determ. 8-86887
 B₂O₃, effect of conc. on mag. props. and defects of YSmLuCaGeIG films grown in PbO-B₂O₃ solvents 8-68321
 B₂O₃, molten, reaction with water, reactor fuel-coolant interaction simulation 8-58363
 B₂O₃, struct. determ., continuous random network approach 8-67693
 B(OH)₃, ¹H/²H quadrupole reson. freqs. detected by double reson. with level crossing 8-84497
 (B(OH)₃)₂, hydrogen bond, ab initio MO calcs. 8-58588
 BP, epitaxial growth on Si substrate, Si impurity profile, ion microanal. 8-78886
 BP, sp. ht., Debye temp., compressibility and Grüneisen coeff. meas. 8-63865

boron compounds continued

- BP, VPE, diffused layers formed in Si substrates, device appls. 8-56585
 B₁₂Si, switching and high field effects, cond. mechanism 8-64048
 CaB₆-SmB₆ system complex borides, prep. and props. 8-52703
 CIBS, form., photoelectron and microwave spectra 8-90214
 Fe-Cr-SiC-B₂C powder mixture, compressibility and elec. cond. in cold pressing under low press. 8-60609
 n-propylboranes, ¹¹B NMR 8-90190
- borosilicate glasses**
 ball mill grinding, rate constant determination (*Japanese*) 8-95828
 ball mill grinding, wet, dry, rate constant determination (*Japanese*) 8-95827
 cladding, for optical fibres of phosphate glasses, transparent in UV region 8-87113
 film, SiO₂ rich, prepared by modified CVD, refr. index behaviour 8-60526
 fluxing material, effect on oxidation of graphite crucibles (*Japanese*) 8-84755
 machinable glass ceramic, elastic moduli, press. and temp. derivatives 8-52873
 optical fibres, low-loss single mode, design, fabrication and transmission characts. 8-71199
 optical fibres, prepared by modified CVD, reproducibility 8-90531
 surface, damage due to impact of small glass and steel spheres 8-52994
 Al₂O₃-SiO₂ clad with B₂O₃-SiO₂ effect of drawing tension on residual stresses 8-64554
 BaO-B₂O₃-SiO₂:Ti³⁺, elec. cond., struct. 8-72148
 BaO-B₂O₃-SiO₂:Ti³⁺, optical absorpt. spectra 8-72564
 CdO-B₂O₃-SiO₂, glass, dielec.-relax. currents 8-52004
 CdO-B₂O₃-SiO₂, phase equilibria at 800°C, photoelectric effects 8-68675
 K₂(F,O)-B₂O₃-SiO₂, effect of replacing B₂O₃ by Al₂O₃ or Ga₂O₃ 8-63677
 K₂O-Al₂O₃-B₂O₃-SiO₂, glass, ESR exam. of paramagnetic centres formed during mech. destruction by grinding 8-88188
 Li₂O-Na₂O-B₂O₃-SiO₃, exam. of metastable phase separation region 8-88450
 Na₂O-Al₂O₃-B₂O₃-SiO₂, glass, ESR exam. of paramagnetic centres formed during mech. destruction by grinding 8-88188
 Na₂O-B₂O₃-SiO₂-Fe glass, near IR optical absorption of Fe (II) 8-84616
 Na₂O-B₂O₃-Bi₂O₃-SiO₂, heterophase glass, diffusion and elec. cond. 8-67858
 Na₂O-BaO-SiO₂, metastable two liquid tie line calc. 8-92246
 Na₂O-PbO-B₂O₃-SiO₂, homogeneous melt formation rate, exam. 8-64520
 SiO₂-Al₂O₃-B₂O₃-Li₂O (Li₂O-Na₂O) (Na₂O) glass exam. of optical props. 8-88277
 SiO₂-GeO₂-B₂O₃, prepared by modified CVD, refr. index behaviour 8-60526
- Borrmann effect** see X-ray crystallography; X-ray diffraction
Bose-Einstein statistics see quantum statistical mechanics
Bose gas see boson systems
boson fluids see boson systems
boson systems
 see also liquid helium-4; quantum statistical mechanics
 Bose 1-D gas with point interaction 8-49762
 Bose condensate, bounds in dimensions ν≥3 8-54294
 Bose description of fermions 8-89402
 Bose electron-hole liquid, existence of states with superfluid flow, Ginzburg-Landau theory (*Russian*) 8-72085
 Bose system functional formulation, renormalisation group approach 8-66026
 Bose-Einstein condensation in an Einstein universe 8-77797
 boson operators, exponential ordering of quadratic forms 8-77800
 bosonization in positive definite Hilbert space 8-49974
 charged Bose gas, optimal BDJ-type ground state props. 8-54295
 cluster expansion formalism, independ. pair correlations 8-73922
 condensed, canonical ensemble approach 8-89400
 condensed Boson hard-sphere system, Jastrow wave function 8-84018
 cosmic coherent avalanche catastrophies, gamma-freq. graviton radiation 8-85844
 created boson multiplicity distrib., method of combinants 8-81917
 excitation spectrum of system of interacting bosons 8-71897
 hard disc Bose gas, ground state energy 8-95196
 Heisenberg eqns. on C* algebra of quasilocal observables, boson and fermion systems 8-57854
 helicity modulus at low temperatures 8-70052
 imperfect Bose gas, quasiparticle sound velocity, temp. depend. 8-51761
 K-flows quasi-free reversible, generalised 8-54297
 Lie group Sp(8,R), Lorentz subgroup anal. and null plane boson realisation 8-62116
 many-body problem, two-dimens., for low-density hard-disc Bose gas 8-95195
 nonlinear Bose systems, Dyson-Wick expansions 8-73921
 normal quantum fluid, kinetic theory, transport props. 8-77799
 nuclear many body problem, boson-fermion descript. (*Chinese*) 8-82297
 one dimensional continuous quantum systems, limit Gibbs state 8-93599
 one-dimensional many boson system, ground-state props., SCF approx. 8-49761
 quadratic boson Hamiltonian, diagonalisation 8-93600
 S-matrix for interacting extended boson fields, scatt. amplitude, self energy 8-66047
 Schwinger boson representation for the quantized rotator 8-93602
 statistical bootstrap model, hadronic mass spectrum, pion condensation, boson gas 8-70345
 two-dimensional nonideal Bose gas, ground state, theory 8-93601
 two-dimensional quantum systems at zero temp., liquid to gas phase transitions 8-77798
 Yukawa potential-ground state boson interaction, Monte Carlo study 8-51768
 π condensation, vacuum instability in external fields 8-50114
⁴He atomic Bose system, equilibrium superradiance 8-55994
 π phase transition and multiplicity distrib. in Feynman gas model with Bose statistics (*Russian*) 8-89683

bosons

- see also *alpha particles; boson systems; deuterons; gravitons; intermediate bosons; meson resonances; mesons; photons*
 conformal relativity, classification of metric bosons 8-93803
 spinor Bethe Salpeter and Goldstein eqns., fermion-boson coupling, numerical soln. 8-86400
 strong external fields, fermion and boson interactions 8-49987
 three-boson stimulated scatt., quantum mechanics (*Russian*) 8-78115
 Young's double beam interference experiment with spinor and vector waves 8-89363
 χ , suggested J^P values, is $\chi(3505)$ a vector boson? 8-62473
 $\mu \rightarrow \nu_e \chi^+$, hypothetical, search for scalar charged boson, apparatus and theoretical aspects 8-58177
 NN interaction,, neutral scalar, pseudoscalar and neutral vector boson radiative corrections, explicit formulae 8-70372

boundaries see *boundary layers; boundary value problems; grain boundaries; metal-insulator boundaries; semiconductor-insulator boundaries; semiconductor-metal boundaries*

boundary layer flow see *boundary layers*

boundary layer turbulence

- ablating plane (axisymmetric) body, turbulent boundary layer with neg. press. gradient 8-79389
 aerodynamically heated body, stable shape during ablation (*Russian*) 8-75162
 aerosol deposition on plate in turbulent flow 8-87380
 atmosphere, above ocean waves, scaling laws for optically relevant turbulent parameter C_2^2 8-85677
 atmosphere, and air-sea interactions 8-92953
 atmosphere, dissipation effects on parallel shear instability near ground 8-69406
 atmosphere, horizontal vel. spectra in unstable surface layer 8-73427
 atmosphere, momentum transfer during abrupt laminar-turbulent transition 8-65365
 atmosphere, multi-component linear digital simulation 8-61513
 atmosphere, neutral wind profile following surface roughness change, calc. 8-73483
 atmosphere, stratified surface layer, turbulence and diffusion, basic Lagrange characts. 8-81270
 atmosphere, surface turbulent fluxes modelling in stable conditions 8-61482
 atmosphere, three dimensional turbulent flow anal. 8-69395
 atmosphere, turbulence and internal waves spectra in stably stratified boundary layer (*Russian*) 8-81297
 atmosphere, turbulent and radiative transport interaction in development of fog and low-level stratus 8-81313
 atmosphere, turbulent interface layers theory 8-71323
 atmosphere-ocean, penetrative convection regime, entrainment rate (*Russian*) 8-69401
 axial turbomachine, cascade and through-flow theories as inner and outer expansions 8-75148
 axisymmetric, weak and strong disturbances effect on skin friction, mean vel. and shear stress 8-90857
 axisymmetric field flow around obstacle, effect on heat transfer (*Russian*) 8-83385
 axisymmetric supersonic turbulent base pressures 8-94764
 blunt-based axisymmetric body, subsonic turbulent near-wake 8-94740
 boiling crisis at concentric (eccentric) annuli with turbulence promoters 8-55639
 buoyancy and extra strain effects, mathematical modelling 8-94674
 bursting, spanwise struct. obs., in turbulent channel wall region 8-90855
 centre plane boundary in sq. duct, side walls effect 8-79311
 channel, with stepwise change in wall roughness, relax. processes 8-90861
 channel flow, velocity correl. function truncation (*Russian*) 8-75124
 coherent motion mechanism in turbulent shear flow wall region 8-90854
 compressible gas with heat transfer, surface roughness 8-90931
 compressible nonadiabatic gas flow in tube, eqns. system numerical integration (*Russian*) 8-83427
 compressible turbulent boundary layer, extended mixing length appls. 8-94655
 convergent and divergent flows, turbulent boundary layer with press. gradient, Reynolds analogy 8-83382
 corrugated wall, exptl. study of flow (*French*) 8-90844
 curved surfaces, turbulence meas. 8-79310
 curved wall, turbulent boundary layer detachment by perpendicular compressive thrust (*German*) 8-94661
 cylinder disturbance 8-67188
 cylinder in cross flow in turbulent pipe flow, heat transfer 8-90874
 cylinders, rot., intervening turbulent flow struct., model eqns. calc. 8-90852
 diffusers, conical, injection for boundary layer control 8-90864
 disperse systems, coagulation, slow, turbulent 8-53259
 dispersed particles steady-state radial distrib., in turbulent vertical gas flow 8-55680
 elastic shells, excitation and stress field in compressible fluid 8-51183
 entrainment in turbulent jets and plumes 8-94781
 final self preserving state of disturbed large 2-dimens. shear layer 8-90851
 flat plate, adiabatically densified fluid film, turbulent two-substance boundary layer (*German*) 8-90845
 flat plate in air flow, heat transfer at inner boundary layer 8-94715
 flat rectangular channel turbulent water flow, free stream and viscous sublayer temp. fluctuations 8-83369
 fluctuating flows near walls, turbulence intensity distrib. Thompson's velocity profiles 8-67189
 free and surface-mounted obstacles, topology, flow visualization 8-51157
 free coaxial jets with independent air supply to nozzles (*Bulgarian*) 8-59436
 free convection, vel. profile 8-94693
 gas, with variable physical props., pipe flow, turbulent momentum and heat transfer calc. 8-90869
 gas-solid particle suspension, turbulent flow in curvilinear channel, local heat exchange 8-63484
 Hassid-Poreh energy model anal., inc. accel. and surface heat transfer step change 8-51158
 heat and mass transfer, at turbulent boundary layer, diffusion model 8-94544

boundary layer turbulence continued

- heat and mass transfer in abruptly changing wall boundary conditions 8-94545
 heat flux equation, turbulent boundary layer, local similarity model 8-75142
 heat pipe, with header and single or two-phase artery systems 8-90981
 heat transfer, turbulent water film, different initial flow conditions, high temp. gradients 8-90862
 heat transfer across boundary layer, external flow turbulence effect 8-94713
 heat transfer across boundary layer, free-stream turbulence effects 8-94714
 heat transfer behaviour, turbulent boundary layer on rough surface with blowing 8-71334
 heat transfer coeff. meas. by dilatometry 8-83388
 heated wall experiments, turbulent field from temp. fluctuations 8-94667
 high-temperature turbulent air flow in round tube, friction resistance, cooling (*Russian*) 8-75135
 hydrofoils, tail-loaded, fully cavitating, avoidance of turbulent separation 8-94659
 incompressible gradient flow before separation and on rough surface, turbulent viscosity 8-87338
 interaction of turbulent spot with turbulent boundary layer, flow struct. obs. 8-90858
 interface layers turbulent flow, appl. to air/sea boundary layer 8-71323
 isotope separation by gaseous diffusion, aerodynamic effects 8-59469
 jet, turbulent, plane, impinging on plane surface, RMS boundary press. pulsations 8-59438
 jet, turbulent wall type, self-preserving flow 8-79352
 jets, radial turbulent, flow, attachment to disc plate, flow patterns, nozzle dimension effects 8-83443
 k- ϵ turbulence model, three dimens. finite difference anal. 8-51154
 large scale eddy destruction effects on skin friction and Clauser shape factor 8-90860
 large scale structure, turbulent spots model, bursts 8-90847
 large-scale turbulence modes obs. using mesh screen and heat wake 8-90859
 law of the wall, appl. to turbulent boundary layer calc. with injection or suction 8-67187
 liquid fuel film, combustion behind shock wave, heat and mass transfer in turbulent boundary layer (*Russian*) 8-71401
 liquid metal, film, turbulent flow down vertical wall under gravity, heat transfer 8-59396
 liquid metal heat transfer in regular fuel element arrays, Nusselt no. calc. 8-89932
 mass transfer, near-wall liq., coherent struct.-caused, numerical computation 8-59379
 mass transfer in viscous sublayer by electrochemical method, expt. 8-83368
 MHD convertor, diagonal channel, conversion efficiency optimisation by sliding descent method, turbulence (*Russian*) 8-75226
 MHD turbulent heat and momentum transfer in 2-dimens. channel with transverse mag. field 8-94848
 mixing, in two-dimens. turbulent layer, initial conditions effect 8-90848
 mixing length determination, from turbulence characts. meas., in tubes and boundary layers (*Russian*) 8-83371
 moving surface, integral and numerical methods 8-63421
 nuclear reactor pin bundle, two-phase flow, eqns. of motion 8-86570
 ocean, turbulent interface layers theory 8-71323
 ogive cylinder, mag. suspended, subsonic flow, reverse Magnus flow, turbulent boundary layer 8-51153
 oscillatory MHD boundary layer flow, free convection effects 8-91018
 particle transverse motion in turbulent boundary layer 8-79358
 periodic intermittent model for wall region 8-87336
 permeable plate, numerical anal. of turbulent boundary layers 8-67186
 permeable surface, turbulent boundary layer, in crossed elec. and mag. fields (*Russian*) 8-94836
 permeable tube with wall injection, transient turbulent boundary layer 8-83486
 pipe, heated, vertical, gas buoyancy effect on downward flow and heat transfer 8-74427
 pipe flow, turbulent, temp.-depend. viscosity effect on convective heat transfer 8-90884
 piped fluids in motion, turbulent flow, direct analytical soln. 8-87393
 plane plate with roughness element, nonsteady flow, numerical calc. (*German*) 8-94663
 plate, flat, turbulent boundary layer, mainstream turbulence, vorticity effects 8-83408
 plate, thin, in gradient current flow, coupled heat exchange (*Russian*) 8-83398
 plate, yawed, flat, leading edge vortex induced 3-dimens. turbulent boundary layer 8-90856
 plate at angle to flow, heat loss meas. for boundary turbulence and separation 8-90846
 plate with simultaneous injection and suction, turbulent layer friction and vel. profile 8-83469
 plume, turbulent, thermal, along vert. wall, struct. and heat transfer 8-90880
 polymer soln., diffusion in boundary layer 8-87368
 polymer solns., turbulent boundary layer in pipe flow 8-67256
 polymer solution, drag reduction in turbulent flows, book contrib. 8-59432
 polymer solution, mass transfer between solid surfaces and drag-reducing fluids 8-79339
 porous plate, suction, turbulent field anisotropy effect (*French*) 8-51156
 pressure fluctuation spectrum, elastic boundary compliance effect 8-63422
 Preston tube calibration in transpired turbulent boundary layer 8-79397
 pulsating turbulent flow onto elastic surface, boundary-value problem (*Russian*) 8-75153
 Reynold's stress tensors, rot. probe meas., in 3-dimens. boundary layer 8-94656
 Reynolds shear stress, turbulent flow over a periodic rough surface 8-71326

boundary layer turbulence continued

- rotating radial convergent duct, air flow heat transfer boundary conditions, turbulent and transition flow 8-83476
- rotational flow between rot. and static discs, with radial flow, numerical method 8-59403
- rough surface, Reynolds analogy extension 8-51159
- rough surface heat transfer in turbulent boundary layer, mixing length hypothesis 8-83378
- rough surface turbulent flow heat and mass transfer, Reynolds analogy deviations 8-83380
- semiempirical calc. using arbitrary free stream press. gradient 8-94640
- separating turbulent shear layers, flow field prediction 8-71321
- separation of subsonic and supersonic flows, ultra-short duration visualisation (*French*) 8-75128
- separation point, turbulent boundary layer numerical prediction, heat transfer (*French*) 8-94657
- separation region, oscillatory flow effects 8-75127
- separation zone behaviour 8-71320
- shallow water basin, wind-driven current, eddy viscosity, bottom friction 8-65319
- shear layer, axisymmetric and plane jet, initial condition effect 8-90850
- ship model, hydrodynamic resistance, analytic calc. (*Russian*) 8-75123
- shock-separated flows, turbulence models 8-71365
- smoke flow visualisation combined with hot-wire anemometry, technique, appl. to turbulent boundary layer 8-91044
- stagnating thermal turbulent boundary layer mean and fluctuating characts., divergent flow heat transfer 8-83370
- steady flows, fully stalled, flow computation in two dims. passages 8-94826
- steam-generating tube, bubble/plug flow boiling regimes, elevated press., drift vel. and void fraction determs. 8-87379
- steam-generating tubes, rough (smooth), post-dryout, heat transfer 8-55678
- step, rearward-facing, downstream turbulent flow 8-59380
- stratified fluid, turbulent layer development (*Russian*) 8-63477
- streamline curvature effects, anal. 8-59382
- structures and mechanisms of turbulence, conference, Berlin, Germany (Aug. 1977) 8-94647
- subcooled forced convection boiling heat transfer at subatmospheric pressure 8-94525
- supersonic, wall temp. effect 8-94765
- supersonic flow, self-induced oscills. 8-67215
- surface roughness and injection 8-94654
- swirling annular capillary jet flow (*Russian*) 8-75180
- Taylor-Görtler instability in turbulent shear flows and boundary layer transitions 8-90836
- temperature profile and Reynolds analogy expressions 8-87337
- three dimensional turbulent boundary layers, turbulence meas. c.f. shear stress hypothesis (*German*) 8-94664
- three-dimensional flow around bodies of arbitrary shapes, soln. method 8-79312
- trailing-edge turbulent flow noise, incident surface pressure field effect 8-90865
- transonic vel. profiles, local skin friction coeff. 8-67214
- tube, annular high Prandtl no. flow, turbulent heat transfer, surface rejuvenation model 8-71333
- tube, vertical, laminar and turbulent heat transfer, air and Ar 8-71332
- tube flow, velocity correl. function truncation (*Russian*) 8-75124
- turbulence characteristics, in separated, reattached, and redeveloped regions of 2-d flow over flat-plate 8-94660
- turbulent flow relaminarisation, flow visualisation 8-75244
- turbulent natural convection boundary layer, space-time correl. meas. 8-71322
- two-dimensional fence flows, wall constraint 8-59381
- two-dimensional turbulence on the surface of a sphere 8-73447
- underground cable system, convectively cooled, vel. distribs., press. drop correlations 8-71330
- unified similarity theory, turbulent convection at vertical surface 8-90890
- unsteady, near separation, oscill. press. gradient effect struct. features 8-75126
- unsteady boundary layers, separated and attached, review 8-71313
- unsteady boundary layers with reversal and separation 8-75163
- unsteady transitional and turbulent boundary layers, expt. and calc. methods (*French*) 8-75125
- velocity profiles over smooth surface 8-67183
- vortex-array representations, interaction, of free-stream turbulence near sem infinite flat plate 8-90842
- wall shear stress prediction in three-dimensional turbulent boundary layers 8-67184
- wall turbulence, turbulent correlation equations 8-94673
- water surface, free, roughness determ., from air flow struct. anal. 8-63441
- wind-wave interaction, two-layer flow, numerical simulation 8-92823
- yawed flat plate at incidence, three-dimens. boundary layer turbulence meas. 8-51160
- He, near-critical, friction factors for flow in curved tubes 8-83367
- N₂O₄, dissociating, turbulent pipe flow, heat transfer, resistance 8-91026

boundary layer turbulent flow see *boundary layer turbulence*

boundary layers

see also *boundary layer turbulence*

- ablating body shape, numerical soln. method (*Russian*) 8-75134
- absorbing-scattering semitransparent planar layer, flat temp. waves 8-90683
- acoustic, enclosure, thermoviscous dissipation at walls, normal mode theory 8-83171
- aerodynamically heated body, stable shape during ablation (*Russian*) 8-75162
- aeroelasticity of unsteady aerodynamics, force calc. methods (*French*) 8-75095
- aerofoil, dynamic forces acting, subsonic instabilities (*French*) 8-67213
- aerofoil, two-dimens., in incompressible flow, unsteady motion 8-67171
- aerofoil in oscillating flow, vel. field, surface press. 8-75164
- aerofoil in unsteady airstream, two-dimens. viscous flow, numerical predictions 8-75166
- aerofoil in unsteady viscous flow, numerical soln. procedures 8-75165

boundary layers continued

- air layer near water surface, diurnal characts., equatorial region, GATE meas. 8-61527
- air-sea interaction, surface drift current speed and direction calc., geostrophic wind factor 8-61422
- air-sea interface, oceanic variability obs. during Project BOMEX 8-69362
- airfoils with oscill. jet flaps, quasisteady theory 8-63467
- alkali metal vapour condensation from gas flow (He, Ar, N₂) heat and mass transfer 8-75192
- angular perturbations, stability and convergence 8-90827
- annular climbing film flow dispersion models 8-83473
- arc, boundary layer cooling of atmospheric arcs, arc interruption by moving rod 8-87545
- asymmetric flow past wings, nonlinear-discrete vortex method 8-71351
- atmosphere, aerodynamic roughness as function of wind direction over asymm. surface elements 8-92890
- atmosphere, convective, temperature-humidity covariance budget 8-73430
- atmosphere, convective matching layer 8-81310
- atmosphere, diabatic baroclinic, parametrisation for circulation modelling (*Russian*) 8-88882
- atmosphere, dissipation modelling under forced convection conditions 8-92900
- atmosphere, eddy convection vel. 8-92894
- atmosphere, eddy flux meas. over ocean, related transfer coeffs. 8-81265
- atmosphere, energy characts. of urban-rural surfaces in greater St. Louis area 8-61484
- atmosphere, evaporation fogs formation theory and prediction 8-61522
- atmosphere, finite amplitude Kelvin-Helmholtz billows, evolution 8-81293
- atmosphere, friction vel. and temp. scale from temp. and wind vel. profiles 8-81268
- atmosphere, geostrophic large-scale drag coefficient estimation 8-61488
- atmosphere, ground level gravity waves occurrence in SE. Australia, microbarographs obs. 8-73439
- atmosphere, heterogeneous surface of large aerodynamic roughness, transfer characts. 8-73487
- atmosphere, local circulation in Rome area, surface obs. 8-81264
- atmosphere, marginally unstable interfacial gravity waves (*French*) 8-92888
- atmosphere, marine, ranked interaction with ocean on sub-semidiurnal time scales (*Russian*) 8-77260
- atmosphere, mass consistent model for wind fields over complex terrain 8-92906
- atmosphere, mechanical effect of urban area on convective precip. 8-81338
- atmosphere, meteorological episodes increasing air pollution in Belgium 8-81374
- atmosphere, mountain ridges effect on frontal waves development, numerical simulation (*Russian*) 8-53701
- atmosphere, Navier-Stokes eqns. soln. 8-92956
- atmosphere, nocturnal, height determ. 8-73450
- atmosphere, over ocean, salt spray contamination of atm. temp. sensors 8-69489
- atmosphere, press. fluctuations, ground effects 8-61498
- atmosphere, radiation balance over salt marsh 8-61481
- atmosphere, radio refr. index struct. parameter height distrib. with lower boundary spatial transition 8-73491
- atmosphere, radio refractive index structure in transitional boundary layer 8-57268
- atmosphere, similarity parameters from first-order closure and data 8-92893
- atmosphere, small-scale wind vars. over water surface, computation model 8-61480
- atmosphere, snow cover energy budget, energy flux meas. 8-92859
- atmosphere, source disturbances simulating orographic effects, upstream boundary values (*German*) 8-65375
- atmosphere, stability, baroclinicity and scale-height ratio effects on drag laws 8-73429
- atmosphere, steady-state characts. of temp. inversions capping well-mixed layer 8-61483
- atmosphere, surface layer press. perturbs. due to ocean swell waves (*Russian*) 8-65362
- atmosphere, surface roughness change effects 8-77306
- atmosphere, temp. and humidity correl. above warm wet surface 8-85646
- atmosphere, three-dimens. model rel. to expt. data 8-73428
- atmosphere, topographic influence on surface wind 8-81266
- atmosphere, vertical currents induced by orography and turbulence 8-96278
- atmosphere, vertical motion in stratified ground layer under coniferous forest canopy (*Russian*) 8-96266
- atmosphere, wind dispersion ellipticity over ocean surface, N. Atlantic example 8-61528
- atmosphere, wind shears and inversions (*German*) 8-81336
- atmosphere ocean interfacial conditions, influence on bulk evaporation coeffs., isotopic method determ. 8-85576
- atmosphere-ocean interaction, sea waves influence on wind profile 8-92895
- atmosphere-ocean interaction parametrisation for storm conditions, atm. circulation models appl. (*Russian*) 8-65359
- atmosphere-ocean interactions along North American west coast, 1965-69 period, preliminary anal. 8-61508
- atmosphere-ocean interface, energy transfers at high wind speeds, effect of spray 8-85574
- atmosphere-ocean interface, wind vel. profiles and drift current along wind-generated wave profile (*Russian*) 8-61429
- atmosphere-vegetation interaction, simplified one-dimens. theory 8-61479
- atmospheric boundary layer physics, conference (Smolenice, Czechoslovakia, 1974 February 18-21) 8-88873
- atmospheric convection in boundary layer, lidar obs. 8-65366
- atmospheric wind profile meas. using acoustic Doppler sounder 8-65413
- axisymmetric boundary layer flow between wall and paraboloid (*Russian*) 8-75121

boundary layers continued

axisymmetric free shear layer, effects of initial momentum thickness 8-71325
 axisymmetric stagnation flow on circ. cyl. 8-79298
 base flow at supersonic vel., rockets and re-entry vehicles appl. 8-67243
 Blasius flow, horizontal, heated from below, longitudinal vortices onset 8-71342
 bluff body, two-dimens., drag and wake (*Japanese*) 8-55647
 body of revolution, slender, nonlinear normal forces, Reynolds no. influence (*German*) 8-51191
 boiling, two-phase boundary layer, temp. fluctuations 8-51222
 boiling and bubbling heat transfer under the conditions of free and forced convection 8-90637
 boiling mechanism during burnout phenomena in subcooled two-phase water flows 8-94529
 boundary layer on conical body with gas injection (*Japanese*) 8-59417
 bubble, of vap., with microlayer, universal growth relations 8-71266
 bubble, rising, hydrodynamic interaction with suspended solid particle 8-51221
 bubble oxygenator, O₂ transfer controlling factors 8-53568
 bubble population prediction, in flow boiling, from gas bubble nucleation expts. 8-90696
 bubbles, active nucleation site spatial distrib., bubble flow density 8-71267
 camphene-coated surface, convective local mass-transfer coeffs., holographic interferometry method 8-75234
 Cartesian model, viscous boundary layer flow over topography 8-92904
 cathodic diffusion boundary layer, free convective flow obs. with shadow Schlieren method 8-68894
 channel, annular, with vortex generators, and uniform (nonuniform) heat injection length, crit. heat flux (*Russian*) 8-83397
 channel, rectangular, laminar forced convective heat transfer for 3rd kind temp. boundary conditions 8-87341
 circulation flows near wall, ideal liq., two-dimens. anal. in Cartesian coords. 8-51173
 combined convective laminar boundary flow, vertical cylinder in horizontal flow, finite difference approx. 8-90893
 compressible boundary layer flows, curvature near separation 8-55661
 compressible flow in rot. cylinder, lineared anal., appl. to gas centrifuges 8-71345
 concentration distribution on models during erosion by air flow 8-67172
 condensate film flow on finned surfaces, heat transfer, heat exchanger design 8-75038
 condenser system, submerged, bubble pumped augmented natural convection 8-94535
 convection, free, and radiative transfer, at vertical plane surface 8-55645
 convection, free, laminar, three-dimens., about surface, numerical anal., visualisation (*French*) 8-87343
 convection, natural, from vert. DC current-heated plate, linear stability anal. 8-90873
 convection, natural, in presence of transverse mag. field similarity soln. 8-67197
 convection, natural, laminar, enclosure with heat source and sink on horiz. boundary 8-90882
 convection, natural, over uniform heat flux vertical surface, higher-order approx. 8-59388
 convection of vertical layer, flow stability, boundary thermal props. effect 8-55644
 cooling efficiency, axisymmetric air flow past rot. cylinder, main flow swirl effect 8-75132
 Couette flow, permeable wall layer, heat transfer and temp. distrib. 8-51165
 Couette flow, striated boundary effect on viscous drag 8-59367
 Couette flow along surface, isothermal slip 8-67220
 counter-current two-phase flow, annuli, rod bundles, liq. film behaviour, flooding 8-59452
 creeping flow about sphere, general soln. of linear Navier-Stokes eqn. 8-71307
 cylinder, circ., separated wake stagnation pt., 2nd order boundary-layer soln. 8-63432
 cylinder, circular, with slit, flow characts., control, patterns, wake flow, vortices 8-83404
 cylinder array, convective mass transfer with surface reaction 8-79369
 cylinder in cross flow, skin friction and vortex shedding freqs. 8-94758
 cylindrical channel walls, adsorption from fluid in Poiseuille flow 8-84048
 cylindrical slab of fluid, in weightlessness condition, surface-tension driven convection (*Russian*) 8-90872
 cylindrical tube, free vibration in viscous incompressible liquid (*Russian*) 8-55636
 deformation section in flow in constricting devices 8-75206
 diffusers, 2-dimens., with suction through porous parallel side walls, characts. (*Japanese*) 8-83492
 diffusers, curved, performance, separation in subsonic, transonic channels (*French*) 8-94818
 dilute suspension, boundary layer in presence of electric field (*Russian*) 8-63503
 disc-halo galaxies gaseous components, boundary layer circulation 8-57627
 disperse system, flotation of fine particles by group of bubbles, kinetics 8-53261
 double-diffuse convection, diffuse interface model, high Rayleigh nos. 8-90963
 drag force on sphere moving in medium with variable viscosity 8-67173
 drag on sphere accelerating rectilinearly in elastico-viscous fluid, Fourier transform technique 8-51145
 duct, circ., laminar convective MHD heat transfer for 3rd kind temp. boundary conditions 8-87342
 duct, narrow, plane, temp. distrib., heat flow to dense blown layer (*Russian*) 8-83402
 ducts with porous walls, Navier-Stokes exact eqns. 8-67266
 dust-liquid channel flow, with varying inlet temp., transient forced convection soln. 8-87375
 dusty fluid, motion induced by impulsive plane boundary motion and cylinder motion 8-79362

boundary layers continued

Earth core, effect of boundary irregularities on fluid speed and geomag. field 8-73333
 elastohydrodynamic point contact, mathematical model for lubricating film thickness (*German*) 8-63464
 falling films, nonisothermal flow (*German*) 8-83439
 finite difference approx., boundary layer flow 8-51155
 flame, laminar mixed-mode forced-free diffusion type, on vert. burning fuel slab 8-91033
 flat duct, inlet zone turbulence under differing boundary layers, heat transfer, expt. 8-83481
 flat plate boundary layer in porous medium, free convection, similarity solns. 8-75199
 flow about arbitrary 2-dimens. boundary, implicit finite difference simulation 8-94628
 flow between rotating spheres, frictional moment 8-79301
 flow over cone, dual-plate holographic interferometry 8-63512
 flow past axially uniform viscous vortex, tornado mathematical model 8-59405
 fluidised beds, heat transfer to horizontal tube (*German*) 8-59387
 forced convection heat transfer in horizontal layers, buoyancy effects 8-90901
 free convection boundary layers on cylinders of elliptic cross section 8-90877
 free convection effects on the Stokes problem for an infinite vertical plate 8-90879
 free convection mass transfer from horizontal surface, electrochemical and holographic interferometric obs. 8-87344
 free convective heat transfer at a vertical semiinfinite plate 8-79318
 free convective heat transfer in fluid confined by wavy wall 8-55642
 free-forced convection from a heated cone, cross flow transition, similarity soln. 8-90892
 freestream turbulence statistical characts., convective heat transfer calc., boundary layer eddy viscosity 8-83366
 grey bodies system, closed combined radiation convection heat transfer, two-layer gas model 8-75052
 ground surface temperature and moisture content, prediction with inclusion of vegetation layer 8-73373
 heat exchange, radiant plate, diametrical Ar gas flow (*Russian*) 8-94565
 heat exchange in dense layer at large Biot no. (*Russian*) 8-83400
 heat flux transducers for local heat exchange meas. of air flow in tube (*Russian*) 8-83509
 heat pipe, heat transfer agent flowrate through porous wick, approx. calc. method 8-75197
 heat transfer augmentation, convective, effect of mech.-produced unsteady boundary layer flow 8-71261
 heat transfer bibliography 8-63425
 heat transfer in laminar freely convecting boundary layer, series soln. predictive capability 8-71335
 high temperature boundary layer mass transfer, nonequib. ionisation effects 8-93634
 horizontal cylinder, laminar free convective heat transfer 8-75130
 horizontal cylindrical surface, free convection, local nonsimilarity anal. 8-75120
 hot surface quenching rate, countercurrent single- and two-phase flow effects 8-59451
 hot wall with impinging liq. droplet, transient temp. profile 8-75050
 hydrodynamic control of increase of diffusional boundary layer upon plate immersed in Ostwald fluid (*French*) 8-87329
 hydroplaning of a rotating cylinder on water 8-63522
 hydroplaning plate, lift, drag 8-63523
 hypersonic gas flow, radiant heat and evaporative cooling 8-91028
 insulated plate thermometer, incompressible boundary layer flow 8-55626
 jet, heavy, flowing into nonmixing medium 8-51212
 jet, supersonic, flowing onto infinite perpendicular barrier, limiting expansion ratio 8-59439
 jet impact system with unilateral outlet, air flow, heat exchange (*Russian*) 8-83449
 Jupiter, atmosphere, subliming boundary layer flow, simulation 8-65545
 laminar, convective diffusion due to incident turbulent jet 8-67242
 laminar, semiempirical calc. using arbitrary free stream press. gradient 8-94640
 laminar, separation at angular inflection on solid surface 8-67169
 laminar boundary layer flow, heat transfer, rel. to vel. fluctuations 8-94710
 laminar boundary flow over spinning blunt body of revolution, Magnus forces 8-94745
 laminar boundary layer, heated, with nonuniform surface temp. distrib., stability 8-67175
 laminar boundary layer, on permeable surface, in crossed elec. and mag. fields (*Russian*) 8-75118
 laminar boundary layer development under continuous incipient separation conditions 8-63415
 laminar boundary layer flow along vaporising liq. layer (*German*) 8-83403
 laminar compressible boundary layer swirling flow in nozzle, flow and heat transfer 8-94795
 laminar convection, heated vertical surface, boundary-layer thickness and Prandtl number 8-51161
 laminar dispersion in rectangular conduits, side wall effects, convection 8-94636
 laminar equalising flow in Couette-type channel flow (*German*) 8-51239
 laminar film, convective coupled heat transfer, Nusselt no. computation 8-59398
 laminar film condensation from moving vapour, with suction 8-59459
 laminar flow along porous vertical wall 8-90825
 laminar flow around free and surface-mounted obstacles, topology, flow visualization 8-51157
 laminar flow instability, nonlinear theory 8-63416
 laminar flow over parabola, second approx. 8-63414
 laminar flow over periodic wavy surface, nonlinear anal. 8-90826
 laminar flow pattern, press., enthalpy, vel. from point source of heat 8-79316
 laminar incompressible boundary layer eqns. finite element soln. 8-79304
 laminar to turbulent transitions, temp. factor effect 8-63417
 laminar vapour flow in film boiling, stability limits 8-90832

boundary layers continued

large Reynolds number, 2-D hydrodynamic lubricating theory (*Russian*) 8-59368
 laser-Doppler technique, local size and vel. probability distrib., two-phase suspension flow 8-59517
 Laval nozzle, surface burning in two-phase flow, boundary layer interaction, Rakhmatulin model 8-83452
 leading edge effect on free-convection heat transfer 8-79319
 Leidenfrost layer, liq. drop falling onto hot liq. surface, boiling instability 8-94588
 liquid film, falling, laminar, transport augmentation by surface waves 8-71343
 liquid fuel droplet heating with internal circulation 8-75194
 liquid layer appl. using rubber roller, nip flow operations anal. 8-71310
 liquid layer creeping over surface, angle of contact, viscous liq. 8-51149
 liquid-vapour flow, heat transfer crisis, wall shear stress 8-90986
 longitudinal and cross flow around heat exchanger tube bundles comparison, heat transfer efficiency aspects 8-94687
 low speed flow up a step 8-79303
 magnetic fluid (cable coolant), natural convection heat transfer 8-94846
 magnetosphere, frontside boundary layer obs. and reconnection problem 8-89010
 magnetotail, hot tenuous plasmas, fireballs and boundary layers 8-77438
 marine, microwave radiometric sensing of atmospheric structure 8-57272
 matched asymptotic expansions method, asymptotic matching principle for higher approx., boundary layer problems appl. 8-94642
 matter-antimatter boundary layers with mag. neutral sheet, model 8-53807
 Maxwell fluid, unsteady flow past flat plate, transform technique 8-59428
 melting surface, air bubble evolution effect on boundary layer separation 8-67015
 melting/freezing interface, annular region, perturbation soln. 8-59286
 MHD, nonsimilar incompressible laminar boundary layers, finite-difference scheme 8-79386
 MHD boundary layer flow, on flat plate, effects of varying velocity 8-67275
 MHD boundary layers, laminar, control problem (*German*) 8-91024
 MHD flow in rot. channel, wall conductances effect on heat transfer 8-51245
 MHD flow over porous plate, Hall effect 8-51246
 MHD generator, electrothermal instability in the seeded combustion gas boundary layer near cold electrodes 8-71547
 MHD thermal boundary layer flow near oscill. limiting surface, stellar atm. appl. 8-94831
 MHD unsteady free convection past a hot vertical plate 8-87396
 micropolar fluid jet normal impingement on curved surface, flow near stagnation point 8-90949
 micropolar fluid on circular cylinder, thermal boundary layer 8-75174
 natural convection flow, nonisothermal flat plate, numerical soln. 8-67194
 natural convection mass transfer along porous vertical plate 8-90876
 natural convection of air over a heated plate with forward-facing step 8-90875
 Navier-Stokes eqns., bluff body aerodynamics, numerical simulation methods 8-75115
 non-Newtonian flow along thin needle, vel. profile, skin friction 8-67229
 non-Newtonian fluid film flow along vertical oscillating plate (*German*) 8-59431
 non-Newtonian fluids, lubrication, elastohydrodynamic, between two rot. cylinders 8-83435
 non-Newtonian fluids in jacketed agitated vessel, heat transfer, viscosity correl. 8-75143
 non-Newtonian non-similar laminar boundary layers, rapid calc. procedure 8-90943
 non-steady boundary layer, turbulence development 8-90829
 nonideal plasma generation, by electrolyte impulse diaphragmic discharge 8-71506
 nonsimilar axisymmetric stagnation flow on a moving cylinder 8-79297
 nonsimilar laminar free convection flow along a nonisothermal vertical plate, finite difference method 8-75119
 nonstationary boundary layer with self-induced press. at transonic external stream vels. 8-83428
 nonsteady MHD thermal boundary layer, in incompressible laminar flow with variable elec. cond., approx. soln. 8-91022
 nozzles, supersonic, thermal protection by gas curtain, vel. gradient 8-51215
 numerical methods, book contrib. 8-59369
 ocean, abyssal shear zone obs. 8-73386
 ocean, hydrodynamic friction layer instability rel. to Langmuir circulation 8-92840
 ocean, two-layer, stable wind-driven equatorial currents theory (*Russian*) 8-61427
 ocean eddies and islands, effects on mixing 8-85572
 ocean upper layer temperature, influence of mesoscale eddies (*Russian*) 8-81191
 oil-cooling baffled shell-and-tube heat exchanger expt. 8-83395
 Oldroyd liquid, unsteady flow between two porous walls 8-63452
 open cavity heat and mass transfer 8-55640
 Orr-Sommerfeld eqn., continuous spectrum and eigenfunctions 8-67176
 oscillating porous flat plate boundary layer, hydromagnetic flow 8-51250
 oscillatory boundary layer, on bed beneath gravity waves, laser Doppler anemometry 8-90929
 Oseen, unsteady three dims., applied conc. force 8-67167
 permeable bed boundary layer flow, temp. distrib. and Nusselt no. 8-51166
 Petrov-Galerkin finite element method, boundary value problem 8-69989
 phase interfaces, balance eqns. and struct. models 8-59453
 pipe, heated, straight, free-forced convection in entry region 8-90883
 plastic disperse systems, generalised flow theory with account of wall effect 8-87320

boundary layers continued

plate, downward-facing, flat, heat transfer augmentation by nonuniform elec. field corona 8-94873
 plate, flat, optically thin boundary layer, of grey medium near leading edge, radiative-convective heat transfer 8-91027
 plate, thin, in gradient current flow, coupled heat exchange (*Russian*) 8-83398
 plate, with suction, three-dimens. fluctuating flow, heat transfer, skin friction 8-87389
 plate at angle to flow, heat loss meas. for boundary turbulence and separation 8-90846
 plate in nonhomogeneous fluid 8-94639
 plate temp. oscillations, response of horizontal free convection boundary layer 8-59391
 plates, collinear, interrupted, flow-aligned, heat transfer and press. drop 8-87232
 plume, above vert. heated plate, development of wall and free types 8-90881
 Poiseuille flow, plane, horiz., rot., stability, effect of Coriolis force 8-67203
 porous plate, with time-varying motion, surrounding liq. MHD flow 8-51251
 positive column, metastable atom radial transport, effect of wall boundary conditions 8-67493
 potential flow, approx. numerical solns. 8-79293
 potential flow around axisymmetric bodies 8-63412
 potential flow over bodies, convective heat transfer 8-59395
 potential flow over wing with free vortex 8-63444
 powder flow over inclined surfaces 8-63488
 power law liquid, comparison of 2-D and axisymmetric jet flows 8-79351
 pseudoplastic fluid, flowing upward in vert. heated tube, variable physical props. 8-90945
 pulsating laminar-boundary layer, heat transfer and skin friction 8-94711
 radiative transfer in expanding homogeneous sphere (*Russian*) 8-73945
 radiative-convective heat transfer, numerical methods 8-94577
 rarefied gas flow induced by thermal stress, imperfect accommodation at boundary 8-87362
 rarefied polyatomic gases, ang. momentum polarisations, boundary layer behaviour 8-51200
 rattle formation model 8-63482
 rigid wall-hot gas stream interaction, heat cond. eqns. soln. 8-79194
 rotating body, axisymmetric, arbitrary surface temp. distrib., thermal boundary layer, exact solns. 8-75133
 rough subliming surface, laminar boundary layer, anal. 8-51148
 saturated liquid, boiling onset, film boiling transition, crit. heat flux densities (*Russian*) 8-83234
 SAW, phase velocities on solid-liquid boundary 8-83151
 separated flow, heat transfer 8-79315
 separated flow with laminar mixing region, heat and mass transfer, math. simulation 8-59397
 ship hydrodynamics, drag on displacement ships, hydrofoils, hovercrafts 8-63423
 shock layer, hypersonic, vibr. nonequilibrium, near stagnation streamline, low Reynolds no. flow 8-87417
 shock wave generation, liq.-liq. interface with temp. discontinuity 8-51197
 shock wave interactions, oblique incidence (*Japanese*) 8-55662
 singular nonlinear differential eqns., boundary layer flow 8-63413
 skewed boundary layers in duct with streamwise press. grad. variation 8-79302
 slip flow, MHD, over porous plate, with variable suction, heat transfer 8-79337
 smectic-A liquid crystal, permeative flow around obstacle, extended boundary layers 8-67644
 solar wind flow past planets, axisymm. implicit blunt body computation technique 8-96370
 spacecraft atmospheric entry, body shape for minimal radiative heat inflow (*Russian*) 8-77457
 sphere in unsteady motion in liq., drag. calc. 8-67170
 sphere surface viscoelastic Prandtl boundary layer flow, separation point 8-63460
 spheroids, harmonically oscillating, unsteady airload prediction, analytical soln. 8-51184
 spillway surfaces, flow around three dims. projections, cavitation 8-67232
 stagnation flow, nonlinear stability 8-90831
 stagnation point boundary layer on subliming surface with roughness elements 8-94635
 stationary boundary layer flow, plane heat balance eqn. asymptotic soln. (*German*) 8-63430
 steam, horizontal flow on cylinder, condensation 8-94550
 steam condensation heat transfer on below-freezing pt. surface 8-75042
 steam-generating tube, bubble/plug flow boiling regimes, elevated press., drift vel. and void fraction determ. 8-87379
 steam-liquid, annular-dispersed flow, hydrodynamic characts. 8-94806
 steam-water, flow characts. at high press. 8-94805
 steam-water mixture, with high vap. content, annular flow, heat transfer, press. loss 8-75193
 sticking condition for fluid at solid boundary, entropy change 8-83359
 stochastic model of fluctuations 8-90818
 Stokes flow, axisymmetric, about body of revolution whose section is cardioid 8-55629
 Stokes flow in a trench between concentric cylinders 8-83360
 Stokes flow past plane with cylindrical ridge or trough, separation 8-55653
 Stokes flow past radially deforming sphere at small Reynolds number 8-67174
 Stokes flow past smooth cylinder 8-55627
 Stokes problem of motion of Cassinian cylinder in viscous fluid 8-71312
 stratification effects in boundary layer flow over hills 8-53707
 streaming, of vel. and temp., in oscill. boundary layers 8-83358
 subsonic flow past pulsating airfoil 8-71348
 supercritical flow of an ideal fluid over a spillway 8-94638
 supersonic flow, self-induced oscils. 8-67215
 supersonic flow past slender cone at high incidence 8-90932
 supersonic flow through cascade, linearised theory (*French*) 8-94766

boundary layers continued

- supersonic separated flow changes, caused by throttling in round duct 8-63446
- supersonic wave drag of planar singularity distributions 8-83430
- surface reactions and mass transport, in Leveque's approx. 8-76907
- surface streamlines, governing eqns. 8-71309
- swirling flow, fluid between rotating discs, nonmonotonicity of solns. 8-59404
- symmetrical flow past double wedge at subsonic Mach nos. 8-51182
- thermal mixing layer development over water and heated land, lab. simulation 8-73449
- thermal response behaviour, laminar flow 8-75136
- thermocapillary convection, unevenly heated liq. stream near gas bubble 8-59460
- three dimensional boundary layer, streamline coords., similarity transforms 8-90816
- three dimensional free convection flow and heat transfer along a porous vertical plate 8-90866
- three dimensional layer theory, using shell geometrical concepts 8-90815
- three-dimens. flow over blunt bodies 8-79296
- Tokamak, neutral injection system, cold gas flow pattern evaluation 8-66397
- transient boundary layer on porous plate, coolant injection, laminar flow stability and heat transfer 8-83389
- translational friction, for arbitrary shaped objects, modified Oseen tensor calcs. 8-71311
- transonic flow around bodies of rotation (*Russian*) 8-87357
- transonic shock-boundary layer interaction, shock obliquity effect 8-90933
- tube, horizontal, laminar combined convection, circumferentially nonuniform heating effect 8-71331
- tube, vertical, laminar and turbulent heat transfer, air and Ar 8-71332
- tube, vertical, steam generating annular flow, dry-out position prediction, computer model 8-59447
- turbulent boundary layer generation in unsteady flow 8-90828
- two-component fluid, laminar boundary layer, temp. and conc. field calcs. (*German*) 8-71386
- two-parameter skin friction formula for adiabatic compressible flow, shocked relaxing boundary layer 8-51188
- two-phase flow, disc straddling interface 8-90971
- two-phase flow instability in parallel channels 8-94810
- two-phase mixture flow in rotary mixer, optimal dimensions 8-63485
- two-phase nonequilibrium flow, spectral characts. 8-94854
- underground cable system, convectively cooled, temp. distribns., heat transfer correlations 8-71262
- unsteady, transitional and turbulent, expt. and calc. methods (*French*) 8-75125
- unsteady boundary layers, separated and attached, review 8-71313
- unsteady boundary layers with reversal and separation 8-75163
- upstream adiabatic zone, subsonic, supersonic downstream boundary layer heat transfer effects 8-83379
- vapour generator, two-phase flow dynamics 8-94808
- visco-elastic liquid, flow past hot porous circular cylinder, free and forced convection 8-83386
- viscoelastic fluid flow in annulus entrance region, boundary layer anal. 8-63459
- viscoelastic fluid unsteady flow through pipes under different press. gradient conditions 8-75172
- viscoelastic free convection boundary layer flow past infinite plate with constant suction 8-90936
- viscoelastic radial flow between parallel discs 8-67223
- viscoelastic squeeze films, effect of normal oscill. and fluid inertia 8-67224
- viscometer, high pressure, non-isothermal flow, thermal boundary conditions (*German*) 8-67292
- viscoplastic liquid film on vertical vibr. wall, with slip, shaking loose 8-59371
- viscous dissipation effect on heat transfer, circ. cylinder axisymmetric stagnation flow 8-51164
- viscous fluid, variable thermal conductivity, variational calc. of vel. profile and temp. in laminar boundary layer (*French*) 8-55625
- viscous fluid flow through slot between fixed and rotating surfaces of revolution (*Polish*) 8-79300
- viscous liquid unsteady flow in annular channel 8-75205
- viscous-inviscid supersonic (transonic) flow matching, two-dimens., numerical method (*French*) 8-79334
- vortex shedding behind circular cylinder, wake 8-75149
- vortex sheet approx. for incompressible boundary layers 8-67201
- vorticity of free stream adjusting to flat plate, Laplace eqn. soln. 8-59406
- wall temperature distributions, in regions of deteriorated heat transfer 8-83377
- water, cooling, boundary layer thermal state during transition from free to forced convection (*Russian*) 8-81192
- water-entrained gas flow, force on moving body 8-63480
- wavy fluid film, instantaneous vel. profile meas. 8-79299
- wind shear fluctuations downwind of surface roughness elements 8-92918
- wind tunnel, wall interference, two-dimens., correction method, examples (*French*) 8-67293
- wing, rectangular, with tip clearance in channel, aerodynamic characts. 8-59415
- wire, in longitudinal laminar air stream, heat exchange (*Russian*) 8-83401
- N₂, cryogenic, shock wave-boundary layer interaction (*German*) 8-71370
- N₂O₄, dissoc. flow in tube, heat transfer and drag 8-71402
- Na, liq., in vert. pipe, hydraulic resistance under boiling conditions 8-90968

boundary-value problems

see also *initial value problems*

- acoustic resonant frequencies in an eccentric spherical cavity 8-90548
- acoustic waveguides, sound pressure field variation as function of refractive index 8-94464
- atmosphere, source disturbances simulating orographic effects, upstream boundary values (*German*) 8-65375
- attenuation of solns. to eqns (*Russian*) 8-65753

boundary-value problems continued

- beam, elastic, on elastic half-space support, forced flexural vibr. 8-63353
- boiling, pool-type, heat transfer stability prediction, finite disturbances 8-75044
- Boltzmann equation, global solutions, bounded convex domain 8-57876
- bubble growth, noncondensing gas-vap. injected into liquid 8-55553
- buried cylindrical heat source, transient temp. distrib., upper and lower bounds 8-75048
- cantilever (Timoshenko), elastically restrained, with attached masses, follower force stability 8-63347
- cantilevers, joined by a rigid connector nat. freq. determ. 8-83298
- capillary-porous body, nonlinear heat/mass transfer problem, soln. using invariant groups 8-55688
- cavitation, acoustic, threshold conditions for onset 8-59433
- Clausius-Mossotti problem for cubic arrays of spheres 8-52422
- complex coord. method, error bounds 8-49705
- concentric shock wave self-similarity exponent approximation 8-75169
- concentric shock waves in inhomogeneous medium, self-similarity exponent 8-75168
- cone/plate system in fluid, friction heating and convection 8-87238
- convection in porous cavity, Darcy medium, 2-dimens. solns. 8-91007
- convergence of perturbation method and boundary conditions at non-canonical surfaces (*Russian*) 8-77696
- convex nonlinear boundary value problems, iterative bounds for stable solns. 8-54167
- crystal optics with spatial dispersion 8-92040
- diffused substance kinetics in biological systems 8-53312
- dipole antenna in warm isotropic plasma, multiple water bag model 8-91115
- Dirichlet problem, response function method for fast soln. of Laplace eqn. 8-86119
- Dirichlet-Neumann boundary-value problems, variational principles and hypercircle 8-57749
- droplet, vaporising, internal temp. field 8-51042
- dual extremum principles for heat eqn. 8-70077
- Earth interior density distrib., determ. from gravity logging data (*Russian*) 8-92999
- ECG forward problem, relationships among Green's theorem, Helmholtz theorem and integral eqn. methods 8-57090
- elastic and acoustic wave equations, absorbing boundary conditions 8-59320
- elastic inextensible material, uniqueness of displacement boundary-value problem 8-54195
- elastic problems for cracks, seepage problems, by direct variational method 8-83331
- elastic waves at frictional boundary, transmission (reflection), approx. anal. method 8-63371
- elasticity, mixed boundary-value problems, orthogonal polynomial solns. 8-54193
- elastohydrodynamic contact optimisation 8-79288
- electric and magnetic fields, 2D open boundary problems, finite element anal. 8-94354
- electrode surface, partially covered, eqns. for chronopotentiometry 8-85236
- electromagnetic scatt., time depend., boundary value formulation, integro-differential eqns. 8-66726
- elliptic, second order, weak hybrid finite element methods, appl. to Dirichlet problem 8-73835
- elliptic problems, representations of first variations, appl. to optimisation and sensitivity anal. 8-77674
- EM field of a homogeneous sphere in an infinite medium, mode decomposition 8-81864
- EM stationary rotationally symm. field representation by superimposing circular aperture and ring fields (*German*) 8-55277
- equivalence of direct and indirect boundary element methods 8-81814
- Euler equations, solid-body boundary conditions, numerical implementation 8-90814
- extremum principles for linear initial and mixed boundary value problems of math. phys. 8-49637
- Feller eqn., generalised, boundary condition solns. 8-62167
- fibre-reinforced composite, quasi-one-dimens. thermal diffusion, mixture theory 8-71271
- finite difference calc., campylotropic coords. for boundary value problems 8-65757
- flow, creeping, about sphere, general soln. of linear Navier-Stokes eqn. 8-71307
- flow, three-dimensional region elliptic transformation 8-55624
- fluid mechanics, boundary element methods versus finite elements 8-73860
- foundation dynamic interaction with viscoelastic half-space (*German*) 8-79228
- Fourier analysis of difference schemes for Laplace eqn. in rot. symm. system 8-77677
- free edge stress fields, in composite laminates 8-67039
- freezing, multidimensional problems in arbitrary domains, numerical method 8-90693
- generalised biharmonic eqn., appl. to hydrodynamic stability using homogeneous boundary conditions 8-90834
- geodesy, boundary value problem from telluroid definition 8-65171
- geodesy, linear boundary value problem and three-dimensional geodesic mapping eqns. (*German*) 8-73304
- geodesy, results from Molodensky's problem in gravity space 8-65173
- geodesy, three dimensional, datum problem rel. to boundary value problem 8-61310
- geodetic boundary-value problem, variational formulation 8-92772
- groundwater two-dimensional unconfined saturated flow, boundary integral solns. 8-77291
- heat and electrical transfer differential eqns. 8-67004
- heat conduction, inverse nonlinear problems, simulation methods 8-94513
- heat conduction, inverse problem, Fourier eqn. Runge-Kutta integration 8-89417
- heat conduction in nonuniform media, boundary-value problems 8-63266
- heat conduction inverse boundary-value problems, finite difference method 8-63263
- heat conduction transient, two-dimens., crit. time step for finite element solns. 8-71260

boundary-value problems continued

- heat conductivity eqns., soln. of boundary value problems by Green's function method (*Russian*) 8-63267
- heat equation involving moving phase boundaries, analytic soln. 8-90694
- heat exchange in complex domains, new soln. techniques 8-94509
- heat transfer, finite element method of calculation (*Japanese*) 8-89414
- heat transfer, laminar, convective, in rectangular channel, for 3rd kind temp. boundary conditions 8-87341
- infinite hollow cylinder with external crack, boundary value problem 8-90712
- infinite solid, elliptical crack under shear 8-75096
- ingot, hollow cylindrical, temp. field and crystallisation front calc. (*Russian*) 8-63690
- integral eqns., numerical soln. to multi-part mixed problems 8-62056
- internal waves at surface between two fluids, velocity potentials for singularities 8-90926
- inverse scattering method for nonlinear evolution eqns. under nonvanishing conditions 8-57808
- Josephson junction, in inhomogeneous field (*Russian*) 8-84350
- Kirchhoff plates, matrix displacement method with parameter transformation by additional compatibility postulation (*German*) 8-79202
- linear differential eqns., fourth order, finite difference formulae for boundary value problems 8-73856
- linear hyperbolic mixed boundary value problem, soln. existence, uniqueness, hydraulics appl. (*German*) 8-93514
- linear transport eqn., asymptotic theory for small mean free paths 8-70078
- linear two-point, with non-separable boundary conditions, reduction to Cauchy systems 8-54158
- magnetic field calc., two-dimens., boundary integral eqn. method 8-94355
- magnetic fields, finite element and finite difference anal. 8-94353
- magneto-elasto dynamics, mixed initial and boundary value problems, vibr. circular plate in mag. field 8-67034
- materials with memory, linear theory of heat cond., final value problem, existence, uniqueness theorems 8-59266
- maximal variational principle for transport theory 8-62166
- Maxwell's eqns., Ewald-Oseen extinction theorem 8-62974
- melting/freezing interface, annular region, perturbation soln. 8-59286
- metallic media, varying loads, elevated temp. inelastic anal. using state variable theories 8-83264
- MHD generator, simplest physical model 8-71548
- MHD laminar convective heat transfer in circ. duct, for 3rd kind temp. boundary conditions 8-87342
- micropolar elasticity theory, uniqueness of 2-D boundary value problems 8-54192
- micropolar fluid with stretch, convection, appl. to Earth mantle 8-51202
- microstrip anisotropic electrostatic field problems, Green's function technique 8-70998
- mixed boundary value problems for Helmholtz eqn., integral eqn. method 8-57751
- mixture, binary, time-depend. solidification, series soln. 8-75058
- nonhomogeneous elastic layer bonded to nonhomogeneous half-space, torsion by circular die 8-87263
- nonlinear heat conduction problems, soln. construction procedure, Kantorovich method 8-59264
- nonlinear reaction-diffusion models for interacting populations 8-65886
- nonlinear singular perturbation problem on a semi-infinite interval 8-94631
- nonlinear wave eqns. in n-dimensional space, periodic solns. 8-93540
- nonlinear waves in dissipative or dispersive media 8-49672
- numerical soln. through integral eqns., review 8-81808
- open resonator with cylindrical confocal mirrors, plane EM wave excitation (*Ukrainian*) 8-55280
- parabolic boundary value problem optimal control, heating process 8-67021
- patch test for nonconforming finite elements, conditions for piecewise polynomial functions 8-77697
- periodic surface scatt., existence theorems (*Russian*) 8-73890
- Petrov-Galerkin finite element method, boundary layer behaviour 8-69989
- piezoelectricity, linear transversely isotropic media, normal mode response, boundary effects 8-52441
- planar body, with circ. boundary and thermally insulated cracks, temp. distrib. 8-67002
- plane elastostatics, boundary value problems, spectra of integral operators 8-57782
- plasma, MHD turbulence, three-dimens. soln. in cylindrical geometry 8-67351
- plastic flow, plane strain and axially symm. problems 8-51089
- plastic flow theory, spatial problems 8-51088
- plate, completely free, rectangular, free vibr. analysis by method of superposition 8-83300
- plate, thick, containing eccentric spherical cavity, transverse bending stresses 8-63288
- plates, rectangular thin, effect of different edge flexibility coeffs. on transverse vibrs. 8-83294
- Poiseuille flow, at large Reynolds numbers, Navier-Stokes eqn. soln. (*Russian*) 8-59364
- Poisson equation over complex domain, finite difference method, Neumann boundary conditions 8-79189
- porous catalyst pellets, singular perturbation anal. of boundary value problems modelling reactions 8-76906
- pulsating turbulent flow onto elastic surface, finite difference method (*Russian*) 8-75153
- quantum statistical mechanics (*Rumanian*) 8-86219
- radiation problem simplified boundary elements 8-86226
- reaction of continuous dynamic systems with complex form under time-space random fields 8-65767
- rigid wall-hot gas stream interaction, heat cond. eqns. soln. 8-79194
- rivers, pollutant dispersion, boundary conditions effect 8-85611
- rod, expanding, conductive heat transfer computation, fast numerical technique 8-75029
- rotating flexible rods, unstable vibration and buckling 8-79242
- Saint-Venant torsion problem, classical, integral and functional eqns. 8-57780

boundary-value problems continued

- saturated porous medium, completely confined, onset of thermal convection 8-83387
- Schrodinger operator spectrum with damped oscill. pots. 8-77748
- Schwinger-DeWitt expansion, boundary terms, flat space results 8-77815
- semishadow field diffraction, boundary wave uniform asymptotics (*Ukrainian*) 8-89350
- shell, spherical, with conical nozzle, thermal stress anal. 8-79204
- shells, two-dimensional eqn. system (*Ukrainian*) 8-89342
- shells of revolution, thin-walled, heated, temp. field, thermostatic control 8-67003
- shock layer, hypersonic, vibr. nonequilib., near stagnation streamline, low Reynolds no. flow 8-87417
- shock tube boundary-value problem global soln. (*French*) 8-63449
- sine-Gordon eqn., Goursat and Cauchy problems 8-77682
- singular nonlinear differential eqns., boundary layer flow 8-63413
- solar evolving force-free magnetic fields, variational formulation 8-93182
- solid, crystalline, finite strain, uniqueness criteria and minimum principles 8-51086
- spatial problems of rigid plastic equilib. 8-55569
- spreading resistance calculations, role of source boundary conditions 8-89499
- stability and convergence 8-90827
- Stefan and dam problems, free boundary convexity 8-83356
- Stefan problem simulation and control, associated variational inequality 8-67009
- stratified shear flow, with nonlinear crit. layer, approx. soln. 8-79357
- structural anal., soln. by orthogonal collocation 8-51063
- structural panel, rectangular, with elastic edge constraints, dynamic response, Bolotin's asymptotic method 8-75091
- Sturm-Liouville, error estimation 8-81818
- supersonic wave drag of planar singularity distributions 8-83430
- temperature field, heat transfer problems, linear algebraic soln. method 8-59281
- thermal resistance minimisation, solid with heat-exchanging surfaces, variational method 8-94512
- thermoelasticity, linear, energy arguments 8-51067
- thermoelectric element, arbitrary shape, cooling efficiency 8-67010
- thermophysics, numerical solutions (*Russian*) 8-55545
- thin circular quadrant, singularly loaded, with clamped radial edges and free circular edge 8-63300
- transient radiation-conductive heat transfer in selectively-absorbing media 8-94572
- transonic flow, similar solns. 8-94762
- transport problem stationary, generalised, Laplace operator eigenfunction series soln. (*Russian*) 8-81931
- tube, circ., entrance region, mass transfer, asymptotic expansion soln. 8-87392
- two-dimensional crystal boundary, oscill. propag. 8-63924
- two-dimensional nonstationary Euler eqn. solution in time-dependent bounded domain (*Italian*) 8-69986
- two-point, statistical variant using Einstein-Fokker-Planck eqn. (*Russian*) 8-81924
- two-point boundary-value problems with eigenvalue parameter in boundary conditions 8-73830
- unclosed shells of revolution with inhomogeneous boundary conditions, two-dimensional statics (*Ukrainian*) 8-89341
- unconstrained variational statements 8-93518
- viscoelasticity, linear, exterior problem 8-71283
- viscoplasticity anal., boundary integral eqn. method (*French*) 8-90728
- viscous dissipation effect on heat transfer, circ. cylinder axisymmetric stagnation flow 8-51164

bowing see bending**brain**

see also neurophysiology

- acoustically dependent latency shifts of brain stem evoked response in man 8-85318
- alpha frequency rel. to head size, implications for brain wave model 8-69035
- cerebral blood flow computer for use in angiogram theatres 8-73227
- cerebral regional blood flow meas. with ^{133}Xe , functional landscapes in brain 8-85356
- cerebral regional O_2 distrib. model during continuous inhalation of $^{15}\text{O}_2$, C^{15}O and C^{15}O_2 8-65108
- complex visual stimuli representation 8-88709
- cortical periodic complex cells, cat, spatial freq. selectivity 8-69057
- electrical sources, human, 3D localisation, quantitative evaluation 8-92613
- epidural intracranial pressure meas. by piezoresist. transducer (*German*) 8-85404
- evoked potentials, processing, computer techniques 8-92728
- evoked potentials and EEG freq. in patients undergoing haemodialysis and kidney transplantation 8-61160
- glucose utilisation meas. by emission tomography 8-69183
- head injury model with viscoelastic brain tissue, mech. response 8-69117
- hippocampus pyramidal cells, somatostatin as excitatory transmitter 8-64973
- human brain functions rel. to foundations of physics, science and technology 8-73823
- hypothalamic neurone spontaneous firing over narrow temp. interval 8-56961
- impedograph, computerised 8-77139
- intracerebral currents, contribs. to EEG and evoked potentials 8-92611
- intracerebral spontaneous haematoma diagnosis and prognosis by computed tomography 8-73195
- intracranial pressure telemetric meas. (*German*) 8-85403
- magnetoencephalogram genesis mechanisms 8-53432
- magnetoencephalography, correl. with EEG for normals and patients 8-65062
- mammalian neuron connectivity estimate 8-77039
- murine brain rapid thermal fixation using microwave device 8-92689
- nonlinear constitutive relations for human brain tissue 8-80910
- optic tectum, IR and visual integration in rattlesnakes 8-69054
- skull-brain system, human, prolate spheroidal viscoelastic shell containing viscoelastic fluid, axisymm. vibrs. 8-80901

brain continued

- superior colliculus directional selectivity in hamster rel. to strobe-rearing and dark-rearing 8-69052
- synaptic vesicle ion content determ. by PIXE 8-61166
- vision with moving eyes, microelectrode studies of single neurons (*German*) 8-53397
- visual cortex, critical period interaction, kitten 8-56972
- visual cortex functional specialisation of rhesus monkey 8-80873
- visual cortex receptive field organisation and spatial freq. characts. 8-69068
- visual cortical area 19 of cat, periodic complex cells 8-56974
- visual cortical neurone orientational prop. recovery and ocular motility in dark-reared kittens 8-53396
- visual cortical neurone reaction patterns to const. illum. 8-80871
- visual evoked cortical potentials in men during compression and saturation in He-O₂ 8-61173
- visual evoked potential evidence of adaptation to spatial Fourier components in humans 8-69051
- visual evoked potential to search in short-term memory, late components 8-61172
- O₂ partial pressure measurement with thin-layer polarographic probe, intracortical appl. (*German*) 8-85410

brain models

see also *neural nets*

- amygdaloid kindling phenomenon extended first approx. model 8-53378
- cognitron, feedback-type, self-organising neural network with associative memory 8-56962
- cortical spreading depression, math. model 8-80857
- injury, pulse loading effect 8-57029
- M-cells, logic cct. model to account for CNS inhibition features 8-64917
- memory model, optimal associative recall by an incomplete key 8-96039
- rhythmic activity generation models (*Dutch*) 8-73150
- scalp potentials, dipole layer model 8-77035
- self-excited wave medium with memory 8-77034
- third intracranial ventricle dynamic displacement detection 8-57035
- visual cortex neurones, rabbit, organisation of background activity 8-69044

brass

- anisotropic bend ductility in single phase alloys 8-60726
- bicrystal, α - β two-phase, plastic deform. and fracture 8-84898
- β -brass, cryst. struct., elastic consts., central force model 8-51637
- α -brass, single crystal, obstacle strength variation during stress relaxation 8-68723
- γ -brass type alloys, faulted defects, nature determ. by image matching technique 8-63777
- cold rolled, optical, X-ray and TEM exam. of deformation struct., and textures 8-88500
- cold worked, or heat treated, or recrystallised wire specimen, damping behaviour (*German*) 8-88489
- corrosion fatigue and stress corrosion cracking in ammoniacal soln. 8-64757
- crack opening displacement, rel. to flow stress 8-68810
- creep fracture of α - β phase, tensile tests 8-88531
- cyclic strain induced creep, relation between modes of stress and strain superposition 8-60733
- defect removal, obs. by positron annihilation 8-84677
- dislocation structure around crack tips in early stage of fatigue 8-60830
- drawability correlation with sheet metal texture 8-60683
- elastic constants, third order, from US velocity meas. 8-76687
- electroforming, study of process variables in the electromagnetic bulging of tubes 8-80582
- electron irradiated, defect production and interdiffusion 8-67739
- electronic momentum densities by two-dimensional angular correlation of annihilation radiation 8-91605
- fracture initiation and propagation during strip drawing 8-64663
- ion beam-produced surface Cu accumulation, ESCA obs. 8-52612
- isotropic plate, noncollinear three phonon interaction 8-66970
- lead brass, mechanical damping in terms of Granato-Lücke theory, comparison with unleaded brass and Cu₃Au 8-95772
- mechanical damping in terms of Granato-Lücke theory, comparison with Cu₃Au and lead brass 8-95772
- mechanical ratcheting, plastic theory 8-76702
- order-disorder transformation temperature effect on quench hardening 8-95745
- orientation change in (211) [111] single crystals during rolling (*Japanese*) 8-60712
- plastic, anisotropic hardening pot., stress/strain relation under combined axial load/torsion 8-52896
- quenched, secondary defect form. during ageing, TEM obs. for α -brass 8-88482
- reversible shape memory effect in β_1 -phase containing α -precipitates (*Japanese*) 8-60711
- sheet, in-plane stretching, limit strain meas. 8-80573
- sheet metal, texture heterogeneity, numerical simulation (*French*) 8-92274
- simulation of rolling and shear texture, using an adapted Taylor theory 8-52835
- steel, austenitic stainless, FCC, fractographic obs. of SCC 8-64786
- strain tempering by rapid heating and cooling of cold drawn wires (*Japanese*) 8-84863
- stress corrosion cracking of α -phase, X-ray study (*Czech*) 8-85043
- superplastic deform. rate rel. to flow stress, determ. methods 8-60709
- surface, contact ang. meas., aq. ethanol (glycerine) solns., 20-70°C 8-56025
- surface, heated, water droplet evaporation, heat transfer characts. 8-59269
- surface, Leidenfrost pt. of drops of water (Freons) (carbon tetrachloride) (chloroform), press. effect 8-87784
- textured thin specimens, fracture 8-60816
- vacancy form. enthalpy, determ. from threshold temp. for positron trapping in vacancies 8-80433
- water/brass interface leaky Rayleigh wave reflectivity loss meas. 8-59187
- wear and cutting surface against acrylic, epoxy and polyamide resins (*Japanese*) 8-56779

brass continued

- yielding of α - β brass two-phase bicrystals, activated slip systems 8-84911
- Al/brass/Al bimetal, three layers, formed by cold rolling, exam. of formation of intermetallic phases at interface 8-56658
- electrical resistivity, relax. time near order-disorder transition 8-87788
- Sn- α brass interface, heat flux rectification, rectification coefficient 8-76048

Bravais lattice see *crystal atomic structure*

brazing bonding see *brazing*

brazing

see also *soldering*

- filler metal, deformation mechanism at brazed joint 8-80616
- particle beam accelerator grid assemblies, 120 keV, fabrication and brazing 8-66379
- TiB₂-Al₂O₃, thermal stability of composite materials 8-60638
- TiB₂-CaO, thermal stability of composite materials 8-60638
- TiB₂-MgO, thermal stability of composite materials 8-60638
- TiB₂-Y₂O₃, thermal stability of composite materials 8-60638
- ZnS/ZnSe composite window, erosion-resistant, fabrication and evaluation 8-71211

breakage see *fracture*

breakdown (electric) see *electric breakdown*

breakdown (mechanical) see *manufacturing processes*

breakdown diodes see *avalanche diodes; Zener diodes*

breeder reactors see *fission reactors*

bremsstrahlung

see also *electron radiation; gamma-ray spectra; gamma-rays; X-ray emission spectra; X-rays*

- afterglow discharge, electron-atom bremsstrahlung, time decay 8-63620
- betatron, 5 MeV, ang. distrib. and penetrating power 8-70657
- betatron bremsstrahlung field shaping apparatus for teletherapy 8-57062
- bulk media, shielding study, Monte Carlo anal. of thick target spectra 8-59839
- cascade showers, three-dimens., Landau-Pomeranchuk-Migdal effect 8-49993
- classical gravitational bremsstrahlung, wave generation 8-93093
- coherent bremsstrahlung from polarised electrons, asymmetry coeff. (*Russian*) 8-92139
- coherent EM radiation intensity, produced by modulated electron/ion beams in gas 8-50686
- computer program for calc. ang. distrib. of nonrelativistic bremsstrahlung intensity 8-87001
- dielectric trapping, bremsstrahlung shielding meas. 8-78507
- electron bremsstrahlung spectrum in point Coulomb field, classical and nonrelativistic quantum theory 8-65792
- electron neutral inverse bremsstrahlung in electron beam sustained discharge 8-63604
- electron-atom-bremsstrahlung standard radiometric source improvement 8-67484
- electron-ion bremsstrahlung with shielding 8-66667
- electron-ion plasma, stimulated bremsstrahlung light absorption (*Russian*) 8-87438
- electronic oscillations in relativistic plasma, hydrodynamic model (*Russian*) 8-79434
- energy spectra, 1 to 2000 keV, neutral atoms Z=2 to 92 8-62920
- fast-pulsed electron beam energy meas. using bremsstrahlung absorption spectroscopy 8-49940
- flow detectors, radiation type, electron bremsstrahlung irradi. field dia. calc. 8-56857
- free-free photoabsorpt. of electron-atom systems 8-62770
- gamma-rays generation by fast electrons travelling through antiferroelectric or antiferromagnetic crystalline structures 8-76545
- hadron multiprod., long-range correl., overlapping independent emission 8-82141
- Higgs boson, bremsstrahlung prod. with heavy fermion pair in e^-e^+ collisions 8-86449
- inverse bremsstrahlung, high energy, nucl. mag. contribs. 8-74350
- inverse bremsstrahlung absorption intensity depend., in inhomogeneous standing wave, laser fusion appls. 8-67382
- ion electron scatt., series expan. for intensity components 8-50648
- meson resonances in nuclear field (*Russian*) 8-78424
- monochromatic photon beam generation by high energy electron beam (*Japanese*) 8-74821
- neutron production by electron linear accelerator beam, bremsstrahlung and (γ ,n) processes (*Japanese*) 8-78532
- neutron star, neutrino-pair bremsstrahlung in hot plasma, strong mag. field 8-61878
- nucleon-nucleon bremsstrahlung expts. review, comparison of results with theory 8-62447
- PIXE trace element anal., new method to determ. concentrations 8-76966
- plasma, inverse bremsstrahlung for intense radn. fields 8-51288
- plasma, laser-produced, spherically symmetric absorption (reflection), simulation 8-51285
- plasma illuminated by strong optical field, electron stimulated bremsstrahlung 8-59623
- plasma spectrum, mag. field effects 8-67323
- quantum optics, phase relations, bremsstrahlung struct. (*Russian*) 8-74870
- reactor shielding materials, Pb and steel, 6 MeV γ penetration bremsstrahlung 8-58350
- relativistic electron collision with heavy ions 8-75376
- resonance absorption, in laser-produced plasma, X-ray bremsstrahlung emission obs. 8-59559
- Rochester cross section, bremsstrahlung study, soft photon region 8-62401
- solar flares fast electrons scatt. in atm., X-ray spectrum 8-77542
- stellar atmospheres, H₂⁻ and N₂⁻ free free absorpt. rel. to opacity 8-81610
- UHF nonequilibrium plasma diagnostics by atomic bremsstrahlung continuum 8-67483
- ultrarelativistic charge collision with atom or diatomic mol., X-ray emission (*Russian*) 8-70776
- universality of multiplicity distrib., hadronic bremsstrahlung 8-70419
- water, distrib. in water, Al, Fe and Pb, 22 MeV electron bombardment 8-59840

bremsstrahlung continued

- $e^+p \rightarrow e^+\gamma + X$, deep-inelastic bremsstrahlung, quark charges, colour gluon mass 8-74216
- NN bremsstrahlung amplitude, sensitivity of observables to short and intermediate distance wavefunctions 8-62449
- np, effects of nonminimal currents and role of various couplings 8-70394
- np bremsstrahlung at 200 MeV 8-66144
- $p+d \rightarrow p+d+\gamma$, 6.3 to 6.9 MeV, bremsstrahlung, cross-sections 8-62429
- pp, bremsstrahlung, field theoretic calc., treatment of OBE external emission processes 8-62451
- pp bremsstrahlung, bounds on external emission amplitude, cross section values 8-62450
- pp bremsstrahlung, ω radiative decay contrib. 8-70386
- pp bremsstrahlung, review of Low theorem soft photon approach 8-62452
- pp \rightarrow pX, bremsstrahlung model and recoil mass distrib. 8-70418
- pp \rightarrow ppy, 200 MeV, cross section meas., bremsstrahlung at small angles 8-62446
- pp \rightarrow ppy, 730 MeV, total and elastic cross sections for bremsstrahlung, Low theorem discussion 8-62448
- pp \rightarrow virtual gamma+hadrons soft bremsstrahlung, external emission dominance model 8-62430
- π^+p , 269 MeV, 298 MeV, bremsstrahlung cross-section and soft-photon theorem 8-89730
- Ag, spectral distrib. of X-ray braking radiation, due to electrons, calc. using Monte Carlo method 8-56538
- Al, 22 MeV electron bombardment, bremsstrahlung distrib. 8-59840
- Al bremsstrahlung, β generated, spectral shape depend. on target thickness 8-56545
- Al, surface, proton bombarded at 450 keV, X-ray bremsstrahlung, 2.5-8.5 keV 8-80436
- Ar, electron scatt., in laser radiation field, free-free cross sections meas. 8-74762
- Ar, electron scatt. in laser radiation field, free-free cross sections, reson. struct. 8-74763
- Ar, electron-atom bremsstrahlung continuum, afterglow decay (*German*) 8-83626
- Au, spectral distrib. of X-ray braking radiation, due to electrons, calc. using Monte Carlo method 8-56538
- ^{45}Ca , internal bremsstrahlung photon intensity and energy yield 8-86509
- Cu bremsstrahlung, β generated, spectral shape depend. on target thickness 8-56545
- Cu, spectral distrib. of X-ray braking radiation, due to electrons, calc. using Monte Carlo method 8-56538
- Fe, 22 MeV electron bombardment, bremsstrahlung distrib. 8-59840
- $^1\text{H}(\text{d},\text{d}\gamma)$ 6.3-7.1 MeV, bremsstrahlung anomaly near breakup threshold 8-89888
- ^3H conc. meas., scintillation detector appl., bremsstrahlung from β -rays 8-55042
- Ne, electron-atom bremsstrahlung continuum, afterglow decay (*German*) 8-83626
- Ne medium-pressure discharge, electron temp. radial profile meas. by electron-atom bremsstrahlung continuum 8-67497
- Pb, 22 MeV electron bombardment, bremsstrahlung distrib. 8-59840
- Pb, bremsstrahlung, β generated, spectral shape depend. on target thickness 8-56545
- pp bremsstrahlung, intermediate nucleon isobars contrib., relativistic model, nuclear force significance 8-93899
- ^{35}S , internal bremsstrahlung photon intensity and energy yield 8-86509
- Sn, bremsstrahlung, β generated, spectral shape depend. on target thickness 8-56545
- ^{90}Y internal bremsstrahlung, evidence for detour transitions in β -decay processes 8-66247

bridge circuits

see also bridge instruments

- AC, for ferromagnetic ring complex reluctivity meas. (*Russian*) 8-54412
- electrical temp. meas. methods and trends (*German*) 8-93681
- electromag. convertor, forming part of unbalanced bridge circuit, exam. of characts. 8-85100
- four-terminal meas. circuit stray-impedance errors 8-77940
- Kelvin bridge, link resistance compensation 8-86292
- p-n junctions capacitance meas., using analogue multiplication (*Bulgarian*) 8-57977
- RC double-balanced bridge analysis (*Polish*) 8-89498
- resistance thermometer, conductor resistance effect compensation using hexagonal bridge (*German*) 8-77910
- strain-gauge dynamometer, effect of temp. on characts. 8-93677
- temperature controller, based on Wheatstone bridge and thermistor, high precision 8-86258
- thermal conductivity of fluid meas., automatic Wheatstone bridge, theory 8-65933
- thermistor thermometer bridge network charact. linearisation (*German*) 8-86271
- thermoelectric thermometer cold junction thermo-EMF compensation, parameter optimisation (*Russian*) 8-86270
- Wheatstone bridge, optimisation of sensitivity 8-86298

bridge instruments

see also bridge circuits

- AC mutual inductance bridge using operational amplifiers, mag. susceptibility meas. 8-89508
- AC thermometry and DC heating circuitry in thermal props. meas. 8-74000
- automatic conductometer, exam. 8-56933
- crystal bridge for equivalent electrical parameters meas. of piezoelectric crystals 8-54404
- industrial resistance thermometers testing using incomplete bridge balancing technique 8-73998
- magnetic susceptibility meas., of Fe alloys, temp.-time instability (*Slovak*) 8-57989
- multi-bridge device, computerised, for capacitance and loss angle meas. (*Russian*) 8-70159
- mutual inductance bridge using operational amplifiers 8-54407
- off balance interferometric bridge, using heterodyne detection for recording vibratory phenomena 8-70119

bridge instruments continued

- plane shearing stress meas. with wired strain gauges (*German*) 8-89471
- RC double-balanced bridge analysis (*Polish*) 8-89498
- RF voltage standard, precision, using thermistor bridge, HF-UHF range 8-89504
- single-ended cavity resonator loaded Q-factor meas. using reflection bridge 8-54405
- small active resistance and inductance meas. AC bridge 8-86299
- thermometric AC bridge for temp. meas., 13.81-273.15K range (*Polish*) 8-93683
- Wheatstone bridge-using thermistors for temp. meas. in calorimeter, optimisation (*German*) 8-86275
- Wien oscillator, low-power, for low-temps. ~ 25 mK 8-93680

Bridgegram method see crystal growth from melt

brightness

see also sky brightness

- 1418+54, new violently variable BL Lacertae object, historical light curve 8-93410
- 1978 SB, asteroid, UBV photometry 8-96422
- 1978 SB, fast-moving object, discovery positions and magnitudes 8-93142
- Abell clusters of galaxies, Westerbork obs. rel. to radio and X-ray luminosity 8-96549
- atmosphere, brightness temps. vars. in H_2O 1.35 cm reson. region (*Russian*) 8-81403
- aureole around UV source at finite distance 8-77320
- aureole radiance field about point source in scatt.-absorbing medium 8-77319
- camera films, automatic exposure, theoretical anal. 8-86363
- cluster galaxies, luminosity function 8-54058
- clusters of galaxies, Bautz-Morgan classes and luminosity function 8-54057
- Comet Machholz (1978I), visual magnitude estimate (1978, September 19) 8-89126
- comets, monochromatic brightness var. 8-81590
- comets, monochromatic brightness vars. core-mantle model 8-81589
- compact galaxies, mean surface brightness and integral brightness relation 8-93412
- compact radio sources, brightness distrib. mapping from VLBI data 8-89266
- cumulus clouds, size and particles effects on satellite-observed reflected brightness 8-73510
- Cygnus Loop, 25 MHz brightness distrib. and total flux density 8-54027
- diamond, round brilliant cut, statistical assessment of brilliance and fire 8-90361
- diamond, round brilliant cut style modifications, brilliance, sparkliness and fire 8-90362
- diamond simulants, brilliance, sparkliness and fire 8-90363
- Fornax cluster of galaxies, bright members surface photometry 8-96548
- Galactic central IR surface brightness obs. by balloon (*Japanese*) 8-61925
- galaxies, bright, in Virgo cluster area, standard total magnitudes and mean errors 8-65685
- galaxies, elliptical, surface photometry 8-57625
- galaxies, low surface brightness, luminosity function, props. 8-96532
- galaxies, redshift-magnitude bands and evolution from Perseus and A1367 clusters obs. 8-54033
- galaxies in field of Abell 1781, photometric obs. 8-77609
- galaxy clusters, brightness spectrum and cosmic luminosity 8-81696
- generalised radiance uniqueness theorem 8-94365
- giant H II regions, radio maps interpretation 8-85994
- HZ Herculis, eclipsing binary, accretion disc brightness distrib. from optical light curve 8-65658
- high-power laser luminance contrast meas. 8-87055
- HVC 132+23-221, small high vel. H I cloud, brightness temp. struct. 8-89241
- image plane irradiance caused by the natural radiation of the objective lens 8-83068
- inhomogeneous source radiant intensity, averaged cross-spectral density concept 8-74958
- interstellar dark globules, IR surface brightness and emergent spectra 8-53999
- LED luminous intensity ang. distrib. and total light flux meas. device (*Chinese*) 8-82018
- light source measurement standard photometric system errors 8-58005
- lunar craters, brightness vars. during eclipses 8-61770
- Mars, integral photometry 8-61780
- meteors, luminous efficiency coeff. from photographic obs. 8-96440
- meteors, television photographs photometry and brightness curves 8-96441
- Moon, brightness at 2 and 6 cm wavelength, centre to limb var. 8-81572
- NGC 2742, spiral galaxy, luminosity and mass/light ratio (*French*) 8-89255
- NGC 4565, spiral galaxy, minor axis brightness profile rel. to massive halos problem 8-93409
- optical ceramic, KO-1, IR scatt. and brightness indicatrices meas. 8-71164
- Periodic Comet Ashbrook-Jackson (1977g), total visual magnitude estimates 8-93169
- Periodic Comet Comas Sola (1977n), total visual magnitude estimate, (1978, October 8) 8-96435
- Periodic Comet Wild 2, (1978b) magnitudes, (1978, February 8 to May 11) 8-53885
- photometric etalons, scatt. matrix and brightness coeffs. of MS-20, MS-14 reflectors 8-82020
- quasars, radio intensity and polarisation distrib. at three freqs. 8-96560
- radiation fields from polygonal sources, Fock method 8-83060
- radio galaxies, radio brightness distrib. obs. with RATAN-600 telescope 8-65698
- radio sources, brightness distrib. investigation via lunar occultations 8-65712
- radio sources, luminosity evolution rel. to source counts freq. depend. and spectral index distrib. 8-96554
- radio sources with short wave radio emission excess, flux densities and variability at 1.35 cm (*Russian*) 8-57666

brightness continued

- random nonGaussian backgrounds, simulation, calc. spatial correl. function 8-79089
 scalar wave fields of fluctuating primary planar sources, coherence and radiant intensity 8-90355
 sea ice, low-salinity, UHF and microwave brightness temps. meas. 8-81175
 Seyfert galaxies, X-ray luminosity function and variability time scale 8-57701
 Seyfert galaxies X-ray emission, luminosity function from Uhur obs. 8-93392
 solar brightness temperature near its minimum, meas. by balloon-borne lamellar-grating interferometer 8-85921
 solar granulation, morphological interpretation of spatial power spectrum 8-65581
 star magnitude simulator, IC device 8-81742
 sun companion star, visible or IR brightness prediction rel. to reality 8-57475
 Uranus, microwave brightness temp. increase 8-93150
 Venus IR brightness, limb darkening and thermal anomalies. obs. 8-85876
 vision, photopigment depletion effects 8-56977
 visual luminance difference threshold, Holladay's principle (*Japanese*) 8-65000
 X-ray sources, extragalactic, luminosity evolution rel. to detect. in deep surveys 8-96567
 zodiacal light brightness rel. to galaxies apparent magnitudes estimation (*Russian*) 8-93389
 H I regions, 21 cm line brightness temp. rel. to galactic shocks 8-54042
 H II regions, anisotropic, with axial symmetry, models and brightness distrib. 8-85993
 H II regions is IC 1795/1805, IR luminosity compared with exciting star total luminosity 8-96519

Brillouin scattering *see* **Brillouin spectra****Brillouin spectra**

- see also stimulated Brillouin scattering*
 cyclohexane-tetrachloromethane, heteromolecular vibr. relax. time, Rayleigh-Brillouin spectra 8-59731
 differential-type Brillouin scattering system, construction (*Japanese*) 8-89562
 ethanol, aq. soln., conc. fluctuations, shear and longit. relax., Brillouin scatt. and pulse techniques 8-71792
 ferromagnetic metallic glasses, Brillouin scattering 8-92085
 fluoride crystals, Brillouin scatt. and high temp. disorder 8-80365
 glass film on substrate, Brillouin scatt. from surface phonons, SAW vel. and attenuation 8-95587
 isotropic metals, theoretical anal. 8-80367
 laser-target interaction expt., backscattered light and harmonic generation, spectral anal. 8-59676
 lineshapes, oblique-incidence Brillouin scatt. by acoustic phonons 8-72534
 lithium ammonium tartrate monohydrate, in paraelec. phase, Brillouin scatt. 8-64373
 metal, light scatt. from surface acoustic phonons 8-76484
 methyl alcohol, liq., ratio of Brillouin to total light scatt. intensity 8-52515
 molecular crystal, orientationally disordered, translation-rot. dynamics, soft modes 8-83906
 nematic liquid crystals, hydrodynamic correlation functions, propagating modes 8-94988
 optical vacuum furnace for Raman and Brillouin spectroscopy 8-58062
 parametric interaction of EM and acoustic waves in solids, theory 8-60166
 plasma, Brillouin backscatt., nonlinear three-wave interaction 8-75356
 plasma, sidescatter threshold, non-resonant EM pump field modification 8-67362
 PMMA, oriented, hypersound propag., elastic props. 8-75737
 polymer, elasticity of bulk and film from multipass Brillouin spectra 8-76485
 polymer, liq., Brillouin scatt. and segmental motion, appl. to polypropylene glycol 8-91217
 resonant scattering, analogy to modulation spectroscopy (*Japanese*) 8-68526
 semiconductor, opaque, light scatt. from surface acoustic phonons 8-76484
 stimulated Brillouin backscatter from theta pinch 8-67359
 styrene, thermal polymerization, Rayleigh-Brillouin light scatt. study 8-53206
 superionics, with fluoride structure, Brillouin scattering and lattice defect energetics 8-80369
 water, liq., ratio of Brillouin to total light scatt. intensity 8-52515
 CS₂, liq., ratio of Brillouin to total light scatt. intensity 8-52515
 CdS, acoustic phonon intensity fluctuations after strong nonlinear amplification 8-59909
 CdS, bulk acoustic phonons, light scatt. from phonon-induced surface ripples 8-75924
 CdS, lattice attenuation meas. by US injection method 8-76480
 CdS, mode corrected TA phonons, reson. Brillouin scatt. 8-72535
 CdS, reson. scatt. of exciton-polaritons by acoustic phonons 8-60482
 CdS, two-phonon resonant Brillouin scatt. 8-84597
 CdS, reson. Brillouin scatt. by piezoelectrically inactive TA phonon domains 8-84593
 Cr (111) surface, acoustic phonons Brillouin scatt. data 8-95222
 Fe, thermal acoustic magnons, Brillouin scatt. meas. 8-95424
 Fe₈₀B₂₀, ferromagnetic metallic glasses, Brillouin scattering 8-92085
 Fe₄₀Ni₄₀P₁₀B₆, ferromagnetic metallic glasses, Brillouin scattering 8-92085
 GaAs, bulk acoustic phonons, light scatt. from phonon-induced surface ripples 8-75924
 GaAs, excitonic polariton reson. interaction with LA phonons 8-60481
 GaAs, phonon surface density, Brillouin elasto-optic cross section 8-72536
 H₂, Rayleigh-Brillouin spectrum at high densities 8-90189
 He, superfluid 8-59991
 KCN, Brillouin line width of phonons 8-80370
 KD₃(SeO₃)₂, central peak, soft acoustic shear mode, light scatt. study, isotope effects 8-52518

Brillouin spectra continued

- KH₂PO₄, dynamic central peak in ferroelectric phase 8-84538
 KH₂PO₄, soft branch Brillouin spectra, quasielastic central peak suppression by annealing 8-95588
 KH₂(SeO₃)₂, slightly deuterated, central peak obs. in Brillouin spectra 8-64374
 Li₂SO₄, molten, Brillouin spectra, refr. index meas., hypersonic vel. 8-68523
 NH₄Br, λ-type phase transition, Brillouin scattering 8-79725
 (NH₄)₂SO₄, Brillouin scatt. from room temp. to -70°C 8-52517
 NaNO₂, mechanism of order-disorder transition, opt. spectra 8-76403
 Ni, thermal acoustic magnons, Brillouin scatt. meas. 8-95424
 Pb₂Ge₂O₁₁, acoustic relax. assoc. with phase transition at hypersonic freq. 8-88267
 Pb₂Ge₂O₁₁, dynamic central peaks and phonon interactions near structural phase transitions 8-83903
 Pb₂MgNb₂O₉, diffuse phase transition, Brillouin scatt. and acoustic phonons 8-76401
 PbMoO₄, Brillouin spectra, photoelastic consts. and optical purity 8-60480
 PbMoO₄, molecular light scattering 8-72537
 Si film, hydrogenated amorphous, Brillouin scatt. 8-72538
 SnCl₂·2H₂O, protonic order-disorder transition, inelastic light scatt. obs. 8-68497
 SrTiO₃, dynamic central peaks and phonon interactions near structural phase transitions 8-83903
 ZnO, acoustic phonon intensity fluctuations after strong nonlinear amplification 8-59909

Brillouin zones*see also band structure*

- alkali metals, thermal properties and Gruneisen parameters, employing model pot. 8-71815
 anisotropic linear spin chain, two-magnon problem with arbitrary interaction radius 8-72320
 chemisorption on Ni (001), electronic struct., KKR model calcs. 8-56200
 diamond, electronic energy bands of diamond-type crystals, appl. of EHT method 8-87907
 FCC, BCC and SC crystals, electronic struct. tight binding model 8-84123
 graphite, electronic props., self consistent LCAO calc., point vacancy in 2-dimens. crystal 8-51932
 graphite, galvanomagnetic effects, trigonal warping of constant energy surfaces 8-87987
 Hume-Rothery alloys, magnetism 8-95417
 III-V semiconductors, effective mass, forbidden bandwidth and lattice constant relation (*Slovak*) 8-51879
 infinite crystal, surface states determ. by complex extension of tight binding 8-80032
 lattice dynamical properties, Brillouin zone summations, convergence 8-91384
 polymethylene chain, vibr. spectra, CH stretching region, struct. and assignments 8-70991
 transition metals, second series, electronic band Brillouin zone APW calc., electronic config. effects 8-51883
 Bi, band structure model parameters, deformation theory (*Russian*) 8-56067
 CdS_{1-x}Se_x, zone edge phonons 8-76475
 n-CdSnAs₂, optical absorption rel. to energy spectra (*Russian*) 8-75994
 Cu, angle-resolved photoemission, band struct. 8-95680
 Cu₂Ni_{1-x} solutions of KKR-CPA equations for paramagnetic alloys 8-95256
 GaAs-AlAs alternating monolayers, zone folding effects on phonons 8-72510
 Ga_{1-x}In_xP, zone edge phonons 8-76475
 Ge, electronic energy bands of diamond-type crystals, appl. of EHT method 8-87907
 Hg₂Cl₂ prototype phase, soft mode, inelastic neutron scattering, Raman effect 8-91411
 In₂Bi, de Haas-van Alphen effect 8-91594
 n-InSb, low temp., spin mag. moment in Brillouin zone (*Russian*) 8-56159
 K_{1-x}Rb_xBr, lattice dynamics on pseudo-crystal model 8-75762
 LiH (D), single crystals, electronic excitations, review (*Russian*) 8-72574
 N₂, solid, lattice dynamical calcs., use of anisotropic at.-at. pot. functions, α-γ transition 8-71811
 NaCl (100) face, angle-resolved photoemission 8-56567
 Ni, angle-resolved photoemission, band struct. 8-95680
 Ni, polarisation-dependent angle-resolved photoemission for band structure studies 8-95678
 Si, electronic energy bands of diamond-type crystals, appl. of EHT method 8-87907
 α-Sn, electronic energy bands of diamond-type crystals, appl. of EHT method 8-87907
 SnSe, electronic band struct. determ. 8-51890
 TiC, Shockley surface states and bonding 8-91739
 W, polarisation-dependent angle-resolved photoemission for band structure studies 8-95678

bristles *see* **fibres****brittle fracture***see also ductile-brittle transition; notch brittleness*

- δ, criterion for BCC single crystals. (*Russian*) 8-56732
 acoustic emission simulation by SiC grain brittle fracture and elastic sphere impact, freq. anal. 8-55504
 alkaline earth fluorides, crack propag., cryst. props. effects 8-75720
 amorphous mat., refraction of propagating crack by stress wave 8-92337
 asbestos fibre reinforced Portland cement analytical fracture resistance curve expression 8-76756
 biocompatible implants, developed for bone fracture prevention, development research criteria 8-77155
 bovine hip bone, compression tests, effect of specimen shape and size on mech. props. and fracture mode 8-69132
 brittle materials, diametral compressive stress considering Hertzian contact, fracture and tensile strength meas. (*Japanese*) 8-72946
 ceramics, fracture toughness, exam. of methods of enhancing, merits and limitations 8-60771
 circular disc under impact loading, fracture mech. 8-88514

brittle fracture continued

cleavage crack extension in brittle material, atomic structure discreteness effect 8-79281
 crack response to impact by caustics 8-56724
 crack system propagation, stability conditions 8-51131
 cracks, stability, propagation, fracture mech. (*Czech*) 8-79257
 Dacron, vascular substitute, exam. of tensile fracture behaviour 8-77157
 deformation instability, soln. to Griffin problem satisfying stability condition 8-63382
 diametral compression tests, tensile strength meas., appl. to biaxial stress fracture (*Japanese*) 8-72840
 ductile metals in liquid metal environments, embrittlement and brittle fracture, exam. 8-60766
 dynamic crack propagation and arrest 8-68758
 edge failures, influence on fracture data, method of correcting 8-83346
 energy criteria in rupture and fatigue (*French*) 8-90771
 epoxy resin, effect of environment on stability of cracking 8-95807
 equilibrium and kinetic aspects of brittle fracture 8-79271
 failure beyond linear elastic regime 8-67141
 fatigue crack growth, mechanisms 8-64703
 fibre reinforced alloys, anal. of fracture process and fibre strength, by Monte Carlo simulation (*Japanese*) 8-80634
 fibre reinforced composite, hybrid C and glass fibre, fracture energy 8-95801
 flat glass in vacuum, exam. of temp. dependence of microhardness and microstrength 8-88532
 float glass, exam. of dynamic fatigue 8-80631
 fracture mechanics, recent theoretical and experimental developments, review 8-60776
 friction in transition from plastic to brittle contact (*Russian*) 8-53000
 glass, strength test, biaxial, use of Weibull statistics 8-68798
 glass, tempered, spontaneous fracture due to NIS inclusions, exam. of behaviour mechanics 8-71294
 glass fibre epoxy cross-ply laminates, multiple transverse cracking 8-95800
 glass plates, effect of localized damage on energy losses, during impact by glass spheres 8-52973
 glass plates, fast crack propagation meas. continuous stress meas., new method 8-73009
 grain boundary, stress induced drift diffusion, appl. to creep and growth of grain boundary voids 8-72811
 grain size dependence 8-80651
 granodiorite, fracture under uniaxial compression, mech. and AE meas. (*Japanese*) 8-56748
 graphite, diametral compressive strength, comparison with uniaxial tensile strength (*Japanese*) 8-72947
 growth dynamics, crack vel. meas. using evaporated thin conducting film 8-83347
 Hastelloy X, relations between weld heat affected zone cracking and microstruct., Gleeble test (*Japanese*) 8-52858
 Haversian bone, exam. of mechanical failure at microstructural level 8-77080
 hot-pressed with crystn. grain boundary phases 8-95716
 ice, rupture mechanism exam. (*German*) 8-52976
 impact damage in elastic response regime 8-71785
 impact fracture in elastoplastic regime 8-51133
 Inconel 706 and 718, relations between weld heat affected zone cracking and microstruct., Gleeble test (*Japanese*) 8-52858
 initiation by ductile tearing 8-64656
 interaction between cracks positioned at an angle, anal. 8-83871
 ionic crystal, exposed to high-current electron beam pulses, min. size of excited region for crack initiation (*Russian*) 8-84961
 laminates, fracture, effect of adhesive layers 8-90791
 limiting stresses for brittle body with elliptical hole with edge cracks, diag. construction (*Russian*) 8-55600
 line crack subject to shear 8-79268
 marble, Italian Ondagata, diametral compressive strength, comparison with uniaxial tensile strength (*Japanese*) 8-72947
 material with heterogeneous struct., fracture mechanism 8-67127
 materials testing under biaxial normal stress 8-68869
 micro and macro fracture mechanics, exam. of brittle fracture and fatigue crack growth 8-60774
 modulus of brittleness, crit. tensile span 8-92318
 monolithic component glasses and rigid sintered fibre-optic elements, microcrack form. during grinding 8-87175
 nonlinear lattice theory 8-67138
 one-dimensional chain, thermal fluctuation induced rupture, computer simulation 8-91378
 overlapping interacting cracks 8-55593
 PMMA, amorphous, structural cause of orientation modification, exam. 8-67664
 PMMA, brittle fracture initiation characts., under biaxial loading, exam. 8-60803
 PMMA, destructive mech. cracks, electron microscope exam. of generation centres 8-68782
 PMMA, fracture toughness under biaxial stress 8-76760
 PMMA, influence of craze configuration on fracture 8-76758
 PMMA, kinetic theory of quasi-brittle fracture (*German*) 8-84991
 PMMA, light absorption, laser crack development 8-68780
 PMMA, optical interference meas. of critical crack tip displacements 8-84964
 PMMA, overlapping skew-parallel crack dynamic propag. and arrest meas., method of caustics 8-84962
 PMMA, rain erosion behaviour, exam. 8-53001
 PMMA, stability of cracking, effect of environment 8-95806
 PMMA, stability of cracking, effect of environment 8-95807
 PMMA based composite (acrylic bone cement), effect of BaSO₄ and glass particle dispersions, on fracture behaviour 8-76753
 PMMA/PVC, cracking in layered composites 8-95808
 polycarbonate, impact behaviour, effects of thermal pre-treatment and mol. wt. 8-95798
 polyethylene, effect of pressure and environment on fracture and yield 8-76757
 polyethylene, high density, environmental stress cracking and morphology 8-68834
 polyoxymethylene, effect of pressure and environment on fracture and yield 8-76757
 polypropylene, crystalline, morphological aspects of crack growth 8-76761

brittle fracture continued

polypropylene, effect of pressure and environment on fracture and yield 8-76757
 polystyrene, amorphous, structural cause of orientation modification, exam. 8-67664
 polystyrene, effect of pressure and environment on fracture and yield 8-76757
 porcelain enamel layers on steel, H₂ induced fracture of layers 8-76752
 pressure vessel, strength analysis, by thermal shock 8-68819
 pressure vessels, brittle fracture probability using reactor surveillance capsule data 8-80641
 pressure vessels, unconditioned probability of brittle fracture 8-78479
 PVC, optical interference meas. of critical crack tip displacements 8-84964
 PVC rigid plate specimens, Charpy impacted, SEM exam. of fracture surface (*Japanese*) 8-52953
 reactor pressure vessel material, radiation embrittlement, current regulation assessment 8-52966
 rock, anisotropic, chip form. 8-61407
 rocks, failure processes and AE under compression (*Japanese*) 8-56749
 S glass-Ni sphere composite, exam. of crack shape and fracture toughness 8-72886
 stability loss near crack 8-55597
 stability problem, three-dimensional linearised theory (*Russian*) 8-55606
 stainless steel brittle fracture resistance improvement by N content reduction 8-95788
 statistical anal., evaluation of a fundamental approach 8-64619
 statistical theory, fracture of brittle solids, under multiaxial stresses (*Japanese*) 8-90788
 steatite, ceramic, exam. of thermal damage by strength meas. 8-84997
 steel, 12Kh18N9T-TiB₂, eutectic alloy, high temp. props. 8-84931
 steel, alloy, Fe-Ni-Cr-Mo-V-C, HY130, effect of H₂ and impurities on brittle fracture, review 8-60765
 steel, alloy, high-temp. combined ht. treatment and mech. working, C content effects (*Russian*) 8-52854
 steel, alloy, Ni-Cr-Mn, type 4340 intergranular brittle fracture, exam. by impact testing and Auger spectroscopy 8-52978
 steel, austenitic stainless, temper embrittled, type 304, Auger spectroscopic exam. of grain boundary surface phases 8-76741
 steel, cast, tendency to brittle fracture (*Russian*) 8-56735
 steel, constructional, fracture toughness in cyclic loading 8-72860
 steel, constructional, impact strength/brittle fracture relationship in ductile-brittle transition zone 8-56740
 steel, Cr-Mo-V, heat treatment and influence of cold plastic deform. 8-72858
 steel, fracture micromechanisms, fracture toughness, exam. 8-56766
 steel, fracture toughness, influence of low-cycle damage 8-72873
 steel, low alloy, cleavage fracture, fine scale precipitation dispersion effect, TEM obs. 8-60788
 steel, low alloys, high strength, stress corrosion cracking in saturated Ca(OH)₂ solns., due to Cl⁻ and SO₄²⁻ additions 8-88567
 steel, low C, martensitic, fracture toughness variations during tempering 8-60812
 steel, low S, ESR and electric arc, notch toughness, interaction between overheating and tempering temp. effects 8-52970
 steel, mild, type SM41, brittle fracture initiation characts., under biaxial loading, exam. 8-60803
 steel, Mn, H₂ embrittlement mechanism (*Korean*) 8-68774
 steel, pearlitic, brittle fracture of structures 8-72869
 steel, pearlitic eutectoid, cleavage fracture, grain size effect 8-60784
 steel, reactor vessel, neutron irradi. effect on brittle fracture characts. (*Slovak*) 8-50254
 steel, structural, brittle fracture, intermediate fracture stress, fracture initiation mode transition 8-60802
 steel, structural, rel. between static and dynamic fracture toughness 8-68815
 steel, structural, unalloyed, brittle fracture, grain size and precipitate thickness effect 8-60786
 steel, structural 8-68808
 steel, type 4340, effect of H₂ and impurities on brittle fracture, review 8-60765
 steel bearings, for gas turbines brittle fracture due to stress combination 8-56771
 steel structural components, flaw assessment based on cleavage fracture hypothesis 8-60804
 steel structures, appl. of risk analysis to brittle fracture and fatigue 8-56768
 strain energy density fracture criteria, extension to brittle and ductile fracture 8-75102
 strain intensity criterion for crack branching in brittle mats. 8-55592
 structure design, method of calculation 8-72869
 styrene-diene triblock copolymer, hexagonal struct., flow props. of melt and fracture 8-76729
 Tetron, vascular substitute, exam. of tensile fracture behaviour 8-77157
 thermoplastic, acrylic, hot stretched, aircraft cabin windows, exam. of anisotropic fracture 8-76763
 thermoplastics, glassy, embrittlement mech. and inelastic deform. criterion for delayed failure 8-52940
 transition metal carbides and nitrides, surface energy for brittle fracture from phonon frequencies 8-67790
 wood, rupture mechanism exam. (*German*) 8-52976
 Zircaloy-2, pressure tube, fragmentation on failure 8-72863
 Al alloys, fracture micromechanisms, fracture toughness, exam. 8-56766
 Al-epoxy adhesive systems, opening and edge-sliding fracture toughness 8-95805
 Al₂O₃, evaluation of crack resistance and crack velocity, using controlled fracture experiments 8-72881
 Al₂O₃ fracture resistance, exam. 8-76826
 Al₂O₃ on Al, anodic oxide film, effect of interface roughness on cracking 8-76755
 Al₂O₃, single crystal, fracture mirror formation, anisotropy of fracture surface energy and elastic constants 8-68824
 Al₂O₃/Nb/Al₂O₃ joint, solid state bonded, exam. of bond fracture strength 8-76826
 C fibres, Al coated, effect of annealing on ultimate tensile strength and fracture 8-56744

brittle fracture continued

- Cr-Cr-Ni-(P), hard alloys, sintered, fracture props., P addition effects 8-60610
 Cu, fracture criterion, expt. verification 8-64648
 Cu-Ni-Zn, microduplex, superplastic deform., cavitation and fracture 8-64640
 Fe based alloys, solute segregation to grain boundaries 8-72780
 Fe-C-Fe₂O₃, cleavage initiation by ductile tearing 8-64656
 Fe-Ni, brittle transgranular and intergranular fatigue crack growth rate, yield strength effect 8-68786
 Fe-Ni-Cr-Ti, superalloy A286, powder, exam. of microstruct. and mech. properties 8-52979
 Ir, impurity segregation to grain boundary effects 8-64637
 LiAlSiO₄ glass-ceramic, fracture phenomena as function of initial flaw size and temp. 8-95797
 Mo, single cryst., δ , criterion for brittle fracture (*Russian*) 8-56732
 NaCl, exposed to high-current electron beam pulses, min. size of excited region for crack initiation (*Russian*) 8-84961
 Na₂O-CaO glass tube, fracture by field assisted ion exchange 8-68771
 Na₂O-CaO-SiO₂, evaluation of crack resistance and crack velocity, using controlled fracture experiments 8-72881
 Na₂O-CaO-SiO₂, lifetime predictions, dependence on crack propag. eqns. 8-72882
 Na₂O-CaO-SiO₂, origins of acoustic emission in fracture 8-72889
 Na₂O-CaO-SiO₂, plates, exam. of Hertz crack branching 8-72887
 Na₂O-CaO-SiO₂ glass, crack nucleation around plastic indents 8-92327
 Na₂O-CaO-SiO₂ glass rods, prediction of thermal fatigue resist. 8-84955
 Ni₃Al, ductility in poly- and single crystals, compressive and tensile tests 8-56715
 Si, monocrystalline, effect of notch root radius on fracture behaviour 8-76751
 Si₃-Al-O-N₂, hot pressed, exam. of fracture mechanisms 8-72879
 SiC, hot pressed, brittle fracture and subcritical crack growth 8-72885
 SiC, meas. of critical stress intensity factor and subcritical crack propag. rates 8-72880
 Si₃N₄, exam. of fracture resistance 8-76826
 Si₃N₄, hot pressed, flawed plate under combined stresses, failure prediction 8-72884
 Si₃N₄, hot pressed, high temp. compressive cracking, optical and electron microscopy exam. 8-76733
 Si₃N₄, hot pressed, slow crack growth from controlled surface flaws 8-80632
 Si₃N₄, meas. of critical stress intensity factor and subcritical crack propag. rates 8-72880
 Si₃N₄, room temp. fracture strength data, statistical anal. 8-64619
 Si₃N₄, struct. of slow crack interface, light and electron microscope obs. 8-68770
 Si₃N₄/Zr joint, solid state bonded, exam. of bond fracture strength 8-76826
 Si₃N₄-Al₂O₃, hot-pressed with crystn. grain boundary phases 8-95716
 SiO₂, crack propag. and bifurcation 8-72888
 Ti-Al-Sn (5, 2.5 wt.%), electron microscope and X-ray diffr. exam., of basal and near basal hydrides 8-80550
 U, two-dimensional expt. fracture map 8-95803
 U-Mo (10 wt.%), gaseous O₂ and hydrogen embrittlement, exam. 8-60811
 W fibre reinforced Ni-Cr alloys, Ni, Co, Co alloys, and Ni alloys, effect of alloying on structural stability, mech. props. 8-56600
 WC-Co, comparison of indentation crack resistance, and fracture toughness 8-76739
 WC-Co alloys, brittle fracture, precision matching of mating fracture surfaces, by SEM fractographs 8-60807
 Zn, electrode, single crystal, fracture surface charge density effect 8-68787
 Zn, pure, polycrystalline, cleavage fracture, hydrostatic tension effect 8-52990
 Zn-Hg(Ga) metal/liquid metal, exam. of crack propag. in liquid metal environment 8-60766
 ZnS, hot pressed, water drop impact damage, SEM exam., IR transmission 8-88543
 ZrNb, pressure tube, fragmentation on failure 8-72863

brittle materials *see* **brittleness****brittleness**

- see also brittle fracture; embrittlement; hydrogen embrittlement; notch brittleness*
 abrasive brittle material, rating capability for elastic deformation 8-56680
 brittle circular disc under impact loading, fracture mech. 8-88514
 compressive strength of brittle material, statistical and micromech. theory 8-64618
 crack extension from flaws under compressive load 8-95812
 diametral compression test, considering Hertzian contact, fracture and tensile strength meas. (*Japanese*) 8-72946
 glass, flat, dependence of microbrittleness on SO₂ conc. 8-84960
 intergranular creep crack growth, diffusion controlled theory 8-84950
 metal, BCC, effect of screw dislocations on mech. props. (*Russian*) 8-60704
 modulus of brittleness, crit. tensile span 8-92318
 nonuniform triaxial compression of brittle materials, material strength gain, exam. 8-76725
 optimal structural design 8-79207
 particles, small, brittleness rel. to impossibility of comminution by compression 8-52709
 refractory metal alloy, heat resistance and cold brittleness, achievements and trends 8-95718
 steel, alloy, Cr-Mo-V-P, quenched, temper brittleness in relation to V and P concs. 8-52986
 steel, prestrained pressure vessel, correl. between dynamical toughness characteristics 8-68816
 strain rate depend. effect of specimen vol. on strength 8-90726
 thermal stress resistance parameters when subject to thermal stress fatigue 8-90787
 vitrocereamic-metal composite materials development, Spacelab appl., mech. props. (*French*) 8-92229
 Cr, optimum alloying with rare earth metals, Ti, Zr, Hf, Nb, Ta 8-68651
 Fe, Armco, screw dislocation effect on mech. props. (*Russian*) 8-60704

brittleness continued

- Fe-Cr alloy, impact strength, rel. to '475°C brittleness' (*Russian*) 8-92323
 Fe-Ni alloy, hot shortness (*Japanese*) 8-84998
 Na₂O-CaO-SiO₂ glass, crack nucleation around plastic indents 8-92327
 W-WC, activated sintering, mech. props. (*Korean*) 8-60622

broadband amplifiers *see* **wideband amplifiers****bromine**

- see also nuclei with*
 alkali metal chloride: F⁻(Br⁻)(I⁻), anion impurities substitution, energies of soln., association and migration 8-83831
 atom, diffusion coeff. in laminar flames 8-51272
 atom, photoelectron spectra, photoionisation cross-sections 8-90131
 benzene-Br₂ charge transfer complex, Raman spectra, bending modes, electronic excited states 8-56485
 fluoromethane+Br, isotope selective photobromination, using c.w. CO₂ laser irradi. in excess inert gas 8-76843
 intercalation process with graphite 8-63965
 lattice dynamics using simple bond charge model 8-55919
 liquid, neutron diffr., evaluation of effective pair pot. 8-75527
 liquid, struct., theory and computer simulation 8-59734
 liquid, struct., X-ray diffr. obs. 8-59733
 methanol-water soln., etching of GaP 8-68833
 molecular crystal, bond charge model, for lattice dynamics 8-79692
 molecule, B³Π_u⁺ state deactivation efficiency, temp. depend. 8-70869
 molecule, dissoci. attachment by 0.8 eV electrons 8-74776
 molecule, dissociative attachment of electrons 8-62931
 molecule, photodissoc., Br*(4²P_{1/2}) yield, wavelength depend., collisional release 8-64857
 in oceans, Cl and Br origin 8-65342
 solution in methyl alcohol InP substrate etching and polishing appl. (*Slovak*) 8-56576
 UV laser possible pumping by synchrotron radiation, NaCl:I(Br) luminesc. 8-66835
 AgCl:Br⁻, EPR of mobile electrons, mechanism for photoinduced decomposition 8-80219
 Br II levels, NF values meas. in Ne-Br₂ mixtures 8-62753
 Br⁻ adsorpt. on Au electrode, specular reflect. investig. 8-61047
 Br+Br, symmetric collisions, MO-2p π radiation anisotropy, quasimolecular nature 8-70924
 Br+Br₂, atom-exchange, rate and activation energy, trajectory model and pot. energy surface 8-64811
 Br+CO₂(HCl), quenching of 4²P_{1/2} state, vib. excitation, temp. depend. 8-58792
 Br+H₂, laser field interacting with collision dynamics, model system 8-62876
 Br+O₂→BrO+O₂, reaction rate constant, 200-360K 8-73024
 Br₂, air pollutant, spectroscopic analysis using scanning tunable dye laser 8-81362
 Br₂, optically pumped at 532 nm, lasing obs. in visible and near IR 8-63094
 Br₂-graphite systems, adsorbed and intercalated, EXAFS 8-72638
 Br₂+Ar, ergodic deactivation, anharmonic effects on transfer rate 8-82818
 Br₂+H, nonreactive scatt., long range anisotropic pot. determ. 8-66626
 Br₂+I(5²P_{1/2}), deactivation kinetics, time-resolved spectrosc. obs. 8-95916
 Br₂+I(5²P_{1/2}), deactivation kinetics, Br(4²P_{1/1}) prod., time-resolved spectrosc. obs. 8-95917
 Br₂+O₂, reaction with W surface, rate of reaction meas., gas flow experiment 8-92510
 Br₂+Sn, reactive scatt., ang. distrib. and time-of-flight spectra 8-64842
 BrF, B³Π(0⁺) states, collision-free lifetimes laser fluoresc. obs. 8-94278
 Br*(4²P_{1/2}) yield, in Br₂(IBr) photodissoc., wavelength depend., collisional release 8-64857
 Br(4²P_{1/2})+N₂O, electronic-vibr. energy transfer obs. 8-55220
 H+Br₂→HBr+Br, pot. energy surface, ab initio generalised valence bond calc. 8-73026
 KCl:Br, colouration under two-photon excitation, absorption spectra 8-84618
 Ne-Br₂ mixture, at. state densities of Ne I levels, NF values of Br II levels 8-62753
 ZnS:Cu, Br based electroluminesc. cells, light, const. field effects on electroluminesc. 8-84658

bromine compounds

- ESCA chemical shift, indirect evaluation of Coulombic contribution to ionis. pots. for nonbonding electrons 8-92572
 ESCA using Au M₄ X-rays (2123 eV) 8-72683
 ethylene+Cl₂(Br₂) complex, intermolecular interaction and struct. SCF-MO-LCAO CNDO/2 calc. 8-58763
 organic π - σ complexes, low freq. spectra 8-78713
 BrCN, general quartic force field, Machina-Overend parameters 8-50532
 BrCN+Ar(N), CN quartet state production, fluoresc. anal. 8-68888
 BrCl, elec. dipole moment, Stark effect meas. 8-90211
 BrCl, excited B³Π(0⁺) state, excitation spectra and predissoc. 8-66593
 BrCl, excited B³Π(0⁺) state, laser-induced fluoresc., steady-state kinetics 8-66594
 BrCl, time-resolved fluoresc. of a³Π₀⁺ state 8-63093
 BrF, predissociation in B³Π(0⁺) state 8-66591
 BrF, stable levels of B³Π(0⁺) state 8-66592
 BrF₃, excited vibr. states, microwave spectrum, rot. const. determ. 8-94237
⁷⁹BrF₆, radical, prep. and EPR comparison with other hexafluoride radicals 8-68381
 BrO+O→Br+O₂, reaction rate constant, 200-360K 8-73024
 BrO₃⁻ in NaClO₃, Raman spectra, fundamental vibr. modes 8-78711
 BrO₃⁻+H₂SO₄+gallic acid system, uncatalysed oscillatory chemical reactions 8-61004
 BrONO₂, stratospheric photolysis, UV and IR spectra 8-53227
 KBr, effect of addition on corrosion of Cu in seawater 8-80670

Brownian motion

- see also colloids*
 anharmonic Brownian oscillator, canonical correlation function based on projection operator technique 8-55926

Brownian motion continued

- charged particles, Brownian motion, long and short range correl. 8-62155
- colloidal systems, stochastic transport eqns. 8-93609
- diffusion equation, derivation from Fokker Planck equation using perturbation methods 8-54117
- diffusion of interacting Brownian particles suspended in fluid 8-54304
- discovery of phenomena, historical review for teachers 8-86090
- EPR and saturation transfer EPR, fast computation, perturbation approx. extension for overmodulation 8-82754
- Feynman path integrals, white noise approx., inertialess Brownian system 8-57859
- Fokker-Planck approach to Brownian rotation 8-62160
- Fokker-Planck equation, systematic soln. for high-friction case 8-49767
- friction coefficient, freq.-depend., spherical Brownian particle in fluid near crit. pt. 8-73929
- heavy particle, quantum Brownian motion, adiabatic expansion 8-49768
- ionic crystal, Brownian sublattice, microscopic theory 8-79681
- Kramer's rate formula 8-83992
- Langevin equation solution, using Wiener's method (*Korean*) 8-49766
- light scattering, correlations for interacting Brownian particles 8-82911
- liquid crystal, uniaxial, polarised fluoresc. emission, orientational distrib. function, rot. Brownian motion 8-80390
- magnetic Brownian particles, theory of Mossbauer effect (*Russian*) 8-68436
- molecular excited states, absorption spectrum, diffusion rot. effects (*Russian*) 8-74641
- multiphase flow diffusion equations 8-94801
- multiple light scattering, Brownian polymer particles in water 8-78912
- multiple light scattering, depolarisation ratio and linewidths 8-78913
- N-particle system, Brownian dynamics with hydrodynamic interactions 8-91209
- nonlinear, and formation of macroscopic order, theory of instability 8-89408
- one-dimensional ionic conductors, cooperative diffusion and soliton Brownian motion 8-95177
- path integrals for inertial classical particles, Brownian motion between capacitor plates 8-57858
- polymer, uniaxial, fluoresc. polarisation, orientation and mol. dynamics effects 8-76516
- polymer chain, of bistable oscillators, Brownian dynamics of transitions 8-86983
- repeated-ring kinetic theory, particle in fluid 8-59729
- revolving particles, solution of Fokker-Planck eqn. (*Russian*) 8-77802
- rod-like macromolecules in conc. soln., basic kinetic eqn. and appl. 8-67637
- sapphire single-crystal clocks and frequency standards 8-57915
- solvent, polar, spherical ion radius and limiting elec. cond. Brownian motion 8-95168
- superionic conductors, dynamic properties 8-79673
- Syton determination of size distribution of submicron particles in colloidal suspension, FODA 8-61057
- threshold-phase transition analogy 8-70081
- time-evolution of non-Markov processes 8-54305
- translational motion, appl. to differential cross-section calc., incoherent scattering of slow neutrons 8-75504
- viscous drag case, Monte Carlo simulation, for teachers 8-61984
- Si single-crystal clocks and frequency standards 8-57915

Brownian movement *see* **Brownian motion****brush discharges** *see* **brushes; discharges (electric)****brushes**

- electrical contacts, for homopolar generators, tests at high surface vels. and current densities 8-54964
- homopolar machine, pulse power current collection system, for fusion research 8-54949
- Cu-graphite starter brushes, effect of high velocities, current densities on wear, friction 8-88544

brushgear *see* **brushes****bubble chambers**

- electromagnetic shower photographs, for teachers' 8-65737
- event recognition by optical correl. (*German*) 8-70704
- film exposure for meas. by HPD 8-58553
- Gargamelle, neutrino physics history, theory and expt. 8-50027
- hybrid devices, recent developments 8-82584
- hybrid systems, characteristics, construction and use, book contrib. 8-82591
- hyperon bubble chamber 11.7 T solenoid 8-50435
- photographic recording feed mechanism 8-78564
- propane, charge particle multiplicity and charge exchange at 40 GeV/c (*Russian*) 8-55118
- signal-processing procedure for inter-image identification of particle tracks in bubble chambers 8-70727
- track extraction using single vidicon tube 8-82580
- track following, predictor-corrector technique 8-90044
- track rescue system for bubble chamber film meas. 8-70728
- track sensitive target expts., automatic film meas. 8-55105
- Ne+ π^- , 25 and 50 GeV, multiplicity of charged particles 8-62575

bubble nuclei *see* **nuclear density****bubble point** *see* **boiling point****bubble points** *see* **bubbles****bubbles***see also* **foams**

- acoustooptical effects in liquid containing gas bubbles 8-50994
- active nucleation site spatial distrib., bubble flow density 8-71267
- air bubble, in hydraulic oil, effect of diffusion on diameter change 8-90966
- blood oxygenator, O₂ transfer controlling factors 8-53568
- boiling, nucleate, subcooled, latent heat transport contrib. 8-75046
- boiling, Reynolds analogy, heat transfer 8-59277
- boiling and bubbling heat transfer under the conditions of free and forced convection 8-90637
- boiling mechanism during burnout phenomena in subcooled two-phase water flows 8-94529
- break-up in stagnant fluids 8-75182
- bubbly flows, simultaneous meas. of local liquid vel. and void fraction by gas laser, accuracy (*Japanese*) 8-67295

bubbles continued

- cavitating bubble model, numerical soln. 8-79347
- cavitation, acoustic, threshold conditions for onset 8-59433
- cavitation bubble collapse in water shock tube 8-67231
- cavitation bubbles, linear stability of growth or collapse, slightly viscous liquid 8-90947
- coalescence rate, ambient liq. viscoelasticity effect 8-67248
- condenser system, submerged, bubble pumped augmented natural convection 8-94535
- convective heat and mass exchange, Pe \leq 1000, in power-law liq. 8-55683
- drift flux field eqns. for churn turbulent bubble flow 8-94807
- dynamics and dissolution of bubbles in viscoelastic fluid 8-90970
- education, bubble cohesion in foam, binding energy calc. 8-61978
- ethyl ether-N₂, bubble homogeneous nucleation in gas-liq. soln., press., expt. and theory 8-91430
- fission gas, steady state behaviour in carbide fuels, modelling 8-78469
- fission gas, transfer between grain faces and edges in UO₂ 8-79815
- fission gas bubble distrib. in mixed oxide fast reactor fuel pin, anal. of TEM obs. 8-58358
- fission gas re-solution, comparison of single knock on and complete bubble destruction models 8-82455
- flashing adiabatic flows, calc. taking into account bubble separation freq. variation under forced flow 8-67258
- flotation of fine particles by group of bubbles, kinetics 8-53261
- flow boiling bubble population prediction, from gas bubble nucleation expts. 8-90696
- flow produced by uniform translation along cylinder vertical axis (*French*) 8-90967
- fluidised bed, nonuniform, force on fixed sphere, rising gas bubble force field 8-59476
- free gas concentration in liquids, rapid anal. by acoustic method 8-91041
- gas, capture by cryst. growing from melt, thermal cond. influence 8-79543
- gas sparged devices for viscous liq. systems, design, bubble size 8-83454
- gas-liquid flow, bubble size and density, void fraction, sifting method meas. (*Japanese*) 8-83462
- glacier structure and flow rel. to elongated air bubbles in ice (*Japanese*) 8-88861
- glass microbubbles, method for polishing bubbles into hemispheres 8-95869
- graphite, pyrolytic, numerical discussion of flaking mechanism from ion bombard. 8-52947
- growth, noncondensing gas-vap. injected into liquid 8-55553
- growth in slow formation regime of nucleate pool boiling 8-90687
- heat conduction, unsteady, in quarter plane, appl. to bubble growth 8-75045
- heat transfer controlled collapse in isothermal tube 8-90979
- homogeneous nucleation in gas-liq. soln., press., expt. and theory 8-91430
- hydrodynamic interaction with suspended solid particle, flotation dynamics 8-51221
- laser breakdown of liquid, dynamics of growth and pulsations 8-51226
- law of metastability, appl. to effect of mag. field on boiling liqs. 8-79199
- liquid, spontaneously evaporating, critical discharge from channel 8-59456
- liquid cavitation and droplet impact erosion, predictability of prototype machine from lab. tests 8-64723
- liquid-gas bubbles system, phase transition kinetics and kinetic eqns. 8-83933
- liquid-vapour critical flow, two-fluid model 8-90973
- liquid-vapour mixture, acoustic wave propag. 8-90972
- magnetic flowmeters, bubble noise effects on output signal, Na loop test 8-91038
- microstreaming influence on growth due to rectified diffusion in sound field 8-51232
- mixture, binary, nucleate boiling heat transfer, conc. depend. 8-87249
- motion in rotating liquid under residual gravity 8-55679
- motion under gravity in rotating fluid, differential equations of motion (*German*) 8-90918
- nonNewtonian lubricant, bubble behaviour 8-56786
- nuclear reactor transit time estimation coolant bubbles appl. 8-94067
- nucleate boiling, single bubble growth at wall, shape and departure 8-90647
- nucleate boiling bubble dynamics, calc. 8-90648
- polymer solution, Denn model 8-79343
- polymer solution, second-order fluid model 8-79344
- pool barbotage, heat transfer coeffs., high-speed cine-photography and oscillography 8-90982
- raise rate in nonuniform fluidised bed 8-67263
- saturated liquid, boiling onset, film boiling transition, crit. heat flux densities (*Russian*) 8-83234
- shock structure in a liquid containing gas bubbles with nonsteady inter-phase heat transfer 8-83424
- size distribution, changes due to interbubble gas diffusion 8-85204
- solidification interface in reduced gravity, bubble interactions 8-84787
- spherically symmetric flow stability 8-83456
- steam-generating tube, bubble/plug flow boiling regimes, elevated press., drift vel. and void fraction determs. 8-87379
- superheated binary liquid mixtures, homogeneous nucleation of bubbles 8-67818
- surface viscosities at high pressure gas-liquid interfaces 8-75907
- thermocapillary convection, unevenly heated liq. stream near gas bubble 8-59460
- transient boiling, bubble nucleation and growth instabilities 8-90649
- transient cavitation-free bubbles, threshold energy 8-75176
- two-phase flow patterns, high pressure water in heated four rod bundle 8-89938
- vapour, in immiscible liquid, collapse 8-94547
- vapour bubble with microlayer, universal growth relations 8-71266
- virtual mass coeff. by Blokh-Ginevskii method (*Russian*) 8-75186
- vitreous enamel, bubble struct. and flaw forecasting 8-53118
- vortex ring formation during large air bubble ascent in water 8-83410
- Al melt, exam. of H₂ bubble origin, using first bubble technique 8-85115
- Ar in PtSi after 20 to 160 keV sputtering, TEM and backscatt. spectrometry obs. 8-64435

bubbles continued

- Fe, cast, Mg treated, graphite modularisation by Mg gas bubbles 8-52867
 Fe, pig, liquid gas bubble form. at nozzles, acoustic exam. 8-52723
 H_2O , squeezed boiling, internal characts. 8-90655
 He blister formation in irradi. Mo, vacancy mutation to divacancies by He trapping 8-51601
 He, growth in Nb-Zr (1 wt.%), α -particle effects 8-67749
 He I, stable microscopic bubbles and evaporation-condensation resonance 8-91381
 He, in Nb-Zr (1%), He bubbles and voids with ringed images, SEM and TEM exam. 8-51529
 He, ion implanted in metals, statistical model of low temp. blister formation 8-67754
 He, liq., bubble formation mechanism, on surface of deformed crystal (*Russian*) 8-85066
 He-assisted, bubble nucleation computer simulation 8-86625
 ^4He , superfluid, superheating and bubble formation 8-56000
 Hg bubble motion with and without mag. field 8-91021
 hydrocarbon-water, emulsions, superheated, bubble nucleation 8-61056
 Na, liquid, local boiling behind local flow blockage, simulated LMFBR fuel subassembly 8-54842
 Na vapour condensation from rising bubble, effects of internal circulation velocity and noncondensable gas 8-50258
 Ni, irradiated, with He^+ bubble depth distrib. meas. by TEM and blister form. mech. 8-95088
 UO_2 , irradiated, spacing of intergranular fission gas bubbles 8-66340
 UO_2 , irradiated sample, 1000 to 2100K, swelling and fission gas obs. 8-78462
 UO_2 vapour condensation from rising bubble, effects of internal circulation velocity and noncondensable gas 8-50258
 $\text{UO}_2\text{-PuO}_2$, mixed oxide fast reactor-fuel pin, fission gas bubble distrib. 8-78459
 W, annealed wire, analytical determ. of K content of single bubbles 8-64909

buckling

- annular plate, algorithm for numerical soln. of critical buckling 8-83275
 axisymmetric buckling of a complete spherical shell under uniform external press. 8-83274
 bifurcation from rotationally invariant states 8-77671
 cantilever cones, buckling under external pressure, exptl. and numerical solns. 8-71287
 ceramics, brittle, post thermal buckling resistance, role of physical props. 8-64585
 channel, straight (buckled), two-dimens. flow, stability anal. 8-59490
 conical shells, axially compressed with edge constraint, elastic and plastic buckling 8-63341
 cylindrical elastic tubes, collapse and buckling under combined bending and pressure loads 8-83277
 cylindrical shell deform., effect of loading history on bifurcation (*Ukrainian*) 8-55578
 cylindrical shell with circumferential notch under axial compression, stability (*Polish*) 8-79239
 cylindrical shells, fluid-filled, vibr. and buckling under torsion 8-79253
 cylindrical shells with small curvature 8-67066
 diagonal braces in building frame, inelastic stability 8-75083
 director rod, elastic instability 8-63292
 flat plate, simply supported, uniaxial compression, secondary buckling anal. 8-55579
 flywheel, buckling and vibr. of rotating spoke, anal. 8-71288
 forced vibrations of freely supported continuous beam (*Rumanian*) 8-75085
 incremental deformations of initially stressed media with couple stresses 8-62077
 intertraced parallel structural columns, buckling loads 8-67064
 metal structures, inelastic anal. 8-70586
 nonconservative autonomous and nonautonomous systems, stability, energy approach 8-51097
 nonlinear elastic stability problems using a finite difference perturbation method 8-83273
 nonlinear post-buckling anal., perturbation approach to imperfect struts. and snap-buckling 8-79244
 nonlinear structural eigenvalue calcs., mode finding 8-51102
 nuclear reactor, coupled cores, calc. of buckling variation and neutron flux, Green's function method 8-74421
 plane frame struts., modified pot. energy approach to post-buckling anal. 8-83276
 plate, obliquely stiffened, subjected to uniform compression, buckling strength (*Japanese*) 8-67067
 plates and shallow shells, approx. methods for linear and nonlinear anal. 8-51101
 plates stiffened, large amplitude flexural vibrs. 8-83307
 pressure vessel, cylindrical, thin torispherical ends, expts. on buckling under internal pressure 8-90736
 prismatic plate assemblies, buckling and vibr. anal. with compact computer program 8-90737
 rectangular plates, orthotropic, buckling determ. using structure smoothing method (*German*) 8-87285
 reverse-buckling safety discs, release pressure 8-89489
 rotating flexible rods, unstable vibration and buckling 8-79242
 rotationally restrained orthotropic plates under uniaxial compression, buckling 8-67065
 shell, cylindrical, nonuniform axial edge load, thermal load, linear buckling 8-63345
 shell, integrally, stringer stiffened circ., cylindrical, buckling under axial compression 8-63346
 shells, truncated conical, thermal buckling, axisymmetric initial deflections 8-79240
 skew plates, simply supported, finite element anal. 8-59319
 steel, shell, circ. integrally stringer-stiffened, buckling under axial compression 8-63346
 steel beams, inelastic, mild, flexural behaviour and lateral buckling anal. under cyclic loads (*Japanese*) 8-87283
 stiffened plates, tests on interactive buckling 8-71286
 structural anal., soln. by orthogonal collocation 8-51063
 structures, computational method 8-63342
 structures with rotational degrees of freedom, large displacement-small strain anal. 8-89310

buckling continued

- superconducting coil, buckling, vibr., lateral constraint and damping effects 8-63344
 symmetric structures, optimal design against postbuckling collapse 8-51100
 tensioned sheet, with central opening, buckling behaviour and parametric reson. investigation 8-90759
 torispherical vessel heads, internally pressurised, elastic-plastic buckling 8-79241
 two-bar frame, eccentrically loaded, nonlinear stability anal. 8-63343
 yielding of plates with hardening and large deformations 8-59311
 Al alloy 7075-T6, buckling under axial compression on circ. integrally stringer-stiffened shell 8-63346

building

see also civil engineering; erection

- BWR power plant, construction experience 8-86673
 CANDU plant construction, Bruce nuclear power development, Ontario Hydro 8-86676
 conference, nuclear power plant construction, operation and development, Tokyo, Japan (Sept. 78) 8-86672
 embedded foundations, soil-structure interaction problem, spring method 8-79216
 environmental noise, study re. nuclear power plant construction 8-87194
 foundation dynamic interaction with viscoelastic half-space (*German*) 8-79228
 heat transfer, fundamentals in reln. to heating and cooling load calcs. 8-90628
 multistorey buildings, reduction of structure-borne sound levels by floors and walls (*German*) 8-94483
 noise insulation near airports 8-55508
 nuclear plant, FUGEN project, Japan, construction and start-up 8-86675
 nuclear power plant (*Korean*) 8-54819
 nuclear power plants, construction and engineering problems, layout aspects 8-86702
 partially buried, heat flux through soil, calc. (*German*) 8-55554
 Taipower, completion of first power plant, construction experience, test- ing and start-up 8-86674
 wind velocity gust factors, analytical approach 8-88897

bulk density *see density*

bulk diffusion *see diffusion in solids*

bundling *see packaging*

burning *see combustion*

burnout *see combustion*

burst noise *see random noise*

bushes *see bushings*

bushings

- HV, high vacuum, for cryogenic appl. 8-81977

BWT *see backward-wave tubes*

C invariance

- disconnected gauge groups and the global violation of charge conservation 8-78086
 electric charge conservation (*Russian*) 8-77739
 pp interactions, test of charge-conjugation invariance 8-66145
 $\pi^0 \rightarrow 3\gamma$, C-noninvariant decay 8-82203

cable insulation

see also insulating oils

- EHD pumping of cable oil 8-87414
 flameproof coating for PVC insulated cables, composition, tests (*Russian*) 8-68828
 polyethylene, elec. trees free radical ESR study 8-60393
 radiation resistance of cable insulating materials for nuclear power stations, expt. 8-59835
 solid dielectrics, treeing 8-80285

cable jointing

- optical fibre, joint and connector losses (*French*) 8-55464
 optical fibre fusion splices by discharge heating 8-75007
 optical fibre splicing techniques 8-79147

cables (electric)

- see also coaxial cables; submarine cables; superconducting cables; underground cables*
 magnetic fluid (cable coolant), natural convection heat transfer 8-94846
 polyethylene, electric cables, anal. of breaking strength distrib. (*Japanese*) 8-84921
 shielded cables, nonlinearities and multiple exposure anomalies at CASINO, MCCABE code verification 8-58502

CAD

- see also circuit CAD; computer-aided analysis; control system CAD; electric machine CAD; power system CAD*
 acoustic design, interior, based on digital meas. techniques (*Polish*) 8-59205
 air pollution density distrib., flow pattern in Tanabe area, Japan, numerical anal. (*Japanese*) 8-96289
 curved electron beam system with strong deceleration at collector region, optimisation 8-74106
 diffuse system design, optimum conditions, appl. to optical system 8-50886
 fusion reactor, TNS, electrical design costing 8-55014
 fusion reactor, Tokamak constant tension D-shaped coils, lateral support struct. 8-55013
 holographic optical element design using analogous lens model 8-58955
 inductive displacement-measuring system synthesis using CAD 8-73982
 ion extractor electrode CAD (*Japanese*) 8-86680
 IR sensor, spinning cryogenic, integrated thermal/structural/optical evaluations 8-82040
 lens, aspheric, stigmatic, for ruby or He-Ne laser (*Czech*) 8-55427
 lens design optimisation, Version 14 program 8-90488
 lens system design with extended depth of focus, Version 14 optimisation program 8-90489
 multislit spectrometer for the night airglow observation 8-73542
 optical design techniques, for desk and pocket calculators 8-71181
 optical system surfaces (*Russian*) 8-74963
 optical system with annular pupil, orthogonal polynomials, appl. to Fraunhofer diffr. 8-50714

CAD continued

- OTF calculation using gaussian quadrature, rel. to lens system design 8-90383
 sound system design aid, HP 97 program 8-75015
 strength of axisymmetric body, optimum shape calc., finite element technique 8-51060

cadmium

see also nuclei with

- anharmonic interactions, elastic X-ray scatt. 8-75755
 atom, 6^3P_1 level, relax. of alignment and population 8-70795
 atom, absolute photoabsorption. cross section, 40-250 eV 8-58613
 atom, absorption spectrum, simultaneous excitation of two electrons 8-58614
 atom, effective core potentials calcs. rel. to bond lengths and energies 8-66464
 atom, integral Compton scatt. cross sections, of γ -rays from K-shell electrons 8-58643
 atom, integral K-shell Compton scattering, cross-section, for 1250 keV photons 8-90128
 atom, photoionisation cross section, many-body perturbation theory, dipole length and vel. calc. 8-78674
 atom, quadrupole antishielding factors, Hartree-Fock perturbation theory 8-62723
 Auger electron spectra, electron impact excited, vap. and solid state differences 8-52603
 concentration in snow of Mt. Blanc rel. to air pollution 8-81258
 cover, effective energy cut-off determ., rel. to neutron flux meas. in high-temp. reactor 8-86573
 cyclotron reson., data inversion 8-91593
 determination, in atmosphere, flameless atomic absorpt. in particle size fractionated aerosols 8-69434
 determination, using modified flameless at. absorpt. spectrophotometer 8-82044
 determination in sea and fresh waters, interlaboratory comparison 8-81209
 differential cathode ray polarograph, exam., determination of Cd, Zn 8-56930
 discharge, low-pressure, high current, intensity in middle UV 8-50878
 discharge lamp, electrodeless, microwave excited, SIMPLEX optimisation 8-83061
 dislocation internal friction, orientation depend., for single crystals 8-52882
 electrodeposition on solid Cd or CdHg amalgam, rate, impedance meas. 8-52693
 electron density at nucleus, press. depend., Hartree SCF calcs. 8-56411
 electron radiation damage, determ. of threshold displacement energy 8-59837
 failure under hydrostatic press., kinetics 8-52944
 Fermi surface, strain depend., from US vel. oscills. 8-84133
 Fermi surface changes under uniaxial compression 8-51876
 gas laser LG-70, specification 8-74889
 grain size effect on acoustic emission generated during plastic deformation 8-80609
 Hall effect and elec. resist., temp. depend. 8-64030
 Hall plasma accelerator, using Cd vap. 8-71553
 hexagonal, temp. depend. anisotropy of phonon scatt. resist. 8-51967
 isotopic abundances in 28 meteorites and three terrestrial rocks 8-53891
 laser, 441.6 nm, positive column He-Cd discharge, excitation mechanism 8-58983
 laser CW oscillation, Cd^+ transitions in He-CdBr₂, He-CdCl₂ and He-CdI₂ discharges 8-50765
 photoelectron spectra, 4d spin-orbit splitting, crystal field and band-broadening effects, CNDO calcs. 8-76577
 polycrystalline, effect of strain rate on stress relaxation behaviour 8-72807
 positron annihilation rates, electron-electron and electron-positron correl. effects 8-76548
 positron-vacancy interactions, equilb. temp. depend. of positron annihilation 8-76547
 roadside soil and plants in Alexandria district, Egypt, contamination with Cd, Ni, Pb and Zn 8-81171
 single crystal, root-mean-square atom displacement, X-ray meas. 8-75624
 ultrafine particle, positron annihilation exam. 8-56542
 US attenuation of conduction electrons, shear waves calc. 8-91589
 US attenuation of conduction electrons calc. 8-91588
 AgCl: Cd^{2+} , EPR of mobile electrons, mechanism for photoinduced decomposition 8-80219
 Al alloys, 7075-T6, H₂ effects and Cd segregation to grain boundaries 8-84764
 Cd I, II, level crossing in gas laser, at. const. and collision cross sections determ. 8-50763
 Cd II lasing action, 441.6 nm, exam. of mechanism for power increase due to I addition, using He-Cd⁺ laser. 8-55344
 Cd, influence of source material and shape on sublimation props. 8-80474
 Cd-Ar low-pressure discharge column, energy balance obs. 8-67504
 Cd-palmitate (arachidate) multilayer struct., hopping rate, direct evaluation 8-88045
 Cd⁺, removal using Itaya-zeolite (Japanese) 8-95951
 CdS:Cd, Cu- or defect-compensated, optical ageing rel. to storage cond. 8-84247
 CdSe:Cd, Cu, photo-induced changes in absorpt. spectra 8-80382
 Cd^{*} excimer, fluoresc. band shape, decay rates 8-70866
 Cu₂O:Cd, dipolar and quadrupolar bound excitons, absorption spectrum (Russian) 8-92099
 Fe_{1-x}Cl₂:Cd_x, randomly disordered, tricrit. behaviour, light scatt. 8-68255
 Hd-Cd hollow cathode laser in mag. field, Cd II stimulated emission 8-79002
 He-Cd hollow cathode laser, laterally emitted light 8-66810
 He-Cd hollow cathode laser, upper level decay rate, mag. field tuning dip meas. 8-87043
 He-Cd II lasers, positive column, hollow cathode types, 4416 Å oscill. characts. (Japanese) 8-94392
 He-Cd laser, intensity fluctuations meas., comparison with 8-71087
 He-Cd⁺ laser, population densities of He excited states in positive column discharge 8-58989

cadmium continued

- He-Cd⁺ laser, upper and lower laser states population densities, simultaneous determ. 8-87042
 KBr:Ca, X-ray re-irradiation effects on Z₁ centres 8-75664
 (NH₄)₂SO₄:Cd⁺, ferroelec. transition, soft mode contrib., EPR obs. 8-72469
 NaCl:Cd²⁺, Z₄-like centre, absorpt. spectra obs. 8-76498
 Na₂O₅-P₂O₅:Cd²⁺, metaphosphate glass, absorpt. spectra of radiation products 8-64865
 Si:Cd, n⁺-n-n⁺ structure, photocond. lifetimes, deep level occupancy in exclusion region 8-72253
 Zn, electron radiation damage in HVEM, nature of defect clusters 8-59838
 ZnS:Cd, Raman spectra, impurity induced first order transitions 8-88310

cadmium alloys

see also cadmium compounds

- α -Ag-Cd, chemical interdiffusion and Kirkendall shifts 8-87829
 Ag-Cd (45 at.%), morphology and crystal struct. of stress-induced martensites 8-68693
 Ag-Cd (approx. 50 at.%), disordered hcp to ordered bcc transition, meas. of activation energy 8-72773
 Ag-Cd alloys, internally oxidised, thermal stability of CdO, exam. of particle coarsening 8-76789
 Al-Cd, containing low melting point inclusions, impact props., temp. depend. 8-60792
 Au-Ag-Cd, martensitic transformation, preceding struct. anomaly 8-68692
 Au-Cd (47.5 at.%), effect of cooling rates on stress-strain behaviour 8-76721
 Au₃Cd, sputtered epitaxial films, order-disorder reaction obs. 8-84092
 Bi-Cd-Sb, calc. of phase equilibria using thermodynamic values from different models 8-60646
 Cd-Ag, polycryst. quenched foil, the influence of Ag on the recovery spectrum 8-76661
 Cd-Ag, polycryst. wire, cold worked, resistivity changes 8-68827
 Cd-Hg, dil., anomalously high elec. field gradients below 0.05K 8-72442
 ω -Cd-Hg alloy, melt-growth, morphology of single crystals. 8-64464
 Cd-In diffusion into Pb_{1-x}Sn_xTe, changes in elec. props. 8-91348
 Cd-Pb-Bi-Sn system, ternary liq. alloys, thermodynamic props. 8-51701
 Cd-Zn, directionally solidified lamellar eutectics, specimen prep. for TEM (German, English) 8-95885
 Cd-Zn, polycryst. wire, cold worked, resistivity changes 8-68827
 Cd-Zn (Ag), annealed, work softened, exam. of crystallographic texture, hardness 8-80559
 Cd-Zn (up to 1.57 at.%), single cryst., precip. hardening, 77-300K 8-60675
 CdHg^{*}, metal vapour exciplex laser, stability criteria 8-66802
 Co-Cd, dil. alloy, impurity hyperfine interactions 8-84416
 Cu-Cd, electron work function, contact pot. difference meas. 8-80041
 Cu-Cd, magnetic susceptibility, comp. and temp. depend., melting effects 8-52202
 Cu-Cd alloy, CA 162, flat spring, mechanical props. in bending, stress relax. test, 23 to 232°C 8-72806
 Cu-Cd alloys obtained by electrolysis, struct. 8-91552
 Fe-Co-Cd, mag. hyperfine field at Cd site, TDPAC meas. 8-60363
 In-Cd, dil., elec. field gradient at Cd impurities, press. depend., TDPAC meas. 8-64302
 Li₂Cd_{1-x}In_x, optical props., struct., energy bands, interband transitions 8-72539
 Mg-Cd, complex energy band, I-depend. pseudopot. 8-84124
 Mg₂Cd, disordering under electron irradi. in electron microscope 8-83849
 Mg₂Cd, effect on order, of compression deformation 8-52924
 Na-Cd, liq., mag. susceptibility, diamagnetism 8-72326
 Ni-Cd, dil., ferromagnetic dynamic crit. exponent, hyperfine interaction vs. neutron scatt. expts. 8-84437
 Ni-Co-Cd alloys, electrodeposition from acetate bath 8-68637
 Sm₁₁Cd₄₅, cryst. struct. similarity with γ -brass and α -Mn clusters 8-75625

cadmium compounds

see also cadmium alloys

- arachidate monolayer, Ag(Au) substrate, reson. surface plasmon reflection 8-56536
 chalcogenides, electronic polarisabilities of ions 8-79559
 dialkylammonium cadmium chloride, soft modes, phase transitions 8-79723
 fluoperovskites, MCdF₃, nonlinear elastic behaviour, US velocity, 1 bar-3 kbar 8-59851
 halides, Mn activated, electron-phonon interaction, lattice vibr. effective energies (Russian) 8-59911
 p-n junction photovoltaic diode, appl. as IR detector 8-86330
 AgNO₃-TiNO₃-Cd(NO₃)₂-H₂O mixtures, Henry's law, excess free energy 8-68908
 Au-CdIn₂S₄, surface-barrier diodes, mech. of current flow 8-56228
 CEr₂S₆, spinel, crystal struct. (French) 8-91326
 (Cd,Tl,Ag)₂NO₃, mixed aq. solns., vapour press., 98.5°C, Brunauer-Emmett-Teller isotherms 8-51655
 Cd complex, (Cd[SC(CH₃)₂CH₂NH₂]₂CdCl₂)₂·2H₂O cryst. and mol. struct. 8-74787
 Cd-As-S chalcogenide glass system, prod. and acoustooptic props. (Russian) 8-63158
 Cd-Sb system, phase diagram, struct. and stability of phases (German) 8-60661
 Cd-Sb thin film prep. by vacuum deposition, elec. props. 8-92194
 Cd_{1-x}Ag_xCr₂Se₄, ferromag., magnetoresistance exam. (Russian) 8-84238
 CdAs₂, single crystals, growth from vapour phase 8-88416
 CdBr₂, vapour grown crystals, polytype formation, effect of mode and conditions of growth 8-72709
 CdBr₂, XPS, satellite of Br 4s line 8-56556
 CdBr₂:Fe²⁺(Co²⁺)(Ni²⁺), charge transfer near UV spectra, 4.2K, mag. circular dichroism 8-80378
 CdBr₂-BiBr₃, molten, elec. cond., 500-870K, composition depend. 8-55965
 CdBr₂(I₂), vapour growth crystals, decomposition, electron microscope study 8-92268
 CdBr₂·4H₂O, NMR, ¹¹³Cd nucl. mag. shielding 8-68395

cadmium compounds continued

- CdCO₃, NMR, ¹¹³Cd nucl. mag. shielding 8-68395
 CdCl₂, aq. soln., Raman spectrum, local order 8-84563
 CdCl₂, effective core potentials calcs. rel. to bond lengths and energies 8-66464
 CdCl₂, NMR, ¹¹³Cd nucl. mag. shielding 8-68395
 CdCl₂:Fe²⁺(Co²⁺)(Ni²⁺), charge transfer near UV spectra, 4.2K 8-80378
 CdCl₂-NaCl, KCl molten salt mixtures, US velocity and adiabatic compressibility obs. 8-75730
 CdCl₂(Br₂)(I₂), adsorption of NO, crit. and triple point temps. of first adsorbed layer 8-91548
 CdCr₂S₄ ferromag. semicond. film, props. 8-76175
 CdCr₂S₄, thermodyn. props. 8-51703
 CdCr₂S₄(Se₄), spin depend. phonon Raman scatt., band struct. 8-68491
 CdCr₂Se, ferromag. semicond., high field effects, magnon carrier scatt. 8-87981
 CdCr₂Se₄, evap., mass spectra 8-53238
 CdCr₂Se₄, ferromag. semicond., properties and use for making devices, review 8-60131
 CdCr₂Se₄, ferromag. semiconductor, light scatt. from magnons under strong fields 8-84554
 CdCr₂Se₄, mag. semicond., photoinduced binding of domain walls (*Russian*) 8-80174
 CdCr₂Se₄, photoferromag. effect quenching, photocond. 8-68488
 CdCr₂Se₄, spinel film, struct. SEM study, props. 8-79905
 CdCr₂Se₄, temp. depend. of resist. and magnetoresist., influence of Se vacancies 8-60130
 CdCr₂Se₄, velocity-field characts., above T_c 8-64049
 CdCr₂Se₄:Ag, ferromag. reson. field and linewidth anisotropy, Se vacancy effects 8-60338
 p-CdCr₂Se₄:Ag, oscillatory magnetoresist., temp. and mag. field depend. 8-52011
 CdCr₂Se₄:Cu, elec. props., temp. depend. (*Russian*) 8-72181
 CdCr₂Se₄:In, ferromag. semicond., carrier mobility, electron-two magnon scatt. Hall effect 8-51992
 CdCr₂Se₄:In(Ga), temp. driven metal-semiconductor transition, temp. and mag. field depend. (*Russian*) 8-88003
 CdCr₂Se₄(S₄), ESR line intensity near Curie point 8-64269
 CdF₂, electrode polarisation 8-76377
 CdF₂, NMR, ¹¹³Cd nucl. mag. shielding 8-68395
 CdF₂:Gd³⁺, hydrostatic press. and temp. effects on EPR spectrum 8-76304
 CdF₂:NaF, formation and reorientation of Na⁺-anion vacancy complexes 8-84516
 CdF₂:Ti²⁺, electronic struct. and EPR of Ti²⁺ 8-76034
 CdFCl, CdFBr, existence and vibr. characterisation, IR and Raman matrix isolation obs. 8-78706
 CdFe(CO)₄, IR and Raman spectra, vibr. anal. 8-66553
 Cd_{1-x}Fe_xCr₂S₄:Cu, effect of doping on elec. props. and Curie temp. 8-84214
 CdGa₂S₄, photoluminesc. and photocond. meas. 8-60159
 CdGa₂S₄:Ag(In), photoluminesc. and photocond. meas. 8-60159
 CdGa₂Se₄, electron traps, energy spectrum, photocurrent decay, TSC temp. depend. (*Russian*) 8-64057
 CdGa₂Se₄, electrophotographic props. (*Russian*) 8-59100
 CdGeAs₂, develop. of tunable coherent radiation at 16 μm 8-90454
 CdGeAs₂, freq. mixing for tunable IR sources 8-59030
 Cd₂Ge₂As₄, band gap, DC cond., elastic consts., and glass transition temp., pressure depend. 8-72064
 CdHg, positive gain measurements or 470 nm continuum band 8-66805
 Cd_{0.2}Hg_{0.8}Se, longitudinal Nernst-Ettingshausen effect, effect of disorder scatt. 8-84240
 Cd_{0.9}Hg_{0.1}Se mixed cryst., electron mobility and electron scatt. 8-95296
 Cd_{0.9}Hg_{0.1}Se type semiconductor, small-gap, electron scatt. and transport props. 8-95294
 Cd_{0.9}Hg_{0.1}Se type semiconductor, small-gap, electron scatt. and transport props. 8-95295
 (CdHg)Te photoconductive detector, thermal figure of merit limit 8-89540
 Cd_{0.9}Hg_{0.1}Te, fine-graded gap struct., electrophysical props. (*Russian*) 8-60144
 Cd_{0.9}Hg_{0.1}Te, gap width temp. depend., absorpt. band edge meas. 8-72521
 Cd_{0.9}Hg_{0.1}Te, IR detector appls., prep., elec. props. (*German*) 8-86332
 n-Cd_{0.9}Hg_{0.1}Te, in strong mag. field, current-voltage characts., current instabilities 8-87980
 Cd_{0.9}Hg_{0.1}Te, isothermal growth of epitaxial layers 8-60577
 n-Cd_{0.9}Hg_{0.1}Te, magnetophonon oscils. of transverse magnetoresist. 8-72177
 Cd_{0.9}Hg_{0.1}Te, photoresistor, performance at large bias currents (*Russian*) 8-76105
 Cd_{0.9}Hg_{0.1}Te, temp. shift of energy gap, contrib. of lattice dilatation 8-51892
 CdHg* excimer, kinetic model of sustained discharge excitation 8-66804
 CdI₂, 2H to 4H structural change, X-ray diffr. study 8-75614
 CdI₂, molten, electrical cond., press. effect, 0-1 kbar 8-55963
 CdI₂, NMR, ¹¹³Cd nucl. mag. shielding 8-68395
 CdI₂ polytypes, crystal structure analysis, refinements for structure determination 8-91312
 CdI₂ polytypes, crystal structures using new refinements for structure determination 8-91313
 CdI₂, polytypism, phase and growth aspects 8-83764
 CdI₂, polytypism and luminesc. (*Russian*) 8-56520
 CdI₂ single cryst., EPR of V²⁺, Mn²⁺, Co²⁺ 8-68362
 CdI₂, soln. grown, rotation twinning, arcing and polytypism 8-51557
 CdI₂, sputtering processes during 6 keV Xe ion bombard. 8-68590
 CdI₂, UV reflectivity meas., band struct., LCAO calcs. 8-72545
 CdI₂, vapour, excited by photodissociation, fluoresc. yields 8-55138
 CdI₂-AgPO₃, glasses, ionic conductivity and structure (*French*) 8-67854
 n-Cd_{0.9}In_{0.1}Cr₂Se₄, effect of doping on elec. cond. and magnetoresist. 8-72174
 CdIn₂S₄, fundamental optical constants 8-84549
 CdIn₂S₄:Co, optical absorption meas. 8-64384
 CdMoO₄, refr. index, single crystals having scheelite struct. 8-79082

cadmium compounds continued

- Cd(NO₃)₂·4H₂O-CoCl₂, melt viscosity, equivalent conductivity, glass transition temp. 8-75855
 Cd(NO₃)₂·4H₂O-NiCl₂, melt viscosity, equivalent conductivity, glass transition temp. 8-75855
 Cd₂Nb₂O₇, Raman-scattering investigation of vibrational structure 8-76441
 Cd₂Nb_{2-2x}Sn_{2x}O_{7-2x}F_{2x}, solid soln., X-ray diffr. and Mossbauer study (*French*) 8-87659
 CdNd₄(SiO₃)₂O, synthesis, cryst. struct. 8-87653
 CdNi_{1-x}Fe_xO₄, mag. behaviour, Mossbauer meas. 8-52390
 CdO, magnetoresistance, temp. depend. of degenerate, narrow and broad samples 8-95306
 CdO, NMR, ¹¹³Cd nucl. mag. shielding 8-68395
 CdO, X-ray determ., Debye-Waller factors, Debye temp. and vibration amplitudes 8-55928
 CdO-B₂O₃-SiO₂, glass, dielec.-relax. currents 8-52004
 CdO-SnO₂ film, DC sputtering prep., visible and near IR transmission, resist. 8-88049
 CdO-TeO₂ system, partial phase diagrams 8-84784
 CdO-WO₃-H₂O, interconnection between kinetics of structure formation and chem. reactions 8-53198
 Cd₂P₂, high press. phase relns. and cryst. structs. 8-59792
 CdR₂S₄, (R=Sc, Yb, Tm), IR and Raman spectra, force consts. 8-68503
 CdS, A-exciton-polariton, time depend. optical spectrosc. obs. 8-80376
 CdS, absorpt. spectra, 400-650 nm, electron irradi. defects and absorpt. edge shift 8-64382
 CdS, acoustic phonon intensity fluctuations after strong nonlinear amplification 8-59909
 CdS, ambipolar diffusion meas. using nonlinear transient gratings 8-80000
 CdS, application in dynamic holographic correction schemes (*Russian*) 8-55326
 CdS, bulk acoustic phonons, light scatt. from phonon-induced surface ripples 8-75924
 CdS, chem. sprayed film, struct. and morphology 8-72020
 CdS, chem. sprayed film growth using centrifugal disc atomiser 8-92189
 CdS, collision controlled light scatt. by electrons, influence of elec. field (*Russian*) 8-64375
 CdS crystal, magnetic field intensity meas. by obs. of Faraday effect 8-93739
 CdS, cubic, ab initio band struct. calcs. within local density functional formalism 8-87910
 CdS cylindrical crystal, transverse SAW obs. 8-84042
 CdS, dry process formation from CdO and S (*Spanish*) 8-56607
 CdS, edge emission spectra alteration by uniaxial stress (*Russian*) 8-72486
 CdS, electrocrystallisation of films on Cd 8-72014
 CdS, epitaxial layers on Cd single crystal, direct synthesis and struct. 8-68628
 CdS, exciton cathodoluminesc. of semicond. with surface pot. barriers 8-88366
 CdS, exciton luminescence, surface recombination, space-charge-layer effects 8-80410
 CdS, exciton-ionised donor complex, binding energy 8-67949
 CdS, excitonic region, nonlinear optical meas., 4.2K 8-68531
 CdS film, double-layered polycrystalline, on LiNbO₃ substrate, fabrication and props. rel. to SAW appl. 8-64480
 CdS film, influence of nonstoichiometric surface layer on props. 8-64148
 n-CdS film, transient photoconductivity effects (*French*) 8-87994
 CdS, film, X-ray diffr. and elec. cond. 8-64149
 CdS, film electrolytically deposited, surface and bulk photocond. props. 8-60154
 CdS, film for solar cells, struct. and elec. props., thickness depend. 8-72289
 CdS films, vac. evaporation from CdS.Cr₂O₃ system, photoelec. props. 8-80074
 CdS, flexural waves in resonator platelets, synchronous amplification and generation 8-84527
 CdS, gain spectroscopy and plasma recomb. 8-88327
 CdS, heterojunctions with InP and GaAs, prep. by CdS CVD and etching 8-52062
 CdS, induced absorption and gain from high density excitons 8-68533
 CdS, induced absorption in energy ranges of exciton and exciton-biexciton transitions 8-72548
 CdS, lattice attenuation meas. by US injection method 8-76480
 CdS layers from CdS+Cr₂O₃ system, effect of heat treatment on spectral distrib. of photosensitivity 8-80017
 CdS, luminesc. data. statistical anal. (*Russian*) 8-68559
 CdS, luminesc. from heavy ion tracks 8-88365
 CdS MIS devices surface states 8-72267
 CdS, mode corrected TA phonons, reson. Brillouin scatt. 8-72535
 CdS, model S=1/2 amorphous antiferromagnet, spin polarisation 8-52288
 CdS, NMR, ¹¹³Cd nucl. mag. shielding 8-68395
 CdS, neutron and fast electron irradi., local centre form., TSC and photoluminesc. meas. 8-87719
 CdS, neutron irradiated, intrinsic defects 8-51599
 CdS, nonlinear refr. index coeffs. meas. by nonlinear refraction method (*Russian*) 8-79066
 CdS, ODMR, bound excitons 8-80253
 CdS, photoanodes in sulphide-polysulphide electrolytes, instability 8-80755
 CdS, photoconducting, surface acoustic noise amplification by carrier drift 8-72208
 CdS, photorefl. in exciton region, surface layer influence 8-76489
 CdS, piezoelec. semicond., piezoresist. of grain boundaries 8-51995
 CdS, pure and Al doped, vacuum deposited film, photoelectric props., optical absorption 8-60162
 CdS, reson. Raman Scatt. under two-photon excitation of excitonic mols. 8-52486
 CdS, reson. Raman scatt., second-order, theory for case of strong excitonic effects 8-76460
 CdS, reson. scatt. of exciton-polaritons by acoustic phonons 8-60482
 CdS Schottky contact, photovoltage 8-95337
 CdS screen for laser CRT, stimulated emission with TV type operation 8-59028

cadmium compounds continued

- CdS, seeded growth from vapour of large single crystals 8-64449
 n-CdS semicond. liq. junction solar cells, photocurrent spectra, carrier recombination 8-76142
 CdS, spatial dispersion effects, exciton decay const. depend. (*Russian*) 8-72086
 CdS, spin-flip line shape 8-88307
 CdS spray pyrolysis film prep. and characterisation 8-64492
 CdS surface, nonequilib. electron effects due to chem. excitation 8-72239
 CdS, surface energy levels, O(C) adsorpt., AES study (*Japanese*) 8-88008
 CdS, surface props., photorefectance spectra in the exciton region 8-95324
 CdS, thin films, deposition onto hot substances, vapour phase method 8-95694
 CdS, two photon absorption relative to Raman cross sections 8-87098
 CdS, two-phonon resonant Brillouin scatt. 8-84597
 CdS, up-conversion and optical storage, spatially modulated band struct. 8-64397
 CdS, vacuum epitaxial growth on CuInSe₂ 8-92193
 CdS, vol. depend. of refr. index 8-88275
 CdS:Bi film, implantation and post annealing, superlinearity 8-52028
 CdS:Cd(In), Cu- or defect-compensated, optical ageing rel. to storage cond. 8-84247
 CdS:Cl, extrinsic, exciton absorption 8-72569
 CdS:Cl, heavily doped, fluoresc. spectrum upper threshold calculated 8-52568
 CdS:Cu, In, Ga, spray deposited film, struct., X-ray obs. 8-71713
 CdS:Cu, photocond. under high excitation intensity 8-52033
 CdS:Cu, spectral sensitisation by cyanine dyes 8-64064
 CdS:Gd³⁺, mag. susceptibility, cryst. field calc. 8-76035
 CdS:In, spin flip Raman scatt., electron dynamics 8-80342
 CdS:In whiskers, prep. by vapour deposition 8-75969
 CdS:Li, anisotropy of the absorption by impurity centers in hexagonal crystals 8-88343
 CdS:Ni, dark cond. and photoconductivity 8-76110
 CdS:Ni, elec., photoelec. and luminesc. props. (*Russian*) 8-84259
 CdS:Ni, exciton reflection spectra 8-72557
 CdS:P, implanted, photoluminesc. and electroreflection spectra (*Russian*) 8-52544
 CdS-CaS, solid soln., rock salt struct., high press. phase equilibrium study 8-52777
 CdS-Cu₂-S, chem. formed heterojunction, photosensitivity characts. of Cu₂-S 8-72199
 CdS-Cu₂-S heterojunction, elec. and photoelec. characts., effect of etching of CdS 8-80048
 CdS-Cu₂-S single cryst. heterojunction, trap depths in depletion region 8-52064
 CdS-Cu₂-S thin film heterojunctions, base doping effect on elec. and photoelec. props. 8-80043
 CdS-CuI film heterojunction photocells, prep., photoelec. props. 8-80044
 CdS-electrolyte contact, electrolytic decomposition and photodecomposition 8-95357
 CdS-InP heterostructure formation and elec. evaluation 8-72738
 CdS-MgS, solid soln., rock salt struct., high press. phase equilibrium study 8-52777
 n-CdS-n-SiC heterojunctions, photoelec. and elec. props. 8-80042
 CdS-Si n-p heterojunction photodetector, fabrication and characts. 8-52068
 CdS-SrS, solid soln., rock salt struct., high press. phase equilibrium study 8-52777
 3CdSO₄·8H₂O, cryst., phonon assisted indirect transitions 8-72559
 CdS(PO₄)₂·OH, single crystals, X-ray struct. anal. 8-95019
 CdS(Se) film, pyroelectric effects, origin 8-88258
 CdS_{0.75}Se_{0.25}, linear electro-optic effect meas., light modulator appl. 8-76434
 CdS_{1-x}Se_x, mixed cryst., electron-hole drops and plasma, luminesc. obs. (*Russian*) 8-92119
 CdS_{1-x}Se_x, spatial distribution and lasing modes under one photon optical excitation (*Russian*) 8-59012
 CdS_{1-x}Se_x, zone edge phonons 8-76475
 CdS,Se_{1-x} laser damage, self-focusing influence 8-50844
 CdS,Se_{1-x} mixed crystals, exciton spectra 8-92131
 CdS,Se_{1-x} photoresistors, cutoff freq. extension by addition of Cr₂O₃, recrystn. (*Russian*) 8-84248
 Cd₃Se₂Ge₃O₁₂, garnet, refined cryst. struct. 8-87654
 CdSe 8-80474
 CdSe, ambipolar diffusion meas. using nonlinear transient gratings 8-80000
 CdSe, charge transport 8-84233
 CdSe crystal, stimulated emission from electron-hole plasma, temp. depend. 8-88331
 CdSe, defect struct. in Se vapour 8-64043
 CdSe, fundamental vibrs., Raman scatt. and IR refl. obs. 8-60451
 p-CdSe, Hall density and mobility, in Se vapour atm., 600-1100K 8-52014
 CdSe, hot carrier distribution, optically excited, picosec. time resolved reflectivity obs. 8-76495
 CdSe, meas. of partial press., by optical absorption method (*Japanese*) 8-51661
 CdSe, NMR, ¹¹³Cd nucl. mag. shielding 8-68395
 CdSe, nonstoichiometry, Cd and Se press. meas., up to 1400K 8-87664
 CdSe, optical parametric devices, freq. tuning possibility by uniaxial press. 8-59084
 CdSe, optically pumped, dynamic polarisation of nucl. moments 8-68411
 CdSe, photoanodes in sulphide-polysulphide electrolytes, instability 8-80755
 CdSe, photosensitivity of elastic properties 8-92049
 n-CdSe semicond. liq. junction solar cells, photocurrent spectra, carrier recombination 8-76142
 CdSe:Cd, Cu, photo-induced changes in absorpt. spectra 8-80382
 CdSe:P, effect of P on edge luminesc. 8-64399
 CdSe-Ge (111) heterojunctions, epitaxial, azimuthal rotation 8-84085
 Cd₂Se₃, elec. resist., thermoelectromotive force, temp. depend. 300 to 1400K (*Russian*) 8-84243
 CdSiP₂, birefringence meas. 8-56455

cadmium compounds continued

- CdSiP₂, bond strengths and bond lengths, thermal expansion coeff. meas. 8-87651
 n-CdSnAs₂, optical absorption rel. to energy spectra (*Russian*) 8-75994
 Cd₂SnO₄, film, spinel struct., X-ray diffr. study 8-75644
 Cd₂SnO₄ selective coatings, optical absorpt. edge 8-83046
 CdSnP₂, Hall mobility of holes 8-52015
 CdSnP₂:Cu, deep centres, emission transitions, polarisation (*Russian*) 8-84650
 CdTe cathodic deposition from aqueous electrolytes 8-64484
 CdTe, creep activation energy and velocity (*Russian*) 8-56716
 CdTe, crystal structure stability, P-T diagrams 8-51886
 p-CdTe, ESR optical detect., Overhauser shift, g-factor 8-80252
 CdTe film, cathode sputtered, chemical composition and struct. 8-84100
 CdTe film, excitation by H of anomalously high voltage (*Russian*) 8-60235
 CdTe, film grown in quasi-closed volume, struct. (*Russian*) 8-75952
 CdTe, growth by travelling heater method, high resistivity charact., γ-ray detector appl. 8-84707
 CdTe, IR transparent materials, forward and backward scatt. data 8-59099
 CdTe, lattice mode, dispersive refl. meas. using modular interferometer 8-89568
 CdTe, meas. of partial press., by optical absorption method (*Japanese*) 8-51661
 CdTe, NMR, ¹¹³Cd nucl. mag. shielding 8-68395
 CdTe negative dielectric relax. of hot electrons 8-52001
 CdTe, plastic deformation activation anal. below room temp. 8-84935
 n-CdTe semicond. liq. junction solar cells, photocurrent spectra, carrier recombination 8-76142
 CdTe, single cryst. IR laser window, low absorption at 10.6 μm 8-79081
 CdTe single-crystal film, switching and memory effects 8-76174
 CdTe, temp.-depend. of root-mean-square dynamic displacements, characteristic temp., X-ray study 8-83895
 CdTe, tunable high efficiency microwave freq. shifting of IR laser 8-71126
 CdTe, use in X-ray detectors 8-86745
 CdTe:Be, impurity modes and IR absorption 8-76506
 CdTe:Cl, single cryst., photo Hall effect obs. 8-76094
 CdTe:Ge, mag. props. 8-56289
 CdTe:In, lightly- and heavily-doped, cathodoluminesc., temp., injection level and freq. depend. 8-52584
 CdTe:Zn, TSC, carrier traps, depth and quenching by IR radiation 8-56420
 CdTe-metal contact, surface barrier exam. 8-64111
 CdTe_{1-x}S_x, long-wavelength optical phonons, composition depend., IR and Raman spectra 8-67788
 CdTe_{1-x}Se_x, Raman scatt. spectra, two-mode behaviour 8-60450
 CdTh(MoO₄)₃, struct., DTA and X-ray diffr. obs. (*French*) 8-95024
 CdTh(WO₄)₃, struct., DTA and X-ray diffr. obs. (*French*) 8-95024
 Cd₂V₂O₇, V-O-V bridge stretching freq. correl. with bond angle 8-74636
 CdX₂ (X=Br, Cl), spectroscopic parameters of mols. from vibr. isotopic effects 8-74798
 CdX₂, CdXY (X,Y=Cl,Br,I), matrix isolated, far IR spectra, thermodynamic props. 8-86869
 CdXY (X, Y=Cl, Br, I), spectroscopic parameters of mols. from vibr. isotopic effects 8-74798
 CdZnS-CdS bifilm solar photocells, feasibility, study 8-76113
 (CdZn)S-Cu₂S solar cell, film form. and characts. 8-68080
 Cd_{1-x}Zn_xS 10 μm film optical and electrical characterisation (*French*) 8-64153
 Cd_{1-x}Zn_xS, electro-optical multilayer film, for data storage and display 8-71176
 Cd_{1-x}Zn_xS, epitaxial growth of single crystal layers on (111) GaAs substrate, close-space geometry 8-92198
 Cd_{1-x}Zn_xS, RF sputtered electro-optical film for data storage and display 8-83047
 Cds, reson. Brillouin scatt. by piezoelectrically inactive TA phonon domains 8-84593
 CsCdCl₃, phase transition under pressure 8-51664
 Cu₂S-CdS film junction formation by dry-barrier process 8-64109
 Cu₂-CdS heterojunctions, nature of longwave photo EMF 8-84284
 HgCdTe IR photovoltaic detectors for 8-14 μm range, review (*Italian*) 8-54451
 HgCdTe MIS structure, modelling and appl. to CCD IR imagery 8-80058
 Hg_{0.4}Cd_{0.6}Te, annealing temp. effect on carrier conc. 8-72167
 Hg_{0.7}Cd_{0.3}Te, 17 to 77K, photo- and cathodoluminesc. 8-52569
 Hg_{1-x}Cd_xTe, Faraday effect at CO₂ laser freq. 8-64348
 Hg_{1-x}Cd_xTe, high intensity IR transmission limit 8-79074
 Hg_{1-x}Cd_xTe, Hooge's flicker noise MIS ext. 8-56233
 n-Hg_{1-x}Cd_xTe, photoconductor, contact noise at 77K 8-88028
 Hg_{1-x}Cd_xTe, zero-gap semicond. with nonparabolic band struct., hot electron mobility and conc. 8-76080
 Hg_{1-x}Cd_xTe, single-LO-phonon and -plasmon recombination channels narrow-bandgaps 8-91728
 HgSe-CdSe pseudobinary alloy, phase diagram and cryst. growth 8-68620
 In-CdS-In Josephson junction, exhibiting nonuniform max. current distrib. self-resonant modes 8-56263
 (InAs)_{1-x}(CdTe)_x, band gap and effective mass, IR spectra obs. 8-56491
 K₂Mn₂Cd_{1-x}F₄, 2-dimens. antiferromag. sidebands on EPR lines 8-56370
 Mn₂Cd_{1-x}Te, far IR refl. spectra, phonon spectra 8-52497
 MnO-CdO, solid solns. prep., struct. 8-95157
 NaBr, XPS, satellite of Br 4s line 8-56556
 Na₂Cd₂Si₂O₁₀, cryst. struct. 8-83801
 NaCl-CdO heterojunction form. in cathode-plasma dyeing, temp. depend. (*Russian*) 8-67710
 Pb-CdS-In Josephson junction, light-sensitive, structural fluctuations (*Russian*) 8-56265
 Pb_{1-x}Cd_xS, epitaxial, resist. and Hall coeff., substrate temp., thickness and comp. depend. 8-72290
 PbS-CdSe, phase boundary processes 8-71857
 RbCdBr₃, polarised Raman spectra 8-76443

cadmium compounds continued

- RbCdCl₃, crystal struct., polarised Raman spectra and X-ray diffraction obs. 8-76443
 Si-CdS heterojunction memory diodes, switching process 8-80046
 Sr_{1-x}Cd_xF₂, lattice dynamics 8-75763
 Te-Se-CdO struct., fabrication and characts. 8-76106
 (ZnCd)S:Ag phosphor, absolute efficiency under fluoroscopy conditions 8-73203
 Zn_{0.1}Cd_{0.9}S-CdTe p-n junction, prep. by spray pyrolysis, photovoltaic props. 8-60196
 Zn_{0.1}Cd_{0.9}S film, prep. by soln. spray method, and struct., optical and elec. props. 8-52666
 Zn_{0.1}Cd_{0.9}S, laser damage, self-focusing influence 8-50844
 Zn_{0.1}Cd_{0.9}S, lasing modes and spatial distrib. under one-photon excitation, cavity model 8-74913
 Zn_{0.1}Cd_{0.9}S:In, low resist. film for solar cell window 8-71200
 Zn_{0.1}Cd_{0.9}Te, reflection spectra, energy band struct. comp. depend. (*Russian*) 8-56500
 Zn_{0.1}Cd_{0.9}Te, relaxation processes, emission spectra (*Russian*) 8-72598
 ZnS-CdS:Ag, Ni, Co, thermoluminesc. glow curves 8-95611

caesium

- see also nuclei with
 6³Si_{1/2}-6²P_{3/2} transition ($\lambda=8521 \text{ \AA}$) with hyperfine splitting, curves of growth 8-66513
 absorption on stainless steel oxides, meas. of contamination using washing test 8-62597
 adsorbed on Si and Ge (100), negative electron affinity surfaces, thermal stability of work fn. 8-92167
 adsorption, on GaP (001), photoemission meas. 8-87874
 adsorption and absorption on oxidised stainless steel 8-84061
 adsorption on GaAs (InSb), LEED, AES, EELS study 8-68068
 adsorption on MoS₂, LEED, Auger and work function meas. 8-71994
 adsorption on Pt, field-emission microscopy 8-51822
 adsorption on ZnO (0001) of alkali metals, anomalous behaviour of Na 8-79883
 atom, 6s, photoelectron ang. distrib., anisotropic effects 8-50514
 atom, 6S-7S, parity violation search in highly forbidden mag. transition 8-82709
 atom, discrete level raising into far continuum, oscillator strength to shape reson. transfer 8-78624
 atom, excited state, two-photon ionisation by ruby laser light 8-74621
 atom, fine-struct. of excited nd and nf states, at. core effect 8-58606
 atom, g-factor anomalies and strongly forbidden M1 transitions 8-78825
 atom, multiphoton ionisation, reson. peak amplitude, temporal effects 8-78760
 atom, optical reson. line electron impact excitation cross sections, polaris. 8-55244
 atom, proportional counter pulse height fluctuations, resonant ionisation studies 8-90025
 atom, reson. multiphoton ionisation by ultrashort laser pulses, 1.06 μm 8-58630
 atom, resonantly excited in cylindrical discharge plasma, effective lifetimes 8-79413
 atom, strongly forbidden M₁ transitions, g-factor anomalies (*Russian*) 8-78648
 atom, superfluorescence, comparison with theory, quantum beat spectroscopy appls. 8-86837
 atom, superfluorescence (*Dutch*) 8-70780
 atom, transition probability of valence shells, relativistic pseudopot. calc. 8-86803
 atom, two-photon spectra, energy levels for highly excited ²F states 8-70805
 atom, XPS, free atom core binding energy 8-74699
 atomic clock, laser synchronisation between observatories of Paris and San Fernando (*French*) 8-89461
 atomic clock, long beam, primary standard, accuracy, reliability 8-89454
 atomic photoionisation, ion alignment, many electron correl. effect 8-74622
 atomic vapour, f-value determ. method using stimulated electronic Raman scatt., appl. to Cs 8-82693
 atoms, HFS, isotope shift related to nucl. charge rad. 8-78826
 beam clock development for satellites 8-57910
 beam deflection system for time and freq. primary standard 8-89453
 beam frequency standard design for satellites 8-57911
 beam frequency standard drift and noise performance rel. to velocity distributions 8-57912
 dense plasma, elec. and radiative heat cond. evaluation 8-71452
 diffusion in high temp. alloys, AES, SIMS depth profile study (*German*) 8-84008
 discharge, hollow cathode, volt-ampere characts. 8-71563
 discharge, hot cathode diode, low-press., initial stage transient processes 8-51382
 discharge plasma, optogalvanic effect characts. 8-63583
 electronic transition from self consistent APW χ_α calcs. 8-51884
 film, on Mo substrate, ang. depend. XPS, depth profile determ. 8-88404
 frequency standard, NRLM-I, improvement of freq. stability 8-62184
 frequency standard, Ramsey cavity and beam optics design, expt. 8-89456
 frequency standards, freq. offset due to spectral impurities 8-89455
 fuel reprocessing waste ¹³⁷Cs, ⁹⁰Sr and rare earth radioisotope separation by cation exchange 8-78486
 fully-ionised plasma hollow-cathode arc discharge theory 8-67533
 gas discharge, two-photon ionis. by laser light 8-87534
 hexamethylphosphoramide-K(Cs)(Rb), low temp. glass, EPR of solvated ats. 8-91927
 intercalation compounds with graphite, low temp. sp. ht. 8-71868
 layer on p-Si(111) surface inversion layer, negative magnetoresist. in 2D impurity band 8-64135
 liquid, meas. of density at high temp. and pressures 8-55903
 liquid, short range order parameters, from information theory 8-83730
 liquid, specific heat meas., at temp. up to 1700K under pressure 8-51696
 LWR fuel-cladding gap, Cs-U-Zr-H-I-O system, chemical thermodynamics 8-82440
 nonideal plasma thermodynamic props., shock wave obs. 8-71434
 nuclear mag:spin-lattice relaxation times 8-86889

caesium continued

- nuclear reactor mixed-oxide fuel, Cs concentration effects 8-82452
 optical functions, effect of surface roughness 8-56447
 photoplasma, optical excitation in radiation diffusion conditions 8-55227
 plasma, excited atomic state inversion obs. 8-71460
 plasma, ohmic heating, electrical conduction temp. depend. 8-71442
 plasma diagnostics by wire explosion 8-71516
 plasma elec. conductivity meas. 8-71450
 plasma probe meas. in mag. field 8-63597
 plasma thermoelectronic laser energy converter 8-90421
 radioactive Cs in seawater, rapid determ. using Cs selective resin 8-85609
 relativistic model pseudopot., appl. to elec. resist. in liq. phase 8-51866
 solubility, diffusion and permeation in ZrC 8-51684
 vapour, coherent anti-Stokes Raman scatt. 8-71146
 vapour, Joule-Thomson effect, 768-1234K 8-71420
 vapour, oscill. in low voltage arc discharge growth 8-51386
 vapour, parametric conversion of 3.39 μm He-Ne laser radiation to visible 8-83036
 vapour, thermodynamic props. calc. from Joule-Thomson data 8-94886
 vapour heat pipe discharge tube pumping for 823 cm⁻¹ tunable IR laser 8-63069
 Cs I, atomic wavefunctions collapse 8-70733
 Cs I, plasma diagnostics, excited level populations, relative spectral line intensities (*Spanish*) 8-51344
 Cs⁺ in He and Ne gas, ion mobility and longit. diffusion coeff. 8-67308
 Cs⁺ internal dialysis in Myxicola giant axons, Na inactivation 8-96036
 Cs⁺, ion mobility in Ar, Kr, Xe, diffusion, generalised Einstein relation 8-67298
 Cs-Ba triode arc switch, high-current, low-voltage, pulsed control 8-71551
 Cs-He, new absorption/emission bands perturbed Cs transitions assignment, pot. energy curves 8-66486
 Cs⁺-Ar(Kr)(Xe), ion mobility and interaction pot., drift tube meas. at 300K 8-59537
 Cs+Ar, two-photon ionisation spectra, satellites, absorption line shape 8-82668
 Cs+Ar(Kr)(Xe), spectral line breadth and shift, Van der Waals pot. calc. 8-90126
 Cs+D₂O, ion-pair form., energy, angle and mass anal. of products 8-70970
 Cs+H₂, rot. excitation, infinite order sudden approx. 8-74740
 Cs+H⁺, elastic and charge exchange collisions, projected valence bond method 8-78804
 Cs+He⁺, 5-100 keV, electron capture form. of fast metastable He 8-74760
 Cs+Xe (neopentane), Cs line shape broadening, satellite data inversion, interaction pot. 8-74608
 Cs⁺+2Cs₂→Cs₃⁺+Cs, gas phase reaction rate const. calc. 8-92457
 Cs⁺+X, X=H, H₂, He, C, N, O, cross-section, closure-Born approx. 8-66630
 Cs₂, laser-excited fluoresc. in Cs-Xe mixture, pumping, level scheme 8-86909
 Cs₂⁺, adiabatic pot. curves, ground and excited state, Hellmann-type model pots. 8-78647
 Cs₂⁺, form. by Cs+Cs assoc. ionisation, dissociation energy 8-58804
 CsAl(SO₄)₂.12H₂O, third order elastic consts. from stress shifted reson. freqs. 8-55905
 CsI, four-photon ionisation near 6f resonance 8-70801
¹³⁷Cs accumulation by marine organisms, sediment and sea water influences 8-80981
¹³⁷Cs accumulation in fruitbodies of Basidiomycetes 8-80977
¹³⁷Cs, fallout effects of Nagasaki atomic bomb 8-85393
¹³⁷Cs immobilisation in cement-waste composites 8-82466
¹³⁷Cs levels in soils and vegetation of W.Malaysia 8-73263
¹³⁷Cs transfer coefficient into cows milk rel. to level of milk prod. 8-80978
 Cs(6s)+H⁺, elastic scatt., pot. determ. from differential cross-sections meas. 8-78778
 Cs(n²D_{3/2})+Cs(6²S_{1/2}) collisions, inelastic cross sections 8-74753
 Cs(nP₁)+Cs(6S), assoc. ionisation, threshold energy, Cs₂⁺ dissociation energy 8-58804
 He-Cs mixture discharge, B-invariant transformation theory 8-67503
 He-Cs plasma, HF instability in crossed fields, obs. 8-75305
 ZrN_{0.5}Cs, thermionic emission, metallic sublattice vacancy effects 8-68597

caesium alloys

- charge transfer insulators, mechanism, resistivity 8-80070
 CsAu, NMR line shape, Knight shift, X-ray diffr. study, struct. props. 8-68402
 CsAu, photoelectron spectroscopy and energy bands calc. 8-76581
 Cs_{1-x}Au_x, liq., metal-nonmetal transition, electronic theory 8-79930

caesium clocks see atomic clocks**caesium compounds**

- see also caesium alloys
 caesium hydrogen tartrate, anomalous dispersion of Cs, refined struct. from modified least squares program 8-51522
 halide, porous layers, electron bombardment induced cond. 8-56550
 halides, F-centres, first excited degenerate states, props. of electron-phonon interaction 8-63824
 CS, heat of formation from electron impact dissociation of CS₂ and OCS 8-73074
 CS, valence electron photoionisation, ionisation pot. and spectral intensities 8-70883
 CSI:Na cryst., V_K-Na⁰ centre pairs, tunnelling recomb. 8-91952
 Ce₂(SO₄)₃, dosimeter, mixed field of fast neutrons and γ -rays, absorbed dose meas. 8-74514
 CsAg₂Se₂, crystal struct., X-ray study (*German*) 8-83795
 CsAl(SO₄)₂.12H₂O:Cr³⁺, ESR spectra 8-91944
 Cs₂Au₂Cl₆, ¹⁹⁷Au Mossbauer high press. study of mixed valence compound 8-52387
 CsBr, electron-phonon interactions of F-centres, first-order Raman scatt. 8-64370
 CsBr, far IR spectra, matrix isolated, monomers, dimers, trimers 8-66545

caesium compounds continued

- CsBr, first-order Raman off- and on-reson. scatt. induced by F-centres 8-92073
 CsBr, hyper-Raman spectra by single channel method 8-84591
 CsBr, self trapped exciton, optical detection of spin relax. processes 8-60358
 CsBr, ZZ 8-75792
 CsBr:NO₂⁻, luminesc. centre polarisation and reorientation (*Russian*) 8-76529
 CsBr:O₂⁻ centres, luminesc., polarisation temp. depend. 8-87943
 CsBr:Ti³⁺, perturbed lattice dynamics, breathing shell model calculation 8-75744
 CsCdCl₃, phase transition under pressure 8-51664
 CsCdF₃, nonlinear elastic behaviour, US velocity, 1 bar-3 kbar 8-59851
 CsCl, CsCl+KCl mixtures, osmotic coeffs. at 298.15K 8-92509
 CsCl, electron-phonon interactions of F-centres, first-order Raman scatt. 8-64370
 CsCl, far IR spectra, matrix isolated, monomers, dimers, trimers 8-66545
 CsCl, first-order Raman off- and on-reson. scatt. induced by F-centres 8-92073
 CsCl, rot. excitation by electron impact, calc. cross sections 8-66670
 CsCl structure, quantifying concept of coordination number 8-95008
 CsCl, thermal expansivity determ. at high press. 8-79787
 CsCl:Cr³⁺, ESR of Cr³⁺ centres, room temp. 8-91943
 CsCl-UCl₃ melts, density, surface tension and viscosity 8-67764
 CsCl+KCl mixtures, osmotic coeffs. at 298.15K 8-92509
 CsCl+SF₆, collision induced dissoci., threshold behaviour 8-88627
 Cs₂Cl₂+SF₆, collision induced dissoci., threshold behaviour 8-88627
 CsCl(Cs₂Cl₂)+Ar(Kr)(Xe), collision-induced ion-pair form., absolute cross sections 8-73029
 CsClO₄-LiClO₄, binary melt, Raman spectra, polarised line width, temp. depend. 8-84578
 CsCoCl₃, anisotropic antiferromag., inelastic neutron scatt. study 8-60274
 CsCrCl₃, co-operative Jahn-Teller distorted struct. determ. 8-63713
 Cs₂CrO₄, ZZ 8-88326
 CsCuCl₃, birefr. and opt. rot. near structural phase transition points 8-75823
 CsD₂AsO₄, high efficiency SHG of Nd:YAG laser radiation 8-59088
 CsD₂AsO₄, high efficiency freq. doubling of Nd:YAG laser light 8-79071
 CsF, doped with F-centres, first order Raman scatt. 8-52492
 CsF, electron impact, elastic scatt., model, static and static exchange calcs. 8-94321
 CsF, electron-phonon interactions of F-centres, first-order Raman scatt. 8-64370
 CsF, far IR spectra, matrix isolated, monomers, dimers, trimers 8-66545
 CsF, muon Coulomb capture ratio 8-62959
 CsF, rot. excitation by electron impact, calc. cross sections 8-66670
 Cs₂FeCl₅·H₂O, mag. phase boundaries, susceptibility, 3D Heisenberg antiferromag. behaviour 8-84420
 CsFeCrF₆, CsFeVF₆, crystal struct., Mossbauer hyperfine spectra 8-52381
 CsH, dissoci. energy calc. 8-90314
 CsH, X¹Σ⁺ and A¹Σ⁺ states, pot. energy curves, Rydberg-Klein-Rees methods 8-50486
 CsH⁺, Σ state pot. energy, Hellman pseudopot. calcs. 8-70764
 CsH₂AsO₄, high temp. phase transition 8-71856
 CsH₂PO₄, high press. phase diagram 8-52457
 CsH₂PO₄, neutron diffraction study of cryst. struct. 8-79592
 CsH₂PO₄, single cryst. growth, struct. and elec. props. 8-71693
 Cs₄Hf(C₂O₄)₄·nH₂O, electric field gradient at metal site, γ-ray perturbed ang. correlation meas. 8-52380
 CsI, acoustic NMR, role of incoherent phonons (*Russian*) 8-80230
 CsI, adsorption of Ar-O₂ mixture, test of eqns. for gas mixture adsorption on heterogeneous surface 8-60030
 CsI, correl. between UV emission band at 300 nm and self-trapped excitons, 4.2K 8-75998
 CsI crystals, in scintillation counters, nonstatistical counting rates due to phosphoresc. 8-95597
 CsI, far IR spectra, matrix isolated, monomers, dimers, trimers 8-66545
 CsI, high mass secondary ion clusters detected by SIMS 8-88400
 CsI, hyper-Raman spectra by single channel method 8-84591
 CsI, isotope diffusion 8-75875
 CsI, prep., 5-30 μ thick single cryst., for channellography appl. 8-80658
 CsI, selective etching, growth and dissolution in alcohols 8-71739
 CsI, ZZ 8-75792
 CsI:NO₂⁻, luminesc. centre polarisation and reorientation (*Russian*) 8-76529
 CsI:Na phosphor screen, absolute efficiency under fluoroscopy conditions 8-82084
 CsI:Ti³⁺, Jahn-Teller split luminesc., high press. study 8-52565
 CsI(Tl) crystal light output when exposed to protons at 3-15 MeV 8-78570
 Cs₂KMO₃F₃, (M=Mo, W), low temp. phase transitions (*French*) 8-92036
 Cs₂LiCr(CN)₆, room temp. struct., phase transitions 8-51491
 CsMnF₃, antiferromagnet, struct. with compensated magnetisation in noncollinear phase (*Russian*) 8-88095
 CsMnF₃, mag. field- and temp.-depend. of light absorption spectra 8-52528
 Cs₂MoO₃F₃, ferroelec. and order-disorder phase transitions 8-92037
 CsNCS, long-wave lattice modes 8-59881
 CsNO₃-LiClO₄, binary melt, Raman spectra, polarised line width, temp. depend. 8-84578
 Cs₂NaAlF₆, cryst. struct. determ. 8-95036
 Cs₂NaBiCl₆, optical props. 8-68549
 Cs₂NaEuCl₆, luminescence Raman spectra, means for localisation of binding energy levels (*German*) 8-88304
 Cs₂NaTbCl₆, Tb³⁺ ⁵D₄→⁷F₃ transitions, mag. and elec. dipole intensities 8-76033
 Cs₂NaYCl₆:Re,Tm, fluorescence, two-step blue up-convertors 8-95603
 CsNiCl₃, antiferromag. coupling in linear chains, molecular orbital approach 8-52239
 CsNiCl₃, nuclear spin-lattice relax., temp. depend., anisotropic effects 8-64293

caesium compounds continued

- CsNiCl₃, one-dimens. antiferromag., US attenuation 8-88156
 CsNiF₃, ¹⁹F NMR, spin fluctuation suppression 8-91970
 CsNiF₃, NMR and relax. exam. 8-52371
 CsNiF₃, solitons in one-dimens. ferromag., inelastic neutron scatt. 8-95450
 CsO₂, X-ray low temp. phase study, crystallographic domains and unit cell dims. 8-63728
 Cs_{1-x}O₂, metallic glass, prep., elec. props. and struct. 8-67652
 Cs₂O-SiO₂-(GeO₂) system glasses, X-ray diffraction anal., electron radial distrib. curves 8-87622
 CsOH, liquid and vaporised, attack on stainless steel 8-68840
 CsPbCl₃, elastic constants and thermal expansion, near struct. transitions 8-59849
 CsPbCl₃, O_h¹-D_{4h} transition, US and thermodynamic props. 8-67826
 CsPbCl₃, phase transition under pressure 8-51664
 CsPbCl₃, struct. phase transitions, NMR obs. 8-83943
 Cs₂PbCu(NO₃)₆, successive Jahn-Teller phase transitions, neutron and X-ray diffraction 8-95154
 Cs₂RbMO₃F₃, (M=Mo, W), low temp. phase transitions (*French*) 8-92036
 Cs₂ReF₆, absorpt. spectra, splitting of Γ₈(⁴A_{2g}) ground state 8-74658
 Cs₂SO₄, IR absorpt. spectra, polymorphism, site group approx. and SO₄ stretching mode 8-52510
 Cs₂SO₄ molecules isolated in inert gas matrices, low freq. IR spectra 8-50547
 Cs₂S₂O₆, hexagonal, piezoelec., electro-optic, dielec., elastic, thermoelastic props., space groups 8-76388
 Cs₂Sb_{0.5}Mo_{0.5}IVCl₆, (M^{IV}=Se, Te, Sn), ¹²¹Sb Mossbauer effect 8-84506
 CsSiF₆Mn³⁺, splitting of vibronic levels 8-60496
 Cs₂SnBr₄:ReBr₆²⁻, luminesc. spectra and relax. processes 8-68552
 Cs₂SO₄:Ti, absorpt. and luminesc. spectra 8-72586
 Cs₂Te, photocathode for proximity focused image converter, field enhancement of photoemission 8-72677
 Cs₂TeI₆, ¹²⁹I Mossbauer spectra, coupling consts. 8-62833
 Cs₂Ti₂O₉, preparation, cryst. struct. determ. 8-75646
 Cs₂UF₆, D_{3d} distortion on octahedral UF₆⁻ complex (*French*) 8-84173
 Cs₄(UO₂)₂F₈·2H₂O, IR absorpt. and Raman spectra, normal coordinate anal. (*French*) 8-52509
 CsVCl₃, antiferromag. coupling in linear chains, molecular orbital approach 8-52239
 Cs₂WO₃F₃, ferroelec. and order-disorder phase transitions 8-92037
 CsXe excimer, laser-excited fluoresc. in Cs-Xe mixture, pumping, level scheme 8-86909
 Cs₂ZrCl₆:Os⁴⁺, multiple state luminesc. 8-72584
 Cs₂[Pt(CN)₄](FHF)_{0.39}, cryst. struct., X-ray diffraction meas. 8-59789
 K₂CsSb photocathodes, prep. and props. 8-84693
 (La,Cs)B₆, single crystal growth for thermionic emission 8-92183
 MgCs₂(SeO₄)₂·6H₂O, EPR, crystal field and hexahydrate distortion 8-91938
 (NH₄,Cs)Cl, negative isotope effect on II-III phase transition (*German*) 8-95155
 NaI(Tl), well-detector, low-background γ-spectrometry, comparison with CsI(Tl) 8-86724

caesium generators see plasma diodes

caesium plasma diodes see plasma diodes

calcium

see also nuclei with

- adsorption on ZnO (0001) of alkali metals, anomalous behaviour of Na 8-79883
 alkali halide:Ca, impurity-vacancy complexes, association and orientation energies 8-51578
 atom, electron impact, 3p⁶ subshell excitation, VUV spectra (*Russian*) 8-90117
 atom, multiphoton ionisation spectroscopy of even- and odd-parity states 8-86973
 atom, transition probability of valence shells, relativistic pseudopot. calc. 8-86803
 atom, X-ray production by protons by 0.5 to 2.0 MeV energy 8-66646
 atom and ion, spectral lines collision broadening and shifts 8-58624
 axon, ATP as energy source for Ca pump in squid giant axons 8-77043
 brine, routine anal. by X-ray fluoresc. spectrometry applying matrix corrections 8-88690
 charge distribution in isotopes 40, 42, 44, 48, Hartree-Fock anal. (*Russian*) 8-70747
 cochlear endolymph Ca content 8-61203
 determination, image vol. samples 8-53308
 determination, in lake sediments, by atomic absorption spectroscopy 8-95970
 diffusion in KCl simultaneously with Sr 8-79813
 film, optical consts. meas., 2 to 5.6 eV (*French*) 8-52586
 in vivo measurement by ³⁷Ar method, inert gas elimination in humans 8-61247
 ion levels in squid axons, influence of pCO₂ 8-56960
 lipid bilayers, Ca²⁺ transport system of rat liver mitochondria 8-64966
 magnetic hyperfine field in Fe, TDPAD meas. 8-52389
 molecule, optical spectra, inert matrices 8-58712
 plasma, Gaunt factor temp. depends., from Ar II and Ca II Stark widths 8-87491
 radiative decay of autoionisation states (*Ukrainian*) 8-82682
 serum automated electroanal. using ion-selective disc electrodes with neutral cation-carriers (*German*) 8-73269
 surface segregation in dense Al₂O₃ exposed to steam and steam-CO 8-85013
 Ca II, in fast sporadic meteor spectrum, low-energy electron excitation 8-93170
 Ca II 3934 Å K-line, temporal var. in solar spectrum 8-93186
 Ca III, atomic structure determ. by model pot. method 8-86777
 Ca XV, transition probabilities, energy spectra calcs. 8-70791
 Ca⁺, transition probability of valence shells, relativistic pseudopot. calc. 8-86803
 Ca²⁺ effect on chromaffin granule electrophoretic mobility meas. by light scatt. 8-53357
 Ca²⁺ intracellular changes in human erythrocyte ghosts, arsenazo III meas., rel. to K permeability 8-96032
 Ca²⁺/Na⁺ extracellular ratio effect on photosensory membrane of Limulus ventral nerve photoreceptor 8-69067

calcium continued

- Ca-N₂O-CO flame, Ca catalyzed, gain meas., emission band assignment 8-66815
 Ca-N₂O-CO flame, candidate chem. laser reactions, intracavity dye laser absorpt. meas. 8-63108
 Ca²⁺-induced luminesc. of aequorin, inhibition by anaesthetics 8-76985
 Ca+HF(DF), beam reaction, vibr. excitation 8-68877
 Ca+O₂(CO₂), CaO form., product states obs. 8-92450
 Ca+O₂(CO₂)(N₂O), reaction, electronic branching, statistical and dynamical influences 8-92451
 Ca₂ in Kr matrix, 1- and 2-photon fluoresc. excitation 8-50567
 Ca₂ laser-excited fluorescence in inert gas matrices 8-94273
 Ca₂, vibr. relax. in rare gas matrices 8-58711
⁴³Ca²⁺, aq. ions, nucl. quadrupole relax. 8-64287
 Ca(4s4p²P)+N₂O, absolute chemiluminesc. cross-section and photon yield 8-53208
 Ge:Ba, Ca, recomb. props. 8-56156
 KCl:Ca²⁺, Ca²⁺ precip., flotation density obs. 8-51690
 NaCl:Ca, light scattering coeff., effect of growing condition 8-55418
 NaCl:Ca²⁺, Mn²⁺, EPR of Mn²⁺, effect of Ca²⁺ on Mn²⁺ vacancy dipole decay 8-56371
 Pb-Ca-Sn, effect of Sn additions on precipitation behaviour, of Pb-Ca alloys (*German*) 8-52821
 YIG: Ca²⁺ epitaxial films, Fe⁴⁺ centres, MCD, optical absorpt., and thermoelectric power meas. 8-95595
 YIG:Ca, epilayer, reversible oxidation, ferromag. reson. 8-76781
 YIG:Ca, O diffusion depend. on defect conc. 8-67857

calcium compounds

- (*Russian*) 8-72403
 α -Ca₃(PO₄)₂, wet-process formation of nonstoichiometric Ca₃(PO₄)₂(OH)₂ (*Japanese*) 8-84752
 cabal glass:SiO₂(TiO₂), microheterogeneity, and elec. cond. 8-83997
 calibo glass:Eu³⁺, Ho³⁺, energy transfer 8-76510
 chabazite, adsorption of Ar-N₂ mixture, test of eqns. for gas mixture adsorption on heterogeneous surface 8-60030
 ettringite, expansion by H₂O adsorption, exam. 8-64806
 halophosphate, thermostimulated luminesc., mech. milling effects (*Russian*) 8-76537
 LPE growth, saturation magnetisation, collapse field, bubble diameter 8-95703
 marble, ball mill grinding, wet, dry, rate constant determination (*Japanese*) 8-95827
 marble, Italian Ondagata, diametral compressive strength, comparison with uniaxial tensile strength (*Japanese*) 8-72947
 marble, powder, ultra fine, surface roughness effect on formation by rotating friction mill (*Japanese*) 8-95709
 particle size measurement by monoparticulate film method (*Japanese*) 8-95874
 soda lime glass, Ag⁺ ion exchanged, planar optical waveguide, manufacturing tolerances 8-71212
 soda-lime glass, depth profiles of Na and Ca by SIMS and AES 8-51805
 steel, sintered, Cr-Mo, CaF addition effects on struct. heterogeneity 8-60611
 tienshanite, cryst. struct. determ. 8-83800
 tris sarcosine calcium chloride:VO²⁺, EPR and absorpt. spectra 8-60330
 (YSmEuCa)₃(FeGe)₅O₁₂, garnet film, ion implanted, bubble domain props. 8-88152
 BaCO₃-SrCO₃-CaCO₃, phase inhomogeneity effects on oxide cathode props. 8-52614
 Ba_{0.92}Ca_{0.08}TiO₃ ceramic, uniaxial stress effects, US dilatometric and dielec. meas. 8-52454
 CaAl₂Si₂O₇, cryst. struct. 8-63700
 Ca₃Al₂Si₂O₁₂, grossular, cryst. struct. and compressibility to 60 kbar 8-63718
 CaB₆-SmB₆ system complex borides, prep. and props. 8-52703
 Ca₂(B₂O₃)Cl₂H₂O, triclinic chilgardite, cryst. struct. determ. 8-63737
 CaB₃O₄(OH)₃·H₂O, order-disorder ferroelec., crit. dynamics, NMR data compared with dielec. data 8-76415
 CaBr₂·4CH₃OH, cryst. struct. determ. (*French*) 8-59788
 CaBr₂·4C₂H₅OH, cryst. struct. determ. (*French*) 8-59788
 CaCO₃, acceleration of growth of particles, Lorentz forces, electric and mag. field effects 8-51455
 CaCO₃, aragonite-calcite transformation, effect of impurities, DTA and IR studies 8-51662
 CaCO₃, ball mill grinding, rate constant determination (*Japanese*) 8-95828
 CaCO₃, calcite, cryst. preferred orientation in marble, mag. susceptibility anisotropy development 8-56286
 CaCO₃, IR reflectivity, oblique phonons 8-60440
 CaCO₃ polydisperse particles, in Ca(HCO₃)₂ soln., growth, soln. in mag. field 8-53260
 CaCO₃, thermal decomp. in vacuo, ultrastruct. and crystallography 8-71864
 CaCO₃-carboxymethylcellulose suspension, filtration eqn. 8-55690
 CaCO₃+SiO₂, in presence of NaF, thermal decomposition of Ca₂SiO₄ formation 8-68889
 CaCl₂, D² Σ and X² Σ , two-photon vis. absorption, vibr. and rot. consts. 8-78764
 CaCl₂, E² Σ -B² Σ system, rot. anal., optical-optical double reson. obs., using two dye lasers 8-70855
 CaCl₂ laser excitation and ODR spectra 8-82757
 CaCl₂ conc. solns., vel. corals. calcs., diffusion, cond. and transference props. 8-85166
 CaCl₂, solns. in methanol, conductance data anal., assoc. consts. 8-71875
 CaCl₂-tryptophan, γ - and UV-irrad. solvent matrices at 77K, H⁺ fluoresc. 8-70779
 CaCl₂·5.99.5.33H₂O, molar cond., compressibility, expansivity 8-51712
 CaCO₃, ball mill grinding, wet, dry, rate constant determination (*Japanese*) 8-95827
 Ca_{1-x}Eu_xSi₂, solid solns., α -ThSi₂ struct. type, comp. and press depend. 8-91322
 CaF, A² Π -X² Σ band system, MODR 8-74685
 CaF₂ (100), elec.-mech. coupling of dislocations 8-75676
 CaF₂, (n, γ) induced point defects, struct. and annealing 8-59842
 CaF₂, achievement of negative temp. (*French*) 8-74009

calcium compounds continued

- CaF₂, bleaching characteristics of crystals coloured by low energy electrons 8-76497
 CaF₂, Brillouin scatt. and high temp. disorder 8-80365
 CaF₂, colour centre thermal stability 8-83811
 CaF₂, cond. meas. under controlled F₂ chem. pot. (*Japanese*) 8-59972
 CaF₂, crack propag., cryst. props. effects 8-75720
 CaF₂, EXAFS, intrinsic UV luminesc. excitation spectra 8-52567
 CaF₂, elec. cond. at high temp. 8-72159
 CaF₂ electrolyte for thermodynamic study of alkaline earth oxide compounds 8-53241
 CaF₂, etching behaviour in HCl vapour 8-59812
 CaF₂, F-centres, muffin-tin approx. inadequacy 8-63761
 CaF₂ film, ionic migration study by Rutherford scatt., defects, secondary emission (*French*) 8-55982
 CaF₂, fluorite, phase relations, to 60 kbar and 1800°C 8-84785
 CaF₂, IR transparent materials, forward and backward scatt. data 8-59099
 CaF₂, linear thermal expansion coeffs. meas., room temp. to 250°C 8-55416
 CaF₂, low symmetry U⁵⁺ centres 8-76307
 CaF₂, muon Coulomb capture ratio 8-62959
 CaF₂, overlaid with Au and CaF₂ films, channelling meas. 8-67762
 CaF₂ photoelastic modulator, for vibrational circular dichroism spectrometer 8-54476
 CaF₂, rigid lattice system, appl. of zero time resolution NMR 8-76325
 CaF₂, slab, surface modes of vibr. 8-71935
 CaF₂, superionic conductor, theoretical investigation of Raman scatt. 8-80351
 CaF₂ trapezoid, ThF₄ and ZnSe coated, IR characterisation by internal-refl. spectra 8-71161
 CaF₂, vol. depend. of refr. index 8-88275
 CaF₂:Ce, Stark struct., phototransitions, g-factors 8-67995
 CaF₂:D²⁺ submm. magnetospectroscopy, tunable far IR laser potential 8-52481
 CaF₂:Dy, colour centres, antiresonance-type phenomenon in external fields 8-68529
 CaF₂:Dy³⁺, high temp. fluorescence using Ar⁺ and N₂ lasers 8-56514
 CaF₂:Dy³⁺, Mossbauer obs. 8-64303
 CaF₂:ErF₃, clustering, defect struct., NMR study 8-80229
 CaF₂:Eu²⁺, nuclear spin diffusion barrier, ¹⁹F NMR Obs. 8-64282
 CaF₂:Gd³⁺, ITC spectra of impurity aggregate 8-71883
 CaF₂:Gd³⁺, ligand ENDOR cubic centres, elec. field effect (*Russian*) 8-60357
 CaF₂:Gd³⁺, S-state splitting, investigation by ESR and ENDOR at high pressure 8-52345
 CaF₂:Gd³⁺-M⁺, (M=Li, Na, K, Rb, Cs, Ag), electric field effect expts., EPR line breadths, lattice distortions 8-80210
 CaF₂:Pb, O, UV absorption, impurity centres 8-68534
 CaF₂:Pr³⁺, multisite system, laser selective excitation and energy transfer 8-84634
 CaF₂:RF₃, colour centre prod. by γ -irrad., absorpt. spectra obs. 8-72565
 CaF₂:Sm, charge transitions, positron annihilation exam. 8-92143
 CaF₂:Ti²⁺, electronic struct. and EPR of Ti²⁺ 8-76034
 CaF₂:Tm²⁺, EPR, optical recording in weak mag. field 8-68376
 CaF₂:Tm²⁺, spin density parameters at ¹⁹F nuclei 8-68001
 CaF₂:Tm³⁺, 8.2 keV excited state, mag. props., Schottky ht. capacity, nucl. quadrupole splitting 8-76037
 CaF₂:U³⁺, cubic site substituent, EPR spectra obs. 8-72392
 CaF₂:U⁵⁺, rhombic centre EPR spectrum, heat treatment effects 8-72407
 CaF₂:Y(La), dielec. relax. spectrum, ion size trends 8-72460
 CaF₂:YbF₃, clustering, defect struct., NMR study 8-80229
 CaF₂-(Y,R)F₃ (R=any lanthanide except Pm, Eu), phase diagrams 8-84783
 CaF₂-SrF₂-BaF₂:Gd³⁺, luminescence spectrum of Gd³⁺ ion and solid solution region obs. 8-84638
 CaF₂-UF₄-CeF₃ solid soln., surface degradation, complex admittance analysis 8-55980
 CaF₂-YF₃:Nd³⁺, spectral migration of electronic excitation, selective laser excitation (*Russian*) 8-80417
 CaF₂·H₂O, solid soln. prep. and struct. determ. (*French*) 8-51505
 CaF₂·3Ca(PO₄)₂, apatite, fission damage detection, absorpt. spectra 8-84617
 CaFe₂·Fe³⁺(OH)(O(Si₂O₇)), ilvaite, IR spectrum and Mossbauer effect obs. (*French*) 8-80321
 Ca₃Fe₂(Mn₂)Ge₃O₁₂, single magnetic sublattice antiferromagnetic garnets 8-52652
 CaFz crystals, grown from synthetic raw materials, quality, effect of impurities, composition 8-79083
 Ca₃Ga₂Ge₃O₁₂, substrate, electron examination of microstruct. and microsegregation 8-67919
 CaH, in RF-excited heat pipe oven, efficient arc source 8-63162
 CaHPO₄·SO₄·4H₂O, synthetic, cryst. struct. and relation to brushite and gypsum 8-83785
 CaI, electronic band spectrum 6100 to 6600 Å 8-90176
 CaI, mol. dissoc. energy, high temp. mass spectra 8-58863
 CaIr_xRe_{1-x}O₃, (0<x<1), sintered, exam. of mag. and electrical props. 8-80135
 CaMg(CO₃), dolomite, kinetics and thermodynamics of decomposition to metastable solid product 8-80740
 CaMgSi₂O₆-Ca₂MgSi₂O₇-KAlSi₂O₆, phase diagram of ternary eutectic system 8-80529
 Ca₃Mn₂Ge₃O₁₂, highly anisotropic garnet, neutron diffr. obs. of mag. struct. 8-68168
 CaMoO₄, refr. index, single crystals having scheelite struct. 8-79082
 Ca₂NaHSi₂O₉, pectolite, TEM obs., of microtwins and stacking faults 8-75677
 Ca(NO₃)₂·3.91H₂O-NiCl₂ melts, glass forming, transport behaviour 8-59963
 CaO, at. charge densities, X-ray struct. factors 8-79566
 CaO, coherent/incoherent scatt. cross-sections of 136-278 keV γ -rays 8-70881
 CaO, dissociation energies, spectrometric determ. 8-74789
 CaO, doped, thermal stability of hole centres and hole recombination luminescence (*Russian*) 8-72614
 CaO, effect on PbO activity in molten PbO-SiO₂ system 8-60663
 CaO, electronic struct., SCF calcs. 8-66462
 CaO, Eu, Eu²⁺ to Eu³⁺ charge transformation (*Russian*) 8-72403

calcium compounds continued

- CaO, F-centres, $^3T_{1g}$ relaxed excited state, uniaxial stress effect and spin-lattice coupling 8-72405
- CaO, form. from $Ca + O_2(CO_2)$, electronic states obs. 8-92450
- CaO, random intrinsic strain effect on ODMR, PMDR, of F-centre in Jahn Teller states 8-84499
- CaO, undoped and Cl-, F- or Al-doped, X-ray and UV luminesc., electron-hole recombination processes (Russian) 8-76528
- CaO:Mn²⁺, impurity pot. well shape calcs. 8-87950
- 5CaO-3Al₂O₃, cryst. struct. determ. 8-55840
- CaO-Al₂O₃, molten binary slag, dissolved C study (Japanese) 8-60662
- CaO-Al₂O₃ based glass development, water removal, use in IR to 5 μ m 8-83052
- CaO-Al₂O₃ melt, solubility of H₂O at 1600°C 8-51687
- CaO-CaF, hot pressed, effects of CaF₂ addition, sintering behaviours and microstructs. investig. (Japanese) 8-95721
- CaO-Li₂O-Al₂O₃-SiO₂:Nd³⁺, CaO enriched, laser-type glasses, spectroscopic behaviour 8-60497
- CaO-MgO-CeO₂, fired, phase equilibrium diagram, 1700 to 1200°C 8-92248
- CaO-MgO-SiO₂, melts, mixing enthalpy, 1700-1873K 8-79785
- CaO-MgO-ZrO₂-SiO₂, phase study, SiO₂ compatibility relationship 8-95734
- CaO-MgO-ZrO₂-SiO₂, phase study, ZrO₂ compatibility relationship 8-95735
- CaO-P₂O₅ glass, diffusion of Cu⁺, fluoresc. meas. 8-59980
- CaO-P₂O₅ glass, pulsed EPR study of Cu 8-84479
- CaO-SiO₂-Al₂O₃, slag phase, activity of components at 1873K (Polish) 8-52775
- CaO-SiO₂-MgO melt, elec. cond. meas., MgO behaviour (Japanese) 8-75857
- CaO+ α -Fe₂O₃, additive in ZrO₂ sintering 8-76617
- β -(CaO₂)-SiO₂-H₂O, SEM and X-ray diff. exam. of structure, crystallisation props. 8-73012
- Ca(OD)₂:Cu²⁺, ESR, secondary spectra 8-88174
- CaOH, dissociation energies, spectrometric determ. 8-74789
- CaOH, laser excited mol. fluorescence, in an air-acetylene flame 8-86908
- Ca(OH)₂, dissociation energies, spectrometric determ. 8-74789
- 3CaO-Al₂O₃ cement, high level radioactive waste disposal 8-78485
- Ca₂P₂O₇:Sb, (Sb,Mn), luminesc., activation, colour centres (Russian) 8-92123
- Ca₃(PO₄)₂, new cryst. phase prep. and struct. (French) 8-83789
- Ca₃(PO₄)₂:Sb, (Sb,Mn), luminesc., activation, colour centres (Russian) 8-92123
- Ca₃(PO₄)₂Cl, structural interaction of Cl 8-55837
- Ca₃(PO₄)₂F, dislocation struct. exam. (Russian) 8-63770
- Ca₃(PO₄)₂F, structural interaction of F 8-55837
- Ca₃(PO₄)₂F:Nd³⁺, optical fluorescence intensity and cryst. field parameters 8-52570
- Ca₁₀(PO₄)₆(OH)₂, dissolution in water at constant pH, exam. of kinetics 8-59949
- Ca₁₀(PO₄)₆(OH)₂ halogenated derivatives, IR absorpt. spectra (Spanish) 8-52489
- Ca₃(PO₄)₂OH, structural interaction of OH 8-55837
- Ca₃(PO₄)₂OH:Mn, synthesized by hydrothermal method in CaO-P₂O₅-H₂O, thermoluminescence study rel. to starting mixture 8-95612
- Ca₃(PO₄)₂(OH)₂, nonstoichiometric, wet-process formation from α -Ca₃(PO₄)₂ (Japanese) 8-84752
- Ca_{1+x}Re₂O₆(OH)_{2x} (x=0,3), high pressure synthesis and structure (French) 8-51511
- CaS discs, sintering method prep., ionic cond. meas., 650 to 900°C (Japanese) 8-75869
- CaS, phosphor, tunnel luminescence (Russian) 8-72577
- CaS, phosphors, hole recombination luminescence (Russian) 8-72576
- CaS, single crystal, reflectance and absorption spectra, at edge of fundamental absorption (Russian) 8-56499
- CaS:Bi, Tm, phosphor sensitisation mechanism, energy transfer 8-60507
- CaS:Cr³⁺(Cr⁺), EPR (Russian) 8-91946
- CaS:Pd phosphor, thermally stimulated elec. cond., kinetics, 300-413K 8-76088
- CaS-Pb,Mn, phosphors, thermoluminesc. and fluoresc. spectra 8-64396
- CaSO₄ TLD disc response to ¹³¹I and ¹²⁵I, influence of thyroid geometry 8-73250
- CaSO₄:Dy, TLD phosphor, gamma-ray induced sensitisation 8-74542
- CaSO₄:Dy, thermolum. dosimetry, high dose behaviour, comparison with trap depth model prediction 8-78588
- CaSO₄:Dy fast-neutron TLD, efficiency increase by mixing with S 8-73251
- CaSO₄:Dy TLD, fading in high γ -dose region 8-90027
- CaSO₄:Dy(Tm) thermoluminescent props. of non-commercial phosphors 8-58550
- CaSO₄:Sm phosphors, mag. susceptibility temp. depend. 300-453K 8-52196
- CaSO₄· $\frac{1}{2}$ H₂O, (α and β -phase), surface chem. and porosity 8-85200
- CaSO₄·2H₂O, ball mill grinding, rate constant determination (Japanese) 8-95828
- Ca₃Sc₂Ge₂O₁₂, garnet, refined cryst. struct. 8-87654
- Ca₃Sc₂Si₂O₁₂, garnet, refined cryst. struct. 8-87654
- Ca₂(Si,Al)₁₂(O,N)₁₆, α' -Sialon ceramics, prep. and characterisation 8-84750
- β -CaSiO₃ fibre, continuous unidirectional crystallisation from melt 8-95739
- Ca₂SiO₄, bredigite-larnite rock from Scawt Hill, electron microprobe anal. 8-68952
- β -Ca₂SiO₄, formation in presence of NaF, under different thermal treatments 8-68889
- Ca₂SiO₄, hydraulic reaction observed by microwave dielectric meas. 8-80745
- Ca₃SiO₅ form. by solid state reaction, mixture and firing condition effects 8-56602
- Ca₂SiO₅Cl₂, cryst. struct. 8-67694
- Ca_{1-x}Sr_xSi₂, solid solns., α -ThSi₂ struct. type, comp. and press depend. 8-91322
- CaTiO₃-Ca₂Fe₂O₅, Mossbauer resonance exam. of structure, phase equilibrium 8-76640

calcium compounds continued

- CaTiO₃-LaAlO₃ solid soln., phase redistrib. during roasting in H₂ 8-52735
- CaTiSiO₅, sphere, effects of thermal annealing on track etching rate 8-65435
- CaV ferrite garnet, large grained, mag. props. 8-64222
- CaWO₄, refr. index, single crystals having scheelite struct. 8-79082
- CaWO₄, scheelite struct., intrinsic hole centres, EPR study 8-64274
- CaWO₄:Er³⁺, phase relaxation, spin echo meas. 8-68375
- CaWO₄:Eu³⁺(Sm³⁺), energy transfer after red edge excitation 8-52552
- Ca₂X₃, α , intermediate phases, cryst. struct. (X=Iib, IIib, IVb, Vb element) 8-83793
- CaY₂Mg₂Ge₂O₁₂:Nd, CW room temp. laser operation, 0.941 and 1.059 μ m 8-66842
- CaZn(SiO₄)₂H₂O, clinohedrite, cryst. struct., H bonds 8-79593
- Ca₂[(UO₂)₃(PO₄)₂(OH)₂(OH)₂·4H₂O], phurcalite, cryst. struct. determ. 8-55849
- CaF₂, UV visible absorpt. by laser calorimetry, wavelength modulation spectroscopy 8-66876
- CdS-CaS, solid soln., rock salt struct., high press. phase equilibrium study 8-52777
- CeF₃, ¹⁹F NMR, free induction decay, initial behaviour 8-80227
- CoO-CaO-P₂O₅ glass devices, memory switching 8-56192
- (EuLuCa)₃(FeGe)₅O₁₂, mag. props. and growth of 2 μ m bubbles 8-91910
- K₂Ca(SO₄)₂·H₂O, syngenite, space group refinement by vibr. spectroscopy methods 8-79507
- K₂O-CaO-B₂O₃:CuII, immiscibility, ESR detect. 8-80200
- (La_{0.8}Ca_{0.2})MnO_{3+y}, sample preparation using O₂ partial pressure controller (Japanese) 8-73977
- LiO₂-CaO-SiO₂, phase equilibria 8-64528
- LiTaO₃-CaZrO₃, struct. and dielec. props. 8-80298
- MgCaH_{3.72}, synthesis and struct. (Japanese) 8-84751
- MgO-CaMgSiO₄, exam. of high temp. creep behaviour 8-80601
- MgO-CaO-SiO₂-Al₂O₃-Na₂O·P₂O₅, effect of NaPO₃ on phase composition rel. to basic refractories 8-80528
- Mg₂SiO₄-Fe₂SiO₄-CaAl₂Si₂O₈-SiO₂ system phase relations rel. to lunar basalts origin 8-65512
- (Na,Ca)₂Zr(Si₆O₁₅)₃·3H₂O, Mongolian elpidite, cryst. struct. 8-95038
- NaCa₂Si₄O₁₀F, agrellite, new type of silicate double chain 8-51514
- Na₂O-CaO-B₂O₃-Fe₂O₃ glass, Mossbauer expts., 85-500K 8-80260
- Na₂O-CaO-SiO₂, foil, exam. of surface plasticity, and cracks, by electron microscopy 8-68733
- Na₂O-CaO-SiO₂, for optical fibres, high purity glass production methods 8-87176
- Na₂O-CaO-SiO₂, glass, light scatt. rel. to heat treatment (German) 8-84598
- Na₂O-CaO-SiO₂, multicomponent liq. state diffusion 8-55962
- Na₂O-CaO-SiO₂ glass, crack nucleation around plastic indents 8-92327
- 2Na₂O-CaO-XSiO₂ glass, He mobility, interconnectivity, miscibility limits, effect of morphology 8-67864
- RbCaF₃, nonlinear elastic behaviour, US velocity, 1 bar-3 kbar 8-59851
- SiO₂-Al₂O₃-B₂O₃-MgO-CaO-Na₂O, strengthened by ion exchange, exam. of internal stresses using polarising microscope 8-88549
- SiO₂-Al₂O₃-CaO-MgO, liq. silicic and slag, struct, density, surface tension (Polish) 8-83711
- SiO₂-NaO-K₂O-CaO-MgO-Al₂O₃ melt, anodic dissolution of Co and Ni in melt 8-88582
- ((SiO₂)₄₅(CaO)₅₅(Fe₂O₃)₃₅ glass, effect of melt atmosphere on mag. props. 8-68299
- SmCaGe garnet LPE bubble film, coercivity, thickness depend. 8-68324
- Sm_{0.3}Lu_{0.7}Tm_{0.2}Y_{1.45}Ca_{0.85}Fe_{4.15}Ge_{0.85}O₁₂, LPE growth, saturation magnetisation, collapse field, bubble diameter 8-95703
- TiB₂-CaO, thermal stability of composite materials 8-60638
- (Y,Eu,Lu,Ca)₃(Fe,Ge)₅O₁₂, bubble memory chip, dynamic conversion comparison with (Y,Sm,Lu,Ca)₃(Fe,Ge)₅O₁₂ 8-68319
- (Y,Eu,Tm,Ca)₃(Fe,Ge)₅O₁₂, Ca, Ge substituted garnet LPE films, elec. props., charge imbalance, Seebeck effect 8-68101
- (Y,Eu,Tm,Ca)₃(Fe,Ge)₅O₁₂ garnet film coercivity, new annealing method 8-84459
- (Y,Sm,Ca)₃(Fe,Ge)₅O₁₂ single-crystal films, props. 8-64247
- (Y,Sm,Lu,Ca)₃(Fe,Ge)₅O₁₂, bubble memory chip, dynamic conversion comparison with (Y,Eu,Lu,Ca)₃(Fe,Ge)₅O₁₂ 8-68319
- (Y,Sm,Lu,Ca)₃(Fe,Ge)₅O₁₂ garnet film coercivity, new annealing method 8-84459
- (Y,Sm)₃(Fe,Ge)₅O₁₂, Ca, Ge substituted garnet LPE films, elec. props., charge imbalance, Seebeck effect 8-68101
- (YCaEuYb)₃(FeGe)₅O₁₂, LPE, stripe end motion, effect of in-plane field 8-68330
- Y_{3-x}Ca_{2x}Fe_{2-x}In_{3-x}V_{3-x}O₁₂, first magnetocryst. anisotropy const., ferrimag. reson obs. 8-68218
- Y_{3-x}Ca_{2x}Fe_{2-x}Zr_{3-x}Fe_{3-x}O₁₂, first magnetocryst. anisotropy const., ferrimag. reson obs. 8-68218
- (YEuLuCa)₃(FeGe)₅O₁₂ film, stable state of bubbles containing Bloch lines 8-76281
- Y_{1.52}Eu_{0.3}Tm_{0.3}Ca_{0.88}Ge_{0.88}Fe_{4.12}O₁₂, bubble translation vel., ion-implantation effects 8-68327
- (YEuYbCa)₃(FeGe)₅O₁₂ film, mag. σ -bubbles, automation props. 8-88150
- (YSmCa)₃(FeGe)₅O₁₂ LPE films, optimum growth conditions for low coercivity 8-95499
- (YSmLuCa)₃(FeGe)₅O₁₂, reproducibility in bubble garnet LPE growth 8-92204
- (YSmLuCa)₃(FeGe)₅O₁₂, mag. props. and growth of 2 μ m bubbles 8-91910
- (YSmLuCa)₃(FeGe)₅O₁₂, LPE growth, growth reproducibility of bubble props. 8-92208
- (YSmLuCa)₃(FeGe)₅O₁₂, garnet film, refractive index dispersion 8-88273
- YSmLuCaGeIG, mag. props. and defects, depend. on B₂O₃ conc. on growth in PbO-B₂O₃ solvents 8-68321
- (YSmTmCa)₃(GeFe)₅O₁₂ film, YY pattern racetrack discrimination and state stability of S=1 and 0 bubbles 8-91908

calculating see calculation

calculating apparatus

slide rule for rot. calcs., optical polarisation appl. 8-49594

calculating machines *see* **calculating apparatus**

calculation

see also **graphs**; **nomograms**
No entries

calculators *see* **calculating apparatus**

calculators (electronic) *see* **electronic calculators**

calculus

see also **differentiation**; **integration**; **variational techniques**
No entries

calibration

see also **measurement standards**; **standardisation**

absolute calibration of grating spectrograph for laser wavelength meas. 8-90528

AC portable digital voltmeter and calibrator 8-74019

aerosol detector, in cryogenic systems 8-81986

air pollution measurement, particulates and gaseous pollutants anal. and calibration techniques 8-69531

angular scales, angle etalon constr. (*German*) 8-77852

apparatus volumetric calibration by cryogenic Xe gas transfer 8-93653

asbestos, airborne, X-ray diff. anal., calibration standards 8-69517

astronomical mm. obs., effect of Earth's atmosphere, two-layer model 8-53691

atmosphere N₂O measurements, laboratory intercalibration 8-81277

atmosphere NO/NO₂/O₃ monitors, intercalibration 8-69529

auto-collimating telescopes, angular measurement appl. (*German*) 8-77848

automatic network analyser, EM reflection coeff. meas. appl. 8-89463

blood gas analysers, review 8-69238

blood pressure instruments, direct systolic/diastolic meas., review 8-69234

bolometer, fast superconducting molecular beam detector 8-86383

bone conduction vibrators, calibration force levels 8-65046

calibrator using band-gap voltage reference, oscilloscope appl. 8-65941

calorimeter, dynamic differential types comparison, in linear macromol. heat capacity meas. 8-89482

calorimetric probes for gas stream enthalpy meas. 8-70126

capacitance transducer, calibrated, for detection of acoustic emission 8-71256

cardiac output analysers, equipment, maintenance and ccts., review 8-69239

cellulose nitrate α -particle detector for Rn short lived daughters, results and calibration (*Czech*) 8-62663

chamber calibration using ruby R₁ luminescence line shift, 80 to 550K 8-86284

chemical anal. by counting meas. calibration determs., statistical uncertainties of anal. 8-92533

colorimetric educational laboratory, calibration of set of surface colour standards 8-49625

convective heat loss assessment from humans in cold water 8-81093

crude-oil hydrometers calibration 8-73969

cryogenic construction material magnetisation meas. (*Slovak*) 8-93693

defibrillators, review of instruments and maintenance 8-69251

digital laser-Doppler velocimeters signal processor accuracy testing (*German*) 8-86242

digital voltmeter (*German*) 8-93723

diode laser, appl. to IR spectra of NH₃ mols. 8-58689

dosimeter, thermoluminesc., calibration, γ -ray irradiator (*Japanese*) 8-66452

double Compton gamma-ray telescope, calibration in neutron beam 8-53827

double constant current source for cryogenic current comparators, standard resistor calibration appl. 8-93731

Dynalizer II, application to X-ray quality control 8-77896

electro-medical servicing, quality maintenance 8-77126

electroacoustic and aerodynamic calibrated sound sources compared 8-55543

electrochemical O₂ meter calibration in 10⁻⁷ bar range 8-80812

F-type stars, absolute luminosity calibration 8-65612

film dosimeters, calorimeter for calibration in high intensity electron fields 8-73257

flowmeter, by electronic weighing 8-55700

fluxmeter measurement range extension 8-57993

gamma-ray spectrometric logging and surface exploration equipment 8-85706

gas flow meas. standard methods review 8-94864

hailpads calibration 8-93001

halofluorocarbons, in ambient air, in situ quantification technique calibration 8-69530

Harwell linac II total scatt. spectrometer, Ni powder diff. data 8-86725

heart volume determination by angiography, X-ray magnification estimation 8-73197

high press. apparatus with shaped Bridgman anvils, calibration 8-49856

high-voltage spark sources, calibration meas. methods 8-49908

hospital test instruments, scientific and medical instrumentation capability 8-69242

hot wire anemometer probes, X-configuration dynamic testing device 8-87421

hot-film anemometer, calibration of low-vel., flow direction 8-91043

inductometer calibrator, U-738, description 8-74034

ion microprobe analysis, calibration using matrix ion species ratios, appls. 8-61070

IR fluctuation hygrometer, design, calibration, field trial results 8-77368

isothermal displacement calorimeter, for positive excess enthalpies 8-89483

laser low level pulse simulation and calibration, tracking system evaluation 8-59074

laser-Doppler technique, local size and vel. probability distrib., two-phase suspension flow 8-59517

linear gauges, high precision, automatic interference comparator appl. (*German*) 8-77847

long slip gauges, Fabry-Perot etalon appl. (*German*) 8-77849

low pressure manometer calibration method using vacuum technique 8-74015

low-impedance microphone calibrator for pressure transducers 8-59212

calibration continued

machinery acoustic noise meas. standards and reference sources (*French*) 8-83185

magnetic induction calibration units, description 8-74035

magnetic resonance spectrometer calibration by EPR spectra recording 8-89513

magnetised Fe-scintillator sandwich total absorption calorimeter, performance at 15-140 GeV 8-55103

mass spectrometer, space-borne, in-flight calibration device 8-93115

mass spectrometers for van der Waals dimers 8-89585

mass standards, calibration by sets of weights intercomparison 8-54342

measurement instruments, optimal intervals determ., generalised method (*Rumanian*) 8-49787

metrology use in material inspection 8-95899

modular electron calorimeter, relative and absolute calibration 8-78578

moisture measurement in porous ceramic components, equipment (*German*) 8-54378

neutron activation in vivo total body anal. using 14 MeV neutrons, calibration and evaluation of system 8-53490

neutron monitor calibration for radiation protection at 24.5 keV and 2 keV 8-89983

neutron precision long counters, calibration for use with filtered neutron beams (*German*) 8-58529

neutron sources, anisotropic neutron emission 8-90009

NMR spectroscopy, low-temp. thermometer for ¹H, ¹⁹F, and ¹³C samples 8-65949

noise source, high-level, for calibration of Johnson noise power thermometers 8-82005

oceanographic radio techniques, calibration and appls. 8-77337

open channel acoustic flowmeters, design, calibration and errors 8-55701

optical fibre absolute power meas. thermistor sensor 8-65971

optical transmittance, inverse-fourth photometric device 8-82021

oximeter calibration, humans exposed to centrifugation 8-92734

pH meters, online, problems and solutions 8-53282

photodiodes, down to 5 nm wavelength, synchrotron UV radiation appl. 8-77959

photometric gas analyser, method 8-49877

photometry of white dwarf stars, calibration 8-85938

plastic scintillators, radioluminesc. absolute output following ⁶⁰Co γ -ray irradi. (*Russian*) 8-92124

portable radiation meters, accuracy checking facility at Berkeley Laboratories, UK 8-74507

precision transducers with pneumatic output signals, reference air/water multibute manometer appl. 8-93717

pressure calibration by resistance-jump transitions up to 500 kilobars 8-54388

Preston tube calibration in transpired turbulent boundary layer 8-79397

proton beam calib., limits on differential hysteresis in Enge split-pole spectrograph 8-55082

pulsed low current source for amplifier calib. in ion-molecule collision expts. 8-93724

radiation-force balance, portable, for diagnostic US transducer output power meas. 8-69163

radiocarbon dates calibration, bristlecone pine and ancient Egypt 8-70234

records, direct-writing analogue type, biomedical appls., techniques and maintenance, review 8-69241

refractive index measurement, calibration substrate for Abeles equipment 8-77965

respiratory monitors, instrumentation and maintenance, review 8-69236

RF voltage standard system for voltages from microvolt to 1 V (*Japanese*) 8-89491

rheometer, high freq., operation, calibration, appls. 8-83345

RMS digital voltmeter calibrator for VLF 8-86293

roentgenocardiograph with photoelectronic sensors, calibration device 8-57061

ruby R₁ fluoresc. press. gauge, calibration, 0.06-1 Mbar, specific vol. meas. for Cu, Mo, Pd, Ag 8-70150

satellite solar cell calibration using high-altitude balloon (*Japanese*) 8-61700

solar EUV output, meas. techniques and instruments recalibration 8-57535

solar magnetograph calibration programme (*Russian*) 8-65499

solar radiation meas. field instrument standard 8-88946

sound pressure in insert earphone couplers and real ears 8-65152

spark-source mass spectroscopic anal. of Al, Al alloys, sensitivity calibration 8-68962

spectral radiance calibration of light sources in vac. UV using synchrotron radiation 8-65954

spectrometer, millimetre-wave astronomical, intensity calibration error evaluation 8-53821

spectrophotometer, four-channel, for stellar Ca II H and K flux meas., calibration obs. 8-73646

spectrophotometric standards, glass filter SRM 930 by NBS, clinical laboratory appl. 8-54331

spinning magnetometer, absolute calibration method 8-54413

stellar spectra, photographic equivalent widths calibration against solar photoelectric equivalent widths, feasibility 8-73658

stellar uvby β photometric system, absolute luminosity calibrations check by means of small trigonometric parallaxes 8-57463

stylus-type surface texture meas. instrument against interferometrically measured step 8-77862

superconducting susceptometer, automatic, sensitivity calibration, biological appl. 8-57154

Tarapur Atomic Power Station radioactive waste discharge monitoring 8-89989

telescopes, auto-collimating, absolute calibration methods (*German*) 8-86239

test gas atmospheres, calibration standards, generated by gas phase titration 8-69507

test leaks 8-53121

thermogravimetric automatic temperature indicator 8-86257

thermometers, time response calibration, concepts and model calcs. 8-54370

thermometers, using Ga melting-point apparatus, enzymologic appl. 8-85460

calibration continued

- thermometry considerations in localised hyperthermia, review 8-53561
 thermopile radiometers for UV spectrum appl. (*Japanese*) 8-54422
 thermosphere, tidal struct. at equinox, model calibration 8-81476
 time meas. system adjustment and calibration signal generator 8-57903
 TIROS N microwave sounder unit, blackbody calibration 8-93016
 transducers, reciprocity calibration in unconventional acoustic geometries 8-83200
 transfer standard radiometric sources and detectors, calibration using synchrotron radiation 8-65967
 two-coordinate measuring device, interference band-object scanning, precision gauge block length standards (*German*) 8-89433
 two-photon absorption calibration via stimulated Raman gain 8-87098
 UHF-plasma torch emission spectrometry by metal hydride generation (*Japanese*) 8-92582
 underwater acoustic transducers using complex exponential signal representation 8-79183
 underwater transducers, steered planar nearfield calibration array 8-59214
 US C-scan grey scale recorder, calibration method 8-95878
 UV double-beam photometer, for atm. O₃ calibration 8-69505
 UV photometer for atmospheric ozone monitors calibration 8-77960
 vacuum gauge calibration, 10⁻⁴ to 10 Pa, by orifice flow method 8-82000
 vacuum monochromator, grazing-incidence, absolute calibration using Tokamak discharges 8-87492
 vacuum press. meas. considerations (*French*) 8-49846
 vector magnetometer sensor orientation, accurate calibration 8-53741
 VUV calibration facility for radiation detector spectral sensitivity meas. (*German*) 8-82037
 weather radar calibration, correl. with rain gauge data (*Japanese*) 8-85670
 wedge opening load specimen, side grooved, stress intensity factor soln. and calibration 8-51130
 Weissenberg rheogoniometer, computerised calib. and meas. of Newtonian fluids 8-87323
 X-ray fluorescence anal. of trace elements, calibration constns. (*French*) 8-61095
 CO₂ laser stability and heterodyne frequency calibration 8-59031
¹⁴¹Ce standard, measured by dose calibrators, simulated ⁹⁹Tc^m standard 8-61261
 Ge-Li spectrom., re-evaluation of precise γ -ray energies for calibration 8-90015
 Ge(Li), spectrometer efficiency, dead time and pulse pile-up correction 8-50442
 H meters, on-line, calibration system 8-86236
 He gas jet noise source, absolute calibr. 8-59228
³He ionisation chamber, calibration for use with filtered neutron beams (*German*) 8-58529
 Ni-Cr foil strain gauge, for cryogenic anal. of supercond. structs. in high mag. fields, fusion reactors 8-54947
 O₂ consumption and CO₂ prod. continuous meas. for men in hyperbaric chambers 8-81008
 O₃ calibration methods, accuracy 8-69506
 O₃ calibration reference instrument calibration 8-73524
 Pt resistance thermometer calibration characts. linearisation methods (*Russian*) 8-70123
 Pt₉₀Rh₁₀/Pt thermocouple, Inconel sheathed, MgO-insulated, decalibrations during 1200°C use, ion microprobe obs. 8-57957
²³⁹Pu, lung burden X-ray counting efficiency, from inhaled ¹⁰³Pd studies 8-85391
 SO₂ small automatic monitoring network calibration and maintenance aspects 8-81462

californium

see also nuclei with

crystal structure at high press., X-ray diffr. 8-83766

californium compounds

- ²⁵²CfCl₃ metabolism in rat and effect of in vivo DTPA chelation therapy 8-85387
 CfI₂, cryst. struct. determ., X-ray diffr., optical spectra 8-75645
 CfI₃, cryst. struct. determ., X-ray diffr., optical spectra, thermal expansion coeffs., 20 to 700°C 8-75645

calling equipment (telephone) see telephone station equipment**calorimeters**

see also calorimetry

- 100 GHz bolometer mount efficiency meas. calorimeter (*Japanese*) 8-54460
 absolute calorimeters for high-power high-energy CO₂ laser 8-93686
 AC, high resolution, for organic liquids 8-70127
 AC calorimeter, construction and design (*Japanese*) 8-89481
 adiabatic scanning microcalorimeter specific heat capacity meas. of small samples 8-86274
 automatic heat flow calorimeter for heats of reaction meas. 8-54373
 BB2 meter, for high-power CW laser energy meas. 8-54372
 bolometer mount, effective efficiency meas. using computerised system 8-86272
 classification, systematic criteria, exam. (*Rumanian*) 8-81975
 differential microcalorimeter for absorbed gamma-radiation dosage, 0.01-10 W (*Russian*) 8-85385
 digital automatic thermodynamic enthalpy and specific heat determ. equipment 8-57951
 dosimetry, total absorption type calorimeter for 25 MeV electron beams (*Japanese*) 8-78501
 dynamic differential calorimeters comparison, in linear macromol. heat capacity meas. 8-89482
 film dosimeters, calorimeter for calibration in high intensity electron fields 8-73257
 fusion reactor neutral beam injector, calorimeter and beam dump design 8-66382
 high pressure liquid thermal capacity meas., design guidelines (*Russian*) 8-74001
 isothermal displacement calorimeter, for positive excess enthalpies 8-89483
 laser absorption calorimeter automation 8-74084
 laser calorimeter for absorpt. coeff. determ. of IR windows and mirrors 8-49838
 laser low energy output meas. with absolute calorimeter 8-55396
 liquids, complex thermophysical studies 8-57953

calorimeters continued

- miniature, fast-acting, with changeable semicond. thermal detector 8-77916
 modular electron calorimeter, relative and absolute calibration 8-78578
 photocalorimeter, to determine moisture content of gases, exam. 8-56936
 plasma diagnostics and laser beam meas. 8-51361
 precision with isothermal jackets, mathematical model for temperature field 8-93687
 pulse gas calorimeter, for vacuum UV radiation meas. (*Russian*) 8-93688
 respiration calorimetry determination of O₂-calorie equivalence of thyroid patients and normal subjects (*German*) 8-85412
 snow melt calorimeter (*Japanese*) 8-88934
 temperature change meas., optimisation of Wheatstone bridge using thermistors (*German*) 8-86275
 transient heat flow anal., features (*Russian*) 8-86273

calorimetry

see also calorimeters; specific heat; thermal analysis

- benzene, vapour-flow calorimetry 8-91058
 convective heat loss assessment from humans in cold water 8-81093
 deformation calorimetry, meas. of energy stored in plastic deform. of Al and Al alloys 8-84894
 differential microcalorimetry for direct meas. of difference between two thermal effects (*French*) 8-57950
 differential scanning, computer-interfaced, heat capacity meas. 8-65935
 emissivity of solids determ. 8-62201
 ethane, solid, thermodynamic props. between double solid-to-solid transition and triple point temp. 8-75828
 ethylene + N₂, gaseous, excess enthalpy, determ. by flow calorimetry 8-91057
 explosives, secondary, thermal decomp., solid-state kinetics, differential scanning calorimetry 8-92449
 fusion reactor 120 keV neutral beam, calorimetric and optical beam diagnostics 8-54933
 inorganic solids, high energy irradiation, energy storage meas. 8-51581
 laser power measurement by thermoelec. meter 8-63124
 light absorption, visible and near-IR for black surfaces 8-93685
 macromolecule, linear, heat capacity meas., dynamic differential calorimeters comparison 8-89482
 nontransition element/alkali metal systems, direct calorimetric exam. 8-84775
 optical fibre ribbons, loss meas. 8-87127
 pacemaker, batteries, characterisation of internal power losses by calorimetry 8-92747
 pacemakers and batteries, microcalorimetric study 8-57130
 polystyrene glasses, transition temp. and thermodynamic state 8-75819
 probes for gas stream enthalpy meas., calibration 8-70126
 pyridine, ethyl pyridine, heat of adsorpt. on sponge Fe, Fe₂O₃, CuO, adhesive wear, flow calorimetry 8-85193
 sheath temp. distrib. for material selection criterion 8-77917
 specific heat meas. method at arbitrary temp., simple and accurate 8-62202
 stearic acid, heat of adsorpt. on Fe₂O₃ powder, surface area meas. by flow calorimetry 8-81974
 steel, reflectivity at 10.6 μ m, calorimeter meas. 8-55393
 transparent solids, absorpt. coeffs. by laser calorimetry, wavelength modulation spectroscopy 8-66876
 Cs, liq., specific heat meas., at temp. up to 1700K under pressure 8-51696
 FeSiF₆.6H₂O, phase transform. exam. by X-ray and DSC methods 8-83948
 Ga/rare earth systems, direct calorimetric exam. 8-84775
 GaAs, absorption coefficients, method of meas. 8-83048
 InSb, heats of transformation for high pressure, orthorhombic modification, exam. 8-56627
 KNO₃, polymorphism, calorimetric investigation 8-75827
 Sn low-temp. specific heat meas. under pressure 8-77915
 V-D, exam. of phase diagram, using DTA and calorimetry, isotope effect 8-80527
 W, sintered metal reference standard, sp. ht. at high temp. 8-89427

calorists see calorimeters**CAMAC**

- dosimetry, automated data acquisition and anal. system at LAMPF pion therapy facility 8-53506
 fusion reactor ignition, eight-beam CO₂ laser system, minicomputer-CAMAC control system 8-58493
 hodoscopic detector registration systems, data coding/reading block 8-78602
 ion mobility measurement, in drift tubes, using CAMAC crate interfaced to microcomputer 8-93661
 JET, control and data acquisition system, CODAS 8-62619
 particle track chamber, semi-automatic meas. instrum. register for camera photograph reduction 8-78575
 pulse sequence fast A/D conversion 8-55119
 Rutherford Laboratory N5 expt. data acquisition system, program struct. and CAMAC hardware 8-90051
 time to digital convertor in real time, low cost 8-55111
 two-channel data gathering and registration system for fast-action experiments 8-77877

camera lenses see photographic lenses**camera tubes, television** see television camera tubes**cameras**

see also coronagraphs; television cameras

- 35 mm camera control cct. for automated time-lapse photography 8-58076
 astronomical Schmidt camera, direct, quasi-telecentric and telecentric combinations of interference filters 8-57441
 automatic exposure of photographic camera films 8-65992
 automatic focusing of cameras using self-contained IC 8-82069
 automatic lens focusing using optolinear chip 8-54480
 cassette film camera for automatic and rapid prod. of colour pictures (*Russian*) 8-93780
 Cine, guide elements, use of powdered polymer coatings 8-78021
 cine, time-lapse mechanism design, clouds and lightning photography appl 8-85747

cameras continued

- cinematography, colour film processes and cameras, review, 1894 to date (*German*) 8-93773
 digital control of Canon A-1 camera 8-70206
 exposure meter for KSR-1M film camera (*Russian*) 8-93779
 field and aperture quantitative determ. (*Spanish*) 8-49921
 gonioscopy, foot-operated camera trip for Nikon photo slit lamp 8-80986
 high-speed photography and photonic recording 8-86367
 holographic grating, calc., for very wide field camera (*French*) 8-81547
 image converter streak camera 8-54484
 International Ultraviolet Explorer (IUE), cameras in-flight photometric performance 8-96383
 intervalometer using two cameras, sampling option 8-77367
 IR single-line scanning 8-58029
 magnetostriction spark cameras data readout cct. 8-78576
 McMullan 4 cm electronographic camera, appl. to high-dispersion stellar spectroscopy 8-73644
 mobile gamma camera with remote image processing computer system, for nuclear medicine 8-92700
 motion picture camera device for shooting in movement (*Russian*) 8-93777
 multipulse lightning discharge oscillogram scanning camera 8-61588
 multiwire proportional gamma camera for imaging $^{99}\text{Tc}^m$ radionuclide distrib. 8-53493
 night identification appl., trade-offs consideration 8-54489
 oscillographs, photographic recording using Polaroid camera (*Italian*) 8-78007
 particle camera, aircraft-borne, for in situ photography of cloud particles 8-85750
 particle track chamber, semi-automatic meas. instrum. register for camera photograph reduction 8-78575
 picture taking parameters display in amateur cameras, review 8-89578
 Polaroid Sonar One-Step camera, US automatic focusing 8-78011
 positron camera, 3-dimens., for nucl. medicine 8-73225
 Radcliffe Cassegrain telescope, d-camera vel. system 8-73645
 scintigraphic camera systems and their assessment by computer 8-57063
 scintillation gamma camera, anal. of basic characts. 8-57059
 spin scan camera system, on geostationary satellite, for global weather monitoring 8-61600
 super-8 silent movie camera (*German*) 8-86365
 transaxial tomography camera, photographic image reconstruction, analogue recording system 8-82085
 underwater radiance scanner, design and implementation 8-61609
 Viking Lander camera, optical system and design 8-53794
 Viking Lander camera, stray light control 8-61713
 X-ray, small angle scattering camera for synchrotron radiation 8-66020
 X-ray and optical cameras, laser fusion appls. 8-59686
 X-ray diffraction camera, method for cryst. mounting on ends of fibres 8-93663

candoluminescence *see luminescence*

canted spin arrangements

- see also weak ferromagnetism*
 ferromagnet, rel. to ZZ 8-68014
 FeGe, hexagonal, low-temp. mag. struct., neutron diff. meas. 8-95418
 KNiF₃, antiferromag. domain wall motion obs. by X-ray synchrotron topography 8-88139
 Li_{0.5(1-x)}Zn_xFe_{2.5-0.5x}O₄, canted spin struct., neutron diff. study 8-68175
 Ni-Mn alloy, disordered, mag. struct., high field twist deform. 8-68166
 YFeO₃, mag. domain walls, photomagnetic effects, ^{57}Fe NMR obs. 8-95464

capacitance

- see also photocapacitance*
 chlorophyll a film, charge injection and storage 8-53317
 4'-4'-cyano-octyl-biphenyl, smectic A liq. cryst., elec. field effects, capacitance meas. 8-91237
 4'-4'-cyano-octyloxy-biphenyl, smectic A liq. cryst., elec. field effects, capacitance meas. 8-91237
 electrode metal-solvent interaction rel. to elec. double layer struct., adsorpt. 8-61023
 free space capacitance calc. for a square cylinder of finite length (*Chinese*) 8-66705
 n-GaAs:O, press. depend. of deep level associated with O, transient capacitance meas. 8-64000
 impedance of a p-n junction by direct currents (*Russian*) 8-84285
 Josephson contact microwave detector sensitivity and cutoff frequency rel. to capacitance 8-49902
 layer of symmetrical spherical dipoles, Poisson-Boltzmann treatment of capacitance 8-64844
 metal-semiconductor junctions, capacitance, temp.-depend., by space-charge methods 8-91758
 microstrip anisotropic electrostatic field problems, Green's function technique 8-70998
 MIS structures with semiconductor layers of critical thickness, potential distrib. and capacitance calc. 8-95381
 MOS C-V data in strong inversion, surface minority carrier redistrib. 8-72266
 MOS structure, generation lifetimes from C-t transients 8-88036
 oxide-electrolyte interface, transition layer model 8-68895
 p-n diode, dynamic base capacitance and time const. 8-68076
 p-n junction, abrupt, depletion layer capacitance, theory 8-52067
 p-n junctions, capacitance, temp.-depend., by space-charge methods 8-91758
 p-n junctions, determ. of arbitrary doping profile, depletion layer capacitance meas. 8-88021
 Ag/(α -AgI) interface, impedance meas., equivalent circuit parameters. calc., electrolyte defect struct. 8-59975
 CdS, film for solar cells, struct. and elec. props., thickness depend. 8-72289
 GaAs MESFET, deep trapping effects at GaAs-GaAs:Cr interface 8-72245
 GaAs MIS capacitor, transient capacitance and C-V characts. 8-95374
 p-InAs-Au contacts, influence of free surface on elec. behaviour 8-95362

capacitance continued

- InP MIS capacitor, transient capacitance and C-V characts. 8-95374
 Pb, small Josephson junction, temp. and mag. field variations in resist., cos ϕ conductance and effective capacitance 8-84357
 PbI₂ single crysts., photo-induced AC impedance meas., photodielec. effect 8-52034
 Si, clean-cleaved, Schottky barrier height meas. accuracy 8-52081
 Si:S, existence of isotope shift for S deep level, isothermal transient capacitance meas. 8-63999
 Si-SiO₂-KCl₄ interface, capacitance meas. 8-80051
 Ta-Ti-O, reactive sputtered film, elec. props. 8-84336
 TiO₂-Si, MIS capacitor, C-V characts. meas. 8-60208
 ZnO pellets, and ZnO:Li single crysts., photo-induced AC impedance meas., photodielec. effect 8-52034

capacitance measurement

- 25 kV bias isolation unit for 1 MHz measurements using commercial C/G meter 8-54401
 accuracy improvement by variable coeff. elimination (*Russian*) 8-49789
 capacitoplethysmography for heart and lung meas. (*Japanese*) 8-53465
 capacitor, by three-voltmeter minicomputer multibridge system (*Russian*) 8-70159
 capacitor transducer, noise-stable meas. cct. (*Russian*) 8-89493
 defibrillator, damped sine wave, intact, evaluation of operating parameters 8-57120
 dielectrography methods and apparatus, recording capacitance changes due to blood vol. fluctuations 8-57046
 dispersion field transducers for granular material exam. 8-85078
 electric double layer capacitance meas., potentiostatic method 8-85169
 Lampard type electrostatic systems, analysis of the effect of the metrological properties (*Polish*) 8-77928
 lumped-capacitance method for complex dielec. permitt. in polar liqs. 8-77936
 MIS structure surface characterisation by C(V) curves 8-72276
 MOS structure dynamic volt-capacitance characteristic meas. 8-60207
 p-n junctions capacitance, using bridge circuit with analogue multiplication (*Bulgarian*) 8-57977
 two plate capacitor with aerostatic electrode regulation for precise determination of capacitor loss factor (*German*) 8-74021
 p-GaP electrode, for solar cell, differential capacitance meas. for flat-band potential determ. 8-72256

capacitance meters *see capacitance measurement*

capacitor storage

- arc gap with displacement by mag. field 8-87513
 banks, optimum design rules, fusion reactor technology 8-74487
 foil-and-paper 10 kV capacitors, low-cost energy storage for fusion reactors 8-74485
 fusion reactor laser, Shiva pulse power, isolation and control system 8-54935
 fusion reactor magnet coil, 125 kG, 1 m, design, fabrication 8-55008
 HV capacitor banks and ccts. initiating by air driven fibre optic coupled pulser system 8-54943
 neutral beam power supply, 40 kV, 25 ms, for fusion reactor 8-62610
 propylene film-paper-phthalate ester capacitors 8-74486
 pulsed electron accelerator current density distrib. multichannel recorder 8-58520
 rail accelerator, ambient medium heating expt. 8-75439
 Shiva laser, 25 MJ energy storage and delivery system 8-55015
 Shiva laser, 25 MJ energy storage and delivery system 8-59038
 solid-state laser miniature power pack 8-59015

capacitor stores *see capacitor storage*

capacitors

- see also electrolytic capacitors; thin film capacitors; varactors*
 aerosol particles sizing, appl. of elec. capacitor 8-81471
 Brownian motion between capacitor plates, path integrals for inertial classical particles 8-57858
 capacitance/loss-tangent meas. by three-voltmeter multi-bridge method (*Russian*) 8-70159
 cylindrical particle analyser, fringing field 8-94165
 dense plasma focus, capacitor bank system design and safety 8-54889
 displacement transducers, effect of tilt and surface damage 8-54356
 ferroelectric films, resonant autothermostabilisation (*Russian*) 8-52451
 foil-and-paper 10 kV capacitors, low-cost energy storage for fusion reactors 8-74485
 PF correction, dielectric fluid test and anal., quality assurance 8-80272
 potential fields calc., plane-parallel, in mixed boundary conditions (*Rumanian*) 8-82877
 propylene film-paper-phthalate ester capacitors, for energy storage 8-74486
 two plate with aerostatic electrode regulation for precise determination of capacitor loss factor, features (*German*) 8-74021
 vibrating-capacitor electrometer, current noise meas. 8-54398
 GaAs crystals appl., with nipi superstructures (*German*) 8-95064

capacity, channel *see channel capacity*

capillarity

- see also bubbles; contact angle; drops; foams; liquid films; surface tension*
 band broadening, in microcapillary tubes, liq. chromatographic appls. 8-61085
 capillary rheometer, viscous heating from power law fluid, perturbation expansion anal. 8-63519
 capillary waves generated by steep gravity waves, meas. 8-59409
 capillary-gravity waves, linear problems 8-51178
 capillary-gravity waves in viscous fluid 8-51177
 capillary-porous bodies, heat and moisture transfer, analytical formulae 8-67013
 capillary-porous body, nonlinear heat/mass transfer problem, soln. using invariant groups 8-55688
 creeping flow over surface, angle of contact, viscous liq. 8-51149
 cumene, films, thin, wetting, rheological characts. determ., capillary method 8-51788
 n-decane, films, thin, wetting, rheological characts. determ., capillary method 8-51788
 drops in immiscible liquid, intermittent elec. field heat transfer augmentation 8-94872

capillarity continued

- dynamic liquid surface tension determ. from drop oscillation frequency and capillary jet instability 8-56026
 dynamic surface tension, meas. by excited capillary jet axisymmetric disturbance growth rate 8-95205
 electrocapillary theory, Lippmann relation, surface thermodynamics 8-61048
 extensional flow capillary rheometer for extensional viscosity meas. 8-55704
 flow of gases and liquids through ultrafine capillaries 8-94822
 flow velocity meas. in capillary using pulsed NMR 8-83506
 fluid interfaces, flotation and mech. manipulation of solid spheres 8-63906
 freesurface breakdown in rot. liq., wavelets 8-59402
 heat pipe, with header and single or two-phase artery systems 8-90981
 heat pipe with capillary struct., amount of coolant effect on operation 8-75037
 jets, capillary instability, determ. of dynamic surface tension of inks 8-84031
 Knudsen to Poiseuille flow transition, capillary model 8-55689
 liquid film, free, squeezing mode relax., laser scatt. rel. to colloid interaction 8-87354
 liquid jet, capillary instability, effect of harmonics 8-71378
 liquid surface shape near stripwise heterogeneous wall, analytical soln. of Laplace eqn. 8-67890
 low-temperature heat pipe wick evaporation (*Ukrainian*) 8-90639
 MHD gravity-capillary waves in liq. film falling by permeable bed 8-67277
 moist materials, drying kinetics calc. method, heat (moisture) transfer 8-55555
 ocean wave detection by microwave radar, gravity-capillary wave modulation 8-77333
 polyethylene capillaries, for polarography in corrosive media, prep. 8-61090
 polymer solns., unstable flow, reservoir to capillary, jet instability onset and flow patterns, obs. 8-87364
 porous body, drying, X-ray absorption obs., radiometry, temp. control 8-67023
 porous media wetting, capillary rise, contact angle effect (*German*) 8-84033
 porous solid with below-freezing pt. adsorbate, isothermal adsorption and dimensional changes obs. 8-75925
 sintered composite-liq. metal interaction, mass transfer eqn. approx. soln. 8-67262
 solid bodies, capillary interaction 8-51792
 solution of diffusion eqn. for capillary method with no external stirring 8-54518
 swirling annular capillary jet flow (*Russian*) 8-75180
 thermocapillary convection, unevenly heated liq. stream near gas bubble 8-59460
 tracer diffusion coefficients, open-ended continuous capillary method determ. 8-75861
 water, films, thin, wetting, rheological characts. determ., capillary method 8-51788
 water drainage, by capillary flow (*Japanese*) 8-95208
 water in capillary, freezing and melting behaviour, dilatometry, elec. cond. meas. 8-75908
 waves, travelling, gravity-capillary, on liq. film surface falling past permeable bed 8-87351
 D₂O, temperature of maximum density in capillaries 8-51801
 Na, vaporisation from capillary-porous structs. (heat tubes, vap. chambers) crit. heat flux 8-90631
 Si, preshaped single crystal prep. by pendant drop method (*French*) 8-64466

capillary phenomena *see capillarity***capture cross-sections, nuclear** *see nuclear reactions and scattering***Carathéodory's principle** *see thermodynamics***carbon***see also nuclei with**see also carbon fibres; charcoal; diamond; graphite*

- activated, adsorption of 0.98 mol.% Ar, vol. adsorption capacity 8-75933
 activated, vol. adsorption capacity for selected trace contaminants 8-56031
 activation analysis by photonuclear reaction (*Japanese*) 8-76945
 adsorption, of Ar (methane), surface excess isotherms, gravimetric determ. 8-51816
 adsorption, of CO₂, surface area meas., temp. and chemisorption effects 8-95225
 adsorption, on CdS, AES study (*Japanese*) 8-88008
 adsorption of gas, rate depend. on granule size and gas flow velocity 8-56033
 adsorption on W, Auger signal comparison using differential and integral Auger spectra 8-76561
 aerosol particles, size-fractionated, C, N and O determ. by particle elastic scatt. anal. 8-81466
 aerosol visibility vs. particle size distrib. 8-88911
 amorphous, elec. cond. and Hall effect, temp. depend. 8-60141
 amorphous, ranges of implanted 10-30 keV D⁺ 8-83858
 atom, CNDO/S nucl. screening const. calcs. 8-86787
 atom, effective valence shell Hamiltonian, ab initio calcs. 8-82611
 atom, electron affinity, modified variational approx. 8-66679
 atom, electron impact ionis., 7-1000 eV, cross-section 8-86956
 atom, electron scatt., at. field bremsstrahlung, photon linear polaris. 8-62927
 atom, electron scatt. and photoionis., correlation effects 8-58842
 atom, excited states, quadrupole moments, Sternheimer shielding factors 8-82630
 atom, ground state energy, HF calc., second-order correction 8-86784
 atom, ground state wavefunction, SCF HF calc. 8-90070
 atom, photoionisation of 2s shell, photoelectron ang. distrib. 8-86833
 atom, radiative lifetimes of visible and near IR transitions, solar abundance 8-50506
 atom, theoretical ionis. energies and oscill. strengths, excited s-, p- and d-levels 8-86823
 atom+H⁺ (He⁺), K-shell ionisation, impact parameter depend. 8-62891
 baked mixes, use of coal tar and petroleum pitches as binders 8-80483

carbon continued

- black, effect on cationic polymerisation of styrene by SnCl₄ 8-68891
 black, pyrocarbon coating (*French*) 8-68921
 black, surface S-containing group complexing 8-68920
 Black Pearls A, in butanol, electrophoretic mobility, charge origin 8-85211
 blacks, surface polarity, surface activity, slurry pH, oxidation effects 8-68915
 catalytic graphitisation, three-phase, of phenolic resin C by Ni particles 8-68922
 cathode damage and vapour/thermionic arc transition obs. 8-71603
 chemisorbed oxygen surface complexes, thermal desorpt. analysis 8-56032
 coating on Pt, temp. depend. of H₂⁺ sputtering 8-95634
 contamination of ion irradi. Th surface, AES obs. 8-71775
 convoy electrons from solids, ion vel. and Z and target material depend. 8-84692
 deposition of columnar and laminar forms on Ni 8-63943
 depth profiling of ³He ion implantation 8-59830
 determination by alpha-induced X-ray spectrometry 8-53275
 determination of C, O₂ purification and flux selection (*Japanese*) 8-92571
 diffusion, in α -Ti, AES meas. 8-51735
 diffusion coeff. in Fe-Ni austenite, 950-1100°C 8-51747
 diffusion into liq. Fe (*Russian*) 8-79791
 diffusion on Pt(111) surface, AES 8-71954
 disordered anthracene char, density fluctuations effect on physical properties 8-51420
 dissolution into Ni through (110) surface, 615-660K, AES, LEED 8-63932
 dissolved in molten CaO-Al₂O₃ binary slag (*Japanese*) 8-60662
 electrical contact generation by tattooing C into skin tissue 8-77122
 electrode breakdown voltage dependence on adsorbed gases 8-75465
 energy levels, position orbital calcs., electron repulsion integrals, teaching appl. 8-93494
 evaporated layers, thickness determ. by objective colorimetry 8-77844
 fibre, Al-coated, stress rupture 8-80628
 film, amorphous, growth under ion impact in butane plasma, and IR transparency 8-52688
 film, deposited on (AlGa)As DH laser facet to prevent deterioration 8-87049
 film, work function, heat treatment 8-64563
 film automatic thickness control in freeze etching and related techniques, resist. monitor 8-49810
 film deposition by ion beam methods 8-72728
 fluorophosphate glasses, C determ. by deuteron activation analysis 8-68961
 foil, heavy ion impact energy loss 8-55902
 foil, secondary electron yield from heavy ion beam-tilted-foil expts. 8-62889
 foil+H₂⁺ (H⁺), 0.5-2.5 MeV, forward electron vel. distrib., peak shape 8-78794
 glassy, electrodes, polymer film coated, prep., characterisation, electrochem. stability 8-76866
 glassy, LMSC process prepared, exam. of props. by TEM and X-ray anal. 8-63675
 grain boundary segregation, in α -Fe 8-72778
 graphitised C black, adsorption of inert gases, gas-solid virial coeffs. 8-75928
 graphon, adsorption of Ar, high press. and temp., gas density profile theory 8-67903
 Graphon, colloidal, in butanol, electrophoretic mobility, charge origin 8-85211
 impregnated, reaction steps in gas sorption 8-68916
 ion bombarded, chemical effects on secondary photon and ion emission 8-95637
 ion energy selection by parallel-plate electrostatic analyser 8-83610
 ions, energy loss in tissue-equivalent gas for elastic nuclear collisions 8-86759
 ions, ionisation equilib. and radiative energy loss rates in low-density plasmas 8-87430
 isotopes, origin and ¹²C/¹³C ratio evolution 8-93201
 isotropic pyrolytic, for biomedical devices, mech. props. 8-65150
 kaonic ¹²C, coupled channel formalism, role of $\Lambda(1405)$, binding effect, Pauli blocking 8-55261
 lattice dynamics of diamond type crystals, Keating's valence force field 8-79687
 monatomic, transport properties, rel. to spacecraft entry into planetary atms. 8-87424
 neutron yield calcs., electron beam incidence 8-95622
 organic, non-methane, C in global troposphere 8-73462
 particle formation, C₂+C₃ as possible first step 8-68876
 particles in flame, laser heating and sublimation 8-61012
 phenolic resin-derived, oxidation, ht. treatment effects 8-56790
 plasma, laser produced, anomalous mag. field reversal, two-dimens. numerical results 8-87471
 plasma extended source for short wavelength amplifiers 8-79447
 plasmas produced by lasers, photoexcitation in the ionisation dynamics 8-91130
 porous particle, internal combustion, model 8-92481
 powder behaviour in vibrating field from cond. obs. (*Japanese*) 8-95711
 proton impact X-ray emission, ang. distrib. and polarisation fraction 8-56546
 pyrocarbon deposition in fluidised bed, qualitative model, investigation with Stromungsröhr 8-56595
 pyrocarbon deposition on C black (*French*) 8-68921
 pyroceramic, sputtering and blistering from H⁺ and He⁺ bombardment 8-79649
 pyrolysed non-graphitising, modified struct. model, interference function 8-67681
 pyrolytic, energy depend. of methane prod. during deuteron bombardment 8-95939
 pyrolytic film electrode, fabrication, electrochem. characterisation 8-92487
 reactivity with Y₂O₃, exam. by thermal anal. 8-85154
 reflection of H, D and He ions 8-95640
 residual carbonaceous material, in urban airborne particulates, Raman microprobe obs. 8-69441
 solar C I multiplets at 1560 and 1657 Å, overlapping emission peaks obs and theory 8-93178

carbon continued

- from solid-state reduction of carbonate ions, X-ray diffr. 8-56594
 solubility in BCC transition metals 8-71861
 soot and benzo(a)pyrene combined aerosol form., rel. to air pollution and health hazards 8-80796
 soot-CO₂-water vap. mixture, in luminous flames and smoke, IR mean absorption coeffs. calc. procedure 8-91061
 soot-gas mixture, in luminous flames and smoke, IR mean absorption coeffs. calc. procedure 8-91061
 sphere radiation in plasma, NRL fusion programme 8-59042
 STEM, bright field single atom images with half plane detectors 8-66010
 stripper foils, lifetime enhancement, heavy ion bombardment 8-94156
 surface, interaction with D⁺ ions, 5-30 keV temp. depend. of methane formation 8-79645
 surface groups, acidimetry, formation of derivatives 8-68918
 surface groups, spectroscopy 8-68919
 surface reconstruction-induced subsurface strain, theory 8-91516
 Swann band profiles in spectra of two comets 8-85909
 terrestrial C reservoir changes rel. to atm. CO₂ 8-57278
 texture change on ht. treatment under press. 8-60687
 vitreous, wetting by Cu-Sn-Ti alloys 8-71904
 zincblende structure group IVA covalent crystals, Murnaghan parameter estimates from Morse pot. 8-95014
 ZZ 8-91367
 C 1s contaminant buildup on conductors (insulators) in X-ray ESCA 8-95981
 C I IR forbidden emission lines obs. in Orion Nebula 8-85987
 C II, III, IV, radiative mean life meas. by beam-foil technique 8-90121
 C III, C IV, electron impact ionisation 8-70941
 C, pyrolysis mechanism, electron microscopy, DTA, IR, ESR obs. 8-56593
 C VI, laser plasma, electron density profile, Stark broadening meas. of vac. UV lines 8-59684
 C⁺, effective valence shell Hamiltonian, ab initio calcs. 8-82611
 C²⁺, dynamic multipole polarisability, coupled Hartree-Fock 8-82858
 C²⁺, Hund's first rule, new interpretation 8-78620
 C³⁺, fine struct. and lifetimes, doubly excited quartet system 8-78827
 C⁴⁺, electron impact excitation, cross-sections, modified Oppenheimer approx. 8-82843
 C⁴⁺ plasma, soft X-ray emission, electron-beam sliding spark device 8-79444
 Cⁿ⁺, (n=1,2,3) effective valence shell Hamiltonian, ab initio calcs. 8-82611
 C-C composites, existence diagram and properties (French) 8-64517
 C-PVC composite, fluctuation induced tunnelling conduction 8-52044
 C+H⁺, electron capture cross sections 8-62912
 C+He (methane), C atom K-shell binding energy by Auger spectra 8-50525
 C+Li⁺(Co⁺)(Au⁺), cross-section, closure-Born approx. 8-66630
 C+N₂ reaction, CNN radial prod., matrix isolation study 8-86880
 C⁺+H₂→CH⁺+H, classical trajectory anal. 8-53192
 Cⁿ⁺+Ar, continuum electron capture, projectile vel. and Z depend. 8-55222
 Cⁿ⁺+H(H₂), q=1-4, single electron capture cross sections 8-55233
 C₂, Swan, Phillips, Deslandes-d'Azambuja, and Fox-Herzberg systems, rotational dependence 8-74701
 C₂, transition moments of Swan band system, SCF-CI calc. 8-58746
 C₃, electron spectrum, ab initio MRD CI calcs. 8-90089
 C₃, matrix isolated, vibr. relax. 8-66637
 (C)_n, cryst. struct. determ. from X-ray photoelectron and X-ray spectra 8-88384
¹²C/¹³C, ratio in atmospheric of cool C star V460 Cygni 8-93223
¹²C/¹³C ratios in Population I K-type giant stars, rel. to CN strengths 8-93229
¹³C, mechanism of spin transfer to next neighbours in complexes 8-86892
¹³C, nuclei in molecules, isotope shifts calcs. 8-86917
¹⁴C concentration in Earth's atmosphere, corrections with astrophysical and geophysical phenomena 8-61477
¹⁴C dating rel. to magnetic and other dating methods 8-57359
¹⁴C in atmosphere content variation, past geomagnetic and cosmic ray intensity variations 8-61691
 C⁺+Ar(H₂)(N₂)(CO)(CO₂)(O₂), charge transfer cross-sections, 0.7-2.4 keV, C⁺(²P) and C⁺(⁴P) 8-58806
 C₂(³Σ_g⁻), collisionless production in IR laser field 8-55206
 C₂(³Π_g⁻) shock wave excitation, emission, excited state populations, in CO-N₂-Ar mixtures (Russian) 8-74638
 Fe:C, decarburisation by H₂, conversion electron Mossbauer obs. 8-85198
 Fe-Al-C, mag. permeability disaccommodation 8-88141
 Fe-C, pearlite, eutectoid alloy, efficiency of directional transformation on orientated growth 8-76642
 GaAs, C, O, Si impurities 8-59832
 GaAs:C⁺, Ga⁺, dual implantation of C⁺ and Ga⁺, sheet resist. and Hall effect meas. 8-67728
 H-C, thermal desorption, one-phonon at. scatt., 3-dimens., continuum model 8-87860
 Ni 200, C interstitial effect of yield point develop. during static strain ageing, model 8-88498
 Pt:C, C layer formation on (111) surface, temp. depend., LEED, AES study 8-71911
 Si:C, vibrational properties of the (001) split interstitial 8-91405
 Si-C, sputtering and blistering from H⁺ and He⁺ bombardment 8-79649

carbon compounds

see also organic compounds

- ¹³C¹⁶O₂, ν₃ band, absorpt. spectrum 8-58693
 carbide coating formation by chromising C steels 8-88571
 carbonate formation in Marslike environments 8-61778
 carbonates dissolved in groundwater, in Edwards artesian aquifer, Texas 8-73416
 CN in Population I K-type giant stars, band strengths rel. to ¹²C/¹³C ratios 8-93229
 CO₂ lasers, CW, high-power appl. of photoinitiated impulse-enhanced electrically excited discharge 8-50785
 CO dose meter for working places exposed to extreme peaks of CO contamination 8-81096
 gas mixture, thermal diffusion const. 8-67300

carbon compounds continued

- graphite monofluoride, surface alteration by interaction with Ar⁺ and Xe⁺ beams 8-91347
 oxides, glow discharge, excitation and ionisation mech., elec. and optical obs. (Russian) 8-59695
 refractory materials, group IVa and Va, slip, microhardness, comments 8-84967
 CH⁺, ground state photodissoc. cross sections into A¹Π state 8-82793
 CH₂SiH₂, ab initio GO calc. 8-94187
 C₈K, intercalation compound, superconductivity 8-91827
 CN (A²Π), chem. prod., CN number densities for gain, emission and absorpt. meas. 8-63112
 CN, A- and B-state lifetimes, collisional transfers and perturbations 8-78756
 CN, r-centroids for B²Σ⁺-X²Σ⁺ transition 8-70811
 CN, radical, nonradiative transition rates, matrix isolated molecule 8-78740
 CN, radical fluoresc. excitation spectrum and laser emission from ICN photolysis 8-76892
 CN radicals, electronic transition laser, using C₃F₇CN and (CN)₂C₄F₈ photodissociation 8-50769
 CN, red and violet band systems, rotational dependence of Franck-Condon factors 8-74701
 CN, solar lines in 7100-7600 Å range, table 8-77495
 CN⁻, finite field method calc., moments, polarisability, field-induced shifts in mol. props. 8-74561
 CN⁻, first hyperpolarisability, Hartree-Fock-Slater calc. (French) 8-78625
 (CN)⁻, monolayer on Ag, Raman spectra 8-72520
 CN⁻, proton affinity, integral Hellmann-Feynman theorem 8-70767
 CN⁺, ab initio full CI calcs. 8-50480
 CN+H⁺, perturbed rotational state approach 8-92469
 C₂N₂, adsorption on stepped Pt (111) surface 8-71992
 C₂N₂, multiphoton UV photodissoc. 8-50602
 CN(B²Σ) shock wave excitation, emission, excited state populations, in CO-N₂-Ar mixtures (Russian) 8-74638
 CNN, matrix isolation spectrum, 2600-1900 Å 8-86880
 CN(v)+O(³P)(O₂) reacts., prod. energy distrib. meas., CO vibr. level population (German) 8-76833
 CO A-X system, rotational dependence of Franck-Condon factors 8-74701
 CO, absorpt. spectra around 2100 cm⁻¹, Fourier transform spectroscopy appl. 8-58068
 CO, acetone decomposition, near IR laser action 8-63055
 CO adsorpt. on Al₂O₃-Ni catalyst in H₂-He, effect of H₂S on IR spectrum 8-71945
 CO, adsorbed gas, on glassy AsSe, surface cond., photocond. 8-80038
 CO, adsorbed on metal surface, collective vibr. modes, dipole interactions 8-50533
 CO, adsorbed on metals, valence photoemission book contrib. 8-95672
 CO, adsorbed on Ni and Cu, bond geometry, determ. using photoemission 8-71951
 CO, adsorbed on Ni(Pt), intermediate UPS/XPS synchrotron radiation study 8-52633
 CO, adsorbed on Pd, photoelectron spectra, 40-180 eV, adsorbate sensitivity enhancement 8-80453
 CO, adsorbed on Pt (111), oxidation process, reflection-absorpt. IR study 8-76468
 CO, adsorbed on stepped Ni, adsorpt.-desorpt. behaviour, LEED, AES, thermal flash desorpt. study 8-71984
 CO, adsorpt. on Cu (100), UV and X-ray photoelectron spectra, LEED 8-56037
 CO, adsorpt. on Mo(100), LEED, AES, study 8-87873
 CO, adsorpt. on Pd(001), LEED, electron energy loss spectra study, surface struct. effect on weak chemisorpt. bonding 8-71987
 CO, adsorption on Cu, angle-resolved UPS and adsorbate induced struct. 8-71983
 CO, adsorption on Fe(001), random occupation of adsorption sites, LEED exam. 8-63930
 CO, adsorption on GaAs(Pt), surface electronic struct. (surface chem.) using synchrotron radiation 8-53254
 CO, adsorption on MgO powder, 77 to 150K, mol. motion anal. 8-84051
 CO, adsorption on Pd (111), catalytic oxidation, mol. beam investig. 8-88656
 CO, adsorption on Pd(111), mutual interactions, transient product formation with O₂ 8-87871
 CO, adsorption on planar and O₂ etched Si (111), AES, SEM, ESD, flash desorption mass spectra 8-63934
 CO, adsorption on Pt (111) and Pt 6(111)×(111), EELS and thermal desorption spectroscopy 8-91547
 CO, adsorption on SnO₂ gas sensor, effect on cond. 8-76067
 CO, adsorption on stepped Pt (111) surface 8-71992
 CO, adsorption on V, effect on extended fine struct. above L-shell appearance pot. thresholds 8-92148
 CO, adsorption on W, surface reflectance spectroscopy on low index planes 8-71965
 CO, adsorption on W (001) surface, electron energy loss spectra 8-71999
 CO, adsorption on W and Ni, mol. orientation, ion scatt. 8-71949
 CO, atmospheric, production from oxidation of vegetation hydrocarbon emissions 8-88881
 CO, atmospheric abundance, geographical, seasonal and secular vars. (Russian) 8-53700
 CO, atmospheric abundance determ. by analysing solar spectra 8-85643
 CO, boiling/condensation heat transfer props., cryogenic appls. 8-79192
 CO CW electric discharge laser, saturation parameter expt. determ. 8-50762
 CO catalytic oxidation on spinel type ferrites, role of mag. exchange interactions 8-56916
 CO, catalytic oxidation over NiO, activated complex struct., rate consts. 8-80786
 CO chemical laser, CS₂-O₂ mixtures in discharge 8-50766
 CO, chemical laser, supersonic combustor driven 8-87047
 CO, chemisorbed and condensed on Rh(111) surface, energy level shifts 8-87865
 CO, chemisorbed on Cu(111), coverage depend. photoelectron spectra, adsorption sites 8-95647

carbon compounds continued

- CO, chemisorbed on IR, electron states, electron field emission 8-84704
 CO, chemisorbed on Ir(111) surface, electron beam induced desorption and dissociation 8-56043
 CO, chemisorbed on Ni, ab initio LCAO MO SCF calc. for NiCO 8-62712
 CO, chemisorbed on Ni (001), site determ. by angle-resolved UPS 8-71970
 CO, chemisorbed on Ni(111), surface optical excitations, reflectance spectra, electron energy loss meas. 8-84064
 CO chemisorbed on Rh/ γ -Al₂O₃ disperse δ -phase, IR spectra, site distrib., mol. mobility 8-72496
 CO, chemisorpt. on Cu(Ni)(Cu-Ni), SIMS, AES, desorpt. meas. 8-87875
 CO, chemisorpt. on Pd particles supported on mica, ultra high vacuum technique 8-71960
 CO, chemisorpt. on W(110), absolute coverage and work function meas. 100 and 300K 8-71986
 CO, chemisorption in Ni(100), mol. levels, angle depend. calcs. 8-90069
 CO, chemisorption on clean Fe (100) and (111) surfaces, LEED and thermal desorption 8-71996
 CO, chemisorption on cleaved Si (111), Ge (111), electron energy loss spectra 8-79885
 CO, chemisorption on Ir (110), preexponential factor and desorption energy 8-71963
 CO, chemisorption on Ni and Cu, electronic struct. of (M)₂CO clusters 8-95948
 CO, chemisorption on Pd(111) surface, mol. beam scatt. expts. 8-79878
 CO, chemisorption on polycryst. Ti surface, secondary electron yield obs. 8-71971
 CO, chemisorption on Si(Ge), surface photoemission, adsorption gate geometry 8-73079
 CO, chemisorption on Ti (0001), LEED struct. anal. 8-71964
 CO, chemisorption on W (100) surface, mol. orbital study 8-71995
 CO, collisional excitation of interstellar molecule 8-81664
 CO covered Ni films, adsorpt. of H, isotherms, resist., work function changes 8-75926
 CO, decomposition in corona discharge, qualitative chemical anal. of reaction products 8-60992
 CO, desorbed from W, thermal desorption and conversion kinetics, AES study 8-71959
 CO, desorpt. from graphite, kinetics 8-60025
 CO, detection by Co₃O₄ MOS device 8-76908
 CO, diffusion coeff. in laminar flames 8-51272
 CO, dipole moment functions for d³ Δ and a² Σ^+ states, MCSCF calc. 8-78636
 CO discharge, low-pressure laser striation obs. 8-66814
 CO, dissoci. chemisorption on Fe(Ni) (*German*) 8-53257
 CO, dissociative excitation by electron impact, metastable fragment energy 8-66672
 CO, Doppler-free two-photon vac. UV absorption spectra 8-86882
 CO, effect on electron loss spectra, Pt(111) surface (*German*) 8-52605
 CO, effect on SnO₂:ThO₂, elec. oscill. phenomenon 8-68032
 CO, efficient self-sustained pulsed laser 8-55377
 CO electric discharge unstable resonator laser, computer model 8-58988
 CO, electron scatt., absolute total cross-section meas. 8-74774
 CO, electron scatt. at low energy, mechanisms (*Russian*) 8-90306
 CO, electrostatic interaction energies for point charge and NaCl (100) surface 8-74592
 CO emission from late-type galaxies 8-89250
 CO, emissivity calc. 8-90675
 CO, equilib. geometry, orbital energies, ab initio rel. to pseudopot. calcs. 8-82613
 CO, finite field method calc., moments, polarisability, field-induced shifts in mol. props. 8-74561
 CO, first hyperpolarisability, Hartree-Fock-Slater calc. (*French*) 8-78625
 CO fluorescence in EUV solar spectrum, obs. 8-93184
 CO, form. in contracting interstellar clouds, thermal instabilities 8-81675
 CO, glow discharge, O atom conc. determ. by mass spectrometry (*Russian*) 8-87512
 CO, ground states, anal. pot. function calcs. 8-78775
 CO, ground-state, absorpt. oscillator strengths for vibr. rot. transitions 8-62846
 CO, high resolution lifetime meas., perturbation and collisional transfer correl. 8-78699
 CO, hydrogenation to methane and higher mol. wt. compounds on Rh(Fe) surface 8-73034
 α -CO, IR and Raman spectra, vibron band, vibron-phonon combination bands 8-68495
 CO, IR band nonrigid rot. absorption 8-91060
 CO, IR radiation spectral absorbance and transmittance, accurate modelling technique 8-91062
 CO in giant stars in globular clusters, IR obs. 8-93339
 CO in Jupiter upper atmosphere, extraplanetary source 8-93144
 CO in molecular cloud complexes, structure of W75-DR 21 region 8-89232
 CO, in Sc galaxy NGC 5236 (M83), radio emission obs. 8-65689
 CO, integrated CARS power, press. depend. 8-59081
 CO, interstellar, time-dependent form. and chem. fractionation 8-57602
 CO, ion transport in electrical discharge 8-87435
 CO laser, CS₂-N₂O-O₂ continuous combustion, performance characts. (*Russian*) 8-55348
 CO laser, high power combustor driven system 8-87065
 CO laser, vibr. distrib., O₂ addition effect 8-50757
 CO, on Pt surface, IR spectrum obs. in presence of free CO 8-74654
 CO, orbital contribs. to relax. energies accompanying core ions., Δ SCF HF calcs. 8-82642
 CO, ordered overlayer on Ni(100) surface, angle resolved UV photoemission 8-56570
 CO, oriented molecules, vibrationally inelastic electron scatt. 8-67907
 CO, oriented mols., inelastic low energy electron scatt. 8-72653
 CO, photoabsorpt. cross-section, 50-340 Å, as sum of empirical at. cross-sections 8-58718

carbon compounds continued

- CO, Photoelectron angular distrib. of C and O K-shell ionisation 8-52628
 CO, proton affinity, integral Hellmann-Feynman theorem 8-70767
 CO, reactions with NO over Rh flash desorption spectra, titration, reaction kinetic calcs. 8-61045
 CO, reson. transitions, radiative lifetimes, astrophys. appls. 8-62767
 CO, rot. population transfer, IR laser double reson. expt. 8-50566
 CO sealed laser, approximate analytic theory 8-58994
 CO, temp. meas. technique using IR tunable diode laser 8-86268
 CO, vibr. excited, in Ar matrix, information theoretic anal. 8-91386
 CO, vibr. population distrib. in supersonic expansion 8-71364
 CO, vibr. struct. of K₂ emission spectra 8-86886
 CO, viscomagnetic heat flux, in a Burnett regime 8-71400
 CO, X-ray K-absorpt. spectra, vibr. fine struct., ab initio restricted HF calc. 8-86883
 CO⁺, appearance potential by anal. of field-dispersed ions 8-85234
¹²C¹⁸O, 8-82768
¹²C¹⁸O, A'¹ π -X'¹ σ^+ (13,0) band, monochromatic excitation 8-82767
¹²C¹⁸O, Herzberg system of C¹ Σ^+ state 8-90185
¹³C¹⁶O, fluoresc. and electronic quenching cross sections 8-82768
¹⁴C¹⁶O, fourth positive band system, near UV meas. 8-66559
¹²C¹⁶O:CO isotopes, IR and Raman spectra, vibron band, vibron-phonon combination bands 8-68495
 CO/H₂ ratio in interstellar dark clouds, meas. 8-96513
 CO/H₂ surface complex, on W (100), flash desorption and AES obs. 8-73083
 CO-Ar mixture non-self-sustained discharge instability obs. 8-71612
 CO-He low press. mixture, CO vibr. distrib. to high level 8-58985
 CO-O₂-SF₆, efficient CO₂ laser radiation 3rd harmonic generation, for fusion ignition 8-59087
 CO-OCS-N₂, liq. mixture, vibr. energy relax. and exchange, laser induced fluoresc. obs. 8-70905
 CO+C⁺, charge transfer cross-sections, 0.7-2.4 keV, C⁺(²P) and C⁺(⁴P) 8-58806
 CO+H₂⁺(He⁺), dissoc. charge transfer, energy transfer processes 8-74759
 CO+He, energy sudden approx., beam scatt. meas. mol. anisotropy effects 8-78802
 CO+He, nuclear mag. shielding const., interaction geometry depend., chemical shift, gauge invariant method 8-62866
 CO+He, rot. excitation, infinite order sudden approx. 8-74740
 CO+I₂(ICl)(NO₂), E-V energy transfer reactions, electronically excited target mol. 8-64814
 CO+inert gas, collision-induced intersystem crossing mechanism 8-74689
 CO+Kr(³P₁)(¹P₁) A'¹ Π -X'¹ Σ^+ and b³ Σ^+ -a³ Π sensitised fluorescence, isotope effects 8-82761
 CO+Li⁺, vibr. excitation, 70 to 1500 eV 8-82824
 CO+N₂O, adsorption on NiO, catalysed reaction in Neel transition region 8-53258
 CO+N₂(CO), ionis. at low energy 8-58791
 CO+NO, electronic energy transfer, spectroscopic obs. 8-82716
 CO+NO+H₂ interaction over Pt, Rh, Ru and Os, NH₄OCN formation 8-73082
 CO+NiF₂ react., Ar matrix isolated, ab initio MO calcs. 8-92458
 CO+O, vibr. deactivation 8-94305
 CO+O₂ interaction on Ag (110), ellipsometry-LEED expts. 8-91542
 CO+O⁺(⁴S)(²D), charge transfer reactions, cross-sections meas. 8-92462
 CO+O(¹D), deactivation rate consts. temp. depend., 113-333K 8-88629
 CO+Xⁿ⁺, X=Ar,Kr,Xe,U, Auger emission line shape after dissoc. 8-86838
 CO+Xe, ¹²⁹Xe chem. shielding, second virial coeff. 8-66563
 CO⁺+CO (methane), charge transfer cross-section, low energy 8-58791
 CO⁺+H₂, ion-molecule reaction detection of laser-induced ion spectrum, rot. components 8-74671
¹³CO⁺+CO, charge-exchange detection of ¹³CO⁺ electronic absorption spectrum, hyperfine consts. calc. 8-70822
 CO₂, ¹³C NMR, chem. shift, determ. of virial coeffs., rovibr. motion 8-58720
 CO₂, 1 mJ line tunable optically pumped laser 8-66840
 CO₂, 100 kJ laser, optical design and components 8-82990
 CO₂, 10.6, 9.4 μ m laser bands high-press. absorpt-spectra 8-66543
 CO₂, 200 J TEA laser, injection mode locking 8-79049
 CO₂, 30¹ Π - ∞ 0⁰ band, meas. at different temps. of absolute intensities, line half-widths and broadening by Ar and N₂ 8-86865
 CO₂, 30¹ Π - ∞ 0⁰ and 30⁰ Π - ∞ 0⁰ bands, absolute intensity meas. at different temps. 8-86864
 CO₂, 7883 Å band in Venus spectrum, high-dispersion obs. 8-53851
 CO₂, (001) \rightarrow (000) fluorescence following dye laser photolysis of s-tetrazine 8-88652
 CO₂ absorption in leaves, sun vs. shade 8-80850
 CO₂, acetone decomposition, near IR laser action 8-63055
 CO₂, adsorbed gas, on glassy AsSe, surface cond., photocond. 8-80038
 CO₂, adsorption on C, surface area meas., temp. and chemisorption effects 8-95225
 CO₂, adsorption on water, 0-50°C, press. effects on surface tension 8-56024
 CO₂, anomalous energy minima surfaces 8-86791
 CO₂, antisymmetric vibr., energy relax. rate, rel. to IR luminesc. kinetics (*Russian*) 8-82826
 CO₂, aqueous solution, photoelectrochemical reduction on p-type GaP in liq. junction solar cells 8-88649
 CO₂, atmospheric, short-term disturbances in record at Mauna Loa Observatory 8-88879
 CO₂, atmospheric input from burning wood 8-81368
 CO₂, atmospheric levels rel. to agricultural expansion in late 19th century 8-53717
 CO₂, atmospheric line freqs. in 4.3 μ region 8-88910
 CO₂ \rightarrow CO+O, dissoc. pathways, pot. energy surface and vibr. anal. of IR and Raman spectra 8-64826
 CO₂, CW gasdynamic mixing lasers, pumped by N₂ or air, low stagnation temp. characts. 8-63053
 CO₂, CW high power lasers, appls. for metal working 8-79026
 CO₂, CW laser, sealed-off design, NaCl Brewster angle mirrors 8-55370

carbon compounds continued

- CO₂ CW laser burning CO in air for pump energy, saturation parameters 8-71077
- CO₂, CW waveguide laser, anodised Al waveguide construction 8-55376
- CO₂, CW waveguide laser, nearly atm. press., using plasma injection technique 8-74925
- CO₂, chemisorption on clean Fe (100) AND (111) surfaces, LEED and thermal desorption 8-71996
- CO₂, collision induced Raman scatt. at ν_2 and ν_3 inactive vibrs. 8-90175
- CO₂, collision-induced absorpt. at 4.6 cm⁻¹ 8-78679
- CO₂, compression to 34 kbar, apparatus and technique, diamond anvil cell 8-74017
- CO₂ conc. increase effects on stratospheric O₃ 8-57250
- CO₂, concs. in lower thermosphere 8-96336
- CO₂, content of atmosphere, role of C storage by forests and oceans 8-53718
- CO₂ convection laser discharge, negative ion effects 8-55335
- CO₂, desorpt. from graphite kinetics 8-60025
- CO₂ dissociation obs. in flow system with cylindrical hollow cathode 8-66674
- CO₂ dissociation obs. in hollow-cathode glow discharge 8-70946
- CO₂ effects on long-term global sea surface temp. vars. 8-73398
- CO₂, elec. discharge, negative ions and volt.-current characts. 8-71574
- CO₂, electric breakdown voltage, 300-2100K (Russian) 8-51370
- CO₂, electric discharge gasdynamic 16 μ m laser, high average power, high repetition rate 8-55381
- CO₂, electric discharge convection laser, saturation characts. (Chinese) 8-90408
- CO₂, electrochem. reduction for use in energy storage 8-92490
- CO₂, electron beam controlled laser with plasma mirror, stimulated emission dynamics 8-50799
- CO₂, electron diffraction cross-section, finite scatt. geom. in mol. beam expt. 8-74803
- CO₂, electron excitation-relax., time resolved Fourier spectra 8-58070
- CO₂, electron impact, transitions, generalised oscill. strengths 8-94327
- CO₂, electron impact excitation, electron cooling in Mars and Venus atmos. 8-57481
- CO₂, electron scatt., absolute total cross-section meas. 8-74774
- CO₂, electron-beam-controlled laser, operation characts., 1 to 10 atm range 8-71118
- CO₂, electron-beam-controlled laser, pulse forming network power source 8-74928
- CO₂, exchange in Mars atmosphere-regolith system, rel. to atm. press. 8-73668
- CO₂ expiratory concentration analysis by computer 8-57106
- CO₂ fast flow laser, combined pulse and DC discharge as pump 8-71117
- CO₂, fast-flow laser, pumping efficiency by AC discharge 8-50801
- CO₂, Franck-Condon transition amplitudes for mol. dissoci., semiclassical evaluations 8-62860
- CO₂, freq. stabilised laser with OsO₄ absorber, output freq. reproducibility 8-50800
- CO₂, from fossil fuel burning, climatic effects, proposed CO₂ disposal in deep ocean 8-57301
- CO₂, future atm. level prediction using atm. and ocean models 8-61549
- CO₂ gas sensing probe, potentiometric, micro-size 8-61071
- CO₂ gasdynamic laser, gain supersonic flow heating effect, condition optimisation 8-82947
- CO₂ gasdynamic laser, two-stage expansion of N₂, supersonic nozzle 8-71076
- CO₂ glow discharge, acoustic wave influence on F⁻ forward ionisation wave 8-67521
- CO₂, glow discharge, O atom conc. determ. by mass spectrometry (Russian) 8-87512
- CO₂ glow discharge chemical processes and rate coefficients 8-63626
- CO₂ H⁺, geom. struct., ab initio mol. orbital study 8-62939
- CO₂ high power elec. discharge laser, multielement cathode design and operational characts. 8-82983
- CO₂ high stability CW waveguide laser, for high resolution saturation spectroscopy 8-71112
- CO₂, high-press. tunable IR lasers 8-59030
- CO₂, IR band nonrigid rot. absorption 8-91060
- CO₂, IR energy levels and line intensities 8-85691
- CO₂ IR laser, transients obs. by modulation of intracavity absorber 8-74933
- CO₂, IR radiation spectral absorbance and transmittance, accurate modelling technique 8-91062
- CO₂ in atmosphere, rel. to C reservoir changes 8-57278
- CO₂ in tropical atm., IR cooling rate rel. to H₂O vapour 8-81405
- CO₂ influence on level of ionised Ca in squid axons 8-56960
- CO₂, ion transport in electrical discharge 8-74435
- CO₂, ionisation current growth, Townsend swarm coeffs. 8-59541
- CO₂, isotope ratios, optical anal. method 8-85228
- CO₂ laser, 16 GHz tunable sideband generation 8-90428
- CO₂ laser, compact flowing gas system 8-87067
- CO₂ laser, convective-cooled, fast-flow, pulse discharge stability 8-94389
- CO₂ laser, double transverse pulsed discharge characteristics 8-71617
- CO₂ laser, E-beam sustained large amplitude discharge, for fusion appls. 8-55382
- CO₂ laser, Faraday effect optical isolation at 10.6 μ m using chalcogenide spinels 8-50816
- CO₂ laser, frequency control by spectrally depleted destructive two-beam interf. 8-74941
- CO₂ laser, gaseous saturable absorber cell to suppress parasitic oscillations 8-87066
- CO₂ laser, glow discharges at high press., voltage-current characts. 8-87036
- CO₂ laser, high power, CW, electron beam sustained, performance, theory and expt. 8-71074
- CO₂ laser, high repetition rate-pulsed, weak shock wave effect 8-90409
- CO₂ laser, high-power high-energy, using an absolute calorimeter 8-93686
- CO₂ laser, high-power photoionisation stabilised, operation at press. up to 13 atm. 8-63131
- CO₂ laser, line selection using metal film reflection filter 8-55368

carbon compounds continued

- CO₂ laser, long and short pulse formation, optimum conditions 8-87037
- CO₂ laser, nsec pulse amplification at efficiencies greater than 20% 8-50818
- CO₂ laser, pulse flow stretching (Chinese) 8-90435
- CO₂ laser, small-gap multiatm. press. system 8-74921
- CO₂ laser, Stark cell noise reduction 8-59059
- CO₂ laser, thermally pumped, output power enhancement by Ar gas addition 8-55336
- CO₂ laser, versatile high-power industrial system 8-55380
- CO₂ laser amplifier, double-discharge at 1800 torr 8-50815
- CO₂ laser amplifier, high power large aperture electron beam controlled, development (Japanese) 8-66846
- CO₂ laser amplifier, short pulse amplification calcs. 8-58979
- CO₂ laser amplifier design, IR laser optical pumping appl. 8-63133
- CO₂ laser beam meas. using pyroelectric vidicons 8-49907
- CO₂ laser discharge, special case of effect of initial conditions on homogeneous discharge development 8-63613
- CO₂ laser discharges, determ. of recombination coeff. 8-90407
- CO₂ laser discharges, electrode surface field and preionisation effects on spatial distrib. of arcs 8-63054
- CO₂ laser electron beam pulsed, sealed electron guns 8-71119
- CO₂ laser frequency measurements: a review, limitations, extension to 197 THz (1.5 μ m) 8-81952
- CO₂ laser generation by pulsed microwave excitation 8-74879
- CO₂ laser intensity distrib., hot spot detect. using Ag halide film 8-82945
- CO₂ laser self-sustained discharge, effect of low-ionisation-potential additives 8-71616
- CO₂ laser stability and heterodyne frequency calibration 8-59031
- CO₂ laser system, eight beam, optical anal. 8-50814
- CO₂ laser systems for laser fusion appls. 8-50817
- CO₂ liq., 100 to 3000 atm., depolarised Rayleigh spectra, orientation dynamics, wings 8-92084
- CO₂ liq., transient stimulated vibr. Raman scatt. 8-71144
- CO₂ mixing gasdynamic laser 8-71073
- CO₂, molecular correlation energies, estimation from semi-transferable orbital correlation energies 8-82650
- CO₂ multiatmospheric UV-preionised lasers 8-50805
- CO₂, negative point-plane corona, electrical characts. 8-71567
- CO₂, negative Van der Waals polymer mols., formed by nozzle expansion 8-90307
- CO₂ partial pressure in blood, meas. by rapid response electrode system (German) 8-85409
- CO₂, periodically operated laser, pulse repetition freq. limits 8-50750
- CO₂ permafrost on Mars, effect on topography 8-65535
- CO₂ photofixation to formic acid in water, photosynthesis mimicking 8-88650
- CO₂, physisorbing on Ni, stay time meas. 8-56044
- CO₂ plasma, 10000-13000K, VUV continuum radiation 8-91152
- CO₂ plasma, surface treatment of polyester fabric, effect on surface struct., props. 8-95831
- CO₂, polymer degradation products, chem. anal. by UV photoelectron spectroscopy 8-53300
- CO₂, press. broadening coeffs. at 4.2 μ m, rot. quantum number 8-74704
- CO₂, pulsed electron-beam-controlled laser, parameters optimisation 8-71116
- CO₂, pulsed laser, high power, oscill. spectrum expansion (Russian) 8-74882
- CO₂, pulsed laser, laser induced medium perturbation 8-58977
- CO₂ pulsed laser beam, thermal coupling 8-63145
- CO₂, radiative transfer, Curtis-Godson approx. 8-67019
- CO₂, radiative transfer in 4.2 μ m band with non-LTE in terrestrial atm. (Russian) 8-88914
- CO₂, rapid wavelength switching probe laser, J-line scan gasdynamic laser diagnostic 8-59044
- CO₂, refr. index and Lorentz-Lorenz functions, 944 cm⁻¹ and 15803 to 22002 cm⁻¹ 8-59543
- CO₂ relativistic electron beam transport at low pressures 8-75373
- CO₂ scatt. electron angular distrib. 8-74766
- CO₂ sealed photoionisation TEA laser, limiting processes 8-82946
- CO₂, solid pellets, for on-top seeding of convective clouds 8-73531
- CO₂, solubility in cellulose acetate, 0-70°C, up to 45 atmos. 8-83957
- CO₂ TE laser, passive mode locking using p-Ge saturable absorber 8-71127
- CO₂ TE laser, performance improvement with tripropylamine additives 8-78991
- CO₂ TEA amplifier, gain meas. on sequence bands 8-78990
- CO₂ TEA laser, compact sealed single mode operation 8-50810
- CO₂, TEA laser, energy extraction improvement in multiline double band mode 8-63129
- CO₂, TEA laser, pulse shape and duration, excitation method (German) 8-83010
- CO₂ TEA laser design and construction (Italian) 8-55360
- CO₂ TEA laser discharge, influence of additives and contaminants evaluated by electrical meas. 8-94388
- CO₂ TEA laser electrical excitation rates, theory and expt. 8-71078
- CO₂ TEA laser emission on sequence bands 8-71075
- CO₂ TEA laser with long optical resonator, mode-locked operation 8-79041
- CO₂ TEA oscillator, simultaneous freq. stabilisation and injection 8-55362
- CO₂, TEA sealed laser, seed gas compatible system with unheated oxide catalyst 8-63130
- CO₂, thermal accommodation coeffs., on Al(Fe), translational (internal) gas-solid energy exchange 8-92506
- CO₂, thermal diffusivity and cond. in crit. region meas. by holographic interferometry (German) 8-59942
- CO₂, transition calibration, rotational constants, absorption spectrum, 4.82- μ m region 8-58868
- CO₂, transition moment of IR band near 7740 cm⁻¹ 8-90224
- CO₂, transition moment of IR band near 7740 cm⁻¹ 8-90225
- CO₂, two-scale factor universality near crit. point 8-55936
- CO₂, vibr. excitation and de-excitation by electronic collisions, calc. of cross section 8-66669
- CO₂ vibr. luminesc., excited by DC discharge, rot. and vibr. mol. const. 8-58867
- CO₂, vibr.-rot. transition overtones, active Raman spectra obs. 8-50550

carbon compounds continued

- CO₂ waveguide high press. laser, line selection and tunability 8-59026
 CO₂ waveguide laser, small signal gain, saturation intensity and volumetric output power 8-74880
 CO₂ waveguide laser, transversely RF excited 8-63127
 CO₂⁺, appearance potential by anal. of field-dispersed ions 8-85234
 CO₂⁺, fluoresc. quantum yields, isotope effects, photon-photoion coincidence meas. 8-90200
 CO₂⁺, thin foil impact, dissociation struct. effects in ionic fragment energy spectra 8-50631
¹²CO₂, absorpt. spectrum at 4.3 microns 8-58692
¹³C¹⁶O₂, ν₃ fundamental at 4.4 μm 8-86862
¹⁴CO₂ breath analysis tests, plastic scintillation filament detector system 8-65122
¹⁴CO₂, in liq. scintillator, determ. of low radiocarbon activity by absorption 8-74550
 C¹⁸O₂, Raman spectra in Fermi reson. region 8-74664
 CO₂-H₂O-peridotite system, phase relationships, rel. to planetary mantles 8-77506
 CO₂-hydrocarbon mixture, phase equilibria and critical phenomena at high press. 8-51648
 CO₂-N₂, gasdynamic laser mixture, vibr.-nonequilib. nozzle flows, numerical and approx. solns. 8-74881
 CO₂-N₂, high temperature gas diagnostics by spectral remote sensing, 700-1350K 8-74002
 CO₂-N₂, ionisation current growth, Townsend swarm coeffs. 8-59541
 CO₂-N₂-H₂, non-self-maintained glow discharges at atm. pressure, elec. characteristics and energy exchange 8-71606
 CO₂-N₂-H₂ electron beam controlled laser, efficiency and output energy depend. on H₂ 8-58978
 CO₂-N₂-He, discharge ionisation growth, diffusion coeffs. 8-83636
 CO₂-N₂-He flowing gas mixture, glow discharge produced population inversion 8-78992
 CO₂-N₂-He gas mixtures, fluorescent IR radiation from glow discharge 8-94386
 CO₂-N₂-He gas mixtures, time-of-flight meas. of electron transport parameters 8-94387
 CO₂-N₂-He mixture volumetric glow discharge formation at atm. pressure 8-71615
 CO₂-SF₆, AC particle initiated breakdown, compressed gas mixture 8-87556
 CO₂-soot-water vap. mixture, in luminous flames and smoke, IR mean absorption coeffs. calc. procedure 8-91061
 CO₂+Ar(N₂), 301_m-000 band, intensities, press.- and self-broadening coeffs. meas. 8-78695
 CO₂+Br, quenching of 4²P_{1/2} state, vib. excitation, temp. depend. 8-58792
 CO₂+C⁺, charge transfer cross-sections, 0.7-2.4 keV, C⁺(²P) and C⁺(⁴P) 8-58806
 CO₂+Ca, CaO form., product states obs. 8-92450
 CO₂+Ca, reaction, electronic branching, statistical and dynamical influences 8-92451
 CO₂+ethane system, isothermal vapour-liq. equilibrium data, 10 to 25°C and high press., critical points 8-79754
 CO₂+H₂O, photoassisted reaction on SrTiO₃ (111) face, methane form. 8-76878
 CO₂+hydrocarbon in mixtures, vibr. energy transfer, laser induced fluoresc. obs. 8-58731
 CO₂+hydrocarbon mixtures, vapour-liq. equilibrium, crit. locus curve, Soave eqn. 8-83913
 CO₂+Kr, collision dynamics, generalised Langevin eqn. approach 8-70900
 CO₂+Li⁺, vibr. excitation, 70 to 1500 eV 8-82824
 CO₂+N₂, ionis. at low energy 8-58791
 CO₂+N₂, semiclassical energy transfer method, Coriolis coupling 8-90266
 CO₂+N₂⁺, reaction rate determ. 8-60985
 CO₂+O⁺(⁴S)(²D), charge transfer reactions, cross-sections meas. 8-92462
 CO₂+OH⁻→HCO₃⁻ react., MO-LCAO-SCF calcs., energy barrier 8-76846
 CO₂+SO₂, collisional quenching of ³B₁ state, 8-1300 torr 8-86906
 CO₂+Xⁿ⁺, (X=Ar,Kr,Xe,U), Auger emission line shape after dissociation 8-86838
 CO₂⁺+Th, charge transfer cross-section, 1-500 eV 8-82835
 CO₂⁺+U, charge transfer cross-section, 1-500 eV 8-82835
 CO₂²⁻, electronic struct., X-ray spectra obs. 8-55185
 CO₂²⁻, X-ray fluorescence, electronic struct. determ. 8-86887
 C₃O₂, far IR and Raman spectra, vibr. mode and quasilinear config. 8-62940
 CO(Σ⁺), total X-ray scatt., two-electron density functions 8-70889
 CO(Σ⁺Σ⁺)+Ar*(²P), differential elastic and quenching cross-sections 8-58773
 CO⁺.CO, lateral diffusion in CO, mass spectra meas. 8-91055
 CS, as origin of 3.9 micron absorpt. band in C stars 8-93231
 CS, collisional excitation of interstellar molecule 8-81664
 CS J=1-0 transition at 49 GHz in southern molecular clouds 8-65674
 CS, presence or absence in solar atm., theory 8-69765
 CS⁺, red emission spectrum, rot. anal. and perturbation effects 8-55193
 CS₂, absorpt. spectra, Rydberg series converging to A²Π_u states of CS₂⁺ 8-90182
 CS₂, amplified phase-conjugate refl. and optical parametric oscill., 4-wave mixing obs. 8-74946
 CS₂, ang. distrib. of stimulated Raman scatt. 8-83039
 CS₂ filled waveguide, time-reversed wave generation by nonlinear refraction 8-90447
 CS₂, liq., ³³S NQR, quadrupole coupling const. from linewidth data 8-91985
 CS₂, liq., Kerr effect in UV region, mol. optical anisotropy dispersion 8-72488
 CS₂, liq., light scatt. intensities, struct. models 8-60476
 CS₂, liq., ratio of Brillouin to total light scatt. intensity 8-52515
 CS₂, non-polar liq., microwave induced Kerr effect meas. 8-76435
 CS₂, ν₃ band, dipole moment correl. function, isotope splitting and band contour 8-74650
 CS₂, ππ* and Rydberg bands, cryogenic solvent effects 8-55182
 CS₂, S atom L_{II,III}-absorption spectra 8-86807
 CS₂, single-photon isotope separation using ArF laser 8-55211
 CS₂, solid, tailoring of potentials, in lattice dynamics 8-79679
 CS₂, spectral splitting of stimulated Raman scatt. 8-50860

carbon compounds continued

- CS₂, vibr.-rot. bands at 46 μm, isotope effects 8-94245
¹³CS₂, laser emission at 6.9 μm, HF laser optical pump 8-58995
 CS₂-acetone, liq. mixture, excess Gruneisen parameter, intermol. interaction 8-67635
 CS₂-ethanol mixture, thermal diffusion ratio determ. by forced Rayleigh scatt. 8-75858
 CS₂-niromethane, crit. resist. of binary liq., 10 Hz-100 kHz 8-76123
 CS₂+acetic anhydride, elec. resist. near crit. soln. temp. 8-71874
 CS₂+He(Ar)(N₂), perturbed rot. diffusion of CS₂, IR spectra 8-75245
 CS₂+OH, flash photolysis reson. fluoresc. rate consts. determ., global S cycle 8-95914
 CS₃+N₂O+O₂ combustion, CO laser performance characts. (Russian) 8-55348
 C₃S₂, electronic struct., optical and photoelectron spectra 8-70745
 C₁₂(SbCl₄), magnetothermal oscill. and electronic struct. 8-84129
¹³C¹⁶O, A¹π-X¹σ⁺(13,0) band, monochromatic excitation 8-82767
 Ca-N₂O-CO flame, Ca catalyzed, gain meas., emission band assignment 8-66815
 Ca-N₂O-CO flame, candidate chem. laser reactions, intracavity dye laser absorpt. meas. 8-63108
 CaCO₃, calcite, spectral splitting of stimulated Raman scatt. 8-50860
 ClO⁻+NO(NO₂)(SO₂)(CO₂), rate consts. at 300K 8-76829
 F₂CS, pot. surfaces, X¹A₁, a³A₂ and a³A₂(b₁) states, ab initio SCF calcs. 8-86795
 H₂-CO₂, turbulent flow heat transfer, expt. and numerical anal. 8-94690
 HCl+O⁻(O₂⁻)(NO₂⁻)(CO₃⁻)(CO₄⁻), rate consts. at 300K 8-76829
 KCl:CO₃²⁻, Sr²⁺(Ba²⁺), shift and broadening of local vibr. bands, temp. depend. 8-87755
 Mg-N₂O-CO flame, efficient chem. generation of Mg(³P) 8-63109
 Mg-N₂O-CO flame, Mg catalyzed, gain meas., emission band assignment 8-66815
 N₂:CO, IR and Raman spectra, vibron band, vibron-phonon combination bands 8-68495
 N₂:CO₂(N₂O)(methane-d₄), liq., vibr. relax., Raman scatt. obs. 8-92061
 N₂-CO₂ mixture non-self-sustained discharge ionisation instabilities, obs. 8-71610
 NH+CO, vibrational energy transfer in solids, rot. mode participation 8-63815
 N₂O+CO, nonequilibrium reaction in shock waves (Russian) 8-76845
 N₂O+Li⁺, vibr. excitation, 70 to 1500 eV 8-82824
 NiCO, hypothetical mol., adsorbate bond geometry, determ. using photoemission 8-71951
 OCS, collisional excitation of interstellar molecule 8-81664
 OCS, dipole moment, laser microwave double reson.-Stark effect meas. 8-55191
 OCS, electron impact dissociation, CS heat of form. determ. 8-73074
 OCS, electron scatt., absolute total cross-section meas. 8-74774
 OCS, IR spectral moments and mean squared torques, rare gas effects 8-62944
 OCS laser, two-quantum excitation, photolysis, energy transfer, for fusion expts. 8-59003
 OCS, microwave rot. lines, self-broadening 8-58668
 OCS photolytic laser, for fusion research 8-59002
 OCS+bromomethane, microwave spectral line width, dipole-dipole interaction calc. 8-74648
 OCS+H₂, rot. excitation, infinite order sudden approx. 8-74740
 O₃O₂, 3ν₁+ν₂←2ν₁⁰ 4ν₁+ν₂←3ν₁¹ Q-branches, diode laser analysis 8-74660
 O(²P)+C₃O₂→3CO, reaction dynamics and monoxide vibr. distrib., laser reson. absorpt. method 8-68882
¹³C¹⁶O and ¹²C¹⁸O, emission bands of E¹Π-A¹Π transition 8-90177
 SCN⁻, associated with metallic cations in aq. soln., press. effect, Raman spectra (French) 8-80333
 SCO, S atom L_{II,III}-absorption spectra 8-86807
 Sr-N₂O-CO flame, candidate chem. laser reactions, intracavity dye laser absorpt. meas. 8-63108
 Sr-N₂O-CO flame, Sr catalyzed, gain meas., emission band assignment 8-66815

carbon fibre reinforced composites

- epoxy matrix, effect of material variability on predicted environmental behaviour, numerical anal. 8-90733
 epoxy resin, diamag. susceptibility as fibre alignment characterisation method 8-84381
 glass matrix, SiC fibre coating, hot pressing production method (German) 8-95724
 glass/C reinforced epoxy resin, hybrid effects, conditions for positive or negative effects vs. rule of mixtures, mech. props. 8-68769
 graphite fibre reinforced Al, temp. and press. effect on interface chemistry, mech. prop. meas. 8-64595
 graphite fibre reinforced epoxy, laminated plate under tension, stacking sequence and lay up angle effect on free edge stresses round hole 8-88524
 graphite fibre reinforced epoxy laminates, expt. investigation of tensile moduli and strength 8-52870
 graphite fibre reinforced panels, low energy impact testing 8-72845
 graphite fibre reinforced Sn-Pb (38 wt.%) alloy, effect of interface on fracture characts. 8-76723
 graphite reinforced epoxy, B fibre addition as radiographic inspection aid 8-95880
 graphite reinforced epoxy resin, average stress failure criterion appl. 8-88519
 graphite reinforced epoxy steel scarf joint, adhesively bonded, exam. of failure 8-92350
 hybrid C and glass fibre, fracture energy 8-95801
 kinking as structural degradation mode 8-52893
 plastic matrix, ±45° orientation, creep, fatigue, repeated loading and crack growth 8-68729
 plastic matrix, strength, specimen size effect, statistical anal. 8-68724
 polyacetal matrix, friction and wear against glass and steel 8-56783
 polyester matrix, interlaminar shear fatigue 8-56742
 PTFE matrix, friction and wear against glass and steel 8-56783
 thermal expansion, in low temp. range 8-83978
 thermal expansion, influence of resin type 8-95164
 thermal expansion, ply multidirectional effects 8-95165
 unidirectional model for longit. tensile strength prediction 8-95778
 C matrix, fibre-matrix interactions 8-84725
 Cu matrix, fatigue strength under constant strain (Russian) 8-95796

carbon fibre reinforced composites continued

- TaC-C fibre composite, neutral beam target appls. 8-66399
 TiC-coated C fibres in Ni, diffusion barrier effectiveness 8-60624
 ZrN-coated C fibres in Ni, diffusion barrier effectiveness 8-60624

carbon fibres

- see also *carbon fibre reinforced composites*
 cathode prebreakdown field emission transition to vacuum breakdown 8-75462
 neutron irradiation effects 8-78496
 oxidation, coated with pyrolytic SiC 8-60857
 struct. and physical props. effects of B additions and heat treatment temp. 8-68715
 Al coated, effect of annealing on ultimate tensile strength and fracture 8-56744

carbon microphones see *microphones***carbon steel**

- accumulation of longitudinal strain under cyclic torsion 8-64615
 acoustic emission characts., effect of pressurisation during tensile testing 8-92304
 austenitic grain size determination, exam. of methods used 8-85071
 bainitic, morphological characteristics 8-68682
 brittle fracture, grain size and precipitate thickness effect 8-60786
 carbide coating formation by chromising C steels 8-88571
 carbide formation during chromising, exam. in terms of ternary phase diagrams 8-56818
 carbide transitions during post-strain ageing and tempering (*Russian*) 8-95741
 casting by C diffusion solidification 8-52792
 cementite decomposition during plastic deform., alloying element effects 8-84768
 coarsening of dispersed particles, in solid matrices 8-56651
 cold deformation hardening, effect of C content and cementite shape 8-92277
 cold formability (*French*) 8-60681
 cold rolled St3Kp, annealed, mag. nondestructive inspection of strip and ribbon 8-60913
 cold-worked, Mossbauer obs. of cementite decomp. and restitution 8-64558
 corrosion by wet elemental S, exam. as function of pH and particle size 8-92388
 corrosion during cyclical exposure, to wet elemental S, and He atmosphere 8-92391
 corrosion fatigue resistance in cavitations, bainitic and martensitic structs. (*Russian*) 8-56815
 corrosion in concentrated H₂SO₄ 8-64767
 crack growth, Weibull analysis 8-92319
 crack opening displacement, rel. to flow stress 8-68810
 crack resistance, preliminary loading condition effects on crack appl. 8-56739
 cumulative damage rule, based on reduction in fatigue limit, experimental confirmation 8-92358
 cyclic strain induced creep, relation between modes of stress and strain superposition 8-60733
 deformation peculiarities at high temp. under superplasticity with cyclic thermal load (*Russian*) 8-95776
 diffusion coating by Cr and Pb melt bath, kinetics (*Korean*) 8-60873
 diffusion of H₂, SCC via martensite form. cooling rate changes on Mn and Ni addition (*Russian*) 8-56813
 dual phase structures (martensite and ferrite), effect of martensite composition on content, mech. props. 8-76717
 ductile fracture under cold forming conditions, press. effect 8-52938
 elastic-plastic plane waves with combined stresses 8-90764
 fatigue, mean stress effects (*German*) 8-56721
 fatigue behaviour of NiAl precipitation hardening 8-84983
 fatigue crack features, in S 35 C and SK 5, anal. by precision matching method (*Japanese*) 8-52955
 fatigue crack growth in air and seawater, under constant amplitude and random loading 8-64679
 fatigue crack plasticity, effect of water vapour 8-64678
 fatigue crack propag. and crack closure, of part through cracks (*Japanese*) 8-72842
 fatigue crack propag. and crack closure behaviour, under various loading conditions 8-68795
 fatigue crack propag. and fractography under periodic oversteering, exam. (*Japanese*) 8-52958
 fatigue crack tip, observation of crack closure phenomena, by electron microscopy 8-68794
 fatigue cracks, transition from initiation to propagation 8-68802
 fatigue damage, under sawtooth wave strain cycling at elevated temp. (*Japanese*) 8-84977
 fatigue deformation, phenomenological exam. 8-64691
 fatigue of AISI 1010, effect of Se, Te additions 8-92359
 fatigue strength, push-pull, effect of high tensile load during stress cycling (*Japanese*) 8-92332
 ferrite-pearlite, cyclic behaviour, fatigue, chem. comp. and microstruct. effects 8-60833
 ferritic, low-C, deform. microstruct., electron microscopy (*German*) 8-64589
 ferritic-pearlitic transform., kinetics, struct. aspects (*French*) 8-68685
 fracture toughness testing, obs. of crack initiation and stable growth processes (*Japanese*) 8-52954
 fretting fatigue, microstructural and environment effects 8-64734
 fretting fatigue damage, SEM exam. 8-88541
 fretting fatigue tests, effects of environmental H₂O, O₂ 8-92407
 hardened and tempered parts, nondestructive magnetic inspection 8-95889
 heat treated, exam. of microfractographic aspects of fatigue cracks (*Japanese*) 8-52959
 high C, high Cr, rapidly quenched, in situ carbide reactions during tempering (*Japanese*) 8-84862
 hydrogen embrittlement, elastic interaction of H₂ with precipitates 8-92340
 hypoeutectic, texture development from frictional stress (*German*) 8-53003
 hypoeutectoid Widmanstätten struct. form., contrib. to the laws (*Slovenian*) 8-84817
 inelasticity in steel 45, under cyclic strain in active media 8-80613
 joints, with interference, increasing supporting capacity, by electrophysical methods, exam. 8-85055

carbon steel continued

- low C, C content effects in corrosion fatigue in nitrate solns. (*Russian*) 8-56811
 low C, capped, cold rolled sheet, deep drawability, effect of carbide size, cold reduction, annealing 8-64559
 low C, fatigue fractographs (*Japanese*) 8-92335
 low C, flow stress variation after unloading, tensile load/strain diagrams (*Russian*) 8-76703
 low C, forming limit diagram, eval. of applicability of theoretical anal. 8-60682
 low C, grain size effect on fatigue strength, high temps. 8-68759
 low C, martensitic, fracture toughness variations during tempering 8-60812
 low C, Mn, laws of banding structure form. (*Slovenian*) 8-83776
 low C, non-ductile transition temp., tensile speed, effect of prestrain (*Japanese*) 8-72839
 low C, oxide scale removal from fractured surfaces, improved techniques 8-95886
 low C, P, plastic anisotropy and mech. props., dynamic strain ageing effect 8-64608
 low C, positron annihilation, influence of fatigue 8-76551
 low C, rimmed, structural damage in sheet metal forming 8-64614
 low C, rimmed and killed, exam. of impact fatigue behaviour (*Japanese*) 8-88528
 low C, thermomechanically processed, martensitic fibre development, fatigue fracture 8-64572
 low C, V(C,N) precipitation and twinning in $\gamma \rightarrow \alpha$ transform. (*Polish*) 8-52807
 low C ductile-brittle transition behaviour, grain size effects 8-52942
 martensite-ferrite combined microstructure, two-phase, tensile fracture strength 8-60783
 mechanical props., DIN ST 35, FBR safety anal. 8-60966
 medium C, interface temp. meas. in fretting 8-64741
 medium C, S45C, hardening temp. determ. using pulsed laser 8-72942
 mild, activation energy for strain ageing 8-56677
 mild, alloying constituents, XES determ. 8-73126
 mild, conical rider on Cu surface, plastic deform. and wear at friction junction, SEM exam. 8-88542
 mild, corrosion behaviour of borided and nitrided steels in aqueous media 8-95837
 mild, corrosion in complex aq. environment, linear polarisation investigation. 8-76782
 mild, corrosion inhibitor, zinc potassium chromate 8-95839
 mild, cylindrical shells, limit loading under loop bending moment 8-80581
 mild, etching method for revealing plastic deformation 8-72825
 mild, exam. of fatigue damage, using thermography 8-92356
 mild, fatigue crack growth from a surface flaw 8-68803
 mild, high temp., generation and reception of US surface waves test head device 8-95901
 mild, high temp. fatigue, effect of temp. variation 8-64685
 mild, inelastic beam flexural behaviour and lateral buckling anal. under cyclic loads (*Japanese*) 8-87283
 mild, mode II fatigue crack growth threshold 8-92362
 mild, nitrided, oxidation resistance 8-95846
 mild, plate, effect of striking velocity on perforation energy 8-68818
 mild, protection by Zn-rich paint in flowing aerated 0.5 M NaCl solution, Zn particle size effect 8-95840
 mild, protection by Zn-rich paint in flowing aerated 0.5 M NaCl solution, exposed area ratio effect 8-95841
 mild, protection by Zn-rich paint in flowing aerated 0.5 M NaCl solution, zinc content effect 8-95842
 mild, protection by Zn-rich paint in flowing aerated 0.5 M NaCl solution, zinc oxide addition effect 8-95843
 mild, resistance to slow stable crack growth, use of J integral 8-68809
 mild, SM41, brittle fracture initiation characts., under biaxial loading, exam. 8-60803
 mild, stress history effect on fatigue crack retardation 8-64627
 mild, stress/strain relation formulation for plastic deform. for strain trajectory 8-52913
 mild, wear mechanism against oriented fibre reinforced plastics 8-56782
 nonmetallic inclusions, improved metallographic technique for examining 8-72956
 notched beam, fatigue crack emanates from notch root, fracture strength 8-72866
 optical constant dispersion and emissivity, up to 900K 8-52464
 pearlite in C steels (0.08 to 1.6 wt.%), exam. of temp. depend. of mag. coercivity 8-52304
 pearlitic eutectoid, cleavage fracture, grain size effect 8-60784
 plates, comparison of dynamic tear and Charpy V notch impact props. 8-92357
 precipitation of VC in ferrite, pearlite, during direct transformation, TEM exam. 8-52812
 prestrain effect on non ductile transition temp. and bending speed relationship (*Japanese*) 8-84919
 prior austenite grain size, effect on near threshold fatigue crack growth 8-92341
 prior austenite grain size, effect on near threshold fatigue cracks growth 8-92342
 push-pull fatigue strength, effect of tensile preload on plastic strain range (*Japanese*) 8-64625
 resistivity, thermal and elec., spin disorder scatt. anal. 8-76063
 reverse flow behaviour in spheroidized 1090, exam. 8-80610
 rimming, effect of addition of Al to Zn on phase composition and morphology (*Polish*) 8-53014
 rotational hysteresis 8-91889
 sheet, thin, residual stresses determ. after bending 8-60708
 solidification singularities in C and low-C steels (*Russian*) 8-80532
 spheroidised, fracture toughness, cementite particle effects, optic and electron obs. 8-60785
 spheroidized, medium C, strain hardening 8-52845
 steel, mild, bolt thread strain meas. 8-60972
 steel C, fatigued, strengthening by surface plastic deformation 8-88505
 strain hardening parameters, determination from stress-strain curves 8-80562
 surface, heated, water droplet evaporation, heat transfer characts. 8-59269
 tensile strength, effect of specimen length (*Japanese*) 8-84920

carbon steel continued

- thermal diffusivity meas., const.-rate heating method (*Japanese*) 8-79976
 thermal fatigue, effect of temp. difference in fatigue tests on fatigue life (*Japanese*) 8-84978
 type S15CK, tuffrided, fatigue strength at elevated temp., under reversed axial strength (*Japanese*) 8-84980
 X-ray stress meas., appl. of position sensitive proportion counter (*Japanese*) 8-64791
 yield strength, anisotropy in relation to temp. of deformation 8-80612
 cold swaged, exam. of H₂ attack mechanisms 8-76791
 Mo coated, fretting wear and fatigue strength assessment 8-88583
 SiO₂ inclusion formation on introduction of solid SiO into molten steel (*Russian*) 8-80530

carbon tetrachloride, CCl₄ *see organic compounds***carcinotrons**

No entries

cardiology

- see also blood; electrocardiography; haemodynamics*
 angiocardiology, quantitative radionuclide, in dogs with atrial septal defects 8-85362
 angiographic images of left ventricle, system for off-line anal. using minicomputer 8-80964
 arrhythmia monitoring, ARGUS/RT microcomputer system 8-81014
 artificial, mitral valves, insufficiency, press. and work losses (*German*) 8-88764
 artificial valve with convex closing body (*German*) 8-81066
 atrial pacing stress test quantification, normal, abnormal values, coronary artery disease in man 8-85449
 atrial trabecula membrane, frog, accommodation, repeat responses and anode-breaking excitation 8-64956
 ballistocardiogram compared with HF ECG 8-77123
 biopotential distribution laws rel. to functional state 8-65142
 birth monitoring by cardiocotography, interference effect by infusion pumps (*German*) 8-85416
 capacitoplethysmography for heart and lung meas. (*Japanese*) 8-53465
 cardiac noise, automatic segment anal. (*German*) 8-88759
 cardiac output analysers, equipment, maintenance and ccts., review 8-69239
 cardiac output and shunt calc. from dye dilution curves using automated catheterisation system 8-81023
 cardiac output automatic determ. by indicator dilution in computerised monitoring system 8-81022
 cardiac output control mechanism modelling (*Japanese*) 8-69133
 cardiac output on-line determ. by thermomodulation in coronary care unit 8-81021
 cardiac-assist in-series devices, controller 8-81075
 cardio-vascular structures, new examination method, short range sonar 8-87221
 cardiovascular research database system 8-53549
 cineangiocardiology, automatic anal. using TV system on-line with minicomputer 8-92699
 computer applications, conf., Rotterdam, Netherlands, (Sep.-Oct. 1977) 8-81013
 computer system SYSCORMORAM for haemodynamic and cineangiographic data treatment 8-81030
 computer-aided monitoring after open-heart surgery, appl. to adrenaline effects meas. 8-81059
 contractility, muscle tissue quality and sliding filament micromechanism (*Dutch*) 8-73171
 contraction kinetics recording using thorax elec. fields (*Czech*) 8-77138
 coronary sinus blood flow on-line computerised assessment by thermomodulation 8-81024
 defibrillation, multiple-shock, effect of shock separation time 8-57053
 defibrillation, myocardial damage rel. to high-energy elec. current 8-57051
 defibrillation, performance characteristics of three commercial instruments in transthoracic ventricular defibrillation of animals 8-57048
 defibrillation, transthest, strength-duration curves for trapezoidal waveforms of various tilts, dogs and ponies 8-57054
 defibrillation, transthest damped sine wave shocks producing cardiac damage 8-57052
 defibrillation, transthest ventricular, comparative efficacy of damped sine wave and square wave in dogs and ponies 8-57055
 defibrillation, transthoracic, square-wave, experience in dog and calf 8-57050
 defibrillation, transthoracic ventricular, in adults, success rate rel. to energy used 8-57049
 defibrillation conference, Lafayette, USA, (Sept. 1977) 8-57047
 echocardiogram, M-mode, computer-assisted anal. 8-80942
 echocardiogram computer-assisted interactive interpretation 8-80938
 echocardiogram on-line computer anal. 8-80941
 echocardiography, 2D, transducer beam profile effects on tissue aperture detection 8-73185
 echocardiography, two-dimens., wall motion and thickening quantification by computer-aided contouring 8-80937
 echographic information related to left ventricle and mitral valve in diastole, anal. by small computer 8-80939
 electrical generator integral characts. in normal humans 8-69244
 ergometric test, computer interpretation of heart-rate var., anal. of cardiac control in exercise 8-85430
 excitable medium self-sustained activity, role of inhomogeneity 8-64968
 fibre optic, catheter transducer, side hole type, for intracardiac press. meas. (*Japanese*) 8-73272
 fibre optic catheter-tip micromanometer as intracardiac press. transducer (*Japanese*) 8-73270
 flowmeters, digital 2D full range Doppler velocity meter for cardiovascular diagnosis 8-88731
 foetal heart rate recording, interference due to infusion pump (*German*) 8-85414
 foetal ventricular ejection time, registration and clinical significance 8-85417
 gammagraphy, 3-dimens. image processing appl. to coded aperture imaging (*French*) 8-57067
 heart imaging from computerized tomography 8-88741
 heart rate meas. (foetal), adaptive correlation ratemeter, US signals 8-88732

cardiology continued

- image description and analysis, interactive knowledge-based systems approach 8-81031
 imaging, comparison of red blood cells labelled with ⁹⁹Tc^m in vitro and in vivo 8-65109
 intravenous antiarrhythmic drug infusion, automated delivery 8-81058
 ischaemic heart disease determ. by heart beat interval anal. and medical questionnaire evaluation 8-65145
 ischaemic heart disease diagnosis using respiratory sinus arrhythmia 8-65147
 isolated heart preparation computer control for biomedical research 8-53603
 left ventricular diameter-time curve shape from M-mode echocardiogram, automated anal. 8-80940
 left ventricular ejection fraction determ. using multicryst. scintillation camera 8-73213
 left ventricular ejection fraction determ. using radionuclides 8-80962
 left ventricular function, normal and abnormal, vel.-strain relationship 8-69119
 left ventricular function evaluation using ECG synchronised scintillation camera 8-65110
 left ventricular regional function anal. from cineangiogram, computer system appl. 8-80963
 left-heart haemodynamics, mathematical model 8-65074
 left-ventricular ejection fraction and segmental wall motion by peripheral first-pass radionuclide angiography 8-61246
 magnetocardiograms from normal hearts, interpretation (*Japanese*) 8-53433
 magnetometry of human heart in small ferromag. enclosure, using SQUID. 8-92726
 mechanics, elastic props., forces, stresses and press. (*Dutch*) 8-73170
 microwave-induced chronotropic effects in isolated rat heart 8-69137
 mitochondria of bovine heart, EPR investigation of two forms of Fe-S centre N-2 8-69014
 muscle, behaviour of myosin projections during staircase phenomenon 8-53362
 muscle cells, paraffin-embedded, cryofracture, SEM and TEM obs. 8-57148
 myocardial contrast accumulation, densitometric evaluation 8-69216
 myocardial imaging with ²⁰¹Tl, interinstitutional study of observer variability 8-85361
 myocardial infarction, topographic relation between myocardial ²⁰¹Tl uptake and left ventricular kinetics 8-61243
 myocardial perfusion scan interpretation, computer technique 8-80960
 myocardial scintigraphy, computerised extraction of organ contours (*German*) 8-88735
 myocardial-stress perfusion scintigraphy, predictive value in patients without previous infarction 8-73205
 myocardium contraction amplitude depend. on freq. of elec. stimulation, frog 8-77027
 myocardium mitochondria lipid composition and phase transitions rel. to depth of hypothermia, rats and dogs 8-53350
 output measurement, in vitro comparison of six commercially available thermomodulation systems 8-77135
 prosthetic heart valves, rigid leaflet and caged-ball types, diastolic ventricular mechs. 8-81079
 QRS-onset and offset in children, detection using parametrised templates 8-85438
 radiographic image sequence analysis and recording 8-57069
 radioisotope functional imaging, clinical experience 8-80958
 radionuclide cardiac motion study, computer-processed, ECG gating device 8-73210
 radionuclide cineangiography, clinical utility of real-time computer-based system 8-80957
 radionuclide computer-assisted cardiology, off-line viewing using videotape 8-65119
 radionuclide images, digital image superposition algorithm, accuracy and reproducibility 8-73209
 rat cardiac muscle, mech. props., effect of 1 MHz ultrasound 8-96062
 RF EM noninvasive transcutaneous measurement technique (*Italian*) 8-85352
 scintigraphy and angiography, equipment for quant. evaluation and off-line operation (*German*) 8-88736
 scintigraphy of cardiac function using Bonn System III 8-73198
 sinatorial node of rabbit heart, vagal stimulation, K⁺ permeability and extracellular transients 8-92608
 submitochondrial particle succinic dehydrogenase, interaction of ubiquinone with Fe-S centre, EPR 8-69016
 surgery, data acquisition and processing during operation by multiplexer (*German*) 8-92743
 surgical aspiration automatic control device for cardiac surgery (*French*) 8-61282
 systolic time interval processing system, STIPS 8-81029
 T-wave rise time rel. to heart rate, exercise vector cardiograms study 8-85434
 thalassaemic tissue, Mossbauer spectra of Fe deposits 8-73202
 three-dimensional image reconstruction for cone-beam X-ray sources 8-77111
 US image feature enhancement via digital processing 8-73183
 US imaging systems, high-resolution, real-time 8-69160
 US imaging techniques and appls. 8-49620
 valve motion obs. CW FM sonar 8-61230
 ventricle volume characts., nuclear medical determ., appl. of computer system (*German*) 8-88737
 ventricular excitation, digital simulation, computer model evaluation 8-85302
 ventricular function computer simulation, development of model and parameter estimation 8-53439
 ventricular pressure and ECG continuous monitoring during angina attacks, computer anal. 8-85436
 ventricular wall dynamics and obs. on blood flow 8-80896
 ventriculography, algorithm for automatic selection of end diastolic and end systolic cine frames 8-88757
 vibration quantitative characterisation by multipolar acoustic heart model, minicomputer method 8-85429
 video processor for computer calc. of press.-vol. indices from left ventriculograms 8-53495
 video-angiocardiac image series storage improvement by digital signal processing (*German*) 8-92723
 volume determination by angiography, X-ray magnification estimation 8-73197

cardiology continued

Ca transients in aequorin-injected frog cardiac muscle 8-61149

³¹P NMR investigations of metabolism, pH and contractile performance 8-69018²⁰¹Tl distribution in stressed rats, imaging, organ uptake and myocardial kinetics 8-65114**carrier avalanches** see impact ionisation**carrier density**

see also current density; electron density; electron density (metals)

chalcogenide lone-pair semicond. charged impurities, effect on carrier concs., Street-Mott model 8-67984

charge carrier conc., temp. depend., computer data anal., effect of band parameter errors (Russian) 8-52006

conducting crystals, kinematical and dynamical inelastic light scatt. 8-80368

defect cluster scatt. and removal of carriers, model 8-76069

distribution function, high energy asymptote in strong elec. field (Russian) 8-72163

drift solutions, discontinuities, hot carriers injection and accumulation 8-51999

ferroelectric and antiferroelectric crystals, perovskite type structure, semiconductor props. (Polish) 8-56437

ferromagnetic semiconductor, electronic spectrum, influence of finite carrier conc. 8-76220

free carrier profile measurement on thin-layers, fast current pulse MOS deep-depletion technique 8-80075

graphite, galvanomagnetic effects, low field data and free carrier densities 8-87986

graphite, galvanomagnetic effects, trigonal warping of constant energy surfaces 8-87987

graphite, neutron irradiated, effect on quantum limit Shubnikov-de Haas oscils. 8-95304

injection laser, reson.-like peak reduction in direct modulation due to carrier diffusion 8-74905

photovoltage for doping factor, mobility ratio and excess conc. determ. extreme band bendings 8-91726

piezoelectric semiconductors, dependence of US attenuation 8-72206

semiconductor, Einstein relation for degenerate carrier concentrations 8-72143

semiconductor, electron distribution function, temp. gradient effect 8-72145

semiconductor, galvanomagnetic-effects in strong elec. field 8-56163

semiconductor, trap-free lifetime and relaxation, bulk boundary conditions for injection and extraction 8-72169

semiconductor containing traps, minority, carrier lifetime 8-60137

semiconductor crystal surface, nonequilib. electron effects due to chem. excitation 8-72238

semiconductor in mag. and US wave fields, electronic density of states (Russian) 8-72056

semiconductor laser, dynamic behaviour, lateral mode and carrier density profile effects 8-82968

sputtered films, optical props. and appls. 8-72623

Bi, diffusion thermoelectric power in mag. field, calcs. 8-56167

Bi film, carrier conc. and mobility, resist., galvanomag. and thermoelec. meas. 8-52111

Bi_{1-x}Sb_x, semicond.-semimetal transition, temp. and press. depend. of transport props. 8-76120Bi₈₈Sb₁₂-Sn, current carrier energy spectrum (Russian) 8-60139CdCr₂Se₄:Cu, elec. props., temp. depend. (Russian) 8-72181Cd_{0.9}Hg_{0.1}Te, fine-graded gap struct., electrophysical props. (Russian) 8-60144

CdS, chem. sprayed film, struct. and morphology 8-72020

CdS, film for solar cells, struct. and elec. props., thickness depend. 8-72289

CdS-type semiconds., Dember effect, theory 8-72189

CdSe, defect struct. in Se vapour 8-64043

p-CdSe, Hall density and mobility, in Se vapour atm., 600-1100K 8-52014

CuInTe₂, grown from near stoichiometric comp., elec. and optical props. 8-68504Cu_{1-x}Mo_xS₈, normal state and superconducting property measurements 8-91660Cu_{1-x}Mo_xS₈, Hall effect and magnetoresistivity 8-95400

Fe-Al-Ni-Co-Cu alloys, Ti alloying and deoxidising addition (Russian) 8-80181

α-Fe₂O₃, polycryst., pure and TiO₂ doped, flatband potentials, donor densities, photocurrent meas. 8-76089Ga_{0.9}Al_{0.1}-As, LPE, charge carrier conc. distrib. (Russian) 8-52694

GaAs, anodic oxide film, annealing effect on carrier density profile 8-88040

p-GaAs, electronic props. 8-68040

GaAs, epitaxy using TMG and AsH₃, chloride etching effect 8-76606

p-GaAs IR plasma reflectivity spectra calc., rel. to carrier conc. 8-52511

GaAs, LPE, charge carrier conc. distrib. (Russian) 8-52694

n-GaAs, proton irradi., E_p=30 MeV, defect form., orientation depend. 8-55898

GaAs, VPE on Ge substrate, and characterisation 8-72736

GaAs:Ge, vap. grown, diatomic complex donor and acceptor model 8-80003

GaAs:Sn, LPE layers, electronic props., depend. on Sn incorporation 8-87883

GaAs_{1-x}P_x based structs., carrier conc., mobility calcs. from Hall effect meas. 8-60138Ga_{0.9}In_{0.1}-PyAs_{1-y}, In rich bulk single crystals, growth from melt via gradient freeze method, and characterisation 8-86618Ga_{1-x}In_xSb, LPE on GaSb by stepwise grading, and characterisation 8-72745

GaP, rare earth doped, photolum. and elec. props. (Russian) 8-52545

GaP, soln. growth of bulk crystals, luminesc. and elec. props. 8-92181

GaP:Te, Hall effect and elec. cond., 80-400K 8-91705

GaP:Zn, Hall effect and elec. cond., 80-400K 8-91705

Ga₂Se₃(1-x) solid solns., electrical props. meas. 8-84216

GdP-GdS systems, mag. exchange interactions, free carrier conc. 8-60278

Ge bicrystal cleavage plane, Shubnikov-de Haas oscils. (Russian) 8-64094

Ge, elec. cond., optically injected carrier density and temp. depend. 8-68046

Ge film, polycrystalline, structural and elec. props. 8-76173

carrier density continued

n-Ge, group V doped, point defect form. due to γ-ray irradi., carrier density, mobility meas. 8-71759

p-Ge:Ga, carrier heating by weak elec. field, hole-hole collision influence 8-72161

Hg_{0.6}Cd_{0.4}Te, annealing temp. effect on carrier conc. 8-72167Hg_{1-x}Cd_xTe, zero-gap semicond. with nonparabolic band struct., hot electron mobility and conc. 8-76080

HgTe, vacancy doping by off-stoichiometry, influence on transport props. 8-55862

InAs, intrinsic point defects, nature and influence on electrophys. props. 8-79609

p-InAs-Au contacts, influence of free surface on elec. behaviour 8-95362

In₂O₃, Seebeck coeff., density of states effective mass 8-56171In₂O₃, transparent electrode deposition on PLZT ceramic, elec. and opt. props. 8-74848In₂O₃:Sn, film, HF sputtered, cond., Hall mobility, oxidation, charge carrier density 8-72287

InP carrier profiling using liq. barrier contact 8-76087

n-InP, epitaxial, Hall effect, electron mobility and density, temp. depend. 8-72288

InP, planar reactive deposition on CdS, heterostruct. formation and elec. evaluation 8-72738

Nd-Gd-Te alloys of R₂Te₃-T₃Te₄ region, physicochem. props. 8-52017Pb_{1-x}Ge_xTe:Ga, Fermi level stabilization, transport props. meas., 77-400K 8-56065PbMo₆S₈, Hall effect and magnetoresistivity 8-95400PbMo₆S₈, normal state and superconducting property measurements 8-91660Pb_{0.99}Sn_{0.01}Se, struct. phase transition, temp and hydrostatic press. influence, Hall effect, resistivity (Russian) 8-51675Pb_{0.8}Sn_{0.2}Te, hole conc. at 77K from room temp. thermoelec. meas. 8-56155p-Pb_{0.82}Sn_{0.18}Te, Hall coeff. sign-inversion temp. 8-52010Pb_{1-x}Sn_xTe, Cd-In diffusion, changes in elec. props. 8-91348

PbTe, carrier conc. inhomogeneity 8-52019

n-PbTe, epitaxial, time dependent negative weak field magnetoresist. 8-64151

p-PbTe MIS capacitors 5 μm IR detector appl. 8-52101

PbTe, solidus line anal., carrier conc. 8-75806

PbTe-SnTe, solid soln. single crystals, TSM growth and elec. characts. 8-68625

SeN₄, region of homogeneity, physicochem. props. 8-52018

Si, carrier conc. determ., electrochem. method 8-60200

Si, laser measurement, of semiconductor materials and devices (Rumanian) 8-52035

p-Si polycrystalline films on graphite substrates (French) 8-64154

Si, radiation-doped and annealed, carrier density and mobility meas. 8-56145

Si:P, carrier mobility and distrib. rel. to annealing, 400-910°C 8-79995

Si-Ge alloy, thermoelec. material, lattice thermal conductivity rel. to grain size and carrier conc. 8-91495

Si-Ge:Al(B)(P), hot-pressed alloy, thermoelec. props. 8-91711

SnO₂, transparent electrode deposition on PLZT ceramic, elec. and opt. props. 8-74848Sn_{1-x}Pb_xTe, elec. and struct. props. of epitaxial layers (Russian) 8-64147

SnSe, sublimation growth, deviation from stoichiometry, elec. props. 8-76594

SnTe, solidus line anal., carrier conc. 8-75806

Te, lightly doped, galvanomagnetic props. in fields up to 140 kOe 8-91707

Te, warm hole conductivity 8-72160

Te:Se, 96 to 500K, cond. Hall const., hole mobility, conc., dislocation effects (Russian) 8-64039

V₂O₅-P₂O₅ glass, dielec. relax. mechanism, SDRC investigation, Schottky barrier formation in metal-glass-metal systems 8-60388ZnGeP₂, synthesis, characts., applic. to laser windows (French) 8-80467ZnP₂, pure and doped, carrier mobility and conc., donor and acceptor energy levels, 190 to 380K 8-84217

ZnSe, laser induced modulation of opt. absorpt. 8-88324

carrier diffusion length see carrier lifetime**carrier lifetime**

alkali halides, F-centre trapping of conduction electrons, photocond. study 8-56179

diffusion length and surface recomb. vel. determ., light excitation 8-91725

injection laser, reson.-like peak reduction in direct modulation due to carrier diffusion 8-74905

insulator, charge carrier injection, Onsager model 8-80001

minority carrier diffusion length, Schottky barriers, electron bombard. investigation 8-68037

minority carriers, spectrometric determ. (Russian) 8-84230

MIS, minority carrier, lifetime and generation determ., graphical technique 8-95378

MOS capacitor, comparison of lifetime meas. techniques 8-56232

MOS capacitor, minority carrier generation time and surface generation rel. determ. from Q-t meas. 8-72265

p-n diode minority carrier storage effect reduction by F ion implantation damage 8-72243

p-n junction, impedance determ. from direct currents (Russian) 8-84285

p-n junctions, photoeffect, quantity effective diffusion length (Russian) 8-56212

pentacene layers, photogeneration, charge carrier transport (Russian) 8-56181

SEM meas. of diffusion const., lifetime and surface recomb. vel. 8-91701

SEM measurement of minority carrier diffusion lengths in semicond. interpretation 8-80002

semiconductor, ambipolar diffusion meas. using nonlinear transient gratings 8-80000

semiconductor, carrier capture cross section by attractive Coulomb centres, piezoelec. scatt. 8-72170

semiconductor, lifetime meas. by photoconductivity null apparatus 8-56184

carrier lifetime continued

- semiconductor, minority carrier injection 8-60136
 semiconductor, nonuniform diffusion length and elec. field determ. 8-72166
 semiconductor containing traps, minority, carrier lifetime 8-60137
 semiconductors, two-photon conductivity calc., nano-pico sec. pulse excitation 8-72188
 shallow junction devices, minority carrier diffusion lengths 8-72168
 tetracene, layers, photogeneration, charge carrier transport (*Russian*) 8-56181
 CdSe, charge transport 8-84233
 GaAlAs DH laser diode, deep level associated with slow degradation 8-87050
 Ga_{1-x}Al_xSb p-n homojunction LPE and photovoltaic effect obs. (*French*) 8-64108
 Ga(As,P)/(In,Ga)P DH laser, red-emitting, optical and elec. characts. 8-66826
 GaAs, illuminated, carrier lifetime profile, depth depend. 8-68036
 GaAs injection lasers, longitudinal mode spectrum, effect of carrier diffusion 8-71099
 GaAs, minority carrier diffusion lengths, contact metal effects 8-72260
 n-GaAs, two-valleyed semicond., hot electron diffusion coeff., random walk calc. 8-68033
 GaAs VPE layers, role of diffused Ga vacancy in degradation 8-95050
 GaAs:Ge, vap. grown, diatomic complex donor and acceptor model 8-80003
 Ga_{1-x}In_xSb, LPE on GaSb by stepwise grading, and characterisation 8-72745
 Ge, charge carrier diffusion coeff. 8-84218
 Ge:Ba, Ca, recomb. props. 8-56156
 InAs, intrinsic point defects, nature and influence on electrophys. props. 8-79609
 InGaAsP-InP DH lasers, carrier lifetimes meas. 8-66828
 Pb_{1-x}Sn_xY, Y=Te, Se, S, photocond. anisotropy rel. to lifetime: 8-52032
 p-PbTe MIS capacitors 5 µm IR detector appl. 8-52101
 Se, amorphous, carrier lifetime and drift mobilities 8-87985
 n-Si, A-centre ionisation energy change due to uniaxial deform. 8-71733
 Si, carrier lifetime, comparison of meas. by photocond. decay and surface photovoltage 8-68038
 Si, carrier lifetime degradation at room temp. 8-95301
 Si, diffused p-n junction, computer calcs. of photoresponse using Gummel-de-Mari algorithm 8-56221
 Si epitaxial film, correlation between electrooptical and electrical props., IR absorpt. spectra (*Russian*) 8-60453
 Si, epitaxial layers, minority carrier lifetime and diffusion length meas., photocurrent technique 8-95302
 Si, film, polycryst., for photovoltaic appl., grain size effects 8-72034
 n-Si, γ-irrad. (E_{max}=100 MeV), carrier recomb. 8-56158
 Si, laser measurement, of semiconductor materials and devices (*Rumanian*) 8-52035
 Si, metallurgical grade, purification and charact. 8-56573
 Si p⁺n diodes, minority carrier lifetimes, gettering of Cu and Au during Ga diffusion 8-91350
 p-Si polycrystalline films on graphite substrates (*French*) 8-64154
 p-Si radiation defects due to 30 MeV proton irrad., rel. to solar energy converters 8-71776
 Si slice, minority carrier diffusion lengths, surface photovoltage meas. 8-72168
 Si: Cd(Zn), n⁺-n-n⁺ structure, photocond. lifetimes, deep level occupancy in exclusion region 8-72253
 Si:Gd, radiation defect form., effect of Gd impurities, elec. and optical meas. 8-71764
 p-ZnF₂:S(Se)(Te), photocond., carrier generation and recomb. at high excitation levels (*Russian*) 8-64059

carrier mean free path

see also *electron mean free path (metals)*

- poly(p-xylylene), electron MFP as function of kinetic energy, XPS 8-52114
 GaAs, surface (111), (111), (110), XPS, photo-Auger ionisation cross section, electron mean free paths 8-56558

carrier mobility

see also *carrier mean free path; carrier relaxation time; current density; electron-hole recombination; electron mobility (metals)*

- alkali halides, F-centre trapping of conduction electrons, photocond. study 8-56179
 amorphous layers, injected charge drift and localisation (*German*) 8-91794
 anthracene, off-diagonal electron mobility and lateral space charge drift 8-72192
 benzophenone, charge carrier generation and mobility 8-84231
 defect cluster scatt. and removal of carriers, model 8-76069
 β-9,10 dichloroanthracene, hole mobility anisotropy and cryst. struct., transient photocond. 8-95310
 dielectric liquids, cond. band minima, rel. to electron mobility maxima 8-80029
 drift solutions, discontinuities, hot carriers injection and accumulation 8-51999
 ferroelectric and antiferroelectric crystals, perovskite type structure, semiconductor props. (*Polish*) 8-56437
 ferromagnetic semiconductors, carrier mobility, electron-two magnon scatt. Hall effect 8-51992
 heterogeneous material, scatt. theory, effective medium approx. 8-56116
 III-V mixed semiconductor, electron mobility theory 8-84210
 III-V semiconductor, anisotropic carrier mobility due to dislocations 8-60124
 III-V semiconductor, low temperature, high mobility transistor materials 8-87970
 ionised impurity scatt. limited mobility in semiconductors with spatially variable dielec. function 8-51986
 MBBA, nematic liq. cryst., charge carrier drift mobility 8-87801
 MIS inversion channel hole mobility rel. to field treatment in active media 8-91774
 MOS inverted-channel carrier scatt., effect of oxidation in Cl media 8-76156
 naphthalene, hole mobility, anomalous current transients 8-76091

carrier mobility continued

- narrow band-gap semiconductor, energy depend. relax. time, EM response of electrons 8-60142
 organic semiconductor layers, injected charge drift and localisation (*German*) 8-91794
 p-n junction, impedance determ. from direct currents (*Russian*) 8-84285
 pentacene layers, photogeneration, charge carrier transport (*Russian*) 8-56181
 photovoltage for doping factor, mobility ratio and excess conc. determ. extreme band bendings 8-91726
 powder combinations, compressed, mixing ruler concerning Hall effect and Hall mobility (*German*) 8-84234
 quantum resonance impedance oscillations (*Russian*) 8-91781
 quasilocal acceptor states, effects on band gap and electron mobility (*Russian*) 8-60082
 semiconductor, amorphous or disordered, cond. mechanisms, model of medium-range comp. disorder 8-79994
 semiconductor, carrier transport, in presence of temp. gradient, flux method 8-72144
 semiconductor, containing screw dislocations, impurity centres 8-72111
 semiconductor, Einstein relation for degenerate carrier concentrations 8-72143
 semiconductor, electron distribution function, temp. gradient effect 8-72145
 semiconductor, models for transport and accumulation 8-87975
 semiconductor with disordered regions, carrier mobility, theory and expt. 8-56166
 semiconductors, relaxation regime, generalised transport eqns. 8-56139
 semimetal, degenerate, anisotropic scattering at low temp. (*Russian*) 8-95298
 SOS, cryst. perfection rel. to MOS transistor mobility 8-75956
 SOS film, electron mobility 8-91792
 SOS MOS devices, hole mobility under residual stress, Hall meas., valence band struct. 8-88039
 sputtered films, optical props. and appls. 8-72623
 stilbene, single cryst., free charges and excitons generated by electron pulses 8-63988
 TCNB complexes, hole mobility, photocurrent meas., 260-300K 8-60161
 TCNQ salt, (NMP)_x(Phen)_{1-x}(TCNQ), band filling and disorder 8-87968
 tetracene, layers, photogeneration, charge carrier transport (*Russian*) 8-56181
 thermopiezosemiconductor critical drift velocity for US amplification 8-60169
 transition metal oxides, 3d-, microwave cond. at high temp. (*Japanese*) 8-91715
 violanthrene-A film, amorphous and crystalline, carrier mobility differences 8-60125
 AlGaAs-GaAs DH laser, carrier leakage, physical mechanisms 8-66824
 As_{0.3}Te_{0.48}Ge_{0.1}Si_{0.12}, amorphous film, transient switching processes 8-84232
 n-BaTiO₃, elec. transport props., theoretical discussion and expt. 8-84215
 Bi film, carrier conc. and mobility, resist., galvanomag. and thermoelec. meas. 8-52111
 Bi, single crystal, drift velocity of charge carriers (*Russian*) 8-84208
 CdCr₂Se₄:In, ferromag. semicond., carrier mobility, electron-two magnon scatt. Hall effect 8-51992
 Cd₂Hg_{1-x}Se mixed cryst., electron mobility and electron scatt. 8-95296
 CdSe, charge transport 8-84233
 CdSe, defect struct. in Se vapour 8-64043
 p-CdSe, Hall density and mobility, in Se vapour atm., 600-1100K 8-52014
 CdSnP₂, Hall mobility of holes 8-52015
 CdTe negative dielectric relax. of hot electrons 8-52001
 CdTe:Cl, single cryst., photo Hall effect obs. 8-76094
 Cr_{1-x}Mn_xSi₂, semicond. props. 8-79992
 CrSi₂, semicond. props. 8-79992
 Cu₂Mo₂S₈, Hall effect and magnetoresistivity 8-95400
 EuO:Gd, electron mobility below Curie temp. 8-91696
 GaAs, CVD in Ga-AsCl₃-H₂ system with different input supersaturations (*Russian*) 8-68098
 GaAs, carrier mobility profiles meas. at room temp. by Corbino effect 8-60128
 GaAs, electron transient vel. characts., Γ-L-X cond. band ordering 8-79997
 p-GaAs, electronic props. 8-68040
 GaAs epitaxial layers, characterisation Hall effect and Schottky diode profile meas. 8-91791
 GaAs, epitaxy using TMG and AsH₃, chloride etching effect 8-76606
 n-GaAs, photo-Hall effect meas. of ionised impurity scatt. 8-56182
 n-GaAs, piezoelectric semiconductor, influence of acoustic phonon disturbances on conductivity 8-91697
 n-GaAs, proton irrad., E_p=30 MeV, defect form., orientation depend. 8-55898
 GaAs VPE layers, role of diffused Ga vacancy in degradation 8-95050
 GaAs:Ge, vap. grown, diatomic complex donor and acceptor model 8-80003
 GaAs:Sn, LPE layers, electronic props., depend. on Sn incorporation 8-87883
 GaAs_{1-x}P_x based structs., carrier conc., mobility calcs. from Hall effect meas. 8-60138
 Ga₂In_{4-x}PyAs_{1-y}, In rich bulk single crystals, growth from melt via gradient freeze method, and characterisation 8-68618
 n-GaP, cryst. growth, synthesis solute diffusion method, elec. characts. (*Korean*) 8-52653
 GaP, rare earth doped, photolum. and elec. props. (*Russian*) 8-52545
 GaP, soln. growth of bulk crystals, luminesc. and elec. props. 8-92181
 GaP:Te, Hall effect and elec. cond., 80-400K 8-91705
 GaP:Zn, Hall effect and elec. cond., 80-400K 8-91705
 Ga₂Se₃(1-x) solid solns., electrical props. meas. 8-84216
 n-GaSb, galvanomagnetic effects 8-72172
 p-GaSb, heavy and light holes scattering 8-91692
 GaSe, Hall mobility anisotropy 8-68041

carrier mobility continued

- Ge film, polycrystalline, structural and elec. props. 8-76173
 n-Ge, group V doped, point defect form. due to γ -ray irradi., carrier density, mobility meas. 8-71759
 Ge, hole drift velocity, effect of impurity scatt. 8-60127
 Ge, ionised impurity scatt. limited mobility in semiconductors with spatially variable dielec. function 8-51986
 He, solid, charge motion, singularities in temp. and time depend. (*Russian*) 8-56019
 He, solid, peculiarities of charge motion (*Russian*) 8-95202
 Hg_{1-x}Cd_xTe, quasi-local acceptor levels and electron mobility 8-67974
 Hg_{1-x}Cd_xTe, zero-gap semicond. with nonparabolic band struct., hot electron mobility and conc. 8-76080
 HgI₂, electrons and holes cyclotron reson. 8-72061
 HgTe, vacancy doping by off-stoichiometry, influence on transport props. 8-55862
 InAs, intrinsic point defects, nature and influence on electrophys. props. 8-79609
 In_{0.9}Ga_{0.1}As, heteroepitaxial, MBE grown, props. 8-84328
 n-In₂O₃ film, RF sputter grown, substrate bias effect on elec. and optical props. 8-64150
 In₂O₃, transparent electrode deposition on PLZT ceramic, elec. and opt. props. 8-74848
 n-InP, epitaxial, Hall effect, electron mobility and density, temp. depend. 8-72288
 n-InP, epitaxial, subthreshold velocity-field charact., 77K 8-64038
 InP, planar reactive deposition on CdS, heterostruct. formation and elec. evaluation 8-72738
 p-InSb film, elec. transport props. 8-72291
 InSb, gamma irradiated, changes in energy spectrum of impurity spectrum 8-51937
 n-InSb, photoconductivity, 1.8K, hot-carrier and free-carrier absorption. effects 8-84254
 InSb:Cr, press. effects on transport props. 8-56146
 InSb-type semiconductor, inelastic scatt. of electrons by optical phonons 8-76073
 MBBA:(TEAI), elec. drift mobility, carrier identification (*Korean*) 8-51998
 β -MnO₂, powders, Hall carrier mobility mixing rule (*German*) 8-52008
 PbMo₆S₈, Hall effect and magnetoresistivity 8-95400
 PbO₂, and pyrolusite compressed powder mixtures, mixing rules concerning Hall effect and Hall mobility (*German*) 8-84234
 Pb_{0.82}Sn_{0.18}Te, carrier tunnelling through potential barrier in p-n junctions (*Russian*) 8-52074
 Pb_{1-x}Sn_xTe, Cd-In diffusion, changes in elec. props. 8-91348
 n-PbTe, epitaxial, time dependent negative weak field magnetoresist. 8-64151
 PbTe-SnTe, solid soln. single crystals, TSM growth and elec. characts. 8-68625
 Se, amorphous, carrier lifetime and drift mobilities 8-87985
 Si epitaxial film, correlation between electrooptical and electrical props., IR absorpt. spectra (*Russian*) 8-60453
 Si, inversion layer, Hall effect meas. 8-56199
 Si inversion layer, press. depend. of struct. of field effect mobility 8-60216
 Si, ionised impurity scatt. limited mobility in semiconductors with spatially variable dielec. function 8-51986
 Si MNOS structures with tunnelling-thickness SiO₂ films, surface channel hole mobility obs. 8-95380
 Si MOS inversion layer, subband struct., many body effects 8-64131
 Si, metallurgical grade, purification and charact. 8-56573
 n-Si, microwave and far IR hot carrier mobility, Monte Carlo calc. appl. to mm. transit time oscill. efficiency 8-72184
 p-Si polycrystalline films on graphite substrates (*French*) 8-64154
 Si, radiation-doped and annealed, carrier density and mobility meas. 8-56145
 Si:Cr, specific resistance, activation energy of deep levels, and carrier mobility (*Russian*) 8-72146
 Si:P, carrier mobility and distrib. rel. to annealing, 400-910°C 8-79995
 Si₃Te₃, passivated single cryst., elec. conductivity 8-95299
 Si₁₂Te₄₈As₃₀Ge₁₀, amorphous film, elec. cond. mechanisms, temp. depend. (*Japanese*) 8-80078
 SnO₂, transparent electrode deposition on PLZT ceramic, elec. and opt. props. 8-74848
 Sn_{1-x}Pb_xTe, elec. and struct. props. of epitaxial layers (*Russian*) 8-64147
 SnS₂, electron mobility, elec. cond. and Hall effect meas. 8-80004
 SnSe, sublimation growth, deviation from stoichiometry, elec. props. 8-76594
 Te, electron irradiated, dose-depend. and recovery behaviour of transport props. 8-71761
 Te, warm hole conductivity 8-72160
 Te:Se, 96 to 500K, cond. Hall const., hole mobility, conc., dislocation effects (*Russian*) 8-64039
 ZnGeP₂, synthesis, characts., applic. to laser windows (*French*) 8-80467
 ZnP₂, pure and doped, carrier mobility and conc., donor and acceptor energy levels, 190 to 380K 8-84217

carrier relaxation time

- see also *electron relaxation time (metals)*
 energy relaxation of photoexcited hot electrons at very low temperatures 8-91724
 III-V mixed semiconductor, electron mobility theory 8-84210
 narrow band-gap semiconductor, energy depend. relax. time, EM response of electrons 8-60142
 piezoelectric semiconductor film, mobility of hot electrons 8-56247
 semiconductors, relaxation regime, generalised transport eqns. 8-56139
 Stark-Ladder current theory 8-68035
 surface electrical resistivity of thin semiconductors, semimetallic films 8-91751
 zincblende narrow-gap mixed crystals, disorder scatt. 8-51985
 Bi, diffusion thermoelectric power in mag. field, calcs. 8-56167
 Bi:Se, semimetallic alloy, microwave spectroscopy 8-87908
 GaAs, film, radiative relax. time, nonequilibrium carriers 8-84657
 Ge bicrystalline cleavage plane, Shubnikov-de Haas oscills. (*Russian*) 8-64094
 Hg_{1-x}Cd_xTe, quasi-local acceptor levels and electron mobility 8-67974

carrier relaxation time continued

- MnP₂, nonequilibrium luminesc. and relaxation processes, 25 to 300K (*Russian*) 8-80415
 Pb_{0.82}Sn_{0.18}Te, narrow, band gap, relax. time for Shubnikov-de Haas effect 8-80006
 Si, (100) surface, effective mass and collision time 8-64081
 p-Si, millimetric and far IR cond., evidence for interband transitions 8-52022
carrier scattering at surfaces see *surface scattering*
carrier scattering by dislocations see *dislocation scattering*
carrier scattering by impurities see *impurity scattering*
carrier scattering by point defects see *point defect scattering*
carrier traps see *electron traps; hole traps*
CARS see *coherent antiStokes Raman scattering*
cartography
 aerial photography rapid screening by optical power spectrum analysis 8-63033
 air pollution effects indicators, provisional map 8-81387
 automated pattern recognition with hybrid optical/digital systems 8-63037
 Earth surface, three-dimensional mapping onto telluroid 8-65171
 GEOSAT, geological industry recommendations on remote sensing from space 8-69495
 gridded data convolution and padding algorithm 8-69475
 holographic terrain displays in 3D 8-78979
 hydraulic fractures mapping technique 8-69543
 ISO FORTRAN IV program for generating isopleth maps on small computers 8-57157
 Lake Lugano, bathymetric map 8-96252
 laser point transfer machine, TRANSMARK, performance testing 8-81438
 macroseismic intensity map of Friuli, 1976 May 6 earthquake 8-65203
 magnetic maps for Italy, regional survey 8-65175
 oceanic rainfall maps, global climatic features 8-65379
 orthomapping review 8-88777
 photogrammetric meas. for field mapping (*German*) 8-92776
 planetary mapping by airbrush technique 8-53833
 radar image interpretation, line detection technique 8-61630
 remote sensing using artificial satellites, Space Shuttle and European Spacelab 8-69494
 resistivity mapping using combined telluric profiling technique (*French*) 8-69285
 solute loading and chem. denudation rate mapping in Devon, England 8-69375
 stereo photogrammetry, prism correlator appl. 8-86368
 stereomapping processes 8-61631
 stereoplotter, orthoprinting system, TOPOMAT, appls., accuracy 8-81437
 stereoplotter, TOPOCART B, accuracy and performance study 8-81436
 thematic map accuracy, statistical testing of remote sensing 8-77372
 three-dimensional geodesic mapping eqns., rel. to Earth best-known figure determ. (*German*) 8-73304
 video stereophotogrammetry, interactive computerised, for Mars Viking 1975 Lander data 8-81557
 wetland mapping in New Jersey and New York 8-77265
cascade showers see *cosmic ray showers and bursts*
Cassegrain antennas see *reflector antennas*
casting
 austenitic crystals, inverted casting process for very rapid growth of large crystals 8-84791
 ceramics, slip moulding method development 8-68661
 epoxy tensile coupons, method for producing silicone rubber moulds 8-72957
 liquid metal continuous casting, solidification process, convective heat transfer, anal. 8-84789
 steel, C, casting by C diffusion solidification 8-52792
 steel, cast struct. form. in continuous casting (*German*) 8-92256
 vacuum melting furnaces and casting techniques 8-84727
 Al alloy, cast struct. form. in continuous casting (*German*) 8-92256
 Al-Si-Cu-Ni alloy casting, thermal props. 8-95814
 β -Al₂O₃, new slip casting technique for fabrication of ceramics 8-84745
 Be, produced in zero gravity environment, BeO particles uniform distrib. 8-72753
 Cu-Nb, exam. of monotectic reaction, using chill casting technique 8-68679
castings
 dimensional instability of CF8 stainless-steel castings at elevated temperatures 8-82448
 fracture toughness characteristics, using double torsion method 8-68863
 ingot, temp. field calc. approx. by equiv. cylinder (*German*) 8-84788
 pressure diecast automatic components, processing condition effect on performance 8-88623
 steel, 12Kh18N9T-TiB₂, eutectic alloy, high temp. props. 8-84931
 steel, effect of non-uniform struct. on props. 8-84850
 steel, rimming, continuously cast, nonmetallic inclusion distrib. (*Russian*) 8-80534
 steel shot, impact fracture (*Japanese*) 8-92338
 Al-Mn alloys, study of solidification by rapid cooling (*Japanese*) 8-88459
 Al-Si, hypereutectic silumins, P and Na modification 8-84792
 B-Al cast braid, crystallisation and structuring of Al matrix (*Russian*) 8-52725
 Cu-Al-Ni-Fe, (10, 5, 5 wt.%), cast microstruct. 8-80535
 Cu-Ni cast alloy, effect of alloying and residual elements 8-85033
catalysis
 see also *catalysts; reaction kinetics*
 acetic acid, chemisorbed on MgO, decomposition mechanism 8-92502
 acetylene, adsorbed on Ni(111), benzene form., vibr. spectra 8-95952
 adsorbed species, catalytic reaction, high temp. IR obs. 8-88655
 autocatalytic reaction system, sustained oscills., deterministic and stochastic theories 8-95922
 cell energy metabolism, ATP effect on initiator stage enzyme activity and conc. 8-64950
 chemisorption on metal films, use of external mag. field, review 8-72003

catalysis continued

- chromatographic reaction and separation in pulse-fed catalytic reactor 8-64880
- β -cyclodextrinylbisimidazole, ribonuclease model, catalysis of cyclic phosphate substrate 8-85287
- cylinder array, convective mass transfer with surface reaction 8-79369
- electronnegativity, spin-orbital, and catalytic activity 8-73078
- enzyme catalysis, electron pairing as source of cyclic instabilities 8-95953
- ethanol, chemisorbed on MgO, decomposition mechanism 8-92502
- ethylene to acetylene conversion on Ni (111), UPS 8-88657
- graphitisation, three-phase, of phenolic resin C by Ni particles 8-68922
- heterogeneous, basic eqns. and examples (*Dutch*) 8-80788
- heterogeneous, bimolecular surface reactions, defect renormalised propagator stochastic theory 8-95955
- heterogeneous, kinetic transport, deactivation rate interactions on steady state and transient response 8-68914
- heterogeneous, research using IR spectroscopy, literature review (*German*) 8-53256
- inelastic electron tunnelling spectroscopy, surface chem. and heterogeneous catalysis appls. 8-92512
- inhibitory additives, for anatase-rutile transition (*Japanese*) 8-95744
- interstellar H_2 , form, by catalysis process 8-54005
- isopropyl alcohol decomposition using $MoO_3:Li$ catalyst 8-60122
- metallic surfaces, thin film appls. 8-75943
- methane, dissoci. by adsorption-desorption process on W 8-92511
- nucleation and growth at surfaces, kinetic studies, review 8-72046
- orbital perturbation approaches 8-80783
- organic compounds, photocatalytic oxidation on Mars 8-85883
- phospholipid vesicle walls, photosensitised electron transport 8-80787
- porous catalyst pellets, singular perturbation anal. of boundary value problems modelling reactions 8-76906
- propanol, chemisorbed on MgO, decomposition mechanism 8-92502
- retinals, catalysed cis-trans isomerisation by crude tissue extracts 8-64925
- steel, superheated-steam oxidation, exam. of catalyst influence 8-85030
- styrene, cationic polymerisation by $SnCl_4$ in presence of C black 8-68891
- urease shear inactivation, metal ion effect, rel. to shear deform. effects in enzyme catalysis 8-76982
- weakly coordinated molecular systems, mutual vibronic effects in chem. reactions and catalysis 8-64821
- Ziegler-Natta type catalysis, reaction pathway, ab initio SCF-LCAO-MO calcs. 8-56891
- BCl_3-H_2 , photochem. with Ti, Pb catalysts, isotopic excitation by laser 8-64882
- BN, cubic, water catalysed form. 8-53199
- CO, adsorbed on Pd (111) surface, catalytic oxidation, mol. beam investig. 8-88656
- CO catalytic oxidation on spinel type ferrites, role of mag. exchange interactions 8-56916
- CO, catalytic oxidation over NiO, activated complex struct., rate const. 8-80786
- $CO+N_2O$, adsorption on NiO, catalysed reaction in Neel transition region 8-53258
- $CINO_2$, catalysed by CINO, thermal decomposition spectral photometric investig. (*German*) 8-95925
- Fe, membranes, effect of electrodeposited metals on H permeation, proposed catalytic mechanism 8-53252
- H_2 , interstellar, form., catalytic prod. on transition metal grains 8-57616
- H_2 , ortho-para conversion on paramagnetic crystal impurity, mag. field effects, theory 8-61050
- N, at. recombination, Smith side tube method obs. 8-68881
- NH_3 on Pt surface, heterogeneous reaction of decomp., stimulation by CO_2 laser 8-61052
- NH_4OCN formation, in interaction of CO, NO and H_2 over Pt, Rh, Ru and Os 8-73082
- N_2O , decomposition on titanate catalyst, energy reson. hypothesis 8-95947
- NiO, adsorption of $CO+N_2O$, catalysed reaction in Neel transition region 8-53258
- O, form. from O_2 adsorbed on reduced $Mo_2O_3-Al_2O_3$ catalysts 8-85197
- O_2+CO interaction on Ag (110), ellipsometry-LEED expts. 8-91542
- Pt, catalysts, supported, characterisation, hydrogenation and H_2-D_1 equilib. 8-76910
- Pt complex, coordinatively unsaturated, electronic struct. and catalytic activity 8-72228
- WO_m ($m=2-3$), adsorption of O_2 (propene), struct., rel. to catalysis 8-51826
- ZrC, whiskers, CVD on Ni, catalytic effect 8-51865

catalysts

see also *catalysis*

- ESCA, quantitative surface anal., limitations, depth profiling, catalyst surface anal. 8-53298
- heterogeneous, energy resonance hypothesis 8-95947
- heterogeneous catalysis, basic eqns. and examples (*Dutch*) 8-80788
- magnetic characterisation, review 8-64881
- metal oxides, thermodesorption of O_2 , expt. technique (*French*) 8-64884
- methanation catalysts, nonreduced, IR spectra 8-88288
- phosphoric acid, for afterpolymerisation of ϵ -caprolactam under reduced press. (*Japanese*) 8-95929
- sodium-naphthalene, catalyst for polymerisation of methacrylamide by H transfer (*Japanese*) 8-95726
- titanites, decomposition of N_2O , energy reson. in catalysis 8-95947
- transition metal complex, surfaces, and supported catalysts, analogies among active sites 8-56917
- zeolite, Faujasite type, varied Si/Al ratio, absorption of H_2S 8-60029
- zeolite, synthetic, ZSM-11, synthesis and struct. 8-87657
- O_2 , adsorption of O_2 , catalytic oxidation mechanism 8-61046
- $\gamma-Al_2O_3$, heat treatment rel. to texture 8-72789
- Al_2O_3 -supported, X-ray fluoresc. anal. using matrix correctional procedure 8-80817
- Bi, molybdates on SiO_2 , EPR rel. to catalytic reactions (*French*) 8-64271

catalysts continued

- $CeRh_{1-x}Pd_x$, electronic and cryst. struct. comparison, catalytic behaviour 8-84398
- Co-Ni, selective catalytic surface behaviour, tight-binding approx. calcs. 8-76924
- Cu, clusters, size, geometric effects, catalysis implications 8-73131
- Fe film, polycryst., heat of adsorpt. of H_2 and D_2 8-91530
- Fe on Al_2O_3 substrate, controlled vapour growth of small particles 8-75958
- In, for Mg/H_2 reaction, kinetics 8-76851
- $K_2O-Al_2O_3-SiO_2$ system, crystallisation of glasses in primary phase field of leucite 8-67658
- MgO powder, decomp. of chemisorbed ethanol, propanol and acetic acid 8-92502
- $MoO_3:Li$, elec., catalytic props. 8-60122
- $Mo_2O_3-Al_2O_3$, reduced catalyst, adsorption of O_2 , O^- form. 8-85197
- Ni, Al_2O_3 supported, CO adsorpt. in H_2 -He, effect of H_2S on IR spectrum 8-71945
- Ni films, CO-covered, adsorpt. of H, isotherms, resist., work function changes 8-75926
- Ni polycrystalline foils, methanation reaction, kinetic information 8-73081
- Ni/ $Al_2O_3(SiO_2)$ methanation catalysts, nonreduced, IR spectra 8-88288
- Os, interaction of CO, NO and H_2 , NH_4OCN formation 8-73082
- Pb, BCl_3-H_2 photochem. with Ti, Pb catalysts, isotopic excitation by laser 8-64882
- Pb,MnO_2 , synthesis, chem. stability, use (*French*) 8-80525
- Pd, catalyst hollow cone dark field microscopy on γ -alumina substrates 8-61049
- Pd, clusters, size, geometric effects, catalysis implications 8-73131
- Pd on Al_2O_3 , controlled vapour growth of small particles 8-75958
- Pt, interaction of CO, NO and H_2 , NH_4OCN formation 8-73082
- Pt polycrystalline foils, methanation reaction, kinetic information 8-73081
- Rh, interaction of CO, NO and H_2 , NH_4OCN formation 8-73082
- Rh/ $\gamma-Al_2O_3$ disperse δ -phase, chemisorpt. of CO, IR spectra, site distrib., mol. mobility 8-72496
- Ru, interaction of CO, NO and H_2 , NH_4OCN formation 8-73082
- SnO_2 , catalyst particles, converger beam electron diffr. 8-83685
- ThNi₅, methanation catalyst, AES and characteristic energy loss spectra 8-56915
- Ti, BCl_3-H_2 photochem. with Ti, Pb catalysts, isotopic excitation by laser 8-64882
- V_2SO_4 , catalyst particles, converger beam electron diffr. 8-83685
- W (100), CO/H_2 surface complex, flash desorption and AES obs. 8-73083
- WC, microcrystalline, mol. dynamics, motion of H_2O and H_2 mols. adsorbed on surface, catalytic activity 8-71941
- ZrNi₅, methanation catalyst, AES and characteristic energy loss spectra 8-56915

cataphoresis see *electrophoresis*

catastrophe theory

- bifurcation from rotationally invariant states 8-77671
- bistable system, catastrophe prediction using externally applied force 8-77823
- flow fields and other vector field struct. and evolution 8-77733
- gases, chem. pot. near crit. density, Thom's catastrophe theory 8-91063
- introduction and appl. 8-69967
- materials testing appls. (*German*) 8-64797
- nonconservative hyperbolic systems, gradient catastrophe in soln. 8-69992
- pituitary thyrotropic responsiveness to protirelin, CUSP catastrophe model 8-81095
- self-immunisation mechanisms of applied mathematics 8-65745
- swallow tail catastrophe and ferromagnetic hysteresis 8-56349

cathode-ray oscilloscopes

see also *oscillographs*

- beam splitter using operational amplifier as square wave generator 8-77884
- circuitry techniques incl. triggering, hold-off, auto-fix and logic control system (*Italian*) 8-77882
- compact, easy to use 8-49814
- design using modular systems 8-93671
- digital storage oscilloscopes, Gould Advance OS4000 using A/D and D/A converters 8-93673
- double time multiplier (*Rumanian*) 8-86252
- FET probes used for reducing rise-time meas. error 8-93667
- HF CRO design, using cold switching for front panel operation 8-93672
- maintenance- and service-types, operation, selection guideline 8-86259
- measuring techniques, trends (*German*) 8-74020
- multipulse lightning discharge oscillogram scanning camera 8-61588
- polar coordinate display CRO 8-86253
- sampling oscilloscope's capabilities extended by adding vertical channels 8-65914
- stochastic instantaneous signal recording, add-on cct. (*German*) 8-74031
- types and props., reviews (*Swedish*) 8-62189
- very short time interval measurement appl. 8-81948
- voltage calibrator using band-gap technique 8-65941

cathode-ray tube displays

see also *cathode-ray oscilloscopes*

- medical, equipment and maintenance, review 8-69240
- nuclear medicine images, minimum detectable grey-scale differences 8-61249
- pseudorelief image of microstructures and photographic images, production on CRT screen (*Russian*) 8-93674
- underwater US video system (*German*) 8-94471
- visual stimulator, computer-controlled, for electrophysiology expts. 8-69230

cathode-ray tube screens see *cathode-ray tubes; fluorescent screens*

cathode-ray tubes

- see also *image converters; image intensifiers; image storage tubes; television camera tubes*
- dome-shaped grid utilisation, thick film losses, and vert. output (*Italian*) 8-77882

cathode-ray tubes continued

- mass spectrometer three-dimens. quadrupole electron gun, compact tube assembly poisoning resistant 8-54493
- SEM positive print photography of CRT image 8-82082

cathode rays

- focusing optimisation with specified image parameters 8-86385

cathodes

- see also electron emission; oxide coated cathodes; photocathodes; thermionic cathodes
- arc, axial flow stability, cathode emission mechanism change effect 8-83638
- Berkeley type ion source, long life cathode 8-66375
- cathode surface heating by high pressure glow discharge, catastrophic bridging 8-87574
- damage from 300 ns, 4.5 A arc, material comparisons 8-87579
- DC vacuum arc emitted particle flux 8-75470
- explosive electron emission, cathode plasma emission surface processes 8-71569
- field emission, oxygen processing method 8-64448
- field emission current density, max., rel. to cathode geometry and kinetic props. 8-72704
- flash X-ray tubes with new type of cathode 8-58101
- glow discharge cathode region microscopic model 8-67524
- hollow-cathode glow discharge with static stepped V-I characteristic (Russian) 8-75443
- hot cathode temperature, thermionic emission meas. method (Czech) 8-70121
- liquid metal, 8-87578
- metallic cathodes, electroluminescent impurities causing vacuum breakdown, obs. 8-84660
- multielement cathode, for high power elec. discharge laser, design and operational characts. 8-82983
- plasmatron, W cathode unit operation 8-75433
- spectroscopic light source cathodes, of Al(graphite), glow discharge and hollow cathode types 8-82047
- twin-hollow-cathode interferometer-spectrometer, discharge characts. for He and Ar (German) 8-67461
- twin-hollow-cathode of interferometer-spectrometer, radial electron temp. (German) 8-67462
- ultrahigh vacuum discharge cathode erosion minimum conditions 8-75461
- vacuum arc cathode plasma interaction with transverse mag. fields 8-75468
- vacuum arc cathode spot dynamic models 8-75481
- vacuum diode, laser produced cathode plasma, streaming, electron emission temp. determ. 8-91162
- Ag cathode, underpotential deposition of Pb 8-52692
- Ag, cathode spots on vac. arc discharge electrodes, model 8-91179
- Al-Si₃N₄-Al thin-film cold cathode, electrical forming, expt. 8-76160
- Al-SiO₂-Au cathode, emitted electron energy distrib. 8-52645
- C cathode damage and vapour/thermionic arc transition obs. 8-71603
- C fibre cathode prebreakdown field emission transition to vacuum breakdown 8-75462
- Cu, cathode spots on vac. arc discharge electrodes, model 8-91179
- Cu, erosion, vacuum to atmospheric press. arcs 8-79482
- Hg DC vacuum arc anchored cathode spot current density obs. 8-75467
- LaB₆ hollow cathode for dense plasma production 8-55729
- LaB₆, single cryst., highly stable, for conventional electron microprobe instruments 8-78043
- Mo cathode surface contamination effect on erosion by nanosecond vacuum discharge 8-75463
- Ni, cathode spots on vac. arc discharge electrodes, model 8-91179
- W, cathode spots on vac. arc discharge electrodes, model 8-91179
- W microneedles, field electron emission, suitability for electron source investigation 8-52644
- W:ThO₂, uncarburized filament activation by sputtering 8-52608

cathodes, electrochemical see electrochemical electrodes**cathodochromism**

- No entries

cathodoluminescence

- cathode fall in electron beam controlled stationary non-self-sustained discharges 8-71613
- diamond, semiconducting, GR1 cathodoluminescence, fine struct. 8-68566
- energy transfer, random walk model, comment 8-72610
- energy transfer, random walk model, reply to comment 8-72611
- ferroelectrics, O-octahedric, cathodolum. spectral and temp. depend. 8-84665
- SEM cathodoluminescence analysis of impurities, localisation and sensitivity 8-95985
- surface plasmon light emission induced by fast electrons on modulated surface 8-80424
- Ag, surface plasmon light emission induced by fast electrons on modulated surface 8-80424
- Al_{1-x}Ga_xAs, LPE, cathodoluminesc. obs. 8-68565
- Ar, liquid, triplet state of self-trapped exciton states, evidence of existence, luminescence meas. 8-72608
- CdS, exciton cathodoluminesc. of semicond. with surface pot. barriers 8-83666
- CdS, Se_{1-x} mixed crystals, exciton spectra 8-92131
- CdTe:In, lightly- and heavily-doped, cathodoluminesc., temp., injection level and freq. depend. 8-52584
- GaAs LPE layers, dopant tracing of terrace growth 8-75948
- GaAs:Cr, fine structure in cathodoluminescence spectrum 8-56524
- GaAs:Si(Ge) LPE layers, luminesc. props. rel. to substrate quality 8-52583
- GaN epitaxial layers, exciton cathodolum. (Russian) 8-76543
- GaN:As(P), implanted single cryst. film, cathodolum. 8-60523
- GaP, dopant dislocations, scanning electron micrographs, cathodoluminesc. 8-91340
- GaP, first order Mott transition of exciton gas 8-76535
- GaP, LEC crystal, cathodolum. and photolum. around dislocations 8-84663
- GaP, SEM, cathodoluminesc., impurity and defect detect. 8-83695
- Hg_{0.7}Cd_{0.3}Te, 17 to 77K, photo- and cathodoluminesc. 8-52569
- α -HgS, natural, yellow emission 8-68567
- In_{1-x}Ga_xP, epitaxial film, cathodolum. obs., recomb. mechanisms 8-72613
- KI, polariton effects in resonant emission 8-76533

cathodoluminescence continued

- Kr, liquid, triplet state of self-trapped exciton states, evidence of existence, luminescence meas. 8-72608
- LiGaO₂:Fe, phosphor, luminesc. 8-92108
- LiH (D), single crystals, electronic excitations, review (Russian) 8-72574
- MgO, electronic excitations and luminescence, review (Russian) 8-72575
- MgO, single crystals, compressed, SEM exam. of cathodoluminescence 8-56525
- Mg₂Zn_{1-x}Te, high purity, luminesc. and band gap 8-68553
- Si:P, excitation density depend. of cathodoluminesc. from bound multiexciton complexes 8-72609
- SiC, cathodoluminescence, comparison with other materials 8-92130
- SnO₂, rare earth ion doped, luminesc. and charge compensation 8-76532
- Xe, liquid, triplet state of self-trapped exciton states, evidence of existence, luminescence meas. 8-72608
- Y₂O₃:Eu³⁺, absorpt. spectra, fluoresc., electron beam excitation 8-92093
- YVO₄:Eu³⁺, absorpt. spectra, fluoresc., electron beam excitation 8-92093
- ZnO, low energy cathodolum., surface effects 8-60522
- ZnS, low voltage cathodoluminescence 8-52585
- ZnSe:Cu, Al, single cryst., low-voltage red cathodolum. 8-80423
- ZnTe:O,Zn, dual ion implantation, luminesc. spectra obs. 8-87697

cathodophosphorescence see cathodoluminescence**cathodothermoluminescence** see cathodoluminescence**catholytes** see electrolytes**causality** see physics fundamentals**causticity** see pH**cavitation**

see also bubbles; vortices

- acoustic, threshold conditions for onset 8-59433
- bubble cavitation problem, numerical soln. 8-79347
- bubble collapse in water shock tube 8-67231
- bubbles, linear stability of growth or collapse, slightly viscous liquid 8-90947
- cavitating fluid model (Russian) 8-55668
- cavitation tunnel, for high-temp. operation 8-63521
- creep damage and rupture criteria, cavity config., use of density meas. 8-60818
- creep failure by cavitation under non-steady conditions, exam. 8-56774
- dynamic instability phenomenon, governing eqn. 8-59434
- fatigue high temp., hold time effects, cavitation nucleation, creep interaction 8-60734
- flow around circular cylinder, pressure distrib. (French) 8-67234
- flow turbulence influence on the inception and growth of cavitation 8-90948
- flow-induced, suppression by dilute polymer solutions 8-67233
- hydrodynamic siren, acoustic excitation of cavitation 8-94776
- hydrofoils, tail-loaded, fully cavitating, avoidance of turbulent separation 8-94659
- ionizing radiation and cavitation threshold 8-94774
- large-scale spatial oscillations of a cavity in a sound field 8-94775
- laser produced water bubbles, behavioural study by holograph cinematography (German) 8-87371
- Laval nozzle, hot water flow 8-75181
- liquid, laser breakdown, photoacoustic and photohydrodynamic parameters 8-52597
- liquid cavitation and droplet impact erosion, predictability of prototype machine from lab. tests 8-64723
- liquid filtration US enhancement 8-59526
- natural flow and US cavitation erosion comparison 8-59435
- Nimonic 80A, intergranular creep fracture under const. cavity density 8-60825
- nonlinear interaction of deformable body with liquid pressure wave (Ukrainian) 8-65777
- nonNewtonian lubricant, bubble behaviour 8-56786
- nucleation at second phase particles in grain boundaries 8-59819
- polyacrylamide, additive to water supply, effect on cavitation and erosion in pipes 8-83441
- polymer solution, bubble behaviour, Denn model 8-79343
- polymer solution, bubble behaviour, second-order fluid model 8-79344
- polythene, finite element anal. of crazing and cavitation by dil. aq. detergent 8-53006
- spillway surfaces, flow around three dimens. projections 8-67232
- steel, C, corrosion fatigue resistance in cavitations, bainitic and martensitic structs. (Russian) 8-56815
- steel, cavitation during superplastic flow, affecting factors 8-60728
- steel Cr-V (1.5, 0.5 wt.%), cavitation effect of temp. and C content 8-64638
- supercavitation mechanisms, isoperimetric problems (Russian) 8-75177
- surface tension and gravity, combined influence, nonlinear theory of perturbed motion (Russian) 8-75178
- US cavitation emission from insonated plant tissues 8-59185
- water, matching optimisation for magnetostrictive transducers 8-94503
- Ag, implanted grain boundary cavities effect on cavity growth kinetics and creep fracture 8-52935
- Ag, large grain boundary cavity coalescence during tension creep 8-52894
- Al-Cu(Mg), age-hardenable, US cavitation erosion mechanisms, effects of comp. and heat treatment 8-53002
- Al-Mg, fracture during superplastic flow 8-60729
- Cu alloys, cavitation during superplastic flow, affecting factors 8-60728
- Cu-Ni-Zn, microduplex, superplastic deform., cavitation and fracture 8-64640
- H₂O, cavitation nuclei conc., holographic and hydrodynamic obs. 8-83440
- He, liq., bubble formation mechanism, on surface of deformed crystal (Russian) 8-85066
- Mo wire, laser shock induced microstructural changes, rel. to explosive shock induced phenomena 8-67768
- NaCl, rock salt, progressively mined soln. cavities, struct. behaviour 8-61409

cavitation continued

- Pb-Sn eutectic, cavitation during superplastic flow, affecting factors 8-60728
 W wire, laser shock induced microstructural changes, rel. to explosive shock induced phenomena 8-67768

cavity resonators

- see also acoustic resonators; laser cavity resonators*
 cylindrical hole in wall of infinite thickness, elec. and mag. polarisabilities determ. 8-71004
 EM spherical cavity resonator, amplitude of standing gravitational waves (*Russian*) 8-73906
 ENDOR cavity for electron spin echo experiments 8-82013
 EPR spectrometer, 2 mm band, with re-entrant resonator 8-86311
 Fabry-Perot nonlinear electro-optic device, using refl. light feedback 8-55457
 Josephson junction, semiconductor-barrier, cavity resonances 8-84352
 microwave, partially filled with temp.-anisotropic uniform hot plasma, eigenmodes 8-75362
 microwave cavity for EPR at high hydrostatic pressures 8-89518
 microwave IC substrate permittivity meas. in cylindrical cavity 8-77942
 open resonator with cylindrical confocal mirrors, plane EM wave excitation (*Ukrainian*) 8-55280
 optical microscope, scanning resonant cavity, nonlinear interaction enhancement 8-93758
 RF cavities for e^+e^- storage rings, damping antennas for spurious RF modes 8-70659
 single-ended cavity resonator loaded Q-factor meas. using reflection bridge 8-54405
 small frequency shifts meas. using two open resonators at mm wavelengths 8-81949
 superconducting X-band Pb cavity expt., closed-cycle mech./adsorption refrigeration appl. 8-93708
 Wonderstone ENDOR cavity 8-70174
 Cu, resonant cavities, RF loss reduction at 35 GHz by cryogenic cooling 8-93761
 Pb-Te-Pb Josephson junction, cavity resonances 8-84352

c.c.d. circuits *see charge-coupled device circuits***CCTV** *see closed circuit television***celestial mechanics**

- see also N-body problems; stellar motion*
 1978 RA (=1975 TB), Apollo object, orbital elements and ephemeris 8-93141
 1978 SB, orbital elements and ephemeris, (1978 September 9 to October 29) 8-93143
 aligned triple collision, new study (*French*) 8-85832
 area-preserving polynomial mapping, instability 8-77463
 Ariel 4 (1971-109A), defensive orbit 8-73604
 artificial satellite motion, orbitally stable multistep methods 8-85834
 artificial satellites, role of orbit determ. in altimeter data anal. 8-77177
 asteroid, mean motion resonant with Jupiter, short-periodic perturbations 8-53803
 asteroid 108 Hecuba, motion in restricted three-body problem, nonlinear oscils. (*German*) 8-57488
 asteroid families, concs. in proper elements space statistics and mapping 8-96420
 asymmetric periodic orbits in three dimensions 8-77476
 autonomous Hamiltonian system near equilib. point, formal integrals 8-89047
 autonomous Hamiltonian systems, orbital stability of periodic Lyapunov motions (*Russian*) 8-69664
 averaging method and two-timescale method, common derivation 8-85835
 bifurcations of straight line oscils., rel. to Stormer and spring pendulum problems 8-71278
 capture problem 8-77477
 circular restricted three-body problem (*French*) 8-93084
 close binary systems, effects of libration on light curves 8-57579
 close-Earth satellite perturbations due to lunar inequalities 8-53786
 Comet Bradfield, parabolic elements and ephemeris, 1978 July 31 to (1979 January 7) 8-65551
 Comet Fujikawa (1978n), orbital elements and ephemeris (1978, October 9 to December 8) 8-93168
 Comet Giclas (1978k), precise positions, orbital elements and ephemeris 8-89122
 Comet Macholz (1978l), orbital elements and ephemeris (1978, September 19 to October 9) 8-89126
 Comet Meier (1978f), precise positions, orbital elements and ephemeris 8-53884
 comet orbits, three-dimenx. model construction 8-61808
 Comet Seargent (1978m), parabolic orbital elements and ephemeris, (1978, September 29 to October 29) 8-93164
 Comet Seargent (1978m), precise positions and parabolic orbital elements 8-96432
 cometary orbits, perihelion distrib. asymmetry 8-96429
 comets and asteroids close approaches to Earth, list of events 8-73621
 comets capture by Laplace scheme, orbital elements statistical consequences 8-53888
 comets motion, correction for nongravitational effects, comparison of methods 8-61811
 complete class of potentials forming vel. field of given multiplicity, determ. method (*Russian*) 8-69665
 P/Daniel, predicted orbital elements 8-53883
 diurnal motion of Sun seen from Mercury, computer aided soln., teaching aspects 8-61969
 dynamical systems, averaging method 8-77469
 early solar system, mass removal by outer planets 8-53841
 Earth orbital elements, periodic vars. influence on insolation (*Russian*) 8-53605
 Earth orbital elements rel. to caloric insolation long-term vars. 8-73502
 education, alternative derivation of Kepler's laws from conservation principles 8-49583
 elliptic restricted three-body problem, invariant relation 8-69662
 elliptic restricted three-body problem, invariant relation for Trojan asteroids 8-69726
 families of three-dimens. periodic orbits bifurcating from plane periodic orbits around both primaries 8-57432

celestial mechanics continued

- force function of two general celestial bodies 8-73620
 Galilean satellites, photometric eclipses anal. rel. to theory of motion 8-53864
 Geminid meteor stream, orbital period 8-53889
 generalised Kepler motion, Lie groups of motor integrals 8-85831
 generalised two-dimens. problem of three fixed centres, classification of motions (*Russian*) 8-77465
 generalized elliptic restricted three-body problem, libration points 8-53799
 geostationary satellites, methods for numerical integration of eqns. of motion 8-69659
 gradient of field of directions normal to trajectory, and forms of potential 8-65662
 gravity potential derivatives evaluation using Bernstein multidimens. inequality (*German*) 8-93081
 gyrostatic satellite in circular orbit, regular precessions 8-93082
 Hamiltonians linear in momenta, note 8-77468
 Hill's curves, geometric prop. 8-77474
 Hill's problem in Lunar theory 8-77473
 initial orbit determ. using angles and angular rates of movement of artificial satellites 8-53795
 integrals of motion, disappearance in multi-resonance conditions 8-77471
 Kepler problem, time transformation stabilisation (*German*) 8-89333
 keplerian motion and gyration 8-77472
 Keplerian orbits, revised flux vector for collisional evolution 8-93080
 Kirkwood Gaps and stability of conservative periodic systems 8-65544
 Kustaanheimo-Stiefel regularizing transformation derivation 8-93086
 Lagrangian solutions stability at critical relation of masses (*Russian*) 8-69666
 Laplace, P.S., chronology and citations of early work, 1770-1773 period 8-93505
 lunar capture hypothesis, effect of planetary bodies deform. energy 8-81570
 lunar centre of mass displacement from geometric centre, comment 8-69937
 Mars, oval orbit construction and rejection by Kepler, physical hypotheses 8-62027
 Mars moons, dynamical evolution and origin 8-89104
 Mars orbit emplacement using atmospheric braking, control algorithm 8-69639
 Mars satellites, orbits and perturbations 8-89100
 Mercury rotational motion theory (*Russian*) 8-93134
 Moon, 18.6 year nodal cycle effect on shallow seas surface temp. due to tidal mixing vars. 8-73387
 Moon, libration in longit. due to Giordano Bruno AD 1178 impact, consistency with laser ranging 8-69717
 Moon, orbit and physical libration rel. to univer al time meas. from lunar laser ranging 8-85854
 motion in spherically symmetric force fields, vector consts. 8-85833
 obliquity of ecliptic in geological time (*Chinese*) 8-69270
 Periodic Comet Giclas (1978k), improved elliptical orbital elements 8-85916
 Periodic Comet Haneda-Campos, orbital elements and ephemeris 8-89121
 Periodic Comet Haneda-Campos (1978j), orbital elements 8-89127
 Periodic Comet Taylor (1916 I), nuclei separation vels. during disintegration 8-61812
 periodic Hamiltonian flows, generalised Bertrand's problem, Kepler system 8-86131
 periodic motions close to Lagrangian solns. of three-body problems, orbital stability 8-53804
 periodic orbits around rotating ellipsoid 8-77464
 periodic three body orbits in the case of small third mass 8-77467
 planar magnetic binaries problem, areas of motion 8-96386
 planar N-body problem, circular-elliptic type periodic solns. 8-93083
 planetary satellites synchronous rotation theory (*Russian*) 8-93134
 planetary theory developments in 1973-6 period 8-77505
 Pluto, 1978 P 1, possible satellite, orbit and eclipses ephemeris 8-93152
 Pluto, long-term motion, semi-analytical theory 8-69741
 Pluto, orbital motion solutions comparison 8-93151
 Poisson's theorem in heliocentric variables, applicability to planetary orbits major axes invariability (*French*) 8-85829
 Quadrantid meteor shower, orbit 8-61815
 quasiperiodic motions stability in Hamiltonian systems 8-93085
 resonances of higher order in conservative Hamiltonian systems 8-53800
 restricted three body problem, stability of second species periodic orbits 8-61717
 restricted three-body problem, numerical extrapolation of periodic solutions 8-69663
 rigid body, motion in Newtonian force field, phase coords. determ. (*Russian*) 8-89049
 rigid body near Earth's surface, stability of flight (*Russian*) 8-89048
 satellite orbital lifetimes, prediction methods 8-73605
 satellite orbital motion, flexible appendage effects 8-77456
 satellite-derived ocean tide parameters, lunar tidal accel. determ. 8-73662
 Schwarzschild field geodesic, Newtonian limit 8-86056
 solid bodies in solar system, gravitational potential 8-77550
 Starlette satellite, precision orbit computation 8-65478
 stationary satellites, equations of motion, numerical integration methods (*Japanese*) 8-85837
 stationary satellites of Earth, Moon and Mars, coordinates of gravit. fields stationary points 8-53805
 Stormer problem, periodic motions in mag. dipole meridian plane 8-85841
 Stormer problem, periodic motions in mag. dipole meridian plane 8-89053
 terrestrial longit. determ., without time, from obs. of lunar altitude 8-85836
 three body problem, Lagrange quadrilateral triangle, Euler collinear solns., generalisation to nongrav. forces 8-54178
 three-body problem, model for close encounters in planetary system 8-61718
 three-body system disruption, statistical theory for three-dimens. motion 8-77475
 three-impulse min.-time orbital transfer generation, numerical method 8-73607

celestial mechanics continued

- time standard differences and celestial mechanics (*Italian*) 8-93087
- time transformations and Cowell's method 8-77466
- trajectory optimisation for ion-propelled space tug 8-53798
- translatory-rotary motion of gravitating spheroids (*Russian*) 8-73841
- translatory-rotary motion of three rigid bodies, Euler solns. (*Russian*) 8-53802
- Trojan asteroids and fictitious objects at 1/1 resonance, long-period effects 8-85830
- two-body orbital mechanics, solution to Kepler's problem for orbital position 8-73622
- two-body problem, general time elements 8-77470
- Uranus, rings origin, orbital reson. effects 8-53874
- Uranus rings, reson. orbit theory and prediction of undiscovered satellite 8-81585
- Uranus rings, three-body resons. rel. to ring radii 8-89117
- Vinti problem, extended phase space formulation 8-53801
- zodiacal light dust, orbits from Doppler shift meas. 8-85904

cell model (liquids) see liquid theory**cell motility**

- bacterial migrating chemotactic bands, quasi-elastic light scatt., *E. coli* 8-77018
- bacterial motility, *E. coli*, struct. effects in quasi-elastic light scatt. 8-77024
- bacterial movement tracking using one-dimens. fringe system 8-73299
- bacterial sensory electrophysiology, motility depend. on membrane pot. and chemotaxis 8-53373
- ciliated cell response during irradiat. at different dose rates 8-61216
- fibroblast spreading kinematics, individual locomotor activity 8-69006
- flagella bend propagation, derivation of eqns. of motion and simulation 8-77074
- sperm flagella equation of motion 8-80895
- spermatozoa swimming in cervix, effects of dynamical interaction and peripheral layer viscosity 8-69126
- Ca-dependent sensory-motor response of marine dinoflagellate to CO₂ 8-57026

cells (electric)

- see also fuel cells; photoelectric cells; photoelectrochemical cells; primary cells; secondary cells
- electrolytic cell resistance meas., differential recorder 8-86297
- fast ionic conductors, review, device appls. 8-51724
- metal/metal ion system, instantaneous corrosion rate deform. by Faradaic rectification 8-80667
- metal/metal ion systems, instantaneous corrosion rate determ. by Faradaic rectification 8-80666
- nuclear energy, nonconventional conversion systems (*Rumanian*) 8-86705
- pacemakers and batteries, microcalorimetric study 8-57130
- Zn(Hg)/KOH, ZnO(sat.), rates, instantaneous, Faradaic rectification, experimental verification part II 8-80667
- Ag sintered electrode production for concentrating cell (*Portuguese*) 8-88637
- AgI-Ag₂O-B₂O₃ system, ionic cond., struct., electrochem. prop. in galvanic cell 8-95181
- AgNbO₃.4AgI room temp. solid electrolyte and galvanic cell performance 8-79803
- β -AgVO₃.4AgI room temp. solid electrolyte and galvanic cell performance 8-79803
- Cu(Hg)/CuSO₄(m)/Hg₂SO₄, Hg, EMF, standard electrode pot. 8-76874
- Fe-thiamine solution, modified, photogalvanic effect 8-91722
- Pb(Sb)/H₂SO₄, PbSO₄(sat.), rates, instantaneous, Faradaic rectification, experimental verification part II 8-80667

cellular biophysics

- see also biomembrane transport; biomembranes; cell motility; cellular effects of radiation; cellular transport and dynamics; lipid bilayers
- adhesion models, reaction kinetics and forces 8-80844
- algal suspensions, light scatt. and absorpt. props., 380-720 nm 8-92604
- ATP, chemiosmotic theory of manufacture in cells 8-61151
- ATPase kinetics in *E. coli* cells, ³¹P NMR meas. 8-77022
- atrial trabecula membrane, frog, accommodation, repeat responses and anode-breaking excitation 8-64956
- bacterial culture, Degn-Harrison reaction scheme, multiple steady state 8-88700
- bacterial sensory electrophysiology, motility depend. on membrane pot. and chemotaxis 8-53373
- bioenergetics and proton-electron systems of membranes, review 8-96030
- biopolymer negative resistance, rel. to living cell props. 8-64923
- birefringence analysis in biological materials 8-56954
- bladder smooth muscle impulse propag., math. anal. (*Japanese*) 8-53359
- blood cell profile direct meas. using SEM beam reference lines 8-81094
- charged disk interactions in various dielectric media, biological cell modelling 8-66706
- chemical reactions and ion transport in brown adipose tissue, network thermodynamics 8-92606
- chemiluminescence of aldehyde-preserved plant tissues on exposure to salts of heavy metals 8-77160
- chlorophyll c absorpt., fluoresc. and fluoresc. excitation spectra in alga cell at -196°C 8-53329
- chloroplast, bean, effect of salts on form of EPR II signal 8-64952
- chloroplast millisecond afterglow, activation and suppression 8-96025
- chloroplasts, EPR investigation of state of Mn²⁺ 8-69008
- chromaffin granule electrophoretic mobility meas. by light scatt., effect of Ca²⁺ and Mg²⁺ 8-53357
- chromosome band online linear scanning, human, BANDSCAN computer program 8-92758
- chromosome examination under light transmission microscope (*German*) 8-92685
- chromosome size meas., fast karyotype approach 8-61153
- chromosomes, banded human, contrast enhancing filter 8-92755
- cultured cell time lapse cinemicrographs, computer-aided analysis 8-92756
- cylindrical surface crystals in biological structures, dislocation interactions 8-95055
- cytophotometric histogram, computer aided analysis of cell-cycle phase 8-92759

cellular biophysics continued

- division control by tension or diffusion 8-64962
- DNA distributions automatic processing and interpretation 8-92757
- electric circuit model, alternating signal interaction 8-77011
- electric circuit model, alternating signal interaction 8-77012
- electron transfer reaction energetic coupling to endergonic reactions, mol. mechanism 8-96026
- embryonic skeletal muscle differentiation, electrophysiological and biochem. membrane props. 8-53363
- energy metabolism, ATP effect on initiator stage enzyme activity and conc. 8-64950
- epithelium of small intestine, mech. props. of intercellular contacts 8-53351
- erythrocyte, human, steady rate of glycolysis rel. to ATP conc., quantitative model 8-53354
- erythrocyte, sectioned, generalised theory of geometrical shape 8-65071
- erythrocyte high gradient magnetic separation 8-53585
- erythrocyte membrane, phys. state of lipids, X-ray diffr. 8-80835
- erythrocyte membranes, ESR study of abnormalities in Duchenne muscular dystrophy 8-96111
- erythrocyte osmotic fragility curve, statistical synthesis 8-65070
- erythrocyte survival after slow freezing in glycerol, temp. depend., human cells 8-77019
- erythrocytes, slowly frozen human cells, phys.-chem. basis of protection by glycerol 8-77020
- erythrocytes, technique for observing 3D dim. struct. with a cryo-SEM 8-92765
- erythrocytes of human blood, diameter meas. by specific elec. cond. 8-53353
- excitable cell model, numerical method 8-53376
- excitable medium self-sustained activity, role of inhomogeneity 8-64968
- eye slow cell responses in insects, colour adaptation 8-64988
- fibroblast spread kinematics, population anal. 8-53352
- fluorescein, excitation and emission polarisation spectra, cell cycle changes 8-96013
- fluorescent probe interaction with surface structs. of *E. coli* 8-69007
- frozen cell structure and function, freezing patterns and post-thaw survival 8-64960
- Halobacterium, Mossbauer spectrum of whole cells and ferredoxin, EPR spectrum of ferredoxin 8-76998
- heart contractility, muscle tissue quality and sliding filament micromechanism (*Dutch*) 8-73171
- heart muscle, behaviour of myosin projections during staircase phenomenon 8-53362
- heart physiology, ³¹P NMR investigations of metabolism, pH and contractile performance 8-69018
- hyperthermia effect on nonhistone proteins isolated with DNA 8-80843
- image anal. in cytology/cytogenetics, using Golay transform processor 8-61152
- kinetic parameters estimation from flow microfluorometry 8-73143
- lecithin-water systems, bilayer connecting passages 8-96028
- leucocyte, human, fluorochromed with acridine orange, spectral char. acts. 8-96024
- light scattering problem, integral formulation, appl. to biological particles 8-63010
- lipid bilayer membrane interaction forces in zone of contact 8-53345
- liver cells, rat, isolate5, ³¹P NMR studies 8-61150
- liver tissue, mouse, appearance of free radical centres on low temp. oxidation 8-69013
- lymphocyte surface morphology, human, SEM obs., review 8-53599
- medically relevant class determ., scatt. light cluster anal., cervical smear tests (*German*) 8-92686
- membrane nuclear hydrodynamic shear, non-equil. Ising model, master eqn. 8-61146
- microtubule structure, temp. depend. 8-85288
- mitochondria and submitochondrial particle membrane pot. generation in anaerobic conditions 8-69015
- mitochondria membrane Ca²⁺ interaction, influence of oestrogens 8-53349
- mitochondria of bovine heart, EPR investigation of two forms of Fe-S centre N-2 8-69014
- mitochondrial membrane pot., respiratory chain study by method of penetrating ions 8-64951
- morphological parameters extraction from diffr. pattern of cells, Fourier optical approach 8-92749
- muscle, active frog skeletal, isometric tension, slow stretch effect, X-ray diffr. study 8-80906
- muscle, fast and slow myosin in developing fibres 8-64961
- muscle, frog, spin-spin relax. times rel. to temp. and water content 8-56952
- muscle, glycerol-extracted fibrillar fibres, cross-bridge slippage induced by AMP-PNP and stretch 8-77075
- muscle, myosin regulated, changes in crossbridge attachment 8-53361
- muscle, skeletal, Na relaxation, spin echo study, evidence of Na ion binding inside a biological cell 8-88698
- muscle, skeletal, tension development, F-actin subunits struct. non-equiv. model 8-64959
- muscle, smooth, effect of hyperosmolar soln. on elec. connections between cells 8-69027
- muscle, striated, reversible loss of Ca control of tension assoc. with removal of regulatory light chains, scallop 8-53360
- muscle, vertebrate striated, thick filament linked Ca²⁺ regulation 8-69020
- muscle crossbridge stroke and activity revealed by optical diffr. 8-69021
- muscle fibre, skeletal, helicoids in T system and striations, HV electron microscopy 8-53356
- muscle mechanics thermodynamic model 8-80908
- muscles, smooth, of elastic arteries, biophys. props. 8-69011
- myocardium mitochondria lipid composition and phase transitions rel. to depth of hypothermia, rats and dogs 8-53350
- oxidative phosphorylation mechanism, depend. of functional indices on mitochondrial incubation medium 8-69009
- oxidative phosphorylation mechanism, role of closed condition of mitochondrial membranes 8-77013
- peripheral polymorphonuclear leucocyte system model, humans 8-56956
- photoreceptor form dichroism in vertebrates 8-56969

cellular biophysics continued

- photosynthesis, biophysical processes, review 8-92605
 physicochemical properties of intra- and extra-cellular media at low temps., effect of non-electrolytes 8-53355
 plant cell wall and cytoplasm refr. index determ. by interference microscopy 8-57151
 population auto-activation, math. model 8-77017
 Purkinje cells of cerebellar cortex, histogram analysis of interpulse intervals 8-96042
 R. spheroides, triplet state electron spin echoes, fluoresc. detection 8-70856
 red blood cell suspensions, haemoglobin NMR relax., T_1 and T_2 meas. 8-80832
 retina of turtle, horizontal cells influence on bipolar cells' membrane pot. 8-88708
 retinal light responses, simultaneous recording by extra- and intracellular electrodes in crayfish 8-69055
 rhodopseudomonas sphaeroides, reaction centre triplet state fluoresc. mag. field depend. 8-53358
 ribosomes of *Escherichia coli*, partially deuterated subunit, protein and RNA distrib., neutron scatt. 8-77021
 rod outer segment, *Rana pipiens*, birefringence meas. of struct. inhomogeneities 8-77048
 skeletal muscle fibre with helicoidal T system, linear elec. props. 8-80852
 solid tumour growth model, apoptosis as volume loss mechanism 8-96027
 spherical three-layer particles as cell models, light scatt. and attenuation, shell effect 8-82913
 spin labels and biomembranes, review 8-69265
 structure and surface, high-speed analysis, laser absorpt. and scatt. meas. (*German*) 8-92687
 submitochondrial particle succinic dehydrogenase, interaction of ubiquinone with Fe-S centre, EPR 8-69016
 thermal injury kinetics, HeLa cells 8-56955
 tissue molecular dynamics and freezing phase transition studied by proton spin relax. 8-68983
 visual cell, proposed role of cyclic GMP 8-64997
 visual cells, daily rhythms and vision research 8-61176
 yeast cells, singular, dielec. props. 8-88699

cellular effects of radiation

- see also biological effects of (type of radiation)*
 abdominal epidermis histogenesis and age depend. of X-ray sensitivity in flesh fly metamorphosis 8-65084
 adoptive antibody responses in DBA/2 and BALB/c mice, differential effects of preirrad. 8-80926
 amino acid stimutable transport system in rat liver after whole-body γ -irrad. 8-65098
 amino acid transport hormonal control in liver of rats exposed to whole-body γ -irrad. 8-65099
 amoeba irradiated by thermal neutrons, absorbed dose estimation 8-53449
 bacterial photosynthesis, primary electron transfer processes, psec. dynamics 8-80841
 beta-emitting radionuclides from reactor accident, ingestion, acute toxicity 8-65082
 bone marrow ^{32}P effects during postnatal development of Swiss albino mice 8-53450
 bone marrow erythrocytes of mice, X-ray induced micronuclei 8-77088
 bronchial cancer induction by α -emitting warm particles 8-96078
 cell permeability polarity and control by phytochrome, red light irrad. of mass 8-77025
 Chinese hamster cells, ^{60}Co -irrad., computer anal. of survival curve data 8-85344
Chlamydomonas reinhardtii, dividing, X-ray and proton-induced ultrastruct. changes 8-65085
Chlorella pyrenoidosa synchronised cultures, effect of extremely low doses of secondary radiation from ^{32}P 8-73176
 chlorophyll, energy trapping dynamics in photosynthetic unit model 8-88697
 chloroplast thylakoid, light-induced absorbancy and scatt. changes about 520 nm rel. to struct. 8-69019
 chloroplasts, EPR investigation of state of Mn^{2+} 8-69008
 chloroplasts, photoinduced dielectric const. shift (*French*) 8-61147
 chloroplasts in pulsed illum. regime, photophosphorylation 8-64958
 chromosome aberration specificity, X-irrad. human T-cell line 8-80921
 chromosome aberrations as dosimetric technique for fission neutrons at 0.2 to 50 rad 8-69145
 chromosome aberrations rel. to overexposure in accidents 8-53519
 ciliated cell response during irrad. at different dose rates 8-61216
 DNA, double strand breaks, recombination, formation of chromosomal rearrangements 8-85289
 DNA, X-ray induced damage in rat cerebellar neurons and brain tumour cells 8-80922
 DNA break rejoining capacity rel. to mouse age 8-69148
 DNA unscheduled synthesis in UV irrad. spleen lymphocytes after X-irrad., rat 8-69156
E. coli K-12 cells, inhibition of X-ray induced UV resistance by nitrofurantoin 8-85342
E. coli strains, two with lambda lysogens, induced radioresist. 8-69140
E. coli AB2463 recA response to fast neutron beams, 4 to 27 MeV, rel. to dosimetry intercomparison 8-65077
 Ehrlich ascites carcinoma cell fluoresc. after X-irrad. 8-69143
 Ehrlich ascites vital cell UV primary fluoresc. rel. to ^{60}Co γ -ray dose 8-69142
 electric circuit model, alternating signal interaction 8-77011
 electric circuit model, alternating signal interaction 8-77012
 EM wave on excitable nerve membrane, surface charge density variation 8-85334
 embryonic bone and cartilage, effects of in vitro gamma irrad. 8-65089
 erythrocyte electrophoretic mobility, effect of UHF EM radiation 8-53442
 erythropoietin action, identification of two components by irrad. in vitro 8-65094
Escherichia coli radiation-damage inducible system, rel. to UV light mutagenesis 8-53458

cellular effects of radiation continued

- fast neutron irradiation of cells cultured in monolayer, dosimetric aspects 8-69218
Halobacterium halobium R_1 cells, photogeneration of two-vector transmembrane gradient of protons 8-80845
 heavy particle comparison for therapy, cell survival, OER and RBE 8-85337
 heavy particle comparison for therapy, cell survival vs. depth 8-85336
 herpesviruses, survival and immunological characts. after gamma irrad. 8-77089
 high LET constraints on low LET survival of cells, RBE theory 8-92679
 hyperthermia and X-ray combined effects on CHO cells, rel. to temp. and order of appl. 8-65088
 laser exposure of mammalian cells using evanescent fields created in optical waveguides 8-73298
 laser flash absorption change kinetics spectroscopy at 820 nm, photosynthesis study appl. 8-92769
 leaf P700^+ reaction centre reduction in higher plants 8-64954
 leucocyte, human, fluorochromed with acridine orange, spectral characts. 8-96024
 leukaemic cell line, mouse, radioprotection by procaine 8-65080
 light response and kinetics in *Aplysia* giant neuron 8-53381
 Light-regulated body ion balance in marine slug *Elysia viridis* (*Montagu*) 8-73146
 lipid photoperoxidation in isolated chloroplasts, role of superoxide anion radicals and superoxide dismutase 8-77016
 liposomal membrane permeability, radioresist. 8-80919
 liposome proton permeability increase on peroxide photo-oxidation of lipids 8-69024
 lung carcinogenesis in rats, induced by inhaled high-fired $^{239}\text{PuO}_2$ BeO 8-96077
 lymphocyte death and transform., effects of X-ray and neutrons 8-69144
 lymphocytes, in vitro ^{60}Co gamma-ray response of leucoagglutinin stimulated human cells 8-57041
 lymphoma cell survival after X-irrad., effect of vitamin E 8-92677
 malignancy analysis based on somatic mutation 8-69147
 mammalian cell, survival of normal and hybrid X-ray resist. lines exposed to X-rays and protons 8-80929
 mammalian cell radiosensitivity, effect of NaCl solns. containing radiosensitisers and radioprotectors 8-69146
 mammalian cells in vitro, 300 keV X-ray, 14 MeV neutron and pion $^-$ effects 8-69155
 mammary adenocarcinoma cell lines, mouse, radiation response and characts. 8-65095
 mammary carcinoma C3H response to fractionated irrad., rel. to fractionation number and intertreatment interval 8-53453
 micellar system, photoinduced redox processes kinetics, intracellular electron transfer 8-92603
 mitochondrial protein synthesis in rat liver after whole-body X-irrad. 8-80925
 mitotic crossover increase in *Nicotiana tabacum* after 150 kVp X-irrad. 8-61219
 mouse ovaries, X-ray effect on population of granulosa cells (*Russian*) 8-73177
 multi-target survival curve linear transform 8-65078
 nerve and muscle isolated preps., 2450 MHz radiation effects 8-53443
 neutrons generated by 70 MeV protons on Li, OER and RBE meas. 8-65079
 photosynthesis, effect of bivalent cations on photo-induced redox conversions of P700 8-77014
 photosynthesis, in vitro models 8-77023
 photosynthesis, interaction of paramag. probe I (12,3) with bean chloroplast membranes 8-77015
 photosynthesis, picosec. spectroscopic investig. 8-68964
 photosynthesis in green plants, principle of nonadditiveness, two photosystem concept 8-80842
 photosynthesis of higher plants, energy migration and electron transport, theoretical results 8-64957
 photosynthetic efficiency of green spectral region for *Chlorella* 8-69010
 photosynthetic electron transport in higher plants, adaptation rel. to light intensity 8-64953
 photosynthetic reactions of leaf discs and chloroplast preps. of crop species, 298 nm radiation effects 8-61220
 photosynthetic systems, computer assisted scanning and kinetic spectrophotometry 8-68963
 postreplication repair enhancement of Chinese hamster cells by UV light 8-92678
 postreplication repair enhancements in UV-irrad. Chinese hamster cells by irrad. in G_2^- or S-phase 8-77085
 postreplication repair in mammalian cells after UV irrad., model 8-80918
 pre-implantation embryos and implantation reaction in mouse, acute X-irrad. effects 8-69154
 primordial germ cells of fish *Oryzias latipes*, nucl. size changes after γ -irrad. 8-53451
 progression, in broad bean roots, monoenergetic neutron effects 8-65086
 pupillary sphincter, light-induced Ca release in photosensitive vertebrate smooth muscle 8-64994
 pyrimidine dimers, excision repair of UV damage in monkey kidney cells 8-53332
 respiration in *Halobacterium halobium* cells, photoinduced inhibition and stimulation 8-96066
 retinal tissue damage, by single ultrashort laser light pulses 8-96065
 RNA, heterogeneous nucl., effects of UV irrad. and postirrad. incubation on size in murine cells 8-69139
 rod outer segment shedding, intraocular initiation 8-85309
 splenic cells, rat, enhanced cytotoxic reactivity after X-irrad. 8-85343
 spores of *Bacillus subtilis*, mutagenic effect of water-t 8-80928
 sterilisation modes, cell killing and early differentiation 8-65093
 subcellular particle membrane pot. diff., proton channels in oxidative phosphorylation 8-64964
 surface photoelectron micrographs and quantum yields 8-61148
 survival model appls., fixation time picture 8-65087
 testes, glucose 6-phosphate dehydrogenase studies following partial body γ -irrad. 8-80924
 testes, isocitrate dehydrogenase studies after partial-body γ -irrad. 8-80923

cellular effects of radiation continued

- thermal neutron beam response of hamster and HeLa cells containing various concs. of ^{10}B 8-73178
 thymine dimer excision from DNA of UV-irrad. plant seedlings 8-61221
 thymine dimer excision kinetics in UV-irrad. human cells 8-53331
 thymocyte membrane props. modification by hyperthermia and gamma-rays 8-69017
 track structure theory in radiobiology and radiation detection 8-50446
 tumour cell survival with fractionated doses, pitfalls in use of in vitro survival curves 8-77084
 tumour X-irrad. in vivo, enhanced lymphocyte-mediated killing of tumour cells 8-77086
 US perturbation obs. at cellular level 8-61214
 yeast, inducible enzyme synthesis, UV effects on regulation and activity per cell 8-69157
 yeast cells, alpha-irrad., UV-induced reactivation 8-80920
 O_2 enhancement effect, photo-reactivation of γ -radiation damage 8-77087
 Pt complex potentiation, of X-irrad. lethal effects, rodent cells 8-85345
 $^{239}\text{PuO}_2$ alpha-particle freq. in lung cells 8-69151

cellular method

- extended rigorous cellular method, theory and appl. to films 8-52055
 nonspherical potential calc., appl. to Cu and graphite 8-56063

cellular transport and dynamics

- acetylcholine receptor electrophoretic movement in embryonic muscle cell membrane 8-85298
 active transport and energy transformation, quantum mechanism 8-53364
 amino acid, permeability of E. coli K-12 8-77029
 amino acid stimutable transport system in rat liver after hole-body γ -irrad. 8-65098
 amino acid transport hormonal control in liver of rats exposed to whole-body γ -irrad. 8-65099
 axon, giant, Myxicola, internal Cs^+ dialysis, Na inactivation 8-96036
 axon, squid giant, temp. effects on gating currents 8-96037
 axon Na conductance and Ca transport, squid, mol. model 8-85305
 axoplasmic transport, slow, asymm. in branches of bifurcating axons 8-80848
 barbiturate-induced slow outward currents in Aplysia neurones 8-80866
 bioenergetics and proton-electron systems of membranes, review 8-96030
 carbohydrate active transport in membrane vesicles of Acholeplasma laidlawii cells 8-64965
 cell permeability polarity and control by phytochrome, red light irrad. of mass 8-77025
 charge transfer in thin membranes, discrete models, nonsteady state at high polarising voltages 8-69023
 chromatophores of photosynthesising purple bacteria, sorption and desorpt. of water 8-69012
 cochlear endolymph Ca content 8-61203
 conductance fluctuations in cultured spinal neurones induced by γ -aminobutyric acid 8-80867
 cortical spreading depression, math. model 8-80857
 digitalis inotropy rel. to enhanced slow inward Ca current 8-61155
 epithelial K active transport system of insect midgut, pump-mediated efflux 8-80846
 epithelium, living, size and shapes of lateral intercellular spaces 8-77032
 erythrocyte Ca transport in myotonic muscular dystrophy patients 8-80849
 erythrocyte ghosts, human, Ca^{2+} intracellular changes, arsenazo III meas., rel. to K permeability 8-96032
 excitable fibre, steady speeds of spread of stable and unstable impulses, depend. on membrane ionic currents 8-53382
 fibroblast spread kinetics 8-64955
 fibroblast spreading kinematics, individual locomotor activity 8-69006
 fusion rosettes in Paramecium, possible function as Ca^{2+} gates 8-56958
 gating charge immobilisation by inactivation-simulating substance 8-61154
 glucose transport in human red cell ghosts, effect of chlorpromazine and temp. 8-77026
 growth regulation, effects of cell density and metabolite flux on dynamics 8-85296
 growth regulation, effects of cell density and metabolite flux on dynamics 8-88701
 haemoglobin, human and Lumbricus terrestris, conc. depend. of self-diffusion 8-68984
 Halobacterium halobium R_1 cells, photogeneration of two-vector transmembrane gradient of protons 8-80845
 ion transport and chem. reactions in brown adipose tissue, network thermodynamics 8-92606
 ionic channel formation in living cell membrane, microelectrode obs. 8-53372
 ionic channels in excitable membranes, current problems and biophysical approaches 8-53369
 junction membrane form., quantum jumps of cond. 8-73145
 leaf CO_2 absorption and diffusion, sun vs. shade leaves 8-80850
 Light-regulated body ion balance in marine slug Elysia viridis (Montagu) 8-73146
 membrane dynamic equation solving, practical algorithm 8-77038
 mitochondria membrane Ca^{2+} interaction, influence of oestrogens 8-53349
 monosynaptic potentials onset and propagation, discrete-dynamic equations 8-77040
 muscle, smooth, effect of hyperosmolar soln. on elec. connections between cells 8-69027
 muscle, smooth, intestinal cell, voltage clamp studies of hyperpolarising inactivation 8-80847
 myocardium contraction amplitude depend. on freq. of elec. stimulation, frog 8-77027
 myotubes, human, cultured, acetylcholine-induced conductance fluctuations 8-61157
 nerve excitability, interactions between intrinsic membrane protein and elec. field 8-53377
 nerve impulse, physical mechs., ion transport through membranes, review 8-85306

cellular transport and dynamics continued

- nerve impulse equation, dynamic responses of impulse 8-64972
 nerve impulse propagation, subthreshold solns. of Hodgkin-Huxley eqns. 8-77044
 neuromuscular blockade by amantadine by suppression of acetylcholine receptor ionic cond. 8-64975
 neuromuscular frequency-depend. block and temp.-induced seizure in ts mutant of Drosophila 8-56963
 neuromuscular junction, snake, synaptic channel gating differences at twitch and slow junctions 8-80868
 neurone Ca conduction units, Helix aspersa 8-77041
 neurones of large horse-leech, electrophysiological characts. rel. to intracellular Na^+ conc. 8-53374
 neurosecretory structure particle motion, effect of increased K^+ concs. 8-77046
 nonspiking neurones, pharmacological evidence for fast Na channels 8-73151
 periodic conversions in biological system solns., optical mixing method obs. 8-96029
 photoreceptor visual response rel. to metarhodopsin transitions, barnacle 8-69050
 photosensory membrane of Limulus ventral nerve photoreceptor, effect of extracellular Ca/Na ratio 8-69067
 photosynthetic electron transport in higher plants, adaptation rel. to light intensity 8-64953
 plants, transfer cells and their roles in transport of solutes 8-73148
 polarised spherical cell, ionic conc. profiles and charge distrib. 8-73144
 protein biosynthesis, role of guanine nucleotides 8-68982
 protein transfer across microsomal membranes reassembled from separated membrane components 8-69029
 retinal on-centre bipolar cell, ionic mechanisms of rod and cone signals 8-61177
 rod network in turtle retina, elec. spread 8-80874
 rod outer segment adaptation anal. based on a simple equiv. cct. 8-73157
 sarcoplasmic reticulum Ca^{2+} , Mg^{2+} -ATPase transient kinetics obs. by fluoresc. 8-61156
 sarcoplasmic reticulum membrane rearrangements on peroxide oxidation of lipids 8-69025
 sinatorial node of rabbit heart, vagal stimulation, K^+ permeability and extracellular transients 8-92608
 single-file ionic transport theory, reduced flow diagrams 8-69022
 subcellular particle membrane pot. diff., proton channels in oxidative phosphorylation 8-64964
 sugar transport system dependent regulation of adenylate cyclase, review 8-69031
 thymocyte membrane props. modification by hyperthermia and gamma-rays 8-69017
 transepithelial ion transport endogenous regulation, implications of ouabain-like activity in toad skin 8-73147
 viral infection, membrane leakiness, rel. to development of antiviral agents 8-53371
 visual cell microvilli membrane fragment protonic and ionic processes, cephalopod 8-73159
 water diffusion meas. by pulsed gradient NMR, cell struct. size determ. 8-77159
 Ca conductance, inactivation without facilitation in Cs-loaded Aplysia neurones 8-56965
 Ca ion levels in squid axons, influence of pCO_2 8-56960
 Ca pump driven by ATP in squid giant axons 8-77043
 Ca transients in aequorin-injected frog cardiac muscle 8-61149
 Cl^- active transport inhibition by piretanide, in teleost intestine cell 8-64967
 K channel blocking agent, 3,4-diaminopyridine 8-69028
 K currents induced by acetylcholine in Aplysia neurones, slow relax. 8-80865
 K^+ ion flux through membrane channels, nerve impulses, random walk anal. 8-77045
 K^+ permeability of mitochondrial and artificial bilayer membranes 8-53365
 Na channel, fully coupled excited state model, conductance in volt. clamped case 8-85297
 Na current in cardiac and nervous tissues, validity of $\text{dV}_{\text{max}}/\text{dt}$ as meas. 8-77037
 Na permeability inactivation in squid giant nerve fibres, review of exptl. work 8-73154

cement industry

- dust generation, peak short term dustfall meas. and effect on residential development 8-81386

cements (building materials)

- used only for those materials which bind together particulate matter so as to form a coherent mass of considerable strength. For cements that cause two or more separate masses to adhere see adhesion*
 alite paste, mature, microstructure study by SEM, TG and X-ray diffr., corrosion 8-92381
 asbestos fibre reinforced Portland cement analytical fracture resistance curve expression 8-76756
 hardened paste, internal stresses and microcrack form. caused by drying 8-92325
 mortar, deform. charact., expt. study (Japanese) 8-56704
 polypropylene fibrillated film reinforced cement, loading capacity, cracking 8-72759
 porous solid with below-freezing pt. adsorbate, isothermal adsorption and dimensional changes obs. 8-75925
 Portland cement clinker, elec. props. 8-59976
 portland cement paste, microstructure study by SEM, TG and X-ray diffr., corrosion 8-92381
 review, physics and chemistry 8-73013
 steel fibre reinforced cementitious material, radiographic anal. of fibre distrib. 8-52747
 steel wire reinforced Portland cement mortar, wire pull out, inelastic behaviour 8-56681
 $3\text{CaO} \cdot \text{Al}_2\text{O}_3$, high level radioactive waste disposal 8-78485
 ^{137}Cs immobilisation in cement-waste composites 8-82466

centrifuges

- dust-air cyclone separator, operation anal. 8-57362
 earthquake modelling, appl. of centrifuge 8-81429
 enrichment by plasma centrifuge, rotational velocity meas. 8-74502
 gas, compressible flow in rot. cylinder, linearised anal. 8-71345

centrifuges continued

- gas centrifuge, effect of compressible flow on max. separating power 8-70644
 high-temperature centrifuge construction 8-57938
 inert gas rotating arc meas. in plasma centrifuge 8-75438
 isotope centrifuge, effect of thermal convection on separative power, numerical anal. 8-58500
 polystyrene monodisperse ^{51}Cr tagged aerosol prod. using aerosol centrifuge 8-92519
 rotating plasma, separation of metals 8-75436
 U enrichment by plasma centrifuge, partial pressure distrib. obs. 8-74501

ceramals see cermet**ceramics**

see also refractories

- alkali metal polyaluminates, synthesis, solar furnace appl. 8-84746
 alkali-alkaline earth ceramic solid solutions, with tetragonal tungsten bronze struct., low freq. optical modes 8-76477
 alumina, multiaxial fracture, general approach to statistical anal. 8-90785
 alumina powder, particle size analysis, using centrifugal sedimentation (*German*) 8-57890
 archaeology, dating by alpha-recoil tracks in mica 8-70237
 brittle, post thermal buckling resistance, role of physical props. 8-64585
 ceramic-metal seal technology, history and trends 8-81992
 chamotte glazed masses, deformation occurring during heat treatment 8-84747
 chemical reactions in plasma generated near ferroelectric surface, obs. 8-68931
 crack and inclusion detection, NDT microwave evaluation 8-95866
 crack tip, process zone, theory for stress field 8-67154
 crystalline materials, IR transmission, review 8-55417
 defects in materials, direct observation and characterisation 8-88617
 electroceramics and magnetoceramics, microstructure and physical props. 8-72756
 engineering materials, nature and props., book 8-72707
 failure prediction under thermal loading, Weibull eqn. 8-88534
 fatigue data analysis, lifetime predictions for ceramic materials 8-95870
 ferroelectric, axially loaded, nature of elec. field and resulting voltage 8-72468
 ferroelectric, dielec. losses due to domain wall oscill. 8-84541
 ferroelectric films, resonant autothermostabilisation (*Russian*) 8-52451
 fluorite ceramics, doped, short range order anal. by electron diffr. 8-83672
 fracture toughness, exam. of methods of enhancing, merits and limitations 8-60771
 fracture toughness specimens, wedge indentation technique for precracking, appl. to Al_2O_3 and SiO_2 8-85087
 fusion reactor materials, effects of radiation on electrical insulators 8-95082
 glass and oxide glasses, microstructure 8-88442
 glass ceramic, machinable, elastic moduli press. and temp. derivatives, specific heat 8-52873
 glass-ceramic machinable, machining techniques 8-77881
 grain and phase boundaries between crystals, conf., Konigstein, Germany (Oct. 1977) 8-72762
 $(\text{H}_2\text{O})_{3-x}\text{Ta}_{11+x}\text{O}_{30}$, synthesis, non-stoichiometry, density and ionic cond. meas. (*French*) 8-52741
 kaolinite to mullite reaction series, reexam. of solid state phase transformations 8-64535
 LV switchgear contacts (*Slovak*) 8-56603
 metallographic method for polishing specimens, of ceramics and metal-ceramic mixtures 8-56850
 microstructure dependence of mechanical behaviour 8-88533
 moisture measurement in porous ceramic components, equipment (*German*) 8-54378
 mullite, polycrystalline, prep. by hot pressing aluminosilicate glasses 8-60639
 mullite fibre reinforced mullite, in vitro degradation, bending strength, Young's modulus, density meas. 8-85011
 optical, KO-1, IR scatt. and brightness indicatrices meas. 8-71164
 piezoceramic articles, nonuniform polarisation investig. by microwave polaris. method 8-72969
 piezoceramic elastic compliance and mechanical Q-factor at high drive levels 8-60395
 piezoelectric, phase method of microwave flaw detection 8-72968
 piezoelectric ceramic vibrator, resonant freq. temp. stability anal. (*Chinese*) 8-68454
 piezoelectric cylindrical shell, longitudinal wave propagation 8-92026
 piezoelectric US transducer, shear-wave vel. meas., bone elastic moduli determ. 8-83201
 porcelain, conventional and rapid fired, comparison of texture and props. (*German*) 8-64510
 porcelain enamel, resistance to aqueous attack, expt. results 8-56788
 porcelain enamel, resistance to aqueous attack, prediction eqn. 8-60853
 porcelain enamel layers on steel, H_2 induced fracture of layers 8-76752
 powders, electron microscope determination of particulate sizes (*German*) 8-57891
 processing before firing, book 8-56608
 quartz porcelain fast fired, development of microstruct. (*German*) 8-60625
 quasibinary and quasiternary ceramic oxide systems, calculation of phase diagrams 8-60660
 rare earth aluminates, effects of roasting in reducing and oxidizing media on elec. props. 8-52736
 recrystallisation and grain growth, survey 8-76660
 rheological meas. device for 20° to 90°C and constant moisture content 8-85079
 sculpture from Oaxaca, Mexico, authentication by thermolum. and style 8-70238
 SEM and anal. techniques (*German*) 8-56832
 slip moulding method development 8-68661
 β -spodumene-mica glass ceramic, thermal expansion thermal shock and moduli of rupture and elasticity 8-60736
 steatite, exam. of thermal damage by strength meas. 8-84997

ceramics continued

- strain intensity criterion for crack branching in brittle mats. 8-55592
 structural stresses measurement using X-ray diffr. meas. (*German*) 8-52744
 suspended particle, effect of electrolyte on charge, in cermet electrode-position 8-68665
 TBK-3, ferroelectric ceramic, 90° electric domain processes, mech. stress, X-ray diffr. 8-72478
 thermal conductivity, effect of decrease in thermal resistance of pores and microcracks 8-75892
 toughened, stress corrosion characts., exam. 8-71295
 transparent glass-ceramics, microstruct. and props. 8-59960
 TsTS polarized ceramic film, Lamb waves near. crit. freq. study (*Russian*) 8-52039
 TsTS-23, ferroelectric ceramic, 90° electric domain processes, mech. stress, X-ray diffr. 8-72478
 ultrasonic NDT techniques, low-frequency 8-80690
 unfired, cavity form. by electron beam machining 8-80660
 unfired, precision e-beam machining, kinetic focusing 8-80661
 US attenuation 8-67772
 vitreous enamel, bubble struct. and flaw forecasting 8-53118
 vitreous enamel coating, method of quantitatively assessing blistered structure 8-53108
 vitroceramic-metal composite materials development, Spacelab appl., mech. props. (*French*) 8-92229
 white Cl-containing slag glass-ceramic, synthesis with nonsulphide catalyst 8-52748
 $\text{AlN-Al}_2\text{O}_3$ powders, hot pressing, crystalline phase obs. 8-95720
 Al_2O_3 , abrasive, wear in simulated hot grinding 8-56784
 $\alpha\text{-Al}_2\text{O}_3$, atomic disorder, dominant type 8-63757
 Al_2O_3 based ceramic sintering conditions effects on props. (*German*) 8-56604
 Al_2O_3 based ceramics, ladder structures, interference phenomena explanation 8-72898
 Al_2O_3 , biaxially stressed, exam. of localised impact damage 8-72846
 Al_2O_3 , cylindrical voids, exam. of instability 8-79603
 Al_2O_3 , D plasma interaction, surface structure, chemistry and resistivity changes 8-53010
 Al_2O_3 , dense, surface segregation of Ca under exposure to steam and steam-CO 8-85013
 Al_2O_3 , evaluation of crack resistance and crack velocity, using controlled fracture experiments 8-72881
 Al_2O_3 for technical ceramics, extraction and prep. (*German*) 8-53200
 Al_2O_3 fracture resistance, exam. 8-76826
 Al_2O_3 , fracture toughness specimen, appl. of wedge indentation technique for precracking 8-85087
 Al_2O_3 , initial sintering, method for obtaining surface diffusion coeffs., appl. to shrinkage data 8-95713
 $\beta\text{-Al}_2\text{O}_3$, new slip casting technique for fabrication of ceramics 8-84745
 $\beta\text{-Al}_2\text{O}_3$ phases, synthesized, effect of starting Al_2O_3 composition and halogen ion additions, on structural state 8-76620
 Al_2O_3 , porous, sintered, delayed failure, static fatigue in distilled water 8-64750
 Al_2O_3 pressing method, for the telecommunications industry (*Hungarian*) 8-52728
 $\alpha\text{-Al}_2\text{O}_3$, rapid firing, XPS study of cryst. struct. 8-68663
 Al_2O_3 , reactive hot pressing, exam. of pressing characteristics 8-80499
 Al_2O_3 , single crystal, fracture mirror formation, anisotropy of fracture surface energy and elastic constants 8-68824
 Al_2O_3 , sinterability, $\text{NH}_4\text{AlO}(\text{OH})\text{HCO}_3$ synthesis conditions effect (*Japanese*) 8-52710
 Al_2O_3 , sinterability, $\text{NH}_4\text{AlO}(\text{OH})\text{HCO}_3$ crystallinity effect (*Japanese*) 8-52711
 Al_2O_3 , sintered, containing MgAl_2O_4 precipitates, Mg distribution at grain boundaries 8-80498
 Al_2O_3 , sintered, MgO-enhanced densification, test of second phase and impurity segregation models 8-64511
 Al_2O_3 , sintering of single phase and multiphase components (*German*) 8-80494
 Al_2O_3 , stress value determination by bending tests, comparison with crack tip theory 8-67154
 Al_2O_3 , vitreous-bonded, eval. of proof testing to assure against delayed failure 8-84954
 Al_2O_3 , wetting by Cu-Sn-Ti alloys 8-71904
 $\text{Al}_2\text{O}_3/\text{Nb}/\text{Al}_2\text{O}_3$ joint, solid state bonded, exam. of bond fracture strength 8-76826
 $\beta\text{-Al}_2\text{O}_3\text{-Na}_2\text{O}$, superionic anisotropic ceramic, prod. by microwave sintering (*French*) 8-52742
 $\beta\text{-Al}_2\text{O}_3\text{-Na}_2\text{O}$, vacuum hot pressed, densification kinetics 8-72758
 $\beta\text{-Al}_2\text{O}_3\text{-Na}_2\text{O}:\text{Mg}$, ionic cond., effect of microstruct. and phase composition 8-67859
 $\text{Al}_2\text{O}_3\text{-Na}_2\text{O-LiO}_2$ (8.8, 0.75 wt.%) exam. of Na^+ resistivity as function of temp. grain size model 8-80654
 $\beta\text{-Al}_2\text{O}_3\text{-Na}_2\text{O-SiO}_2$, solid electrolytes, exam. of microstruct. ionic resistivity 8-80566
 $\text{Al}_2\text{O}_3\text{-TiC}$, multiphase ceramics, mech. strengthening due to dispersion of non-metallic particles (*German*) 8-60674
 $\text{Al}_2\text{O}_3\text{-ZrO}_2$, microstructure effect on friability 8-64515
 $\text{Al}_2\text{O}_3\text{-ZrO}_2$, multiphase ceramics, mech. strengthening due to dispersion of non-metallic particles (*German*) 8-60674
 BN, production kinetics of gasification of organosilicon binders 8-60635
 BN, toughening by stress-induced phase transforms. 8-80635
 $\text{BaCO}_3\text{-SrCO}_3\text{-TiO}_2(\text{ZrO}_2)$, ternary systems, solid-phase synthesis 8-52733
 BaF_2 , optical ceramic, hot pressing in vacuum, rel. to spectral transmission 8-52730
 BaO-SiO_2 glass ceramic, nucleation, effect of electric fields 8-83742
 $\text{Ba}_2\text{TiGe}_2\text{O}_8\text{-Ba}_2\text{TiSi}_2\text{O}_8$, pseudobinary system, pyroelectricity and related props. 8-95553
 BaTiO_3 , 90° electric domain processes, mech. stress, X-ray diffr. 8-72478
 BaTiO_3 ceramics, calcination effects, TiO_2 powder eval. (*Japanese*) 8-64516
 BaTiO_3 , dielec. and elastic const., temp. depend. (*Russian*) 8-64307
 BaTiO_3 , ferroelec. ceramic, mech. strength, for single crystals and Ca and Co modified specimens 8-64332
 BaTiO_3 , ferroelectric ceramic, dielec., piezoelec. and elastic props., orientational contrib. 8-68468

ceramics continued

- BaTiO₃, positive temp. coeff. resistivity as function of Ti-Ba ratio 8-72151
- BaTiO₃-Ni(Co, Mn)Fe₂O₄, ceramic, exam. of prep. and physical props. 8-68655
- C pyroceramic, sputtering and blistering from H⁺ and He⁺ bombardment 8-79649
- CaO-CaF, hot pressed, effects of CaF₂ addition, sintering behaviours and microstructs. investig. (*Japanese*) 8-95721
- CaO-MgO-CeO₂, fired, phase equilibrium diagram, 1700 to 1200°C 8-92248
- CaO-MgO-ZrO₂-SiO₂, phase study, SiO₂ compatibility relationship 8-95734
- CaO-MgO-ZrO₂-SiO₂, phase study, ZrO₂ compatibility relationship 8-95735
- CaS discs, sintering method prep., ionic cond. meas., 650 to 900°C (*Japanese*) 8-75869
- Ca₃(Si₂Al₂)₁₂(O,N)₁₆, α'-Sialon ceramics, prep. and characterisation 8-84750
- Ca₃SiO₅ form. by solid state reaction, mixture and firing condition effects 8-56602
- CaTiO₃-LaAlO₃ solid soln., phase redistrib. during roasting in H₂ 8-52735
- CdS, dry process formation from CdO and S (*Spanish*) 8-56607
- Co_{1-x}Fe_{2x+1}O₄, prep. by wet and ceramic methods, struct., mag. and surface props. 8-52307
- Cr₂O₃-WO₃, phase relations 8-92249
- Eu_{0.5}Ba_{0.5}TiO₃, ferromag., ferroelec., ceramic, Curie temps. determ. 8-68230
- Eu₂O₃-Ta₂O₅, microcracking, elastic props., internal friction 8-92326
- Fe₂O₃, diffusion in gas phase during firing of MgO-Cr₂O₃ bricks (*French*) 8-80495
- Fe₂O₃-WO₃, phase relations 8-92249
- Fe₃O₄, low temp. sintering 8-92221
- Gd₃Al₂O₁₂ phase obtained by crystallisation of amorphous Gd₂O₃-5/3Al₂O₃ by quenching 8-92224
- HfO₂-Gd₂O₃, phase relations 8-72769
- K₂O-Al₂O₃ system, high temp. thermodynamics and phase equilibria 8-80521
- KTaO₃, defect struct. and elec. props. 8-91695
- LaB₆, chemical vapour growth of whiskers, and single crystals 8-72710
- LiAlSiO₄ glass-ceramic, fracture phenomena as function of initial flaw size and temp. 8-95797
- LiF, ceramic, characts. on pressing in vacuum and in air 8-52734
- LiF compact, particle size rel. to pore characts. 8-60631
- LiF tile and sheet for thermal neutron shielding (*Japanese*) 8-74510
- Li₂O-Al₂O₃-SiO₂, glass ceramic, elastic props. at high press., US meas. 8-83863
- Li₂(Si₂Al₂)₁₂(O,N)₁₆, α'-Sialon ceramics, prep. and characterisation 8-84750
- LiTiZn ferrites, elec. resist., mag. props., effect of Bi addition 8-95474
- MgAl₂O₄, powder effect of precursory sulphate solution anion on sintering 8-56605
- MgF₂, optical ceramic, synthesis 8-52729
- MgO bicrystals, formed by welding single crystals with H₃PO₄, exam. 8-56796
- MgO brick, particle-size distrib. depend. of texture and struct. (*Japanese*) 8-84753
- MgO, EPR of Mn²⁺ diffusion 8-91477
- MgO, effect of Cl⁻ and F⁻ ions on calcination and sintering (*Japanese*) 8-95719
- MgO, lattice misorientation and displaced vol. for microhardness indentation 8-64617
- MgO, plastically deformed, recovery of internal friction at room temp. (*French*) 8-80577
- MgO single crystal, absorbed fluid effect on rolling contact deform. 8-64719
- MgO, single crystal, wear damage, surface cracks 8-68825
- MgO-Al₂O₃-Cr₂O₃, vacuum vaporisation, Langmuir method 8-95149
- MgO-Al₂O₃-SiO₂ glass ceramic, nucleation, effect of electric fields 8-83742
- MgO-Cr₂O₃, vaporisation rate, O₂ partial press. effect (*Japanese*) 8-63848
- Mo-Mn-Fe-Si/Al₂O₃ ceramic seal, interfacial phases 8-72011
- Na_{3-x}Ta_{11+x/5}O₃₀, synthesis, non-stoichiometry, density and ionic cond. meas. (*French*) 8-52741
- Na₃YSi₄O₁₂, high Na⁺ ion conduct. 8-91479
- PLZT ceramic, possible construction of matrix-addressable controlled transparency 8-71222
- PLZT ceramic birefringence props., transverse electro-optical meas. 8-72487
- PLZT, electro-optical, physical, elec. and optical props. and fabrication (*Polish*) 8-56458
- PLZT, ferroelectric devices for optical systems 8-90473
- PLZT-ceramics, cathodolum. spectral and temp. depend. 8-84665
- PZT, PbO content estimation using analytical procedure (*German*) 8-53279
- (Pb_{0.71}Ba_{0.285})_{0.991}(Zr_{0.707}Ti_{0.293})_{0.981}Bi_{0.019}O₃, slim loop ferroelec. ceramic, shock wave compressed, elec. response 8-80293
- PbBi₄Ti₄O₁₅, dielec. props., temp. depend. 8-95561
- Pb(Mg_{1/3}Nb_{2/3})O₃-PbTiO₃-PbZrO₃, piezoceramics for high frequency use 8-95555
- PbTiO₃, ferroelec. ceramic, mech. strength 8-64332
- PbTiO₃, ferroelectric ceramic, dielec., piezoelec. and elastic props., orientational contrib. 8-68468
- PbTiO₃, piezoceramics for high frequency use 8-95555
- PbTiO₃-PbZrO₃-In(Li₃/W₂/O₃), piezoelec. ceramic characteris. for surface wave filters 8-95215
- Pb(Zn_{1/3}Nb_{2/3})O₃, perovskite type, high-press. high temp. synthesis (*Chinese*) 8-68654
- Pb(Zr,Ti,Ge)O₃, antiferro-ferroelectric transition 8-95565
- Pb(Zr,Ti)O₃, axially loaded, nature of elec. field and resulting voltage 8-72468
- Pb(Zr,Ti)O₃ ceramic-polyvinylidene fluoride composite film, complex piezoelec. props. 8-64323
- Pb(Zr,Ti)O₃, ferroelec. ceramic, mech. strength 8-64332
- Pb(Zr,Ti)O₃, prep. and reactivity from butoxide precursors 8-84749
- PbZr_{0.95}Ti_{0.05}O₃, impact loading, mech. and elec. response, elec. state effect 8-64317
- ceramics continued
- Pr₂NiO₄, elec. props., 300 to 1000°C 8-91694
- PrFeO₃, elec. props., 300 to 1000°C 8-91694
- Rb_{5-x}Ga_{11+x/5}O₃₀, synthesis, non-stoichiometry, density and ionic cond. meas. (*French*) 8-52741
- Si-Al-O-N system, TEM exam. of X phase structure 8-56606
- Si-C-Al-O-N and related systems, new materials 8-95159
- Si₃-Al-O-N₂, hot pressed, exam. of fracture mechanisms 8-72879
- SiAlON system, β', 15 R phases, oxidation resist. (*French*) 8-72899
- SiC, exam. of T₂ diffusion coeffs. and D₂ solubility 8-79816
- SiC, fracture toughness specimen, appl. of wedge indentation technique for precracking 8-85087
- SiC, hot pressed, brittle fracture and subcritical crack growth 8-72885
- SiC, meas. of critical stress intensity factor and subcritical crack propag. rates 8-72880
- SiC, reaction sintered, TEM exam. of recrystallisation, phase transformation 8-80567
- SiC surface, H⁺, D⁺ and Ar⁺ bombardment, 5 to 15 keV, meas. of erosion yield 8-79647
- SiC, uncommon mode of morphological development among coherent phases, optical and electron microscope exam. 8-80544
- Si₃N₄, biaxially stressed, exam. of localised impact damage 8-72846
- Si₃N₄ ceramic, surface and subsurface struct. by photoacoustic spectroscopy 8-68481
- Si₃N₄, exam. of fracture resistance 8-76826
- Si₃N₄, growth of α and β phases 8-95717
- Si₃N₄, hot pressed, flawed plate under combined stresses, failure prediction 8-72884
- Si₃N₄, hot pressed, high temp. compressive cracking, optical and electron microscopy exam. 8-76733
- Si₃N₄, hot pressed, slow crack growth from controlled surface flaws 8-80632
- Si₃N₄, meas. of critical stress intensity factor and subcritical crack propag. rates 8-72880
- Si₃N₄, reaction bonded, exam. of strength as function of nitrated density, microstruct. design 8-68731
- Si₃N₄, reaction bonded, Na assisted oxidation, exam. 8-56795
- Si₃N₄, reaction bonded and hot pressed, exam. of thermal shock behaviour (*German*) 8-64561
- Si₃N₄, room temp. fracture strength data, statistical anal. 8-64619
- Si₃N₄, static fatigue, fitting of data to iterative trivariate analysis 8-76732
- Si₃N₄/Zr joint, solid state bonded, exam. of bond fracture strength 8-76826
- Si₃N₄-Al₂O₃-Y₂O₃, sintered, observation of a noncrystalline phase 8-64536
- Si₃N₄+MgO, reaction during hot pressing 8-68658
- SiO₂, crack propag. and bifurcation 8-72888
- SiO₂, molten, struct., X-ray radial distrib. anal. 8-67651
- SiO₂, surface reactivity modification by Ar/O₂ plasma treatment 8-64890
- Si₃ON₂ needle crystal growth by nitriding Si-SiO₂ system in powder compacts (*Japanese*) 8-68609
- SrFe₁₂O₁₉ ceramic compact, sublattice magnetisation and textures 8-68426
- ThO₂-based ceramic impurity diffusion, electrotransport method 8-67869
- TiB₂, hardness of sintered material 8-60636
- TiB₂-Al₂O₃, thermal stability of composite materials 8-60638
- TiB₂-CaO, thermal stability of composite materials 8-60638
- TiB₂-MgO, thermal stability of composite materials 8-60638
- TiB₂-Y₂O₃, thermal stability of composite materials 8-60638
- TiN, ultra-fine powder prep. by reaction in N₂ plasma jet (*Japanese*) 8-72757
- TiO₂, rutile, ageing in strong electric field TiO₂ (*Polish*) 8-52869
- TiO₂, rutile, ferroelectric ceramic, dielec., piezoelec. and elastic props., orientational contrib. 8-68468
- TiO₂, sintering, hardness, density, elec. cond. and colour (*Japanese*) 8-68659
- TiO₂-containing slag-glasses, phase separation and glass-ceramic formation 8-51424
- TiO₂-SiO₂ powders, anatase-rutile transition, mechanism investigation (*Japanese*) 8-95746
- Tl_{3-x}Ta_{11+x/5}O₃₀, synthesis, non-stoichiometry, density and ionic cond. meas. (*French*) 8-52741
- UC-(PuC), ceramic fission reactor fuels, fabrication and performance, review 8-58392
- UN-(PuN), ceramic fission reactor fuels, fabrication and performance, review 8-58392
- UO₂, sintered pellets, relationship between intercept length and grain diameter 8-52743
- UO₂-(PuO₂)(BeO), ceramic fission reactor fuels, fabrication and performance, review 8-58392
- Y₂O₃, U, C interactions, thermal anal. 8-85154
- Y₂O₃-Nb₂O₅, solid state reactions, 1275 to 1350°C, electron microscopy, EPMA, X-ray diff., dilatometry (*Japanese*) 8-63883
- Y₂O₃-TiB₂ ceramic, production by sintering in vacuo, or hot moulding at 1500°C 8-60629
- Y₂(Si₂Al₂)₁₂(O,N)₁₆, α'-Sialon ceramics, prep. and characterisation 8-84750
- Y₂Si₂O₇Cl; Ce phosphor, prep. and luminescence props. 8-52740
- ZnO, adsorp. of H₂O vapour, annealing and grinding effects 8-68656
- ZnO ceramics, non-Ohmic, cond. mech. 8-68034
- ZnO, wurtzite structure, hydrothermally grown exam. of thermal expansion coefficient 8-75854
- ZnO-Al₂O₃-SiO₂, transparent glass-ceramics, EPR obs. of glass crystallisation 8-80507
- ZnO-Al₂O₃-SiO₂, transparent glass ceramics, heat treatment effect on microstruct. 8-56667
- ZnO-Al₂O₃-SiO₂, transparent glass-ceramic, microstruct., physical props., crystallisation ht. treatment depend. 8-80506
- ZrC, solubility, diffusion and permeation of Cs 8-51684
- ZrO₂, containing metastable tetragonal phase, stress induced phase transform. effect on props. 8-68683
- ZrO₂, cubic, nitride stabilised 8-92223
- ZrO₂, obtained by coprecipitation with different oxides, props. 8-64514
- ZrO₂ powders, vapour phase reaction production 8-68660

ceramics continued

- ZrO₂, technical grade containing CaO, polymorphic transform. up to 1200°C 8-64539
 ZrO₂-ZrO₂, multiphase ceramics, mech. strengthening due to dispersion of non-metallic particles (*German*) 8-60674

Cherenkov counters see *Cherenkov counters*

Cherenkov radiation see *Cherenkov radiation*

cerium

see also *nuclei with*

- aluminates:Ce³⁺, luminesc. exam. 8-56513
 electrical resistance, temp. coeff., 20 kbar at 300K 8-83973
 FCC, ground-state props. 8-75989
 ground state properties of f band metals 8-91607
 phase transition, high press., $\alpha \rightarrow \alpha'$, volumetric study 8-83940
 photometric determ. in cast Fe and steel (*German*) 8-68955
 specific heat, up to 20 kbar at 300K 8-83973
 valence mixed state, Kondo lattice, Anderson localisation models (*Japanese*) 8-51945
 CaF₂:Ce, Stark struct., phototransitions, g-factors 8-67995
 γ -Ce, field induced mag. form factor 8-68151
 Ce II, isotope shift and screening, pseudo-relativistic HF calc. 8-90096
 Ce⁴⁺/Ce³⁺ dosimeter, adsorbed doses, potentiometric determ. 8-94146
¹⁴¹Ce, diffusion behaviour in SiC, 1650 to 1850°C 8-79814
¹⁴¹Ce standard, measured by dose calibrators, simulated ⁹⁹Tc^m standard 8-61261
¹⁴⁴Ce inhalation effect of influenza virus infection on pulmonary retention and mouse survival 8-85340
 La₂Mg₃(NO₃)₁₂·24H₂O:Co²⁺, Ce³⁺, relax. and ESR in magnetically cooled systems 8-88225
 YAG:Ce³⁺, new fast scintillator for SEM 8-86394
 YAG:Ce³⁺, excited state absorpt. loss, 5d \rightarrow 4f rare earth lasers 8-90417
 Y₃Si₂O₈Cl; Ce phosphor, prep. and luminescence props. 8-52740

cerium alloys

- Al₃Ce, Al₃Ce, nucl. orientation exam. of Ce ground state at very low temp. 8-67999
 Ce-Co, liq., charge transfer effect 8-94967
 Ce-Co-Si system, mag. props. in 77-300K range (*Russian*) 8-56290
 Ce-Cu, liq., charge transfer effect 8-94967
 Ce-Fe-Si system, mag. props. in 77-300K range (*Russian*) 8-56290
 Ce-La, mag. ordering, sp. ht., susceptibility and resist. 8-68238
 Ce-Ni, hydriding characts., applicability for H₂ storage material 8-83955
 Ce-Ni-Si system, mag. props. in 77-300K range (*Russian*) 8-56290
 CeAg(Mg)(Zn), magnetic struct. and cryst. field, neutron diffr. exam. 8-72328
 CeAl₂, anisotropic magnetostriction near antiferromagnetic transition 8-88157
 CeAl₂, conf. Kondo system, sp. ht. meas. 8-52210
 CeAl₂, low temp. mag. behaviour, neutron diffr. 8-84395
 CeAl₂, mag. anisotropy, transition, crystal field splitting 8-52243
 CeAl₂, NMR, cryst. field effects and mag. order in low temp. phase 8-68391
 CeAl₂, sp. ht. in high mag. fields, Kondo effect 8-52284
 CeAl₃, anomalous resistivity maxima in metallic magnetic system 8-79977
 CeAl₃, singlet ground state at T=0, mag. ordering 2.5-6K 8-84388
 CeAl₃, valence mixed state, Kondo lattice, Anderson localisation models (*Japanese*) 8-51945
 Ce₃₀Au₂₀, amorphous, cryst. field effects and mag. interactions, magnetoconduction and transport props. meas. 8-68191
 Ce₂Co, absorpt. of D, heats of reaction and equil. press., T-getters for CTR 8-51683
 Ce₃Co, absorpt. of D, heats of reaction and equil. press., T-getters for CTR 8-51683
 CeCu₂Si₂, resistivity, thermal conductivity and thermopower between 1.5 and 300K 8-87963
 Ce₈Fe, absorpt. of D, heats of reaction and equil. press., T-getters for CTR 8-51683
 CeFe₄Al₈, mag. props. 8-52250
 CeGa₂, mag susceptibility, 1.5-300K and Neel temp. 8-68184
 Ce_{1-x}Gd_xRu₂, superconductivity and ferromagnetism coexistence, 60 mK-4.2K, spin echo NMR 8-84349
 Ce_{1-x}La_xAl₂, extraordinary Hall effects, 4.2-300K, cryst. field interaction 8-79980
 CeMn₂Si₂, cryst. and mag. struct. determ. 8-52225
 Ce₄Ni, absorpt. of D, heats of reaction and equil. press., T-getters for CTR 8-51683
 CePd₃-Gd, EPR of Gd³⁺ impurities in host with interconfig. fluctuations 8-56377
 Ce_{1-x}Pr_xAl₂, mixed mag. phase at low temp. 8-68228
 CeRh_{3-x}Pd_x, electronic and cryst. struct. comparison, catalytic behaviour 8-84398
 Ce_{1-x}Th_x, mixed valence systems, spin dynamics and mag. ordering 8-68162
 CeZn, mag. struct. and cryst. field effects 8-52223
 (Co, Cu, Fe)₂Ce, sintered permanent magnets, magnetic charact. 8-60608
 (Co,Cu,Fe)₂Ce, sintered, mag. props. 8-68302
 Co-Cu-Fe-Ce, mag. characteristics of sintered permanent magnets 8-60312
 Fe, cast, Ce hypoeutectic, new phase formation sequence during crystallisation, X-ray obs. (*Russian*) 8-95731
 (La,Ce)Al₂, conf. Kondo system, sp. ht. meas. 8-52210
 (La,Ce)Sn₃, dil. alloys, supercond. and normal state props. 8-76184
 LaAl₂-Ce, dil., linewidth of cryst. field excitations 8-67988
 Mg-Mn-Ce, MA8, dislocations at grain boundaries and grain-boundary glide 8-64605
 Y-Ce, Kondo syst m, spatial extent of Ce moment, neutron diffr. meas. 8-68159

cerium compounds

see also *cerium alloys*

- alkaline earth fluoride solid solns., MF₂-UF₄-CeF₃, surface degradation, complex admittance anal. 8-55980
 chalcogenides, low temp. thermal props. 8-84445
 halides and oxides, stability study, energy difference between trivalent and tetravalent Ce states 8-79553
 pnictides, low temp. thermal props. 8-84445

cerium compounds continued

- CaO-MgO-CeO₂, fired, phase equilibrium diagram, 1700 to 1200°C 8-92248
 Ce complex, Ce (III) 1,2-dioxy-3-sulphoanthraquinone, soln., absorpt. spectra (*Russian*) 8-76975
 CeAs, evidence for valence fluctuations, ⁷⁵As Knight shift data 8-91966
 CeB₆, single crystal growth for thermionic emission 8-92183
 Ce(CO₃)₂²⁺, in Na and guanidinium salts, struct./props. correlation (*French*) 8-95032
 CeCl₃(Br₃), interaction parameters, high freq. meas. of adiabatic differential susceptibility 8-68211
 Ce₂La_{1-x}F₃, paramag. mixed crystal, scattering of optical phonons by rare earth ions 8-68518
 Ce₆(MoO₄)₃(Mo₂O₇), X-ray examination crystal struct. 8-67687
 CeN, optical props. and valence mixture 8-56450
 Ce₂Ni₆P₁₇, synthesis and cryst. struct. 8-75634
 CeO, fabrication of Fresnel lens for thin-film waveguide 8-94452
 CeO₂, chemisorption of H₂, kinetics and characts. at different pressures and temps. 8-51821
 CeO₂, elec. cond. and dielectric props. at low temp. 8-72447
 CeO₂:Yb³⁺, ENDOR, evidence for covalency 8-80247
 CeO₂-Mo-CeO₂ thin-film selective coatings for solar energy collectors 8-94422
 CeO₂-Y₂O₃ film, surface characterisation, XPS, ESCA, and AES expts. 8-72028
 Ce₂O₃-S-Ga₂S₃, exam. of preparation and props. (*French*) 8-80504
 CeP₅O₁₄, photoemission spectra, 4f, 5p and 5s giant reson. enhancement 8-95660
 CeS, mag. props., sp. ht. and thermal expansion 8-60292
 Ce₂(SO₄)₃ soln., adiabatic and apparent molal compressibility determ. from US vel. meas. 8-63797
 CeSe, mag. props., sp. ht. and thermal expansion 8-60292
 CeTe, mag. props., sp. ht. and thermal expansion 8-60292
 SrF₂:CeF₃, absorpt. spectra of γ -irrad. cryst., 77K, 200-700 nm 8-84615

cermets

- effective bulk dielec. const., analytical props. 8-56414
 electrodeposition, effect of electrolyte in charge carried by suspended ceramic particle 8-68665
 small particle composite, optical properties from periodic multiple scatt. theory 8-56444
 Ag-SiO₂ film, elect. and struct. props., ion beam sputtering 8-80071
 Al₂O₃-Au cermet, optical constants, incl. proximity effects 8-56446
 Al₂O₃-W cermet, phase bonding 8-52745
 Au-dielectric cermets, optical constants, incl. proximity effects 8-56446
 Cr-SiO film, RF sputtered, substrate bias effect obs., on electrical resistivity 8-60573
 (Fe-Ni)_{1-x}(SiO)_x, cermet film, internal stresses (*Russian*) 8-75951
 KCl-Al composite, optical and IR reflectance 8-56465
 KCl-Al(Pd) composite, far IR absorption 8-56466
 Mg-MgF₂, sputtered films, opt. props. 8-80430
 Ni-Cr-MgO system, elec. resist. variation with comp. and prep. method 8-60637
 Pb₂Rh₂O₅, thick film, temp. coeff. of resist., cond. mech. 8-84315
 SiC, wetting by Cu-Ti and Cu-Sn-Ti melts 8-68664
 (Ti,V)C carbides, prep. and mech. props. 8-64518
 TiC-Mo₂C-Ni cermets, influence of anomalous phases on strength 8-92228
 TiC-Ni, reaction kinetics under simulated liq.-phase sintering 8-52746

cesium see *caesium*

CESR

- density matrix formalism for coupled dynamical systems 8-95522
 III-V semiconductors, optical detect. of CESR, giant Overhauser shifts 8-80251
 metal, CESR for arbitrary probability of scattering at surface (*Russian*) 8-68378
 metal, CESR line shape, strong surface relax. case (*Russian*) 8-56378
 metals, surface relax. time of conduction electron spins 8-91814
 rare earth alloys, cryst. field effect on EPR and NMR 8-56391
 semiconductor, conduction electron paramag. relax., Coulomb mechanism 8-88191
 semiconductor without inversion centre, conduction electrons spin relaxation (*Russian*) 8-52355
 AgCl: Cd²⁺, Pb²⁺, Br⁻, mechanism for photoinduced decomposition 8-80219
 Cu, surface spin-flip probability from TESR 8-91953
 n-InSb, effective g-value of electrons determ. by spin flip Raman scatt. and electric-dipole-excited ESR 8-52494
 Li/Sr(Cu) interface, CESR meas. 8-80218
 Pd, expts. using transmission technique 8-91954
 Si:P, ion implanted, resist. changes induced by ESR 8-68377

chalcogenide glasses

- AC conductivity, temp. dependence 8-72153
 chalcogenide lone-pair semicond. charged impurities, effect on carrier concs., Street-Mott model 8-67984
 electrical conductivity, percolation-controlled 8-72150
 electrical conductivity, press. effects 8-56142
 electron-hole recombination, mech. 8-72196
 layered acoustic waveguide, group delay time, temp. coeff. var. 8-83152
 luminescence centres, evidence for neutrality 8-88356
 optical grating direct writing using SEM 8-83121
 optimal polynomials in calcs. of complex glass's properties 8-68026
 photoconductivity, analysis 8-72197
 photoelastic properties, optimum glasses for acoustic delay lines and deflectors 8-55420
 point defect exam. by positron annihilation 8-72637
 quartz-chalcogenide glass IKS-25 system, mech. of contact interaction, mech. and optical props. 8-88375
 radiative emission during threshold ON-state 8-76119
 switches, relaxation processes in memory and threshold switches 8-60172
 thermopower in Anderson model 8-84241
 threshold switching mechanism in chalcogenide glass thin films, review 8-76122
 As-S system, glass forming ability and phase diagram 8-59760
 As-Se system glasses, point defects, positron lifetime spectra meas. 8-88380

chalcogenide glasses continued

- As₂(S,Se,Te)₃ glasses, Hall mobility composition depend. 8-68042
 As₂S₃, amorphous, electrodiffusion profile meas. of Ag migration 8-87822
 As₂S₃, amorphous film, photooxidation, substrate depend. 8-64866
 As₂S₃, amorphous thin films resonant Raman scattering 8-68505
 As₂S₃ glass, localised paramag. states, As₄S₆, As₄S₄ units, mol. analogue models 8-60087
 As₂S₃:Ag, amorphous US props. 8-51616
 As₂S₃-AsBr₃, glass, exam. of combination scatter spectra in IR 8-88315
 As₂S₃, thin film optical waveguide, for acoustooptic modulators 8-83051
 As₂S₃, Raman and IR spectra, struct. model 8-80330
 As₂S_{1-x} glass, Raman spectra, chem. struct. (Russian) 8-76469
 (As₂S₃)_{1-x}(AsI₃)_{1-x} glass, Raman spectra, chem. struct. (Russian) 8-76469
 As₂S₃(Se₃), thermal expansion at low temperatures 8-83982
 As₂S₃(Se₃), X-ray induced paramag. states and luminesc. 8-95520
 As₂Se₃, amorphous, electrophotographic props., photodecomp. effect 8-49918
 As₂Se₃, contact influence on AC cond. 8-76076
 As₂Se₃, glass, density of optically induced localised paramagnetic states 8-52354
 As₂Se₃, glassy, dielectric const. determ. 8-72449
 As₂Se₃, glassy, with adsorbed H₂O(NH₃)(NO₂)(O₂)(CO₂)(CO), surface cond., photocond. 8-80038
 As₂Se₃, neutrality of luminescence centres 8-88356
 As₂Se₃, struct. changes, Mn²⁺ EPR expts. 8-79534
 As₂Se₃:Ag, amorphous, US props. 8-51616
 As₂Se₃-InI₃, glass system, IR spectra 8-64365
 As₂Se₃-Ti₃Se (Ti₂Se₂) (Ti), glass, hot pressed, temp. dependence of optical absorption edge 8-88328
 As₆₀Se₄₀, amorphous films, spectral characts. of photodarkening 8-76494
 As₄Se₃Ge, glass, light irradi. induced changes in optical and elec. props. (Japanese) 8-68031
 As₄Se₃Ge, struct. changes, Mn²⁺ EPR expts. 8-79534
 As₄₀Se_{50-x}S_xGe₁₀ film strip-loaded waveguide formed in graded-index LiNbO₃ planar waveguide 8-74965
 AsSe_{1.5-x}Te_x glasses, physical props. 8-68028
 As₂Se₃Te_{3-x} chalcogenide glasses, cond. meas., field strength and temp. depend. 8-84225
 As₂Te₃+Ti_x, glassy system, composition depend. of activation energy, thermopower meas. 8-64052
 As₈Te_{100-x} glassy system, composition depend. of activation energy, thermopower meas. 8-64052
 AsTeCu_x (0≤x≤0.4) glass, effect of Cu on elec. cond. and thermoelectricity, 100 to 370K 8-87978
 As₄Te₃Ge(Si), struct. changes, Mn²⁺ EPR expts. 8-79534
 As₅₀Te₄₅I₅, glass, semicond., elec. switching, high press. effects 8-72212
 As₂Te_{3-x}Se_x, ¹²⁵Te Mossbauer expts., comparison of amorphous and cryst. samples 8-88232
 Cd-As-S, prod. and acoustooptic props. (Russian) 8-63158
 Cu-As-Se glasses, recording and erasure by laser beam (Russian) 8-71170
 Cu₄(As_{0.4}Se_{0.6})_{1.37} amorphous, ⁷⁷Se NMR, comp. depend. 8-76329
 Cu₁₀As₃Se₃₈O₂₁, chalcogenide glass, exam. of electron mechanism of photo induced changes 8-87998
 Ge-As-Te system, glasses, magnetochemical exam. 8-88092
 Ge-Se, elastic props. under press., US interferometry 8-79658
 Ge-Se, glassy, photoinduced photolum. fatigue (Russian) 8-60520
 Ge-Se glass system, effect of changes in local surrounding of atoms on optical props. (Russian) 8-80414
 GeS₂, thermal expansion at low temperatures 8-83982
 GeS₈ glass, activation energies after neutron irradiation, elec. cond. and transmission coeff. 8-83850
 GeSe amorphous films, photoconductivity measurements, recombination model 8-64061
 GeSe₂ film, glassy, self-controlled laser-beam chopping effect 8-60528
 Ge₂Se_{1-x} 0<x<0.2, crystallisation in amorphous bulk and thin films 8-55813
 Ge₄Se_{1-x} amorphous semicond., elec. props. 8-84219
 Ge₂Se_{1-y} glass, bulk and film, IR transmission and reflectivity meas., struct. mode assignments 8-79537
 α-Ge₂Se_{1-y} photoluminescence and fatigue effects 8-84648
 Te film, amorphous, evaporated and annealed, variable range hopping cond. 8-80077
 Hg-As-S, prod. and acoustooptic props. (Russian) 8-63158
 Hg-As-S modulating glasses, optical parameters and struct. (Russian) 8-63159
 In₂Se_{1-x}SnO₂ heterostructure, anomalous temp. depend. obs. on photo-voltage 8-56209
 P-As-Se glasses, mag. susceptibility, dielec. const., opt. props. 8-64184
 P-Se glass system, IR spectra 8-64365
 P-Se-Te system glasses, vitrification region 8-51425
 PbS-As₂S₃ glass, elastic props. temp. depend. 8-71780
 Sb₂Se₃-Se-SbSeI, exam. of glass formation, IR transmission spectra 8-88452
 Se-based, band gap variation 8-90461
 Se-Ge, lattice vibr. spectra, photostruct. change, far IR absorpt. 8-72494
 Se-S, glassy alloy, order-disorder transition kinetics 8-67650
 Si-As-Te glasses, crystallisation kinetics under influence of water vapour 8-59762
 Si-Te system, structural changes rel. to memory effect (Russian) 8-71679
 SnTe film, amorphous, evaporated and annealed, variable range hopping cond. 8-80077
 Te₈₀Ge_{12.5}Pb_{7.5} phase-separated system, overlapping effects of glass transition and crystn., DSC results 8-83739
 Ti₃SeAs₂Te₃, amorphous semicond., nuclear spin-lattice relaxation by localised electronic states, modification by spin diffusion 8-52372
 Zn-As-S, prod. and acoustooptic props. (Russian) 8-63158

change of state *see phase transformations***channel capacity**

- electrocuteaneous stimulation, energy threshold meas. and channel capacity estimation (Japanese) 8-53573
 multilevel pulsed phase modulation in optical links 8-78934

channeling *see channelling***channelling**

- see also energy loss of particles*
 atomic collisions in solids, book contrib. 8-75697
 Bloch wave channelling as electron diffr. 8-83860
 coherent Roentgen radiation prod. from channelled charged particles in a monocrystal (Russian) 8-92138
 curved crystal, charged particle channelling, EM radiation emission 8-75698
 diffraction of radiation from channelled charged particles 8-75699
 doping of channelled ion implantations, apparatus for spatial uniformity 8-51569
 electron channelling, induced radiation (Russian) 8-64425
 electron channelling band width, SEM study (Chinese) 8-91366
 electrons and positrons, quantum theory of spontaneous and stimulated emission (Russian) 8-49999
 energy loss of channelled ions, effect of screw dislocations 8-67761
 fast channelled particles with low charge, energy loss calcs. 8-55899
 metal, solute atom displacement in mixed dumbbell interstitials for FCC lattice 8-79631
 molecular-type states in fast-electron channelling 8-87731
 nuclear inelastic channel suppression, nuclear reson. and electronic scatt. of γ-quanta, hyperfine transitions 8-60361
 planar, α-particles, 1 to 5 MeV, stopping power of solids, effect of extended defects 8-51602
 radiation spectrum of relativistic channelled particles, theory 8-83859
 radiative damping effect for ultrarelativistic channelled particles 8-67758
 relativistic electrons, spontaneous EM emission in channel pot. 8-83848
 Rutherford scattering of fast electrons during channelling, temp. depend. (Russian) 8-83857
 SEM, electron channelling patterns 8-83697
 trajectory focusing of channelled ions, surface scatt. and surface struct. anal. 8-68594
 Al-Mn(Cu)(Ag), solute atom displacement in mixed dumbbell interstitials for FCC lattice 8-79631
 Be, oscillatory channelled ⁴He⁺ ion scatt. yield 8-52610
 CaF₂, overlaid with Au and CaF₂ films, channelling meas. 8-67762
 CsI, prep. 5-30 μ thick, preparation for channellography 8-80658
 Cu metastable alloy layers, Ag⁺ and Ta⁺ implanted, structure obs. by MeV He⁺ channelling 8-71709
 Cu-Be, solute atom displacement in mixed dumbbell interstitials for FCC lattice 8-79631
 GaAs(P), ion irradi. damage, strain effect contrib., channelling meas. 8-67752
 Ge, stopping power for fast channelled α-particles 8-79654
 KBr, 5-30 μ thick, preparation for channellography 8-80658
 KCl, radiation damaged, proton and ⁴He⁺ channelling, F-centre production, optical absorpt. meas. 8-79656
 LiF, radiation damaged, proton and ⁴He⁺ channelling, F-centre production, optical absorpt. meas. 8-79656
 NaCNaCl, 5-30 μ thick, preparation for channellography 8-80658
 NaCl, radiation damaged, proton and ⁴He⁺ channelling, F-centre production, optical absorpt. meas. 8-79656
 NaCl:Ti, luminesc. yield, effect of fast electron channelling 8-84646
 NaF, radiation damaged, proton and ⁴He⁺ channelling, F-centre production, optical absorpt. meas. 8-79656
 Ni, (110), surface relaxation and composition, medium energy ion scatt. spectra 8-63916
 (Pd_{0.2}Au_{0.2})D_{0.04}, lattice location of D, ion channelling obs. 8-67708
 Pt (111) and (100), surface struct. anal. by MeV ion backscatt. and channelling 8-71916
 Si, amorphous, Si implanted, substrate-orientation depend. of epitaxial regrowth rate, channelling effect meas. 8-79900
 Si, channelled and random proton stopping power, 30-1000 keV 8-67760
 Si, channelled-ion implantation of group III and group IV ions 8-75682
 Si detector, ionisation energy for channelled 160 MeV α-particles 8-62680
 Si, elec. activation of implanted As during low temp. anneal, channelling meas. 8-51571
 Si, implanted, dechannelling of MeV He ions by twinned regions 8-75700
 Si, ion irradi. damage, strain effect contrib., channelling meas. 8-67752
 Si, polycrystalline layer, laser-induced single cryst. transition, RHEED and backscatt. obs. 8-87704
 Si:B, implanted laser annealed samples, unidirectional contraction 8-71747
 TaD_{0.10}, lattice location of D, ion channelling obs. 8-67708
- characteristic temperature** *see Debye temperature*
- characteristics measurement**
see also headings for specific characteristics, e.g. gain measurement; viscosity measurement
 turbine blade arrays, turbulence characts. of stream, obs. 8-71319
- charcoal**
see also carbon
 activated charcoal with oxine, adsorption of ⁶⁰Co waste water 8-58365
 thermal conductivity meas. at room temp. 8-63889
- charge (electric)** *see electric charge*
- charge compensation**
see also crystallography
 plasma, streaming, in laser vac. diode, electron emission temp. 8-91162
 polyacetylene, n- and p-type doping, and compensation, p-n junction formation 8-76070
 semiconductor, compensated, solid-state inductance, theory and expt. 8-56138
 TGS, vacuum-cleaved cryst., charge compensation, ferroelec. field effect obs. 8-95556
 BaF₂:Er³⁺, single-site multiphonon and energy transfer relax. 8-52547
 CaF₂:Ce, Stark struct., phototransitions, g-factors 8-67995

charge compensation continued

- CaF₂:Gd³⁺-M⁺, (M=Li, Na, K, Rb, Cs, Ag), electric field effect expts., EPR line breadths, lattice distortions 8-80210
 CdS:Cd(In), Cu- or defect-compensated, optical ageing rel. to storage cond. 8-84247
 GaAs, dual implantation of C⁺ and Ga⁺, sheet resist. and Hall effect meas. 8-67728
 n-GaAs, melt-grown, stoichiometry, photolum. obs. 8-72583
 n-GaAs:Cu, contaminated single cryst., deep level photoluminesc. model 8-68554
 GaN:As(P), implanted single cryst. film, cathodolum. 8-60523
 n-Ge:Sb, fast neutron irradi. effects on donor conc., and annealing 8-56107
 n-Ge:Sb, γ -irrad. effects on donor conc. and compensation by acceptors 8-56106
 Ge:Sb, neutron irradi., carrier mobility theory and expt. 8-56166
 Ge:Sb,Cu, exactly compensated, impurity absorpt. and photocond. spectra 8-56189
 n-InP, Hall effect, 10-300K, thermal activation energy and influence of compensation 8-72171
 KBr, electron irradi. at 4K, role of V_k centres in equilib. among centres 8-67712
 Na₂HAsO₄·7H₂O:Cu²⁺, ESR, Cu lattice location 8-52342
 SiO₂:Na, film, depth profiling by SIMS 8-79624
 SnO₂, rare earth ion doped, luminesc. and charge compensation 8-76532
 V₂O₅-Fe₂O₃-Li₂O ternary system, charge compensation of Fe ions, Mossbauer obs. 8-52410
 YIG: Ca²⁺ epitaxial films, Fe⁴⁺ centres, MCD, optical absorpt., and thermoelectric power meas. 8-95595
 ZnSe:In, heavily doped, Hall effect and DC cond. expts., compensating acceptors 8-52013
 ZnSe:In, heavily doped, impurity band cond., Hall coeff. and cond. expts. 8-72147

charge-coupled device arrays *see charge-coupled device circuits***charge-coupled device circuits**

- body motion computer-aided tracking using CCD image sensor 8-61269
 control system for Si cryst. growth 8-68623
 ECG signal automatic evaluation using analogue circuits (*German*) 8-92717
 IR charge transfer device imaging arrays 8-77990
 IR image sensors, operation (*German*) 8-63190
 IR imagery, modelling and appl. of HgCdTe MIS struct. 8-80058
 multichannel photon counting image detector arrays 8-65970
 pattern recognition, transversal filter anal. 8-71052
 sleep EEG automatic K-complex detector 8-53557
 solid-state imaging devices, conference, San Diego (1977) 8-66944
 star pattern sensors for real time spacecraft attitude determination 8-96380
 star tracker, microprocessor controlled CCD, STELLAR design 8-53792

charge-coupled devices*see also charge-coupled device circuits*

- MOS structure, n-channel, evidence for impact ionised electron injection in substrate 8-88031

charge density waves

- chain conductors, CDW ordering 8-79731
 commensurability effects and collective excitations in systems with CDWs (*Russian*) 8-60074
 commensurate-incommensurate CDW phase transition in one-dimensional electron-phonon system 8-67959
 commulene type infinite chain cryst., energy bands, ab initio Hartree-Fock orbital calc. 8-60066
 electron gas, two-dimens., polarisability, many-body correction 8-60071
 electron gas instability in strong mag. field 8-79950
 electron-phonon scattering, effect on CDW phase transition 8-95265
 frictional force on drifting CDW 8-56123
 Ginzburg-Landau theory of weakly coupled metallic chains 8-60068
 hexagonal layers, lattice distortions, chem. bond model 8-79560
 isotropic metals, CDW, Fermi-surface instability 8-79947
 jellium, attenuation of collective excitations 8-84157
 layered compounds, effect of exchange on CDWs 8-60078
 lock-in and onset transitions of CDWs, triple point 8-67960
 many-electron system, Wigner cryst., electron chain and CDW in strong mag. fields 8-60067
 metal simple, CDW detection by angle-resolved photoemission 8-95658
 metallic chain, weakly coupled, Ginzburg-Landau theory 8-91626
 MOS, n-type inversion layers, two-valley model low temp. phase study, CDW coupling consts. 8-72275
 one-dimensional lattice, props. of commensurate CDW system 8-75796
 polyacetylene type infinite chain cryst., energy bands, ab initio Hartree-Fock orbital calc. 8-60066
 quasi one-dimensional conductor, phonon drag conductivity in Frohlich Peierls phase, effect of impurities 8-60114
 quasi-one-dimensional conductor, impurity effects, interchain interaction 8-72138
 quasi-one-dimensional conductors, review 8-60070
 quasi-one-dimensional electron systems, effect of interchain electron transfer on phase transition 8-51911
 quasi-one-dimensional system, Frohlich cond. in fluctuation region 8-84203
 rare earth compounds, valence mixed state, Kondo lattice, Anderson localisation models (*Japanese*) 8-51945
 TCNQ salt, acridizinium, one-dimens. cond., permittivity 25 to 60 GHz, 4.2K 8-88248
 TCNQ salt, quinolinium, one-dimens. cond., permittivity 25 to 60 GHz, 4.2K 8-88248
 TCNQ-HMTTF, struct. evidence of CDW 8-51912
 TTF_{0.97}Se_{0.03}-TCNQ, Peierls-superlattices and soft phonon anomalies, X-ray scatt. meas. 8-75795
 TTF(SCN)_{0.588}, Peierls instability, strain coupled charge density waves, X-ray scatt. obs. 8-79949
 TTF-TCNQ, collective-mode conductivity in metallic phase 8-64031
 TTF-TCNQ, Peierls-superlattices and soft phonon anomalies, X-ray scatt. meas. 8-75795
 TTF-TCNQ, struct. phase transitions, coupled phasons model 8-83942

charge density waves continued

- tunnelling of solitons and CDWs through impurities 8-51913
 two-dimensional layer, model, electron-correlated density-wave states 8-51919
 Wigner crystal, two-dimens., in strong mag. field, classical and quantum theory 8-79948
 Cr, spin density wave, CDW and strain wave, effect of spin polarisation of reservoir and imperfect nesting 8-56284
 Hg₃₋₈AsF₆, one-dimens. fluctuations and chain ordering transform., neutron scatt. calc. 8-59923
 Na₂VS₂(Se₂), mag. and elec. props. rel. to struct. transitions 8-91848
 NbSe₂, 2H polytype, effect of incipient CDW on second-order Raman spectra 8-80357
 NbSe₂ (2H), effect of CDW fluctuations on Raman active optic phonon freq. 8-87750
 NbSe₃, linear-chain metal, Hall effect meas. 8-76058
 NbSe₃, non-ohmic transport props. near phase transitions 8-72213
 NbSe₃, satellite electron diffr. below 59K, Fermi surface features 8-84136
 NbSe₂ (2H), effect of electron-phonon scattering on CDW phase transition 8-95265
 NbSe₂ (2H) microscopic theory of charge density wave instability 8-79732
 NbTe₂, CDW and accompanying periodic structural distortions 8-72094
 nbSe₂ (2H) single crystal, elec. resistivity, effect of hydrogen intercalation (*Russian*) 8-84338
 n-Si (111) MOS charge layer, optical spectrum of inter-subband transition 8-64133
 n-Si inversion layer, exchange instabilities 8-52052
 n-Si, inversion layers, many-valley electron-phonon interactions, piezoresistance, anisotropic cond., Shubnikov-de Haas oscillations 8-52096
 Si inversion layers, random pair attractive interaction model of carrier correl., compared with expt. 8-60212
 Si(III) inversion layers, CDW induced cyclotron reson. harmonics 8-64085
 TTF-TCNQ single crystal, nonlinear electronic transport, microwave harmonic mixing 8-91684
 TaS₂, 1T, anomalous magnetoresist., CDW state 8-72173
 TaS₂ (1T), CDW and accompanying periodic structural distortions 8-72094
 4Hb-TaS₂, Fermi surfaces and charge transfer 8-79926
 TaS₂, non-linear conduction in two-dimensional CDW 8-91685
 TaS₃, CDW state, Raman spectroscopy obs. 8-60439
 TaS_{2-x}Se_x, layer compound, Hall coeff., 4-200K 8-95305
 TaS₂(Se₂), 1T phase, CDWs, electronically driven phonon anomalies and phase transforms. 8-63834
 TaS₂(Se₂), 2H polytype, effect of incipient CDW on second-order Raman spectra 8-80357
 TaSe₂ (2H), CDW and accompanying periodic structural distortions 8-72094
 TaSe₂ (2H), domain-like incommensurate CDW and first order commensurate-incommensurate transitions 8-56084
 TaSe₂ (2H), effect of CDW fluctuations on Raman active optic phonon freq. 8-87750
 TaSe₂ (2H), softening of CDW excitation, at superstructure transition 8-79728
 TaSe₂(2H), effect of electron-phonon scattering on CDW phase transition 8-95265
 TiSe₂ (1T), structurally induced semimetal-to-semicond. transition, ab initio LCAO calc. 8-51896
 TiSe₂ (1T), lattice dynamics and phase transitions 8-79727
 TiSe₂, CDW and accompanying periodic structural distortions 8-72094
 TiSe₂, semimetallic behaviour band struct. from local-density functional approach 8-56070
 VSe₂ (1T), deform. modulated superstruct., electron diffr. expts. 8-51515
 VSe₂, CDW and accompanying periodic structural distortions 8-72094
 VSe₂, CDW states, intrinsic mag. props., mag. susceptibility and NMR obs. 8-68397
 VSe₂, press. depend. of CDW transitions, role of Coulomb correlations, elec. props. 8-87927
 V₃Si, anharmonic mode softening effects 8-79734

charge exchange

- for charge exchange in particle and nuclear physics see elementary particle interactions and nuclear reactions and scattering*
see also charge transfer states; ionisation
 N-acetylglucosamide, substrate-inhibitor of lysozyme, localisation of unpaired electrons 8-68992
 alkali atom+hexafluoride molecule, collisional ionisation 8-55226
 alkali atom+methane derivative, collisional ionisation, nitromethane, perfluoromethyl bromide (iodide) electron affinities 8-66639
 anthracene-dimethylpyromellite-imide, CT complex, reaction yield detect. double reson., delayed fluoresc. quenching (*Russian*) 8-88230
 aqueous soln., ion luminesc. quenching by electron transfer 8-76511
 atom+multiply charged ion, charge exchange 8-58813
 bacteriochlorophyll a, bacterial photosynthesis primary electron transfer processes, psec. dynamics 8-80841
 bacteriopheophytin, bacterial photosynthesis primary electron transfer processes, psec. dynamics 8-80841
 benzene, cation radical, charge exchange reagent appls. 8-70929
 carrier-molecule complexes, probability description of electron transport processes 8-53314
 9,10-diphenylanthracene, electrogenerated chemiluminescence, T₂ state emission 8-60524
 electrode-redox system electron transfer reacts. time-depend. perturbation theory 8-61027
 electron and exciton transfer rates, effect of nucl. degrees of freedom 8-60057
 F ions recoiling in gases, hyperfine interactions 8-74735
 fast ion+atom collisions, one electron charge transfer and capture 8-70931
 highly charged ions in neutral atoms 8-62913
 inert gas ion, in parent gas, transverse diffusion coeff., reson. charge exchange effects 8-63533
 interstellar ion-dust grain collisions, electron transfer 8-77591
 ion equilibrium negative charge state fractions 8-90288
 ion pair forming collisions, dynamics 8-66661
 ion-atom collision, radiative charge exchange, high energy 8-55234

charge exchange continued

ion-ion collisions, crossed beam expts. 8-58843
 ion-metal atom processes, charge exchange cross sections, calcs. and computer program 8-55236
 mesosphere, ion-neutral bunches charge exchange rel. to ion bunching 8-73424
 methane+N₂⁺(CO⁺), charge transfer cross-section, low energy 8-58791
 micellar system, photoinduced redox processes kinetics, intramolecular electron transfer 8-92603
 multiply charged heavy ions, charge exchange, and prod. method 8-58816
 nitronaphthylamines, ESCA and UV photoelectron spectra, assignments 8-50588
 octane-water interface, water photo-oxidation in presence of adsorbed porphyrins 8-64933
 oxide electrodes, electron transfer reactions, tunnelling through a space charge barrier 8-80050
 particle beam, flux control, charge exchange method (*Russian*) 8-70662
 photo-copiers, organic photoconductors, charge acceptance calc. 8-80020
 plasma, axially symmetric, Doppler broadened optical line emission interpretation model 8-75276
 plasma, ion drift velocity in EM fields, charge transfer effect 8-83527
 proteins, folded, models for H exchange 8-76981
 reactive and charge transfer collisions, between ions and molecules 8-62914
 ring current ions+geocoronal H, charge exchange rel. to low-latit. E-region ionisation 8-77415
 thionine-mono-haloaniline triplet exciplex, quenching position dependent heavy atom effect, intersystem crossing 8-53197
 trypsin inhibitor, soybean, folded, models for H exchange 8-76981
 two-level atomic collision system 8-62893
 ubiquinone-Fe complex, bacterial photosynthesis primary electron transfer processes, psec. dynamics 8-80841
 upper atmosphere H escape flux, charge exchange induced, diurnal and solar cycle vars. 8-93022
 Ag, population mechanism, highly-excited states, hollow cathode discharge (*Russian*) 8-63610
 Ar⁺, in Ar, transverse diffusion coeff., reson. charge exchange effects 8-63533
 Ar⁺+Ar, elastic scatt. and charge exchange, differential cross section, 2.7-20 eV 8-66660
 Ar⁺+Kr(Xe), thermal energy charge transfer reaction rates, mass spectrometric obs. 8-61000
 Ar⁺+N₂, energy transfer, vibronic excitation, emission spectra 8-66578
 Ar²⁺+He(Ne)(Ar)(Kr), electron transfer cross-section, <100 eV 8-66654
 Ar²⁺+Kr(Xe), thermal energy charge transfer reaction rates, mass spectrometric obs. 8-61000
 Ar³⁺+He, electron transfer cross-section, <100 eV 8-66654
 CH₄⁺+CH₄(CH₂D₂), dissoci. charge transfer reactions, H and D atoms elimination 8-85141
 CO+H₂⁺(He⁺), dissoci. charge transfer, energy transfer processes 8-74759
 CO⁺+CO (methane), charge transfer cross-section, low energy 8-58791
¹³CO⁺+CO, charge-exchange detection of ¹³CO⁺ electronic absorption spectrum, hyperfine consts. calc. 8-70822
 C⁺+Ar(H₂)(N₂)(CO)(CO₂)(O₂), charge transfer cross-sections, 0.7-2.4 keV, C⁺(P) and C⁺(⁴P) 8-58806
 Ce-Co, liq., charge transfer effect 8-94967
 Ce-Cu, liq., charge transfer effect 8-94967
 Cl⁻, far UV spectra in solns. 8-94208
 Cs₁-Au₁, liq., metal-nonmetal transition, electronic theory 8-79930
 Cu, population mechanism, highly-excited states, hollow cathode discharge (*Russian*) 8-63610
 D+M→D⁺+M⁺ (M=alkali metal atom), ion-pair form. 8-58779
 D₃⁺+inert gas, ion decay, 1-40 eV (*Russian*) 8-90286
 FeAl B2 struct., band struct. and density of states, KKR calc. 8-63969
 H, change in spectral line intensity of multiply charged ions (*Russian*) 8-58814
 H-like atom+bare ion, electron capture to continuum, cross-section cusp 8-90289
 H-like ions, electron impact excitation to S states exchange effects 8-58835
 H+He(N₂), stripping cross-section, 0.3 to 3 keV 8-78807
 H+O⁺, in upper atm., rel. to H⁺ loss during solar cycle 8-93021
 H+positron, charge exchange, excited positronium states form. 8-58873
 H⁺+Cs, elastic and charge exchange collisions, projected valence bond method 8-78804
 H⁺+D→H+D⁺ near threshold rel. to HD molecule formation in interstellar medium 8-89239
 H⁺+H, charge transfer cross section calc., up to 100 keV 8-55235
 H⁺+H(D), elastic scatt. and charge exchange, resonances 8-78777
 H⁺+H(O), in upper atm., rel. to H⁺ loss during solar cycle 8-93021
 H⁺+H(1s), radiative charge exchange, 1-50 MeV 8-55234
 H⁺+He⁺, charge transfer and ionis. cross sections, coincidence meas. 8-50634
 H⁺+He(Ar) electron transfer cross sections 8-58809
 H⁺+inert gas, 4s-state electron capture cross-section meas. 8-82836
 H⁺+O₂, energy transfer, vibronic excitation, emission spectra 8-66578
 H₂⁺+Ar(He)(H₂), 10 keV dissoci. charge exchange collisions 8-94319
 H₃⁺+Ar(H₂)(air), dissoci., 400-800 keV, product charge state distrib. model 8-82838
 H(D)+Cs, 40 keV, prod. of polarised H⁻ or D⁻ ions, low emittance 8-55078
 HNC⁺, radical cation, charge exchange mass spectrometry, HNC⁺ ion recombination and ionisation pot. 8-76838
 He (2³P)+Ca(Sr), collisional quenching of metastable states, excitation transfer cross sections 8-66653
 He⁺, electron impact excitation to S states exchange effects 8-58835
 He+He⁺, resonant charge transfer cross sections, 2 to 100 eV 8-66655
 He⁺+acetylene-d₀(-d₂), CH⁺(CD⁺), A-X luminesc., in near-thermal charge exchange 8-50632

charge exchange continued

He⁺+Ar, charge transfer cross section, kinetic energy dependence in low energy region (*Japanese*) 8-90100
 He⁺+Ar, low energy charge transfer collisions, kinetic energy depend. 8-86947
 He⁺+H₂, charge transfer at 1.5 and 3 keV, He(³P) excitation 8-66658
 He⁺+He, 2¹P level, direct and charge-exchange excitation, 150-1000 keV 8-70913
 He⁺+He, elastic scatt. and charge exchange, differential cross-section, 0.4-30 eV 8-66659
 He⁺+N₂, charge exchange, time-resolved emission probe 8-86946
 He⁺+Pb, at. beam and surface interaction, scatt. ion yield oscils. 8-55221
 He²⁺+H₂→He⁺H⁺+H⁺, two-electron capture 8-58811
 He²⁺+He, 5 to 100 keV, elastic and double charge exchange, mol. treatment 8-82813
 He²⁺+N₂, 200-600 eV, 0-20°, comparison with He²⁺+Ne(Ar) 8-74732
 He²⁺+Ne(He), electron transfer cross-section, <100 eV 8-66654
 He₂⁺, rate coeffs. for bimol. and termol. ion-mol. reactions 8-53188
 He₂⁺+O₂ charge exchange laser 8-50759
 Kr²⁺+Kr, symm. reson. double charge transfer, 0.04-20 eV 8-66657
 Li⁺+Na, charge transfer and elastic scatt., two state model 8-58805
 Li_{1-x}Pb_x, liq., metal-nonmetal transition, electronic theory 8-79930
 Mg+He⁺(He₂⁺), inelastic collisions, 2-800 eV, excited state form. 8-94312
 N⁻, form., by double electron transfer, cross-section meas. 8-78806
 N²⁺+He, electron transfer cross-section, <100 eV 8-66654
 N₂⁺+methane, charge transfer cross-section, low energy 8-58791
 NH₄F, electron distribution and charge transfer in NH₄⁺ ion 8-91291
 Ne⁺+Kr(Xe), thermal energy charge transfer reaction rates, mass spectrometric obs. 8-61000
 Ne⁺+N₂, charge exchange, time-resolved emission probe 8-86946
 Ne²⁺+He(Ne)(Ar), electron transfer cross-section, <100 eV 8-66654
 Ne₂⁺+Kr(Xe), thermal energy charge transfer reaction rates, mass spectrometric obs. 8-61000
 O²⁺+He, electron transfer cross-section, <100 eV 8-66654
 O₂⁺, symmetric charge transfer reactions, selected states, photo-ion, electron coincidence 8-73028
 O⁺(²D)+N₂, charge exchange rate coefficient, effect of N₂⁺ recomb. on aeromonic determ. 8-88954
 O⁺(⁴S)(²D)+Ar(H₂)(N₂)(O₂)(CO)(NO)(CO₂), charge transfer reactions, cross-sections meas. 8-92462
¹⁶O³⁺+Al, energy-loss straggling, charge exchange effects 8-58799
 SF₆, equilib. electron-transfer reactions in gas phase involving long-lived neg. ion radicals 8-58807
 Th+X⁺, X=O, N, N₂, CO₂, charge transfer cross-section, 1-500 eV 8-82835
 TiC, TiN and VC, charge distrib. and bond ionicity 8-63961
 U ion beam prod. at 50 keV by charge exchange in gas and metal vapour targets 8-70675
 U+X⁺, X=O, N, N₂, CO₂, charge transfer cross-section, 1-500 eV 8-82835
 U³⁶⁺+N(Ne)(Ar)(Kr), radiative charge exchange, 16, 64, 256 MeV/amu 8-55234
 Uf₆ on C-coated Pt(Pt-W), mol. negative surface ionisation 8-56913
 VC, TiC and TiN, charge distrib. and bond ionicity 8-63961
 Xe²⁺+Xe, symm. reson. double charge transfer, 0.04-20 eV 8-66657
 Xe⁺(²P)+Ca(Sr), collisional quenching of metastable states, excitation transfer cross sections 8-66653

charge measurement

see also electrometers

aerosols, meas. via variable freq. electrostatic mobility analyser 8-77945
 electron beam charge monitor, single pulse toroidal coil type 8-78036
 nucleonic dual charge sensitive preamplifier 8-55110
 plasma density IF phase meas. using three-mirror interferometer 8-75414
 polymer foil, charge distrib. determ., thermal pulse technique, meas. accuracy 8-80287
 surface charge measurement by electrostatic induction 8-49807

charge-ordered states

narrow partially filled S-band, charge ordering (*Russian*) 8-76015
 nonconducting linear chain systems, 3D Coulomb coupling and charge ordering 8-60075
 (Ti_{1-x}V_x)₄O₇, mag. susceptibility calcs. 8-91850

charge storage diodes

dual dielectric charge storage cells, writing and erasing, differential studies 8-80059
 laser diode 1ns pseudo-random pulse modulation cct. 8-50836

charge transfer see charge exchange

charge transfer states

A15 compound trends, self consistent band calcs. 8-79925
 alkylammonium iodides, solns., MCD spectra of iodide ions 8-94268
 anthracene:cylohexadienyl type radicals, charge transfer reactions 8-52535
 anthracene-d₁₀-s-tetracyanobenzene, rotational mode coupling in phase transition 8-71827
 anthracene-pyromellitic dianhydride, cryst., charge transfer exciton transitions, refl. spectra obs. 8-72540
 anthracene-tetracyanobenzene, magnetic resonant modulation of photoconductivity 8-64062
 benzene-Br₂ charge transfer complex, Raman spectra, bending modes, electronic excited states 8-56485
 benzene-I₂, binary soln., charge transfer spectrum 8-90183
 chlorides, I⁻ or Br⁻ doped, optical investigation of atomic hydrogen centres 8-88351
 chloroaluminium phthalocyanine, sublimed layer, IR absorption, vibr. assignments 8-55174
 chymotrypsin, charge relay system, H-bond models, IR spectra 8-64935
 copper phthalocyanine, polycryst. film, charge transfer state and optical spectra (*Russian*) 8-84607
 diamagnetic susceptibility, interatomic charge transfer in diatoms, mol. second moments, additivity formulas 8-70961
 p-dichlorobenzene, charge transfer complexes, NQR shifts 8-55186
 electron and exciton transfer rates, effect of nucl. degrees of freedom 8-60057

charge transfer states continued

- EPR conversion-rate meas., charge transfer band identification 8-76297
 excited charge transfer systems, in polar solvents, dynamic behaviour obs. 8-58772
 impurity centre-external elec. field interaction, charge transfer processes influence 8-87944
 inter-electron repulsion integrals for three open shell configurations in cubic symmetry 8-90061
 ion equilibrium negative charge state fractions 8-90288
 mixed donor-acceptor stacks, mag. gap and partial charge transfer, VB calc. 8-76008
 mixed valence system, far IR intervalence tunnelling transition, vibronic coupling model 8-58646
 molecular charge transfer complexes, mol. and cryst. struct. 8-62942
 molecular crystal, Frenkel excitons, effect on charge carrier transfer 8-79936
 quartz, rose, charge transfer mechanism for origin of colour, EPR and optical expts. 8-52537
 TCNQ-NMP, nucl. relax. and spin dynamics 8-52370
 tetracyanoethylene-benzene(-toluene), and isotopic forms, excited charge-transfer state nonrad. decay, vibr. role 8-82765
 TNF-carbazolyl compound charge transfer complexes, equilib. consts. 8-64877
 vanadyl phthalocyanine, sublimed layer, IR absorption, vibr. assignments 8-55174
 BaO-B₂O₃-SiO₂:Ti³⁺, optical absorpt. spectra 8-72564
 CdBr₂:Fe²⁺(Co²⁺)(Ni²⁺), charge transfer near UV spectra, 4.2K, mag. circular dichroism 8-80378
 CdCl₂:Fe²⁺(Co²⁺)(Ni²⁺), charge transfer near UV spectra, 4.2K 8-80378
 Co_{49.6}Al_{50.4}, Compton scatt., 59.54 keV γ -rays, charge transfer study 8-68578
 Co_{1-y}Fe_{2+y}O₄, role of vacant and chemisorbed O and charge transfer effect 8-79868
 Cs alloys, charge transfer insulators, mechanism, resistivity 8-80070
 Fe_{40.7}Al_{59.3}, Compton scatt., 59.54 keV γ -rays, charge transfer study 8-68578
 Ga complex, photoluminesc. spectra, $\pi \rightarrow \pi^*$ and charge transfer L \rightarrow M transitions, Stokes shift 8-64407
 H_n⁺ (n=3,5,7,9,11), stability, struct., ab initio MO calcs. 8-74810
 In complex, photoluminesc. spectra, $\pi \rightarrow \pi^*$ and charge transfer L \rightarrow M transitions, Stokes shift 8-64407
 IrF₆, in mixed crystals, Jahn-Teller effect, $\Gamma_{8g}(t_{2g})^3$ state, 6800 Å 8-76032
 KCN, ionic mol. cryst., exciton struct. 8-79935
 LaCoO₃, structural phase transition involving changes in spin and valency 8-79765
 LuPO₄:Yb³⁺, charge transfer type luminesc. 8-64392
 PbI₂ intercalated with organic mols., energy band splitting (*Russian*) 8-76027
 PdBr₂(H₂O)_{4-n}²⁻ⁿ, electronic absorpt. spectra, band assignments 8-50553
 PdCl₂(H₂O)_{4-n}²⁻ⁿ, electronic absorpt. spectra, band assignments 8-50553
 PtCl₂(H₂O)_{4-n}²⁻ⁿ, electronic absorpt. spectra, band assignments 8-50553
 TTF-TCNQ, transport props. of dynamically disordered chains 8-72137
 4Hb-TaS₂, Fermi surfaces and charge density waves 8-79926
 TaS₂ intercalated with NH₃, charge transfer, PAC meas. 8-76366
 UF₆, neat and mixed cryst. emission spectra, lowest charge transfer state, Jahn-Teller effect 8-67992
 Xe-MF₆, M=W, Mo, U, Re, Ir, charge transfer interactions, VUV and IR obs. 8-50664
 YPO₄:Yb³⁺, charge transfer type luminesc. 8-64392
 ZnO, surface charge transfer in presence of photosensitising dyes 8-68049
 ZnO, surfaces, charge transfer in presence of photosensitising dyes, photovoltage spectra 8-72193

charge transfer transitions see *charge transfer states*

charged dislocations see *dislocation dipoles*

charm particles

see also *D mesons; psi mesons*

- asymptotic freedom and charmonium 8-54534
 baryon semi-leptonic decay and quark effective masses, SU₄ symmetry 8-58185
 baryons, dipole mag. moments, new U₃ scheme using u, d, c quarks 8-58165
 baryons, inclusive yields of \bar{p} and λ as function of energy 8-78199
 baryons, magnetic moments by SU₃ and SU₄ symmetry 8-82209
 baryons, nonleptonic decays 8-66118
 charm quark prod., scaling violation as threshold effect 8-66088
 charmonium, ¹P₁ state, mass, branching ratios, decay rates 8-62370
 charmonium, rel. to gluons, quantum chromodynamics theory 8-62362
 charmonium, review of exptl. results and theoretical advances (*German*) 8-66184
 charmonium and QCD, review 8-82157
 charmonium model of ψ family 8-78143
 charmonium narrow states, hadronic and EM decays 8-70343
 charmonium photoprod., gluon-exchange model 8-74214
 charmonium potential, variation-iteration principle 8-54227
 charmonium singlet state, possible resolution 8-74225
 charmonium spectrum, relativistic and nonrelativistic theory 8-50010
 charmonium state decay, nonrelativistic and relativistic theory 8-58221
 charmonium states, multimesonic decays, statistical quark model 8-82171
 D and F charmed meson decay and evidence for (ts), current 8-58167
 dilepton and trilepton production in neutrino experiments (*Polish*) 8-89704
 discoveries during 1974-7, and associated theory (*Czech*) 8-86103
 EM properties of charmed hadrons, SU₄×U_c calcs., mag. moments, mass differences 8-70368
 fragmentation function for charmed quarks from $\mu^+\mu^-$ and μ^-e^+ event data 8-62355
 Gargamelle, neutrino physics history, theory and expt. 8-50027
 gluon fusion model, hadronic charm prod. 8-66081
 hadron production and decay, book contrib. 8-82208

charm particles continued

- hadronic charm prod. cross section and particle lifetimes, Monte Carlo anal. 8-89679
 hadronic multiparticle reactions, models, prod. of strangeness, baryon number, charm 8-74286
 high-energy (>10 GeV) neutrino physics, review of development, book contrib. 8-82201
 history of search for fundamental constituents of matter (*Polish*) 8-54588
 inclusive semileptonic decay, struct. functions, scaling limits 8-82165
 inverted charmed meson multiplets as a test for scalar quark confinement 8-70325
 mass spectra, SU(4) and SU(3)×SU(3)' theories comparison (*Chinese*) 8-82127
 masses of new mesons and effects of the fifth flavour 8-66098
 mesons, dynamic SU(4,1) symmetry, mass spectra, anal. (*Russian*) 8-70350
 multiparticle decay theoretical models for heavy hadrons containing charmed quarks 8-70344
 parity-violating amplitude of charmed-baryon nonleptonic decays 8-62398
 photoproduction processes of charm particles with charm nonconservation (*Russian*) 8-74201
 QCD, charm contrib. to electroprod. struct. functions 8-58170
 QCD, charm photoprod., ψ , D, F etc. prod., sum rules, cross sections 8-58169
 QCD, two-dimens. extrapolation to four-dimens. 8-78081
 QCD estimates for associated charm production by weak neutral currents 8-78169
 QCD quark-gluon plasma, hadronic prod. of leptons, photons charm and ψ 8-89669
 quark fusion model, strange and charmed quark numbers, vector meson description 8-58158
 quark line rule, generalised, SU₄ symm. scheme, reaction of hadrons containing charm quarks 8-54614
 quark-antiquark pot., charmonium model modifications, spin forces and instantons 8-93842
 scaling, nonrelativistic Schrodinger eqn. charmonium 8-54613
 semileptonic decay, effective chiral Lagrangian method 8-74254
 semilocal duality constraints for mesons, on-shell particles, masses, couplings 8-58174
 stable charmed hyperfragments containing charmed baryon+nucleons, binding energies, lifetimes 8-89815
 SU(4,1) hadron dynamical symm. anal., charmed 1/2⁺ baryon and 0⁻ meson mass (*Russian*) 8-74237
 SU(4) symmetric 20-plet representation of charmed baryons, mass, EM splitting 8-54615
 SU(4) symmetry breaking pattern and baryon masses 8-89690
 tensor force effects on ψ family in charmonium model 8-89675
 C \rightarrow $\Lambda(K^0)$ +hadrons, charm prod. cross section, new particle search (*Russian*) 8-89711
 cc bound states, e⁺e⁻ decay processes, relativistic harmonic oscillator model 8-62393
 $\chi(3,45)$, γ -transitions in charmonium system 8-78138
 χ particles, radiative decay widths calc., broken SU(4) model 8-62395
 D⁺-D⁰, D⁺-D⁰ mass differences using modified nonrelativistic Schrodinger eqn. 8-58186
 e⁺e⁻ annihilation, anomalous lepton prod., charmed mesons and heavy leptons 8-66134
 e⁺e⁻ annihilation, resonance decays above charm prod. threshold, single channel dominance 8-66133
 e⁺e⁻ inclusive electron prod., in multiprong events, charmed particle decay 8-66136
 η_c , predictions of existence by extrapolation methods 8-93863
 $\eta_c \rightarrow \gamma + \text{anything}$, OZI rule violating decay in QCD 8-89709
 η_c mass determ. from QCD sum rules 8-74223
 η_c mass from dispersion sum rules in QCD, identification with $\chi(2,83)$ (*Russian*) 8-89681
 F, F*, Schwinger phenomenological and dyon description 8-82109
 F, search in e⁺e⁻ annihilation, preliminary results 8-78199
 F(0⁻), F*(1⁻), charmed strange mesons, weak decays 8-74249
 F and F* from e⁺e⁻ annihilation 8-78198
 F mesons, semileptonic decay const., D and F decay const. ratio determ. 8-62392
 F-meson masses and leptonic decay consts. 8-66087
 F $\rightarrow \tau \bar{\nu}_\tau$, charmed mesons, heavy lepton decays, ν_τ neutrino mass depend. (*Russian*) 8-62394
 F $\rightarrow \pi^+e^+e^-$, enhancement due to π^+ EM form factor, generalised PCAC applicability 8-82164
 F* meson and anomalous $e\mu$ events 8-66108
 $\gamma\bar{p}$ total cross sections, 18 to 185 GeV, charm-anticharm contrib. 8-54635
 $\gamma\bar{p}$ at threshold, source of charm production 8-70379
 $\nu(\bar{\nu})N$, high energy dimuon prod., consistency with charm particle prod. 8-89697
 $\bar{\nu}N$, ratio of μ^+e^- events to μ^+ events, charmed particle prod. model 8-89702
 νN tetramuon prod. sources, heavy quark and lepton cascades, charm prod. 8-70356
 pp, prompt lepton emission, 53 GeV, e/π ratio, charm particle total inclusive cross section 8-93914
 pp, prompt μ and $\mu\mu$ prod. 400 GeV, possible charm prod. 8-89750
 pp $\rightarrow e^+\mu^++X$, charmed meson pair semileptonic decay, inclusive charm prod. cross section 8-89759
 ψ to charm particles, 1975 and 1976, e⁺e⁻ colliding beam technique (*Polish*) 8-74297
 $\psi/\psi\pi\pi$, charm model 8-74250
 Y(9.54) and broken SU₃ in nonstrange quark sector, vector mesons 8-58166
 X(2.82), γ -transitions in charmonium system 8-78138

charring see *combustion*

Chebyshev approximation

- B-splines basis, Galerkin method for soln. of one-dimens. primitive eqns. 8-49650
 circular disc, stress intensity factors and crack energy 8-79260
 cracks, curvilinear, star-shaped array in infinite isotropic elastic medium 8-55609
 plate, elastic, under uniform twisting, periodic collinear cracks (*Japanese*) 8-67097

Chebyshev approximation continued

- polynomial method for computing analytic solns. to eigenvalue problems, appl. to anharmonic oscillator 8-62058
- polynomials, appl. of method of double application 8-81843
- shifted Chebyshev polynomials, soln. of second kind operation eqns., convergence 8-62059

chelates see coordination complexes**chemical analysis**

- see also *chemical analysis by nuclear reactions and scattering; chromatography; electrochemical analysis; electron probe analysis; ion microanalysis; mass spectroscopic chemical analysis; polarimetry; pollution detection and control; radioactive chemical analysis; spectrochemical analysis; thermal analysis; X-ray chemical analysis*
- aerosol S compounds, techniques for chem. comp. determ. 8-95976
- air pollution measurement, particulates and gaseous pollutants anal. and calibration techniques 8-69531
- alloys, local composition determ., assessment of TEM direct lattice imaging technique 8-53294
- alloys, surface segregation, atom-probe FIM quantification investig. 8-62263
- analyser design impact of microprocessors (*German*) 8-61096
- anodic film, automated interpretation of ellipsometer obs. 8-56902
- arteriovenous O₂ difference, noninvasive meas. method (*German*) 8-85441
- atmosphere, NO/NO₂/O₃ monitors intercalibration 8-69529
- atmosphere, non-methane hydrocarbons monitoring via photoionisation 8-73549
- atmosphere high acidity analysers, comparative tests near industrial installations in Fos-Etang de Berre region 8-81464
- atmospheric aerosol, N.Z.Z. 8-85645
- atmospheric aerosols, chemical characterisation, progress and problems 8-68969
- atmospheric particulates, chemical characterisation via light scatt. method 8-69533
- automated rapid system for anal. of dissolved organic N in natural waters 8-93014
- automatic gas/gaseous mixture thermal cond. analyser (*Spanish*) 8-76972
- automatic system using microwave heating device 8-88666
- biological samples, trace metals determ., microwave oven-based wet digestion technique 8-92542
- blood gas analysers, review 8-69238
- bone mineral concentration estimation by beta-ray backscatt. (*German*) 8-69179
- bytownite megacrysts., study of trapped basaltic melts, petrogenetic process study 8-95688
- CO dose meter for working places exposed to extreme peaks of CO contamination 8-81096
- coal, mag. and Mossbauer characterisation 8-64903
- composition variation determ. using electrolyte electroreflectance 8-80809
- concentration meas. by portable optoelectronic convertor 8-80820
- depth profiles, ion scatt. technique, digital data collection 8-56942
- electron microscopy techniques, review, 1976-77 8-82077
- ellipsometry of electrochem. surface layers 8-56874
- experimental data interpretation 8-77827
- fission reactor spent fuel γ -ray spectrometry and chemical analysis 8-54841
- gas analyser, portable, 1920 to 1978 development 8-61124
- gases, moisture content determ. using photocolormeter 8-56936
- gases, thermophysical props. tabulated for mixture composition certification 8-80818
- glass surfaces, corrosion, passivation and anal. 8-60854
- halofluorocarbons, in ambient air, background levels in situ quantification 8-69530
- heavy metals, in aquatic systems, distrib. and speciation techniques 8-69390
- high freq. induction melting and centrifugal casting, working curve sample prep. photoemission anal. (*Japanese*) 8-53050
- industrial flare flames, smoke detection and control by electric fields 8-81360
- inorganic micro and trace analysis, historical perspectives 8-81784
- instrument use and planned acquisitions 8-88684
- intravascular O₂ saturation continuous meas. using fibre optic catheter (*German*) 8-85411
- kinetic aspects, review 1975-1977 8-85216
- light element chemistry of Apollo 12 site regolith samples 8-65515
- lung gas analysis using redox gas sensors (*German*) 8-85440
- magnetic susceptibility applications, review of literature 1975-1977 8-82006
- marine atmosphere, SO₂ meas. at concs. lower than ppb 8-81340
- medicine, paramag. O₂ analyser, for teaching 8-49622
- metal, microdetermination of C, purification of O₂ and flux selection (*Japanese*) 8-92571
- microchemical techniques, conf., Davos, Switzerland, (May 1977) 8-85254
- microchemistry, history (*German*) 8-81785
- microcomputer system for automating analytical instrumentation 8-73127
- microcomputer-based digital titrator 8-80805
- microscopy applications, review of literature 1976-1977 8-85221
- minicomputer appls., errors 8-92543
- monitoring laboratory, installation 8-61123
- multi-purpose instrument for biochemical and related undergraduate studies 8-73816
- nuclear fuel reprocessing, input analysis, verification (*German*) 8-70623
- organic compounds, trace analysis 8-85255
- oxides, stoichiometry meas. and control 8-51694
- pollution control, polarisation and interference microscopy appls. 8-61544
- polyethylene terephthalate fibres, high freq. US effects on physical and chem. structs. (*Polish*) 8-51446
- ponderomatic meas. for fluid detection in chem. anal. 8-68953
- preconcentration in inorganic trace analysis 8-85256
- radiation chemistry instrumentation, in Inst. Nuclear Res., Warsaw 8-76888
- schorl tourmaline, elastic const. 8-68718
- SEM, automation, quant. anal. of elementary images (*French*) 8-78045

chemical analysis continued

- silica gel, skeletal struct. modification with alcohols and water vap., thermal analysis obs. 8-88659
- standard gas mixture preparation at high pressures certification 8-93718
- static methods for certifying composition of binary gas mixtures 8-76961
- steel, Mn-Cr-V, structural changes during solution annealing (*Czech*) 8-84864
- stopped-flow systems, automated, for fast react. rate anal. methods, review 8-95971
- sulphate aerosol, individual submicron particles detect. technique 8-69527
- superalloys, phase extraction, chemical and X-ray diffr. anal. 8-72951
- surface analysis, review of AES technique and applications 8-68946
- surface analysis, review of ion scattering spectroscopy 8-68948
- surface analytical instruments, present status (*Japanese*) 8-80823
- teaching, problems 8-81736
- thin film structures, chemical anal. by Auger spectroscopy (*Russian*) 8-92581
- tissue-equivalent plastic A-150, density and composition uniformity 8-73252
- trace analysis, state and development (*German*) 8-68956
- trace element analysis, pH adjustment by gaseous reagents 8-73094
- transition metal disilicides, powdered, determ. of free metals, oxides, photometric method 8-61101
- ultra high vacuum technology developments (*Japanese*) 8-49845
- urban plume particulates collected on Anderson 8-stage impactor stages, chemical anal. 8-69433
- user-oriented software Fourier spectrum display 8-64896
- vapour dynamic diffusion batcher with porous partition 8-79404
- wear debris anal., quantitative methods 8-64912
- Al saponite, differential thermal anal., IR absorpt. spectra, chlorite-like mineral 8-88816
- As determ. in ores of reduced heteropoly acids, photometric method 8-61103
- C, surface groups, acidimetry, formation of derivatives 8-68918
- CO₂ expiratory concentration analysis by computer 8-57106
- CaO-Al₂O₃, molten binary slag, dissolved C study (*Japanese*) 8-60662
- Cd, determ. in sea and fresh waters, interlaboratory comparison 8-81209
- Ce, photometric determ. in cast Fe and steel (*German*) 8-68955
- Cr (III), (VI), determ. in industrial wastes 8-61105
- Fe, dissolved organic, determ. in seawater 8-81208
- Fe III, high-spin, in cancer, EPR 8-53466
- α -Fe₂O₃, analysis of car exhaust by Mossbauer spectroscopy 8-92963
- GaAs_{1-x}P_x, heterogeneous struct. obs. by anodisation-electrorefl. technique 8-84088
- GaAs_{1-x}P_x:Zn, diffusion profile determ., ³²P/⁶⁵Zn double tracer technique 8-55888
- GaP:Zn, diffusion profile determ., ³²P/⁶⁵Zn double tracer technique 8-55888
- HCl gas in ambient air, detection using coated piezoelec. quartz cryst. 8-92532
- H₂S in air, precon., determ. by flame photometric detection 8-92535
- He in breath, determ. using acoustic analyser, for closing vol. meas. 8-61223
- Hg determ. in sea and fresh waters, interlaboratory comparison 8-81209
- Hg-vapour gas analysers testing using Zarzma equipment 8-76962
- K₂Pt(C₂O₄)₂.nH₂O, chem. analysis and elec. cond. meas. 8-76060
- Mn (III), determ. in industrial wastes 8-61105
- NO, calibration standards, generated by gas phase titration 8-69507
- NO₂, calibration standards, generated by gas phase titration 8-69507
- α -NaFe₂O₃:Mg²⁺(Co²⁺)(Zn²⁺), substitution of Fe²⁺ (*French*) 8-95034
- O₂ analyser instrumentation and operation 8-69237
- O₃, calibration standards, generated by gas phase titration 8-69507
- O₂(¹ Δ) content determ. in chemical generator gaseous effluents, ratiometric system 8-76970
- P determ. in ores of reduced heteropoly acids, photometric method 8-61103
- PZT ceramics, PbO content estimation using analytical procedure (*German*) 8-53279
- Pb, determ. in blood, haematofluorometric method 8-53554
- Pt, catalysts, supported, characterisation, hydrogenation and H₂-D₁ equilib. 8-76910
- S compounds, water-soluble, anal. of atmospheric aerosols 8-96282
- Si (111) surface, anal. by ion-electron spectroscopy 8-72670
- SiO₂-Na₂O-CaO, electrochemically coloured, chemical composition and structure of surface layers 8-84758
- Ti (III), (IV), simultaneous photometric determ. 8-61102

chemical analysis by mass spectrometry see mass spectroscopic chemical analysis**chemical analysis by nuclear reactions and scattering**

- see also *chemical effects of nuclear reactions and scattering; neutron activation analysis*
- aerosols, atm., instrumental anal. of light element comp. 8-69516
- charged particle activation anal., are energy in ave. stopping power method 8-76963
- charged particle chemical analysis, two reactions method 8-76964
- cyclotron, small, applications (*Hungarian*) 8-70656
- development trends and appl. 8-55041
- fluorophosphate glasses, C determ. by deuteron activation analysis 8-68961
- ion induced γ -rays, thick sample reaction yields, energies, appl. in prompt nuclear anal. 8-62502
- NBS reactor, summary of activities, (July 1976 to June 1977) 8-82435
- nuclear medicine diagnostics, for teaching 8-49618
- organic materials, nuclear backscattering using cyclotron 8-80807
- particle elastic scattering analysis, appl. to C, N and O determ. in size fractionated urban aerosols 8-81466
- proton activation analysis, 11 MeV protons 8-88686
- (γ , γ'), reaction activation anal. of elements using ¹⁶N γ -rays 8-88689
- B, neutron irradiated, quantitative anal. using cellulose nitrate solid state track detectors 8-56937
- Bi determ. by photon activation anal. 8-85273
- C, activation anal. by photon-nucleus reaction (*Japanese*) 8-76945

chemical analysis by nuclear reactions and scattering continued

- F determ. in atm. samples by $^{19}\text{F}(\text{p},\alpha)^{16}\text{O}$ react. using low energy accelerator 8-85239
 H depth profiling in materials, use of $^1\text{H}(^{15}\text{N},\alpha\gamma)$ resonant reaction (*French*) 8-91357
 H, determ. by simultaneous heavy-ion induced nuclear reacts. and at X-ray emission 8-85240
 Hg, determ., in Pb, radioactivation and other methods 8-76952
 Mg alloy scales, F conc. profiles determ. using $^{19}\text{F}(\text{p},\alpha\gamma)$ 8-88678
 N, activation anal. by photon-nucleus reaction (*Japanese*) 8-76945
 Nb-Ti, film, composition determ. by ^3He elastic scatt. 8-76974
 NbTi, chemical comp., supercond. films and bulk surfaces 8-76973
 O, activation anal. by photon-nucleus reaction (*Japanese*) 8-76945
 Si:B, conc. profile of implanted cryst., by $^{11}\text{B}(\text{p},\alpha)$ chem. anal., annealing (*German*) 8-83843
 SiN_x , plasma deposited, H content meas. 8-63949
 Ta film, determ. of thickness and O, N content 8-80824
 U, determ. in environmental samples, neutron activation, neutron assay and fluorometric methods 8-61087

chemical association *see association***chemical batteries** *see cells (electric)***chemical bonding** *see bonds (chemical)***chemical bonds** *see bonds (chemical)***chemical composition** *see chemical analysis***chemical diffusion** *see diffusion***chemical effects of nuclear reactions and scattering**

- see also chemical analysis by nuclear reactions and scattering; radiation chemistry*
 No entries

chemical effects of radiation *see radiation chemistry***chemical elements** *see elements (chemical)***chemical engineering** *see chemical technology***chemical equilibrium**

- see also chemical reactions; reaction kinetics*
 chemical instabilities, rel. to equilibrium phase transitions 8-65897
 complex ions, mobility and stability const., counter-current ion migration determ. (*German*) 8-56900
 constants determination, projection map technique 8-53240
 cycling zone adsorption, travelling wave, continuous flow equil. staged model 8-64874
 dimers, dissociating, in nonisothermal ideal gas phase, stationary state anal. 8-76848
 liquid nuclear waste, simulated, ion exchange equilibration, radiotracer obs. 8-74444
 metal complexes, solns., activity correction in thermodynamic stepwise stability constant expression 8-56912
 MHD generator, supersonic, working body thermodynamic props., chem. kinetics effect 8-91163
 microemulsions, thermodynamic stability 8-95962
 polycaprolactam characteristics dependence, at equilibrium state, on polymerisation conditions, in closed system (*Japanese*) 8-95928
 slags, application of activity concept to physical chemistry 8-53243
 specific equil. recombination rate coeffs., Laplace transform calcs. of temp. depend. 8-60989
 TCNE, K salt, in nematic liq. crystal solvent, ion pairing, EPR spectra 8-73020
 TNF-carbazoyl compound charge transfer complexes, equil. const. 8-64877
 Cu-KELEX 100 (alkyl β -hydroxy quinoline), distribution coeffs., model 8-53244
 Cu-LIX 65N (β -hydroxy benzophenone oxime) distribution coeffs., model 8-53244
 GdS, vaporisation thermodynamics and dissoc. energy obs. 8-67822
 $\text{H}_2\text{CO}^+ + \text{H}_2\text{S} \rightleftharpoons \text{H}_3\text{S}^+ + \text{HCHO}$, chemical equil. const., proton affinity of HCHO and H_2S 8-85189
 $\text{H}_2\text{CO}^+ + \text{HCN} \rightleftharpoons \text{H}_2\text{CN}^+ + \text{HCHO}$, chemical equil. const., proton affinity of HCHO and HCN 8-85189
 $\text{H}_2\text{O} + \text{H}^+ \rightleftharpoons \text{H}_3\text{O}^+$, equil., H_2O proton affinity calc. 8-92497
 $\text{H}_3\text{S}^+ + \text{HCN} \rightleftharpoons \text{H}_2\text{CN}^+ + \text{H}_2\text{S}$, equil., rate coeffs. and proton affinity, flowing afterglow 8-56885
 I partition equilibrium between air and NaOH aq. effect of CO_2 conc. 8-78474
 Mo-Fe-O-H system, thermodynamic equil. 8-60657

chemical exchanges

- see also ion exchange; isotope exchanges*
 acetylacetonatobutyl halides, equil. reacts. redistribution of -F, -Cl monofunctional groups (*French*) 8-64816
 atom+diatom, transition states, trapped trajectories and classical bound states in continuum 8-88630
 ATPase kinetics in *E. coli* cells, ^{31}P NMR meas. 8-77022
 butyl boron halides, equil. reacts., redistribution of -F, -Cl monofunctional groups (*French*) 8-64816
 N-5-chlorosalicylideneaniline, $\text{H}^+ \cdot ^{14}\text{N}$ double reson. NQR spectra temp. depend. thermochromism and tautomeric mech. 8-70849
 exothermic triatomic exchange reactions, prod. energy distrib., statistical dynamic model 8-92455
 extended diffusion and 'sticky' collisions 8-86940
 methane, H abstraction by thermal H, 10-30K, ESR evidence 8-76839
 methylene + $\text{H}_2 \rightarrow \text{CH}_3 + \text{H}$, triplet methylene abstraction, partial open shell FSGO calc. 8-80719
 NMR spin echo, chemical exchange and T_2 relax., multiple sites 8-78727
 $\text{BCl}_3 + \text{H}_2$ laser induced chemistry, theory 8-76884
 Bi_2Te_3 , chemical bonding models, correctness test using mag. susceptibility, and chemical substitution 8-67680
 $\text{Br} + \text{Br}_2$, atom-exchange, rate and activation energy, trajectory model and pot. energy surface 8-64811
 $\text{Cl} + \text{H}(\text{D})\text{I}$, exothermic triatomic exchange reactions, prod. energy distrib., statistical dynamic model 8-92455
 $\text{D} + \text{F}_2(\text{Cl}_2)$, exothermic triatomic exchange reactions, prod. energy distrib., statistical dynamic model 8-92455
 $\text{F} + \text{H}_2 \rightarrow \text{HF} + \text{H}$ energy profile, minimal basis ab initio VB calcs. 8-50477
 Fe-Zn, liquid-solid reaction in Zn bath, effect of Fe concentration, alloy layer growth, exam. (*Japanese*) 8-85037
 $\text{H} + \text{F}_2(\text{Cl}_2)$, exothermic triatomic exchange reactions, prod. energy distrib., statistical dynamic model 8-92455
 $\text{H} + \text{H}_2$, Cl calc. of three dims. pot. energy surface 8-56882

chemical exchanges continued

- $\text{H} + \text{H}_2$, least squares fit to ab initio pot. energy function 8-56883
 $\text{H} + \text{H}_2(\nu=1) \rightarrow \text{H}_2 + \text{H}$, exchange reaction, classical trajectory method, vibr. excitation, partial rate const. 8-60993
 $\text{H}^+ + \text{methane} \rightarrow \text{methane} + \text{H}^+$, nucleophilic substitution, ab initio pot. energy classical trajectory anal. 8-68886
 $\text{H}_2 + \text{D}_2$, exchange reaction, steady-state, surface reaction effects (*French*) 8-85148
 $\text{H}_2 + \text{D}_2$, exchange reaction, gas phase, heterogeneous initiation (*French*) 8-85149
 $\text{HF} + \text{D}$, vibr. threshold energies, reagent energy effects 8-85145
 HI, H abstraction by thermal H, 10-30K, ESR evidence 8-76839
 $\text{H}_3\text{S}^+ + \text{HCN} \rightleftharpoons \text{H}_2\text{CN}^+ + \text{H}_2\text{S}$, equil., rate coeffs. and proton affinity, flowing afterglow 8-56885
 $\text{HgH} + \text{NO} \rightarrow \text{HNO} + \text{Hg}$, reaction rate temp. depend., chemiluminescence 8-68885
 NaAsO_2 aq. solns., O exchange between $\text{AsO}_2(\text{OH})_2^-$ and water 8-92459
 TiCl_3 , (TiCl_3), labelled, exchange of Ti ats. rel. to γ -irrad., heat treatment, grinding 8-92470
 $\text{V}_2\text{O}_{3-x}\text{F}_x$ ($0 \leq x < 0.3$), preparation and physical props. 8-76619

chemical industry

- nuclear fuel reprocessing, on-line control (*Russian*) 8-74460
 particle size measurement techniques, rapid response, online methods, pharmaceutical, agricultural products appl. 8-89429
 residence time measurement, magnetic recording and hybrid computers appl. 8-81953
 synthetic chemicals production, multiple digital differential thermal analysis instrumentation 8-77902

chemical kinetics *see reaction kinetics***chemical lasers**

- combustion driven nozzle, F_2 absorption meas. 8-79011
 electronic chemical laser pot. systems, intracavity dye laser monitoring technique 8-62239
 electronic transition lasers, conf., Snowmass Village, USA (Sept. 1976) 8-63076
 fluoride- H_2 system, F quantum yield in photodissociation, stimulated emission delay meas. 8-58753
 Group IV photolytic laser expts., for fusion research 8-63101
 Group VIA photolytic laser systems, for fusion research 8-59002
 highly viscous chemical laser nozzles flow, two dims. Navier Stokes eqns., implicit marching method 8-63506
 inert gas hydrides, laser active media, feasibility, energy storage 8-79014
 mercuric halide dissociation lasers, discharge pumping 8-79009
 metal atom oxidation reactions, kinetics of chemilum. emitter form. and quenching 8-63107
 metal oxide, temp. depend. of chemilum. reactions, activation energies for excited state form. 8-66818
 methyl isocyanide photodissoc., cyanide radical energy partitioning chemical laser determ. 8-73063
 molecular collisions in intense laser field, visible chem. laser possibility 8-62876
 photorecombination reactions initiated by shock wave, light amplification (*Russian*) 8-63100
 power spectral performance, coupled fluid dynamic, kinetic and physical optics model 8-79040
 $\text{Ba-N}_2\text{O}$ flame, candidate chem. laser reactions, intracavity dye laser absorpt. meas. 8-63108
 CN ($\text{A}^2\P$), chem. prod., CN number densities for gain, emission and absorpt. meas. 8-63112
 CN, radical fluoresc. excitation spectrum and laser emission from ICN photolysis 8-76892
 CN radicals, electronic transition laser, using $\text{C}_3\text{F}_7\text{CN}$ and $(\text{CN})_2\text{C}_4\text{F}_8$ photodissociation 8-50769
 CO chemical laser, $\text{CS}_2\text{-O}_2$ mixtures in discharge 8-50766
 CO, chemical laser, supersonic combustor driven 8-87047
 CO, high power combustor driven system 8-87065
 CO laser, $\text{CS}_2\text{-N}_2\text{O-O}_2$ continuous combustion, performance characts. (*Russian*) 8-55348
 $\text{CO} + \text{O}$, vibr. deactivation 8-94305
 $\text{Ca-N}_2\text{O-CO}$ flame, Ca catalyzed, gain meas., emission band assignment 8-66815
 $\text{Ca-N}_2\text{O-CO}$ flame, candidate chem. laser reactions, intracavity dye laser absorpt. meas. 8-63108
 $\text{Cl} + \text{HI}$, chem. laser, energy distrib., spectrosc. obs. 8-71096
 DF chemical laser, jet curtains for gas containment 8-63099
 DF, F_2 absorption diagnostic, sensitive technique 8-74896
 DF laser, pulsed unstable resonator, mode control and performance studies 8-82995
 DF, pulsed microwave discharge 8-58998
 DF-HF CW lasers, performance, computer modelling 8-71094
 $\text{Ge-N}_2\text{O}$, rate coeff. meas. for $\text{Ge} + \text{N}_2\text{O} \rightarrow \text{GeO} + \text{N}_2$ reaction 8-63110
 GeO , produced in $\text{Ge} + \text{N}_2\text{O}$ reaction, kinetics of chemilum. emitter form. and quenching 8-63107
 H halides, $\text{I}^*(5^2\text{P}_{1/2})$ quenching, electronic-vibr. energy transfer 8-63114
 $\text{H}_2\text{-F}_2\text{-He}$ chemical CW laser, flows (*Russian*) 8-74895
 $\text{H}_2\text{-F}_2\text{-O}_2$, chem. laser mixture, multiatm., spontaneous explosions 8-73044
 HBr, electronic to vibr. energy transfer from excited halogen atoms, IR fluoresc. 8-63113
 HCl cryosorption-pumped CW chemical laser 8-74894
 HCl, electronic to vibr. energy transfer from excited halogen atoms, IR fluoresc. 8-63113
 HCl laser, V=3 to V=2 band process, computer simulation 8-71095
 HF CW laser with cylindrical telescopic resonator, flame front model 8-59001
 HF chemical laser, laminar flow pattern (*Russian*) 8-87048
 HF cryosorption-pumped CW chemical laser 8-74894
 HF, cw chem. diffusion laser, amplifier operation 8-79015
 HF, F_2 absorption diagnostic, sensitive technique 8-74896
 HF, high-energy laser, energy extraction, beam quality, for fusion ignition 8-63102
 HF laser, pulsed unstable resonator, mode control and performance studies 8-82995
 HF laser, spherical telescopic resonator, design 8-71120
 HF, pulsed $\text{H}_2 + \text{F}_2$ chain reaction laser, rot. nonequil. mechanisms effect on performance 8-82958
 HF, pulsed microwave discharge 8-58998

chemical lasers continued

- HF, rot. population transfer effect obs. 8-79013
 HF, stable discharges, with large electrode separation 8-55371
 HF-DF, CW laser, specie conc. and temp. by Raman spectra 8-58999
 HgBr dissociation laser is elec. discharge 8-50768
 I, Asterix III and German laser fusion programme 8-63136
 I chem. produced $^2P_{1/2}$ state, gain meas. 8-63115
 I, continuously pumped continuous flow photodissociation laser 8-59027
 I, continuously variable water filter for linearity testing of photoresistors 8-55397
 I, electronic transition chemical laser 8-55347
 I electronically excited atom prod., collisional release and photocomp. kinetics of I_2 8-66819
 I laser, high-power, beam quality, gain saturation effect, for fusion ignition 8-63149
 I laser, smooth pulse oscillator for single mode operation 8-59057
 I laser medium, CF_3I , UV absorption modification, by vibr. excitation for fusion ignition 8-58717
 I, photodissociation laser, 1.315 μm transition line struct. 8-59000
 I, pulsed photodissociation laser, based on methyl iodide 8-50767
 I, using ICF_3CN photodissociation 8-50769
 La-F $_2$ (ClF)(Cl $_2$)(SF $_6$), visible chem. laser development from reactions yielding visible chemilum. 8-63111
 Mg-N $_2$ O-CO flame, efficient chem. generation of Mg(3P) 8-63109
 Mg-N $_2$ O-CO flame, Mg catalyzed, gain meas., emission band assignment 8-66815
 NF, b $^1\Sigma^+$ state, enhancement by I laser pumping, lasing potential 8-79012
 NF, chem. pumped electronic transition laser system, chem. and scale-up 8-63103
 NF, excited, lasing potential, prod. by N+O $_2$ F reaction 8-63106
 NF($\Delta^1\Delta$)+I($^2P_{1/2}$) system, electronic angular momentum transfer, chem. kinetic model 8-63104
 NF(b $^1\Sigma^+$) enhancement by I laser pumping 8-63105
 NO, electronic to vibr. energy transfer from excited halogen atoms, IR fluoresc. 8-63113
 O $_2$, high energy pulsed laser feasibility at 1.27 μm , O $_3$ photolysis 8-63117
 OCS laser, two-quantum excitation, photolysis, energy transfer, for fusion expts. 8-59003
 OD laser, pure rot. lasing intensity, pumping by collision induced energy transfer 8-74897
 O $_2$ (Δ_g)+I($^2P_{3/2}$), possible electronic transition chem. laser 8-63116
 OH laser, pure rot. lasing intensity, pumping by collision induced energy transfer 8-74897
 Se-F $_2$ (ClF)(Cl $_2$)(SF $_6$)(Br $_2$), visible chem. laser development from reactions yielding visible chemilum. 8-63111
 SCF supersonic mixing flame, spontaneous emission, electronic transition chem. laser pot. 8-66817
 Se, OCSe photodissoc., forbidden at. transitions 8-79010
 SiF, chemilum. obs. of $A^2\Sigma^+$ and $a^4\Sigma^-$ states 8-66816
 SnO, produced in Sn+N $_2$ O(O $_2$)(O) reactions, kinetics of chemilum. emitter form. and quenching 8-63107
 Sr-N $_2$ O-CO flame, candidate chem. laser reactions, intracavity dye laser absorpt. meas. 8-63108
 Sr-N $_2$ O-CO flame, Sr catalyzed, gain meas., emission band assignment 8-66815
 SrF, temp. depend. of chemilum. reactions, activation energies for excited state form. 8-66818
 XeF, from photodissoc. of XeF $_2$, B(1/2)-X $^2\Sigma^+$ transition, stimulated emission 8-71097
 Y-F $_2$ (ClF)(Cl $_2$)(SF $_6$)(Br $_2$)(IBr), visible chem. laser development from reactions yielding visible chemilum. 8-63111
 YCl supersonic mixing flame, spontaneous emission, electronic transition chem. laser pot. 8-66817
 YO, temp. depend. of chemilum. reactions, activation energies for excited state form. 8-66818

chemical reactions

- see also association; atom-atom collisions; atom-ion collisions; atom-molecule reactions; atomic inelastic collisions; catalysis; charge exchange; chemical exchanges; chemically reactive flow; chemiluminescence; chemisorption; CIDEP; CIDNP; corrosion; dissociation; electrolysis; free radical reactions; heat of reaction; ion-molecule reactions; isomerisation; molecule-molecule reactions; oxidation; photochemistry; polymerisation; pyrolysis; radiolysis; reaction kinetics; reduction (chemical); solvation
 air pollution control, venturi-jet scrubber, gas absorpt. with chem. reaction, performance study 8-81393
 angular momentum disposal, information theory anal. 8-80730
 Arrhenius equation and accel. testing 8-53182
 automatic detection of chemical reaction sites 8-92476
 bases, K $^+$ affinities ab initio SCF calc. 8-58585
 benzenes, trisubstituted, dil. solns., relax. mech., Debye relax. times 8-80744
 chromatographic reaction and separation in pulse-fed catalytic reactor 8-64880
 comet comae, gas-phase chemistry in one dimension 8-93154
 composition centre waves, periodic chaotic, Pade approximant scheme 8-80716
 conference, electronic and atomic collisions, Paris (July 1977) 8-58758
 dense plasma, coaxial acceleration and plasmochimistry (Russian) 8-92482
 dynamical correlations near instabilities in nonlinear chemical reaction systems 8-80715
 EHF theory in chem. reactions, wave functions symmetry props. 8-92447
 electron kinetics in nonpolar liquids 8-95918
 electron pair mechanism, non-specialist teaching appl. 8-89279
 elimination reaction, D kinetic isotope effects, tunnelling, zero-point energy effects 8-56889
 energy barrier location, sudden and gradual late barriers, classical trajectory method 8-92454
 estuary and river sited power plants, water discharge and chlorination, simulation 8-96250
 gallic acid+BrO $_3^-$ +H $_2$ SO $_4$ system, uncatalysed oscillatory chemical reactions 8-61004
 gas absorption with second-order irreversible chem. reaction, enhancement factors 8-80727

chemical reactions continued

- grain and phase boundaries between crystals, conf., Konigstein, Germany (Oct. 1977) 8-72762
 hot gas thermodynamics and diagnostics 8-76865
 interstellar diffuse clouds, chemistry rel. to OH and HD column densities and temps. 8-93385
 ion transport and chem. reactions in brown adipose tissue, network thermodynamics 8-92606
 lacustrine sediments, selective chem. extraction of CO $_3^{2-}$ associated metals 8-65406
 law of mass action, first order phase transition, chemical instability 8-80778
 methanation over polycrystalline Ni(Pt) foils, kinetic information 8-73081
 methane, conversion in H $_2$ plasma flow, Monte Carlo study 8-61010
 micellar system, photoinduced redox processes kinetics, intramolecular electron transfer 8-92603
 molecular collisions, joint products' state distrib. 8-64807
 molecular geometry, mass spectrometric investigation, using mol. rearrangement 8-86972
 in molten salts, acidity effects 8-73039
 montmorillonite, dehydration kinetics 8-76857
 nonequilibrium solutions, conf. Leeds, England (July 1976) 8-73036
 nonequilibrium phase transitions in chemical systems 8-54325
 nuclear fuel processing solutions, interactions 8-78487
 orbital correspondence anal. in max. symm., appl. to spin-forbidden processes 8-78631
 orbital interaction and chemical bonds. Exchange repulsion and rehybridization in chemical reactions 8-85142
 organic chemistry, textbook, undergraduate level 8-57711
 phenomenological relations, linear network thermodynamics 8-95905
 plasma chemistry, status and trends 8-76864
 polymer reactants in organic reactions, review 8-95923
 polymers, struct., bonding, reactivity by ESCA 8-53299
 potential energy barrier position between initial and final states 8-76831
 propan-1,3-dioic acid, H $_2$ O $_2$, KIO $_3$, MnSO $_4$, HClO $_4$, I $_2$, periodic chem. reactions, bi- and tristability, rel. to biological mech. (French) 8-80726
 REACT program for computer-assisted simulation of chemical reaction sequences, structure elucidation applications 8-92477
 reactivity with Y $_2$ O $_3$, exam. by thermal anal. 8-85154
 Schotten-Baumann esterification, teaching, use of positive photoresist 8-89284
 semiconductor metal interface, Schottky barrier, chemical reaction and charge redistrib. 8-95365
 L-serine, in aqueous solns., US spectra using automatic recording spectrometer 8-75735
 shock tube unsteady expansion wave technique, applic. 8-61011
 solid-solid pellet systems, diffusion and reaction 8-85139
 solid-state redox reaction, electron tunnelling rate, transfer model 8-76844
 solvated electron+ion, in ethanol, reactivity, ion pairing effects 8-85147
 solvation, classical mean space charge model 8-76841
 steel, alloy, Fe-C-Si-S, liquid, desulphurisation with CaO, exam. of reaction mechanisms 8-80742
 stochastic process description, props. 8-60991
 transient diffusion with n-order irreversible chem. reaction, finite element method 8-85122
 transition metal carbides, solid-phase reacts., effect of nonstoichiometry, thermodynamic evaluation 8-60632
 unimolecular reactions, induced by monochromatic IR radiation 8-88645
 unimolecular reactions, reformulation of theory 8-80712
 unimolecular reactions, vibrational collisional energy transfer efficiencies 8-80714
 vibrational distribution, rot. effects 8-80717
 weakly coordinated molecular systems, mutual vibronic effects in chem. reactions and catalysis 8-64821
 Wolff rearrangement, teaching, use of positive photoresist 8-89284
 Al $_2$ O $_3$ (H $_2$ O) $_3$, gibbsite, synthetic, crystallinity and topotactic reactions, X-ray diff. obs. 8-63851
 BaCO $_3$ -SrCO $_3$ -TiO $_2$ (ZrO $_2$), ternary systems, solid-phase synthesis 8-52733
 CO, decomposition in corona discharge, qualitative chemical anal. of reaction products 8-60992
 CO $_2$ glow discharge chemical processes and rate coefficients 8-63626
 Ca $_3$ (PO $_4$) $_2$ (OH) $_2$, nonstoichiometric, wet-process formation from α -Ca $_3$ (PO $_4$) $_2$ (Japanese) 8-84752
 CdO-WO $_3$ -H $_2$ O, interconnection between kinetics of structure formation and chem. reactions 8-53198
 CoFe $_2$ O $_4$ formation rate consts. meas. by Mossbauer effect 8-68875
 F, with Ta, appl. of modulated mol. beam mass spectrometry anal. 8-56944
 Fe:C, decarburisation by H $_2$, conversion electron Mossbauer obs. 8-85198
 H+H $_2$, finite element methods for reactive scattering 8-92453
 K $_2$ (F,O)-B $_2$ O $_3$ -SiO $_2$, effect of replacing B $_2$ O $_3$ by Al $_2$ O $_3$ or Ga $_2$ O $_3$ 8-63677
 M $_2$ O-MnO-B $_2$ O $_3$ glasses, M=Li, Na, K, glass-forming region and physicochem. props. 8-63678
 N+H $_2^+$, triplet state ab initio CI pot. energy surfaces 8-74729
 $^{14}N^{15}N$ +O plasma reaction system, isotope fractionation under simulated space conditions 8-73623
 NO $_x$ plasma chemistry (Russian) 8-92482
 Na $_2$ O-Al $_2$ O $_3$ -SiO $_2$ glass, formation from alkoxides, phys. and chem. evolution 8-80503
 O $_2^+$, symmetric charge transfer reactions, selected states, photo-ion, electron coincidence 8-73028
 Si nitridation, Fe-contaminant effects, mechanism 8-80496
 Si, powder compact, nitriding, growth of α and β phases 8-95717
 Si $_3$ N $_4$ +MgO, reaction during hot pressing 8-68658
 Sn-Ni, equiatomic, metastable, transformation kinetics, Avrami parameters calc. method 8-92239
 T+O $_2$ high energy reaction, excitation function 8-68907
 UAl $_2$ +2Al \rightarrow UAl $_3$, effect on Young's modulus and rupture strength in dispersion reactor fuel (German) 8-62596
 Y $_2$ O $_3$, U, C interactions, thermal anal. 8-85154
 ZnO-Sb $_2$ O $_3$ -O $_2$ system, cpd. forming reactions 8-52699

chemical reactivity *see* **chemical reactions****chemical relaxation**

- benzenes, trisubstituted, dil. solns., relax. mech., Debye relax. times 8-80744
 gas dynamics with relaxation effects, acoustic waves, nonequilibrium atmosphere effects, review 8-79390
 micelle formation, in aq. solns., kinetics relax. process 8-76928
 pulses and waves, lowest order multiple time scale exspn. 8-68874
 subpicosecond relax. time meas. using pulsed lasers (*Czech*) 8-78838
 O₂ dissociation relaxation behind regular reflected and stationary oblique shocks 8-85159

chemical shift*see also* **isomer shift**

- atomic chemisorption, chemical trends, core-hole relax. effects, jellium model 8-76909
 atomic effective charge distrib. in cpds., chem. shift of electron levels 8-86785
 benzenoid hydrocarbons, atom numerical code scheme for classification of chemical shifts 8-94205
 t-butanol-acetone-cyclohexane, complexation, thermodynamic parameters (*Russian*) 8-76905
 bytropic liquid crystals:Cs⁺, ¹³³Cs NMR, chemical shift anisotropies 8-79525
 chloromethanes, Auger electron spectra and chem. shift 8-90231
 p-dichlorobenzene, charge transfer complexes, NQR shifts 8-55186
 ESCA chemical shift, indirect evaluation of Coulombic contribution to ionis. pots. for nonbonding electrons 8-92572
 ESCA studies of Ga, As, GaAs₂Ga₂O₃, As₂O₃ and As₂O₅ 8-92171
 ESCA using X-ray photons >1500 eV, Au M_α X-rays (2123 eV) 8-72683
 haloalkanes, ¹⁹F chem. shielding, temp. depend., FT NMR obs. 8-86888
 halomethanes, ¹³C chemical shifts, diamag. susceptibility, effect of non-bonded interactions 8-78726
 hexafluoride radicals, prep. and EPR spectra comparison, hyperfine splitting 8-68381
 hydrocarbons, α-substituent effects in ¹³C NMR, quantum chem. calcs. 8-74680
 III-V semiconductors, chemical shifts of NMR lines of Ga nuclei 8-88201
 keratin-NaCl, Na Auger electron spectra 8-53339
 light elements, Z>10, K-L Auger process, review 8-50523
 metalloenzymes, ¹¹³Cd as NMR active site probe 8-68999
 methane, NMR chem. shift., temp. depend., virial coeffs. 8-58722
 monohalobenzenes, inner shell excitation and ionis., electron energy loss spectra, XPS, assignments 8-62934
 p-nitrofluorobenzene, nematic phase NMR, ¹⁹F shielding anisotropy 8-62824
 NMR, quadrupole coupling const. and chem. shift, from single-cryst. data 8-91982
 NMR chem. shift., temp. depend., virial coeffs. 8-58722
 oxalic and dihydrate, monocrystals, high resolution PMR 8-64283
 paramagnetic metal ions as structural probes for NMR investigation of inorganic and bioinorganic compounds 8-62828
 pentacoordinated ferrous porphyrins, ¹H and ¹⁹F NMR, hyperfine shift, π electron binding 8-78719
 peptide, NMR spectroscopy study 8-88694
 polymer primary structures ESCA and EHCO methods 8-52630
 protein, NMR spectroscopy study 8-88694
 quasiatomic theory, complexation, thermodynamic parameters calcs., spectroscopic appls. (*Russian*) 8-76905
 solid, H-bonded, NMR chem. shift tensors (*German*) 8-84489
 squaric acid, ¹³C chemical shift tensor study of antiferroelec. second order phase transition 8-52462
 tris(dimethylamino)phosphorus, ¹⁵N and ³¹P NMR aligned in liq. cryst., geom. struct. 8-82751
 two internal-vacancy atoms, Green function calcs. (*Russian*) 8-50451
 vanadyl triisopropylate, chem. shifts, NMR line widths, temp. and solvent depend. 8-70853
 X-ray absorption edge-shifts, empirical relations, effective ionic charge for isoelectronic series 8-55136
 [N(CH₃)₂H]₂SnF₆, phase transition and temp. effects, Mossbauer and NMR spectra 8-88236
 AuF₃, ¹⁹F NMR chemical shift, crystal chemistry 8-87645
 CO₂, ¹³C NMR, chem. shift., determ. of virial coeffs., rovibr. motion 8-58720
 Cl compounds, chemical shifts of X-ray electron and Auger lines 8-86912
 Co(ethylenediamine)₃(ClO₄)₃, ESCA chem. shift meas., internal standards 8-50585
 Cs perfluoro-octanoate, amphiphilic liq. cryst., ¹⁹F multipulse NMR study 8-76328
 Cu complexes, FT NMR, ⁶³Cu and ⁶⁵Cu chemical shifts and coupling constants 8-94260
 Cu compounds, chemical shifts of X-ray electron and Auger lines 8-86912
 Cu₂(As₂O₄Se_{0.6})_{1.8}, amorphous, ⁷⁷Se NMR, comp. depend. 8-76329
 CuBr, NMR chemical shifts, temp. depend. 8-68401
 CuCl, NMR chemical shifts, temp. depend. 8-68401
 CuI, NMR chemical shifts, temp. depend. 8-68401
¹⁹F, chem. shielding in isolated haloalkanes, temp. depend. 8-86888
 GaAs (110)-Al(Ga) interface, interface states, photoemission study 8-95359
 GaAs, transmutation doped, shallow donors, magneto-optical study, photocond. meas. 8-87996
 GaAs-Ga, (110) interface electron states, photoemission study, chemical shift, surface charge redistrib. 8-72259
 H₂SeO₄, NMR of ⁷⁷Se, chemical shift and screening tensors (*Russian*) 8-64285
 He+CO, nuclear mag. shielding const., interaction geometry depend., chemical shift, gauge invariant method 8-62866
 InCl, InBr, InI, UV photoelectron spectra of valence d shells, gas-phase 8-62845
 KD₂PO₄, ferroelec. transition, ³¹P chem. shift obs. 8-76414
 LiNO₃, electron irradi. damage, XPS obs. 8-64444
 Li₂SO₄, electron irradi. damage, XPS obs. 8-64444
⁷Li₂O, β-radiation detected NMR of ⁶Li obs., double freq. irradiation, ⁷Li hyperfine struct. anomaly 8-91994
⁷Li₂S, β-radiation detected NMR of ⁶Li obs., double freq. irradiation, ⁷Li hyperfine struct. anomaly 8-91994

chemical shift continued

- MgO, from Mg+O₂ matrix reaction, IR spectra, isotope shifts and blue matrix shift 8-80736
 Mg₃P₂, ³¹P multiple pulse NMR, chem. shift anisotropy 8-52369
 NH₄ perfluoro-octanoate, amphiphilic liq. cryst., ¹⁹F multipulse NMR study 8-76328
 N₂O, ¹⁵N NMR, chem. shift., determ. of virial coeffs., rovibr. motion 8-58720
 β-Na₂O·Al₂O₃, high-field ²³Na NMR 8-64284
 Nb complexes, F-containing, X-ray K absorption edges, chem. interpretation 8-74676
 PH₃, ³¹P NMR chem. shift, virial coeff. determ. 8-58721
 PH₃(D₃), ³¹P NMR, chemical shielding, centrifugal distortion, anharmonic vibr., cubic force const. 8-82752
 P₄S₁₀, ³¹P multiple pulse NMR, chem. shift anisotropy 8-52369
³¹P, in inorganic solids, multiple pulse NMR 8-52369
 PbCl₂, PbBr₂, PbI₂, UV photoelectron spectra of valence d shells, gas-phase 8-62845
 RbF(Cl)(Br)(I), chem. shift in X-ray absorpt. spectra, correl. with ion contrib. to bond 8-76559
 Se compounds, chemical shifts of X-ray electron and Auger lines 8-86912
⁷⁷Se, FT NMR in solns., chem. shift, I₁ relax. times, NOE enhancement 8-95528
 SnCl₂, SnBr₂, UV photoelectron spectra of valence d shells, gas-phase 8-62845
 Te, NMR spectrum, electron paramagnetism and atomic self-diffusion mechanism 8-72426
 Te, Te cpds., Auger spectra 8-58638
 TlCl, TlBr, TlI, UV photoelectron spectra of valence d shells, gas-phase 8-62845
²⁰⁵Tl⁺ adsorbed on hydrated silica, NMR relax. chem. shift 8-72427
 U complex, U(acac)₄, cryst. fields, mag. susceptibility, chem. shift (*French*) 8-84179
 Xe+CO(N₂), ¹²⁹Xe chem. shielding, second virial coeff. 8-66563
 Zn₃P₂, ³¹P multiple pulse NMR, chem. shift anisotropy 8-52369

chemical structure

- see also* **bonds (chemical)**; **crystal atomic structure**; **crystal chemistry**; **molecular configurations**
 chemistry, macromolecules, and the needs of man 8-95907
 epoxy resin, low temp. thermal props., phonon states and crosslinked struct. (*German*) 8-75846
 Kevlar-49, chemical characterisation 8-95725
 polymer, crosslinked (*German*) 8-75584
 polymer, degradation, mol. mechanisms (*German*) 8-76860
 polymer, glassy, elastic moduli, calc. method from chem. struct. (*Russian*) 8-75707
 quantum mechanics, replacement of chemical bond concept by loge theory 8-54243
 REACT program for computer-assisted simulation of chemical reaction sequences, structure elucidation applications 8-92477
 silane, coupling agent on E-glass fibre, structure, Fourier transform infrared spectroscopy 8-60643
 silane, coupling agent on porous silica, Fourier transform infrared spectroscopy 8-60642
 structural search codes for on-line compound registration 8-90319
 As₂S_{3-x} glass, Raman spectra, chem. struct. (*Russian*) 8-76469
 (As₂S₃)_x(AsI₃)_{1-x} glass, Raman spectra, chem. struct. (*Russian*) 8-76469
 Fe₂N₃, prep. by reactive sputtering, struct. and props. (*Japanese*) 8-92190
 Fe₇₀Ni₃₀, short range order, diffuse elastic neutron scatt. study 8-52219
 Fe₂O₃, prep. by reactive sputtering, struct. and props. (*Japanese*) 8-92190
 Fe_{1-x}Pd_x film, air-exposed, comp. profiles by AES, ESCA and ion sputtering 8-95245
 GaAs_{1-x}P_x, heterogeneous struct. obs. by anodisation-electrorefl. technique 8-84088
 Gd-Co film, amorphous, Ar sputtered, struct. 8-63946
 Gd-Co-Mo film, amorphous, Ar sputtered, struct. 8-63946
 Na₂O-B₂O₃-Na₂SO₄, glass, exam. of chemical differentiation, using Cu ion segregation 8-87625
 Nb film, ion bombardment with N₂⁺, Ar⁺, struct. changes, chemical compound formation (*Russian*) 8-95084
 Si-SiO₂ interface, chem. struct. of transitional region 8-95824
 SiO_x film, vacuum evaporated, phase comp., electron spectroscopy obs. 8-60042
 SiO₂, on Si exposed to O₂, phase comp., electron spectroscopy obs. 8-60042
 SnF₂, α and γ modifications, elec. cond., α→γ phase transitions, structs. 8-75867
 Ta film, ion bombardment with N₂⁺, Ar⁺, struct. changes, chemical compound formation (*Russian*) 8-95084
 Ti film, ion bombardment with N₂⁺, Ar⁺, struct. changes, chemical compound formation (*Russian*) 8-95084
 Zn₇Sb₂O₁₂, Zn₄Sb₂O₉, and conditions of formation 8-52699

chemical technology

- see also* **chemical industry**; **chemical variables control**; **chemical variables measurement**; **oil refining**
 continuous flow stirred tank reactor, mixing model 8-63508
 inert gas liberation in multiposition metallic reactor 8-59978
 liquid-liquid extraction column online control by modal control techniques 8-54865
 non-Newtonian fluids in jacketed agitated vessel, heat transfer, viscosity correl. 8-75143
 nuclear chemical-bound energy system, short term market prospects (*German*) 8-82505
 pulsed perforated plate column, mass transfer direction rel. to efficiency 8-71385
 two-phase mixture flow in rotary mixer, optimal dimensions 8-63485
 water splitting thermochemical cycle for synthetic fuel prod. at fusion reactors 8-58458

chemical vapour deposited coatings *see* **CVD coatings****chemical vapour deposition**

- see also* **vapour phase epitaxial growth**
 controlled nucleation thermochemical deposition, improvements over chemical vapour deposition 8-92387
 interface morphology on profiled substrates, calc. of development 8-60040

chemical vapour deposition continued

- morphological stability analysis 8-92200
 optical fibre, fabrication, low OH content, vapour phase axial deposition method 8-83125
 optical fibre refractive index change due to external forces 8-74971
 optical fibres, multimode graded index, modified process, reproducibility 8-90531
 plasma deposition and plasma stream transport (*Japanese*) 8-92199
 plasma stream transport method 8-52684
 protective glassy layers at 500°C for Cu passivation 8-76785
 steel, C, carbide formation during chromising, exam. in terms of ternary phase diagrams 8-56818
 steel, high alloy ledeburitic, wear and corrosion resistant coating by chemical vapour deposition 8-92403
 surface treatment by gas plasma (*Japanese*) 8-92386
 wear resistant surface, review 8-72938
 $\text{Al}_x\text{Ga}_{1-x}\text{As-GaAs-Al}_x\text{Ga}_{1-x}\text{As}$ photopumped quantum-well laser, room temp. CW operation 8-74908
 Al_2O_3 , CVD, props. rel. to deposition parameters 8-92197
 Al_2O_3 , coating, wear characteristics, comparison of coated and uncoated WC hard metals 8-92365
 B, chem. transport with I_2 , BI_3 synthesis 8-52682
 $\text{B}_2\text{O}_3\text{-SiO}_2$ low-loss single mode fibres, design, fabrication and transmission characts. 8-71199
 C, columnar and laminar forms, deposition on polycrystalline Ni foils 8-63943
 CdS, heterojunctions with InP and GaAs, prep. by CdS CVD and etching 8-52062
 Cr_2S_3 , single crystal, exam. of unit cell structures by interference contrast microscopy 8-67670
 Fe whiskers grown from $\text{FeCl}_2\cdot 4\text{H}_2\text{O}$, exam. of growth morphology 8-72051
 Fe-Cr-C, steel carbide formation during chromising, exam. in terms of ternary phase diagrams 8-56818
 Fe-Si layer, growth kinetics and morphology 8-95700
 FeCr_2S_4 , vapour grown, growth mechanism of multisteps on surface 8-75605
 Fe_2TiO_5 , pseudobrookite, single cryst. growth by chem. transport 8-80464
 $\text{Ga}_{1-x}\text{Al}_x\text{As-GaAs}$ DH lasers, very low threshold, grown by metalorganic CVD 8-55365
 $\text{Ga}_{1-x}\text{Al}_x\text{As-GaAs}$ laser, distributed Bragg confinement, room temp. operation 8-74907
 $\text{Ga}_{1-x}\text{Al}_x\text{As-GaAs}$ low threshold room temp. DH lasers grown by metalorganic CVD 8-50804
 GaAs- Br_2 (-Zn) system, filamentary cryst. prep. 8-52650
 $\text{Ga}_{1-x}\text{In}_x\text{Sb}$, vapour phase epitaxial growth by open tube method 8-84109
 Ge, vapour transport rate, Ge- I_2 equilib. 700 to 1300K (*French*) 8-64476
 In_2O_3 , transparent electrode deposition on PLZT ceramic 8-74848
 InP film, CVD on preferentially etched Mo, initial growth behaviour 8-51855
 LaB_6 , chemical vapour growth of whiskers, and single crystals 8-72710
 Mo_2C , from $\text{Mo}(\text{CO})_6$ pyrolysis, laser fusion target appls. 8-60861
 Ni dendrites on Al, CVD, selective solar photothermal absorber 8-52683
 $\text{Nb}_5\text{Cr}_{1-x}\text{O}_2$, cryst. prep. and struct., mag. props. 8-52198
 Nb_3Ge film, CVD fabrication of supercond. tape for high-field magnets 8-95698
 Nb_3Ge tape, prepared continuously by CVD, props. 8-60257
 Si CVD of polycrystal on liquid Sn layer 8-64479
 Si, CVD using CO_2 laser 8-56589
 Si, film deposition, growth kinetics under low H_2 press. 8-56586
 Si, polycryst., growth, props. and MIS appl. (*Slovak*) 8-92196
 SiCl_4+O_2 in modified CVD process for optical fibre prod., reaction IR spectra 8-80472
 Si_3N_4 , investigation of gas phase of CVD reaction 8-52681
 Si_3N_4 , separation, effect of reactor geometry (*German*) 8-60583
 Si_3N_4 , Si rich, CVD film prep. and props. 8-76607
 SiO_2 film, CVD on GaAs using tetraethoxysilane oxidation 8-60582
 SiO_2 layers, passivating, deposition by plasma decomp. in planar reactor 8-88430
 SiO_2 , Si rich, CVD film prep. and props. 8-76607
 $\text{SiO}_2\text{:F}$ layers, deposition from $\text{SiCl}_4\text{-SiF}_4\text{-O}_2$ gas mixture by plasma CVD method 8-95699
 SnO_2 , crystal growth habits (*Japanese*) 8-95686
 SnO_2 film, CVD using $\text{SnCl}_4\text{-H}_2\text{O}$ and $\text{SnCl}_4\text{-H}_2\text{O}_2$ systems, elec. and optical props. 8-52686
 SnO_2 , transparent electrode deposition on PLZT ceramic 8-74848
 Ti-Zr-B system 8-60581
 TiB_2 , chemical vapour growth by modified hot wire method 8-60555
 TiC, coating, wear characteristics, comparison of coated and uncoated WC hard metals 8-92365
 $\text{Ti}(\text{N,C,O})$, wear resistant coating for cemented carbides and high speed steels 8-92406
 $\text{U}_{1-x}\text{Th}_x\text{O}_2$, solid solution, single crystal growth by chemical transport reactions 8-72708
 W_2C , W_3C , wear resistant coatings, low temp. form., on steel substrate 8-92404
 ZnO , CVD films on sapphire substrates, use as optical waveguide 8-90500
 ZrC, whiskers, CVD on Ni, catalytic effect 8-51865
 ZrO_2 powders, vapour phase reaction production 8-68660

chemical variables control

- see also *pollution detection and control*
 crystallizer for growing single crystals from solutions with precision control of supersaturation 8-80465
 liquid mixture composition, using high-precision gas chromatograph 8-53283
 particle size, rapid response, online method for continuous industrial processes 8-89429
 CO_2 conc. regulation in climatic cabinets for corrosion testing (*German*) 8-53069

chemical variables measurement

- see also *chemical analysis*; *moisture measurement*; *pollution detection and control*
 salinity in ocean, Kiel multi-purpose sea probe microprocessor-based data acquisition system (*German*) 8-85701

chemical variables measurement continued

- trace analysis, state and development (*German*) 8-68956
 O_2 meter, type 648, mains-free, features (*German*) 8-94858
 O_2 partial pressure and bioelectric potential simultaneous meas. in living tissue (*German*) 8-85453
- chemically reactive flow**
 ablating plane (axisymmetric) body, turbulent boundary layer with neg. press. gradient 8-79389
 arc-heated gas flow, ion saturation current fluctuation probe 8-63574
 axisymmetric confined flame, aerodynamic and heat transfer, finite difference scheme, program 8-94689
 axisymmetric laminar jet diffusion flame, split operator finite difference solns. 8-51252
 burner with diffusive control, intermixing of gas streams with transverse swirled air flow 8-87418
 chemical reactions, lattice model, coupling of translational and reactive dynamics 8-55696
 condation, gas with chemically reacting noncondensable components 8-51258
 confined burning jet, droplet vaporisation, expt. and theory 8-94855
 continuous flow stirred tank reactor, mixing model 8-63508
 cylinder array, convective mass transfer with surface reaction 8-79369
 detonation sputtering, exp. determ. of dynamic characts. of two-phase flow (*Russian*) 8-94852
 diffusion flames, laminar and planar, large activation energies, asymptotic development (*German*) 8-91035
 flame, diffusion type, oppositely directed jets, elec. props. 8-56896
 flame, laminar mixed-mode forced-free diffusion type, on vert. burning fuel slab 8-91033
 flame, turbulent diffusing, analytic incorporation of probability density functions 8-75232
 flame front, laminar, hydrodynamic instability, nonlinear integro-differential eqn. 8-51253
 flame front, laminar, hydrodynamic instability, numerical solns. 8-51254
 flame stabilisation behind bluff-body flame holder (*Japanese*) 8-67284
 flames, premixed, laminar, time-depend. soln. determ. 8-67282
 flow velocity, field induced by flame spreading over fuel, laser velocimeter meas. 8-59529
 fluidised bed, reaction near grid, two-phase model 8-67280
 furnace heat transfer, 3-dimens. computer model predictions test 8-59504
 gas dynamics with relaxation effects, acoustic waves, nonequilibrium atmosphere effects, review 8-79390
 gas flow in catalytic convertor, numerical soln. 8-67281
 gas mixture turbulent concurrent double pipe heat exchanger equilib. and nonequib. reaction 8-94856
 n-hexane, tank flame, turbulence, holographic interferometric synchronous photography (*German*) 8-51255
 highly viscous chemical laser nozzles flow, two dimens. Navier Stokes eqns., implicit marching method 8-63506
 hydrocarbon diffusional combustion in air, finite activation energy anal. 8-95930
 isobaric turbulent reacting jet issuing into costream 8-63509
 jet flame, props. and mixing process in recirculation zone 8-91025
 Laval nozzle, surface burning in two-phase flow, boundary layer interaction, Rakhmatulin model 8-83452
 liquid fuel droplets, transient heat flow in combustion gases, models 8-63507
 particle in gas stream, convective, diffusion with nonlinear kinetics of heterogeneous chem. reaction 8-83499
 photosensitised reacts. in continuous chem. processes, scatt. effects 8-73057
 premixed turbulent flame combustion, heat transfer obs. and calc. (*French*) 8-94688
 pressure waves interaction with combustion field 8-63504
 solute dispersion in porous medium in MHD flow between parallel plates, homo- and heterogeneous reaction effects 8-55697
 supersonic nozzle, chem. nonequib. flow, specific momentum losses 8-59505
 surface reactions and mass transport, in Leveque's approx. 8-76907
 thermal instability of vibr.-excited mol. gas, appl. to surface ignition (*Russian*) 8-56895
 transonic nozzle flow of vibr. relax. or chem. reacting gases 8-59506
 turbulent pipe flow with heat transfer and chem. reaction 8-51257
 turbulent premixed flame, theoretical predictions (*French*) 8-94853
 vortex ring, turbulent, acoustic emission accompanying burning 8-94676
 $2\text{NO}_2 \rightleftharpoons 2\text{NO} + \text{O}_2$, gas mixture turbulent concurrent double pipe heat exchanger equilib. and nonequib. reaction 8-94856
 $\text{Br}_2 + \text{O}_2$, reaction with W surface, rate of reaction meas., gas flow experiment 8-92510
 $\text{H}_2\text{-F}_2\text{-He}$ chemical CW laser, flows (*Russian*) 8-74895
 N_2O_4 , dissoc. flow in tube, heat transfer and drag 8-71402
 N_2O_4 , dissociating, turbulent pipe flow, heat transfer, resistance 8-91026
 $\text{N}_2\text{O}_4 \rightleftharpoons 2\text{NO}_2$, gas mixture turbulent concurrent double pipe heat exchanger equilib. and nonequib. reaction 8-94856
 O_3 , decomposition flame, flat, laminar, vel., struct. 8-51256

chemiluminescence

- aequorin, Ca^{2+} -induced luminesc., inhibition by anaesthetics 8-76985
 albumin, human serum, kinetics of eosin-sensitised photochemilum. of solns. 8-68991
 alkali halide crystal, irradi., chemiluminesc. process during dissolution (*Russian*) 8-92133
 analytical, flow cell design 8-73090
 bromomethane, VUV laser multiphoton dissoc., CH excited state branching ratio, chemiluminesc. 8-70884
 9,10-diphenylanthracene, electrogenerated chemiluminescence, T_2 state emission 8-60524
 5-hydroxy-2,3-dihydro-1,4-phthalazindione, electron beam excited chemiluminesc., chem. and light yields 8-53209
 infrared, detection, in ion-molecule reactions, vibrational product states appl. 8-88625
 ion-molecule reactions, anal. of spectra 8-64832
 luminol, electron beam excited chemiluminesc., chem. and light yields 8-53209
 metal atom oxidation reactions, kinetics of chemilum. emitter form. and quenching 8-63107

chemiluminescence continued

- metal oxide, temp. depend. of chemilum. reactions, activation energies for excited state form. 8-66818
 PVC, ozonized, decomposition of peroxides, chemilum. meas. 8-68893
 CH, chemiluminesc. in flowing afterglow of Ar+methane 8-64839
 CN ($A^2\Pi$), chem. prod., CN number densities for gain, emission and absorpt. meas. 8-63112
 Ca-N₂O-CO flame, Ca catalyzed, gain meas., emission band assignment 8-66815
 Ca(4s4p²P)+N₂O, absolute chemiluminesc. cross-section and photon yield 8-53208
 Cl+H₂S→HCl+HS, laser-initiated chain reactions, rate consts., product energy distrib. 8-85144
 F+formic acid (formaldehyde), microscopic reaction dynamics, branching ratio, IR chemiluminesc. 8-73021
 Fe(CO)₅+Ar*(³P), chemiluminesc. 8-61014
 GeO, produced in Ge+N₂O reaction, kinetics of chemilum. emitter form. and quenching 8-63107
 H+Cl₂(SCl₂)(S₂Cl₂)(SOCl₂)(SO₂Cl₂), energy disposal, HCl IR chemiluminesc. obs. 8-92484
 HCl laser, V=3 to V=2 band process, computer simulation 8-71095
 HF+D, vibr. threshold energies, reagent energy effects 8-85145
 HN₃+NH₃*, intermediate reaction of laser photolysis of HN₃ 8-61037
 Hg+2NH₃→HgNH₃+NH₃, photosensitized, HgNH₃ complex lifetime 8-53193
 HgH+M→Hg+H+M, reaction rate temp. depend., chemiluminescence 8-68885
 HgH+NO→HNO+Hg, reaction rate temp. depend., chemiluminescence 8-68885
 Ho+N₂O→HoO*+N₂, chemiluminesc. reaction, cross-section 8-76847
 I chem. produced ²P_{1/2} state, gain meas. 8-63115
 La-F₂(ClF)(Cl₂)(SF₆), visible chem. laser development from reactions yielding visible chemilum. 8-63111
 Li+Cl₂(SF₆) (dichlorofluoromethane) (*German*) 8-92485
 LiF, γ-irradiated, chemilum. during dissolution (*Russian*) 8-80427
 Mg-N₂O-CO flame, efficient chem. generation of Mg(³P) 8-63109
 Mg-N₂O-CO flame, Mg catalyzed, gain meas., emission band assignment 8-66815
 MgCl spectra obs. in Mg*-Cl₂ crossed beams, metastable Mg as new light source of forbidden lines 8-90112
 ND*+DN₃→ND₂*+N₃, chemiluminesc. reaction of electronically excited species, rate const. 8-80771
 NF(a'⁴Δ)+I(²P_{1/2}) system, electronic angular momentum transfer, chem. kinetic model 8-63104
 NF(b'³Σ⁺) enhancement by I laser pumping 8-63105
 NH*+HCl(methane)(ethylene)(cyclopropane) (cyclohexane), rate const., time resolved chemiluminesc. 8-60982
 NH*+HN₃→NH₂*+N₃*, rate const., time resolved chemiluminesc. 8-60982
 O+NO binary reaction, crossed beams, NO₂ chemiluminesc. 8-64843
 O+O→O₂, matrix reaction, diffusion controlled, 8-20K 8-61013
 O₂+La(Y)(Sc), crossed beam chemiluminescence reaction, spectral simulation, hyperthermal energy meas. 8-80732
 O*+H₂S, matrix reaction, diffusion controlled, 8-20K, O(³P) 8-61013
 S+O₂→SO₂, matrix reaction, diffusion controlled, 8-20K 8-61013
 S+S→S₂, matrix reaction, diffusion controlled, 8-20K 8-61013
 Sc-F₂(ClF)(Cl₂)(SF₆)(Br₂), visible chem. laser development from reactions yielding visible chemilum. 8-63111
 ScF supersonic mixing flame, spontaneous emission, electronic transition chem. laser pot. 8-66817
 SiF, chemilum. obs. of A²Σ⁺ and A⁴Σ⁻ states 8-66816
 Sn+N₂O, chemiluminesc., high temp. fast flow reactor kinetics obs. 8-88636
 SnO, produced in Sn+N₂O(O₂) reactions, kinetics of chemilum. emitter form. and quenching 8-63107
 Sr-N₂O-CO flame, Sr catalyzed, gain meas., emission band assignment 8-66815
 SrF, temp. depend. of chemilum. reactions, activation energies for excited state form. 8-66818
 Sr*+N₂O→SrO*+N₂, visible chemiluminescence, absolute cross section and photon yields 8-92463
 Te(P₁)+inert gas, gas phase flash photolytic deexcitation obs., 1000K (*Russian*) 8-50626
 Y-F₂(ClF)(Cl₂)(SF₆)(Br₂)(IBr), visible chem. laser development from reactions yielding visible chemilum. 8-63111
 YCl supersonic mixing flame, spontaneous emission, electronic transition chem. laser pot. 8-66817
 YO, temp. depend. of chemilum. reactions, activation energies for excited state form. 8-66818

chemisorption

- acetylene, chemisorption on Pt (111), ethylidyne group form., LEED and ELS obs. 8-73075
 activated chemisorption kinetics, differential heat of adsorption meas. 8-84062
 alloy, binary, atomic roughness and chemical adsorption at solid-liquid interface (*French*) 8-51787
 atomic chemisorption, chemical trends, core-hole relax. effects, jellium model 8-76909
 catalyst, mag. characterisation, review 8-64881
 chemisorbed atoms and mols., vibrational motion dynamics, infrared absorpt. line shape 8-51814
 chemisorption, of H(O), on electrode, volume of adsorbed species, temp. and press. effects 8-84060
 electrolyte-solid interface, electrochemistry of surface 8-80798
 electronegativity, spin-orbital, and catalytic activity 8-73078
 electronic excitations of chemisorbed molecules, selection rule effects, EELS 8-76566
 embedding problem, SCFMO formalism 8-71977
 ethylene, chemisorption on Pt (111), ethylidyne group form., LEED and ELS obs. 8-73075
 graphite, of O, CO-NDO calcs. 8-75937
 Green's function methods for substrates with complex band. struct. 8-71961
 1-hexene-water(-D₂O), field-induced surface reactions, field ionis. mass spectra obs. 8-95949
 interstellar transition metal grains; of H. rel. to H₂ catalytic form. 8-54005
 kinetics, heterogeneity effects (*German*) 8-85202
 metal, chemisorbed O₂ and H₂O effect on surface props. 8-60187

chemisorption continued

- metal, intra-adsorbate Coulomb correl. and surface struct. roles 8-71979
 metal, intra-adsorbate Coulomb correl. and surface struct. roles 8-71980
 metal, narrow d-band, semiempirical theory, H and O chemisorpt. 8-75927
 metal, vac. UV photoelectron spectrometer appl. (*Japanese*) 8-78044
 metal films, evaporated, with BCl₃, HCl, interaction, adsorpt. 8-75945
 metal films, use of external mag. field, review 8-72003
 metal surface, chemisorption, vac. UV photoelectron spectrometer for study (*Japanese*) 8-62264
 metal surface, electron correl. in chemisorbed H atom, friction coeff. 8-60026
 metal surface, jellium, H chemisorption, linear response theory 8-91543
 metal surface, jellium, H chemisorption, relax. energies in UPS 8-91544
 metals, theoretical models, review (*Russian*) 8-84071
 photographic stabilisers, of yellow colloidal Ag, semiconductor props. (*German*) 8-86369
 polystyrene substrate, Cu vapour deposition, surface complex, XPS obs. 8-72026
 semiconductor, of H₂, effect of surface states 8-51823
 semiconductor crystal surface, nonequilib. electron effects due to chem. excitation 8-72238
 semiconductor crystal surface, nonequilib. electron effects due to chem. excitation 8-72239
 semiconductor surface, clean and with chemisorbed species, atomic and electronic struct. 8-72223
 simple metals, atomic chemisorption, atom-jellium model 8-84066
 site geometry, detector integrated angular distrib., photoexcitation depend. on target orientation, anal. 8-56564
 theory, inverse matrix diagonal and off diagonal elements, self energy perturbation theory 8-82607
 transition metal (001) surface, model, chemisorption, coverage depend. of adsorption behaviour 8-71976
 transition metals, of H, Hubbard-type surface mol. model binding energy calcs. 8-71990
 UPS, angle-resolved, chemisorption site determ. 8-71970
 Ag (110), adsorption of O₂ and CO-O₂ interaction, ellipsometry-LEED expts. 8-91542
 Ag(110), of ethanol, chemisorption and oxidation 8-61044
 Al (100), of O, photoemission ang. depend., MO cluster model calc. 8-76576
 Al film, polycryst., of O₂, synchrotron radiation photoemission expts., 70-150 eV 8-95228
 Al, of dibenzotetrathiafulvalene, ionisation and polarisation energies of mol., UPS meas. 8-79886
 Al, of formic acid, electron tunnelling spectra study 8-84049
 Al, of O₂ (NO), 80 to 290K, 10⁻⁶ to 10⁻² Pa, XPS study 8-95657
 Al₂O₃, of formic acid, electron tunnelling spectra study 8-84049
 Al₂O₃, of monocarboxylic acids, tunnelling spectroscopy 8-91545
 Au-Al₂O₃, of propylene, desorption and D exchange obs. 8-51827
 Au, of dibenzotetrathiafulvalene, ionisation and polarisation energies of mol., UPS meas. 8-79886
 C, chemisorbed oxygen surface complexes, thermal desorpt. analysis 8-56032
 C, of CO₂, surface area meas., temp. and chemisorption effects 8-95225
 CO, on Ni(111), surface optical excitations, reflectance spectra, electron energy loss meas. 8-84064
 CeO₂, chemisorption of H₂, kinetics and characts. at different pressures and temps. 8-51821
 Cl, chemisorbed layer on Si (111), SCF LCAO calcs. of Si band struct. 8-88010
 Co, of O, LEED anal. of Co(001)c(2×2)-O struct. 8-91546
 Cu (001), electronic struct. of (M)₂CO clusters 8-95948
 Cu (100) surface, of O₂, angularly resolved UPS meas. 8-71956
 Cu (111), of CO, coverage depend. photoelectron spectra, adsorption sites 8-95647
 Cu, chemisorpt. of CO, SIMS, AES, desorpt. meas. 8-87875
 Cu-Al, surface segregation during adsorption and low pressure oxidation (*French*) 8-75932
 Cu-Ni, chemisorpt. of CO, SIMS, AES, desorpt. meas. 8-87875
 Cu(110), of ethanol, chemisorption and oxidation 8-61044
 Fe (100) and (111) surfaces, of CO, CO₂, acetylene, ethylene, H₂ and NH₃ 8-71996
 Fe, cryst. of CO(H₂)(N₂), dissoc. chemisorpt. (*German*) 8-53257
 α-Fe, of acetylene, (ethylene), struct., bonding, dissoc., UPS obs., MO calcs. 8-84050
 GaAs (110), chemisorbed O₂, extrinsic surface states 8-91535
 GaAs (110), electronic states and initial steps in oxidation 8-91534
 Ge (111), of CO, on cleaved surface, electron energy loss spectra 8-79885
 Ge, of CO(Cl), surface photoemission, adsorption gate geometry 8-73079
 IR, chemisorption electron states for CO and O, electron field emission 8-84704
 Ir (110), of CO, preexponential factor and desorption energy 8-71963
 Ir (111) surface, electron beam induced desorption and dissociation of chemisorbed CO 8-56043
 LaB₆ (100), of O₂, LEED, AES, work function meas. 8-71989
 Mg film, polycryst., of O₂, synchrotron radiation photoemission expts., 70-150 eV 8-95228
 MgO powder, decomp. of chemisorbed ethanol, propanol and acetic acid 8-92502
 Mo(100), of O₂, low-energy SIMS, ion yields depend. on surface chem. and primary ion energy 8-73105
 NO, adsorbed on Cu, species identification, struct., dissoc. chemisorption, desorption, UV photoelectron spectroscopy 8-52635
 Nb film, of SO₂, adsorpt., corrosion 8-79897
 Nb, of O₂, electronic struct., UPS meas. 8-95682
 Ni (001), chemisorption site determ. for S and CO, angle-resolved UPS 8-71970
 Ni (001), electronic struct. of (M)₂CO clusters 8-95948
 Ni (001), of O, electronic struct., KKR model calcs. 8-56200
 Ni (100), of ethylene and acetylene, angular resolved UPS exam. 8-72685
 Ni (100), of O, bonding model 8-79889

chemisorption continued

- Ni (110) surface, of H_2 , demagnetisation, positive spin polarisation in electron field emission 8-52646
 Ni, chemisorpt. of CO, SIMS, AES, desorpt. meas. 8-87875
 Ni, chemisorption of S, ang. depend. of multicentre Auger matrix element for Ni (100)-c(2×2)S 8-92151
 Ni film, of H_2 , effect on ferromag. reson. 8-72375
 Ni foil, of H_2 , surface states and thermo EMF 8-91674
 Ni, of CO, ab initio LCAO MO SCF calc. for NiCO 8-62712
 Ni, of CO, on (100) surface, mol. levels, angle depend. calcs. 8-90069
 Ni, of H, surface magnetism 8-95510
 Ni, of H, X_α cluster calcs. (Japanese) 8-72002
 Ni, polycryst., of O_2 , SIMS and flash desorption obs. 8-76568
 Ni(Ni)₂-ethylene cluster complex 8-82641
 PbS(Se)(Te), of O_2 , room temp., UPS and XPS obs. 8-91529
 PbSe surface, clean and O_2 -exposed, XPS (UPS) obs., electronic struct. 8-52637
 Pb_{1-x}Sn_xTe, MBE, O_2 uptake, AES, XPS and UPS expts. 8-95227
 Pd (100), of acetylene, substrate effects on bonding, electronic spectrum 8-63933
 Pd, of CO, ultra high vacuum technique 8-71960
 Pd, of He(CO)(O₂), mol. beam study 8-79878
 Pt electrode, of H, entropy, temp. and press. effects 8-84059
 Pt electrode, of H(O), volume of adsorbed species, temp. and press. effects 8-84060
 Pt electrode surfaces, of H_2 , electrochem. activity comparison 8-61015
 Pt, of O_2 , thermomag. effect, temp. depend. (Russian) 8-60034
 Rh, of NO, reaction with CO, obs., reaction kinetics calcs. 8-61045
 Rh/ γ -Al₂O₃ disperse δ -phase, chemisorpt. of CO, IR spectra, site distrib., mol. mobility 8-72496
 Rh(111), of CO, energy level shifts of CO 8-87865
 Ru (0001), of acetylene, substrate effects on bonding, electronic spectrum 8-63933
 Si (111), Cl₂ chemisorption, ang. resolved UPS and LEED meas. using Vidicon intensity processor 8-71972
 Si (111), electronic states and initial steps in oxidation 8-91534
 Si (111), of CO, on cleaved surface, electron energy loss spectra 8-79885
 Si (111), of Cl, LCAO calcs., Auger line shapes, localized density of states 8-56202
 Si (111), of Cl, surface energy bands and atomic position of Cl 8-56041
 Si (111), of H(Cl), conduction-band surface resonance 8-52051
 Si, acetone layer, CH radical production by sputtering, rot. and vibr. population distrib. 8-64436
 Si, bonding states of adsorbed O_2 , photoemission obs. 8-92170
 Si, of CO(Cl), surface photoemission, adsorption gate geometry 8-73079
 Si, of H_2 , atom-probe FIM obs. 8-71968
 Si, of organic solvents (Russian) 8-91537
 Sn, O_2 precursor adsorption, chemisorption activation energy 8-71950
 Ta film, of SO₂, adsorpt., corrosion 8-79897
 Ti (0001), of CO, LEED struct. anal. 8-71964
 Ti film, of SO₂, adsorpt., corrosion 8-79897
 Ti, of N₂, O_2 and CO on polycryst. surfaces, secondary electron yield obs. 8-71971
 TiO₂, of H₂O, differential heat of chemisorption 8-84052
 TiO₂, of O_2 , phase investig. by UPS 8-72684
 TiO₂, X-irrad., adsorpt. of O_2 , EPR meas. 8-80211
 W (001), of H_2 , angle-resolved photoemission, symmetry-related polarisation effects 8-56566
 W (100), CO/H₂ surface complex, flash desorption and AES obs. 8-73083
 W (100) surface, of CO, mol. orbital study 8-71995
 W (110), chemisorption of O, Monte Carlo modelling of phase changes 8-71969
 W, of O, as (110) surface, adatom-adatom interaction energies determ. 8-67904
 W, of O, on (110) surface, phase transitions, coverage effects 8-79879
 WC, microcrystalline, mol. dynamics, motion of H₂O and H₂ mols. adsorbed on surface, catalytic activity 8-71941
 W(100), of O_2 , low-energy SIMS, ion yields depend. on surface chem. and primary ion energy 8-73105
 W(110), of CO and O_2 , absolute coverage and work function meas. 100 and 300K 8-71986
 Zn surface, O_2 interaction, chemisorpt. and oxidation 8-64886
 ZnO 1010 surface, reaction of O_2 , AES, LEED, EPR, desorpt., surface cond. and work function expts. 8-95950
 ZnO, of H, electrical cond. exam. adsorption centres 8-67913
 ZnO, of H₂O, differential heat of chemisorption 8-84052
 ZnO, of pyridine, acetone, dimethyl sulphoxide, UPS, mol. orbitals effect on bonding 8-72699
 ZnS, of O_2 , after illumination and in presence of CO and O_2 8-87877

chemistry

- see also atmospheric chemistry
 biochemistry and biophysics horizons, book 8-68977
 formulae, historical development, review 8-73822
 organic chemistry, textbook, undergraduate level 8-57711
 post-graduate educational system in North America rel. to Muslim graduate student 8-65736
 pure and applied chemistry, conf., Tokyo, Japan (Sept. 1977) 8-95906
 undergraduate education, future changes 8-69929
 Z=106, atomic and chemical props. by gas chromatography and aqueous chemistry, book contrib. 8-85121
 Ha, (element 105), atomic and chemical props. by gas chromatography and aqueous chemistry, book contrib. 8-85121
 Ir, recovery from laboratory residues 8-81957
 Rf, (element 104), atomic and chemical props. by gas chromatography and aqueous chemistry, book contrib. 8-85121

chemistry, physical see physical chemistry**chemistry computing**

- see also computerised instrumentation; spectroscopy computing
 analysis, instrumental, minicomputer appls., errors 8-92543
 analytical chemistry, user-oriented software Fourier spectrum display 8-64896
 applications in organic struct. chem. and mol. spectroscopy in USSR 8-88624

chemistry computing continued

- atom numerical code scheme for classification of chemical shifts 8-94205
 binary solid-liquid equilibria, student experiment, phase diagram computer program 8-89285
 electron integrals transformation method, program in FORTRAN IV H 8-82603
 element distributions obtained by ion microprobe, images quantification 8-73101
 estuary and river sited power plants, water discharge and chlorination, simulation 8-96250
 gas chromatography, data acquisition and use of microwave plasma detector as element analyser (German) 8-64895
 hydrocarbon combustion products, 1400-2600K, minimisation of NO, computer model 8-85161
 ion-selective electrode measurements in flowing system, computer-controlled interference correction 8-92527
 MNDO calculations, total energy, anal. first derivatives 8-86763
 molecular spatial models, Stuart-Briegleb type, computer construction 8-86970
 molecular systems including up to 232 orbitals, CNDO calcs., computer program 8-86788
 particle size measurement techniques, rapid response, online methods, continuous industrial processes appl. 8-89429
 polystyrene solutions, US degradation obs. 8-95989
 potentiometric titration system, microcomputer controlled, for soln. equilb. obs. 8-92522
 quasimolecules, electronic struct. calc., CNDO approx., computer program 8-86789
 REACT program for computer-assisted simulation of chemical reaction sequences, structure elucidation applications 8-92477
 reaction sites automatic detection 8-92476
 SCF calculations, simplified extrapolation procedure 8-82604
 solutions, dilute, Monte Carlo free energy calcs. in isothermal-isobaric ensemble 8-92498
 steroids, mass spectra, computer-aided interpretation by pattern recognition methods 8-64898
 structural formulae for chem. cpds., program for detecting presence or absence of struct. fragments 8-62941
 structural search codes for on-line compound registration 8-90319

Cherenkov counters

- $\psi(J)$ particle, discovery, props., experimental apparatus develop. (Czech) 8-78232
 beta-emitter radioassay, prep. of plant samples 8-81088
 Darmstadt linear accelerator, detector system and performance of elec. scatt. system 8-70680
 deep water muon and neutrino detection using Cherenkov light gathering systems (Russian) 8-55109
 EAS, duration of atmospheric Cherenkov pulses 8-73595
 high-speed pulse shaper/discriminator for scintillation and Cherenkov counters 8-86748
 large solid angle counter for DELCO expt. at SPEAR 8-86729
 liquid-filled, for gamma-ray counting of large samples 8-53491
 photographic detector appl. to search for Dirac monopole 8-70700
 silica aerogel counter test results from CERN PS 8-86731
 telescope for α -particle and proton-spectroscopy on GOES and TIROS spacecraft 8-86734
 transition radiation effects on efficiency of particle detection 8-58893
 Pb glass EM shower detector, test results 8-70689

Cherenkov detectors see Cherenkov counters**Cherenkov radiation**

- see also Cherenkov counters; electron radiation
 atmospheric Cherenkov pulse duration, depend. on cosmic ray shower parameters 8-89025
 cosmic rays, γ primaries meas., 10 to 100 GeV, using air showers Cherenkov light distrib., detector system 8-73597
 electron bunch coherent radiation, electron distrib. effects 8-66734
 electrons in mica target, 140-250 keV, ang. distrib. of radiation at 4000 Å and 5000 Å (Russian) 8-55291
 gamma-ray resonance frequency range (Russian) 8-80432
 inhomogeneous medium, geometric optics description 8-66766
 large cosmic ray showers, Cherenkov radiation computer simulation using hadronic collisions models 8-57415
 plasma, three-dimens. vel. diffusion, in two-stream turbulence 8-59595
 synchrotron-Cherenkov radiation, angular distribution 8-62998
 threshold behaviour of Vavilov-Cherenkov radiation 8-82895
 transition radiation from Cherenkov charge in nonstationary medium (Russian) 8-50694
 vacuum UV Cherenkov source as radiation standard (Russian) 8-63164

chilling see cooling**chiral symmetries**

- see also S_N theory
 bound states from instantons 8-78087
 broken isospin symmetry in chiral SU(4)⊗SU(4) and D⁺-D⁰ mass difference 8-89691
 chiral nonlinear field eqns., exact solns. 8-54527
 classical Euclidean 2-D nonlinear σ -models, continuity eqns. 8-54210
 conserved chiral charge on Schwinger model 8-49961
 dual chiral pion model, partially conserved axial-vector current 8-58175
 gauge chiral U(1) symmetry and CP invariance in presence of instantons 8-78075
 homogeneous Lorentz group, chirality, Weyl spinors 8-93810
 index theorem, axial-vector anomalies, in Schwarzschild and Taub-NUT spaces 8-93832
 kink solns. of extended nonlinear model and particle interpretation 8-89612
 lattice Schwinger model, massive QED for fermions in 1+1 dimens. 8-78121
 lightlike chiral structure of hadrons, nonleptonic hyperon decays 8-74253
 method of action-angle variables and the classical dynamics of a nonlinear Lagrangian 8-77702
 QCD, strong interaction gauge theory, SU(3) colour gauge vector mesons, confinement 8-78136
 QCD phase transitions, chiral symmetry breaking, confinement, as tunnelling through singular barriers 8-82145

chiral symmetries continued

- relativistically invariant two-dimens. models, classification method (*Russian*) 8-70291
 Schwinger model, $A=0$ gauge, breaking of chiral symm. 8-62307
 Schwinger model, chiral symm. breaking and vac. struct. 8-89615
 $SU(4) \times SU(4)$ broken chiral symm. 8-74176
 $SU(4) \times SU(4)$ broken symm. in quartet model, D- and F-meson masses and decay consts. 8-66087
 supergravity, chirally extended, Maxwell-Einstein, auxiliary field struct. 8-78126
 supersymmetric nonlinear σ model, S-matrix determ. 8-66052
 supersymmetric nonlinear σ model, spontaneous breakdown of chiral symmetry 8-54549
 transverse pure gauge fields and nonlinear chiral solitons, Coulomb condition 8-78068
 U(1) problem and zero-mass quarks 8-82124
 K_1^0 , weak radiative decays in chiral theory using virtual π^0 and η pole diagrams (*Russian*) 8-78172
 NN interactions and chiral symm., dispersion relation anal. 8-66048
 $\varphi \rightarrow \pi\gamma$, $SU(3) \times SU(3)$ algebra, appl. to ground state mesons, coupling constraints and decay rate 8-58183

chlorine

see also nuclei with

- adsorbed, on Ag(111), props., struct., AES study 8-72024
 adsorption, on Al(Fe), thermal accommodation coeffs., translational (internal) gas-solid energy exchange 8-92506
 adsorption and reaction with InP surface, electron spectroscopic obs. 8-56036
 atom, form. from HCl dissoc. excitation in afterglow, light emission 8-90115
 atom, L X-ray emitting levels, lifetimes 8-66493
 atom, MINDO parameters 8-86786
 atom, photoelectron spectra, photoionisation cross-sections 8-90131
 atom diffusion in Ar and He gas, diffusion const. 8-71417
 atomic K α X-ray satellite spectra, gas phase meas. 8-66496
 brine, routine anal. by X-ray fluoresc. spectrometry applying matrix corrections 8-88690
 chemisorbed layer on Si (111), SCF LCAO calcs. of Si band struct. 8-88010
 chemisorbed on Si (111) surface, surface energy bands and atomic position of Cl 8-56041
 chemisorption on Si(111), conduction-band surface resonance 8-52051
 chemisorption on Si(Ge), surface photoemission, adsorption gate geometry 8-73079
 chemisorption on Si (111), ang. resolved UPS and LEED meas. using Vidicon intensity processor 8-71972
 chemisorption on Si (111), LCAO calcs., Auger line shapes, localized density of states 8-56202
 diffusion, in α -Ti, AES meas. 8-51735
 energy straggling of Cl ions+Ar-methane, (isobutane) 8-58785
 isotope enrichment using laser photolysis of dichlorodifluoromethane 8-58859
 lattice dynamics using simple bond charge model 8-55919
 liquid, transient stimulated vibr. Raman scatt. 8-71144
 molecular crystal, bond charge model, for lattice dynamics 8-79692
 molecule, absorption in ultrasoft X-ray region 8-90187
 molecule, dissoc. attachment by 0-8 eV electrons 8-74776
 molecule, dissociation, weak bias and anharmonicity effects 8-82661
 molecule, effective core potentials, all-electron calcs. 8-62704
 molecule, photochemical reaction using Ar ion laser, Cl isotope enrichment 8-74780
 molecule, rot. relax. classical trajectory computation, using Lennard-Jones pot. 8-62880
 molecule in Ar matrix, MCD, emission spectrum at 13600 cm^{-1} , Zeeman anisotropy 8-82057
 in oceans, Cl and Br origin 8-65342
 CaO:Cl , X-ray and UV luminesc., electron-hole recombination processes (*Russian*) 8-76528
 CdS:Cl , extrinsic, exciton absorption 8-72569
 CdS:Cl , heavily doped, fluoresc. spectrum upper threshold calculated 8-52568
 Cl I, photoionisation cross section, calc. by many-body perturbation theory 8-62771
 Cl II in CuCl and FeCl_2 vapours, pulse generation at 5218 Å, 5221 Å 8-58990
 Cl VIII, Ne I like reson. and Na I-like satellite lines, relativistic HF calc., beam-foil spectra 8-94210
 Cl XIII-XV, $\Delta n=0$ transitions, lifetime meas. beam-foil spectra 8-78798
 Cl⁻, far UV spectra in solns. 8-94208
 Cl⁻ free-bound continuum radiation threshold broadening obs. in plasma 8-71579
 Cl⁻, pair polarisability, ab initio SCF MO energies 8-70741
 Cl⁻ radiative detachment threshold effect of plasma microfield 8-71580
 Cl+Al, molecular K X-ray transitions, mol. radiative electron capture effect 8-58802
 Cl+D₂→DCl+Cl, LEPS pot. energy surface, rate consts., isotope effect, quasiclassical trajectory calc. 8-56887
 Cl+formaldehyde, rate const. 8-85136
 Cl+H₂S→HCl+HS, laser-initiated chain reactions, rate consts., product energy distrib. 8-85144
 Cl+HBr, ZZ 8-80729
 Cl+HI, chem. laser, energy distrib., spectrosc. obs. 8-71096
 Cl+HNO(H₂O₂)(HO₂), rate consts., stratospheric appl. 8-85125
 Cl+HO₂ react. rate const. determ. at 298K (*French*) 8-64817
 Cl+H(D)I, exothermic triatomic exchange reactions, prod. energy distrib., statistical dynamic model 8-92455
 Cl+NO+N₂→NOCl+N₂, rate const. temp. depend. 8-76828
 Cl⁻+chloromethane, S₂ reaction, local orbital description ab initio FSGO method 8-76842
 Cl₂ in Ar matrix, vibr. relax., stochastic classical trajectory approach 8-79707
 Cl₂+H, activation energy and trajectory calcs., temp. and isotope effects 8-76835
 Cl₂+H, energy disposal, HCl IR chemiluminesc. obs. 8-92484
 Cl₂+H, nonreactive scatt., long range anisotropic pot. determ. 8-66626
 Cl₂+H(D), exothermic triatomic exchange reactions, prod. energy distrib., statistical dynamic model 8-92455

chlorine continued

- Cl₂+Li, chemiluminescence spectra, excited Li (*German*) 8-92485
 Cl₂+Sn, reactive scatt., ang. distrib. and time-of-flight spectra 8-64842
 Cl(²P)+methane, absolute rate and temp. depend. 8-80731
³⁷Cl₂, pure rot. Raman spectrum 8-94252
³⁸Cl+H₂(D₂) reactions, characterisation, effect of ethylene-I₂ scavenger 8-73071
 Cu+Cl¹⁺, X-ray cross sections, projectile fluoresc. yields 8-74751
 H+Cl₂, impulsive triatomic reaction, vibr. state distrib., impulsive energy release model 8-92456
 HCl+Cl, vibr. energy transfer to oscillatory, restricted rot. and translational motion 8-70908
 NaI:Cl⁻, anharmonic effects on low-frequency impurity phonon resonances 8-75771
 Se:Cl, trigonal, defect and impurity electron levels, surface photovoltage spectra 8-72108
 Si-SiO₂ interface, with Cl⁻ incorporated, characterisation by low temp. cond. meas. 8-60220
 ZnS:Cl⁻, Cu⁺(Ag⁺), phosphor, high press. effect on thermoluminesc. 8-64419
 ZnS:Cu(Cl), electroluminesc. and photoluminesc. spectra, fine struct. (*Russian*) 8-84661

chlorine compounds

- ESCA chemical shift, indirect evaluation of Coulombic contribution to ionis. pots. for nonbonding electrons 8-92572
 ethylene+Cl₂(Br₂) complex, intermolecular interaction and struct. SCF-MO-LCAO CNDO/2 calc. 8-58763
 organic π - σ complexes, low freq. spectra 8-78713
 ozoneosphere, CIX content rel. to temp. struct. and O₃ distrib. 8-57246
 volatile chlorides, adsorption isotherms meas. using radionuclides and chromatography 8-76902
 AgClO₃, ClO₂ spin Hamiltonian 8-60326
 CIBS, form., photoelectron and microwave spectra 8-90214
 ClCN, and isotopic derivatives, rot. depend. of Fermi resonance 8-94227
 ClCN, general quartic force field, Machina-Overend parameters 8-50532
 ClF, gas, rot. frame NMR, reorientational and ang. correl. times 8-78721
 ClF+Ar, shock wave, vibr. relax., laser schlieren meas. 8-90267
³⁵ClF₆, radical, prep. and EPR comparison with other hexafluoride radicals 8-68381
 ClHCl⁻, deuteron quadrupole coupling const., nuclear mag. shielding, geometry depend. 8-58586
 ClNO+ClONO₂ react., gas phase, kinetics, mechanism, IR photometric investig. (*German*) 8-76834
 ClNO₂, catalysed by ClNO, thermal decomposition spectral photometric investig. (*German*) 8-95925
 ClNO₂, kinetics of thermal decomposition (*German*) 8-95924
 ClNO₂, standard enthalpies of form. determ. (*German*) 8-53235
 ClO, A²II-X²II, UV absorpt. spectrum 8-74673
 ClO, bandstrength determ. of fundamental vibr.-rot. spectrum 8-70872
 ClO, laser spectroscopy relevant to stratospheric photochemistry 8-88951
 ClO radical, IR vibr.-rot. spectra, background data for atm. meas. 8-58679
 ClO, rot. spectrum, mol. parameters in $v=0$, $v=1$ states 8-70821
 ClO⁻+NO(NO₂)(SO₂)(CO₂), rate consts. at 300K 8-76829
 ClO₂, gas-phase electron g-tensor, magic doublet rot. Zeeman spectra 8-90212
 ClO₂ radical, laser mag. reson., ν_1 band 8-94263
 ClO₂, standard enthalpies of form. determ. (*German*) 8-53235
 ClO₂⁻, Cl L_{IIIII} fluoresc. X-ray spectra, mol. orbital struct. 8-70848
 ClO₃⁻, Cl L_{IIIII} fluoresc. X-ray spectra, mol. orbital struct. 8-70848
 ClO₃⁻, in KClO₄, detection by EPR of ClO₃ radicals created by X-irrad. 8-76311
 ClO₃⁻ in NaBrO₃, Raman spectra, fundamental vibr. modes 8-78711
 ClO₄⁻, Cl L_{IIIII} fluoresc. X-ray spectra, mol. orbital struct. 8-70848
 Cl₂O, standard enthalpies of form. determ. (*German*) 8-53235
 ClO₂F, cryst. struct., X-ray and neutron diff., Raman spectra (*French*) 8-83788
 ClO₂F, ¹⁹F NMR line shape temp. depend. and spin-lattice relax. 8-91969
 ClO₂F, vap. phase Raman spectrum, single isotopic species bands 8-78712
 ClONO₂, laser spectroscopy relevant to stratospheric photochemistry 8-88951
 ClONO₂+NO(ClNO) react., gas phase, kinetics, mechanism, IR photometric investig. (*German*) 8-76834
³⁵ClF(³⁷ClF)+Kr potential, asymmetric, isotope substitution effect, Legendre expansion coord. transformation 8-70894
 Cu compounds, chemical shifts of X-ray electron and Auger lines 8-86912
 CuCl, pulse generation of Cl II at 5218 Å, 5221 Å 8-58990

cholesteric liquid crystals

- acoustical activity 8-83880
 BMAOB-cholesteryl caprinate mixture, spiral pitch temp. depend. 8-79529
 boojums, analogy with behaviour in superfluid ³He-A 8-56014
 cholesteric-nematic liq. cryst. mixtures, electro-optic charact., light scatt. modes (*Japanese*) 8-79527
 cholesteric pelargonate, liq. cryst., crystallisation rate const. and Avrami index 8-94994
 cholesteryl azo dyes, prep., DSC, struct. props. 8-51412
 cholesteryl benzoate, orientational order, EPR study 8-75540
 cholesteryl caprilate, conduction mechanism 8-64046
 cholesteryl chloride-cholesteryl crotonate (75:25% wt.) mixture, cholesteric-nematic transition field effect temp. depend. 8-75813
 cholesteryl chloride-cholesteryl pelargonate mixture, cholesteric-nematic transition 8-91244
 cholesteryl laurate, conduction mechanism 8-64046
 cholesteryl oleate-MBBA mixture, memory effect characts., crit. freq. rel. to erase voltage 8-94993
 cholesterylalkanoates, liq. cryst., optical anisotropy and struct. ordering (*Russian*) 8-87616
 COC, shear flow, helix distortion, optical meas. 8-94982
 disclinations, generation process, matrix representation 8-59743

cholesteric liquid crystals continued

- EHD instability with isotropic mechanism (*Russian*) 8-87617
 electric field induced nematic to cholesteric transition, transient phenomena of relax. 8-75811
 Grandjean lines, flow induced 8-71670
 helical sense and pitch from birefringence meas. 8-59744
 helix period, mag. field strength depend. near phase transition to smectic A (*Russian*) 8-59754
 light refraction, by a cholesteric prism under applied mag. field (*French*) 8-80319
 mixture, optical activity (*Russian*) 8-71677
 mixture, with positive dielectric anisotropy influence of external fields (*Rumanian*) 8-59751
 nematic-cholesteric mixture with positive dielectric anisotropy, light scatt. characts. 8-75537
 network polymers, heterogeneous, from partially hydrolysed poly(methyl D-glutamate) and poly(oxyethylene glycol), mesophase struct. (*Japanese*) 8-95002
 planar texture instability for cholesteric-nematic mixture with negative dielec. anisotropy 8-59739
 screw sense, form of spiral disclination lines calc. 8-67643
 semiconductor-liquid crystal interface props. (*Rumanian*) 8-83723
 shear electricity, symmetry considerations 8-60394
 thermosensitive, props. (*Hungarian*) 8-59755
 topological classification of distortions 8-79523
 transient electrodynamic instability, for system with positive anisotropic dielec. permeability (*Russian*) 8-51418
 uncompensated system, increase in pitch of cholesteric helix with temp. 8-71676
 US propagation, mesophases and phase transitions 8-79667
 visualisation of microwave fields 8-58031

chondrites *see meteorites***choppers (circuits)**

- low-power UV source, with electronic chopper 8-79087

chopping *see cutting***chromatic aberration** *see aberrations***chromatography**

- acetylene-NO₂, combustion products, 1400-2600K, minimisation of NO, computer model 8-85161
 affinity, calf lymph nodes, X-irrad. interaction between histone F2b and DNA 8-85346
 air pollution, vertical diffusion study using airborne gas-chromatography and numerical modelling 8-69435
 alkyl Pb compounds, in atmosphere, detect. via gas chromatograph-microwave plasma detector 8-68975
 alkyl Se compounds, in atmosphere, detect. via gas chromatograph-microwave plasma detector 8-68975
 atmosphere organic pollutants, determ. via gas chromatography after cryogenic sampling 8-81468
 benzene production, monitoring procedure for pure product 8-92583
 biological fluorocarbon detection by gas chromatography (*German*) 8-96117
 blood gas sampler, for gas chromatography, design, construction and characteristics (*Japanese*) 8-85458
 breath anal. by gas chromatography, use of relative time programming 8-61268
 capacitor dielectric fluid test and anal., quality assurance 8-80272
 capillary gas, mass spectroscopy and computer techniques, organic compound analysis in environmental samples appl. 8-80799
 carotenoid pigments, in geochem. systems, HPLC determ. 8-61078
 charcoal tube sampling technique, meas. accuracy 8-69508
 chrysotile, adsorpt. of organic micropollutants, XPS and gas solid elution chromatography exam. 8-80790
 coiled glass columns, for gas chromatography, rapid packing system 8-73095
 column switching technique for gas chromatographic analysis 8-92530
 crocidolite, adsorpt. of organic micropollutants, XPS and gas solid elution chromatography exam. 8-80790
 cytidine-5'-monophosphate, γ -irrad. aq. soln., spin-trapped radicals, liq. chromatography and EPR spectroscopy 8-53340
 data processor, microprocessor based, appls. to chromatography (*Japanese*) 8-61131
 density detector operation, mathematical modelling (*Russian*) 8-92580
 Du Pont DP-1, gas chromatograph/mass spectrometer, sub-picogram detection, wide dynamic range and automatic source rejuvenation 8-93782
 field flow fractionation, macromolecules appl. 8-90327
 Fourier transform gas chromatograph-IR system, trace organic pollutants detect. 8-68967
 gas, automatic, vapour-liquid equilb. meas., appls. (*German*) 8-88667
 gas, combined with mass spectrometry, forensic laboratory appl. 8-92556
 gas, comparison of quenching effects in single-, dual-flame photometric detection 8-61072
 gas, Fourier transform IR detector system, programmable 8-92560
 gas, graphitised C black packed columns, efficiency rel. to particle size 8-92536
 gas, high-precision on-stream instrument, process control appl. 8-53283
 gas, influence of temp. programming 8-68958
 gas, infrared group specific detectors 8-92557
 gas, mass spectrometer anal. system, ion multiplier noise filter 8-92541
 gas, multicolumn, multidetector chromatographic reactor, appls. 8-92590
 gas, photoionisation detector appl. 8-92561
 gas, quantitative, errors, efficiency 8-92538
 gas, quantitative, unrecognised systematic errors 8-92537
 gas chromatographic detectors, errors in operation 8-92554
 gas chromatographic effluents, FT IR spectrometric identification 8-73091
 gas chromatography, data acquisition and use of microwave plasma detector as element analyser (*German*) 8-64895
 gas chromatography, for determ. of halocarbons in air 8-85739
 gas chromatography, laser optoacoustic spectroscopic detection 8-92521
 gas-liquid, computing integrator correction factor 8-76960
 gas-solid, using radiotracers, appl. to adsorption meas. of volatile chlorides 8-76902

chromatography continued

- gas/photoionisation mass spectrometry, organic compds. anal. appl. 8-92531
 gel permeation, combined with low angle laser light scatt., polymer molecular weight distrib. appl. 8-92230
 gel permeation chromatography of interacting multicomponent systems, protein isomerisation study 8-68950
 gel permeation chromatography of interacting multicomponent systems, protein isomerisation kinetic consts. determ. 8-68951
 gel-permeation, mol. wt. distrib. of polymer films (*German*) 8-85252
 glass capillary columns and specification of dedicated instrument 8-80804
 halogen leak detection, reduction of background effects by means of chromatographic columns 8-70110
 high performance liquid, flow measurement, control system for reciprocating pumps, HPLC detectors appl. 8-92559
 high performance liquid chromatography, automation 8-80806
 high performance low pressure liquid chromatography, laboratory appl. 8-80801
 high-sensitivity autoionography, detection of radioactive spots on thin-layer chromatograms 8-86960
 hydrocarbon resin, mol. wt., chem. constitution investigation by gel permeation chromatography (*German*) 8-64910
 ion chromatography, new analytical technique for sulphate and nitrate assay in ambient aerosols 8-68974
 ion-exchange, enzymatic digestion of γ -irradiated DNA 8-85290
 ionising radiation decomposition of chromatographic support materials (*German*) 8-92587
 Kevlar-49, chemical characterisation 8-95725
 liquid, band broadening, in microcapillary tubes 8-61085
 liquid, differential deviation refractometer appl., high sensitivity and time response conditions (*Czech*) 8-80810
 liquid, high performance, liq. sample loop geometry 8-92539
 liquid, high performance, solute elution behaviour on porous polystyrene gel 8-92524
 liquid, high performance in-house slurry packing of columns, advantages 8-92555
 liquid, high press., pulse dampening system 8-92540
 liquid, packed microcapillary columns 8-61069
 liquid, pump design review for HPLC apparatus 8-80800
 liquid, reverse phase, resolution change with column temp. 8-92525
 liquid, sorption materials characteristics and development trends (*Czech*) 8-64904
 liquid, using volatile solvents, effluent detector 8-92529
 liquid chromatography, real time Fourier transform IR detector 8-86357
 metal species, identification and determ. by chromatographic-at. spectrosc. method 8-68972
 mixtures, universal gas chromatographic system, based on frontal anal. 8-61114
 nonrecursive, based on analogue delay device, for mass spectrometer ion multiplier 8-92541
 nylon 6,6, drawn fibre, selective degradation, gel permeation chromatography, TEM 8-71683
 nylon 6,6, selective degradation, mol. wt. determ., gel permeation chromatography, TEM 8-71682
 organic solids, photoproduced in simulated Jovian atmosphere, mol. anal. 8-69740
 papain inactivated by OH radicals and H₂O₂, optical density, amino acid composition and fluoresc. 8-53344
 plasma chromatograph-mass spectrometer, H₂O determ. in electronic component packages 8-86379
 poly [2-(p-azidobenzoyloxy)ethyl methacrylate], MW distrib. effects on photosensitivity (*Japanese*) 8-94418
 polymer films, mol. wt. distrib. by gel-permeation chromatography (*German*) 8-85252
 polymers, paints, testing, modern analytical methods appl. (*Polish*) 8-85253
 polystyrene solutions, US degradation obs. 8-95989
 porphyrin pigments, in geochem. systems, HPLC determ. 8-61078
 positive pressure columns 8-73092
 Quadmagnova, GC/MS system, computer scanning and control 8-76946
 radial, high performance, apparatus and techniques 8-80802
 radiochromatograms, thin-layer, anal. by proportional chamber 8-77174
 reaction and separation in pulse-fed catalytic reactor 8-64880
 silica gels, surface treatment, adsorption properties (*Japanese*) 8-95855
 solution adsorption, from liq. chromatography 8-84054
 stability criteria, appl. to gas chromatography 8-62049
 supercritical fluid chromatograph, pneumatic amplifier pump 8-88665
 teaching, mobile spectroscopy, chem. anal. laboratory 8-93502
 thin layer, luminesc. meas. methods 8-53305
 thin layer, luminescence quantitation, solvent effects 8-53306
 thin layer, quantitative photometric scanning, analysis of organic substances appl. 8-92558
 thin-layer, amino acid and urea anal. of samples obtained by percutaneous electrophoresis 8-61237
 thymidine-5-monophosphate, γ -irrad. aq. soln., spin-trapped radicals, liq. chromatography and EPR spectroscopy 8-53340
 transition metal complex ions in aq. HCl, temp. gradient chromatography (*Japanese*) 8-61120
 vacuum gas chromatography-mass spectrometry, using short gas capillary columns 8-95968
 Viking lander gas chromatograph-mass spectrometer 8-77460
¹⁸B separation using anion exchange resin, isotopic plateau holding displacement chromatography (*Japanese*) 8-56886
 C black with pyrocarbon coating, surface props. (*French*) 8-68921
 H₂, determ. in H₂O after photolysis, gas chromatography 8-61089
 H₂SO₄, air pollution, new detector, aerosol mobility chromatograph 8-96297
 O₂, determ. in H₂O after photolysis, gas chromatography 8-61089
 S, SO₂²⁻ and related species, sampling and anal. of atm. aerosols 8-96283
 SF₆ insulated switching installations and devices, gas chromatography appl. (*German*) 8-88668
³⁵S content of coolant gas in Windscale AGR, gas chromatographic and radiochemical anal. 8-73125

chromium

see also nuclei with

abundance in stars, Utrecht UV spectrophotometer obs. 8-69793
 alloying with rare earth metals, Ti, Zr, Hf, Nb, Ta 8-68651
 antiferromagnetic, polarisation domain effects on US velocity 8-52329
 atom, double K-shell ionisation by electron impact, X-ray spectra 8-62928
 atom, double K-shell ionisation by electron impact 8-62929
 atom, X-ray production by protons by 0.5 to 2.0 MeV energy 8-66646
 atom, X-ray spectra, chemical bonding and multiple ionis. effects 8-50630
 atomic transition probabilities, oscill. strengths 8-74601
 concentration determ. in atm. and rainwater in Vizcaya, Spain (*Spanish*) 8-57264
 concentration in atmospheric sedimentable powder, in Vizcaya, Spain (*Spanish*) 8-57265
 contact to GaAs, effect on minority carrier diffusion length 8-72260
 crystal structure below Neel temp., X-ray diff. study 8-83772
 Debye-Waller factor, temp. variation, lattice dynamical calc. 8-55925
 distribution in alloy steel welds, laser emission microanal. method 8-61110
 DMSO:Cr³⁺, Nd³⁺, energy transfer and migration, donor-acceptor interaction, phosphoresc. quenching conc. depend. 8-64403
 electrodeposit, formation of axial texture (111) [hkl], math. model (*Russian*) 8-84082
 electrodeposition, high purity 8-84724
 electrolytic oxidation in SO₂ atmosphere, CrO₃ ionic defect effects (*Ukrainian*) 8-92504
 evaporated film, refl. and struct. 8-72021
 Fermi surface, stress depend., from quantum oscill. effects 8-91597
 ferromagnetic surface layer on antiferromag. bulk, determ. by surface magnetoplasma wave detect. 8-68356
 film, beam splitter phase coatings, for producing phase quadrature interferometer outputs 8-77974
 film, vacuum deposited, O⁺ bombardment sputtering rates 8-88390
 film sandwich structures Auger anal. 8-72030
 fine particles, δ- and BCC, mag. props. 8-52314
 galactic cosmic rays, isotopic composition, balloon meas. 8-89024
 guanidinium aluminium sulphate hexahydrate:Cr³⁺, EPR, 295.5, 78.45, 1.61K, zero field splitting 8-68359
 implantation in mild steel, annealing and rolling behaviour of conc. profile 8-75684
 island film photoconductivity obs. 8-95392
 lattice vibrations, Debye temp., freq. wave vector dispersion relations 8-63818
 linear expansion coefficient, at low temp. 8-83977
 liquid, multiple scatt. calcs. of resist. 8-76039
 oxidation, combination anal. using ESCA, AES and SIMS 8-72924
 particles, ultrafine, for photothermal conversion of solar energy 8-71163
 particulate layer on Cr₂O₃, high solar absorpt. characts., selective surface electroplating 8-87111
 phonon dispersion, Debye temp. and Debye-Waller factors, lattice dynamical model 8-55920
 plated steel, H₂ distrib., laser-mass spectrometer investig. 8-61113
 plating thickness meas. with MIP-10 8-53144
 ruby:Cr³⁺, exchange integral, pressure depend., test of theory 8-87741
 single modulation state, temp. limits of cryomagnetic method 8-72374
 sliding charact., friction and wear (*Japanese*) 8-56778
 solar abundance from photospheric spectra and oscillator strengths 8-69757
 source material, partial press. anal. 8-72731
 spin density wave, CDW and strain wave, effect of spin polarisation of reservoir and imperfect nesting 8-56284
 spin density waves detected by Ta mag. hyperfine field meas. 8-60364
 surface, (111), acoustic phonons Brillouin scatt. data 8-95222
 surface electronic struct., tight-binding approx. calcs. 8-64090
 vacuum-chromized Ti alloy VT3-1, fretting corrosion in couple with unprotected alloys (*Russian*) 8-56804
 vapour deposition, columnar struct. rel. to deposition conditions 8-52675
 X-ray K_β emission spectrum, unpaired electrons and plasmon correlation 8-88383
 X-ray K absorpt. discontinuities 8-60532
 Al_{0.9}Ga_{0.1}As:Cr, high resist. film, photolum. and photocond. meas. 8-72596
 Al₂O₃:Cr²⁺, Jahn-Teller study, EPR data anal. 8-84172
 BiI₃:Cr³⁺, ESR, spin-lattice relax., temp. depend. 8-88178
 CaS:Cr³⁺(Cr⁺), EPR (*Russian*) 8-91946
 Cr (III), (VI), determ. in industrial wastes 8-61105
 Cr³⁺, efficient cross pumping of Nd³⁺ in Nd(Al,Cr)₃(BO₃)₄ laser 8-59010
 Cr³⁺, electronic states interactions with crystal odd vibrs., R-lines vibr. recurrences 8-84639
 Cr³⁺ hydration model, external water interactions 8-78772
 Cr³⁺ impurity spectra anal. with Trees' correction 8-68539
 Cr/Cu/Cr layer composite, influence of phase boundary on flow stress 8-60717
 Cr₂O₃-Cr film, optical props., rel. to chemical/metallurgical constitution, appl. as solar absorber 8-56531
⁵⁵Cr, 7p states HFS, level crossing technique, core polarisation, spin orbit interaction, config. mixing 8-78668
 CsAl(SO₄)₂.12H₂O:Cr³⁺, ESR spectra 8-91944
 CsCl:Cr³⁺, ESR of Cr³⁺ centres, room temp. 8-91943
 GaAs:Cr, fine structure in cathodoluminescence spectrum 8-56524
 GaAs:Cr, IR spectral detectivity 8-70184
 GaAs:Cr, luminesc. stress splitting, 4.2K 8-84627
 GaAs:Cr, semi-insulating, characterisation by photoelectronic data 8-68051
 GaAs:Cr, semiinsulating solid-state inductance, theory and expt. 8-56138
 GaAs:Cr, Si, deep centre photoluminescence spectra 8-95601
 GaAs:Cr, site symmetry of Cr ions, ground-state splitting, ballistic phonon expts. 8-95273
 GaAs:Cr, VPE grown, exam. of doping GaAs using Cr(CO)₆ 8-72737
 GaAs:Si, Cr, carrier concs. from Hall effect, microscopy, localised vibrational modes absorption meas. 8-56104
 GaP:Cr, ESR of doubly ionised Cr acceptor and IR luminesc. 8-56374

chromium continued

InSb:Cr, press. effects on transport props. 8-56146
 KH₃(SeO₃)₂:Cr³⁺, ferroelastic material, EPR, 77-300K 8-60331
 KLiSO₄:Cr; optical activity characts. cryst.-chem. exam. 8-95569
 KMgF₃:Cr³⁺, EPR spectrum, effect of external elec. field 8-68368
 KMgF₃:Cr³⁺, trigonal centres, EPR lines, pseudo-Stark splitting 8-68367
 α-LiIO₃:Cr³⁺, EPR of impurity ion and radn. induced defects (*German*) 8-84480
 MgO:Cr²⁺, critically coupled spin-phonon mode 8-67779
 MgO:Cr²⁺, redox behaviour, ESR and X-ray diff. 8-52341
 MgO:Cr³⁺, strain modulated ESR 8-88175
 MgO:Cr³⁺, valence conversion in single crystals, by UV irradiation (*German*) 8-84620
 Mo, arc, steady, vac., plasma ion mass and energy diagnostics 8-51385
 NH₄Cl:Cr³⁺, ESR of Cr³⁺ centres, room temp. 8-91943
 NH₄H₂AsO₄:Cr³⁺, fast and slow dynamic reorientation 8-80306
 NH₄H₂AsO₄:Cr³⁺, ENDOR spectra 8-88224
 (NH₄)₂H₂PO₄:Cr³⁺, EPR exam. above and below T_c 8-68363
 (NH₄)₂SO₄:Cr³⁺, EPR study of ferroelec. phase transition 8-64337
 Si:Cr, specific resistance, activation energy of deep levels, and carrier mobility (*Russian*) 8-72146
 Si:Cr, spin-lattice relax. of Jahn-Teller Cr⁰ centre (*Russian*) 8-72402
 TiO₂:Cr³⁺, rutile, temp. depend. of EPR 8-76299
 YAG:Cr³⁺, ESR absorption spectra, line broadening 8-91940
 ZnS:Cr, vibr. modes of transition element impurities 8-76472
 ZnS(Se)(Te):Cr²⁺, Jahn-Teller coupling 8-67997

chromium alloys

see also chromium compounds

alloying with rare earth metals, Ti, Zr, Hf, Nb, Ta 8-68651
 chromindur, origin of coercivity, Lorentz microscopy, magnetisation and Mossbauer effect 8-64219
 chromindur, phase separation, Mossbauer obs. 8-88116
 Cr-Au alloys, dil., elec. resist., 77-700K 8-64035
 cyclic oxidation, static and dynamic, high temp. alloys 8-88576
 Hastelloy N, Si additions, comp. of eta carbide after ageing 8-52816
 Haynes alloy 188, SEM exam. of fracture surface, due to low cycle fatigue at 700°C (*Japanese*) 8-52963
 Haynes Stellite 6B, Al₂O₃ particle erosion of surface, SEM obs. 8-88545
 Haynes Stellite 6B, particle erosion damage, TEM obs. 8-88546
 Incoloy 800, 600 and 718, press. vessel, fatigue design criteria 8-60758
 Incoloy 800, austenitic, creep fatigue interaction at 600°C 8-64672
 Inconel, sputtering and blistering from H⁺ and He⁺ bombardment 8-79649
 Inconel 600, equilibrium surface bombarded with high dose He⁺ ions 8-95091
 Inconel 600, fusion reactor vac. vessel, air, N, adsorpt., thermal desorpt., heat treatment effects 8-54880
 Inconel 718, superalloy, wear of superhard tool during cutting, SEM and metallographic obs. 8-64720
 Inconel alloy 718, exam. of struct., properties and continuum synthesis of ductile fracture 8-76736
 Inconel-sheathed MgO-insulated Pt₉₀Rh₁₀/Pt thermocouple, decalibrations during 1200°C use, ion microprobe obs. 8-57957
 Kh20N40 alloys, phase composition after quenching, tempering 8-60650
 Mn_{1.98-x}Cr_xFe_{0.02}Sb, Mossbauer effect exam. 8-68432
 Nichrome, Kh20N80, varying porosity, effective thermal cond., 373-1400K, meas. method 8-75053
 Nicrosil-Nisil, thermocouple appl. for digital furnace control system 8-49831
 Nimocast, diffusion of Cs, AES, SIMS depth profile study (*German*) 8-84008
 steel, alloy, cluster formation susceptibility in 40 KhN, influence of isothermal working in H₂ (*Russian*) 8-56643
 steel, alloy, Cr-Cu-Mn-C, HT80, effect of grain size on sensitivity to reheat cracking (*German*) 8-72856
 steel, alloy, Cr-Mo, alloy SCM3, hydrogen embrittlement, delayed fracture, exam. (*Japanese*) 8-64620
 steel, alloy, Cr-Mo, pitting and crevice corrosion, exam. (*Japanese*) 8-64769
 steel, alloy, Cr-Mo-V, fatigue, failure probability based on residual strength 8-68797
 steel, alloy, Cr-Mo-V-P, quenched, temper brittleness in relation to V and P concs. 8-52986
 steel, alloy, Fe-Cr-Mo-Si-V, various steels, short rod stress intensity factor tests up to 700K, exam. 8-60815
 steel, alloy, Fe-Cr-Ni-Mo-Al, (13, 8, 2, 1, wt.%), H₂ effects on fracture, exam. 8-60809
 steel, alloy, Fe-Ni-Cr-Mo-V-C, H₂S stress corrosion cracking, effects of overload, exam. 8-60886
 steel, alloy, Fe-Ni-Cr-Mo-V-C, HY130, effect of H₂ and impurities on brittle fracture, review 8-60765
 steel, alloy, Fe-Ni-Cr-Sb-C effect of Ni, Sb, on temper embrittlement 8-60813
 steel, alloy, Fe-Ni-Mn-Si-Cr-Ni-Mo, effect of metallurgy on stress corrosion cracking, and hydrogen embrittlement 8-60885
 steel, alloy, Mn-Si-C, exam. of fracture toughness for sheets, using linear elastic fracture mechanics 8-56762
 steel, alloy, Ni-Cr-Mn, type 4340 intergranular brittle fracture, exam. by impact testing and Auger spectroscopy 8-52978
 steel, alloy, Ni-Cr-Mo, alloys SNCM8, SAE 4161, heat treated, residual stress at fatigue fracture surface (*Japanese*) 8-64622
 steel, alloy, Ni-Cr-Mo, SNCM8, mech. strength under combined alternating strength 8-64690
 steel, alloy, Si-Mn-Cr, heat treated, exam. of microfractographic aspects of fatigue cracks (*Japanese*) 8-52959
 steel, alloy, softening process in deformed type 15GYuT, metallographs (*Russian*) 8-52840
 steel, austenitic, mechanical props. of DIN X8 CRNIMONB 1616 and DIN X2 CRNI 189, FBR safety anal. 8-60966
 steel, austenitic, Ni-Cr high alloy, N₂, P and Ni effect on stress corrosion cracking and stacking fault energy (*Czech*) 8-60875
 steel, austenitic stainless, Cr-Ni-Ti, creep deform. effects on intergranular TiC dispersion stability 8-84912
 steel, austenitic stainless, influence of varying Cr, Mo, N contents on resist. to pitting corrosion 8-80668

chromium alloys continued

- steel, Cr-Mo-V, stress-fatigue interaction 8-64681
 steel, Cr-Mo-V, stress-fatigue interaction 8-64682
 steel, Cr-Mo-V, low alloy, creep-fatigue interaction 8-64673
 steel, Cr-Mo-V, stress-relief cracking mechanism 8-64669
 steel, Cr-Mo-V, press. vessel, crack growth under creep 8-64627
 steel, Cr-Mo, welding at forging temp., effect on struct. and mech. props. (Czech) 8-64624
 steel, Cr-Mo, Ni-Cr and Ni-Cr-Mo, quenched and tempered struct., effect on H diffusion coeff. and solution (Japanese) 8-64657
 steel, Cr 10 wt.%, SiO₂, vapour deposited coatings, exam. of corrosion protective props. 8-64651
 steel, Cr-C, (1.14, 1.16 wt.%) tempered, resistance to small plastic deformation, strain relaxation (Russian) 8-64648
 steel, Cr-C (0.5, 0.65 wt.%) and 45.4, 0.15 wt.%, rapidly quenched, in situ carbide reactions during tempering (Japanese) 8-64651
 steel, Cr-Mo, powder forged, fracture processes and fracture toughness 8-72870
 steel, Cr-Mo (2.25, 1 wt.%), relationship between minimum creep rate and time to fracture 8-64754
 steel, Cr-Mo-V, brittle fracture resistance obs., influence of cold plastic deform. 8-72868
 steel, Cr-Mo-V, creep crack growth temp. depend., 525 to 600°C 8-64634
 steel, Cr-Mo-V, creep fracture, microstruct. effects 8-64668
 steel, Cr-Mo-V, fracture toughness data, comparison with equivalent energy and energy per unit area data 8-52965
 steel, Cr-Mo-V, medium strength, correlation between crack initiation, propag. and microstruct. 8-60787
 steel, Cr-Mo-V, normalised and tempered, size and geometry effect on creep cracking behaviour 8-64630
 steel, Cr-Mo-V, press. vessel, fracture, effect of tempering 8-60799
 steel, Cr-Mo-V, thermal fatigue and rupture strength 8-72857
 steel, Cr-Mo-V (0.5, 0.5, 0.25 wt.%), comparison of methods of correlating creep crack growth 8-60826
 steel, Cr-Mo-V (0.5, 0.5, 0.25 wt.%), creep crack growth, temp. effect 8-64667
 steel, Cr-Mo-V (0.5, 0.5, 0.25 wt.%), heat treated, microstructure effect on threshold region fatigue 8-56757
 steel, CrMoV, compact tension specimen, thickness effect 8-68764
 steel, CrMoV, failure in post yield regime using single edge notched tension specimens 8-68765
 steel, CrMoV, low alloy, dispersed phase of VC, hardening mechanism (Czech) 8-60676
 steel, ledeburite, fracture during hot plastic deformation exam. 8-56755
 steel, low C, Cr-Ni (25, 25 wt.%), σ phase form., prestrain effects (Japanese) 8-92260
 steel, maraging, investigation with lower Ni and Co contents (Chinese) 8-84812
 steel, Mn-Cr-Ni-N, N effect on relaxation behaviour, internal friction temp. depend. (Russian) 8-52872
 steel, Mn-Cr-V, structural changes during solution annealing (Czech) 8-84864
 steel, MnCr (16, 5 wt.%), bending fatigue behaviour improvement by surface treatment (German) 8-84957
 steel, Ni-Cr, (4.1, wt.%), isothermal embrittlement, AES exam. of grain boundary segregation 8-60814
 steel, Ni-Cr-Mo, exam. of delayed fracture using fracture mechanics (Japanese) 8-52961
 steel, Ni-Cr-Mo-V, turbine rotor shaft, fracture toughness, validity criterion for K_{IC} 8-72861
 steel, Ni-Cr-P (0.06 wt.%), influence of intercritical heat treatment on temper embrittlement susceptibility 8-52863
 steel, NiCr, random load fatigue crack propag. 8-64692
 steel, Si-Mn-Ni-Cr-Mo, acoustic emission during stress corrosion cracking appl. to materials testing 8-53042
 steel, sintered, Cr-Mo, CaF addition effects on struct. heterogeneity 8-60611
 steel, stainless, surface cleaning by H⁺ bombard., AES study 8-53022
 steel, stainless, type Kh17N13M2T, strengthening by plastic deformation and cold working (Russian) 8-52839
 steel, X5CrNiTi26.6, ferrite-austenitic struct., optical and electron microscopy 8-84848
 steel, Cr-Mo low-alloy, material selection for nuclear steam generator 8-54834
 steel, Cr-V (1.5, 0.5 wt.%), cavitation effect of temp. and C content 8-64638
 steel, Ni-Cr, Sb doped, temper embrittlement susceptibility, intercritical heat treatment effect 8-64570
 strengthening by modified austempering 8-76665
 Al-Cr, dil., electron irradiated, interaction of self interstitials with undersized solute atoms 8-63789
 Al-Zn-Mg-Cu-Cr, (5.6, 2.5, 1.6, 0.3 wt.%), laminates, 8 and 22 layers, adhesively bonded exam. of fatigue crack propag. 8-92345
 Al-Zn-Mg-Cu-Cr, (5.6, 2.5, 1.6, 0.3 wt.%), alloy 7075, plates, adhesively bonded, exam. of fatigue crack growths 8-92348
 Au-Cr, dil., spin glass, elec. resist., press. and conc. effects 8-52278
 Au-Cr alloy pressure gauges, annealing effects 8-49854
 Au-Cr Kondo alloy, effect of press. on resistivity 8-79978
 B-Cr, diffusion coatings on alloy steel U8, wear resistance 8-56823
 Co-Al-Cr, eutectic alloys, charact. by melting, oxidation resistance and composition 8-52768
 Co-Cr, high temp. sulphide corrosion 8-64775
 Co-Cr recording films, perpendicular mag. anisotropy, hysteresis loop, microstruct., TEM obs. 8-95491
 Co-Cr system, phase diagram re-determ. from thermodynamic data 8-76631
 Co-Cr-Al, eutectic alloy, unidirectional solidification, oxidation and tensile tests 8-52790
 Co-Cr-Al, exam. of cyclic oxidation resistance at 1100 and 1200°C, comparison with Ni-Cr-Al system 8-88572
 Co-Cr-Mo (Zr)(Nb)(Ta), eutectic alloys, charact. by melting, oxidation resistance and composition 8-52768
 Co-Cr-Ni-TaC, directionally solidified eutectic, mech. props. and struct., thermal cycling effects (Russian) 8-92282
 Co-Cr-Ni-W-Ta-C, alloy Mar M-509, TEM exam. of thermal fatigue crack propag. in cast alloy 8-76740
 Co-Cr-WC, corrosion and corrosive wear in sea water 8-92408
 Co-W-Cr (15, 20 wt.%), surgical implant ion beam textured, stress/strain relations, fatigue characts. 8-73297

chromium alloys continued

- (Cr, Mn)-As, mag. props. and struct. 8-64190
 Cr-Al, disordered alloy, effect of high press. on resistivity 8-95286
 Cr-Co, dil., Neel temp., impurity conc. depend. calc. 8-68232
 Cr-Co-Ga systems, phase equilibria diagrams at 800 and 600°C (Ukrainian) 8-92236
 Cr-Fe, antiferromag. phase boundary, neutron diff. meas. 8-95437
 Cr-Fe, dil., Neel temp., impurity conc. depend. calc. 8-68232
 Cr-Fe, low conc. alloys, coexistence of itinerant antiferromagnetism with paramagnetism 8-84586
 Cr-Fe (30 wt.%) alloys, refined fine comminution 8-60598
 Cr-Fe-V, calc. of phase equilibria using thermodynamic values from different models 8-60646
 Cr-Fe-V, dil., V effect on para- to incommensurate and commensurate transitions 8-68260
 Cr-Mn, strain wave and spin density wave intensities, neutron diff. 8-80266
 Cr-Mo-V, steamline bends, restorative heat treatment effects 8-68716
 Cr-Ni-Ga systems, phase equilibria diagrams at 800 and 600°C (Ukrainian) 8-92236
 Cr-Pt, dil., effect of Pt on itinerant antiferromagnetism 8-64191
 Cr-Re, dil. alloy, mag. susceptibility temp. depend., thermal expansion coeff. (Russian) 8-76225
 Cr-Si-V, dil., V effect on para- to incommensurate and commensurate transitions 8-68260
 Cr-V, strain wave and spin density wave intensities, neutron diff. 8-80266
 CrAl, semicond. solid solns., temp. depend. of elec. resist. at high temp. 8-87341
 Cr-C-Ni-(P), hard alloys, sintered, fracture props., P addition effects 8-60610
 Cr₁₁Ge₈, CrGe, and Cr₁₁Ge₁₈, amorphous films, short-range order, electron diff. obs. (Russian) 8-56050
 CrNi₂, type alloys, ordering, influence of static stresses (Russian) 8-56631
 Cr₂Pd₂-Ge₁₈, amorphous, RF sputtered, elec. resist. and magnetoresist., Kondo type behaviour 8-76066
 Cr₂Pd₂-Ge₁₈, amorphous alloys, magnetoresist., mag. susceptibility, magnetisation 8-80148
 CrSi, NMR and μ SR, microscopic mag. props. (Japanese) 8-52368
 Cu-Cr, dil., NMR data, ionic model and Kondo temp. 8-68399
 Cu-Cr, dil., NMR satellite data, rel. to electronic struct. 8-68398
 Cu-Cr, dil., spin glass, elec. resist., press. and conc. effects 8-52278
 Cu-Cr, dil. alloy, Knight shift temp. depend., electronic struct. 8-84488
 Cu-Cr (1 wt.%), exam. of low cycle fatigue props. at elevated temp. 8-64674
 Cu-Cr-Zr-Mg (0.5, 0.1, 0.03 wt.%), exam. of low cycle fatigue props. at elevated temp. 8-64674
 Cu-Ni-Cr, lattice imaging and optical microanalysis of spinodal decomp. 8-52754
 Cu-Ni-Cr system, coarsening in the (γ_1 , γ_2) region, metallographic study 8-84762
 Cu-Cr-Pb, proximity effect, tunnelling conductance 8-52160
 Fe, cast, white Cr alloyed, wear resistance, effect on abrasive hardness 8-64722
 Fe-Al-Cr (10, 5 to 10, wt.%), corrosion by coal char, SEM and X-ray diff. exam. 8-88573
 Fe-Cr-Mo(Ni)(V), white cast, effect of abrasion on carbide microstructure (German) 8-88540
 Fe-C-Ni-Cr, athermal alloy, exam. of martensite transformation kinetics 8-80545
 Fe-C(graphite)-Ni-Cr, dynamically hot pressed mech. props., effect of Ni-Cr additions 8-60620
 Fe-Cr, amorphous alloy, effect of metalloid impurities on corrosion resistance and electrochem. behaviour 8-72925
 Fe-Cr, BCC, ferromag., spin wave stiffness constant 8-91851
 Fe-Cr, dil., high freq. induction melting and centrifugal casting, working curve sample prep. photoemission anal. (Japanese) 8-53050
 Fe-Cr, from ore reduction, metallographic investigation, optical microscopy and SEM (French) 8-68648
 Fe-Cr, hardness after nitriding, metallographic, electron microscopic and microprobe anal. 8-51608
 Fe-Cr, high purity binary alloy, isothermal decomp. of austenite 8-64525
 Fe-Cr, impact strength, rel. to '475°C brittleness' (Russian) 8-92323
 Fe-Cr, Invar alloy, explanation of phys. anomalies (Russian) 8-88112
 Fe-Cr, layers formed by reaction with molten Al, X-ray, EPMA and hardness meas. (Japanese) 8-72926
 Fe-Cr, mag. moments and Fe site hyperfine fields, magnetis. obs. 8-76276
 Fe-Cr, oxidation, in H₂/H₂O vapour mixtures, epitaxial oxide phase formation, effect on oxidation 8-88568
 Fe-Cr, role of C in transform. by heating in (α + γ) phase (French) 8-52798
 Fe-Cr, XPS obs. of Fe 2p states 8-52625
 Fe-Cr (20 wt.%) high temp. oxidation behaviour with small La additions (0 to 1.3 wt.%) (Japanese) 8-85039
 Fe-Cr (26 wt.%) effect of Ni content and austenite phase, on low temp. toughness and embrittlement 8-60754
 Fe-Cr-Al, attenuation and vel. of acoustic shock waves, amplitude depend. 8-63810
 Fe-Cr-Al, elec. heating alloy, effect of rare earth additives on quality (Chinese) 8-84825
 Fe-Cr-Al (14, 0.1 to 2 wt.%), oxidation at high temps. (Japanese) 8-60872
 Fe-Cr-Al alloys, low temp. sp. ht., resistivity and coercive force 8-63866
 Fe-Cr-Al-Y (Y-Al₂O₃)(Y₂O₃), preparation and exam. of mech. props. 8-52720
 Fe-Cr-C, steel carbide formation during chromising, exam. in terms of ternary phase diagrams 8-56818
 Fe-Cr-Co, effect of heat treatment on strain gauge factor 8-72802
 Fe-Cr-Co (31 wt.%, 23 wt.%), microstruct. and mag. props., ageing and thermomag. treatment effects 8-76769
 Fe-Cr-Co alloys, permanent magnet material development 8-91895
 Fe-Cr-Co-Al (27.5, 17.5, 0.5) alloy, magnetic props. and microstructure 8-72367
 Fe-Cr-Co-Al (27.5, 17.5, 0.5 wt.%) alloy, induced anisotropy 8-76239

chromium alloys continued

- Fe-Cr-Co-Si alloy, interaction domains after heat treatment in mag. fields (*Russian*) 8-68286
 Fe-Cr-Co-V alloy, microstruct. and mag. props. 8-68221
 Fe-Cr-Mo-C, X-ray investigation after friction and oxidation 8-52997
 Fe-Cr-Nb-C, X-ray microanal. of carbide phases rel. to Nb conc. (*Russian*) 8-88467
 Fe-Cr-Ni, electron irradiated, resistivity during annealing, 4.2-1300K 8-87962
 Fe-Cr-Ni, irradiated, Ni segregation to sinks 8-91472
 Fe-Cr-Ni, mag. state at low temps. (*Russian*) 8-56298
 Fe-Cr-Ni, textured ($\alpha+\gamma$) alloy, α' lath martensite formation 8-95749
 Fe-Cr-Ni alloy, dual-ion-irradiated, swelling anal. 8-86600
 Fe-Cr-Ni alloys, oxidation-sulphidation in gas mixture, parabolic kinetics, thermochem. diagram 8-72932
 Fe-Cr-Ni-C (23.19, 4.91, 0.025 wt.%), two phase alloy, effect of prestrain above Md temp. on Ms temp. 8-80543
 Fe-Cr-Ni-Cu-Sn, Cu and Sn effect on Cr and Ni segregation (*German*) 8-72777
 Fe-Cr-P-C, amorphous, corrosion resist. in 1N HCl 8-80678
 Fe-Cr-SiC-B₃C powder mixture, compressibility and elec. cond. in cold pressing under low press. 8-60609
 Fe-Cr-Ta, eutectic alloy, exam. of eutectic temp., composition, and oxidation resistance 8-52767
 Fe-Cr-V-C, X-ray microanal. of carbide phases rel. to V conc. (*Russian*) 8-88467
 Fe-Cr-(Co), decomposition of solid soln. in mag. field, neutron and X-ray diff. study (*Russian*) 8-68694
 Fe-Mn-Co-Ni-Cr, antiferromag. props., Neel temp. determ. 8-88124
 γ -Fe-Ni-Cr, mag. struct., neutron scatt. study (*Russian*) 8-68160
 Fe-Ni-Cr (25, 15 wt.%), high temp. creep, dispersed γ' -Ni₃(Al, Ti) effects (*Czech*) 8-64590
 Fe-Ni-Cr austenitic steel, martensitic transform. kinetics, metastability criterion (*French*) 8-68690
 Fe-Ni-Cr coating, electrodeposited, exam. of passivity 8-80655
 Fe-Ni-Cr-C, effect of austenite yield strength, stacking fault energy, on martensite morphology 8-80546
 Fe-Ni-Cr-Mn-Al-Ti Incoloy 800, exam. of scale morphology, alloying element distrib. after oxidation 8-80677
 Fe-Ni-Cr-P-B, Metglas 2826A, hardness, elastic moduli, density, cryst. temp., mech. props. for flywheel appl. (*Dutch*) 8-52878
 Fe-Ni-Cr-Ti, superalloy A286, powder, exam. of microstruct. and mech. properties 8-52979
 Fe-Ni-Cr-Ti-Mn-Mo, (25.8, 14.04, 2.17, 1.27, 1.30 wt.%), superalloy A-286, precipitation hardening, exam. of fracture toughness and mech. props. 8-92355
 Fe-W-Cr-Mo-Co with austenitic phase, magnetic and mech. props., cold working and ageing effects (*Japanese*) 8-60678
 Fe₆₅(Ni_{1-x}Cr_x)₃₅, remanent magnetisation, temp. depend., anomalies near Curie temp. (*Russian*) 8-60310
 Fe₃₃Ni₃₅Cr₁₄P₁₂B₆, Metglas 2826A, Hall resistivity, effect of thermal cycling and annealing 8-56125
 Fe₃₃Ni₃₅Cr₁₄P₁₂B₆, shear band form. 8-68756
 Ni superalloy Mar-M200, slow fatigue crack propagation rate meas. using high freq. resonant technique 8-52983
 Ni-(W,Cr)C, corrosion and corrosive wear in sea water 8-92408
 Ni-Al-Cr, precipitation-strengthened, mechanical props. 8-84968
 Ni-Al-Cr-Co-Ti, Waspaloy, exam. of dislocation-precipitate interaction, cyclic stress-strain behaviour 8-84925
 Ni-Co-Cr-Mo-Ti-Al Nimonic 105, loading frequency and environmental effects on high temp. fatigue crack growth 8-64675
 Ni-Co-Cr-Ta-Al-W-Mo-Ti, cast, phase volume fraction determ. using manual point count practice 8-53052
 Ni-Cr, film, quantitative anal. by DC arc optical emission spectroscopy 8-68940
 Ni-Cr, solid soln., exam. of back stress role in creep behaviour of particle strengthened alloys 8-52889
 Ni-Cr (20 wt.%), CC W fibre reinforced, alloy by effect on struct. stability, mech. props., metallographic exam. 8-56600
 Ni-Cr (20 wt.%), reinforced by coated Mo filaments, effect of coating on composite strength 8-56710
 Ni-Cr (20 wt.%) based composite, use of SiC fibres with protective Al₂O₃ coating, IR investigation 8-60623
 Ni-Cr alloy, KhN70VMTYu, gas turbine blades, thermocyclic strength characts., exam. 8-60743
 Ni-Cr foldfoil strain gauge, for cryogenic anal. of supercond. structs. in high mag. fields, fusion reactors 8-54947
 Ni-Cr surface, chemisorption, appl. of vac. UV photoelectron spectrometer (*Japanese*) 8-62264
 Ni-Cr-Al (15, 5 wt.%), oxide dispersion strengthened, effect of dispersoids on oxidation 8-80679
 Ni-Cr-Al-Ti (Ti-Co), exam. of back stress role in creep behaviour of particle strengthened alloys 8-52889
 Ni-Cr-Co-Al-Ti-W-Ta-Mo, IN 738 LC, loading frequency and environmental effects on high temp. fatigue crack growth 8-64675
 Ni-Cr-Co-Mo-Al-Ti alloys, Waspaloy, Astroloy, exam. of microstruct. effect on crack growth 8-52977
 Ni-Cr-Fe (15.7, 7.63 wt.%), Inconel 600, anal. of pit generation by 3.5% NaCl by stochastic theory (*Japanese*) 8-85038
 Ni-Cr-Fe-Mo-Co (21.41, 19.28, 8.64, 2.16 wt.%), Hastelloy alloy X, exam. of thermal stability 8-84865
 Ni-Cr-MgO system, elec. resist. variation with comp. and prep. method 8-60637
 Ni-Cr-Nb-Al eutectic alloys, sulphidation/oxidation at high temps., corrosion mechanism 8-72934
 Ni-Cr-Ti-Al-Fe-Co (19.65, 2.40, 1.37, 0.78, 0.52 wt.%), strength of γ' hardened alloy, ageing exam. 8-88501
 Ni-Cr-Ti-Al-Mo-Nb-Fe (13-16, 2.35-2.75, 1.3-1.7, 2.8-3.2, 1.8-2.2, 2.0 wt.%), heat resistant props, mech. props. struct., stepwise ageing effects (*Russian*) 8-76666
 Ni-Cr-Ti(Nb)(Zr), eutectic alloy charact. by melting temp., composition and oxidation resistance 8-52771
 Ni-Cr-W (20, 3 wt.%), high temp. creep, atmospheric effect on anomalous behaviour 8-80617
 Ni-Cr-W-Cr(Si) hardness, corrosion resistance, wear resistance tests in 10% HCl (*German*) 8-92368
 NiAl-Cr eutectic alloy, directional solidification singularities (*Russian*) 8-68678
 NiCr-AlY sintered fibre metal struct. abrasible seal material, friction and wear 8-56785
 NiCr-MoAl-ThO₂ (13.3 wt.%), powder, mech. alloying 8-84744

chromium alloys continued

- Ni₂Cr, neutron irradiat., point defect prod. and annealing 8-87718
 Ni₃(Fe,Cr), kinetic phenomena rel. to ordering and electron struct. (*Russian*) 8-76043
 Pt-Cr dil. alloy, 0.5 at.%, ¹⁹⁵Pt NMR for local mag. susceptibility 8-84484
 Rh-Pd-Cr, dil. alloy, mag. moment 8-95416
 steel, austenitic stainless, 18 Cr-11 Ni, effect of boron on nucleation of M₂₃C₆ carbides (*Polish*) 8-84808
 Te-Cr, dil. liq. alloy, elec. cond. at high temp. and press. 8-87959
 Ti alloy VT3-1, large forgings, heat treatment, struct. and mech. props. 8-52864
 Ti-Al-Cr-Mo-Fe(V)(Zr), effect of structure and heat treatment on tensile strength, ductility, fatigue limit and notch sensitivity 8-56711
 Ti-Al-Mo-Cr (4.5, 5, 1.5 wt.%), CORONA-5, effect of microstructure and heat treatment on fracture 8-60805
 Ti-Al-Mo-Cr-Fe, effect of heating on thermal stability of phases, lattice constants and chem. comp. 8-56672
 Ti-Al-V-Cr, electrochemical behaviour under tensile stress in boiling H₂SO₄ and acidic chloride solns. 8-95851
 Ti-Cr, sintered, friction and wear, structural factors 8-60843
 Ti-Cr (15 at.%), aged omega phase, electron microscope exam. 8-72783
 Ti-Cr (6 wt.%), alpha precipitation kinetics 8-68697
 U-Cr-Al (0.2, 0.1 at.%) precip. elem. with high swelling resistance for KS-150 reactor 8-78471
 V-Cr, elastic moduli, US pulse echo meas. 8-84881
 V-Cr alloys, absorption of H₂, thermodynamic parameters 8-87862
 V-Cr-Ti, fusion reactor first wall structural materials, prediction of life limiting props. 8-62605
 Zn-Cr, dil., mag. anisotropy, 0.001 to 2K 8-68157
 Zr-W-Cr, Zr-rich corner of phase diag. (*Russian*) 8-80517

chromium compounds

see also *chromium alloys*

- chromate salts, ZZ 8-88326
 magnesite-chromite powder, exam. of rheological characts., compaction 8-60628
 Al₂O₃-Cr₂O₃, microstrain correction 8-59852
 Cd_{1-x}Ag_xCr₂Se₄, ferromag., magnetoresistance exam. (*Russian*) 8-84238
 CdCr₂Se₄(Se₄), spin depend. phonon Raman scatt., band struct. 8-68491
 CdCr₂Se₄, photoferromag. effect quenching, photocond. 8-68488
 CdCr₂Se₄, velocity-field characts., above T_c 8-64049
 p-CdCr₂Se₄:Ag, oscillatory magnetoresist., temp. and mag. field depend. 8-52011
 CdCr₂Se₄:Cu, elec. props., temp. depend. (*Russian*) 8-72181
 CdCr₂Se₄:In(Ga), temp. driven metal-semiconductor transition, temp. and mag. field depend. (*Russian*) 8-88003
 CdCr₂Se₄(S₄), ESR line intensity near Curie point 8-64269
 CoCr₂S₄, Faraday effect, appl. to CO₂ laser systems, radiation damage resist. 8-95579
 Cr complex, Cr(V)-dimethylformamide, proton dynamic polaris. and relax. 8-91988
 Cr complex, Cr(V)-fluoroorganics, proton and ¹⁹F dynamic polaris. and relax. 8-91989
 Cr complex, dimer, di- μ -diphenylphosphinatoacetylacetonatochromium(III), EPR of exchange coupled Cr³⁺ pairs 8-88172
 Cr complex, trimeric clusters, low temp. mag. props. 8-76261
 CrAs, heat capacity, enthalpy increments, thermodynamic props., 5 to 1280K 8-91450
 CrB₂, NMR of ¹¹B meas. 8-56397
 CrB₂, RF sputtered, comp. by XPS 8-51839
 CrB₃, crit. spin-relax. in hard mag. direction 8-72390
 CrBr₃, parametric representation of the equation of state of a Heisenberg system in the critical region 8-79741
 CrBr₃, XPS, satellite of Br 4s line 8-56556
 CrBr₄, Raman spectra, struct. and thermodynamic functions 8-60443
 CrC, plasma sprayed coating 8-68835
 Cr₃C₂, form. from Cr₂O₃/graphite mixture in H₂ atmos. (*Japanese*) 8-92225
 Cr(CO)₃, bond angles, hybrid bond orbital calcs. 8-94188
 Cr(CO)₆, relative intensities of ν (CO) and ν (MC) Raman bands 8-55176
 CrCl₃, optical absorpt. spectra, spin-allowed transitions 8-52527
 CrCl₃, Raman spectra, struct. and thermodynamic functions 8-60443
 CrF₃-BaF₂-NiF₂, X-ray crystallography study, phase identification at 700°C, cryst. symm. (*French*) 8-95733
 Cr_{1-x}Fe_xS₆, metal-dielect. transition, X-ray, thermal anal., elec. cond. temp. depend. 8-67942
 CrI₃, ferromagnetic, origin of magnetic hyperfine field transferred at iodine 8-92000
 Cr_{1-x}Mn_xSi₂, semicond. props. 8-79992
 e-Cr₂N phase, analysis of expt. results of Mills and Schwerdtfeger to yield partial enthalpy and entropy 8-52783
 Cr(NH₃)₃ONOC₂, cryst. struct. determ. at 245K 8-75637
 CrO₂, single mag. particle, remanent coercive force and remanent loop meas. 8-95480
 CrO₂, single particle material for tape and disc manufacture, prep., props., and appls. 8-52308
 CrO₃, ionic defects, influence of S during Cr electrolytic oxidation in SO₂ atmosphere (*Ukrainian*) 8-92504
 CrO₃⁻ radical in K₂CrO₄ and KCrO₃Cl, g-factor anisotropy 8-67994
 CrO₂²⁻, electronic struct. determ. from X-ray spectra 8-86885
 CrO₂²⁻ in halide salt aqueous solution, absorpt. spectra, 4.2 to 290K (*Russian*) 8-60499
 CrO₃ addition to CdS_{1-x}Se_x photoresistors, extension of cutoff freq. (*Russian*) 8-84248
 Cr₂O₃, adsorption of Cs, meas. of contamination using washing test 8-62597
 Cr₂O₃, corrosion product in LMFBR type mixed oxide fuel pins 8-70599
 Cr₂O₃ effect of addition on crystallisation of Na₂O-Al₂O₃-SiO₂-TiO₂ glass 8-87626
 Cr₂O₃ substrate for CdS photoresistors, effect of heat treatment 8-80017
 Cr₂O₃, thin plate single crystal, vapour phase growth 8-64450
 Cr₂O₃, US wave vel. near mag. transition 8-84263

chromium compounds continued

- Cr₂O₃-Al₂O₃ solid solns., effect of Cr on point of zero charge 8-61021
 Cr₂O₃-Cr film, optical props., rel. to chemical/metallurgical constitution, appl. as solar absorber 8-56531
 Cr₂O₃-TiO₂ system, phase relations 8-80523
 Cr₂O₃-WO₃, phase relations 8-92249
 Cr₂O₃(S₂), spectrally selective EM wave absorber, solar energy collector material, props. (*Duich*) 8-50872
 Cr₂O₃-SH₂O, heat-treated, narrow particle size distrib., surface props. 8-85210
 Cr₂S₃, single crystal, exam. of unit cell structures by interference contrast microscopy 8-67670
 CrS_{1-x}Se_x, antiferromag. props., struct., variations near Neel temp. 8-64199
 CrSi₂, formation on Pd₂Si and PtSi, radioactive Si tracer obs. 8-60578
 CrSi₂, semicond. props. 8-79992
 Cr₂Si₂(C₂), sputtered films, microstruct. and wear props. 8-64733
 CrTe, effect of high pressures on magnetic properties 8-52238
 CrThS(Se)₃, synthesis, cryst. characts. (*French*) 8-51517
 Cr₁₂-W₂P₇, solid solns., prep., cryst. struct. (*French*) 8-63723
 CsCrCl₃, co-operative Jahn-Teller distorted struct. determ. 8-63713
 Cu₂Cr₂Se_{4-x}Br_x, ferromag. magneto-resistance exam. (*Russian*) 8-84238
 (Fe,Cr)₃C, reln. between bond energy and X-ray emission line shifts 8-50555
 Fe_{1-x}Cr_xBO₃, magnetisation, 4.2-600K 8-68187
 (Fe_{1-x}Cr_x³⁺Cr_{3-x}³⁺)₂O₇²⁻, γ to α transform. elec. cond. study, oxidation initial stage kinetics, lacunar spinel form. 8-92384
 FeCr₂S₄, vapour grown, growth mechanism of multisteps on surface 8-75605
 HgCr₂Se₄, ESR line intensity near Curie point 8-64269
 MgCr₂Fe_{2-x}O₄, comp. effects on ferrite characts. 8-52305
 MgO-Al₂O₃-Cr₂O₃, vacuum vaporisation, Langmuir method 8-95149
 MgO-Cr₂O₃, diffusion of Cr₂O₃ and Fe₂O₃ in gas phase during firing (*French*) 8-80495
 MgO-Cr₂O₃, vacuum vaporisation 8-91434
 MgO-Cr₂O₃, vaporisation rate, O₂ partial press. effect (*Japanese*) 8-63848
 MnCrF₅, antiferromag., mag. struct. (*French*) 8-52211
 Mn₃Cr₂Ge₂O₁₂, garnet, antiferromag. ordering (*Russian*) 8-80146
 NaCl-AlCl₃-CrCl₃, molten, electrochemical exam. of Cr 8-56939
 Nb₂Cr_{1-x}O₂, cryst. prep. and struct., mag. props. 8-52198
 Pb₂-Sr_{1-x}(Zr_{1-x}Ti_x)₂O₇:Cr₂O₃, ferroelec. ceramic, reversible characts. and dielectric losses (*Russian*) 8-84517
 Pb(Zr_{0.47}Ti_{0.43}Sn_{0.10})O₃:Cr₂O₃, ferroelec. ceramic, reversible characts. and dielectric losses (*Russian*) 8-84517
 β-RbCrCl₃, co-operative Jahn-Teller distorted struct. determ. 8-63713
 TiC-Cr₃C₂(Cr₃C₂-WC), powder mixture, steel bonded, exam. of sintering behaviour 8-52712
 ZnCr₂Se₄, magnetoelastic coupling, mag. suscept. meas. 8-76288

chromosphere

- acoustic dissipation and H⁺ radiation, rel. to heating 8-96454
 active regions on solar limb, 1175 to 1940 Å emission-line spectra 8-96446
 chromosphere-corona transition region, nonequilib. plasma density diagnostics via C III EUV Lines 8-53899
 convective noise waves, dissipation in mag. struct. rel. to chromosphere heating 8-65600
 corona-chromosphere transition region, EUV models 8-69767
 downflow in supergranulation network rel. to transition region models 8-61838
 dynamic response to soft X-rays from flares 8-65580
 Evershed flow in chromosphere-photosphere transition region 8-65593
 filaments and flare obs. 1967-9, Hα monochromatic light 8-61836
 flares, chromosphere 3835 Å emission rel. to soft X-ray flux 8-89156
 flares, optical thickness and H ionization degree from Balmer line obs. 8-73694
 flares and associated radio emission (*Italian*) 8-96457
 flares fast electrons scatt. in atm., X-ray spectrum 8-77542
 heating by solar flares, charged particles beam collisional interaction with H target 8-93095
 magnetic fields of active regions, zero points 8-96465
 magnetic structures, models (*Italian*) 8-81603
 microwave bursts, polarisation features interpretation 8-96468
 modelling, hydrodynamic and mag. features (*Italian*) 8-81599
 models, survey of last 30 years' research 8-69764
 motions, EUV obs. by OSO-8 (*Italian*) 8-81602
 network, evolution during active regions development (*Russian*) 8-57531
 network, photospheric layers models from Mg II h and k line wings 8-57518
 observations and interpretation (*Italian*) 8-81604
 plages, physical props. models based on Ca II and Mg II obs. 8-89153
 radiative equilibrium departures, grey absorpt. 8-81531
 resonance line scatt. from optically thin structs. located above solar limb 8-65591
 short period acoustic heating theory appl. to chromospheric models (*Italian*) 8-85926
 spectral line formation, C II reson. lines obs. rel. to temp. struct. 8-53896
 sunspot umbrae, Ca II H, K and IR lines interpretation 8-53901
 temperature and electron density above sunspot umbrae 8-53908
 transition region, Bowen fluoresc. rel. to electron density determ. 8-93179
 transition region and chromosphere, OSO-8 obs. of wave propag. 8-93183
 transition zone, area var. of supergranule network features with temp. 8-89152
 velocity fields, observations (*Italian*) 8-81601
 velocity fields, theory (*Italian*) 8-81600
 C I multiplets at 1560 and 1657 Å, overlapping emission peaks obs. and theory 8-93178
 Ca II H and K lines cores in integrated sunlight, rel. to solar activity 8-77535
 Ca II K and Hα obs. during 1969 at Kodaikanal Obs. 8-61832
 Ca II K line and Hα obs. of filaments, flocculi and prominences, during 1969 at Kodaikanal Obs. 8-61833

chromosphere continued

- H I Lα/Hα ratio for flares, quasars and prominences 8-61826
 Hα, seven components form. rel. to 9873 MHz line appearance 8-89151
 He I, He II XUV emission lines, intensity ratios and distrib. functions 8-57516
 He I D₃ line obs. of spicules, photoionisation model 8-65592
 S I 1807 Å and 1900 Å lines, anal. of profiles 8-57517

chronographs *see* **chronometers****chronometers**

- Re-Os nuclear chronometer, reliability, rel. to element rel. abundance 8-85919

CIDEP

- benzophenone in isopropanol, submicrosecond time resolved EPR, lser photolysis, CIDEP polarisation mech. 8-80764
 p-benzosemiquinone monoprotonated radical, submicrosecond time resolved EPR, lser photolysis, CIDEP polarisation mech. 8-80764
 duro-semiquinone monoprotonated radical, submicrosecond time resolved EPR, lser photolysis, CIDEP polarisation mech. 8-80764
 pulse radiolysis study, examples of S-T₁ polarisation 8-86891
 theory, stochastic-Liouville vector model with asymptotic soln. 8-66567

CIDNP

- methanol, aq., radiolysis, CIDNP, methoxy radical involvement 8-53223
 pancreatic trypsin inhibitor tyrosine residues in soln., laser photo-CIDNP as surface probe 8-73138
 proteins in solution, laser photo-CIDNP as surface probe 8-73138

cinemifilming *see* **cinematography****cinematography**

- see also cameras*
 additional meas. flashing technique (*Russian*) 8-54486
 additive film copying machine, modulator mechanodigital design (*German*) 8-65987
 Beaulieu cine camera, 16 mm, time lapse apparatus 8-74089
 camera supply, control and synchronisation systems (*Russian*) 8-49936
 cameras, guide elements, use of powdered polymer coatings 8-78021
 chemical-photographical processing influence on physical-mechanical props. of motion picture materials (*Russian*) 8-93778
 cinerointerferometry, quantitative biplane method, error propag. 8-73224
 colour atlas for colour organisation in film production (*Russian*) 8-93776
 colour film processes and cameras, review, 1894 to date (*German*) 8-93773
 colour negative motion picture process, latensification representation (*Russian*) 8-86373
 digital photographic sound track recording optimisation (*Russian*) 8-89580
 film grain multiplicative noise anal. 8-58932
 film slitting in the laboratory 8-93770
 high-speed, high-intensity lighting 8-54483
 high-speed photography and photonic recording 8-86367
 holocinematography, high speed, acousto-optic beam deflection for spatial freq. multiplexing 8-74860
 holographic cinematography in USSR 8-78976
 image intensifiers for rapid filming, microchannel proximity tubes characts. (*French*) 8-49917
 information eval. of image quality for cinematographic systems (*Russian*) 8-54485
 instant cine film development and projection 8-78012
 laser produced cavitation in water, behavioural study by holocinematography (*German*) 8-87371
 liquid crystal indicator of variable light-reading angle 8-57932
 marksmanship training, moving target screen system with laser beam firing 8-54488
 metal plate high-gradient transverse deformation interferometry 8-82024
 motion picture camera device for shooting in movement (*Russian*) 8-93777
 pool barbotage, heat transfer coeffs., high-speed cine-photography and oscillography 8-90982
 review of technical progress in 1977 in USSR (*Russian*) 8-89579
 single-frame, automation (*Russian*) 8-86374
 stereo film projection, in 3D motion picture theatre (*Russian*) 8-86371
 time lapse cinemicrographs of cultured cells, computer-aided analysis 8-92756
 ventriculography, algorithm for automatic selection of end diastolic and end systolic cine frames 8-88757
 X-rays, pulsed and continuous, motion picture filming of moving objects 8-57057

circuit analysis *see* **network analysis****circuit analysis computing**

- see also circuit CAD*
 fusion reactor, Shiva Faraday rot. coils, circuit and mag. anal. 8-54951

circuit breakers

- see also circuit breaking arcs; gas blast circuit breakers*
 analogue safety data link, for Princeton Large Torus control room 8-54938
 ASDEX circuit breaker system, design, calcs. and tests 8-55032
 current measurement, using electron beam deflection tube 8-54393
 high current switch, fast closing, for fusion reactor field coils 8-74484
 HVDC interrupter test facility, dual 30 kA systems 8-55035
 liquid metal plasma valve, 15 kA-30 kV, fusion reactor application 8-74488
 toroidal field system on TEXT Tokamak, DC regulation 8-55038
 vacuum interrupter, for high voltage DC current, for fusion reactors 8-74489
 Al, foil, elec. explosion, immersion medium effects 8-67389

circuit-breaking arcs

- see also circuit breakers; sparks*
 AC arc, axially blown with N₂, field strength and energy balance eqn. 8-87523
 air blast circuit breaking arcs, elec. grad. using plasma probe methods 8-87527

circuit-breaking arcs continued

- gas blast arcs, very high current, elec. conductance of arc gap 8-87524
- gas blast circuit breakers, current zero period, boundary layer integral method 8-87522
- gas blast circuit breaking arc, arc diameter, RF technique 8-87528
- gas blast circuit breaking arc, thermal disturbances in hot gas surround 8-87529
- gas blast circuit breaking arcs, air and SF₆, energy clogging 8-87531
- gas blast circuit breaking arcs, electron temp. at current zero, 3 kA arc 8-87526
- high-current vacuum arc in a magnetic field 8-71572
- radiative transfer, magnetic stability, and turbulent heat exchange 8-75482
- weak mag. field driven arc velocity and configuration obs. 8-71596
- SF₆, 20 kA arc, electrode vap. contamination, time depend. energy balance 8-87525
- SF₆ arc field distrib. and conductance in current-zero region 8-71590
- SF₆, gas blast circuit breaking arc, clogging transition 8-87530
- SF₆ high-current arc props., influence of electrode material 8-71592
- SF₆, optically thick, convection-loss dominated model 8-87519
- SF₆, plasma diagnostic techniques (*Japanese*) 8-55768

circuit CAD

- see also *circuit analysis computing*
- bandpass filters, SAW, withdrawal weighted CAD 8-66991

circuit oscillations

- see also *circuit resonance*
- Josephson junction, long, oscills., exact solns. of sine-Gordon eqn. 8-68115

circuit resonance

- see also *circuit oscillations*
- No entries

circuit theory

- see also *filters; network analysis; network topology*
- angular spectrum of EM field, elec. network equivalent 8-78867
- dissipative slowly modulated steady state, dQ=TdS far from equilib. 8-81934
- education, electrical circuit equivalent resistance and capacitance 8-69938

circuit topology see *network topology***circuits** see *networks (circuits)***circular polarisation** see *polarisation***circular waveguides**

- 100 GHz bolometer mount efficiency meas. calorimeter (*Japanese*) 8-54460
- EM scattering by spherical shell with arbitrarily located circular aperture, anal. 8-62989
- laser, construction and operation characteristics (*Rumanian*) 8-59049
- X-ray transmission, curved Pb glass capillaries 8-86395

citation analysis see *information analysis***civil engineering**

- see also *building; dams*
- elastic-plastic finite element analysis, interpolation vs. iterative soln. for Tresca yield condition 8-59312
- fibre reinforced composites, apparent fibre spacing 8-79222
- flood control planning 8-81245
- FRC, reinforcement parameter 8-79223
- mechanical dished supports, oscillation and stability conditions based on mixed finite elements (*German*) 8-87299
- seismic Rayleigh surface waves, interaction with structures 8-81109
- structural anal., soln. by orthogonal collocation 8-51063

civil engineering computing

- see also *town and country planning*
- anisotropic solid fluid flow with free or artesian surface analysis, finite element method appl. 8-92872
- crack growth in concrete, computer simulation using Monte Carlo method 8-76764
- dam groundwater flow anal. by finite element method 8-92875
- dam porous media unsteady flow calculation, combined finite element/characteristics methods appl. 8-91012
- dynamics of shells of revolution under axisymmetric load involving shear deformation 8-79210
- earthquake wave analysis program WAVE, DEMOS-E library program 8-92800
- elastoplastic anal. using ASKA program system, bending, isotropic/kinematic hardening, tunnel construction 8-63312
- elastoplastic arches, shakedown anal. 8-51091
- embedded foundations, soil-structure interaction problem, spring method 8-79216
- free surface flow digital simulation by finite element method 8-90819
- frictionless tidal channel behaviour digital simulation by finite element and finite difference methods 8-92876
- groundwater discrete kernel generator digital simulation using finite element method 8-92873
- groundwater flow calc. by finite element Galerkin method 8-89320
- groundwater flow model using finite element method 8-92874
- groundwater two-dimensional flow digital simulation using finite element method 8-93018
- high precision triangular laminated anisotropic cylindrical shell finite element 8-79206
- linear strain triangular element solns. 8-90719
- modal anal., formulations for numerical calcs. 8-57767
- nonlinear free surface flow digital simulation by boundary integral eqn. method 8-92850
- optimal water distribution systems design 8-61457
- plastic buckling of structures 8-63342
- porous media one-dimensional unsteady drainage digital simulation, finite element method appl. 8-91011
- shallow water with moving boundaries digital simulation by finite element method 8-92847
- strain hardening structures under repeated loading, deflection analysis 8-63313
- stratified turbulent flow digital simulation using finite element method 8-90964
- thermal problems, one-dimens., with phase change, efficient numerical technique 8-59270
- time split finite element algorithm for environmental release prediction digital simulation 8-92880

civil engineering computing continued

- two-dimensional flow with singularities digital simulation by finite element method 8-90822
- two-dimensional hydrodynamics and water quality digital simulation by finite element method 8-92877
- unsaturated soil simultaneous heat and moisture transport analysis by finite element method 8-92868
- variable domain finite element model for dam unsteady compressible fluid flow digital simulation 8-90820
- water network anal. using node recording algorithms and admittance matrix 8-85613
- water network anal. using sparse matrix and successive linearisation methods 8-85614
- well flow anal. using finite element method 8-92870

cladding techniques

No entries

claddings

- biaxial creep behaviour, ribbed GCFR cladding at 650C 8-86597
- fuel-cladding chem. interactions at high burnup 8-86584
- irradiation expt. 8-86587
- kohlestein insulation for use in HTR systems, further investigations (*German*) 8-66346
- LWR, stress conc. in cladding produced by cracked fuel pellets 8-50260
- LWR fuel-cladding gap, Cs-U-Zr-H-I-O system, chemical thermodynamics 8-82440
- mixed-oxide fuel, cladding breaches 8-82450
- mixed-oxide fuel pin, cladding breaches 8-82451
- nuclear advanced reactors, materials and design 8-78452
- nuclear fuel element model for cladding performance during power changes, strain defects 8-58359
- nuclear reactor fuel cladding tubes, 20/25/Nb stainless steel, biaxial creep meas. 8-82442
- nuclear reactor structural materials, WR-1 irradiation facility 8-89945
- pellet-cladding interaction, irradiation tests 8-86588
- PWR, peak cladding temp. sensitivity to LOCA reflood parameters 8-86639
- reactor cladding waste, spent fuel contamination, composition and amounts arising in EC 8-66360
- SGHWR fuel pins, fuel cladding ratchetting study 8-54855
- stainless steel, cold-worked Type 316, transient mechanical behaviour 8-86598
- steel, stainless, 316, nuclear fuel cladding, crack nucleation 8-72864
- steel, stainless, type 316, cold worked effect of prior neutron induced creep on burst strength 8-62599
- steel antioxidation protective glass enamel cladding exam. of development 8-85031
- stoichiometry effects on cladding attack on mixed oxide fuel 8-86583
- stresses in fuel rod cladding, effect of fuel-pellet chips 8-86589
- Zircaloy fuel cladding, O embrittlement obs. 8-89947
- Zircaloy-2 cladding, beta-phase, creep and creep rupture props., 1000 to 1500°C 8-78470
- U-Si-Al fuel rods, Zr-Nb cladding, irradiation behaviour with peripheral voidage 8-54835
- ZnS, on ZnSe substrate, erosion-resistant composite window fabrication and evaluation 8-71211

classical algebra see *algebra***classical field theory**

- see also *classical mechanics; electromagnetic field theory; gravitation; special relativity*
- action functional in distrib. spaces 8-54207
- affine motion in recurrent Finsler space 8-57797
- chromodynamics, SU(n), classical noncommuting quark source charges 8-78144
- classical angular momentum of an electron-magnetic monopole (*Chinese*) 8-86460
- coupled field theory, classical perturbation theory appl. 8-57799
- coupled fields in one dimension: cross-over from a continuous symmetry to a discrete one 8-87758
- dyon solns. for classical Yang-Mills field eqn. 8-54560
- education, Lienard-Wiechert field expression, circulating charge in static mag. field 8-69933
- education, Lorentz theory for classical radiation reaction of accel. charged particle, dumbell model 8-49592
- electrodynamics, covariant formulation for charges of finite extension 8-77731
- electrodynamics, energy tensor definition for system of charged particles and EM fields 8-77734
- embedding classical fields in QFT, electrodynamics, Yang-Mills theories, gravit. appls. 8-54223
- Euclidean 2-D nonlinear σ -models, continuity eqns. 8-54210
- Euclidean field theory, nonclassical configs. as minima of constrained systems 8-70256
- Euler-Lagrange eqns., generalised solns. 8-54206
- Euler-Lagrange hyperbolic systems of second order, relativistic strings 8-54209
- Fermion contribution to instantons 8-78079
- fermions on the hypertorus 8-74149
- flow fields and other vector field struct. and evolution 8-77733
- general relativity singularity-free extended particle model 8-54255
- general vector fields, classical theory, internal symmetries and conservation laws (*Russian*) 8-62328
- generalised Fourier transforms 8-54205
- generalised Parseval eqn. 8-54204
- homogeneous massive scalar field model, existence of nonsingular isotropic cosmological soln. (*Russian*) 8-77635
- induced potential problem in 3-D, functional analytic approach 8-58880
- interdigital transducers, quasiacoustic wave propagation, field theory anal. 8-66998
- Klein Gordon lattice field eqn. in 4-D space-time, Lorentz covariance 8-54184
- limit theorems for random fields 8-81860
- Lippmann-Schwinger type integral eqn. of motion, quantum corrections 8-62318
- Lorentz groups on skew symmetric tensor space, nonlinear realisations of direct product 8-62329
- meson fields, classical coherent component 8-78082
- nonlinear, relativistic new solutions, charge barrier mechanism 8-54211

classical field theory continued

- nonlinear σ -model, two, dimens., scatt. of massless lumps, nonlocal charges 8-62300
- nonlinear one-dimensional model with internal degrees of freedom 8-49684
- nonlinear scalar field, time-dependent solns. 8-81865
- ordered physical line structures, nonlinear local field theory, appl. to high polymers, supercond. flux line lattices 8-81859
- Pauli exclusion principle proof from self-consistent field theory of electrodynamics 8-49683
- plane-symmetric cosmological model, Einstein eqn. solns. for dust 8-49733
- polynomial conservation laws in (1+1) dimens. classical and quantum field theory, nonlinear Schrödinger eqn. 8-54224
- quick-change fields in continua, regularisation 8-49663
- radiating point charge, energy and ang. momentum splitting 8-69996
- real-time approach to instanton phenomena, multidimensional pots. with degenerate absolute minima 8-78067
- relativistically invariant two-dimens. models, classification method (*Russian*) 8-70291
- Schwarzschild sphere and classical electron self-energy 8-49681
- sine Gordon equation, exact time depend. solns. in 2+1 and 3+1 dimens. 8-78074
- sine-Gordon supersymmetric theory, infinite set of bosonic conserved currents 8-62313
- SO_4 , SL_{2C} classical gauge field eqns., isotropic and solitary-wave solns. 8-93795
- spin in kink-type classical field theories 8-81861
- spontaneous particle creation in strong gravitational field, semiclassical theory 8-54281
- stable limit cycles of vector fields, new negative criteria 8-57756
- statistical mechanics, classical, universal features for continuum-field nonlinear Hamiltonians 8-93543
- teaching, curl operator when $A \cdot \text{curl } A \neq 0$ 8-62020
- Thirring model, 2-D, complete integrability 8-49685
- topology, propagation of surfaces of weak discontinuity, broken extremes in classical field theory 8-93541
- twisted products for cotangent bundles of classical groups and Stiefel manifolds 8-49680
- twisted scalar field, vacuum solns. 8-93804
- variational principles on rth order jets of fibre bundles in field theory 8-86168

classical mechanics

- see also classical mechanics of continuous media; classical mechanics of discrete systems; classical theories of fluid structure*
- arithmetic models formulation 8-86130
- autonomous Hamiltonian system near equilib. point, formal integrals 8-89047
- canonical formalism, Bose type classical Hamilton algebra, phase space variables 8-54170
- crossbowl, by cone over thread, numerical solution (*Russian*) 8-55612
- dimensional base selection in expt. design and planning 8-49636
- education, dynamics of variable mass system, flexible inextensible rope 8-86071
- education, Maxwell fish-eye pot. and Coulomb pot. from mechanics 8-49585
- implicit finite element algorithm for geometrically nonlinear problems of struct. dynamics, stability anal. 8-86157
- implicit finite element algorithms for geometrically nonlinear problems of struct. dynamics, accuracy anal. 8-86158
- inertial frames in classical space time 8-81826
- Laplace operator in 2-D, coordinate transform., for teachers 8-61999
- multiple parameter system vibrations and stability, book 8-93532
- Newtonian mechanics, inverse problem, Lagrangian computation method 8-89329
- nonlinear systems, asymptotic stability, geom. props. of Lyapunov functions (*German*) 8-87286
- twisted products for cotangent bundles of classical groups and Stiefel manifolds 8-49680

classical mechanics of continuous media

- see also elasticity; fluid mechanics; plasticity*
- Airy functions, stress problem solns., teaching appl. 8-86063
- anisotropic constitutive equations and Schur's lemma 8-89337
- anisotropic layered medium, plane wave transmission 8-83150
- anisotropic solids with magnetic symm., unified dynamic theory 8-77713
- beam, large displacement-small strain anal., finite elements with rot. degrees of freedom 8-86161
- beam, rigid plastic, stepped, impulsively loaded, optimal design for asymmetric mode motions 8-90723
- bifurcation from rotationally invariant states 8-77671
- bodies with binary material and kinematic-kinetic structure 8-73848
- book, relativistic theories of materials 8-81907
- cantilever beam shape optimisation (*Polish*) 8-79203
- catastrophe theory, symmetry and higher order cuspsoids 8-62079
- cell collocation method in continuum mechanics 8-77711
- column design, optimisation of support conditions and segmentation 8-51062
- composite media, Green's functions 8-77712
- conjugate gradient solutions, finite element elastic problem with high Poisson ratio 8-90707
- continuum model of a particle system with three-point interactions 8-73852
- cylindrical shell with circumferential notch under axial compression, stability (*Polish*) 8-79239
- cylindrical shell-filler system, natural and parametric vibrations, taking tangential interaction into account 8-67085
- deformable media, perturbation method in 3-D problems (*Russian*) 8-49660
- density determ. of body from given potential (*Russian*) 8-77710
- discontinuity surface model, balance eqn. and phase transition 8-73850
- faceless linear cones, orders, gauge, and distance, appl. to continuum mechanics and special relativity 8-57753
- filled polymer, mathematical model of strengthening (*German*) 8-63279
- finite element grids, optimal choice 8-77698
- flow-induced oscillations, bifurcation to divergence and flutter, infinite dimensional anal. 8-89336

classical mechanics of continuous media continued

- foil bearing, deflection due to finite width bump, iterative methods 8-77691
- frameworks' stability analysis appl., w.r.t. sway excess of columns 8-51098
- frameworks calc., composed of thin-walled open sections, with aid of computer 8-51059
- fuel element spacers, structural anisotropic plates composed of cylindrical shells 8-89940
- Gauss-Hertz principle, extension of continuum form to time domain 8-73851
- granular materials, void compaction and material nonuniformity, influence on acceleration waves, addendum 8-83280
- Hamiltonian continuum mechanics, differential geom. foundation 8-77708
- imperfection sensitivity of N-degree-of-freedom system with coincident critical points, symm. effects, stability props. 8-79236
- interdigital transducers, quasicoustic wave propagation, field theory anal. 8-66998
- Kirchhoff plates, matrix displacement method with parameter transformation by additional compatibility postulation (*German*) 8-79202
- limit analysis, comparison of static and kinematic approaches (*French*) 8-86156
- macroscopic determinancy principle corollaries (*Russian*) 8-77714
- membranes, optimised dishes, strength and stability (*German*) 8-87256
- mesh analysis processes, convergence (*German*) 8-87257
- microstructure with finite deformations, reciprocity theorem, stored energy function (*Italian*) 8-81836
- mixed continuous mechanics problems, orthogonal functions (*Russian*) 8-49659
- non-local continuum mechanics, conservation laws 8-65770
- nonideal realisations of constraints and loosenesses 8-73849
- nonlinear elliptic problems for doubly connected domains, heuristic method (*Russian*) 8-86159
- nuclear power plant, aircraft impact, simplified derivation of reaction-time history 8-89958
- plate, elastic, under tension stress conc. due to surface pit 8-83243
- plate, flexural motion, effect of accelerometer mass 8-90741
- plate thick, circular hole under axisymm. radial load, stress anal., displacements 8-79201
- polar materials, restrictions on boundary conditions 8-54186
- quasi-Newtonian force 8-63765
- quick-change fields in continua, regularisation 8-49663
- Rayleigh-Taylor instability, method of generalised coords. 8-65771
- ring shaped bodies, collapse (*German*) 8-87258
- Saint-Venant torsion problem, classical, integral and functional eqns. 8-57780
- shallow thin shell finite element, stiffness matrix development 8-90705
- shell, spherical, with conical nozzle, thermal stress anal. 8-79204
- shell structures, thin, curved finite element 8-79205
- shells, conoid, parabolic, with vertical director line, stress analysis 8-51058
- shells, nonlinear geometrical anal. 8-77709
- shells of revolution, geom. characteristics, congruence of finite deform. (*Russian*) 8-86160
- shells of revolution with variable geometry, optimisation of mass 8-67030
- skew plate, soln. of infinite matrix 8-75064
- skew plates, large amplitude bends., including shear and rotatory inertia effects 8-90743
- slender damped structures, vortex excited aeroelastic oscills., mathematical model (*German*) 8-94616
- stability criteria, intrinsic, relative strengths 8-90738
- static fields in inhomogeneous anisotropic medium (*Ukrainian*) 8-81837
- stress tensor in nematic liquid crystals, micropolar continuum mechanics 8-67647
- stress tensor in nematic liquid crystals, micropolar continuum theory 8-67648
- structural anal., soln. by orthogonal collocation 8-51063
- structural panel, rectangular, with elastic edge constraints, dynamic response, Bolotin's asymptotic method 8-75091
- structures of discontinuous shape, finite element analysis of bending behaviour (*Japanese*) 8-83238
- structures with rotational degrees of freedom, large displacement-small strain anal. 8-89310
- suction force, interpretation of Rice integral 8-49658
- surfaces, relativistic, classical theory (*Russian*) 8-69984
- tensor equation $AX + XA = H$, explicit soln. (*French*) 8-86155
- thermoelasticity theory with appl., book 8-79219
- thermomechanics, introduction, book 8-54187
- thin cylindrical shell, compression dynamics, nonlinear evolution of Rayleigh-Taylor instability 8-79243
- thin cylindrical shells subjected to transient inner pressures, dynamic stress anal. 8-89344
- thin shell forming processes, geom. props. (*Russian*) 8-51061
- Timoshenko beam theory, natural frequency of continuous beam 8-83322
- transport processes, relativistic generalisation in continuum (*Hungarian*) 8-89383
- two-component materials, thermo-viscoelastic theory 8-73854
- wave-power devices, Salter duck, two-pontoon system, operating efficiency comparison 8-94591
- weakly nonlinear systems, props., discussion 8-93535

classical mechanics of discrete systems

- see also N-body problems*
- approximately relativistic Lagrangians for classical interacting point particles 8-54179
- arbitrarily slow irreversibility, example 8-70083
- arithmetic models formulation 8-86130
- associative Hamiltonian algebras 8-69975
- asymptotic expansions in motion of two electrons in nuclear field 8-66459
- asymptotically uniform rotation of rigid body about fixed point (*Ukrainian*) 8-65761
- autonomous Hamiltonian systems, orbital stability of periodic Lyapunov motions (*Russian*) 8-69664

classical mechanics of discrete systems continued

- axisymmetric rigid body in air, stability of unperturbed motion (*Russian*) 8-86146
- ball, radius of gyration determ., using air track, undergrad. demonstration 8-49606
- bipedal walking, linear stabilisation (*Russian*) 8-51055
- bouncing ball, student expt. 8-54122
- classical systems with regular or irregular motion, advances in understanding 8-93522
- collision processes, information theoretic maximal entropy theory, rel. to scatt. theory 8-81888
- complex plane motions of a point (*Russian*) 8-86129
- conference proceedings, nonlinear dynamics, tribute to Sir Edward Bullard 8-93603
- conformal invariant model of localised spinning test particles 8-49729
- conservative dynamic systems, search for cyclic coords. (*Russian*) 8-65764
- conservative finite dimensional system, stability of equilb. branching points (*Russian*) 8-86143
- crawl swimmer, six-stroke, dynamics, mathematical model (*German*) 8-90702
- driven oscillator motion with nondecreasing input vels., use in inertia actuated fuse 8-59293
- dynamics, fundamental principles generalisation, appl. to motion of disc on ice surface (*Russian*) 8-65762
- education, cart wheels on inclined plane, theory and expt. 8-61977
- education, Coriolis machine, inertial motion viewed from rot. reference frame, coordinate transformation 8-69934
- education, mechanical mutual inertia in spring coupled system, mutual inductance analogue 8-49590
- education, quantum mechanics, mechanical model 8-49591
- eikonal function for two classical relativistic particles 8-81828
- elastic mechanical systems, design sensitivity analysis, adjoint variable methods 8-90706
- flexible strings mechanism, variational principle in Euler representation (*Russian*) 8-54172
- flotation of solid body on liquid surface, equilb. state (*Russian*) 8-67029
- flutter-unstable dynamical system with gyroscopic (circulatory) forces, nonlinear behaviour 8-63276
- fundamental constants introduction (*French*) 8-62071
- Galilei relativity in Newtonian mechanics, possible Lie admissible covering 8-73838
- Gauss and Mainardi-Codazzi eqns. generalisations, appls. to quantum and classical mechanics 8-62092
- gravity acceleration as a function of mass, for teachers 8-81766
- gyroscopic system, linear, damped, modal anal., appl. to satellite 8-63275
- gyrostat, nonregular precessions in a Newtonian central field (*Italian*) 8-81825
- Hamiltonian dynamics, for closed system of N particles in mutual interaction 8-62070
- Hamiltonian dynamics, integrable and nearly integrable systems historical review 8-93521
- Hamiltonian systems, additional integrals of motion 8-49711
- Hamiltonians linear in momenta, note 8-77468
- harmonic oscillator, two dims., q equivalent particle Hamiltonian 8-93525
- ideal constraints, generalisation 8-65759
- impact phenomena with elastically deformable stricker and solid obstacle 8-77703
- impulse dynamical equations, nonholonomic system, solid on plane, rolling without slipping (*Italian*) 8-57769
- inertia ball demonstration, theory 8-73811
- interacting particles system, nonrelativistic classical and quantum mechanics conservation laws 8-89328
- interconnected dynamical systems on Banach spaces, well posedness, instability, Lagrange stability 8-69976
- intermediate-axis theorem, undergraduate demonstration expt. 8-61990
- iterative procedures for penalty function solns. of algebraic systems 8-57770
- Kepler problem, time transformation stabilisation (*German*) 8-89333
- Lagrange formalism, direct and inverse variational characterisation of linear non conservative systems 8-93527
- Lagrangian mechanics, consts. of motion anal. 8-81829
- Lagrangian systems with one degree of freedom, invariance and conservation laws 8-62067
- Lagrangians and Hamiltonians, constructed from eqn. of motion, for teachers 8-62016
- libration in systems of many degrees of freedom (*Russian*) 8-86141
- linear systems, stability of motion rel. to part of variables (*Russian*) 8-86144
- linked rigid body systems, nonlinear eqns. of motion (*German*) 8-87254
- mass point displacement under effect of forcing conditions (*German*) 8-86149
- masses of two bodies in dynamic interaction constituting an isolated system (*French*) 8-89326
- matrix differential equation, rotations as solns., for teachers 8-62021
- method of action-angle variables and the classical dynamics of a nonlinear Lagrangian 8-77702
- mooring cable in nonuniform stream, equilb. shape and tension (*French*) 8-63277
- Morse oscillator, classical motion, calcs. 8-73796
- motion in spherically symmetric force fields, vector consts. 8-85833
- motion integral disappearance in multi-resonance conditions 8-77471
- motion of solid body with elastic and dissipative elements (*Russian*) 8-65763
- multidimensional two particle problem with noncentral pot. 8-54174
- multimass undamped vibration system, decoupling from large struct. 8-57774
- Nambu mechanics, relation to generalised Hamiltonian mechanics 8-93526
- Nambu mechanics, reln. to Lagrange, and Hamilton-Dirac mechanics 8-54180
- Newton's 2nd law, spatial translation symmetry, for teaching 8-54129
- Newton's law, introduction of a repulsive force 8-73839
- non-holonomic constraints, existence of potential function (*French*) 8-86128

classical mechanics of discrete systems continued

- nonconservative systems, integration of motion eqns. (*Ukrainian*) 8-81827
- nonlinear mechanical system with time optimal condition, synthesis 8-54176
- nonlinear mechanical systems of arbitrary order, stationary oscillations (*Russian*) 8-65765
- nonlinear oscillator, stroboscopic phase portrait and strange attractors 8-54177
- optimal motion stabilisation (*Russian*) 8-86145
- particle motion in central force, without orbit precession 8-86057
- passive vibr. isolation, shock absorber selection 8-55556
- pendulum-gyroscopic platform stabilised in inertial space, autonomous determ. of coords. (*Ukrainian*) 8-65760
- periodic Hamiltonian flows, generalised Bertrand's problem 8-86131
- periodic orbits, simple time independent Hamiltonian system, general results 8-93523
- plane periodic motion of two rigid bodies (*Russian*) 8-73840
- Poincare canonical momenta and Nambu mechanics 8-77701
- pseudocoervative systems, effect of damping on stability 8-81832
- pseudowork-energy principle nonrigid or rot. bodies, for teaching 8-49602
- quasistationary motions of mechanical systems (*Russian*) 8-62066
- random excitation of harmonic oscillations of single degree of freedom systems 8-54175
- Rayleigh's principle for simply supported beam, energy considerations 8-83322
- reaction of continuous dynamic systems with complex form under time-space random fields 8-65767
- relativistic string with massive ends, classical and quantum theory 8-62073
- Riemann curvature of conservative systems 8-89332
- rigid asymmetric body in Newtonian force field, motion (*Italian*) 8-81822
- rigid body with discrete symmetry, conditionally-linear integration of eqns. of motion (*Russian*) 8-86135
- rigid motion, canonical treatment for rigidly connected point systems 8-69972
- rolling coin, computer anal. of motion (*Hungarian*) 8-73837
- Signorinis perturbation scheme for a general reference config. in finite elastostatics 8-83241
- spinning tops, mechanics (*German*) 8-87253
- string vibr. against point shaped obstacle, energy theorem 8-81824
- string vibr. through moving ring 8-81823
- string vibrating against rigid wall, partially elastic or anelastic impact, energy calcs. 8-67028
- SU(2) symmetry group generators for classical Calogero system 8-62332
- third-order nonlinear systems with aperiodic excitations, Laplace transform technique 8-81830
- thrown string problem 8-89331
- top rising by friction, exact mathematical soln. 8-83343
- transitive dynamic systems, polhode concept generalisation (*French*) 8-62065
- translatory-rotary motion of gravitating spheroids (*Russian*) 8-73841
- wheeled vehicle with nonholonomic couplings, eqns. of motion (*Russian*) 8-59292

classical theories of fluid structure

see also kinetic theory; liquid theory

- adsorption, Percus-Yevick and hypernetted chain theories, second and third virial coeffs. for hard-sphere gas 8-60031
- area of intersection of n equal circular discs, appl. to hard-disc fluid model 8-57755
- Brownian motion in fluid, repeated-ring kinetic theory 8-59729
- n-butane, intermol. pair corrls., RISM integral eqn. 8-63656
- collective motion and effective potential 8-79513
- Enskog equation, modified, approach to equilb. 8-94957
- fluid-solid surface interaction, two-particle correlation function 8-79880
- graph theoretic techniques 8-71662
- hard disc fluid, sixth and seventh virial coeffs. 8-91047
- hard sphere fluid contacting soft repulsive wall, Monte-Carlo method 8-67632
- hard sphere system, second-order perturbation theory 8-79516
- hard spheres, partition functions, Miller's method 8-71828
- hard spherocylinders, Monte Carlo simulation 8-91046
- hard-sphere fluid near hard wall, Monte Carlo calcs. 8-55795
- ionic solution, in mol. polar solvent, charged sphere model, statistical mechs. 8-71655
- Lennard-Jones fluid, hypernetted-chain eqn. of state 8-67800
- liquid mixtures, local mole fractions consistency 8-83702
- molecular fluid perturbation theory, Pople expansion third order term, anisotropic pot. 8-79510
- molecular liquid, thermodynamic functions, interaction site model calc. 8-71661
- nonadditive hard spheres, scaled particle theory, positive nonadditive solns. 8-79515
- Percus-Yevick equation, nonequilibrium analogue 8-55797
- Percus-Yevick equation, square-well pot., perturbation version 8-63648
- polyelectrolyte, 1-1 soln., excluded vol. theory, Khun statistical segment basis 8-83716
- polymer chain dynamics, in soln., computer simulation 8-83718
- polymer solution, conc., rheological props., rod-like mol. model 8-75114
- rigid spherocylinder fluid, virial eqn. of state 8-63836
- solid substrate interaction, comparison of theories 8-63655
- square-well fluid, using corrected integral eqns. 8-79511
- statistical mechanics of small chain mols. packing effect 8-71656
- statistical thermodynamics, review 8-83703
- Stockmayer fluid, mol. dynamics and thermodynamic perturbation theory, mol. polarisability effects 8-71419
- tricritical phenomena, ternary, quaternary fluid mixtures, classical models 8-91416
- two dimensional radial distrib. function 8-67629
- CS₂, liq., light scatt. intensities, struct. models 8-60476
- N₂, liq., dephasing of mol. vibr. related to corrl. functions 8-75523

classification

see also indexing

- recurrent Lie group classification (*French*) 8-62047

classification, pattern *see pattern recognition*

clathrates *see molecules; organic compounds*

clay

- Al(1) clay of Frankische Alb, slope forms statistical investigation (*German*) 8-57211
dispersion and swelling, effect on soil hydraulic cond. 8-53668
Grote Nete basin, Belgium, geomorphology (*Flemish*) 8-61452
groundwater flow anal. by finite element method 8-92875
halloysite, $\text{Al}_2\text{O}_3(\text{SiO}_2)(\text{H}_2\text{O})_2$, NMR study of adsorbed water, molecular motions 8-95226
landscapes, soils and erosion, Wither Hills, New Zealand 8-88864
Mars, clay minerals prod. by alteration of glass 8-89097
minerals, distrib. in sediments of Bay of Bengal 8-81146
montmorillonite, dehydration kinetics 8-76857
montmorillonite neoformation by post-depositional subsurface weathering in slope deposit 8-73367
remoulded, shear stress path, stress history rel. to shear strength characts. 8-77219
sediment, artificial, const. vol. deform. effects on magnetisation 8-65265
soils, cracking and swelling dynamics 8-73359
soils, sandy and clay, microwave absorption (*Russian*) 8-81162
thermoluminescence dating of sediments baked by Chaîne des Puys lava flows 8-92808
 $\text{Fe}_2\text{Si}_4\text{O}_{10}(\text{OH})_8$, greenalite, metagag. clay mineral, mag. props. (*French*) 8-88817
H isotope exchange between clay minerals and seawater 8-69329

cleaning *see surface treatment*

cleanliness *see hygiene*

cleavage, crystal *see crystal cleavage*

Clebsch-Gordan coefficients

- see also elementary particle theory*
biatomic molecular gas, quantum kinetic theory (*Rumanian*) 8-91053
calculation program ANGOM 8-89359
functions on tableaux and frames of the symmetric group S_n , determined by computer program 8-86173
Gel'fand lattice polynomials and irreducible representations of $U(n)$ 8-49700
gradient formula for the $O(5) \supset O(3)$ chain of groups 8-78285
induced projective unitary-antiunitary representations, selection rules, Clebsch-Gordan series 8-54214
intelligent states, computation of Clebsch Gordan coeff. 8-62101
isoscalar factors, on noncanonical bases 8-81797
meson sector in $SO(8)$ model of elementary particles 8-58135
multiplicity free 6-j symbols and Weyl coeff. of $U(n)$ 8-65809
polarisation in heavy ion reactions, Strutinsky model, asymptotic Clebsch-Gordan coeffs. 8-74391
projective Lie algebra of Lorentz group, homographic transform. 8-57739
 S_n group coeffs. generation by computer program 8-86172
 SU_m containing $SU_n \times SU_n$, irreducible bases (*Chinese*) 8-66049
 SU_n C-G coeffs., contiguous relns., derivation method 8-74171
sums of products, for Clebsch-Gordan and Wigner coeffs., rel. between diagrams 8-81879
 SU_{m+n} containing $SU_m \otimes SU_n$, irreducible bases (*Chinese*) 8-66049

climatology

- see also atmospheric humidity; atmospheric precipitation; sunlight; wind*
aerosols from Mount Agung eruption as test of global climatic perturbation 8-69440
albedo modification due to intensive solar energy production 8-85680
N America, late Pleistocene palaeoclimates inferred from speleothems stable isotope studies 8-57297
N. American glacial history extended to 75000 years ago 8-77284
American Southwest, evidence for cold, dry full-glacial climate 8-57296
atmosphere parameters relevant to helicopter icing problems, need for improved climatology 8-85657
atmosphere particulate pollution, climatological effects 8-85678
British Columbia, S central, late Pleistocene stratigraphy and climates 8-92804
coastal California, late Quaternary climate and evidence for Ice Age refugium 8-57293
caloric insolation long-term vars. resulting from Earth orbital elements 8-73502
Canadian haze climatology 8-57304
causes of climatic change 8-73499
cirque glaciations, Holocene and latest Pleistocene, in Shuswap Highland, British Columbia, ages 8-92856
climatic change effects on food production, statistical models limitations 8-57303
climatic optimum, rel. to insular phosphorite form. on Ebon atoll, Micronesia 8-81121
Clyde Foreland, Baffin Is., last interglacial-glacial cycle, stratigraphy, biostratigraphy and chronology 8-61536
confusion in terminology (*German*) 8-65380
Corsica (France), Quaternary alluvial deposits rel. to paleoclimates 8-57234
diffusive nonlinear heat transport in simple climate model 8-81349
drought effects on agriculture in United Kingdom, 1975-76 period 8-57298
Earth global heat balance, annual var. 8-73300
Earth insolation, influence of orbital elements periodic vars. (*Russian*) 8-53605
El Nino, climatic research project at Scripps Institution of Oceanography 8-69464
elm tree rings as rainfall record 8-65381
energy balance model, sensitivity and role of cloudiness (*Russian*) 8-88902
energy contribution to anthropogenic climatic fluctuations, 21st century problem 8-57299
energy policy, climatic effects 8-61538
England, decreasing wetness in 1969-77 period 8-65377
NW Europe, appl. of extended ^{14}C time scale by isotope enrichment 8-77314
European agriculture rel. to climatic change 8-85679
European air temperature change patterns 8-92957
fluctuations, relation of moistening to thermal regime 8-92937
geomagnetic field reversals and climatic change, statistical correl. 8-61537

climatology continued

- global mass and energy requirements for glacial oscills. rel. to mean ocean temp. oscills. 8-81351
historic climate correl. with wheat prices and wages 8-81346
Holocene climatic fluctuations, evidence from rock glaciers in Jasper National Park, Alberta 8-77276
Holocene palaeo-winds, evidence from palynology in Baffin Island 8-57262
ice age in northeast county Wicklow, climatic environment rel. to ice wedges form. 8-69379
ice ages, prod. by Earth encounter with interstellar cloud 8-57292
ice ages and ecological catastrophes, prod. by Earth-comet close approach 8-53714
ice ages rel. to Earth's obliquity and eccentricity in orbit 8-53715
impact of large solar energy systems 8-81358
insolation rel. to climate, normal incidence solar intensity rel. to weather at Fort Hood, Texas 8-57240
insolation rel. to climatological variables, solar energy availability estimation 8-81344
Institute of Meteorology and Climatology, Slovak Acad. Sci. (1964-74) (*Russian*) 8-88920
interannual cloud-cover vars. in contiguous United States 8-92909
interglacial episode termination and Wilson Antarctic surge hypothesis 8-53669
IR cooling rates, effect of tropospheric aerosols 8-88886
Italy, vorticity generation and energy budget, 1961-65 period 8-81350
karst landscapes, origin of labyrinth and tower styles, necessary climatic conditions 8-96208
large scale solar energy conversion effects, conf., Laxenburg, Austria, Dec. 1976 8-81352
Late Quaternary climatic changes, W. Africa, from deep sea sedimentation 8-73355
local energy exchange dynamics and climatic boundary conditions, solar energy conversion effects, preliminary examination 8-81355
long-term climatic change, appls. to hydrometeorology 8-96240
long-term climatic change numerical modelling 8-77315
model experiments, simulated changes in albedo, surface roughness, surface hydrology, solar energy conversion effects 8-81354
models, stability and extremal props. (*Russian*) 8-53716
natural disaster fallacies, Sahel drought example 8-57302
nondeterministic theories of climatic change, comments 8-73503
northern hemisphere annual temperature approximation, simple method 8-81345
Norway Station/Sanae (Antarctica), surface temp. and sea-level press. 8-81324
numerical prediction, weather and climate, recent advances 8-96276
ocean data and information services, appl. to climatic problems 8-69463
oceanic rainfall maps, global climatic features 8-65379
S. Pacific, hydroclimatic anomalies 8-65335
Pacific Pleistocenes palaeoclimatic stratigraphies, comparative anal. of results 8-57295
palaeoclimatology, record of E. Mediterranean Sea deep sea sediment core 8-57294
palaeoclimatology and vegetation ecology (*French*) 8-88901
pleistocene, southern trade winds and oceanic upwelling during last 75000 years 8-57217
Pleistocene-Holocene transition, W. Pacific, from stable isotopes anal. in deep sea carbonates 8-73354
Pliocene and Pleistocene glaciations rel. to Barents Ice Sheet, evidence from Barents Sea 8-57227
central Sahel, Neolithic hyperarid period 8-73500
simulation of geophysical fluid system rel. to climatic var. 8-81353
solar activity, long-period vars. correl. with terrestrial climate (*French*) 8-73695
solar energy conversion, possible effects 8-81356
solar intensity model year construction rel. to climate 8-57241
solar thermal energy production, large scale, possible climatic effects 8-81357
stability of simple climate models, variational estimate (*Russian*) 8-69437
stratosphere, intense ionisation events, effects on NO_2 , O_3 and climate, rel. to life extinction 8-96273
stratospheric aerosol layer and climatic effects 8-81331
structural and stochastic anal. of zero-dimens. climate system 8-73501
sunspots and volcanic dust effects on climate, statistical evidence from long-term temp. records 8-69439
surface temperature changes nonlinear response in climate model, ice-albedo, lapse-rate and cloud-top feedbacks 8-69438
temperature and precipitation, temporal fluctuations averaging for continents Europe and N. America 8-92958
Texas High Plains, precipitation climatology 8-92959
thermal pollution from fuel and energy consumption, effects on weather and climate 8-61539
two-level primitive eqn. atm. model for climatic sensitivity expts. 8-81348
watershed geomorphology, relative scales of time and effectiveness of climate 8-81229
World Meteorological Organisation programme activity development 8-61531
world predicament and climatic change, need for interdisciplinary research 8-57300
zonally averaged climate model 8-81347
 CO_2 content of atmosphere, role of C storage by forests and oceans 8-53718
 CO_2 from fossil fuel burning, climatic effects, proposed CO_2 disposal in deep ocean 8-57301
 CO_2 levels rel. to agricultural expansion in late 19th century 8-53717
O isotope palaeotemperatures, from Tertiary period in North Sea area 8-88903
 ^{18}O stratigraphy in deep-sea sediments, evidence for deglacial meltwater effect 8-85530

climb, dislocation *see dislocation climb*

clock paradox *see special relativity*

clocks

- see also atomic clocks; chronometers; time measurement*
digital, control by signals from standard freq. transmitter (*German*) 8-57902
energy efficiency, mains and battery operated clocks, for teachers 8-81773

clocks continued

- precision, synchronisation and time/frequency dissemination 8-49803
- radio time signal coding and clocks for private and industrial use (*German*) 8-89445
- random perturbations, absolute continuity theorem (*French*) 8-62150
- sapphire, single-crystal clocks and frequency standards 8-57915
- simple darkroom timer design and construction 8-89577
- sundials to atomic clocks for understanding time and freq., book 8-57904
- synchronisation cct. for error monitoring, correction 8-73970
- NH₃ special-purpose frequency standard and clock 8-57913
- Si single-crystal clocks and frequency standards 8-57915

closed circuit television

- colour single-tube camera, SICOLOR, appl. to endoscopy (*German*) 8-88758

closed loop control systems *see closed loop systems***closed loop systems**

- see also feedback*
- active optical systems, real-time control over optical wave fronts 8-71187
- dimensional gauging using scanning laser beam 8-57898
- stochastic approx. procedures in continuous time 8-69969
- thermal-blooming compensation, using closed-loop adaptive single parameter system 8-94407

cloud chambers

- expansion cloud chamber with thermoelectric cooling 8-90034
- NO₂ in nonane, supersaturated gas, photoinduced nucleation 8-80760

cloud physics *see clouds***clouds**

- see also atmospheric precipitation; sky*
- atmosphere, radiation modulation of aerosol state by moving clouds (*Russian*) 8-88916
- beam broadening in randomly inhomogeneous cloudy aerosol medium (*Russian*) 8-58911
- boundary layer near water surface, diurnal characts., equatorial region, GATE meas. 8-61527
- cirrus, influence on IR cooling rate 8-73455
- classification from visible and IR SMS-1 data 8-77309
- climate model, sensitivity and role of cloudiness (*Russian*) 8-88902
- cloudiness correl. with ozone vars. rel. to UV radiation protection 8-73456
- colour guide, book 8-92952
- condensation nuclei counters, comparison of two instruments 8-61598
- convective clouds, dry ice appls. for on-top seeding 8-73531
- convective clouds, three dimensional turbulent flow anal. 8-69395
- convective shallow cloud model, precip. mechanisms 8-81311
- cooling tower plumes from energy centres, predicted climatology 8-61541
- cumulonimbus clouds, elec. field strength and raindrop spectra, study from mobile ground station 8-92943
- cumulus, size and particles effects on satellite-observed reflected brightness 8-73510
- cumulus and cumulonimbus forms and patterns 8-57289
- cumulus congestus, NE Colorado, graupel particles characts. 8-81312
- cumulus convection initiation mechanisms and development 8-69410
- cumulus seeding technique, preliminary tests 8-57352
- cyclonic storm, rainbands, precip. cores and generating cells 8-81307
- drop spectrum evolution for condensed stage in turbulent atm. 8-81325
- drop spectrum evolution rel. to collision efficiency 8-69415
- droplet coalescence growth, fast computational method for Telford's theory 8-69486
- droplet growth and initial dew point temp. accuracy in cloud chamber on space shuttle 8-96268
- droplets size distrib. in cloud bases 8-73458
- drops, crystallisation on CuS aerosol prepared by burning pyrotechnic mixture 8-96279
- extinction meas. using electronic chopper for UV source 8-79087
- F-region plasma clouds, high altitude limit of gradient drift instability 8-88984
- F-region striated Ba clouds, electron density struct. meas. 8-88974
- funnel cloud in Trinidad, West Indies 8-73498
- funnel clouds, characts. from obs. during sailplane flights 8-69396
- global middle UV radiation meas. at ground, cloud effects 8-92882
- Hampstead storm, London, numerical simulation of quasistationary cumulonimbus system 8-77308
- N.Hemisphere, cloud cover correl. with middle troposphere organised vertical vels. 8-92939
- hurricane modification expts. by cloud seeding, evaluation 8-85654
- hydrometeor clouds, thermal microwave radiances 8-85638
- ice, growth beneath water film, air bubble precipitation 8-83922
- ice and water content from Nimbus 6 IR sounder data 8-92925
- ice particles, depolarisation of 19 and 28 GHz Earth-space signals 8-73492
- ice splinter production during riming, possible mechanism 8-85662
- insolation over tropical Pacific Ocean, cirrus cloud effects 8-92914
- interannual cloud-cover vars. in contiguous United States 8-92909
- IR radiation, cloud height, thickness and overlap effects 8-57252
- Israel and Jordan, rainfall fields, cloud seeding effects 8-73452
- lidar backscatter from horizontal ice crystal plates 8-92984
- lidar polarisation meas. for cloud phase discrimination 8-86269
- lidar probing of fogs and clouds, double scatt. approx. 8-73512
- lidar scattering from clouds at 347, 694 nm, polarisation props. 8-85689
- light beam coherence through optically dense turbid layer 8-55300
- light reflection, path length difference and wavelength correl. (*Russian*) 8-69447
- light scattering, directional scatt. coefficients meas. in droplet and cryst. clouds (*Russian*) 8-96292
- light scattering effects on satellite aurora and nightglow obs. 8-77385
- liquid water content, organic aerosol effects 8-73465
- liquid water content meas. of lab. supercooled clouds, instrument design 8-96316
- liquid water content rel. to atm. visibility 8-81404
- marine atmosphere, ranked interaction with ocean on sub-semidiurnal scales (*Russian*) 8-77260
- mesoscale downdraughts, assoc. with cool ocean surface waters, GATE results 8-69365
- mesosphere ice clouds production by Earth encounter with interstellar cloud, climatic effects 8-57292

clouds continued

- microphysics, book 8-88896
- multiburst cloud rise after nuclear explosion 8-94142
- noctilucous, particle sizes rel. to available mesospheric H₂O vapour 8-57248
- noctilucous clouds, 1977 obs. over W.Europe and Atlantic 8-92929
- ocean skin temperature, effects of clouds, hydrodynamic model (*Russian*) 8-65331
- organic material impact on fog and cloud processes 8-73467
- orographic, air-truth lidar polarisation studies 8-73454
- particle camera, aircraft-borne, for in situ photography of cloud particles 8-85750
- raindrop size distributions parameterisation 8-77301
- Raman rotational and double scatt., lidar meas. 8-77318
- reflectance with laser beam illum., multiple scatt. contrib. 8-85686
- satellite cloud picture recorder for reception of APT pictures 8-81434
- satellite derived cloud imagery, optical Fourier transform anal. 8-85749
- snowflakes, vapour deposition and aggregation growth, analytical model 8-73433
- solar radiation absorption, cloud and aerosol effects on heating rate 8-57319
- stationary homogeneous shallow cumulus cloud field, statistical props. 8-73434
- stochastic coagulation clouds, kinetic eqn. 8-92944
- supercooled, drop size distrib. influence on secondary ice particles prod. during graupel growth 8-73481
- supercooled cloud, induced snowfall due to power plant plume 8-81284
- surface radiative flux, clear and cloudy conditions, parametrisation accuracy 8-77325
- surface temperature changes nonlinear response in climate model, ice-albedo, lapse-rate and cloud-top feedbacks 8-69438
- thunderstorms, elec. fields, precip. elements charge and size, airborne obs. 8-73485
- Transcaucasia, cloud field statistical struct. 8-92942
- tropical iridescent cloud occurrence rel. to tropopause temp. 8-85675
- turbulent and radiative transport interaction in development of fog and low-level stratus 8-81313
- turbulent atmosphere, pollution release, exposure freq. distrib. from multiple cloud sources 8-57255
- Typhoon June (1975), water vapour and clouds liq. water meas. by scanning microwave spectrometer 8-73436
- volcanic plume height, control by eruption energetics and dynamics 8-61381
- warm cumulus, three-dimens. numerical model with microphysical processes (*Russian*) 8-88884
- water metastable states, phase diagram (*Russian*) 8-95129
- waterspout statistics for Nassau, Bahamas 8-92919
- Wilson Cloud form. by low altitude nuclear explosions, water aerosol and droplets characts. 8-53704
- winter orographic cloud seeding project, predictor control for evaluation 8-92922
- winter thunderclouds of Hokuriku coast, Japan, elec. dipole struct. 8-73443
- H₂O vapour and cloud liquid determ. by dual freq. ground-based microwave radiometry 8-93007

Clusius-Dickel columns *see isotope separation***cluster analysis** *see pattern recognition***cluster approximation**

- alkali halides, F-centre, cluster-Bethe lattice treatment 8-63762
- alloys, density of electronic states, dressed-cluster approx. 8-95249
- classical canonical ensemble 8-49752
- cluster expansion formalism, independ. pair correlations 8-73922
- covalent crystals, defect states, many-electron approach 8-67980
- defect, energy of formation, Gibbs free energy 8-91332
- disordered systems, short-range order and off-diagonal randomness 8-75782
- electron correlation problems, lattice statistical aspects, Gutzwiller approx. 8-84160
- electron correlations, ground state results in high density regime 8-72097
- electron density of states, self consistent cluster-Bethe lattice calc. 8-67930
- electron gas, correlation energy, appl. of coupled cluster approx. 8-72102
- electronic transport in substitutionally disordered system, derivation of cluster approx. 8-84184
- FCC clusters, size and shape depend., tight binding approximation 8-79920
- FCC Ising ferromagnet., cluster variation approx. 8-68278
- fermion clusters, many particle correlations, method of transition density operators 8-49763
- ferromagnet with random anisotropy, Curie temp., constant coupling approx. 8-76264
- graphite, electronic props., self consistent LCAO calc., point vacancy in 2-dimens. cryst. 8-51932
- Heisenberg ferromagnet, structurally disordered, variational method for cluster model 8-91839
- Heisenberg magnet, constant coupling approx., derivation 8-76213
- HF approach, cluster-environment interaction 8-84117
- Ising model, two-dimensional renormalisation group approach 8-52261
- itinerant ferromagnet in disordered phase, energy band struct. 8-68141
- narrow band systems, momentum distrib., cluster var. method 8-72060
- random walk, self-avoiding, direct renormalisation group approach 8-73933
- symmetry-adapted-cluster expansion, variational determ., open-shell orbital theory applic. 8-54213
- three-state Potts model variant, phase behaviour 8-68259
- transition metal surface, electron states at steps, cluster-Bethe lattice approx. 8-52045
- transition-metal compounds, effects of electron transfer on shake-up satellites, model calc. 8-95650
- Al, adsorption of O₂, relation between energy-band and cluster model 8-52048
- Fe, ferromagnetic, cluster method, environmental effects 8-95405
- GaAs surface, cluster model approach for electronic struct. 8-56205

cluster approximation continued

- Ge, surface, cluster model approach for electronic struct. 8-56205
 $\text{LaCl}_3\text{:Pr}^{3+}$, crystal field parameters using multiple-scatt.- X_α method 8-95271
 Li (100), O adsorption, cluster models, ab initio HF LCAO theory 8-71978
 Li, entropy and enthalpy of solution of H 8-51692
 LiCl:Cu^{+} , luminescent centre, cluster MO calculation of energy levels 8-64411
 Na entropy and enthalpy of solution of O(N)(C)(H) 8-51692
 Ni, chemisorption of H, X_α cluster calcs. (*Japanese*) 8-72002
 $\beta\text{-NiAl}$, self-consistent embedded-cluster model for mag. impurities 8-67973
 Si, surface, cluster model approach for electronic struct. 8-56205
 SiO_2 clusters, CNDO/2 calc., appl. of cyclic boundary conditions 8-72110
 VO , octahedral clusters, electronic struct., X_α discrete variation and SW methods 8-63976
 VO_2 clusters in metallic and semiconductor phases, electronic struct., X_α calcs. 8-63977

cluster model (nuclear) see *nuclear cluster model***clustering, impurity** see *segregation***clustering, solute** see *segregation***clusters, atomic** see *atomic clusters***clusters, globular (stellar)** see *globular star clusters***clusters, metal** see *metal clusters***clusters, molecular** see *molecular clusters***clusters, stellar** see *stellar clusters and associations***clusters of galaxies**

see also *galaxies; intergalactic matter*

- 0915+320, wide-angle-tail radio source in group of galaxies, 4.9 GHz map 8-93441
 Abell 1367, obs. rel. to galaxies redshift-magnitude bands and evolution 8-54033
 Abell 1781, photometry of field galaxies 8-77609
 Abell 2118 cluster, extent of hot intergalactic gas 8-86021
 Abell 2634, radiosources around 3C 465, continuum maps 8-73764
 Abell 426 and 1367, surface brightness and colour distrib. of elliptical galaxies 8-81681
 Abell 643, 1562, rich clusters with classical double radio sources, interferometric obs. 8-57662
 Abell clusters and superclusters, search for X-ray emission 8-54091
 Abell clusters fields, Westerbork obs. 8-96549
 association with QSOs, radio source morphology appl. 8-93434
 Bautz-Morgan classes, distrib. rel. to clusters luminosity function and brightest galaxies 8-54057
 Big Bang model, galaxy cluster missing mass from massive leptons, additional ν species 8-81719
 binary galaxies, axis ratios and posn. angles for galaxies in pairs 8-93430
 binding mass, contrib. of heavy stable neutral leptons 8-93091
 bright galaxies membership, optical redshifts results 8-89252
 brightness spectrum, number-luminosity relation and cosmic luminosity 8-81696
 catalogue of galaxies and clusters of galaxies in SMC direction 8-96410
 Centaurus, spiral and elliptical galaxies distrib. rel. to Virgo cluster redshifts 8-54061
 close pairs of galaxies, excess radio emission 8-57658
 clumps, formation and evolution in expanding Universe 8-93432
 Coma, central regions struct. from equidensity diagrams 8-93435
 Coma, new stellar standard sequence 8-93436
 Coma cluster, halo radio source meas. by Westerbork survey 8-86027
 Coma cluster, low energy X-ray absorpt. obs. 8-86025
 Coma cluster, ratio of escape vel. to mean vel. (*German*) 8-53995
 Coma/A1367 supercluster and environment 8-65700
 compact groups, distrib. of compact galaxies (*Russian*) 8-61926
 compact groups of compact galaxies, eighth list, 32 objects (*Russian*) 8-93125
 core condensation in heavy haloes rel. to galaxy formation and clustering 8-54051
 cosmological N-body simulation, rel. to galaxy clustering evolution 8-96550
 covariance function, explanation for 9 Mpc break 8-65688
 covariance function, Limber's relativistic formula, relativistic inversion 8-69891
 density perturbations in expanding universe, three-point correl. function and higher order functions prediction 8-65730
 emission-line galaxies in dense clusters 8-65703
 enriched gas in clusters and dynamics of galaxies and clusters rel. to galaxy formation 8-77596
 extragalactic objects clustering in Universe (*Polish*) 8-96580
 formation, violet gas dynamics 8-86018
 formation in expanding universe, new model 8-93489
 formation in self-similar space-times, perturbation scheme 8-54099
 Fornax cluster, bright members surface photometry 8-96548
 galaxies, Hubble's law as laboratory exercise in astronomy 8-65740
 gas content meas. by obs. of microwave background at 10.6 GHz 8-96551
 gaseous protoclusters spatial struct. and galaxy form. 8-93415
 giant galaxies in clusters, radioactive accretion flow 8-93433
 gravitational instability in early Universe, cluster-sized perturbations 8-93487
 head-tail radio galaxies, galaxy counts in surrounding region rel. to tail orientation 8-54060
 head-tail radio galaxies in poor clusters, radio and optical obs. 8-96530
 Hercules supercluster, galaxy distrib. in field 8-93437
 hierarchical clustering pattern, stability 8-86026
 Hubble constant determ., large turbulent Universe model 8-96578
 Hydra I, ram-pressure sweeping, optical evidence 8-93429
 integrated Brandt masses for spiral and irregular galaxies in groups 8-93398
 intergalactic dust, evidence from Zel'dovich effect 8-54041
 intracluster Fe-enriched gas, origin and evolution 8-93390
 intracluster gas flow patterns and X-ray emission 8-65705
 isolated pairs of galaxies, radio continuum survey 8-57657
 large-scale distribution and motion, in adiabatic theory of form. 8-54056

clusters of galaxies continued

- Local Group, angular momentum of galaxies 8-93400
 Local Group, colour-magnitude data, Virgo I cluster distance determ. 8-73763
 Local Group, distances for six nearest galaxies 8-89247
 Local Group, H I content of dwarf spheroidal galaxies, upper limit 8-57633
 local group, high sensitivity survey of high vel. H I clouds 8-65686
 Local Group, predominantly normal matter from primary cosmic rays antihelium abundance 8-73594
 Local Group, secondary distance indicators 8-93402
 Local Group, UKS 1927-177 and 2323-326, 21 cm. obs. of new dwarf irregular galaxies 8-65697
 Local Group galaxies, progression in Cepheid period-amplitude diagram characts. 8-53956
 local space density, of galaxy clusters, active nuclei and quasars 8-57676
 luminosity functions, derivation 8-54058
 mass spectrum, low mass portion anal. 8-81695
 missing dark mass rel. to primordial star generation 8-61946
 morphological evolution and galactic cannibalism 8-93404
 NGC 4631 group, tidal interactions model 8-54059
 NGC 4631/NGC 4656 group, neutral H aperture synthesis obs. 8-54043
 number density distribution of galaxy clusters 8-81693
 number-density distrib. from red Palomar Sky Survey prints 8-57659
 Perseus, energy-dependent map of X-ray emission, SAS 3 obs. 8-65702
 Perseus, obs. rel. to galaxies redshift-magnitude bands and evolution 8-54033
 Perseus cluster, low energy X-ray absorpt. obs. 8-86025
 primordial heavy leptons halos, annihilation contrib. to cosmic gamma-ray background 8-93479
 quintets of galaxies, statistical anal. of discrepant redshifts 8-65701
 radio and cD galaxies, optical props. 8-93413
 radiosources with complex morphology in galaxy clusters 8-93443
 redshift-magnitude bands and galaxies evolution, data anal. 8-57629
 redshifts of radio tail galaxies in clusters 8-69889
 relaxation from aspherical initial conditions 8-96538c
 rich Abell clusters, survey at 408 and 1407 MHz 8-81694
 rich clusters, form. times and gravit. const. var. 8-69892
 rich clusters, morphology and peculiar vels. of radiosources 8-77610
 rich clusters, photometric technique and luminosity function 8-89264
 Shakhbazian I, compact cluster, photometry of compact galaxies (*Russian*) 8-93428
 supercluster membership rel. to Abell cluster richness 8-65704
 superclusters reality, influence of intragalactic factors on external objects apparent distrib. 8-96552
 supernova explosions, microwave pulsed emission upper limit 8-69890
 tidally interacting galaxies, evolution of mass and tidal radius 8-65699
 universe inhomogeneities, power law relating mass fraction to density enhancement 8-57656
 Virgo, obs. of NGC 4472, very weak radio galaxy 8-65708
 Virgo cluster, distance and redshift rel. to Hubble's const. 8-89265
 Virgo cluster, low energy X-ray absorpt. obs. 8-86025
 Virgo cluster, X-ray source struct. 8-54090
 Virgo cluster area, standard total magnitudes of 139 bright galaxies 8-56685
 Virgo cluster redshift controversy, evidence from Centaurus cluster 8-54061
 Virgo I, distance modulus from colour-magnitude data of Local Group 8-73763
 Virgo region, new velocities 8-86028
 Weyl's geometry rel. to dynamical mass excess 8-69919
 X-ray and radio emission, intracluster gas heating by relativistic electrons 8-57655
 X-ray clusters, radio limits on ionised gas 8-89243
 X-ray emission, origin 8-57660
 X-ray emission detectability, deep surveys predictions and strategies 8-96567
 X-ray luminosity-richness relation 8-93431
 X-ray sources, props. 8-96565
 X-ray sources correl. with radiosources from 26.3 MHz survey 8-65707
 H I absorption in QSO spectra, search for cluster effects 8-93448

clutter

see also *radar clutter; radar displays; radar interference*

IR background suppression algorithm 8-77985

CNDO calculations

- p-benzoquinone, electronic struct., CNDO/S calcs. 8-70754
 1,1'-binaphthyl, electronic struct., fluorene, CNDO/S CI calcs. 8-90084
 bridging bond angle variations in siloxanes, silicates, Si nitrides and sulphides, mol. orbital calc. on model systems 8-55125
 carbonyl groups, intermol. interactions in $\text{H}_2\text{CO-H}_2\text{CO}$ system, quantum chem., classical calcs. 8-86932
 chemisorption, embedding problem, SCFMO formalism 8-71977
 chemisorption of O on graphite CO-ND0 calcs. 8-75937
 cyclopropane- d_6 , d_6 , absolute IR intensities, dipole moment derivatives and polar tensors 8-90165
 diamond, relaxation about the vacancy 8-71722
 dimethyl cadmium, photoelectron spectra, 4d spin-orbit splitting, crystal field and band-broadening effects, CNDO calcs. 8-76577
 α,ω -diphenyl-trans-polyenes, 1st excited singlet valence states, CI and extended CNDO/S calcs. 8-74807
 electronegativity of atoms, correl. of CNDO-bonding parameters 8-74577
 ethylene+ $\text{Cl}_2(\text{Br}_2)$ complex, intermolecular interaction and struct. SCF-MO-LCAO CNDO/2 calc. 8-58763
 ethylenes, substituted, He I and He II photoelectron spectra, CNDO/S calcs. 8-55201
 force constants, semiempirical quantum mechanical method 8-62947
 formaldehyde, ground and low lying excited states, CNDO/ V^{n-1} method (*Russian*) 8-74576
 molecular electronic structure, semiempirical CNDO method, calc. program 8-86782
 molecular systems including up to 232 orbitals, CNDO calcs., computer program 8-86788
 nitroanilines electronic states, CNDO/s-CI correlative calcs. 8-58604
 oxalyl chloride, rot. isomerism, CNDO and EHT-type methods 8-58591

CNDO calculations continued

- phosphatidyl ethanolamine, charge distrib., dipole moment, CNDO calcs. 8-80840
 trans-polyenes, 1st excited singlet valence states, CI and extended CNDO/S calcs. 8-74807
 polyenes, twisting force consts., CNDO theory potential energy surface 8-50474
 quasimolecules, electronic struct. calc., CNDO approx., computer program 8-86789
 Ag clusters, charge distrib., density of states, CNDO calcs. 8-70995
 As₂O₃, electronic struct., X-ray emission, XPS, UPS obs., CNDO cluster calc. 8-52638
 C, CNDO/S nucl. screening const. calcs. 8-86787
 Cd, photoelectron spectra, 4d spin-orbit splitting, crystal field and band-broadening effects, CNDO calcs. 8-76577
 H₂SO₄ and SO₃.H₂O, CNDO/2 calc. of thermal stability 8-76840
 Li(CO)_n (n=1,2,3,4,5,6,8), semiempirical CNDO calcs., solvation struct. 8-82649
 N, CNDO/S nucl. screening const. calcs. 8-86787
 N₂O₂, localised mol. orbitals from semiempirical CNDO calcs. 8-62726
 N₂O₃, localised mol. orbitals from semiempirical CNDO calcs. 8-62726
 N₂O₄, localised mol. orbitals from semiempirical CNDO calcs. 8-62726
 O, CNDO/S nucl. screening const. calcs. 8-86787
 P₂O₄(OH)₄²⁻ group, electronic struct. calcs. 8-67971
 S₂N₂, electronic struct. by CNDO/2 calcs. 8-62727
 S₂N₂, electronic struct. by CNDO/2 calcs. 8-62727
 SO₃+H₂O→H₂SO₄, gas phase kinetics, CNDO/2 calc. of H₂SO₄ and SO₃.H₂O struct. 8-76840
 Sb₂O₃, electronic struct., X-ray emission, XPS, UPS obs., CNDO cluster calc. 8-52638
 Si, semivacancy and pair of semivacancies calc. by CNDO/2 method 8-51537
 SiO₂ clusters, CNDO/2 calc., appl. of cyclic boundary conditions 8-72110
 Si₂O₆(OH)₂⁶⁻ group, electronic struct. calcs. 8-67971

coagulation

- blood clotting, Fourier transform. IR obs. 8-68945
 dispersion, coagulating, light scatt. data, Fourier inversion anal. 8-76932
 dispersion, coagulating, light scatt. for close range struct. determ. 8-53273
 finite system 8-68933
 integrodifferential equation, exact soln., breakdown effect 8-53272
 magnetic powder-liquid suspension, rel. to NDT by magnetic powder method 8-60942
 polymer coatings, chemiphoretic deposition without electric current onto metal 8-64763
 polystyrene, sol, light scatt. data, Fourier inversion anal. 8-76932
 sheared coagulated sols, energy dissipation during sheared flow 8-63461
 suspension, flow equation 8-63487
 Ti⁴⁺ hydroxide, coagulation struct. effects on particle size of TiO₂ 8-52732

coal

- see also mining*
 analysis, neutron activation, using standard reference materials as multi-element irradi. standards 8-80815
 brown, pulverised, SO₂ emission reduction by limestone-additive process (German) 8-53724
 brown coal, adsorption and binding of U from seawater, IR spectroscopic obs. 8-82855
 conversion plants, exam. of corrosion and wear of steels, review 8-53012
 dipping seams, seismic reflection method using Rayleigh channel waves 8-69471
 electrostatic precipitation technology development, stack gas ionisation by electron beams 8-57346
 fast-neutron activation anal. 8-85742
 layer thickness meas., EM technique 8-53740
 magnetic and Mossbauer characterisation 8-64903
 magnetic susceptibility anisotropy meas. as banding-plane indicator 8-77221
 neutron activation anal. 8-85265
 neutron activation anal. 8-85740
 nuclear process steam for coal gasification 8-78488
 nuclear techniques, characterisation of trace elements 8-85744
 prompt-neutron activation anal., system optimisation 8-85743
 seam thickness meas. using resonant loop as EM sensor 8-57366
 seams with discontinuities, SH channel wave attenuation 8-69292
 seismic response of carboniferous rock, synthetic seismograms 8-69293
 slurry diagnostics by US transmission 8-87216
 Fe-containing minerals, in coals, mag. hyperfine fields meas. 8-88234
 Fe-containing minerals in coals, magnetic hyperfine fields meas. 8-68427

coating processes *see coating techniques***coating techniques**

- see also anodisation; cladding techniques; coatings; electrodeposition; electrophoretic coating techniques; encapsulation; epitaxial growth; metalisation; spray coating techniques; vapour deposition*
 automatic RF sputtering system for multicomponent film production 8-52672
 boronising sintering of stainless steel 8-60594
 glass shells, for laser fusion targets, plasma polymerisation coating method 8-60859
 graphite tubes, for at. absorpt. spectroscopy, pyrolytic coating method optimisation 8-76940
 hard overcoats in replicated optics 8-66968
 laser fusion targets, plating methods 8-60862
 optical coatings, problems of application technology 8-83069
 polymer coatings, chemiphoretic deposition without electric current onto metal 8-64763
 polymer film deposition onto steel, Pt and glassy C electrodes 8-76866
 pyrocarbon deposition in fluidised bed, qualitative model, investigation with Stromungsrohr 8-56595
 pyrocarbon deposition on C black (French) 8-68921

coating techniques continued

- sand, resin-coated, curing effects on physicomach. props. (Korean) 8-60855
 p-xylene, plasma polymerised films on glass, as laser fusion targets, deposition method 8-60860
 C, pyrolytic film electrode, fabrication, electrochem. characterisation 8-92487
 Fe, Fe-C, diffusion coating by Cr and Pb melt bath, kinetics (Korean) 8-60873

coatings

- see also anodised layers; antireflection coatings; claddings; decorative coatings; electrodeposits; electrophoretic coatings; epitaxial layers; insulating coatings; protective coatings; spray coatings; sputtered coatings; vapour deposited coatings; varnish*
 carbide coating formation by chromising C steels 8-88571
 coated inclusion in elastic medium 8-79215
 composite, development and use in USSR (Russian) 8-52696
 depth profiles, SIMS technique (Japanese) 8-85246
 diamond indentation and draw tester, for meas. of ultra-adherence in films 8-72944
 dielectric coatings, for laser mirrors, surface optoacoustic spectrometry 8-87085
 electrode coating effects on elec. breakdown voltage hysteresis in air and SF₆ 8-87553
 electrode surface and coating effect on DC breakdown voltages in SF₆ 8-87557
 ethylene polymer films, highly fluorinated, exam. of wetting props. 8-60856
 laminated coatings, for fuel confinement, fusion reactor target appls. 8-60883
 medullary implants with porous coating, stress distrib. 8-69256
 melt-spread, contact reactions of Fe-group metals with Al base melts 8-60879
 methacrylic polymer films, highly fluorinated, exam. of wetting props. 8-60856
 oxide film on metallic glass, removal using US oscill. energy (Russian) 8-72935
 partially film coated crystal, strain field, deform. model and X-ray topography (German) 8-83653
 Permalloy coated garnet films, bubble statics, dynamics (Japanese) 8-52326
 plastic surface coatings as alternative to standard thin section cover glass in microscopy 8-73974
 points, testing, modern analytical methods appl. (Polish) 8-85253
 polymer coating, creep determ. by impression of rigid sphere 8-85084
 polymer film coated steel, Pt and glassy C electrodes, prep., charact., stability 8-76866
 porcelain enamel layers on steel, H₂ induced fracture of layers 8-76752
 pyrocarbon deposition on C black (French) 8-68921
 pyrocarbon fuel coating, irradiation tests 8-86594
 steel, Si killed, effect of Al addition to Zn on phase composition and morphology of products of Fe-Zn reaction (Polish) 8-85021
 thickness measurement, methods and instrumentation for measuring, review 8-73000
 trimethylamine.HCl coated piezoelec. quartz cryst. for HCl gas determ. in air 8-92532
 triphenylamine coated piezoelec. quartz cryst. for HCl gas determ. in air 8-92532
 viscoelastic hollow cylinder, elastic coating, thermomech. responses 8-79230
 vitreous enamel coating, method of quantitatively assessing blistered structure 8-53108
 Be coatings, α-radiation meas. of thickness 8-82600
 C, isotropic pyrolytic, for biomedical devices, mech. props. 8-65150
 Cu, fatigue behaviour effect of Zn, Au diffused coatings 8-72850
 Fe-Ni-Cr coating, electrodeposited, exam. of passivity 8-80655
 Mo, coating, soldered to diamond surface, contact strength, device 8-60910
 Mo-Zr-C (0.12, 0.002 wt.%), prep. of diffusion metal coating on alloy, oxidation rates (Russian) 8-56816
 MoSe₂, lubricating coatings, texture, prep. by Se_(g)+Mo 8-53018
 Na₂O-SiO₂ glass, coated with SnO coeff. of friction and fracture toughness 8-80657
 Ni coating on mag. steel, thickness measurement of coating 8-76821
 SiC, for C fibres in glass composite, hot pressing production method (German) 8-95724

coatings, protective *see protective coatings***coaxial cables**

- lumped-capacitance method for complex dielec. permitt. in polar liqs. 8-77936
 shielded cables, nonlinearities and multiple exposure anomalies at CASINO, MCCABE code verification 8-58502

coaxial lines *see coaxial cables***cobalt**

- see also nuclei with*
 anodic dissolution into silicate glass melt, exam. 8-88582
 atom, X-ray spectra, chemical bonding and multiple ionis. effects 8-50630
 atomic layers, Pauli paramagnetism to band ferromagnetism transition thickness depend. 8-72377
 atomic magnetic moments comparison to values of ferromagnetic metal 8-52244
 chemisorption of O, LEED anal. of Co(001)c(2×2)-O struct. 8-91546
 concentration determ. in atm. and rainwater in Vizcaya, Spain (Spanish) 8-57264
 concentration in atmospheric sedimentable powder, in Vizcaya, Spain (Spanish) 8-57265
 de Haas van Alphen oscill., effective mass 8-87900
 diffusing out of high current density plated Au, oxidation kinetics 8-92393
 diffusion in Pb, exam. by activation analysis 8-91488
 diffusion in Si layers heavily diffusion-doped with P or B 8-59982
 electrical resistivity, effect of domain wall orientation at 4K 8-91662
 electrodeposited film, saturation magnetisation and perpendicular anisotropy meas. 8-76277
 electromigration and residual resistivity, in Au 8-71881
 FCC, modified Krebs model, phonon dispersion relations 8-79682
 FCC, selected area diff. pattern indexing, graphical technique, for teaching 8-54132

cobalt continued

- ferromagnetic, EMF generation by pulsed laser irradi. 8-68021
 film, Kerr magneto-optical const. 8-76541
 foil, wall struct., bubble, plate domains, 1 MeV electron microscope study 8-84463
 fractionation of Co and Sc versus Fe content for crystalline phases of ultramafic nodules 8-65306
 growth of single crystals by electron-beam floating zone method 8-68624
 HCP to FCC transition, mag. domain nucleation 8-64218
 internal fields, positive muon investigation 8-68438
 ion in crystal, Racah parameter 8-56110
 liquid, density of states of d-band, heat of vaporisation 8-95253
 liquid, multiple scatt. calcs. of resist. 8-76039
 modulus defect due to internal strain 8-76286
 monolayer, oxidation, quasisimultaneous SIMS, AES, XPS 8-72919
 NMR of ^{59}Co in metal, temp. depend. 8-52364
 oxidation at high temps., parabolic rate const. determ. 8-64779
 oxide surface layer, TOF atom probe anal. 8-64766
 powders, rapidly solidified, nucleation, undercooling and homogeneous struct. 8-52708
 radioactive release from reactor cooling water, fixation by sandy soil (*Japanese*) 8-74443
 self-powered flux detectors, response charact. in CANDU reactors 8-82594
 self-powered neutron flux detector response in mockup Bruce reactor core 8-58391
 small magnetic particles, anisotropy field, resonance meas. 8-64227
 steady creep rate, stress depend., exam. at phase transformation at 390°C 8-52923
 steady state creep rate, stress depend. rel. to FCC to HCP phase change 8-64598
 stopping power for 28 MeV α -particles, re-evaluation 8-79651
 strontium tartrate tetrahydrate Co^{2+} electronic absorpt. spectrum 8-92098
 surface, electron spin polarisation, electron capture spectroscopy 8-95645
 surface, magnetic order 8-95439
 surface, O_2 layer thickness, reson. α -scatt. from ^{16}O 8-64778
 surface structure in HCP and FCC bulk phases 8-51807
 trace element anal. by (p,X,X) expt. 8-61128
 tunnelling electron spin polarisation rel. to band struct. 8-68095
 $\text{BaTiO}_3\cdot\text{Co}$, charact. behaviour of spontaneous polarisation and dielec. const. 8-60382
 $\text{CdBr}_2\cdot\text{Co}^{2+}$, charge transfer near UV spectra, 4.2K, mag. circular dichroism 8-80378
 $\text{CdCl}_2\cdot\text{Co}^{2+}$, charge transfer near UV spectra, 4.2K 8-80378
 $\text{CdI}_2\cdot\text{Co}^{2+}$, EPR 8-68362
 $\text{CdIn}_2\text{S}_4\cdot\text{Co}$, optical absorption meas. 8-64384
 $\text{Co-Al}_2\text{O}_3$ catalysts, reducing and sulphiding treatments, XPS obs. 8-85196
 Co-Fe(Ni) system, interdiffusion zone growths (*Czech*) 8-84009
 Co-Si film system, diffusion marker expts. 8-79824
 Co-Si film system, interaction kinetics 8-79823
 ^{57}Co , disintegrating nucleus, energy absorpt. by mol. environment 8-80775
 ^{59}Co , mag. hyperfine struct. analysis, spectral lines 4000 to 4300 Å 8-62752
 ^{60}Co gamma ray absorbed-dose standards comparison 8-74512
 ^{60}Co removal from waste water, adsorption on activated charcoal with oxine 8-58365
 ^{60}Co -charging of γ -irradiation installation (*Bulgarian*) 8-82558
 $\text{Cu}_2\text{O}\cdot\text{Co}^{2+}$, photomemory effect, EPR expts. 8-52353
 Fe-Co, bimetallic molecule, matrix isolated, Mossbauer spectrum 8-68425
 Fe-Co, bimetallic molecule, matrix isolated, Mossbauer spectrum 8-88233
 GaAs: Co^{2+} , EPR expts., γ -factor determ. 8-76301
 $\text{La}_2\text{Mg}_3(\text{NO}_3)_{12}\cdot 24\text{H}_2\text{O}\cdot\text{Co}^{2+}$, Ce^{3+} , relax. and ESR in magnetically cooled systems 8-88225
 $\text{Li}_9\text{Fe}_{17}\text{Al}_{103}\text{O}_4\cdot\text{Co}$, single cryst., domain struct., mag. annealing effect depend. on induced anisotropy 8-68290
 $\text{Li}_1\text{Fe}_{11}\text{O}_8\cdot\text{Co}$, single cryst., domain struct., mag. annealing effect depend. on induced anisotropy 8-68290
 $\text{LiNbO}_3\cdot\text{Co}$, optical props. 8-64383
 $\text{MgO}\cdot\text{Co}^{2+}$, strain modulated ESR, extensional and flexural modes 8-68365
 $\text{MgO}\cdot\text{Co}^{2+}$, strain modulated ESR, extensional and flexural modes 8-68366
 $\text{PbI}_2\cdot\text{Co}^{2+}$, EPR 8-68362
 Si: Co , influence of neutron irradiation on elec. props. 8-55895
 Si: Co , study of impurity states 8-76020
 $\text{SrCl}_2\cdot\text{Fe}^{2+}(\text{Co}^{2+})$ electronic absorption spectra in far and middle infrared 8-68537
 $\text{SrCl}_2\cdot\text{Mn}^{2+}(\text{Co}^{2+})$, cubic impurity EPR spectra, elec. field effect, mechanism 8-68361
 W fibre reinforced, alloy by effect on struct. stability, mech. props., metallographic exam. 8-56600
 WC-Co composite, surface anal. by quantitative AES 8-76622
 WC-Co composite chemical characterisation by AES and ISS 8-76621
 WC-Co sputter deposited film, struct. and comp. 8-72023
 WC-Co sputter deposited film, friction and wear 8-72918
 $\text{YFeO}_3\cdot\text{Co}$, NMR of ^{57}Fe , spin echo 8-91987
 YIG: Co^{2+} , mag. permeability, illumination and impurity depend. (*Russian*) 8-64220
 ZnS:Lo, vibr. modes of transition element impurities 8-76472
 ZnS-CdS:Ag, Ni, Co, thermoluminesc. glow curves 8-95611

cobalt alloys

see also cobalt compounds

- Alnico 5, thermal treatment in mag. field, mag. props. 8-91905
 chromindur, origin of coercivity, Lorentz microscopy, magnetisation and Mossbauer effect 8-64219
 chromindur, phase separation, Mossbauer obs. 8-88116
 $\text{Fe}_2\text{Co}_{1-x}\text{Ti}_x$ ferromag., high-field and high-pressure mag. behaviour 8-91919
 Haynes alloy 188, SEM exam. of fracture surface, due to low cycle fatigue at 700°C (*Japanese*) 8-52963
 Haynes Stellite 6B, Al_2O_3 particle erosion of surface, SEM obs. 8-88545
 Haynes Stellite 6B, particle erosion damage, TEM obs. 8-88546

cobalt alloys continued

- Heusler alloys, hyperfine fields and mag. interactions, NMR spectra 8-88222
 metalloid-transition metal amorphous surface alloys formed by ion implantation, TEM study 8-67730
 rare earth intermetallic RCO_2 , itinerant system, weak ferromagnetism 8-52191
 rare earth intermetallics, permanent magnet material development 8-91895
 rare earth intermetallics, permanent magnet production and props. 8-52309
 rare earth intermetallics, RCO_2 , elastic moduli, 4.2-300K 8-52332
 rare earth- Co_{17} , mag. anisotropy 8-84414
 rare earth- $\text{Co}_2\text{-Al}$, dil., nonmag. impurities effect on ordering temp. 8-84427
 rare earth-Co alloy, electron microscopy exam. 8-67722
 rare earth-Co alloys, spin wave spectra 8-56304
 rare earth-Co permanent magnets, microstruct., TEM obs., magnetisation 8-91901
 rare earth-Co-Si(Ge), ThCu_2Si_2 type, lattice parameters 8-51469
 resistivity magnetoresistance, s,p impurities in ferromag. host 8-68008
 steel, alloy, maraging, 250-grade, ductility and toughness of hot isostatically pressed powder 8-52925
 steel, maraging, grain refinement due to cyclic heat treatment 8-52971
 steel, maraging, investigation with lower Ni and Co contents (*Chinese*) 8-84812
 steel, maraging, type 200, effect of freq. on cyclic crack growth in salt water environment 8-64680
 steel, maraging 250-grade, fatigue crack growth model, notch analysis of fracture approach 8-52984
 steel, martensitic, high C, Co addition effect on strength (*Korean*) 8-68736
 steel, stainless, Cr-Ni, maraging, effect of Mo, Co additions on hardening 8-84835
 super alloy X-40, creep-fatigue interaction at high-temp. 8-84958
 transition metal alloy, ferromag., H-impurity complex obs. by magnetic aftereffect 8-72373
 Au-Co, dil. local moments, third harmonic de Haas-van Alphen wave shape anal. 8-84127
 Be-Co (0-50 at.%) alloys, thermal, metallographic and X-ray anal., phase diagram (*Russian*) 8-56611
 CaSb, resist., susceptibility and thermopower rel. to electronic struct. 8-67935
 Ce-Co, liq., charge transfer effect 8-94967
 Ce-Co-Si system, mag. props. in 77-300K range (*Russian*) 8-56290
 Ce_2Co , absorpt. of D, heats of reaction and equilib. press., T-getters for CTR 8-51683
 Ce_3Co , absorpt. of D, heats of reaction and equilib. press., T-getters for CTR 8-51683
 (Co, Cu, Fe) $_5\text{Ce}$, sintered permanent magnets, magnetic charact. 8-60608
 (Co,Cu,Fe) $_5\text{Ce}$, sintered, mag. props. 8-68302
 Co base superalloy, rupture life, prior temperature cycling effect 8-60840
 Co based amorphous alloy, mag. ordered, hyperfine field distrib., NMR meas. 8-68409
 Co-Al, mag. struct. of Co rich intermetallic cpd., neutron scatt., cluster model 8-80130
 Co-Al-Cr(Nb)(Ta), eutectic alloys, charact. by melting, oxidation resistance and composition 8-52768
 Co-Al-Nb, monovariant directionally solidified eutectics, struct. and mech. props. (*Russian*) 8-92254
 Co-C interstitial alloys, electronic struct. and ordering of sp defects 8-91639
 Co-Cd, dil. alloy, impurity hyperfine interactions 8-84416
 Co-Cr, high temp. sulphide corrosion 8-64775
 Co-Cr recording films, perpendicular mag. anisotropy, hysteresis loop, microstruct., TEM obs. 8-95491
 Co-Cr system, phase diagram re-determ. from thermodynamic data 8-76631
 Co-Cr-Al, exam. of cyclic oxidation resistance at 1100 and 1200°C , comparison with Ni-Cr-Al system 8-88572
 Co-Cr-Mo (Zr)(Nb)(Ta), eutectic alloys, charact. by melting, oxidation resistance and composition 8-52768
 Co-Cr-Ni-TaC, directionally solidified eutectic, mech. props. and struct., thermal cycling effects (*Russian*) 8-92282
 Co-Cr-Ni-W-Ta-C, alloy Mar M-509, TEM exam. of thermal fatigue crack propag. in cast alloy 8-76740
 Co-Cr-WC, corrosion and corrosive wear in sea water 8-92408
 Co-Cr(VC)(Ti,V)C-(Al), eutectic alloy, unidirectional solidification, oxidation and tensile tests 8-52790
 Co-Cu-Fe-Ce, mag. characteristics of sintered permanent magnets 8-60312
 Co-Fe alloy, HCP and DHCP, magnetostriction const. determ. 8-80184
 Co-Fe alloys, FCC structure, average mag. moment, conc. depend. 8-88099
 Co-Fe-Mn, dil. ferromag. alloy, mag. moment, saturation magnetisation meas. 8-64195
 Co-Fe-Nb alloy, mag. precipitation-hardening and Bloch wall pinning 8-80173
 Co-Fe-Nb-Mo, semihard magnetic alloy, magnetic props. 8-95469
 Co-Fe-Ti (12.6 wt.%), semihard permanent magnet, magnetic precipitation hardening 8-52830
 Co-Fe-Ti alloy, precipitation hardened, rel. between struct. and mag. props. 8-95470
 Co-Ga system, exam. of thermodynamics of α and β' phases 8-71870
 Co-Ga-B, phase diagram, metallographic, X-ray and electron probe anal. 8-92241
 Co-Gd-Mo-Ar film, amorphous, mag. props. 8-80182
 Co-Mn alloys, FCC, mag. moments of Mn atoms 8-76226
 Co-Ni, electrodeposition, mag. props. (*French*) 8-64488
 Co-Ni (33 wt.%), FCC deform. twinning kinetics, relationship to stress-strain behaviour 8-52887
 Co-Ni alloys, electrodeposited, struct., internal stress, and mag. props. 8-95471
 Co-P, amorphous alloy, domain struct., effect of annealing 8-60304
 Co-P, amorphous electrodeposited films, domain wall motion, Kerr effect 8-60322

cobalt alloys continued

- Co-P, cryst. and amorphous mag. films, ferromag. resonance line width (*Russian*) 8-88192
 Co-P, electrodeposited amorphous alloy, mag. permeability 8-52310
 Co-P, metallic glass, phonon propagation at low temp. 8-87756
 Co-P electroless film on Al base disc substrate, microstruct. rel. to mag. props. 8-68304
 Co-P film, amorphous, spin wave dispersion law, spin wave reson. obs. (*Russian*) 8-88196
 Co-P metallic glasses, crystn. kinetics by differential scanning calorimetry 8-91257
 Co-Pt, struct. and mag. props. rel. to degree of order 8-72368
 Co-Se, P-T diagram and structural study 8-56622
 Co-Si film system, diffusion marker expts. 8-79824
 Co-Si film system, interaction kinetics 8-79823
 Co-Si-Ge system, X-ray diffr. exam., band struct. (*Russian*) 8-56623
 Co-Si-Nb(Zr), eutectic alloys, charact. by melting, oxidation resistance and composition 8-52768
 Co-W-Cr (15,20 wt.%), surgical implant ion beam textured, stress/strain relations, fatigue characts. 8-73297
 Co-WC, corrosion and corrosive wear in sea water 8-92408
 CoAl, bonding, self-consistent energy bands 8-91610
 $\text{Co}_{0.9}\text{Al}_{0.1}$, Compton scatt., 59.54 keV γ -rays, charge transfer study 8-68578
 $\text{Co}_{1-x}\text{Au}_x$, amorphous, elec. resist., temp. depend., spin wave contrib. and resist. minimum 8-51961
 $\text{Co}_{0.8}\text{B}_{0.2}$ alloy amorphous thin films, anisotropic mag. and microstruct. props. 8-95487
 $\text{Co}_{1-x}\text{Fe}_x\text{Si}$, solid solution, optical props. 8-72556
 $\text{Co}_2\text{Ga}_{2-x}\text{Cu}_x$, mag. and struct. phases from magnetisation, neutron, X-ray diffr. techniques 8-52253
 $\text{Co}_2\text{Ga}_{2-x}\text{Ni}_x$, mag. and struct. phases from magnetisation, neutron, X-ray diffr. techniques 8-52253
 $\text{Co}_2\text{HfSn-Fe}$, dil., Heusler alloy, Fe hyperfine fields, Mossbauer obs. 8-68424
 Co_2MM , (MM+mischmetal), coercive force, effect of preparation conditions 8-95467
 $\text{Co}_{40}\text{Ni}_{40}\text{B}_{20}$, magnetostriction, temp. depend. 8-91921
 $\text{Co}_{1-x}\text{Ni}_x\text{Si}$, solid solution optical props. 8-72556
 Co_2P , amorphous, mag. excitations and static struct., neutron scatt. obs. 8-68204
 CoSi , NMR and μSR , microscopic mag. props. (*Japanese*) 8-52368
 CoSi solid solution, optical props. 8-72556
 $\text{Co}_2\text{Si-Si}$, CoSi-Si , and $\text{CoSi}_2\text{-Si}$ interfaces, chemical state, AES expts. 8-91767
 $\text{Co}_{74}\text{Si}_{10}\text{B}_6$, amorphous toroidal core, switching characts. and domain structures. 8-95477
 $\text{Co}_2\text{TiSn-Fe}$, dil., Heusler alloy, Fe hyperfine fields, Mossbauer obs. 8-68424
 CoZn β - and γ -intermetallic compounds, thermodynamics (*German*) 8-92242
 $\text{Co}_2\text{ZrSn-Fe}$, dil., Heusler alloy, Fe hyperfine fields, Mossbauer obs. 8-68424
 Cr-Co, dil., Neel temp., impurity conc. depend. calc. 8-68232
 Cr-Co-Ga, phase equilibria diagrams at 800 and 600°C (*Ukrainian*) 8-92236
 Cu-Al-Si-Co (2.8, 1.8, 0.4 wt.%), superplastic phase, exam. of mech. props. 8-52891
 Cu-Co , dil., Kondo system, host NMR exam. 8-80246
 DyCo_2 , field induced vol. magnetostriction 8-91920
 Dy_4Co_3 , cryst. field effect on mag. moment direction, neutron diffr. meas. 8-80132
 ErCo_2 , field induced vol. magnetostriction 8-91920
 $\text{ErCo}_{5.6}$, easy magnetisation direction 8-84415
 Er_4Co_3 , cryst. field effect on mag. moment direction, neutron diffr. meas. 8-80132
 $\text{Er}_{65}\text{Co}_{35}$, amorphous, amg. ordering, susceptibility, magnetisation and hysteresis meas. 8-68190
 $(\text{ErCo}_2)_x(\text{ErAl}_2)_{1-x}$, mag. and struct. investigations of intermetallic systems 8-95440
 $\text{ErCo}_{5-x}\text{Ni}_x$, ferrimagnetic series, magnetisation, coercive field meas. 8-91896
 $(\text{Fe,Co})\text{PBAI}$, metallic glass, viscous flow, alloying effect 8-79793
 Fe-Al-Ni-Co-Cu alloys, Ti alloying and deoxidising addition (*Russian*) 8-80181
 Fe-Co , annealing of point defects produced by plastic deform. (*French*) 8-72829
 Fe-Co , BCC, ferromag., spin wave stiffness constant 8-91851
 Fe-Co , damping capacity of Gentalloy, internal friction meas., mech. and mag. depend. (*Japanese*) 8-52875
 Fe-Co , dil., high freq. induction melting and centrifugal casting, working curve sample prep. photoemission anal. (*Japanese*) 8-53050
 Fe-Co , hyperfine field distrib., temp. and press. depend. 8-91651
 Fe-Co , local environment effect on atomic moments, itinerant model 8-68188
 Fe-Co , partially ordered, elec. cond. 8-91663
 Fe-Co (35 wt.% and 52 wt.%), heat treated, decrease in sensitivity of mag. props. to mech. stresses (*Russian*) 8-56363
 Fe-Co (5 to 25 wt.%), exam. of damping capacity of Gentalloy 8-72800
 Fe-Co alloy, diffusion of H_2 , diffusion coefficient and permeability (*Russian*) 8-79819
 Fe-Co alloy particles for mag. tapes, mag. props. 8-95479
 Fe-Co alloys, optical and spectrosc. props. (*Russian*) 8-72529
 Fe-Co-B , metallic glass, Mossbauer investigation of electronic struct. 8-92009
 Fe-Co-C-B , amorphous, room-temp. saturation induction 8-95476
 Fe-Co-Cd(Sn) , mag. hyperfine fields at Fe, Cd and Sn sites, Mossbauer and TDPAC meas. 8-60363
 Fe-Co-Mn , dil. alloys, NMR freq. temp. depend., spin echo meas. 8-64296
 Fe-Co-Ni-W alloy, 45KKhVN, plastic deform., electron microscope obs. (*Russian*) 8-80584
 Fe-Co-V , anelastic phenomena, related to atomic order, exam. of magnetostriction (*French*) 8-80579
 Fe-Co-V (2%), annealing of point defects produced by plastic deform. (*French*) 8-72829
 Fe-Co-V (2%) alloy, correl. of resistivity with microstructure 8-72896
 Fe-Cr-Ce , decomposition of solid soln. in mag. field, neutron and X-ray diffr. study (*Russian*) 8-68694
 Fe-Cr-Co , effect of heat treatment on strain gauge factor 8-72802

cobalt alloys continued

- Fe-Cr-Co (31 wt.%, 23 wt.%), microstruct. and mag. props., ageing and thermomag. treatment effects 8-76769
 Fe-Cr-Co alloys, permanent magnet material development 8-91895
 Fe-Cr-Co-Al (27.5, 17.5, 0.5) alloy, magnetic props. and microstructure 8-72367
 Fe-Cr-Co-Al (27.5, 17.5, 0.5 wt.%) alloy, induced anisotropy 8-76239
 Fe-Cr-Co-Si alloy, interaction domains after heat treatment in mag. fields (*Russian*) 8-68286
 Fe-Cr-Co-V alloy, microstruct. and mag. props. 8-68221
 Fe-Mn-Co-Ni-Cr , antiferromag. props., Neel temp. determ. 8-88124
 Fe-Ni-Co , rel. between induced uniaxial anisotropy and coercive force 8-91904
 Fe-Ni-Co-B-C-Si , amorphous, room-temp. saturation induction 8-95476
 Fe-Ni-Co-B-P soft magnetic metallic glasses, status report 8-64226
 Fe-Ni-V-Co , Co influence on age hardening (*Russian*) 8-68703
 Fe-W-Cr-Mo-Co with austenitic phase, magnetic and mech. props., cold working and ageing effects (*Japanese*) 8-60678
 FeCo , ordered alloy, 550°C change, study through elec. cond. and specific heat meas. 8-56633
 $\text{Fe}_{0.65}\text{Co}_{0.35}\text{B}$, crystalline disordered, evaluation of complex Mossbauer spectra 8-60370
 $(\text{FeCoNi})_8\text{B}_{20}$, glass, evidence supporting split-band model from magnetostriction 8-95509
 $(\text{Fe}_{0.9}\text{Co}_{0.1})_x\text{Si}_y\text{B}_z$, $(\text{Fe}_{1-x}\text{Co}_x)_{78}\text{Si}_{14}\text{B}_8$ amorphous ribbons, magnetomech. coupling and saturation magnetostriction 8-68353
 $\text{Fe}_2\text{Co}_{70}\text{Si}_{10}\text{B}_{10}$, amorphous toroidal core, switching characts. and domain structures. 8-95477
 $(\text{Fe}_x\text{Co}_{100-x})_{100-(y+z)}\text{Si}_y\text{B}_z$ amorphous ribbon, mag. moment and Curie temp., comp. depend. 8-95421
 $\text{Fe}_2\text{Si-Co}$, dil., cond. electron polarisation and moment perturbations 8-68224
 Gd-Co , and Gd-Co-Mo films, amorphous, mag. props., annealing effects 8-64235
 Gd-Co , CPA calcs., moments and transition temps. 8-52252
 Gd-Co alloy amorphous thin films, anisotropic mag. and microstruct. props. 8-95487
 Gd-Co amorphous films, model calculations for anisotropy formation induced by resputtering processes 8-64242
 Gd-Co amorphous sputtered films, magnetoelastic contrib. to perpendicular anisotropy, internal stress meas. 8-95490
 Gd-Co film, amorphous, Ar sputtered, struct. 8-63946
 Gd-Co film, amorphous, microstruct. and magnetism 8-64230
 Gd-Co film, amorphous, phase separation as source of perpendicular anisotropy 8-64244
 Gd-Co film, amorphous, preferential resputtering effect induced anisotropic distrib. of atomic pairs 8-63950
 Gd-Co film, amorphous, selective resputtering-induced anisotropy 8-72376
 Gd-Co film, amorphous, stability of small bits to temp. and mag. field changes 8-68314
 Gd-Co film, bias-sputtered, dipolar mechanisms for mag. anisotropy 8-64233
 Gd-Co film, homogeneity of films prepared by bias sputtering 8-72379
 Gd-Co film, sputtered, inert gas incorporation effect on uniaxial anisotropy 8-64232
 Gd-Co-Fe film, amorphous, bias-sputtered, uniaxial perpendicular anisotropy 8-64234
 Gd-Co-Mo film, amorphous, Ar sputtered, struct. 8-63946
 Gd-Mo-Mo film, amorphous, in-plane susceptibility near compensation point 8-64238
 Gd-Mo-Mo amorphous film, domain drag effect obs. 8-91911
 GdCo film, amorphous, sputtered, in-plane anisotropy induced by rare gas annealing 8-84458
 $\text{Gd}_{1-x}\text{Co}_x$, film, resistivity, Hall effect, domain wall density 8-76169
 $\text{Gd}_{25}\text{Co}_{75}$, amorphous film, ZZ 8-68014
 $\text{Gd}_{65}\text{Co}_{35}$, amorphous, amg. ordering, susceptibility, magnetisation and hysteresis meas. 8-68190
 GdCoMo film, amorphous, sputtered, ferrimag., in-plane susceptibility near compensation point 8-64240
 $\text{Gd}(\text{Fe}_x\text{Co}_{1-x})_2$, ferromag. reson. of pseudobinary cubic compounds 8-91961
 Hf-Co , phase diagram, X-ray diffr., thermal anal. and metallography obs. 8-60652
 Hf-Co-Ga system, crystal atomic struct. and phase equilibria (*Ukrainian*) 8-84772
 $(\text{Ho, Y})\text{Co}_2$, first order phase transitions 8-84426
 $(\text{Ho, Y})\text{Co}_2$, mag. props., elec. resist. and thermal expansion 8-76246
 Ho-Co alloy amorphous thin films, anisotropic mag. and microstruct. props. 8-95487
 Ho-Co film, amorphous, microstruct. and magnetism 8-64230
 HoCo film, amorphous, sputtered, in-plane anisotropy induced by rare gas annealing 8-84458
 HoCo_2 , field induced vol. magnetostriction 8-91920
 Ho_4Co_3 , cryst. field effect on mag. moment direction, neutron diffr. meas. 8-80132
 $\text{La}_{1-x}\text{Co}_x$, amorphous, conc. depend. of Co moment 8-56300
 MnSi-CoSi solid solution, mag. props. 8-56403
 Nd-Co film, amorphous, exam. of domain struct. 8-68336
 NdCo_5 , single ion anisotropy const. temp. depend. effect of spatial variation of mag. moment 8-91864
 $\text{Nd}_{64}\text{Co}_{36}$, amorphous, amg. ordering, susceptibility, magnetisation and hysteresis meas. 8-68190
 NdCo_{1-x} film, amorphous, mag. props. meas. 8-68312
 Ni superalloy Mar-M200, slow fatigue crack propagation rate meas. using high freq. resonant technique 8-52983
 Ni-Al-Cr-Co-Ti , Waspaloy, exam. of dislocation-precipitate interaction, cyclic stress-strain behaviour 8-84925
 Ni-Co , ferromag. films, magnetoresistance effect, crystal struct. 8-68017
 Ni-Co , ferromagnetic resonance, surface anisotropy 8-95526
 Ni-Co-Cd alloys, electrodeposition from acetate bath 8-68637
 Ni-Co-Cr-Mo-Ti-Al Nimonic 105, loading frequency and environmental effects on high temp. fatigue crack growth 8-64675
 $\text{Ni-Co-Cr-Ta-Al-W-Mo-Ti}$, cast, phase volume fraction determ. using manual point count practice 8-53052
 Ni-Co-H system, phase transform. under high H_2 press., Co additive effects (*Russian*) 8-60645

cobalt alloys continued

- Ni-Co-Mn, dil. alloys, NMR freq. temp. depend., spin echo meas. 8-64296
- Ni-Co-Mn, dil. ferromag. alloy, mag. moment, saturation magnetisation meas. 8-64195
- Ni-Co-P, amorphous alloy, electrical and mag. props. 8-95281
- Ni-Co-P, amorphous electrodeposited films, domain wall motion, Kerr effect 8-60322
- Ni-Co-P, ferromag. film, amorphous to cryst. transition, diffraction and resistivity meas. 8-60587
- Ni-Cr-Al-Ti-Co, exam. of back stress role in creep behaviour of particle strengthened alloys 8-52889
- Ni-Cr-Co-Al-Ti-W-Ta-Mo, IN 738 LC, loading frequency and environmental effects on high temp. fatigue crack growth 8-64675
- Ni-Cr-Co-Mo-Al-Ti alloys, Waspaloy, Astroloy, exam. of microstruct. effect on crack growth 8-52977
- Ni-Cr-Fe-Mo-Co (21.41, 19.28, 8.64, 2.16 wt.%), Hastelloy alloy X, exam. of thermal stability 8-84865
- Ni-Cr-Ti-Al-Fe-Co (19.65, 2.40, 1.37, 0.78, 0.52 wt.%), strength of γ' hardened alloy, ageing exam. 8-88501
- Ni-Fe-Co film, magnetoelastic vibr. generation during high freq. mag. reversals (Russian) 8-60320
- Ni_{1-x}Co_xAl, self-consistent embedded-cluster model for mag. impurities 8-67973
- Pd-Co, dil., ferromag., magnetoresist. 8-91665
- Pd-Co, dil., Mossbauer emission spectra, fast relaxation regime, ⁵⁷Co hyperfine field 8-60362
- Pr₂Sm_{1-x}Co_x, magnetisation and magnetocryst. anisotropy 8-68215
- Pt-Co, dil, magnetopower, magnetoresistivity 8-68016
- Pt-Co alloys, crit. neutron scatt. in crit. conc. region for onset of ferromagnetism 8-72347
- Pt-Co resistance thermometer, for low temp. appl. 8-73994
- Rh-Pd-Co, dil., local environment and mag. props. 8-64187
- Rh-Pd-Co, dil. alloy, mag. moment 8-95416
- Rh₂CoSn, ferromag., crit. exponent of ¹¹⁹Sb hyperfine field, Mossbauer obs. 8-92008
- Rh₂CoSn, metallic ferromagnet, hyperfine mag. field temp. depend. (Russian) 8-80265
- Sm-Co, alloy powders and sintered magnets, effect of chem. treatment on mag. props. 8-60311
- Sm-Co, decomp. kinetics when aged, X-ray mag. props. and metallography study (Russian) 8-56644
- Sm-Pr-Co, added Fe, Sn, permanent magnets, demagnetisation curves, X-ray obs. 8-91900
- SmCo₅ hydride films, mag. props. 8-68306
- SmCo₅, intrinsic coercivity losses, temp. depend. 8-95468
- SmCo₅, isotropic plasma sprayed magnet, high coercivity 8-68295
- SmCo₅, magnetic alloys, pressed, sintering rel. to mag. props., cryst. struct. 8-60600
- SmCo₅, sintered alloy magnetic properties (Russian) 8-72369
- SmCo₅ spheres, exam. of sintering in vacuum and Ar atmospheres 8-84738
- SmCo₅, substituted alloy, low reversible temp. coeff. 8-68178
- Sm₂Co₇, mag. and struct. investigations of intermetallic systems 8-95440
- Sm₂(Co_{1-x}Al_x)₁₇ (Russian) 8-64202
- Sm(Co_{1-x}Cu_x)_{7.8} alloys, coercive fields, domain wall energies, mag. and metallographic exam. 8-91897
- SmCo_{3.5}Cu_{1.5}, time dependent magnetisation 8-80176
- SmCo_{5-x}Cu_x, giant intrinsic magnetic hardness, high field meas. 8-68289
- Sm₂(Co_{1-x}Fe_x)₁₇, anisotropy consts., conc. and temp. depend. (Russian) 8-64202
- Sm(CoFeCuMn)₇, coercive force and anisotropy temp. depend. 8-68297
- SmCo₂Ni₃-Y(Pr)(Gd)(Tb)(Er), giant intrinsic magnetic hardness 8-56347
- SmCo_{5-x}Ni_x, giant intrinsic magnetic hardness, high field meas. 8-68289
- SmCo_{5-x}Ni_x, giant intrinsic magnetic hardness analysis 8-88146
- SmCo₅Ni₅₋₅₀, exchange fluctuations and giant intrinsic mag. hardness 8-56310
- Sm₂Co_{17-x}Ni_x, effect of Ni on mag. props. 8-68296
- Sm₂Dy_{1-x}Co_x, temp. compensated magnetic material, mag. and struct. characterisation 8-68177
- Sm₂Er_{1-x}Co_x, temp. compensated magnetic material, mag. and struct. characterisation 8-68177
- Sm_{1-x}Nd_xCo₅ alloys, magnetisation, magnetocrystalline anisotropy, 4.2 to 280K 8-91863
- Sm₂Tb_{1-x}Co_x, temp. compensated magnetic material, mag. and struct. characterisation 8-68177
- TbCo₂, X-ray obs. of low temp. modifications of crystal struct. (Russian) 8-75632
- Tb₄Co₃, cryst. field effect on mag. moment direction, neutron diffraction meas. 8-80132
- Te-Co, dil. liq. alloy, elec. cond. at high temp. and press. 8-87959
- Ti(Fe_{1-x}Co_x), density of states estimation from magnetisation and resistivity meas. 8-84119
- TiFe_{1-x}Co_x, mag. props., under high press. and in high mag. fields 8-95423
- TmCo₅, easy magnetisation direction 8-84415
- Tm₄Co₃, cryst. field effect on mag. moment direction, neutron diffraction meas. 8-80132
- UCo₂, mag. props., ferromag. transition (Russian) 8-68148
- UMn₂-UCo₂, mag. props., ferromag. transition (Russian) 8-68148
- W fibre reinforced, alloy by effect on struct. stability, mech. props., metallographic exam. 8-56600
- W-Co, dil., excess resistivity, temp. depend., Kondo effect 8-68011
- WC-Co, comparison of indentation crack resistance, and fracture toughness 8-76739
- WC-Co, exam. of effect of continuous carbide phase, on hardness, and deformation 8-52974
- WC-Co, sintered, obs. of spinel particles by TEM 8-95714
- WC-Co, sintered hard alloy, mechanism of penetration of liquid metals 8-60619
- WC-Co, various combinations, fracture characts. in bending, compression, and toughness tests 8-60808
- WC-Co alloys, brittle fracture, precision matching of mating fracture surfaces, by SEM fractographs 8-60807
- WC-Co alloys, single edge notched beams, exam. of fracture toughness 8-52975

cobalt alloys continued

- WC-Co cemented carbide, fracture toughness meas., model for variation with microstruct. 8-60806
- WC-Co cemented carbides, high temp. transverse rupture strength, effect of domain size of binder phase (Japanese) 8-92329
- WC-Co mixed powder prod. by rotary kiln, new continuous process 8-64502
- WC-Co(TiC-Co), powder compacts, effect of additional pressing at hydrostatic pressures on props. 8-56596
- WC-TaC-Co, cemented carbide, strength improvement by hot isostatic pressing 8-84969
- Y-Co, amorphous alloy film, spin reson. meas., exchange stiffness 8-68389
- Y-Co, CPA calcs., moments and transition temps. 8-52252
- YCo₃, amorphous ferromagnet, exchange dominated surface modes 8-52359
- YCo₃ film, amorphous, DC sputtered, easy axis and easy plane magnetisation 8-64237
- YCo₃ film, amorphous, sputtered, in-plane anisotropy induced by rare gas annealing 8-84458
- Y_{1-x}Co_x, amorphous, conc. depend. of Co moment 8-56300
- Y₂(Co₂Fe_{1-x})₁₇, mag. anisotropy assoc. with Fe substitution 8-76240
- Y₂Co_{17-x}Ni_x, effect of Ni on mag. props. 8-68296
- Y(Fe₂Co_{1-x})₂, ferromag. reson. of pseudobinary cubic compounds 8-91961
- Y_{1-x}Gd_xCo₂, NMR of ⁵⁹Co 8-52376
- (Y_{1-x}Co_x)₂Co₅, anisotropy fields, coercivities, annealing effects 8-91898
- Zr-Co, amorphous alloy film, spin reson. meas. 8-68389
- Zr(Al_{1-x}Co_x)₂, Laves phase, H₂ absorption capacity meas. 8-87866
- Zr_{1-x}Co_x, amorphous, conc. depend. of Co moment 8-56300
- Zr₃Co_{1-x}M_x, M=Cu, Ni, Fe, Mn, Ag, and Ru, phase stability and supercond. T_c 8-80519
- Zr(Fe_{1-x}Co_x)₂, density of states estimation from magnetisation and resistivity meas. 8-84119

cobalt compounds

see also cobalt alloys

- boranes, $\text{OCH}_3(\text{B}_9\text{C}_2\text{H}_{10})_2\text{Co}$ and $(\text{C}_2\text{H}_5)_2\text{Co}_2\text{CB}_9\text{H}_{10}^-$, cryst. struct. (Czech) 8-87649
- ferrite, spinel type catalytic oxidation of CO, role of mag. exchange interactions 8-56916
- oxide surface layer, TOF atom probe anal. 8-64766
- phthalocyanine film, sorption of O₂ and water, AES obs. 8-91531
- tetramethylammonium tetrachlorocobaltate, ferroelectricity 8-76408
- vanadates, elec. and mag. props., stoichiometry 8-51991
- [Co(NH₃)₄Cl]₂Cl, cis and trans isomers, XPS, shake-up satellites 8-82783
- BaCo_{1.5}Fe_{16.5}O₂₇, type W ferrite, spin reorientation 8-60301
- Ba_{0.138}Co_{0.62}Fe₁₆O₂₇, W-type hexaferrite cryst., first order magnetisation processes 8-95472
- CaO-Al₂O₃-SiO₂ glass, remanent magnetisation, log t low 8-68300
- Co complex, bis(N-b-naphthyl-salicylaldehyde) Co (II), space group, lattice consts., X-ray diffraction obs. 8-51496
- Co complex, bisdimethylglyoxime (thiosemicarbazide)-cobalt (III) nitrate, mol. and cryst. struct. of dihydrate 8-83803
- Co complex, dipyrindine chloride, single crystal metamagnetism 8-72345
- Co salts: M²⁺, M=Mn, VO, EPR, spin-lattice relax. time meas., 180-380K 8-64268
- Co-H, solid soln., magnetisation curve 8-84452
- CoAl₂O₄, cation distribution, Mossbauer and X-ray diffraction obs. 8-95532
- CoAl₂O₄, electron density distrib. 8-51481
- Co₃B₂O₁₃, intermediate phase between paraelectric and ferroelectric phase (Russian) 8-68465
- CoBr₂, XPS, satellite of Br 4s line 8-56556
- CoCO₃, birefringence of light (Russian) 8-56456
- Co(CO)₃, bond angles, hybrid bond orbital calcs. 8-94188
- CoCO₃, weak ferromag., antiferromag. reson., phenomenological theory 8-60339
- CoCO₃, weakly ferromag., light scatt. on spin waves (Russian) 8-72419
- CoCl₂, lattice dynamics, static displaced shell model 8-79689
- CoCl₂-Cd(NO₃)₂·4H₂O, melt viscosity, equivalent conductivity, glass transition temp. 8-75855
- CoCl₂²⁻, electronic energy levels calc. by conventional and X alpha Hartree-Fock methods 8-66470
- CoCl₂·6H₂O, albitronite, new mineral from Llano County, Texas 8-65286
- CoCl₂·6H₂O, paramag., PMR 8-91962
- CoCr₂S₄, Faraday effect, appl. to CO₂ laser systems, radiation damage resist. 8-95579
- CoF₂, domain formation in staggered field induced by uniaxial stress, neutron diffraction exam. 8-76289
- CoF₂, muon Coulomb capture ratio 8-62959
- Co_(1-x)Fe_xCl₂·2H₂O, random mixture of anisotropic antiferromags., isotropic state obs. 8-84396
- Co₂Fe_{3-x}Cr_xO₈, epitaxial, magneto-optical props., effect of Cr³⁺ 8-52590
- Co₂²⁺Fe_{1-x}²⁺Fe_x³⁺O₄ ferrites, effect of Fe²⁺ on Mossbauer parameters 8-76360
- CoFe₂O₄ formation rate consts. meas. by Mossbauer effect 8-68875
- Co_{1-x}Fe_{2+x}O₄, prep. by wet and ceramic methods, struct., mag. and surface props. 8-52307
- Co_{1-y}Fe_{2+y}O₄, equilib. surface comp., cation comp. with stoichiometric oxygen content 8-79867
- Co_{1-y}Fe_{2+y}O₄, role of vacant and chemisorbed O and charge transfer effect 8-79868
- Co₂Fe_{3-x}O₈, single cryst. mag. films, holograms recording and thermomagnetic writing 8-55324
- CoK₂(P₂O₇)₂·7H₂O, cryst. data (French) 8-79568
- Co(NO₃)₃·6H₂O addition to molten salt heat transfer fluid, solar absorbing properties enhancement 8-87112
- Co₃Ni_{1-x}Cl₂·6H₂O, calorimetry, γ -type transitions of sp. ht. 8-68256
- Co_{3-x}Ni_xO₄, 0 ≤ x ≤ 1.1, struct., semicond.-semimetal transition, Seebeck coeff. 8-87972
- CoO (100), electron energy loss spectra exam. 8-72652
- CoO, collinear antiferromag., equiv. type-II mag. struct. 8-56296
- CoO, defect struct. and self-diffusion 8-63759
- CoQ film, growth kinetics on high current density plated Au 8-92393

cobalt compounds continued

- CoO, ionisation, electron density relax. effects. ab initio calcs. 8-50466
 CoO on Co₃O₄, oriented growth following Co₃O₄ pyrolysis 8-80739
 CoO, solubility of S at 1000°C 8-63858
 CoO₆¹⁰⁻, ionisation, electron density relax. effects. ab initio calcs. 8-50466
 Co₃O₄ addition to molten salt heat transfer fluid, solar absorbing properties enhancement 8-87112
 Co₃O₄, detector of CO, appl. in MOS device 8-76908
 Co(OH)₂(SiF₆), phase transitions, spectrometric exam. (*French*) 8-88291
 Co₃S₄, Cu_{0.5}Co_{2.5}S₄, CuCo₂S₄, spinels, ht. of formation 8-53237
 Co₂S₃, exam. of thermodynamic activity, for several phases, using gas equilibration technique 8-52785
 CoSO₄ soln. in H₂O, methanol-H₂O, US dispersion, 3-60 MHz (*German*) 8-59862
 CoSO₄·H₂O, IR spectra, H₂O external modes temp. depend. 8-58683
 CoSi, thermoelectric and optical props. 8-91714
 CoSiF₆·6H₂O, paramag., nucl. and electron spin lattice relax. 8-84494
 Co₂V₂O₇, V-O-V bridge stretching freq. correl. with bond angle 8-74636
 Co(ethylenediamine)₃³⁺, charge distrib., ESCA, internal standards 8-50585
 Co(ethylenediamine)₃(ClO₄)₃, ESCA chem. shift meas., internal standards 8-50585
 CsCoCl₃, anisotropic antiferromag., inelastic neutron scatt. study 8-60274
 dibarium cobalt formate tetrahydrate Cu²⁺ doped, EPR of Cu-Co interactions 8-60334
 HgCo(NCS)₄, calibration standard, low temp. molar mag. suscept. meas. 8-59947
 KCoF₃, antiferromag., ⁵⁹Co NMR exam. 8-76332
 K₂Co₂(SO₄)₃, cubic langbeinite struct., low temp. mag. susceptibility 8-56299
 Mn_{1.18}Zn_{0.06}Co_{0.01}Fe_{1.75}O₄, transport props. near Curie points 8-88100
 (NH₄)₂Co(SO₄)₂·6H₂O, submillimeter ESR meas., SH² term of effective spin Hamiltonian 8-64264
 NdCo(BO₂)₃, cryst. struct. 8-63735
 NiCo ferrite, induced mag. anisotropy, hysteresis loops, Barkhausen effect (*Russian*) 8-64203
 PrCo₅, heat treated, coercive force exam. 8-68298
 Rb₂CoF₄, two dimens. Ising like antiferromag., spin wave excitations 8-72342
 Rb₂CoMg_{1-x}F₄, magnetic specific heat, dilution on a two-dimensional Ising-like antiferromagnet 8-91871
 Rb₂CoMg_{1-x}F₄, neutron scatt. exam., obs. of two dimens. mag. long range order 8-56295
 ScCoSi, X-ray determ. of struct., new representative of struct. type TiNiSi 8-79595
 ScCo_{0.25}Si_{1.75}, X-ray determ. of struct., new representative of struct. type ZrSi₂ 8-79595
 SmCo₅, heat treated, coercive force exam. 8-68298
 SrCo_{3-x}, XPS spectra, shake-up satellite of Co2p 8-52617
 V(VI) peroxo complex ion precipitation with Co(III) complex cation 8-80728
 V₂O-Co₂O, solid solutions, exam. of thermal conductivity 8-79827

cochlea see ear

codes

see also encoding

- criticality anal. using KENO and SU-HAMMER codes, for U-233 and U-235 solns. 8-89949
 sensory feedback code comparison using electrocutaneous tracking, for prosthetics 8-69255

coding see encoding

coding errors

see also error correction

- Hadamard transform optical instrument, systematic errors 8-94375

coefficient of thermal expansion see thermal expansion

coercive force

see also magnetic hysteresis

- Alnico 5, thermal treatment in mag. field, mag. props. 8-91905
 anisotropic materials, magnetisation reversal, 1/H law 8-84454
 chromindur, origin of coercivity, Lorentz microscopy, magnetisation and Mossbauer effect 8-64219
 chromindur, phase separation, Mossbauer obs. 8-88116
 coercimeter, with cylindrical attachable electromagnet, exam. of design 8-76809
 ferrite, connection between limiting hysteresis loops and number of easy magnetisation axes (*Russian*) 8-72364
 ferrites, soft and microwave, grain-size effects on mag. props., review 8-64222
 ferromagnetic crystal, domain wall pinning effect and intrinsic coercivity, computer simulation 8-64217
 ferromagnetic probe coercive force meter, different heads, for tubing inspection 8-60943
 hard magnetic material, micromagnetism, theory 8-52301
 magnetic hysteresis curve, multiple particle model (*German*) 8-80178
 measurement with superimposed sensor 8-88612
 NDT coercivity meter with portable display system 8-53135
 pearlite in C steels (0.08 to 1.6 wt.%), exam. of temp. depend. of mag. coercivity 8-52304
 permanent magnet ferrites, forming 8-64495
 rare earth intermetallics, RFe_{5-x}Ni_x, giant intrinsic mag. hardness 8-56354
 rare earth iron alloy, amorphous film, cosputtered, struct. and mag. props. 8-60323
 rare earth-Co amorphous film, sputtered, in-plane anisotropy induced by rare gas annealing 8-84458
 Recalloy, Fe-Nb, semihard magnetic alloy, magnetic props., hardness, microstruct. 8-56660
 semiautomatic digital coercimeter, exam. of design 8-76817
 steel, C, cold rolled St3Kp, annealed, mag. nondestructive inspection of strip and ribbon 8-60913
 steel, low alloy, type 3sp, effect of temp. at end of rolling on mech. props., and coercive force 8-72799
 steel, low alloy and C, hardened and tempered parts, nondestructive magnetic inspection 8-95889

coercive force continued

- steel bearing parts, magnetic inspection of heat treatment quality 8-73007
 (Ba,Sr)Fe₁₂O₁₉, Ferroxdure, developments and research 8-84455
 (Co, Cu, Fe)₃Ce, sintered permanent magnets, magnetic charact. 8-60608
 (Co,Cu,Fe)₃Ce, sintered, mag. props. 8-68302
 Co-Cu-Fe-Ce, mag. characteristics of sintered permanent magnets 8-60312
 Co-Fe-Nb alloy, mag. precipitation-hardening and Bloch wall pinning 8-80173
 Co-Fe-Nb-Mo, semihard magnetic alloy, magnetic props. 8-95469
 Co-Fe-Ti (12.6 wt.%), semihard permanent magnet, magnetic precipitation hardening 8-52830
 Co-Fe-Ti alloy, precipitation hardened, rel. between struct. and mag. props. 8-95470
 Co-Ni alloys, electrodeposited, struct., internal stress, and mag. props. 8-95471
 Co-P, electrodeposited amorphous alloy, mag. permeability 8-52310
 Co-P electroless film on Al base disc substrate, microstruct. rel. to mag. props. 8-68304
 Co-Pt, struct. and mag. props. rel. to degree of order 8-72368
 Co_xMM, (MM+mischmetal), coercive force, effect of preparation conditions 8-95467
 CrO₂, single mag. particle, remanent coercive force and remanent loop meas. 8-95480
 (ErCo₂)(ErAl₂)_{1-x}, mag. and struct. investigations of intermetallic systems 8-95440
 ErCo_{5-x}Ni_x, ferrimagnetic series, magnetisation, coercive field meas. 8-91896
 (EuLu)₂Fe₂O₁₂, Ga, Al or (Ca,Ge) substituted, mag. props. and growth of 2 μm bubbles 8-91910
 Fe alloys, anisotropic precipitation struct. in external mag. field (*German*) 8-72785
 Fe, cast, grey, pearlitic relationship of magnetic props. to condition of C 8-56353
 Fe, deformed, dislocation structure determ. from magnetic props. 8-5874
 Fe-Al-Ni-Co-Cu alloys, Ti alloying and deoxidising addition (*Russian*) 8-80181
 Fe-Co alloy particles for mag. tapes, mag. props. 8-95479
 Fe-Cr-Al alloys, low temp. sp. ht., resistivity and coercive force 8-63866
 Fe-Cr-Co-Al (27.5, 17.5, 0.5) alloy, dependence on shape anisotropy and effective particle size 8-72367
 Fe-Ni-Al alloys, phase diagram, miscibility gap, mag. props. 8-92237
 Fe-Ni-Co, rel. between induced uniaxial anisotropy and coercive force 8-91904
 Fe-Ni-Co-B-P soft magnetic metallic glasses, status report 8-64226
 Fe-Si-Al (6.4 wt.%), Sendust alloy, effect of Ni content on mag. props. 8-72897
 Fe-Si-Mn, effect of Mn addition on mag. props. and elec. resist. 8-91890
 Fe_{100-x}B_x, mag. and struct. props., comp. depend. 8-60314
 Fe₈₀B₂₀, sputter deposited amorphous, low field mag. props. 8-68335
 Fe₂C_{1-x} amorphous sputtered film, mag. props. 8-68311
 Fe₄₀Ni₃₀Mo₆B₁₈ glassy alloy, high permeability, low field mag. characts. 8-68301
 α-Fe₂O₃ film, prep. by reactive condensation and mag. props. 8-64241
 γ-Fe₂O₃ powders, influence of densification on mag. props. 8-95481
 γ-Fe₂O₃, prep. from thermal decomp. of [Fe₃(HCOO)₆(OH)₂]HCOO.4H₂O and characterisation 8-80741
 γ-Fe₂O₃, single mag. particle, remanent coercive force and remanent loop meas. 8-95480
 Fe₃O₄ film, prep. by reactive condensation and mag. props. 8-64241
 Fe₃O₄, spherulitic film growth, elec. and mag. props. 8-68627
 FePd epitaxial film, vacuum-deposited, for thermomag. recording, mag. and magneto-optical props. (*Russian*) 8-60319
 FePt epitaxial film, vacuum-deposited, for thermomag. recording, mag. and magneto-optical props. (*Russian*) 8-60319
 Fe_{2.6-x}Ti_{0.4}Al_{0.4}O₄, Fe_{2.4-x}Ti_{0.6}Al_{0.4}O₄, titanomagnetite, monodomain, mag. props. 8-56346
 (Gd,Bi)₃(Fe,Ga)₅O₁₂ magneto-optic film, ion irradi. effect on storage props. 8-52324
 Gd-Co film, amorphous, stability of small bits to temp. and mag. field changes 8-68314
 (GdMn)₂(GdAl)_{1-x}, mag. and struct. investigations of intermetallic systems 8-95440
 MgM²⁺Fe_{2-x}O₄, M=In,Al,Cr,Sc, comp. effects on ferrite characts. 8-52305
 Mn-Ga, DO₂₂ type alloys, magnetic props., crystal struct. (*Japanese*) 8-59784
 Mn₅₅Al₄₅ alloy, permanent mag. props., depend. on particle size 8-91899
 Ni-Co-P, amorphous alloy, electrical and mag. props. 8-95281
 Ni-Fe-Nb, Hardperm alloy, sheets, effect of sheet thickness, and annealing, on mag. props. 8-76772
 Ni-Fe-Nb alloys, mag. permeability and struct. (*Chinese*) 8-84450
 Ni-Fe-Nb-Al alloys, mag. permeability and struct. (*Chinese*) 8-84450
 Ni-P electrodeposit, magnetisation coercivity and magnetostriction 8-68338
 NiFe soft magnetic alloys, magnetic props., effect of annealing and fabrication (*German*) 8-53004
 Ni_{1-x}P_x, electrodeposited, amorphous, mag. and transport props. 8-52106
 Pb₂Sr_{1-x}(Zr_{1-x}Ti_x)O₃:Cr₂O₃, ferroelec. ceramic, reversible characts. and dielectric losses (*Russian*) 8-84517
 (Pb_{1-x}Ba_x)₂Ge₃O₁₁, ferroelec. transition blurring, US relax., dielec. and opt. props. 8-95559
 Pb(Zr_{0.47}Ti_{0.43}Sn_{0.10})O₃:Cr₂O₃, ferroelec. ceramic, reversible characts. and dielectric losses (*Russian*) 8-84517
 PrCo₅, heat treated, coercive force exam. 8-68298
 Sm-Co, alloy powders and sintered magnets, effect of chem. treatment on mag. props. 8-60311
 Sm-Pr-Co, added Fe₂Sn, permanent magnets, demagnetisation curves, X-ray obs. 8-91900
 SmCaGe garnet LPE bubble film, coercivity, thickness depend. 8-68324
 SmCo₅, heat treated, coercive force exam. 8-68298
 SmCo₅, intrinsic coercivity losses, temp. depend. 8-95468

coercive force continued

- SmCo₅ isotropic plasma sprayed magnet, high coercivity 8-68295
 Sm₂Co₇, mag. and struct. investigations of intermetallic systems 8-95440
 Sm(Co_{1-x}Cu_x)_{7.8} alloys, coercive fields, domain wall energies, mag. and metallographic exam. 8-91897
 SmCo₅Cu_{1.5}, time dependent magnetisation 8-80176
 Sm(CoFeCuMn)₇, coercive force and anisotropy temp. depend. 8-68297
 SmCo₂Ni₃-Y(Pr)(Gd)(Tb)(Er), giant intrinsic magnetic hardness 8-56347
 SmCo_{5-x}Ni_x, giant intrinsic magnetic hardness analysis 8-88146
 Tb₂Fe_{1-x} film, amorphous, magnetostriction and magnetisation 8-68305
 Ti-Permalloy thin film diffusion couples, low temp. interdiffusion interdiffusion 8-71889
 (Y,Eu,Tm,Ca)₃(Fe,Ge)₅O₁₂ garnet film coercivity, new annealing method 8-84459
 (Y,Sm,Lu,Ca)₃(Fe,Ge)₅O₁₂ garnet film coercivity, new annealing method 8-84459
 YFeO₃ platelets, domain wall mobility, dynamic coercivity 8-91884
 YIG, bulk, low mag. domain wall mobility 8-95463
 (YSmCa)₃(FeGe)₅O₁₂ LPE films, optimum growth conditions for low coercivity 8-95499
 YSmLuCaFeGe garnets, growth and temp. characts. of small bubbles 8-80183
 (YSmLuCa)₃(FeGe)₅O₁₂, mag. props. and growth of 2 µm bubbles 8-91910
 (Y₁₋₂Co₂)Co₅, anisotropy fields, coercivities, annealing effects 8-91898

coercivity *see coercive force***cognitive systems**

- see also adaptive systems; artificial intelligence*
 cognitron, feedback-type, self-organising neural network with associative memory 8-56962

coherence

- see also light coherence*
 at-power reactor noise, second-order coherent functions 8-94070
 coherent state, necessary condition to remain coherent 8-73879
 cosmic coherent avalanche catastrophies, gamma-freq. graviton radiation 8-85844
 Dicke-maser model dynamics, phase transition to the spontaneous coherent state 8-66792
 electron diffraction line patterns, scattering model (French) 8-51397
 electron storage ring coherent microwave emission fine struct. 8-78875
 EM radiation intensity, produced by modulated electron/ion beams in gas 8-50686
 field emission electron beams, two beam interference 8-63002
 one-mode fields, greatest lower bounds for degree of coherence of higher order 8-71068
 pulsar coherent radiation, relativistic soliton model (Russian) 8-77568
 two-level system in radiation field, dynamics, temp. depend. props. 8-66793

coherence distance *see coherence length***coherence length**

- Cu₂Mo₆S₈, normal state and superconducting property measurements 8-91660
 NbN, supercond. props., SQUID behaviour 8-72311
 PbMo₆S₈, normal state and superconducting property measurements 8-91660
coherent antiStokes Raman scattering
 absolute Raman cross sections determ. by indirect meas. of stimulated Raman gain, technique 8-66864
 acetylene, computer controlled CARS spectra of Q branches 8-62241
 benzene, second order CARS, dispersion curves 8-58707
 β-carotene, ν₁ line shape, CARS and CSRS 8-82727
 gas quantitative analysis 8-68968
 hexafluoride molecule selective excitation via Doppler free multiphoton process 8-55178
 integrated power, press. depend. 8-59081
 isotropic liquid, polarisation props. 8-80334
 lasers application in Raman spectroscopy, review 8-65979
 liquid, dephasing of coherently excited mol. vibrs. (Dutch) 8-72505
 polarised coherent active Raman spectroscopy and coherent Raman ellipsometry (Russian) 8-55414
 pulsed dye laser system, computer controlled 8-62241
 resonance-enhanced CARS, and coherent anti-Stokes hyper-Raman spectroscopy 8-86980
 rhodamine 6G, lasing, reson. CARS spectra in methanol, ethanol, acetonitrile, H₂O 8-74948
 second order, mechanisms 8-58707
 spectrometer system for chemists, using freq. doubled Nd+YAG laser 8-64906
 Cs vapour, coherent anti-Stokes Raman scatt. 8-71146
 D₂, absolute Raman cross sections determ. by indirect meas. of stimulated Raman gain 8-66864
 N₂, computer controlled CARS spectra of Q branches 8-62241
 N₂, crossed-beam phase-matched CARS generation 8-50850
 NH₃, computer controlled CARS spectra of Q branches 8-62241
 O₂, computer controlled CARS spectra of Q branches 8-62241

coherent potential approximation *see CPA calculations***cohesive energy** *see binding energy***coils**

- see also inductors; solenoids; windings*
 ampere absolute value improved realisation 8-93737
 fusion reactor, doublet Tokamak, parallel connected ohmic heating coil 8-54930
 fusion reactor, Princeton large torus 3-coil test 8-54945
 fusion reactor, T-10M Tokamak, normal and supercond. inductive energy storage and switching 8-55018
 fusion reactor, TMX, magnets, mech. design 8-58494
 fusion reactor, Tokamak constant tension D-shaped coils, lateral support struct. 8-55013
 fusion reactor, toroidal device with nonplanar mag. axis, magnet and coil engineering 8-55009
 fusion reactor coil, multilayer structs., laminated beam theory anal. 8-55011

coils continued

- fusion reactor coil design, cost anal., for neutral beam magnets 8-55005
 fusion reactor coil design codes 8-66367
 fusion reactor implosion heating coil, radially fed, design, fabrication 8-55006
 fusion reactor magnet coil, 125 kG, 1 m, design, fabrication 8-55008
 fusion reactor RFC-XX, coil system, design, fabrication, testing 8-55007
 fusion-fission breeder reactor, supercond. poloidal field coil design 8-70640
 glass fibre reinforced epoxy prepreg, PDX TF coil insulation 8-62656
 Helmholtz coil and fluxmeter system for magnetic saturation meas. 8-93738
 magnetic field induction vector remote meas. of 0.01 to 5 T, mag. induction Hall probe 8-93659
 Marshall coil, epoxy-insulated, fabrication 8-66388
 Oak Ridge National Laboratory superconducting coil fabrication development 8-50370
 plasma, high density, in mag. mirror, RF plugging coils 8-83604
 Q-factor measurement by damped oscillation method (Japanese) 8-89492
 RF field coils for Petula Tokamak compressional transit time mag. pumping heating 8-70634
 Rogowski coil for current and voltage meas. in pulsed X-ray devices (Japanese) 8-93788
 superconducting coil, buckling, vibr., lateral constraint and damping effects 8-63344
 Tokamak fusion, Impurity Study Experiment, mag. field calcs. using GFUN-3D programme 8-66368
 toroidal field coil construction and appl. (German) 8-54877
 toroidal field coils, bending-free, for Tokamak reactor 8-55012

coincidence circuits

- see also counters*
 anticoincidence gated scaler and live timer, counting loss correction for Geiger counter 8-86737
 digital multidiscriminator for use in gamma-gamma coincidence experiments 8-70707
 three level coincidence-correlator detectors, underwater sound appls. 8-63245
 e⁺e⁻→2γ, ang. correl. meas. device (German) 8-86726

coincidence counters *see coincidence circuits; counters***cold-cathode tubes**

- see also counting tubes; photomultipliers; phototubes*
 controlled gas discharge switch 8-86300
 negative glow plasma, contact electrode charging time meas. 8-67525

cold rolling

- α-brass, drawability correlation with sheet metal texture 8-60683
 α-brass, FCC, fractographic obs. of SCC 8-64786
 brass (70:30), cold rolled, optical, X-ray and TEM exam. of deformation struct., and textures 8-88500
 machine for cold rolling, deformed concrete reinforcing bars for model tests 8-60924
 metal, friction and slip 8-64707
 rolls, US monitoring of hardened thickness with low hardness gradient 8-60955
 sheet, texture form., model (French) 8-68705
 steel, alloy, low C, effects of pre-treatment on graphitisation behaviour (Japanese) 8-84860
 steel, austenitic stainless, FCC, fractographic obs. of SCC 8-64786
 steel, C, cold rolled St3Kp, annealed, mag. nondestructive inspection of strip and ribbon 8-60913
 steel, low C, capped, cold rolled sheet, deep drawability, effect of carbide size, cold reduction annealing 8-64559
 steel, Nb-V, cold rolled, HSLA, prod. by precipitation hardening, annealing 8-88471
 steel, sheet structural changes during rolling influence of lubricants on friction and wear 8-95815
 steel, stainless, maraging, type 03Kh11N10M2T2, exam. of thermal embrittlement 8-84986
 steel, stainless, recrystallisation texture, effect of Cu, Ti additions on development (Japanese) 8-80558
 Ag, deformed bars, cold rolled, exam. of microstruct. by thin foil TEM 8-88502
 Ag-Ni, two ductile phase, exam. of rolling deformation 8-72819
 Ag-Ni, two ductile phase alloy, exam. of softening behaviour after cold rolling 8-72847
 Al, cold rolled, X-ray diffr. and optical microscope exam. of fatigue damage (Japanese) 8-84976
 Al, cold rolled and annealed, substruct. near fatigue crack tip, X-ray microbeam technique exam. (Japanese) 8-64621
 Al/brass/Al bimetal, three layers, formed by cold rolling, exam. of formation of intermetallic phases at interface 8-56658
 Al-Ag, nonhomogeneity of deform. 8-84888
 Al-Mg (5 wt.%) deformed bars, cold rolled, exam. of microstruct. by thin foil TEM 8-88502
 Al-Zn, nonhomogeneity of deform. 8-84888
 Au, deformed bars, cold rolled, exam. of microstruct. by thin foil TEM 8-88502
 α-brass, defect removal, obs. by positron annihilation 8-84677
 Cd-Zn (Ag), annealed, work softened, exam. of crystallographic texture, hardness 8-80559
 Cu annealed and cold rolled, with bamboo structure, exam. of grain boundaries as vacancy sources in diffusional creep 8-88508
 Cu, defect removal, obs. by positron annihilation 8-84677
 α-Cu-Al, FCC, fractographic obs. of SCC 8-64786
 Cu-Mn(Fe)(Ni)(Zn)(Ge), dilute solid soln., exam. of recrystallisation and stored energy 8-52836
 Cu-Ni (10 wt.%), deformed bars, cold rolled, exam. of microstruct. by thin foil TEM 8-88502
 Cu-Ni-Fe (26.8 wt.%), microduplex struct. form., recrystn. annealing (Japanese) 8-76659
 Fe-Co-Cr-W-Ni-C, alloy KKhVN, transforms. during annealing and nature of hardening (Russian) 8-56653
 Fe-Co-Ni-W alloy, 45KKhVN, plastic deform., electron microscope obs. (Russian) 8-80584
 Fe-Mn, γ to ε phase transform. induced by high press. and plastic deform. 8-68686
 Fe-Si (3 wt.%), orientation development during secondary recrystallisation, primary matrix effect, magnetic props. (Czech) 8-60679

cold rolling continued

- Fe-Si (6.5 wt.%), ductility and mag. props., Ni and Mn addition effects 8-76704
 Gd, texture formation during cold rolling (*Russian*) 8-92275
 Mg, recrystallisation after cold rolling 8-72790
 Mo, hardened sub-structure, high-temp. radiation resist. (*Russian*) 8-56654
 Ni, defect removal, obs. by positron annihilation 8-84677
 Ni, deformed bars, cold rolled, exam. of microstruct. by thin foil TEM 8-88502
 Re, metallo-ceramic, deform. and cold working by cold rolling (*Russian*) 8-56655
 α -Ti alloy, VT1-1, cold rolled, recrystn. texture and prop. anisotropy 8-52846
 Ti-Mo, metastable β -phase, stress induced products formed by cold rolling (*Japanese*) 8-88483
 Ti-V, metastable β -phase, stress induced products formed by cold rolling (*Japanese*) 8-88483
 Y, texture formation during cold rolling (*Russian*) 8-92275

cold shortness see brittleness**cold working**

- see also bending; cold rolling; plastic deformation; slip; work hardening
 alloy, cold-worked, particle size and strain determ. from X-ray diffr. profiles 8-88588
 elastoplastic material, dynamic cold working, struct. modification (*French*) 8-52847
 fracture criterion for bulk cold working processes 8-56775
 metal, cold-worked, particle size and strain determ. from X-ray diffr. profiles 8-88588
 Recalloy, Fe-Nb, semihard magnetic alloy, magnetic props., hardness, microstruct. 8-56660
 refractory composites, fibre reinforced, directionally solidified tensile tests, in HVEM, deform. and fracture (*French*) 8-68785
 steel, alloy, carburized case parameters, effect on props. of 20Kh3MVFA and 12Kh2N4A 8-52989
 steel, austenitic, 16H2NMB, struct., texture and mech. props. of product of transform. 8-92273
 steel, austenitic, 800H, effect of hardening processes on initial stress-strain curve 8-84846
 steel, austenitic stainless, irradiation induced creep, AISI 316, 20% cold worked effect of temp. change 8-72816
 steel, austenitic stainless, welded joints, cold working effects on mech. and corrosion props. (*Hungarian*) 8-52838
 steel, austenitic-ferritic Ni-Cr, 12Kh21NST, phase and struct. transform. (*Russian*) 8-95748
 steel, C, ductile fracture under cold forming conditions, press. effect 8-52938
 steel, C, transition from initiation to propagation of fatigue cracks 8-68802
 steel, C and alloy, cold formability (*French*) 8-60681
 steel, cold deformation hardening, effect of C content and cementite shape 8-92277
 steel, cold-worked, Mossbauer obs. of cementite decomp. and restitution 8-64558
 steel, prestrained pressure vessel, correl. between dynamical toughness characteristics 8-68816
 steel, stainless, type 316, 20% cold worked, exam. of creep 8-72817
 steel, stainless, type 316, neutron-irrad., void size reduction 8-79636
 steel, stainless, type Kh17N13M2T, strengthening by plastic deformation and cold working (*Russian*) 8-52839
 steel SS-41, plastic working with vibr., US hardness tester 8-53044
 Ag-Ga solid soln., internally oxidised, hardness (*Japanese*) 8-60744
 Ag-Sb, cold-worked, lattice defects, convolution relations for X-ray line breadth calcs. 8-51394
 Ag-Zn, cold-worked, lattice defects, convolution relations for X-ray line breadth calcs. 8-51394
 Al alloy 7075, fracture props., effect of thermomechanical treatment 8-60793
 Al and Al-Mn (1 wt.%), subgrain growth during annealing after cold work 8-56656
 Al, dislocation substructure formation under hydrostatic extrusion 8-56696
 Al-Ge alloy, Ge precip., ion irrad., dose rate and temp. depend. 8-79642
 Al-Zn-Mg (6.15%), influence of ageing and cold work on tensile and fracture props. (*Japanese*) 8-52842
 B₂C rings, Al bonded, exam. of fabrication techniques 8-72748
 Cd-Ag, polycryst. wire, cold worked, resistivity changes 8-68827
 Cd-Zn, polycryst. wire, cold worked, resistivity changes 8-68827
 Cu, cold worked, determ., of dislocation pinning and unpinning stages, using internal friction meas. 8-92278
 Cu, cold worked, grain size effects on short-term strength (*Russian*) 8-56693
 Cu, dislocation substructure formation under hydrostatic extrusion 8-56696
 Cu, wires, effect of heat treatment during drawing 8-56659
 Cu-Al, internally oxidised, structural, elec. and mech. characts. 8-60761
 α -Cu-Ni-Zn-Pb, fire cracking and ordering (*German*) 8-60760
 Cu-Sb, cold-worked, lattice defects, convolution relations for X-ray line breadth calcs. 8-51394
 Cu-Zn, cyclic stress/strain curves in monocrystalline and polycrystalline samples, cold work and Zn addition effects 8-95786
 Fe, cold work stored energy effects on mag. moment vs. temp. curve 8-95419
 Fe-H system, cold work internal friction peak, appl. of Schoeck's model 8-95771
 Fe-Ni alloy, cold work stored energy effect on mag. moment vs. temp. curve 8-95419
 Fe-W-Cr-Mo-Co with austenitic phase, magnetic and mech. props., cold working and ageing effects (*Japanese*) 8-60678
 Nb, H₂ loaded, cold worked, plastic deformation, exam. of α internal friction peak 8-92307
 Nb₃Al, BCC struct., cold working and converting to A-15 struct. 8-64553
 Ni cold worked, annealed, exam. of anelastic relaxation at low temp. 8-84877
 Ni, dislocation substructure formation under hydrostatic extrusion 8-56696

cold working continued

- Pb-Sn, eutectic alloy, plastic deform., work hardening (*German*) 8-92279
 Ti-Mo(Nb)(Ta), BCC struct., tetragonal phase form. by cold deform. (*Russian*) 8-88462
 Ti-Nb-Mo(V)(Ta)(Al)(Zr), BCC struct., tetragonal phase form. by cold deform. (*Russian*) 8-88462
 Zr base alloys, irradiation growth, dislocation model 8-51595

collections of physical data

- A=18-20, light nuclei, compilation of energy levels, nuclear struct. information 8-62478
 A=215, nuclear data sheets, decay characteristics and level struct. 8-58224
 A=219, nuclear data sheets, decay characts. and level struct. 8-58225
 A=223, nuclear data sheets, decay characts. and level struct. 8-58226
 A=227, nuclear data sheets, decay characts. and level struct. 8-58227
 A=48, nuclear data sheets, to September 1977 8-82266
 acetic (ethanoic) acid, ideal gas thermodynamic props. 8-51275
 actinide sensitivities, analytic evaluation 8-82427
 alkaline earth halides, aq. solns., activity and osmotic coeffs. 8-53242
 alloy, multicomponent phase diagram calc., NPL alloy data bank 8-92243
 atmospheric chemistry, reaction rates and photochemical data 8-77312
 atomic mass evaluation, input values 8-70949
 atomic spectral lines, 10000-40000 Å 8-50490
 ATS-6 electron content data presentation 8-61593
 Auger electron energies, elements 10 \leq Z \leq 100 8-62774
 binary alloys, thermal conductivity, data anal. and synthesis 8-95284
 cresols, ideal gas thermodynamic props. 8-75250
 cyanoacetylene, microwave spectrum, mol. consts. 8-74647
 electron bremsstrahlung energy spectra, 1 to 2000 keV, neutral atoms Z=2 to 92 8-62920
 electron inelastic mean free paths of solids, data tables 8-84686
 electron repulsion integrals for p-block ats., teaching appl. 8-93494
 elementary particle properties review, leptons, mesons, baryons 8-66179
 ferroelectric, Debye temp., tabulation of calorimetric values 8-51639
 fission prod. conc., sensitivity anal. 8-82428
 fission product gamma-ray and half-life 29 \leq A \leq 69, data collection 8-50134
 flame calculations, list of rate coeffs. 8-85160
 formic (methanoic) acid, ideal gas thermodynamic props. 8-51275
 gases, thermophysical props. tabulated for mixture composition certification 8-80818
 geology, adequacy of non-metric data 8-81413
 halomethanes, liquid densities, data tables 8-75703
 heat capacities, molar, correlation coeffs., data collection 8-85188
 injected ion drift tube mass spectrometer ionic mobility data in non-parent gas 8-87428
 ion induced γ -rays, thick sample reaction yields, energies, appl. in prompt nuclear anal. 8-62502
 JANAF thermochemical tables, 1978 supplement 8-93637
 Japanese Evaluated Nuclear Data Library, first version evaluation (*Japanese*) 8-74428
 light noble gases in chondrites, achondrites and ureilites, anal. compilation 8-65574
 liquid water, viscosity, -8°C to 150°C, anal. of data 8-95101
 materials handbook, industrial 8-56571
 methane+H(HO)(O)(O₂), H abstraction, rate consts. calcs. 8-95921
 motorway free-flow traffic noise obs. 8-90591
 MSDC/EPA/NIH mass spectral search system 8-65912
 muonic atoms, energy-level values, electrodynamic corrections 8-62956
 nuclear data files of UK Chemical Committee, summary of data, available in ENDF/B format 8-82425
 nuclear data for space technology 8-82407
 nuclear data sheets for A=110 8-66189
 nuclear data sheets for A=237 to November 1977 8-82267
 nuclear data sheets for A=241 to November 1977 8-82268
 nuclear data sheets for A=45 8-66187
 nuclear data sheets for A=47 8-66188
 nuclear structure, even-even nuclei, quasi-bands 8-82265
 nuclei, even-even, 58 \leq A \leq 150, E₂, M1 multipole mixing ratios 8-50118
 nuclei with A=194, review of struct. information to July (1977) 8-89769
 nuclei with A=207, review of struct. information to August (1977) 8-89770
 nuclei with A=209, review of struct. information to September (1977) 8-89771
 oceanographic data, global analysis 8-65316
 organic compounds, crit. temps. correl. with boiling pts. 8-91421
 organic compounds, hydrolysis in water, rate consts. 8-76856
 phenol, ideal gas thermodynamic props. 8-75250
 plasma, radiative cooling rates, high-temp. low-density plasma 2 \leq Z \leq 92 8-83534
 rare earth elements, atomic energy levels, data tables 8-86805
 rocks and minerals, lattice conds. at mantle press. and temp. 8-69338
 streamflow, empirical data, multivariate gamma distrib. fitting 8-81240
 surface tension, pure liqs., temp. depend. correl. 8-91512
 transition metal, polynary oxocompounds, struct. data, book 8-51521
 ultrasonic materials testing reference blocks and transducers, survey 8-68858
 US props of mammalian tissues 8-88727
 US vel. and atten. in mammalian tissues 8-57044
 Ag, projectile range for Z=8-20, 0.0125-12.0 MeV/nucleon 8-83856
 Au, projectile range for Z=8-20, 0.0125-12.0 MeV/nucleon 8-83856
 Cr, atomic transition probabilities, oscil. strengths 8-74601
 Cu, γ -ray absorption cross-sections, 10-160 MeV 8-90136
 Cu, projectile range for Z=8-20, 0.0125-12.0 MeV/nucleon 8-83856
 Fe, projectile range for Z=8-20, 0.0125-12.0 MeV/nucleon 8-83856
 He ion stopping powers and ranges in all elements 8-58565
 He isoelectronic sequences, screening constants, ground and excited states 8-62701
 He isoelectronic series, energy level and classifications of doubly-excited states 8-62736
 Li isoelectronic sequences, screening constants, ground and excited states 8-62701
 Mn, atomic transition probabilities, oscil. strengths 8-74601

collections of physical data continued

- NH₃, thermodynamic props., anal. of data 8-93636
 Ni, projectile range for Z=8-20, 0.0125-12.0 MeV/nucleon 8-83856
 O₂, density of solid in equil. with vapour 8-93656
 OH radicals, microwave spectra data tables 8-50542
 Pb, γ -ray absorption cross-sections, 10-160 MeV 8-90136
 Sn, γ -ray absorption cross-sections, 10-160 MeV 8-90136
 Ta, γ -ray absorption cross-sections, 10-160 MeV 8-90136
 Ti, projectile range for Z=8-20, 0.0125-12.0 MeV/nucleon 8-83856
 V, atomic energy levels in all stages of ionisation, data anal. 8-94207
 V, atomic transition probabilities, oscill. strengths 8-74601

collective states, nuclear see *nuclear collective states and giant resonances*
collimators (optical) see *optical collimators*

collision processes

see also *atom-surface impact; atomic inelastic collisions; charge exchange; chemical reactions; elastic scattering of atoms and molecules; elastic scattering of electrons by atoms and molecules; electron attachment; electron impact; elementary particle interactions; intermolecular mechanics; ion-surface impact; molecular inelastic collisions; molecule-surface impact; negative ions; Penning ionisation; plasma collision processes; potential energy surfaces for collision processes; quantum field theory; quasimolecules; radiation quenching*

- agglomeration, computer simulation (Japanese) 8-95706
 agglomeration, Monte Carlo simulation (Japanese) 8-95707
 aligned triple collision in celestial mechanics, new study (French) 8-85832

artificial satellites, collision freq. and debris belt creation 8-89035
 chemical reactions and reactive collision phenomena, props. of stochastic process description 8-60991

classical trajectory calcs., empirical testing of nonrandom integration method 8-50607

cosmology, bound condensations collisions rel. to struct. development in expanding model 8-93489

curve-crossing collisions, scatt. matr. 8-70891

Earth-comet close approach, rel. to ice ages and ecological catastrophes 8-53714

Earth/comet collisions, rel. to origin of terrestrial life 8-73660

education, binary elastic collision in rel. space, isosceles trapezoid representation 8-61981

heavy-ion collisions, QED, strong and supercritical fields, book contrib. 8-74193

information theoretic maximal entropy theory, rel. to scatt. theory 8-81888

M31+M32, gravit. perturbations effects rel. to galaxies relative position 8-93394

meteorites parent bodies, collisions rel. to origin of polymict brecciated meteorites 8-57513

multiple scattering formalism, time depend. generalisation 8-86518

near-adiabatic collisions, theory, electron translation factor method 8-81889

near-adiabatic collisions, theory, scatt. coord. method 8-81890

NGC 4631 group of galaxies, tidal interactions model 8-54059

NGC 7822 (W1), supernova remnant/H II region collision from kinematics studies 8-54028

nonresonant, possible relax.-time comparisons failure for local thermodynamic equil. 8-81935

null event method in simulation, ion collision appl. 8-90262

particle scattering from target, spin-spin interaction calcs. 8-81730

Phobos, dynamical evolution and time to collision with Mars 8-89104

planetesimal aggregation during solar system system form., collisions rel. to jetstream configuration 8-69713

R-matrix theories 8-58760

R-matrix theory 8-58761

Schrodinger equation, time-depend., explicit integration method 8-57805

solar system/interstellar cloud impending encounter, evidence 8-93352

stars in galactic nucleus, collisions rel. to black hole sustenance 8-57632

three-level system, stimulated Raman scatt. and stimulated collision induced fluoresc. 8-87103

two Coulomb centres problem at small inter-centre separations 8-70892

collision sequences, focused see *sputtering*

colloid chemistry see *colloids*

colloids

see also *Brownian motion; coagulation; electrophoresis; electroviscous effect; emulsions; gels; magnetic fluids; thixotropy*
 aerocolloidal suspension of solid particles, shock wave entering aerocolloid domain 8-51227

arene, photophysics, functionalised micellar assembly, phosphoresc. and triplet Ag⁺ enhancement 8-95598

cholesterol+water, interaction in organic media, dielec. and NMR spectroscopy 8-76979

CIDEP, examples of S-T₊ polarisation 8-86891

copolymer, graft or block, multiphase composite systems, struct., colloidal behaviour (Chinese) 8-73088

dispersion, coagulating, light scatt. for close range struct. determ. 8-53273

double-layer structure, electrohydrodynamic determination 8-95960

electro-optical phenomena, induced dichroism rel. to elec. field calc. 8-50699

electrophoresis, mass transport, apparatus 8-85168

excimer formation in micellar surfactant solns., distributional effects 8-64855

ferrofluids, exptl. obs. of agglomeration in presence of mag. field (French) 8-92514

ferromagnetic colloids, helical flow in mag. field (Russian) 8-75213

floculation, book 8-92520

fractionation and size analysis using flow field-flow fractionation 8-61062

Hamaker const. and combining rules for model oil-water systems 8-68934

intervascular lipid transfer, direct fusion of phospholipid vesicles, kinetic basis comparison 8-96034

isoprene-styrene copolymer latexes, film-forming properties 8-53266

latex polymer, electrodeposition on metal 8-53015

light scattering, Percus-Yevick approx., for spherical particles 8-94368

liquid film, free, squeezing mode relax., laser scatt. rel. to colloid interaction 8-87354

micellar system, naphthalene as fluoresc. probe 8-95599

colloids continued

micelle formation, in aq. solns., kinetics relax. process 8-76928

microemulsions, stability, thermodynamic approach 8-95959

microemulsions of micelles, interpretation of second virial coeff. of osmotic press. (French) 8-64891

oil in water microemulsion, added NaCl, light beating spectroscopy of micelles mutual diffusion coefficient 8-80793

Ostwald ripening and its application to precipitates and colloids in ionic crystals and glasses [Review] 8-80548

particle size distribution, reduced electric dipole moments, polarisabilities using electric birefringence 8-95958

particles in colloidal state, refr. index, theory 8-95567

polystyrene, in butanol, electrophoretic mobility, charge origin 8-85211

polystyrene particles flocculation, light scatt. for close range struct. determ. 8-53273

PTFE, in butanol, electrophoretic mobility, charge origin 8-85211

pyrene excimer formation in micellar surfactant solns., distributional effects 8-64855

sedimentation through polyethylene oxide semidilute aq. soln. 8-95965

silica, fractionation and size analysis using flow field-flow fractionation 8-61062

sodium dodecyl sulphate micelles, diarylalkane intramolecular excimer formation, microfluidity and fluoresc. meas. 8-80791

sodium dodecyl sulphate NaCl aq. soln., micellar props., laser light scatt. exam. 8-92513

solution droplets, solid, particle form., heat and mass transfer 8-95967

stochastic transport eqns. 8-93609

superheated supercond. colloid as a total absorption detector preliminary calcs. 8-78579

superheated supercond. colloid neutron detector, detection and background rejection tests 8-78580

Syton determination of size distribution of submicron particles in colloidal suspension, FODA 8-61057

Ag, colloidal, reaction with photographic stabilisers, equil. conditions (German) 8-61067

Au sol, grain boundary struct. obs. and boundary diffusion 8-51552

C blacks, in butanol, electrophoretic mobility, charge origin 8-85211

Cu, metal cluster, optical spectroscopy, atom to bulk 8-95591

colour see *colour*

colorimeters

see also *colorimetry*

reflectance spectrophotometers, old geometry problems (German) 8-54431

review of modern instrums. 8-93747

single-beam photoelectric colorimeter (KFO), meas. transmission coeffs. in visible spectrum 8-77963

spectrophotometer, ACS Spectra Sensor 8-54429

spectrophotometer, Zeiss DMC 25 automatic recording instrument errors 8-54430

spectrophotometer for colour measurement, flexible instrument with microprocessor 8-54428

spectrophotometer with pulsed Xe flashtube and parallel wavelength sensing 8-54427

tristimulus for PVC system plate-out testing (Hungarian) 8-93751

Zeiss Automatic Colorimeter RFC-3, colour-meas. performance 8-54426

Zeiss DMC 26 universal model (German) 8-54432

colorimetry

see also *colorimeters; spectrochemical analysis; spectrophotometry*

CIE-UCS system, determ. of most similar temp. (German) 8-54433

colour matching, review of basic laws and progress during the last 15 years 8-65955

colour negative films (high speed), testing 8-86364

colour vision testing, colorimetric assessment of Holmgren wool test 8-53409

conference, Troy, NY, USA (July 1977) 8-49882

correlated colour temp. determ. (Hungarian) 8-93749

correlated colour temperature and colour-difference formula 8-54424

educational colorimetric laboratory, calibration of set of surface colour standards 8-49625

fluorescent dye colour coords., spectroradiometric meas. (Spanish) 8-49880

fluorescent material colour meas. (Spanish) 8-49879

laser heated surface colour temp. meas. pyrometer 8-57956

light source brightness measurement, standard photometric system errors 8-58005

mathematical determination of colour contrast, uniform chromaticity scale construction 8-49881

photographic papers, colorimetric evaluation of colour separation (Russian) 8-49926

Polaroid photography colour reproduction 8-54490

polychromatic line spread function colour meas., colorimetric MTF 8-50712

proton radiography, solid state detectors 8-92424

PVC near-colourless transparent film, colorimetric determ. of colour 8-49884

repeatability (Hungarian) 8-93748

spectral sensitivities of colour-reproduction systems 8-49883

spectrophotometric for 0° illumination/diffuse observation measuring geometry (Hungarian) 8-93750

uniform colour scales of OSA samples, colorimetric specification 8-65952

C thin layers, thickness determ. by objective colorimetry 8-77844

Mn VI, colorimetric determ., appl. to Egyptian Mn ores 8-53285

colour

see also *colour vision*

colour matching, review of basic laws and progress during the last 15 years 8-65955

conference, Troy, NY, USA (July 1977) 8-49882

minerals, physical theories for origin of colour 8-69323

multi-quark hadrons in two dims. QCD, asymptotic solns. with Regge trajectory spectra 8-66085

ocean, Monte Carlo model including atm. and ocean scatt., absorpt. 8-61421

picture colour component detection in SAW scanning 8-59149

pseudocolour encoding of holographic images using single wavelength 8-87025

pseudocolour encoding of spatial frequency information 8-87018

colour continued

quartz, rose, charge transfer mechanism for origin of colour, EPR and optical expts. 8-52537
seawater off Ireland west coast, surface waters colour, UV absorbance and salinity 8-85603

colour blindness see *colour vision*

colour cameras, television see *colour television cameras*

colour centres

see also *F-centres; OH⁻-centres; paramagnetic resonance of colour centres; U-centres; V-centres*

alkali halides, radiolysis, growth of colloidal metal inclusions 8-92493
alkaline earth fluoride crystals, colour centre thermal stability 8-83811
KBr, thermally processed cryst., optical absorption bands (*Russian*) 8-76513
minerals, physical theories for origin of colour 8-69323
nonmetal, impurity optical absorption and emission, anharmonic effects 8-56503
quartz, electron irradiated, optical and anelastic absorptions and resonator freq. 8-64385
quartz, smoky, HF US relax. 8-71796
quartz, synthetic, fading rel. to lattice deformation (*German*) 8-63760
review of colour and symm. in imperfect crystals 8-72562
sapphire, radiation-coloured, vacuum UV spectra 8-84605
semiconductor, optical absorption by impurities, phonon-electron interaction 8-56502
semiconductor, Raman scattering from impurities 8-56468
semiconductor, Raman scattering from impurities 8-56469
silicate glass darkening due to UV radiation from laser produced plasma jet 8-52598
AgCl, colloid centres induced by reactor neutrons at 20K 8-72560
AlH₃, photoelectric effect spectra and kinetics, photochem. mechanism colour centres 8-56506
BaF₂:Er³⁺, single-site multiphonon and energy transfer relax. 8-52547
CaF₂, bleaching characteristics of crystals coloured by low energy electrons 8-76497
CaF₂:Dy, colour centres, antiresonance-type phenomenon in external fields 8-68529
CaF₂:RF₃, colour centre prod. by γ -irrad., absorpt. spectra obs. 8-72565
Ca₂P₂O₇:Sb, (Sb,Mn), luminesc., activation, colour centres (*Russian*) 8-92123
Ca₃(PO₄)₂:Sb, (Sb,Mn), luminesc., activation, colour centres (*Russian*) 8-92123
CsBr:NO₂⁻, luminesc. centre polarisation and reorientation (*Russian*) 8-76529
CsI:NO₂⁻, luminesc. centre polarisation and reorientation (*Russian*) 8-76529
CuGaS₂, coloration, pure and Fe doped, EPR and optical absorpt. obs. 8-88336
KBr, efficiency of creation of X₃⁻ centres in X-rayed alkali halides (*Russian*) 8-71731
KBr, substrate, with colloidal centre vacuum deposition of Au particles (*Rumanian*) 8-60579
KBr, X-irrad., I-centre activation energy and thermal diffusion 8-72606
KBr(Cl)(I):O₂⁻ centres, luminesc., polarisation temp. depend. 8-87943
KCl, efficiency of creation of X₃⁻ centres in X-rayed alkali halides (*Russian*) 8-71731
KCl, H₂O-related centres 8-67711
KCl, substrate, with colloidal centre vacuum deposition of Au particles (*Rumanian*) 8-60579
KCl, X-irrad., I-centre activation energy and thermal diffusion 8-72606
KCl, X-irradiated, formation of cation defects 8-91359
KF:Hg²⁺, electrolytic colouration 8-75665
KI, efficiency of creation of X₃⁻ centres in X-rayed alkali halides (*Russian*) 8-71731
KI:S₂⁻ centres, luminesc., polarisation temp. depend. 8-87943
LiF:Hg²⁺, electrolytic colouration 8-75665
LiTaO₃:M, optical damage of transition-metal-doped ferroelectric 8-95571
MgO, implanted K aggregates, TEM and optical spectra obs. 8-83838
MoO₃, film, colour centre studies, optical absorpt. spectra 8-71724
NaBr, thermally processed cryst., optical absorption bands (*Russian*) 8-76513
NaCl crystal, radiation coloured by electron beam, holographic lattice recorded by He-Ne laser 8-58950
NaCl, efficiency of creation of X₃⁻ centres in X-rayed alkali halides (*Russian*) 8-71731
NaCl, influence of coloration on intrinsic luminesc. 8-80399
NaCl, substrate with colloidal centre, vacuum deposition of Au particles (*Rumanian*) 8-60579
NaCl-CdO heterojunction form. in cathode-plasma dyeing, temp. depend. (*Russian*) 8-67710
NaF:Hg²⁺, electrolytic colouration 8-75665
RbBr:O₂⁻ centres, luminesc. polarisation temp. depend. 8-87943
RbCl:Sn, Sn-centres study, X-ray and coloration effects 8-76500
Si, A-centres, electron irrad., influence on positron annihilation spectra 8-76552
SiO₂, vitreous, colour centres, dangling bond defects, radiation effects 8-71732
SiO₂, vitreous, exam. of electron excitations and intrinsic defects 8-87905
TiO₂, anatase single crystals, switching, coloration and memory effect 8-72216
TiO₂, rutile, deuteron and alpha-particle implantation, chemical effects, optical and cond. meas. 8-67755
YAG, colour centres conceived as bound polarons 8-63990

colour filters see *optical filters*

colour model

algebra of colour 8-62354
asymptotic fields, colour confinement in QFT 8-70331
axion mass in extended SU(2)×U(1) colour gauge theory 8-78080
bag model, spectroscopic appls., baryonium, gluonium, quark phase of matter, review 8-50008
baryonium, review of QCD, duality, string models and bag models 8-78135
baryonium model from qq $\bar{q}\bar{q}$ hadron spectrum, T- and M-diquonium 8-58172

colour model continued

broken supersymmetry, existence of massless colour octet quarks and unstable hadrons 8-89631
charmonium, rel. to gluons, quantum chromodynamics theory 8-62362
charmonium and QCD, review 8-82157
charmonium model of ψ family 8-78143
charmonium photoprod., gluon-exchange model 8-74214
chromodynamics, SU(n), classical noncommuting quark source charges 8-78144
colour octet weak current induced by quark mixing, consequences of possible existence 8-58161
currents in Su(5) and E₇ unified gauge theories 8-54600
deep inelastic lepton-hadron scatt. in massive vector gauge models 8-74262
discrete finite nilpotent Lie analogs: new models for unified gauge field theory 8-66025
electric confinement and magnetic superconductors, appl. of QCD 8-58157
Feynman diagrams, colour group indices, IR divergences in Yang-Mills theories 8-54547
gauge theories, an introduction for experimental particle physicists 8-82119
gluon field condensation, instability of Yang-Mills level (*Russian*) 8-70289
gluon jets from QCD, jet ang. radius and energy depend. 8-89662
gluonic decay of heavy quarkonium states, QCD test, three jet struct. 8-62365
hadron collisions, theory and phenomenology of lepton pair production, review 8-82159
hadronic massive lepton pair prod., theory review, Drell-Yan model, QCD predictions 8-89752
heavy quark prod. in photoproduction, QCD model, possible large p_t process connection 8-78137
impulse approximation in QCD, partons p_t distrib., appl. to deep inelastic electron scatt. 8-62368
instanton effective size estimate from gluon field strength tensor vacuum expectation value 8-70326
instanton effects on quark-antiquark potential 8-93847
instantons and infrared divergences 8-70284
inverted charmed meson multiplets as a test for scalar quark confinement 8-70325
jet processes in QCD 8-82104
large p_t jet prod. in hadronic collisions, QCD calc. for inclusive cross section 8-86439
lepton-hadron deep inelastic scatt., massive vector gauge model (*Russian*) 8-89720
leptonic colour model, expt. evidence 8-62350
Lorentz structure of confining quark-quark interaction, asymptotic freedom, new particle spectroscopy 8-66077
mass splittings of heavy mesons and baryons (*Chinese*) 8-78146
massless chromodynamics, vacuum rearrangement 8-70327
massless QCD 8-78093
meson wave functions in 1+1 dimens. QCD 8-54559
metastable multi-quark states, colour chemistry 8-74212
Moufang plane and octonionic quantum mechanics 8-69999
multi-jet structure of hadronic final states and trajectory slope 8-93843
multiparticle production on nuclei, role of colour 8-93981
nonabelian gauge theories, coherent state approach to IR behaviour 8-82107
nonperturbative QCD effects at large momentum transfers, e⁺e⁻ annihilation to hadrons 8-82226
nonrelativistic colour quark model, meson and baryon masses 8-50014
nonrelativistic pot. models for heavy quark systems, Y and ψ hadronic decay 8-89688
nonrelativistic quark model with one gluon exchange pot., baryon spectroscopy in SU(6)⊗O(3) 8-78147
perturbative QCD and expt. signatures of weak bosons 8-93916
positive parity excited baryons in quark model with hyperfine interactions 8-82161
potentially CP violating phase in QCD, alleged axion mass, PCAC quark masses 8-66080
proton fragmentation functions, Q² depend., lowest order QCD calcs. 8-62359
Q² dependent parton distribution function on QCD 8-93857
Q² resonances in baryon-antibaryon systems, NN scattering and NN→ $\pi^+\pi^-$ 8-58171
QCD, μ pair transverse momentum distrib. in Drell-Yan processes 8-62374
QCD, axial gauge, mass shell behaviour 8-49966
QCD, charm contrib. to electroprod. struct. functions 8-58170
QCD, charm photoprod., ψ , D, F etc. prod., sum rules, cross sections 8-58169
QCD, dynamical props. 8-70332
QCD, e⁺e⁻ annihilation energy, asymptotically free perturbation theory 8-66045
QCD, electric field representation without gauge field constraints 8-93846
QCD, factorisation and the parton model 8-93848
QCD, field strength and action copies in any axial-like gauge 8-82143
QCD, gauge independence of IR cancellation, fermion-fermion scatt. 8-50006
QCD, gluon colour screening by Higgs mechanism 8-93861
QCD, hard processes, universality of mass singularities 8-82101
QCD, hard semi-inclusive processes 8-93862
QCD, inclusive production at large transverse momentum, cross section 8-62369
QCD, infinite-mass limit determ. 8-66039
QCD, lattice-gauge theory calc. of π and ρ -meson decay consts. 8-74154
QCD, massless, two dimens., bound states 8-62371
QCD, OZI rule violating radiative decays of heavy pseudoscalars 8-89709
QCD, perturbation theoretic parameter Λ 8-89667
QCD, positivity constraints on quark and gluon momentum distrib. 8-74205
QCD, strong interaction gauge theory, SU(3) colour gauge vector mesons, confinement 8-78136
QCD, transverse momentum distrib. of μ pairs from pN interactions, p-nucleus study 8-62375

colour model continued

- QCD, transverse momentum of jets in electrod. of hadrons 8-62367
- QCD, two-dimens. extrapolation to four-dimens. 8-78081
- QCD, universal multiplicity hypothesis, bounds on quark gluon coupling, quark mass, and confinement region 8-74213
- QCD and polarised quarks (*Russian*) 8-74217
- QCD effects, parton transverse momenta, large- p_t hadron prod. 8-66083
- QCD estimates for associated charm production by weak neutral currents 8-78169
- QCD estimates for heavy-particle prod. 8-82108
- QCD invariant charge, study of gauge theory by Lipatov's method (*Russian*) 8-74220
- QCD jets, algorithm for parton spectra 8-89680
- QCD of hadron struct. 8-93849
- QCD of quark matter to nuclear matter transition at neutron star density 8-54608
- QCD perturbation theory, asymmetries in inclusive hadron prod. 8-50057
- QCD perturbation theory, quark decay functions, heavy hadron prod. 8-62364
- QCD phase transitions, chiral symmetry breaking, confinement, as tunnelling through singular barriers 8-82145
- QCD predictions for large p_t hadron prod. by polarised hadrons 8-82148
- QCD quark-gluon plasma, hadronic prod. of leptons, photons and ψ (*Russian*) 8-89672
- QCD quark-gluon plasma, hadronic prod. of leptons, photons charm and ψ 8-89669
- QCD two virtual gluon exchange force, using quark van der Waals force 8-82152
- quantum chromodynamics, hadronprod. of lepton pairs and real photons 8-50056
- quark confinement in condensate of non-Abelian vortices 8-70328
- quark fragmentation into mesons, statistical model, vector meson contrib. 8-54639
- quarkonium decay, gluon jets and gluonic resonances, QCD test 8-93841
- quarkonium decay into heavy quark flavours, ψ (J) energy distrib., QCD perturbation theory 8-82146
- radiative corrections in gauge theories, QCD current algebra formulation, weak interaction universality 8-93883
- right handed colour octet currents for charm and colour excitation in $\nu\bar{\nu}$ reactions 8-93874
- S-wave colour singlet states, multi-quark configurations, determ. and systematic labelling 8-58155
- semiempirical mass formula for hadrons in quark model and QCD 8-74236
- solutions of Yang-Mills eqns. with external sources, colour charged particles 8-89624
- SU(3) \times SU(3) c scheme of three triplet model, colour symm. ψ -mesons descript. 8-78151
- SU(3) gauge fields, colour screening 8-82102
- SU(4) \times S $_3^c$, straton model, meson classification (*Chinese*) 8-78145
- SU(6) unified gauge group, neutral current coupling to ν_μ and ν_e 8-54626
- SU(N) scalar QCD in two dimens., and the parton model 8-93856
- sum rules and moments of dimuon prod., valence quark transverse moments 8-54660
- superoperator generalisation of dual model with coloured quarks, three reggeon vertex (*Russian*) 8-74234
- supersymmetric new hadronic states, production, decay and detection 8-70302
- three triplet quark model with observable colour, hadron weak current, $\Delta T=1/2$ rule (*Russian*) 8-74219
- two jet model, large p_t hadronic multiplicity, colour octet exchange 8-62377
- van der Waals forces in QCD colour singlets 8-86441
- Wilson operator formalism, generalised parton model equivalence 8-93855
- Yang-Mills theory, conserved flux, elimination of colour charge from gauge field 8-89659
- Zweig suppressed decay of heavy 1^{--} vector mesons, two gluon exchange 8-54616
- $e^+e^- \rightarrow HX$, associated production of gluonic jets and heavy mesons 8-93892
- $e^+e^- \rightarrow$ hadrons, asymptotically free QCD perturbation theory for multi-jet final states 8-74267
- $e^+e^- \rightarrow$ hadrons, azimuthal correlations, quantum chromodynamics anal. 8-70382
- $e^+e^- \rightarrow$ hadrons, finite energy sum rules, cross section, QCD calcs. 8-62413
- $e^+e^- \rightarrow$ hadrons, inclusive distrib., jets, 1+1 dimens. QCD 8-66137
- $e^+e^- \rightarrow Y$, suggested search for gluon hadronic states in collinear gluon jets 8-89663
- ep deep inelast. scatt., QCD perturbative corrections 8-74263
- $e^+p \rightarrow e^+\gamma + X$, deep-inelastic bremsstrahlung, quark charges, colour gluon mass 8-74216
- η , η' and η_c , mixing and decays in nonrelativistic quark model for QCD idea 8-82166
- η Dalitz decays, excitable colour gluons 8-58181
- η_c mass determ. from QCD sum rules 8-74223
- η_c mass from dispersion sum rules in QCD, identification with $X(2.83)$ (*Russian*) 8-89681
- μ pair prod., QCD ang. correl. 8-49976
- μ pair production in hadron-hadron collisions, gluon effects, QCD predictions 8-78148
- $\nu(\bar{\nu})N$ inclusive scatt., scaling violation evidence, QCD test 8-89701
- pN , μ pair prod., QCD predictions for zero and nonzero rapidities 8-89674
- $pp \rightarrow \mu^+\mu^-$ + anything, Drell-Yan formalism 8-78229
- ψ hadronic production, gluon contrib. in QCD framework 8-78139
- $\psi \rightarrow \psi + \eta$, two gluon mechanism, Y dynamics test 8-89665
- ρ form factors ratio, high momentum transfer behaviour in QCD 8-70340
- Y(9.4) family, gauge theory mass anal., harmonic oscillator pot. 8-82186
- Y(9.5) hadronic prod., parton distrib. and QCD 8-78142
- Y(9.5), possible colour-excited states (*Chinese*) 8-82169
- $Y \rightarrow Y + \eta$, two gluon mechanism, Y dynamics test 8-89665

colour perception see colour vision

colour photography

- aerial photography, multispectral, soil survey in New Zealand 8-85728
- cassette film camera for automatic and rapid prod. of colour pictures (*Russian*) 8-93780
- cinematography, colour film processes and cameras, review, 1894 to date (*German*) 8-93773
- colorimetric evaluation of colour separation (*Russian*) 8-49926
- colour atlas for colour organisation in film production (*Russian*) 8-93776
- colour mixing and colour films (*German*) 8-93774
- dye-releasing compounds, colour imaging technology for instant photography 8-62247
- ecosystem succession detection by aerial IR photography 8-81459
- image sharpness rel. to spatial freq. for Ag and dye (*Russian*) 8-49933
- lens transmittance 8-62250
- negative films (high speed), colorimetric testing 8-86364
- Polaroid photography colour reproduction 8-54490
- printing and processing efficiency improvement for motion pictures 8-78023
- spectral sensitivities of colour-reproduction systems 8-49883

colour television

- image coloration psychophysics 8-65025
- spectral sensitivities of colour-reproduction systems 8-49883

colour television cameras

- lens testing, meas. of spectral transmission and modulation transfer function 8-94456
- single tube SICOLOR, appl. to endoscopy (*German*) 8-88758

colour tv see colour television

colour vision

- see also eye
- accommodation response, effects of colour 8-69042
- appearance specification, terms and formulae 8-56995
- brightness under contrast, psychophys. functions 8-57000
- cat, effect of stimulus size 8-69076
- chromatic adaptation, review 8-53403
- chromatic adaptation effects and colour appearance at various illum. levels (*Japanese*) 8-92628
- chromatic border perception, role of red- and green-sensitive cones 8-69091
- chromatic stereopsis, opposition of photometric and dioptric factors (*Italian*) 8-56986
- colour matching at moderate to high levels of retinal illuminance 8-56981
- colourfulness, new concept 8-56996
- conference, Troy, NY, USA (July 1977) 8-49882
- contrast sensitivity, achromatic and colour, instrument for testing 8-73275
- countercolour system and colour vision eqns. for arbitrary colour (*German*) 8-57007
- crustacea with scotopic eyes, screening pigment effects on spectral sensitivity 8-65009
- deuteranomalous trichromats, locus if unique green 8-53400
- dichoptic colour and brightness combinations 8-53407
- dichromat long-wavelength-sensitive photoreceptor spectral sensitivity determ. by border percept elimination 8-69092
- discrimination by Bering Sea spotted seal 8-69077
- distinctness of borderline rel. to Natural Colour System 8-57002
- equal saturation contours for surface colours 8-57001
- evoked potentials and latent chromatic response, reproducibility (*Japanese*) 8-92629
- foveally viewed yellow target, chromatic uncertainty effect on detectability 8-65005
- haploscopic apparatus for study of colour perception under different adaptation conditions 8-56997
- Holmgren wool test, colorimetric assessment 8-53409
- hue response recovery following chromatic adaptation 8-53404
- image coloration psychophysics 8-65025
- insect eye slow cell responses, colour adaptation 8-64988
- interocular light adaptation effect on Lie specific threshold 8-69079
- interocular transfer of colour-contingent motion positive aftereffects 8-69100
- Mach bands, definitions 8-69096
- McCollough aftereffects, colorimetric matches 8-65026
- motion perception, role of colour 8-85312
- multidimensional scaling 8-64979
- Munsell colours, principal hue components 8-56999
- opponent processes, psychophysical and electrophysiological studies 8-53402
- opposite colour difference and anti-colour in human visual system 8-65004
- orthogonal systems generating hypersensitivity, colour and depth 8-80881
- parafoveal stimuli, spectrally different, psychophysical tests of equiv. luminance 8-53414
- perception, colour changes due to distance and lighting, direct assessment using Natural Colour System 8-57004
- perception, human, graphic model (*German*) 8-57005
- perception fundamentals 8-77054
- perception of coloured field, effect of subtense and surround luminance 8-57003
- photocoagulation using ruby laser, colour discrimination time variability 8-53401
- photoreceptor spectral sensitivity on-line computation using programmable pocket calculator 8-69264
- physiological basis of trichromatic to tetrachromatic colour scheme transition 8-53406
- physiological measurement facility, monkey detected responses (*Japanese*) 8-92752
- pigeon, *Columba livia*, spectral sensitivity of red and yellow oil droplet fields 8-80876
- prime colour theory of human vision 8-53410
- reflected light common and relative components as information about illum., colour and 3-dimens. form 8-56982
- retinula peripheral cells within *Drosophila* visual mutants, response to monochromatic white-noise 8-69078
- rhabdom spectral absorption, crayfish visual pigment, photoproduct and pH sensitivity 8-65008
- selective chromatic adaptation at different spatial freqs. 8-65006

colour vision continued

- simultaneous colour contrast, deviations of induced colours from directions of complementary colours 8-56998
 spectral response of human eye, rhodopsin thermal activation energy 8-92630
 statistical study of colour matching functions 8-53408
 Stiles II-mechanisms candidacy for colour-matching fundamentals 8-56980
 Stiles-Crawford function peak shift with wavelength 8-92631
 tetrachromatic matching, additivity and Maxwell spot 8-53405
 tilt after-effect magnitude, colour and contour rivalry influence 8-69098
 trichromatic theory and time vector in relativity theory (*French*) 8-57006
 vector algebra description of operations with colour, human visual system 8-96047
 vernier-horopter and colour 8-65007

columbium *see niobium***coma** *see aberrations***combinational mathematics** *see combinatorial mathematics***combinatorial mathematics**

- see also graph theory; trees (mathematics)*
 dimer config. enumeration, n-dimensional theory, graph paths 8-54315
 isomers, enumeration by combinatorics, Polya's theorem 8-93501
 porphyrins, isomers, enumeration by combinatorics, Polya's theorem 8-93501

combustion

- see also explosions; flames; heat of combustion; reaction kinetics*
 acetylene-NO-O₂, combustion products, 1400-2600K, minimisation of NO, computer model 8-85161
 aerosols, particle size distrib., health hazards 8-81394
 anthropogenic combustion, as source of polycyclic aromatic hydrocarbons in recent sediments 8-57192
 ball lightning explanation by water electrolysis and combustion 8-69436
 burner with diffusive control, intermixing of gas streams with transverse swirled air flow 8-87418
 chamber of TPP 210 A steam generator, radiant heat flux distrib., light model simulation 8-94567
 concentration fluctuations in turbulent gas flows, by Fourier analysis of Raman signals, nonintrusive measurement technique 8-92564
 convex nonlinear boundary value problems, iterative bounds for stable solns. 8-54167
 detonation of unmixed liq.-gas mixture with surface evap., fluid dynamical characts. (*Russian*) 8-55630
 diagnostics, laser Raman and fluoresec. techniques 8-88635
 fuel droplet, deflagration and extinction in weakly reactive atoms. 8-64840
 gas, boundary layer combustion, combined heat transfer 8-91029
 gas jets, laminar homogeneous, combustion process (*Russian*) 8-94850
 hydrocarbon combustion products, 1400-2600K, minimisation of NO, computer model 8-85161
 laminar diffusion boundary layers, ignition and extinction 8-64838
 laser Doppler velocimeter with variable frequency shift for combustion flow meas. (*Japanese*) 8-67294
 liquid fuel droplets, transient heat flow in combustion gases, models 8-63507
 liquid fuel film, combustion behind shock wave, heat and mass transfer in turbulent boundary layer (*Russian*) 8-71401
 methyl radical+O₂ (NO), mass spectra, absence of reaction in combustion system 8-53195
 MHD generator, electrothermal instability in the seeded combustion gas boundary layer near cold electrodes 8-71547
 mixture burning in Soundhaus' tube, radial self excited vibr. regimes (*Ukrainian*) 8-68892
 oil-fired burners, particle size distrib. characterisation using Beta distrib. 8-81384
 plasma, combustion product plasma, near-electrode contraction conditions 8-94946
 PMMA, spreading of two-phase film of melt, heat and mass exchange, ignition and combustion (*Russian*) 8-76861
 pressure waves interaction with combustion field 8-63504
 radiative heat transfer, Milne-Eddington absorpt. coeff. 8-90680
 shock waves, starvation kinetics 8-64841
 solid rocket propellant combustion, holographic recording 8-82935
 thermal instability of vibr.-excited mol. gas, appl. to surface ignition (*Russian*) 8-56895
 tubular reactor, model calc. with longitudinal transfer and heat losses through sides (*Russian*) 8-73043
 turbulent, averaging of pulsed laser Raman signals 8-70839
 turbulent, model for molecular mixing of unmixed gases (*Russian*) 8-94849
 vortex ring, turbulent, acoustic emission accompanying burning 8-94676
 Al particulate combustion process model (*Russian*) 8-85164
 C₃ porous particle, internal combustion, model 8-92481
 CS₃+N₂O+O₂ combustion, CO laser performance characts. (*Russian*) 8-55348
 H+O₂→OH+O, combustion, quasiclassical trajectory calcs. 8-53201
 H₂-N₂O-CO-Ar, conc.-time data for O and CO₂, 2000-2850K 8-85162
 H₂-O₂-CO-Ar, conc.-time data for O and CO₂, 2000-2850K 8-85162
 hydrocarbon-water, emulsions, superheated, bubble nucleation 8-61056
 N₂O+H→N₂+OH, rate const., 2000-2850K, combustion of H₂/N₂O/CO/Ar 8-85162

comets

- 1974 observations, discoveries and recoveries 8-73682
 1975 observations, discoveries and recoveries 8-73683
 P/Arend-Rigaux (1977k), precise positions for 1977 Oct.-1978 Mar. 8-65548
 P/Ashbrook-Jackson (1977g), magnitude estimates (1978 Aug.-Sept.) 8-85912
 P/Ashbrook-Jackson (1977g), precise position for 1978 Apr. 5 8-53887
 P/Ashbrook-Jackson (1977g), spectroscopic obs. 8-96437
 P/Ashbrook-Jackson (1977g), total visual magnitude estimate for 1978 July 1 8-73679

comets continued

- P/Ashbrook-Jackson (1977g), total visual magnitude estimates 8-93169
 P/Ashbrook-Jackson (1977g), total visual magnitude estimates 1978 July 8-77519
 P/Ashbrook-Jackson (1977g), visual magnitude estimates (1978 September 7 and 10) 8-89128
 Bradfield (1978c), precise positions, parabolic elements and ephemeris 8-65551
 Bradfield (1978o), discovery and positions 8-93165
 Bradfield (1978o), precise position for 1978 Oct. 18 8-96439
 Bradfield (1978o), precise positions for 1978 Oct., parabolic elements, ephemeris 8-96433
 capture by Laplace scheme, orbital elements statistical consequences 8-53888
 capture problem in celestial mechanics 8-77477
 chemistry, organic mol. rel. to origin of life and transfer to Earth 8-73660
 P/Chernykh (1977l), precise positions 1977 Aug.-1978 Mar. 8-53886
 P/Chernykh (1977l), precise posns., improved elements and ephemeris 8-69747
 close approaches to Earth, list of events 8-73621
 comae model, gas-phase chemistry in one dimension 8-93154
 p/Comas Sola (1977n), ephemeris for 1978 July-1979 June period 8-69749
 P/Comas Sola (1977n), total visual magnitude estimate, (1978, October 8) 8-96435
 cosmic dust, book 8-57498
 P/d'Arresi (1976 XI), meteoroids characts. 8-53876
 P/d'Arresi (1976 XI), nucleus light curve and rotation 8-53877
 P/Daniel, predicted orbital elements 8-53883
 digital image enhancement 8-81556
 discovery and positions for 1977 July 18-19 8-77518
 Donati (1858 VI), rot. period of nucleus 8-57506
 dust, low vel. particle meas. during cometary fly-by mission using capacity type detector 8-93113
 dust particles, impact mass spectrometer for chemical analysis on fly-by mission 8-93112
 dynamic processes on Earth, extraterrestrial causes, rel. to extinction of life 8-92820
 Earth close approach, rel. to ice ages and ecological catastrophes 8-53714
 P/Encke dust, large grains in short supply 8-85908
 P/Encke fragment as possible Tunguska object 8-89120
 ephemerides on minor planet circulars 4425-4482 for four objects 8-85886
 formation and primitive solar nebula evolution rel. to solar accretion disk 8-81566
 Fujikawa (1978n), discovery and positions (1978, October 9 and 10) 8-96431
 Fujikawa (1978n), precise position, (1978, October 10) 8-93166
 Fujikawa (1978n), precise position for 1978 Oct. 11 8-96434
 Fujikawa (1978n), precise positions, orbital elements and ephemeris 8-93168
 P/Gehrels 3 (1975o), precise positions for 1978 Feb.-Mar. 8-73677
 P/Giacobini-Zinner (1972 VI), brightness rel. to 1972 August solar flares 8-57534
 Giclas (1978k), discovery report 8-85915
 P/Giclas (1978k), precise position and improved orbital elements 8-85916
 Giclas (1978k), precise positions, orbital elements and ephemeris 8-89122
 P/Giclas (1978k), precise positions 1978 Sept., elliptical elements, ephemeris 8-93162
 P/Giclas (1978k), spectroscopic obs. 8-96437
 P/Gunn, ephemeris continuation for 1978 July-1979 April period 8-61805
 P/Gunn, precise positions for 1977 Oct. and Dec. 8-69750
 Haneda-Campos (1978j), discovery and initial posns. 8-85911
 P/Haneda-Campos (1978j), precise position for 1978 Sept. 29 8-93167
 P/Haneda-Campos (1978j), precise positions, (1978 September 2 and September 8) 8-89124
 Haneda-Campos (1978j), precise positions, magnitude, orbital elements, ephemeris for 1978 Sept. 8-85913
 P/Haneda-Campos (1978j), precise positions, orbital elements and ephemeris 8-89121
 P/Haneda-Campos (1978j), precise positions 1978 Aug.-Sept., ephemeris for 1978 Sept.Oct. 8-89131
 P/Haneda-Campos (1978j), precise positions (1978, September 6 and 8) 8-85914
 P/Haneda-Campos (1978j), precise positions and orbital elements 8-89127
 historical records, comets obs. in Greek and Roman sources before 410 AD 8-77658
 P/Jackson-Neujmin, ephemeris for 1978 June 21-1979 January 7 period 8-53878
 Kobayashi-Berger-Milon (1975IX), Swann band profiles 8-85909
 Kohler (1977m), precise positions, (1977 October 4 to 1978 April 8) 8-73680
 Kohler (1977m), precise posns. for 1977 October-1978 March period 8-61806
 Kohoutek (1973 XII), precise posns. (1974 Jan. 17-20) (*French*) 8-81577
 Kohoutek (1973XII), Swann band profiles 8-85909
 P/Kojima (1977r), precise positions for 1978 Jan. and Mar. 8-65549
 Machholz (1978l), discovery report 8-89123
 Machholz (1978l), elliptical elements and total visual magnitude estimate 8-89129
 Machholz (1978l), orbital elements and ephemeris (1978, September 19 to October 9) 8-89126
 Machholz (1978l), positional obs., (1978, September 14 and 15) 8-89125
 Machholz (1978l), precise positions, total visual magnitude estimates, 1978 Sept. 8-89130
 Machholz (1978l), precise positions 1978 Sept.-Oct., magnitudes, parabolic orbital elements, ephemeris 8-93163
 Machholz (1978l), total visual mags. and ephemeris continuation 8-93159
 Meier (1978f), OH emission at 1665 and 1667 MHz 8-61800

comets continued

- Meier (1978f), positions, elements, ephemeris, magnitudes and spectrum 8-53881
 Meier (1978f), posns., elements, ephemeris and magnitudes 8-61801
 Meier (1978f), precise positions, (1978, May 2 to June 9) 8-69751
 Meier (1978f), precise positions, orbital elements and ephemeris 8-53884
 Meier (1978f), precise positions and magnitude estimates (1978 May-June) 8-69748
 Meier (1978f), precise positions for 1978 Apr.-May, total visual magnitude estimates 8-57505
 Meier (1978f), precise posns. (1978 May-July) 8-77520
 Meier (1978f), precise posns. and total visual mag. estimates (1978 Aug.-May) 8-57504
 Meier (1978f), total visual magnitude estimates for 1978 July 8-85910
 monochromatic brightness var. 8-81590
 monochromatic brightness variations, appl. of core-mantle model 8-81589
 nongravitational effects in orbital motion, comparison of correction methods 8-61811
 Oort cloud, form. from mass removed from early solar system by outer planets 8-53841
 Oort cloud, origin 8-57502
 orbital accelerations caused by solar companion star 8-81567
 orbits, perihelion distrib. asymmetry 8-96429
 orbits, three-dimens. model construction 8-61808
 origins, research and interplanetary relationships 8-57507
 Palomar Sky Survey record of probable comet, posn. and daily motion 8-69752
 plasma tail disconnection events, mag. field line reconnection at interplanetary sector boundaries 8-93155
 plasma tails disruption, triggering by flute instability 8-93156
 population in circumterrestrial space 8-73599
 precise posns. on Minor Planet Circulars 4391-4424 for 15 objects 8-81578
 precise posns. on minor planet circulars 4425-4482 for eight objects 8-85886
 precise posns. on Minor Planet Circulars 4483-4520 for 13 objects 8-93140
 P/Sanguin (1977p), precise posns. (1977 Nov.-1978 Jan.) 8-73685
 P/Schuster (1977o), precise positions, 1977 October 16 and (1978 January 2) 8-65550
 P/Schwassmann-Wachmann 1, 1978 September 13-14 magnitude 8-93160
 P/Schwassmann-Wachmann 1, 1978-9 ephemeris 8-77521
 P/Schwassmann-Wachmann 1, precise posns. (1977 Dec.-1978 March) 8-69746
 Seargent (1978m), discovery, posns. and appearance 8-93158
 Seargent (1978m), positions 1978 Oct. 8-93161
 Seargent (1978m), precise positions, 1978, October 6, and parabolic orbital elements 8-96432
 Seargent (1978m), precise positions, parabolic orbital elements and ephemeris 8-93164
 Seargent (1978m), precise positions for 1978 Oct., parabolic elements, ephemeris, UV spectra 8-96436
 Seargent (1978m), precise positions for 1978 Oct. 8-96438
 P/Shajn-Schaldach, ephemeris for 1978 June-1979 March period 8-53879
 P/Shajn-Schaldach (1978i), recovery positions 8-73678
 short-period, with large perihelion distances, search, unidentified asteroids obs. 8-85907
 tail magnetic field magnitude estimation 8-93157
 P/Taylor (1916 I), nuclei separation vels. during disintegration 8-61812
 theories and observations 8-69753
 Tsuchinshan (1977g), precise posns. (1977 Nov.-1978 Jan.) 8-61804
 Tunguska, 1908, catastrophe, cosmochemical anomaly in silicate microspherules comp. 8-96430
 Tunguska cosmic body, chemical comp. and nature 8-61810
 Tunguska event, thermal explosion of porous meteoroid, model 8-61813
 P/Tuttle-Giacobini-Kresak, 1978-9 ephemeris 8-73684
 P/Van Biesbroeck (1977s), precise posns. (1978 April-May) 8-73686
 P/Van Biesbroeck (1977s), precise posns. (1978 Jan.-May) 8-61802
 West (1976 VI), dust tail striae, propagating inhomogeneities 8-61809
 West (1976 VI), IR obs., dust model 8-81592
 West (1976 VI), IR obs., results 8-81591
 West (1976 VI), spectrophotometry after perihelion passage, emission features vars. 8-57503
 West (1978a), ephemeris, (1978, June 11 to September 9) 8-61807
 West (1978a), precise positions for 1978 Jan.-May 8-61799
 P/Whipple (1977h), ephemeris (1978 June 21 to 1979 April 17) 8-53882
 P/Wild 2, (1978b), precise positions, (1978 February 8 to April 12) 8-53885
 P/Wild 2 (1978b), precise positions (1978 Feb.-Apr.) 8-53880
 P/Wild 2 (1978b), precise positions for 1978 Mar.-May, ephemeris 8-73676
 P/Wild 2 (1978b), precise posns. (1978 February-April) 8-73681
 P/Wild 2 (1978b), precise posns. and magnitudes (1978 Jan.-May) 8-61803
 CN radicals, newly created, possible detect. in spectra 8-61798

commissioning

- Calcutta variable energy cyclotron vacuum system design, testing and commissioning 8-86707

communication networks

- see also computer networks
 conference, EUROCON, Venice, 1977, May 8-53552

communication systems see telecommunication systems**communication theory** see information theory**communications applications of computing** see communications computing**communications computer control**

- see also communications computing
 automated meteorological data transmission from commercial aircraft via satellite 8-57327

communications computing

- see also communications computer control
 IEEE International EMC Symposium, Atlanta (1978) 8-82876

communications computing continued

- optical signal receivers, optimal and nonoptimal, logical structs. efficiency comparison, simulation (*Russian*) 8-71041
 troposphere, radio propag. characts. prediction using FORTRAN computer programs (*Italian*) 8-85666

community planning see town and country planning**commutation**

- see also commutators
 arc quenching system for transient and statistical flashover, fusion reactor systems 8-75455
 six-channel MOSFET commutator, monopolar mass spectrometer appls. (*Russian*) 8-74099

commutators

- see also commutation
 Kalousek commutator, appl. to electrochem. stripping anal. 8-53290

compacting see densification**comparators (circuits)**

- see also phase comparators
 double constant current source for cryogenic current comparators, standard resistor calibration appl. 8-93731
 gated constant-fraction discriminator for use with fast-focused photomultiplier tubes 8-58063
 least or greatest interval timer 8-62183
 microwave moisture content-attenuation-voltage convertor with time-domain attenuation comparisons (*Polish*) 8-70131
 photon count cct. using high-speed comparator in discriminator 8-77979
 Q-meter, digital, automatic, design procedure 8-70155

compasses

- see also navigation
 No entries

compensation

- see also error compensation
 electrolyte electrical conductivity meas., voltage amp. for temp. compensation (*German*) 8-54399
 flow meas., hot wire and hot film temperature compensating circuits, temp. probe appl. 8-59510
 galvanomagnetic semiconductor voltage and current transducers, Gauss effect compensation 8-77892
 high-speed pulse shaper/discriminator for scintillation and Cherenkov counters 8-86748
 hot-wire anemometer temp. compensation errors estimation (*Russian*) 8-57345
 Kelvin bridge, link resistance compensation 8-86292
 light divider phase distortion compensation improvement 8-58073
 magnetic induction, stabilised source 8-94360
 multichannel temperature recorder, Thermodac II with 24 channels, thermocouples 0 degree C compensation 8-65930
 near IR absorption analysis, differential compensation method 8-80819
 photomultiplier modulating cct. with spurious signal compensation 8-58033
 radiometer, absolute differential, compensation cct., features 8-65956
 resistance thermometer, conductor resistance effect compensation using hexagonal bridge (*German*) 8-77910
 shading effects and countermeasures 8-78922
 temperature during illumination measurement using photoresistors, digital linearisation using microprocessors (*German*) 8-77961
 thermal compensator for diode laser closed-cycle refrigerator stabilisation 8-50797
 thermal-blooming compensation, using closed-loop adaptive single parameter system 8-94407
 thermoelectric thermometer cold junction thermo-EMF compensation, parameter optimisation (*Russian*) 8-86270
 wideband AC electronic voltmeter (*Spanish*) 8-86304
 Se photocells, temp. coeff. of sensitivity 8-82033
 Si resistors, both p-type and n-type 8-91698

compensation, charge see charge compensation**complementarity**

- quantum mechanics, development and Heisenberg's role (*Polish*) 8-89291

complete computer programs

- see also subroutines
 cylindrical demagnetisation matrix computation, FORTRAN IV program 8-76274
 EEG bispectra computation computer program, in FORTRAN 8-92727
 exploratory drilling exhaustion sequence plot program in FORTRAN 8-57334
 FORTRAN 336 statement program for prismatic plate assembly anal. 8-90737
 FORTRAN least-squares approx. for lateral absorbed dose distrib. for 25 MeV electrons appl. (*Japanese*) 8-74505
 Lagrange's interpolation formula program for Texas Instruments SR-56 8-77699
 volcanic rocks classification using Irvine and Baragar classification scheme, FORTRAN IV program 8-57203

complex angular momentum plane

- see also angular momentum theory; Pomeranchuk poles and trajectories; Regge poles and trajectories
 complex momenta eikonal approx., hadron-nucleus collisions at asymptotically high energies (*Russian*) 8-74294
 Coulomb amplitude, integral representations 8-78118
 Faddeev eqns., pole approx. (*Russian*) 8-49986
 T-matrix, perturbation formalism for complex poles and widths, appl. to intermediate struct. 8-66255

compliance constants see elastic constants**composite insulating materials**

- glass fibre reinforced epoxy, as electrical insulation for Tokamak toroidal field coils, mech. props. 8-64610
 glass fibre reinforced epoxy prepreg, PDX TF coil insulation 8-62656
 glass fibre reinforced epoxy resin, mech. props. 8-64582
 polymer-TiO₂ composite, dielec. props. (*Japanese*) 8-95540
 Pb(Zr,Ti)O₃ ceramic-polyvinylidene fluoride composite film, complex piezoelec. props. 8-64323

composite materials

see also *cermets*; *composite insulating materials*; *composite superconductors*; *concrete*; *eutectic alloys*; *fibre reinforced composites*; *fibres*; *filled polymers*; *laminates*

aligned composites, in-situ growth by disproportionation of amorphous metal systems 8-72755

alloy, disperse state formation (*Russian*) 8-52757

bearing capacity of designs, subject to intense surface heating 8-67057

bi-material, elastic composite, Southwell's analogues for plane and bending problems 8-87265

bimaterial plate, cracked, finite element anal. of stress distribution 8-75104

binary mixture theory for thermal diffusion in unidirectional fibrous composites 8-87230

cellulose, fibres, membranes and composites, polystyrene used for modification of props. 8-95727

cemented carbides, wear resistant coating of Ti(N,C,O), CVD 8-92406

composite material, cubic arrangements of spherical particles in isotropic matrix, effective conductivities 8-55547

composite medium, two-component residually stressed, elastoplastic crack model (*German*) 8-90790

connectivity and piezoelectric-pyroelectric composites 8-80290

copolymer, graft or block, multiphase composite systems, struct., colloidal behaviour (*Chinese*) 8-73088

cubic arrays of spheres in dielectric matrix, permittivity 8-56415

cylinder, circular transient thermal stress anal. 8-79217

development and use in USSR (*Russian*) 8-52696

diamond composite with Cu-Ti matrix, microstresses, X-ray diffr. exam. 8-56679

dispersion hardened metallic matrix composite, powder metallurgically produced effective interparticle distance effects (*German*) 8-52727

double-skinned composite circular cylindrical shells failure under external press. 8-75078

double-skinned composite circular cylindrical shells under external press., experimental behaviour 8-75077

effective bulk dielec. const., analytical props. 8-56414

elastic longitudinal waves, diffr. at elastic circular inclusions (fibres) (*Russian*) 8-63368

elastic properties, self-consistent field approx. 8-51078

electrophotographic two-component developer discharge and contact interaction (*German*) 8-62258

electrostrictive resonators, finite element simulation 8-59237

EM wave propagation, self-consistent theory 8-56442

epoxy, Ag powder filled, thermal cond. below 3K 8-51757

epoxy resin cured with composite curing agents, arc resistance (*Japanese*) 8-92371

fibre reinforced plastics, exam. of strength criteria 8-75105

flat belt drive material, tension relaxation under simulated drive conditions 8-56688

fluid impregnated solids, elastic and dynamic response regimes 8-90713

fracture and fatigue, review 8-68781

fracture time under tensile loading 8-88521

fusion reactor, three-dimens. solid finite element anal. for simulating composite windings 8-55003

glass ceramic, machinable, elastic moduli press. and temp. derivatives, specific heat 8-52873

glass microsphere reinforced, composite, mech. charact. calc. 8-64578

glued members, low frequency acoustic flaw detector inspection 8-60954

grain and phase boundaries between crystals, conf., Konigstein, Germany (Oct. 1977) 8-72762

graphite-based, survey 8-56609

graphite-SiC-FeSi crucible mat., oxidation loss and wettability of inorganic fluxing materials (*Japanese*) 8-84755

Green's functions 8-77712

Griffith crack, interface of layer bonded to half plane, approx. method 8-79258

heat conductance, combined numerical method 8-63261

heat transfer on layered composites 8-71264

high precision triangular laminated anisotropic cylindrical shell finite element 8-79206

inhomogeneous systems, hysteresis of phase transitions, general soln. 8-59926

insulating and conducting particles mixture, percolation problem 8-60097

isotropic composite material containing spherical inclusions at nondilute concs., effective elastic moduli 8-67037

laminated half space under influence of vibrations (*Russian*) 8-63370

linearized theory of elastic wave propagation in initially stressed bodies (*Russian*) 8-83318

mechanical strength, density depend. (*German*) 8-94592

membranes, composite, relaxation time, network thermodynamics formalism 8-68926

metal gauze reinforced porous permeable mats. with prearranged struct., prep. 8-68652

metal matrix, state of the art review, book 8-72706

metal particle composite, physical and optical props. 8-56528

metal-glass mats. alloyed with Cu, powder prep. and props. 8-72912

metal-insulator composite films, optical props., rel. to solar collector appls. 8-72622

nonlinear elasticity, extremum principles, appl. to composites 8-51072

nylon-quartz fibre support for low temp. mag. suscept. meas. 8-65947

optical properties, review 8-56496

orthotropic materials design for stress optimisation 8-63291

particulate, mechanical model 8-51105

particulate reinforced epoxy resin model specimens, Young's modulus, expt. study (*Japanese*) 8-56683

physical nature of fracture 8-80653

plane deformation for composite with longitudinal cracks 8-67096

plates and shells, construction elements, review of physical props. 8-67056

PMMA based composite (acrylic bone cement), effect of BaSO₄ and glass particle dispersions, on fracture behaviour 8-76753

PMMA-metal oxide composite powder, prep. and props. (*Japanese*) 8-95708

PMMA/PVC, cracking in layered composites 8-95808

polyethylene-Fe, wear resistance on steel counterbody, exam. 8-68826

polyhedral sandwich domes, elastic behaviour, failure, practical investigation and numerical simulation 8-59309

composite materials continued

polymer blends and composites, behaviour, review 8-76626

polystyrene composite with mica flakes, TDC meas., interfacial polarisation 8-64316

polystyrene-wood, polymer composite, dielec. props. at low temperature range (*Japanese*) 8-95541

powder reinforced metal composite with glass microsphere filler prod. in space 8-52726

PTFE impregnated porous bronze, coeff. of friction, temp. effect 8-64737

PVC composite, MBS type multifunctional impact modifier effect on mech. and rheological props. (*Polish*) 8-52751

PVC-Cu composite, annealing effects on elec. resist. 8-68060

random functions theory appl. to microinhomogeneous media (*Russian*) 8-63280

reinforced plastics, low frequency acoustic flaw detector inspection 8-60954

reinforced tube, bending and flexure 8-51076

resin, Langmuir type model for anomalous moisture diffusion 8-67867

rod, small deformations, initial stresses effect 8-63284

S glass-Ni sphere composite, exam. of crack shape and fracture toughness 8-72886

simulation of tensile behaviour and fracture void initiation (*Japanese*) 8-52948

sintered composite-liq. metal interaction, mass transfer eqn. approx. soln. 8-67262

small particle composite, optical properties from periodic multiple scatt. theory 8-56444

small particle composites, optical props. 8-56445

solid propellants, fracture criterion, fracture time computation 8-75106

steel, austenitic, heat-resisting, deformation and fracture rel. to grain-boundary reaction nodules 8-80591

Timoshenko type shells of composite material, nonlinear theory (*Russian*) 8-63283

transport properties of arrays of spheres, exact solns. 8-56120

two-component materials, thermo-viscoelastic theory 8-73854

viscoelastic properties modelling 8-75082

viscous composite, steady creep bending stresses 8-71280

vitroceramic-metal, development, Spacelab appl., mech. props. (*French*) 8-92229

wood-polymer composite, dynamic viscoelasticity and modulus (*Japanese*) 8-59356

zircon bricks, thermal conductivity meas. up to 1200°C (*Japanese*) 8-95193

Al-graphite particulate composite, exam. of friction, wear and tensile props. 8-72890

C-C composites, existence diagram and properties (*French*) 8-64517

C-PVC composite, fluctuation induced tunnelling conduction 8-52044

Cr₂O₃-Cr film, optical props., rel. to chemical/metallurgical constitution, appl. as solar absorber 8-56531

Cu-Al composite, simulation of tensile behaviour and fracture void initiation (*Japanese*) 8-52948

Cu-Fe, composite, simulation of tensile behaviour and fracture void initiation (*Japanese*) 8-52948

Fe-B alloy reinforced polysulphone exam. of tensile and flexure props. 8-72823

Fe-Fe₂O₃ composite films, structural props., microhardness, 250 to 700K 8-84095

γ-Fe₂O₃, small particle composite, preparation methods, superparamagnetism, optical transparency 8-60315

KCl-Al composite, optical and IR reflectance 8-56465

KCl-Al(Pd) composite, far IR absorption 8-56466

PVC-Cu, particulate composite, mech. props. effect of particle size 8-95799

PZT-polymer flexible composite transducer 8-80291

Pb-Al₂O₃ composites, mech. alloyed, hot hardness meas. (*Japanese*) 8-84830

Si-Al, composite, simulation of tensile behaviour and fracture void initiation (*Japanese*) 8-52948

Si-based, survey 8-56609

SiO₂ powder filled epoxy resin, flow props. during curing (*Japanese*) 8-59355

SiO₂-Ni granular metal films, minimum metallic cond. 8-56241

TiB₂-Al₂O₃, thermal stability of composite materials 8-60638

TiB₂-CaO, thermal stability of composite materials 8-60638

TiB₂-MgO, thermal stability of composite materials 8-60638

TiB₂-Y₂O₃, thermal stability of composite materials 8-60638

W-Cu composite materials, vel. dispersion and scatt. of transverse US waves 8-91383

W-ThO₂ composite, struct., lamination tendency, effects of method of manuf. 8-68653

WC-Co, sintered hard alloy, mechanism of penetration of liquid metals 8-60619

WC-Co composite, surface anal. by quantitative AES 8-76622

WC-Co composite chemical characterisation by AES and ISS 8-76621

WCuB prep. by infiltration of W skeleton by CuB, hardness meas. (*German*) 8-64508

Y₂O₃-TiB₂, ceramic, production by sintering in vacuo, or hot moulding at 1500°C 8-60629

ZrC-C composite system, electrical resist. meas., percolation theory anal. 8-84269

composite models of hadrons

see also *parton model*; *quark models*

Bethe-Salpeter wave function divergence at origin 8-74147

bilocal fields, ϕ^3 vertex, unitary S-matrix 8-62323

constituent rearrangement model, nonleptonic hyperon decay 8-62357

dual topological unitarisation, review of S-matrix developments for hadron bootstrap theory 8-62381

fixed angle and Regge behaviour, hard scatt., fragment x-distrib. 8-78154

hadronic resonance props., consideration as compound of bradyons and tachyons 8-58163

hadrons as compounds of bradyons and tachyons, ground state and decay anal. 8-58156

lepton bound states of sub-hadronic dimens., quark lepton relation 8-54609

meson bound state eqn. and solutions 8-78101

meson structure wave functions in relativistic straton model, Bethe-Salpeter eqn. (*Chinese*) 8-50011

composite models of hadrons continued

- MIT bag model for vector meson and baryon radiative decays 8-66110
 perturbation expansion of quantised composite field theory, gauge invariance (*Chinese*) 8-82156
 preon model for hadron and lepton struct. 8-78124
 rest-mass level density, statistical model of hadrons, non-interacting pions 8-62353
 straton model, bound states of mesons, average radii, pion appl. (*Chinese*) 8-78150
 straton model, near-flat-bottom interaction pot., wave function of pseudoscalar meson (*Chinese*) 8-82167
 straton model, SU(5) extension, descript. of new Y particles near 9.5 GeV (*Chinese*) 8-82168
 string type solns., in classical gauge field theories, broken gauge symmetry 8-62317
 SU(4)×S₃, straton model, meson classification (*Chinese*) 8-78145
 Δ(1232) isobar in nuclei, one-boson-exchange and straton model anal. (*Chinese*) 8-78275
 K⁺p→hyperon+X, 4-16 GeV/c, unified descript. of Λ, Λ, Σ⁺, Ξ⁻ prod., urbaryon model 8-66173
 p struct. anal. from high-energy pp expts. 8-62457
 pp scatt., high energy, impact picture for polarisation and rotation parameter 8-70341
 π, wave function renormalisation const., upper bounds 8-74215

composite particles

- see also alpha-particles; deuterons; nuclei with mass number 1 to 5; tritons
 No entries

composite superconductors

- continuous resistive transition self-field instability depend. 8-50369
 eddy current losses 8-62636
 effect of axial conduction and metal-helium heat transfer 8-91832
 integrated composite conductor for fusion program 8-62631
 multifilamentary, current transfer, expt. results for NbTi- and Nb₃Sn 8-72316
 multifilamentary, current transfer, theory 8-72315
 multifilamentary, losses in coil 8-62637
 multifilamentary superconductor, current distrib. close to input leads 8-84363
 partial quench and recovery, simulation, transient heat transfer expt. 8-83219
 technical superconductors, requirements and basic properties (*Slovak*) 8-88069
 Ag-Nb-Ga, phase relations, A15 phase diffusion layer formation 8-52764
 Cu, electrical conductivity, effect of cyclic strains and work hardening at 4.2K 8-91655
 Nb alloys, for appl. in magnets, technology (*Dutch*) 8-49871
 Nb wire, Cu clad, supercond., Meissner effect in Cu meas. 8-64166
 Nb-Ti, Cu clad, Meissner effect in Cu Meas. 8-64166
 Nb-Ti, multi-filamentary superconducting wires, mag. field dependence of AC losses 8-60256
 Nb₃Ge, supercond. tape, growth technique via amorphous state 8-84708
 Nb₃Sn, filamentary segments, flux pinning, proximity effects, percolation thresholds 8-56269
 Nb₃Sn composite processes with Cu-Sn-Zn matrix, superconducting props. 8-84370
 Nb₃Sn, current transfer, theory 8-72315
 Nb₃Sn, current transfer, expt. results 8-72316
 Nb₃Sn, filamentary, fatigue tests on small coils 8-64652
 Nb₃Sn, filamentary conductors, type-II, low temp. 30 GeV proton effects on critical props. 8-52178
 Nb₃Sn, multifilament conductors, strain-crit. current meas. 8-64174
 Nb₃Sn multifilament conductors, strain effect on crit. props. 8-80108
 Nb₃Sn, neutron irradi. effect on supercond. fusion magnet props. 8-52128
 NbTi, current transfer, theory 8-72315
 NbTi, current transfer, expt. results 8-72316
 NbTi filament reinforced Cu, superconducting composite, elastic const., temp. depend. 8-68717
 NbTi, filamentary conductors, type-II, low temp. 30 GeV proton effects on critical props. 8-52178
 NbTi, neutron irradi. effect on supercond. fusion magnet props. 8-52128
 V-Al/Cu-Ge composite tape, transition temp., upper crit. field 8-68126
 V₃Ga, filamentary conductors, type-II, low temp. 30 GeV proton effects on critical props. 8-52178
 V₃Ga, high current density multifilament wire, neutron effects on equilibrium and transport props. 8-52126
 V₃Ge, bronze-processed, stress-induced enhancement of supercond. T_c 8-64159
 V₃HfZr, C-15 cryst. struct. supercond. props. 8-64173
 V₃Si, supercond. tape, growth technique via amorphous state 8-84708

composition measurement see chemical analysis**compressibility**

- see also compressibility of gases; compressibility of liquids; compressive strength
 alkali hydrides, bulk props. prediction from molecular behaviour 8-51468
 alkali metal, model potential calculation of binding energy and compressibility 8-91632
 bar (tube), compressible, combined loading, elastic-plastic problem 8-63311
 bovine hip bone, compression tests, effect of specimen shape and size on mech. props. and fracture mode 8-69132
 calcite rock, compression wave studies 8-81151
 chlorite, cryst. struct. and compressibility at high press. 8-63717
 hard-alloy powder mixtures, compressibility in hydrostatic working 8-68645
 intermetallic phases with L1₂ and D0₁₉ struct., atom incompressibility, lattice parameter approach 8-91294
 Kaprolon, compressibility, elec. cond., sound vel. behind shock front 8-95105
 metal, BCC, neutron irradiated, spontaneous recombination volumes of Frenkel defects, rel. to compressibility 8-71765
 modelling by steel spheres, packing density coeff. 8-84916

compressibility continued

- partially ionised fluid, thermal instability, compressibility and collisional effects 8-55693
 particles, small, impossibility of comminution by compression 8-52709
 phlogopite, cryst. struct. and compressibility at high press. 8-63717
 spatial elastica theory with centrelinc compressibility 8-79211
 zincblende structure group IVA covalent crystals, Murnaghan parameter estimates from Morse pot. 8-95014
 Ag, isothermal compression curves to 120 kbar, X-ray diffr. study 8-83876
 AgBr(Cl), formation vol. of Frenkel defect 8-79606
 Al, isothermal compression curves to 120 kbar, X-ray diffr. study 8-83876
 BP, sq. ht., Debye temp., compressibility and Gruneisen coeff. meas. 8-63865
 CF, X-ray diffr., high press. effect 8-83766
 Ca₃Al₂Si₂O₁₂, grossular, cryst. struct. and compressibility to 60 kbar 8-63718
 CdCr₂S₄, thermodyn. props. 8-51703
 Fe and related compounds, hydrostatic compression expts. 8-83862
 Fe, atomised powder compacts for mag. cores, oxidation, compressibility, heat treatment (*Japanese*) 8-72752
 Fe based porous metals, exam. of volume change under high pressure 8-52906
 α-Fe₂O₃ (haematite), X-ray diffr. compression studies under hydrostatic isothermal conditions 8-85539
 KCN, crystal props., log potential model calc. 8-63829
 Mg₃Al₂Si₂O₁₂, pyrope, cryst. struct. and compressibility to 60 kbar 8-63718
 Mg₂Cd, effect on order, of compression deformation 8-52924
 MgIn, X-ray diffr. exam. of compressibility 8-51610
 NaCN, crystal props., log potential model calc. 8-63829
 NaF, ab-initio calc. of cohesion energy, compressibility and density 8-71782
 α-NbD₃, under hydrostatic press., γ ray diffr., Bragg refls. 8-75726
 Ni based porous metals, exam. of volume change under high pressure 8-52906
 RbCN, crystal props., log potential model calc. 8-63829
 Se, vitreous, mech. props. at temps. <300K, uniaxial compression tests (*French*) 8-55908
 SmS, vol. changes at press. up to 20 kbar 8-71791
 SnS₂ berndite, cryst. struct. and compressibility at high press. 8-67685
 WC-Co, various combinations, fracture characts. in bending, compression, and toughness tests 8-60808
- compressibility of gases**
 see also high pressure phenomena and effects
 high pressure physics and technology, conf., Moscow, Russia (May 1975) 8-51611
 mixtures, thermodynamic props. prediction 8-83512
 thermal-diffusion coupled appl. to gas compression and decompression with porous material 8-94882
 thermophysical props. tabulated for mixture composition certification 8-80818
 N₂, thermodynamic and transport props., consistent correlation using Lennard-Jones (12-6) and Buckingham (exp-6) pots. 8-91045
- compressibility of liquids**
 acetonitrile-methanol, excess vol. and isentropic compressibility, from density and US vel. meas. 8-79776
 aqueous non-electrolytes, solution structure, adiabatic compressibility studies 8-87605
 benzene-ethanol, excess vol. and isentropic compressibility, from density and US vel. meas. 8-79776
 benzene-n-heptane, excess vol. and isentropic compressibility, from density and US vel. meas. 8-79776
 benzyl alcohol-n-butanol, excess vol. and isentropic compressibility, from density and US vel. meas. 8-79776
 binary liquid alloys, surface tension, compressibility and surface segregation 8-67889
 bromobenzene+m-xylene, US vel. and adiabatic compressibility 8-51614
 n-butyl alcohol, dil. aq. soln., US vel., 4.04 MHz 8-67770
 ethyl alcohol, dil. aq. soln., US vel., 4.04 MHz 8-67770
 glycerol, influence of electrolytes on acoustic props. 8-75728
 hexantriol-1,2,6, influence of electrolytes on acoustic props. 8-75728
 metal, long wavelength limit of liquid struct. factor, compressibility 8-67633
 metals, compressibility calc. by struct. factor (*Russian*) 8-59847
 metals, liq., compressibilities, surface tension at melting temp. 8-91370
 methyl alcohol, dil. aq. soln., US vel., 4.04 MHz 8-67770
 polythene melts of high density, viscosity meas., entropy and compressibility (*German*) 8-67162
 polyvalent electrolyte apparent molal adiabatic compressibility and US vel. obs. 8-61028
 n-propyl alcohol, dil. aq. soln., US vel., 4.04 MHz 8-67770
 rare gases, liquid, long wavelength limit of liquid struct. factor, compressibility 8-67633
 ternary liquid mixtures, molecular interaction and thermodynamic props. 8-59861
 ternary liquid mixtures, nonlinear effects with high amplitude US prop. 8-51613
 thermophysical properties rel. to compressibility 8-83964
 water, compressibility modulus 8-75701
 Al, liquid, dynamical struct. factor 8-71667
 Al₂(SO₄)₃ soln., adiabatic and apparent molal compressibility determ. from US vel. meas. 8-63797
 CaCl₂×5.99.5.33H₂O, molar cond., compressibility, expansivity 8-51712
 CdCl₂-NaCl, KCl molten salt mixtures, US velocity and adiabatic compressibility obs. 8-75730
 Ce₂(SO₄)₃ soln., adiabatic and apparent molal compressibility determ. from US vel. meas. 8-63797
 NiCl₂, aq. soln., viscosity meas., struct. props. 8-75863
- compressible flow**
 see also compressibility
 axial-flow compressor cascade flows computer simulation 8-79333
 axisymmetric confined flame, aerodynamic and heat transfer, finite difference scheme, program 8-94689
 blunt-based axisymmetric body, subsonic turbulent near-wake 8-94740

compressible flow continued

- boundary layer flow, laminar, thermal response behaviour 8-75136
- boundary layer flow singular nonlinear differential eqns. 8-63413
- casades with different trailing edge thicknesses, vortex shedding freq. determ. 8-75152
- cavitating fluid model (*Russian*) 8-55668
- curved wall, turbulent boundary layer detachment by perpendicular compressive thrust (*German*) 8-94661
- elastic porous media, transient compressible liq. flow, linearisation of nonlinear partial differential eqn. 8-63490
- elastic shells, excitation and stress field in compressible fluid 8-51183
- expansion of compressible fluid in venturi, critical rate determ. (*French*) 8-55659
- flow around lattice, calc. by successive approxs. (*Russian*) 8-63443
- gas centrifuge, effect of compressible flow on max. separating power 8-70644
- gas flow in catalytic convertor, numerical soln. 8-67281
- gas jet transport system, steady state, radioactive distrib. in compressible stream tube (*German*) 8-90007
- hodograph eqn., numerical soln. 8-51179
- jet, circ., controlled perturbation, smoke visualisation 8-90956
- jet, circ., free shear layer transition wave development 8-94643
- jet, supersonic, flowing onto infinite perpendicular barrier, limiting expansion ratio 8-59439
- jet, turbulent, plane, impinging on plane surface, RMS boundary press. pulsations 8-59438
- laminar compressible boundary layer swirling flow in nozzle, flow and heat transfer 8-94795
- MHD shear flow stability 8-51244
- Navier-Stokes equations, Lighthill's theory to non-adiabatic cases 8-83372
- nonadiabatic compressible gas flow in tube, eqns. system numerical integration (*Russian*) 8-83427
- perfect fluid, irrotational stationary flows, unicity condition (*French*) 8-87356
- plane plastic flow of compressible solids 8-55575
- Rankine-Hugoniot jump conditions, viscous and thermal effects 8-59418
- rotating cylinder, linearsed anal., appl. to gas centrifuges 8-71345
- shock layer, hypersonic, vibr. nonequib., near stagnation streamline, low Reynolds no. flow 8-87417
- sound amplification in nonuniform flow 8-83158
- spheroids, harmonically oscillating, unsteady airload prediction, analytical soln. 8-51184
- study, gas dynamics method based on iterative techniques (*Hungarian*) 8-94757
- supersonic flow, wake of axisymmetric body, ideal gas, numerical anal. 8-59420
- turbulent boundary layer, compressible, extended mixing length appls. 8-94655
- turbulent boundary layer, supersonic, wall temp. effect 8-94765
- turbulent boundary layer generation in unsteady flow 8-90828
- turbulent boundary layer with heat transfer, surface roughness 8-90931
- turbulent tube flow, heat transfer 8-71314
- turbulent vel. profiles at transonic vels., local skin friction coeff. 8-67214
- two-dimensional gas flow model, comparison of two methods of computation (*Russian*) 8-59413
- two-dimensional jet flow in ideal compressible gas, calc. method 8-83448
- two-parameter skin friction formula for adiabatic compressible flow, shocked relaxing boundary layer 8-51188
- two-phase flow, compressibility effect on hydrodynamics, resistance coeff. 8-55684
- variable domain finite element model for dam unsteady compressible fluid flow digital simulation 8-90820
- variational principle for compressible heavy fluid 8-83426
- viscous compressible fluid, wave perturbations (*Russian*) 8-75161
- water-entrained gas flow, force on moving body 8-63480
- waves on axisymm. mean flows in compressible atms., generalised Elias-sen-Palm and Charney-Drazin theorems 8-81306
- N₂, cryogenic, shock wave-boundary layer interaction (*German*) 8-71370

compression, bandwidth see *bandwidth compression*

compressive strength

- see also *compressibility*
- anvil, truncated, compressive strength, high press. apparatus appl. 8-84906
- brittle material, statistical and micromech. theory 8-64618
- brittle materials, diametral compression tests, tensile strength meas., appl. to biaxial stress fracture (*Japanese*) 8-72840
- brittle materials, diametral compressive stress considering Hertzian contact, fracture and tensile strength meas. (*Japanese*) 8-72946
- brittle materials, strength in nonuniform triaxial compression 8-76725
- cement mortar, deform. charact., expt. study (*Japanese*) 8-56704
- ceramics, microstructure dependence of mechanical behaviour 8-88533
- compact bone, empirical strength theory, biaxial stress characts. 8-77081
- compression failure anal., glassy materials investigation 8-55608
- concrete, US testing of compressive strength (*German*) 8-68847
- concrete masonry units, mixed with pelletised slag 8-52707
- epoxy, Al₂O₃-filled, shock-wave compression, 0.4-3.7 GPa 8-59856
- epoxy resin, low temp. irradiation effects on mechanical props., use in superconducting magnets 8-60737
- epoxy resin adhesives, crack propag. and mech. props. 8-68783
- furan resin, effect of silica fillers (*Polish*) 8-68740
- glass fibre reinforced epoxy, as electrical insulation for Tokamak toroidal field coils, mech. props. 8-64610
- glass fibre reinforced plastics, under compressive load (*Japanese*) 8-92301
- glass fibre reinforced polymer matrix laminates, compressive strength 8-64609
- glass microsphere reinforced, composite, mech. charact. calc. 8-64578
- granite, weathered, bearing capacity determined by graphical soln. of pole trail method (*Japanese*) 8-56706
- granodiorite, fracture under uniaxial compression, mech. and AE meas. (*Japanese*) 8-56748

compressive strength continued

- graphite, diametral compressive strength, comparison with uniaxial tensile strength (*Japanese*) 8-72947
- graphite, structural, impact toughness, reln. to compressive strength 8-88605
- graphite/epoxy laminates fatigue characts. under compression loading 8-84971
- marble, Italian Ondagata, diametral compressive strength, comparison with uniaxial tensile strength (*Japanese*) 8-72947
- nylon, oriented, transverse compression 8-68728
- plate, obliquely stiffened, subjected to uniform compression, buckling strength (*Japanese*) 8-67067
- polyethylene, high density, crystalline, flat stressed state, yield point time-temp. factors 8-64601
- polyethylene, orientated, var. of yield stress with orientation, yield criteria exam. 8-52900
- polyethylene extrudate, transverse compression 8-68728
- polyurethane foam, rigid integral, effect on flexural and compressive strength, due to tall oil oligoether 8-68743
- rings, bearing capacity under compression 8-83256
- rock, deformation and fracture under general triaxial stress states, anisotropic dilatancy (*Japanese*) 8-56750
- rock materials, strength determ. in triaxial compression, suggested methods 8-81432
- rocks, failure processes and AE under compression (*Japanese*) 8-56749
- rotationally restrained orthotropic plates under uniaxial compression, buckling 8-67065
- rubber, creep processes associated with uniaxial compression 8-68734
- sea ice, failure by compression (*Japanese*) 8-88841
- steel, alloy, static and fatigue strength, tension and compression test results 8-95810
- steel, high-speed, quenched and tempered notch toughness, ultimate and yield strength in tension and compression 8-95782
- steel, shell, circ. integrally stringer-stiffened, buckling under axial compression 8-63346
- steel plate collapse, anal. by live energy minimisation 8-52910
- thick-walled tubes, compression by external pressure, expt. data, modified plasticity theory 8-59316
- tuff, deform. charact., expt. study (*Japanese*) 8-56704
- Al alloy 7075-T6, buckling under axial compression on circ. integrally stringer-stiffened shell 8-63346
- Cu₂O, creep substruct. under compression, X-ray diff. study 8-95785
- Fe, cast, pearlitic, residual compressive stress distrib. effect on resultant stress conc. in notched samples 8-92336
- Mo, polycrystalline, fracture and ductile-brittle transition, hydrostatic press. effects 8-60735
- Nb₃Sn, filamentary, fatigue tests on small coils 8-64652
- Ni₃Al, ductility in poly- and single crystals, compressive and tensile tests 8-56715
- Sb-Ge, unidirectionally solidified, exam. of compressive props. and struct. 8-68730
- Si₃N₄, hot pressed, high temp. compressive cracking, optical and electron microscopy exam. 8-76733
- W-WC, activated sintering, mech. props. (*Korean*) 8-60622
- WC-Co (TiC-Co), powder compacts, effect of additional pressing at hydrostatic pressures on props. 8-56596

compressors

- axial-flow compressor cascade flows computer simulation 8-79333
- manifold, fluid induced damping 8-83164
- membrane compressor for inert gas and mixtures 8-86286
- vapour compression distillation unit, compressor and flow system matching 8-83931
- zero mechanical work thermal compressor or pump, in high speed rotating frame 8-57962

Compton effect

- adjoint photon transport, Monte Carlo biasing scheme, Compton scatt. and absorpt. 8-77819
- atmosphere, γ -radn. EM effects, Compton electron currents 8-93020
- benzene, mol., directional Compton profile, ab initio SCF LCAO MO calc. 8-62857
- bound and free electron Compton scatt. in coherent EM field 8-94225
- cis- and trans-2-butene, Compton profiles, theory and expt. 8-50597
- α Carinae (Canopus), generalised Compton effect in spectrum 8-53938
- Compton currents, historical aspects and recollections 8-80018
- diamond, Compton profiles, X-ray struct. factors, band struct., LCAO calc. 8-51889
- education, Compton collision formula and Klein-Nishina formula ang. depend. verification, undergraduate expt. 8-62010
- electron mass operator in plane wave field, near cyclotron reson. region (*Russian*) 8-86432
- form factors, off-shell, use of Ward identity for Compton scatt. polarisability 8-66120
- gamma ray spectrometer, collimator system, intensity profile meas., construction 8-90013
- induced Compton scattering in pulsar winds 8-96497
- intermediate-Z elements, γ -ray scatt. from K-shell electrons, Compton scatt. cross-sections 8-58643
- kinetic energy in Compton profiles 8-72628
- low energy proton Compton scattering, p polarisabilities 8-93886
- microwave background radiation spectrum, evidence for Compton distortions 8-86039
- molecular isoelectronic series, Compton profile, empirical correlation with energy 8-78758
- monochromatic photon beam generation by high energy electron beam (*Japanese*) 8-74821
- moving mirror reflection analogy to the Compton effect 8-82218
- nonlinear inverse Compton radiation spectrum, deepest descents method 8-85840
- proton differential cross sections, 450 to 950 MeV 8-93885
- protons, Compton scatt., Regge pole model 8-93884
- pulsar synchro-Compton radiation damping of linearly polarised plasma waves 8-61877
- QSOs and BL Lacertae type objects, physical problems 8-57649
- radiative transitions, classical theory appl. 8-74597
- relativistic Compton laser, power potentiality (*Russian*) 8-90405
- scintigraphy, multichannel, collimated, Compton effect on spatial resolution, digital spatial filtering 8-69182

Compton effect continued

- stimulated Compton scattering and related phenomena, book contrib. 8-82219
 thermodynamic data determ. by X-ray and neutron scatt. 8-83974
 transition metal, 3d, paramag., energy band calcs. 8-91608
 urea, single crystal Compton profiles, H-bonding and dimer config. effects, calc. and meas. 8-80431
 X-ray emission spectrum, multiple Compton scatts. effect, Monte Carlo calcs. 8-96389
 Ag, integral K-shell Compton scattering, cross-section, for 1250 keV photons 8-90128
 Al, Compton profile from 662 keV γ -ray spectroscopy 8-56539
 Ar, Compton profile, local density approx., Kohn-Sham self consistent scheme 8-94193
 Ar, impulse Compton profiles, atomic optimised pot. model 8-74618
 Be, anisotropy, theoretical investigation by K-emission, APS, and Compton profiles 8-63970
 Cd, integral K-shell Compton scattering, cross-section, for 1250 keV photons 8-90128
 Co_{49.6}Al_{50.4}, Compton scatt., 59.54 keV γ -rays, charge transfer study 8-68578
 F₂, Compton scatt. profile, SCF MO theory calcs. 8-58577
 Fe, Compton profile from 662 keV γ -ray spectroscopy 8-56539
 Fe_{49.7}Al_{50.3}, Compton scatt., 59.54 keV γ -rays, charge transfer study 8-68578
 H₂, electron impact spectroscopy for Compton profile meas. 8-90299
 He, electron impact spectroscopy for Compton profile meas. 8-90299
 In, integral K-shell Compton scattering, cross-section, for 1250 keV photons 8-90128
 KBr, Compton profile, 59.54 keV γ -rays 8-64426
 KCl, Compton profile, 59.54 keV γ -rays 8-64426
 KF, Compton profile, 59.54 keV γ -rays 8-64426
 Kr, Compton profile, local density approx., Kohn-Sham self consistent scheme 8-94193
 Kr, impulse Compton profiles, atomic optimised pot. model 8-74618
 Mo, integral K-shell Compton scattering, cross-section, for 1250 keV photons 8-90128
 NaBr, Compton profile, 59.54 keV γ -rays 8-64426
 NaCl, Compton profile, 59.54 keV γ -rays 8-64426
 NaF, Compton profile, 59.54 keV γ -rays 8-64426
 Nb, integral K-shell Compton scattering, cross-section, for 1250 keV photons 8-90128
 Ne, Compton profile, local density approx., Kohn-Sham self consistent scheme 8-94193
 Ne, impulse Compton profiles, atomic optimised pot. model 8-74618
 Pd, Compton profiles, comparison with band struct. calcs. 8-84675
 PdH_{0.72}, Compton profiles, comparison with band struct. calcs. 8-84675
 PdH_{0.72}, Compton profile, electronic struct. (German) 8-92140
 Sb, integral K-shell Compton scattering, cross-section, for 1250 keV photons 8-90128
 SiO₂, amorphous and cryst., Compton profile study 8-88378
 Sn, integral K-shell Compton scattering, cross-section, for 1250 keV photons 8-90128
 V, Compton profiles, comparison with band struct. calcs. 8-84675
 V, energy bands, calcs. using LCGO method 8-91608
 VD_{0.77}, Compton profile, electronic struct. (German) 8-92140
 VD_{0.77}, Compton profiles, comparison with band struct. calcs. 8-84675
 VH_{0.71}, Compton profile, electronic struct. (German) 8-92140
 VH_{0.71}, Compton profiles, comparison with band struct. calcs. 8-84675

Compton profile *see* Compton effect

Compton scattering *see* Compton effect

computation *see* calculation

computer-aided analysis

- see also analogue simulation; CAD; circuit analysis computing; digital simulation; electric machine analysis computing; hybrid simulation*
 analytical chemistry, user-oriented software Fourier spectrum display 8-64896
 axially symmetric hollow collectors for high temp. solar installations, radiative heat transfer computation 8-79093
 cultured cells time lapse cinemicrographs 8-92756
 electrical conductivity and threshold switching in non-cryst. semiconds. of computer simulation 8-88002
 human gait, representation by 4 dimens. vectors (German) 8-88723
 Japanese kinki dialect, anal. and perception of two-mora word accent types (Japanese) 8-92659
 memory function, transverse current correlations in classical one component plasma 8-94892
 optical fibre connector, using resilient alignment method, finite element program 8-71230
 photon correlation in nanosecond range using programmable digital counter, photomultiplier evaluation 8-54464

computer-aided circuit analysis *see* circuit analysis computing

computer-aided circuit design *see* circuit CAD

computer-aided design *see* CAD

computer-aided instruction

- see also education*
 atomic orbitals, hydrogen-like, shape, teaching appl. 8-93496
 binary solid-liquid equilibria, student experiment, phase diagram computer program 8-89285
 celestial mechanics, diurnal motion of Sun seen from Mercury, computer aided soln. 8-61969
 computer physics, elementary concentrated one-week course 8-73799
 differential eqn. teaching with interdisciplinary models 8-77640
 educational technology and the computer 8-49615
 frontiers in education, conference, Urbana-Champaign (1977) 8-81779
 graphics for numerical analysis tuition 8-81817
 HMO theory, student use, computerised visual aids 8-77649
 microcomputer-based multiboard communication system for nonverbal handicapped children 8-57126
 Personalised System of Instruction, feedback with computer generated tests 8-69950
 physics CAL packages at Univ. of Surrey 8-81756
 programs for high-school expts. 8-86094
 simulated laboratory exercises, validity of graphic approach 8-81780
 teaching machines and conversation theory 8-49614

computer applications

see also CAD; complete computer programs; computer-aided analysis; computerised control; computerised instrumentation; computerised signal processing; engineering computing; natural sciences computing; subroutines
 resource management, conf., Alamogordo, NM, USA, 1978 8-69541

computer-generated holography

- n-colour complex kinoform, distortions in reconstructed image (Russian) 8-66790
 fast Fourier transform holography method 8-71064
 Fourier hologram machine synthesis (Czech) 8-66784
 gratings, prod. of two-dimens. laser beam deflections 8-58956
 phase determination of amplitude modulated complex wavefront 8-55305
 phase error reduction 8-74863
 scanner, computer produced hologram, with auxiliary reflector 8-71054
 space-variant holographic systems using phase-coded reference beams 8-74868
 volume holograms constructed from computer-generated masks 8-87026
 wave field three-dimensional energy distrib. 8-71009

computer graphic equipment

- see also interactive terminals; plotters*
 ECG 22 8-81027
 spectral data analysis using graphics display terminal 8-54473

computer graphics

- see also curve fitting*
 biostereochemical modelling, interactive computer graphics, appl. to DNA-protein interaction 8-88693
 graphics interface package for the HBOOK histogramming routine; subroutine package HPLLOT 8-89465
 gravity studies using the facilities of UMRCC and the Computer Graphics Unit 8-77878
 macromolecules, graphics model building and refinement system 8-75505
 meteorology, data editing and validation using interactive graphics 8-77330
 Mirror Fusion Test Facility, neutral beam injection, optimisation by computer graphics 8-66376
 molecular spatial models, Stuart-Briegleb type, computer construction 8-86970
 neurophysiology, computer assisted unit data acquisition/reduction 8-61266
 numerical anal. tuition, computer-aided 8-81817
 particle track data in plastics, rapid anal. using interactive programming and graphic displays 8-66456
 PDP-15 interactive graphics, appl. to seismic surface waves anal. 8-81427
 phase diagrams, computer generated for ethylene and propylene 8-83928
 simulated laboratory exercises, validity of graphic approach 8-81780
 TRIPLLOT, APL program for plotting triangular diagrams 8-57335
 X-ray tomography dynamic boundary surface detection 8-53479

computer interfaces

- see also CAMAC; data communication equipment*
 Barkhausen effect, mag. thin films, statistical anal., instrumentation, computer interfacing 8-82008
 Cary 118C spectrophotometer, universal computer interface 8-73972
 microcomputer-based data acquisition system for NMR spectrometer interfacing 8-74042
 Varian EM-360 NMR spectrometer interface with Altair 8800B microcomputer 8-89519
 visual stimulator for electrophysiology expts. 8-69230
 X-Y recorder for Auger spectrometer using pulse height analyser 8-49942

computer networks

- King Faisal Specialist Hospital (Saudi Arabia) information system 8-57105

computer operator training *see* training

computer printers *see* printers

computer programming *see* programming

computer programs, complete *see* complete computer programs

computer programs (listings) *see* complete computer programs

computer science education

- computer physics, elementary concentrated one-week course 8-73799

computer software

- not used for applications software for which see specific applications*
see also programming
 reliability and maintainability symposium, Los Angeles (1978) 8-50250

computer storage devices *see* storage devices

computer subroutines *see* subroutines

computerised communications control *see* communications computer control computerised control

- see also communications computer control; control engineering computing; direct digital control; electrical engineering computing; mechanical engineering computing; nuclear engineering computing*
 annealing of electron field emitters and multiple multichannel analyser, precision temp. regulator 8-86384
 biomedical applications of microprocessors 8-57095
 CERN proton synchrotron, stand alone control system for continuous transfer ejection to SPS 8-82552
 digital thermal field analysers 8-82034
 drip feed unit microprocessor control development 8-53563
 fusion reactor, 2XIIB, neutral beam injector system, automated control 8-62620
 fusion reactor, pulsed expts., computer-based control systems 8-62624
 isolated heart preparation appl. for biomedical research 8-53603
 JET, control and data acquisition system, CODAS 8-62619
 manipulator, computer controlled, for use as remotely controlled arm 8-81083
 microcomputer-aided arm prosthesis using myoelectric pattern recognition 8-53576
 microcomputer-controlled instrument for electrochemical studies 8-73128
 microprocessor control systems for nuclear power plants, program reliability (Spanish) 8-58369

computerised control continued

- multiple projector presentation, slide projection control using microprocessor 8-55425
- nuclear fuel reprocessing facilities continuous criticality control, dynamic approach 8-50291
- on-line ECIL TDC-312 computer-controlled four-circle neutron diffractometer 8-55787
- paraplegics' multitask exoskeleton computer control 8-53580
- particle size meas. by laser beam expt. 8-70098
- PLT, neutral beam test stand, data acquisition system 8-62622
- polisher, controlled, for optical fabrication 8-75006
- robots and manipulators, symposium, Warsaw (Sept., 1976) 8-53574
- Scylla IV-P, computer-based control and data acquisition system for CTR 8-62621
- sonar, fibre optic system, geological and hydrographic survey applications 8-88947
- tetraplegics' jointed manipulator with joystick control 8-53581
- Tokamak plasma equilibrium, feedback control 8-55738
- underwater robot/manipulator, development and remote control 8-77356
- upper-limb prostheses multifunctional control microprocessor system, myoelectric signal identification method 8-88766
- Wyoming Infrared Telescope (Jelm Mountain), computer control 8-85848

computerised instrumentation

- see also *astronomy computing; astrophysics computing; automatic test equipment; biology computing; chemistry computing; computerised monitoring; computerised spectroscopy; computerised tomography; electrical engineering computing; electronic engineering computing; geophysics computing; nuclear engineering computing; physics computing*
- acoustic excitation impulse generator 8-90618
- astronomical laser ranging equipment, computer system (*Japanese*) 8-89080
- audiometer, screening, and real-time computer techniques 8-81009
- auditory evoked responses, computer driven bipolar stimulator 8-57011
- automated shipboard acquisition and processing of offshore geophys. data (*Russian*) 8-53750
- automated visual edge match system for image quality assessment 8-62218
- automatic calorimeter system for bolometer mount effective efficiency meas. in 35 GHz band 8-86272
- automatic evaluation of isotope anal. of nuclear fuels, isotope dilution, mass and α spectrometry 8-55120
- automatic network analyser, EM reflection coeff. meas., calibration 8-89463
- biomedical applications of microprocessors 8-57095
- blink comparator, semi-automated, for large photographic plates (*Japanese*) 8-89081
- body motion computer-aided tracking using CCD image sensor 8-61269
- body radioactivity measurement, SABRE 3 computer system 8-85425
- brain impedograph 8-77139
- cardiac output measurement, in vitro comparison of six commercially available thermodilution systems 8-77135
- cardiac radionuclide cineangiography, clinical utility of real-time computer-based system 8-80957
- cardiology, conf., Rotterdam, Netherlands, (Sep.-Oct. 1977) 8-81013
- chemical, analyser design impact of microprocessors (*German*) 8-61096
- chromatography, microprocessor based low cost data processor (*Japanese*) 8-61131
- co-ordinate reader, using X-Y plotter and HP 9830A calculator (*French*) 8-77886
- colorimeter, Zeiss DMC 26 universal model (*German*) 8-54432
- conference, Gaithersburg, MD, USA (1978) 8-70104
- coordinate measurement, computerised, problem oriented language MAUS (*German*) 8-89432
- coordinate measurement, mating simulation (*German*) 8-77846
- coronary sinus blood flow on-line computerised assessment by thermodilution 8-81024
- CRO design using modular system 8-93671
- data logger, YODAC-8, microprocessor controlled, for temp. data acquisition 8-49813
- dielectric loss meas., on-line calculator-based system 8-54397
- digital transient recorders, enhancement of signal averaging using microcomputer 8-57930
- dosimetry, automated data acquisition and anal. system at LAMPF pion therapy facility 8-53506
- drift tubes, ion time of arrival spectra determ., using CAMAC crate interfaced to microcomputer 8-93661
- ECG analysis system, application to hypoxic rat ECGs 8-57088
- ECG microcomputer-based evaluation system, improving diagnostic capabilities 8-88761
- EEG frequency analyser, real-time, microprocessor monitored 8-57092
- EEG phasic event detection by microprocessor 8-57091
- effective annealing time determ. using analogue computer 8-88475
- electric impedance meas., microprocessor-based, advantages 8-89501
- electron microprobe, automated, evolution of quantitative elementary point anal. in geosciences (*French*) 8-78046
- electron spectroscopy, features 8-86390
- electron test accelerator, Chalk River, control computer 8-90004
- electronic microbalance and precision balance design (*German*) 8-57935
- exercise ECG computer-assisted anal., implementation and clinical anal. 8-81051
- eye refractor, automatic, optical system 8-61274
- Fabry-Perot interferometer, microcomputer stabilisation 8-74055
- faradaic admittance, rapid drop time on-line FFT meas. 8-92544
- film, large format, for use with laser scanning system 8-62260
- Fizeau wavelength meter, laser and other monochromatic sources, digital display 8-89450
- foot/floor contact temporal patterns during walking, automated on-line meas. system 8-77128
- force distribution under human foot, online meas. system 8-96110
- forward scattered light system for optical fibre diameter meas. 8-62176
- fusion reactor ignition, eight-beam CO₂ laser system, minicomputer-CAMAC control system 8-58493

computerised instrumentation continued

- hardwired image analyser software control 8-57917
- high performance liquid chromatography, automation 8-80806
- holographic interferograms evaluation, of thermal boundary layers (*Czech*) 8-62220
- hybrid computer for chemical reaction residence time meas. 8-81953
- illumination measurement using photoresistors, digital linearisation using microprocessors (*German*) 8-77961
- interferometer phase detection using LSI-11 microcomputer and high-speed digital techniques 8-71545
- intravenous antiarrhythmic drug infusion, automated delivery 8-81058
- isochronous cyclotron mag. field automatic meas. system 8-82547
- laser data acquisition/analysis system for Si vidicon optical detector 8-58041
- laser wavemeter, inexpensive broadband optics and minicomputer interface 8-89448
- local circulatory system characterisation by CW Doppler US flow meas. 8-57109
- medical US imaging, digital scan convertor system using microprocessor 8-96082
- microcomputer system for automating analytical instrumentation 8-73127
- microcomputer-based data acquisition system for NMR spectrometer interfacing 8-74042
- microcomputer-based digital titrator 8-80805
- microcomputers in biomedical and clinical applications 8-73283
- microprocessor based instrument, Dinamap, for arterial press. automatic determ. 8-96108
- microprocessor based system for ECG analysis, design and development 8-73287
- microprocessor for optical processing system noise analogue signals 8-81955
- microprogrammable integrated meteorological data acquisition system 8-77374
- minicomputer for condenser capacitance and loss tangent meas. (*Russian*) 8-70159
- mobile gamma camera with remote image processing computer system, for nuclear medicine 8-92700
- motor unit recruitment and firing freq. control in elec. stimulated muscles of cat 8-81092
- multichannel precision temperature measuring device, minicomputer, Pt 100 resistance thermometer appl. (*German*) 8-77914
- multichannel system for radioastronomical data recording and processing in real time (*Russian*) 8-65507
- multiple response parameters meas. 8-57136
- multivariate discrete information analyser, particle recording appl. 8-78601
- neutral beam system, 120 keV, for fusion reactor ignition 8-66377
- nuclear medicine, sequential method for high 3D resolution imaging 8-53489
- nuclear medicine diagnostics, for teaching 8-49618
- nuclear reaction thresholds and half-life meas., computer controlled system 8-55114
- nuclear reactor in-core meas. (*Czech*) 8-86637
- oceanographic, Kiel multi-purpose sea probe microprocessor-based data acquisition system (*German*) 8-85701
- oil prospecting, new seismic reflection techniques 8-73541
- on-line ECIL TDC-312 computer-controlled four-circle neutron diffractometer 8-55787
- optical plotter, computer controlled, for filter generation (*French*) 8-90538
- phase-locked interferometry 8-58022
- phoneme recognition system based on human audition, psychophysical expts. 8-69115
- plasma electron temp. and density meas., semiautomatic system for double probe anal. 8-87490
- polarimeter, elliptical, for astronomy and atm. sciences 8-61745
- potentiometer, microprocessor-controlled, for nanovolt meas. 8-89502
- potentiometric titration system, microcomputer controlled, for soln. equilib. obs. 8-92522
- potentiostat, computer interfaceable 8-57976
- pulse radiolysis system 8-64862
- quadrupole gas analyser with integral microprocessor 8-73109
- radiation absorption measuring instrument characs. evaluation with reference to information theory (*German*) 8-86753
- radioastronomical data reduction, via digital electronic integrator (*Russian*) 8-74465
- radionuclide cardiology, off-line viewing using videotape 8-65119
- rapid temperature change measurement, computerised thermistor cct. 8-49829
- real time moire topography equipment controlled by microcomputer 8-89441
- real-time ECG contour anal. program using microprocessor system 8-73288
- recorder, six colour, six channel, synchronised by a microprocessor (*French*) 8-77885
- reference averaging radiometer using microprocessor 8-70176
- scintigraphy and angiography, equipment for quant. evaluation and off-line operation (*German*) 8-88736
- SEM, automation, quant. anal. of elementary images (*French*) 8-78045
- solar acousto-optical radio spectrograph, data correction and calibration 8-73631
- solar data collection system using microprocessors 8-69542
- Solar Thermal Test Facility, 5 MW, heliostat focus and alignment system 8-50894
- spectrophotometer for colour measurement, flexible instrument with microprocessor 8-54428
- ST-segment response in exercise ECG, accurate automatic measurements 8-77140
- stopped-flow apparatus, data acquisition and processing using minicomputer (*German*) 8-53190
- stopped-flow systems, automated, for fast react. rate anal. methods, review 8-95971
- telescope control, zenithal blind spot of altazimuth-mounted equipment 8-53823
- temperature-jump apparatus, data acquisition and processing using minicomputer (*German*) 8-53190
- theodolites, electrooptical and microprocessor-based (*Czech*) 8-77860
- thermogravimetric data acquisition and reduction program 8-64901
- tomography, computerised, axial, for teaching 8-49619

computerised instrumentation continued

- tomography with X-ray beams (*German*) 8-53480
- TRIUMF biomedical pion beam automated dose mapping system 8-73254
- two-string balance microprocessor operation (*German*) 8-57936
- UTR-2 radiotelescope northern sky survey, expt. techniques and data processing 8-57461
- ventricle volume characts., nuclear medical determ., appl. of computer system (*German*) 8-88737
- video stereophotogrammetry, interactive computerised, for Mars Viking 1975 Lander data 8-81557
- video-tracking of micro-circulation, appl. of bit-slice processors (*German*) 8-88749
- visual evoked potential on-line evaluation by sliding average form. (*German*) 8-85402
- visual stimulator for electrophysiology expts. 8-69230
- voltammetry, cyclic differential pulse, computerised instrumentation 8-85235
- voltmeter, LF, fast response, microprocessor-based, for true RMS value 8-89503
- writing aid for motor handicapped, microprocessor-based device, LOGOS 8-81077
- X-ray diagnostic table, computer controlled, multidirectional, CAS-SETELESS spotfilm device (*Japanese*) 8-61278
- xerographic copy line profile meas. using microcomputer/microdensitometer system 8-74088
- H meters, on-line, calibration system 8-86236
- Rn-Th monitor for earthquake prediction research 8-73532

computerised monitoring

- air pollution, CO₂ laser long-path absorption system, automation 8-92971
- air pollution, on site automatic analysers review (*French*) 8-81451
- air pollution monitoring system, program system (*Japanese*) 8-81414
- arrhythmia detection using a low-power, CMOS processor 8-73276
- arrhythmia monitoring, ARGUS/RT microcomputer system 8-81014
- arrhythmia monitoring using interactive computer system, clinical evaluation 8-81028
- cardiac output and shunt calc. from dye dilution curves using automated catheterisation system 8-81023
- cardiac output automatic determ. by indicator dilution in computerised monitoring system 8-81022
- cardiac output on-line determ. by thermodilution in coronary care unit 8-81021
- cardiacirculatory computer-aided monitoring after open-heart surgery, appl. to adrenaline effects meas. 8-81059
- ECG, interactive analysis techniques with Random Access Mass Storage ECG Analysis System 8-81034
- ECG, monitoring abnormal QRS events, sequential improvements in on-line algorithm 8-81026
- ECG arrhythmia classification in context, extension of single-beat algorithm 8-85426
- intensive care in paediatrics (*German*) 8-88754
- intensive care unit, use and acceptance of automated monitoring systems 8-81057
- intensive monitoring computer system, SOLO, one-patient multiparameter bedside monitor 8-81053
- interactive lake survey programme for water resource surveillance 8-81257
- intravenous antiarrhythmic drug infusion, automated delivery 8-81058
- labour ward information and monitoring system (*German*) 8-88750
- microcomputer system for on-line analysis of electroencephalographic data 8-73277
- microcomputers for bedside monitoring of patients (*German*) 8-88751
- microcomputers in biomedical and clinical applications 8-73283
- motion online detection in digital video images, mice identification in labyrinth expts. (*German*) 8-92754
- n 8-85431
- nuclear power plants, diagnostic system using noise anal. 8-50279
- nuclear reactor pump coolant tests 8-70585
- oil spills remote monitoring, computer controlled laser radar system (*Japanese*) 8-92994
- oxyhaemoglobin dissociation curve direct obs. in man in vivo, computer investigation 8-85433
- particle size distrib., on-line measurement techniques, instruments (*German*) 8-60895
- patient monitoring, multi-microprocessor system (*German*) 8-88752
- radioactive effluent monitoring, symposium, Portoroz (1977) 8-89985
- remote diagnostic techniques used in Viking lander operations 8-57426
- spectrometer, semiconductor mosaic type, amplification-conversion tract meas./monitoring automation 8-78547
- steel weld fatigue life estimation, multichannel NDT monitor 8-56846
- systolic time interval processing system, STIPS 8-81029
- transcutaneous pO₂ measurement in computer-assisted monitoring of infants 8-85432
- vascular interface system for automation of haemodynamic monitoring and therapy 8-81054
- ventricular arrhythmia on-line study 8-81060
- ventricular fibrillation recognition using ECG power spectrum 8-81032
- vertebrate cornea, transparent layered structure thickness monitor 8-92737
- vibration, rotating laser light beam appl. (*Russian*) 8-71299

computerised navigation

- artificial satellites autonomous navigation problems, shoreline information 8-53732

computerised pattern recognition

- aerial photography rapid screening by optical power spectrum analysis 8-63033
- arrhythmia detector evaluation, ECG database development 8-81018
- arrhythmia monitoring using interactive computer system, clinical evaluation 8-81028
- automated pattern recognition with hybrid optical/digital systems 8-63037
- biological specimen pattern recognition via matched spatial filtering 8-69261
- blood cell differential counter, ADC 500, pattern recognition based image processing system 8-73282
- bubble chamber film, track rescue system 8-70728

computerised pattern recognition continued

- bubble chamber tracks, signal processing procedure for interimage identification 8-70727
 - cardiac arrhythmias diagnosis, online real-time pattern recognition (*Italian*) 8-85439
 - cardiac image description and analysis, interactive knowledge-based systems approach 8-81031
 - cell recognition and counting using adaptive coherent optical processor 8-77120
 - computerised tomographic scan data format 8-73243
 - continuous ECG processing program 8-92725
 - data extraction and classification from film, conf., San Diego, USA (Aug. 1977) 8-63023
 - ECG, ambulatory arrhythmia quantification by correl. technique 8-81020
 - ECG, computerised Holter tape processing systems for drug testing, validation technique 8-81017
 - ECG, Holter recording processing, computer system 8-81015
 - ECG, Holter tape dual-channel anal. system, ARGUS/2H 8-81016
 - ECG, monitoring abnormal QRS events, sequential improvements in on-line algorithm 8-81026
 - ECG and VCG, wave recognition algorithms for automatic QRS meas. (*German*) 8-69225
 - ECG arrhythmia classification in context, extension of single-beat algorithm 8-85426
 - ECG Holter analysis, appls. of Dyna-Gram IIIB system 8-81019
 - ECG/VCG, rhythm diagnosis using statistical signal anal., identification of transient rhythms 8-77142
 - ECG/VCG rhythm diagnosis using statistical signal anal., identification of persistent rhythms 8-77141
 - EEG epileptic transient detect. 8-53542
 - EEG sleep pattern feature extraction and recognition by real-time anal. (*Japanese*) 8-73271
 - EEG standardised classification, sequential epoch method 8-57101
 - electromyography, clinical, computer anal. 8-80985
 - electrophoretic waveform analysis for blood serum protein composition determ. 8-64928
 - gastric Ba-filled X-ray films, computer screening (*Japanese*) 8-73211
 - histology appl. of interactive pattern recognition system PEEP/DECIDE/GRAPH 8-73291
 - image anal. in cytology/cytogenetics, using Golay transform processor 8-61152
 - lung tissue stereological parameter computer anal. 8-73280
 - microcomputer-aided arm prosthesis using myoelectric pattern recognition 8-53576
 - optical power spectrum sampling and nonparametric pattern recognition algorithms 8-63032
 - piecewise-linear approximated ECG waveform recognition 8-57119
 - polar reference texture in radiocolloid liver images 8-73241
 - steroids, mass spectra, computer-aided interpretation by pattern recognition methods 8-64898
 - structure extraction, search-free technique, appl. to M-mode echocardiogram and chromosome image 8-81025
 - ventricular arrhythmia on-line study 8-81060
 - ventricular fibrillation recognition using ECG power spectrum 8-81032
- computerised picture processing**
see also computer-generated holography
- acoustic holographic image reconstruction for moving objects 8-75019
 - adaptive binarisation using hybrid image processing system 8-87019
 - analytical video stereoscopy, extended images, real-time photogrammetry 8-88926
 - angiographic images of left ventricle, system for off-line anal. using minicomputer 8-80964
 - astronomical image processing digital techniques 8-81555
 - astronomical telescope speckle interferometry, online digital autocorrelator 8-81548
 - astronomy, photon counting and analogue TV systems with digital real time image processing 8-96402
 - blood cell differential counter, ADC 500, pattern recognition based image processing system 8-73282
 - body surface potential distribution map recording and processing 8-57116
 - cardiac function scintigraphy using Bonn System III 8-73198
 - cardiac radiographic image sequence analysis and recording 8-57069
 - cardiac radionuclide cineangiography, clinical utility of real-time computer-based system 8-80957
 - cartography radar image interpretation, line detection technique 8-61630
 - chromosome autoradiograph analysis by computer 8-57071
 - computerised tomographic scan data format 8-73243
 - computerised tomography image reconstruction, interpolation effect 8-77110
 - conference, Bonas, France (June 1976) 8-58927
 - cytofluorometer, imaging system for correlating fluoresc. cell meas. in flow 8-61240
 - data extraction and classification from film, conf., San Diego, USA (Aug. 1977) 8-63023
 - data extraction from film using optical and/or digital and/or electronic devices 8-63024
 - digital image processing applications, conference, San Diego (1977) 8-81528
 - digital thermal field analysers 8-82034
 - display system using computer generated integral photograph 8-87021
 - dynamic random-dot stereograms, computer generated, binocular depth perception 8-80879
 - ECG surface potential map reconstruction from limited no. of leads 8-57117
 - echocardiogram computer-assisted interactive interpretation 8-80938
 - echocardiography, two-dimens., wall motion and thickening quantification by computer-aided contouring 8-80937
 - film-grain noise, low-contrast image detection 8-94370
 - geometrical anal. of image parts, CLIP parallel processor, algorithm implementation 8-58936
 - glaucoma diagnosis by digital processing of optic nerve head images 8-81043
 - half-tone images, spatial resolution and tone reproduction 8-63016
 - high-speed X-ray cylindrical scanning multiaxial computerised tomography unit 8-80956

computerised picture processing continued

- histology appl. of interactive pattern recognition system PEEP/DECIDE/GRAPH 8-73291
- hospital integral picture processing and communication system 8-57104
- hybrid optical correlator system for automated stereo compilation 8-63035
- image matching using struct. information, edge vector correlation 8-63036
- Image mensuration by maximum a posteriori probability estimation 8-63015
- image processing and eigen representation 8-55312
- image reconstruction from projections, freq. domain techniques 8-58935
- image segmentation and feature extraction, overview 8-58937
- images degraded by spatially varying pointspread functions, 2D digital restoration 8-78920
- interactive image digital/optical processing system development problems 8-74855
- interactive software, structure and design philosophy 8-58940
- kidney membrane conformational changes anal. after renal ischemia 8-73142
- LANDSAT imagery processing and enhancement 8-69545
- LANDSAT images and appls. 8-65404
- LANDSAT multispectral data classification algorithms 8-61629
- LANDSAT ratio image dynamic range reduction technique 8-69547
- leg long bone growth meas. in children from radiogram, error reduction using computer processing 8-77103
- lung tissue stereological parameter computer anal. 8-73280
- microprocessor-based optical/digital processor 8-63027
- multiply-exposed radiograph digital image restoration improvement 8-78054
- multispectral remote sensing ratio image digital processing and interpretation 8-81461
- myocardial infarction, topographic relation between myocardial ²⁰¹Tl uptake and left ventricular kinetics 8-61243
- myocardial perfusion scan interpretation 8-80960
- myocardial scintigraphy, computerised extraction of organ contours (German) 8-88735
- nonlinear image restoration with signal-dependent noise, decomposed local algorithm 8-78951
- nuclear medicine, sequential method for high 3D resolution imaging 8-53489
- optical computing for image bandwidth compression, analysis and simulation 8-94373
- optical power spectrum sampling and nonparametric pattern recognition algorithms 8-63032
- pockels readout optical modulator, for optical/digital processing systems 8-79125
- polar reference texture in radiocolloid liver images 8-73241
- pseudo-colour images, microprocessor controlled method for electronic image processing (German) 8-92724
- radioastronomical aperture synthesis imagery data optical reconstruction 8-69702
- radiogram, stomach contour extraction (Japanese) 8-53482
- radiographic image anal., patient diagnosis appl. 8-61256
- radiographic image analogue processing by photographic spatial filtering 8-57070
- radiographic imaging, digital video acquisition system for extraction of subvisual information 8-69208
- radioisotope subtraction technique in diagnosis of abdominal abscesses 8-73212
- radionuclide angiography determ. of left-ventricular ejection fraction and segmental wall motion 8-61246
- radionuclide cardiac motion study, computer-processed, ECG gating device 8-73210
- radionuclide images, digital image superposition algorithm, accuracy and reproducibility 8-73209
- random nucleated halftone screen 8-62192
- real-time spatial modulators for optical/digital processing systems 8-63025
- reconstruction spots for digital sampled images 8-63034
- recursive digital filtering method, two-dimensional, problems 8-58933
- remote-sensed data texture anal. 8-61628
- restoring with maximum entropy, Poisson sources and backgrounds 8-66769
- SAW device for optical image processing 8-71051
- scintigram change obs. by crosscorrelation 8-80961
- scintigraphy, medical, digital image processing methods 8-80947
- signal detection methods, optical/digital components evaluation in hybrid processor 8-63026
- smoothing and image noise 8-69190
- solar corona and comet digital image enhancement 8-81556
- stereophotogrammetry, automatic, using structural pattern recognition techniques 8-61632
- three-dimensional image reconstruction for cone-beam X-ray sources 8-77111
- tissue section electron microscope image texture discrimination and automated meas. 8-57099
- tomography, basic physics, mathematics and data reconstruction 8-73218
- tomography with X-ray beams (German) 8-53480
- TV-microprocessor system, for high speed image counting and sizing 8-94377
- US image feature enhancement via digital processing 8-73183
- US ophthalmological signal acquisition and image enhancement 8-57045
- Viking Orbiter and Lander stereo image processing 8-81554
- X-ray computed tomographic image optimal processing 8-80955
- X-ray computed tomography, aspects 8-53481
- X-ray tomography, noise power spectrum 8-53492

computerised power station control *see power station computer control*

computerised process control *see process computer control*

computerised signal processing

- see also biology computing; computerised pattern recognition; computerised picture processing; medical diagnostic computing*
- acoustical data anal. using digital techniques 8-83193
- analytical chemistry, user-oriented software Fourier spectrum display 8-64896

computerised signal processing continued

- biomedical signal processing and telemetry, digital bandpass analysis 8-57107
- biomedical signal processing microcomputer development 8-81012
- blood flow measurement by US Doppler method, computer-aided determ. of angles (German) 8-80931
- body surface potential mapping, automated acquisition and processing system 8-81033
- Bryn processor, acoustic array gain, sampling error effect 8-66975
- ECG, digital filters, implemented on microprocessor 8-85428
- ECG analysis system as part of regional cardiovascular information system 8-81049
- ECG analysis system oriented toward polarcardiology 8-85447
- ECG microcomputer-based evaluation system, improving diagnostic capabilities 8-88761
- ECG monitoring by contour comparison, QRS triggering with real-time correlator (German) 8-92715
- echocardiogram, M-mode, computer-assisted anal. 8-80942
- echocardiogram on-line computer anal. 8-80941
- echographic information related to left ventricle and mitral valve in diastole, anal. by small computer 8-80939
- EEG, dynamic anal. of event-related vars. (German) 8-85400
- EEG dynamic evolutionary spectral analysis 8-57102
- EEG epileptic transient detect., pattern recognition techniques 8-53542
- EEG nonstationary point automatic detect. (French) 8-57112
- EEG slope descriptor computation, time and frequency domain comparison 8-57115
- haemodynamic and cineangiographic data treatment, computer system SYSCORMORAM 8-81030
- LANDSAT data high-level computer processing 8-69546
- left ventricular diameter-time curve shape from M-mode echocardiogram, automated anal. 8-80940
- microprocessor for optical processing system noise analogue signals 8-81955
- nuclear power plant diagnostic system using noise anal. 8-50279
- ophthalmological tissue differentiation, digitisation of HF US signals 8-80935
- particle track data in plastics, rapid anal. using interactive programming and graphic displays 8-66456
- radar and sonar coherent optical processing techniques 8-75018
- representation of gait by 4-dimensional vectors (German) 8-88723
- sonar signal processor, 36-channel, programmable 8-66976
- synthetic aperture radar underwater mapping, array processing 8-69549
- systolic time interval processing system, STIPS 8-81029
- time-domain wave-shaping filter weights computation 8-77351
- tissue characterisation by computer-aided US method (German) 8-80932
- tissue characterisation by computer-aided US method (German) 8-80933
- upper-limb prostheses multifunctional control microprocessor system, myoelectric signal identification method 8-88766
- Varian EM-360 NMR spectrometer interface with Altair 8800B microcomputer 8-89519
- video-angiocardigraphic image series storage improvement by digital signal processing (German) 8-92723
- visual evoked potential on-line evaluation by sliding average form. (German) 8-85402

computerised spectroscopy

- see also spectroscopy computing*
- astronomical spectroscopy, appl. of general image anal. system 8-53834
- atomic absorption spectrophotometer, two-channel, microcomputer-based, appls. 8-56926
- automated correlation spectrometer with two Ge(Li) detectors 8-82562
- automatic precision wavelength comparator for spectrograms 8-82042
- Cary 118C spectrophotometer, universal computer interface 8-73972
- compilation of computer-readable spectroscopic reference data 8-64894
- computer compatible conversion for printing multichannel analysers 8-90036
- cooled and intensified array detectors 8-65983
- Darmstadt linear accelerator, detector system and performance of elec. scatt. system 8-70680
- Darmstadt linear accelerator electron scatt. facility, data processing 8-70681
- deconvolution of spectra by least-squares fitting 8-64897
- digital modulator and synchronous demodulator system: an alternative to the analog phase detector 8-70107
- digital multidiscriminator for use in gamma-gamma coincidence experiments 8-70707
- dye CW laser, on-line computer control, laser isotope separation appl. 8-70948
- emission spectrophotometry, review of data processing systems (Japanese) 8-88685
- ESCA for nondestructive charact. using TV type position sensitive detector 8-76969
- Febry-Perot interferometer, with automated data acquisition and stabilisation system 8-70180
- flow microfluorometry instrumentation, rapid data collection, analysis and graphics 8-86348
- gas analysis by computer-controlled microwave rotational spectrometry 8-85227
- graphics display terminal for spectral data analysis 8-54473
- Leuven isotope separator on-line at CYCLONE cyclotron 8-70682
- mass spectrometer for isotopic solids anal. 8-78026
- mass spectrometer ion multiplier noise filter based on analogue delay device, anal. appl. 8-92541
- microcomputer based scanning instrument controller, for optical spectroscopy 8-93764
- microcomputer scanning system for respiratory mass spectrometer 8-88756
- microprocessor controlled data acquisition system, for pulsed laser spectroscopy 8-86341
- minicomputer driven microprobe (French) 8-74111
- Mossbauer data acquisition system using minicomputer 8-90050
- Mossbauer spectroscopy, automated complex, information retrieval and processing (Russian) 8-82091

computerised spectroscopy continued

- multichannel scaling using 8-bit microcomputer 8-82595
- neutron diffractometer, reflection centring algorithm 8-75503
- NMR spectrometer, pulse, controlled by programmable digital unit (Czech) 8-77952
- nonflame atomiser, programmed unit for at. absorpt. anal. 8-54462
- optical multichannel spectrometric detectors, vidicon, online data handling capability 8-74077
- photon correlation in nanosecond range using programmable digital counter, photomultiplier evaluation 8-54464
- photon counting spectrometer, computer controlled, rapid scanning of low light level spectra 8-86338
- programmable multielement atomic absorption system 8-80803
- Quadmagnova, GC/MS system, computer scanning and control 8-76946
- Raman spectrometer, digital control system, appl. to soft mode spectroscopy 8-86345
- rocks, minerals, anal. of small samples using X-ray quantometer 8-61112
- TOF spectrum, computer interaction through direct memory access and with buffer memory 8-70685
- two-photon spectrometer for organic crystals 8-58064
- voltammetry, cyclic, AC, on-line digital FFT faradaic admittance data acquisition 8-61118
- X-ray analysis, high-speed, profile fitting method 8-75492
- X-ray fluorescence analyser with minicomputer (German) 8-88677
- Si(Li) electron spectrometer on-line with an automatic irradiation apparatus 8-90014

computerised test equipment *see automatic test equipment***computerised tomography**

- abdominal diseases diagnosis and management 8-88739
- abdominal infection evaluation, complementary role of ⁶⁷Ga-citrate imaging and computed tomography 8-73207
- accurate fan-beam reconstruction 8-78931
- anatomical cross-section determ. using radiotherapy simulator, for treatment planning 8-61244
- beam hardening correction 8-65125
- beam hardening reduction, calc. method 8-80951
- body scanners, comparison of translate-rotate, pure rotary types 8-69211
- congenital intracranial vascular malformation detect., scintigraphy vs. tomography and angiography 8-77104
- cost-effectiveness considerations in evaluation of new technology 8-69192
- craniofacial anomaly assessment, computerised versus conventional tomography 8-73239
- density reconstruction using arbitrary ray-sampling schemes 8-80954
- divergent beam X-ray transform, math. theory 8-96088
- dosimetry, exposure meas. techniques 8-69212
- dual-energy scans, data processing 8-69215
- dynamic emission computed tomography, quantitative pots. 8-77105
- elemental anal., usefulness of photon mass attenuation coeff. 8-77108
- emission computed tomography, CCA system 8-73285
- first image reconstruction based on Radon inversion formula 8-77109
- heart imaging from computerized tomography 8-88741
- high-speed X-ray cylindrical scanning multiplanar computerised tomography unit 8-80956
- image noise and smoothing in scanners 8-85368
- image reconstruction, basic physics and maths. 8-73218
- image reconstruction, Fourier techniques evaluation in relation to number of X-ray sums 8-77112
- image reconstruction, interpolation effect 8-77110
- image reconstruction principles in X-ray tomography 8-88745
- incomplete geometries in fast X-ray scanner 8-80952
- intracerebral spontaneous haematoma diagnosis and prognosis 8-73195
- iterative three dimensional reconstruct. from twin cone beam projections, simulation study 8-80949
- neutron radiography for nucl. fuel 8-82529
- outline, physics aspects in medical engineering (German) 8-92735
- positron emission transaxial tomograph, PETT IV and computer system 8-80959
- radiographic contrast agent techniques applied to computerised tomography examination 8-65105
- radiotherapy treatment planning using the ACTA-scanner 8-65104
- reconstruction noise rel. to detectability 8-69213
- reconstruction simulation, no. of rays versus no. of views 8-69214
- review, principles, development and situation in Sweden (Swedish) 8-65106
- scan data format considerations 8-73243
- scanner development for head and neck diagnosis (Japanese) 8-61277
- scanner resolution, geometrical limitations 8-73237
- scintillation camera single-photon computed tomography, optimised collimator 8-77106
- sensitometry, definitions and practical techniques 8-69194
- skeletal system CT examination 8-88740
- smoothing and image noise 8-69190
- Somatom, rapid image reconstruction and examination speed 8-92693
- three-dimensional image reconstruction for cone-beam X-ray sources 8-77111
- three-dimensional visualisation of anatomic sites and radiation dosimetry contours 8-77113
- TOMAX autostereoscopic display, three-dimens. viewing of tomographic data 8-85446
- transaxial scanning X-ray tomography, oblique viewing plane reconstruction 8-77114
- transmission and emission computed tomography, review (Japanese) 8-81042
- ultrafast scanners, picture reconstruct. techniques for incomplete data 8-80950
- urological diagnosis, possibilities and limitations (German) 8-85369
- X-ray, dynamic boundary surface detection 8-53479
- X-ray computed tomographic image optimal processing 8-80955

computing applications to aerospace engineering *see aerospace computing***computing applications to art** *see art***computing applications to astronomy** *see astronomy computing***computing applications to astrophysics** *see astrophysics computing***computing applications to biology** *see biology computing***computing applications to biomedical engineering** *see medical computing***computing applications to chemistry** *see chemistry computing***computing applications to circuit analysis** *see circuit analysis computing***computing applications to circuit design** *see circuit CAD***computing applications to civil engineering** *see civil engineering computing***computing applications to communications engineering** *see communications computing***computing applications to control engineering** *see control engineering computing***computing applications to control system design** *see control system CAD***computing applications to education** *see educational computing***computing applications to electric machine analysis** *see electric machine analysis computing***computing applications to electric machine design** *see electric machine CAD***computing applications to electrical engineering** *see electrical engineering computing***computing applications to electronic engineering** *see electronic engineering computing***computing applications to engineering** *see engineering computing***computing applications to geophysics** *see geophysics computing***computing applications to history** *see history***computing applications to linguistics** *see linguistics***computing applications to literature** *see literature***computing applications to mathematics** *see numerical analysis***computing applications to mechanical engineering** *see mechanical engineering computing***computing applications to medical administration** *see medical administrative data processing***computing applications to medical diagnostics** *see medical diagnostic computing***computing applications to medicine** *see medical computing***computing applications to music** *see music***computing applications to natural sciences** *see natural sciences computing***computing applications to nuclear engineering** *see nuclear engineering computing***computing applications to physics** *see physics computing***computing applications to power system design** *see power system CAD***computing applications to psychology** *see psychology***computing applications to town and country planning** *see town and country planning***concrete***see also cement industry*

- acceptance tests comparability for separation charact., quality control (German) 8-68848
- Berger coeffs. for Eisenhower-Simmons γ -ray buildup factors in concrete 8-78510
- CANDU irradiated fuel storage, concrete canister programme, heat transfer and shielding effectiveness 8-58388
- crack growth, computer simulation using Monte Carlo method 8-76764
- cylinders, fracture, fluid pressure testing using H₂O and N₂ gas 8-60750
- dam construction elements, appl. of fracture mechanics to thermal stress cracking 8-76766
- elastic modulus variations, gauge meas. by embeddable-strain-units 8-84878
- endochronic model for nonlinear triaxial behaviour 8-51095
- fatigue strength obs., of unreinforced concrete, cyclic loads testing (Dutch) 8-52945
- FRC, reinforcement parameter 8-79223
- gamma-ray linear attenuation coeff., radiation protection at γ -irradiation installation, GOU-1 (Bulgarian) 8-82530
- holographic interferometry study of chemical bond of concrete to smooth steel rods 8-88593
- joints glued with reaction resinous mortar, photoelastic exam. (German) 8-76825
- leachability determ., radioactive tracer method 8-61135
- LMFBR, pool-type, dried hot concrete vessel design 8-50248
- LMFBR prestressed concrete reactor vessels, analytical model and code applications 8-74448
- masonry units, splitting tensile test 8-53061
- masonry units, use and production of pelletised slag, mech. props. 8-52707
- moisture content meas. by 4 electrodes (German) 8-60929
- piezoelectric transducers, prep. method problems for UF-90PTs instrument, for US testing of concrete 8-90622
- plasticity theory anal. of shear 8-83270
- plates, cracked, and beams existence of critical strain energy release rate 8-76765
- prestressed members, creep fracture during manufacture 8-76767
- reinforced concrete structural integrity assessment, NDT method 8-56847
- review, physics and chemistry 8-73013
- short steel wire reinforced (polymer impregnated) concretes, cracking and toughening 8-80626
- steel bar reinforced concrete member, effect of steel bars on US testing 8-60923
- steel reinforced concrete beams, mech. strength determ. under combined bending and tension 8-60749
- US testing of compressive strength (German) 8-68847
- US testing of deep foundations 8-88585
- water transport, neutron radiography study, results review 8-59961

concurrency (computers) *see multiprocessing systems***condensation***see also clouds; drops; fog*

- accommodation coefficients, effects on evaporation and condensation (Japanese) 8-81933
- aerosol, heteromolecular nucleation and condensation, multi-dimens. theory 8-92518
- air-steam mixtures, heat transfer to moving droplets 8-90997
- alkali metal vapour condensation from gas flow (He, Ar, N₂) heat and mass transfer 8-75192
- benzene, benzene-d₆, vibrational anharmonicity, condensation effect, vap. press. isotope effect 8-58657
- binary mixture flow in vertical channel, film condensation 8-75139
- channel, local (total) heat transfer coeffs., friction factors 8-51045

condensation continued

chemically reacting gas, chemically reacting noncondensable components 8-51258
 cloud, warm cumulus, three-dimens. numerical model with microphysical processes (*Russian*) 8-88884
 contact angle hysteresis, dropwise condensation heat transfer 8-71273
 convection, augmented, bubble pumped, in submerged condenser system 8-94535
 dielectric liquid, film condensation, heat transfer enhancement in elec. field 8-55551
 drop electrification by evaporation or vapour condensation (*French*) 8-61511
 droplet growth and initial dew point temp. accuracy in cloud chamber on space shuttle 8-96268
 drops, noncirculating, direct contact condensation 8-94548
 dropwise condensation, max. drop size rel. to heat transfer coeff. 8-94559
 dropwise condensation of Hg, heat transfer meas. 8-94560
 enhanced film condensation by surface forces, optimum condenser tube fin geometry 8-75039
 ethylene, condensation, zero point energy shift, isotope effects 8-95147
 extended surface heat transfer with condensation on to fin 8-94551
 film condensation in three dimens. flows 8-94692
 film condensation of steam in vertical Cu tube, heat transfer coeff. 8-94553
 film flow, of condensate on finned surfaces, heat exchanger design 8-75038
 filmwise condensation, onto vertical fluted plate, numerical anal. 8-94552
 flow, transient, two-phase, flow reversal prediction LOCA conditions 8-94811
 fluoromethanes, condensation, zero point energy shift, isotope effects 8-95147
 fluted tube, condensation heat transfer, Gregorig model 8-87236
 free jet, homogeneous nucleation of clusters, noncryst. struct. (*French*) 8-79760
 free molecular vapour flow, mass transfer during condensation in channel 8-51198
 gas bubble nucleation, exptl. data use in flow boiling bubble population prediction 8-90696
 gas-liquid droplet system, phase transition kinetics and kinetic eqns. 8-83933
 gas-vapour droplets, nonuniform mixture, acoustic wave attenuation 8-83154
 heat transfer, condensate pattern for condensation of immiscible liquid binary vapour 8-94558
 heat transfer augmentation, in horizontal tube condensation, using twisted-tape inserts and internal fins 8-71265
 heat transfer by condensation of gas-vap. mixture, in high-press. pipe 8-94589
 homogeneous condensation, from supersaturated vapour, stochastic simulation 8-51657
 ice, electrical effects during condensation and phase transitions 8-67821
 kinetic theory, evaporation, condensation, linear, nonlinear problems 8-75802
 kinetic theory, hydrodynamic eqn. and slip boundary condition 8-63903
 kinetic theory of one-dimensional evaporation and condensation problem (*Japanese*) 8-81932
 laminar condensation, intermittent charact. 8-94555
 laminar film condensation, non-condensing gas in tube 8-94554
 laminar film condensation, on vertical plate, surface tension effects 8-95148
 laminar film condensation from moving vapour, with suction 8-59459
 laminar film condensation of mixed vapours, combined body force and forced convection 8-51162
 methane, condensation, zero point energy shift, isotope effects 8-95147
 nucleation, microscopic theory (*Russian*) 8-67801
 nucleation, microscopic theory (*Russian*) 8-67802
 organic compound, two-dimensional condensation with adsorbed mol. reorient. 8-61051
 plate condenser with grid pattern slotlike channels, low-press. steam condensation, heat transfer 8-75040
 rotating heat pipes, condensation heat transfer, noncondensable gas effects 8-51167
 shape of drop on inclined plane, solar still aspects 8-79856
 shock compression of condensing media, relax. processes kinetics 8-94610
 spherical liquid droplets, nonlinear condensation and evaporation 8-63902
 steam, annular duct flow, heat transfer to condensate film 8-94709
 steam, dropwise condensation, effect of condenser tube material on heat transfer 8-75059
 steam, film condensation in tube, heat transfer, vibr. effect 8-51044
 steam, horizontal flow on cylinder, condensation 8-94550
 steam, tube condensation, augmented internal geom., and press. drop 8-94556
 steam condensation heat transfer on below-freezing pt. surface 8-75042
 steam jet condensation, dynamical pressure pulse effects 8-94549
 steam-inert gas, uncondensable gas content effect on steam condensation heat transfer in vert. tube 8-75041
 superheated vapour in vertical tube 8-87783
 supersaturated gas condensation kinetic model, cluster nucleation assoc. and dissoc. 8-85151
 surface suction effect on condensation in presence of noncondensable gas 8-90691
 tubes with in-line static mixers, surface renewal model 8-75060
 turbulent annular-mist flow, wall and interfacial shear stress 8-94812
 turbulent filmwise condensation heat transfer coeffs. 8-63429
 vapour bubble, in immiscible liquid, collapse 8-94547
 vapour condensation on vertical surface, laminar flow in film condensate 8-75057
 vibrational anharmonicity, condensation effect, vap. press. isotope effect 8-58657
 water condensation on charged centres 8-51791
 water vapour, condensation in presence of H_2SO_4 and HNO_3 pollutants 8-81343

condensation continued

water vapour in rectangular channel, partially cooled perimeter, heat transfer 8-94557
 Ar nucleation, Ar in He carrier gas, supersonic nozzle flow 8-94871
 BF_3 , boiling/condensation heat transfer props., cryogenic appls. 8-79192
 C particle formation, $\text{C}_2 + \text{C}_3$ as possible first step 8-68876
 CO_2 , boiling/condensation heat transfer props., cryogenic appls. 8-79192
 H_2O , condensation via rarefaction wave 8-71847
 He condensation forevacuum pump 8-86282
 He, condensing on positron, Monte Carlo lifetime spectra, temp. and elec. field effects 8-55263
 N_2 -He mixture, film condensation, appls. to condensers for cryogenic installations 8-59941
 NO, boiling/condensation heat transfer props., cryogenic appls. 8-79192
 NO_2 in nonane, supersaturated gas, photoinduced nucleation 8-80760
 Na vapour condensation from rising bubble, effects of internal circulation velocity and noncondensable gas 8-50258
 Ni-W (2%), Mg diffusion meas., 970-1330K, appl. of vapour collect and AES method 8-75876
 O_2 bidimensional condensation on lamellar halide (*French*) 8-75941
 UO_2 vapour condensation from rising bubble, effects of internal circulation velocity and noncondensable gas 8-50258

condensers (electric) see capacitors**condensers (steam plant)**

enhanced film condensation by surface forces, optimum condenser tube fin geometry 8-75039
 plate condenser with grid pattern slotlike channels, low-press. steam condensation, heat transfer 8-75040
 supersonic nozzle discharge, heat transfer and gas dynamics 8-55671
 turbulent flat jet condenser, nozzle hydraulic and heat transfer characts. 8-94793

condensing see condensation**conductance, electric** see electric admittance**conductance, electric, measurement** see electric admittance measurement**conductance measurement, electric** see electrical conductivity measurement**conducting materials**

see also bimaterials; electrolytes; metals; semiconductor materials; superconducting materials
 ESCA, X-ray type, C 1s contaminant buildup on conductors and insulators 8-95981

conduction, heat see heat conduction**conduction bands**

see also Fermi level; semiconductor materials
 dielectric liquids, cond. band minima, rel. to electron mobility maxima 8-80029
 glasses and amorphous semiconductors, band struct. and forbidden gap, review 8-75987
 heavily doped, Raman phonons, interband excitation effects 8-52501
 hybridization effect on phase transitions in the Falicov-Kimball model 8-91617
 OPW method, instability rel. to error in core eigenvalues 8-63963
 semiconductor, zinc blende struct., cond. band nonparabolicity and cyclotron reson. linewidth (*German*) 8-75993
 tight binding calc., overlap and next-nearest-neighbour interaction effects 8-72059
 x-ray edge singularities of relaxed-out bound states and relaxed-in band states 8-92173
 Bi electron properties, carrier spectrum 8-84137
 n-Cd SnAs_2 , optical absorption rel. to energy spectra (*Russian*) 8-75994
 Cu, Bloch states, photoelectron spectra, angle resolved 8-92175
 EuS, conduction band density of states, redistrib. near ferromag. saturation 8-67939
 GaAs, electron transient vel. characts., Γ -L-X cond. band ordering 8-79997
 GaAs, piezoresistance and conduction band minima 8-51993
 GaAs-Ga $_{1-x}$ Al $_x$ As, superlattice umklapp processes in resonant Raman scattering 8-64362
 GaAs $_{1-x}$ P $_x$ based structs., carrier conc., mobility calcs. from Hall effect meas. 8-60138
 N-InAs, Moss-Burstein effect, S, Sn, Te dopants 8-64389
 In $_{1-x}$ Ga $_x$ As-GaSb $_{1-y}$ As $_y$, new heterostruct. characts. 8-72247
 In $_2\text{O}_3$ -SnO $_2$ -Si heterojunctions, elec. and photovoltaic characts. 8-52070
 InSb, cyclotron harmonic transitions, warping and inversion asymm. effects 8-68383
 KBr, electronic states at (100) surface, accounting for spin-orbit interaction (*Russian*) 8-91750
 KCl, electronic states at (100) surface, accounting for spin-orbit interaction (*Russian*) 8-91750
 KI, electronic states at (100) surface, accounting for spin-orbit interaction (*Russian*) 8-91750
 Na $_2\text{WO}_4$, vacuum UPS exam. 8-84700
 PbI $_2$ intercalated with organic mols., energy band splitting (*Russian*) 8-76027
 Pd, hydride and alloys, electronic band struct., comparative study of electric and mag. props. 8-95259
 Si (111), chemisorption of $\text{H}_2(\text{Cl})$, conduction-band surface resonance 8-52051
 Si, exchange and correlation pot., band struct. calc. 8-56068
 Si, with non-spherical pots. for two basis atoms, electronic struct. 8-72069
 Si(111), conduction-band surface resonance 8-52051
 TiO $_{2+x}$, conduction band determ. 8-60055
 ZnO (1010) surface bias voltage effect on hardness, charge exchange near dislocations 8-52078

conduction electron spin resonance see CESR**conduction in solids, ionic** see ionic conduction in solids**conductivity, electrical** see electrical conductivity**conductivity, thermal** see thermal conductivity**conductors (electric)**

see also bimaterials; wires (electric)
 cylindrical conductor carrying AC, temp. and stresses 8-82875
 film conductor, pulse nonlinearity meas. 8-56242
 heterogeneous, planar nonstationary EM field anal. in transient state (*Polish*) 8-71000

confinement, plasma *see plasma confinement*

connecting *see joining processes*

connectors (electric) *see electric connectors*

conservation laws

see also C invariance; CP invariance; CPT invariance; elementary particle symmetry; P invariance; T invariance
artificial compression method for shocks and contact discontinuities 8-70298

continuum mechanics, discontinuity surface model, balance eqn. and phase transition 8-73850

electromagnetism in non-Riemannian space, Maxwell's equations as conservation laws 8-77737

energy momentum tensor symmetries, concomitant conservation laws, Einstein massless scalar meson field appl. 8-86205

Euclidean invariance, spontaneous breaking, long range ordered media, defect, config. classification 8-59748

G conjugate invariance of current matrix elements in $v(\vec{v})N$ elastic scatt. 8-54627

general vector fields, classical theory, internal symmetries and conservation laws (Russian) 8-62328

Hamiltonian eqns., infinite-dimens., integrable 8-57744

ideal vortex motion, two dimens., symms., conservation laws 8-87349

interacting particles system, nonrelativistic classical and quantum mechanics conservation laws 8-89328

Lagrangian mechanics, consts. of motion anal. 8-81829

Lagrangian systems with one degree of freedom, invariance and conservation laws 8-62067

lepton number conservation, double beta decay 8-58256

matrix theory of elastic wave scatt., conservation law 8-63217

Newton's 2nd law, spatial translation symmetry, for teaching 8-54129

non-local continuum mechanics, conservation laws 8-65770

nonlinear difference-difference equations, derivation of infinite number of conservation laws 8-89324

nonsymmetric unified field theory, conservation laws, Bianchi type identities 8-73910

photoproduction processes of charm particles with charm nonconservation (Russian) 8-74201

planet formation process, conservation laws and mass distrib. 8-81565

polynomial conservation laws in (1+1) dimens. classical and quantum field theory, nonlinear Schrodinger eqn. 8-54224

quantum theory consequences of more general theory of symmetries, conservation laws 8-49718

scale and conformal invariance, scalar currents, theory with continuous mass spectrum 8-62335

sine-Gordon supersymmetric theory, infinite set of bosonic conserved currents 8-62313

stationary Einstein-Maxwell space-times, conserved quantities determ. 8-49737

strong P and T noninvariances in a superweak theory 8-82123

symmetries of energy momentum tensor, concomitant conservation laws 8-57831

vN interactions, quasielastic scatt., book contrib. 8-78171

constant current modulation *see amplitude modulation*

constant current sources

double, for cryogenic current comparators, standard resistor calibration appl. 8-93731

iontophoresis, gated HV system with accurate current monitoring 8-69259

pulsed low current, at acoustic freq., using LED and photomultiplier 8-93724

constant voltage diodes *see avalanche diodes; Zener diodes*

constants

see also elastic constants; gravitational constant; lattice constants; optical constants

International Astronomical Union 1976 system of constants (Russian) 8-73611

molecular size and Avogadro's number, determ., student expt. 8-81741

Planck's constant, and finite struct. const. calc. 8-82135

Planck's constant, time invariance 8-93556

Stephan's constant determ., student expt. 8-69948

e/p mass ratio, direct determ. using cyclotron resonance technique 8-70093

constitution diagrams *see phase diagrams*

constraint theory

bodies with binary material and kinematic-kinetic structure 8-73848

continuum mechanics, nonideal realisations of constraints and loosenesses 8-73849

construction *see building*

construction industry

see also civil engineering

materials evaluation using high temp. thermal analysis 8-80687

noise abatement, legal considerations, statutory law 8-87197

reinforced concrete structural integrity assessment, NDT method 8-56847

constructional engineering *see civil engineering*

contact angle

see also capillarity; surface tension; wetting

brass, contact ang. meas., aq. ethanol (glycerine) solns., 20-70°C 8-56025

creeping flow over surface, angle of contact, viscous liq. 8-51149

Duralumin, contact ang. meas., aq. ethanol (glycerine) solns., 20-70°C 8-56025

ethanol, aq. solns., contact ang. with metals, 20-70°C 8-56025

fingerprint/surface, contact angle meas. 8-78056

glycerine, aq. solns., contact ang. with metals, 20-70°C 8-56025

homogeneous surface, hysteresis of contact angle 8-51793

hysteresis, dropwise condensation heat transfer 8-71273

liquid spreading, edge effect for zero contact angle 8-84032

liquid surface shape near stripwise heterogeneous wall, analytical soln. of Laplace eqn. 8-67890

microdrop, two-dimensional, on solid body surface, stability dynamics 8-51790

mixture, binary, nucleate boiling heat transfer, conc. depend. 8-87249

nitrobenzene, contact angle on pretreated polyethylene, H_2O environment (Japanese) 8-79858

poly(ethylene terephthalate), surface props. rel. to UV irr. (Japanese) 8-79859

contact angle continued

porous media wetting, capillary rise, contact angle effect (German) 8-84033

ring tensiometry, effect of contact angle 8-60011

solid bodies, capillary interaction 8-51792

spreading phenomenon in dry powder electrophotography 8-63904

steel, contact ang. meas., aq. ethanol (glycerine) solns., 20-70°C 8-56025

styrene-tetrahydrofuran block copolymer, H_2O contact angle and surface struct. (Japanese) 8-79861

Al-graphite adhesion and contact angle, effects of metal additives (Japanese) 8-60008

Be, contact ang. meas., aq. ethanol (glycerine) solns., 20-70°C 8-56025

Cu, aq. ethanol (glycerine) solns. contact ang., 20-70°C 8-56025

Ga, contact angle meas. between melt and crystal during Czochralski growth 8-64461

Ge, contact angle meas. between melt and crystal during Czochralski growth 8-64461

H_2O , contact angle measurement, effect of acoustic energy 8-95207

H_2O , contact angle on polystyrene, cause of hysteresis 8-95206

Ni, contact ang. meas., aq. ethanol (glycerine) solns., 20-70°C 8-56025

contact e.m.f. *see contact potential*

contact potential

see also contact resistance

Kelvin method contact PD meas. manipulator 8-57979

Cu-Cd(In)(Sb), electron work function, contact pot. difference meas. 8-80041

Mo (110), oxidation exam. of LEED 8-92402

$Na_2SO_4 \cdot 10H_2O$, solid-liq. transform., solar energy conversion applicability 8-60155

$Na_2S_2O_3 \cdot 5H_2O$, solid-liq. transform., solar energy conversion applicability 8-60155

W (100), adsorbed La, depend. of work function, heat of adsorpt. on surface coverage, contact potential study 8-67912

ZnO, electron beam induced decomposition and desorption, AES and contact pot. difference meas. 8-79893

ZnS, chemisorption of O_2 after illumination and in presence of CO and O_2 8-87877

contact resistance

see also contact potential

four-terminal meas. circuit stray-impedance errors 8-77940

III-V multilayer structs., contact resistance profiling method 8-56213

impedance meter, AC, battery-operated, for contact resist. determ. before patient monitoring 8-81006

low temperature characts. 8-68072

metallic foil contact resistance transducers, thermochemical method of oxide film formation 8-89466

metallic point contacts, nonlinear resist. rel. to phonon emission and background effects 8-68074

planar devices, contact resistance derivation 8-60205

semiconductor-metal contacts, contact resist. and bulk resist. of semiconductor samples, pulse method 8-52083

spheres at high pressure, contact stresses and spreading resistance 8-71296

Au electrodeposited coating properties obs., Cu diffusion under high temperature (Czech) 8-91486

Cu-Ni thin film couples, interfacial reactions, contact resistance meas. 8-63882

GaAs transferred electron devices, ohmic contacts 8-52082

HfP_3 , corrosion resist. and elec. cond., bulk and film samples 8-72285

$ZrPt_3$, corrosion resist. and elec. cond., bulk and film samples 8-72285

contactors

see also relays

high current switch, fast closing, fusion reactor fast discharge expt. 8-74483

contacts, electrical *see electrical contacts*

continuous creation hypothesis *see cosmology*

continuum hypothesis *see set theory*

continuum mechanics *see classical mechanics of continuous media*

contours, surface *see surface contours*

contrast transfer function *see optical transfer function*

control devices, electric *see electric final control devices*

control engineering applications of computing *see control engineering computing*

control engineering computing

see also computerised control; control system CAD

mechanical actuator, stepper motor, appl. to control of scientific apparatus 8-62683

control equipment

see also actuators; controllers; electric control equipment; relays; telecontrol equipment; thermostats; valves

photographic film copying, control mechanism to reduce waste quota (German) 8-93772

pollution control equipment operation and maintenance 8-61615

control gear, electric *see electric control equipment*

control rooms, radio *see radio studios*

control system analysis

see also correlation methods; describing functions; frequency response; linearisation techniques; perturbation techniques; phase space methods; piecewise-linear techniques; poles and zeros; sensitivity analysis; stability; state-space methods; step response; three term control; transfer functions

Tokamak plasma equilibrium, feedback control 8-55738

control system CAD

nuclear channel reactors, automatic control system design for energy distrib. 8-82475

thermal regenerator, with variable mass flow rate, computer model 8-75047

control system computer aided design *see control system CAD*

control system synthesis

see also correlation methods; describing functions; frequency response; linearisation techniques; perturbation techniques; phase space methods; piecewise-linear techniques; poles and zeros; sensitivity analysis; stabil-

control system synthesis continued

- ity; state-space methods; step response; three term control; transfer functions
 astronaut transfer in weightlessness, biomechanical model 8-96106
 BWR load following plant, low sensitivity design to controller 8-78473
 nuclear reactor distributed parameter optimal control methods 8-54858
 PWR steam supply control system optimisation 8-50251
 Tokamak, ISX, dynamics and feedback control 8-71528

control systems

- see also adaptive systems; closed loop systems; distributed parameter systems; multidimensional systems; optimal control; physical instrumentation control; sampled data systems; time-varying systems
 plasma instability, suppression by feedback method automatic control, stabilisation methods 8-63564

control theory

- see also control system analysis; control system synthesis; optimal control; stability
 irreversible energy conversion processes, information model (Ukrainian) 8-89419
 porous media, miscible or immiscible displacements, identification and modelling 8-69392

controllability

- see also stability
 biological compartmental systems, multi-input and multi-output, controllability, observability and structural identifiability 8-76978

controllers

- see also cryostats; instruments; servomechanisms; thermostats
 annealing of electron field emitters and multiple multichannel analyser, precision temp. regulator 8-86384
 astronomical laser ranging equipment, system controller (Japanese) 8-89079
 cardiac-assist in-series devices, controller 8-81075
 cryogenic pressure regulator 8-57963
 crystal oven pilot-lamp stability controller 8-54374
 driven oscillator motion with nondecreasing input vels., use in inertia actuated fuse 8-59293
 gas flow control, automated, transducer 8-59508
 gyrostabilizer, nonlinear suspension bearing, dynamic error (Russian) 8-75063
 microcomputer based scanning instrument controller, for optical spectroscopy 8-93764
 neutral beam filament supply, 15 V 10^3 A, programmable, regulated, for fusion reactor 8-70630
 noise reduction in steam power, chemical, petrochemical industries 8-51002
 pneumatic amplifier pump, for supercritical fluid chromatography, control and programming 8-88665
 pressure regulator device, behaviour anal. 8-93668
 pressure regulator for proportional regulation of two gas pressures, anaesthetic appl. 8-53560
 rapid-scan spectrometer control unit 8-74067
 resistance furnace programmed temperature regulator 8-86256
 time-lapse apparatus for 16 mm Beaulieu cine camera 8-74089

convection

- see also convection in liquids
 ablating body shape, numerical soln. method (Russian) 8-75134
 absorbing-scattering infinite slab, combined conductive and radiative heat transfer 8-71269
 advection processes, finite difference method, balanced expansion technique 8-77719
 aerosol precipitation from laminar gas stream, free convection effect 8-83459
 air jet, vertical axisymmetric buoyant, profile meas. 8-90906
 annulus with permeable insulator, radiative and free convective transfer 8-94575
 arc, high press., convection 8-59701
 atmosphere, dry penetrative convection 8-92889
 atmosphere, Lorenz system, 14-D generalization 8-75131
 atmosphere, parametrisation, conditional instability of second kind hypothesis appl. 8-61530
 atmosphere, wave generation and frontal collapse 8-77300
 atmosphere convective precipitation, mechanical effect of urban area 8-81338
 atmosphere-ocean, penetrative convection regime, entrainment rate (Russian) 8-69401
 atmospheric boundary layer, convective matching layer 8-81310
 atmospheric boundary layer, temperature-humidity covariance budget 8-73430
 atmospheric boundary layer, three-dimens. model rel. to expt. data 8-73428
 atmospheric convective diffusion from nuclear power station spray cooling 8-94078
 bed of inductively-heated particles, water-cooled, natural convection heat transfer 8-71396
 Benard, generalised problem with viscosity variations 8-71329
 Benard convection, in heat conducting media (German) 8-79308
 bibliography of heat transfer 8-63425
 boiling, nucleate, subcooled, latent heat transport contrib. 8-75046
 boiling, subcooled, nucleate, mechanistic model 8-90697
 boiling, sustained and transient, inlet subcooling effect on flow instabilities 8-94809
 boiling and bubbling heat transfer under the conditions of free and forced convection 8-90637
 Boussinesq equation, finite element anal. 8-79292
 bubble in power-law liq., convective heat and mass exchange, $Pe \leq 1000$ 8-55683
 buried cylindrical heat source, transient temp. distrib., upper and lower bounds 8-75048
 camphene-coated surface, convective local mass-transfer coeffs., holographic interferometry method 8-75234
 cataclysmic binaries accretion discs, convection as viscosity source 8-93307
 centrifugally driven thermal convection in rot. cylinder 8-51172
 Cepheid variables, double-mode and bump, rot. and convection effects on period ratios 8-93249
 channel flows of high temp. gases, heat transfer 8-94722
 chimney, thermally isolated, convective heat outflow, mathematical model soln. (German) 8-90887

convection continued

- circular channel with laminar flow, convective heat transfer (French) 8-63424
 circular fins with triangular profile, convective efficiency 8-67007
 cloud, warm cumulus, three-dimens. numerical model with microphysical processes (Russian) 8-88884
 cloud model, shallow convective, precip. mechanisms 8-81311
 clouds, three dimensional turbulent flow anal. 8-69395
 columns convecting over linear heat sources, interaction, wind effect (Russian) 8-55637
 combined convection heat transfer in rod arrays, numerical anal. 8-90898
 combined convective laminar boundary flow, vertical cylinder in horizontal flow, finite difference approx. 8-90893
 compressible convection in stellar interiors 8-89183
 condensation of chemically reacting gases, chemically reacting noncondensable components 8-51258
 condenser system, submerged, bubble pumped augmented natural convection 8-94535
 convective dynamo, models for planetary and solar magnetism 8-89090
 corona wind cooling of flat surface, convective heat transfer coeffs. 8-87234
 Couette flow, permeable wall layer, heat transfer and temp. distrib. 8-51165
 coupled conduction-turbulent convection in a circular tube 8-94691
 critical point hydrodynamics 8-59361
 critical radius effect with a variable heat transfer coefficient 8-83205
 cylinder array, convective mass transfer with surface reaction 8-79369
 cylinders of limited dimensions in cylindrical housings, heat transfer 8-67008
 cylindrical cavity, thermal convection with uniform volumetric energy generation 8-94541
 cylindrical slab of fluid, in weightlessness condition, surface-tension driven convection (Russian) 8-90872
 difference schemes and Hermite interpolation 8-63268
 diffusion-convection eqn. anal. with explicit difference methods 8-62165
 diffusion-convection eqn. soln. 8-90888
 diffusion-convection partial differential equations, finite element method soln. 8-90889
 double-diffuse convection, diffuse interface model, high Rayleigh nos. 8-90963
 drop evaporation rate in forced convective flow with transverse sound fields 8-51224
 drop in uniform (shear) stream, convective heat and mass exchange, $Pe \leq 1000$ 8-55683
 drying, heat and mass transfer, optimal control 8-67006
 dryout characts. of steam generator 8-90990
 duct flow, turbulent convective heat transfer 8-94719
 ducts and pipes intricately shaped cross section, heat transfer, Laplace and structural method 8-83477
 dust laden gas in channel, combined heat transfer 8-91031
 dust-liquid channel flow, with varying inlet temp., transient forced convection soln. 8-87375
 Earth deep mantle convection and lithosphere basal shear stress, roles in plate tectonics 8-57188
 Earth mantle, Benard problem with viscosity depend. on temp. and press. 8-69317
 Earth mantle, creep laws 8-69305
 Earth mantle, roll cell convection under Pacific plate 8-73345
 Earth mantle, spin-symmetric convection rel. to Phanerozoic plate tectonics 8-92812
 Earth mantle, two-scale convection rel. to global gravity anomalies 8-85528
 Earth mantle, two-scale flow model rel. to plate tectonics 8-73348
 EHD augmented baking, corona wind impingement effects 8-87235
 electrically conducting rarefied gas, oscill. flow, past vertical porous plate, free convection 8-90830
 finite amplitude two dimensional Benard convection, in finite rot. system, weakly nonlinear theory 8-83394
 fire in polytropic atmosphere, gas flow in convection plume (Russian) 8-96262
 flame, laminar mixed-mode forced-free diffusion type, on vert. burning fuel slab 8-91033
 flat plate, in forced flow, approx. method for heat transfer calc. 8-94682
 flat plate boundary layer in porous medium, free convection, similarity solns. 8-75199
 fluid layer, selection mechanisms for convective motion pattern form. 8-54316
 fluid layer stability, under general convective boundary conditions 8-94683
 forced, heat propagation eqn. (Italian) 8-83375
 forced convection heat transfer in horizontal layers, buoyancy effects 8-90901
 forced convection in annuli and rod bundles with variable heat flux distribution 8-94082
 forced convection in flows through rows of surface protrusions 8-94732
 forced convection quench data rel. to steady-state nucleate boiling data 8-90995
 forced convection within straight noncircular ducts 8-90878
 free convection and radiative transfer, at vertical plane surface 8-55645
 free convection boundary layers on cylinders of elliptic cross section 8-90877
 free convection effect on Stokes problem for vertical plate in elastoviscous fluid 8-67226
 free convection effects on the Stokes problem for an infinite vertical plate 8-90879
 free convection laminar flow, viscous dissipation and pressure stress effects importance 8-63428
 free convective flow in porous medium, longit. vortices, onset, linear stability anal. 8-94813
 free convective heat transfer at a vertical semiinfinite plate 8-79318
 free convective heat transfer, external surface of vertical isothermal cylinder 8-83390
 free convective heat transfer in fluid confined by wavy wall 8-55642
 free laminar convection, three-dimens., about surface, numerical anal., visualisation (French) 8-87343

convection continued

free MHD convection, near plane and axisymmetric bodies, approx. soln. (*Russian*) 8-94832
 free-forced convection from a heated cone, cross flow transition, similarity soln. 8-90892
 Free-forced convection in the entry region of a heated straight pipe 8-90883
 freestream turbulence statistical characts., convective heat transfer calc., boundary layer eddy viscosity 8-83366
 fully developed laminar flow with internal heat generation between horizontal parallel plates, thermal instability 8-90899
 gas, boundary layer combustion, combined heat transfer 8-91029
 gas flow patterns in furnaces, composite heat transfer 8-90677
 gas pipe flow, turbulent Graetz problem, Joule-Thomson effect 8-75204
 gas tube flow, radiative and convective transfer 8-94576
 gas-filled cavities with baffles, free convection 8-94702
 grey bodies system, closed combined radiation convection heat transfer, two-layer gas model 8-75052
 heat transfer and flow instability of natural convection over upward-facing horizontal surfaces 8-94698
 heat transfer augmentation, convective, effect of mech.-produced unsteady boundary layer flow 8-71261
 heat transfer conference, Aug. 78, Toronto, Canada 8-90624
 heat transfer from cylinders in vertical cyclone chambers 8-90870
 heat transfer from porous sphere in low Reynolds number flow 8-59482
 heated cylinder in radial elec. field, corona characts. power freq. variation effects 8-87538
 Hele-Shaw cell, permeability determ., geothermal modelling appl. 8-59466
 helical coiled tubes, laminar convective heat transfer 8-94678
 heterogeneous liquid stream, stress diffusion effect, molar diffusion coeff. 8-79338
 HGTR core, multiregional coupled conduction-convection model 8-94083
 horizontal cylinder, laminar free convective heat transfer 8-75130
 horizontal cylindrical surface, free convection, local nonsimilarity anal. 8-75120
 horizontal tube, fully developed laminar flow, combined free and forced convection, expt. 8-87391
 horizontal tube turbulent flow secondary current struct., thermogravitation effects 8-90902
 human convective heat loss assessment in cold water 8-81093
 ionosphere, polar cap connection during Tordo 1 polar cusp Ba plasma injection expt. 8-77402
 ionosphere, rocket-borne meas. of ion convection in dayside aurora 8-77391
 isothermal vertical plate, natural convection, leading edge geometry effects, expt. 8-87346
 isotope centrifuge, effect of thermal convection on separative power, numerical anal. 8-58500
 jet, buoyant, turbulent in cross flow, finite difference method 8-90907
 jet array impinging surface, convective heat transfer 8-90953
 jet incident on plate, convective diffusion in boundary layer 8-67242
 laminar channel flow, heat transfer 8-79317
 laminar convection, heated vertical surface, boundary-layer thickness and Prandtl number 8-51161
 laminar cyclone, free and forced convection 8-55548
 laminar film condensation of mixed vapours, combined body force and forced convection 8-51162
 laminar flow in internally finned tubes 8-94724
 laminar flow pattern, press., enthalpy, vel. from point source of heat 8-79316
 laminar free convection boundary layer heat transfer, series solution predictive capability 8-71335
 laminar heat transfer from perforated surfaces 8-94727
 laminar natural convection heat transfer to a viscoelastic fluid 8-83436
 laminar plume above a line heat source in a transverse magnetic field 8-67269
 laser-beam induced heat and mass transfer 8-93635
 layer, dense, large Biot no., heat exchange (*Russian*) 8-83400
 layer with nonlinear density temp. relation 8-94697
 leading edge effect on free-convection heat transfer 8-79319
 line thermal numerical model, initial conditions influence 8-92932
 local mass-transfer coeffs. meas. by holographic interferometry, vortex instability effect 8-75234
 low thermal cond. materials, anal. of optimum method of inspecting by active thermal method 8-72996
 magnetic flux ropes and convection 8-71399
 magnetosphere, polar cap convection rel. to boundary mag. fields, laboratory simulation 8-57396
 magnetosphere convection, one-dimensional gasdynamical model 8-81508
 magnetosphere electric convection field, model 8-89004
 magnetosphere midlatitude convection elec. fields, rel. to ring current development 8-57395
 measurement by differential light interferometer with achromatic $\lambda/2$ compensation 8-87419
 melting surface, air bubble evolution effect on boundary layer separation 8-67015
 meteorology, aspects relevant to astrophysics 8-88898
 MHD unsteady free convection past a hot vertical plate 8-87396
 micropolar fluid with stretch, convection, appl. to Earth mantle 8-51202
 mixed, over semi-infinite vertical flat plate 8-55646
 mixed convection heat transfer rates in vertical tubes, expt. 8-90897
 mixed convection on a horizontal plate with uniform surface heat flux 8-90903
 mixed convection to air in a vertical pipe 8-90896
 mixed-convection heat transfer around an isothermal flat surface of finite length 8-90891
 Moon, distortion due to convection unlikely 8-61761
 multidimensional body, radiative-convective heating, unsteady temp. calc. method 8-90640
 natural, from vert. DC current-heated plate, linear stability anal. 8-90873
 natural, in presence of transverse mag. field similarity soln. 8-67197
 natural, over uniform heat flux vertical surface, higher-order approx. 8-59388

convection continued

natural convection, heat transfer in rectangular cavity with vertical walls of different temps. 8-67195
 natural convection flow, nonisothermal flat plate, numerical soln. 8-67194
 natural convection for three dimens. flows 8-94692
 natural convection from heated submerged cylinder 8-94704
 natural convection heat transfer in closed gas-filled tubes 8-94703
 natural convection in air-filled enclosure 8-94707
 natural convection in doubly inclined rectangular boxes 8-94708
 natural convection in enclosure, ventilation effect on temp. 8-94705
 natural convection in region between concentric cylinders (*French*) 8-94700
 natural convection mass transfer along porous vertical plate 8-90876
 natural convection of air over a heated plate with forward-facing step 8-90875
 natural convection transport to air above heated ridge, expt. 8-94680
 natural thermoconvective filtration in circular porous interlayers 8-94817
 needles, nonisothermal, forced convective heat transfer 8-90636
 Neptune thermal evolution, convective cooling model and comparison with Uranus 8-85903
 nonsimilar laminar free convection flow along a nonisothermal vertical plate, finite difference method 8-75119
 nonstationary MHD convection, in vertical circular channel (*Russian*) 8-94833
 nonstationary one-dimensional diffusion under forced convection, Omega functions as auxiliary functions 8-93631
 numerical methods in convection theory 8-89058
 onset with spatially periodic heating, nonreson. wavelength excitation 8-94699
 oscillatory flow, line heat source in horizontal rectangular chamber 8-90868
 oscillatory MHD boundary layer flow, free convection effects 8-91018
 oscillatory, in porous medium heated from below 8-79320
 overstable convection in horizontally treated rotating fluid 8-67202
 E.Pacific Rise-Galapagos Rise system, seawater circulation rel. to convective heat loss 8-73331
 particle in gas stream, convective, diffusion with nonlinear kinetics of heterogeneous chem. reaction 8-83499
 pipe, heated, vertical, gas buoyancy effect on downward flow and heat transfer 8-74427
 pipe, rotating, curved, convection heat transfer, appl. to spacecraft spin system 8-94737
 plane channel of variable cross-section, conjugate heat transfer (*French*) 8-59386
 plasma sheet, adiabatic accel. of ions induced by convection 8-88997
 plate, downward-facing, flat, heat transfer augmentation by nonuniform elec. field corona 8-94873
 plate, flat, optically thin boundary layer, of grey medium near leading edge, radiative-convective heat transfer 8-91027
 plate, multiply connected, convective heat exchange, small parameter method for thermoelastic equilib. problems. (*Russian*) 8-63301
 plate melting in free convection flow 8-94531
 plate temp. oscillations, response of horizontal free convection boundary layer 8-59391
 plume, above vert. heated plate, development of wall and free types 8-90881
 plume, turbulent, thermal, along vert. wall, struct. and heat transfer 8-90880
 porous cavity, Darcy medium, 2-dimens. solns. 8-91007
 porous medium, deep evaporation characterisation, of water (*French*) 8-59468
 porous medium, horizontal, subjected to end-to-end temp. difference, natural convection 8-91010
 potential flow over bodies, convective heat transfer 8-59395
 radial heat transfer, conduction, convection and heat of phase change 8-90700
 radiative-convective heat transfer, numerical methods 8-94577
 radiative-convective heat transfer from extended surface, Monte Carlo method 8-67005
 radioactive gas adsorpt. in porous medium, convective diffusion (*Russian*) 8-87387
 Rayleigh-Benard convection, crit. effects 8-71328
 Rayleigh-Benard convection, periodic thermal perturbation, chaotic response 8-94685
 rectangular cavity packed with porous media, heat transfer 8-71392
 river/atmosphere time dependent, single dimensional heat exchange, analysis (*Bulgarian*) 8-57221
 rod cluster assembly, forced convection heat transfer, Poisson eqn. by finite difference scheme 8-79189
 rotating annulus with negative radial temp. gradient 8-90912
 roughened rod in smooth channel, turbulent convective heat transfer 8-51241
 saturated porous material in box, three-dimens. convection 8-71393
 sea water, haline connection induced by freezing (*Japanese*) 8-88843
 semiconvection in stars, semitheory 8-69787
 shear flow, stratified, free-turbulent, buoyancy effects on large scale struct. 8-90849
 slab with temp. depend. thermal cond., convective boundary, transient cond., finite difference method 8-75031
 solar corona, mag. loops, downflows and convection 8-93175
 solar cosmic rays propag., diffusion in mag. fields, convection in solar wind, dimens. method soln. (*Chinese*) 8-81511
 solar energy compound parabolic concentrator, natural convection, finite element soln. 8-90634
 solar granulation, Benard cell convection model rel. to spatial power spectrum 8-65581
 solar photosphere, convective correction to spectral lines measured wavelengths 8-93181
 solar photosphere, small-scale mag. fields and convection 8-53906
 solid laser planar active element convective cooling (*Russian*) 8-82978
 sphere in power-law fluid, convective heat transfer 8-87340
 stars, compressible convection onset in model atmospheres 8-65605
 stars, convection and magnetic fields 8-89185
 stars, convection in rotating spheres and spherical shells 8-89184
 stars, convective zone boundaries 8-89187
 stars, penetrative convection 8-89186
 stars, URCA convection 8-89189
 steady and time dependent convection in a rectangular box 8-94706

convection continued

- steam-water mixture, with high vap. content, annular flow, heat transfer, press. loss 8-75193
- Stefan problem simulation and control, associated variational inequality 8-67009
- stellar atmosphere, thermal-convective instability, radiative transfer effects 8-53929
- stellar convection, energy transport 8-89180
- stellar convection, hydrodynamics rel. to solar obs. 8-89182
- stellar convection, IAU Colloquium 38 (Nice, France, 1976 August 16-20) 8-89176
- stellar convection, mixing-length theory rel. to physical models 8-89179
- stellar convection 8-89194
- stellar convection theory (1930-1945) 8-89177
- stellar cores, He flash and convection 8-89191
- stellar dynamical instabilities at start of convection 8-89181
- stellar mixing-length theory 8-89178
- stellar photoconvection 8-89190
- stellar structure models, convection theory including turbulent kinetic energy flux 8-57543
- subcooled forced convection boiling heat transfer at subatmospheric pressure 8-94525
- submerged jet closed vessel recirculation flow, temp. distrib. and buoyancy 8-90958
- Sun, axisymmetric convection with a magnetic field 8-89165
- Sun, convective noise waves dissipation in solar upper atmosphere mag. struct. 8-65600
- Sun, convective zone cophasal regions model 8-96469
- sunspots, running penumbral waves origin 8-93188
- thermal convection in a large box with imperfectly insulated sidewalls 8-59399
- thermal convection onset under const. flux boundary conditions, mag. field effect 8-69676
- thermal convection with spatially periodic boundary conditions: resonant wavelength excitation 8-59392
- thermally driven shear flow heated from below, stability 8-67177
- thermogravitational convection asymmetry, finite difference method 8-59267
- thermosiphon, inverse, thermo-hydraulic design 8-94534
- thermosolutal convection rel. to stellar convection 8-89188
- three dimensional free convection flow and heat transfer along a porous vertical plate 8-90866
- tissue, microwave heating, effect of surface cooling and blood flow 8-57038
- tissue, perfused, macroscopic temp. distrib. 8-64944
- transient convective turbulent heat transfer in tubes, thermal and hydrodynamic instability 8-83485
- tube, horizontal, laminar combined convection, circumferentially nonuniform heating effect 8-71331
- tube, vertical, laminar and turbulent heat transfer, air and Ar 8-71332
- turbomachines heat transfer, unsteady 8-67198
- turbulent boundary layer, vel. profile 8-94693
- turbulent buoyancy convection heat transfer, two-dimens., with internal heat sources 8-94540
- turbulent convection within rapidly rotating superadiabatic fluids with horizontal temperature gradients 8-90913
- turbulent free convection heat transfer from flat vertical plate to power law fluid 8-67225
- turbulent vertical buoyant jet decay in uniform environment, unified scaling law 8-90905
- two-fluid system, in horizontal layer, with internal heat sources, natural convection 8-94539
- two-phase flow, dryout region of forced convection evaporation, heat transfer coeff. 8-90988
- two-phase flow instability in parallel channels 8-94810
- unified similarity theory, turbulent convection at vertical surface 8-90890
- upper atmosphere, ion convection momentum sources in thermosphere neutral comp. 8-77380
- Uranus thermal evolution, convective cooling model and comparison with Neptune 8-85903
- variable viscosity fluid, convective heat transport 8-55641
- velocity field amplitude, convection rolls, wavenumber dependence 8-71327
- vertical layer, steady convective flow stability, boundary thermal props. effect 8-55644
- vertical surface against stably stratified fluid, heat transfer 8-90885
- viscoelastic free convection boundary layer flow past infinite plate with constant suction 8-90936
- viscous flow, 2nd order upwind scheme critique 8-94744
- vortex filament form. from ascending flows over evap. liquid 8-63440
- wall temperature distributions, in regions of deteriorated heat transfer 8-83377
- water, cooling, boundary layer thermal state during transition from free to forced convection (*Russian*) 8-81192
- whirlwind, ring-shaped, onset caused by rising air in stratified atmosphere (*Russian*) 8-77298
- CO₂ laser, convective-cooled, fast-flow, pulse discharge stability 8-94389
- Fe₂O₃, hematite, reduction, exam. of role of convective mass transfer 8-52724
- H₂-CO₂, turbulent flow heat transfer, expt. and numerical anal. 8-94690
- He, supercritical, natural convection heat transfer 8-94694

convection in liquids

- Alad'ev wall superheat correl., expt. validity test 8-83393
- cathodic diffusion boundary layer, free convective flow obs. with shadow Schlieren method 8-68894
- channel, rectangular, laminar forced convective heat transfer for 3rd kind temp. boundary conditions 8-87341
- complex domain heat exchange, new soln. techniques 8-94509
- cone/plate system in fluid, friction heating and convection 8-87238
- duct, circ., laminar convective MHD heat transfer for 3rd kind temp. boundary conditions 8-87342
- embedded heater in solid, melting and natural convection 8-90646
- enclosure with heat source and sink on horiz. boundary, laminar natural convection 8-90882

convection in liquids continued

- film boiling under natural convection conditions, heat transfer 8-83231
- fine particle deposition, on rotating disc surface, convective diffusion under elec. double layer forces 8-61060
- free convection in finite vertical channel, magnetic field effects 8-67270
- free convection mass transfer from horizontal surface, electrochemical and holographic interferometric obs. 8-87344
- Freon-11, pool-boiling, heat transfer from inclined plate 8-51046
- hydrodynamic stability open disc theorem, thermal and thermohaline convection 8-59370
- incipient boiling, transition to film boiling 8-90660
- laminar dispersion in rectangular conduits, side wall effects, convection 8-94636
- laminar film, convective coupled heat transfer, Nusselt no. computation 8-59398
- laminar fluid convection, liq. flowing in annular channel with const. heat flux, numerical soln. 8-83392
- liquid, dielectrophoretic heat transfer 8-94874
- liquid fuel droplet heating with internal circulation 8-75194
- liquid metal continuous casting, solidification process, convective heat transfer, anal. 8-84789
- magnetic fluid, thermoconvective instability, with mag. field perturbations 8-94847
- magnetic fluid (cable coolant), natural convection heat transfer 8-94846
- measurement by differential light interferometer with achromatic $\lambda/2$ compensation 8-87419
- melting, of substrate into different miscible liq. layer, hydrodynamic instability, heat transfer 8-90695
- melting solid, role of natural convection 8-71275
- MHD convective viscous flow past porous plate with suction, mass transfer effects 8-87398
- mixed laminar convection in vertical tube, thermophysical prop. temp. depend., effects 8-90895
- mixture, binary, oscillatory convective instability, thermodynamic anal. 8-94753
- multilayer flow, thermoconductive waves, interaction with radiation induced waves (*German*) 8-94803
- natural convection in liquids with temperature dependent viscosity 8-94695
- non-Newtonian fluid, effective diffusion of impurity in laminar flow of liquid 8-67228
- non-Newtonian fluid, hydrodynamic stability of free convection in vertical layer 8-59430
- open channel thermally stratified flow, eddy diffusivity buoyancy effects, obs. 8-90904
- pipe, horizontal, with different end temps., fully developed natural counterflow, temp. distrib. 8-75137
- pipe flow, turbulent, temp.-depend. viscosity effect on convective heat transfer 8-90884
- polyary mixtures, natural convection boiling, heat transfer 8-90658
- pool boiling heat transfer from horizontal plates (*Japanese*) 8-67016
- pool heated volumetrically, reactor accident condition, phase change, free surface, thermal instability 8-89960
- porous cylinder, water-saturated, heated, natural convection onset 8-59478
- porous media of low permeability, heat transfer in forced convection 8-83472
- pseudoplastic fluid, flowing upward in vert. heated tube, variable physical props. 8-90945
- rotating horizontal fluid layer, thermal instability 8-63438
- saturated porous medium, completely confined, onset of thermal convection 8-83387
- silicone oil thin films, convective heat transfer, surface tension effect 8-94681
- surface-tension induced convection at reduced gravity 8-83374
- suspension, dielectric, convective heat transfer, rheodynamics, in horizontal coaxial cylindrical channel 8-59494
- thermal instability anal. for horizontal liq. layers with a density max. 8-67193
- thermocapillary convection, unevenly heated liq. stream near gas bubble 8-59460
- transformer, oil-cooled, heat exchange anal., network method (*Russian*) 8-83399
- turbulence, free-stream, near semiinfinite flat plate, vortex array representations interaction 8-90842
- turbulent liquid flow in heated tube at supercritical press., heat transfer 8-71316
- turbulent natural convection boundary layer, space-time correl. meas. 8-71322
- turbulent natural convection in liq. metals in narrow cell (*French*) 8-94701
- underground cable system, convectively cooled, temp. distrib., heat transfer correlations 8-71262
- underground cable system, convectively cooled, vel. distrib., press. drop correlations 8-71330
- vertical tube with laminar combined convection, water, finite difference anal. 8-90894
- visco-elastic liquid, flow past hot porous circular cylinder, free and forced convection 8-83386
- viscous fluid, smooth transition to convection 8-83396
- water, forced laminar convection in horizontal pipe, density inversion effects, numerical anal. 8-90900
- water, natural convection at density extremum 8-94696
- water, transition boiling under forced convective conditions, reactor accident condition 8-89961
- water cooling through free surface, critical value of boundary Rayleigh number (*Russian*) 8-61426
- Al₂O₃, floating zone melting, forced convection, computer simulation 8-88422
- He distrib. system for Large Coil Test Facility 8-55001
- *He, superfluid, thermo-osmotic convection, at incipient lambda transition, above crit. press. 8-95199
- NaClO₃, growth and dissolution kinetics, diffusion and convection regimes 8-63684
- Si, floating zone melting, forced convection, computer simulation 8-85422

convergence

see also *convergence of numerical methods*

biorthogonal series convergence, biharmonic and Stokes flow edge problems 8-81847
eigenfunction expansions assoc. with vector-matrix differential eqn., convergence 8-69965
multiple Fourier series, convergence of rectangular partial sums 8-73831
off shell scattering amplitude, S-matrix, pot. scatt., Mittag-Leffler expansions of Green's function, convergence 8-73874
stochastic approx. procedures in continuous time 8-69969
Wigner-Kirkwood expansion of second virial coeff., convergence accel. 8-91052

convergence of numerical methods

approximation method for solution of nonlinear integral equation with error estimation for problems in heat or mass transfer (*Russian*) 8-57879
aqueous solutions, Monte Carlo simulation, convergence of new algorithm 8-63649
atomic struct., numerical HF radial function during SCF iteration, convergence 8-58574
Bayesian deconvolution, convergent props. 8-57861
Bayesian deconvolution, noise props. 8-57862
boundary layer problems, singular perturbations, stability and convergence 8-90827
CLEAN method, iterative beam removal, mathematical-statistical description 8-57464
collocation finite element method for groundwater flow simulation 8-93018
collocation variational method for solving Fredholm integral eqns., convergence condition 8-57764
constrained finite element solns., convergence proof 8-54168
continued fractions method for Mie scatt. calcs. 8-82914
cooperative stereo algorithm anal. 8-53413
cylinder, infinite, solid, diametrically opposite conc. load deform. and stress 8-63287
density series, analysis of tail for Coulomb crystal energy 8-91300
diatomic molecule vibr. pots., representations accuracy 8-66531
differential equations, first order, convergence of averaging method and two-timescale method 8-85835
direct gravity formula for 1967 Geodetic Reference System 8-92775
fibrous materials, chain of bundles probability model for strength, numerical study of convergence 8-88496
finite element anal. of buckling of simply supported skew plates 8-59319
finite element method groundwater two-dimensional flow digital simulation 8-93018
fracture mechanics, appl. of method of pots. 8-51121
function minimum norm approximation 8-54166
Galerkin's method, non-uniform convergence 8-83304
heat exchanger true vibrations numerical soln. 8-75094
heat transfer, nonlinear, iterative-variational method 8-94511
heat transfer in laminar freely convecting boundary layer, series soln. predictive capability 8-71335
implicit finite element algorithms for geometrically nonlinear problems of struct. dynamics, accuracy anal. 8-86158
ionospheric data processing, improvement of convergence of least squares method (*Russian*) 8-85700
iterative procedures for penalty function solns. of algebraic systems 8-57770
laminar flow with separation, successive approx. algorithm, convergence (*Russian*) 8-75117
MC-SCF theory, orthonormality-constrained orbital optimisations 8-86766
mesh analysis processes (*German*) 8-87257
molecular orbital CI calcs., convergence rate 8-70750
molecular orbital SCF calcs., accel. convergence using reverse level shifting technique 8-70735
Navier-Stokes equations, theory and numerical analysis, book 8-77721
nonlinear free surface flow problems, divergent low Froude number series expansion 8-51146
nonlinear variation eqns., convergence of finite element solns. 8-86127
orthogonal polynomials expansions, summation procedure 8-81805
Pade approximants, punctual, partial wave expansion summations in scatt. by long range pots. 8-49707
perturbation method and boundary conditions at noncanonical surfaces (*Russian*) 8-77696
plate, rectangular, with clamped simply supported edge conditions, free-vibr. anal. 8-59340
radiowave propagation, numerical approximations of Sommerfeld integral for fast convergence 8-66727
Seidel's process for linear eqns. with non-negative elements (*Ukrainian*) 8-54165
shifted Chebyshev polynomials, soln. of second kind operation eqns., convergence 8-62059
spherical dome, three-dimens. elasticity soln. and edge effects 8-59306
stable operational processes appl. to inverse geophys. problems 8-85718
Stoke's problem in velocity pressure formulation, mixed finite element approx. (*French*) 8-86164
two-dimensional neutron diffusion eqn. for triangular region, finite Fourier transform soln. 8-78432
viscous flow, 2nd order upwind scheme critique 8-94744
water, liq., Monte Carlo simulation, convergence of new algorithm 8-63649

conversion electron spectra

conversion electron Mossbauer spectroscopy down to 4.2K, applications to thin film and surface studies 8-84504
double focusing Fe core electron spectrometer BILL for (n_e^-) meas. 8-82566
high-spin states, means and methods of investig. 8-86722
microfoil conversion electron detector for Mossbauer spectroscopy 8-70698
Mossbauer spectroscopy, electron transport anal. 8-94159
polarisation of conversion electrons, parity violating nuclear forces 8-50125
 $^{157}\text{Gd}(n,\gamma)$, γ and conversion electron spectra, ^{158}Gd collective bands 8-89819

conversion electron spectra continued

^{180}Hf , polarisation of internal conversion electron calc. 8-50125
Hg, $A=191,2,3,5,7,9$, rot. aligned bands, high spin states, energy levels $B(E2)$ values 8-70483
 ^{208}Pb , obs. of levels in $^{198}\text{Hg}(\alpha,2n)$ 8-66192
 $^{207}\text{Po}^m(2.79\text{ s})$, $^{207}\text{Po}^s$ decay, spin from conversion electrons meas. 8-58252
 ^{191}Pt , $A=190-193$, lifetimes of rotation-aligned states 8-93969
 $^{121}\text{Sb}(n,\gamma)$, γ and conversion electron spectra, ^{122}Sb energy level scheme 8-54721
 $^{205}\text{Tl}(\alpha,3n)$, 35-51 MeV, ^{206}Bi high-spin states anal. 8-82368
 ^{165}Tm , levels from ^{165}Yb β -decay, γ and conversion electron spectra 8-74334

converters see converters**convertors**

see also *analogue-digital conversion; digital-analogue conversion; direct energy conversion; frequency converters; image converters; magnetohydrodynamic converters; magnitude converters; power converters; solar absorber-convertors*
charge to voltage convertor, for ionisation chamber dosimeters 8-78505
frequency-voltage convertor for angular velocity meas. (*Polish*) 8-70101
Pt-Rh resistance thermometer temp. convertor for nonlinearity error correction (*Russian*) 8-70124

cooling

see also *Joule-Thomson effect; low-temperature production; magnetic cooling; refrigeration; supercooling*
ablation of elastic solid, variational principle 8-90698
air, radiative cooling behind strong shock waves 8-91030
atmosphere, IR cooling rates, effect of tropospheric aerosols 8-88886
bubble growth, noncondensing gas-vap. injected into liquid 8-55553
cable oil, EHD pumping 8-87414
circulating cooling system, based on commercial 6.3 helium liquefier 8-57961
condenser system, submerged, bubble pumped augmented natural convection 8-94535
cryogenics, a critical review 8-89485
deflecting septum magnet for cyclic accelerator 8-78525
dendritic ice form. in pipe, cooling rate effect 8-90690
electrical circuit, slowly modulated dissipative steady state, $dQ=TdS$ far from equilib. 8-81934
electronic components cooling tube, calc. method (*Russian*) 8-59271
electronic cooling, developments (*Russian*) 8-86712
electrophotographic copier photoconductor drum cooling methods 8-62245
expansion cloud chamber with thermoelectric cooling 8-90034
explosive r process cooling process 8-69791
fibre optic image tube, cooling effect 8-96401
film cooling efficiency, axisymmetric air flow rot. cylinder, main flow swirl effect 8-75132
flow rates through porous media, heat and mass transfer (*Russian*) 8-59479
fluidised bed, plasma jet cooling mechanism 8-79371
frost growth rate prediction eqn. for cooled surfaces 8-87248
fusion reactor magnet coil, 125 kG, 1 m, design, fabrication 8-55008
gas, with variable physical props., pipe flow, turbulent momentum and heat transfer calc. 8-90869
gas-solid particle suspension, turbulent flow in curvilinear channel, local heat exchange 8-63484
heavy particle beam cooling in an electron flux, mag. field effects 8-82557
hexahedrite meteorites, cooling rates 8-57511
hot wall with impinging liq. droplet, transient temp. profile 8-75050
hypersonic gas flow, radiant heat and evaporative cooling 8-91028
jet cooling on heated plate, surrounding fluid effect 8-79350
land basin with snow, radiative cooling 8-88872
magnetic fluid (cable coolant), natural convection heat transfer 8-94846
Manicouagan impact melt sheet, Quebec, thermal history 8-81167
metal growth in space, theoretical models, comparison with ground expts. 8-84786
mixture, binary, time-depend. solidification, series soln. 8-75058
Neptune thermal evolution, convective cooling model and comparison with Uranus 8-85903
nuclear power station spray cooling, heat and mass atmospheric transfer 8-94078
oil-cooling baffled shell-and-tube heat exchanger expt. 8-83395
orbiting astronomical telescopes, IR detector cryogenic cooling requirements 8-96400
photomultiplier cooling by semiconductor microrefrigerators 8-57942
pipe, of variable thermal and elec. conds., elec.-heated, flow-cooled, temp. distrib. 8-90626
plate, downward-facing, flat, heat transfer augmentation by nonuniform elec. field corona 8-94873
quenching temperature, 0.03-1.3 MPa, base material thermal props. depend. 8-94587
radiation press cooling of ions in Penning EM trap 8-66527
resin slab, stress response, fluctuating external moisture (temp.) effects 8-55620
rod, expanding, conductive heat transfer computation, fast numerical technique 8-75029
solid laser active element, circular, cooling process, variation in ambient temp. (*Russian*) 8-74915
solid laser planar active element convective cooling (*Russian*) 8-82978
spectroscopic cooled and intensified array detectors 8-65983
stable low-temperature source to test for cold urticaria 8-61276
steam condenser, supersonic nozzle discharge, heat transfer and gasdynamics 8-55671
steel, magnetite film formation at metal scale interface, during cooling 8-88575
stochastic cooling tests on proton beams, initial cooling expt. 8-90006
superconducting magnet circulation cooling system based on He liquefaction apparatus 8-57992
superconducting magnets, cooling system using liquid He 8-54998
superconducting magnets, force-cooled conductors design 8-54999
superconducting magnets, hollow conductors, cooled by supercritical He 8-54997
temperature cycling apparatus using liquid He storage Dewar 8-65938

cooling continued

- thermoelectric, rectangular monolithic infinite cascade thermojunctions 8-57944
 thermoelectric element, arbitrary shape, cooling efficiency 8-67010
 thermoelement cooling control by variation of geometric shape 8-62195
 tissue, microwave heating, effect of surface cooling and blood flow 8-57038
 transformer, oil-cooled heat exchange anal., network method (*Russian*) 8-83399
 turbulent air flow in round tube, high-temp., friction resistance, cooling (*Russian*) 8-75135
 turbulent water film, with different initial flow conditions and high temp. gradients, heat transfer 8-90862
 two-phase porous cooling system development 8-59477
 underground cable system, convectively cooled, temp. distrib., heat transfer correlations 8-71262
 underground cable system, convectively cooled, vel. distrib., press. drop correlations 8-71330
 Uranus thermal evolution, convective cooling model and comparison with Neptune 8-85903
 vaporising coolant enthalpy for cryodevice initial cooling (*Russian*) 8-70130
 water cooling through free surface, critical value of boundary Rayleigh number (*Russian*) 8-61426
 Ag composite, SiC whisker-reinforced, prep. aboard Skylab. 8-84741
 Al-In (40, 70 wt.%), liq. phase immiscible system, solidification in microgravity 8-84770
 Au-Cd (47.5 at.%), effect of cooling rates on stress-strain behaviour 8-76721
 Ba⁺ ion cloud containment in RF trap, <50 ions, optical sideband cooling 8-75407
 countercurrent single- and two-phase flow effects on hot surface quenching rate 8-59451
 Fe, cast, dispersed with interdendritic graphite, eutectoid transformation of austenite during cooling 8-84800
 GaAs n-n⁺ epitaxial structure for CW microwave electroacoustic amplifier 8-59235
²H-¹H molten-salt-cooled fusion reactor blankets, nuclear heating and radiation leakage 8-78490
 He distrib. system for Large Coil Test Facility 8-55001
 Li, liq. cooled pulsed fusion reactor blanket heat transfer, numerical calc. 8-94141
 N cooled discharge plasma electron energy distrib. function 8-63633
 N₂O₄ dissociating coolant, chemical reaction kinetics in transient regimes (*Russian*) 8-58344
 N₂O₄ dissociating coolant, O₂ generation time constant, enthalpy change (*Russian*) 8-58345
 Si/Li spectrometer, using Peltier elements (*Czech*) 8-49947

cooling towers

- see also water supply
 with column supports, free vibration analysis 8-83292
 model and full-scale cooling tower resonance tests 8-83291

Cooper Hewitt lamps see mercury vapour lamps**Cooper pairing** see Cooper pairs**Cooper pairs**

- see also BCS theory; Josephson effect
 AC Josephson-Fiske effect, coherence 8-88082
 multi-valley semimetals with Coulomb interaction between electrons (*Russian*) 8-64165
 self-consistent selection of a superconducting representation for the BCS model 8-88067
 two-band systems, BCS pairing and Peierls distortion compatibility 8-88068

coordination complexes

- inorganic complexes are indexed under the appropriate metal compound headings
 EPR of doped mag. centres 8-64259
 nuclear power station decontamination, chelating agent appl. 8-50280
 oxine, impregnation of activated charcoal, adsorption of ⁶⁰Co from waste water 8-58365
 radiolytically formed chelating agents, corrosion prevention appls. 8-64745
 transition metal, electronic energy transfer process 8-56907

copolymerisation see polymerisation**copper**

- see also nuclei with
 absorbed O₂, ion-bombardment, ejected particle ang. distrib. 8-95643
 acoustic velocity, shock-compressed uniform solid, lateral discharge ang. semiempirical formula (*Russian*) 8-55910
 activity distrib., UO₂ natural reactor fuel in ZED-2 hot loop facilities 8-58347
 adsorption, of H, potential energy curves, pairwise additive model calcs. 8-73087
 adsorption of CO, angle-resolved UPS and adsorbate induced struct. 8-71983
 adsorption of O₂ on (210) surface, LEED and AES meas. 8-71998
 adsorption of O, on (001) surface, deep core level XPS anisotropy 8-72690
 AES, valence band spectra, solid-state and atomic features 8-72646
 alkali silicate glass, CuO doped, ESR spectra of Cu²⁺, quadrupole effects 8-64265
 amplitude depend. modulus effect 8-64573
 angle-resolved photoemission, band struct. 8-95680
 angle-resolved photoemission, prediction of spectral peak intensities 8-72695
 annealed, cyclic plasticity under cyclic nonproportional strain histories, cyclic hardening, memory erasure, strain hardening 8-88510
 annealed and cold rolled, with bamboo structure, exam. of grain boundaries as vacancy sources in diffusional creep 8-88508
 annealed O free, high cond., proportional biaxial cyclic hardening 8-84844
 anode spot form., in vac. arc, threshold current time depend. 8-87515
 atom, γ -ray absorption cross-sections, 10-160 MeV 8-90136
 atom, beam foil spectra, 20 to 350 nm wavelength, 16 to 110 MeV beam energy 8-78655
 atom, electron impact, excitation function (maxima, cross-sections) 8-50650
 atom, large angle K-shell ionisation probabilities, projectile charge and mass depend. 8-74750

copper continued

- atom, oscillator strengths, relativistic HF, core-polarisation model pot. 8-86818
 atom, semiempirical, relativistic oscillator strengths including core polarisation for p-, s-, d-series 8-74609
 atom K-shell ionis., X-ray prod. cross section for incident H⁺, ⁴He and ¹⁴N ions 8-70923
 atomic ground and metastable populations, buffer gas effect 8-82955
 atomic oscillator strengths, formula for cancellation disappearances 8-90124
 atomistic images of field ion microscopy at high temps. 8-55792
 Auger spectra, L_{2,3}VV and MVV 8-68583
 Auger spectra, MVV, atomic model and valence band features 8-72644
 bicrystals, effect of grain boundary on tensile deformation (*Japanese*) 8-88495
 Bloch states, photoelectron spectra, angle resolved 8-92175
 Bragg diffraction, anharmonic contributions, Mossbauer study 8-76358
 bremsstrahlung, β generated, spectral shape depend. on target thickness 8-56545
 cathode spots on vac. arc discharge electrodes, model 8-91179
 cathodes, erosion, vacuum to atmospheric press. arcs 8-79482
 cellular method calc. for nonsppherical potential 8-56063
 chemisorption, of CO, SIMS, AES, desorp. meas. 8-87875
 chemisorption and oxidation of ethanol on (110) surface 8-61044
 chemisorption of CO, coverage depend. photoelectron spectra, adsorption sites 8-95647
 chemisorption of CO, on (001) face, electronic struct. of (M)₂CO clusters 8-95948
 cluster, and bulk, struct. and electronic props. 8-95592
 cluster, optical spectroscopy, atom to bulk 8-95591
 clusters, size, geometric effects, catalysis implications 8-73131
 coalescence of SiO₂ particles 8-92271
 cold worked, determ. of dislocation pinning and unpinning stages, using internal friction meas. 8-92278
 cold worked, grain size effects on short-term strength (*Russian*) 8-56693
 collection mirrors for synchrotron radiation, Cu material 8-62275
 commercial pure, creep-rupture props., vacuum, (*Japanese*) 8-72843
 concentration in atmospheric sedimentable powder, in Vizcaya, Spain (*Spanish*) 8-57265
 concentration in snow of Mt. Blanc rel. to air pollution 8-81258
 corrosion, effect of addition of bromides and iodides, in seawater 8-80670
 crack nucleation and stage I propag. in high strain fatigue, microscopic and interferometric obs. 8-52936
 crack nucleation and stage I propag. in high strain fatigue, mechanism 8-52937
 creep curves, comparison with theory 8-79232
 crystal potential in electron diff. and band theory 8-83677
 cutting of bicrystal to compare mechanism for large crystals and polycrystals (*Japanese*) 8-60871
 cyclic hardening role in crack nucleation at high strain amplitude 8-64633
 cyclically deformed, nucleation of persistent slip bands 8-72830
 cylindrical metal liners, explosion-accelerated, form stability anal. 8-83425
 Debye Waller determ. from modified Cheveau model 8-59918
 defect annealing study by positron annihilation, and elec. resistivity meas. 8-51584
 defect removal, obs. by positron annihilation 8-84677
 deformed, intensity and lattice strain distrib., exam. (*German*) 8-52885
 determination, in powder rock samples, by at. absorpt. (*Russian*) 8-85278
 determination, separation from Sb in Cu alloys, inverse voltammetry method 8-61099
 dibarium cobalt formate tetrahydrate:Cu, EPR of Cu-Co interactions 8-60334
 diffusion, in Al, isotope effect 8-84006
 diffusion coefficients calc. for H and D (*Russian*) 8-91483
 diffusion in Au electrodeposited coating, under high temperature, influence on contacts performance (*Czech*) 8-91486
 diffusion in Ga_{1-x}In_xP, epitaxial film, effect of intrinsic impurities 8-87825
 diffusion in P₂O₅-glass, fluoresc. meas. 8-59980
 diffusion of ¹¹⁰Ag, activation energy, form. enthalpy of vacancies 8-51736
 diffusivity and solubility in LEC GaP 8-51743
 dislocation damping during electron irradiation, new model for peaking effect 8-87683
 dislocation substructure formation under hydrostatic extrusion 8-56696
 drawing deform. band form., axial orientation force meas., X-ray pole figure determ., on single crystal (*Japanese*) 8-76710
 dynamic material behaviour under nearly uniaxial strain conditions, modified Kolsky apparatus 8-85070
 electrical conductivity, effect of cyclic strains and work hardening at 4.2K 8-91655
 electrical resistivity, electron-electron scatt. and Fermi surface calc. 8-64023
 electrical resistivity, press. variation 8-84193
 electrical resistivity of dislocations, calc. (*Russian*) 8-60117
 electrodeposited coating, annealing effect on struct. and microhardness (*Russian*) 8-76668
 electrodeposited coating on Fe membrane, effect on H permeation, proposed catalytic mechanism 8-53252
 electrodeposited single crystal film, fatigue cracking investigation (*Japanese*) 8-84975
 electrodeposition on Cu single crystal (100) face, in presence of Br ions 8-84723
 electroforming, study of process variables in the electromagnetic bulging of tubes 8-80582
 electrolytic deposition, collagen and chloride additions effects obs., on morphology and crystal orientation 8-51852
 electrolytic deposition from CuSO₄ solns. 8-61022
 electromigration, thermomigration, and solubility, in Pb 8-71882
 electromigration in Pb 8-84003
 electron beam reflection, high current (*Russian*) 8-84690
 electron irradi., very low atomic displacement threshold energy obs. 8-95078

copper continued

- electron irradiated, stage III recovery kinetics 8-63792
 electron states, parametrised, separable potential for band structure calculations 8-79912
 electron transmission and absorption, 70 keV initial energy 8-71777
 electronic props., pseudopotential calc. 8-51960
 electronic structure, empirical parametrisation scheme 8-91585
 electroplated coating, levelling kinetics, interferometric investigation (*Bulgarian*) 8-79864
 energy reflection coefficient for 5 to 10 keV He ions 8-95639
 epitaxial, on (111) Au, periodic arrays of misfit dislocations, electron diffr. 8-51857
 epitaxy on W (001) 8-60041
 equation of state, isentropic expansion method 8-91414
 in estuarine environments, inorganic speciation 8-69371
 evaporated layer on Ge, RHEED Kikuchi bands, anomalous contrast 8-87597
 EXAFS in photoelectron yield spectra and optimisation of the photon glancing angle 8-80435
 exploding foils, rapid mag. energy transfer, conductivity law (*French*) 8-91135
 explosive compaction of metal powders 8-64501
 facing Cr steel, thermodynamic anal. 8-60878
 failure under hydrostatic press., kinetics 8-52944
 fatigue behaviour effect of Zn, Au diffused coatings 8-72850
 fatigue crack initiation, model using probabilistic technique 8-68800
 FCC, appl. of model for lattice dynamics 8-91387
 film, aggregated, absorpt. peaks, collective oscills. of electrons 8-80428
 film, annealing effect on grain size 8-72015
 film, APW band struct. calc., muffin-tin potential 8-87899
 film, band struct., appl. of extended rigorous cellular method 8-52055
 film, deposited on polystyrene substrate formation of Cu-O-polymer complex 8-92372
 film, electrodeposited, recrystallisation kinetics, X-ray scatt. (*Russian*) 8-60045
 film, energy losses of 20-40 keV electrons 8-92153
 film, epitaxial on Mo, S impurity segregation at interface 8-84076
 film, evaporated, interaction with BCl_3 , HCl, adsorpt. 8-75945
 film, ion-plated, stainless steel, porosity depend. on process parameters 8-84720
 film, polycryst., nodule mechanism of diffusion-induced disintegration (*Russian*) 8-51829
 film, vacuum deposited, O^+ bombardment sputtering rates 8-88390
 film continuity, observations by Auger spectroscopy 8-64433
 film sandwich structures Auger anal. 8-72030
 flow detector tube filter use 8-56857
 foil, elec. explosion, dielec. breakdown 8-67388
 foil, energy straggling of 6.74 MeV protons 8-79641
 foil, role of grain-boundary porosity in superplasticity (*Russian*) 8-56690
 foil, sputtering with ^{252}Cf fission products, desorbed secondary ions 8-68596
 fracture criterion, expt. verification 8-64648
 fracture due to shock waves leaving surface, shear stresses 8-51128
 Frenkel pair production threshold energy, temp. depend., exam. 8-51530
 friction props. of surface films in air and high vacuum 8-60850
 friction under electrolyte immersion condition 8-64738
 fusion reactor shield, neutron induced activity and γ -ray source investigation 8-54872
 geochemistry in sediments of Gulf of St. Lawrence and estuary 8-92855
 grain boundary sliding and intergranular fracture, in bicrystals 8-75717
 grain size effect on acoustic emission generated during plastic deformation 8-80609
 Gruneisen parameter, behaviour at high press. 8-83899
 high conductivity, high sp. ht., for cryogenic appl., prep. 8-76670
 hollow cathode discharge population mechanism for highly-excited states (*Russian*) 8-63610
 horizontal plate, pool-boiling heat transfer, nucleation centre size, surface roughness 8-90652
 implantation in mild steel, annealing and rolling behaviour of conc. profile 8-75684
 implanted ion detection by X-ray emission anal. in TEM 8-51575
 initial sintering, method for obtaining surface diffusion coeffs., appl. to shrinkage data 8-95713
 interaction of annealing twins in fcc metals and alloys 8-68712
 interatomic potential from intermediate and low energy data 8-55829
 interatomic potentials from experimental phonon spectra 8-75621
 interdiffusion with sintered Al powder, struct. effect at high press. 8-60606
 internal stress meas. by decremental unloading technique 8-64576
 internal stresses in plastically deformed crystals (*Russian*) 8-79615
 ion impact phenomena, computer simulation 8-88396
 irradiated, containing self-interstitials and vacancies, electronic transport props. 8-60105
 irradiated, exam. of dislocation bias for interstitials to edge dislocations 8-79612
 irradiation induced defects, electron microscope images 8-83854
 isochronal recovery of high energy d-Be neutron damage 8-51592
 kfor=for 8-80822
 laser, CuBr lasant, continuously pulsed, long duration, high efficiency operation 8-79029
 laser, discharge heated longit., scaling 8-50790
 laser, using Cu acetylacetonate as Cu atom donor 8-82956
 laser impact, multiple crater refl., effect on refl. props. 8-52596
 lattice and grain boundary diffusion of P, exam. of diffusion rates by tracer sectioning technique 8-79817
 lattice atom displacements near end of implanted μ^+ tracks 8-55890
 LEED anal. of surface struct. 8-71914
 liquid, absorption of gaseous O_2 8-51686
 liquid, diffusion of Tl, Ir, Pb and Bi (*Japanese*) 8-59962
 liquid, multiple scatt. calcs. of resist. 8-76039
 liquid surface tension meas. with levitated metal droplets, influence of oscill. amplitude 8-51798
 metabolic model and dosimetric data 8-65130
 mirror, diamond turned, surface and optical studies 8-79098
 monolayer, (001), level ordering of states 8-91748
 monolayer, electronic struct. 8-72233

copper continued

- monopyrazine zinc sulphate trihydrate: Cu^{2+} , ESR meas. 8-84478
 muonic Coulomb capture, ionic charge effect 8-66694
 neutron yield calcs., electron beam incidence 8-95622
 nitroxide free radical mag. interaction with lanthanides or Cu^{2+} in liqs., ESR 8-68380
 noncrystalline, electronic density of states, multiple scatt. calcs. 8-91578
 O free, annealing in photoemission electron microscope, twin density recrystallised grain size relation (*German*) 8-52850
 OFHC, creep and relaxation curves for torsion-tension members at elevated temps. 8-83260
 ore, leaching, effects of ultrasonics and their appls. 8-92214
 ore processing materials, nondispersive X-ray fluoresc. anal. 8-92575
 oxidation in CO_2 , 800-1000°C 8-76784
 oxidation of (111) single cryst. surface, laminar Cu_2O growth 8-72025
 partial densities of states, electron-phonon interaction 8-51869
 passivation by protective glassy layers at 500°C 8-76785
 phonon dispersion relations and Debye-Waller factor calcs. 8-51630
 phosphate glasses: Cu^{2+} , EPR, optical spectra 8-72399
 photoemission, bulk versus surface effects 8-52626
 photoemission, temp. and photon-energy induced breakdown of direct transition model 8-95681
 pipe carrying potable water, corrosion 8-92409
 planar channelling of α -particles, stopping power of solids 8-51602
 plastic strain meas. due to sliding wear 8-64731
 plastically deformed crystals, SEM exam. of light and dark etch pits, dislocation arrangements 8-87679
 polishing in H_3PO_4 , polarisation curves 8-56851
 polycryst. surface, Ar^+ sputtered, ion to neutral yield ratio, SIMS anal. 8-72659
 polycrystalline, Ar ion double scatt. 8-88399
 polycrystalline, effect of grain size, specimen thickness, on mech. props. 8-84945
 polycrystalline, magnetoresist. due to crystal defects 8-56128
 polycrystalline target back sputtering of 100 to 500 eV Ne ions, computer simulation 8-60537
 polymer laminate, fracture surface exam. by XPS (*German*) 8-84992
 porous, sintered, deform. diagram based on theory of plasticity (*Russian*) 8-88494
 positron annihilation characteristics, effect of temp. 8-64427
 positron-vacancy interactions, equilb. temp. depend. of positron annihilation 8-76547
 powder compact, elec. resistivity 8-64028
 powders, prep. of spherical starting particles, for suspension electrolysis 8-60689
 protective coating on Al powder (*Russian*) 8-60881
 proton impact X-ray emission, ang. distrib. and polarisation fraction 8-56546
 proton irradiated, muon spin rotation study at low temps. 8-92011
 PVC:Cu film, struct. and optical props., soln. growth technique 8-51837
 PVC-Cu composite, annealing effects on elec. resist. 8-68060
 radiation induced low-energy collision cascades, effects of thermal vibr. and zero-point motion 8-87705
 reference standards for radiation pyrometry, silver and copper freezing points 8-57888
 resonant cavities, RF loss reduction at 35 GHz by cryogenic cooling 8-93761
 saturation resistivity charges, ion and fission fragment irradi. induced 8-79643
 secondary ion emission, chain effect for fast recoils Ar^+ ion beam impact 8-56554
 SEM, electron channelling patterns 8-83697
 sheet metal, texture heterogeneity, numerical simulation (*French*) 8-92274
 single crystals, effect of stacking fault energy on extrusion and intrusion development 8-72826
 single crystals, in high temp. creep, meas. of internal stress 8-80608
 single crystals, influence of friction and geometry of deformation, on texture inhomogeneities during rolling 8-72792
 single crystals, positron trapping by edge dislocations, producing by bending 8-80606
 sintering, cold working, recrystn. annealing, mech. props. and microstruct., porosity recrystallisation and grain growth, survey 8-76660
 sliding charact., friction and wear (*Japanese*) 8-56778
 slip line length for single crystals, oriented along [100] and [111] 8-76664
 smelting, exam. of vacuum lift refining 8-60621
 specific volume meas., for ruby R_1 fluoresc. press. gauge calibration, 0.06-1 Mbar 8-70150
 spectral distrib. of X-ray braking radiation, due to electrons, calc. using Monte Carlo method 8-56538
 spheres, electrically augmented pneumatic transport at low particle and duct Reynolds numbers 8-87409
 sputtered with 15 or 30 keV H^+ , He^+ and Ar^+ ions, energy and angular distrib. 8-95625
 sputtering by Ar, Brinkman cross section, approx. for sputtering yield 8-76571
 steel fibre reinforced Cu, exam. of creep behaviour (*German*) 8-52931
 stimulated emission from explosively formed vapour, apparatus for obs. 8-50764
 stopping power for 28 MeV α -particles, re-evaluation 8-79651
 stopping power meas. for 4-5 MeV/N ^{16}O , ^{40}Ar , ^{65}Cu , and ^{84}Kr 8-70720
 stopping powers, projectile range for $Z=8-20$, 0.0125-12.0 MeV/nucleon 8-83856
 strain tempering by rapid heating and cooling of cold drawn wires (*Japanese*) 8-84863
 structure changes in single cryst. under influence of static and dynamic stresses (*Russian*) 8-92300
 substrate for solar selective surfaces, graphite coating props. 8-74952
 surface, (001), intensity profiles, barrier reson. features, LEED 8-64089
 surface, (001), scatt. of He and Ne atoms at 20K 8-80451
 surface, (001) and (111), angular resolved photoelectron spectroscopy 8-95652
 surface, (100), adsorpt. of CO, UV and X-ray photoelectron spectra, LEED 8-56037
 surface, (100), adsorption and incorporation of O_2 8-56042

copper continued

- surface, (100), adsorption of O_2 , angularly resolved UPS meas. 8-71956
- surface, (111), polarisation depend. of angle resolved photoemission spectra 8-56557
- surface, (311), struct. determ. by multiple scatt. calcs. of LEED intensities 8-56028
- surface, active nucleation site spatial distrib., bubble flow density 8-71267
- surface, adsorbed H_2 , adsorbate induced photoemission, book contrib. 8-95668
- surface, adsorbed monolayer of Kr, many-body interactions 8-84068
- surface, adsorbed N_2 , H, O and ethylene monolayers, UV-visible polarised modulation spectra obs. 8-72619
- surface, adsorbed NO , species identification, struct., dissociation, desorption, UV photoelectron spectroscopy 8-52635
- surface, adsorption of Sr^{2+} , ^{90}Sr tracer expt., immersion time, conc. and temp. depends. 8-87863
- surface, boiling props. of H_2O rel. to organics 8-90654
- surface, contact angs. meas., aq. ethanol (glycerine) solns., 20-70°C 8-56025
- surface, dissociation of H_2 , effect of surface roughness, classical trajectory calcs. 8-76925
- surface, excited state formed by B^+ impact, light emission coeffs. 8-64417
- surface, $H^+(H_2^+)$ ion impact, energy refl. coeffs. 8-54969
- surface, heated, water droplet evaporation, heat transfer characts. 8-59269
- surface, horiz., min. film boiling temp. of saturated ethanol-water mixture 8-90692
- surface, intermediate UPS/XPS synchrotron radiation study 8-52633
- surface, ion impact, mol. effects in electron emission 8-80446
- surface, photoelectron spectra electron refraction and light polarisation effects 8-72700
- surface, photoemission 8-52619
- surface, polished, with H_2O cryofilm, bidirectional visible and near IR reflectance 8-88274
- surface, polycrystalline, Ar ion bombard., regular pyramid production 8-59843
- surface, stay time meas. for physisorbing Xe 8-56044
- surface (100), oxidation electron spectroscopic study 8-64782
- surface (111), epitaxial growth of Pb and Ti, LEED, RHEED, AES study 8-84090
- surface cleaning by H^+ bombard., AES study 8-53022
- surface electron states, (111) terrace of stepped (211) face, photoemission meas. 8-84697
- surface energy band calc., significance for photoemission 8-95330
- surface sliding damage, no lubrication, materials depend. (Japanese) 8-56780
- surface spin-flip probability from TESR 8-91953
- surfaces, O_2 adsorbed, exam. of structure by LEED, O_2 pressure-temp. diagram (Japanese) 8-79884
- tellurite glass, Cu^{2+} and Ni^{2+} doped, band-pass filters for 550 to 616 nm, transmission characts. 8-71166
- TEM exam. of ion damage in FCC metals 8-87727
- tetramethylammonium manganous chloride:Cu, impure Heisenberg chain paramagnet, EPR sidebands, intensity, linewidths 8-76300
- thermal conductivity maximum, temp. range 4.2 to 70K, plastic deform. influence 8-76049
- thermal expansion coeff. meas. using strain gauges and thermocouple 8-53059
- thermal oxidation, influence of ion implantation 8-64768
- thin conductor, dynamic moduli of elasticity meas. by travelling normal wave method 8-53110
- tracer diffusion, atom size effect 8-84005
- vacancy, mechanical multipole moments determ. 8-55868
- vacancy formation and migration, entropy factors 8-75866
- vacuum deposited on Al substrate, recrystallisation 8-60044
- valence band Auger spectra 8-76563
- vapour deposition on polystyrene surface complex, XPS obs. 8-72026
- vapour electron energy distrib. function computation 8-71091
- vapour laser emission, pulse characteristics rel. to plasma parameters 8-71090
- vapour production method, hollow cathode arc, Ar buffer gas 8-86981
- void growth and localisation of shear in plane strain tension 8-64613
- wall-stabilised arc conductivities with Cu vapour contamination 8-75458
- wear and deform. of surface against conical mild steel rider 8-88542
- wick, sintered, effective thermal cond. meas. 8-94582
- wire, polycryst., internal friction, ultrasonic vibrations effect (Russian) 8-76685
- wire, residual elec. resist., size effect and grain boundary contribs., heat treatment effects (Russian) 8-56126
- wire, stranded and solid, rel. stability of thermal EMF in cryogenic environment 8-60111
- wires, effect of heat treatment during drawing 8-56659
- work function, influence of cryst. orientation with and without adsorbed S (French) 8-76134
- X-ray absorption edge, chem. shift, electron binding energy in compounds 8-62822
- X-ray K-absorption discontinuity, extended fine struct. 8-76556
- X-ray photoelectron spectra ang. depend. (German) 8-72679
- X-ray studies of fusion energy neutron damage 8-51593
- XPS, angle-resolved, interpretation 8-72696
- yield stress variation 8-56652
- Ag-Cu, composite, fibre and layer structs., anomalous props. caused by internal phase boundaries 8-72754
- BaS:Cu, thermoluminesc. and decay 8-80426
- BaTiO₃:Cu, photoferroelec. props., Jahn-Teller effect, laser irradiation effect on pyroelec. props. 8-60400
- C fibre reinforced Cu composite, fatigue strength under constant strain (Russian) 8-95796
- Ca(OD)₂:Cu²⁺, ESR, secondary spectra 8-88174
- CdCr₂Se₄:Cu, elec. props., temp. depend. (Russian) 8-72181
- Cd_{1-x}Fe_xCr₂S₄:Cu, effect of doping on elec. props. and Curie temp. 8-84214
- CdS:Cd(In), Cu- or defect-compensated, optical ageing rel. to storage cond. 8-84247
- CdS:Cu, In, Ga, spray deposited film, struct., X-ray obs. 8-71713
- CdS:Cu, photocond. under high excitation intensity 8-52033

copper continued

- CdS:Cu, spectral sensitisation by cyanine dyes 8-64064
- CdSe:Cd, Cu, photo-induced changes in absorpt. spectra 8-80382
- CdSnP₃:Cu, deep centres, emission transitions, polarisation (Russian) 8-84650
- Cr/Cu/Cr layer composite, influence of phase boundary on flow stress 8-60717
- Cu complex, with acetylene, Ar matrix-isolated EPR obs., bonding 8-50564
- Cu film, stability and rupture using perturbation analysis 8-79911
- Cu II, 1 W continuous output from 780.8 nm transition 8-82953
- Cu, ultra-microhardness testing for vacuum deposited film and bulk specimen 8-79910
- Cu^{2+} , dopant, ground state wavefunctions and Δg 8-64012
- Cu^{2+} ions, influence on IR spectra of H_2O 8-72501
- Cu^{2+} , removal using Itaya-zeolite (Japanese) 8-95951
- Cu:H, interaction of H and vacancies, positron annihilation, Doppler broadening 8-80434
- Cu: μ^+ , lattice distortions, microscopic calc. 8-87665
- Cu/Au+0.03 at.% Fe, thermocouple characteristics, in mag. field at low temps. (Russian) 8-54365
- Cu/Zn galvanic couple, potential distrib. meas. technique, appl. to corrosion study, apparatus (Japanese) 8-53049
- Cu-Be-O surface, O(¹⁸S) impact, secondary electron yield 8-58797
- Cu-Fe, composite, fibre and layer structs., anomalous props. caused by internal phase boundaries 8-72754
- Cu-graphite starter brushes, effect of high velocities, current densities on wear, friction 8-88544
- Cu-H₃PO₄ system, instability and oscillations (French) 8-64850
- Cu-In solid/liquid interface, laws governing diffusive interaction (Russian) 8-91516
- Cu-KELEX 100 (alkyl β -hydroxy quinoline), distribution coeffs., model 8-53244
- Cu-LIX 65N (β -hydroxy benzophenone oxime) distribution coeffs., model 8-53244
- Cu-N₂, effect of Cu vapour on wall stabilised arc extinguishing times 8-87548
- Cu-Ne mixture, 3-20 kHz pulse discharge obs. 8-71092
- Cu-Ni biccrysal, misfit dislocation config., moire patterns, interdiffusion effects 8-84110
- Cu-Ni bimetallic films, dislocation wall form. during interdiffusion, TEM obs. 8-51856
- Cu-Ni system, X-ray diffr. line broadening from small subgrains containing gradients of spacing 8-67612
- Cu-Ni thin film couples, interfacial reactions, contact resistance meas. 8-63882
- Cu-Plexiglas double layer barrier, deform. of electron spectra (Russian) 8-84292
- Cu-SiO₂ single crystals, dispersion hardened, exam. of yield stress between 77 to 1200K 8-76720
- Cu+Cl⁺, X-ray cross sections, projectile fluoresc. yields 8-74751
- Cu+H⁺, X-ray emission, optical transition radn. 8-58618
- Cu_n, cluster formation, by ion bombardment of single cryst. surface 8-92157
- Cu(I) olfactory binding site 8-96060
- Cu(II), selective separation from rare earth elements on chelate ion exchangers 8-58861
- ⁶³Cu, ⁶⁵Cu, Fourier transform NMR studies 8-94262
- Fe-Cu, bimetallic molecule, matrix isolated, Mossbauer spectrum 8-68425
- Fe-Cu, bimetallic molecule, matrix isolated, Mossbauer spectrum 8-88233
- Fe-Ni-Cu, composite fibre and layer structs., anomalous props. caused by internal phase boundaries 8-72754
- n-GaAs:Cu, contaminated single cryst., deep level photoluminesc. model 8-68554
- GaAs:Cu, in MSM struct., phototrigger effect 8-56238
- GaAs:Cu, supersaturated solid solns., decomp., surface impurity content 8-51681
- GaP:Cu, thermally and optical excited cond., deep level centres 8-72190
- GaP:Cu p⁺-n junction, deep level parameters, TSC meas., rel. to photo-current techniques 8-72249
- GaP:Cu-Ni, Schottky barrier, TSC meas., trap levels 8-91709
- n-Ge:Cu, characts. of radiation defects 8-55893
- Ge:Cu, IR detector, impurity photoconductivity (German) 8-82036
- Ge:Cu, quenched, interaction between shallow-level defects and Cu atoms, Hall effect meas. 8-64002
- Ge:Cu photoresistor, liquid H₂ cooled, detectability 8-80019
- Ge:Si:Cu, exactly compensated, impurity absorpt. and photocond. spectra 8-56189
- He conc. profile meas. rel. to blistering 8-95089
- HgCl₂, reaction on metallic Cu, reaction velocities, effect of neutral salt addition 8-64887
- K₂O-B₂O₃:Cu II, glass, O basicity, ESR study 8-80199
- K₂O-CaO-B₂O₃:CuII, immiscibility, ESR detect. 8-80200
- K₂SO₄-ZnSO₄:Cu II, glass, O basicity, ESR study 8-80199
- Li/Cu interface, CESR meas. 8-80218
- LiCl:Cu⁺, luminescent centre, cluster MO calculation of energy levels 8-64411
- Mo, arc, steady, vac., plasma ion mass and energy diagnostics 8-51385
- NH₄Br:Cu²⁺, ESR and absorpt. spectra, 300-1500 nm 8-60492
- NaCl:Cu⁺, X-irrad. at room temp., ESR of Cu²⁺ centres 8-52343
- NaCl:Cu⁺, X-ray irradiation, role of Cu⁺ in thermoluminesc. 8-56526
- Na₂HAsO₄·7H₂O:Cu²⁺, ESR, Cu lattice location 8-52342
- NaI:Cu⁺, luminesc. of isolated V_k-centres 8-84641
- Na₂O-P₂O₅:Cu II, glass, O basicity, ESR study 8-80199
- NbTi filament reinforced Cu, superconducting composite, elastic const., temp. depend. 8-68717
- Ne-Cu hollow-cathode laser discharge sputtering obs. 8-66800
- Ne-Cu pulsed discharge, electron energy distrib., ionis. rate 8-51387
- Ne-Cu UV laser, spectral range, threshold, power output 8-66809
- Si:Cu, interaction between vacancy emitting absorbing precipitates and dislocations, TEM obs. 8-71755
- Si:Cu, recoil implantation from thin surface films, backscatt. obs. 8-63783
- Si:Ga, Cu, Au, gettering of Cu and Au during Ga diffusion 8-91350
- SrS:Cu, phosphor, photolum. meas. 8-80393
- W-Cu composite materials, vel. dispersion and scatt. of transverse US waves 8-91383

copper continued

- ZnO:Cu,H, motional effects in EPR spectra 8-80207
 ZnS:Cl⁻, Cu⁺, phosphor, high press. effect on thermoluminesc. 8-64419
 ZnS:Cu, Br based electroluminesc. cells, light, const. field effects on electroluminesc. 8-84658
 ZnS:Cu, effect of elec. field on photoluminescence, model of luminogen centre 8-76522
 ZnS:Cu(Cl), electroluminesc. and photoluminesc. spectra, fine struct. (Russian) 8-84661
 ZnS-Cu, comet shaped electroluminesc. lines 8-52578
 Zn_{0.9}Se_{0.1}:Mn(Cu), luminesc. obs. 8-60519
 ZnSe:Cu, Al, single cryst., low-voltage red cathodolum. 8-80423
 ZnSe:Cu, double comet shaped electroluminesc. 8-52577
 ZnSiF₆:Cu²⁺, spin-spin interactions of impurity pairs (Russian) 8-72397

copper alloys

see also brass; copper compounds

- analysis by ion microprobe, quantitative, using matrix ion species ratios 8-61070
 brass (70/30), interaction of annealing twins in fcc metals and alloys 8-68712
 bronze, anisotropic bend ductility in single phase alloys 8-60726
 bronze P, friction with steel, boundary lubrication conditions, element conc. anal. of films 8-85001
 bronze porous, PTFE impregnated, coeff. of friction, temp. effect 8-64737
 bronze-steel, phase composition and struct. of diffusional interlayer in fusion zone, X-ray analysis 8-56821
 cavitation during superplastic flow, affecting factors 8-60728
 compositional modulation spectra, line shape 8-76491
 Cu₂Ni_{1-x}, soft X-ray emission spectra 8-95620
 Cu₂Ni_{1-x}, magnetism of surface 8-95511
 cyclic hardening and saturation behaviour of single crystals 8-64555
 determination of Cu, Sb, inverse voltamperometry method 8-61099
 dilute, containing rare earth impurities, magneto-transport props. 8-68015
 dilute, size effect of impurity atoms rel. to trapping radii for migrating self-interstitials 8-75690
 dilute, transport props. 8-76046
 F 8-84820
 inelastic electron scattering by dislocations (Russian) 8-79988
 magnetic susceptibility, correl. with lattice parameter for α -phase alloys 8-68154
 manganin pressure gauges, effects of shock compression and relief (Russian) 8-70149
 metal-glass mats. alloyed with Cu, powder prep. and props. 8-72912
 Monel, in thermoluminesc. dosimeter, low dose meas. (Japanese) 8-86696
 Monel, Ni-Cu-Fe-Mn, resistance spot weld quality evaluation, using stress wave emission technique 8-53066
 mutual alloying behaviour of the elements straddling the line Li-Mg-Cu-Au in the long periodic table 8-84769
 Nilomag alloy 771 coloured, X-ray photoelectron spectroscopy of surface film 8-64899
 permeation in Cu alloys, Cu-Au and Au, growth of permeation barriers 8-75883
 phosphor bronze, beam, cylindrical, flexurally vibrating, Timoshenko's shear coeff. 8-83866
 purification of solid metals by electrotransport (German) 8-51745
 steel, alloy, Cr-Cu-Mn-C, HT80, effect of grain size on sensitivity to reheat cracking (German) 8-72856
 steel, stainless, recrystallisation texture, effect of Cu, Ti additions on development (Japanese) 8-80558
 superplastic, activation energy of plastic flow 8-64584
 thermal conductivity measurement, cryostat for meas. of plastically deformed specimens at liq. He temps. 8-81985
 thermopower and resistivities, validity of Nordheim-Gorter relation 8-91671
 Ag-Cu, α -phase alloy, thermopower at low temps. 8-84196
 Ag-Cu (6.2 at.%), tricrystalline specimens, fine lamellar discontinuous precipitation (German) 8-52822
 Ag-Cu-Sn(Zn)(Au), effect of additions on eutectic and peritectic temp., of binary alloys 8-84801
 Ag-Pd-Cu alloys, contact-spring props. and age hardening 8-88473
 Al bronze, anisotropic bend ductility in single phase alloys 8-60726
 Al bronze, O free, annealing in photoemission electron microscope, twin density recrystallised grain size relation (German) 8-52850
 Al-Al₂ eutectic, abrasive fragmentation (Czech) 8-64715
 Al-Cu, age-hardenable, US cavitation erosion mechanisms, effects of comp. and heat treatment 8-53002
 Al-Cu, Al₂O₃ fibre reinforced, exam. of interface interactions during fabrication 8-76616
 Al-Cu, dil., deviation from Matthiessen's rule at high temps. 8-64025
 Al-Cu, electric discharge sintering of powder mixtures 8-60605
 Al-Cu, O transport during fatigue crack growth 8-52981
 Al-Cu, solute atom displacement in mixed dumbbell interstitials for FCC lattice 8-79631
 Al-Cu, US wave propag. velocity, exam. 8-72982
 Al-Cu (10 wt.%), inverse segregation 8-52819
 Al-Cu (2.12 at.%), irradiated by 8J CO₂ laser pulses, metastable precipitate and amorphous phase (French) 8-80552
 Al-Cu (3.71 wt.%), stress oriented precipitation of Guinier-Preston zones and θ' 8-52809
 Al-Cu (4 wt.%), AE during deform., effect of ageing at 170°C 8-64597
 Al-Cu (4 wt.%), age hardening, conditions leading to localised plastic deform. and fracture in slip bands during fatigue 8-64670
 Al-Cu (4 wt.%), aged to contain Guinier Preston zones, crystallographic fatigue crack growth 8-60832
 Al-Cu (4 wt.%), elastic accommodation of semicoherent θ' 8-64543
 Al-Cu (4 wt.%), enhanced precipitation under electron irradiation in HVEM 8-52818
 Al-Cu (4% wt.), single crystals, positron trapping at precipitates 8-76554
 Al-Cu (4.5 wt.%), volume contraction accompanying solidification 8-52791
 Al-Cu (up to 0.5 at.%), neutron damage rate, interpretation of results 8-63794

copper alloys continued

- Al-Cu alloy prod., Cu interdiffusion with sintered Al powder, struct. effect at high press. 8-60606
 Al-Cu alloy RR58, high strain fatigue life, prior treatment effect 8-60835
 Al-Cu alloys, quenched rapidly, microstruct. 8-56668
 Al-Cu film, galvanostatic formation anodic oxide, Rutherford backscattering and depth profiling 8-92395
 Al-Cu film bilayers, growth kinetics of θ phase, He⁺ backscatt. and X-ray exam. 8-84105
 Al-Cu-Fe alloys, solid and liquid, exam. of constitution and mag. props. (German) 8-52206
 Al-Cu-Mg, alloys A-U4, A-U4G1, A-U2GN, effect of environment on fatigue crack growth 8-64677
 Al-Cu-Mg alloy, influence of plastic deformation on fatigue limits, for prestrained components 8-68799
 Al-Cu-Mg alloy RR58, comparison of methods of correlating creep crack growth 8-60826
 Al-Cu-Mg-Mn (4.5, 1.5, 0.6 wt.%), alloy 2024-T3, exam. of residual strength of plate containing crack, fracture anal. 8-90792
 Al-Cu-Mg-Mn (4.5, 1.5, 0.6, wt.%), alloy 2024-T81, plates, adhesively bonded, exam. of fatigue crack growth 8-92349
 Al-Cu-Mg-Mn (4.5, 1.5, 0.6 wt.%), thin sheet, exam. of fracture toughness, and fatigue crack growth 8-92353
 Al-Cu-Mg-Mn-Fe-Si, alloy D16, effect of mechanothermal treatment on mech. props. 8-56674
 Al-Cu-Mg-Si-Mn (2.5, 0.7, 0.7, 0.5 wt.%), alloy AK6, US inspection of heat treatment quality 8-76681
 Al-Cu-Mg-(Si), inclusions, oriented distrib. metallography and effects on anisotropy (Russian) 8-80589
 Al-Cu-Ni, directionally solidified, exam. of struct. of two phase alloys 8-80537
 Al-CuAl₃ eutectic, thermal instability in temp. gradient 8-52851
 Al-Mg-Cu, Al₂O₃ fibre reinforced, exam. of interface interactions during fabrication 8-76616
 Al-Mg-Zn-Cu, exam. of precipitation struct. by neutron scattering 8-92270
 Al-Si-Cu-Mg, alloy AL32, ageing of castings produced by pressure die castings 8-56650
 Al-Si-Cu-Ni alloy casting, thermal props. 8-95814
 Al-Zn-Mg-Cu, alloy 7075, hydrostatic pressure effects on ductile fracture 8-60779
 Al-Zn-Mg-Cu, alloy 7075, fatigue, loading sequence, normal and reversed sequence effect 8-68791
 Al-Zn-Mg-Cu, alloy 7075, effect of purity level, dispersoid type, heat treatment, on fracture toughness 8-80636
 Al-Zn-Mg-Cu, alloy 7075-T6, corrosion in halide solutions, exam. of anion dependency 8-60867
 Al-Zn-Mg-Cu, alloy 7075-T6, fatigue crack closure with negative stress ratio, following single tensile overloads 8-64687
 Al-Zn-Mg-Cu, inclusions, oriented distrib. metallography and effects on anisotropy (Russian) 8-80589
 Al-Zn-Mg-Cu alloy, laminated, adhesively bonded alloy 7075-T6, exam. of fracture resistance 8-76754
 Al-Zn-Mg-Cu alloys, effect of alloying elements as stress corrosion failure using regression analysis 8-80669
 Al-Zn-Mg-Cu-Cr, (5.6, 2.5, 1.6, 0.3 wt.%), laminates, 8 and 22 layers, adhesively bonded exam. of fatigue crack prop. 8-92345
 Al-Zn-Mg-Cu-Cr, (5.6, 2.5, 1.6, 0.3 wt.%), alloy 7075, plates, adhesively bonded, exam. of fatigue crack growths 8-92348
 Al₂Cu, single cryst. elastic consts., 4.2-300K 8-72803
 Au-Ag-Cu, chem. surface anal., low energy ISS compared with SIMS 8-64908
 Au-Cu, refr. index and absorpt. coeff., 1-5 eV (Russian) 8-60484
 Au-Cu, surface comp. as function of temp., AES expts. 8-95212
 Au-Cu-Ag dental alloy, age-hardened, struct. and morphology 8-92272
 Au-Ni-Cu phase diagrams, thermodynamic calc. (Korean) 8-68672
 Au-Zn(Cu), electrolytic thinning for use in transmission electron microscopy 8-57918
 Au₂Cu, ht. of order-disorder transform., differential microcalorimetry (French) 8-57950
 Be bronze, electrolytic polishing using cylindrical stationary electrode 8-64783
 Be bronze, electropolishing using cylindrical electrode moving forwards 8-64784
 Be bronze, struct. and props. after ageing under load 8-84932
 Be bronze BrB2, quenched deformed, substruct. and props., effect of prerecrystallisation annealing (Russian) 8-60677
 Be-Cu surface, secondary electron yield, for electron multiplier ion detector 8-74094
 Ce-Cu, liq., charge transfer effect 8-94967
 CeCu₂Si₂, resistivity, thermal conductivity and thermopower between 1.5 and 300K 8-87963
 (Co, Cu, Fe)₂Ce, sintered permanent magnets, magnetic charact. 8-60608
 (Co,Cu,Fe)₂Ce, sintered, mag. props. 8-68302
 Co-Cu-Fe-Ce, mag. characteristics of sintered permanent magnets 8-60312
 Co-Ni, selective catalytic surface behaviour, tight-binding approx. calcs. 8-76924
 Co₂Ga_{2-x}Cu_x, mag. and struct. phases from magnetisation, neutron, X-ray diffr. techniques 8-52253
 Cu-(Sn-Ti) melts, wetting of SiC 8-68664
 Cu-Ag, dil., dose depend. of impurity detrapping stages after electron irradiation 8-51582
 Cu-Ag, metastable alloy layer formed by Ag⁺ ion implantation 8-71709
 Cu-Ag, solid soln., nonhomogeneity of deform. 8-84889
 α -Cu-Al, binary substitutional, short-range ordering kinetics, vacancy behaviour 8-55867
 Cu-Al, change in force constant due to volume effects 8-75778
 Cu-Al, dispersion hardening by internal oxidation 8-56649
 Cu-Al, eutectic composition, exam. of high temp. mechanical behaviour (French) 8-72818
 α -Cu-Al, FCC, fractographic obs. of SCC 8-64786
 Cu-Al, faulted dipoles, geometry and form. 8-59809
 Cu-Al, impurity concentration effects 8-75777
 Cu-Al, internally oxidised, structural, elec. and mech. characts. 8-60761
 Cu-Al, intrinsic temp. depend. of stacking-fault energy 8-51564

copper alloys continued

- Cu-Al, magnetic susceptibility, comp. and temp. depend., melting effects 8-52202
 α -Cu-Al, short range ordered, struct. and new superlattice phase 8-52756
 Cu-Al, sulphurisation solid state phenomena 8-64781
 Cu-Al, surface segregation during adsorption and low pressure oxidation (French) 8-75932
 Cu-Al, thermal conductivity, data anal. and synthesis 8-95284
 Cu-Al (10 wt.%), water-quenched, tensile fatigue strength at high temp. in vacuo (Japanese) 8-72837
 Cu-Al (10.4%), creep, absence of instantaneous plastic strain upon stress changes 8-75718
 Cu-Al (11.6 wt.%), mech. props., tempering temps. effects 8-76669
 Cu-Al (13 at.%), polycryst., effect of grain size, specimen thickness, on mech. props. 8-84945
 Cu-Al (14.8 at.%), vacancy formation energy determ. 8-63756
 Cu-Al (6.4 wt.%), rolled low stacking fault energy alloy, struct. and texture 8-52844
 α -Cu-Al alloy, short range order structure 8-91303
 Cu-Al composite, simulation of tensile behaviour and fracture void initiation (Japanese) 8-52948
 Cu-Al powder mixture, elec. discharge reaction sintering 8-64507
 Cu-Al-Ni, habit plane for SIM $\gamma' \rightleftharpoons \beta_1'$ transform. 8-56640
 Cu-Al-Ni-Fe, (10, 5, 5 wt.%), cast microstruct. 8-80535
 Cu-Al-Si-Co (2.8, 1.8, 0.4 wt.%), superplastic phase, exam. of mech. props. 8-52891
 Cu-Al(Au), critical voltage effect (Japanese) 8-91206
 Cu-Al(Ge)(Sn) film, thermoelec. power, 80-350K 8-68096
 Cu-Al(In), lamellar eutectoids, calorimetric determ. of interfacial enthalpy 8-60668
 Cu-Au, dil., dose depend. of impurity detrapping stages after electron irradiation 8-51582
 Cu-Au, dil., enhanced lattice sp.ht. 8-51699
 Cu-Au, dil., O₂ solubility, thermodynamic and residual resist. study 8-59952
 Cu-Au, order-disorder transform, influence of strain energy 8-84796
 Cu-Au, thermal conductivity, data anal. and synthesis 8-95284
 Cu-Au (50 at.%), ordered, influence of elastic stresses on mech. props. (Russian) 8-92298
 Cu-Au alloy, ZZ 8-75883
 Cu-Be, impurity concentration effects 8-75777
 Cu-Be, solute atom displacement in mixed dumbbell interstitials for FCC lattice 8-79631
 Cu-Be (0.99 wt.%), direct obs. of small Guinier-Preston zones 8-72776
 Cu-Be alloy, CA 172, flat spring, mechanical props. in bending, stress relax. test, 23 to 232°C 8-72806
 Cu-Be alloy, X-ray diff. pattern singularities (Russian) 8-67682
 Cu-Be-Ni-Zr, anodic behaviour of intermetallic phase 8-72895
 Cu-Cd, magnetic susceptibility, comp. and temp. depend., melting effects 8-52202
 Cu-Cd alloy, CA 162, flat spring, mechanical props. in bending, stress relax. test, 23 to 232°C 8-72806
 Cu-Cd alloys obtained by electrolysis, struct. 8-91552
 Cu-Cd(In)(Sb), electron work function, contact pot. difference meas. 8-80041
 Cu-Cr, dil., spin glass, elec. resist., press. and conc. effects 8-52278
 Cu-Cr, dil. alloy, Knight shift temp. depend., electronic struct. 8-84488
 Cu-Cr (1 wt.%), exam. of low cycle fatigue props. at elevated temp. 8-64674
 Cu-Cr-Zr-Mg (0.5, 0.1, 0.03 wt.%), exam. of low cycle fatigue props. at elevated temp. 8-64674
 Cu-Cr(Mn)(Fe), dil., NMR satellite data, rel. to electronic struct. 8-68398
 Cu-Cr(Mn)(Fe), dil., NMR data, ionic model and Kondo temp. 8-68399
 Cu-Fe, composite, simulation of tensile behaviour and fracture void initiation (Japanese) 8-52948
 Cu-Fe, dil., transmission ESR meas. 2 to 40K 8-68364
 Cu-Fe, mixed cryst., Debye-Waller factors, Mossbauer spectra obs. (German) 8-52412
 Cu-Fe, supersaturated, spontaneous magnetisation region development, Mossbauer obs. (German) 8-64306
 Cu-Fe (1 wt.%), stress induced martensitic transformation of spherical Fe particles, exam. 8-52803
 Cu-Fe phase diagram, 650 to 1050°C (German) 8-60658
 Cu-Fe-P alloy, CA 196, flat spring, mechanical props. in bending, stress relax. test, 23 to 232°C 8-72806
 Cu-Ga, liq., mag. susceptibility, diamag. 8-72326
 Cu-Ga, magnetic susceptibility, comp. and temp. depend., melting effects 8-52202
 Cu-Ge, liq., mag. susceptibility, diamag. 8-72326
 Cu-Ge (8.7 wt.%) pulse duration effects on shock hardening 8-80561
 Cu-Ge (8.7 wt.%) shock hardening behaviour at very short pulse durations 8-80560
 Cu-Hg amalgam electrode, standard pot. 8-76874
 β -Cu-In, directionally transformed eutectoid, morphology exam. by metallography (German) 8-92257
 Cu-In, magnetic susceptibility, comp. and temp. depend., melting effects 8-52202
 β -Cu-In, unidirectionally transformed eutectoid, lamellar microstructure, influence of grain boundaries on thermal stability 8-72795
 Cu-Ir, dil., impurity diffusion, temp. depend. (Russian) 8-67851
 Cu-M alloys (M=Zn, Al, Sn, Mn, Pb), diffusive redistrib. during friction (Russian) 8-52999
 Cu-MgO, dispersion hardened, prep. by milling Cu and Mg oxidising atmos. (German) 8-64509
 Cu-Mn, dil., anomalous thermal expansion below 50K 8-51710
 Cu-Mn, dil., spin glass, thermopower, rel. to spin glass freezing temp. 8-79983
 Cu-Mn, impurity spin dynamics in magnetic glasses at low frequencies (French) 8-88126
 Cu-Mn (3 to 20 at.%), high temp. steady state tensile deform. (Japanese) 8-52917
 Cu-Mn (38 to 58 wt.%), age hardened, exam. of precipitation and strengthening 8-72782
 Cu-Mn alloy, classical RKKY model, zero temp. dynamic struct. factor 8-68271
 Cu-Mn alloy, spin glass, neutron scatt. 8-68265

copper alloys continued

- Cu-Mn alloy, spin-glass, US exam. 8-68351
 Cu-Mn Kondo system, ⁵⁴Mn nucl. orientation 8-68421
 Cu-Mn(Fe)(Co), Kondo system, host NMR exam. 8-80246
 Cu-Mn(Fe)(Ni)(Zn)(Ge), dilute solid soln., exam. of recrystallisation and stored energy 8-52836
 Cu-Nb, exam. of monotectic reaction, using chill casting technique 8-68679
 Cu-Nb, supercond. wire, directional solidification of melts, supercond. ionisation temp. (Russian) 8-76596
 Cu-Ni, alloys, electronic states, KKR-CPA calc. 8-84125
 Cu-Ni, chemisorpt. of CO, SIMS, AES, desorpt. meas. 8-87875
 Cu-Ni, diffusional homogenisation in compacted powder blends, X-ray diff. line profile analysis 8-80491
 Cu-Ni, dil., electronic struct., virtual bound state due to s-d hybridisation 8-75990
 Cu-Ni, effect of alloying and residual elements 8-85033
 Cu-Ni, film, compositionally modulated, enhanced magnetisation density 8-84460
 Cu-Ni, film, preferential sputtering due to altered layer struct., AES meas. 8-76573
 Cu-Ni, oscills. in composition depth profile, UPS meas. 8-71919
 Cu-Ni, sulphidation between 653 to 770K, exam. of scale morphologies, using X-ray diff., and electron microprobe anal. 8-88559
 Cu-Ni, surface composition cluster size distrib., Monte Carlo method calc. 8-63915
 Cu-Ni, thermal conductivity, data anal. and synthesis 8-95284
 Cu-Ni (10 wt.%), deformed bars, cold rolled, exam. of microstruct. by thin foil TEM 8-88502
 Cu-Ni (20 and 50 wt.%), sulphidation, exam. of scale growth kinetics 8-88560
 Cu-Ni dil. paramagnetic alloys, sp. elec. resist., effect of Ni clusters (German) 8-95293
 Cu-Ni-Cr, lattice imaging and optical microanalysis of spinodal decomp. 8-52754
 Cu-Ni-Cr system, coarsening in the ($\gamma_1 + \gamma_2$) region, metallographic study 8-84762
 Cu-Ni-Fe (26.8 wt.%), microduplex struct. form., hardness meas., optical and electron microscopy (Japanese) 8-76659
 Cu-Ni-Nb-Al, formation of γ' and γ'' precipitates 8-76655
 Cu-Ni-Sn (15, 9 wt.%), age hardening accompanying phase transition 8-64551
 Cu-Ni-Sn (4.4 wt.%) resistance spot weld quality evaluation, using stress wave emission technique 8-53066
 Cu-Ni-Sn alloy, flat spring, mechanical props. in bending, stress relax. test, 23 to 232°C 8-72806
 Cu-Ni-Zn, microduplex, superplastic deform., cavitation and fracture 8-64640
 α -Cu-Ni-Zn-Pb, fire cracking and ordering (German) 8-60760
 Cu-Pb liquid alloys, exam. of O diffusivity at 1430K using electrochemical cell 8-51713
 Cu-Pd, thermal conductivity, data anal. and synthesis 8-95284
 Cu-Pd alloy, singularities of physical props. and ordering (Russian) 8-76643
 Cu-Pt, order-disorder transform, influence of strain energy 8-84796
 Cu-Pt existence regions of FCC superstructs. (Russian) 8-52760
 Cu-Sb, cold-worked, lattice defects, convolution relations for X-ray line breadth calcs. 8-51394
 Cu-Si, change in force constant due to volume effects 8-75778
 Cu-Si, impurity concentration effects 8-75777
 Cu-Si, stacking fault energy meas. by tensile deform. of polycrystalline samples 8-95060
 Cu-Si (up to 4.75 wt.%), exam. of high temp. oxidation in low O₂ and pure CO₂ atmospheres, by thermogravimetry 8-88574
 Cu-SiO₂, dispersion hardened, surface plasticity effect 8-52832
 Cu-Sn (15 at.%), temp. depend. of elastic consts. above martensitic transition temp., US exam. 8-76695
 Cu-Sn (2 wt.%), effect of undercooling on crystal multiplication 8-84866
 Cu-Sn (25 wt.%), struct. after ultrahigh-speed quenching (Russian) 8-80563
 Cu-Sn liquid alloys, thermodynamic meas. 8-52765
 Cu-Sn-Ti, wetting of alumina and vitreous C 8-71904
 Cu-Ta, metastable alloy layer formed by Ta⁺ ion implantation 8-71709
 Cu-Ti, liquid phase sintering, metallographic electron beam microanalytical investigation 8-95888
 Cu-Ti (1.07 wt.%), containing coherent precipitation, observations of flow and fracture 8-80643
 Cu-Ti (4 wt.%), aged, stress corrosion cracking in Cu-NH₃ solutions, effect of pH, Cu and NH₃ conc. 8-88562
 Cu-Ti matrix of diamond composite, microstresses, X-ray diff. exam. 8-56679
 Cu-Ti system, diffusion obs. (German) 8-63881
 Cu-Zn, cyclic stress/strain curves in monocrystalline and polycrystalline samples, cold work and Zn addition effects 8-95786
 Cu-Zn, magnetic susceptibility, comp. and temp. depend., melting effects 8-52202
 Cu-Zn, order-disorder transform, influence of strain energy 8-84796
 Cu-Zn, thermal conductivity, data anal. and synthesis 8-95284
 Cu-Zn (30 wt.%), rolled, electron microscope exam. of recrystallisation 8-76663
 α -Cu-Zn (5.3 to 21.8 wt.%), single crystals, effect of stacking fault energy on extrusion and intrusion development 8-72826
 β -Cu-Zn-Al, electron microscope exam. of premartensitic state 8-72801
 β -Cu-Zn-Al, ordering 8-68687
 Cu-Zn-Al, pseudoelastic alloy, exam. of fatigue props. 8-76744
 Cu-Zn-Al (19.3, 13.0 wt.%), effect of hydrostatic or uniaxial stress on elastic consts., near martensitic transformation point 8-76697
 β -Cu-Zn(-Ni)(-Mn), order-disorder transformation temperature effect on quench hardening 8-95745
 Cu-Zr, intermediary phases of equilib. diagram 8-84771
 γ -Cu₃Al₄, struct. refining from diff. meas. 8-55834
 CuAu, calc. of elastic interaction between locally transformed regions with screw and edge dislocations 8-83844
 CuAu-type superstructure, interaction of reacting dislocations (Russian) 8-83814
 Cu₃Au, fast neutron irradiation, displacement cascades 8-83852
 Cu₃Au, mechanical damping in terms of Granato-Lücke theory, comparison with leaded and unleaded brass 8-95772

copper alloys continued

- CuCr-Pb, proximity effect, tunnelling conductance 8-52160
 Cu₂MnAl, ferromag. Heusler alloy, polarised neutron study of mag. moment density 8-84391
 Cu₂Mn_{0.98}Al_{1.02}, Heusler alloy, hyperfine fields at sp elements, spin echo NMR meas. 8-84496
 Cu_{2.0}Mn_{0.94}In_{1.0}, In-Heusler single crystal, elec. resist. 8-60107
 Cu₂Ni_{1-x}, solutions of KKR-CPA equations for paramagnetic alloys 8-95256
 Cu₂Ni_{1-x}, Fermi surface of concentrated paramag. alloys 8-95257
 Cu₂Ni_{1-x}, random alloy, angle-resolved photoemission 8-95683
 Cu₂NiZn, superlattice dislocations 8-83816
 CuPt, specific heat, Debye temp. below 30K 8-55956
 Cu_{82.5}Sb_{17.5}, X-ray K-absorption discontinuity, extended fine struct. 8-76556
 η-Cu₃Si precipitates in Si, cryst. struct. 8-91304
 Cu₃Sn, one-dimens. long period superstructs. with Zn and Ni additions 8-83777
 CuSnMg, crystal struct. anal. 8-91306
 Cu₃SnMg, crystal struct. anal. 8-91306
 Cu₆₀Zr₄₀, amorphous, elec. resist. calc. and temp. coeff., using t-matrix 8-72130
 Dy-Cu amorphous mag. alloy, linear sp. ht. due to single-ion excitation 8-91874
 Dy₂Cu_{1-x}, amorphous film, magnetisation meas., local anisotropy effects 8-68309
 ErCu, cubic antiferromag., mag. excitations inelastic neutron scatt. meas. 8-72341
 Eu(Ni_{1-x}Cu_x)₅, mixed valency, isomer shift temp. depend. 8-84511
 EuNi₂Cu_{8-x}, mixed valency of Eu, Mossbauer expts. 8-52407
 Fe, grey cast, corrosion resist., Cu alloying additions effect (Russian) 8-56807
 Fe-Al-Ni-Co-Cu alloys, Ti alloying and deoxidising addition (Russian) 8-80181
 Fe-Cu (0.21, 0.2 wt.%), neutron irradiated, torsional props. effect of Cu additions and annealing temp. 8-56699
 Fe-C(graphite)-Ni-Cu, dynamically hot pressed mech. props., effect of Ni-Cu additives 8-60620
 Fe-Cr-Ni-Cu-Sn, Cu and Sn effect on Cr and Ni segregation (German) 8-72777
 Fe-Cu, dissolution rate into molten Al, convection mass transfer (Japanese) 8-71858
 Fe-Cu, layers formed by reaction with molten Al, X-ray, EPMA and hardness meas. (Japanese) 8-72926
 Fe-Cu, protective coating on Al powder (Russian) 8-60881
 Fe-Cu (1.2 wt.%) effect of precipitation on recrystallisation, texture 8-88476
 Fe-Cu (30 wt.%) alloy, dendrite remelting during isothermal holding, microspin obs. (Japanese) 8-71836
 Fe-Cu metastable dil. alloy film, hyperfine interactions 8-52398
 Fe-Cu-C, sintered parts, struct. stabilisation with C potential control of protective atmosphere 8-60614
 Gd-Cu, amorphous alloy, mag. coupling 8-88108
 Gd-Cu, amorphous alloy films, mag. phase diagram, spin glass and ferromag. regions 8-68234
 Gd-Cu alloy film, amorphous, struct. and mag. props. 8-52318
 Gd₂Cu_{1-x}, amorphous film, magnetisation meas., fully aligned moment 8-68309
 Ge-Cu (0, 23, 40 at.%), amorphous film struct. (German) 8-95391
 Ge-Cu film, amorphous, EPR meas. 8-80212
 Ho₂Cu_{1-x}, amorphous film, magnetisation meas., local anisotropy effects 8-68309
 LaCu₂Si₂, resistivity, thermal conductivity and thermopower between 1.5 and 300K 8-87963
 La(Ni_{1-x}Cu_x)₅, H₂ sorption props. 8-91533
 Mg-Cu, binary system, nonstoichiometry, of Laves phases, MgCu₂ (French) 8-52770
 Mg-Cu-Pb system, phase equilibria in Mg-rich corner (French) 8-76630
 Mn-Cu, plastic deform. mechanism and shape-memory effect, mag. struct. obs. (Russian) 8-60705
 Mn-Cu-Al alloy under torsion, anomalous elasticity and transformation plasticity obs. (Russian) 8-78334
 Nb-Cu-Sn, cast supercond. alloy, crit. current, degradation resistance 8-76203
 Nb-Ga-Cu, phase diagram, metallographic and X-ray study, annealed and as-cast supercond. crit. temp. (Russian) 8-56617
 Ni-Cr, O transport, during fatigue crack growth, exam. 8-52981
 Ni-Cu, low field magnetisation meas., mag. props. comp. depend. 8-91879
 Ni-Cu, protective coating on Al powder (Russian) 8-60881
 Ni-Cu, sp. ht. in mag. field, 1.2-15K 8-68262
 Ni-Cu alloy, asymmetry of XPS of shell electrons (Russian) 8-76579
 Ni-Cu-Mn, dil. alloys, NMR freq. temp. depend., spin echo meas. 8-64296
 Ni₃(Fe,Cu), kinetic phenomena rel. to ordering and electron struct. (Russian) 8-76043
 Pd-Cu, T diffusion, effect on freq. factor and activation energy 8-63880
 Pd-Cu alloy, asymmetry of XPS of shell electrons (Russian) 8-76579
 Pd_{77.5}Cu_{22.5}Si_{16.5}, metallic glass, diffusion of Au 8-55983
 Pd_{0.775}Si_{0.165}Cu_{0.06}, metallic glass, intensity-depend. US attenuation at low temps. 8-79671
 Pd_{0.78}Si_{0.16}Cu_{0.06}, phonon propagation below 1K 8-71824
 Pd_{1-x}Si_xCu_y, glassy, low temp. specific heat 8-83969
 Pr-Cu-Al system, X-ray and microscopic anal. (Ukrainian) 8-84774
 PrCu₂, cryst. field transitions near cooperative Jahn-Teller transition 8-84178
 PrCu₃, cryst. field effects on transport props. 8-72133
 Pt-Cu alloy, asymmetry of XPS of shell electrons (Russian) 8-76579
 Sm(Co_{1-x}Cu_x)_{7.8} alloys, coercive fields, domain wall energies, mag. and metallographic exam. 8-91897
 SmCo₃Cu_{1.5}, time dependent magnetisation 8-80176
 Sm(CoFeCuMn)₇, coercive force and anisotropy temp. depend. 8-68297
 SmNi_{1-x}Cu_x, giant intrinsic mag. hardness due to randomised cryst. field interactions 8-68208
 Tb₂Cu_{1-x}, amorphous film, magnetisation meas., local anisotropy effects 8-68309
 TbNi_{2-x}Cu_x, elec. resist. and mag. props. 8-72348,

copper alloys continued

- Ti-Cu-Al(Zr)(Sn)(Nb)(Mo), heat treatable alloys, effect of alloying on strength, tensile props. 8-56671
 V-Al/Cu-Ge composite tape, transition temp., upper crit. field 8-68126
 W-Cu composite materials, vel. dispersion and scatt. of transverse US waves 8-91383
 WCuB prep. by infiltration of W skeleton by CuB, hardness meas. (German) 8-64508
 YbCuAl, mixed valence behaviour, mag. props. 8-68150
 Zn-Cu system, sputtering during atomic diffusion, UPS meas. 8-92159
 Zr-Cu (1.6 wt.%), mechanical equation of state, stress relax. meas. 8-52880
 Zr₃Co_{1-x}Cu_x, phase stability and supercond. T_c 8-80519
 Zr₄₀Cu_{60-x}M_x (M=Fe,Mn,Gd,Tb), amorphous, mag. ordering and local random anisotropy 8-68273
 Zr₄₀Cu_{60-x}M_x (M=Gd, Tb, Fe or Mn), amorphous alloy, mag. interactions 8-95432

copper compounds

- see also copper alloys
 benzoate trihydrate, half-field EPR, 1.5-300K 8-60333
 bis(triethylbenzylammonium)tetrachlorocuprate(II), mag. anisotropy, susceptibility, EPR of Cu²⁺ 8-52344
 bis(trimethylbenzylammonium)tetrachlorocuprate(II), mag. anisotropy, susceptibility, EPR of Cu²⁺ 8-52344
 determination, in seawater, chromatographic-at. spectrosc. method 8-68972
 diammonium layer compound, ND₃-(CH₃)₂-ND₃CuCl₄, antiferromag., magneto-optical meas. birefringence 8-68483
 dipyrindinium copper bromide, Py₂Cu₃Br₇, Cu⁺ ion conductor, cryst. struct. 8-51527
 ESCA shake-up satellites, spin density intensity ratio relation 8-50590
 EXAFS investigation of Cu-O, Cu-N, Cu-Br bond lengths 8-52593
 ferrite, spinel type catalytic oxidation of CO, role of mag. exchange interactions 8-56916
 ferrites, crystallisation of monocrystals from high temp. soln. 8-60561
 formate.4D₂O, field-induced antiferromag. order above T_a 8-84389
 halide lasers, transverse excitation, large active volume 8-59021
 matte converting, thermodynamics of process, Noranda process, exam. using computer model 8-80492
 molybdates, valence band X-ray induced Auger spectra and XPS 8-80813
 oxalate, decomposition kinetics, in polymeric medium, thermogravimetry and DTA 8-52749
 oxides, valence band X-ray induced Auger spectra and XPS 8-80813
 phthalocyanine, polycryst. film, charge transfer state and optical spectra (Russian) 8-84607
 pyridinium cuprous bromide, solid electrolyte, crystal growth from melt 8-64462
 vanadates, elec. and mag. props., stoichiometry 8-51991
 AgCuSe, X-ray photoelectron and Auger spectra 8-56561
 Al₂O₃/CuO, thin film interaction, CuAl₂O₄ form. (Russian) 8-52697
 AsTeCu_x (0≤x≤0.4) glass, effect of Cu on elec. cond. and thermoelectricity, 100 to 370K 8-87978
 BaCu_{2+x} (0≤x≤0.12), study of mag. and elec. props. rel. to the non-stoichiometry (French) 8-95051
 CdS-Cu₂S single cryst. heterojunction, trap depths in depletion region 8-52064
 CdS-CuI film heterojunction photocells, prep., photoelec. props. 8-80044
 (CdZn)S-Cu₂S solar cell, film form. and characts. 8-68080
 CoU₂S₅, mag. struct., exchange energy, magnetisation and neutron diffr. expts. 8-68170
 Cu complex, acetylacetone, appl. as Cu atom donor in 5106 Å Cu laser 8-82956
 Cu complex, bis-(alkylammonium) (11) tetrachloride, perovskite, lattice perfection 8-87633
 Cu complex, bis-(alkylammonium) Cu(11)tetrachloride, perovskite, face struct. and growth rate 8-87634
 Cu complex, bis-ethylene diamine copper(II) sulphate, dielectric relaxation studies 8-84519
 Cu complex, Cu(II) acetylacetonates, X-ray K-absorpt. edges, edge widths and shifts 8-50556
 Cu complex, Cu(en)₃Cl₂·0.75 en, X-ray and ESR data, Jahn-Teller distortions 8-80206
 Cu complex, with Schiff base of o-aminobenzaldehyde and S-methyldithiocarbamate, cryst. struct. 8-95040
 Cu, complexes, FT NMR, ⁶³Cu and ⁶⁵Cu chemical shifts and coupling constants 8-94260
 Cu compounds, chemical shifts of X-ray electron and Auger lines 8-86912
 Cu²⁺ complex, in water-ethanol soln., struct., EPR 8-50565
 Cu-Al₂O₃ powder, electrolytic deposition 8-84743
 Cu-As-Se glasses, recording and erasure by laser beam (Russian) 8-71170
 Cu-O system, liq., thermodynamic study (Japanese) 8-64529
 CuAl₂Cl₆, Raman resonance spectra of vapour 8-94251
 Cu₄(As_{0.6}Se_{0.4})₁₂, amorphous, ⁷⁷Se NMR, comp. depend. 8-76329
 Cu₁₀As₃Se₃O₂₁, chalcogenide glass, exam. of electron mechanism of photo induced changes 8-77998
 CuBr, continuously pulsed laser, cable-capacitor Blumlein discharge circuit, expt. characts. 8-82981
 CuBr, Debye-Waller factors and Debye temp., powder neutron diffr., 295K 8-91407
 CuBr, evaporated film, magneto-optical effects on exciton bands 8-72624
 CuBr laser, bubble gas effects on ground and metastable populations 8-82955
 CuBr, multiphonon far IR absorpt., 2-80K 8-60462
 CuBr, NMR chemical shifts, temp. depend. 8-68401
 CuBr, phonon dispersion 9-parameter shell model, compared with expt., and Debye temp. evaluation 8-59891
 β-CuBr, phonon spectra, dispersion curves parameter calc. from zinc blende zone boundary conditions 8-51632
 CuBr, two-phonon optical absorpt. spectra 8-52485
 CuBr, XPS, satellite of Br 4s line 8-56556
 CuBr-Ag system, spectral distrib. of photosensitivity (Russian) 8-56535
 CuBr₂, highly conc. aqueous soln., local ordering, extended X-ray absorb. fine struct. spectra 8-79520

copper compounds continued

- (CuBr), photoelectron spectrum and valence shell struct. 8-62843
 CuBr(Cl), biexcitons, many exciton effects 8-51901
 CuCl, biexciton luminescence and two photon Raman emission, polarisation props. 8-80406
 CuCl, continuously pulsed laser, cable-capacitor Blumlein discharge circuit, expt. characts. 8-82981
 CuCl, evaporated film, magneto-optical effects on exciton bands 8-72624
 CuCl, exciton mol. creation by pure and phonon-assisted two-photon transitions 8-63987
 CuCl, excitonic mol. luminesc. spectra, picosecond time anal. 8-52548
 CuCl, existence of charged excitons 8-76496
 CuCl laser, potential, high-energy large vol. device 8-50807
 CuCl, multiphonon far IR absorpt., 2-80K 8-60462
 CuCl, NMR chemical shifts, temp. depend. 8-68401
 CuCl, phonon dispersion 9-parameter shell model, compared with expt., and Debye temp. evaluation 8-59891
 CuCl pulsed laser, time depend. of Cu-atom conc. in ground and metastable states 8-66806
 CuCl, reson. two-photon Raman scatt., excitonic polariton dispersion 8-72509
 CuCl, reson. two-photon excitation of excitonic mol. using circ. polarised light 8-84566
 CuCl, resonantly excited excitonic molecules, time resolved spectroscopy 8-92109
 CuCl, two-phonon optical absorpt. spectra 8-52485
 CuCl, Z₃-exciton, temp. dependent TPA linewidth 8-67946
 CuCl, zincblende struct., high press. Raman scatt., 77K 8-60463
 CuCl-TiCl system, phase diagram and high ionic cond. obs. 8-79802
 CuCl₂, aq. soln., Raman spectrum, local order 8-84563
 (CuCl₂) photoelectron spectrum and valence shell struct. 8-62843
 CuCl₂, electronic energy levels calc. by conventional and X alpha Hartree-Fock methods 8-66470
 CuCl₂TMSO, ferromag. spin 1/2 linear chain, mag. susceptibility 8-68180
 CuCl₂·2H₂O, antiferromag. to paramag. transition, high field magnetisation meas. 8-64204
 CuCo₂S₄, Cu_{0.5}Co_{2.5}S₄, spinels, ht. of formation 8-53237
 CuCr₂Se₄, magnetic properties obs. 8-76227
 Cu₂Cr₂Se₄₋₁Br_x, ferromag. magneto-resistance exam. (Russian) 8-84238
 CuFe₂O₄, LPE grown, domain struct. rel. to tetragonal distortion 8-92205
 CuFe₂O₃, cation substitution effect on eutectoid decomposition 8-68890
 Cu_{1-x}Fe_{2+x}O₄, cation distrib. and valence state 8-63732
 CuFeS₂, chalcopyrite, electrode surface reduction kinetics 8-56897
 CuFeS₂, explosive-shock deform. 8-95108
 CuGa_{1-x}In_xS₂, solid soln., IR refl. spectra, comp. depend. 8-52498
 CuGaS₂, coloration, pure and Fe doped, EPR and optical absorpt. obs. 8-88336
 CuGaS₂, crystal growth by I₂ vapour transport, using temperature variation method 8-68610
 CuGaS₂, single cryst., photocond. spectra 8-84252
 CuGaSe₂, crystals, I₂ vapour transport grown, luminesc. spectra 8-88349
 CuGaSe₂, obs. of energy transitions from lower valence band states 8-95576
 CuGaSe₂, temp. depend. of fundamental absorpt. edge 8-92090
 CuH, electronic struct., heat of formation, single particle lifetimes, Din-gle temp. meas. 8-51923
 Cu₂HgI₂, ZZ 8-52639
 CuI, elec. props. 8-56193
 CuI, NMR chemical shifts, temp. depend. 8-68401
 CuI, phonon dispersion 9-parameter shell model, compared with expt., and Debye temp. evaluation 8-59891
 CuI, superionic conductor, Raman study 8-80353
 (CuI)₃, photoelectron spectrum and valence shell struct. 8-62843
 γ-Cu(IO₃)₂, cryst. struct. and mag. behaviour 8-79571
 Cu_{1-x}In_xCrS₄, light induced magnetisation 8-76275
 CuInS₃, crystal growth by I₂ vapour transport, using temperature variation method 8-68610
 CuInS₂(Se₂) film, vacuum deposited, absorpt. coeff. 8-72621
 CuInS₂(Se₂)(Te₂), thin films and photovoltaic devices, AES evaluation 8-67928
 CuInS₂(Se₂)(Te₂), thin film, bulk polycryst. and single cryst. samples, AES 8-72648
 CuInSe₂ epitaxial growth on GaAs 8-84104
 CuInSe₂, polycrystalline thin film anomalous photovoltaic effect (German) 8-68102
 CuInTe₂, grown from near stoichiometric comp., elec. and optical props. 8-68504
 Cu₂Mo₆S₈, normal state and superconducting property measurements 8-91660
 Cu₂Mo₆S₈, evaporated two-phase, crit. current and scaling laws 8-91831
 Cu₂Mo₆S₈, Hall effect and magnetoresistivity 8-95400
 Cu₂Mo₆S₈, thin films, low temp. normal state, resist., temp. depend. 8-91783
 Cu(NH₃)₄PtCl₆, Cu(NH₃)₄²⁺ cation mol. orbital parameters 8-64011
 Cu(NH₃)₄(H₂O)²⁺ solns., effect on working of Ti-Ni alloy (Russian) 8-53017
 Cu(NO₃)₂, aq. soln., Raman spectrum, local order 8-84563
 CuO, ²Σ_g⁻/_u⁻ transition, rot. anal. 8-82748
 CuO addition to molten salt heat transfer fluid, solar absorbing properties enhancement 8-87112
 CuO, C²II-X²II, and D²A-X²II, band systems, rot. anal. 8-82747
 CuO, colorant, bandpass filter glass, 550-616 nm, transmission characts. 8-66919
 CuO, effect on PTFE-Al adhesion joints 8-53183
 CuO surface, contaminated, cleaning treatments, ion scatt. anal. 8-53307
 CuO-CaO-P₂O₅, glass devices, memory switching 8-56192
 Cu₂O, 1s yellow exciton, lineshape studies by reson. Raman scatt. 8-76465
 Cu₂O, Auger quantitative anal. 8-73104
 Cu₂O, creep substruct. under compression, X-ray diffr. study 8-95785
 Cu₂O, electric field screening by surface electron states 8-52058
 Cu₂O, exciton spectrum, effect of isotopic substitution 8-67955
 Cu₂O, excitons and structural defects at low temp. 8-84255

copper compounds continued

- Cu₂O, form. by Cu oxidation in CO₂, 800-1000°C 8-76784
 Cu₂O, growth by melting, photocond. spectra 8-52029
 Cu₂O, heat of adsorpt. of pyridine and ethyl pyridine, flow microcalorimetry 8-85193
 Cu₂O, laminar growth on (111) Cu single cryst. surface, microstruct. 8-72025
 Cu₂O, photomemory effect, EPR expts. 8-52353
 Cu₂O polycrystalline and single cryst. mech. behaviour 8-95777
 Cu₂O, refl.-absorpt. IR spectroscopy 8-84555
 Cu₂O, reson. Raman scatt., yellow and green excitonic series 8-72511
 Cu₂O, single crystal, thermoelectric behaviour (French) 8-71786
 Cu₂O, theory of lattice dynamics 8-59896
 Cu₂O, thermal expansion at low temp. 8-59959
 Cu₂O, thermal switching, resist.-temp. charact. 8-64071
 Cu₂O, yellow exciton series, silver impurity influence on spectrum 8-64388
 Cu₂O, yellow exciton series, 1s paraexciton levels, phonon assisted transitions, optical absorpt. edge 8-79934
 Cu₂O:Ag⁺, yellow series line width, exciton-impurity scatt. 8-64386
 Cu₂O:Cd, dipolar and quadrupolar bound excitons, absorption spectrum (Russian) 8-92099
 Cu₂O-electrolyte contact, electrolytic decomposition and photodecomposition 8-95357
 Cu₂O, film, thermolec. power, activation energy variation with electrode spacing in DC sputtering 8-76099
 Cu₂(OH)₂CO₃, malachite, vibr. assignments, force consts., coincidence method appl. 8-62953
 Cu₂P, Cu₃P, electronic struct. of valence bands, X-ray spectra and XPS 8-92176
 Cu₄(PO₄)₂O, cryst. struct. (French) 8-55854
 Cu₄(PO₄)₂O, cryst. struct. 8-55855
 CuS aerosol prepared by burning pyrotechnic mixture, crystallisation activity 8-96279
 Cu₂S, epitaxial layers grown from liq. soln. RHEED obs. 8-91558
 Cu₂S, epitaxial overgrowths on Cu films, characts., TEM and RHEED obs. 8-84101
 Cu₂S, film preparation for solar cells, elec., optical, struct. props. 8-76602
 Cu₂S layer spray preparation and CuCl-thiourea complex formation 8-64471
 Cu₂S, solid, oxidation mechanism, kinetic factors 8-85133
 Cu₂S, threshold photoelectric emission (French) 8-60549
 Cu₂S, ZZ 8-52639
 Cu₂S-CdS film junction formation by dry-barrier process 8-64109
 Cu₂S-CdS heterojunction, elec. and photoelec. characts., effect of etching of CdS 8-80048
 Cu₂S-CdS thin film heterojunctions, base doping effect on elec. and photoelec. props. 8-80043
 Cu₂-S films, vacuum deposited, electrical conduction and phase transitions 8-84332
 Cu₂-S in chem. formed Cu_{2-x}S-CdS heterojunction, photosensitivity characts. 8-72199
 Cu_{2-x}S-CdS heterojunctions, nature of longwave photo EMF 8-84284
 Cu₂S layer, on CdS, electron diffr. obs. of phases 8-51847
 CuSCN, Cu(SCN)₂, muonic Coulomb capture, ionic charge effect 8-66694
 CuSO₄, effect of press. on ion pair dissoc., cond. of aq. solns. 8-53218
 CuSO₄, solution, activity coeff. determ. 8-76874
 CuSO₄, solution, dielectric relaxation studies 8-84519
 CuSO₄·3CO(NH₂)₂, X-ray determ. of electron density distrib. 8-67699
 CuSe, X-ray photoelectron and Auger spectra 8-56561
 Cu₁₈Se, I-V characts., switching effects, nonstoichiometry effects (Russian) 8-84266
 Cu₂Se, X-ray photoelectron and Auger spectra 8-56561
 CuSiF₆·6H₂O, paramag., nucl. and electron spin lattice relax. 8-84494
 CuSiO₃·2H₂O, chrysocolla, electronic absorpt. spectra 8-92087
 p-Cu₂Sn-n-ZnS heterojunction, I-V characts., photocond. and electrolum. 8-72251
 CuTa₂O₆, cryst. struct. (French) 8-51497
 Cu₁Te, and Cu₂Te, I-V characts., switching effects, nonstoichiometry effects (Russian) 8-84266
 CuTeO₄, cryst. struct. determ. 8-55845
 Cu₂V₂O₅, metallic, Raman scatt. 8-80358
 Cu₂V₂O₅, nonmetallic bronze, low field sp. ht. and mag. suscept. 8-72357
 Cu₂VS₄, mixed conductor, fast ion transport at room temp. 8-72214
 Cu₂Zn_{1-x}ZrF₆·6H₂O, distortions of nearest Jahn-Teller [Cu(H₂O)₆]²⁺ centres 8-68000
 Fe₂Cu_{1-x}Rh_xS₄, mag. tetrahedral intrasublattice interaction, X-ray, magnetisation and Mossbauer expts. 8-52241
 FeS-Ni₃S₂-Cu₂S melt, enthalpy (Russian) 8-95730
 Ga₂Te₃-Cu system solid solns., elec. cond. 8-51988
 K₂Cu(CN)₄, isotopic mixed crystal with ¹²C and ¹³C, Raman scattering 8-76476
 K₂Cu_{1-x}Zn_xF₄, two-dimens., ferromag., spin wave excitations 8-80140
 K₂PbCu(NO₂)₆, incommensurate Jahn-Teller phase transition 8-79730
 K₂PbCu(NO₂)₆, Jahn-Teller phase transitions, order-disorder model 8-79762
 Li_{0.5}Fe_{2.5}O₄-CuFe₂O₄-ZnFe₂O₄, order-disorder transition, quadratic transformation (French) 8-76447
 Li_{0.5}Ga_{2.5}O₄-CuCr₂O₄ system, phase diagrams, IR spectra, Cu²⁺ electronic spectra (French) 8-51461
 MgTaCuO₄, cryst. struct., synthesis 8-83790
 (NH₄)₂(Cu(H₂O)₆)(CuSO₄)₄, cryst. struct. determ. by X-ray diffr. 8-55839
 Na₂[Mⁿ(NH₃)₄][M'(S₂O₃)₂]₂·L, (Mⁿ=Cu, Ni), (M'=Cu, Ag), (L=H₂O, NH₃), IR spectra, vibr. anal. (French) 8-52477
 (NdCu₂)(Ti₃Fe)O₁₂, synthesis, cryst. struct. and Mossbauer exam. 8-84505
 PbMo₆S₈, Hall effect and magnetoresistivity 8-95400
 Rb₂Cu(SO₄)₂·6H₂O, single cryst., fine struct., mag. dipole coupling, EPR obs. 8-68360
 (ThCu₃)(Mn₂Fe₃)O₁₂, synthesis, cryst. struct. and Mossbauer exam. 8-84505
 ThCu₃Mn₂O₁₂, mag. struct. of new perovskite-type ferrimag. 8-52222
 TiCuD_{0.90}, neutron powder diffr. study for cryst. struct. refinement 8-95018

copper-oxide rectifiers

No entries

copper zinc alloys *see brass***copying** *see reproduction (copying)***Corbino effect***see also Hall effect*

GaAs, carrier mobility profiles meas. at room temp. by Corbino effect 8-60128

Coriolis force*see also rotation*

acetonitrile, soln., IR perpendicular bands, profiles, rot. models 8-58695

coupling constants, spectroscopic determ., extremal props., book contrib. 8-78678

1,1'-dicyanoethene(-d₂), microwave spectrum, Coriolis interaction, rot. assignments 8-82721

education, Coriolis machine, inertial motion viewed from rot. reference frame, coordinate transformation 8-69934

fluid motion within ellipsoidal cavity, influence of Coriolis force field (Russian) 8-81296

formaldehyde(-d₁, d₂), and isotopic forms, microwave spectrum, ν_4 - ν_6 vibr. states Coriolis reson. 8-82719

hot-wire sensor, effect of centrifugal and Coriolis forces on rotating probe 8-94862

influence on LF waves in rotating plasmas 8-75309

ketene, IR spectra, rot.-vibr. anal. of Coriolis coupled bands 8-86859

liquid films, thin, effect of Coriolis force on film dynamics 8-94747

methyl fluoride, second-order Coriolis resonance between ν_2 and ν_5 states, microwave spectra 8-74646

methylene fluoride, excited vibr. state, microwave spectrum 8-58672

molecular, symmetry coordinates construction, arbitrariness limitation 8-55252

odd nuclei states, Coriolis mixing, phonon admixture and non-adiabatic effects in even-even core 8-74310

pipes carrying fluid flow, oscillation stability (German) 8-87298

Poiseuille flow, plane, horiz., rot., stability, effect of Coriolis force 8-67203

ring, oscillatory behaviour, influence of Coriolis forces on power transmission belts (German) 8-87255

tetrafluoromethane, ν_4 fundamental of three isotopic species 8-70835

tetrahalide of group IV A, molecular const. 8-66528

tsunami type plane wave, Coriolis force effect (Russian) 8-77193

XY₆-type molecules, Coriolis coupling const., at. mass effect, XCl₆ appls. 8-66684BHBr₂, and isotopic forms, mol. pot. const., amplitudes, Coriolis coupling, centrifugal distortion 8-50662BHCl₂, and isotopic forms, mol. pot. const., amplitudes, Coriolis coupling, centrifugal distortion 8-50662BHF₂, and isotopic forms, mol. pot. const., amplitudes, Coriolis coupling, centrifugal distortion 8-50662BrF₃, excited vibr. states, microwave spectrum, rot. const. determ. 8-94237CO₂+N₂, semiclassical energy transfer method, Coriolis coupling 8-90266HfBr₄(HfI₄), struct., force field and Coriolis const. calcs. 8-86843

ONCN, far IR spectra, pure rot. and vibr.-rot. bands 8-82731

TiBr₄(TiI₄), struct., force field and Coriolis const. calcs. 8-86843ZrBr₄(ZrI₄), struct., force field and Coriolis const. calcs. 8-86843**cornea** *see eye***corona***see also electric breakdown; flashover; solar corona*

aerosol particle neutralisation to Boltzmann's equilib. by corona discharge 8-61064

air, negative point-plane corona, electrical characts. 8-71567

air, pulsed corona discharge channel fast heating process 8-67560

air corona discharge ion density and mobility obs. 8-67594

air gap discharge zone probabilistic features 8-67582

air HF corona discharge ignition characteristics 8-67589

air positive point corona current continuous component 8-67586

charging props. of PMMA-metal oxide composite powder (Japanese) 8-95708

convective heat transfer coeffs. for corona wind cooling of flat surface 8-87234

corona to spark transition, cathode zone activity, Schlieren obs. 8-87585

counter resolution rel. to current, gas pressure and anode wire diameter (Russian) 8-90018

DC corona Trichel pulse development at atm. pressure, obs. 8-67588

discharge, decomposition of CO, qualitative chemical anal. of reaction products 8-60992

discharge, spherical probe I-V characts., electrostatic precipitator testing appl. 8-79467

discharges from ice points on metal electrodes 8-67587

EHD augmented baking, corona wind impingement effects 8-87235

EHD study of corona wind between wire and plate electrodes 8-71561

electrification of objects under DC transmission lines, charge simulation calcs. 8-78853

energy spectrum of corona impulses generated from insulated wires under high AC voltages 8-71621

heat transfer augmentation around downward facing flat plate by nonuniform elec. field 8-94873

heated cylinder in radial elec. field, corona characts. power freq. variation effects 8-87538

high-pressure corona discharge current oscillations and role of excited atoms 8-67590

homopolar corona, plane parallel field, outer region electrical characts. calc. (Russian) 8-67447

impulse corona development in rod/plane gaps-negative polarity 8-87541

needle-to-plane electrode corona inception voltage and streamer length 8-67583

negative corona discharge in air, current distrib. 8-87539

negative impulse corona and sparkover, background ionisation effects 8-87540

onset voltage in bipolar fields 8-67580

point-to-plane gap corona and breakdown in supersonic airstream 8-67573

point-to-plane negative corona discharge in axial airstream 8-67585

corona continued

polyethylene films, adhesive props. improvement by corona discharge appl. (French) 8-92438

polyvinylidene fluoride, corona charging at 12.5 kV, obs. 8-92027

rod-to-plane air gap breakdown under negative impulse voltage 8-67563

secondary electron emission due to negative corona discharges 8-67592

sphere-plane gap avalanche current pulse meas. in nonuniform fields 8-67556

thundercloud elec. field meas. by balloon-borne coronasonde 8-61577

Trichel corona, negative ion mass spectra 8-87537

CO₂, negative point-plane corona, electrical characts. 8-71567He-O₂ corona discharge CV characteristics 8-91168O₂, negative point-plane corona, electrical characts. 8-71567SF₆ and SF₆-N₂ mixture, elec. breakdown and corona stabilisation obs. 8-87582SF₆, negative point-plane corona, electrical characts. 8-71567SF₆ rod-to-plate corona discharge characteristic obs. 8-67584SF₆-air mixture impulse discharge characteristics of 30 cm gaps 8-67572**coronagraphs***see also solar corona*

No entries

corpuscular streams *see cosmic rays; solar wind***correlation methods***see also correlators*

acoustic emission sources, localisation 8-87220

acoustics, correlation coeff. meas. for signals with stationary additive noise 8-94489

altimetric data file acquisition automatic digital correlation method 8-61633

astronomical H₂O radio sources, autocorrel. anal. of spectra 8-65713

blood velocity, catheter meas., cross correl. technique 8-80943

coherent Doppler anemometer for turbulent vel. meas., potential accuracy anal. (Russian) 8-71406

coherent radiation beams, parameters from correlation method (Russian) 8-50705

Continental Shelf sediment sonar signal processing 8-61622

cross correlation techniques for remote river velocity and level meas. 8-57328

data extraction from film using optical and/or digital and/or electronic devices 8-63024

ECG, ambulatory arrhythmia quantification by correl. technique 8-81020

ECG body surface potential map estimation, limited lead selection 8-57111

ECG monitoring by contour comparison, QRS triggering with real-time correlator (German) 8-92715

echolocation, bat, accuracy of meas. of target angular coords. using equi-signal zone 8-77071

gravitational waves, possible detection using correlation techniques 8-89393

hydrometeorologic elements in coastal zone, long-term var. from correl. anal. (Russian) 8-77258

image correlation with geometric distortion acquisition performance 8-71039

image correlation with geometric distortion effect on local accuracy 8-71040

image degradation identification 8-58941

image matching using struct. information, edge vector correlation 8-63036

ionosphere sounding, filtering effect on drift parameters determined by full correl. anal. 8-65450

laser scattered light intensity, recurrence rate correl. 8-66760

meteorology, optimum difference schemes, synthesis on sphere 8-93011

multiband image spatial domain filtering by Karhunen-Loeve transform 8-78952

northern hemisphere annual temperature approximation, simple method 8-81345

nuclear reactor transit time estimation coolant bubbles appl. 8-94067

oblique incidence sound absorpt. characts. of materials using cross-correlation methods (Japanese) 8-83172

optical analogue computer performance advantages 8-78949

optical space-variant pattern recognition, using polar camera 8-66767

Photoelectric recording of optical fields by correlation processing 8-71048

photon correlation in nanosecond range using programmable digital counter, photomultiplier evaluation 8-54464

positive column, striation dynamics, velocity/amplitude correlation 8-67517

power curve regression equations for Ohio River, statistical computer program 8-61472

precipitation over Central Europe, large-scale field components extraction for forecasting purposes 8-92940

PWR neutron noise interpretation by vibration analysis 8-94073

radar ambiguity function display and one-dimensional correlation/convolution by coherent optical processors 8-78950

ripple noise pitch detection by human, adaptive model 8-73166

scintigram change obs. by crosscorrelation 8-80961

semiconductor junction noisy transient meas. 8-62205

semielliptic notch with crack, micro- and macro-stress concentration correlation (German) 8-83330

sideways-looking radar using synthetic aerial, remote sensing appl. 8-69537

spatial convolution and correlation of optical fields via degenerate four-wave mixing 8-71044

statistical treatment of experimental data, book 8-77834

stereophotogrammetry, automatic, using structural pattern recognition techniques 8-61632

underwater sound arrival angle estimation by multiple cross-correlation meas. 8-66978

US filtering and correlation by SAW devices 8-60969

velocity measurement by light scattering techniques, digital correlation appl. 8-57916

visual evoked response of humans, nonlinear anal. 8-92622

correlation theory

see also *correlators; information theory*

- biomedical signals, development of common struct. for filters, correlators and Fourier analysers (*German*) 8-88748
- expanding universe, density perturbations three-point correl. function and higher order functions prediction 8-65730
- galaxy pair-correlation function, clustering evolution effects, cosmological N-body simulations 8-96550
- geomagnetic field quiet time var. rel. to interplanetary mag. field, autocorrel. effects 8-61697
- interferometer model for binaural perception and resolving power of bats (*French*) 8-80883
- statistical treatment of experimental data, book 8-77834
- surface roughness estimation using linear FM signal (*Russian*) 8-77353
- underwater sound propagation in presence of randomly perturbed parabolic profile 8-94477

correlators

see also *correlation methods; correlation theory; information theory*

- acousto-optic memory correlator, long duration, using 'acousto-photorefractive effect' 8-79124
- acousto-optic memory correlator using acousto-photorefractive effect 8-71248
- astronomical telescope speckle interferometry, online digital autocorrelator 8-81548
- automated correlation spectrometer with two Ge(Li) detectors 8-82562
- biomedical signals, development of common struct. for filters, correlators and Fourier analysers (*German*) 8-88748
- holographic interference correlators, theory 8-78969
- hybrid optical correlator system for automated stereo compilation 8-63035
- imaging system using intensity triple correlator 8-74846
- kit of instruments for statistical research 8-87215
- memory-correlator cells employing acoustically induced charge hologram in piezoelectric semiconductors 8-86290
- optical convolvers and correlators, generalised model 8-55303
- optical image and signal processing, United States Air Force programmes 8-74854
- optical matched filter image correlator, for aerial reconnaissance film screening 8-94371
- optical wideband ambiguity function generator with Doppler compensation 8-78936
- pressure modulator radiometer for atm. gas emission meas. 8-81457
- SAW monolithic storage correlator, appl. to adaptive filter 8-87208
- tracking correlation receiver with feedback for radio astronomical interferometry 8-57445
- video correlating system for blood flow vel. meas. in microvessels 8-53543

correspondence principle

- general system quantisation, rigid sphere appl., wave eqn. using correspondence principle 8-57801
- Liouville mechanics for systems with singular Lagrangian, quantisation 8-62096
- orbital correspondence anal. in max. symm., appl. to spin-forbidden processes 8-78631
- quantisation as a nontrivial deformation of classical mechs. (*Czech*) 8-86171
- quantum mechanics, development and Heisenberg's role (*Polish*) 8-89291

corrosion

see also *corrosion protection; corrosion testing; electrochemistry; stress corrosion cracking; surface chemistry*

- alite paste, mature, microstructure study by SEM, TG and X-ray diffr., corrosion 8-92381
- alloy, high temperature, mechanical, thermal and corrosion props. 8-95763
- alloy steel, austenitic, Ni free, TEM exam. of corrosion process 8-85029
- alloys, corrosion resistance in geothermal brine environments 8-85032
- butadiene coatings, on steel, delamination by corrosion 8-64765
- coal conversion plant material, corrosion and wear 8-53012
- commercial refractories, soln. in soda-lime glass, 1200-1350°C 8-95821
- electronic device dendritic growth mechanisms 8-56058
- examination, appl. of small cyclotrons (*Hungarian*) 8-70656
- fission reactor materials, UO₂ high temp. reaction with Zr-Nb 8-66344
- glass surfaces, corrosion, passivation and anal. 8-60854
- graphite, oxidation, corrosion resistance, bend strength, assessment for rotary glass fibre making apparatus 8-64753
- high temperature corrosion, review (*Japanese*) 8-72911
- ion implantation surface alloy creation, corrosion resistance 8-88569
- LMFBR, H burden from steam side corrosion in Na heated steam generators 8-58355
- LMFBR type mixed oxide fuel pins, composition of corrosion product oxide phases in pin gaps 8-70599
- materials interactions, stability, phase transformations, thermodynamics and corrosion 8-88444
- metal-glass mats. alloyed with Cu, powder prep. and props. 8-72912
- metal/metal ion system, instantaneous corrosion rate determ. by Faradaic rectification 8-80667
- metal/metal ion systems, instantaneous corrosion rate determ. by Faradaic rectification 8-80666
- metals, scaling, theory, electrochem. transport model 8-64761
- mullite fibre reinforced mullite, in vitro degradation, bending strength, Young's modulus, density meas. 8-85011
- noble metal, interfacial corrosion in metal to ceramic reaction welding 8-53035
- nuclear power station corrosion research, review of problems (*Czech*) 8-62598
- nuclear reactors, steam generator tube survey, causes of failures, repair procedure 8-54826
- nucleation and growth at surfaces, kinetic studies, review 8-72046
- ohmic potential drop, rel. to crit. pitting and protection pots. 8-72900
- parylene polymers, synthesis, elec., phys., corrosion props. (*German*) 8-64521
- polarisation resistance measurements, determ. of corrosion mechanis. 8-80656

corrosion continued

- polarography, in glass-corroding media, using polyethylene capillary tubes 8-61090
- porcelain enamel, resistance to aqueous attack, expt. results 8-56788
- porcelain enamel, resistance to aqueous attack, prediction eqn. 8-60853
- portland cement paste, microstructure study by SEM, TG and X-ray diffr., corrosion 8-92381
- PWR, in-reactor loop expts. on corrosion product transport and water chemistry 8-58335
- silicate glass, IR reflection spectra relation to corrosion state of surface (*Japanese*) 8-88554
- silicate glass corroded by moisture, IR refl. spectra change (*Japanese*) 8-53013
- silicate glasses, corrosion by aq. solns. 8-64752
- silicate glasses, exam. of chemical stability, in alkali solns. 8-88557
- sintered mats., complex diffusion alloying 8-68650
- steel, 12Kh18N9T-TiB₂, eutectic alloy, high temp. props. 8-84931
- steel, alloy, Cr-Mo, pitting and crevice corrosion, exam. (*Japanese*) 8-64769
- steel, alloy, Fe-Cr-Ni-Mo-Al, (13, 8, 2, 1, wt.%), H₂ effects on fracture, exam. 8-60809
- steel, austenitic, intergranular defectiveness determ. using inductive instruments 8-53075
- steel, austenitic, stainless, pitting and crevice corrosion, effect of Mo, Si and N (*Japanese*) 8-92399
- steel, austenitic stainless, influence of Cr, Mo, N, content on resist. to pitting corrosion 8-80668
- steel, austenitic stainless, influence of steel comp. on corrosion in high temp. Na 8-80675
- steel, austenitic stainless, welded joints, cold working effects on mech. and corrosion props. (*Hungarian*) 8-52838
- steel, C, corrosion by wet elemental S, exam. as function of pH and particle size 8-92388
- steel, C, corrosion during cyclical exposure, to wet elemental S, and He atmosphere 8-92391
- steel, C, corrosion in concentrated H₂SO₄ 8-64767
- steel, C, fatigue crack growth in air and seawater, under constant amplitude and random loading 8-64679
- steel, case-hardened cast, contact endurance rel. to austenizing (*Russian*) 8-56805
- steel, corrosion, Na loop system, analysis of radioactive corrosion product transfer 8-78464
- steel, Cr (9 wt.%), SiO₂ vapour deposited coatings, exam. of corrosion protective props. 8-88563
- steel, Cr-Mo-(Nb)-(Ni)(Ti), low-alloy selection for nuclear steam generator tubes 8-54834
- steel, deformed and welded mild, potential distrib. meas. technique, appl. to corrosion study, apparatus (*Japanese*) 8-53049
- steel, ferritic, Cr-Mo, containing less than 12 wt.% Cr, sensitisation during welding, to intergranular corrosion 8-88566
- steel, ferritic stainless, Cr-Mo, Mo effect on pitting pot., AES anal. 8-95852
- steel, galvanised, pipe carrying potable water 8-92409
- steel, martensitic, low C, nitriding, exam. of case props. 8-85045
- steel, mild, corrosion in complex aq. environment, linear polarisation investig. 8-76782
- steel, stainless, 95Kh18, vacuum quenching 8-85047
- steel, stainless, attack by liquid and vapourised CsOH 8-68840
- steel, stainless, corrosion due to molten LiF-LiCl-LiBr, fusion reactor appl. 8-53217
- steel, stainless, corrosion resistance in sea water 8-85028
- steel, stainless, crevice corrosion, mathematical model 8-95834
- steel, stainless, Li compatibility, H₂ influence 8-68844
- steel, stainless, radiation-thermal treatment, N₂O₄ coolant action, intergranular corrosion (*Russian*) 8-58357
- steel, stainless, sintered Kh18N10T, friction and corrosion props. for frictional units of nuclear plants 8-60845
- steel, stainless, sputtering and chem. attack by H ions of 100 eV energy 8-95635
- steel, stainless, type 12Kh18N10T, US inspection for intergranular corrosion 8-60912
- steel, stainless, type Kh17N13M2T, strengthening by plastic deformation and cold working (*Russian*) 8-52839
- steel, stainless 310, sulphidation kinetics temp. effect and Cr role 8-64773
- surface science, rel. to energy development and technology 8-88553
- thermodynamics and electrochemistry, energy considerations 8-88643
- Zircaloy heated surface, FeO deposition in boiling water 8-58353
- Al alloys, pit propagation, influence of anions in halide solution 8-72917
- Al alloys, pitting corrosion rel. to load-carrying capacity of sheets (*Russian*) 8-56806
- Al, sputtering and chem. attack by H ions of 100 eV energy 8-95635
- Al-Sn, (<0.28 wt.%) corrosion behaviour in 16% HCl 8-85054
- Al-Zn-Mg-Cu, alloy 7075-T6, corrosion in halide solutions, exam. of anion dependency 8-60867
- Au, sputtering and chem. attack by H ions of 100 eV energy 8-95635
- Au-In, electrodeposited from acid cyanide electrolyte, exam. of wear and corrosion resistance 8-80482
- Co-Cr, high temp. sulphide corrosion 8-64775
- Co-Cr-WC, corrosion and corrosive wear in sea water 8-92408
- Co-WC, corrosion and corrosive wear in sea water 8-92408
- Cu, effect of addition of bromides and iodides on corrosion in seawater 8-80670
- Cu, pipe carrying potable water 8-92409
- Cu/Zn galvanic couple, potential distrib. meas. technique, appl. to corrosion study, apparatus (*Japanese*) 8-53049
- Cu-Ni, sulphidation between 653 to 770K, exam. of scale morphologies, using X-ray diffr., and electron microprobe anal. 8-88559
- Cu-Ni (20 and 50 wt.%), sulphidation, exam. of scale growth kinetics 8-88560
- Cu-Ni cast alloy, effect of alloying and residual elements 8-85033
- Fe, anodic dissolution in acidic chloride solns., exam. 8-92389
- Fe, Armo, corrosion and mechanical behaviour in liquid Li 8-53036
- Fe, corrosion and electrochem. behaviour in NaOH soln. containing ClO₃⁻ (*Japanese*) 8-72928
- Fe, grey cast, corrosion resist., Cu alloying additions effect (*Russian*) 8-56807
- Fe-(Mo)-CaF₂, sintered, friction and corrosion props. for frictional units of nuclear plants 8-60845

corrosion continued

- Fe-Al-Cr (10, 5 to 10, wt.%), corrosion by coal char, SEM and X-ray diff. exam. 8-88573
- Fe-Cr, amorphous alloy, effect of metalloid impurities on corrosion resistance and electrochem. behaviour 8-72925
- Fe-Cr-Ni alloys, oxidation-sulphidation in gas mixture, parabolic kinetics, thermochem. diagram 8-72932
- Fe-Cr-P-C alloy, amorphous, corrosion resist. in 1N HCl 8-80678
- Fe-Mo-P-C alloy, amorphous, corrosion resist. in 1N HCl 8-80678
- Fe-Ni-Cr-Mn-Al-Ti Incoloy 800, exam. of scale morphology, alloying element distrib. after oxidation 8-80677
- Fe-W-P-C alloy, amorphous, corrosion resist. in 1N HCl 8-80678
- Fe-Zn, stable and metastable alloys, order-disorder, mag. interactions and corrosion behaviour 8-68422
- HfPt₃, corrosion resist. and elec. cond., bulk and film samples 8-72285
- InP surface, interaction with Cl, electron spectroscopic obs. 8-56036
- K₂O-SiO₂ glass, improvement in water resist. by ion exchange 8-85012
- Li₂O-SiO₂ glass, improvement in water resist. by ion exchange 8-85012
- Mo, film, vacuum deposited, elec. cond., internal stresses, surface corrosion, MOS gate appl. (*Japanese*) 8-80073
- Na₂O-FeO-Fe₂O₃-SiO₂, chemical durability at different pH values 8-72902
- Na₂O-MgO-Al₂O₃-SiO₂, chemical durability at different pH values 8-72902
- Na₂O-SiO₂ glass, improvement in water resist. by ion exchange 8-85012
- Nb, film, evaporated, adsorpt. of SO₂, corrosion 8-79897
- Ni, bright, rest potential meas. and interpretation in NaCl and dil. H₂SO₄ (*French*) 8-85056
- Ni, corrosion in LiCl-KCl eutectic melt containing nitrate ions (*Japanese*) 8-92398
- Ni, S penetration of NiO scales 8-64776
- Ni-(W,Cr)C, corrosion and corrosive wear in sea water 8-92408
- Ni-based superalloys, mechanical integrities of surface scales, contaminant corrosion 8-95845
- Ni-Cr-Fe (15.7, 7.63 wt.%), Inconel 600, anal. of pit generation by 3.5% NaCl, by stochastic theory (*Japanese*) 8-85038
- Ni-Cr-Nb-Al eutectic alloys, sulphidation/oxidation at high temps., corrosion mechanism 8-72934
- Ni-Cr-W-C(Si) hardness, corrosion resistance, wear resistance tests in 10% HCl (*German*) 8-92368
- Pb/PbCl₂ electrode, in chloride media, low temp. props. 8-68899
- PbO-K₂O-SiO₂-(Al₂O₃) glass, corrosion in acid, leaching kinetics 8-92378
- PbO-SiO₂ glass, corrosion in acid, conc. profile meas. 8-92379
- PbO-SiO₂-(Al₂O₃) glass, corrosion in acid, leaching kinetics 8-92378
- Pb(Sb)/H₂SO₄, PbSO₄(sat.), rates, instantaneous, Faradaic rectification, experimental verification part II 8-80667
- Pt electrode, electrochemical studies in NaHCO₃ solutions at elevated temps. 8-85026
- Si, ion-implanted surface, profiling method 8-95075
- SiAlON system, β', 15 R phases, oxidation resist. (*French*) 8-72899
- Sn powder, incorporated into lacquers, applied to tinplate containers 8-80671
- Ta, film, evaporated, adsorpt. of SO₂, corrosion 8-79897
- Th-U alloy fuel behaviour in organic-cooled reactor 8-86605
- Ti alloy, VT3-1, vacuum-chromized, fretting-corrosion in couple with unprotected BT3-1 and steel 40KhNMA (*Russian*) 8-56804
- Ti, crevice corrosion in NaCl soln., 100 to 250°C (*Japanese*) 8-72927
- Ti, film, evaporated, adsorpt. of SO₂, corrosion 8-79897
- Ti-Pd, crevice corrosion in NaCl soln., 100 to 250°C (*Japanese*) 8-72927
- TiO₂, anodically formed layers, film instability obs. 8-72916
- V-Mo, effect of ion plated Mo on corrosion in liquid Na, mech. props. 8-53020
- Zn(Hg)/KOH, ZnO(sat.), rates, instantaneous, Faradaic rectification, experimental verification part II 8-80667
- Zr-Al(8.6 wt.%), mech. props., corrosion and fast neutron irradiation influence 8-84948
- Zr(HPO₄)₂, cryst., heat treated, acid strength distrib. 8-92377
- ZrPt₃, corrosion resist. and elec. cond., bulk and film samples 8-72285

corrosion control see *corrosion protection*

corrosion fatigue see *stress corrosion cracking*

corrosion fatigue testing see *corrosion testing*

corrosion prevention see *corrosion protection*

corrosion protection

- see also *anodisation; corrosion; corrosion protective coatings; packaging; pH control*
- Al, electrodes, use of soluble corrosion inhibitors to suppress electrode dissolution 8-88565
- metal surfaces, laser heat treatment, wear resist., corrosion protection, hardening, review 8-72939
- in nuclear reactor, radiolytically formed chelating agents appl. 8-64745
- painting (*Japanese*) 8-95829
- plastics, managing problems of corrosion (*Japanese*) 8-92382
- pollution control equipment appl. 8-77317
- steel, austenitic, corrosion-resistant, strengthening by alloying with N₂ 8-95757
- steel, borided, nitrided, corrosion behaviour in aqueous media 8-95837
- steel, corrosion protection, NAA obs. 8-53038
- steel, mild, corrosion inhibitor, zinc potassium chromate 8-95839
- steel, mild, protection by Zn-rich paint in flowing aerated 0.5 M NaCl solution, Zn particle size effect 8-95840
- steel, mild, protection by Zn-rich paint in flowing aerated 0.5 M NaCl solution, exposed area ratio effect 8-95841
- steel, mild, protection by Zn-rich paint in flowing aerated 0.5 M NaCl solution, zinc content effect 8-95842
- steel, mild, protection by Zn-rich paint in flowing aerated 0.5 M NaCl solution, zinc oxide addition effect 8-95843
- steel, protective props. of N-containing inhibitors (*Russian*) 8-56809
- steel, rusted, exam. of tannin treatment action mode 8-88564
- steel, stainless, 18-8 Ti and 18-8 Nb, against stress corrosion cracking in polythionic acid solution 8-56824

corrosion protection continued

- steel, stainless, sensitised surface normalisation by laser melting 8-60869
- steel 20, protective props. of diammonium salt-based inhibitors (*Russian*) 8-56808
- Cu, passivation by protective glassy layers at 500°C 8-76785
- Fe, corrosion pitting in acid, alkaline solution, gelatin effect 8-95838
- Fe surface, purposeful modification by gas adsorption, charact. by photoemission 8-71955

corrosion protective coatings

- anticorrosive and antifouling coatings, laboratory and environmental testing 8-64746
- benzoic acid inhibitor film on Fe, passivation and inhibitor props., X-ray photoemission spectroscopy exam. 8-88561
- boride on stainless steel, mech., elec. props., boronising sintering method investig. 8-60594
- controlled nucleation thermochemical deposition, improvements over chemical vapour deposition 8-92387
- organic, performance evaluation of adhesion and permeability 8-64764
- paint, zinc-rich, for protection of mild steel, dust particle size effect 8-95840
- paint, zinc-rich, for protection of mild steel, Zn content effect 8-95842
- paint, zinc-rich, for protection of mild steel, ZnO addition effect 8-95843
- paint, zinc-rich for protection of mild steel, exposed area ratio effect 8-95841
- semiconductor, implantation of Si, Al, Hf, Ta into InP and GaAs, form. of protective oxide 8-79622
- steel, butadiene coatings, delamination by corrosion 8-64765
- steel, high alloy ledeburitic, wear and corrosion resistant coating by chemical vapour deposition 8-92403
- steel, organic, adhesion and permeability 8-64764
- steel, stainless, corrosion protection by heat treatment method 8-68836
- steel antioxidant protective glass enamel cladding exam. of development 8-85031
- surface alloys prod. by ion implantation 8-88569
- Al alloys, stress corrosion cracking protection, by γ₁Al₂O₃ anodic film 8-95836
- Al, ion plated coating on steel (*Japanese*) 8-80477
- Al-Zn coated steel sheet, chromate passivation protection against wet-storage stain 8-95854
- Fe-Zn, on low C rimming steel, effect of addition of Al to Zn on phase composition and morphology (*Polish*) 8-53014
- FeO inhibitor film on Fe, passivation and inhibitor props., X-ray photoemission spectroscopy exam. 8-88561
- Ni base superalloy IN 100, corrosion resistant intermetallic coating, microstruct. effect on mech. props. 8-85058
- SiC, pyrolytic, on C fibres, rate of oxidation 8-60857
- SiO₂ 9% Cr steel, vapour deposited, exam. of corrosion protection props. 8-88563
- Ti alloy, VT3-1, vacuum-chromized, fretting-corrosion in couple with unprotected BT3-1 and steel 40KhNMA (*Russian*) 8-56804
- V-Mo, effect of ion plated Mo on corrosion in liquid Na, mech. props. 8-53020
- Zn coated steel sheet, chromate passivation protection against wet-storage stain 8-95854

corrosion testing

- alloys, corrosion resistance in geothermal brine environments 8-85032
- eddy current monitoring 8-88584
- fatigue crack arrest, corrosive environment, at low stress intensities 8-92415
- glass bottles, qualitative method for monitoring chemical corrosion 8-85068
- heat exchange tube thickness meas. by eddy current for corrosion testing, computer study 8-68852
- mechanicochemical testing of metals, electrochemical cell for mechanicochem. behaviour determ. 8-60905
- monitoring review 8-68849
- nuclear reactor structural materials, WR-1 irradiation facility 8-89945
- simulated boiling water reactor conditions 8-80696
- steel, austenitic stainless, tube carburised layer metallographic determ. 8-85077
- steel, low alloy, constructional, fatigue cracking in corrosive media 8-85081
- steel, Si-Mn-Ni-Cr-Mo, acoustic emission during stress corrosion cracking appl. to materials testing 8-53042
- steel, stainless, US methods for intergranular corrosion inspection 8-95898
- CO₂ conc. regulation in climatic cabinets for corrosion testing (*German*) 8-53069
- Fe-Ni-Cr-Mo, exam. of tapered tensile specimen, for stress corrosion threshold stress testing 8-53055
- Ti alloys, structural materials for liquid metal radiation loops 8-72958

corundum

- see also *ruby; sapphire*
- doped, induced absorption spectra, low temp. irradiation effects (*Russian*) 8-72570
- fusion cast refractory, effects of glassy phase on thermal cycling resist. 8-84956
- ion bombarded, vol. expansion, annealing compaction, surface props. 8-67748
- spherical ground samples, extinction effects, inhomogeneous mosaicity 8-75494
- Al₂O₃:Ni²⁺, corundum, phaser production of transverse phonons by impurity centres (*Russian*) 8-91390

cosmic dust

- see also *meteoroids*
- atmospheric cosmogenic radioisotope flux variation due to cosmic dust and meteoritic matter 8-61634
- black hole, thin spherical dust shell, dynamics, Russner-Nordstrom geometry 8-77481
- black spherules collected at Mt. Norikura, Japan, accretion rate 8-96445
- book, general aspects 8-57498
- η Carinae, IR ang. diameter 8-93271
- chemistry, organic compounds and relation to origin of life 8-73660

cosmic dust continued

- circumstellar clouds, scattered stellar radiation circular polarisation theory 8-96428
 circumstellar dust shells, contrib. to young stars reddening and polarisation 8-93199
 circumstellar dust shells, Monte Carlo simulation of polarised light transfer 8-81608
 circumstellar dust shells and mass loss, from luminous O-B3 stars in open clusters (*German*) 8-53925
 clouds rel. to diffuse galactic light and Milky Way brightness fluctuations 8-61921
 comet dust particles, impact mass spectrometer for chemical analysis on fly-by mission 8-93112
 comet low vel. particle meas. during fly-by mission using capacity type detector 8-93113
 Comet West (1976 VI), IR obs., dust model 8-81592
 cometary dust in atmosphere, rel. to ice ages and ecological catastrophes 8-53714
 comets, dust mantle model rel. to monochromatic brightness vars. 8-81589
 comets, origins, research and interplanetary relationships 8-57507
 CRL 2104, CRL 2179, late WC stars, 2 to 4 μ m spectrophotometry and circumstellar dust 8-96491
 CH Cygni, dust grains form. in circumstellar shell from linear polarisation vars. 8-69808
 V1016 Cygni, IR spectrum and circumstellar dust shell 8-93266
 30 Doradus complex, in LMC, UV reddening law 8-96516
 dust grains in early solar system, formation of planets with Fe cores 8-85869
 Einstein eqns., nonexistence of solns. 8-49736
 galactic centre, distrib. of stars and dust, black hole hypothesis 8-86010
 galactic centre direction, near IR polarisation due to aligned interstellar grains 8-96534
 galactic dust globules, microwave spectral lines obs. 8-57609
 galactic interstellar extinction law, vars. 8-85990
 giant stars with IR excesses, gas-dust shells rel. to optical emission linear polarisation 8-96481
 globular clusters, UBVR photometric obs., dust patches 8-81662
 grain accretion in protoplanetary nebula, liquid drop effects 8-85862
 HD 45677 or 50138, hot Bep stars with circumstellar dust IR excesses, UV obs. 8-93250
 intergalactic dust in galaxy clusters, evidence from Zel'dovich effect 8-54041
 interplanetary, large fluffy particles as explanation of optical props. 8-57499
 interplanetary, orbit distribution, Pioneer 8 and 9 obs. 8-89031
 interplanetary, scatt. meas. of irregular particles versus Mie theory 8-58918
 interplanetary dust, zodiacal light circular polarisation theory 8-96428
 interplanetary dust, zodiacal light indications 8-57500
 interplanetary dust grains, H-implanted, role in upper atmosphere H chemistry 8-65445
 interplanetary particle dynamics 8-57501
 interplanetary particles, sampling techniques 8-57459
 interplanetary, causing dark patches in zodiacal light 8-93153
 interstellar, Apollo 17 far UV search for starlight scatt. 8-65726
 interstellar dark dust cloud model, lifetime of molecules 8-85999
 interstellar dust, chemical composition 8-57624
 interstellar dust, IR extinction meas. rel. to diffuse interstellar bands strengths 8-93198
 interstellar grain destruction by chemical reactions, collisions and photodesorption 8-54021
 interstellar grain destruction by sputtering 8-54020
 interstellar grain mantle growth in UV-shielded dense clouds 8-54022
 interstellar grain motions, role in star form. 8-69788
 interstellar grains, carbyne as major constituent 8-69859
 interstellar grains in interplanetary space, optical detection during out-of-ecliptic mission 8-85906
 interstellar plasma clouds, dust sedimentation rel. to star form. 8-73744
 interstellar transition metal grains, of H, rel. to H₂ catalytic form. 8-54005
 interstellar UV extinction obs. in galactic plane from TD1 satellite 8-93382
 intracluster dust, contrib. to Orion young stars reddening and polarisation 8-93199
 IR sources, 10 μ m silicate absorpt. band equivalent widths and dust temps. 8-57614
 IR sources assoc. with double-lobed refl. nebulae, far IR obs. rel. to dust emissivity 8-54009
 M17, Platt particles and spatial temp. fluctuations 8-61907
 Mars atmosphere, solar heating rates during global dust storm 8-85878
 microparticle studies by space-borne instrumentation 8-57460
 nebulae, dusty, non on-the-spot (OTS) models 8-85995
 NGC 1068, Seyfert galaxy, silicate emission feature from IR photometry 8-54035
 NGC 2264, young open cluster, differential reddening due to intra-cluster dust clouds 8-53996
 NGC 4151, Seyfert galaxy, optical polarimetry, circumnuclear dust envelope 8-61916
 NGC 7027, 16-38 μ m spectral obs. and dust model of planetary nebula 8-93354
 λ Orionis H II region, absorption shell and core 8-77590
 Periodic Comet Encke dust, large grains in short supply 8-85908
 PHL 938, quasar, continuum spectrum reddening due to dust 8-96561
 plane-symmetric cosmological model, Einstein eqn. solns. for dust 8-49733
 polysaccharide grain model for galactic IR sources, IR fluxes calcs. 8-54008
 reflection nebulae, simplified models rel. to dust comp. and particle size 8-96526
 relativistic dust universes, comoving metrics, Newtonian interpretation 8-65732
 HM Sagittae, IR spectrum and circumstellar dust shell 8-93266
 sedimentation of grains in interstellar clouds 8-93349
 Seyfert galaxies, dust thermal emission contrib. to IR energy distrib. 8-57645
 Seyfert galaxies nuclei, dust effects on continuous optical spectra 8-57644

cosmic dust continued

- silicate grain condensation, laboratory expt. 8-54015
 silicates, optical props. in far UV 8-53875
 stratosphere, upper, evidence for extraterrestrial dust layers 8-73445
 thermal emission spectrum from small interstellar grains with temp. fluctuation 8-69864
 X-ray burst propag. through interstellar dust, small-angle scatt. effects 8-57433
 zodiacal light, wavelength dependent model, Mie scatt. and thermal emission 8-81587
 zodiacal light dust, orbits from Doppler shift meas. 8-85904
⁵⁹Ni formation cross section in Fe+ α at 7-24 MeV, poss. prod. in cosmic dust 8-78399
- cosmic radiation** *see cosmic rays*
cosmic radiations, radiofrequency *see radiofrequency cosmic radiation*
cosmic radio waves *see radiofrequency cosmic radiation*
cosmic ray absorption
 No entries
- cosmic ray alpha-particles and helium nuclei**
 antihelium, relative abundance in primary cosmic radiation 8-73594
 solar flares, energetic particle composition temporal development 8-89148
 solar protons and α particles, rigidity-independent coronal propag. and escape 8-77444
 sunward flowing moderate intensity proton and alpha particle fluxes, characts. 8-89016
- cosmic ray apparatus**
see also particle detectors
 background radiation, meas. methods 8-82588
 Cerenkov counter for spacecraft application 8-86734
 Cherenkov photographic detector appl. to search for Dirac monopole 8-70700
 Cherenkov pulse duration during EAS 8-73595
 electrons and nuclei expt. on International Sun-Earth, Explorer C spacecraft 8-85792
 energetic particle flux meas. in magnetosphere and interplanetary space, International Sun-Earth Explorer A and B spacecraft 8-85799
 gamma-ray Compton telescope, high ang. resolution, 0.3-10.0 MeV directivity (*Portuguese*) 8-85847
 gamma-ray detectors, counters and telescopes (*Polish*) 8-96394
 gamma-ray telescope in 10-30 MeV range 8-73638
 inclined muon monitors, muon spectra, generating functions, rel. to diurnal variation at Kiruna 8-85783
 International Sun-Earth Explorer spacecraft, expts. and instruments 8-85785
 interplanetary and solar electrons meas. instrumentation on International Sun-Earth Explorer spacecraft 8-85786
 ion sensor, low-energy, for space meas. with reduced photosensitivity 8-53764
 isotope spectrometer on International Sun-Earth Explorer C spacecraft 8-85797
 low energy proton expt. on International Sun-Earth Explorer C spacecraft 8-85791
 manned submersibles for cosmic ray detect. in deep sea 8-81510
 medium energy expt. on International Sun-Earth Explorer C spacecraft 8-85798
 multidetector telescope expt. on International Sun-Earth Explorer C spacecraft for isotopic abundance determ. 8-85789
 MUTRON, cosmic ray mag. spectrometer, MWPC trigger system 8-55081
 neutron detector, large underground telescope, Russia (*Russian*) 8-73589
 nuclear and ionic charge distrib. particle expts. on International Sun-Earth Explorer spacecraft 8-85790
 pellicle stack, γ -ray family from cosmic-ray hadron reactions, accelerated scanning method 8-78546
 plastic total absorption track detector of high energy particles 8-55107
 scintillation counter hodoscopes, LED test system 8-58556
 scintillation counters, large area, light collection 8-74538
 scintillation time-of-flight telescope for cosmic γ -ray preselection 8-82572
 solar wind ion comp. expt. on International Sun-Earth Explorer C spacecraft 8-85793
 spacecraft expt. determ. of cosmic-ray particle fluxes 8-85778
 superheavy primary cosmic ray nuclei, obs. with solid-state track detectors and X-ray films (*Japanese*) 8-61688
 upper atmosphere, background effects in scintillation telescopes 8-85823
 CsI crystals, in scintillation counters, nonstatistical counting rates due to phosphoresc. 8-95597
 Fe-liquid scintillator multilayer calorimeter transition effects, muon burst rates 8-90019
 H₂O, acoustic rad. from ionising particles 8-71793
- cosmic ray composition**
see also cosmic ray alpha-particles and helium nuclei; cosmic ray deuterons; cosmic ray electrons; cosmic ray mesons; cosmic ray muons; cosmic ray neutrinos; cosmic ray nuclei; cosmic ray photons
 antiprotons and antihelium, relative abundance in primary cosmic radiation 8-73594
 Dirac monopole, search with Cherenkov photographic detector 8-70700
 galactic proton/electron ratio 8-69633
 hadron unaccompanied flux at depth 730 g cm⁻², energy spectra in range 10²-10⁴ GeV 8-73593
 heavy leptons in cosmic radiation underground, search using scintillation+Cherenkov detectors 8-65470
 isotopic composition, rel. to cosmic ray origin and containment time 8-53781
 isotopic composition of B, C, N, Ne, Mg and Si, mean mass determ. 8-93060
 medium energy expt. on International Sun-Earth Explorer C spacecraft 8-85798
 nuclei, low energy, props., Skylab expt. 8-69632
 nuclei from 3000 MeV to 50 GeV per nucleon, charge comp. and energy spectra 8-93059
 pion spectrum, at top of atmosphere 8-53780
 solar flares, energetic particle composition temporal development 8-89148
 solar flares, particle emission comp. (*Italian*) 8-96461

cosmic ray composition continued

sunward flowing proton and alpha particle fluxes, comp. and spectra 8-89016

^7Be , cosmic ray accel. probe 8-81512

cosmic ray deuterons

No entries

cosmic ray effects and interactions

see also *high-energy cosmic ray interactions*

atmosphere, ion-pair production rate above 18 km altitude, parametrization 8-65469

atmospheric nucleon and charged pion unidirectional diffusion eqns. 8-57417

Barwell meteorite, preatmospheric size, particle track study 8-53893

charged cosmic ray scatt. in stochastic mag. field, above 1 GeV 8-61689

clusters of galaxies, intracluster gas heating by relativistic electrons rel. to X-ray and radio emission 8-57655

EAS, muon spectrum at sea-level, Maeda's model, using pion-kaon ratio 8-85781

fragmentation parameters meas. in nuclear emulsions, validity 8-90017

gamma-rays origin in cosmic ray interactions with matter (Polish) 8-96571

hadron interactions, violation of scaling model (Russian) 8-78231

intercloud cosmic ray ionisation rate 8-85989

ionisation events in stratosphere, effects on NO_2 , O_3 and climate, rel. to life extinction 8-96273

meteorites, ^{39}Ar prod. as evidence for Maunder minimum in solar activity 8-57529

meteorites, mass ablation, cosmic-ray track study 8-53894

nuclide production in Fe meteorites, rare gas concs. 8-65473

one-dimensional diffusion eqn. integration, one-fireball model 8-57416

San Juan Capistrano meteorite, cosmic ray record 8-57512

solar system ^{16}O and ^{26}Al isotopic anomalies, local proton irradiation model 8-93128

spaceflight, radioactivity induced in scintillator materials 8-85822

CsI crystals, in scintillation counters, nonstatistical counting rates due to phosphoresc. 8-95597

H_2O , acoustic rad. from ionising particles 8-71793

^{15}N , enrichment in Mars atm. due to cosmic ray interactions in early solar system 8-73669

SF_6 , breakdown at high pressure, possible cosmic ray effects 8-87577

cosmic ray electrons

clusters of galaxies, intracluster gas heating by relativistic electrons rel. to X-ray and radio emission 8-57655

cosmic rays propagation and distribution in Galaxy 8-69621

EAS near core, struct. of electron-photon component (Russian) 8-57414

energy spectrum, theory of lifetime distrib. of particles 8-96368

galactic halo, relativistic electrons spectrum from radio obs. 8-96544

galactic proton/electron ratio 8-69633

interplanetary, detect. expt. on International Sun-Earth, Explorer C spacecraft 8-85792

interplanetary and solar, meas. instrumentation on International Sun-Earth Explorer spacecraft 8-85786

interplanetary propagation, Mars spacecraft meas. 8-53779

interstellar local electron spectrum determ. from galactic radio background 8-93056

modulation of Jupiter electrons, Pioneer 10 and 11 obs. 8-61690

polar, magnetotail lobe and interplanetary low energy electrons, satellite obs. 8-73587

primary electrons, detect. by synchrotron radiation in geomag. and interstellar mag. fields 8-57412

propagation in Galaxy, leaky-box model 8-57409

solar electrons from September and November 1977, flares, spectra and time profiles 8-77446

solar flare electrons, peculiarity of ejection into interplanetary space (Russian) 8-77445

solar flare energetic particles, interplanetary propag. model 8-65468

solar wind, very low electron and proton temps., statistical anal., origin 8-65477

splash and re-entrant albedo electrons, energy spectra 8-69630

cosmic ray energy spectra

electron spectrum determ. from galactic radio background 8-93056

electrons and nuclei expt. on International Sun-Earth, Explorer C spacecraft 8-85792

galactic cosmic rays, propag. and spectra in finite solar cavity 8-69623

galactic halo, relativistic electrons spectrum from radio obs. 8-96544

gamma-ray background, spectrum rel. to primordial heavy leptons annihilation contrib. 8-93479

gamma-ray bursts, multiple Compton scatts. effect on X-ray emission spectrum 8-96389

hadron unaccompanied flux at depth 730 g cm^{-2} , energy spectra in range 10^2 - 10^4 GeV 8-73593

inclined muon monitors, muon spectra, generating functions, rel. to diurnal variation at Kiruna 8-85783

leakage error in cosmic ray spectra 8-89023

muon spectrum at sea-level, Maeda's model, using pion-kaon ratio 8-85781

nuclei, low energy, props., Skylab expt. 8-69632

nuclei from 3000 MeV to 50 GeV per nucleon, charge comp. and energy spectra 8-93059

pion spectrum, at top of atmosphere 8-53780

pion and galactic subcosmic rays; interstellar space spectrum of role in cosmos 8-61693

solar energetic particle events following September and November, 1977, flares, proton and electron spectra 8-77446

spacecraft expt. determ. of cosmic-ray particle fluxes 8-85778

splash and re-entrant albedo electrons, energy spectra 8-69630

sunward flowing proton and alpha particle fluxes, comp. and spectra 8-89016

theory of lifetime distrib. of particles 8-96368

cosmic ray geophysical effects see *geophysical aspects of cosmic rays*

cosmic ray jets see *cosmic ray showers and bursts*

cosmic ray mesons

atmospheric nucleon and charged pion unidirectional diffusion eqns. 8-57417

axion, astrophysical limitations on mass (Russian) 8-61835

cosmic ray mesons continued

meson-neutrino spectrum from GSFC 8-85782

pion spectrum, at top of atmosphere 8-53780

cosmic ray muons

detection in deep sea using manned submersibles 8-81510

EAS, ave. lateral muon density distrib., arrival direction studies 8-73596

EAS, method of searching for anomalous muon generation 8-89026

EAS, muon spectrum at sea-level, Maeda's model, using pion-kaon ratio 8-85781

EAS high energy muons, array and data analysis 8-89027

EM interactions of muons and muon pairs, 5-1200 GeV (Russian) 8-73598

inclined muon monitors, muon spectra, generating functions, rel. to diurnal variation at Kiruna 8-85783

large cosmic ray showers, muon component computer simulation using hadronic collisions models 8-57415

scintillation detector system, cosmic ray muon lifetime, undergraduate teaching 8-81752

sea-level muon charge ratio, energy up to 1 TeV 8-89029

sea-level muon spectra, model using kaon-pion ratio 8-93064

sea-level spectrum, Dao scaling model for $\text{pp} \rightarrow \pi^+ \text{X}$ 8-61694

stellar daily variation, semiannual modulation 8-69626

temperature variations, spectrographic obs. of secondary cosmic rays 8-69628

$\mu^+ \mu^-$ ratio, calc. from pp inclusive reactions at ISR energies 8-58212

cosmic ray neutrinos

background neutrinos and Friedmann model (Polish) 8-89276

Bianchi type IX universes, neutrino viscosity 8-77633

detection in deep sea using manned submersibles 8-81510

lepton mixing and neutrino oscillations, cosmic neutrinos, heavy leptons, μ decay 8-82193

lepton mixing and neutrino oscills. review, 'solar neutrino puzzle' 8-66182

meson-neutrino spectrum from GSFC nucleon spectrum 8-85782

solar neutrino problem rel. to Fe limited solubility in central Fe-H plasma 8-89149

solar neutrino problem rel. to solar interior struct. (Italian) 8-81598

ultrahigh energy neutrino emission from cosmic ray sources 8-65723

cosmic ray neutrons

aircraft altitudes, Ames collaborative study on mid-latitude flights 8-53538

detector, large underground telescope, Russia (Russian) 8-73589

cosmic ray nuclei

see also *cosmic ray alpha-particles and helium nuclei; cosmic ray neutrons; cosmic ray protons*

cosmic rays propagation and distribution in Galaxy 8-69621

emulsion plastic sandwich stack event, cosmic ray nucleus interpretation 8-69635

energy loss params., appl. on mass determ. of cosmic ray nuclei in nuclear emulsion 8-94175

fragmentation parameters meas. in nuclear emulsions, validity 8-90017

interplanetary, detect. expt. on International Sun-Earth, Explorer C spacecraft 8-85792

isotopic composition of B, C, N, Ne, Mg and Si, mean mass determ. 8-93060

isotopic composition of Fe-group elements, galactic cosmic rays 8-89024

low energy, ionisation states and origin 8-69634

low energy, props., Skylab expt. 8-69632

multidetector telescope expt. on International Sun-Earth Explorer C spacecraft 8-85789

propagation in Galaxy, leaky-box model 8-57409

superheavy primary cosmic ray nuclei, obs. with solid-state track detectors and X-ray films (Japanese) 8-61688

cosmic ray-nucleus reactions

for inelastic cosmic ray-nucleus scattering, see "*cosmic ray-nucleus scattering*"

atmospheric nucleon and charged pion unidirectional diffusion eqns. 8-57417

high-energy cosmic-ray components in atmosphere, scaling features 8-93062

one-dimensional diffusion eqn. integration, one-fireball model 8-57416

protons, local irradiation model for solar system ^{16}O and ^{26}Al isotopic anomalies 8-93128

$\text{pp} \rightarrow \pi^+ \text{anything}$, pion spectrum at top of atmosphere 8-53780

^{15}N , enrichment in Mars atm. due to cosmic ray interactions in early solar system 8-73669

cosmic ray-nucleus scattering

No entries

cosmic ray origin

see also *cosmology; element origin*

Fermi acceleration, effects of particle pitch angle scatt. 8-53775

galactic gamma radiation, possible origin, data from COS-B and SAS-2 satellites (French) 8-85776

gamma-ray burst sources, new limits on distrib. 8-93465

gamma-ray bursts, multiple Compton scatts. effect on X-ray emission spectrum 8-96389

injection into dense supernova shells by pulsars 8-65638

interstellar matter acceleration, evidence from cosmic rays isotopic comp. 8-53781

neutron star, episodic accretion of gas and cosmic Γ -ray bursts 8-69824

nuclei, low energy, ionisation states and origin 8-69634

nuclei and electrons propag. and distrib. in Galaxy, rel. to origin 8-69621

review of past and present research (Russian) 8-73590

source spectrum and abundances, evidence from nuclei charge comp. and energy spectra 8-93059

sources of ultra-high energy cosmic rays 8-61941

steady state Universe using stochastic electrodynamics, cosmic background radiation and red shift 8-77631

^7Be , cosmic ray accel. probe 8-81512

cosmic ray photons

see also *cosmic ray X-rays; solar cosmic ray photons*

γ -rays ultra-high energy, emulsion chamber anal. (Chinese) 8-89028

cosmic ray photons continued

- atmospheric Cherenkov radiation in large cosmic ray showers, computer simulation using hadronic collisions models 8-57415
- condensation in hot Universe, longitudinal relict. rad. (*Russian*) 8-65734
- diffuse gamma radiation, galactic and isotropic components 8-65725
- EAS near core, struct. of electron-photon component (*Russian*) 8-57414
- galactic gamma radiation, possible origin, data from COS-B and SAS-2 satellites (*French*) 8-85776
- gamma-ray astronomy, review (*Polish*) 8-96394
- gamma-ray background, prod. by annihilation of primordial stable neutral heavy leptons 8-93479
- gamma-ray burst sources, new limits on distrib. 8-93465
- gamma-ray bursts, multiple Compton scatts. effect on X-ray emission spectrum 8-96389
- gamma-ray families from hadron reactions, accel. scanning in X-ray pellicle stack 8-78546
- gamma-rays origin in cosmic ray interactions with matter (*Polish*) 8-96571
- ionising background radiation, influence on H at periphery of galaxies 8-65729
- neutron star, episodic accretion of gas and cosmic Γ -ray bursts 8-69824
- scintillation time-of-flight telescope for cosmic γ -ray preselection 8-82572
- γ , primaries meas., 10 to 100 GeV, using air showers Cherenkov light distrib., detector system 8-73597

cosmic ray propagation

- anisotropic propag., transport eqn., Green's function 8-77441
- atmospheric nucleon and charged pion unidirectional diffusion eqns. 8-57417
- galactic cosmic rays, propag. in finite solar cavity 8-69623
- galactic dynamical halo, retrodictive probability approach 8-65467
- galactic propagation and distribution 8-69621
- interplanetary, Mars spacecraft meas. 8-53779
- interplanetary propagation, origin of transient cosmic ray intensity vars. 8-89021
- interplanetary propagation, quiet time anisotropies obs. from Pioneer 10 and 11 8-77442
- interstellar propagation, evidence from 3000 MeV to 50 GeV nuclei charge comp. and energy spectra 8-93059
- leaky-box model for galactic propag. 8-57409
- medium energy expt. on International Sun-Earth Explorer C spacecraft 8-85798
- primary cosmic radiation, antiprotons relative abundance rel. to galactic propag. model 8-73594
- solar cosmic rays propag., diffusion in mag. fields, convection in solar wind, dimens. method soln. (*Chinese*) 8-81511
- solar energetic particle events following September and November, 1977, flares, diffusion model 8-77446
- solar equator vicinity, daily cosmic ray flows during solar cycle 8-69622
- solar flare electrons, peculiarity of ejection into interplanetary space (*Russian*) 8-77445
- solar flare energetic particles, interplanetary propag. model 8-65468
- solar particle event, 1973 April 29, mean free paths near Earth 8-89017
- solar proton and electron events, interplanetary scatt. mean free path 8-57421
- statistical particle acceleration models for Cassiopeia A supernova remnant 8-57606
- streaming perpendicular to mean mag. field, gyrophase distrib. function 8-53778
- sunward flowing proton and alpha particle fluxes, interplanetary propag. model 8-89016
- transport eqn., steady-state, nonenergetic-source soln. 8-96366
- turbulent diffusion, partially averaged field approach 8-53776
- velocity diffusion, turbulent mag. field, Monte Carlo calc. 8-53777
- ^7Be , cosmic ray accel. probe 8-81512

cosmic ray protons

- antiprotons, relative abundance in primary cosmic radiation 8-73594
- galactic proton/electron ratio 8-69633
- galactic protons, as extraterrestrial source of atmospheric water vapour 8-69416
- interplanetary corotating regions, nucleon accel. and modulation of Jupiter electrons 8-61690
- interplanetary propagation, Mars spacecraft meas. 8-53779
- low energy proton expt. on International Sun-Earth Explorer C spacecraft 8-85791
- solar energetic proton events at large heliocentric distances, shock-assoc. 8-77451
- solar flare energetic particles, interplanetary propag. model 8-65468
- solar flare protons, Mars 7 probe meas. 8-69624
- solar flares, energetic particle composition temporal development 8-89148
- solar proton flares, temporal ref. functions from microwave radio bursts 8-73591
- solar proton fluxes at 1 AU during solar min., Prognost 3 obs. 8-69769
- solar proton irradiation model for solar system ^{16}O and ^{26}Al isotopic anomalies 8-93128
- solar protons, as extraterrestrial source of atmospheric water vapour 8-69416
- solar protons and α particles, rigidity-independent coronal propag. and escape 8-77444
- solar protons from September and November, 1977, flares, spectra and time profiles 8-77446
- solar wind, very low electron and proton temps., statistical anal., origin 8-65477
- sunward flowing moderate intensity proton and alpha particle fluxes, characts. 8-89016

cosmic ray showers and bursts

- see also cosmic ray electrons; cosmic ray X-rays
- atmospheric Cherenkov pulse duration, depend. on cosmic ray shower parameters 8-89025
- EAS, atomic nuclei fragmentation, analytical method (*Russian*) 8-65472
- EAS, ave. lateral muon density distrib., arrival direction studies 8-73596

cosmic ray showers and bursts continued

- EAS, duration of atmospheric Cherenkov pulses 8-73595
- EAS, results of highest energy nuclei 8-57413
- EAS near core, struct. of electron-photon component (*Russian*) 8-57414
- EAS radio emission, electric field strength (*Russian*) 8-93061
- high-energy cosmic-ray components in atmosphere, scaling features 8-93062
- inclined muon monitors, muon spectra, generating functions, rel. to diurnal variation at Kiruna 8-85783
- large cosmic ray showers, computer simulation using models of hadronic collisions 8-57415
- lateral electron structure in EAS, simulation study 8-81513
- muon charge ratio, energy up to 1 TeV 8-89029
- muon generation, anomalous, method of searching in EAS 8-89026
- muon spectrum at sea-level, Maeda's model, using pion-kaon ratio 8-85781
- muons in EAS, array and data analysis 8-89027
- neutron star, episodic accretion of gas and cosmic Γ -ray bursts 8-69824
- path fluctuations in EM cascade in infinite medium (*Russian*) 8-65471
- pellicle stack, γ -ray family from cosmic-ray hadron reactions, accelerated scanning method 8-78546
- γ cascade widths, review of expt. evidence and calcs. 8-85779
- γ , primaries meas., 10 to 100 GeV, using air showers Cherenkov light distrib., detector system 8-73597
- μ burst rates, Fe-liquid scintillator multilayer calorimeter transition effects 8-90019

cosmic ray solar modulation

- 27-day modulation with solar wind radial attenuation 8-73592
- galactic cosmic rays, propag. in finite solar cavity 8-69623
- galactic cosmic rays north-south gradient rel. to solar polar coronal holes 8-89019
- intensity var. rel. to solar activity 8-69625
- interplanetary corotating regions, nucleon accel. and modulation of Jupiter electrons 8-61690
- Maunder minimum in solar activity, meteoritic evidence for reduced cosmic ray modulation 8-57529
- nuclei, low energy, ionisation states and origin 8-69634
- past solar activity by means of cosmogenic isotope conc. in lunar samples 8-61828
- solar equator vicinity, daily cosmic ray flows during solar cycle 8-69622
- stellar daily variation, semiannual modulation 8-69626
- storm, symmetrical equator-pole anisotropy rel. to solar plasma regime 8-89020
- sunward flowing proton and alpha particle fluxes, solar wind vel. depend. 8-89016
- transient cosmic ray intensity vars., solar flare origin 8-89021
- transient cosmic ray intensity vars., solar source 8-89022

cosmic ray variations

- see also geomagnetism
- 1972, August cosmic ray storm, north-south anisotropies and related phenomena 8-89018
- active solar processes, manifestation in interplanetary space from data of cosmic ray variations 8-57411
- altitude differences and geomag. field secular changes effects 8-93058
- inclined muon monitors, muon spectra, generating functions, rel. to diurnal variation at Kiruna 8-85783
- intensity solar diurnal variation, interplanetary mag. field north-south component correl. 8-93057
- meteorological conditions determ. from cosmic ray obs., spectrographic method 8-69627
- past cosmic ray intensity using time variations of tree ring stable isotope conc. 8-61692
- recurrent Forbush decreases and solar active regions rel. to M-regions 8-96367
- solar activity rel. to intensity vars. 8-69625
- spectrographic investigation method and mean-mass temp. 8-73588
- stellar daily variation, semiannual modulation 8-69626
- temperature variations, spectrographic obs. of secondary cosmic rays 8-69628
- transient cosmic ray intensity vars., solar flare origin 8-89021
- transient cosmic ray intensity vars., solar source 8-89022
- unusual cosmic ray storm (1978, February), symmetrical equator-pole anisotropy 8-89020
- ^{14}C concentration in Earth's atmosphere, corrections with astrophysical and geophysical phenomena 8-61477
- ^{14}C in atmosphere content variation, past geomagnetic and cosmic ray intensity variations 8-61691

cosmic ray X-rays

- background sources, detectability in deep X-ray surveys 8-96567
- diffuse 2 to 10 keV background, contrib. from, Seyfert galaxies emission 8-93392
- diffuse X-radiation background above 20 keV, balloon obs. 8-54096

cosmic rays

- see also cosmic ray absorption; cosmic ray apparatus; cosmic ray composition; cosmic ray effects and interactions; cosmic ray energy spectra; cosmic ray origin; cosmic ray propagation; cosmic ray showers and bursts; cosmic ray solar modulation; cosmic ray variations; galactic cosmic rays; geophysical aspects of cosmic rays; high-energy cosmic ray interactions; primary cosmic rays; radiofrequency cosmic radiation; solar cosmic ray particles; solar radiation
- nature and astrophysical sources, review 8-77486
- space sciences, conf., Trivandrum, India (Jan. 1977) 8-69586

cosmic X-rays see cosmic ray X-rays**cosmogony** see cosmology**cosmology**

- see also black holes; element origin; general relativity; red shift
- accelerating Universe models 8-57707
- adiabatic regularisation, quantum field in Robert-Walker metric 8-73916
- aether drift experiments, nonuniformity of background radiation 8-93482
- age of Universe, impossibility of an infinite past 8-62029
- anisotropic uniform model universes with cosmical const., flat space 8-73788
- anisotropic universe, scalar particle creation 8-77487

cosmology continued

- anisotropy damping through quantum effects in early universe 8-57708
- background radiosources, Westerbork survey, angular size distrib. and source count 8-96553
- baryon symmetric big bang cosmology 8-61945
- baryon-symmetric, cosmic microwave background distortions 8-65727
- Bianchi type IX universes, neutrino viscosity 8-77633
- Bianchi VIII/IX cosmological models, anisotropic, with matter and EM fields 8-73784
- Big Bang model, galaxy cluster missing mass from massive leptons, additional ν species 8-81719
- big bang theory and phys. singularities in general relativity theory (*Russian*) 8-81893
- big-bang model and ^4He abundance, review, book contrib. 8-89277
- bimetric gravitation theory, cosmological basis, closed universe 8-65844
- black holes, cosmological density 8-77573
- Bose-Einstein condensation in an Einstein universe 8-77797
- Brans-Dicke closed space cosmology, exact soln. for radiation-filled era 8-93488
- Brans-Dicke theory, cosmological solns. for homogeneous isotropic universe 8-96579
- Cauchy problem for general relativistic perfect magnetofluid 8-70024
- charge in cosmological models, effect on curvature parameter 8-69921
- chronometric redshift theory, erroneous presentation correction 8-85839
- composite particle formation in explosive nucleosynthesis 8-69678
- contracting and expanding universe without singularity, thermal particle prod. 8-73785
- cosmological principle, new look 8-86042
- cosmological red shift, Doppler and gravitational components using Birkhoff's theorem 8-86041
- 3CR radiosources, source counts and V/V_{max} tests for complete sample 8-77613
- dark night sky paradox, expansion and hierarchical struct. of the universe 8-86055
- density perturbations in expanding universe, three-point correl. function and higher order functions prediction 8-65730
- dynamical space and gravitation within a purely geometrical framework including Machian ideas 8-93587
- early Universe, EM and gravit. Green's functions 8-73786
- education, nonscience majors, innovative course based on mass-radius diagram of states of matter 8-62002
- education, Olbers' paradox, comment 8-86070
- Einstein-Cartan, Friedmann-like cosmological models without singularities 8-77632
- Einstein-Cartan theory, bounce of spheres 8-93572
- elastic spacetime rel. to black holes and gravitational waves 8-73625
- expanding universe effect on quantum mechanics of electromag. bounded spin $1/2$ particles 8-54271
- expanding universe with bulk and shear viscosity in conformally flat coords. 8-96575
- extragalactic distance scale, review of distance indicators 8-93396
- extragalactic distance scale applied to galaxies in Local Group 8-89247
- extragalactic objects clustering in Universe (*Polish*) 8-96580
- extragalactic radiosource counts rel. to big bang model 8-69920
- fine-scale anisotropy of microwave background, long-wavelength gravitational wave effects 8-81535
- formation of galaxies and clusters: violent gas dynamics 8-86018
- Friedmann cosmological models, relativity of space finiteness-infiniteness 8-96582
- Friedmann model, large distance meas. by triangulation 8-86047
- Friedmann models, fermion pair creation by gravit. field and singularity (*Russian*) 8-93493
- galaxies, redshift-magnitude bands and evolution from Perseus and A1367 clusters obs. 8-54033
- galaxies active nuclei, local space density 8-57676
- galaxies and clusters form., large-scale distrib. and motion in adiabatic theory 8-54056
- galaxies covariance function, explanation for 9 Mpc break 8-65688
- galaxies distribution, hierarchical clustering pattern stability 8-86026
- galaxy clumps, formation and evolution in expanding Universe 8-93432
- galaxy clustering evolution, cosmological N-body simulations 8-96550
- galaxy clustering spectrum, low mass portion anal. 8-81695
- galaxy clusters, brightness spectrum and cosmic luminosity 8-81696
- galaxy clusters, covariance function, Limber's relativistic formula, relativistic inversion 8-69891
- galaxy development in expanding Universe (*Danish*) 8-86019
- GB2 sky survey at 1400 MHz, differential radiosource counts 8-54063
- general relativistic hierarchical cosmology, exact model 8-69917
- general relativity, big bang model, nucleosynthesis, scale covariant theory, review 8-73789
- geometrodynamics, inclusion of observer in wave function 8-54234
- Godel's metric 8-62125
- Godel universe, scalar perturbations 8-57709
- gravitating sphere in Lyra's geom., thermodynamic equilb. 8-65840
- gravitation wave propagation in expanding universe 8-73787
- gravitational collapse, classical and quantum, problems (*Russian*) 8-53815
- gravitational constant possible var., cosmological limit 8-93492
- gravitational inertial field and critical systems, free motion 8-93484
- gravitational inertial field eqns., Lagrangian density, Hubble law 8-93483
- gravitational instability in early Universe, cluster-sized perturbations 8-93487
- gravitational radiation, high freq., cosmological field, energy 8-57837
- gravitational-inertial field of Universe, generalised metric tensor theory 8-89275
- gravitationally nondegenerate Bianchi type I cosmological model, in general relativity 8-93490
- gravito-C-field, in cylindrically symmetric space-time, rigorous solns. 8-69926
- Hagedorn's bootstrap model of early Universe, dense matter eqn. of state, external mag. field 8-86044
- Hawking effect, thermal nature of the density matrix for black hole particle prod. (*Russian*) 8-89644
- Hawking mini black-holes origin and cold early Universe 8-93298

cosmology continued

- heavy stable neutral lepton, astrophysical consequences of existence 8-93091
- hierarchical and relativised models of Universe (*Russian*) 8-86043
- hot universe with primordial black holes, neutrino radiation kinetics (*Russian*) 8-93485
- Hoyle's hypothesis, cosmological models 8-86045
- Hubble's constant, doubling rel. to superluminal radio sources model 8-81722
- Hubble's law, laboratory exercise in astronomy 8-65740
- Hubble constant, from late-type galaxies H I obs. 8-86015
- Hubble constant, value from Virgo cluster distance and redshift 8-89265
- Hubble constant determ., large turbulent Universe model 8-96578
- Hubble diagram for QSOs 8-77616
- inhomogeneous cosmological models containing spacelike and timelike singularities alternately 8-69925
- ionising background radiation, meas. from effects on H at periphery of galaxies 8-65729
- IR night sky background, $2.4 \mu\text{m}$ meas. 8-81715
- isotropic models of Universe, regularisation of fermion stress-energy tensor 8-81725
- isotropic Universe, kinetics of small perturbations (*Russian*) 8-54102
- isotropic Universe, kinetics of small perturbations (*Russian*) 8-54103
- isotropic universe, kinetics of small perturbations (*Russian*) 8-65731
- JBD theory, exact cosmological soln. with particle creation 8-96576
- Killing vectors in plane HH spaces 8-54104
- locally rotationally symm., spatially homogeneous cosmological model, decomposable differential operators 8-57825
- Mach's principle equivalence principle, violation, for teachers 8-61998
- matter-antimatter antiproton studies 8-54654
- matter and antimatter cosmological separation 8-69918
- matter-antimatter boundary layers with mag. neutral sheet, model 8-53807
- matter-antimatter hydrodynamics, annihilation rate calc. 8-73780
- matter-antimatter symmetric universe, random geometry 8-86046
- matter-filled universe, relativity of space and time finiteness-infiniteness 8-96581
- metric tensor components interpretation, astrophys. implications 8-93097
- metrical connection in space-time, Newton's and Hubble's laws 8-57435
- microwave background radiation polarisation, anisotropic cosmological expansion 8-73778
- microwave background radiation polarisation, IR survey 8-73779
- microwave background radiation spectrum, statistical anal. of data 8-86039
- missing dark mass rel. to primordial star generation 8-61946
- models, obs. and theoretical approaches and expectations 8-77636
- neutrino background radiation, cosmological significance 8-77486
- neutrino stability and cosmological He production 8-73783
- neutrinos and Friedmann model (*Polish*) 8-89276
- Newtonian cosmology with time-varying gravitational constant 8-65733
- Newtonian model with diminishing gravitational constant 8-54100
- Newtonian model with varying gravitational constant, alternative approach 8-54101
- nonsingular isotropic cosmological model, physical reality (*Russian*) 8-77635
- nonsymmetric unified field theory of Einstein, cosmological implications, Universe expansion 8-73911
- parallaxes of objects at cosmological distances, meas. via radiointerferometric techniques 8-53796
- particles and fields conference, Argonne, IL, USA (Oct. 1977) 8-78130
- photon condensation in hot Universe, longitudinal relic rad. (*Russian*) 8-65734
- Planck's constant, time invariance 8-93556
- plane-symmetric cosmological model, Einstein eqn. solns. for dust 8-49733
- pregalactic microwave background, origin 8-86040
- primaeval giant elliptical galaxies, observable props. 8-89260
- primordial background radiation, temp. fluctuations due to gravit. waves 8-65728
- primordial black hole development 8-93299
- primordial black holes, upper bound on number density calc. 8-65649
- primordial low mass black holes evaporation and H recomb. kinetics (*Russian*) 8-61943
- primordial microwave radiation, recomb. lines calc. 8-54097
- primordial nucleosynthesis, limits on props. of massive neutral leptons 8-57438
- QSO redshifts and field galaxies 8-89271
- quarks, unbound, attempts to reconcile recent evidence for existence in stable matter 8-58160
- quasar absorption lines origin, cosmological hypothesis predictions and observational evidence 8-57684
- quasar evolution 8-57688
- quasars, flat spectrum, evidence for cosmological evolution 8-54074
- quasars, Hubble diagrams 8-57691
- quasars, Hubble diagrams and optical luminosity functions 8-61930
- quasars, local space density 8-57676
- quasars, redshift-magnitude relation, statistical study and chronometric cosmology 8-93455
- quasars, redshifts and Hubble diagrams 8-96559
- quasars relative luminosities determ. from emission line strengths, rel. to Universe model 8-61931
- quasi-stellar objects, variable, photometry and completeness of faint blue objects in Sandage-Luyten field 8-54069
- quasi-stellar radio sources from 4C and Parkes catalogues, cosmological implications 8-65714
- radiation damping in universe with topologically closed space sections 8-57828
- radiation era, magnetic field amplification 8-96577
- radio sources, cosmological evolution rel. to source counts freq. depend. and spectral index distrib. 8-96554
- radial field theory, corpuscular theory, origin of natural forces 8-77785
- radiosources, statistical test on complete sample of identified sources 8-89269
- radiosources isotropy in B2 catalogue 8-73766
- redshift-magnitude bands and galaxies evolution, data anal. 8-57629

cosmology continued

- relativistic, radiative transfer for polarized light, eqn. soln. method 8-73781
- relativistic dense matter, statistical mechanics using phenomenological quantum field model 8-89814
- relativistic dust universes, comoving metrics, Newtonian interpretation 8-65732
- relativistic mechanics, generalised, spacetime quantisation and Mach's principle 8-73867
- relic radiation, as possible product of quantum era in universe expansion (*Russian*) 8-81717
- relict black-body radiation temp. fluctuations prod. by cosmological turbulence (*Russian, English*) 8-77630
- rich clusters of galaxies, form. times and gravit. const. var. 8-69892
- rival cosmologies to big bang, review 8-57705
- Robertson-Walker expanding universe, energy spectrum of H-atom 8-73869
- rotating black hole, Kerr metric, spontaneous creation of massive spin 1/2 particles 8-89217
- rotating pressure-free space-time, thin self-similar disc config. 8-96387
- scale covariant gravitation theory, rel. to stellar vel. dispersion age depend. 8-65661
- scale covariant models and early Earth temp. 8-57704
- scale-covariant, 3K background and Large Numbers Hypothesis 8-93480
- self-similar space-times, perturbation scheme 8-54099
- self-similar space-times, solutions to general relativity eqns. 8-54098
- semiclassical theory of scalar field in globally hyperbolic universe 8-54250
- Seyfert-like galaxies, medium-redshift, redshift-magnitude-ang. dia. data statistical anal. 8-86016
- solar system formation, re-evaporation of condensed matter, evidence from meteorite mineral content 8-85864
- space-time infinity of Universe, various problems (*Polish*) 8-61948
- space-time properties, local and global, Einstein's eqns., Universe matter density 8-61942
- spatial conformal flatness in homogeneous and inhomogeneous cosmologies 8-69924
- spectral lines of prestellar origin, prediction in cosmic relic radiation (*Russian*) 8-77628
- standard hot big bang model of Universe, dynamics 8-69922
- star formation before galaxies, missing mass soln. 8-57654
- static and near-static semiclosed configs. and cosmological term (*Russian*) 8-93486
- static Universe model with two centres, red shift explanation 8-57706
- steady state Universe using stochastic electrodynamics, cosmic background radiation and red shift 8-77631
- structure development in expanding universe, new model 8-93489
- superdense nonequilibrium cosmic objects, coherent boson graviton avalanche catastrophes 8-85844
- supergravity, local supersymmetry in (2+1) dims., differential forms. 8-49980
- symmetry restoration in the early Universe 8-73782
- thermal particle production in a radiation dominated Robertson-Walker universe 8-81721
- time varying Newtonian gravity, Q 8-77634
- time-asymptotic particle interpretation in the Friedman-de Sitter space 8-81720
- trace anomalies in a two-dimensional de Sitter metric and black-body radiation 8-65841
- turbulence in cosmology, non-linear interactions rel. to universe expansion, quantum turbulence 8-77629
- Type V_L cosmologies, tilting and viscous models 8-57703
- unidentified high latitude radiosources 8-57672
- unified gauge theories and the baryon number of the universe 8-85842
- uniform gravitational collapse, lepton pair creation, macroscopic gauge theory of gravity 8-81724
- universal CP noninvariant superweak interaction and baryon asymmetry of the universe 8-66072
- Universe, consistent age 8-81723
- universe, history from origin to earliest geological times, rel. to origin of life 8-69923
- Universe expansion 8-93491
- universe inhomogeneities, power law relating mass fraction to density enhancement 8-57656
- universe model, computer simulation of galaxy distrib. in Lick catalogue 8-81718
- Universe structure, open and closed curved spaces 8-77652
- vacuum state, influence of gravitation and cosmological effects on symmetry breaking (*Chinese*) 8-65858
- viscous fluid cosmological model in general relativity 8-61944
- weak interaction and isotropy of Universe 8-61947
- Weyl's geometry rel. to dynamical mass excess in clusters of galaxies 8-69919
- D abundance in Galaxy rel. to cosmology 8-69883
- Re-Os, rel. abundance, rel. to nuclear chronometer reliability 8-85919

cosmotrons

No entries

Costa Ribeiro effect see *dielectric phenomena; phase transformations***Cotton-Mouton effect** see *birefringence; magneto-optical effects***Cottrell atmospheres**

No entries

Cottrell locking see *Cottrell atmospheres***Couette flow**see also *jets*

- cone/plate system in fluid, friction heating and convection 8-87238
- dusty gas between two infinite coaxial cylinders 8-55685
- gas creep along solid surface, half-space moments method calcs. 8-67222
- hydrodynamic instabilities, transition to turbulence, Couette flow, vortex streets, Rayleigh-Benard instability 8-83362
- hydrodynamic thermal breakdown in viscous fluid, Couette flow between cylinders 8-83391
- laminar equalising flow in Couette-type channel flow (*German*) 8-51239
- MHD, effects of couple stresses for electrically conducting fluid, skin effect 8-91020
- nematic liquid crystals, book contrib. 8-59531
- permeable wall layer, heat transfer and temp. distrib. 8-51165

Couette flow continued

- pipe flow, finite amplitude stability theory 8-63498
- porous annular region, steady flow 8-75201
- rarefied gas mixture flow along surface, isothermal slip 8-67220
- striated boundary effect on viscous drag 8-59367
- symmetric Couette and Taylor flow between rotating coaxial cylinders, Navier-Stokes eqn. solns. (*German*) 8-94750
- viscometer measurement error correction, non-Newtonian liquids appl. (*German*) 8-94868

counter accessoriessee also *counting circuits*

No entries

counters

- see also *Cherenkov counters; counting tubes; fission counters; Geiger counters; proportional counters; scintillation counters; semiconductor counters; spark counters*
- condensation nuclei, counter with inherent size resolution capability 8-81470
- dead time correction for a counting rate measured with a system of buffer memories 8-86756
- lossy integrator, response for time variable counting rate (*Rumanian*) 8-90045
- paralysable event detectors, improved counting technique 8-57928
- X-ray detectors, counting losses, electron storage ring synchrotron radiation 8-86752

counters (circuits) see *counting circuits***counting circuits**

- see also *coincidence circuits; pulse height analysers; scaling circuits*
- drift chamber counter, missed counts and registration efficiency calc. 8-78594
- hybrid impedance matching circuit for surface barrier detectors (*French*) 8-90035
- lightning ground-flash multiple-stroke discriminator cct. 8-81446
- lossy integrator, response for time variable counting rate (*Rumanian*) 8-90045
- magnetostriction spark cameras data readout cct. 8-78576
- multiwire proportional chamber, shift register read out system 8-86736
- multiwire proportional chamber with analogue data plotting 8-78566
- nucleonic dual charge sensitive preamplifier 8-55110
- particle simulation unit for counter circuitry testing 8-81002
- photon count cct. using high-speed comparator in discriminator 8-77979
- pulse discriminator, timing distrib., effect of randomizing time 8-58555
- scintillation counter hodoscopes, LED test system 8-58556
- time to digital convertor in real time, low cost 8-55111
- triple const. fraction discriminator evaluation 8-70708
- $H(n, \gamma)$, parity violation study, high-rate counting circuitry for γ -rays 8-62527
- Pr wire thermal cond. automatic meas. device 8-54362

counting tubessee also *dekstrons*

No entries

country planning see *town and country planning***county planning** see *town and country planning***coupled circuits**

four-terminal meas. circuit stray-impedance errors 8-77940

coupled networks see *coupled circuits***coupled superconductor devices** see *superconducting junction devices***couplers (electric connectors)** see *electric connectors***coupling (process)** see *joining processes***coupling circuits** see *coupled circuits***CP invariance**

- axion, Gargamelle beam dump expt. 8-50003
- Cabibbo current and CP violation in a six quark gauge model 8-70329
- gauge chiral $U(1)$ symmetry and CP invariance in presence of instantons 8-78075
- historical introduction, weak interactions, book 8-78133
- left-right symm. gauge theories, CP violation, absolutely stable hadrons 8-74155
- nonleptonic hyperon decays, CP violation, deviations from $\Delta I = 1/2$ rule 8-70367
- potentially CP violating phase in QCD, alleged axion mass, PCAC quark masses 8-66080
- quark electric dipole moment from CP noninvariant gauge theory, left handed currents (*Russian*) 8-74218
- quarks and leptons, fermion physics in terms of $SU(2) \times SU(1)$ gauge theory 8-74197
- quaternion model, gauge theory for leptons and quarks (*Russian*) 8-62315
- self-coupled vector fields, calcs. using Dirac quantisation procedure 8-89610
- soft CP violation, renormalisable gauge model for strong, weak and EM interactions 8-74196
- strong P and T noninvariances in a superweak theory 8-82123
- universal CP noninvariant superweak interaction and baryon asymmetry of the universe 8-66072
- weak interaction, vector-like theories, CP violation, spontaneous breaking 8-62333
- K_1^0 - K_2^0 system, violation, CPT conservation, book contrib. 8-78173

CPA calculations

- alloys, disordered, orbital mag. susceptibility of conduction electrons CPA calc. 8-76217
- alloys, highly resistive, temp. depend. on elec. resist. 8-91657
- binary alloy, model substitutionally disordered, electron momentum density 8-56061
- binary alloy, short range order effect on density of states (*Russian*) 8-67929
- binary alloys, random, dielec. matrix and related props. 8-51916
- cluster, at., homomorphic CPA analyticity 8-82872
- cluster, at., homomorphic CPA for off-diagonal randomness 8-82873
- Cu_3Ni_{1-x} , soft X-ray emission spectra 8-95620
- dilute ferromagnet, spin wave excitations, multicomponent CPA theory 8-68135
- disordered alloys, electronic struct., CPA calcs., short-range order 8-63964

CPA calculations continued

- disordered alloys, transport phenomena theory, coherent pot. approx. 8-87958
- disordered quasi-one-dimensional systems with electron correlation, electronic properties 8-87966
- electronic transport in substitutionally disordered system, derivation of cluster approx. 8-84184
- electronic transport in substitutionally disordered systems, MCPA and Monte Carlo calc. 8-84185
- ferromagnetic alloys, conc., spin fluctuations, SCR theory and CPA calcs. 8-64290
- ferromagnetic random binary alloys, elastic neutron scatt. cross section 8-91845
- Heisenberg antiferromagnet, dil., CPA calc. 8-68263
- Heisenberg antiferromagnet, dil. with random first- and second-neighbour exchange bonds, CPA theory 8-52187
- Heisenberg model, amorphisation (*Russian*) 8-80118
- Hubbard model, local moments 8-95414
- magnetic ternary alloys, statistical theory of electrical resistivity 8-87969
- metallic alloys, ordered and disordered, positron localisation 8-79962
- n-type semiconductors, plasmon-local phonon mode interaction, RPA, CPA theory 8-87932
- rare earth alloys, CPA calc. of mag. moments and transition temps. 8-84423
- rare earth compound, intermediate valence induced by alloying, CPA calculations 8-67986
- rare earth-transition metal alloys, CPA calcs., moments and transition temps. 8-52252
- transition metal alloy, electronic structure, mag. props. 8-95254
- transition metal alloys, spin glass behaviour, simple itinerant model 8-84436
- two-dimensional white noise problem and inversion layer localisation 8-84271
- Au-Cu alloy, rel. to refr. index and absorpt. coeff., 1-5 eV (*Russian*) 8-60484
- Cu-Ni, alloys, electronic states, KKR-CPA calc. 8-84125
- $\text{Cu}_x\text{Ni}_{1-x}$, Fermi surface of concentrated paramag. alloys 8-95257
- $\text{Fe}_x\text{Zn}_{1-x}\text{F}_2$, Neel temp., CPA calc. 8-68233
- $\text{Fe}_x\text{Zn}_{1-x}\text{F}_2$, Neel temp. mag. cone depend., CPA calcs. 8-88122
- GaAs, valence band structure, CPA, bond orbital calcs. 8-87909
- GaP, valence band structure, CPA, bond orbital calcs. 8-87909
- GaSb, valence band structure, CPA, bond orbital calcs. 8-87909
- Gd-Co, CPA calcs., moments and transition temps. 8-52252
- Gd-Fe, CPA calcs., moments and transition temps. 8-52252
- Gd-Ni, CPA calcs., moments and transition temps. 8-52252
- InAs, valence band structure, CPA, bond orbital calcs. 8-87909
- InP, valence band structure, CPA, bond orbital calcs. 8-87909
- InSb, valence band structure, CPA, bond orbital calcs. 8-87909
- $\text{Mn}_x\text{Zn}_{1-x}\text{F}_2$, CPA estimate for Neel temp. 8-76245
- $\text{Mo}_x\text{Nb}_{1-x}$, is the rigid-band model valid? 8-95258
- Pd-Pt, resonant modes, rel. to CPA predictions 8-75757
- Pr-Nd (5%), impurity modes and mag. ordering 8-84422
- Y-Co, CPA calcs., moments and transition temps. 8-52252

CPT invariance

- book, axiomatic QFT, PCT, spin and statistics 8-78102
- Lagrangian formalisms with CPT violation, causal Lagrangian, gauge theories 8-62303
- modular operator, local observables, in von Neumann algebras, duality in QFT, CPT invariance 8-81793
- $\nu(\bar{\nu})$ N elastic scatt., symmetry relations CPT invariance of current matrix elements 8-54627
- p-p symmetry, mass difference, Dirac and CPT theory test 8-82125

crack detection

see also cracks

- acoustic flow detection, contactless electrogasdynamics 8-53120
- acoustic flow detector with sound indicator 8-53140
- acoustic signalling unit for US echo type flow detector 8-53117
- acoustic wave scattering by flaws, reciprocity theory appl. 8-72941
- automatic US equipment for monitoring drill and casing tubes 8-53085
- boundaries, effect on cylindrical defect field 8-53093
- ceramics, crack and inclusion detection, NDT microwave evaluation 8-95866
- cold strip surface, flaw inspection with optoelectronic equipment 8-60967
- contact tip of transducer, method of joining 8-53086
- crack polarisation when magnetised in a longitudinal alternating field, detection method 8-53094
- crack scattering in polycrystalline media 8-75089
- cylindrical defect detection, boundary effect calc. during magnetic study 8-53150
- dielectric material, electro-optical inspection of internal defects 8-56869
- echo type flow detector, frontal resolution investigation 8-53109
- eddy current tester, for nonferrous tubes and rods 8-85099
- eddy current through type transducer, operating condition simulation when inspecting ferromagnetic rods 8-53077
- elastic wave radiation, rel. to AE signal charact. 8-60952
- electrically welded tubes, magnetic method with ferroprobe 8-53080
- electromagnetic NDT, digital method of edge effect suppression 8-56866
- electromagnetic transducer for crack exam. 8-76816
- electron radiography, feasibility for microcrack detection 8-72967
- failed steam accumulator anal., role of NDT 8-95877
- fatigue crack growth in aircraft wing test, AE detection 8-60925
- ferrite, US testing 8-53084
- ferrites, microwave flow detection 8-53122
- ferromagnetic probe inspection unit for automatic inspection of welded tubing 8-56860
- ferroprobe, basic concepts 8-60959
- ferroprobe flow detector with RF pulse excitation 8-53081
- field meas. by Hall probes, accurate estimate 8-53155
- flow detection during leak tests, mech. treatment effects 8-60956
- flow detection using optical filters 8-53163
- flow detector magnetizing units with semiconductor rectifiers, magnetic field meas. 8-53076
- flow sizing of real defects, review 8-53041
- flow detectors, radiation type, electron bremsstrahlung irr. field dia. calc. 8-56857

crack detection continued

- fracture mechanics evaluation, role of NDT 8-68862
- glued members, low frequency acoustic flow detector inspection 8-60954
- gradiometer, ferromagnetic probe, fault detection optimisation 8-53096
- growth gauge ffr assessing flow growth potential in structural components 8-68859
- holographic interferometry and speckle 8-60933
- hot-rolled rods, surface defect detection without scale removal by NDT 8-95890
- impedance flow detector, acoustic, feasibility of standardless check 8-53158
- insulating material monitoring by electroluminescent screens, defect imaging 8-53083
- IR defectoscopy, optimum algorithm in case of noncontent temp. meas. 8-60947
- laser speckle interferometry for nondestructive evaluation 8-60976
- local magnetic field image recording on magnetic tape without bias 8-53129
- magnetic powder, circulation method/magnetic field effect (*German*) 8-60928
- magnetic powder flow detection, contact recording of patterns 8-53102
- magnetizing flow detection system for underground pipeline inspection 8-53103
- moire method, speckle shearing, qualitative appl. for structural flow detect. (*German*) 8-82015
- optical instrument, for measuring depth and dimensions of surface microdefects 8-76812
- phase sensitive eddy current detectors, effect of compensation conditions, on transducer-product clearance inductions 8-85103
- piezoelectric ceramics, using phase method of microwave flow detection 8-72968
- pressure vessels, probability of flow nondetection 8-78479
- pressure vessels weld quality assessment, NDT methods and equipment 8-56871
- radiation crack detection, use of luminescent convertors 8-53125
- rate meter-type flow detector, measuring circuits 8-60963
- reinforced plastics, low frequency acoustic flow detector inspection 8-60954
- remote sensing of flaws in solids using laser system 8-60975
- resonant radio flow detector, 2 mm band for low temp. investigations 8-53115
- scan control unit, BUS-1 8-53143
- sensitivity, of various nondestructive inspection methods 8-72974
- sheet samples, crack length automatic recording 8-60907
- small surface cracks, size estimation using SAW 8-76793
- steel, stainless, US methods for intergranular corrosion inspection 8-95898
- steel, statistical methods in US anal. of real defects 8-72976
- steel band used as pulling member, device for inspecting mechanical state 8-76810
- transducers, applied, resistance due to cracks, eddy current calc. and hodograph 8-53095
- tube flow detection by annular US transducers 8-60971
- US automatic inspection of tubing 8-56865
- US echo pulse flow detectors, use of auxiliary sensitivity regulation 8-60951
- US flow detect., tolerance on operating freq., sensitivity standardisation 8-53089
- US flow detection sensitivity enhancement by focusing system, theory 8-53112
- US flow detection sensitivity enhancement by focusing system 8-53113
- US flow detection, mirror shadow method sensitivity expression and analysis 8-53088
- US inspection, automatic, thin walled large diameter pipes, flaw size classification 8-60949
- US spectral anal. of flaws, theoretical study 8-95897
- US spectroscopic NDT 8-76805
- vitreous enamel, bubble struct. and flaw forecasting 8-53118
- weld flow study using ultrasonic holography (*Dutch*) 8-68855
- weld joint, furnace welded pipe inspection unit for above 1000°C 8-53134
- Al alloy cylindrical parts, crack detection by two channel eddy current inspection unit 8-72998
- Al, US and X-ray testing of castings, moulds and die-casting machines 8-53097
- Nb ingot, US flow detection sensitivity enhancement by focusing system 8-53113
- SiO_2 film, local defects detection by electrolytic decoration (*Bulgarian*) 8-60896

crack-edge stress field analysis

see also penny-shaped cracks

- I-shaped crack elastic energy evolution rate in laminate determ. by pliability vibr. meas. 8-83348
- adhesive fracture specimen, DCB, crack tip stress field anal. 8-55602
- adhesively bonded metallic panels, 2-ply, finite element and integral eqns. anal. of fatigue crack growth 8-92347
- beam (plate) pure bending, dynamic fracture, axial force effect 8-63385
- biaxial load effects 8-55594
- body force method, to calculate stress intensity factors, for crack, in arbitrarily shaped plate 8-90775
- bonded dissimilar materials, crack along bond, stress intensity factors 8-55607
- brittle cracks, stability, propagation, fracture mech. (*Czech*) 8-79257
- brittle fracture from loss of stability near crack 8-55597
- brittle materials, intergranular creep crack growth, diffusion controlled theory 8-84950
- Cauchy type singular integral eqns. with complex singularities, numerical soln., stress intensity factors 8-55611
- ceramics, process zone surrounding crack tip, theory 8-67154
- circular disc, stress intensity factors and crack energy 8-79260
- closure of crack related to crack propag., prediction method for crack growth 8-67099
- component containing cracks, critical review of creep 8-63321
- composite materials, bimaterial plate, cracked, finite element anal. of stress distribution 8-75104

crack-edge stress field analysis continued

- coplanar cracks in infinite transversely isotropic medium, stress distrib. 8-51122
- corrosion-fatigue crack propagation modelling 8-90779
- crack extension criterion of maximum shear or principal stress 8-79278
- crack-tip, from field values of displacements using complementary energy 8-67114
- crack-tip problems and quarter-point triangular elements 8-83333
- curvilinear cracks, star-shaped array in infinite isotropic elastic medium 8-55609
- cylindrical shell, transverse shear effect on axial crack 8-67090
- Dugdale model, calcs. using weight functions 8-55590
- Dugdale model solution, of cracked bodies, finite element analysis 8-67116
- edge notch stress anal., book contrib. 8-94621
- elastic solid, cracked or notched, general numerical method for three dimensional singularities 8-67137
- elastic-plastic crack tip characterisation, relation to R-curves 8-56767
- elastic-plastic materials, finite deformation anal. of crack-tip opening 8-51126
- elasto-plastic flow in computer simulated, A533 steel 8-56720
- elastodynamic anal. by finite element method using singular element 8-55603
- elastodynamic effects on crack branching 8-67113
- elastodynamics, stress and crack-displacement intensity factors 8-67112
- elliptic crack and punch problems, Lamé polynomial solns. 8-75069
- energy-balance approach to fatigue crack growth 8-90773
- extension due to nonuniform internal press. 8-51124
- fatigue crack growth, threshold 8-63392
- fatigue crack growth in notched components 8-83329
- fatigue crack propagation, theoretical expl. of delaying effects of overloads 8-67093
- fatigue crack propagation theory, threshold derivation 8-83337
- fatigue cracks in side notches, stress intensity factor formula 8-79264
- fatigue cracks threshold stress intensity for crack growth, prediction using dislocation model 8-83870
- fibre reinforced composites, exam. of thermal stress fracture 8-75103
- fracture, arbitrary criterion, weakest link theory reformulated 8-90786
- glass plate, flexure crack propag., expt. and anal. 8-80620
- graphite, pyrolytic, ion bombard., flaking, stress fields around penny-shaped cracks 8-52946
- Green's function for thru-crack emanating from fastener holes 8-67118
- Griffith crack, interface of layer bonded to half plane, approx. method 8-79258
- griffith crack in an infinite nonhomogeneous elastic medium under shear 8-87300
- Griffith crack problems in non local elasticity, solutions for one and two dimensional problems 8-51125
- growth determination, in mixed mode loading system 8-67105
- hollow elastic solid, cracked, torsion anal. 8-51134
- infinite hollow cylinder with external crack, boundary value problem 8-90712
- infinite solid, elliptical crack under shear 8-75096
- intensive finite element grading for stress concs. 8-55587
- interface crack, incompletely open, nonsocil. singularities 8-59346
- interface penny-shaped crack, Fredholm integral eqn. soln. 8-90784
- laminates, fracture, effect of adhesive layers 8-90791
- limiting stresses for brittle body with elliptical hole with edge cracks, diag. construction (Russian) 8-55600
- line crack subject to shear 8-79268
- metal elements, adhesively bonded, cracked or with discontinuities, analysis procedures 8-90793
- metal panels, adhesively bonded, cracked, fracture anal., crack tip stress intensity factors 8-90792
- method of potentials, appl. to fracture mechanics 8-51121
- mixed boundary-value problems soln. by direct variational method 8-83331
- notch problems, book 8-94617
- numerical model analysis of stable crack growth 8-55596
- optically transparent materials, evaluation of elastic ratio by interferometry 8-90804
- Paris differential eqn. for fatigue cracks, numerical calc. of eqn. parameters 8-63384
- penny-shaped crack, sudden twisting in a finite elastic cylinder, stress calcs. 8-67110
- perforated plate, stretched, cracks emerging from circular openings 8-51129
- photoelastic determination, of mode I stress intensity factors 8-90781
- plate, asymmetric crack branching under plane stress and loading 8-59344
- plate, elastic, under uniform twisting, periodic collinear cracks (Japanese) 8-67097
- plate, wide, analysis on crack in high strain zone (Chinese) 8-83326
- plate structures, two-dimensional, computer program based on superposition method (Japanese) 8-51123
- PMMA, methanol crazes, mech. props., craze-strain profile 8-72844
- propagating rectangular fracture in semi-infinite elastic medium 8-57168
- quarter elliptical cracks in irregular bodies, exam. using finite element alternating method 8-90796
- quasi static crack growth, in sheet materials 8-67106
- quasibrittle body with internal determ. of crack growth kinetics and life expectancy 8-63383
- reactor pressure vessel, stress intensities for nozzle cracks 8-70583
- ring segments, radially cracked, displacement coeffs. from boundary collocation anal. 8-71298
- rock, symmetrically extending plane crack, self-similar pressure profiles 8-69340
- rubber, peeling initiation and propag. 8-76824
- running crack tip, effect of strain rate depend. Young's modulus on stress and strain fields 8-75097
- semielliptic notch with crack, micro- and macro-stress concentration correlation (German) 8-83330
- separation energy rate for crack advance 8-56765
- shadow methods, reflected, transmitted, obs. of sharp V-notched plates, under pure bending 8-90777
- shear crack, stress distrib., finite elastic anal. 8-51119
- singularity at corner of wedge shaped punch or crack 8-83252

crack-edge stress field analysis continued

- singularity at crack tip, order changing at discontinuity 8-59345
- slitlike crack arrays, plastic and strain hardened materials, fracture characts. 8-90798
- stable crack-growth, fracture criteria, numerical approach 8-67104
- state of stress in vicinity of crack, approx. three dimensional 8-67135
- steel, 0.40/0.50 C, crack growth, Weibull analysis 8-92319
- steel, structural, slow stable crack growth, exam. of crack profile 8-84965
- strain energy density and surface layer energy for blunt cracks or notches, book contrib. 8-94618
- strain intensity criterion for crack branching in brittle mats. 8-55592
- stress intensity factor calc., infinite similar element method 8-79277
- stress intensity factor crack opening displacement relationship for compact tension specimen 8-90778
- stress intensity factor from stress conc. factor, calc. 8-55588
- stress intensity factors, anal. determ. by variational method for eccentric cracks 8-67115
- stress intensity factors, single-edge cracked bar loaded by in-plane transverse forces (Chinese) 8-83327
- stress intensity factors, UNCLE finite element system calcs., appls. in fracture mechanics 8-67098
- stress intensity factors by enriched finite elements 8-90774
- subcritical crack growth depend. on effective stress intensities 8-56726
- thermal stresses in elastic plane with circular boundary and thermally isolated cracks (Russian) 8-55599
- thermoelastic semiinfinite solid with heated boundary, thermally insulated line crack 8-55610
- three dimensional cracks, stress intensity factors 8-55601
- three-dimensional crack anal. by finite element method 8-83332
- tip opening displacement by finite element anal. (Czech) 8-59343
- transitions elements for use with quarter point crack-tip elements 8-63376
- viscoelastic, crack growth relations, for orthotropic, prestrained media 8-90772
- wedge loading of a semi-infinite strip with an edge crack 8-79270
- wedge opening load specimen, side grooved, stress intensity factor soln. and calibration 8-51130
- weight function calcs. from stress intensity factor 8-55591
- weight function concept, crack closure method, method, stress intensity factors calcs. in plane or axisymm. problems 8-67102
- Al alloys selection using fracture mechanics 8-56725
- Al-Zn-Mg-Cu-Cr, (5.6, 2.5, 1.6, 0.3 wt.%), alloy 7075, plates, adhesively bonded, exam. of fatigue crack growths 8-92348
- Ti-V (40 at.%), microcracks intersecting fatigue crack, exam of origin 8-80638

crack inspection see *crack detection***crack-tip stress field analysis** see *crack-edge stress field analysis***cracking** see *fracture***cracks**

- see also *crack detection; crack-edge stress field analysis; crazing; fatigue cracks; penny-shaped cracks; stress corrosion cracking; thermal stress cracking*
- Γ -shaped crack elastic energy evolution rate in laminate determ. by pliability vibr. meas. 8-83348
- aircraft parts, microfractographic fracture analysis exam., SEM exam. (Japanese) 8-52950
- alkali halide crystals, defect state change during electrolysis 8-95057
- anvil, truncated, compressive strength, high press. apparatus appl. 8-84906
- Araldite B, crack arrest toughness determination 8-72867
- axisymmetrical homogeneous elastic solid with internal circular cracks, energy release rates 8-67139
- biaxially fibre reinforced composites, two dims. mixture theory, dynamic crack appl. 8-87301
- bonded dissimilar half planes having Griffith crack at interface, elastic wave interaction 8-67091
- borosilicate glass surface, damage due to impact of small glass and steel spheres 8-52994
- branched crack, under biaxial stress 8-67125
- brass, crack opening displacement, rel. to flow stress 8-68810
- brass, fracture initiation and propagation during strip drawing 8-64663
- brittle fracture, structure design, method of calculation 8-72869
- brittle material, compressive strength, statistical and micromech. theory 8-64618
- brittle material under compressive load, crack extension from flaws 8-95812
- brittle solid, crack system propagation, stability conditions 8-51131
- case hardened components, exam. of fracture surface by TEM. (Japanese) 8-52949
- cement, hardened paste, internal stresses and microcrack form. caused by drying 8-92325
- circumferentially notched tensile specimen, finite element anal. 8-67150
- closed cylindrical shell with insulated cross crack (Ukrainian) 8-90638
- combined mode cracks, fracture criteria 8-79285
- composite material, longitudinally cracked, exam. of plane deformation 8-67096
- compression failure anal., glassy materials investigation 8-55608
- continuous plastic cracks in ordered alloys, discrete dislocation analysis 8-80625
- crack branching, elastodynamic effects 8-67113
- crack tip disintegration by strong EM field 8-83339
- crack tip opening displacement, rel. to J-integral, discussion (Chinese) 8-83328
- cracked elastic body statics, three-dimensional problem (Russian) 8-73858
- cracked thick walled cylinder, elastic plastic fracture anal. under displacement controlled loading 8-67119
- crystal cleavage due to dislocation tilt wall splitting 8-91377
- defected stripe, current crowding and flux divergence 8-71885
- deposited film thickness and grain size determ. on non-conductive SEM specimens 8-77170
- depth measurement, ultrasonic techniques, review 8-95903
- directivity pattern of radiation 8-87305
- dislocation model for interaction between tensile crack and hole 8-67092
- doubly-periodic array of cracks in an infinite isotropic medium 8-87303

cracks continued

- Dugdale model solution, of cracked bodies, finite element analysis 8-67116
- dynamic crack propagation and arrest 8-68758
- dynamically loaded in strain rate sensitive materials 8-60820
- elastic material, finite element anal. of crack problems 8-67146
- elastic strip, arbitrarily oriented, crack distrib. (*Russian*) 8-63378
- elastic strip debond dynamics, simple transient motion 8-67040
- elastic-perfectly plastic material, theory of stable crack growth 8-79272
- elastic-plastic crack problem, comparison of finite element soln. 8-79263
- elastodynamic anal. by finite element method using singular element 8-55603
- elastic-plastic crack and hole interaction in elastic medium under uniform shear load 8-51117
- epoxy resin, thermoelastic stress creation and motion picture recording of interaction with dynamic crack 8-56697
- epoxy resin adhesives, crack propag. and mech. props. 8-68783
- equilibrium and kinetic aspects of brittle fracture 8-79271
- equivalent inclusion method for a three-dimensional lens-shaped crack in anisotropic media 8-67123
- extension, initial stage in time depend. and/or ductile fracture 8-67107
- extension due to nonuniform internal press. 8-51124
- fibre reinforced composites, cracking and fracture, review 8-60772
- fibrous composite, short steel wire reinforced (polymer impregnated) concretes, cracking and toughening 8-80626
- fracture, appl. of continuum theory of dislocations fracture mechanics 8-67767
- fracture mech., linear elastic, appl. to crack stability in brittle struct., elastic-plastic conditions 8-90800
- fracture mech. during creep, interference microscopy exam. of 12Kh18N9, 08Kh18N10T 8-56756
- fracture mechanism 8-63380
- fracture resistance, dependence on crack length 8-67120
- fracture toughness parameters J and G^A , effect of load biaxiality 8-67128
- fusion reactor materials, material requirements exam., review 8-50257
- glass fibre reinforced plastics, under compressive load (*Japanese*) 8-92301
- glass plate, flexure crack propag., expt. and anal. 8-80620
- glass plates, effect of localized damage on energy losses, during impact by glass spheres 8-52973
- grain boundary estimation of creep rupture time (*Chinese*) 8-83325
- granite plate, crack propagation by projectile impact load 8-60741
- graphite, pyrolytic, numerical discussion of flaking mechanism from ion bombard. 8-52947
- Green's function for thru-crack emanating from fastener holes 8-67118
- growth, three-dimensional problem 8-79266
- growth determination, in mixed mode loading system 8-67105
- growth in conditions of creep (*Russian*) 8-63379
- growth prediction in nonhomogeneous viscoelastic media 8-75098
- Haynes Stellite 6B, particle erosion damage, TEM obs. 8-88546
- hot-pressed with crystn. grain boundary phases 8-95716
- HSLA steel 8-52943
- ice, Antarctic deep core, X-ray diffr. topographic studies 8-63803
- ice shelves, floating, tidal flexure cracks, fracture mechanics 8-69368
- impacted pretensioned plate, dynamic finite element and photoelastic analyses 8-67111
- instability, directional criteria 8-90789
- integral J_1 , calculation by finite element analysis 8-67129
- interaction between cracks positioned at an angle 8-83871
- ionic crystals, fracture in mag. field 8-59855
- kinetic model of crack propagation (*Russian*) 8-63381
- layered cylinder, axisymmetric delaminations 8-79269
- limestone plate, crack propagation by projectile impact load 8-60741
- line crack subject to shear 8-79268
- linear elastic solids, time-depend. crack propag. 8-75099
- LMFBR, effect of cracks in fast neutron embrittled hexagonal subassembly ducts 8-74446
- LMFBR materials, exam. of material requirement 8-50256
- lug, test and analysis 8-67153
- metal weld, submerged arc, metallographic study of chevron cracking 8-56761
- microcracks, statistical linking theory consistent with classical reliability theory 8-84952
- mixed boundary-value problems, orthogonal polynomial solns. 8-54193
- model, deduced from thermodynamics (*French*) 8-63386
- modified Westergaard equations 8-67122
- monolithic component glasses and rigid sintered fibre-optic elements, microcrack form. during grinding 8-87175
- nonhomogeneous medium under shear, elasticity theory 8-86166
- nuclear fuel element model for cladding performance during power changes, strain defects 8-58359
- nuclear fuel-cladding interaction between cracked surfaces, mechanical and temp. contact 8-66341
- nuclear reactor, cracked fuel elements, temp. distrib. calc. 8-78446
- overlapping interacting cracks 8-55593
- periodic curvilinear cracks in isotropic medium, integral eqn. soln. 8-51118
- pin loaded single edge notched tension specimens, K-COD relationship 8-67133
- planar body, with circ. boundary and thermally insulated cracks, temp. distrib. 8-67002
- plane, arbitrary shape, soln. of three dimensional problem 8-79265
- plane crack problems in micropolar theory of elasticity 8-54191
- plane notch and crack problems, appl. of displacement and hybrid stress methods 8-63375
- plane stress to plane strain thickness dependent transition, anal. model 8-67126
- plastic flow round crack under friction and combined stress 8-79280
- plastic materials, crack resistance (*Russian*) 8-63377
- plate, three dimensional theories 8-67136
- plate, wide, analysis on crack in high strain zone (*Chinese*) 8-83326
- PMMA, overlapping skew-parallel crack dynamic propag. and arrest meas., method of caustics 8-84962
- PMMA, rain erosion behaviour, exam. 8-53001

cracks continued

- polycrystalline material, diffusional growth of cracks (*Russian*) 8-91376
- polymer crystals, deform. and fracture, submicrocrack nucleation and supermod. struct. 8-52918
- pressure vessel, strength analysis, by thermal shock 8-68819
- propag. simulation, using moving grid based finite difference scheme 8-83334
- propagation and arrest, in plates, pipes and pressure vessels 8-56770
- propagation under compression, finite element analysis 8-67148
- propylene, isotactic, crack propag. rel. to morphology (*German*) 8-76749
- pulsed stress effects 8-56724
- PVC sheet, notched, yielding 8-56708
- quarter elliptical cracks in irregular bodies, exam. using finite element alternating method 8-90796
- quasi static crack growth, in sheet materials 8-67106
- quasi-Newtonian force 8-63765
- quasistatic crack growth, nonlocal model, thermodynamics of irreversible processes basis 8-83324
- refraction of propagating crack by stress wave, brittle amorphous mat. 8-92337
- Rochelle salt, mechanoluminescence and crack mobility, charge prod. during fracture 8-88370
- rock, symmetrically extending plane crack, self-similar pressure profiles 8-69340
- rocks, oriented cracks, differential strain analysis 8-53647
- running crack tip, effect of strain rate depend. Young's modulus on stress and strain fields 8-75097
- sheet, misfitting inclusion and circular arc cracks 8-67117
- sheet metals, ductile, shearing process 8-84841
- singular crack borders, constitutive preps. 8-67108
- slender Z-crack, elasticity problems 8-87304
- small particles, crack propag. rel. to impossibility of comminution by compression 8-52709
- soda-lime glass surface, damage due to impact of small glass and steel spheres 8-52994
- stable crack-growth, fracture criteria, numerical approach 8-67104
- steady state crack propagation, media with variable elastic moduli 8-90783
- steel, A533B, crack branching 8-64705
- steel, alloy, crack arrest toughness determination 8-72867
- steel, austenitic, precipitation hardened, ductility of grain boundaries and crack propag. (*German*) 8-52834
- steel, austenitic stainless, propagation 8-60797
- steel, C, crack opening displacement, rel. to flow stress 8-68810
- steel, C, crack resistance, preliminary loading condition effects in crack appl. 8-56739
- steel, C, ductile fracture under cold forming conditions, press. effect 8-52938
- steel, CC Cr-Mo-V, stress relief cracking mechanism 8-64669
- steel, CC Cr-Mo-V press. vessel, crack growth under creep 8-60827
- steel, Cr-Mo-V, medium strength, correlation between crack initiation, propag. and microstruct. 8-60787
- steel, Cr-Mo-V, normalised and tempered, size and geometry effect on creep cracking behaviour 8-64630
- steel, Cr-Mo-V (0.5, 0.5, 0.25 wt.%), comparison of methods of correlating creep crack growth 8-60826
- steel, Cr-Mo-V (0.5, 0.5, 0.25 wt.%), creep crack growth, temp. effect 8-64667
- steel, crack tip studies, stretched zone and COD 8-68812
- steel, ductile struct., crack propag. 8-68805
- steel, fracture toughness testing, obs. of crack initiation and stable growth processes (*Japanese*) 8-52954
- steel, high strength, alloy, initiation of cracks at delayed fracture, AE study 8-72868
- steel, high strength, low alloy, plate, impaired ductility in sheared edges 8-60727
- steel, high strength, weld cold cracking, anal. of fracture morphology, using SEM (*Japanese*) 8-52960
- steel, low alloy, high strength, correlation between fracture toughness, tensile props., fracture morphology 8-60789
- steel, low alloy, naval, stretch zone width meas., COD for ductile crack initiation 8-68813
- steel, low alloy creep resisting, causes of weldment cracking 8-56760
- steel, martensitic, grinding crack formation, impingement cracks and strain influence (*Japanese*) 8-56747
- steel, mild, resistance to slow stable crack growth, use of J integral 8-68809
- steel, Ni-Cr-Mo, exam. of delayed fracture using fracture mechanics (*Japanese*) 8-52961
- steel, pressure vessel, A533B, ductile, plane strain crack growth 8-80621
- steel, stainless, 316, nuclear fuel cladding, crack nucleation 8-72864
- steel, stainless, duplex, hot ductility and fracture mechanism 8-60731
- steel, structural, rel. between static and dynamic fracture toughness 8-68815
- steel, type A508, C1 2, microcrack formation during stress-relief annealing of a weldment 8-80629
- steel structural components, flaw assessment based on cleavage fracture hypothesis 8-60804
- strain energy density and surface layer energy for blunt cracks or notches, book contrib. 8-94618
- stress analysis of crack, elastoplastic range 8-67144
- stress and crack-displacement intensity factors, in elastodynamics 8-67112
- stress intensity factor, near doubly riveted stiffeners 8-67152
- stress intensity factor formula for side notches 8-79264
- stress intensity factors, anal. determ. by variational method for eccentric cracks 8-67115
- stress intensity factors, single-edge cracked bar loaded by in-plane transverse forces (*Chinese*) 8-83327
- stress intensity factors at the tips of kinked and forked cracks 8-67124
- sulphide group minerals, effects of cracks on electrical conductivity 8-64045
- thermoelastic periodic problems for infinite solid with disc shaped cracks, integral eqn. solns. (*Ukrainian*) 8-55559
- three dimensional, stress intensity factors 8-55601
- tip opening displacement by finite element anal. (*Czech*) 8-59343

cracks continued

- transversely isotropic medium with cylindrical cavity and external crack, stress distrib. 8-79259
 tube with hexagonal bore, crack formation during rolling (*Russian*) 8-80622
 two-dimensional, in plate structures, stress analysis, computer program based on superposition method (*Japanese*) 8-51123
 underground nuclear explosion, gas flow in permeable Earth formation with crack 8-61372
 US scattering of elastic waves, quasistatic approx. 8-67080
 virtual extension method for combined tensile and shear loading 8-67149
 viscoelastic, crack growth relations, for orthotropic, pretrained media 8-90772
 wedge loading of a semi-infinite strip with an edge crack 8-79270
 yield zone form., fracture resistance, influence of specimen configuration 8-68817
 Al alloy, crack tip studies, stretched zone and COD 8-68812
 Al alloy 6061-T6, fracture initiation and propagation during strip drawing 8-64663
 Al alloys, fracture toughness under plane stress 8-92316
 Al, fracture due to shock waves leaving surface, shear stresses 8-51128
 Al, liquid metal embrittlement by Ga 8-64653
 Al, step coverage optimisation by computer simulation and SEM 8-51838
 Al-Cu-Mg alloy RR58, comparison of methods of correlating creep crack growth 8-60826
 Al-Cu-Mg-Mn (4.5, 1.5, 0.6 wt.%), thin sheet, exam. of fracture toughness, and fatigue crack growth 8-92353
 Cr-Mo-V, steamline bends, restorative heat treatment effects 8-68716
 Cu, fracture due to shock waves leaving surface, shear stresses 8-51128
 α -Cu-Ni-Zn-Pb, fire cracking and ordering (*German*) 8-60760
 $\text{Eu}_2\text{O}_3\text{-Ta}_2\text{O}_5$, microcracking, elastic props., internal friction 8-92326
 Fe, cast, rare-earth-Mg nodular, fracture toughness and fatigue (*Chinese*) 8-95791
 H embrittlement cracking at notches 8-84985
 KCl, spontaneous cleavage, step line propag., macroscopic defects 8-87662
 LiAlSiO_4 glass-ceramic, fracture phenomena as function of initial flaw size and temp. 8-95797
 MgO, lattice misorientation and displaced vol. for microhardness indentation 8-64617
 MgO, single crystal, wear damage, surface cracks 8-68825
 $\text{Na}_2\text{O-CaO-SiO}_2$ glass, crack nucleation around plastic indents 8-92327
 Ni-Cr-Co-Mo-Al-Ti alloys, Waspaloy, Astroloy, exam. of microstruct. effect on crack growth 8-52977
 Ni-Mo-Cr steel, elastic-plastic material characterisation 8-72854
 Si, dangling bonds, EPR, localised states and unpaired electrons on microcrack surfaces 8-52351
 $\text{Si}_3\text{N}_4\text{-Al}_2\text{O}_3$, hot-pressed with crystn. grain boundary phases 8-95716
 Zn, liquid metal embrittlement 8-64653
 Zr and Zr alloys, cracking, H_2 induced delay, strain energy effect on H_2 solubility 8-92364
 Zr-Nb alloy, pressure tubes of PWR reactor, cracks identification and avoidance 8-82472

cranking model

- back bending, Hartree-Fock Bogolyubov approach, cranking method 8-58228
 back bending effect, Hartree-Fock-Bogolyubov treatment of cranking method, yrast states 8-82264
 cranked Hartree-Fock-Bogolyubov wave functions, ang. momentum distrib. at band crossings 8-93956
 giant resonance description, RPA, GCM, and semiclassical theories unification 8-54671
 Hartree Fock Bogolyubov method, high nuclear spins, quadrupole pairing, moment of inertia, yrast traps 8-54712
 rotating nuclei, selfconsistency conditions in cranked harmonic oscillator model, HF calcs. 8-58239
 yrast spectroscopy, nuclei with high angular momentum, review 8-50063
 ^{158}Er , moment of inertia anomaly at ang. momentum of 26 to 30 8-62496
 $^{\text{A}}\text{Hf}$, $\text{A}=172\text{-}180$, prolate isotopes, Yrast traps using cranked modified oscillator pot. 8-93923
 ^{240}Pu , moments of inertia of fissioning isomers 8-74299
 ^{236}U , moments of inertia of fissioning isomers 8-74299

crazing

- see also stress corrosion cracking
 dicyano bisphenol polycarbonate, crazing, polar group incorporation 8-85017
 PMMA, effect of surface finish on strength, and craze resistance 8-76724
 PMMA, fracture surface parabola markings, temp. 8-52969
 PMMA, influence of craze configuration on fracture 8-76758
 PMMA, methanol crazes, mech. props., craze-strain profile 8-72844
 PMMA, struct.-prop. relationship between mol. wt. and fracture surface energy 8-80633
 polycarbonate, cyclic deformation and craze growth 8-76759
 polycarbonate, environmental stress crazing 8-68832
 polycarbonate, impact behaviour, effects of thermal pre-treatment and mol. wt. 8-95798
 polycarbonate, plane strain fracture energy instability and mixed mode crack propag. 8-68775
 polycarbonate, stress crazing, liq. environment effects 8-84970
 polycarbonate, yielding and crazing behaviour in torsion under superimposed hydrostatic press. 8-52898
 polyethylene, low density, SEM exam. of environmental stress cracking 8-53011
 polyethylene terephthalate, crazing and shear deformation on stretching in air and liquids (*Russian*) 8-88558
 polymers, glassy, initiation and growth of crazes 8-60767
 polymers, stress analysis of circular craze, extension of linear membrane model 8-75081
 polystyrene, effect of pressure and environment on fracture and yield 8-76757
 polystyrene, high-impact type, deformation and microvoid form. 8-80602

crazing continued

- polystyrene-poly(styrene-*b*-butadiene-*b*-styrene) polyblends, electron micrographs for struct. 8-51442
 polythene, finite element anal. of crazing and cavitation by dil. aq. detergent 8-53006
 styrene-acrylonitrile copolymer swelling, glass transition and crazing, polar group incorporation 8-85017
 thermoplastics, homogeneous, fracture under plane strain and plane stress conditions 8-52941
- creation hypothesis, continuous** see cosmology
- creation of electron pairs** see electron pair production
- creep**
 see also creep fracture; creep testing; diffusion creep; elastic aftereffect; irradiation induced creep; recovery-creep; stress relaxation
 ageing bodies, with growing slit, creep theory 8-63329
 ageing media, thermodynamic pots. in creep theory (*Russian*) 8-63318
 Al alloy, type AK4-1T1, effect of high temp. ageing, on endurance of thin welded joints 8-80570
 alloy, high temperature, mechanical, thermal and corrosion props. 8-95763
 ampule for inside fission reactor exam. of materials, examining creep, long term strength in plane stress state 8-85098
 austenitic stainless steel, type 316, anelasticity and creep transients 8-84880
 baddeleyite-corundum refractories, creep and annealing 8-84907
 biaxial creep behaviour, ribbed GCFR cladding at 650°C 8-86597
 brass, cyclic strain induced creep, relation between modes of stress and strain superposition 8-60733
 carboxyl terminated butadiene nitrile-diglycidyl ether of bisphenol A epoxy resin, struct. and mech. props. 8-52901
 ceramics, microstructure dependence of mechanical behaviour 8-88533
 component containing cracks, critical review 8-63321
 composite, steady creep bending stresses 8-71280
 composite spherical shells under uniform internal pressure, transition theory of creep 8-90724
 constitutive equations of continuum creep damage mechanics 8-67054
 Cotac 74, directionally solidified composite, creep behaviour prediction (*French*) 8-68754
 crack growth in conditions of creep (*Russian*) 8-63379
 curves, theoretical exam. of curve shape, comparison with Cu creep curves 8-79232
 deformation, effect of damage 8-79664
 Earth mantle, creep laws 8-69305
 fatigue high temp., hold time effects, cavitation nucleation, creep interaction 8-60734
 fibre reinforced metals, creep behaviour exam. (*German*) 8-52931
 fracture mechanics parameters, applicability to creep, fatigue crack propag., at evaluated temp., exam. using various materials (*Japanese*) 8-52962
 fusion reactor blanket, thermal stresses and cyclic creep-fatigue 8-62655
 gabbro, long-term creep, large and small specimen results obtained over 20 and 3 years respectively (*Japanese*) 8-56705
 galena, polycryst. synthetic, stress relax. 500 to 800°C 8-87737
 geological faults, fracture, creep and strain 8-69345
 grain and phase boundaries between crystals, conf., Königstein, Germany (Oct. 1977) 8-72762
 granite, long-term creep, large and small specimen results obtained over 20 and 3 years respectively (*Japanese*) 8-56705
 granodiorite, fracture under uniaxial compression, mech. and AE meas. (*Japanese*) 8-56748
 graphite fibre reinforced Al, temp. and press. effect on interface chemistry, mech. prop. meas. 8-64595
 Incoloy 800, austenitic, creep fatigue interaction at 600°C 8-64672
 independent and sequential processes, charact. 8-52921
 inelastic solids, anelastic relaxation anal., extended to creep at high temp., appl. to internal friction (*French*) 8-63806
 independent processes, analysis 8-80594
 LMFBR materials, exam. of material requirement 8-50256
 metal, hardening due to increased subgrain boundary stability 8-52934
 metal, stress conc. caused by grain boundary sliding under power law creep 8-60732
 metal, surface energy meas. by zero creep method at extremely low O_2 partial press. (*Czech*) 8-63926
 metal failure, due to hydrostatic pressure, exam. of kinetics 8-52944
 metal structures, inelastic anal. 8-70586
 metal wire, influence of grain boundaries on high temp. creep (*German*) 8-72812
 metallic media, varying loads, elevated temp. inelastic anal. using state variable theories 8-83264
 metals, BCC, effect of screw dislocations, on mech. props. (*Russian*) 8-60704
 metals, creep prediction using analytical tabular method (*Ukrainian*) 8-68725
 metals, recrystallisation during hot deform. 8-68714
 metals, time depend. inelastic deform., boundary integral eqn. calcs. 8-51090
 microcreep, low temp., quantum effects (*Russian*) 8-71784
 natural rubber vulcanisates, creep under tension, O_2 effects 8-92302
 non-linear viscoelastic behaviour, numerical anal. 8-59318
 nuclear fuel cladding, slightly oval cylindrical shells, creep anal. 8-78468
 nuclear fuel element model for cladding performance during power changes, strain defects 8-58359
 nuclear reactor structural materials assessment, AISI 316 and 9Cr-1Mo steels, for UK LMFBR 8-86581
 nylon-6,6, creep meas. at const. temp., humidity 8-95883
 olivine, creep mechanisms 8-69332
 PMMA, in distilled water, influence of liquid environmental media on mech. behaviour 8-52902
 PMMA, influence of craze configuration on fracture 8-76758
 polyamide coating on steel roller, experimental exam. of contact parameters 8-68842
 polyarylate, F-2 influence of water on mech. props. (*Russian*) 8-88513
 polycrystalline wires, small dia., formulation of zero creep method 8-52922

creep continued

polyethylene, high density, creep, computer program calc. (*German*) 8-60715
 polyethylene, high density, creep curves, exponential functions for description (*German*) 8-90732
 polyethylene, high density, fracture buildup due to prolonged loading, exam. 8-68779
 polyethylene, low density, shear and tensile creep at finite strains 8-52903
 polymer, creep curves, correl. between isothermal and thermomech. 8-64587
 polymer films and sheets 8-80590
 polymeric systems, rheology, review 8-87317
 polypropylene, creep curves (*German*) 8-64599
 polypropylene, linear viscoelastic region, creep prediction using temp. pulse technique 8-68732
 polypropylene, shear and tensile creep at finite strains 8-52903
 polystyrene, Millar interpenetrating network, viscoelasticity and phase domain form. 8-83749
 polyurethane, dithiodiglycol-plasticised, time-crosslinked density reduction, photochem. scission obs. 8-52920
 PVC, amorphous, orientation study by creep thermomechanical method, computer anal. 8-75561
 PVC, antiplasticisation rel. to ageing and nonlinear viscoelasticity 8-52929
 PVC, plasticised, history-independent recovery, creep, stress relaxation 8-80607
 rapid cycling problems, finite element soln. 8-63317
 relaxation and creep curves for torsion-tension members, at elevated temps. 8-83260
 rotating discs, variable thickness, transition theory of creep, stress determ. 8-90725
 rubber, creep processes associated with uniaxial compression 8-68734
 soil, viscous nonlinear, stresses and strains 8-73363
 stationary creep in structures with random material props. 8-67053
 steel, austenitic, grain boundary sliding, exam. by tensile creep tests 8-76715
 steel, austenitic stainless, Cr-Ni-Ti, creep deform. effects on intergranular TiC dispersion stability 8-84912
 steel, austenitic stainless, grain boundary migration during high temp. creep, TEM exam. 8-88509
 steel, austenitic stainless, type 316, effect of hold times on fatigue life, explanation in terms of grain boundary sliding damage 8-72851
 steel, C, accumulation of longitudinal strain under cyclic torsion 8-64615
 steel, CC Cr-Mo-V, creep fatigue interaction 8-60841
 steel, CC Cr-Mo-V, creep/fatigue interaction 8-64632
 steel, CC Cr-Mo-V, low alloy, creep fatigue interaction 8-64673
 steel, Cr-Mo, constitutive eqn. model for high temp. behaviour of fast reactor structural alloys 8-66343
 steel, Cr-Mo-V, steamline bends, restorative heat treatment effects 8-68716
 steel, creep and fatigue fracture prevention 8-60837
 steel, low C and mild, fatigue deformation, phenomenological exam. 8-64691
 steel, medium C and austenitic stainless, cyclic strain induced creep, relation between modes of stress and strain superposition 8-60733
 steel, stainless, 316, creep fatigue interaction failure 8-80652
 steel, stainless, type 316, 20% cold worked, exam. of creep 8-72817
 steel, stainless 8-64583
 steel, stainless 20/25/Nb, biaxial creep meas., reactor fuel cladding tubes performance obs. 8-82442
 steel, stainless 316, creep under high stress 8-52892
 steel fibre reinforced Cu, exam. of creep behaviour (*German*) 8-52931
 structural anal., underlying concepts of finite element analysis 8-66337
 structures subjected to arbitrary cyclic loading, creep life estimation 8-90722
 superplasticity, mechanism rel. to hyperfine grain struct. 8-84930
 Teflon, creep under joint action of tension, hydrostatic pressure 8-68750
 thin walled tubes, exam. of steady creep under combined loading 8-83269
 torsional creep problem, appl. of maximum principle 8-71284
 transition behaviour, exam. of diffusion term significance in criteria 8-75719
 tubes, thin wall, model for collapse due to creep (*Spanish*) 8-87276
 two-phase structures, high-temp. deform. 8-68738
 visceral smooth muscles in vertebrates, viscoelastic and plastic props. 8-73169
 viscoelastic materials with fading memory, thermodynamics of relaxation and creep processes 8-71282
 viscoelasticity, linearised theory, variational principles (*Russian*) 8-87279
 Zircaloy-4 fuel sheathing, inverted primary creep 8-86615
 Zircaloy 4, stress relaxation in bending 8-68719
 Zircaloy creep collapse, hot cell examination 8-86596
 β -Zircaloy-2, tensile creep and creep rupture props. under vacuum 8-52915
 Zircaloy-2 cladding, beta-phase creep and creep rupture props., 1000 to 1500°C 8-78470
 Ag, large grain boundary cavity coalescence during tension creep 8-52894
 Al, creep and dislocation distribution, influence of electron irradiation (*Russian*) 8-95775
 Al-Cu-Mg-Mn-Fe-Si, alloy D16, effect of mechanothermal treatment on mech. props. 8-56674
 Al-Mg (2 wt.%) subgrain formation at low stresses 8-84928
 Al-Mg (5.5%), creep, absence of instantaneous plastic strain upon stress changes 8-75718
 α -Al₂O₃, atomic disorder, dominant type 8-63757
 (Al₂O₃)₂MgO, n=1.1, high temp. creep, dislocation behaviour 8-80593
 C fibre reinforced plastic, $\pm 45^\circ$ orientation, creep, fatigue, repeated loading and crack growth 8-68729
 CdTe, creep activation energy and velocity (*Russian*) 8-56716
 Co alloy, X-40, creep-fatigue interaction at high-temp. 8-84958
 Co, steady creep rate, stress depend., exam. at phase transformation at 390°C 8-52923

creep continued

Co, steady state creep rate, stress depend. rel. to FCC to HCP phase change 8-64598
 Cu alloy, superplastic, activation energy of plastic flow 8-64584
 Cu, commercial, pure, creep-rupture times and creep rate, in vacuum (*Japanese*) 8-72843
 Cu, creep curves, comparison with theory 8-79232
 Cu foil, role of grain-boundary porosity in superplasticity (*Russian*) 8-56690
 Cu single crystals, in high temp. creep, meas. of internal stress 8-80608
 Cu, wire, polycryst., internal friction, ultrasonic vibrations effect (*Russian*) 8-76685
 Cu-Al, eutectic composition, exam. of high temp. mechanical behaviour (*French*) 8-72818
 Cu-Al (10.4%), creep, absence of instantaneous plastic strain upon stress changes 8-75718
 Cu-Al-Si-Co (2.8, 1.8, 0.4 wt.%), superplastic phase, exam. of mech. props. 8-52891
 Cu₂O, creep substruct. under compression, X-ray diffr. study 8-95785
 Fe, Armco, corrosion and mechanical behaviour in liquid Li 8-53036
 Fe, Armco, screw dislocation effect on mech. props. (*Russian*) 8-60704
 Fe, Armco and carbonyl, kinetic singularities of plastic deform. during $\gamma \rightarrow \alpha$ transform. (*Russian*) 8-92262
 α -Fe, hydrostatic pressure effect on creep rate and failure time 8-92306
 α -Fe-C (0.03 wt.%), structural singularities of transition from thermally activated to force-induced fracture (*Russian*) 8-56731
 Fe-Mo (1.8%), creep, absence of instantaneous plastic strain upon stress changes 8-75718
 Fe-Ni-Cr (25, 15 wt.%), high temp. creep, dispersed γ' -Ni₃(Al, Ti) effects (*Czech*) 8-64590
 GaAs cryst., creep and dislocation vel. at different doping and temps. 8-95783
 HgTe, creep activation energy and velocity (*Russian*) 8-56716
 KCl single crystal, dislocation velocity stress exponent estimation by stress relaxation and creep tests (*Japanese*) 8-55875
 Li₂O-Al₂O₃-4SiO₂, glass-ceramic, tensile creep and high temp. fracture 8-52914
 MgO-CaMgSiO₄, exam. of high temp. creep behaviour 8-80601
 MgO(Al₂O₃)_{1.8}, spinel, X-ray refl. topography, dislocation substructures during creep form. (*French*) 8-68737
 Mg₂SiO₄, forsterite, glissile splitting of dislocations, cross-slip-controlled creep and mantle rheology 8-61406
 Mo, monocrystalline, exam. of microplasticity at ambient temps. (*French*) 8-52888
 NaCl, rock salt, progressively mined soln. cavities, struct. behaviour 8-61409
 Nb-Zr-C alloy, creep in vacuum, prolonged high-temp. ageing effects (*Russian*) 8-56692
 NbC_x, creep-comp. curves for homogeneous region 8-52911
 Ni base superalloy IN 100, corrosion resistant intermetallic coating, microstruct. effect on mech. props. 8-85058
 Ni-based alloys, binary, ternary, complex, TiC additions, effects 8-92305
 Ni-Cr, solid soln., exam. of back stress role in creep behaviour of particle strengthened alloys 8-52889
 Ni-Cr alloy, KhN70VMTYu, gas turbine blades, thermocyclic strength characts., exam. 8-60743
 Ni-Cr-Al-Ti (Ti-Co), exam. of back stress role in creep behaviour of particle strengthened alloys 8-52889
 Ni-Cr-Co-Mo-Al-Ti alloys, Waspaloy, Astroloy, exam. of microstruct. effect on crack growth 8-52977
 Ni-Cr-W (20, 3 wt.%), high temp. creep, atmospheric effect on anomalous behaviour 8-80617
 Ni-ThO₂, dispersion hardened, fracture mechanism map 8-60823
 Pb-Al₂O₃ composites, creep rate and creep behaviour (*Japanese*) 8-84830
 Si₃N₄, reaction bonded, creep, internal oxidation effects 8-56701
 Ta-W-Hf (8.2 wt.%), T-111, O₂ absorption, effect on lattice parameter and specimen dilation 8-83958
 W, wire, doped, high temp. creep behaviour 8-88499
 Zr-Nb (1 wt.%) exam. of creep behaviour, 373 to 773K 8-80599
 ZrC_x, creep-comp. curves for homogeneous region 8-52911

creep fracture

α - β brass, exam. of creep fracture by tensile tests 8-88531
 brittle materials, intergranular creep crack growth, diffusion controlled theory 8-84950
 composite, fracture time under tensile loading 8-88521
 concrete prestressed members, creep fracture during manufacture 8-76767
 Cotac 74, directionally solidified composite, creep behaviour prediction (*French*) 8-68754
 crack growth, model, diffusion of vacancies along grain boundaries 8-75716
 damage criteria, cavity config., use of density meas. 8-60818
 damage parameter, energy based, for fatigue and creep-fatigue appl. 8-59347
 engineering alloys, prediction of creep fracture, exam. 8-56776
 failure by cavitation under non-steady conditions, exam. 8-56774
 fracture mech., during creep, interference microscopy exam. of 12Kh18N9, 08Kh18N10T 8-56756
 fusion reactor first wall/blanket system, thermal-hydraulics and fatigue life modelling 8-58453
 grain boundary estimation of creep rupture time (*Chinese*) 8-83325
 granodiorite, fracture under uniaxial compression, mech. and AE meas. (*Japanese*) 8-56748
 Larson-Miller parameter, exam. 8-76742
 Larson-Miller parameter, exam. 8-76743
 like improvement mechanism, reheat treatment 8-64666
 macroscopic growth 8-79282
 metals, fracture during creep 8-68778
 microcracks, statistical linking theory consistent with classical reliability theory 8-84952
 Nimonic 80A, intergranular creep fracture under const. cavity density 8-60825
 polycrystalline material, diffusional growth of cracks (*Russian*) 8-91376

creep fracture continued
polystyrene fibre, ageing effects on elongation to fracture (*German*) 8-76750
steel, austenitic Cr-Ni (18,12 wt.%), containing coarse irregular carbide precipitates along grain boundaries, ductility 8-60718
steel, austenitic stainless, fast neutron irradiation, effect on mech. props. 8-92309
steel, CC Cr-Mo-V press. vessel, crack growth under creep 8-60827
steel, Cr-Mo (2.25, 1 wt.%), relationship between minimum creep rate and time to fracture 8-56759
steel, Cr-Mo-V, creep crack growth temp. depend., 525 to 600°C 8-64634
steel, Cr-Mo-V, creep fracture, microstruct. effects 8-64668
steel, Cr-Mo-V, normalised and tempered, size and geometry effect on creep cracking behaviour 8-64630
steel, Cr-Mo-V (0.5, 0.5, 0.25 wt.%), comparison of methods of correlating creep crack growth 8-60826
steel, Cr-Mo-V (0.5, 0.5, 0.25 wt.%), creep crack growth, temp. effect 8-64667
steel, ferritic, low alloy, effect of microstruct. on creep fracture 8-80640
steel, low alloy creep resisting, causes of weldment cracking 8-56760
steel, Mo-V, creep rupture strength, heat treatment effects (*German*) 8-72834
steel, stainless, Cr-Ni-Nb-Ti, effect of I₂ vapour on creep fracture props. 8-72814
steel, stainless, type DIN 1.4970 exam. of creep fracture in vacuum at 923 to 1073K 8-72817
strip yield models for crack incubation and growth 8-55605
styrene-butadiene rubber, fracture time variability, endochronic prediction 8-76734
β-Zircaloy-2, tensile creep and creep rupture props. under vacuum 8-52915
Zircaloy-2 cladding, beta-phase, creep and creep rupture props., 1000 to 1500°C 8-78470
Ag, gas bubble embrittlement mechanism 8-60824
Ag, implanted grain boundary cavities effect on cavity growth kinetics and creep fracture 8-52935
Al-Cu-Mg alloy RR58, comparison of methods of correlating creep crack growth 8-60826
C fibre, Al-coated, stress rupture 8-80628
Cu bicrystals, grain boundary sliding and intergranular fracture studies 8-75717
Cu, commercial, pure, creep-rupture times and creep rate, in vacuum (*Japanese*) 8-72843
Cu-Cr (1 wt.%), exam. of low cycle fatigue props. at elevated temp. 8-64674
Cu-Cr-Zr-Mg (0.5, 0.1, 0.03 wt.%), exam. of low cycle fatigue props. at elevated temp. 8-6674
α-Fe, hydrostatic pressure effect on creep rate and failure time 8-92306
α-Fe-C (0.03 wt.%), structural singularities of transition from thermally activated to force-induced fracture (*Russian*) 8-56731
Fe-Cr-Al-Y (Y-Al₂O₃)(Y₂O₃), preparation and exam. of mech. props. 8-52720
Ni, deformed in uniaxial tension, fracture map 8-56764
Ni-based alloys, binary, ternary, complex, TiC additions, effects 8-92305
creep-recovery see recovery-creep
creep testing
canisters for radioactive waste vitrification 8-86648
device for examining under radiation, -196 to 250°C 8-60920
polymer, creep tests for determining degree of cross-linking (*German*) 8-76822
polymer coating, creep determ. by impression of rigid sphere 8-85084
polymers, hygroscopic, creep testing machines in environmental chamber, nylon-6,6 appl. 8-95883
rate determination using Michelson interferometer 8-68856
SAE 1045, creep and relaxation curves for torsion-tension members at elevated temps. 8-83260
crestatrons see travelling-wave-tubes
crimping
No entries
critical constants, thermal see critical points
critical current density (superconductivity)
A15 films, electron beam codeposition, synthesis and props. 8-72296
compound superconductors, radiation effects on critical currents 8-52175
film, inversion temp. in pinning of vortices by periodic struct. 8-56274
type II superconductor, neutron irradiation effects (*Rumanian*) 8-52144
vortex array, pinning of flux lines by randomly-spaced pinning centres 8-52172
Nb, superconductor, neutron irradiation, low temp., effect on critical current 8-52180
Nb-Ti, radiation effects on critical currents 8-52175
Nb-Zr sputtered films on Ta, struct. and supercond. props. (*Japanese*) 8-52138
Nb₃Ge, CVD, impurity doping effect on supercond. crit. props. 8-52174
Nb₃Ge film, prep. by coevaporation, supercond. props. 8-91830
Nb₃Ge tape, prepared continuously by CVD, props. 8-60257
Nb₃Sn composite processes with Cu-Sn-Zn matrix, superconducting props. 8-84370
Nb₃Sn, critical current density 8-52176
Nb₃Sn, neutron irradiation, crit. current change rel. to temp. and metallurgy 8-80109
Nb₃Sn superconductor, low temp. deuteron irradiation 8-52182
NbTi wire, supercond., magnetisation rel. to field orient. 8-52151
PbMo_{0.5}S₈, supercond. wire prep. by powder technique 8-52705
PbMo_{0.5}S₈, sputtered film, critical current density meas. 8-84369
V, superconductor, neutron irradiation, low temp. effect on critical current 8-52180
critical currents
see also critical current density (superconductivity); flux creep; flux flow; flux pinning
coupled Josephson weak links, phase locking 8-72309
definitions of terms for supercond. phenomenology, meas. practices 8-52117

critical currents continued
Josephson junction, barrier inhomogeneities, effect on junction behaviour (*German*) 8-91818
MB DC-SQUID, crit. current mag. modulation, logic device appl. 8-84371
multifilamentary superconductor, current transfer, expt. results for NbTi and Nb₃Sn 8-72316
multifilamentary superconductor, current transfer, theory 8-72315
SQUID, with V-VO_x-Pb Josephson tunnel junctions, quantum interference, critical currents 8-91821
superconducting bridge, DC Josephson effect, microscopic theory (*Russian*) 8-56258
superconducting contact, effect of UHF field (*Russian*) 8-72313
superconductor-degenerate semiconductor-superconductor structures, critical Josephson current calc. 8-52162
type I superconductor, critical current, in circ. mag. field 8-68124
type II superconductors, flux pinning investigation using one-dimens. analogue model 8-88086
Ag-Sn proximity effect bridge, crit. current anomaly 8-76194
Cu_{2.5}Mo_{0.5}S₈, evaporated two-phase, crit. current and scaling laws 8-91831
In, film, embedded with He particles, superconductor ion implantation study of inhomogeneities 8-52181
Nb and Nb alloys, superconductor, flux pinning under heavy ion irradiation 8-52167
Nb, neutron irradiation, low temp., 15 MeV, effect on superconducting props. 8-52179
Nb₂O, type II supercond., radiation-induced flux pinning 8-80106
Nb-Cu-Sn, cast supercond. alloy, crit. current, degradation resistance 8-76203
Nb-Zr, type II supercond., radiation-induced flux pinning 8-80106
Nb₃Ge, supercond. film, CVD, crit. temp., crit. current density 8-76204
Nb₃Sn composite supercond., current transfer, theory 8-72315
Nb₃Sn composite supercond., current transfer, expt. results 8-72316
Nb₃Sn, critical current enhancement by low temp. fast neutron induced flux pinning centres 8-52177
Nb₃Sn, filamentary, fatigue tests on small coils 8-64652
Nb₃Sn, filamentary conductors, type-II, low temp. 30 GeV proton effects on critical props. 8-52178
Nb₃Sn, multifilament conductors, strain-crit. current meas. 8-64174
Nb₃Sn multifilament conductors, strain effect on crit. props. 8-80108
Nb₃Sn, radiation damage effect on superconducting props. 8-52127
Nb₃Sn superconducting layers, struct. and prep. (*Slovak*) 8-56273
Nb₃Sn, superconducting props., effect of radiation induced atomic disorder 8-52133
Nb₃Sn superconductors, bronze-processed, effect of Ta additions 8-95404
NbTi composite supercond., current transfer, theory 8-72315
NbTi composite supercond., current transfer, expt. results 8-72316
NbTi, filamentary conductors, type-II, low temp. 30 GeV proton effects on critical props. 8-52178
Pb_{0.87}Sn_{0.129}, supercond., hysteresis in flux flow characts., normal metal precipitates 8-80107
V₂Ga, filamentary conductors, type-II, low temp. 30 GeV proton effects on critical props. 8-52178
critical field, superconducting see superconducting critical field
critical fluctuations
see also fluctuations in superconductors
azoxy-4,4'-(diundecyl α-methylcinnamate), smectic A to smectic C phase transition, optical tilt angle meas. 8-95141
binary mixture, high-frequency sound absorpt. near crit. separation point 8-83881
CBOOA, liq. cryst., mag. aligned, smectic A-nematic transition, US absorpt meas. 8-95137
CBOOA, liq. cryst., nematic to smectic A transition, high resolution X-ray scatt. exam. 8-94984
CBOOA, liq. cryst., smectic A to nematic phase transition, crit. neutron scatt. 8-95135
CBOOA, US attenuation near nematic-smectic A transition 8-87773
ferroelectric, uniaxial, static and dynamic crit. phenomena, Larkin-Khmelnitzkii theory 8-64327
ferroelectrics, sp. ht. calc., soft mode contrib., near T_c 8-64338
gels, crit. conc. fluctuation dynamics, near phase separation 8-56921
Ising system, finite, statistically layered, crit. phenomena 8-95446
liquid-liquid mixtures, critical region fluctuations, centrifuging effects 8-63850
magnetic material, fluctuational breakdown of metastable states at phase transitions (*Russian*) 8-52245
magnetic systems, effect on resistivity 8-87955
magnetic transition at T=0, impurity effects 8-76259
nematic liquid crystal, acoustic attenuation anomaly above clearing point 8-75816
nematic liquid crystal, quasi-elastic light scatt. near instability point, dielec. regime 8-75535
nonequilibrium phase transitions in chemical systems 8-54325
p-nonyloxybenzoate p-butyloxyphenol, smectic A to smectic C transition, crit. fluctuations, Rayleigh scatt. obs. 8-95140
pentane-o-nitrotoluene critical solution, nonlinear dielectric effect 8-55952
spin glass, theory 8-52279
TBBA, liq. cryst., smectic A-nematic transition, cybotactic cluster form., X-ray obs. 8-95138
TBBA, smectic C to smectic A transition, crit. exponent, neutron diff. obs. 8-95143
KH₂PO₄:SeO₄³⁻, slowing down of fluctuations near T_c, EPR obs. 8-60403
NH₄Br(Cl), anomalous sound attenuation above lambda point 8-51617
Sr₂Ba_{1-x}Nb₂O₆, neutron and light scatt. in phase transition region 8-64336
critical mixtures
alkali metal vapour-He(Ar)(N₂), alkali condensation in flow, heat and mass transfer 8-75192
binary, latent heat of vaporisation, prediction 8-83930
binary mixture, high-frequency sound absorpt. near crit. separation point 8-83881
binary mixture, nucleate boiling heat transfer, conc. depend. 8-87249
binary mixture, time-depend. solidification, series soln. 8-75058
binary mixture in external field, crit. opalescence 8-84595

critical mixtures continued

- binary mixture near crit. point, singly and multiply scattered light distrib. 8-56494
 cyclohexane+acetic anhydride, elec. resist. near crit. soln. temp. 8-71874
 ethanol-water mixture, saturated, min. film boiling temp. on horiz. stainless steel and Cu surfaces 8-90692
 ethanol-water-chloroform mixture, light scatt. near plait point 8-72532
 fluid near crit. point, rapid evaluation of multiple scatt. 8-84594
 n-heptane+acetic anhydride, elec. resist. near crit. soln. temp. 8-71874
 n-heptane-nitrobenzene, US study of crit. mixing 8-75732
 liquid-liquid mixtures, critical region fluctuations, centrifuging effects 8-63850
 2,6-lutidine-H₂O, phase separation, hydrodynamic effects 8-83960
 methanol-cyclohexane, mixture, thermal expansion near crit. soln. point 8-71871
 nitrobenzene, solns., elec. permittivity near crit. point 8-76372
 pentane-o-nitrotoluene critical solution, nonlinear dielectric effect 8-55952
 polyethylene oxide, aq. salt soln., meas.-based thermodynamic quantities 8-75525
 solutions with closed loop coexistence curves, directionality depend. of lattice models 8-95158
 steam-inert gas, uncondensable gas content effect on steam condensation heat transfer in vert. tube 8-75041
 triethylamine-H₂O, crit. phenomena, US vel. and absorpt. 8-91382
 water, subcooled, choked expansion and the isentropic homogeneous equilib. model for 2-phase flow 8-91034
 CS₂+acetic anhydride, elec. resist. near crit. soln. temp. 8-71874
³He-⁴He, tricritical normal phase liq., ion mobility 8-79850
²³⁵U, ²³⁵U systems, criticality anal. using KENO and SU-HAMMER codes 8-89949

critical opalescence

- binary mixture in external field, crit. opalescence 8-84595

critical phenomena

- see also *critical fluctuations; critical mixtures; magnetic transitions; phase equilibrium; phase transformations; renormalisation*
 ϵ expansion for critical amplitude ratio 8-65896
 σ model, two dims., nonlinear, three loop calc., minimal subtraction method 8-62289
 asymptotic number of lattice animals in bond and site percolation 8-54310
 bistable system, catastrophe prediction using externally applied force 8-77823
 bond percolation processes in d dimensions 8-70066
 Bose condensate, bounds in dimensions $\nu \geq 3$ 8-54294
 Brownian particle, freq.-depend. friction coeff. in fluid near crit. pt. 8-73929
 cell membrane nuclear hydrodynamic shear, non-equil. Ising model, master eqn. 8-61146
 chemical instabilities, rel. to equilibrium phase transitions 8-65897
 continuous renormalisation transformation, variational calcs., rel. to Potts model 8-93618
 correlation functions in X-Y models and step free energies in roughening models 8-67675
 cylindrical shell deform., effect of loading history on bifurcation (*Ukrainian*) 8-55578
 dual resonance amplitudes, satisfactory invariant measure 8-66093
 dynamic critical phenomena, real-space renormalisation group methods, appl. two-dims. kinetic Ising model 8-77810
 dynamic critical phenomena closed-form differential renormalisation group generator 8-86413
 electronic transport coeff., soln. between Mori-Green-Kubo formulae and Boltzmann approx. 8-79971
 exponent renormalisation, first order transition 8-70085
 field-theory renormalization and critical dynamics above T_c: helium, antiferromagnets, and liquid-gas systems 8-87767
 gases, chem. pot. near crit. density, Thom's catastrophe theory 8-91063
 Gaussian random field, ferromagnets in 4+ ϵ space dims. 8-73954
 Glauber-Ising model, 2-dims., crit. dynamics, real-space renormalisation group theory 8-70070
 Glauber-Ising model, real space-time depend. renormalisation group 8-49774
 graph-like state of matter, electrical cond. of random networks, gelation and elasticity 8-65875
 interline region heat transfer, London-Van der Waals dispersion force effect 8-71276
 Ising ferromagnet, crit. correlation-function approxs. 8-56324
 Ising ferromagnet, rectangular, n-point functions 8-76250
 Ising model, correlation length, renormalisation group calc. (*Russian*) 8-77811
 Ising model, spin-one system, correlation functions with bilinear and biquadratic interactions 8-91876
 Ising models, three-dims., renormalisation group transform. 8-62163
 Ising site model, random mixtures, Monte Carlo simulation 8-73935
 Ising site model, random mixtures, Monte Carlo simulation 8-73936
 Ising system, two-state, crit. behaviour, Bragg-Williams approx. calcs. 8-86223
 Ising system, with lattice anisotropy, two dims., crit. props. 8-73932
 Ising system on triangular lattice, critical dynamics, time dependent real-space renormalisation group 8-60289
 Ising-system, two-state, crit. behaviour, Monte Carlo calcs. 8-86222
 kinetic Ising model of ferromagnetism, simulation of equilib. critical props. 8-89410
 lattice gas model, critical cond., rel. to cond. in superionic conductors 8-93614
 lattice Schwinger model, massive QED for fermions in 1+1 dims. 8-78121
 lattice-lattice scaling, reln. to scaled eqn. of state, appl. to Ising model 8-70067
 Lifshitz point, low-temp. renormalisation group 8-65898
 logarithmic corrections to a simple power law at d=4 in 1/n expansion 8-65895
 neutron star matter at high temp. and density, bulk props. 8-89812
 nonequilibrium critical phenomena, probability density functions, fluctuations 8-54327

critical phenomena continued

- nuclear critical opalescence, precursor to pion condensation 8-62498
 $O(1/n^2)$, critical indices for 3-dimens. system with short range forces 8-49775
 percolation problem, high order behaviour in O^3 field theories 8-65883
 percolation theory, bond problem, critical probabilities, bond clusters 8-86224
 Potts model, appl. of Legendre transformation 8-80156
 Potts model, zero state, in 2+ ϵ dimensions, crit. exponents 8-77809
 Potts model and percolation 8-54312
 pseudocritical phenomena near the spinodal point 8-65894
 quenched critical fluid, time evolution of fluctuation spectrum 8-65893
 random resistor networks, critical behaviour near percolation threshold 8-87956
 random spin system, 1/n expansion 8-62173
 real-space renormalisation group study of crit. dynamics 8-49785
 Reggeon quantum spin model, critical exponents 8-62338
 renormalisation group, scale breaking model 8-49972
 renormalisation group transformations (*Chinese*) 8-95128
 renormalisation theory, variational principles 8-73951
 segregation of two molten polymers of different lengths, critical props. 8-55801
 spin lattice models, continuous-integral method 8-93615
 spin system, isotropic, N-component, with long- and short-range interactions, crit. behaviour 8-76256
 spin-1/2 models, on square lattice, sublattice renormalisation transformations 8-65878
 thermal radiation, critical phenomena for periodically rough water surface (*Russian*) 8-81188
 threshold-phase transition analogy 8-70081
 topological excitations in Abelian Higgs model 8-70275
 transformation methods in anal. of crit. prop. 8-49771
 tricritical behaviour, nonuniversality 8-93640
 two-dimensional quantum systems at zero temp., liquid to gas phase transitions 8-77798
 zero field susceptibility in d=4, n=0 limit, confluent logarithmic singularities 8-54308
⁴He, superfluid, thermo-osmotic convection, at incipient lambda transition, above crit. press. 8-95199
 NH₄Cl, molar heat capacity near order-disorder transform. under high press. 8-51697

critical points

- see also *boiling point; melting point*
 chlorotrifluoromethane, self-diffusion coeff. near crit. temp., density depend. obs. 8-95530
 cubic margules solution model, miscibility gap and crit. point behaviour 8-59925
 elements and refractories with high crit. temp., review 8-59931
 ethane, solid, thermodynamic props. between double solid-to-solid transition and triple point temp. 8-75828
 ethane+CO₂ system, isothermal vapour-liq. equilibrium data, 10 to 25°C and high press., critical points 8-79754
 fluid near crit. point, rapid evaluation of multiple scatt. 8-84594
 HMTTF-TCNQ chain, three dimensional ordering critical temp. 8-95152
 hydrodynamics of fluid near critical points 8-59361
 Ising ferromagnet, 2-D, with quenched bond disorder, critical temp. 8-56328
 Lennard-Jones (100) crystal-liquid interface, structure 8-91284
 Lennard-Jones system, molecular dynamics simulation of interfacial and co-existence props. at triple point 8-83916
 Lifshitz point, critical exponents, ϵ -expansion 8-65899
 magnetic disordered system, critical phenomena 8-52269
 metastable states near tricritical point (*Russian*) 8-63841
 methane, effects of impurities and annealing on triple point 8-83919
 mixtures, analogy with pure fluids 8-67819
 nitrobenzene:n-hexane, depolarised Rayleigh scatt., crit. anomalies 8-68524
 nonequilibrium phase transition, dynamical features (*Chinese*) 8-83030
 organic compounds, crit. temps. correl. with boiling pts. 8-91421
 planar rotator model, one-hypercube renormalisation group transform. 8-72353
 polymer, flexible chain collapse 8-87628
 polymer mixtures, molten, interface props. near consolute point 8-87792
 polymer solution, semidilute, chain size 8-87607
 reference standards for radiation pyrometry, silver and copper freezing points 8-57888
 rigid-rod fluid, thermodynamic props., crit. points and transitions 8-73919
 tricritical phenomena, ternary, quaternary fluid mixtures, classical models 8-91416
 triple points cells, Ar, O₂, comparison 8-73996
 triple points of Kr, Ar, N₂, Ne, reference temperature appl. 8-73997
 Yang-Lee edge singularity and ϕ^3 field theory 8-65882
 Ar, triple point, depolarized Rayleigh scattering from fluids of spherical molecules 8-88319
 Ba₂TiGe₂O₈-Ba₂TiSi₂O₈, pseudobinary system, pyroelectricity and related props. 8-95553
 CO₂, thermal diffusivity and cond. in crit. region meas. by holographic interferometry (*German*) 8-59942
 Fe-H system, influence of H press. on Fe crit. points and H solubility 8-52758
 FeCl₂, magnetic phase diagram, optical studies 8-88121
 GeH₄, Lorenz-Lorentz coeff., refr. index, crit. const. and density depend. 8-92041
 Hg, liq.-vap. interface, density profile near triple point, X-ray refl. 8-75821
 Mo, liq., exptl. determ. of crit. data 8-75531
 NH₄Cl, order parameter, electro-optic measurement 8-88280
 NH₄Cl, order-disorder phase transition, type of multicritical point, nonlinear quadratic susceptibility 8-83947
 Ne, vapour press. and triple point, influence of impurities 8-79756
 PbZr_xTi_{1-x}O₃ solid solutions, tricritical behaviour 8-80296

critical temperature, superconducting see *superconducting transition temperature*

CRO see *cathode-ray oscilloscopes*

crocidolite *see asbestos*

cross-sections (nuclear) *see nuclear reactions and scattering*

crosstalk
bidirectional optical fibre, crosstalk, review 8-66901
optical fibre 8-50923
optical fibre link, end-to-end cross coupling loss meas. 8-90502

crowdions
Ag, TEM exam. of ion damage in FCC metals 8-87727
Au, TEM exam. of ion damage in FCC metals 8-87727
Cu, TEM exam. of ion damage in FCC metals 8-87727
Ni, pure and doped, mech., mag. relax. meas. dumb-bell self-interstitial reorientation (*German*) 8-52879
Ni, TEM exam. of ion damage in FCC metals 8-87727
Pt, TEM exam. of ion damage in FCC metals 8-87727
W, split crowdion interstitial, (111), computer simulation of TEM imaging 8-71723

CRT *see cathode-ray tubes*

crushing
particles, small, impossibility of comminution by compression 8-52709
U ore, ²²²Rn release 8-89970

crushing strength *see compressive strength*

cryogenic pumps *see cryopumping*

cryogenics
see also cryopumping; cryoscopy; cryostats; cryotrons; Joule-Thomson effect; low-temperature production; low-temperature techniques; magnetic cooling; refrigeration
biological material, prep. for X-ray microanal. of diffusible elements, methods of drying ultrathin cryosections 8-77166
biological material prep. for X-ray microanal. of diffusible elements, rapid freezing and ultrathin section prep. 8-77165
boiling of cryogenic liquids, crit. heat flux, heating surface props. effects 8-90662
closed cycle refrigerator, low power, SQUID's appl. 8-77921
construction material magnetisation meas. (*Slovak*) 8-93693
contact heat transfer between heat-liberating element and surface of subliming solid cryoagent 8-81987
density reference system for cryogenic fluids 8-54344
energy technology relationship 8-88053
epoxy resin, low temp. irradiation effects on mechanical props., use in superconducting magnets 8-60737
flange joint design and characteristics 8-86277
force cooled superconductor cryostability expt. 8-50378
fusion reactor toroidal field coil thermal design and anal. 8-50368
heat influx through electrical cable, calc. 8-81988
heat pipe, cryogenic, gas-controlled performance anal. 8-75034
heat pipe, internal heat transfer visualisation 8-94533
heat pipe/radiator dynamic testing 8-94532
laminar-vacuum insulation, nonstationary heat and mass transfer 8-59279
laminar-vacuum insulation, nonstationary heat and mass transfer 8-59280
laser fusion targets, fabrication 8-58485
laser fusion targets, fabrication and characterisation 8-58484
laser fusion targets, irradiation systems 8-58486
liquid methane density meas. at cryogenic temp., commercial densimeters eval. 8-54343
nuclear cryogenically pumped gas target for γ -ray ang. distrib. meas. 8-55076
polymeric cryoprotectants in preservation of biological ultrastruct., aq. soln. low temp. states 8-65157
polymeric cryoprotectants in preservation of biological ultrastructure, physiological effects 8-65158
polymeric cryoprotectants in preservation of biological ultrastructure, morphological aspects 8-65159
radioactive waste, gaseous, cryogenic rectification system for ⁸⁵Kr and ¹³³Xe removal 8-50268
review, of low temp. physics and technology 8-89485
review of investigations near absolute zero early investigation to present day discoveries 8-69958
Santleben-Beenakker thermal conductivity effect apparatus 8-81989
space research appls., 1 mK to 10K temp. range, survey 8-93712
superconducting magnets, cooling system using liquid He 8-54998
superconducting magnets, force-cooled conductors design 8-54999
superconducting magnets, hollow conductors, cooled by supercritical He 8-54997
superconducting magnets cryostabilisation using superfluid He 8-54996
supercritical liquid air storage plant for elec. energy 8-74006
target, cryogenic, produced for laser-driven fusion, frozen H₂ 8-86688
temperature cycling apparatus using liquid He storage Dewar 8-65938
TFT, neutral beam line cryopanel, cryogenic supply systems 8-55027
triple point cells, Ar, O₂, comparison 8-73996
triple points of Kr, Ar, N₂, Ne, reference temperature appl. 8-73997
two-stage solid cryogen cooler development, orbital operation, IR radiometer for spacecraft appl. 8-89040
Cu, high-cond., high spt. ht., for cryogenic appl., prep. 8-76670
He cryogenic discharge, current oscills. 8-67463
He leak detection in large cryogenic vessels 8-93694
He, liq., narrow channel flow and heat transfer characts., void fraction in steady and transient states 8-55000
He, thermally induced oscills. in cryogenic apparatus 8-67875
N₂-He mixture, film condensation, appls. to condensers for cryogenic installations 8-59941

cryopumping
balloon borne mass spectrometer, liquid He cryopump and opening device 8-77370
deposition system using liq. He cooled cryopumping panel 8-56581
freeze-drying technique for prep. biological tissue for electron microscopy 8-65164
fusion reactor, cryosorption pumping, D₂-He (5 at.%), on mol. sieve, 5A, 4.2K 8-74499
fusion reactor and injector devices, large cryopumps 8-50399
fusion reactor high power neutral injector cryopumps, design and performance 8-74494
ion pump-cryopump system, performance 8-70142
liquid He cryopump, for fusion machines, degassing 8-54382
liquid He cryopumps for PLT neutral beam injectors 8-58439

cryopumping continued
neutral beam injection system cryopump, liq. He-cooled, for fusion reactor H₂ pumping 8-74495
neutral beam injection vac. components, for fusion reactor 8-74493
neutral beam line injectors, cryopumping system, for Tokamak Fusion Test Reactors 8-55028
ultrahigh vacuum pumps 8-89488
D, cryosorption pumping, 6 to 20K, fusion reactor appl. 8-70626
I₂, cryocondensation pumping, smooth surface at 4.2K, fusion reactor application 8-74492

cryoscopes *see cryoscopy*

cryoscopy
No entries

cryosorption *see sorption*

cryostats
adiabatic demagnetisation of nucl. spins, refrigeration 8-49844
continuous flow helium cryostat for optical studies at fixed high pressure 8-81984
with continuous He flux, for optical investigations, construction 8-74008
device for obtaining temperatures of 4.2-300K with considerable heat flow into specimen 8-77922
EPR spectroscopy in strong elec. fields at 77 and 4.2K 8-86310
fibreglass insert to liquid He Dewar 8-57967
gas high pressure cell for optical studies at low temp. and hydrostatic pressure 8-82016
glass He cryostat for optical and magneto-optical investigations 8-74007
glass helium cryostat for optical and magneto-optical studies 8-81981
matrix isolation apparatus for magneto-optical obs. 8-82057
normal boiling point determination for Ne 8-79757
reentrant Dewar, modified, for magneto-optical flux detection in superconductors 8-89486
silica windows in liquid He cryostat, unwanted birefringence 8-66926
small flow-through cryostat for polarization microscope 8-86327
temperature field inhomogeneity in cooled screen, effect on efficiency 8-62204
thermal conductivity measurement, of plastically deformed specimens at liq. He temps. 8-81985
thermal load by radiation from the neck (*German*) 8-86276
vapour pumping system, for obtaining temps. of 4.2 to 300K 8-81980
He cryostat modification for asymm. Michelson interferometer 8-74053
He immersion and gas-flow optical cryostat system 8-77923
³He liquid target for scatt. expts. 8-70663
⁴He, isotopically pure, apparatus for preparation 8-57959

cryotrons
No entries

crystal atomic structure
see also crystal atomic structure of alloys; crystal atomic structure of elements; crystal atomic structure of inorganic compounds; crystal atomic structure of organic compounds; electron diffraction crystallography; lattice constants; neutron diffraction crystallography; space groups; superlattices; X-ray crystallography
binary crystals, stability and average structure factors 8-91297
electron density maps, extrapolative filtering, resolution maximisation 8-75506
homogeneous linear structures, systemisation according to charact. numbers of position symbols 8-95009
noncentrosymmetric structures, correlation between third cumulants in refinement 8-91288
point groups, symmetry, teaching aid 8-77650
quasisymmetry (P-symmetry) groups in crystallography, semidirect products method 8-51457
space groups, triclinic, cryst. struct. refinement by least squares 8-75607
structure factor moduli, estimates from negative intensity obs. 8-75486
structure semiinvariants, extension concept, role in probabilistic theory 8-75608
symmetry adaptation, operator equivalence, mag. reson., operator equivalent formalism (*French*) 8-84374
unit cell, determinantal eqns. for scale factor, temp. factors, quantitative chem. contents 8-75609

crystal atomic structure of alloys
inhomogeneous binary alloys, X-ray diffr. profile calc. 8-67609
intermetallic phases with L1₂ and D0₁₉ struct., atom incompressibility, lattice parameter approach 8-91294
Kh20N40 alloys, phase composition after quenching, tempering 8-60650
martensite crystal, struct. X-ray diffr. study 8-79565
nonstoichiometric solid solutions, ordering 8-87794
rare earth alloys, RFe₄Al₈, cryst. struct. mag. props. and hyperfine interactions 8-87648
rare earth intermetallics, RMg₂, cryst. and mag. props., ordering 8-68185
rare earth intermetallics, RMn₂Si₂ and RMn₂Ge₂ 8-59782
rare earth ternary alloys with Fe or Co and Si or Ge, ThCu₂Si₂ type 8-51469
rare earth trialuminides, long period polytypes, electron diffr., high resolution imaging 8-83781
steel, thermodynamic props. of C in austenite, relationship with cryst. lattice anomalies of martensite (*Russian*) 8-59781
transition metal alloy, ground state properties, self-consistent calc. 8-91587
transition metal alloys, BCC crystal struct. dependence on band struct. 8-83778
transition metal-group IIIB alloys, relationship between struct. and thermodynamic props. (*German*) 8-91307
Ag-Nd (*German*) 8-51472
Ag-Pr (*German*) 8-51472
Al-Ag alloy, second ageing stage, diffuse electron and X-ray scatt. (*Russian*) 8-68711
Au-Ge (27 at.%), metastable phase struct. determ. by electron diffr. 8-83780
Au-Mg (18 at.%) alloy, superstruct. determ., electron microscope obs. 8-75630
Au-Mn alloys, equiatomic region of phase diagrams crystallographic and mag. exam. 8-52755

crystal atomic structure of alloys continued

- Au-Mn system, AAB₂ struct., experimental evidence for occurrence 8-63698
- Au₁₁Mn₄, ordering, electron diffr. and high resolution TEM obs. 8-71707
- Au₂Mn₂, electron microscope exam. of ordering 8-63697
- Au(Pd)-Zn, martensitic transformation, Hall coeff., specific elec. resistivity and X-ray powder diffraction 8-72774
- AuSn₄-Sn, unidirectionally solidified, X-ray diffr. anal. of crystal struct. 8-91308
- BaNiSn₃, cryst. struct. rel. to ThCr₂Si₂ type (*German*) 8-51470
- BaPtSn₃, cryst. struct. rel. to ThCr₂Si₂ type (*German*) 8-51470
- CeMn₂Si₂, cryst. and mag. struct. determ. 8-52225
- CeRh₃-Pd, electronic and cryst. struct. comparison, catalytic behaviour 8-84398
- Co₂Ga_{2-x}Cu_x, mag. and struct. phases from magnetisation, neutron, X-ray diffr. techniques 8-52253
- Co₂Ga_{2-x}Ni_x, mag. and struct. phases from magnetisation, neutron, X-ray diffr. techniques 8-52253
- α -Cu-Al, short range ordered, struct. and new superlattice phase 8-52756
- α -Cu-Al alloy, short range order structure 8-91303
- Cu-Be alloy, X-ray diffr. pattern singularities (*Russian*) 8-67682
- γ -CuAl₄, struct. refining from diffr. meas. 8-55834
- η -Cu₃Si precipitates in Si, cryst. struct. 8-91304
- Cu₃Sn, one-dimens. long period superstructs. with Zn and Ni additions 8-83777
- CuSnMg, crystal struct. anal. 8-91306
- Cu₃SnMg, crystal struct. anal. 8-91306
- (ErCo₂)₂(ErAl₂)_{2-x}, mag. and struct. investigations of intermetallic systems 8-95440
- Eu₂As₃, cryst. struct. of high and low temp. phases 8-75626
- Fe-Al eutectic alloy, duplex crystals, unit cell parameters, appl. of Weissenberg technique 8-67684
- Fe-Mn, effect of N on cryst. lattice parameter of austenite (*Russian*) 8-67683
- Fe-Mn-As, crystal struct. and magnetic props. of intermetallic cmpds. with Cu₂Sb type struct. (*Japanese*) 8-59785
- Fe-Ni, taenite, superstruct. in Fe meteorites 8-61820
- FeSb₂, phase structure, X-ray crystallography (*French*) 8-91305
- Fe_{1-x}Sb_x, phase structure, X-ray crystallography (*French*) 8-91305
- (GdMn₂)₂(GdAl₂)_{2-x}, mag. and struct. investigations of intermetallic systems 8-95440
- Hf-Co-Ga system, crystal atomic struct. and phase equilibria (*Ukrainian*) 8-84772
- Hf_{1-x}Zr_xV₂, lattice const. at 4K and room temp., phase division at $x=0.4$ 8-51474
- Hg-Tl, metastable system, prep. by quenching, phase struct. 8-52762
- Li₂Ag_{2-x}In_x, optical props., struct., energy bands, interband transitions 8-72539
- Li₂Cd_{2-x}In_x, optical props., struct., energy bands, interband transitions 8-72539
- LiIr, struct. and props. exam. 8-92245
- Mn-Ga, DO₂₂ type alloys, magnetic props., crystal struct. (*Japanese*) 8-59784
- Mn-H(D), ferromag., thermal, struct. mag. props. 8-88145
- Mo-ZrC, internal oxidation, struct. formation law, microstruct. examination 8-84836
- Nb-Ga-Fe, phase equilib. at 1000°C, cryst. data for intermediate phases 8-52763
- Nb₃Si, high press. phase, prod. by recryst. of metastable sputter deposits, struct. and supercond. props. 8-60571
- Nb₃Sn, X-ray study of fission fragment induced structural damage 8-51589
- Ni-base cost multicomponent alloy, γ' , carbide, boride phases, quantities, composition (*Russian*) 8-75627
- Ni-Cr-Ti-Al-Mo-Nb-Fe (13-16, 2.35-2.75, 1.3-1.7, 2.8-3.2, 1.8-2.2, 2.0 wt%), heat resistant props, mech. props. struct., stepwise ageing effects (*Russian*) 8-76666
- Ni₃Sb₂, cryst. struct. (*German*) 8-83775
- Pb-Sb, crystal struct., supercond. after subjection to high press. 8-88064
- Pd-Ag-Au, temp. effect on lattice parameters and thermal expansion 8-51473
- Pd-Zn system, phase characterisation (*German*) 8-60654
- Pd₂Se₄, cryst. struct. determ. (*German*) 8-75628
- Pd₂Te₄, cryst. struct. and binding (*German*) 8-51471
- Pr-Cu-Al system, X-ray and microscopic anal. (*Ukrainian*) 8-84774
- Pt₁₃In₉, exam. of crystal structure, and phase diagrams (*German*) 8-83779
- PtPb₂Bi (*German*) 8-59783
- Pu-Pt(Rh)(Pt-Rh), exam. of phases and crystal structure 8-80518
- Pu₂Pt, cryst. struct. determ. 8-79564
- Sm₁₁Cd₄₅, cryst. struct. similarity with γ -brass and α -Mn clusters 8-75625
- Sm₂Co₂, mag. and struct. investigations of intermetallic systems 8-95440
- SnNiSn₃, cryst. struct. rel. to ThCr₂Si₂ type (*German*) 8-51470
- TbCo₂, X-ray obs. of low temp. modifications of crystal struct. (*Russian*) 8-75632
- TbFe₂, X-ray obs. of low temp. modifications of crystal struct. (*Russian*) 8-75632
- α , α + β Ti alloys, structural instability during prolonged periods of heating (*Russian*) 8-56664
- Ti-Mo(Nb)(Ta), BCC struct., tetragonal phase form. by cold deform. (*Russian*) 8-88462
- Ti-Nb-Mo(V)(Ta)(Al)(Zr), BCC struct., tetragonal phase form. by cold deform. (*Russian*) 8-88462
- Ti₃Ga, lattice period and crystallographic struct., temp. depend. (*Russian*) 8-55835
- U₄(Re_{0.17}Si_{0.83})₁₃, X-ray diffraction anal. of crystal struct. (*Ukrainian*) 8-83773
- U₄Re₂Si₆, X-ray diffraction anal. of crystal struct. (*Ukrainian*) 8-83773
- U₃Si, X-ray diffr. exam. 8-75629
- V-Rh alloys, short range atomic order exam. (*Russian*) 8-63696
- V₂Si, electron charge distrib., martensitically transforming single cryst., X-ray diffr. meas. 8-75631
- Zr-Os quenched alloys, metastable phases (*Ukrainian*) 8-84804
- ZrCoSi, crystal struct. (*Ukrainian*) 8-83774
- ZrRh_{3-x}Pd_x, electronic and cryst. struct. comparison 8-84398

crystal atomic structure of elements

- actinides, struct. props. rel. to F electrons 8-83951
- diamond, Compton profiles, X-ray struct. factors, band struct., LCAO calc. 8-51889
- rare earths, struct. props. rel. to F electrons 8-83951
- transition metal clusters, cohesive energy and level statistics 8-95267
- B, α , and β -rhombohedral, struct. changes on Zn incorporation 8-79596
- (C)_n, cryst. struct. determ. from X-ray photoelectron and X-ray spectra 8-88384
- CF, X-ray diffr., high press. effect 8-83766
- Cd, single cryst., root-mean-square atom displacement, X-ray meas. 8-75624
- Ce, α - α' high press. transition, volumetric study 8-83940
- Cr, crystal structure below Neel temp., X-ray diffr. study 8-83772
- Dy, crystal structure, P-T phase diagram 8-84776
- Gd, crystal structure, P-T phase diagram 8-84776
- Ge (111) surface, annealed, atomic structure 8-75916
- I, metallic solid, high press. struct., phase transition, X-ray diffr. study 8-87647
- β -Mn, struct., polyhedron model 8-79563
- Nd, crystal structure, P-T phase diagram 8-84776
- α -S, monoclinic allotrope, thermal behaviour 8-67813
- β -S, X-ray powder diffr. pattern at -150, -75, 100°C 8-95015
- α -Se, monoclinic allotrope, thermal behaviour 8-67813
- Sm, crystal structure, P-T phase diagram 8-84776
- U, field emission microscopy, emissive props. 8-88409
- V, single cryst., (110) scatt. factor, absolute meas. 8-71706

crystal atomic structure of inorganic compounds

- alkali bromide-VBr₂ systems, cryst. struct., DTA investig. (*German*) 8-72766
- alkali hydrides, bulk props. prediction from molecular behaviour 8-51468
- alkaline earth halides, thermodynamic and structural props., computer simulation 8-75849
- barium mordenite, dehydrated, position of cations and molecules, electron probe anal. 8-51509
- carbonate mineral, (Si, Cl)-bearing, from limestone-granite contact zone, X-ray powder diffr. pattern (*French*) 8-69339
- chevkinite from Oslo region, Norway, cryst. struct. and chemical comp. 8-85533
- chlorite, cryst. struct. and compressibility at high press. 8-63717
- 1,5-diazo-3,7-dithiabicyclo (3,3,1) nonane, molecular and cryst. struct. 8-51528
- dickite occurrence in Jamaica, ordered and disordered varieties 8-83786
- garnets, cation-anion distances, Poix formula 8-67701
- graphite intercalation compounds, props. and appls. 8-71711
- halide compounds ABX₃ with perovskite struct., cryst. chem., X-ray diffr. anal. 8-95042
- humite, real struct., mixed layer characts. 8-79567
- metal-rich compounds, struct. and props. 8-95045
- mixed oxides, cryst. struct., electron microscopy study 8-91310
- molybdates (double), of mono- and tri-valent metals, polymorphism, X-ray diffr. obs. 8-87642
- MX₄ molecules, distortion from T_d symm. appl. to PO₄, SO₄, AlCl₄ 8-63706
- MX₄ molecules, distortion from T_d symm. kernel, co-kernel and averaged configs. 8-63705
- neutron, construction, appl. to cation distrib. determ. in nonstoichiometric MnZn ferrite (*Bulgarian*) 8-83656
- orthopyroxene from lunar anorthosite 15415, crystal structure and thermal history 8-53842
- oxides, superstruct. based on fluorite lattice, conc. wave method 8-51393
- paragonite, 2M₁, cryst. struct. refinement by HV electron diffr. 8-67696
- paragonite, 3T, cryst. struct., oblique texture electron diffr. 8-67697
- perovskite-like oxides, high-pressure series, rel. between structure and physical properties 8-51493
- perovskites with space group I4/mcm, determ. by cryst. struct. 8-75643
- perrierite from Oslo region, Norway, cryst. struct. and chemical comp. 8-85533
- phlogopite, cryst. struct. and compressibility at high press. 8-63717
- polysilicic acid, IR spectra, struct., crystallisation effects (*Russian*) 8-72528
- rare earth compounds, R₂MoO₅, preparation, exam. of higher oxygen pressure limit, mag. susceptibility (*French*) 8-76618
- rare earth compounds, RThNbTiO₈, synthesis and cryst. struct. (*French*) 8-83799
- rare earth sulphides, R₂S₃-In₂S₃, intermediate combinations, description of crystal types (*French*) 8-75648
- rare earth-transition metal pnictides of ThCr₂Si₂ type 8-51502
- ruby, single cryst. struct. determ. for press. up to 90 kbar 8-83875
- stishovite (SiO₂), single cryst. anal. of struct. 8-53648
- struct. and props. exam. 8-92245
- structural diagram of compounds ABO₄ 8-79548
- synthesis, structs. (*French*) 8-51519
- taenite lamellae in Fe meteorite, Mossbauer study 8-65575
- tetraferriphlogopite, cryst. struct. refinement using least squares approx. 8-79594
- tetratitanates, M₂Ti₄O₉ (M=Li, Na, K, Rb, Cs, Tl, Ag), preparation, cryst. struct. determ. 8-75646
- tienshanite, X-ray determ. 8-83800
- titanomagnetite, synthetic, cation distrib. 8-55856
- transition metal, polynary oxocompounds, struct. data, book 8-51521
- transition metal dicalcogenides, deform. modulated superstruct., model explaining results for VSe₂ 8-51515
- transition metal dioxides, elec. struct. props., two-band model calcs. 8-67934
- TTT-(I₃)_{0.5}, one-dimens. metal, mag. susceptibility, elec. resist., thermopower meas. 8-87967
- tungstates (double), of mono- and tri-valent metals, polymorphism, X-ray diffr. obs. 8-87642
- zeolite, synthetic, ZSM-11, synthesis and struct. 8-87657
- ABCl₃ cpds., basic struct. types and polymorphisms 8-79583
- AgI, structural model for superionic conduction 8-79797
- AgI type solid electrolytes, expt. props. 8-63877

crystal atomic structure of inorganic compounds continued

- AgNO₃, struct. at room temp. and press., perfect cryst. (French) 8-55846
 Ag₃Nb₂O₇F₂, cryst. struct. determ. from single cryst. diff. data (French) 8-95030
 Ag₃P₂Se₆ (French) 8-63703
 α-Ag₂S, structure, comment on coherent scattering intensity 8-95027
 Ag₂SI, superionic conductor, ordered phase struct. 8-83792
 Al₂Nb₂O₇, new phase of mixed oxide 8-59787
 β-Al₂O₃ phases, synthesized, effect of starting Al₂O₃ composition and halogen ion additions, on structural state 8-76620
 Al(OH)₃, unit cell, determinantal eqns. for scale factor, temp. factors, quantitative chem. contents 8-75609
 Al₂(OH)₄(SO₄)₇·7H₂O, aluminite, cryst. struct. determ. and refined 8-83782
 AlO₂N₂ spinel, crystal struct. model 8-91333
 γ-AlOOD, boehmite, hydrogen bond, neutron profile refinement of struct. 8-71701
 AuTeI 8-51504
 B hydrides and related cpds., cryst. struct., secondary and multi-centre bonding 8-63751
 B-Zn solid soln., struct. changes on Zn incorporation into α- and β-rhombohedral B 8-79596
 B₁₀H₁₄, cryst. struct. (Czech) 8-87649
 B₂O₃, cryst. struct. determ., continuous random network approach 8-67693
 BaBrF, struct. at. struct. by X-ray diff. 8-75641
 BaCl₂·2H₂O, cryst. struct. determ. by neutron diff. 8-75639
 Ba₂Fe₂BO₆, (B=Re, Te, W, Mo), siegnette magnets with hexagonal barium titanate structure 8-76397
 β-Ba₂Fe₂Si₅, and low temp. α polymorph., cryst. struct. 8-67690
 Ba₂FeSbO₆, siegnette magnets with hexagonal barium titanate structure 8-76397
 Ba(H₂PO₄)₂, triclinic, cryst. struct. (French) 8-55848
 BaKPO₃·H₂O (French) 8-51480
 BaO, at. charge densities, X-ray struct. factors 8-79566
 BaSO₄, barite, crystal struct. and sulphate force consts. 8-83784
 Ba₂Sb₂NiO₉, 6H, cation ordering, powder neutron diff. obs. 8-55852
 Ba_{0.2}Sr_{0.75}Nb₂O₆, quadratic susceptibility dispersion meas., oscillator model including structure 8-59078
 Ba_{1-x}Sr_xNiO_{3-y}, Sr substitution effect, powder X-ray diff. 8-51498
 Ba₂X₃, α, intermediate phases, cryst. struct. (X=IIb, IIIb, IVb, Vb element) 8-83793
 α-BaZrF₆ with [Zr₂F₁₂]⁴⁻ complex (French) 8-51477
 BiOI-2Bi₂O₃, prep., cryst. struct. (French) 8-53205
 Bi₂Sn₂O₇, prep., stability, and crystallographic exam. (French) 8-51510
 BiTiNbO₆, cryst. struct. determ. (German) 8-79570
 CEr₂S₄, spinel, crystal struct. (French) 8-91326
 CaAl₂Si₂O₈, anorthite, quenched from 1530°C 8-63700
 Ca₃Al₂Si₂O₁₂, grossular-, cryst. struct. and compressibility to 60 kbar 8-63718
 Ca₂(B₂O₃)Cl₂·H₂O, triclinic chilgardite, cryst. struct. determ. 8-63737
 CaBr₂·4CH₃OH, cryst. struct. determ. (French) 8-59788
 CaBr₂·4C₂H₅OH, cryst. struct. determ. (French) 8-59788
 CaCO₃, thermal decomp. in vacuo, ultrastruct. and crystallography 8-71864
 Ca_{1-x}Eu_xSi₂, solid solns., α-ThSi₂ struct. type, comp. and press depend. 8-91322
 CaF₂·(Y,R)F₃ (R=any lanthanide except Pm, Eu), phase diagrams 8-84783
 CaF₂·H₂, solid soln. prep. and struct. determ. (French) 8-51505
 Ca₂HPO₄SO₄·4H₂O, synthetic, cryst. struct. and relation to brushite and gypsum 8-83785
 CaO, at. charge densities, X-ray struct. factors 8-79566
 5CaO·3Al₂O₃, cryst. struct. determ. 8-55840
 β-(CaO₂)·SiO₂·H₂O, SEM and X-ray diff. exam. of structure, crystallisation props. 8-73012
 Ca₃(PO₄)₂, new cryst. phase prep. and struct. (French) 8-83789
 Ca₃(PO₄)₂Cl, structural interaction of Cl 8-55837
 Ca₃(PO₄)₂F, structural interaction of F 8-55837
 Ca₃(PO₄)₂OH, structural interaction of OH 8-55837
 Ca_{1-x}Re_xO₆(OH)_{2x} (x=0,3), high pressure synthesis and structure (French) 8-51511
 Ca₂Sc₂Si₃(Ge₃)O₁₂, garnets, refined cryst. struct. 8-87654
 Ca₂(Si₂Al₂)₁₂(O,N)₁₆, α'-Sialon ceramics, prep. and characterisation 8-84750
 Ca₂SiO₃Cl₂ 8-67694
 Ca_{1-x}Sr_xSi₂, solid solns., α-ThSi₂ struct. type, comp. and press depend. 8-91322
 CaTiO₃-Ca₂Fe₂O₃, Mossbauer resonance exam. of structure, phase equilibrium 8-76640
 Ca₂X₃, α, intermediate phases, cryst. struct. (X=IIb, IIIb, IVb, Vb element) 8-83793
 CaZn(SiO₄)₂·H₂O, clinohedrite, cryst. struct., H bonds 8-79593
 Ca₂[(UO₂)₃(PO₄)₂(OH)₂](OH)₂·4H₂O, phurcalite, cryst. struct. determ. 8-55849
 Cd complex, [Cd(SC(CH₃)₂CH₂NH₂)₂CdCl₂]₂·2H₂O cryst. and mol. struct. 8-74787
 Cd-Sb system, phase diagram, struct. and stability of phases (German) 8-60661
 CdCr₂Se₄, spinel film, struct. SEM study, props. 8-79905
 CdI₂ polytypes, crystal structure analysis, refinements for structure determination 8-91312
 CdI₂ polytypes, crystal structures using new refinements for structure determination 8-91313
 Cd₂Nb_{2-2x}Sn_{2x}O_{7-2x}F_{2x}, solid soln., X-ray diff. and Mossbauer study (French) 8-87659
 CdNd₄(SiO₄)₃O, synthesis, cryst. struct. 8-87653
 CdP₂, high press. phase relns. and cryst. struct. 8-59792
 CdS(PO₄)₃OH, single crystals, X-ray struct. anal. 8-95019
 Cd₃Se₂Ge₂O₁₂, garnet, refined cryst. struct. 8-87654
 CdSiP₂, bond strengths and bond lengths, thermal expansion coeff. meas. 8-87651
 Cd₂SnO₄, film, spinel struct., X-ray diff. study 8-75644
 CdTh(MoO₄)₃, struct., DTA and X-ray diff. obs. (French) 8-95024
 CdTh(WO₄)₃, struct., DTA and X-ray diff. obs. (French) 8-95024
 Ce(CO₃)₂, in Na and guanidinium salts, struct./props. correlation (French) 8-95032
 Ce₆(MoO₄)₃(Mo₂O₇), X-ray examination crystal struct. 8-67687
 Ce₆Ni₆P₁₇, synthesis and cryst. struct. 8-75634

crystal atomic structure of inorganic compounds continued

- CFI₂ and CFI₃, cryst. struct. determ., X-ray diff., optical spectra 8-75645
 ClO₂F, cryst. struct., X-ray and neutron diff., Raman spectra (French) 8-83788
 Co complex, bis(N-β-naphthyl-salicylaldiminato) Co (II), space group, lattice consts., X-ray diff. obs. 8-51496
 Co complex, bis(N-p-tolyl-salicylaldiminato) Co (II), space group, lattice consts., X-ray diff. obs. 8-51496
 Co complex, bisdimethylglyoxime (thiosemicarbazide)-cobalt (III) nitrate, mol. and cryst. struct. of dihydrate 8-83803
 CoAl₂O₄, cation distribution, Mossbauer and X-ray diff. obs. 8-95532
 CoAl₂O₄, electron density distrib. 8-51481
 CoCl₂·6H₂O, albritonite, new mineral from Llano County, Texas 8-65286
 CoK₄(P₂O₉)₂·7H₂O, cryst. data (French) 8-79568
 Co_{3-x}Ni_xO₄, 0≤x≤1.1, struct., semicond.-semimetal transition, Seebeck coeff. 8-87972
 CrBr₄, CrCl₄, Raman spectra, struct. and thermodynamic functions 8-60443
 Cr(NH₃)₃ONOC₂, cryst. struct. determ. at 245K 8-75637
 CrS_{1-x}Se_x, antiferromag. props., struct., variations near Neel temp. 8-64199
 CrThS(Se)₃, synthesis, cryst. characts. (French) 8-51517
 Cr_{12-x}W_xP₇, solid solns., prep., cryst. struct. (French) 8-63723
 CsAg₃Se₂, crystal struct., X-ray study (German) 8-83795
 CsAu, semicond. and metallic, NMR line shape, Knight shift, X-ray diff. study 8-68402
 CsCdCl₃, phase transition under pressure 8-51664
 CsCrCl₃, co-operative Jahn-Teller distorted struct. determ. 8-63713
 CsFeCrF₆, CsFeVF₆, crystal struct., Mossbauer hyperfine spectra 8-52381
 CsH₂PO₄, cryst. struct., neutron-diffraction study 8-79592
 Cs₂LiCr(CN)₆, room temp. struct., phase transitions 8-51491
 Cs₂NaAlF₆, cryst. struct. determ. 8-95036
 Cs₂O, low temp. phase study, crystallographic domains and unit cell dimens. 8-63728
 CsPbCl₃, phase transition under pressure 8-51664
 Cs₁₀Ta₂₀O₇₈, cationic exchanger with crossed tunnel struct., cryst. struct. (French) 8-83797
 Cs₂[Pt(CN)₄](FHF)_{0.39}, cryst. struct., X-ray diff. meas. 8-59789
 Cu complex, with Schiff base of o-aminobenzaldehyde and S-methylthiocarbamate, cryst. struct. 8-95040
 Cu_{1-x}Fe_{2x+3}O₄, cation distrib. and valence state 8-63732
 γ-Cu(IO₃)₂, cryst. struct. and mag. behaviour 8-79571
 Cu₄(PO₄)₂O (French) 8-55854
 Cu₄(PO₄)₂O, X-ray obs. 8-55855
 CuSO₄·3CO(NH₂)₂, X-ray determ. of electron density distrib. 8-67699
 CuTa₂O₆ (French) 8-51497
 CuTeO₄, cryst. struct. determ. 8-55845
 γ-DBa(PO₃)₂, polyphosphate, crystal structure determination (French) 8-91314
 Eu₅As₄, cryst. struct. determ., symmetrical version of Sm₅Ge₄-type struct. 8-63710
 EuB₆-C₂, magnetic and elec. props. 8-91842
 Eu_{1-x}Sr_xSi₂, solid solns., α-ThSi₂ struct. type, comp. and press depend. 8-91322
 FeCl₂-graphite, intercalation compound, formation by reduction of Fe(III) compounds with Fe(CO)₅ 8-63721
 Fe₂Cu_{1-x}Rh_xS₄, mag. tetrahedral intrasublattice interaction, X-ray, magnetisation and Mossbauer expts. 8-52212
 FeIn₂S₄, indite, thiospinel, cation ordering in tetrahedral sites, X-ray diff. meas. 8-95028
 FeMnGaO₄, X-ray study of cryst. struct. and ionic config. 8-55851
 Fe₂O₃-TiO₂ system, high temp. intergrowth struct., metal atom ordering in intergrowth boundaries 8-79573
 Fe₃O₄, magnetite, electronic struct. at low temps., NMR anal. 8-67686
 FeOCl intercalation cpds. with Li and amines, cryst. struct. 8-51512
 FeOOH, high-pressure phase, neutron diffraction study 8-52212
 FeS, zinc blende type, crystallographic and Mossbauer obs. 8-87650
 FeS₂ (pyrite), glide elements study by electron microscopy and electron diff. 8-83817
 FeTh₂S(Se)₃, synthesis, cryst. characts. (French) 8-51517
 FeThSe₃, synthesis, cryst. characts. (French) 8-51517
 Ga₂Nb₂O₇, and Ga₂Nb₂O_{7.25}, new phase of mixed oxide 8-59787
 Gd₂Ge₂O₇(OH)₂ 8-71714
 GeO₂, new high-pressure modification 8-75825
 GeS (German) 8-51484
 GeTe, X-ray emission spectra, amorphous and cryst. struct. (Russian) 8-88385
 HCl·2ZnCl₂·2H₂O, struct. refinement 8-51488
 HCl·6H₂O, cryst. struct., H bonds, X-ray determ. 8-83783
 HgCrO₄, cryst. struct. determ. 8-63712
 HgSeO₄·H₂O, cryst. struct. determ. by neutron diff. 8-55838
 InF₃·3H₂O, cryst. struct. by X-ray diff. 8-63729
 InPS₄, In₄(P₂Se₆), In₄(P₂Se₆), struct. chem. 8-51482
 InSb, polymorphism and cryst. struct. at high temp. and press. 8-95026
 In₂Ta₂O₇, new phase of mixed oxide 8-59787
 In_{0.30}WO₃, struct. anal. (French) 8-59786
 K₂AgO₂, determ. of cryst. struct. X-ray diff. (French) 8-95029
 K₂Ag₂Se₃, crystal struct., X-ray study (German) 8-83795
 KAlCl₄ 8-51487
 KAlSiO₄, metastable polymorph, prep. by ion exchange with RbAlSiO₄, struct. 8-79585
 K₂CO₃-Sr-CO₃ phase diagrams, evidence of new compound (French) 8-95033
 KClO₃, refinement of cryst. struct. 8-55850
 α-K₂Cr₂O₇, symmetry centres exam. by morphological methods 8-59796
 KD₂PO₄, IR and Raman polarised spectra, rel. to crystal struct. 8-56489
 β-KER₃F₁₀ (French) 8-51500
 K₂Hf(MoO₄)₆, X-ray structural investigation 8-79597
 K₂Li(Pt(CN)₄)₂·2H₂O, cryst. struct., polarised emission obs. 8-52538
 K₂Mg(S₂O₃)₂·6H₂O, isolation, struct., decomposition (French) 8-52506
 K₃N(SO₃)₃·2H₂O, cryst. binding of H₂O, IR spectra 8-75620

crystal atomic structure of inorganic compounds continued

- KNbW₂O₉, crystallography, polymorphism and phys. props. 8-79599
 K(Ni(CN)₂HN₂S₂), cryst. struct. determ. 8-63715
 KO₂, low temp. phase study, crystallographic domains and unit cell dimens. 8-63728
 K₂O-Ta₂O₅ mixed oxides, cryst. struct., electron microscopy study 8-91309
 K₂O-Ta₂O₅ mixed oxides, cryst. struct., electron microscopy study 8-91310
 K₂O.3MoO₃.3H₂O, fibrillar crystals, morphology and struct. 8-63959
 K₂P₂O₇.F₂ (French) 8-51501
 K₂(Pt(CN)₄)(FHF)_{0.3}.3H₂O, struct. determ., X-ray diffr. exam. 8-63711
 K₂PtS₅, synthesis and cryst. struct. (German) 8-79588
 KSbO₃, cubic, K⁺ ion ordering, electron microscopy 8-79550
 K₂SnCl₆, structural phase transition exam. by neutron powder diffr. 8-55940
 K₂TeO₃.3H₂O, X-ray cryst. struct. determ. 8-95017
 K₂Te^{IV}Te^{VI}O₁₂, cryst. struct., Te IV pentacoordination by O 8-63704
 K₂Zn(NH₂)₄, cryst. struct. determ. (French) 8-79590
 K₈Zr(MoO₄)₆, X-ray structural investigation 8-79597
 K[B(SO₃Cl)₄] 8-63701
 K₆[Si₂Te₆], cryst. struct. (German) 8-79569
 La-Fe, liquid quenched, X-ray diffr. and Mossbauer effect exam. of structure 8-76678
 LaB₆ film, structure, stoichiometry, elec. properties 8-60043
 LaCoO₃, synthesis and characterisation by powder X-ray diffr. 8-79580
 La₂CoO₄, synthesis and characterisation by powder X-ray diffr. 8-79580
 La₄Co₃O₁₀, synthesis and characterisation by powder X-ray diffr. 8-79580
 LaCuO₃, struct. rel. to phys. props., high-pressure series of perovskite-like oxides 8-51493
 La₂Fe_{1.76}S₅ (French) 8-51499
 LaGaO₃, cryst. struct. determ. (French) 8-79575
 LaKFe(CN)₆.4H₂O, cryst. struct. determ. 8-55844
 La₆Ni₆P₁₇, synthesis and cryst. struct. 8-75634
 La₃RuO₁₁, prep. and struct. study, metal-metal bonding (French) 8-91325
 La₃Ru₃O₁₁, crystal struct., X-ray diffr. study 8-67688
 La₄Ru₄O₂₁, mixed valence oxide of new hexagonal struct. type 8-51503
 La₂Zr₂O₇-La₂Hf₂O₇ system, cryst. struct., phase diagram 8-83806
 LiBa₃Nb₃(Ta₃)(Sb₃)Ti₅O₂₁, insertion of Li, X-ray and neutron diffr. study (French) 8-91324
 LiEu(SO₄)₂ 8-67695
 Li_{0.5}Ga_{2.5}O₄-CuCr₂O₄ system, phase diagrams, IR spectra, Cu²⁺ electronic spectra (French) 8-51461
 LiH, density matrix, factor X-ray struct. factor 8-67692
 LiN₃, evidence for N₃⁻ from static and dynamic props. 8-60465
 Li₂O.3MoO₃.5.7H₂O, fibrillar crystals, morphology and struct. 8-63959
 Li₃Pr₂(BO₃)₃, cryst. struct. 8-87655
 (Li_{0.5}R_{0.5})TiO₃, distorted perovskite struct. 8-83791
 Li₂(Si,Al)₁₂(O,N)₁₆, α'-Sialon ceramics, prep. and characterisation 8-84750
 LiSiON, allotropes, powder diffr. obs. (French) 8-63726
 Li₃ThF₇ 8-63702
 Li₁₄Zn(GeO₄)₄, crystal struct. and ionic conductivity 8-51728
 Mg₃Al₂SiO₁₂, pyrope, cryst. struct. and compressibility to 60 kbar 8-63718
 MgCaH₃.7₂, synthesis and struct. (Japanese) 8-84751
 Mg₃Nb₆O₁₁, struct. determ. and refinement from X-ray 8-91319
 MgO, at. charge densities, X-ray struct. factors 8-79566
 MgO, electron diffr., dynamical effects for cryst. struct. determ. 8-83679
 MgSiO₃, perovskite, synthesis and cryst. chem. charact., rel. to mantle mineralogy 8-65266
 MgTaCuO₄, cryst. struct., synthesis 8-83790
 Mn aluminosilicate, ganophyllite, cryst. struct. 8-75633
 Mn_{0.75}Ga_{2.17}S₄, twinning and cryst. struct. determ. (French) 8-83798
 MnGd₂S₄, mag., struct. and Mossbauer effect study 8-51507
 Mn(PO₃)₃, cryst. struct. determ. (French) 8-55843
 MnTa₂O₆, columbite struct., X-ray diffr., IR and Raman spectra (French) 8-63727
 MnThSe₃, synthesis, cryst. characts. (French) 8-51517
 Mn₁₂-W₂P₇, solid solns., prep., cryst. struct. (French) 8-63723
 Mo₂Cl₁₀S, struct., dielec. and diamag. props. (French) 8-67691
 Mo₂Cl₁₀Se, struct., dielec. and diamag. props. (French) 8-67691
 Mo₂Cl₁₀Te, struct., dielec. and diamag. props. (French) 8-67691
 MoSi₃, integrated intensities and lattice parameters, X-ray anal. 8-63733
 NH₄AlCl₄, crystal struct., X-ray, Raman, IR and NMR 8-63720
 (NH₄)₂BeF₂, paraelec. phase 8-95025
 (NH₄)₂(Cu(H₂O)₆)(CuSO₄)₄, cryst. struct. determ. by X-ray diffr. 8-55839
 (NH₄)₂Mg(S₂O₃)₂.6H₂O, isolation, struct., decomposition (French) 8-52506
 NH₄N₃, cryst. struct. determ. by neutron diffr. 8-79574
 (NH₄)₂PO₃F, H₂O, X-ray diffraction and Raman spectra struct. determ., external mode temp. depend. (French) 8-52507
 (NH₄)₂PtS₅, synthesis and cryst. struct. (German) 8-79588
 (NH₄)₂SeO₄.2NH₄HSeO₄ 8-71715
 (NH₄)₂Te₂O₅.2H₂O, crystal structure determination 8-91317
 (Na,Ca)₂Zr(Si₆O₁₅).3H₂O, Mongolian elpidite, cryst. struct. 8-95038
 (Na,K)(V,P)O₃ system, cation substitutions, crystallographic studies 8-79581
 Na polysilicates, IR spectra, struct., crystallisation effects (Russian) 8-72528
 Na₈Al₆Ge₆O₂₄.CO₃.2H₂, cryst. struct. 8-83805
 NaCN.2H₂O, cryst. struct. determ. 8-75635
 NaCa₂Si₁₀F₆, agrellite, new type of silicate double chain 8-51514
 Na₂Cd₃Si₃O₁₀, X-ray obs. 8-83801
 NaCl, struct. refinement at 32 kbar, using single-crystal diamond cell 8-67610
 α-NaFe₂O₃.Mg²⁺(Co²⁺)(Zn²⁺), substitution of Fe²⁺ (French) 8-95034
 Na₂Fe₃(PO₄)₃, synthetic alluaudite 8-83802
 Na₂Fe₂(PO₄)₃, polymorphism and ionic conduction (French) 8-67678
 Na₂GeO₃ 8-51489
 Na₃La(AsO₄)₂, allotropes, prep. and cryst. struct. (French) 8-63724

crystal atomic structure of inorganic compounds continued

- NaLiZrSi₆O₁₅, zektzerite, silicate mineral with six-tetrahedral-repeat double chains 8-63719
 Na₂MnFeF₇, trigonal webberite variant, X-ray and neutron diffr. (German) 8-51508
 Na₃Nd(AsO₄)₂, allotropes, prep. and cryst. struct. (French) 8-63724
 Na₃Nd(PO₄)₃, laser mat., cryst. struct. 8-79582
 Na₃NdSi₆O₁₃(OH)₂.nH₂O, cryst. struct. determ. 8-63738
 Na₃NiO₄, crystallographic data (German) 8-63736
 Na₃Pr(AsO₄)₂, allotropes, prep. and cryst. struct. (French) 8-63724
 4Na₂SO₄.2H₂O.NaCl, cryst. struct. determ. 8-55841
 Na₂S₂O₃.5H₂O, cryst. struct. determ. by neutron diffr. 8-63714
 Na₂Ti₂Si₂O₆.Na₃PO₄, lomonosovite, cryst. struct. determ. 8-51520
 Na₂TiZn₂[GeO₄]₃, cryst. struct. determ. 8-63734
 Na₂Zn₂Si₂O₇, cryst. struct. refinement 8-87652
 Na₂[B₄O₆(OH)₂] 8-51479
 Na₈[Si₆Al₆O₂₄](OH)₂.1.7H₂O, hydrosodalite, cryst. struct. by neutron diffr. 8-95039
 Na₃[V(NCS)₆].12H₂O, single crystals, X-ray diffr. cryst. struct. anal. 8-95021
 Nb-H system, NMR evidence for low temp. pseudo-cubic phase 8-80526
 Nb₂Cr_{1-x}O₂, cryst. prep. and struct., mag. props. 8-52198
 NbS₂, high pressure polymorphs 8-51459
 NbSe₂, high pressure polymorphs 8-51459
 NbTe₂, high pressure polymorphs 8-51459
 NdAs₂, single-cryst. struct. refinement 8-63709
 NdCo₂B₄, and its analogues, struct. determ. (Ukrainian) 8-91320
 NdCo(BO₂)₅, cryst. struct. 8-63735
 (NdCu₃)(Ti₃Fe)O₁₂, synthesis, cryst. struct. and Mossbauer exam. 8-84505
 NdFeTiO₅, magnetic props. and crystal growth 8-92185
 Nd₂O₄.4TiO₂, growth from soln., struct. 8-83794
 Nd₂Si₂, cryst. struct. determ. 8-95037
 Nd₂(SO₄)₃, anhydrous, cryst. struct. determ. 8-79598
 Ni(NH₄)₂(SO₄)₂.6H₂O, electron density distrib., X-ray diffr. 8-95035
 NiO-TiO₂, solid soln. series, between rocksalt and spinel structure 8-51513
 Ni(S₂N₂H₂)₂, cryst. struct. determ., new β modification 8-63716
 Np(VO₃)₄, crystallographic data (French) 8-63725
 α-P₂S₄ 8-51486
 Pb₄In₂S₁₇, Pb₂Tn₆S₁₃ (French) 8-63707
 Pb(Mg_{0.5}W_{0.5})O₃-BiFeO₃, dielec. props., cryst. struct. 8-84534
 Pb₂Mn₂O₁₅ (French) 8-80525
 Pb₃O₄, isomorphous with ZnSb₂O₄, cell parameters evolution with temp. (French) 8-75642
 γ-4PbO.SiO₂, synthesis and struct. 8-71716
 Pb₃(P₂V_{1-x}O₄)₂, phase diagram and crystallography (French) 8-92252
 PbSO₄, anglesite, crystal struct. and sulphate force consts. 8-83784
 PbTiO₃, neutron powder profile refinement, temp. depend. 8-51476
 PbZr_{0.9}Ti_{0.1}O₃, neutron powder profile refinement, temp. depend. 8-51475
 PdBi₂O₄, cryst. struct. (French) 8-51516
 Pr₆Ni₆P₁₇, synthesis and cryst. struct. 8-75634
 PrOI, X-ray diffr. coord. parameter determ. 8-87656
 PrP₂O₁₄, chemical synthesis and crystal growth of laser quality 8-92184
 Pt(SeC(NH₂)₂)₄Cl₂, crystal and mol. struct. 8-59794
 RbAg₂Se₂, crystal struct., X-ray study (German) 8-83795
 RbAu, NMR line shape, Knight shift, X-ray diffr. study, struct. props. 8-68402
 Rb₂BiBr₆, cryst. struct. determ. 8-75638
 RbCdCl₃, crystal struct., polarised Raman spectra and X-ray diffraction obs. 8-76443
 β-RbCrCl₃, co-operative Jahn-Teller distorted struct. determ. 8-63713
 RbF.H₂O₂, X-ray and neutron diffr. struct. determ. 8-67698
 Rb₃Mn₂Cl₇, cryst. struct. 8-79578
 Rb₁₀Nb₂O₇₈, cationic exchanger with crossed tunnel struct., cryst. struct. (French) 8-83797
 RbO₂, low temp. phase study, crystallographic domains and unit cell dimens. 8-63728
 Rb₂O-Nb₂O₅ mixed oxides, cryst. struct., electron microscopy study 8-91309
 Rb₂O-Ta₂O₅ mixed oxides, cryst. struct., electron microscopy study 8-91309
 Rb₂O-Ta₂O₅ mixed oxides, cryst. struct., electron microscopy study 8-91310
 Rb₂PTl₃, synthesis and cryst. struct. (German) 8-79588
 Rb₁₀Ta₂₀O₇₈, cationic exchanger with crossed tunnel struct., cryst. struct. (French) 8-83797
 Rb₃₀WO₃, struct. anal. (French) 8-59786
 S₂Se₂, s=6-3, y=2-5, thermal behaviour 8-67813
 SbF₃.(NH₂)₂CS and SbF₃[(NH₂)₂CS]₂, X-ray cryst. struct., IR spectrum (French) 8-87643
 Sb₂O₃Cl₂, cryst. struct. refined 8-79572
 2MASb₂O₇, polytype, crystal structure determination 8-91316
 ScCoSi, X-ray determ. of struct., new representative of struct. type TiNiSi 8-79595
 ScCo_{0.25}Si_{1.75}, X-ray determ. of struct., new representative of struct. type ZrSi₂ 8-79595
 ScFe_{0.25}Si_{1.75}, X-ray determ. of struct., new representative of struct. type ZrSi₂ 8-79595
 Sc(HSeO₃)₃ 8-51485
 ScH(SeO₄)₂.2H₂O, single crystals, X-ray diffr. struct. anal. 8-95020
 ScMn_{0.25}Si_{1.75}, X-ray determ. of struct., new representative of struct. type ZrSi₂ 8-79595
 ScNiSi, X-ray determ. of struct., new representative of struct. type TiNiSi 8-79595
 ScNi_{0.25}Si_{1.75}, X-ray determ. of struct., new representative of struct. type ZrSi₂ 8-79595
 ScNi₂Si₃, cryst. struct., X-ray structural anal. 8-95044
 Sc(PO₃)₃, cryst. struct. determ. from X-ray intensity data 8-95043
 Sc₂(P₂O₇)₃, cryst. struct. determ. (French) 8-55842
 Sc₂(SeO₄)₃, cryst. struct. determ. 8-63708
 SeMOCl₂, prep., cryst. struct., characterisation (French) 8-63722
 SeOCl₂dioxane, cryst. struct., secondary and multi-centre bonding 8-63751
 Se₂TiO₃, cryst. struct. (French) 8-95023
 Si-C-Al-O-N and related systems, new materials 8-95159
 SiC, one dimensional disorder 8-51492
 SiO₂, new high-pressure modification 8-75825

crystal atomic structure of inorganic compounds continued

SiO₂, pseudopotential study of bonding and structure 8-75622
SiO₄ tetrahedra, mean Si-O bond lengths var. 8-63699
SmS, semicond.-metal transition, phase struct. determ. 8-91618
Sm₃S₄, cryst. struct. and valence state of Sm (*German*) 8-75636
Sn₂Br₂F₆, cryst. struct. determ. (*French*) 8-79591
SnO₂ fluorite isotype, implications for Earth's lower mantle 8-61371
SnS₂ berndtite, cryst. struct. and compressibility at high press. 8-67685
SnS_{2-x}Se_x solid soln., resistivity, lattice parameter, comp. and temp. depend. 8-91693
SrCl₂, superionic, quasielastic neutron scatt. 8-79504
α-SrHPO₄, triclinic, crystal structure determination (*French*) 8-91315
SrO, at. charge densities, X-ray struct. factors 8-79566
SrSO₄, celestite, crystal struct. and sulphate force const. 8-83784
SrSb₂O₅, SrSb₄O₉, SrSb₆O₁₀, mixed valence cpds., prep., IR and X-ray investigation (*French*) 8-88292
SrTiO_{3-x}, anion deficiency and anion vacancy ordering 8-51532
Sr₂X₃, α, intermediate phases, cryst. struct. (X=IIb, IIb, IVb, Vb element) 8-83793
Sr₂Zr₂O₇·2H₂O, cryst. struct. and thermal stability, X-ray characterisation 8-83796
Sr[Fe(CN)₅NO]·2H₂O, cryst. and mol. struct. 8-91311
TaH₃(D_{3h}), cryst. struct., phase diagrams, order-disorder transition 8-55836
TaS₂/pyridine intercalated, struct. and bonding 8-91323
Te(OH)₆, X-ray diffr. cryst. struct. refinement 8-95022
ThBC, crystal struct. 8-55853
Th(CO₃)₂⁶⁻, in Na and guanidinium salts, struct./props. correlation (*French*) 8-95032
(ThCu₃)(Mn₂Fe₂)O₁₂, synthesis, cryst. struct. and Mossbauer exam. 8-84505
ThSiO₄, huttonite and thorite polymorphs 8-51478
Th(VO₃)₄, crystallographic data (*French*) 8-63725
TiC_{1-x}N_x, lattice distortion of ordered phase (*Ukrainian*) 8-68680
TiCuD₉₀, neutron powder diffr. study for cryst. struct. refinement 8-95018
TiO, ordered phase, vacancy-strain coupling 8-79549
TiO₂ film, electron diffr. exam. 8-79906
TiO₂, hexagonal, implications for Earth's lower mantle 8-61371
TiSi₂, crystal atomic struct., X-ray diffr. exam., lattice parameters and integrated intensities 8-75647
TiAsS₄, struct. and soft mode behaviour 8-91327
TiBr-VBr₂ system, cryst. struct., DTA investig. (*German*) 8-72766
Ti₄Ge₂S₆, cryst. struct. determ. (*German*) 8-79577
Ti₂MoO₄, prep., characterisation 8-63731
Ti(NO₃)₃(H₂O)₃, cryst. struct. determ. 8-59790
TiNbO₃ and Ti₂Nb₁₆O₄₁, new phase of mixed oxide 8-59787
Ti₂Nb(Ta)₆TiO₁₈, structs. with intersecting tunnels, TI distrib. (*French*) 8-79586
Ti₃PSe₄, struct. and soft mode behaviour 8-91327
TiRO₃ (Ln=La, Nd, Sm, Eu, Gd), determ. of lattice parameters (*French*) 8-95031
Ti₂TeO₃, Ti₂Te₂O₇, Ti₂Te₂O₅, Ti₂TeO₆, Ti₂TeO₁₂, synthesis, thermal stability, crystallographic data (*French*) 8-51518
Ti_{0.3}WO₃, struct. anal. (*French*) 8-59786
U-C-N system, high temp. X-ray diffr. exam. of structure (*French*) 8-72765
UBr₃, cryst. struct. investig., powder neutron diffr. 8-91321
U₂SeO₃ 8-51490
UO₂TeO₃ 8-51490
UScS₃, cryst. struct. determ. (*French*) 8-79576
V₂D, single crystal, superstructure modulation and long range order, X-ray obs. 8-71712
VO₂, doped, morphology, structure and props. (*German*) 8-59823
VSe₂ (1T), deform. modulated superstruct., electron diffr. expts. 8-51515
V-Si-M, M=Hf, Nb, Ta, Mo, W, Ni, Ge, Sb, cryst. struct., supercond. T_c comp. depend. 8-51494
VaH₃(D_{3h}), cryst. struct., phase diagrams, order-disorder transition 8-55836
WC, electrochem. separation from W alloys, phase anal. 8-60651
WCl₅, crystal structure determination 8-91318
WO₃, trigonal 8-51483
WSeF₄, cryst. struct., and preparation 8-63730
Y₄(Si,Al)₁₂(O,N)₁₆, α'-Sialon ceramics, prep. and characterisation 8-84750
YThNbTiO₈, synthesis and cryst. struct. (*French*) 8-83799
Y₆WO₁₂·Eu³⁺, crystal struct., fluorescence spectra, exam. 8-52558
YbB₁₂, mag. props., cryst. struct., valence of Yb (*Russian*) 8-60263
Zn complex, ZnS₂O₄·pyridine, cryst. struct., nature of S-S bonds 8-55847
Zn-Sb system, phase diagram, struct. and stability of phases (*German*) 8-60661
Zn_xFe_{0.85-x}O, prep. and struct., mag. and semicond. props. (*French*) 8-51506
ZnGeP₂, P vacancies, lattice parameters, optical props. depend. on thermal treatment (*Russian*) 8-71729
ZnHPO₄·H₂O=(H₂O)ZnPO₄, cryst. struct. determ. 8-63739
Zn₃P₂, high press. phase relns. and cryst. structs. 8-59792
Zn₃(PO₄)₂·4H₂O, hopeite, cryst. struct. redeterm. 8-75640
Zn₄(P₂S₆)₃, monoclinic system (*French*) 8-59791
ZnSb₂O₄, isomorphous with Pb₂O₄, cell parameters evolution with temp. (*French*) 8-75642
Zn₂SiO₄, willemite, cryst. struct. 8-83804
ZrD_{1.82x} and ZrD_{1.06x}, struct. and phase equilib., neutron diffr. obs. (*Russian*) 8-92244
ZrO₂, technical grade containing CaO, polymorphic transform. up to 1200°C 8-64539
ZrO₂·UF₄, orthorhombic struct., X-ray and electron diffr. study (*French*) 8-67689

crystal atomic structure of organic compounds

acetic acid, deuterated, neutron powder diffr. anal. at 4.2 and 12.5K 8-75649
L-alanine, solid, H bonding, wide line NMR obs. 8-52362
1-amino-2-phenyl benzocycloheptanol-hydrobromide monohydrate, cryst. struct., heavy atom method 8-79601
ammonium uranyl formate, struct. determ. from X-ray diffr. and IR spectrum (*French*) 8-75653

crystal atomic structure of organic compounds continued

anthanthrene, mol. imaging by high resolution electron microscopy 8-79600
barium beauvericin complex, appl. of cryst. struct. refinement technique based on fast Fourier transform algorithm 8-91197
benzil, crystallographic study of solid-solid phase transition (*French*) 8-55939
benzonitrile, 198K (*French*) 8-51524
β-bis(ethylammonium)tetrachloromanganate, cryst. struct. refinement, neutron diffr. 8-55858
bis(propylammonium)tetrachlorocadmate, first-order phase transition, X-ray diffr. meas. 8-55826
boranes, B₉H₁₂OCH₃S(CH₃)₂, C₂B₁₀H₁₀Br₂, B₁₈C₄H₂₂, cryst. struct. (*Czech*) 8-87649
boranes, OCH₃(B₉C₂H₁₀)₂Co and (C₂H₅)₂Co₂CB₉H₁₀, cryst. struct. (*Czech*) 8-87649
bromoacetic acid, cryst., films, polarised IR spectra, struct. 8-72502
cadmium histidine, unique phase determination, two-wavelength Bijvoet pair method, reson. neutron scatt. 8-91201
caesium hydrogen tartrate, anomalous dispersion of Cs, refined struct. from modified least squares program 8-51522
o-chlorobenzoic acid, solid, H bonding, wide line NMR obs. 8-52362
p-(N-chlorobenzylidene)-p-chloraniline, cryst., polymorphism, cryst. struct. rel. to mol. conform. 8-75611
4-chlorophenoxyacetyl-4-propenyl benzene 8-63750
cholesteryl chloroformate, crystal structure 8-91331
β-choline chloride, X-ray diffr. 8-55861
cis-3,5-dibromo-4-oxo-2,2,6,6-tetramethylpiperidin-1-yloxy, cryst. struct., secondary and multi-centre bonding 8-63751
copper tetra-4-dimethylaminophthalocyanine intercalated with TaS₂, layered cpd., struct. and supercond. 8-84342
β-cyclodextrin dimeric complexes as models for lipid bilayer diffusion transport 8-80838
bis-π-cyclopentadienyltitanium dichloride, struct. parameter refinement 8-87660
bis-π-cyclopentadienylzirconium dichloride, struct. parameter refinement 8-87660
3,5-di-tert-butyl-4-hydroxybenzylidenemalononitrile, excited-state proton transfer, cryst. and mol. struct. 8-84630
2,4-dibromo-1,5-diphenylpenta-3-one, cryst. struct., secondary and multi-centre bonding 8-63751
β-9,10 dichloroanthracene, hole mobility anisotropy and cryst. struct., transient photocond. 8-95310
dichlorodurene, order-disorder phase transition, struct. from neutron diffr. at 70K 8-55825
diethyl tin dihalides, cryst. struct., secondary and multi-centre bonding 8-63751
dipyridinium copper bromide, Py₂Cu₃Br₇, Cu⁺ ion conductor, cryst. struct. 8-51527
durene-p-dibromobenzene system, phase diagram and X-ray diffr. expts. 8-79774
ethane, single cryst. X-ray struct. determ., plastic and monoclinic forms 8-63744
ferrocene, ordered, disordered phases, structs. (*French*) 8-63749
formic acid, deuterated, neutron powder diffr. exam. at 4.5K 8-75650
glycogen phosphorylase b activity, struct. of cryst. and complexes 8-80830
guanido iodate, X-ray obs. 8-83807
guanyl ribonucleases of fungi, crystn. and X-ray diffr. 8-71718
gummosine, cryst. and mol. structs., and absolute config., X-ray expts. 8-79602
N-hydro-N'-methylphenaziniumyl cation in HMP-ClO₄, mol. config. 8-62938
insulin, appl. of cryst. struct. refinement technique based on fast Fourier transform algorithm 8-91197
iodobenzene bis(dichloroacetate), cryst. struct., secondary and multi-centre bonding 8-63751
iodobenzene diacetate 8-63751
iodoxybenzene, cryst. struct., secondary and multi-centre bonding 8-63751
lithium formate monohydrate, non-centrosymmetric struct., X-N and multiple deform. electron density maps 8-91328
methane-d₄, solid, lattice parameters and thermal expansion for different phases 8-51526
p-methoxy-XY-p'-alkyl tolanes, mol. struct., packing coeffs., and thermal stability 8-95046
methyl meristotropate, mol. and cryst. struct. 8-95047
molecular charge transfer complexes, mol. and cryst. struct. 8-62942
myoglobin, appl. of cryst. struct. refinement technique based on fast Fourier transform algorithm 8-91197
o-nitrophenol, cryst. and mol. struct., H bond distance 8-51523
2-nitroso-2-bromo-3,3-dimethyl-butane, cryst. data 8-67703
octafluoronaphthalene, high press. struct., neutron powder diffr. 8-63743
organic ortho compounds, solid, H bonding, wide line NMR obs. 8-52362
organonitrogen derivatives of Si, Ge and Sn, prep. and props. 8-60456
orthocyanobenzyl bromide, lattice const., space group, density, X-ray obs. 8-51525
p-phenylenediacrylic acid dimethyl ester, photopolymerisable cryst., struct. determ. 8-63747
phosphorylase b, structure factor moduli, estimates from negative intensity obs. 8-75486
piperazinium Ag₁₀I₂·4-dimethylformamide, exam. of electrical cond. and crystal structure 8-75871
potassium formate, IR absorpt. spectra, sampling effects, Davydov splitting and struct. 8-52508
prostratin derivative, cryst. struct., overlapping Patterson peaks and direct methods 8-55779
PTS, pyroelectric effect 8-95554
TCNQ(perylene)₂, cryst. struct. determ. 8-75651
TCNQ 1:3 radical salt, [Pt(dipy)₂]²⁺[TCNQ]₃²⁻, cryst. struct. 8-63741
TCNQ salt, NH₄-TCNQ, crystal structure and phase transition 8-91330
TCNQ salt, [Pt(NH₃)₄]²⁺[(TCNQ)₂]²⁻ cryst. and mol. struct. and EPR props. 8-55860
tetrabutylammonium hexatungstate (*German*) 8-63740
tetraethylammonium acetate tetrahydrate, stoichiometry and cryst. data 8-67702

crystal atomic structure of organic compounds continued

- tetraethylammonium chloride tetrahydrate, stoichiometry and cryst. data 8-67702
 tetraethylammonium fluoride hydrate, stoichiometry and cryst. data 8-67702
 tetraethylammonium sulphate monohydrate, stoichiometry and cryst. data 8-67702
 tetramethylammonium manganese(II) tribromide, cryst. struct. at 235 and 115K 8-63745
 tetramethylammonium salt of $[\text{Me}_2\text{N}(\text{ICl})_2]^-$, cryst. struct., secondary and multi-centre bonding 8-63751
 tetrapotassium tetrakis(oxalato)zirconate (IV) pentahydrate, cryst. struct. determ. 8-63746
 p-thiocyanatoaniline 8-71717
 thiourea, bond charges, comparison of exptl. and theoretical X-ray scatt. curves 8-55782
 TMTSF-DMTCNQ, cryst. and mol. struct. 8-63742
 tolan-mercury diphenyl solid soln., anal. of diffusely scatt. intensity distrib. of X-rays 8-95048
 s-triazine, structural transitions, low temp. phase 8-55943
 triethylamyllose-solvent complexes, conform. and packing analysis 8-75654
 triphenyl tin isocyanate, struct. determ. and refinement 8-67704
 TTF-TCNQ, crystal and molecular structure determination (*French*) 8-91329
 urea, bond charges, comparison of exptl. and theoretical X-ray scatt. curves 8-55782
 urea, bond electron density distrib., 123K, simple refinement 8-55857
 urea-uranyl sulphate, $\text{UO}_2\text{SO}_4 \cdot 2\text{CO}(\text{NH}_2)_2$, lattice parameters, space groups, X-ray crystallography 8-59798
 urea-uranyl sulphate, $\text{UO}_2\text{SO}_4 \cdot 3\text{CO}(\text{NH}_2)_2$, lattice parameters, space groups, X-ray crystallography 8-59798
 2-zinc insulin, rhombohedral, cryst. struct. refinement, experience with fast Fourier least squares 8-92595
 zinc malonate dihydrate, cryst. struct., X-ray refl. obs. 8-75652
 p-phenylenediacrylic acid diphenyl ester, photopolymerisable cryst., struct. determ. 8-63748

crystal binding

see also *binding energy*; *lattice energy*

- A15 struct., stabilized by crystal field distortion of exotic elements at chain sites 8-79555
 alkali chlorides, modified electronic charge density 8-79554
 alkali halide, exchange charge polarisation, dielectric const., Dick and Overhauser model 8-55832
 alkali halide, lattice energy, binding, indeterminacy principle theory 8-59777
 alkali halide, second-neighbour interaction potential 8-91298
 alkali halide crystals, evaluation of van der Waals interaction energies 8-71705
 alkali halides, exchange charge shell model analysis of strain derivatives of static polarisability, effective charge parameter 8-91296
 alkali halides, interionic potentials, completely independent specification of Born-Mayer potentials 8-55828
 alkali halides, interionic potentials, cryst. independent shell parameters and fitted Born-Mayer pots. 8-55827
 alkali halides, short range interactions, static polarisabilities 8-71702
 alkali halides, static polarisability, vol. depend. 8-52428
 alkali halides, three body interaction effects on cohesive props. 8-83770
 alkali hydrides, bulk props. prediction from molecular behaviour 8-51468
 alkaline earth fluorides, vol. depend. of refr. index 8-88275
 alloy, AB type, equilib. props. by Markovian simulation 8-91302
 alloys, CsCl type, nearest neighbour distance and atomic props. 8-51465
 Anderson-Gruneisen parameter for cubic crystals 8-79672
 anthracene, electron diffr. of topochem. conversion and phase transition 8-83680
 binary crystals, stability and average structure factors 8-91297
 coordination number, quantifying concept for irregular coordination polyhedra 8-95008
 covalent elements, cohesion in condensed phases, corrections to simple Huckel approx. 8-59779
 covalent elements, cohesion of σ and π bonds in condensed phases, simple Huckel approx. 8-59778
 covalent semiconductor, electronic and struct. energies calc. 8-59874
 diamond, relaxation about the vacancy 8-71722
 1,5-diazo-3,7-dithiabicyclo (3,3,1) nonane, molecular and cryst. struct. 8-51528
 dispersion force calculations, use of finite atomic radius 8-51467
 effective ion-ion interaction, third-order contrib., ang. forces, tetrahedral solids 8-67970
 electron plasma of crystal, interactions of classical charges 8-79561
 electronic polarizabilities of ions in doubly refracting crystals 8-79551
 force constants, diamond and sphalerite struct. crystals 8-91408
 II-VI and III-V, ion effective charge parameter, electronic polarisability 8-51463
 II-VI partially covalent crystals., vol. depend. of refr. index 8-88275
 III-V semiconductors, chemical shifts of NMR lines of Ga nuclei 8-88201
 interatomic potentials from experimental phonon spectra 8-75621
 intermetallic phases with LiI_2 and D_{019} struct., atom incompressibility, lattice parameter approach 8-91294
 ionic crystals, van der Waals potentials 8-83767
 ionic radius, electronic polarisability and effective nucl. charge, correl. 8-63694
 ionic solids, deformation dipole model 8-72454
 ionic systems, simple, stability and melting 8-71839
 ionicity, Pauling's and Phillips' comparison by empirical LCAO band theory 8-51464
 Morse function, one-dimens. cryst. stability, for teaching 8-54134
 quantum static multipole polarisabilities 8-82859
 quantum-defect theory of heats of formation and struct. transition energies 8-55830
 rare earth and actinide halides and oxides stability study, energy difference between trivalent and tetravalent metal states 8-79553
 semiconductor, lone pair, defect chemistry 8-51935
 shortened intermolecular contacts 8-63695
 sigma phase structure, ionicity modified pair pot. model anal. 8-51466

crystal binding continued

- spinel, MgCr_2O_4 and MgV_2O_4 , valency and ionicity rel. to magnetism 8-52229
 sulphides of nonmagnetic transition metals, semicond. props. rel. to at. vol. 8-64037
 transition metal, eqn. of state, s- and d-contribs. 8-91633
 transition metal oxides, energy loss spectra, ion polarisability 8-68585
 transition metal pnictides, atomic volume, semicond. props. 8-59780
 urea, density distributions of bonding electrons 8-75616
 valence electron distribution and 'size of atoms' in crystals (*Russian*) 8-87644
 zincblende structure group IVA covalent crystals, Murnaghan parameter estimates from Morse pot. 8-95014
 AgBr, exchange charge polarisation 8-92016
 AgCl, exchange charge polarisation 8-92016
 alkali halides, interatomic forces, Born model anal. on US data 8-55833
 Au, lattice vibr., electron press., central pair pot. model calc. 8-75749
 B_2H_6 , mol., static electron densities 8-79552
 BaO, at. charge densities, X-ray struct. factors 8-79566
 Ca, FCC, ground-state props. 8-75989
 CaO, at. charge densities, X-ray struct. factors 8-79566
 Cd chalcogenides, electronic polarisabilities of ions 8-79559
 CdSiP₂, bond strengths and bond lengths, thermal expansion coeff. meas. 8-87651
 CrO_2 , band struct., cryst. binding and ESCA spectra, X_α cluster calc. 8-64443
 Cu, cryst. pot. in electron diffr. and band theory 8-83677
 Cu, interatomic potential from intermediate and low energy data 8-55829
 $\text{Cu}(\text{NH}_3)_4\text{PtCl}_4$, $\text{Cu}(\text{NH}_3)_4^{2+}$ cation mol. orbital parameters 8-64011
 $\text{Ga}_{1-x}\text{In}_x\text{P}$, Delta lattice parameter model, correl. with electronic props. 8-91560
 H, metallic, Coulomb crystal energy 8-91300
 H_2 , metallic interion interaction (*Russian*) 8-91299
 $\text{K}_3\text{N}(\text{SO}_3)_2 \cdot 2\text{H}_2\text{O}$, cryst. binding of H_2O , IR spectra 8-75620
 KNa_2 , binding energy and lattice const., nonparametric calc. (*Russian*) 8-51462
 La, FCC, ground-state props. 8-75989
 $\text{La}_2\text{RuO}_{11}$, prep. and struct. study, metal-metal bonding (*French*) 8-91325
 MgO, at. charge densities, X-ray struct. factors 8-79566
 NaCl, polarisation mechanism and lattice mechanics, microscopic approach 8-59888
 Nb_3Al , metallic bonding, electronic states calcs. 8-79916
 Nb_3Au , A-15 struct. supercond., microhardness, bonding 8-76199
 Nb_3Ge , metallic bonding, electronic states calcs. 8-79916
 Nb_3Ir , A-15 struct. supercond., microhardness, bonding 8-76199
 Nb_3Sn , A-15 struct. supercond., microhardness, bonding 8-76199
 OHO bonds, O-H vs. O...O distance correlation and geometric isotope effect 8-75615
 PbCl_2 , binding, ionicity, covalent contrib., Madelung const., cohesive energy 8-79558
 $\text{Pb}_{1-x}\text{Sn}_x\text{Te}$, lattice instability and phonon lifetimes, neutron scatt. 8-55932
 Pd_3Te_4 , cryst. struct. and binding (*German*) 8-51471
 Pt_3In_9 , exam. of crystal structure, and phase diagrams (*German*) 8-83779
 $\text{RbF}(\text{Cl})(\text{Br})(\text{I})$, chem. shift in X-ray absorpt. spectra, correl. with ion contrib. to bond 8-76559
 Se, effective charge tensor, microscopic treatment 8-59879
 SiC single crystals., polytypism obs. by high temp. oxidation expts. 8-59797
 SrO, at. charge densities, X-ray struct. factors 8-79566
 Th, FCC, ground-state props. 8-75989
 TlBr, CsCl and NaCl phases, atomic interactions and lattice statics and dynamics 8-83889
 V_3Ge , A-15 struct. supercond., microhardness, bonding 8-76199
 V_3Si , A-15 struct. supercond., microhardness, bonding 8-76199
 Zn chalcogenides, electronic polarisabilities of ions 8-79559
 Zn complex, ZnS_2O_4 -pyridine, cryst. struct., nature of S-S bonds 8-55847

crystal chemistry

see also *crystallography*

- alloys, CsCl type, nearest neighbour distance and atomic props. 8-51465
 halide compounds ABX_3 with perovskite struct., cryst. chem., X-ray diffr. anal. 8-95042
 molecular charge transfer complexes, mol. and cryst. struct. 8-62942
 nonstoichiometric solid solutions, ordering 8-87794
 oxides, stoichiometry meas. and control 8-51694
 silicates, layered, not containing Al, synthesis and cryst. chem. 8-51495
 ABCl_3 cpds., basic struct. types and polymorphisms 8-79583
 AuF_3 , ^{19}F NMR chemical shift, crystal chemistry 8-87645
 B_2C , thermal cond., nonstoichiometry effect 8-63887
 BaCuO_{2+x} ($0 \leq x \leq 0.12$), study of mag. and elec. props. rel. to the non-stoichiometry (*French*) 8-95051
 BaF_2 - NiF_2 - CrF_3 , X-ray crystallography study, phase identification at 700°C, cryst. symm. (*French*) 8-95733
 BaTiO_3 , single cryst., elec. cond., 800-1200°C, nonstoichiometric disorder 8-51989
 CdSe, nonstoichiometry, Cd and Se press. meas., up to 1400K 8-87664
 CsAuF_4 , ^{19}F NMR chemical shift, crystal chemistry 8-87645
 Cu_{1-x}Se , I-V characts., switching effects, nonstoichiometry effects (*Russian*) 8-84266
 Cu_{1-x}Te , and Cu_2Te , I-V characts., switching effects, nonstoichiometry effects (*Russian*) 8-84266
 Fe_{1-x}O , wustite phase, surface elec. props. 8-76133
 n-GaAs, melt-grown, stoichiometry, photolum. obs. 8-72583
 Hg-Tl, metastable system, prep. by quenching, phase struct. 8-52762
 InAs, intrinsic point defects, nature and influence on electrophys. props. 8-79609
 KLiSO_4 :Cr, optical activity characts. cryst.-chem. exam. 8-95569
 NaPF₆, high press. phase diagram, vibr. spectra 8-60446
 Se_2TiO_6 , cryst. struct. (*French*) 8-95023
 SmS, cryst. struct. in homogeneity region 8-91334
 SnO_2 :Sb, and pure cryst., microstruct., X-ray diffr., optical and electron microscope studies 8-79619

crystal chemistry continued

SrTiO_{3-x}, anion deficiency and anion vacancy ordering 8-51532
 Ti₂TeO₃, Ti₂Te₂O₇, Ti₂Te₂O₅, Ti₂TeO₆, Ti₆TeO₁₂, synthesis, thermal stability, crystallographic data (*French*) 8-51518
 US₂N₂O₈, neutron diffraction exam. of structure 8-79777
 ZrS(Se)₂, nonstoichiometry 8-75841

crystal classes *see crystal symmetry***crystal cleavage**

crack propag. due to dislocation tilt wall splitting 8-91377
 TGS, vacuum-cleaved cryst., charge compensation, ferroelec. field effect obs. 8-95556
 BaSO₄, single cryst., neutron bombard. effect on struct. 8-63793
 KCl, spontaneous cleavage, step line propag., macroscopic defects 8-87662
 LiF, electrification of crystals by cleavage 8-60189
 Mo, single cryst., δ , criterion for brittle fracture (*Russian*) 8-56732
 Se₉₀-Te₁₀ alloy crystals, growth and cleavage 8-88421
 Si, (111) cleavage, Kikuchi pattern, 40 keV incident electrons, electron energy loss spectra (*French*) 8-87594

crystal defects

see also Cottrell atmospheres; crowdions; crystal inclusions; crystal microstructure; defect electron energy states; disclinations; dislocations; grain boundaries; impurity-defect interactions; phonon-defect interactions; point defects; stacking faults; twinning

A15 supercond. with defects 8-76183
 alkali halide crystals, defect state change during electrolysis 8-95057
 anharmonic lattice with defects 8-73937
 anharmonic system, generalisation of CPA 8-75783
 γ -brass type alloys, faulted defects, nature determ. by image matching technique 8-63777
 1,4-dibromonaphthalene, optical props., struct. disorder effects 8-52525
 direct observation and characterisation 8-88617
 displacive phase transitions, localised modes, central peak, influence of defects 8-83905
 effective annealing time determ. using analogue computer 8-88475
 electron microscope diffr. contrast 8-83700
 Euclidean invariance, spontaneous breaking, long range ordered media, defect, config. classification 8-59748
 formation energy of defects, Gibbs free energy 8-91332
 insulating crystals, conf., Gatlinburg, USA (Oct. 1977) 8-63755
 ionic crystals, transport phenomena, appl. to solid state devices 8-55976
 line defects, X-ray topography (*French*) 8-79502
 metal, positron annihilation study of neutron damage, review 8-71769
 metals, defects in structure of lattice 8-88617
 misfit boundary, X-ray diffr., general soln. 8-51562
 misfit boundary, X-ray diffr., special cases 8-63776
 molecular crystals, optical props., struct. disorder effects 8-52525
 multicomponent solid solutions, defect formation in heteroepitaxial structures 8-83825
 nuclear fuel element model for cladding performance during power changes, strain defects 8-58359
 optical, of laser active materials, ruby and garnet, influence on energetic effectiveness obs. (*Czech*) 8-79022
 plastic behaviour in terms of defect motions 8-95104
 polyethylene, solid, nucl. spin-lattice relax. time, freq. depend. defect diffusion, 77-373K 8-72428
 polymers, crystalline, with lattice defects, exam. of plastic deformation for 2-d models 8-68747
 quartz synthetic crystals, observation of growth defects by light scatt. tomography 8-71743
 radiation damage, imitation by action of shock waves (*Russian*) 8-95107
 Rayleigh and hyper-Rayleigh light scatt. 8-60478
 scattering phaseshifts and resonances for line defects 8-51953
 semiconductor, model describing removal and scattering of charge carriers by defect clusters 8-76069
 semiconductor materials, noise models for investigation of defects (*German*) 8-87661
 stationary lattice defects as sources of elastic singularities 8-59800
 steel, stainless, low energy D implanted, microstruct. 8-95073
 topography settings, white beam X-ray, for cryst. defects, synchrotron radiation 2-axis spectrometer 8-67619
 transition metal oxides, extended defects, review 8-63753
 X-ray characterisation of single crystals for devices with multiple crystal arrangement 8-83651
 X-ray line breadth calculations, convolution relations 8-51394
 Ag film, annealing study of elec. resist. and defect density 8-76167
 AgI, defects rel. to elastic behaviour near phase transitions with negative dP/dT 8-83885
 Al, dynamic defect annealing during plastic deform. 8-88478
 α -Al₂O₃, ion bombard., vol. expansion, annealing compaction, surface props. 8-67748
 β -Al₂O₃-Na₂O-MgO, blocking defects observed by high resolution electron microscopy 8-55879
 Bi_{1-x}GeO_{20x}, single crystals, optical homogeneity depend. on growth conditions 8-95007
 CaF₂:ErF₃, clustering, defect struct., NMR study 8-80229
 CaF₂:YbF₃, clustering, defect struct., NMR study 8-80229
 Cu complex, bis-(alkylammonium) (11) tetrachloride, perovskite, lattice perfection 8-87633
 Cu, polycryst. magnetoresist. due to crystal defects 8-56128
 Cu-Ag (Au), dil., dose depend. of impurity detrapping stages after electron irradiation 8-51582
 Cu₂O, growth by melting, photocond. spectra 8-52029
 EuO, quadrupole coupling due to lattice imperfections 8-76347
 KCl, spontaneous cleavage, step line propag., macroscopic defects 8-87662
 K₂SO₄.Al₂(SO₄)₃.24H₂O, stirring effect on crystalline quality of soln. grown crystals 8-91281
 β -Ni₃S₂, defect struct. 8-63754
 PbCO₃, neutron diffr. topographic study of growth defects 8-91282
 Se, photoconductive film, field instability, Ar⁺ ion irradiation-induced defects 8-87997
 Si, Czochralski cryst., hillock etching of microdefects, TEM obs. 8-87678
 Si, electron irradiated, positron annihilation 8-87713
 Si integrated circuits, effects of introduction, review 8-88547

crystal defects continued

Si, ion-implanted layers, crystalline-to-amorphous transition, radiation defect prod. 8-87696
 Si, swirl defects, gettering effects, obs. by photoluminesc. meas. 8-84623
 Si wafers, etched in HCl, exam. of bunch formation 8-68831
 Si:Na, quantitative analysis of residual impurities with SIMS 8-87688
 TbVO₄, Jahn-Teller phase transition, γ -ray diffractometry 8-91205
 YSmLuCaGeIG, mag. props. and defects, depend. on B₂O₃ conc. on growth in PbO-B₂O₃ solvents 8-68321
 Zn-Cu system, sputtering during atomic diffusion, UPS meas. 8-92159

crystal dislocations *see dislocations***crystal electron states** *see electron energy states (condensed matter)***crystal energy** *see lattice energy***crystal etching** *see etching***crystal faces**

nucleation rate equation, generalisation of nucleus shape depend. parameters 8-84765
 sapphire, profiled growth, struct. perfection 8-68621
 Al₃Ni dendrite facets, determ. cryst. direction by SEM (*French*) 8-87893
 Cu complex, bis-(alkylammonium) Cu(11)tetrachloride, perovskite, face struct. and growth rate 8-87634
 ErAG, facet formation 8-63687
 GaAs-AlGaAs DH laser with buried facet 8-55373
 GaSb, pulled crystal, microfacet obs. near irregularly remelted surfaces 8-91278
 YAG, facet formation 8-63687

crystal field interactions

see also crystal hyperfine field interactions

A15 struct., stabilized by crystal field distortion of exotic elements at chain sites 8-79555
 alkali bromide-VBr₂ systems, cryst. struct., DTA investig. (*German*) 8-72766
 alkali halide:Sn²⁺, V_c-centres, vacancy induced splitting of excited states, Sn²⁺ structure 8-51931
 alkali metal-hexamethylphosphoramide, low temp. glass, EPR of solvated K, Cs and Rb 8-91927
 antiferromagnetic semiconductor, magnon-plasmon interaction and its effect on Raman scatt., theory 8-56302
 p-benzoquinone(-d₄), n- π^* excited states, distant intramol. interaction between identical chromophores 8-90203
 Berthollides, chaotic mag. states 8-56330
 biological systems, containing Fe, electronic and mag. struct., semiempirical MO cluster calcs. 8-62733
 calcium tartrate tetrahydrate:Ni²⁺, optical absorpt. spectrum 8-84610
 carbazoyl substituted diacetylene monomer cryst., ODMR and triplet state kinetics 8-76355
 chemical state effects in AES 8-92566
 close-packed metals, elec. field gradients, vol. and struct. depend. 8-64014
 cryst. with defects 8-60478
 cubic metal:Gd, influence of cryst. field on EPR 8-52346
 d^{3,7}-configurations, weak field energy matrices calcs. with nonzero spin-orbit coupling 8-76029
 d^{4,6}-configurations, weak field energy matrices calcs., spin-orbit coupling effects 8-76030
 d⁵-configurations, weak field energy matrices calcs. 8-76031
 diacetylene, single cryst., EPR of low-temp. photoproducts, photopolymerisation 8-85175
 diagrammatic Green function technique appl. to cryst. field systems with exchange 8-68130
 dimethyl cadmium, photoelectron spectra, 4d spin-orbit splitting, crystal field and band-broadening effects, CNDO calcs. 8-76577
 ferromagnet, internal fields, positive muon investigation 8-68438
 fluorene, lowest singlet state, exciton band struct. calc. 8-63983
 fluorite type crystal, Ti²⁺ doped, electronic struct. and EPR of Ti²⁺ 8-76034
 garnet:Nd³⁺, spectral, structural regularities, anal. 8-51948
 graphite, adsorbed o-H₂ (p-D₂), NMR, orientational behaviour, weak crystal field 8-75935
 guanidinium aluminium sulphate hexahydrate:Cr³⁺, EPR, 295.5, 78.45, 1.61K, zero field splitting 8-68359
 guanidinium aluminium sulphate hexahydrate:Mn²⁺, NMR 8-91939
 heat magnetization in the singlet-triplet model 8-64211
 hindered rotational energy levels of a linear ion in octahedral and tetrahedral crystalline fields 8-59767
 1-hydronaphthyl radical, in naphthalene single cryst., anisotropic oscill. strength 8-50591
 hydrostatic pressure shifts of Van Vleck susceptibilities and Knight shifts, appl. of parametrisation 8-72120
 II₂V₂ semiconductors, spin-orbit and cryst. field splittings of valence band 8-63980
 impurity molecules in crystals, exclusion rules for librational-tunnelling states 8-84174
 intercombination transition intensities in strong crystal fields, symmetry reduction method 8-84175
 ion with dⁿ config., level splitting in trigonal and tetragonal cryst. field symm. 8-51949
 ionic crystals, surface F centres, electronic struct., numerical soln. of one electron Schrodinger eqn. 8-64091
 Jahn-Teller system, octahedral T₁, ligand trajectories 8-76028
 ligand field theory, energy matrices checking method (*Russian*) 8-72123
 magnetic 3d impurity in non-magnetic metal, effective ion Hamiltonian 8-64016
 magnetic form factor meas. by inelastic neutron scatt. 8-52221
 magnetic symmetry and spin-wave Hamiltonian struct. 8-84373
 magnets, EPR line shape 8-91926
 manganese minerals, photoluminesc., cryst. field theory (*Russian*) 8-84654
 metal, antishielding effects and temp. depend. of field gradients 8-51951
 metal, conduction electron coupling with moments of 3d and 4f ions 8-60090
 metal, elastically strained, elec. field gradients on nuclei, calc. (*Russian*) 8-60096
 metals, close-packed, elec. field gradients, vol. and struct. depend. 8-51947
 microcrystals, magnetically ordered, high temp. behaviour 8-84456

crystal field interactions continued

- minerals, physical theories for origin of colour 8-69323
 1,4-naphthoquinone, $T_1 \leftarrow S_0$ transition, elec. and mag. field spectra 8-88322
 NQR, steady-state, basic principles 8-76349
 NQR spectroscopy, elec. field gradient tensor parameters 8-72432
 palladiumporphyrin, in n-alkane, $S_1 \leftarrow S_0$ absorpt. spectrum, vibronic coupling and avoided crossing, field splitting 8-84613
 parametrisation of temp. depend. of splitting of axial 8S state ions 8-91652
 phosphorescent triplet state, spin-lattice relax. mechanism (Russian) 8-68542
 plagioclase: $Mn^{2+}(Fe^{3+})$, ligand field bands of impurity luminesc. centres and their site occupancy 8-88350
 quantum mechanics, use in magnetism and crystal field theory, review 8-76215
 rare earth alloys, cryst. field effect on EPR and NMR 8-56391
 rare earth alloys, R_2Co_{17} , formation of mag. anisotropy role of rare earth ions (Russian) 8-76238
 rare earth amorphous alloys, antiferromagnetism, mol. field approx. 8-80142
 rare earth and rare earth intermetallic hydrides, magnetic properties, effect of hydrogenation 8-68210
 rare earth garnets, appl. of superposition model to cryst. field 8-68132
 rare earth intermetallics, $RFe_{5-x}Ni_x$, giant intrinsic mag. hardness 8-56354
 rare earth ions, energy transfer rates, unified method using standard tensor calc. (French) 8-79965
 rare earth metallic systems, linewidth of cryst. field excitations 8-67988
 rare earth metals and alloys 8-84177
 rare earth perrenates, $(ReO_4)^-$ ion vibr. rel. to static field, Raman investig. (Russian) 8-76470
 rare earth series, variation of fourth and sixth order cryst. field parameters 8-72122
 rare earth systems, crystal field effects 8-67987
 rare earth-Fe-Al alloys, RFe_2Al_3 , mag. props. 8-52250
 rare earths, spin waves and excitations 8-84407
 scheelite-type species, magnitude of cation fields 8-80111
 semiconductor, diamond structure, plasmon line shape, local field effects 8-76011
 semiconductor, zinc-blende structure, plasmon line shape, local field effects 8-76011
 sigma phase structure, ionicity modified pair pot. model anal. 8-51466
 simple ionic crystals, ion transport 8-63878
 spin echo, rot., in solids, anisotropic interaction recovery 8-68410
 strontium tartrate tetrahydrate Co^{2+} electronic absorpt. spectrum 8-92098
 transition metal compounds, intensity of Laporte forbidden transitions, ligand polarisation model 8-64378
 transition metal ions in amorphous compounds, crystal field theory and mag. props. 8-72318
 transition metal ions in HCP hosts, energy splittings 8-67989
 transition metal oxides, crystal field effect on isothermal bulk moduli 8-61364
 transition metal oxides, pressure-induced high-spin-low-spin transitions 8-85549
 Yang-Lee edge singularity and q^3 field theory 8-65882
 Ag, electron density at nucleus, press. depend., Hartree SCF calcs. 8-56411
 $AgClO_3$, ClO_2 spin Hamiltonian 8-60326
 Al, electron-irrad., NQR, EFG around vacancies and interstitials 8-88220
 $Al^{13}B$, relax. mechanism for polarised implant 8-87693
 Al-Al oxide- $Bi_{1-x}Pr_x$ tunnel junction, cryst. field struct. obs. in conductance 8-84358
 Al_2Ce , Al_3Ce , nucl. orientation exam. of Ce ground state at very low temp. 8-67999
 $Al_2O_3:Fe^{2+}$, phonon spectroscopy using superconducting tunnel junctions 8-91389
 $BaClF:Sm^{2+}$, energy levels, optical props. 8-84631
 Ba_2EuNbO_6 , luminescence Raman spectra, means for localisation of binding energy levels (German) 8-88304
 Ba_2EuTaO_6 , luminescence Raman spectra, means for localisation of binding energy levels (German) 8-88304
 $BaO:Mn^{2+}$, impurity pot. well shape calcs. 8-87950
 $BaTbO_3$, perovskite struct., Tb^{4+} EPR obs., cryst. field parameters determ. (Italian) 8-52350
 $Ba[Fe(CN)_6] \cdot 2H_2O$, NMR, H_2O orient. (French) 8-52366
 $Be_2SiO_4:F$, EPR and ENDOR 8-76295
 $CaF_2:Eu^{2+}$, nuclear spin diffusion barrier, ^{19}F NMR Obs. 8-64282
 $CaF_2:Gd^{3+}$, S-state splitting, investigation by ESR and ENDOR at high pressure 8-52345
 $CaF_2:Tm^{3+}$, 8.2 keV excited state, mag. props., Schottky ht. capacity, nucl. quadrupole splitting 8-76037
 $CaO:Mn^{2+}$, impurity pot. well shape calcs. 8-87950
 $Ca_3(PO_4)_2:F:Nd^{3+}$, optical fluorescence intensity and cryst. field parameters 8-52570
 Cd, electron density at nucleus, press. depend., Hartree SCF calcs. 8-56411
 Cd, photoelectron spectra, 4d spin-orbit splitting, crystal field and band-broadening effects, CNDO calcs. 8-76577
 Ce compounds, rocksalt type, low temp. thermal props. 8-84445
 $CeAg(Mg)(Zn)$, magnetic struct. and cryst. field, neutron diff. exam. 8-72328
 $CeAl_2$, mag. anisotropy, transition, crystal field splitting 8-52243
 $CeAl_2$, NMR, cryst. field effects and mag. order in low temp. phase 8-68391
 $Ce_{30}Au_{20}$, amorphous, cryst. field effects and mag. interactions, magnetisation and transport props. meas. 8-68191
 $Ce_{1-x}La_xAl_2$, extraordinary Hall effects, 4.2-300K, cryst. field interaction 8-79980
 $CeO_2:Yb^{3+}$, ENDOR, evidence for covalency 8-80247
 CeS, mag. props., sp. ht. and thermal expansion 8-60292
 CeSe, mag. props., sp. ht. and thermal expansion 8-60292
 CeTe, mag. props., sp. ht. and thermal expansion 8-60292
 CeZn, mag. struct. and cryst. field effects 8-52223
 Co^{2+} in crystal, Racah parameter 8-56110
 $CoAl_2O_4$, electron density distrib. 8-51481

crystal field interactions continued

- Cr^{3+} , electronic states interactions with crystal odd vibr., R-lines vibr. recurrences 8-84639
 Cr^{3+} impurity spectra anal. with Trees' correction 8-68539
 CrO_2 radical in K_2CrO_4 and $KCrO_3Cl$, g-factor anisotropy 8-67994
 $Cs_2Hf(C_2O_4)_4 \cdot nH_2O$, electric field gradient at metal site, γ -ray perturbed ang. correlation meas. 8-52380
 $Cs_2NaEuCl_6$, luminescence Raman spectra, means for localisation of binding energy levels (German) 8-88304
 $Cs_2NaTbCl_6$, $Tb^{3+} \rightarrow ^5D_4 \rightarrow ^7F_1$ transitions, mag. and elec. dipole intensities 8-76033
 $CsUF_6$, D_3d distortion on octahedral UF_6^- complex (French) 8-84173
 Cu^{2+} , dopant, ground state wavefunctions and Δg 8-64012
 Cu-Cr, dil. alloy, Knight shift temp. depend., electronic struct. 8-84488
 $Cu(NH_3)_4PtCl_4$, $Cu(NH_3)_4^{2+}$ cation mol. orbital parameters 8-64011
 $CuSiO_3 \cdot 2H_2O$, chrysocolla, electronic absorpt. spectra 8-92087
 Dy, magnetic anisotropy and ^{161}Dy Mossbauer effect 8-92001
 Dy-Cu amorphous mag. alloy, linear sp. ht. due to single-ion excitation 8-91874
 Dy_2Co_3 , cryst. field effect on mag. moment direction, neutron diff. meas. 8-80132
 DyH_2 , mag. and electronic props., ^{161}Dy Mossbauer spectroscopy 8-80262
 $DyIG$, mol. field coeffs., magnetisation and mag. susceptibility anal. 8-95406
 $ErAl_2$, crystal field study rel. to $La_{0.9}Er_{0.1}Al_2$ 8-76036
 Er_2Co_3 , cryst. field effect on mag. moment direction, neutron diff. meas. 8-80132
 $ErCu$, cubic antiferromag., mag. excitations inelastic neutron scatt. meas. 8-72341
 $ErFe_2$, excited state spin waves inelastic scatt. meas. 8-76234
 $ErFe_2$, Laves phase, cryst. field effects on spin wave dispersion relations 8-84408
 $ErFeO_3$, far IR spectra 8-88303
 ErH_3 , cryst. fields and mag. props. 8-68181
 $ErSb$, cryst. field effects on transport props. 8-72133
 Eu complex, $(Et_4N)_3[Eu(NCS)_6]$, Eu^{4+} ion site symm. 8-84656
 $(EuX_6)_3$, (X=Br, Cl), spectral hypersensitive intensity, ligand polarisability contrib. 8-51946
 Fe complex, $Fe(III)$ tris diseleno chelates, sextet doublet Boltzmann equilib. Mossbauer spectra 8-60366
 Fe complexes, electronic and mag. struct., semiempirical MO cluster calcs. 8-62733
 Fe^{3+} -doped crystals, mag. susceptibility, cryst. field calc. 8-76035
 $FeCl_2 \cdot 2D_2O$, magnon-phonon coupling 8-72530
 $FeCl_2 \cdot 2H_2O$, also deuterated, electronic transitions in Raman spectra 8-80337
 $FeFe_2$, theory of Raman scattering, coupled phonon-magnon excitations 8-72531
 $Fe_3Mg_{1-x}SO_4 \cdot 7H_2O$, EFG tensor evaluation, ^{57}Fe single crystal Mossbauer meas. 8-88237
 Fe_3O_4 , Mossbauer spectra above Verwey transition 8-68415
 Fe_3O_6 , O_2 annealed, optical absorpt., spin struct., polaronic absorpt., cryst. field transitions 8-68493
 $Fe_{0.996}S$, $Fe_{0.93}S$, determination of quadrupole splitting sign, ground state appl. 8-76363
 Gd^{3+} -doped crystals, mag. susceptibility, cryst. field calc. 8-76035
 $Gd_3Ga_5O_{12}:Nd^{3+}$, cryst. field anal. 8-64013
 $(Gd_0.5Y_{0.5})_3Ni$, FeB struct., cryst. field effects on mag. struct. 8-52226
 H linear chain of atoms, electronic struct. calc. 8-79969
 H_2 monolayer, on triangular lattice, orientational phases 8-75934
 HfO_2 , chem. induced elec. field gradient, perturbed ang. correl. obs. 8-80257
 $HfO(H_2PO_4)_2 \cdot H_2O$, chem. induced elec. field gradient, perturbed ang. correl. obs. 8-80257
 HfF_6 , chem. induced elec. field gradient, perturbed ang. correl. obs. 8-80257
 $HfSiO_4:U^{4+}(U^{5+})$, opt. spectra 8-88334
 Ho_2Co_3 , cryst. field effect on mag. moment direction, neutron diff. meas. 8-80132
 $HoFe_2$, spin wave and cryst. field excitations, neutron scatt. 8-68196
 $HoIG$, mol. field coeffs., magnetisation and mag. susceptibility anal. 8-95406
 $Ho_2Tb_{1-x}Fe_2$, single crystals, continuous spin orientations, magnetisation easy direction 8-84453
 $Ho_2Y_{1-x}F_3$, calc. of $Ho^{3+} \rightarrow Ho^{3+}$ energy transfer rates (French) 8-79966
 ^{181}Ho , ^{181}Ta , dil., elec. field gradient at impurity, anomalous temp. depend., host 4f levels, γ - γ correls. 8-95272
 In, electron density at nucleus, press. depend., Hartree SCF calcs. 8-56411
 IrF_6 , in mixed crystals, Jahn-Teller effect, $\Gamma_8(t_{2g})^3$ state, 6800 Å 8-76032
 IrO_2 , electronic struct., XPS obs., rel. to TiO_2 , RuO_2 8-52632
 KCl, cluster expansion of density matrix and crystal energy 8-87952
 $KCl:Pb^{2+}(0.005\% Pb)$, A band fine structure, electron-phonon interaction 8-60491
 $K_4Fe(CN)_6 \cdot 3H_2O$, internal field and ferroelec. ordering 8-76406
 $K_4Hf(C_2O_4)_4 \cdot nH_2O$, electric field gradient at metal site, γ -ray perturbed ang. correlation meas. 8-52380
 $KMgF_3:Cr^{3+}$, trigonal centres, EPR lines, pseudo-Stark splitting 8-68367
 $KY_3F_{10}:Eu^{3+}$, fluoresc. intensity, 77 to 4K, cryst. field parameters of Eu^{3+} 8-72580
 $KY_3F_{10}:Eu^{3+}$, fluoresc. decay, radiative and nonradiative transition probabilities 8-72581
 La, ground state, two band Hubbard model, for almost mixed valence system 8-84171
 La-Pr, superconductive tunnelling, cryst. field effects 8-88085
 $LaAl_2$, cryst. field splitting and spin-spin interaction of Eu^{2+} and Gd^{3+} , ESR meas. 8-68370
 $LaAl_2:Gd^{3+}(Eu^{2+})$, cryst. field parameters, relax. rates 8-84482
 $LaAl_3$ -Ce, dil., linewidth of cryst. field excitations 8-76988
 $LaBe_{13}:Er(Dy)(Gd)$, ESR, crystalline field single ion effects 8-84481
 $LaBe_{13}:Er(Dy)$, dil., ESR, crystalline elec. field splitting, exchange parameters 8-52348
 $LaCl_3:Pr^{3+}$, crystal field parameters using multiple-scatt.- X_α method 8-95271
 $La_{0.9}Er_{0.1}Al_2$, crystal field study rel. to $ErAl_2$ 8-76036
 $LaF_3:Ho^{3+}$, site symmetry and selection rules 8-60514

crystal field interactions continued

- La_{1-x}Pr_xSn₃, supercond., 0.6 meV cryst. field transitions, neutron spectroscopy 8-67991
 LaPt₃, cryst. field effects on transport props. 8-72133
 LaSb, cryst. field effects on transport props. 8-72133
 La_{1-x}Tb_xAg, supercond., 0.6 meV cryst. field transitions, neutron spectroscopy 8-67991
 La_{1-x}Tb_xAl₂, supercond., 0.6 meV cryst. field transitions, neutron spectroscopy 8-67991
 La_{1-x}Tb_xSn₃, supercond., 0.6 meV cryst. field transitions, neutron spectroscopy 8-67991
 LiNbO₃:Co, optical props. 8-64383
 LiTbF₄, Tb³⁺ absorption spectra, 4000 to 25000 cm⁻¹ 8-72550
 Lu-rare earth, dil., cryst. fields 8-80127
 LuAG:Nd³⁺, cryst. field anal. 8-64013
 LuBe₁₃:Er(Dy)(Gd), ESR, crystalline field single ion effects 8-84481
 LuBe₁₃-Er, dil., ESR, crystalline elec. field splitting, exchange parameters 8-52348
 Lu₃Ga₅O₁₂:Nd³⁺, cryst. field anal. 8-64013
 Mg, electric field gradient and Knight shift, temp. depend., OPW calcs. 8-56387
 MgCs₂(SeO₄)₂·6H₂O, EPR, crystal field and hexahydrate distortion 8-91938
 MgK₂(SeO₄)₂·6H₂O:Mn²⁺, EPR, crystal field and hexahydrate distortion 8-91938
 Mg₂MnO₈, EPR in magnesium-manganese spinel (*Russian*) 8-91936
 MgO:Cr³⁺, strain modulated ESR 8-88175
 Mn complex, MnCl₂·3,5-lutidine hydrochloride complex, photoluminesc. and photoexcitation 8-92106
 MnBr₂, vibr. struct. in cryst. field electronic transitions 8-59895
 MnCl₂, vibr. struct. in cryst. field electronic transitions 8-59895
 MnO-Al₂O₃-SiO₂ glass, spin freezing, muon spin depolarisation, superparamag. domain model 8-68272
 N₂, dynamically induced electronic transitions of matrix isolated atom 8-63825
 (NH₄)₄Hf(C₂O₄)₄·nH₂O, electric field gradient at metal site, γ-ray perturbed ang. correlation meas. 8-52380
 NaCl:Cu⁺, X-irrad. at room temp., ESR of Cu²⁺ centres 8-52343
 Na₄Hf(C₂O₄)₄·nH₂O, electric field gradient at metal site, γ-ray perturbed ang. correlation meas. 8-52380
 Na₂S:Gd³⁺ crystal field splitting, parametrisation of temperature dependence 8-91652
 Nd³⁺:scheelite-type crystals, magnetic, thermal properties, cryst. field calcs. 8-91875
 NdP₂O₁₄, laser site-selection time-resolved spectroscopy 8-76524
 (NdX₃)₃, (X=Br, Cl, I), spectral hypersensitive intensity, ligand polarisability contrib. 8-51946
 NiBr₂, photoconductivity spectrum meas. using rate of charge method, transport props. 8-60160
 NiBr₂, vibr. struct. in cryst. field electronic transitions 8-59895
 NiCl₂, vibr. struct. in cryst. field electronic transitions 8-59895
 Ni(CIO₄)₂·6H₂O, EPR and IR spectra, 98-298K, phase transition at 224K 8-84477
 PbFCl:Gd³⁺(Eu²⁺), crystal field splitting, parametrisation of temperature dependence 8-91652
 PbF₂(Cl₂)(Br₂) 8-72082
 Pr pnictides and chalcogenides, press. depend. of cryst. field splitting 8-68392
 Pr³⁺, configuration interaction contrib. to correlation cryst. field 8-56111
 Pr-Nd (5%), impurity modes and mag. ordering 8-84422
 PrAl₃, crystal field splitting of Pr³⁺, inelastic thermal neutron scattering 8-67996
 PrCu₂, cryst. field transitions near cooperative Jahn-Teller transition 8-84178
 PrCu₅(Pt₅), cryst. field effects on transport props. 8-72133
 PrD₂, neutron scatt. and cryst. fields 8-79970
 PrD_{2.5}, neutron scatt. and cryst. fields 8-79970
 Pr₃Tl, induced ferromag., mag. props. under hydrostatic press. 8-56315
 Pr₃Tl, linewidth of cryst. field excitations 8-67988
 PrVO₄, energy levels, opt. and NMR meas. 8-80226
 Rb₂Cu(SO₄)₂·6H₂O, single cryst., fine struct., mag. dipole coupling, EPR obs. 8-68360
 Rb₄Hf(C₂O₄)₄·nH₂O, electric field gradient at metal site, γ-ray perturbed ang. correlation meas. 8-52380
 RuO₂, electronic struct., XPES obs., rel. to TiO₂, IrO₂ 8-52632
 Sb, electron density at nucleus, press. depend., Hartree SCF calcs. 8-56411
 SmH₂, low temp. sp.ht., antiferromag. ordering and cryst. field splitting effects 8-84439
 Sn, electron density at nucleus, press. depend., Hartree SCF calcs. 8-56411
 SrCl:Mn²⁺, shape of potential well, calc. 8-87951
 SrCl₂:Fe²⁺(Co²⁺) electronic absorption spectra in far and middle infrared 8-68537
 SrCl₂:Mn²⁺(Co²⁺), cubic impurity EPR spectra, elec. field effect, mechanism 8-68361
 SrO:Mn²⁺, impurity pot. well shape calcs. 8-87950
 SrO₂:Fe²⁺(Fe³⁺), EPR spectra, evidence for off-centre displacement of Fe²⁺ 8-72398
 Tb₄Co₃, cryst. field effect on mag. moment direction, neutron diff. meas. 8-80132
 TbIG, appl. of superposition model to cryst. field 8-68132
 TbIG, mol. field coeffs., magnetisation and mag. susceptibility anal. 8-95406
 Te, electron density at nucleus, press. depend., Hartree SCF calcs. 8-56411
 ThBe₁₃:Er(Dy)(Gd), ESR, crystalline field single ion effects 8-84481
 ThSiO₄:U⁴⁺(U⁵⁺), opt. spectra 8-88334
 TiO₂, electronic struct., XPES obs., rel. to RuO₂, IrO₂ 8-52632
 TiBr-VBr₂ system, cryst. struct., DTA investig. (*German*) 8-72766
 Tm₄Co₃, cryst. field effect on mag. moment direction, neutron diff. meas. 8-80132
 TmSb, cryst. field effects on transport props. 8-72133
 TmSe, mixed valence systems, spin dynamics and mag. ordering 8-68162
 TmZn, cooperative Jahn-Teller effect 8-67998
 U complex, U(acac)₃, cryst. fields, mag. susceptibility, chem. shift (*French*) 8-84179
 U³⁺, screening factors (*French*) 8-72119

crystal field interactions continued

- U⁴⁺, cryst. field effects and screening factors (*French*) 8-72119
 UO₂, optical props. and electronic struct. 8-68527
 U(OH)₂SO₄, cooperative Jahn-Teller effect, mag. susceptibility meas. 8-72121
 UPd₃, crystalline electric field levels of U, neutron scatt. exam. 8-60267
 Y-rare earth, dil., cryst. fields 8-80127
 YAG:M³⁺, ESR absorption spectra, line broadening of Fe³⁺, Cr³⁺, Gd³⁺ 8-91940
 YAG:Nd³⁺, cryst. field anal. 8-64013
 Y₃Ga₅O₁₂:Nd³⁺, cryst. field anal. 8-64013
 Y₂O₃:Eu²⁺, absorpt. spectra, fluoresc., electron beam excitation 8-92093
 YVO₄:Eu³⁺, absorpt. spectra, fluoresc., electron beam excitation 8-92093
 YVO₄:Eu³⁺, laser site-selection spectroscopy investigation 8-68556
 Zn-Cr, dil., mag. anisotropy, 0.001 to 2K 8-68157
 ZnO, light sensitivity rel. to local internal fields (*Russian*) 8-49932
 ZrSiO₄:U⁴⁺(U⁵⁺), opt. spectra 8-88334

crystal field splitting *see* **crystal field interactions****crystal field theory** *see* **crystal field interactions****crystal fields** *see* **crystal field interactions****crystal filters**

- 220 MHz acoustic bulk wave resonator and filter realisation 8-59245
 SAW in-line chirp filter applications 8-59207
 LiNbO₃ UHF SAW filters using group-type unidirectional interdigital transducers 8-59252

crystal growth

see also **crystal growth from melt**; **crystal growth from solution**; **crystal growth from vapour**; **crystal purification**; **crystallisation**; **dendrites**; **epitaxial growth**; **nucleation**

- actinide metal preparation and refining 8-84705
 n-alkenes, n even, interaction energy at twin boundary, dihedral reentrant, salient angle effect on growth morphology 8-55876
 dendrites, growth models, steady state, exam. 8-72052
 generalised kinetic equation, growth spiral in chem. pot. gradient 8-87631
 Lennard-Jones (100) crystal-liquid interface, structure 8-91284
 polytypism, some aspects in crystals, rel. to growth 8-83764
 preparatory experiments for first Spacelab flight 8-88414
 quartz, dissolution of grown synthetic quartz inside the autoclaves 8-63911
 quartz, synthetic, growth boundary between -X and Z sectors 8-59775
 quartz, synthetic, growth sector boundary between -X and Z sectors 8-59774
 roughening models, step free energies, and correlation functions in X-Y models 8-67675
 solid-on-solid model, screw dislocations, rel. to correl. in X-Y model 8-63691
 Spacelab, crystal growth expts. 8-52647
 Spacelab, past and future cryst. growth in space 8-80462
 Spacelab crystal growth expts. 8-52648
 stress in growing crystals, effects of radial and axial temp. gradients (*German*) 8-67672
 temperature field for crystal growing, electrical analogue model (*German*) 8-63688
 BN, cubic, water catalysed form. 8-53199
 (Ba₃Nb₆Si₄O₂₆)_n.Ba₃Nb₄Ti₄O₁₁, n=3/2 to 29/2, intergrowth series, electron microscope obs. (*French*) 8-83762
 Cd₁Hg_{1-x}Te, IR detector appls., prep., elec. props. (*German*) 8-86332
 Cr_{12-x}W_xP₇, solid solns., prep., cryst. struct. (*French*) 8-63723
 α-Fe single crystal whiskers, controlled growth by H reduction of ferrous halides, X-ray and SEM exam. of crystals 8-60554
 Mn_{12-x}W_xP₇, solid solns., prep., cryst. struct. (*French*) 8-63723
 Nd, single crystal prep. by solid state electrotransport 8-84709
 Pr, single crystal prep. by solid state electrotransport 8-84709
 SeMoOCl₄, prep., cryst. struct., characterisation (*French*) 8-63722
 Si₃ON₂ needle crystal growth by nitriding Si-SiO₂ system in powder compacts (*Japanese*) 8-68609
 Sn₂Pb_{1-x}Te mixed cryst., cryst. growth and assessment 8-80463

crystal growth from gel

- KClO₄, single crystals, growth by modified gel technique 8-72711
 PbCO₃ whiskers, growth kinetics in silica gel 8-75971
 ZnS, cubic, expt. conditions 8-68614

crystal growth from melt

- see also* **liquid phase epitaxial growth**; **zone melting**
 alkali halide crystals, optical components, melt growth conditions 8-50955
 anthracene, prep. and growth of single cryst. 8-64463
 Burton-Prim-Slichter equation, interpret. of diffusion boundary layer thickness 8-87636
 bytownite megacrysts., study of trapped basaltic melts, petrogenetic process study 8-95688
 Chevrel type compounds, single crystals, growth, stoichiometry, elec. resist. 8-92187
 dilute binary alloy monocrystal, thermodynamics of growth, model (*French*) 8-87635
 disjoining pressure repulsion of macroscopic particle ahead of crystn. front. 8-95005
 duren-p-dibromobenzene system, phase diagram and X-ray diff. expts. 8-79774
 high pressure chamber, for cryst. growth, temp. field distrib. determ. 8-82001
 high temperature reaction cell for microscopic obs. 8-64457
 horizontal ribbon growth from melt, theoretical anal. 8-75604
 ice-water interface struct., fluctuations during solidification 8-59935
 impurity incorporation, kinetic factor effects 8-52656
 impurity incorp., effect of crystallisation front oscils. 8-52657
 liquid encapsulated Czochralski crystal growth, pressurised chambers 8-64459
 low-melting point materials, appl. of Czochralski method 8-76599
 macroparticle capture by growing cryst., influence of particle thermal cond. 8-79543
 magnetic garnet, comp. anal. by AAS 8-92585
 metals, crystal growth, electrochem. Czochralski method, growth rate limitations 8-88433

crystal growth from melt continued

- organic compounds grown by Czochralski technique, assessment of perfection 8-64460
oxide single crystals, Czochralski grown, thermoelectric stresses 8-55822
particle trapping in cryst. growing from melt at variable rate 8-67676
polyethylene oxide, melt grown single crystal, isothermal growth, thickening and melting 8-51432
pyridinium cuprous bromide, solid electrolyte 8-64462
rare earth $Zr_{1-x}O_{2-x/2}$ growth from skull melting, directional solidification 8-60567
ribbon-form material, rapid quenching from melt (*Japanese*) 8-92210
ruby, cryst., optical properties, effect of annealing near melting point 8-90419
ruby rod, EPR study, comparison of Verneuil and Czochralski grown crystals 8-91945
sapphire, profiled growth, struct. perfection 8-68621
secondary nucleal birth and growth rate in single-seeded batch crystalliser 8-83759
semiconductor single crystals, melt grown, dislocation creation by thermal stresses 8-83825
thermoelastic stress distribution in single cryst. pulling by Czochralski technique 8-63681
vertical directional crystallisation device, heat transfer, analytical investigation. (*Russian*) 8-52654
wide ribbon growth by multiple inert gas jet thermal profile control 8-64458
AgGaS₂, optical quality, grown from melt, EPR characterisation 8-64260
Ba₂Na(Nb,Ti)₂O₁₅, prep. and electro-opt. props. 8-76432
Ba₂TiGeO₈-Ba₂TiSiO₈, pseudobinary system, pyroelectricity and related props. 8-95553
Bi, growth of single cryst. wires with high resistivity ratios 8-68622
Bi₃B₅O₁₂, crystal growth from melt, exam. of growth kinetics 8-72717
Bi₂GeO₂₀, single crystals. optical homogeneity depend. on growth conditions 8-95007
CaF₂ crystals, grown from synthetic raw materials, quality, effect of impurities, composition 8-79083
 ω -Cd-Hg alloy, melt-growth, morphology of single crystals. 8-64464
Cu-Nb, supercond. wire, directional solidification of melts, supercond. ionisation temp. (*Russian*) 8-76596
Cu₂O, growth by melting, photocond. spectra 8-52029
DyAG, single cryst. growth by Czochralski method 8-95690
Dy₂Al₂O₁₂, Czochralski growth, interface shape transitions 8-59772
DyF₃, crystal growth by Bridgman-Stockbarger method and Czochralski method 8-52660
ErAG, facet formation 8-63687
ErF₃, crystal growth by Bridgman-Stockbarger method 8-52660
Ga, contact angle meas. between melt and crystal during Czochralski growth 8-64461
GaAs, grown-in dislocation density, impurity effect 8-51543
n-GaAs, melt-grown, stoichiometry, photolum. obs. 8-72583
Ga_{0.4}In_{0.6}PyAs_{1-y}, In rich bulk single crystals. growth from melt via gradient freeze method, and characterisation 8-68618
GaSb, pulled crystal, microfacet obs. near irregularly remelted surfaces 8-91278
GdF₃, crystal growth by Bridgman-Stockbarger method 8-52660
GdGa garnet, Czochralski grown, substrate material dislocation propagation 8-59771
Gd₂Ga₂O₁₂, Czochralski grown, effect of melt flow phenomena on perfection 8-88419
Gd₂Ga₂O₁₂, growth of 3" diameter crystals 8-68616
Gd₂Ga₂O₁₂:Nd³⁺, growth, stimulated emission, spectral props. 8-95593
Gd₂(MoO₄)₃, and isotypes exam. of crystal growth, and defect generation 8-68617
Ge, contact angle meas. between melt and crystal during Czochralski growth 8-64461
Ge:Ga, effects of destabilising vertical thermal gradients on cryst. growth and segregation 8-52659
HgSe-CdSe pseudobinary alloy, phase diagram and cryst. growth 8-68620
HoF₃, crystal growth by Bridgman-Stockbarger method and Czochralski method 8-52660
In_{0.4}Ga_{0.6}Sb, vertical Bridgman Stockbarger growth, magnetic field effect 8-60565
InP, grown-in dislocation density, impurity effect 8-51543
InSe, layered crystalline slabs, growth by Czochralski method 8-68619
KCl, Czochralski-grown, dislocation subboundary characts. 8-67718
KCl, spiral growth, screw dislocation mechanism, phase-contrast microscopy obs. 8-76737
KNbO₃, single domain crystal growth, SHG with Nd:YAG laser 8-74954
KNbO₃ single crystals, preparation of pure, Fe doped, and reduced crystals 8-60564
Li₂N single crystals, Czochralski growth, exam. 8-56574
Mg, melt grown by Bridgman method, X-ray topography 8-59770
NaCl:Ca, light scattering coeff., effect of growing condition 8-55418
NaCl:LiCl, melt, semiperiodic closed growth lamellae on crystal-melt interface 8-67668
NiO, oriented bicrystal growth by floating zone and Verneuil's method (*French*) 8-92186
PbWO₄, growth by Czochralski method, props. 8-60566
Pb(WO₄)_{1-x}(MoO₄)_x mixed crystal, growth by Czochralski method, props. 8-60566
Se_{0.9}-Te_{0.1} alloy crystals, growth and cleavage 8-88421
Si, carrier lifetime degradation at room temp. 8-95301
Si continuous polycrystalline films on C substrates 8-64490
Si, crystal defects in integrated circuits, review 8-88547
Si, Czochralski growth with automatic diam. control 8-52658
Si, metallurgical grade, purification and charact. 8-56573
Si plate prod. by Stepanov method, stability analysis (*Russian*) 8-52655
Si, polycryst. manufacturing methods for photovoltaic energy prod., solar cells, grain growth from melt (*Dutch*) 8-52661
Si, preshaped single crystal prep. by pendant drop method (*French*) 8-64466
Si ribbon, crystal characterisation, growth with dies 8-76598
Si, ribbon, impurity distrib. in EFG 8-91280
Si, ribbon edge-defined film-fed growth control using C-CD imagers 8-68623

crystal growth from melt continued

- Si, ribbon growth via RTR technique, process update and material characterisation 8-76597
Si ribbon parallel twinned structure development by shaped crystallisation 8-64465
Si wafers, Czochralski, gettering of surface and bulk impurities 8-64456
Sn, crystn., mechanism of influence of soluble impurities 8-71692
Sr_{0.75}Ba_{0.25}Nb₂O₆, large cryst. growth, control of opt. defects 8-76595
Tb-Y, single crystal growth from melt, X-ray obs., props. (*Russian*) 8-95689
TbF₃, crystal growth by Bridgman-Stockbarger method 8-52660
TiO₂, plasma growth, photoelectronic props. 8-52662
YAG, Czochralski grown crystals, interface shape change 8-83760
YAG, facet formation 8-63687
Zn, bicrystals grown by modified Bridgman technique 8-60563
ZnGeP₂, synthesis, characts., applic. to laser windows (*French*) 8-80467
ZnSe_{0.9}S_{0.1}, melt grown, 10K, band edge photoluminesc. 8-84628

crystal growth from solution

- see also *crystal growth from gel; liquid phase epitaxial growth*
cellulose II, preparation and crystal growth, electron diff. obs. 8-91285
citric acid monohydrate, crystallisation and cryst. growth rate 8-87638
crystalliser, with precision control of supersaturation 8-80465
diffusive mass transfer in crystal growth, exam. 8-67669
dipropylammonium manganese chloride, layer perovskite, step bunching obs. by compound holographic microscopy 8-63682
glutamic acid hydrochloride, L(+), solution growth of large single crystals, using cylindrical seeds 8-60556
hydrothermal synthesis and growth, selection of mineralisers 8-72715
interface reaction const., correl. with elementary surface process 8-63683
low gravity growth 8-84706
metal ion adsorption, nucleation effects (*German*) 8-68635
polymer nucleation, bundle-like and longit. growth of fibrillar crystal from flowing soln. 8-51433
proteins, effect of protein conc. and solubility on nucleation rate 8-87632
PVC:Fe(Cu) film, struct. and optical props., soln. growth technique 8-51837
 α -quartz dislocation free and low dislocation, prep. by hydrothermal crystallisation 8-72712
quartz synthetic crystals, observation of growth defects by light scatt. tomography 8-71743
rate constant of reaction, determ. from overall crystal growth coeff. 8-59773
rubidium acid phthalate, solution growth of large single crystals, using cylindrical seeds 8-60556
stearic acid, grown from benzene soln., etch pit obs. of dislocations 8-87676
succinonitrile, undercooled, analysis of dendritic growth 8-75970
TGS, soln. growth of large single crystals, using cylindrical seeds 8-60556
triglycine fluoroberyllate, solution growth of large single crystals, using cylindrical seeds 8-60556
Ag, single crystal, adsorption of metal ions on (111) and (100) surfaces (*German*) 8-68636
AlPO₄ hydrothermal synthesis 8-60562
BaB₆, (La,Ba)₆, (Ea,Ba)₆, single crystal growth for thermionic emission 8-92183
BaSO₄, crystal growth, effect of nitrilotri (methylenephosphonic acid) adsorption 8-88417
Bi₂WO₆ single crystal, growth from flux in Bi₂WO₆-Na₂WO₄, below transformation temperature 8-72713
CaCO₃, acceleration of growth of particles, Lorentz forces, electric and mag. field effects 8-51455
Ca₂Fe₂(Mn₂)Ge₂O₁₂, single magnetic sublattice antiferromagnetic garnets 8-52652
CdI₂, soln. grown, rotation twinning, arcing and polytypism 8-51557
CdNd₄(SiO₄)₃O, synthesis, cryst. struct. 8-87653
CdTe cathodic deposition from aqueous electrolytes 8-64484
CdTe, growth by travelling heater method, high resistivity charact., γ -ray detector appl. 8-84707
CeB₆, single crystal growth for thermionic emission 8-92183
CsH₂PO₄, single cryst. growth, struct. and elec. props. 8-71693
CsI, selective etching, growth and dissolution in alcohols 8-71739
Cu complex, bis-(alkylammonium) (11) tetrachloride, perovskite, lattice perfection 8-87633
Cu complex, bis-(alkylammonium) Cu(11)tetrachloride, perovskite, face struct. and growth rate 8-87634
Cu ferrites, crystallisation of monocrystals from high temp. soln. 8-60561
ErOHCO₃, synthesis of rare earth carbonates under hydrothermal conditions 8-72714
EuB₆, (La,Eu)₆, (Eu,Y)₆, (Eu,Ba)₆, single crystal growth for thermionic emission 8-92183
n-GaP, cryst. growth, synthesis solute diffusion method, elec. characts. (*Korean*) 8-52653
GaP, soln. growth of bulk crystals., luminesc. and elec. props. 8-92181
GdOHCO₃, Gd₂O₃, CO₃, synthesis of rare earth carbonates under hydrothermal conditions 8-72714
InP, crystal growth by synthesis solute diffusion method 8-64454
K₂Al₂(SO₄)₄.24H₂O, growing in aqueous solution, observation of secondary nuclei production 8-68613
 α -K₂Cr₂O₇, symmetry centres exam. by morphological methods 8-59796
K(H,D)₂PO₄ crystals, effect of isotopic replacement on growth kinetics 8-95006
KH₂(D_{1-x})₂PO₄, X-ray topographic study of growth strains in single crystal 8-91279
KH₂PO₄, liq. inclusion formation during large cryst. growth 8-64455
K₂SO₄.Al₂(SO₄)₃.24H₂O, stirring effect on crystalline quality of soln. grown crystals 8-91281
(La,Cs)₆, single crystal growth for thermionic emission 8-92183
(La,Y)₆, (Eu,Y)₆, single crystal growth for thermionic emission 8-92183
LaB₆, (La,Eu)₆, (La,Y)₆, (La,Ba)₆, (La,Cs)₆, single crystal growth for thermionic emission 8-92183

crystal growth from solution continued

- LaOHCO₃, La₂Cl(CO₃)₄, synthesis of rare earth carbonates under hydrothermal conditions 8-72714
 α -LiIO₃, cryst. growth by conc. convection of soln. 8-72716
 MgSO₄, rate constant of reaction, determ. from overall crystal growth coeff. 8-59773
 MgSO₄·7H₂O, growing in aqueous solution, observation of secondary nuclei production 8-68613
 (NH₄)₂SO₄, single crystal growth from aq. soln. (*Japanese*) 8-92182
 NaBO₂·H₂O·3H₂O, crystallisation from aq. soln., nucleation rates with surfactant 8-91276
 NaBO₂·2H₂O·3H₂O, crystallisation from aq. soln., growth kinetics with surfactant 8-91277
 NaClO₃, growth and dissolution kinetics, diffusion and convection regimes 8-63684
 Na₂O·3MoO₃, nucleation of fibrillar crystals, effect of surface layer, growth on air bubbles 8-60559
 NdFeTiO₃, magnetic props. and crystal growth 8-92185
 Nd₂O₃·4TiO₂, growth from soln., struct. 8-83794
 Pb-S-I-X-H₂O, (X=solvent) crystallisation conditions 8-80466
 Pb₂MgNb₂O₉, crystal growth procedure, meas. electro-optic and dielectric props. 8-88418
 Pb₂MgTa₂O₉, crystal growth procedure, meas. electro-optic and dielectric props. 8-88418
 γ -4PbO·SiO₂, synthesis and struct. 8-71716
 PrP₂O₁₄, chemical synthesis and crystal growth of laser quality 8-92184
 RPO₄-Pb₂P₂O₇, R=Tb-Lu, solubility curves for high temp.-melts for growth of single crystals. 8-95687
 SrSO₄, mass transfer in precip. from mixed solvents (*German*) 8-67674
 Tm₂O₃, mineraliser effect on growth morphology 8-91283
 YOHCO₃, synthesis of rare earth carbonates under hydrothermal conditions 8-72714
 YPO₄-Pb₂P₂O₇, solubility curves for high temp.-melts for growth of single crystals. 8-95687
 YSmLuCaGeIG, mag. props. and defects, depend. on B₂O₃ conc. on growth in PbO-B₂O₃ solvents 8-68321
 ZnO, wurtzite structure, hydrothermally grown exam. of thermal expansion coefficient 8-75854
 ZnS cubic single crystals, growth by double decomposition reaction in melt 8-60557
 ZnSO₄, rate constant of reaction, determ. from overall crystal growth coeff. 8-59773
 ZnSnP₂-ZnSiP₂, heterocombination simultaneous crystallisation 8-60560

crystal growth from vapour

see also vapour phase epitaxial growth

- acetylene, spherical cryst. grown in situ for low-temp. X-ray work 8-68612
 alkali halide, morphology of growth and evaporation surface 8-79544
 carbon tetrabromide, vapour deposition for optical studies, Raman spectra 8-64451
 ethane, spherical cryst. grown in situ for low-temp. X-ray work 8-68612
 ethylene spherical cryst. grown in situ for low-temp. X-ray work 8-68612
 frost growth rate prediction eqn. for cooled surfaces 8-87248
 GeO₂, hexagonal needle crystals, vapour growth 8-52651
 methane-d₄, solid, sound velocity meas., 4-77K 8-75734
 AgInS₃, crystal growth by I₂ vapour transport, using temperature variation method 8-68610
 Au crystallites, formation in flowing Ar system, density, size distrib. and size dispersion 8-88415
 CdBr₂, vapour grown crystals, polytype formation, effect of mode and conditions of growth 8-72709
 CdBr₂(I₂), vapour growth crystals, decomposition, electron microscope study 8-92268
 CdS, seeded growth from vapour of large single crystals 8-64449
 CdS:In whisker prep. 8-75969
 CoO on Co₂O₄, oriented growth following Co₂O₄ pyrolysis 8-80739
 Cr₂O₃, thin plate single crystal, vapour phase growth 8-64450
 Cr₂S₃, single crystal, exam. of unit cell structures by interference contrast microscopy 8-67670
 CuGaS₂, crystal growth by I₂ vapour transport, using temperature variation method 8-68610
 CuInS₂, crystal growth by I₂ vapour transport, using temperature variation method 8-68610
 Fe whiskers grown from FeCl₂·4H₂O, exam. of growth morphology 8-72051
 FeCr₂S₄, vapour grown, growth mechanism of multisteps on surface 8-75605
 Fe₂TiO₅, pseudobrookite, single cryst. growth by chem. transport 8-80464
 GaS, optimisation of crystal growth conditions by I₂ vapour transport 8-68611
 GaSe, optimisation of crystal growth conditions by I₂ vapour transport 8-68611
 GdAs₃, single crystals 8-88416
 Ge, ultrafine multiply twinned particles, form. by gas-evaporation technique 8-63685
 LaB₆, chemical vapour growth of whiskers, and single crystals 8-72710
 LaB₆ film, structure, stoichiometry, elec. properties 8-60043
 Nb₂Cr_{1-x}O₂, cryst. prep. and struct., mag. props. 8-52198
 Si monocrystalline rod growth from gas phase 8-64453
 SnO₂, crystal growth habits (*Japanese*) 8-95686
 Sn_{2-x}Se_x solid soln., resistivity, lattice parameter, comp. and temp. depend. 8-91693
 SnSe, sublimation growth, deviation from stoichiometry, elec. props. 8-76594
 TiB₂, chemical vapour growth by modified hot wire method 8-60555
 U_{1-x}Th_xO₂, solid solution, single crystal growth by chemical transport reactions 8-72708
 ZnAs₂, single crystals 8-88416
 ZnIn₂S₄ film, photoluminesc. and photocond. 8-52677
 ZnO, single cryst. growth in ZnO-H₂-H₂O-O₂ vapour, morphology, electrophys. and opt. props. 8-52649

crystal growth from vapour continued

- Zn₃P₂, photovoltaic material and Schottky diode characteristics 8-64066
 ZnSiP₂, conc. profiles during gas phase transport (*German*) 8-64452
- crystal hyperfine field interactions**
- alkali bromide (chloride):V²⁺, electron spin transfer 8-87949
 alkali halide:Hg, EPR and optical props. 8-91933
 alkali metal salts, NMR spectra of alkali metal nuclei, shielding and quadrupole coupling consts. 8-84487
 allowed β - γ angular correlations induced by mag. interactions 8-68419
 alloy, elec. field gradient analysis 8-51950
 antiferromagnet, local field at positive muon 8-92010
 diamagnetic lattice, EPR parameters of V⁴⁺, cryst. field effects 8-64263
 EPR of heteropairs with strong exchange coupling, hyperfine struct. 8-72395
 ferromagnet, amorphous and crystalline, evaluation of complex Mossbauer spectra 8-60370
 ferromagnet, local field at positive muon 8-92010
 ferromagnetic alloys, hyperfine field systematics of nonmag. ions 8-60093
 ferromagnetic metal-rare earth, dil., hyperfine fields 8-87947
 garnets, mag. props. of V⁴⁺ ion, effect of covalency 8-64010
 group IV elements, ⁵⁷Fe isomer shift, quadrupole coupling and interat. distance correl. 8-52408
 guanidinium aluminium sulphate hexahydrate:Mn²⁺, NMR 8-91939
 halides, NMR spectra of halogen nuclei, shielding and quadrupole coupling consts. 8-84487
 HCP metal, naive model for electric field gradient, numerical results for Zn 8-91650
 Heusler alloys, hyperfine fields and mag. interactions, NMR spectra 8-88222
 liquid crystals, lyotropic, ²³Na NMR quadrupole splittings, elec. double layers 8-76345
 magnetic insulators, indirect exchange interactions, polar model study 8-88110
 metal, antishielding effects and temp. depend. of field gradients 8-51951
 metal, elec. field gradient analysis 8-51950
 nuclear inelastic channel suppression, nuclear reson. and electronic scatt. of γ -quanta, hyperfine transitions 8-60361
 polarised ferromagnetic media, decelerating ion, transient field phenomena 8-72445
 press. depend. of effective mag. fields on ⁵⁷Fe nuclei 8-52383
 rare earth alloys, RAl₂, RZn, ordered, NMR determ. of hyperfine fields 8-84180
 rare earth alloys, RFe₂Al₃, cryst. struct. mag. props. and hyperfine interactions 8-87648
 rare earth intermetallics, R_xFe_y, conc. depend. of Fe moments 8-56413
 rare earth metals, heavy, NMR exam. of electric field gradient 8-52363
 rare earth-Au, dil., Mossbauer exam. of mag. hyperfine field at ¹⁹⁷Au impurity 8-88244
 rare earth-Fe alloy, RFe₂ (R=Tb, Dy, Ho and Y) crit. phenomena, Mossbauer exam. 8-52403
 rare-earth alloys, quadrupole scatt. anisotropy, magnetically ordered material 8-64034
 Si:Sb(P)(As), shallow donor states with strong central cell perturbation theory 8-51933
 spin Hamiltonian, higher order hyperfine terms, transition metal ion in octahedral symmetry field 8-79967
 superhyperfine structures, paramagnetic impurity, ligand nuclei interaction, calcs. 8-80195
 symmetry of lattice with hyperfine interactions at atomic nuclei 8-67677
 transient ESR line profiles, S=I=1/2, system, calcs. 8-88170
 transition metal-rate earth alloy, dil., hyperfine fields, theory 8-68226
 Ag-Pd, dil., elec. field gradient, conc. and temp. effects 8-68416
 AgClO₃, ClO₂ spin Hamiltonian 8-60326
 Al, hyperfine interactions of implanted Fe, conversion electron Mossbauer spectroscopy 8-52391
 Al:¹¹¹In, electron irradiat., defect trapping at impurities 8-55892
 Al₂O₃:V³⁺, frequency crossing signals of V³⁺ ions, conc. depend. study using thermal phonons 8-95115
 As₂Te_{3-x}Se_x, ¹²⁵Te Mossbauer expts., comparison of amorphous and cryst. samples 8-88232
 BaGeF₆, Group IV hexafluoride anion radical γ -irrad., EPR spectra 8-72411
 BaO-B₂O₃-SiO₂:Ti³⁺, optical absorpt. spectra 8-72564
 BaPbF₆, Group IV hexafluoride anion radical γ -irrad., EPR spectra 8-72411
 Be-Ru, dil., quadrupole interactions at ⁹⁹Ru, TDPAC meas. 8-91996
 CaF₂:Dy³⁺, Mossbauer obs. 8-64303
 CaF₂:Gd³⁺, ligand ENDOR cubic centres, elec. field effect (*Russian*) 8-60357
 Cd-Hg, dil., anomalously high elec. field gradients below 0.05K 8-72442
 CdI₂:M²⁺, M=V, Mn, Co, EPR 8-68362
 Cd_{1-x}Ni_xFe₂O₄, mag. behaviour, Mossbauer meas. 8-52390
 CeAl₃, NMR, cryst. field effects and mag. order in low temp. phase 8-68391
 CeO₂:Yb³⁺, ENDOR, evidence for covalency 8-80247
 Co based amorphous alloy, mag. ordered, hyperfine field distrib., NMR meas. 8-68409
 Co-Cd, dil. alloy, impurity hyperfine interactions 8-84416
 Co₂HfSn-Fe, dil., Heusler alloy, Fe hyperfine fields, Mossbauer obs. 8-68424
 Co₂TiSn-Fe, dil., Heusler alloy, Fe hyperfine fields, Mossbauer obs. 8-68424
 Co₂ZrSn-Fe, dil., Heusler alloy, Fe hyperfine fields, Mossbauer obs. 8-68424
 Cr, spin density waves detected by Ta mag hyperfine field meas. 8-60364
 CrI₃, ferromagnetic, origin of magnetic hyperfine field transferred at iodine 8-92000
 CsFeCrF₆, CsFeV₆, crystal struct., Mossbauer hyperfine spectra 8-52381
 CsNiF₃, ¹⁹F NMR, spin fluctuation suppression 8-91970

crystal hyperfine field interactions continued

- Cu-Mn Kondo system, ^{54}Mn nucl. orientation 8-68421
 $\text{Cu}_2\text{Mn}_{0.98}\text{Al}_{1.02}$, Heusler alloy, hyperfine fields at sp elements, spin echo NMR meas. 8-84496
 DyAl_2 , conduction electron spin and orbital polarisation effects 8-80228
 DyF_3 , transferred hyperfine interaction, NMR study 8-68393
 $\text{Dy}(\text{Fe}_x\text{Ni}_{1-x})_2$, mag. behaviour, susceptibility and Mossbauer expts., 4.2-1300K 8-52235
 DySb , quadrupole scatt. anisotropy, magnetically ordered material 8-64034
 ErAl_2 , conduction electron spin and orbital polarisation effects 8-80228
Eu, Mossbauer isomer shift and magnetic hyperfine field, press. effect 8-52386
 EuM_2Ge_2 , M=Mn, Fe, Co, Ni, Cu, magnetism and hyperfine interactions 8-76228
 $\text{EuNi}_{1-x}\text{Cu}_x$, mixed valency of Eu, Mossbauer expts. 8-52407
 $\text{EuNi}_{1-x}\text{Zn}_x$, mixed valency of Eu, Mossbauer expts. 8-52407
 EuO , quadrupole coupling due to lattice imperfections 8-76347
Fe based amorphous alloy, mag. ordered, hyperfine field distrib., NMR meas. 8-68409
Fe, hyperfine fields at impurities in ferromag. metal 8-52244
Fe, mag. hyperfine field of K, Ca and Ti, TDPAC meas. 8-52389
Fe, Mossbauer energy shift near Curie temp. 8-52388
Fe, transient mag. field, vel. and atomic number depend. 8-91999
Fe: ^{119}Sn , pressure dependence of effective magnetic fields 8-52382
Fe: ^{172}Yb , hyperfine mag. field, TDPAC meas. 8-52394
Fe: I, ^{131}I NMR, vacancy associated impurity sites 8-91964
Fe:K(Ar), mag. hyperfine interaction, temp. depend. 8-68420
 α -Fe-based dil. solid solutions, electronic struct., hyperfine interactions 8-79968
Fe-Co, hyperfine field distrib., temp. and press. depend. 8-91651
Fe-Co-Cd(Sn), mag. hyperfine fields at Fe, Cd and Sn sites, Mossbauer and TDPAC meas. 8-60363
Fe-containing minerals, in coals, mag. hyperfine fields meas. 8-88234
Fe-containing minerals in coals, magnetic hyperfine fields meas. 8-68427
Fe-Cr alloy, mag. moments and Fe site hyperfine fields, magnetis. obs. 8-76276
Fe-Cu metastable dil. alloy film, hyperfine interactions 8-52398
Fe-Dy, dil., implanted impurity hyperfine interaction 8-68417
Fe-Ir, hyperfine field distrib., spin echo NMR meas. 8-76351
Fe-Mo, hyperfine field distrib., spin echo NMR meas. 8-76351
Fe-Ni, hyperfine field distrib., temp. and press. depend. 8-91651
Fe-Pt, Invar type, strong ferromagnetism, mag. props. 8-64197
Fe-Rh, hyperfine field distrib., spin echo NMR meas. 8-76351
Fe-Zn, stable and metastable alloys, order-disorder, mag. interactions and corrosion behaviour 8-68422
 $\text{Fe}_{80}\text{B}_{20}$ Metglass, Mossbauer spectra line broadening 8-52400
 $\text{Fe}_3\text{-Mn}_2\text{Si}$, evidence for the ang. depend. of the hyperfine interactions 8-76241
 $\text{Fe}_{3-x}\text{Ni}_x\text{O}_4$, low temp. Mossbauer spectra, electron transfer and spin density distribution 8-52404
 Fe_2O_3 , amorphous, temp. depend. of hyperfine field, Mossbauer spectroscopy 8-84508
 Fe_3O_4 , hyperfine fields and spin densities below 20K 8-52405
 Fe_3O_4 , Mossbauer spectra above Verwey transition 8-68415
 Fe_3O_4 , NMR exam. of low temp. phase 8-56401
 Fe_3O_4 , NMR of low temp. phase, electron ordering anal. 8-56402
 $\text{Fe}_3\text{O}_4\text{-xF}_x$, low temp. Mossbauer spectra, electron transfer and spin density distribution 8-52404
 β - FeOOH , Mossbauer investigation of the quadrupole splitting 8-76370
 FeSb_2O_6 , Mossbauer spectra, molecular field effects 8-91997
 Fe_3Si -based alloy, dil., cond. electron polarisation and moment perturbations 8-68224
 Fe_3Si -based dil. alloys, conduction electron polarisation, moment perturbations 8-68225
 $\text{Fe}_{3-x}\text{Zn}_x\text{O}_4$, low temp. Mossbauer spectra, electron transfer and spin density distribution 8-52404
 FeZrF_6 , phase transition at 212.3K, Mossbauer, EPR study, quadrupole splitting, Jahn-Teller effect (German) 8-68430
GaP:S, ENDOR meas., symmetries, hyperfine parameters 8-72435
GaP:Zn, isolated Ga vacancy due to electron irradi., EPR study 8-95519
Gd-Hg, dil., mag. hyperfine field, TDPAC meas. 8-52414
Gd-Ir, dil., hyperfine interaction of ^{193}Ir , Mossbauer effect meas. 8-52413
 GdM_2Ge_2 , M=Mn, Fe, Co, Ni, Cu, magnetism and hyperfine interactions 8-76228
Ge: ^{77}Fe , quadrupole interac. 8-92005
Ho-Sn, dil. alloy, hyperfine interaction of ^{119}Sn , Mossbauer meas. 8-91998
 $\text{Ho}(\text{Fe}_x\text{Ni}_{1-x})_2$, mag. behaviour, susceptibility and Mossbauer expts., 4.2-1300K 8-52235
 HoSb , quadrupole scatt. anisotropy, magnetically ordered material 8-64034
KBr, H-centre struct., hyperfine interactions 8-79611
KCl, H-centre struct., hyperfine interactions 8-79611
KCl, press. shifts of F-centre hyperfine interaction parameters 8-79957
 $\text{KCl:K}_2\text{Os}^{IV}(\text{CN})_6$, electron irradi., EPR, ligand hyperfine struct. 8-60335
 KCoF_3 , antiferromag., ^{59}Co NMR exam. 8-76332
 $\text{KD}_3(\text{SeO}_3)_2$, D NMR above and below ferroelec. transition, H-bond behaviour 8-52460
 KFeS_3 , quadrupolar and mag. hyperfine anisotropy, Mossbauer meas. 8-56408
 K_2SnF_6 , Group IV hexafluoride anion radical γ -irrad., EPR spectra 8-72411
LiCl, press. shifts of F-centre hyperfine interaction parameters 8-79957
LiF:Mg(Ag), electron spin-lattice relax. of V_i -centre 8-95518
LiF:Na $^+$ H_a -centre struct., hyperfine interaction 8-79611
Lu, electric field gradient, at ^{181}Ta substitutional atoms, pressure dependence 8-52385
 LuIr-Nd^{3+} , dil., ESR, hyperfine crystals. of $^{143,145}\text{Nd}$, g-factor, crystalline field splitting 8-52349
 $\text{LuRh}_2\text{-Nd}^{3+}$, dil., ESR, hyperfine crystals. of $^{143,145}\text{Nd}$, g-factor, crystalline field splitting 8-52349

crystal hyperfine field interactions continued

- MnSi-CoSi solid solution, mag. props. 8-56403
NaCl, press. shifts of F-centre hyperfine interaction parameters 8-79957
 $\text{Na}_2\text{Zn}(\text{SO}_4)_2 \cdot 4\text{H}_2\text{O}$:Ni, optical absorpt. and EPR obs. 8-76501
 NdAl_2 , conduction electron spin and orbital polarisation effects 8-80228
Ni: ^{119}Sn , 8-52382
Ni: ^{172}Yb , hyperfine mag. field, TDPAC meas. 8-52394
Ni-Dy, dil., implanted impurity hyperfine interaction 8-68417
 $\text{Ni}_2\text{Mn}_{0.9}\text{Fe}_{0.1}\text{Sn}$, Fe site hyperfine field and mag. moment, Mossbauer effect meas. 8-76365
NiO: ^{67}Zn , perturbed ang. correl. 8-95535
 PbHfO_3 , elec. field gradient, crit. behaviour, DPAC meas. 8-80303
 $\text{PbI}_2\text{-M}^{2+}$, M=V, Mn, Co, EPR 8-68362
Pd-Co, dil., Mossbauer emission spectra, fast relaxation regime, ^{57}Co hyperfine field 8-60362
Pd-Fe, Mossbauer spectra, scatt. and transmission geometries, differences in crit. behaviour near T_c 8-76367
Pd-Ni, local susceptibilities, ^{61}Ni Mossbauer spectroscopy 8-95536
Pd $_3$ Fe, hyperfine interactions during atomic ordering, Mossbauer obs. (Russian) 8-56630
PdMnSb, Heusler alloy, hyperfine fields of 5sp shell impurities substituting Sb, Mossbauer spectra 8-80261
Pd $_2$ MnSb, Heusler alloy, hyperfine fields of 5sp shell impurities substituting Sb, Mossbauer spectra 8-80261
 $\text{Pd}_2\text{Mn}_{0.98}\text{Sn}_{0.02}\text{In}_{0.02}$, Heusler alloy, hyperfine fields at sp elements, spin echo NMR meas. 8-84496
PrCl $_3$, one-dimensional X-Y system, far IR absorpt. spectra, cooperative spin excitations 8-95584
PtMnSn, ^{197}Au and ^{119}Sn hyperfine fields, Mossbauer expt. 8-72439
 $\text{Rb}_2\text{Cu}(\text{SO}_4)_2 \cdot 6\text{H}_2\text{O}$, single cryst., fine struct., mag. dipole coupling, EPR obs. 8-68360
 Rb_2FeF_6 , 1D antiferromagnetic system, Mossbauer investigation 8-95533
Re-Hg, dil., anomalously high elec. field gradients below 0.05K 8-72442
 ReNCl_4 , EPR in $\text{Ph}_4\text{As}[\text{RuNCl}_4]$, hyperfine splitting and spin Hamiltonians 8-64272
 Rh_2CoSn , ferromag., crit. exponent of ^{119}Sn hyperfine field, Mossbauer obs. 8-92008
Sc, electric field gradient of ^{181}Ta substitutional atoms, press. depend. 8-52385
Si, extended Huckel theory calculations for positive divacancy 8-87938
Si, muon state, muon spin rot. exam. 8-60373
Si: ^{57}Fe , quadrupole interac. 8-92005
Si:Sb(P)(As), shallow donor electrons, hyperfine interactions, reply to Onffroy's calcs. 8-51934
Sn complex containing P, $\text{L}_2\text{Sn}(\text{CH}_3)_2\text{Cl}_{4-m}$, Mossbauer parameters, quadrupole splittings (Russian) 8-76362
TaS $_2$ intercalated with NH_3 , charge transfer, PAC meas. 8-76366
TbAl $_2$, conduction electron spin and orbital polarisation effects 8-80228
TbF $_3$, transferred hyperfine interaction, NMR study 8-68393
 $\text{Tm}_2\text{Al}_2\text{O}_{12}$:Yb $^{3+}$, g-shift meas., EPR 8-56376
TmTe, hyperfine struct. of Tm^{2+} , Mossbauer spectra 8-76368
U complex, U(acac) $_4$, cryst. fields, mag. susceptibility, chem. shift (French) 8-84179
U, electric field gradient, of ^{181}Ta substitutional atoms, press. depend. 8-52385
VO $_2$, electronic struct., quadrupole coupling, Mulligen-Wolfsberg-Helmholtz calcs. 8-87948
 mV_2O_5 (100-m) P_2O_5 , (m=100-2), V(IV) complexes conc., absorpt. and ESR spectra 8-64266
YAG:Gd $^{3+}$, EPR absorpt. spectrum 8-76305
 $\text{Y}_{1-x}\text{Gd}_x\text{Co}_2$, NMR of ^{59}Co 8-52376
YIG, press. depend. of effective mag. fields on ^{57}Fe nuclei 8-52383
YbAl $_3$, Mossbauer effect obs. of induced hyperfine field 8-52396
Yb $_2\text{Ti}_2\text{O}_7$, cryst. field props., Yb $^{3+}$ hyperfine spectra, Mossbauer effect meas. 8-67990
Zn, naive model for electric field gradient 8-91650
Zn, quadrupole interaction at ^{181}Ta , TDPAC meas. 8-52392
Zn-Hg, dil., anomalously high elec. field gradients below 0.05K 8-72442
ZnO:Cu,H, motional effects in EPR spectra 8-80207
 ω -Zr, electric field gradients at substitutional Ta atoms, TDPAC high-pressure study 8-52384
 $\text{Zr}_{0.9}\text{Fe}_{0.1}\text{V}_2$, NMR and mag. susceptibility 8-95527
 $\text{Zr}_{0.99}\text{Pt}_{0.01}\text{V}_2$, NMR and mag. susceptibility 8-95527
 ZrV_2 , NMR and mag. susceptibility 8-95527

crystal imperfections see crystal defects**crystal inclusions**

- alkali halides, radiolysis, growth of colloidal metal inclusions 8-92493
alloy, disperse state formation (Russian) 8-52757
anisotropic ellipsoidal inclusion, polynomial eigenstrain problem 8-83808
anisotropic media, elastic strain energy of precipitates, and periodic distrib. inclusions 8-84810
oblate spheroidal inclusion, internal stress, misfit, inhomogeneity and plastic deform. 8-60701
particle trapping in cryst. growing from melt at variable rate 8-67676
porous rigid-plastic material containing rigid inclusions, yield function, plastic potential, void nucleation 8-64612
purification, inclusion emersion in vertical zone refining 8-52663
quartz, synthetic influence of hydrostatic pressure on precip. of structure-bound water in microinclusions 8-75838
quartz inclusion morphology for thermolum. dating, effect of HF etching 8-70240
shear stresses induced by hydrostatic pressure near the surface of an inclusion 8-75074
solid surface, point defects, inclusion and separation zones, elastic energies determ. (German) 8-95054
steel, 12X2H4A, nonmetallic inclusion effect on plasticity and impact strength (Ukrainian) 8-92296
steel, cast high-strength, local intergranular fractures, formation mechanism (Russian) 8-95795
steel, inclusions effect on distrib. of local microheterogeneous deform. (Russian) 8-80586
steel, molten, deoxidised, reaction with oxidising gas bubbles 8-88438

crystal inclusions continued

- steel, molten deoxidised, reaction with oxidising gas bubbles 8-84739
 steel, rimming, continuously cast, nonmetallic inclusion distrib. (*Russian*) 8-80534
 steel, rolled, effect of inclusions on torsional fatigue 8-92314
 steel, SiO₂ inclusion formation on introduction of solid SiO into molten steel (*Russian*) 8-80530
 steel, steam turbogenerator rotors, fatigue crack initiation and growth, from macroscopic slag inclusions 8-64681
 steel, transformer, formation of perfect cubic texture in thin sheets (*Russian*) 8-80557
 stress concentration due to oblate spheroid inclusion, exam. 8-71281
 surface, point defects, inclusion and segregation zone, elastic energies (*German*) 8-95049
 Al alloys, inclusions, oriented distrib. metallography and effects on anisotropy (*Russian*) 8-80589
 Al alloys, preliminary forging effects on struct. and mech. props. of extruded sections (*Russian*) 8-80564
 Al-Pb(Bi)(Cd), containing low melting point inclusions, impact props., temp. depend. 8-60792
 Cu complex, bis-(alkylammonium) (11) tetrachloride, perovskite, lattice perfection 8-87633
 Cu, fatigue behaviour effect of Zn, Au diffused coatings 8-72850
 Fe, cast, Mg, despheroidising effect of Bi, Sn on graphite in alloy 8-56670
 Fe, pure, ductile fracture, effect of nonmetallic inclusions 8-64660
 Fe-C-Fe₂O₃, cleavage initiation by ductile tearing 8-64656
 Gd₂(MoO₄)₃, and isotypes exam. of crystal growth, and defect generation 8-68617
 KH₂PO₄, liq. inclusion formation during large cryst. growth 8-64455
 MgO, implanted K aggregates, TEM and optical spectra obs. 8-83838
 Nb alloys, non-metallic inclusion form. during quenching from liquid state 8-95766
 Ni alloy, ZrS₆K, diffusion layer form. on Nb addition, struct., comp. (*Russian*) 8-56814
 SmCo₅ magnetic alloys, pressed, sintering rel. to mag. props., cryst. struct. 8-60600
 Ti-B, binary inclusions, interaction with diamond in polycryst. diamond sintering (*Chinese*) 8-80484
 Ti-Cr, sintered, friction and wear, structural factors 8-60843
 Ti-Cr-TiC, sintered, friction and wear, structural factors 8-80843
 Ti-Si, binary inclusions, interaction with diamond in polycryst. diamond sintering (*Chinese*) 8-80484
 Ti-TiC system, sintered, friction and wear, structural factors 8-60843

crystal internal fields see crystal field interactions

crystal interstitials see interstitials

crystal lattice structures see crystal atomic structure

crystal microphones see microphones

crystal microstructure

- for microstructural changes, see also phase transformations, hardening, heat treatment, metalworking
 see also crystal defects; crystal inclusions; crystallites; dendritic structure; domain boundaries; domains; electron microscope examination of materials; eutectic structure; grain boundaries; grain size; Guinier-Preston zones; mosaic structure (microstructure); noncrystalline state structure; precipitation; segregation; subboundary structure; superlattices; texture; X-ray diffraction examination of microstructure
 alite paste, mature, microstructure study by SEM, TG and X-ray diff., corrosion 8-92381
 cellular microstructure, 3-dimens. anal. by computer simulation 8-87640
 ceramic, ferrimag. or ferroelec., microstructure and physical props. 8-72756
 ceramics, microstructure dependence of mechanical behaviour 8-88533
 ceramics, US attenuation 8-67772
 cold rolling, texture form., model (*French*) 8-68705
 ferrite, microstruct. depend. of props. and applics., review 8-88548
 garnet:Nd³⁺, spectral, structural regularities, anal. 8-51948
 graphite intercalation cpds., struct. and order-disorder transforms. 8-71710
 high strength structural mats., microstruct. influences on fatigue and fracture resist. 8-56728
 magnetic materials, psarks rel. to pseudo-single domain behaviour 8-65274
 martensite crystals, orientation relationship definition, anal. method 8-60670
 martensite layers, external stress effects on equilibrium morphology, thermodynamic model (*Russian*) 8-52804
 materials props. depend., book 8-88470
 metals, recrystallisation during hot deform. 8-68714
 opal, ordered arrangements of SiO₂ spheres of two different sizes 8-87658
 polyethylene, pyramidal crystals, soln.-grown, collapse mechanics 8-76713
 polyethylene, single cryst. and spherulites, microstruct., deform. micromechanisms 8-83758
 polyethylene terephthalate, mech. props., influence of cryst. arrangement and noncryst. region struct. 8-76707
 polymer, drawing properties, role of interfibrillar tie mols. 8-76706
 polymer, recrystallisation during drawing 8-76658
 polymer, soln.-grown cryst., diff. line-broadening, bending contrib. 8-75574
 polymer microstructure morphogenesis, book contrib. 8-83757
 polymers, solid, orientation effects, conf., Budapest, Hungary (April 1976) 8-75557
 polypropylene, cold-drawn isotactic bars and thin films, microstruct. and annealing 8-95760
 portland cement paste, microstructure study by SEM, TG and X-ray diff., corrosion 8-92381
 quartz porcelain fast fired, development of microstruct. (*German*) 8-60625
 quartz-feldspar mylonite, microstruct. and fabric development 8-96201
 rare earth-Co permanent magnets, microstruct., TEM obs., magnetisation 8-91901
 sapphire, profiled growth, struct. perfection 8-68621
 steel, alloy, low C, effects of pre-treatment on graphitisation behaviour (*Japanese*) 8-84860
 steel, alloy, maraging, 18% Ni, effect of solution and ageing treatments, on microstruct., tensile props., fracture toughness 8-80648

crystal microstructure continued

- steel, alloy, Mn-Si-C, exam. of fracture toughness for sheets, using linear elastic fracture mechanics 8-56762
 steel, alloy, transform. kinetics of supercooled austenite in 12Kh1MF, structural method 8-52801
 steel, alloy, type 52100, exam. of microstruct. and fracture, as function of austenitising in temp. range 800 to 1100°C 8-76673
 steel, alloy, U20Kh6T2D, structural transformations during heat treatment, and wear resistance 8-88484
 steel, austenitic, AISI 4340, effect of step quenching on microstruct. and fracture toughness 8-84834
 steel, austenitic, Kh12N20T3R, ageing, submicroscopic struct. role in dispersion hardening (*Russian*) 8-64549
 steel, C, fretting fatigue damage, SEM exam. 8-88541
 steel, C, type S15CK, tuffrided, fatigue strength at elevated temp., under reversed axial strength (*Japanese*) 8-84980
 steel, case-hardened cast, contact endurance rel. to austenizing (*Russian*) 8-56805
 steel, cementite coarsening in type 1080 in a temp. gradient 8-88486
 steel, Cr, influence of ultrasound on tempering processes (*Russian*) 8-52827
 steel, Cr-Mo-V, creep fracture, microstruct. effects 8-64668
 steel, Cr-Mo-V, medium strength, correlation between crack initiation, propag. and microstruct. 8-60787
 steel, Cr-Mo-V (0.5, 0.5, 0.25 wt.%), heat treated, microstructure effect on threshold region fatigue 8-56757
 steel, Cr-Ni-Mo-V, quenched, morphology, structural constitution after austenite form. by heating (*Russian*) 8-68709
 steel, ferrite-pearlite, cyclic behaviour, fatigue, chem. comp. and microstruct. effects 8-60833
 steel, ferritic, low alloy, effect of microstruct. on creep fracture 8-80640
 steel, high-speed, eutectic carbide structure, determ. by SEM 8-85075
 steel, low alloy, eutectoid pearlitic, exam. of microstructures dominating ductility (*Japanese*) 8-84917
 steel, low alloy, exam. of fatigue crack growth, and Paris Law parameter relationship 8-92343
 steel, low alloy, high strength, correlation between fracture toughness, tensile props., fracture morphology 8-60789
 steel, low alloy, pearlite block, exam. of crystallographic features, formation processes (*Japanese*) 8-84799
 steel, low alloy and C, bainite morphology 8-68682
 steel, low C, C content effects in corrosion fatigue in nitrate solns. (*Russian*) 8-56811
 steel, low C, Mn, laws of banding structure form. (*Slovenian*) 8-83776
 steel, martensite-ferrite combined microstructure, two-phase, tensile fracture strength 8-60783
 steel, martensitic, fatigue crack form. associated with cyclic slip deform. along prior austenite grain boundaries 8-60831
 steel, Mn, as rolled bainitic, tensile, impact and machinability props., transport appl. 8-88503
 steel, Mn, influence of ultrasound on tempering processes (*Russian*) 8-52827
 steel, Ni, microstruct., plastic zone size and crack propag. 8-60790
 steel, pearlitic, fatigue, metallographic aspects 8-60828
 steel, stainless, fatigue crack morphology of type 304 cycled at const. stress amplitude at elev. temps. 8-64671
 steel, stainless, Kh18N10T, substructure after high-temp. thermomechanical treatment with high deformation rates (*Russian*) 8-76657
 steel, stainless, low energy D implanted, microstruct. 8-95073
 steel, stainless, maraging, Cr-Co, effect of ageing on microstruct., TEM and neutron diffraction exam. 8-84867
 steel, stainless, orthopaedic fixation devices, failure, SEM exam. of fatigue crack surfaces and microstructure 8-77156
 steel, tool, NC6, carbide lattice, kinetics of its destruction (*Polish*) 8-92280
 steel 30Kh2NMFA, microstructure of cup and cone fracture surface, effect of size of disperse phase particles (*Russian*) 8-68762
 steel fibre reinforced Ag, exam. of recrystallisation behaviour (*German*) 8-84849
 steel U8, hydrogenation effects on fatigue crack propag. (*Russian*) 8-56800
 tetrakaidecahedra as grain models 8-51458
 α+β Ti alloys, prior β grains and α platelet morphology, exam. 8-76679
 titanomagnetites, domain struct. var. with temp. 8-65272
 vacuum deposited metal film, elec. field effect on residual struct. 8-51836
 X-ray laser holography, possible appl. to crystal and biological microstructure 8-55322
 Al alloy, sheets, type 7004, asymmetrical solidification structures, fluid flow, in W arc welds 8-84794
 Al alloys, preliminary forging effects on struct. and mech. props. of extruded sections (*Russian*) 8-80564
 Al alloys, stress corrosion cracking protection, by γ₁Al₂O₃ anodic film 8-95836
 Al and Al alloys, plastically deformed, influence of microstruct. on energy stored 8-84894
 Al-Cu (4 wt.%), AE during deform., effect of ageing at 170°C 8-64597
 Al-Cu alloys, quenched rapidly, microstruct. 8-56668
 Al-Cu-Ni, directionally solidified, exam. of struct. of two phase alloys 8-80537
 Al-Mg-Ti(Zr), struct. and factors determining brittle intermediate compound form. 8-52817
 Al-Si, hypereutectic silumins, P and Na modification 8-84792
 Al-Si eutectic, Na, Sb and Sr alloying addition effects on microstructure (*French*) 8-64548
 Al-Zn-Mg, effect of microstruct. on localised shear failure 8-52996
 Al-Zn-Mg-Ti, Ti effect on microstructure during ageing 8-64568
 β-Al₂O₃-Na₂O:Mg, ionic cond., effect of microstruct. and phase composition 8-67859
 β-Al₂O₃-Na₂O-SiO₂, solid electrolytes, exam. of microstruct. ionic resistivity 8-80566
 Al₂O₃-SiO₂ heat insulating refractories, prep., physical, thermal, structural props. 8-68662
 Al₂O₃-ZrO₂, microstructure effect on friability 8-64515
 Au-Al system, influence of current on phase form. in diffusion layer (*Russian*) 8-52826
 C-C composites, existence diagram and properties (*French*) 8-64517

crystal microstructure continued

- CaCO₃, thermal decomp. in vacuo, ultrastruct. and crystallography 8-71864
 Ca₃Ga₂Gc₂O₁₂, substrate, electron examination of microstruct. and microsegregation 8-67919
 CaTiO₃-LaAlO₃ solid soln., phase redistrib. during roasting in H₂ 8-52735
 Co-Cr recording films, perpendicular mag. anisotropy, hysteresis loop, microstruct., TEM obs. 8-95491
 Co-P electroless film on Al base disc substrate, microstruct. rel. to mag. props. 8-68304
 Cr, columnar struct. rel. to deposition conditions 8-52675
 Cr-Fe (30 wt.%) alloys, refined fine comminution 8-60598
 Cr-Ni-(P), hard alloys, sintered, fracture props., P addition effects 8-60610
 Cr₃Si₂(C₂), sputtered films, microstruct. and wear props. 8-64733
 Cu complex, bis-(alkylammonium) (11) tetrachloride, perovskite, lattice perfection 8-87633
 Cu-Al-Ni-Fe, (10, 5, 5 wt.%), cast microstruct. 8-80535
 β-Cu-In, directionally transformed eutectoid, morphology exam. by metallography (*German*) 8-92257
 Cu-Ni-Cr system, coarsening in the (γ₁+γ₂) region, metallographic study 8-84762
 Cu-Ni-Nb-Al, formation of γ' and γ'' precipitates 8-76655
 Cu₂O, creep substruct. under compression, X-ray diffr. study 8-95785
 Fe alloys, anisotropic precipitation struct. in external mag. field (*German*) 8-72785
 Fe alloys, influence of plastic deform. on twinned martensite struct. (*Russian*) 8-88493
 Fe, Armo, microstruct., effect of strain rate on change, due to tension-compression 8-80614
 Fe, cast, rare-earth-Mg nodular, fracture toughness and fatigue (*Chinese*) 8-95791
 Fe, columnar struct. rel. to deposition conditions 8-52675
 Fe-Al(Cr)(V)(Ti), hardness after nitriding, metallographic, electron microscopic and microprobe anal. 8-51608
 Fe-C-Cr-Mo(Ni)(V), white cast, effect of abrasion on carbide microstructure (*German*) 8-88540
 Fe-C-Si, effects of Si on matrix struct. of spheroidal graphite cast iron (*Korean*) 8-60666
 Fe-Co-V(2%) alloy, correl. of resistivity with microstructure 8-72896
 Fe-Cr-Co (31 wt.%, 23 wt.%), microstruct. and mag. props., ageing and thermomag. treatment effects 8-76769
 Fe-Cr-Co-Al (27.5, 17.5, 0.5) alloy, rel. to mag. props. 8-72367
 Fe-Ni-C alloy, external stress effects on equilibrium morphology, thermodynamic model (*Russian*) 8-52804
 Fe-Ni-C alloy, N31, austenite state in premartensitic temp. interval (*Russian*) 8-56634
 Fe-Si (3 wt.%), grain oriented, MnS precipitate distribution, electron microscope observation (*Chinese*) 8-95751
 Gd₃Ga₂O₁₂, substrate, electron examination of microstruct. and microsegregation 8-67919
 In₂Ga_{1-x}Sb, influence of annealing on microstruct., exam. 8-56669
 InP, microstructs. assoc. with hardness indentations 8-80627
 LaB₆ film, structure, stoichiometry, elec. properties 8-60043
 Li₂O pellets, sintered, exam. of microstructure 8-72749
 MgO-Al₂O₃-SiO₂, exam. of microstructure and crystallisation kinetics 8-80501
 MnZn ferrite, appreciable SiO₂ content, origin of core losses, microstructure and mag. props. 8-64225
 MnZn ferrites, impurity induced exaggerated grain growth 8-92222
 Mo-ZrC, internal oxidation, struct. formation law, microstruct. examination 8-84836
 MoSi₂, sputtered films, microstruct. and wear props. 8-64733
 Na₂-SiO₂ glass, prep. by metallic-organic derived method, phase separation 8-56610
 Nb₃Ge, CVD, impurity doping effect on supercond. crit. props. 8-52174
 Ni base superalloy IN 100, corrosion resistant intermetallic coating, microstruct. effect on mech. props. 8-85058
 Ni, polycryst., hydrogenation rel. to fine struct. 8-59950
 Ni-Cr-Co-Mo-Al-Ti alloys, Waspaloy, Astroloy, exam. of microstruct. effect on crack growth 8-52977
 Ni-Cr-Fe-Mo-Go (21.41, 19.28, 8.64, 2.16 wt.%), Hastelloy alloy X, exam. of thermal stability 8-84865
 Ni-Ti, near equiatomic alloy, TEM exam. of austenite-martensite interface 8-51401
 Pb-Bi, peritectic reaction, microstruct. changes 8-52753
 SiC fibre reinforced Ni-Cr alumina coated fibres, hot pressed, annealed, IR study 8-60623
 SiC, reaction sintered, TEM exam. of recrystallisation, phase transformation 8-80567
 SiC, uncommon mode of morphological development among coherent phases, optical and electron microscope exam. 8-80544
 Si₃N₄, hot pressed, Y₂O₃ fluxed, microstruct. 8-64512
 SmCo₅ magnetic alloys, pressed, sintering rel. to mag. props., cryst. struct. 8-60600
 Sn, molten rotating stream, vortical filament generation during solidification (*Russian*) 8-88460
 Sn-Pb eutectic, struct. and plasticity, thermomech. treatment effects (*Russian*) 8-60686
 SnO₂, crystal growth habits, CVD method (*Japanese*) 8-95686
 SnO₂:Sb, and pure cryst., microstruct., X-ray diffr., optical and electron microscope studies 8-79619
 Ti, fatigue fracture surface microstruct., electron microscope obs. 8-60834
 Ti-11, unstable shear modes in fatigued β-annealed specimens 8-84984
 Ti-alloy, IMI-685, unstable shear modes in fatigued β-annealed specimens 8-84984
 UO₂, commercial fuel pin, irradiation induced volume changes, comparison with model 8-78465
 V-N, BCC solid soln., superperiodicity of lattice in quenched ordered struct. (*Russian*) 8-56662
 W fibre, KSiAl doped, recrystallisation, Li diffusion effects, hardness, strength, microstructure meas. (*German*) 8-64644
 W-ThO₂ composite, struct., lamination tendency, effects of method of manuf. 8-68653
 WC, plasma sprayed coating 8-68835
 WC-Co, exam. of effect of continuous carbide phase, on hardness, and deformation 8-52974

crystal microstructure continued

- WC-Co, sintered, obs. of spinel particles by TEM 8-95714
 Zn, film, vac. deposited, X-ray diffr. study of microstruct. 8-75966
 ZnO-Al₂O₃-SiO₂, transparent glass-ceramics, EPR obs. of glass crystallisation 8-80507
 ZnO-Al₂O₃-SiO₂, transparent glass ceramics, heat treatment effect on microstruct. 8-56667
 ZnO-Al₂O₃-SiO₂, transparent glass-ceramic, microstruct., physical props., crystallisation ht. treatment depend. 8-80506
 Zr(HPO₄)₂·H₂O-Kynar membranes, struct., ion mobility 8-76915
 ZrO₂, optimum sintering characts., density, X-ray diffr., IR spectrum, UV spectrum obs. 8-76617
- crystal morphology**
 alkali halide, morphology of growth and evaporation surface 8-79544
 n-alkenes, n even, interaction energy at twin boundary, dihedral reentrant, salient angle effect on growth morphology 8-55876
 austenitic stainless steel, 18 Cr-11 Ni, directly aged, nucleation of M₂₃C₆ carbides (*Polish*) 8-52806
 film, morphology and morphological changes 8-72043
 film, ultrathin, effort of optical radiation on growth and struct. 8-72045
 martensite crystal, struct. X-ray diffr. study 8-79565
 martensite layers, external stress effects on equilibrium morphology, thermodynamic model (*Russian*) 8-52804
 MBBA, solid, NMR and thermal behaviour, cooling and mag. field effects 8-76336
 nucleation rate equation, generalisation of nucleus shape depend. parameters 8-84765
 poly(chlorotrifluoroethylene) films, crystalline superstruct., mol. orientation, X-ray diffr., depolarised light scatt. 8-71685
 polyethylene, high density, environmental stress cracking and morphology 8-68834
 polymer morphology and lamellas in bulk and oriented linear high polymer 8-51434
 sapphire, profiled growth, struct. perfection 8-68621
 steel, low C rimming, effect of addition of Al to Zn on phase composition and morphology (*Polish*) 8-53014
 steel, Si killed, effect of Al addition to Zn on phase composition and morphology of products of Fe-Zn reaction (*Polish*) 8-85021
 tetrakaidecahedra as grain models 8-51458
 Ag electrodeposits, dendritic growth inhibition by tartaric acid and tartarates (*French*) 8-87894
 Al-Al₄Ca, eutectic alloy, unidirectionally solidified, exam. of growth and crystallography 8-72771
 Al_{0.3}Ga_{0.7}As:Te(SN), impurity effects on interface morphology of LPE films on corrugated GaAs substrates 8-88435
 C, columnar and laminar forms, deposition on polycrystalline Ni foils 8-63943
 CaF₂, etching behaviour in HCl vapour 8-59812
 ω-Cd-Hg alloy, melt-growth, morphology of single crystals. 8-64464
 CsH₂PO₄, single cryst. growth, struct. and elec. props. 8-71693
 Cu electrodeposits, collagen and chloride additions effects obs. 8-51852
 Fe-Ni-C alloy, external stress effects on equilibrium morphology, thermodynamic model (*Russian*) 8-52804
 Ga-Al, effect of Al on solidification kinetics, and morphology of Ga 8-56628
 α-K₂Cr₂O₇, symmetry centres exam. by morphological methods 8-59796
 K₂O.3MoO₃.3H₂O, fibrillar crystals, morphology and struct. 8-63959
 Li₂O.3MoO₃.5.7H₂O, fibrillar crystals, morphology and struct. 8-63959
 MgO-Al₂O₃-SiO₂, exam. of microstructure and crystallisation kinetics 8-80501
 NaCl:BaCl₂, oriented growth of BaCl₂ phases, platelet-matrix interface structure and energy 8-87793
 Ni, fine particles, prep. by vacuum evaporation, crystal habits 8-88437
 Ni sulphide ores from Kambalda, W.Australia, sulphide fabrics 8-77229
 Pd growth on MoS₂, reorientation of small particles 8-84103
 SiO₂-Al₂O₃ based minerals, phase equilib., struct., comp. (*French*) 8-60659
 Tm₂O₃, mineraliser effect on growth morphology 8-91283
 VO₂, doped, morphology, structure and props. (*German*) 8-59823
 WC₂, electrochem. separation from W alloys, phase anal. 8-60651
 ZnO, rate of deposition and morphology 8-84719
 ZnO, single cryst. growth in ZnO-H₂O-O₂ vapour, morphology, electrophys. and opt. props. 8-52649
 ZnS cubic single crystals, growth by double decomposition reaction in melt 8-60557
 ZrC, whiskers, CVD on Ni, catalytic effect 8-51865
- crystal orientation**
 distribution determ. from incomplete pole figures, computer program 8-64804
 low quartz crystal setting, enantiomorphism 8-79496
 quartz, (a) axes preferred orientations in tectonites, flow kinematics 8-96200
 quartz in shear zone from Castell Odair, Scotland, orientation re-investigation 8-77216
 schreibersite, platelike, in hexahedrites, habit planes 8-65572
 texture anal., three dimensional, computer simulation of errors 8-64805
 thermoelectric convertor error due to crystallographic misorientation anisotropy 8-77904
 Ag, single cryst. film, cryst. orientation effect on EELS 8-80442
 AgMg single crystals, orientation and temp. depend. of slip 8-87682
 Al, anodisation, influence of substrate orientation 8-88581
 Cd, dislocation internal friction, orientation depend., for single crystals. 8-52882
 CoO on Co₃O₄, oriented growth following Co₃O₄ pyrolysis 8-80739
 Cu, influence of cryst. orientation on work function, with and without adsorbed S (*French*) 8-76134
 α-Fe single crystal whiskers, controlled growth by H reduction of ferrous halides, X-ray and SEM exam. of crystals 8-60554
 Fe₂Al, slip geometry and pseudoelastic behaviour, effect of crystal orientation (*French*) 8-87681
 Mg, dislocation internal friction, orientation depend., for single crystals. 8-52882
 Nb, surface oxide softening, anisotropy 8-60716
 Ni sulphide ores from Kambalda, W.Australia, sulphide fabrics 8-77229

crystal orientation continued

- α -Si₃N₄, hardness anisotropy 8-95804
- Ta-N, domain configurations of new phase (*French*) 8-56648
- Zn, dislocation internal friction, orientation depend., for single crystals 8-52882

crystal oscillators *see crystal resonators***crystal properties**

see also crystal chemistry

No entries

crystal purification

see also zone refining

- alkali metals, distiller for purification, construction, operation 8-80490
- inclusion emersion in vertical zone refining 8-52663
- Gd, fused salt electrorefining, evaluation of electrolytes 8-92215
- InP, LPE, high purity, use of baking to reduce Si contamination 8-72744
- Si:P, Au gettering by P diffusion and P-induced dislocations 8-91346

crystal resonant gamma-ray interactions *see Mossbauer effect***crystal resonators**

see also piezoelectric oscillators

- 31st Annual Frequency Control Symposium, Atlantic City (1977) 8-57905
- 32.768 kHz X-Y flexure watch crystal as pressure-force transducer 8-57934
- 300 MHz oscillators using SAW resonators and delay lines 8-59255
- AT-cut quartz plate vibration anal. using light modulated oscillator 8-71255
- digital thermometers using quartz crystal oscillator high accuracy achieved 8-65932
- horizontal-shear surface wave grating resonators 8-59249
- microwave Q-factor meas. system 8-54396
- piezoceramic elastic compliance and mechanical Q-factor at high drive levels 8-60395
- quartz, electron irradiated, optical and anelastic absorptions and resonator freq. 8-64385
- quartz, second-order phenomena and polarising effect with plates of orientation 8-72463
- quartz, synthetic, growth boundary between -X and Z sectors 8-59775
- quartz, synthetic, growth sector boundary between -X and Z sectors 8-59774
- quartz cryst., piezoelec., coated, detection of HCl gas in ambient air 8-92532
- quartz oscillator plate, surface treatment by 100 keV B ion implantation (*Japanese*) 8-59826
- α -quartz plate frequency changes rel. to electroelastic tensor and second-order phenomena 8-60398
- quartz SAW resonator deep etching 8-59248
- quartz SAW resonator tuning by shorted reflector opening 8-59246
- SAW resonators, comparison of metal strip and waffle iron arrays 8-51030
- surface-skimming bulk wave controlled quartz crystal oscillator 8-59250
- thin film thickness measurements, instrumentation system 8-89436
- tunable variable bandwidth/frequency SAW resonator 8-59247
- CdS, flexural waves in resonator platelets, synchronous amplification and generation 8-84527
- LiTaO₃, piezoelectric resonator characterisation 8-95550
- Pb(Mg_{1/3}Nb_{2/3})O₃-PbTiO₃-PbZrO₃, piezoceramics for high frequency use 8-95555
- PbTiO₃, piezoceramics for high frequency use 8-95555

crystal structure

- see also crystal atomic structure; crystal microstructure; crystal morphology; crystal orientation; crystal symmetry; crystallography; granular structure; polymorphism*
- classical octopolar solid, temp. effect, Monte Carlo calc. 8-75598
- NBS reactor, summary of activities, (July 1976 to June 1977) 8-82435
- orthosilicate chloritoid, layered, disordered, electron microscopic and X-ray anal. 8-75511
- planetary system evolution from preplanetary gas disc, rel. to crystallisation and cryst. struct. (*German*) 8-93129
- CrC, plasma sprayed coating 8-68835

crystal surface and interface vibrations

- alkali halides, absorpt. in molecules, clusters and microcrystals 8-80363
- chemisorbed atoms and mols., vibrational motion dynamics, infrared absorpt. line shape 8-51814
- conference on lattice dynamics, Paris, France (Sept. 1977) 8-59869
- density response, transition-metal slab 8-71930
- desorption, laser stimulated, quantum theory 8-79876
- desorption, thermal, one-phonon at. scatt., 3-dimens., continuum model 8-87860
- desorption kinetics, Kramers-Langevin stochastic eqn., heavy-atom limit, adatom-phonon coupling 8-84065
- dynamical properties of solid surfaces, analytic approach 8-71929
- FCC, self-consistent Einstein model of anharmonic surface vibr. 8-75920
- ferroelectrics, surface sound waves on domain boundaries, low temp. sp. ht. 8-71937
- glass film on substrate, Brillouin scatt. from surface phonons, SAW vel. and attenuation 8-95587
- Green function method for electronic struct. and vibr. modes calc. at surfaces 8-88012
- hemicylinder-air-quartz system, semi-infinite crystal, dispersion of surface phonon polaritons 8-71939
- inelastic scattering of low energy electron beams by surface vibrs., nature of image force 8-91527
- ionic crystal, surface vibrational properties, review 8-71928
- ionic crystals, surface polaron 8-60020
- lattice force constant determination 8-71933
- LEED, anisotropic vibr. effects 8-71650
- localised, resonant and antiresonant modes (*French*) 8-71938
- metal, light scatt. from surface acoustic phonons 8-76484
- metal-liquid He interface, thermal boundary resistance, determ. in transport approach 8-51815
- quartz, amorphous and crystalline, surface polaritons and splitting of optical frequencies 8-72090
- response functions for cryst. and surfaces, appl. to surface scatt. 8-72669

crystal surface and interface vibrations continued

- roughness effects on dynamical props. 8-75923
- semiconductor, opaque, light scatt. from surface acoustic phonons 8-76484
- slab or semi-infinite solid, electronic contributions to lattice vibr. 8-71932
- transition metal, surface lattice dynamics 8-95224
- two-dimensional crystal boundary, oscill. propag. 8-63924
- Ar, monolayer adsorbed on graphite, lattice dynamics 8-75946
- CaF₂, slab, surface modes of vibr. 8-71935
- CdS, bulk acoustic phonons, light scatt. from phonon-induced surface ripples 8-75924
- Cr (111) surface, acoustic phonons Brillouin scatt. data 8-95222
- Cu, adsorbed mol. monolayers, UV-visible spectra 8-72619
- Fe, surface lattice dynamics 8-95224
- Fe, surface phonon spectra 8-71934
- GaAs, bulk acoustic phonons, light scatt. from phonon-induced surface ripples 8-75924
- GaAs, phonon surface density, Brillouin elasto-optic cross section 8-72536
- GaP, Raman scattering selection rules for surface polaritons 8-72091
- K halides, surface lattice dynamics, by Green's function method 8-71936
- LiF, 63 meV He atom scatt., single Rayleigh phonon interaction 8-80447
- methane-I plastic crystal, surface modes 8-71926
- MgO (001), surface relax. influence on surface vibr. modes, bulk shell model calcs. 8-71927
- MgO, reconstruction of the (001) surface 8-75922
- N₂, monolayer adsorbed on graphite, lattice dynamics 8-75946
- NaCl (001), surface relax. influence on surface vibr. modes, bulk shell model calcs. 8-71927
- NaI (001), surface relax. influence on surface vibr. modes, bulk shell model calcs. 8-71927
- Pt (111), surface reaction with acetylene ethylene, and H₂, EELS 8-71947
- Pt (111) stepped surface, localised surface phonons obs. 8-95223
- Pt(111), adsorption of NO, anal. of adsorption processes and surface reactions, vibration spectroscopy 8-87868
- Rh(111), surface geometry, vibrational props., Debye temp., LEED study 8-87852
- Sb₂S₃, layered biaxial cryst., surface phonon polaritons (*Russian*) 8-60021
- Si-³He interface, phonon reflection 8-84043
- Si-SiO₂, surface and interface phonons in bonded solids 8-71931
- SiO₂, amorphous, surface phonon theory 8-84044
- SiO₂, amorphous and crystalline, surface polaritons and splitting of optical frequencies 8-72090
- SiO₂ powder, surface modes, IR spectra 8-92063
- SiO₂, surface and interface phonons in bonded solids 8-71931
- W (001) surface, long-wavelength surface phonon spectrum 8-75921
- W, surface phonon spectra 8-71934
- WC, microcrystalline, mol. dynamics, motion of H₂O and H₂ mols. adsorbed on surface, catalytic activity 8-71941
- W(100), adsorbed H, nondipole electron impact vibr. excitations obs. 8-63922
- ZnO, small crystal, optical surface phonon modes 8-71940

crystal symmetry

see also crystallography; group theory

- algebraic definition of cryst. symmetry on n-dimens. space (*French*) 8-55824
- anisotropic constitutive equations and Schur's lemma 8-89337
- classification of crystals by acoustic props. 8-79547
- coordination number, quantifying concept for irregular coordination polyhedra 8-95008
- elastically bent single cryst., right-left asymmetry due to anisotropy on diffraction (*Russian*) 8-71699
- ethylene, isotopically mixed, crystal, dilute guest probe orientational energy, IR, Raman spectra 8-68496
- garnets, doped, site symm. exam., ang. variation of induced linear dichroism 8-95429
- homogeneous linear structures, systematisation according to charact. numbers of position symbols 8-95009
- implications in charge density studies 8-71694
- mixed metal chloride acousto-optical props. (*Russian*) 8-60419
- molecule struct., shapes symmetry 8-71697
- Mossbauer nuclei lattice with hyperfine interactions 8-67677
- normal mode calcs. of crystals and molecules, coordinates and force matrices generation, computer program 8-91393
- OD-groupoid families, complete list for OD-structures consisting of equivalent layers 8-59776
- point groups, symmetry, teaching aid 8-77650
- pseudo-centrosymmetry destruction by direct method 8-91286
- stereographic projection model, construction, teaching appl. 8-86086
- structural diagram of compounds ABO₄ 8-79548
- BaF₂-NiF₂-CrF₃, X-ray crystallography study, phase identification at 700°C, cryst. symm. (*French*) 8-95733
- (Ba_{1-x}Nb_xSi₄O₂₆)_n-Ba₃Nb₄Ti₄O₁₁, n=3/2 to 29/2, intergrowth series, electron microscope obs. (*French*) 8-83762
- K₃AgO₂, determ. of cryst. struct. X-ray diff. (*French*) 8-95029
- K₂CO₃-Sr-CO₂ phase diagrams, evidence of new compound (*French*) 8-95033
- KNO₃, Raman spectroscopic study of NO₃⁻ component with temp. 8-76458
- LiNO₃, Raman spectroscopic study of NO₃⁻ component with temp. 8-76458
- Mn₂GaC, mag. symmetry of ordered phases, mag. modes for point groups 8-71698
- NaNO₃, Raman spectroscopic study of NO₃⁻ component with temp. 8-76458

crystal whiskers *see whiskers (crystal)***crystallisation**

- see also crystal growth; dendrites; heat of crystallisation; nucleation*
- activation energies of mass transfer at phase boundaries, quantum theoret. calcs. (*German*) 8-67671
- aligned composites, in-situ growth by disproportionation of amorphous metal systems 8-72755
- α,ω -alkoxypolyethylene oxide, low mol. wt., crystallinity and fusion 8-51448

crystallisation continued

alloys, binary, nonequilib. dynamics, eqns. for supercooling, supersaturation of melt (*Russian*) 8-95736
 batch agitated crystalliser, design 8-60558
 borophosphate glasses, effect of F on props. 8-67657
 bytownite megacrysts., study of trapped basaltic melts, petrogenetic process study 8-95688
 cholesterol pelargonate, liq. cryst., crystallisation rate const. and Avrami index 8-94994
 citric acid monohydrate, crystallisation and cryst. growth rate 8-87638
 crystallisation, activation energies of mass transfer at phase boundaries, quantum theoret. calcs. (*German*) 8-67673
 cumulate nodules from Lesser Antilles island arc, crystallisation conditions 8-65267
 directional, techniques for calc. distrib. coeffs. from expt. data 8-75606
 disjoining pressure repulsion of macroscopic particle ahead of crystn. front. 8-95005
 electrocrystallisation, galvanostatic transients, crystn. overvoltage 8-76867
 electrocrystallisation, impedance frequency dependence, in the case of DC superposition 8-51844
 electrocrystallisation, nucleation and growth mechanism, ohmic overpotential effects, simulation 8-51842
 electrocrystallisation, nucleation and growth mechanism, ohmic overpotential effects determ. 8-51843
 electrocrystallisation noise, phenomenological model 8-51845
 ethanol-water system, metastable states, hydrates existence and props., low temp. 8-71835
 glass, crystallisation and opacity, exam. by high temp. viscometry and X-ray diffr. (*Polish*) 8-84875
 guanyl ribonucleases of fungi, crystn. and X-ray diffr. 8-71718
 hardness, elastic moduli, density, cryst. temp., mech. props., for flywheel appl. (*Dutch*) 8-52878
 ice, growth beneath water film, air bubble precipitation 8-83922
 ice, on CuS aerosol prepared by burning pyrotechnic mixture, freezing temps. 8-96279
 ingot, hollow cylindrical, temp. field and crystallisation front calc. (*Russian*) 8-63690
 interface morphology during crystallisation, single filament unconstrained growth from pure melt 8-52787
 interface morphology during crystallisation, single filament unconstrained growth from binary alloy melt 8-52788
 Landau theory, solidification and cryst. nucleation 8-83761
 liquid metal continuous casting, solidification process, convective heat transfer, anal. 8-84789
 macromolecules, crystallisation thermodynamics, various degrees of coiling 8-51445
 metal, FCC, modelling of growth from melt (*Russian*) 8-60664
 metal and alloy crystallisation, apparatus for decanting solid and liquid phases 8-56597
 metallic glass, density and Young's modulus, struct. relax. effects 8-72804
 metallic glass, hardness, elastic moduli, density, cryst. temp., mech. props., for flywheel appl. (*Dutch*) 8-52878
 metals, crystal growth, electrochem. Czochralski method, growth rate limitations 8-88433
 migration of salts in a porous medium allowing for their crystallisation (*Russian*) 8-87388
 minerals, magnetic trends on alkali-Fe-Mg diagrams 8-85551
 naphthalene-p. chloronitrobenzene system, eutectic, solidification 8-64530
 planetary system evolution from preplanetary gas disc, rel. to crystallisation and cryst. struct. (*German*) 8-93129
 polyester filaments, solvent-induced crystallisation 8-83754
 polyesters, epitaxial crystallisation, on organic and inorganic substrates 8-91565
 polyethylene, lamellar structs. nucleated onto fibrous substrates for high modulus 8-75578
 polyethylene, oxidation rel. to spherulitic crystn. (*Russian*) 8-71689
 polyethylene, spherulitic, nonexponential transformation equation 8-67662
 polyethylene melt spinning, extensional flow induced crystallisation 8-55818
 polyethylene oxide trioxane mixtures, eutectic crystallisation 8-56626
 polyethylene terephthalate, crystallisation kinetics from glassy state 8-75579
 polyethylene terephthalate, effects of preliminary ht. treatment on crystallisation (*German*) 8-75593
 polyethylene terephthalate, uni- and biaxially drawn films, preferred planar orientation 8-80590
 polyhexamethylene sebacate-poly 2-methyl-2-ethyl-1,3-propylene sebacate, cryst. multiblock copolymers, crystallisation 8-91269
 polyhexamethylene terephthalate/polyoxytetramethylene block copolymers, melting and crystallisation 8-91260
 polymer, fibrous crystallisation, chain extension and fibre form. 8-75573
 polymer, mixed heterogeneous homogeneous nucleation and nonintegral exponents of time 8-55820
 polymer, orientational ordering rel. to mech. props. (*Russian*) 8-59766
 polymer crystallisation, growth rates, nucleation, annealing and random copolymer crystallisation 8-51435
 polymer crystallisation, natural and artificial heterogeneous nucleation 8-51431
 polymer crystallisation, review 8-51430
 polymer crystallisation and fusion, conf., Louvain-la-Neuve, Belgium (1976) 8-51429
 polymer microstructure morphogenesis, book contrib. 8-83757
 polymers, amorphous, segmental distrib., crystallisation and viscoelastic relax. meas. 8-51443
 polypropylene, impurities redistribution during crystn. 8-75577
 polypropylene, shear effect on crystallisation (*German*) 8-75586
 polysilicic acid, IR spectra, struct., crystallisation effects (*Russian*) 8-72528
 polystyrene, isotactic, morphology and growth of chain struct. (*German*) 8-75597
 polystyrene blends, isotactic and atactic, small-angle X-ray scattering 8-55817
 polystyrene-polyethylene oxide, cryst. multiblock copolymers, crystallisation 8-91269

crystallisation continued

polyvinylidene fluoride, high-press. melting and crystallisation 8-91422
 proteins, effect of protein conc. and solubility on nucleation rate 8-87632
 quartz, growth from soln., mechanism 8-83763
 rare earth glasses, $R_2O_3-S-Ga_2S_3$, ($R=La$ to Nd), exam. of preparation and props. (*French*) 8-80504
 rare earth oxide (R_2O_3)- M_2O , glassy systems ($M=Ti, Nb, Ta$), rapid quenching by laser beam, exam. of composition and crystallization 8-52856
 rubber, natural, oriented, crystallisation kinetics and melting 8-75554
 spherulitic, nonexponential transformation equation 8-67662
 steel, alloy, high C, amorphous, produced by rapid quenching from melt, hardness and strength 8-59764
 ZZ 8-88057
 AgBr, thin layers, evaporation conditions, photoresponse (*Bulgarian*) 8-78017
 $Al_2O_3-B_2O_3-P_2O_5$ glasses, formation and props. 8-83737
 $Al_2O_3-SiO_2$ glass powder, mullite crystallisation during hot pressing 8-60639
 $Al_2O_3-SiO_2-P_2O_5$, refractory glasses, exam. of liquid immiscibility and crystallisation 8-55814
 $BaClO_3 \cdot H_2O \rightarrow BaClO_3$, dehydration process 8-59932
 $BaO-Fe_2O_3$, splat quenching struct. and crystn. mechanism (*French*) 8-51426
 $BaO-La_2O_3-GeO_2$, exam. of glass forming region, properties and crystallisation 8-88454
 $BaSO_4$, crystal growth, effect of nitrilotri (methylenephosphonic acid) adsorption 8-88417
 $CaO-Al_2O_3-SiO_2-ZnO$, continuous unidirectional crystn. of fibrous metasilicates from melt 8-95739
 $CaO-MgO-Al_2O_3-SiO_2-ZnO$, continuous unidirectional crystn. of fibrous metasilicates from melt 8-95739
 $CaO-SiO_2-ZnO$ continuous unidirectional crystn. of fibrous metasilicates from melt 8-95739
 $\beta-(CaO_2)-SiO_2-H_2O$, SEM and X-ray diffr. exam. of structure, crystallisation props. 8-73012
 $\beta-CaSiO_3$ fibre, continuous unidirectional crystallisation from melt 8-95739
 CdS, electrocrystallisation of films on Cd 8-72014
 $Ce(CO_3)_2^{5-}$, in Na and guanidinium salts, struct./props. correlation (*French*) 8-95032
 Co-P metallic glasses, crystn. kinetics by differential scanning calorimetry 8-91257
 $CuO-CaO-P_2O_5$ glass devices, memory switching 8-56192
 $(Fe, Mo)_{80}B_{20}$, glassy alloy, Curie temp. and crystn. temp., Mo additions effect, Mossbauer spectra 8-68428
 Fe, cast, with Mn, high S, exam. of sulphide phases, cocrystallisation during solidification 8-56646
 Fe meteorites, crystallisation rel. to origin of magnetisation 8-65564
 Fe-B amorphous metallic glasses, high-temp. mag. anal. 8-91258
 Fe-B amorphous alloy, crystallisation kinetics 8-83736
 Fe-B glass, crystallisation kinetics, elec. resist. meas. 8-83741
 Fe-B metallic glass, hardness, elastic moduli, density, cryst. temp., mech. props., for flywheel appl. (*Dutch*) 8-52878
 Fe-B metallic glass, role of Fe_3B in crystn., mag. and Mossbauer expts. 8-94997
 Fe-B metallic glasses, crystn. kinetics by differential scanning calorimetry 8-91257
 Fe-Si amorphous film, conversion electron Mossbauer effect 8-72440
 Fe-Si film, amorphous, conversion electron Mossbauer study, crystallisation obs. 8-84507
 $Fe_{80}B_{20}$, crystallisation of amorphous alloys, TEM and X-ray diffr. exam. of struct., growth characts. 8-79539
 $Fe_{40}Ni_{40}B_{20}$, metallic glass, embrittlement kinetics and crystn., quenching influence 8-68766
 $Fe_{50}Ni_{30}B_{20}$, crystallisation of amorphous alloys, TEM and X-ray diffr. exam. of struct., growth characts. 8-79539
 $Gd_3Al_2O_{12}$ phase obtained by crystallisation of amorphous $Gd_2O_3 \cdot 5/3 Al_2O_3$ by quenching 8-92224
 Ge, evaporated film, lattice parameters and phase transition temp., phase influence of glass substrates 8-94996
 Ge_2Se_{1-x} , $0 < x < 0.2$, crystallisation in amorphous bulk and thin films 8-55813
 $HfO_2/ErO_3/FeO_3$, crystn. on seeds, layer morphology 8-72041
 (In, Ga)Sb, sputter deposited amorphous film, impulse stimulated explosive crystallisation 8-84098
 $K_2O-Al_2O_3-SiO_2$ system, crystallisation of glasses in primary phase field of leucite 8-67658
 $LiO_2 \cdot 2SiO_2$, glass, devitrification with ageing 8-79536
 $Li_2O-Fe_2O_3-SiO_2$ glass, struct. and crystallisation behaviour 8-83738
 Mg-Zn metallic glass, hardness, elastic moduli, density, cryst. temp., mech. props., for flywheel appl. (*Dutch*) 8-52878
 $MgO-Al_2O_3-SiO_2$, exam. of microstructure and crystallisation kinetics 8-80501
 $MgO-Al_2O_3-SiO_2$ glass, features of crystallisation, in the presence of the thermal decomposition of tetrabutoxytitanium 8-87627
 $Mg_{74}Zn_{26}$ glass, exam. of crystallisation 8-71681
 Mn-Al alloy, vacuum codeposited, disorder of $MnAl_6$ phase in recovery process 8-51854
 Na polysilicates, IR spectra, struct., crystallisation effects (*Russian*) 8-72528
 $NaBO_2 \cdot H_2O \cdot 3H_2O$, crystallisation from aq. soln., nucleation rates with surfactant 8-91276
 $NaBO_2 \cdot 2H_2O \cdot 3H_2O$, crystallisation from aq. soln., growth kinetics with surfactant 8-91277
 $Na_2O-Al_2O_3-SiO_2-TiO_2$, effect of Cr_2O_3 , NiO, and MgO additions on crystallisation 8-87626
 $Na_2O-B_2O_3$ melt, crystallisation of $Na_2B_6O_{13}$ 8-59763
 Na_2O-SiO_2 glass, devitrification with ageing 8-79536
 Nb-Ni metallic glass, hardness, elastic moduli, density, cryst. temp., mech. props., for flywheel appl. (*Dutch*) 8-52878
 Nb_3Ge , RF and DC sputtered films comparison, O content effect 8-72022
 Nb_3Ge , supercond. tape, growth technique via amorphous state 8-84708
 Ni-Co-P, ferromag. film, amorphous to cryst. transition, diffr. and resistivity meas. 8-60587
 Ni-P metallic glasses, crystn. kinetics by differential scanning calorimetry 8-91257

crystallisation continued

- (Ni₂Pd)₈₂P₁₈, phase separated, exam. of crystallisation by differential thermal analysis 8-87623
 PbO-ZnO-B₂O₃, Corning 7575 seal glass, devitrification 8-79532
 Pd₇₀Fe₁₀Si₂₀ alloy, amorphous to cryst. transition, 350 to 450°C, Mossbauer spectra 8-59758
 Pd₈₀Si₂₀, amorphous alloy crystn., high press. effect 8-95001
 SS_{ex} (x=10, 15, 40), amorphous crystal transition, appl. of Kolmogorov-Avrami equation 8-67649
 Sb electrodeposit, amorphous, explosive crystn., semicond-semimetal transition and IR absorpt. 8-51849
 Se, crystallisation kinetics, correlation with molecular structure 8-94998
 Se-S, glassy alloy, order-disorder transition kinetics 8-67650
 Si, amorphous films, crystallisation kinetics and morphology, TEM obs. 8-84093
 Si, crystn. front face effect on at displacements (*Russian*) 8-67781
 Si ribbon parallel twinned structure development by shaped crystallisation 8-64465
 Si, self-implanted layer, grain size, laser irradi. energy density depend. 8-72012
 Si-As-Te glasses, crystallisation kinetics under influence of water vapour 8-59762
 Si₃N₄-Al₂O₃-Y₂O₃, sintered, observation of a noncrystalline phase 8-64536
 Si₃ON₂, needle crystals, growth by nitriding process in powder compacts (*Japanese*) 8-76601
 Sn, mechanism of influence of soluble impurities 8-71692
 SrO-Fe₂O₃, splat quenching struct. and crystn. mechanism (*French*) 8-51426
 SrSO₄, activation energies for mass transfer during crystallisation, surface active agent effects (*German*) 8-63689
 SrSO₄, mass transfer in precip. from mixed solvents (*German*) 8-67674
 Te₈₀Ge_{12.5}Pb_{7.5}, phase-separated system, overlapping effects of glass transition and crystn., DSC results 8-83739
 Th(CO₃)₆³⁻, in Na and guanidinium salts, struct./props. correlation (*French*) 8-95032
 YAG, solubility in solvent PbO_x-PbF₂, phase form. in system Y₂O₃-Fe₂O₃-PbO-PbF₂-B₂O₃ 8-95247
 ZnO-Al₂O₃-SiO₂, transparent glass-ceramics, EPR obs. of glass crystallisation 8-80507
 ZnO-Al₂O₃-SiO₂, transparent glass-ceramic, microstruct., physical props., crystallisation ht. treatment depend. 8-80506
 ZnO-La₂O₃-GeO₂, exam. of glass forming region, properties and crystallisation 8-88454

crystallite texture see texture**crystallites**

see also crystal microstructure

- AgBr, thin layers, struct. and photographic characts. 8-49919
 carnauba wax, orientation prod., by mech. press. or US waves 8-64314
 catalyst, mag. characterisation, review 8-64881
 concentration variations, X-ray diffraction line profile anal. 8-75491
 disordered cylindrical lattices, diffracted X-ray intensities 8-79493
 electrophotographic KC film digital recording performance 8-78024
 fibrillas, crystallite shear deforms. rel. to small-angle X-ray scatt. pattern (*Russian*) 8-71690
 ionic rectangular crystallites, IR absorpt. calcs. 8-95583
 poly(chlorotrifluoroethylene) films, crystalline superstruct., mol. orientation, X-ray diffr., depolarised light scatt. 8-71685
 poly-p-phenylene terephthalate, high modulus fibre, struct. obs. 8-75564
 polyethylene, linear, solution-crystallized, NMR anal. of phase struct. 8-71684
 polyethylene, Young's modulus, crystallite thickness 8-76689
 polymer, oriented, amorphous-crystalline low ang. X-ray diagrams, supermol. struct. models, schematic representation (*Russian*) 8-87630
 polypropylene-nylon 11 fibres, bimodal cryst. texture, X-ray diffr. and electron microscopy 8-75567
 polyvinylidene fluoride, X-ray diffr. evidence for ferroelectricity 8-60399
 Al, cryst. and polycryst., inhomogeneity effects on galvanomagnetic props. 8-60109
 Au, formation in flowing Ar system, density, size distrib. and size dispersion 8-88415
 Au, polycryst. film, RF bias-diode and triode sputtered, resist. and microstruct. 8-80072
 C, glassy, LMSC process prepared, exam. of props. by TEM and X-ray anal. 8-63675
 CdBr₂(I₂), vapour growth crystals, decomposition, electron microscope study 8-92268
 Co-P electroless film on Al base disc substrate, microstruct. rel. to mag. props. 8-68304
 Cu-Cd alloys obtained by electrolysis, struct. 8-91552
 Cu₂O, form. by Cu oxidation in CO₂, 800-1000°C 8-76784
 Fe₂O₃ crystallite formation in B₂O₃ and Na₂O.B₂O₃ glasses, Mossbauer obs. 8-68429
 Fe₃O₄, magnetite, oxidation kinetics, influence of cryst. size 8-79778
 KCl, IR absorpt. calcs. in rectangular crystallites 8-95583
 Mg(OH)₂, decomposition to MgO, mechanism, product crystallite size rel. to reaction rate 8-85152
 PbO-2B₂O₃-Fe₂O₃ glass, Mossbauer study, struct., crystallite formation, broadened quadrupole doublet 8-59761
 Pt, surface area loss, on graphite support, in H₃PO₄ 8-73076
 Zr₂O₃ microcrystals, tetragonal struct. stabilisation, crystallite size effect 8-51670

crystallographic shear

- brass, orientation change in (211) [111] single crystals during rolling (*Japanese*) 8-60712
 brass, simulation of rolling and shear texture, using an adapted Taylor theory 8-52835
 ductile single crystals, exam. of strain localisation 8-52912
 lithium ammonium tartrate monohydrate, spontaneous shear strain, X-ray obs. 8-56433
 plastic deformation mechanism, meas. of microplasticity 8-60720
 polyethylene, crysts. subject to fold-surface tensile stress, elastic deform. 8-76712

crystallographic shear continued

- polyethylene, pyramidal crysts., soln.-grown, collapse mechanics 8-76713
 polypropylene, shear effect on crystallisation (*German*) 8-75586
 steel, high strength, low alloy, plate, impaired ductility in sheared edges 8-60727
 Al-Zn-Mg, effect of microstruct. on localised shear failure 8-52996
 Cu, void growth and localisation of shear in plane strain tension 8-64613
 Cu-Al (6.4 wt.%), rolled low stacking fault energy alloy, struct. and texture 8-52844
 Fe, single crystals, work hardening and behaviour and dislocation struct. during simple shear tests 8-95762
 Fe₂O₃-TiO₂ system, high temp. intergrowth struct., metal atom ordering in intergrowth boundaries 8-79573
 Nb, surface oxide softening, anisotropy 8-60716
 Si, ion implantation damage, annealing, role of stresses 8-75679
 Ti-11, unstable shear modes in fatigued β -annealed specimens 8-84984
 Ti-alloy, IMI-685, unstable shear modes in fatigued β -annealed specimens 8-84984
 Ti₂O_{2n-1}, reduced rutile, elastic strain energy due to crystallographic shear plane arrays 8-55880
 Zr(Ca)O_{2-x}, internal, external distortion mechanisms, neutron diffr. study 8-83946
 Zr(Y)O_{2-x}, internal, external distortion mechanisms, neutron diffr. study 8-83946

crystallography

- see also crystal atomic structure; electron diffraction crystallography; gamma-ray diffraction; isomorphism; lattice constants; neutron diffraction crystallography; space groups; X-ray crystallography
 algorithms, mol. fragment recognition in E maps and electron density maps 8-55772
 charge deform. models 8-71695
 charge density mapping, limitations, appls. 8-71696
 electron density, minimising variance in integrals and derivatives 8-91195
 molecular geometry, computer retrieval and anal., general principles and methods 8-83643
 molecular geometry, computer retrieval and anal., geometry of β -1'-aminofuranoside fragment 8-83645
 molecular geometry, computer retrieval and anal., variance and interpretation 8-83644
 molecular systems, electron density, spatial, rel. to conform. props., computer simulation 8-70763
 one-phase structure seminvariants of first rank, estimation 8-79545
 optical crystallography techniques, advances in spindle stage methods 8-85702
 optimized conjugate gradient solution for least-squares equations 8-79495
 phase determination physical significance of triplets in direct methods 8-55776
 pseudo-extinctions, interpretation 8-55780
 reciprocal lattice in crystallography, undergraduate demonstration 8-61989
 reflexion intensity, probability of meas. as negative 8-55781
 thermal-motion correction for bond angles, harmonic approx. 8-55777
 vectors, best proper rotation to relate two sets 8-91184

crystals

see also bicrystals; crystal structure; crystallography; dendrites; epitaxial layers; liquid crystals; plastic crystals; whiskers (crystal)
 No entries

Curie point see Curie temperature**Curie point writing** see thermomagnetic recording**Curie temperature**

see also ferroelectric Curie temperature

- alloys, amorphous, mag. props., review (*Japanese*) 8-52259
 amorphous magnet, Bethe-Peierls-Weiss approx. 8-76263
 biotite, thermal decomposition, stability of ferromag. products 8-57195
 concentrated alloys, ferromag., spin fluctuations 8-64290
 FCC alloys, atomic ordering and antiferromagnetism 8-72330
 ferromagnet with random anisotropy, Curie temp., constant coupling approx. 8-76264
 ferromagnetic materials, Curie point determ. from saturation magnetisation-temp. charact. 8-60281
 ferromagnetic metal, itinerant electron model, for US propagation and structural instabilities 8-95508
 ferromagnetic semiconductor, optical transparency, photoferromag. effect, Curie temp. shift (*Russian*) 8-72387
 Ising model, Curie point in quenched bond model 8-56318
 itinerant electron ferromagnetism, spin fluctuation theory 8-80151
 liquid ferromagnet, model calculation 8-88088
 metal, amorphous ferromagnetic, paramagnetic Curie temp. determ. 8-76242
 pearlite in C steels (0.08 to 1.6 wt.%), exam. of temp. depend. of mag. coercivity 8-52304
 rare earth alloys, R-3d alloys (3d=Mn,Fe,Co,Ni), magnetic properties 8-52231
 rare earth intermetallics, RAu_{3.6}, ordering temps. and effective moments 8-60283
 rare earth intermetallics, RMg₂, cryst. and mag. props., ordering 8-68185
 rare earth iron alloy, amorphous film, cosputtered, struct. and mag. props. 8-60323
 rare earth sesquioxides, 300 to 900K, mag. susceptibility and Curie temp. meas. 8-56288
 rare earth-Co₂-Al, dil., nonmag. impurities effect on ordering temp. 8-84427
 rare earth-Fe, intermetallic compounds, mag. props. (*Rumanian*) 8-92007
 TGS, gamma irradi. effects on heat capacity, Curie temp., permittivity 8-67737
 titanomagnetites, Curie temps. rel. to domain struct. temp. var. 8-65272
 transition metal-metalloid amorphous alloys, mag. props. review 8-52300
 CdCr₂Se₄(S₄), ESR line intensity near Curie point 8-64269
 Cd_{1-x}Fe_xCr₂S₄:Cu, effect of doping on elec. props. and Curie temp. 8-84114

Curie temperature continued

- CrTe, effect of high pressures on magnetic properties 8-52238
 Cu-Fe, supersaturated, spontaneous magnetisation region development, Mossbauer obs. (*German*) 8-64306
 CuCr₂Se₄, experimental obs. 8-76227
 Dy(Fe_{1-x}Ni_x)₂, mag. behaviour, susceptibility and Mossbauer expts., 4.2-1300K 8-52235
 Dy₂O₃, 300 to 900K, mag. susceptibility and Curie temp. meas. 8-56288
 (ErCo₂)_{1-x}(ErAl₂)_{1-x}, mag. and struct. investigations of intermetallic systems 8-95440
 Er₂O₃, 300 to 900K, mag. susceptibility and Curie temp. meas. 8-56288
 EuB_{6-x}C_x, magnetic and elec. props. 8-91842
 Eu_{0.5}Ba_{0.5}TiO₃, ferromag., ferroelec., ceramic, Curie temps. determ. 8-68230
 (EuLu)₃(Fe₂O₁₂), Ga, Al or (Ca,Ge) substituted, mag. props. and growth of 2 μ m bubbles 8-91910
 EuNi₂Cu_{1-x}, comp. depend., Mossbauer obs. of mixed valency of Eu 8-52407
 EuNi₂Zn_{1-x}, comp. depend., Mossbauer obs. of mixed valency of Eu 8-52407
 EuO, mag. struct. and transition temp., indirect exchange 8-91860
 EuO:La, photothreshold reduction by mag. induced space charge layer 8-72692
 EuO_{1-x}N_x, ferromag. semicond., elec. and mag. props. (*French*) 8-79993
 EuS, mag. struct. and transition temp., indirect exchange 8-91860
 (Fe,Mo)₈₀B₂₀, glassy alloy, Curie temp. and crystn. temp., Mo additions effect, Mossbauer spectra 8-68428
 Fe, cold work stored energy effects on mag. moment vs. temp. curve 8-95419
 Fe, ferromagnetic, cluster method, environmental effects 8-95405
 Fe, whisker, mag. crit. phenomena, size effects 8-68258
 Fe-B, amorphous metallic glasses, high-temp. mag. anal. 8-91258
 Fe-Cr-Co (31 wt.%, 23 wt.%), microstruct. and mag. props., ageing and thermomag. treatment effects 8-76769
 Fe-Ni alloy, cold work stored energy effect on mag. moment vs. temp. curve 8-95419
 Fe-Ni-Al alloys, phase diagram, miscibility gap, mag. props. 8-92237
 Fe-Ni-Co-B-P soft magnetic metallic glasses, status report 8-64226
 Fe-Si-Al (6.4 wt.%), Sendust alloy, effect of Ni content on mag. props. 8-72897
 Fe-Si-B powders, prep. by atomisation technique 8-92213
 Fe_{100-x}B_x (11.5 $\leq x \leq 22$), magneto-volume effect 8-91922
 (Fe_xCo_{100-x})_{100-(y+z)}Si_yB_z, amorphous ribbon, mag. moment and Curie temp., comp. depend. 8-95421
 Fe₇₈Mo₂₂, exam. of mag. props. between 300 and 900K 8-85010
 Fe₆₅(Ni_{1-x}Cr_x)₃₅, remanent magnetisation, temp. depend., anomalies near Curie temp. (*Russian*) 8-60310
 Fe₃₂Ni₃₆Cr₁₄P₁₂B₆, Metglas 2826A, Hall resistivity, effect of thermal cycling and annealing 8-56125
 Fe₄₀Ni₄₀P₁₄B₆, (Metglas 2826), ferromag. Curie temp. determ. 8-64206
 (Fe_{0.5}Ni_{0.5})₇₅P₁₆B₆Al₃ glass, struct. relax. as origin of Curie temp. ageing 8-84418
 Fe₂Sn_{1-x}, amorphous, mag. behaviour 8-95478
 Fe₂TiO₄, ulvospinel, containing magnetized inclusions, mag. behaviour, cooling through Curie point 8-56314
 Fe₂TiO₄-Fe₂O₄, titanomagnetite, prepared at different oxidation conditions, hysteresis props. 8-56352
 Gd, EPR linewidth and spin-spin relax. near T_c 8-68369
 Gd-Ag, vap. quenched alloys, struct. and mag. props. 8-84461
 Gd-Ag(Cu) alloy film, amorphous, struct. and mag. props. 8-52318
 Gd-Al, amorphous film, microwave mag. reson. 8-91948
 Gd-Al, amorphous film, microwave mag. reson. 8-92060
 Gd-Al(Cu)(Ga)(Rh)(Pd), amorphous alloys, mag. coupling of rare earth moments 8-88108
 Gd-Co, CPA calcs., moments and transition temps. 8-52252
 Gd-Fe, CPA calcs., moments and transition temps. 8-52252
 Gd-Ni, CPA calcs., moments and transition temps. 8-52252
 GdAg_{1-x}In_x, magnetic transition temp., effect of hydrostatic press. 8-76244
 (GdMn₂)_{1-x}(GdAl₂)_{1-x}, mag. and struct. investigations of intermetallic systems 8-95440
 GdNi₅, anomalous behaviour near Curie point 8-91880
 GdNi_{1-x}, sputtered amorphous films, mag. props. and Hall meas. 8-95488
 GdY_{1-x}Fe_x, saturation magnetisation, magnetostriction, Curie temp., ferrimag. ordering, exchange field (*Russian*) 8-68343
 HgCr₂Se₄, ESR line intensity near Curie point 8-64269
 (Ho,Y)Co₂, first order phase transitions 8-84426
 Ho particles, effect of size on paramag. Curie temp. 8-60317
 Ho(Fe_{1-x}Ni_x)₂, mag. behaviour, susceptibility and Mossbauer expts., 4.2-1300K 8-52235
 Ho₂O₃, 300 to 900K, mag. susceptibility and Curie temp. meas. 8-56288
 KFeS₂, magnetic reson. meas. 8-95524
 La_{0.65}Pb_{0.35}MnO₃, transport props. near Curie points 8-88100
 Li ferrite, fine particle, for arc plasma spraying mm-wave phase shifter 8-64469
 LiTiZn ferrites, elec. resist., mag. props., effect of Bi addition 8-95474
 Lu₂V₂O₇, pyrochlore struct., mag. props. 8-72335
 MRh₂B₄ (M=trivalent transition metal, usually rare earth) supercond. and ferromagnetism, role of Sc 8-95438
 Mn-Bi eutectic alloy, mag. anisotropy 8-68220
 Mn₂As-Mn₂Sb, structural and magnetic props. determ. 8-76248
 Mn_{1-x}Sb_{1-x}Sn_x, magnetisation and Curie temp., prep. and comp. depends. 8-64200
 Mn₁₈Zn_{0.06}Co_{0.01}Fe_{1.75}O₄, transport props. near Curie points 8-88100
 Na_{1-x}Li_xNbO₃, dielec. const. and X-ray diffr., for Curie temp. and phase diagrams 8-72768
 NaNH₄SeO₄·2H₂O, ferroelectric crystal, effect of hydrostatic pressure on phase transition 8-52453
 Ni, amorphous film, getter sputtered at 25K, resistivity, Curie temp. 8-52673
 Ni, anomalous resistivity near Curie temp., band theoretical calc. 8-56127
 Ni, high purity single cryst., sp. ht. near crit. temp. 8-64212

Curie temperature continued

- Ni, oxidation kinetics near Curie temperature 8-88578
 Ni, photoelectric effect in paramag. and ferromag. states, Auger spectra 8-95649
 Ni-Mn disordered alloys, mag. moment and Curie point 8-76243
 NiS₂, neutron diffr. anomaly at Curie temp., antiferromag. refl. 8-76260
 NiSiF₆·6H₂O, ESR spectra at low temperatures and high pressures 8-52339
 Pb₂Ge₃O₁₁:BaO, impurities, static central peak 8-92079
 Pd-Fe, Mossbauer spectra, scatt. and transmission geometries, differences in crit. behaviour near T_c 8-76367
 Pd-Ni, local susceptibilities, ⁶¹Ni Mossbauer spectroscopy 8-95536
 Pd-Ni alloy, dil., ferromagnetism, local moments, susceptibility, magnetisation and Curie temp. (*Russian*) 8-88115
 Pr₂Tl, induced ferromag., mag. props. under hydrostatic press. 8-56315
 ROsB₄, R=Y, Gd, Tb, Dy, Ho, Er, Tm, struct. and mag. props. 8-79584
 RRuB₄, R=Y, Cd, Tb, Dy, Ho, Er, Tm, struct. and mag. props. 8-79584
 (Sc,M)Rh₂B₄, M=Ca, Th or rare earth, supercond. and ferromagnetism 8-95438
 Sm₂Co₇, mag. and struct. investigations of intermetallic systems 8-95440
 Sm₂Dy_{1-x}Co₅, temp. compensated magnetic material, mag. and struct. characterisation 8-68177
 Sm₂Er_{1-x}Co₅, temp. compensated magnetic material, mag. and struct. characterisation 8-68177
 Sm₂Tb_{1-x}Co₅, temp. compensated magnetic material, mag. and struct. characterisation 8-68177
 TbB₂, mag. props. and neutron diffr. 8-84401
 Tb₂O₃, 300 to 900K, mag. susceptibility and Curie temp. meas. 8-56288
 TiFe_{1-x}Co_x, mag. props., under high press. and in high mag. fields 8-95423
 Tm₂O₃, 300 to 900K, mag. susceptibility and Curie temp. meas. 8-56288
 Tm₂V₂O₇, pyrochlore struct., mag. props. 8-72335
 U₂N₂Bi(Sb)(Te), mag. props. 8-72333
 (Y,Sm,Lu)₃(Fe,Ga)₅O₁₂, LPE mag. film, suitability for 1 to 3 micron bubble devices 8-68323
 Y-Co, CPA calcs., moments and transition temps. 8-52252
 Y-Ni amorphous alloy, spontaneous magnetisation, Curie temp. and paramag. susceptibility 8-68189
 Y₂(Fe_{1-x}N_x)₁₇, magnetic properties, Mossbauer spectra (*Chinese*) 8-95433
 (YSmLuCa)₃(FeGe)₅O₁₂, mag. props. and growth of 2 μ m bubbles 8-91910
 YbCuAl, mixed valence behaviour, mag. props. 8-68150
 Yb₂O₃, 300 to 900K, mag. susceptibility and Curie temp. meas. 8-56288
 Yb₂V₂O₇, pyrochlore struct., mag. props. 8-72335
 ZrZn₂, high purity, mag. props., pulsed fields up to 17 T 8-64198

curium

- see also nuclei with
 antiferromag. state, paramag. suscept. meas., electronic struct. (*Czech*) 8-80133
 movement through food chain 8-61264
²⁴²Cm and ²⁴⁴Cm in global fallout, lichen sample results 8-57263
²⁴⁴Cm, biological availability, influence of DTPA at soil-plant and plant-animal interfaces 8-73264

curium compounds

- CmO₂, band struct., cryst. binding and ESCA spectra, X_α cluster calc. 8-64443

current (electric) see electric current**current algebra**

- see also elementary particle theory; hadron current; light cones; quantum field theory
 anomalous currents in curved space 8-62336
 axial anomalies and index theorems on open spaces 8-93821
 Cabibbo current and CP violation in a six quark gauge model 8-70329
 current-current interaction, general props., book contrib. 8-78163
 dual chiral pion model, partially conserved axial-vector current, S-matrix theory 8-58175
 dual current vertex, group theoretical struct. 8-74229
 Gell-Mann-Nishijima formula for EM current operator generalised 8-78109
 hadroproduction of quark flavours, extension of conserved vector current hypothesis to gluons 8-58159
 mass-sum rule, Veneziano-type amplitudes π and K mesons 8-74180
 neutrino as axial EM field source, symm. P-invariant broadened Maxwell eqns. (*Russian*) 8-58141
 neutrinos, gauge theories, EM props., forbidden processes and currents with anomalous Lorentz struct. 8-54599
 nuclear currents, microscopic anal. of elementary particle description 8-82304
 oriented nuclei, β - γ ang. correl., G-parity nonconservation 8-54723
 P-state particle, field current reln. and total width (*Chinese*) 8-82188
 potentially CP violating phase in QCD, alleged axion mass, PCAC quark masses 8-66080
 pseudoparticle fields, role of fermionic zero modes 8-74159
 QCD, gauge independence of IR cancellation, fermion-fermion scatt. 8-50006
 radiative corrections in gauge theories, QCD current algebra formulation, weak interaction universality 8-93883
 relativistic harmonic oscillator quark model, N and $\Delta(1236)$ form factors 8-93852
 relativistic quantum fields, particles and currents, book 8-82117
 right handed colour octet currents for charm and colour excitation in $v(\bar{v})$ reactions 8-93874
 scalar and conformal invariance, scalar currents, theory with continuous mass spectrum 8-62335
 second class currents on nuclei, effective two-body operator approach 8-54694
 semi-leptonic weak interactions, book contrib. 8-78162
 sine-Gordon supersymmetric theory, infinite set of bosonic conserved currents 8-62313

current algebra continued

- strong localised EM potential interactions with charged leptons or vac. state, critical pots., weak currents 8-54597
 $SU(4) \times U(1)$ as gauge symm. for quark, lepton quartets, weak and EM interactions, weak currents 8-74174
 $SU(5)$ and E_7 unified gauge theories 8-54600
 supercurrent, existence and deduction from an arbitrary superfield Lagrangian (*Russian*) 8-89633
 two-photon decays, weak, Hamiltonian derived in model with right-handed currents (*Russian*) 8-66119
 up-quark zero mass, critical anal. in current algebra framework 8-82144
 weak charged V-A current 8-74179
 $D(1865) \rightarrow e\nu K^*(890)$, right handed current, eK^* ang. correl., energy spectra 8-74248
 D mesons, decay const. using current algebra with Lagrangian model 8-58176
 F mesons, mass and decay const. using current algebra with Lagrangian model 8-58176
 $F^+ \rightarrow \pi^+ e^+ e^-$, enhancement due to π^+ EM form factor, generalised PCAC applicability 8-82164
 $K_s \rightarrow 2\gamma$ decay, contribution of Hamiltonian derived for weak two-photon decays (*Russian*) 8-66119
 K_μ decay in relativistic quark model, axial vector form factors and decay rate 8-66109
 $\nu(\bar{\nu})N$ elastic scatt., symmetry relations, current matrix elements 8-54627
 νN interactions, CVC and PCAC tests, book contrib. 8-78171
 $\varphi \rightarrow \pi\gamma$, $SU(3) \times SU(3)$ algebra, appl. to ground state mesons, coupling constraints and decay rate 8-58183
 π photoproduction near threshold, interior dispersion relations appls. 8-93889
 $\pi^- p \rightarrow e^+ e^- n$, induced pseudoscalar nucleon form factor, current algebra appl. (*Russian*) 8-78212
 τ decay, large timelike Q^2 , conservation of vector current and current algebra 8-78155
 $^{12}N \rightarrow ^{12}C(g.s.)$, second-class axial current, meas. alignment-positron-momentum correl. 8-82317

current control, electric *see electric current control***current density**

- see also critical current density (superconductivity); electron density*
 electrocrystallisation, galvanostatic transients, crystn. overvoltage 8-76867
 electrolyte conductivity rel. to electrode current density (*Russian*) 8-64847
 electromagnet windings with constant current density, maximum permissible mag. field 8-57990
 field emission current density, max., rel. to cathode geometry and kinetic props. 8-72704
 pulsed electron accelerator current density distrib. multichannel recorder 8-58520
 Stark-Ladder current theory 8-68035
 steel, mild, corrosion in complex aq. environment, linear polarisation investig. 8-76782
 surface scattering from piecewise planar surfaces, algorithm 8-62983
 thermionic convertor, long, cylindrical, current density distrib. 8-71552
 wave diffraction on circular cylinder with longitudinal slot (*Ukrainian*) 8-90345
 AlGaAs-GaAs DH laser, carrier leakage, physical mechanisms 8-66824
 C cathode damage and vapour/thermionic arc transition obs. 8-71603
 Cs fully-ionised plasma hollow-cathode arc discharge theory 8-67533
 Hg DC vacuum arc anchored cathode spot current density obs. 8-75467
 Zn electrodeposit dendritic growth control using impedance meas. 8-84721

current distribution

- see also current density*
 diagonal-type nonequilibrium plasma MHD generator, electrode internal and external connection effects 8-91165
 Fredholm eqn. of the second kind for current distrib. in antenna theory (*Chinese*) 8-66708
 Josephson junction, finite size, current distribution (*Russian*) 8-80103
 magnetic field calc. from current distrib., finite element techniques 8-94358
 multifilamentary superconductor, current distrib. close to input leads 8-84363
 negative corona discharge in air, current distrib. 8-87539
 pulsed electron accelerator current density distrib. multichannel recorder 8-58520
 solenoid, semiinfinite, thin, mag. field and current density distrib. near edge Wiener-Hopf calc. 8-70999

current fluctuations

- see also noise*
 BWR in-core instrument tube vibration obs. by reactor noise techniques 8-94064
 chemically reactive arc-heated gas flow, ion saturation current fluctuation probe 8-63574
 laser heterodyne signals from moving object, bandpass filtering by finite apertures 8-55306
 metal film resistor, resistance fluctuations from spontaneous enthalpy fluctuations 8-72217
 myotubes, human, cultured, acetylcholine-induced conductance fluctuations 8-61157
 neurone Ca conduction units, Helix aspersa 8-77041
 GaAs, epitaxial layers, low freq. current noise between 4.4 and 300K 8-95388

current measurement, electric *see electric current measurement***current transformers**

- see also electric current control; electric current measurement*
 low leakage for Tokamak devices series coupled power crowbar system (*Japanese*) 8-55755

current transients *see transients***currents algebra** *see current algebra***curvature measurement**

- large curved surface coordinate determ. apparatus 8-77863
 Moire topographic method, anal., concave convex region discrimination 8-65901

curvature of field *see aberrations***curve fitting**

- degree of fit, new criteria 8-57758
 hard magnetic materials, demagnetisation curve, single function approx. using computer (*Hungarian*) 8-60307
 ionosphere, analytic partial derivatives for incoherent scatter data least-squares fitting 8-73581
 parabola fitting, filtering characts. of smoothing method (*Japanese*) 8-89084
 vision, Stiles II-mechanisms candidacy for colour-matching fundamentals 8-56980

cutting

- see also machine tools; machining*
 cine-film slitting in the laboratory 8-93770
 diamond, polycrystalline tool, wear in rock removal processes 8-64724
 glass fibre cutting device (*Italian*) 8-50951
 Inconel 718, superalloy, wear of superhard tool during cutting, SEM and metallographic obs. 8-64720
 metal, appl. of Taylor eqn. for different cutting speeds (*German*) 8-72915
 plasma cutting at elevated press., underwater appl. 8-87507
 steel, stainless, austenitic, CC Ni-Al, γ -phase, fracture mechanical aspects of abrasive friction, wear, chip formation 8-72865
 steel 1Kh18N9T, physico-mech. props. after boring in metallic melts (*Russian*) 8-56736
 steel 40Kh, surface working effects on crack resist. (*Russian*) 8-56734
 Al, cutting of bicrystal to compare mechanism for large crystals and polycrystals (*Japanese*) 8-60871
 Al, orthogonal cut surface, effect of cutting condition on residual stress (*Japanese*) 8-85035
 Al, orthogonal cut surface, relations between residual stress and moire strain, exam. (*Japanese*) 8-85036
 Al, reverse finish cutting, exam. (*Japanese*) 8-85034
 Cu, cutting of bicrystal to compare mechanism for large crystals and polycrystals (*Japanese*) 8-60871
 Fe-Si (3.5 wt.%), cutting of bicrystal to compare mechanism for large crystals and polycrystals (*Japanese*) 8-60871
 Si, carrier lifetime degradation at room temp. 8-95301
 Ti-Ni alloy, effect on $[Cu(NH_3)_4(H_2O)]^{2+}$ solns. on drilling (*Russian*) 8-53017
 WC base alloys, uncoated and TiC or Al_2O_3 coated, wear charact. 8-92365
 Zn, cutting of bicrystal to compare mechanism for large crystals and polycrystals (*Japanese*) 8-60871

CVD *see chemical vapour deposition***CVD coatings**

- glass film, SiO_2 rich, prepared by modified CVD, refr. index behaviour 8-60526
 multilayer optical interference coatings via glow discharge polymerization techniques 8-87170
 tribology appl. 8-64743
 BN, pyrolytic, diffusion source for Si 8-91352
 C, columnar and laminar forms, deposition on polycrystalline Ni foils 8-63943
 In_2O_3 , transparent electrode deposition on PLZT ceramic, elec. and opt. props. 8-74848
 InP, on preferentially etched Mo, initial growth behaviour 8-51855
 Mo, deposited by low temp. carbonyl pyrolysis, struct. 8-72039
 Nb₃Ge, CVD, impurity doping effect on supercond. crit. props. 8-52174
 Nb₃Ge film, nucleation of high- T_c phase in presence of impurities 8-88054
 Nb₃Ge, supercond. film, CVD, crit. temp., crit. current density 8-76204
 Re, on cemented carbides, hardness (*German*) 8-64777
 (SN)_x fbms, electrical properties 8-91782
 Si CVD grown polycrystal recrystallisation 8-64560
 Si, film, CVD, low press., struct. and stability, X-ray diffr. and TEM obs. 8-91559
 Si, zone refined, prep. of solar cells 8-64475
 Si:H amorphous, elec. cond., effect of adsorbed gases and illumination 8-88048
 Si:O film, near IR absorption, O impurity states 8-88333
 Si-C films, plasma deposition with neutralisation 8-88429
 Si-N films, reactive plasma deposited for MOS-LSI passivation 8-56584
 SiC, diffusion behaviour of fission products, 1650 to 1850°C 8-79814
 Si₃N₄, encapsulant for annealing for implanted GaAs:Se 8-83834
 Si₃N₄, low temp. deposition using microwave-excited active N₂ 8-84718
 Si₃N₄, on Si, implantation effects on substrate hardening and film stress reduction 8-71748
 Si₃N₄, with varying refr. index, AES and XPS 8-72029
 Si₃O₂N₂, pyrolytic, on GaAs, evidence for growth-induced damage from photolum. expts. 8-75953
 (SiO₂)_x(Si₃N₄)_{1-x} on GaAs, deposition method and props. 8-91796
 SnO₂ film, CVD using SnCl₄-H₂O and SnCl₄-H₂O₂ systems, elec. and optical props. 8-52686
 SnO₂, transparent electrode deposition on PLZT ceramic, elec. and opt. props. 8-74848
 Ti-Zr-B system 8-60581
 W, deposited by low temp. carbonyl pyrolysis, struct. 8-72039
 W on Si, properties and kinetic parameters for deposition 8-91570

CVD epitaxial growth *see vapour phase epitaxial growth***CVD thin films** *see CVD coatings***cyanogen, C₂N₂** *see carbon compounds***cybernetics**

- see also artificial intelligence; biocybernetics; information theory; man-machine systems; pattern recognition*
 education, pupil learning and teacher activity algorithms 8-49577
 education, suggested uses of algorithms 8-49578

cyclopentadienylides *see organometallic compounds***cyclotron resonance**

- for ion cyclotron resonance spectroscopy *see mass spectroscopy*; for ion cyclotron resonance heating *see plasma heating*
see also diamagnetism; dopplers
 Azbel-Kaner, surface impedance of a metal in magnetic field 8-87901
 electron beam, high-current, stability in mag. field in waveguide 8-66742

cyclotron resonance continued

- electron gas, two dimens., Coulomb interaction effects 8-60073
 electron liquid, cyclotron reson. at skipping orbits (*Russian*) 8-72240
 Fermi-liquid parameter determ. from cyclotron reson. meas. 8-60069
 gases, electron cyclotron resonance absorpt. signals 8-51278
 inversion layers, carrier effective mass, contribs. of electron-electron and electron-phonon interactions 8-64087
 inversion layers, mag. field depend. of reson. line width 8-56380
 inversion-layer electrons, temp. depend. cyclotron reson. lineshape, theory 8-64086
 laser illumination, additional, effect on reson. effects in mag. field 8-72417
 magneto plasma half space, reflected pulse, cyclotron and upper hybrid resonance freq. 8-63569
 maser amplifier with freq. conversion 8-55329
 metal spherical Fermi surface, cyclotron reson. line shape and cyclotron waves 8-95251
 metals, compensated, Gantmakher-Kaner effect in strong mag. fields 8-91595
 quadratic grouping of electrons directed by transversely inhomogeneous magnetostatic fields (*Russian*) 8-74822
 semiconductor, intervalley cyclotron-phonon reson., IR absorption in mag. field 8-60448
 semiconductor, pinning struct. of cyclotron reson. lines 8-72414
 semiconductor, zinc blende struct., cond. band nonparabolicity and cyclotron reson. linewidth (*German*) 8-75993
 semiconductor-insulator boundary, space charge layers, HF magnetoconductivity 8-60231
 spatially inhomogeneous system, galvanomagnetic effects (*Russian*) 8-72129
 thin conductors, SHG and size cyclotron reson. 8-72186
 two dimensional electrons interacting with surface and volume phonon 8-80221
 two-dimensional electron impurity system, quantum theory of cyclotron reson. lineshape 8-64083
 e⁻p mass ratio, direct determ. using cyclotron resonance technique 8-70093
 AgBr, cyclotron reson. of polarons at high microwave fields 8-67958
 Bi, Azbel-Kaner type cyclotron reson. obs. 8-56379
 Bi:Sb, semimetallic alloy, microwave spectroscopy 8-87908
 Bi-Sb narrow gap semiconductor, EM wave propagation in direction parallel to mag. field 8-80014
 BiSb, Azbel-Kaner type cyclotron reson. obs. 8-56379
 Cd, inversion of cyclotron resonance data 8-91593
 Ge, irrad., electron scatt., 36 GHz, 1.8 to 4.2 K 8-72416
 HgI₂, electrons and holes cyclotron reson. 8-72061
 InSb, cyclotron harmonic transitions, warping and inversion asymm. effects 8-68383
 p-InSb, cyclotron reson. of nonequilib. photoelectrons, distrib. function and line profile 8-60336
 n-InSb, directional temp. of hot electrons under elec. and mag. fields 8-84135
 InSb film, threshold singularity on quantising mag. fields 8-87904
 InSb, magneto-optical anomalies of impurity electrons, two-LO-phonon region 8-72415
 K-Na, dil., dynamical props. of quasiparticle excitations, de Haas-van Alphen effect meas. 8-84128
 PbTe, magnetorefectance of surface space charge layers 8-52475
 Rb-K, dil., dynamical props. of quasiparticle excitations, de Haas-van Alphen effect meas. 8-84128
 Re, RF size effect, Fermi surface dimensions determ. 8-91598
 Si, inversion layer, interacting electron system, cyclotron reson. 8-87902
 Si inversion layer surface cyclotron resonance, temp. and stress effects 8-60229
 Si inversion layers, far IR reson. magnetotransmission, temp. and band gap light depend. 8-64363
 n-Si, surface space-charge layer, intersubband-cyclotron combined reson. 8-68063
 Si(III) inversion layers, CDW induced cyclotron reson. harmonics 8-64085
 Te, surface cyclotron resonance, freq. depend. 8-64084

cyclotrons

see also *microtrons; synchrocyclotrons*

- Berkeley 88 inch cyclotron, systematics in the control settings, beam parameter prediction 8-78526
 Calcutta variable energy cyclotron vacuum system design, testing and commissioning 8-86707
 compact, applications (*Hungarian*) 8-74517
 electrostatic inflector and extractor for cyclic accelerators, HV expts. 8-50421
 GANIL system, two separated sector cyclotrons, status report 8-55058
 Hamburg isochronous cyclotron, influence of phase or time struct. of internal beam on extraction conditions (*German*) 8-94155
 heavy element mass spectroscopy with the Berkeley 88-inch cyclotron 8-70217
 heavy-ion accelerators, book contrib., review 8-90003
 isochronous cyclotron mag. field automatic meas. system 8-82547
 isochronous meas. of phase angle variations of beam pulses by sampling technique (*German*) 8-74520
 Leuven isotope separator on-line at CYCLONE cyclotron 8-70682
 magnetic analyser for compact cyclotron 8-66439
 mass analysis, high-energy, appl. to chem. anal., radioactive dating, and quark detection (*Czech*) 8-86375
 minicomputer data acquisition system for Princeton cyclotron facility 8-90048
 Polarised beam from the University of Manitoba spiral ridge cyclotron 8-70660
 PTB, emittance measuring instrumentation, program for phase ellipse area (*German*) 8-58512
 SIN injector cyclotron, RF system improvements 8-90005
 small, applications (*Hungarian*) 8-70656
 superconducting heavy ion cyclotron, proposed for Chalk River, mag. field related mech. tolerances 8-58511
 TRIUMF biomedical negative pion beam line, tuning 8-96113
 variable energy cyclotron at Calcutta 8-74518
¹⁵N cpds., for environmental and biological research, cyclotron prod. 8-82551

Czochralski method see *crystal growth from melt*

D-layer see *D-region*

D mesons

- axial vector mesons, three body decays, rel. between D(1285) and A₁(JP=1⁺⁺) 8-78176
 charmonium narrow states, hadronic and EM decays 8-70343
 decay at $\psi(3772)$, inclusive props. 8-93876
 discovery, review of exptl. results and theoretical advances (*German*) 8-66184
 EM mass splittings, Born-term contribs. 8-78181
 EM properties of charmed hadrons, SU₆×U_c calcs., mag. moments, mass differences 8-70368
 hadronic decay and evidence for (cs), current 8-58167
 hadronic decays of charmed D meson, MIT bag model calcs. 8-82207
 heavy hadronic meson theory, gauge theoretic formulation of SU₂×U₁ model, D-meson mass limit 8-70316
 mass formulae and mixing in SU(8) and SU_w(8) symmetries (*Russian*) 8-66097
 masses and leptonic decay consts. 8-66087
 masses of new mesons and effects of the fifth flavour 8-66098
 semileptonic decay, effective chiral Lagrangian method 8-74254
 semileptonic decay const., D and F decay const. ratio determ. 8-62392
 semileptonic decays, K-e correl. anal. 8-78179
 spin tests for charmed mesons produced in e⁺e⁻ annihilation at $\sqrt{s}=4.028$ GeV 8-74269
 D, D*, Schwinger phenomenological and dyon description 8-82109
 D(1285) from $\bar{p}p \rightarrow KK\pi\pi\pi$, 700-760 MeV/c, spin-parity assignment, dominant decay mode 8-54646
 D(1865)→ $\nu\bar{\nu}K^*(890)$, right handed current, eK* ang. correl., energy spectra 8-74248
 D(1.87) isomultiplet, mass differences, effect of EM mixing on mass splitting (*Russian*) 8-89714
 D→e⁺e⁻ branching ratio from e⁺e⁻ annihilation multiprong data 8-78200
 D→K⁺π⁻, branching ratios, isospin anal. 8-70363
 D→K⁺π⁻, branching ratios, charged and neutral D-meson lifetimes 8-62396
 D→ $\nu\bar{\nu}K(K^*)$ at $\psi'(3770)$ from e⁺e⁻ interaction 8-89693
 D→ $\tau^+\bar{\nu}_\tau$, charmed mesons, heavy lepton decays, ν_τ neutrino mass depend. (*Russian*) 8-62394
 D⁰ and D⁺, 3.772 GeV, mass and decay branching ratios 8-78199
 D⁰→K⁺π⁻π⁰, nonleptonic charm decay, branching ratio 8-70364
 D⁰→K⁰π⁺π⁻, prod. and decay from νN interaction 8-89700
 D⁺-D⁰, Coulomb and tadpole contributions to EM mass differences 8-89713
 D⁺-D⁰ mass difference, broken isospin symmetry in chiral SU(4)⊗SU(4) 8-89691
 D⁺-D⁰ mass splitting and and forbidden decays $\psi' \rightarrow \eta\psi$, $\psi' \rightarrow \pi^0\psi$ 8-66114
 D[±](1870)→Λ(K⁰)+hadrons, charm prod. cross section upper bounds (*Russian*) 8-89711
 D[±](2.01) isomultiplet, mass differences, effect of EM mixing on mass splitting (*Russian*) 8-89714
 μN deep inelastic scatt., D-meson muon progenitor 8-62407
 ν production of charmed D mesons and D⁰→K⁰π⁺π⁻ 8-70354
 pN interactions, 400 GeV, D-prod., muon polarisation meas. 8-70413
 pp→DD cross sections, Monte Carlo anal., particle lifetime for detection in emulsion 8-82229
 pp→DD+X, upper limit for DD prod. at 55 GeV 8-89758
 pp→ $\mu^+\mu^-X$, possible charmed meson pair prod., DD cross section 8-89751
 Cu+p, 400 GeV, dimuon and trimuon prod., prompt ν source, DD prod., axions 8-89860

D-region

- daytime solar proton event-disturbed model 8-93038
 diffusion of weakly ionized multiconstituent plasma 8-57384
 electron concentrations, diurnal vars. during storm after-effect 8-65451
 electron density and recomb. coeff. profiles calc. rel. to absorpt. and rocket meas. 8-69559
 electron density variation obs. (*Russian*) 8-61652
 electron loss coefficient, review (*Russian*) 8-85756
 ion bunching, model 8-73424
 ionisation, effects of solar flares Fe XXV 1.87 Å line emission 8-65588
 layer structures, density response to gravity waves 8-81290
 LF/VLF radiowave propag. characts. anal. 8-93049
 MF pulsed transmissions, method for separating D- and E-region contribs. to total absorpt. 8-69593
 partial reflections, filtering effect on drift parameters determined by full correl. anal. 8-65450
 partial reflections electron density profiles, sensitivity to irregularity comp. 8-81495
 radio wave absorption, riometer meas. 8-85763
 radiowave absorption, effect on forward scatter radiometer amplitude distrib. index 8-65552
 radiowave anomalous absorpt. during sudden disturbances, solar zenith angle depend., electron loss coeff. 8-69568
 review 8-77392
 water cluster ions, mass spectrometer results analysis 8-61659

D/A conversion see *digital-analogue conversion*

damage, radiation see *radiation effects*

damming see *dams*

damping

see also *dislocation damping; internal friction*

- acoustic, impedance of closed front fibre masses 8-83144
 aeroelasticity, active control and suppression of flutter in aircraft (*Russian*) 8-67079
 beams, large amplitude vibration damping by viscoelastic layers 8-63363
 brass, cold worked, or heat treated, or recrystallised wire specimen (*German*) 8-88489
 brass, mechanical damping in terms of Granato-Lucke theory, comparison with Cu₃Au and leaded brass 8-95772
 channel, straight (buckled), two-dimens. flow, stability anal. 8-59490
 cushion dynamic props. by mech. impedance method 8-72953
 dissipative circulatory structural systems, dynamic behaviour 8-63364
 dye laser, N₂ laser-pumped, subns. relax. oscills. 8-82959

damping continued

- elasticity, St. Venant planar theory, nonhomogeneous problem, logarithmic decrement (*French*) 8-49664
- fluid induced, in refrigeration machinery manifolds 8-83164
- forced vibration prevention by damped dynamic absorber 8-63355
- forced vibrations of continuous systems with damping Rayleigh-Ritz-Galerkin approx. 8-59332
- forced vibrations of systems with retardation and damping 8-83290
- foundation dynamic interaction with viscoelastic half-space (*German*) 8-79228
- gyroscopic system, linear, damped, modal anal., appl. to satellite 8-63275
- hand-arm system, distributed-parameter dynamic model 8-92663
- heavily damped waves, method for determ. wave number and damping coeff. 8-63557
- hysteresis damping, continuum description 8-67078
- Langmuir waves, modulated, nonlinear Landau damping effect 8-81849
- lead brass, mechanical damping in terms of Granato-Lucke theory, comparison with unleaded brass and Cu₃Au 8-95772
- long-wave oscillation damping calc. (*Russian*) 8-75302
- Lorenz model, chaos and limit cycles 8-57787
- machine vibrations anal. and obs. block deformability influence (*Italian*) 8-51108
- model and full-scale cooling tower resonance tests 8-83291
- molecule above metal surface, damping of mechanism for excited state 8-92160
- non-linear dispersive wave, coupled modes approach, effect of dissipation on recurrence 8-49670
- passive vibr. isolation, shock absorber selection 8-55556
- plastics, fatigue fracture props. correl. with viscoelastic damping 8-52993
- plates and shells, internal damping, influence of geometry 8-50996
- polymer, dynamic mech. anal. 8-60697
- polymeric materials, engineering structures, design and meas. 8-87185
- pressure-force transducer using 32.768 kHz X-Y flexure watch crystal 8-57934
- pseudoconservative systems, effect of damping on stability 8-81832
- radiation damping in universe with topologically closed space sections 8-57828
- radioactive fallout damping coefficients 8-92961
- rotor, flexible, on flexible bearing, viscous-damping, vibr. and balancing 8-63352
- rotor, passing through crit. speed, with gyroscopic effect, asymptotic calc. 8-63354
- rotors, elastic wave stability 8-87297
- satellite attitude control system, gyrodampers appl. 8-96379
- satellite rotation, exponential damping, magnetic field effects 8-69645
- satellite rotation, shielding effects on magnetic damping 8-69646
- sea surface waves, attenuation by energy transfer to sediment motion 8-73389
- shaft, symmetrical, nonlinear elastic and internal damping props., flexural vibrations 8-71290
- shock isolator for closed-cycle refrigerator of diode laser 8-50796
- short wave generation by cylinder oscillating at liquid interface 8-79331
- sound generation and transmission in flow ducts with axial temperature gradients 8-90551
- sound transmission into heavily-damped cylindrical fuselage 8-83166
- speech, vocal tract losses, influence on damping of reson. freqs. 8-85325
- spinning tops, mechanics (*German*) 8-87253
- stochastic excitation systems, identification of damping and stiffness parameters (*Polish*) 8-69973
- tapered unconstrained beams, vibration damping 8-51106
- viscosity, of water-fluidised bed, by oscills. damping meas. 8-59475
- zero sound, in classical liq., excitation, damping, memory function approach 8-67771
- Cu₃Au, mechanical damping in terms of Granato-Lucke theory, comparison with leaded and unleaded brass 8-95772
- Fe-Co, damping capacity of Gentalloy, internal friction meas., mech. and mag. depend. (*Japanese*) 8-52875
- Fe-Co (5 to 25 wt.%), exam. of damping capacity of Gentalloy 8-72800

dams

see also civil engineering; hydroelectric power stations

- concrete dam construction elements, appl. of fracture mechanics to thermal stress cracking 8-76766
- hydraulic conductivity clay mineral dispersion and swelling effects on earthen dams 8-53668
- hydrodynamic press. on sloping dams during earthquake, momentum method 8-73412
- hydrodynamic press. on sloping dams during earthquake exact theory 8-73413
- porous media unsteady flow calc. by combined finite element/characteristics methods 8-91012
- Stefan and dam problems, free boundary convexity 8-83356
- two-dimensional flow with singularities digital simulation by finite element method 8-90822
- variable domain finite element model for dam unsteady compressible fluid flow digital simulation 8-90820

dark space see discharges (electric)

data acquisition

see also CAMAC; data handling; indicators; recorders

- altimetric data file acquisition automatic digital correlation method 8-61633
- Auger and line optical data acquisition, synchrotron radiation source 8-63019
- automated correlation spectrometer with two Ge(Li) detectors 8-82562
- automated shipboard acquisition and processing of offshore geophys. data (*Russian*) 8-53750
- automatic evaluation of isotope anal. of nuclear fuels, isotope dilution, mass and α spectrometry 8-55120
- autoranging, in high speed systems 8-85233
- body radioactivity measurement, SABRE 3 computer system 8-85425
- body surface potential mapping, automated acquisition and processing system 8-81033
- BWR neutron noise source identification, stochastic model data anal. 8-94106

data acquisition continued

- cardiac surgery, data acquisition and processing during operation by multiplexer (*German*) 8-92743
- chemical identification of substances fixed on silica gel, using Raman spectroscopy (*French*) 8-88664
- dead time correction for a counting rate measured with a system of buffer memories 8-86756
- digital data collection for ion scattering depth profiles 8-56942
- digital data store for radio monitoring of patients (*German*) 8-80998
- dosimetry, automated data acquisition and anal. system at LAMPF pion therapy facility 8-53506
- Earth tides, tilts, parallel recording through digital print-out and photorecording channels (*Russian*) 8-88785
- ECG body surface potential map estimation, limited lead selection 8-57111
- ECG digital recording by mobile cart with microprocessor and DC 300 cartridge recorder 8-85427
- echocardiogram, M-mode, computer-assisted anal. 8-80942
- echocardiogram on-line computer anal. 8-80941
- echographic information related to left ventricle and mitral valve in diastole, anal. by small computer 8-80939
- EEG phasic event detection by microprocessor 8-57091
- EEG standardised classification, sequential epoch method 8-57101
- electron test accelerator, Chalk River, control computer 8-90004
- emission spectrophotometry, review of data processing systems (*Japanese*) 8-88685
- EXAFS and photo-electron spectroscopy expts., flexible data acquisition system 8-62676
- exponential decays analogue anal. using transient recorder 8-86244
- Febry-Perot interferometer, with automated data acquisition and stabilisation system 8-70180
- flow, combined visualisation-anemometry technique, appl. to turbulent boundary layer 8-91044
- flow microfluorimetry instrumentation, rapid data collection, analysis and graphics 8-86348
- fusion reactor, beam-profile fast scan monitor 8-54941
- fusion reactor, diagnostics of radial plasma transport rate, data acquisition and handling system 8-54937
- fusion reactor, Tokamak data acquisition, multichannel A/D subsystem 8-54936
- gas chromatography, data acquisition and use of microwave plasma detector as element analyser (*German*) 8-64895
- hodoscopic detector registration systems, data coding/reading block 8-78602
- Hydrometeorological monitoring in weather modification programs 8-69544
- instrumentation tape recorders 8-49817
- intensified-Si intensity target vidicon application to IR astronomy 8-81544
- intrinsic semiconductor IR detector array data acquisition system 8-77991
- ionosonde, digital universal, operation modes 8-73577
- JET, control and data acquisition system, CODAS 8-62619
- laser data acquisition/analysis system for Si vidicon optical detector 8-58041
- magnetic susceptibility instrument, supercond., automatic, biological appl. 8-57153
- mass spectrometer with computer controlled data collection 8-82071
- mass spectroscopy computer acquisition and analysis of metastable transition data using electric sector voltage variation 8-70102
- meteorological real-time data acquisition and anal. 8-69466
- meteorological radar data acquisition system at Spino d'Adda ground station 8-69468
- microcomputer system for automating analytical instrumentation 8-73127
- microcomputer-based data acquisition system for NMR spectrometer interfacing 8-74042
- microcomputers in biomedical and clinical applications 8-73283
- microprogrammable system, MIDAS IIA, meteorological appl. 8-77374
- minicomputer data acquisition system for Princeton cyclotron facility 8-90048
- minicomputer driven microprobe (*French*) 8-74111
- Mississippi River computerized data bank 8-73520
- mobile gamma camera with remote image processing computer system, for nuclear medicine 8-92700
- Mossbauer data acquisition system using minicomputer 8-90050
- multiple detector data acquisition system, microcomputer based 8-90049
- multiplexing systems, microprocessor-based, remote- and central-type comparison, cost anal., appl. 8-89971
- multivariate discrete information analyser, particle recording appl. 8-78601
- MWPC, correcting codes for information registration 8-94176
- neurophysiology, computer assisted unit data acquisition/reduction 8-61266
- neutron standard cross section expts., flux monitor, source, data acquisition and anal. 8-90039
- nuclear medicine, data evaluation system for use with gamma cameras 8-92732
- nuclear medicine, Janus III, computer system for acquisition, processing of diagnostic units data 8-80948
- nuclear reaction on-line data acquisition system for monitoring high resolution multidimensional spectra 8-58567
- nuclear research reactor program 8-86679
- oceanography, information exchange between probe and computer during R/V 'Akademik Vernadsky' cruise (*Russian*) 8-77363
- oceanography, Kiel multi-purpose sea probe microprocessor-based data acquisition system (*German*) 8-85701
- Omo River project (Ethiopia) data management system appraisal 8-57326
- particle track chamber, semi-automatic meas. instrum. register for camera photograph reduction 8-78575
- photoionisation mass spectrometer, balloon-borne for stratospheric gas meas. 8-85732
- plasma diagnostics, Thomson scatt. system, analogue data processing circuits 8-87488
- plasma electron temp. and density meas., semiautomatic system for double probe anal. 8-87490
- plot system developed for nondestructive materials testing exam. 8-53067

data acquisition continued

- PLT, neutral beam test stand, data acquisition system 8-62622
- pulsed electrostatic probes as diagnostic for transient plasma 8-94937
- PWR, thermohydraulic processes obs. in high press. water loop (*Hungarian*) 8-82432
- radioactivity meas., statistical distrib. accumulation in real time 8-94178
- radiographic imaging, digital video acquisition system for extraction of subvisual information 8-69208
- real time data acquisition system for controlling and collecting data from laboratory instruments 8-54348
- remote sensing image data processing/acquisition techniques 8-61627
- Rutherford Laboratory N5 expt. data acquisition system, program struct. and CAMAC hardware 8-90051
- Shiva laser beam diagnostics 8-59037
- Shiva laser computer control system 8-59034
- Shiva laser fusion facility, target diagnostic system, data acquisition and anal. 8-51366
- signature analysis systems with Fourier analyzer 8-87195
- solar data collection system using microprocessors 8-69542
- spectroscopy, compilation of computer-readable reference data libraries 8-64894
- thermogravimetric data acquisition and reduction program 8-64901
- TRIUMF biomedical pion beam automated dose mapping system 8-73254
- two-channel data gathering and registration system for fast-action experiments 8-77877
- vascular interface system for automation of haemodynamic monitoring and therapy 8-81054
- voltammetry, cyclic, AC, on-line digital FFT faradaic admittance data acquisition 8-61118
- X-ray diffraction data acquisition using position-sensitive counter (*Japanese*) 8-88774
- Pr wire thermal cond. automatic meas. device 8-54362

data communication equipment

- see also *data transmission equipment*
- optical fibre data bus, active fail-safe terminal 8-55438

data communication systems

- aircraft satellite data link, for meteorological reconnaissance data transmission 8-96299
- automated meteorological data transmission from commercial aircraft via satellite 8-57327
- Hermes, geostationary communications satellite, Canadian design 8-93068
- oceanography, data exchange between probe and computer (*Russian*) 8-77363
- optical fibre, communication link between computer units, using LED-photodiode pair 8-71224
- optical fibre communication, cabling, light source and receiver technology, review 8-59125
- Vela seismological network, datacomputer communications protocols 8-81411

data compression

- see also *information theory*
- code delta-modulation for standard hydrophysical information compression (*Russian*) 8-65432
- medical US data compression 8-77093
- remote sensing image data processing/acquisition techniques 8-61627
- thin-film distributed optically excited laser, signal suppression by superluminescence radiation (*Russian*) 8-87091

data dictionaries see *database management systems***data handling**

- fusion reactor, diagnostics of radial plasma transport rate, data acquisition and handling system 8-54937
- geodetic data base, basic entities definition 8-65392
- International Sun-Earth Explorers 1 and 2, fluxgate magnetometers command and data handling 8-85804

data loggers

- electron test accelerator, Chalk River, control computer 8-90004
- interfacing and control of portable data loggers 8-93662
- multichannel digital temp. recorder, TR-2711, measuring 100 channels in 10 s 8-65931
- multichannel temperature recorder, Thermodac II with 24 channels using thermocouples 8-65930
- optical multichannel anal., data microprocessing of thermally stimulated luminescence 8-54347
- punched-tape recording system, radioastronomy appl. (*Russian*) 8-65501
- YODAC-8, microprocessor controlled, for temp. data acquisition 8-49813

data reduction and analysis

- see also *data acquisition*
- acoustical data anal. using digital techniques 8-83193
- air pollution data obtained near refineries, interpretation via pollution roses 8-81379
- air pollution effects indicators, provisional map 8-81387
- astrometry using Palomar Schmidt plates, reduction procedures accuracy 8-57455
- astronomical images, general anal. system 8-53834
- astronomical laser ranging equipment, computer system (*Japanese*) 8-89080
- astronomical photographs, reduction via intensity microphotometer with step-drives (*Russian*) 8-57457
- astronomy, semi-automated blink comparator for large photographic plates (*Japanese*) 8-89081
- atmosphere O₃ profile determ., outgoing thermal radiation meas. regression anal. 8-92945
- automated shipboard acquisition and processing of offshore geophys. data (*Russian*) 8-53750
- automatic curve slope meter for physical or chemical quantities 8-49812
- automatic evaluation of isotope anal. of nuclear fuels, isotope dilution, mass and α spectrometry 8-55120
- Bayesian deconvolution, appl. and algorithm implementation 8-70103
- binary stars orbital solutions, derivation for unseen companions 8-93313
- bubble chamber film, track rescue system 8-70728
- calorimetry, differential scanning, computer-interfaced, heat capacity meas. 8-65935

data reduction and analysis continued

- cardiocirculatory computer-aided monitoring after open-heart surgery, appl. to adrenaline effects meas. 8-81059
- CESSNA interactive spectrum anal. program on minicomputer 8-94177
- compact radio sources, mapping from VLBI data 8-89266
- deconvolution of experimental outcomes, program DEO 8-70729
- digital diurnal ionograms (*Italian*) 8-85699
- digital radar data computer processing for High Plains Coop. Program (HIPLEX) 8-92989
- digital seismic data processing, struct. anal. of graphs (*Russian*) 8-53749
- dosimetry, automated data acquisition and anal. system at LAMPF pion therapy facility 8-53506
- Earth tide observations processing, individual monthly sets weightings (*Russian*) 8-88789
- Earth tides observations, monthly data set anal. (*Russian*) 8-88786
- electro-optical phenomena of disperse systems, computer calc. method 8-50699
- electron test accelerator, Chalk River, control computer 8-90004
- emission spectrophotometry, review of data processing systems (*Japanese*) 8-88685
- epitaxial growth expt. data, of GaAs in Ga-AsCl₃-He₂ system (*Bulgarian*) 8-60580
- fatigue data analysis, lifetime predictions for ceramic materials 8-95870
- flow, two-phase, nonequilib., spectral characts. 8-94854
- flow, unsteady, transitional and turbulent boundary layers, expt. and calc. methods (*French*) 8-75125
- Fourier spectroscopy in far IR 8-62240
- galactic plane survey at 5 GHz, computer reduction of data 8-81686
- gamma-ray multiplicity meas., fast converging bootstrap method for data anal. 8-70730
- geophysical data reduction on arbitrary surface in regions of high topographic relief 8-61298
- giant H II regions, radio maps interpretation 8-85994
- gravity anomalies measured in Krivoj Rog basin (Krivbas) underground workings, interpretation (*Russian*) 8-85466
- histogram plotting, FORTRAN program 'HIST' 8-77876
- holographic interferograms evaluation, of thermal boundary layers (*Czech*) 8-62220
- image reconstruction from incomplete and noisy data, examples and appls. 8-53837
- interferometry, multiwavelength testing using modified Twyman-Green interferometer 8-59169
- International Ultraviolet Explorer (IUE), ground data processing system performance 8-96383
- ionsphere incoherent scatter data, analytic partial derivatives for least-squares fitting 8-73581
- ionsphere sounding, filtering effect on drift parameters determined by full correl. anal. 8-65450
- ionspheric data processing, improvement of convergence of least squares method (*Russian*) 8-85700
- jet, free, turbulent flow, large scale struct., discrete values meas. 8-90840
- latitude observations, technique for Earth daily free nutation, determ. 8-96126
- macroseismic data processing and interpretation 8-61583
- mass spectroscopy computer acquisition and analysis of metastable transition data using electric sector voltage variation 8-70102
- materials testing, nondestructive, radiometry methods, automatic data processing, development of models and algorithms 8-72991
- metal, positron annihilation, ang. correl. data analysis 8-52592
- meteorological real-time data acquisition and anal. 8-69466
- meteorological radar data acquisition system at Spino d'Adda ground station 8-69468
- microearthquake network data, automatic anal. 8-81412
- minicomputer driven microprobe (*French*) 8-74111
- neurophysiology, computer assisted unit data acquisition/reduction 8-61266
- neutron activation analysis, data reduction, computer language MUL-TELMT 8-85241
- neutron activation analysis, gamma-ray spectra prediction, detection limits, computational procedure 8-85242
- NMR spectrometer, pulse, controlled by programmable digital unit (*Czech*) 8-77952
- nuclear medicine, data evaluation system for use with gamma cameras 8-92732
- oceanographic multi-freq. microwave radiometer, data processing and performance evaluation 8-81417
- optical crystallography computer anal. of spindle stage data 8-85702
- parallel surface continuation, appl. to reduction of terrain induced aeromagnetic anomalies 8-61316
- particle size anal. using optical counting data 8-77842
- particle track data in plastics, rapid anal. using interactive programming and graphic displays 8-66456
- polymer, noncrystalline solid, preferred orientation from scatt. ang. distrib. 8-75560
- probe data reduction in axially symmetric expts. 8-89464
- programs for high-school expts. 8-86094
- radio astronomy, direct transform hardware processing of rot. synthesis data 8-85856
- radio astronomy, direct transform hardware processing of rot. synthesis data 8-85857
- radio meteor wind data, anal. using finite element approximation 8-81475
- radioastronomical data recording and processing, real-time, multichannel system (*Russian*) 8-65507
- radioastronomical data reduction, via digital electronic integrator (*Russian*) 8-57465
- reflection seismic recordings, minimum entropy deconvolution 8-81423
- reflection seismograms signal anal., use of kepstrum 8-81425
- rocks, minerals, anal. of small samples using X-ray quantometer 8-61112
- Rutherford Laboratory N5 expt. data acquisition system, program struct. and CAMAC hardware 8-90051
- satellite altimeter data analysis, role of orbit determ. 8-77177
- seismic cross sounding, data interpretation via reflected wave method (*Russian*) 8-92796

data reduction and analysis continued

- seismic exploration, iterative identification of non-invertible autoregressive moving-average systems 8-81422
- seismic pattern recognition, fundamental problems 8-81428
- seismic surface waves, anal. using PDP-15 interactive graphics 8-81427
- seismic wavelet estimation, short-time homomorphic signal anal. appls. 8-81426
- Shiva laser fusion facility, target diagnostic system, data acquisition and anal. 8-51366
- solar radio bursts, recording instrumentation and data reduction (*Italian*) 8-96458
- solar type IV radio events, FFT anal. rel. to pulsating structs. 8-96455
- spectrograms, automatic precision wavelength comparator 8-82042
- thermogravimetric data acquisition and reduction program 8-64901
- tilt meter observations harmonic anal., influence of S_1 diurnal meteorological wave (*Russian*) 8-88788
- US flowmeter data processing, transfer function modelling of arteries 8-61225
- vapour-liquid equilibrium, data reduction, extension of Barker's method 8-79735
- weighted entropy method for clinical data reduction 8-92742
- X-ray fluoresc. anal., energy dispersive, least squares, Monte Carlo methods, mathematical anal. techniques 8-85243
- X-ray fluoresc. anal. line intensities calc., computer program, appls. 8-61107
- X-ray fluoresc. element anal. in pulps, conc. calcs., iterative method 8-61109
- X-ray spectra, energy-dispersive, nongaussian peak overlap problem 8-78050
- F III, IV, beam-foil spectra, mean lives, 2150-3200 angstrom 8-55224
- H II regions radio emission analysis, consequences of improper analytic methods 8-54000
- H₂O sources spectra, autocorrel. anal. 8-65713
- Hg vapour-gas mixture, Hg diffusion, data correlation 8-79403

data tables *see collections of physical data***data transmission equipment**

- see also data communication equipment; telemetering equipment*
- duoPIGatron ion source, optical telemetry and data transfer system 8-66443
- fibre-optic integral data source/receiver package 8-63179
- optical fibre eight-terminal data bus, using T-couplers 8-59129
- plasma diagnostics, Thomson scatt. system, analogue data processing circuits 8-87488

data transmission systems *see data communication systems***database management systems**

- cardiovascular research database system 8-53549
- chemical reaction sites automatic detection 8-92476
- CLAIR data system overview 8-57325
- geological and geochemical data management and processing 8-57324
- MSDC/EPA/NIH mass spectral search system 8-65912
- Omo River project (Ethiopia) data management system appraisal 8-57326
- Vela seismological network, use of datacomputer 8-81411

dating, Earth *see geochronology***dating, radioactive** *see radioactive dating***Davydov splitting**

- fluorene, lowest singlet state, exciton band struct. calc. 8-63983
- fluorene, near 6K, two-photon excitation spectrum, g-exciton states location 8-64393
- potassium formate, IR absorpt. spectra, sampling effects, Davydov splitting and struct. 8-52508
- rhodamine B, double Davydov's splitting of visible absorpt. band 8-82746
- KCN, ionic mol. cryst., exciton struct. 8-79935

Davydov states *see Davydov splitting***dawn** *see twilight***dawn chorus** *see atmospherics***dayglow** *see airglow***d.c. amplifiers**

- circuit design, to record heat pulse during material fracture 8-60921
- digital automatic thermodynamic enthalpy and specific heat determ. equipment 8-57951
- digital electrometer appl., cct. 8-77933

d.c. generators

see also homopolar generators

- disc dynamo, pseudo-stochastic behaviour in circuits with shunt, couple and series resistance 8-93608

d.c. power transmission

- electrification of objects under DC transmission lines, charge simulation calcs. 8-78853

d.c. sputtering

- ion beam sputtering, glow discharge source for nuclear thin film target prep. 8-55067
- magnetron sputtering, basic physics appl. to cylindrical magnetrons 8-72664
- negative ion sources, role of alkali metal 8-74526
- planar magnetron sputtering 8-72725
- planar-magnetron sputtering source, modified 8-95693
- polymer layer, glow deposition rate obs. in DC discharges 8-68633
- sputter electrode preparation for multiply charged heavy ion sources 8-66009
- steel, stainless, ground surface ion bombardment, in DC glow discharge 8-95098
- steel, stainless, vacuum components, sputtering and reactive effects during glow discharge treatment 8-70141
- Al₁In_{1-x}Sb, DC sputtering and struct. 8-52674
- CdO-SnO₂ film, DC sputtering prep., visible and near IR transmission, resist. 8-88049
- Cu₂O, film, thermoelec. power, activation energy variation with electrode spacing in DC sputtering 8-76099
- In₂O₃-SnO₂ film, reactive DC diode sputtering, using large scale system 8-72723
- Nb₃Ge, RF and DC sputtered films comparison, O content effect 8-72022
- Ni₂O, film, thermoelec. power, activation energy variation with electrode spacing in DC sputtering 8-76099

d.c. sputtering continued

- Si, amorphous, dark conductivity and photocond. obs. (*French*) 8-64155
 - SnO₂, two-step deposition process using DC sputtering and oxidation, and characterisation 8-95691
 - WC-Co sputter deposited film, struct. and comp. 8-72023
- DDA** *see digital differential analysers*
- DDC** *see direct digital control*
- de Haas-van Alphen effect**
see also diamagnetic properties of substances; diamagnetism
 bound state induced scattering reson. at dislocations, effect on de Haas-van Alphen freq. 8-76019
 electronic properties harmonic content of de Haas-van Alphen effect, appl. to dil. mag. alloys 8-84127
 graphite-Br₂, intercalation process 8-63965
 metal, dislocation scatt. and de Haas-van Alphen amplitudes 8-63967
 quasiparticle picture 8-91592
 transition metal, anal. by linearly recursive approx. 8-91603
 transition metal, Fermi surface, stress depend., from quantum oscill. effects 8-91597
 β' -AgMg, de Haas-van Alphen effect, LMTO band struct. and Fermi surface 8-75984
 Al, Fermi surface, scattering anisotropy of conduction electrons on dislocations (*Russian*) 8-60051
 Cd, Fermi surface, strain depend., from US vel. oscills. 8-84133
 Cd, Fermi surface changes under uniaxial compression 8-51876
 Co, de Haas van Alphen oscill., effective mass 8-87900
 Fe, de Haas-van Alphen effect and exchange splitting, effect of pressure (*Russian*) 8-95252
 Ga, expt. and interpretation 8-84132
 Gd, Fermi surface determ. 8-84138
 Hg, single cryst., electron-phonon interactions, departure from LK theory 8-84130
 In₂Bi, de Haas-van Alphen effect 8-91594
 K₂Na, dil., dynamical props. of quasiparticle excitations, de Haas-van Alphen effect meas. 8-84128
 Mg, Fermi surface changes under uniaxial compression 8-51876
 Mg-Mn, dil. alloy, de Haas-van Alphen effect, exchange interaction, Kondo effect 8-88093
 Nb₃Sn, A-15 superconductor, dHvA effect 8-75985
 Ni, anal. by linearly recursive approx. 8-91603
 Pb, effective cyclotron masses of central and noncentral ξ orbits, de Haas-van Alphen effect 8-63968
 Pb, mag. interaction, de Haas-van Alphen effect 8-79921
 Pd, Fermi surface, stress depend., oscillatory magnetostriction and de Haas-van Alphen torque obs. 8-91602
 Pt, Fermi surface obs. 8-91601
 Rb-K, dil., dynamical props. of quasiparticle excitations, de Haas-van Alphen effect meas. 8-84128
 Re, Fermi surface, strain depend., from US vel. oscills. 8-84133
 Re, Fermi surface, stress depend., quantum oscills. obs. 8-91599
 ReO₃, anal. by linearly recursive approx. 8-91603
 Sb, de Haas-van Alphen effect, effective mass, Fermi levels 8-75982
 Sb, spin splitting meas. from de Haas-van Alphen effect, g-factors 8-51881
 Sb₂Te, de Haas-van Alphen effect, effective mass, Fermi levels 8-75982
 Sb-Sn, dil., de Haas-van Alphen effect, effective mass, Fermi levels 8-75982
 UGe₃, meas. comparison with band struct. calc. 8-72068
 URh₃, magnetisation density 8-52203
 V₃Si, A-15 superconductor, dHvA effect 8-75985
 W, anal. by linearly recursive approx. 8-91603
 Y, Fermi surface and de Haas-van Alphen effect 8-75983
 YAl₂, de Haas-van Alphen effect 8-91590
 Zn, Fermi surface changes under uniaxial compression 8-51876
 ZrB₂, Fermi surface, de Haas-van Alphen effect meas. 8-84134

Debye-Huckel theory

- ionic conductor, quasielastic scatt. of light, neutrons and electrons, Debye-Huckel eqn. (*Chinese*) 8-68521
- polyelectrolytes in soln., electrostatic persistence length rel. to unified theory 8-95932
- polyvalent electrolyte apparent molal adiabatic compressibility and US vel. obs. 8-61028

Debye-Scherrer cameras *see cameras; X-ray crystallography apparatus***Debye temperature**

see also specific heat

- adamantane, Lennard-Jones (6-12) interaction pot., Debye temp. calc. 8-63828
- bicyclo [222] octane, Lennard-Jones (6-12) interaction pot., Debye temp. calc. 8-63828
- bulk moduli, Wachtman's eqn., and temp. depend. 8-75799
- electron-proton interaction, two-body sum over states of static screened Coulomb pot. 8-55714
- ferroelectric, tabulation of calorimetric values 8-51639
- high temperature variation (*French*) 8-63831
- metal, BCC, lattice dynamical calc. 8-55925
- metal, Debye charact. temp. and fusion transitions 8-63864
- methane and methane-d₄, Lennard-Jones (6-12) interaction pot., Debye temp. calc. 8-63828
- Nb₃Ge, supercond., single phase, sp. ht. meas., 4-29K 8-72307
- neopentane, Lennard-Jones (6-12) interaction pot., Debye temp. calc. 8-63828
- nitrides, surface energy for brittle fracture from phonon frequencies 8-67790
- rare earth metals, thermodynamic props. determ. form US vel. meas. 8-55912
- solid, thermal expansion at high temp. (*French*) 8-55960
- transition metal binary alloy, amorphous and crystalline, superconducting transition temp. correlation with solute conc. 8-52139
- Al₂Cu, single cryst. elastic const., 4.2-300K 8-72803
- Al_{0.95}Ga_{0.05}V, low temp. thermal expansion 8-95167
- Al_{0.9}V, low temp. thermal expansion 8-95167
- Am, Debye-Waller factor, temp. depend. 8-83902
- Au, effect of press. on resistivity 8-79978
- Au, var. at high temp. (*French*) 8-63831
- BP, sp. ht., Debye temp., compressibility and Gruneisen coeff. meas. 8-63865
- Ba, elastic properties, Debye temp., 20°C, 20 to 70 kbar, US wave velocity meas. 8-87735

Debye temperature continued

- CdO, X-ray determ., Debye-Waller factors, Debye temp. and vibration amplitudes 8-55928
 Cr, lattice vibrations, Debye temp., freq. wave vector dispersion relations 8-63818
 Cr, phonon dispersion, Debye temp. and Debye-Waller factors, lattice dynamical model 8-55920
 CsBr(I), ZZ 8-75792
 Cu-Al(Au), critical voltage effect (*Japanese*) 8-91206
 CuBr, Debye-Waller factors and Debye temp., powder neutron diffr., 295K 8-91407
 CuCl(Br)(I), phonon dispersion, 9-parameter shell model, compared with expt., and Debye temp. evaluation 8-59891
 CuPt, specific heat, Debye temp. below 30K 8-55956
 Fe-Ni, FCC and BCC lattices, X-ray characteristic temp. (*Russian*) 8-67797
 GaAs, Debye temperature, atomic mean square displacement 8-87757
 GaP, Debye temperature, atomic mean square displacement 8-87757
 GaS, sp. ht., vibr. spectra and Debye temp. 8-87796
 GaSb, Debye temperature, atomic mean square displacement 8-87757
 GaSe, sp. ht., vibr. spectra and Debye temp. 8-87796
 GaTe, sp. ht., vibr. spectra and Debye temp. 8-87796
 InSb, Debye temperature, atomic mean square displacement 8-87757
 KCN, crystal props., log potential model calc. 8-63829
⁶LiH(D), cryst., cohesive energy, force const., lattice freq., Debye temp., Gruneisen parameters, calc. 8-91293
 Mg, phonon spectrum and thermodynamic functions, inelastic coherent cold neutron scatt. (*Russian*) 8-55917
 MnS, X-ray determ., Debye-Waller factors, Debye temp. and vibration amplitudes 8-55928
 Mo, phonon dispersion, Debye temp. and Debye-Waller factors, lattice dynamical model 8-55920
 NH₄Cl(Br), ZZ 8-75792
 NaCN, crystal props., log potential model calc. 8-63829
 PbF₂, lattice dynamics 8-79697
 PbS, X-ray determ., Debye-Waller factors, Debye temp. and vibration amplitudes 8-55928
 Pt, specific heat meas., 0.4 to 30K, Debye temp. 8-55955
 RbCN, crystal props., log potential model calc. 8-63829
 Rh(111), surface geometry, vibrational props., Debye temp., LEED study 8-87852
 Sc, sp. ht. data rel. to electronic props. 8-83971
 n-Si, electronic effect 8-83901
 Sn, monocrystals with impurities, temp. depend. of Debye temp. 8-79975
 Ta, lattice vibrations, Debye temp., freq. wave vector dispersion relations 8-63818
 TiN, Raman scatt. supercond. transition temp., phonon density of states, Debye temp. 8-52499
 Ti, hexagonal lattice equilibrium, electron gas model with noncentral forces, lattice dynamics 8-95123
 TiCl(Br), ZZ 8-75792
 V, lattice dynamics and cryst. equil. 8-75753
 W, phonon dispersion, Debye temp. and Debye-Waller factors, lattice dynamical model 8-55920
 Y_{0.7}Th_{0.3}C_{1.58}, specific heat 8-91813
 Zn, hexagonal lattice equil., electron gas model with noncentral forces, lattice dynamics 8-95123

Debye-Waller factors

- see also lattice dynamics*
 anharmonicity, low-temp. model, Debye-Waller factors of Mossbauer effect 8-55927
 atom-surface scattering 8-92164
 tert-butanol, mol. dynamics, liq. and cryst. states, neutron inelastic scatt. obs. 8-75599
 metal, BCC, temp. variation, lattice dynamical calc. 8-55925
 metal, FCC, phonon dispersion relations and Debye-Waller factor calcs. 8-51630
 monolayers of adsorbed atoms, props. 8-84057
 statistical crystal model, small amplitude acoustic perturbations 8-55930
 transition metal surface (adsorbate), intermediate UPS/XPS synchrotron radiation study 8-52633
 X-ray and neutron scatt. determ. methods 8-83974
 (K⁺, π⁻) on light nuclei, recoilless Λ prod. strength from DW factor 8-50116
 Ag, Debye Waller determ. from modified Cheveau model 8-59918
 Ag, phonon dispersion relations and Debye-Waller factor calcs. 8-51630
 Al, Debye Waller determ. from modified Cheveau model 8-59918
 Al, phonon dispersion relations and Debye-Waller factor calcs. 8-51630
 Am, temp. depend., Mossbauer effect meas. 8-83902
 Au, Debye Waller determ. from modified Cheveau model 8-59918
 Au, phonon dispersion relations and Debye-Waller factor calcs. 8-51630
 BaTiO₃, struct. changes due to cubic-tetragonal phase transition 8-60407
 CdO, X-ray determ., Debye-Waller factors, Debye temp. and vibration amplitudes 8-55928
 Cr, phonon dispersion, Debye temp. and Debye-Waller factors, lattice dynamical model 8-55920
 CsBr(I), ZZ 8-75792
 Cu, Debye Waller determ. from modified Cheveau model 8-59918
 Cu, phonon dispersion relations and Debye-Waller factor calcs. 8-51630
 Cu, photoemission, temp. and photon-energy induced breakdown of direct transition model 8-95681
 Cu-Fe, mixed cryst., Debye-Waller factors, Mossbauer spectra obs. (*German*) 8-52412
 CuBr, Debye-Waller factors and Debye temp., powder neutron diffr., 295K 8-91407
 Fe complex, Fe(papt)₂, high spin ⁵T₂ \rightleftharpoons low spin ¹A₁ transition, Debye-Waller factors and magnetism 8-80259
 Fe_{1-x}Ni_x (x<29at.%), γ -phase dispersion, Mossbauer spectra 8-52399
 MgO, electron diffr., dynamical effects for cryst. struct. determ. 8-83679
 MnS, X-ray determ., Debye-Waller factors, Debye temp. and vibration amplitudes 8-55928

Debye-Waller factors continued

- Mo, phonon dispersion, Debye temp. and Debye-Waller factors, lattice dynamical model 8-55920
 NH₄Cl(Br), ZZ 8-75792
 Ni, Debye Waller determ. from modified Cheveau model 8-59918
 Ni, phonon dispersion relations and Debye-Waller factor calcs. 8-51630
 PbS, X-ray determ., Debye-Waller factors, Debye temp. and vibration amplitudes 8-55928
 TiCl(Br), ZZ 8-75792
 V, lattice dynamics and cryst. equil. 8-75753
 W, phonon dispersion, Debye temp. and Debye-Waller factors, lattice dynamical model 8-55920

decay periods (radioactive) *see* radioactive decay periods

decay schemes (radioactive) *see* radioactive decay schemes

decay theory (nuclear) *see* nuclear decay theory

decision theory *see* decision theory and analysis

decision theory and analysis

- see also Bayes methods; dynamic programming*
 cervical cancer automatic cytoscreening, stypical cells classification 8-73289
 clinical diagnostic method effectiveness, decision probability calc. (*Hungarian*) 8-65146
 digital seismic data processing, struct. anal. of graphs (*Russian*) 8-53749
 optical noise, Schade detail S/N ratio derived from decision theory 8-63022
 pattern recognition theory and application, book 8-64927

decoding

- see also demodulation*
 gammagraphy, 3-dimens. image processing appl. to coded aperture imaging (*French*) 8-57067
 matched filters, using optical delay line provide encoding or decoding structures 8-74983
 optical coding and decoding operations, parallel image transmission by single fibre 8-71216
 particle track data in plastics, rapid anal. using interactive programming and graphic displays 8-66456
 space-frequency conversions for image transmission and processing 8-71046
 synthetic aperture radar, satellite-borne, optical decoding 8-90384

decomposition

- microstructure features and processes only; for other aspects see dissociation and pyrolysis*
see also spinodal decomposition
 quenched binary alloy at low temps., time evolution, phase separation 8-68670
 semiconductor supersaturated solid solns., decomp., surface impurity content 8-51681
 steel, austenitic, high speed, supercooled, austenite decomposition kinetics 8-92233
 steel, austenitic heat-resisting, deformation and fracture rel. to grain-boundary reaction nodules 8-80591
 steel, austenitic supercooled, transformation kinetics into spheroidised pearlite (*Russian*) 8-95742
 steel, cementite decomposition during plastic deform., alloying element effects 8-84768
 steel, cold-worked, Mossbauer obs. of cementite decomp. and restitution 8-64558
 supersaturated solid solution, diffusive decomposition 8-76653
 YN, decomp. press.-temp. relations 8-52780
 YN-UN, solid soln., decomp. press.-temp. relations 8-52780
 Al-Ag, discontinuous decomposition (*Polish*) 8-52808
 Al-Li solid soln., decomposition exam. by secondary ion ion emission (*Russian*) 8-68696
 Al-Mn alloys, study of solidification by rapid cooling (*Japanese*) 8-88459
 Al-Zn, discontinuous decomposition (*Polish*) 8-52808
 Al-Zn alloys, room temp. decomp. of metastable phases precipitated at 200°C 8-84814
 Al-Zn-Mg alloys, decomp. kinetics from Young's modulus obs., microprocesses (*German*) 8-64522
 Al-Zn-Mg alloys, decomposition kinetics, resistivity meas., extended jump model 8-84766
 CdBr₂(I₂), vapour growth crystals, decomposition, electron microscope study 8-92268
 Ce-Ni, hydriding characts., applicability for H₂ storage material 8-83955
 CrC, plasma sprayed coating 8-68835
 CuFe₂O₃, cation substitution effect on eutectoid decomposition 8-68890
 Fe-Cr, high purity binary alloy, isothermal decomp. of austenite 8-64525
 Fe-Cr-(Co), decomposition of solid soln. in mag. field, neutron and X-ray diffr. study (*Russian*) 8-68694
 GaAs:Cu, supersaturated solid solns., decomp., surface impurity content 8-51681
 Ge:Li, supersaturated solid solns., decomp., surface impurity content 8-51681
 Hf-Co, phase diagram, X-ray diffr., thermal anal. and metallography obs. 8-60652
 Hf-Nb (30 to 50 at.%) exam. of beta phase decomposition processes 8-76674
 La-Ni, hydriding characts., applicability for H₂ storage material 8-83955
 La₂Ni₂D₂ storage material, neutron, X-ray diffr. study 8-83954
 Ti alloy VT16, decomposition of metastable β -phase (*Russian*) 8-68710
 α Ti-Al-(Zr), embrittlement due to ageing 8-56673
 Ti-Cr(Mo), alpha precipitation kinetics 8-68697
 β -Ti-Fe, (7.1 wt.%) exam. of ω phase formation, by X-ray diffr. and Mossbauer spectroscopy 8-52800
 WC, plasma sprayed coating 8-68835
 ZnS cubic single crystals, growth by double decomposition reaction in melt 8-60557
 Zr-Y (15 wt.%) solid solution, decomp., during heating and cooling cycles (*Russian*) 8-92267

decomposition, spinodal *see spinodal decomposition*

decomposition, thermal *see pyrolysis*

decorative coatings

No entries

deep levels

- amorphous solid, abnormal bonding and electronic states in forbidden energy gap 8-51942
- diamond Schottky barriers, photocapacity meas. 8-52057
- n-GaAs:O, press. depend. of deep level associated with O, transient capacitance meas. 8-64000
- high resistivity material, deep level spectroscopy 8-72165
- impurity centre conc. meas., junction capacitance technique, review (*Japanese*) 8-79958
- semiconductor, deep level parameters, TSC meas., rel. to photocurrent techniques 8-72249
- semiconductor, Faraday rotation in presence of attractive traps 8-76081
- semiconductor, photoionisation of deep impurity centres, drag of electrons 8-51938
- semiconductor diode, with deep impurity levels, diffusion effect on negative resist. 8-56217
- semiconductor diode, with overcompensated semicond., deep centres, isothermal relax. of current 8-52072
- semiconductor with highly anisotropic bands, photoionisation cross section of deep impurity centres 8-56510
- CdS, up-conversion and optical storage, spatially modulated band struct. 8-64397
- CdS:Li, anisotropy of the absorption by impurity centers in hexagonal crystals 8-88343
- CdSe, optically pumped, dynamic polarisation of nucl. moments 8-68411
- CdSnP₂:Cu, deep centres, emission transitions, polarisation (*Russian*) 8-84650
- CuGaS₂, single cryst., photocond. spectra 8-84252
- GaAlAs DH laser diode, deep level associated with slow degradation 8-87050
- GaAs, deep level trap emission identification by indirect conduction minima technique 8-84163
- GaAs, deep trapped impurities, photocond. spectra, interpretation 8-52030
- GaAs, epitaxial layers, elec. characterisation 8-91791
- GaAs MESFET, deep trapping effects at GaAs-GaAs:Cr interface 8-72245
- GaAs:Cr, Si, deep centre photoluminescence spectra 8-95601
- n-GaAs:Cu, contaminated single cryst., deep level photoluminesc. model 8-68554
- GaAs:O, photocond., electron traps, level-broadening, 90 to 150K 8-60158
- GaAs:Si, Cr, carrier concs. from Hall effect, microscopy, localised vibrational modes absorption meas. 8-56104
- GaAs-(GaAl)As epitaxial layers and DH lasers, deep centre 1.02 eV luminesc. 8-80387
- GaAs-Al_{0.5}Ga_{0.5}As-Cr/Au MIS capacitors, characts. meas. 8-95371
- GaAs-GaAlAs DH LED, transient current trap spectroscopy 8-80049
- GaAs-GaAlAs LEDs, deep levels (*French*) 8-56218
- GaP p-n junction, capacitance-freq. dispersion and electroluminescence efficiency 8-64101
- GaP:Cr, ESR of doubly ionised Cr acceptor and IR luminesc. 8-56374
- GaP:Cu, thermally and optical excited cond., deep level centres 8-72190
- GaP:Cu p⁺-n junction, deep level parameters, TSC meas., rel. to photocurrent techniques 8-72249
- GaP:O, optical transitions via deep levels, phonon interaction 8-87939
- GaP:O, optical transitions via deep levels, cross section temp. depend. 8-87940
- GaP:s, elec. props. following 1.7 MeV electron irradiation 8-80005
- Ge, slow surface, states, optical excitation investigation 8-76129
- InSb:Cr, press. effects on transport props. 8-56146
- InSb_{1-x}Bi_x disordered solid solns, ionisation energy of fluctuation levels 8-72116
- KBr:LiP(Na⁺), electronic struct. of (V_k)_s 8-95269
- LiF, thermoluminescence intensity depend. on heating rate and deep trap 8-56527
- Se, photoconductive film, field instability, Ar⁺ ion irradiation-induced defects 8-87997
- n-Si, A-centre ionisation energy change due to uniaxial deform. 8-71733
- Si, evaporated heteroepitaxial film, deep states obs. 8-72292
- Si, ion implantation, TSC meas. of coupled levels 8-84165
- Si ion implanted p-n junction, cryst. damage influence on elec. props. 8-56219
- Si, neutral undistorted vacancy 8-91638
- p-Si, neutron irradi. effects, admittance meas. of n⁺-p diode 8-51587
- Si:Au, degeneracy factor of acceptor level 8-51927
- Si:B, laser damage obs. by DLTS 8-76023
- Si:Cd(Zn), n⁺-n-n⁺ structure, photocond. lifetimes, deep level occupancy in exclusion region 8-72253
- Si:Cr, specific resistance, activation energy of deep levels, and carrier mobility (*Russian*) 8-72146
- Si:P, neutron transmutation doped, radiation damage exam., elec. props. 8-95080
- Si:S, existence of isotope shift for S deep level, isothermal transient capacitance meas. 8-63999
- Si-SiO₂ interface in MIS struct., B⁺ ion implanted, elec. props. due to laser irradi. 8-72272
- ZnS:Ag film, evaporated, IR quenching of photocapacitance, deep levels obs. 8-56180
- p-ZnSiP₂, single cryst., recomb. processes, photoelec. props. (*Russian*) 8-68053

defect electron energy states

see also colour centres; deep levels

- alkali halide, with oppositely charged defect centres, autoionisation-tunnel relax. of electron excitation 8-72117
- anthracene, monocryst., additional absorpt. spectrum at low temp. 8-92096
- BCC transition metals, screw dislocations, electronic theory, Peierls stress, core energy calc. 8-71737
- bound state induced scattering reson. at dislocations 8-76019

defect electron energy states continued

- chalcogenide glass, mech. for electron-hole recomb. 8-72196
- covalent crystals, defect states, many-electron approach 8-67980
- D⁺-centre electronic struct. in strong mag. field 8-51928
- diamond, Jahn-Teller coupling at ND1 and GR1 centres 8-56103
- diamond, relaxation about the vacancy 8-71722
- elemental semiconductors, hybridisation effect on dislocation electronic states 8-51936
- graphite, electronic props., self consistent LCAO calc., point vacancy in 2-dimens. cryst. 8-51932
- II-VI semiconducting phosphors, ODMR, defect excited states 8-80254
- insulating crystals, conf., Gatlinburg, USA (Oct. 1977) 8-63755
- interdislocation interaction on account of carriers bound with dislocations 8-75670
- light scattering by excitons localised at dislocations 8-60479
- metal, electrons around vacancies, electron density calc. 8-64003
- one-electron approximation effect of corals. and defects 8-63960
- sapphire, F-type centre induction, 6.1 eV optical absorpt. band 8-88332
- semiconductor, lone pair, defect chemistry 8-51935
- semiconductor neutral point defect electronic struct., self consistent method 8-91641
- semiconductors, multicharged defects, screening of electrostatic fields 8-79959
- thermal neutrons, inelastic scattering by one-dimens. defecton (*Russian*) 8-84169
- vacancy, Green's function calc. (*Russian*) 8-56101
- vacancy formation energy, nonspherical contribution 8-83810
- vacancy formation energy calc. within density functional and second order perturbation formalisms 8-67975
- AgCl, colloid centres by heavy ion implantation 8-63780
- BaS:Cu, thermoluminesc. and decay 8-80426
- BaSO₄, barytes, with large magnitude of emitted light, thermolum. curves 8-88368
- Bi, neutral point defect electronic struct., self consistent method 8-91641
- CaF₂:Dy³⁺, Mossbauer obs. 8-64303
- CdO-B₂O₃-SiO₂, glass, dielec.-relax. currents 8-52004
- CdS, neutron irradiated, intrinsic defects 8-51599
- CdS:Cd(In), Cu- or defect-compensated, optical ageing rel. to storage cond. 8-84247
- p-CdSe, Hall density and mobility, in Se vapour atm., 600-1100K 8-52014
- FeSb₃O_{4-y}, defect struct. and mag. transition, elec. transport and Mossbauer expts. 8-59803
- n-GaAs, heat treated, origin of 1.41 eV emission band, photolum. expt. 8-72579
- GaAs, radiation defect obs. using Schottky diode characts. 8-76024
- n-GaAs:Te, heavily doped, interband luminesc. intensity, heat treatment effect 8-72593
- Ga₂Se_(1-x) solid solns., electrical props. meas. 8-84216
- N-Ge, pressure influence on photoconductivity temp. dependence 8-76109
- n-Ge:Sb, fast neutron irradi. effects on donor conc., and annealing 8-56107
- n-Ge:Sb, γ -irradi. effects on donor conc. and compensation by acceptors 8-56106
- LiF-Li₂O, F-aggregate centres (*Russian*) 8-64394
- N₂:N, dynamically induced electronic transitions of matrix isolated atom 8-63825
- NaClO₃, reson. Raman scatt. from metastable O₂ produced by γ -irradi. 8-60432
- SeN₃, region of homogeneity, physicochem. props. 8-52018
- Se:As(Cl), trigonal, defect and impurity electron levels, surface photovoltage spectra 8-72108
- Si, amorphous electron-hole recomb. mech. 8-72196
- Si, extended Huckel theory calculations for positive divacancy 8-87938
- p-Si, fast electron irradi., Hall mobility, temp. depend. 8-56165
- Si film, amorphous and polycrystallised, localised states, elec. and optical props. 8-64008
- Si, ideal vacancy, self consistent Green's function calc. 8-91640
- Si, neutral undistorted vacancy 8-91638
- p-Si, neutron irradi. effects, admittance meas. of n⁺-p diode 8-51587
- p-Si, neutron irradiated, elec. props. 8-51939
- n-Si, sputtering-induced defects, elec. characts. 8-51941
- Si:B, laser damage obs. by DLTS 8-76023
- Si:Co, study of impurity states 8-76020
- SiO₂ clusters, CNDO/2 calc., appl. of cyclic boundary conditions 8-72110
- ZnO, surface phenomena, interpretation by compensation model 8-95323

defects, crystal *see crystal defects*

defibrillators

see also patient treatment

- conference, Lafayette, USA, (Sept. 1977) 8-57047
- damped sine wave, intact, evaluation of operating internal resist., inductance and capacitance 8-57120
- delivered energy measurement methods, DC defibrillators appl. 8-61281
- electrode gel testing, meas. of impedance to transthoracic DC discharge 8-57056
- multiple-shock defibrillation, effect of shock separation time 8-57053
- myocardial damage rel. to high-energy elec. current 8-57051
- performance characteristics of three commercial instruments in transthoracic ventricular defibrillation of animals 8-57048
- review of instruments and maintenance 8-69251
- thoracic impedance of humans, meas. using automatic recording device on defibrillator 8-61239
- transchest damped sine wave shocks producing cardiac damage 8-57052
- transchest defibrillation, strength-duration curves for trapezoidal wave-forms of various tilts, dogs and ponies 8-57054
- transchest ventricular defibrillation, comparative efficacy of damped sine wave and square wave in dogs and ponies 8-57055
- transthoracic square-wave defibrillation experience in dog and calf 8-57050
- transthoracic ventricular defibrillation in adults, success rate rel. to energy used 8-57049

deformation

- see also bending; cold working; creep; drawing (mechanical); elastic deformation; elongation; ferroelasticity; plastic deformation; shape memory effects; thermomechanical treatment
- Adirondack anorthosite, deform. characts. 8-61399
- alkali halides, exchange charge shell model analysis of strain derivatives of static polarisability, effective charge parameter 8-91296
- armour material, selection criterion 8-53063
- bone mechanical model with appl. to human upper tibia, porous material, deform. (*Japanese*) 8-88724
- chamotte glazed masses, deformation occurring during heat treatment 8-84747
- creep deformation, effect of damage 8-79664
- cylindrical shell, dynamic response to concentrated impact load, radial displacement, stresses 8-67072
- displacement fields, strain state determ., using moire bands and deformed raster 8-63404
- dynamics of shells of revolution under axisymmetric load involving shear deformation 8-79210
- Earth, strain-tide spectroscopy 8-73301
- Earth, three-dimensional geodesic mapping eqns. and best-known figure for non-rigid models (*German*) 8-73304
- Earth crust, Central Alps structural zones and continental collisions 8-81124
- Earth crust, foreland folding model 8-81141
- Earth crust, shear deform. zones along major transform faults and subducting slabs 8-73330
- extensible string motion in nonviscous fluid (*Russian*) 8-77718
- fluid impregnated solids, elastic and dynamic response regimes 8-90713
- glass, flat, air cooled, duration of inelastic deformation 8-84908
- glass fibre reinforced composite, semifinished product nonlinearity model, force anal. of winding 8-63325
- glass fibre reinforced plastics, under compressive load (*Japanese*) 8-92301
- HMTTF-TCNQ chain, three dimensional ordering, HMTTF chain deform. temp. var. 8-95152
- ideal fibre reinforced composites, finite plane deformation and energy dissipation 8-79274
- incremental deformations of initially stressed media with couple stresses 8-62077
- laminated half space under influence of vibrations (*Russian*) 8-63370
- Late Palaeozoic slate belt, structural succession and tectonic significance 8-81140
- machine vibrations anal. and obs. block deformability influence (*Italian*) 8-51108
- metal plate high-gradient transverse deformation interferometry 8-82024
- metals, ferrous and non ferrous, exam. of abnormal deformations and transformations (*French*) 8-60714
- microstructure with finite deformations, reciprocity theorem, stored energy function (*Italian*) 8-81836
- nonlinear interaction of deformable body with liquid pressure wave (*Ukrainian*) 8-65777
- nuclear reactor core mats., constitutive eqn. 8-80598
- optical fibre refractive index change due to external forces 8-74971
- periodotite xenoliths of Massif Central, deform. rel. to upper mantle struct. and geodynamics 8-81120
- plane strain problem of hardening and softening plastic materials, theory 8-83869
- plate thick, circular hole under axisymm. radial load, stress anal., displacements 8-79201
- PMMA, kinetic theory of quasi-brittle fracture, crack tip inelastic deform. (*German*) 8-84991
- polyhedral sandwich domes, elastic behaviour, failure, practical investigation and numerical simulation 8-59309
- polypropylene, shear effect on crystallisation (*German*) 8-75586
- quartz, synthetic, fading rel. to lattice deformation (*German*) 8-63760
- rock failure precursors during anelastic deformation 8-61405
- rocks, effect of stress cycling and inelastic volumetric strain on remanent magnetisation 8-88820
- rubber, natural, stretching effects on glass transition, sp. ht. obs. (*German*) 8-79753
- sea ice field of Okhotsk Sea coast of Hokkaido, divergence and rot. meas. (*Japanese*) 8-96223
- slope forms in Al(1) clay of Franksche Alb, statistical investigation of deform. (*German*) 8-57211
- steel, sheet, effects of strain rate and deformation heating in tensile testing 8-85089
- α Ti, work hardened in tension, developed of internal strain (*French*) 8-76716
- urease shear inactivation, metal ion effect, rel. to shear deform. effects in enzyme catalysis 8-76982
- viscoelastic, crack growth relations, for orthotropic, prestrained media 8-90772
- viscoelastic deformation of incompressible material, thermomechanical theory (*Russian*) 8-63327
- viscoelastic multiple filament yarn, finite extension, slender curved rods theory 8-75076
- X-ray diffr. line profile analysis, on-line computer routine, microstrain determ. 8-79498
- ZTL-180 zenith telescope, objective distortion determ. from visual obs. of star pairs (*Russian*) 8-89068
- Ag, electron irradi., elastic moduli and internal function (*French*) 8-87703
- Ag:Er(Dy), orbit-lattice coupling, nonuniform strain effects 8-88182
- Al alloys, thermally activated deformation, exam. of hypothesis 8-72820
- Al, polycrystalline, abrasion, deform., fatigue, study by exoelectron microscope (*Japanese*) 8-74108
- Al:Er(Dy), orbit-lattice coupling, nonuniform strain effects 8-88182
- Al₂O₃-Cr₂O₃, microstrain correction 8-59852
- Cu-Mn (3 to 20 at.%), high temp. steady state tensile deform. (*Japanese*) 8-52917
- Fe, grey cast, deform. and fracture regions in microzones (*Russian*) 8-80585
- LaAg_{1-x}In_x alloys, structural instability 8-79562
- LiF, single crystal, dislocation generation, beneath static and rolling contact with sphere 8-87671

deformation continued

- Nb₃Sn, A-15 compounds, interlattice displacements, elastic consts. 8-55906
- V₃Si(Ge), A-15 compounds, interlattice displacements, elastic consts. 8-55906

deformation lines see *Luder's bands***degenerate semiconductor materials** see *degenerate semiconductors***degenerate semiconductors**

- see also heavily doped semiconductors; superconducting semiconductors
- chalcogenide lone-pair semicond. charged impurities, effect on carrier concs., Street-Mott model 8-67984
- EM wave absorption, depend. on external quantising mag. field 8-95308
- ferromagnetic, electric field response and electrofluctuation instability (*Russian*) 8-56083
- galvanomagnetic phenomena, model, transport phenomena in presence of medium range disorder (*French*) 8-56162
- many-valley degenerate semiconds., supercond. transition temp. (*Russian*) 8-56254
- nonlinear current density, theory 8-56149
- nonparabolic, acoustic wave absorption/amplification coefficient 8-64069
- plasma, Fermi energy determ., Coulomb collisions in quantising mag. field (*Russian*) 8-55715
- quasi-two-dimensional, warm electrons 8-60222
- recombination-generation currents derivation 8-52007
- EuO:La, photothreshold reduction by mag. induced space charge layer 8-72692
- GaAs, excitons, diamond like semiconductor, variational calculation of binding energies 8-79938
- p-GaAs:Zn, Mn, degenerate, tunnel p-n junction and semicond.-metal struct., I-V characts. 8-72252
- n-GaSb, galvanomagnetic effects 8-72172
- GeTe:Mn, thermoelec. power, 2.5-25K, magnon drag effect 8-56169
- n-InSb, acoustomagnetoec. effect obs. 8-72207
- n-InSb, photoconductivity, 1.8K, hot-carrier and free-carrier absorption. effects 8-84254
- n-InSb, reson. excitation of Kondo effect and negative magnetoresist. (*Russian*) 8-56159
- Pb_{1-x}Sn_xTe, absorption edge shift, energy gap determ. 8-88308
- Pb_{1-x}Sn_xTe, electron-phonon interaction 8-71819
- TiS₂, carrier-lattice coupling 8-63822

dekattrons

No entries

delay circuits

- see also delay lines; phase shifters
- high-speed rotational vacuum tap for discharge gas sampling 8-57969

delay elements (circuits) see *delay circuits***delay lines**

- see also acoustic delay lines
- EM delay lines readout in spark, proportional, and drift chamber appl. 8-74547
- matched filters, using optical delay line provide encoding or decoding structures 8-74983
- MWPC, improvement of position resolution from delay line readout 8-74543
- proportional wire devices with resistive cathodes, detection of induced pulses 8-70691
- rods and clad rods, elastic waves anal., tutorial review 8-94608

delayed neutrons

- explosive r process cooling process 8-69791
- fast critical expts., effective delayed neutron fractions and central reactivity worths 8-62602
- fissile materials, anal. by cyclic activation of delayed neutrons 8-53296
- fissionable isotopes in aq. soln., assay by pulsed neutron interrogation 8-68966
- multigroup-multipoint diffusion operator spectrum with delayed n 8-74430
- pulse height spectra 8-78328
- spectra, gross props. 8-78327
- β -delayed neutron decay, statistical model, Monte Carlo techniques, fictional pandemonium nucleus calcs. 8-89830
- ⁸⁵As, A=85-7, mass chain, half lives and n-emission probabilities of delayed-n precursors 8-70497
- ⁹²Br mass chain, half lives and n-emission probabilities of delayed-n precursors 8-70497
- ¹⁴⁵Cs, mass chain, half lives and n-emission probabilities of delayed-n precursors 8-70497
- ¹²⁰In, A=120-129, total β -decay energies and masses of strongly neutron rich isotopes 8-86512
- Na neutron rich isotopes, β -delayed emission of n, 2n, α , t 8-74343
- ²³⁹Pu, anal. by cyclic activation of delayed neutrons 8-53296
- ²³⁹Pu muonic atom, n emission, bound μ influence on fission barrier 8-89845
- ⁸⁵Sb, A=135-6, mass chain, half lives and n-emission probabilities of delayed-n precursors 8-70497
- ²³²Th muonic atom, n emission, bound μ influence on fission barrier 8-89845
- ²³⁵U, anal. by cyclic activation of delayed neutrons 8-53296

delayed protons

- Ba, A=117, 119, 121, delayed proton emitters, positron-proton coincidence meas. 8-78326
- Cd, A=97, 99, β delayed proton emission, spectra, branching ratio, half life 8-86517
- Cs, A=114-118, neutron deficient isotopes, half lives, β^+ , γ , delayed p and α meas. 8-70489
- ¹⁴³Gd^{m+}, β^+ and EC decay 8-50130

delays

- see also delay circuits; distributed parameter systems
- acoustics, echo time delay detection, effect of zero singularity smoothing 8-90605
- acoustics, time delay meas. in noise identification problems 8-83193
- low-pass, nonrecursive filter based on analogue delay device, mass spectrometer appl. 8-92541
- round-the-world signal group delay, frequency dependence calc. (*Russian*) 8-61654

delta modulation

code delta-modulation for standard hydrophysical information compression (*Russian*) 8-65432

demagnetisation

see also magnetisation

adiabatic of nucl. spins, refrigeration 8-49844
curves, approximate graphic construction method for permanent mag. materials (*Chinese*) 8-80175
cylindrical demagnetisation matrix computation, FORTRAN IV program 8-76274
domain wall micromagnetic dynamics, numerical model 8-72381
ferromagnetic materials, grain-oriented demagnetisability 8-84449
film, rel. to micromagnetic dynamics in domain walls, numerical model 8-72382
hard magnetic materials, demagnetisation curve, single function approx. using computer (*Hungarian*) 8-60307
multidomain grains, demagnetisation field 8-65273
multidomain magnetic disc, ferromagnetic reson. 8-68386
palaeointensity methods using AF demagnetisation and anhysteretic remanence, reliability 8-77352
piezomagnetic rod, demagnetizing field effect, longitudinal-effect extensional vibration 8-95504
Co-Cu-Fe-Ce, mag. characteristics of sintered permanent magnets 8-60312
La₂Mg₃(NO₃)₁₂·24H₂O:Co²⁺, Ce³⁺, relax. and ESR in magnetically cooled systems 8-88225
Ni (110) surface, positive spin polarisation in field emission and demagnetisation by H₂ adsorption 8-52646
Sm-Co, alloy powders and sintered magnets, effect of chem. treatment on mag. props. 8-60311
Sm-Pr-Co, added Fe₂Sn, permanent magnets, demagnetisation curves, X-ray obs. 8-91900

demagnetisation, adiabatic *see magnetic cooling*

demagnetization *see demagnetisation*

Dember effect

CdS-type semiconds., Dember effect, theory 8-72189
LiH (D), single crystals, electronic excitations, review (*Russian*) 8-72574
ZnO, particulate, Dember effect, rel. to electrography 8-95314
Zn₃P₂, photocond. and Dember effect meas., 0.5 to 1.2 µm, possible detector appl. 8-91721

demodulation

see also demodulators; modulation
heterodyne correlation radiometry 8-77980
infrared heterodyne spectroscopy in astronomy 8-85859
IR discretely tunable gas lasers and heterodyne detect. techniques for atm. monitoring 8-61605
IR laser heterodyne spectroscopy for trace gases remote detect. in planetary atms. 8-61606
laser heterodyne signals from moving object, bandpass filtering by finite apertures 8-55306
optical field distribution, heterodyne reception of information 8-87024
submillimeter wave heterodyne detection, with a laser LO 8-70183

demodulators

see also demodulation; discriminators; modems
low-distortion FM demodulator using SAW delay device 8-51014
PLL, ECG-telemetry apparatus appl. (*German*) 8-57097

demonstrations

includes student experiments
see also student laboratory apparatus
α-particle in air, range, energy and range straggling, stopping power meas. 8-73815
acoustical second-order Doppler effect, introductory expt. for special relativity 8-49584
astronomy, Hubble's law as laboratory exercise 8-65740
ball, radius of gyration determ., using air track, undergrad. demonstration 8-49606
binary solid-liquid equilibria, student experiment, phase diagram computer program 8-89285
biomechanics using a crane boom 8-81759
bouncing ball, student expt. 8-54122
Brewster's angle measurement using ordinary lab. apparatus, for high-school students 8-86097
cart wheels on inclined plane, theory and expt. 8-61977
coefficient of restitution of bouncing ball expt. 8-86074
coherence, simulation expt. 8-73810
Compton collision formula and Klein-Nishina formula ang. depend. verification, undergraduate expt. 8-62010
Coriolis machine, inertial motion viewed from rot. reference frame, coordinate transformation 8-69934
cornea, radius of curvature, quantitative geometric optics expt. 8-62004
dielectric surface, reflectances, undergraduate exptl. meas. 8-73809
diffraction pattern display using photodiode array 8-86069
digital display for lecture hall use 8-86075
Doppler shift of laser beam 8-69939
dye laser, tunable, undergraduate demonstration expts. 8-61988
Earth resistivity surveying, apparatus, interpretation, undergrad. field-work 8-49623
electrical circuit equivalent resistance and capacitance 8-69938
electron interference using standard electron microscope and electron biprism as interferometer 8-62005
elliptically polarised light, quantitative anal., $\frac{1}{4}$ -wave plate, student expt. 8-49608
energy expts. for interdisciplinary general science course 8-65738
falling domino chain, expt. and computer program 8-62009
Faraday generator, one piece, paradoxical expt. from 1851 8-73813
force vectors, modified force table expt., load cells and hanging students 8-69947
Fourier transform spectroscopy for students 8-57722
fresh river water-estuary halocline, expt. simulation, salt diffusion in tap water 8-61980
Hero's engine, constructional details 8-69946
human eye, artificial model, physics laboratory for medical students 8-62003
human retina model for props. of vision 8-77655
image light reflection, optical illusion 8-49604
inertia ball demonstration, theory 8-73811
Josephson tunnel junction, Nb-PbSn, 3rd yr undergrad. expt. 8-54126
Leidenfrost effect, demonstrations 8-81744

demonstrations continued

light transmission, through reflecting cylindrical tubes, demonstration 8-73812
Lissajous figures, generation tech. 8-77656
magnetic domains, dynamic behaviour, struct., rel. to ferromag., teaching appls. 8-86080
magnetic domains, using Kerr magneto-optical effect 8-69949
magnetic field lines, rot. mag.-Cu disc interaction 8-54131
materials sci., undergraduate creative project 8-86082
molecular models based on Petri dishes stereochem. appls. 8-73817
molecular size and Avogadro's number, determ., student expt. 8-81741
neutron activation analysis, student experiment 8-77651
nuclear fallout radioactivity γ-ray detection and anal., Chinese fission bomb anal. 8-49596
photoelectric effect and electron diffusion in gases 8-81745
photoresist, positive, formulation, photochem. props., chem. teaching appl. 8-89284
prism, min. ang. deviation, school corridor demonstration 8-81760
pulsars, suggested expts. 8-61982
reciprocal lattice in crystallography, undergraduate demonstration 8-61989
reflectivity, quantitative meas., undergrad. lab. expt. 8-49624
refractive index of beer, lecture room demonstration 8-54128
retinal internal circulation visualisation using Purkinje's methods 8-69043
rotating bodies, intermediate-axis theorem 8-61990
Rutherford scattering, analogous demonstration by mech. expt. using mag. disc (*German*) 8-81778
scientific investigation experiment, development of theoretical model 8-86066
slide preparation techniques for audio visual aids 8-54139
solar system model 8-86095
spectroscopy, chem. anal., mobile laboratory 8-93502
Stefan's law, W filament elec. lamp, student expt. 8-54125
Stephan's constant determ. 8-69948
stimulated Raman effect, electromagnetic-mechanical model experiment (*German*) 8-86077
stroboscopes appl. 8-55453
thermoelectric effects, low-temperature measurements, undergraduate lab. project 8-54119
uncertainty principle using single-slit diffraction pattern 8-69953
undergraduate experiments for applied physics laboratories (*Japanese*) 8-57724
NaI:Ti scintillator response, γ-ray, (X-ray) rel. $\frac{1}{2}$ -width energy depend., undergrad. expt. 8-49600

dendrites

see also crystal growth

Alnico 8 permanent magnet, magnetic props. rel. with crystallographic texture 8-95483
dilute binary alloy monocrystal, thermodynamics of growth, model (*French*) 8-87635
electronic device dendritic growth mechanisms 8-56058
growth models, steady state, exam. 8-72052
interface morphology during crystallisation, single filament unconstrained growth from pure melt 8-52787
interface morphology during crystallisation, single filament unconstrained growth from binary alloy melt 8-52788
metal crystals, electrolytic growth, CCTV obs. 8-51863
metal growth in space, theoretical models, comparison with ground expts. 8-84786
solidification interface in reduced gravity, bubble interactions 8-84787
steady state growth models 8-91576
succinonitrile, undercooled, analysis of dendritic growth 8-75970
Ag electrodeposits, dendritic growth inhibition by tartaric acid and tartrates (*French*) 8-87894
Al₃Ni dendrite facets, determ. cryst. direction by SEM (*French*) 8-87893
Cu₂O, form. by Cu oxidation in CO₂, 800-1000°C 8-76784
Ni, on Al, CV, selective solar photothermal absorber 8-52683
Ni-C, quenched, struct. of graphite precipitates, TEM obs. (*Russian*) 8-68695
Zn electrodeposit dendritic growth control using impedance meas. 8-84721

dendritic crystals *see dendrites*

dendritic structure

alkali halide crystals, dendrite formation during electrolysis 8-95057
repeated precipitation on edge dislocations, micromechanisms 8-95752
steel, cast, effect of non-uniform struct. on props. 8-84850
Al-Mg-Si alloys, dendritic non-homogeneity 8-56641
Cu-Sn (2 wt.%), effect of undercooling on crystal multiplication 8-84866
Fe-Cu (30 wt.%) alloy, dendrite remelting during isothermal holding, microspion obs. (*Japanese*) 8-71836
Sn-Bi (Pb) alloys, supercooled, dendritic growth rates (*Russian*) 8-80533

dense fluids, theory *see liquid theory*

densification

see also density; powders; sintering

hard-alloy powder mixtures, compressibility in hydrostatic working 8-68645
liquid phase sintering, role of grain and phase boundaries 8-72747
magnetite-chromite powder, exam. of rheological characts., compaction 8-60628
magnesium stearate-containing powder mixtures, bonding 8-84731
metal powder, sintering, with intense energy release of interparticle contacts 8-60615
nonisothermal sintering, densification of powder compacts 8-60596
PMMA, oriented, hypersound propag., elastic props. 8-75737
polymer glasses, thermodynamics of densification process 8-95723
porous solid, mixture theory of thermomechanics 8-63315
powder, under uniform directional loading 8-68644
powder compacts, effect of additional pressing at hydrostatic pressures on props. 8-56596
powder metallurgy compact, elec. resistivity 8-64028
powdered compact, densification model with simultaneous grain growth 8-80486
pressing dies, dimensions of hard-alloy inserts calc. 8-60593
steel, high speed, powder, cold isostatic compaction effect on thermophysical props. 8-52717

densification continued

- vacuum techniques' contribution to powder metallurgy 8-84736
 vibrational compaction, of bulk materials 8-52701
 Al, 78% dense porous, dynamic compaction 8-63315
 AlN-Al₂O₃ powders, hot pressing, crystalline phase obs. 8-95720
 Al₂O₃, sintered, MgO-enhanced densification, test of second phase and impurity segregation models 8-64511
 β -Al₂O₃-Na₂O, vacuum hot pressed, densification kinetics 8-72758
 CaO-CaF₂, hot pressed, effects of CaF₂ addition, sintering behaviours and microstructs. investig. (*Japanese*) 8-95721
 Cu, powder compact, elec. resistivity 8-64028
 Fe compacts, porous, dynamic hot pressing, press. rel. to density, time 8-60599
 Fe-Cr-SiC-B₄C powder mixture, compressibility and elec. cond. in cold pressing under low press. 8-60609
 Fe-S-C (1.3 wt.%), sulphidised Fe-graphite bearing materials, sintering, struct. form. 8-60601
 γ -Fe₂O₃ powders, influence of densification on mag. props. 8-95481
 MgO, effect of Cl⁻ and F⁻ ions on calcination and sintering (*Japanese*) 8-95719
 Mo, powder, cold isostatic compaction effect on thermophysical props. 8-52717
 Si, nitridation kinetics, combined effect of Fe and H₂ 8-95722
 Si₃N₄, hot pressing with Y₂O₃ and Li₂O additives 8-92220
 Si₃N₄, hot-pressed with crystn. grain boundary phases, prep. 8-95715
 Si₃N₄-Al₂O₃, hot-pressed with crystn. grain boundary phases, prep. 8-95715
 SiO₂, vitreous, compaction dependence on ionisation dose 8-67738
 Ti, strip prod. by powder rolling 8-80493
 UO₂, irradiation induced vol. change 8-67740
 UO₂, thermal and in-reactor densification 8-66364
 W, powder, cold isostatic compaction effect on thermophysical props. 8-52717
 ZnO, segregation of Li₂O at grain boundaries 8-64513

densimeters *see densitometry***densitometers** *see densitometry***densitometry**

- see also photometry*
 accurate fan-beam reconstruction 8-78931
 automated visual edge match system for image quality assessment 8-62218
 compensation densitometer servosystem using integrated operational amplifiers 8-89525
 electrophoretic waveform analysis for blood serum protein composition determ. 8-64928
 flare light in microdensitometer, simple model 8-58008
 glaucoma diagnosis by digital processing of optic nerve head images 8-81043
 hardwired image analyser software control 8-57917
 intensity microphotometer with step-drives, for negatives transparency conversion (*Russian*) 8-57457
 myocardial contrast accumulation, densitometric evaluation 8-69216
 photographically recorded spectral lines, of nonuniform half-width, microphotometric errors 8-86337
 processor control using preexposed control strips and visual comparative densitometry 8-69210
 SEM, photographic densitometry, appl. to chromosomes 8-77168
 smoke plume concentration meas. by optical radar (*Chinese*) 8-58006
 solar corona and comet digital image enhancement 8-81556
 spectrophotometer kinetic curve recording unit 8-86352
 TEM, thin section uniform region quantitative meas. 8-58097
 turbid media, approx. linear relationship for optical response 8-90371
 water penetration imagery, surface/depth data separation by multispectral scanning 8-69539
 xerographic copy line profile meas. using microcomputer/microdensitometer system 8-74088

density

see also atmospheric pressure and density; density measurement; density of gases; density of liquids; density of solids

- Earth interior, density distrib. from gravity logging data (*Russian*) 8-92999
 globular clusters, star space densities from multicolour strip photometry 8-89229
 gravimetric density formula for Earth of spherical shells 8-61303
 neopentane, critical, electron mobility, gravity effect 8-91738
 N Pacific Ocean waters, density 8-73391
 sea ice near Showa Station, Antarctica, density and salinity meas. (*Japanese*) 8-96226
 seawater, density field calc. in Kuroshio jet current region 8-92843
 sheet material, radioisotope method for measurement of average value, and dispersion in surface density 8-76811
 solar coronal loops, temp. and density struct. 8-89155
 H II regions, influence of gas density on ionisation and temp. struct. 8-61911
 (MgO)_x-(Al₂O₃)_y, formation of nonstoichiometric spinel on heating hydrous MgAl₂O₄ 8-76672
 Ni-ZrO₂, thin layers, vapour deposited, dispersion strengthened, exam. of struct., mech. props. 8-80554

density, atmospheric *see atmospheric pressure and density***density, vapour** *see density of gases***density measurement**

see also hydrometers

- blood sedimentation rate free from gravity influence, rapid determ. from density meas. (*German*) 8-81085
 bone mineral concentration estimation by beta-ray backscatt. (*German*) 8-69179
 cryogenic fluids, density reference system 8-54344
 dilatometry with pressure transducing instrumentation, apparent molar vol. of NaOH in water 8-75702
 fluid density measurement techniques, biological macromolecules in solution appl. 8-92751
 gas, by multibeam interferometry 8-58016
 gas, low density meas. by reson. fluoresc. 8-54341
 gas flow application of shearing interferometers 8-55706
 gas-liquid mixtures, flowing, gas conc. meas., acoustic method 8-59448
 gravimetric measurement of sorption isotherms, errors 8-67905
 liquid, piezoelectric transducer appl. (*Russian*) 8-49799
 liquid methane density meas. at cryogenic temp., commercial densimeters eval. 8-54343

density measurement continued

- magnetic float densimeter for measuring liquid density 8-49801
 plasma, Thomson scatt. diagnostics using optical multichannel analyser 8-67432
 plasma density fluctuation evaluation by microwave interferometry 8-67437
 plasma wall sputtered metal density meas. by atomic fluorescence spectroscopy 8-67422
 polymers, cryst. density, X-ray diffr. determ. 8-91273
 water, saline and pure max. density points meas. 8-57900
 N₂, density measurement up to 1800K and 8 kbar, procedure 8-81947

density of gases

- air pollution density distrib., flow pattern in Tanabe area, Japan, numerical anal. (*Japanese*) 8-96289
 molar volumes microscopic insight from macroscopic data, teaching appl. 8-69930
 thermophysical props. tabulated for mixture composition certification 8-80818
 transport coefficients density expansion, 1st logarithmic term, moderately dense gas 8-94878
 He, electron mobility, anomalous density and temp. depend. at low temp. 8-75253
⁴He vapour, thermal cond. as function of density 8-55712
 Kr, viscosity coeff., density expsn. 8-91054
 N₂, density up to 2000K and 6 kbar by displacement method 8-51266
 N₂, molar volume measured by adiabatic compression 8-51267
 UF₆, temp. and density profiles in freely expanding gas for laser enrichment 8-74458

density of liquids

see also hydrometers

- acetonitrile-methanol, excess vol. and isentropic compressibility, from density and US vel. meas. 8-79776
 anisylidene-p-aminophenyl acetate, nematic liq. cryst., refractive index, density, orientational order 8-76419
 anisylidene-p-aminophenyl butyrate, nematic liq. cryst., refractive index, density, orientational order 8-76419
 benzene-ethanol, excess vol. and isentropic compressibility, from density and US vel. meas. 8-79776
 benzene-n-heptane, excess vol. and isentropic compressibility, from density and US vel. meas. 8-79776
 benzyl alcohol-n-butanol, excess vol. and isentropic compressibility, from density and US vel. meas. 8-79776
 binary mixtures, US props., excess density, interaction between components 8-63657
 4,4'-bis(heptyloxy)azoxybenzene, nematic liq. cryst., refractive index, density, orientational order 8-76419
 4,4'-bis(hexyloxy)azoxybenzene, nematic liq. cryst., refractive index, density, orientational order 8-76419
 p,p'-diheptylazobenzene, nematic, physical props. 8-79524
 p(p-ethoxyphenylazo)phenyl undecylenate, nematic liq. cryst., refractive index, density, orientational order 8-76419
 p(p-ethoxyphenylazo)phenyl heptanoate, nematic liq. cryst., refractive index, density, orientational order 8-76419
 p(p-ethoxyphenylazo)phenyl hexanoate, nematic liq. cryst., refractive index, density, orientational order 8-76419
 p(p-ethoxyphenylazo)phenyl valerate, nematic liq. cryst., refractive index, density, orientational order 8-76419
 fluctuation effect on Brownian particle freq.-depend. friction coeff., near crit. pt. 8-73929
 halomethanes, liquid densities, data tables 8-75703
 Hildebrand's law, fluidity as a function of molar vol. (*French*) 8-63872
 hydraulic characts. of liqs. flowing through porous metal fibre mats., permeability laws 8-67848
 laminar convection in vertical tube, thermophysical prop. temp. depend., effects 8-90895
 lecithin bilayers, density and mol. interactions 8-80837
 measurement using piezoelectric transducer (*Russian*) 8-49799
 metal, density determ. by X-ray diffr. (*Russian*) 8-75529
 methane-propane(pentane)(n-heptane)(n-decane)(H₂S) mixtures, densities calc., van der Waals model 8-79740
 molar volumes microscopic insight from macroscopic data, teaching appl. 8-69930
 polyethylene melt spinning, extensional flow induced crystallisation 8-55818
 PVC, density rel. to rheological, surface props. of PVC pastes (*Polish*) 8-85212
 seawater in Canaries Current, density-depth relation rel. to current tidal component (*Russian*) 8-77263
 ternary liquid mixtures, molecular interaction and thermodynamic props. 8-59861
 toluene, relationships between thermal cond., dynamic viscosity and density, high state parameters 8-83861
 transport properties, relationships between thermal cond., dynamic viscosity and density, high state parameters 8-83861
 water, forced laminar convection in horizontal pipe, density inversion effects, numerical anal. 8-90900
 water, relationships between thermal cond., dynamic viscosity and density, high state parameters 8-83861
 water, saline and pure max. density points meas. 8-57900
 Al, density fluctuations 8-55806
 Ca(NO₃)₂·3.91H₂O-NiCl₂ melts, glass forming, transport behaviour 8-59963
 Cs, liquid, meas. of density at high temp. and pressures 8-55903
 CsCl-UCl₃ melts, density, surface tension and viscosity 8-67764
 D₂O, temperature of maximum density in capillaries 8-51801
 Fe, cast, grey, density variation during slow crystallisation (*Russian*) 8-95737
 FeO-SiO₂, molten, viscosity and density 8-59965
 H₂O-acetic acid-silver acetate, ternary liq., elec. cond. and density 8-91464
 He, equations of state, 3.3 to 14K (*Russian*) 8-83912
³He, equations of state, 3.3 to 14K (*Russian*) 8-83912
³He, significant structure theory, thermodynamic props. 8-51774
⁴He, superfluid density depression by velocity 8-51760
 K, liq., density, 1640-2030K, 36.1-100.2 atm 8-91369
 NaOH, in water, apparent molar vel. determ., dilatometry with pressure transducing instrumentation 8-75702
 NiCl₂, aq. soln., viscosity meas., struct. props. 8-75863

density of liquids continued

- RbCl- UCl_3 melts, density, surface tension and viscosity 8-67764
 $\text{SiO}_2\text{-Al}_2\text{O}_3\text{-CaO-MgO}$, liq. silicic and slag, struct, density, surface tension (*Polish*) 8-83711
 Te, liquid, meas. of viscosity, density and surface tension (*French*) 8-91371

density of solids

- acoustic velocity, shock-compressed uniform solid, lateral discharge ang. semiempirical formula (*Russian*) 8-55910
 borophosphate glasses, effect of F on props. 8-67657
 ceramic, ferrimag. or ferroelec., microstructure and physical props. 8-72756
 Chevrel type compounds, single crystals, growth, stoichiometry, elec. resist. 8-92187
 creep damage and rupture criteria, cavity config., use of density meas. 8-60818
 cubic crystals, theoretic props. at arbitrary press., density and bulk modulus 8-51606
 fluorophosphate glasses, rare-earth activated, luminesc., bonding 8-64415
 glass, tempered, density and refractive index variation 8-64564
 glass-ceramics, transparent, microstruct. and props. 8-59960
 $\text{LiNO}_3\cdot 3\text{H}_2\text{O}$ ($3\text{D}_2\text{O}$), density, thermal expansion coeff., isotope effect 8-87733
 metal powder explosive compaction 8-64501
 metallic glass, hardness, elastic moduli, density, cryst. temp., mech. props., for flywheel appl. (*Dutch*) 8-52878
 metallic glass, struct. relax. effects 8-72804
 mixed metal chloride acousto-optical props. (*Russian*) 8-60419
 molar volumes microscopic insight from macroscopic data, teaching appl. 8-69930
 polycarbonate fibre, highly-oriented, drawing behaviour and mech. props. 8-76708
 polyconjugate system, interrelation between physicochem. props. and microstruct. 8-55816
 polypropylene, cold-drawn isotactic bars and thin films, microstruct. and annealing 8-95760
 PTFE fibres, US effects on structure (*Polish*) 8-68702
 sintered material, relation between density and sound velocity 8-53173
 sintering, packing fraction effects (*German*) 8-64494
 steel, cavitation during superplastic flow, affecting factors 8-60728
 steel, solidification singularities in C and low-C steels (*Russian*) 8-80532
 technological strength and nondestructive methods of testing during heat treatment 8-85090
 thermal penetration property ρ ck meas. instrum. 8-70120
 tissue-equivalent plastic A-150, density and composition uniformity 8-73252
 transition metal, 3d and 4d, local density theory, mech. and mag. props. evaluation 8-91630
 transition metal-group IIIB alloys, relationship between struct. and thermodynamic props. (*German*) 8-91307
 Ag composite, SiC whisker-reinforced, prep. aboard Skylab. 8-84741
 Ag specific volume meas., for ruby R_1 fluoresc. press. gauge calibration, 0.06-1 Mbar 8-70150
 Al-Si (8 wt.%), threshold H_2 for pore form. during solidification 8-52794
 $\text{Al}_2\text{O}_3\text{-B}_2\text{O}_3\text{-P}_2\text{O}_5$ glasses, formation and props. 8-83737
 $\beta\text{-Al}_2\text{O}_3\text{-Na}_2\text{O-SiO}_2$, solid electrolytes, exam. of microstruct. ionic resistivity 8-80566
 Ar, solid, density at melting and isochoric equations of state 8-83915
 $\text{AsSe}_{1.5}\text{-Te}_x$ glasses, physical props. 8-68028
 $\text{BaO-La}_2\text{O}_3\text{-GeO}_2$, exam. of glass forming region, properties and crystallisation 8-88454
 $\text{BaPO}_3\text{-F-Al}_2\text{O}_3\text{-B}_2\text{O}_3$ glasses, phys. props. 8-63676
 C, anthracene char, density fluctuations effect on physical properties 8-51420
 C, baked mixes, use of coal tar and petroleum pitches as binders 8-80483
 Cu alloys, cavitation during superplastic flow, affecting factors 8-60728
 Cu, specific volume meas., for ruby R_1 fluoresc. press. gauge calibration, 0.06-1 Mbar 8-70150
 Eu_2O_3 , sintering kinetics 8-52731
 Fe compacts, porous, dynamic hot pressing, press. rel. to density, time 8-60599
 Fe, porous, density, elec. cond., Young's modulus, toughness 8-64645
 Fe-B metallic glass, hardness, elastic moduli, density, cryst. temp., mech. props., for flywheel appl. (*Dutch*) 8-52878
 Fe-Ni-Cr-P-B, Metglas 2826A, hardness, elastic moduli, density, cryst. temp., mech. props., for flywheel appl. (*Dutch*) 8-52878
 Fe-Si (6.5 wt.%) steel, core mat. development (*Korean*) 8-60852
 FeF_2 (rutile), high press. phase transform. and zero-press. density increase 8-79761
 InAs, intrinsic point defects, nature and influence on electrophys. props. 8-79609
 $\text{KCl:Ca}^{2+}(\text{Sr}^{2+})$, impurity precip., flotation density obs. 8-51690
 $\text{K}_2(\text{F}_2\text{O})\text{-B}_2\text{O}_3\text{-SiO}_2$, effect of replacing B_2O_3 by Al_2O_3 or Ga_2O_3 8-63677
 Kr, solid, density at melting and isochoric equations of state 8-83915
 LiF compact, particle size rel. to pore chars. 8-60631
 $\text{M}_2\text{O-MnO-B}_2\text{O}_3$ glasses, M=Li, Na, K, glass-forming region and physicochem. props. 8-63678
 Mg-Zn metallic glass, hardness, elastic moduli, density, cryst. temp., mech. props., for flywheel appl. (*Dutch*) 8-52878
 Mo, specific volume meas., for ruby R_1 fluoresc. press. gauge calibration, 0.06-1 Mbar 8-70150
 NaF, ab-initio calc. of cohesion energy, compressibility and density 8-71782
 $\text{Na}_2\text{O-Al}_2\text{O}_3\text{-SiO}_2$ glass, formation from alkoxides, phys. and chem. evolution 8-80503
 Nb-Ni metallic glass, hardness, elastic moduli, density, cryst. temp., mech. props., for flywheel appl. (*Dutch*) 8-52878
 Ni-Fe alloy, FCC, density, lattice parameters, X-ray diffr. and hydrostatic weighing 8-55904
 $\beta\text{-Ni}_3\text{S}_2$, defect struct. 8-63754
 O_2 , density of solid in equilib. with vapour 8-93656
 P-As-Se glasses, mag. susceptibility, dielec. const., opt. props. 8-64184

density of solids continued

- Pb-Sn eutectic, cavitation during superplastic flow, affecting factors 8-60728
 Pd specific volume meas., for ruby R_1 fluoresc. press. gauge calibration, 0.06-1 Mbar 8-70150
 ScN_x , region of homogeneity, physicochem. props. 8-52018
 Se-S, glassy alloy, order-disorder transition kinetics 8-67650
 SiC, powder mixtures, composition vs. apparent density diagrams construction, model 8-60633
 SiC, self-bonded, statistical distrib. of values of apparent density 8-68657
 $\text{SiO}_2\text{-Al}_2\text{O}_3\text{-B}_2\text{O}_3\text{-Li}_2\text{O}$ ($\text{Li}_2\text{O-Na}_2\text{O}$) (Na_2O) glass exam. of optical props. 8-88277
 $\text{Ta}_{16}\text{W}_{18}\text{O}_{94}$, characterisation of thermally contracting tungstates 8-63869
 Ta_2WO_6 , characterisation of thermally contracting tungstates 8-63869
 $\text{Ta}_{22}\text{W}_{67}$, characterisation of thermally contracting tungstates 8-63869
 Ti-Be-Si glass ribbons, physical and mech. props. 8-95767
 TiO_2 , sintering, hardness, density, elec. cond. and colour (*Japanese*) 8-68659
 Ti_2MoO_4 , prep., characterisation 8-63731
 $\text{V}_2\text{O}_5\text{-P}_2\text{O}_5$ glass, density and O molar volume 8-59759
 W alloys, sintered relation between density and sound velocity 8-53173
 $\text{ZnO-La}_2\text{O}_3\text{-GeO}_2$, exam. of glass forming region, properties and crystallisation 8-88454
 ZrO_2 , optimum sintering characts., density, X-ray diffr., IR spectrum, UV spectrum obs. 8-76617
- density of states, electron** see *electronic density of states*
deoxyribonucleic acids see *DNA*
deperming see *demagnetisation*
describing functions
 see also *control system analysis*
 visual evoked response of humans, nonlinear anal. 8-92622
- design aids**
 see also *design engineering; nomograms*
 capacitor banks, optimum design rules 8-74487
 graphs for optical system design, multi-layer, using equivalent films (*Czech*) 8-90486
- design engineering**
 see also *project engineering; systems engineering*
 475 MVA pulsed motor generators for TFTR 8-58498
 600 kW repetitive stacked line transformer pulse generator 8-77935
 600 MW pulsed energy convertors for toroidal field coil, design philosophy 8-58496
 ASDEX circuit breaker system, design, calcs. and tests 8-55032
 axial flow fan, control of tip-vortex noise 8-90593
 buried pipeline transient temp. distrib. estimation 8-75048
 Calcutta variable energy cyclotron vacuum system design, testing and commissioning 8-86707
 capacitor banks, optimum design rules 8-74487
 cryopumps for fusion reactor high power neutral injectors, design and performance 8-74494
 double helix vacuum resistance heater element design and construction details 8-49839
 electrostatic precipitator, free-fall, design and operating modes 8-71020
 EM instruments for use in liquid sodium, theoretical anal. 8-54857
 frontiers in education, conference, Urbana-Champaign (1977) 8-81779
 fusion reactor, JET, high voltage network to load AC/DC pulse power conversion 8-58497
 fusion reactor, T-10M Tokamak, normal and supercond. inductive energy storage and switching 8-55018
 fusion reactor, TEXT, pulsed homopolar generator power supply, engineering and design 8-55016
 fusion reactor, TMX, magnets, mech. design 8-58494
 fusion reactor, TNS, electrical design costing 8-55014
 fusion reactor, Tokamak constant tension D-shaped coils, lateral support struct. 8-55013
 fusion reactor, toroidal device with nonplanar mag. axis, magnet and coil engineering 8-55009
 fusion reactor coil design, cost anal., for neutral beam magnets 8-55005
 fusion reactor design and economics, confinement physics effects 8-50358
 fusion reactor magnet coil, 125 kG, 1 m, design, fabrication 8-55008
 fusion reactor neutral beam injection system cryopump, liq. He-cooled, for H_2 pumping 8-74495
 fusion reactor RFC-XX, coil system, design, fabrication, testing 8-55007
 fusion reactor solenoid, orthotropic, finite element stress anal. 8-55010
 fusion-fission breeder reactor, supercond. poloidal field coil design 8-70640
 heat exchanger design eqn., condensate film flow on finned surfaces 8-75038
 homopolar generator, fast discharge machine, design, fabrication, testing, for fusion reactor 8-54952
 homopolar machine, 10 MJ, fast-discharging, for fusion reactor 8-54950
 implosion heating coil, radially fed, design, fabrication and appl. 8-55006
 ion beam accelerator, multimegawatt, high-voltage power system, design philosophy, for fusion reactor 8-62613
 laser amplifier design using generalised experimental data 8-66836
 maintenance-free water test stations, design aspects (*German*) 8-65403
 MW impulse generator system, for ion cyclotron heating, fusion reactor 8-70635
 neutral beam, pulsed, arc (arc filament) power supplies, for fusion reactor 8-70637
 neutral beam accelerator electrodes, spark discharge protection, for fusion reactor 8-62609
 neutral beam injection vac. components, for fusion reactor 8-74493
 neutral beam power supply, series switch/regulator system, 40 kV, 80 A, 10 ms, for fusion reactor 8-66366
 open channel acoustic flowmeters, design, calibration and errors 8-5701

design engineering continued

- open channel acoustic flowmeters, design, meas. errors and operation 8-63516
 polymeric materials, vibration damping and control, design and meas. 8-87185
 radome and backstructure design improvements 8-57449
 refrigerator, closed-cycle, for supercond. electronic systems, design 8-93711
 Shiva laser, 25 MJ energy storage and delivery system 8-55015
 Shiva laser, 25 MJ energy storage and delivery system 8-59038
 space antenna, self-deploying large parabolic antenna and array design 8-57450
 spring, complex arch type, movable, snap-through action characts., appl. to microswitches 8-63339
 spring, complex arch type, movable, snap-through action characts., microswitch appls. 8-63340
 thermal regenerator, with variable mass flow rate, computer model 8-75047
 toroidal field coils, bending-free, for Tokamak reactor 8-55012
 Viking lander radar system mechanical design 8-57427

desk calculators see *calculating apparatus; electronic calculators*

desk-top computers see *minicomputers*

desorption

- atom-surface one phonon scatt., 3-dimens., continuum model of thermal desorption 8-87860
 dielectric solid surface breakdown in vac., desorption mechanism 8-67464
 electrolyte aqueous soln. drops, ion emission due to laser heating 8-59063
 electron stimulated, reneutralisation 8-79894
 electron stimulated, reneutralisation 8-84070
 epitaxial growth, vapour phase, growth mode characterisation 8-87885
 fission fragment induced desorption, method for correlated events in TOF mass spectrometry 8-58089
 graphite, energetic ion sputtering, appl. of AES-SIMS (IMA)-FDS combined systems to physical and chemical processes 8-95636
 graphite, of CO, CO₂, kinetics 8-60025
 graphite, surface alteration by interaction with Ar⁺ and Xe⁺ beams, thermal desorpt. mass spectroscopy 8-91347
 graphite monofluoride, surface alteration by interaction with Ar⁺ and Xe⁺ beams, thermal desorpt. mass spectroscopy 8-91347
 homogeneous surfaces, statistical mech. of collisions which lower desorption rate (German) 8-84072
 Inconel 600, fusion reactor vac. vessel, air, N, adsorpt., thermal desorpt., heat treatment effects 8-54880
 inert gas liberation in multiposition metallic reactor 8-59978
 kinetics, Kramers-Langevin stochastic eqn., heavy-atom limit, adatom-phonon coupling 8-84065
 laser stimulated desorption, quantum theory 8-79876
 Macrotron Tokamak, laser-induced desorption of impurities from walls, spectral anal. 8-59681
 metal oxides, thermodesorption of O₂, expt. technique (French) 8-64884
 metal-H₂ systems, determ. of absorption/desorption isotherms, high press. 8-51679
 microscopic models of desorption spectra 8-71946
 phosphonium cations, quaternary, produced by field desorption, collisional activation spectra 8-56946
 photochemistry and photodesorption, isotope separation aspects 8-64863
 positive ion photoemission, vacuum UV quantum yield limit 8-79896
 precursor intermediates, desorption kinetics 8-87876
 steel, stainless, 321 and 304, D implanted, thermal desorption and bombardment induced release 8-95072
 steel, stainless, D implanted, thermal desorption 8-71750
 steel, stainless, ion induced release of trapped D 8-95095
 steel, stainless, type 304, electron stimulated desorption rel. to CTR first wall appl. 8-51818
 sulphonium cations, tertiary, produced by field desorption, collisional activation spectra 8-56946
 Teflon, surface alteration by interaction with Ar⁺ and Xe⁺ beams, thermal desorpt. mass spectroscopy 8-91347
 thermal, generalised Langevin theory for surface dynamics 8-60024
 thermal desorption mass spectra, activation energy, rate coeff., analytic expressions 8-60022
 thermal desorption mass spectra, effect of heating rate and pumping speed, quantitative anal. 8-60023
 thermal desorption model analysis (German) 8-63940
 thermal desorption with large variable friction constant 8-71974
 thermodesorption, temp. control device (German) 8-86251
 time dependent escape rate from potential well 8-79888
 W, oxidised polycryst. kinetics 8-75939
 Al alloy, 6061, vacuum material, desorpt. of neutral mols. by electron and ion bombardment 8-95229
 Al foil, sputtering with ²⁵²Cf fission products, desorbed secondary ions 8-68596
 η-Al₂O₃, chemisorption of propylene, desorption and D exchange obs. 8-51827
 Ar, solid, of He, appl. of simplified continuum model 8-87860
 Ar surface, spin aligned condensed atomic H 8-63929
 C, chemisorbed oxygen surface complexes, thermal desorpt. analysis 8-56032
 C, of H, astrophysical system, appl. of simplified continuum model 8-87860
 Ce-Ni, hydriding characts., applicability for H₂ storage material 8-83955
 Cu foil, sputtering with ²⁵²Cf fission products, desorbed secondary ions 8-68596
 Cu, of NO, species identification, struct., dissociation, chemisorption, desorption, UV photoelectron spectroscopy 8-52635
 Fe (100) and (111) surfaces, chemisorption of CO, CO₂, acetylene, ethylene, H₂ and NH₃, LEED and thermal desorption 8-71996
 Ge (111) of K and O₂, rel. to work function, K thermodesorpt. spectra 8-79874
 H₂ surface, spin aligned condensed atomic H 8-63929
³He, specific heat second layer adsorbed on Grafoil 8-87843
 InSb, irrad. real and clean surfaces, work function 8-95336
 Ir (111) surface, electron beam induced desorption and dissociation of chemisorbed CO 8-56043
 Kr, solid, of He, appl. of simplified continuum model 8-87860

desorption continued

- La-Ni, hydriding characts., applicability for H₂ storage material 8-83955
 La₂Ni₃D₂ storage material, neutron, X-ray diffr. study 8-83954
 MgO powder, decomp. of chemisorbed ethanol, propanol and acetic acid 8-92502
 Mo, electron stimulated desorption of negative ions from adsorbed gases 8-91549
 Mo, surface, electron-stimulated desorption of negative ions, work function 8-72654
 NaCl, deform. process, exoemission and desorption meas. (Russian) 8-75708
 Ni foil, sputtering with ²⁵²Cf fission products, desorbed secondary ions 8-68596
 Ni, polycryst., O₂ interaction obs. 8-76568
 Ni surface, polycrystalline, adsorbed S, H₂⁺ ion induced desorption 8-84069
 Ni, trapping and release of inert gases, thermal evolution mass spectrometry 8-95077
 NiH₂, of H₂, effect of hydrogenation on fine struct. of polycryst. Ni 8-59950
 Ni(111), adsorption of acetylene, evolution of adsorber species, rel. to vibr. spectra 8-95952
 PbS, of SO₂, optical excitation meas. of trap charging (Russian) 8-76180
 Pt (111) stepped surface, adsorption of O₂, CO, C₂N₂ and ethylene 8-71992
 Pt, of acetone, photoion emission, quantum yield limit 8-79896
 Pt, surfaces (111) and 6(111)×(111), CO adsorption, EELS and thermal desorption spectroscopy 8-91547
 Pt(111), adsorption of NO, anal. of adsorption processes and surface reactions, vibration spectroscopy 8-87868
 Re, coadsorption of ethylene and O₂, thermal desorption study (French) 8-85194
 Si film, amorphous, plasma-deposited, H₂ evolution, mass spectrometry and RHEED obs. 8-72050
 SiC, energetic H and Ar ion sputtering, AES-SIMS-FDS combined obs. 8-80444
 SiC, energetic ion sputtering, appl. of AES-SIMS (IMA)-FDS combined systems to physical and chemical processes 8-95636
 SnO₂:ThO₂, exposed to CO gas, self-oscill. phenomenon 8-68032
 W (001) surface, adsorption of CO, electron energy loss spectra and thermal desorption 8-71999
 W (100), CO/H₂ surface complex, flash desorption and AES obs. 8-73083
 W (100), laser induced desorption, mirror electron microscopy 8-84067
 W (100), of O, electron stimulated desorption ion energy distrib. and surface struct. 8-75940
 W, methane dissociation by adsorption-desorption process 8-92511
 W, of CO, thermal desorption and conversion kinetics, AES study 8-71959
 W surface, adsorbed H₂, energy spectra for electron stimulated desorption of H⁺ calc. 8-79892
 Xe, solid, of He, appl. of simplified continuum model 8-87860
 ZnO 1010 surface, reaction of O₂, AES, LEED, EPR, desorpt., surface cond. and work function expts. 8-95950
 ZnO (1010) surface, of Zn, O₂, nonstationary sublimation (German) 8-60035
 ZnO, electron beam induced decomposition and desorption, AES and contact pot. difference meas. 8-79893
 ZnO, of H₂O(NH₃)(NO)(acetone), photoion emission, quantum yield limit 8-79896

detection (demodulation) see *demodulation*

detector circuits

see also *demodulation; demodulators*

- Josephson junction current-voltage charact., resonance detection cct. 8-54406
 peak detector extremator, cct. 8-74096
 submillimeter wave heterodyne detection, with a laser LO 8-70183

detectors

see also *electric sensing devices; hydrophones; infrared detectors; microwave detectors; nonelectric sensing devices; particle detectors; photodetectors; ultraviolet detectors*

- periodic magnetic signal detection by magnetoresistance sensor (Japanese) 8-57997
 US beam detector, two-dimensional 8-94495

determinants

see also *matrix algebra*

- fermion determinant in QED, asymptotic estimates 8-54593
 Lanczos method, method of moments, tri-diagonalisation of a matrix 8-58240
 quantum fluctuations of instantons 8-54530
 S-matrix theory, determinant and its relation to number of eigenvalues due to perturbation 8-58132

detonation

see also *explosions; shock waves*

- laser supported detonation wave, Whitham's rule anal. 8-59423
 oxyacetylene, critically-initiated detonation waves, quasi-steady regime 8-90930
 plane hyperdetonation shock wave reflection from rigid wall 8-75167
 shock waves, starvation kinetics 8-64841
 sputtering, exp. determ. of dynamic characts. of two-phase flow (Russian) 8-94852
 Al₂O₃(-TiO₂) coatings, detonation deposited on steel, prep., wear resist., antifriction props. 8-60877

deuterium

- absolute Raman cross sections determ. by indirect meas. of stimulated Raman gain, technique 8-66864
 absorption by Ce binary alloys, T-getters for CTR evaluation 8-51683
 abundance in Galaxy rel. to cosmology 8-69883
 adsorption on graphite of p-D₂, NMR, orientational behaviour, weak crystal field 8-75935
 atom, detection by resonant three photon ionisation 8-74624
 atom, ground state Lamb shift, isotope shift and relativistic nuclear recoil correction 8-82696
 atom, Lamb shift, from elec. field quenching radiation anisotropy 8-66502
 compressed-D₂-filled glass microspheres for multibeam laser-target expts. 8-82509

deuterium continued

compression to 44.7 kbar, apparatus and technique, diamond anvil cell 8-74017
 deuterium-tritium thermonuclear ignition, high current density approach, expt. 8-54874
 deuteron bombardment of pyrolytic C, methane form., energy depend. 8-95939
 diffusion and permeability in Fe at 49 to 506°C 8-59977
 diffusion and solubility in PTFE, activation enthalpy 8-79775
 diffusion coefficients, Pd, Ni, and Cu, calc. (*Russian*) 8-91483
 diffusion in hydrogenated amorphous Si, SIMS anal. 8-75877
 diffusion in No, Pd, Va, quantum rate theory for symmetric double well pot. 8-55970
 duopigatron gas discharge ion source, perform. characts. 8-54505
 duoplasmatron gas discharge ion source, plasma expansion cup effects 8-58092
 electric breakdown, Paschen's law violations 8-87570
 electron surface barriers for dense phases 8-91754
 fluid n-D₂, eqn. of state from P-V-T and US vel. meas. up to 20 kbar 8-63837
 fusion reactor, cryosorption pumping, D₂-He (5 at.%), on mol. sieve, 5A, 4.2K 8-74499
 fusion reactor, D-T to catalysed-D operation, trapped ion scaling law 8-66419
 hailstone trajectories determ. from crystallography, D content and radar backscatt. 8-61614
 heat of adsorption on polycryst. Fe film 8-91530
 implanted in pyrolytic graphite, depth profiles 8-95071
 implanted into stainless steel, 321 and 304, thermal desorpt. and bombardment induced release 8-95072
 implanted into Zr, temp. depend. depth profiles 8-95076
 implanted stainless steel, TEM obs. of defect struct. 8-95073
 interstellar absorption line at 327 MHz, search towards galactic centre 8-77599
 ion implantation into solids, ranges of implanted 10-30 keV D⁺ 8-83858
 laser isotope separation, reaction chamber 8-55040
 liquid, US vel., 22-35K (*Russian*) 8-75731
 liquid n-H₂, n-D₂, Ne mixtures, deviation from Rao-Wada rule 8-75729
 magnetic relaxation study in Fe 8-64228
 molecular photodissoc., D(2p) dissoc. products detection 8-50605
 molecule, dissociative electron attachment, Faddeev calcs. of cross sections (*Russian*) 8-70945
 molecule, photoionisation, body-frame Hund's case b description 8-94295
 molecule, Raman spectra, vibr. freq. press. shifts 8-78703
 permeability, diffusivity and solubility in pure Fe at 10 to 60°C 8-75887
 permeation, in Pd, comparison to H₂ (*Russian*) 8-75881
 permeation in Cu alloys, Cu-Au and Au, growth of permeation barriers 8-75883
 plasma, beam-heated, in Princeton Large Tokamak, neutron emission profiles 8-63588
 plasma, inertial confinement, reaction gains, reheat calcs., collective model 8-59664
 plasma, neutron generation by CO₂ laser implosion of polyethylene shell into conical region 8-87468
 plasma diagnostic technique using self reversed deuterium D_α line 8-55746
 prep. by electrolysis of heavy water using self-controlled cell 8-80752
 pumping by Ti film, pumping speed comparison between H₂ and D₂ 8-51819
 radiation induced exchange reaction kinetics of H₂, D₂ and T₂, review 8-61005
 solid, 0.5-3 keV electron penetration depth 8-56549
 solid, far IR absorption by phonons and librions in ordered state 8-80331
 solid, librion spectra and conversion as function of ortho-para conc., Raman scatt. spectra 8-84570
 solid, para, roton dragging librions 8-67886
 solid-liquid coexistence curve anomaly (*Russian*) 8-75824
 solubility in SiC, exam. 8-79816
 storage, in La₂Ni₃, neutron, X-ray diff. study 8-83954
 tracing in Icelandic hydrothermal systems 8-69386
 trapped in stainless steel, ion induced release 8-95095
 trapping and replacement of 1 to 14 keV H and D in stainless steel 8-95070
 trapping in irradiated stainless steel 316 8-95069
 trapping up to 7 eV in austenitic stainless steel 316, depth profiles 8-71751
 D-T pellet, ideal gas treatment, implosion and shock waves 8-55735
 Cl+D₂→DCl+Cl, LEPS pot. energy surface, rate const., isotope effect, quasiclassical trajectory calc. 8-56887
 D NMR, hydrocarbon chain ordering in model membrane, D quadrupole splitting 8-64947
 D⁺, polarised prod. in ¹H+Cs atomic collision at 40 keV, 3.1 μA 8-55078
 D/H ratio in Uranus atmosphere, meas. 8-57497
 D-³He satellite fusion reactor, field-reversed mirror confinement 8-70643
 D-D fusion reactor blanket, nucl. characts., summary 8-89973
 D-plasma, interaction with Al₂O₃, surface effects 8-53010
 D-T ball, compressive plasma fusion using CO₂ lasers 8-82507
 D-T charges, explosion-induced compression for thermonuclear microfusion, power station parameters 8-82508
 D-T layer implosion through nonhomogeneous transition layer 8-74465
 D-T plasma, ion-cyclotron wave spectra dispersion eqn. numerical soln. (*Russian*) 8-59561
 D-T plasma, kinetics of compression induced fusion chain reaction 8-50297
 D-T plasma ball, critical continuously shaped concentric explosive compression, approx. estimate 8-87473
 D+F₂, impulsive triatomic reaction, vibr. state distrib., impulsive energy release model 8-92456
 D+F₂(Cl₂), exothermic triatomic exchange reactions, prod. energy distrib., statistical dynamic model 8-92455
 D+H⁺→H+D⁺ near threshold rel. to HD molecule formation in interstellar medium 8-89239
 D+HCl(HBr)(HI), abstraction and exchange reactions 8-73025

deuterium continued

D+HF, kinetic isotope effect and temp. depend. 8-53202
 D+HF, vibr. threshold energies, reagent energy effects 8-85145
 D+HI→H+DI, Franck-Condon theory 8-60984
 D+M→D⁺+M⁺ (M=alkali metal atom), ion-pair form. 8-58779
 p-D₂, order-disorder phase transition 8-79726
 D₂, quadrupole mass filter sensitivities and β-particle induced exchange kinetics 8-58090
 p-D₂, solid, librion spectrum calc. 8-79677
 D₂, collision induced dissoc., positive and negative ions form. 8-50612
 D₂⁺, expectation values, Born-Oppenheimer, adiabatic and non-adiabatic results 8-82624
 D₂-³He, filled microspheres, implosion expts. 8-59672
 D₂-DT-T₂ mixture, solid and liq., props. for fusion reactor applications 8-66415
 D₂-filled cone, fusion neutron generation using explosive implosion of polyethylene shell 8-82510
 D₂+³⁸Cl, reactions, characterisation, effect of ethylene-I₂ scavenger 8-73071
 D₂+H₂, exchange reaction, gas phase, heterogeneous initiation (*French*) 8-85149
 D₂+H₂, reactive and inelastic scatt. using repulsive model pot. energy surface 8-66620
 D₂+H₂, exchange reaction, steady-state, surface reaction effects (*French*) 8-85148
 D₂+H₂→2HD, transition state, study of Jahn-Teller instability of H₄ 8-60995
 D₂+H⁺, differential inelastic and reactive scatt., low energies 8-62911
 D₂+He, vibr. deexcitation, cross sections, rate const., vibr. rot. model 8-62879
 D₂+He, vibr.-rot. transitions, optical potential approach 8-62885
 D₂+Ne⁺, elastic scatt. at small angles, 1.3-3.5 keV, scaling law 8-82812
 D₃, collision induced dissoc., positive and negative ions form. 8-50612
 D₃⁺+inert gas, ion decay, 1-40 eV (*Russian*) 8-90286
 D(⁶Li)-T, inertially-confined, high thermonucl. gain with low T inventory 8-58403
 DT, solid and liq., fusion reactor applications 8-66415
 F+D₂, electronic-to-rot. energy transfer cross sections 8-86935
 H/D ratio in planetary atmospheres, determ. from CH₃D 9613 Å band 8-86861
 H⁺+H(D), elastic scatt. and charge exchange, resonances 8-78777
 HCl-D₂-He mixture, gasdynamic laser theory, gain depend. on parameters 8-50761
 HD, detect. in Saturn and Uranus atms., D/H abundance ratio calc. 8-57495
 HD+D₂, rot. inelastic differential cross sections, diffr. oscils. in 8lastic and inelastic scatt. 8-74743
²H-²H molten-salt-cooled fusion reactor blankets, nuclear heating and radiation leakage 8-78490
 N₄⁺+D₂, reaction rate determ. 8-60985
 O⁺+D₂→OD⁺+D, crossed beam studies product ang. and energy distrib. 8-53203

deuterium compounds

see also heavy water

DBR, vibr. energy transfer, laser selective isotope excitation 8-82790
 DCN, photodissoc., vibr. energy states population meas. 8-58751
 DCN, self-assoc. in matrices, IR vibr. spectra of multimers 8-86858
 DCl, isotope exchange reactions, equilib. const., adiabatic correction, electron correl. effects 8-88626
 DCl, two photon reson.-enhanced third harmonic generation 8-87094
 DCl, vibr. energy transfer, laser selective isotope excitation 8-82790
 DCl(HCl)+Ar potential, asymmetric, isotope substitution effect, Legendre expansion coord. transformation 8-70894
 DF chemical laser, jet curtains for gas containment 8-63099
 DF laser, pulsed unstable resonator, mode control and performance studies 8-82995
 DF, laser action by pulsed microwave discharge 8-58998
 DF-HF CW lasers, performance, computer modelling 8-71094
 DF+Ca(SR), beam reaction, vibr. excitation 8-68877
 DN₃, IR multiphoton dissoc., form. and reaction of electronically excited ND 8-80771
 DN₃+ND⁺→ND₂⁺+N₃, chemiluminesc. reaction of electronically excited species, rate const. 8-80771
 DNC, anharmonic force field, equilib. struct., rot. const. and bond lengths 8-90147
 D₂O ice, thermal cond., H and D order effects 8-67871
 D₂O, saturated and superheated steam, eqn. of state up to 500°C 8-79401
 D₂O-H₂O ice, thermal cond., H and D order effects 8-67871
 D₂O₂, lattice phonons by neutron scatt., covalent force model 8-67782
 D₂O₂⁺, isotope effects, easily polarisable H and D bonds 8-94231
 D₂SiCl₃, Raman and IR spectra, mol. motion 8-64353
 D₃SiNCO, low freq. bending mode, pot. function 8-82728
 DX+F, (X=I, Br, Cl), H abstraction, absolute reaction rate, H/D isotope effect 8-80721
 HD, quadrupole mass filter sensitivities 8-58090
 H(D)I+Cl, exothermic triatomic exchange reactions, prod. energy distrib., statistical dynamic model 8-92455

deuteron effects

refractories, swelling on proton, deuteron and He ion bombardment 8-67750
 silicate glasses, swelling on proton, deuteron and He ion bombardment 8-67750
 Nb₃Sn superconductor, low temp. deuteron irradiation 8-52182
 Ni, irradi. induced creep, defect investigation 8-80597
 Pt, deuteron irradi., close Frenkel pair recomb. during annealing 8-87716

deuteron interactions see deuteron-nucleus reactions; hadron-deuteron interactions; lepton-deuteron interactions; meson-deuteron interactions; photon-deuteron interactions; proton-deuteron interactions

deuteron-nucleus reactions

for inelastic deuteron-nucleus scattering, see 'deuteron-nucleus scattering'
 see also nuclear fusion
 cumulative effects, phenomenological model for pion prod. and elastic scattering involving deuterons 8-58267
 (d,p) off-shell effects 8-62545

deuteron-nucleus reactions continued

- light ion direct reactions, polarisation expts., tensor polarised deuteron beams 8-54732
- multi-nucleon transfer and direct reactions, nuclear struct., review 8-50060
- rare earth nuclei (d,t) reactions, band heads, two-step process 8-62551
- spallation in d+nucleus reactions distrib. of spectator neutrons, theory and expt. comparison (*Russian*) 8-58290
- (d,³He) on ¹²C, ¹⁶O, ²⁴Mg, ⁴⁰Ca, 29 MeV, polarised d, low lying analogue states, DWBA anal. 8-82285
- (d,p), reduced normalisations 8-86522
- (d,p) reactions, stripping of relativistic deuterons, Glauber theory 8-94014
- (d,t) anomalous transitions in rare earths, inadequacy of CCBA 8-70543
- (d,t) on ¹²C, ¹⁶O, ²⁴Mg, ⁴⁰Ca, 29 MeV, polarised d, low lying analogue states, DWBA anal. 8-82285
- ²⁷Al(d,³He)²⁶Mg, 12.4 MeV, tensor analysing power, D-state component in ³He wave function 8-54769
- Al(d,p), 6.3 GeV/c, p momentum spectra from d breakup 8-89887
- ³⁸Ar(d,pv), 4.4 MeV, ³⁹Ar, energy level spin and parity assignments, level spectroscopy 8-93943
- ⁴⁰Ar(d,p) and ⁴⁰Ar(d,n), lifetime meas. of ⁴¹Ar, ⁴¹K, by DSA method 8-78308
- ¹⁹⁷Au(d, f), 2.1 GeV, binary and ternary fission kinetics (*French*) 8-70577
- ¹⁰B(d,α), cross-section contrib. from ⁸Be 3⁺ states, isospin mixing model 8-89789
- Be+d neutron source, material damage study, He prod. and neutron fluence per neutron obs. in irradiated material 8-86710
- ⁹Be (d,t), cross-section contrib. from ⁸Be 3⁺ states, isospin mixing model 8-89789
- ⁹Be(d,α)⁷Li 12.17 to 14.43 MeV, α ang. distrib., excitation functions 8-54770
- ⁹Be(d,py)¹⁰Be, 1.5 MeV, angular correlation meas. 8-94015
- ⁹Be(d,t)⁸Be 12.17 to 14.43 MeV, t ang. distrib., excitation functions, spectroscopic factor 8-54770
- Bi (d,p), 6.3 GeV/c, p momentum spectra from d breakup 8-89887
- ²⁰⁸Bi(d,f), 2.1 GeV, binary and ternary fission kinetics (*French*) 8-70577
- ¹²C+d, 1.1-4.6 GeV/nucleon, nuclear fragmentation meas. (*Russian*) 8-54773
- ¹²C(d,α)¹⁰B(1.74 MeV, T=1), coupled channel anal. of energy depend. isospin violation 8-70541
- ¹²C(d,p)¹²C*, reaction mech., relation to ¹²C(d,d), S-matrix theory, 1.63 to 2.05 MeV (*Chinese*) 8-78393
- ⁴¹Ca(d,p), wave functions of O⁺ states in ⁴²Ca 8-74308
- ⁴¹Ca(d,p)⁴²Ca, 11 MeV, cross section, vector analysing power, spectroscopic strengths 8-74374
- ⁴⁸Ca(d,p), 11.9 MeV, analysing power, cross section, ⁴⁹Ca levels, spins, parities, spectroscopic factors 8-78391
- C(d,p), 6.3 GeV/c, p momentum spectra from d breakup 8-89887
- ⁵⁹Co(d,p), 14 MeV, ⁶⁰Co, level struct., spectroscopic factors, DWBA anal. 8-86478
- D+d reaction, 6.8 to 11.1 MeV, beam dosimetry 8-53509
- D(d,n)³He, 1.1 to 2.5 GeV/c, energy depend., cross sections, reaction mech. 8-54643
- ¹⁶⁸Er(d,t)¹⁶⁷Er, 17 MeV, band heads, two-step process 8-62551
- ⁴⁶Ge(d,³He) 26 MeV, A=70, 72, ⁴⁶Ge, A=69, 71, spectroscopic factors, occupation number anomalies 8-82279
- ⁴⁶Ge(d,³He) 26 MeV A=74, 76, ⁴⁶Ge, A=73, 75, deduced levels, occupation number anomalies, spectroscopic factors 8-82279
- ²H(d,n)³He, 6 to 17 MeV, n prod. absolute differential cross sections 8-74373
- ²H(d,pnd), 52 MeV, breakup mechanism 8-74375
- ²H(d,t)³H, differential cross sections calc. using DWBA, distortions 8-54772
- ³H(d,n)⁴He, 150 keV, vector polarised deuterons, n-p analysing power 8-62544
- ³H(d,n)⁴He, 6 to 17 MeV, n prod. absolute differential cross sections 8-74373
- ³H(d,n)⁴He, 700 keV, n polarisation meas., scintillation + TOF technique 8-86538
- H(d,p), A=1,2, 6.3 GeV/c, p momentum spectra from d breakup 8-89887
- ³He(d,α)³H, use in depth resolution by ³He profiling 8-58557
- ⁴He(d, n), 50 MeV, neutron polarisation meas. 8-70726
- ⁴He(d,p)³He n, 15 MeV polarised deuterons, differential cross sections, vector analysing powers 8-89884
- ⁶Li+d→αα*→αtp, 1.2-8 MeV, ⁸Be, highly excited αα* states 8-78262
- ⁶Li(d,α)⁴He*, 13.6 MeV, α spectra, excited state of ⁴He, spin, parity 8-54771
- ⁷Li(d,α)⁴He, E_d=250 to 750 keV, cross section determ. in absolute current meas. reaction chamber (*French*) 8-78388
- ⁷Li(d,αn), 7.0 MeV, prevalence of ⁸Be formation 8-82357
- ²⁴Mg(d,⁶Li)²⁰Ne, 28 MeV, α pick up, angular distrib. and spectroscopic factors 8-78352
- ²⁴Mg(d,n)²⁵Al, stripping reactions to unbound states from p-n correlations, spin, parity and widths 8-62547
- ²⁴Mg(d,p)²⁵Mg, stripping reactions to unbound states from p-n correlations, spin, parity and widths 8-62547
- ²³Mg(d,α), 12.07 to 11.57 MeV, angle-integrated cross section, ²³Na, spin, parity, energy levels 8-50179
- ¹⁴N(d,p)¹⁵N*, Q-value, test of differential hysteresis in Enge split-pole spectrograph 8-55082
- ¹⁵N(d,p)¹⁵N off-shell effects 8-62545
- ¹⁴⁴Nd(d,t)¹⁴³Nd, 12.1 MeV, ¹⁴³Nd nucleus levels, intermediate coupling unified model calcs. 8-89791
- ²⁰Ne(d,α), 10.5 to 12.0 MeV, tensor analysing power meas., ¹⁸F level spin, isospin and parity assignments 8-74305
- ¹⁶O(d,⁶Li), 80 MeV, ¹²C deduced levels and spectroscopic factors, ang. distrib., DWBA anal. 8-94013
- ¹⁶O(d,⁶Li)¹²C, 50, 65, 80 MeV, energy depend., spectroscopic factors 8-74372
- ¹⁶O(d,p)¹⁷O, coupled channel variational method for multi-step direct nuclear reactions. II. Test on a (d,p) reaction 8-66259
- ¹⁷O(d,t) and (d,τ) pick-up reactions, particle-hole spectra of ¹⁶O, ¹⁶N, spectroscopic strengths 8-58288
- ¹⁸O(d,α), 8.5 to 11.3 MeV polarised deuterons, ¹⁶N levels, spin parity assignments 8-89886

deuteron-nucleus reactions continued

- ¹⁸O(d,t), 17 MeV, ¹⁸O ground state wave function 8-66287
- ³¹P(d,p), 1.5-2.5 MeV, ³²P spectroscopic factors and level transition excitation function anal. 8-74371
- ²⁰⁷Pb(d,f), 2.1 GeV, binary and ternary fission kinetics (*French*) 8-70577
- ²⁰⁸Pb(d,3n)²⁰⁷Bi, spin and parity assignment of ²⁰⁷Bi levels 8-89788
- ²⁰⁸Pb(d,nv), half life of ²⁰⁹Bi 2442.8 keV lowest 2p 1h state 8-74331
- ¹⁴¹Pr(d,3n), simple formula for excitation functions 8-93978
- ¹⁹⁶Pt(d,t), A=192-198, even, 26 MeV, levels obs. 8-50089
- ¹⁹⁶Pt(d,p) 13.5 MeV, ¹⁹⁷Pt states from ang. distrib. and spectroscopic factors 8-78267
- ¹⁹⁶Pt(d,t) 13.5 MeV, ¹⁹⁷Pt states from ang. distrib. and spectroscopic factors 8-78267
- ²³⁹Pu(d,p), 4.0-6.2 MeV, reson. in fission probabilities of ²⁴⁰Pu 8-78429
- ³²S(d,α)³⁰P, statistical fluctuations at 135°, 2.0-2.5 MeV 8-89882
- ³²S(d,p)³³S, statistical fluctuations, at 135°, 2.0-2.5 MeV 8-89882
- Se (d,p), 12.5 MeV, ^{77,79,81,83}Se level struct., spins, parities, cross section, vector analysing power 8-89885
- ⁷⁴Se(d,p), 6 MeV, ⁷⁵Se energy levels, DWBA, sum rule anal., spectroscopic factors 8-66285
- ²⁸Si(d,p), 6 to 10.46 MeV polarised d, study of Ericson fluctuations 8-54735
- ²⁸Si(d,p)²⁹Si, 1.0 to 2.5 MeV, excitation functions and angular distrib., DWBA anal. 8-62543
- ⁸⁸Sr(d,p)⁸⁹Sr, 12 MeV polarised d, ⁸⁹Sr level transitions and spin assignments 8-66286
- ²³²Th(d,f), 2.1 GeV, binary and ternary fission kinetics (*French*) 8-70577
- ²³⁸U(d,f), A=235, 238, 2.1 GeV, binary and ternary fission kinetics (*French*) 8-70577
- ²³⁴U(d,t), 14 MeV, states in ²³³U 8-66208
- ²³⁵U(d,pf), 23 MeV, total KE release 8-78426
- ²³⁸U(d,p), 12 MeV, ²³⁹U level assignments 8-66209
- ¹⁷⁶Yb(d,nv), 14 MeV, gamma-ray spectra (*Russian*) 8-54720
- Zr+d, excitation functions and thick target yields 8-50182

deuteron-nucleus scattering

- antisymmetrisation effects on d-heavy nucleus scattering, nuclear matter model 8-70545
- eikonal approx. and distortions in heavy particle stripping mechanism (*Russian*) 8-78337
- elastic deuteron-nucleus scattering, breakup corrections to spin depend. 8-58289
- inelastic reactions at 3.6 GeV/nucleon 8-82358
- (d,d) 12 MeV, tensor polarised, differential cross section, vector and tensor analysing power 8-78357
- ⁴⁰Ar(d,d), optical model parameter investigation using 9-12 MeV polarised d 8-94016
- ⁹Be(d,d), 12.17 to 14.43 MeV, elastic and inelastic scatt., optical model anal. 8-89883
- ¹²C(d,d)¹²C, reaction mech., relation to ¹²C(d,p), S-matrix theory, 1.63 to 2.05 MeV (*Chinese*) 8-78393
- ¹H+d, polarised projectile, parity nonconservation in low energy scatt. 8-66271
- ¹H(d,dy) 6.3-7.1 MeV, bremsstrahlung anomaly near breakup threshold 8-89888
- ²H(d,f), 4.3, 6.3 and 8.9 GeV/c, struct. of secondary d spectra high momentum parts (*Russian*) 8-78394
- ³H(d,d), elastic scatt. √s=53 GeV, narrow min, and inelastic shadow effects, Glauber theory 8-89740
- ⁴He(d,d), Faddeev Lovelace eqn. soln. 8-54767
- ²⁴Mg+d, 10 MeV vector polarised deuterons scatt., nuclear shape effects, optical pot., analysing power 8-54768
- Mo(d,d), A=92, 94, 96, 98, 100, elastic, inelastic scatt., coupled channel, optical model anal., deformation parameters 8-94017
- ²⁰⁸Pb(d,d'), 14, 17 MeV, direct population of collective states, multiplets, deform. parameters 8-74376
- ³S+d, 10 MeV vector polarised deuterons scatt., nuclear shape effects, optical pot., analysing power 8-54768
- Se(d,d), polarised deuterons, vector analysing power, optical model calcs. 8-62550
- ²⁸Si+d, 10 MeV vector polarised deuterons scatt., nuclear shape effects, optical pot., analysing power 8-54768
- ²⁸Si(d,d'), 6 to 10.46 MeV polarised d, study of emission fluctuations 8-54735

deuteron photodisintegration

- γd→pn, 350-700 MeV, p polarisation meas. 8-82215
- γd→ppn*, cross section, double pion photoprod. on one nucleon 8-70378
- ²H photodisintegration and electrodisintegration, weak interaction and P nonconservation 8-89849
- ²H(γ, pp)π⁻, high momenta of emitted nucleons 8-70512
- ²H(γ,p)n, forward proton prod., low energy theorems 8-70510

deuteron polarisation

- depolarisation during acceleration and storage of polarised protons and deuterons 8-58519
- polarimeter designs for high energy p and d beams, polarised beam spin anal. 8-58516
- vector polarised deuterons in ³H(d,n)⁴He at 150 keV, n-p analysing power 8-62544
- γd→n⁰d, recoil deuteron polarisation statistical tensors anal. 8-74348
- πd scatt., 142 MeV, polarisation observables 8-78210

deuteron scattering see *deuteron-nucleus scattering; hadron-deuteron scattering; lepton-deuteron scattering; meson-deuteron scattering; photon-deuteron scattering; proton-deuteron scattering*

deuterons

- see also *cosmic ray deuterons*
- 6 quark system, wave function, elastic form factor, NN forces, spectroscopy (*Russian*) 8-50015
- beam production, by localised source in focused discharge 8-58093
- break-up effect in two-step process 8-62534
- charge form factor accompanying high imparted momentums (*Russian*) 8-58189
- D-state about 4%, appl. to reaction data anal. 8-70461
- D-state probability, review of spin, binding energy, magnetic and quadrupole moment 8-62488
- EM form factors at large transferred momentum, six-quark state (*Russian*) 8-89715

deuterons continued

- EM quadrupole form factor peak value, determination of percentage D-state 8-93950
- form factors relation to wave functions 8-70462
- propagation in nuclear matter, spin depend. of d optical pot. and binding energy 8-70545
- stripping cross sections to a resonance, exact and DWBA anal. comparison 8-93985

developers (photographic) see photographic materials**development, photographic see photographic process****development management see research and development management****diagnosis, patient see patient diagnosis****diagnostics, plasma see plasma diagnostics****diagrams**

- see also Feynman diagrams; nomograms; Nyquist diagrams; phase diagrams
- high cycle fatigue diagram based on dynamic severity criterion 8-60759

dialogue programming see interactive programming**diamagnetic properties of substances**

- see also de Haas-van Alphen effect; diamagnetism
- aromatic compounds, diamag. susceptibility 8-80123
- glass, small ang. optical beam polariz., by Faraday rot. (Korean) 8-50918
- graphite ribbon, interlayer interaction effects on diamagnetism London theory 8-52201
- halomethanes, ^{13}C chemical shifts, diamag. susceptibility, effect of non-bonded interactions 8-78726
- marble, mag. susceptibility anisotropy development through cryst. preferred orientation of calcite 8-56286
- mesomorphic mixtures, binary phase diagrams, thermodynamic props., diamag. anisotropy 8-95139
- 4-octyloxy-4'-heptyl- α -cyanstilbene liquid cryst., mag. props. 8-87615
- PAA, nematic liq. cryst., thermomagnetic behaviour (French) 8-87612
- PAP, nematic liq. cryst., thermomagnetic behaviour (French) 8-87612
- poly- γ -benzyl-L-glutamate, soln., liq. film, diamagnetic susceptibility 8-74794
- BaTiO_3 , magnetochemical exam. of phase transition, mag. suscept. meas. 8-88265
- C fibre reinforced epoxy resin, diamag. susceptibility as fibre alignment characterisation method 8-84381
- C-C composites, existence diagram and properties (French) 8-64517
- CaCO_3 , calcite, cryst. preferred orientation in marble, mag. susceptibility anisotropy development 8-56286
- CdTe:Ge , mag. props. 8-56289
- Cu-Ga(Ge) , liq., mag. susceptibility 8-72326
- $\text{Cu}_x\text{V}_2\text{O}_5$, nonmetallic bronze, low field sp. ht. and mag. suscept. 8-72357
- Ge-As-Te system, glasses, magnetochemical exam. 8-88092
- $\text{IrGe}_{1.5}\text{S}_{1.5}(\text{Se}_{1.5})$, new skutterudite relation compounds, prep. and charact. 8-52700
- $\text{IrSn}_{1.5}\text{S}_{1.5}$, new skutterudite relation compounds, prep. and charact. 8-52700
- $\text{Mo}_6\text{Cl}_{10}\text{S}$, struct., dielec. and diamag. props. (French) 8-67691
- $\text{Mo}_6\text{Cl}_{10}\text{Se}$, struct., dielec. and diamag. props. (French) 8-67691
- $\text{Mo}_6\text{Cl}_{10}\text{Te}$, struct., dielec. and diamag. props. (French) 8-67691
- Na-Cd, liq., mag. susceptibility 8-72326
- Na-Tl, liq., mag. susceptibility 8-72326
- $\text{Na}_2(\text{Fe}(\text{CN})_5\text{NO})\cdot 2\text{H}_2\text{O}$, powder, Mossbauer absorption in mag. field 8-68418
- $\text{Na}_x\text{V}_2\text{O}_5$, nonmetallic bronze, low field sp. ht. and mag. suscept. 8-72357
- P-As-Se glasses, mag. susceptibility, dielec. const., opt. props. 8-64184
- $\text{RhGe}_{1.5}\text{S}_{1.5}$, new skutterudite relation compounds, prep. and charact. 8-52700
- ScN_x , region of homogeneity, physicochem. props. 8-52018
- Si, liq., mag. susceptibility and diamag.-paramag. transition at melting pt. 8-95415
- YbCl_2 , mag. props., 77-292K 8-52197

diamagnetic resonance see cyclotron resonance**diamagnetism**

- see also cyclotron resonance; de Haas-van Alphen effect; diamagnetic properties of substances
- electron gas, classical diamagnetism, Gibbs method (Russian) 8-73918
- EPR of V^{4+} in diamagnetic lattice, cryst. field effects 8-64263
- ionic cubic lattice in homogeneous mag. field, oscillations 8-91868
- molecular diamagnetic susceptibility, interatomic charge transfer in diatoms, mol. second moments, additivity formulas 8-70961
- simple metals, solid and liq., electronic struct., mag. susceptibilities calc. 8-52204
- two-phase conducting diamagnetic system, coeff. of EM ejection of particles (Russian) 8-94364
- type II superconductors, fluctuation induced diamagnetism above H_2 8-80097
- Ba, diamag. quasi-Landau spectrum near ionis. threshold, two-photon ionis. spectra obs. 8-58642
- Na, Rydberg states, diamag. struct. 8-50484
- ^{85}Rb , ground state dipole HFS diamagnetic shift, high field optical pumping expt. 8-90129
- Sr, diamag. quasi-Landau spectrum near ionis. threshold, two-photon ionis. spectra obs. 8-58642

diameter measurement

- cortical bone diameter meas., manual and computer-aided methods comparison 8-85376
- dimensional gauging using scanning laser beam 8-57898
- droplet, transparent, diameter meas. by side reflection 8-59518
- electrically conductive filaments, fine and superfine, instrument for contact free measurement 8-93655
- erythrocytes of human blood, diameter meas. by specific elec. cond. 8-53353
- internal gauge, microinterferometer IZK-61 8-89438
- optical fibre, computerised forward scattered light system appl. 8-62176
- Pioneer images of Galilean satellites, edge-finding technique for dias. determ. 8-85893
- specimen cross section during low temp. compression, apparatus design 8-57940

diameter measurement continued

- tape-controlled remote automatic diameter meas. machine, report 8-86241
- threads, meas. by three wire method, influence of shape deviation of taut measuring wires (German) 8-77845

diamond

- artificially coloured diamonds, spectroscopic diagnostic technique 8-65281
- brilliance, sparkliness and fire of diamond simulants 8-90363
- composite with Cu-Ti matrix, microstresses, X-ray diffr. exam. 8-56679
- Compton profiles, X-ray struct. factors, band struct., LCAO calc. 8-51889
- core electron expansion, kinetic energy in Compton profiles 8-72628
- diamond:B, thermoluminesc., TSC, correlation meas. 8-88369
- diamond:B hopping conductivity in range 12 to 1300K 8-51994
- diamond, pseudopotential method of band struct. anal. 8-51886
- diamond, radiation detector for light and charged particles 8-49900
- dielectric breakdown, two-photon absorpt. and other optical damage mechanisms 8-84684
- dielectric function, optical frequency model calcs. 8-51921
- dielectric properties, mean point value calc. 8-87930
- electron irradiated, type Ib, migration of N, optical absorption meas. 8-56505
- electronic energy bands of diamond-type crystals, appl. of EHT method 8-87907
- elementary excitations in crystals, dielectric theory 8-60076
- enthalpy of solution at 1320K, heat of transformation to graphite 8-59945
- EPR, of electron irradi. type IIa diamond at liquid N_2 temp. 8-76310
- erosion impact of annealed 310 stainless steel, SEM and TEM study 8-64725
- ESR studies, review 8-95521
- Fresnel diffraction at platelets, defect struct. anal. by 3 Å phase-contrast microscopy 8-87701
- GR defect, high resolution optical spectra after electron irradi. 8-56515
- high pressure cell used in automatic diffractometer up to 90-kilobars 8-54387
- identification from reflection pattern photographs 8-54481
- ion implantation, review 8-87698
- Jahn-Teller coupling at ND1 and GR1 centres 8-56103
- lattice dynamical calc. using extended Born-von Karman scheme 8-59889
- linewidth of GR2-8 transition 8-60488
- magnetic field and stress splitting of GR1 line 8-60095
- metal-diamond interface, Schottky barrier theory, ionicity depend. 8-52086
- natural, N3 luminesc. decay time 8-76520
- phonon frequencies, model calc. using tight binding Hamiltonian 8-59894
- plastic deformation at room temperature 8-52927
- plastically deformed, EPR of two N atom centre 8-72408
- powder, rapid oxidation development, kinetic model (French) 8-68917
- pressure calibration by resistance-jump transitions up to 500 kilobars 8-54388
- resonant Raman scatt., first and second order 8-60471
- round brilliant cut diamond, statistical assessment of brilliance and fire 8-90361
- round brilliant cut diamond style modifications, brilliance, sparkliness and fire 8-90362
- Schottky barrier, electronic struct., pseudopot. calc. 8-95364
- Schottky barriers, photocapacity meas. 8-52057
- semiconducting, depend. of energy gap on short-range order 8-84142
- semiconducting, GR1 cathodoluminescence, fine struct. 8-68566
- semiconductor properties and use for making devices, review 8-60131
- sintering under high press., binary inclusion-diamond interaction (Chinese) 8-80484
- spin-spin interaction of N_2 and Ni centres, temp. effects 8-83177
- stress effects on GR 2-3 absorption lines 8-72563
- surface soldered to metal film, contact strength determ. device 8-60910
- synthetic, carbonado type, struct. and microhardness 8-84994
- synthetic, elec. cond. 8-56144
- synthetic, electroluminescence excitation mechanism, role of defects 8-52581
- synthetic and natural, neutron irradi., optical and elec. props. (Russian) 8-59841
- synthetic micropowder, degree of charging of polished Ti and Fe surfaces 8-60880
- thermal conductivity of single cryst. 8-65921
- tool, polycrystalline, wear in rock removal processes 8-64724
- vibrating suspension, defective surface layer formation on transparent materials (Russian) 8-53007
- wear on steel, effects of clean surface reactions 8-85008
- X-ray diffraction, three and four wave, comparison of diamond type crystals. 8-67608
- zone-centre optical phonon, effect of uniaxial stress, elastic consts. determ. 8-91399
- Fe/Mg partitioning between coexisting olivines and orthopyroxenes (Portuguese) 8-65284
- N_2^{+} + Group IV elements and oxides, XPS and UPS prod. determ. 8-73084

diaphragms**see also valves**

- pressure-force transducer using 32.768 kHz X-Y flexure watch crystal 8-57934

dichroism**see also magnetic circular dichroism; pleochroism**

- acridine C-radical, polarised absorpt. and ESR spectra, dichroism and HF-Cl calc. 8-50563
- adipic acid, monoclinic crystals, IR absorption and dichroism 8-88293
- alkali halides, photodichroic, as optical processing elements 8-83056
- atomic degenerate system, Doppler-free laser-induced dichroism and birefringence 8-82711
- 1,1'-bianthryl derivatives, dimer optical activity, vibronic circ. dichroism, theoretical anal. 8-62821
- biaryls, dimer optical activity, vibronic circ. dichroism, theoretical anal. 8-62821
- Bowman-Birk soybean proteinase inhibitor, gamma irradi. 8-53343

dichroism continued

- butadiene chromophores, *cis*- and *trans*- (α - and β -phellandrene) absorpt. and CD spectra 8-62834
 (X)-D-camphor, circularly dichroic band at 3000 Å, RPA calc. 8-94267
 chiral molecule, interference effects, natural dichroism line shape 8-82758
 cholesterylalkanoates, liq. cryst., optical anisotropy and struct. ordering (*Russian*) 8-87616
 circular dichroism meas. in vacuum UV 8-49913
 composite thermal/visual display superposition technique 8-77992
 condensed phases, picosec. relax. polarisation spectrosc. meas. 8-68530
 conjugated molecules, linear and mag. cir. dichroism interpretation 8-62835
 cyanine dyes, J-aggregates, swirl-induced optical activity 8-72482
 β -cyclodextrin-azulene complex, circular dichroism spectra 8-58713
 cylinder, optically active, EM wave scatt. 8-82912
 disperse systems, electro-optical phenomena, induced dichroism rel. to elec. field calc. 8-50699
 DNA, monodisperse, rod-like mols., transient elec. dichroism 8-94344
 ferricytochrome c structure, effect of different phospholipids 8-68981
 form dichroism, theoretical treatment, determ. of macromol. shape 8-60417
 garnets, doped, site symm. exam., ang. variation of induced linear dichroism 8-95429
 gas, reson. optical activity induced by right-left nonsymm. mol. collisions 8-75254
 liquid crystals, guest-host interaction, optical shutter appl. 8-74988
 macromolecular, solutions, mol. orientation, time-depend. torque, rot. diffusion eqn. 8-68471
 MBBA, electronic spectra 8-52530
 β -naphthol, IR dichroic ratio, oriented gas and effective charge models calcs. 8-60437
 photoacoustic spectroscopy, dichroism meas. 8-62227
 photoreceptor form dichroism in vertebrates 8-56969
 planar molecules in stretched polymer films, solute orientation, transition moment direction, dichroic spectra 8-58742
 polycarbonate, glassy, IR dichroism at small strains 8-56475
 polyethylene, polarised Raman studies of crystalline and amorphous orientation 8-67660
 polymer orientation measurement, in solid, by spectroscopic techniques, mech. anisotropy 8-75558
 polytetramethylene oxide-polytetramethylene terephthalate, block copolymer, props. 8-51438
 pressure jump method for fast kinetics using optical rotation and circular dichroism 8-77175
 ribosomal protein S4 from *Escherichia coli*, circular dichroism obs. of conformation 8-96003
 spectroscopy, circular dichroism sum rules, SCF mol. orbital theory 8-58059
 twisted anisotropic media, light propag., appl. to photoreceptors 8-63004
 vibrational circular dichroism spectrometer, using CaF₂ photoelastic modulator and Xe lamp 8-54476
 KCl:I crystals, V-band development using X-rays 8-88337
 KCl:Na, photoinduced reorientation of A-centres near room temp. 8-64344
 KF:LiF, photodichroic, real time recording medium, for optical spectrum analyzer 8-71174
 LiNbO₃:Co, optical props. 8-64383
 MoS₂(Se₂), effect of uniaxial stress on excitonic optical spectra 8-84606
 NdMoO₄, photoacoustic spectroscopy, dichroism meas. 8-62227
 Ne, two and three level systems, laser induced dichroism and birefr. 8-79065
 WS₂(Se₂), effect of uniaxial stress on excitonic optical spectra 8-84606
 ZnSiP₂, photocond. and photolum. spectra, optical anisotropy 8-72200

dictionaries *see glossaries***dielectric breakdown** *see electric breakdown***dielectric constant** *see permittivity***dielectric depolarisation**

- composite media, dielec. and optical props. 8-84546
 electret discharge model, injection relaxation mechanism, space-charge cond. 8-80279
 piezoelectric rod, depolarising-field effect, longitudinal effect extensional vibration 8-95551
 polyvinylacetate film, effect of electrode metals on depolarisation current characts. 8-76387
 TGS, vacuum-cleaved cryst., charge compensation, ferroelec. field effect obs. 8-95556
 H₂SO₄, solns., static permittivity, kinetic depolarisation, time-domain spectroscopy 8-68440
 PbZr_{0.95}Ti_{0.05}O₃, impact loading, mech. and elec. response, elec. state effect 8-64317

dielectric devices

- see also capacitors; ferroelectric devices; insulators; piezoelectric devices; pyroelectric devices; space-charge limited devices*
 particle track detector, for neutron dosimetry (*Czech*) 8-66425

dielectric function

- alloy, dil., wave-vector-nonconserving optical transitions 8-72100
 binary alloys, random, dielec. matrix and related props. 8-51916
 Brillouin scattering, resonant, analogy to modulation spectroscopy (*Japanese*) 8-68526
 n-butanol, dielectric response function, by lumped capacitance method 8-95539
 charged fluids near freezing point, static dielectric behaviour 8-56417
 complex reflection amplitudes of photons, sum rules 8-63006
 composite materials, small particle, optical props. 8-56445
 composite media, dielec. and optical props. 8-84546
 data presentation and interpretation 8-76376
 diamond, dielectric function, optical frequency model calcs. 8-51921
 diamond, dielectric properties, mean point value calc. 8-87930
 dispersion of dielectric axes in monoclinic and triclinic crystals related to lattice dynamics 8-87920
 electron dielectric function, second-order RPA 8-49753
 electron gas, generator coordinate method 8-60077
 electron liquid, density response function 8-67961

dielectric function continued

- elemental semiconductor, electric susceptibility from chemical-bond approach 8-51922
 elemental semiconductor, local field effects in static response 8-76010
 elementary excitations in crystals, dielectric theory 8-60076
 EM wave propag., self-consistent approach 8-51920
 ferromagnet, harmonic rotator, Coulomb plasma and related model, two dimens. case 8-88137
 ferromagnetic conductor, electric field response and electrofluctuation instability (*Russian*) 8-56083
 frequency dependent dielectric constant, rel. to dielec. polarisation 8-56425
 frequency dependent dielectric function of gapless semiconductors in a magnetic field 8-63994
 graphite, electronic props., self-consistent LCAO calc. 8-51887
 heavily doped semiconductor, n-type, Mott transition, dielec. enhancement and conduction electron screening, unified treatment 8-72073
 hemicylinder-air-quartz system, semi-infinite crystal, dispersion of surface phonon polaritons 8-71939
 Hubbard model, electrical conductivity calculation, dielectric function and plasma oscillations 8-64020
 Hubbard model, strong correlation limit 8-87929
 III-V semiconductors, ionic tetrahedral, electrical susceptibility, chemical bond approach 8-87931
 inhomogeneous media, elec. transport, optical props., exact theory 8-56119
 ionised impurity scatt. limited mobility in semiconductors with spatially variable dielec. function 8-51986
 Li, elec. resist., effects of core and correl. corrections 8-64026
 metal, highly reflecting, determ. of IR optical constants by surface plasmon excitation 8-76418
 metal, memory function for response of conduction electrons 8-56096
 metal, normal and magnetic, temp. depend. of plasma freq. 8-56100
 metal, optical functions, effect of surface roughness 8-56447
 metal, static dielectric permittivity sign (*Russian*) 8-76012
 metal surface electronic struct., linear response theory, appl. to Na 8-56197
 metallic particles, ultrafine, far IR absorpt. calc. 8-60454
 noble metals, pseudopot. exam. of electronic props. 8-51960
 phenanthrene, cryst., refl. spectra of first singlet transition 8-88323
 phonon-magnon interactions, dielectric function, theoretical anal. 8-80275
 polariton modes at interface between two conducting or dielec. media, review 8-87922
 polyethylene oxide, aq. soln., dielec. relax., interferometric transmission obs. 8-52437
 polyvinyl methyl ether, aq. soln., dielec. relax., interferometric transmission obs. 8-52437
 power law frequency dependent dielectric function and nonanalyticity properties 8-60387
 PVA, aq. soln., dielec. relax., interferometric transmission obs. 8-52437
 reflection spectra, Kramers-Kronig anal. with preliminary dispersion anal. 8-49915
 relativistic degenerate electron plasma, dielec. response function 8-71529
 sea ice, complex dielec. const., 0.1-40 GHz 8-61430
 semiconductor, reson. in fundamental absorpt. region, quasi-mol. model interpretation 8-76490
 static electron gas dielectric function, simple useful anal. form 8-79953
 surface, lattice force constant determination 8-71933
 thiourea, soft mode and Debye relaxations 8-80347
 transition metal oxides, dielec. behaviour 8-71703
 TTF-TCNQ, conductivity and dielec. permeability, freq. depend. 8-79984
 valence electrons, finite energy, f-sum rules 8-88276
 water-in-hexadecane, microemulsion, dielectric behaviour, Cole-Cole type relax., temp. depend. 8-56426
 zinc blende semiconductors, small-gap, electron scatt. and transport props. 8-95294
 zinc blende semiconductors, small-gap, electron scatt. and transport props. 8-95295
 zz 8-91367
 Ag particles, lattice defect influence on size effect 8-88329
 Ag surface, inert gases adsorption, physisorption energies 8-71944
 Cd_{1-x}Hg_xSe mixed cryst., electron mobility and electron scatt. 8-95296
 Cd_{1-x}Zn_xS 10 μ m film optical and electrical characterisation (*French*) 8-64153
 CeN, optical props. and valence mixture 8-56450
 Fe-Co alloys, optical and spectrosc. props. (*Russian*) 8-72529
 GaAs-AlAs and related monolayer heterostructures, pseudopot. calc. 8-60198
 GaP, upper polariton branch obs. by ATR 8-68510
 Ge, dielectric properties, mean point value calc. 8-87930
 Ge, IR absorption and scatt. by electron-hole drops 8-51903
 Ge, ionised impurity scatt. limited mobility in semiconductors with spatially variable dielec. function 8-51986
 GeSe₂, IR and Raman spectra 8-95585
 HgSe(Te), dynamic dielectric function, IR absorpt. meas. 8-68508
 p-HgTe, dynamic dielectric function, experimental and theoretical study 8-92069
 InSb inversion layer, electromagnetic mode 8-60080
 InSb-type semiconductor, spatial dispersion of permittivity 8-67967
 KNbO₃, complex electronic dielectric const. from tight binding energy bands 8-60054
 KTaO₃, complex electronic dielectric const. from tight binding energy bands 8-60054
 La, soft phonons, f-band induced instability 8-83907
 MgAl₂O₄, IR spectrum exam. 8-76454
 MgO, dielectric properties, mean point value calc. 8-87930
 Na (001) surface electronic struct., linear response theory 8-56197
 NaCl, dielectric properties, mean point value calc. 8-87930
 Na₂WO₃, intra- and interband plasmons, inelastic electron scatt. exam. 8-72098
 Pb₃(Ge_{1-x}Si_x)₂O₁₁, dielec. spectra, ferroelec. behaviour 8-60406
 Pd, optical properties, 0.1 to 6 eV 8-92092
 ReO₃, intra- and interband plasmons, inelastic electron scatt. exam. 8-72098
 Si, dielectric properties, mean point value calc. 8-87930

dielectric function continued

- Si, dielectric screening and zone-centre phonons 8-67785
 Si, ionised impurity scatt. limited mobility in semiconductors with spatially variable dielec. function 8-51986
 SiC, refractive index dispersion, 0.4-50 μm , 105-297K 8-84548
 α -Sn, dielectric properties, mean point value calc. 8-87930
 UO_2 , optical props. and electronic struct. 8-68527
 WO_3 film, intra- and interband plasmons, inelastic electron scatt. exam. 8-72098

dielectric hysteresis

- ferroelectric crystals, parameter meas. (*Polish*) 8-88272
 ferroelectric liquid crystals, temp. depend. of elec. susceptibility and spontaneous polarisation (*Japanese*) 8-68467
 ferroelectric materials, high press. studies, rel. to Earth and planetary interiors 8-69334
 ferroelectric thin film hysteresis, electronic system for display on CRO 8-89496
 polyvinylidene fluoride film, cryst. dipole orientation in elec. field 8-80286
 reversible nonlinearity in dielectric films 8-92024
 $\text{Ba}_{0.92}\text{Ca}_{0.08}\text{TiO}_3$ ceramic, uniaxial stress effects, US dilatometric and dielec. meas. 8-52454
 BaTiO_3 , doped, loss mechanism and domain stabilisation 8-84542
 $\text{KTa}_{1-x}\text{Nb}_x\text{O}_3$ film, RF sputtering, structural and electrical properties obs. 8-88426
 PLZT, transparent ferroelec., RF sputtering and film characterisation 8-72727
 $\text{Pb}(\text{Ti}_{1-x}\text{Zr}_x[\text{Fe}_{1/2}\text{Ta}_{1/2}])\text{O}_3$, pyroelec. props. at transition between ferroelec. phases 8-52447
 Rb_2ZnBr_4 , dielectric const. and ferroelectric hysteresis 8-84535

dielectric-loaded waveguides

- arbitrarily shaped dielectric body inside waveguide, three-dimensional anal. 8-71005
 complex dielectric constant of semiconductors as SHF, measurement techniques 8-95542
 EM field calc., produced by transverse electric waves (*Russian*) 8-82884

dielectric loss angle see *dielectric losses***dielectric loss-angle measurement** see *dielectric loss measurement***dielectric loss measurement**

- see also *dielectric losses*
 combined total reflection-transmission method, appl. to dielec. spectroscopy 8-86295
 glass-plastic, engineering, nondestructive structural identification 8-92422
 loss-angle meas. at 100 GHz range, precision, Fabry-Perot resonator 8-70163
 micrometer electrode for improved meas. in 1-200 MHz range 8-49864
 microwave resonator bridge method 8-54391
 on-line calculator-based meas. system 8-54397
 polar liqs. using a lumped-capacitance method for coaxial lines 8-77936
 procedure for measurement, using Q meter in freq. range 50 to 35 MHz 8-54394
 solid dielec., high sensitivity, using supercond. high-Q resonator 8-93733

dielectric losses

- see also *loss angle*
 aliphatic ethers, dil. solns., dielec. loss meas. for dielec. relax. 8-68451
 aminobenzotrifluoride, benzene soln., permittivity and dielec. loss 8-64320
 aminopyridines, in 1,4-dioxane soln., dielec. consts., losses and relax. 8-64319
 2,3-butanediol, dielectric dispersion 8-72455
 cellulose fibre, moist, dielec. props. 8-76380
 ceramics, ferroelec., dielec. losses due to domain wall oscill. 8-84541
 chloral, liq., permittivity, dielec. loss, up to 60 GHz 8-60384
 chlorobenzotrifluoride, benzene soln., permittivity and dielec. loss 8-64320
 dichloromethane-decalin glass, mol. dynamics, from dielec. loss meas., 107-148K, 293K 8-76379
 dicyanoalkanes, in benzene soln., microwave absorption, internal rot. 8-60385
 1,3-dihalopropane, dielectric permittivity and loss, dipole moment 8-60383
 EBBA, solid and liquid states, temp. and freq. depend. (*Russian*) 8-72450
 EBBA, stable and metastable solid phases, dielec. dispersion meas. 8-60390
 ester-imide varnishes, electroinsulating, thermal resist. (*Polish*) 8-84014
 4-ethylaminobenzil, dil. soln. in benzene, cyclohexane and dioxane, dielectric behaviour 8-52421
 ethyltrichloroacetate, liq., permittivity, dielec. loss, up to 60 GHz 8-60384
 explosive mixtures, dielec. consts. and losses below 100 kHz 8-56422
 nitrobenzotrifluoride, benzene soln., permittivity and dielec. loss 8-64320
 oxide glasses, elec. cond. and dielec. relax., correl. 8-79801
 parylene polymers, synthesis, elec., phys., corrosion props. (*German*) 8-64521
 polyester varnishes, electroinsulating, thermal resist. (*Polish*) 8-84014
 polyethersulphone, dielectric γ losses 8-68449
 polyethylene, dielec. relax. mechanism, 1-80K (*German*) 8-76384
 polyethylene, gamma radiation effects on dielect. parameters, expt. (*Hungarian*) 8-59836
 polyethylene, high-density, dielec. loss, below 4.2K, antioxidant, annealing and drawing effects 8-84518
 polyethylene, low density, dielec. behaviour, struct. props. influence (*German*) 8-92017
 polyferrocene film, plasma polymerised, dielec. props., 40 kHz to 50 MHz, 30-400°C 8-52439
 polymer, glass transition under high-press., dielec. loss method obs. (*Russian*) 8-71841
 polymer glass transition, dynamic props., mol. model (*Russian*) 8-87777
 polymer- TiO_2 composite, dielec. props. (*Japanese*) 8-95540

dielectric losses continued

- polypyromellitimide, low temperature relax., NMR, dielec. and mech. losses 8-71686
 polysulphone, dielectric γ losses 8-68449
 power law frequency dependent dielectric function and nonanalyticity properties 8-60387
 PVC, gamma radiation effects on dielect. parameters, expt. (*Hungarian*) 8-59836
 PVC-polyvinylidene chloride copolymer, dielectric loss at low-temp 8-95543
 solids and liquids, dielectric loss characterisation 8-88252
 styrene-butadiene-styrene triblock copolymers, dielec. props. 8-95545
 styrene-butyl vinylpyridinium-TCNQ copolymer, dielectric const. (*Japanese*) 8-60375
 styrene/n-butyl-2-vinylpyridinium-TCNQ copolymer, dielec. permittivity (*Japanese*) 8-56416
 transient excitation, energy flow analysis 8-80282
 tremolite asbestos, fibrous. elec. anisotropy 8-80273
 Ag_3SbS_3 , dielec. and acoustic props. (*German*) 8-64335
 $\text{Al-Al}_2\text{O}_3$ -Al, thin film capacitors, dielec. losses 8-76382
 Al_2O_3 film, dielec. props., AC and DC elec. characts. 8-68445
 $\text{Ba}_3\text{Fe}_2\text{ReO}_9$, siegnette magnets with hexagonal barium titanate structure 8-76397
 $\text{Ba}_3\text{Fe}_2\text{TeO}_9$, siegnette magnets with hexagonal barium titanate structure 8-76397
 $\text{Ba}_{0.54}\text{Sr}_{0.46}\text{Nb}_2\text{O}_6\text{:Y}(\text{La})(\text{Tm})$, dielectric and electrooptic props. 8-68466
 BaTiO_3 , c-domain cryst., HF dispersion of permittivity 8-60379
 BaTiO_3 , doped, loss mechanism and domain stabilisation 8-84542
 BaTiO_3 , monocrystalline, superposition of unidirectional electric field effect, time depend. (*Slovak*) 8-52435
 BaTiO_3 type perovskite ferroelectric, neutron irradiated, amplification of freq. dispersion of permittivity (*Russian*) 8-52419
 Ca_2SiO_3 , hydraulic reaction observed by microwave dielectric meas. 8-80745
 CeO_2 , elec. cond. and dielectric props. at low temp. 8-72447
 $\text{FeO-P}_2\text{O}_5$ glasses, electrical and mechanical losses 8-80283
 H_2O , adsorbed on kaolinite clays, dielec. props. 8-76381
 KNbW_2O_9 , crystallography, polymorphism and phys. props. 8-79599
 $\text{Li}_2\text{O-B}_2\text{O}_3$ glass, conductivity, permittivity, and dielectric loss obs., mixed isotope effect 8-95182
 $\text{Pb}_2\text{-Sr}_{1-x}(\text{Zr}_x\text{-Ti}_{1-x})\text{O}_3\text{:Cr}_2\text{O}_3$, ferroelec. ceramic, reversible characts. and dielectric losses (*Russian*) 8-84517
 $\text{PbBi}_4\text{Ti}_4\text{O}_{15}$ ceramic, dielec. props., temp. depend. 8-95561
 $\text{Pb}_3(\text{Ge}_{1-x}\text{Si}_x)_2\text{O}_{11}$, dielec. spectra, ferroelec. behaviour 8-60406
 PbI_2 single crystals, photo-induced AC impedance meas., photodielec. effect 8-52034
 $\text{Pb}(\text{Zr,Ti})\text{O}_3$ thin layers, tan δ temp. dependence obs. (*Bulgarian*) 8-88259
 $\text{Pb}(\text{Zr}_{0.47}\text{Ti}_{0.43}\text{Sn}_{0.10})\text{O}_3\text{:Cr}_2\text{O}_3$, ferroelec. ceramic, reversible characts. and dielectric losses (*Russian*) 8-84517
 rubber, gamma radiation effects on dielect. parameters, expt. (*Hungarian*) 8-59836
 SrTiO_3 , dielectric loss at microwave frequencies (*Russian*) 8-52440
 Ta-Ti-O, reactive sputtered film, elec. props. 8-84336
 TiO_2 film, RF sputtering, dielec. props. and X-ray phase analysis 8-80288
 ZnO pellets, and ZnO:Li single crystals, photo-induced AC impedance meas., photodielec. effect 8-52034

dielectric materials

- see also *antiferroelectric materials*; *dielectric thin films*; *electrets*; *ferroelectric materials*; *glass*; *insulating materials*; *insulation*; *piezoelectric materials*
 capacitor dielectric fluid test and anal., quality assurance 8-80272
 electro-optical inspection of internal defects 8-56869
 solid dielectrics, treing 8-80285
 thermal method of investigating hidden nonuniformities in flat dielectric materials 8-56868

dielectric measurement

- see also *dielectric loss measurement*; *permittivity measurement*
 conductive liquid Kerr constant meas. 8-88279
 electrospark inspection unit for tube defect obs. 8-92431
 fluids and dispersions, dielec. meas. using cell 8-93725
 microwave Q-factor meas. system 8-54396
 permeability of dielectrics with one sided access to part 8-89500
 Q-meter measurement range expansion method 8-74023

dielectric phenomena

- see also *dielectric hysteresis*; *dielectric losses*; *dielectric properties of substances*; *dielectric relaxation*; *dielectric resonance*; *electric strength*; *ferroelectricity*; *piezoelectricity*; *solvated electrons*
 apolar viscoelastic dielectrics, thermodynamic theory, linear effects 8-67059
 geminate recombination, time depend. Onsager problem anal. soln., critical elec. field 8-72446
 metal-semiconductor junction photoelec. phenomena, effect of dielectric gap and surface states (*Russian*) 8-84299
 plasma (fluid), hydrogenic, transverse dielec. function, excitation spectrum 8-67311
 radiative transfer in plane stratified dielectric 8-51050
 sphere, dielectric, motion in travelling elec. field 8-50685
 surface with accumulated air positive ions, vacuum breakdown obs. 8-75464
 wedge, review of theory of EM field behaviour 8-66712

dielectric polarisation

- see also *Barkhausen effect*
 alkali halide, exchange charge polarisation, dielectric const., Dick and Overhauser model 8-55832
 butanediol terephthalate-polytetramethylene oxide terephthalate copolymers, dielec. props. 8-95546
 chiral smectic C, ferroelec. props., dielec. meas. 8-52463
 composite media, dielec. and optical props. 8-84546
 education, homogeneous ellipsoidal inclusions, general theorems, Poisson theorem, dielectric polarisation, conduction and elasticity 8-61979
 electrical response of relaxing dielectrics compressed by shock waves, axial mode problem 8-80280
 ferroelectric crystals, parameter meas. (*Polish*) 8-88272
 ferroelectric liquid crystals, temp. depend. of elec. susceptibility and spontaneous polarisation (*Japanese*) 8-68467

dielectric polarisation continued

- frequency dependent dielectric constant, rel. to dielec. polarisation 8-56425
 glass, dielectric instabilities in high permittivity glass 8-52433
 ionic solid, deformation dipole model 8-72454
 molecular solid, electronic polaris. energy, quantum dynamic rel. to classical microelectrostatic approach 8-52427
 nonlinear dielectric relaxation 8-60389
 PAN, spectroscopic analysis of electrically polarised films 8-68443
 plastics, radio and light polarisation stress analysis 8-68857
 polyacrylonitrile, film, dielectric polarisation 8-52431
 polyester foil, static polarisation depend. on heat ageing 8-60688
 polypeptides, helical, dielectric polarisability, side chain motions 8-76378
 polypyrrolimittide, thermal depolarisation current 8-52429
 polystyrene composite with mica flakes, TDC meas., interfacial polarisation 8-64316
 polyvinylidene fluoride film, cryst. dipole orientation in elec. field 8-80286
 powder, three pulse echo, mechanism contrbs. 8-68444
 α -quartz, obs. of reversible elastic Dauphine twinning 8-87684
 α -quartz plate frequency changes rel. to electroelastic tensor and second-order phenomena 8-60398
 Rochelle salt, polarisation echo, near ferroelec. transition 8-88266
 sisal wax, electronic conduction and persistent internal polarisation 8-80277
 smectic helixing crystal, dielec. props., temp. and freq. depends. (*Russian*) 8-60380
 sodium ammonium tartrate, polarisation, improper ferroelec. transition 8-72477
 styrene-butadiene-styrene triblock copolymers, dielec. props. 8-95545
 TGSe, dielectric const. near ferroelec. transition temp., effect of surface capacitance 8-56438
 TTF-TCNQ crystal, antiferroelec. ordering of electronic polarisation, simple model anal. 8-92028
 AgBr, exchange charge polarisation 8-92016
 AgCl, exchange charge polarisation 8-92016
 BaTiO₃, doped, loss mechanism and domain stabilisation 8-84542
 BaTiO₃, LF relaxational polarisation 8-68460
 BaTiO₃:Co, charact. behaviour of spontaneous polarisation and dielec. const. 8-60382
 CdF₂ crystals, electrode polarisation 8-76377
 KD₂PO₄, polarisation echo, near ferroelec. transition 8-88266
 K₄Fe(CN)₆·3H₂O, ferroelec., s.p.h.t. and spontaneous polarisation, -65 to 0 degrees C, mol. field model 8-64333
 KH₂PO₄, central components in ferroelec. phase 8-56436
 KH₂PO₄, dynamic central peak in ferroelectric phase 8-84538
 LiNbO₃, band struct. and spontaneous polarisation calcs. 8-95261
 NH₄Br, self-polarisation at order-disorder transition 8-52432
 NH₄Cl, self-polarisation at order-disorder transition 8-52432
 (NH₄)₂SO₄, ferroelec., dielec. behaviour and nature of phase transition 8-88262
 NaCl, polarisation mechanism and lattice mechanics, microscopic approach 8-59888
 NaF, reversible optical storage element using M-centre polarisation 8-94416
 NaNO₂, band struct., polarisation and piezoelec. const. calc. 8-52448
 Pb₂-Sr_{1-x}(Zr_xTi_{1-x})O₃:Cr₂O₃, ferroelec. ceramic, reversible characts. and dielectric losses (*Russian*) 8-84517
 Pb₂Ge_{3-x}Si_xO₁₁, ferroelec., switching vel. and spontaneous polarisation 8-84543
 PbTiO₃, cryst., polarisation and resistivity, elec. field effects 8-64313
 PbZrO₃-monocryst., elec. cond., permittivity, polarisation, para- and ferro- to antiferroelec. phase transitions 8-60402
 PbZr_{1-x}Ti_xO₃ solid solutions, tricritical behaviour 8-80296
 Pb(Zr_{0.47}Ti_{0.43}Sn_{0.10})O₃:Cr₂O₃, ferroelec. ceramic, reversible characts. and dielectric losses (*Russian*) 8-84517
 SbSI, abrupt polarisation changes under influence of external forces 8-68459
 SbSI, max. vel. of domain boundaries in polarisation reversal, Barkhausen effect meas. 8-60411
 SbSI, paraelectric phase, jump-like switching processes, ferroelec. surface layer 8-92038
 SiO₂:OH⁻, vitreous, elec. dipolar echoes 8-52430
 ZnO, piezoelec. powder, dynamic polarisation echoes 8-52443

dielectric properties of gases

No entries

dielectric properties of liquids and solutions

- aliphatic ethers, dil. solns., dielec. loss meas. for dielec. relax. 8-68451
 trans-p-n-alkoxy- α -methyl-p'-cyanophenyl cinnamates, nematic liq. cryst., static dielec. props. 8-60376
 aminobenzotrifluoride, benzene soln., permittivity and dielec. loss 8-64320
 aminopyridines, in 1,4-dioxane soln., dielec. const., losses and relax. 8-64319
 associated solutions, H bonding and anomalous saturation 8-52426
 benzenes, substituted, dielectric absorpt. and NMR 8-88251
 benzophenone, in o-terphenyl soln., dielectric absorpt. studies, molecular relax. 8-95544
 biphenyl-4-p-n-alkoxybenzoates, nematic liq. cryst., static dielec. props. 8-60376
 bis-heptyloxy-azoxybenzene, tilt angle in C-phase, dielectric measurements 8-63673
 2,3-butanediol, dielectric dispersion 8-72455
 n-butanol, dielectric response function, by lumped capacitance method 8-95539
 capacitor dielectric fluid test and anal., quality assurance 8-80272
 charged fluids near freezing point, static dielectric behaviour 8-56417
 chloral, liq., permittivity, dielec. loss, up to 60 GHz 8-60384
 chlorobenzotrifluoride, benzene soln., permittivity and dielec. loss 8-64320
 cholesteric liquid crystal with anisotropic dielec. permeab., transient electrodynamic instability (*Russian*) 8-51418
 dextran aqueous solutions, microwave dielec. behaviour 8-92018
 DHAB, nematic, ordering change due to external DC elec. field, permittivity obs. 8-94990
 dicyanoalkanes, in benzene soln., microwave absorption, internal rot. 8-60385

dielectric properties of liquids and solutions continued

- 1,3-dihaloopropane, dielectric permittivity and loss, dipole moment 8-60383
 dipole, spherical, steadily rot., dielec. friction 8-87600
 DOBAMBC, and DOBAMBCC, chiral smectic C liq. cryst., dielec. const., electroclinic effect 8-94980
 EBBA, solid and liquid states, temp. and freq. depend. (*Russian*) 8-72450
 electrolyte solutions, dielec. dispersion and dielec. friction 8-52436
 ethanol, assoc. in dil. soln., dielec. obs., dipole moment meas. 8-83714
 ethyl-3-chloropropionate, liq., microwave absorption and relax. 8-60386
 ethyl-(methoxybenzylidene-amino)cinnamate, low freq. dielec. constant meas. in cryst. and liq. cryst. phase 8-91226
 4-ethylaminobenzil, dil. soln. in benzene, cyclohexane and dioxane, dielectric behaviour 8-52421
 ethylene-maleic acid copolymer 8-84515
 ethyltrichloroacetate, liq., permittivity, dielec. loss, up to 60 GHz 8-60384
 film condensation, heat transfer enhancement in elec. field 8-55551
 fluids and dispersions, dielec. meas. using cell 8-93725
 9-fluorenone, in o-terphenyl soln., dielectric absorpt. studies, molecular relax. 8-95544
 heat transfer in liquids by dielectrophoresis 8-94874
 heterocyclic compounds in dilute solutions, dielectric relax., microwave technique 8-84520
 HOBACPC, chiral smectic C liq. cryst., dielec. const., electroclinic effect 8-94980
 liquid dielec. permittivity meas., sub-mm wave, using laser- and Fourier transform-spectrometry 8-95568
 losses in solids and liquids, characterisation 8-88252
 MBBA, nematic liq. cryst., flexoelectric and dielec. relax. behaviour 8-94979
 MBBA binary mixtures with a nematogenic or nonmesogenic cpd., dielec. relax. 8-72457
 merocyanine dye, solvent-depend. hyperpolarisability, polar (nonpolar) solvents 8-70962
 methyl methacrylate, oligomers, dielectric relax., end-group effects 8-92019
 methyl-3-bromopropionate, liq., microwave absorption and relax. 8-60386
 methyl-4-chlorobutyrate, liq., microwave absorption and relax. 8-60386
 molecular reorientation, dielec. friction theory 8-87599
 naphthalenes, substituted, dielec. relax. and permittivity in pure liqs. 8-64318
 nematic liquid crystal mixtures with low-freq. dielec. relax., phase behaviour 8-91246
 nematic-isotropic mixture, dielec. props., phase diagram 8-52424
 nitrobenzene, solns., elec. permittivity near crit. point 8-76372
 nitrobenzotrifluoride, benzene soln., permittivity and dielec. loss 8-64320
 4-nitrophenyl-4-octyloxybenzoate, nematic and smectic-A phase, dielec. meas. 8-60392
 nonlinear rigid polar molecular fluid, dielec. const. 8-72451
 4-octyl-4'-cyanobiphenyl, liq. cryst. phases, dielec. relax. meas., short range interactions 8-94976
 octyl-cyano-biphenyl, nematic and smectic-A phase, dielec. meas. 8-60392
 PCB, nematic, smectic phases, dielec. and optical props. 8-60377
 4-n-pentyl phenyl-4-(4-pentyl benzoxyloxy)3-chlorobenzoate, liq. cryst., flexoelectric and dielec. relax. behaviour 8-94979
 polar fluid of heteronuclear molecules, dielectric const. 8-84514
 polar liquid, complex permittivity meas., lumped capacitance method 8-77936
 polar liquid, relative permittivity, dielectric and Kerr effect relaxation in alternating elec. fields 8-80284
 polydiethylsiloxane chains, dipole moments 8-78844
 polyethylene oxide, aq. soln., dielec. relax., interferometric transmission obs. 8-52437
 polypeptides, helical, dielectric polarisability, side chain motions 8-76378
 polyvinyl methyl ether, aq. soln., dielec. relax., interferometric transmission obs. 8-52437
 PVA, aq. soln., dielec. relax., interferometric transmission obs. 8-52437
 PVA, liq., mobilities at const. temp., vol. 8-95174
 sea water, dielectric permeability calc. (*Russian*) 8-77261
 smectic helixing crystal, dielec. props., temp. and freq. depends. (*Russian*) 8-60380
 smectic liquid crystal, A phase, dielec. permittivity 8-71673
 solvation, classical mean space charge model 8-76841
 solvent, polar, spherical ion radius and limiting elec. cond. Brownian motion 8-95168
 solvent effects, virtual charge model representation of solvent polaris. 8-74593
 spheruloids, in streaming suspension, dynamics, dielectric const. 8-76374
 suspension, dielectric, convective heat transfer, rheodynamics, in horizontal coaxial cylindrical channel 8-59494
 TDOBAMBC, chiral smectic C liq. cryst., dielec. const., electroclinic effect 8-94980
 vinyl acetate, oligomers, dielectric relax., end-group effects 8-92019
 water, heavy water, and ionic solns., high-field nonlinear effect, Piekara factor meas. 8-68441
 water, supercooled emulsified droplets, relative permitt. and cond., Maxwell-Wagner interfacial polarisation 8-52423
 Cu complex, bis-ethylene diamine copper(II) sulphate, dielectric relaxation studies 8-84519
 CuSO₄, dielectric relaxation studies 8-84519
 H₂O₂ aq. solns., struct. and dielec. props. 8-63659
 H₂SO₄, solns., static permittivity, kinetic depolarisation, time-domain spectroscopy 8-68440
 KCl aqueous solution emulsions, complex permittivity meas., dielec. relax. 8-72459
 K₂SO₄, dielectric relaxation studies 8-84519
 Ni(ClO₄)₂, dielectric relaxation studies 8-84519
 Ni(NH₃)₆SO₄ solution, dielectric relaxation studies 8-84519
 NiSO₄, dielectric relaxation studies 8-84519

dielectric properties of solids

absorption band struct. resolution by using complex dielectric const. 8-72546

alkali halide, exchange charge polarisation, dielectric const., Dick and Overhauser model 8-55832

alkali halides, Mott-Littleton dielectric theory 8-80274

alkali halides, static polarisability, vol. depend. 8-52428

alkali halide, optic mode Gruneisen parameters and strain derivatives, Born-Mayer and Szigeti model 8-55929

amorphous solid, very far IR props. 8-80344

aromatic aldehydes, in polystyrene matrix, group relax., weight factor effects determ. 8-68446

4-bromobiphenyl, dielectric const., mol. reorientation in solid 8-72448

butanediol terephthalate-polytetramethylene oxide terephthalate copolymers, dielec. props. 8-95546

data presentation and interpretation 8-76376

diamond, dielectric properties, mean point value calc. 8-87930

4,4-dibromobiphenyl, dielectric const., mol. reorientation in solid 8-72448

dichloromethane-decalin glass, mol. dynamics, from dielec. loss meas., 107-148K, 293K 8-76379

EBBA, stable and metastable solid phases, dielec. dispersion meas. 8-60390

glass, dielectric instabilities in high permittivity glass 8-52433

heterocyclics, in polystyrene matrices, energy barriers, dielec. absorpt. meas. 8-70958

ice, Ih phase, dielec. anisotropy 8-64310

ice microcrystals, NH_4Cl doped, activation energy of Debye's dipolar relax., influence of salt content (French) 8-56424

laser-induced evaporation of nonlinearly absorbing dielectric surface 8-80438

losses in solids and liquids, characterisation 8-88252

OHMBBA, solid phase dielectric relax. times and strength, mol. rot. 8-72456

oxide glasses, elec. cond. and dielec. relax., correl. 8-79801

polyacrylonitrile, film, dielectric polarisation 8-52431

polydiethylene glycol terephthalate, relaxation, dielectric prop. 8-68447

polyethylene, gamma radiation effects on dielect. parameters, expt. (Hungarian) 8-59836

polyethylene, low density, dielec. behaviour, struct. props. influence (German) 8-92017

polyferrocene film, plasma polymerised, dielec. props., 40 kHz to 50 MHz, 30-400°C 8-52439

polymer, amorphous, segmental distrib., light-, neutron- and X-ray scatt., piezooptical and dielec. meas., review 8-51444

polymer, glass transition under high-pressure, dielec. loss method obs. (Russian) 8-71841

polypentamers, phosphorylated, hydrogenated derivatives, dynamic mech. and dielectric props. 8-68448

polystyrene-wood, polymer composite, dielec. props. at low temperature range (Japanese) 8-95541

PVC, gamma radiation effects on dielect. parameters, expt. (Hungarian) 8-59836

PVC-polyvinylidene chloride copolymer, dielectric loss at low-temp 8-95543

rare earth aluminates, effects of roasting in reducing and oxidizing media on elec. props. 8-52736

squaric acid, hydrostatic press. effect on phase transition, dielec. and dilatometric meas. 8-55941

statistical test of solid dielectrics in pulse irradiation regime 8-95548

styrene-butadiene-styrene triblock copolymers, dielec. props. 8-95545

styrene-butyl vinylpyridinium-TCNQ copolymer, dielectric const. (Japanese) 8-60375

styrene/n-butyl-2-vinylpyridinium-TCNQ copolymer, dielec. permittivity (Japanese) 8-56416

TCNQ salt, NMP-TCNQ, realisation of disordered Hubbard model, dielec. props. 8-79917

TCNQ salts, $\text{Qn}(\text{TCNQ})_2$ and $\text{NMeAd}(\text{TCNQ})_2$, dielec. const. and elec. cond. 8-60116

TCNQ salts with asymmetric donors, transport props. 8-60115

transition metal oxides, dielec. behaviour 8-71703

tremolite asbestos, fibrous. elec. anisotropy 8-80273

triethylene, in polystyrene matrix, energy barriers, dielec. absorpt. meas. 8-70958

US Gruneisen parameter for nonconducting cubic crystals 8-87744

AgBr, dielectric behaviour under hydrostatic press. 8-52420

AgBr, exchange charge polarisation 8-92016

AgCl, dielectric behaviour under hydrostatic press. 8-52420

AgCl, exchange charge polarisation 8-92016

Ag_2SbS_4 , dielec. and acoustic props. (German) 8-64335

Al_2O_3 film, dielec. props., AC and DC elec. characts. 8-68445

$\beta\text{-Al}_2\text{O}_3\text{-Na}_2\text{O}$, microwave absorpt., low-temp. dielectric props. anomalies, ion tunnelling states 8-92013

As_2Se_3 , glassy, dielectric const. determ. 8-72449

BaTiO_3 , ferroelectric ceramic, dielec., piezoelec. and elastic props., orientational contrib. 8-68468

BaTiO_3 type perovskite ferroelectric, neutron irradiated, amplification of freq. dispersion of permittivity (Russian) 8-52419

$\text{BaTiO}_3\text{:Co}$, charact. behaviour of spontaneous polarisation and dielec. const. 8-60382

$\text{Bi}_{12}\text{GeO}_{20}$, electrophys., props. determ. (Russian) 8-51987

$\text{Bi}_2\text{Sb}_{1-x}\text{SI}_x$, atomic substitution and ferroelec. phase transition 8-68464

$\beta\text{-AgI}$, ionic cond. and dielec. meas., Frenkel defect formation energy 8-87814

Ca_2SiO_5 , hydraulic reaction observed by microwave dielectric meas. 8-80745

CeO_2 , elec. cond. and dielectric props. at low temp. 8-72447

DyAsO_4 , cooperative Jahn-Teller phase transitions, dielec. anomalies 8-64312

DyVO_4 , cooperative Jahn-Teller phase transitions, dielec. anomalies 8-64312

Fe_2O_4 , dielec. props. of low temp. phase, at microwave freq. 8-64309

GaN, preparation variables rel. to dielectric data, GaAs conversion 8-60591

Ge, dielectric properties, mean point value calc. 8-87930

GeH_4 , heat capacity, dielectric const., thermodynamic props. 8-83967

Li_3N , superionic conductor, local ionic motion, anisotropic dielec. behaviour 8-87817

dielectric properties of solids continued

$\text{Li}_2\text{O-B}_2\text{O}_3$ glass, conductivity, permittivity, and dielectric loss obs., mixed isotope effect 8-95182

$\text{LiTaO}_3\text{-CaZrO}_3$, struct. and dielec. props. 8-80298

MgO , dielectric properties, mean point value calc. 8-87930

$\text{Mo}_6\text{Cl}_{10}\text{S}$, struct., dielec. and diamag. props. (French) 8-67691

$\text{Mo}_6\text{Cl}_{10}\text{Se}$, struct., dielec. and diamag. props. (French) 8-67691

$\text{Mo}_6\text{Cl}_{10}\text{Te}$, struct., dielec. and diamag. props. (French) 8-67691

$(\text{NH}_4)_2\text{SO}_4$, ferroelec., dielec. behaviour and nature of phase transition 8-88262

NaCl , dielectric properties, mean point value calc. 8-87930

$\text{Na}_{0.33}\text{V}_2\text{O}_5$, dielec. const. and microwave cond. 8-60378

$(\text{Pb}_{1-x}\text{Ba}_x)_2\text{Ge}_2\text{O}_{11}$, ferroelec. transition blurring, US relax., dielec. and opt. props. 8-95559

$\text{Pb}(\text{Mg}_{0.5}\text{W}_{0.5})\text{O}_3\text{-BiFeO}_3$, dielec. props., cryst. struct. 8-84534

PbTiO_3 , cryst., polarisation and resistivity, elec. field effects 8-64313

PbTiO_3 , ferroelectric ceramic, dielec., piezoelec. and elastic props., orientational contrib. 8-68468

$\text{Pb}(\text{Zr,Ti})\text{O}_3$ ceramic-polyvinylidene fluoride composite film, complex piezoelec. props. 8-64323

rubber, gamma radiation effects on dielect. parameters, expt. (Hungarian) 8-59836

Si, dielectric properties, mean point value calc. 8-87930

$\text{SiO}_2\text{:OH}^-$, vitreous, elec. dipolar echoes 8-52430

SiO_2 film, MIM struct., DC bias dependent dielectric dispersion props. 8-76178

$\alpha\text{-Sn}$, dielectric properties, mean point value calc. 8-87930

Ta_2O_5 , film, dielec. props. meas., two layer Maxwell-Wagner model 8-76373

TiO_2 , rutile, ferroelectric ceramic, dielec., piezoelec. and elastic props., orientational contrib. 8-68468

TlBr, dielectric behaviour under hydrostatic press. 8-52420

TlCl, dielectric behaviour under hydrostatic press. 8-52420

$\text{V}_2\text{O}_5\text{-P}_2\text{O}_5$ glass, dielec. relax. mechanism, SDRC investigation, Schottky barrier formation in metal-glass-metal systems 8-60388

dielectric properties of substances

see also antiferroelectricity; dielectric depolarisation; dielectric function; dielectric materials; dielectric measurement; dielectric phenomena; dielectric polarisation; dielectric properties of gases; dielectric properties of liquids and solutions; dielectric properties of solids; electric strength; optical susceptibility; permittivity; piezoelectricity; pyroelectricity

adsorbed layers near λ -transition, thermodynamic relns. of Pippards type for dielectric and mag. props. 8-79881

geminate recombination, time depend. Onsager problem anal. soln., critical elec. field 8-72446

dielectric relaxation

see also dielectric resonance

aliphatic ethers, dil. solns., dielec. loss meas. for dielec. relax. 8-68451

aminobenzotrifluoride, benzene soln., permittivity and dielec. loss 8-64320

aminopyridines, in 1,4-dioxane soln., dielec. const., losses and relax. 8-64319

aromatic aldehydes, in polystyrene matrix, group relax., weight factor effects determ. 8-68446

benzenes, nitrohalide substituted, microwave absorpt., mol. struct. 8-75522

benzenes, substituted, dielectric absorpt. and NMR 8-88251

benzophenone, in o-terphenyl soln., dielectric absorp. studies, molecular relax. 8-95544

butanediol terephthalate-polytetramethylene oxide terephthalate copolymers, dielec. props. 8-95546

chiral smectic C, ferroelec. props., dielec. meas. 8-52463

chlorobenzotrifluoride, benzene soln., permittivity and dielec. loss 8-64320

cyanobiphenyl liq. cryst. mixtures, mol. mechanism producing dielec. relax. 8-84521

dextran aqueous solutions, microwave dielec. behaviour 8-92018

1,3-dihalopropane, dielectric permittivity and loss, dipole moment 8-60383

dipole-orientation relaxation times, meas., temp. depend. 8-84512

disperse system, diphasic struct., systematic anal. to determ. permittivity and elec. cond. from dielec. relax. 8-56423

electret discharge model, injection relaxation mechanism, space-charge cond. 8-80279

electrical response of relaxing dielectrics compressed by shock waves, axial mode problem 8-80280

electrolyte solutions, dielec. dispersion and dielec. friction 8-52436

electrolytic solutions, dielectric relaxation studies 8-84519

enzyme activity rate reduction by EM fields (Russian) 8-61142

ethyl-3-chloropropionate, liq., microwave absorption and relax. 8-60386

4-ethylaminobenzil, dil. soln. in benzene, cyclohexane and dioxane, dielectric behaviour 8-52421

9-fluorenone, in o-terphenyl soln., dielectric absorp. studies, molecular relax. 8-95544

frequency dependent dielectric constant, rel. to dielec. polarisation 8-56425

heterocyclic compounds in dilute solutions, dielectric relax., microwave technique 8-84520

ice microcrystals, NH_4Cl doped, activation energy of Debye's dipolar relax., influence of salt content (French) 8-56424

inhomogeneous isotropic dielectric, anal. 8-68450

ionic conductive crystal, statistical theory of relaxation current and low-freq. dielectric dispersion 8-60391

ketone-paraffin solid soln., dielec. relax., temp. and lattice const. depend. (German) 8-76383

Langmuir film, dark and photo-stimulated relaxation similarity 8-92021

liquid crystals, nematic and smectic mol. dynamical investigation 8-91252

MBBA, nematic liq. cryst., flexoelectric and dielec. relax. behaviour 8-94979

MBBA binary mixtures with a nematogenic or nonmesogenic cpd., dielec. relax. 8-72457

methyl methacrylate, oligomers, dielectric relax., end-group effects 8-92019

methyl-3-bromopropionate, liq., microwave absorption and relax. 8-60386

dielectric relaxation continued

- methyl-4-chlorobutyrate, liq., microwave absorption and relax. 8-60386
 naphthalenes, substituted, dielec. relax. and permittivity in pure liqs. 8-64318
 nematic liquid crystal mixtures with low-freq. dielec. relax., phase behaviour 8-91246
 nematic-isotropic mixture, dielec. props., phase diagram 8-52424
 nitrobenzotrifluoride, benzene soln., permittivity and dielec. loss 8-64320
 4-nitrophenyl-4-octyloxybenzoate, nematic and smectic-A phase, dielec. meas. 8-60392
 non-Markovian effects 8-52434
 nonlinear, rotational Brownian motion of symmetrical top 8-60389
 4-octyl-4'-cyanobiphenyl, liq. cryst. phases, dielec. relax. meas., short range interactions 8-94976
 octyl-cyano-biphenyl, nematic and smectic-A phase, dielec. meas. 8-60392
 OHMBBA, solid phase dielectric relax. times and strength, mol. rot. 8-72456
 oxide glasses, elec. cond. and dielec. relax., correl. 8-79801
 4-n-pentyl phenyl-4(4-pentyl benzyloxy)3-chlorobenzoate, liq. cryst., flexoelectric and dielec. relax. behaviour 8-94979
 piezoelectric and dielectric relax., difference between 8-72458
 piezostimulated current curves, theoretical and exptl. anal. methods, for dielec. relax. time determ. 8-92020
 PMMA, shock-wave compressed, dielectric props. 8-80281
 polar liquid, relative permittivity, dielectric and Kerr effect relaxation in alternating elec. fields 8-80284
 polycarbonate, dielec. relax. and ductile brittle transition 8-52438
 polydiethylene glycol terephthalate, relaxation, dielectric prop. 8-68447
 polyethylene, dielec. relax. mechanism, 1-80K (German) 8-76384
 polyethylene oxide, aq. soln., dielec. relax., interferometric transmission obs. 8-52437
 polymer dynamics simulation, relax. rates and dynamic viscosity 8-91211
 polypentenamers, phosphonylated, hydrogenated derivatives, dynamic mech. and dielectric props. 8-68448
 polyvinyl methyl ether, aq. soln., dielec. relax., interferometric transmission obs. 8-52437
 polyvinylacetate film, effect of electrode metals on depolarisation current characts. 8-76387
 power law frequency dependent dielectric function and nonanalyticity properties 8-60387
 PVA, aq. soln., dielec. relax., interferometric transmission obs. 8-52437
 PVA, liq., mobilities at const. temp., vol. 8-95174
 styrene-butadiene-styrene triblock copolymers, dielec. props. 8-95545
 vinyl acetate, oligomers, dielectric relax., end-group effects 8-92019
 vinyl chloride:vinyl acetate copolymer film dipole continuous relax. spectrum 8-91700
 water-in-hexadecane, microemulsion, dielectric behaviour, Cole-Cole type relax., temp. depend. 8-56426
 Al-Al₂O₃-M, thin film sandwich, leakage current and dielec. relax., 80-500K 8-76158
 Al-Si₃N₄-SiO₂-Si capacitors with optical data writing 8-76154
 Al₂O₃-loaded epoxy, shock-wave compressed, dielectric props. 8-80281
 BaTiO₃, c-domain cryst., HF dispersion of permittivity 8-60379
 BaTiO₃, LF relaxational polarisation 8-68460
 CaF₂:Y(La), dielec. relax. spectrum, ion size trends 8-72460
 CdO-B₂O₃-SiO₂, glass, dielec.-relax. currents 8-52004
 CdTe negative dielectric relax. of hot electrons 8-52001
 Fe(CO)₅, microwave dielec. relax., fluxional mechanism 8-94235
 H₂O, adsorbed on kaolinite clays, dielec. props. 8-76381
 H₂O, dielectric relaxation in plant tissues 8-88692
 H₂O₂ aq. solns., struct. and dielec. props. 8-63659
 KCl aqueous solution emulsions, absorption band determination 8-72459
 KCl:SrCl₂, Z₁-centres, dipolar relax., ITC meas. 8-75660
 α-LiIO₃, statistical theory of relaxation current and low-freq. dielectric dispersion 8-60391
 Li₃N, superionic conductor, local ionic motion, anisotropic dielec. behaviour 8-87817
 NaCl:Mn²⁺, dimer detection, EPR and ITC expts. 8-59833
 Pb(Zr,Ti)O₃ ceramic-polyvinylidene fluoride composite film, complex piezoelec. props. 8-64323
 Pb(Zr,Ti)O₃ thin layers, tan δ temp. dependence obs. (Bulgarian) 8-88259
 Si-SiO₂ interface traps energy distribution meas., in MOS devices, under non-steady-state (Korean) 8-64119
 SiO₂, evaporated film, Debye-type dielec. dispersion props. 8-56421
 SiO₂ film, MIM struct., DC bias dependent dielectric dispersion props. 8-76178
 V₂O₅-P₂O₅ glass, dielec. relax. mechanism, SDRC investigation, Schottky barrier formation in metal-glass-metal systems 8-60388

dielectric resonance

see also *dielectric relaxation; paraelectric resonance*
 No entries

dielectric strength see *electric strength***dielectric susceptibility** see *optical susceptibility***dielectric thin films**

- see also *ferroelectric thin films; insulating thin films; optical films; piezoelectric thin films*
 cathodic sputtering deposition of oxides and oxyfluorides (French) 8-80468
 ellipsometry for semiconductor process control, dielec. layers meas. 8-49887
 MIS structures, elec. strength (Slovak) 8-56231
 multilayer thin films, spin wave resonance, model 8-76316
 planar magnetron sputtering 8-72725
 polyferrocene film, plasma polymerised, dielec. props., 40 kHz to 50 MHz, 30-400°C 8-52439
 reversible nonlinearity analysis 8-92024
 MgO, intrinsic surface states at (100) and (110) surfaces 8-91740
 SiO₂, elec. strength in Al-SiO₂-Si MOS structures meas. (Slovak) 8-56231

dielectric thin films continued

- Ta-Ti-O, reactive sputtered film, elec. props. 8-84336
 TiO₂ film, RF sputtering, dielec. props. and X-ray phase analysis 8-80288

dielectric triodes see *space-charge limited devices***dielectric waveguides**

- see also *optical waveguides*
 rod waveguide in magnetoplasma, TM mode propag. 8-51314
 scattering from arbitrarily located inhomogeneity 8-87161

dielectrics see *dielectric materials***diesel engines** see *internal combustion engines***difference amplifiers** see *differential amplifiers***difference equations**

- ablation, multidimens., embedding in inverse heat cond. problem, finite difference method 8-94508
 aerofoil in unsteady viscous flow, numerical soln. procedures 8-75165
 annular turbulent flows with heat transfer 8-94718
 atoms and ions, valence region energies, electronegativity, Politzer-Parr partitioning, finite difference approx. 8-78612
 axisymmetric confined flame, aerodynamic and heat transfer, finite difference scheme, program 8-94689
 boundary layer flows, finite difference method 8-51155
 centred finite difference scheme for 3-D eqns. of elastodynamics, stability 8-63294
 chaotic behaviour of physical and biological systems 8-62158
 combined convective laminar boundary flow, vertical cylinder in horizontal flow, finite difference approx. 8-90893
 compartmental models with delays, phys. realisability 8-53313
 computational methods, book 8-81820
 conducting slab response to source fields, EM analogue model and finite difference calcs. 8-61329
 convective difference schemes and Hermite interpolation 8-63268
 crack propag. simulation, using moving grid based finite difference scheme 8-83334
 Darcy flow, chilled pipe freezing zone, finite difference method 8-94734
 diffusion coefficient time depend. from single (de)sorption expt., step-by-step calc. method 8-87859
 diffusion-convection eqn. anal. with explicit difference methods 8-62165
 duct rotating around perpendicular axis, flow and heat transfer, finite difference method 8-94752
 elementary length and time interval (French) 8-77743
 elliptic PDE with discontinuous coeff., finite difference soln. 8-89347
 equilibrium equations soln. for rapidly rot. stars 8-65601
 F₂-layer, plasma continuity eqn., comparative anal. of numerical soln. methods 8-69578
 fibreglass composite, oriented, model, conditions of monolithicity, exam. 8-67044
 finite difference calc., campyloptropic coords. for boundary value problems 8-65757
 finite difference evaluation of heat transfer in nucl. fuel pins 8-82419
 finite difference method, appl. to bodies in non-planar stream (Russian) 8-75116
 finite difference method, appl. to thermal stress anal. with phase changes 8-79218
 finite difference method appl. to advection processes, balanced expansion technique 8-77719
 flame, laminar mixed-mode forced-free diffusion type, on vert. burning fuel slab 8-91033
 flow, transient boiling in duct, dynamics 8-94528
 flow about arbitrary 2-dimens. boundary, implicit finite difference simulation 8-94628
 flow depend. expansion process, initial value problem, two step difference method (German) 8-57877
 Fourier analysis of difference schemes for Laplace eqn. in rot. symm. system 8-77677
 frictionless tidal channel behaviour 8-92876
 gas body, low-density, entry motion in exponential atmosphere (Russian) 8-77376
 heat cond. eqn., synthesis of optimum boundary control (Ukrainian) 8-55544
 heat conduction inverse boundary-value problems, finite difference method 8-63263
 heat flow eqn., different schemes 8-90627
 heat transfer, nonlinear, iterative-variational method 8-94511
 helical springs, numerical soln. of dynamic response 8-67026
 hydrodynamics models, nonstationary gas flow, two dimens., variational approach to finite difference scheme 8-51147
 intense laser beam diffraction by long US wave in liquid column 8-60421
 jet, buoyant, turbulent in cross flow, finite difference method 8-90907
 jets, turbulent two-dimens., parallel, mixing 8-51209
 Lax-Wendroff difference scheme, appl. in fluid dynamics 8-65758
 linear differential eqns., fourth order, finite difference formulae for boundary value problems 8-73856
 magnetic fields, boundary-value problems, finite element and finite difference anal. 8-94353
 magnetic problems, grid and metric optimisation, finite difference and finite element methods 8-94352
 meteorology, optimum difference schemes, synthesis on sphere 8-93011
 MHD, nonsimilar incompressible laminar boundary layers, finite-difference scheme 8-79386
 MHD axial flow in triangular pipe, finite difference method 8-59498
 Navier-Stokes eqn., steady, numerical soln. by highly accurate finite-difference method (French) 8-86163
 Navier-Stokes eqns., finite difference scheme 8-71306
 Navier-Stokes eqns., finite difference schemes, stability anal. 8-89346
 Navier-Stokes equations, theory and numerical analysis, book 8-77721
 non-Newtonian flow in pipe, finite difference methods 8-94770
 nonlinear, partial difference eqn., Backlund transformation, discrete-time Toda eqn. 8-73829
 nonlinear difference-difference equations, derivation of infinite number of conservation laws 8-89324
 nonlinear elastic stability problems using a finite difference perturbation method 8-83273
 nonlinear hyperbolic conservation laws, finite difference methods 8-49649

difference equations continued

- nonsimilar laminar free convection flow along a nonisothermal vertical plate, finite difference method 8-75119
 nuclear mass relations and eqns. 8-66194
 numerical method, fast, iterative, implicit, for solving multidimensional partial differential eqns. 8-93519
 parabolic partial differential equations, operator compact implicit soln. methods 8-89348
 partial differential eqns. reduction by Galerkin, collocation, and method of lines 8-77693
 partial differential equations, time depend., Method of Lines compared to finite difference scheme 8-79291
 particle, spherical, convective heat and mass exchange, $Pe \leq 1000$ 8-55683
 Poisson equation over complex domain, finite difference method, Neumann boundary conditions 8-79189
 polymer dynamics simulation, general theory 8-91210
 pulsating turbulent flow onto elastic surface, finite difference method (Russian) 8-75153
 reactor neutron field analogue simulation (Russian) 8-74416
 shells, truncated conical, thermal buckling, axisymmetric initial deflections 8-79240
 shock wave ionisation in transverse magnetic field, finite-difference methods 8-51249
 slab with temp. depend. thermal cond., convective boundary, transient cond., finite difference method 8-75031
 soil, unsaturated, coupled heat and water movement prediction, math. model 8-61446
 soil water flow modelling, finite difference and Galerkin techniques 8-81249
 spectral transform method extension for solving nonlinear differential difference eqns. 8-81804
 stability theory (Chinese) 8-81803
 steady-state response of difference eqns., digital computation schemes 8-57718
 supersonic flow, wake of axisymmetric body, ideal gas, numerical anal. 8-59420
 supersonic three-dimens. flow, finite difference method 8-51190
 thermal regenerator, with variable mass flow rate, computer model 8-75047
 thermogravitational convection asymmetry, finite difference method 8-59267
 transient 1-D two-phase flow eqns., finite difference approx. 8-51229
 turbulent air flow in round tube, high-temp., friction resistance, cooling (Russian) 8-75135
 turbulent boundary layer, Hassid-Poreh energy model anal., inc. accel. and surface heat transfer step change 8-51158
 turbulent channel flow, secondary current numerical simulation 8-94828
 uncertainty analysis of P input into a lake 8-81262
 vertical tube with laminar combined convection, water, finite difference anal. 8-90894
 viscous flow, 2nd order upwind scheme critique 8-94744
 water wave propag., long-period, finite difference-element integration scheme 8-75157
 wave diffraction by thin phase grating, difference eqn. solns. 8-54198
 N_2O_4 , dissoc. flow in tube, heat transfer and drag 8-71402

differential amplifiers

- wideband isolated for biological signals, cct. 8-57089

differential calculus *see* differentiation**differential equations**

- see also boundary-value problems; difference equations; Green's function methods; integro-differential equations; linear differential equations; Navier-Stokes equations; nonlinear differential equations; partial differential equations*
 abstract evolution eqns., almost automorphic solns. 8-65754
 Alfvén ion cyclotron waves, in finite length plasma, differential eqn. 8-91097
 biochemical multiple-loop negative feedback control networks, oscills., periodic metabolic systems 8-85285
 boundary layer problems, singular perturbations, stability and convergence 8-90827
 bubble motion under gravity in rotating fluid, differential equations of motion (German) 8-90918
 Chebyshev polynomial method for computing analytic solns. to eigenvalue problems, appl. to anharmonic oscillator 8-62058
 condensate film flow on finned surfaces, heat transfer, heat exchanger design 8-75038
 decomposable differential operators in cosmological context 8-57825
 diffusion, multi-group, FBR neutron-physical calc. (Czech) 8-66332
 Duffing's eqn. forced by periodic impulses, harmonic solns. 8-89325
 dusty gas, two fluid model field eqn., time interval for soln., iteration method (German) 8-63489
 dusty gas, unsteady flow in cylinders, numerical soln. 8-51231
 electrostatic precipitator, free-fall, motion of charged particles, determ. 8-71020
 EM wave propagation in ionosphere, generalised differential eqn. 8-53770
 energy-absorbent media, wave theory generalisation (Russian) 8-77725
 Euler's method, computer programs for high-school expts. 8-86094
 fatigue crack growth, model prediction, two coupled differential equations 8-67103
 first-order differential eqns., common derivation of averaging method and two-timescale method 8-85835
 flow, in annulus, axial, numerical stability anal. 8-83363
 fluid flow, boundary elements method soln. 8-90821
 forced vibrations of freely supported continuous beam (Rumanian) 8-75085
 gyroscopic system, linear, damped, modal anal., appl. to satellite 8-63275
 Hamiltonian eqns., infinite-dimens., integrable 8-57744
 heat exchange in dense layer at large Biot no. (Russian) 8-83400
 higher monotonicity properties of certain Sturm-Liouville functions 8-57750
 highly-ionised free-fall positive column, differential eqn. system 8-67489
 hydrology, modified Richards' eqn., oscill. of numerical soln. 8-81243
 inverse problem for general first order differential eqn. systems 8-74181

differential equations continued

- Kepler problem, time transformation stabilisation (German) 8-89333
 left-heart haemodynamics, mathematical model 8-65074
 light ellipticity, azimuth and system parameters linking eqns., 3-dimens. model propag. 8-50695
 Lorentz-Dirac eqn. for classical charged particle, mass renormalisation 8-62007
 lossy integrator, response for time variable counting rate (Rumanian) 8-90045
 metal cutting appl. of Taylor eqn. for different cutting speeds (German) 8-72915
 multilayered cylinders, nonstationary temp. fields with rotational symmetry (German) 8-79190
 non-Newtonian fluid, effective diffusion of impurity in laminar flow of liquid 8-67228
 nonhomogeneous elastic rods, similarity soln. of wave propagation 8-59323
 Painlevé second transcendent, numerical and asymptotic approx. 8-49675
 parameter sensitivity analysis method for differential eqn. models 8-81453
 Paris differential eqn. for fatigue cracks, numerical calc. of eqn. parameters 8-63384
 plasma, rapidly changing, numerical integration of ionisation rate eqns. 8-55734
 pointlike and nonpointlike transforms of differential eqns. in cartesian coords., geometrical treatment 8-54159
 polymer dynamics simulation, general theory 8-91210
 real-space renormalisation giving differential renormalisation-group eqns., two-dimens. triangular Ising lattice 8-65881
 Riccati eqns. depending on parameter, soln. of Fredholm integral first kind eqn. (Russian) 8-54153
 self-adjointness of Schrödinger-type operator powers 8-81877
 solution righthand part in form of second order homogeneous multinomial (Russian) 8-54157
 step operators, Lie algebraic props. 8-62052
 stochastic constraints on iterative maximisation of system of differential eqns. 8-57757
 stochastic differential equations, solns., splitting corrls. 8-49770
 stochastic functional differential eqns. and systems of differential inequalities 8-77801
 supersonic wave drag of planar singularity distributions 8-83430
 teaching with interdisciplinary models and computer 8-77640
 time depend. diffusion eqn. for neutronic calcs., use of exterior differential forms 8-54871
 two-phase flow in a nozzle, max. mass flow rate determ. 8-71384
 Volterra eqns., generalised, stability theorem 8-86116
 Volterra soliton, collapse into weak monotone shock wave 8-49673
 wave processes description (Russian) 8-81850
 H_2 , diffusion in interstitials, master equation equivalence 8-79794

differential scanning calorimetry *see* thermal analysis**differential thermal analysis** *see* thermal analysis**differentiation**

see also differential equations

No entries

diffraction

- see also acoustic wave diffraction; diffraction gratings; diffractometers; electromagnetic wave diffraction; electron diffraction; neutron diffraction*
 diffraction of plane shock wave at angle in ideal compacting medium (Russian) 8-63357
 elastic longitudinal waves, diffr. at elastic circular inclusions (fibres) (Russian) 8-63368
 linear viscoelastic waves, theory of diffraction (Russian) 8-65787
 NMR determination of phys. and biological struct. (Rumanian) 8-49874
 scalar wave diffraction by two parallel slits in plane 8-49671
 semishadow field diffraction, boundary wave uniform asymptotics (Ukrainian) 8-89350
 shear waves, diffr. at row of round elastic fibres 8-67083
 shock wave diffraction at small angles in ideal compacting medium (Russian) 8-67082
 water-wave diffr. by semi-infinite vertical barrier on rotating Earth 8-83417

diffraction gratings

see also holographic gratings

- aberration balancing for grating mountings with large aberrations 8-66906
 absolute calibration of grating spectrograph for laser wavelength meas. 8-90528
 aspheric grating for EUV astronomy 8-57451
 beam splitter using diffr. grating combination, for Michelson interferometer 8-70205
 Bragg and Raman-Nath diffr. regimes rel. to grating thickness 8-71028
 chalcogenide amorphous film, grating direct writing using SEM 8-83121
 coded grating method for measuring three dimensional objects 8-86240
 coherent synthesized aperture system, image form., resolution improved by diffr. grating 8-50715
 concave grating mounting, for visible spectroscopy 8-50913
 conducting rectangular bar transmission gratings 8-62993
 crossed lamellar transmission grating, exam. of diffr. props. 8-59139
 dielectric coated gratings, general integral theory 8-66909
 echelle spectrograph for high-resolution stellar spectra 8-96396
 edge-type reflection gratings, anal. algorithms 8-86998
 embossable surface relief structures for black and white, colour reproduction, ZOD images 8-65990
 energy absorption and anomalies, rel. to surface waves, general theory 8-94447
 etching monitoring using grating test pattern, appl. to SiO_2 and Si_3N_4 8-76775
 filter with surface corrugated diffr. grating, characts. for oblique incidence 8-50949
 Fredholm integral eqn. formalism 8-63192
 grazing incidence diffraction gratings, efficiency in soft X-ray region 8-63187
 illuminator using laser light source, geometrical optical anal. (Russian) 8-79094

diffraction gratings continued

- interferometer-grating spectrograph for high resolution spectroscopy in middle UV 8-77490
 lamellar reflection grating, theory 8-74982
 laser beam modulator using rotary diffraction grating 8-87080
 laser beam multiplication, interferometric method (*Ukrainian*) 8-90442
 magnetic diffraction gratings with alterable magnetic domains for optoelectronics 8-63197
 Moire contouring using virtual moving gratings simulated on computer 8-73968
 moire fringes, profile prediction method, fringe sharpening 8-87009
 monochromator for UV-visible spectrophotometer, stray light 8-94445
 monochromators of concave grating mounting for space telescopes, VUV region 8-73629
 multiple imaging with thin phase filters, signal processing approach 8-66772
 multiprofile buried gratings, dielec. coated metallic, use as beam sampling mirrors, theory 8-79120
 non-optical surface topography, by oblique fringe projection from diffr. gratings 8-89437
 parallel plate grating, freq. modulation non-redundant scanning of light beam 8-78907
 periodic grating reflector array for thin film Fabry-Perot laser 8-55471
 periodic surface characterisation by US diffraction spectroscopy 8-60974
 phase shifts and resonances 8-94446
 replication process 8-66962
 ruled blazed plane gratings, efficiency, synchrotron radiation monochromisation 8-63189
 ruling engine with piezoelec. control 8-83128
 scalar domain, asymptotic theory 8-66910
 scattered light, specification and meas. from diffr. gratings 8-78905
 semi-infinite solid-state phase grating, optical props. 8-87155
 semiconductor, ambipolar diffusion meas. using nonlinear-transient gratings 8-80000
 servosystem, opto-electronic, correction of nonrectilinearity of ruling engine 8-87174
 sieve screens, two-dimens. array, diffr.-interf. patterns, Kirchhoff approx. 8-83088
 thin phase grating diffr. eqn. solns. 8-54198
 thin phase gratings with arbitrary grating shape, diffr. efficiency 8-66911
 toroidal diffraction grating, spectral image at point at spectrometer entrance slit (*Russian*) 8-57452
 transmission grating, facet-type, aberrations for cosmic X-ray and XUV spectroscopy 8-85851
 transmission grating diffraction regimes 8-66912
 transmission lamellar grating theory, diffracted light intensity anal. 8-74981
 UV region, 300 to 2000 Å, simple selection rules 8-55435
 vacuum UV efficiency, conference on synchrotron radiation instrumentation, Orsay, France (Sept. 1977) 8-62999
 volume diffraction gratings as filter, for image restoration 8-94378
 XUV gratings, classical and ionic mountings, EM diffraction 8-63188
 Al, Au coatings, UV light polarisation at grazing incidence 8-87129
 LiNbO₃, waveguide, corrugated, electro-optic scanning of light diffr. from grating output coupler 8-63172

diffraction instruments see diffractometers**diffraction model**

- diffractive states, large mass, forward prod., multichannel eikonal model 8-82181
 Neveu-Schwarz dual model for $p\pi$ system 8-82175
 scattering amplitudes satisfying geometrical scaling, low and high-energy props. 8-86447
 secondary particle multiplicity distribution in nuclei, 200 and 800 GeV (*Russian*) 8-89879
 K⁺p interactions, 14.3 GeV/c, two body diffraction dissociations, cross sections, mass spectra 8-62464
 N diffraction dissociation into N π system, near threshold calcs., appl. to $pn \rightarrow pp\pi^-$ (*Russian*) 8-54623
 Np \rightarrow (N π)p, double peripheral description in diffraction model 8-58204
 p+emulsion nuclei diffractive coherent prod., inclusive and exclusive channels 8-62530
 $pp \rightarrow (p\pi^+\pi^-)(p\pi^+\pi^-)$, 24 GeV/c, double diffraction dissociation reaction, cross sections, mass spectra 8-93908
 pp diffraction dissociation, 25 and 200 GeV/c, parameter invariant quantities (*Russian*) 8-54655
 pp elastic scatt., high energy, large momentum transfer, diffraction model with nucleon core 8-74281
 $pp \rightarrow pp2\pi^+2\pi^-$, 100 GeV/c, diffraction and p^0 prod. in exclusive interactions 8-93909
 $pp \rightarrow pp\pi^+\pi^-$, 100 GeV/c diffraction and Δ^{++} prod. in exclusive interactions 8-93909
 pp scatt., absence of multiple-dip struct. in differential cross section 8-82246
 π diffr. dissoci. into 5π at 16 GeV/c 8-82252
 π^+p , 14 GeV/c, N diffr. dissoci., bubble-chamber anal. 8-66175

diffractometers

see also X-ray diffractometers

- gamma-ray, using ¹⁹⁸Au source at FRM reactor 8-54514
 neutron, construction, appl. to cation distrib. determ. in nonstoichiometric MnZn ferrite (*Bulgarian*) 8-83656
 neutron, flat-cone, utilising linear position-sensitive detector 8-67624
 on-line ECIL TDC-312 computer-controlled four-circle neutron diffractometer 8-55787
 optical, indexing of spiral biological objects on microphotographs 8-96121

diffusion

- see also biotransport; diffusion in gases; diffusion in liquids; diffusion in solids; electromigration; membranes; osmosis; permeability; self-diffusion; surface diffusion; thermal diffusion; turbulent diffusion
 aerosol, polydispersity, unipolar charging, charging mobility analysis 8-61059
 aerosol, unipolar diffusion charging, particle dielectric constant and ion mobility effects 8-61058

diffusion continued

- aerosol particle deposition in channel due to diffusion and electric charge 8-90978
 aerosol particles diffusion and gravitational settling in tube 8-90976
 Brownian particles, diffusion of interacting spherical particles suspended in fluid 8-54304
 chemical reactions, lattice model, coupling of translational and reactive dynamics 8-55696
 concentration dependence of diffusion coeff. from single (de)sorption expt., step-by-step calc. method 8-87859
 conformational dynamics and the rotational isomeric state model 8-90315
 convection-diffusion eqn. soln. 8-90888
 convection-diffusion partial differential eqns., finite element method soln. 8-90889
 cooperative diffusion in temporary network 8-77820
 cylinder array, convective mass transfer with surface reaction 8-79369
 diffusion-convection eqn. anal. with explicit difference methods 8-62165
 dissociation, diffusion-controlled reaction, theory 8-64820
 double-diffuse convection, diffuse interface model, high Rayleigh nos. 8-90963
 electrical circuit analogue, for teachers 8-86089
 excitable medium diffusion discrete models and spatial patterns 8-93629
 fine particle deposition, on rotating disc surface, convective diffusion under elec. double layer forces 8-61060
 flame, laminar mixed-mode forced-free diffusion type, on vert. burning fuel slab 8-91033
 flow depend. expansion process, initial value problem, two step difference method (*German*) 8-57877
 gas transport, in synthetic polymer membranes, history 8-76912
 geometric approach to diffusion eqns., equivalent set of differential forms 8-54321
 heat and mass transfer, at turbulent boundary layer, diffusion model 8-94544
 hydrocarbon gas, sorption and transport in ethyl cellulose membrane 8-76913
 inhomogeneous films and membranes, diffusion, theory 8-76914
 ion flow through membrane, effect of chem. reaction on time depend., binding of mobile ion 8-95954
 isolated pairs in condensed media, partially diffusion controlled reaction 8-92441
 Kawasaki inequality generalisation for diffusion consts. 8-70076
 Lennard-Jones (100) crystal-liquid interface, structure 8-91284
 local fluctuations in chemical reactions, nonlinear master eqn., dimensional expansions, augmented mean field theory 8-73019
 magnetodiffusion of charged particle in unpolarised electromag. beam 8-57858
 many-particle system, generalised diffusion processes 8-73942
 Markov processes, extremal paths 8-73944
 meteor plasma diffusion, geomagnetic field effect expt. (*Russian*) 8-61814
 meteor trails, atmospheric ambipolar diffusion coeff. meas. errors 8-88952
 modelling, equivalence of different methods 8-57818
 multiple scatt. of particle beams, axial mag. field effect 8-70712
 non-stationary one-dimensional, psi-functions 8-54322
 nonlinear diffusion process, path integral evaluation, by Fourier series 8-70075
 nonlinear reaction-diffusion models for interacting populations 8-65886
 nonstationary one-dimensional diffusion under forced convection, Omega functions as auxiliary functions 8-93631
 one group, integral transport eqn. for homogeneous sphere, neutron scatt., classical diffusion, anal. 8-62589
 Onsager-Machlup formula for 1-D nonlinear diffusion processes 8-77816
 Onsager-Machlup function, Lagrangian for diffusion process most probable path 8-73940
 orientational time correlation functions for J and M diffusion models 8-73939
 particle growth, mathematical modelling, continuity eqns. for particle distrib. 8-65863
 permeable barrier transient diffusion, applied to NMR with pulsed field grad. 8-91986
 phenomenological theory 8-93626
 plasma diffusion, rates, automatic computation, stellar interiors appl. 8-57434
 probabilistic anal. of Lagrangian of diffusion process 8-62170
 quasideterministic Fokker-Planck dynamics 8-93627
 radiation belts, particles radial diffusion from geomagnetic field fluctuations at synchronous orbit 8-96359
 reacting-diffusing system, turbulent spatio-temporal dynamics 8-56880
 reaction-diffusion eqns., axis-symmetric time periodic solns. 8-81930
 Rossby wave critical layer, evolution, vorticity outward diffusion 8-79329
 Schwinger-DeWitt expansion, boundary terms, flat space results 8-7815
 Smoluchowski equation, derivation from Fokker Planck equation using perturbation methods 8-54117
 Smoluchowski process, number fluctuation anal. of random locomotion 8-54318
 solar cosmic rays propag., diffusion in mag. fields, convection in solar wind, dimens. method soln. (*Chinese*) 8-81511
 stars in main sequence, diffusion and turbulence rel. to abundance anomalies 8-89198
 thin-layer cell, fast reaction, kinetic consts., diffusion and conc. impedance 8-73053
 transient diffusion with n-order irreversible chem. reaction, finite element method 8-85122
 viscoelastic media, deform. theory with account of thermodiffusion (*Ukrainian*) 8-67052
 Al, of Cu(Zn), isotope effect 8-84006
 Cu-In solid/liquid interface, laws governing diffusive interaction (*Russian*) 8-95156

diffusion coefficient see diffusion**diffusion creep**

- bound theorems and large strain diffusion flow 8-84895

diffusion creep continued

- grain boundary, stress induced drift diffusion, appl. to creep and growth of grain boundary voids 8-72811
 grain boundary sliding, stresses and deform. 8-68739
 grain rearrangement, solids with hexagonal grain struct. 8-84896
 power law creep, exam. of whether creep is diffusion controlled 8-52890
 voids, review of diffusional growth of creep voids 8-71720
 Cu annealed and cold rolled, with bamboo structure, exam. of grain boundaries as vacancy sources in diffusional creep 8-88508
 W, filament, incandescent lamps, creep, failure, life prediction 8-84927

diffusion in gases

- see also self-diffusion in gases; thermal diffusion in gases*
 aerosol, ambient, sulphate particles diffusion sampling for size discrimination and chemical comp. 8-69528
 aerosol, diffusion and sedimentation in Poiseuille tube flow 8-59463
 aerosol dry deposition, filtration model rel. to trace metal deposition from atmosphere 8-73441
 air pollution density distrib., flow pattern in Tanabe area, Japan, numerical anal. (Japanese) 8-96289
 alkali metal vapour-He(Ar)(N₂), alkali condensation in flow, heat and mass transfer 8-75192
 atmosphere, stratified surface layer, turbulence and diffusion, basic Lagrange characts. 8-81270
 atmosphere, vertical diffusion study using airborne gas-chromatography and numerical modelling 8-69435
 atom distribution, in flame spectrometry, moving point source model 8-61084
 atomic diffusion in diatomic gases, dominant coupling limit 8-63524
 binary mixtures, nonreacting, nonlocal continuum 8-51268
 bubble size distribution, changes due to interbubble gas diffusion 8-85204
 cell design for diffusion coeff. meas. in gas phase 8-55709
 dense gases, mutual diffusion coeff., spin-echo meas. 8-67303
 dimers, dissociating, in nonisothermal ideal gas phase, stationary state anal. 8-76848
 electron diffusion in gas, Maier-Leibnitz expt. reexamined 8-83516
 fast diffusion meas., nondestructive, using positron emitter as tracer 8-54519
 hydrocarbon diffusional combustion in air, finite activation energy anal. 8-95930
 intermolecular pair pot. energy function from gaseous transport coeffs., unlike monatomic interactions 8-62871
 mass spectrometer sample line diffusion processes 8-64907
 methane-ethane-propane-butane, binary and multicomponent mixtures, viscosity, diffusion coeffs. 8-94883
 naphthalene sublimation, radial diffusion rate, mothball lifetime, for teaching 8-54124
 particle in gas stream, convective, diffusion with nonlinear kinetics of heterogeneous chem. reaction 8-83499
 teaching, relax. approx. to Boltzmann eqn. approach 8-73804
 upper atmosphere, ambipolar diffusion wavenumber regions rel. to meteor trails electron density fluctuations 8-73687
 vapour dynamic diffusion batcher with porous partition 8-79404
 Ar+Ar(³P₂)(³P₀), flowing afterglow metastable decay rates, diffusion, two- and three-body rate consts. 8-73027
 Ar+Kr(³P₂), flowing afterglow metastable decay rates, diffusion, two- and three-body rate consts. 8-73027
 Ar+Xe(³P₂), flowing afterglow metastable decay rates, diffusion, two- and three-body rate consts. 8-73027
 Br, diffusion coeff. in laminar flames 8-51272
 CO, diffusion coeff. in laminar flames 8-51272
 CO⁺.CO, lateral diffusion in CO, mass spectra meas. 8-91055
 CS₂+He(Ar)(N₂), perturbed rot. diffusion of CS₂, IR spectra 8-75245
 Cl in Ar and He gas, diffusion const. of atom 8-71417
 Cs⁺ in He and Ne gas, ion mobility and longit. diffusion coeff. 8-67308
 Cs⁺, ion mobility in Ar, Kr, Xe, diffusion, generalised Einstein relation 8-67298
 H₂(²Σ_u⁺)-He(2³S), discharge ionisation growth, diffusion coeffs. 8-83636
 Hg vapour-gas mixture, Hg diffusion, data correlation 8-79403
 Hg(6³P₂)+inert gas, diffusion in low-current discharge 8-63618
 I, diffusion coeff. in laminar flames 8-51272
 N₂-He-CO₂, discharge ionisation growth, diffusion coeffs. 8-83636
 N₂-NO(He), discharge ionisation growth, diffusion coeffs. 8-83636
 N₂⁺, N₂⁺, lateral diffusion in N₂, mass spectra meas. 8-91055
 O₂⁺, lateral diffusion in O₂, mass spectra meas. 8-91055
 Ti, diffusion coeff. in laminar flames 8-51272

diffusion in liquids

- see also electromigration; self-diffusion in liquids; thermal diffusion in liquids*
 1:2 electrolytes, conc. solns., vel. correls. calcs., diffusion, cond. and transference props. 8-85166
 air bubble, in hydraulic oil, effect of diffusion on diameter change 8-90966
 biological material, prep. for X-ray microanal. of diffusible elements, methods of drying ultrathin cryosections 8-77166
 biological material prep. for X-ray microanal. of diffusible elements, rapid freezing and ultrathin section prep. 8-77165
 carbon tetrachloride-benzene-cyclohexane system, quaternary diffusion, capillary-cell method using ¹⁴C labelling 8-87800
 cathodic diffusion boundary layer, free convective flow obs. with shadow Schlieren method 8-68894
 cyclodextrins, diffusion in aq. polymer solns., complex form. 8-91460
 diffusive mass transfer in crystal growth, exam. 8-67669
 p-dodecanoylbenzylidene-p'-aminoazobenzene, smectic A mesophase, diffusion of trichlorotrifluoroethane, NMR spin echo obs. 8-94975
 electrochemical converters, conc. type, for elec. signals, diffusion theory of conc. networks 8-61026
 electrolyte, diffusion interactions between electrodes spaced on oscillating cylinder (French) 8-64849
 estuary halocline, expt. simulation, salt diffusion in tap water, educational aspects 8-61980
 fast diffusion meas., nondestructive, using positron emitter as tracer 8-54519
 gels, dynamic light scattering in poor solvent 8-88318
 glass phase separating, interpretation of temp. dependence of transport process 8-87806

diffusion in liquids continued

- glycerol solutions, diffusion coeffs., viscosity 8-51711
 glycol solutions, diffusion coeffs., viscosity 8-51711
 gravity wave, liquid with superficial film and diffusion effect (French) 8-75156
 heterogeneous liquid stream, stress diffusion effect, molar diffusion coeff. 8-79338
 p-hexanoylbenzylidene-p'-aminoazobenzene, smectic A mesophase, diffusion of trichlorotrifluoroethane, NMR spin echo obs. 8-94975
 ionic diffusion in naturally-occurring aqueous solns., use of activity coeffs. in transition-state models 8-57224
 Kuroshio jet current region, nonlinear density diffusion rel. to density field calc. 8-92843
 Liesegang rings demonstration of transient state pot. flow 8-63408
 LMFBFR, yield characts. of short-lived fission products in Na heat-transfer agent 8-66338
 macromolecules in soln., sedimentation, expt. determ., errors due to diffusion (Russian) 8-76934
 mass transfer inside drops in continuous fluid, effect of pulsation (French) 8-55686
 MBBA, liq. cryst., mass diffusion meas., tracer dye-laser method 8-59738
 measurement, apparatus and appl. to ⁸⁵Kr in fluid Kr 8-54520
 metals and alloys, book 8-51406
 molten salts, transport coeffs., integral representations 8-67842
 non-Newtonian fluid, effective diffusion of impurity in laminar flow of liquid 8-67228
 Norwegian Sea pycnocline, apparent vertical eddy diffusion rates from T vertical distrib. 8-81185
 ocean, relative diffusion meas. at small scales 8-88838
 ocean microstructure, double-diffusive intrusions into density gradient 8-85569
 oil in water microemulsion, added NaCl, light beating spectroscopy of micelles mutual diffusion coefficient 8-80793
 polymers in dilute solutions, diffusion and relaxation time 8-55964
 polystyrene, melt, bulk diffusion, local diffusion (Japanese) 8-95170
 polystyrenes, toluene soln., diffusion through cellulose membrane, friction coeffs. 8-73085
 quiescent two-phase systems, interfacial resistance to interphase mass transfer 8-67828
 rate constant of reaction, determ. from overall crystal growth coeff. 8-59773
 rotational tunnelling and diffusion in condensed mol. systems, neutron scatt. 8-63658
 sodium dodecyl sulphate NaCl aq. soln., micellar props., laser light scatt. exam. 8-92513
 solution of diffusion eqn. for capillary method with no external stirring 8-54518
 steel, alloy, Fe-C-Si-S, liquid, desulphurisation with CaO, exam. of reaction mechanisms 8-80742
 tetrachloromethane-cyclohexane system, interdiffusion, ternary diffusion eqn., radioactive tracer obs. 8-79792
 tetrafluoromethane, Kr diffusion, 243.15K, density depend., size effect 8-75859
 thin-layer cell, concentration impedance, unequal diffusion coeffs. and 2nd-order reactions effects (French) 8-53214
 thin-layer cell, concentration impedance reactive and nonreactive diffusion effects (French) 8-53213
 three-component liquids, analysis of measured values of coeffs. (Japanese) 8-91463
 tracer diffusion coefficients, capillary method determ. calcs. 8-91462
 tracer diffusion coefficients, open-ended continuous capillary method determ. 8-75861
 water, of H, review of neutron radiography results 8-59961
 Cu, of Ti, Ir, Rb and Bi (Japanese) 8-59962
 Cu-Pb liquid alloys, exam. of O diffusivity at 1430K using electrochemical cell 8-51713
 Fe, of alloying elements (Russian) 8-79791
 Fe-based solns., liq., diffusion of N 8-75862
 Fe-C, levitated drops, carburisation and decarburisation in CO-CO₂ gas mixture, exam. of reaction kinetics 8-85053
 Fe-Ni liquid alloy, physical and chemical props. deviations from Raoult's law (Russian) 8-95729
 KF-H₂O, diffusion coeffs., diaphragm cell expts. (German) 8-83986
 MgCl₂-NaCl-H₂O, ionic diffusion theory, use of activity coeffs. in transition-state models 8-57224
 NaCl-KCl-H₂O, ionic diffusion theory, use of activity coeffs. in transition-state models 8-57224
 NaClO₃, growth and dissolution kinetics, diffusion and convection regimes 8-63684
 Na₂O-CaO-SiO₂, multicomponent liq. state diffusion 8-55962
 O₂, diffusion coeff. in liqs. determ. by ESR line widths 8-91929
 Si:As, melting by high power ns laser pulsing, As diffusion 8-79789
 SiO₂-NaO-K₂O-CaO-MgO-Al₂O₃ melt, anodic dissolution of Co and Ni in melt 8-88582

diffusion in plasma *see plasma transport processes***diffusion in solids**

- see also electromigration; ionic conduction in solids; self-diffusion in solids; surface diffusion*
 A15 compound formation by diffusion from ternary bronzes, thermodynamics 8-84740
 alkali metal chloride: F⁻(Br⁻)(I⁻), anion impurities substitution, energies of soln., association and migration 8-83831
 alloy, role of phase boundaries in phase transformations 8-72772
 alloys, irradiated, segregation, inverse Kirkendall effect, effect of constitution on void swelling 8-91472
 anisotropic diffusion in stress fields 8-55973
 batch adsorption for pore diffusion with film resistance and an irreversible isotherm 8-84047
 BCC metal, of H isotopes, self-capture effect and activation energy (Russian) 8-75879
 bimetallic epitaxial film, modification of interfaces during interdiffusion 8-71890
 brittle materials, intergranular creep crack growth, diffusion controlled theory 8-84950
 bronze-steel, phase composition and struct. of diffusional interlayer in fusion zone, X-ray analysis 8-56821
 cellophane membrane, transient diffusion of unstirred polystyrene solns. 8-92508
 Clausius-Mossotti problem for cubic arrays of spheres 8-52422

diffusion in solids continued

composite material, cubic arrangements of spherical particles in isotropic matrix, effective conductivities 8-55547
 composite resin, Langmuir type model for anomalous moisture diffusion 8-67867
 defects, radiation effects 8-87827
 diamond and HCP lattices, random walks 8-71876
 diffusion into Si, in open tube, high vacuum system 8-91349
 discontinuous swelling, type II diffusion as particular soln. of conventional eqn. 8-91471
 dispersion hardened alloy, calc. of back stress decrease, due to Orowan dislocation loop climb 8-83812
 enhanced diffusion mechanisms, review 8-67847
 film, effect of surface condition at low temps. 8-91469
 fission reactor materials, UO_2 high temp. reaction with Zr-Nb 8-66344
 flow of solute atoms near crack tip, time dependent, exam. 8-75722
 formation kinetics of solid layer on surface in reaction diffusion 8-63938
 gas, thermal evolution from solid following detrapping and diffusion during linear tempering schedule 8-75889
 gas in porous medium, continuity of soln. in n space dimensions 8-95130
 gases in metals, detection by vacuum spark technique, appl. to Al wire 8-61094
 glass, nonequilib. thermodynamics (German) 8-83746
 glass membranes, transient diffusion of sucrose, mannitol, pentaerythritol stirred aq. solns., thermodynamics 8-92507
 glassy polymers, powders, transport props., vapour sorption expts. 8-76919
 grain boundary diffusion with radioactive decay 8-59967
 grain rearrangement, solids with hexagonal grain struct. 8-84896
 Hastelloy X, H permeability using permeation method (Japanese) 8-51740
 heteronuclear system, spin diffusion, NMR 8-88213
 high strength steels HT80, HY130, quenching and tempering effect on H_2 diffusion (Japanese) 8-64565
 hopping of a pair of distinguishable particles on uniform one dimensional chain, time-dependent correlations 8-88212
 impurities, Kramer's rate formula 8-83992
 impurity diffusion profiles, influence of limited solubility 8-55989
 insulating film, detection of self-diffusion of ionic charges by surface potential decay method 8-72295
 interstitial diffusion, nonadiabatic quantum theory 8-79818
 ionised impurity, diffusion, in semi-infinite semiconductor 8-75886
 kinetic model for solid diffusion with competing surface reaction 8-51719
 lattice atom displacements near end of implanted μ^+ tracks 8-55890
 lattice diffusion, Heisenberg ferromagnet 8-88090
 liquid metal wire, thermomigration through a solid in thermal gradient, force model 8-67870
 metal, clean surface, H release rate 8-95187
 metal, FCC, H isotope diffusion coeffs. calc. (Russian) 8-91483
 metal, grain boundary diffusion, temp. depend. and activation energy 8-95191
 metal, oxide film growing by cation diffusion, stress generation 8-60865
 metals diffusion thermodynamics, kinetics and mechanism 8-95179
 metals irradiated, heavily, exam. of percolative mass transfer 8-79639
 Mossbauer line broadening, influence of diffusion (German) 8-84510
 noble metals, divacancy contrib. to impurity diffusion 8-79812
 nonuniformly stressed crystal, statics and kinetics of vacancies (Russian) 8-55863
 NQR caused by vacancy diffusion of impurities, spectral density 8-68408
 one-dimensional hopping, moment expansions and occupancy (site) correlation functions 8-55972
 path independent integral for symmetric stress-diffusion fields surrounding line cracks 8-67130
 pentacene, in p-terphenyl, electronic excitation transport, acousto-optical effects 8-72079
 PMMA, diffusion-controlled penetration by monohydric normal alcohols 8-76918
 point defect diffusion in stress field of edge dislocation of irradiated solid 8-51720
 polyethylene, diffusion of long molecules, meas. and results 8-55987
 polyethylene, diffusion of long molecules, topological constraints 8-55986
 polyethylene, solid, nucl. spin-lattice relax. time, freq. depend. defect diffusion, 77-373K 8-72428
 polymers, diffusion coeffs. of gases, sorption, permeation investigs., review 8-67868
 power law frequency dependent dielectric function and nonanalyticity properties 8-60387
 precipitate migration in applied field by vol. diffusion 8-64545
 PTFE, $\text{H}_2(\text{D}_2)$ solubility and diffusion, activation enthalpy 8-79775
 quantum rate theory for symmetric double well pot. 8-55970
 rare earth-Se film couple, formation and crystallographic charact. of thin film phase 8-91574
 refractory metal, generalised model for prediction of periodic trends in sintering activation 8-64498
 rotational tunnelling and diffusion in condensed mol. systems, neutron scatt. 8-63658
 semiconductor doping diffusion process, built-in elect. field diffusion enhancement factor, anal. 8-55985
 sintered mats., complex diffusion alloying 8-68650
 size variation technique for diffusion coeff. determ. 8-83991
 solid solution, diffusion, influence of conc.-induced stresses (Russian) 8-55969
 solid-solid pellet systems, diffusion and reaction 8-85139
 spheroidal precipitate motion in temp. gradient by vol. diffusion 8-64544
 steel, C, diffusion of H_2 , SCC via martensite form. cooling rate changes on Mn and Ni addition (Russian) 8-56813
 steel, C, hydrogen embrittlement, elastic interaction of H_2 with precipitates 8-92340
 steel, stainless, 304L, T grainboundary diffusion and trapping, autoradiographic exam. 8-51738
 steel Cr-Mo, Ni-Cr, Ni-Cr-Mo, Cr, quenched and tempered struct. effect on H diffusion coeff. and solubility (Japanese) 8-52857
 strong drift effects 8-87808

diffusion in solids continued

superlattice thin films, sputtered, ion-bombardment-enhanced diffusion during growth 8-87882
 supersaturated solid solution, diffusive decomposition 8-76653
 surface-moving grain boundary interaction, anal. (Russian) 8-67721
 thermoelastic stressed solid, gaseous diffusion, thermodynamic struct., transport theory 8-51065
 thermoelastic stressed solid, gaseous diffusion, thermomech. formulation 8-51064
 tracer diffusion via vacancy mechanism, correlation factor, modified derivation 8-87809
 vacancies, formation volume, anal. of diffusion expts. under press. 8-55971
 X-ray diffraction line broadening from small subgrains containing gradients of spacing 8-67612
 Zircaloy, steam oxidised, partitioning behaviour of O_2 8-68839
 α -Zircaloy-4, O stabilized, O diffusion using ^{18}O tracer 8-51737
 α -Ag-Cd, chemical interdiffusion and Kirkendall shifts 8-87829
 AgBr, Na^+ , NQR caused by vacancy diffusion of impurities, spectral density 8-68408
 AgCl:Si, effect of impurity doping on Sr^{2+} diffusion 8-84002
 Al, dissolution rate of amorphous Si 8-95188
 Al: ^{12}B , relax. mechanism for polarised implant 8-87693
 Al: ^{24}Na , diffusion of Na, determ. of diffusion coeff. and activation energy 8-51746
 Al/brass/Al bimetal, three layers, formed by cold rolling, exam. of formation of intermetallic phases at interface 8-56658
 Al-Au bimetal thin film interdiffusion zone, intermetallic phase form kinetics, 70-160°C 8-75891
 Al-CuAl, eutectic, thermal instability in temp. gradient 8-52851
 Al-Mg-Zn, interdiffusion 8-51751
 Al-Ta-poly-Si interdiffusion, Ta barrier effect, Auger anal. 8-71888
 Al-Zn, dil., grain boundary diffusion 8-91475
 Al_2O_3 , initial sintering, method for obtaining surface diffusion coeffs., appl. to shrinkage data 8-95713
 Au films on Si substrate, solid-solid reactions 8-95369
 Au, of Pd and Pt, 700-1000°C (Russian) 8-91484
 Au/AuPb₂ interface, Pb and Au diffusion, LEED, AES study 8-71988
 Au-Ag bilayers, conc. profile by AES, interdiffusion coefficient determ. (French) 8-84077
 Au-Al system, influence of current on phase form. in diffusion layer (Russian) 8-52826
 AuGe/n-GaAs, SIMS study Au behaviour during annealing 8-75947
 BaO crown and flint glasses, Ag and Cu diffusion for optical waveguide fabrication 8-59166
 C, columnar and laminar forms, deposition on polycrystalline Ni foils 8-63943
 C fibre, of Ni, ZrN (TiC) diffusion barrier effectiveness 8-60624
 Co-Fe(Ni) system, interdiffusion zone growths (Czech) 8-84009
 Co-Si film system, diffusion marker expts. 8-79824
 Co-Si film system, interaction kinetics 8-79823
 Cs, diffusion in high temp. alloys, AES, SIMS depth profile study (German) 8-84008
 Cu, atom size effect in tracer diffusion 8-84005
 Cu, diffusion coeffs. calc. for H and D (Russian) 8-91483
 Cu, fatigue behaviour effect of Zn, Au diffused coatings 8-72850
 Cu in Au electrodeposited coating, under high temperature, influence on contacts performance obs. (Czech) 8-91486
 Cu, initial sintering, method for obtaining surface diffusion coeffs., appl. to shrinkage data 8-95713
 Cu, interdiffusion with sintered Al powder, struct. effect at high press. 8-60606
 Cu, lattice and grain boundary diffusion of P, exam. of diffusion rates by tracer sectioning technique 8-79817
 Cu, of ^{110}Ag , activation energy, form. enthalpy of vacancies 8-51736
 Cu-alloys, ZZ 8-75883
 Cu-Fe phase diagram, 650 to 1050°C (German) 8-60658
 Cu-M alloys (M=Zn,Al,Sn,Mn,Pb), diffusive redistrib. during friction (Russian) 8-52999
 Cu-Ni, diffusional homogenisation in compacted powder blends, X-ray diffr. line profile analysis 8-80491
 Cu-Ni (20 and 50 wt.%), sulphidation, exam. of scale growth kinetics 8-88560
 Cu-Ni bicrystal, misfit dislocation config., moire patterns, interdiffusion effects 8-84110
 Cu-Ni bimetallic films, dislocation wall form. during interdiffusion, TEM obs. 8-18586
 Cu-Ni thin film couples, interfacial reactions, contact resistance meas. 8-63882
 Cu-Ti system, diffusion obs. (German) 8-63881
 CuInTe_2 :Zn, donor impurity in diffusion, elec. and optical props. 8-68504
 Fe, annealed, Hz permeation, 230 to 300K (Japanese) 8-84004
 Fe, cast, diffusion saturation and form. of FeB and Fe_2B coatings 8-53032
 Fe, diffusion and solid solubility of Sb, 773-873K, ion backscatt. anal., rel. to intergranular embrittlement 8-71880
 Fe, Fe-C, diffusion coating by Cr and Pb melt bath, kinetics (Korean) 8-60873
 Fe, lattice distortions due to H, X-ray diffr. exam. 8-79629
 Fe, motion of H and D, mag. relax. meas. 8-64228
 Fe, $\mu^+\text{SR}$, theory of spin depolarisation rate 8-80271
 Fe, of H_2 and D_2 , at 49 to 506°C 8-59977
 α -Fe, of Zn, multiphase diffusion 8-79822
 Fe, pure, of H and D at 10 to 60°C 8-75887
 Fe-Al (40 at.%) B₂ type ordered alloy, C migration, resistivity meas. (French) 8-52868
 Fe-Co alloy, of H_2 , diffusion coefficient and permeability (Russian) 8-79819
 Fe-Cr, role of C in transform. by heating in (α + γ) phase (French) 8-52798
 Fe-Ni (20 to 100 wt.%), exam. of C diffusion coeff., in temp. range 950 to 1100°C 8-51747
 Fe-Ni mixed powders, effect of Ni particle size and unequal interdiffusion, on sintering process (Japanese) 8-84728
 Fe-Ni system, interdiffusion zone growths (Czech) 8-84009
 Fe_3O_4 - $\text{Fe}_{2.8}\text{Ti}_{0.2}\text{O}_4$, interdiffusion expts. 8-55991
 $\text{Ga}_{1-x}\text{Al}_x\text{As}$, of Zn, depend. on Al content 8-59981
 GaAs, heavy metal migration, ESCA study (French) 8-75885

diffusion in solids continued

- GaAs, minority carrier diffusion lengths, contact metal effects 8-72260
 GaAs:Be, annealing effect during MBE 8-79898
 GaAs_{1-x}P_x, diffusion of implanted Zn ions, ion microprobe analysis 8-95190
 GaIn_{1-x}P_x, epitaxial film, diffusion of Cu(Au)(Zn), intrinsic impurity effects 8-87825
 Ga₂O₃-Fe₂O₃ system, anomalous Mossbauer line shapes, incomplete annealing 8-92006
 GaP, diffusivity and solubility of Cu 8-51743
 GaP, LEC, SSD and CVD samples, Zn tracer diffusion profiles in solids 8-95189
 GaP:Au, diffusion, solubility, and electrotransport of Au 8-91489
 Ge, effect of Au on film props. 8-76161
 Ge:P, conc. depend. of diffusion coeff. at P diffusion 8-95185
 Ge-GaAs (110), heterojunction chemistry, photoemission expts., inter-diffusion obs. 8-95244
 H embrittlement cracking at notches 8-84985
 H₂, random walk models, generalisation to correlations over two jumps 8-79794
³He, quantum diffusion in solid ⁴He, tunnelling jumping approx. (*Russian*) 8-87844
⁴He, of ³He, quantum diffusion, pulsed NMR exam. (*Russian*) 8-71902
⁴He, quantum diffusion of ³He, tunnelling jumping approx. (*Russian*) 8-87844
 β-Hf, electrotransport and diffusion of Ta impurities (*German*) 8-87826
 Hf, thermotransport and thermopower of O₂ 8-76055
 In, of Pb, diffusion coeff. determ., RF size effect meas. (*Russian*) 8-91717
 InP, of Ag, low temp. 8-75884
 InSb/GaSb superlattice thin films, sputtered, ion-bombardment-enhanced diffusion during growth 8-87882
 KCl, of Sr and Ca, simultaneous diffusion coeffs. 8-79813
 KCl single crystals, thermal stability of neutron induced damage 8-79634
 KCl:Ba²⁺, precipitation kinetics, supersaturation effects, geometry of formed heterophase struct. (*Russian*) 8-84824
 LiNbO₃ planar waveguide, refractive index rel. to Ti diffusion (*Russian*) 8-59120
 LiNbO₃:Fe, ferroelectric, treated in Li₂CO₃, formation of Fe²⁺ state, Mossbauer effect 8-92003
 LiNbO₃:Ti waveguide, diffused, Mg diffusion effects on chars. 8-66905
 MgO, EPR of Mn²⁺ diffusion 8-91477
 MnZn ferrite, gas phase fluorination for improved props. 8-52306
 MnZn ferrites, impurity induced exaggerated grain growth 8-92222
 Mo, adsorption of N₂, surface coverage and diffusion in bulk 8-60036
 Mo, of H₂, 900-1100°C (*Russian*) 8-79811
 Mo, of Li, mechanism 8-84007
 Mo, of volatile fission products ¹⁴⁰Ba and ¹³²Te, 1400-2000K (*Russian*) 8-91485
 Mo, RF sputtered, diffusion barrier props. 8-71887
 Mo, vacancy mutation to divacancies by He trapping, percolation onset 8-51601
 Mo:N, ion implanted proton-irradiated, annealing behaviour 8-91362
 MoSi₂, diffusion marker for backscatt. studies of W+Mo bilayer film 8-87828
 Na₂O-B₂O₃ glass, covered with PbO film, deep penetration of Pb²⁺ ions 8-79535
 2Na₂O-CaO-XSiO₂ glass, He mobility, interconnectivity, miscibility limits, effect of morphology 8-67864
 Nb, diffusion of H, influence of H-H pairing, jump model 8-75878
 Nb, diffusivity of O, N, exam. 8-51741
 Nb, review of neutron radiography results 8-59961
 Ni alloy, of aluminide coating, spontaneous form. of diffusion barrier (*German*) 8-71886
 Ni alloy, ZrS₆K, diffusion layer form. on Nb addition, struct., comp. (*Russian*) 8-56814
 Ni, diffusion coeffs. calc. for H and D (*Russian*) 8-91483
 Ni, effect of plastic deform. and martensite transformation on Fe atom mobility (*Ukrainian*) 8-55974
 Ni ferrite, gas phase fluorination for improved props. 8-52306
 Ni foil, of H₂, surface states and thermo EMF 8-91674
 Ni, H permeability using permeation method (*Japanese*) 8-51740
 Ni, of Ag, volume and grain-boundary, diffusion parameter temp. depend. meas. (*Russian*) 8-67863
 Ni, of H, permeability and diffusivity (*Japanese*) 8-66345
 Ni, of H (*Japanese*) 8-51739
 Ni, of In, temp. depend. (*Russian*) 8-75880
 Ni/Pt double layers on Si substrate, silicide formation 8-84010
 Ni-Se interface, reactive diffusion, electronic struct., UPS study 8-51748
 Ni-Si film system, silicide first phase form., reaction kinetics 8-79821
 Ni-Si interface, NiSi formation from Ni₂Si, Pt marker study 8-87830
 Ni-V, interdiffusion coeffs. in phase transform. range, 810-1175°C (*Russian*) 8-91490
 Ni-W (2%), Mg diffusion meas., 970-1330K, appl. of vapour collect and AES method 8-75876
 Ni-Zn diffusion couple, annealing and reaction diffusion (*Japanese*) 8-51749
 NiO, single cryst., of S 8-95186
 No, H₂(D₂) diffusion model, quantum rate theory for symmetric double well pot. 8-55970
 P₂O₅-glass, of Cu⁺ ion, fluoresc. meas. 8-59980
 Pb, atom size effect in tracer diffusion 8-84005
 Pb, ion implanted, diffusion of Co, exam. by activation analysis 8-91488
 Pb, of ⁶⁴Cu, electromigration, thermomigration, and solubility 8-71882
 PbO film, on vitreous SiO₂, interdiffusion reactions, UV spectroscopy obs. 8-51750
 Pb_{1-x}Sn_xTe, Cd-In diffusion, changes in elec. props. 8-91348
 Pb_{1-x}Sn_xTe-PbTe heterojunction, Sn diffusion profile, X-ray diffr. data interpretation 8-51832
 Pd, diffusion coeffs. calc. for H and D (*Russian*) 8-91483
 α-Pd, H₂ diffusion by galvanostatic charging 8-84001
 Pd, H₂(D₂) diffusion model, quantum rate theory for symmetric double well pot. 8-55970

diffusion in solids continued

- α-Pd, next-neighbour jumps of H in quasi-elastic neutron scattering 8-91487
 Pd-Pt, of T, effect on freq. factor and activation energy 8-63880
 Pd₇₅Cu₂₅Si_{16.5} metallic glass, diffusion of Au 8-55983
 Pt membranes, of H₂, diffusion at high press. and temps. 8-55984
 Pt-Si film system, silicide first phase form., reaction kinetics 8-79821
 Pt₉₀Rh₁₀/Pt thermocouple, Inconel sheathed, MgO-insulated, decalibrations during 1200°C use, ion microprobe obs. 8-57957
 Pu-Cu, of T, effect on freq. factor and activation energy 8-63880
 Si, amorphous, hydrogenated, of D₂, SIMS anal. 8-75877
 Si, diffusion of B,P and Sb, implantation damage effects 8-55988
 Si, diffusion of Ga in closed capsule, surface damage elimination 8-87691
 Si, diffusion of Ga through SiO₂ layer, junction depth 8-51574
 Si, of P(B)(As), proton enhanced diffusion and vacancy migration 8-67747
 Si, P diffused sample, stacking faults and dislocations formation from interstitials 8-95059
 Si, rel. to oxidation stacking faults and microdefects, growth behaviour during high temp. annealing 8-72901
 Si, sputtered, cluster formation, influence of HF plasma interaction 8-64441
 Si, stress enhanced diffusion of B, using SiO₂ diffusion masks, photo-diode fabrication 8-67865
 Si substitutional diffusion model 8-71884
 Si, vacuum deposition, combined with Sb ion implantation (*Japanese*) 8-88428
 Si: (B, P, Ge), impurity-pair diffusion, influence of elastic stresses 8-87824
 Si:Au, impurity capture cross section and generation lifetime determ., MOS expts. 8-91772
 Si:Au, neutron irradiated, penetration of Au into Si 8-59984
 Si:B, near intrinsic (100) and (111) samples, inert and oxidising ambients, diffusion, segregation 8-75882
 Si:B, p-n junction form. by B deposition and laser-induced diffusion 8-87690
 Si:B(P), diffusion induced imperfections, laser annealing, rel. to junction chars. 8-75678
 Si:B(P), heavily diffusion-doped layers, Co diffusion 8-59982
 Si:Fe, EPR and neutron activation anal. of thermal defects 8-91355
 Si:Ga, gettering of Au and Cu during Ga diffusion 8-91350
 Si:P, electrostatic field on impurity atoms, heavy doping effects 8-51570
 Si:P, emitter-misfit dislocation formation during P diffusion 8-91338
 Si:Pb, implanted and annealed, impurity redistrib. 8-75689
 Si-B, P diffusion and activity after Ar ion bombardment 8-95192
 Si-B, using BN, expt. (*Bulgarian*) 8-59824
 Si-Rh interface, RhSi form. by lattice diffusion 8-71891
 SiC, diffusion behaviour of fission products, 1650 to 1850°C 8-79814
 SiC, diffusion tracer deposition, using travelling solvent zone 8-51742
 SiC, exam. of T₂ diffusion coeffs. and D₂ solubility 8-79816
 SiC, of B, polycryst. struct. effect 8-59983
 SiC:Be, film donor impurity, diffusion influence on elec. and optical props. 8-87942
 Si₃N₄ film, diffusion of Al, AES and depth profiling 8-51744
 SmCo₅ spheres, exam. of sintering in vacuum and Ar atmospheres 8-84738
 Ta, internal friction meas. of O, N diffusion 8-75888
 Ta, review of neutron radiography results 8-59961
 Ta, single cryst., positive muon diffusion 8-80267
 Th metal, diffusion and electrotransport of Th metal 8-86611
 ThO₂-based ceramic impurity diffusion, electrotransport method 8-67869
 Ti, review of neutron radiography results 8-59961
 α-Ti, S, C and Cl diffusion, AES meas. 8-51735
 Ti-Permalloy thin film diffusion couples, low temp. interdiffusion inter-diffusion 8-71889
 TiCuH, H-atom diffusion, PMR obs. 8-91978
 TiO₂, of Na and H from Na amalgam, room temp. coloration technique 8-84611
 UO₂, irradiated, spacing of intergranular fission gas bubbles 8-66340
 UO₂, neutron irradiated, diffusion of fission product T 8-67866
 UO₂, transfer of fission gas between grain faces and edges 8-79815
 V, review of neutron radiography results 8-59961
 V-SiO₂ interface reaction, identification of diffusion species 8-75890
 Va, H₂(D₂) diffusion model, quantum rate theory for symmetric double well pot. 8-55970
 W fibre, KSiAl doped, recrystallisation, Li diffusion effects, hardness, strength, microstructure meas. (*German*) 8-64644
 WC-Co, sintered hard alloy, mechanism of penetration of liquid metals 8-60619
 WSi₂, diffusion marker for backscatt. studies of W+Mo bilayer film 8-87828
 Y₂O₃-Nb₂O₅, solid state reactions, 1275 to 1350°C, electron microscopy, EPM, X-ray diffr., dilometry (*Japanese*) 8-63883
 Zn:Al, ion implantation of Al, defect flow induced outdiffusion 8-63779
 ZnS,Se_{1-x} layer on ZnS, ZnSe, growth by solid-state diffusion technique 8-56578
 ZnSe, charged dislocation motion mechanism (*Russian*) 8-79820
 α-Zr, atom size effect in tracer diffusion 8-84005
 α-Zr, O stabilized, O diffusion using ¹⁸O tracer 8-51737
 Zr-Zr₂Al₃, diffusion weldings between 1000 and 1300°C, electron microprobe anal. (*German*) 8-84011
 ZrC, solubility, diffusion and permeation of Cs 8-51684

diffusion pumps

- jet assembly and vaporiser design optimisation 8-81999
 ultrahigh vacuum pumps 8-89488
 Hg use and abuse for vacuum production and meas. 8-81998

diffusivity see diffusion**diffusivity, thermal see thermal diffusivity****digital-analog converters see digital-analogue conversion****digital-analogue conversion**

- see also analogue-digital conversion
 CRO storage, Gould Advance OS4000 using A/D and D/A converters 8-93673

digital arithmetic

linear eqns. integral soln. using integer arithmetic 8-69960
numerical optical data processor, representation and implementation 8-78947

digital circuits

see also digital integrated circuits; pulse circuits; switching circuits
astronomical laser ranging equipment, telescope drive (*Japanese*) 8-89078
dual integrated gate generator 8-55112
integrator, for radioastronomical obs. processing (*Russian*) 8-57465
magnetic stirrer with no external moving parts appl. 8-93666

digital communication systems

31st Annual Frequency Control Symposium, Atlantic City (1977) 8-57905
fibre-optic digital transmission, shot noise probability distribution function 8-50717
gigabit laser communication 8-66860
medium and long distance digital optical fibre communication systems 8-50941
multilevel pulsed phase modulation, channel capacity in optical links 8-78934
optical, GaAlAs laser transmitter 8-90423
optical fibre, expt. 8-66943
optical fibre 32 Mbit/s non-repeated 50 km transmission expt. 8-79108
optical fibre cable links installed in operational ducts, transmission meas. 8-50928
optical fibre transmission capability expansion 8-66914
optical fibre transmission experiment, 800 Mbit/sec at 1.05 μm 8-83075
optical space communications with Nd:YAG laser 8-66859
optical waveguides using silica fibre for wavelengths beyond 1 μm 8-50907
X-ray picture digital transmission over voice-grade telephone channels, laser scanning system 8-80953

digital control

see also numerical control
camera, Canon A-1, digital logic principles 8-70206
digital computer control in Canadian nuclear plants, past performance and future outlook 8-58383
electrostatic generator terminal voltage on-line feedback stabilisation using digital computer 8-82004
mechanical actuator, stepper motor, appl. to control of scientific apparatus 8-62683
neutral beam filament supply, 15 V 10^3 A, programmable, regulated, for fusion reactor 8-70630
particle size meas. by laser beam expt. 8-70098
particle track chamber, semi-automatic meas. instrum. register for camera photograph reduction 8-78575
programmable for Fresnel lenses manufacture (*Russian*) 8-50884
Raman spectrometer, digital control system, appl. to soft mode spectroscopy 8-86345
stepping motor control system for repetitive scanning of a monochromator 8-54355

digital differential analysers

blood cell differential counter, ADC 500, pattern recognition based image processing system 8-73282

digital filters

see also signal processing; two-dimensional digital filters
basilar membrane model for voice features extraction 8-77069
biomedical signal processing and telemetry, digital bandpass analysis 8-57107
ECG, implemented on microprocessor 8-85428
electron micrograph optical and digital spatial freq. filtering 8-70231
hydrophysical nonstationary processes, real time digital filtration (*Russian*) 8-65425
linear filters for transformation of apparent electrical resistivities 8-96304
microcomputer based digital filter for electroencephalogram processing 8-73278
random pulse train inputs (*Japanese*) 8-53547
recursive filter, generation of 1/3 octave data 8-87211
scintigraphy, multichannel, collimated, Compton effect on spatial resolution, digital spatial filtering 8-69182
seismic data, optimum mixed delay spiking filters appls. 8-77346
speckle image digital processing 8-71053
two-dimensional, image enhancement appl. (*Italian*) 8-53539

digital instrumentation

see also digital readout; digital voltmeters
5 MHz digital frequency meter (*German*) 8-62206
AC voltmeter type F4850 and wattmeters type F4860, operational principles (*Russian*) 8-70158
acoustic excitation impulse generator 8-90618
aerosol classification pulse amplitude analyser 8-61587
averaging meter for nonelectric periodic quantities, dual slope principle (*German*) 8-73983
Barkhausen computer interface for thin mag. film props. anal. 8-82008
bellow-type transducer for pressure meas. (*Polish*) 8-93719
bubble chamber film, track rescue system 8-70728
clocks, standard-freq. controlled, for high precision time meas. (*German*) 8-77871
contactless for production process linear dimensions meas. (*Polish*) 8-93652
crystalline sample fusion temp. meas. automatic instrument 8-57945
digital dynamic method for precise meas. of static characteristics 8-54389
digital lineariser for nonlinear transducers 8-57931
electron microscope image enhancement, digital processing method (*German*) 8-89599
electronic digital thermometer (*German*) 8-54368
electronic microbalance and precision balance design (*German*) 8-57935
electronic scales and precision instrum. (*German*) 8-70100
Fizeau wavelength meter, laser and other monochromatic sources, digital display 8-89450
frequency meter, for LF meas., using TTL ICs 8-86296
frequency meter, using variable measuring times and automatic scale conversion (*Spanish*) 8-49862
ionosonde, universal, for multi-parameter ionograms 8-73577

digital instrumentation continued

laboratory automated systems and digital techniques 8-57922
least or greatest interval timer 8-62183
meteorology and oceanology (*German*) 8-53745
micrometer, development and appl. 8-65902
million channel 300 MHz bandwidth digital spectrum analyser for Deep Space Network and SETI 8-73642
modulator and synchronous demodulator system, alternative to analogue phase detector 8-70107
multimeters, Gould Alpha III, features (*French*) 8-77943
multichannel digital temp. recorder, TR-2711, measuring 100 channels in 10 s 8-65931
multichannel temperature recorder, Thermodac II with 24 channels using thermocouples 8-65930
multidiscriminator for use in γ - γ coincidence expts. 8-70707
multimeter, with LED or LCD display (*French*) 8-57986
multimeter Quadriovometer MX 737A (*German*) 8-57988
multimeters, microprocessor controlled 8-93721
multiple digital differential thermal analysis instrumentation, synthetic chemicals production appl. 8-77902
noise and vibration measurement, Bruel & Kjaer products review 8-94493
open channel acoustic flowmeters, design, calibration and errors 8-55701
phase meter, 2 Hz to 200 kHz, without freq. tuning (*German*) 8-54409
photometric meas., digital meter, cct. and operation (*Polish*) 8-65943
punched register for astronomical elec. photometer (*Russian*) 8-93117
Q-meter, automatic, design procedure 8-70155
refractometer for atmospheric radiowave refractive index meas. 8-86321
resistance bridge type thermometer, operational principles (*Polish*) 8-49834
respiratory rate and ventilation digital recorder 8-81005
scanning electron diffractometer, appl. to radiation sensitive materials 8-87596
semiautomatic digital coercimeter, exam. of design 8-76817
single-sweep waveform recorder with automatic range selection 8-77889
six-channel scanning thermometer type AD2036 operational principles 8-86269
storage instrum. and function generator electronic modelling appls. 8-77937
storage oscilloscopes, Gould Advance OS4000, using A/D and D/A converters 8-93673
thermal meas. using data logger and computer 8-81966
thermodynamic enthalpy and specific heat determ. equipment 8-57951
thermometer, linear, 0 to 99.9°C range (*German*) 8-93684
thermometer, process meas. control appl. 8-49833
thermometer, type 2572, with temp. range 4K to 1760°C with 0.1°C resolution 8-65929
thermometers, 300°C-1800°C range, features (*Russian*) 8-65926
thermometers using quartz crystal oscillator high accuracy achieved 8-65932
thin film thickness measurements, instrumentation system 8-89436
time interval meas. instrument with 2 nsec accuracy 8-77867
transient recorders, enhancement of signal averaging using microcomputer 8-57930
two-channel data gathering and registration system for fast-action experiments 8-77877
US thickness gauge, portable 8-92427
wavemeter for CW lasers 8-89447

digital instruments *see digital instrumentation***digital integrated circuits**

see also integrated logic circuits; integrated memory circuits
laboratory automated systems and digital techniques 8-57922
miniature pressure-frequency convertor with pulse output 8-57926

digital readout

see also digital instrumentation
display for lecture hall use 8-86075
Earth tides, tilts, parallel recording through digital print-out and photorecording channels (*Russian*) 8-88785
electrophotographic KC film digital recording performance 8-78024
nuclear track sensitive target expts., automatic film meas. 8-55105
recording system, for automatic US flaw detection system 8-76815
X-ray tube kVp indirect determ. using digital readout device 8-53486

digital signals

reflection seismograms signal anal., use of kepsrum 8-81425

digital simulation

agglomeration, computer simulation (*Japanese*) 8-95706
agglomeration, Monte Carlo simulation (*Japanese*) 8-95707
air pollution density distrib., flow pattern in Tanabe area, Japan, numerical anal. (*Japanese*) 8-96289
amygdaloid kindling phenomenon extended first approx. model 8-53378
anisotropic solid fluid flow with free or artesian surface analysis, finite element method appl. 8-92872
astronomical spectra obtained with low-dispersion Fehrenbach prism, computer simulation 8-57468
atmospheric boundary layer turbulence, multi-component linear digital simulation 8-61513
atomic dislocation modelling, flexible boundary conditions and nonlinear geometric effects 8-75667
axial-flow compressor cascade flows computer simulation 8-79333
biological evoked potentials, single trial, S/N ratio and response variability 8-61159
biostereochemical modelling, interactive computer graphics, appl. to DNA-protein interaction 8-88693
biped locomotion control 8-80904
bladder smooth muscle impulse propag., math. anal. (*Japanese*) 8-53359
blood pulsative flow, finite element method appl. 8-92670
brain rhythmic activity generation models (*Dutch*) 8-73150
composite electrostrictive resonators, finite element simulation 8-59237
composite superconductors, stability anal. by thermal analyser digital computer program 8-54995
computer applications to process control, conference, The Hague (1977) 8-49808

digital simulation continued

- computer simulated laboratory exercises, validity of graphic approach 8-81780
- computerised tomography, iterative three dimensional reconstruct. from twin cone beam projections, simulation study 8-80949
- computerised tomography, reconstruction simulation, no. of rays versus no. of views 8-69214
- crack growth in concrete, computer simulation using Monte Carlo method 8-76764
- crack propag. simulation, using moving grid based finite difference scheme 8-83334
- digestive tract electrical rhythms simulation 8-64970
- direction-sensitive displacement analysis by multiple freq. holographic interferometry 8-54338
- ductile-brittle transition, atomistic simulation by computer, exam. of thermal activation of crack tip plasticity 8-60801
- dynamic emission computed tomography, quantitative pots. 8-77105
- eddy current through type transducer, operating condition simulation when inspecting ferromagnetic rods 8-53077
- elasto-plastic flow in computer simulated, A533 steel 8-56720
- EMG, surface, digital simulation, spectral anal. 8-80863
- EMG, surface, model for digital simulation 8-80862
- environmental release prediction, time split finite element algorithm 8-92880
- EPR, rat liver and hepatoma mitochondrial lipids, stochastic anal. 8-76984
- EPR and saturation transfer EPR, fast computation, perturbation approx. extension for overmodulation 8-82754
- EPR powder spectral simulation, paramagnetic ions 8-80194
- fatigue crack propag., computer simulation based on crack closure concept 8-68793
- ferromagnetic crystal, domain wall pinning effect and intrinsic coercivity, computer simulation 8-64217
- flagella bend propagation, derivation of eqns. of motion and simulation 8-77074
- flow about arbitrary 2-dimens. boundary, implicit finite difference simulation 8-94628
- fluid velocity vector and temp. fields reconstruction, three-dimens., from acoustic transmission meas. 8-51261
- fracture processes and fibre strength, in brittle fibre reinforced alloys, anal. by Monte Carlo computer simulation (*Japanese*) 8-80634
- free surface flow, finite element method appl. 8-90819
- frictionless tidal channel behaviour, finite element and finite difference methods appl. 8-92876
- fusion reactor design and performance requirements, cost and systems anal. 8-50357
- gamma camera scintigrams, influence of digital representation on image quality (*German*) 8-88738
- gamma-ray spectral anal. using FFT (*Japanese*) 8-90047
- gammagraphy, 3-dimens. image processing appl. to coded aperture imaging (*French*) 8-57067
- general heat transfer, CSMF package 8-75145
- groundwater discrete kernel generator, finite element method appl. 8-92873
- groundwater flow model using finite element method 8-92874
- groundwater two-dimensional flow, finite element method appl. 8-93018
- hard rod system, initially ordered, one-dimens., mol. dynamics computer simulations 8-71658
- heat conduction, inverse nonlinear problems, simulation methods 8-94513
- HTGR steam power plant, nonlinear dynamic model 8-78437
- human respiratory system, role of the Van der Pol oscillator 8-65073
- hydrological system tracer, finite element method appl. 8-92881
- image reconstruction, Fourier techniques evaluation in relation to number of X-ray sums 8-77112
- ingot, temp. field calc. approx. by equiv. cylinder (*German*) 8-84788
- inter/cross modulation levels for GaAlAs diode laser 8-55455
- ion bombardment collision cascades, computer simulation, Monte Carlo code 8-67756
- Ising model, nonequilib. intensive parameters and detailed balance, computer simulation calcs. 8-76208
- JET, synchronous generator, bridge convertor and ohmic heating systems, digital simulation 8-54960
- lakes or bay landslide wave generation, Galerkin finite element appl. 8-92879
- large amplitude water wave, finite element method appl. 8-92851
- large cosmic ray showers, computer simulation using models of hadronic collisions 8-57415
- left-heart haemodynamics, mathematical model 8-65074
- leucine aminopeptidase crystalline aggregates, interpretation of electron microscope images 8-68988
- mass spectrometer, quadrupole mass filter with flat electrodes, computer simulation 8-54492
- measurement errors, random, simulation (Monte Carlo) method, teaching appl. 8-86062
- metal crystal, lattice defects, relax. studies 8-79604
- Moire contouring using virtual moving gratings simulated on computer 8-73968
- molecular dynamics of liqs., neutron scatt. and computer simulation 8-63650
- molecular fluids, translational motion, Mori three variable theory and mol. dynamics simulation 8-63651
- molecular systems, electron density, spatial, rel. to conform. props., computer simulation 8-70763
- MOS transmission line, resistive, free charge transport, simulation, distrib. model 8-68092
- multislit spectrometer for the night airglow observation 8-73542
- neuromuscular system output response, effect of correlated adjacent interspike interval sequences of input 8-80858
- neuronal populations, diffusely-connected, computer simulation 8-53384
- nonlinear free surface flow, boundary integral eqn. method appl. 8-92850
- nuclear plant risks assessment, of accidents and normal operation 8-50281
- oil spill simulation in Florida Gulf outer continental shelf 8-73406
- one-dimensional chain, thermal fluctuation induced rupture, computer simulation 8-91378
- optical computing for image bandwidth compression, analysis and simulation 8-94373

digital simulation continued

- optical signal receivers, optimal and nonoptimal, logical structs. efficiency comparison, simulation (*Russian*) 8-71041
- optimal numerical filters fitted for noise damping, atm. circulation simulation appl. 8-92997
- oxyhaemoglobin dissociation curve direct obs. in man in vivo, computer investigation 8-85433
- polymer, amorphous, conform. from simulation of filling diamond lattice with chains (*German*) 8-75595
- polymer, amorphous, conform. from simulation of thermal motion (*German*) 8-75594
- polymer chain, of bistable oscillators, Brownian dynamics of transitions 8-86983
- polymer chain dynamics, in soln., computer simulation 8-83718
- polymer dynamics simulation, general theory 8-91210
- polymer dynamics simulation, relax. rates and dynamic viscosity 8-91211
- polymer solution, simulation of macromol. dynamics, Monte-Carlo method, conc. depend. (*Polish*) 8-51404
- porous media one-dimensional unsteady drainage, finite element method appl. 8-91011
- radiation induced low-energy collision cascades in Cu, computer simulation 8-87705
- radionuclide mean clearance time transverse section imaging 8-73222
- REACT program for computer-assisted simulation of chemical reaction sequences, structure elucidation applications 8-92477
- repetitive firing computer models nonlinear systems anal. 8-80854
- road traffic acoustic behaviour near traffic lights, computer simulation 8-90597
- rotating disc electrode, with optically transparent ring, digital simulation 8-53210
- sedimentology, Rayleigh-Ritz method appl. 8-92878
- shallow water with moving boundaries, finite element method appl. 8-92847
- Solar Thermal Test Facility, 5 MW, heliostat focus and alignment system 8-50894
- sonar signal processor, 36-channel, programmable 8-66976
- speckle image digital processing 8-71053
- speckle interferometry of binary stars, computer simulations in photon-counting mode 8-53836
- steel, stainless, hot rolling resist., multistage mode of deform. effects (*Russian*) 8-80583
- stratified turbulent flow, finite element method appl. 8-9f964
- stray light phenomena, GUERAP III Monte Carlo simulation 8-58907
- stray light simulation with advanced Monte Carlo techniques 8-58906
- TEM imaging of W(111) split crowdion interstitial, computer simulation 8-71723
- temperature and EM fields simulation, inductively heated semiconductor 8-55961
- thermal conductivity prediction of heterogeneous mixture, digital simulation technique 8-87247
- thermal regenerator, with variable mass flow rate, computer model 8-75047
- tidal estuary two-dimensional hydrodynamic model using finite element method 8-92846
- transmitter kinetics model computer simulation results 8-92617
- transonic flow, unsteady, implicit shock-fitting computational scheme 8-94763
- tsunami long wave propagation analysis, finite element method appl. 8-92849
- tsunami wave propagation, finite element method appl. 8-92848
- two-dimensional flow with singularities, finite element method appl. 8-90822
- two-dimensional hydrodynamics and water quality by finite element method 8-92877
- ultrasonic sound field, in air, quantitative visualisation (*French*) 8-87212
- underwater acoustic holographic image reconstruction for moving objects 8-75019
- US attenuation measurement of soft tissues, signal processing of broadband pulsed US 8-77094
- vacuum system transient simulator, appl. to Princeton TFTR 8-74496
- variable domain finite element model for dam unsteady compressible fluid flow 8-90820
- ventricular excitation, digital simulation, computer model evaluation 8-85302
- ventricular function computer simulation, development of model and parameter estimation 8-53439
- vortices, in mixing layer, numerical simulation 8-90853
- water quality modelling of high mountain stream of Bishop Creek, California 8-53666
- water resource finite element anal., conf. at London, England 1978 8-92867
- well flow analysis, finite element method appl. 8-92870
- wind-wave interaction, two-layer flow, numerical simulation 8-92823
- writing aid for motor handicapped, microprocessor-based device, LOGOS 8-81077
- Al, step coverage optimisation by computer simulation and SEM 8-51838
- AlF, hyperfine structure simulated by computer programme 8-50538
- Al₂O₃, sintering of single phase and multiphase components (*German*) 8-80494
- Br₂, liq., struct., theory and computer simulation 8-59734
- Cu, polycryst., back sputtering of 100 to 500 eV Ne ions, computer simulation 8-60537
- Fe, amorphous, realistic structural model, search for Bernal holes 8-83734
- Fe, BCC, computer simulation of entropy of 1/2{111}{110} edge dislocation 8-67716
- α-Fe, BCC, migration of vacancies near twin boundaries 8-51535
- Fe, BCC, vib. entropy of 1/2{111}{110} edge dislocations 8-63768
- Fe-N single crystals, solid soln. stress assisted nucleation of α' precipitates 8-52810
- Fe_{1-x}Mg_xCl₂, magnetic excitations 8-91852
- HCl laser, V=3 to V=2 band process, computer simulation 8-71095
- (H₂O)₂, dimer intermolecular pot., liq. struct. mol. dynamics simulation 8-71657
- Xe anode-directed streamer propagation simulation 8-67591

digital storage

see also cryotrons; optical stores; read-only storage
CRO storage, Gould Advance OS4000 using A/D and D/A converters 8-93673
heart-rate store, PLL circuit, portable (*German*) 8-65139

digital systems

see also computer networks; fast-response computer systems; multiprocessing systems; real-time systems; sampled data systems
frontiers in education, conference, Urbana-Champaign (1977) 8-81779
image processing applications, conference, San Diego (1977) 8-81528
plot system developed for nondestructive materials testing exam. 8-53067

digital to analogue converters see digital-analogue conversion**digital voltmeters**

AC measurement, using digital instruments 8-93726
AC portable voltmeter and calibrator 8-74019
AC type F4850, operational principles (*Russian*) 8-70158
capacitance/loss tangent of capacitor meas., three voltmeter method (*Russian*) 8-70159
measurement errors reduced by user-controllable filtering 8-77931
miniature, for battery and mains supply (*German*) 8-86289
miniature, mains/battery, construction and calibration (*German*) 8-93723
for noise and vibration meas. 8-55538
programmable, microprocessor controlled, features 8-93720
RMS digital voltmeter calibrator for VLF 8-86293

digitisers see analogue-digital conversion**dilatometers** see extensometers**dilute alloys**

see also impurity electron states; Kondo effect; magnetic properties of dilute systems

atomic displacements around impurity and three body interaction 8-91406
binary alloy monocrystal, thermodynamics of growth, model (*French*) 8-87635

electrical resistivity, Kondo effect vs. spin glass behaviour 8-68269

formation energy, lattice relax. and zero-point vibrations 8-83771

formation energy, lattice relax. and zero-point vibrations 8-87646

Kondo alloys, calc. of host nucl. spin-lattice relax. 8-88215

magnetic 3d impurity in non-magnetic metal, effective ion Hamiltonian 8-64016

magnetic alloys, dil., transition metal hosts, props. review 8-84417

magnetism of dilute and conc. alloys (*Rumanian*) 8-91843

noble metals containing rare earth impurities, magneto-transport props. 8-68015

rare earth alloys, dil., ESR linewidth of rare-earth ions 8-68373

rare earth-Au, dil., Mossbauer exam. of mag. hyperfine field at ¹⁹⁷Au impurity 8-88244

superconducting dilute alloys, eqn. for crit. temp. 8-72300

ternary, substitutional solute element effect on diffusivity of interstitial solute element 8-59969

thermopower and resistivities, validity of Nordheim-Gorter relation 8-91671

transition and noble metal dilute alloys, Einstein's temp. and vibrational entropy, rel. to electronic struct. 8-83900

transition metal impurities in transition and noble metal hosts, electronic struct. 8-75990

wave-vector-nonconserving optical transitions 8-72100

A-Mn, dil., mag. susceptibility and single impurity effects 8-64186

Ag-Au, dil., low temp. elec. resist. 8-51964

Ag-Mn alloys, dilute, low temp. elec. resist. (*Russian*) 8-68024

Al alloys, dil., size effect of impurity atoms rel. to trapping radii for migrating self-interstitials 8-75690

Al-based, Hall coeff., calc. by 4-OPW approx. 8-76052

Al-Cr(V)(Ti), dil., electron irradiated, interaction of self interstitials with undersized solute atoms 8-63789

Al-Cu(Ag)(Ge), dil., deviation from Matthiessen's rule at high temps. 8-64025

Al-Fe, electron irradiated, interstitial-solute complexes, internal friction spectra 8-92289

Al-Li, quenched and irradiated, recovery, resist. and internal friction obs. 8-52848

Al-M, dil. alloy, electronic states of 3d-transition metal (M) impurities 8-64005

Al-Mg, dil., long-range solute-host interactions 8-95062

Al-Mn, dil., ⁵⁴Mn Knight shift meas. using nucl. orientation 8-68396

Al-Mn, dil., coherent propag. and strain-induced localisation of muons 8-95537

Al-Sn, dil. alloy, vacancy-impurity interaction, exam. by electrical resistivity meas. at 77K (*German*) 8-83846

Al-Zn, dil. alloy, ageing and reversion, annealing curves, X-ray obs. 8-88485

Au-Co, dil., local moments, third harmonic de Haas-van Alphen wave shape anal. 8-84127

Au-Cr Kondo alloy, effect of press. on resistivity 8-79978

Au-Fe, dil., approach to saturation of magnetisation 8-56293

Au-Fe, dil., local moments, third harmonic de Haas-van Alphen wave shape anal. 8-84127

Au-Fe, very dil. alloy, Kondo temp. 8-91688

Au-Sn (100 ppm), quenched and aged, small vacancy clusters, electron microscope obs. 8-76671

Be-Ru, dil., quadrupole interactions at ⁹⁹Ru, TDPAC meas. 8-91996

Bi-Te, dil. alloy, elec. cond. depend. on Te conc. (*Russian*) 8-76042

Ce_{1-x}La_xAl₃, extraordinary Hall effects, 4.2-300K, cryst. field interaction 8-79980

Co-Cd, dil. alloy, impurity hyperfine interactions 8-84416

Co-Fe-Mn, dil. ferromag. alloy, mag. moment, saturation magnetisation meas. 8-64195

Cr-Pt, dil., effect of Pt on itinerant antiferromagnetism 8-64191

Cr-Re, dil. alloy, mag. susceptibility temp. depend., thermal expansion coeff. (*Russian*) 8-76225

Cu alloys, dil., size effect of impurity atoms rel. to trapping radii for migrating self-interstitials 8-75690

Cu-Al, change in force constant due to volume effects 8-75778

Cu-Al, impurity concentration effects 8-75777

Cu-Au, dil., enhanced lattice sp.ht. 8-51699

Cu-Au, dil., O₂ solubility, thermodynamic and residual resist. study 8-59952

Cu-Be, impurity concentration effects 8-75777

dilute alloys continued

Cu-Cr, dil. alloy, Knight shift temp. depend., electronic struct. 8-84488

Cu-Cr(Mn)(Fe), NMR data, ionic model and Kondo temp. 8-68399

Cu-Cr(Mn)(Fe), NMR satellite data, rel. to electronic struct. 8-68398

Cu-Fe, dil., transmission ESR meas. 2 to 40K 8-68364

Cu-Ir, dil., impurity diffusion, temp. depend. (*Russian*) 8-67851

Cu-Mn, dil., anomalous thermal expansion below 50K 8-51710

Cu-Mn(Fe)(Co), Kondo system, host NMR exam. 8-80246

Cu-Ni, dil., electronic struct., virtual bound state due to s-d hybridisation 8-75990

Cu-Ni dil. paramagnetic alloys, sp. elec. resist., effect of Ni clusters (*German*) 8-95293

Cu-Si, change in force constant due to volume effects 8-75778

Cu-Si, impurity concentration effects 8-75777

α-Fe-based dil. solid solutions, electronic struct., hyperfine interactions 8-79968

Fe-Co-Mn, dil. alloys, NMR freq. temp. depend., spin echo meas. 8-64296

Fe-N alloy, dil., galvanomag. effects, 4.2-250K 8-87964

Fe-Ni-Mn, dil. alloys, NMR freq. temp. depend., spin echo meas. 8-64296

Fe-Ni-Si, double spontaneous reversible deformation during thermal cycling 8-84942

α-Fe-V, dilute alloy, Mossbauer diffusion line broadening, exponential fitting evaluation 8-52379

Fe₂Si-based dil. alloys, conduction electron polarisation, moment perturbations 8-68225

Ga-In, dil., elec. resist., temp. and impurity depend., deviation from Matthiessen's b-axis crystals 8-51970

Ga-Sn, dil., elec. resist., temp. and impurity depend., deviation from Matthiessen's b-axis crystals 8-51970

Ga-Zn, dil., elec. resist., temp. and impurity depend., deviation from Matthiessen's b-axis crystals 8-51970

Ge-Si, impurity concentration effects 8-75777

Hg-Au(Tl)(Bi), liquid dilute amalgams, elec. cond. and thermoelec. power 8-51976

Ho-Sn, dil. alloy, hyperfine interaction of ¹¹⁹Sn, Mossbauer meas. 8-91998

¹⁸¹Ho-¹⁸¹Ta, dil., elec. field gradient at impurity, anomalous temp. depend., host 4f levels, γ-γ corrs. 8-95272

In-Cd, dil., elec. field gradient at Cd impurities, press. depend., TDPAC meas. 8-64302

K-Na, dil., dynamical props. of quasiparticle excitations, de Haas-van Alphen effect meas. 8-84128

(La, Ce)₂Sn₃, dil. alloys, supercond. and normal state props. 8-76184

(La_{1-x}Gd_x)Al₂, dil., reverse resistance anomaly 8-76054

Lu-rare earth, dil., cryst. fields 8-80127

LuRh₂-Nd³⁺, dil., ESR, hyperfine crysts. of ^{143,145}Nd, g-factor, crystal-line field splitting 8-52349

Mg-Mn, dil. alloy, de Haas-van Alphen effect, exchange interaction, Kondo effect 8-88093

Mo-C dilute alloy defect cluster nucleation and growth under 1250 keV electron microscope (*Japanese*) 8-87663

Ni-Au, dil., orientation depend. of surface segregation, AES and SEM obs. 8-71908

Ni-Co-Mn, dil. alloys, NMR freq. temp. depend., spin echo meas. 8-64296

Ni-Co-Mn, dil. ferromag. alloy, mag. moment, saturation magnetisation meas. 8-64195

Ni-Cu-Mn, dil. alloys, NMR freq. temp. depend., spin echo meas. 8-64296

Pd based 3d metal alloys, mag. phase diagram calc. 8-80144

Pd-Co, dil., Mossbauer emission spectra, fast relaxation regime, ⁵⁷Co hyperfine field 8-60362

Pd-Fe(Co)(Ni) dilute alloys, ferromag., magnetoresist. 8-91665

Pd-transition metal, dil., itinerant versus localised magnetism 8-64188

Pr-rare earth dilute alloy, low field magnetic props. 8-84443

Pt-Co, dil. magnetopower, magnetoresistivity 8-68016

Pt-Cr(Nb)(Re)(Rh)(V), dil. alloy, 0.5 at.%, ¹⁹⁵Pt NMR for local mag. susceptibility 8-84484

Rb-K, dil., dynamical props. of quasiparticle excitations, de Haas-van Alphen effect meas. 8-84128

Ru-Fe, dil., localised spin fluctuation system, supercond. transition temp., conc. depend. 8-56253

Sb-Sn, dil., de Haas-van Alphen effect, effective mass, Fermi levels 8-75982

Sc-Dy(Er)(Tb), dil. alloy, high field magnetisation 8-56292

Sn-In dil. liq. alloy, electrodiffusion and electroconvection, effective diffusion coeff., apparent effective valence 8-87802

Sn-Pb, lattice dynamics, sp. ht., resist., thermal expansion and nuclear γ reson. expts. (*Russian*) 8-87749

Sn-Sb dil. liq. alloy, electrodiffusion and electroconvection, effective diffusion coeff., apparent effective valence 8-87802

Te-Co(Cr)(Au)(Ag), dil. liq. alloy, elec. cond. at high temp. and press. 8-87959

V₂Hf_{1-x}Ta_x, C15 supercond., electronic and lattice props. 8-68110

W-Co, dil., excess resistivity, temp. depend., Kondo effect 8-68011

W-Fe, dil., excess resistivity, temp. depend. 8-68011

W-Fe, dil., spin glass props., DC mag. susceptibility meas. 8-68283

W-Re, dil., excess resistivity, temp. depend. 8-68011

Y-rare earth, dil., cryst. fields 8-80127

Zn-Fe, dil., ⁵⁷Fe Mossbauer effect meas. 8-95534

dimensions

No entries

dimers see molecules**dineutrons** see neutrons**Dingle temperature**

graphite, neutron irradiated, effect on quantum limit Shubnikov-de Haas oscills. 8-95304

metal, dislocation scatt. and de Haas-van Alphen amplitudes 8-63967

transition metal hydrides, electronic struct., heat of formation, single particle lifetimes, Dingle temp. meas. 8-51923

CuH, electronic struct., heat of formation, single particle lifetimes, Dingle temp. meas. 8-51923

Mg-Mn, dil. alloy, de Haas-van Alphen effect, exchange interaction, Kondo effect 8-88093

NbSe₃, oscillatory magnetotransport, Fermi surface anisotropy, Hall effect, g-factor, Dingle temp. 8-51975

Dingle temperature continued

- Pb_{0.92}Sn_{0.08}Te, narrow band gap, relax. time for Shubnikov-de Haas effect 8-80006
PdH, electronic struct., heat of formation, single particle lifetimes, Dingle temp. meas. 8-51923
TaSe₃, oscillatory magnetotransport, Fermi surface anisotropy, Hall effect, g-factor, Dingle temp. 8-51975

diode lasers see semiconductor junction lasers

diode sputtering

- deposition rates calc., at. scatt. in system 8-52670
negative ion MFP in diode sputtering 8-95641
Au, polycryst., RF bias-diode and triode sputtered, resist. and microstruct. 8-80072
Gd-Co film, amorphous, selective resputtering-induced anisotropy 8-72376
In₂O₃-SnO₂ film, reactive DC diode sputtering, using large scale system 8-72723
SmAu, negative ion MFP 8-95641

diode tubes see diodes

diodes

- see also plasma diodes; rectifier tubes; semiconductor diodes
foil-less diodes, relativistic electron beam generation 8-89593
gas-filled diode, rarefied gas breakdown time delay statistics 8-87571
noncylindrical symmetric space-charge flow, Coriolis and centripetal accel. 8-91182
noncylindrical symmetric space-charge flow, momentum eqns. 8-91181
self-scanning linear diode array, appl. to laser bandwidth and wavelength stability meas. 8-86343

dipole antennas

- boundary-value problem, dipole in warm isotropic plasma, multiple water bag model 8-91115

dipole moment, electric see electric moments

dipole moments, magnetic see magnetic moments

Dirac electron theory see Dirac equation; electron theory

Dirac equation

- see also electron theory
algebraic struct., rel. of Pauli and Dirac eqns., from geometric interp. of Heisenberg's commutation rule 8-93549
axial anomalies and index theorems on open spaces 8-93821
canonical formalism for Dirac field, Lagrangian formalism basis 8-49989
conformal invariant 2- and 3-point functions for tensor fields with arbitrary spin 8-49977
Dirac essentially self adjoint operator, resolvent estimator near infinity 8-49992
Dirac S-matrix in k-plane 8-54577
Einstein-Dirac eqns., ν radiation in general relativity (Russian) 8-49727
exact solutions of eqns. of motion of charge (Russian) 8-49954
expanding universe effect on quantum mechanics of electromag. bounded spin 1/2 particles 8-54271
extended electron model, quantum and classical theory elaboration 8-82134
free massive anticommuting spin 3/2 field, quantisation using Dirac's Hamiltonian method 8-58113
index theorem, axial-vector anomalies, in Schwarzschild and Taub-NUT spaces 8-93832
instanton soln. 8-82100
instantons, local supersymmetry transf. and fermion solns. 8-74177
intrinsic SO(2,1) \times GL(1,R) invariance of Dirac eqn. 8-93826
invariance groups for class of countable systems of first-order partial differential eqns. 8-49635
K-shell atomic ionisation by heavy particle, electronic relativistic effects, Dirac wavefunctions, semiclassical effects 8-78792
Lagrangian field theory, vector bundles, rth order Noether invariants and canonical symmetries 8-86409
Lorentz-Dirac eqn. constraints 8-77736
ME-EM field model of free electron state 8-49988
nonlinear, interpretation of Backlund transformations 8-49965
nonlinear spinor eqns. with localised solns. 8-49964
Pauli matrix algebra formulation, 1-by-4 Dirac field as 2-by-2 matrix 8-74185
polarisation in external EM field 8-58116
polarised light beams in gravitational fields, Dirac-spinor form of Maxwell's eqns. 8-50696
quantum Dirac field, scatt. automorphisms, external field perturbations 8-58112
relativistic electron scattering from a two-centre potential 8-66058
relativistic electrons, radiation in periodic mag. array, wavelength and polarisation 8-58149
relativistic field equations with 2(2j+1) components derived from Bargmann-Wigner wavefunction 8-58105
relativistic scattered wave theory, normalisation and symmetrisation 8-62694
Rutherford scattering with radiation reaction, Lorentz-Dirac eqn. soln. for opposite point charges 8-55289
scalar potential inter-relation between non-relativistic and relativistic wave eqns. 8-58110
semiclassical approx. for Dirac eqn. in strong fields (Russian) 8-89645
single particle state obeying Dirac eqn., new bound state to continuum formulation 8-78335
solution of the Dirac equation with anomalous magnetic moment 8-82133
spinning electron, quantum mech. rotor, dynamics, invariance requirements 8-70250
spinning particles interacting with external fields, invariance groups of relativistic eqns., SU₃ symm. 8-49962
spinor electrodynamics, quasiclassical approx. (Russian) 8-49996
spinor function, covariant derivative in Minkowski space with torsion 8-57824
strong external fields, fermion and boson interactions 8-49987
strong localised EM potential interactions with charged leptons or vac. state, critical pots., weak currents 8-54597
p-p symmetry, mass difference, Dirac and CPT theory test 8-82125
H, atomic struct., relativistic Dirac eqn., for teachers 8-62019

direct coupled amplifiers see d.c. amplifiers

direct current amplifiers see d.c. amplifiers

direct current generators see d.c. generators

direct current power transmission see d.c. power transmission

direct digital control

- see also control systems
gas flow control, automated, transducer 8-59508

direct energy conversion

- see also cells (electric); magnetohydrodynamic conversion; photothermal conversion; plasma diodes; solar energy conversion; thermionic conversion; thermoelectric conversion
thermal plasma energy, direct conversion to electrical energy (Russian) 8-87502
X-rays to electricity conversion scheme for advanced fusion reactors 8-70641

direct nuclear reactions and scattering

- see also pick-up reactions; stripping reactions
break up process as three body problem, Faddeev eqns. 8-89842
coupled channel Born approximation code, OUKID, finite range heavy ion direct reactions, appls. 8-89832
coupled channel variational method for multi-step direct nuclear reactions. I. Formalism and numerical test 8-66258
deformed nuclei, single nucleon form factor for knockout and pick-up reactions, (p,2p) calcs. 8-93999
DWBA computer program for heavy-ion transfer reactions 8-50145
E1-E2 direct-semidirect model for fast nucleon radiative capture, γ ang.-distrib. 8-62536
giant dipole resonance region radiative nucleon capture, expt. ang. distrib. coeffs., direct-semidirect theory 8-74354
heavy ion induced direct reactions and scatt., multi-step processes 8-50190
light ion direct reactions, polarisation expts., tensor polarised deuteron beams 8-54732
light ion reactions, two step processes, effective interaction, CC and DWBA 8-54733
plane wave description, DWBA 8-54734
Sturm-Liouville expansion method, one- and two-particle transfer form (Russian) 8-89844
(N, α) knock on reactions, final nucleus polarisation, polarised N capture 8-74352
(π , γ), unified description of direct and resonance processes 8-86551
(π , π), strong absorpt. model for π induced knockout reactions 8-74404
¹²C(⁶Li, α)¹⁴N, E(⁶Li)=20 MeV, using polarised ⁶Li source, exact finite range DWBA anal. 8-58293
¹²C(π , π)⁹Be, 112 MeV, pole approx. anal., knock out reaction mechanism (Russian) 8-86553
⁴⁰Ca(¹⁶O, ¹⁶O), 60 MeV, direct reaction calcs., ang. distrib. 8-58298
⁵⁰Co(n,2n) direct process contrib., cross section and secondary n spectrum (Russian) 8-78386
⁵⁴Fe(n,2n) direct process contrib., cross section, DWTA and DWBA anal. (Russian) 8-78386
⁵⁶Fe(n,2n), direct process contrib., cross section, DWTA and DWBA anal. (Russian) 8-78386
⁴He+ π , 110, 160 MeV, cross section ratio of (π , π) to (π , π) + (π , π) reactions 8-74403
⁶Li(p,p)³He, 1 GeV, knock-out of clusters, distorting factors, microscopic approach (Russian) 8-58285
¹⁶O(d,p)¹⁷O, coupled channel variational method for multi-step direct nuclear reactions. II. Test on a (d,p) reaction 8-66259
¹⁶O(p,2p), 320 MeV polarised protons, quasifree scatt., spin orbit coupling 8-66272
²⁰⁸Pb(n,Zn) direct process contrib. n angular correlations (Russian) 8-78386
²⁰⁸Pb(N, γ), 6 to 40 MeV, dipole/quadrupole interference, direct-semidirect model, γ ang. distrib. 8-93994
²⁰⁸Pb(p, γ) fast capture, direct-semidirect model excitation function calcs. 8-94004
²⁸Si+⁹Be, localisation of direct reaction processes, fusion and total cross sections 8-78353
¹¹⁸Sn(¹⁸O, ¹⁶O)¹²⁰Sn, 53 to 62 MeV, optimum Q value at the Coulomb barrier 8-78413
²³⁸U(n, γ), 5-20 MeV, direct and collective capture, excitation curve, γ -spectra 8-94001

direction finders, radio see radio direction-finding

directional antennas see directive antennas

directional couplers

- integrated optical switch, optically controlled two channel, based on directional coupler 8-83116
modulator switch, balanced bridge, using Ti-diffused LiNbO₃ strip waveguides 8-63201
optical tunable switched directional couplers of two thin film waveguides using SAW 8-75003
rib waveguide switches with MOS electrooptic control, monolithic integrated optics in GaAs-Al_xGa_{1-x}As 8-87168
Ga_{1-x}Al_xAs-GaAs injection laser, branching waveguide coupler fabrication by LPE 8-63202
GaAs directional couplers and electrooptic switches, wavelength depend. 8-79143
GaAs rib-waveguide directional-coupler switch with Schottky barriers 8-63204
LiNbO₃:Ti optical waveguide directional coupler type modulator 8-66951

directional patterns see antenna radiation patterns

directive antennas

- electron, excitation by three-ring antenna, radiation characts. 8-91107

dirty superconductors

- electron-hole coupling, dynamic behaviour (Russian) 8-76187
type II superconductors, fluctuation induced diamagnetism above H_{c2} 8-80097
Cu₂Mo₆S₈, normal state and superconducting property measurements 8-91660
Pb, crit. mag. field, functional derivatives 8-91798
PbMo₆S₈, normal state and superconducting property measurements 8-91660

discharge lamps

- see also arc lamps; flash lamps; fluorescent lamps; metal vapour lamps
electron-atom-bremsstrahlung standard radiometric source improvement 8-67484
LV deuterium lamp, stabilised, as secondary radiation standard in 220-360 nm 8-77998

discharge lamps continued

- microwave discharge lamp for atomic resonance absorption/fluorescence spectrometry 8-89586
- pulsed hollow cathode lamp characteristics 8-67530
- UV, rotating triple-reflection polariser 8-94443
- UV inert gas monochromated discharge lamp, addition to XPS spectrometer 8-89601
- vacuum UV pulsed controlled source 8-87115
- VUV He reson. line radiation source, for UHV photoelectron spectroscopy 8-89602
- Ar lamp, pulse-operated, for VUV irr. (*Russian*) 8-75453
- D, transfer standards for UV spectral emission scales determination 8-78001
- He I polarised radiation source for surface studies 8-74959
- He, with Be film optical filter, for photoelectron spectroscopy 8-79115
- Xe motion picture switching projection lamp, transfer processes from thyristor rectifiers (*Russian*) 8-94421
- Xe optical discharge radiation source 8-87116
- Xe-Kr-Ar mixtures, VUV continuous spectrum prod. in low volt. lamp (*Russian*) 8-75451

discharge lasers see gas lasers**discharge tubes** see gas discharge tubes**discharges (electric)**

- see also arcs (electric); electric breakdown; flashover; glow discharges; high-frequency discharges; lightning; partial discharges; positive column; sparks; surface discharges; Townsend discharge
- air, predischARGE-stabilised breakdown voltage (*German*) 8-63608
- air diffuse discharge, gasdynamic effects 8-81294
- air discharge, sputtered cathode metal atoms, time-resolved light emission 8-71601
- air high-current discharge cond. zone, HF mag. field probe 8-71589
- air high-current pulse discharge, near-electrode process dynamics 8-71602
- aircraft skin, lightning damage simulation 8-87575
- anode-directed streamer maximum velocity estimation 8-67593
- atmospheric negative ions, electron detachment rates, time lags to breakdown 8-87564
- atomic O, form. and recomb. in U-tube downstream from DC discharge 8-67333
- avalanche discharge model, unstable boundary layer in crossed fields 8-83641
- ball lightning, elec. discharge into sand layer expts., erosion-discharge model 8-81322
- capillary, with evaporable wall, plasma parameters axial distrib. (*Russian*) 8-75280
- cathode directed streamer propagation, charge sheath model 8-67459
- cathode fall in electron beam controlled stationary non-self-sustained discharges 8-71613
- charged particle beam production, in variable density gas discharge 8-51381
- CO₂ lasers, CW, high-power appl. of photoinitiated impulse-enhanced electrically excited discharge 8-50785
- cold-cathode controlled gas discharge switch 8-86300
- combined pulse and DC discharge to pump fast-flow CO₂ laser 8-71117
- combustion product plasma, near-electrode contraction conditions 8-94946
- conference, Liverpool, England, Sep. 1978 8-87521
- continuous optical discharge convective flow, thermogasdynamic instability 8-75397
- contraction in inert gas discharge, electron distrib. (*Russian*) 8-91176
- corona discharge, decomposition of CO, qualitative chemical anal. of reaction products 8-60992
- cylindrical discharge plasma, radial electron density gradient in electronegative gas 8-87433
- diatomic species nonequilibrium dissociation, numerical and analytical results compared 8-71428
- discharge cleaning in JFT-2 Tokamak, AES 8-51316
- dye gas laser, excitation by elec. discharge, electron beams, optical stimulation (*Czech*) 8-79016
- electric strength and elec. cond. 8-91180
- electron beam plasma discharge, in crossed elec. and mag. field (*Russian*) 8-87458
- electron beam stabilised discharge in flowing medium, numerical calc. 8-94943
- electron drift tube, photon emission investig. 8-87566
- electron energy distribution in positive column 8-67465
- electron neutral inverse bremsstrahlung in electron beam sustained discharge 8-63604
- electrovortical flow, in discharge between hyperboloidal electrodes (*Russian*) 8-75217
- explosive electron emission, cathode plasma emission surface processes 8-71569
- focused discharges, electron beam and deuteron beam prod. 8-58093
- gas, homogeneous discharge, development, effect of initial conditions 8-63613
- gas discharge between coaxial electrodes with dielectric layer 8-75476
- gas discharge in crossed fields, obs. 8-75471
- gaseous dielectric, discharge development, relative motion between gas and electrode, theory 8-63616
- gases as electrical insulators, nature and practice 8-83632
- geometrically extended electrode, charged particle and energy fluxes 8-79442
- guiding effect, laser produced plasma channels 8-71568
- halide vapour, discharge, potential fusion laser systems 8-63074
- high-current pulsed discharge, plasma props., spectral meas. 8-87535
- high-density electrode discharge stability in very strong mag. field 8-75478
- high-power non-self-sustained discharge with ionisation by repetitive electrodeless pulses in closed-cycle laser 8-71514
- high-speed rotational vacuum tap for discharge gas sampling 8-57969
- hollow cathode discharge as negative ion source 8-82072
- hollow cathode discharge ion source, with drift tube, for reaction rate consts. meas. 8-64834
- hollow cathode spectroscopic light source, characts. using Ar(He) carrier gases, Al(graphite) cathodes 8-82047
- homopolar corona, plane parallel field, outer region electrical characts. calc. (*Russian*) 8-67447
- hot cathode reflex discharge in cusp and uniform mag. fields 8-67456
- discharges (electric)** continued
- HV AC Penning discharge, vacuum pumping characts. 8-93713
- HV nonosecond transient meas. from pulsed low inductance gas discharge, Kerr effect 8-51380
- hypersonic plasma jet discharge, pulsed radiation source (*Russian*) 8-74073
- inert gas mixtures for particle detection, high-pressure discharges in nonuniform elec. fields. 8-74545
- ion exchange currents (microdischarges), in vacuum accelerator tube 8-55057
- ion transport 8-87435
- ion-acoustic instability suppression by microwave field 8-71466
- ionised gases, conf., Berlin, E.Germany (Sept. 1977) 8-63615
- Jupiter Voyager electrostatic discharge protection 8-89042
- laser triggered fast-response sealed dischargers 8-51391
- LF waves, plasma ionisation instability, dispersion rel. (*Russian*) 8-83519
- limiting current in steady state diffusion-recombination discharge 8-67466
- liquid metal cathodes, nanosec. discharge form. in H₂ atmosphere 8-87578
- low-pressure discharge, restriction of current with hollow cathode (*Russian*) 8-94944
- low-pressure discharge anode sheath in crossed fields, electron density distrib. 8-75424
- low-pressure discharge electron kinetics 8-75483
- low-pressure discharge striking in axisymmetric elec. and mag. fields 8-75472
- low-voltage pulse discharge plasma, radial temp. distrib. and chem. comp. determ. (*Russian*) 8-71544
- magnetised DC discharge plasma, pot. difference meas., anomalous resist. 8-87434
- maser dissociator, H beam production performance characts. 8-87034
- metal vapour laser discharges, stability criteria 8-66802
- MHD flow due to an electric discharge from a finite size electrode 8-79388
- MHD generator, discharge struct. 8-91166
- non-self-maintained discharge, plasma probe currents 8-63631
- non-self-sustained discharge plasma, thermal instability development, laser appls. 8-71611
- nonideal plasma generation, by electrolyte impulse diaphragmic discharge 8-71506
- nonpolar electrolyte, on anode, ion attachment and ion emission 8-65998
- optogalvanic effect characts. in discharge plasmas 8-63583
- parallel discharge growth during impulse breakdown in air, mechanism (*German*) 8-63607
- Penning, hot plasma devices, ion heating mechanism (*Rumanian*) 8-59710
- photoionisation, at low intensity illumination, nonlinearities, effective cross section 8-87517
- plasma return current discharge, prod. and heating of large-volume plasmas 8-94920
- positive leader, in long nonuniform air gap, growth 8-75444
- positive leader propagation mechanism 8-79483
- prebreakdown ionisation current spatial growth expts., initial photoelec. current changes 8-67566
- radiation temp. of weakly ionised gas discharge (*Russian*) 8-59697
- ring discharge, 1st to 2nd stage transition obs., press. and freq. depends. 8-83635
- rod-to-plane air gap impulse-voltage delayed streamer and leader formation 8-67570
- rod-to-plane air gap impulse-voltage primary and secondary streamer obs. 8-67569
- semi-self-maintained gas discharge, ionisation instability theory 8-67511
- simulation of the growth of axially symmetric discharges between plane parallel electrodes 8-91173
- sintering of metal powder, with intense energy release of interparticle contacts 8-60615
- sparking potential dependence on nature of the wall 8-67552
- striking in highly inhomogeneous axisymmetric mag. field 8-75473
- sustained by uniform ionisation source, props. 8-71605
- theory of the main discharge of lightning (*French*) 8-92887
- Tokamak discharge gas breakdown time model 8-67555
- toroidal discharge, dynamic stabilisation in weak longit. mag. field (*Russian*) 8-87476
- transient electric discharge power and energy meas. using wideband ICs 8-87520
- ultrahigh vacuum discharge cathode erosion minimum conditions 8-75461
- underwater electric discharge, acoustic, hydraulic and total efficiency 8-51388
- vacuum gap electrode surface sorption, mass spectroscopic obs. 8-75466
- Ag, population mechanism, highly-excited states, hollow cathode discharge (*Russian*) 8-63610
- Ar, 3p²5p config. aligned in discharge, interf. signals, lifetimes and collision cross sections 8-70796
- Ar constricted discharge, electron density and temp. and gas temp., iterative method (*German*) 8-83627
- Ar continuous optical discharge maintenance in applied mag. field 8-75396
- Ar discharge rotating plasma column LF oscillations 8-71481
- Ar, high press. gas discharge form. 8-87567
- Ar, plasma, electron-ion recombination, 300 to 500K, in discharge tube 8-59714
- Ar plasma interaction with flat anode 8-71497
- Ar, twin-hollow-cathode interferometer-spectrometer, discharge characts. (*German*) 8-67461
- Ar, weakly ionised, energy transfer at high press. 8-58845
- Ar-SF₆ mixture, space discharge excited by electron beam (*Russian*) 8-83629
- Ar-SF₆ mixture, space discharge excited by electron beam (*Russian*) 8-83630
- CO discharge, low-pressure laser striation obs. 8-66814
- CO-Ar mixture non-self-sustained discharge instability obs. 8-71612
- CO₂ laser, double transverse pulsed discharge characteristics 8-71617
- CO₂ laser self-sustained discharge, effect of low-ionisation-potential additives 8-71616
- CO₂, negative ions and volt.-current characts. 8-71574

discharges (electric) continued

- Cd, low-press., high current, intensity in middle UV 8-50878
 CdHg*, metal vapour exciplex laser, stability criteria 8-66802
 Ce, gas discharge, two-photon ionis. by laser light 8-87534
 Cs, discharge, hot cathode diode, low-press., initial stage transient processes 8-51382
 Cs discharge plasma, optogalvanic effect characts. 8-63583
 Cs hollow cathode discharge, volt-ampere characts. 8-71563
 Cu, population mechanism, highly-excited states, hollow cathode discharge (*Russian*) 8-63610
 Cu-Ne mixture, 3-20 kHz pulse discharge obs. 8-71092
 HF chemical laser, stable discharges, with large electrode separation 8-55371
 HF, nonequilibrium dissociation in electric discharge, vibrational excitation 8-94306
 H₂(³Σ_g⁺)-He(2³S), discharge ionisation growth, diffusion coeffs. 8-83636
 He cryogenic discharge, current oscills. 8-67463
 He DC discharge electron free streaming wave propagation obs. 8-75314
 He, gas discharge, high voltage, low current, anal. of cathode fall 8-51375
 He high-current pulse discharge plasma kinetic and dynamic processes 8-67601
 He, plasma, non-equilib., of strong current pulse discharge, diagnostics (*Russian*) 8-75271
 He pulsed discharge, He₂ mol. formation in early afterglow, time-resolved spectra 8-63585
 He, radiation from hollow-cathode discharge in weak mag. field 8-70789
 He, twin-hollow-cathode interferometer-spectrometer, discharge characts. (*German*) 8-67461
 He, twin-hollow-cathode of interferometer-spectrometer, radial electron temp. (*German*) 8-67462
 Hg, high-pressure discharge, temp. and electron density meas. (*French*) 8-59705
 HgCl*, metal vapour excimer laser, stability criteria 8-66802
 Kr discharge, secondary ionisation processes 8-59711
 KrF*, waveguide laser excited by capacitively coupled discharge 8-94391
 MgO-Ag porous layer, secondary electron emission from ion impact, gas discharge device appl. 8-68586
 N₂ electron-beam-sustained discharge stability model 8-71608
 N₂, high-speed Raman spectroscopy, condensed discharge vibr. excitation, vibr. temp. 8-82740
 N₂ laser discharge emission model and meas. 8-71093
 N₂ non-LTE, pulsed discharge, I-V characteristic obs. 8-71618
 N₂-Ar mixture non-self-sustained discharge instability obs. 8-71612
 N₂-He-CO₂, discharge ionisation growth, diffusion coeffs. 8-83636
 N₂-NO(He), discharge ionisation growth, diffusion coeffs. 8-83636
 Na-Xe, high-pressure discharge, electron density, interferometric meas. 8-75415
 Na-Xe vapour, high power discharge, potential excimer laser 8-82957
 Ne discharge, wavenumber spectra of turbulent ionisation waves 8-71541
 Ne flash tube, investigation of forms. and decay mech. of internal fields 8-58552
 Ne, laser irradi. and voltage changes 8-63606
 Ne, metastable level deactivation by electron collision in low press. discharge 8-83520
 Ne, radiation from hollow-cathode discharge in weak mag. field 8-70789
 Ne, thermalisation of level populations, occurrence in elec. discharge 8-66649
 Ne, weakly ionised, energy transfer at high press. 8-58845
 Ne-Ar, high press. mixture, AC discharges, one-dimensional numerical simulation 8-67451
 Ne-Cu pulsed discharge, electron energy distrib., ionis. rate 8-51387
 Ne-HCl(CH₄) mixture breakdown obs. 8-67553
 Nz, electron beam sustained discharge, performance 8-75365
 O plasma electron energy distribution obs. 8-63595
 O₂, discharge development, relative motion between gas and electrode, theory 8-63616
 O_x metastable and O₃ production in electron-beam-controlled high-pressure discharge 8-71607
 Pb-He discharge, excitation process, Pb⁺ emission lines 8-66803
 SF₆, compressed, negative ion drift in applied field 8-87565
 SF₆, discharge development, relative motion between gas and electrode, theory 8-63616
 SF₆, electric strength, electrode surface roughness effects, model (*German*) 8-63609
 SF₆, predischARGE-stabilised breakdown voltage (*German*) 8-63608
 SF₆-N₂-Ar mixture high-current multispark discharge switching characteristic 8-67444
 U, vapour prod. by sputtering, Ne, Ar, Kr, carrier agents, density meas. (*French*) 8-86967
 Xe discharge plasma spectral and integral characteristics calc. 8-71583
 XeF*, waveguide laser excited by capacitively coupled discharge 8-94391

discharges (partial) *see partial discharges***disclinations**

- cholesteric liquid crystals, topological classification of distortions 8-79523
 cholesteric screw sense, form of spiral disclination lines calc. 8-67643
 Cosserat's medium, linear and surface defects, stresses 8-83813
 ferromagnet, local variation in mag. anisotropy due to linear defects (*Russian*) 8-68214
 kinematics, continuous distrib. of disclinations and dislocations 8-63764
 nematic and cholesteric liquid crystals, disclinations, generation process, matrix representation 8-59743
 nematic liquid crystals, acoustic emission, appl. to defect dynamics study 8-91232
 nematics, topological instability of singularities at small distances (*Russian*) 8-79531
 smectic C liquid crystals, chiral, defects induced by planar anchoring (*French*) 8-94978
 smectic C liquid crystals, elasticity and defects 8-91233
 stationary lattice defects as sources of elastic singularities 8-59800

disclinations continued

- theory, rel. to X-ray topography data 8-64254
 two-dimensional triangular lattice, melting theory 8-71833
discontinuous control systems *see sampled data systems*
discontinuous metallic thin films
 electric field distrib. and emission currents of island condensates 8-88047
 electrical conduction and current noise mechanism, theory 8-56244
 metal particle composite, physical and optical props. 8-56528
 noble metal aggregated film, absorpt. peaks, collective oscills. of electrons 8-80428
 noble metal aggregated film, light scatt. 8-64423
 nucleation, oriented island growth on point defects 8-87889
 Ag, granular films, optical props., depend. on refractive index of surrounding medium 8-84672
 Ag, on mica, microstruct. changes 8-72013
 Al, granular, hopping cond., supercond., magnetoresist., Zeeman splitting 8-60243
 Au, diffusion on atomically clean Si (111) surface 8-72037
 Au, discontinuous film, optical transmittance 8-56529
 Au, elec. cond. and current noise, temp. depend. meas. 8-56245
 Au films, optical transmittance, effect of island morphology 8-84673
 Cr island film photoconductivity obs. 8-95392
 Cu, vapour deposited, on polystyrene, surface complex, XPS obs. 8-72026
 Ni film on leucosapphire, island growth as annealing in Ag vapour (*Russian*) 8-51830
 Ni-SiO₂, granular film, hopping cond., magnetoresist. 8-56240
 Pd, chemisorpt. of CO, ultra high vacuum technique 8-71960
 Pt, elec. cond. and current noise 8-72286
 Pt island film photoconductivity obs. 8-95392
 Pt, ultrathin film, elec. cond., amorphous Ge overlayer thickness depend. 8-72284
 W-Al₂O₃, granular film, percolation conductivity 8-84319

discrete symmetries

- see also C invariance; CP invariance; CPT invariance; P invariance; parity; T invariance*
 disconnected gauge groups and the global violation of charge conservation 8-78086
 gauge model with six quarks, discrete symmetries, Cabibbo universality, flavour mixing angles 8-62346
 SU(2)×U(1) model, quark mass matrix and discrete symmetries 8-54607

discrete systems

- see also sampled data systems*
 Markov system, nonstationary, profit accumulation process (*Ukrainian*) 8-89308

discriminators

- see also demodulators*
 direct meas. of β absorbed dose rate by discriminator and filter (*Japanese*) 8-74511
 gated constant-fraction discriminator for use with fast-focused photomultiplier tubes 8-58063
 high-speed pulse shaper/discriminator for scintillation and Cherenkov counters 8-86748
 lightning ground-flash multiple-stroke discriminator cct. 8-81446
 multimode optical fibre phase modulators and discriminators, theory 8-55446
 multimode optical fibre phase modulators and discriminators, expts. 8-55449
 photon count cct. using high-speed comparator 8-77979
 PLL for automatic observation of whistlers 8-89014
 ten-channel differential discriminator for radiation detection spectra 8-78593
 X-ray proportional counter background reduction by leading-edge discriminator 8-78561

disinclinations *see disclinations***disintegration (radioactive)** *see radioactivity***disintegration energies** *see radioactivity***dislocation anchoring** *see dislocation pinning***dislocation arrays**

- coherent motion, lattice dynamics 8-71738
 edge dislocation interactions in infinite array, elastic energy 8-55871
 electron dynamical diffraction from periodic arrays of dislocations 8-83669
 plate, elastic, under uniform twisting, periodic collinear cracks (*Japanese*) 8-67097
 polyethylene, crystals, subject to fold-surface tensile stress, elastic deform. 8-76712
 Cu, epitaxial, on (111) Au, periodic arrays of misfit dislocations, electron diffr. 8-51857
 Cu-Ni bimetallic films, dislocation wall form. during interdiffusion, TEM obs. 8-51856
 GaAs,Sb_{1-x}, epitaxial layer, struct. defects rel. to luminesc. 8-72040
 Pd, epitaxial, on (111) Au, periodic arrays of misfit dislocations, electron diffr. 8-51857
 Si:P, emitter-misfit dislocation formation during P diffusion 8-91338
 Ta-N, domain configurations of new phase (*French*) 8-56648

dislocation breakaway, pinned *see dislocation damping***dislocation climb**

- dispersion hardened alloy, calc. of back stress decrease, due to Orowan dislocation loop climb 8-83812
 edge dislocation climb, numerical anal. 8-71736
 repeated precipitation on edge dislocations, micromechanisms 8-95752
 steel, stainless 316, creep under high stress 8-52892
 two phase polycrystals, grain size stability and switching, dislocation climb and glide, computer model 8-75715
 Al-Mg (2 wt.%) subgrain formation at low stresses 8-84928
 (Al₂O₃)_nMgO, n=1.1, high temp. creep, dislocation behaviour 8-80593
 GaAs laser material, secondary dislocation climb during optical excitation 8-75672
 GaAs-GaAlAs DH material, dislocation glide and climb, electron diffr. 8-83824
 MgO, climb of a(100) dislocations, TEM obs. 8-71741
 Ni, transient irradi.-induced creep under D bombardment, mechanism 8-80597

dislocation climb continued

- Si, single crystals, dynamical recovery and self-diffusion 8-87816
 Si:Cu, interaction between vacancy emitting absorbing precipitates and dislocations, TEM obs. 8-71755

dislocation damping

- see also *Bordoni effect*
 dislocation damping during electron irradiation, new model for peaking effect 8-87683
 Nb, plastically deformed, hydrostatic pressure effect on dislocation relaxation, US exam. 8-76696

dislocation density

- alkali halide crystals, defect state change during electrolysis 8-95057
 β -copper phthalocyanine, dislocation detection (*German*) 8-63773
 fracture, appl. of continuum theory of dislocations fracture mechanics 8-67767
 heterojunction devices, double and triple layer, density of misfit dislocations 8-51850
 ice, Antarctic deep core, X-ray diffr. topographic studies 8-63803
 metal, near surface microstructure effect, on wear 8-64730
 MOS structure, surface charge, effect of process induced defects in Si 8-72274
 nucleation, criterion for dynamic recrystallisation during hot working 8-52852
 obstacle strength determ. in solid soln. 8-68704
 olivine, naturally deformed, recovery process, rel. to Earth upper mantle mech. state 8-96202
 oxide single crystals, Czochralski grown, thermoelastic stresses 8-55822
 plastic zone, direct meas. in side grooved fracture toughness specimens 8-68864
 plate, elastic, under uniform twisting, periodic collinear cracks (*Japanese*) 8-67097
 polycrystalline aggregate, continuous distrib. of dislocations, stress fields, movements in elastic-plastic deform. 8-75709
 steel, hypoeutectoid Widmanstätten struct. form., contrib. to the laws (*Slovenian*) 8-84817
 steel, low-C, ferritic, deform. microstruct., electron microscopy (*German*) 8-64589
 steel, stainless, electron irradiated, dislocation assisted vacancy diffusion 8-55891
 steel cylindrical bar loaded by longitudinal impact, dislocation struct. and plastic deform. (*Czech*) 8-60713
 Ag-Cu, composite, fibre and layer structs., anomalous props. caused by internal phase boundaries 8-72754
 Ag-Ge (4.5 at.%), FCC, vapour-deposited, lattice imperfections, X-ray diffr. 8-72032
 Ag-Ni, composite, fibre and layer structs., anomalous props. caused by internal phase boundaries 8-72754
 Al, struct. changes in single cryst. under influence of static and dynamic stresses (*Russian*) 8-92300
 Al, thin foil, adhesion and friction, rel. to observed dislocation density 8-64706
 Bi, US propagation anomalies, under hydrostatic press. (*Russian*) 8-83884
 Cu, amplitude depend. modulus effect 8-64573
 Cu, commercial pure, creep-rupture props., vacuum, dislocation density increase (*Japanese*) 8-72843
 Cu, struct. changes in single cryst. under influence of static and dynamic stresses (*Russian*) 8-92300
 Cu-Fe, composite, fibre and layer structs., anomalous props. caused by internal phase boundaries 8-72754
 CuFeS₂, explosive-shock deform. 8-95108
 Fe, deformed, dislocation structure determ. from magnetic props. 8-55874
 Fe, zone refined, strained, substructural changes during annealing (*Slovenian*) 8-84845
 FeNi-Cu, composite fibre and layer structs., anomalous props. caused by internal phase boundaries 8-72754
 GaAs, grown-in dislocation density, impurity effect 8-51543
 GaAs VPE layers, role of diffused Ga vacancy in degradation 8-95050
 Ga₂In_{1-x}PyAs_{1-y}, In rich bulk single crystals, growth from melt via gradient freeze method, and characterisation 8-68618
 GaP, LEC, SSD and CVD samples, Zn tracer diffusion profiles in solids 8-95189
 Ge, deformation, annealing characts., X-ray study 8-75713
 Ge, epitaxial growth from monogermane at 685°C 8-51833
 Ge, influence of dislocations on free-exciton lifetime 8-60064
 Ge, phonon scattering and dislocation effect on low temp. phonon cond. 8-51754
 InP, grown-in dislocation density, impurity effect 8-51543
 InSb, plastically bent single crystals, dislocation struct. obs. 8-59816
 KBr, quench hardening related to dislocation density and slip 8-52855
 KCl-BaCl₂ supersaturated solid soln., deformed, BaCl₂ precipitation kinetics, metastable region (*Russian*) 8-60673
 NaCl, deform. process, exoemission and desorption meas. (*Russian*) 8-75708
 NaCl, polishing of single crystals, kinetics of defect formation (*Russian*) 8-95819
 NaCl, quench hardening related to dislocation density and slip 8-52855
 Ne, solid, lattice thermal cond. 0.5 to 10K, dislocation densities, average grain sizes 8-79830
 Ni, decrease due to D bombardment, 22 MeV 8-80597
 Ni, polycryst., hydrogenation rel. to fine struct. 8-59950
 Se, undeformed rhombohedral, dislocations, electron microscope obs. (*French*) 8-51548
 Si, deformation, annealing characts., X-ray study 8-75713
 Si, deformed crystal, faulted dipoles 8-59814
 Si monocrystalline rod growth from gas phase 8-64453
 Sr_{0.2-0.7}Ba_{0.25-0.75}Nb₂O₆, large cryst. growth, control of opt. defects 8-76595
 Zn, film, vac. deposited, X-ray diffr. study of microstruct. 8-75966

dislocation dipoles

- ionic crystal, point defect-dislocation interactions 8-63787
 ionic single crystals, elec.-mech. coupling of dislocations 8-75676
 melting, cooperativity in dislocation theory 8-59934
 narrow dipoles, high density, electron diffr. numerical eval. 8-71645
 two dimensional crystal, rel. to melting transition 8-51645
 Cu-Al, faulted dipoles, geometry and form. 8-59809
 GaP, dislocation loops and bipolar obs. by chemical etching 8-55873

dislocation dipoles continued

- KCl (100), elec.-mech. coupling of dislocations 8-75676
 KCl, dislocation motion in micro-plastic region, direct obs. via charged dislocation p.d. 8-91341
 LiF (100), elec.-mech. coupling of dislocations 8-75676
 NaCl (100), elec.-mech. coupling of dislocations 8-75676
 NaCl, dislocation motion in micro-plastic region, direct obs. via charged dislocation p.d. 8-91341
 Si, deformed crystal, faulted dipoles 8-59814
 Si:Cu, interaction between vacancy emitting absorbing precipitates and dislocations, TEM obs. 8-71755

dislocation drag

- Si:Cu, interaction between vacancy emitting absorbing precipitates and dislocations, TEM obs. 8-71755

dislocation energy

- Ni 200, C interstitial effect of yield point develop. during static strain ageing, model 8-88498

dislocation etching

- amethyst crystals, dislocations, selective etch method 8-75674
 β -copper phthalocyanine, dislocation detection (*German*) 8-63773
 β -copper phthalocyanine, dislocation etching kinetics (*German*) 8-67719
 α -quartz dislocation free and low dislocation, prep. by hydrothermal crystallisation 8-72712
 stearic acid, etch pit obs. of dislocations 8-87676
 CaF₂, etching behaviour in HCl vapour 8-59812
 CsI, selective etching, growth and dissolution in alcohols 8-71739
 Cu plastically deformed crystals, SEM exam. of light and dark etch pits, dislocation arrangements 8-87679
 Fe₃Si, etching of slip produced antiphase domain boundaries 8-63769
 GaAs {001} layer, LPE, dislocation etch pits revealed by molten KOH 8-63772
 GaAs cryst., creep and dislocation vel. at different doping and temps. 8-95783
 GaAs, structural defects, detection by electrochemical etching 8-55872
 GaP, dislocation loops and bipolar obs. by chemical etching 8-55873
 GaP, LEC crystal, cathodolum. and photolum. around dislocations 8-84663
 InSb, plastically bent single crystals, dislocation struct. obs. 8-59816
 KBr, quench hardening related to dislocation density and slip 8-52855
 KBr, rot. of vacuum thermal etch pits 8-87674
 KCl-KBr mixed crystals, microhardness studies, nonlinear depend. on composition 8-83872
 MgO, precipitation on dislocations, ultramicroscopy and chem. etching 8-67720
 MgO, single crystals, compressed, SEM exam. of cathodoluminescence 8-56525
 NaCl, motion of individual surface dislocation semi loops (*Russian*) 8-51542
 NaCl, quench hardening related to dislocation density and slip 8-52855
 Nb, surface oxide softening, anisotropy 8-60716
 NdGa₂O₁₂ wafer, dislocations, etch pits and birefr. obs. 8-83818
 Si, Czochralski cryst., hillock etching of microdefects, TEM obs. 8-87678
 Zn, dislocation etch pits on (0001) surface of single crystal (*Japanese*) 8-59811

dislocation glide see *slip***dislocation interactions**

- see also *impurity-dislocation interactions*; *vacancy-dislocation interactions*
 antiferromagnet, moving dislocations, interaction with spin waves (*Russian*) 8-56303
 collective dislocation motion, dynamic effects 8-79632
 critical resolved shear stress, from misfitting particles 8-79613
 cylindrical surface crystals, dislocation interactions 8-95055
 edge dislocation interactions in infinite array, elastic energy 8-55871
 glide, interacting dislocation motion, resisted by point-like barriers, computer simulation 8-71742
 interaction force between dislocation, and misfitting ordered particle, calc. 8-83815
 interdislocation interaction on account of carriers bound with dislocations 8-75670
 ionic crystal, point defect-dislocation interactions 8-63787
 metal, stress-induced EM effect, phys. model 8-55909
 plastic deformation, phenomenological theory, with mobile and immobile dislocations 8-75714
 point defect-dislocation interaction, radiation-induced creep, rate expression 8-87706
 spin wave resonance line broadening by dislocations 8-64275
 stressed crystal, dislocation superradiance collapse (*Russian*) 8-79706
 two-dimensional triangular lattice, melting theory 8-71833
 void swelling, rate theory, effect of recombination on sink strengths 8-87712
 Zircaloy-4, quenched, strain ageing behaviour, ageing time and temp. effects 8-56657
 Ag, neutron irradiation, low temp. recovery, effect of plastic deform. 8-51588
 Al alloys, age-hardening, resistivity change by low temp. deform., GP zone cutting (*Japanese*) 8-84831
 Au bicrystals, interaction of lattice dislocations with grain boundaries, electron microscope obs. 8-51579
 Cu single crystals, positron trapping by edge dislocations, produced by bending 8-80606
 CuAu, calc. of elastic interaction between locally transformed regions with screw and edge dislocations 8-83844
 CuAu-type superstructure, interaction of reacting dislocations (*Russian*) 8-83814
 Fe-Ni (29 at.%), calc. of elastic interaction between locally transformed regions with screw and edge dislocations 8-83844
 Fe-Ni alloy, N27T2 and N28, internal friction peaks after reverse martensitic transform. (*Russian*) 8-92287
 Ge, phonon scattering and dislocation effect on low temp. phonon cond. 8-51754
 Mg-Mn-Ce alloy, MA8, dislocations at grain boundaries and grain-boundary glide 8-64605
 NbS₃, Peierls distortion, chain polytypism and dislocation coupling 8-79589
 Ni, neutron irradiation, low temp. recovery, effect of plastic deform. 8-51588

dislocation interactions continued

- Ni-Al-Cr-Co-Ti, Waspaloy, exam. of dislocation-precipitate interaction, cyclic stress-strain behaviour 8-84925
 Pt, neutron irradiation, low temp. recovery, effect of plastic deform. 8-51588
 Pt₂Mo-type superstructure, interaction of reacting dislocations (*Russian*) 8-83814
 Si, plastically deformed, dislocations reactions obs. by X-ray topography 8-75691
 Zn, single crystals, positron trapping by edge dislocations, produced by bending 8-80606
 Zn-Al alloys, dislocations obs. in superplastic deformation 8-51549

dislocation jog motion *see* **dislocation jogs****dislocation jogs**

- repeated precipitation on edge dislocations, micromechanisms 8-95752
 Schmid's law deviations, in uni-directional strain 8-71783
 Se, undeformed rhombohedral, dislocations, electron microscope obs. (*French*) 8-51548
 Si, single crystals, dynamical recovery and self-diffusion 8-87816

dislocation locking

see also **Cottrell atmospheres**

No entries

dislocation loops

see also **vacancy condensation loops**

- acoustic emission from moving dislocations near crystal surface 8-87856
 BCC materials, small dislocation loop images 8-83823
 α -brass, quenched, secondary defect form. during ageing, TEM obs. 8-88482
 cryst. with defects 8-60478
 dispersion hardened alloy, calc. of back stress decrease, due to Orowan dislocation loop climb 8-83812
 electron microscope diffr. contrast 8-83700
 FCC metals and alloys, elastic energies of dissociated Frank loops 8-75671
 graphite, point defects and self diffusion 8-63758
 metal, hardening due to increased subgrain boundary stability 8-52934
 metals, mechanical multipole moments determ. 8-55868
 tetrahedral semiconductor, interstitial type dislocation loop form. by vacancy precipitation 8-67715
 Al, [111] single crystal, in situ deform., HVEM obs. 8-52886
 Al foil, quenched, anomalous annealing phenomena, quantitative study 8-80565
 Al, mechanical multipole moments determ. 8-55868
 Al:¹²⁵B, relax. mechanism for polarised implant 8-87693
 Al-Li alloy, dil., quenched and irradi., recovery, resist. and internal friction obs. 8-52848
 Bi, US propagation anomalies, under hydrostatic press. (*Russian*) 8-83884
 Cd, electron radiation damage in HVEM, nature of defect clusters 8-59838
 Cu, Frenkel pair production threshold energy, temp. depend., exam. 8-51530
 Cu, irradiation induced defects, electron microscope images 8-83854
 Cu, X-ray studies of fusion energy neutron damage 8-51593
 Cu₂Au, fast neutron irradi., displacement cascades 8-83852
 Ga₂-Al₂As DH injection laser diode, long-term-degraded, TEM obs. 8-71102
 GaAs, ion implantation damage, TEM exam. of variation with ion species and stoichiometry 8-59827
 GaAs:Te, heavily-doped, annealing-induced prismatic dislocation loops and elec. changes 8-51546
 GaP, dislocation loops and bipolar obs. by chemical etching 8-55873
 KCl, motion of dislocation half-loops, influence of prestart loading and ensemble nature 8-71745
 Mg, electron irradi. damage, dislocation loop growth, in situ obs. 8-87715
 Mg, melt grown by Bridgeman method, X-ray topography 8-59770
 MgO, precipitation on dislocations, ultramicroscopy and chem. etching 8-67720
 Mo, irradiation induced defects, electron microscope images 8-83854
 NaCl, dislocation half loop mobility 8-59817
 NaCl, motion of individual surface dislocation semi loops (*Russian*) 8-51542
 Nb and Nb alloys, superconductor, flux pinning under heavy ion irradiation 8-52167
 Nb, irradiated superconductor, fluxoid defect interactions 8-52166
 NdGa₂O₁₂ wafer, dislocations, etch pits and birefr. obs. 8-83818
 Ni, transient irradi.-induced creep under D bombardment, mechanism 8-80597
 Ni-Al-Cr-Co-Ti, Waspaloy, exam. of dislocation-precipitate interaction, cyclic stress-strain behaviour 8-84925
 PbNb₂O₆, ferroelectric thick crystals, domain formation and dislocation loops 8-60410
 Si, ion-implanted, secondary defects development, three-stage model 8-87725
 Si, ion-implanted layers, residual defects after high temp. annealing 8-87695
 Si:B, ion implanted, localised defects, TEM study 8-87699
 Si:B, ion implanted, struct. of rod defects, TEM obs. 8-71744
 Si:B, TEM study of stacking fault form. and annealing 8-51566
 Si:B(P), diffusion induced imperfections, laser annealing, rel. to junction characts. 8-75678
 Si:Cu, interaction between vacancy emitting absorbing precipitates and dislocations, TEM obs. 8-71755
 Si:O, cryst., annealed, struct. defects 8-75673
 Zn, electron radiation damage in HVEM, nature of defect clusters 8-59838
 Zr base alloys, irradiation growth, dislocation model 8-51595
 Zr, irradiation induced defects, electron microscope images 8-83854

dislocation motion

for **dislocation relaxation** *see* **dislocation damping**

see also **dislocation climb**; **slip**

- acoustic emission from moving dislocations near crystal surface 8-87856
 alkaline earth fluorides, crack propag., cryst. props. effects 8-75720
 antiferromagnet, moving dislocations, interaction with spin waves (*Russian*) 8-56303

dislocation motion continued

- β_1 brass containing α -precipitates, reversible shape memory effect (*Japanese*) 8-60711
 coherent motion, lattice dynamics 8-71738
 collective dislocation motion, dynamic effects 8-79632
 crystal cleavage due to dislocation tilt wall splitting 8-91377
 dislocation damping during electron irradiation, new model for peaking effect 8-87683
 dissociated dislocations in diamond cubic struct. 8-59806
 dynamic Peierls stress in cryst. model with slip anisotropy, screw dislocation motion 8-95056
 elasto-plastic metal-dislocation system, stress-activated dislocation motion, thermodynamic theory (*Chinese*) 8-83868
 fatigue crack, dislocation diffusion mech. of form. 8-60829
 fatigue crack propag., low temp. 8-72876
 ferromagnet, dislocation motion, mag. moments around screw dislocations, spin waves retarding dislocations 8-87670
 geological materials, dislocation dynamics studies via stress relaxation testing method 8-96309
 H₂O:HF ice, single crystal, velocity of individual dislocations by X-ray topography (*French*) 8-87677
 Haynes Stellite 6B, particle erosion damage, TEM obs. 8-88546
 high pressure effects on dislocation mobility 8-55869
 ice, quantum mechanical approach to velocity of dislocations 8-91339
 impact testing, investigation of dislocation dynamic props. (*Russian*) 8-85069
 ionic crystal, point defect-dislocation interactions 8-63787
 kinematics, continuous distrib. of disclinations and dislocations 8-63764
 metal, flow stress relation with thermal conductivity discontinuity at supercond. transition 8-60246
 metal bicrystal, mech. behaviour, continuous theory of dislocations appl. 8-67717
 metals, BCC, effect of screw dislocations, on mech. props. (*Russian*) 8-60704
 metals irradiated, heavily, exam. of percolative mass transfer 8-79639
 multiple dislocation motion, exam. 8-51541
 nonuniformly moving dislocations, elastic half space response to realistic faulting model 8-85486
 plastic deformation, cyclic, exam. of reversible strain, effect on dislocation motion 8-84892
 plastic deformation, phenomenological theory, with mobile and immobile dislocations 8-75714
 plastic deformation, steady-state, irreversible thermodynamic description 8-72831
 polycrystalline aggregate, continuous distrib. of dislocations, stress fields, movements in elastic-plastic deform. 8-75709
 Schmid's law deviations, in uni-directional strain 8-71783
 steel, austenitic stainless, Cr-Ni-Ti, creep deform. effects on intergranular TiC dispersion stability 8-84912
 steel, Cr-C, (2.14, 1.08 at.%) tempered, resistance to small plastic deformation, strain relaxation (*Russian*) 8-56698
 steel, stainless, creep 8-64583
 stress field, diffusing elastic fluid, mechanical interaction effects 8-63766
 thermally activated motion of dislocation group, exam. 8-87669
 Al, [111] single crystal, in situ deform., HVEM obs. 8-52886
 Al, acoustic emission under plastic deform., spectral anal., dislocation mean free path 8-84934
 Al and Al-Mn (1 wt.%), subgrain growth during annealing after cold work 8-56656
 Al, dynamic defect annealing during plastic deform. 8-88478
 Al foil, quenched, anomalous annealing phenomena, quantitative study 8-80565
 Al-Mg (5.5%), creep, absence of instantaneous plastic strain upon stress changes 8-75718
 Al-Mg solid soln., AE during plastic deform. 8-64592
 Al-Zn-Mg alloys, decomp. kinetics from Young's modulus obs., microprocesses (*German*) 8-64522
 Be, forest dislocation effect on single twin layer development in single crystals 8-63775
 Cu, internal stresses in plastically deformed crystals (*Russian*) 8-79615
 Cu-Al (10.4%), creep, absence of instantaneous plastic strain upon stress changes 8-75718
 Fe, cast, spherical, mech. behaviour, continuous theory of dislocations appl. 8-67717
 Fe dislocation dynamics, HVEM in situ obs. 8-83822
 Fe-Mo (1.8%), creep, absence of instantaneous plastic strain upon stress changes 8-75718
 Fe-Si, low-temperature fatigue crack propagation 8-72876
 Fe-Ti (0.056 at.%), mobile dislocations during stress relaxation 8-68721
 Fe-Ti (0.056 at.%), mobile dislocations during stress relaxation 8-68722
 GaAs cryst., creep and dislocation vel. at different doping and temps. 8-95783
 GaP:N LED, acoustic emission, NDT of dislocation motion 8-91759
 KCl, dislocation motion in micro-plastic region 8-91341
 KCl, motion of dislocation half-loops, influence of prestart loading and ensemble nature 8-71745
 KCl single crystal, dislocation velocity stress exponent estimation by stress relaxation and creep tests (*Japanese*) 8-55875
 LiF, single crystal, dislocation generation, beneath static and rolling contact with sphere 8-87671
 Mo, dislocation dynamics, HVEM in situ obs. 8-83822
 NaCl, dislocation half loop mobility 8-59817
 NaCl, dislocation motion in micro-plastic region 8-91341
 NaCl, motion of individual surface dislocation semi loops (*Russian*) 8-51542
 Nb, neutron irradi. effects on mech. props. 8-91361
 Nb, surface oxide softening, anisotropy 8-60716
 Ni, dislocation dynamics, HVEM in situ obs. 8-83822
 Ni-Cr-Ti-Al-Fe-Co (19.65, 2.40, 1.37, 0.78, 0.52 wt.%), strength of γ' hardened alloy, ageing exam. 8-88501
 Ni₃ (Al,Ti), flow stress and work hardening, exam. of temp. depend. by tensile tests 8-84839
 Si:P, high dose implantation, outside dislocation generation 8-87672
 Zn, forest dislocation effect on single twin layer development in single crystals 8-63775
 ZnSe, charged dislocation motion mechanism (*Russian*) 8-79820

dislocation motion, nonconservative *see* **dislocation climb**

dislocation motion hindrance *see* **dislocation drag**

dislocation multiplication

- slip band broadening, computer model 8-59808
- steel, St3 and KhVG, rel. to strength variation under influence of shock waves (*Russian*) 8-92299
- Ag and Ag alloys, yield stress temp. variation hysteresis (*Russian*) 8-52905
- Ge epitaxial layers, on GaAs substrate, misfit dislocation multiplication mechanism 8-87673
- Mg₂SiO₄, forsterite, glissile splitting of dislocations, cross-slip-controlled creep and mantle rheology 8-61406
- Ti-Al alloy, VT5-1, rel. to strength variation under influence of shock waves (*Russian*) 8-92299

dislocation nucleation

- dissociated dislocations in diamond cubic struct., movement 8-59806
- fatigue cracks threshold stress intensity for crack growth, prediction using dislocation model 8-83870
- glass surface, peeling of rubber film, spontaneous creation of interfacial dislocations 8-73011
- semiconductor single crystals, melt grown, dislocation creation by thermal stresses 8-83825
- steel, St3 and KhVG, rel. to strength variation under influence of shock waves (*Russian*) 8-92299
- Al, dislocation generation from grain boundary, in situ obs. 8-51547
- Ti-Al alloy, VT5-1, rel. to strength variation under influence of shock waves (*Russian*) 8-92299
- Zr, dissolution of γ -ZrH, in situ study, HVEM obs. 8-55951

dislocation pile-ups

- β_1 brass containing α -precipitates, reversible shape memory effect (*Japanese*) 8-60711
- cubic crystal, distrib. of dislocations in intersecting pile-ups (*Russian*) 8-87668
- filler metal, deformation mechanism at brazed joint 8-80616
- refractory composites, fibre reinforced, directionally solidified tensile tests, in HVEM, deform. and fracture (*French*) 8-68785
- steel, cold-worked, state of cementite, nucl. gamma reson. meas., plastic deform. (*Russian*) 8-68706
- steel, inclusions effect on distrib. of local microheterogeneous deform. (*Russian*) 8-80586
- steel, martensitic, delayed fractures suppression, by neutron irradiation (*Czech*) 8-67743
- Al-Cu (4 wt.%), AE during deform., effect of ageing at 170°C 8-64597
- α -Fe, distrib. of dislocations in intersecting pile-ups (*Russian*) 8-87668
- KCl-KBr, dislocation rosettes, diffusion origin 8-83820
- KCl-NaCl, dislocation rosettes, diffusion origin 8-83820
- Ti-11, unstable shear modes in fatigued β -annealed specimens 8-84984
- Ti-alloy, IMI-685, unstable shear modes in fatigued β -annealed specimens 8-84984

dislocation pinning

- see also* **dislocation damping**
- metals irradiated, heavily, exam. of percolative mass transfer 8-79639
- microcreep, low temp., quantum effects (*Russian*) 8-71784
- Ag, electron irradi., elastic moduli and internal function (*French*) 8-87703
- Al alloys, inelastic electron scattering by dislocations (*Russian*) 8-79988
- Cu alloys, inelastic electron scattering by dislocations (*Russian*) 8-79988
- Cu, cold worked, determ., of dislocation pinning and unpinning stages, using internal friction meas. 8-92278
- Cu-Ni-Fe (26.8 wt.%), microduplex struct. form., recrystn. annealing (*Japanese*) 8-76659
- KCl, dislocation motion in micro-plastic region 8-91341
- NaCl, dislocation motion in micro-plastic region 8-91341
- NaCl, strain ageing exam. 8-56661
- NbN_x, solid soln, strain ageing, internal friction, elec. cond. kinetics (*Russian*) 8-76667
- NbN_xO_y, solid soln, strain ageing, internal friction, elec. cond. kinetics (*Russian*) 8-76667
- NbO_x, solid soln, strain ageing, internal friction, elec. cond. kinetics (*Russian*) 8-76667
- Ni 200, C interstitial effect of yield point develop. during static strain ageing, model 8-88498

dislocation relaxation *see* **dislocation damping**

dislocation scattering

- used for carrier scattering by dislocations*
- helical electric current flowing along screw dislocation 8-51959
- III-V semiconductor, anisotropic carrier mobility due to dislocations 8-60124
- III-V semiconductor, local resist. near dislocations, eqns. 8-60123
- junction current, luminesc. near dislocation, surface, integral representations, appl. to LED's 8-68079
- metal, dislocation scatt. and de Haas-van Alphen amplitudes 8-63967
- noble metal, elec. resist. of dislocations, calc. (*Russian*) 8-60117
- scattering phaseshifts and resonances for line defects 8-51953
- screw dislocation, electron scattering 8-60101
- semiconductor, model describing removal and scattering of charge carriers by defect clusters 8-76069
- Ag, strained, anisotropic electron scatt. in elec. resist. 8-91656
- Al alloys, inelastic electron scattering by dislocations (*Russian*) 8-79988
- Al, Fermi surface, scattering anisotropy of conduction electrons on dislocations (*Russian*) 8-60051
- Al, strained, anisotropic electron scatt. in elec. resist. 8-91656
- Cu alloys, inelastic electron scattering by dislocations (*Russian*) 8-79988
- K, electrical resistivity below 2K, temp. depend. 8-51969
- Mo, film, vacuum deposited, elec. cond., internal stresses, surface corrosion, MOS gate appl. (*Japanese*) 8-80073
- Pd, strained, anisotropic electron scatt. in elec. resist. 8-91656
- Te:Sb, 96 to 500K, cond. Hall const., hole mobility, conc., dislocation effects (*Russian*) 8-64039

dislocation sources

- see also* **Frank-Read sources**
- local heating in crystals during low-temperature deformation 8-67766
- Si, initial stage of plastic flow 8-64602

dislocation structure

- amethyst crystals, dislocations, selective etch method 8-75674
- asymmetric Bragg condition for thick real crystals, applic. to dislocation networks (*German*) 8-67607
- BCC metals, vacancy-edge dislocation interactions, computer simulation 8-83845
- Bordoni relaxation, theoretical aspects, numerical calcs. from thermally activated double kink formation 8-63805
- α -brass, dislocation structure around crack tips in early stage of fatigue 8-60830
- γ -brass type alloys, faulted defects, nature determ. by image matching technique 8-63777
- continuum approach of physical line structs., appl. to dislocations 8-81859
- electron microscope diffr. contrast 8-83700
- grain boundary dislocations, Burgers vectors, grain boundary dislocations 8-87680
- ice, Antarctic deep core, X-ray diffr. topographic studies 8-63803
- III-V quaternary-binary heterojunction, X-ray characterisation of defects 8-95239
- model for interaction between tensile crack and hole 8-67092
- obstacle strength determ. in solid soln. 8-68704
- olivine, naturally deformed, recovery process, rel. to Earth upper mantle mech. state 8-96202
- periodic misfit-dislocation networks, electron diffr. 8-59815
- polyethylene crystal, preferred orientation relationship, epitaxy 8-67923
- sapphire, profiled growth, struct. perfection 8-68621
- steel, low C, P, plastic anisotropy and mech. prop. dynamic strain ageing effect 8-64608
- steel, low-C, ferritic, deform. microstruct., electron microscopy (*German*) 8-64589
- steel, maraging, investigation with lower Ni and Co contents (*Chinese*) 8-84812
- steel, stainless 316, creep under high stress 8-52892
- steel cylindrical bar loaded by longitudinal impact, dislocation struct. and plastic deform. (*Czech*) 8-60713
- X-ray distrib. function (*German*) 8-63767
- Ag and Ag alloys, yield stress temp. variation hysteresis (*Russian*) 8-52905
- Ag film, epitaxial growth, characterisation of [001] tilt boundaries 8-84097
- Al, creep and dislocation distribution, influence of electron irradiation (*Russian*) 8-95775
- Al, dislocation substructure formation under hydrostatic extrusion 8-56696
- Al, fatigue induced dislocation struct. and hardening, exam. (*Japanese*) 8-64624
- Al, screw dislocation core, atomic struct. calc., modified lattice-statics approach 8-75669
- Al-Cu (4 wt.%), elastic accommodation of semicoherent θ' 8-64543
- (Al₂O₃)_nMgO, n=1.1, high temp. creep, dislocation behaviour 8-80593
- Au bicrystal, dislocation networks in twin boundaries, TEM obs. 8-51556
- Au film, epitaxial growth, characterisation of [001] tilt boundaries 8-84097
- Ca₃Ga₂Ge₃O₁₂, substrate, electron examination of microstruct. and microsegregation 8-67919
- Ca₃(PO₄)₂F, dislocation struct. exam. (*Russian*) 8-63770
- CdSe-Ge (111) heterojunctions, epitaxial, azimuthal rotation 8-84085
- Cu and Cu-Al alloys, mech. props. effect of free mean path 8-84945
- Cu, dislocation substructure formation under hydrostatic extrusion 8-56696
- Cu-Ni bicrystal, misfit dislocation config., moire patterns, interdiffusion effects 8-84110
- Fe, BCC, computer simulation of entropy of $\frac{1}{2}\{111\}\{110\}$ edge dislocation 8-67716
- Fe, deformed, dislocation structure determ. from magnetic props. 8-58874
- Fe, dislocation struct. around fatigue cracks, exam. (*Japanese*) 8-64623
- Fe, single crystals, work hardening and behaviour and dislocation struct. during simple shear tests 8-95762
- α -Fe-C (0.03 wt.%), structural singularities of transition from thermally activated to force-induced fracture (*Russian*) 8-56731
- Fe-Co-Ni-W alloy, 45KKhVN, plastic deform., electron microscope obs. (*Russian*) 8-80584
- Fe-Ni-Cr (25, 15 wt.%), high temp. creep, dispersed γ' -Ni₃(Al, Ti) effects (*Czech*) 8-64590
- Fe-Pt, nearly thermoelastic, irreversible lattice defects formed by martensitic transform. cycles 8-60671
- FeS₂ (pyrite), glide elements study by electron microscopy and electron diffr. 8-83817
- Ga_{1-x}Al_xAs_{1-y}P_y-GaAs quaternary heterojunction, misfit dislocation charact. by synchrotron radiation white beam topography 8-63771
- Gd₃Ge₂O₁₂, substrate, electron examination of microstruct. and microsegregation 8-67919
- InSb, plastically bent single crystals, dislocation struct. obs. 8-59816
- KCl, Czochralski-grown, dislocation subboundary characts. 8-67718
- KCl-KBr, dislocation rosettes, diffusion origin 8-83820
- KCl-NaCl, dislocation rosettes, diffusion origin 8-83820
- Mg, cyclic hardening of single crystal 8-64552
- Mg, melt grown by Bridgeman method, X-ray topography 8-59770
- MgO(Al₂O₃)_{1.8}, spinel, X-ray refl. topography, dislocation substructures during creep form. (*French*) 8-68737
- Mo, foil dislocation struct. of rolling texture (*Russian*) 8-59810
- Mo single crystals, substruct. variation during fatigue, kinetics (*Russian*) 8-60742
- NbN_x, solid soln, strain ageing, internal friction, elec. cond. kinetics (*Russian*) 8-76667
- NbN_xO_y, solid soln, strain ageing, internal friction, elec. cond. kinetics (*Russian*) 8-76667
- NbO_x, solid soln, strain ageing, internal friction, elec. cond. kinetics (*Russian*) 8-76667

dislocation structure continued

- Ni, dislocation substructure formation under hydrostatic extrusion 8-56696
 Ni single crystals, cyclically deformed, behaviour during annealing 8-71740
 Sb, epitaxial growth on Bi substrate 8-95246
 Si, 60° dislocation, X-ray diffraction contrast, section topography 8-83819
 Si, plastically deformed monocrystal, X-ray topographical study (*German*) 8-59813
 Sms, mechanical polishing, stabilisation mechanism for metallic phase on surface 8-60015
 UO₂, compressed, dislocation substructure obs. (*French*) 8-78461
 Y₂O₃, plastically deformed, dislocations obs. by TEM (*French*) 8-51545
 Zn, dislocation struct. stability, effect of deformational and thermal annealing 8-64567
 Zr base alloys, irradiation growth, dislocation model 8-51595
 α-Zr, polycrystalline, cyclic deformation (*Japanese*) 8-68757

dislocation translation *see slip***dislocations**

- For pipe diffusion, see diffusion in solids. See also dislocation
 see also Bordoni effect; Cottrell atmospheres; disclinations; edge dislocations; grain boundaries; screw dislocations*
 antiferromagnet, phase transformations in strong mag. fields, mag. moments collapse, strengthened magnetoelastic links (*German*) 8-68227
 atomic dislocation modelling, flexible boundary conditions and nonlinear geometric effects 8-75667
 austenitic stainless steel, type 316, anelasticity and creep transients 8-84880
 compressed crystals, dislocations and point defects (*Russian*) 8-75666
 continuous plastic cracks in ordered alloys, discrete dislocation analysis 8-80625
 Cosserat's medium, linear and surface defects, stresses 8-83813
 crystal under high pressure, dislocation theory 8-55870
 4-cyano-4-n-cyanobiphenyl, smectic A mesophase, plasticity anal., defects motion, Grandjean wall form. 8-91227
 defect diffusion, radiation effects 8-87827
 dissociated, stacking fault width determ. from 224 reflections with $g \cdot b = 0$ 8-59722
 Earth mantle peridotites, stress estimates from structural studies 8-69330
 elemental semiconductors, hybridisation effect on dislocation electronic states 8-51936
 elimination by recrystallisation (*German*) 8-51559
 fatigue crack, blunting and growth, prediction of threshold stress intensity using dislocation model 8-79662
 ferromagnet, local variation in mag. anisotropy due to linear defects (*Russian*) 8-68214
 N-p-heptyloxybenzylidene-p-heptylaniline, liq. cryst., dislocations obs. in smectic A and C mesophases 8-91230
 homotopy groups of condensed matter physics 8-63752
 III-V semiconductor, temp. distrib. around dislocations, due to Joule heating, calc. 8-71734
 III-V semiconductors, manifestation of local vibr. of dislocations in IR spectra 8-88339
 n-decyl-p-azoxy-α-methyl cinnamate, dislocations obs. in smectic A and C mesophases 8-91230
 light scattering by excitons localised at dislocations 8-60479
 melting, dislocation generation, anharmonicity and solitons 8-79746
 melting, dislocation model, theory 8-83923
 metal, dislocations rel. to electron gas thermodynamics at 2¹/₂th order transition (*Russian*) 8-51910
 ordered alloy, with L₁ structure, dissociation of superdislocations and plastic deform. mech. (*Russian*) 8-52909
 piezoelectric crystal, Gulyaev-Blustein wave excitation by developing defects (*Russian*) 8-56030
 quasi-Newtonian force 8-63765
 semiconductor light source degradation, review of recent expts. 8-82970
 smectic C liquid crystals, elasticity and defects 8-91233
 smectic liquid crystals, acoustic emission, appl. to defect dynamics study 8-91232
 stationary lattice defects as sources of elastic singularities 8-59800
 superconductor, flux pinning summation curves 8-52165
 theory, rel. to X-ray topography data 8-64254
 twin interfaces, obs. using relative translations of adjacent crystals in TEM 8-75675
 two-phase structures, high-temp. deform. 8-68738
 vacancy loss during quenching of low dislocation density cryst. 8-75656
 X-ray plane wave topography, observation of dislocation in Si single cryst. 8-91342
 Ag, finite dislocation elements, isostress contours 8-71735
 Ag plastically deformed crystal, exam. of dislocation dynamics during strain rate changes 8-88506
 Ag, plastically deformed crystals, exam. of dislocation dynamics during strain rate changes 8-88507
 Cu complex, bis-(alkylammonium) (11) tetrachloride, perovskite, lattice perfection 8-87633
 Cu single crystals, in high temp. creep, meas. of internal stress 8-80608
 Cu₂NiZn, superlattice dislocations 8-83816
 GaP, dopant dislocations, scanning electron micrographs, cathodoluminesc. 8-91340
 GaP, SEM, cathodoluminesc., impurity and defect detect. 8-83695
 n-GaSb, temp. distrib. around dislocations, due to Joule heating, calc. 8-71734
 GdGa garnet, Czochralski grown, substrate material dislocation propagation 8-59771
 Gd₃Ga₂O₁₂, Czochralski grown, effect of melt flow phenomena on perfection 8-88419
 Gd₂(MoO₄)₃, and isotypes exam. of crystal growth, and defect generation 8-68617
 LiF, manifestation of local vibr. of dislocations in IR spectra 8-88339
 MgO, lattice misorientation and displaced vol. for microhardness indentation 8-64617
 Nb, supercond., field history effect of flux gradient 8-91828
 Nb-H, behaviour of H in Nb, relation to mech. props. 8-80572

dislocations continued

- Si, 60° dislocation, X-ray diffraction contrast, section topography 8-83819
 Si, crystal defects in integrated circuits, review 8-88547
 Si, epitaxial film, struct. defects, effects on planar diffused p-n junction elec. props. (*Russian*) 8-60195
 Si, P diffused sample, stacking faults and dislocations formation from interstitials 8-95059
 Si, structural defects on (115) plane 8-87675
 Si:B, SEM obs. of dislocations using Schottky barrier EBIC technique 8-79614
 Sn, superconducting and normal phases, damping of dislocations and supercond. attenuation 8-52155
 TiCl₃, (TiCl)₃, labelled, exchange of Ti ats. rel. to γ-irrad., heat treatment, grinding 8-92470
 V₃Si plastically deformed cryst., lattice transform., Kossel technique 8-95153
 ZnO (1010) surface bias voltage effect on hardness, charge exchange near dislocations 8-52078

disordered systems, vibrational states *see vibrational states in disordered systems***disperse systems**

- see also aerosols; Brownian motion; colloids; dust; emulsions; foams; fog; gels; powders; smoke; sols; suspensions*
 adsorption on hydrated solid phase surface exchange cations effect 8-64893
 agitated dispersion, droplet breakage and coalescence rates during mixing 8-85205
 alloy, disperse state formation (*Russian*) 8-52757
 atomisation of liquid by impinging jets, expt. and theory 8-87373
 butyl rubber dispersion, electron-microscopic investigation 8-53268
 coagulating dispersions, light scatt. data, Fourier inversion anal. 8-76932
 coagulation, slow, turbulent 8-53259
 coagulation, with breakdowns, exact solution of integrodifferential equation 8-53272
 coagulation in finite systems 8-68933
 collection efficiency of grid filters, effect of Stokes and Reynolds numbers 8-61592
 dielectrophoretic forces, expt. anal. 8-64892
 diphasic structure, systematic anal. to determ. permittivity and elec. cond. from dielec. relax. 8-56423
 dispersed flow, heat and mass transfer, phase transition effect 8-67252
 electrosurface properties measurement 8-53249
 filtration coeffs. of polymer-modified disperse systems 8-67264
 fine particle deposition, on rotating disc surface, convective diffusion under elec. double layer forces 8-61060
 flame, containing light scatt. particles, optical props. and temp. meas. method (*Russian*) 8-56894
 fluorescence from molecules embedded in small particles, angular distrib. 8-76926
 ice microcrystal dispersions, dielec. props. (*French*) 8-60374
 latex, monodisperse, phase diagram, spectroscopic study 8-85209
 latex, monodisperse, short-range order, spectroscopic study 8-85208
 lecithin-cholesterol interaction, equilib., stoichiometry of complexes in bulk systems 8-68985
 lecithin-cholesterol interaction, equilib., surface film phase relations and cholesterol condensing effect 8-68986
 light scattering data analysis for very polydisperse samples 8-50702
 liquid-liquid dispersion, droplet size spectra in turbulent pipe flow 8-67247
 lyotropic liquid crystal, struct. rel. to amphiphilic structure 8-51416
 macromolecular absorbed layer, energy of interaction between two spherical particles 8-53271
 macromolecules, polydispersity in nonlinear electric methods, nonlinear dielec. effect formulas derived 8-59730
 magnetic separation, particle capture in axial filters, theory and performance 8-92515
 maleate-acrylate polyester resin, with phenol and glass microspheres, rheological behaviour 8-53267
 metallic particles, anomalous absorpt. in far IR region 8-56464
 metals separated by dielectric, electronic component of metal-metal interaction force, calc. 8-52056
 monodispersed particles, angular distrib. of fluoresc. 8-76927
 multispectral extinction data, analytic inversion in anomalous diffr. approx. 8-87016
 N-particle system, Brownian dynamics with hydrodynamic interactions 8-91209
 optical extinction measurements, forwardscattering corrections in aerosol media, monodispersions 8-94367
 particle and pore size distrib. curves quantitative evaluation, Fortran program (*Czech*) 8-80795
 particle growth, mathematical modelling, continuity eqns. for particle distrib. 8-65863
 plastic non-Newtonian fluids in circular pipes, laminar flow stability loss 8-79342
 PMMA latex particles, laser light scatt. for visualisation in EHD 8-75236
 polydisperse droplets, produced by EHD method, charge-to-mass ratio 8-76931
 polydisperse hard-disc systems, equations of state, particle size effects 8-73947
 polydisperse hard-sphere systems, equations of state, particle size effects 8-73947
 polydisperse particles, fractional anal. by ring method (*Russian*) 8-71035
 polymeric systems, rheology, review 8-87317
 polymers, heterophase mixtures, excess energy 8-53264
 polystyrene latex, grain boundary struct. obs. and boundary diffusion 8-51552
 polystyrene latex dispersions, aqueous, in presence of poly(vinyl alcohol), stability, crit. flocculation temp. 8-85207
 polystyrene latex particles from water, adsorption of poly(vinyl alcohol), influence of temp. 8-85206
 polystyrene latexes, soft X-ray scatt., struct. determ. 8-51395
 spherulids in shear flow, light scatt., orientation correlation 8-76481
 sterically stabilised dispersions, critical flocculation temperature, effect of dipolar substituent groups 8-61061
 surface area meas. by light transmission (*German*) 8-89431

disperse systems continued

- suspended spheres, effective shear viscosity of regular array 8-51718
- thermal conductivity prediction of heterogeneous mixture, digital simulation technique 8-87247
- transport in heterogeneous media, random dispersed phase model 8-65885
- turbidity spectrum for parameters determ., allowance for nonspherical particles 8-55302
- two-phase conducting diamagnetic system, coeff. of EM ejection of particles (*Russian*) 8-94364
- vibrational compaction, of bulk materials 8-52701
- waves, plane, nonlinear viscous multicomponent media 8-51228
- Ag particles, lattice defect influence on size effect 8-88329
- Al_3N_4 , dispersion in transformer steel for cubic texture formation (*Russian*) 8-80557
- Au sol, grain boundary struct. obs. and boundary diffusion 8-51552
- C particle formation, C_2+C_3 as possible first step 8-68876
- $Cr_2O_3 \cdot SH_2O$, heat-treated, narrow particle size distrib., surface props. 8-85210
- Cu- Al_2O_3 powder, electrolytic deposition 8-84743
- Fe oxides, disperse, chemical reduction in discharges (*Russian*) 8-95915
- Ge, ultrafine multiply twinned particles, form. by gas-evaporation technique 8-63685
- Hg+water systems, drop fragmentation rel. to thermal explosion detonation requirements 8-71368

dispersion (wave)

- see also *acoustic dispersion*; *optical dispersion*
- composite, fibre-reinforced, layered, harmonic elastic waves, dispersion 8-63223
- dispersive wave trains, near-linear, two-time procedure for higher order modulation 8-65788
- Earth, surface waves phase vel. and attenuation simultaneous inversion, Love waves appl. 8-85491
- EM monochromatic wave energy density in nonabsorbent medium with freq. and space dispersion (*Russian*) 8-74818
- granular solid, one-dimens., small amplitude wave behaviour 8-59339
- groups of waves, dispersion rel. to vels. and refr. laws 8-85575
- magneto-acoustic macroscopic soliton instability growth rate, dispersion eqn. (*Russian*) 8-59562
- non-linear dispersive wave, coupled modes approach, effect of dissipation on recurrence 8-49670
- nonlinear dispersive system with small dissipation, statistical theory 8-70058
- nonlinear dispersive wave eqns., modulational instability and envelope solns. 8-54199
- ocean trapped waves, wavenumber/freq. spectrum anal. and dispersion relations (*Russian*) 8-81189
- plasma, ion-cyclotron wave spectra dispersion eqn. numerical soln. (*Russian*) 8-59561
- seismic surface waves anisotropic dispersion, isotropic inversion significance 8-96156
- solid, phase and group vels. determ. for dispersive waves 8-81848
- surface waves, inhomogeneous liq.-vap. interface, origin 8-75158
- thin walled elastomer tubes, dispersive effects in wave propag. 8-87289
- three-frequency soliton solns. in second approximation (*Russian*) 8-57789
- unsteady waves from initial, periodic and travelling disturbances, asymptotic anal. (*Russian*) 8-77254
- waveguide, plasma filled, EM wave freq. spectra dispersion eqn. numerical anal. (*Russian*) 8-59605
- whistler dispersion, group delay automatic meas., ionosphere and magnetosphere electron density 8-93050
- zero sound, in classical liq., excitation, damping, memory function approach 8-67771
- Co-P film, amorphous, spin wave dispersion law, spin wave reson. obs. (*Russian*) 8-88196
- GaAs thin films, differential mobility anisotropy effect on wave propag. 8-88050
- YIG film, dielec. layered struct., magnetostatic volume wave propag., dispersion eqn. 8-95426

dispersion hardening

- see also *precipitation hardening*
- coarsening of dispersed particles, in solid matrices 8-56651
- dispersion hardened metallic matrix composite, powder metallurgically produced effective interparticle distance effects (*German*) 8-52727
- steel, austenitic, Kh12N20T3R, ageing, submicroscopic struct. role in dispersion hardening (*Russian*) 8-64549
- steel, C, coarsening of dispersed particles, in solid matrices 8-56651
- steel, CrMoV, low alloy, dispersed phase of VC, hardening mechanism (*Chinese*) 8-60676
- Ag-MgO, laws of plasticity of dispersion strengthened materials 8-84832
- Al_2O_3 -TiC, multiphase ceramics, mech. strengthening due to dispersion of non-metallic particles (*German*) 8-60674
- Al_2O_3 -ZrO₂, multiphase ceramics, mech. strengthening due to dispersion of non-metallic particles (*German*) 8-60674
- Cu-Al, dispersion hardening by internal oxidation 8-56649
- Cu-MgO, dispersion hardened, prep. by milling Cu and Mg oxidising atmos. (*German*) 8-64509
- Cu-SiO₂, dispersion hardened, surface plasticity effect 8-52832
- Cu-SiO₂ single crystals, dispersion hardened, exam. of yield stress between 77 to 1200K 8-76720
- Fe-Cr-Al-Y ($Y-Al_2O_3$)(Y_2O_3), preparation and exam. of mech. props. 8-52720
- Mo-TiN (3.5 vol.%), failure characts. exam. 8-68788
- Mo-ZrC, internal oxidation, struct. formation law, microstruct. examination 8-84836
- Ni-Cr, solid soln., exam. of back stress role in creep behaviour of particle strengthened alloys 8-52889
- Ni-Cr-Al (15, 5 wt.%), oxide dispersion strengthened, effect of dispersoids on oxidation 8-80679
- Ni-Cr-Al-Ti (Ti-Co), exam. of back stress role in creep behaviour of particle strengthened alloys 8-52889
- Ni-Cr-Ti-Al-Fe-Co (19.65, 2.40, 1.37, 0.78, 0.52 wt.%), strength of γ' hardened alloy, ageing exam. 8-88501
- Ni-SiC, electrodeposited, oxidation 8-64756
- Ni-ThO₂, dispersion hardened, fracture mechanism map 8-60823
- Ni-ThO₂, irradiated with 5 MeV Ni⁺⁺, ThO₂ redistrib. 8-71771

dispersion hardening continued

- Ni-ZrO₂, thin layers, vapour deposited, dispersion strengthened, exam. of struct., mech. props. 8-80554
- NiCr-MoAl-ThO₂ (13,3 wt.%), powder, mech. alloying 8-84744
- Pb-Al₂O₃ composites, mech. alloyed, hot hardness meas. (*Japanese*) 8-84830
- W, wire, doped, high temp. creep behaviour 8-88499
- W-WC, activated sintering, mech. props. (*Korean*) 8-60622
- ZrO₂-ZrO₂, multiphase ceramics, mech. strengthening due to dispersion of non-metallic particles (*German*) 8-60674

dispersion power, rotatory see optical rotation**dispersion relations**

- see also *dispersion (wave)*; *Kramers-Kronig relations*; *Mandelstam representation*; *N/D method*; *phonon dispersion relations*; *phonons*; *plasma instability*; *plasma waves*; *S-matrix theory*
- atom, forward elastic electron scatt. amplitude, dispersion relation 8-90263
- bounded skewed shear flow, tensor form of bulk dispersion coeff. 8-73393
- circumferential waves, cylindrical shell supported by a continuum 8-90564
- elastic wave propagation, influence of random porosity 8-90552
- electronuclear sum rules, generalised, from EM structure functions 8-89806
- haeme proteins, inversely polarized modes in reson. Raman scatt., depolarisation dispersion curves, vibronic interactions 8-78676
- high-density pulsed plasma, laser interferometry 8-67430
- interior dispersion relations appls. to π photoprod. near threshold 8-93889
- internal waves excited by travelling forcing effects, compressibility influence 8-61495
- metal particles, spherical, surface plasmon dispersion relation, hydrodynamical model 8-84277
- nuclear fission, Sommerfeld-Watson transformation (*Rumanian*) 8-86526
- nuclear matter, dispersion relations, HF method for hard core interactions (*German*) 8-54713
- phase transition, 1st order, ageing stage, kinetic instabilities 8-87765
- plasma electrostatic heat flux instabilities, linear Vlasov dispersion relation 8-79420
- plasmon dispersion in simple metals 8-91629
- pseudoscalar Dalitz decays, form factor slopes, VDM with subtracted dispersion relation 8-58181
- relativistic particle ring, coherent oscillations, radial mode dispersion relations 8-55060
- surface waves in prestressed body with cylindrical cavity (*Russian*) 8-63369
- thin stretched foils, membrane wave excit. 8-90578
- unidirectional wave motions, book 8-77730
- US excitation and detection in mag. polarised nonferromagnetic metals. 8-56856
- velocity dispersion of missing mass in solar neighbourhood, stability of N-component stellar disc 8-69886
- cross sections in dispersion-relation anal., geometrical scaling 8-74260
- D-meson, gauge theoretic formulation of $SU_2 \times U$, model, mass limit 8-70316
- $\gamma N \rightarrow \pi N$, resonance region photoprod., dispersion model, M1 and E2 photoexcit. $N \rightarrow \Delta(1236)$ 8-70377
- KN interactions, low energy, K matrix and dispersion relns., $\Gamma(1405)$ resonance 8-70408
- NN and NN forward scatt. amplitudes 8-62337
- NN I=1 amplitudes struct. at 6 GeV/c 8-70395
- NN interactions, conf., Vancouver, Canada (July 1977) 8-62418
- NN interactions and chiral symm., dispersion relation anal. 8-66048
- NN systems, resonances due to annihilation, baryonium states, many channel N/D method 8-66143
- pp helicity amplitudes at $t=0$, dispersion theoretic anal. 8-62340
- πN S-matrix, inelastic effects in sidewise dispersion relations for nucleon EM form factors 8-82212
- $\pi\pi$, coupled integral eqns. for scatt. at all energies 8-49982
- $\psi \rightarrow 3\gamma$, dispersion sum rule charmonium theory, decay probability lower bound (*Russian*) 8-89716
- $\psi \rightarrow 3\gamma$, dispersion theory of charmonium, self consistency test, decay probability (*Russian*) 8-89717
- Σ^- mag. moment calc. from dispersion relations in t 8-82257
- Y particle at 9.4 GeV, differential dispersion relations theory of I^+I^- annihilation 8-86424
- H, elastic electron scattering, static exchange amplitude, dispersion rels. 8-66664
- H electron scatt. forward elastic exchange amplitudes and forward dispersion relations, anal. props. 8-78812
- $^3He + \pi^+$, dispersion relations, determ. of π^3He^3H coupling constant 8-58307

dispersions see disperse systems**dispersoids see disperse systems****displacement measurement**

- 90° phase shift beam splitter for displacement interferometer 8-87145
- biaxial laser-based displacement transducer 8-73967
- capacitance displacement transducers, effect of tilt and surface damage 8-54356
- capacitive transducers, manufacturing error effect on accuracy 8-89467
- circular hole, normal surface displacement, reflection holographic interferometry 8-57893
- contour holography of moving object, using injection locked flash pumped dye laser 8-50737
- differential frequency angular rate and displacement sensor, construction (*Russian*) 8-70106
- direction-sensitive displacement analysis by multiple freq. holographic interferometry 8-54338
- double beam Michelson interferometer meas. of small linear displacements 8-73966
- holographic interferometry, errors in small vector displacements meas., statistical anal. 8-78953
- holographic interferometry appl. to displacement, deformation and vibration meas. (*Italian*) 8-54337
- holographic interferometry with continuously scanning reconstruction beam 8-71055
- holographic techniques, expt. comparison 8-71057

displacement measurement continued

- holographic vibration analysis, computer-aided, for vectorial displacements of bladed discs 8-71056
- holographic zero order fringe identification, direction of motion detection 8-63044
- impact force vs. displacement curves, expt. determ. 8-83344
- inductive displacement-measuring system synthesis using CAD 8-73982
- interferometry, automatic fringe counting, independ. of signal level changes 8-58018
- linear variable differential transformer method 8-73978
- loudspeaker signal displacement meas., optical method 8-51023
- microinterferometer transducer, air-bearing, for use with universal inspection machines 8-57899
- moving coil linear variable differential transformer for displacement meas. at liquid helium temps. in strong magnetic fields 8-54415
- speckle interferometry, real-time meas. of vibrations and displacements (*Italian*) 8-54336
- speckle pattern TV interferometer, principle and appl. 8-58014
- strain measurement, full field optical method having postrecording sensitivity and directional selectivity 8-57892
- stress analysis using holographic interferometry and speckle photography 8-70095
- third intracranial ventricle dynamic displacement detection 8-57035
- ultraprecision spindle unit construction on aerostatic supports 8-77880
- ultrasmall displacement meas. by interferometry 8-57897

displacive transformations

- see also *martensitic transformations; polymorphic transformations; soft modes*
- anharmonic Brownian oscillator, canonical correlation function based on projection operator technique 8-55926
- coupled fields in one dimension: cross-over from a continuous symmetry to a discrete one 8-87758
- crystal clasification by transition mechanisms (*Russian*) 8-60401
- defects, localised modes and central peak 8-83905
- dialkylammonium metal chlorides, soft modes, phase transitions 8-79723
- displacive type ferroelectric, thermal expansion and effect of press. on transition temp. 8-72471
- dynamic aspects, nuclear quadrupole relax. studies 8-76344
- ferroelectric, unified theory, quantum limit, zero point energy 8-68461
- Hamiltonian model with scalar displacive transition, crit. dynamics, renormalisation 8-87766
- lattice defects, behaviour models at structural phase transitions 8-83904
- lattice mode softening by high-power visible and IR laser radiation 8-71825
- soft mode, dipole relaxation 8-91409
- squaric acid, struct. transition, US vel. meas. 8-79770
- vibronic theory of antiferroelec. and struct. modulated transitions, soft modes 8-79719
- $\text{Bi}_2\text{Bi}_2\text{Fe}_2\text{Ti}_2\text{O}_8$, dielec. and magnetoelec. props. 8-95562
- $\text{Cs}_2\text{LiCr}(\text{CN})_6$, room temp. struct., phase transitions 8-51491
- K_2OsCl_6 , ferrorotative transition, neutron scatt. expt., consistency with displacive and order-disorder models 8-51673
- K_2SnBr_6 , transform. dynamics probed by Raman scatt. and microscopy 8-63832
- NH_4LiSO_4 , NH_4IO_3 , phase transitions, SHG obs. 8-76398
- $\text{Pb}_2\text{Ge}_2\text{O}_{11}$, dynamic central peaks and phonon interactions 8-83903
- RbCaF_3 , thermal props. near phase transition 8-75850
- SrTiO_3 , anharmonic motion rel. to struct. transition 8-79718
- SrTiO_3 , dynamic central peaks and phonon interactions 8-83903
- SrTiO_3 under [111] uniaxial stress, neutron scatt. 8-67798
- TiCdF_3 , thermal props. near phase transition 8-75850
- TiN_3 , press. induced transition dynamics, light scatt. 8-80362

display devices

- AC plasma display panel wall charge magnitude and distribution probe 8-67487
- electrochromic displays, technical aspects 8-65917
- garnet film, magnetic rag-domains, appl. to magneto-optical displays 8-91912
- garnet film, numerical display element exploiting rag domains 8-68339
- gas discharge cells in colour display panels, comparison of light output (*Japanese*) 8-62191
- liquid crystal, alignment of director using submicrometre periodicity gratings 8-63666
- liquid crystal, smectic A phase, electrically induced scatt. texture and elec. reversal 8-83725
- liquid crystal display technique 8-51419
- liquid crystal indicator of variable light-reading angle 8-57932
- liquid crystal properties rel. to molecular structure 8-55807
- picture taking parameters display in amateur cameras, review 8-89578
- pulsed Doppler blood velocity meter readout 8-69158
- smectic A liquid crystal, scattering textures, appl. to display device 8-91236
- smectic displays, thermo-optic and elec. field effects (*French*) 8-91223
- three-dimensional display improvement 8-59225
- $\text{Cd}_{1-x}\text{Zn}_x\text{S}$, electro-optical multilayer film, for data storage and display 8-71176
- $\text{Cd}_{1-x}\text{Zn}_x\text{S}$, RF sputtered electro-optical film for data storage and display 8-83047
- $\text{In}_2\text{O}_3\text{-SnO}_2$, magnetron RF sputtered electro-optical film for data storage and display 8-83047
- $\text{In}_2\text{O}_3\text{-SnO}_2$ electro-optical film, for data storage and display 8-71176
- $\text{In}_{2-x}\text{Sn}_x\text{O}_{3-y}$ film, deposited from organometallic composition, transparent cond. appl. 8-91793

display equipment see *display instrumentation***display instrumentation**

- see also *cathode-ray tube displays; display devices; radar displays; screens (display)*
- astronomy, photon counting and analogue TV systems with digital real time image processing 8-96402
- biostereometrics, three dimens. displays 8-81010
- composite thermal/visual display superposition technique 8-77992
- diffraction pattern display using photodiode array 8-86069
- digital display for lecture hall use 8-86075
- display design, visual psychophysics appl. 8-65017
- ECG data interactive display system 8-53550

display instrumentation continued

- emission spectrometry, current developments (*Japanese*) 8-86356
- holographic display, large scale, in photographic emulsion, image reconstruction 8-78974
- holographic projection-type displays 8-78972
- holographic stereogram imagery 8-78978
- holographic terrain displays in 3D 8-78979
- holography, large-scale reflection and transmission, for displays 8-78975
- image evaluation, psychophys. and visual aspects, conf., Rochester, USA, (Oct. 1977) 8-65016
- impedance camera for spatially specific meas. of thorax 8-53464
- laser recorder of video signals, on dry-developed photosensitive paper (*French*) 8-92998
- SEM modification for simultaneous exposure numbering 8-62266
- three dimensional imaging, conf., San Diego, USA (Aug. 1977) 8-78971
- TOMAX autostereoscopic display, three-dimens. viewing of tomographic data 8-85446
- US multiple section tomogram simultaneous display equipment 8-61227
- US real-time B-scan machine attachment for three-dimensional display 8-61229
- video displays, conventional or stereo, operator performance for perceptual tasks 8-80882
- video displays, conventional or stereo, operator performance for perceptual tasks 8-85314

display instruments see *display instrumentation***display systems** see *display instrumentation***displays, radar** see *radar displays***disruptive voltage** see *electric breakdown***dissipation (heat)** see *cooling***dissociation**

- see also *electrolytic dissociation; heat of dissociation; ionisation; molecular dissociation; molecular dissociation energies; photodissociation*
- cellulose fibre, moist, dielec. props. 8-76380
- chromatographic support materials decomposition by ionising radiation (*German*) 8-92587
- desorption kinetics with precursor intermediates 8-87876
- dolomite, $\text{CaMg}(\text{CO}_3)_2$, kinetics and thermodynamics of decomposition to metastable solid product 8-80740
- excited charge transfer systems, in polar solvents, dynamic behaviour obs. 8-58772
- explosives, secondary, thermal decomp., solid-state kinetics, differential scanning calorimetry 8-92449
- inorganic solid, interfacial endothermic reaction, abnormal thermal decomp. rate 8-76852
- metal ion hydrolysis (*Chinese*) 8-85153
- organic compounds, hydrolysis in water, rate consts. 8-76856
- pentlandite, prep., H_2 reduction with lime, to yield Fe-Ni alloy 8-85018
- polyethylene, fine struct., prep., O_3 selective degradation, chromatographic obs. 8-92475
- polymethylstyrene, mech. scission by US irradiation (*Japanese*) 8-59190
- radioactive waste, vitrification, thermal decomp. of nitrates and additives in glass-making (*Korean*) 8-86638
- steel, cold-worked, state of cementite, nucl. gamma reson. meas., plastic deform. (*Russian*) 8-68706
- tetrabutyltitanium, thermal decomposition in $\text{MgO-Al}_2\text{O}_3\text{-SiO}_2$ glass, effect on crystallisation 8-87627
- water, dissociation under solar illumination, band bend of surface of n-TiO₂ photoanode 8-91765
- $\text{AlFeF}_5\cdot 7\text{H}_2\text{O}$, Mossbauer spectra, thermal decomp. products 8-80258
- BF_3OH , transient mol. form., microwave spectroscopic obs. 8-74643
- $\text{BH}(\text{OH})_2$, transient mol. form., microwave spectroscopic obs. 8-74643
- $\text{Ba}(\text{N}_3)_2$, thermal decomp., role of defects 8-73033
- $\text{CaCO}_3\text{-SiO}_2$, in presence of NaF, thermal decomposition of Ca_2SiO_4 formation 8-68889
- CdSe, meas. of partial press., by optical absorption method (*Japanese*) 8-51661
- CdTe, meas. of partial press., by optical absorption method (*Japanese*) 8-51661
- $\text{FeMF}_3\cdot 7\text{H}_2\text{O}$ (M=Zn, Co, Fe), Mossbauer spectra, thermal decomp. products 8-80258
- Li_2ZrO_3 , thermal decomposition, enthalpy of formation 298.15K 8-61003
- Li_4ZrO_4 , thermal decomposition, enthalpy of formation 298.15K 8-61003
- Li_2ZrO_3 , thermal decomposition, enthalpy of formation 298.15K 8-61003
- $\text{Mg}(\text{OH})_2$, decomposition to MgO, mechanism, product crystallite size rel. to reaction rate 8-85152
- Mn_2O_3 , thermal decomposition, exam. by thermogravimetric methods 8-80743
- NO, in AC field, kinetics and energetics (*French*) 8-64824
- NO_2 , in AC field, kinetics and energetics (*French*) 8-64824
- N_2O , decomposition on titanate catalyst, energy reson. hypothesis 8-95947
- N_2O_4 dissociating coolant, chemical reaction kinetics in transient regimes (*Russian*) 8-58344
- N_2O_4 dissociating coolant, O_2 generation time constant, enthalpy change (*Russian*) 8-58345
- N_2O_4 , dissociating system, dynamic sorption of ^{131}I from gas phase (*Russian*) 8-58356
- Na vapour, heat cond., temp. discontinuity for dissociating gas 8-94887
- Ni_3C film, thermal decomposition, AES meas. 8-56056
- PbO_2 , thermal decomposition, heating rate effect, kinetics, mechanism, struct. 8-92473
- Re_2 , adsorbed on W (211) surface, dissoc., thermodynamics 8-87861
- $\gamma\text{-TiH}_2$, dissociation pressure, 20 to 70°C 8-85150
- ZrSiO_4 , mechanochemical effect by mechanical grinding (*Japanese*) 8-84754

dissolution *see dissolving***dissolving**

- see also solubility; solutions; solvation*
alkali halide crystal, irradi., chemiluminesc. process during dissolution (*Russian*) 8-92133
calcite, marine, dissolution by fossil fuel CO₂, effect of sediment mixing 8-81212
kinetics of dissolution 8-63686
polycarbonate, decomposition by H₂SO₄ and grinding by ball mill, exam. of molecular chain scission (*Japanese*) 8-64827
polyoxyethylene aq. soln., kinetics of soln. form. 8-64913
quartz, dissolution of grown synthetic quartz inside the autoclaves 8-63911
salts, dissolving and outwashing from soil and rock, hydromechanical treatment (*Russian*) 8-77279
steel, stainless, stabilised, knife line attack phenomenon, dissoln. of carbides in thermal cycles (*Japanese*) 8-68701
steel, stainless stabilised, knife line attack phenomenon, dissoln. of carbide during isothermal heat treatment (*Japanese*) 8-72784
Ca₁₀(PO₄)₆(OH)₂, dissolution in water at constant pH, exam. of kinetics 8-59949
Co, anodic dissolution into silicate glass melt, exam. 8-88582
CsI, selective etching, growth and dissolution in alcohols 8-71739
Fe, anodic dissolution in acidic chloride solns., exam. 8-92389
Fe-Si(Ni)(Cu)(Mn)(C), dissolution rate into molten Al, convection mass transfer (*Japanese*) 8-71858
LiF, γ -irradiated, chemilum. during dissolution (*Russian*) 8-80427
MgO, etching in acids, kinetics and mechanism of dissolution 8-85014
NaCl, rock salt, progressively mined soln. cavities, struct. behaviour 8-61409
NaClO₃, growth and dissolution kinetics, diffusion and convection regimes 8-63684
Ni, anodic dissolution into silicate glass melt, exam. 8-88582
Ni, dissolution and passivation in acid medium, effect of S in solid solution (*French*) 8-64771
Pb/PbCl₂ electrode, in chloride media, low temp. props. 8-68899
PuO₂-Na₂O, biological solubility of aerosols in rats 8-96096
(Th,U)O₂ reactor fuel, dissolution in HNO₃-HF mixtures, fuel reprocessing study 8-59951

distance measurement

- astronomical laser ranging equipment, computer system (*Japanese*) 8-89080
astronomical laser ranging equipment, photoelectric circuit (*Japanese*) 8-89075
astronomical laser ranging equipment, range gate (*Japanese*) 8-89076
astronomical laser ranging equipment, system controller (*Japanese*) 8-89079
astronomical laser ranging equipment, telescope drive (*Japanese*) 8-89078
astronomical laser ranging equipment, timing system (*Japanese*) 8-89077
cosmology, Friedmann model, large distance meas. by triangulation 8-86047
critical gap meas. and adjustment instrument 8-62177
direction scintillation meas. with split image range finder (*German*) 8-83076
electro-optical distance measurement, appl. to water levels surveying obs. (*German*) 8-69280
laser interferometer, principles and performance 8-89442
laser rangefinder, AN/GVS-5 hand-held, production engineering techniques 8-59018
laser ranging equipment, range meas. system (*Japanese*) 8-89074
laser ranging systems, NASA applications 8-81527
lunar laser ranging, polishing and Foucault test of receiving telescope mirror (*Japanese*) 8-89065
lunar laser ranging obs., universal time meas. results 8-85854
modular multi-axis laser distance measuring system of high accuracy (*German*) 8-77856
optical path difference meas. by double diffraction interferometer (*Japanese*) 8-82025
parallaxes of objects at cosmological distances, meas. via radiointerferometric techniques 8-53796
phototachymeter, pulsed phase, distance meas. accuracy, semicond. laser temporal characts. effect 8-70097
refraction-free direction meas., coincidence method (*German*) 8-87124
refraction-free directions, coincidence procedure 8-87125
satellite range measurements, formula for refr. effects computation 8-73609
triangulation, microwave distance meas. in German net (*German*) 8-88792
US time-coordinated convertor appl., design aspects (*Russian*) 8-77857
Virgo galaxy cluster, distance and redshift rel. to Hubble's const. 8-89265

distillation

- see also isotope separation*
benzene production, using process chromatographs, monitoring procedure for pure product 8-92583
biological materials continuous flow electrophoretic separator, for sounding rocket expts. 8-85398
biological materials fractionation in space by deflected lamina electrophoresis 8-85397
distiller of alkali metals, construction, operation 8-80490
radioactive liquid scintillation counting waste vol. reduction by distillation 8-78556
vapour compression distillation unit, compressor and flow system matching 8-83931
- distortion, electric** *see electric distortion*
distortion measurement, electric *see electric distortion measurement*
distortive transformations *see solid-state phase transformations*
distributed Bragg reflector lasers
corrugated waveguides and lasers, improved coupled mode analysis for TM mode 8-83117
grating reflector for thin film Fabry-Perot laser 8-55471
optical resonator with distributed Bragg reflectors, response to light pulses 8-63141
two-dimensional DFB laser with acoustic wave and Bragg reflectors 8-79043
Ga_{1-x}Al_xAs-GaAs laser, distributed Bragg confinement, room temp. operation 8-74907

distributed Bragg reflector lasers continued

- GaAs, periodic surface corrugation generation by holography 8-55469
GaAs-(Ga,Al)As light modulators and distributed Bragg reflector laser, monolithic integration 8-50944
GaAs-(Ga,Al)As LOC-DBR laser, high differential quantum efficiency 8-79031
GaAs-Al_xGa_{1-x}As, optically pumped taper coupled laser, second order Bragg reflector 8-50788
GaAs-AlGaAs integrated twin-guide laser, temp. characts. 8-87064
Ga_{1-x}In_xAs-P_{1-y}As_{1-y}InP injection laser, partially loaded with distributed Bragg reflector 8-82986

distributed feedback lasers

- Bragg interactions in active medium, first and second order 8-50747
corrugated waveguides and lasers, improved coupled mode analysis for TM mode 8-83117
fibre waveguide photosensitivity, appl. to refr. filter fabrication 8-63171
grating reflector for thin film Fabry-Perot laser 8-55471
periodic corrugated waveguides, grating coupled radiation and distrib. feedback 8-59161
semiconductor acoustic DFB laser, high speed repetitive Q-switching 8-83007
semiconductor heterostructures, elec. and optical phenomena, discrete devices, review 8-72250
thin-film periodic structures, optoelectronic devices appls. (*Polish*) 8-50947
Ga_{1-x}Al_xAs, channelled substrate, planar struct. and DFB lasers 8-79032
GaAs, optically pumped laser with acoustic distributed feedback 8-82977
GaAs, periodic surface corrugation generation by holography 8-55469
GaAs-GaAlAs optically pumped DFB laser, wavelength tuning effect 8-82979

distributed parameter systems

- hand-arm system, distributed-parameter dynamic model 8-92663
heat exchangers, approx. of dynamics of method of weighted residuals (*Japanese*) 8-67024
identification using doubly cubic spline, underground aquifer appl. 8-69391
nuclear reactor distributed parameter optimal control methods 8-54858
nuclear reactor system pointwise control and observation problems 8-54859
optimal control of 1-D linear distributed parameter systems with cost functionals 8-59257
parabolic boundary value problem optimal control, heating process 8-67021
self-excited wave medium with memory 8-77034
Shiva laser computer control system 8-59034

distribution networks

- fusion reactor auxiliaries, power distrib. system 8-54962
Tokamak fusion test reactor, AC distrib. system for pulsed loads 8-54963

distributions, statistical *see statistics***district heating**

- BWR, safety study of district heating network 8-62600

diversity reception

- see also fading*
COMSTAR beacon receiver diversity experiment 8-73421
optical heterodyne receivers in turbulent atm., signal current probability distrib., theory 8-78916
optical heterodyne receivers in turbulent atm., signal current probability distrib., expt. 8-78917
satellite links rain attenuation and site diversity effect, statistical studies 8-88892

dividers, voltage *see voltage dividers***DNA**

- amoeba irradiated by thermal neutrons, absorbed dose estimation 8-53449
atom-atom potential functions method, improved definition of A and B forms 8-96000
bacteriophage DNA and protein cross-linkage by ⁶⁰Co gamma-rays 8-77002
calf thymus binding to cis- and trans-dichlorodiammineplatinum(II) extended X-ray absorpt. spectra 8-85291
cell distributions automatic processing and interpretation 8-92757
cetavlon salt, twin struct. obs. 8-71746
chromatin extracted from cultured mammalian cells, gamma radiolysis, DNA alkali-labile strand damage 8-77003
chromosome autoradiograph analysis by computer 8-57071
cytidine monophosphate, aq. soln., spectra, 300-450 nm, polarisation study 8-96015
cytidyl-3',5'-cytidine, aq. soln., spectra, 300-450 nm, polarisation study 8-96015
deoxyribonucleoprotein, gamma-ray protein damage 8-53338
gamma-irradiated, enzymatic digestion, separation by ion exchange chromatography 8-85290
histone F2b-DNA interaction studied by X-irrad. of calf lymph nodes 8-85346
inelastic electron tunnelling spectroscopy appls. 8-92770
lymphocytes, in vitro ⁶⁰Co gamma-ray response of leucoagglutinin stimulated human cells 8-57041
molecular electrostatic pots. of complementary base pairs 8-92597
molecular shape, form dichroism of cryst. 8-60417
monodisperse, rod-like mols., transient elec. dichroism 8-94344
polytene chromosome, stretched, stained with acridine orange, fluoresc. polarisation rel. to DNA packing 8-76995
postreplication repair enhancements in UV-irrad. Chinese hamster cells by irradi. in G₂- or S-phase 8-77085
prealbumin-DNA-hormone interactions, X-ray studies, review 8-53322
protein-DNA interaction, biostereochem. modelling, interactive computer graphics 8-88693
proton transfers between base pairs, LCAO SCF all-electron PRDO method 8-80829
pyrimidine dimers, excision repair of UV damage in monkey kidney cells 8-53332
pyrimidines, cryst., lattice dynamics 8-75766

DNA continued

- radiation induced double strand breaks, recombination, formation of chromosomal rearrangements 8-85289
 radiation-induced 8-69147
 radiation-induced break rejoining capacity rel. to mouse age 8-69148
 replicon autoradiograms, computer-assisted measurement 8-92692
 single-stranded, alkali-labile sites and post-irrad. effects induced by H radicals 8-68994
 solution, conc.-depend. collapse in presence of second polymer 8-56949
 sugar ring non-standard conforms. in A and B structs. 8-80827
 thermal properties in wide range of concs. of ions of neutral salts and of polymer 8-80833
 thymine dimer excision from DNA of UV-irrad. plant seedlings 8-61221
 thymine dimer excision kinetics in UV-irrad. human cells 8-53331
 transcription, UV and incubation effects on heterogeneous nucl. RNA size in murine cells 8-69139
 transforming, X-ray sensitivity rel. to presence of free radicals 8-68995
 unscheduled synthesis in UV irradi. spleen lymphocytes after X-irrad., rat 8-69156
 UV damage, postreplication repair in mammalian cells, model 8-80918
 UV irradiation of Chinese hamster cells, postreplication repair enhancement 8-92678
 X-ray induced damage in rat cerebellar neurons and brain tumour cells 8-80922
 CsDNA, absorpt. factor, X-ray diffr. study using 1.2 Å synchrotron radiation 8-76988

document retrieval *see information retrieval*

Doherty amplifiers *see power amplifiers*

domain boundaries

- for boundaries between magnetic domains and electric domains see magnetic domain walls and electric domains walls respectively*
see also antiphase boundaries
 liquid phase sintering, role of grain and phase boundaries 8-72747
 Ag film, on mica, microstruct. changes 8-72013
 (Ba₃Nb₂Si₄O₂₆)_n.Ba₃Nb₄Ti₄O₂₁, multiple intergrowth and microdomains obs. by electron diffr. and microscopy (French) 8-95160
 Ta-N, domain configurations of new phase (French) 8-56648

domains

- see also antiphase domains; crystal microstructure; domain boundaries; electric domains; magnetic domains*
 polyether-amidourethane, segmented, polymer domain struct., IR spectra and optical microscope (Russian) 8-51453
 polyethylene, uniaxially stretched, density fluctuations 8-75587
 polystyrene, Millar interpenetrating network, viscoelasticity and phase domain form. 8-83749
 polystyrene-poly(styrene-*b*-butadiene-*b*-styrene) polyblends, electron micrographs for struct. 8-51442
 TMMC, one-dimensional, EPR at HF and low temp. 8-80205
 Ag-Ge (4.5 at.%), FCC, vapour-deposited, lattice imperfections, X-ray diffr. 8-72032
 GaAs:O, slow domains, origin 8-60132
³He, superfluid B-phase, domain struct., derived from Ginzburg-Landau eqns. 8-63896
 Pb₃(PO₄)₂, ferroelastic, switching processes in pulse mech. field 8-59853
 V₂O₃, low temp. crystallographic struct. domains 8-83765
 Zn, film, vac. deposited, X-ray diffr. study of microstruct. 8-75966

domestic appliances

- see also ovens; refrigerators*
 pacemaker interference, body potentials and currents from ELF elec. fields and household appliances 8-88770

doping, semiconductors *see semiconductor doping*

doping profiles

- channelled ion implantations, apparatus for spatially uniform doping 8-51569
 chemical analysis, by secondary-ion mass spectrometry (German) 8-95978
 dose depend. in laser annealing 8-91354
 III-V multilayer structs., contact resistance profiling method 8-56213
 melt-grown crystal, effect of crystallisation front oscils. 8-52657
 p-n junctions, determ. of arbitrary doping profile, depletion layer capacitance meas. 8-88021
 p-n junctions, determ. of doping levels using nondestructive IR emission meas. 8-95338
 stripe optical waveguide, formed by ion exchange, diffusion profile 8-87137
 BP, epitaxial growth on Si substrate, Si impurity profile, ion microanal. 8-87886
 GaAs, dual implantation of C⁺ and Ga⁺, sheet resist. and Hall effect meas. 8-67728
 GaAs, with nipi superstructures, production and appl. (German) 8-95064
 GaAs:Si, Cr, carrier concs. from Hall effect, microscopy, localised vibrational modes absorption meas. 8-56104
 GaAs:Zn, depth profile, photoluminesc. obs., LED applic. 8-72587
 GaAs_{1-x}P_x:Zn, diffusion profile determ., ³²P/⁶⁵Zn double tracer technique 8-55888
 GaP, dopant dislocations, scanning electron micrographs, cathodoluminesc. 8-91340
 p-GaP, epitaxial layers grown from liq., overcompensated, doping levels 8-91353
 GaP, LEC, SSD and CVD samples, Zn tracer diffusion profiles in solids 8-95189
 GaP:Zn, diffusion profile determ., ³²P/⁶⁵Zn double tracer technique 8-55888
 LiNbO₃:Fe, ferroelectric, treated in Li₂CO₃, formation of Fe²⁺ state, Mossbauer effect 8-92003
 Mg:H, solid soln. produced by ion implantation 8-67733
 PbTe, ion-implanted, doping profile evaluation by Hall effect and sheet resist. meas. 8-59831
 Si, amorphous layer, ion-implanted, spatially controlled cryst. regrowth by laser irradiation 8-55810
 Si doping by ion implantation, atomic collision theory and range-energy relations 8-71753
 Si, ion implanted, laser-annealed, theoretical anal. of thermal and mass transport 8-91364

doping profiles continued

- Si, ion-implanted layers, impurity profile meas. after laser annealing 8-87702
 Si, ion-implanted surface, profiling method 8-95075
 Si polycrystalline solar cells, ion implantation method and results 8-63784
 Si:B, conc. profile of implanted cryst., by ¹¹B(p,α) chem. anal., annealing (German) 8-83843
 Si:B, dopant density determ. by nucl. track technique 8-55886
 Si:B, p-n junction form. by B deposition and laser-induced diffusion 8-87690
 Si:B, polycrystalline, depth profiles of implanted B atoms, meas. by secondary ion mass spec. (Japanese) 8-67734
 Si:H, ion implanted Monte Carlo calcs. of profiles of H ions 8-55889
 Si:P, Au gettering by P diffusion and P-induced dislocations 8-91346
 Si:P, carrier mobility and distrib. rel. to annealing, 400-910°C 8-79995
 Si:P, characterisation by IR reflectivity 8-56501
 Si:P, ion implanted, lattice damage and electrical activation correlation 8-67726
 Si:Te, ion implanted, laser annealed, lattice location of Te 8-67725
 Si-SiO₂ interface, Au conc., effective impurity doping 8-52094
 Si-SiO₂ interface, Auger-sputter profiling obs. of P pileup 8-95240
 Si-SiO₂-Si structures, P, As depth profiles, ion microanal. (Japanese) 8-85251

Doppler broadening *see Doppler effect*

Doppler effect

- see also atomic spectra; red shift; spectral line breadth*
 4 MHz range-gated US Doppler flowmeter design and application 8-59527
 accelerated dielectric medium, relativistic study 8-81862
 arterial haemodynamic transfer function calc. from Doppler US flowmeter waveforms 8-61235
 atomic degenerate system, Doppler-free laser-induced dichroism and birefringence 8-82711
 broadened laser amplification line frequency characteristics meas. 8-59060
 cosmological red shift, Doppler and gravitational components using Birkhoff's theorem 8-86041
 de Broglie wave, relativistic Doppler shift for teaching 8-49613
 DSA study of ²⁸Si lifetimes in selected materials, theoretical stopping power predictions 8-74329
 education, acoustical second-order Doppler effect, introductory expt. for special relativity 8-49584
 education, Doppler shift of laser beam, expt. 8-69939
 F₂-layer vertical sounding, radio signal Doppler spectrum and arrival angle meas. (Russian) 8-61651
 flowmeters, digital 2D full range Doppler velocity meter for cardiovascular diagnosis 8-88731
 forbidden decay modes of one- and two-electron ions, book contrib. 8-82679
 heart rate meas. (foetal), adoptive correlation ratemeter, US signals 8-88732
 heterodyne correlation radiometry 8-77980
 HF Doppler method studies of high-latitude ionospheric dynamics 8-73569
 HF Doppler obs. over S.E. Australia during 1976 Oct. 23 total eclipse 8-61662
 holography through fog, coherence requirements for light source 8-58949
 ionosphere, Doppler fluctuations and angle-of-arrival var. caused by scintillation 8-77411
 ionospheric EM wave propagation in HF and MF bands, Doppler meas. accuracy 8-77417
 laser anemometer Doppler system, optics and signal processor for turbulent low speed flows (French) 8-59521
 laser Doppler velocimeter with variable frequency shift for combustion flow meas. (Japanese) 8-67294
 laser velocimeter instrumentation developed by Electricite de France Optical Applications Division (French) 8-75233
 light Doppler effect, absolute spacetime theory 8-69979
 Loran-A (1.85 MHz) radio wave backscatter from ocean waves, Doppler spectra (Japanese) 8-85737
 molecular beam RF spectroscopy, interference effects (French) 8-58669
 opt. freq. shifting of light and laser beams for Rayleigh scatt. spectroscopy 8-79392
 optical Doppler instrument for measuring small turbulent flow velocities 8-90838
 optical Ramsey fringes in two-photon spectroscopy, time delayed pulsed Doppler free technique 8-82708
 optical wideband ambiguity function generator with Doppler compensation 8-78936
 plasma, axially symmetric, Doppler broadened optical line emission interpretation model 8-75276
 polyoxyethylene aq. soln., kinetics of soln. form. 8-64913
 positron annihilation, 2-D Doppler broadened technique 8-70722
 positron annihilation γ-ray spectra, deconvolution using solid state detector 8-72631
 positron annihilation γ-ray spectra, Doppler broadening, parameters 8-72630
 positron annihilation in rare gases, Doppler broadening meas., electron mom. distrib. 8-55131
 relativistic gas, Doppler shift distrib. 8-65492
 sea echo radar spectra resolution limitation inferred from ionospheric Doppler broadening 8-81489
 solar oscillations, Fe I 5124 Å Doppler shift obs. 8-53905
 sonar fish counting system, feasibility study 8-50980
 spectral line collisional broadening, classical and quantum theories, radiator motion effect 8-86822
 spectral line profile, saturation, influence of atomic collisions 8-70792
 spectrum profiles in the presence of Stark, Lorentz and Doppler broadenings 8-86820
 stellar spectra, differential Doppler shifts rel. to atmospheres vel. gradients determ. 8-57538
 sub-Doppler line shapes, saturation and two-photon spectra, elastic collisions, review 8-82697
 Sun, Doppler shifts meas. rel. to 7 to 70 minutes periods pulsations 8-93180
 superradiance, Doppler beat observation 8-66794

Doppler effect continued

- three-level coupled Doppler-broadened system, optical time-delayed laser saturation spectroscopy 8-54472
 two-level system, saturation kinetics after Doppler broadening (*Russian*) 8-86921
 two-photon absorpt., collisionally perturbed, reson. profile and strengths, degeneracy and Doppler shift 8-55156
 US blood velocity meas., phase-locked loop technique 8-61234
 US Doppler velocimetry for 3D blood flow meas. 8-88730
 US wave 3D meas. in transparent solids, Doppler-shifted light scatt. technique 8-90613
 X-ray sources, binary detect. via Doppler effect (*Russian*) 8-77623
 zodiacal light spectrum, Doppler shifts meas. 8-85904
 Ag, Doppler factor, comparison between calculated values and measured results 8-54811
⁴¹Ar states from ⁴⁰Ar(d,p), lifetimes meas. by DSA method 8-78308
 Au, Doppler factor, comparison between calculated values and measured results 8-54811
 Ba⁺ ion cloud containment in RF trap, <50 ions, optical sideband cooling 8-75407
 Be, Doppler effects in X-ray spectra excited by accelerated ions 8-86808
 Cs, photoplasma, optical excitation in radiation diffusion conditions 8-55227
 Cu:H, interaction of H and vacancies, positron annihilation, Doppler broadening 8-80434
 Ge, electron-hole drop velocities as probe of phonons 8-68517
 He II, Doppler and Stark broadened lines, electron density and ion temp. meas. 8-67407
³He-⁴He mixtures Doppler shift in third and fourth sound 8-56017
⁴¹K states from ⁴⁰Ar(d,n), lifetimes meas. by DSA method 8-78308
 Mg, Doppler effects in X-ray spectra excited by accelerated ions 8-86808
 Mg II, radiation press cooling of ions in Penning EM trap 8-66527
 Na₂, TOF spectra, molecular beam diagnostics with internal state selection 8-86968
 Na(³P_{1/2}) + Ar → Na(³P_{3/2}) + Ar, angular scatt. distrib., Doppler spectrosc. obs. 8-94309
 Se, Doppler effects in X-ray spectra excited by accelerated ions 8-86808
 Si, electron-irradiated, annihilation of positrons, broadening measurements 8-87713
 Xe + Bi, Bi K α X-ray lines, Doppler broadening 8-62759

Doppler shift see *Doppler effect***dopplersons**

- metal, Gantmakher-Kaner effect in strong mag. field (*Russian*) 8-80015
 metal film, surface impedance oscills. in perpendicular mag. field (*Russian*) 8-76165
 metals, compensated, Gantmakher-Kaner effect in strong mag. fields 8-91595
 W, alternating sign Hall effect and dopplerson spectrum 8-79981

dosimeters

- see also *dosimetry*; *thermoluminescent dosimeters*
 Andersson-Braun remmeter modifications for improved directional depend. and thermal neutron sensitivity 8-53499
 capacitor chamber appl. 8-78509
 cellulose nitrate α -particle detector for Rn short lived daughters, results and calibration (*Czech*) 8-62663
 charge to voltage convertor, for ionisation chamber dosimeters 8-78505
 direct meas. of β absorbed dose rate by discriminator and filter (*Japanese*) 8-74511
 electron linear accelerator, dose monitoring system 8-92710
 EM radiation probes, implantable, design factors 8-73258
 film, calorimeter for calibration in high intensity electron fields 8-73257
 Fricke type, mixed field of fast neutrons and γ -rays, absorbed dose meas. 8-74514
 gamma-radiation absorbed dosage, differential microcalorimeter 0.01-10 W (*Russian*) 8-85385
 Geiger-Mueller counter γ dosimeters, fast neutron sensitivities, mixed field dosimetry 8-92705
 ionisation chamber ion collection efficiencies in pulsed and continuous radiation beams 8-53505
 Keithley diagnostic ion chambers, energy depend. of correction factors 8-53507
 liquid scintillator determ. of dose rates from homogeneously distrib. β , γ - and EC, γ -emitters in phantom organs 8-53501
 neutron monitor calibration for radiation protection at 24.5 keV and 2 keV 8-89983
 polycarbonate foil electrochemical etching for dosimetry, bulk etching rate evaluation 8-78506
 portable radiation meters, accuracy checking facility at Berkeley Laboratories, UK 8-74507
 radiation protection instruments for personnel dosimetry, area and environmental monitoring 8-66427
 REM ratemeter, for mixed radiation, using two spherical ionisation chambers 8-96100
 REM ratemeter for direct reading of dose equivalent rate 8-53502
 semiautomatic device for relative dose distrib. recording 8-85380
 semiconductor devices, dose meas. using radiation induced changes (*Japanese*) 8-78504
 thermoluminescence, calibration, γ -ray irradiator (*Japanese*) 8-66452
 thermoluminescence reader, high sensitivity (*Japanese*) 8-66426
 TLD, automatic readers for personnel monitoring 8-50408
 UV, semiconducting dosimeter 8-74059
 whole body counter, portable chair type for in vivo internal contamination monitoring 8-61260
 Al₂O₃:Si,Ti photostimulated thermolum., and appl. to UV dosimetry 8-53511
 Ce⁴⁺/Ce³⁺ dosimeter, adsorbed doses, potentiometric determ. 8-94146
 Ce₂(SO₄)₃ type, mixed field of fast neutrons and γ -rays, absorbed dose meas. 8-74514
 In₂Te₃-type semicond. radiation-resistant fast-electron detectors 8-78559
⁷LiF TLD, efficiency for H⁺ and Ar¹⁸⁺ detect. 8-53504
 Mg₂SiO₄:Tb TLD, supralinearity of response to electrons and X-rays (*Japanese*) 8-78503

dosimeters continued

- Mg₂SiO₄:Tb thermoluminescence phosphor, response to high energy electrons (*Japanese*) 8-78502
²³⁷Np dosimeter and spark counting system, for routine personnel monitoring 8-89984
²²²Rn, passive environmental monitor based on exoelectron dosimeter 8-82523
- dosimetry**
 see also *dosimeters*; *radiation detection and measurement*; *radiation monitoring*
 accident features affecting emergency measures 8-55055
 actinide nuclear transmutation, photon and neutron surface dose rates for actinide containing fuel 8-66428
 airborne radionuclide release assessment, importance of vars. in deposition vel. 8-80979
 alpha particle stopping cross-sections in ethylene and polyethylene, 1.5 to 4.2 MeV 8-53510
 alpha particle stopping power and straggling in liqs., determ. by Si spectrometer 8-82563
 amoeba irradiated by thermal neutrons, absorbed dose estimation 8-53449
 atmospheric emissions from nuclear plants, applications related concept for radiation exposure calc. (*German*) 8-82531
 Berger coeffs. for Eisenhauer-Simmons γ -ray buildup factors in concrete 8-78510
 beta emitters, insoluble, ingested, dose to gastrointestinal tract 8-65134
 beta-emitting radionuclides from reactor accident, ingestion, acute toxicity 8-65082
 beta-emitting volume-seeking radionuclides in human bone, mean skeletal dose factors 8-77115
 beta-rays, high-energy, hazards to eye lens and gonads 8-65131
 biological dose rates in and around JAERI fusion reactor shielding 8-54872
 bone radiosensitive tissues irradiated by surface deposited radionuclides, calc. dose factors 8-53512
 brachytherapy, radiation exposure of nursing personnel to patients 8-85384
 breast dose and cancer risk due to fluoroscopic chest exams. of women with tuberculosis 8-65128
 breast radiography with Mammomat, skin exposure and absorbed dose 8-73245
 C_K and C_L reevaluation using extended cavity ionisation theory, ferrous sulphate G-values appl. 8-92706
 cellulose nitrate solid state nucl. track detector, gamma dose meas. 8-73247
 cervical stage III carcinoma treatment, two regimes with same TDF but differing morbidity 8-53474
 charged heavy particle therapy, desirability of treatment with multiple fields 8-73220
 charged particle beam, influence of thin inhomogeneities 8-69219
 charged particle beam, influence of thin inhomogeneities 8-69220
 chromosome aberrations as dosimetric technique for fission neutrons at 0.2 to 50 rad 8-69145
 cloud dose data file fast correction for changes in dispersion parameters 8-80969
 collective dose commitment for estimate of radioactive pollution, concept and calcs. (*German*) 8-74504
 colonic diverticular disease population survey, patient X-ray dose 8-61259
 computerised tomography dosimetry, exposure meas. techniques 8-69212
 cosmic ray neutrons, Ames collaborative study on mid-latitude flights 8-53538
 craniofacial anomaly assessment, computerised versus conventional tomography 8-73239
 criticality accidents at facilities processing fissile material, characts., detect. and action procedures (*French*) 8-55054
 cylindrical source shielding eqns. including buildup, lateral dose rate, compact function use 8-89982
 dental X-ray photographs, comparative study of patient exposure to radiation 8-92702
 diagnostic radiology, mean active bone marrow dose to USA adult population 8-85382
 dosimetry, automated data acquisition and anal. system at LAMPF pion therapy facility 8-53506
 electron beam dose distrib. modification by transverse mag. fields 8-65132
 electron dose reduction coeff., internal radionuclides, source free target, cylindrical geometry 8-92704
 electrons, 25 MeV, absolute meas. of absorbed dose in water in total absorption type calorimeter (*Japanese*) 8-78501
 electrons, 25 MeV, lateral absorbed dose distrib. in water, least-squares fitting FORTRAN program (*Japanese*) 8-74505
 electrons, high energy, depth absorbed dose distrib. 8-73256
 EM, non-ionising, hazards in the laboratory and effects on skin and eyes 8-96064
 EM energy deposition in biological tissue at 900 and 450 MHz 8-69222
 emergency conditions, monitoring and handling 8-57082
 environmental external radiation levels in N Carolina 8-80968
 environmental pollution by nuclear fission products 8-85607
 European neutron dosimetry intercomparison project results, recommendations for biological and medical appls. 8-82532
 fast neutron dosimetry using S activation in CaSO₄:Dy and Teflon dosimeters 8-70648
 fast neutron irradiation of cells cultured in monolayer, dosimetric aspects 8-69218
 fast neutron research reactor YAYOI core absorbed dose meas. by chemical dosimeters (*Japanese*) 8-86695
 fast neutron therapy, use of ¹⁰B to enhance tumour dose 8-73249
 fast neutrons, 4 to 27 MeV, dosimetry using response of E.coli AB2463 recA 8-65077
 fluoroscopy, organ dose per unit exposure, estimation method for artificial pneumothorax 8-96097
 frame recording method for intermittent X-ray TV to reduce exposure dose in fluoroscopy (*Japanese*) 8-89607
 gonadal doses to 78070 patients undergoing diagnostic X-ray exam. 8-53503

dosimetry continued

- graphite ionisation chamber with CO₂ filling, Monte Carlo anal. of fast neutron irradiation 8-82583
- heavy particle comparison for therapy, depth-dose distrib. for π^- , n, p, He, C, Ne and Ar ions 8-85379
- high LET constraints on low LET survival of cells, RBE theory 8-92679
- inner radiation belt, max. radiation dose following 1962 STARFISH explosion 8-69612
- intracavitary therapy, dosimetry of Cathetron applicators 8-69217
- ionizing radiation and cavitation threshold 8-94774
- IR spectroscopy appl. to charged part. dose meas. in cellulose triacetate 8-94145
- IRT 2000 reactor in Sofia, neutron spectra and doses in exptl. canals (*Bulgarian*) 8-82489
- liquid air, transport of neutron and secondary γ -rays from 14 MeV source 8-50234
- Lucens reactor accident, alarm and surveillance 8-50283
- LWR core meltdown, activity release and aerosol characts. 8-82469
- maximum permissible conc. calc. using absorbed dose data of MIRD pamphlet 11 8-53516
- maximum tolerable radiation doses recommended by Israel Advisory Committee on Nucl. Safety 8-53517
- Maxwell method for rapid neutron dose evaluation in overexposure cases 8-62664
- multi-channel meas. device for environmental control network (*Hungarian*) 8-57072
- natural radiation exposure, New Zealand, soil survey and air doses for ²²⁶Ra and ²³²Th daughters and ⁴⁰K 8-88747
- neutron, dielectric track detectors appl. (*Czech*) 8-66425
- neutron beams from D+d reaction, 6.8 to 11.1 MeV, dosimetric props. 8-53509
- neutron beams prod. by Be+p, 30 and 40 MeV, polyethylene filtration 8-53494
- neutron dose levels of 8 MeV linear accelerator and 18 MeV betatron used in radiotherapy (*German*) 8-69221
- neutron dose measurements in a dummy for test animal irradiation in a reactor 8-61218
- neutron dosimetry methods for accidental exposures, Czechoslovak intercomparison 8-57075
- neutron flux density determ., thermal and intermediate energy, using Au foils 8-82536
- neutron leakage spectra from critical assemblies, depth dose, dose equiv. and quality factor 8-58504
- neutron radiotherapy, nature and significance of radiation outside beam 8-53477
- neutron source, 14 MeV, skyshine anal., Monte-Carlo computer code 8-66429
- neutron source for radiotherapy, gas target, energy spectra, flux, dose rates 8-92698
- neutron spectra from reactor, depth dose, dose equivalent, quality factor for various reactors and shields 8-94143
- neutron spectra in stopping pion field, meas. with multiple foil activation method 8-73248
- neutron therapy hospital staff, occupational exposure report 8-96098
- nuclear energy production, research review (*Hungarian*) 8-74414
- nuclear power station, radiation protection, recommendations review (*Hungarian*) 8-74508
- output factors, scatter ratios, for radiotherapy units, ⁶⁰Co γ -ray and MV X-ray calcs. 8-92708
- personal dosimetry service testing and evaluation in 1976 in Michigan 8-53498
- personal dosimetry in USA, survey results 8-53500
- photon beam 18 MV, from Philips SL/75-20 linear accelerator, fast and slow neutron contamination 8-65127
- photon dose rate from induced activity in the beam stop of a 400 GeV proton accelerator 8-94144
- photons, monoenergetic, microdosimetric meas. of ionisation 8-65133
- pion⁻ beam stopping distrib. determ. by charge collector 8-53513
- pion⁻ irradiation, dose outside treatment volume 8-53508
- pion⁻ therapy, neutron energy spectrum in stopping pion field 8-85386
- pion radiotherapy studies with nucl. emulsions 8-73219
- plexiglass, red, gamma dose meas. by optical absorpt., elec. conductivity, and mechanical hardness 8-55045
- pollutant release assessment, JEREMIAH computational system environmental transport and dose calcs. 8-94150
- population dose from atm. dispersion of radioactivity, calc. method 8-85381
- portable radiation meters, accuracy checking facility at Berkeley Laboratories, UK 8-74507
- radiation field of extended rectangular source, numerical integration 8-66424
- radiation protection instruments for personnel dosimetry, area and environmental monitoring 8-66427
- radiation testing of materials in reactors, measure of radiation effect, dosimetric information 8-79640
- radioactive waste, land disposal, repository, packaging and cost estimate, internal radiation dose (*Japanese*) 8-66351
- radiographic film/screen combinations and patient exposure, Nationwide Survey of X-ray Trends 8-73233
- radiographic magnification technique for gallbladder imaging 8-69186
- radiography, quantitative meas. for estimating patient dose (*German*) 8-57073
- radiology diagnostic facilities, quality assurance programme, proposed recommendation 8-73235
- radionuclide airborne release assessment, determ. of atm. stability categories 8-73504
- radiotherapy 25 MV X-ray beam, fast and thermal neutron profiles 8-73246
- radiotherapy beam-flattening filter calcs. for high-energy X-ray machines 8-65126
- radiotherapy by external ionising radiation beams, for teaching 8-49616
- radiotherapy treatment plan selection, complication probability factor 8-53476
- reactor near-stack dose calc., diffusion model applicability 8-94147
- Reactor Safety Study (Wash-1400) and implications for radiological emergency response planning 8-50284
- restricted energy absorption coefficients 8-80971
- review of nuclear fuel cycles and waste management 8-54863

dosimetry continued

- rodents inhabiting radioactive waste receiving area 8-85383
- semiconductor detector for ionising radiation dosimetry, anisotropy of dose sensitivity 8-70705
- SI units in radiological protection 8-86235
- solid state track detectors, use in neutron dosimetry, verification of possibilities (*Czech*) 8-82574
- steam generator, multiple tube rupture, radiological consequences 8-74452
- stopping power for low energy heavy charged particles, similarity treatment of phase effects 8-50447
- teletherapy, implementation of Philips treatment planning system 8-73244
- terrestrial beta radiation field in natural environment, numerical evaluation 8-81161
- thermal neutron beam response of hamster and HeLa cells containing various concs. of ¹⁰B 8-73178
- thermoluminescence dating of pottery, ⁸⁷Rb dose-rate contrib. 8-70242
- thorotrast and ²²⁴Ra radiobiological significance 8-96076
- thorotrast biological effects, conf., Alta, USA (July 1974) 8-96068
- thorotrast cases, bone irradiation meas. results 8-96092
- thorotrast patients, α -ray tissue dose 8-96093
- thorotrast patients, Danish, malignancies 8-96074
- thorotrast patients, endosteal α -particle dose 8-96094
- thorotrast patients, German, malignancies and estimated tissue dose 8-96072
- thorotrast patients, Portuguese, malignancies 8-96073
- thymic region shielding in radiobiology expts., dosimetry in irradiated mouse cadavers 8-61257
- thyroid irradiation and 1977 ICRP dose limits for medical radioisotopes 8-65135
- thyrotoxicosis therapy, dose determ. by thyroid uptake meas., effect of gland parameters 8-61245
- tissue-air ratios for whole body irradiation with ⁶⁰Co gamma-rays 8-61258
- tissue-equivalent plastic A-150, density and composition uniformity 8-73252
- TLD, use in high level photon dosimetry 8-74503
- track structure theory in radiobiology and radiation detection 8-50446
- TRIUMF biomedical pion beam automated dose mapping system 8-73254
- TSC in human nail, for dose estimation after accidental exposure 8-73253
- UK nuclear power station radioactive effluent monitoring and public information 8-89992
- UV radiation source output monitoring detector for psoriasis photochemotherapy 8-53473
- X-ray attenuation coeffs. of materials meas. 8-84680
- Al min. activity blanket design for TFTR upgrade 8-58460
- Al₂O₃, UV dosimetry grade, thermolum. glow curves and emission spectra, 90-500K 8-72615
- Be+d neutron source, material damage study, He prod. and neutron fluence per neutron obs. in irradiated material 8-86710
- ¹⁴¹Cs standard, measured by dose calibrators, simulated ⁹⁹Tc^m standard 8-61261
- ⁶⁰Co gamma ray absorbed-dose standards, comparison 8-74512
- ⁶⁰Co, shutdown dose rate prediction in BWR primary coolant circuit 8-74445
- ⁶⁰Co-charging of γ -irradiation installation (*Bulgarian*) 8-82558
- Cs, in seawater, rapid determ. using Cs selective resin 8-85609
- ¹³⁷Cs contamination of external-radiation doses in USSR territory 8-86698
- Cu, metabolic model and dosimetric data 8-65130
- ¹⁴⁴e inhalation effect of influenza virus infection on pulmonary retention and mouse survival 8-85340
- HT single release in a room, radiation dose 8-74513
- HTO potential radiation dose to man, HT gas escape into forest ecosystem 8-96101
- I radioisotopes, high efficiency mixed species air sampling, readout and dose assessment system 8-57074
- I radioisotopes, meas. of crit. environmental exposure for reactor accidents 8-57081
- ¹²⁵I insulin, labelling using dimethylsulphoxide as labelling agent (*Korean*) 8-88746
- ¹³¹I measurement in human thyroid gland, use of NaI(Tl) scintillation survey meter 8-80970
- ¹³¹I population thyroid dose in USA after Chinese atm. nucl. weapons tests 8-77116
- ¹³¹I, radiation exposure dose determ., hot particle model 8-82520
- ¹⁹²Ir radiographic source, radiation accident 8-53514
- ³²P-diphosphonate dose determ. in patients with bone metastases from prostatic carcinoma 8-61251
- PuO₂, multiple low level exposure, case study 8-80967
- PuO₂-Na₂O, biological solubility of aerosols in rats 8-96096
- ²³⁷Pu, ²³⁹Pu, citrate, early retention in mature beagles 8-96095
- ²³⁸Pu IV citrate chronic exposure effect on embryonic development of fish eggs 8-53447
- ²³⁹Pu, endosteal cell dose and relative distrib. factors compared to ²²⁶Ra 8-96091
- ²²⁶Ra, ²²⁸Ra in humans, radiation induced malignancies 8-96075
- Ra and daughter products, personal dosimetry and area monitoring (*Japanese*) 8-55044
- ²²⁴Ra and daughters, radioactive props. and biological behaviour 8-96090
- ²²⁴Ra biological effects, conf., Alta, USA (July 1974) 8-96068
- ²²⁴Ra, endosteal cell dose and relative distrib. factors compared to ²²⁶Ra 8-96091
- Rn daughter concentrations in air of dwellings in Great Britain 8-77118
- ²²²Rn concentration in N.Carolina groundwater supplies rel. to stomach dose and conc. standards 8-85612
- ²²²Rn daughter dose estimates from area sources 8-94151
- ¹⁰⁶RuO₄ in lung, in vivo meas. and dosimetry 8-53515
- ⁹⁰Sr contamination of external-radiation doses in USSR territory 8-86698
- T, release from CTR, radiological dose calc. 8-78511
- U, miners Rn daughter inhalation and pulmonary cancer incidence 8-96080
- ¹²⁷Xe maximum permissible conc. in air 8-61262

double nuclear magnetic resonancesee also *ENDOR*

bacteriochlorophyll cation in soln., N atom ENDOR and proton triple resonance 8-96018

benzene-d₆, NMR double-quantum spin decoupling 8-88227

book, principles of magnetic reson. 8-80189

N-5-chlorosalicylideneaniline, H⁺-¹⁴N double reson. NQR spectra temp. depend. thermochromism and tautomeric mech. 8-70849

coupled spin systems, relax. mechanisms and multiple quantum transitions 8-88211

dimethylsulphoxide-d₆, NMR double-quantum spin decoupling 8-88227

double-quantum spin decoupling 8-88227

formic acid(-d₁), dilute deuterated mixture, high-sensitivity NQR, double quadrupole reson. 8-68412

heteronuclear double-resonance spectra, modulations 8-86897

N-(2-hydroxythiobenzoyl)morphiline, ¹H NMR, spin decoupling by torsional transitions 8-62832

iodomethane, IR-RF double reson., NQR of spin-rot. coupling consts. 8-66569

motional effect 8-68413

NQR double resonance detection, principles and appl. to D 8-76354

nuclear spin systems dynamics, review (*Rumanian*) 8-55189

solid-state expts., theoretical concepts and expt. results 8-76353

spin 1/2 system, nuclear double resonance by longitudinal detection 8-78733

TBBA, smectic phases, orientational order, ¹⁴N NQR and double NMR obs. 8-94974p-terephthal-bis-aminocinnamate, smectic phases, orientational order, ¹⁴N NQR and double NMR obs. 8-94974

thermodynamic influence of spin-spin energy on cross-relax. and spin diffusion 8-76343

two-dimensional, state-of-the-art 8-74044

B(OH)₃, ¹H/²H quadrupole reson. freqs. detected by double reson. with level crossing 8-84497HIO₃, ¹H/²H quadrupole reson. freqs. detected by double reson. with level crossing 8-84497H₂SeO₃, ¹H/²H quadrupole reson. freqs. detected by double reson. with level crossing 8-84497²H-¹H, double-quantum spin decoupling 8-88227KAl₂Br₇, NQR double-reson., Al₂Br₇⁻ ion in cryst. 8-91993KHCO₃, ¹H/²H quadrupole reson. freqs. detected by double reson. with level crossing 8-84497KHSO₄, ¹H/²H quadrupole reson. freqs. detected by double reson. with level crossing 8-84497⁷Li₂O, β-radiation detected NMR of ⁸Li obs., double freq. irradiation, ⁷Li hyperfine struct. anomaly 8-91994⁷Li₂S, β-radiation detected NMR of ⁸Li obs., double freq. irradiation, ⁷Li hyperfine struct. anomaly 8-91994NaHCO₃, ¹H/²H quadrupole reson. freqs. detected by double reson. with level crossing 8-84497Te(OH)₆, ¹H/²H quadrupole reson. freqs. detected by double reson. with level crossing 8-84497**double refraction** see *birefringence***double refraction, electric** see *electro-optical effects***double refraction, magnetic** see *magneto-optical effects***double resonance, electron nuclear** see *ENDOR***doublet antennas** see *dipole antennas***DPPH, diphenylpicrylhydrazyl** see *organic compounds***drag reduction**

drag-reducing polymers aqueous solutions, turbulent bursts rel. to wall friction 8-63454

pipe flow turbulent entrance region, drag reducing fluid, expt. and anal. 8-63458

plate, with suction, three-dimens. fluctuating flow, heat transfer, skin friction 8-87389

polymer solution, drag reduction, laminar to turbulent transition, rot. disc expt. 8-75173

polymer solution, drag reduction in turbulent flows, book contrib. 8-59432

polymer solution, mass transfer between solid surfaces and drag-reducing fluids 8-79339

polymer solution, molecular weight distrib. effect on drag reduction in turbulent stream 8-83437

ship hydrodynamics, drag on displacement ships, hydrofoils, hovercrafts 8-63423

turbulent energy dissipation model 8-79345

drawability see *ductility***drawing (mechanical)**

α-brass, drawability correlation with sheet metal texture 8-60683

brass, fracture initiation and propagation during strip drawing 8-64663

draw resonance theory, Newtonian fluids 8-83350

draw resonance theory, power-law and Maxwell fluids 8-83351

E-glass fibre strength, effect of forming and ageing atmos. 8-92283

nylon 66, doubly oriented, annealing of drawn and rolled samples, struct. 8-52859

optical, fibres with high tensile strength, furnace drawing method 8-68666

optical fibre drawing technique for bundle of 19 fibres drawn from double crucible 8-55480

optical fibre formation of microcapillary by pulling from billet, azimuthal asymmetry effects, theory 8-87172

optical fibres, drawing conditions influence on attenuation 8-68667

optical fibres, UV curable epoxy acrylate coated, long-term mech. behaviour 8-95802

PA-6, polymer fibre, orientation changes during stretching, IR spectra 8-75568

PET, filament form. from gels 8-80508

PMMA, oriented, hypersound propag., elastic props. 8-75737

PMMA, uniaxially drawn, shrinkage, continuum model (*German*) 8-76722

polyamide-6, fibrillar struct. and annealing, small-angle X-ray diffr. 8-75565

polycarbonate fibre, highly-oriented, drawing behaviour and mech. props. 8-76708

polyethylene, drawn polymer, fibre composite model 8-76719

polyethylene, filled with glass particles, uniaxially drawn, elastic constants, filler addition effect (*Japanese*) 8-95780**drawing (mechanical) continued**

polyethylene, high-density, dielec. loss, below 4.2K, antioxidant, annealing and drawing effects 8-84518

polyethylene, oriented, elastic stiffness constants, US meas. 8-76690

polystyrene melt, drawing filaments, surface instabilities 8-71305

polyethylene terephthalate, uni- and biaxially drawn films, preferred planar orientation 8-80590

polyethylene ultradrawn fibres, Poisson ratio from Michelson interferometry 8-80596

polymer, drawing properties, role of interfibrillar tie mols. 8-76706

polymer, recrystallisation during drawing 8-76658

polypropylene, cold-drawn isotactic bars and thin films, microstruct. and annealing 8-95760

polypropylene, drawn polymer, fibre composite model 8-76719

polypropylene, monofilaments, drawing behaviour, melt-induced orientation effects 8-84922

polypropylene, reasons for disintegration under tension 8-84940

polypropylene, stretching flow for film prod., stretching over canonical mandrel 8-71304

polypropylene, ultradrawn fibres, Poisson ratio from Michelson interferometry 8-80596

polystyrene-poly(styrene-b-butadiene-b-styrene) polyblends, mech. props. 8-52919

PTE, polymer fibre, orientation changes during stretching, IR spectra 8-75568

PVC, uniaxial tension, deep drawing, rigidity (*German*) 8-64556

Recalloy, Fe-Nb, semihard magnetic alloy, magnetic props., hardness, microstruct. 8-56660

short tube drawing from thin metal sheets 8-86248

silica fibre, plastic coated, furnace drawing technique (*Italian*) 8-55475steel, C and alloy, cold formability (*French*) 8-60681

steel, low C, capped, cold rolled sheet, deep drawability, effect of carbide size, cold reduction annealing 8-64559

steel, quenched and tempered sheet, first operation cupping (*German*) 8-72788

styrene-diene triblock copolymer, hexagonal struct., flow props. of melt and fracture 8-76729

tube wall heating during steady state tube drawing (*German*) 8-84899

Al alloy 6061-T6, fracture initiation and propagation during strip drawing 8-64663

Al₂O₃-SiO₂ clad with B₂O₃-SiO₂ effect of drawing tension on residual stresses 8-64554β-CaSiO₃ fibre, continuous unidirectional crystallisation from melt 8-95739Cu single cryst., drawing deform. band form., axial orientation force meas., X-ray pole figure determ. (*Japanese*) 8-76710

Cu, wires, effect of heat treatment during drawing 8-56659

SiO₂, laser drawn fibers, tension rel. to drawing vel. and ultimate strength 8-74986SiO₂, optical fibre, phys. behaviour of neck-down region during furnace drawing 8-83127SiO₂, silica, optical fibre-drawing, vac. furnace 8-66960W fibre, KAl, KSi, KSiAl and KSiGa, addition effects on workability (*German*) 8-64557**drives**see also *electric drives; propulsion*

propulsion protection drive, optimum ratio between operational component times 8-82474

intra-aortic balloon heart assist device fluidic drive system 8-53566

repetitive photoelec. scanning system for high resolution optical spectra accumulation 8-54456

drop model (nuclear) see *nuclear liquid drop model***droplets** see *drops***drops**

agitated dispersion, droplet breakage and coalescence rates during mixing 8-85205

air-steam mixtures, heat transfer to moving droplets 8-90997

atomisation of liquid by impinging jets, expt. and theory 8-87373

boiling, gradient explosion, under conditions of bulk heat release 8-83226

break-up in stagnant fluids 8-75182

breakup, rel. to liquid jet penetration 8-94798

California coastal eog and stratus microstruct. 8-61505

carbon tetrachloride, drops, on brass surface, Leidenfrost pt., press. effect 8-87784

carbon tetrachloride-I₂-water system, mass transfer in pulsed perforated plate column 8-71385

chloroform, drops, on brass surface, Leidenfrost pt., press. effect 8-87784

cloud development in turbulent atm., drop spectrum evolution 8-81325

cloud drop spectrum evolution rel. to collision efficiency 8-69415

cloud droplet coalescence growth, fast computational method for Telford's theory 8-69486

cloud drops spectrum, kinetic eqn. of stochastic coagulation clouds 8-92944

clouds, directional light scatt. coeffs. in droplet and cryst. clouds (*Russian*) 8-96292

coalescence, film drainage 8-71387

coalescence rate, ambient liq. viscoelasticity effect 8-67248

condensation, max. drop size rel. to heat transfer coeff. 8-94559

condensation nuclei, size resolution via humidity gradient counter 8-81470

confined burning jet, droplet vaporisation, expt. and theory 8-94855

convective heat and mass exchange, Pe≤1000, in uniform (shear) stream 8-55683

cumulonimbus clouds, elec. field strength and raindrop spectra, study from mobile ground station 8-92943

deformation and breakup of a single slender drop in an extensional flow 8-67250

diameter, hold-up and backmixing coeffs. in liq-liq. spray columns 8-75183

disperse drop composition meas. in two-phase stream 8-55682

droplet growth and initial dew point temp. accuracy in cloud chamber on space shuttle 8-96268

dynamic liquid surface tension determ. from drop oscillation frequency and capillary jet instability 8-56026

electrification by evaporation or vapour condensation (*French*) 8-61511

drops continued

electrified pendent drops, axially symmetric, equilb. profiles 8-87846
 electrolyte aqueous soln. drops, ion emission due to laser heating 8-59063
 emulsion, inverse-type, coalescence of drops in uniform elec. field 8-53265
 evaporation, modelled by wet porous sphere, heat-transfer meas. 8-59268
 evaporation on heated surfaces, theory 8-87785
 evaporation rate in forced convective flow with transverse sound fields 8-51224
 falling into still liq., vortex ring formation 8-90946
 film boiling destabilisation, liq. drop falling onto hot liq. surface 8-94588
 flow produced by uniform translation along cylinder vertical axis (*French*) 8-90967
 fluid-liquid interface, approach of close-packed arrays of drops and spheres 8-84030
 formation of drops with non-wetting liqs. in capillaries and bores (*German*) 8-87370
 Freons, C51-12, 113, drops, on brass surface, Leidenfrost pt., press. effect 8-87784
 gas-liquid droplet system, phase transition kinetics and kinetic eqns. 8-83933
 gas-liquid flow in triangular ducts, two-phase wall layers 8-90999
 gas-vapour droplets, nonuniform mixture, acoustic wave attenuation 8-83154
 glycerine-water drops, collision dynamics, ang. of incidence influence (*Russian*) 8-83461
 heat and mass transfer during vapour absorpt. 8-63427
 heat transfer, electric field effect 8-59276
 heat transfer in immiscible liquid, intermittent elec. field augmentation 8-94872
 hot wall with impinging liq. droplet, transient temp. profile 8-75050
 inorganic emulsions, hydrophile lipophile balance temperature 8-95961
 laser anemometry, size and velocity meas. equipment 8-86238
 law of metastability, appl. to effect of mag. field on boiling liqs. 8-79199
 liquid, evaporation, idealised models for preheat stage 8-94586
 liquid drop motion in non-Newtonian media 8-75184
 liquid droplet, direct contact with high temp. surface, Leidenfrost temp. model 8-90666
 liquid droplet, surface thickness and surface oscillations, quantum and classical calcs. 8-91511
 liquid fuel droplet heating with internal circulation 8-75194
 liquid fuel droplets, transient heat flow in combustion gases, models 8-63507
 liquid-liquid dispersion, droplet size spectra in turbulent pipe flow 8-67247
 magnetic fluid, spherical drop, motion in rot. mag. field (*Russian*) 8-75212
 mass transfer inside drops in continuous fluid, effect of pulsation (*French*) 8-55686
 mass transfer to ambient liq., combination of resistances 8-83458
 microdrop, two-dimensional, on solid body surface, stability dynamics 8-51790
 motion in flow with varying vel. 8-59457
 motion in immiscible liquid, integral eqn. for Stokes flow 8-71389
 noncirculating, direct contact condensation 8-94548
 ocean spray, effect on energy transfers across air-water interface at high wind speeds 8-85574
 oil droplets, motion and optical props. by interf. method 8-67893
 optically dense liquid crops, motion in laser radiation field 8-50842
 oscillating drop, immersed in 2nd fluid, induced flow field streaming 8-59454
 pendant, profile area meas. 8-81943
 pneumatic nebuliser efficiency enhancement through appl. of elec. field 8-95966
 polydisperse droplets, produced by EHD method, charge-to-mass ratio 8-76931
 polymer drop wetting solid surface, spreading index for polymer surface props. (*Russian*) 8-51802
 rain drop spectra and fine structure on different time bases (*French*) 8-53681
 raindrop size distributions parameterisation 8-77301
 raindrops, EM scattering by dielectric spheroids and ellipsoids 8-85622
 reaction between water droplets and molten sodium 8-71263
 shape of drop on inclined plane, solar still aspects 8-79856
 size and dielectric const. determ., active microwave system 8-54339
 colloidal solution droplets, solid, particle form., heat and mass transfer 8-95967
 solution droplets in gas flow, heat and mass transfer during evaporation 8-90998
 solution droplets vaporisation, in high-temp. gas flow, heat and mass transfer 8-75191
 steam-water mixture, upward flow in tube, liq. film-core mass transfer, liq. distrib. 8-75189
 supercooled cloud, drop size distrib. influence on secondary ice particles prod. during graupel growth 8-73481
 supercooled droplets, bursting rel. to ice splinter production during riming 8-85662
 superheated droplets, flash boiling, undergraduate student expt. 8-81748
 suspension of spherical drops, mean drag and ave. velocity (*Russian*) 8-67259
 transparent droplet diameter meas. by side reflection 8-59518
 vaporisation in two-phase, gas+solid particle, flow 8-55677
 vaporising, internal temp. field 8-51042
 vapour-droplet flow field, one-dimens. motion eqn. 8-59455
 vapour-droplet mixtures, small perturbation propagation 8-95111
 viscous fluid drop, induced flow field in oscillating fluid 8-90980
 water, drops, on brass surface, Leidenfrost pt., press. effect 8-87784
 water, large drops accel. to terminal vel., drag coeff. 8-61506
 water, optical props., comparison with atmospheric aerosols (*Russian*) 8-77328
 water, sessile drops on inclined plane surfaces, shape 8-67891
 water and ice particles, interpretation of foil impactor impressions, rel. to hail research 8-57356

drops continued

water droplet evaporation, heat transfer characts., on heated surfaces 8-59269
 water droplets, atmospheric, sources and effects of surface organic monolayers 8-69412
 water droplets size distrib. in cloud bases 8-73458
 water drops, crystallisation on CuS aerosol prepared by burning pyrotechnic mixture 8-96279
 wetting, mechanism, mol. dynamics 8-51789
 Wilson Cloud form. by low altitude nuclear explosions, water aerosol and droplets characts. 8-53704
 H₂O, sessile drop impinging on heated surface, heat and mass transfer mechanism 8-90908
 He, condensing on positron, Monte Carlo lifetime spectra, temp. and elec. field effects 8-55263
 He, superfluid, laser light scatt., multiplicative and additive stochastic processes 8-84596
⁴He, droplets, surface energy, tension, thickness 8-84015
⁴He, heavy nucleus analogue 8-59992
 Hg+water systems, drop fragmentation rel. to thermal explosion detonation requirements 8-71368
 Si, preshaped single crystal prep. by pendant drop method (*French*) 8-64466

drying

biological material, prep. for X-ray microanal. of diffusible elements, methods of drying ultrathin cryosections 8-77166
 biological material prep. for X-ray microanal. of diffusible elements, rapid freezing and ultrathin section prep. 8-77165
 capillary porous body, drying, X-ray absorption obs., radiometry, temp. control 8-67023
 critical point dryer, low-cost, with continuous flow dehydration attachment, for electron microscopy 8-53595
 diffusion coefficient time depend. from single (de)sorption expt., step-by-step calc. method 8-87859
 droplet, vaporising, internal temp. field 8-51042
 evaporation of organic solvents, internal heating by IR irradiation 8-87237
 gelatin hardened layer structuralisation, kinetic anal. using swelling 8-62255
 heat and mass transfer, optimal control 8-67006
 insulating element, laminated, vac. drying in inert heat-transfer vap. 8-56875
 moist material, external heat transfer, calc. methods, drying kinetics 8-59467
 moist materials, drying kinetics calc. method, heat (moisture) transfer 8-55555
 oscillatory drying process optimisation 8-83215
 porous bodies, drying, internal mass transfer coeffs. calc. 8-67011
 porous bodies, theory and expt. verification 8-59278
 spray drying, of highly viscous conc. solns., heat and mass transport (*Russian*) 8-83230
 sublimation drying in UHF EM field 8-83936
 temperature coeff. depend. on heat and mass transfer similarity criteria 8-83214
 ultrathin cryo-section stabilization by freeze-drying 8-54349

dual resonance model see duality and dual models**duality (mathematics)**

dual extremum principles for heat eqn. 8-70077
 dual extremum principles for heat transfer problems with variable thermal props. 8-66999
 dual variational principles 8-77676
 modular operator, local observables, in von Neumann algebras, duality in QFT, CPT invariance 8-81793
 self duality in 4-dimens. Riemannian geometry, Yang-Mills eqns. 8-78073
 X-Y model, vortices and low temp. struct. 8-49777

duality and dual models

see also Veneziano model

1/N dual unitarisation, triple bare pomeron parameters of Gribov's Lagrangian 8-74232
 $\lambda\varphi^4$ field theory with internal symm., string representation 8-70266
 $\lambda\varphi^4$ theory, dual string theory from Feynman graph expansion 8-54544
 Adler zero and dual peripheral model 8-78153
 baryonium, review of QCD, duality, string models and bag models 8-78135
 baryonium, spectrum and prod. mechanisms 8-74295
 baryonium interactions, string model, dual amplitudes (*Russian*) 8-54620
 current-induced reactions, dual unitarisation 8-74233
 deep inelastic processes book contrib. 8-82222
 dual models of weak interactions of leptons and quarks 8-66070
 dual multiperipheral model, Pomeron and Reggeon slopes 8-62379
 dual resonance amplitudes, satisfactory invariant measure 8-66093
 dual topological unitarisation, review of S-matrix developments for hadron bootstrap theory 8-62381
 dual-resonance model, M-loop amplitudes for excited states 8-50019
 duality and dual models rho mesons diffraction model [Neveu-Schwarz dual model for $\rho\pi$ system] 8-82175
 elementary length and time in the strong interaction, meson reson. width data 8-82189
 group theoretical structure of dual current vertex 8-74229
 hadronic amplitudes, diffractive contrib., Chew Rosenzweig pomeron soln. 8-62382
 high energy behaviour of a double discontinuity and the bare Pomeron 8-82179
 instanton soln., Dirac eqn. 8-82100
 integral representation of dual resonance amplitudes with two off mass shell states 8-66094
 intermediate mass distribution of dual resonance pomeron, rel. to multiperipheral processes 8-50020
 isomorphic function and Fock space representations of dual model superconformal group 8-74230
 Klein-Gordon equation, stringlike solns. 8-82114
 mass-sum rule, Veneziano-type amplitudes π and K mesons 8-74180
 meson radiative transition, symm. and duality constraints 8-78178
 narrow states in pp, qq $\bar{q}\bar{q}$ mesons, BB bound states, duality, expt. 8-62378
 Neveu-Schwarz Ramond dual fermion model, inclusive single particle distribts 8-86446
 partition functions of dual strings, functional evaluation 8-74231

duality and dual models continued

- relativistic motion of massive quarks joined by massive string 8-74206
- s-channel discontinuities of torus insertion, dual unitarisation scheme, p - A_2 exchange degeneracy breaking 8-93866
- S-matrix, planar, building of cylinder correction in topological expansion or dual unitarisation 8-62321
- S-matrix theory dual chiral pion model, partially conserved axial-vector current 8-58175
- self-dual gauge field, Green function 8-82099
- self-dual SU(2) gauge field, Pontryagin density 8-66044
- semilocal duality constraints for mesons, on-shell particles, masses, couplings 8-58174
- spinning string, quantisation by Grassmann variables conversion to Clifford algebra elements 8-66095
- string junction model, large p , hadron prod. 8-62380
- string theory solns., in classical gauge field theories, broken gauge symmetry 8-62317
- SU(4) broken symm., duality, baryon+baryon and baryon+antibaryon exotic mesons prod. 8-89629
- superoperator generalisation of dual model with coloured quarks, three reggeon vertex (*Russian*) 8-74234
- topological excitations in Abelian Higgs model 8-70275
- U₁ gauge field in SU₃ gauge field, dual charges (*Chinese*) 8-86417
- unified theory of direct interaction between particles, strings and membranes 8-86433
- vortex strings, mag. monopoles in gauge field theory 8-70283
- Yang's R gauge for self-dual SU(3) gauge fields 8-78088
- NN interaction, low energy, meson exchange forces, one boson exchange potential, dual quark models 8-62444
- pp, dual model, vacuum exchanges, double pomeron poles with exotic Regge poles 8-89686
- v prod. from duality and new quark charge 8-74224

ductile-brittle transition

- see also embrittlement
- atomistic simulation by computer, exam. of thermal activation of crack tip plasticity 8-60801
- cleavage initiation by ductile tearing 8-64656
- complex loading, exam. of ductile-brittle failure 8-79664
- ductile-brittle transition pressure, grain size effect (*Japanese*) 8-60745
- polycarbonate, dielec. relax. and ductile brittle transition 8-52438
- polycarbonate, impact behaviour, effects of thermal pre-treatment and mol. wt. 8-95798
- polystyrene, effect of pressure and environment on fracture and yield 8-76757
- small particles, ductile-brittle transition rel. to impossibility of comminution by compression 8-52709
- steel, austenitic, fracture toughness props. of A533B, prior austenite grain size effect 8-60780
- steel, C, prestrain effect on non ductile transition temp. and bending speed relationship (*Japanese*) 8-84919
- steel, constructional, impact strength/brittle fracture relationship in ductile-brittle transition zone 8-56740
- steel, low C, ductile-brittle transition behaviour, grain size effects 8-52942
- steel, low C, non-ductile transition temp., tensile speed, effect of prestrain (*Japanese*) 8-72839
- thermoplastics, glassy, embrittlement mech. and inelastic deform. criterion for delayed failure 8-52940
- Al-Zn-Mg (6.1.5%), influence of ageing and cold work on tensile and fracture props. (*Japanese*) 8-52842
- Fe, cast, nodular graphite, annealed, fracture behaviour at low temps. 8-72875
- Fe-Al-Si, bending test, mech. props. under high press. and temp. (*Japanese*) 8-76711
- Fe-C-Fe₂O₃, cleavage initiation by ductile tearing 8-64656
- Fe-Cr alloy, impact strength, rel. to '475°C brittleness' (*Russian*) 8-92323
- Fe-Ni, fracture toughness at cryogenic temp. 8-72878
- Fe-Ni-C (9, 0.1 wt.%), effect of intercritical tempering on impact energy, exam. of mech. props. 8-52861
- Fe₄₀Ni₄₀P₂₀, amorphous alloy, ductile-brittle transition temp., relation to composition 8-52972
- Fe₄₀Ni₄₀P₂₀, amorphous alloy, ductile-brittle transition temp., relation to composition 8-52972
- Fe₄₀Ni₄₀P₁₄B₆, amorphous alloy, ductile-brittle transition temp., relation to composition 8-52972
- Mo, polycrystalline, fracture and ductile-brittle transition, hydrostatic press. effects 8-60735
- Mo-TiN (3.5 vol.%), failure characts. exam. 8-68788

ductile fracture

- see also ductile-brittle transition; notch ductility
- beam (plate) pure bending, dynamic fracture, axial force effect 8-63385
- cast Fe, spheroidal graphite, hydrostatic pressure effects on ductile fracture 8-60779
- circumferentially notched tensile specimen, finite element anal. 8-67150
- crack extension, evaluation of resistance in single notch edge specimens 8-68807
- crack extension, initial stage in time depend. and/or ductile fracture 8-67107
- criteria for blunting cracks 8-64657
- cup and cone fatigue fracture, electron fractographic obs. (*Japanese*) 8-72838
- elastic contact problems, in fracture mech., friction effects 8-67142
- engineering structures, welded exam. of fracture processes, review 8-60777
- epoxy resins, exam. of fracture energy above glass transition temps. 8-56743
- fibrous polymeric material, molecular model of fracture 8-60768
- fracture toughness parameters J and G^A , effect of load biaxiality 8-67128
- glass fibre reinforced plastic/polyurethane foam/Al sandwich, flexural props. (*Japanese*) 8-56707
- hydrostatic pressure effects on fracture, exam. 8-60779
- Inconel alloy 718, exam. of struct., properties and continuum synthesis of ductile fracture 8-76736
- metal, ductile fracture criterion 8-60817
- metal, fracture and ductile deform., microprobabilistic approach 8-64665

ductile fracture continued

- metal panels, adhesively bonded, cracked, fracture anal., crack tip stress intensity factors 8-90792
- method of potentials, appl. to fracture mechanics 8-51121
- PMMA, impact testing, elastic analysis of conventional test, reassessment of testing 8-60770
- polyethylene, high density, fracture buildup due to prolonged loading, exam. 8-68779
- polyethylene, medium density, impact testing, elastic analysis of conventional test, reassessment of testing 8-60770
- polymers, fracture, molecular interpretation 8-60769
- polymers, fracture and fatigue, review 8-68781
- polystyrene, effect of pressure and environment on fracture and yield 8-76757
- PTFE, impact testing, elastic analysis of conventional test, reassessment of testing 8-60770
- rotating discs, burst strength and necking 8-79226
- rubber, peeling initiation and propag. 8-76824
- steel, alloy, C-Cr-Mo-V, exam. of fracture toughness and critical flow anal. 8-72848
- steel, alloy, Cr-Mo, alloy SCM3, hydrogen embrittlement, delayed fracture, exam. (*Japanese*) 8-64620
- steel, alloy, ductility, hydrostatic press. effects 8-80615
- steel, alloy, HY130, temper embrittlement due to Si intergranular segregation, effect on H₂ induced cracking 8-76735
- steel, alloy, toughness evaluation inconsistency of AISI 4340 austenitised at increasing temp. 8-52982
- steel, alloy, type 52100, exam. of microstruct. and fracture, as function of austenitising in temp. range 800 to 1100°C 8-76673
- steel, austenitic stainless, type 304, intergranular H₂ assisted fracture, exam. of mechanism 8-80644
- steel, C, ductile fracture under cold forming conditions, press. effect 8-52938
- steel, cast high-strength, local intergranular fractures, formation mechanism (*Russian*) 8-95795
- steel, cavitation during superplastic flow, affecting factors 8-60728
- steel, ductile struct., crack propag. 8-68805
- steel, high strength, low alloy, rare earth treated, ductile fracture mech. 8-64658
- steel, inclusions effect on distrib. of local microheterogeneous deform. (*Russian*) 8-80586
- steel, ledeburite, fracture during hot plastic deformation exam. 8-56755
- steel, low alloy, naval, stretch zone width meas., COD for ductile crack initiation 8-68813
- steel, mild, plate, effect of striking velocity on perforation energy 8-68818
- steel, mild, resistance to slow stable crack growth, use of J integral 8-68809
- steel, pressure vessel, A533B, ductile, plane strain crack growth 8-80621
- steel, reheat cracking in weld zone, method for evaluating sensitivity to cracking 8-72855
- steel, stainless, type 304, exam. of H₂ induced cracking 8-76738
- steel, structural, slow stable crack growth, exam. of crack profile 8-84965
- steel 30Kh2NMFA, microstructure of cup and cone fracture surface, effect of size of disperse phase particles (*Russian*) 8-68762
- steel Cr-V (1.5, 0.5 wt.%), cavitation effect of temp. and C content 8-64638
- steel fibre reinforced Ag, exam. of recrystallisation behaviour (*German*) 8-84849
- steel low alloy, high strength, ductile failure criteria for blunting crack 8-64657
- steel plates, C and alloy steels, comparison of dynamic tear and Charpy V notch impact props. 8-92357
- steel spheroidised type AISI 1090, hot rolled H₂ promotion of plastic instability 8-60725
- steels, structural, fracture initiation, exam. 8-60778
- strain energy density fracture criteria, extension to brittle and ductile fracture 8-75102
- strain gauge method for detecting initiation 8-85085
- stress analysis of cracks, elastoplastic range 8-67144
- styrene-diene triblock copolymer, hexagonal struct., flow props. of melt and fracture 8-76729
- unstable fracture criteria under large plastic deformation 8-67143
- viscoelastic system, fracture mechanics 8-67145
- void-containing materials, ductile fracture, conditions for shear localisation 8-79663
- Al alloy 6061-T6 cylinder, dynamic fracture, expt. rel. to Mott's theory 8-64651
- Al alloys grain size effect 8-60781
- Al-Cu(Zn-Mg), age hardening, conditions leading to localised plastic deform. and fracture in slip bands during fatigue 8-64670
- Al-Mg, fracture during superplastic flow 8-60729
- Al-Mg-Si-Mn, Mn addition effects on fracture 8-60791
- Al-Zn-Mg-Cu, alloy 7075, hydrostatic pressure effects on ductile fracture 8-60779
- Al-Zn-Mg-Cu alloy, laminated, adhesively bonded alloy 7075-T6, exam. of fracture resistance 8-76754
- Al-Zn-Mg-Mn, correlation of microscopic features, with macroscopic crack propagation 8-60800
- Cr-C-Ni-(P), hard alloys, sintered, fracture props., P addition effects 8-60610
- Cu alloys, cavitation during superplastic flow, affecting factors 8-60728
- Cu-Al composite, simulation of tensile behaviour and fracture void initiation (*Japanese*) 8-52948
- Cu-Fe, composite, simulation of tensile behaviour and fracture void initiation (*Japanese*) 8-52948
- Cu-Ti (1.07 wt.%), containing coherent precipitation, observations of flow and fracture 8-80643
- Fe, cast, ferritic, ductile fracture initiation and propag. 8-84966
- Fe, cast, ferritic SG ductile fracture initiation and propagation 8-64661
- α -Fe, plastic deform. in neck leading to fracture 8-64655
- Fe, pure, ductile fracture, effect of nonmetallic inclusions 8-64660
- Fe-C-Fe₂O₃, cleavage initiation by ductile tearing 8-64656
- Fe-Ni-Al, correlation of microscopic features, with macroscopic crack propagation 8-60800

ductile fracture continued

- Fe-Si (2.35 wt.%), misorientation dependence of grain boundary segregation, Auger spectroscopy exam. 8-76629
 Li₂O-Al₂O₃-4SiO₂, glass-ceramic, tensile creep and high temp. fracture 8-52914
 Ni, deformed in uniaxial tension, fracture map 8-56764
 Ni-ThO₂, dispersion hardened, fracture mechanism map 8-60823
 Ni₃Al, ductility in poly- and single crystals, compressive and tensile tests 8-56715
 Pb-Sn eutectic, cavitation during superplastic flow, affecting factors 8-60728
 Si-Al, composite, simulation of tensile behaviour and fracture void initiation (*Japanese*) 8-52948
 Si₃N₄, struct. of slow crack interface, light and electron microscope obs. 8-68770
 Ti-Al (6.1 wt.%), hot rolled sheet, ductile fracture nuclei, SEM obs. 8-64654
 Ti-Al-Sn (5, 2.5 wt.%), ductile fracture at low temps. 8-64659
 Ti-Al-Sn (5, 2.5 wt.%), fracture mechanism at cryogenic temps. 8-64642
 Ti-Al-V (6, 4 wt.%), void formation and growth, tensile fracture, exam. 8-80637
 Ti-Al-Zr (6.5 wt.%), alloy IMI 685, SEM exam. of crack growth 8-72849
 U, two-dimensional expt. fracture map 8-95803
 U-Mo (10 wt.%), commercial alloys, influence of metallurgical factors on fracture processes (*French*) 8-60751
 Zn, single cryst., in metal melt, plastic deform. and fracture obs. by acoustic emission (*Russian*) 8-56737
 Zn-Al (22 wt.%), superplastic, eutectoid alloy, ductility and fracture 8-60819
 Zr₃Al, ordered polycrystals, ductile fracture 8-64641

ductility

- see also ductile fracture; notch ductility*
 alloy, heat-resistant, alloying and heat treatment effects on struct. and strength 8-95758
 alloy, high temperature, mechanical, thermal and corrosion props. 8-95763
 brass, anisotropic bend ductility in single phase alloys 8-60726
 bronze, anisotropic bend ductility in single phase alloys 8-60726
 criterion 8-63336
 Hastealloy X, relations between weld heat affected zone cracking and microstruct., Gleeble test (*Japanese*) 8-52858
 Inconel 706 and 718, relations between weld heat affected zone cracking and microstruct., Gleeble test (*Japanese*) 8-52858
 limiter materials, for Doublet III fusion research machine, selection 8-55026
 measurement technique for high-strain rate ductility of metals 8-80694
 metal, BCC, effect of screw dislocations on mech. props. (*Russian*) 8-60704
 metal, fracture and ductile deform., microprobabilistic approach 8-64665
 polycarbonate, dielec. relax. and ductile brittle transition 8-52438
 PVC sheet, notched, yielding 8-56708
 rock, deformation and fracture under general triaxial stress states, anisotropic dilatancy (*Japanese*) 8-56750
 sheet metals, ductile, shearing process 8-84841
 steel, 12Kh18N9T-TiB₂, eutectic alloy, high temp. props. 8-84931
 steel, alloy, ductility, hydrostatic press. effects 8-80615
 steel, alloy, maraging, 18% Ni, effect of solution and ageing treatments, on microstruct., tensile props., fracture toughness 8-80648
 steel, alloy, maraging, 250-grade, ductility and toughness of hot isostatically pressed powder 8-52925
 steel, alloy 4340, fracture and high temp. props., 533K to 1255K 8-60821
 steel, austenitic, precipitation hardened, ductility of grain boundaries and crack propag. (*German*) 8-52834
 steel, austenitic Cr-Ni (18,12 wt.%), containing coarse irregular carbide precipitates along grain boundaries, ductility 8-60718
 steel, austenitic heat-resisting, deformation and fracture rel. to grain-boundary reaction nodules 8-80591
 steel, austenitic stainless, fast neutron irradi., effect on mech. props. 8-92309
 steel, CrMoV, failure in post yield regime using single edge notched tension specimens 8-68765
 steel, high strength, fatigue crack growth 8-64697
 steel, high strength, low alloy, plate, impaired ductility in sheared edges 8-60727
 steel, low alloy, eutectoid pearlitic, exam. of microstructures dominating ductility (*Japanese*) 8-84917
 steel, low C, dual phase structures (martensite and ferrite), effect of martensite composition on content, mech. props. 8-76717
 steel, low C, thermomechanically processed, martensitic fibre development, fatigue fracture 8-64572
 steel, maraging, (18 wt.% Ni), solution annealed, exam. of cryogenic tensile, fatigue, and fracture props. 8-92311
 steel, Mo-bearing, intercritically annealed dual-phase strip, props. and appl. 8-84858
 steel, Ni, sintered, relation between microstruct., microchemistry and mech. props. 8-64504
 steel, silver, elastic limit, bending strength, and ductility rel. to tempering temp. after quenching 8-95764
 steel, stainless, 304 and 316 elev. temp. tensile ductility minima 8-60730
 steel, stainless, duplex, hot ductility and fracture mechanism 8-60731
 steel, stainless, type AISI 316, effect on props. of Zn transfer from galvanised wire at 550°C 8-88527
 steel, stainless, type Kh17N13M2T, strengthening by plastic deformation and cold working (*Russian*) 8-52839
 steel, strengthening by rapid electrothermal treatment 8-84870
 steel, TRIP, powder processing, tensile strength, ductility 8-64499
 uniaxial tension, effect of material strain rate sensitivity and specimen heterogeneity (*Polish*) 8-84887
 Ag composite, SiC whisker-reinforced, prep. aboard Skylab. 8-84741
 Al alloy, heat treatment of semifinished products of alloy 01420 before cold deformation 8-84873
 Al alloys, preliminary forging effects on struct. and mech. props. of extruded sections (*Russian*) 8-80564
 Al bronze, anisotropic bend ductility in single phase alloys 8-60726

ductility continued

- Al-graphite particulate composite, exam. of friction, wear and tensile props. 8-72890
 Al-Mg alloy AMg6, mech. props. of welded joints, impurity effects 8-95789
 Al-Zn-Mg (6,1.5%), influence of ageing and cold work on tensile and fracture props. (*Japanese*) 8-52842
 Co-Cr(V)(Ti,V)C-(Al), eutectic alloy, unidirectional solidification, oxidation and tensile tests 8-52790
 Cr, optimum alloying with rare earth metals, Ti, Zr, Hf, Nb, Ta 8-68651
 Cu, cold worked, grain size effects on short-term strength (*Russian*) 8-56693
 Cu-Ni cast alloy, effect of alloying and residual elements 8-85033
 Fe, Armco, screw dislocation effect on mech. props. (*Russian*) 8-60704
 Fe, Armco, texture role in prestrain embrittlement 8-60796
 α-Fe, hydrostatic pressure effect on creep rate and failure time 8-92306
 Fe-Al-Si, bending test, mech. props. under high press. and temp. (*Japanese*) 8-76711
 Fe-Ni-Cr-Ti-Mn-Mo, (25.8, 14.04, 2.17, 1.27, 1.30 wt.%), superalloy A-286, precipitation hardening, exam. of fracture toughness and mech. props. 8-92355
 Fe-Ni-Mo, ferrite plus martensite structures, exam. of mech. props. 8-856709
 Fe-Si (6.5 wt.%), ductility and mag. props., Ni and Mn addition effects 8-76704
 Ir-W (0.3 wt.%), P segregation to grain boundaries, effect on high temp. ductility 8-95754
 Ni carbonyl powder, sheet filtration materials with metallic gauze backing layers, bending strength and ductility 8-60613
 Ni-Al-Cr, precipitation-strengthened, mechanical props. 8-84968
 Ni-B, hydrogen embrittlement, effect of B additions (*Japanese*) 8-84973
 Ni₃Al, ductility in poly- and single crystals, compressive and tensile tests 8-56715
 Ti alloy, VT23, ht. treatment effects on fracture (*Russian*) 8-80623
 Ti alloy VT3-1, large forgings, heat treatment, struct. and mech. props. 8-52864
 Ti alloys, AT3 and AT6, tensile props. prolonged oxidation effects 8-85050
 Ti-Al-Cr-Mo-Fe(V)(Zr), effect of structure and heat treatment on tensile strength, ductility, fatigue limit and notch sensitivity 8-56711
 Ti-TiO₂-ZrO₂-Mo, sintered struct. and mech. props. 8-60618
 Zr-Al(8.6 wt.%), mech. props., corrosion and fast neutron irradi. influence 8-84948
 Zr-Ru(Pd), heat treated, mech. props. and struct. 8-80571

duplicating *see reproduction (copying)*

dusk *see twilight*

dust

see also cosmic dust

- AC test dust, particle size distrib. for filter media testing 8-53060
 actinide industrial dusts, lung clearance studies at NRPB 8-65137
 aeolian sediments, Mahalanobis' D² distance appl. (*Portuguese*) 8-61388
 air pollution, dust cyclone operation, anal. 8-57362
 airborne, respirable fraction, performance characts. of samplers matched to them 8-53438
 atmosphere, effect on IR cooling rates 8-88886
 atmosphere, peak short term dustfall meas. from dust generating industry 8-81386
 atmosphere, propagation calcs., use of average complex refr. index 8-57314
 atmosphere, SO₂ adsorpt. and oxidation on particles 8-96287
 atmosphere dust, meas. via personal CIP type sampler 8-81469
 back discharge, flashover meas., streamer or steady glow mode, dust layer effects 8-59708
 NW British Isles, dust fall on 1977 March 6 assoc. with short rain shower 8-57287
 Couette flow, of dusty gas between two infinite coaxial cylinders 8-55685
 lidar obs. at 0.7 and 10.6 μm wavelength 8-69459
 Liege industrial region, five year record of atmospheric fall-out 8-81375
 loess geological environments, China (*Chinese*) 8-81156
 marine atmosphere, lightly polluted, dust gravimetric determ. rel. to dark smokes 8-81376
 optical depth of Saharan dust, NOAA 3 VHRR reflected radiance meas. 8-65390
 pollution control, polarisation and interference microscopy apps. 8-61544
 raingauge dust excluder 8-73548
 respirable aerosol mass conc. meas., using piezoelec. microbalance 8-69518
 rotating charged dust, Newtonian and general relativistic treatments 8-73908
 spark generator for dust explosion hazard assessment and gas ignition 8-57983
 storms, aerosol and momentum mixing, fast-response meas. 8-65364
 stratosphere, dust meas., (1970-1977) 8-73445
 troposphere, Sahara dust cont. over N.Atlantic from air cond. meas. 8-92897
 unsteady flow of dusty viscous fluid through uniform pipe 8-59450
 volcanic, effects on climate, statistical evidence from long-term temp. records 8-69439
 Fe, tribothermoluminescence of flakes in grinding wheel, rel. to solar coronal dust radiation 8-68570

dust storms *see storms*

dwarf stars

see also white dwarfs

- λ Aurigae, in ε Indi moving group, detailed anal. 8-85982
 Barnard's star, spectrophotometry with Carnegie image tube 8-57466
 BD+75°325, hot subdwarf, UV spectrum obs. by International Ultraviolet Explorer (IUE) 8-96474
 brown dwarfs and black holes rel. to missing mass 8-61879
 YZ Canis Minoris, red dwarf star, weak radio flares interferometric obs. 8-65633
 α Canis Minoris (Procyon), CNO abundances from near IR spectrum 8-93222

dwarf stars continued

- CD-42°14462 (V3885 Sagittarii), dwarf nova in permanent outburst 8-53966
 CD -31°622 as metal-deficient subdwarf 8-65618
 UV Ceti, anomalous flare activity obs. 8-89202
 Z Chamaeleontis, monitoring of southern dwarf nova, 1954-76 period 8-93272
 BY Draconis stars, photometric radii compared with luminosity class V stars (*Russian*) 8-57564
 ε Eridani, model chromosphere of K-type dwarf 8-65610
 ε Eridani, UV spectrum obs. by International Ultraviolet Explorer 8-96475
 extreme subdwarfs molecular band strengths, theoretical approach 8-93221
 F-, G- and K-type, in solar neighbourhood, absolute magnitudes 8-81632
 flare stars, identification with transient soft X-ray sources questioned 8-96485
 G-type, macroturbulence and age anticorrel. 8-93226
 HD 17576, UV subdwarf companion discovery from uvby β photometry 8-96479
 HD 27561, Hyades cluster star, CNO abundances from near IR spectrum 8-93222
 HD 40409, in ε Indi moving group, detailed anal. 8-85982
 14 Herculis, C/Fe ratio of K-type dwarf 8-93227
 high-velocity metal-poor dwarfs, blue spectra abundance anal. 8-53933
 K- and M-type, space motions rel. to stellar age 8-69846
 late-type main-sequence stars near Sun, intermediate-band photometry 8-53934
 LB 3459, short period eclipsing binary system containing two O-type subdwarfs, uvby photometry 8-53987
 LTT 2437, most metal-deficient subdwarf, spectrum, photometry and Ca/H ratio 8-69797
 in M31, inner nuclear regions, spectral features and dwarf content 8-86005
 M-type, in solar neighbourhood, absolute magnitudes 8-81631
 M-type, spectrophotometry with Carnegie image tube 8-57466
 Me-type dwarf stars, long-term variability 8-93254
 novae, nature, H accretion, mag. field, radiation mechanisms (*Russian*) 8-93277
 70 Ophiuchi A, model chromosphere of K-type dwarf 8-65610
 SX Phoenixis, short period dwarf Cepheid, UV photometric obs. 8-57561
 45 Tauri, Hyades cluster star, CNO abundances from near IR spectrum 8-93222
 UV 1758+36, He deficient hot subdwarf B star, atm. parameters, radial vel. 8-53944

dye lasers

- active medium, hydroacoustical perturbations (*Russian*) 8-82966
 amplified spontaneous emission with picosecond light pulses 8-82965
 BBO solution, induced pump absorption, lasing threshold and efficiency 8-50773
 beam divergence, transverse mode saturation, kinetics (*Russian*) 8-74931
 beam expansion with diffr. grating in dye laser cavity 8-66858
 bicyclic dye, stability, photodegradation parameters 8-71098
 bicyclic dye stability, photodegradation relationships 8-55349
 carbocyanine dye CW laser emission, spectral range extension up to 1020 nm 8-74901
 complex organic laser active substances, props. (*Russian*) 8-74904
 continuous jet dye laser, appl. to intracavity spectrometer (*Russian*) 8-70197
 continuously scanned tunable laser, for atmospheric pollutants detection 8-81362
 coumarin 6 dye mols. in liq. cryst., fluoresc. intensity, orientation control 8-82759
 coumarin derivatives in simple dye laser, pumping by N_2^+ ion laser 8-74903
 coupling reflector, involute-related, for flash lamp pumped laser systems 8-90425
 CW, on-line computer control, laser isotope separation appl. 8-70948
 CW, tuning and spectral narrowing using low-loss diffr. grating 8-71109
 CW digital wavemeter, moving cube-corner interferometer system 8-50840
 double pumping source (*Chinese*) 8-82960
 dyes, absorption edge struct. in stimulated fluorescence spectra, Raman scatt. 8-55350
 energy transfer laser, intermol. interactions and spectral shifts 8-74902
 flash lamp pumped, mode locking, picosecond, pulse generation 8-71131
 flashlamp pumped, SHG (*Japanese*) 8-90459
 flashlamp pumped dye laser synchronisation, CW laser injection, spectral purity (*French*) 8-63118
 flashlamp pumped intense subnanosecond pulse generation, 0.58 to 0.80 μ m 8-90422
 flashlamp-pumped, birefr. filter for tuning, theory and design 8-74914
 flashlamp-pumped, two-stage amplification, for SHG 8-74922
 frequency locking by intracavity stimulated Raman scatt. 8-79050
 frequency locking to Na flame atomic transitions 8-50795
 gas, excitation by elec. discharge, electron beams, optical stimulation (*Czech*) 8-79016
 grazing-incidence pulsed, operation in single longit. cavity mode 8-94398
 high power CW dye laser configuration 8-50806
 hydroxycoumarin dyes, laser emission 8-82962
 induced pump absorption, lasing threshold and efficiency 8-50773
 injection locked flash pumped, for contour holography of moving object 8-50737
 intracavity dye laser technique for spectroscopic and kinetic meas. of transients 8-62239
 intracavity enhancement of absorpt. in nanosecond regime 8-78839
 IR, pulsed, tunable, pumped by flashlamp-driven dye laser 8-94400
 jet stream, thickness meas. in real time, by optical technique 8-82975
 ketocyanine dye, lasing under lamp excitation 8-82964
 longitudinal mode selection due to saturable absorpt. 8-63143
 α -NPO solution, induced pump absorption, lasing threshold and efficiency 8-50773

dye lasers continued

- α -NPO-Ar mixture, vapour phase laser, electron beam pumping 8-63097
 optical, gain and saturation considerations 8-94393
 perylene, vapour phase, N_2 laser excited, quantum efficiency and thermal stability 8-50771
 photonic efficiency of dye laser amplifiers (*French*) 8-59004
 POPOP, vapour phase, N_2 laser excited, quantum efficiency and thermal stability 8-50771
 POPOP solution, induced pump absorption, lasing threshold and efficiency 8-50773
 POPOP vapour, electron beam excited superradiance 8-66820
 POPOP-Ar- N_2 , electron beam pumped, intense laser emission at 381 nm 8-74898
 prism used as beam expander in N_2 laser pumped dye laser, dispersion 8-74924
 pulse generation and meas., 0.2 psec., from passively mode locked dye laser 8-50830
 pulse generation- subpicosecond relax. times meas. in rhodamine 6G, B (*Czech*) 8-78838
 pulsed, light polarisation with thin wedge plate in cavity 8-55394
 pumping by Nd:YAG laser freq. doubled output 8-59090
 pyrene, vapour phase, N_2 laser excited, quantum efficiency and thermal stability 8-50771
 rate equations, spiking phenomenon 8-55351
 rate equations 8-82961
 reference wavelengths, two-photon transitions to Rydberg levels 8-94221
 rhodamine 6G, amplifier system, pumped by TEA N_2 laser 8-82984
 rhodamine 6G, CW synchronously mode-locked, subpicosecond pulse generation 8-71128
 rhodamine 6G jet stream CW laser, tuning range, mode competition effects 8-50791
 rhodamine 6G solution, induced pump absorption, lasing threshold and efficiency 8-50773
 rhodamine 6G synchronously mode locked CW laser, pulse width depend. on intracavity bandwidth 8-66821
 rhodamine 6G water soln. laser with spatial lamp pumping, spatial coherent emission 8-82963
 rhodamine B and 6G, laser wavelength and dye conc. 8-50770
 rhodamine dye soln. series, flashtube-pumped, calc. and expt. generated quantum power 8-50772
 spectrally narrow pulsed, without beam expander 8-79028
 spectroscopic light source appl. (*German*) 8-89552
 stability conditions for laser cavities with two foci 8-66850
 subnanosecond single photon counting fluorescence spectroscopy using tunable dye laser excitation 8-86355
 subpicosecond spectroscopy by passively modelocked continuously operated dye lasers 8-58066
 superluminescent source of optical noise for nonlinear optics (*Russian*) 8-79033
 synchronous mode locking, composite gain and absorber medium, sub ps pulses 8-79046
 TP-C-DMP, new bifluorophoric laser dye with intramolecular energy transfer, lasing characts. 8-74899
 TP-CSC-DMP, bifluorophoric mol. ultrafast intramolecular energy transfer 8-74900
 tunable, opto-galvanic effect in plasma, spectroscopy appl. 8-95977
 tunable dye laser, for picosec. spectroscopy, 400-500 nm 8-82988
 tunable dye laser fast light deflection, ultrahigh resolution 8-63178
 tunable laser, undergraduate demonstration expts. 8-61988
 tunable ps high efficiency system for 340 nm to near IR 8-50789
 tunable UV and visible lasers 8-59029
 two wavelength outputs with orthogonal polarisations 8-50792
 N_2 laser pumped, single mode operation 8-87060
 N_2 laser-pumped, subns. relax. oscils. 8-82959
 Na fluorescein, laser wavelength and dye conc. 8-50770

dyeing

- non-Newtonian fluids, particle movement, appl. to dyeing and haematology (*German*) 8-87369

dynamic nuclear polarisation

- see also CIDNP; Overhauser effect; solid effect
 1H and ^{19}F dynamic polarisation, Cl scalar coupling enhancement 8-66568
 aromatic molecules in cryst. lattice, phosphoresc. intensity and optical nuclear polarisation, level anticrossing effects 8-91992
 dichlorofluoromethane, 1H and ^{19}F dynamic polarisation, Cl scalar coupling enhancement 8-66568
 dynamic polarisability, TDHF theory and RPA sum rules 8-78292
 nuclear relaxation, spin temperature, solid effect, and thermal mixing, review of principles 8-64297
 organic free radical solutions, mol. motions 8-91991
 ruby, correlated ESR and NMR c-axis variation effect, dynamic nuclear polarisation 8-72436
 single crystal, correlated ESR and NMR c-axis variation effect, dynamic nuclear polarisation 8-72436
 speed of DNP, impurity acting as centre of polarisation coinciding with reson. freq. of distant nuclei (*French*) 8-91990
 CdSe, optically pumped, dynamic polarisation of nucl. moments 8-68411
 Cr complex, Cr(V)-dimethylformamide, proton dynamic polaris. and relax. 8-91988
 Cr complex, Cr(V)-fluoroorganics, proton and ^{19}F dynamic polaris. and relax. 8-91989
 Fe complex $Fe(NO)[S_2C_2N(C_2H_5)_2]_2$ in frozen toluene, for dynamically proton polarised target 8-52378
 LiH, nucl. antiferromag. struct., neutron diffr. and dynamic polarisation (*French*) 8-88226
 Mg_2SiO_4 , NMR of ^{29}Si and ^{25}Mg with dynamic polarisation technique 8-56405

dynamic programming

- classical relativistic dynamics fundamentals revisited (*French*) 8-62074
 multispectral radiance method for temp. distribution meas. (*Japanese*) 8-77912
 PWR steam supply control system optimisation 8-50251
 respiratory airflow pattern modelling by optimisation criteria 8-80898

dynamic response

- beam dynamic deflection under external force of time-dependent frequency 8-83289
 cylindrical shell to conc. impact load 8-67072

dynamic response continued

- fluidic element nonstationary flow meas. by laser Doppler velocimeter with frequency tracker (*Japanese*) 8-55707
- foundation dynamic interaction with viscoelastic half-space (*German*) 8-79228
- helical springs, numerical soln. of dynamic response 8-67026
- high cycle fatigue diagram based on dynamic severity criterion 8-60759
- LMFBR, dynamic response of containment vessel and coolant wave propag., REXCO-EUR code manual 8-58349
- loaded thin circular plate stability criterion 8-77700
- model and full-scale cooling tower resonance tests 8-83291
- nerve impulse equation, dynamic responses of impulse 8-64972
- nuclear plant design, seismic response spectrum normalisation 8-50415
- nuclear plant equipment response to aircraft impact 8-50416
- peak harmonic response of locally non-linear systems 8-51109
- structural panel, rectangular, with elastic edge constraints, dynamic response, Bolotin's asymptotic method 8-75091
- submerged hemispherical shells, dynamic response to earthquake motions 8-51110

dynamic stability *see stability***dynamic testing**

- see also fatigue testing*
- alloy testing for use in heat treatment furnace, disc tribometer with high temp. pin 8-95900
- apparatus, for adherence, wear resist. and thermal shock meas. of thin films 8-72943
- cryogenic heat pipe/radiator dynamic testing 8-94532
- cushion dynamic props. by mech. impedance method 8-72953
- electromagnetic device for loading and measuring wear in vacuum 8-56841
- experimental device for measuring friction between ski and snow 8-92410
- fibres, high-strength and high tensile, equipment for testing elongation 8-56844
- fracture toughness determination, by instrumented impact tests 8-68861
- friction and wear testing equipment for use at high temp. in air 8-56839
- hot twisting, shearing stresses, anal. determ. 8-60900
- metal thermoelastic coeff. meas. by strain gauges 8-56853
- metals, alloys, unit for dynamic testing over wide temp. range 8-60908
- MOS structure dynamic volt-capacitance characteristic meas. 8-60207
- nonlinear materials, dynamic testing using harmonic excitation, jump phenomena 8-51141
- particulate materials, dynamic shear strength and flow behaviour, shear cell meas. 8-53048
- phenolformaldehyde resin moulding compounds, dynamic testing (*German*) 8-76699
- piezoelectric dynamometer for dynamic force meas. (*Hungarian*) 8-65918
- plastic ligaments and tendons, dynamic motion simulator for testing (*German*) 8-81070
- polymer, wear testing of bearing material, new sliding bearing test facility 8-95862
- shock-loaded material, self-consistent technique for estimating dynamic yield strength 8-80692
- uniaxial strain conditions in modified Kolsky apparatus, dynamic material behaviour meas. 8-85070
- US grey scale scanner dynamic range testing 8-69169
- vibration test rig for wear meas. of granules 8-56840
- Al-Si-Mg (1, 0.6 wt.%), plasticity due to superimposed macrosonic and static strains 8-60719
- K, device for press. variation of yield stress, elastic constants 8-53047

dynamical symmetry

- narrow resonances, dynamical model, mass mixing and splitting in degenerate multiplet states 8-93813
- rotational symmetry in Hamiltonian dynamics 8-74134
- unitary representations of general covariant group algebra, Lie algebra 8-58136
- weak interaction theory review, dynamical symmetry breaking 8-78131

dynamics

- see also ballistics; fluid dynamics; force; friction; haemodynamics; impact (mechanical); kinematics; resonance; rotating bodies; rotation; vibrating bodies; vibrations*
- astatic gyroscope with elastic cardan suspension, dynamics (*Russian*) 8-63273
- Centaurus galaxy cluster, galaxy dynamics rel. to Virgo cluster redshifts 8-54061
- connectance of dynamical systems with increasing no. of degrees of freedom 8-81831
- conservative dynamic systems, search for cyclic coords. (*Russian*) 8-65764
- coupled linear chains, dynamics 8-89403
- crawl swimmer, six-stroke, dynamics, mathematical model (*German*) 8-90702
- education, dynamics of variable mass system, flexible inextensible rope 8-86071
- education, falling domino chain, expt. and computer program 8-62009
- elastodynamics, vel. pots., stress functions 8-93534
- fundamental principles generalisation, appl. to motion of disc on ice surface (*Russian*) 8-65762
- galaxies, cool stellar discs equilib. 8-54037
- galaxies, free collapse of stars rotating sphere 8-93325
- galaxies, radial oscill. modes of cool stellar discs 8-57628
- galaxies distribution, N-body model computations rel. to hierarchical clustering pattern stability 8-86026
- galaxy clustering evolution, cosmological N-body simulations 8-96550
- genetic systems, dynamics of neutral mutation 8-86220
- Hamiltonian dynamics, for closed system of N particles in mutual interaction 8-62070
- impulse dynamical equations, nonholonomic system, solid on plane, rolling without slipping (*Italian*) 8-57769
- interplanetary particle dynamics 8-57501
- interstellar medium, two-phase model and intercloud wind 8-85991
- Kepler problem, formal equivalence with Maxwell fish-eye theory 8-81733

dynamics continued

- Lagrangian mechanics, consts. of motion anal. 8-81829
- linked rigid body systems, nonlinear eqns. of motion (*German*) 8-87254
- mass point displacement under effect of forcing conditions (*German*) 8-86149
- method of action-angle variables and the classical dynamics of a non-linear Lagrangian 8-77702
- motion of solid body with elastic and dissipative elements (*Russian*) 8-65763
- Orion Molecular Cloud, new dynamical model 8-93373
- Periodic Comet Taylor (1916 I), nuclei separation vels. during disintegration 8-61812
- periodic solns., numerical extrapolation 8-69663
- Poincare canonical momenta and Nambu mechanics 8-77701
- projectile motion, computer programs for high-school expts. 8-86094
- statistical mechanical relation 8-49748
- stellar clusters, nonexistence of additional integral of motion of star 8-65663
- Virgo galaxy cluster, galaxy dynamics rel. to redshift controversy, evidence from Centaurus 8-54061
- viscoelastic body with stripwise loading (*German*) 8-87281

dynamometers*see also force measurement*

- piezoelectric dynamometer for dynamic force meas. (*Hungarian*) 8-65918
- strain gauge, effect of temp. on characts. 8-93677
- strain gauge, wind tunnel dynamometer, five component 8-54361
- strain-gauge type for aircraft rudder-bars (*French*) 8-49825
- two-string balance microprocessor operation (*German*) 8-57936

dynamos *see d.c. generators***dysprosium***see also nuclei with*

- crystal structure, P-T phase diagram 8-84776
- film, elec. resist. results 8-84326
- film, magnetoelastic waves, GHz, excitation, field depend. 8-72378
- film, vacuum deposition, using liq. He cooled cryopumping panel 8-56581
- foil, average thermal neutron flux determ. method 8-73112
- galvanomagnetic effect, longit., in single crystals (*Russian*) 8-56132
- helical antiferromagnetic phase, basal plane anisotropy 8-84412
- internal fields, positive muon investigation 8-68438
- magnetic anisotropy and ^{161}Dy Mossbauer effect 8-92001
- magnetic phase transitions, helical state, field induced 8-72349
- spin wave exam. 8-56306
- thermal expansion, interferometric meas. 8-52333
- Ag:Dy, orbit-lattice coupling, nonuniform strain effects 8-88182
- Al:Dy, orbit-lattice coupling, nonuniform strain effects 8-88182
- Al-Al₂O₃-Al junctions, Dy doped at Al₂O₃-Al interface, electron transport mechanisms and barrier height 8-91778
- CaF₂:Dy²⁺ submm. magnetospectroscopy, tunable far IR laser potential 8-52481
- CaF₂:Dy, colour centres, antiresonance-type phenomenon in external fields 8-68529
- CaF₂:Dy³⁺, high temp. fluorescence using Ar⁺ and N₂ lasers 8-56514
- CaF₂:Dy³⁺, Mossbauer obs. 8-64303
- CaSO₄:Dy thermoluminescent props. of non-commercial phosphors 8-58550
- Dy I excited states, lifetime meas. using single photon counting method 8-70793
- Dy II spark spectrum, isotope shift, config. mixing 8-58628
- Dy³⁺, free-radical relax. agent in biological tissues 8-81090
- LaBe₁₃:Dy, ESR, crystalline field single ion effects 8-84481
- LuBe₁₃:Dy, ESR, crystalline field single ion effects 8-84481
- SnO₂:Dy³⁺, luminesc. and charge compensation 8-76532
- ThBe₁₃:Dy, ESR, crystalline field single ion effects 8-84481
- ZnO:Dy, phosphor, electrolum. and photolum. spectra 8-80421

dysprosium alloys

- dilute, ESR linewidth of rare-earth ions 8-68373
- Dy₁₂Fe₂O₂, anomalous magnetisation, compensated to uncompensated mag. arrangement transition 8-52254
- Dy-Au, dil., Mossbauer exam. of mag. hyperfine field at ^{197}Au impurity 8-88244
- Dy-Cu amorphous mag. alloy, linear sp. ht. due to single-ion excitation 8-91874
- Dy-Fe, amorphous, random anisotropy effects 8-68223
- DyAl₂, conduction electron spin and orbital polarisation effects 8-80228
- DyAu_{3.6}, ordering temps. and effective moments 8-60283
- DyCo₂, field induced vol. magnetostriction 8-91920
- Dy₂Co₃, cryst. field effect on mag. moment direction, neutron diffr. meas. 8-80132
- Dy₂Cu_{1-x}, amorphous film, magnetisation meas., local anisotropy effects 8-68309
- DyFe₂, amorphous, struct. determ. EXAFS exam. 8-51421
- DyFe₂, crit. phenomena, Mossbauer effect 8-52403
- DyFe₂, high field magnetostriction and magnetisation 8-84471
- DyFe₂, magnetisation and magnetic anisotropy 8-91862
- Dy_{1-x}Fe_x, amorphous film, cosputtered, struct. and mag. props. 8-60323
- DyFe₄Al₈, mag. props. 8-52250
- Dy(Fe,Ni_{1-x})₂, mag. behaviour, susceptibility and Mossbauer expts., 4.2-1300K 8-52235
- DyGa₂, mag susceptibility, 1.5-300K and Neel temp. 8-68184
- DySb, quadrupole scatt. anisotropy, magnetically ordered material 8-64034
- Dy_{0.7}Tb_{0.3}Fe₂, magnetostrictive material, liq. phase sintering 8-64493
- Dy_xTb_{1-x}Fe₂ and Ho_xTb_{1-x}Dy_{1-x-y}Fe₂, high magnetostriction cpd., mag. anisotropy origins 8-68217
- Fe-Dy, dil., implanted impurity hyperfine interaction 8-68417
- Gd-Dy, galvanomag. effect, longit., in single crystals (*Russian*) 8-56132
- Ni-Dy, dil., implanted impurity hyperfine interaction 8-68417
- Sc-Dy, dil., high field magnetisation 8-56292
- Sm₂Dy_{1-x}Co₃, temp. compensated magnetic material, mag. and struct. characterisation 8-68177
- Tb_{0.27}Dy_{0.73}Fe₂, domain configurations, obs. by Kerr effect and synchrotron radiation topographs 8-64215
- Tb_{0.27}Dy_{0.73}Fe₂, LF magnetoelastic effects 8-68348
- Tb_{0.3}Dy_{0.73}Fe₂, magnetisation and magnetic anisotropy 8-91862

dysprosium alloys continued

- Tb_{0.27}Dy_{0.73}Fe₂, perpendicular suscept., magnetomechanical coupling and shear modulus 8-91918
 Tb_{0.3}Dy_{0.7}Fe₂, elastic vs. magnetoelastic anisotropy 8-68347
 Tb_{0.3}Dy_{1-x}Fe₂, Laves phase alloy, magnetostriction depend. on powder orientation before sintering 8-76284
 Y_{0.98}Dy_{0.02}, spin glass, calorimetric exam. 8-68270

dysprosium compounds

see also *dysprosium alloys*

- Dy complex, acetoacetic ether, luminesc. spectral band intensities, solvent effects (*Russian*) 8-84653
 DyAG, adiabatic magnetisation, optical obs. 8-88283
 DyAG, crit., tricit., and crossover phenomena, light scatt. 8-68251
 DyAG, forced magnetostriction meas. 8-68349
 DyAG, single cryst. growth by Czochralski method 8-95690
 Dy₃Al₂O₁₂, Czochralski growth, interface shape transitions 8-59772
 DyAsO₄, cooperative Jahn-Teller phase transitions, dielec. anomalies 8-64312
 DyB₃, mag. behaviour, in strong mag. field (*Russian*) 8-88119
 DyBi, thermal expansion, thermal cond., 300-900K 8-91453
 DyF₃, crystal growth by Bridgman-Stockbarger method and Czochralski method 8-52660
 DyF₃, transferred hyperfine interaction, NMR study 8-68393
 DyFeO₃, spin reorientation near Morin temp., magneto-optical exam. 8-68284
 DyH₂, mag. and electronic props., ¹⁶¹Dy Mossbauer spectroscopy 8-80262
 DyIG, mol. field coeffs., magnetisation and mag. susceptibility anal. 8-95406
 DyMo₆S₈, supercond. and antiferromag. coexistence, neutron study 8-95401
 Dy₂O₃, 300 to 900K, mag. susceptibility and Curie temp. meas. 8-56288
 c-Dy₂O₃, transmitted intensity depend. on thickness, incident beam parallel to crystallographic axis 8-63644
 DyPO₄, susceptibility near mag. phase boundaries 8-52258
 DyPO₄-Pb₂P₂O₇, solubility curves for high temp.-melts for growth of single crystals. 8-95687
 Dy(ReO₄)₃·4H₂O, (ReO₄)⁻ ion vibrs. rel. to static field, Raman investig. (*Russian*) 8-76470
 DySe, formation and crystallographic charact. of thin film phase 8-91574
 DyVO₄, basal plane magnetisation anisotropy under Jahn-Teller distortion 8-68222
 DyVO₄, cooperative Jahn-Teller phase transitions, dielec. anomalies 8-64312
 DyVO₄, Jahn-Teller distortion, mag. field depend. 8-79733
 DyVO₄, Jahn-Teller phase transition and improper antiferroelectricity (*Japanese*) 8-80294
 KDy(WO₄)₂, low temp. phase transitions (*Russian*) 8-87787
 RbDy(MoO₄)₂, low temp. phase transitions (*Russian*) 8-87787

E-layer see *E-region***E-region**

see also *sporadic-E layer*

- auroral E-region, Pc 5 micropulsation reson. region examination by dual auroral radar system 8-65454
 cosmic noise absorption, F-lacuna and slant-E condition rel. to E-region Farley-Buneman instability 8-73563
 cross polar cap horizontal currents, rel. to mag. disturbances and elec. fields 8-77405
 disturbances induced by F-region ion cloud releases 8-61657
 E-layer crit. freq., geomagnetic east component, and sunspot number relationships 8-65461
 electrodynamical state, horizontal mag. field component influence (*Russian*) 8-73556
 electron density and recomb. coeff. profiles calc. rel. to absorpt. and rocket meas. 8-69559
 electron density variations during geomag. disturbances 8-69567
 equatorial electrojet, equivalent circuit anal. of neutral wind effects 8-57392
 general circulation at altitudes >100 km, empirical model 8-61664
 height variations, influence of lunar tides 8-77382
 HF oscillating echoes from polar E-region 8-57390
 layer structures, density response to gravity waves 8-81290
 low-latitude E-region, ionisation by energetic ring current particles 8-77415
 MF pulsed transmissions, method for separating D- and E-region contri- butions, to total absorpt. 8-69593
 radiowave scatt. by anisotropic inhomogeneities oriented along geomag- netic field 8-53771
 radiowave scintillation studies using ATS-6 radio beacons at Delhi 8-69600
 time comparison of JJY signal reception via the E-region 8-65910
 NO density in lower E-region, diurnal and seasonal effects at low lat- ities. 8-88976
 NO global morphology in lower E-region 8-88975

ear

see also *hearing*

- artificial ear for sensitivity/frequency meas. for telephone use 8-63255
 basilar membrane model using digital filter for voice features extrac- tion 8-77069
 behavioural, unit and AP thresholds, relationship in normal and abnor- mal ears 8-92642
 cat eardrum model as thin shell using finite element method 8-65036
 cochlea, 3-dim. model, point-impedance charact. of basilar membrane 8-57009
 cochlea, two dimensional model, method for computing motion 8-65037
 cochlear endolymph Ca content 8-61203
 cochlear excitation, electric circuit model and overpressure meas. in guinea pigs (*French*) 8-85316
 cochlear fluid mechanics, kinetic theory 8-53440
 cochlear inner and outer hair cell selective destruction, freq. discrimina- tion 8-77067
 cochlear mechanics, some obs. 8-92643
 earplugs, real-ear noise attenuation and effectiveness 8-87199
 frequency discrimination capacities in goldfish, phase-locking in saccular nerve fibres 8-88720
 guinea pig, method for gaining access to auditory nerve 8-85455

ear continued

- middle-ear muscle contraction, influence on auditory threshold 8-85319
 minimum audible pressure, revised estimate 8-65040
 oculomotor control system, expt. set-up for clinical investigation, visual, acoustic, vestibular stimulations 8-80990
 semicircular canal primary afferents, impulse weight functions, frog 8-69116
 sound pressure in insert earphone couplers and real ears 8-65152
 vestibular nystagmus, computer anal. of irregularities indicating central vestibular disorders 8-81036
- ear microphones** see *microphones*
- earphones**
 see also *hearing aids*
 group delay distortions in electroacoustical systems 8-69105
 sound pressure in insert earphone couplers and real ears 8-65152

Earth

- see also *Earth composition; Earth rotation; Earth structure; earthquakes; geochemistry; geochronology; geodesy; geomagnetic variations; geomagnetism; terrestrial atmosphere; terrestrial electricity; terrestrial heat*
- attenuation models 8-61367
 best-known figure, three-dimensional geodesic mapping equations for non-rigid Earth models (*German*) 8-73304
 circumterrestrial debris belt, creation by artificial satellites collisions 8-89035
 daily free nutation parameters, determ. technique 8-96126
 density distrib., inverse problems, max. entropy method, extreme models 8-65230
 dynamic processes, extraterrestrial causes, rel. to extinction of life 8-92820
 dynamical evolution of Earth-Moon system from shell growth rings 8-96122
 early regolith formation 8-85698
 external gravitational fields screening by Earth's mass, effects on Earth tides obs. (*Russian*) 8-88787
 free oscillations, perturb. theory, surface waves group vel. formulae 8-61349
 global heat balance, annual var. 8-73300
 gravimetric density formula for Earth of spherical shells 8-61303
 gravitational field, stationary points coordinates 8-53805
 hydraulic fractures mapping technique 8-69543
 interstellar cloud encounter, terrestrial consequences 8-57292
 local vectors connection in actual gravity field of Earth, model field, disturbing pot. 8-61297
 E.Mediterranean and Levant fracture zone, tectonics of continental col- lision 8-69319
 monitoring environment, Earthnet satellite programme 8-88921
 natural freq. spectra, information content of different angular numbers 8-61344
 normal modes of laterally homogeneous Earth, one dims. example 8-88797
 normal modes of rotating Earth model, excitation by earthquake fault 8-73312
 nutation, appl. to latti. var. and national ephemerides calc. 8-88776
 obliquity of ecliptic in geological time (*Chinese*) 8-69270
 optical-mechanical scanners for Earth observation (*Russian*) 8-96321
 orbital elements, periodic vars. influence on insolation (*Russian*) 8-53605
 orbital elements rel. to caloric insolation long-term vars. 8-73502
 origin and history to earliest geological times, rel. to origin of life 8-69923
 polar g-values 8-81727
 shell of uniform layers, asymptotic distrib. of torsional eigenfreqs. 8-92797
 shoreline information in artificial satellites autonomous navigation prob- lems 8-53732
 solotone effect and torsional eigenfreqs. of spherical shell 8-92798
 statistical model from gravity anomalies and HB₁ model 8-61306
 thermal history, rel. to time-varying gravitation in Newtonian theory 8-93592
 tidal deformations and pot. vars., relation between Love numbers and load factors 8-61305
 tides in new USSR Universal Time system, 1955-74 period (*Russian*) 8-69279
 torsional eigenfreqs. of spherical shell, asymptotic distrib. 8-88800

earth (electric) see *earthing***earth (soil)** see *soil***Earth age** see *geochronology***Earth atmosphere** see *terrestrial atmosphere***Earth composition**

see also *Earth structure*

- Alpine tectonite lherzolites, Sr isotope comp., evidence for mantle ori- gin 8-65302
 anorthosite gneisses, trace element comp. rel. to petrogenesis 8-65224
 Archaean plutonic rocks, Pb isotope comp. 8-65223
 Archaean volcanic rocks S content rel. to ocean floor basalts 8-88824
 basalts, deep sea, statistical anal. of clinopyroxenes 8-88828
 basalts, oceanic, noble gas abundance patterns controlling factors 8-65220
 basalts from E.Pacific Rise-Galapagos Rise system, major element comp. rel. to mag. anomalies 8-73331
 chevkinite from Oslo region, Norway, cryst. struct. and chemical comp. 8-85533
 Clearwater Lake impact structures, Quebec, meteoritic component and impact melt comp. 8-65314
 continental crust, evolution age and isotope evidence 8-65233
 continental crust, heat-producing radioactive elements distrib. and redis- trib. 8-65232
 continental tectosphere comp. and development 8-81133
 isotopic equilibrium, regional and local, in mantle, from volcanic rocks comp. 8-65216
 Japan, granitic rocks rel. to country rocks 8-81119
 kimberlite nodules, upper mantle petrology and geotherms 8-65310
 large impact craters, meteoritic material detect. and chemistry 8-57208
 Loc Uisg granophyre, Isle of Mull, isotopic and chem. evidence for ori- gin 8-65303
 Manicouagan impact melt, Quebec, chemical interrelationships with basement rel. to form. processes 8-81165

Earth composition continued

- Manicouagan impact melt, Quebec, stratigraphy, petrology and chemistry 8-81164
 mantle, mixed oxide and perovskite structure model 8-85507
 mantle, noble gases, abundances and isotopic compositions 8-85521
 mantle composition from Pacific Ocean Basin basalts Sr isotope comp. 8-65218
 mantle composition rel. to ocean ridge basalts trace elements 8-65219
 mantle melting, past and present, isotope and trace element evidence 8-65238
 metals, pressure depend. of melting 8-85517
 methane, outgassing from Earth interior 8-92809
 minerals, magnetic trends on alkali-Fe-Mg diagrams 8-85551
 ocean floor basalts and ferromanganese deposits, Pb, Nd and Sr isotope comp. 8-61395
 oceanic basalts, differential Sm/Nd evolution 8-61391
 orthopyroxene, occurrence and origin in some lavas from the French Massif central 8-96203
 perrierite from Oslo region, Norway, cryst. struct. and chemical comp. 8-85533
 pigeonite, occurrence and origin in some lavas from the French Massif central 8-96203
 planetary-type rare gases in an upper mantle derived amphibole 8-96167
 plutonic granitic rocks, O and H isotope comps. 8-65221
 polycyclic aromatic hydrocarbons in recent sediments, global distrib. 8-57192
 sphalerite, FeS content as geobarometer, experimental extension to 10 kbar 8-85703
 tholeiitic basalts, rare earth elements behaviour during submarine weathering 8-73369
 tholeiitic basalts from Japan, geochemical types 8-96206
 volcanic rocks, Tetagouche Group, Canada, geochem. rel. to origin 8-65298
 volcanic rocks from Aleutian Islands and Pribilof Islands, Alaska, Pb and Sr isotopes 8-57185
 MgSiO₃, perovskite, synthesis and cryst. chem. charact., rel. to mantle mineralogy 8-65266
 Sr evolution in W.Greenland-Labrador craton, early Rb depletion in mantle 8-69304
 Sr, Pb, isotope geochemistry rel. to catastrophic or continuous core form. 8-57178
 Xe, fissionogenic isotopes in CO₂ well gas 8-73374

Earth core

- catastrophic or continuous formation, Sr and Pb isotope geochemistry constraints 8-57178
 convective dynamo, models 8-89090
 core-mantle boundary irregularities, effect on fluid speed and geomag. field 8-73333
 early Earth, core form. rel. to Moon fission origin timing 8-85867
 equation of state fit to outer core 8-85522
 geomagnetic dynamo theory, MHD, book contrib. 8-61331
 gravitationally powered dynamo 8-77199
 inner core rel. to nutation in obliquity and longitude 8-85510
 models, core form. effects 8-61368
 outer core structure from SKS amplitudes and travel times 8-65208
 seismic wave scattering by rough core-mantle boundary 8-61345
 structure vars. due to evolution 8-85512
 Fe, thermodynamical Gruneisen function 8-61361

Earth crust

- see also geology; oceanic crust*
 active faults, aerial photographs interpretation (*Japanese*) 8-96124
 active margins 8-57191
 Aegean region, crust and upper mantle struct. from deep seismic sounding 8-69308
 Aegean region, geodynamics 8-69307
 Aegean Sea and surrounding regions, active tectonics 8-96181
 Alabama Piedmont, structural development 8-65290
 Alpine metamorphism, thermal budget 8-61373
 Alps, foreland folding model 8-81141
 N.American Cordillera near Fortieth Parallel, tectonics and chronology 8-81138
 andesitic volcanism and crustal evolution 8-85524
 Antarctica, palaeomag. results and test for oroclinal bending 8-73311
 Archaean lithospheric/crustal thickness from volcano spacings 8-65225
 Archaean continental crust, magma genesis by crustal anatexis, garnet-pyroxene thermometry and barometry 8-65236
 ascending andesitic magma, cooling model 8-65239
 Asia, evidence for large Cainozoic crustal shortening from palaeomag. data 8-57189
 Atlantic equatorial fracture zone trends, plate kinematic implications 8-85527
 Mid-Atlantic Ridge, geophysical and petrological constraints 8-85508
 Aulneau batholith, Ontario, subcritical seismic crustal refl. survey 8-65213
 Australia, isostasy and evolution of compensation mechanism 8-65252
 Australia continental slope and shelf, sedimentary basins evolution from Mesozoic times 8-96175
 average dislocation temporal and spatial vars. before and after large earthquakes (*Chinese*) 8-61334
 Balcones Fault Zone Texas, fracture patterns, field study 8-73337
 Baltic shield and Barents Sea, crust and upper mantle struct., Rayleigh waves dispersion 8-77204
 Banda Sea (E.Indonesia), subducted lithosphere geometry from seismicity and fault plane solns. 8-81131
 basic intrusions emplacement mechanism 8-61374
 Benue Trough, Nigeria, early Cretaceous basalt volcanism and initial continental rifting 8-61417
 Black Sea crust, nature of mag. anomalies (*Russian*) 8-85473
 Botswana, dyke swarm interpretation as failed Gondwana spreading axis 8-57180
 Brevard ductile deformation zone, N.Carolina, struct. and seismic refl. study 8-65289
 Briones Hills, California, geodolite meas. near earthquake 8-92803
 Briones Hills, California, tilt obs. near earthquake 8-92802
 N.Britain, crustal struct. from Lithospheric Seismic Profile in Britain (LISPB) 8-73329
 Canadian Shield, structure of Archaean basin-craton complexes 8-61412
 E.Carthians, complex model of lithosphere (*Russian*) 8-85511
 Earth crust continued
 Central Alps, structural zones and continental collision 8-81124
 Cerro Galan Caldera, NW.Argentina, tectonic setting 8-85523
 chemical evolution from Early Archaean rocks comp. 8-65222
 Clearwater Lake impact structures, Quebec, meteoritic component and impact melt comp. 8-65314
 Colorado plateau, crustal struct. from seismic waves high-resolution group vel. anal. 8-81111
 continental basement exploration by seismic reflection profiling 8-96172
 continental blocks rotational motions, evidence from terrestrial objects astronomical azimuths 8-53613
 continental crust, evolution age and isotope evidence 8-65233
 continental crust, heat-producing radioactive elements distrib. and redistribution. 8-65232
 continental drift mechanisms, review 8-92813
 continental lithosphere, vertical temp. distrib. limits 8-65207
 continental lithosphere thermal evolution 8-65234
 continental lithosphere thickening model 8-77200
 continental margin, possible mode conversion between Rayleigh and Love waves 8-73314
 continental shelf and slope deep terraces off N Labrador 8-65255
 continental tectosphere comp. and development 8-81133
 convective hydrothermal geothermal reservoirs, balance laws and constitutive relations 8-61379
 Coosa Valley, Alabama, struct., folding and thrust faulting 8-65291
 crystalline foundation, anomalous high conductivity bands discovery (*Russian*) 8-96137
 Denali fault system, Alaska and Canada, displacement history 8-88805
 Denali fault system, geological history rel. to S.Alaska tectonic development 8-81137
 descending lithosphere thermal regime, effect of varying angle and rate of subduction 8-77206
 Devonian alkalic basalt dykes, NE.Newfoundland, tensional environment 8-88826
 Devonian Millboro Shale, Appalachian Plateau, slip planes, discfold anal. 8-65293
 dilatancy-magnetic effect, local mag. vars. assoc. with earthquakes (*Chinese*) 8-61333
 dislocation modelling of creep-related tilt changes 8-92801
 Dnieper-Donets depression, deep struct. from magnetotelluric sounding data (*Russian*) 8-96170
 Dnieper-Donets depression, sedimentary cover struct. along Jagotin-Baturin profile (*Russian*) 8-92806
 doming and rifting mechanism, Upper Rhinegraben rift development appl. 8-61387
 Donets Basin, crustal evolution (*Russian*) 8-69302
 dynamic rupture on three-dimens. fault with non-uniform frictions 8-77186
 earthquake cycle, asthenosphere readjustment effects on free surface deform. 8-85490
 earthquakes, centrifuge modelling 8-81429
 W.Europe and E.Canadian continental shelves, basement fractures, transAtlantic correls. 8-73327
 evolution in silicate planets, review 8-61774
 Fairweather fault Late Quaternary offsets and crustal plate interactions in S.Alaska 8-88804
 Farallon plate fragmentation by pivoting subduction 8-77208
 faulting analysis in three dimens., strain field 8-77225
 Franciscan melanges, comparison with olistostromes of Taiwan and Italy 8-81159
 Frankische Alb, slope forms in Al(1) clay, statistical investigation (*German*) 8-57211
 free surface, effects on seismic moments and corner freqs. determ. 8-85492
 free surface effect on calculated stress drops 8-65193
 geological faults, fracture, creep and strain 8-69345
 geological-geophysical zoning possibility 8-57342
 geosyncline processes, energy aspects (*Russian*) 8-96182
 geothermics, Southwestern Germany and Switzerland (*German*) 8-53633
 global plate tectonics, rel. to pole secular motion 8-65172
 Gondwana, tectonics from Alcaparrosa Formation (Argentina) palaeomagnetism and K-Ar age 8-96135
 Gran Canaria/Tenerife mag. discordance rel. to NW.African continental margin form. 8-85478
 granite magmatism initiation and thermal diversity 8-65240
 gravity secular variations, due to water quantity vars. in lithosphere (*Russian*) 8-53609
 Great Basin of Nevada and W.Utah, struct. from seismic surface waves 8-73336
 E.Greenland, Jurassic basin evolution 8-73344
 E.Greenland dyke swarm offshore continuation, rel. to N.Atlantic Ocean formation 8-73352
 greenstone belts, ancient marginal basins or ensialic rift zones 8-61418
 Hinterland Belt, Canadian Cordillera, deformation episodes 8-88825
 Iceland, geothermal activity rel. to geological struct. 8-61376
 Iceland, lateral magma flow within rifted crust 8-73339
 Iceland-Faeroe Ridge, subsidence history rel. to Lower Tertiary laterite and Thulean land bridge 8-85514
 inter-arc basins, kinematic model 8-81127
 intraplate volcanism, geological and geophysical parameters 8-65243
 intraplate volcanism, magma flow through lithospheric fractures, tensional tectonics 8-65242
 Iran plateau, crustal struct. from seismic waves high-resolution group vel. anal. 8-81111
 isostasy of plain regions (*Russian*) 8-85525
 Italy, fault-plane solns. and stress regime 8-69299
 Izu Peninsula, Japan, active faults in Amagisan area (*Japanese*) 8-96164
 Izu Peninsula, Japan, crustal uplift, Mogi model, related gravity change (*Japanese*) 8-96165
 Izu Peninsula, Japan, earthquake swarm epicentres distrib. rel. to Bouguer anomaly (*Japanese*) 8-96144
 Izu Peninsula, Japan, geodimeter surveys, horizontal strain meas. (*Japanese*) 8-96163
 Izu Peninsula, Japan, gravity change assoc. with earthquake swarm (*Japanese*) 8-96123

Earth crust continued

- Izu Peninsula, Japan, resistivity meas. in crustal uplift area (*Japanese*) 8-96127
- Izu-Tokai District, Japan, tectonic activity rel. to earthquake prediction (*Japanese*) 8-96145
- NE Japan Arc, deep seismic zone double-planed struct. 8-77203
- Japan geosyncline outer margin, structural characts. and tectonisms around microcontinent 8-81139
- Japan islands and Sea of Japan, seismic structure 8-92807
- Kupjansk-Novozovskoe profile quasiperiodic gravity anomalies and structural confinement (*Russian*) 8-85465
- Kuril Trench, lithosphere elastic-perfectly plastic bending under generalised loading 8-73341
- Labrador Trough, Canada, early recumbent folds in northeastern part 8-65300
- Lachlan Fold Belt in New South Wales, description, tectonic history 8-96211
- Lageos for crustal movement meas. 8-65441
- Lake Eyre North, S.Australia, bottom profile and tectonic grooves 8-69376
- Ligurian Sea area, crustal and upper mantle structure 8-65209
- lithosphere, heterogeneities rel. to P-wave time and amplitude anomalies interpretation 8-96153
- lithosphere bending at trench, elastic-perfectly plastic anal. 8-81135
- Lithospheric Seismic Profile in Britain (LISPB), crustal shear waves studies 8-73313
- lithospheric strain model using generalised Norton-Hoff law (*French*) 8-88809
- loading effects of quarter-diurnal oceanic tides by Ligurian Sea 8-61308
- magnetic anomalies caused by two-dimens. vertical faults, direct interpretation method 8-77181
- magnetic model under Ukrainian Shield 8-61313
- Manicouagan impact crater, gravity study and upper crust density contrasts 8-81170
- Manicouagan impact crater, Quebec, investigation 8-81163
- Manicouagan impact melt, Quebec, chemical interrelationships with basement rel. to form. processes 8-81165
- Manicouagan impact melt, Quebec, stratigraphy, petrology and chemistry 8-81164
- Manicouagan impact melt sheet, Quebec, thermal history 8-81167
- Manicouagan impact structure, Quebec, melt rocks petrogenesis 8-81166
- Manicouagan melt sheet, Rb-Sr isochron age 8-81168
- Manicouagan structure, Quebec, central mag. anomaly 8-81169
- E.Mediterranean, crustal struct., sedimentary layers 8-69311
- E.Mediterranean, deep struct. and tectonics 8-69309
- E.Mediterranean, struct. and tectonic setting of Levant continental margin 8-69310
- Mediterranean and marginal seas origin 8-69322
- E.Mediterranean gravity anomalies, volcanic activity rel. to tectonic development 8-69318
- Mediterranean region, Holocene eustatic changes and coastal tectonics, crustal consumption 8-81201
- Mediterranean region, struct. and tectonics, conf., Haifa, Israel (Aug.-Sep. 1976) 8-69306
- metadolerite dykes and assoc. folds, Caledonides of Finnmark, Norway 8-61375
- metamorphic bathozones and bathograds, meas. of regional scale post-metamorphic uplift and erosion 8-81113
- meteorite craters, form., props. and catalogue 8-96411
- Middle America arc, focal mechanism solns. and tectonics 8-77191
- models with single crust-mantle discontinuities, ray-mode duality for SH waves 8-77183
- Mole (Haute-Savoie, France), geological profile of south flank rel. to struct. and tectonics (*French*) 8-69348
- Motagua Fault and Guatemala earthquake (1976, February 4), seismological aspects 8-85493
- motions detect. using spaceborne laser ranging systems 8-92995
- mountain ridges, effect on atmosphere frontal waves development, numerical simulation (*Russian*) 8-53701
- Nain anorthosite (Labrador), palaeomagnetic results and tectonic implications 8-77178
- Nambucca slate belt, plate tectonic significance of structural succession 8-81140
- New Hebrides island arc, fracture zone and aseismic ridge subduction rel. to 1969 January 19 earthquake 8-73342
- E. Newfoundland, aborted Proterozoic rifting 8-57200
- Newfoundland lithosphere structure from teleseismic PP-wave refls. 8-65210
- Nova Scotia, tidal loading response, results from improved ocean tide models 8-92821
- ore-deposition through geological time, review 8-77235
- Otago schist megaculmination, origins and tectonic significance in New Zealand Rangitata Orogen 8-81142
- Pangaea and movement of crustal fragments on shrinking Earth 8-57187
- Papua New Guinea, delayed partial melting of subduction-modified mantle 8-57183
- Pearson Formation (Great Slave Supergroup, NWT), palaeomagnetism and Coronation loop 8-77179
- Peking-Tientsin area, China, crustal struct. from gravity data, rel. to seismicity (*Chinese*) 8-61357
- permeable formation with crack, nucl.-explosion induced, gas flow 8-61372
- Phanerozoic sedimentary basins, Australia, tectonic implications 8-96174
- phase boundary under surface loads, dynamics 8-85509
- plate motions, rel. to asthenosphere flow model 8-96180
- plate tectonics, roles of boundary friction, basal shear stress and deep mantle convection 8-57188
- plate tectonics in Phanerozoic 8-92812
- plates ridge and trench boundaries, appl. to individual plate absolute motion determ. 8-85529
- point pulse source in elastic anisotropic half-space, propag. of vibrs. 8-57174
- Precambrian dykes, preferred orientation of intrusion 8-88829
- Precambrian thermal regimes 8-65235
- pressure-temperature conditions modelling, appl. of rocks elastic props. experimental studies (*Russian*) 8-96207

Earth crust continued

- proterozoic intraplate deformation, comparison with SE Asian neotectonics 8-65250
- quartzites, microscopic deform. and flow laws, South Mountain Anticline 8-77220
- rift structure in S.Ethiopia 8-61377
- rifting and volcanism relative timing and tectonic implications 8-81129
- rock bodies, cooling, residual stress development 8-88819
- San Andreas Fault, vel. contrast, P-wave nodal plane distortion 8-65188
- Scandinavian Caledonides, nappe displacement 8-81143
- seismic wave reflection at wide angles, travel times 8-65202
- sequential deformation in central Appalachians 8-65294
- shear deformation zones, along major transform faults and subducting slabs 8-73330
- soils electrical properties, investigation of seasonal variations, in 10-1000 kHz band 8-88796
- South America, origin of compressional intraplate stresses 8-61385
- South Fork Mountain Schist (N Coast Ranges, California), early Cretaceous metamorphic age 8-81114
- southern continents palaeopositions, revised reconstruction 8-92805
- statistical model from gravity anomalies and HB₁ model 8-61306
- stress field, in situ determ. via hydrofracturing, fracture mechanics approach 8-81435
- stress field of Tangshan area before and after 1976 July 28 earthquake (*Chinese*) 8-61358
- structure from seismic surface wave obs. 8-73323
- structure rel. to quasi-periodic gravity vars. (*Russian*) 8-69275
- surface tidal tilts, influence of atmospheric press. fluctuations (*Russian*) 8-88790
- Tashkent Palaeozoic crystalline basement, tectonic struct., gravity survey (*Russian*) 8-53610
- Tasman Fold Belt System in New South Wales, description 8-96210
- Tasman Fold Belt System in Tasmania, description 8-96209
- Tasman Fold Belt System in Victoria, evolution, tectonics, deform. 8-96212
- Tasman Orogenic Zone, description of eastern part 8-96214
- Tasman Orogenic Zone, Thomson Orogen, tectonically active area 8-96213
- temperature distrib. and electrically conducting zone formation 8-85519
- E.Tennessee, palinspastic map 8-65295
- Tennessee Valley and Ridge, folding 8-65292
- tidal tilts, parallel recording through digital print-out and photorecording channels (*Russian*) 8-88785
- tilt meter observations at Berezhovaya Rudka station, results (*Russian*) 8-88783
- tilt meter observations harmonic anal., influence of S₁ diurnal meteorological wave (*Russian*) 8-88788
- topography effects on ionospheric electron density inhomogeneities, airborne soundings 8-69579
- Trivandrum, crust-mantle structure from Indian geomagnetic data 8-85520
- W.Turkmenistan, density model of crustal structure (*Russian*) 8-69303
- Umfraville gabbro, Ontario, palaeomagnetism rel. to Grenvillian plate tectonics 8-92777
- vertical movements, rel. to surface relief in Bulgaria, statistical investig. 8-81126
- vertical orogenetic profile, relation between terrestrial heat flux and rocks mechanical characts. (*German*) 8-81123

Earth electricity *see terrestrial electricity***Earth heat** *see terrestrial heat***Earth interior**

- see also Earth core; Earth crust; Earth mantle; tectonics; volcanology*
- attenuation models 8-61367
- daily rotation variations, correl. with secular geomag. field vars. 8-73302
- density distribution, determ. from gravity logging data (*Russian*) 8-92999
- dynamic shear modulus corrections for Love numbers 8-85513
- elastic prestress in Earth interior, effects 8-77202
- ferroelectric phases, high press. studies 8-69334
- global problems of fluid dynamics 8-96173
- magnetothermoelastic plane Lamb's problem in initially stressed conducting medium 8-67077
- melting of metals, pressure depend. 8-85517
- methane, outgassing rel. to geological phenomena and pot. fuel supplies 8-92809
- Mie-Gruneisen eqn. of state, generalisation 8-96194
- models, core form. effects 8-61368
- seismic wave reflectivity, information extraction via minimum entropy deconvolution 8-81423
- structure vars. due to evolution 8-85512

Earth lower mantle *see Earth mantle***Earth magnetic field** *see geomagnetism***Earth magnetic field variations** *see geomagnetic variations***Earth mantle**

- Aegean region, crust and upper mantle struct. from deep seismic sounding 8-69308
- Aegean region, geodynamics 8-69307
- Alpine tectonite lherzolites, Sr isotope comp., evidence for mantle origin 8-65302
- anomalous regions from S times for deep-focus Indian earthquakes 8-77188
- Apennines, Rayleigh wave phase vels. rel. to upper mantle struct. 8-53618
- ascending andesitic magma, cooling model 8-65239
- asthenosphere, electrical conductivity data and partial melt content 8-85518
- asthenosphere, flow rel. to plate motions 8-96180
- asthenosphere, stresses and effective viscosities 8-65229
- asthenosphere readjustment during earthquake cycle, effects on free surface deform. 8-85490
- attenuation models 8-61367
- Baltic shield and Barents Sea, crust and upper mantle struct., Rayleigh waves dispersion 8-77204
- Banda Sea (E.Indonesia), subducted lithosphere geometry from seismicity and fault plane solns. 8-81131

Earth mantle continued

Black Sea, mantle material intrusion age rel. to mag. anomalies nature (*Russian*) 8-85473
 N.Britain, upper mantle struct. from Lithospheric Seismic Profile in Britain (LISPB) 8-73329
 chemical evolution from Early Archaean rocks comp. 8-65222
 composition, rel. to ocean ridge basalts trace elements 8-65219
 composition from Pacific Ocean Basin basalts Sr isotope comp. 8-65218
 continental basement exploration by seismic reflection profiling 8-96172
 convection, Benard problem with viscosity depend. on temp. and press. 8-69317
 convection in Canadian Shield, structure of Archean basin-craton complexes 8-61412
 convection pattern and subcrustal stress field under Asia, rel. to seismicity 8-57190
 convection system, spin-symmetric, rel. to Phanerozoic plate tectonics 8-92812
 core-mantle boundary irregularities, effect on fluid speed and geomag. field 8-73333
 creep laws 8-69305
 deep mantle convection and lithosphere basal shear stress, roles in plate tectonics 8-57188
 degassing by volcanism, rel. to oceanic Cl and Br origin 8-65342
 descending lithosphere thermal regime, effect of varying angle and rate of subduction 8-77206
 equation of state fit to lower mantle 8-85522
 evolution model, from oceanic basalts Pb isotope comp. data 8-65217
 ferroelectric-like phase transformation of pyroxene in mantle 8-61362
 Fogo seamounts, anomalous upper mantle struct. indicated by P-wave rel. delays 8-85515
 forsterite, glissile splitting of dislocations, cross-slip-controlled creep and mantle rheology 8-61406
 global tectonics rel. to mantle flow pattern 8-88810
 Gorringer Bank, oceanic mantle and crust, geological survey 8-53632
 Great Basin of Nevada and W Utah, struct. from seismic surface waves 8-73336
 guide channels for seismic energy, transverse waves in upper mantle (*Italian*) 8-61355
 horizontal inhomogeneities influence on tidal oscill. amplitudes 8-57159
 intraplate volcanism, magma flow through lithospheric fractures, tensional tectonics 8-65242
 isotopic equilibrium, regional and local, in mantle, from volcanic rocks comp. 8-65216
 NE Japan Arc, double-planed deep seismic zone and upper mantle structure 8-77198
 kimberlite nodules, upper mantle petrology and geotherms 8-65310
 Ligurian Sea area, crustal and upper mantle structure 8-65209
 lithosphere, heterogeneities rel. to P-wave time and amplitude anomalies interpretation 8-96153
 lithosphere bending at trench, elastic-perfectly plastic anal. 8-81135
 long-period reflected and converted upper mantle phases 8-92786
 low velocity zone, interpretation in terms of thermally activated point defects 8-88806
 lower, implications of fluorite isotype of SnO_2 and new modification of TiO_2 8-61371
 magma generation, evidence from ophiolite suites, oceanic lithosphere generation appl. 8-65311
 Massif Central, upper mantle regional struct. and geodynamics 8-81120
 E.Mediterranean, deep struct. and tectonics 8-69309
 melting, past and present, isotope and trace element evidence 8-65238
 micropolar fluid with stretch, convection, appl. to asthenosphere 8-51202
 Mid-Atlantic Ridge, crust and upper mantle struct. at 45°N 8-73332
 mixed oxide and perovskite structure model 8-85507
 models with single crust-mantle discontinuities, ray-mode duality for SH waves 8-77183
 noble gases, abundances and isotopic compositions 8-85521
 normal mode attenuation, Q mode of mantle 8-61343
 W North America, low-Q and low-vel. zones from surface wave vel. and attenuation inversion 8-85491
 ocean basins upper mantle, isotropic inversion of anisotropic surface-wave dispersion 8-96156
 oceanic upper mantle, seismic anisotropy of ophiolite peridotite 8-53645
 olivine, creep mechanisms 8-69332
 olivine, naturally deformed, recovery process, rel. to Earth upper mantle mech. state 8-96202
 W.Pacific, HF P_n and S_n phases obs. at great distances, spectral anal. 8-77195
 Papua New Guinea, delayed partial melting of subduction-modified mantle 8-57183
 partial melting under oceanic spreading ridges 8-65237
 peridotites, origin of olivine subgrain boundaries 8-85544
 Peru-Chile Trench basalts, fractionation and mantle heterogeneity 8-53626
 phase boundary under surface loads, dynamics 8-85509
 planetary-type rare gases in an upper mantle derived amphibole 8-96167
 point pulse source in elastic anisotropic half-space, propag. of vibrs. 8-57174
 radioactivity, rel. to geosynclinal processes energy sources (*Russian*) 8-96182
 rheology of upper mantle, micromechanisms of flow and fracture 8-69331
 rocks physical props. under mantle conditions, conf., Durham, England (Aug. 77) 8-69333
 roll cell convection under Pacific plate, evidence from bathymetry and heat flow 8-73345
 seismic compressional and shear vels. in lower mantle, radial var. 8-73316
 seismic wave reflection at wide angles, travel times 8-65202
 seismic wave scattering by rough core-mantle boundary 8-61345
 seismic waves absorption in partially melted medium 8-85488
 spin-pairing transition favours small mean atomic weight 8-61364
 spinel lherzolite nodules from Pleistocene cinder cone, upper mantle origin 8-65299

Earth mantle continued

spinel-garnet peridotite transitions in upper mantle, evidence from harzburgite xenolith 8-65309
 stishovite (SiO_2), single cryst. anal. of struct. 8-53648
 stress estimates from structural studies in some mantle peridotites 8-69330
 stress measurement, applicability limits of grain size geopiezometer 8-85715
 structure beneath Japan Sea 8-81118
 structure from seismic surface wave obs. 8-73323
 structure of upper mantle beneath Eurasia and N.Atlantic and Arctic Oceans 8-85506
 structure peculiarities rel. to nature of excess quadrupole moment 8-73334
 structure vars. due to evolution 8-85512
 subcrustal earthquake location and mislocation 8-85498
 subducting oceanic crust, thermodynamic consequences of minerals dehydration, high press. and temp. 8-69301
 temperature distrib. and electrically conducting zone formation 8-85519
 thermal convection, two-scale flow model rel. to plate tectonics 8-73348
 Trivandrum, crust-mantle structure from Indian geomagnetic data 8-85520
 two-scale convection, rel. to global gravity anomalies 8-85528
 W.United States, upper mantle P-wave vel. structure 8-61363
 upper, thermomechanical models, plate vel. changes rel. to magnetic activity 8-65231
 upper, travel-time branches from Yellowknife seismic array data 8-65211
 MgSiO_3 , perovskite, synthesis and cryst. chem. charact., rel. to mantle mineralogy 8-65266
 Sr evolution in W.Greenland-Labrador craton, early Rb depletion in mantle 8-69304

Earth rotation

see also time and latitude
 acceleration, nontidal secular vars. correl. with secular geomag. field vars. 8-73302
 angular velocity variations, influence of geosynclines pot. energy changes (*Russian*) 8-96182
 atmosphere, ang. rot. vars. rel. to zonal circulation model, numerical expts. (*Russian*) 8-81295
 axis of figure, precession and nutation 8-65167
 Chandler wobble, optimal complex ARMA model 8-61304
 daily free nutation parameters, determ. technique 8-96126
 day length tidal fluctuations, comparison with self-consistent equilib. ocean tides 8-96218
 early Earth, dynamical and secular stability rel. to Moon fission origin 8-85867
 effect on long baseline radio interferometer, classical response 8-61733
 geodesy, Molodensky's problem in gravity space for rot. Earth 8-65173
 geodetic reference frames, polar motion effects 8-69272
 Greenwich Obs. Time and Latitude Service, Time Report (April-June, 1977) 8-69661
 Greenwich Obs. Time and Latitude Service, Time Report (January-March 1977) 8-57431
 Greenwich Obs. Time and Latitude Service, Time Report (July-September 1977) 8-73619
 Greenwich Obs. Time and Latitude Service, Time Report (October to December, 1977) 8-89046
 latitude variation, computation for national ephemerids calc. 8-88776
 normal modes of rotating Earth model, excitation by earthquake fault 8-73312
 nutation in obliquity and longitude rel. to nature of inner core 8-85510
 plate tectonics, Phanerozoic, control by spin-symmetric mantle convection 8-92812
 polar movements, sea level response 8-53608
 polar wander paths, palaeomagnetic, deficiency of high-latit. poles 8-65181
 pole secular motion, rel. to global plate tectonics 8-65172
 pole-tide signal at low-latitude coastal station 8-61322
 positional astronomy and definition of ephemeris pole 8-93078
 precession determ. from Lick proper motions referred to galaxies 8-65487
 quadrupole moment excess and mantle struct. peculiarities 8-73334
 solar hour angle, formula rel. to latit.-independ. sundial construction 8-81549
 time adjustment on 1978 December 31, positive leap second 8-93079
 Tokyo Astronomical Obs., Time and Latitude Bulletins (July-September 1977) 8-73618
 universal time system (TU2), differences anal. rel. to Earth rotation nonuniformities 8-65174
 VLBI appl. to geodesy, Earth rot. and network geometry optimisation 8-92996

Earth satellites *see artificial satellites; Moon*

Earth structure

see also Earth composition; Earth interior
 active margins 8-57191
 Aegean region, crust and upper mantle struct. from deep seismic sounding 8-69308
 Alabama Piedmont, structural development 8-65290
 Alboran Sea, crustal seismic profiles 8-61370
 ancient Earth elastic parameters, appl. to lunar capture hypothesis 8-81570
 anelasticity model constraints rel. to complex propag. function 8-88802
 Antarctic plate boundary near Bouvet triple junction, tectonic structure 8-53639
 Apennines, Rayleigh wave phase vels. rel. to upper mantle struct. 8-53618
 Archaean lithospheric/crustal thickness from volcano spacings 8-65225
 asthenosphere, stresses and effective viscosities 8-65229
 attenuation models 8-61367
 Aulneau batholith, Ontario, subcritical seismic crustal refl. survey 8-65213
 Balcones Fault Zone Texas, fracture patterns, field study 8-73337

Earth structure continued

- Baltic shield and Barents Sea, crust and upper mantle struct., Rayleigh waves dispersion 8-77204
 Brevard ductile deformation zone, N.Carolina, struct. and seismic refl. study 8-65289
 SE Canadian Cordillera, structural evolution 8-88808
 Canadian Shield, structure of Archean basin-craton complexes 8-61412
 E.Carpathians, complex model of lithosphere (*Russian*) 8-85511
 Central Alps, structural zones and continental collision 8-81124
 continental basement exploration by seismic reflection profiling 8-96172
 Coosa Valley, Alabama, struct., folding and thrust faulting 8-65291
 core catastrophic or continuous formation, Sr and Pb isotope geochemistry constraints 8-57178
 crust, quasi-periodic gravity vars. (*Russian*) 8-69275
 crust and upper mantle structure from seismic surface wave obs. 8-73323
 crustal geological-geophysical zoning possibility 8-57342
 Danakil Depression and Dead Sea Rift, comparative study of sedimentary fills 8-69347
 early Earth, dynamical and secular stability rel. to Moon fission origin 8-85867
 elastodynamic propag. matrices, stratified Earth models 8-77197
 Great Basin of Nevada and W Utah, struct. from seismic surface waves 8-73336
 impulse response, seismic wavelet estimation via short-time homomorphic signal anal. 8-81426
 inclined media interface, effects on ground surface displacements due to longit. incident wave (*Russian*) 8-85485
 internal structure vars. due to evolution 8-85512
 island arcs, curvature rel. to convergence vel. and subduction angle 8-81128
 NE Japan Arc, deep seismic zone double-planed struct. 8-77203
 NE Japan Arc, double-planed deep seismic zone and upper mantle structure 8-77198
 Japan geosyncline outer margin, structural characts. and tectonisms around microcontinent 8-81139
 Japan islands and Sea of Japan, seismic structure 8-92807
 lateral variations from free oscills. and surface waves 8-88799
 Ligurian Sea area, crustal and upper mantle structure 8-65209
 lithosphere, heterogeneities rel. to P-wave time and amplitude anomalies interpretation 8-96153
 Manicouagan impact crater, gravity study and upper crust density contrasts 8-81170
 mantle, lower, compressional and shear vels. radial var. 8-73316
 mantle structure beneath Japan Sea 8-81118
 mantle structure peculiarities rel. to nature of excess quadrupole moment 8-73334
 media with inclined boundaries, seismic screening (*Russian*) 8-92794
 E.Mediterranean, crustal struct., sedimentary layers 8-69311
 E.Mediterranean, deep struct. and tectonics 8-69309
 E.Mediterranean, struct. and tectonic setting of Levant continental margin 8-69310
 Mediterranean region, struct. and tectonics, conf., Haifa, Israel (Aug.-Sep. 1976) 8-69306
 Mid-Atlantic Ridge, struct. at 45°N 8-73332
 models with single crust-mantle discontinuities, ray-mode duality for SH waves 8-77183
 Newfoundland lithosphere structure from teleseismic PP-wave refls. 8-65210
 north magnetic pole, 1975 position analytical determ. 8-92778
 outer core structure from SKS amplitudes and travel times 8-65208
 Peking-Tientsin area, China, crustal struct. from gravity data, rel. to seismicity (*Chinese*) 8-61357
 sedimentary layers, energy resource exploration via refl. seismology, book 8-96162
 seismic reflecting-refracting surface, binary holography kinematic principle (*Russian*) 8-92795
 shear deformation zones along major transform faults and subducting slabs thermal-mechanical struct. 8-73330
 shear wave phase velocity and Q^{-1} , determ. from surface wave vel. and attenuation inversion 8-85491
 strain tides, spectroscopy rel. to struct. and reson. behaviour 8-73301
 surface-wave phase vel. inversion for anisotropic structure 8-85482
 Tashkent Palaeozoic crystalline basement, tectonic struct., gravity survey (*Russian*) 8-53610
 Trivandrum, crust-mantle structure from Indian geomagnetic data 8-85520
 W.Turkmenistan, density model of crustal structure (*Russian*) 8-69303
 upper mantle, travel-time branches from Yellowknife seismic array data 8-65211
 upper mantle beneath Eurasia and N.Atlantic and Arctic Oceans 8-85506
 upper mantle of W.United States, P-wave vel. structure 8-61363

Earth third layer see *Earth mantle***Earth upper layer** see *Earth mantle***earthring**

- birth monitoring by cardiocography, interference effect by infusion pumps (*German*) 8-85416
 ECG, grounded, resistance to coherent mains interference, exptl. evaluation 8-85419
 ECG, grounded, standardisation of resist. to external cophasal power line interference for isolated patients 8-57085
 Shiva laser, 25 MJ energy storage and delivery system 8-59038
 PbSnTe-PbTe heterostructs., effect of electrical grounding on electron irradi. 8-60194

earthquake recorders see *seismometers***earthquakes**

- see also *seismology*
 Aegean Sea and surrounding regions, earthquakes rel. to active tectonics 8-96181
 aftershock sequences, sidereal periods, χ^2 test 8-53622
 Alaska, 1964 March 28, aquifer response to tidal forcing 8-73407
 anomalous aftershock sequences, physical model 8-77194
 antiseismic calc., stochastic model appl. 8-96139
 average dislocation temporal and spatial vars. before and after large earthquakes (*Chinese*) 8-61334

earthquakes continued

- Banda Sea (E.Indonesia), seismicity and fault plane solns. rel. to subducted lithosphere geometry 8-81131
 Brawley, California, 1976 November 4, strong ground motion modelling 8-92782
 Briones Hills, California, 1977 January 8, locations and magnitudes of earthquake swarm 8-65187
 Briones Hills, California, geodolite meas. near earthquake 8-92803
 Briones Hills, California, tilt obs. near earthquake 8-92802
 Canada, 1971 catalogue 8-85500
 centrifuge modelling, experimental results 8-81429
 China, isoseisms for large magnitude earthquakes 8-92788
 Chu basin, weak earthquakes focal parameters spatial distrib. rel. to strong earthquakes 8-61348
 Collin, GDR, microearthquake records, event criteria (*German*) 8-57170
 Dagestan, 1970 May 14, precision in hypocentre and dimens. determ. 8-57172
 deep-focus earthquakes, GH branch confirmed from PKP obs. 8-61341
 dilatancy-magnetic effect, local mag. vars. assoc. with earthquakes (*Chinese*) 8-61333
 displacement field close to focus of earthquake, calc. (*Russian*) 8-65204
 dynamic rupture on three-dimens. fault with non-uniform frictions 8-77186
 earthquake wave analysis program WAVE, DEMOS-E library program 8-92800
 elastic half space response to realistic faulting model 8-85486
 elastic prestress in Earth interior, effects 8-77202
 elastodynamic radiation from slip zone, ray method 8-73322
 energy and prediction rel. to quasi-periodic gravity vars. (*Russian*) 8-69275
 energy coupling between tectonic processes and earthquakes 8-73321
 faulting, simulation, expt. thermal fragmentation 8-96160
 focal mechanism effect on P-waves dynamic parameters and magnitudes from longit. waves 8-73318
 foci motion, typification technique, seismotectonic problems soln. 8-61350
 foreshocks spectral features 8-96147
 fracture at weak shock sources before and after strong earthquake 8-85487
 Friuli, 1976 May 6, German macroseismic intensity map 8-65203
 geodesy contributions to geodynamics (*German*) 8-81101
 geological faults, fracture, creep and strain 8-69345
 Gorda Ridge spreading centre, microearthquakes and active faulting, sonobuoy array meas. 8-85494
 gravity effects on earthquake sources exhibiting anelastic vol. changes 8-57176
 Guatemala (1976, February 4), seismological aspects 8-85493
 Haicheng, 1975 February 2, associated gravity field vars. (*Chinese*) 8-61332
 hydrodynamic press. on sloping dams during earthquake, momentum method 8-73412
 hydrodynamic press. on sloping dams during earthquake exact theory 8-73413
 hypocentre and dimensions determ., precision 8-57172
 hypocentre location, resolution of small ocean bottom seismic networks 8-85713
 Iceland, weak earthquakes in northern part of rift zone 8-85496
 Indian deep-focus earthquakes, S times 8-77188
 S.Iran (1976, March 16), seismic waves group vel. anal. rel. to crustal struct. 8-81111
 Italy, isoseismic area and earthquake magnitude relations 8-65196
 Izu Peninsula, Japan, active faults in Amagisan area (*Japanese*) 8-96164
 Izu Peninsula, Japan, crustal uplift, Mogi model, related gravity change (*Japanese*) 8-96165
 Izu Peninsula, Japan, earthquake swarm epicentres distrib. rel. to Bouguer anomaly (*Japanese*) 8-96144
 Izu Peninsula, Japan, field work on recent crustal activity, rel. to earthquake prediction (*Japanese*) 8-96140
 Izu Peninsula, Japan, gravity change assoc. with earthquake swarm (*Japanese*) 8-96123
 Izu Peninsula, Japan, groundwater geochem. in crustal uplift area, rel. to earthquake prediction (*Japanese*) 8-96242
 Izu Peninsula, Japan, obs. of earthquake swarm, 1975-77 period (*Japanese*) 8-96141
 Izu-Tokai District, Japan, tectonic activity rel. to earthquake prediction (*Japanese*) 8-96145
 Japah, earthquake records in 'Diary of Librarians of Edo Bakufu (Feudal Government)' 8-65200
 NE Japan Arc, deep seismic zone double-planed struct. 8-77203
 Japan Sea, historical tsunamis behaviour and source areas 8-65198
 Jordan Rift Valley, macroseismic study and structural damage of major earthquakes 8-65190
 Kalapana earthquake, Hawaii, localised compressional vel. decrease 8-65206
 Kanto district, definition and characts. of seismically active regions (*Japanese*) 8-96148
 Kawazu, Japan, 1976 August 18, damage and seismic intensity (*Japanese*) 8-96142
 Kawazu, Japan, 1976 August 18, damage and seismic intensity distrib. (*Japanese*) 8-96143
 Kinnaur, Himachal Pradesh, India, 1975 January 19, fault-plane soln. 8-96161
 macroseismic data processing and interpretation 8-61583
 magnitude determ. from surface and body waves, calibrating curves for different instruments 8-57173
 micro, space time correlations anal. 8-65184
 microearthquake activity adjacent to Rockin pluton, California 8-92791
 microseisms at Palisades, source location and propag. 8-85495
 Mid-Atlantic Ridge, ocean-bottom seismograph obs. near 45°N, results 8-96157
 Middle America arc, focal mechanism solns. and tectonics 8-77191
 moments and corner freqs., effects of free surface on body waves 8-85492
 Moxa, GDR, microearthquake records, event criteria (*German*) 8-57170

earthquakes continued

- New Hebrides (1969, January 19), focal mechanism and source char-
acts. rel. to fracture zone subduction 8-73342
Ninetyeast Ridge area, seismicity and tectonics, Indian plate internal
deform. 8-73343
nuclear power station design engineering for earthquake loads
8-66431
oceanic transform earthquakes, source parameters rel. to plate vel. and
transform length 8-53620
Odawara City, Japan, 1853 March 11, intensity, damage and magnitude
from old documents (*Japanese*) 8-96146
W.Pacific, HF P_n and S_n phases obs. at great distances, spectral anal.
8-77195
periodicities of Alaskan and central American earthquakes 8-53621
periodicity rel. to lunar sidereal period 8-53844
precursors, seismic wave propag. through cracked solid, model
8-61342
prediction, continuous method for Rn measurement in groundwater and
springs 8-88924
prediction, radio emergency warning system (*Japanese*) 8-85497
prediction, using He/Ar and N₂/Ar ratio vars. in fault zone groundwater
air bubbles 8-88803
prediction based on tectonics (*Chinese*) 8-61335
prediction information classification for practical use 8-57177
prediction using automated Rn-Th monitor 8-73532
premonitory processes, fluid-infiltrated rock 8-51073
ray parameter-epicentral distance curves for point source on boundary
8-61336
Rayleigh, surface waves, principal mode and harmonics obs. for focal
depth determ. 8-61351
RESMAC seismic array, interactive epicentre location procedure
8-65395
response of nonlinear plates to random loads 8-94604
Rumania, 1977 March 4, rupture process, fault-plane soln. 8-65201
San Fernando, 1971 February 9, source finiteness, teleseismic body
waves 8-92781
San Francisco, 1906, source mechanism 8-85499
Sanriku district coast, earthquake fault models from tsunamis simula-
tion (*Japanese*) 8-65199
seismic pattern recognition, fundamental problems 8-81428
seismic waves attenuation and azimuthal depend. in SE United States
8-65185
seismicity, model and observed, represented in two-dimens. space
8-53619
shallow earthquakes occurrence, statistical study 8-96155
Shikotan, 1968 January 29, surface waves initial phase and phase vel.
8-92793
Sinkiang, China, earthquake swarm (1974), source mechanisms from
surface waves anal. 8-81427
source parameters, relation to magnitude 8-96154
source parameters rel. to tectonic field, dynamical process of fault
motion 8-88801
source spectra scaling law, regional var. 8-92783
source time function depend. on tectonic field 8-92799
South America, origin of compressional intraplate stresses 8-61385
statistics, truncated exponential frequency-magnitude relationship
8-65191
stress concentration mechanism for intraplate earthquakes 8-81112
strong earthquake foci dynamic parameters, from longit. wave spectra
8-57171
strong ground motion characterisation, uniform risk functionals
8-92789
strong volcanic earthquakes assoc. with lateral eruptions, dynamic focal
parameters 8-61347
subcrustal, location and mislocation 8-85498
Sweden, seismicity map, earthquake catalogue for 1951-76 period
8-96159
Tango, 1927, conjugate fault system model, geodetic data inversion
8-88779
Tangshan, 1976 July 28, stress field of area before and after earth-
quake (*Chinese*) 8-61358
tectonic patterns and earthquakes, central Mississippi valley 8-85504
Tohoku, Japan, intraplate seismicity correl. with interplate earthquakes
8-92787
tsunami type plane wave, Coriolis force effect (*Russian*) 8-77193
United Kingdom, perceptible earthquakes 8-77189
Ust'-Kamchatka, 1971 December 15, P-wave study 8-73317
Vladivostok, 1973 September 29, seismic moment from P-waves and
mantle Rayleigh waves 8-61354
Vrancea, 1977 March 4, multiple seismic event 8-65205
Vrancea, Rumania, 1977 March 4, seismic waves and intensity recorded
in Poland 8-92779
Yellowstone, Wyoming, 1975 June 30, event and precursive spectral
stability 8-61352

EAS see cosmic ray showers and bursts

Eberhard effect see photographic materials

ebullition see boiling

e.c.g. see electrocardiography

echelons see diffraction gratings

echo

- see also anechoic chambers; architectural acoustics; clutter; reverberation;
sonar
auroral radar echoes drift meas. using radar auragraph 8-65436
circumglobal signals in Atlantic equatorial zone (*Russian*) 8-69585
electroacoustic echo in piezoelectric and ferroelectric materials
8-95549
HF oscillating echoes from polar E-region 8-57390
HF peculiar lunar echoes, guided wave propag. in ionosphere and mag-
netosphere 8-93032
ionosphere, equatorial, theoretical model of spread-F echoes in HF and
VHF bands 8-85764
piezoelectric powder, echos, theory (*French*) 8-72462
powder, three pulse echo, mechanism contribs. 8-68444
powdered materials, nonlinear mechanism leading to polarisation
echos 8-87739
pulse Doppler radar obs. of severe thunderstorms 8-85651
radio auroral signals, maximum entropy spectral anal. 8-93006
radio sources, superluminal, energy echo model rel. to Hubble's const.
doubling 8-81722

echo continued

- rectangular room, instantaneous excitation of one-dim. sound
waves (*German*) 8-87201
sea echo radar spectra resolution limitation inferred from ionospheric
Doppler broadening 8-81489
signals propag. characts., 10 and 15 MHz 8-69574
single-transducer coupler for diagnostic pulsed Doppler or pulse-echo
US instrumentation 8-61236
sounder transducer field plotter 8-59238
time delay detection, effect of zero singularity smoothing 8-90605
US liver sector scans, echoes across diaphragm 8-69165
VHF radar signals, partial refl. and scatt. from clear atmosphere
8-81278
VHF radar signals partial refl. from troposphere 8-85656
VHF radiowave ionospheric propag., equatorial spread-F scattering
8-61661
SiO₂:OH⁻, vitreous, elec. dipolar echoes 8-52430

echo suppression

- cartography radar image interpretation, line detection technique
8-61630

eclipses

see also solar eclipses

- Galilean satellites, photometric eclipses anal. rel. to theory of motion
8-53864
Jupiter inner satellites, mutual eclipses and occultations in 1979,
ephemerides 8-53866
lunar eclipses, transitory phenomena obs. on Moon 8-61770
Pluto, 1978 P 1, possible satellite, orbit and eclipses ephemeris
8-93152
Saturn satellites, mutual eclipses and occultations in 1979-1980,
ephemerides 8-53868

ecology

- biosphere and active solar processes link, role of Earth's natural electro-
mag. field 8-61211
catastrophes, comets and ice ages 8-53714
compartmental analysis in biology, medicine and ecology, mathematical
foundations 8-68978
cone pigment ecology in teleost fish 8-69041
dynamic processes on Earth, extraterrestrial causes, rel. to extinction of
life 8-92820
ecosystem succession detection by aerial IR photography 8-81459
palaeoclimatology and vegetation ecology (*French*) 8-88901
system model sampling/identification, input signal anal. 8-69267
thermal insulation of animal coats and human clothing, review
8-73139
Pu dynamics in deciduous forest ecosystem, linear compartment
donor-controlled model 8-85392
Pu ecological export from reprocessing waste pond 8-53533

economic and sociological effects

see also personnel; social aspects of automation

- academic physics community and industrial perspective 8-62032
academic research and graduate education, effect of Department of
Defense funding 8-62031
agricultural effects of 1975-76 drought in United Kingdom 8-57298
chemistry, macromolecules, and the needs of man 8-95907
climatic change effects on food production, statistical models limita-
tions 8-57303
crop response to hail suppression seeding, Nelspruit project, South
Africa 8-57257
energy contribution to anthropogenic climatic fluctuations, 21st century
problem 8-57299
energy crisis, exponential growth 8-86049
energy modelling and forecasting at US ERDA 8-49629
European agriculture rel. to climatic change 8-85679
Federal funding policy in physics and politics 8-62033
French plan VII, energy forecasting 8-49628
graduate PhD student subfield choice and employment prospects
8-65747
high school mathematics and science courses, participation rates
8-81737
historic climate correl. with wheat prices and wages 8-81346
Israel, water shortage and supply, long-run policy for agriculture
8-61454
natural disaster fallacies, Sahel drought example 8-57302
science and society, AAAS president's lecture 8-77660
science anxiety, a course for university entrants 8-77637
tornadoes, distrib. of death and damage in United States 8-69397
water pollution abatement benefits in Merrimack River Basin, survey
results 8-61456
weather forecasting, prospects and methods of improvement 8-69394
world predicament and climatic change, need for interdisciplinary
research 8-57300

economics

- CANDU PHWR, Wolsung nuclear power plant, fuel cost anal.
8-54832
Elmo bumpy torus reactor, economics 8-54994
environment monitoring system, benefit assessment 8-73507
flat solar collector, energy and economic analyses 8-83236
fusion plant, inertial confinement, commercialisation anal. 8-58410
fusion power, parametric anal. of utility operations 8-58409
fusion power plant, inertial confinement type, target prod., costs
8-58488
fusion power plants, engineering limitations 8-74473
fusion reactor, ohmic heating energy storage for power reactor, costing
8-58495
fusion reactor, TNS, electrical design costing 8-55014
fusion reactor coil design, cost anal., for neutral beam magnets
8-55005
fusion reactor design and economics, confinement physics effects
8-50358
fusion reactor toroidal field coil stress anal., cost effective procedures
for TFTR 8-50379
geophysics, reflection seismic exploration 8-96325
Go-ri nuclear power plant, fuel cycle schemes, economic comparison
8-54831
hail-prevention operations, cost effectiveness estimation methods anal.
8-93013
industrial cost-effective noise control 8-55515
integrated energy systems, environment impacts 8-73506
laser fusion breeder, impact on nuclear economy 8-50336

economics continued

- linear accelerator, energy doubling using coupled cavities (*Russian*) 8-70652
- LMFBR, energy investment 8-78512
- low-level radioactive waste management complexity and cost-effectiveness 8-94117
- LWR 1300 MWe system, design of containment to withstand core melt 8-66335
- LWR diversion resistant processes and cycles 8-86677
- LWR plant, economic effect of increased seismic load on design and construction costs 8-66432
- monetary system, analogy with electric current flow in circuit 8-54144
- NASA remote sensing technology transfer to State of Georgia, cost anal. 8-73519
- neutral beam, pulsed, arc (arc filament) power supplies, for fusion reactor 8-70637
- neutral beam filament supply, 15 V 10³ A, programmable, regulated, for fusion reactor 8-70630
- nuclear fuel cycle, core design optimisation 8-82420
- nuclear fuel transport by air, feasibility and economics 8-94154
- nuclear power plant siting evaluation, w.r.t. safety, comparison with coal-fired power station (*Czech*) 8-50266
- nuclear reactor, fuel savings by 'stretch out' operation (*German*) 8-86632
- nuclear reactor pump coolant tests, computerised monitoring 8-70585
- optical fibre, cost models for A-7 aircraft ALOFT project 8-59131
- PWR, optimal fuel loading and operation planning 8-50276
- radiograph quality control programme, economic analysis 8-73236
- radiographic equipment servicing by hospital-based group 8-69247
- radiography, cost-effectiveness considerations in evaluation of new technology 8-69192
- radiology diagnostic facilities, quality assurance programme, proposed recommendation 8-73235
- relativistic electron beam hybrid reactor, economic model 8-58412
- Shiva laser, 25 MJ energy storage and delivery system 8-55015
- thermocouple alloys, Microsil-Nisil, for furnace control Chromel-Alumel thermocouple replacement 8-49831
- Tokamak fusion power generation 8-74472
- tokamak fusion power plants, major cost drivers 8-58443
- Tokamak fusion reactors, commercial feasibility 8-58406
- tokamak next step designs, system size and cost trends 8-58416
- Tokamak power systems, economics 8-54993
- T breeding costs in critical fission reactor 8-58456

eddy current losses

- long magnetic conductors, estimation of TE- and TM-mode losses 8-91891
- plane loop, power dissipation and inductance calc. method (*German*) 8-58881
- superconducting coil, multifilamentary composite losses 8-62637
- superconducting composite 8-62636
- thin laminations, minor loop hysteresis loss calc. 8-90342
- transformer, EM losses, effect of degree of perfection of crystallographic texture (*Russian*) 8-60309
- Fe-Ni, low frequency power losses 8-95466
- Fe-Si, low frequency power losses 8-95466
- Fe-Si (3 wt.%), domain wall drift due to nucleation during cyclic magnetisation 8-95461
- Fe-Si (3 wt.%), grain oriented, domain wall variation throughout magnetisation cycle 8-95459
- Fe-Si (3 wt.%), grain oriented, power loss depend. on domain wall bowing 8-95460
- Fe-Si (3 wt.%), loss prediction, from distorted waveforms 8-76273
- Nb-Ti, multi-filamentary superconducting wires, mag. field dependence of AC losses 8-60256

eddy currents

- see also induction heating*
- amplitude phase methods of testing, design relationship for eddy current transducers 8-53152
- conducting cylinder with transverse mag. field, eddy current induction 8-74815
- conducting liquid, eddy current induced pumping, longit. current in corrugated tube (*Russian*) 8-75216
- conductors in steady motion, solution in theory of eddy currents and forces 8-62970
- corrosion monitoring 8-88584
- defectoscope performance analysis with series tank circuit in input stage 8-53106
- dual energy methods of calculation 8-78859
- eddy current inspection, possibilities of phase generator circuits 8-88614
- education, eddy currents, levitation, metal detectors and induction heating 8-61967
- electrically conducting spherical specimens, electromagnetic control 8-53138
- electromag. convertor, forming part of unbalanced bridge circuit, exam. of characts. 8-85100
- EM wave propag., self-consistent approach 8-51920
- fastener hole inspection, computer automation of eddy current inspection, exam. 8-53040
- ferromagnetic half space, density induced by a transient magnetic field 8-71002
- ferromagnetic probe, with square cross section, numerical computation (*German*) 8-77951
- fusion reactor eddy current analysis, finite element circuit method 8-66373
- fusion reactor eddy currents, 3-dimens., perturbation-polynomial expansion calcs. 8-66372
- heat exchange tube thickness meas. by eddy current for corrosion testing, computer study 8-68852
- hot-rolled rods, surface defect detection without scale removal by NDT 8-95890
- inspection equipment, circuit for selecting signals in specified phase range 8-56863
- moving conducting ribbon, interaction with ferromag. inductor field (*Russian*) 8-94359
- NDT, detection limit, comparison with US methods 8-60957
- nondestructive inspection unit of petroleum pipes, based on eddy current modulation unit 8-76814
- nonmagnetic electrically conducting rod, section shape effect on eddy current transducer parameters with uniform field 8-53132

eddy currents continued

- nonmagnetic strip in transverse uniform alternating magnetic field 8-94362
- numerical anal. of eddy-currents induced within a metal cylinder by parallel ACs (*Polish*) 8-78856
- numerical solution eddy-current problems, including moving Fe parts 8-90340
- phase sensitive eddy current detectors, effect of compensation conditions, on transducer-product clearance inductions 8-85103
- pressure transducer elastic elements characts. optimisation (*Russian*) 8-77890
- soft magnetic metals, ideal, AC response 8-64223
- spatial harmonics, spectra density meas. 8-53141
- stamped disc surface inspection by automated eddy current unit 8-92430
- tester for crack detection, of nonferrous tubes and rods 8-85099
- thin conducting plates, variational techniques for eddy current calc. 8-90341
- thin film, integro-differential eqns. soln. by finite element method 8-90343
- thin walled bearing races eddy current inspection of hardening and tempering quality 8-95892
- through tube transducer, operating condition simulation when inspecting ferromagnetic rods 8-53077
- Tokamak, Texas exptl., homopolar generator, eddy currents, EM forces (torques), due to misalignment 8-54953
- Tokamak machines, eddy currents, numerical and exptl. anal. 8-66374
- transducer, part geometry effect on inspection 8-53078
- transducers, applied, resistance due to cracks, eddy current calc. and hodograph 8-53095
- transducers, for meas. thickness of lacquer coloured coating on mag. base 8-85101
- tube flaw detection by annular US transducers 8-60971
- Al alloy cylindrical parts, crack detection by two channel eddy current inspection unit 8-72998
- Ni, magnetoelastic effects, ΔE -effect and macroeddy current damping, internal friction meas. 8-64253
- Ti-Al-V (6, 4 wt.%) effect of high temp. oxidation on eddy current conductivity 8-76770

edge dislocations

- alkali halide, morphology of growth and evaporation surface 8-79544
- alkanes, thin plate microcrystals, transmission electron diffraction intensities 8-83821
- BCC metals, vacancy-edge dislocation interactions, computer simulation 8-83845
- 4-n-butyloxyphenyl-4'-nonyloxybenzoate, edge dislocations in smectic C mesophase 8-91231
- climb, numerical anal. 8-71736
- collective dislocation motion, dynamic effects 8-79632
- β -copper phthalocyanine, dislocation detection (*German*) 8-63773
- critical resolved shear stress, from misfitting particles 8-79613
- III-V semiconductor, anisotropic carrier mobility due to dislocations 8-60124
- III-V semiconductor, local resist. near dislocations, eqns. 8-60123
- III-V semiconductor, temp. distrib. around dislocations, due to Joule heating, calc. 8-71734
- interactions in infinite array, elastic energy 8-55871
- metal, dislocation scatt. and de Haas-van Alphen amplitudes 8-63967
- metal, FCC and BCC, self-diffusion along edge dislocations by vacancy mech. (*Russian*) 8-87810
- 4-n-octyloxy-4'-cyanobiphenyl, smectic A liq. cryst., elastic modulus determ., stress/strain relationships 8-91229
- point defect diffusion in stress field of edge dislocation of irrad. solid 8-51720
- repeated precipitation on edge dislocations, micromechanisms 8-95752
- type II superconductor, dielectric interaction of flux line lattice with internal stresses of cryst. imperfections 8-56270
- Ca₃(PO₄)₂F, dislocation struct. exam. (*Russian*) 8-63770
- Cu irradiated, exam. of dislocation bias for interstitials to edge dislocations 8-79612
- Cu single crystals, positron trapping by edge dislocations, produced by bending 8-80606
- CuAu, calc. of elastic interaction between locally transformed regions with screw and edge dislocations 8-83844
- Cu₂O, laminar growth on (111) Cu single cryst. surface, microstruct. 8-72025
- α -Fe, atomic dislocation modelling, flexible boundary conditions and nonlinear geometric effects 8-75667
- Fe, BCC, computer simulation of entropy of $\frac{1}{2}\{111\}\{110\}$ edge dislocation 8-67716
- Fe, BCC, vib. entropy of $\frac{1}{2}\{111\}\{110\}$ edge dislocations 8-63768
- Fe, deformed, dislocation structure determ. from magnetic props. 8-55874
- α -Fe:He, impurity clustering in vacancies bound to edge dislocations 8-91358
- Fe-Ni (29 at.%), calc. of elastic interaction between locally transformed regions with screw and edge dislocations 8-83844
- Fe-Si (3 wt.%), degeneration of slip on (211) planes (*Russian*) 8-80587
- n-GaSb, temp. distrib. around dislocations, due to Joule heating, calc. 8-71734
- InSb, plastically bent single crystals, dislocation struct. obs. 8-59816
- Mo, monocrystalline, exam. of microplasticity at ambient temps. (*French*) 8-52888
- NaCl, dislocation half loop mobility 8-59817
- Nb, surface oxide softening, anisotropy 8-60716
- Sr_{0.75}Ba_{0.25}Nb₂O₆, large cryst. growth, control of opt. defects 8-76595
- Zn, single crystals, positron trapping by edge dislocations, produced by bending 8-80606

education

- see also computer science education; educational aids; educational courses; teaching; training*
- academic research and graduate education, effect of Department of Defense funding 8-62031
- algorithms, implication for instructional design 8-81735
- algorithms, suggested uses 8-49578
- alternative energy sources, solar and atmospheric 8-69951
- Aristotle's theory of falling bodies, pre-sixteenth century objections, for teachers 8-62026
- astronomy, test item file construction and use 8-86054

education continued

- atomic fluorescence spectroscopy, review of principles, instrumentation, methodologies, appls., teacher education appl. 8-69927
 career opportunities for physicists, discussion 8-61966
 chemistry, undergraduate education, future changes 8-69929
 class notetaker, rotating assignment of student 8-81734
 computers in educational technology 8-49615
 crisis question technique 8-81738
 cybernetic methods, pupil learning and teacher activity algorithms 8-49577
 elementary particles, individual properties, theory 8-57721
 energy crisis, exponential growth 8-86049
 examinations, two-trial system, general physics course 8-49612
 fluorescence spectrometry, anal. appls., historical review 8-93507
 frontiers in education, conference, Urbana-Champaign (1977) 8-81779
 group problem-solving sessions, in personalised system of instruction courses 8-61954
 hydrology of unsaturated zone, United States educational effort 8-81224
 Millikan, Robert A., contribs. to physics teaching 8-69956
 models and their use in chemistry teaching 8-86064
 models as a pedagogical tool 8-86065
 models in science, philosophical discussion 8-86108
 oral examination as follow up to written exam., report 8-61953
 participation rates in high school mathematics and science courses 8-81737
 personalised system of instruction, for low-enrolment years 8-61955
 physical understanding or mindless programming of students? 8-81739
 physics, education and employment, situation and prospects 8-61963
 physics, human resources and career opportunities 8-61962
 physics careers, employment and education, conf., Pennsylvania, USA (Aug. 1977) 8-62034
 physics education versus job training 8-61965
 Physics Manpower Panel of American Physical Society, employment and education trends 8-65735
 post-doctoral appointments, tenure and multiple appointments 8-61964
 PSI system for reducing teaching loads in small depts. 8-49575
 PWR pressure vessel safety, term paper from course at Georgia Tech 8-58379
 science, engineering, post-graduate educational system in North America rel. to Muslim graduate student 8-65736
 science anxiety, a course for university entrants 8-77637
 science career facilitation project in energy-related fields 8-61959
 science education, computers and intuition 8-81740
 scientific investigation experiment, development of theoretical model 8-86066
 Scripps Institution of Oceanography, research projects and education review 8-69464
 student and teacher perception of physicist's image 8-62030
 teacher effectiveness, self-determined change 8-54106
 test-taking techniques, multiple-choice and advanced placement exams. 8-77654
 Universe structure, open and closed curved spaces 8-77652
 university lecturer, volunteer, experience in Fiji 8-61961
 University physics education, South-East Asian Regional Conf., Penang, Malaysia (May 1977) 8-81732
 Universum, Swedish astronomical information project (Swedish) 8-86048
 USSR, educational TV and radio programme development (French) 8-89286

educational aids

see also *student laboratory apparatus*

- astronomy, Hubble's law as laboratory exercise 8-65740
 atomic orbital cross-sections, bonding interactions, spring model, teaching aid 8-93503
 calculator, programmable, as physics teaching aid, numerical intergation appl. 8-86083
 crystallographic point groups, symmetry, teaching aid 8-77650
 Einstein, Albert, colour film footage 8-62001
 fracture, recognition from stereo photographs 8-54140
 HMO theory, student use, computerised visual aids 8-77649
 human retina model for props. of vision 8-77655
 Lissajous figures, generation tech. 8-77656
 microcomputer-based multiboard communication system for nonverbal handicapped children 8-57126
 molecular models based on Petri dishes stereochem. appls. 8-73817
 neurophysiology, electronic model of neuron 8-85301
 photosynthesis, carbon fixation cycle, model, teaching appl. 8-73806
 planetarium design, model from Mesquite Schools, near Dallas 8-81777
 resource letter on environmental noise control 8-61949
 spark tape anal. and mech. energy expts. 8-81758
 stereographic projection model construction, for cryst. symmetry demonstration 8-86086
 video recorders (German) 8-69954

educational computing

see also *computer-aided instruction*

- calculator, programmable, as physics teaching aid, numerical integration appl. 8-86083
 Kirchoff's laws of spectral analysis, computer laboratory exercises 8-73790
 science education, computers and intuition 8-81740
 test scoring system, micro-computer based 8-81757

educational courses

- astronomy, university courses and career prospects 8-69931
 biomedical engineering, France 8-73807
 biomedical engineering undergraduate degree program, state university approach 8-77646
 computer physics, elementary concentrated one-week course 8-73799
 course development by team, human factors 8-49580
 engineering and physical science careers advisory program 8-69932
 environmental sciences, curricula for undergraduate courses 8-77644
 forced pacing method of instruction calculus-based freshman physics course 8-61951
 fusion design team, undergraduate education 8-58469
 health physics, Faculty Institute in Applied Health Phys. at Oak Ridge National Lab. 8-49581

educational courses continued

- interdisciplinary, physics, energy and environmental technology 8-61958
 introductory physics, core plus branch struct., self selection 8-61950
 liberal arts physics course in holography 8-73798
 liberal arts technology, history 8-86061
 lower division physics, multiple level lecture series 8-61952
 macromolecular solns., educational courses, integration with phys. chem. 8-77642
 marine science courses evaluation 8-53657
 mathematics courses, effect of class evaluation method on learning 8-57719
 mathematics for engineering students, student and teacher perceptions of degree of difficulty 8-57712
 medical physics, four year baccalaureate course (undergraduate) 8-54107
 M.Sc. theses, for pedagogical direction of studies (Polish) 8-73808
 musical acoustics, role of demonstrations, source material 8-49576
 nonscience majors, innovative course based on mass-radius diagram of states of matter 8-62002
 nuclear reactor safety, nucl. engineering programme at UCLA 8-58377
 nuclear reactor safety education at Northwestern Univ. 8-58376
 nuclear reactor safety educational programme at Purdue 8-58380
 nuclear reactor safety instructional programs at RPI, LWR and FBR appl. 8-58375
 nuclear reactor safety teaching, MIT nucl. engineering dept. courses, USA 8-58378
 personalised system of instruction, for low-enrolment years 8-61955
 physical chemistry teaching, macromol. principles 8-77643
 physical science, undergraduate major course, broadening 8-61960
 physics, future changes, discussion 8-61956
 physics, philosophical approaches 8-81791
 physics, Piaget-type questionnaire assessment 8-81731
 physics, teacher effectiveness, self-determined change 8-54106
 physics for liberal arts majors, Piagetian styled process-based course 8-73800
 physics Ph.D., industrial training option 8-61957
 PSI introductory physics, comparison with lecture-discussion method, long range effects 8-49574
 science anxiety, a course for university entrants 8-77637
 secondary-school students, talented, university summer science course 8-89282
 solar energy concepts, in chem. teaching 8-73805
 special relativity for general students 8-73791
 spectroscopy quantum chem. teaching, fluctuating elec. dipoles, light absorpt. 8-73802
 wind energy as alternative energy source, energy science course material 8-61973

e.g. see *electroencephalography*

effective mass (band structure)

- electron specific heat and effective mass, temp. depend. (Russian) 8-59958
 graphite, neutron irradiated, effect on quantum limit Shubnikov-de Haas oscils. 8-95304
 III-V semiconductors, spherulitic structure, relation with forbidden bandwidth and lattice constant (Slovak) 8-51879
 inert gas solids, exciton states, nonstructural theory using effective mass approx. 8-84147
 inert gases, solid, electronic excitations, nonstructural theory 8-79942
 insulators, improved effective mass for impurity levels 8-87941
 interface effect on effective mass approximation 8-64082
 inversion layers, carrier effective mass, contribs. of electron-electron and electron-phonon interactions 8-64087
 rare-earth, light-heavy alloys, resistivity, mag. contrib. to resist. and Neel temp. 8-51971
 semiconductor, zincblende-type, valence band effective mass strain depend. 8-51880
 semiconductor solid solution, compositional disorder, free carrier absorpt. 8-64387
 semiconductor-insulator boundaries, impurity electron states near interface 8-95320
 Si:Sb(P)(As), shallow donor states with strong central cell perturbation theory 8-51933
 singularities of the small polaron effective mass 8-63989
 Wannier-Mott exciton decay, on acoustic phonons, in thin semicond. wire (Russian) 8-72075
 n-CdSnAs₂, optical absorption rel. to energy spectra (Russian) 8-75994
 Co, de Haas van Alphen oscill., effective mass 8-87900
 Cr_{1-x}Mn_xSi₂, semicond. props. 8-79992
 CrSi₂, semicond. props. 8-79992
 Cu₂MoS₈, normal state and superconducting property measurements 8-91660
 n-Ga_{1-x}Al_xSb, transport phenomena in low and high mag. fields 8-80007
 GaAs, electron effective mass, temp. depend. for various degrees of doping and compensation (Russian) 8-79923
 GaAs, hole effective mass, press. depend., theory and tunnelling expts. 8-75986
 Ge, magnetoplasma resonance in electron-hole drops (Russian) 8-79944
 Ge, valence band effective mass strain depend. 8-51880
 HgI₂, electrons and holes cyclotron reson. 8-72061
 HgI₂, stimulated emission at high exciton density, temp. depend. 8-84608
 (InAs)₂(CdTe)_{1-x}, band gap and effective mass, IR spectra obs. 8-56491
 In₂O₃, Seebeck coeff., density of states effective mass 8-56171
 K-Na, dil., dynamical props. of quasiparticle excitations, de Haas-van Alphen effect meas. 8-84128
 Pb, effective cyclotron masses of central and noncentral ξ orbits, de Haas-van Alphen effect 8-63968
 PbMoS₈, normal state and superconducting property measurements 8-91660
 Pb_{1-x}Sn_xTe, electron-phonon interaction 8-71819
 Pt, rel. to de Haas van Alphen obs. of Fermi surface 8-91601
 Rb-K, dil., dynamical props. of quasiparticle excitations, de Haas-van Alphen effect meas. 8-84128
 Re, RF size effect, Fermi surface dimensions determ. 8-91598

effective mass (band structure) continued

- Sb, carrier energy spectrum, effect of hydrostatic pressure 8-87903
 Sb, de Haas-van Alphen effect, effective mass, Fermi levels 8-75982
 Sb:Te, de Haas-van Alphen effect, effective mass, Fermi levels 8-75982
 Sb-Sn, dil., de Haas-van Alphen effect, effective mass, Fermi levels 8-75982
 SeN₄, region of homogeneity, physicochem. props. 8-52018
 Si, (100) surface, effective mass and collision time 8-64081
 Si:Sb(P)(As), shallow donor electrons, hyperfine interactions, reply to Onffroy's calcs. 8-51934
 Si-Al₂O₃, inversion layer subbands, magnetocond. oscills. 8-64124
 SiC:N, refr. index dispersion, effective electronic mass determ. 8-84548

effusion

- Langmuir torsion effusion meas., recoil force correction factors 8-75929
 Ni-S system, Knudsen effusion and thermodynamics 8-79759

EHD see electrohydrodynamics**EHT calculations**

- AB₄, non-transition element complexes, shapes and other props. 8-82648
 AB₅, non-transition element complexes, shapes and other props. 8-86790
 AB₆, non-transition element complexes, shapes and other props. 8-82647
 diamond, electronic energy bands of diamond-type crystals, appl. of EHT method 8-87907
 haloalkanes, max. overlap approx., heat of form. and dipole moment 8-94198
 nicotinamide, and related compounds, dipole moments, electronic transitions, chemical and biological activity 8-90086
 nicotinic acid, and related compounds, dipole moments, electronic transitions, chemical and biological activity 8-90086
 oxalyl chloride, rot. isomerism, CNDO and EHT-type methods 8-58591
 polymer primary structures ESCA and EHT methods 8-52630
 transition metal complexes, counterintuitive orbital mixing in semiempirical, ab initio MO calcs. 8-90078
 CO₂, anomalous energy minima surfaces 8-86791
 Cu, clusters, size, geometric effects, catalysis implications 8-73131
 GaAs surface, cluster model approach for electronic struct. 8-56205
 Ge, electronic energy bands of diamond-type crystals, appl. of EHT method 8-87907
 Ge, surface, cluster model approach for electronic struct. 8-56205
 Pd, clusters, size, geometric effects, catalysis implications 8-73131
 Pt(O)-Pt(O) dimers, bonding in a d¹⁰-d¹⁰ system 8-74579
 Si, electronic energy bands of diamond-type crystals, appl. of EHT method 8-87907
 Si, extended Huckel theory calculations for positive divacancy 8-87938
 Si, surface, cluster model approach for electronic struct. 8-56205
 α-Sn, electronic energy bands of diamond-type crystals, appl. of EHT method 8-87907
 W (100) surface, chemisorption of CO, mol. orbital study 8-71995

eigenfunctions see eigenvalues and eigenfunctions**eigenvalues and eigenfunctions**

- acoustic motional source transfer function characts., ocean profile anal. appl. 8-66982
 Anderson localisation, transport props. of 2D disordered electron systems in strong mag. fields 8-95318
 anharmonic oscillator, quantum mechanical, eigenvalues of secular eqns. 8-49698
 anharmonic potential models, exactly soluble, const. and soln. 8-54221
 basis states generation by variational methods 8-78295
 beam, subjected to elastic constraints, free vibrs. 8-83309
 bimolecular reactions, rot.-vibr. symmetry correlation, building-up principle from mol. fragments 8-76849
 cantilevers, joined by a rigid connector nat. freq. determ. 8-83298
 Chebyshev polynomial method for computing analytic solns. to eigenvalue problems, appl. to anharmonic oscillator 8-62058
 clamped rectangular orthotropic plates, natural freqs. of vibr. upper and lower bounds 8-83284
 classical nonlinear σ-model, two dims., scatt. of massless lumps, non-local charges 8-62300
 composite wall, constant props., transient heat cond. problem (French) 8-87229
 confined solutions of multidimensional inversion equations 8-77678
 convection, natural, over uniform heat flux vertical surface, higher-order approx. 8-59388
 convergence of eigenfunction expansions assoc. with vector matrix differential eqn. 8-69965
 Coulomb potential with cut-off, exact eigenvalues 8-62692
 covariant EM projection operators, covariant description of charged particle guiding centre motion 8-58145
 crystal symmetry, implications in charge density studies 8-71694
 crystal vibrations, matrix paradox, for teaching 8-49611
 cylinder, circ., elastic, axial eigenfunctions orthogonality 8-51080
 cylindrical shell with elastic filler, eigenfrequency spectra, dynamic instability regions, nonaxisymmetrical vibrations 8-63367
 double well anharmonic oscillator, no horn of singularities 8-73884
 Earth, shell of uniform layers, asymptotic distrib. of torsional eigenfreqs. 8-92797
 eigenvalue eqns., appl. to fast and thermal neutron systems 8-50231
 eigenvalue perturbation theory, remarkable examples 8-93558
 Einstein eqns., classification system for one Killing vector solns. 8-93579
 elastic wave scatt. from cylindrical cavity, nuclear resonance theory 8-87290
 elastoplastic non-isothermal deform., bifurcation of equilib. 8-79220
 elastostatic anal. of transversely isotropic finite cylinders 8-51074
 electrohydrodynamic stability in rigid cylinder, dielectric viscous fluids, eigen wavenumbers 8-59497
 EM wave in random media, degeneracy and inhomogeneity in transport theory 8-62982
 energy eigenvalue problem, adiabatic perturbation theory using QFT techniques 8-93551
 ensemble of two-body random Hamiltonians, nonzero mean matrix elements, eigenvalue density, Monte Carlo calcs. 8-81920

eigenvalues and eigenfunctions continued

- factorization theorems, stability and repeated bifurcation 8-65751
 flow, in annulus, axial, numerical stability anal. 8-83363
 flywheel, buckling and vibr. of rotating spoke, anal. 8-71288
 four vector components, eigenvalues and -functions for spin 0 and 1 8-49720
 Galerkin's method, non-uniform convergence 8-83304
 gravitational radiation and invariants of curvature tensor in general relativity 8-57836
 ground state properties of Lipkin Meshkov Glick model using atomic coherent states, nuclear phase transitions 8-62489
 Hamiltonian of single variable systems, asymptotic behaviour of bound eigenfunctions 8-77754
 hydrodynamic oscillations in Gentilly-I steam mains by inertial analysis 8-89944
 hydrodynamic stability, open disc theorem, upper bound of eigenvalues 8-59370
 image processing and eigen representation 8-55312
 induced potential problem in 3-D, functional analytic approach 8-58880
 infinite sector problems, direct method of calc. of eigenvalues 8-81807
 Jacobi matrices, rational, asymptotical eigenvalue density 8-81794
 jet, free, turbulent flow, large scale struct., discrete values meas. 8-90840
 Jost functions, S-matrix of massive Thirring model, relativistic field theoretic model 8-54552
 JWKB quantisation condition, appl., breakdown and near-dissoc. behaviour 8-58571
 Kalman filter technique, eigenfunction expansion, neutron flux core distrib. 8-54839
 laminate, 3-phase, longitudinal heat propag. at high exciting freqs. 8-90684
 Lanczos method, method of moments, tri-diagonalisation of a matrix 8-58240
 large scale general eigenvalue problem iterative method for soln. 8-89318
 laser modelocking, soln. of 2nd order integro-differential eqns. 8-66796
 linear harmonic oscillator on lattice, wave functions, energy eigenvalues, Pade approximant method 8-57817
 loaded thin circular plate stability criterion 8-77700
 lower bounds to ground state eigenvalues, Pade approximants 8-49722
 massless electrodynamics, vacuum instability, bare coupling constant Gell-Mann-Low eigenvalue condition 8-89643
 matrix eigenvalues sensitivity 8-89295
 meson wave functions in 1+1 dims. QCD 8-54559
 mixtures of reacting gases, extension of Chapman Enskog method (Russian) 8-57878
 multilayered cylinders, nonstationary temp. fields with rotational symmetry (German) 8-79190
 N-electron atomic Hamiltonian first eigenvalue, Hartree-Fock approx. method 8-90062
 N-mode laser, emitted light correlations 8-63051
 neutron diffusion modelisation, optimal design and eigenvalue problems 8-66329
 neutron hot perfect fluid relativistic stars, asymptotic eigenfrequency distrib. for even parity perturbations 8-49668
 neutron pulse behaviour in multizone breeder system, two-zone system pulse method 8-86574
 nonlinear structural eigenvalue calcs., mode finding 8-51102
 normal modes of laterally homogeneous Earth, one dimens. example 8-88797
 numerical inversion of Laplace transform and Fredholm integral eqns., eigenvalues and eigenfunctions 8-81800
 optical resonator nonsymm. eigenvalue problems, numerical solns., Prony method 8-82992
 optical system, noisy image restoration, eigenfunction expansion technique 8-63020
 OPW method, instability rel. to error in core eigenvalues 8-63963
 plasma, collisionless universal instability, stability of bound eigenmode solns., convective modes 8-71472
 plasma, MHD turbulence, three-dimens. soln. in cylindrical geometry 8-67351
 plasma, Vlasov type, inhomogeneous, localised modes 8-83563
 plasma MHD waves segregation in ideal medium 8-87440
 plate, completely free, rectangular, free vibr. analysis by method of superposition 8-83300
 plate, orthotropic multilayered, acoustic transmission loss 8-83143
 plate, orthotropic multilayered, vibr. modes, acoustic transmission 8-83142
 plate, rectangular, with clamped simply supported edge conditions, free-vibr. anal. 8-59340
 plates, rectangular stepped thickness, with edges elastically restrained against rotation, vibrations 8-90740
 plates, rectangular thin, effect of different edge flexibility coeffs. on transverse vibrs. 8-83294
 Poiseuille flow, at large Reynolds numbers, Navier-Stokes eqn. soln. (Russian) 8-59364
 Poiseuille flow, plane, horiz., rot., stability, effect of Coriolis force 8-67203
 polyatomic molecules, isotopic reduced partition function ratio approx., by polynomial perturbation method 8-66530
 PWR core, variational estimate of eigenvalue of neutron diffusion eqn. 8-58322
 reflected cylindrical reactor, eigenfunction and numerical solns. to critical problem 8-58326
 rigid rotor in electric field, energy eigenvalues, Brillouin-Lowdin perturbation expansion 8-62690
 rigorous lower bounds to energy levels, Brillouin Wigner perturbation theory, finite summations 8-54216
 S-matrix theory, determinant and its relation to number of eigenvalues due to perturbation 8-58132
 scalar wave scatt. by slender body of revolution 8-81857
 Schrodinger eigenstates, pointwise bounds, probabilistic approach 8-93544
 Schrodinger eqn., one dimensional, gap between asymptotic degenerate eigenvalues, quantum and semiclassical methods 8-57803
 Schrodinger eqn. with double-minimum potential, numerical integration 8-58573

eigenvalues and eigenfunctions continued

- Schrodinger eqn. with singular pots., scatt. phase shifts and eigenvalues 8-62102
 Schrodinger eqns. in exterior domains, nonexistence of nontrivial solns. 8-65819
 Schrodinger operator eigenvalues, proof of nonexistence 8-81878
 self-avoiding random walks, eigenvalues Monte Carlo determ. 8-57849
 self-conjugate and positive definite operator, simultaneous calc. of eigenvalues (*Ukrainian*) 8-54154
 semi-classical bounds for eigenvalues of Schrodinger operators 8-70010
 shell, cylindrical, nonuniform axial edge load, thermal load, linear buckling 8-63345
 shell model eigenvector components, distrib., invariance props. of random matrices ensemble 8-62492
 singularity at corner of wedge shaped punch or crack 8-83252
 skew-symmetric eigenvalue problem, algorithmic formulations 8-77673
 solotone effect and torsional eigenfreqs. of spherical shell 8-92798
 solution of the Dirac equation with anomalous magnetic moment 8-82133
 spectral modal analysis program DYNA-M, structures containing up to 40 lumped masses, DEMOS-E library program 8-92800
 spherical dome, three-dimens. elasticity soln. and edge effects 8-59306
 spin system, isotropic, N-component, with long- and short-range interactions, crit. behaviour 8-76256
 stationary axially symmetric Einstein eqns., linear eigenvalue problem, complete integrability 8-77780
 Stokes flow in a trench between concentric cylinders 8-83360
 Stokes flow in conical trenches 8-83413
 SU(2), eigenstates of complex linear combinations of J_1 , J_2 , J_3 8-58139
 SU(2) gauge fields, eigenspinor-eigenvalue eqn. 8-78076
 surface waves, existence in nonhomogeneous elastic semi-space 8-67071
 torsional eigenfreqs. of spherical shell, asymptotic distrib. 8-88800
 transport problem stationary, generalised, Laplace operator eigenfunction series soln. (*Russian*) 8-81931
 two-point boundary-value problems with eigenvalue parameter in boundary conditions 8-73830
 variational interpolation of linear functionals of inhomogeneous eqns. 8-49638
 vibrating plates, reposing on springs, numerical solutions and eigenvalues (*French*) 8-79245
 WKB approx. and scaling behaviour for Helmann-Feynman and virial theorems 8-86193
 H, eigenvalue resonances in Stark effect and perturbation theory 8-90118
 NO, $v=0,1$ states, spectroscopic data calc. 8-86851

eigenvectors see *eigenvalues and eigenfunctions***eightfold way** see *SU₃ theory***Einstein-de Haas effect**

see also *gyromagnetic ratio*
 measurement, balance appl., thermal noise effect 8-65906

einsteinium

see also *nuclei with*

No entries

einsteinium compounds

No entries

elastic aftereffect

Ag-Zn (30 at.%), electron irradiated, atomic mobility, elastic aftereffect meas. (*French*) 8-63874

elastic constants

see also *elastic moduli*

- alkali halides, interionic potentials, completely independent specification of Born-Mayer potentials 8-55828
 alkali hydrides, bulk props. prediction from molecular behaviour 8-51468
 alkali metals, elastic constants, temp. depend. 8-51603
 alkali metals, electron fluid model 8-75738
 Anderson-Gruneisen parameter for cubic crystals 8-79672
 β -brass, cryst. struct., elastic consts., central force model 8-51637
 brass, elastic constants, third order, from US velocity meas. 8-76687
 cholesteric liquid crystal mixture, with positive dielectric anisotropy influence of external fields (*Rumanian*) 8-59751
 compliance and K_1 calibration of double cantilever beam specimens 8-55598
 conical inclusions, singularity values for ranges of elastic constants 8-51071
 cyanobiphenyls, 80CB and its mixtures with 7CB, orientational order and elastic consts. 8-91245
 diamond, zone-centre optical phonon, effect of uniaxial stress, elastic consts. determ. 8-91399
 dicalcium lead propionate, ferroelec., piezoelec. and elastic props. 8-84528
 p,p'-diheptylazobenzene, nematic, physical props. 8-79524
 fatigue crack growth, mechanisms 8-64703
 ferroelectrics, low lying vibrational modes, crit. behaviour of uniaxial materials 8-84539
 fibre reinforced composites calculation of stress distrib. and X-ray elastic consts. (*German*) 8-52883
 fluorite crystals, Brillouin scatt. and high temp. disorder 8-80365
 forsterite, elastic constants of single crystal, temp. var. 8-92818
 incoherent ellipsoidal precipitate, re-exam. of elastic strain energy 8-51676
 laminate, calculation of stress distrib. and X-ray elastic consts. (*German*) 8-52883
 liquid crystal, tensor field of weak inhomogeneous orientational ordering (*Russian*) 8-67640
 metallic materials, mech. stressed, lattice strain distrib., X-ray elastic const. calc. (*German*) 8-52884
 methylammonium aluminium sulphate, third order elastic consts. from stress shifted reson. freqs. 8-55905
 microinhomogeneous media, appl. of random functions theory (*Russian*) 8-63280
 nematic liquid crystals, IR absorption, strong positive dielec. anisotropy, elastic consts. 8-75545
 octyl-cyanobiphenyl, elastic props. near nematic-smectic A transition 8-59756

elastic constants continued

- orthoentstatite 8-85546
 partially disordered crystal, lattice dynamic model 8-83897
 phenomenological theory of elastic constants anomalies near struct. transition 8-67765
 piezoceramic elastic compliance and mechanical Q-factor at high drive levels 8-60395
 polyethylene, oriented, elastic stiffness constants, US meas. 8-76690
 polymer complex dielec. permittivity and compliance, algorithm for calc. freq. dependence 8-68442
 Potts model, three state, order-disorder structural transform. exam. 8-83918
 α -quartz plate frequency changes rel. to electroelastic tensor and second-order phenomena 8-60398
 rare earth-iron alloys, elastic vs. magnetoelastic anisotropy 8-68347
 rocks, meas. at high press. in cubic press. 8-69337
 semiconductor alloy, pseudobinary, phase diagram calc. 8-52786
 shallow thin shell finite element, stiffness matrix development 8-90705
 sintered two phase material, calculation of stress distrib. and X-ray elastic consts. (*German*) 8-52883
 steel, austenitic stainless, X-ray elastic constants, determination by ψ_0 oscillation method (*Japanese*) 8-64575
 steel plates, hot rolled, anisotropic texture, exam. of elastic deformation behaviour (*Japanese*) 8-64586
 stress intensity factors, UNCLE finite element system calcs., appls. in fracture mechanics 8-67098
 stress intensity factors in plane or axisymmetric problems, calc. using weight function concept and crack closure 8-67102
 transition metal, BCC, phonon dispersion curves and elastic, calc. using cohesive energy 8-59885
 Al, elastic properties (*Russian*) 8-56678
 Al₂Cu, single cryst. elastic consts., 4.2-300K 8-72803
 Al₂O₃, single crystal, fracture mirror formation, anisotropy of fracture surface energy and elastic constants 8-68824
 Al₂(SO₄)₃ soln., adiabatic and apparent molal compressibility determ. from US vel. meas. 8-63797
 As, zone centre phonons and elastic consts., hydrostatic press. depend. 8-59905
 Au, pseudopotential, fitted to elastic data 8-75705
 BN, hexagonal, long optical vibrs., elastic consts. from valence force consts. 8-51621
 Ba(NO₂)₂·H₂O, hexagonal, piezoelec., electro-optic, dielec., elastic, thermoelastic props., space groups 8-76388
 BaTiO₃, dielec. and elastic consts., temp. depend. (*Russian*) 8-64307
 BaTiO₃, ferroelectric ceramic, dielec., piezoelec. and elastic props., orientational contrib. 8-68468
 Bi, US propagation anomalies, under hydrostatic press. (*Russian*) 8-83884
 Bi, zone centre phonons and elastic consts., hydrostatic press. depend. 8-59905
 Cd₂Ge₃As₁₁, press. depend. 8-72064
 Ce₂(SO₄)₃ soln., adiabatic and apparent molal compressibility determ. from US vel. meas. 8-63797
 CsAl(SO₄)₂·12H₂O, third order elastic consts. from stress shifted reson. freqs. 8-55905
 CsCdF₃, nonlinear elastic behaviour, US velocity, 1 bar-3 kbar 8-59851
 CsPbCl₃, elastic constants and thermal expansion, near struct. transitions 8-59849
 Cs₂S₂O₆, hexagonal, piezoelec., electro-optic, dielec., elastic, thermoelastic props., space groups 8-76388
 Cu-Sn (15 at.%), temp. depend. of elastic consts. above martensitic transition temp., US exam. 8-76695
 Cu-Zn-Al (19.3, 13.0 wt.%), effect of hydrostatic or uniaxial stress on elastic consts., near martensitic transformation point 8-76697
 Fe, elevated temps., US vel. obs., transmitting receiving pulse method 8-75830
 Fe-B, binary alloys, giant ΔE effect and Elinvar characts. 8-76291
 Fe₃Pt, Invar alloy, theory of elastic-anomalies 8-95505
 GaN, elastic constant calc., elastic wave propag. vel. 8-87734
 Ho, magnetoelastic interactions 8-64252
 HoAl₂, magnetoelastic effects on elastic consts., 4.2-280K 8-72385
 K, device for press. variation of yield stress, elastic constants 8-53047
 KAl(SO₄)₂·12H₂O, third order elastic consts. from stress shifted reson. freqs. 8-55905
 KCN, Brillouin line width of phonons 8-80370
 KCN, dipolar impurity tunnelling model, elastic interaction and const. 8-71826
 KCN, order-disorder transition, press. and temp. depend. of soft elastic const. 8-79769
 KCl_{1-x}CN_x, dipolar impurity tunnelling model, elastic interaction and const. 8-71826
 LaAg_{1-x}In_{1-x} alloys, structural instability 8-79562
 LiClO₄·3D₂O, hexagonal, piezoelec., electro-optic, dielec., elastic, thermoelastic props., space groups 8-76388
 LiClO₄·3H₂O, hexagonal, piezoelec., electro-optic, dielec., elastic, thermoelastic props., space groups 8-76388
 metals, model pseudopotential calcs., elastic consts., spin susceptibility, Fermi surface distortions 8-79922
 ND₄Cl, order-disorder transformation, elasticity and heat capacity temp. depend., US obs. 8-71851
 NH₄Al(SO₄)₂·12H₂O, third order elastic consts. from stress shifted reson. freqs. 8-55905
 NH₄H₂PO₄, improper antiferroelec. phase transition, elastic props., free energy, thermodynamic theory 8-80299
 NaCN, order-disorder transition, press. and temp. depend. of soft elastic const. 8-79769
 NaClO₃, single crystals, change of elastic constants by gamma radiation 8-63800
 NaNO₂, adiabatic and isothermal elastic compliances, critical behaviour 8-92031
 NaNO₂, elastic constants and US attenuation coeffs., anisotropic charact. 8-63809
 Nb third-order elastic consts. using nonlinearity parameter 8-75733
 Nb-Zr(Hf)(W) alloys, single cryst. elastic consts. 77-298K 8-84879
 Nb₃Sn, A-15 compounds, interlattice displacements, elastic consts. 8-55906
 NbTi filament reinforced Cu, superconducting composite, elastic const., temp. depend. 8-68717
 Nd, elastic constants, low-temp., mag. field depend. 8-76290

elastic constants continued

- Pb, elastic properties (*Russian*) 8-56678
 Pb₃MgNb₂O₉, diffuse phase transition, Brillouin scatt. and acoustic phonons 8-76401
 PbS-As₂S₃, glass, elastic props. temp. depend. 8-71780
 PbTiO₃, ferroelectric ceramic, dielec., piezoelec. and elastic props., orientational contrib. 8-68468
 Pr, elastic constants, magnetic effects 8-68355
 RbAg₂I₃, third order elastic constns. at room temp. using 110 cut 8-59848
 RbCaF₃, nonlinear elastic behaviour, US velocity, 1 bar-3 kbar 8-59851
 RbCdF₃, nonlinear elastic behaviour, US velocity, 1 bar-3 kbar 8-59851
 RbI, elastic constants determ. by inelastic neutron scatt. 8-79659
 Sb, zone centre phonons and elastic constns., hydrostatic press. depend. 8-59905
 Sc, lattice dynamics, sp.ht. and bulk modulus 8-71814
 SiO₂, fused, US study by harmonic generation, elastic constns., Gruneisen parameters 8-83735
 Tb_{0.3}Dy_{0.7}Fe₂, elastic vs. magnetoelastic anisotropy 8-68347
 TiO₂, rutile, ferroelectric ceramic, dielec., piezoelec. and elastic props., orientational contrib. 8-68468
 TiCdF₃, nonlinear elastic behaviour, US velocity, 1 bar-3 kbar 8-59851
 TmPO₄, Jahn-Teller induced elastic constant changes, 4.2 to 300K 8-79657
 V₂Ge, third order elastic constns. 8-88490
 V₃Si, third order elastic constns. 8-88490
 V₂Si(Ge), A-15 compounds, interlattice displacements, elastic constns. 8-55906
 ZnS struct. solids, second and third order 8-63799

elastic deformation

- see also bending; elasticity; electrostriction; stress/strain relations; torsion
 aeolotropic cylindrical shell, nonhomog., hollow, thick-walled, torsional stresses 8-75068
 anisotropic media, elastic strain energy of precipitates, and periodic distrib. inclusions 8-84810
 annular plate of inhomogeneous material, variable loading and heated conditions 8-94594
 antiphase problems in linear elasticity theory (*French*) 8-87268
 anvil, truncated, compressive strength, high press. apparatus appl. 8-84906
 arterial wall axial deform. and anisotropy (*Japanese*) 8-53437
 axisymmetrical homogeneous elastic solid with internal circular cracks, energy release rates 8-67139
 bar with space curve axis, loaded bar shape calc. 8-51069
 beam, elastic, on elastic half-space support, forced flexural vibr. 8-63353
 beam dynamic deflection under external force of time-dependent frequency 8-83289
 beams, 1-D, stability in torsional extension (*German*) 8-87270
 beams, straight, finite displacements and small deform., asymptotic anal. (*French*) 8-90716
 bi-material, elastic composite, Southwell's analogues for plane and bending problems 8-87265
 Boussinesq problem for material with different moduli in tension and compression 8-55564
 brittle abrasive material, rating capability for elastic deformation 8-56680
 brittle solids, unstable growth of thermally induced interacting cracks 8-63374
 cantilever (Timoshenko), elastically restrained, with attached masses, follower force stability 8-63347
 channel, straight (buckled), two-dimens. flow, stability anal. 8-59490
 circular cylinder, micropolar, elastic, flexure problem 8-51083
 composite material, longitudinally cracked, exam. of plane deformation 8-67096
 composite rod, small deformations, initial stresses effect 8-63284
 conical shells, axially compressed with edge constraint, elastic and plastic buckling 8-63341
 consolidating semi-space, axisymmetric punch problem with mixed boundary, permeability conditions 8-51087
 contact problem with friction, solution using nodal parameters (*French*) 8-63401
 contact stress minimisation by contour design 8-63396
 crack tip singularity, order changing at discontinuity 8-59345
 cracks, curvilinear, star-shaped array in infinite isotropic elastic medium 8-55609
 cracks, model deduced from thermodynamics (*French*) 8-63386
 crystalline solids, absolute strain rate in elastic deformation, model 8-75073
 crystalline solids, discontinuous nature of elastic deformation 8-75072
 crystals, device for low temp. uniaxial compression 8-49809
 cubic boxes subjected to pressure, exptl. stress and strain anal. 8-59307
 cylinder, circ., elastic, axial eigenfunctions orthogonality 8-51080
 cylinder, compressible, under uniform compression, stability (*Russian*) 8-55577
 cylinder, infinite, solid, diametrically opposite conc. load deform. and stress 8-63287
 cylinder, thin, deformation due to band press. 8-94595
 cylindrical elastic tube torsional oscillations under large internal and external press. 8-79249
 cylindrical shell, transverse shear effect on axial crack 8-67090
 cylindrical shell with circular cut out, uniform bending, strength and flexural rigidity 8-87282
 diamond composite with Cu-Ti matrix, microstresses, X-ray diff. exam. 8-56679
 director rod, elastic instability 8-63292
 discs, anisotropic, singular integral eqn. anal. (*German*) 8-87272
 dynamic rigid indentation induced by sliding frictionless contact 8-75107
 Earth, surface waves phase vel. and attenuation simultaneous inversion, Love waves appl. 8-85491
 Earth crust, free surface deform. during earthquake cycle, asthenosphere readjustment effects 8-85490
 Earth lithosphere bending at trench, elastic-perfectly plastic anal. 8-81135

elastic deformation continued

- elastic solid, cracked or notched, general numerical method for three dimensional singularities 8-67137
 elliptic crack and punch problems, Lamé polynomial solns. 8-75069
 elliptic infinite bar, impulsive loads, three dimens. elastic stress-strain anal. 8-87259
 elliptical contact deform. between elastic solids, simplified soln. 8-55616
 Euler column Lyapunov stability analysis 8-71285
 exceptional wave propagation in continuous medium, finite deform., evolution of discontinuities, elastic pot. determ. (*Italian*) 8-54202
 eye, elasticity of sclera and choroid in humans, rel. to scleral rigidity and accommodation 8-80907
 fibreglass composite, oriented, model, conditions of monolithicity, exam. 8-67044
 fluid-infiltrated elastic materials, deformation of cavities and inclusions 8-51073
 fusion reactor coil, multilayer structs., laminated beam theory anal. 8-55011
 glued joint, axially symmetric, stress determ. for torque loading (*Polish*) 8-79287
 half-space, coupled thermoelastic problems 8-59300
 hyperelastic compressible medium with cylindrical cavity, finite dynamic expansion under sudden press. 8-79213
 hyperelastic isotropic behaviour laws for large deform. (*French*) 8-77715
 ice, floating sheet, viscoelastic response under prolonged loading 8-51093
 incoherent ellipsoidal precipitate, re-exam. of elastic strain energy 8-51676
 incompressible isotropic material, speed of propagation of waves 8-54201
 indentation testing, mech. characts. calcs. inc. elastic strains (*Russian*) 8-95863
 inextensible material, uniqueness of displacement boundary-value problem 8-54195
 infinite elastic solid with spherical inclusions, linear elasticity eqns., stresses, displacements 8-65773
 integral equation formulation of plane deform. of isotropic incompressible solid 8-51081
 interface separation for elastic layer on rigid plane, loaded by rigid stamp 8-87307
 laminated composite, dynamic response under large deformation, nonlinear mixture theory 8-56717
 laminated rectangular antisymmetric angle ply plates, shear deform. effects on vibr. 8-63356
 large deflection of a shallow spherical shell subjected to uniform normal pressure and heating 8-94593
 linear elastic half-space, frictional unloading problem, variational soln. for stress analysis 8-59350
 liquid-filled circular cylinder, influence of bulge terms on section and deform. (*German*) 8-90717
 lithosphere, elastic-perfectly plastic bending under generalised loading, appl. to Kuril Trench 8-73341
 lithosphere, subducting, dynamic support of ocean trench outer rise 8-81116
 long-wave quasiparticle states localized at screw dislocation (*Russian*) 8-95126
 membrane, elastic support, mixed boundary-value problems, variational principles and hypercircle 8-57749
 membrane, rectangular under uniform pressure, large deflections 8-55560
 membranes, elastic, universal deforms. 8-67048
 metal, elastically strained, elec. field gradients on nuclei, calc. (*Russian*) 8-60096
 metallic materials, mech. stressed, lattice strain distrib., X-ray elastic const. calc. (*German*) 8-52884
 metallic structures, magnetostriction method of measuring elastic stresses 8-72985
 metals and alloys, polycrystalline, LF viscosity meas. 8-80576
 microhardness, Knoop numbers, correction factors, elastic recovery 8-72952
 mixed boundary-value problems soln. by direct variational method 8-83331
 non-linear viscoelastic behaviour, numerical anal. 8-59318
 nonhomogeneous elastic layer bonded to nonhomogeneous half-space, torsion by circular die 8-87263
 nonlinear dynamic mech. moduli 8-60693
 nonlinear elastic stability problems using a finite difference perturbation method 8-83273
 nonlinear finite elasticity, uniqueness condition, work theorem 8-57784
 nonlinear isotropic medium, symmetric spherical wave propagation eqns., permissible transform. (*Russian*) 8-87292
 nylon, oriented, transverse compression 8-68728
 orthotropic cantilever beams, Rayleigh-Ritz determ. of upper and lower bounds 8-59298
 piezoelectric plate, infinite, on elastic medium, transient response to pot. pulse 8-52442
 piezoelectric thin plates, integer polynomial solns. (*Russian*) 8-52444
 planetary bodies, ancient, deform. energy rel. to lunar capture hypothesis 8-81570
 plate, deformation instability in brittle fracture mechs. problems 8-63382
 plate, elastic deform. due to axisymmetric punch 8-75065
 plate, heated equilateral triangular, large deflection, uniform load, temp. distrib. 8-83250
 plate, homogeneous high-order deformation theory 8-63308
 plate, laminated, high-order deformation theory 8-63309
 plate, orthotropic, irregular, on elastic foundation, vibrs. under in-plane forces 8-79251
 plate, right angled isosceles triangle, on Pasternak-type viscoelastic foundation, deflection 8-75075
 plate, thin circular, bending, parabolic loading over concentric elliptic limaçon 8-59299
 plate bending theory, optimal thickness distrib. (*Russian*) 8-63295
 plates, tapered, circular, with affine imperfections, large deflections, stresses 8-75070
 PLT toroidal field coils, operational deflection meas. 8-62627
 PMMA, nonlinear dynamic mech. moduli 8-60693

elastic deformation continued

- polycrystals, intensity and lattice strain distrib., calc. from inverse pole figures (*German*) 8-52885
 polyethylene, crystals, subject to fold-surface tensile stress, elastic deform. 8-76712
 polyethylene, hard elastic fibres, deform. and struct., -196 to 80°C 8-51437
 polyethylene extrudate, transverse compression 8-68728
 polyhedral sandwich domes, elastic behaviour, failure, practical investigation and numerical simulation 8-59309
 polysilicane gel on glass plate, elastic deformation in adhesion of solids 8-60010
 pre-stress, influence on imperfection sensitivity 8-67035
 prism bending to helical form, formal perturbation scheme 8-55558
 propagating rectangular fracture in semi-infinite elastic medium 8-57168
 punch-elastic body dynamic contact, superseismic stage, exact soln. 8-55614
 quartz, synthetic, growth boundary between -X and Z' sectors 8-59775
 quartz, synthetic, growth sector boundary between -X and Z sectors 8-59774
 rectangular bar, semi-infinite, longitudinal impact, elasticity eqns. anal. 8-90703
 rubber stress/strain relations, uniaxial extension and compression 8-80578
 rubbers vulcanized, biaxial finite deformation props. (*Japanese*) 8-84939
 semiconductors, subsurface strain, reconstruction induced, theory, appl. to Si (100) 8-63914
 shafts, with abrupt changes of section, flexibility of shafts 8-90711
 shear deformations, generalised, for isotropic incompressible hyperelastic materials 8-94599
 shell, nonlinear elastic cylindrical biharmonic excitation, parametric vibrations (*French*) 8-87294
 shell theory (*Ukrainian*) 8-83244
 singularity at corner of wedge shaped punch or crack 8-83252
 solid lubrications dynamics, obs. using Micro Contact Imager 8-85002
 spherically symmetric elasticity problems, finite element soln. 8-63293
 spring, complex arch type, movable, snap-through action characts., appl. to microswitches 8-63339
 spring, complex arch type, movable, snap-through action characts., microswitch-appls. 8-63340
 springs, thin, of constant cross section, elastic behaviour calc. and obs. (*German*) 8-87269
 square plate, large deflection, behaviour according to Foepl and Von Karman 8-63296
 steadily moving load, elastic strip on rigid foundation, noncontact regions, displacements, contact press. 8-87264
 steel plates, hot rolled, anisotropic texture, exam. of elastic deformation behaviour (*Japanese*) 8-64586
 strain energy of solids with different moduli in tension and compression, small strain theory (*French*) 8-87261
 stretched plates weakened by inner curvilinear holes 8-55567
 strip, arbitrarily oriented crack distrib. (*Russian*) 8-63378
 surface deform. of opt. flats and Fizeau method for film thickness meas. 8-77970
 tensile conc. optimisation using iterative method (*German*) 8-87271
 thermoelastoplastic medium, variables for universal deform. representation 8-49666
 thin circular quadrant, singularly loaded, with clamped radial edges and free circular edge 8-63300
 transverse deformations associated with rectilinear shear in elastic solids 8-86162
 transverse flexure of rectangular plate of arbitrary stiffness (*Russian*) 8-51084
 tube, cylindrical, thick-walled, finite twist and external press., stability, vibrs. 8-83286
 turbulent flow, press. fluctuation spectrum, elastic boundary compliance effect 8-63422
 viscoelastic deformation, finite, one-dimens., impulsive response, constraints (*French*) 8-51092
 viscoelastic media, deform. theory with account of thermodiffusion (*Ukrainian*) 8-67052
 viscoelasticity, nonlinear, estimate for work 8-55572
 wedge stroke blow, along membrane at surface of incompressible liquid (*Russian*) 8-55561
 wood particle board, method of mech. testing, elastic deform. meas. 8-56837
 (Al,Ga)As/GaAs, LPE grown heterostructures, X-ray diff. exam. of interfacial elastic strains 8-72019
 Al, US velocity, anomalous response to applied stress 8-63811
 Cu, deformed, intensity and lattice strain distrib., exam. (*German*) 8-52885
 Fe, elastoresistivity effect, meas. of resistance at 4.2K and 300K, using mag. field method 8-72132
 Fe-Co-Cr-W-Ni-C, alloy KKhVN, transforms. during annealing and nature of hardening (*Russian*) 8-56653
 Fe-Ni-Si, double spontaneous reversible deformation during thermal cycling 8-84942
 Ge, deformation, annealing characts., X-ray study 8-75713
 Nb, elastically deformed, quadrupole effects, NMR line intensity (*Russian*) 8-56400
 Si, deformation, annealing characts., X-ray study 8-75713
 Si, plastically deformed, hot-exciton luminesc. as function of strain 8-88361
 V, elastically deformed, quadrupole effects, NMR line intensity (*Russian*) 8-56400
 Zr-Sn alloys, mathematical models for transient deform. 8-86616

elastic hysteresis

- cyclic plasticity and masing behaviour in metals and alloys 8-64616
 glass fibre reinforced vinyl ester matrix, axial fatigue failure sequence and mechanism 8-68773
 impact vibration, steady, body with impact hysteresis characts., stability anal. 8-51099
 rubber, hysteretic behaviour, thermomech. study 8-76692
 screw connections, bend and tension loaded, hysteresis (*German*) 8-87312

elastic hysteresis continued

- shafts, noncircular cross section, effect of external forces and internal friction on rotary motion (*French*) 8-63274
 steady state response of systems with hardening hysteresis 8-60680

elastic limit

- brass sheet, in-plane stretching, limit strain meas. 8-80573
 resolution method for second problem of elastic limits for plane (*French*) 8-57779
 steel, low alloy, type 4340, quenched and tempered, effect of plastic strain followed by ageing, on torsion fatigue resistance 8-92360
 steel, sheet, in-plane stretching, limit strain meas. 8-80573
 steel, silver, elastic limit, bending strength, and ductility rel. to tempering temp. after quenching 8-95764
 Al sheet, in-plane stretching, limit strain meas. 8-80573
 Be bronze, str. and props. after ageing under load 8-84932
 Be bronze, BrB2, quenched deformed, substruct. and props., effect of prerecrystallisation annealing (*Russian*) 8-60677
 Ta wire, strain ageing by return of elastic limit method (*French*) 8-68713

elastic moduli

- see also Poisson ratio; shear modulus; Young's modulus
 alkali halide crystal, fourth order elastic moduli 8-91373
 alkali metals, third order elasticity moduli, temp. depend. (*Russian*) 8-63798
 Anderson-Gruneisen parameter for cryst. of cubic symmetry, determ. using elastic moduli 8-79713
 bone, US transducer, shear-wave vel. meas. 8-83201
 Boussinesq problem for material with different moduli in tension and compression 8-55564
 bovine hip bone, compression tests, effect of specimen shape and size on mech. props. and fracture mode 8-69132
 bulk moduli, Wachtman's eqn., and temp. depend. 8-75799
 compressed crystals, dislocations and point defects (*Russian*) 8-75666
 concrete, elastic modulus variations, gauge meas. by embeddable-strain-units 8-84878
 covalent crystal, resistance to microindentation 8-60753
 crystal classification by acoustic props. 8-79547
 crystals, strain wave vels., Poisson ratios and elastic moduli 8-51609
 cubic crystals, theoretic props. at arbitrary press., density and bulk modulus 8-51606
 cushion dynamic props. by mech. impedance method 8-72953
 dental restorative materials, empirical eqn. including fracture toughness for friction 8-61283
 double lapped composite joints, efficiency in bending, of steel/B reinforced Al or epoxy adherends 8-68870
 E-glass fibre reinforced epoxy, room temp. curable, mech. props. and thermal conductivity 8-68669
 enstatite, elastic modulus and internal friction in single crystal 8-85550
 Epon 828 epoxy, composite three dimensional model for photoelasticity 8-52871
 epoxy resin, low temp. irradiation effects on mechanical props., use in superconducting magnets 8-60737
 epoxy structural adhesives, tensile tests, stress/strain relations, stress relaxation 8-60702
 ethylene copolymers, partially crystallised, quasistatic moduli at small strains (*German*) 8-76700
 FCC lattice, uncorrelated-pairs approximation for anharmonic free energy, tests 8-59920
 fibre reinforced ionomer composites, fatigue strength, dynamic viscoelastic props. and fracture surface exam. (*Japanese*) 8-92339
 fibrous composite material, estimate for composites isotropic on the average 8-51077
 film on cylinder, calc. of moduli (*Russian*) 8-63304
 forsterite, elastic modulus and internal friction in synthetic polycrystal 8-85550
 gels, dynamic light scattering in poor solvent 8-88318
 glass ceramic, machinable, elastic moduli press. and temp. derivatives, specific heat 8-52873
 glass fibre reinforced plastics, under compressive load (*Japanese*) 8-92301
 glass microsphere reinforced, composite, mech. charact. calc. 8-64578
 glass/C reinforced epoxy resin, hybrid effects, conditions for positive or negative effects vs. rule of mixtures, mech. props. 8-68769
 graphite fibre reinforced epoxy laminates, expt. investigation of tensile moduli and strength 8-52870
 hardened components, residual stress, elastic characts. after surface plastic stress 8-60901
 hardness, elastic moduli, density, cryst. temp., mech. props., for flywheel appl. (*Dutch*) 8-52878
 II-VI semiconductors, electronic theory, cryst. energy and bulk modulus 8-72104
 III-V semiconductor, electronic theory, cryst. energy and bulk modulus 8-72104
 incoherent ellipsoidal precipitate, re-exam. of elastic strain energy 8-51676
 intervertebral joint, systems identification for material props. 8-69125
 isotropic composite material containing spherical inclusions at nondilute concs., effective elastic moduli 8-67037
 metallic glass, hardness, elastic moduli, density, cryst. temp., mech. props., for flywheel appl. (*Dutch*) 8-52878
 muscle, glycerol-extracted fibrillar fibres, cross-bridge slippage induced by AMP-PNP and stretch 8-77075
 muscle, mech. pulse propag. vel. meas. using piezoelectric crystals, elastic moduli 8-92668
 oblate spheroidal inclusion, internal stress, misfit, inhomogeneity and plastic deform. 8-60701
 4-n-octyloxy-4'-cyanobiphenyl, smectic A liq. cryst., elastic modulus determ., stress/strain relationships 8-91229
 peridotite, elastic modulus and internal friction 8-85550
 plastic powder compact rheological characteristics (*Japanese*) 8-95770
 PMMA, viscoelastic props., γ -irrad. influence (*Russian*) 8-88492
 poly(p-phenylene terephthalamide) fibres, chain orientation distrib., and elastic props. 8-75566
 polyacrylamide-water gels, copolymerised with N,N-methylene bisacrylamide, dynamic light scatt. 8-60477
 polycrystalline material, scatt., lattice representation 8-65774
 polyethylene, dynamic mech. behaviour, longitudinal cryst. thickness 8-76691

elastic moduli continued

- polyethylene, filled, model, effect of stiff fillers on elastic modulus 8-68720
- polyethylene, filled with glass particles, uniaxially drawn, elastic constants, filler addition effect (*Japanese*) 8-95780
- polyethylene, lamellar structs. nucleated onto fibrous substrates for high modulus 8-75578
- polymer, particle-filled, elastic moduli, interfacial slippage effect anal. 8-76688
- polymer films and sheets 8-80590
- polymers, composite three dimensional model for photoelasticity 8-52871
- polymers, elastic moduli, press. depend. 8-52877
- polymers, mech. props., temp. dependence of polymers of different struct., 4.2 to 300K 8-68746
- polymers in glassy state, calc. method from chem. struct. (*Russian*) 8-75707
- polymethylpentene, viscoelastic props., γ -irrad. influence (*Russian*) 8-88492
- polypropylene fibres, homologue mixtures, props. 8-76709
- polystyrene, microcryst. cellulose filled, glass transition temp. shifts 8-95144
- polyvinylidene fluoride, film, piezoelec., pyroelec., thermal expansion, elastic const. 8-84529
- prolate spheroidal inclusion, stress conc. 8-67042
- PVA, microcryst. cellulose filled, glass transition temp. shifts 8-95144
- random media, effective moduli, unified calc. of bounds and self-consistent values 8-91372
- rare earth cobalt intermetallics, RCO_2 , elastic moduli, 4.2-300K 8-52332
- schorl tourmaline, elastic const. 8-68718
- soft elastic material dynamic props. determ. (*German*) 8-71297
- β -spodumene-mica glass ceramic, thermal expansion thermal shock and moduli of rupture and elasticity 8-60736
- steel, 12X2H4A, nonmetallic inclusion effect on plasticity and impact strength (*Ukrainian*) 8-92296
- steel, austenitic stainless, fast neutron irrad., effect on mech. props. 8-92309
- steel wire reinforced Portland cement mortar, wire pull out, inelastic behaviour 8-56681
- technological strength and nondestructive methods of testing during heat treatment 8-85090
- TGS, large scale inhomogeneity effect on ferroelectric transition (*Russian*) 8-76411
- TGS, sound group vel. vector direction, temp. depend. 8-67774
- transition metal, 3d and 4d, local density theory, mech. and mag. props. evaluation 8-91630
- transition metal alloys, elastic properties, vol. depend. 8-95103
- transition metals, solubility of H_2 and bulk modulus 8-55950
- Ag, electron irrad., elastic moduli and internal function (*French*) 8-87703
- AgBr, bulk modulus fall, curvature of conductivity plots, consequence of anharmonicity 8-79800
- AgCl, bulk modulus fall, curvature of conductivity plots, consequence of anharmonicity 8-79800
- AgI, sound vels. and bulk moduli near phase transitions with negative dP/dT 8-83885
- Al, elastic properties (*Russian*) 8-56678
- Al, mechanical deformation with superimposed insonation, volume effects 8-60723
- As_2Se_3 :Ag, amorphous US props. 8-51616
- As_2Se_3 :Ag, amorphous, US props. 8-51616
- Au, lattice vibr., electron press., central part pot. model calc. 8-75749
- Ba, elastic properties, Debye temp., 20°C, 20 to 70 kbar, US wave velocity meas. 8-87735
- $\text{Ba}(\text{NO}_3)_2$, press. derivatives of elastic-moduli, ultrasonic velocity meas. 8-95102
- C, isotropic pyrolytic, for biomedical devices, mech. props. 8-65150
- β - CaSiO_3 fibre, continuous unidirectional crystallisation from melt 8-95739
- CsPbCl_3 , O_h - D_{4h} transition, US and thermodynamic props. 8-67826
- Cu alloys, flat spring, mechanical props. in bending, stress relax. test, 23 to 232°C 8-72806
- Cu, amplitude depend. modulus effect 8-64573
- Eu_2O_3 - Ta_2O_5 , microcracking, elastic props., internal friction 8-92326
- Fe and related compounds, bulk moduli from hydrostatic compression 8-83862
- Fe, cast grey, effect of quenching conditions, on elastic modulus 8-56675
- Fe, glassy, heat of crystn., and bulk modulus, calc. using struct. model 8-51428
- Fe-Al (12 wt.%) alloy 23 kHz US transducer piezomagnetic props. 8-59240
- Fe-B alloy reinforced polysulphone exam. of tensile and flexure props. 8-72823
- Fe-B metallic glass, hardness, elastic moduli, density, cryst. temp., mech. props., for flywheel appl. (*Dutch*) 8-52878
- Fe-Co-Cr-W-Ni-C, alloy KKhVN, transforms. during annealing and nature of hardening (*Russian*) 8-56653
- α - Fe_2O_3 (haematite), X-ray diff. compression studies under hydrostatic isothermal conditions 8-85539
- Ge-Se glass, elastic props. under press., US interferometry 8-79658
- LiNbO_3 , LF sound attenuation, internal friction 8-63804
- $\text{Li}_2\text{O-Al}_2\text{O}_3\text{-SiO}_2$, glass ceramic, elastic props. at high press., US meas. 8-83863
- Mg-Zn metallic glass, hardness, elastic moduli, density, cryst. temp., mech. props., for flywheel appl. (*Dutch*) 8-52878
- γ -Mn-Ni-C, elastic anomalies, martensitic transformation in Mn rich alloys 8-84807
- Mo, elastic moduli meas. (*Russian*) 8-75704
- Nb-Ni metallic glass, hardness, elastic moduli, density, cryst. temp., mech. props., for flywheel appl. (*Dutch*) 8-52878
- PVC-Cu, particulate composite, mech. props. effect of particle size 8-95799
- Pb, elastic properties (*Russian*) 8-56678
- $\text{Pb}(\text{NO}_3)_2$, press. derivatives of elastic-moduli, ultrasonic velocity meas. 8-95102
- PbS, thermomech. props., SCF $X\alpha$ scatt. wave theory 8-71704
- p-Si, photosensitivity of elastic moduli and surface tension 8-83864
- SmS, f-d hybridisation, valence fluctuation and phonon spectrum, Raman scatt. expts. 8-60464

elastic moduli continued

- $\text{Sr}(\text{NO}_3)_2$, press. derivatives of elastic-moduli, ultrasonic velocity meas. 8-95102
- $\text{Tb}_{0.27}\text{Dy}_{0.73}\text{Fe}_2$, perpendicular suscept., magnetomechanical coupling and shear modulus 8-91918
- (Ti,V)C carbides, prep. and mech. props. 8-64518
- α -Ti alloy, VT1-1, cold rolled, recrystn. texture and prop. anisotropy 8-52846
- Ti, mechanical deformation with superimposed insonation, volume effects 8-60723
- V-Cr, elastic moduli, US pulse echo meas. 8-84881
- V_3Si , neutron irrad., sound velocity, magnetic susceptibility and upper critical field 8-88074
- ZnSe, elastic moduli, temp. depend., 293-973K, electrostatic reson. determ. 8-59850

elastic moduli measurement

- concrete, elastic modulus variations, gauge meas. by embeddable-strain-units 8-84878
- education, coefficient of restitution of bouncing ball expt. 8-86074
- glass fibre reinforced plastics, effect of deform. rate (*German*) 8-64796
- muscle, skeletal, deriving viscoelastic modulus from transient pulse propagation 8-77077
- Poisson's ratio determ. by Moire method 8-51137
- polymer, precision meas. using reson. method (*German*) 8-76823
- polymers, dynamic shear modulus 8-60916
- rocks elastic properties determination, modified borehole jack method 8-81448
- steel, wire, dynamic moduli of elasticity meas. by travelling normal wave method 8-53110
- 4-sulphone diglycidyl ether, on Al alloy D16T alloy base, dynamic shear modulus determ., -80 to -180°C 8-60916
- travelling normal wave method for thin wire 8-53110
- Cu, thin conductor, dynamic moduli of elasticity meas. by travelling normal wave method 8-53110

elastic scattering of atoms and molecules

- asymmetric scattering, spin-1 particle by non-central field 8-55214
- atom+diatom, body-fixed formulation for close-coupling calc. 8-78768
- atom+diatom, scatt., L_z -conserving sudden approx. calcs. 8-66628
- diatomic one-electron mols., wavefunction calc., collision matrix elements, computer program 8-50457
- gas kinetic theory, elastic cross-section analytical approximation (*Russian*) 8-75248
- ion+molecule, classical differential cross-sections, anisotropic pots. 8-66627
- molecular scattering wavefunctions, algebraic approx. 8-78780
- near-adiabatic collisions, theory, electron translation factor method 8-81889
- near-adiabatic collisions, theory, scatt. coord. method 8-81890
- prior statistical distributions implied by dynamical threshold laws for molecular collisions 8-86928
- quantum-mechanical streamlines and classical trajectories in elastic scattering 8-78098
- rainbow scattering, Regge pole anal. 8-58774
- scattering amplitudes, Regge representation calcs. 8-58770
- scattering cross sections, phase shift calc. 8-78767
- spectral line shapes, linear and nonlinear, atom or mol. cross sections 8-70899
- sub-Doppler line shapes, saturation and two-photon spectra, elastic collisions, review 8-82697
- Ar, collision induced light scatt. spectra, pair polarisability 8-55135
- Ar+methane, low energy collision, close coupling and coupled states, rot. transitions 8-78784
- Ar+N₂(TIF), scatt., L_z -conserving sudden approx. calcs. 8-66628
- Ar⁺+Ar, elastic scatt. and charge exchange, differential cross section, 2.7-20 eV 8-66660
- Au⁺+X, X=H, H₂, He, C, N, O, cross-section, closure-Born approx. 8-66630
- B⁺+inert gas atom, pot. interactions 8-55219
- Cs⁺+X, X=H, H₂, He, C, N, O, cross-section, closure-Born approx. 8-66630
- H+H₂, elastic differential cross section high resolution meas. 8-50610
- H+He(Ne)(Ar)(Kr)(Xe), low energy elastic scatt. cross section MCSCF calc., van der Waals forces 8-70897
- H⁺+Cs, elastic and charge exchange collisions, projected valence bond method 8-78804
- H⁺+Cs(6s), elastic scatt., pot. determ. from differential cross-sections meas. 8-78778
- H⁺+H(D), elastic scatt. and charge exchange, resonances 8-78777
- H₂+Kr, elastic total cross section, orbiting effects, Regge theory 8-82814
- HD+D₂, rot. inelastic differential cross sections, diffr. oscills. in elastic and inelastic scatt. 8-74743
- H(1s), electron impact, elastic phase shift, post-adiabatic approx. calcs. 8-58827
- He+Ne pot., differential cross section, quantum mechanical inversion 8-70896
- He⁺+H, unpolarised and spin-change collision, low energy 8-86943
- He⁺+He, elastic scatt. and charge exchange, differential cross-section, 0.4-30 eV 8-66659
- He²⁺+He, 5 to 100 keV, elastic and double charge exchange, mol. treatment 8-82813
- He²⁺+N₂, 200-600 eV, 0-20°, comparison with He²⁺+Ne(Ar) 8-74732
- He(2³S) collisions, elastic scatt., Penning ionisation, polarisations (*Russian*) 8-70922
- I₂, angular momentum transfer, elastic, inelastic collisions, orientation and polarised fluoresc. 8-90271
- Kr⁺+He, persistence of velocity following elastic collisions 8-78779
- Li⁺+Na, charge transfer and elastic scatt., two state model 8-58805
- Li⁺+X, X=H, H₂, He, C, N, O, cross-section, closure-Born approx. 8-66630
- N₂+Ar, total differential cross section, diffr. oscills. quenching 8-66625
- Na+Ar, differential cross-section at thermal energy, Na-Ar ground state pot. 8-58769
- Ne+Ar(Kr)(Xe), elastic scatt. absolute total cross section, long range interaction 8-58768

elastic scattering of atoms and molecules continued

- Ne⁺+D₂, elastic scatt. at small angles, 1.3-3.5 keV, scaling law 8-82812
 Xe+He, saturated absorpt. of 3.51 μ m line, vel. changing collisions by line width 8-86819

elastic scattering of electrons by atoms and molecules

- see also gas phase electron diffraction*
 alkali halides, electron impact, elastic scatt., model, static and static exchange calcs. 8-94321
 atom, forward elastic electron scatt. amplitude, dispersion relation 8-90263
 atom, one-electron, scatt. asymmetry and spin polaris. 8-58820
 atomic continuum processes, R-matrix method, program 8-74558
 atoms, electron and positron forward scatt. amplitudes, anal. behaviour 8-58829
 atoms, scattering of fast electrons and positrons 8-62918
 butane, gas, electron drift vel., Ramsauer-Townsend minima in electron scatt. 8-87427
 conference, electronic and atomic collisions, Paris (July 1977) 8-58758
 DC Fano effect polarised electron source appl. to electron-atom scatt. 8-66689
 diatomic molecules, equilibrium parameters and Morse anharmonic consts., electron diffr. determ. 8-58818
 dichlorodinitromethane, mol. struct., electron diffr. investig. 8-86950
 electron and positron scatt. by atoms, cross sections, review and expt. conditions 8-58828
 electron scatt. using dilatation transforms., restricted perturbation methods 8-50639
 electron-atom collision theory, soln. of coupled integro-differential eqns. by computer program 8-86948
 ESP detector for 300-2000 eV electron, optimum conditions theory (*Japanese*) 8-66693
 ethane, gas, electron drift vel., Ramsauer-Townsend minima in electron scatt. 8-87427
 Feshbach resonances at 1 meV resolution 8-58831
 hydrocarbons, gas phase, thermal electron interactions, drift vel. meas. 8-62919
 light elements, electron backscatt. rates, Moliere approx. calcs. (*German*) 8-82841
 metal vapour, elastic and inelastic scatt. 8-58830
 methane, gas, electron drift vel., Ramsauer-Townsend minima in electron scatt. 8-87427
 molecular electron scatt., ab initio theory including polarisation 8-50640
 molecule, semiclassical perturbation theory 8-58825
 multiphoton free-free transitions in scatt. electrons induced by laser pulses 8-62917
 neopentane, gas, electron drift vel., Ramsauer-Townsend minima in electron scatt. 8-87427
 phase shifts calc. perturbation theory, one-electron target computer program 8-50637
 photoelectric effect and electron diffusion in gases 8-81745
 polar molecule electron scatt., excitation and scatt. cross sections 8-58826
 polar molecules, elastic and inelastic electron scatt. 8-94322
 propane, gas, electron drift vel., Ramsauer-Townsend minima in electron scatt. 8-87427
 R-matrix method, application to atoms and ions 8-58833
 R-matrix method, appls. to electron mol. collisions 8-58834
 R-matrix method, basic concepts, rel. to other theories 8-58832
 second Born approx., small angle elastic electron scatt. from atoms, high energy limit 8-78811
 soft photon approx. accuracy for resonances in electron scatt. in laser field 8-70935
 variational methods, appl. to at. scatt., review 8-86951
 Ar, electron and positron scattering, elastic, 100 and 500 eV, second-order eikonal approx. 8-78814
 Ar, electron scatt., in laser radiation field, free-free cross sections meas. 8-74762
 Ar, electron scatt. in laser radiation field, free-free cross sections, reson. struct. 8-74763
 Ar, electron scattering, elastic, at low-energy, polarised orbital calc. 8-82840
 Ba, electron scatt., elastic and inelastic (5'D, 6'P) cross sections, 20-100 eV 8-74769
 Ba, scatt. from excited atoms, 30 and 100 eV, inelastic and superelastic 8-86933
 CO, electron scatt., absolute total cross-section meas. 8-74774
 CO, electron scatt. at low energy, mechanisms (*Russian*) 8-90306
 CO₂, electron scatt., absolute total cross-section meas. 8-74774
 CO₂, scatt. electron angular distrib. 8-74766
 CsF, electron impact, elastic scatt., model, static and static exchange calcs. 8-94321
 H (2s) metastable state elastic electron scatt. 8-55238
 H, differential cross sections calc. 8-90293
 H, elastic electron scattering, static exchange amplitude, dispersion rels. 8-66664
 H, electron and positron scattering, elastic, 100 and 500 eV, second-order eikonal approx. 8-78814
 H, electron scatt. in presence of a laser field, theory 8-74767
 H, forward elastic exchange amplitudes and forward dispersion relations, anal. props. 8-78812
 H, forward scatt. amplitude, dispersion relation 8-58823
 H, logarithmic ang. depend. at small scatt. angles 8-50638
 H, positron elastic scattering, low-energy S-wave phase shifts calcs. 8-78813
 H-like atom or ion, electron-electron interaction operator, dipole approx. 8-58821
 H₂, electron elastic scatt., free-electron-gas model exchange pot. 8-58824
 H₂, electron scatt., ab initio theory, elastic scatt. and rot. excitation 8-50640
 H₂, modified Glauber theory 8-94320
 H₂⁺, electron scatt. eqns. convergence, H₂ continuum states, appl. to photoionis. 8-66663
 H₂+e, elastic scatt., incident energies, 100-2000 eV, calcs. 8-55237
 HBr, electron scatt., elastic rot. scatt. and vibr. excitation 8-58822
 HCN, elastic electron scatt. differential cross section, 3-50 eV, 20-130°, rel. to He 8-90291

elastic scattering of electrons by atoms and molecules continued

- He, absolute total scatt. cross sections, 0.5 to 50 eV 8-74765
 He, electron and positron total scatt. cross sections, positronium form. 8-62916
 He, electron scattering, elastic, at low-energy, polarised orbital calc. 8-82840
 He, modified Glauber approx. 8-74764
 He, positron scatt., total cross section 8-70933
 He⁺, modified Coulomb-Glauber approx. 8-86949
 Hg, electron impact spectra, intermediate energy 8-82842
 I₂, equilibrium parameters and Morse anharmonic consts., electron diffr. determ. 8-58818
 KI, electron impact, elastic scatt., model, static and static exchange calcs. 8-94321
 LiF, electron elastic scatt. cross sections 8-50641
 LiF, electron impact, elastic scatt., model, static and static exchange calcs. 8-94321
 Mg, cross sections 10, 20, 40 eV 8-70940
 Mn, elastic and inelastic electron scatt. 10 to 100 eV 8-70934
 N₂, differential cross-section, 0-30 eV 8-78815
 N₂, electron elastic scatt., free-electron-gas model exchange pot. 8-58824
 N₂, electron impact, differential cross-section, converged close-coupling calcs. 8-90290
 Na, 54.4-150 eV differential cross-sections, 12-140°, optical model calcs. 8-74761
 Ne, electron and positron total scatt. cross sections, positronium form. 8-62916
 Ne, electron scattering, elastic, at low-energy, polarised orbital calc. 8-82840
 Ne, positron elastic scatt., close-coupling calc. 8-90292
 O, low-energy electrons integral scatt. cross section 8-69556
 OCS, electron scatt., absolute total cross-section meas. 8-74774

elastic waves

- see also acoustic waves; Love waves; magnetoelastic waves; Rayleigh waves; seismic waves; vibrations*
 absorbing boundary conditions for wave equation 8-59320
 bar, nonuniform elastic, longit. vibr. dynamics of impact excitation 8-75086
 bonded dissimilar half planes having Griffith crack at interface, elastic wave interaction 8-67091
 bone, wave propag. in piezoelectric two-layered cylindrical shell with hexagonal symmetry 8-55487
 circumferential waves, cylindrical shell supported by a continuum, dispersion relations 8-90564
 classical Lamb problem, time-harmonic soln. for elastic head waves 8-63215
 composite, fibre-reinforced, layered, harmonic elastic waves, dispersion 8-63223
 compressional wave vel. temp. depend. in anisotropic dunite 8-77224
 coupled solid/fluid/surface wave dynamic interaction problem, improved fluid superelement 8-81108
 crack scattering in polycrystalline media, ultrasonic attenuation meas. 8-75089
 cracks, action as elastic wave radiation, rel. to AE signal charact. 8-60952
 crystals, strain wave vels., Poisson ratios and elastic moduli 8-51609
 cylindrical cavity in absorptive medium, elastic wave reflection 8-55582
 cylindrical shear wave propag., inhomogeneous viscoelastic solids 8-75090
 deformed material, speed of propagation of waves 8-54201
 diffraction by cracks, surface-wave rays 8-79161
 diffraction by semi-infinite solid's periodic rigid boundary 8-90768
 diffraction of longitudinal waves at elastic circular inclusions (fibres) (*Russian*) 8-63368
 dislocations moving nonuniformly, elastic half space response to realistic faulting model 8-85486
 edge waves under biaxial initial stresses 8-79248
 elastic media, longit. shear fracture, dynamical problem for region with curvilinear cuts 8-81842
 elastic wave propagation, influence of random porosity 8-90552
 elliptical cylinders, scatt. matrix for elastic waves 8-59324
 exceptional wave propagation in continuous medium, finite deform., evolution of discontinuities, elastic pot. determ. (*Italian*) 8-54202
 ferromagnets, higher order surface couplings 8-79212
 fibre reinforced composites, wave guide-type propag., microstruct. theory 8-83279
 frictional boundary, transmission (reflection), approx. anal. method 8-63371
 gas filled tube, pressure waves (*German*) 8-87295
 half-space containing cylindrical inclusion, dynamic surface stresses 8-90748
 interface of two solids, sliding mechanism without slipping 8-51136
 laminated rectangular antisymmetric angle ply plates, shear deform. effects on vibr. 8-63356
 linear viscoelastic waves, theory of diffraction (*Russian*) 8-65787
 linearized theory of elastic wave propagation in initially stressed bodies (*Russian*) 8-83318
 longitudinal propag. theory in solid cylinder under initial stress 8-51116
 matrix theory of scatt., conservation law 8-63217
 micropolar elastic cylinder, free vibrs., wave propag., asymptotic anal. 8-51111
 micropolar elastic waves in cylindrical bore containing fluid 8-51107
 multiple scattering by elastic ellipsoidal inclusions, self-consistent approach 8-63372
 nonhomogeneous elastic rods, similarity soln. of wave propagation 8-59323
 nonlinear isotropic medium, symmetric spherical wave propagation eqns., permissible transform. (*Russian*) 8-87292
 piezoelectric plate, infinite, on elastic medium, transient response to pot. pulse 8-52442
 plane harmonic elastic P and S wave scatt. by spherical inclusions and cavities 8-89353
 plane wave reflection under initial stresses at free surface 8-55581
 poro-elasticity, disturbance due to expanding ring and disc load 8-79250
 propagation in cylindrical coord. systems 8-88798
 propagation in infinite bar, elliptical cross section 8-67073

elastic waves continued

- propagation when negative slope region in stress/strain diagram (*Russian*) 8-79255
 Rayleigh wave, propag., isotropic elastic material with homog. strain 8-94460
 rectangular bar, semi-infinite, longitudinal impact, elasticity eqns. anal. 8-90703
 refracted transverse, influence of adjoining media characts., on the amplitude 8-94614
 rocks, longitudinal wave vels. during nonelastic deform. 8-61402
 rocks sound velocity determination, suggested methods 8-81433
 rods, elastic, linear, nonhomogeneous, propag. and decay of shock and accel. waves 8-83278
 rods and clad rods, elastic waves anal., tutorial review 8-94608
 rotors, elastic wave stability 8-87297
 scattering from cylindrical cavity, nuclear resonance theory 8-87290
 sea ice in Gulf of Bothnia, flexural waves meas. (*Japanese*) 8-96225
 SH waves, multiple scatt. by arbitrary cross section cylinders 8-63216
 shear waves, diffr. at row of round elastic fibres 8-67083
 solids, transition matrix for correl. scatt. wave coeffs. to incident wave coeffs., using Betti's identity 8-90744
 Stoneley wave meas. using differential interferometric optical scanning system 8-75919
 strain measurement in rod, electron inertial effect, shock loaded rod 8-51139
 stress wave propagation calcs., effect of material constitutive models 8-90769
 surface waves, existence in nonhomogeneous elastic semi-space 8-67071
 surface waves in generalized thermoelasticity 8-87291
 surface waves in prestressed body with cylindrical cavity (*Russian*) 8-63369
 surface waves in two component mixture of elastic materials (*Russian*) 8-59335
 thin stretched foils, membrane wave excit. 8-90578
 thin walled elastomer tubes, dispersive effects in wave propag. 8-87289
 transient disturbance prod. in elastic half-space by impulsive shearing traction 8-57786
 tube, cylindrical, thick-walled, finite twist and external press., stability, vibrs. 8-83286
 unconsolidated porous sand reservoirs, elastic props. 8-61400
 viscoelastic fluid flow between parallel plates, inertia elasticity and shear thinning props. (*German*) 8-55665
 viscoelastic surface waves on clamped boundary 8-90767
 Al alloy 6061-T6 cylinder, dynamic fracture, expt. rel. to Mott's theory 8-64651
 CdS, flexural waves in resonator platelets, synchronous amplification and generation 8-84527
 Cu₂O, single crystal, thermoelectric behaviour (*French*) 8-71786
 GaN, elastic constant calc., elastic wave propag. vel. 8-87734
 LiNbO₃, ion implanted, acoustic model of SAW delay lines (*French*) 8-55540
 LiTaO₃, near ferroelec. transition, elasticity, photoelasticity 8-88268

elasticity

- for crack problems in elasticity see *crack-edge stress field analysis*
 see also *elastic constants*; *elastic moduli*; *elasticity of liquids*; *elastoplasticity*; *photoelasticity*; *rheology*; *thermoelasticity*
 adhesive bonded lap joints, elastic stresses theory 8-55563
 aeroelasticity, active control and suppression of flutter in aircraft (*Russian*) 8-67079
 aeroelastic vibr. elimination, appl. of Pontriagin max. principle 8-55584
 aeroelasticity of unsteady aerodynamics, force calc. methods (*French*) 8-75095
 anisotropic material, different moduli in traction and compression, stress-strain laws in small strain theory (*French*) 8-90704
 anisotropic media oscillations (*Russian*) 8-87293
 anisotropic nonhomogeneous elastic media, radial deform. and stresses 8-51079
 astatic gyroscope with elastic cardan suspension, dynamics (*Russian*) 8-63273
 axisymmetric disturbance due to shearing stress discontinuity propag. in elastic medium 8-67075
 bar, impact excitation, longitudinal vibr. 8-94606
 bar with space curve axis, loaded bar shape calc. 8-51069
 beam, flexural vibrs., method of asymptotic expansions (*French*) 8-51112
 beam, large displacement-small strain anal., finite elements with rot. degrees of freedom 8-86161
 beam of stepped thickness, Timoshenko theory 8-94600
 beams, elastic structures, optimal rigidity (*French*) 8-59305
 cantilever beam shape optimisation (*Polish*) 8-79203
 cantilever column, elastically restrained, subjected to follower force, instability 8-63299
 centred finite difference scheme for 3-D eqns. of elastodynamics, stability 8-63294
 ceramics, effects of additives on elastic properties, elastic property-porosity data 8-88533
 classical elastodynamics as linear symm. hyperbolic system, differentiability of solns. 8-57783
 coated inclusion in elastic medium 8-79215
 composite, steady creep bending stresses 8-71280
 composite media, self-consistent field approx. for elastic props. 8-51078
 conical inclusions, elastic stress singularity 8-51071
 conical shell, anisotropic, stress conc. new hole (*Ukrainian*) 8-83247
 conjugate gradient solutions, finite element elastic problem with high Poisson ratio 8-90707
 connectivity theory for formally symmetric operators 8-49651
 contact problem for dissimilar semi-infinite elastic strips 8-55615
 Cosserat's medium, linear and surface defects, stresses 8-83813
 cracked elastic body statics, three-dimensional problem (*Russian*) 8-73858
 cracked hollow elastic solid, torsion anal. 8-51134
 cuboid surrounded by infinite elastic space, stress field due to initial strains 8-55565
 cylinder, thin, deformation due to band press. 8-94595
 cylinder on elastic support, excitation by harmonic Rayleigh waves, free surface effects (*German*) 8-87296

elasticity continued

- cylinders, noncompressible, under all-round compression (*Ukrainian*) 8-90708
 cylindrical elastic tubes, collapse and buckling under combined bending and pressure loads 8-83277
 cylindrical shell, thin, instability rel. to mechanical anal. of geologic struts. (*Chinese*) 8-73364
 debond dynamics of elastic strip, simple transient motion 8-67040
 discrete equations of fluid flow and elasticity 8-65781
 discs, axisymmetric planar vibr. HF spectrum (*Ukrainian*) 8-83283
 dislocation stress field, diffusing elastic fluid, mechanical interaction effects 8-63766
 dynamical problem for region with curvilinear cuts 8-81842
 edge dislocation interactions in infinite array, elastic energy 8-55871
 education, homogeneous ellipsoidal inclusions, general theorems, Poisson theorem, dielectric polarisation, conduction and elasticity 8-61979
 elastic mechanical systems, design sensitivity analysis, adjoint variable methods 8-90706
 elastic-liquid systems, dynamical strength (*Russian*) 8-51085
 elastodynamics, vel. pots., stress functions 8-93534
 ellipsoidal inclusion, external elastic field 8-55566
 elastic-plastic crack and hole interaction in elastic medium under uniform shear load 8-51117
 epoxy resin, low temp. thermal props., phonon states and crosslinked struct. (*German*) 8-75846
 expansion of thin-walled hyperelastic spherical shell 8-55576
 ferromagnets, higher order surface couplings 8-79212
 fibre reinforced composites, wave guide-type propag., microstruct. theory 8-83279
 fibre reinforced materials, macroscopic elastic props. (*Russian*) 8-59304
 fibre reinforced prestressed elastic circular cylinder, stability 8-79234
 film on cylinder, calc. of moduli (*Russian*) 8-63304
 finite element anal. of crack problems 8-67146
 finite element formulation, variational technique 8-69985
 finite element method, reduced integration, appl. to elastostatics 8-75066
 flagella bend propagation, derivation of eqns. of motion and simulation 8-77074
 fluid impregnated solids, elastic and dynamic response regimes 8-90713
 fluid saturated porous solid, eqns. of motion 8-79208
 frameworks' stability analysis, w.r.t. sway excess of columns 8-51098
 frictionless contact problem for elastic layer under axisymm. loading 8-83341
 general relativistic elastomechanics, compatibility relations (*German*) 8-81902
 general relativity 8-70025
 geometry of motion of single elastic body point 8-49662
 glass, narrow sandwich seals, shape factor, finite element anal. 8-75111
 glass narrow sandwich seal, correction factor for thermal expansion mismatch 8-75110
 graph-like state of matter, electrical cond. of random networks, gelation and elasticity 8-65875
 gravitational wave effects (*German*) 8-81904
 Green's matrix for two elastic half-spaces, frictionless sliding (*German*) 8-62083
 griffith crack in an infinite nonhomogeneous elastic medium under shear 8-87300
 Griffith crack problems in non local elasticity, solutions for one and two dimensional problems 8-51125
 hollow elastic cylinder, axisymmetric mixed problem, Legendre polynomial soln. 8-81840
 hyperelastic compressible medium with cylindrical cavity, finite dynamic expansion under sudden press. 8-79213
 hyperelastic rod dynamics, second-order theory 8-77717
 hysteresis damping, continuum description 8-67078
 impact damage in elastic response regime 8-71785
 impact phenomena with elastically deformable stricker and solid obstacle 8-77703
 infinite elastic solid with spherical inclusions, linear elasticity eqns., stresses, displacements 8-65773
 inhomogeneous medium, high freq. Reissner-Sagocci problem, exam. of stress singularity 8-83239
 inhomogeneously compressed rods, crit. loads, two-sided estimates 8-62082
 interface separation for elastic layer on rigid plane, loaded by rigid stamp 8-87307
 isotropic composite material containing spherical inclusions at nondilute concs., effective elastic moduli 8-67037
 lattice shells under axially symmetric load, field eqns. 8-79209
 layered rod on sagging elastic supports, aeroelastic stability, vibr. modes 8-51115
 linear, two dimens., Saint-Venants principle for non-striplike domains 8-54188
 linear dynamic theory of elasticity, minimum principles 8-57781
 linear hemitropic micropolar isotropic elastostatics, Green functions 8-49661
 machine vibrations anal. and obs. block deformability influence (*Italian*) 8-51108
 magneto-elasto dynamics, mixed initial and boundary value problems, vibr. circular plate in mag. field 8-67034
 membrane, prestressed, dynamic loading 8-51068
 metal specimen, ultrasonic technique for stress anal. 8-64790
 micropolar elastic cylinder, free vibrs., wave propag., asymptotic anal. 8-51111
 micropolar elasticity, mixed problem 8-54189
 micropolar elasticity theory, uniqueness of 2-D boundary value problems 8-54192
 mixed boundary-value problems, orthogonal polynomial solns. 8-54193
 motion of solid body with elastic and dissipative elements (*Russian*) 8-65763
 nonconservative autonomous and nonautonomous systems, stability, energy approach 8-51097
 nonhomogeneous elastic layer bonded to nonhomogeneous half-space, torsion by circular die 8-87263
 nonhomogeneous medium under shear, elasticity theory 8-86166

elasticity continued

- nonlinear discrete-continuous model of an elastic layered medium 8-81844
- nonlinear elastic continuum, comparison of Runge-Kutta-Nystrom method and Newmark method (*German*) 8-87273
- nonlinear elasticity, extremum principles, appl. to composites 8-51072
- nonlinear finite elasticity, uniqueness condition, work theorem 8-57784
- one-dimens. problems, diagonal mass matrices and finite element eqns. 8-73857
- optimal control of dynamically controllable motions, appl. to hollow cylinder deform. 8-79214
- optimal design of freely vibr. elastic bodies (*German*) 8-65775
- optimality criteria methods in elastic struct. design 8-83253
- orthotropic shell with tangential and normal strain, engineering theory eqn. 8-63303
- penny-shaped crack, sudden twisting in a finite elastic cylinder, stress calcs. 8-67110
- plane, inclusion problem, numerical soln. of Cauchy-type integral eqn. 8-54194
- plane crack problems in micropolar theory of elasticity 8-54191
- plane elastostatics, boundary value problems, spectra of integral operators 8-57782
- plane shearing stress meas. with wired strain gauges (*German*) 8-89471
- plane theory, singular integral eqn. for mixed problem soln. (*Ukrainian*) 8-89339
- plate, high freq. long wave vibrs., two-dimens. eqns. 8-83321
- plate, obliquely stiffened, subjected to uniform compression, buckling strength (*Japanese*) 8-67067
- plate, thick, containing eccentric spherical cavity, transverse bending stresses 8-63288
- plate bending elements, quadrilateral, finite element anal. with reduced integration 8-75071
- plate theory, high order, stress soln. determ. 8-83248
- plate theory, nonlinear eqn., Cauchy problem, existence and uniqueness of smooth global soln. (*French*) 8-93513
- plate with aperture, bending moments, exact. soln. 8-94598
- plate with circular hole, axisymmetric stress distrib. 8-51066
- plates, rectangular stepped thickness, with edges elastically restrained against rotation, vibrations 8-90740
- plates, thin heterogeneous, and sloping shells, elastic materials, exam. of theory 8-63307
- PMMA, oriented, hypersound propag., elastic props. 8-75737
- polymer, elasticity of bulk and film from multipass Brillouin spectra 8-76485
- polymer glass, isothermal struct. relax., in high elasticity transition region, mol. model (*Russian*) 8-87629
- polymer networks, effect of geometric constraints on junctions 8-75711
- polymer structure and mech. props., book 8-83756
- polymer with spherical inclusions, slope discontinuity prediction in stress/strain behaviour 8-94596
- poro-elasticity, disturbance due to expanding ring and disc load 8-79250
- propagation of elastic waves in infinite bar, elliptical cross section, linear elasticity 8-67073
- reinforced shell under external press., max. stability 8-94597
- reinforced tube, bending and flexure 8-51076
- relativistic theories of materials, book 8-81907
- resolution method for second problem of elastic limits for plane (*French*) 8-57779
- ring sector, mixed plane elasticity theory problem (*Russian*) 8-62080
- rock bodies, cooling, residual stress development 8-88819
- rocks, elastic props. experimental studies rel. to Earth crust press.-temp. conditions modelling (*Russian*) 8-96207
- rod, fixed-free circular, soln. under various bad conditions 8-67047
- rubber elasticity, molecular aspects book contrib. 8-84886
- rubber tube, inflation and extension, biaxial strain studies 8-83251
- rubber-like elastic materials, stress-strain behaviour 8-67049
- sandwich plates, finite element anal. 8-67046
- screw dislocation in nonlocal hexagonal elastic crysts. 8-59807
- semi-infinite plate subjected to increasing boundary force, dynamic response, ice sheets 8-83254
- semi-infinite strip under symmetric load, stresses, elastic plane theory 8-59301
- shaft, symmetrical, nonlinear elastic and internal damping props., flexural vibrations 8-71290
- shallow shells, force loading and temp. field effects, algorithm construction (*Ukrainian*) 8-89338
- shallow thin shell finite element, stiffness matrix development 8-90705
- shear crack, stress distrib., finite elastic anal. 8-51119
- shear stresses induced by hydrostatic pressure near the surface of an inclusion 8-75074
- shell theory, momentless (*Russian*) 8-51075
- shells, two-dimensional eqn. system (*Ukrainian*) 8-89342
- short column vibrator, apparent elasticity analysis and applications 8-59242
- Signorinis perturbation scheme for a general reference config. in finite elastostatics 8-83241
- slender damped structures, vortex excited aeroelastic oscils., mathematical model (*German*) 8-94616
- slender Z-crack, elasticity problems 8-87304
- spatial elastica theory with centreline compressibility 8-79211
- spherical dome, three-dimens. elasticity soln. and edge effects 8-59306
- spherical shell, axisymmetric forms of equilibrium (*Russian*) 8-87262
- St. Venant planar theory, nonhomogeneous problem, logarithmic decrement (*French*) 8-49664
- stability theory for plates with inhomogeneous precritical states (*Russian*) 8-49665
- static fields in inhomogeneous anisotropic medium (*Ukrainian*) 8-81837
- steadily moving load, elastic strip on rigid foundation, noncontact regions, displacements, contact press. 8-87264
- steady state crack propagation, media with variable elastic moduli 8-90783
- steel, austenitic, martensitic transform, temp., singularities in 50Kh2N22 (*Russian*) 8-68689

elasticity continued

- steel, austenitic, type of Kh15N27T3MR, exam. of elasticity props. 8-56687
- stochastic excitation systems, identification of damping and stiffness parameters (*Polish*) 8-69973
- stress analysis, improved equilibrium finite elements 8-75067
- stress and crack-displacement intensity factors, in elastodynamics 8-67112
- stress separation in photo-orthotropic elasticity, numerical method 8-59296
- string vibrating against rigid wall, partially elastic or anelastic impact, energy calcs. 8-67028
- structures with rotational degrees of freedom, large displacement-small strain anal. 8-89310
- tapered beams, stress trajectories, stress contours 8-63305
- thermomechanics, introduction, book 8-54187
- thick-walled shells of revolution, axisymmetric problems soln. by design and exptl. methods (*Russian*) 8-73853
- thin hyperelastic spherical shell, finite amplitude oscillations 8-93533
- three dimensional notch problems, elastic medium, book contrib. 8-94622
- three-dimensional bodies with rigid inclusion or periodically spaced holes, macroscopic behaviour (*French*) 8-87260
- three-phase anisotropic medium, antipane line force 8-67041
- Timoshenko type shells, nonlinear theory (*Russian*) 8-63283
- transversely isotropic finite cylinders, elastostatic analysis 8-51074
- transversely isotropic medium with cylindrical cavity and external crack, stress distrib. 8-79259
- transversely isotropic half-space, Boussinesq and Cerruti solns. 8-55568
- two-component systems, elastic moduli 8-59302
- wave propagation in fluid saturation porous medium (*French*) 8-86165
- weakly rigid motions in linear kinematics of Cosserat surfaces, elastostatics 8-87267
- wedge-shaped straight elastic bars, new method for longitudinal and torsional vibration freq. calc. 8-59338
- Al-Cu (4 wt. %), elastic accommodation of semicoherent θ' 8-64543
- Al-Mn alloys, study of solidification by rapid cooling (*Japanese*) 8-88459
- CdSe, photosensitivity of elastic properties 8-92049
- Fe-Si, polycrystalline, exam. of stress-strain state of individual grains 8-80580
- Mn-Cu-Al alloy under torsion, anomalous elasticity and transformation plasticity obs. (*Russian*) 8-75834

elasticity of liquids

see also *compressibility of liquids*

- CBOOA, liq. cryst., twist viscosity and mech. props. near smectic A-nematic transition 8-95136
- hexyl-azoxybenzene, liq. cryst., twist viscosity and mech. props. near smectic A-nematic transition 8-95136
- lipid bilayers, saddle-splay elasticity and mol. asymmetry 8-92594
- octyloxycyanobiphenyl, liq. cryst., twist viscosity and mech. props. near smectic A-nematic transition 8-95136
- polymer, isotropically swollen networks, vol. depend. of elastic eqn. of state 8-67832
- smectic C liquid crystals, elasticity and defects 8-91233
- $Al_2(SO_4)_3$ soln., adiabatic and apparent molal compressibility determ. from US vel. meas. 8-63797
- $Ce_2(SO_4)_3$ soln., adiabatic and apparent molal compressibility determ. from US vel. meas. 8-63797

elasto-optical effects see *photoelasticity; piezo-optical effects*

elastomers

see also *rubber*

- butadiene, durability, influence of intermol. interaction (*Russian*) 8-76746
- polytetramethylene oxide-polytetramethylene terephthalate, block copolymer, props. 8-51438
- polyurethane, dithiodiglycol-plasticised, time-crosslinked density reduction, photochem. scission obs. 8-52920
- prosthetics, in vivo method for evaluation of effects of materials on arterial thrombosis 8-81071
- radiation vulcanisation, continuous, exam. (*German*) 8-92231
- Ruticon optical processing capabilities 8-79140
- TCNQ, elastomeric complexes, doped with pure TCNQ, elec. conductivity 8-84220
- thin walled elastomer tubes, dispersive effects in wave propag. 8-87289
- B filled elastomer mould, surface coating for wear prevention in mould 8-64728

elastoplasticity

- approximation functionals, simplification in elastoplasticity theory (*Russian*) 8-63328
- arches, shakedown anal., linear programming appl. 8-51091
- axisymmetric large elastoplastic strain problems, natural finite element anal. 8-83259
- bar, elastic-plastic, large deform. anal. under repeated axial loading, small deform. theory correl. 8-59310
- bar (tube), compressible, combined loading, elastic-plastic problem 8-63311
- beams, impulsively loaded, higher modal dynamic plastic behaviour 8-90721
- bending, isotropic/kinematic hardening 8-63312
- bifurcation in elastic-plastic solids, perturbed motion of stress axes 8-90730
- carbon steel, elastic-plastic plane waves with combined stresses 8-90764
- cold working, dynamic, struct. modification (*French*) 8-52847
- composite medium, two-component residually stressed, elastoplastic crack model (*German*) 8-90790
- compound rotor, exam. of stress state, taking account of interference stresses, contact stresses 8-83342
- crack growth, numerical model 8-55596
- crack tip characterisation, relation to R-clusters 8-56767
- cracked bodies, plane stress to plane strain thickness dependent transition, anal. model 8-67126
- cracked thick walled cylinder, elastic plastic fracture anal. under displacement controlled loading 8-67119
- cylinder, elastoplastic, necking under uniaxial tension 8-63335
- cylinder expansion under finite plane strain 8-51094

elastoplasticity continued

- double-skinned composite circular cylindrical shells failure under external press. 8-75078
- double-skinned composite circular cylindrical shells under external press., experimental behaviour 8-75077
- elastic-perfectly plastic material, theory of stable crack growth 8-79272
- elastic-perfectly plastic von Mises material, accuracies of numerical soln. constitutive eqns. 8-59315
- elastic-plastic crack problem, comparison of finite element soln. 8-79263
- elasto-plastic flow in computer simulated, A533 steel 8-56720
- elasto-plastic metal-dislocation system, stress-activated dislocation motion, thermodynamic theory (*Chinese*) 8-83868
- elasto-viscoplastic analysis of large deform. problems, natural finite element formalism 8-83258
- elastoviscoplastic analysis for spherical or cylindrically symm. cavities in infinite media 8-79229
- elstic-plastic crack and hole interaction in elastic medium under uniform shear load 8-51117
- finite element analysis, interpolation vs. iterative soln. for Tresca yield condition 8-59312
- fracture mech., linear elastic, appl. to crack stability in brittle struct., elastic-plastic conditions 8-90800
- fracture toughness parameters J and G^A , effect of load biaxiality 8-67128
- hardening elastoplastic material, variational inequality 8-63320
- ideal elastic-plastic materials, constitutive eqns. and thermodynamics 8-71272
- impact fracture in elastoplastic regime 8-51133
- incremental formulation in nonlinear mechanics, large strain elastoplasticity 8-77692
- integral I and elastic-plastic fracture criteria (*Chinese*) 8-75100
- integral J_I , calculation by finite element analysis 8-67129
- internal struct. tensor 8-79227
- large deformation elastoplastic analysis of arbitrary shells, triangular finite element 8-83257
- linear strain triangular element solns. 8-90719
- LMFBR, dynamic response of containment vessel and coolant wave propag., REXCO-EUR code manual 8-58349
- matched asymptotic expansions, in nonlinear fracture mechanisms 8-51127
- metal, stress-induced EM effect, phys. model 8-55909
- metals, residual stress and deformation, due to quenching, elastic-plastic anal. (*Japanese*) 8-83268
- non-isothermal deform., bifurcation of equilb. 8-79220
- notched plates, monotonic and cyclic loaded, exam. of elastic-plastic stress-strain behaviour 8-63390
- perforated plane, thermoelastic-plastic problem (*Russian*) 8-55571
- PLASTEF code, numerical simulation of thermoelastoplastic behaviour using finite element method 8-90731
- polycrystals, constitutive relns. in elastic-plastic range 8-63801
- polymer, elastoplasticity theory 8-75712
- rotating discs, burst strength and pecking 8-79226
- screw connections, bend and tension loaded, hysteresis (*German*) 8-87312
- separation energy rate for crack advance 8-56765
- shallow shells elastoplastic anal. using laminated element (*Japanese*) 8-63323
- soil, deformation of compressible elastoplastic ground 8-96198
- soil, pulverulent, homogeneous, stresses due to vertical local load (*French*) 8-61398
- soil-struct., interaction initial stress finite element method 8-59313
- solid, crystalline, finite strain, uniqueness criteria and minimum principles 8-51086
- solid containing holes in vicinity of crack tip, finite element anal. 8-67147
- sphere under external press., stability 8-94603
- stability condition for elastic plastic structures 8-87284
- steel, Cr-Mo, constitutive eqn. model for high temp. behaviour of fast reactor structural alloys 8-66343
- steel, free plate elastoplastic stress condition during phase transformation 8-95781
- steel, notched bar, plastic zone determ. near rupture (*French*) 8-88515
- steel, plates, thin, welding residual stresses calc., elastoplastic thermal stress anal. 8-83262
- steel, stainless, type 304, elastoplastic fracture mechanics for reactor piping 8-68777
- steel, stainless type 316, monotonic and cyclic biaxial loading at room temp. 8-52928
- steel, structural, J -integral fracture toughness, specimen size effect, extension to elastoplastic region 8-68808
- steel shaft, residual tangential stress determ. after elastoplastic twisting 8-60902
- strain hardening structures under repeated loading, deflection analysis 8-63313
- stress analysis of crack, elastoplastic range 8-67144
- thermal stresses in axisymm. problems (*Japanese*) 8-51096
- thermoelastoplastic medium, variables for universal deform. representation 8-49666
- thermoelastoplasticity three-dimensional integral eqns. (*French*) 8-90718
- thick-walled tube, two segment elastic plastic processes (*Russian*) 8-67063
- thin skin structures, residual strength prediction, using crack resistance curves 8-90795
- torispherical vessel heads, internally pressurised, elastic-plastic buckling 8-79241
- torsion problems, zone estimates 8-67058
- trusses, with unstable bars, collapse anal. 8-90729
- visco-elastoplastic medium mechanical birefringence in loading and unloading processes 8-59314
- viscoplasticity anal., boundary integral eqn. method (*French*) 8-90728
- Al, alloys, limiting plastic props. (*Russian*) 8-88504
- Ni-Mo-Cr steel, elastic-plastic material characterisation 8-72854

elastoresistance

- Al film, single cryst., elastoresist. effect 8-84321
- Fe, elastoresistivity effect, meas. of resistance at 4.2K and 300K, using mag. field method 8-72132

ELDOR

- 4-methyl-2,6-di-tert-butylphenol, γ -irrad. cryst., ENDOR transitions, ELDOR detect. 8-95531

electrets

- see also dielectric devices; electrostatics; photoelectrets; thermoelectrets*
- carnauba wax, orientation prod., by mech. press. or US waves 8-64314
- carnauba wax magneto-electret, Struve function 8-76287
- discharge model, injection relaxation mechanism, space-charge cond. 8-80279
- ferroelectrics, phenomenological theory of electret effects 8-88260
- foil transducer eqns. using Lagrange's eqn. 8-83202
- PMMA, tubular magnetoelectrets, TSC obs. 8-88250
- polymer foil, charge distrib. determ., thermal pulse technique, meas. accuracy 8-80287
- polyvinylacetate film, effect of electrode metals on depolarisation current characts. 8-76387
- PTFE film electret, optical spectra, band theory interpretation (*Russian*) 8-88376
- silastic, magneto-electret of tubular shape, surface charge 8-56419
- US transducer performances and prospects 8-59244

electric actuators

- drip feed unit microprocessor control development 8-53563

electric admittance

- air blast circuit breaker, near current zero, local elec. props. 8-87516
- alkaline earth fluoride solid solns., $\text{MF}_2\text{-UF}_4\text{-CeF}_3$, surface degradation, complex admittance anal. 8-55980
- composite electrostrictive resonators, finite element simulation 8-59237
- impedance of a p-n junction by direct currents (*Russian*) 8-84285
- CdS-Cu₂S single cryst. heterojunction, trap depths in depletion region 8-52064
- GaAs-Al_{0.5}Ga_{0.5}As-Cr/Au MIS capacitors, characts. meas. 8-95371
- GaP, p^+-n diode junction, admittance meas. and carrier traps 8-91757
- p-Si, neutron irrad. effects, admittance meas. of n^+ -p diode 8-51587

electric admittance measurement

- faradaic admittance, rapid drop time on-line FFT meas. 8-92544

electric amplifiers *see amplifiers***electric arc furnaces** *see arc furnaces***electric arc welding** *see arc welding***electric arcs** *see arcs (electric)***electric breakdown**

- see also electric breakdown of gases; electric breakdown of liquids; electric breakdown of solids*
- cathode prebreakdown field emission transition to vacuum breakdown 8-75462
- dielectric surface with accumulated air positive ions, vacuum breakdown obs. 8-75464
- vacuum breakdown initiation, 4.2K, critical field emission currents 8-75459
- vacuum gap with processed electrodes, atm. effects on dielectric strength 8-51389
- C electrode breakdown voltage dependence on adsorbed gases 8-75465

electric breakdown of gases*see also electron avalanches*

- air, breakdown potential, pulse lamp irrad. effects (*Russian*) 8-83518
- air, breakdown voltages, from normal to cryogenic temps. 8-59692
- air, elec. discharge, effect of long laser spark ionis. channel 8-67468
- air, electric breakdown voltage hysteresis, electrode coating effects 8-87553
- air, high temp. elec. breakdown characts., theory and obs. 8-87581
- air, negative point-plane corona, electrical characts. 8-71567
- air, positive point-plane gap, critical press. prediction, v_p /press. characts. 8-87583
- air, submillimetric laser induced breakdown 8-67446
- air breakdown in superimposed DC and HF electric fields 8-67571
- air gaps, schlieren studies of impulse breakdown 8-87518
- atmospheric negative ions, electron detachment rates, time lags to breakdown 8-87564
- benzonitrile, anodic polymer growths during electrical breakdown conditions, TEM study (*French*) 8-75960
- breakdown voltage of air, effect of sand particle pollution 8-81363
- butene-1, Townsend primary and secondary ioniz. coeffs. and sparking voltages 8-51372
- electric strength 8-83631
- ethylene, Townsend primary and secondary ioniz. coeffs. and sparking voltages 8-51372
- Freons and their mixtures with N_2 and SF_6 , breakdown voltage in uniform electric field (*German*) 8-71423
- gap between two spherical electrodes, breakdown voltage calc. 8-55763
- gas-filled diode, rarefied gas breakdown time delay statistics 8-87571
- gases as electrical insulators, nature and practice 8-83632
- high temp., 300-2100K, formulae and graphs for breakdown voltage (*Russian*) 8-51370
- large-area nanosecond discharge breakdown 8-71614
- laser triggered fast-response sealed dischargers 8-51391
- laser-induced breakdown phenomena 8-75390
- liquid metal cathodes, nanosec. discharge form. in H_2 atmosphere 8-87578
- long air gap minimum breakdown voltage and time estimation 8-67575
- long rod-to-plane air gap voltage/time characteristic for switching impulses 8-67576
- minimum breakdown potentials in crossed elec. and mag. fields 8-67554
- photon-photon scattering, effective-photon theory for cross-section 8-58962
- point-to-plane gap corona and breakdown in supersonic airstream 8-67573
- positive leader, in long nonuniform air gap, growth 8-75444
- predischarge current meas. in compressed air 8-87555
- propylene, Townsend primary and secondary ioniz. coeffs. and sparking voltages 8-51372
- RF breakdown, time-resolved studies 8-79485
- rod-to-plane air gap breakdown under negative impulse voltage 8-67563

electric breakdown of gases continued

- SF₆ compressed, breakdown threshold, surface roughness and pressure effects 8-75449
 Tokamak discharge gas breakdown time model 8-67555
 D₂, elec. breakdown, Paschen's law violations 8-87570
 Ar breakdown in superimposed DC and HF electric fields 8-67571
 Ar gap, low-press., with thermionic cathode, upper and lower breakdown voltages 8-79405
 Ar, high press. gas discharge form. 8-87567
 Ar, high temperature, up to 2400°C, breakdown voltage and voltage-current characts. obs. 8-87510
 Ar, microwave breakdown of nanosecond duration, calc. of threshold fields 8-94948
 Ar, plasma, ion energy level populations in crossed elec. and mag. fields 8-67428
 CO₂, negative point-plane corona, electrical characts. 8-71567
 H₂, elec. breakdown, Paschen's law violations 8-87570
 He, breakdown by alternating electric field near ion cyclotron freq. 8-55765
 He, dielectric breakdown across epoxy insulation 8-62658
 He, microwave breakdown of nanosecond duration, calc. of threshold fields 8-94948
 N, compressed, breakdown at cryogenic temp., obs. (Russian) 8-67448
 N₂ breakdown in superimposed DC and HF electric fields 8-67571
 N₂, breakdown voltages, from normal to cryogenic temps. 8-59692
 N₂, compressed, insulation breakdown at cryogenic temp., obs. 8-51368
 N₂, elec. breakdown at high press. and field strengths, steady-state expts. 8-79488
 N₂, high temp. elec. breakdown characts., theory and obs. 8-87581
 N₂, high temperature, up to 2400°C, breakdown voltage and voltage-current characts. obs. 8-87510
 NO in AC field, kinetics and energetics (French) 8-64824
 NO₂, in AC field, kinetics and energetics (French) 8-64824
 Ne flash tube, investigation of forms. and decay mech. of internal fields 8-58552
 Ne microwave breakdown field calc., Monte Carlo method 8-67551
 Ne-HCl mixture breakdown obs. 8-67553
 Ne-methane mixture breakdown obs. 8-67553
 O₂, negative point-plane corona, electrical characts. 8-71567
 S₆, partial discharge disintegration product meas. (Czech) 8-67450
 SC₆, electric breakdown voltage hysteresis, electrode coating effects 8-87553
 SF₆ and SF₆-N₂ mixture, elec. breakdown and corona stabilisation obs. 8-87582
 SF₆ avalanche breakdown as stochastic process 8-67574
 SF₆ breakdown at high pressure, possible cosmic ray effects 8-87577
 SF₆ breakdown characts. for 0.8 to 2.6 MV range 8-87552
 SF₆ breakdown distributions, low-value fracture determ. 8-67578
 SF₆ breakdown field strength, electrode surface roughness tolerance 8-67577
 SF₆ breakdown mechanisms, review 8-59699
 SF₆ coaxial gap breakdown probability determ., influence of meas. procedure 8-67579
 SF₆, discharge development, high speed elec. and optical temporal resolution 8-87584
 SF₆ electric strength, electrode surface roughness effects (German) 8-63609
 SF₆, electrode surface and coating effect on DC breakdown voltages 8-87557
 SF₆, first breakdown voltages 8-87554
 SF₆ high-temp. electrical breakdown parameters 8-67567
 SF₆, negative point-plane corona, electrical characts. 8-71567
 SF₆, positive point-plane gap, critical press. prediction, v_c/press. characts. 8-87583
 SF₆-air mixture impulse discharge characteristics of 30 cm gaps 8-67572
 SF₆-He(N₂)(CO₂), AC particle initiated breakdown, compressed gas mixture 8-87556
 Xe anode-directed streamer propagation simulation 8-67591

electric breakdown of liquids

- dielectric fluid, electro-dielectrophoretic forces acting on spherical impurity particles, analytical evaluation 8-88641
 dielectric tracking, in liq. He, supercond. magnet coolant 8-92022
 electrical dispersion in different gaseous environments 8-88254
 n-hexane, impurity particle motion, under DC and AC conditions, expt. results and computer simulation 8-88642
 hydrocarbons, liq., dynamics of elec. breakdown 8-88253
 mineral oil, breakdown voltage, live electrode polarity depend. for non-uniform field 8-75450
 organic purified dielectric liquids, expt. 8-84523
 D₂O laser induced breakdown, comparison with H₂O 8-68453
 H₂O, laser induced breakdown, comparison with D₂O 8-68453
 He, dielectric breakdown across epoxy insulation 8-62658

electric breakdown of solids

- see also impact ionisation; partial discharges; Zener effect*
 diamond, dielec. breakdown, two-photon absorpt. and other optical damage mechanisms 8-84684
 dielectric, in vacuum, surface breakdown 8-64321
 donors with excited states, non-equilibrium phenomena, theory of kinetics of electron transitions 8-79961
 electret discharge model, injection relaxation mechanism, space-charge cond. 8-80279
 epoxy resin, electroluminesc. 8-56522
 epoxy resin, partial discharge initiation phase, effects of field strength, temp. and internal mech. stresses (German) 8-72461
 film, breakdown mechanisms 8-76385
 III-V semiconductor, avalanche breakdown voltage for p-n junction, calc. 8-88020
 insulating solid, elec. strength and degradation 8-83631
 insulator, transparent absorpt. wave struct. associated with optical breakdown 8-68581
 one-sided abrupt junctions, distinction between avalanche and tunnelling breakdown 8-56211
 p-n junction, planar, junction breakdown walkout exam. 8-60199
 Perspex, breakdown by treeing 8-84526
 polycaprolactam film, temperature-time dependence (Russian) 8-76386

electric breakdown of solids continued

- polyethylene, artificial voids, partial discharge charact. (German) 8-92023
 polyethylene, elec. trees free radical ESR study 8-60393
 polyimide film, in high-temperature region 8-84522
 polymer breakdown plasma analysis, mass-spectrometric installation 8-88670
 PVC films, temperature-time dependence (Russian) 8-76386
 solid dielectrics, treeing 8-80285
 statistical test of solid dielectrics in pulse irradiation regime 8-95548
 transparent solids, role of thermal stresses in optical breakdown (Russian) 8-95547
 treeing in organic insulating materials, tutorial 8-84524
 Al foil, elec. explosion, dielec. breakdown 8-67388
 Al, foil, elec. explosion, immersion medium effects 8-67389
 Al_{0.9}Ga_{0.1}As native oxide, low leakage, MOS characterisation 8-91795
 Al₂O₃ composite films, elec. instability 8-68452
 Cu foil, elec. explosion, dielec. breakdown 8-67388
 LiNbO₃, light emission from surface on heating or cooling 8-64416
 SiO₂ film, electric strength in MOS structures obs., under unidirectional, alternating and combined voltages (Slovak) 8-88034
 SiO₂, thermal, elec. stressed film, dielec. breakdown 8-64322

electric cables *see cables (electric)***electric capacity** *see capacitance***electric cells** *see cells (electric)***electric charge***see also space charge*

- aerosol, polydispersity, unipolar charging, charging mobility analysis 8-61059
 aerosol, unipolar diffusion charging, particle dielectric constant and ion mobility effects 8-61058
 conducting body charge distrib. computation (Polish) 8-78850
 force exerted when immersed in polarised nonconducting dielec. fluid 8-78872
 observable phase factors and symmetry of electric and magnetic charges 8-86428
 C blacks, surface polarity, surface activity, slurry pH, oxidation effects 8-68915
 LiF, electrification of crystals by cleavage 8-60189
 O ions, energetic, in radiation belts, charge states theory 8-77427

electric coils *see coils***electric condensers** *see capacitors***electric conductance** *see electric admittance***electric conductance measurement** *see electric admittance measurement***electric conduction processes** *see electrical conductivity***electric conductors** *see conductors (electric)***electric connectors***see also cable joining*

- 600 MW pulsed energy converters for toroidal field coil, design philosophy 8-58496
 BNC-JJ coaxial floating shield bakable and coolable vacuum feed-through useful from dc to 4 GHz 8-54381
 fusion reactor magnet coil, 125 kG, 1 m, design, fabrication 8-55008
 inlet for elec. conductor into high-pressure chamber 8-74016
 moulding compound, glass fibre reinforced low press. diallyl phthalate, props. 8-52750

electric control equipment*see also controllers; electric actuators; electric final control devices; electric sensing devices; switches; telecontrol equipment; telemetering equipment*

- 35 mm camera control cct. for automated time-lapse photography 8-58076
 above-knee prosthesis, myoelectric control system development 8-53575
 bilateral shoulder disarticulated children's jaw-controlled manipulator 8-53578
 resistance furnace programmed temperature regulator 8-86256

electric control gear *see electric control equipment***electric current***see also arcs (electric); corona; critical currents; current density; current distribution; current fluctuations; eddy currents; electrojets; fault currents; leakage currents; short-circuit currents; sparks*

- ionosphere, currents distrib. rel. to polar-equatorial currents 8-93029
 limiting current of electron in mag. field of conical electron beam 8-90348
 metallic tethers in ionospheric plasma, current and pot. distrib. 8-69652
 prebreakdown ionisation current spatial growth expts., initial photoelec. current changes 8-67566
 solar corona, plasma heating by anomalous current dissipation 8-53895

electric current control*current-supply stabiliser, adjustable, for magnetic lens β spectrometers*

- 8-74528
 neutral beam, pulsed, arc (arc filament) power supplies, for fusion reactor 8-70637
 phototransducers in tide-recording equipment, current and light output ratio stabilisation (Russian) 8-88949

electric current measurement*see also ammeters; galvanometers*

- AC, precision direct meas. facility 8-49863
 AC measurement, using digital instruments 8-93726
 ampere absolute value improved realisation 8-93737
 atmospheric conduction current, direct meas. 8-85637
 coronascope, balloon-borne, for thundercloud elec. field meas. 8-61577
 cylindrical probe, electron current second derivative calc. algorithm 8-63594
 digital dynamic method for precise meas. of static characteristics 8-54389
 electrometer/ratiometer of high sensitivity and precision 8-70154
 electron beam deflection tube, circuit breaker current meas. 8-54393
 Faraday cup for simultaneous ion-beam current obs. and meas. 8-49865
 galvanomagnetic semiconductor voltage and current transducers, Gauss effect compensation 8-77892
 lightning stroke current meas. using optical fibre cable and optoelectronic conversion, rocket launched 8-92930

electric current measurement continued

- minivoltmeter, electronic, in 10 nA range (*Spanish*) 8-54408
in pulsed X-ray device, voltage divider and Rogowski coil (*Japanese*) 8-93788
servo-controlled balance, absolute ampere determ. 8-82003
SQUID for AC current meas. down to 10^{-14} A 8-49859

electric discharge machining see *spark machining***electric discharges** see *discharges (electric)***electric distortion**

- see also *fading*
low-distortion FM demodulator using SAW delay device 8-51014

electric distortion measurement

- waveform distortion anal. due to recording and playback speed instability 8-73981

electric domain walls

- ceramics, ferroelec., dielec. losses due to domain wall oscill. 8-84541
coupled fields in one dimension: cross-over from a continuous symmetry to a discrete one 8-87758
ferroelectrics, surface sound waves on domain boundaries, low temp. sp. ht. 8-71937
guanidinium aluminium sulphate, domain wall energies and domain structures 8-92039
quartz ferroelastic twinning coercive stress obs. 8-59854
TGS, X-ray topography 8-60409
uniaxial ferroelectric, static and dynamic crit. phenomena, Larkin-Khmelnitzkii theory 8-64327
 $Gd_2(MoO_4)_3$, prismatic domain exam. 8-56441
 $NaNO_2$, rel. to thermal history effects on temp. range of modulated struct. for 163°C transition 8-95563
SbSI, max. vel. of domain boundaries in polarisation reversal, Barkhausen effect meas. 8-60411
 $Sr_{0.5}Ba_{0.5}Nb_2O_6$, ferroelec., dielec. behaviour 8-80309

electric domains

see also *electric domain walls; ferroelectric materials*

- ferroelectric domain equilibrium configuration near Curie temp. 8-88270
guanidinium aluminium sulphate, domain wall energies and domain structures 8-92039
maximum electric field in high-field domain in Gunn devices 8-79996
metals, electrical domains at low temps. (*Russian*) 8-91687
TBK-3, ferroelectric ceramic, 90° electric domain processes, mech. stress, X-ray diffr. 8-72478
TST-23, ferroelectric ceramic, 90° electric domain processes, mech. stress, X-ray diffr. 8-72478
 $Ba_{0.92}Ca_{0.08}TiO_3$ ceramic, uniaxial stress effects, US dilatometric and dielec. meas. 8-52454
 $Ba_2NaNb_2O_{15}$, ferroelec. conversion to single domain, elec. and photoelec. props. 8-88271
 $BaTiO_3$, 90° electric domain processes, mech. stress, X-ray diffr. 8-72478
 $BaTiO_3$, doped, loss mechanism and domain stabilisation 8-84542
 $BaTiO_3$, ferroelectric ceramic, dielec., piezoelec. and elastic props., orientational contrib. 8-68468
 $BaTiO_3$, martensite type phase transition 8-64326
CdS, lattice attenuation meas. by US injection method 8-76480
n-GaAs, diffusion coeff., Monte Carlo calc., rel. to trapped domain behaviour 8-56152
 $Gd_2(MoO_4)_3$, domain structure obs. by GdF_3 decoration 8-84544
 $Gd_2(MoO_4)_3$, prismatic domain exam. 8-56441
 $LiTiO_3$, light scatt. from ferroelec. domains 8-80310
 NH_4Cl , order parameter, electro-optic measurement 8-88280
 $NaNH_4SeO_4 \cdot 2H_2O$, ferroelectric crystal, effect of hydrostatic pressure on phase transition 8-52453
 $Pb_2Ge_{1-x}Si_xO_{11}$, ferroelec., switching vel. and spontaneous polarisation 8-84543
 $PbNb_2O_6$, ferroelectric thick crystals, domain formation and dislocation loops 8-60410
 $PbNb_2O_6$ ferroelectric single crystals, domain struct., cryst. planes, twinning 8-64340
 $PbTiO_3$, domain struct. formation during jump motion of phase front 8-64339
 $PbTiO_3$, ferroelectric ceramic, dielec., piezoelec. and elastic props., orientational contrib. 8-68468
n-Si, current-voltage characts., static high field domains 8-84223
 $Sr_{1-x}Ba_xNb_2O_6$, neutron and light scatt. in phase transition region 8-64336
 TiO_2 , rutile, ferroelectric ceramic, dielec., piezoelec. and elastic props., orientational contrib. 8-68468
 VO_2 single cryst., switching, visual obs. of metallic and semicond. domains 8-52041

electric double refraction see *electro-optical effects***electric drives**

see also *electric propulsion*

- astronomical laser ranging equipment, telescope drive (*Japanese*) 8-89078
Fourier spectrometer, electrodynamic drive system 8-82059
telescope drive, controlled 300 Hz freq. supply 8-61746

electric field effects

see also *acoustoelectric effects; discharges (electric); electrical conductivity; electro-optical effects; electrochemistry; electrodynamics; electrokinetic effects; electroluminescence; electromechanical effects; electromigration; electron field emission; electrophoresis; field emission ion microscopy; field evaporation; field ion emission; field ionisation; high field effects; magnetoelectric effects; particle optics*

- cholesteric liquid crystal mixture, with positive dielectric anisotropy influence of external fields (*Rumanian*) 8-59751
cholesteryl chloride-cholesteryl crotonate (75:25% wt.) mixture, cholesteric-nematic transition field effect temp. depend. 8-75813
4-4'-cyano-octyl-biphenyl, smectic A liq. cryst., elec. field effects, capacitance meas. 8-91237
4-4'-cyano-octyloxy-biphenyl, smectic A liq. crystelec. field effects, capacitance meas. 8-91237
dielectric liquid, film condensation, heat transfer enhancement in elec. field 8-55551
drop, heat transfer, electric field effect 8-59276
drops in immiscible liquid, intermittent elec. field heat transfer augmentation 8-94872
electron mobility, trajectory curvature effect in strong elec. field 8-83517

electric field effects continued

- electrostatic precipitator, free-fall, motion of charged particles, determ. 8-71020
emulsion, inverse-type, coalescence of drops in uniform elec. field 8-53265
flames, propag. rate and precombustion Joule heating 8-53207
HV transmission line elec. and mag. field exposure effects and hazards 8-77083
ionic conductor, quasielastic scatt. of light, neutrons and electrons, Debye-Huckel eqn. (*Chinese*) 8-68521
linear response theory, macroscopic vs. microscopic, appl. to electron in periodic pot. 8-65813
positron in condensing He, Monte Carlo lifetime spectra, temp. and elec. field effects 8-55263
powder, disintegration of powder particle agglomerates under the action of an alternating electric field 8-68642
semiconductor, paramagnetism switching off in strong electric field (*Russian*) 8-80124
superionic conductor, phase transitions induced by elec. field 8-63856
surface tension of polar liq., elec. field effect 8-51791
swine, exposure method for vertical 60 Hz elec. fields 8-53587
vacuum deposited metal film, elec. field effect on residual struct. 8-51836
Ar gas, high press., recombination luminescence in scintillation induced by alpha particles 8-50441
Au-Al system, influence of current on phase form. in diffusion layer (*Russian*) 8-52826
 $BaO-SiO_2$ glass ceramic, nucleation, effect of electric fields 8-83742
 $CaCO_3$, acceleration of growth of particles, Lorentz forces, electric and mag. field effects 8-51455
 $CaF_2:Gd^{3+}-M^+$ ($M=Li, Na, K, Rb, Cs, Ag$), electric field effect expts., EPR line breadths, lattice distortions 8-80210
 $Ga_2O_3-Fe_2O_3$ system, anomalous Mossbauer line shapes, incomplete annealing 8-92006
 $\alpha-LiIO_3$, in electrostatic field, X-ray double cryst. spectrometric investigation (*Chinese*) 8-67666
 $\alpha-LiIO_3$, lattice consts. variation due to electrostatic field (*Chinese*) 8-83787
 $MgO-Al_2O_3-SiO_2$ glass ceramic, nucleation, effect of electric fields 8-83742
Se, crystallisation kinetics correlation with molecular structure 8-94998
p-Si, positron annihilation, effects of applied elec. field (*German*) 8-72634
 $SrCl_2:Mn^{2+}(Co^{2+})$, cubic impurity EPR spectra, elec. field effect, mechanism 8-68361

electric field measurement

see also *field plotting*

- coronasonde, balloon-borne, for thundercloud elec. field meas. 8-61577
electrostatic intensity, electroluminescence method (*Russian*) 8-77934
International Sun-Earth Explorer 1 and 2, plasma wave investigation 8-85802
magnetosphere, DC and low-freq. field instrumentation on International Sun-Earth Explorer A 8-85807
magnetosphere, quasi-static and low-freq. fields meas. by International Sun-Earth Explorer-1 8-85808
miniature ELF electric field probe 8-70160
miniature probe, 60 Hz, laboratory investigation of electric fields generated by electrode systems appl. 8-77930
ocean electric fields, EM phenomena accompanying movement of current fairing in sea water (*Russian*) 8-77361
scanning mirror electron microscopy, quantitative evaluation of elec. microfields 8-74110
solar wind, DC and low-freq. field instrumentation on International Sun-Earth Explorer A 8-85807
solar wind, quasi-static and low-freq. fields meas. by International Sun-Earth Explorer-1 8-85808

electric field strength measurement see *electric field measurement***electric fields**

see also *electric field effects; electric field measurement; electromagnetic fields; electromagnetic waves; field plotting*

- auroral zone electric fields at 1 R_E altitude 8-57397
auroral zone electric fields rel. to interplanetary magnetic field vars. 8-77431
charge distortion on a wire in a warm plasma 8-55274
conducting body charge distrib. computation (*Polish*) 8-78850
cylindrical particle analyser, fringing field 8-94165
dayside magnetopause, electric field topology 8-57398
dielectric, inhomogeneous nonmatrix type, elec. field and effective dielec. tensor eqns. 8-52425
Einzel-type electrostatic field with rot. symmetry, Fourier-Bessel soln. 8-82878
electrode fields calc., blade-type (*Czech*) 8-55273
electron microscopy using electrostatic field on electron-charged dielec. (*German*) 8-82081
EPR spectroscopy in strong elec. fields at 77 and 4.2K 8-86310
F-region convective electric field determ. from rocket meas. of thermal ion spectra 8-57386
flame, diffusion type, oppositely directed jets, elec. props. 8-56896
insulating and semiconducting media, electric field numerical soln. (*Slovak*) 8-66710
interplanetary elec. field penetration of magnetosphere, balloon meas. 8-57408
ionosphere, auroral zone electric fields, conductivities and currents, latitudinal distrib. 8-77399
ionosphere, transverse electric fields rel. to field aligned currents, model 8-77397
ionosphere equatorial field, coupling to high-latit. mag. vars. 8-93029
LF and MF ground waves in realistic terrain, field strength meas. at LF and MF 8-88795
magnetosphere, transverse electric fields rel. to field aligned currents, model 8-77397
magnetotail, substorm electric field effects on charged particles 8-77425
Maxwell's equations as one quaternion eqn., appl. to wave propag., for teaching 8-54133
microstrip anisotropic electrostatic field problems, Green's function technique 8-70998
monochromatic parallel beam uniformly polarised (*French*) 8-90339

electric fields continued

- multilayer resonance elements, elec. field distribution calc. (*Russian*) 8-78854
- nonlocal electrostatics, spherical interface 8-82880
- permittivity meas., lumped-capacitance method, fringing field effect anal. 8-54392
- plasma, collisionless, signature of parallel elec. fields 8-77439
- plotting, computer programs for high-school expts. 8-86094
- potential fields calc., plane-parallel, in mixed boundary conditions (*Rumanian*) 8-82877
- pulsar magnetospheres with parallel electric fields 8-65643
- quadrupole lens spatial field determ. 8-55292
- in quiet plasmasphere, dynamo origin, whistler data 8-77426
- surface scattering from piecewise planar surfaces, algorithm 8-62983
- thunderstorm electric fields, 10-year study of Minneapolis area 8-57253
- two-dimensional open boundary problems, finite element anal. 8-94354
- weakly conducting layer, elec. field transient penetration 8-84525
- LiNbO₃ crystal, different interdigital electrode struct., electric field distrib. obs. 8-76433

electric filters *see filters***electric final control devices**

- see also electric actuators; electric motors; switches*
- static interruptor cct., triac, thermostatic and lighting control appl. (*Italian*) 8-73984

electric furnaces

- see also arc furnaces; resistance furnaces*
- plasma generation, investig. of gas conditions (*Russian*) 8-94921
- toroidal ellipsoid furnace, narrow zone heating by new radiation focusing 8-88424
- vacuum furnace, optical fibre-drawing 8-66960
- vacuum furnaces for quenching developed in USSR 8-84872

electric fuses

- metal-filled epoxy resin, temp. variation, current interruption appl. 8-76124

electric generators

- see also a.c. generators; d.c. generators; magnetohydrodynamic converters; Van de Graaff generators*
- generator-motor model for physics classes 8-65739
- impulse current generators, H₂O as electrical insulator (*Russian*) 8-75430

electric glow *see corona***electric heaters** *see electric heating***electric heating**

- see also domestic appliances; drying; electric furnaces; heating elements; induction heating; ovens; radiofrequency heating; space heating*
- blanking resistive heating for Auger spectroscopy and LEED using retarding field analyzer 8-54509
- double helix vacuum resistance heater element design and construction details 8-49839
- fluid heating mantle using heat-exchanger principles 8-93665
- metal wire, heated by electrical current, steady-state thermal cond. 8-59285
- ohmic heating system for TFTR Tokamak 8-55017
- parallel connected ohmic heating coil for double Tokamak fusion reactor 8-54930
- pipe, of variable thermal and elec. conds., elec.-heated, flow-cooled, temp. distrib. 8-90626
- SEM/STEM cold stage thick specimen heating model 8-61289
- thermal length control, for lasers and etalons 8-87056

electric heating elements *see heating elements***electric ignition**

- discharge striking in highly inhomogeneous axisymmetric mag. field 8-75473
- low-pressure discharge striking in axisymmetric elec. and mag. fields 8-75472
- spark generator for dust explosion hazard assessment and gas ignition 8-57983

electric impedance

- see also electric reactance; electric resistance*
- characteristic impedance of double line in front of dielec. wedge (*German*) 8-78855
- dipole antenna in warm isotropic plasma, boundary-value problem, multiple water bag model 8-91115
- eddy current transducer, impedance introduced by nonmagnetic plate 8-60939
- eddy currents, calculation by dual energy methods 8-78859
- electrocrystallisation, impedance frequency dependence, in the case of DC superposition 8-51844
- glow discharge, tube impedance with and without metal cover 8-67508
- hollandites, ionic cond., impedance, struct. 8-67856
- hollow-cathode arc discharge impedance/frequency characteristic obs. 8-67536
- impedance of a p-n junction by direct currents (*Russian*) 8-84285
- Josephson-effect absolute noise thermometer, resolution of unmodelled errors 8-62196
- liquid, small signal AC response, mobile charge recomb., theory 8-52005
- metal, surface impedance in magnetic field, Azbel-Kaner cyclotron resonance 8-87901
- metal film, surface impedance oscils. in perpendicular mag. field (*Russian*) 8-76165
- piezoelectric transducers, input electrical impedance expression, internal loss correction 8-53101
- plane wave at skew incidence on right-angled impedance wedge 8-90346
- radiation and scatt. from wires and surfaces, free space impedance functions 8-86999
- solid, small signal AC response, mobile charge recomb., theory 8-52005
- thin-layer cell, concentration impedance, unequal diffusion coeffs. and 2nd-order reactions effects (*French*) 8-53214
- thin-layer cell, concentration impedance reactive and nonreactive diffusion effects (*French*) 8-53213
- thin-layer cell, fast reaction, kinetic const., diffusion and conc. impedance 8-73053

electric impedance continued

- Ag/(α -AgI) interface, impedance meas., equivalent circuit parameters. calc., electrolyte defect struct. 8-59975
- Cd, electrodeposition on solid Cd or CdHg amalgam, rate, impedance meas. 8-52693
- GaAs-metal Schottky barrier diodes, impedance, freq. and voltage depend. 8-64114
- Ni_{1-x}O, electronic cond. at high temp., complex impedance study, effect of defects (*French*) 8-79990
- PbI₂ single crystals, photo-induced AC impedance meas., photodielec. effect 8-52034
- Si, surface characterisation by Si-electrolyte interface impedance meas. 8-84291
- ZnO pellets, and ZnO:Li single crystals, photo-induced AC impedance meas., photodielec. effect 8-52034

electric impedance measurement

- see also electric reactance measurement; electric resistance measurement*
- AC impedance meter, battery-operated, for contact resist. determ. before patient monitoring 8-81006
- biological tissue, vector impedance meter 8-57138
- brain impedograph, computerised 8-77139
- defibrillator electrode gel testing, meas. of impedance to transthoracic DC discharge 8-57056
- microprocessor-based instrument, method, advantages 8-89501
- plethysmography, influence of erythrocyte vel. 8-61238
- thoracic impedance of humans, meas. using automatic recording device on defibrillator 8-61239
- thorax, impedance camera for spatially specific meas. 8-53464
- thrombophlebitis diagnosis, reliability of Doppler and impedance techniques 8-77144
- tissue impedance meas. by phase-sensitive voltage and current detection 8-53602
- Zn electrodeposit dendritic growth control using impedance meas. 8-84721

electric load *see load (electric)***electric machine analysis computing**

- Faraday-type MHD generator optimisation, using a computer method (*Polish*) 8-79476

electric machine CAD

- diagonal-wall MHD generator design optimisation by nonlinear programming (*Polish*) 8-79477

electric machine computer aided design *see electric machine CAD***electric machine testing** *see machine testing***electric machine theory** *see machine theory***electric machines**

- see also electric generators; electric motors; machine bearings; machine testing; machine theory; rotors; superconducting machines*
- vibrations anal. and obs., block deformability influence (*Italian*) 8-51108

electric moments

- see also atomic electric moment; molecular moments; nuclear electric moment*
- colloids, macromolecules, particle size distribution, reduced electric dipole moments, polarisabilities using electric birefringence 8-95958
- neutron dipole moments and spin rotations 8-74296
- nonpolar molecules, adsorbed on metal surface, depolarisation interaction 8-51820
- nucleon structure function, quark and gluon moments, gauge theory 8-50036
- polar liquid, electric double layer at surface 8-53212
- quark electric dipole moment from CP noninvariant gauge theory, left handed currents (*Russian*) 8-74218
- thermodynamic properties of permanent dipoles on lattice 8-88246
- $\Delta(1236)$ M1 and E2 photoexcitation $N \rightarrow \Delta$ in $\gamma N \rightarrow \pi N$ 8-70377
- KCl:Li⁺, coherent excitation by EM and acoustic waves, induction and echo signal study 8-67773

electric motors

- see also stepping motors*
- generator-motor model for physics classes 8-65739

electric networks *see networks (circuits)***electric noise measurement**

- 300 MHz oscillators using SAW resonators and delay lines 8-59255
- automatic anomalous noise meas. for ferroelectric capacitor parameters, not in equil. (*French*) 8-74029
- microwave noise standards, Japanese, 10 GHz system (*Japanese*) 8-57985

electric potential

- see also contact potential; overvoltage; surface potential; voltage control; voltage measurement*
- anodic film form., electrode pot. variation rel. to nucleation, growth 8-68634
- Earth surface hydraulic fractures mapping technique 8-69543
- limited ion-dipole system, screened pot. (*Russian*) 8-66707
- metal-polyethylene terephthalate-metal struct., electrochem. effects as source of EMF 8-72278
- metallic tethers in ionospheric plasma, current and pot. distrib. 8-69652
- oxide-electrolyte interface, transition layer model 8-68895
- plane-parallel potential fields calc., in mixed boundary conditions (*Rumanian*) 8-82877
- Procopiu effect EMF in ferromag. material under torsion (*Rumanian*) 8-86986
- pulsar polar caps, pot. drops and ultrarelativistic particle accel. along curved mag. field 8-53970
- two-dimensional potential fields in complex media (*Slovak*) 8-94351
- Cu-Hg amalgam electrode, standard pot. 8-76874
- Fe-Mo systems, galvanic cell meas., 1160 to 1366K 8-61042

electric power generation

- see also direct energy conversion; power stations; wave power generation*
- diagonal-wall MHD generator design optimisation by nonlinear programming (*Polish*) 8-79477
- energy efficiency, problems and solns. 8-81762
- energy policy, climatic effects 8-61538
- fusion, inertial confinement, electric power generation 8-50314
- laser fusion, electric power generation 8-50315
- PULSAR, pulsed power conversion system with inductive storage 8-58029

- electric power generation** continued
thermonuclear power plants, problems and perspectives (*Polish*) 8-54876
Tokamak fusion power generation 8-74472
- electric propulsion**
see also *electric drives*
marine reactor systems, Monte Carlo reliability anal. of power and heat removal systems (*Japanese*) 8-58396
- electric reactance**
see also *capacitance; inductance*
eddy currents, calculation by dual energy methods 8-78859
- electric reactance measurement**
see also *capacitance measurement; inductance measurement*
Q-meter, digital, automatic, design procedure 8-70155
- electric relays** see *relays*
- electric resistance**
Josephson tunnel junctions, fabrication and four terminal resistance study (*Chinese*) 8-68116
micro plastic strain energy criterion applied to reversed biaxial fatigue 8-63391
transducers, applied, resistance due to cracks, eddy current calc. and hodograph 8-53095
n-GaAs, AuGe contact, temp. dependence meas. 8-76146
- electric resistance furnaces** see *resistance furnaces*
- electric resistance measurement**
see also *ohmmeters*
12 kHz IC resistance-frequency convertor (*Russian*) 8-81963
DC standard materials, physical and technological props. (*German*) 8-54400
defibrillator, damped sine wave, intact, evaluation of operating parameters 8-57120
double constant current source for cryogenic current comparators, standard resistor calibration appl. 8-93731
freeze etching and related techniques, resist. monitor for automatic film thickness regulation 8-49810
gigaohmmeter, electronic, with controllable threshold sensitivity 8-74024
high resistance measurement, for radiation detectors (*French*) 8-77929
human body resistance measurements (*German*) 8-53541
Kelvin bridge, link resistance compensation 8-86292
metal samples high precision meas. and control in He II environment 8-54403
ohm SI unit realisation at National Physical Laboratory 8-89505
piezoelectric crystals, crystal bridge for equivalent electrical parameters meas. 8-54404
probe, ultra-high vacuum compatible, thin film supercond. meas. 8-49867
semiconductor resistivity, spreading resist. calcs., role of source boundary conditions 8-89499
small active resistance and inductance meas. AC bridge 8-86299
soil resistance meter, geological and archaeological applications (*German*) 8-57361
GaAs, epitaxial layers on conductive substrate, elec. characterisation 8-91790
W, sintered metal resist. standard, resist. at high temp. 8-89427
- electric resistors** see *resistors*
- electric sensing devices**
see also *instruments; measurement*
balance, mechanical, with electronic displacement sensor, precision 8-77866
crack length automatic recording in sheet samples 8-60907
differential frequency angular rate and displacement sensor, construction (*Russian*) 8-70106
EEG automatic sleep staging detectors 8-53551
EM device, noncontacting, for bone mech. props. in vivo determ. 8-77133
EM instruments for use in liquid sodium, theoretical anal. 8-54857
ferromagnetic pick-up for iron sheet local magnetic properties (*Russian*) 8-77946
for quartz thermometer 8-81967
level detector for pumped bath of He II 8-49843
nasal air emission in speech disorders, electrodynamic evaluation 8-77134
porosity meas. device for fluidised beds, exam. 8-60911
redox gas sensor of sintered SnO₂, for anal. of pathological lung gases (*German*) 8-85440
sleep EEG automatic K-complex detector 8-53557
temperature sensors, elec. Japanese and international standards 8-65928
As₁₀Ge₁₅Te₇₅, thermal memory switch development 8-89468
SnO₂, gas sensor, CO, H₂O vapour, surface temp. effect on cond. 8-76067
- electric shielding, nuclear** see *nuclear screening*
- electric shocks**
see also *electrical faults; protection; safety*
electroconvulsive therapy pulse instrument 8-53562
intensive care unit/coronary care unit safety 8-69252
- electric spark machining** see *spark machining*
- electric sparks** see *sparks*
- electric strain gauges** see *strain gauges*
- electric strength**
see also *electric breakdown*
air, predischARGE-stabilised breakdown voltage (*German*) 8-63608
dielectric films in MIS structures (*Slovak*) 8-56231
discharge with external ionis., electric strength and elec. cond. 8-91180
epoxy resin, mech. and thermal props., amine hardeners, added softeners and filter effects (*Polish*) 8-68741
epoxy resin cured with composite curing agents, arc resistance (*Japanese*) 8-92371
Freons and their mixtures with N₂ and SF₆, breakdown voltage in uniform electric field (*German*) 8-71423
gas in crossed electric and magnetic fields, elec. strength calcs. 8-87568
gaseous dielectrics, electron-molecule interactions and negative ion resonances 8-75480
gases as electrical insulators, nature and practice 8-83632
insulating solid, elec. strength and degradation 8-83631
- electric strength** continued
moving gas, electric strength calcs., gas vel. effects 8-87568
oil for switching surges and long flash-over distances, expt. (*Czech*) 8-56427
organic purified dielectric liquids, expt. 8-84523
polycaprolactam film, temperature-time dependence (*Russian*) 8-76386
PVC films, temperature-time dependence (*Russian*) 8-76386
spark gap electric strength recovery after impulse current passage 8-67565
statistical test of solid dielectrics in pulse irradiation regime 8-95548
vacuum gap with processed electrodes, atm. effects on dielectric strength 8-51389
Al₂O₃, film, CVD, props. rel. to deposition parameters 8-92197
N₂, compressed, insulation breakdown at cryogenic temp., obs. 8-51368
N₂, gas, in crossed elec. and mag. fields, elec. strength calcs. 8-87568
SF₆ breakdown field strength, electrode surface roughness tolerance 8-67577
SF₆, compressed, electrode surface roughness effects, model (*German*) 8-63609
SF₆, predischARGE-stabilised breakdown voltage (*German*) 8-63608
SiO₂ film, in MOS structures, under unidirectional alternating and combined voltages (*Slovak*) 8-88034
- electric susceptibility** see *electric admittance*
- electric susceptibility** see *optical susceptibility*
- electric switchgear** see *switchgear*
- electric transformers** see *transformers*
- electric utilities** see *electricity supply industry*
- electric variables measurement**
see also *attenuation measurement; capacitance measurement; charge measurement; dielectric measurement; electric admittance measurement; electric current measurement; electric distortion measurement; electric field measurement; electric impedance measurement; electric noise measurement; electric reactance measurement; electric resistance measurement; electrical conductivity measurement; frequency measurement; gain measurement; inductance measurement; phase measurement; power factor measurement; power measurement; Q-factor measurement; voltage measurement*
free carrier profile measurement on thin-layers, fast current pulse MOS deep-depletion technique 8-80075
Hall coeff. contactless meas. in materials of small Hall angle in skin depth regime 8-86303
null apparatus for minority carrier lifetime meas. 8-56184
piezoelectricity, reson. method for determ. of small piezoelec. consts. (*German*) 8-92025
Seebeck coefficient, AC method of meas. using laser beam, for semiconductor. 8-76096
semiconductor junction noisy transient meas. 8-62205
- electric welding**
see also *arc welding; electron beam welding; resistance welding*
quality monitoring, US testing 8-56854
- electric wiring** see *wiring*
- electrical conduction in condensed matter**
see also *carrier density; carrier lifetime; carrier mean free path; carrier mobility; carrier relaxation time; dislocation scattering; electrical conductivity of liquids; electrical conductivity of solids; electrical conductivity transitions; electron density (metals); electron mean free path (metals); electron mobility (metals); electron-phonon interactions; electron relaxation time (metals); high field effects; hopping conduction; impurity scattering; Lorenz number; minority carriers; mixed conductivity; negative resistance effects; one-dimensional conductivity; photoconductivity; point defect scattering; size effect; skin effect; small polaron conduction; space-charge-limited conduction; spin disorder resistivity; surface conductivity; surface scattering; thermally stimulated currents; tunnelling*
Hubbard model, electrical conductivity calculation, dielectric function and plasma oscillations 8-64020
isothermal local resistivity, theory 8-72128
noninteracting electrons in correlated arrays of fixed scatterers, AC and DC cond. 8-51955
Swiss Physical Society, autumn sessions 8-72053
- electrical conductivity**
see also *electrical conduction in condensed matter; electrical conductivity of gases; electron mobility; ion mobility; space-charge-limited conduction*
disperse system, diphasic struct., systematic anal. to determ. permittivity and elec. cond. from dielec. relax. 8-56423
electron transport over barriers of fluctuating height 8-56122
erythrocytes of human blood, diameter meas. by specific elec. cond. 8-53353
graph-like state of matter, electrical cond. of random networks, gelation and elasticity 8-65875
heat and electrical transfer differential eqns. 8-67004
Kubo-Greenwood formula for teachers 8-62017
multistate trapping model, rel. to continuous-time random walk model 8-93624
nonlinear electrical conductivity theory based on integral Boltzmann eqn. 8-72125
quantum theory, appls. 8-84181
- electrical conductivity measurement**
25 kV bias isolation unit for 1 MHz measurements using commercial C/G meter 8-54401
automatic conductometer, exam. 8-56933
chemical monitoring laboratory, installation 8-61123
cryostat, for meas. on plastically deformed specimens at liq. He temps. 8-81985
electrolytes in H₂O, voltage amp. for temp. compensation (*German*) 8-54399
electrolytic cell resistance meas., differential recorder 8-86297
four-probe method for up to 50 kbar and 1000°C 8-57978
glasses, sources of error in AC cond. meas. 8-76076
inductive oscillometry, field difference theory 8-51342
instrument for loose materials 8-54395
polymeric insulators, controlled current DC meas. 8-57982
seawater, using meters with automatic correction of characts. (*Russian*) 8-65426
semiconductor film X-ray and electrical characteristics meas. chamber 8-86396
semiconductor layers, resistivity meas. by four point contacts arbitrarily spaced on circumference 8-51983

electrical conductivity measurement continued

- semiconductor resistivity, spreading resist. calcs., role of source boundary conditions 8-89499
 semiconductor samples pulse method for contact resist. and bulk resist. 8-52083
 semiconductors, SHF waveguide methods 8-95542
 six solenoid oscilloscope for non-intrusive LF positive-glow plasma diagnostics 8-51343
 skin conductivity measurement, electrode materials (*German*) 8-85406
 spherical metallic specimens, eddy-current probe method 8-53138
 CaF_2 , elec. cond. at high temp. 8-72159
 Mo, neutron irradiation temp. determ. by electrical resistivity meas. 8-58354
 Si plate resistivity meas. using constriction resistance method (*Rumanian*) 8-54390
 W, neutron, irradiation temp. determ. by electrical resistivity meas. 8-58354
 ZrO_2 , elec. cond.-nonstoichiometry relationship, direct determ. 8-76079

electrical conductivity of amorphous metals and alloys

- see also dislocation scattering; electron density (metals); electron mean free path (metals); electron mobility (metals); electron relaxation time (metals); electronic conduction in metallic thin films; impurity scattering; point defect scattering; surface scattering
 alloys, highly resistive, temp. depend. on elec. resist. 8-91657
 diffraction model, critical test, elec. resistivity of amorphous and liq. metals 8-84191
 ferromagnet, amorphous, resist. 8-64021
 low-temp. resistivity in mag. field 8-91667
 metal film, amorphous, structural and amorphous props. 8-84323
 metallic conductors, disordered and non-crystalline, anomalous elec. cond. 8-95279
 metallic glasses, elec. and thermal props. 8-72131
 metallic glasses, electrical conductivity, phenomenological theory 8-60102
 metallic glasses, physical principles, manufacture, mech. and mag. props. (*French*) 8-83744
 metglas type system, structural and amorphous props. 8-84323
 saturation effects in electron transport 8-76065
 transition in metals and alloys 8-95280
 transition metal alloys, anomalous behaviour of resist., alternative mechanism to spin scatt. 8-91690
 transition metals and their alloys, amorphous, elec. resist. 8-60103
 Au-Si, amorphous sputtered film, elec. props. 8-68006
 Be-Nb-Zr alloys, glassy and partially crystalline; supercond. T_c and struct. props. 8-60239
 $\text{Be}_{40}\text{Ti}_{50}\text{Zr}_{10}$, metallic glass, thermoelectric power and resist. 8-95289
 CC Fe-B glass, crystallisation kinetics, elec. resist. meas. 8-83741
 $\text{Ce}_{30}\text{Au}_{70}$, amorphous, cryst. field effects and mag. interactions, magnetisation and transport props. meas. 8-68191
 $\text{Co}_{1-x}\text{Au}_x$, elec. resist., temp. depend., spin wave contrib. and resist. minimum 8-51961
 $\text{Cr}_{1-x}\text{Pd}_{2-x}\text{Ge}_{18}$, RF sputtered, elec. resist. and magnetoresist., Kondo type behaviour 8-76066
 $\text{Cs}_{1-x}\text{O}_x$, metallic glass, prep., elec. props. and struct. 8-67652
 $\text{Cu}_{60}\text{Zr}_{40}$, amorphous, elec. resist. calc. and temp. coeff., using t-matrix 8-72130
 Fe film, amorphous and polycrystalline, Hall effect, resistivity and mag. moment 8-91786
 Fe-Y, amorphous, resist. and magnetoresist. meas., local moment system 8-68018
 $\text{Fe}_{1-x}\text{Au}_x$, elec. resist., temp. depend., spin wave contrib. and resist. minimum 8-51961
 $\text{Fe}_{1-x}\text{Au}_x$, amorphous ferromagnetic, resistivity, anisotropic, field dependence 8-87960
 $\text{Fe}_{32}\text{Ni}_{36}\text{Cr}_{14}\text{P}_{12}\text{B}_6$, Metglas 2826A, Hall resistivity, effect of thermal cycling and annealing 8-56125
 $\text{Fe}_{1-x}\text{Ni}_{1-x}\text{P}_{1-x}\text{B}_6\text{Al}_3$, amorphous alloy, low temp. elec. resist. saturation 8-68005
 $\text{Fe}_{29}\text{Ni}_{49}\text{P}_{14}\text{B}_6\text{Si}_2$, Metglas 2826B, Hall, elec. resist., magnetisation and heat capacity meas. 8-68019
 $\text{Fe}_{34}\text{Pd}_{46}\text{P}_{20}$, amorphous, sp. ht. and resist. near ferromag. phase transition 8-56333
 Ge-Al film, elec. resist. and IR transmission, comp. and substrate temp. depend. 8-52112
 Ge-Se-Fe films, metallic and semicond., amorphous, mag. and elec. props. 8-52319
 Mg-Zn, amorphous sputtered film, elec. props. 8-68006
 Ni, amorphous film, getter sputtered at 25K, resistivity, Curie temp. 8-52673
 Ni-B amorphous alloy film, atomic and electronic transport (*French*) 8-84325
 Ni-Co-P, amorphous alloy, electrical and mag. props. 8-95281
 Ni-Co-P, ferromag. film, amorphous to cryst. transition, diff. and resistivity meas. 8-60587
 Ni-P, metallic glass, elec. resistivity 8-91654
 Ni-Y, amorphous, resist. and magnetoresist. meas., weak itinerant ferromagnet 8-68018
 $\text{Ni}_{1-x}\text{Au}_x$, elec. resist., temp. depend., spin wave contrib. and resist. minimum 8-51961
 Pt-Sb, amorphous sputtered film, elec. props. 8-68006
 $\text{Rb}_{1-x}\text{O}_x$, metallic glass, prep., elec. props. and struct. 8-67652

electrical conductivity of amorphous semiconductors and insulators

- see also carrier density; carrier lifetime; carrier mean free path; carrier mobility; carrier relaxation time; dislocation scattering; electrical conductivity transitions; electronic conduction in insulating thin films; high field effects; hopping conduction; impurity scattering; minority carriers; negative resistance effects; photoconductivity; point defect scattering; small polaron conduction; surface scattering
 carrier pulse propagation, macroscopic theory 8-72154
 chalcogenide glass, AC conductivity, temp. depend. 8-72153
 chalcogenide glasses, elec. cond., press. effects 8-56142
 chalcogenide glasses, percolation-controlled elec. cond. 8-72150
 epoxy resin, mech. and thermal props., amine hardeners, added softeners and filler effects (*Polish*) 8-68741
 fluorinated copolymers, mech. and elec. props., processing and appls. 8-84760
 glasses, contact influence on AC cond. 8-76076
 hopping conduction, DC, pre-exponential factor 8-76074

electrical conductivity of amorphous semiconductors and insulators continued

- Kaprolon, compressibility, elec. cond., sound vel. behind shock front 8-95105
 optimal polynomials in calcs. of complex glass's properties 8-68026
 oxide glasses, elec. cond. and dielec. relax., correl. 8-79801
 plexiglass, red, gamma dose meas. by optical absorpt., elec. conductivity, and mechanical hardness 8-55045
 poly-aryl-acetylene, elec. cond. of cis- and trans- stereo isomers (*German*) 8-84221
 polyacrylonitrile, pyrolyzed, elec. cond. and dielec. const. in AC regime 8-60173
 polyethylene, conduction mechanism, expt. determ. (*German*) 8-76086
 polyethylene, low density, dielec. behaviour, struct. props. influence (*German*) 8-92017
 polymers, nonlinear electric behaviour interpreted through free vol. changes 8-84226
 PTFE, mech. and elec. props., processing and appls. 8-84760
 relaxation regime, generalised transport eqns. 8-56139
 semiconductor, amorphous or disordered, cond. mechanisms, model of medium-range comp. disorder 8-79994
 teflon, measuring technique (*French*) 8-77929
 threshold switching by computer simulation 8-88002
 violanthrene-A film, amorphous and crystalline, carrier mobility differences 8-60125
 $\text{Al}_2\text{O}_3\text{-B}_2\text{O}_3\text{-P}_2\text{O}_5$ glasses, formation and props. 8-83737
 As_2Se_3 , glassy, with adsorbed $\text{H}_2\text{O}(\text{NH}_3)(\text{NO}_2)(\text{O}_2)(\text{CO}_2)(\text{CO})$, surface cond., photocond. 8-80038
 $\text{As}_4\text{Se}_3\text{Ge}_2$, glass, light irradi. induced changes in optical and elec. props. (*Japanese*) 8-68031
 $\text{AsSe}_{1.5-x}\text{Te}_x$ glasses, physical props. 8-68028
 $\text{As}_2\text{Se}_3\text{Te}_{3-x}$ chalcogenide glasses, cond. meas., field strength and temp. depend. 8-84225
 $\text{As}_2\text{Te}_3\text{-Ti}_x$, glassy system, composition depend. of activation energy, thermopower meas. 8-64052
 $\text{As}_x\text{Te}_{100-x}$, glassy system, composition depend. of activation energy, thermopower meas. 8-64052
 AsTeCu_x ($0 \leq x \leq 0.4$) glass, effect of Cu on elec. cond. and thermoelectricity, 100 to 370K 8-87978
 $\text{BaO-B}_2\text{O}_3\text{-SiO}_2\text{:Ti}^{3+}$, elec. cond., struct. 8-72148
 n-BaTiO₃, elec. transport props., theoretical discussion and expt. 8-84215
 C, elec. cond. and Hall effect, temp. depend. 8-60141
 CC NiO, amorphous, charge transport in band tails 8-76026
 Cd-Sb thin film prep. by vacuum deposition, elec. props. 8-92194
 $\text{Cd}_3\text{Ge}_3\text{As}_{11}$, DC cond., press. depend. 8-72064
 $\text{Cu}_{10}\text{As}_{31}\text{Se}_{38}\text{O}_{21}$, chalcogenide glass, exam. of electron mechanism of photo induced changes 8-87998
 CuO-CaO- P_2O_5 glass devices, memory switching 8-56192
 FeO- P_2O_5 glasses, electrical and mechanical losses 8-80283
 $\text{Fe}_2\text{O}_3\text{-B}_2\text{O}_3\text{-PbO}$ glass, semicond., elec. resist. meas. 8-95300
 GaP film, deposited by RF sputtering (*Czech*) 8-52667
 GaP, plasma deposition and elec. cond. 8-60585
 GaSe film, I-V characts. in strong elec. fields, 173-373K 8-56248
 Ge, effect of Au, fresh and aged samples 8-76161
 Ge film, DC cond., Meyer-Neldel rule 8-64152
 Ge, film, variable range hopping 8-76176
 Ge:Al(Sb) film, amorphous, ion implantation, effect on cond. 8-83839
 Ge:Mn, amorphous, cond. increase by Mn doping 8-72155
 Ge-Al film, elec. resist. and IR transmission, comp. and substrate temp. depend. 8-52112
 GeS₈ glass, activation energies after neutron irradiation, elec. cond. and transmission coeff. 8-83850
 $\text{Ge}_2\text{Se}_{1-x}\text{S}_x$, amorphous semicond., elec. props. 8-84219
 GeTe film, amorphous, evaporated and annealed, variable range hopping cond. 8-80077
 H_2WO_4 film, effect of struct. on optical and electrical props. 8-84671
 $\text{In}_2\text{O}_3\text{:Sn}$, sputtered film, optical and elec. props. 8-76177
 $\text{La}_2\text{O}_3\text{-S-AgS-Ga}_2\text{S}_3$, ionic conducting glasses (*French*) 8-79804
 $\text{Na}_2\text{O-Al}_2\text{O}_3\text{-SiO}_2$ glasses, elec. cond. and cation mobility 8-59973
 (SN)_x polymer, elec. props. of amorphous thin film and single crystal, role of chain breaks (*Japanese*) 8-68104
 Se, amorphous, carrier lifetime and drift mobilities 8-87985
 Se-S, glassy alloy, order-disorder transition kinetics 8-67650
 Si DC sputtered, amorphous, dark conductivity and photocond. obs. (*French*) 8-64155
 Si film, amorphous, effects of annealing of gap states 8-72115
 Si film, variable range hopping 8-76176
 Si:Al(Sb) film, amorphous, ion implantation, effect on cond. 8-83839
 Si:H film, elec. cond., effect of adsorbed gases and illumination 8-88048
 Si:Mn, amorphous, cond. increase by Mn doping 8-72155
 Si_3N_4 , amorphous, charge transport in band tails 8-76026
 Si_3N_4 , unsteady cond. in high elec. fields 8-76152
 SiO amorphous thin film capacitor, EPR, elec. cond. 8-68358
 $\text{Si}_{12}\text{Te}_{48}\text{As}_{30}\text{Ge}_{10}$, amorphous film, elec. cond. mechanisms, temp. depend. (*Japanese*) 8-80078
 SnTe film, amorphous, evaporated and annealed, variable range hopping cond. 8-80077
 $\text{Ta}_{16}\text{W}_{18}\text{O}_{94}$, characterisation of thermally contracting tungstates 8-63869
 Ta_2WO_6 , characterisation of thermally contracting tungstates 8-63869
 $\text{Ta}_{22}\text{W}_4\text{O}_{67}$, characterisation of thermally contracting tungstates 8-63869
 $\text{TiO}_2\text{-SiO}_2$, semicond. glass, small polaron hopping cond. 8-60126
 WO_3 amorphous film, elec. cond. and dielec. const. 8-60238

electrical conductivity of crystalline metals and alloys

- see also dislocation scattering; electron density (metals); electron mean free path (metals); electron mobility (metals); electron relaxation time (metals); electronic conduction in metallic thin films; impurity scattering; point defect scattering; surface scattering
 actinide systems, nearly magnetic, thermoelectric power determ. 8-56133
 alkali metal, ideal electrical resistivity, temp. depend. 8-64022
 alloy,dil., electrical resistivity, Kondo effect vs. spin glass behaviour 8-68269
 alloys, highly resistive, temp. depend. on elec. resist. 8-91657
 binary alloy, electronic transport in substitutionally disordered systems, MCPA and Monte Carlo calc. 8-84185

electrical conductivity of crystalline metals and alloys continued

- α -brass, electron irradiated, defect production and interdiffusion 8-67739
- β_1 brass containing α -precipitates, reversible shape memory effect (*Japanese*) 8-60711
- Cr-Au alloys, dil., elec. resist., 77-700K 8-64035
- disordered system, residual resistivity 8-87954
- electrical domains at low temps. in metals (*Russian*) 8-91687
- electrically conducting spherical specimens, electromagnetic control 8-53138
- ferromagnet, anisotropic, spin-fluctuation resist. 8-56137
- ferromagnetic metal, with domain struct., resistivity 8-95285
- irradiated metal, containing self-interstitials and vacancies, electronic transport props. 8-60105
- magnetic ternary alloys, statistical theory of electrical resistivity 8-87969
- metal, BCC, temp. depend., anharmonic effects 8-76045
- metal, defect annealing study by positron annihilation, and elec. resistivity meas. 8-51584
- metal, ferromagnetic, dynamic scatt. effects on crit. transport props. 8-84239
- metal, impure elec. conductivity calc., effect of electron-electron correlation (*Russian*) 8-68010
- metal, kinetic effects at high anisotropic strains, elec. transport props. meas. 8-54384
- metal, quantum kinetic equation for electrons 8-91686
- metal wires, DC resistance, size effect correction 8-91679
- metal with unfilled f-shell, elec. resist. (*Russian*) 8-72141
- metals, normal hexagonal, temp. depend. anisotropy of phonon scatt. resist. 8-51967
- noble metal, elec. resist. of dislocations, calc. (*Russian*) 8-60117
- nonlinear effects due to coherent mag. breakdown (*Russian*) 8-76062
- powder metallurgy compact, elec. resistivity 8-64028
- rare earth metals, anisotropy of elec. resist., scatt. mechanism 8-72134
- rare-earth, light-heavy alloys, resistivity, mag. contrib. to resist. and Neel temp. 8-51971
- rare-earth alloys, quadrupole scatt. anisotropy, magnetically ordered material 8-64034
- Recalloy, Fe-Nb, semihard magnetic alloy, magnetic props., hardness, microstruct. 8-56660
- resistivity anomalies of ferromag. metals near Curie temp., itinerant mag. electron theory 8-95292
- resistometric studies of lattice defects review (*Japanese*) 8-59799
- saturation effects in electron transport 8-76065
- saturation resistivity charges, ion and fission fragment irradi. induced 8-79643
- spin glass, resistivity below ordering temp. 8-51980
- spin glasses under high press., resist. meas. 8-52277
- steel, alloy, Fe-C-Zn (0.45, 1.56 wt.%), pearlite transformation during continuous cooling 8-80538
- steel, alloy, thermal and electro-physical props. of various heat resisting stampings (*Russian*) 8-51698
- steel, alloy, type HSLA, exam. of NbCN precipitation by elec. resistivity meas. 8-84822
- steel, C, resistivity, thermal and elec., spin disorder scatt. anal. 8-76063
- steel, type 55SM5FA, formation of hardened layer during burnishing 8-85046
- superconducting B-W type compounds, resist. characts. in normal state 8-51963
- thermopower and resistivities, validity of Nordheim-Gorter relation 8-91671
- transition metal alloys, anomalous behaviour of resist., alternative mechanism to spin scatt. 8-91690
- transition metal double oxides, exam. of elec. cond. 8-51990
- transition metals, McMillan-Hopfield factor and ideal phonon limited resist. 8-64024
- two-component layered system, with interpenetrating components, thermoelec. and galvanomag. props. 8-79982
- Ag alloys, dil., transport props. 8-76046
- Ag, elec. resist., press. variation 8-84193
- Ag, low temp. elec. resist. 8-51964
- Ag, strained, anisotropic electron scatt. in elec. resist. 8-91656
- Ag-Au, dil., low temp. elec. resist. 8-51964
- Ag-Cu, composite, fibre and layer structs., anomalous props. caused by internal phase boundaries 8-72754
- Ag-Mn alloys, dilute, low temp. elec. resist. (*Russian*) 8-68024
- Ag-Ni, composite, fibre and layer structs., anomalous props. caused by internal phase boundaries 8-72754
- Al alloys, age-hardening, resistivity charge by low temp. deform. (*Japanese*) 8-84831
- Al, strained, anisotropic electron scatt. in elec. resist. 8-91656
- Al-Ag, discontinuous decomposition (*Polish*) 8-52808
- Al-Ag (up to 40 at.%), exam. of anelastic phenomena and structural state 8-76693
- Al-Cu(Ag)(Ge), dil., deviation from Matthiessen's rule at high temps. 8-64025
- Al-Li alloy, dil., quenched and irradi., recovery, resist. and internal friction obs. 8-52848
- Al-Mg-Ag, age effect on age hardening (*Japanese*) 8-52831
- Al-Mn (0.35 wt.%), quenched exam. of Mn-vacancy interaction 8-76676
- Al-Sn, dil. alloy, vacancy-impurity interaction, exam. by electrical resistivity meas. at 77K (*German*) 8-83846
- Al-Zn, dil. alloy, ageing and reversion, annealing curves, X-ray obs. 8-88485
- Al-Zn, discontinuous decomposition (*Polish*) 8-52808
- Al-Zn, formation of Guinier-Preston zones, and their limit temp. (*Japanese*) 8-84861
- Al-Zn, precipitation struct. and phys. props. effect of miscibility gap (*German*) 8-92265
- Al-Zn-Mg alloys, decomposition kinetics, resistivity meas., extended jump model 8-84766
- Au alloys, electrical resistivity, deviations from Matthiessen rule and scattering anisotropy 8-76051
- Au, elec. resist., press. variation 8-84193
- Au polycrystalline wire, internal oxidation of impurities, rel. to resist. and magnetoresist. 8-83842
- Au, residual resistivity of ^{57}Co 8-71881

electrical conductivity of crystalline metals and alloys continued

- Au-Cd (47.5 at.%), effect of cooling rates on stress-strain behaviour 8-76721
- Au-Cr, dil., spin glass, elec. resist., press. and conc. effects 8-52278
- Au(Pd)-Zn, martensitic transformation, Hall coeff., specific elec. resistivity and X-ray powder diffraction 8-72774
- BaVS₃, quasi-one-dimensional ferromag. or antiferromag., metallic cond. and mag. meas. 8-52233
- Bi-Te, dil. alloy, elec. cond. depend. on Te conc. (*Russian*) 8-76042
- CaSb, resist., susceptibility and thermopower rel. to electronic struct. 8-67935
- Cd, Hall effect and elec. resist., temp. depend. 8-64030
- Cd-Ag, polycryst. quenched foil, the influence of Ag on the recovery spectrum 8-76661
- Cd-Ag, polycryst. wire, cold worked, resistivity changes 8-68827
- Cd-Zn, polycryst. wire, cold worked, resistivity changes 8-68827
- Ce, sp. ht. and temp. coeff. of resist., 20 kbar at 300K 8-83973
- Ce-La, mag. ordering, sp. ht., susceptibility and resist. 8-68238
- CeCu₂Si₂, resistivity, thermal conductivity and thermopower between 1.5 and 300K 8-87963
- Co based alloys, resistivity magnetoresistance, s,p impurities in ferromag. host 8-68008
- Co, electrical resistivity, effect of domain wall orientation at 4K 8-91662
- Cr-Al, disordered alloy, effect of high press. on resistivity 8-95286
- Cr-Fe-V, dil., V effect on para- to incommensurate and commensurate transitions 8-68260
- Cr-Si-V, dil., V effect on para- to incommensurate and commensurate transitions 8-68260
- Cu alloys, dil., transport props. 8-76046
- Cu, effect of cyclic strains and work hardening at 4.2K 8-91655
- Cu, elec. resist., electron-electron scatt., Fermi surface calc. 8-64023
- Cu, elec. resist., press. variation 8-84193
- Cu, high-cond., high spt. ht., for cryogenic appl., prep. 8-76670
- Cu wire, residual elec. resist., size effect and grain boundary contribs., heat treatment effects (*Russian*) 8-56126
- α -Cu-Al, binary substitutional, short-range ordering kinetics, vacancy behaviour 8-55867
- Cu-Al, internally oxidised, structural, elec. and mech. characts. 8-60761
- Cu-Au, dil., O₂ solubility, thermodynamic and residual resist. study 8-59952
- Cu-Cr, dil., spin glass, elec. resist., press. and conc. effects 8-52278
- Cu-Fe, composite, fibre and layer structs., anomalous props. caused by internal phase boundaries 8-72754
- Cu-Ni dil. paramagnetic alloys, sp. elec. resist., effect of Ni clusters (*German*) 8-95293
- Cu₂₀Mn₉₄In₀₁, In-Heusler single crystal, elec. resist. 8-60107
- Cu₂Mo₈S₈, normal state and superconducting property measurements 8-91660
- DySb, quadrupole scatt. anisotropy, magnetically ordered material 8-64034
- electrical resistivity, relax. time near order-disorder transition 8-87788
- Er, Hall const. and elec. resist., 80-700K (*Russian*) 8-60110
- ErSb, metallic, cryst. field effects on transport props. 8-72133
- Fe, appl. of KUR LINAC to radiation damage studies 8-71760
- Fe based alloys, resistivity magnetoresistance, s,p impurities in ferromag. host 8-68008
- Fe, elasto-resistivity effect, meas. of resistance at 4.2K and 300K, using mag. field method 8-72132
- Fe, highly pure, temp. depend. 1.6 to 298K 8-84194
- Fe, porous, density, elec. cond., Young's modulus, toughness 8-64645
- Fe, powder, consolidated, exam. of mech. and electrical props. 8-56599
- Fe-Al (40 at.%) B₂ type ordered alloy, C migration, resistivity meas. (*French*) 8-52868
- Fe-C (0.52 wt.%), FCC structure, exam. of electromigration of C by steady state method 8-75865
- Fe-Co, partially ordered, elec. cond. 8-91663
- Fe-Co alloy, annealing of point defects produced by cold working (*French*) 8-72829
- Fe-Co-V (2%), annealing of point defects produced by cold working (*French*) 8-72829
- Fe-Co-V(2%) alloy, correl. of resistivity with microstructure 8-72896
- Fe-Cr-Al alloys, low temp. sp. ht., resistivity and coercive force 8-63866
- Fe-Cr-Co, effect of heat treatment on strain gauge factor 8-72802
- Fe-Cr-Ni, electron irradiated, resistivity during annealing, 4.2-1300K 8-87962
- Fe-Cr-SiC-B₄C powder mixture, compressibility and elec. cond. in cold pressing under low press. 8-60609
- Fe-N alloy, dil., galvanomag. effects, 4.2-250K 8-87964
- Fe-Ni, (35 wt.%), transport props. and Invar features (*Russian*) 8-51973
- Fe-Ni, elect. phenomena rel. to martensitic avalanche (*French*) 8-68691
- Fe-Si-Al (6.4 wt.%), Sendust alloy, effect of Ni content on mag. props. 8-72897
- Fe-Si-Mn, effect of Mn addition on mag. props. and elec. resist. 8-91890
- FeCo, ordered alloy, 550°C change, study through elec. cond. and specific heat meas. 8-56633
- FeNi-Cu, composite fibre and layer structs., anomalous props. caused by internal phase boundaries 8-72754
- Fe₃₋₄Si₁₋₃, electron transport 8-91669
- Ga-In, dil., elec. resist., temp. and impurity depend., deviation from Matthiessen's b-axis crystals 8-51970
- Ga-Sn, dil., elec. resist., temp. and impurity depend., deviation from Matthiessen's b-axis crystals 8-51970
- Ga-Zn, dil., elec. resist., temp. and impurity depend., deviation from Matthiessen's b-axis crystals 8-51970
- GdNi₅, anomalous behaviour near Curie point 8-91880
- HfPt₃, corrosion resist. and elec. cond., bulk and film samples 8-72285
- (Ho,Y)Co₂, mag. props., elec. resist. and thermal expansion 8-76246
- Ho, Hall const. and elec. resist., 80-700K (*Russian*) 8-60110
- HoSb, quadrupole scatt. anisotropy, magnetically ordered material 8-64034
- K, electrical resistivity below 2K, temp. depend. 8-51969
- LaCu₂Si₂, resistivity, thermal conductivity and thermopower between 1.5 and 300K 8-87963

electrical conductivity of crystalline metals and alloys continued

- LaPt₅, cryst. field effects on transport props. 8-72133
 LaSb, metallic, cryst. field effects on transport props. 8-72133
 Li, effects of core and correl. corrections 8-64026
 Lu-Gd, dil., positive exchange Kondo system, magnetisation and resist. 8-68158
 Mg, Hall effect and elec. resist., temp. depend. 8-64030
 Mg, recrystallisation after cold rolling 8-72790
 Mg-Nd-Zr, phase diagram, Mg rich region, microscopic anal. and elec. resistivity meas. (*Russian*) 8-56619
 Mg₂Sn, phase transition under hydrostatic pressure, Mossbauer effect and electric resistance 8-51665
 Mn-Pt, exam. of Elinvar props., from -150 to 500°C 8-76684
 MnSb, resist., susceptibility and thermopower rel. to electronic struct. 8-67935
 Mo, liquid and solid, thermophysical props. 8-75808
 Mo, temp. depend., electron-electron scatt. 8-68025
 Mo-Ni two phase alloys, elec. and mass transport (*Russian*) 8-76044
 Nb, high-temperature nonlinear electrical resistivity, supposed failure of Boltzmann eqn. 8-91664
 Nb₃Ge(Al), anomalous resistivity, insight from band theory 8-60106
 Nb₃Sn, highly disordered, elec. resist. and supercond. T_c 8-52142
 Nd-La, mag. ordering, sp. ht., susceptibility and resist. 8-68238
 Ni, anomalous resistivity near Curie temp., band theoretical calc. 8-56127
 Ni based alloys, resistivity magnetoresistance, s,p impurities in ferromag. host 8-68008
 Ni, resistivity, thermal and elec., spin disorder scatt. anal. 8-76063
 Ni-Co-H system, phase transform. under high H₂ press., Co additive effects (*Russian*) 8-60645
 Ni-Co-P, ferromag. film, amorphous to cryst. transition, diff. and resistivity meas. 8-60587
 Ni-Cr-MgO system, elec. resist. variation with comp. and prep. method 8-60637
 Ni-Re, dil. alloys, two-band Mott conductivity (*Russian*) 8-60118
 Ni-Ti (51.5 at.% Ni) metallide, thermal cond., elec. resistivity, 90-450K 8-68009
 Ni₂Cr, neutron irradi., point defect prod. and annealing 8-87718
 Ni₃(Fe,M), M=Cu, Cr, Mo, W, kinetic phenomena rel. to ordering and electron struct. (*Russian*) 8-76043
 Ni₃Mn, elec. resist., relax. time near order-disorder transition 8-87788
 NiSb, resist., susceptibility and thermopower rel. to electronic struct. 8-67935
 PbMo₆S₈, normal state and superconducting property measurements 8-91660
 Pd, hydride and alloys, electronic band struct., comparative study of electric and mag. props. 8-95259
 Pd, liq. and solid, thermophysical props. 8-75808
 Pd, strained, anisotropic electron scatt. in elec. resist. 8-91656
 Pd, transport props. 40 mK-6K 8-51968
 Pr-rare earth dilute alloy, low field magnetic props. 8-84443
 PrCu₂(Pt₃), cryst. field effects on transport props. 8-72133
 Pt foil, quenched, 1.2 MeV electron irradi., subthreshold irradi. effects 8-51585
 Re, electrical resistance anisotropy, temp. depend. (*Russian*) 8-76041
 Re, electron-electron scatt. 8-68025
 Re, single crystal, size effect in elec. resistivity (*Russian*) 8-87961
 Re, specific heat, elec. cond., emissivity, 1600-2400K 8-67835
 Ru, electrical resistance anisotropy, temp. depend. (*Russian*) 8-76041
 Ru, single crystal, size effect in elec. resistivity (*Russian*) 8-87961
 Sc, sp. ht. data rel. to electronic props. 8-83971
 Sm, resistivity and thermopower anomalies at high temp. 8-64027
 Sn, monocrystals with impurities, elec. resist. anisotropy 8-79975
 Sn-Pb alloy, dil., lattice dynamics, sp. ht., resist., thermal expansion and nuclear γ reson. expts. (*Russian*) 8-87749
 Sn_xPg_{1-x}, thermal cond. and Lorenz function 8-51966
 Ta, electrical and thermal resistance at low temp. (*Russian*) 8-68007
 Ta-O solid soln., interstitial ordering and precipitation at 100 to 270°C, exam. 8-52813
 Tb-Y, single crystal growth from melt, X-ray obs., props. (*Russian*) 8-95689
 TbNi_{1-x}Cu_x, elec. resist. and mag. props. 8-72348
 Ti 8-60602
 α -Ti alloy, VT1-1, cold rolled, recrystn. texture and prop. anisotropy 8-52846
 Ti, melting point, normal spectral emittance and elec. resistivity, pulse heating method 8-91423
 Ti-Al-V alloy, thermophysical meas. above 1450K, using subsecond transient technique 8-95161
 Ti-V, anomalous elec. resistivity, mag. susceptibility, soft-phonon induced structural inhomogeneities 8-60104
 Ti(Fe_{1-x}Co_x), density of states estimation from magnetisation and resistivity meas. 8-84119
 TmSb, metallic, cryst. field effects on transport props. 8-72133
 TmZn, cooperative Jahn-Teller effect 8-67998
 V₂(Hf,Zr), Laves phase compounds, temp. dependence with composition 8-76047
 VO₂, metallic phase, electronic props., plasma freq., Hall coeff. 8-84195
 V₃Si, neutron irradiated single crystal, superconducting transition temp. widths, resistivity and heat capacity meas. 8-91802
 V₃Si, neutron-irrad., ht. capacity and resistivity 8-88075
 W, electrical resistivity-temperature scale and vacancy parameters 8-71727
 W, electron-electron scatt. 8-68025
 W, single crystals, electron irradiated, recovery of resistivity, 4.5-380K (*German*) 8-87714
 W, sintered metal resist. standard, resist. at high temp. 8-89427
 W, thermal neutron irradiated, radiation damage and stage III defect annealing 8-51586
 W, wire, elec. resistance, low-temp. continuous and cyclic heating effects, compared with W-Re 8-92370
 W-Co, dil., excess resistivity, temp. depend., Kondo effect 8-68011
 W-Fe, dil., excess resistivity, temp. depend. 8-68011
 W-Re, dil., excess resistivity, temp. depend. 8-68011
 W-Re, wire, elec. resistance, low-temp. continuous and cyclic heating effects, compared with W 8-92370
 W-Zr (2.92, 7.42 and 10.02 wt.%), and W₂Zr, thermal expansion, elec. resistance, 100-900°C, crystallisation 8-91455
 Zn, Hall effect and elec. resist., temp. depend. 8-64030
 Zr-Nb(2.5 wt.%) alloy, effect of pre-irradiation on oxidation 8-88580

electrical conductivity of crystalline metals and alloys continued

- Zr(Fe_{1-x}Co_x), density of states estimation from magnetisation and resistivity meas. 8-84119
 ZrPt₃, corrosion resist. and elec. cond., bulk and film samples 8-72285
 ZrV₂, Laves-phase, cubic to rhombohedral transition, lattice electron instability 8-92261
- electrical conductivity of crystalline semiconductors and insulators**
see also carrier density; carrier lifetime; carrier mean free path; carrier mobility; carrier relaxation time; dislocation scattering; electronic conduction in crystalline semiconductor thin films; electronic conduction in insulating thin films; high field effects; hopping conduction; impurity scattering; minority carriers; negative resistance effects; photoconductivity; point defect scattering; small polaron conduction; surface scattering
 alkali halides, premelting elec. cond., heat capacity 8-91445
 alkali perchlorates, elec. transport during struct. transforms. 8-59971
 anthracene, off-diagonal electron mobility and lateral space charge drift 8-72192
 Chevrel type compounds, single crystals, growth, stoichiometry, elec. resist. 8-92187
 defect cluster scatt. and removal of carriers, model 8-76069
 diamond:B hopping conductivity in range 12 to 1300K 8-51994
 diamond, synthetic, elec. cond. 8-56144
 diamond, synthetic and natural, neutron irradi., optical and elec. props. (*Russian*) 8-59841
 EBBA, solid and liquid states, temp. and freq. depend. (*Russian*) 8-72450
 ferroelectric and antiferroelectric crystals, perovskite type structure, semiconductor props. (*Polish*) 8-56437
 graphite, grain boundary scattering effect on temp. depend. of electroresistivity, galvanomagnetic effect (*Russian*) 8-56148
 III-V semiconductor, temp. distrib. around dislocations, due to Joule heating, calc. 8-71734
 α -MnS, elec. props. meas. 8-87971
 polyethylene, inverse currents, applied voltage, electrode material depend. 8-84206
 potassium acetylacetonate, polycryst., elec. cond., pyroelectricity, phase transition, UV spectrum 8-76392
 rare earth aluminates, effects of roasting in reducing and oxidizing media on elec. props. 8-52736
 rare earth tungstates and molybdates, A₂BO₆ type, elec. cond., and Meyer-Neldel rule 8-72157
 relaxation of nonequib. electrons at very low temps. 8-60121
 relaxation regime, generalised transport eqns. 8-56139
 semiconductor, carrier transport, in presence of temp. gradient, flux method 8-72144
 semiconductor galvanomagnetic-effects in strong elec. field 8-56163
 semiconductors, kinetic effects at high anisotropic strains, elec. transport props. meas. 8-54384
 semimetal, degenerate, anisotropic scattering at low temp. (*Russian*) 8-95298
 semimetals, exciton phase, transport effect in strong mag. fields 8-87977
 sisal wax, electronic conduction and persistent internal polarisation 8-80277
 spinel structures, electroconductivity and electron exchange 8-84207
 Stark-Ladder current theory 8-68035
 stilbene, single cryst., free charges and excitons generated by electron pulses 8-63988
 sulphide group minerals, using four point probe technique, effects of cracks 8-64045
 transition metal double oxides, exam. of elec. cond. 8-51990
 transition metal pnictides, atomic volume, semicond. props. 8-59780
 transition metal vanadates, elec. and mag. props., stoichiometry 8-51991
 urea nitrate single cryst., elec. cond. anisotropy 8-79807
 violanthrene-A film, amorphous and crystalline, carrier mobility differences 8-60125
 zinc blende semiconductors, small-gap, electron scatt. and transport props. 8-95294
 zincblende narrow-gap mixed crystals, disorder scatt. 8-51985
 Ag₃AsS₃, proustite, residual conductivity and low-temp. phase transitions 8-91729
 α -Ag₂S, electronic and electrogalvanic props. (*French*) 8-84237
 Ag₃SbS₃, piezoelec. semicond., residual cond., ultrasound photoabsorpt. (*Russian*) 8-72465
 Ag₂Te-Ag₂S system, elec. and thermal props. at 300K 8-64044
 Al₂O₃, elec. props. under isentropic compression up to 500 GPa 8-71789
 Al₂O₃ film, Al embedded, non-ohmic conduction behaviour 8-64157
 B, purity evaluation by elec. meas. 8-59822
 BaCuO_{2+x} (0 \leq x \leq 0.12), study of mag. and elec. props. rel. to the non-stoichiometry (*French*) 8-95051
 BaTiO₃ ceramic, positive temp. coeff. resistivity, investigation as function of Ti-Ba ratio 8-72151
 BaTiO₃, donor doped, elec. props., effect of kinetic processes 8-64042
 BaTiO₃, perovskite structure, semiconductor props. (*Polish*) 8-56437
 BaTiO₃, single cryst., elec. cond., 800-1200°C, nonstoichiometric disorder 8-51989
 BaTiO₃-Ni(Co, Mn)Fe₂O₄, ceramic, exam. of prep. and physical props. 8-68655
 Bi, growth of single cryst. wires with high resistivity ratios 8-68622
 Bi microcontact, resistivity at low temp. (*Russian*) 8-80054
 Bi, polycryst., grain boundary scattering effect on temp. depend. of electroresistivity, galvanomagnetic effect (*Russian*) 8-56148
 Bi, quenching and annealing of defects, elec. resist. meas. 8-87973
 Bi, recrystn., effect of Sb, Sn and Pb 8-52841
 Bi, single crystal, drift velocity of charge carriers (*Russian*) 8-84208
 Bi, whiskers, hardness, elec. props. (*Russian*) 8-51874
 Bi: Sb(Te), quenching and annealing of defects, elec. resist. meas. 8-87973
 Bi₁₂GeO₂₀, electrophys., props. determ. (*Russian*) 8-51987
 Bi_{1-x}Sb_x, semiconductor, anomalous conductance in strong electric and longit. quantised mag. field (*Russian*) 8-76084
 C fibre reinforced epoxy phenol plastic, resistance to interlayer shear and elec. resistivity 8-68752
 C-C composites, existence diagram and properties (*French*) 8-64517
 CaF₂, elec. cond. at high temp. 8-72159
 CdCr₂S₄, ferromag. semicond. film, props. 8-76175

electrical conductivity of crystalline semiconductors and insulators continued

- CdCr₂Se₄, temp. depend. of resist. and magnetoresist., influence of Se vacancies 8-60130
- CdCr₂Se₄In(Ga), temp. driven metal-semiconductor transition, temp. and mag. field depend. (Russian) 8-88003
- Cd_{1-x}Fe_xCr₂S₄:Cu, effect of doping on elec. props. and Curie temp. 8-84214
- Cd₂Hg_{1-x}Te, fine-graded gap struct., electrophysical props. (Russian) 8-60144
- Cd₂Hg_{1-x}Te, IR detector appls., prep., elec. props. (German) 8-86332
- n-Cd₂Hg_{1-x}Te, in strong mag. field, current-voltage characts., current instabilities 8-87980
- n-Cd_{1-x}In_xCr₂Se₄, effect of doping on elec. cond. and magnetoresist. 8-72174
- CdS:Cd(In), Cu- or defect-compensated, optical ageing rel. to storage cond. 8-84247
- CdS:Cl, impurity conductivities 8-91691
- CdS:Ni, dark cond. and photoconductivity 8-76110
- CdS:Ni, elec., photoelec. and luminesc. props. (Russian) 8-84259
- Cd₂Se₃, elec. resist., thermoelectromotive force, temp. depend., 300 to 1400K (Russian) 8-84243
- CdSnF₂:Cu, deep centres, emission transitions, polarisation (Russian) 8-84650
- CdTe, growth by travelling heater method, high resistivity charact., γ-ray detector appl. 8-84707
- CeO₂, elec. cond. and dielectric props. at low temp. 8-72447
- Co_{2-x}Ni_xO₄, 0 ≤ x ≤ 1.1, struct., semicond.-semimetal transition, Seebeck coeff. 8-87972
- CrAl, semicond. solid solns., temp. depend. of elec. resist. at high temp. 8-67941
- Cr_{1-x}Mn_xSi₂, semicond. props. 8-79992
- CrSi₂, semicond. props. 8-79992
- Cu_{1-x}Se, I-V characts., switching effects, nonstoichiometry effects (Russian) 8-84266
- Cu_{1-x}Te, and Cu₂Te, I-V characts., switching effects, nonstoichiometry effects (Russian) 8-84266
- Er₂Se₃, elec. resist., thermoelectromotive force, temp. depend., 300 to 1400K (Russian) 8-84243
- EuB_{6-x}C_x, magnetic and elec. props. 8-91842
- EuO_{1-x}N_x, ferromag. semicond., elec. and mag. props. (French) 8-79993
- EuS, pure and Gd doped, electronic struct., mag. exchange and elec. transport props. 8-87974
- Eu_{1-x}Yb_xO(S), solid soln., ferromag. semicond., increase of exchange interaction 8-88109
- (Fe_{1-x}³⁺Al_x³⁺)₂O₃²⁻, γ to α transform. elec. cond. study, oxidation initial stage kinetics, lacunar spinel form. 8-92384
- (Fe_{1-x}³⁺Cr_x³⁺)₂O₃²⁻, γ to α transform. elec. cond. study, oxidation initial stage kinetics, lacunar spinel form. 8-92384
- FeMnGaO₄, X-ray study of cryst. struct. and ionic config., elec. resist. meas. 8-55851
- Fe₂N₃, prep. by reactive sputtering, struct. and props. (Japanese) 8-92190
- α-Fe₂O₃, polycryst., pure and TiO₂ doped, flatband potentials, donor densities, photocurrent meas. 8-76089
- FeSb₂O₇, defect struct. and mag. transition, elec. transport and Mossbauer expts. 8-59803
- GaAs, disordered, ion implanted, elec. props. 8-84212
- GaAs, dual implantation of C⁻ and Ga⁺, sheet resist. and Hall effect meas. 8-67728
- n-GaAs, piezoelectric semiconductor, influence of acoustic phonon disturbances on conductivity 8-91697
- n-GaAs, proton irradi., E_p = 30 MeV, defect form., orientation depend. 8-55898
- n-GaAs:O carrier removal profiles meas. 8-56154
- GaAs_{0.6}P_{0.4}Be, implanted annealing studies, elec. resist., Hall effect meas. 8-84213
- Ga_{1-x}Mn_xSb alloys, mag. phase transition obs. 8-52248
- GaP:Si, elec. props. following 1.7 MeV electron irradiation 8-80005
- GaP:Te, Hall effect and elec. cond., 80-400K 8-91705
- GaP:Zn, Hall effect and elec. cond., 80-400K 8-91705
- Ga₂Se₃(1-x) solid solns., electrical props. meas. 8-84216
- n-GaSb, temp. distrib. around dislocations, due to Joule heating, calc. 8-71734
- Ga₂Te₃-Cu system solid solns., elec. cond. 8-51988
- Ga_xV_{1-x}O₂, resistivity, EPR, enthalpy and entropy meas., rel. to semicond.-metal transition 8-88004
- GdP, electronic struct., mag. exchange and elec. transport props. 8-87974
- GdS, electronic struct., mag. exchange and elec. transport props. 8-87974
- n-Ge, elec. cond., effect of shock waves (Russian) 8-87979
- Ge film, polycrystalline, structural and elec. props. 8-76173
- Ge, optically injected carrier density and temp. depend. 8-68046
- Ge:Sb, impurity conductivities 8-91691
- HfS₂, equilibria, nonstoichiometry and elec. props. temp. depend. (French) 8-64053
- HgCr₂Se₄, ferromag. semicond., transport props. 8-68039
- Ho₂Se₃, elec. resist., thermoelectromotive force, temp. depend., 300 to 1400K (Russian) 8-84243
- InAs, intrinsic point defects, nature and influence on electrophys. props. 8-79600
- InSb, high-purity specimen irradiated at 80K, transport prop. and defect annealing 8-95307
- InSb:Cr, press. effects on transport props. 8-56146
- InSb-type semiconductor, inelastic scatt. of electrons by optical phonons 8-76073
- n-InSe, optical spectra, photocond. and resistivity 8-88321
- IrGe_{1.5}S_{1.5}(Se_{1.5}), new skutterudite relation compounds, prep. and charact. 8-52700
- IrSn_{1.5}S_{1.5}, new skutterudite relation compounds, prep. and charact. 8-52700
- K, electrical conductivity, Toya's theory 8-51965
- KNbO₃, perovskite structure, semiconductor props. (Polish) 8-56437
- KTaO₃, defect struct. and elec. props. 8-91695
- LaB₆ film, structure, stoichiometry, elec. properties 8-60043
- La_{0.65}Pb_{0.35}MnO₃, transport props. near Curie points 8-88100
- LiNbO₃, anomaly in elec. resist. 8-68030
- LiNbO₃-3(Li₂O).Nb₂O₅ eutectic, anomaly in elec. resist. 8-68030

electrical conductivity of crystalline semiconductors and insulators continued

- LiTiZn ferrites, elec. resist., mag. props., effect of Bi addition 8-95474
- Lu₂Se₃, elec. resist., thermoelectromotive force, temp. depend., 300 to 1400K (Russian) 8-84243
- MgM²⁺Fe_{2-x}O₄, M = In, Al, Cr, Sc, comp. effects on ferrite characts. 8-52305
- Mn₂As₂Sb_{1-x}, x < 0.5, temp. dependence, 78 to 400K 8-76248
- MnZn ferrite, gas phase fluorination for improved props. 8-52306
- Mn_{1.18}Zn_{0.06}Co_{0.01}Fe_{1.75}O₄, transport props. near Curie points 8-88100
- MoO₃:Li, elec., catalytic props. 8-60122
- Na, electrical conductivity, Toya's theory 8-51965
- NaF:U, single crystals, variation with preparation procedure 8-72588
- NaNbO₃, perovskite structure, semiconductor props. (Polish) 8-56437
- Na₂VS₂(Se₂), mag. and elec. props. rel. to struct. transitions 8-91848
- NbN₂, solid soln., strain ageing, internal friction, elec. cond. kinetics (Russian) 8-76667
- NbN₂O₃, solid soln., strain ageing, internal friction, elec. cond. kinetics (Russian) 8-76667
- NbO₃, solid soln., strain ageing, internal friction, elec. cond. kinetics (Russian) 8-76667
- Nd-Gd-Te alloys of R₂Te₃-T₃Te₄ region, physicochem. props. 8-52017
- Nd₂(MoO₄)₃, mag. susceptibility, elec. cond. and thermolec. power 8-88091
- Nd₂O₃, A-type, thermoelectric power, AC cond. 8-68044
- Ni ferrite, gas phase fluorination for improved props. 8-52306
- NiO, elec. cond. under low O₂ press. 8-64041
- NiO, localised charge carrier transport, Seebeck, resistivity meas. 8-72152
- Ni_{1-x}O, electronic cond. at high temp., vacancies and interstitials effect (French) 8-79990
- NiSO₄:Li (10 at.%), powder, semiconducting, exam. of freeze drying rate in cryochemical prep. method 8-52706
- Pb₂Sr_{1-x}(Zr_xTi_{1-x})O₃:Cr₂O₃, ferroelec. ceramic, reversible characts. and dielectric losses (Russian) 8-84517
- PbF₂, superionic, electrical conductivity at high temp. 8-79798
- Pb_{1-x}Ge_xTe:Ga, Fermi level stabilization, transport props. meas., 77-400K 8-56065
- Pb_{0.55}Sn_{0.45}Se, struct. phase transition, temp. and hydrostatic press. influence, Hall effect, resistivity (Russian) 8-51675
- Pb_{1-x}Sn_xTe, Cd-In diffusion, changes in elec. props. 8-91348
- PbTiO₃, cryst., polarisation and resistivity, elec. field effects 8-64313
- PbTiO₃, perovskite structure, semiconductor props. (Polish) 8-56437
- PbTiO₃, struct. changes with temp. variation, rel. to elec. cond. 8-91437
- PbZrO₃, perovskite structure, semiconductor props. (Polish) 8-56437
- PbZrO₃-monocoryst., elec. cond., permittivity, polarisation, para- and ferro- to antiferroelec. phase transitions 8-60402
- Pb(Zr_{0.47}Ti_{0.43}Sn_{0.10})O₃:Cr₂O₃, ferroelec. ceramic, reversible characts. and dielectric losses (Russian) 8-84517
- Pr₂NiO₄, elec. props., 300 to 1000°C 8-91694
- PrFeO₃, elec. props., 300 to 1000°C 8-91694
- RhGe_{1.5}S_{1.5}, new skutterudite relation compounds, prep. and charact. 8-52700
- (SN)_x polymer, elec. props. of amorphous thin film and single crystal, role of chain breaks (Japanese) 8-68104
- ScN_x, region of homogeneity, physicochem. props. 8-52018
- Sc₂Se₃, elec. resist., thermoelectromotive force, temp. depend., 300 to 1400K (Russian) 8-84243
- Se, crystallisation kinetics correlation with molecular structure 8-94998
- Si, γ-ray induced elec. cond. at low temps. 8-52002
- n-Si, inversion layers, many-valley electron-phonon interactions, piezoresistance, anisotropic cond., Shubnikov-de Haas oscillations 8-52096
- Si, metallurgical grade, purification and charact. 8-56573
- Si monocrystalline rod growth from gas phase 8-64453
- p-Si, neutron irradiated, elec. props. 8-51939
- Si, neutron transmutation doped, zero-bias resist. of grain boundaries 8-76072
- Si, polymorphism under high press. (Russian) 8-59947
- Si wafer, colour-banded, sheet resist. variation following high dose implantation at high dose rates 8-95074
- Si:As, implanted, spatially varied activation during regrowth of amorphous layers, sheet resist. and backscatt. obs. 8-71749
- Si:As, ion implanted, anomaly of elec. activation by additional Ne irradiation 8-84211
- Si:Cr, specific resistance, activation energy of deep levels, and carrier mobility (Russian) 8-72146
- Si:Ni(Co)(Mn), influence of neutron irradiation as elec. props. 8-55895
- Si:P, annealing characteristics at low temp., elec. props. 8-63781
- Si:P, carrier mobility and distrib. rel. to annealing, 400-910°C 8-79995
- Si:P, impurity conductivities 8-91691
- Si-Ge:Al(B)(P), hot-pressed alloy, thermolec. props. 8-91711
- β-SiC, cubic, elec. props. 8-51996
- Si₃Te₃, passivated single cryst., elec. conductivity 8-95299
- Sms, first-order transition from semiconducting to metallic state 8-52040
- SnO₂, gas sensor, CO, H₂O vapour, surface temp. effect on cond. 8-76067
- SnO₂:ThO₂, exposed to CO gas, self-oscill. phenomenon 8-68032
- SnS₂, electron mobility, elec. cond. and Hall effect meas. 8-80004
- SnS_{2-x}Se_x solid soln., resistivity, lattice parameter, comp. and temp. depend. 8-91693
- SnSe, sublimation growth, deviation from stoichiometry, elec. props. 8-76594
- SnTe, isothermal meas. of galvanomag. and thermomag. effects (Russian) 8-56160
- SrCl₂, superionic, electrical conductivity at high temp. 8-79798
- Te:Sb, 96 to 500K, cond. Hall const., hole mobility, conc., dislocation effects (Russian) 8-64039
- TiB₂, low-temp. neutron irradi., electrical resistance and stored energy 8-67744
- TiO₂, rutile, deuteron and alpha-particle implantation, chemical effects, optical and cond. meas. 8-67755

electrical conductivity of crystalline semiconductors and insulators continued

- TiO₂, sintering, hardness, density, elec. cond. and colour (*Japanese*) 8-68659
 TiS₂, resistivity, Hall effect and mag. suscept. 8-79991
 TiSe₂:Ta(V), transport props. and phase transition 8-72149
 Ti_{1-x}V_xS₂, resistivity, Hall effect and mag. suscept. 8-79991
 Ti₂MoO₄, prep., characterisation 8-63731
 Tm₂Se, 0.87< χ <1.05, mag., thermal and transport props., comp. depend. 8-68239
 U dipnictides, elec. and mag. props. 8-84399
 UO_{2+x}, elec. cond. and thermoelectric power 8-52020
 Y₂S₃, elec. cond. and thermoelectric power, p-n transition (*French*) 8-84264
 Yb₂Se₃, elec. resist., thermoelectromotive force, temp. depend., 300 to 1400K (*Russian*) 8-84243
 ZnGeP₂, synthesis, characts., applic. to laser windows (*French*) 8-80467
 ZnO ceramics, non-Ohmic, cond. mech. 8-68034
 ZnO, single cryst. growth in ZnO-H₂-H₂O-O₂ vapour, morphology, electrophys. and opt. props. 8-52649
 ZnP₂, pure and doped, carrier mobility and conc., donor and acceptor energy levels, 190 to 380K 8-84217
 Zn₃P₂ photovoltaic material and Schottky diode characteristics 8-64066
 ZnSe, effect of In-doping and Zn-annealing, 300 to 77K 8-76075
 ZnSe:In, heavily doped, Hall effect and DC cond. expts., compensating acceptors 8-52013
 ZnSe:In, heavily doped, impurity band cond., Hall coeff. and cond. expts. 8-72147
 ZnSe-HgSe, solid soln., defect distrib., elec. props., Hagemark's theory 8-64040
 ZnSiP₂:Ga, effect of doping conc. on elec. cond. and Hall coeff. 8-76077
 ZrO₂, elec. cond.-nonstoichiometry relationship, direct determ. 8-76079
 ZrO₂:Nd₂O₃, in contact with NdCrO₃, electrical cond. meas. 8-76071
 ZrO₂:Y₂O₃, in contact with YCrO₃, electrical cond. meas. 8-76071
 ZrS, equilibria, nonstoichiometry and elec. props. temp. depend. (*French*) 8-64053

electrical conductivity of electrolytic liquids

- see also *electrochemical analysis; electrolytic ion mobility; Wien effect*
 1:2 electrolytes, conc. solns., vel. correls. calcs., diffusion, cond. and transference props. 8-85166
 alkaline earth halides, solns. in methanol, conductance data anal., assoc. const. 8-71875
 aqueous solutions, naturally recurring, activity coeffs. rel. to ionic diffusion 8-57224
 rel. to electrode current density (*Russian*) 8-64847
 electrolyte solns., particle-particle interactions, velocity correl. coeffs. 8-64852
 mixed electrolytes, conductance, relax. terms 8-67840
 molten salts, transport coeffs., integral representations 8-67842
 multicomponent electrolyte systems, elec. cond. and diffusion 8-71872
 polar solvent, spherical ion radius and limiting elec. cond. Brownian motion 8-95168
 symmetrical electrolytes, conductance, relax. terms 8-67840
 tetrabutylammonium picrate, elec. cond. in nematic (smectic) 4-alkyloxy-4'-cyanobiphenyls, temp. (conc.) depends. (*German*) 8-55966
 unsymmetrical electrolytes, conductance, relax. terms 8-67840
 AlI₃, molten, electrical cond., press. effect, 0-1 kbar 8-55963
 Ba soln. in liq. ammonia, conductance at -62.37°C 8-91459
 Ba(ClO₄)₂, soln. in liq. ammonia, conductance at -62.37°C 8-91459
 BiI₃, molten, electrical cond., press. effect, 0-1 kbar 8-55963
 CaCl₂×5.99, 5.33H₂O, molar cond., compressibility, expansivity 8-51712
 CdBr₂-BiBr₃, molten, elec. cond., 500-870K, composition depend. 8-55965
 CdI₂, molten, electrical cond., press. effect, 0-1 kbar 8-55963
 Cd(NO₃)₂·4.1H₂O-CoCl₂, melt viscosity, equivalent conductivity, glass transition temp. 8-75855
 Cd(NO₃)₂·4.1H₂O-NiCl₂, melt viscosity, equivalent conductivity, glass transition temp. 8-75855
 CuSO₄, effect of press. on ion pair dissoc., cond. of aq. solns. 8-53218
 GaI₃, molten, electrical cond., press. effect, 0-1 kbar 8-55963
 HgBr₂-BiBr₃, molten, elec. cond., 500-870K, composition depend. 8-55965
 I₂, molten, electrical cond., press. effect, 0-1 kbar 8-55963
 InI₃, molten, electrical cond., press. effect, 0-1 kbar 8-55963
 KClO₄ soln. in liq. ammonia, conductance at -62.37°C 8-91459
 LiBr, in anhydrous acetone, elec. conductance at high press., Shvedlovsky method 8-53219
 MnSO₄, effect of press. on ion pair dissoc., cond. of aq. solns. 8-53218
 ZnSO₄, effect of press. on ion pair dissoc., cond. of aq. solns. 8-53218

electrical conductivity of gases

- see also *space-charge-limited conduction*
 butane, gas, electron drift vel., Ramsauer-Townsend minima in electron scatt. 8-87427
 electron drift velocities as function of elec. and mag. variables in several gas mixtures 8-71424
 ethane, gas, electron drift vel., Ramsauer-Townsend minima in electron scatt. 8-87427
 methane, gas, electron drift vel., Ramsauer-Townsend minima in electron scatt. 8-87427
 neopentane, gas, electron drift vel., Ramsauer-Townsend minima in electron scatt. 8-87427
 propane, gas, electron drift vel., Ramsauer-Townsend minima in electron scatt. 8-87427
 Ramsauer-Townsend effect, partially ionised gas elec. cond. 8-67458
 teaching, relax. approx. to Boltzmann eqn. approach 8-73804
 CO₂ laser, glow discharges at high press., voltage-current characts. 8-87036
 H₂, electron swarms, anisotropic scatt. model 8-91059

electrical conductivity of gases continued

- N₂O, mech. of thermal electron attachment, microwave cond. meas. 8-59536
 N₂O-hydrocarbon mixtures, mech. of thermal electron attachment, microwave cond. meas. 8-59536
electrical conductivity of liquids
 see also *electrical conductivity of electrolytic liquids*
 albumin, human serum, elec. cond. and dielec. const., 1 to 15 MHz 8-53315
 alkali metal-Au alloys, elec. props. 8-84187
 alloys, highly resistive, temp. depend. on elec. resist. 8-91657
 cholesteryl caprilate, conduction mechanism 8-64046
 cholesteryl laurate, conduction mechanism 8-64046
 cyclohexane+acetic anhydride, elec. resist. near crit. soln. temp. 8-71874
 dielectric liquids, cond. band minima, rel. to electron mobility maxima 8-80029
 diffraction model, critical test, elec. resistivity of amorphous and liq. metals 8-84191
 EBBA, liq. crystals, thin layers, addition of iminoxyl radicals, effect on elec. cond. (*Russian*) 8-67641
 EBBA, solid and liquid states, temp. and freq. depend. (*Russian*) 8-72450
 electrophotographic liquid developer, permittivity and conductivity meas. (*German*) 8-62257
 n-heptane+acetic anhydride, elec. resist. near crit. soln. temp. 8-71874
 n-heptane-methyl alcohol, crit. resist. of binary liq., 10 Hz-100 kHz 8-76123
 HEXOAB/7CBP, mixed crystals, induced smectic A phases, elec. cond. 8-76068
 homogeneous solid, small signal AC response, mobile charge recomb., theory 8-52005
 MBBA, liq. crystals, thin layers, addition of iminoxyl radicals, effect on elec. cond. (*Russian*) 8-67641
 MBBA, nematic liq. cryst., charge carrier drift mobility 8-87801
 metal, tight binding theory of transport props., Ishida-Yonezawa approx. for single-band model 8-84190
 metallic liquids, resistivity, struct. factor calcs. 8-51962
 metals, resistivity as function of press., nearly-free-electron model 8-84192
 metals and alloys, book 8-51406
 nematic liquid crystal mixtures, charge carrier transport 8-51413
 nitromethane-CS₂, crit. resist. of binary liq., 10 Hz-100 kHz 8-76123
 noble metals, pseudopot. exam. of electronic props. 8-51960
 PCB liquid crystal, conductivity depend. on thickness and electrode molecular orientation 8-91248
 PEBAB/HEXOAB, mixed crystals, induced smectic A phases, elec. cond. 8-76068
 transition metals and alloys, elec. resistivity, Hall coeff., mag. susceptibility 8-95280
 water, supercooled emulsified droplets, relative permitt. and cond., Maxwell-Wagner interfacial polarisation 8-52423
 Al, model pseudopotential 8-91582
 Bi, electrical resistivity with spin-orbit scatt. 8-64018
 Bi, liquid, elec. cond. and assoc. optical scattering 8-76040
 CS₂+acetic anhydride, elec. resist. near crit. soln. temp. 8-71874
 Ca-Ag(In), liquid alloy, thermodynamic exam 8-75848
 Ca(NO₃)₂·3.91H₂O-NiCl₂ melts, glass forming, transport behaviour 8-59963
 CaO-SiO₂-MgO melt, elec. cond. meas., MgO behaviour (*Japanese*) 8-75857
 Cs, relativistic model pseudopot., appl. to elec. resist. calc. in liq. phase 8-51866
 Cs_{1-x}Au_x, liq., metal-nonmetal transition, electronic theory 8-79930
 D₂-DT-T₂ mixture, solid and liq., props. for fusion reactor applications 8-66415
 Ga, elec. resist. calc., 19 and 35°C, using calc. and expt. struct. factors (*Russian*) 8-56124
 H₂O-acetic acid-silver acetate, ternary liq., elec. cond. and density 8-91464
 Hg-Au(Tl)(Bi), liquid dilute amalgams, elec. cond. and thermoelec. power 8-51976
 Ir complexes with adenosine, xanthosine, prep., elec. cond., IR spectra, characterisation 8-92065
 K, liq. elec. resistivity calcs. 8-79974
 Li_{1-x}Pb_x, liq., metal-nonmetal transition, electronic theory 8-79930
 MBBA(:TEAI), elec. drift mobility, carrier identification (*Korean*) 8-51998
 Mo, liquid and solid, thermophysical props. 8-75808
 Na, liq., elec. resistivity calcs. 8-79974
 Na₂O-SiO₂-MgO melt, elec. cond. meas., MgO behaviour (*Japanese*) 8-75857
 Pb, electrical resistivity with spin-orbit scatt. 8-64018
 Pb, relativistic model pseudopot., appl. to elec. resist. and phonon spectra calc. 8-51866
 Pd, liq. and solid, thermophysical props. 8-75808
 Rh complexes with adenosine, xanthosine, prep., elec. cond., IR spectra, characterisation 8-92065
 Ru complexes with adenosine, xanthosine, prep., elec. cond., IR spectra, characterisation 8-92065
 S, conductivity meas. from melting point to 900°C 8-84209
 Sn, elec. resist. calcs., 232, 450 and 650°C, using calc. and expt. struct. factors (*Russian*) 8-56124
 Sn, electron transfer of rare earth impurities (*Russian*) 8-95278
 Sr, soln. in liq. Na., elec. resistivity, conc. depend. 8-84188
 Te-Co(Cr)(Au)(Ag), dil. liq. alloy, elec. cond. at high temp. and press. 8-87959
 Te-Sb, liq., elec. cond. 8-84186
 Ti, molten, reson. model calc. of elec. resist. 8-84189
 V₂O₅, type liquid semiconductor, elec. props. control, by O₂ partial press. (*Russian*) 8-72142

electrical conductivity of one-dimensional systems see *one-dimensional conductivity***electrical conductivity of plasmas** see *plasma transport processes***electrical conductivity of solids**

see also *electrical conductivity of amorphous metals and alloys; electrical conductivity of amorphous semiconductors and insulators; electrical conductivity of crystalline metals and alloys; electrical conductivity of crystalline semiconductors and insulators; electronic conduction in crystalline*

electrical conductivity of solids continued

- semiconductor thin films; *electronic conduction in insulating thin films; electronic conduction in metallic thin films; ionic conduction in solids; recovery; superconductivity*
 Anderson localisation, transport props. of 2D disordered electron systems in strong mag. fields 8-95318
 antiferromagnet, crit. resist. below T_c 8-68004
 basalts, Indian, elec. cond. meas., 475-1100K 8-69336
 Clausius-Mossotti problem for cubic arrays of spheres 8-52422
 composite material, cubic arrangements of spherical particles in isotropic matrix, effective conductivities 8-55547
 conference on elec. transport and optical props. of inhomogeneous media, Columbus, USA (Sep. 1977) 8-56114
 DC electrical conductivity, microscopic fields and currents 8-56121
 disordered alloys, transport phenomena theory, coherent pot. approx. 8-87958
 disordered system, conductivity near mobility edges 8-76038
 disordered system, residual resistivity 8-87954
 dunite, elec. cond during shock compression from 12.5 to 45 GPa 8-85536
 electric current, determ. by time correlation functions force-force and force-momentum 8-95274
 electric current, determ. by time correlation functions force-force and force-momentum, pseudopot. method 8-95275
 electron gas, interacting, elec. cond. 8-95276
 electron scattering due to screw dislocations 8-60101
 electronic transport coeff., soln. between Mori-Green-Kubo formulae and Boltzmann approx. 8-79971
 fatty acid, AC and DC cond. 8-56239
 film, Cottey conduction model extension 8-84183
 film, physical interpretation of specularly parameter 8-72282
 graphite intercalation compounds, props. and appls. 8-71711
 inhomogeneous conductors, resistor networks, cooperative phenomena 8-56118
 inhomogeneous media, elec. transport, optical props., exact theory 8-56119
 inhomogeneous media, electrical cond., review 8-56115
 insulating and conducting particles mixture, percolation problem 8-60097
 lattices of spheres, elec. cond. calcs., BCC, FCC, disordered array 8-72126
 linear response theory and area preserving mappings, review 8-62174
 magnetic systems, anomalous resistivity maxima 8-79977
 magnetic systems, crit. behaviour 8-87955
 percolation lattice, diffusion, random walk method, Monte Carlo method 8-60098
 percolation model, three component, reactive, conductivity calc., $\text{Na}_2(\text{NH}_4)_{1-x}$ appl. 8-68003
 percolation threshold, computer generated pictures of infinite clusters 8-56117
 polyacetylene- I_2 , highly conducting, Raman, XPS and X-ray diffr. obs. 8-80454
 powder behaviour in vibrating field from cond. obs. (Japanese) 8-95711
 PVC-Cu composite, annealing effects on elec. resist. 8-68060
 quantum mechanical theory, uncertainty principle 8-84182
 random conductance lattices, conduct., renormalisation group approach 8-60100
 random resistor network, 6- ϵ dimensions, renormalisation group treatment 8-51956
 random resistor network, mean field theory and crit. exponents 8-79973
 random resistor networks, critical behaviour near percolation threshold 8-87956
 random-phase model, electrical conductivity of bond-type disordered system 8-51952
 resistor lattice conductivity exponent, position space renormalisation, decimation, dimensionality depend. 8-60099
 rocks, conductivity of cylindrical cores, porosity effects 8-61401
 semiconductors, temp. rise due to nonlinear heat generation 8-87983
 single-impurity Kondo system, fluctuation conductivity 8-76064
 substitutionally disordered system, derivation of cluster approx. 8-84184
 substitutionally disordered systems, MCPA and Monte Carlo calc. 8-84185
 TCNQ, elastomeric complexes, doped with pure TCNQ, elec. conductivity 8-84220
 transition metals, liq., multiple scatt. calcs. of resist. 8-76039
 tremolite asbestos, fibrous, elec. anisotropy 8-80273
 ultramafic rocks, elec. cond. meas., 670-1820K 8-69335
 Ag-SiO₂ film, elect. and struct. props., ion beam sputtering 8-80071
 BaO-BaX₂-P₂O₅ glass, X=F, Cl, Br, conductivity 8-67862
 BaPO₃-F-Al₂O₃-B₂O₃ glasses, phys. props. 8-63676
 Ba₂TiGe₂O₈-Ba₂TiSi₂O₈, pseudobinary system, pyroelectricity and related props. 8-95553
 C, baked mixes, use of coal tar and petroleum pitches as binders 8-80483
 C-PVC composite, fluctuation induced tunnelling conduction 8-52044
 CaB₆-SmB₆ system complex borides, prep. and props. 8-52703
 Cr-SiO film, RF sputtered, substrate bias effect obs. 8-60573
 Cu₂MoS₈, thin films, low temp. normal state, resist., temp. depend. 8-91783
 D₂-DT-T₂ mixture, solid and liq., props. for fusion reactor applications 8-66415
 Hf_{1-x}Ta_x-C, thermal cond. and diffusivity, 1000-2200°C, elec. cond. 8-91491
 In₂O₃, transparent electrode deposition on PLZT ceramic, elec. and opt. props. 8-74848
 Na-NH₃ solid mixture, cond., three component reactive percolation model 8-68003
 Na₂O-NaF-B₂O₃ glass, nature of conductivity 8-63876
 Ne, solid, elec. cond. obs., insulating up to 500 GPa 8-95315
 PbMoS₈, thin films, low temp. normal state, resist., temp. depend. 8-91783
 (SN)_x films, electrical properties 8-91782
 SmB₆, mixed valent, DC transport props., metallic or insulating props. 8-68029
 SmS, mixed valent, DC transport props., metallic or insulating props. 8-68029
 SnO₂, transparent electrode deposition on PLZT ceramic, elec. and opt. props. 8-74848

electrical conductivity of solids continued

- TaS₂, non-linear conduction in two-dimensional CDW 8-91685
 ZrC-C composite system, electrical resist. meas., percolation theory anal. 8-84269
 ZrC-ZrN system, solid solns., elec. resist., thermo EMF, thermal cond., expansion coeffs. 8-60176
- electrical conductivity transitions**
see also metal-insulator transition
 alkali metal-NH₃ solutions, metal-nonmetal transition Hall mobility, electrodeless meas. 8-56194
 chalcogenide film, threshold switching mechanism, review 8-76122
 chalcogenide glass, radiative emission during threshold ON-state 8-76119
 chalcogenide switch, relaxation processes in memory and threshold switches 8-60172
 inhomogeneous materials, electronic props., metal-nonmetal transitions, review 8-56073
 maximum metallic resistance, in two dimensions as 30000 ohms 8-95335
 metal-filled epoxy resin, temp. variation, current interruption appl. 8-76124
 MIM structure, new switching effect at atmos. press. 8-80067
 PMMA, threshold switching effects 8-84270
 polyacrylonitrile, pyrolyzed, elec. cond. and dielec. const. in AC regime 8-60173
 potassium acetylacetonate, polycryst., elec. cond., pyroelectricity, phase transition, UV spectrum 8-76392
 semiconductor, switching under impact ionisation 8-72215
 sulphide group minerals, using four point probe technique, metallic to semicond. 8-64045
 thermal switching, resist.-temp. charact. 8-64071
 threshold switching in non-cryst. semiconds. by computer simulation 8-88002
 Ag-BN-Si-Al sandwich, humidity sensitive threshold switching 8-88046
 Ag₃AsS₃, proustite, residual conductivity and low-temp. phase transitions 8-91729
 As₂₀Te₄₅I₃, glass, semicond., elec. switching, high press. effects 8-72212
 Bi_{1-x}Si_x, switching and high field effects, cond. mechanism 8-64048
 Bi_{1-x}Sb_x, semicond.-semimetal transition, temp. and press. depend. of transport props. 8-76120
 CdCr₂Se₄:Cu, elec. props., temp. depend. (Russian) 8-72181
 CdCr₂Se₄:In(Ga), temp. driven metal-semiconductor transition, temp. and mag. field depend. (Russian) 8-88003
 CdTe single-crystal film, switching and memory effects 8-76174
 Co_{3-x}Ni_xO₄, 0≤x≤1.1, struct., semicond.-semimetal transition, Seebeck coeff. 8-87972
 Cr_{1-x}Fe_xS, metal-dielec. transition, X-ray, thermal anal., elec. cond. temp. depend. 8-67942
 CuO-CaO-P₂O₅ glass devices, memory switching 8-56192
 Cu_{1-x}Se, I-V characts., switching effects, nonstoichiometry effects (Russian) 8-84266
 Cu_{1-x}Te, and Cu₂Te, I-V characts., switching effects, nonstoichiometry effects (Russian) 8-84266
 EuO_{1-x}N_x, ferromag. semicond., elec. and mag. props. (French) 8-79993
 EuS-metal contact, electrical switching exam. 8-68085
 Fe₂O₄, finely dispersed, electronic phase transition, cond. and DTA meas. 8-91736
 Fe₂O₄, photocond. 70-130K, temp. range including metal-semicond. transition (Russian) 8-56178
 Ga-NaX zeolite system, press. depend. of metal-insulator transition 8-88005
 n-GaAs, metal-insulator transition in impurity band induced by mag. field and loss of dimens. 8-52042
 Ga₂V_{1-x}O₂, resistivity, EPR, enthalpy and entropy meas., rel. to semicond.-metal transition 8-88004
 H₂, isotropically compressed, elec. cond. at Mbar press. 8-95315
 K₂Pt(CN)₄Br_{0.3}·3H₂O, one-dimens. cond. transition, spin suscept. and DC cond. temp. depends. 8-84198
 LiNbO₃·3(Li₂O)·Nb₂O₅ eutectic, anomaly in elec. resist. 8-68030
 Na_{1-x}V₁₂O₂₉, press. depend. of elec. cond., semicond.-metal phase transition obs. 8-64072
 NbSe₃, non-ohmic transport props. near phase transitions 8-72213
 PbAr, metal-insulator transition, resistivity meas. 8-80028
 Pb_{0.59}Sn_{0.41}Se, struct. phase transition, temp and hydrostatic press. influence, Hall effect, resistivity (Russian) 8-51675
 Ru_{1-x}Ti_xO₂ solid solns., metal-nonmetal transition 8-91735
 (SN)_x and S₂N₄, high press. study 8-52782
 SSe_x (x=10, 15, 40), amorphous crystal transition, appl. of Kolmogorov-Avrami equation 8-67649
 Sb amorphous film, elect. resist. 8-95390
 Sb electrodeposit, amorphous, explosive crystn., semicond-semimetal transition and IR absorpt. 8-51849
 Sb-Au amorphous film, elec. resist. 8-95390
 Si diodes, p⁺-i-n⁺ struct., double-injection switching, effect of surface recomb. 8-88025
 Si-SiO₂-SnO₂ structure, switching props. 8-76138
 Si-transition metal metastable films as temp. independent resistors 8-68097
 Sm₂Bi₃, press. induced valence instability, elec. resist. transition 8-95317
 Sm_{1-x}Gd_xS, press. induced electronic transitions 8-68058
 SmS, crit. point for isostructural black to metallic phase transition, thermolec. power meas. 8-60174
 SmS, first-order transition from semiconducting to metallic state 8-52040
 SmS, semicond.-metal transition, phase struct. determ. 8-91618
 (TSeT)₂Cl, high press. metallic phase (Russian) 8-95316
 TiO₂, anatase single crystals, switching, coloration and memory effect 8-72216
 VO₂, doped, morphology, structure and props. (German) 8-59823
 VO₂, interference film, colour and elec. resist. changes at phase transition temp. (German) 8-56533
 VO₂, semiconductor-metal transition, effect of ¹⁸O substitution 8-84268
 VO₂ single cryst., switching, visual obs. of metallic and semicond. domains 8-52041
 VO₂:Ga, Mo, temp. variation with impurity content 8-76121

electrical conductivity transitions continued

- V_2O_5 , semiconductor-metal transition, effect of ^{18}O substitution 8-84268
 V_2O_5 , switching mech. 8-60175
 V_3O_5 , semiconductor-metal transition, effect of ^{18}O substitution 8-84268
 V_2O_5 film, prep. by thermal decomp. of vanadium naphthenate, and elec. props. (*Japanese*) 8-88425
 Y_2S_3 , p-n transition, elec. cond. and thermoelectric power (*French*) 8-84264
 ZrC-C composite system, electrical resist. meas., percolation theory anal. 8-84269

electrical contacts

- see also *contact potential*; *contact resistance*; *ohmic contacts*; *point contacts*
 Josephson contact microwave detector sensitivity and cutoff frequency rel. to capacitance 8-49902
 low temperature resist. characts. 8-68072
 LV switchgear contacts, AgMgO properties (*Slovak*) 8-56603
 metal-insulator contacts, model of charge injection 8-68088
 rotating systems, temp. meas., minimisation of contact drop error 8-73991
 skin tissue C tattoo for generation of permanent dry elec. contacts 8-77122
 surface damage caused by closing voltages, field-ion microscopic studies 8-64098
 Ag-Pd-Cu alloys, contact-spring props. and age hardening 8-88473
 Al-Au bimetal thin film interdiffusion zone, intermetallic phase form kinetics, 70-160°C 8-75891
 Au alloy electrodeposits, for electronics industry, characts. 8-52695
 Au coated, Cu diffusion under high temperature obs., effects on mech. and elec. props. (*Czech*) 8-91486
 Au-As $_2$ Se $_3$ contact, model of charge injection 8-68088
 Bi microcontact, resistivity at low temp. (*Russian*) 8-80054
 GaAs, minority carrier diffusion lengths, contact metal effects 8-72260
 n-Hg $_{1-x}$ Cd $_x$ Te, photoconductor, contact noise at 77K 8-88028

electrical engineering applications of computing see *electrical engineering computing***electrical engineering computing**

- see also *computerised control*; *computerised instrumentation*; *electric machine analysis computing*; *electric machine CAD*; *power system CAD*
 fusion reactor, TNS, electrical design costing 8-55014
 fusion reactor, Tokamak, commercial, plasma driving system requirements 8-54954
 fusion reactor coil design codes 8-66367

electrical fault location see *fault location***electrical faults**

- see also *accidents*; *discharges (electric)*; *electric distortion*; *fault currents*; *fault location*; *flashover*; *insulation*; *losses*; *overvoltage*; *protection*; *testing*; *transients*
 analogue safety data link, for Princeton Large Torus control room 8-54938
 PbSnTe-PbTe heterostructs., effect of electrical grounding on electron irradi. 8-60194

electrical forming see *electroforming***electrical insulation** see *insulation***electrical noise** see *noise***electrical power systems** see *power systems***electrical properties of substances**

- see also *dielectric properties of substances*; *discharges (electric)*; *electrical conductivity*; *thermoelectricity*
 materials, electronic, optical, magnetic and thermal props., rel. to energy technology 8-88412

electrical resistance measurement see *electric resistance measurement***electrical transport processes** see *electrical conductivity***electricity**

- see also *atmospheric electricity*; *electric charge*; *electric current*; *electric impedance*; *electrical properties of substances*; *electromagnetism*; *terrestrial electricity*; *triboelectricity*
 energy efficiency, problems and solns. 8-81762

electricity supply industry

- nuclear waste disposal problems, present and future trends 8-66350

electro-optical devices

- see also *liquid crystal devices*; *optical modulation*; *Q-switching*
 A/D conversion using channel waveguide modulators 8-66898
 array processor for complex signals 8-94428
 Bragg switch for optical channel waveguides 8-75002
 broadband travelling wave modulator, expt. design principle 8-94438
 channel waveguide double-pole double-throw switch/coupler, using total internal refl. 8-71233
 deflectors, boundary effects, pot. distrib. (*Russian*) 8-71228
 deflectors for laser beam scanning 8-79060
 dielectric resonator, trapped mode, coupling and tuning for laser beam modulation 8-55389
 differential electro-optic shutter with ns pulse operation 8-74994
 distance measurement device, appl. to water levels obs. (*German*) 8-69280
 Fabry-Perot nonlinear electro-optic device, using refl. light feedback 8-55457
 gate for nonpolarised emission (*Russian*) 8-59132
 guided wave, for logic and computation 8-66946
 holographic phase distributions, linear and nonlinear, determ. using electro-optical system 8-58954
 image detail enhancement system with PROM, for photographic recording 8-58086
 image evaluation, subjective effects of electronic and turbulent noise 8-65023
 integrated optical switch, optically controlled two channel, based on directional coupler 8-83116
 Kerr cell for anal. of very short laser impulses (*Italian*) 8-54477
 light modulator, phase matched 8-83089
 liquid crystal electro-optical modulators for two-dimensional data processing 8-79141
 modulator, large bandwidth, using min-wave drivers 8-87164
 modulator switch, balanced bridge, using Ti-diffused LiNbO $_3$ strip waveguides 8-63201

electro-optical devices continued

- modulator using electro-optic phase shifter pair with optical waveguide couplers 8-66952
 modulator-based instrument, for polarisation dependent light scatt. meas. 8-58010
 multimode fibre bussing, active fail-safe terminal 8-55438
 optical modulator, coupled-waveguide with pn junction 8-71235
 optical waveguide switch, 3×3, for optical switching system 8-55470
 photoelectronic phase and frequency modulation 8-79131
 photometric device for arterial thrombosis investigations 8-85456
 Pockels cell, variable length subnanosecond laser pulse prod. 8-94405
 Pockels readout optical modulator, acoustooptic snapshot, optical, signal spectrum analyser 8-90494
 pockels readout optical modulator, for optical/digital processing systems 8-79125
 Pockels readout optical modulator, image and signal processing appls. 8-79123
 Pockels readout optical modulator, optical processing appls. 8-83100
 real-time spatial modulators for optical/digital processing systems 8-63025
 rib waveguide switches with MOS electrooptic control, monolithic integrated optics in GaAs-Al $_x$ Ga $_{1-x}$ As 8-87168
 space qualification of optical instruments, using long duration exposure facility 8-85826
 switch, bistable, multimode integrated 8-79145
 systems integration and optical design, conference, Reston, VA, USA (Apr. 1977) 8-50783
 tacheometer, electrooptical, EOT 2000, design parameters, performance figures 8-77858
 thermoplastic light modulators, status and prospects 8-79138
 total internal reflection modulator, small glancing angles 8-74987
 tunable optical waveguide directional coupler filter 8-79144
 tuning element, for spectrometer wavelength modulation, using CW dye laser 8-61083
 ultralinear bistable electro-optic polarization modulator based on Pockels cell 8-83077
 VHF resonator radiant energy meas. (*Russian*) 8-77944
 wideband thin film modulators and switches, for optical communication 8-63206
 Al $_x$ Ga $_{1-x}$ As $_y$ Sb $_z$ -Ga $_{1-x}$ Sb $_z$ buried heterojunction electroabsorption modulation 8-55439
 Cd $_{1-x}$ Zn $_x$ S, electro-optical multilayer film, for data storage and display 8-71176
 Ga $_{1-x}$ Al $_x$ As, metal-gap channel waveguides, intensity modulation 8-66899
 GaAs directional couplers and electrooptic switches, wavelength depend. 8-79143
 GaAs, electroabsorpt. avalanche photodiode waveguide detectors 8-65965
 GaAs rib-waveguide directional-coupler switch with Schottky barriers 8-63204
 In $_2$ O $_3$ -SnO $_2$ electro-optical film, for data storage and display 8-71176
 KD $_2$ PO $_4$, electron beam addressed light valve, optical processing appl. 8-83099
 KD $_2$ PO $_4$ electrooptic modulator, field of view extension 8-94429
 KD $_2$ PO $_4$, optically addressed light valve, optical processing appl. 8-83101
 LiNbO $_3$, anisotropic multilayer waveguide for electro-optical modulator, propag. characts. (*Italian*) 8-50904
 LiNbO $_3$, light modulator with interdigital electrodes, operating characts. 8-90511
 LiNbO $_3$ optical waveguides, electrooptic modulation and switching, recent progress 8-50945
 LiNbO $_3$ phase modulator, axial mode locking of CW Nd $^{3+}$:YAG ring laser 8-50835
 LiNbO $_3$ phase modulator, freq. shift device for optical range 8-59147
 LiNbO $_3$ travelling wave optical waveguide modulator, 10 GHz bandwidth 8-59134
 LiNbO $_3$ waveguide, corrugated, electro-optic scanning of light diffr. from grating output coupler 8-63172
 LiNbO $_3$:Ti, electro-optic waveguide modulator, temp. stabilisation 8-50926
 LiNbO $_3$:Ti waveguide directional coupler type modulator 8-66951
 LiTaO $_3$, multimode electro-optical 2×2 crossbar switch 8-55473
 LiTaO $_3$ zig-zag reflection interferometric light modulator 8-90527
 PLZT ceramic, possible construction of matrix-addressable controlled transparency 8-71222
 PLZT ceramics, optical information storage and spatial light modulation 8-83097
 ZnSe, absorpt. modulation of light, and its appl. to page composer (*Japanese*) 8-83083

electro-optical effects

- see also *electroabsorption*; *electrochromism*; *electroluminescence*; *electrorefractance*; *Kerr electro-optical effect*; *photorefractive effect*; *Pockels effect*; *Stark effect*
 anthracene:tetracene (pentacene), effect of elec. field on fluoresc. (*Russian*) 8-56521
 atomic spectra, Rydberg states, simultaneous strong elec. and mag. fields 8-78663
 cholesteric-nematic liq. cryst. mixtures, electro-optic charact., light scatt. modes (*Japanese*) 8-79527
 dicalcium strontium, propionate, thermodynamics of props. 8-76426
 disperse systems, electro-optical phenomena, induced dichroism rel. to elec. field calc. 8-50699
 ferroelectric mats., conf., Novosibirsk, USSR (Sep. 1976) 8-76393
 field induced twisted structure with quasihomotropic boundary conditions, electro-optic behaviour 8-60424
 fluid, rarefied, symmetries of static elec. field induced opt. effects 8-55713
 Franz-Keldysh, optically enhanced for n $^+$ -p-n $^+$ phototransistor struct. 8-60423
 gas in applied elec. field, IR transmission modulation (*French*) 8-50912
 HF high voltage meas. 8-86301
 HOBA, smectic C liq. cryst., EHD instabilities 8-91238
 holographic parameters, set up for meas. on electro-optic crystals 8-87031
 improper ferroelectrics, thermodynamics of props. 8-76426
 large-molecule system, field-induced birefringence theory 8-76421

electro-optical effects continued

- liquids, transparent isotropic, electro-optical and magneto-optical effects, review 8-84553
- macromolecules, polydispersity in nonlinear electric methods, nonlinear dielec. effect formulas derived 8-59730
- matrix theory fundamentals of active electrooptic and magneto-optic media (*Russian*) 8-63005
- MBBA-cholesteryl oleate mixture, memory effect characts., crit. freq. rel. to erase voltage 8-94993
- MBBA-PCB (41 wt.%) + pleochroic dye, electrothermo-optic effect, optical storage device appl. 8-87611
- molecular electro-optical emission, for excited state dipole moment determ. 8-62230
- nematic liq. crystal, dielectric anisotropy, IR spectra, effect of AC elec. field 8-64355
- nematic liquid crystal twisted layer, light transmission 8-68476
- nematic-cholesteric mixture with positive dielectric anisotropy, light scatt. characts. 8-75537
- optical recording media, review 8-71172
- perovskite and tungsten bronze cryst. struct. types, ionic grouping theory, electrooptical, nonlinear optical effects (*Chinese*) 8-52472
- polymethacrylic acid, dye-tagged, electrically oriented solns., fluoresc. polaris. changes 8-76523
- racemic liq. soln., mirror isomeric mol. separation by RF rot. polarisation elec. field 8-80317
- smectic A phase, variable tilt, electro-optic effect giving stored colours 8-51415
- sodium polystyrene sulphonate, dye-tagged, electrically oriented solns., fluoresc. polaris. changes 8-76523
- submillimetre monochromatic spectroscopic determination of dielec. props. of electro-opt. materials 8-76428
- tanane, crit. behaviour near ferroelec.-ferroelastic transition 8-52459
- tetracene, fluorescence, effect of weak external electric field (*Russian*) 8-80416
- N,N,N',N'-tetramethylparaphenylenediamine, recomb. fluoresc., elec. field quenching 8-92107
- TGS, electrooptic switching anomalies 8-52473
- two-level system in sinusoidal elec. field (*Russian*) 8-58966
- uniaxial noncentrosymmetric crystals, with intersecting dispersion curves, external actions effect 8-84552
- ABO₃-type crystal, electro-opt. effect, theoretical treatment 8-76427
- ADP-type crystals, electrooptic effect in ultraviolet region 8-76431
- Ba(NO₂)₂·H₂O, hexagonal, piezoelec., electro-optic, dielec., elastic, thermoelastic props., space groups 8-76388
- Ba₂Na(Nb,Ti)₂O₁₅, prep. and electro-opt. props. 8-76432
- Ba_{0.5}Sr_{0.46}Nb₂O₆·Y(La)(Tm), dielectric and electrooptic props. 8-68466
- BaTiO₃, electro-opt. effect, theoretical treatment 8-76427
- Bi₁₂SiO₂₀, volume hologram polarisation props. and appls. 8-74859
- CdS, collision controlled light scatt. by electrons, influence of elec. field (*Russian*) 8-64375
- CdTe, tunable high efficiency microwave freq. shifting of IR laser 8-71126
- Cd_{1-x}Zn_xS, RF sputtered electro-optical film for data storage and display 8-83047
- Cs₂S₂O₆, hexagonal, piezoelec., electro-optic, dielec., elastic, thermoelastic props., space groups 8-76388
- D, Lamb shift, from elec. field quenching radiation anisotropy 8-66502
- Fe₃B₇O₁₃I, thermodynamics of props. 8-76426
- GaSe(Te)-SnO₂ spray heterojunction, electro-optical props. 8-64102
- Gd₂(MoO₄)₃ 8-88281
- Gd₂(MoO₄)₃, spontaneous electrooptic effect, role of induced birefringence 8-68480
- Gd₂(MoO₄)₃, thermodynamics of props. 8-76426
- In₂O₃-SnO₂, magnetron RF sputtered electro-optical film for data storage and display 8-83047
- KDP-type crystals, electrooptic effect in ultraviolet region 8-76431
- KDP-type crystals, phase transitions, quadratic electrooptical coeff., electrostriction 8-76430
- KH₂PO₄, Pockels' const., linear electro-optic const., sign of piezoelectric const. 8-60425
- KI:Eu²⁺(S²⁺)(Mn²⁺), elec. field effect on mech. of recomb. 8-80397
- KTa_{1-x}Nb_xO₃, local polarisability in quantum paraelec. and quantum ferroelec. phases 8-64325
- KTaO₃, SHG and quadratic electrooptic effect 8-76429
- La₂Pb_{1-x}Zr_xTa_{1-y}O₃, ferroelec. with diffuse phase transition, electrostriction-optical props. 8-68457
- LiClO₄·3D₂O, hexagonal, piezoelec., electro-optic, dielec., elastic, thermoelastic props., space groups 8-76388
- LiClO₄·3H₂O, hexagonal, piezoelec., electro-optic, dielec., elastic, thermoelastic props., space groups 8-76388
- LiNH₄SO₄, LiNH₄SeO₄, nonlinear opt. props. including SHG 8-76396
- LiNH₄SO₄, phase transitions and phys. props. 8-76399
- LiNbO₃ crystal, different interdigital electrode struct., electric field distrib. obs. 8-76433
- LiNbO₃, LiNbO₃:Fe, amplification of laser beams by ferroelectrics 8-90393
- LiNbO₃, LiNbO₃-Fe, photorefractive in ferroelectrics rel. to electro-opt. effects 8-92048
- LiNbO₃ photorefractive reversible optical memory (*Russian*) 8-58943
- LiNbO₃ transparency with vacuum-deposited electrodes (*Russian*) 8-60422
- NH₄Cl, order parameter, electro-optic measurement 8-88280
- NaNH₄SO₄·2H₂O, NaNH₄SeO₄·2H₂O, nonlinear opt. props. including SHG 8-76396
- Ne, gas discharge, laser irr. and voltage changes 8-63606
- Ne, glow discharge, voltage change due to laser irr., 572-654 nm 8-63605
- PLZT ceramic birefringence props., transverse electro-optical meas. 8-72487
- PLZT ceramics, physical, elec. and optical props. and fabrication (*Polish*) 8-56458
- PLZT, transparent ferroelec., RF sputtering and film characterisation 8-72727
- PbMg_{1/3}Nb_{2/3}O₃, electro-opt., elasto-opt., opt. and photo-induced props. 8-95560
- PbMg_xNb_{1-x}O₃, ferroelec. with diffuse phase transition, electrostriction-optical props. 8-68457
- Pb₃MgNb₂O₉, crystal growth procedure, meas. electro-optic and dielectric props. 8-88418

electro-optical effects continued

- PbMg₂Ta₂O₉, crystal growth procedure, meas. electro-optic and dielectric props. 8-88418
- PbZn_{1/3}Nb_{2/3}O₃, electro-opt., elasto-opt., opt. and photo-induced props. 8-95560
- SnCl₃⁻, harmonic approx., force const., electro-optical parameters and normal vibrs 8-62790
- SnI₃⁻, harmonic approx., force const., electro-optical parameters and normal vibrs 8-62790
- SrClF, cryst., Raman intensity anal., normal coord. anal. 8-72493
- SrTiO₃, SHG and quadratic electrooptic effect 8-76429
- ZnSe, linear electro-optic coeff. dispersion, relation to reson. Raman scatt. 8-56459
- ZnSe, twinning effect on electro-optical props. 8-68478
- electroabsorption**
- anthracene crystals, and thin films, electroabsorption in disordered solids 8-95590
- impurity centres in crystals, quadratic Stark effect, Jahn-Teller effect 8-68536
- semiconductor with nonspherical bands, diamag. excitons and Franz-Keldysh effect 8-72554
- Al_{1-x}Ga_{1-y}As_{1-x-y}Sb_x-Ga_{1-z}Sb_z buried heterojunction electroabsorption modulation 8-55439
- GaAs, electroabsorpt. avalanche photodiode waveguide detectors 8-65965
- GaAs, optical modulation spectra, proton damage effect 8-76487
- electroacoustic effects** see *acoustoelectric effects*
- electroacoustic generators** see *acoustic generators*
- electrocaloric effects** see *pyroelectricity*
- electrocardiogram** see *electrocardiography*
- electrocardiography**
- see also *bioelectric potentials; biomagnetism; cardiology*
- ambulatory arrhythmia quantification by correl. technique 8-81020
- amplifiers, instruments and maintenance, review 8-69232
- analysis system oriented toward polarcardiology 8-85447
- arrhythmia classification in context, extension of single-beat algorithm 8-85426
- arrhythmia detection using a low-power, CMOS processor 8-73276
- arrhythmia detector evaluation, ECG database development 8-81018
- arrhythmia monitoring, ARGUS/RT microcomputer system 8-81014
- arrhythmia monitoring using interactive computer system, clinical evaluation 8-81028
- arrhythmia monitors, review 8-69233
- arrhythmia simulator for monitor testing 8-61270
- arrhythmia studies, interactive graphics system for quantitative data extraction 8-81027
- automatic ambulatory rhythm monitoring 8-85431
- automatic evaluation of ECG signals using analogue circuits (*German*) 8-92717
- biopotential distribution laws rel. to functional state 8-65142
- body surface potential distribution map recording and processing 8-57116
- body surface potential map estimation, limited lead selection 8-57111
- body surface potential mapping, automated acquisition and processing system 8-81033
- cardiac arrhythmias diagnosis, online real-time pattern recognition (*Italian*) 8-85439
- cardiac output determ. using Kubicek formula and integration method (*German*) 8-92720
- cardiotachygram, anal. of recurring beat sequences (*German*) 8-88753
- clinical ECG real-time telephone transmission usefulness and reliability 8-57108
- clinical electrophysiology laboratory automatic control system 8-57110
- computer analysis program capable of serial comparison, 1976 IBM program description and performance 8-57086
- computer display of serial changes in hypertensive cardiovascular disease 8-81047
- computer program performance in separating normals from non-normals 8-81046
- computer programs, differences in meas. results 8-81048
- computer-assisted ECG anal. system as part of regional cardiovascular information system 8-81049
- computerised ECG analysis system, application to hypoxic rat ECGs 8-57088
- computerised Holter tape processing systems for drug testing, validation technique 8-81017
- computerised interpretation, automatic protection against diagnostic errors due to wrong electrode placement 8-81052
- computerised quantitative evaluation of cardiac arrhythmias 8-85435
- cordless, and heart rate meter (*Japanese*) 8-80984
- data interactive display system 8-53550
- digital filters, implemented on microprocessor 8-85428
- digital recording by mobile cart with microprocessor and DC 300 cart-ridge recorder 8-85427
- dipole crosstalk in inverse cardiac generator 8-92615
- electrical contact generation by tattooing C into skin tissue 8-77122
- electrical generator integral characts. in normal humans 8-69244
- epicardial and body surface pot. meas. in intact dog, transfer coeffs. calc. 8-92614
- ergometric test, computer interpretation of heart-rate var., anal. of cardiac control in exercise 8-85430
- exercise ECG automated anal., clinical experience 8-81050
- exercise ECG computer-assisted anal., implementation and clinical anal. 8-81051
- fine structure analysis by noise reduction (*German*) 8-73268
- foetal heart rate non-invasive registration by transabdominal ECG (*German*) 8-85418
- foetal heart rate recording, interference due to infusion pump (*German*) 8-85414
- forward problem, relationships among Green's theorem, Helmholtz theorem and integral eqn. methods 8-57090
- grounded, resistance to coherent mains interference, exptl. evaluation 8-85419
- grounded, standardisation of resist. to external cophasal power line interference for isolated patients 8-57085
- heart frequency monitor in microprocessor technology (*German*) 8-92718
- heart-rate store, PLL circuit, portable (*German*) 8-65139
- HF ECG compared with ballistocardiogram 8-77123
- Holter analysis, appls. of Dyna-Gram IIIB system 8-81019

electrocardiography continued

- Holter recording processing, computer system 8-81015
 Holter tape dual-channel anal. system, ARGUS/2H 8-81016
 impedance cardiogram integration method for cardiac output automatic determ. 8-92719
 information content improved by turning reference axes by 20°, Frank system processing (*German*) 8-92713
 interactive analysis techniques with Random Access Mass Storage ECG Analysis System 8-81034
 ischaemic heart disease determ. by heart beat interval anal. and medical questionnaire evaluation 8-65145
 ischaemic heart disease diagnosis using respiratory sinus arrhythmia 8-65147
 lead system information content (*German*) 8-69226
 left ventricular function evaluation using ECG synchronised scintillation camera 8-65110
 microcomputer-based evaluation system, improving diagnostic capabilities 8-88761
 microprocessor based system for ECG analysis, design and development 8-73287
 monitoring, long-term, with contourgraphic signal representation (*German*) 8-92714
 monitoring abnormal QRS events, sequential improvements in on-line algorithm 8-81026
 monitoring by contour comparison, QRS triggering with real-time correlator (*German*) 8-92715
 myocardial infarction, topographic relation between myocardial ^{201}Tl uptake and left ventricular kinetics 8-61243
 oesophageal multiprobe for temp., ECG and heart and lung sound meas. 8-77146
 optimum data processing and storage design 8-57118
 pattern recognition program for continuous ECG processing in accelerated time 8-92725
 piecewise-linear approximated ECG waveform recognition 8-57119
 QRS automatic meas. in children's ECG and VCG, wave recognition algorithms (*German*) 8-69225
 QRS-onset and offset in children, detection using parametrised templates 8-85438
 radionuclide cardiac motion study, computer-processed, ECG gating device 8-73210
 real-time ECG contour anal. program using microprocessor system 8-73288
 rhythm diagnosis using statistical signal anal., identification of persistent rhythms, ECG/VCG 8-77141
 rhythm diagnosis using statistical signal anal., identification of transient rhythms, ECG/VCG 8-77142
 single-channel electrocardiograph with telephone transmission attachment 8-88760
 slew rates in adult and infant ECG 8-53544
 ST-segment response in exercise ECG, accurate automatic measurements 8-77140
 surface mapping recordings registered at rest and during exercise, diagnostic value 8-81044
 surface potential map reconstruction from limited no. of leads 8-57117
 systolic time interval processing system, STIPS 8-81029
 T-wave rise time rel. to heart rate, exercise vector cardiograms study 8-85434
 telemetry apparatus, single-channel, PLL demodulator appl. (*German*) 8-57097
 trigger circuits, QRS, reliability and precision tests using synthetic ECG (*German*) 8-92716
 vectocardiogram analysis program for children, with multivariate diagnostic classification 8-81045
 vectocardiogram, computer treated, discrimination between normals, LBBB with and LBBB without myocardial infarction 8-85448
 vectocardiogram computer system for anal., display and storage 8-85437
 vectocardiography display and rate analysis, minicomputer system 8-92738
 ventricular arrhythmia on-line study, computer system 8-81060
 ventricular fibrillation recognition using ECG power spectrum 8-81032
 ventricular pressure and ECG continuous monitoring during angina attacks, computer anal. 8-85436

electrocataphoresis *see electrophoresis***electrochemical analysis**

- see also electrochemistry; polarography; voltammetry (chemical analysis)*
 carboxyhaemoglobin, redox investig. using reson. Raman, visible absorption and electrochem. methods 8-76832
 chalcopryite oxidation, in acidic chloride medium electrochem. study 8-95817
 coulometric impulse technique, review 8-73048
 cytochrome c, redox investig. using reson. Raman, visible absorption and electrochem. methods 8-76832
 derivative neopolarograms, shapes, theory 8-53289
 differential pulse chronoamperometry 8-73111
 electroanalytical chemistry, 1952-1977, review 8-92567
 electrolyte-solid interface, electrochemistry of surface 8-80798
 faradaic admittance, rapid drop time on-line FFT meas. 8-92544
 first-order electrochemical analysis, reversible pot. and rate const., chronoamperometric determ. 8-61086
 gases in metals, detection by vacuum spark technique, appl. to Al wire 8-61094
 ion selective electrodes, review 8-85165
 ion-selective electrode, flowing systems meas. 8-92527
 ion-selective membrane electrodes, selectivity, statistical calcs. 8-92549
 mechanicochemical testing of metals, electrochemical cell for mechanicochem. behaviour determ. 8-60905
 microcomputer-controlled instrument for electrochemical studies 8-73128
 potentiometric gas sensing probes, micro-size, for ammonia, CO_2 8-61071
 potentiometric titration system, microcomputer controlled, for soln. equilib. obs. 8-92522
 reference electrode arrangement, high temp. polarisation study 8-64845
 review of instrumentation and dynamic techniques over past 4 years 8-85215

electrochemical analysis continued

- serum automated electroanal. using ion-selective disc electrodes with neutral cation-carriers (*German*) 8-73269
 stripping analysis, Kalousek polarography appls. 8-53290
 titration using automatic conductometer, exam. 8-56933
 toxic compounds, enzymatic sensor for continuous determ. (*French*) 8-73099
 CO_2 partial pressure in blood, meas. by rapid response electrode system (*German*) 8-85409
 Fe, annealed, H₂ permeation, 230 to 300K (*Japanese*) 8-84004
 Fe-Ni-Cr (40, 20 wt.%), Kh20N40 alloys, phase composition after quenching, tempering 8-60650
 Mn (II), determ. in industrial wastes 8-61105
 O_2 meter calibration in 10^{-7} bar range 8-80812
 O_2 meter for O_2 meas. in liquid Na 8-58337
 O_2 partial pressure determ. in biological fluids, electrochem. cell 8-85420
 S, probe for coal gasification systems 8-76947
 S²⁻ ion-selective electrode, sensitivity, surface heterogeneity effects 8-92526
 W alloys, phase anal., electrochem. separation of carbides 8-60651
 WO_3 electrode, surface growth of ternary compds., in electrolyte containing redox couples 8-61016
 ZrO_2 , elec. cond.-nonstoichiometry relationship, direct determ. 8-76079

electrochemical batteries *see cells (electric)***electrochemical electrodes**

- see also electrochemistry*
 arterial pO_2 intravascular monitoring using catheter-tip polarographic electrode (*German*) 8-85408
 cathodic diffusion boundary layer, free convective flow obs. with shadow Schlieren method 8-68894
 concentration polarisation, convectionless steady state, interferometric investig. 8-68896
 converters, electrochem., conc. type, for elec. signals, diffusion theory of conc. networks 8-61026
 diffusion between electrodes spaced on cylinder oscillating in electrolyte (*French*) 8-64849
 effective area determination 8-73045
 electrocrystallisation, galvanostatic transients, crystn. overvoltage 8-76867
 electrolyte conductivity rel. to electrode current density (*Russian*) 8-64847
 electron transfer to redox system time-depend. perturbation theory 8-61027
 electrophoretic force along equipot. electrode 8-61024
 endogastric probe for telemetric pH meas. (*German*) 8-85452
 gas discharge between coaxial electrodes with dielectric layer 8-75476
 gas-evolving electrodes, mass transfer, superposition of hydrodynamic flow 8-73047
 heterogeneous, current and pot. distrib., surface section equilib. pot. 8-53221
 interface with electrolyte, orient. models for solvent 8-61017
 ion-selective disc electrodes with neutral cation-carriers for automated electroanal. of serum (*German*) 8-73269
 ion-selective electrode, flowing systems meas. 8-92527
 ion-selective membrane electrodes, selectivity, statistical calcs. 8-92549
 Kel-F-graphite composition electrode, voltammetric appls. 8-92489
 metal, interaction with solvent rel. to elec. double layer struct., adsorpt. 8-61023
 oxide electrodes, electron transfer reactions, tunnelling through a space charge barrier 8-80050
 oxide-covered metal electrodes, direct elastic electron tunnelling, calcs. 8-52085
 oxide-electrolyte interface, transition layer model 8-68895
 polyethylene capillary dropping mercury electrodes, for corrosive media appls., prep. 8-61090
 polymer film coated steel, Pt and glassy C electrodes, prep., charact., stability 8-76866
 reference electrode for automated in situ hydrochemical meas. (*Russian*) 8-65430
 review, ion selective electrodes 8-85165
 ring-disc electrodes, collection efficiency for high freq. AC 8-64853
 rotating disc electrode, with optically transparent ring, digital simulation 8-53210
 rotating ring-disc electrode with pyrolytic graphite end-plane sections 8-92488
 solid, behaviour in normal and differential pulse voltammetry 8-73055
 surface, covalently bound molecules, redox reactions, steric effects 8-73077
 surface, partially covered, eqns. for chronopotentiometry 8-85236
 Ag, metal ion adsorption, kinetics, surface struct. 8-79873
 Ag sintered electrode production for concentrating cell (*Portuguese*) 8-88637
 Al alloys, pit propagation, influence of anions in halide solution 8-72917
 Al- Al_2O_3 -electrolyte, electroluminesc., nondestructive electronic avalanche 8-68563
 Au, chemisorption of H(O), volume of adsorbed species, temp. and press. effects 8-84060
 Au electrodes, adsorpt. of Br⁻, specular reflect. investig. 8-61047
 Au, metal ion adsorption, kinetics, surface struct. 8-79873
 C, pyrolytic film electrode, fabrication, electrochem. characterisation 8-92487
 CO_2 partial pressure in blood, meas. by rapid response electrode system (*German*) 8-85409
 n-CdS(Se)(Te) semicond. liq. junction solar cells, photocurrent spectra, carrier recombination 8-76142
 Cu- H_3PO_4 system, instability and oscillations (*French*) 8-64850
 Cu-Hg amalgam electrode, standard pot. 8-76874
 CuFeS₂, chalcopryite, electrode surface reduction kinetics 8-56897
 $\alpha\text{-Fe}_2\text{O}_3$, pure and TiO₂ doped, electrode, photooxidation of H₂O appl. 8-76886
 n-GaAs semicond. liq. junction solar cells, photocurrent spectra, carrier recombination 8-76142
 p-GaP electrode, for solar cell, differential capacitance meas. for flat-band potential determ. 8-72256
 Li, electrochemical behaviour, in propylene carbonate, SEM study (*French*) 8-56899

electrochemical electrodes continued

- O₂ electrode, membrane-covered catheter-tip system, construction and performance 8-81003
 O₂ partial pressure determ. in biological fluids, electrochem. cell 8-85420
 O₂ partial pressure measurement with thin-layer polarographic probe, intracortical appl. (*German*) 8-85410
 Pb, passivation in H₂SO₄ soln. 8-76871
 Pb/PbCl₂ electrode, in chloride media, low temp. props. 8-68899
 Pt, chemisorption of H, entropy, temp. and press. effects 8-84059
 Pt, chemisorption of H(O), volume of adsorbed species, temp. and press. effects 8-84060
 Pt electrode, in Na₂SO₄-NaCl melt, polarisation meas., reactions 8-68898
 Pt electrode, multilayer oxides, electrochem. reduction mechanism, kinetics 8-61019
 Pt electrode (100), (111), polycryst. surfaces, comparison of electrochem. activity 8-61015
 Pt electrodes, platinised, adsorpt. of Au in aq. HCl 8-56914
 Pt-electrolyte interface, electron states, photoemission studies 8-85171
 Ru electrodes, adsorption and surface reactions, cyclic voltammetry and X-ray emission spectrometry 8-61018
 S⁻ ion-selective electrode, sensitivity, surface heterogeneity effects 8-92526
 Si, carrier conc. determ., electrochem. method 8-60200
 Ta electrode, anodised, meas. of electrochem. reactions, appl. to time stimulation 8-95931
 Ti/RuO₂/MnO₂ electrode, anode characts. 8-68897
 WO₃ electrode, surface growth of ternary compds., in electrolyte containing redox couples 8-61016
 Zn electrode, passive film form. by chrono-ellipsometry (*Japanese*) 8-68900
 Zn, electrode, single crystal, fracture surface charge density effect 8-68787
 Zn-tetraphenylporphine/metal electrode, photocurrent generation mechanism 8-76868
 ZnO electrode, reson. Raman spectra of adsorbed rose bengal 8-76446
 ZnO electrode, role of triplet states in xanthene dye sensitisation 8-76869

electrochemical machining *see electrolytic machining*

electrochemical polishing *see electrolytic polishing*

electrochemistry

- see also Debye-Huckel theory; electrical conductivity of electrolytic liquids; electrochemical analysis; electrochemical electrodes; electrolysis; electrolytic devices; electrophoresis*
 acetate, aq. soln. current-potential curve, influence of NO₃⁻, SO₄²⁻, PO₄³⁻ and Cl⁻, obs. (*Japanese*) 8-85172
 adhesive joint failure, adhesive/electronically conducting substrate, exam. of electrochemical aspects 8-60979
 bone healing, use of anodised Ta electrode, meas. of electrochem. reactions 8-95931
 carboxylate, aq. soln. current-potential curve, influence of NO₃⁻ and SO₄²⁻, obs. (*Japanese*) 8-85173
 coulometric impulse technique, review 8-73048
 double-layer structure, electrohydrodynamical determination 8-95960
 electric double layer capacitance meas., potentiostatic method 8-85169
 electric double layer capacity, chronopotentiometric meas., reversible electrochem. reaction effects 8-80753
 electrochemical overpotential phenomena, appls. 8-64846
 ellipsometry of electrochem. surface layers 8-56874
 energy considerations 8-88643
 excited electronic state, photoelectrochemistry 8-76872
 fast ionic conductors, review, device appls. 8-51724
 first order reaction, reversible pot. and rate const., chronoamperometric determ. 8-61086
 free convection mass transfer from horizontal surface, electrochemical and holographic interferometric obs. 8-87344
 gas-liquid interface, mass transfer, ultramicroprobe method obs. 8-63901
 heat and mass transfer rates at high Pr, electrochemical modelling 8-83383
 1-hexene-water-(D₂O), field-induced surface reactions, field ionis. mass spectra obs. 8-95949
 indifferent salts, acid conc. aq. solns., H evolution at Hg electrode 8-53215
 layer of symmetrical spherical dipoles, Poisson-Boltzmann treatment of capacitance 8-64844
 mechanisms studied by parameter sensitivity functions and zone diagrams (*French*) 8-88638
 metal-water systems at elevated temps., thermodynamic props. 8-76898
 metals, scaling, theory, electrochem. transport model 8-64761
 mixed electrolytes, conductance, relax. terms 8-67840
 nonpolar molecules, ionis. by alkali ion attachment at electrolyte surface 8-65998
 ohmic potential drop, rel. to crit. pitting and protection pots. 8-72900
 photographic developer activity, rel. to difference of electrochem. and redox potentials (*Russian*) 8-62243
 polar liquid, electric double layer at surface 8-53212
 polycarbonate foil electrochemical etching for dosimetry, bulk etching rate evaluation 8-78506
 PTFE/graphite bond in H₃PO₄ environment, electrochemical exam. of joint failure 8-60979
 reaction intermediates, at rot. disc. electrodes, spectroscopic obs. 8-53210
 reference electrode arrangement, high temp. polarisation study 8-64845
 rotating disc-ring electrode equipment, automated, appls. 8-95933
 semiconductor-electrolyte boundary, current flow, study of semicond. using electrochem. techniques 8-95356
 sensitised photocurrents, temp. depend., electrochem. meas. 8-72205
 Smoluchowski equation, with Coulomb pot., appl. to fluoresc. quenching 8-73051
 Smoluchowski equation with Coulomb pot., time-depend., soln. 8-73050
 solid state, teaching approach 8-93498
 steel, mild, corrosion in complex aq. environment, linear polarisation investig. 8-76782

electrochemistry continued

- surface thermodynamics, Lippmann relation, electrocapillary theory 8-61048
 symmetrical electrolytes, conductance, relax. terms 8-67840
 thin-layer cell, concentration impedance, unequal diffusion coeffs. and 2nd-order reactions effects (*French*) 8-53214
 thin-layer cell, concentration impedance reactive and nonreactive diffusion effects (*French*) 8-53213
 thin-layer cell, fast reaction, kinetic consts., diffusion and conc. impedance 8-73053
 turbulent mass transfer in viscous sublayer by electrochemical method, expt. 8-83368
 two-dimensional nucleation and growth, double potentiostatic step response, perturbation effects calcs. 8-51841
 two-layer baths, dynamic rectification effect calcs. 8-95934
 unsymmetrical electrolytes, conductance, relax. terms 8-67840
 vitamin B₁₂, electrochemical reduction of methylcobalamin and methylcobinamide, one electron intermediates 8-85286
 Ag, single crystal, electrochem. grooving, gross linear defect obs. 8-67894
 AgI, interfacial electrochem., review 8-80748
 AgI-Ag₂O-B₂O₃ system, ionic cond., struct., electrochem. prop. in galvanic cell 8-95181
 Ag₂V₂O₅, thermodynamic, elec. and electrochem. props. 8-84265
 Al-Zn-Mg-Cu, alloy 7075-T6, corrosion in halide solutions, exam. of anion dependency 8-60867
 AlH₃, photographic processes, thermo- and electrochemical transformations 8-89576
 Au(CN)₂⁻, electrochemical reduction kinetics 8-73052
 CO₂, electrochem. reduction for use in energy storage 8-92490
 Cd, electrodeposition on solid Cd or CdHg amalgam, rate, impedance meas. 8-52693
 Cr₂O₃-Al₂O₃, solid soln., effect of Cr on point of zero charge 8-61021
 Cu, friction under electrolyte immersion condition 8-64738
 Cu-Be-Ni-Zr, anodic behaviour of intermetallic phase 8-72895
 Cu-H₃PO₄ system, instability and oscillations (*French*) 8-64850
 CuFeS₂, chalcopyrite, electrode surface reduction kinetics 8-56897
 Fe, corrosion and electrochem. behaviour in NaOH soln. containing ClO₃⁻ (*Japanese*) 8-72928
 Fe, pitting in Na₂SO₄-NaCl solns. (*Japanese*) 8-85042
 Fe₂O₃-Al₂O₃, solid solns., effect on Fe on point of zero charge 8-61021
 H, extraction from LiF-LiCl-LiBr melt, appls. to fusion reactor blanket processing 8-53217
 Hg-aqueous electrolyte interface, double layer charge relax., thermal jump meas. 8-53216
 Hg-electrolyte interface, with imposed temporal and spatial periodicity, double-layer transduction 8-88639
 IrO₂, anodic films, electrochem. characts., electrochromic system 8-80316
 Mg-Al-Ti(Pb) systems, phase diag., electrode pots. (*Russian*) 8-80516
 MoSe₂, layer cryst., electrochem. solar cell, electron transfer mechanism 8-52077
 Na conductive glass-Na amalgam interface, electrochem. obs. 8-76870
 NaCl-graphite interface, elec. cond. 8-52060
 Pd-Al alloys, Fermi level position rel. to mixing behaviour, Al activity, thermodynamic props. (*German*) 8-75835
 Pt electrode, in Na₂SO₄-NaCl melt, polarisation meas., reactions 8-68898
 Pt electrode, multilayer oxides, electrochem. reduction mechanism, kinetics 8-61019
 Si, doped and intrinsic, chemomech. effect 8-64751
 SiO₂-Na₂O-CaO, electrochemically coloured, chemical composition and structure of surface layers 8-84758
 SiO₂-NaO-K₂O-CaO-MgO-Al₂O₃ melt, anodic dissolution of Co and Ni in melt 8-88582
 TiO₂, anodically formed layers, film instability obs. 8-72916
 WO₃ electrochromic film in liq. electrolyte, chem. and electrochem. stability 8-73054
 Zn electrode, passive film form. by chrono-ellipsometry (*Japanese*) 8-68900
- electrochromic devices**
see also electrochromic devices
 displays, technical aspects 8-65917
 picture taking parameters display in amateur cameras, review 8-89578
- electrochromism**
 electrolytic double layer, light absorpt., electrochromic changes 8-84551
 formaldehyde, electrochromism of 1749 Å band, electric dipole moment and polarisability 8-66572
 polymers, network, low freq. mol. mobility, quadratic electrochromism method (*Russian*) 8-71688
 Rydberg transitions, field effects in vacuum UV region 8-66561
 H₂WO₄ film, effect of struct. on optical and electrical props. 8-84671
 IrO₂, anodic films, electrochem. characts., electrochromic system 8-80316
 WO₃ electrochromic film in liq. electrolyte, chem. and electrochem. stability 8-73054
 WO₃-BaO film, electrochromic coloration and decoloration, BaO additive effects 8-72620
- electrodeposited coatings** *see electrodeposits*
- electrodeposited films** *see electrodeposits*
- electrodeposited layers** *see electrodeposits*
- electrodeposition**
see also electrodeposits; electroplating
 alpha activity electrodeposition onto Au foil, use in Si surface barrier detector 8-82565
 anodic film form., electrode pot. variation rel. to nucleation, growth 8-68634
 cermet, effect of electrolyte in charge carried by suspended ceramic particle 8-68665
 dendritic metal crystals, electrolytic growth, CCTV obs. 8-51863
 electrocrystallisation, galvanostatic transients, crystn. overvoltage 8-76867
 electrocrystallisation, impedance frequency dependence, in the case of DC superposition 8-51844
 electrocrystallisation, nucleation and growth mechanism, ohmic overpotential effects, simulation 8-51842

electrodeposition continued

- electrocrystallisation, nucleation and growth mechanism, ohmic over-potential effects determ. 8-51843
 electrocrystallisation noise, phenomenological model 8-51845
 electrolytic nucleation at high supersaturation 8-61025
 latex polymer, electrodeposition on metal 8-53015
 metal ion adsorption, nucleation effects (*German*) 8-68635
 metal layers, underpot. deposition, mechanisms, phase transitions, nucleation 8-60590
 metals, crystal growth, electrochem. Czochralski method, growth rate limitations 8-88433
 Permalloy, electrodeposition, mag. props. (*French*) 8-64488
 two-dimensional nucleation and growth, double potentiostatic step response, perturbation effects calcs. 8-51841
 Ag cathode, underpotential deposition of Pb 8-52692
 Ag, electrocrystallisation, in pulse electrolysis, expt. 8-64489
 Ag, single crystal, adsorption of metal ions on (111) and (100) surfaces (*German*) 8-68636
 Ag-Zn alloy, controlled-potential, spontaneous transformations obs. 8-51853
 Au, by electrochemical reduction of dicyanoaurate, reaction kinetics 8-73052
 Au, electrodeposited, struct., texture, influence of As on brightness (*Bulgarian*) 8-79862
 Au-In, electrodeposited from acid cyanide electrolyte, exam. of wear and corrosion resistance 8-80482
 Cd, electrocrystallisation, in pulse electrolysis, expt. 8-64489
 Cd, electrodeposition on solid Cd or CdHg amalgam, rate, impedance meas. 8-52693
 CdS, electrocrystallisation of films on Cd 8-72014
 CdTe cathodic deposition from aqueous electrolytes 8-64484
 Co-Ni, electrodeposition, mag. props. (*French*) 8-64488
 Cr, high purity 8-84724
 Cu, electrocrystallisation, in pulse electrolysis, expt. 8-64489
 Cu, electrodeposition on Cu single crystal (100) face, in presence of Br ions 8-84723
 Cu, electrolytic deposition from CuSO₄ solns. 8-61022
 Cu powder with homogeneous dispersion of Al₂O₃ particles 8-84743
 Fe-Ni, electrodeposition, mag. props. (*French*) 8-64488
 Fe-Ni-Cr coating, electrodeposited, exam. of passivity 8-80655
 GaAs, synthesis by molten salt electrolysis 8-64486
 Gd, purification by electrorefining, exam. 8-52721
 In from acid sulphate solns., electrode reactions 8-88436
 In-Tl, electrodeposition from aq. sulphate soln., X-ray struct. 8-84722
 Ni (*Spanish*) 8-92486
 Ni-Co-Cd alloys, electrodeposition from acetate bath 8-68637
 Pb, passivation in H₂SO₄ soln. 8-76871
 Si, electrodeposited film, appl. in solar cell fabrication 8-76611
 Si preparation by electrolysis of fluorosilicate solns. in molten alkali halide mixtures (*French*) 8-64491
 Ti anode, surface deposit from NaCl electrolysis, elemental anal. 8-73117

electrodes

see also *electroplated coatings*

- Ag, dendritic growth inhibition by tartaric acid and tartrates (*French*) 8-87894
 Ag-Zn alloy, deposited under controlled potential, spontaneous transformations obs. 8-51853
 Au alloys for electronics industry, characts. 8-52695
 Au coating, Cu diffusion process obs., under high temperature (*Czech*) 8-91486
 Au, electrodeposit, struct., texture, influence of substrate (*Bulgarian*) 8-79863
 CdS, film electrolytically deposited, surface and bulk photocond. props. 8-60154
 Co, electrodeposited film, saturation magnetisation and perpendicular anisotropy meas. 8-76277
 Co-Ni alloys, electrodeposited, struct., internal stress, and mag. props. 8-95471
 Cr, formation of axial texture (111) [hkl], math. model (*Russian*) 8-84082
 Cu, annealing effect on struct. and microhardness (*Russian*) 8-76668
 Cu, collagen and chloride additions effects obs., on morphology and crystal orientation 8-51852
 Cu film, electrodeposited, recrystallisation kinetics, X-ray scatt. (*Russian*) 8-60045
 Cu single crystal film, electrodeposited, fatigue cracks (*Japanese*) 8-84975
 Cu-Cd alloys obtained by electrolysis, struct. 8-91552
 Fe, cast, noise reduction by electrolytic coating 8-80681
 Fe-Zn, stable and metastable alloys, order-disorder, mag. interactions and corrosion behaviour 8-68422
 Ni, electrodeposit structure, rel. to electrochem. noise 8-67916
 Ni, electrodeposited, oxidation 8-64756
 Ni, electrodeposited film, saturation magnetisation and perpendicular anisotropy meas. 8-76277
 Ni film, electrodeposited, recrystallisation kinetics, X-ray scatt. (*Russian*) 8-60045
 Ni-Co-P, ferromag. film, amorphous to cryst. transition, diff. and resistivity meas. 8-60587
 Ni-P, magnetisation coercivity and magnetostriction 8-68338
 Ni-SiC, electrodeposited, oxidation 8-64756
 Ni_{1-x}P_x, electrodeposited, amorphous, mag. and transport props. 8-52106
 Sb, amorphous, explosive crystn., semicond-semimetal transition and IR absorpt. 8-51849
 Zn electrodeposit dendritic growth control using impedance meas. 8-84721
 Zn, electrodeposit structure, rel. to electrochem. noise 8-67916

electrodes

see also *anodes; cathodes; electrochemical electrodes; microelectrodes*

- air high-current pulse discharge, near-electrode process dynamics 8-71602
 Al, electrodes, use of soluble corrosion inhibitors to suppress electrode dissolution 8-88565
 bioelectric signal recording using surface electrodes, methods of reducing movement interference (*German*) 8-85405
 blade, electrical and magnetic circuits calc. (*Czech*) 8-55273
 boundary conditions for space charge surface layer at electrode plasma boundary, particle flux (*Russian*) 8-55736

electrodes continued

- capacitive dispersion field transducers for granular material exam. 8-85078
 cardiac pacemaker electrode threshold current and optimal design (*Japanese*) 8-53569
 ceramic-based, in MHD channel, temp. distrib. 8-59258
 coaxial cylindrical discs, radial heat flow 8-75032
 defibrillator electrode gel testing, meas. of impedance to transthoracic DC discharge 8-57056
 diagonal-type nonequilibrium plasma MHD generator, electrode internal and external connection effects 8-91165
 dielectric constant and dissipation factor meas. in 1-200 MHz range 8-49864
 electric breakdown voltage hysteresis, electrode coating effects in air and SF₆ 8-87553
 electrodes, laminated, for nerve biopotential recording 8-92760
 EMG surface electrode, for motor unit action potential duration meas. 8-81039
 free-burning arc continuous radiation rel. to electrode erosion 8-71578
 geometries for various dielectrophoretic force laws 8-88640
 graphite electrode open channel config. for N₂ laser 8-55379
 high-current photomultiplier with disc electrode leads 8-58032
 HV heavy-current arc gap 8-87514
 ion extractor electrode CAD (*Japanese*) 8-86680
 Kelvin method contact PD meas. manipulator 8-57979
 MHD generator, Faraday type, current profile optimisation, electrode cond. profile 8-94939
 minerals, electrodes and paste specimens for emission spectrographic anal. (*French*) 8-92563
 negative glow plasma, contact electrode charging time meas. 8-67525
 pacemaker lead failure type discrimination 8-53570
 plasma-electrode interface, geom. extended electrode, charged particle and energy fluxes 8-79442
 pressurised field distortion spark gaps, arc voltage waveforms, electrode material effects 8-87549
 rotating electrode, for improved reproducibility in spark source mass spectrometry 8-93781
 SAW scattering in piezoelectric material, by metallic electrodes anal. 8-83157
 skin conductivity measurement, electrode materials (*German*) 8-85406
 sputter electrode preparation for multiply charged heavy ion sources 8-66009
 surface and coating effect on DC breakdown voltages in SF₆ 8-87557
 surface plasma source, H⁻ ion form. and secondary electrons (*Russian*) 8-71503
 transparent electrode deposition on PLZT ceramic, elec. and opt. props. 8-74848
 vacuum gap electrode surface sorption, mass spectroscopic obs. 8-75466
 Au-Si-Al structure electrode mass transfer and switching with meeroxy 8-95389
 C electrode breakdown voltage dependence on adsorbed gases 8-75465
 α-Fe₂O₃, polycryst., pure and TiO₂ doped, flatband potentials, donor densities, photocurrent meas. 8-76089
 Gd small ion-getter pump 8-89487
 In_{2-x}Sn_xO_{3-y} film, deposited from organometallic composition, transparent cond. appl. 8-91793
 Ni alloy, thermionic electron emission into Cs vapour, for thermionic converters 8-60540
 PbS, nonstoichiometric, increase of rest pot. with p-type semicond. character 8-56170
 SF₆ high-current arc props., influence of electrode material 8-71592
 ZnO binder electrophotography, tone reproduction and copy quality (*German*) 8-62259

electrodynamics

see also *electron beams; electron optics; electron tubes; ion beams; ion optics; ion sources; quantum electrodynamics*

- accelerated point charge, bound and emitted four-momentum, retarded integration 8-66738
 adiabatic invariant of charged particle spiralling in longit. mag. field 8-58892
 astrophysics, electrodynamic and gravit. effects of Proca stresses 8-93098
 atmosphere electrodynamic state, horizontal mag. field component influence (*Russian*) 8-73556
 bodies at rest including quadrupoles, theory (*German*) 8-81858
 cause and effect relationship 8-54108
 charged liquid, SCF equation, partial soln. (*Russian*) 8-74823
 charges of finite extension, generally covariant formulation 8-77731
 classical charged particles with spin 8-65790
 coherent EM radiation intensity, produced by modulated electron/ion beams in gas 8-50686
 coherent radiation, from electron bunch, electron distrib. effects 8-66734
 cyclotron radiation from oppositely directed electron beams 8-78874
 deformable media, electrodynamics, nonrelativistic classical field eqns. 8-49679
 deformable media, electrodynamics, relativistic field equations 8-49678
 dielectric sphere, motion in travelling elec. field 8-50685
 dynamical and kinematical charges in classical nonlinear scalar field 8-54208
 dyon field, extended Yang-Mills formalism, Mandelstam's path depend. formalism 8-62288
 education, charge hyperbolic motion and radiation 8-49587
 education, Lienard-Wiechert field expression, circulating charge in static mag. field 8-69933
 education, Lorentz theory for classical radiation reaction of accel. charged particle, dumbell model 8-49592
 education, Lorentz-Dirac eqn. for classical charged particle, mass renormalisation 8-62007
 electric charge conservation (*Russian*) 8-77739
 electron acceleration by inhomogeneous electrostatic RF field 8-82538
 electron beams, electrodynamic principles of rotating relativistic types 8-71019
 electron bremsstrahlung spectrum in point Coulomb field, classical and nonrelativistic quantum theory 8-65792

electrodynamics continued

- electron in magnetic field, induced angular momentum, classical and quantum calcs. 8-86060
- EM radiation-charged particle stimulated interaction, classical and quantum theory study (*Russian*) 8-86431
- embedding classical fields in QFT, electrodynamics, Yang-Mills theories, gravit. appls. 8-54223
- energy tensor definition for system of charged particles and EM fields 8-77734
- fields generated by charged particle in vac., zero vel. limit, electrostatics solns. 8-82881
- free-electron momentum modulation, limited interaction length with light 8-62995
- gyrating charged particle in EM field, adiabatic invariance of mag. moment 8-78873
- Hamiltonians, stochastic character effect on particle accelerator design 8-93606
- HF fields, charged particles relativistic motion (*Russian*) 8-62996
- hidden variables, quantum mechanics, and stochastic electrodynamics (*French*) 8-62107
- homogeneous conducting medium, transformed eqn. (*Russian*) 8-81866
- ionosphere plasma, long metallic tethers electrodynamics 8-69652
- ions, trajectory in const. mag. field plus orthogonal sinusoidal elec. field 8-50687
- Jupiter-Io electrodynamic interaction, theory 8-81583
- Lorentz-Dirac eqn. constraints 8-77736
- marine electrodynamics, magnetostatics problems and appl. to water masses movement (*Russian*) 8-77259
- Maxwellian electrodynamic theory, history from eqn. discovery to mag. monopoles (*German*) 8-65791
- metric free, with electric and mag. charges, field eqn. general solns. 8-69994
- monopole, accelerated, field strength determ. (*Chinese*) 8-77740
- multidimensional two particle problem with noncentral pot. 8-54174
- mutually interacting charge fields, gauge theoretical formulations of elementary particle processes 8-58122
- nonadiabatic losses of particles in a dipole trap (*Russian*) 8-87002
- noninertial reference system, electrodynamics eqns. (*Russian*) 8-81895
- nonlinear approach to electrodynamics spin and stability props. anal. 8-49682
- nonlinear electrodynamics, Birkhoff's theorem analogue (*Russian*) 8-54273
- particle motion in EM field at relativistic speeds (*German*) 8-90350
- Pauli exclusion principle proof from self consistent field theory of electrodynamics 8-49683
- plasma, fluctuation-dissipative relation in nonlinear electrodynamics (*Russian*) 8-79410
- polarised nonconducting dielectric fluid, anal. of force exerted on immersed elec. charge 8-78872
- quaternionic notation for classical electrodynamics extension, Lagrangian formulation and canonical formalism 8-81863
- radiating electron, stability of motion 8-65789
- radiating point charge, energy and ang. momentum splitting 8-69996
- radiation from charge moving in randomly inhomogeneous media, fluctuation effects (*Russian*) 8-71017
- relativistic charged particle in nonuniform mag. field (*Russian*) 8-78876
- relativistic electron beam, 'peeling' on entering mag. field 8-66741
- relativistic electron beam, crit. current in mag. field in vacuum channel (*Russian*) 8-71016
- relativistic transformations, Newtonian force and EM field, for teaching 8-49601
- relativistic two-body electrodynamics 8-54112
- resonant wave-particle interaction, at half-integer cyclotron harmonics 8-78871
- rotating dielectric column, EM scatt., relativistic soln. 8-50681
- Rutherford scattering with radiation reaction, Lorentz-Dirac eqn. soln. for opposite point charges 8-55289
- Schwarzschild electrodynamics, rel. to black holes and neutron stars 8-77480
- Schwarzschild sphere and classical electron self-energy 8-49681
- self-resonant electron motion in monochromatic wave 8-66737
- Smith-Purcell radiation generated by electron beam, non-redundant spectral tunnelling 8-78906
- stationary levels of electron in field of polarised neutral particle (*Russian*) 8-66733
- steady state Universe using stochastic electrodynamics, cosmic background radiation and red shift 8-77631
- synchrotron radiation field, statistical states 8-66736
- transition radiation, classical theory 8-82896
- vacuum, transition radiation and scatt. in strong EM field (*Russian*) 8-58895
- X-ray scattering by free and bound electrons in strong laser field 8-58148

electrodynamometers see *dynamometers*

electroencephalograms see *electroencephalography*

electroencephalography

see also *bioelectric potentials; biomagnetism; brain*

- adaptive matched filters for the measurement of acoustically evoked potentials in the EEG (*German*) 8-88755
- alpha and non-alpha intervals alternation, queueing theory model 8-96040
- alpha frequency rel. to head size, implications for brain wave model 8-69035
- amygdaloid kindling phenomenon extended first approx. model 8-53378
- automatic sleep staging detectors 8-53551
- autoregressive models usefulness for EEG segments classification 8-80989
- bispectra computation computer program, in FORTRAN 8-92727
- dynamic evolutionary spectral analysis 8-57102
- electrical contact generation by tattooing C into skin tissue 8-77122
- epileptic transient detect., pattern recognition techniques 8-53542
- event-related variations, dynamic computer anal. (*German*) 8-85400
- evoked potential on-line statistical detect., appl. to audiometry 8-69245
- evoked potentials, processing, computer techniques 8-92728

electroencephalography continued

- evoked potentials and EEG freq. in patients undergoing haemodialysis and kidney transplantation 8-61160
- frequency analyser, real-time, microprocessor monitored 8-57092
- intracerebral currents, contribs. to EEG and evoked potentials 8-92611
- microcomputer based digital filter for electroencephalogram processing 8-73278
- microcomputer system for on-line analysis of electroencephalographic data 8-73277
- non-convulsive response induced by intermittent photic stimulation, clinical usefulness 8-69246
- nonstationary, anal. by approx. canonical expansion method 8-53555
- nonstationary point automatic detect. (*French*) 8-57112
- phasic event detection by microprocessor 8-57091
- photic one-second stimulation, on/off effects in background EEG activity 8-69047
- respirometer, noncommercial respiratory transducer for EEG laboratory 8-65138
- rhythmic activity generation models (*Dutch*) 8-73150
- scalp potentials, dipole layer model 8-77035
- scalp recorded potentials, intracranial sources, 3D localisation, quantitative evaluation 8-92613
- signal processing and telemetry, digital bandpass analysis 8-57107
- sleep EEG automatic K-complex detector 8-53557
- sleep pattern feature extraction and recognition by real-time anal. (*Japanese*) 8-73271
- slope descriptor computation, time and frequency domain comparison 8-57115
- spike detection using combined inverse and matched filter techniques 8-61267
- standardised classification, sequential epoch method 8-57101
- stationarity and normality of EEG data during sleep stages 8-92610
- stimulus artifact suppression, sample and hold amplifier system 8-77163
- visual evoked cortical potentials in men during compression and saturation in He-O₂ 8-61173
- visual evoked potential to search in short-term memory, late components 8-61172
- visually evoked elec. and mag. response simultaneous recording for diagnosis 8-53558

electroendosmosis see *electrophoresis*

electroerosive machining see *spark machining*

electrofluidynamics see *electrohydrodynamics*

electrofluorescence see *electroluminescence*

electroforming

- brass, study of process variables in the electromagnetic bulging of tubes 8-80582
- Al alloy, study of process variables in the electromagnetic bulging of tubes 8-80582
- Cu, study of process variables in the electromagnetic bulging of tubes 8-80582

electrofluidynamics see *electrohydrodynamics*

electrohydrodynamics

- aerosol, β -active, emission electrification in external field 8-83497
- aerosols, charging migration and EHD transport 8-88660
- anthracene, liq., EHD transit flow 8-75895
- baking, EHD augmented, corona wind impingement effects 8-87235
- boundary layer of dilute suspension during application of elec. field (*Russian*) 8-63503
- bubbling electrofluidised bed, heat transfer rates 8-87242
- bulk-coupled normal field interfacial instability 8-87407
- cable oil, EHD pumping 8-87414
- cholesteric liquid crystal, EHD instability with isotropic mechanism (*Russian*) 8-87617
- cholesteric liquid crystal with anisotropic dielec. permeab., transient electrodynamic instability (*Russian*) 8-51418
- conducting fluid, laminar rot. in cylindrical vessel, elec. and mag. field effects (*Russian*) 8-75222
- conducting liquid, eddy current induced pumping, longit. current in corrugated tube (*Russian*) 8-75216
- conducting liquid, plane-parallel shear flow, elec. current and mag. field effects (*Russian*) 8-75221
- converter or nozzle for jet printer, output parameter exact solns. (*Russian*) 8-75230
- corona wind between wire and plate electrodes 8-71561
- corona wind cooling of flat surface, convective heat transfer coeffs. 8-87234
- DHAB, nematic, ordering change due to external DC elec. field, permittivity obs. 8-94990
- dielectric fluid, space charge transfer by slow flow, in strong nonuniform elec. field (*Russian*) 8-75223
- dielectric liquid, elec. dispersion in different gaseous environments 8-88254
- dielectric liquid, film condensation, heat transfer enhancement in elec. field 8-55551
- dielectric liquid in electric field, two-dimensional vel. field stochastic charact. (*Russian*) 8-75208
- dielectric viscous fluids, electrohydrodynamic stability in rigid cylinder 8-59497
- double injection with recombination, EHD linear and nonlinear stability 8-87412
- double-layer structure, electrohydrodynamical determination 8-95960
- electrostatic spraying of liquids 8-67274
- electrovortical flow, in discharge between hyperboloidal electrodes (*Russian*) 8-75217
- flow visualisation by laser light scatt. from PMMA latex particles 8-75236
- Freon-113, pure and mixed with methanol, EHD coupled minimum film boiling, surface wave model 8-87240
- heat pipe designs, performance characts. 8-87241
- heat transfer in liquids by dielectrophoresis 8-94874
- HOBA, smectic C liq. cryst., EHD instabilities 8-91238
- hydrocarbons flowing through circular pipe, streaming currents developed in laminar and turbulent flows 8-87413
- impact charging of an isolated cylinder with skewed field and flow 8-87404
- insulating liquid subject to unipolar injection, EHD stability, nonlinear phenomena 8-87411

electrohydrodynamics continued

- insulating liquids, electroconvection, uni- and bi-polar injection 8-87405
 laminar boundary layer, on permeable surface, in crossed elec. and mag. fields (*Russian*) 8-75118
 linear induction MHD pump, cylindrical, electrodynamic forces (*Russian*) 8-94843
 liquid crystal, dissipative structures in turbulent movement (*Russian*) 8-55808
 liquid film, free, stabilised with ionic surfactants, EHD 8-87403
 liquid film, thin, free, stabilised with ionic surfactants, dynamics 8-87416
 mass spectrometry, EHD ionisation, instrumentation, mechanisms and appls., review 8-86378
 Maxwell stress, deformable surface, general case 8-59501
 MBBA, nematic liq. cryst., dynamically excited, transversal EHD instabilities and umbilics 8-94983
 MBBA, nematic liq. cryst., electroviscous effect, electrohydrodynamic investigation 8-87804
 naphthalene, liq., EHD transit flow 8-75895
 nematics, nonlinear effects above electrohydrodynamic instability threshold (*Russian*) 8-75551
 nitrobenzene, steady state electroconvection, self beating laser spectroscopy 8-87408
 organic liquids, electrohydrodynamic ionisation, solvated ion mass spectroscopy, anal. appl. 8-73102
 polydisperse droplets, produced by EHD method, charge-to-mass ratio 8-76931
 polyethylenoxide, flow rate increase by electric field 8-75210
 smectic A liquid crystal, EHD instability and elec. cond. anisotropy (*Russian*) 8-59753
 solid aerosol collection in spouted bed, electric field effect 8-91019
 solid spacer influence on liq. motion induced by unipolar injection 8-87406
 spectral anemometer, electrogasdynamic 8-87422
 subsonic grid turbulence, diffusion processes of small spots of electrostatically charged mols. 8-87410
 surface wave propagation, nonlinear effects 8-67278
 suspension, dielectric, convective heat transfer, rheodynamics, in horizontal coaxial cylindrical channel 8-59494
 Symposium, Colorado, USA (Jan. 1978) 8-87402
 Taylor, G.I., contrib. to EHD 8-86099
 turbulent boundary layer, at permeable surface, in crossed elec. and mag. fields (*Russian*) 8-94836
 Cu spheres, electrically augmented pneumatic transport at low particle and duct Reynolds numbers 8-87409
 Hg-electrolyte interface, with imposed temporal and spatial periodicity, double-layer transduction 8-88639

electrojets

- see also ionosphere*
 auroral currents, magnetometer array and radar backscatt. joint obs., N.Scandinavia 8-85768
 auroral region, elec. fields and mag. effects of solar flares 8-69576
 auroral westward electrojet, rel. to Pc 5 activity in morning sector 8-61685
 counter-electrojet, search for correl. with interplanetary mag. field 8-88983
 equatorial, equivalent circuit anal. of neutral wind effects 8-57392
 equatorial, neutral winds and phase vel. of instabilities 8-57388
 equatorial, theory 8-69607
 equatorial electrojet, changes during mag. storm correlated with interplanetary mag. field 8-85766
 equatorial electrojet, vars. rel. to interplanetary mag. field vars. 8-77413

electrokinetic effects

- see also electrodynamics; electrophoresis*
 capillary surface, zeta potential determ. method using oscillating laminar flow streaming pot. meas. 8-76873
 interfaces, with two types of ionising group, electrokinetic and surface pots. 8-76136
 porous materials, thermal diffusion based on electrokinetic effect, coefficient determ., calc. and obs. (*Russian*) 8-90641
 Cr electrolytic oxidation in SO₂ atmosphere, CrO₃ ionic defect effects (*Ukrainian*) 8-92504
 Si, doped and intrinsic, chemomech. effect 8-64751

electroluminescence

- see also phosphors*
 anthracene: 1-chloroanthracene, electrolum. meas. 8-84659
 diamond, synthetic, electroluminescence excitation mechanism, role of defects 8-52581
 diode, laser measurement, of semiconductor materials and devices (*Rumanian*) 8-52035
 9,10-diphenylanthracene, electrogenerated chemiluminescence, T₂ state emission 8-60524
 electrostatic intensity appl. (*Russian*) 8-77934
 epoxy resin, electroluminesc. 8-56522
 fluorene, electroluminesc. (*Russian*) 8-92129
 insulating material monitoring by electroluminescent screens, defect imaging 8-53083
 metallic cathodes, electroluminescent impurities causing vacuum breakdown, obs. 8-84660
 metallic particle tunnel junctions, light emission 8-80066
 radiation crack detection, use of luminescent convertors 8-53125
 Al-Al₂O₃-electrolyte, electroluminesc., nondestructive electronic avalanche 8-68563
 Al-oxide-electrolyte system, luminesc. spectra (*Russian*) 8-76539
 Al-SiO₂-Au, thin layer struct., electroluminesc. (*French*) 8-76531
 p-Cu₂Sn-n-ZnS heterojunction, I-V characts., photocond. and electrolum. 8-72251
 Ga_{1-x}Al_xSb p-n structure, variable-gap, electroluminescence 8-52582
 GaAs:Si p-n structure, radiative recombination region 8-52071
 GaAs-InSe p-n junctions, 'optical' contacts, elec. props. 8-56222
 GaAsSb_{1-x}, epitaxial layer, struct. defects rel. to luminesc. 8-72040
 p-Ga_{1-x}In_xAs, Auger recomb., theory and luminesc. expts. 8-56518
 GaP LED degradation, effect of γ -irradiation 8-95610
 GaP p-n junction, capacitance-freq. dispersion and electroluminescence efficiency 8-64101
 GaP:Zn, growth, I-V characts., electroluminesc. (*Korean*) 8-52653
 GaSb, photolum., electrolum. meas. in p-n junction, temp. influence 8-72594

electroluminescence continued

- GaSe, additional IR electrolum. band obs. at 77K 8-72607
 GaSe(Te)-SnO₂ spray heterojunction, electro-optical props. 8-64102
 p-InAs, Auger recomb., theory and luminesc. expts. 8-56518
 In₂Ga_{1-x}As p-n homojunction, MBE grown, electrolum. meas. 8-84328
 In₂Ga_{1-x}As, thick LPE growth, electrolum. obs. 8-60589
 In₂Se-InSe p-n junctions, 'optical' contacts, elec. props. 8-56222
 InTe-InSe p-n junctions, 'optical' contacts, elec. props. 8-56222
 LiH₃, evidence for N₂⁻ from static and dynamic props. 8-60465
 NH₄NO₃, intrinsic electroluminescence obs. 8-80420
 (NH₄)₂SO₄, intrinsic electroluminescence obs. 8-80420
 PbTiO₃ single crystals, electroluminesc., elec. field, freq. and temp. depend. 8-80422
 Si inversion layers, cyclotron and subband emission 8-64128
 SiC, surface luminesc. in presence of anodisation 8-52579
 Ta-Ta₂O₅-ZnS:TbF₃-Au thin films, MIS struct., DC electrolum. obs., Poole-Frenkel effect 8-88038
 ZnO:Dy(Nd)(Sm), phosphor, electroluminesc., photoluminesc. spectra 8-80421
 ZnO:La phosphor, electrolum. brightness waves, -168 to +85°C 8-52580
 ZnS, electroluminesc. and photoluminesc. spectra, fine struct. (*Russian*) 8-84661
 ZnS, electroluminophor, ageing rate, voltage effects (*Russian*) 8-84662
 ZnS:Cu, Br based electroluminesc. cells, light, const. field effects on electroluminesc. 8-84658
 ZnS:Cu, effect of elec. field on photoluminescence, model of luminogen centre 8-76522
 ZnS:Cu(Cl)₂ electroluminesc. and photoluminesc. spectra, fine struct. (*Russian*) 8-84661
 ZnS:Mn film, emission centres of DC electrolum. 8-68564
 ZnS:Mn film device, laser modulation of electrolum. 8-52576
 ZnS:Pb phosphor mech. of elec. field liberation of electrons from traps 8-72616
 ZnS-Cu, comet shaped electroluminesc. lines 8-52578
 ZnSe-GaAs thin film DE electroluminescent cell with 20 V threshold voltage 8-76141
 ZnSeCu, double comet shaped electroluminesc. 8-52577

electrolysis

- see also anodisation; electrical conductivity of electrolytic liquids; electrodeposition; electroforming; electrolytic dissociation; electrolytic ion mobility; electrolytic machining; electrolytic polishing*
 alkali halide crystals, defect state change during electrolysis 8-95057
 cathodic diffusion boundary layer, free convective flow obs. with shadow Schlieren method 8-68894
 concentration polarisation at electrode, convectionless steady state, interferometric investig. 8-68896
 electronic device dendritic growth mechanisms 8-56058
 ferricyanide bleach regeneration, simplified electrolytic method 8-74090
 ferrous material fractured surface exam., oxide scale removal 8-95886
 hydroxyapatites, elec. cond., charge carrier identification 8-67855
 ion separation, by ion exchange membranes 8-53247
 lamellar eutectic, specimen thinning for TEM (*German, English*) 8-95885
 nonaqueous solution cell, heat transfer through diaphragm 8-73049
 polymer film coated steel, Pt and glassy C electrodes, prep., characts., stability 8-76866
 ring-disc electrodes, collection efficiency for high freq. AC 8-64853
 steel, MnCr (16, 5 wt.%), bending fatigue behaviour improvement by surface treatment (*German*) 8-84957
 transition metal foil-electrolyte interface, optical and elec. expts. 8-88644
 water, decomposition by fusion energy, H₂ prod., synthetic fuel 8-50335
 Ag/α-Ag₂S, interface, electrochemical transfer across phase boundaries 8-73046
 C, prod. from solid-state reduction of carbonate ions, X-ray diffr. 8-56594
 CO₂, aqueous solution, photoelectrochemical reduction on p-type GaP in liq. junction solar cells 8-88649
 Cu, powders, prep. of spherical starting particles, for suspension electrolysis 8-60689
 Li, electrochemical behaviour, in propylene carbonate, SEM study (*French*) 8-56899
 NaCl soln., electrolysis, surface deposit on Ti anode anal. 8-73117
 Ni, powders, prep. of spherical starting particles, for suspension electrolysis 8-60689
 Pb, powders, prep. of spherical starting particles, for suspension electrolysis 8-60689
 Pt surface, electrochem. oxidation and reduction, XPS obs. 8-95653
 ZrO₂, elec. cond.-nonstoichiometry relationship, direct determ. 8-76079

electrolytes

- for solid electrolytes see superionic conducting materials*
see also electrolysis; superionic conducting materials
 1:2 electrolytes, conc. solns., vel. corrs. calcs., diffusion, cond. and transference props. 8-85166
 aqueous solns., IR librational bands, struct. making and breaking 8-56476
 aqueous solutions, ion-solvent interactions, transport props. (*German*) 8-79790
 aqueous solutions, naturally recurring, activity coeffs. rel. to ionic diffusion 8-57224
 aqueous solutions, self-diffusion of H₂O, NMR spin-echo obs. 8-80243
 binary electrolyte solns. thermodynamics using US props. 8-73946
 cermet electrodeposition, effect of electrolyte in charge carried by suspended ceramic particle 8-68665
 charge fluctuations, two-component ionic conductor, collective dynamics 8-67841
 concentrated aqueous electrolyte solutions, transport props. (*German*) 8-80750
 Coulombic systems, HNC and RHNC eqns. for restricted primitive model 8-67630
 Debye screening length, solvent effect in diffuse double layer problem 8-53211

electrolytes continued

- dilute systems of dipoles and dipolar charged particles, Mayer resummation method 8-83710
 electrical conductivity meas., voltage amp. for temp. compensation (*German*) 8-54399
 electrohydrodynamic ionisation, solvated ion mass spectroscopy, anal. appl. 8-73102
 electrophoretic force along equipot. electrodes 8-61024
 fluid systems, thermodynamic props., activity expansions 8-76901
 formamide, partly deuterated, in electrolytic soln., IR spectra, anion-solvent H-bonding 8-84558
 geminate recombination, time depend. Onsager problem anal. soln., critical elec. field 8-72446
 high energy primary cell electrolytes (*German*) 8-80751
 interface with electrode, orient. models for solvent 8-61017
 ion distribution near phase boundary (*German*) 8-56901
 ionic conductivity, phenomenological theory 8-83994
 ionic solutions, elec. field statistics 8-87601
 liquid-air interface, dipole layer, electrolyte effect 8-51796
 liquid-liquid interface, adsorbed monolayer mol. orientation, electrolyte effects, reson. Raman obs. 8-60430
 maleic acid-styrene copolymer, aq. soln., conform. transition 8-75526
 multicomponent systems, velocity correl. coeffs. 8-85167
 polar liquid, solvated electron optical props. and thermodynamic char-acts., polaron model 8-85170
 polarisable fluid containing charged particles, mol. dynamics theory 8-91214
 polarisable spheres model 8-56898
 poly-1,4-phenylene terephthalamide, in H_2SO_4 , dilute soln. viscosity 8-75524
 polyelectrolyte, 1-1 soln., excluded vol. theory, Khun statistical segment basis 8-83716
 polyelectrolyte aqueous salt soln., inelastic light scatt. obs., conformational changes 8-60474
 polyelectrolyte solutions, apparent ionic charge 8-76875
 polyelectrolyte solutions, colligative props., chain flexibility influence 8-94962
 polyelectrolytes in soln., electrostatic persistence length rel. to unified theory 8-95932
 polyvalent electrolyte apparent molal adiabatic compressibility and US vel. obs. 8-61028
 porous cellulose acetate membranes for mixed uni-valent electrolytes in aqueous solns. reverse osmosis predictability 8-53250
 propylene carbonate, SEM study of electrochem. behaviour of Li (*French*) 8-56899
 reverse osmosis transport processes at membranes (*German*) 8-95946
 solution, streaming at neg. polarographic maximum 8-61020
 solutions, apparent ionic charge 8-76875
 solutions, dielec. dispersion and dielec. friction 8-52436
 solutions, diffraction expts. and theory (*German*) 8-95935
 solutions, preferential solvation, NMR obs. 8-95919
 solutions, preferential solvation and mol. motion, NMR obs. 8-95920
 strong II-I electrolytes, aq. soln., Raman spectrum, local order 8-84563
 transition metal foil-electrolyte interface, optical and elec. expts. 8-88644
 velocity correlation coeffs., particle-particle interactions 8-64852
 viscosity of conc. solns., temp. depend. 8-80749
 Wien effect in mixed strong electrolytes 8-75856
 $BaCl_2$, conc. solns., vel. correls. calcs., diffusion, cond. and transference props. 8-85166
 $CaCl_2$, conc. solns., vel. correls. calcs., diffusion, cond. and transference props. 8-85166
 CaF_2 , elec. cond. at high temp. 8-72159
 $CsCl$, $CsCl+KCl$ mixtures, osmotic coeffs. at 298.15K 8-92509
 $CsCl+KCl$ mixtures, osmotic coeffs. at 298.15K 8-92509
 $CuSO_4$, solution, activity coeff. determ. 8-76874
 Hg-electrolyte interface, with imposed temporal and spatial periodicity, double-layer transduction 8-88639
 Ni coating hardness rel. to sulphamate electrolyte selection (*Bulgarian*) 8-88552
 $NiCl_2$, aq. soln., viscosity meas., struct. props. 8-75863

electrolytes, solid see superionic conducting materials

electrolytic capacitors

No entries

electrolytic conductivity of liquids see electrical conductivity of electrolytic liquids

electrolytic deposition see electrodeposition

electrolytic devices

- electrochemical convertors, conc. type, for elec. signals, diffusion theory of conc. networks 8-61026
 S probe, coal gasification systems appl. 8-76947

electrolytic dissociation

see also electrolytic ions

- ball lightning explanation by water electrolysis and combustion 8-69436
 heavy water, prep. of D_2 using self-controlled cell 8-80752
 semiconductor-electrolyte contact, electrolytic decomposition and photodecomposition 8-95357
 stretched dipoles, in applied elec. field, distrib. function 8-64851

electrolytic ion mobility

see also electrophoresis

- complex ions, mobility and stability constns., counter-current ion migration determ. (*German*) 8-56900
 diagram expansions for systems with Coulomb interaction, removal of divergences 8-73056
 electrolyte, and polyelectrolyte solns., apparent ionic charge 8-76875
 parallel-plate channel wall solution in electrolyte laminar flow (*Russian*) 8-64848
 water, MHD motion meas. by microfluxmeter 8-79384

electrolytic ions

- see also electrical conductivity of electrolytic liquids; electrolytic dissociation; electrolytic ion mobility
 acetate, aq. soln. current-potential curve, influence of NO_3^- , SO_4^{2-} , PO_4^{3-} and Cl^- , obs. (*Japanese*) 8-85172
 carboxylate, aq. soln. current-potential curve, influence of NO_3^- and SO_4^{2-} , obs. (*Japanese*) 8-85173
 stretched dipoles, in applied elec. field, distrib. function 8-64851

electrolytic machining

see also electrolytic polishing

- Ag, single crystal, electrochem. grooving, gross linear defect obs. 8-67894

electrolytic polishing

see also electrolytic machining

- metal, polarisation curves in polishing solns. 8-56851
 steel, stainless, Cr-Ni-Mo, surface, scraping, mech. (electrolytic) polishing, ion etching, effects on ESCA 8-53037
 thin foils, electropolishing technique for transmission electron microscope specimen preparation 8-57919
 transition metals and compounds, electromechanical polishing method 8-53073
 Ag, electropolishing, cyanide-free solution 8-88603
 Au, thin disc prep. and electropolishing for TEM 8-88601
 Au-Zn(Cu) alloys, electrolytic thinning for use in transmission electron microscopy 8-57918
 Be bronze, using cylindrical stationary electrode 8-64783
 Be bronze, using cylindrical electrode moving forwards 8-64784
 Cu- H_3PO_4 system, instability and oscillations (*French*) 8-64850
 SiO_2 film, local defects detection by electrolytic decoration (*Bulgarian*) 8-60896
 Ta and Ta alloys, use of pure FSO_4H 8-85094
 Ti, metallographic specimen prep. for chem., mech. electrolytic polishing 8-80705
 V, blister form and stress build-up, under the bombardment, surface prep. effects 8-95094

electrolytic tanks

- heat conduction of metallic joints determ., for single spot and conical constrictions 8-83207

electromagnetic absorption see electromagnetic wave absorption

electromagnetic compatibility

see also frequency allocation

- biomedical telemetry, transmission and reception with embedded antennae 8-77125
 cardiac pacemaker responses to power frequency signals 8-88771
 EM wave scattering by conducting cylinder arrays interspaced by inhomogeneous dielec. 8-78862
 GEOS booms and mechanisms 8-85825
 IEEE International EMC Symposium, Atlanta (1978) 8-82876
 Jupiter Voyager electrostatic discharge protection 8-89042
 LF EM shielding props. of arbitrary cross-section conducting cylindrical shells 8-55283
 lightning return stroke channel, transmission line model, computer soln. 8-85644
 pacemaker interference simulation by models 8-81069
 shielded cables, nonlinearities and multiple exposure anomalies at CASINO, MCCABE code verification 8-58502
 shielding theory of metallic enclosures with apertures 8-55282
 thermometry considerations in localised hyperthermia, review 8-53561

electromagnetic corrections

"electromagnetic corrections" is distinguished in use from "radiative corrections" by application to elementary particle and nuclear interactions see also radiative corrections

- Coulomb corrections in pp scatt., phase shift contrib. 8-70391
 deep inelastic scatt. and e^+e^- annihilation, EM corrections to asymptotic freedom predictions 8-62403
 radiative corrections in gauge theories, QCD current algebra formulation, weak interaction universality 8-93883
 radiative corrections to parity violation in atoms in $SU(3) \times U(1)$ gauge theory 8-62402
 $e^- +$ nucleus parity violating neutral current interaction, gauge theory predictions, radiative corrections 8-86436
 $K \rightarrow 3\pi$, radiative correction amplitudes from Ke_4 decay anal. 8-86451
 $K \rightarrow \pi\nu$, radiative correction amplitudes from Ke_4 decay anal. 8-86451
 $K \rightarrow \pi\pi\nu$, Ke_4 decay, radiative correction amplitudes 8-86451
 NN interaction, neutral scalar, pseudoscalar and neutral vector boson radiative corrections, explicit formulae 8-70372
 πN coupling constant from simultaneous anal. of all invariant amplitudes using rational series 8-58199
 πN scatt., EM effects at high energies 8-93906
 π^+n backward elastic scatt. 20-40 GeV, Regge theory description, angular distrib., radiative corrections 8-62461

electromagnetic decays

- charmonium narrow states, hadronic and EM decays 8-70343
 charmonium state decay, nonrelativistic and relativistic theory 8-58221
 radially excited states, photon and hadron interactions 8-82170
 two-photon decays, weak, Hamiltonian derived in model with right-handed currents (*Russian*) 8-66119
 $\Delta^+ \rightarrow p + \gamma$, radiative decay in the MIT bag model 8-66110
 K_1 , weak radiative decays in chiral theory using virtual π^0 and η pole diagrams (*Russian*) 8-78172
 $K_1 \rightarrow 2\gamma$ decay, contribution of Hamiltonian derived for weak two-photon decays (*Russian*) 8-66119
 $K^* \rightarrow K + \gamma$, radiative decay in the MIT bag model 8-66110
 $\omega \rightarrow \pi + \gamma$, radiative decay in the MIT bag model 8-66110
 pn mass difference, effects of EM mixing, $\Lambda \rightleftharpoons \Sigma^0$, $\eta \rightleftharpoons \pi^0$, $\omega \rightleftharpoons \rho^0$ (*Russian*) 8-74255
 $\pi^0 \rightarrow 4\gamma$, upper limit to branching ratio 8-93882
 $\psi \rightarrow 3\gamma$, dispersion sum rule charmonium theory, decay probability lower bound (*Russian*) 8-89716
 $\psi \rightarrow 3\gamma$, dispersion theory of charmonium, self consistency test, decay probability (*Russian*) 8-89717
 ψ particles, off-mass-shell coupling constns. and radiative decays in VDM 8-70371
 $\rho \rightarrow \pi + \gamma$, radiative decay in the MIT bag model 8-66110

electromagnetic energy see electromagnetic waves

electromagnetic field theory

see also electromagnetic waves; electromagnetism

- anisotropic solids with magnetic symm., unified dynamic theory 8-77713
 black holes, magnetosphere, charge particle trapping 8-57573
 black-hole evaporation unified gravit. and electromag. field theory 8-53979
 boundary coupling of gravitational wave and EM radiation in cavity 8-54267
 Brans-Dicke theory, EM solns. 8-57841

electromagnetic field theory continued

- Casimir effect, EM waves near perfect conductors 8-55278
 causality and relativity 8-81901
 cavity with cylindrical hole in wall of infinite thickness, elec. and mag. polarisabilities determ. 8-71004
 characteristic impedance of double line in front of dielec. wedge (*German*) 8-78855
 charged fluid, orthonormal tetrads in general relativity 8-54269
 circular bundle of relativistic particles (*Czech*) 8-66711
 conducting rectangular bar transmission gratings 8-62993
 corner diffraction coeff. anal., Albertsen's formulae 8-62978
 coupling through azimuthally symmetric apertures in bodies of revolution 8-62984
 Debye pot., scalar factorisation for Maxwells eqns. 8-77732
 deformable media, electrodynamics, nonrelativistic classical field eqns. 8-49679
 deformable media, electrodynamics, relativistic field equations 8-49678
 dielectric scattering alternative surface current formulation 8-62991
 diffraction convex, smooth, ideally conducting and electrically large surfaces 8-94363
 discontinuous surface in EM field (*Italian*) 8-50676
 dyon field, extended Yang-Mills formalism, Mandelstam's path depend. formalism 8-62288
 education, EM vector pot. and its physical reality 8-61974
 education, homogeneous ellipsoidal inclusions, general theorems, Poisson theorem, dielectric polarisation, conduction and elasticity 8-61979
 education, Maxwell's eqns., Lorentz and conformal covariance, normal transformation rules 8-49589
 eigensolutions of field strength operator, nonlinear and linear processes (*German*) 8-83028
 electric dyadic Green's functions derivation, report 8-86169
 EM instruments for use in liquid sodium, theoretical anal. 8-54857
 EM radiation near black holes and neutron stars 8-53978
 EM scattering from corrugated conducting surfaces with inhomogeneous surface impedance, anal. 8-62987
 EM two-body interaction theory 8-49739
 EM/acoustic waves variational expressions systematic derivation 8-93536
 field penetration into thick, finitely conducting shell, anal. 8-62990
 field radiation by mag. dipole on smooth convex surfaces 8-62977
 field sources on conducting concentric sphere, dipole approx. (*Russian*) 8-86991
 forward scattering anomaly in hollow penetrable body 8-62986
 H-field, E-field, and combined-field solns. for conducting bodies of revolution 8-55275
 intrinsic coupling between gravitational wave and quantised EM radiation 8-54268
 LF EM shielding props. of arbitrary cross-section conducting cylindrical shells 8-55283
 lossy anisotropic inhomogeneous media, variational solns. of EM problems 8-77735
 magnetic, interior force field, for teaching 8-54123
 magnetic shielding barrier LF field penetration 8-82886
 magnetoelastic force convertor operation anal. (*Russian*) 8-70166
 Maxwell's equations as conservation laws, electromagnetism in non-Riemannian space 8-77737
 Maxwell's equations as one quaternion eqn., appl. to wave propag., for teaching 8-54133
 mode decomposition of EM field of a homogeneous sphere in an infinite medium 8-81864
 monochromatic wave energy density in nonabsorbent medium with freq. and space dispersion (*Russian*) 8-74818
 net cohomology over Minkowski space 8-93561
 neutrino as axial EM field source, symm. P-invariant broadened Maxwell eqns. (*Russian*) 8-58141
 noncompletely reducible representations of the Poincare group associated with the generalised Lorentz gauge 8-70249
 nonrelativistic transformations giving invariant Maxwell's EM theory laws 8-77738
 numerical techniques for conformal transformation 8-74816
 observable phase factors and symmetry of electric and magnetic charges 8-86428
 one-mode fields, greatest lower bounds for degree of coherence of higher order 8-71068
 penetration and shield performance calc. 8-82885
 penetration into conducting region, soln. of reverse problem by Fredholm integral eqn. 8-94357
 penetration into conductive spherical cavity 8-86990
 perihelion precession rate in system of two charged masses 8-73897
 planar nonstationary EM field in conducting medium, transient state anal. (*Polish*) 8-71000
 polarised light beams in gravitational fields, Dirac-spinor form of Maxwell's eqns. 8-50696
 quantum field theory of electrostatic potential in gravitational field 8-54270
 radiation with spin, minimum size using special relativistic centroid theorem 8-69995
 relativistic transformations, Newtonian force and EM field, for teaching 8-49601
 Robinson's theorem, shear free condition 8-93586
 scalar and EM fields struct. in tangent bundle of spacetime with absolute parallelism (*Russian*) 8-49741
 scattering by corrugated periodic trapezoidal conducting surface, TE/TM polarisation 8-62994
 scattering by multiple rectangular cylinders, numerical anal. 8-62992
 scattering current/aperture coupling relationship for thin finite cylinders 8-62988
 scattering from thin and finite dielec. fibres 8-62972
 shielding theory of metallic enclosures with apertures 8-55282
 sphere, method of variation of const. appl. to excitation by elec. and mag. currents 8-86989
 spinless particle interaction with electromag. field, path integrals, Klein-Gordon eqn. 8-58144
 spinor eqn. of pure EM field 8-86429
 stationary rotationally symm. field representation by superimposing circular aperture and ring fields (*German*) 8-55277
 tetrad formalism of Maxwell equations with effect of gravitation. II 8-77784

electromagnetic field theory continued

- time domain reflection from inhomogeneous and dispersive slabs 8-62985
 wave diffraction calc. generalised shift operator (*Russian*) 8-78868

electromagnetic fields

- angular spectrum of EM field, elec. network equivalent 8-78867
 axially symmetric linear homogeneous media, modal EM field solns. 8-78857
 biological effects, state of research (*German*) 8-88728
 biosphere and active solar processes link, role of Earth's natural electromag. field 8-61211
 Casimir forces, appl. of analytic regularisation 8-81887
 coil above ferromagnetic half space, expressions for nonstationary electromagnetic field 8-74817
 contactless method of measuring components of complex shape, gap transducer appl. 8-93648
 dielectric wedge, review of theory of EM field behaviour 8-66712
 dipole in boundary between two half-spaces (*Russian*) 8-78858
 Earth, natural EM field short period vars. anal. for wave type and direction determ. (*Russian*) 8-85474
 freely gravitating charge, radiation, in field of weak plane gravitational wave (*Russian*) 8-89381
 fusion reactor magnetic coil systems, EM field, force and inductance calc. by EFFI code 8-62648
 heat front in weak mag. field, EM field perturbation (*Russian*) 8-94835
 horizontal electric dipole, quasi-static subsurface-to-subsurface and subsurface-to-air 8-73375
 intensity distribution, in focal region of wide-angular annular lens and mirror systems 8-90485
 Lagrangian function for intense field, dispersive representation (*Russian*) 8-94361
 lightning return stroke, EM fields radiation, Maxwell eqns. exact soln. appl. 8-73442
 metal surface, semiclassical infinite barrier model 8-64079
 metal surface exposed to external radiation, solns. of Maxwell's eqns. 8-52054
 Mezen' Bay (White Sea), marine tides EM fields 8-73378
 nerve excitable membrane, EM wave effect on surface charge density 8-85334
 ocean, magnetostatics problems in electrodynamics of sea (*Russian*) 8-77259
 precision meas., conf., Ottawa, Canada 1978 8-89462
 RF, transverse linearly polarised, effect on parametric resonator line characts. (*Russian*) 8-82883
 semiconductor, inductively heated, computer simulation of temperature and EM fields 8-55961
 slender void, in homogeneous cond. wire rope, NDT applic. 8-74813
 spatial spectra in millimetre and submillimetre wave ranges (*Ukrainian*) 8-90344
 spherical, reproduction by real meas. devices, from combined radiating sources (*Russian*) 8-85729
 symmetries of generalised electromagnetic fields 8-86988
 Tokamak magnets, EM forces, TORMAC computer program 8-62647
 waveguide radiated, rectangular, in dielectric medium (*Russian*) 8-82884

electromagnetic induction

- see also inductance*
 asteroids primordial metamorphism via elec. induction in T Tauri-like solar wind 8-69728
 circular bundle of relativistic particles, EM field (*Czech*) 8-66711
 coal layer, thickness meas., EM technique 8-53740
 coal seam thickness meas. using resonant loop as EM sensor 8-57366
 conducting cylinder with transverse mag. field, eddy current induction 8-74815
 conducting slab response to source fields, EM analogue model and finite difference calcs. 8-61329
 conductors in steady motion, solution in theory of eddy currents and forces 8-62970
 diamagnetic sphere supported by field from annular current 8-66714
 drill-rod telemetry, calcs. for toroidal coil source 8-85710
 E-polarisation, numerical soln., improved geomagnetic boundary conditions 8-77182
 Earth, geomag. induction vectors local time var. 8-85477
 Earth, transient EM response from irregular surface models 8-57165
 Earth EM fields of horizontal electric dipole on polarisable half-space surface 8-69283
 eddy currents, levitation, metal detectors and induction heating 8-61967
 eddy-currents induced within a metal cylinder by parallel ACs, numerical anal. (*Polish*) 8-78856
 Faraday generator, one piece, paradoxical expt. from 1851 8-73813
 fusion reactor eddy current analysis, finite element circuit method 8-66373
 fusion reactor eddy currents, 3-dimens., perturbation-polynomial expansion calcs. 8-66372
 fusion reactor mechanical diagnostics, techniques in fluctuating mag. fields 8-54946
 ground subsurface, EM transient response 8-57166
 induced polarisation meas. using discharge transient recorder 8-65398
 infinitely conducting oceans of arbitrary shape 8-61318
 magnetic field calc. from current distrib., finite element techniques 8-94358
 magnetic fields, quasi-stationary, finite element anal. 8-94356
 magnetic shielding barrier LF field penetration 8-82886
 MHD, moving conducting fluid inductive interaction with external main windings, config. effects (*Russian*) 8-75225
 MHD generator, simplest physical model 8-71548
 MHD generators, coaxial, magnetic field distrib. (*French*) 8-55758
 MHD induction pump with side bars, thrust-flow characts. at large Re_m (*Russian*) 8-75231
 microwave induced DC voltage phenomenon (*Chinese*) 8-50677
 moving conducting ribbon, interaction with ferromag. inductor field (*Russian*) 8-94359
 Newfoundland, geomag. sounding near northern termination of Appalachian System 8-61314
 ocean currents velocity profiler based on geomag. induction principles 8-61569
 ocean wave motion, assoc. electrokinetic phenomena 8-69351
 ocean-coast model, EM response to E-polarisation induction 8-61321

electromagnetic induction continued

- planar nonstationary EM field in conducting medium, transient state anal. (Polish) 8-71000
 plane eddy current problems, power dissipation and inductance calc. (German) 8-58881
 point charge near cond. plane, force acting, for teaching 8-49605
 polarisable half-space, current pulses, transient EM field 8-96130
 principle of equivalence, expt. test (Russian) 8-77795
 Procopiu effect EMF in ferromag. material under torsion (Rumanian) 8-86986
 RF energy coupling into cylindrical enclosure 8-87000
 RF fields, transverse linearly polarised, effect on parametric resonator line characts. (Russian) 8-82883
 solenoid deceleration in conducting tube 8-50678
 sphere, method of variation of consts. appl. to excitation by elec. and mag. currents 8-86989
 surface charge measurement by electrostatic induction 8-49807
 Tokamak machines, eddy currents, numerical and exptl. anal. 8-66374
 underground quarries, EM detection (French) 8-96306
 underground quarries, EM transmission meas. 8-57365
 VHF radiowave induction heating of biological tissue from portable transmitter, expt. 8-57039
 Fe alloys, amorphous, room-temp. saturation induction 8-95476
 $MgM^{2+}Fe_{2-x}O_4$, $M=In, Al, Cr, Sc$, comp. effects on ferrite characts. 8-52305

electromagnetic interference

- see also radiofrequency interference; telephone interference; television interference
 discharges for sputter deposition and sputter etching, RFI/EMI 8-71566
 IEEE International EMC Symposium, Atlanta (1978) 8-82876
 ocean electric fields measurement, EM phenomena accompanying movement of current fairing (Russian) 8-77361
 pacemaker interference, 60 Hz field and current effects 8-88769
 pacemaker interference, body potentials and currents from ELF elec. fields and household appliances 8-88770
 ventricular synchronous demand cardiac pacemaker advances 8-77152

electromagnetic lenses see magnetic lenses**electromagnetic oscillations**

- see also cavity resonators; lasers; masers; ring lasers
 cavity with cylindrical hole in wall of infinite thickness, elec. and mag. polarisabilities determ. 8-71004
 semiconductor, generation in LF electric field 8-64068

electromagnetic radiation see electromagnetic waves**electromagnetic theory of light**

- isotropic-anisotropic media boundary, light refl. and refr., Maxwell theory (German) 8-87007

electromagnetic wave absorption

- see also electromagnetic wave propagation in plasma; gamma-ray absorption; light absorption; spectra; X-ray absorption
 atmosphere, radiances in absorpt. bands, calc. methods including multiple scatt. 8-61554
 atmosphere, solar radiation absorpt. by H_2O vapour, including multiple scatt. 8-61553
 atmospheric attenuation of 230 GHz, meas. 8-73425
 D-region, radio wave absorpt. diurnal vars. during storm after-effect 8-65451
 D-region absorption, effect on forward scatter radiometer amplitude distrib. index 8-65552
 degenerate semiconductor, depend. on external quantising mag. field 8-95308
 Earth-space communication links, rain attenuation rel. to path diversity 8-69424
 ionosphere, daytime absorpt. surges rel. to substorm phase and interplanetary mag. field direction 8-73575
 ionosphere, equatorial, seasonal var. of radio waves absorpt. 8-85762
 ionosphere, lower, shortcomings in understanding revealed by radiowave absorpt. meas. 8-81492
 ionosphere, radiowaves attenuation rel. to oblique-incidence sporadic-E propag. 8-73578
 ionosphere, sudden commencement absorpt. events at S. pole rel. to lower cleft boundary latit. 8-77437
 ionosphere radio wave absorption, riometer meas. 8-85763
 magnetosphere, auroral absorpt. substorm onset obs. 8-96362
 metallic particles, low-freq. EM absorption, particle size depend. 8-88311
 particles, small, spherical, reformulation of radiation laws 8-87246
 plasma (fluid), hydrogenic, transverse dielec. function, excitation spectrum 8-67311
 radio waves, rain attenuation on terrestrial and Earth-space propag. paths 8-73490
 rain attenuation at 11 GHz (French) 8-77292
 sandy and clay soils microwave absorption (Russian) 8-81162
 solid surface response to high-power incident flux, with temperature dependent absorptivity 8-51038
 sublimation drying in UHF EM field 8-83936
 H_2O vapour laser 118.6 μm radiation absorption by H_2O vapour, temp. and press. effects meas. 8-75255

electromagnetic wave attenuation see electromagnetic wave absorption; electromagnetic wave scattering**electromagnetic wave diffraction**

- see also electromagnetic wave propagation in plasma; gamma-ray diffraction; light diffraction; X-ray diffraction
 circular cylinder with longitudinal slot (Ukrainian) 8-90345
 concave bodies of rotation, asymptotic field determination method (Russian) 8-82888
 conducting rectangular bar transmission gratings 8-62993
 convex, smooth, ideally conducting and electrically large surface 8-94363
 corner diffraction coeff. anal., Albertsen's formulae 8-62978
 crossed lamellar transmission grating, exam. of diffr. props. 8-59139
 edge diffraction, path integral technique 8-62975
 edge-type reflection gratings, anal. algorithms 8-86998
 field radiation by mag. dipole on smooth convex surfaces 8-62977
 filament moving near metal band (Ukrainian) 8-66709
 generalised shift operator (Russian) 8-78868
 Green's function moment method for solution of two Pocklington type integral equations 8-55279

electromagnetic wave diffraction continued

- hybrid diffraction coefficients for first and second order discontinuities of two-dimensional scatterers 8-82892
 inverse diffraction problem of determining inhomogeneity parameters, solvability (Russian) 8-82889
 Maxwell eqns., asymptotic soln. near caustic edge (Russian) 8-58882
 open cylindrical surfaces, numerical soln. 8-58890
 pattern approximation by laser simulation 8-55287
 periodically rough water surface, thermal radiation critical phenomena (Russian) 8-81188
 planar, asymptotic theory of diffraction by ideally conducting solid of revolution 8-86994
 ponderomotive effect, props. for power meas. appl. 8-71014
 radiation fields in biaxially anisotropic media 8-66723
 scattering pattern calc., diffr. on slit and on strip, asymptotic methods 8-86993
 by small apertures in conducting surfaces 8-82893
 solar radiowaves diffraction and refl. from lunar limb during solar eclipses (Russian) 8-65586
 source dimension estimation from diffraction image using Chebyshev approx. (Russian) 8-82903
 sphere with circular opening, vector problem soln. 8-82891
 thin periodic slab, classical EM wave diffraction, rigorous approach using Green's function 8-82890
 thin phase grating diffr. eqn. solns. 8-54198
 ultrashort-wave diffraction field in shadow of ridge-crests, simulation using dielectric prism 8-86995
 unidirectionally cond. strip, electromag. wave diffr., Wiener-Hopf technique 8-58883
 wide-angle spherical mirror under oblique illum., EM diffr. in focal region 8-58888
 XUV gratings, classical and ionic mountings, EM diffraction 8-63188

electromagnetic wave diffusion see electromagnetic wave scattering**electromagnetic wave interference**

- see also atmospheric; electromagnetic wave interferometers; electromagnetic wave interferometry; electromagnetic wave propagation in plasma; light interference; Moire fringes
 monochromatic wave energy density in nonabsorbent medium with freq. and space dispersion (Russian) 8-74818
 radiowave propagation, tropospheric and precipitation scatter, rel. importance in interference and coordination calcs. 8-73423
 whistler-mode waves focusing and interference in spatially varying mag. field 8-65465

electromagnetic wave interferometers

- see also electromagnetic wave interferometry; light interferometers
 digital interferometer, 2 mm wave, for Tokamak discharges in upgraded DIVA 8-75417
 incoherent energy and coherent time of depolarised microwaves meas. 8-96277
 microwave, electron density meas. on T-II plasma device 8-55754
 microwave plasma diagnostic interferometer with fourfold signal passage 8-87487
 off balance interferometric bridge, using heterodyne detection for recording vibratory phenomena 8-70119
 polarising submillimetric Fourier interferometer with achromatic internal modulation 8-65959
 radio interferometer with long baseline, classical response 8-61733
 radio telescope, amateur, interferometer design 8-85849
 radiowave correlation interferometers rel. to binaural perception and resolving power of bats (French) 8-80883

electromagnetic wave interferometry

- see also light interferometry; Moire fringes
 Australian synthesis telescope, design, array config. 8-69690
 Crimea-Haystack VLBI instrument operation (Russian) 8-69693
 Fabry-Perot interferometer transients, for ultrashort laser pulse generation 8-58019
 fusion reactors, interferometric phase detection system, using high speed digital techniques 8-62629
 microwave for biological movements (French) 8-53469
 radar, linear phase detect. (Italian) 8-85855
 radio sources, compact, mapping from VLBI data 8-89266
 radioastrometric technique, for meas. of parallaxes of objects at cosmological distances 8-53796
 radiowave propag. through turbulent atmosphere, phase difference and derivative fluctuations 8-92951
 Tidbinbilla two-element interferometer system design 8-69692
 tracking correlation receiver with feedback for radioastronomical interferometry 8-57445
 VLBI appl. to geodesy, Earth rot. and network geometry optimisation 8-92996

electromagnetic wave propagation

- see also atmospheric electromagnetic wave propagation; atmospheric light propagation; backscatter; electromagnetic wave absorption; electromagnetic wave diffraction; electromagnetic wave interference; electromagnetic wave propagation in plasma; electromagnetic wave reflection; electromagnetic wave refraction; electromagnetic wave scattering; guided electromagnetic wave propagation; light propagation; light transmission; radiowave propagation
 accelerated dielectric medium, relativistic study 8-81862
 analysis, wave-kinetic method, phase-space path integrals 8-62088
 composite media, EM wave propagation, self-consistent theory 8-56442
 dielectric slab, reflection and transmission coefficients with sinusoidal permittivity variation 8-71011
 Earth, wave type and propag. direction from EM field short-period vars. anal. (Russian) 8-85474
 energy-absorbent media, wave theory generalisation (Russian) 8-77725
 exponential amplification in gravitational field of ultrarelativistic rotating body 8-93594
 ferromagnetic material, nonlinear waves and strong discontinuities (Russian) 8-74819
 ferromagnetic medium, penetration depth calc. (Bulgarian) 8-50679
 field penetration into thick, finitely conducting shell, anal. 8-62990
 homogeneous layer, transmission and refl. coeffs., integral eqn. (German) 8-82907
 Maxwell's equations as one quaternion eqn., appl. to wave propag., for teaching 8-54133
 metal, granular, EM wave propag., self-consistent approach 8-51920

electromagnetic wave propagation continued

- metal-metal interface, plasmon polaritons, computer simulation 8-84276
- metallic rod, uniformly corrugated, E_{01} mode-excited, equiv. dielec. const., simulation 8-78864
- microwave scatter and sea state estimation, ocean wave models 8-77244
- multiple freq. mutual coherence functions for beams in random media 8-66720
- null point source intensity in stationary spherically symmetric space-time 8-57839
- periodic medium, fourth-order Bragg interaction 8-58889
- piezoelectric rods, hexagonal crystal symmetry, wave propagation 8-56429
- plane, waves obliquely incident on moving media, radiation press. 8-71007
- plane wave at skew incidence on right-angled impedance wedge 8-90346
- planetary atmospheres, turbulent, effects of inhomogeneous background on radiation propag. 8-69679
- pulse propag. in random media 8-66715
- quantum mechanics for propagator derivation 8-73886
- radiation fields in biaxially anisotropic media 8-66723
- radiation from charge moving in randomly inhomogeneous media, fluctuation effects (*Russian*) 8-71017
- in random media, degeneracy and inhomogeneity in transport theory 8-62982
- random medium with finite inhomogeneity correl. range, EM wave fluctuations (*Russian*) 8-78870
- semiconductor with superlattice, EM wave propagation, solitons (*Russian*) 8-79999
- slow leaky waves, props. 8-78863
- solid, phase and group vels. determ. for dispersive waves 8-81848
- superconductor, surface EM waves 8-88072
- surface wave propagation through gap between oppositely magnetised ferrite substrates 8-50680
- tensorial permeability and conductivity medium, EM wave propag., ferromag. resonance, spin waves (*French*) 8-74820
- time-harmonic wave propag. in random media problems 8-62980
- transport equations for waves in random media 8-62981
- MnFe ferrites, reson., effect of EM propagation 8-64277

electromagnetic wave propagation in plasma

- see also *ionospheric electromagnetic wave propagation*; *light propagation in plasma*; *magnetospheric electromagnetic wave propagation*
- absorption in randomly inhomogeneous collisionless plasma at resonance frequencies (*Russian*) 8-59598
- absorption near electron cyclotron freq. 8-55723
- amplified scattering of EM waves, in presence of singular point, exptl. obs. (*Russian*) 8-79439
- amplitude modulation anal. 8-75346
- anisotropic collisional plasma half space, interaction of penetrating EM waves 8-55724
- antenna probe, circular aperture, induced HF thermal noise calc. 8-87496
- antenna system, dual integral eqn. method 8-75361
- beam generation of EM waves in plasma (*Russian*) 8-75364
- Brillouin backscatt., nonlinear three-wave interaction 8-75356
- Brillouin sidescatter threshold, non-resonant EM pump field modification 8-67362
- coherent parametric instabilities excited by two or more pump waves, theory 8-57381
- cold lossless plasma half-space, transient response in presence of transverse static mag. field 8-67361
- cold magnetised plasma, radiation pressure forces 8-79437
- collisional effects on low-freq. EM wave propag. 8-75349
- cyclotron absorption in plasma-filled waveguide in nonuniform mag. field 8-51315
- cylindrical plasma, excitation with ring of magnetic currents 8-75347
- dense plasma clarification by strong EM wave self-action 8-75360
- dielectric rod waveguide in magnetoplasma, TM mode propag. 8-51314
- dipole antenna in warm isotropic plasma, boundary-value problem, multiple water bag model 8-91115
- echo oscillations, generated by distributed sources, rel. to exciting field type (*Russian*) 8-71485
- electric current generation by EM radiation 8-71492
- electron cyclotron harmonic waves excitation, lab. expt., rel. to topside ionosphere RF sounder expt. 8-93042
- electron energy distribution, in r.f. elec. field 8-67363
- electron gyroresonance cyclotron oscillation propagation obs. in nonuniform mag. field 8-75351
- electron in monochromatic wave, self-reson. motion 8-66737
- electron wave, transform. into ion wave in multicomponent plasma during quasilongit. propag. 8-73572
- electron-cyclotron resonance, wave propag. at angle to non-uniform mag. field (*Russian*) 8-71487
- electron-ion plasma, stimulated bremsstrahlung light absorption (*Russian*) 8-87438
- enhanced line radiation from active molecular plasmas due to electron collision induced instability 8-71491
- excitation of coherent EM radiation by relativistic beam in plasma surrounded by wall 8-67370
- Faraday rotation, effects of pulsewidth 8-71540
- filamentation instability, temporal growth, EM beam of freq. up to plasma reson. freq. 8-51304
- filamentation instability in magnetoplasma, spatial growth 8-51311
- filamentation instability of extraordinary and ordinary modes in a magnetoplasma 8-83575
- Goos Haenchen negative shifts 8-78865
- heating by microwave absorption, expt. 8-75383
- hydrogenic plasmas and fluids, transverse dielec. function, excitation spectrum 8-67311
- inhomogeneous overdense plasma, nonlinear penetration of strong EM waves 8-75355
- inhomogeneous plasma, self-induced reson. absorption of intense EM wave 8-51306
- inhomogeneous stationary laser plasma, stimulated Raman spectra 8-83578
- ion-acoustic instability suppression by microwave field 8-71466

electromagnetic wave propagation in plasma continued

- laser beam interaction, weakly nonlinear systems, props., discussion 8-93535
- LF wave propag. in relativistic electron gas, rel. to Crab Nebula (*Chinese*) 8-67356
- limit polarisation of EM waves escaping inhomogeneous layer of magnetoactive layer (*Russian*) 8-83570
- linear resonant absorpt., analytic theory 8-51310
- linearised plasma nonstationary signal transition 8-71493
- magnetic plasma layer, echo propag. (*Russian*) 8-75345
- magneto plasma half space, reflected pulse, cyclotron and upper hybrid resonance freq. 8-63569
- magnetoactive plasma parametric instability in HF wave generated field (*Russian*) 8-59566
- magnetoionic plasma, hyperbolic eqn. system, inverse problem 8-75354
- magnetoparametric instabilities, appl. to Crab Nebula 8-61727
- microwave generation by negative-mass instability in ultrarelativistic plasma 8-51289
- microwave high-power absorption localisation, cold cylindrical plasma column 8-51319
- microwave plasma diagnostic interferometer with fourfold signal passage 8-87487
- microwave trajectory and electron cyclotron heating, toroidal plasma 8-59628
- microwaves, critical surface phenomena 8-51313
- monochromatic EM wave excitation by relativistic charge particle beam in magnetoactive plasma (*Russian*) 8-87464
- multiple pump ionospheric heating expt. plasma instabilities obs. 8-57382
- nonlinear absorption in moving plasma, dynamics (*Russian*) 8-91111
- nonlinear bleaching effect in plasma layer, EM freq. below plasma freq. (*Russian*) 8-71488
- nonlinear mixing as a plasma density probe 8-77406
- nonlinear penetration of powerful EM radiation in parametrically absorbing plasma 8-83577
- nonlinear transparency due to modulation instability (*Russian*) 8-59604
- nonlinear transparency of dense plasma layer 8-87454
- plasma sounding with finite-radiation-pattern source (*Russian*) 8-59606
- population inversion, soft X-ray transitions in cooling plasma, H-like ions 8-87437
- radiation pattern of open ended waveguide in air core surrounded by annular plasma column 8-67366
- radiation scattering due to cylindrical plasmas excited by ring of elec. currents 8-67357
- radio waves interaction in ionospheric plasma, nonstationary processes (*Russian*) 8-93028
- reflection of impulsive plane wave by plasma half-space moving perpendicular to incident plane 8-67360
- reflection of resonance cone and plasma-filled waveguide modes 8-67365
- reflection process from nonhomogeneous plane stratified plasma 8-87453
- resonance absorption, in laser-produced plasma, X-ray bremsstrahlung emission obs. 8-59559
- resonant absorption, theory and expt. 8-75353
- resonant absorption of laser light, by magnetised plasma 8-51309
- resonant wave-particle interaction at ion gyroharmonic freq. 8-83574
- RF plugging, nonadiabatic, in cusped field, ion heating effect 8-59656
- RF wave heating of 26 keV ion beam trapped in Tokamak 8-59627
- scattering by moving plasma column, cross-polarisation analysis 8-75352
- second harmonic generation by Gaussian beam 8-91112
- self-focusing, plasma flowing transverse to EM beam, kinetic approach 8-59602
- self-focusing 8-75357
- selflocalised EM fields in dense plasma 8-75350
- skin effect of microwaves and transverse pseudowaves 8-59600
- slab-shaped magnetoplasma excitation by magnetic current line sources 8-55717
- spiral electromagnetic waves, Landau and Cerenkov damping in mag. plasma, theory (*Russian*) 8-71486
- stimulated combinational scatt. and particle trapping 8-75358
- stimulated incoherent EM wave scattering on enhanced fluctuations in bounded plasmas 8-83576
- stimulated Raman and Thomson scatt., beat-wave electron trapping 8-51308
- stimulated Raman backscatt. of circ. polarised EM wave 8-91113
- stimulated Raman backscattering from preformed underdense plasma 8-71490
- stimulated Raman scattering, of finite length EM waves (*Russian*) 8-83571
- stimulated scattering, polarisation effects (*Russian*) 8-79440
- strong EM waves in collisionless homogeneous plasma, waveform, polarisation and nonlinear effects 8-53809
- strong waves in collisionless homogeneous plasma, waveform, polarisation and nonlinear effects 8-53809
- surface wave propagation along lossy cylindrical plasma column 8-75315
- thermal modulational instability and stratification 8-75332
- third harmonic generation by Gaussian EM beam in magnetoplasma 8-83572
- Thomson scattering of EM pulses by random fluctuations, self-focusing effects 8-83573
- two dimens. supersonic plasma frontwave propag., intense laser on gas 8-87470
- wave packet self focusing in medium with striction nonlinearity, numerical simulation 8-83042
- waveguide, plasma-filled, propag. and attenuation characts. 8-67367
- whistler wave ducting caused by antenna actions 8-59586
- whistler waves in finite plasma, dispersion and attenuation 8-63570
- whistler-mode waves focusing and interference in spatially varying mag. field 8-65465
- whistlers, group vel. in two-ion plasma 8-87452
- Ar plasma, electron density, microwave refl. meas. 8-59674
- Ne discharge, wavenumber spectra of turbulent ionisation waves 8-71541

electromagnetic wave reflection

- see also electromagnetic wave propagation in plasma; light reflection; X-ray reflection*
 accelerated dielectric medium, relativistic study 8-81862
 D-region, partial reflections, sensitivity to irregularity comp. 8-81495
 dielectric slab, 3 cm microwave refl., longit. displacement 8-62973
 dielectric slab, reflection and transmission coefficients with sinusoidal permittivity variation 8-71011
 E-layer, oblique incidence propag. and ionospheric attenuation 8-73578
 ferrite, magnetised, nonreciprocal refl. of EM waves 8-71006
 ferrites, mag. permeability meas. method, UHF wave total internal reflect. 8-57994
 Goos Haenchen negative shifts 8-78865
 homogeneous layer, transmission and refl. coeffs., integral eqn. (*German*) 8-82907
 inhomogeneous medium with permitt. perturbation 8-86996
 ionosphere, equatorial, theoretical model of spread-F echoes in HF and VHF bands 8-85764
 ionosphere, polarisation of reflected SW radio waves on slant path 8-73573
 nonlinear medium, plane boundary, simple wave theory appl. 8-78866
 radar, differential reflectivity and differential phase shift 8-57270
 radar reflections in rock salt 8-96215
 radar reflectivity variations with height due to wind shear on rain cells (*French*) 8-53682
 radiation fields in biaxially anisotropic media 8-66723
 reflection coeff. meas., computer controlled network analyser calibration 8-89463
 reflection coefficient discontinuity in total internal refl. from inverted population region (*Russian*) 8-58891
 semi-infinite solid-state phase grating, optical props. 8-87155
 solar radiowaves diffraction and refl. from lunar limb during solar eclipses (*Russian*) 8-65586
 time domain reflection from inhomogeneous and dispersive slabs 8-62985
 VHF radar signals, partial refl. and scatt. from clear atmosphere 8-81278
 VHF radar signals partial refl. from troposphere 8-85656

electromagnetic wave refraction

- see also electromagnetic wave propagation in plasma; light refraction*
 atmosphere, microwave refraction coeff. rel. to humidity 8-69398
 atmosphere, radio refr. index struct. parameter height distrib. with lower boundary spatial transition 8-73491
 atmosphere, refr. index struct. parameter from refractivity and amplitude scintillation meas. at 36 GHz 8-81316
 atmospheric radiowave refractive index meas. using digital refractometer 8-86321
 EHF clear air refractivity calc. procedure 8-57266
 inhomogeneous stratified atmosphere, normal-wave soln. 8-53710
 microwave birefringence at gyrotropic boundary by inclined plane wave (*Slovak*) 8-55281
 nonlinear medium, plane boundary, simple wave theory appl. 8-78866
 radiation fields in biaxially anisotropic media 8-66723
 radiowave refraction during transillumination of planetary atmospheres 8-96413
 troposphere, radiowaves refr. rel. to oblique-incidence sporadic-E propag. 8-73578
 troposphere, refr. theories of radio wave propag., review 8-69425
 troposphere, refraction effects on satellite range meas. 8-73609
 tropospheric range correction algorithm 8-61591

electromagnetic wave scattering

- see also backscatter; electromagnetic wave propagation in plasma; gamma-ray scattering; light scattering; X-ray scattering*
 arbitrarily shaped dielectric body inside waveguide, three-dimensional anal. 8-71005
 atmosphere, radiances in absorpt. bands, calc. methods including multiple scatt. 8-61554
 atmosphere, solar radiation absorpt. by H₂O vapour, including multiple scatt. 8-61553
 attenuation caused by rain above 10 GHz freq. (*French*) 8-53686
 azimuthal angle of T-D mode induced scatt. from parametric ion-acoustic wave 8-75322
 backscatter matrix of dielectric spheroids 8-66716
 boundary element calculation method 8-90347
 classical system, stimulated emission and absorpt., appl. to free electron laser 8-63047
 conducting cylinder arrays interspaced by inhomogeneous dielec. 8-78862
 conducting half plane below stratified overburden 8-57167
 from corrugated conducting surfaces with inhomogeneous surface impedance, anal. 8-62987
 by corrugated periodic trapezoidal conducting surface, TE/TM polarisation 8-62994
 dielectric scattering alternative surface current formulation 8-62991
 dielectric spheroids and ellipsoids, integral eqn. soln. 8-85622
 differential attenuation at 13 GHz and 20 GHz on 53 km link (*French*) 8-53684
 diffraction on slit and on strip, scatt. pattern calc., asymptotic methods 8-86993
 by E-region anisotropic inhomogeneities oriented along geomag. field 8-53771
 echo cross-section of longitudinally slotted cylinder, method of moments anal. 8-86992
 EM wave rain induced attenuation and cross-polarization calcs. (*French*) 8-53677
 Ewald-Oseen extinction theorem, Maxwell's eqns., boundary-value problem 8-62974
 finite cylindrical scatterer near imperfectly conducting ground 8-71003
 forward scattering anomaly in hollow penetrable body 8-62986
 forward scattering in random media, path integral approach 8-62979
 grating of parallel conductors scattering anal. 8-50682
 Green's function moment method for solution of two Pocklington type integral equations 8-55279
 incoherent backscatter from rough surfaces, two-scale model re-examined 8-71013
 inhomogeneous media, characterisation via space-variant transfer functions 8-71012
 inhomogeneous sphere, system of p-tuple series eqns., iterative soln. 8-62976

electromagnetic wave scattering continued

- ionosphere, auroral, field-normal plasma-line scatt. detect. expt. 8-73580
 ionosphere, incoherent scatter radar meas. at Arecibo Observatory 8-81488
 ionosphere, intersatellite whistler-mode pulses scatt. 8-69605
 ionosphere, stimulated Brillouin scatt. detect. by Jicamarca radar 8-77412
 microwave attenuation due to rainfall, rain fine structure meas. (*French*) 8-53680
 microwave backscatter modulation by shoaling ocean waves 8-57212
 microwave cross-polarization due to precipitation in atmosphere (*French*) 8-53674
 Mie series solution for sphere, computer program 8-66721
 mode-matching method for two-dimens. scatt., smoothing process 8-58886
 by multiple rectangular cylinders, numerical anal. 8-62992
 multiple scattering of classical EM waves by fixed dielectric obstacles, Fredholm's method 8-71008
 noise field scatt. by large cylinder of finite length (*Russian*) 8-55284
 non-spherical hydrometeors scattering properties (*French*) 8-53676
 ocean surface, radar backscatter rel. to wind speed and fetch 8-77247
 ocean wave scattering theories, review 8-77243
 offset two-dimensional Gaussian beam wave by cylinder, anal. 8-86997
 particles, small, spherical, reformulation of radiation laws 8-87246
 penetrable inhomogeneous scatterer, numerical comp. of scatt. 8-66719
 perfectly conducting spherical shell with circular aperture 8-71015
 periodic dielectric struct., appl. of unimoment method 8-66725
 periodic surface, uniqueness theorems for scattering (*Russian*) 8-49677
 radar backscatter from ocean surface, friction vel. depend. 8-77246
 radiation and scatt. from wires and surfaces, free space impedance functions 8-86999
 radiotelescope, chromatism due to blocking and feed scatt. 8-73630
 radiowave from semi-infinite plate, linear algebraic eqns. infinite system soln. 8-55286
 radiowave propagation, tropospheric and precipitation scatter, rel. importance in interference and coordination calcs. 8-73423
 radiowave studies of ionosphere, incoherent scatter technique development, review 8-81503
 rain attenuation and depolarization of Earth-satellite transmissions at freq. greater than 10 GHz (*French*) 8-53689
 rain attenuation distribution distribution (*French*) 8-53688
 rain depolarization statistical distribution for microwave signal propag. (*French*) 8-53673
 rain induced attenuation and cross-polarization calcs. (*French*) 8-53677
 rain induced signal fluctuations, incoherent effects investigation (*French*) 8-53679
 rain-induced polarization, theoretical model of wind gust effects (*French*) 8-53678
 random media, wave propag. and weak scatt. 8-66722
 random rough-surface model, comparison of variational, perturbational and exact solns. 8-66724
 rotating dielectric column, EM scatt., relativistic soln. 8-50681
 rough dielectric surface, EM wave scatt. 8-58885
 rough semi-infinite dielectric plane 8-58884
 rough surfaces, full wave and physical optics solns. 8-66717
 scattering current/aperture coupling relationship for thin finite cylinders 8-62988
 sea ice, scattering from slightly rough boundary 8-77266
 by spherical shell with arbitrarily located circular aperture, anal. 8-62989
 subsurface line conductor, multiple EM scatt. 8-61317
 surface scattering from piecewise planar surfaces, algorithm 8-62983
 symmetric cylindrical conductor, mode-matching method calc., smoothing process 8-58887
 thin finite dielectric fibres, scatt. analysis 8-62972
 time depend., boundary value formulation, integro-differential eqns. 8-66726
 two-dimensional transient scattering, new space-time integral eqn. 8-78861
 UHF/SHF tropospheric scatter radio links, scanning beams 8-81276
 vacuum, transition radiation and scatt. in strong EM field (*Russian*) 8-58895
 variational principle for random rough surface scattering 8-55285
 VHF ionospheric forward scattering, effect of meteors (*Japanese*) 8-81504
 VHF radar signals, partial refl. and scatt. from clear atmosphere 8-81278
 Wiener-Hopf matrix factorisation for problems solvable with Hurd's method 8-66718
- electromagnetic waves**
see also bremsstrahlung; Cherenkov radiation; electromagnetic field theory; electromagnetism; gamma-rays; heat radiation; light; microwaves; radiofrequency cosmic radiation; solar radiofrequency radiation; sunlight; synchrotron radiation; transition radiation; undulator radiation; whistlers; X-rays
 biological effects, state of research (*German*) 8-88728
 charged particle beam interaction, localised disturbances development (*Russian*) 8-88377
 closed region problems, singularity extraction in kernel functions 8-66728
 conversion of gravitational waves into electromagnetic waves by a moving charge 8-93584
 cyclotron radiation from oppositely directed electron beams 8-78874
 dielectric materials, electromagnetic radiation in crack formation process, exam. 8-76771
 field calculation using integral eqn. method (*Russian*) 8-82887
 field structure spatial spectra in millimetre and submillimetre wave ranges (*Ukrainian*) 8-90344
 field three-dimensional energy distrib. 8-71009
 HF discharge, EM wave ionisation instability model 8-67512
 nonlinear medium nondegenerated wave interaction with amplification, stochasticity occurrence (*Russian*) 8-83027
 radiant-energy exchange by small objects using continuum fields 8-82894
 radiation fields in biaxially anisotropic media 8-66723

electromagnetic waves continued

- Smith-Purcell radiation generated by electron beam, non-redundant spectral tunnelling 8-78906
- spherical, reproduction by real meas. devices, from combined radiating sources (*Russian*) 8-85729
- time-domain electromagnetics and its appl. 8-71010

electromagnetism

- see also *electric fields; electrodynamics; electromagnetic field theory; electromagnetic induction; electromagnetic oscillations; electromagnetic waves; magnetic fields; magnetism*
- Biot Savar law, quantum mechanical generalisation, mag. field from current of assigned geometry 8-70997
- closed region problems, singularity extraction in kernel functions 8-66728
- Coulomb's law in moving medium, Maxwell's eqns. and Dirac function, for teachers 8-61987
- Helmholtz equation, soln. in neighbourhood of corner 8-90335
- Helmholtz homogeneous equation, numerical soln. methods (*German*) 8-90337
- isotropic-anisotropic media boundary, light refl. and refr., Maxwell theory (*German*) 8-87007
- lightning return stroke, EM fields radiation, Maxwell eqns. exact soln. appl. 8-73442
- magnetic field calc., two-dimens., boundary integral eqn. method 8-94355
- Maxwell's eqns., boundary-value problem, Ewald-Oseen extinction theorem 8-62974
- Maxwell's eqns. in matter, covariant formulation 8-57798
- Maxwell's equations, derivation from local gauge invariance 8-54109
- Maxwell's equations, exact soln. for isotropic nonlinear medium (*Russian*) 8-62971
- Maxwell's equations, inside and outside of source, vector spherical harmonics, for teachers 8-81747
- Maxwell's equations in ferromagnetic materials, asymptotic solns. (*Italian*) 8-78860
- Maxwell equations, time-invariant, theory in arbitrary dimensional fields (*German*) 8-90336
- H.C. Oersted, first spark of electrotechnology, biography (*French*) 8-69955
- photoelastic stress anal., relationship between optical theories 8-63302
- rotating charged dust, Newtonian and general relativistic treatments 8-73908
- six dimensional space time formalism of electromagnetism, mag. monopole behaviour of electrically charged tachyons 8-54182
- spherical laser plasma, classical optics and light press. 8-59601
- Stormer problem, periodic motions in mag. dipole meridian plane 8-85841
- Stormer problem, periodic motions in mag. dipole meridian plane 8-89053
- two-phase conducting diamagnetic system, coeff. of EM ejection of particles (*Russian*) 8-94364
- vector fields, Debye pot. representation 8-73797

electromagnets

- see also *coils; superconducting magnets*
- betatron electromagnet pulsed power supply 8-82546
- Bitter coils, axial compression of a coreless mag. coil by fibreglass cylindrical housing 8-93741
- coercimeter, with cylindrical attachable electromagnet, exam. of design 8-76809
- deflecting septum magnet for cyclic accelerator 8-78525
- eddy-current problems, including moving Fe parts, numerical soln. 8-90340
- ferromagnetic parts, magnetisation by use of applied electromagnets 8-72999
- fusion reactor, JET, inner poloidal field coil mechanical design 8-50387
- fusion reactor, JT-60, poloidal field coil internal voltage oscills. 8-50386
- fusion reactor, PDX canned poloidal coils, design, fabrication and mag. alignment 8-50385
- fusion reactor, PDX poloidal field coil power tests 8-50384
- fusion reactor, RFC-XX, coil system, design, fabrication, testing 8-55007
- fusion reactor, TEXT toroidal field coil stress anal. 8-50381
- fusion reactor, TFTR poloidal field coils design details 8-50383
- fusion reactor, three-dimens. solid finite element anal. for simulating composite windings 8-55003
- fusion reactor, TMX, magnets, mech. design 8-58494
- fusion reactor, toroidal device with nonplanar mag. axis, magnet and coil engineering 8-55009
- fusion reactor anisotropic B_z-coil two-dimens. finite element anal. of laminate sliding 8-50382
- fusion reactor B_z-coil stress anal., constraint finite element anal. for contact problem 8-55004
- fusion reactor coil design, cost anal., for neutral beam magnets 8-55005
- fusion reactor coil design codes 8-66367
- fusion reactor magnet coil, 125 kG, 1 m, design, fabrication 8-55008
- fusion reactor toroidal field coil stress anal., cost effective procedures for TFTR 8-50379
- geometrical design expressions, for electromag. used in NDT equipment 8-85102
- inhomogeneous magnetic field from electromagnet produced by parallel shift of central axis of one pole 8-55276
- insulation systems, features 8-89506
- magnetic induction stabilised source 8-94360
- megagauss field production by Cnare effect 8-93739
- miniature, liquid N₂ cooled, features 8-74036
- NMR radiospectrometer electromagnet field uniformity rel. to pole piece shape and material 8-86309
- PDX toroidal field coil mag. force distrib. anal. 8-50380
- poloidal field coils for Tokamak 8-62645
- semiautomatic digital coercimeter, exam. of design 8-76817
- shell-type, with supersaturated polepieces, field topography 8-74033
- Tokamak fusion, Impurity Study Experiment, mag. field calcs. using GFUN-3D programme 8-66368
- toroidal field ripple for Tokamaks, magnetics design 8-62643

electromagnets continued

- windings with constant current density, maximum permissible mag. field 8-57990
- ZGS beam transport for transverse and longitudinally polarised protons 8-55074

electromechanical effects

- articular cartilage, electromechanical props. during compression and stress relaxation 8-92667
- cholesteric liquid crystal, shear electricity, symmetry considerations 8-60394
- electron inertial effect, shock loaded rod, meas. of strain produced 8-51139
- nematogen, flexoelectricity in isotropic phases 8-63672
- PMMA, shock-wave compressed, dielectric props. 8-80281
- protein membrane, double layer mediated energy conversion using imposed freq. and wavelength 8-88695
- TBK-3, ferroelectric ceramic, 90° electric domain processes, mech. stress, X-ray diffr. 8-72478
- TsTS-23, ferroelectric ceramic, 90° electric domain processes, mech. stress, X-ray diffr. 8-72478
- Al₂O₃-loaded epoxy, shock-wave compressed, dielectric props. 8-80281
- BaTiO₃, 90° electric domain processes, mech. stress, X-ray diffr. 8-72478
- KTaO₃, light-sensitive surface-barrier generation of acoustic vol. waves 8-63252
- Pb_{0.95}KNb_{0.05}O₁₅, strong electromechanical coupling of SAW 8-63919
- PbZr_{0.95}Ti_{0.05}O₃, impact loading, mech. and elec. response, elec. state effect 8-64317

electromechanical filters

- α-quartz SAW temp. depend. 8-51813

electrometers

- see also *charge measurement*
- DC amplifier using MOS transistor, features 8-77933
- electrometer/ratiometer of high sensitivity and precision 8-70154
- fast response electrometer for pulse reactor experiments 8-70157
- logarithmic, fast response, for pulse-reactor expts. 8-86291
- MOS transistor electrometer, current noise meas. 8-54398
- vibrating-capacitor electrometer, current noise meas. 8-54398

electrometry see electrometers**electromigration**

- concentration profiles produced by thermo- and electrotransport, calc. (*German*) 8-83995
- defected stripe, current crowding and flux divergence 8-71885
- dipole translation between crystallographic sites, absence of direct force 8-83993
- excited atomic states in EM field, ionisation by electron diffusion (*Russian*) 8-86798
- grain-boundary electromigration, anal., composition profiles from steepest descent methods 8-67849
- liquid alloys, driving force expression 8-51714
- metal, isotope enrichment by combined elec. migration and zone melting 8-76600
- metallic thin films, electromigration, and diffusion, new examination technique 8-67852
- resin particles, dispersed, precipitation on cellulose fibre in elec. field 8-53262
- Schottky-barrier metal-semiconductor junction carrier migration and equivalent cct. analysis (*Russian*) 8-84294
- Ag alloys, purification of solid metals by electrotransport (*German*) 8-51745
- As₂S₃, amorphous, electrodiffusion profile meas. of Ag migration 8-87822
- Au, of ⁵⁷Co, profile shift and steady state methods at different temps. 8-71881
- Cu alloys purification of solid metals by electrotransport (*German*) 8-51745
- Fe-C (0.52 wt.%), FCC structure, exam. of electromigration of C by steady state method 8-75865
- GaP: Au, diffusion, solubility, and electrotransport of Au 8-91489
- β-Hf, electrotransport and diffusion of Ta impurities (*German*) 8-87826
- α-Hf, electrotransport of O impurities (*German*) 8-87826
- Na-K, liq. alloys, electromigration driving force expression 8-51714
- Na-Rb, liq. alloys, electromigration driving force expression 8-51714
- Nd, single crystal prep. by solid state electrotransport 8-84709
- Pb, of ⁶⁴Cu, investigation by steady state method 8-71882
- Pb, of Cu, isothermal conditions, steady state method 8-84003
- Pb, of Ni, steady-state method 8-87820
- Pb, single crystal prep. by solid state electrotransport 8-84709
- Sn-In dil. liq. alloy, electrodiffusion and electroconvection, effective diffusion coeff., apparent effective valence 8-87802
- Sn-Sb dil. liq. alloy, electrodiffusion and electroconvection, effective diffusion coeff., apparent effective valence 8-87802
- Th metal, diffusion and electrotransport of Th metal 8-86611
- Th, of V, Nb and Ta, 1370-1665°C 8-59979
- ThO₂-based ceramic impurity diffusion, electrotransport method 8-67869
- TiO₂, rutile ceramic, ageing in strong elec. field (*Polish*) 8-52869

electromotive force see electric potential**electron absorption**

- see also *beta-ray absorption*
- metals, electron absorpt. and transmission characts., 5 to 30 keV, film-massive block method 8-88387
- semiconductors, electron absorpt. and transmission characts., 5 to 30 keV, film-massive block method 8-88387
- water, distrib. in water, Al, Fe and Pb, 22 MeV electron bombardment 8-59840
- Al, 22 MeV electron bombardment, bremsstrahlung distrib. 8-59840
- Fe, 22 MeV electron bombardment, bremsstrahlung distrib. 8-59840
- Pb, 22 MeV electron bombardment, bremsstrahlung distrib. 8-59840

electron accelerators

- see also *betatrons; electron ring accelerators; microtrons*
- charged transmission line for pulsed high current accelerators, energy transfer 8-78519
- colliding e⁺e⁻ beams accelerator expts., 100 GeV, particle prod., weak currents, etc. (*Russian*) 8-58194
- computerised pulse radiolysis system 8-64862

electron accelerators continued

- Darmstadt linear accelerator, detector system and performance of elec. scatt. system 8-70680
 Darmstadt linear accelerator electron scatt. facility, beam transport and spectrom. 8-70679
 Darmstadt linear accelerator electron scatt. facility, data processing 8-70681
 Darmstadt linear accelerator high resolution scatt. facility 8-70653
 diode type, with large-beam cross section 8-78517
 electron guns, high-current, laminar beam formation 8-74516
 ETL linear accelerator, energy increased up to 40 MeV by improvement of klystron efficiency (*Japanese*) 8-78515
 GELINA, electron linac, neutron time of flight meas. appl. 8-90002
 high current electron beam of TONUS accelerator, time struct. (*Russian*) 8-66434
 high energy low running cost linac, proposed design (*Japanese*) 8-78516
 linear, high-current injector 8-70655
 linear, pion production and appls. (*Japanese*) 8-78533
 linear, radioisotope production, review (*Japanese*) 8-78534
 linear, status, uses, 500 MeV 100 kW linac design (*Japanese*) 8-78514
 linear accelerator, dose monitoring system 8-92710
 Mainz 300 MeV linear accelerator, energy loss system of electron scatt. facility 8-58524
 neutron production by electron linear accelerator beam (*Japanese*) 8-78532
 neutron yield calcs., electron beam incidence, radiation protection implications for accelerators 8-95622
 pulsed electron accelerator current density distrib. multichannel recorder 8-58520
 pulsed giving 20 ps 300 A electron pulses, radiation chem. appls. (*Japanese*) 8-80754
 radiotherapeutic linear electron accelerator NEPTUN-10p 8-88744
 relativistic electron beam accelerator, FX-75, 1-D coaxial transmission line model, FXPULSE program 8-58506
 self-magnetic insulation in vacuum for coaxial geometry 8-78520
 standing wave linear high gradient structure, design concept 8-50423
 synchrotron, electron beam spot, photographic obs., rel. to amplitude of betatron oscillation 8-55059
 synchrotron radiation formation, role of betatron vibrs. (*Russian*) 8-50684
 Tohoku 300 MeV Linac, energy compressing system 8-74515
 undulator linac, electron dynamics, coherent radiation source 8-82539
 ep colliding beams 8-78531
 H₂O, dielectric insulation for electron accelerators and impulse current generators (*Russian*) 8-75430

electron affinity

- alkali atom+methane derivative, collisional ionisation, nitromethane, perfluoromethyl bromide (iodide) electron affinities 8-66639
 atomic electronegativity scale rel. to work function 8-64096
 diatomic molecules, containing elements from Li to F and Na to Cl, calc. from mol. dissoc. energies 8-62943
 formaldehyde, and cation, vertical proton affinity in singlet and triplet states 8-90079
 formaldehyde, proton affinity determ. from chem. reaction equilib. const. 8-85189
 hexafluorides, MF₆, M=S, Se, Te, Mo, W, Re, Ir, Pt ionisation 8-55226
 insulator, rel. to secondary electron escape probabilities 8-72651
 methoxide-d₀(-d₃) anion, electron affinity, vibr. struct., photodetachment electron spectra 8-94282
 methylene, electron affinity, ¹A₁-³B₁ T₀-value, ab initio MRD-CI method calcs. 8-50478
 methylene anion, electron affinity, ¹A₁-³B₁ T₀-value, ab initio MRD-CI method calcs. 8-50478
 MNDO semi-empirical SCF-MO calcs. for atoms, mols., negative ions 8-74578
 open shell systems, coupled cluster approach 8-58595
 thiomethoxide anion, electron affinity, vibr. struct., photodetachment electron spectra 8-94282
 water, proton affinity, many-body Rayleigh-Schrodinger perturbation theory 8-92497
 B, electron affinity, modified variational approx. 8-66679
 C, electron affinity, modified variational approx. 8-66679
 CH₃, experimental determ. of the geometry and electron affinity 8-82860
 F, electron affinity, modified variational approx. 8-66679
 HC₂ radical, electron affinity, ab initio SCF and CI calcs. 8-50468
 HCN, proton affinity determ. from chem. reaction equilib. const. 8-85189
 HCN⁻, SCF ab initio ground state pot. energy surface, geometry, rel. to HCN 8-78646
 H₂O, electron affinity, mol. geom. effects calcs. 8-82618
 H₂O⁻, electron affinity, mol. geom. effects calcs. 8-82618
 H₂S, proton affinity determ. from chem. reaction equilib. const. 8-85189
 K+halogenated methane, negative ion form., electron affinities, bond dissoc. energies 8-82827
 LiH, positron affinity, ab initio LCAO MO SCF calc. 8-82870
 N, electron affinity, modified variational approx. 8-66679
 O, electron affinity, modified variational approx. 8-66679
 Rb⁻, photodetachment, electron affinity 8-90132
 Rb-tetrahydrofuran soln., photolysis, photoelectron emissive EPR signal, scavenger electron affinity reactivity 8-53224
 Xe-MF₆, M=W, Mo, U, Re, Ir, charge transfer interactions, VUV and IR obs. 8-50664

electron annihilation *see electron-positron interactions***electron attachment**

- atomic electron scatt., correlation effects 8-58842
 ion-ion collisions, crossed beam expts. 8-58843
 molecular electron scatt., dissoc. attachment, resonant states 8-58851
 molecular electron scatt., dissoc. attachment 8-58849
 molecular electron scatt., dissoc. attachment 8-58850
 molecule, dissociative attachment of electrons 8-62931
 two-particle-hole Tamm-Dancoff approximation (2ph-TDA) equations for closed-shell atoms and molecules 8-70937
 Br₂, dissoc. attachment by 0-8 eV electrons 8-74776
 CH⁺, continuum electron wavefunction, electron capture width 8-78805

electron attachment continued

- CO₂, gas ionis. by nozzle expansion, negative Van der Waals polymer mols. form. 8-90307
 Cl₂, dissoc. attachment by 0-8 eV electrons 8-74776
 D₂, dissociative electron attachment, Faddeev calcs. of cross sections (*Russian*) 8-70945
 F₂, dissoc. attachment by 0-8 eV electrons 8-74776
 F₂-inert gas mixtures, transport and attachment processes 8-59542
 H₂, dissociative electron attachment, Faddeev calcs. of cross sections (*Russian*) 8-70945
 HBr, dissociative attachment of electrons 8-62931
 HCl, dissoc. electron attachment kinetics in flame, mass spectra obs. 8-68872
 HCl-N₂ mixture, electron swarm, Cl⁻-HCl cluster formation, dissoc. attachment, drift tube mass spectra 8-68884
 HD, dissociative electron attachment, Faddeev calcs. of cross sections (*Russian*) 8-70945
 H₂O, Van der Waals polymer mols., negative ions formed in nozzle expansion 8-90296
 I₂, dissoc. attachment by 0-8 eV electrons 8-74776
 I₂, dissociative attachment, thermal energy electrons 8-82850
 N₂, dissociative electron attachment, N⁻(³P) form. 8-90308
 NH₄⁺, dissoc. electron recombination cross-sections, 0.065-2 eV 8-66671
 NO, dissociative electron attachment, N⁻(³P) form. 8-90308
 N₂O, gas ionis. by nozzle expansion, negative Van der Waals polymer mols. form. 8-90307
 N₂O, mech. of thermal electron attachment, microwave cond. meas. 8-59536
 N₂O-hydrocarbon mixtures, mech. of thermal electron attachment, microwave cond. meas. 8-59536
 SO₂XY, (X,Y=Cl,F), positive and negative ion chemistry 8-85140

electron avalanches

- dielectric solid surface breakdown in vac., desorption mechanism 8-67464
 electron swarm develop., Boltzmann eqn. anal. 8-79487
 gas mixture electron avalanche multiplication in cylindrical elec. field 8-67557
 MWPC, avalanche ang. localisation 8-50434
 one-sided abrupt junctions, distinction between avalanche and tunnelling breakdown 8-56211
 proportional counter, methane filled, influence of electron avalanche KE on gas amplification factor 8-50439
 proportional counters, avalanche spatial distrib. 8-58543
 sphere-plane gap avalanche current pulse meas. in nonuniform fields 8-67556
 Al-Al₂O₃-electrolyte, electroluminesc., nondestructive electronic avalanche 8-68563
 SF₆ avalanche breakdown as stochastic process 8-67574

electron beam absorption *see electron absorption***electron beam applications**

- see also electron beam deposition; electron beam machining; electron beam welding; radiation therapy*
 collective ion acceleration, by temporally modulated relativistic electron beam 8-50422
 compact source for neutral beam production of very low vapour press. materials 8-70225
 dye gas laser, excitation by elec. discharge, electron beams, optical stimulation (*Czech*) 8-79016
 foilled anode electron-beam laser with chopper-wheel gas pulser 8-63122
 GEOS electron beam experiment S 329 8-93075
 holography, appls. and theory review, background and current status 8-74866
 ionisation in electrostatic precipitators, coal processing technology appl. 8-57346
 multigas electron beam pumped lasers 8-94396
 relativistic electron beam Raman laser 8-74877
 surface thickness monitoring, object accessible from one side 8-60944
 thermoplastic light modulators, status and prospects 8-79138
 VHF resonator radiant energy meas. (*Russian*) 8-77944
 CO₂ laser amplifier, high power large aperture electron beam controlled, development (*Japanese*) 8-66846
 CO₂ laser electron beam pulsed, sealed electron guns 8-71119
 Co, growth of single crysts. by electron-beam floating zone method 8-68624
 N₂ electron-beam-sustained discharge stability model 8-71608

electron beam deposition

- glass films, struct. mech. and optical props. (*Czech*) 8-80469
 metal-semiconductor thin film preparation under UHV conditions 8-72733
 MIS structure, Al₂O₃ insulating layer, electron gun evaporated, HF C-V characts. and surface state density 8-84310
 multisource deposition rate control using mass spectrometer as sensing element 8-72730
 scale-up problems 8-72722
 scale-up problems in electron-beam evaporation and sputtering 8-95695
 SOS structure, radiation dose at interface due to electron beam aluminisation 8-68089
 superconducting compound film, electron beam codeposition, synthesis and props. 8-72296
 wear resistant surface, review 8-72938
 Al film, vacuum deposited, rate and press. depend. of contamination 8-72732
 Al film deposition on Kapton laminates by electron beam evaporation 8-76603
 Al, on SiO₂ in FET, effect on electron trapping 8-80060
 Al, step coverage optimisation by computer simulation and SEM 8-51838
 Al₂O₃ film deposition, heating of multiple layer structs. (*Russian*) 8-92192
 Al₂O₃, thick vacuum condensates, electron microscopy struct. investig. (*Russian*) 8-95242
 CdS-Si n-p heterojunction photodetector, fabrication and characts. 8-52068
 Cr, columnar struct. rel. to deposition conditions 8-52675
 Fe, columnar struct. rel. to deposition conditions 8-52675
 Mo film, vacuum deposited onto SiO₂-Si substrates, elec. resist. 8-76166

electron beam deposition continued

- Si electron beam deposited film, epitaxy by pulsed laser annealing 8-56055
- Si, polycrystalline ribbon prep. by electron bombardment (*French*) 8-64474
- TiO₂, metal-TiO₂-Si structure, I-V characteristics, deposition, post-deposition oxidation effects 8-80063
- ZrO₂, film, refr. index and microporosity 8-90467

electron beam effects

- see also *beta-ray effects; cathodochromism; cathodoluminescence; electron impact; plasma-beam interactions*
- alkali halides, influence of purity of crystals on stability of F-centres and interstitials 8-91336
- anthracene, electron irradi., creation and evolution of excited states, scintillation obs. 8-92128
- α -brass, electron irradiated, defect production and interdiffusion 8-67739
- closed liquid Ar circuit for electron irradi. of LiH at 90K (*French*) 8-62214
- diamond, type Ib, electron irradiated, migration of N, optical absorption meas. 8-56505
- dislocation damping during electron irradiation, new model for peaking effect 8-87683
- energy loss in electron beam lithography, Bethe and Spencer-Fano theories 8-87728
- film dosimeters, calorimeter for calibration in high intensity electron fields 8-73257
- gas laser operation, fast electron beam irradi. effects (*Russian*) 8-74878
- heavy particle beam cooling in an electron flux, mag. field effects 8-82557
- ionic crystal, exposed to high-current electron beam pulses, min. size of excited region for crack initiation (*Russian*) 8-84961
- mag. limiter plate, electron irradi. and thermal shock 8-66416
- magnetosphere, high-latitude, Echo 4 beam interactions from artificial auroral streaks obs. 8-89036
- metal, defect annealing study by positron annihilation, and elec. resistivity meas. 8-51584
- metals, appl. of KUR LINAC to radiation damage studies 8-71760
- minority carrier diffusion length, Schottky barriers, electron bombard. investigation 8-68037
- MOS devices with 500 Å and 700 Å thick oxides, saturation radiation effects 8-60209
- piezoelectric ceramic, excitation of acoustoelectric oscills. by ionising radiation 8-56191
- piezoelectric crystal surface, periodic film form. due to SAW 8-72038
- plasma return current discharge, prod. and heating of large-volume plasmas 8-94920
- plastic fibre-optic waveguide, effect of ionising radiation on optical attenuation 8-63170
- polycarbonate, impact behaviour, effects of thermal pre-treatment and mol. wt. 8-95798
- polyethylene, pretreated surface, nitrobenzene contact angle, H₂O environment (*Japanese*) 8-79858
- polystyrene-wood, polymer composite, dielec. props. at low temperature range (*Japanese*) 8-95541
- quartz, cultured cryst., vacuum UV transmittance before and after electron irradi. 8-83044
- quartz, electron irradiated, optical and anelastic absorptions and resonator freq. 8-64385
- relativistic electrons, spontaneous EM emission in channel pot. 8-83848
- SEM/STEM cold stage thick specimen heating model 8-61289
- semiconductor-metal structure, electron bombarded, energy dissipation 8-87732
- steel, ferritic, FV607, void swelling, theory 8-71763
- steel, ferritic, FV607, void swelling in 1 MeV electron irradiation 8-71762
- steel, stainless, type 316, electron irradiated, void swelling 8-55891
- stilbene, single cryst., free charges and excitons generated by electron pulses 8-63988
- surface, rough, optical emission due to electron irradi. 8-60529
- surface layer thickness-composition monitoring by high energy electron backscattering 8-53146
- Ag, electron irradi., elastic moduli and internal function (*French*) 8-87703
- Ag-Zn (30 at.%), electron irradiated, atomic mobility, elastic after-effect meas. (*French*) 8-63874
- Al alloys, dil., size effect of impurity atoms rel. to trapping radii for migrating self-interstitials 8-75690
- Al, creep and dislocation distribution (*Russian*) 8-95775
- Al, electron-irrad., NQR, EFG around vacancies and interstitials 8-88220
- Al:¹¹¹In, electron irradi., defect trapping at impurities 8-55892
- Al-Cr(V)(Ti), dil., electron irradiated, interaction of self interstitials with undersized solute atoms 8-63789
- Al-Cu (4 wt.%), enhanced precipitation under electron irradiation in HVEM 8-52818
- Al-Fe, electron irradiated, interstitial-solute complexes, internal friction spectra 8-92289
- β -Al₂O₃-Na₂O-MgO, blocking defects prod. by electron beam heating 8-55879
- As, amorphous, electron irradi.-induced paramag. centres, 77K 8-88187
- As₂Se₃, amorphous, electron irradi.-induced paramag. centres, 77K 8-88187
- CaF₂, bleaching characteristics of crystals coloured by low energy electrons 8-76497
- Cd, electron radiation damage, determ. of threshold displacement energy 8-59837
- Cd, electron radiation damage in HVEM, nature of defect clusters 8-59838
- CdBr₂(I₂), vapour growth crystals, decomposition, electron microscope study 8-92268
- CdS, absorpt. spectra, 400-650 nm, electron irradi. defects and absorpt. edge shift 8-64382
- CdS, neutron and fast electron irradi., local centre form., TSC and photoluminesc. meas. 8-87719
- CdSe, charge transport 8-84233

electron beam effects continued

- Cu alloys, dil., size effect of impurity atoms rel. to trapping radii for migrating self-interstitials 8-75690
- Cu, electron transmission and absorption, 70 keV initial energy 8-71777
- Cu, Frenkel pair production threshold energy, temp. depend., exam. 8-51530
- Cu, irradi., stage III recovery kinetics 8-63792
- Cu, very low atomic displacement threshold energy obs. 8-95078
- Cu-Ag (Au), dil., dose depend. of impurity detrapping stages after electron irradiation 8-51582
- D₂, solid 0.5-3 keV electron penetration depth 8-56549
- Fe, appl. of KUR LINAC to radiation damage studies 8-71760
- Fe-Cr-Ni, electron irradiated, resistivity during annealing, 4.2-1300K 8-87962
- Fe₆₅⁶⁰Ni₃₅, electron irradiated, small angle neutron scatt. 8-52218
- n-GaAs, electron and gamma ray irradiated, introduction and annealing of defects 8-67736
- GaAs, radiation defect obs. using Schottky diode characts. 8-76024
- GaAs:B, electron or neutron irradiated, low symmetry interstitial B centre 8-79605
- GaP:s, elec. props. following 1.7 MeV electron irradiation 8-80005
- GaP:Zn, isolated Ga vacancy due to electron irradi., EPR study 8-95519
- Ge, amorphous layer, epitaxial recrystn. by electron irradi., solar cell appl. 8-84079
- n-Ge:Cu, characts. of radiation defects 8-55893
- GeO₂, radiation damaged, paramag. point defects, F-centres, ESR, absorpt. spectra 8-80213
- H₂, solid, 0.5-3 keV electron penetration depth 8-56549
- InSb, high-purity specimen irradiated at 80K, transport prop. and defect annealing 8-95307
- InSb, irradi. real and clean surfaces, work function 8-95336
- KBr, electron irradi. at 4K, role of V_k centres in equilib. among centres 8-67712
- KBr:Eu(Yb), electron-irrad., photostimulated luminesc., ionic processes 8-52561
- KCl crystal, F-H centre formation by opt. conversion of self-trapped excitons 8-91335
- KCl, electron injection, F-centre formation efficiency 8-63790
- KCl:K₂Os^{III}(CN)₆, electron irradi., EPR, ligand hyperfine struct. 8-60335
- KI:Eu, electron-irrad., photostimulated luminesc., ionic processes 8-52561
- KSeO₃, cubic, K⁺ ion ordering, electron microscopy 8-79550
- LiCl, irradi., F-centre emission 8-60501
- LiNO₃, electron irradi. damage, XPS obs. 8-64444
- Li₂SO₄, electron irradi. damage, XPS obs. 8-64444
- Mg, electron irradi. damage, dislocation loop growth, in situ obs. 8-87715
- Mg, electron radiation damage, determ. of threshold displacement energy 8-59837
- Mg₃Cd, disordering under electron irradi. in electron microscope 8-83849
- Mo, Tokamak reactor, mag. limiter plate, electron irradi. and thermal shock 8-66416
- Mo-C dilute alloy defect cluster nucleation and growth under 1250 keV electron microscope (*Japanese*) 8-87663
- MoO₃, reduction to MoO₂, by electron beam, electron diffr., microscope investigs. (*French*) 8-95945
- NO, oxidation by electron beam irradi., appl. to exhaust gas treatment 8-80765
- NO₂, reduction by electron beam irradi., appl. to exhaust gas treatment 8-80765
- NaCl, exposed to high-current electron beam pulses, min. size of excited region for crack initiation (*Russian*) 8-84961
- NaCl:Ti, luminesc. yield, effect of fast electron channelling 8-84646
- Nb₃Ge(Sn), electron irradiation at cryogenic temps., effect on T_c and transport props. 8-52122
- Ni, electron irradiated, temp. depend. positron trapping 8-91360
- Ni, pure and doped, mech., mag. relax. meas. dumb-bell self-interstitial reorientation (*German*) 8-52879
- Pb-Ni-Si, metallic glass, electron irradi., positron annihilation radiation, angular correlation study 8-84678
- PbSnTe-PbTe heterostructs., effect of electrical grounding on electron irradi. 8-60194
- Pt, electron irradi., close Frenkel pair recomb. during annealing 8-87716
- Pt foil, quenched, 1.2 MeV electron irradi., subthreshold irradi. effects 8-51585
- RbCl:Eu, electron-irrad., photostimulated luminesc., ionic processes 8-52561
- SO₂, oxidation in moist O₂-N₂ mixture by electron irradi., appl. to exhaust gas treatment 8-80766
- Se, amorphous, electron irradi.-induced paramag. centres, 77K 8-88187
- Si, electron irradiated, high resist. surface layer, Schottky barrier meas. 8-64093
- Si, electron irradiated, positron annihilation 8-87713
- p-Si, fast electron irradi., Hall mobility, temp. depend. 8-56165
- Si:Gd, radiation defect form., effect of Gd impurities, elec. and optical meas. 8-71764
- Si-SiO₂ charge accumulation during low energy electron bombardment 8-64142
- Si-SiO₂ interface, in MOS struct., fast surface states density, electron irradi. effects 8-88042
- SiC, Tokamak reactor, mag. limiter plate, electron irradi. and thermal shock 8-66416
- SiO₂, doped, fibre-optic waveguide, effect of ionising radiation on optical attenuation 8-63170
- SiO₂, electron-beam irradi., electron trapping, MOS capacitor expts. 8-72268
- SiO₂ gate insulators in radiation-hard MOS capacitors, charge relaxation 8-60206
- SiO₂, vitreous, compaction dependence on ionisation dose 8-67738
- Te, electron irradiated, dose-depend. and recovery behaviour of transport props. 8-71761
- Ti, electron radiation damage, determ. of threshold displacement energy 8-59837
- V, electron irradiated, positron study 8-76555

electron beam effects continued

- W (100), adsorbed O, electron stimulated desorption ion energy distrib. and surface struct. 8-75940
 W, single crystals, electron irradiated, recovery of resistivity, 4.5-380K (*German*) 8-87714
 Zn, electron radiation damage, determ. of threshold displacement energy 8-59837
 Zn, electron radiation damage in HVEM, nature of defect clusters 8-59838
 Zr, dissolution of γ -ZrH, in situ study, HVEM obs. 8-55951
 Zr₃Al, disordering by 1 MeV electron irradiation 8-51583

electron beam impact *see* electron impact**electron beam machining**

- ceramic, unfired, cavity form. by electron beam machining 8-80660
 ceramic unfired, precision e-beam machining, kinetic focusing 8-80661
 conference on electron, ion and photon beam technology, Palo Alto, CA, USA (May 1978) 8-74827
 micromachining, imaging conditions, illumination system 8-82899

electron beam welding

- tetrode gun, transport of high-energy, high-power electron beams 8-89587

electron beams

- see also* electron impact; electron optics; Schwarz-Hora effect
 aberration averaging, image and deflection component design 8-74830
 absolute dose rate determ. 8-74103
 auroral electron beam, electrostatic noise generation 8-85759
 bounded electron beam, quasilinear relaxation model (*Russian*) 8-78891
 charge monitor, single pulse toroidal coil type 8-78036
 coaxial autoaccelerator, klystron instability of relativistic electron beam, stability criterion 8-82541
 coaxial autoaccelerator, resonant instabilities of relativistic electron beams 8-82540
 coherent EM radiation intensity, produced by modulated electron/ion beams in gas 8-50686
 collective and single-electron interactions of electron beams with EM waves and free-electron lasers 8-55330
 compact source for neutral beam production of very low vapour press. materials 8-70225
 curved electron beam system with strong deceleration at collector region, optimisation 8-74106
 cyclotron radiation from oppositely directed electron beams 8-78874
 cyclotron wave coupling, interpenetrating electron waves 8-66735
 Deflection distortion in scanning electron-beam systems 8-74835
 distribution function in focusing mag. field (*Russian*) 8-82898
 dynamic beam shaping, electron-beam lithography appl. 8-74834
 dynamic deflection sensitivity in transverse magnetic field 8-86386
 electron storage ring coherent microwave emission fine struct. 8-78875
 electron-photon cascades separation by scintillation counter system 8-78563
 Excede 2 test, artificial auroral expt., ground-based optical meas. 8-89038
 fast-pulsed, energy meas. bremsstrahlung absorption spectroscopy 8-49940
 field emission electron beams, two beam interference 8-63002
 focusing by laser beam fields 8-74833
 gas neutralised, self focusing, effect of self-elec. and mag. fields 8-50692
 generalised relativistic Brillouin theory, appl. to infinite vacuum transmission line 8-87004
 glow discharge generated high-power pulsed beams, gas dynamics diagnostics appls. 8-63515
 gun design for producing high-intensity beam with rectangular cross section 8-93785
 high current electron beam of TONUS accelerator, time struct. (*Russian*) 8-66434
 high energy deposition from pulsed electron beams 8-54500
 high-current electron beam stability in mag. field in waveguide 8-66742
 intense pulsed ion beam meas. by nuclear activation 8-74104
 ionosphere injection expts., electric potential of rocket (*Russian*) 8-93069
 iris-loaded waveguide, inhomogeneous ferrite filled, autoacceleration 8-79441
 laminar using high-current electron guns, formation for linear accelerators 8-74516
 limiting current of electron in mag. field of conical electron beam 8-90348
 linear accelerator production of intense ns beam, space charge and radiation field effects 8-70654
 magnetically isolated annular relativistic electron beam 8-78037
 monochromatic photon beam generation by high energy electron beam (*Japanese*) 8-74821
 pinching from discrete cathodes, for interially confined fusion 8-50318
 polarised by radiative separation in inhomogeneous mag. field practically 8-82076
 Precede, artificial auroral expt., summarised results 8-89037
 production, by localised source in focused discharge 8-58093
 pulsar radio signals spectra and microstruct., relativistic electron beam model 8-65639
 quadratic grouping of electrons directed by transversely inhomogeneous magnetostatic fields (*Russian*) 8-74822
 quantum modulation in field of opposite EM waves 8-74188
 radiation flux parameters meas. by diaphragm method 8-86387
 radiative damping effect for ultrarelativistic channelled particles 8-67758
 relativistic, crit. current in mag. field in vacuum channel (*Russian*) 8-71016
 relativistic, high current, pulse length adjustment 8-65997
 relativistic, intense, ion collective acceleration, localised pinch model 8-87460
 relativistic, technique for amplitude and phase vel. meas. of slow space charge wave 8-54508
 relativistic beam through metallic boundary, self-consistent pot. 8-82900
 relativistic charged particle beams in storage rings, soliton soln., phase locked states 8-50425
 relativistic electron beam, 'peeling' on entering mag. field 8-66741

electron beams continued

- relativistic electron beam dissipative Cerenkov instability, oscill. modes, quasi-linear theory (*Russian*) 8-59564
 relativistic electron beam pinching and combination for inertial confinement fusion 8-50319
 relativistic self-focused electron beam, hose instability meas. 8-83544
 relativistic self-pinch electron beam, Bennett profile, resistive hose instability 8-83543
 ribbon electron beams, equilib. and stability conditions (*Russian*) 8-70220
 rotating relativistic electron beams, electrodynamic principles 8-71019
 scanning system, variable-aperture projection, design 8-74836
 secondary emission monitor of accelerated electron beam current 8-78033
 solar flares, electron beam characts. rel to X-ray and UV emission 8-65598
 solar flares, electron fluxes rel. to optical, X-ray and radio emission 8-89156
 solar flares, hard X-ray sources diagnostics 8-89159
 solar wind, nonlinear Langmuir waves during Type III radio bursts 8-93173
 storage rings, VEPP-2M, -3 and -4 as synchrotron radiation sources, beam characts. 8-62667
 subpicosecond pulse generation and meas. 8-65996
 tetrode gun, transport of high-energy, high-power electron beams 8-89587
 thermal sensitive paper for intense, relativistic electron beam dynamics diagnostic 8-83619
 threshold temp. sensitivity of interelectrode gap determination 8-78890
 Torus accelerator, transport of high current relativistic electron beams in large vols. (*Russian*) 8-82544
 two-beam gain saturation in an electron-ion beam without capture of electrons 8-94919
 uncompensated, slipping flux instability due to transverse potential drift (*Russian*) 8-71026
 LaB₆ cathode, directly heated, for electron beam instruments, design and optimisation 8-93783

electron capture

- see also* charge exchange; electron attachment
 atom+ion collisions, electron capture, quasi-molecular binding corrections 8-90287
 atoms and highly charged ions, charge exchange 8-62913
 bare ion+hydrogenic ion, forward electron capture, third Born approx. calcs. 8-58782
 electron capture processes in ion-atom collisions 8-70930
 fast ion+atom collisions, one electron charge transfer and capture 8-70931
 H⁺+Mg collisions double electron capture 8-58777
 heavy ion+atom, radiative electron capture, target thickness depend. 8-58778
 highly charged atom+ion, slow collisions, one-electron capture 8-58776
 ion-atom collision, radiative charge exchange, high energy 8-55234
 second Born contribution, obs. methods for high impact vels. 8-78803
 C^{q+}+Ar, continuum electron capture, projectile vel. and Z depend. 8-55222
 C^{q+}+H(H₂), q=1-4, single electron capture cross sections 8-55233
 CH⁺, continuum electron wavefunction, electron capture width 8-78805
 H⁺, electron capture from Si foil, cross-section calcs. 8-95623
 H-like atom+bare ion, electron capture to continuum, cross-section cusp 8-90289
 H⁺+He²⁺, electron capture at impact energies below 10 keV 8-50633
 H+heavy charged ion, total electron capture cross section charge depend. oscill. behaviour 8-66656
 H+positron, charge exchange, excited positronium states form. 8-58873
 H⁺+H⁺, electron capture, continuum distorted wave calcs. 8-50635
 H⁺+atom, electron capture, two-state atomic expansion 8-62912
 H⁺+C(N)(O)(Ne)(Ar), electron capture cross sections 8-62912
 H⁺+multielectron atom, fast collision, electron capture, differential cross section calcs. 8-94318
 H₂+³He²⁺, electron capture at impact energies below 10 keV 8-50633
 H₂+H⁺, electron capture probability 8-58808
 H(1s)+p→p+H(1s), 15-200 keV, ang. distrib., differential cross sections calc. 8-82839
 He⁺+Ar(N₂)(He), up to 70 keV, symmetric (antisymmetric) reson. charge transfer cross sections (*Korean*) 8-50636
 He⁺+Na(K)(Cs), 5-100 keV, electron capture form. of fast metastable He 8-74760
 He²⁺+H₂(O₂), electron capture collisions, spin conservation 8-82837
 He²⁺+He, He⁺ form. in various electron states (*Russian*) 8-58815
 He²⁺+He(Ne), electron capture collisions, spin conservation 8-82837
 Li⁺+Ar, up to 70 keV, symmetric (antisymmetric) reson. charge transfer cross sections (*Korean*) 8-50636
 N^{q+}+H(H₂), q=1-5, single electron capture cross sections 8-55233
 O^{q+}, electron loss, forward peak oscill. struct. 8-78796
 O^{q+}+Ar, continuum electron capture, projectile vel. and Z depend. 8-55222
 O^{q+}+H(H₂), q=1-5, single electron capture cross sections 8-55233
 Si^{q+} electron loss, forward peak oscill. struct. 8-78796
²⁸Si+H(H₂), single electron capture cross sections 8-58812

electron capture, nuclear *see* nuclear electron capture**electron density**

- see also* carrier density; current density; electron density (metals)
 air, RF discharge, electron temp. and density 8-51371
 alkanes, electron density, bond order, hydrogen suppressed graphs, extended Huckel theory 8-90088
 arc plasma, low-temp. diagnostics by scatt. and resonance fluorescence 8-67482
 ATS-6 electron content data presentation 8-61593
 aurora, incoherent scatter radar meas. rel. to precipitating electrons energy distrib. 8-77390
 conical laser plasma tube, electron density distrib. 8-58981
 Crab pulsar, high energy electrons density and momentum distrib. 8-73727
 D-region, daytime solar proton event-disturbed model 8-93038
 D-region, diurnal vars. during storm after-effect 8-65451

electron density continued

- D-region, partial refls. density profiles sensitivity to irregularity comp. 8-81495
- D-region electron density variation obs. (*Russian*) 8-61652
- E-region, variations during geomag. disturbances 8-69567
- F₂-layer, plasma continuity eqn., comparative anal. of numerical soln. methods 8-69578
- F₂-layer of ionosphere, comparison of CCIR predictions with in situ meas. 8-57394
- F-region, equatorial, irregularity patches localised origin 8-77404
- F-region, incoherent scatter radar meas. of electron density and ion vel. during isolated substorm 8-65452
- F-region, n₂F₂ annual vars. with latit. and solar activity level 8-69577
- F-region, nighttime seasonal electron density anomaly 8-69566
- F-region, polar cap and auroral zone, math. model 8-65458
- F-region density max., harmonic analysis and periodicities 8-57383
- F-region striated Ba clouds, electron density struct. meas. 8-88974
- Faraday rotation, effects of pulsewidth 8-71540
- flame, diffusion type, oppositely directed jets, elec. props. 8-56896
- free plasma column in gas at high pressure 8-75477
- FT-1 Tokamak, electron density and temp. radial distrib. laser scatt. obs. (*Russian*) 8-59666
- glow discharge, electric probe diagnostics, sputtering of appl. 8-71537
- glow discharges, atomic and ionic spectral line excitation in cathodic region (*Russian*) 8-63611
- H₂ line profile for plasma microfield distrib. function reconstruction 8-71539
- high-density effects on plasma spectroscopy 8-75429
- interplanetary scintillation meas. of electron density power spectrum in solar wind 8-77448
- ion-acoustic plasma turbulence, two-dimensional electron density spectra 8-75479
- ionosphere, antenna in plasma, Debye screening and electron conc. nonuniformity 8-69563
- ionosphere, by automatic meas. of whistler dispersion 8-93050
- ionosphere, density and recomb. coeff. profiles calc. rel. to absorpt. and rocket meas. 8-69559
- ionosphere, effect of radio wave heating on electron densities and temps. 8-77403
- ionosphere, electron density irregularities rel. to intersatellite whistler-mode pulses propag. 8-69605
- ionosphere, equatorial, correl. with seasonal var. of radio waves absorpt. 8-85762
- ionosphere, inhomogeneities, Earth surface topography effects, airborne soundings 8-69579
- ionosphere, lower, effects of solar flares Fe XXV 1.87 Å line emission 8-65588
- ionosphere, lower, electron density profile controls from radiowave absorpt. meas. 8-81492
- ionosphere, mid-latitude F₂-layer, electron density oscils. rel. to lunar tide 8-61655
- ionosphere, noon and midnight mid-latit. trough obs. by Ariel 4 8-85765
- ionosphere, quiet nighttime, electron total content and density rel. to decay rates 8-81493
- ionosphere, temp. and electron density relaxation rel. to radiowave interaction nonstationary processes (*Russian*) 8-93028
- ionosphere, total electron content diurnal and seasonal trends, obs. at Waltair 8-69596
- ionosphere, total electron content meas. at Gauhati, using ATS-6 140 MHz transmissions 8-69598
- ionosphere, total electron content numerical model, corrections for satellite tracking systems 8-69587
- ionosphere, total electron content obs. at Kurukshetra, using ATS-6 140 MHz transmissions 8-69597
- ionosphere, total electron density nighttime behaviour 8-69570
- ionosphere, travelling disturbances, electron density spectra 8-77398
- ionosphere, travelling disturbances characts. over Thumba 8-69590
- ionosphere plasma, electron densities and temps. meas. by Injun 5 during major mag. storm 8-88987
- ionosphere total electron content at Sagamore Hill, solar cycle var. 8-81496
- laser plasma, electron density determ. from X-ray spectra of multiply charged K ions 8-94938
- laser plasma density profile modification by ponderomotive force 8-59634
- laser produced plasma expansion, ion emission, hot, cold electron density, temp. ratios 8-71513
- low-pressure discharge anode sheath in crossed fields, electron density distrib. 8-75424
- magnetosphere, by automatic meas. of whistler dispersion 8-93050
- magnetosphere, electron density meas. via International Sun-Earth Explorers 8-85803
- metal, charge screening and Friedel oscillations of electron density (*Russian*) 8-79951
- meteor trails, causes of fluctuations in effective linear electron density 8-73687
- microwave interferometer for electron density meas. on T-II plasma device 8-55754
- midlatitude plasmasphere, trapped photoelectrons and secondary electrons 8-69565
- multidipole plasma density 8-94929
- nighttime ionospheric intermediate layer obs. by rocketborne impedance probe (*Japanese*) 8-61646
- plasma, dense, fast interferometer diagnostics using N₂ laser 8-87489
- plasma, highly-dispersed aerosol, nonisothermal, thermionic electron density function determ. 8-91066
- plasma, nonequilibrium, electron density diagnostics via C III EUV Lines 8-53899
- plasma, Princeton large torus, multi-channel TV-Thomson scatt., apparatus, mech. aspects 8-54932
- plasma, turbulently heated, electron distrib. anisotropy, X-ray diagnostics 8-59682
- plasma column electron density radial profile, modified laser interferometry 8-67429
- plasma conical waves from scatt. laser radiation, pot. electron density determ. (*Russian*) 8-59667
- plasma density fluctuation evaluation by microwave interferometry 8-67437
- plasma diagnostic technique using self reversed deuterium D₂ line 8-55746

electron density continued

- plasma electron density, interferometric meas. 8-67479
- plasma electron density determ. by CO₂ laser 90° collective scatt. 8-67433
- plasma focus, electron density distrib., N₂ laser interferometric study, X-ray and neutron emission 8-87479
- plasma production modified magnetron discharge facility 8-75380
- plasma with negative cond., electron conc. distrib., stability (*Russian*) 8-55722
- plasmopause, radio sounding by geostationary satellite (*Japanese*) 8-85770
- plasmasphere electron density, whistler data on solar cycle, annual and diurnal vars. 8-88985
- positive column, irregular ionisation wave electron density rel. to light intensity variations 8-67520
- RF discharge in mag. field, plasma rate equation 8-67455
- solar inner corona density distrib. from Fe XIV 5303 Å line intensity obs. 8-61843
- solar limb active regions, electron densities from 1175 to 1940 Å emission-line spectra 8-96446
- solar transition zone, electron density determ. from O III Bowen fluorescence meas. 8-93179
- solar wind, electron density meas. via International Sun-Earth Explorers 8-85803
- solar wind, electron density small-scale fluctuations, interplanetary scintillation obs. 8-96376
- spatial distrib. in nighttime polar ionosphere 8-73570
- steady state plasma, electron temp. and density meas. system 8-87490
- Sun, chromosphere above sunspot umbrae, temperature and electron density 8-53908
- Sun, electron density at 10⁵K from O IV intersystem line obs. in EUV 8-53903
- thermosphere, electron temp. and density relationship in daytime at solar minimum, model 8-61638
- theta-pinch, nonthermal density fluctuations, laser scatt. diagnostics 8-59679
- Tokamak, JFT-2, scrape-off layer, particle and energy fluxes, probe and IR obs. 8-59690
- Wolf-Rayet stars, electron density in emission-line region 8-93263
- Z-pinch, plane, mag. field null region parallel current effect (*Russian*) 8-91137
- Z-pinch discharge, electron temp. and density variation obs. 8-75426
- Al plasma, hot dense homogeneous, X-ray production rate and ionisation state density, calc. 8-71458
- Al XIII, hot pinched plasma, Lyman series Stark profiles, electron density determ. 8-51348
- Ar atmospheric arc plasma deviation from LTE 8-67604
- Ar constricted discharge, electron density and temp. and gas temp., iterative method (*German*) 8-83627
- Ar ion laser, collisional radiative model and expt. 8-55338
- Ar negative glow fast electron density rel. to discharge pressure and current 8-67528
- Ar plasma, electron density, microwave refl. meas. 8-59674
- Ar, precursor shock waves, electron density and assoc. ionisation 8-67217
- C VI, laser plasma, electron density profile, Stark broadening meas. of vac. UV lines 8-59684
- CO₂, laser discharges, determ. of recombination coeff. 8-90407
- Cd-Ar low-pressure discharge column, energy balance obs. 8-67504
- Cl⁻ free-bound continuum radiation threshold broadening obs. in plasma 8-71579
- H II regions, electron density errors from radio emission improper anal. 8-54000
- H₂ line Stark profiles in low-density arc, exptl. discrepancies 8-67470
- He II, Doppler and Stark broadened lines, electron density and ion temp. meas. 8-67407
- He plasma He I 4471 Å line profile obs. at high electron density 8-67472
- He-Ne plasma He I 4471 Å line profile obs. at high electron density 8-67472
- Hg, high-pressure discharge, temp. and electron density meas. (*French*) 8-59705
- Hg low-pressure pulse-modulated discharge optical and electrical parameters 8-67491
- Ru complex, HF calc., electron densities and Mossbauer isomer shift, chemical binding 8-50470
- SF₆ high-current arc props., influence of electrode material 8-71592
- electron density (crystallography)** *see crystallography*
- electron density (metals)**
- liquid metal, surface ion density, nonmonotone, perturbative discrete ion introduction into jellium 8-72222
- Ag clusters, charge distrib., density of states, CNDO calcs. 8-70995
- Fe-Ni alloy, optical and electronic characts., 20-1750°C, comp. depend. (*Russian*) 8-84601
- electron density of states** *see electronic density of states*
- electron density of states (condensed matter)** *see electronic density of states*
- electron detachment**
- atmospheric negative ions, electron detachment rates, time lags to breakdown 8-87564
- atmospheric negative ions, photodissoc. and photodetachment 8-66609
- electron-ion collisions, crossed beam expts. 8-58843
- glow discharge, non self-sustained, detachment process effects 8-59713
- methoxide-d₀(-d₃) anion, electron affinity, vibr. struct., photodetachment electron spectra 8-94282
- open shell systems, coupled cluster approach 8-58595
- thiomethoxide anion, electron affinity, vibr. struct., photodetachment electron spectra 8-94282
- Ar+H⁺, collisional electron detachment, complete ang. distrib. 8-66650
- Cl⁻ radiative detachment threshold effect of plasma microfield 8-71580
- Cl⁻+Ar, detachment energy threshold from ArCl pot. energy curve 8-62745
- F⁻, photodetachment cross section, Stieltjes imaging method 8-55149
- H⁺, electron detachment by electron impact, 1s state product, Born approx. 8-78816
- H+Ar, detachment energy threshold from ArH pot. energy curve 8-62745
- H⁺+H(He), electron detachment cross sections 8-90265

electron detachment continued

- H⁺-He, detachment energy threshold from HeH pot. energy curve 8-62745
 H⁺-He(Ar), electron detachment cross sections 8-58810
 O⁻, photodetachment, fine struct. transitions, photoelectron spectra 8-55151
 Rb⁺, photodetachment, electron affinity 8-90132
 S⁺, photodetachment, fine struct. transitions, photoelectron spectra 8-55151
 S⁻, photodetachment cross section mag. field depend. struct., obs. 8-55148

electron detection and measurement

- absorbed dose in water, absolute meas. using total absorpt. type calorimeter and dose detectors (*Japanese*) 8-78501
 accelerated electron beam current monitor using secondary emission detection 8-78033
 bubble chamber electromagnetic shower photographs, for teachers 8-65737
 double focusing Fe core electron spectrometer BILL for (n,e⁻) meas. 8-82566
 electron-photon cascades separation by scintillation counter system 8-78563
 EM shower sampling counters, characteristics of plastic scintillator and radiator layers 8-58530
 ESP detector for 300-2000 eV electron, optimum conditions theory (*Japanese*) 8-66693
 modular electron calorimeter, relative and absolute calibration 8-78578
 proportional counter, energy loss of relativistic electrons and its fluctuation 8-94171
 single isolated electron measuring technique, resource letter for teachers 8-81776
 spark chamber, electron-photon shower recording, single-particle background suppressing method 8-78573
 In₂Te₃ type semiconductors, basis of ionising radiation detectors 8-86743
 In₂Te₃-type semicond. radiation-resistant fast-electron detectors 8-78559
 Mg₂SiO₄:Tb TLD, response to high energy electrons (*Japanese*) 8-78502
 Mg₂SiO₄:Tb TLD, supralinearity of response to electrons and X-rays (*Japanese*) 8-78503
 Ne flash tube chambers for electron and photon detection 8-58552

electron device noise

- 1/f noise, theoretical analysis (*Polish*) 8-91737
 cryogenically cooled C-band p-i-n diode integrated switch matrix for radio astronomy applications 8-96392
 IR charge transfer device imaging arrays 8-77990
 laser diode characterisation, for multichannel applic. 8-87165
 MOS transistor electrometer, current noise meas. 8-54398
 photomultipliers noise figure, secondary electron emission model 8-86336
 single injection diodes, 1/f noise 8-60204
 vibrating-capacitor electrometer, current noise meas. 8-54398
 Si extrinsic photoconductive IR detectors, VLF behaviour 8-81542

electron diffraction

- see also *electron diffraction crystallography; electron diffraction examination of materials; gas phase electron diffraction; high energy electron diffraction; low energy electron diffraction*
 conference, London, England (Sept. 1977) 8-83657
 supersonic stream flow in vacuum meas., instrument 8-75235

electron diffraction crystallography

- see also *crystal atomic structure; Debye-Waller factors*
 algebraic approaches to N-beam theory 8-83663
 amorphous and gaseous states, philosophical problems in struct. determ. 8-50665
 atom images under dark field, STEM and TEM comparison 8-83696
 BCC materials, small dislocation loop images 8-83823
 Bloch wave channelling as electron diff. 8-83860
 Bravais lattice and reduced cells determ., programs for electron diffraction pattern indexing (*Chinese*) 8-67625
 computer indexing of diff. spots, appl. to bicryst. (*French*) 8-75507
 conference, London, England (Sept. 1977) 8-83657
 contrast in non-symmetric Laue case 8-83666
 cross grating orientation, patterns in axial direction, dispersion surfaces 8-83660
 crystal defects, electron microscope diff. contrast 8-83700
 crystallographic struct. factor phases from electron-microscope dark-field moiré patterns 8-51396
 defect Kikuchi band from thin cryst. 8-83668
 diffraction patterns, extinction problem, automatic indexing program (*Chinese*) 8-91204
 digital scanning electron diffractometer, appl. to radiation sensitive materials 8-87596
 dislocation dipoles, high density, numerical eval. 8-71645
 double crystal interferometer 8-83687
 dynamical diffraction from periodic arrays of dislocations 8-83669
 dynamical theory, perturbation calcs. 8-83665
 dynamical theory 8-83658
 dynamically forbidden lines obs. in 2-D and 3-D diff. 8-83675
 electron density maps, extrapolative filtering, resolution maximisation 8-75506
 experimental limitations on cryst. struct. determ. 8-83678
 HCP metals, systematic electron diff., main beam transmission 8-63643
 image computation for high-resolution TEM 8-71653
 indexing of selected area diff. pattern, graphical technique, for teaching 8-54132
 instrumentation, review 8-83683
 interferometer diffraction pattern, amplitude modulated beam 8-63641
 Kossel pattern anal. 8-83676
 line diffraction patterns, scattering model (*French*) 8-51397
 liquids, expt. developments 8-83686
 macromolecules, graphics model building and refinement system 8-75505
 medium energy, theory and appl. 8-83682
 metal, electron wave flux distrib. fine struct. near Bragg refl. 8-83670
 metal cluster generator for gas-phase electron diff., variation of microcryst. with size 8-63645

electron diffraction crystallography continued

- multilayer close-packed structures, identification possibilities, X-ray and electron diff. patterns 8-94951
 multiple inelastic scattering and dynamical diffraction 8-83667
 multislice and many beam calculations comparison 8-83664
 optical selected-area diff. patterns of high-resolution electron-microscopic images for cryst. anal. 8-55789
 organic molecular crystals, topochem. conversions and phase transitions 8-83680
 periodic misfit-dislocation networks 8-59815
 photographic emulsion response to electrons in gas-phase electron diffraction expts. 8-54482
 protein structure determination, crystal bending, electron-diffraction data 8-53325
 sector device for electron diffraction studies on liquids 8-55788
 string integrals rel. to BC and CB zone axis patterns 8-83681
 structure factor and symm. determ. 8-83673
 twinned crystal, diffracted electron beams, equality of intensities 8-79506
 c-Dy₂O₃, transmitted intensity depend. on thickness, incident beam parallel to crystallographic axis 8-63644
 MgO, dynamical effects for cryst. struct. determ. 8-83679

electron diffraction examination of materials

- see also *gas phase electron diffraction; high energy electron diffraction; low energy electron diffraction; reflection high energy electron diffraction*
 alkanes, thin plate microcrystals, transmission electron diffraction intensities 8-83821
 amorphous materials, microdiffraction patterns from the Finney model 8-63642
 anthracene, electron diff. of topochem. conversion and phase transition 8-83680
 cellulose II, preparation and crystal growth, electron diff. obs. 8-91285
 dichlorodinitromethane, mol. struct., electron diff. investig. 8-86950
 disordered alloys, short range order diffuse electron scatt. 8-87595
 electron sensitive materials 8-83701
 fluoride ceramics, doped, short range order anal. by electron diff. 8-83672
 free jet, homogeneous nucleation of clusters, noncryst. struct. (*French*) 8-79760
 graphite intercalation cpds., struct. and order-disorder transforms. 8-71710
 HCP metals, critical voltages, using n-beam dynamical theory 8-71644
 ionic conductor, quasielastic scatt. of light, neutrons and electrons, Debye-Huckel eqn. (*Chinese*) 8-68521
 Kevlar 49 high modulus polyaromatic fibre, supramolecular struct. 8-55819
 laser evaporated film, morphological features struct. defects 8-67926
 liquids, expt. developments 8-83686
 martensite crystals, orientation relationship definition, anal. method 8-60670
 materials problems and basic research needs rel. to energy resources and storage 8-86703
 paragonite, 2M₁, cryst. struct. refinement by HV electron diff. 8-67696
 paragonite, 3T, cryst. struct., oblique texture electron diff. 8-67697
 perfluoroneopentane, geom. struct. of mol., gas phase electron diff. 8-78810
 poly-N-vinylcarbazole, struct. model, using NMR and diff. data 8-83750
 poly-p-phenylene terephthalate, high modulus fibre, struct. obs. 8-75564
 polyethylene, single cryst. and spherulites, microstruct., deform. micromechanisms 8-83758
 polyethylene sulphide, cryst. struct. by electron diff. 8-51441
 polymer, soln.-grown cryst., diff. line-broadening, bending contrib. 8-75574
 polymethylene compounds, continuous diffuse electron scattering, oblique layer cryst. 8-95004
 polyoxymethylene, epitaxial growth on KBr single crystal (*Japanese*) 8-56054
 polyphenylene terephthalamide, fibril form. from nascent spherulite formed during polymerisation in hexamethylphosphorotriamide (*Japanese*) 8-56893
 rare earth trialuminides, long period polytypes, electron diff., high resolution imaging 8-83781
 rare earth-transition metal alloys amorphous thin films, anisotropic mag. and microstruct. props. 8-95487
 steel, C, tempered martensite embrittlement, and retained austenite, exam. 8-56754
 steel, stainless, Cr-Ni, maraging, effect of Mo, Co additions on hardening 8-84835
 wear study, analytical surface tool, review 8-64718
 ZnO, film, reactively RF sputtered, anal. of texture 8-67921
 ZZ 8-88057
 Ag, adsorption of O₂⁻, catalytic oxidation mechanism 8-61046
 Ag on W (001), geom. factors of FCC-BCC epitaxy 8-60041
 Ag-Cd (45 at.%), morphology and crystal struct. of stress-induced martensites 8-68693
 Al, dislocation substructure formation under hydrostatic extrusion 8-56696
 Al film, vacuum deposited, structural changes during annealing at temp. near melting point 8-84096
 Al, liq. film 8-83721
 Al, MEED, multilayer scatt. effects 8-83682
 Al, vacuum deposited, structural singularities and porosity (*Russian*) 8-75950
 Al-Ag alloy, ageing exam. by X-ray electron spectroscopy and electron diff. exam. (*Russian*) 8-60685
 Al-Ag alloy, second ageing stage, diffuse electron and X-ray scatt. (*Russian*) 8-68711
 Al₂O₃/CuO, thin film interaction, CuAl₂O₄ form. (*Russian*) 8-52697
 Au on W (001), geom. factors of FCC-BCC epitaxy 8-60041
 Au, twinned crystals, epitaxial growth on KCl crystals, electron microscopic study of microstructure 8-91566
 Au, vacuum deposition, on (100) surfaces of KBr, KCl and NaCl substrates with colloidal centres (*Rumanian*) 8-60579
 Au-Cu-Ag dental alloy, age-hardened, struct. and morphology 8-92272

electron diffraction examination of materials continued

- Au-Ge (27 at.%), metastable phase struct. determ. by electron diff. 8-83780
- Au-Mn system, AAB_B struct., experimental evidence for occurrence 8-63698
- Au₃Cd, sputtered epitaxial films, order-disorder reaction obs. 8-84092
- Au₁₁Mn₄, electron diffraction and microscopy obs. 8-75512
- Au₁₁Mn₄, ordering obs. 8-71707
- (Ba₂Nb₂Si₂O₂₆)_n, Ba₂Nb₄Ti₄O₂₁, multiple intergrowth and microdomains obs. by electron diff. and microscopy (*French*) 8-95160
- CdS, epitaxial layers on Cd single crystal, direct synthesis and struct. 8-68628
- CdTe, film grown in quasi-closed volume, struct. (*Russian*) 8-75952
- Co-Se, P-T diagram and structural study 8-56622
- Cr₁₁Ge₈, CrGe, and Cr₁₁Ge₁₉, amorphous films, short-range order, electron diff. obs. (*Russian*) 8-56050
- Cr₃Si₂(C₂), sputtered films, microstruct. and wear props. 8-64733
- Cu, cryst. pot. in electron diff. and band theory 8-83677
- Cu, dislocation substructure formation under hydrostatic extrusion 8-56696
- Cu, epitaxial, on (111) Au, periodic arrays of misfit dislocations, electron diff. 8-51857
- Cu on W (001), geom. factors of FCC-BCC epitaxy 8-60041
- α-Cu-Al, short range ordered, struct. and new superlattice phase 8-52756
- Cu-Pd alloy, singularities of physical props. and ordering (*Russian*) 8-76643
- CuInSe₂, epitaxial growth on GaAs 8-84104
- CuO-CaO-P₂O₅, glass devices, memory switching 8-56192
- Cu₂O, laminar growth on (111) Cu single cryst. surface, microstruct. 8-72025
- Cu₂S layer, on CdS, electron diff. obs. of phases 8-51847
- η-Cu₃Si precipitates in Si, cryst. struct. 8-91304
- Cu₂Sn, one-dimens. long period superstructs. with Zn and Ni additions 8-83777
- Fe, cast, high Mg content (0.33%), exam. of phase composition characts. 8-84780
- Fe, triboelectric charging, effects of fluorinated compounds 8-60188
- Fe-Fe₂O₃ composite films, structural props., microhardness, 250 to 700K 8-84095
- Fe-Ni, martensitic transform. dynamic, quasi-static atomic displacements, NGR, X-ray and electron scatt. meas. (*Russian*) 8-68688
- Fe-Ni alloys, struct. of γ and α-phases near martensitic transform. point (*Russian*) 8-64541
- Fe-Ni-Al-Ti alloy, N27Yu2T2, aged austenite, diffuse electron scatt. distrib. during martensitic deform. (*Russian*) 8-60669
- Fe-Ni-Cr-C, effect of austenite yield strength, stacking fault energy, on martensite morphology 8-80546
- Fe-Ni-Mn, martensitic transforms. electron diff. studies of γ solid soln. (*French*) 8-84803
- Fe-Si (3 wt.%), exam. of plastic deformation, slip band dislocation, under hydrostatic pressure 8-56695
- Fe₃Al, ordered alloys, atomic order parameters from topology of electron-microscope diff. contrast from antiphase boundaries, quantitative determ. 8-95016
- α-Fe₂O₃ film, prep. by reactive condensation and mag. props. 8-64241
- Fe₂O₃-TiO₂ system, high temp. intergrowth struct., metal atom ordering in intergrowth boundaries 8-79573
- Fe₃O₄ film, prep. by reactive condensation and mag. props. 8-64241
- Fe₃O₄, spherulitic film growth, elec. and mag. props. 8-68627
- FeS₂ (pyrite), glide elements study by electron microscopy and electron diff. 8-83817
- Fe₂Si_{1-x}, amorphous, struct. and mag. props., giant moment form. at mag. ordering 8-68192
- GaAs_{1-x}Sb_x, MBE grown, surface struct. exam. by MEED 8-87847
- Gd-Co film, amorphous, Ar sputtered, struct. 8-63946
- Gd-Co film, amorphous, phase separation as source of perpendicular anisotropy 8-64244
- Gd-Co-Mo film, amorphous, Ar sputtered, struct. 8-63946
- Gd-Fe film, amorphous, in-situ ion beam sputtered, microstruct. and Lorentz mag. struct. 8-63947
- Ge amorphous film, effects of ion implantation on structure 8-55881
- Ge, stacking fault width determ. from 224 reflections with g.b.=0 8-59722
- Ge-Cu (0, 23, 40 at.%), amorphous film struct. (*German*) 8-95391
- Hf-Nb (30 to 50 at.%) exam. of beta phase decomposition processes 8-76674
- MgO, dynamical effects for cryst. struct. determ. 8-83679
- Mn-Al alloy, vacuum codeposited, disorder of MnAl₆ phase in recovery process 8-51854
- Mo film deposited by low temp. carbonyl pyrolysis, struct. 8-72039
- MoO₃, film, colour centre studies, optical absorpt. spectra 8-71724
- MoO₃ reduction to MoO₂ by electron beam, electron diff., microscope investigs. (*French*) 8-95945
- MoSi₂, sputtered films, microstruct. and wear props. 8-64733
- Na₈Al₆Ge₆O₂₄.CO₃.2H₂O, cryst. struct. 8-83805
- Nb₃Ge, RF and DC sputtered films comparison, O content effect 8-72022
- NbSe₃, satellite electron diff. below 59K, Fermi surface features 8-84136
- Ni, dislocation substructure formation under hydrostatic extrusion 8-56696
- Ni on W (001), geom. factors of FCC-BCC epitaxy 8-60041
- Ni, sputtered, on Si, annealing effects on transmission electron diff. patterns, silicide form. 8-91562
- Ni-Co-P, ferromag. film, amorphous to cryst. transition, diff. and resistivity meas. 8-60587
- Pb, liq. film 8-83721
- Pd, epitaxial, on (111) Au, periodic arrays of misfit dislocations, electron diff. 8-51857
- Pd particles formed by evaporation on alkali halide crystals, orientation and struct. 8-84108
- PuO₂-UO₂-Na aerosol, from LMFBR HCDA conditions, characterisation 8-94104
- Rh, film, annealing effect on struct., TEM, electron diff. study 8-76682
- Si (111), MEED, secondary electron emission under surface state reson. 8-84688
- Si, (111) cleavage, Kikuchi pattern, 40 keV incident electrons, electron energy loss spectra (*French*) 8-87594

electron diffraction examination of materials continued

- Si, epitaxial regrowth and grain struct. of Al metallisation on (100)Si 8-79901
- Si, ion-implanted layers, radiation defect prod., refl. electron diff. obs. 8-87696
- SiC, one dimensional disorder 8-51492
- SiC, polytypism, reflection electron diff. 8-83694
- SnO₂, catalyst particles, converger beam electron diff. 8-83685
- Ta-O solid soln., interstitial ordering and precipitation at 100 to 270°C, exam. 8-52813
- Te film, growth on (111) KBr films deposited on mica, TEM and electron diff. obs. (*Japanese*) 8-64473
- Ti alloys, twinned hexagonal α phase crystals, electron diff. pattern analysis 8-56647
- Ti, exam. of oxidation kinetics, and oxide film structure 8-56822
- Ti:N surface, ion nitriding by a DC glow discharge method, surface anal. 8-80672
- TiO₂ film, electron diff. exam. 8-79906
- TiRO₃ (Ln=La, Nd, Sm, Eu, Gd), determ. of lattice parameters (*French*) 8-95031
- V₂O₅, low temp. crystallographic struct. domains 8-83765
- V₂O₅ film, prep. by thermal decomp. of vanadium naphthenate, and elec. props. (*Japanese*) 8-88425
- VSbO₄, catalyst particles, converger beam electron diff. 8-83685
- VSe₂ (1T), deform. modulated superstruct., electron diff. expts. 8-51515
- W film deposited by low temp. carbonyl pyrolysis, struct. 8-72039
- Y film, struct. and elec. resist., electron diff. meas. 8-87888
- Yb₂O₃, merohedral twins, many beam diff. contrast 8-83829
- Zr:N surface, ion nitriding by a DC glow discharge method, surface anal. 8-80672
- Zr-Al martensite, DO₁₉ phase formation, selected area diff. obs. 8-84779
- Zr-Nb, singularities of β→ω transform. in alloy, with high content of β-stabiliser (*Russian*) 8-76644
- Zr-Nb-Ge, singularities of β→ω transform. in alloy, with high content of β-stabiliser (*Russian*) 8-76644
- ZrO₂-UF₆, orthorhombic struct., X-ray and electron diff. study (*French*) 8-67689
- electron-electron double resonance** *see* ELDOR
- electron-electron interactions**
see also electron-electron scattering
 itinerant electron ferromagnetism at zero temp. 8-56285
 relativistic barriers for two spin-1/2 particles, from Breit eqn. 8-62339
 transition metal alloy, electronic structure, mag. props. 8-95254
 e⁺e⁻→τ⁺τ⁻, neutral-current effects on ψ-like resonance 8-74239
- electron-electron scattering**
see also electron-electron interactions
 No entries
- electron emission**
see also cathodes; electron field emission; exoelectron emission; photoemission; secondary electron emission; spin polarised electron emission; thermionic electron emission; work function
 cathode plasma explosive emission surface processes 8-71569
 cylindrical hollow cathode negative glow, fast electron angular distrib. obs. 8-67529
 polycaprolactam, stretched sheets, electron emission 8-88411
 polyethylene, stretched sheets, electron emission 8-88411
 D₂, electron surface barriers for dense phases 8-91754
 H₂, electron surface barriers for dense phases 8-91754
- electron energy bands** *see* band structure
- electron energy loss spectra**
 acetylene, chemisorption on Pt (111), ethylidyne group form., LEED and ELS obs. 8-73075
 bremsstrahlung, 1 to 2000 keV, neutral atoms Z=2 to 92 8-62920
 1,3-butadiene, excited singlet states, vibronic struct., electron impact energy loss spectra, 35-90 eV 8-62932
 chemisorbed molecules, electronic excitations, selection rule effects, EELS 8-76566
 chlorofluoromethanes, electron energy loss spectra, oscill. strengths 8-58846
 p-difluorobenzene, electron impact singlet-singlet transition generalised oscill. strength 8-66668
 ethylene, chemisorption on Pt (111), ethylidyne group form., LEED and ELS obs. 8-73075
 graphite, C K-absorpt. edge, EELS meas. 8-56551
 metal surface, chemisorption, vac. UV photoelectron spectrometer for study (*Japanese*) 8-62264
 metal-semiconductor thin film preparation under UHV conditions 8-72733
 microanalysis by energy loss spectrometry (*Japanese*) 8-85244
 microanalysis of light elements by electron energy loss spectrometry 8-80441
 microanalysis using field emission STEM 8-53286
 monohalobenzenes, inner shell excitation and ionis., electron energy loss spectra, XPS, assignments 8-62934
 oriented molecules, inelastic low energy electron scatt. 8-72653
 semiconductor surface electronic structure determ. by low energy electron loss spectroscopy (*Japanese*) 8-88007
 surfaces, electron spectroscopy, review 8-92169
 thiophosgene, triplet state, detected by electron energy-loss spectra 8-78808
 transition metal oxides, energy loss spectra, ion polarisability 8-68585
 Ag, adsorbed on Si (111), electronic and cryst. struct., Schottky barrier form. obs. 8-84091
 Ag film, energy losses of 20-40 keV electrons 8-92153
 Ag, single cryst. film, cryst. orientation effect on EELS 8-80442
 Al film, energy losses of 20-40 keV electrons 8-92153
 Al film, mean free path for plasmon excitation, 1.5 to 10.9 keV 8-51915
 Al, plasmon and phonon excitation 8-72682
 Ar, electron scatt., in laser radiation field, free-free cross sections meas. 8-74762
 Ar, electron scatt. in laser radiation field, free-free cross sections, reson. struct. 8-74763
 Au film, energy losses of 20-40 keV electrons 8-92153
 Ba, electron scatt., elastic and inelastic (5'D, 6'P) cross sections, 20-100 eV 8-74769
 BaO, electron energy loss and secondary emission mechanisms, plasmon losses 8-76565

electron energy loss spectra continued

- BaTiO₃, phonon spectroscopy, amorphous versus crystalline material 8-83898
 Be, inelastic electron scattering near K-edge 8-52606
 CO, chemisorbed on Ni(111), surface optical excitations, reflectance spectra, electron energy loss meas. 8-84064
 CoO (100), electron energy loss spectra exam. 8-72652
 Cu film, energy losses of 20-40 keV electrons 8-92153
 GaAs, electronic surface structure Cs(Rb)(Na) adsorpt. processes, AES, LEED, EELS, study 8-68068
 GaSe, plasmon and phonon excitation 8-72682
 Ge (111), CO adsorption on cleaved surface, electron energy loss spectra 8-79885
 InSb, electronic surface struct., Cs(Rb)(Na) adsorpt., AES, LEED, EELS study 8-68068
 MnO, electron energy loss spectra exam. 8-72652
 Mo, plasmon and phonon excitation 8-72682
 N₂, rot. excitation by electron impact 1-4 eV 8-55248
 NO, adsorbed on Ru (001), inelastic electron scatt. dissoc. energies adsorbed state depend. 8-95956
 NO, doublet-quartet transitions, low energy variable-ang. electron scatt. obs. 8-62933
 Na₂WO₃, intra- and interband plasmons, inelastic electron scatt. exam. 8-72098
 Ni film, inelastic electron scattering 8-92155
 NiO (100), electron energy loss spectra exam. 8-72652
 Ni(111), adsorption of acetylene, evolution of adsorber species, rel. to vibr. spectra 8-95952
 Pd(001), adsorpt. of CO, LEED, electron energy loss spectra study, surface struct. effect on weak chemisorpt. bonding 8-71987
 Pt, 5d band structure effects on line shapes and intensities of core electron excitations 8-92177
 Pt (111), surface reaction with acetylene ethylene, and H₂, EELS 8-71947
 Pt, (111) surface, characteristic loss of electrons (*German*) 8-52605
 Pt, surfaces (111) and 6(111)×(111), CO adsorption, EELS and thermal desorption spectroscopy 8-91547
 Pt(111), adsorption of NO, anal. of adsorption processes and surface reactions, vibration spectroscopy 8-87868
 ReO₃, intra- and interband plasmons, inelastic electron scatt. exam. 8-72098
 Si (111), CO adsorption on cleaved surface, electron energy loss spectra 8-79885
 Si, (111) cleavage, Kikuchi pattern, 40 keV incident electrons, electron energy loss spectra (*French*) 8-87594
 Si, annealed crystal, oxide precipitates identification by electron loss spectra 8-83952
 Si, phonon spectroscopy, amorphous versus crystalline material 8-83898
 Si, volume plasmon dispersion at large wave vectors, EELS 8-56094
 Si(Li) detectors, electron counting, appl. to electron energy loss spectra, by high voltage electron microscopy (*French*) 8-54511
 SiO₂, phonon spectroscopy, amorphous versus crystalline material 8-83898
 SiO₂, phase comp., electron spectroscopy obs. 8-60042
 SrTiO₃ (111), surface struct., electronic props., LEED, AES, UPS study, photoelectrochem. cell anode appl. 8-84035
 SrTiO₃, surface defects, electronic struct., LEED, AES, UPS study 8-84273
 Te, film, AES, LEED, XPS, energy loss spectra studies oxidation effects 8-73086
 TeO₂, film, AES, LEED, XPS, energy loss spectra studies 8-73086
 Th, absorption coefficients, near O_{IV} O_V thresholds, 5d cross sections calc. 8-90134
 ThNi₅, methanation catalyst, AES and characteristic energy loss spectra 8-56915
 TiO, electronic excitations, electron energy loss spectra in 3 to 60 eV range (*French*) 8-80440
 TiO₂, electronic excitations, electron energy loss spectra in 3 to 60 eV range (*French*) 8-80440
 TiO₂, phonon spectroscopy, amorphous versus crystalline material 8-83898
 U, absorption coefficients, near O_{IV} O_V thresholds, 5d cross sections calc. 8-90134
 UIr₃, (100) surface reconstruction, LEED, AES, electron energy loss spectra study 8-75918
 W (100) surface, adsorption of Co, electron energy loss spectra 8-71999
 WO₃ film, intra- and interband plasmons, inelastic electron scatt. exam. 8-72098
 W(100), adsorbed H, nondipole electron impact vibr. excitations obs. 8-63922
 ZnO, polar surface, clean (O₂-H-exposed), reflection energy loss spectra, 2-30 eV 8-64434
 ZnO, Zn 3d core-level transition in electron energy loss spectra, rel. to ZnSe (111) surface 8-68584
 ZrNi₅, methanation catalyst, AES and characteristic energy loss spectra 8-56915

electron energy states (condensed matter)

- see also band structure; band theory models and calculation methods; deep levels; defect electron energy states; dopplers; electron energy states of amorphous solids; electron energy states of liquid metals; electron energy states of liquid semiconductors; electron gas; electron traps; electronic density of states; exchange interactions (electron); excitons; Fermi level; Fermi surface; field interactions (condensed matter); heli-cons; hole traps; impurity electron states; Landau levels; localised electron states; magnetic breakdown; magnons; metal-insulator transition; metal theory; plasmons; polar semiconductors; polarons; positron states; ripplons; spin-orbit interactions; spin-phonon interactions; surface electron states; triplet state*
 alloy, disordered, spectral functions, augmented space formalism 8-84126
 binary substitutional alloy, with long range order, electron energy spectrum (*Russian*) 8-84121
 binary substitutional alloy with long range order, electron energy spectra (*Russian*) 8-75974
 Bloch electrons, behaviour in mag. field, rationality non dependence 8-79914
 dipole density wave state in electron-hole junction system, existence 8-76009

electron energy states (condensed matter) continued

- electron in field of small-radius pot. well and attractive Coulomb pot., energy spectrum 8-56059
 electron motion in one-dimens. periodic pot. under influence of uniform elec. and mag. fields 8-75972
 III-V semiconductors, electronic dielec. const., interionic separation d-core effect 8-60046
 metal, d-electrons, electron density model 8-91580
 multiple scattering in condensed media, calc. of density of states for noncrystn. Cu and Fe 8-91578
 multiple scattering in condensed media, embedding field and effective medium 8-51867
 semiconductor, Benard effect (*Russian*) 8-84122
 semiconductor solid solution, compositional disorder, free carrier absorpt. 8-64387
 Swiss Physical Society, autumn sessions 8-72053
 TCNQ salts, Qn(TCNQ)₂ and NMeAd(TCNQ)₂, rel. to dielec. const. and elec. cond. 8-60116
 TCNQ salts with asymmetric donors, rel. to mag. susceptibility 8-60264
 transfer integral method, three dims., appl. to harmonic cryst. 8-84161
 Fe-Ni alloy, optical and electronic characts., 20-1750°C, comp. depend. (*Russian*) 8-84601
 Na particle, consisting of ats., metallic Na, model, electronic levels 8-50673

electron energy states of amorphous solids

- see also Anderson model*
 alkali borate glass networks, π -electron distrib. SCF INDO LCAO-MO calc., O basicity 8-79924
 alloy, amorphous, electronic struct. 8-72062
 covalent amorphous semiconductors, local struct., bonding and electronic props. 8-51882
 glasses and amorphous semiconductors, band struct. and forbidden gap, review 8-75987
 metallic glasses, ferromag., Mossbauer investigation of electronic struct. 8-92009
 noncrystalline materials, personal review by Sir Nevill Mott 8-55811
 polyethylene disordered chains, electron localisation 8-87945
 polymer primary structures ESCA and ECHO methods 8-52630
 semiconductor, amorphous or disordered, cond. mechanisms, model of medium-range comp. disorder 8-79994
 semiconductor, light irradiation, nonequilib. electron distrib. function in forbidden gap (*Russian*) 8-75988
 As, amorphous, electron and phonon density of states calcs., comp. to XPS 8-56066
 As, phonon density of states compared to electronic density of states 8-55924
 C, amorphous, elec. cond. and Hall effect, temp. depend. 8-60141
 Cu, noncrystalline, electronic density of states, multiple scatt. calcs. 8-91578
 Fe, noncrystalline, electronic density of states, multiple scatt. calcs. 8-91578
 GeSe amorphous films, photoconductivity measurements, recombination model 8-64061
 K₂O-B₂O₃:Cu II, glass, O basicity, ESR study 8-80199
 K₂SO₄-ZnSO₄:Cu II, glass, O basicity, ESR study 8-80199
 (Mo_{1-x}Ru_x)₈₀P₂₀, supercond., mag. susceptibility 8-88057
 Na₂O-P₂O₅:Cu II, glass, O basicity, ESR study 8-80199
 Ni-Pd-P, Ni-Pt-P, amorphous and electronic structs., NMR Knight shifts and linewidths meas. 8-68400
 Si-H, amorphous, energy gap negative-U states, Si-H-Si three centre bond model 8-91606
 SiO₂, amorphous, effect of second nearest neighbour forces on vibr. 8-59915

electron energy states of glassy solids *see electron energy states of amorphous solids***electron energy states of liquid metals**

- book 8-51406
 surface ion density, nonmonotone, perturbative discrete ion introduction into jellium 8-72222
 transition metal, 3d, density of states of d-band, heat of vaporisation 8-95253
 Al, electron momentum density, correlations and ionic potentials 8-60052
 Al, model pseudopotential 8-91582
 Co, density of states of d-band, heat of vaporisation 8-95253
 Sn, electron transfer of rare earth impurities (*Russian*) 8-95278
 Ti, density of states of d-band, heat of vaporisation 8-95253

electron energy states of liquid semiconductors

No entries

electron field emission

- cathode, oxygen processing method 8-64448
 cathode prebreakdown field emission transition to vacuum breakdown 8-75462
 current density maximum, rel. to cathode geometry and kinetic props. 8-72704
 current fluctuation, power spectral density (*Japanese*) 8-88407
 energy distribution meas., analyser system 8-89605
 explosive emission regime, quasiplane cathode processes 8-75460
 n-hexane, field emission into liq., 275-334K 8-88406
 nonpolar organic liquids 8-88406
 single electron field emission non-destructive SEM method 8-88410
 steel, stainless, electrode material, annealing temp. cycle which improves emission props. 8-95858
 tetramethylsilane, field emission into liq., 275-334K 8-88406
 2,2,4-trimethylpentane, field emission into liq., 275-334K 8-88406
 two beam interference with field emission electron beams 8-63002
 ultrahigh vacuum discharge cathode erosion minimum conditions 8-75461
 vacuum arc cathode spot dynamic models 8-75481
 vacuum breakdown initiation, 4.2K, critical field emission currents 8-75459
 Al-SiO₂-Au cathode, emitted electron energy distrib. 8-52645
 Fe (100), (111), (110), spin polarised field emitted electrons 8-60553
 Fe, electron spin polarisation surface magnetism 8-68607
 He Townsend discharge field emission by higher-order ion clusters 8-67550
 InP/InGaAs/InP field assisted photocathode, minority carrier electron transport across p-p heterojunction 8-95651

electron field emission continued

- Ir, chemisorption levels of CO and O on (100) and (110) faces 8-84704
 Mo (100) face, surface reson. 8-72226
 Ni (110) surface, positive spin polarisation in field emission and demagnetisation by H₂ adsorption 8-52646
 Ni, electron spin polarisation surface magnetism 8-68607
 Si, moderately doped, ohmic contact electron emission, quantum calc. 8-68087
 Si photofield cathode, BaO adsorbed layer, work function and emission props. (Russian) 8-68608
 W (100) face, surface reson. 8-72226
 W, adsorption of Fe (Japanese) 8-91536
 W, field emission currents, modified by external mag. fields 8-88408
 W field emitter, strong polarisation effect in photoinduced field emission 8-95684
 W microneedles, field electron emission, suitability for electron source investigation 8-52644
 W, surface pot. barrier effect on photofield emission 8-60551
 W whisker, energy spread meas. of thermal field-emitted electron flow 8-92168

electron gas

- see also cathode ray tubes; electron optics
 Bloch wave effects in density response function 8-56092
 bound electron gas, static semiclassical response 8-56089
 CDW instability of electron gas in a strong magnetic field 8-79950
 classical diamagnetism, Gibbs method (Russian) 8-73918
 Compton scatt., bound and free electron Compton scatt. in coherent EM field 8-94225
 core hole relaxation energies 8-80439
 correlation energy, appl. of coupled cluster approx. 8-72102
 cyclotron resonances, Coulomb interaction effects in 2-dimens. 8-60073
 delta function fermion gas, solitons and HF solns. 8-49755
 dense high-temperature, classical modelization of symmetry effects 8-65869
 dislocations rel. to electron gas thermodynamics at 2^{1/2}th order transition (Russian) 8-51910
 effective ion-ion interaction, third-order contrib., ang. forces, tetrahedral solids 8-67970
 electrical conductivity of an interacting electron gas 8-95276
 electron dielectric function, second-order RPA 8-49753
 energy loss of correlated charges 8-87729
 free lattice electron gas with nearest and second nearest neighbour hopping 8-51873
 galvanomagnetic effects in spatially inhomogeneous system (Russian) 8-72129
 generator coordinate method 8-60077
 ground state, functional spin-density method (Russian) 8-51914
 hexagonal lattice equilibrium, electron gas model with noncentral forces, Ti, Zn, lattice dynamics 8-95123
 inhomogeneous, nonlocal approximation to exchange potential and kinetic energy 8-72096
 ion-ion interaction, third-order contribution, total energy calc. 8-63998
 layered compounds, effect of exchange on CDWs 8-60078
 light scattering, inelastic, photon-electron interactions 8-80368
 metal, damping of excited molecules located above surface 8-92160
 metal, normal and magnetic, temp. depend. of plasma freq. 8-56100
 metal, quantum kinetic equation for electrons 8-91686
 metal, simple, electronic struct. of H impurity 8-67978
 metals separated by dielectric, electronic component of metal-metal interaction force, calc. 8-52056
 noble metal, van der Waals forces and their contrib. to vacancy form. energy and phonon dispersion 8-91635
 nonlocal exchange-correlation pot. for inhomogeneous electron gas and quantum fields 8-65870
 photoemission, many-body effects, book contrib. 8-95667
 plasmon dispersion 8-56099
 polarisability, many-body correction 8-60071
 positron correlation energy, annihilation rate 8-92142
 quasi-one-dimensional electron gas with strong on-site interaction 8-67966
 relativistic degenerate electron plasma, dielec. response function 8-71529
 semiconductor, nonlinear current density, theory 8-56149
 semiconductor solid solution, compositional disorder, free carrier absorpt. 8-64387
 shielding of electric fields by surface electron states in an ionic lattice 8-52059
 short range correlations 8-84156
 short range order, many electron effects, pseudopotential method 8-79954
 spin density functional theory, linear response functions 8-67965
 static electron gas dielectric function, simple useful anal. form 8-79953
 surface magnetic props. of Bloch electron gas in opposing elec. and mag. fields at 0K 8-63992
 surface photoemission of model system, book contrib. 8-95665
 two dimensional, classical, hypernetted chain solns. 8-67963
 two dimensional, collective excitations and electrodynamic behaviour in three layer structure 8-60079
 two dimensional, correlations 8-63996
 two dimensional, ferromagnetism 8-60258
 two dimensional, in strong mag. field, Wigner solidification 8-60005
 two dimensional, mag. props. 8-56095
 two-dimensional electron-impurity system in strong mag. field, electron spectrum and cond. (Russian) 8-88016
 Wigner crystal, two-dimensional, possible re-evaporation at extremely low densities 8-56085
 e⁻e⁻ pairs and equilb. radiation in quantising mag. fields (Russian) 8-49990
 Bi, electron gas heating at low temp. 8-60133
 n-Si inversion layer, electron mag. suscept. 8-52009
 Si inversion layer, influence of natural superlattice on 2-dimens. electron gas spectrum (Russian) 8-68064
 Si, screening of ions, band struct. calcs. with screening variants 8-67938

electron guns

- design for producing high-intensity beam with rectangular cross section 8-93785
 electrostatic einzel lenses, reduced spherical aberration field emission guns appl. 8-74831
 glow discharge generated high-power pulsed beams, gas dynamics diagnostics appls. 8-63515
 high current density, axially symmetric, synthesis 8-55063
 high-current, laminar beam formation for linear accelerators 8-74516
 high-power long-pulse thyatron modulator with small off-duty factor 8-86380
 intensity regulator for 5 to 50 keV electron guns (French) 8-54499
 ionospheric rocket expt. high-power electron gun (Japanese) 8-61566
 mass spectrometer three-dimens. quadrupole electron gun, compact tube assembly poisoning resistant 8-54493
 plasma emitter, electron optical system simulation 8-67442
 plasma production modified magnetron discharge facility 8-75380
 point cathode type, electron-optical props. (German) 8-82901
 portable, containing source, monochromator, counters, for particle detector calibration 8-78539
 tetrode gun, transport of high-energy, high-power electron beams 8-89587
 LaB₆ three-electrode 250 A pulsed electron gun 8-82553
 W tip, use of focused laser beam for cathode heating (German) 8-89591

electron-hole avalanches see impact ionisation**electron-hole drops**

- antiferromagnet, existence of states with superfluid flow, Ginzburg-Landau theory (Russian) 8-72085
 condensation and liquefaction in strong mag. field, RPA and variational calcs. 8-63984
 electron-hole drops, surface struct. 8-60058
 far IR radiation from electron-hole drops (Russian) 8-72600
 Fermi liquid, two component, with electron-hole pairing, microscopic theory (Russian) 8-51905
 motion damping, deform. pot. scatt. 8-67950
 motion damping, impurity and piezoelec. scatt. 8-67951
 noncrystalline system, continuous and discontinuous metal insulator transitions 8-56076
 phase transition during formation of exciton condensate (Russian) 8-60060
 semiconductor, collective excitations of electrons and holes in strong EM field and absorpt. of light (Russian) 8-79945
 semiconductor, electron-hole droplet nucleation and stability, hydrodynamic approach 8-72080
 semiconductor, electron-hole drops under microwave radiation, kinetics of instabilities 8-60059
 semiconductor, optical props. under intense laser fields 8-72513
 semiconductor, temp. of moving electron hole drop (Russian) 8-67953
 semiconductors, basic principles (Russian) 8-72081
 semiconductors, electron-hole liquid theory, generalised RPA 8-87914
 shape in magnetic fields, anal. 8-67954
 size effects, work function determ. 8-72077
 spectrum of electron-hole system in one-dimensional infinitely deep potential well (Russian) 8-67944
 two-dimensional dielectric electron-hole liquid, feasibility 8-87917
 CdS, gain spectroscopy and plasma recomb. 8-88327
 CdS_{1-x}Se_x, mixed cryst., electron-hole drops and plasma, luminesc. obs. (Russian) 8-92119
 GaP, electron-hole plasma photolum. obs. 8-52559
 GaP, motion damping, impurity and piezoelec. scatt. 8-67951
 GaSe exciton absorpt., change under a pulsed dye laser 8-92088
 Ge, compressed electron hole plasma, luminesc. 8-72592
 Ge, electron-hole drop magnetostriction 8-87912
 Ge, electron-hole drop phase separation due to uniaxial stressing 8-84145
 Ge, electron-hole drop velocities as probe of phonons 8-68517
 Ge, electron-hole drop velocities, excitation wavelength depend. 8-88358
 Ge, electron-hole droplet, attachment to donor 8-87916
 Ge, electron-hole droplets, surface props., SCF calc. 8-51904
 Ge, electron-hole droplets, transient photoluminesc. intensities 8-88353
 Ge, electron-hole drops, accel. by IR radiation field 8-95264
 Ge, electron-hole drops, far IR absorption 8-56467
 Ge, electron-hole drops, far IR magneto-optical effects 8-84565
 Ge, electron-hole drops, spatial distrib., time and spatially resolved absorption at 3.4 μm 8-92075
 Ge, electron-hole drops, surface struct. 8-60058
 Ge, electron-hole liquid, luminesc. under infinite uniaxial compression 8-87915
 Ge, electron-hole liquid, pinch effect 8-87993
 Ge, electron-hole-droplet cloud, photoluminesc. of laser excited surface, phonon wind 8-84146
 Ge, high density electron-hole plasma, infrared absorpt. at low temp. 8-92078
 Ge, IR absorption and scatt. by electron-hole drops 8-51903
 Ge, interaction of electron-hole drop with crystal surface 8-79941
 Ge magnetoacoustic effects in the drag of electron-hole drops by phonons 8-68057
 Ge, magnetoplasma resonance (Russian) 8-79944
 Ge, motion damping, impurity and piezoelec. scatt. 8-67951
 Ge, phonon drag of electron-hole drops in longit. quantizing mag. field (Russian) 8-64070
 Ge, uniformly stressed, density and binding energy of electron-hole droplets, photolum. meas. 8-60062
 MgO, electronic excitations and luminescence, review (Russian) 8-72575
 Si:P heavily-doped, photoluminescence 8-72572
 ZnSe, single cryst., electron-hole drops, boundary luminesc. (Russian) 8-80412

electron-hole recombination

- see also carrier mobility
 ambipolar diffusion meas. using nonlinear transient gratings 8-80000
 chalcogenide glass, mech. for electron-hole recomb. 8-72196
 decay kinetics in diffusion approx. in presence of particles pair correlation 8-80398
 degenerate semiconductor, recombination-generation currents derivation 8-52007

electron-hole recombination continued

- diffusion length and surface recomb. vel. determ., light excitation 8-91725
- electron-hole transitions, nonstationary processes, numerical anal. (*Ukrainian*) 8-84229
- n-GaP, quasidirect radiative recombination of free holes at neutral shallow donors 8-64410
- heterostructure laser, elec. characterisation 8-79020
- insulator, charge carrier injection, Onsager model 8-80001
- p^+i-n^+ structure, double-injection negative differential resist. problem, surface recomb. effects 8-88024
- pair correlation of particles under decay conditions, recomb. kinetics in diffusion approximation 8-91702
- photovoltaic effect, impurity centre models (*Russian*) 8-60153
- SEM meas. of diffusion const., lifetime and surface recomb. vel. 8-91701
- semi-infinite direct-gap semiconductor optically generated minority carriers 8-95312
- semiconductor, diamond-like narrow-gap, Auger recomb. calc. 8-63978
- semiconductor-electrolyte functions, photocharacts. 8-91764
- variable gap semiconductor, photolum. emission and excitation spectra 8-76526
- AgCl, cryst. luminesc. and photovoltaic effect kinetics 8-64391
- n-AlGa_{1-x}As, epitaxial, photolum. emission and excitation spectra 8-76526
- AlGa_{1-x}As p-n junction, photolum. and current, interface recomb. effects 8-95346
- CaO, doped, thermal stability of hole centres and hole recombination luminescence (*Russian*) 8-72614
- CaO, undoped and Cl-, F- or Al-doped, X-ray and UV luminesc., electron-hole recombination processes (*Russian*) 8-76528
- CaS, phosphors, hole recombination luminescence (*Russian*) 8-72576
- CdS, exciton luminescence, surface recombination, space-charge-layer effects 8-80410
- CdS:Cu, photocond. under high excitation intensity 8-52033
- n-CdS(Se)(Te) semicond. liq. junction solar cells, photocurrent spectra, carrier recombination 8-76142
- CdSe, charge transport 8-84233
- GaAlAs-GaAs double heterostructure, interfacial recomb. velocity, photolum. meas. 8-68075
- Ga_{0.5}Al_{0.5}As-GaAs, DH, interfacial recomb., photolum. time decay meas. 8-95347
- GaAs, film, radiative relax. time, nonequilibrium carriers 8-84657
- GaAs, illuminated, carrier lifetime profile, depth depend. 8-68036
- n-GaAs:Te, heavily doped, interband luminesc. intensity, heat treatment effect 8-72593
- p-Ga_{1-x}In_xAs, Auger recomb., theory and luminesc. expts. 8-56518
- Ga_{1-x}In_xSb:Zn(Te), photolum. and stimulated emission obs. 8-72595
- β -Ga₂O₃, intrinsic UV emission obs. 8-80396
- GaP:N, photoluminesc., temp. depend., exciton recombination mechanism 8-88355
- GaSb, photolum., electrolum. meas. in p-n junction, temp. influence 8-72594
- n-GaSb:Te, heavily doped, photoluminesc. spectra 8-84644
- Ge, near intrinsic, negative differential cond., ambipolar size effect due to hot carriers 8-72185
- Ge:Ba, Ca, recomb. props. 8-56156
- GeSe amorphous films, photoconductivity measurements, recombination model 8-64061
- Hg_{1-x}Cd_xTe, single-LO-phonon and -plasmon recombination channels narrow-bandgaps 8-91728
- p-InAs, Auger recomb., theory and luminesc. expts. 8-56518
- In_{1-x}Ga_xP, epitaxial film, cathodolum. obs., recomb. mechanisms 8-72613
- KBr:Eu(Yb), electron-irrad., photostimulated luminesc., ionic processes 8-52561
- KCl:AgCl, tunnelling-recombination luminesc. 8-88354
- KI, recomb. luminesc. of H-centre and F-centre electrons (*Russian*) 8-80402
- KI:Eu, electron-irrad., photostimulated luminesc., ionic processes 8-52561
- KI:Eu²⁺(Sr²⁺)(Mn²⁺), elec. field effect on mech. of recomb. 8-80397
- MgO, doped, thermal stability of hole centres and hole recombination luminescence (*Russian*) 8-72614
- NaI:Cu⁺, luminesc. of isolated V_K-centres 8-84641
- PbTe epitaxial film, stimulated emission, absorption spectra and recombination 8-80409
- RbCl:Eu, electron-irrad., photostimulated luminesc., ionic processes 8-52561
- Si, amorphous, electron-hole recombination, mech. 8-72196
- n-Si, γ -irrad. (E_{\max} =100 MeV), carrier recomb. 8-56158
- Si, intrinsic semiconductor, radiative recombination probability (*German*) 8-95608
- Si p^+i-n^+ diodes, double-injection switching, effect of surface recomb. 8-88025
- Si, recombination luminescence, electron-hole drop, excitons orientation in mag. field 8-88362
- SiO₂, doped, thermal stability of hole centres and hole recombination luminescence (*Russian*) 8-72614
- n-SnO₂, high resist., photoelectronic processes 8-60157
- TiSe₂, UPS, excitonic instability indicated from study of band struct. 8-56069
- p-ZnSiP₂, single cryst., recomb. processes, photoelec. props. (*Russian*) 8-68053

electron impact

- see also atomic electron impact excitation; atomic electron impact ionisation; molecular electron impact dissociation; molecular electron impact excitation; molecular electron impact ionisation; secondary electron emission
- bulk plasmon excitation due to electron scatt. from single crystals 8-87933
- doubly truncated spherical electrostatic energy analyser for (e, 2e) expts. 8-58872
- metal ion source using high power density electron impact 8-54497
- neutron yield calcs., on C, Al, Fe, Ni, Cu, Ag, Ba, Ta, W, Au, Pb, U 8-95622
- steel, stainless, type 304, electron stimulated desorption rel. to CTR first wall appl. 8-51818

electron impact continued

- Al alloy, 6061, vacuum material, desorpt. of neutral mols. by electron and ion bombardment 8-95229
- Al, high-current electron beam refl. coeffs. (*Russian*) 8-84690
- Cu, high-current electron beam refl. coeffs. (*Russian*) 8-84690
- GaP, surface sensitivity, low energy electron transmission optical modulation 8-76567
- Mo, electron backscatter fractions 8-87717
- Mo, electron stimulated desorption of negative ions from adsorbed gases 8-91549
- Mo, surface, electron-stimulated desorption of negative ions, work function 8-72654
- Ni:K⁺(Ba⁺), ion implantation, effect on inelastic refl. and energy losses of fast primary electrons 8-55900
- Ni/Au film on silicon vacuum deposited, electron impact mass spectrometric exam. of surface contaminants 8-75957
- Pb, high-current electron beam refl. coeffs. (*Russian*) 8-84690
- Si, surface, optical modulation of low energy electron reflection and transmission 8-88388
- Si thin crystal, electron backscatt. in electron microscope 8-75510
- W, electron backscatter fractions 8-87717

electron interactions see elastic scattering of electrons by atoms and molecules; electron-electron interactions; electron impact; electron-nucleon interactions; electron-nucleus reactions; electron-positron interactions; hadron electroproduction; neutrino-electron interactions

electron ionisation see electron impact

electron lenses

see also aberrations; electron microscopes; electron optics; electrostatic lenses; magnetic lenses

electron-beam focusing optimisation with specified image parameters 8-86385

scanning beam system, moving objective lens design 8-74829

electron lifetime (metals) see electron relaxation time (metals)

electron lithography see electron resists

electron mean free path (metals)

film, calc. 8-72283

metal, theory of electronic transport of sound packets in parallel mag. field (*Russian*) 8-84261

metal wires, DC resistance, size effect correction 8-91679

metallic film, grain boundary electron scattering by effective mean free path 8-84320

Al, film, photoelectron-grain boundary scatt. in Al-SiO₂-Si struct. 8-64120

Au-Fe film spin glass, low temp. resistivity, mean free path effects 8-80163

Cu₂Mo₆S₈, normal state and superconducting property measurements 8-91660

Ga, supercond. thin film, tunnelling meas. in high mag. field 8-68120

Gd, spin wave temp. depend., exchange coupling role 8-68199

Hf, rel. to high temperature thermophysical properties 8-91404

Nb₃Ge(Al), anomalous resistivity, insight from band theory 8-60106

PbMo₆S₈, normal state and superconducting property measurements 8-91660

Ti, rel. to high temperature thermophysical properties 8-91404

Zr, rel. to high temperature thermophysical properties 8-91404

electron micrographs see electron microscope examination of materials; electron microscopy

electron microprobe analysers see electron probe analysis

electron microprobes see electron probes

electron microscope applications

see also electron microscope examination of materials; scanning electron microscope applications

convergent beam diffraction in HV electron microscope 8-83674

education, electron interference using standard electron microscope and electron biprism as interferometer 8-62005

electron diffraction instrumentation 8-83683

ferromagnetic film thickness meas. by diffraction electron microscopy 8-86392

photomicrography of marine microorganisms on submerged surfaces 8-85454

electron microscope examination of materials

see also electron microscope applications; electron microscopy; scanning electron microscope examination of materials; scanning-transmission electron microscope examination of materials; transmission electron microscope examination of materials

alkali halide, morphology of growth and evaporation surface 8-79544

anthracene, mol. imaging by high resolution electron microscopy 8-79600

asbestos fibres identification, electron microscope techniques comparison 8-66012

benzonitrile, anodic polymer growths during electrical breakdown conditions, TEM study (*French*) 8-75960

β_1 brass containing α -precipitates, reversible shape memory effect (*Japanese*) 8-60711

butadiene, styrene, 4-vinylpyridine terpolymer, cross-linked by coordination with Fe (III) chloride, ion clustering 8-83748

butyl rubber dispersion, electron-microscopic investigation 8-53268

carboxyl terminated butadiene nitrile-diglycidyl ether of bisphenol A epoxy resin, struct. and mech. props. 8-52901

cell, surface photoelectron micrographs and quantum yields 8-61148

ceramic powders, electron microscope determination of particulate sizes (*German*) 8-57891

chromindur, origin of coercivity, Lorentz microscopy, magnetisation and Mossbauer effect 8-64219

crystal analysis, optical selected-area diff. patterns of high-resolution electron-microscopic images 8-55789

cup and cone fatigue fracture, electron fractographic obs. (*Japanese*) 8-72838

diamond, Fresnel diffraction at platelets, defect struct. anal. by 3 λ phase-contrast microscopy 8-87701

dislocation generation from grain boundary, in situ obs. 8-51547

electron sensitive materials 8-83701

failure analysis, fault tree technique and electron fractography 8-53071

ferrite powder grain size meas., sample prep. (*German*) 8-56833

ferromagnetic ordered structures, domain structure, effect of defects, electron microscopy 8-64214

film, epitaxial crystal growth, electron microscope obs. (*Japanese*) 8-91568

electron microscope examination of materials continued

- fracture mechanics parameters, applicability to creep, fatigue crack propag., at evalated temp., exam. using various materials (*Japanese*) 8-52962
- Kevlar 49 high modulus polyaromatic fibre, supramolecular struct. 8-55819
- leucine aminopeptidase crystalline aggregates, interpretation of electron microscope images 8-68988
- metal, hardening due to increased subgrain boundary stability 8-52934
- muscle fibre, skeletal, helicoids in T system and striations, HV electron microscopy 8-53356
- myelin structure, of sciatic nerve from bull frog, melamine resin as embedding medium 8-92764
- opal, ordered arrangements of SiO₂ spheres of two different sizes 8-87658
- PMMA, destructive mech. cracks, electron microscope exam. of generation centres 8-68782
- poly-p-phenylene terephthalate, high modulus fibre, struct. obs. 8-75564
- polyconjugate system, interrelation between physicochem. props. and microstruct. 8-55816
- polyethylene, crystals, subject to fold-surface tensile stress, elastic deform. 8-76712
- polyethylene, pyramidal crystals, soln.-grown, collapse mechanics 8-76713
- polyhexamethylene terephthalate/polyoxytetramethylene block copolymers, supramolecular texture 8-91261
- polymer blend morphology, methods for study and specimen prep. 8-75580
- polymer film, supermolecular structure and mech. stress distrib. among chem. bonds 8-75562
- polymeric cryoprotectants in preservation of biological ultrastruct., aq. soln. low temp. states 8-65157
- polyoxymethylene, epitaxial growth on KBr single crystal (*Japanese*) 8-56054
- polypropylene, cold-drawn isotactic bars and thin films, microstruct. and annealing 8-95760
- polypropylene, monofilaments, drawing behaviour, melt-induced orientation effects 8-84922
- polystyrene, isotactic, morphology and growth of chain struct. (*German*) 8-75597
- polystyrene, Millar interpenetrating network, viscoelasticity and phase domain form. 8-83749
- PTFE fibres, US effects on structure (*Polish*) 8-68702
- PVC:Fe(Cu) film, struct. and optical props., soln. growth technique 8-51837
- quartz, ion-etching of grooves for SAW devices 8-95822
- quartz grains, from coastal plain of Rio Grande do Sul, Brazil, coaxial crescentic marks (*Spanish*) 8-92816
- radioactive waste, solidified, composition, structure and properties of final product obs. (*Czech*) 8-66353
- rare earth Zr_{1-x}O_{2-x/2} growth from skull melting, directional solidification 8-60567
- refractory composites, fibre reinforced, directionally solidified tensile tests, in HVEM, deform. and fracture (*French*) 8-68785
- S glass-Ni sphere composite, exam. of crack shape and fracture toughness 8-72886
- stearic acid cryst., etch pit obs. of dislocations 8-87676
- steel, alloy, Cr-C (12, 0.2 wt.%) growth of grain boundary ferrite allotriomorphs, photoemission electron microscope exam. 8-88468
- steel, alloy, Fe-C-Zn (0.45, 1.56 wt.%), pearlite transformation during continuous cooling 8-80538
- steel, alloy, Fe-Cr-Ni-Mo-Al, (13, 8, 2, 1, wt.%), H₂ effects on fracture, exam. 8-60809
- steel, alloy, Mn (Ni), Mossbauer, X-ray and electron microscope studies of martensite 8-56621
- steel, austenitic, 16H2NMB, struct., texture and mech. props. of product of transform. 8-92273
- steel, austenitic stainless, structural inhomogeneity, electron and optical microscope exam. 8-72827
- steel, C, fatigue crack features, in S 35 C and SK 5, anal. by precision matching method (*Japanese*) 8-52955
- steel, C, fatigue crack propag. and fractography under periodic over-stressing, exam. (*Japanese*) 8-52958
- steel, C, ferritic-pearlitic transform., struct. study by optical and electron microscopy (*French*) 8-68685
- steel, C, spheroidised, fracture toughness, cementite particle effects, optic and electron obs. 8-60785
- steel, C, tempered martensite embrittlement, and retained austenite, exam. 8-56754
- steel, high strength, fatigue crack propag. and fractography under periodic over-stressing, exam. (*Japanese*) 8-52958
- steel, high strength, weld cold cracking, anal. of fracture morphology, using SEM (*Japanese*) 8-52960
- steel, high tensile strength, base plate and welded joints, exam. of fatigue crack growth rate (*Japanese*) 8-52956
- steel, hypoeutectoid Widmanstätten struct. form., contrib. to the laws (*Slovenian*) 8-84817
- steel, low alloy and C, bainite morphology 8-68682
- steel, low C, fatigue crack tip, observation of crack closure phenomena, by electron microscopy 8-68794
- steel, low-C, ferritic, deform. microstruct., electron microscopy (*German*) 8-64589
- steel, maraging low-Ni, isothermal martensitic transformations (*Russian*) 8-88465
- steel, mild, fatigue crack initiation, fractographic exam. (*Japanese*) 8-52957
- steel, Mn-Cr-V, structural changes during solution annealing (*Czech*) 8-84864
- steel, stainless, C-Cr-Ni-Mn-V, non mag., aged, struct. and mech. props. (*Russian*) 8-56666
- steel, stainless, precipitate crystallography using electron microscopy 8-83698
- steel, stainless, type Kh17N13M2T, strengthening by plastic deformation and cold working (*Russian*) 8-52839
- steel, tool, NC6, carbide lattice, kinetics of its destruction (*Polish*) 8-92280
- steel, W and Mo, quantitative anal. of carbides formed during tempering 8-64571

electron microscope examination of materials continued

- steel, X5CrNiTi26.6, ferrite-austenitic struct., optical and electron microscopy 8-84848
- steel nitride phase hardening, precipitation and solution kinetics after heat treatment 8-95756
- styrene-tetrahydrofuran block copolymer, H₂O contact angle and surface struct. (*Japanese*) 8-79861
- wear debris anal., quantitative methods 8-64912
- Ag, colloidal, lattice defects, X-ray diffr. and electron microscopy exam. 8-51567
- Ag film, on mica, microstruct. changes 8-72013
- Ag films, UV photostimulated oxidation (*Russian*) 8-95850
- Ag on W (001), geom. factors of FCC-BCC epitaxy 8-60041
- Ag, pure, temp. depend. of stacking fault energy 8-51565
- Ag ultra-thin film, deposited on MgF₂ and SiO substrates, struct. and internal stress 8-91572
- Ag-Cd (45 at.%), morphology and crystal struct. of stress-induced martensites 8-68693
- Al, [111] single crystal, in situ deform., HVEM obs. 8-52886
- Al alloy, fatigue crack propag. and fractography under periodic over-stressing, exam. (*Japanese*) 8-52958
- Al and Al-Mn (1 wt.%), subgrain growth during annealing after cold work 8-56656
- Al, anodic film, formed in H₂SO₄, electron microscopy 8-68843
- Al, dislocation generation from grain boundary, in situ obs. 8-51547
- Al film, vacuum deposited, structural changes during annealing at temp. near melting point 8-84096
- Al, porous anodic film, ion beam thinned, electron microscopy 8-92390
- Al, thin foil, adhesion and friction, rel. to observed dislocation density 8-64706
- Al, vacuum deposited, structural singularities and porosity (*Russian*) 8-75950
- Al-Ag (up to 40 at.%), exam. of anelastic phenomena and structural state 8-76693
- Al-Cu (4 wt.%), elastic accommodation of semicoherent θ' 8-64543
- Al-Cu-Mg-Mn-Fe-Si, alloy D16, effect of mechanothermal treatment on mech. props. 8-56674
- Al-Mg-Ag, age effect on age hardening (*Japanese*) 8-52831
- Al-Sn, (<0.28 wt.%) corrosion behaviour in 16% HCl 8-85054
- Al-Ti-B alloys, segregation of Ti, electron microscope exam. 8-52820
- Al-Zn-Mg, precipitation of η' phase, heat treatment, electron microscope obs. 8-68699
- Al₂O₃, anodic film transient pitting during film growth 8-56817
- Al₂O₃, thick vacuum condensates, struct. (*Russian*) 8-95242
- β -Al₂O₃-Na₂O-SiO₂, solid electrolytes, exam. of microstruct. ionic resistivity 8-80566
- Al₂O₃-SiO₂-P₂O₅, refractory glasses, exam. of liquid immiscibility and crystallisation 8-55814
- Au bicrystals, interaction of lattice dislocations with grain boundaries, electron microscope obs. 8-51579
- Au crystallites, formation in flowing Ar system, density, size distrib. and size dispersion 8-88415
- Au film, on Si, coincidence site phase boundaries 8-67927
- Au on W (001), geom. factors of FCC-BCC epitaxy 8-60041
- Au, pure metal and Au-Sn dil. alloy, vacancy clusters, quenching and ageing 8-76671
- Au, VPE on NaCl, role of surface steps 8-79902
- Au, vacuum deposition, on (100) surfaces of KBr, KCl and NaCl substrates with colloidal centres (*Rumanian*) 8-60579
- Au-Ag-Cd, martensitic transformation, preceding struct. anomaly 8-68692
- Au-Mn system, AABF struct., experimental evidence for occurrence 8-63698
- Au₂Mn₃, electron microscope exam. of ordering 8-63697
- (Ba₂Nb₂Si₂O₂₆)_n.Ba₃Nb₂Ti₄O₁₁, n=3/2 to 29/2, intergrowth series, electron microscope obs. (*French*) 8-83762
- (Ba₃Nb₂Si₄O₂₆)_n.Ba₃Nb₂Ti₄O₁₁, multiple intergrowth and microdomains obs. by electron diffr. and microscopy (*French*) 8-95160
- Be bronze BrB2, quenched deformed, substruct. and props., effect of prerecrystallisation annealing (*Russian*) 8-60677
- C particle formation, C₁+C₃ as possible first step 8-68876
- C, pyrolysis mechanism, electron microscopy, DTA, IR, ESR obs. 8-56593
- C, texture change on ht. treatment under press. 8-60687
- Ca₃Ga₂Ge₂O₁₂, substrate, electron examination of microstruct. and microsegregation 8-67919
- CaO-Al₂O₃-SiO₂-ZnO, continuous unidirectional crystn. of fibrous metasilicates from melt 8-95739
- CaO-MgO-Al₂O₃-SiO₂-ZnO, continuous unidirectional crystn. of fibrous metasilicates from melt 8-95739
- Cd, electron radiation damage in HVEM, nature of defect clusters 8-59838
- CdS, epitaxial layers on Cd single crystal, direct synthesis and struct. 8-68628
- Co, foil, wall struct., bubble, plate domains, 1 MeV electron microscope study 8-84463
- Co-Cr(VC)(Ti,V)C-(Al), eutectic alloy, unidirectional solidification, oxidation and tensile tests 8-52790
- Cr-C-Ni-(P), hard alloys, sintered, fracture props., P addition effects 8-60610
- Cr₂O₃.SH₂O, heat-treated, narrow particle size distrib., surface props. 8-85210
- Cu, Frenkel pair production threshold energy, temp. depend., exam. 8-51530
- Cu on W (001), geom. factors of FCC-BCC epitaxy 8-60041
- Cu-Al, faulted dipoles, geometry and form. 8-59809
- Cu-Al, intrinsic temp. depend. of stacking-fault energy 8-51564
- α -Cu-Al, short range ordered, struct. and new superlattice phase 8-52756
- Cu-Al-Ni-Fe, (10, 5, 5 wt.%), cast microstruct. 8-80535
- Cu-Al(Au), critical voltage effect (*Japanese*) 8-91206
- Cu-Be (0.99 wt.%), direct obs. of small Guinier-Preston zones 8-72776
- Cu-Ni-Cr system, coarsening in the ($\gamma_1 + \gamma_2$) region, metallographic study 8-84762
- Cu-Ni-Fe (26.8 wt.%), microduplex struct. form., hardness meas., optical and electron microscopy (*Japanese*) 8-76659
- Cu-SiO₂, dispersion hardened, surface plasticity effect 8-52832
- Cu-SiO₂ single crystals, dispersion hardened, exam. of yield stress between 77 to 1200K 8-76720

electron microscope examination of materials continued

- Cu-Sn (25 wt.%), struct. after ultrahigh-speed quenching (*Russian*) 8-80563
- Cu-Ti, liquid phase sintering, metallographic electron beam microanalytical investigation 8-95888
- Cu-Zn (30 wt.%), rolled, electron microscope exam. of recrystallisation 8-76663
- β -Cu-Zn-Al, electron microscope exam. of premartensitic state 8-72801
- Cu-Zn-Al, pseudoclastic alloy, exam. of fatigue props. 8-76744
- Cu_3Sn , one-dimens. long period superstructs. with Zn and Ni additions 8-83777
- Fe, degree of charging of surfaces polished by TiC and synthetic diamond micropowders 8-60880
- Fe-Al(Cr)(V)(Ti), hardness after nitriding, metallographic, electron microscope and microprobe anal. 8-51608
- α -Fe-C (0.03 wt.%), structural singularities of transition from thermally activated to force-induced fracture (*Russian*) 8-56731
- Fe-C-Mo, dynamics of transform. interface, ferrite-austenite interface 8-52795
- Fe-C-Mo, dynamics of transform. interface, at intermediate temps. 8-52796
- Fe-Co-Ni-W alloy, 45KKhVN, plastic deform., electron microscope obs. (*Russian*) 8-80584
- Fe-Cr, role of C in transform. by heating in ($\alpha+\gamma$) phase (*French*) 8-52798
- Fe-Ni-Cr coating, electrodeposited, exam. of passivity 8-80655
- Fe-Ni-Cr-Ti-Mn-Mo, (25.8, 14.04, 2.17, 1.27, 1.30 wt.%), superalloy A-286, precipitation hardening, exam. of fracture toughness and mech. props. 8-92355
- Fe-Si (3 wt.%), grain oriented, MnS precipitate distribution, electron microscope observation (*Chinese*) 8-95751
- Fe_3Al , ordered alloys, atomic order parameters from topology of electron-microscope diffr. contrast from antiphase boundaries, quantitative determ. 8-95016
- γ - Fe_2O_3 , prep. from thermal decomp. of $[\text{Fe}_3(\text{HCOO})_6(\text{OH})_2]\text{HCOO} \cdot 4\text{H}_2\text{O}$ and characterisation 8-80741
- Fe_2O_3 -TiO₂ system, high temp. intergrowth struct., metal atom ordering in intergrowth boundaries 8-79573
- FeS_2 (pyrite), glide elements study by electron microscopy and electron diffr. 8-83817
- GaAs:Si, Cr, carrier concs. from Hall effect, microscopy, localised vibrational modes absorption meas. 8-56104
- Gd, mag. domains, Lorentz microscopy obs. 8-84448
- Gd-Co film, amorphous, Ar sputtered, struct. 8-63946
- Gd-Co film, amorphous, phase separation as source of perpendicular anisotropy 8-64244
- Gd-Co-Mo film, amorphous, Ar sputtered, struct. 8-63946
- Gd-Fe film, amorphous, in-situ ion beam sputtered, microstruct. and Lorentz mag. struct. 8-63947
- $\text{Gd}_3\text{Ga}_2\text{O}_{12}$, substrate, electron examination of microstruct. and microsegregation 8-67919
- Ge epitaxial layers, on GaAs substrate, misfit dislocation multiplication mechanism 8-87673
- Ge, evaporated film, lattice parameters and phase transition temp., surface influence of glass substrates 8-94996
- Ge film, amorphous, ^{74}Ge ion implanted, defect struct. obs. 8-51848
- KBr, single crystal, preirradiation and radiation defects, electron microscopical estimation (*Russian*) 8-75695
- KCl, single crystal, preirradiation and radiation defects, electron microscopical estimation (*Russian*) 8-75695
- KCl:Ba²⁺, precipitation kinetics, supersaturation effects, geometry of formed heterophase struct. (*Russian*) 8-84824
- $\text{K}_2\text{O-Ta}_2\text{O}_5$ mixed oxides, cryst. struct., electron microscopy study 8-91309
- $\text{K}_2\text{O-Ta}_2\text{O}_5$ mixed oxides, cryst. struct., electron microscopy study 8-91310
- KSbO_3 , cubic, K⁺ ion ordering, electron microscopy 8-79550
- LiFe_2O_4 , material loss and high-temp. phase transition 8-64534
- LiTaO_3 - SiO_2 - Al_2O_3 , transparency in relation to microstruct. 8-53005
- Mg, electron irradi. damage, dislocation loop growth, in situ obs. 8-87715
- Mg_3Cd , disordering under electron irradi. in electron microscope 8-83849
- MgO, electron diffr., dynamical effects for cryst. struct. determ. 8-83679
- MgO, precipitation on dislocations, ultramicroscopy and chem. etching 8-67720
- $\text{MgO-Al}_2\text{O}_3$ - SiO_2 , metastable liq. phase separation region, electron microscope exam. 8-88451
- Mo, foil dislocation struct. of rolling texture (*Russian*) 8-59810
- Mo-C dilute alloy defect cluster nucleation and growth under 1250 keV electron microscope (*Japanese*) 8-87663
- Mo-ZrC, internal oxidation, struct. formation law, microstruct. examination 8-84836
- MoO_3 reduction to MoO_2 by electron beam, electron diffr., microscope investigations. (*French*) 8-95945
- $\text{Na}_2\text{O-CaO-SiO}_2$, foil, exam. of surface plasticity, and cracks, by electron microscopy 8-68733
- NaSbSe_2 films, struct., photoelec. and opt. props. 8-51834
- Nb_3Ge , RF and DC sputtered films comparison, O content effect 8-72022
- Nd-Co film, amorphous, exam. of domain struct. 8-68336
- Ni alloy 718, fatigue crack growth at 298 and 823K, frequency and wave form effects 8-64636
- Ni on W (001), geom. factors of FCC-BCC epitaxy 8-60041
- Ni-based alloys, binary, ternary, complex, TiC additions; effects 8-92305
- Ni-Cr-Ti-Al-Fe-Co (19.65, 2.40, 1.37, 0.78, 0.52 wt.%), strength of γ' hardened alloy, ageing exam. 8-88501
- Ni-In, FCC, cellular precipitation kinetics 8-52823
- Pd, catalyst hollow cone dark field microscopy on γ -alumina substrates 8-61049
- Pd particles formed by evaporation on alkali halide crystals, orientation and struct. 8-84108
- $\text{Rb}_2\text{O-Nb}_2\text{O}_5$ mixed oxides, cryst. struct., electron microscopy study 8-91309
- $\text{Rb}_2\text{O-Nb}_2\text{O}_5$ mixed oxides, cryst. struct., electron microscopy study 8-91310
- $\text{Rb}_2\text{O-Ta}_2\text{O}_5$ mixed oxides, cryst. struct., electron microscopy study 8-91310

electron microscope examination of materials continued

- Sb, epitaxial growth on Bi substrate 8-95246
- Se, undeformed rhombohedral, dislocations, electron microscope obs. (*French*) 8-51548
- Si, deformed crystal, faulted dipoles 8-59814
- Si, ion implanted, laser annealing, periodic regrowth phenomena 8-67724
- Si, ion implanted, voids, electron microscopy 8-67757
- Si, ion-implanted, secondary defects development, three-stage model 8-87725
- Si, solid-phase-epitaxial, deposited above 380°C, defects obs. 8-63942
- Si thin crystal, electron backscatt. in electron microscope 8-75510
- Si-SiO₂ interface, high-resolution electron microscopy study 8-56046
- $\text{Si}_3\text{-Al-O-N}_3$, hot pressed, exam. of fracture mechanisms 8-72879
- Si_3N_4 , struct. of slow crack interface, light and electron microscope obs. 8-68770
- SnO_2 :Sb, and pure cryst., microstruct., X-ray diffr., optical and electron microscope studies 8-79619
- Tb, mag. domains, Lorentz microscopy obs. 8-84448
- $\text{TeO}_2\text{-P}_2\text{O}_5$, electron microscope exam. of phase equilib. and immiscibility 8-52779
- Ti anodic film, growth kinetics, determ. (*French*) 8-76788
- Ti, degree of charging of surfaces polished by TiC and synthetic diamond micropowders 8-60880
- Ti, electron microscope specimen prep. technique for dynamic straining expt. 8-88602
- Ti, fatigue fracture surface microstruct., electron microscope obs. 8-60834
- Ti-Al-Sn (5, 2.5 wt.%), electron microscope and X-ray diffr. exam., of basal and near basal hydrides 8-80550
- α -Ti-Al-Zr (6.16, 5.23 wt.%), alloy IMI 685, electron microscope observations of strain induced hydrides 8-72828
- Ti-Cr (15 at.%), aged omega phase, electron microscope exam. 8-72783
- Ti-Mo(Nb)(Ta), BCC struct., tetragonal phase form. by cold deform. (*Russian*) 8-88462
- Ti-Nb-Mo(V)(Ta)(Al)(Zr), BCC struct., tetragonal phase form. by cold deform. (*Russian*) 8-88462
- TiO₂, anodically formed layers, film instability obs. 8-72916
- TiO₂, sintering, hardness, density, elec. cond. and colour (*Japanese*) 8-68659
- UO₂, commercial fuel pin, irradiation induced volume changes, comparison with model 8-78465
- V, annealing after irradiation with 210 keV He at 625°C at high fluences 8-67751
- V_2O_5 , low temp. crystallographic struct. domains 8-83765
- $\text{V}_2\text{O}_5\text{-Fe}_2\text{O}_3\text{-Li}_2\text{O}$ system, physical properties 8-84503
- W (100), laser induced desorption, mirror electron microscopy 8-84067
- $\text{Y}_2\text{O}_3\text{-Nb}_2\text{O}_5$, solid state reactions, 1275 to 1350°C, electron microscopy, EPMA, X-ray diffr., dilatometry (*Japanese*) 8-63883
- Zn, electron radiation damage in HVEM, nature of defect clusters 8-59838
- Zr, dissolution of $\gamma\text{-ZrH}$, in situ study, HVEM obs. 8-55951
- $\gamma\text{-ZrH}$, precipitation in Zr, exam. of precipitation mechanism due to shears, electron microscope exam. 8-84809
- ZrO₂, neutron irradi., monoclinic to cubic transform. 8-87720

electron microscopes

- see also *electron microscopy; field emission electron microscopes; scanning electron microscopes; scanning-transmission electron microscopes; transmission electron microscopes*
- exoelectron microscope, appl. to study of damaged metal surface (*Japanese*) 8-74108
- high voltage, Si(Li) detector, electron counting, appl. to electron energy loss spectra (*French*) 8-54511
- high voltage electron microscope, constructed for high resolution crystal struct. images obs. 8-89600
- HV, accurate stigmating using optical diffr. pattern of micrograph 8-49941
- image formation, partial coherence and inelastic scatt. 8-58897
- imaging mechanism, 1 MV high-resolution microscope, crystal struct. anal. (*Japanese*) 8-74113
- microprobe instrument evolution, SEM and STEM 8-70233
- raster electron microscope test object 8-86393
- specimen holders, Philips, in high-resolution stage, restoration of damage 8-62265

electron microscopy

- see also *electron microscope applications; electron microscope examination of materials; electron microscopes; field emission electron microscopy; metallography; scanning electron microscopy; scanning-transmission electron microscopy; specimen preparation; transmission electron microscopy*
- accurate fan-beam reconstruction 8-78931
- Auger electron microscopy, instrumental capabilities 8-70227
- autoradiography, direct deposition method, radioactivity detect. 8-77167
- computer indexing of diffr. spots, appl. to bicryst. (*French*) 8-75507
- critical point dryer, low-cost, with continuous flow dehydration attachment 8-53595
- cryo-ultramicrotomy and myofibrillar fine struct., review 8-53592
- crystallographic struct. factor phases from electron-microscope dark-field moiré patterns 8-51396
- density reconstruction using arbitrary ray-sampling schemes 8-80954
- dielectric surface, electron-charged, microscopy using electrostatic field (*German*) 8-82081
- electron microscope, fluoro-autoradiography, improvement of efficiency 8-65162
- embedding with GMA and Quetol 523 for electron microscopic obs. on semi-thin sections for light microscopy 8-53588
- epitaxial growth process at UHV 8-55790
- freeze etching and related techniques, resist. monitor for automatic film thickness regulation 8-49810
- freeze-drying technique for prep. biological tissue without chem. fixation 8-65164
- freeze-fracture electron microscopy freezing method evaluation by low temp. X-ray diff. 8-57145
- freeze-fracture image enhancement by reversal processing of sheet film 8-62267
- freeze-fracture specimen temp. changes during rapid quenching in liq. coolants 8-57140

electron microscopy continued

- GMA-Quetol 523, ultraviolet polymerisation in embedding procedure for semithin sections prod. 8-92767
 grid handling, of semi-thin sections of GMA-Quetol 523 embedded tissue, with reference to O_2O_4 8-92766
 image enhancement, digital processing method (*German*) 8-89599
 image reconstruction, 3-dimens. with Fourier method (*Japanese*) 8-78048
 image restoration of weak phase objects, digital technique 8-58098
 lattice imaging, introductory paper 8-79508
 light microscope attachment for isolating small specific areas from slide embedded monolayers 8-53596
 magnetic domain walls, off-axis electron microholography 8-82080
 metal shadowed objects, low cost interneegative prod. 8-74109
 mirror microscopy, with monochromatic electron beams (*German*) 8-89598
 molecular imaging, photographic averaging technique 8-79600
 optical and digital spatial freq. filtering of electron micrographs, expt. results 8-82079
 ordered alloys, atomic order parameters from topology of electron-microscope diffr. contrast from antiphase boundaries, quantitative determ. 8-95016
 phase evaluation by electron diffr. by electron interf. (*German*) 8-74112
 phase problems, image recovery from Fourier transform modulus 8-82918
 phase problems 8-70230
 phase retrieval algorithms for semi-weak objects, from noisy electron micrographs 8-78047
 photoemission in high vacuum region, influence of residual atm. and other parameters on image brightness and contrast 8-55791
 postcontamination avoidance using room with controlled microclimate 8-54350
 precipitates, effect of diffuse scatt. on dark field contrast 8-67627
 review, 1976-77 8-82077
 spatial frequency filtering by optical and digital means 8-70231
 specimen temp. meas. using opt. pyrometer, controlled atmosphere 8-93690
 stacking fault width determ. from 224 reflections with $g.b=0$ 8-59722
 tissue section electron microscope image texture discrimination and automated meas. 8-57099
 ultrathin serial section transfer and orientation, accessory equipment 8-73976
 Si thin crystal, electron backscatt. in electron microscope 8-75510

electron mobility

- see also carrier mobility; electron mobility (metals)
 butane, gas, electron drift vel., Ramsauer-Townsend minima in electron scatt. 8-87427
 ethane, gas, electron drift vel., Ramsauer-Townsend minima in electron scatt. 8-87427
 ethane, liq., excess electron mobility, elec. field depend. 8-72218
 gas mixtures, drift velocities as function of elec. and mag. variables 8-71424
 hydrocarbons, gas phase, thermal electron interactions, drift vel. meas. 8-62919
 methane, gas, electron drift vel., Ramsauer-Townsend minima in electron scatt. 8-87427
 methane- $d_0(-d_4)$, electron drift and diffusion, elec. field effects 8-63531
 methylpentanes, electron mobilities and penetration ranges in liq. and crit. regions 8-72220
 neopentane, critical, electron mobility, gravity effect 8-91738
 neopentane, gas, electron drift vel., Ramsauer-Townsend minima in electron scatt. 8-87427
 neopentane, photoinjected electrons, escape probability, field depend. mobility effect 8-72219
 one-component molecular solution, excess electron diffusion 8-52043
 propane, gas, electron drift vel., Ramsauer-Townsend minima in electron scatt. 8-87427
 trajectory curvature effect in strong elec. field 8-83517
 two-component molecular solution, excess electron diffusion 8-52043
 Ar, back diffusion of electrons, in the presence of an electric field 8-75251
 Ar, compressed gas, electron drift vel., density depend. 8-63534
 H_2 , gas, electron swarms, anisotropic scatt. model 8-91059
 He, gas, electron mobility, anomalous density and temp. depend. at low temp. 8-75253
 He, liq., hot electrons on surface (*Russian*) 8-87832
 NH_3 , compressed gas, electron drift vel., density depend. 8-63534
 Xe, electron mobilities in various phases, density, elec. field and temp. effects, quasilocalisation 8-59535

electron mobility (metals)

- asymmetric electron scatt., anomalous Hall effect in ferromags. (*Slovak*) 8-79986
 transition metals and alloys, d electrons as current carriers and electron scatterers 8-91689
 ZZ 8-88057

electron multipliers

- channel electron multiplier appl. to gas electron diffr. 8-83684
 Faraday cup for simultaneous ion-beam current obs. and meas. 8-49865
 high gain, mass spectrometric positive ion detect. 8-74095
 high-conductivity channel electron multipliers, performance characts. 8-86334
 neutral particle detection, channel electron multiplier characteristics 8-58554
 scintillator detector-electron multiplier system, for positive/negative ions pulse counting, mass spectrometer appl. 8-89583
 Be-Cu surface, secondary electron yield, for electron multiplier ion detector 8-74094

electron nuclear double resonance see ENDOR**electron-nucleon interactions**

- see also electron-nucleon scattering; electron-proton interactions
 deep inelastic eN scatt., EM corrections to asymptotic freedom predictions 8-62403
 hadronic final states in deep inelastic scatt., vector meson prod. 8-78184
 parton model anal. of deep inelastic scatt. 8-62405
 residual proton production in deep inelastic electron scatt. 8-70381

electron-nucleon interactions continued

- ed, K^{\pm}/π^{\pm} ratio and symmetry props. of quark-parton model, fragmentation functions 8-93888
 $ed \rightarrow e^+X$, polarised e, parity non-conservation in inelastic scatt. 8-89719
 $eN \rightarrow e\pi\Delta$, low energy, ΔN axial form factors soft-pion theory 8-70380
 $eN \rightarrow e\pi N$, π form factor determ. 8-66128

electron-nucleon scattering

- see also electron-nucleon interactions; electron-proton scattering
 asymmetry predictions for deep inelastic and elastic scatt. and Δ electroproduction 8-58193
 light-cone field-theory and the parton model, book contrib. 8-82220
 ed, quasi-elastic scatt. and form factor of n 8-82210

electron-nucleus reactions

- for inelastic electron-nucleus scattering, see "electron-nucleus scattering"
 see also electron-nucleon interactions; nuclear electron capture
 deep inelastic hadron leptonproduction on nuclei, inclusive hadron final states 8-54741
 hadron electroproduction from nuclei 8-66267
 inner shell core struct. of nuclei from high energy electron elastic scatt. and knockout reactions 8-54739
 low level excitation, inelastic electron scatt. (*Russian*) 8-58265
 parity violating neutral current interaction, gauge theory predictions, radiative corrections 8-86436
 positron energy spectra and ang. distrib., 0.2-2 GeV electron conversion on W targets 8-86713
 spallation reaction and its appls. (*Japanese*) 8-74345
 threshold pion electroproduction, nuclear response surface 8-93989
 (e,e'), cross sections, short range correls. in nuclei, two body density 8-54743
 (e,e'), wave function orthogonality, bound state to continuum transitions 8-78335
 $^{27}Al(e,e'\pi^+)$, energy and ang. distrib. of π s, low lying residual states 8-54740
 $^9Be(e,e'\pi^+)$, energy and ang. distrib. of π s, low lying residual states 8-54740
 $^{12}C(e,e')^{11}B$, nonorthogonality of initial and final nucl. states (*Russian*) 8-66265
 $^{12}C(e,e'\pi^+)$, energy and ang. distrib. of π s, low lying residual states 8-54740
 $^{12}C(e,n)^{11}C$, 30 MeV, cross section absolute meas., corresponding (γ,n) cross section 8-66270
 $^{12}C(e,\pi)$, charged π electroprod. near threshold, data anal. 8-66266
 $^{59}Co(e,e')$, isospin effects in GDR region 8-78344
 2H photodisintegration and electrodisintegration, weak interaction and P nonconservation 8-89849
 $^4He(e,e')^3H$, 1186 MeV, recoil nucleus momentum distrib. (*Russian*) 8-54748
 Li($e,e'\pi^+$), $A=6,7$, energy and ang. distrib. of π s, low lying residual states 8-54740
 $^{238}U(e,e')$, 21 to 32 MeV, E0 and E2 excitations, fission into two $^{12}Cg.s.$ nuclei 8-54744
 $^{16}O(e,e')$, energy and ang. distrib. of π s, low lying residual states 8-54740
 $^{16}O(e,\pi)$, charged π electroprod. near threshold data anal. 8-66266
 $^{238}U(e,e')^{234}Th$, cross section, α -spectra, γ -spectra of ^{234}Th decay 8-58262
 $^{51}V(e,e')$, isospin effects in GDR region 8-78344
 $^{89}Y(e,e'\pi^+)$, energy and ang. distrib. of π s, low lying residual states 8-54740
 ^{64}Zn , electroexcitation of giant multipole reson. (*Russian*) 8-58264

electron-nucleus scattering

- see also electron-nucleon scattering
 $A=40-100$, charge distrib. from (e,e) and muonic X-ray meas. 8-54679
 collective props. of nuclei deduced from electron scatt., deformed nuclei, review 8-50064
 deep inelastic, meson exchange currents from Fermi gas model 8-66268
 few-nucleon systems, energy-weighted longit. sum rule for electron-nucleus scatt. and nuclear forces 8-58238
 high energy elastic scatt., prediction from nucleon density distrib. 8-54738
 interacting boson model, electron scatt. data anal., Sm-Nd region 8-62522
 inverse bremsstrahlung, high energy, nucl. mag. contribs. 8-74350
 isovector M6 excitations, open shell RPA calcs., appl. to electron scatt. form factors 8-50112
 magnetic dipole and quadrupole state excitation, inelastic electron scatt., various nuclei 8-50154
 $^{10}B(e,e)$, 140 MeV, resonances in e spectra (*Russian*) 8-78367
 B(e,e), $A=10, 11$, form factors, Hartree Fock calcs. 8-58263
 ^{209}Bi , charge distrib. from elastic electron scatt. and muonic X-ray data anal. 8-54681
 ^{12}C , elastic and inelastic scatt., resonating group method calc. of form factors 8-50108
 $^{12}C(e,e')$, 500 KeV inclusive scatt., plane wave impulse approx. 8-50214
 $^{12}C(e,e)$ 140 MeV, resonances in e spectra (*Russian*) 8-78367
 $^{40}Ca(e,e')$, microscopic model of isovector multipole giant resonances (*Russian*) 8-54747
 $^{40}Ca(e,e)$, high energy differential cross sections, nucleon density distrib. 8-54738
 $^{59}Co(e,e)$, valence nucleon orbit determ. 8-54669
 $^{Cr}(e,e)$, $A=50,52,53,54$, 226.7 MeV, charge density distrib. (*Russian*) 8-86473
 $^{50}Cr(e,e)$, 227 MeV, differential cross sections, Fermi charge density distrib. (*Russian*) 8-89785
 $^{52}Cr(e,e')$, 90-226 MeV, excitation of low-lying states (*Russian*) 8-54746
 $^{53}Cr(e,e')$, 90-226 MeV, excitation of low-lying states (*Russian*) 8-54746
 D+e scattering, neutron struct. function extraction, space-time descript. 8-62404
 ^{19}F , electroexcitation of ground state rotational band 8-66191
 $^{Fe}(e,e)$, $A=54,56$, 226.7 MeV, charge density distrib. (*Russian*) 8-86473
 $^2H(e,e')$ d bag, nuclear bag states containing quarks, detection 8-70465

electron-nucleus scattering continued

- ³He(e,e), elastic and deep inelastic, nuclear matter density at large momentum transfers (*Russian*) 8-86529
³He(e,e') 1000-1100 MeV, differential cross section for quasi-elastic scatt. (*Russian*) 8-86528
³He(e,e), form factors and dimensional scaling quark model 8-93991
³He(e,e), model depend. of charge densities 8-78248
⁴He(e,e), form factors and dimensional scaling quark model 8-93991
He(e,e), A=3 and 4, high momentum transfer, elastic struct. functions 8-62521
³⁹K(e,e'), mag. dipole and quadrupole state excitation 8-50154
⁹³Nb(e,e), valence nucleon orbit determ. 8-54669
²⁰Ne quadrupole transitions, electron scatt. form factors, shell model calcs. 8-62523
²⁰Ne(e,e'), E1 and E2 giant resonances excitation at 60-120 MeV 8-50144
¹⁴Ni(e,e'), mag. dipole and quadrupole state excitation 8-50154
⁵⁸Ni(e,e'), mag. dipole and quadrupole state excitation 8-50154
¹⁶O(e,e), high energy differential cross sections, nucleon density distrib. 8-54738
Pb, A=204-208, charge distrib. from elastic electron scatt. and muonic X-ray data anal. 8-54681
²⁰⁷Pb+e, high resolution inelastic scatt. cross sections, induced charge of neutron, form factors 8-78366
²⁰⁸Pb(e,e'), 50 to 335 MeV, 12⁻ mag. spin state excitations 8-50155
²⁰⁸Pb(e,e'), cross section calc. using microscopic wave functions 8-50142
²⁰⁸Pb(e,e'), M2 giant resonance excitation, spin-magnetism mass depend. quenching, M1 strength reduction 8-86521
²⁰⁸Pb(e,e'), mag. dipole and quadrupole state excitation 8-50154
¹⁰⁸Pd, vibr. states study, elastic and inelastic electron scatt., anharmonic vibrator model 8-62520
²⁸Si(e,e'), M2 giant resonance excitation, spin-magnetism mass depend. quenching, M1 strength reduction 8-86521
²⁸Si(e,e'), mag. dipole and quadrupole state excitation 8-50154
¹²⁴Sn(e,e) ^{150,225}MeV giant multipole resonances, positions and half widths (*Russian*) 8-78349
⁸⁷Sr(e,e), valence nucleon orbit determ. 8-54669
⁴⁸Ti(e,e), 227 MeV, differential cross sections, Fermi charge density distrib. (*Russian*) 8-89785
Tl, A=205,203, charge distrib. from elastic electron scatt. and muonic X-ray data anal. 8-54681
⁵¹V(e,e), valence nucleon orbit determ. 8-54669
⁹⁰Zr(e,e'), M2 giant resonance excitation, spin-magnetism mass depend. quenching, M1 strength reduction 8-86521
⁹⁰Zr(e,e'), mag. dipole and quadrupole state excitation 8-50154

electron optics

- see also beta-ray spectrometers; electron beams; electrostatic lenses; ion optics; magnetic lenses; particle optics*
aberration, spherical, for teaching 8-54135
aberration correction, mag. deflection systs. 8-66740
beam dynamic deflection sensitivity in transverse magnetic field 8-86386
combined system of electrostatic round lens and mag. deflector, electron-optical characteristics (*Chinese*) 8-82897
conference on electron, ion and photon beam technology, Palo Alto, CA, USA (May 1978) 8-74827
crossed-field energy analyser, stigmatic, focusing and dispersing props. 8-74832
curved electron beam system with strong deceleration at collector region, optimisation 8-74106
education, electron interference using standard electron microscope and electron biprism as interferometer 8-62005
electron gun, with point cathode, electron-optical props. (*German*) 8-82901
electron guns, high-current, laminar beam formation for linear accelerators 8-74516
electron-beam focusing optimisation with specified image parameters 8-86385
ESCA spectrometer operation, using monochromated UV discharge lamp with XPS spectrometer 8-89601
image deflection system, crossed elec. and mag. field, intensity modulation 8-89592
image formation, partial coherence and inelastic scatt. 8-58897
image formation in scanning microscopes with partially coherent source and detector 8-58923
lenses, crossed, electron optical image position, ang. magnification aberration 8-50691
magnetic domain walls, off-axis electron microholography 8-82080
magnetic spectrometer design with corrected second-order aberrations, theory 8-89604
micromachining, imaging conditions, illumination system 8-82899
microscopy, phase contrast transfer with different imaging modes 8-70232
p-n junctions, TEM, defocused images, stationary field approx. 8-67628
plane-symmetric optical systems, equilib. and stability conditions (*Russian*) 8-70220
plasma emitter, electron optical system simulation 8-67442
prism, cone-shaped, combined elec./mag. fields, relativistic particle optics 8-50690
prism, wedge-shaped, combined elec./mag. fields, relativistic particle optics 8-50689
radiation flux parameters meas. by diaphragm method 8-86387
rotation-free mag. lens for transmission electron microscope 8-78042
single beam collective phenomena 8-78893
single-particle dynamics, electron motion 8-78892
stimulated diffr. effects on aperture in non-transparent screen (*Russian*) 8-71018
synchrotron radiation source, X-ray monochromatisation, phase space analysis 8-62276
Young-Fresnel double-mirror interference experiment with electrons (*German*) 8-90351
e⁺e⁻ storage rings, beam-beam interactions 8-78894

electron pair annihilation *see electron-positron interactions***electron pair production**

- compact extragalactic radio sources, electron-positron pair prod. rel. to Faraday rot. 8-73770
Drell-Yan contrib. to lepton pair prod., incident hadron qq correlation function 8-89668

electron pair production continued

- Friedmann cosmological models, fermion pair creation by gravit. field and singularity (*Russian*) 8-93493
heavy ion collisions, positron prod. 8-50198
heavy ion collisions, positron prod. meas. 8-50197
internal pair formation following heavy ion collisions, conversion coeff. calcs. 8-50135
nucleus+ γ , screening corrections for intermediate, high energies, using relativistic form factors 8-93986
QED, strong and supercritical fields, book contrib. 8-74193
QED in an external gravitational field, S-matrix evaluation, pair prod. 8-82131
 α -decay, e⁺e⁻ pair production probability determ. 8-50133
 $\gamma p \rightarrow e^+e^-p$, reson. struct. obs. background process (*Russian*) 8-89722
 μ +atom, e⁺e⁻ pair prod., energy spectrum, screening effects (*Russian*) 8-55250
pp $\rightarrow e^+e^-X$, large p_T reference to Y(9.5), $\zeta(3.5)$ and direct γ -prod. 8-89749
pp interactions, 12 GeV/c, direct e⁺e⁻ prod. 8-78221
pp \rightarrow virtual gamma+hadrons soft bremsstrahlung, external emission dominance model 8-62430
²⁴¹Am, α -decay, e⁺e⁻ pair production probability determ. 8-50133
Be+p, 12 GeV/c, direct e⁺e⁻ prod. 8-78221

electron pairs

- see also electron pair production; positronium*
Weinberg-Salam theory 8-82194

electron paramagnetic resonance *see paramagnetic resonance***electron-phonon interactions**

- see also phonon drag; strong-coupling superconductors; tunnelling spectra; tunnelling spectroscopy; Umklapp process*
1/f noise, originating from lattice scatt., expts. on p-Ge and n-GaAs 8-64074
adsorbed layer, struct. and electron alterations, electron-phonon interaction effects (*Russian*) 8-87880
alkali halides, resonance Raman scattering, electron-phonon interaction for F centres 8-68519
alkali halides, review 8-63991
amorphous solids, electron-phonon interactions, fluoresc. line broadening and spectral diffusion 8-84655
1,12-benzoperylene in n-alkane, zero-phonon lines in luminesc. spectra 8-56512
1, 12-benzperylene, in alkane matrices, zero-phonon lines, press. shifts (*Russian*) 8-76502
CDW phase transition, effect of electron-phonon scattering 8-95265
commensurate-incommensurate CDW phase transition in one-dimensional electron-phonon system 8-67959
conference on lattice dynamics, Paris, France (Sept. 1977) 8-59869
cooperative Jahn-Teller systems of T nature, electron-phonon excitation branches 8-63823
coronene, in alkane matrices, zero-phonon lines, press. shifts (*Russian*) 8-76502
crystal lattice dynamics, microscopic theory 8-87746
cyclotron resonance, two dimensional electrons interacting with surface and volume phonon 8-80221
degenerate electron-phonon system, non-linear ultrasound absorption 8-87745
diamond, resonant Raman scatt., first and second order 8-60471
durene:naphthalene, spin-lattice relax. in photo-excited triplet states, spin axes rot. on thermal excitation 8-76294
electron subsystem, steady-state statistical equilib. conditions, adiabatic approx. 8-87754
electron-hole droplet, motion damping, deform. pot. scatt. 8-67950
electron-hole droplet, motion damping, impurity and piezoelec. scatt. 8-67951
elementary excitations in crystals, dielectric theory 8-60076
energy relaxation of photoexcited hot electrons at very low temperatures 8-91724
heavily doped, Raman phonons, interband excitation effects 8-52501
interimpurity tunnelling of electrons in solids, theory 8-88019
intermediate valence compounds, phonon produced instabilities, periodic Anderson model 8-79964
inversion layers, carrier effective mass, contribs. of electron-electron and electron-phonon interactions 8-64087
inversion layers, mag. field depend. of reson. line width 8-56380
inversion-layer electrons, temp. depend. cyclotron reson. lineshape, theory 8-64086
ionic crystals, surface polaron 8-60020
long-wave quasiparticle states localized at screw dislocation (*Russian*) 8-95126
matrix element calculation, phase transitions 8-79703
metal, BCC, elec. cond. temp. depend., anharmonic effects 8-76045
metal, temp. depend. of low freq. surface impedance 8-56207
metal, thermoelectricity, electron-phonon enhancement 8-56135
metal surface, adsorbed layer, structural and electronic reconstruction 8-84280
metal-insulator transition, anharmonism effects 8-56072
metal-liquid He interface, electron-phonon interaction, thermal boundary resistance 8-67899
metal-liquid He interface, thermal boundary resistance, determ. in transport approach 8-51815
metallic point contacts, nonlinear resist. rel. to phonon emission and background effects 8-68074
metals, normal hexagonal, temp. depend. anisotropy of phonon scatt. resist. 8-51967
microscopic theories of lattice dynamics, developments 8-59870
non-stationary density matrix, representation by function integral 8-71818
one dimension, electron-optical phonon interaction with strong coupling via deform. potential, vibr. excitations 8-51907
one-dimensional conductor, phonon dynamics 8-79704
one-dimensional systems, electron trapping and transport by supersonic solitons 8-72139
Peierls-Hubbard model, quasidegenerate dimens., antiferromagnetism and Peierls distortion 8-67931
perylene in n-alkane, zero-phonon lines in luminesc. spectra 8-56512
phonon spectroscopy, spectral, spatial and temporal 8-83892
photovoltaic effect mechanism, expt. obs. of thermal and spectral variations in the photovoltaic current in ferroelectrics 8-91719
piezoelectric semiconductor, cascade capture of carriers by attractive impurity centres, cross section 8-56157

electron-phonon interactions continued

- polar semiconductor, impurity levels, influence of electron-phonon coupling 8-64007
- polaron, bound, variational calc. of ground state energy 8-84152
- quantum system interacting with nonequilibrium phonons, light absorption props. 8-88340
- quasi one-dimensional conductor, phonon drag conductivity in Frohlich Peierls phase, effect of impurities 8-60114
- quasione dimensional compound, commensurability effect 8-72095
- rare earth compounds, spinless periodic Anderson model with phonons, appl. to mixed valence systems 8-84153
- relaxation of nonequilib. electrons at very low temps. 8-60121
- ruby, high energy phonon spectroscopy 8-83893
- ruby, phonon bottleneck effect, 29 cm^{-1} phonons 8-68562
- saturation effects in electron transport 8-76065
- semiconductor, absorption line profile in static elec. field, effect of impurities 8-92101
- semiconductor, anal. using photoacoustic cell 8-68027
- semiconductor, carrier capture cross section by attractive Coulomb centres, piezoelec. scatt. 8-72170
- semiconductor, conduction electron scattering by vibrating impurities 8-95297
- semiconductor, doped, reson. scatt. theory 8-64036
- semiconductor, doped lattice thermal cond., role of electron-phonon interactions and peripheral phonons, appl. to Ge:P 8-79702
- semiconductor, electron distribution function, temp. gradient effect 8-72145
- semiconductor, electron trap, positively charged, hot electron capture coeff. 8-52003
- semiconductor, excitation spectrum and optical props. in field of standing EM wave and homogeneous field 8-91625
- semiconductor, intervalley cyclotron-phonon reson., IR absorption in mag. field 8-60448
- semiconductor, optical absorption by impurities, phonon-electron interaction 8-56502
- semiconductor, quasi-two-dimensional, electron scatt. by polar optical phonons 8-72237
- semiconductor, Raman scattering from impurities 8-56468
- semiconductor, Raman scattering from impurities 8-56469
- semiconductor, statistical theory of multiple-phonon scattering 8-67794
- semiconductor, zincblende struct., phonon attenuation in presence of internal strains and mag. field 8-76118
- semiconductors, anomalous phonon induced light transmission below plasma edge 8-80368
- singularities of the small polaron effective mass 8-63989
- solitons in a one-dimensional modified Hubbard model 8-87895
- sound velocity, amplitude dependent, in collisionless regime (Russian) 8-52037
- Stark-Ladder current theory 8-68035
- structural phase transitions in crystals, effect of high-power visible and IR laser radiation 8-71825
- superconducting B-W type compounds, resist. characts. in normal state 8-51963
- superconducting dilute alloys, eqn. for crit. temp. 8-72300
- superconducting transition temperature, A15 cpds. 8-91801
- superconductor, elastic tunnelling spectroscopy of single-particle excitations 8-56260
- superconductors, relaxation processes, nonequilib. electrons and phonons 8-91807
- transient resonance Raman scatt., quantum theory, appl. to strongly coupled localised electron-phonon system 8-94412
- transition metal binary alloy, amorphous and crystalline, superconducting transition temp. correlation with solute conc. 8-52139
- transition metals, conf., Toronto, Canada (Aug. 1977) 8-91577
- transition metals, McMillan-Hopfield factor and ideal phonon limited resist. 8-64024
- TTF-TCNQ, conductivity and dielec. permeability, freq. depend. 8-79984
- tunnel self-trapping of electrons or Frenkel excitons, theory (Russian) 8-60192
- unfilled f-shell, elec. resist. (Russian) 8-72141
- vibronic splitting and Zeeman effect for $^4A_{2g} \rightarrow ^2E_g$ transition 8-60495
- vibronic theory of antiferroelec. and struct. modulated transitions, soft modes 8-79719
- zero-point energy of electrons and phonons 8-78603
- zinc blende semiconductors, small-gap, electron scatt. and transport props. 8-95294
- zinc blende semiconductors, small-gap, electron scatt. and transport props. 8-95295
- SnTe-PbTe-GeTe, alloy semiconductor, phase transition (Japanese) 8-91443
- Ag alloys, dil., transport props. 8-76046
- Ag, Fermi velocity from proximity effect tunnelling 8-51875
- Ag halides, review 8-63991
- Al, electron-phonon scattering rates, anisotropic, meas. on Fermi surface 8-87753
- Al, magnetoresist., linear growth in strong. mag. fields (Russian) 8-51972
- Al, supercond., appl. of non-local extension to Gaspari-Gyorffy theory 8-80093
- Al₂O₃, exoelectron emission, energy and ang. distrib. anal. (German) 8-92180
- Au, effect of press. on resistivity 8-79978
- BaTiO₃, phonon spectroscopy, amorphous versus crystalline material 8-83898
- Bi, nonequilibrium phonons, negative differential cond., life time oscills. (Russian) 8-76117
- Ca, FCC, ground-state props. 8-75989
- CdBr₂(I₂), Mn activated, electron-phonon interaction, lattice vibr. effective energies (Russian) 8-59911
- Cd₂Hg_{1-x}Se mixed cryst., electron mobility and electron scatt. 8-95296
- Ce₂La_{1-x}F₃, paramag. mixed crystal, scattering of optical phonons by rare earth ions 8-68518
- CoSi, Mn₂Si_{2-x-m}, thermoelectric and optical props. 8-91714
- Cs halides, F-centres, first excited degenerate states, props. of electron-phonon interaction 8-63824
- CsBr, electron-phonon interactions of F-centres, first-order Raman scatt. 8-64370

electron-phonon interactions continued

- CsCl, electron-phonon interactions of F-centres, first-order Raman scatt. 8-64370
- CsF, doped with F-centres, first order Raman scatt. 8-52492
- CsF, electron-phonon interactions of F-centres, first-order Raman scatt. 8-64370
- CsSiF₆:Mn²⁺, splitting of vibronic levels 8-60496
- Cu alloys, dil., transport props. 8-76046
- Cu, partial densities of states, electron-phonon interaction 8-51869
- Cu₂O, exciton spectrum, effect of isotopic substitution 8-67955
- Fe, highly pure, phonon contrib. to elec. resist., 1.6-298K 8-84194
- Fe, partial densities of states, electron-phonon interaction 8-51869
- FeF₂, absolute first order Raman polarisabilities 8-64369
- n-GaAs, coupled plasmon-LO phonon modes, Raman scatt. meas. 8-60472
- GaAs, forbidden Raman scatt. by LO phonons 8-64367
- n-GaAs, piezoelectric semiconductor, influence of acoustic phonon disturbances on conductivity 8-91697
- GaAs, Raman scatt., electron-phonon deformation potential coupling 8-52502
- GaAs:Cr, site symmetry of Cr ions, ground-state splitting, ballistic phonon expts. 8-95273
- GaAs-Ga_{1-x}Al_xAs, superlattice umklapp processes in resonant Raman scattering 8-64362
- n-GaSb, galvanomagnetic effects 8-72172
- GaSb, reson. two phonon Raman scatt. near E₁ and E₁+Δ₁ gaps 8-60470
- GaSe, Hall mobility anisotropy 8-68041
- Ge, amorphous, thermoelec. power in phonon-assisted hopping regime, Coulomb effects 8-76097
- Ge, electron-hole drop velocities as probe of phonons 8-68517
- Ge, phonon scattering and dislocation effect on low temp. phonon cond. 8-51754
- Ge:P, lattice thermal cond., role of electron-phonon interactions and peripheral phonons 8-79702
- Ge:P, lattice thermal resistivity due to electrons 8-51756
- Hg, single cryst., de Haas-van Alphen effect 8-84130
- InAs, second order Raman scatt., electron-two phonon deform. pots. determ. 8-60473
- InP, reson. Raman scatt., deformation pots. 8-52495
- n-InSb, acoustoelectric gain coeff., nonlinear elec. field depend. 8-76115
- p-InSb, cyclotron reson. of nonequilib. photoelectrons, distrib. function and line profile 8-60336
- InSb film, threshold singularity on quantising mag. fields 8-87904
- InSb, magneto-optical anomalies of impurity electrons, two-LO-phonon region 8-72415
- InSb-type semiconductor, inelastic scatt. of electrons by optical phonons 8-76073
- InSe, excitonic absorpt. edge 8-88352
- K, electrical conductivity, Toya's theory 8-51965
- K, thermoelectric power, high-temp., first-principles calc. 8-91672
- KCl:Pb²⁺(0.005% Pb), A band fine structure, electron-phonon interaction 8-60491
- La, DHCP and FCC phases, phonon density of states 8-67791
- La, FCC, ground-state props. 8-75989
- La, hydrostatic press. depend. in superconducting phase 8-80087
- γ-La₂S₃, indirect electron transitions, diffuse refl. and vibr. spectra 8-84576
- MgF₂, absolute first order Raman polarisabilities 8-64369
- MnF₂, absolute first order Raman polarisabilities 8-64369
- N₂:N, dynamically induced electronic transitions of matrix isolated atom 8-63825
- Na, electrical conductivity, Toya's theory 8-51965
- Nb, plastically deformed, changing lattice dynamics 8-67793
- NbC, superconductor, appl. of non-local extension to Gaspari-Gyorffy theory 8-80093
- Nb₃Ge, amorphous and crystalline A-15 phases 8-83896
- Nb₃Ge(Al), anomalous resistivity, insight from band theory 8-60106
- NbMo₂Be, predicted A15 struct. and T_c=30K 8-76182
- Nb₃Si, Nb₃Sn, Nb₃Ge, Nb₃Ga, Nb₃Al, ZZ 8-91613
- Ni-Fe, film, anomalous Hall and Nernst-Ettingshausen effect, contribution of phonon and impurity scatt. (Russian) 8-64145
- Pb, phonon softening, neutron scatt. at high press. 8-80091
- Pb_{1-x}Ge_xTe, electron-phonon interaction effect on ferroelec. transition 8-76416
- Pb_{1-x}Sn_xSe, band inversion effect on phonon spectra 8-79699
- Pb_{1-x}Sn_xTe, electron-phonon interaction 8-71819
- PbTe, TO phonon softening, free carriers and defects effects 8-79720
- Pd, elec. resist. and supercond. transition temp., electron-phonon contrib. 8-80085
- Pd_{1-x}Ag_xH₂, superconducting transition temp., APW band struct. calcs. 8-95393
- PdH(D₂), optical mode phonons, nonadiabaticity 8-55916
- Re, electrical resistance anisotropy, temp. depend. (Russian) 8-76041
- Ru, electrical resistance anisotropy, temp. depend. (Russian) 8-76041
- Sb, magnetoresistivity, mutual drag effect, temp. depend 8-52012
- Si (100) inversion layer, hot electron drift velocity, Monte Carlo calcs. inc. 3 subbands 8-91752
- Si, amorphous, thermoelec. power in phonon-assisted hopping regime, Coulomb effects 8-76097
- Si, anal. using photoacoustic cell, in pulsed elec. field 8-68027
- n-Si, heavily doped, self energy of phonons interacting with free electrons, Raman scatt. 8-64366
- n-Si, inversion layers, many-valley electron-phonon interactions, piezoresistance, anisotropic cond., Shubnikov-de Haas oscillations 8-52096
- Si, phonon spectroscopy, amorphous versus crystalline material 8-83898
- Si, phonon-mediated intervalley electron-electron interaction 8-95125
- p-Si, Raman scattering by phonons and electrons, interference effects 8-60469
- n-Si-Ge, phonon thermal cond. of hot-pressed alloy, 300-1100K 8-91494
- SiC (6H), phonon drag and phonon-electron interaction (Russian) 8-79701
- SiC, absorption of US waves 8-72210
- SiO₂, phonon spectroscopy, amorphous versus crystalline material 8-83898
- SmB₆, f-d hybridisation, optic phonon anomalies 8-92080
- SmS, f-d hybridisation, optic phonon anomalies 8-92080

electron-phonon interactions continued

- SnTe, electron-phonon interaction effect on ferroelec. transition 8-76416
 SrF₂:Eu²⁺, spectral, spatial and temporal phonon spectroscopy, new spectrometer 8-83892
 Th, FCC, ground-state props. 8-75989
 Ti, partial densities of states, electron-phonon interaction 8-51869
 Ti-V, anomalous elec. resistivity, mag. susceptibility, soft-phonon induced structural inhomogeneities 8-60104
 TiO₂, phonon spectroscopy, amorphous versus crystalline material 8-83898
 TiO₂, unambiguous assignment of fund. absorpt. edge 8-71817
 TiS₂, carrier-lattice coupling 8-63822
 TiSe₃, carrier-lattice coupling 8-63822
 V, partial densities of states, electron-phonon interaction 8-51869
 VO₂, diffuse X-ray scatt. due to lattice instability near metal-semiconductor transition 8-56074
 VO₂, semiconductor-metal transition, effect of ¹⁸O substitution 8-84268
 VO₂, thermal cond. meas., metal-dielectric phase transition, phonon scatt. mechanism 8-87831
 V₂O₃, semiconductor-metal transition, effect of ¹⁸O substitution 8-84268
 V₂O₃, thermal cond. meas., metal-dielectric phase transition, phonon scatt. mechanism 8-87831
 V₃O₅, semiconductor-metal transition, effect of ¹⁸O substitution 8-84268
 V₂O₅, thermal cond. meas., metal-dielectric phase transition, phonon scatt. mechanism 8-87831
 V₃Si, V₃Sn, V₃Ge, V₃Ga, V₃Al, ZZ 8-91613
 ZnS(Se)(Te):Cr²⁺, Jahn-Teller coupling 8-67997

electron-positron inclusive interactions

- charmonium model of ψ family 8-78143
 current-induced reactions, dual unitarisation 8-74233
 D-meson decay at $\psi(3772)$, inclusive props. 8-93876
 hadron decay from jet, transverse momentum 8-74268
 jet angular distrib. eccentricity, technique for detecting new quark flavours 8-70383
 Landau's hydrodynamic model, further aspects 8-82173
 multiprong events, inclusive electron prod., 3.9-7.4 GeV, charmed particle decay 8-66136
 QCD, hard semi-inclusive processes 8-93862
 resonance decays above charm prod. threshold, single channel dominance 8-66133
 $e^+e^- \rightarrow e^+K^+ + \text{anything}$, D-meson decay, K-e correl. anal. 8-78179
 $e^+e^- \rightarrow e^+X^+$, 3.1 to 7.4 GeV, threshold behaviour of $\tau^+\tau^-$ prod. 8-70351
 $e^+e^- \rightarrow eX$, τ branching ratio and e momentum spectrum, D decay 8-89693
 $e^+e^- \rightarrow \gamma\pi^0$, inclusive production, 4.9 to 7.4 GeV, cross sections 8-89723
 $e^+e^- \rightarrow HX$, associated production of gluonic jets and heavy mesons 8-93892
 $e^+e^- \rightarrow \text{hadrons}$, 3.6 to 5.2 GeV, total cross sections, resonance peaks 8-62416
 $e^+e^- \rightarrow \text{hadrons}$, 53 GeV², π^+ and K^+ cross sections, scaling 8-78201
 $e^+e^- \rightarrow \text{hadrons}$, asymptotically free QCD perturbation theory for multi-jet final states 8-74267
 $e^+e^- \rightarrow \text{hadrons}$, azimuthal correlations, quantum chromodynamics anal. 8-70382
 $e^+e^- \rightarrow \text{hadrons}$, EM corrections to asymptotic freedom predictions, gluon corrections 8-62403
 $e^+e^- \rightarrow \text{hadrons}$, finite energy sum rules, cross section, QCD calcs. 8-62413
 $e^+e^- \rightarrow \text{hadrons}$, inclusive distrib., jets, 1+1 dims. QCD 8-66137
 $e^+e^- \rightarrow \text{hadrons}$, jet struct., three-hadron-ball model 8-82224
 $e^+e^- \rightarrow \text{hadrons}$, jet struct. in the energy range 3.1-9.5 GeV 8-89725
 $e^+e^- \rightarrow \text{hadrons}$, multiplicity, scaling, inclusive spectrum, simple hadron cascade model 8-66135
 $e^+e^- \rightarrow \text{hadrons}$, narrow resonance at 9.46 GeV 8-62415
 $e^+e^- \rightarrow \text{hadrons}$, search for narrow resonances in 1.45-1.92 GeV mass region 8-89724
 $e^+e^- \rightarrow \mu^3\pi$, above 6 GeV, inference of τ decay 8-50042
 $e^+e^- \rightarrow n\bar{n}$, pp, simultaneous meas. of decay channels at J/ψ resonance 8-93893
 τ decay involving hadronic vector current 8-66101
 Y, narrow high mass resonance formation in e^+e^- annihilation at 9.46 GeV, heavy qq bound state 8-62414
 Y' at $M(Y')=10.02$ GeV in e^+e^- annihils. using NaI lead-glass det. 8-93894
 Y' obs. at $M(Y')=10.01$ GeV in e^+e^- annihils. using DASP det. 8-93895

electron-positron interactions

- see also *electron-positron inclusive interactions; electron-positron scattering; positron annihilation in liquids and solids*
 annihilation, in university science course for talented high-school students 8-89282
 anomalous e^+ prod. in e^+e^- annihilation, two charged and multi-prong events 8-78200
 anomalous lepton prod., charmed mesons and heavy leptons 8-66134
 charmed particle prod. in e^+e^- annihilation 8-78199
 colliding e^+e^- beams accelerator expts., 100 GeV, particle prod., weak currents, etc. (Russian) 8-58194
 hadronic cross section, hadronic effects 8-70339
 heavy quark and gluon two jet prod. in e^+e^- annihilation (Russian) 8-89696
 heavy quark fragmentation and parton transverse momentum in annihilation 8-82150
 Higgs boson, bremsstrahlung prod. with heavy fermion pair in e^+e^- collisions 8-86449
 Higgs meson prod., possible signals in high energy collisions, gauge groups 8-89649
 multihadron annihilation anomalous behaviour, resonant $K^*(892)$ prod. 8-66132
 nonperturbative QCD effects at large momentum transfers, e^+e^- annihilation to hadrons 8-82226
 particles and fields conference, Argonne, IL, USA (Oct. 1977) 8-78130
 QCD, e^+e^- annihilation energy, asymptotically free perturbation theory 8-66045

electron-positron interactions continued

- resonance states below 2.2 GeV observed in e^+e^- annihilations 8-78197
 spin tests for charmed mesons produced in e^+e^- annihilation at $\sqrt{s}=4.028$ GeV 8-74269
 sum rules, semiclassical method, bound state energy relations 8-70308
 total annihilation cross section, new meas. F, F* discovery, inclusive particle prod. 8-78198
 Weinberg-Salam theory 8-82194
 E⁰, neutral electron-type heavy lepton, and W-boson mass 8-66100
 $e^+e^- \rightarrow 1^{++}$ resonance states, direct production through neutral currents 8-93891
 e^+e^- annihilation in upsilon region, quark model predictions 8-54640
 $e^+e^- \rightarrow e^+e^- \gamma \gamma$, $\mu^+\mu^-$, 5.2 GeV, tests of QED 8-66064
 $e^+e^- \rightarrow e^+e^-$, implications of light neutral gauge boson 8-58154
 $e^+e^- \rightarrow e^+e^-$ or $\mu^+\mu^-$, decay products from new charged heavy lepton pair prod. 8-74238
 $e^+e^- \rightarrow e^+(\mu^+)+1$ charged track, cross section energy depend., τ mass 8-89695
 e^+e^- inclusive hadron prod., neutral weak currents 8-50041
 $e^+e^- \rightarrow \mu^+\mu^-$, 5.8-7.4 GeV, neutral currents strength limit, pole angle asym. 8-78157
 $e^+e^- \rightarrow \mu^+\mu^-$, contribution of weak neutral currents (Russian) 8-62383
 $e^+e^- \rightarrow \mu^+\mu^-$, contribution of weak neutral currents (Russian) 8-62384
 $e^+e^- \rightarrow \mu^+\mu^-$, implications of light neutral gauge boson 8-58154
 $e^+e^- \rightarrow \mu^+\mu^-$ 6.2-7.4 GeV CM, comparison with QED predictions 8-74194
 $e^+e^- \rightarrow \nu\bar{\nu}\gamma$, formula for differential cross-section, including weak interaction and V-A interaction (Russian) 8-62385
 $e^+e^- \rightarrow p\bar{p}$, asym. and polarisation of p, \bar{p} , neutral weak currents (Russian) 8-58195
 $e^+e^- \rightarrow \pi^+\pi^-$, vector meson dominance anal. for π form factor 8-70370
 $e^+e^- \rightarrow \tau^+\tau^-$, heavy leptons discovery and props., review 8-89694
 $e^+e^- \rightarrow \tau^+\tau^-$, $\tau \rightarrow p\nu\pi$, halflife and mass determination, e^+e^- hadronic cross section 8-89765
 $e^+e^- \rightarrow Y$, suggested search for gluon hadronic states in collinear gluon jets 8-89663
 $e^+e^- \rightarrow V\pi \rightarrow \pi^+\pi^-\pi^0$, EM mixing effects, dynamics of vector meson prod. (Russian) 8-58191
 $e^+e^- \rightarrow X$, (X=system of hadrons) 8-82222
 γ polarisation correl. function. 8-78158
 μ^+ -e events, alternative heavy-lepton model 8-66102
 $\mu^+\mu^-$ anomalous prod. from e^+e^- annihilation, heavy lepton prod. and decay 8-82190
 ψ to charm particles, 1975 and 1976, e^+e^- colliding beam technique (Polish) 8-74297
 τ decay, large timelike Q^2 , conservation of vector current and current algebra 8-78155
 Y flavoured vector mesons, production in e^+e^- annihilation at DORIS energies 8-93890
 v prod. from duality and new quark charge 8-74224
 Ar, clustering of atoms around positron and positive ions 8-55270
 Ar, positron annihilation decay consts., temp., elec., and mag. field depend., computer anal. 8-78809
 He, clustering of atoms around positron and positive ions 8-55270
 He, positron annihilation decay consts., temp., elec., and mag. field depend., computer anal. 8-78809
 He-Ar mixture, positron annihilation decay consts., temp., elec., and mag. field depend., computer anal. 8-78809
 Ne, clustering of atoms around positron and positive ions 8-55270

electron-positron scattering

see also *electron-positron interactions*

- Federbush model, absence of induced counterterms e^+e^- scatt. amplitudes 8-50023

electron probe analysers see *electron probe analysis***electron probe analysis**

- archaeometry, sampling stylus 8-70246
 barium mordenite, dehydrated, position of cations and molecules, electron probe anal. 8-51509
 biological fluids, ultramicroanal., by energy dispersive X-ray spectrometry 8-92768
 biological frozen hydrated bulk specimens instrumentation and specimen prep. for electron beam X-ray anal. 8-57142
 biological material, prep. for X-ray microanal. of diffusible elements, methods of drying ultrathin cryosections 8-77166
 biological material prep. for X-ray microanal. of diffusible elements, rapid freezing and ultrathin section prep. 8-77165
 biological samples charging effect in electron-irrad. ice 8-57141
 biological specimens, X-ray micro anal., iso-atomic droplets as models 8-53598
 bytownite megacrysts., study of trapped basaltic melts, petrogenetic process study 8-95688
 ceramic materials, SEM and anal. techniques (German) 8-56832
 correction procedure, microanalysis meas., conversion to elemental weight concentrations 8-76950
 diffusion model for electron probe into solid target, energy depend. 8-71652
 implanted ion detection by X-ray emission anal. in TEM 8-51575
 LMFBF type mixed oxide fuel pins, composition of corrosion product oxide phases in pin gaps 8-70599
 metallic surfaces, adsorption of inorganic and organic molecules, mechanism and effects, exam. (German) 8-51828
 microprobe instrument evolution, SEM and STEM 8-70233
 particle analysis and identification in pharmaceutical industry 8-61125
 proustites, optical props. and chem. comp. rel. to pyrrargyrites 8-95566
 pyrrargyrites, optical props. and chem. comp. rel. to pyrrargyrites 8-95566
 SEM cathodoluminescence analysis of impurities, localisation and sensitivity 8-95985
 SEM-AES-IMA combination with SIM spectrometer, Si device anal. appls. (Japanese) 8-85249
 skeletal muscle bulk specimen, quantitative X-ray microanal. of diffusible ions 8-57143
 steel, high speed, annealed, carbide determ. by anodic oxidation technique (Japanese) 8-85040
 steel, rusted, exam. of tannin treatment action mode 8-88564

electron probe analysis continued

- superalloys, phase extraction, chemical and X-ray diffr. anal. 8-72951
thin films, localised elemental anal. of microphases and inclusions 8-85261
X-ray absorption edges, emission wavelengths, analytic expressions 8-61111
Ag₂S, distrib. on sensitised AgBr emulsion grains, X-ray microanalysis 8-62248
Al-Ag₂Al, eutectic alloy, exam. of terminal solid solubility limits 8-76633
B-C system, region of existence of B₄C phase 8-76636
B₄C, quantitative electron microanalysis (*French*) 8-76948
Bi_{0.5}Sb_{1.48}Te₃ thermoelec. solid soln., homogeneity, effects of prep. method 8-52698
Bi₂Te₃-Se_x thermoelec. mat., prep. effects on inhomogeneities 8-51576
Ca₂SiO₄, bredigite-larnite rock from Scawt Hill, electron microprobe anal. 8-68952
Co-Ga-B, phase diagram, metallographic, X-ray and electron probe anal. 8-92241
Cr-Fe (30 wt.%) alloys, refined fine comminution 8-60598
Cu-Al-Ni-Fe, (10, 5, 5 wt.%), cast microstruct. 8-80535
Cu-Fe phase diagram, 650 to 1050°C (*German*) 8-60658
Cu-Ni, sulphidation between 653 to 770K, exam. of scale morphologies, using X-ray diffr., and electron microprobe anal. 8-88559
Fe, cast, Mg, despheroidising effect of Bi, Sn on graphite in alloy 8-56670
Fe, cast, with Mn, high S, exam. of sulphide phases, cocrystallisation during solidification 8-56646
Fe-Al(Cr)(V)(Ti), hardness after nitriding, metallographic, electron microscopical and microprobe anal. 8-51608
Fe-Mn(Sb)(Sn), additive effect, on eutectoid transformation of Fe 8-52799
Fe-Ni (19wt.%) alloy, oxidation in CO₂, 700 to 1000°C, thermal and metallographic anal., EPMA 8-72931
Fe-Ni (3 wt.%), grain boundary segregation of Sn and P embrittling additions, STEM microanal. 8-76654
Fe-Ni (3 wt.%), grain boundary segregation microanal. using X-ray (STEM) and AES 8-87685
Fe-Ni mixed powders, effect of Ni particle size and unequal interdiffusion, on sintering process (*Japanese*) 8-84728
Fe-Ni-Cr-Mn-Al-Ti Incoloy 800, exam. of scale morphology, alloying element distrib. after oxidation 8-80677
Fe-Si(Cr)(Ni)(Mn)(C), alloy layers formed by reaction with molten Al, X-ray, EPMA anal., hardness meas. (*Japanese*) 8-72926
Mo-Mn-Fe-Si/Al₂O₃ ceramic seal, interfacial phases 8-72011
Na₂O-CaO-SiO₂, multicomponent liq. state diffusion 8-55962
Pu-Pt(Rh)(Pt-Rh), exam. of phases and crystal structure 8-80518
SiC fibre reinforced Ni-Cr alumina coated fibres, hot pressed, annealed, IR study 8-60623
Si₃N₄, reaction bonded, creep, internal oxidation effects 8-56701
Ta-Pd system, phase diagram exam. of composition by X-ray diffr., electron microprobe anal., and metallography 8-76632
(U,Pu)CNO irradiated fuel, electron microprobe anal. 8-70601
U minerals, quantitative microprobe anal. 8-61126
W, annealed wire, analytical determ. of K content of single bubbles 8-64909
(Y_{1-x}Co_x)Co₂, mag. props. annealing effects, phase segregation, EPMA 8-91898
ZnSnP₂-ZnSiP₂, heterocombination simultaneous crystallisation 8-60560
Zr-Zr₂Al₃, diffusion weldings between 1000 and 1300°C, electron microprobe anal. (*German*) 8-84011

electron probe microanalysis see *electron probe analysis*

electron probe microscopy see *electron probe analysis*

electron probes

see also *electron probe analysis*

- automated, evolution of quantitative elementary point anal. in geo-sciences (*French*) 8-78046
minicomputer driven microprobe (*French*) 8-74111
LaB₆ highly stable single cryst. cathode for conventional electron microprobe instruments 8-78043

electron-proton interactions

see also *electron-proton scattering*

- CERN proton synchrotron, electron ring addition, proposal for weak interaction study 8-55062
deep inelastic asymmetry meas., Bjorken sum rule, p spin struct. models 8-70376
deep inelastic scatt., nucleon structure functions 8-50036
deep inelastic scattering, rest frame quark-parton model of proton, scaling 8-70374
QCD perturbative corrections 8-74263
ep deep inelastic inclusive K_s⁰ and Λ electroproduction, quark fragmentation 8-66123
ep $\rightarrow e\Delta^+$ scatt. asymmetry predictions, SU(2) gauge theory 8-58193
ep $\rightarrow e^+X$, polarised e, parity non-conservation in inelastic scatt. 8-89719
ep $\rightarrow e^+nX$, π exchange, π EM struct. functions calcs. 8-70375
ep $\rightarrow e\eta$, meas. in S₁₁ (1535) reson. region 8-50038
ep $\rightarrow e\eta$ at S₁₁(1535) resonance, longit. to transverse cross sections ratio 8-78194
ep $\rightarrow e\pi^0$, elastic π^0 electroprod. above resonance region, cross section, direction 8-62412
ep $\rightarrow e\pi^0$ or $\pi\pi^+$, threshold cross section slope, form factors, π axial mass and radius 8-62411
ep $\rightarrow e\pi^+n$, longitudinal and transverse contrbs., π^+ EM form factor 8-66126
e $^+p\rightarrow e^+\gamma+X$, deep-inelastic bremsstrahlung, quark charges, colour gluon mass 8-74216
K electroproduction, K $^{\pm}/\pi^{\pm}$ ratio and symmetry props. of quark-parton model, fragmentation functions 8-93888

electron-proton scattering

see also *electron-proton interactions*

- deep inelastic scatt. in $\omega=1$ region, field theory and parton model anal. (*Russian*) 8-78190
lepton production, azimuthal depend., parton model calcs. 8-93887

electron radiation

- bremsstrahlung, ang. distrib. of nonrelativistic intensity calcs., program 8-87001

electron radiation continued

- QED calculation of radiation from electron in quantised field of non-monochromatic EM wave (*Russian*) 8-82132
storage ring, SHF radiation, coherent synchrotron vibr. effect (*Russian*) 8-66438
UHF nonequilibrium plasma diagnostics by atomic bremsstrahlung continuum 8-67483

electron relaxation time (metals)

- Al alloy, dil., Hall coeff. calc. by 4-OPW approx. 8-76052
Cu₂Mo₈S₈, normal state and superconducting property measurements 8-91660
electrical resistivity, relax. time near order-disorder transition 8-87788
Fe-Ni alloy, optical and electronic characs., 20-1750°C, comp. depend. (*Russian*) 8-84601
Ni₃Mn, elec. resist., relax. time near order-disorder transition 8-87788
PbMo₆S₈, normal state and superconducting property measurements 8-91660

electron resists

- conference on electron, ion and photon beam technology, Palo Alto, CA, USA (May 1978) 8-74827
energy loss in electron beam lithography, Bethe and Spencer-Fano theories 8-87728
lithography, dynamic beam shaping, advantages, system design 8-74834
vector scan electron beam lithographic system, deflection distortion 8-74835

electron ring accelerators

- beam-beam interactions in e-p storage rings 8-78889
mirror system, wideband, for electron ring diagnostics, using synchrotron radiation 8-78518
relativistic particle ring, coherent oscillations, Vlasov eqn. 8-55060
relativistic ring with discrete and continuous eigenvalue spectrum, resonance crossing 8-58507
e $^+e^-$ storage ring, PETRA 8-78530
e $^+e^-$ storage rings, beam-beam interactions 8-78894

electron scattering see *elastic scattering of electrons by atoms and molecules; electron-electron scattering; electron impact; electron-nucleon scattering; electron-nucleus scattering; electron positron scattering; electron-proton scattering; neutrino-electron scattering*

electron solvation see *solvation*

electron spectra

- see also *Auger effect; conversion electron spectra; electron energy loss spectra; electron impact; electron spectroscopy; photoelectron spectra*
atom+atom collision, Penning and assoc. ionisation, complex. pot. and electron spectrum 8-94310
auroral electrons energy distrib., incoherent scatter radar and photometric meas. comparison 8-77390
magnetosphere, International Sun Earth Explorer 1 electron spectrometer expt. 8-85809
Rydberg states, fine struct. splitting, quantum beat and double reson. spectroscopy 8-86979
solar wind, International Sun Earth Explorer 1 electron spectrometer expt. 8-85809
solid, electron MFP determ. by depth and ang. depend. of inelastically scatt. electron spectra 8-92154
Al, electron MFP determ. by depth and ang. depend. of inelastically scatt. electron spectra 8-92154
Ge, electron MFP determ. by depth and ang. depend. of inelastically scatt. electron spectra 8-92154
H $^+$ +N₂ collisions, proton energy deposition and secondary electron spectra calcs. 8-74746
He, electron impact ionisation, emitted electron ang. distrib. 8-55241
He $^+$ +Ar, Penning ionisation, laser modified collisional effects in electron energy spectrum 8-90278
Hg, electron impact spectra, intermediate energy 8-82842
Mo [110], metastable He impact, secondary electron spectra 8-95642
Na, 54.4-150 eV differential cross sections, 12-140°, optical model calcs. 8-74761
Ne, autoionising states, scatt. electron spectra, post collision interaction effects 8-58819
¹⁸²Ta-containing Ta sheet, radioactive electron emission spectrum (exoelctrons), surface elec. field and Auger effects 8-72705

electron spectrometers

see also *beta-ray spectrometers*

- double focusing Fe core electron spectrometer BILL for (n,e $^-$) meas. 8-82566
doubly truncated spherical electrostatic energy analyser for (e, 2e) expts. 8-58872
electrostatic spectrometer, for conversion electron Mossbauer spectroscopy 8-88238
magnetic, with directional sensitivity, for GEOS-1 satellite appl. 8-94161
magnetic spectrometer design with corrected second-order aberrations, theory 8-89604
Mollenstedt electron vel. analyser high-order energy loss lines removal 8-93786
vacuum UV photoelectron spectrometer for metal chemisorption studies (*Japanese*) 8-78044
wideband electron spectrum analyser, 10 to 275 keV electron energy 8-86719
In₂Te₃-type semicond. radiation-resistant fast-electron detectors 8-78559
Si(Li) electron spectrometer on-line with an automatic irradiation apparatus 8-90014

electron spectroscopy

see also *electron spectra*

- AES, chemical-state effects 8-92566
AES, convolution and deconvolution 8-52601
AES, microarea anal. system with submicron anal. capacity, performance tests 8-73106
analyser for inelastically scatt. electrons from atoms 8-70936
biology research, impact of photoelectron spectroscopy 8-65156
for chemical anal., appls. to materials for electrophotography 8-92565
computer controlled ESCA for nondestructive surface characterization utilizing a TV-type position sensitive detector 8-76969
computerised approach 8-86390
conversion electron Mossbauer spectroscopy, electron transport anal. 8-94159

electron spectroscopy continued

- conversion electron Mossbauer spectroscopy down to 4.2K, applications to thin film and surface studies 8-84504
 conversion electron spectrometer, in-beam use 8-55086
 Darmstadt linear accelerator, detector system and performance of elec. scatt. system 8-70680
 Darmstadt linear accelerator electron scatt. facility, beam transport and spectrom. 8-70679
 Darmstadt linear accelerator electron scatt. facility, data processing 8-70681
 double focusing Fe core electron spectrometer BILL for (n, e^-) meas. 8-82566
 EM shower sampling counters, characteristics of plastic scintillator and radiator layers 8-58530
 ESCA, conf., Uppsala, Sweden (May 1977) 8-53297
 ESCA, quantitative surface anal., limitations, depth profiling, catalyst surface anal. 8-53298
 ESCA, X-ray type, C 1s contaminant buildup on conductors and insulators 8-95981
 ESCA chemical shift, indirect evaluation of Coulombic contribution to ionis. pots. for nonbonding electrons 8-92572
 ESCA photoionisation cross section, relative intensities calcs., comparisons 8-50464
 ESCA using monochromated UV discharge lamp and XPS spectrometer 8-89601
 inelastic mean free paths of solids, data tables 8-84686
 International Sun Earth Explorer 1, electron spectrometer expt. 8-85809
 metal surfaces, clean, AES anal., contamination effects obs. 8-53293
 microanalysis by energy loss spectrometry (*Japanese*) 8-85244
 microfilm conversion electron detector for Mossbauer spectroscopy 8-70698
 mini-orange spectrometers, wedge shaped SmCo_5 magnets 8-58531
 molecular photoelectron spectroscopy, review 8-94283
 molecule, free, ultra-soft X-ray emission spectroscopy, correl. with electron spectroscopy 8-50558
 momentum filter for separation of electrons and negative ions 8-78034
 optical Be filter in He discharge lamp for photoelectron spectroscopy 8-79115
 photoelectron, energy analysis of trapped ions, strong mag. field, elastic scatt. effects 8-62950
 photoelectron spectrometer, vac. UV, for study of chemisorption on metal surfaces (*Japanese*) 8-62264
 photoelectron spectroscopy in strong mag. field, trapped ions, with ion cyclotron reson. 8-50666
 photoelectron spectroscopy using rotating triple-reflection polariser 8-94443
 polymers, struct., bonding, reactivity by ESCA 8-53299
 retardation system for Auger electron spectroscopy 8-50654
 steel, stainless, Cr-Ni-Mo, surface, scraping, mech. (electrolytic) polishing, ion etching, effects on ESCA 8-53037
 surface analysis, quantitative, by electron spectroscopy 8-92552
 surface analysis, review of ESCA technique, instrumentation, and appl. 8-68947
 surface analysis, system, modular combined ESCA, UPS, AES, and SIMS 8-73107
 surface characterisation, multiple technique instrument, ESCA, scanning Auger, UPS and SIMS 8-73108
 surface structure analysis at high press. 8-73103
 surfaces, electron spectroscopy, review 8-92169
 UV photoelectron chemical anal., appl. to conjugated carbonyl cpds. (*French*) 8-90215
 UV photoelectron spectrometer, gas and vap. phase operation 8-82865
 vacuum UV line source, He lamp, for photoelectron spectroscopy 8-94419
 VUV He reson. line radiation source, for UHV photoelectron spectroscopy 8-89602
 X-ray conversion electron spectroscopy using modified photoelectron spectrometer 8-50557
 GaAs oxide, plasma grown, semiquantitative chemical depth profiles, Auger spectroscopy and neutron activation anal. 8-53284
 He I polarised radiation source for surface studies 8-74959
 Si(Li) detectors, electron counting, appl. to electron energy loss spectra, by high voltage electron microscopy (*French*) 8-54511

electron spin

- charge current density of Pauli eqn. using vel. operator method, nonrelativistic derivation 8-73872
 education, electron spin, nonrelativistic quantum mechanics derivation from Schrodinger eqn. 8-69942
 nonlinear effects in theory of erratic electron 8-93825

electron spin-lattice relaxation

- di-*t*-butylnitroxide radical, solid, nucl. and electron spin relax. times meas. 8-60350
 durene:naphthalene, spin-lattice relax. in photo-excited triplet states, spin axes rot. on thermal excitation 8-76294
 lanthanum ethyl sulphate nonahydrate: Tb^{3+} , ESR spectrum, spin lattice relax., effect of hydrostatic compression 8-88185
 liquid, APR line form. induced by anisotropic spin-lattice interactions (*Russian*) 8-52338
 melanin, relax. times, saturation recovery meas. 8-96017
 methyl radical in glassy organic matrices, electron spin-lattice relax. 8-76312
 polycarbonate, irr., electron spin-lattice relax. at low temp. 8-68382
 semiconductor, conduction electron paramag. relax., Coulomb mechanism 8-88191
 semiconductor without inversion centre, conduction electrons spin relaxation (*Russian*) 8-52355
 transient ESR line profiles, $S=1=1/2$ system, calcs. 8-88170
 trissarcosine calcium chloride: Mn^{2+} , ferroelec., electron spin-lattice relax. 8-80208
 TlF halides, spin-lattice relax. 8-88190
 unordered solids, EPR spin lattice relax., dipole induced contrib. 8-80193
 Ag, adsorption of O_2^- , catalytic oxidation mechanism 8-61046
 Co salts: M^{2+} , $\text{M}=\text{Mn}, \text{VO}$, spin-lattice relax. time meas., 180-380K 8-64268
 $\text{CoSiF}_6 \cdot 6\text{H}_2\text{O}$, paramag., nucl. and electron spin lattice relax. 8-84494
 $\text{CuSiF}_6 \cdot 6\text{H}_2\text{O}$, paramag., nucl. and electron spin lattice relax. 8-84494

electron spin-lattice relaxation continued

- Dy^{3+} , free-radical relax. agent in biological tissues 8-81090
 $\text{FeSiF}_6 \cdot 6\text{H}_2\text{O}$, paramag., nucl. and electron spin lattice relax. 8-84494
 $\text{Gd}, \text{La}, \dots, \text{Pd}$, ESR linewidths, g-shifts, effective electron interaction, spin-lattice relax., spin-flip scatt. 8-68372
 $\text{KBr}(\text{Cl})$, $\text{F}_s(\text{Li})$ -centre spin-lattice relax. at 4.2K 8-91950
 $\text{KCl}:\text{V}^{2+}$ 8-91941
 $\text{LiF}:\text{Mg}(\text{Ag})$, electron spin-lattice relax. of V_k -centre 8-95518
 $\text{MgO}:\text{Fe}^{2+}$, intrinsic spin-lattice relaxation rates, nonresonant US meas. 8-80203
 $\text{NaCl}:\text{V}^{2+}$ 8-91941
 $\text{NiSiF}_6 \cdot 6\text{H}_2\text{O}$, paramag., nucl. and electron spin lattice relax. 8-84494
 $\text{RbCl}:\text{V}^{2+}$ 8-91941
 $\text{Si}:\text{As}(\text{P})$, Orbach spin-lattice relax. rate, uniaxial stress depend. 8-72391
 $\text{SrF}_2:\text{Gd}^{3+}$, spin-lattice relax. of Gd^{3+} , EPR line shifts meas. 8-72404
 $\text{TiO}_2:\text{Mn}^{4+}(\text{Cr}^{3+})$, rutile, temp. depend. of EPR 8-76299

electron spin polarisation

- see also *CIDEP*; spin polarised electron emission
 atomic electron scatt., optical model 8-50646
 detector for 300-2000 eV electron, optimum conditions theory (*Japanese*) 8-66693
 ferroelectric crystal without centre of symmetry, photo-Hall effect (*Russian*) 8-60152
 ferromagnetic transition metals, review 8-76591
 ferromagnetic transition metals, review 8-76592
 photoemission of spin polarised electrons, book contrib. 8-95675
 polarised LEED using a GaAs spin polarised electron source 8-83693
 rare earth ferromagnets, spin polarised electron tunnelling 8-68094
 secondary electron emission, theory 8-76564
 Au (110), electron spin polarisation in LEED 8-83692
 Co, tunnelling electron spin polarisation rel. to band struct. 8-68095
 Co, ZZ 8-68014
 Fe, ferromagnetic, cluster method, environmental effects 8-95405
 Fe, field emission, surface magnetism 8-68607
 Fe, tunnelling electron spin polarisation rel. to band struct. 8-68095
 Fe, ZZ 8-68014
 Fe_3Si -based alloy, dil., cond. electron polarisation and moment perturbations 8-68224
 Fe_3Si -based dil. alloys, conduction electron polarisation, moment perturbations 8-68225
 $\text{Gd}_{25}\text{Co}_{75}$, amorphous film, ZZ 8-68014
 Ni and Ni alloys, tunnelling electron spin polarisation rel. to band struct. 8-68095
 Ni, ferromagnetic, electron-magnon interactions 8-68205
 Ni, field emission, surface magnetism 8-68607
 Ni, ZZ 8-68014
 Rb-tetrahydrofuran soln., photolysis, photoelectron emissive EPR signal, scavenger electron affinity reactivity 8-53224
 Xe, electron scatt., optical model for electron spin polaris. 8-50646

electron spin relaxation see electron spin-lattice relaxation**electron spin resonance** see paramagnetic resonance**electron states, impurity** see impurity electron states**electron states, surface** see surface electron states**electron streams** see electron beams**electron structure of solids (crystallography)** see crystallography**electron structure of solids and liquids (energy structure)** see electron energy states (condensed matter)**electron theory**

- see also Dirac equation; quantum electrodynamics
 chronon in quantum theory of electron, existence of heavy leptons, neutrino spectrum 8-70008
 Dirac's extended electron model, quantum and classical theory elaboration 8-82134
 Dirac essentially self adjoint operator, resolvent estimator near infinity 8-49992
 electric charge conservation (*Russian*) 8-77739
 experimental verification of special relativity 8-57777
 finite self-mass in nonperturbative iterative scheme of QED 8-89641
 magnetic moment anomaly determ. using two level dual vac. polarisation model 8-54632
 ME-EM field model of free electron state 8-49988
 monopole pot., wave function for electron motion (*Chinese*) 8-77768
 nonlinear effects in theory of erratic electron 8-93825
 relativistic electron model from the introduction of the chronon 8-93827
 Schwarzschild sphere and classical electron self-energy 8-49681
 spinning electron, quantum mech. rotor, dynamics, invariance requirements 8-70250

electron theory of metals see metal theory**electron traps**

- see also colour centres; hole traps; impurity electron states
 alcohols, trapped electron spectral relax., random-walk model 8-60493
 alkali halides, F-centre trapping of conduction electrons, photocond. study 8-56179
 anthracene, thermally stimulated currents from shallow trapping centres (*Japanese*) 8-92015
 anthracene, triplet exciton trapping, structural imperfections and delayed fluorescence 8-68551
 anthracene crystals, superficial trapping levels, pulsed photocurrent transients 8-76021
 $\text{L}(+)\text{arabinose}$, irradiated single crystals, electron trapping, ESR obs. 8-88646
 chlorophyll-a, microcryst., trapped-electron doping in photovoltaic sandwich cells 8-53334
 cyclodextrin, trapped electrons in cryst. matrices, ESR, optical absorption spectra 8-80768
 defect dielectrics containing electron trap centres, transient current model (*Russian*) 8-60134
 degenerate semiconductor, recombination-generation currents derivation 8-52007
 diamond:B, thermoluminesc., TSC, correlation meas. 8-88369
 $n\text{-GaAs}:\text{O}$, press. depend. of deep level associated with O, transient capacitance meas. 8-64000
 insulators, noncryst., electron density captured at traps, liberated to conduction band 8-87946
 3-methylpentane, γ -irradiated, isothermal luminescence in presence of aromatic solutes at 77K 8-76519

electron traps continued

- MIS solar cell, effects of pinholes, oxide traps and surface states 8-80055
 MNOS structures with tunnelling-thickness SiO_2 films, charge trapping obs. 8-95379
 molecular crystal/electrolyte interface, illuminated, space charge behaviour 8-84290
 MOS capacitor, nonequilib. response to linearly varying voltages 8-52091
 MOS elements in depletion, interfacial tunnel interaction anal. 8-64121
 naphthalene, surface pot. decay, trap modulated mobility 8-72164
 one-carrier SCL currents in solid with two sets of traps distributed in energy 8-72158
 one-dimensional systems, electron trapping and transport by supersonic solitons 8-72139
 organic compounds, irradiated single crystals, electron trapping, ESR obs. 8-88646
 piezoelectric semiconductor, cascade capture of carriers by attractive impurity centres, cross section 8-56157
 polyethylene, high density, TSC field depend. 8-76090
 polypyromellitimide, thermal depolarisation current 8-52429
 quartz, impurity microdefects. electron capture cross-sections (*Russian*) 8-76025
 quartz, trapping levels 8-91703
 Schottky diode, trap refilling, depth and capture cross section determ. 8-80052
 SCL current-voltage charact. of homogeneous solid, arbitrary energetic trap distrib. 8-84224
 semiconductor, electron trap, positively charged, hot electron capture coeff. 8-52003
 semiconductor, Faraday rotation in presence of attractive traps 8-76081
 semiconductor, high resist., continuous energy distrib. of trapping centres, dynamic charact. of SCL current 8-56153
 semiconductor containing traps, minority, carrier lifetime 8-60137
 sisal wax, electronic conduction and persistent internal polarisation 8-80277
 thermostimulated recombination, reaction order (*Russian*) 8-76536
 AgCl-AgI , mixed cryst., trap distrib., thermolum. 8-68568
 As_2S_3 glass, localised paramag. states, As_4S_6 , As_4S_4 units, mol. analogue models 8-60087
 BaS:Cu , thermoluminesc. and decay 8-80426
 $\text{Bi}_{12}\text{GeO}_{20}$ vacuum-deposited film elec. and photoelec. props. (*Russian*) 8-60237
 CaS-Pb,Mn , phosphors, thermoluminesc. and fluoresc. spectra 8-64396
 CdGa_2Se_4 , electron traps, energy spectrum, photocurrent decay, TSC temp. depend. (*Russian*) 8-64057
 n-CdS film, transient photoconductivity effects (*French*) 8-87994
 CdS, neutron irradiated, intrinsic defects 8-51599
 $\text{CdS-Cu}_2\text{S}$ single cryst. heterojunction, trap depths in depletion region 8-52064
 CdTe:Zn , TSC, carrier traps, depth and quenching by IR radiation 8-56420
 $\text{Cd}_{1-x}\text{Zn}_x\text{S}$ 10 μm film optical and electrical characterisation (*French*) 8-64153
 GaAs, deep level trap emission identification by indirect conduction minima technique 8-84163
 GaAs:O, photocond., electron traps, level-broadening, 90 to 150K 8-60158
 GaAs:O, slow domains, origin 8-60132
 GaAs-GaAlAs DH LED, transient current trap spectroscopy 8-80049
 GaAs-GaAlAs LEDs, deep levels (*French*) 8-56218
 GaP p-n junction, capacitance-freq. dispersion and electroluminescence efficiency 8-64101
 Ge, donor-acceptor electron transfer at low temps., photocond. tail 8-84249
 Ge-pyrolytic SiO_2 system, carrier trapping, GeO_2 sublayer effect 8-91775
 Ge-S film, amorphous, photo-induced ESR and optical absorption edge shift 8-88374
 $\text{Ge}_2\text{Se}_{1-x}$, amorphous semicond., elec. props. 8-84219
 He, liq., surface with trapped electron, parallel mag. field effect on interband transition 8-87835
 KCl, F-F' conversion at room temp. 8-51539
 $\text{KI:Eu}^{2+}(\text{Sr}^{2+})(\text{Mn}^{2+})$, elec. field effect on mech. of recomb. 8-80397
 LiCl aqueous glass, X-irradiated, localised electron optical, IR and photoconductivity spectra 8-73064
 LiF, thermoluminescence mechanism, extension of Mayhugh-Christy model 8-80425
 LiH (D), single crystals, electronic excitations, review (*Russian*) 8-72574
 MgWO_4 , luminesc. and capture centres (*Russian*) 8-52543
 PbS oxide, optical excitation meas. of trap charging surface film (*Russian*) 8-76180
 Si ion implanted p-n junction, cryst. damage influence on elec. props. 8-56219
 Si:Au, electron capture cross section, energy level of Au acceptor centre 8-51926
 Si:Co, study of impurity states 8-76020
 Si:P, doped by neutron transmutation, electron traps 8-84164
 Si- SiO_2 interface traps energy distribution meas., in MOS devices, under non-steady-state (*Korean*) 8-64119
 SiO_2 , electron-beam irradi., electron trapping, MOS capacitor expts. 8-72268
 SiO_2 film on Si, negative bias instability 8-91773
 SiO_2 in FET, electron trapping due to electron beam deposited Al 8-80060
 SiO_2 , thermal, elec. stressed film, dielec. breakdown 8-64322
 $\text{SiO}_2\text{:Al}$ film, ion-implanted, electron trapping behaviour 8-67729
 n- SnO_2 , high resist., photoelectronic processes 8-60157
 TiO_2 , plasma growth, photoelectronic props. 8-52662
 YAG, colour centres conceived as bound polarons 8-63990
 YIG, LPE film, non-Ohmic currents 8-68099
 ZnS:Cl^- , $\text{Cu}^+(\text{Ag}^+)$, phosphor, high press. effect on thermoluminesc. 8-64419
 ZnS:Pb phosphor mech. of elec. field liberation of electrons from traps 8-72616
 ZnSe, laser induced modulation of opt. absorpt. 8-88324

electron traps continued

- ZnSiP_2 , photocond. under laser excitation (*Russian*) 8-84258
 ZnWO_4 , luminesc. and capture centres (*Russian*) 8-52543
electron tube diodes see diodes
electron tube manufacture
 ceramic-metal seal technology, history and trends 8-81992
 microchannel plate surface finishing using liquid 8-90544
electron tube rectifiers see rectifier tubes
electron tubes
 see also cold-cathode tubes; diodes; electron emission; microwave tubes; nuvistors; pentodes; relativistic electron beam tubes; tetrodes; thermionic tubes; triodes; ultra-high frequency tubes; X-ray tubes
 electron beam deflection tube, for current and mag. induction meas. 8-54393
electron tunnelling see tunnelling
electron valves see electron tubes
electron-wave tubes
 see also klystrons; magnetrons; travelling-wave-tubes
 No entries
electronegativity
 acetaldehyde, proton affinity, geom. and basis set depend., MO calcs. 8-50461
 atomic electronegativity scale rel. to work function 8-64096
 atoms, correl. of CNDO-bonding parameters 8-74577
 atoms and ions, valence region energies, electronegativity, Politzer-Parr partitioning, finite difference approx. 8-78612
 bases, K^+ affinities ab initio SCF calc. 8-58585
 density functional viewpoint 8-66485
 diatomic molecules, containing elements from Li to F and Na to Cl, calc. from mol. dissociation energies 8-62943
 formaldehyde, proton affinity, geom. and basis set depend., MO calcs. 8-50461
 formic acid, proton affinity, geom. and basis set depend., MO calcs. 8-50461
 molecular reactivities rel. to struct., Taft and Kirkwood-Westheimer eqns. 8-62738
 spark breakdown current growth gas dynamic processes, electronegative gas mixture 8-87588
 spin-orbital, and catalytic activity 8-73078
 tertiary phosphine oxide+aliphatic alcohol, $\pi\text{-}\pi$ conjugation, electronegativity and H-bond energy 8-82863
 CN^- , proton affinity, integral Hellmann-Feynman theorem 8-70767
 CO, proton affinity, integral Hellmann-Feynman theorem 8-70767
 N_2 , proton affinity determ. from N_2H^+ appearance pot. from N_2H_2 8-58869
 OH $^-$, proton affinity, integral Hellmann-Feynman theorem 8-70767
electronic calculators
 for calculator applications see under relevant applications e.g. engineering computing; natural sciences computing
 programmable pocket calculator as physics teaching aid, numerical integration appl. 8-86083
electronic conduction in crystalline semiconductor thin films
 for electronic conduction in amorphous thin films, see "electrical conductivity of amorphous semiconductors and insulators"
 see also electrical conductivity of amorphous semiconductors and insulators; electrical conductivity of crystalline semiconductors and insulators; electrical conductivity transitions
 compensated semicond. film, jump-over cond., control by external field 8-80080
 electron spin orientation in quantum size effect conditions 8-68575
 Al-GaAs-Al sandwich-type sputtered film, elec. props. 8-91780
 Al-lead stearate-Hg, transient and alternating electric currents 8-84311
 Bi, carrier conc. and mobility, resist., galvanomag. and thermoelec. meas. 8-52111
 Bi, elec. cond., obs. of epitaxial growth mechanism (*French*) 8-84329
 Bi film, charge carrier scatt. (*Russian*) 8-80079
 Bi, film, size effect on electrical cond. 8-84331
 $\text{Bi}_{1-x}\text{Sb}_x\text{Te}_3$, solid soln. film on mica substrate, effect of stresses on elec. cond. 8-51859
 $\text{Bi}_2(\text{Te}_{1-x}\text{Sb}_x)_3$, thin cryst. two-dimens. system, electronic props. 8-60181
 Cd-Sb thin film prep. by vacuum deposition, elec. props. 8-92194
 CdO-SnO_2 film, DC sputtering prep., visible and near IR transmission, resist. 8-88049
 CdS, film, X-ray diffr. and elec. cond. 8-64149
 CdS, film electrolytically deposited, surface and bulk photocond. props. 8-60154
 CdS, film for solar cells, struct. and elec. props., thickness depend. 8-72289
 CdS films, vac. evaporation from $\text{CdS.Cr}_2\text{O}_3$ system, photoelec. props. 8-80074
 $\text{Cd}_{1-x}\text{Zn}_x\text{S}$ 10 μm film optical and electrical characterisation (*French*) 8-64153
 CuInSe, epitaxial growth on GaAs 8-84104
 Cu_2S , film preparation for solar cells, elec., optical, struct. props. 8-76602
 Cu_{2-x}S films, vacuum deposited, electrical conduction and phase transitions 8-84332
 GaAs, minority carrier diffusion lengths, contact metal effects 8-72260
 GaAs:Be, annealing effect during MBE 8-79898
 GaAs:Ge, LPE, on semi-insulating GaAs, film-substrate interface characterisation 8-72017
 GaN, plasma deposition and elec. cond. 8-60585
 GaP film, deposited by RF sputtering (*Czech*) 8-52667
 GaSe film, charge transport models (*Russian*) 8-60233
 Ge film, polycrystalline, structural and elec. props. 8-76173
 Ge:Sb(In), film, electronic props. 8-84330
 Ge-Al, elec. resist. and IR transmission, comp. and substrate temp. depend. 8-52112
 n- In_2O_3 film, RF sputter grown, substrate bias effect on elec. and optical props. 8-64150
 $\text{In}_2\text{O}_3\text{:Sn}$, film, HF sputtered, cond., Hall mobility, oxidation, charge carrier density 8-72287
 $\text{In}_2\text{O}_3\text{:Sn}$, HF sputtered films, temp. depend. studies of the elec. transport props. 8-76170
 $\text{In}_2\text{O}_3\text{:Sn}$, sputtered film, optical and elec. props. 8-76177
 $\text{In}_2\text{O}_3\text{-SnO}_2$, stress, and elec. and optical props. 8-51861

electronic conduction in crystalline semiconductor thin films continued

- n-InP, epitaxial, Hall effect, electron mobility and density temp. depend. 8-72288
 n-InP, epitaxial, subthreshold velocity-field charact., 77K 8-64038
 InP, planar reactive deposition on CdS, heterostruct. formation and elec. evaluation 8-72738
 p-InSb film, elec. transport props. 8-72291
 InSb film, quantum size effects, transport props. 8-76171
 Pb_{1-x}Cd_x, epitaxial, resist. and Hall coeff., substrate temp., thickness and comp. depend. 8-72290
 PbS, polycryst., chem. deposition from soln. and characterisation 8-72743
 PbTe, ion-implanted, doping profile evaluation by Hall effect and sheet resist. meas. 8-59831
 Si, electrodeposited film, appl. in solar cell fabrication 8-76611
 Si, epitaxial layers, minority carrier lifetime and diffusion length meas., photocurrent technique 8-95302
 Si, polycryst., growth, props. and MIS appl. (Slovak) 8-92196
 p-Si polycrystalline films on graphite substrates (French) 8-64154
 Si:O, O rich polycryst. film, carrier transport 8-80076
 Si:P(B), film, electronic props. 8-84330
 SmS, first-order transition from semiconducting to metallic state 8-52040
 SnO₂, CVD using SnCl₄-H₂O and SnCl₄-H₂O₂ systems, elec. and optical props. 8-52686
 SnO₂, two-step deposition process using DC sputtering and oxidation, and characterisation 8-95691
 TiGaS₂(Se₂), elec. and photoelec. props. (Russian) 8-52109
 (Y,Eu,Tm,Ca)₃(Fe,Ge)₅O₁₂, Ca, Ge substituted garnet LPE films, elec. props., charge imbalance, Seebeck effect 8-68101
 (Y,Sm)₃(Fe,Ge)₅O₁₂, Ca, Ge substituted garnet LPE films, elec. props., charge imbalance, Seebeck effect 8-68101
 YIG, LPE film, non-Ohmic currents 8-68099
 Zn,Cd_{1-x}S, prep. by soln. spray method, and struct., optical and elec. props. 8-52666
 Zn,Cd_{1-x}S:In, low resist. film for solar cell window 8-71200
 ZnO film, chemisorption of H, electrical cond. exam. adsorption centres 8-67913
 ZnO thin film SAW device manufacture, sputtering system and film characterisation 8-95692
 ZnSe, high conductivity films appl. to p.n. heterojunctions 8-68100
 ZnTe:Sb, as function of growth temp. 8-76172

electronic conduction in insulating thin films

- see also *electrical conductivity of amorphous semiconductors and insulators; electrical conductivity of crystalline semiconductors and insulators*
 chlorophyll-a, microcryst., trapped-electron doping in photovoltaic sandwich cells 8-53334
 polyferrocene, in MIM sandwich, I-V and I-d characts. 8-80064
 polymer foil, charge distrib. determ., thermal pulse technique, meas. accuracy 8-80287
 polypropylene film, evaporated, elec. props. 8-84335
 polyvinyl alcohol films, pure and doped, elec. cond. temp. depend. 8-88052
 Al-Al₂O₃-Al junctions, Dy doped at Al₂O₃-Al interface, electron transport mechanisms and barrier height 8-91778
 Al-Al₂O₃-Al structure, tunnel I-V characts., transmission coeffs. 8-80068
 Al-SiO-Al structure, tunnel I-V characts., transmission coeffs. 8-80068
 Al,Ga_{1-x}As native oxide, low leakage, MOS characterisation 8-91795
 Al₂O₃, amorphous film, non-thermal switching in Al-Al₂O₃-Al struct. (Russian) 8-80069
 Al₂O₃, anodised film, in strong elec. field, pulsed V-I characteristics (Russian) 8-64156
 Al₂O₃ composite films, elec. instability 8-68452
 Al₂O₃ film, CVD, props. rel. to deposition parameters 8-92197
 Al₂O₃ film, dielec. props., AC and DC elec. characts. 8-68445
 Al₂O₃ plasma-anodised, current efficiency 8-91797
 Al₂O₃, porous film, elec. cond. charact. 8-76179
 Al₂O₃, RF sputtered film, transient current meas. 8-52113
 Bi₁₂GeO₂₀ vacuum-deposited film elec. and photoelec. props. (Russian) 8-60237
 Fe₂O₃, prep. by reactive sputtering, struct. and props. (Japanese) 8-92190
 GaP, anodically grown insulating layers, prep. and props. (German) 8-64158
 MgO thin film, DC conduction 8-88051
 (SN)_x polymer, elec. props. of amorphous thin film and single crystal, role of chain breaks (Japanese) 8-68104
 SiN_x plasma deposited dielectric film, elec. props. 8-68103
 Si₃N₄ film, pyrolytically deposited, AC cond. at low freq. 8-84334
 Si₃N₄, Si rich, CVD film prep. and props. 8-76607
 Si₃N₄O₂ film, band diagram, optical props. and elec. cond. meas. 8-84333
 SiO amorphous thin film capacitor, EPR, elec. cond. 8-68358
 SiO₂, electron-beam irradi., electron trapping, MOS capacitor expts. 8-72268
 SiO₂ film, plasma grown, thermally stimulated depolarisation current meas. (Russian) 8-80082
 SiO₂, Si rich, CVD film prep. and props. 8-76607
 SiO₂, thermally grown films, LF conductance 8-80081
 SiO₂ film, MIM struct., DC bias dependent dielectric dispersion props. 8-76178
 Ta-Ti-N, reactive sputtered film, elec. props. 8-84336
 Ta₂O₅ anodic film with Au counterelectrodes, conduction process 8-84312
 TiO₂, metal-TiO₂-Si structure, I-V characteristics, deposition, post-deposition oxidation effects 8-80063
 YH₂, struct. and elec. resist., electron diff. meas. 8-87888
 Y₂O₃, struct. and elec. resist., electron diff. meas. 8-87888

electronic conduction in metallic thin films

- see also *discontinuous metallic thin films; electrical conductivity of amorphous metals and alloys; electrical conductivity of crystalline metals and alloys*
 amorphous, structural and amorphous props. 8-84323
 discontinuous film, elec. cond. and current noise mechanism, theory 8-56244
 electron MFP calc. 8-72283
 grain boundary electron scattering by effective mean free path 8-84320

electronic conduction in metallic thin films continued

- granular metal films, minimum metallic cond. 8-56241
 magnetomorph oscillations, thin films with unlike surfaces, generalised Sondheimer model 8-56243
 metallic thin films, electric field distrib. and emission currents of island condensates 8-88047
 metglas type system, structural and amorphous props. 8-84323
 monocrystalline, size and grain boundary effects in elec. cond. 8-76164
 oscillation kinetic effects, boundary electron scatt. (Russian) 8-52104
 size effect, total resistance temp. coeff. 8-84318
 size effect conductivity in transverse mag. field, Hall coeff. (French) 8-91787
 size effects, anal. 8-76162
 size effects, resistivity derivation 8-76163
 strain coefficients of resistivity, general Fuchs-Sondheimer expressions 8-52107
 thermoelectric power, Fuchs-Sondheimer eqns. for film with grain boundary scatt. 8-52108
 thermoelectric power and temp. coeff. of resistivity 8-91788
 transverse E-type quantum waves (Russian) 8-91785
 Ag film, annealing study of elec. resist. and defect density 8-76167
 Ag, vacuum deposited on Al substrate, recrystallisation 8-60044
 Al film, single cryst., elastoresist. effect 8-84321
 Au discontinuous film, elec. cond. and current noise, temp. depend. meas. 8-56245
 Au, polycryst., RF bias-diode and triode sputtered, resist. and microstruct. 8-80072
 Au-Fe film spin glass, low temp. resistivity, mean free path effects 8-80163
 Cu film, annealing effect on grain size 8-72015
 Cu, vacuum deposited on Al substrate, recrystallisation 8-60044
 Dy film, elec. resist. results 8-84326
 Er film, elec. resist. results 8-84326
 Fe film, amorphous and polycrystalline, Hall effect, resistivity and mag. moment 8-91786
 Fe, Hall resist., effect of N impurity codeposition 8-64146
 Fe, polycryst., heat of adsorpt. of H₂ and D₂, calorimetric and resist. expts. 8-91530
 Fe-Si amorphous film, Hall const. and magnetoresistive effect 8-52105
 Gd film, elec. resist. results 8-84326
 Gd_{1-x}Co_x film, resistivity, Hall effect, domain wall density 8-76169
 Ge-Al, elec. resist. and IR transmission, comp. and substrate temp. depend. 8-52112
 HfPt₃, corrosion resist. and elec. cond., bulk and film samples 8-72285
 Mn, anomalous low temp. resistivity 8-91789
 Mo, film, vacuum deposited, elec. cond., internal stresses, surface corrosion, MOS gate appl. (Japanese) 8-80073
 Mo film, vacuum deposited onto SiO₂-Si substrates, elec. resist. 8-76166
 Na-NH₃ film, vapour deposited, elec. resistivity, metal-nonmetal transition 8-84317
 Nb, ion bombardment with N₂⁺, Ar⁺, struct. changes, chemical compound formation (Russian) 8-95084
 Ni, amorphous film, getter sputtered at 25K, resistivity, Curie temp. 8-52673
 Ni films, CO-covered, adsorpt. of H, isotherms, resist., work function changes 8-75926
 Ni-B amorphous alloy film, atomic and electronic transport (French) 8-84325
 Ni-Co, ferromag. films, magnetoresistance effect, crystal struct. 8-68017
 Ni-Fe, film, anomalous Hall and Nernst-Ettingshausen effect, contribution of phonon and impurity scatt. (Russian) 8-64145
 Ni_{1-x}P_x electrodeposited, amorphous, mag. and transport props. 8-52106
 PZT, ferroelec. film, elec. props., composition anal., AES 8-84530
 Pd, film, on ZnO, struct., elec. props., AES, UPS study 8-76168
 Pt, ultrathin film, elec. cond., amorphous Ge overlayer thickness depend. 8-72284
 SiO₂-Ni granular metal films, minimum metallic cond. 8-56241
 Sm film, elec. resist. results 8-84326
 Sn film, substrate dependent excess electrical conductivity above superconducting transition temp. 8-84324
 Ta, ion bombardment with N₂⁺, Ar⁺, struct. changes, chemical compound formation (Russian) 8-95084
 Ti, ion bombardment with N₂⁺, Ar⁺, struct. changes, chemical compound formation (Russian) 8-95084
 Ti, vacuum deposited, cryst. struct. and elec. props. 8-79908
 Ti-Permalloy thin film diffusion couples, low temp. interdiffusion interdiffusion 8-71889
 W-Al₂O₃ granular film, percolation conductivity 8-84319
 Y, struct. and elec. resist., electron diff. meas. 8-87888
 Zn film, RF sputtered, ageing processes 8-84322
 ZrPt₃, corrosion resist. and elec. cond., bulk and film samples 8-72285

electronic density of states

- A15 compound trends, self consistent band calcs. 8-79925
 AES, obtaining density of states information from self-deconvolution of Auger band-type spectra 8-92150
 alloys, dressed-cluster approx. 8-95249
 amorphous metal, electronic density of states 8-51868
 Anderson model, one dimensional site disordered lattice, AC conductivity 8-84199
 binary alloy, short range order effect on density of states (Russian) 8-67929
 binary alloy model, 2D disordered system, chain-like localisation 8-91646
 binary alloys, electronic density of states in Bethe lattice, using Weaire-Thorpe Hamiltonian 8-51870
 α-brass, electronic momentum densities by two-dimensional angular correlation of annihilation radiation 8-91605
 charge carrier conc., temp. depend., computer data anal., effect of band parameter errors (Russian) 8-52006
 Cr-Au alloys, dil., elec. resist., 77-700K 8-64035
 d-band metals and alloys, s-d hybridisation 8-91644
 disorder and single electron spectrum, in linear chain (Russian) 8-56060

electronic density of states continued

- disordered alloys, electronic struct., CPA calcs., short-range order 8-63964
- disordered system, Coulomb gap, Monte-Carlo simulation 8-84168
- disordered system, four dimens., electron density of states determ. 8-72057
- disordered systems, spectral density of electronic states calcs. 8-72055
- graphite, electronic props., self-consistent LCAO calc. 8-51887
- heavily doped semiconductor, density of eigenvalues, localisation, general disordered system 8-56109
- Heisenberg antiferromagnet, dil., CPA calc. 8-68263
- insulators, noncryst., electron density captured at traps, liberated to conduction band 8-87946
- Lenz-Jensen pot. calc. using third order approx. for electron density, in amorphous material 8-95099
- metal, dislocations rel. to electron gas thermodynamics at $2\frac{1}{2}$ th order transition (*Russian*) 8-51910
- metal, inhomogeneous electron system, nonlocal exchange and correlation 8-56097
- metal, narrow band, quasilocal Auger spectra 8-60536
- metal surface, narrow band, self consistent model calc. of electronic states 8-95333
- MNOS structures with tunnelling-thickness SiO_2 films, charge trapping obs. 8-95379
- multi-Lagrangian interpolation for evaluation of density of states 8-84118
- multiple scattering in condensed media, calc. of density of states for noncrystn. Cu and Fe 8-91578
- polyenes, model results for π electrons 8-55128
- polymer primary structures ESCA and EHC methods 8-52630
- random impurity system, density of states tails, fluctuations and mobility edges 8-67983
- self consistent cluster-Bethe lattice calc. 8-67930
- semiconductor, quasilocal acceptor states, effects on band gap and electron mobility (*Russian*) 8-60082
- semiconductor in mag. and US wave fields, electronic density of states (*Russian*) 8-72056
- superconducting transition temperature, electronic density of states depend. 8-76186
- TCNQ, dimer gas model 8-87926
- TCNQ salt, NMP-TCNQ, realisation of disordered Hubbard model, dielec. props. 8-79917
- tight binding calc., overlap and next-nearest-neighbour interaction effects 8-72059
- tight-binding chains, off-diagonal disorder, density of states, localisation length 8-88247
- transition metal, 3d, liq., density of states of d-band, heat of vaporisation 8-95253
- transition metal, 3d, paramag., energy band calcs. 8-91608
- transition metal, 4d, photoabsorption spectra near K-edge 8-92144
- transition metal, disordered, multiple scattering theory, optical theorem 8-95250
- transition metal, surface electronic structure calculations 8-95329
- transition metal alloys, density of states and complex band struct. for one-dimens. model 8-79919
- transition metal surface, electron states at steps, cluster-Bethe lattice approx. 8-52045
- TTF-TCNQ, band struct., Fermi surface and density of states, LCAO calc. 8-60048
- type II semiconductor, A15 struct., electronic density of states and T_c changes with atomic ordering 8-91800
- V_2V_3 compounds, electronic struct., X-ray emission, XPS, UPS obs. 8-52638
- ZZ 8-88057
- Ag clusters, charge distrib., density of states, CNDO calcs. 8-70995
- Al, adsorption of O_2 , relation between energy-band and cluster model 8-52048
- Al, electronic momentum densities by two-dimensional angular correlation of annihilation radiation 8-91605
- AlAs-GaAs (100) interface, tight binding calc. of electronic struct. 8-95342
- AlAs-GaAs (110) interface, self-consistent calc. of interface states and electronic struct. 8-52066
- As, amorphous, electron and phonon density of states calcs., comp. to XPS 8-56066
- As, phonon density of states compared to electronic density of states 8-55924
- As_2Se_3 , glass, density of optically induced localised paramagnetic states 8-52354
- BaTiO_3 , XPS, band struct., density of states, photoionisation cross sections 8-52629
- Be, inelastic electron scattering near K-edge 8-52606
- n-CdSnAs₂, optical absorption rel. to energy spectra (*Russian*) 8-75994
- CeAs, evidence for valence fluctuations, ^{75}As Knight shift data 8-91966
- Co, liq., density of states of d-band, heat of vaporisation 8-95253
- CoAl, bonding, self-consistent energy bands 8-91610
- $\text{Cs}_{1-x}\text{Au}_x$, liq., metal-nonmetal transition, electronic theory 8-79930
- Cu, clusters, size, geometric effects, catalysis implications 8-73131
- Cu, noncrystalline, multiple scatt. calcs. 8-91578
- Cu, partial densities of states, electron-phonon interaction 8-51869
- Cu-Ni, alloys, electronic states, KKR-CPA calc. 8-84125
- EuS, conduction band density of states, redistrib. near ferromag. saturation 8-67939
- Fe, noncrystalline, multiple scatt. calcs. 8-91578
- Fe, partial densities of states, electron-phonon interaction 8-51869
- Fe, UPS, density of states determ. 8-52623
- FeAl, B2-cpd., band struct. and density of states, KKR calc. 8-63969
- FeAl, bonding, self-consistent energy bands 8-91610
- FeAl, isomer shift, electronic charge density 8-80264
- $\text{Fe}_{0.65}\text{Ni}_{0.35}$, UPS, density of states determ. 8-52623
- GaAs (110), valence band Auger spectra, from Ga and As CCV transitions 8-92149
- n-GaAs, absorption tails in surface depletion layer and bulk 8-64379
- GaAs-Ga_{1-x}Al_xAs superlattice, sub-band dimensionality 8-63981
- GaS, XPS and valence band density of states, tight binding approx. 8-63974
- Ge-GaAs (110) interface, self-consistent calc. of interface states and electronic struct. 8-52066
- KCl, cluster expansion of density matrix and crystal energy 8-87952

electronic density of states continued

- KNbO_3 , XPS, band struct., density of states, photoionisation cross sections 8-52629
- La hydrides, S conduction electrons at Fermi level, depend. on H concentration 8-88217
- LaF_3 , quantum yield, photoelectron spectra, density of states struct. 8-68601
- LiOH , electron distrib. of OH^- 8-75973
- $\text{Li}_{1-x}\text{Pb}_x$, liq., metal-nonmetal transition, electronic theory 8-79930
- Lu, band structure, influence of relativistic effects 8-75991
- Na_2WO_3 enhanced T_c , interband coupling 8-91804
- Nb-Mo-Tc alloys, supercond., point-group symmetry 8-64163
- Nb-Zr(Hf)(W) alloys, rel. to single cryst. elastic consts. 77-298K 8-84879
- Nb_2Al , metallic bonding, electronic states calcs. 8-79916
- Nb_2Au , BCC, density of states, comparison with A-15 8-80095
- Nb_2Ge , metallic bonding, electronic states calcs. 8-79916
- $\text{Nb}_2\text{Ge(Al)}$, anomalous resistivity, insight from band theory 8-60106
- Nb_2Si , Nb_2Sn , Nb_2Ge , Nb_2Al , ZZ 8-91613
- Ni, UPS, density of states determ. 8-52623
- Ni-Pd-P, Ni-Pt-P, amorphous and electronic structs., NMR Knight shifts and linewidths meas. 8-68400
- NiAl, bonding, self-consistent energy bands 8-91610
- PbI_2 , tight binding band structure using scaled parameters 8-79927
- Pd (111), electronic states calc. and adsorbate-induced photoemission struct. interpretation 8-60179
- Pd, clusters, size, geometric effects, catalysis implications 8-73131
- Pd, electronic struct., effects of press. and alloying with Ru, Rh, Ag, and Rh+Ag 8-91581
- $\text{Pd}_{1-x}\text{Ag}_x$, superconducting transition temp., APW band struct. calcs. 8-95393
- PdH , electronic struct. and proton spin-lattice relax. calc. 8-67937
- PdSb , electronic struct., optical transitions, Fermi surface 8-51885
- (SN)₂, XPS calc. using photoionisation cross sections 8-72697
- Si, AES, convolution and deconvolution 8-52601
- Si surface, valence band Auger line shape, corrected numerical results 8-52602
- SiO_2 , O rich polycryst. film, carrier transport 8-80076
- SiO_2 , new interpretation of structure 8-84120
- SrTiO_3 , XPS, band struct., density of states, photoionisation cross sections, theoretical determ. 8-52629
- Ti, liq., density of states of d-band, heat of vaporisation 8-95253
- Ti, partial densities of states, electron-phonon interaction 8-51869
- TiC, TiN and VC, charge distrib. and bond ionicity 8-63961
- $\text{Ti(Fe}_{1-x}\text{Co}_x)$, density of states estimation from magnetisation and resistivity meas. 8-84119
- TiO_{1+x} , conduction band determ. 8-60055
- UGe_3 , de Haas-van Alphen effect, band struct. calc. 8-72068
- V, energy bands, calcs. using LCGO method 8-91608
- V, partial densities of states, electron-phonon interaction 8-51869
- VC, TiC and TiN, charge distrib. and bond ionicity 8-63961
- V_3Si , neutron irradiat., sound velocity, magnetic susceptibility and upper critical field 8-88074
- V_3Si , neutron-irrad., ht. capacity and resistivity 8-88075
- V_3Si , V_3Sn , V_3Ge , V_3Ga , V_3Al , ZZ 8-91613
- WO_3 amorphous film, elec. cond. and dielec. const. 8-60238
- $\text{Y}_{0.7}\text{Th}_{0.3}\text{C}_{1.58}$, specific heat 8-91813
- $\text{Zr(Fe}_{1-x}\text{Co}_x)_2$, density of states estimation from magnetisation and resistivity meas. 8-84119
- electronic density of states of amorphous solids** see *electron energy states of amorphous solids*
- electronic density of states of liquid semiconductors** see *electron energy states of liquid semiconductors*
- electronic desk calculators** see *electronic calculators*
- electronic engineering computing**
see also *circuit analysis computing; circuit CAD; computerised instrumentation*
magnetic hysteresis, vector model, based on interacting dipoles 8-76271
p-n-n⁺ junctions, epitaxial planar, two-dimensional anal. of breakdown 8-80045
Si, diffused p-n junction, computer calcs. of photoresponse using Gummel-de-Mari algorithm 8-56221
- electronic equipment testing**
cardiac pacemaker leak testing methods 8-57133
electro-medical servicing, quality maintenance 8-77126
particle simulation unit for counter circuitry testing 8-81002
raster electron microscope test object 8-86393
- electronic music**
see also *musical acoustics; musical instruments*
electronic music, keyboards for pure music, use of consonant chords 8-83183
microcomputers developments and appl. 8-90610
quadruphonic, Interface 227 multiple function generator 248 appl. (*German*) 8-66993
- electronic structure, atomic** see *atomic structure*
- electronic structure, molecular** see *molecular electronic states*
- electronics applications of computing** see *electronic engineering computing electronics*
see also *beta-rays; cosmic ray electrons; positrons*
intrinsic magnetic moment of free electron in mag. field, meas. possibility (*Russian*) 8-86430
ionsphere photoelectrons flux, low-altitude plasma line anisotropy theory 8-77414
magnetosphere energetic electrons, chorus generation during substorms 8-96356
mass calc. in terms of meas. quantities 8-66180
mass operator in plane wave field, near cyclotron reson. region (*Russian*) 8-86432
QED, one loop effective potential with anomalous moment, electron Lagrangian 8-58146
single isolated electron measuring technique, resource letter for teachers 8-81776
solar corona, fast electrons from hard X-ray bursts rel. to type III-V radio bursts 8-89157
steady state plasma, electron temp. and density meas. system 8-87490
e-p mass ratio, direct determ. using cyclotron resonance technique 8-70093

electrooptics *see electro-optical effects*

electroosmosis *see osmosis*

electrophoresis

see also electrophoretic coating techniques

- albumin, bovine serum, solutions, fluctuation transport theory 8-70057
- biological materials continuous flow electrophoretic separator, for sounding rocket expts. 8-85398
- biological materials fractionation in space by deflected lamina electrophoresis 8-85397
- chromaffin granule electrophoretic mobility meas. by light scatt., effect of Ca^{2+} and Mg^{2+} 8-53357
- deoxyribonucleoprotein, gamma-ray protein damage 8-53338
- dielectric fluid, electro-dielectrophoretic forces acting on spherical impurity particles, analytical evaluation 8-88641
- dielectrophoretic forces, expt. anal. 8-64892
- electrode, equipot., electrophoretic force 8-61024
- electrode geometries for various dielectrophoretic force laws 8-88640
- erythrocyte electrophoretic mobility, effect of UHF EM radiation 8-53442
- heat transfer in liquids by dielectrophoresis 8-94874
- n-hexane, impurity particle motion, under DC and AC conditions, expt. results and computer simulation 8-88642
- mass transport, apparatus 8-85168
- particles suspended in low-cond. liqs., field depend. of electrophoretic mobility 8-56919
- percutaneous electrophoresis of amino acids and urea 8-61237
- polystyrene spheres suspended in isodecane, field depend. of electrophoretic mobility 8-56919
- PtFE, colloidal, in butanol, electrophoretic mobility, charge origin 8-85211
- pulsed DC glow discharge, cataphoresis eqns. 8-67506
- resin particles, dispersed, precipitation on cellulose fibre in elec. field 8-53262
- solutions, fluctuation transport theory 8-70057
- transition metal complex ions in aq. HCl, temp. gradient chromatography (Japanese) 8-61120
- C blacks, colloidal, in butanol, electrophoretic mobility, charge origin 8-85211
- $\text{Cr}_2\text{O}_3\text{-Al}_2\text{O}_3$, solid soln., effect of Cr on point of zero charge 8-61021
- $\text{Fe}_2\text{O}_3\text{-Al}_2\text{O}_3$, solid solns., effect on Fe on point of zero charge 8-61021
- He-Na mixture, low-pressure discharge, radial cataphoresis obs. 8-67507
- He-Ne laser, output power, unsaturated gain distrib. 8-50751

electrophoretic coating techniques

No entries

electrophoretic coatings

- waveform analysis for blood serum protein composition determ. 8-64928
- ThO_2 electrophoretic coating for poisoning resistant Ir filament electron gun 8-54493

electrophotography

- copier photoconductor drum cooling methods 8-62245
- development of electrostatic images, high speed 8-62249
- electron spectroscopy for chemical anal., appls. to materials for electrophotography 8-92565
- electroradiography, image quality, charge transport random fluctuations influence 8-66015
- electrostatic readout, use of powder or liquid toners 8-70212
- imaging process efficiency and quality, electrophotographic process, electronographic cameras and image intensifiers 8-78932
- KC film digital recording performance 8-78024
- liquid developer, permittivity and conductivity meas. (German) 8-62257
- optical storage materials and methods, conf., San Diego, USA (Aug. 1977) 8-71171
- organic photoconductors, charge acceptance calc. 8-80020
- photo migration imaging, anal. 8-86370
- photo-response characts. of electrophotographic plates in nanosecond periods 8-62251
- photoconductor for charge transfer electrophotography 8-65989
- polyvinylidene fluoride, corona charging at 12.5 kV, obs. 8-92027
- recording media, high resolution, expt. characts. 8-70208
- gamma-Ruticon image buffer, imaging props. 8-66915
- semiconductor amorphous and organic layers, injected charge dirft and localisation (German) 8-91794
- solid state camera speed electrophotographic KC film 8-70211
- spreading phenomenon in dry powder electrophotography 8-63904
- thermoplastic layers with fast heating, discharge process 8-49920
- transparent electrophotographic films, information recording 8-70210
- two-component developer discharge and contact interaction (German) 8-62258
- vacuum deposition, from strip source, onto arbitrarily oriented rotating cylinder, for xerography appl. 8-95696
- xerographic copy line profile meas. using microcomputer/microdensitometer system 8-74088
- xerographic development, transfer function model 8-65991
- xerographic papers, electrostatic props. 8-78852
- As_2Se_3 , amorphous, electrophotographic props., photodecomp. effect 8-49918
- CdGa_2Se_4 , electrophotographic props. (Russian) 8-59100
- LiNbO_3 , photovoltaic effect, latent-image formation kinetics, electrophotography appl. 8-84246
- Se spheres embedded in polymer matrix, electrophotographic film, optical props. 8-83055
- ZnO binder electrophotography, tone reproduction and copy quality (German) 8-62259
- ZnO , light sensitivity rel. to local internal fields (Russian) 8-49932
- ZnO , particulate, Dember effect, rel. to electrophotography 8-95314

electrophotoluminescence *see electroluminescence; photoluminescence*

electrophysiology *see bioelectric phenomena*

electroplated coatings

- stresses meas., internal, effects in Ni and Zn (German) 8-56049
- wear resistance, appl., survey 8-72913
- Cu, levelling kinetics, interferometric investigation (Bulgarian) 8-79864

electroplated coatings continued

- Fe, membranes, effect of electrodeposited metals on H permeation, proposed catalytic mechanism 8-53252
- Ni coating hardness rel. to sulphamate electrolyte selection (Bulgarian) 8-88552
- Ni, electroless plating, oxidation kinetics 8-95847
- Sn-Ni, equiatomic, metastable, transformation kinetics, Avrami parameters calc. method 8-92239
- Sn-Ni metastable alloy, surface film comp., time depend., XPS 8-60870
- SnNi electroplate, anal. by SIMS, ion scatt. spectrometry, and Rutherford backscatt. 8-95979

electroplating

- electrocoating, cell design, Fourier transform soln. of Laplace eqn. 8-76609
- Cr particulate layer on Cr_2O_3 , high solar absorpt. characts., selective surface electroplating 8-87111
- Ni plating, surface props. of Ni after each step of activation process 8-95243

electropolishing *see electrolytic polishing*

electroreflectance

- nematic liquid crystal, spontaneous polarisation, rel. to mol. orientation, electro-reflection meas. (Russian) 8-55809
- semiconductors, ternary and binary, composition variation determ. using electrolyte electroreflectance 8-80809
- CdS:P , implanted, photoluminesc. and electroreflection spectra (Russian) 8-52544
- CuGaSe_2 , obs. of energy transitions from lower valence band states 8-95576
- GaAs, implantation disorder, flux and fluence depend., electrorefl. expts. 8-83833
- GaAs, k-linear coupling, E_1' transitions 8-91583
- GaAs, optical modulation spectra, proton damage effect 8-76487
- $\text{GaAs}_{1-x}\text{P}_x$, heterogeneous struct. obs. by anodisation-electrorefl. technique 8-84088
- Ge, effect of surface and nonuniform fields 8-68511
- Si epitaxial film, correlation between electrooptical and electrical props., IR absorpt. spectra (Russian) 8-60453
- Si, polarisation dependent electrorefl. spectra, surface phenomena 8-68479

electrospark machining *see spark machining*

electrostatic accelerators

see also Van de Graaff accelerators

- direct current accelerator for 14 MeV neutron prod., thermal-mech. design 8-66383
- electron acceleration by inhomogeneous electrostatic RF field 8-82538
- electrostatic inflector and extractor for cyclic accelerators, HV expts. 8-50421
- Hall accelerator, four-lens, pure ion beam struct. 8-66441
- heavy-ion accelerators, book contrib., review 8-90003
- multiply charged ion prod. at low energy 8-66437
- neutral beam system, 120 keV, for fusion reactor ignition 8-66377
- Scandinavian low output isotope separator, upgrading to 300 kV 8-66008
- tandem electrostatic 30 MV accelerator, nuclear struct. facility at Daresbury Lab. 8-55056
- TFTR type neutral beam system, ion accelerator design and fabrication 8-66381
- two-grid accelerator systems, ion beam divergence characts. 8-82074
- two-stage ion beam optics for accelerator 8-50418
- ^{14}C , beam production for Munich tandem 8-90008

electrostatic coating techniques

- painting on Al foil using Van de Graaff generator, teaching demonstration 8-54136
- powder coating, parametric study, charging, transport, deposition props. 8-80662

electrostatic coatings

No entries

electrostatic devices

see also capacitors; dielectric devices; electrostatic accelerators; electrostatic generators; electrostatic lenses; electrostatic precipitators

- charge mobility analyser, variable freq., appl. to latex aerosols 8-77945
- circular neutraliser of static electricity, field anal. (Czech) 8-55272
- electron oscillator design optimisation, ion source and vacuum gauge 8-74107
- Faraday cup for simultaneous ion-beam current obs. and meas. 8-49865
- gyroscope, geometry of suspension, max. rigidity case 8-62072
- industrial flare flames, smoke detection and control by electric fields 8-81360
- Lampard type electrostatic systems, analysis of the effect of the metrological properties (Polish) 8-77928
- mass spectrometer electrostatic analyser attachment 8-86377
- mirror, axisymmetric, two-electrode paraxial props., aberrations 8-71025
- neutral beam injectors, electrostatic energy recovery system 8-66400
- parallel-plate analyser for ion energy selection 8-83610
- precipitator, free-fall, motion of charged particles, determ. 8-71020
- pulsed electrostatic probes as diagnostic for transient plasma 8-94937
- spherical plate electrostatic analyser, long entrance aperture effects on azimuthal response 8-89494

electrostatic fields *see electric fields*

electrostatic generators

see also Van de Graaff generators

- high voltage generator for TEM, stability improvement (French) 8-62268
- rotating ball pulse generator, up to 1 kV 8-49866
- terminal voltage on-line feedback stabilisation using digital computer 8-82004

electrostatic lenses

see also aberrations; focusing; particle beams

- charged-particle beam, axisymmetric, focusing in hyperbolic electrostatic field 8-50688
- combined system of electrostatic round lens and mag. deflector, electron-optical characteristics (Chinese) 8-82897
- crossed lenses, electron optical image position, ang. magnification aberration 8-50691
- Einzel lens with curved electrodes, Fourier-Bessel soln. 8-82878

electrostatic lenses continued

- einzel lenses, reduced spherical aberration field emission guns appl. 8-74831
 electron field emission energy distribution meas., analyser system 8-89605
 Faraday double transmitting cup, ion optical control device 8-82556
 heavy ion beam focusing, accelerating, decelerating beams 8-89588
 ion microscope aberrations and image form., study by magnetic anal. of beam from HF source 8-55293
 mass spectrum, second order image aberration correction by electrostatic hexapole lens 8-70216
 quadrupole lens spatial field determ. 8-55292
 retarding electrostatic prism, with increased transmission 8-71022
 round lenses, asymptotic aberration coeffs., systematic transformations 8-74828
 scanning electron beam instrument for studying metals/alloys thermoe-mission props. 8-74025
 space charge lens for high current ion beams 8-55075
 two element lens, acceleration and deceleration of high intensity ion beams 8-89595

electrostatic microphones *see* **microphones**

electrostatic precipitation *see* **electrostatic precipitators; precipitation (physical chemistry)**

electrostatic precipitators

- aerosols, charging migration and EHD transport 8-88660
 back discharge, flashover meas., streamer or steady glow mode, dust layer effects 8-59708
 corona discharge, spherical probe, I-V characts., precipitator testing appl. 8-79467
 electron beam ionisation, coal processing technology appl. 8-57346
 precipitator, free-fall, motion of charged particles, determ. 8-71020
 pulsed electrostatic precipitator and flame photometer for total S aerosol conc. meas. 8-95975
 Hg, atoms, collection by electrostatic precipitators 8-95964

electrostatics

- see also* **electrets; electric charge; electric fields; electrostatic devices; static electrification; triboelectricity**
 aerosol particle charging in continuum regime 8-90349
 aerosol particle deposition in channel due to diffusion and electric charge 8-90978
 aerosols, charge distrib., appl. of four-parameter distrib. model 8-85213
 air, electrostatic forces effect on thermodynamic props. and equilibrium composition 8-55710
 auroral electron beam, electrostatic noise generation 8-85759
 axisymmetric torus electrostatic problem, perturbation method soln. 8-78851
 Brans-Dicke theory, charged particle field 8-65849
 Brownian motion of charged particles, long and short range correlations 8-62155
 cathode directed streamer propagation, charge sheath model 8-67459
 characteristic impedance of double line in front of dielec. wedge (*German*) 8-78855
 charged disk interactions in various dielectric media, biological cell modelling 8-66706
 charged droplets metastable state (*Czech*) 8-86231
 circular neutraliser of static electricity, field anal. (*Czech*) 8-55272
 classical Yang-Mills theory, screening solns., static external source 8-62302
 dipole correlations in conducting media 8-62969
 double layers, review 8-67368
 drops, electrified, pendent, axially symmetric, equilib. profiles 8-87846
 electrification of objects under DC transmission lines, charge simulation calcs. 8-78853
 fields generated by charged particle in vac., zero vel. limit, electrostatics solns. 8-82881
 free space capacitance calc. for a square cylinder of finite length (*Chinese*) 8-66705
 gramicidin A ion channel kinetic behaviour, electrostatic calcs. 8-53368
 induced potential problem in 3-D, functional analytic approach 8-58880
 inertialess charged particles, collection on elliptical and irregular cylinders by elec. forces and gravitation 8-68924
 ion channel, energy and pot. profiles and interactions between ions 8-53367
 nonlocal electrostatic 8-82879
 point charge near cond. plane, force acting, for teaching 8-49605
 point-multipole expansion, charge distrib., for teachers 8-61992
 two point charge system, electrostatic pot. energy and inertial mass change 8-54116
 variational technique for solving two-dimensional problems (*Hungarian*) 8-58879
 weakly ionised gases, in electrostatic field, Maxwell model, ion vel. distrib. and moments 8-94879
 xerographic papers, electrostatic props. 8-78852

electrostriction

- see also* **piezoelectric materials; piezoelectricity**
 composite electrostrictive resonators, finite element simulation 8-59237
 long rods, radial motion under axial mag. field 8-68456
 polarised nonconducting dielectric fluid, anal. of force exerted on immersed elec. charge 8-78872
 solid, anomalously high permitt., acoustic to EM wave conversion 8-91734
 BaTiO₃, Rayleigh wave generation by surface piezoelectricity 8-71925
⁴He, liq., phase transitions, positive and negative ion mobilities meas. 8-87833
 KTaO₃, Rayleigh wave generation by surface piezoelectricity 8-71925
 La_{0.8}Pb_{0.2}Zr_{0.8}Ta_{0.2}O₃, ferroelec. with diffuse phase transition, electrostriction-optical props. 8-68457
 PbMg_{0.5}Nb_{0.5}O₃, ferroelec. with diffuse phase transition, electrostriction-optical props. 8-68457
 W, anodic oxidation, effect of electrostriction, ellipsometry meas. 8-92394

electrosynchronisation *see* **synchronisation**

electroviscous effect

- see also* **colloids; viscosity**
 MBBA, nematic liq. cryst., electroviscous effect, electrohydrodynamic investigation 8-87804

element origin

- see also* **cosmic ray origin; cosmology**
 antimatter model for galactic nuclei and quasars (*Chinese*) 8-73771
 big-bang model and ⁴He abundance, review, book contrib. 8-89277
 Galaxy, chemical evolution rel. to metals distrib. among stellar populations 8-96545
 heavy and neutron-rich elements synthesis by rapid neutron capture process 8-77488
 light elements formation, thermal cycle, isotopic abundances problem (*French*) 8-96574
 metals, explosive nucleosynthesis rel. to Al/Fe ratio in metal-poor-stars 8-57549
 r-process, astrophysical, implications of fission mass distrib. 8-93204
 Ba, Y, s-process elements, abundance in old halo stars rel. to nucleosynthesis in Galaxy 8-65616
 CNO, isotopes origin and isotopic abundance ratios evolution 8-93201
 Eu, r-process element, abundance in old halo stars rel. to nucleosynthesis in Galaxy 8-65616
⁷Li, prod. in nova explosions 8-57555
 Te isotopic composition in meteoritic and terrestrial materials 8-82856

element relative abundance

- see also* **isotope relative abundance**
 Adelaide meteorite, member of new carbonaceous chondrites subgroup, comp. and mineralogy 8-65573
 aerosols, atm., instrumental anal. of light element comp. 8-69516
 alkaline earths, cosmic abundances rel. to oxides occurrence in cool stars and sunspots 8-85933
 Ankara atmosphere aerosol, trace elements and size distrib. determ. by thermal neutron activation anal. 8-81377
 Bench Crater meteorite, member of new carbonaceous chondrites subgroup, comp. and mineralogy 8-65573
 Bencubbin polymict meteoritic breccia, elements concs. rel. to form. 8-96443
 chondritic meteorites, trace element anal. 8-69756
 Earth mantle melting, past and present, isotope and trace element evidence 8-65238
 elliptical galaxies, metal abundance rel. to giant stars population evolutionary synthesis 8-57626
 eucrite parent body, chondritic comp., inference from trace elements 8-69755
 G333.6-0.2, G298.2-0.3, compact H II regions, IR emission lines rel. to elemental abundances 8-96522
 galactic stellar populations, metals distrib. rel. to Galaxy chemical evolution 8-96545
 galaxies, metal abundances rel. to progression in Cepheids period-amplitude diagrams 8-53956
 gaseous nebulae, model anal. of ionisation correction formulae 8-57623
 geothermometry, chemical and isotopic techniques 8-69501
 hailstone samples, Project DUSTORM, microprobe anal., element abundances 8-73453
 heavy element depletion unlikely in Orion Nebula 8-69854
 heavy metal pollution detection in estuarine sediments 8-73546
 Helix Nebula, abundance anomalies in planetary nebula 8-86001
 Holbrook chondrite, vapour phase comp. from mass spectrometry 8-65568
 Iceland high-temperature geothermal systems, aquifer chemistry 8-96245
 intergalactic gas, Fe-enriched, in clusters of galaxies, origin and evolution 8-93390
 ion microprobe analysis, calibration using matrix ion species ratios, appls. 8-61070
 Kakangari meteorite, unique chondrite, noble gases abundances and isotopic comps. 8-65570
 large impact craters melt, Ge, Ir, Ni, Os, Pd, Re abundances rel. to meteorite types 8-57208
 light noble gases in chondrites, achondrites and ureilites, anal. compilation 8-65574
 lunar regolith, light element chemistry of Apollo 12 site 8-65515
 RR Lyrae stars in ω Centauri, Fe/H ratios from UVB photometry 8-73719
 M87 halo globular clusters, metallicity meas. 8-89244
 Magellanic Clouds, chem. comp. of H II regions, photoelec. spectrophotometry 8-77607
 Magellanic Clouds, H II regions chem. comps. 8-93381
 metal-deficiency of NGC 2243, old open star cluster 8-93333
 meteorites of British Museum (Natural History) collection, chemical anal. 8-65569
 minerals, magnetic trends on alkali-Fe-Mg diagrams 8-85551
 minor metals in surface seawater particulates and organic-rich shelf sediments 8-92853
 Moore County, eucrite meteorite, comp. rel. to quench temp. 8-96444
 N132D, supernova remnant in LMC, O/H ratios rel. to supernova nucleosynthesis 8-93345
 noble gases, abundances and isotopic compositions in Earth mantle 8-85521
 nuclear matter with neutrinos retention, eqn. of state and chemical comp. 8-96390
 oceans, Cl/Br ratio rel. to origin 8-65342
 old halo stars, chemical comp. rel. to nucleosynthesis in Galaxy 8-65616
 organic materials, nuclear backscattering using cyclotron 8-80807
 p-nuclei, abundances produced by low-temp. photonuclear nucleosynthesis in degenerate H burning zones 8-57540
 in photoelectric spectrophotometry of emission lines, abundances, from photoelectric spectrophotometry of emission lines 8-81677
 planetary nebulae, CNO abundances rel. to central stars masses and Population II planetary origins 8-85992
 planetary-type rare gases in an upper mantle derived amphibole 8-96167
 QSOs, element abundances from emission-line spectra 8-57677
 r-process elements, implications of fission mass distrib. 8-93204
 rare earth elements in tholeiitic basalts, behaviour during submarine weathering 8-73369
 rare earths, cosmic abundances rel. to oxides occurrence in cool stars and sunspots 8-85933
 rocks, trace element content, direct-reading spectrometer 8-85738
 Saguenay Fjord, suspended particulate matter geochemistry 8-92852
 snow, natural enrichment of elements 8-77303

element relative abundance continued

- solar O, N and C abundances, new radiative lifetimes and oscill. strengths in visible and IR spectra 8-50506
 solar system formation, re-evaporation of condensed matter, evidence from meteorite mineral content 8-85864
 solar wind, α -particle/proton abundance ratio anticorrel. with particle flux in three-fluid model 8-57418
 solar wind, He abundance long-term vars., Imp 6, 7 and 8 results 8-77452
 solar wind, plasma comp. expt. on International Sun-Earth Explorer A 8-85810
 stars, red giants, abundances in M3 and 13 globular clusters 8-93334
 stars in main sequence, diffusion and turbulence rel. to abundance anomalies 8-89198
 superheavy elements in primaevial Moon 8-96412
 supernova remnants, H abundance rel. to H deficiency in Type I supernovae 8-53969
 Tunguska cosmic body, chemical comp. and nature 8-61810
 Tunguska cosmic body, silicate microspherules chemical comp. and cosmochemical anomaly 8-96430
 III Zw 77, compact galaxy with broad emission lines, Fe/Ne ratio 8-73760
 Al/Fe, ratio in metal-poor stars 8-57549
 B abundance determ. in rocks, soils, plants, waters and fertilisers 8-85559
 B, inorganic, in St. Lawrence Estuary, determ. (French) 8-77274
 Ba conc. determ. in stony meteorites 8-65557
 C/Fe ratio of K-type dwarf star 14 Herculis 8-93227
 CNO in main-sequence stars, meas. in α Canis Minoris, 45 Tauri and HD 27561 8-93222
 CNO, initial stellar abundances rel. to CN strengths and $^{12}\text{C}/^{13}\text{C}$ ratios in K-type giants 8-93229
 Ca/H, ratio in two extremely metal-deficient stars 8-69797
 Cd, determ. in sea and fresh waters, interlaboratory comparison 8-81209
 Cr in stars, Utrecht UV spectrophotometer obs. 8-69793
 Cr, solar abundance from photospheric spectra and oscillator strengths 8-69757
 Cu, geochemistry in sediments of Gulf of St. Lawrence and estuary 8-92855
 D abundance in Galaxy rel. to cosmology 8-69883
 Fe abundances in gaseous nebulae, from forbidden Fe III and Fe VI lines intensities 8-53806
 Fe group elements abundances in Sun from singly-ionised lines 8-93189
 Fe in stars, Utrecht UV spectrophotometer obs. 8-69793
 Fe/H ratio for metal-poor stars and globular clusters 8-53937
 H II regions, abundance determ., empirical method test 8-61908
 H II regions, influence of chemical comp. on ionisation and temp. struct. 8-61911
 H/D ratio in planetary atmospheres, determ. from CH_3D 9613 Å band 8-86861
 ^3H , limits on heavy neutrino props. from primordial nucleosynthesis 8-57438
 He/Ar and N_2/Ar ratio vars. in fault zone groundwater air bubbles for earthquake prediction 8-88803
 He/H abundance ratio in H II regions 8-86000
 He/H ratio in planetary nebulae 8-93376
 Hg determ. in sea and fresh waters, interlaboratory comparison 8-81209
 Hq, abundance in Greenland Ice Sheet 8-65349
 Li, determ. in weak-G band giant stars 8-53948
 Mn in Jervis Inlet, British Columbia, distrib. rel. to Mn deposition and nodule growth 8-96187
 Mn nodules, from sea-bed, isotopic and elemental composition, U, Pa, Th, radiochem. anal. 8-77215
 N abundance and isotopic comp. in stony meteorites 8-65558
 N, overabundance in nucleus of NGC 6946 spiral galaxy (French) 8-89257
 N/O ratio in planetary nebulae 8-93376
 Ne in gas-rich samples of carbonaceous chondrite meteorites 8-65559
 O/C in red giants, abundance ratio from TiO absorpt. bands 8-96480
 P, uncertainty analysis of lake loading 8-81262
 Pb, geochemistry in sediments of Gulf of St. Lawrence and estuary 8-92855
 Rb/Sr whole-rock systems and chemical control 8-61366
 Re-Os, rel. abundance, rel. to nuclear chronometer reliability 8-85919
 Rn concs. in geothermal reservoirs 8-69381
 S and trace elements in aerosols from South American continent, conc. relationships 8-57245
 Se in estuarine water in Solent area 8-57230
 Th/U ratio in Archaean granites from NE-Minnesota 8-61356
 Ti, interstellar, depletion from Ti II 3384 Å line obs. 8-57611
 U in volcanic rocks of E. Avoca-Ballard mineralised belt 8-69346
 U-Th-Pb of Saint Severin amphoterite meteorite 8-65560
 Zn, geochemistry in sediments of Gulf of St. Lawrence and estuary 8-92855

elemental semiconductors

- (Russian) 8-52416
 crystal defects in integrated circuits, review 8-88547
 diamond:B, thermoluminesc., TSC, correlation meas. 8-88369
 diamond:B hopping conductivity in range 12 to 1300K 8-51994
 diamond, Compton profiles, X-ray struct. factors, band struct., LCAO calc. 8-51889
 diamond, covalent semicond., depend. of energy gap on short-range order 8-84142
 diamond, dielectric function, optical frequency model calcs. 8-51921
 diamond, electronic energy bands of diamond-type crystals, appl. of EHT method 8-87907
 diamond, elementary excitation in crystals, dielectric theory 8-60076
 diamond, GR 2-3 absorpt. line, uniaxial stress effects 8-72563
 diamond, GR defect, high resolution optical spectra after electron irradiation 8-56515
 diamond, ion implantation, review 8-87698
 diamond, Jahn-Teller coupling at ND1 and GR1 centres 8-56103
 diamond, linewidth of GR2-8 transition 8-60488
 diamond, magnetic field and stress splitting of GR1 line 8-60095
 diamond, plastically deformed, EPR of two N atom centre 8-72408
 diamond, relaxation about the vacancy 8-71722

elemental semiconductors continued

- diamond, semiconducting, GR1 cathodoluminescence, fine struct. 8-68566
 diamond, synthetic, elec. cond. 8-56144
 diamond, synthetic, electroluminescence excitation mechanism, role of defects 8-52581
 diamond, synthetic and natural, neutron irradiation, optical and elec. props. (Russian) 8-59841
 diamond Schottky barrier, electronic struct., pseudopot. calc. 8-95364
 diamond Schottky barriers, photocapacity meas. 8-52057
 diamond structure, plasmon line shape, local field effects 8-76011
 diamond type crystals, semicond.-metal transition 8-72072
 diamond type materials, lattice dynamical calc. using extended Born-von Karman scheme 8-59889
 diamond-type crystal, lattice dynamics from Keating's valence force field 8-79687
 diffusion of Al in open tube high vacuum system 8-91349
 dislocation electronic states, effect of hybridisation 8-51936
 dose depend. in laser annealing 8-91354
 electric susceptibility from chemical-bond approach 8-51922
 electron-hole liquid theory, generalised RPA 8-87914
 electronic states and initial steps in oxidation 8-91534
 electronic struct. from SCF calc. using intersecting spheres model 8-51888
 film, evaporated amorphous, hydrogenation by plasma treatment 8-91555
 fundamental absorpt. spectra, direct interband transitions 8-63972
 p-Ge, 2 mm wave radiation interaction with charge carriers (Russian) 8-87991
 graphite, electronic props., self consistent LCAO calc., point vacancy in 2-dimens. cryst. 8-51932
 graphite, electronic props., self-consistent LCAO calc. 8-51887
 ion implanted, laser-annealed, theoretical anal. of thermal and mass transport 8-91364
 polycrystalline, grain growth study 8-92188
 positron thermalisation, theory (Russian) 8-84170
 properties and use for making devices, review 8-60131
 Si-Al₂O₃-SiO₂ in MIS struct., charge accumulation and spreading (Russian) 8-64116
 SOS, cryst. perfection rel. to MOS transistor mobility 8-75956
 SOS MOS devices, hole mobility under residual stress, Hall meas., valence band struct. 8-88039
 SOS structure, radiation dose at interface due to electron beam aluminisation 8-68089
 static response, local field effects 8-76010
 zincblende structure group IVA covalent crystals, Murnaghan parameter estimates from Morse pot. 8-95014
 Al-nSi-Al, p⁺n⁺p⁺ reach through structs., electronic cond. mechanism 8-64103
 Al-Si, ion plated contacts (Rumanian) 8-88029
 Au-Ge Schottky diode, phonon energies, barrier heights, photovoltage spectra 8-64112
 B, purity evaluation by elec. meas. 8-59822
 Bi, neutral point defect electronic struct., self consistent method 8-91641
 C, reconstruction-induced subsurface strain, theory 8-91516
 Ge (100) with Cs and Cs+O₂ overlayers, negative electron affinity surface, thermal stability of work fn. 8-92167
 Ge (111), CO adsorption on cleaved surface, electron energy loss spectra 8-79885
 Ge (111) coadsorption of K and O₂, rel. to work function, K thermodesorption spectra 8-79874
 Ge (111) surface, 500 eV Ar⁺ bombard., high temp. annealing, recovery, RHEED obs. 8-87723
 Ge (111) surface, annealed, atomic structure 8-75916
 p-Ge, adsorption of Au, effect on I-V characteristics field emission study 8-67925
 Ge, amorphous, EPR expts. 8-88167
 Ge, amorphous, far IR absorption 8-88306
 Ge, amorphous, thermoelec. power in phonon-assisted hopping regime, Coulomb effects 8-76097
 Ge, amorphous film, DC cond., Meyer-Neldel rule 8-64152
 Ge amorphous film, effects of ion implantation on structure 8-55881
 Ge, amorphous film, variable range hopping 8-76176
 Ge, amorphous layer, epitaxial recrystn. by electron irradiation, solar cell appl. 8-84079
 Ge, amorphous overlayer on ultrathin Pt film, effect on cond. 8-72284
 Ge, anomalous X-ray transmission in the presence of four-wave diffraction (111, 200, 311) 8-79494
 Ge, Au-migration at room temp. 8-76161
 Ge bicrystal cleavage plane, Shubnikov-de Haas oscills. (Russian) 8-64094
 Ge, charge carrier diffusion coeff. 8-84218
 Ge, chemical etching processes, review 8-95832
 Ge, chemisorption of CO(Cl), surface photoemission, adsorption gate geometry 8-73079
 Ge, cold semiconductor, Mott transition 8-91616
 Ge, compressed electron hole plasma, luminesc. 8-72592
 Ge, deformation, annealing characts., X-ray study 8-75713
 Ge detector for X-ray and gamma-ray spectroscopy, high-purity, preparation and properties 8-86723
 Ge, dielectric properties, mean point value calc. 8-87930
 Ge, donor-acceptor electron transfer at low temps., photocond. tail 8-84249
 n-Ge, elec. cond., effect of shock waves (Russian) 8-87979
 Ge, electron scattering, inelastic, 70-1400 eV, mean free path 8-84696
 Ge, electron-hole drop magnetostuction 8-87912
 Ge, electron-hole drop phase separation, due to uniaxial stressing 8-84145
 Ge, electron-hole drop velocities as probe of phonons 8-68517
 Ge, electron-hole drop velocities, excitation wavelength depend. 8-88358
 Ge, electron-hole droplet, motion damping, impurity and piezoelec. scatt. 8-67951
 Ge, electron-hole droplet, attachment to donor 8-87916
 Ge, electron-hole droplets, surface props., SCF calc. 8-51904
 Ge, electron-hole droplets, transient photoluminesc. intensities 8-88353
 Ge, electron-hole drops, accel. by IR radiation field 8-95264

elemental semiconductors continued

- Ge, electron-hole drops, far IR absorption 8-56467
 Ge, electron-hole drops, far IR magneto-optical effects 8-84565
 Ge, electron-hole drops, spatial distrib., time and spatially resolved absorption at 3.4 μm 8-92075
 Ge, electron-hole drops, surface struct. 8-60058
 Ge, electron-hole liquid, luminesc. under infinite uniaxial compression 8-87915
 Ge, electron-hole liquid, pinch effect 8-87993
 Ge, electron-hole-droplet cloud, photoluminesc. of laser excited surface, phonon wind 8-84146
 Ge, electronic energy bands of diamond-type crystals, appl. of EHT method 8-87907
 Ge, epitaxial, on n-GaAs, with Ni overlayer, smooth and continuous ohmic contact form. by solid-state diffusion 8-68086
 Ge epitaxial film, ohmic contacts for GaAs devices 8-88027
 Ge, epitaxial growth from monogermane at 685°C 8-51833
 Ge, epitaxial layer deposition by vacuum pyrolysis 8-52676
 Ge epitaxial layer on GaAs tetragonal distortion in heteroepitaxial layer, X-ray diff. exam. 8-67922
 Ge epitaxial layers, on GaAs substrate, misfit dislocation multiplication mechanism 8-87673
 Ge eqn. of state, under press. 8-75801
 Ge, evaporated film, lattice parameters and phase transition temp., surface influence of glass substrates 8-94996
 Ge, far IR magnetoabsorption of free and bound excitons 8-52474
 Ge film, amorphous, ^{74}Ge ion implanted, defect struct. obs. 8-51848
 Ge film, polycrystalline, structural and elec. props. 8-76173
 p-Ge film, transverse magnetoresist. meas. 8-72293
 Ge, film on Si, influence of fragmentary struct. on galvanomag. effects (*Ukrainian*) 8-84327
 n-Ge, group V doped, point defect form. due to γ -ray irradi., carrier density, mobility meas. 8-71759
 n-Ge, H-linear planar Hall effects of hot electrons 8-76082
 Ge, Hall effect in finite specimens of arbitrary lifetime and trap content 8-72175
 n-Ge, heavily doped, extrinsic sp. ht. in metallic regime 8-59956
 Ge, high density electron-hole plasma, infrared absorpt. at low temp. 8-92078
 Ge, hole drift velocity, effect of impurity scatt. 8-60127
 Ge, hot-electron diffusion coefficient 8-87982
 Ge, IR absorption and scatt. by electron-hole drops 8-51903
 Ge, impurity photocond., temp. elec. field and impurity centre conc. effects 8-56190
 Ge, influence of dislocations on free-exciton lifetime 8-60064
 Ge, interface structural model between amorphous and crystalline phase 8-63941
 Ge, intervalley diffusion of hot electrons 8-84227
 Ge, ionised impurity scatt. limited mobility in semiconductors with spatially variable dielec. function 8-51986
 Ge, irradi., cyclotron resonance 8-72416
 Ge, lattice dynamics, inversion matrix, approx. inversion 8-71797
 p-Ge, lattice scatt. identified as cause of 1/f noise 8-64074
 n-Ge, longit. piezoresist., in strong elec. field 8-56147
 Ge magnetoacoustic effects in the drag of electron-hole drops by phonons 8-68057
 Ge, magnetoplasma resonance in electron-hole drops (*Russian*) 8-79944
 Ge, momentum distrib. of electrons, anisotropy, positron annihilation (*Russian*) 8-84676
 Ge, monocryst., for IR optics, prod. techniques and characts. 8-50873
 n-Ge, Mott transition, dielec. enhancement and conduction electron screening 8-72073
 Ge, near intrinsic, negative differential cond., ambipolar size effect due to hot carriers 8-72185
 n-Ge, noise spectra of hot carriers 8-76083
 p-Ge, odd magnetoresist., ionised impurity scatt., theory 8-72178
 Ge, p-n homojunction breakdown voltage for onesided abrupt junctions (*German*) 8-56210
 Ge, phonon boundary scatt., reduction of lattice thermal cond. 8-55921
 Ge, phonon dispersion curves, appl. of deformable-ion model 8-59887
 Ge, phonon drag of electron-hole drops in longit. quantizing mag. field (*Russian*) 8-64070
 Ge, phonon scattering and dislocation effect on low temp. phonon cond. 8-51754
 Ge, photoelastic consts. determ. 8-68474
 N-Ge, pressure influence on photoconductivity temp. dependence 8-76109
 Ge, pseudopotential method of band struct. anal. 8-51886
 Ge, reconstruction-induced subsurface strain, theory 8-91516
 Ge, Schottky barrier, electronic struct., pseudopot. calc. 8-95364
 Ge, slow surface, states, optical excitation investigation 8-76129
 Ge, spectrally selective EM wave absorber, solar energy collector material, props. (*Dutch*) 8-50872
 Ge, supecond, friction layer formed during friction between Ge and Pb (*Russian*) 8-52143
 Ge, surface, cluster model approach for electronic struct. 8-56205
 Ge surface, nonequilib. electron effects due to chem. excitation 8-72239
 Ge surface states, Tamm-like and field sustained, model studies, localisation props. 8-64092
 n-Ge thin plate, transverse magnetoresist. meas., size effect 8-72179
 Ge, two-phonon difference absorption spectra 8-76452
 Ge, ultra high vac. cleaved, photolum., role of intrinsic surface states 8-52571
 Ge, ultrashort optical pulse transmission, pulse-width depend. 8-55403
 Ge, uniformly stressed, density and binding energy of electron-hole droplets, photolum. meas. 8-60062
 Ge, vacancy paradox 8-59804
 Ge, valence band effective mass strain depend. 8-51880
 Ge, vapour transport rate, Ge- I_2 equilib. 700 to 1300K (*French*) 8-64476
 Ge:Al(Sb) film, amorphous, ion implantation, effect on cond. 8-83839
 Ge:As(Ga), photoconductivity oscillation with respect to applied mag. field (*Russian*) 8-80026
 Ge:As, IR detector, impurity photoconductivity (*German*) 8-82036
 Ge:Ba, Ca, recomb. props. 8-56156
 n-Ge:Cu, characts. of radiation defects 8-55893
 Ge:Cu, IR detector, impurity photoconductivity (*German*) 8-82036

elemental semiconductors continued

- Ge:Cu, quenched, interaction between shallow-level defects and Cu atoms, Hall effect meas. 8-64002
 Ge:Cu photoresistor, liquid H_2 cooled, detectability 8-80019
 p-Ge:Ga, carrier heating by weak elec. field, hole-hole collision influence 8-72161
 Ge:Ga, effects of destabilising vertical thermal gradients on cryst. growth and segregation 8-52659
 Ge:Hg photoconductive detector, laser damage thresholds calc. 8-90443
 Ge:inert gas, ion implantation, UV photoemission exam. 8-80457
 Ge:Li, supersaturated solid solns., decomp., surface impurity content 8-51681
 Ge:Mn, amorphous, cond. increase by Mn doping 8-72155
 Ge:Na (111) surface, O_2 adsorpt., work function, surface cond. changes meas. 8-79875
 Ge:P, conc. depend. of diffusion coeff. at P diffusion 8-95185
 Ge:P, lattice thermal cond., role of electron-phonon interactions and peripheral phonons 8-79702
 Ge:P, lattice thermal resistivity due to electrons 8-51756
 Ge:S, photoionisation cross section of deep impurity centres 8-56510
 Ge:Sb, acoustic attenuation, uniaxial stress effects 8-59863
 n-Ge:Sb, fast neutron irradi. effects on donor conc., and annealing 8-56107
 n-Ge:Sb, γ -irrad. effects on donor conc. and compensation by acceptors 8-56106
 Ge:Sb, neutron irradi., carrier mobility theory and expt. 8-56166
 Ge:Sb, phonon thermal cond. calc. 8-71893
 Ge:Sb,Cu, exactly compensated, impurity absorpt. and photocond. spectra 8-56189
 Ge:Sb(In), film, electronic props. 8-84330
 Ge:Si, impurity lattice modes due to single and paired defects 8-75780
 Ge:Si, impurity modes and IR absorption 8-76506
 Ge-CdSe heterojunctions, epitaxial, azimuthal rotation 8-84085
 Ge-electrolyte contact, current-voltage characts., effect of mechanical deform. 8-68082
 Ge-GaAs, n-n isotype heterojunctions, fixed-interface-charge model 8-56215
 Ge-GaAs (100) interface, electronic struct., scattering-theoretic approach 8-95340
 Ge-GaAs (110), heterojunction chemistry, photoemission expts. 8-95244
 Ge-GaAs (110) interface, self-consistent calc. of interface states and electronic struct. 8-52066
 Ge-GaAs abrupt (110) interface, electronic struct. 8-95339
 Ge-GaAs interface, XPS obs. of electronic struct. 8-95341
 Ge-GaAs superlattice and interface, electronic struct. 8-52065
 p-Ge-mn $^{+}$ -Si, heterojunction, γ -radiation effect on forward I-V characteristics (*Russian*) 8-72255
 Ge-Pb $_{1-x}$ Sn $_x$ Te, amorphous/crystalline heterojunction, rectification props., IR detector appl. (*Japanese*) 8-60197
 Ge-pyrolytic SiO_2 system, carrier trapping, GeO_2 sublayer effect 8-91775
 Ge-Sb, D^- complexes and band form., photocond. 8-84251
 Ge-SiO $_2$ -Al, vacuum heating effect on stability 8-64143
 Ge-YIG structure, profile and position of reson. galvanomag. effect curve 8-72242
 Ge-ZnS p-n heterojunction, epitaxial, elec. props. (*Russian*) 8-88023
 Ge-ZnSe abrupt (110) interface, electronic struct. 8-95339
 Ge-ZnSe interface, electronic struct., self-consistent pseudopot. calc. 8-91747
 Ge(100) surface, Ar ion bombarded, determ. of atomic steps, LEED 8-63913
 Ge(111)2 \times 1, surface electron states detected by external reflectivity 8-80036
 In-Ge:As, Schottky barrier tunnel junction, zero bias resistance, temp. depend. 8-72258
 Si:Si, implanted, defect signature by thermally stimulated meas. 8-91643
 Se, amorphous, carrier lifetime and drift mobilities 8-87985
 Se, amorphous, photoinjection of holes into triphenylamine doped bisphenol-A-polycarbonate polymer 8-72191
 Se, amorphous film, photodeposition by Selor process, kinetics 8-75963
 Se, amorphous film, photodeposition by Selor process, struct. and kinetics 8-75964
 Se amorphous layer structure, influence of vacuum deposition conditions (*German*) 8-63957
 Se, amorphous film, photodeposition by Selor process struct. 8-75962
 Se, and related materials, historical study, 1833-1919 8-57727
 Se, crystallisation kinetics correlation with molecular structure 8-94998
 Se, effective charge tensor, microscopic treatment 8-59879
 p-Se film, photocond., phase-memory effect 8-91723
 Se, photoconductive film, field instability, Ar $^+$ ion irradi.-induced defects 8-87997
 Se, red amorphous film, textural change, thermal and photo effects 8-63951
 Se, Se:Te, amorphous, negative magnetoresist., doping depend. 8-56161
 Se, trigonal, model of lattice dynamics using long and short range interactions 8-59893
 Se, undeformed rhombohedral, dislocations, electron microscope obs. (*French*) 8-51548
 Se, vitreous, mech. props. at temps. <300K, uniaxial compression tests (*French*) 8-55908
 Se:As(Cl), trigonal, defect and impurity electron levels, surface photovoltage spectra 8-72108
 Si, 100 keV Sb ion irradiated, disorder accumulation, saturation and sputter limitation 8-67753
 Si, 60° dislocation, X-ray diffraction contrast, section topography 8-83819
 Si (100), oxidation induced stacking fault retrogrowth, O_2 press. depend. 8-64747
 Si, (100), reconstruction induced subsurface strain, appl. of theory 8-63914
 Si (100), struct., LEED study, atomic arrangement model 8-71922
 Si (100) inversion layer, hot electron drift velocity, Monte Carlo calcs. inc. 3 subbands 8-91752
 Si (100) surface, diff. of He atoms obs. 8-52609

elemental semiconductors continued

- Si, (100) surface, effective mass and collision time 8-64081
 Si (100) surface, LEED meas. 8-60016
 Si (100) surface, models of (2×1) surface struct., quasidynamical calc. of LEED intensities 8-71921
 Si (100) with Cs and Cs+O₂ overlayers, negative electron affinity surface, thermal stability of work fn. 8-92167
 Si (110), chemisorption of Cl, LCAO calcs., Auger line shapes, localised density of states 8-56202
 Si (111), 2×1 reconstructed, self-consistent anal. 8-91518
 Si (111), CO adsorption on cleaved surface, electron energy loss spectra 8-79885
 Si (111), chemisorbed Cl layer, SCF LCAO band struct. calcs. 8-88010
 Si (111), chemisorption of H₂(Cl), conduction-band surface resonance 8-52051
 Si (111), Cl₂ chemisorption, ang. resolved UPS and LEED meas. using Vidicon intensity processor 8-71972
 Si (111), cleaved, geometrical struct., LEED expts. 8-91517
 Si (111), surface relax., mol. SCF calcs. 8-91522
 Si, (111) cleavage, Kikuchi pattern, 40 keV incident electrons, electron energy loss spectra (French) 8-87594
 n-Si (111) MOS charge layer, optical spectrum of inter-subband transition 8-64133
 Si (111) surface, 500 eV Ar⁺ bombard., high temp. annealing, recovery, RHEED obs. 8-87723
 Si (111) surface, Al overlayers, theoretical study 8-95366
 Si (111) surface, anal. by ion-electron spectroscopy 8-72670
 Si (111) surface, atomic and electronic struct. 8-72223
 Si (111) surface, atomically clean, diffusion of adsorbed Au 8-72037
 Si (111) surface, clean, ESCA obs., Ni(Au) surface impurities 8-52640
 Si (111) surface, clean, new diffr. phenomena in RHEED 8-63910
 Si (111) surface, oxidised, energy depend. of photoelectron attenuation length 8-52643
 Si (111) surface, surface energy bands and atomic position of chemisorbed Cl 8-56041
 n-Si, A-centre ionisation energy change due to uniaxial deform. 8-71733
 Si, AES, convolution and deconvolution 8-52601
 Si, AES examination of Ar⁺ ion retention during Ar sputtering 8-56552
 Si, AES quantitative anal. of impurities (Japanese) 8-91356
 Si, adsorption of organic solvents (Russian) 8-91537
 Si, amorphous, dissolution with Al 8-95188
 Si, amorphous, EPR expts. 8-88167
 Si, amorphous, electron-hole recombination, mech. 8-72196
 Si, amorphous, epitaxial regrowth by pulsed laser beam 8-91554
 Si, amorphous, glow discharge deposited, photolum. decay 8-72590
 Si, amorphous, hydrogenated, spin depend. photoluminesc. 8-72589
 Si, amorphous, hydrogenated, diffusion of D₂, SIMS anal. 8-75877
 Si, amorphous, hydrogenated, work function and Auger spectroscopy of initial oxidation 8-76132
 Si, amorphous, optically detected ESR obs. 8-84500
 Si, amorphous, photoconductivity, mag. field depend. 8-80023
 Si, amorphous, photovoltaic characts., rel. to appl. in solar cells 8-84253
 Si, amorphous, Si implanted, substrate-orientation depend. of epitaxial regrowth rate 8-79900
 Si, amorphous, thermoelec. power in phonon-assisted hopping regime, Coulomb effects 8-76097
 Si, amorphous and crystalline, hydrogenation and dehydrogenation 8-51677
 Si amorphous film, crystallisation kinetics and morphology, TEM obs. 8-84093
 Si, amorphous film, epitaxial laser crystallisation 8-84078
 Si, amorphous film, variable range hopping 8-76176
 Si amorphous film effect of gas exposure on EPR signal 8-84475
 Si, amorphous heavy ion ranges, He⁺ backscatt. obs. 8-63796
 Si, amorphous layer, epitaxial growth by laser annealing 8-79899
 Si, amorphous layer, ion-implanted, spatially controlled cryst. regrowth by laser irradiation 8-55810
 Si amorphous sputtered film, solar energy selective absorber, spectral emissivity 8-83045
 Si, amorphous thin films, appl. in solar cells, recent developments 8-80016
 n-Si, anisotropy of differential conductivity and transverse diffusion coefficient 8-76078
 Si, annealed crystal, oxide precipitates identification by electron loss spectra 8-83952
 Si, Ar bombarded, blistering effects, SEM obs. 8-67745
 Si, Auger lineshape, one-electron theory for L₂₃VV and L₁L₂₃V 8-72645
 Si, band struct., modulation spectroscopy, two-ray methods (Russian) 8-54469
 Si, bonding states of adsorbed O₂, photoemission obs. 8-92170
 Si, Bragg-case X-ray thin cryst. rocking curves, theory and expt. comparison 8-55785
 Si CVD grown polycrystal recrystallisation 8-64560
 Si CVD of polycrystal on liquid Sn layer 8-64479
 Si, CVD using CO₂ laser 8-56589
 n-Si, capture cross section and generation lifetime determ. of Au, MOS expts. 8-91772
 Si, carrier conc. determ., electrochem. method 8-60200
 Si, carrier lifetime, comparison of meas. by photocond. decay and surface photovoltage 8-68038
 Si, carrier lifetime degradation at room temp. 8-95301
 Si, channelled and random proton stopping power, 30-1000 keV 8-67760
 Si, channelled-ion implantation of group III and group IV ions 8-75682
 Si, characterisation by photoluminescence method (Japanese) 8-80404
 Si, chemical etching processes, review 8-95832
 Si, chemically etched, metal contact, electron and hole currents correl. 8-91769
 Si, chemisorption of CO(Cl), surface photoemission, adsorption gate geometry 8-73079
 Si, chemisorption of H₂, atom-probe FIM obs. 8-71968
 Si, clean-cleaved, Schottky barrier height meas. accuracy 8-52081
 Si continuous polycrystalline films on C substrates 8-64490
 Si, crystal structure stability, P-T diagrams 8-51886

elemental semiconductors continued

- Si, crystn. front face effect on at displacements (Russian) 8-67781
 n-Si, current-voltage characts., static high field domains 8-84223
 Si, Czochralski cryst., hillock etching of microdefects, TEM obs. 8-87678
 Si, Czochralski growth with automatic diam. control 8-52658
 Si DC sputtered, amorphous, dark conductivity and photocond. obs. (French) 8-64155
 Si, dangling bonds, EPR, localised states and unpaired electrons on microcrack surfaces 8-52351
 n-Si, Debye temperature, electronic effect 8-83901
 Si, deformation, annealing characts., X-ray study 8-75713
 Si, deformed, ENDOR of dislocation centre 8-72434
 Si, deformed surface, defect struct. rel. to elec. props. 8-72231
 Si detector, ionisation energy for channelled 160 MeV α -particles 8-62680
 Si, dielectric properties, mean point value calc. 8-87930
 Si, dielectric screening and zone-centre phonons 8-67785
 Si, diffused p-n junction, computer calcs. of photoresponse using Gummel-de-Mari algorithm 8-56221
 Si, diffusion of B,P and Sb, implantation damage effects 8-55988
 Si, diffusion of Ga in closed capsule, surface damage elimination 8-87691
 Si, diffusion of Ga through SiO₂ layer, junction depth 8-51574
 Si, donor ground state wave functions 8-87937
 Si, electrical characterisation, review 8-60120
 Si, electrodeposited film, appl. in solar cell fabrication 8-76611
 Si, electron beam deposited film, epitaxy by pulsed laser annealing 8-56055
 Si, electron irradiated, high resist. surface layer, Schottky barrier meas. 8-64093
 Si, electron-hole drops, surface struct. 8-60058
 Si, electron-phonon interaction anal. using photoacoustic cell 8-68027
 Si, electronic energy bands of diamond-type crystals, appl. of EHT method 8-87907
 Si, electronic screening of lattice vibrs. 8-59875
 Si, electronic struct. from SCF calc. using intersecting spheres model 8-51888
 Si, epitaxial, optical constants meas. by far IR ellipsometry 8-93753
 Si epitaxial film, correlation between electrooptical and electrical props., IR absorpt. spectra (Russian) 8-60453
 Si, epitaxial growth chambers cleaning, improved method using KOH solution 8-64478
 Si, epitaxial layers, minority carrier lifetime and diffusion length meas., photocurrent technique 8-95302
 Si epitaxial p-i-n photoconverter characteristic deterioration at high illumination 8-89536
 Si, epitaxial regrowth and grain struct. of Al metallisation on (100)Si 8-79901
 Si epitaxy and oxidation, first-order process models 8-72049
 Si eqn. of state, under press. 8-75801
 Si, etching by CF₄ plasma, mechanisms 8-72907
 Si, evap. heteroepitaxial film, deep defect states obs. 8-72292
 Si, exchange and correlation pot., band struct. calc. 8-56068
 Si, exciton and deformation pot. fine struct. 8-88301
 Si, exciton-impurity complexes, emission spectra, Zeeman splitting (Russian) 8-64413
 Si extrinsic photoconductive IR detector, counterdoping scheme 8-49896
 Si extrinsic photoconductive IR detectors, VLF behaviour 8-81542
 Si, extrinsic stacking faults, core struct., TEM obs. 8-55878
 Si, far IR impurity spectra, effects of high uniaxial stress 8-56508
 Si, fast electron channelling, quantum-mechanical approx. 8-87731
 p-Si, fast electron irradi., Hall mobility, temp. depend. 8-56165
 Si filamentary piezoresistor for pulsed wave process meas. 8-57980
 Si film, amorphous, effects of annealing of gap states 8-72115
 Si film, amorphous, plasma-deposited, H₂ evolution, mass spectrometry and RHEED obs. 8-72050
 Si film, amorphous and polycrystallised, localised states, elec. and optical props. 8-64008
 Si, film, CVD, low press., struct. and stability, X-ray diffr. and TEM obs. 8-91559
 Si film, hydrogenated amorphous, Brillouin scatt. 8-72538
 Si, film, polycryst., for photovoltaic appl., grain size effects 8-72034
 Si, film deposition, growth kinetics under low H₂ press. 8-56586
 Si film on sapphire, electron mobility 8-91792
 Si, gettering effects, of P ions and P induced dislocations for Au impurities 8-91346
 n-Si, γ -irrad. (E_{max}=100 MeV), carrier recomb. 8-56158
 Si, γ -ray induced elec. cond. at low temps. 8-52002
 Si, HCl oxidation conditions for stacking fault nuclei gettering and undesirable etching 8-68830
 n-Si, heavily doped, extrinsic sp. ht. in metallic regime 8-59956
 n-Si, heavily doped, Raman phonons, interband excitation effects 8-52501
 n-Si, heavily doped, self energy of phonons interacting with free electrons, Raman scatt. 8-64366
 Si, heavily doped implantation layers, laser beam annealing 8-88481
 Si high-resistivity structure, photoelec. props. 8-91730
 n-Si high-temp. vacuum etching, p-n junction photodetectivity 8-95355
 Si, highly transparent semicond., multiphonon IR absorpt. 8-60461
 n-Si, horizontal ribbon growth from melt, theoretical anal. 8-75604
 n-Si, hot-electron diffusion, effect of ionised impurity scatt. 8-56151
 Si, hyperpure, large scale prod. and prep. (German) 8-95704
 Si, ideal vacancy, self consistent Green's function calc. 8-91640
 n-Si, in MOSFET inversion layer, Gunn instability 8-84305
 Si, interface structural model between amorphous and crystalline phase 8-63941
 Si, intrinsic semiconductor, radiative recombination probability (German) 8-95608
 Si inversion layer, elec. break-through, exactly solvable model 8-56234
 Si inversion layer, elec. cond., freq. depend. 8-72270
 n-Si inversion layer, electron mag. suscep. 8-52009
 n-Si inversion layer, electronic bound states, theory 8-60217
 n-Si inversion layer, exchange instabilities 8-52052
 Si, inversion layer, Hall effect meas. 8-56199
 Si inversion layer, high freq. cond., Drude relax., 2D plasmons and minigaps in surface lattice 8-60230
 Si inversion layer, in strong mag. fields, electron localisation 8-60219

elemental semiconductors continued

- Si inversion layer, influence of natural superlattice on 2-dimens. electron gas spectrum (*Russian*) 8-68064
 Si, inversion layer, interacting electron system, cyclotron reson. 8-87902
 Si inversion layer, negative differential resist. 8-60225
 Si inversion layer, obs. of localisation ion two-dimens. systems 8-60213
 Si inversion layer, press. depend. of struct. of field effect mobility 8-60216
 Si inversion layer, random attractive electron-electron interactions in two-dimens. systems 8-60183
 n-Si inversion layer, resist. minima in surface quantum oscils. 8-60215
 Si inversion layer, surface quantum oscillation under pressure 8-60228
 n-Si inversion layer, thermal activation of two-dimens. Shubnikov de Haas cond. extrema 8-60218
 Si inversion layer, transient response under hot electron conditions 8-60223
 Si inversion layer, warm electrons 8-60222
 Si inversion layer (100), wavevector, depend. of the 2D plasmon disp. relationship 8-76101
 Si inversion layer surface cyclotron resonance, temp. and stress effects 8-60229
 Si inversion layers, cyclotron and subband emission 8-64128
 Si inversion layers, far IR reson. magnetotransmission, temp. and band gap light depend. 8-64363
 n-Si inversion layers, in strong mag. field, quantum galvanomag. expts. 8-60214
 n-Si, inversion layers, many-valley electron-phonon interactions, piezoresistance, anisotropic cond., Shubnikov-de Haas oscillations 8-52096
 Si inversion layers, random pair attractive interaction model of carrier correl., compared with expt. 8-60212
 Si inversion layers, stress and intersubband correlation 8-60227
 Si, inversion layers, two-subband screening and transport 8-64126
 Si inversion-layer electrons, temp. depend. cyclotron reson. lineshape, theory 8-64086
 Si, ion implantation, atomic collision theory and range-energy relations 8-71753
 Si, ion implantation, TSC meas. of coupled levels 8-84165
 Si, ion implantation damage, annealing, role of stresses 8-75679
 Si, ion implantation radiation damage, SEM electron beam absorpt. meas. 8-75696
 Si, ion implanted, laser annealing, periodic regrowth phenomena 8-67724
 Si, ion implanted, photovoltaic effect related to annealing 8-76111
 Si, ion implanted, voids, electron microscopy 8-67757
 Si, ion implanted layers, laser annealing 8-67732
 Si ion implanted p-n junction, cryst. damage influence on elec. props. 8-56219
 Si, ion irradi. damage, strain effect contrib., channelling meas. 8-67752
 Si, ion-implanted, cryst. to amorphous transform., ESR expts. and composite model 8-59825
 Si, ion-implanted, disorders, nature and annealing behaviour, review 8-83836
 Si, ion-implanted, secondary defects development, three-stage model 8-87725
 Si, ion-implanted layers, crystalline-to-amorphous transition, radiation defect prod. 8-87696
 Si, ion-implanted layers, impurity profile meas. after laser annealing 8-87702
 Si, ion-implanted layers, residual defects after high temp. annealing 8-87695
 Si, ion-implanted surface, profiling method 8-95075
 Si, ionised impurity scatt. limited mobility in semiconductors with spatially variable dielec. function 8-51986
 Si, LPE growth from supersaturated Sn melt 8-56592
 Si, laser assisted doping, ohmic contacts and p-n junction form. 8-79621
 Si, laser measurement, of semiconductor materials and devices (*Rumanian*) 8-52035
 Si, lattice dynamics, inversion matrix, approx. inversion 8-71797
 Si layer, neutron activation analysis, contamination and cross-contamination 8-83837
 Si, MIS photocapacitive IR detector 8-62223
 Si MNOS structures with tunnelling-thickness SiO₂ films, surface channel hole mobility obs. 8-95380
 Si MOS (111) inversion layers, angular dependent negative magnetoresist. 8-80062
 Si MOS inversion layer, subband struct., many body effects 8-64131
 Si, MOS inversion layers, Hall effect 8-64118
 Si MOSFET, electron and hole drift velocities in high elec. field, Monte Carlo calc. 8-60224
 Si MOSFET, spin orbit interaction and many body effects in surface states 8-64132
 Si MOSFET inversion layers, IR photocond. and absorption 8-64123
 Si MOSFET structures, photocond. rel. to intersubband transitions 8-64127
 Si, metallisation, CrSi₂ formation on Pd₂Si and PtSi 8-60578
 Si, metallurgical grade, purification and charact. 8-56573
 n-Si, microwave and far IR hot carrier mobility, Monte Carlo calc. appl. to mm. transit time oscill. efficiency 8-72184
 Si, microwave oxidation, negative role of fast electrons 8-64744
 p-Si, millimetric and far IR cond., evidence for interband transitions 8-52022
 Si, minority carrier diffusion length, Schottky barriers, electron bombard. investigation 8-68037
 Si, momentum distrib. of electrons, anisotropy, positron annihilation (*Russian*) 8-84676
 Si monocrystalline rod growth from gas phase 8-64453
 n-Si, Mott transition, dielec. enhancement conduction electron screening 8-72073
 Si, muon state, muon spin rot. exam. 8-60373
 Si, μ^+ spin relaxation in longitudinal mag. fields (*Russian*) 8-88245
 Si, n⁺p junction, spin dependent recombination (*French*) 8-80047
 Si n-type, electron irradi., positron annihilation, effect of high-temp. annealing 8-76552
 Si, negative conductivity due to hot electrons transfer in geometric space (*German*) 8-56150
 Si, neutron irradi., internal friction obs. of defects 8-51597

elemental semiconductors continued

- p-Si, neutron irradi. effects, admittance meas. of n⁺-p diode 8-51587
 p-Si, neutron irradiated, elec. props. 8-51939
 Si, neutron irradiated, intrinsic defect exam. by IR spectra 8-52534
 Si, neutron transmutation doped, zero-bias resist. of grain boundaries 8-76072
 p-Si, ohmic contact formation method 8-76137
 Si, optical constants at 5461 Å 8-92043
 Si, oxidation, masking effect of thermal oxidation rate of covering Si₃N₄ film 8-64749
 Si, oxidation, phase comp. of SiO₂, electron spectroscopy obs. 8-60042
 Si, oxidation, thermal growth kinetics, SiO₂ profile meas. 8-88551
 Si, oxidation in presence of Cl and Cl cpds. 8-53009
 Si oxidation mechanism and kinetics 8-95833
 Si, oxidation of dry O₂, revised model 8-92373
 Si, oxidation stacking faults and microdefects, growth behaviour during high temp. annealing 8-72901
 Si, oxidation-induced stacking fault form., by high press. steam oxidation 8-83830
 Si, P diffused sample, stacking faults and dislocations formation from interstitials 8-95059
 Si, p⁺-n-n⁺ high efficiency back surface field solar cells, design and fabrication 8-84283
 Si, p-n homojunction breakdown voltage for onesided abrupt junctions (*German*) 8-56210
 Si, p-n junction, plasmon mechanism for secondary breakdown 8-95352
 Si p-n junction diodes, reversed-biased, permanently induced negative resist., expt. 8-56214
 Si p-n junction made by ruby laser pulses, characts. (*Polish*) 8-84286
 Si, p-n-n⁺ structure, external resistance effect on current-mode second breakdown 8-56216
 Si, p-type and n-type, temp. coeff. of resist. calc. 8-91698
 Si, phonon boundary scatt., reduction of lattice thermal cond. 8-55921
 Si, phonon-mediated intervalley electron-electron interaction 8-95125
 Si photodiode saturation at high modulation freq. 8-54453
 Si, photoemission electron microscopy in high vacuum region, image brightness and contrast 8-55791
 p-Si, photosensitivity of elastic moduli and surface tension 8-83864
 Si, piezo-optical consts., Raman meas. 8-65951
 Si, planar and O₂ etched (111) surface, CO adsorption, AES, SEM, ESD, flash desorption mass spectra 8-63934
 Si, plasma etching, effect of O₂ additions to CF₄ plasmas 8-72908
 Si, plastically deformed, hot-exciton luminesc. as function of strain 8-88361
 Si plate prod. by Stepanov method, stability analysis (*Russian*) 8-52655
 Si, polarisation dependent electrorefl. spectra, surface phenomena 8-68479
 Si, polycryst., growth, props. and MIS appl. (*Slovak*) 8-92196
 Si, polycryst. manufacturing methods for photovoltaic energy prod., solar cells, grain growth from melt (*Dutch*) 8-52661
 Si, polycrystalline, p-n junctions, solar cell appls. 8-56220
 p-Si polycrystalline films on graphite substrates (*French*) 8-64154
 Si, polycrystalline layer, laser-induced single cryst. transition, RHEED and backscatt. obs 8-87704
 Si, polycrystalline ribbon prep. by electron bombardment (*French*) 8-64474
 Si, polymorphism under high press. (*Russian*) 8-59947
 p-Si, positron annihilation, effects of applied elec. field (*German*) 8-72634
 Si, powdered, microwave propag. 8-56175
 Si, reshaped single crystal prep. by pendant drop method (*French*) 8-64466
 Si, pure and heavily doped, 2p core levels and core excitation binding energy, photoemission obs. 8-76583
 Si, pyrolytic BN wafer as diffusion source characterisation 8-91352
 p-Si radiation defects due to 30 MeV proton irradi., rel. to solar energy converters 8-71776
 Si, radiation-doped and annealed, carrier density and mobility meas. 8-56145
 p-Si, Raman scattering by phonons and electrons, interference effects 8-60469
 Si, recombination luminescence, electron-hole drop, excitons orientation in mag. field 8-88362
 Si, reconstruction-induced subsurface strain, theory 8-91516
 Si reverse-biased p-n junction DC characteristics interpretation (*Polish*) 8-91761
 Si ribbon, crystal characterisation, growth with dies 8-76598
 Si, ribbon, impurity distrib. in EFG 8-91280
 Si, ribbon growth, via RTR technique, process update and material characterisation 8-76597
 Si ribbon parallel twinned structure development by shaped crystallisation 8-64465
 Si, ring shaped stacking faults induced by oxide precipitates 8-67723
 Si, screening of ions, band struct. calcs. with screening variants 8-67938
 Si, self-implanted layer, grain size, laser irradi. energy density depend. 8-72012
 Si, semivacancy and pair of semivacancies calc. by CNDO/2 method 8-51537
 Si, shallow donors, Zeeman interaction, relativistic corrections and very small g-shifts, contrib. to EPR 8-72393
 Si, single crystal, kinetics of annealing of vacancy complexes 8-87666
 Si slice, minority carrier diffusion lengths, surface photovoltage meas. 8-72168
 Si, Sn or Ge complex with vacancy, many-electron approach 8-67980
 Si, solid-phase-epitaxial, deposited above 380°C, defects obs. 8-63942
 Si, solubility of Au, gettering by P 8-83961
 Si, sputtered, cluster formation, influence of HF plasma interaction 8-64441
 n-Si sputtering-induced defects, elec. characts. 8-51941
 Si, stacking fault formation, elimination by preoxidation annealing in N₂/HClO₂ mixtures 8-88550
 Si, strain meas. by Pendellosung effect after P ion bombard. 8-55773
 Si, stress enhanced diffusion of B, using SiO₂ diffusion masks, photo-diode fabrication 8-67865
 Si, structural defects on (115) plane 8-87675
 Si substitutional diffusion model 8-71884

elemental semiconductors continued

- Si substrate, implantation effects on hardening and Si_3N_4 film stress reduction 8-71748
 Si, superlattice and 2-D electron gas 8-64080
 Si surface, (111), metastable 2×1 reconstructed, dangling bond mediated attractive electron-electron model 8-91520
 Si, surface, cluster model approach for electronic struct. 8-56205
 Si, surface, energy-minimisation approach to atomic geometry 8-95213
 Si surface, ideal and 2×1 chain-reconstructed, electronic struct. determ. 8-52050
 Si surface, interaction of oxygen gas discharge plasma 8-83840
 Si, surface, optical modulation of low energy electron reflection and transmission 8-88388
 Si, surface, stressed, n-inversion layers, Hartree calc. 8-68066
 Si surface, valence band Auger line shape, corrected numerical results 8-52602
 Si surface (100), vicinal plane surface band struct. electron inversion layers, minigaps 8-68062
 Si, surface (100)(1×1)H struct., LEED study 8-67910
 Si, surface characterisation by Si-electrolyte interface impedance meas. 8-84291
 Si surface doped channels, gate controlled, quantum galvanomagnetic effects 8-64134
 Si, surface final-state effects on core electron transition energies 8-91745
 n-Si, surface quantum oscills. in inversion layers under uniaxial press. 8-88041
 Si, surface self-diffusion, investigation by slow electron diffraction method (Russian) 8-51808
 n-Si, surface space-charge layer, intersubband-cyclotron combined reson. 8-68063
 Si, swirl defects, gettering effects, obs. by photoluminesc. meas. 8-84623
 Si, TO and TA phonons, electronic and struct. energies calc. 8-59874
 Si, thermal oxidation kinetics in pyrogenic water and $\text{HCl-H}_2\text{O}$ mixture 8-64748
 Si, two-dimensional electrons in superlattice, HF cond. 8-64055
 Si, VPE, stationary model, appl. to $\text{SiCl}_4\text{-H}_2$ system 8-52679
 Si, VPE via SiH_2Cl_2 in barrel reactor 8-52685
 Si, vacancy paradox 8-59804
 Si, vacuum deposition, combined with Sb ion implantation (Japanese) 8-88428
 Si vacuum sublimated thin film structure impurity distrib. 8-95354
 Si, valence bond Wannier functions calcs. 8-60053
 Si, van der Waals electron correlation energy 8-95013
 Si, vapour epitaxy, optimum growth conditions 8-76608
 Si, volume plasmon dispersion at large wave vectors, EELS 8-56094
 Si wafer, colour-banded, sheet resist. variation following high dose implantation at high dose rates 8-95074
 Si wafer, high resolution SIMS 8-56929
 Si wafer, migration of fine molten Al rich wires, vertical p-n junction fabrication 8-68077
 Si wafer, stress meas. in film, X-ray method 8-51860
 Si wafer surface sputtering, secondary positive ion mass and kinetic energy anal. 8-88391
 Si wafers, Czochralski, gettering of surface and bulk impurities 8-64456
 Si wafers, etched in HCl, exam. of bunch formation 8-68831
 Si wafers, N heat-treatment effects, stacking faults formation 8-85016
 Si whisker, amorphous, meas. of Young's modulus 8-83865
 Si, whisker growth in amorphous state, in $\text{SiH}_4\text{-Ar}$ atmosphere, visual obs. 8-84112
 Si, with non-spherical pots. for two basis atoms, electronic struct. 8-72069
 Si, work function and Auger spectroscopy of initial oxidation 8-76132
 Si, X-ray intensity anomalously transmitted, ϵ_{220} values 8-83650
 Si, zone refined, prep. of solar cells 8-64475
 Si: (B, P, Ge), impurity-pair diffusion, influence of elastic stresses 8-87824
 Si:Al, absorpt. line broadening 8-95594
 Si:Al, bound-exciton absorption 8-56507
 Si:Al(B)(P), bound multiexciton complexes, work function thermodynamic determ. 8-72078
 Si:Al(In), acceptor levels, IR spectra 8-67972
 Si:Al(Sb) film, amorphous, ion implantation, effect on cond. 8-83839
 Si:As, elec. activation of implanted As during low temp. anneal, Hall effect meas. 8-51571
 Si:As, implanted, spatially varied activation during regrowth of amorphous layers, sheet resist. and backscatt. obs. 8-71749
 Si:As, ion implanted, anomaly of elec. activation by additional Ne irradiation 8-84211
 Si:As, melting by high power ns laser pulsing, As diffusion 8-79789
 Si:As, time-resolved reflectivity during laser annealing 8-92086
 Si:As(P), Orbach spin-lattice relax. rate, uniaxial stress depend. 8-72391
 Si:Au, degeneracy factor of acceptor level 8-51927
 Si:Au, electron capture cross section, energy level of Au acceptor centre 8-51926
 Si:Au, neutron irradiated, penetration of Au into Si 8-59984
 Si:Au, nonequilibrium population of electron states and photomemory of surface pot. 8-56206
 Si:B, conc. profile of implanted cryst., by $^{11}\text{B}(p,\alpha)$ chem. anal., annealing (German) 8-83843
 Si:B, diffusion with BN, expt. (Bulgarian) 8-59824
 Si:B, dopant density determ. by nucl. track technique 8-55886
 p-Si:B, high temp. treatment, effects on ion implanted impurity distrib. profile 8-79625
 Si:B, implanted laser annealed samples, unidirectional contraction 8-71747
 Si:B, impurity conc. from photoluminesc. anal. 8-63785
 Si:B, impurity excited state lifetimes 8-60083
 Si:B, ion implanted, laser and thermal annealing compared, TEM obs. 8-75681
 Si:B, ion implanted, localised defects, TEM study 8-87699
 Si:B, ion implanted, struct. of rod defects, TEM obs. 8-71744
 Si:B, laser damage obs. by DLTS 8-76023
 Si:B, near intrinsic (100) and (111) samples, inert and oxidising ambients, diffusion, segregation 8-75882
 Si:B, p-n junction form. by B deposition and laser-induced diffusion 8-87690

elemental semiconductors continued

- Si:B, piezothermoelec. power 8-56173
 Si:B, polycrystalline, depth profiles of implanted B atoms, meas. by secondary ion mass spec. (Japanese) 8-67734
 Si:B, predeposition of B using BBr_3 8-55882
 Si:B, SEM obs. of dislocations using Schottky barrier EBIC technique 8-79614
 Si:B, TEM study of stacking fault form. and annealing 8-51566
 Si:B(P), diffusion induced imperfections, laser annealing, rel. to junction characts. 8-75678
 Si:B(P), heavily diffusion-doped layers, Co diffusion 8-59982
 Si:B(P)(Sb), multiparticle impurity complexes (Russian) 8-72601
 Si:Cd(Zn), n^+-n-n^+ structure, photocond. lifetimes, deep level occupancy in exclusion region 8-72253
 Si:Co, study of impurity states 8-76020
 Si:Cr, specific resistance, activation energy of deep levels, and carrier mobility (Russian) 8-72146
 Si:Cr, spin-lattice relax. of Jahn-Teller Cr^0 centre (Russian) 8-72402
 Si:Cu, interaction between vacancy emitting absorbing precipitates and dislocations, TEM obs. 8-71755
 Si:Cu(Au), recoil implantation from thin surface films, backscatt. obs. 8-63783
 Si:Fe, EPR and neutron activation anal. of thermal defects 8-91355
 Si:Ga, bound-exciton absorption 8-56507
 Si:Ga, gettering of Au and Cu during Ga diffusion 8-91350
 Si:Ga, LPE growth on Si substrate, melt-back approach 8-80481
 Si:Ga(Al), edge luminesc. spectra of acceptors, multiexciton complexes 8-56517
 Si:Gd, radiation defect form., effect of Gd impurities, elec. and optical meas. 8-71764
 Si:H, amorphous, rehydrogenation, photoluminesc. recovery 8-72571
 Si:H, ion implanted Monte Carlo calcs. of profiles of H ions 8-55889
 Si:H film, amorphous, elec. cond., effect of adsorbed gases and illumination 8-88048
 Si:In, bound exciton photolum. obs. 8-95607
 Si:In, bound-exciton absorption 8-56507
 Si:Ir S-type diodes, characts. 8-56224
 Si:Mn, amorphous, cond. increase by Mn doping 8-72155
 Si:N, amorphous, DC sputtered, enhanced, photocond. 8-56183
 Si:Na, quantitative analysis of residual impurities with SIMS 8-87688
 Si:Ni(Co)(Mn), influence of neutron irradiation as elec. props. 8-55895
 Si:O, cryst., annealed, struct. defects 8-75673
 Si:O, O rich polycryst. film, carrier transport 8-80076
 Si:O film, near IR absorption, O impurity states 8-88333
 Si:O film, near IR reflectivity at high temps. 8-56532
 Si:O film, thermally deposited, semi-insulating, crystallographic study 8-75954
 Si:P, annealing characteristics at low temp., elec. props. 8-63781
 Si:P, Au, neutron irradiated, distrib. of P and Au determ. 8-79627
 Si:P, carrier mobility and distrib. rel. to annealing, 400-910°C 8-79995
 Si:P, characterisation by IR reflectivity 8-56501
 Si:P, doped by neutron transmutation, electron traps 8-84164
 Si:P, electrostatic field on impurity atoms, heavy doping effects 8-51570
 Si:P, emitter-misfit dislocation formation during P diffusion 8-91338
 Si:P, excitation density depend. of cathodoluminesc. from bound multiexciton complexes 8-72609
 Si:P, Hall effect 8-72176
 Si:P, heavily doped, thermal oxidation 8-56793
 Si:P, high dose implantation, outside dislocation generation 8-87672
 Si:P, IR absorpt. and D⁺-band 8-52533
 Si:P, impurity conc. from photoluminesc. anal. 8-63785
 Si:P, ion implantation, effects of high dose rate 8-83835
 Si:P, ion implanted, lattice damage and electrical activation correlation 8-67726
 Si:P, ion implanted, resist. changes induced by ESR 8-68377
 Si:P, ion-implanted, optical refl. obs. of damage 8-55883
 Si:P, luminesc. lines, multiexciton complexes and uniaxial stress 8-92114
 Si:P, neutron transmutation doped, radiation damage exam., elec. props. 8-95080
 Si:P, optically induced divacancy reorientation, EPR spectra 8-80216
 Si:P, polycryst. etching characts. in CF_4 plasma 8-76777
 Si:P, polycrystalline, thermal oxidation in wet O_2 8-92376
 Si:P heavily-doped, photoluminescence 8-72572
 Si:P(B), film, electronic props. 8-84330
 Si:Pb, implanted, laser annealing 8-75685
 Si:Pb, implanted and annealed, impurity redistrib. 8-75689
 Si:S, existence of isotope shift for S deep level, isothermal transient capacitance meas. 8-63999
 Si:Sb, ion implanted, annealing behaviour of stress 8-63778
 Si:Sb(P)(As), shallow donor states with strong central cell perturbation theory 8-51933
 Si:Sb(P)(As), shallow donor electrons, hyperfine interactions, reply to Onffroy's calcs. 8-51934
 Si:Te, ion implanted, laser annealed, lattice location of Te 8-67725
 Si:Ti, IR excitation spectra 8-88289
 Si:Ti, optical absorption and photolum. of bound exciton 8-88359
 Si/SiO₂ interface, slow-trapping instability, kinetics 8-76151
 Si-He interface, phonon reflection 8-84043
 Si-Ag boundary, electronic and cryst. struct. of Ag adsorbed on Si (111), Schottky barrier form. obs. 8-84091
 n-Si-Ag Schottky-barrier diodes, excess current mechanism under uniaxial press. 8-91771
 Si-Al₂O₃, inversion layer subbands, magnetocond. oscills. 8-64124
 Si-Au, spatial origin of electrons in internal photoemission struct. (French) 8-91770
 Si-Au Schottky-barrier, formation process anal., V-I characts. (French) 8-91768
 Si-B, diffusion-free annealing, use of scanning CW Kr laser 8-91345
 Si-B, P diffusion and activity after Ar ion bombardment 8-95192
 Si-CdS p-n heterojunction photodetector fabrication and characts. 8-52068
 Si-electrolyte contact, current-voltage characts., effect of mechanical deform. 8-68082
 Si-Ni interface, NiSi formation from Ni_2Si , Pt marker study 8-87830
 Si-Ni substrate-film interface, annealing effects on transmission electron diff. patterns, silicide form. 8-91562

elemental semiconductors continued

- Si-PbS heterojunction, characts. and operation, IR detector appls. 8-52075
 Si-Si₃N₄ interface, effect of F ions on props. and stability, expt. 8-64141
 Si-SiO₂, inversion layer, electronic ground state, stress, temp., mag. field and gate voltage depend. 8-60226
 Si-SiO₂, charge accumulation during low energy electron bombardment 8-64142
 Si-SiO₂ interface, Auger-sputter profiling obs. of P pileup 8-95240
 Si-SiO₂ interface, chem. struct. of transitional region 8-95824
 Si-SiO₂ interface, high-resolution electron microscopy study 8-56046
 Si-SiO₂ interface, impurity electron states near interface 8-95320
 Si-SiO₂ interface, Na⁺ drifted, impurity bands in inversion layers 8-60211
 Si-SiO₂ interface, relax. of injected charge, temp. depend. 8-72269
 Si-SiO₂ interface, stacking fault-free region formation by annealing 8-51561
 Si-SiO₂ interface, thermally oxidised, oxide thickness effects on electron scatt. 8-88033
 Si-SiO₂ interface, with Cl⁻ incorporated, characterisation by low temp. cond. meas. 8-60220
 Si-SiO₂-Al structure, mechanical stress at Si(111) surface 8-63921
 Si-SiO₂-Si structures, P, As depth profiles, ion microanal. (*Japanese*) 8-85251
 Si-thermal SiO₂-electrolyte system, cond. in superhigh elec. field 8-52080
 Si-transition metal metastable films as temp. independent resistors 8-68097
 Si-transition metal silicide interface, chemical state, AES expts. 8-91767
 Si-ZnS n-n heterojunction, epitaxial, elec. props. (*Russian*) 8-88023
 Si(III) inversion layers, CDW induced cyclotron reson. harmonics 8-64085
 SiO₂-Si, film-substrate, single reflection retarders for different Hg spectral lines 8-79122
 SiO₂-Si:P, P pile-up at interface 8-84303
 Si(111), conduction-band surface resonance 8-52051
 p-Si(111) surface inversion layer, Cs covered, negative magnetoresist. in 2D impurity band 8-64135
 Si(111)2×1, surface electron states detected by external reflectivity 8-80036
 α-Sn, electronic energy bands of diamond-type crystals, appl. of EHT method 8-87907
 Te crystal, photo-EMF obs., depend. on sign of circular polarisation of light (*Russian*) 8-80025
 Te, electron irradiated, dose-depend. and recovery behaviour of transport props. 8-71761
 Te, film, AES, LEED, XPS, energy loss spectra studies oxidation effects 8-73086
 Te film growth on KBr (111) on mica (*Japanese*) 8-79903
 Te in MIS structure, impurity photocond. 8-72203
 Te intrinsic, intermediate IR optical absorpt., 5-20 μm 8-84562
 Te inversion layers, surface quantum transport 8-64088
 Te, lightly doped, galvanomagnetic props. in fields up to 140 kOe 8-91707
 Te, NMR spectrum, electron paramagnetism and atomic self-diffusion mechanism 8-72426
 Te, photocurrent generated by polarised light, direction depend. on polarisation (*Russian*) 8-64065
 Te, self-defocusing of CO₂ laser radiation under phase matched SHG conditions 8-83043
 Te, surface cyclotron resonance, freq. depend. 8-64084
 p-Te, transverse and longit. Nernst-Ettingshausen effect, theory and expt. 8-76095
 Te, trigonal, model of lattice dynamics using long and short range interactions 8-59893
 Te, valence-band X-ray emission spectrum 8-84682
 Te, warm hole conductivity 8-72160
 Te:I, semicond., elec. efficiency (*German*) 8-84166
 Te:Sb, 96 to 500K, cond. Hall const., hole mobility, conc., dislocation effects (*Russian*) 8-64039

elementary particle coupling constants

- baryon resonance photocoupling anal. in relativistic quark model 8-66086
 ge⁴ theory, strong coupling limit of Green functions, anharmonic oscillator appl. 8-78071
 massless electrodynamics, vacuum instability, bare coupling constant Gell-Mann-Low eigenvalue condition 8-89643
 narrow resonances, dynamical model, mass mixing and splitting in degenerate multiplet states 8-93813
 O(3) σ-model, nonlinear, quantum fluctuations of instanton solns. (*Russian*) 8-74161
 phenomenological analysis of single pion photoproduction in the first resonance region 8-89721
 pseudoscalar transition between spin-J and spin 5/2 baryon 8-50032
 radiation gauge static pot. between fermion and antifermion, non Abelian gauge fields 8-89621
 Regge pole model, NN pots., one boson exchange, coupling consts. masses 8-70346
 semilocal duality constraints for mesons, on-shell particles, masses, couplings 8-58174
 spontaneous generation of renormalisation invariant mass in IR stable theories 8-86411
 SU₂×U(1) gauge models and neutral current reacts. 8-89648
 β decay of closed shell ± one nucleon nuclei, axial vector coupling const. quenching 8-89824
 NN nonrelativistic 1-boson exchange potentials based on generalised meson field theory 8-70459
 νν effective coupling constant upper limit from high energy beam data (*Russian*) 8-89706
 p^{pp}, const. determ. from anal. of pp elastic scatt. from 150-515 MeV 8-70396
 π nuclear coupling const., review 8-89835
 π³He coupling constant determ. from ³H(p,n)³He differential cross section 8-89801
 πN coupling const. determ. in MIT bag model 8-78149

elementary particle coupling constants continued

- πN coupling constant from simultaneous anal. of all invariant amplitudes using rational series 8-58199
 ψ particles, off-mass-shell coupling consts. and radiative decays in VDM 8-70371

elementary particle decay

- see also *electromagnetic decays; elementary particle coupling constants; hadron decay; leptonic decays; muon decay; nonleptonic decays; semileptonic decays*
 charmonium and QCD, review 8-82157
 lepton-quark system, quantum number laws, classification of weakly interacting particles, decays 8-82138
 three particle decay, two body resonance approx., Veneziano amplitude expansion 8-82174
 unstable particle decay, Trieste theory, rigorous inequalities 8-93869
 τ decay involving hadronic vector current 8-66101
 τ→νππ, π invariant mass distrib. predictions, hadronic decay rates 8-70352
 τ→πν, decay observation, branching ratio 8-89766
 τ→ππππ, π invariant mass distrib. predictions, hadronic decay rates 8-70352

elementary particle electromagnetic interactions

- see also *Weinberg model*
 baryon resonance photocoupling anal. in relativistic quark model 8-66086
 bremsstrahlung study, Rochester cross section, soft-photon region 8-62401
 bubble chamber, electromagnetic shower photographs, for teachers 8-65737
 Cargese lectures in physics, book 8-82130
 cosmic ray muons and muon pairs, EM interactions, 5-1200 GeV (*Russian*) 8-73598
 deep inelastic scatt., covariant parton model, Feynman integrals of perturbation theory 8-82221
 Higgs-Kibble mechanism and electron-muon mass ratio 8-66065
 High energy behaviour of weak interactions and renormalisable theories, book contrib. 8-78164
 Nambu-Jona-Lasinio type unified model for gravitational and EM forces 8-65850
 particles and fields conference, Argonne, IL, USA (Oct. 1977) 8-78130
 radiative corrections to parity violation in atoms in SU(3)×U(1) gauge theory 8-62402
 SU₂ gauge model, light neutral gauge boson, consequences for e⁺e⁻ and pp(p) 8-58154
 SU(2)⊗U(1) gauge model of EM and weak interactions, fermion mass restriction (*Russian*) 8-89650
 unified theories of weak and electromagnetic interactions 8-81908
 e⁺e⁻→1⁺⁺ resonance states, direct production through neutral currents 8-93891
 NN interaction, EM phase shift calc. within relativistic model, isospin non-conservation 8-62438
 np bremsstrahlung, effects of nonminimal currents and role of various couplings 8-70394
 pp→virtual gamma+hadrons soft bremsstrahlung, external emission dominance model 8-62430

elementary particle gravitational interactions

- classical pseudoparticle solutions in general relativity 8-89390
 classical quark confinement from general relativity 8-58162
 Einstein relativistic particles, construction of quantal theories, appl. to two particle system 8-62347
 fermion and boson fields interacting with gravitational fields 8-86208
 gravitational instantons and universal spin structs. 8-78128
 hadron gravitational interaction, band spinor representation of GL(n,R) 8-50000
 MIT confinement scheme, geometrodynamical approach 8-89657
 Nambu-Jona-Lasinio type unified model for gravitational and EM forces 8-65850
 particles in curved space-time, group of parallel transports 8-54602
 quark confinement, event horizons around a particle surrounded by a static confinement potential 8-66075
 soft graviton emission in scatt. processes, linearised gauge theory 8-49746
 supergravity, unified theory of basic forces 8-50001

elementary particle inclusive interactions

- see also *electron-positron inclusive interactions; elementary particle large momentum transfer interactions; pion-proton inclusive interactions; proton-proton inclusive interactions*
 ν deep inelastic scatt. in SKAT bubble chamber, 2-30 GeV 8-62390
 π⁺π⁻ semi-inclusive distrib. anal. using Kopylov-Podgoretsky-Cocconi formulation, fireball 8-89761
 anomalous lepton signals and inclusive particle prod. in e⁺e⁻ annihilation 8-78198
 asymptotic evaluation of high energy cross sections, functional integration method 8-54551
 C Ne+ν_μ(ν_μ), inclusive distrib. of produced hadrons 8-89854
 charge particle multiplicity and charge exchange at 40 GeV/c, effect of bubble chamber errors (*Russian*) 8-55118
 charge transfer in multiparticle production processes and the quark cluster model 8-93858
 charmed particles, inclusive semileptonic decay, struct. functions, scaling limits 8-82165
 cluster concept in multiple hadron prod. 8-66177
 collective tube model, credibility of criticism by Azimov et al., effects of target fragmentation 8-93982
 complex momenta eikonal approx., hadron-nucleus collisions at asymptotically high energies (*Russian*) 8-74294
 cross-section in region of large transverse momenta and singularity interaction 8-54661
 DC K⁺p, 32 GeV/c, resonance inclusive prod. cross sections, quark model comparison 8-93913
 deep inelastic hadron leptonproduction on nuclei, inclusive hadron final states 8-54741
 deep inelastic processes book contrib. 8-82222
 dimuon prod., sum rules and moments, valence quark transverse moments 8-54660
 dual fermion model, inclusive single particle distrib., πN→πX appl. 8-86446
 electroproduction of hadrons, virtual photon prod., quark fragmentation region 8-54634

elementary particle inclusive interactions continued

gluon properties in high energy hadron reactions 8-66076
 hadron+hadron interactions, Drell-Yan dynamics, lepton pair from qq collision, energy scaling breakdown 8-54610
 hadron interactions, multiplicity, semi-empirical formula 8-58210
 hadron total cross section, role of string junction 8-89676
 hadronic massive lepton pair prod., theory review, Drell-Yan model 8-89752
 hadronic multiparticle reactions, models, prod. of strangeness, baryon number, charm 8-74286
 hadroproduction of μ pairs, 39.5 GeV/c π^\pm , K^\pm , p, \bar{p} beams on Cu target 8-62470
 high energy inelastic hadron reactions, π prod., scaling law, fireball model 8-74287
 high-energy hadronic collisions, classical space-time concepts 8-70420
 high-energy inclusive spectra near phase-space boundary using quark fragmentation model 8-89658
 inclusive Coulomb scatt. cross section in 4th order of QED 8-78117
 large p_t jet prod. in hadronic collisions, QCD calc. for inclusive cross section 8-86439
 large transverse momentum trigger, multiplicities and rapidity distrib. 8-62376
 Lepton pair production cross section using Drell Yan formula, sum rules, moments 8-54611
 massive lepton pairs, transverse momentum distrib. from inclusive hadron prod. 8-89760
 meson resonance and pion simultaneous production, correl. jet model 8-86456
 meson-nucleon collisions, pion spectra forward-backward asymmetry, fragmentation effects, meson reson. decay 8-86457
 multiparticle production, large transverse momenta, momentum conservation, independ. emission model 8-50055
 multiplicity distrib. and correl. at high energies, statistical treatment 8-89682
 polarisation in hadron cumulative prod. and large transverse momentum processes (Russian) 8-74293
 Pomeranchuk theorem inverse, proof for logarithmically rising total cross sections, 10-2000 GeV 8-86425
 pomeron building mechanism, in fragmentation region 8-89687
 QCD, factorisation and the parton model 8-93848
 QCD, hard semi-inclusive processes 8-93862
 QCD, inclusive production at large transverse momentum, cross section 8-62369
 QCD, transverse momentum of jets in electroprod. of hadrons 8-62367
 quark recombination model, vector meson prod., effect on π^\pm and K^\pm fragments from proton 8-82160
 quark-antiquark annihilation, small momentum transfer inclusive spectra 8-58158
 rapid pionisation model, inclusive spectra height and average multiplicity growth (Russian) 8-89763
 rising π inclusive cross section as series of threshold effects, multiperipheral model 8-93918
 s-dependence of proton fragmentation by hadrons, 30-250 GeV/c 8-74291
 s-dependence of proton fragmentation by hadrons 4-24 GeV/c 8-74290
 scaling low for inclusive production of hadrons in particle-particle collisions at high energies 8-54656
 seagull effect in π semi-inclusive distrib. by information theory, p_t - p_t correlations 8-86458
 single particle inclusive distributions, momentum transfer components, phenomenological approach 8-89754
 SU(4) broken symm., duality, baryon+baryon and baryon+antibaryon exotic mesons prod. 8-89629
 transverse momentum distribution of particles, hydrodynamical model calcs. 8-93865
 triple jet production in hadronic collisions at large transverse momentum 8-93919
 two jet model, large p_t hadronic multiplicity, colour octet exchange 8-62377
 two-hadrons inclusive reactions and correl., large p_t , scale-violating quark model 8-74292
 universality of multiplicity distrib., hadronic bremsstrahlung 8-70419
 vector meson production in triple Regge region, absorpt. corrections 8-93867
 $ed \rightarrow e' + X$, polarised e, parity non-conservation in inelastic scatt. 8-89719
 eN deep elastic scatt., hadronic final states 8-78184
 $eN \rightarrow e\pi^\pm X$, sum rules for polarised N 8-89718
 ep deep inelastic inclusive K_s^0 and Λ electroproduction, quark fragmentation 8-66123
 $ep \rightarrow e' + X$, polarised e, parity non-conservation in inelastic scatt. 8-89719
 $ep \rightarrow e' n X$, π exchange, π EM struct. functions calcs. 8-70375
 $e^+p \rightarrow e^+ \gamma + X$, deep-inelastic bremsstrahlung, quark charges, colour gluon mass 8-74216
 K^0 meson production cross section (Russian) 8-82394
 $K^\pm n$, high-energy, react. differences and annihilation 8-74279
 $Kp \rightarrow \pi X$, central region, Regge Mueller approach, inclusive cross sections (Russian) 8-58218
 $K^- p \rightarrow \Delta^{*-}(1232) + X$, 16 GeV/c, cross sections 8-66169
 $K^- p$ inclusive interactions, 10, 16 GeV/c, polarisation of forward produced Λ 8-62466
 $K^- p \rightarrow K^0 X$, pseudoscalar meson prod. in triple Regge region, absorpt. corrections 8-78228
 $K^- p \rightarrow \Lambda^0 + \text{pions}$, 8.25 GeV/c, resonance prod., fluctuations cluster emission model 8-93904
 $K^- p \rightarrow \rho^0 + \text{anything}$, or $f + \text{anything}$, 10, 16 GeV/c, central and fragmentation contribs., quark model predictions 8-62467
 $K^+ p \rightarrow K^0 X$, pseudoscalar meson prod. in triple Regge region, absorpt. corrections 8-78228
 $K^\pm p$, high-energy, react. differences and annihilations 8-74279
 $K^\pm p \rightarrow \text{hyperon} + X$, 4-16 GeV/c, unified descript. of $\Lambda, \Lambda, \Sigma^+, \Xi^-$ prod., urbaryon model 8-66173
 $lp \rightarrow l' h X$, azimuthal depend., parton model calc. 8-93887
 μ pair production in hadron-hadron collisions, gluon effects, QCD predictions 8-78148
 μN deep inelastic scatt., hadronic final states 8-78184
 $\mu p \rightarrow \mu X$, deep inelastic processes, nucleon struct. function, scale breaking 8-78185

elementary particle inclusive interactions continued

NN, πN , KN, cross-sections related by sum rules, pomeron hypothesis, heavy-quark channels and threshold predictions 8-89755
 $np \rightarrow pX$, 800 MeV, proton spectra, $\pi N(1232)$ resonance 8-62437
 ν inclusive cross section on nuclei, ν_μ representation in SU(6) 8-54626
 $\nu(\bar{\nu})N$ inclusive scatt., scaling violation evidence, QCD test 8-89701
 νN charged current reacts., appl. of new scaling rule 8-89703
 $\nu N \rightarrow \mu^\pm \mu^\mp \mu^\pm X$, internal Drell-Yan mechanism, parton model approach 8-89656
 νp high energy interactions, vector meson diffr. prod., charged and neutral current 8-54625
 $p + \text{emulsion nuclei}$, 300 GeV, inclusive correl. functions 8-58279
 $p + \text{emulsion nuclei}$ diffractive coherent prod., inclusive and exclusive channels 8-62530
 $p + \text{nucleus}$, 200 GeV/c, relative yields of π^\pm , K^\pm , p, \bar{p} 8-93995
 $p + \text{nucleus}$, inclusive π prod., 0.78 to 5 GeV, relation to NN π prod. 8-78384
 pd , 200 GeV/c, multiplicity distrib., and rescatt. effects 8-82255
 $pn \rightarrow \mu^+ \mu^- + \text{anything}$, review of data, explanation using quark models, new quarks 8-74202
 $pn \rightarrow p_{\text{slow}} + x$, 195 GeV/c, triple Regge model anal., dominant π exchange 8-54657
 $pN \rightarrow pX$, 28.3 GeV/c, Pt target, polarisation of inclusively produced protons at $p_t=1.5$ GeV/c 8-93917
 $pn \rightarrow \pi X$, central region, Regge Mueller approach, inclusive cross sections (Russian) 8-58218
 $p^+ n$, high-energy, react. differences and annihilation 8-74279
 π^0 inclusive photoprod. and quark-parton model 8-78189
 $\pi^- A \rightarrow \pi^0 X$ with $\Delta(1240)$ slow isobar intermediate prod. in heavy nuclei, cross section (Russian) 8-89917
 $\pi^- N$ interactions, 50 GeV/c, inclusive charged π prod. in nuclear emulsion anal. 8-66168
 $\pi^- N \rightarrow \mu^+ \mu^- X$, 27, 40 GeV, cross sections and differential distrib. (Russian) 8-89919
 $\pi^- n \rightarrow p_{\text{slow}} + x$, 195 GeV/c, triple Regge model anal., dominant π exchange 8-54657
 $\pi^- n$, high-energy, react. differences and annihilation 8-74279
 $\pi^- \pi^- \pi^-$ correlation functions, Mueller scheme with Bose-Einstein statistics 8-93915
 ψ inclusive production on 43 GeV/c π^- on Be, Cu, W, A-depend. 8-62581
 $^{12}\text{C} + \pi^-$, 40 GeV/c, secondary charged particle inclusive spectra, π^\pm struct. functions (Russian) 8-89921
 $\text{Cu} + \pi^-$, 27, 40 GeV, cross sections and differential distrib. for muon pair prod. (Russian) 8-89919
 $h + A \rightarrow h' + \text{anything}$, colour in production on nuclei 8-93981
 $K^- p$, 100 and 175 GeV/c, inclusive scatt. results from Fermilab single arm spectrometer 8-89746
 $\text{Ne} + \nu_\mu(\bar{\nu}_\mu)$, inclusive prod. of hadrons, preliminary data 8-89853

elementary particle interaction models

see also bootstrapping; composite models of hadrons; diffraction model; duality and dual models; peripheral models; statistical models; vector meson dominance model; Weinberg model
 Bounds on slope of diffraction peak and zeros of absorptive differential cross sections 8-74282
 broken SU(3) gauge model of strong and EM interactions, scatt. lengths, baryon mag. moments 8-74133
 deep inelastic scattering, contrib. of twist-four operators, struct. functions 8-78187
 droplet model for high energy pp elastic scatt., ang. depend. 8-82243
 Federbush model, absence of induced counterterms e^+e^- scatt. amplitudes 8-50023
 hadron interactions, multiplicity, semi-empirical formula 8-58210
 hadron multiprod., long-range correl., overlapping independent emission 8-82141
 hadronic multiparticle reactions, models, prod. of strangeness, baryon number, charm 8-74286
 iteration models, elastic reactions beyond diffraction peaks 8-93839
 potential model, πN local phenomenological potentials, 0-250 MeV scatt. 8-70400
 potential model anal. of EM effects in precision anal. of low-energy np interaction data 8-93896
 seven lepton model, quantum flavour dynamics, mixing angle, masses, spontaneous symmetry breaking 8-89652
 vector meson $\rightarrow e^+e^-$, standard leptonic decay width correction, effecting pot. model predictions 8-89707
 d breakup, exotic final state interaction, intermediate Δ , ΔN threshold parameters 8-50043
 $e^+e^- \rightarrow \mu^+ \mu^-$, contribution of weak neutral currents (Russian) 8-62383
 $K^+ +$, 32 GeV/c, 4 and 6 body final states, principal-axis variables anal. 8-58206
 NN interaction, EM phase shift calc. within relativistic model, isospin non-conservation 8-62438
 ν -induced associated production, Born term model 8-58179
 $\nu_e \rightarrow \nu_e e$, weak vector-like models, induced axial vector coupling 8-50025
 $pn \rightarrow d(\pi\pi)^0$, effective two body interaction Hamiltonian, missing mass, ABC effect 8-70388
 pp inelastic scatt., parity violation, $\Delta(1232)$ prod. model 8-62435
 pp large-angle elastic scatt., 1.5-2.06 GeV/c, optical model anal. 8-74270
 pp opaqueness at high energy, factorisable eikonal model and scaling hypothesis comparison 8-74280
 pp total cross section, spin dependence, relativistic model of $\Delta(1232)$ prod. 8-62436
 pp-virtual gamma+hadrons soft bremsstrahlung, external emission dominance model 8-62430
 $\bar{p}p \rightarrow \pi\pi$, model of excited hadronic matter 8-74288

elementary particle interactions

see also cosmic ray effects and interactions; elementary particle coupling constants; elementary particle electromagnetic interactions; elementary particle gravitational interactions; elementary particle inclusive interactions; elementary particle large momentum transfer interactions; elementary particle scattering; elementary particle strong interactions; elementary particle weak interactions; hadron-deuteron interactions; hadron-hadron interactions; high-energy cosmic ray interactions; lepton-deuteron interactions; lepton-hadron interactions; lepton-lepton interactions; photon-deuteron interactions; photon-hadron interactions; photon-lepton interac-

elementary particle interactions continued

tions; *photon-photon interactions; quantum field theory of interactions; unified field theories; vertex functions*
No entries

elementary particle large momentum transfer interactions

see also *elementary particle inclusive interactions*
composite model of quarks, large p_t hadron prod. 8-62472
diquark jets in lepton prod. and large p_t reactions, fragmentation functions 8-82149
elastic quark-quark scatt. model, relations for hadron pairs 8-66092
hadron jet struct. at large transverse momentum in $\gamma\gamma$ interactions 8-82225
heavy quark prod. in photoproduction, QCD model, possible large p_t process connection 8-78137
high transverse momentum processes, quark-parton model anal. 8-82163
high transverse momentum scatt., two particle correlations and ϕ prod., jet trigger 8-78225
inclusive cross-section in region of large transverse momenta and singularity interaction 8-54661
large p_t jet prod. in hadronic collisions, QCD calc. for inclusive cross section 8-86439
large transverse momentum physics review, diagnosis and prognosis 8-78215
large transverse momentum trigger, multiplicities and rapidity distrib. 8-62376
multiparticle production, large transverse momenta, momentum conservation, independ. emission model 8-50055
nonperturbative QCD effects at large momentum transfers, e^+e^- annihilation to hadrons 8-82226
polarisation in hadron cumulative prod. and large transverse momentum processes (Russian) 8-74293
QCD, inclusive production at large transverse momentum, cross section 8-62369
QCD, transverse momentum distrib. of μ pairs from pN interactions, p-nucleus study 8-62375
QCD and polarised quarks (Russian) 8-74217
QCD effects, parton transverse momenta, large- p_t hadron prod. 8-66083
QCD predictions for large p_t hadron prod. by polarised hadrons 8-82148
string function model, large p_t hadron prod. 8-62380
structure function relations, lepton pair processes at large transverse momenta 8-82214
transverse momentum distribution of particles, hydrodynamical model calcs. 8-93865
triple jet production in hadronic collisions at large transverse momentum 8-93919
two jet model, large p_t hadronic multiplicity, colour octet exchange 8-62377
two-hadrons inclusive reactions and correl., large p_t , scale-violating quark model 8-74292
d EM form factors at large transferred momentum, six-quark state (Russian) 8-89715
dd collisions, 4.3, 6.3, 8.9 GeV/c, d spectra high momentum struct., multiple NN scatt. model 8-89727
ed, elastic and deep inelastic scatt. at large momentum transfer, quark model (Russian) 8-86529
 e^+e^- annihilation, DD τ decay, large timelike Q^2 , conservation of vector current and current algebra 8-78155
np, elastic scatt. at large transverse momentum, spin-spin forces 8-78216
p+H target, high transverse momentum π^0 and jets prod. 8-70417
pp collisions, high momentum π^\pm and K^\pm prod., 45 GeV, cross sections 8-93910
pp collisions, large transverse momentum pions prod., correls., fireball model 8-66174
pp collisions at CERN ISR, charged hadron of high transverse momentum at 90° , forward particles 8-58214
pp $\rightarrow e^+e^-X$, large p_t , reference to $Y(9.5)$, $\zeta(3.5)$ and direct γ -prod. 8-89749
pp elastic scatt., high energy, diffraction model with nucleon core 8-74281
pp elastic scatt. at high energy and large momentum transfer, cross-sections 8-62460
pp elastic scatt. at large transverse momentum, spin-spin forces 8-78216
pp interactions, hadron prod. 23.4 to 63.4 GeV, charged multiplicity density for various p_t 8-70414
pp \rightarrow jets, 400 GeV, p_t plots, Monte Carlo and parton model predictions 8-89747
pp $\rightarrow\pi^0+X$, large p_t , π^0 spectra, quark model anal. 8-89756
pp $\rightarrow\pi^0$ +anything, $\sqrt{s}=52.7$ and 62.4 GeV, prod. of high transverse momentum π^0 's 8-78226
pp $\rightarrow\pi^0\pi^0X$, large p_t , azimuthal correlations 8-89749
pp scatt., eikonal mechanisms at high energy 8-82256
 π +H target, high transverse momentum π^0 and jets prod. 8-70417

elementary particle scattering

see also *bootstrapping; elementary particle interactions; hadron-deuteron scattering; hadron-hadron scattering; lepton-deuteron scattering; lepton-hadron scattering; lepton-lepton scattering; Mandelstam representation; photon-deuteron scattering; photon-hadron scattering; photon-lepton scattering; photon-photon scattering; Pomeranchuk poles and trajectories; quantum field theory of elastic scattering; Regge poles and trajectories; relativistic scattering theory; S-matrix theory*
finite geometry effects in scatt. expts., numerical integration method 8-82596
hadron constituent models review, fixed angle and Regge behaviour, hard scatt., fragment X-distrib. 8-78154
off-shell, nonrelativistic two-body amplitudes, generalisation of Jost formalism 8-49687
particles and fields conference, Argonne, IL, USA (Oct. 1977) 8-78130
Pomeranchuk theorem inverse, proof for logarithmically rising total cross sections, 10-2000 GeV 8-86425
pomeron flip-non-flip interference term in elastic polarisation, s-channel helicity 8-50021
representation by Penrose graphs 8-49983

elementary particle scattering continued

three-boson stimulated scatt., quantum mechanics (Russian) 8-78115
Yukawa pot. scatt., separable expansion method, off-shell T matrix 8-93564

elementary particle strong interactions

see also *composite models of hadrons; duality and dual models; hadron classification schemes; peripheral models; quantum field theory of strong interactions*
broken SU(3) gauge model of strong and EM interactions, scatt. lengths, baryon mag. moments 8-74133
Cabibbo angle and quark spectroscopy (Russian) 8-62351
classical quark confinement from general relativity 8-58162
composite hadrons, spin depend., S-matrix theory, TeV energy range 8-58164
Einstein's field eqns., possible generalisation to strong interactions 8-53979
elementary length and time in the strong interaction, meson reson. width data 8-82189
lepton-hadron model, determ. of N form factors 8-74256
lightlike chiral structure of hadrons, nonleptonic hyperon decays 8-74253
master eqn. for quantum systems with strong interactions (Chinese) 8-86229
particles and fields conference, Argonne, IL, USA (Oct. 1977) 8-78130
relativistic dense matter, statistical mechanics using phenomenological quantum field model 8-89814
spin dependence in strong interactions at very high energy 8-58203
dd \rightarrow He n, 1.1 to 2.5 GeV/c, energy depend., cross sections, reaction mech. 8-54643
NN low energy scatt., parity violating observables, strong potentials 8-50045
 $^3\text{He}+\pi^+$, strong interaction shift, multiple scatt. and absorptive effects, calc. 8-62958

elementary particle symmetry

see also *chiral symmetries; conservation laws; discrete symmetries; dynamical symmetry; helicity (elementary particles); isotopic spin (elementary particles); nonlinear symmetries; spontaneous symmetry breaking; SU_n theory; supersymmetry*
atomic parity conservation, left-right symm. unified theories 8-70306
classical and prequantised mechanics without Lagrangians or Hamiltonians for relativistic particles 8-74126
Clebsch Gordan coefficients for meson sector in SO(8) model of elementary particles 8-58135
conformal relativity, classification of metric bosons 8-93803
conformal relativity, kinematic theory of mass 8-77706
conformal relativity, particle species classification, symms., space time origin of isospin 8-93815
dual symmetry of general type vector field, quaternion formulation (Russian) 8-58107
ghost and internal symm., models on Hermitian spheres 8-70304
history of search for fundamental constituents of matter (Polish) 8-54588
internal symmetries, invariant theoretical consideration of nonlinear realizations 8-93817
Lie admissible algebra and nilalgebra, recent developments 8-74168
line reversal symmetry test in baryon exchange processes 8-78202
massive Schwinger model, consistency and Lorentz invariance 8-89613
Moufang plane and octonionic quantum mechanics 8-69999
nuclearity of C^∞ vector spaces in induced inhomogeneous Lie group representations 8-86422
ordered hadron S-matrix, quark interpretation, selection rules 8-62322
renormalisation group transformations as symm. mappings, local Lagrangian density (German) 8-49953
spinning electron, quantum mech. rotor, dynamics, invariance requirements 8-70250
spinning particles interacting with external fields, invariance groups of relativistic eqns., SU₃ symm. 8-49962
supergravity, unified theory of basic forces 8-50001
trichromatic theory and time vector in relativity theory (French) 8-57006
B-B, B-B scattering, models of line reversal symmetry breaking 8-62326
 $\nu(\bar{\nu})N$ elastic scatt., symmetry relations, current matrix elements 8-54627
 ν -induced associated production, Born term model 8-58179

elementary particle theory

see also *Bethe-Salpeter equation; complex angular momentum plane; current algebra; dispersion relations; electron theory; elementary particle interaction models; elementary particle symmetry; Feynman diagrams; form factors; group theoretical schemes; helicity (elementary particles); isotopic spin (elementary particles); Lee model; mass formulae; quantum field theory; S-matrix theory; scaling phenomena; structure functions; sum rules; vertex functions*
charmonium state decay, nonrelativistic and relativistic theory 8-58221
discoveries during 1974-7, and associated theories (Czech) 8-86103
education, elementary particles, quarks and the concept of particle, Richtmyer memorial lecture 8-62286
exclusion principle extended, particle classification anal. 8-49690
five-dimens. model of scalar bosons, O(N) symm. 8-70307
free relativistic spin-1/2 particle energy-momentum invariants and kinetic moment (French) 8-62287
general relativistic particle models, and effective radius (German) 8-86198
individual properties of individual particles, theory, teaching approach 8-57721
meson model based on superposition of Klein-Gordon eqns., ϕ , ϕ' , F, K spectrum 8-58121
meson structure model with covariant oscillator potentials (Chinese) 8-82180
mesonic topological amplitude products, an algebraic soln. 8-81884
microphysics, towards an elemental grounding 8-86106
mutually interacting charge fields, gauge theoretical formulations of elementary particle processes 8-58122
narrow resonance in an open channel 8-66099
neutrino as axial EM field source, symm. P-invariant broadened Maxwell eqns. (Russian) 8-58141

elementary particle theory continued

nonlinear field theory, path integrals definition, rules for transform. of variables 8-78072
 nuclei and particles, introductory text book 8-78234
 P-state particle, field current rela. and total width (*Chinese*) 8-82188
 particle model based on stringlike solitons 8-62294
 relativistic quantum mechanics formulation of space and time 8-65796
 statistics, quantum characts. 8-70297
 e mass calc. in terms of meas. quantities 8-66180

elementary particle weak interactions

see also neutral currents; quantum field theory of weak interactions; Weinberg model

$\Delta I = 1/2$ rule, six dominance, parity violation, weak interaction theory review 8-78131
 axion, Gargamelle beam dump expt. 8-50003
 CERN proton synchrotron, electron ring addition, proposal for weak interaction study 8-55062
 dual models of weak interactions of leptons and quarks 8-66070
 Eotvos expts. and weak interactions, anal. 8-78129
 Fermi weak interaction theory, consistent renormalisation scheme, Yang-Mills theory parallel 8-66071
 fermions, ultra heavy, weak interactions, high energy scattering, low energy renormalisation corrections 8-93838
 Gargamelle, neutrino physics history, theory and expt. 8-50027
 heavy atoms, P-odd effects, weak interaction eqn., SU(2) theory, four fermion theory (*Russian*) 8-93820
 Higgs boson, spontaneously broken gauge theory phenomenon, possible weak interaction model 8-74200
 Higgs-Kibble mechanism and electron-muon mass ratio 8-66065
 High energy behaviour of weak interactions and renormalisable theories, book contrib. 8-78164
 historical introduction, weak interactions, book 8-78133
 isotropy of Universe, entropy prod. in lepton era 8-61947
 lepton mixing and neutrino oscillations, cosmic neutrinos, heavy leptons, μ decay 8-82193
 lepton-quark system, quantum number laws, classification of weakly interacting particles, decays 8-82138
 leptonic weak interactions, book contrib. 8-78161
 non-leptonic weak interactions, book contrib. 8-78163
 nuclear structure, conf. 8-50059
 parity violation, correl. with biomolecules optical asymm. 8-69000
 particles and fields conference, Argonne, IL, USA (Oct. 1977) 8-78130
 photoproduction processes of charm particles with charm nonconservation (*Russian*) 8-74201
 radiative corrections in gauge theories, QCD current algebra formulation, weak interaction universality 8-93883
 radiative corrections to parity violation in atoms in SU(3) \times U(1) gauge theory 8-62402
 second class current in β decay of ^{20}Fe 8-50127
 semi-leptonic weak interactions, book contrib., strangeness-conserving current, strangeness-changing decays 8-78162
 seven lepton model, quantum flavour dynamics, mixing angle, masses, spontaneous symmetry breaking 8-89652
 SU₂ gauge model, light neutral gauge boson, consequences for e^+e^- and $pp(\bar{p})$ 8-58154
 SU(2) \otimes U(1) \otimes U(1) gauge model without parity violation in heavy atoms 8-82097
 SU(2) \otimes U(1) gauge model of EM and weak interactions, fermion mass restriction (*Russian*) 8-89650
 SU(3) \times U(1) modified model, quark and lepton mass hierarchy 8-89653
 theory and phenomenology, graduate textbook 8-78160
 unified theories of weak and electromagnetic interactions 8-81908
 β decay of ^{12}B and ^{12}N , second class currents 8-50126
 $e^+e^- \rightarrow \nu\bar{\nu}$, formula for differential cross-section, including weak interaction and V-A interaction (*Russian*) 8-62385
 $K^0 \rightarrow 3\pi$, CP violation, book contrib. 8-78173
 NN low energy scatt., parity violating observables weak potentials 8-50045
 $\nu(\bar{\nu})N$ elastic scatt., symmetry relations, current matrix elements 8-54627
 νN interactions, book contrib. 8-78171
 τ lepton, search in neutrino expts., neutrino mixing (*Russian*) 8-54604

elementary particles

see also bosons; charm particles; composite particles; cosmic rays; fermions; gamma-rays; hadrons; hypothetical particles; leptons; mass differences; quantum field theory; strange particles
 review of particle props., leptons, mesons, baryons 8-66179

elements (chemical)

for specific metals and non-metals see appropriate chemical names
see also element origin; element relative abundance; periodic system of elements

covalent elements, cohesion in condensed phases, corrections to simple Huckel approx. 8-59779
 covalent elements, cohesion of σ and π bonds in condensed phases, simple Huckel approx. 8-59778
 critical consts., review 8-59931
 Z=106, atomic and chemical props. by gas chromatography and aqueous chemistry, book contrib. 8-85121
 Ha, (element 105), atomic and chemical props. by gas chromatography and aqueous chemistry, book contrib. 8-85121
 Rf, (element 104), atomic and chemical props. by gas chromatography and aqueous chemistry, book contrib. 8-85121

Eliashberg strong-coupling model *see strong-coupling superconductors*

Elinvar

Fe-B, binary alloys, giant ΔE effect and Elinvar characts. 8-76291

ellipsometers

see also ellipsometry

automated device, performance characts. 8-49885
 automated Fourier-Stokes analyser ellipsometer system for in situ investigations 8-49886
 conference, San Diego, CA, USA (Aug. 1977) 8-54437
 Fourier photoellipsometers and photopolarimeters based on modulated optical rot. 8-54439
 IR laser, for Si epitaxial layers meas., expt. 8-62219
 manual to semiautomatic conversion using inexpensive mech. device 8-89526

ellipsometers continued

modulated light system, for substrate and thin film meas. at 10.6 μm 8-54442
 photometric, drift stabilization and photomultiplier linearization with feedback cct 8-54436
 photometric return path ellipsometers, for isotropic and anisotropic surfaces 8-58009
 photometric system, photomultiplier linearisation and system stabilisation 8-54441
 self-nulling stepping-motor driven ellipsometer, design and performance 8-54440

ellipsometry

see also ellipsometers; polarimetry

anodic film, automated interpretation of ellipsometer obs. 8-56902
 atmosphere, boundary layer turbulence, birefringence, ellipsometric meas. 8-69453
 azimuth response function, linear nondepolarising optical system 8-65957
 conference, San Diego, CA, USA (Aug. 1977) 8-54437
 dielectric thin film, thickness measurements determ. using ellipsometer with nonmonochromatic source (*Russian*) 8-51862
 electrochemical surface layer obs. 8-56874
 epitaxial growth, vapour phase, growth mode characterisation 8-87885
 halfshade analyser using two polariser sheets 8-54434
 interferometer double beam, interferometric determ. of ellipsometric phase shift 8-93757
 palmitic acid monolayer on water, characterisation by multiple wavelength ellipsometry 8-92136
 Raman, coherent, and polarised coherent active Raman spectroscopy (*Russian*) 8-55414
 semiconductor epitaxial film optical constants meas. by far IR ellipsometry 8-93753
 semiconductor process control, dielec. layers meas. 8-49887
 steel, austenitic stainless, passive film meas., optical constants (*Japanese*) 8-85041
 surface anisotropy measurement by ellipsometry 8-56452
 uniaxial film on nonabsorbing substrates, characterisation by multiple wavelength ellipsometry 8-92136
 VPE of III-V ternary layers, on-time comp. determ. 8-67915
 Ag (110), adsorption of O₂ and CO-O₂ interaction, ellipsometry-LEED expts. 8-91542
 AgI film, light-induced changes, ellipsometric meas. 8-56537
 Al₂O₃, composite film, barrier layer, ellipsometric meas. 8-67918
 Fe₂O₃, film, quantitative sputter rates, AES, ellipsometry determ. 8-72661
 Ge, rough surface, polarisation angles, ellipsometric meas. 8-56449
 In₂O₃, elec. conducting film on glass substrate, measurement of optical constants and thickness 8-60525
 KCl IR window material, polish layer effect, ellipsometric meas. 8-55419
 KCl surface, vacuum UV radiation damage, spectroscopic study 8-71758
 Ni plating, surface props. of Ni after each step of activation process 8-95243
 Si, film on Al-Cu, ellipsometric meas. technique, comparison to X-ray fluoresc. anal. 8-51840
 Si, rough surface, polarisation angles, ellipsometric meas. 8-56449
 SiC, ellipsometric exam. of polytypes 8-92044
 Si₃N₄ film, thermal oxidation rate and masking effect against Si oxidation, ellipsometry meas. 8-64749
 SnO₂, elec. conducting film on glass substrate, measurement of optical constants and thickness 8-60525
 W, anodic oxidation, effect of electrostriction, ellipsometry meas. 8-92394
 Zn electrode, passive film form. by chrono-ellipsometry (*Japanese*) 8-68900

elliptical polarisation *see polarisation*

elongation

see also deformation; thermal expansion

butadiene-styrene block copolymer, oriented, isotropic, struct. changes during deformation (*Russian*) 8-88512
 Dacron, vascular substitute, exam. of tensile fracture behaviour 8-77157
 fatigue crack growth, mechanisms 8-64703
 fibres, high-strength and high tensile, equipment for testing elongation 8-56844
 Nimonic 80A, intergranular creep fracture under const. cavity density 8-60825
 nylon-6 fibre, chain rupture and tensile deform. viscosity-av. mol. wt. obs. 8-76714
 polyalkylene terephthalates, amorphous and cryst., durability under stretching (*Russian*) 8-88511
 polyethylene, high-density, effect of fillers and moulding process parameters on strength (*Russian*) 8-60640
 polyethylene, welded, exam. of neutron irradi. effects on tensile characts. (*Japanese*) 8-84918
 polyethylene film, chain rupture and tensile deform., viscosity-av. mol. wt. obs. 8-76714
 polyethylene terephthalate, chain rupture and tensile deform., viscosity-av. mol. wt. obs. 8-76714
 polyethylene terephthalate, mech. props., influence of cryst. arrangement and noncryst. region struct. 8-76707
 polymer, plastoelasticity theory 8-75712
 polymer films and sheets 8-80590
 polymers, mech. props., temp. dependence of polymers of different struct., 4.2 to 300K 8-68746
 polypropylene, film and fibre, chain rupture and tensile deform., viscosity-av. mol. wt. obs. 8-76714
 PVC, amorphous, orientation study by creep thermomechanical method, computer anal. 8-75561
 rubber, natural, stretching effects on glass transition, sp. ht. obs. (*German*) 8-79753
 rubber, peeling initiation and propag. 8-76824
 shaped strip, tension during rolling 8-84890
 steel, 12Kh18N9T-TiB₂, eutectic alloy, high temp. props. 8-84931
 steel, austenitic stainless, 316, surgical implant ion beam textured, stress/strain relations, fatigue characts. 8-73297
 steel, austenitic stainless, Cr-Ni (18.8 wt.%), stress-corrosion cracking 8-85057

elongation continued

- steel, low alloy, type 3sp, effect of temp. at end of rolling on mech. props., and coercive force 8-72799
- steel, maraging, (18 wt.% Ni), solution annealed, exam. of cryogenic tensile, fatigue, and fracture props. 8-92311
- steel, martensitic, high C, Co addition effect on strength (*Korean*) 8-68736
- steel, stainless, even elongation and relative hardening in martensitic, transition and austenitic 8-52926
- steel, stainless, ferritic, subjected to 475°C embrittlement, exam. of fracture toughness 8-84982
- steel, structural, unalloyed, brittle fracture, grain size and precipitate thickness effect 8-60786
- steel, TRIP, powder processing, tensile strength, ductility 8-64499
- steel Cr-V (1.5, 0.5 wt.%), cavitation effect of temp. and C content 8-64638
- Tetron, vascular substitute, exam. of tensile fracture behaviour 8-77157
- Al, alternating bending of single crystals, shear strain accumulation and microstrain distrib. (*Russian*) 8-60706
- Al-Mg alloy AMg6, mech. props. of welded joints, impurity effects 8-95789
- Al-Mn alloys, study of solidification by rapid cooling (*Japanese*) 8-88459
- Al-Zn-Mg, plastic instability rel. to grain boundary failure at low temps. 8-56702
- Co-W-Cr (15.20 wt.%), surgical implant ion beam textured, stress/strain relations, fatigue characts. 8-73297
- Fe-C-Ni-Cr(Cu), dynamically hot pressed, mech. props., additives effect 8-60620
- Fe-Cr-Al-Y (Y-Al₂O₃)(Y₂O₃), preparation and exam. of mech. props. 8-52720
- Fe-Ni-Cr-Ti, superalloy A286, powder, exam. of microstruct. and mech. properties 8-52979
- Fe-Si (3 wt.%), exam. of plastic deformation, slip band dislocation, under hydrostatic pressure 8-56695
- Fe-TiB₂, eutectic alloy, high temp. props. 8-84931
- Fe-W-Cr-Mo-Co with austenitic phase, magnetic and mech. props., cold working and ageing effects (*Japanese*) 8-60678
- Ni₃Al, ductility in poly- and single crystals, compressive and tensile tests 8-56715
- Ti alloys, β -annealing and controlled rate quenching effects 8-80568
- Ti-Al-V (6.4 wt.%), surgical implant ion beam textured, stress/strain relations, fatigue characts. 8-73297
- Ti-TiO₂-ZrO₂-Mo, sintered struct. and mech. props. 8-60618
- Zn, alternating bending of single crystals, shear strain accumulation and microstrain distrib. (*Russian*) 8-60706
- Zn-Al (22 wt.%), meas. of plasticity parameters under superplastic flow 8-60710
- Zn-Al (22 wt.%), superplastic, eutectoid alloy, ductility and fracture 8-60819
- Zr-Al (8.6 wt.%), mech. props., corrosion and fast neutron irradiation influence 8-84948
- Zr-O-N system, struct. and plastic deform. (*Russian*) 8-80588
- Zr-Ru(Pd), heat treated, mech. props. and struct. 8-80571

e.m. waves see *electromagnetic waves*

embrittlement

see also *ductile-brittle transition; hydrogen embrittlement*

- ductile metals in liquid metal environments, embrittlement and brittle fracture, exam. 8-60766
- fracture, intergranular, low temp. mechanism 8-60795
- LMFBR, effect of cracks in fast neutron embrittled hexagonal subassembly ducts 8-74446
- LMFBR materials, exam. of material requirement 8-50256
- metal induced embrittlement of metals, evaluation of embrittlement transport mechanisms 8-52980
- steel, alloy, Fe-Ni-Cr-Sb-C effect of Ni, Sb, on temper embrittlement 8-60813
- steel, alloy, HY130, temper embrittlement due to Si intergranular segregation, effect on H₂ induced cracking 8-76735
- steel, alloy, maraging 250 grade, hot isostatically pressed powder, Ti segregation embrittlement 8-52925
- steel, alloy, Ni-Cr-Mn, type 4340 intergranular brittle fracture, exam. by impact testing and Auger spectroscopy 8-52978
- steel, alloy, Ni-Cr-Mo-V, exam. of temper embrittlement susceptibility 8-76737
- steel, austenitic stainless, temper embrittled, type 304, Auger spectroscopic exam. of grain boundary surface phases 8-76741
- steel, C, tempered martensite embrittlement, and retained austenite, exam. 8-56754
- steel, low C, martensitic, fracture toughness variations during tempering 8-60812
- steel, Ni-Cr, (4.1, wt.%), isothermal embrittlement, AES exam. of grain boundary segregation 8-60814
- steel, Ni-Cr-P (0.06 wt.%), influence of intercritical heat treatment on temper embrittlement susceptibility 8-52863
- steel, stainless, ferritic, subjected to 475°C embrittlement, exam. of fracture toughness 8-84982
- steel, stainless, ferritic and duplex, Mossbauer effect study of 475°C embrittlement 8-52933
- steel, stainless, maraging, high strength, exam. of ageing embrittlement (*Japanese*) 8-84972
- steel, stainless, maraging, type 03Kh11N10M2T2, exam. of thermal embrittlement 8-84986
- steel, stainless, maraging, type 03Kh11N10M2T, exam. of thermal brittleness 8-88526
- steel, temper control progress 8-72797
- steel Ni-Cr, Sb doped, temper embrittlement susceptibility, intercritical heat treatment effect 8-64570
- steel pearlitic, statistical anal. of joint effect of Ni, Cu, P on irradiation embrittlement 8-71770
- temper embrittlement kinetics, ternary and binary alloys, computer simulation 8-84953
- thermoplastics, glassy, embrittlement mech. and inelastic deform. criterion for delayed failure 8-52940
- Zircaloy fuel cladding, O embrittlement obs. 8-89947
- Ag, gas bubble embrittlement mechanism 8-60824
- Al, liquid metal embrittlement by Ga 8-64653
- Al single crystals, effect of environment on liquid-metal embrittlement, stress corrosion cracking and corrosion fatigue 8-64676

embrittlement continued

- Al-Mg-Ti(Zr), struct. and factors determining brittle intermediate compound form. 8-52817
- Al-Pb(Bi)(Cd), containing low melting point inclusions, impact props., temp. depend. 8-60792
- Al-Zn-Mg (6.27, 2.94 wt.%), single crystals, effect of environment on liquid-metal embrittlement, stress corrosion cracking and corrosion fatigue 8-64676
- Fe, Armco, texture role in prestrain embrittlement 8-60796
- Fe, diffusion and solid solubility of Sb, 773-873K, ion backscatt. anal., rel. to intergranular embrittlement 8-71880
- Fe-Cr (26 wt.%) effect of Ni content and austenite phase, on low temp. toughness and embrittlement 8-60754
- Fe-Mn (8 wt.%), quenched, exam. of intergranular embrittlement 8-76745
- Fe-Ni (3 wt.%), grain boundary segregation of Sn and P embrittling additions, STEM microanal. 8-76654
- Fe-Ni (3 wt.%), influence of temper embrittlement, on stress corrosion susceptibility 8-85023
- Fe-Ni base metallic glass, annealing embrittlement 8-64635
- Fe₄₀Ni₄₀B₂₀, amorphous alloy, ductile-brittle transition temp., relation to composition 8-52972
- Fe₄₀Ni₄₀B₂₀, metallic glass, embrittlement kinetics and crystn., quenching influence 8-68766
- Fe₄₀Ni₄₀P₂₀, amorphous alloy, ductile-brittle transition temp., relation to composition 8-52972
- Fe₄₀Ni₄₀P₁₄B₆, amorphous alloy, ductile-brittle transition temp., relation to composition 8-52972
- Ti-Al-Sn-Cu-Zn, (5, 2.5, 3, 1.5 wt.%), embrittlement after high temperature long-time exposure (*Chinese*) 8-95792
- α Ti-Al-(Zr), embrittlement due to ageing 8-56673
- U-Mo (10 wt.%), gaseous O₂ and hydrogen embrittlement, exam. 8-60811
- Zn, liquid metal embrittlement 8-64653

e.m.c. see *electromagnetic compatibility*

e.m.f. see *electric potential*

emission nebulae see *nebulae*

emission spectra see *spectra*

emissivity

see also *brightness*

- angular and overall emissivities for halfspace geometry, variational procedure 8-87245
- atmospheric radiative flux, IR cooling rates, study of dust layer regions 8-88886
- 'blackbody' IR sources 8-83059
- blackbody spectrum, interpretation of quantum theory, for teaching 8-54130
- butane, total emissivity, press. depend. 8-90673
- chalcogenide glass, radiative emission during threshold ON-state 8-76119
- diatomic gases, emissivities calc. 8-90675
- Earth IR emission, Lambertian, of spherical surface, radiation press. on satellite (*French*) 8-81529
- metal, interference phenomena and integral emittance, during high temp. oxidation (*Russian*) 8-91458
- meteors, luminous efficiency coeff. from photographic obs. 8-96440
- nebulae, dusty, emissivities of non on-the-spot (OTS) models 8-85995
- ocean surface, microwave thermal radiation and radiometry appls. 8-81415
- p-n junctions, determ. of doping levels using nondestructive IR emission meas. 8-95338
- particles, small, spherical, reformulation of radiation laws 8-87246
- propane, total emissivity, press. depend. 8-90673
- randomly inhomogeneous stratified media, thermal radiation calc., appl. to Earth surface (*Russian*) 8-96312
- solid, calorimetric method for emissivity determ. 8-62201
- sputtered metal silicide solar selective absorbing surfaces 8-52671
- steam, total emissivity, press. depend. 8-90673
- steel, stainless, hard, and mild, optical constant dispersion and emissivity, up to 900K 8-52464
- steel stainless, solar energy collector optical props. rel. to heat treatment 8-94455
- Stefan's law, W filament elec. lamp, student expt. 8-54125
- CeO₂-Mo-CeO₂ thin-film selective coatings for solar energy collectors 8-94422
- Fe, optical constant dispersion and emissivity, up to 900K 8-52464
- KBr(l), oscillatory and diffusive regime, above and below melting point, IR thermal emission spectra 8-83985
- N₂-propane mixture, total emissivity, press. depend. 8-90673
- Ni dendrites on Al, CVD, selective solar photothermal absorber 8-52683
- NaCl(Br), oscillatory and diffusive regime, above and below melting point, IR thermal emission spectra 8-83985
- Re, specific heat, elec. cond., emissivity, 1600-2400K 8-67835
- Si amorphous sputtered film, solar energy selective absorber, spectral emissivity 8-83045
- SiO₂-Mo-SiO₂ thin-film selective coatings for solar energy collectors 8-94422
- Ti, melting point, normal spectral emittance and elec. resistivity, pulse heating method 8-91423
- Ti-Al-V alloy, thermophysical meas. above 1450K, using subsecond transient technique 8-95161
- ZrC, stoichiometric, emissivity, integral hemispherical and monochromatic, N₂ content effect 8-91457

emitters see *television camera tubes*

employees see *personnel*

employment

see also *personnel*

- career changes from physics, at Ph.D. level 8-62045
- career opportunities for physicists, changes, role of American Physics Society 8-62046
- career opportunities for physicists, discussion 8-61966
- career patterns of post 1970's USA physicists 8-62037
- dynamics of funding, enrollments, curriculum and employment 8-65746
- graduate PhD student subfield choice and employment prospects 8-65747
- life in a multidisciplinary government laboratory 8-62043

employment continued

- manpower studies relating to college physics teaching in the midwest 8-62059
- non-PhD physicists, USA employment survey 8-62035
- nonacademic physics employment, survey of employee attitudes 8-62056
- physicists, career development 8-62044
- physics, education and employment, situation and prospects 8-61963
- physics, human resources and career opportunities 8-61962
- physics careers, employment and education, conf., Pennsylvania, USA (Aug. 1977) 8-62034
- physics careers at Westinghouse Research 8-62041
- physics education versus job training 8-61965
- Physics Manpower Panel of American Physical Society, employment and education trends 8-65735
- post-doctoral appointments, tenure and multiple appointments 8-61964
- prospects for would be PhD physicists 8-62040
- science career facilitation project in energy-related fields 8-61959
- supply and demand for PhD physicists, 1975 to 1986 projection 8-62038
- unconventional jobs in unconventional companies 8-62042

emulsions

- see also nuclear track emulsions; photographic emulsions
- flotation of fine particles by group of bubbles, kinetics 8-53261
- inorganic emulsions, hydrophile lipophile balance temperature 8-55961
- inverse-type, coalescence of drops in uniform elec. field 8-53265
- methacrylic acid-methyl methacrylate statistical copolymer suspension, polymerisation, stabilisation effects, viscosity 8-55157
- microemulsion, viscosity meas. (French) 8-60155
- microemulsion structural changes, light scatt. obs. 8-56920
- microemulsions, stability, thermodynamic approach 8-95959
- microemulsions, thermodynamic stability, theory 8-85203
- microemulsions, thermodynamic stability 8-95962
- microemulsions of micelles, interpretation of second virial coeff. of osmotic press. (French) 8-64891
- nonpolar electrolyte, on anode, ion attachment and ion emission 8-65998
- oil in water microemulsion, added NaCl, light beating spectroscopy of micelles mutual diffusion coefficient 8-80793
- poly(vinyl alcohol)-based membranes for haemodialysis (Japanese) 8-96115
- polymerisation, particle size calc., applicability of Gardon's eqns. 8-92479
- PVC composite, MBS type multifunctional impact modifier effect on mech. and rheological props. (Polish) 8-52751
- stability, interfacial phenomena interpretation using schematic density profiles 8-66012
- tissue dispersions, unglycerinated, freeze-etching by appl. of oil emulsion technique 8-53594
- water, supercooled emulsified droplets, relative permitt. and cond., Maxwell-Wagner interfacial polarisation 8-52423
- water-in-hexadecane, microemulsion, dielectric behaviour, Cole-Cole type relax., temp. depend. 8-56426
- AgBr-Ag light sensitive system, diffusion of excited states (Russian) 8-59101
- Al-In emulsion, solidification mechanisms at zero gravity, review 8-88458
- hydrocarbon-water, emulsions, superheated, bubble nucleation 8-61056
- KCl aqueous solution emulsions, complex permittivity meas., dielec. relax. 8-72459

emulsions (nuclear track) see nuclear track emulsions

emulsoids see emulsions

encapsulation

- see also packaging
- GaAs, anodic oxide film, annealing effect on carrier density profile 8-88040
- GaAs:Se, implanted, annealing with O-free CVD Si_3N_4 encapsulant 8-83834

encoding

- see also codes; decoding
- drift chamber counter, missed counts and registration efficiency calc. 8-78594
- hodoscopic detector registration systems, data coding/reading block 8-78602
- image coding with far-field holograms 8-90389
- image processing, two dimensional unitary transforms appl. 8-58928
- line scan sensor, spatial and temporal coding of GaAs laser 8-83022
- matched filters, using optical delay line provide encoding or decoding structures 8-74983
- monochrome picture signal, digitally coded, level reassignment technique 8-55307
- nerve cell impulse flows, determ. of quantity of useful information 8-69038
- optical coding and decoding operations, parallel image transmission by single fibre 8-71216
- optical coding method, scene analysis 8-82924
- optical pseudocolour encoding of spatial frequency information 8-87018
- patterned optical filters for solid-state imager spectral encoding 8-66945
- PCM telemetry systems, air pollution detection/control appl. (German) 8-93003
- pseudocolour encoding, of holographic imaging, new technique 8-78963
- pseudocolour encoding of holographic images using single wavelength 8-87025
- radio time signal coding and clocks for private and industrial use (German) 8-89445
- repetitive photoelec. scanning system for high resolution optical spectra accumulation 8-54456
- space-frequency conversions for image transmission and processing 8-71046
- space-variant holographic systems using phase-coded reference beams 8-74868
- US time-coordinate convertors for distance meas., design aspects (Russian) 8-77857
- Vibroscis system, encoding techniques 8-69474

ENDOR

- alkoxy free radicals, produced by X-irrad. of hydroxy containing cpds., characterisation by ESR and ENDOR 8-95938
- bacteria, photosynthesis, primary electron acceptor, EPR, ENDOR investigs. 8-77004
- bacteriochlorophyll cation in soln., N atom ENDOR and proton triple resonance 8-96018
- benzophenone, triplet, optically detected EPR, ENDOR and ODMR, HFS, isotope and spin-orbit effects 8-86898
- creatine monohydrate, single cryst., radiation damage, ENDOR obs. 8-96016
- dicarboxylic acids, D quadrupole coupling constants, ENDOR study 8-90195
- hydroxyproline HCl, X-irrad., free radical products, ENDOR meas. 8-76883
- inositol, X-irrad., deuteration effects, ENDOR and ESR meas. 8-73067
- 4-methyl-2,6-di-tert-butylphenol, γ -irrad. cryst., ENDOR transitions, ELDOR detect. 8-95531
- microwave cavity for electrons spin-echo experiments 8-82013
- microwave preamplifier for ESR/ENDOR spectrometer sensitivity enhancement 8-82014
- phenoxyl type radical, ^1H and ^{13}C ENDOR studies in soln. 8-94266
- Si:Sb(P)(As) , shallow donor states with strong central cell perturbation theory 8-51933
- strong saturation of NMR of adjacent nuclei, influence on ESR 8-60356
- Wonderstone ENDOR cavity 8-70174
- BaClF , two types of F-centres, identification by ENDOR 8-60355
- Be_2SiO_4 , EPR and ENDOR 8-76295
- ^{13}C -labelled organic radicals, ^{13}C - and proton-ENDOR in soln. 8-55190
- $\text{CaF}_2:\text{Gd}^{3+}$, ligand ENDOR cubic centres, elec. field effect (Russian) 8-60357
- $\text{CaF}_2:\text{Gd}^{3+}$, S-state splitting, investigation by ESR and ENDOR at high pressure 8-52345
- $\text{CeO}_2:\text{Yb}^{3+}$, evidence for covalency 8-80247
- GaP:S , ENDOR meas., symmetries, hyperfine parameters 8-72435
- KBr(Cl) , $\text{F}_2(\text{Li})$ -centre spin-lattice relax. at 4.2K 8-91950
- KCl:Ca,H , studies of localised vibrations of substitutional atomic H 8-80248
- $\text{La}_2\text{Mg}_3(\text{NO}_3)_{12}\cdot 24\text{H}_2\text{O}:\text{Mn}^{2+}$, linear electric field effect on ground state splitting, EPR 8-80198
- $\text{La}_2\text{Mg}_3(\text{NO}_3)_{12}\cdot 24\text{H}_2\text{O}:\text{Co}^{2+}$, Ce^{3+} , relax. and ESR in magnetically cooled systems 8-88225
- $\text{NH}_4\text{H}_2\text{AsO}_4:\text{Cr}^{3+}$, ENDOR spectra 8-88224
- RbCl:Ca,H , studies of localised vibrations of substitutional atomic H 8-80248
- Si, deformed, ENDOR of dislocation centre 8-72434
- Si:Sb(P)(As) , shallow donor electrons, hyperfine interactions, reply to Onfroy's calcs. 8-51934

energies, molecular dissociation see molecular dissociation energies

energy, binding see binding energy

energy, lattice see lattice energy

energy, surface see surface energy

energy bands see band structure

energy bands, electron see band structure

energy control see power control

energy conversion, direct see direct energy conversion

energy gap

see also superconducting energy gap

- adsorption rel. to dopant admixture 8-95596
- Al (001) surface, nearly-free-electron metal, origin of surface reson. states 8-95322
- alkali metal salts with aromatic hydrocarbons, photoelectron emission and optical absorption (Russian) 8-80456
- amorphous solid, abnormal bonding and electronic states in forbidden energy gap 8-51942
- anthracene, solid, electronic struct., comparative ESCA study of polyacenes 8-52631
- benzene, solid, electronic struct., comparative ESCA study of polyacenes 8-52631
- binary crystals, stability and average structure factors 8-91297
- chalcogenide lone-pair semicond. charged impurities, effect on carrier concs., Street-Mott model 8-67984
- diamond, covalent semicond., depend. of energy gap on short-range order 8-84142
- electronic structure of solids under laser irradiation 8-91614
- GaP, reevaluation of bandgap and free exciton binding energy 8-60061
- glasses and amorphous semiconductors, band struct. and forbidden gap, review 8-75987
- III-V quaternary alloys, energy bandgap and lattice const. 8-67940
- insulator, rel. to secondary electron escape probabilities 8-72651
- metal-semiconductor interface, Schottky barrier formation, microscopic model 8-52087
- metal-semiconductor junction photoelec. phenomena, effect of dielectric gap and surface states (Russian) 8-84299
- naphthalene, solid, electronic struct., comparative ESCA study of polyacenes 8-52631
- nearly free electron model, vertex corrections 8-72054
- polyenes, model results for π electrons 8-55128
- PTFE film electret, optical spectra, band theory interpretation (Russian) 8-88376
- quasilocal acceptor states, effects on band gap and electron mobility (Russian) 8-60082
- Schottky-barrier diode wavelength-modulated photoresponse spectra (Russian) 8-84300
- sputtered films, optical props. and appls. 8-72623
- TCNQ salt, $(\text{NMP})_x(\text{Phen})_{1-x}(\text{TCNQ})$, band filling and disorder 8-87968
- tetracene, noncryst., localised valence states in forbidden gap 8-72113
- tetracene, solid, electronic struct., comparative ESCA study of polyacenes 8-52631
- Ag-Te-AgS system, elec. and thermal props. at 300K 8-64044
- AlAs-GaAs monolayer crystal, two-photon absorpt. spectrum 8-52589
- $\text{Al}_2\text{Ge}_{1-x}\text{Sb}_x$, photolum. spectra 8-95602
- AIN, VPE by closed space vapour process, and optical absorpt. edge 8-88371

energy gap continued

- BN, cubic, energy band and piezoelec. calcs. 8-72071
 Bi, band structure model parameters, deformation theory (Russian) 8-56067
 Bi₂O₃ film, optical energy gap, transmission spectra obs. 8-76440
 CC NiO, amorphous, charge transport in band tails 8-76026
 Cd₆Ge₃As₁₁, press. depend. 8-72064
 Cd_{1-x}Hg_xTe, gap width temp. depend., absorpt. band edge meas. 8-72521
 Cd_{1-x}Hg_xTe, temp. shift of energy gap, contrib. of lattice dilatation 8-51892
 CrAl, semicond. solid solns., depend. on antiferromag. ordering 8-67941
 Cr_{1-x}Mn_xSi₂, semicond. props. 8-79992
 CrSi₂, semicond. props. 8-79992
 CuGaSe₂, temp. depend. of fundamental absorpt. edge 8-92090
 CuInS₂(Se₂) film, vacuum deposited, absorpt. coeff. 8-72621
 GaAs, electron-hole plasma, ground state energy 8-84244
 Ga_{1-x}In_xP:N, Delta lattice parameter model, correl. with electronic props. 8-91560
 Ga_{1-x}In_xSb, LPE on GaSb by stepwise grading, and characterisation 8-72745
 GaP:Cu, thermally and optical excited cond., deep level centres 8-72190
 GaSb, electron-hole plasma, ground state energy 8-84244
 n-GaSb:Te(Se), forbidden optical band gap, Moss-Burstein effect 8-88335
 N-Ge, pressure influence on photoconductivity temp. dependence 8-76109
 N-InAs, Moss-Burstein effect, S, Sn, Te dopants 8-64389
 (InAs)_{1-x}(CdTe)_x, band gap and effective mass, IR spectra obs. 8-56491
 In_{1-x}Ga_xP-GaAs heterojunction, VPE, energy band gap and lattice parameter, lattice mismatch effects 8-95345
 InP, electron-hole plasma, ground state energy 8-84244
 InP, reson. Raman scatt., deformation pots. 8-52495
 LiN₃, evidence for N₃⁻ from static and dynamic props. 8-60465
 Mg₂Zn_{1-x}Te, high purity, luminesc. and band gap 8-68553
 Nd₂O₃, A-type, thermoelectric power, AC cond. 8-68044
 Pb_{1-x}Sn_xTe, absorption edge shift, energy gap determ. 8-88308
 Pb_{1-x}Sn_xTe, band struct. and phonon energies, tunnelling spectroscopy 8-72070
 Se-based chalcogenide glasses, band gap variation 8-90461
 Si film, amorphous, effects of annealing of gap states 8-72115
 Si:O, O rich polycryst. film, carrier transport 8-80076
 Si-H, amorphous, energy gap negative-U states, Si-H-Si three centre bond model 8-91606
 Si₃N₄, amorphous, charge transport in band tails 8-76026
 SiO₂, thermally grown film, optical absorption and photocond. 8-64421
 Sn₂P₂S₆, ferroelec., IR and Raman spectra, photocond., edge absorpt. spectra, spontaneous polarisation, forbidden gap 8-68514
 Sn_{1-x}Pb_xTe, elec. and struct. props. of epitaxial layers (Russian) 8-64147
 SrTiO₃, optical absorpt. edge, absorption coeff., reflectivity, 293-853K 8-64342
 TiO₂, UPS meas. of band struct., energy gap 8-72698
 TiGaS₂(Se₂) film, elec. and photoelec. props. (Russian) 8-52109
 UO₂, optical props. and electronic struct. 8-68527
 Zn_{1-x}Cd_xS film, prep. by soln. spray method, and struct., optical and elec. props. 8-52666
 ZnS_{1-x}Se_x, comp. depend., exciton refl. spectrum obs. 8-56071

energy gap, superconducting see superconducting energy gap**energy level crossing**

see also Hanle effect

- anharmonic oscillators, quantum theory, independent to spherically coupled, level crossing 8-77747
 anticrossing effect, levels with different widths 8-55145
 aromatic molecules in cryst. lattice, phosphoresc. intensity and optical nuclear polarisation, level anticrossing effects 8-91992
 atomic spectroscopy, appl. of terms level-crossing and line-crossing 8-70799
 4,4'-dibromodiphenylether:benzophenone-d₁₀, optical decay constants, photoexcited triplet state near level anticrossing field 8-80250
 gas laser, atomic constants and collision cross sections determ. by level crossing 8-50763
 harmonic oscillator model in predissoc., level widths, shifts and curve crossing 8-90239
 laser excitation (Rumanian) 8-50510
 molecular pot. energy curves, non non-crossings, comment 8-78770
 palladiumporphyrin, in n-alkane, S₁←S₀ absorpt. spectrum, vibronic coupling and avoided crossing, field splitting 8-84613
 xanthione, optically detected mag. reson. study of lowest excited triplet state of aromatic thioketones 8-86901
⁴He(3P), fine struct., level crossing obs. 8-82686
 CO₂, anomalous energy minima surfaces 8-86791
³⁵Cr, ⁷P states HFS, level crossing technique, core polarisation, spin orbit interaction, config. mixing 8-78668
 H₂, singlet-triplet anticrossings, doubly excited 3¹K-g(3d)³Σ_g⁺ states 8-50598
⁷Li, HFS and at. lifetimes 8-66678
²¹Ne, 2p³3p config., hyperfine mag. const. by laser level-crossing technique 8-50509
 O₂, harmonic oscillator model in predissoc., level widths, shifts and curve crossing 8-90239

energy level transitions, atomic see atomic spectra**energy level transitions, molecular** see molecular spectra**energy level transitions, nuclear** see nuclear energy level transitions**energy levels** see energy states**energy levels, atomic** see atomic structure**energy levels, molecular** see molecular energy levels**energy levels, nuclear** see nuclear energy levels**energy levels in solids and liquids** see electron energy states (condensed matter)**energy loss of particles**

see also channelling; electron energy loss spectra; radiation effects

α-particle in air, range, energy and range straggling, stopping power meas. 8-73815

energy loss of particles continued

- acetaldehyde, gas, stopping cross section for 0.3 to 2.0 MeV He⁺ ions 8-63537
 aldehydes, molecular stopping cross section of He⁺ ions and atomic stopping cross section of O 8-67746
 alpha-particles, stopping power and straggling in liq. N₂ semicond. detect. spectrometer 8-82565
 atom-electron collisions, stopping cross section (Russian) 8-55990
 atomic collisions in solids, book contrib. 8-78957
 Bethe theory, inelastic collisions of fast charged particles 8-56793
 bremsstrahlung, ang. distrib. of nonrelativistic intensity calcs., program 8-87001
 bremsstrahlung distrib. in water, Al, Fe and Pb, 22 MeV electron bombardment 8-59540
 bremsstrahlung in bulk media, shielding study, Monte Carlo anal. of thick target spectra 8-59839
 bremsstrahlung radiation, ang. distrib. and penetrating power 8-78657
 1,3-butadienes, methyl substituted, singlet-triplet transitions, energies, relative cross-sections, He⁺(H₂⁺) impact spectra 8-86942
 channelled ions, effect of screw dislocations 8-67781
 charged particle activation anal., are energy in ave. stopping power method 8-76965
 charged particle chemical analysis, two reactions method 8-76664
 charged particle telescope TOF system, elemental assignments of reaction products 8-86720
 Cherenkov radiation from electrons in mica target, 140-250 keV (Russian) 8-55291
 coherent bremsstrahlung from polarised electrons, asymmetry coeff. (Russian) 8-92139
 convoy electrons from solids, ion vel. and Z and target material depend. 8-84692
 cosmic ray nuclei in nuclear emulsion, appl. of energy loss params. on mass determ. 8-94175
 dielectric trapping, bremsstrahlung shielding meas. 8-78507
 DSA study of ²⁸Si lifetimes in selected materials, theoretical stopping power predictions 8-74329
 effective charge theory and electronic stopping power of solids 8-67759
 electron beam lithography, energy loss calcs., Bethe and Spencer-Fano theories 8-87728
 electron gas, energy loss of correlated charges 8-87729
 electron probe into solid target, diffusion model energy depend. 8-71652
 electron transport in air and N₂, Monte Carlo calcs. 8-90062
 energy loss and angular spread, review 8-71778
 epoxides, atomic stopping cross section of O 8-67746
 ethylene, stopping cross-sections using alpha particles in energy range 1.5 to 4.2 MeV 8-53510
 ethylene oxide, stopping cross section for 0.3 to 2.0 MeV He⁺ ions 8-63537
 fast channelled particles with low charge, energy loss calcs. 8-55890
 foil, energy loss and straggling of proton and He⁺ ions 8-95100
 gamma-rays generation by fast electrons travelling through antiferroelectric or antiferromagnetic crystalline structures 8-76545
 hadronic transmission through Fe absorbers, 0.8 to 100 GeV calcs. 8-90041
 heavy charged particle penetration phenomena 8-71779
 heavy ion impact on C foil, energy loss 8-55902
 heavy protons, energy-range relns., use in detection 8-58566
 heavy quarks, energy-range relns., use in detection 8-58566
 heterogeneous medium, ion implantation and energy deposition, path length approx. 8-87694
 inert gas ion+oxides, energy loss spectra 8-58798
 ionizing radiation and cavitation threshold 8-94774
 IR spectroscopy appl. to charged part. dose meas. in cellulose triacetate 8-94145
 ketones, molecular stopping cross section of He⁺ ions and atomic stopping cross section of O 8-67746
 Lenz-Jensen pot. calc. using third order approx. 8-95099
 mesonic particles, Coulomb capture in inhomogeneous matter 8-55116
 metals, stopping power for 28 MeV α-particles, re-evaluation, Be, Al, Ti, V, Fe, Co, Ni, Cu, Mo, Rh, Ag, Ta, Au 8-79651
 methane+Ne ion, nuclear stopping power and interatomic potentials 8-74549
 methylpentanes, electron mobilities and penetration ranges in liq. and crit. regions 8-72220
 multiple scatt. of particle beams, axial mag. field effect 8-70712
 multiple scattering of charged particles in thin layer, Monte Carlo method, ang. deflection 8-79650
 negative mesons, capture fractions conc. depend. 8-78600
 nonstationary distribution functions calc. 8-86758
 nuclear filters, prep. from polymers using Ar ions 8-86714
 nuclear stopping power and interatomic potentials 8-74549
 pion⁺ beam stopping distrib. determ. by charge collector 8-53513
 planar channelling of α-particles, stopping power of solids 8-51602
 plasma electrons, stopping power, quantum diffraction effects 8-91064
 polarised ferromagnetic media, decelerating ion, transient field phenomena 8-72445
 polycarbonate thin film, determ. of fission barrier in region Z=82, N=126, using electron linear accelerators 8-55104
 polyethylene, stopping cross-sections using alpha particles in energy range 1.5 to 4.2 MeV 8-53510
 polystyrene, stopping power for 2.2 to 5.9 MeV protons 8-90040
 projectile charge dependence of stopping power 8-79655
 proportional counter, energy loss of relativistic electrons and its fluctuation 8-94171
 propylene oxide, stopping cross section for 0.3 to 2.0 MeV He⁺ ions 8-63537
 proton stopping cross-section within wide energy range, semiempirical formula (Russian) 8-67763
 radiative damping effect for ultrarelativistic channelled particles 8-67758
 recoil range distrib. of heavy mass products in deep inelastic reacts., with Au and U targets 8-66309
 semiconductor-metal structure, electron bombarded, energy dissipation 8-87732
 solid, depth profiling of ³He ion implantation 8-59830
 stable law with index α=1 in fluctuations of ionisation loss of energy of charged particles (Russian) 8-62682
 stopping cross-sections, for nucl. energy level lifetimes 8-70725

energy loss of particles continued

- stopping power for low energy heavy charged particles, similarity treatment of phase effects 8-50447
 stopping-power formula, fast heavy ions 8-59846
 superheated supercond. colloid as a total absorption detector preliminary calcs. 8-78579
 surface chemical analysis, low energy ISS compared with SIMS 8-64908
 thick-target thick catcher nucl. recoil expts., anal. 8-55115
 thin sample, structural change obs. by transmitted fission fragment energy 8-83853
 tissue-equivalent gas, energy loss of H, C, N and O ions for elastic nuclear collisions 8-86759
 vinyl methyl ether, stopping cross section for 0.3 to 2.0 MeV He⁺ ions 8-63537
 Ag, projectile range for Z=8-20, 0.0125-12.0 MeV/nucleon 8-83856
 Ag, stopping power meas. for 4-5 MeV/N ¹⁶O, ⁴⁰Ar, ⁶⁵Cu, and ⁸⁴Kr 8-70720
 Al, heavy ion ranges, He⁺ backscatt. obs. 8-63796
 Al, ranges of implanted 10-30 keV D⁺ 8-83858
 Al, stopping power meas. for 4-5 MeV/N ¹⁶O, ⁴⁰Ar, ⁶⁵Cu, and ⁸⁴Kr 8-70720
 Ar, nuclear emulsion track width by photometric meas. 8-94167
 Au, electron beam energy losses 8-91368
 Au, projectile range for Z=8-20, 0.0125-12.0 MeV/nucleon 8-83856
 Au, stopping power meas. for 4-5 MeV/N ¹⁶O, ⁴⁰Ar, ⁶⁵Cu, and ⁸⁴Kr 8-70720
 C, amorphous, ranges of implanted 10-30 keV D⁺ 8-83858
 C, energy loss of fast H₂⁺ ions 8-79653
 C, stopping power meas. for 4-5 MeV/N ¹⁶O, ⁴⁰Ar, ⁶⁵Cu, and ⁸⁴Kr 8-70720
²⁵²Cf, spontaneous fission, fragment ranges and kinetic energies in Al 8-94037
 Cl ions+Ar-methane, (isobutane), energy straggling 8-58785
 Cu, electron transmission and absorption, 70 keV initial energy 8-71777
 Cu, energy straggling of 6.74 MeV protons 8-79641
 Cu, projectile range for Z=8-20, 0.0125-12.0 MeV/nucleon 8-83856
 Fe, neutron ns. slowing down time, expt. obs. 8-58319
 Fe, projectile range for Z=8-20, 0.0125-12.0 MeV/nucleon 8-83856
⁵⁶Fe ions relativistic nuclei stopping power, Bethe theory higher order corrections 8-78599
 Ge, stopping power for fast channelled α -particles 8-79654
 H₂⁺, fast ions, stopping power of carbon foils 8-79653
 H₂⁺, fast ions, thin solids 8-79652
 He ion stopping powers and ranges in all elements 8-58565
³He profiling, depth resolution using ³He(d, α)¹H reaction 8-58557
⁴He stopping cross sections, 1-8.5 MeV, in H₂, He, N₂, O₂, Ne, Kr, and Xe 8-58558
 In₂Te₃ type semiconductors, basis of ionising radiation detectors 8-86743
 LiF, neutron ns. slowing down time, expt. obs. 8-58319
 Mn, stopping power of 0.5-2.0 MeV ⁴He ions, elastic backscatt. meas. 8-87730
 N₂, energy loss of H, C, N and O ions for elastic nuclear collisions 8-86759
¹⁵N 6.5 MeV ions in solids, energy loss distrib. meas. 8-59845
 Ne, nuclear emulsion track width by photometric meas. 8-94167
 Ni, projectile range for Z=8-20, 0.0125-12.0 MeV/nucleon 8-83856
 Ni, ranges of implanted 10-30 keV D⁺ 8-83858
 Ni, stopping power meas. for 4-5 MeV/N ¹⁶O, ⁴⁰Ar, ⁶⁵Cu, and ⁸⁴Kr 8-70720
 Ni, stopping power of 0.5-2.0 MeV ⁴He ions, elastic backscatt. meas. 8-87730
 Ni:K⁺(Ba⁺), ion implantation, effect on inelastic refl. and energy losses of fast primary electrons 8-55900
¹⁶O⁺⁺+Al, energy-loss straggling, charge exchange effects 8-58799
 Si, amorphous, heavy ion ranges, He⁺ backscatt. obs. 8-63796
 Si, channelled and random proton stopping power, 30-1000 keV 8-67760
 Si thin detector, ionisation energy loss of relativistic electrons 8-55117
 Si+C ion, nuclear stopping power and interatomic potentials 8-74549
 Ti, projectile range for Z=8-20, 0.0125-12.0 MeV/nucleon 8-83856
 Ti, stopping power of 0.5-2.0 MeV ⁴He ions, elastic backscatt. meas. 8-87730
 UO₂ film, vacuum evaporated, He⁺ ion energy loss parameter 8-50253
²³⁵U, fission recoils, chem. effects, energy deposition efficiencies, surface conditions depend. 8-80776
 Zn, stopping power of 0.5-2.0 MeV ⁴He ions, elastic backscatt. meas. 8-87730
 Zr, ranges of implanted 10-30 keV D⁺ 8-83858

energy measurement *see power measurement***energy-range relations** *see energy loss of particles***energy resources**

- see also fuel; solar energy concentrators; solar power; wind power*
 coal and hydrocarbons, exploration via refl. seismology, book 8-96162
 coal gasification and liquefaction 8-53012
 development and technology, surface science rel. problem areas 8-88553
 development role of Sandia Laboratories' photometrics division 8-58077
 education, alternative energy sources, solar and atmospheric 8-69951
 education, conservation effects on resource usage, integral expressions 8-69941
 energy modelling and forecasting at US ERDA 8-49629
 French plan VII, energy forecasting 8-49628
 fusion technology progress 8-62607
 geothermal energy, heat extraction from hot dry rock masses 8-61378
 geothermal research in Netherlands (*Dutch*) 8-61415
 materials problems and basic research needs 8-86703
 ocean thermal energy, HNO₃ cycle process for extraction 8-53660
 rate of consumption, exponential growth 8-86049
 review, worldwide variation of energy production, future Hungarian energy requirements (*Hungarian*) 8-70580
 review of energy resources, reactor accidents, radioactive waste disposal 8-50413
 solar energy availability estimation 8-81344
 solar intensity obs., global insolation on horizontal and tilted surfaces 8-81275

energy resources continued

- tides as alternative energy sources, appraisal 8-86091
 unconventional energy systems, exam. of material requirements 8-50255
 wave energy convertor array power available 8-81216
 wind power potential estimation using power laws 8-92912
 U resources, consumption and 30 year fuel commitments for Canada and the world, 1975-2025 8-82456
 U supply, Canada's role 8-86627

energy states

- see also atomic structure; electron energy states (condensed matter); energy level crossing; molecular energy levels; nuclear energy levels; population inversion*
 education, quantum mechanics, spherically symmetric pots., ladder operators, energy levels and degeneracy 8-62013
 Fermi gas, slightly non-ideal one-dimens., spectral ground state, energy determ. method (*Russian*) 8-62149
 flat rotator in field of circularly polarised wave, quasienergy states 8-54596
 loss energy states of nonstationary quantum systems 8-49719
 oscillator in coherent state, quantum nondemolition meas. 8-54228
 tensor virial theorem, quantum mechanical generalisation for Born-Oppenheimer approx., atoms, mol. 8-86182
 weak external gauge fields, energy levels, modified functional measure 8-49973

energy states in solids and liquids *see electron energy states (condensed matter)***energy storage**

- see also capacitor storage; direct energy conversion; energy storage devices*
 fusion reactor, ohmic heating energy storage for power reactor, costing 8-58495
 fusion reactor, T-10M Tokamak, normal and supercond. inductive energy storage and switching 8-55018
 fusion reactor, TEXT, pulsed homopolar generator power supply, engineering and design 8-55016
 fusion reactor, Tokamak, commercial, plasma driving system requirements 8-54954
 fusion reactor inductive storage technology, new applications, review 8-55019
 materials problems and basic research needs 8-86703
 micellar system, photoinduced redox processes kinetics, intracellular electron transfer 8-92603
 oceans, heat storage rel. to Earth global heat balance annual var. 8-73300
 pulsed power conversion with inductive storage 8-55029
 supercritical liquid air storage plant for elec. energy 8-74006
 thermal regenerator, periodic flow type, transient performance 8-59389
 Tokamak reactor cycles 8-62661
 transfer from low voltage capacitor bank to high inductance with air pulse transformer 8-49860
 unconventional energy systems, exam. of material requirements 8-50255
 unit helium requirements for superconductive energy applications in the USA 8-89999
 CO₂, electrochem. reduction for use in energy storage 8-92490

energy storage devices

- Argonne National Laboratory energy storage and transfer program 8-55031
 flywheel energy storage system for JT-60 toroidal field coil 8-62662
 fusion reactor, Shiva Faraday rot. coils, circuit and mag. anal. 8-54951
 fusion reactor, use of homopolar generator for inductive energy storage 8-54948
 high energy gas laser facility, energy storage system design 8-55030
 homopolar machine with superconducting field coils, design and appl. 8-54927
 inductive, two-stage opening switch technique, for high inductive voltage generation 8-55034
 inductive storage systems motor-generator sets, voltage protection scheme 8-55037
 inductor for high power impulse production, features (*German*) 8-50293
 pulsed, DC vacuum interrupter, tests 8-74489
 Tokamak, Texas exptl., homopolar generator, eddy currents, EM forces (torques), due to misalignment 8-54953
 Tokamak energy storage superconducting solenoids 8-66369

energy transfer collisions, molecular *see molecular inelastic collisions***engineering applications of computing** *see engineering computing***engineering computing**

- see also aerospace computing; civil engineering computing; communications computing; control engineering computing; electrical engineering computing; electronic engineering computing; mechanical engineering computing; nuclear engineering computing*
 applications of finite-element and finite-difference methods 8-57765
 axially symmetric hollow collectors for high temp. solar installations, radiative heat transfer computation 8-79093
 lens design optimisation, Version 14 program 8-90488
 lens system design with extended depth of focus, Version 14 optimisation program 8-90489
 OTF calculation using gaussian quadrature, rel. to lens system design 8-90383
 steam pressure and temp. in relation to enthalpy and entropy (*German*) 8-59532
 zoom lens design by pocket calculator 8-55423

engineering societies *see societies***entertainment** *see sports and entertainment***enthalpy***see also heat of*

- 3,4-benzo-1,6-methano(10)-annulene, mol. geom. and gas phase thermodynamic props., minimisation scheme 8-78829
 brass, vacancy form. enthalpy, determ. from threshold temp. for positron trapping in vacancies 8-80433
 calorimetric probes for gas stream enthalpy meas., calibration 8-70126
 computer generated phase diagrams 8-83928
 cresols, ideal gas thermodynamic props. 8-75250
 cubic margules solution model, miscibility gap and crit. point behaviour 8-59925

enthalpy continued

- digital automatic thermodynamic enthalpy and specific heat determ. equipment 8-57951
 dimers, dissociating, in nonisothermal ideal gas phase, stationary state anal. 8-76848
 ethylene + N₂, gaseous, excess enthalpy, determ. by flow calorimetry 8-91057
 flame, laminar mixed-mode forced-free diffusion type, on vert. burning fuel slab 8-91033
 flow, transient, two-phase, flow reversal prediction LOCA conditions 8-94811
 hydrocarbons, thermodynamic props., optimum incremental diagram calc. method (*German*) 8-51702
 isothermal displacement calorimeter, for positive excess enthalpies 8-89483
 liquid mixture, adsorption on solid, equil., thermodynamics correlations 8-84045
 metal film resistor, resistance fluctuations from spontaneous enthalpy fluctuations 8-72217
 1,5-methano(10)-annulene, mol. geom. and gas phase thermodynamic props., minimisation scheme 8-78829
 PET, thermodynamic equil. melting parameters, effect of annealing 8-71837
 phenol, ideal gas thermodynamic props. 8-75250
 polystyrene glasses, transition temp. and thermodynamic state 8-75819
 propylene, computer generated phase diagrams 8-83928
 PTFE, H₂(D₂) solubility and diffusion, activation enthalpy 8-79775
 TBBA, liq. cryst., metastable phase, thermodynamic props., differential scanning calorimetry meas. 8-94985
 vaporising coolant enthalpy for cryodevice initial cooling (*Russian*) 8-70130
 AgBr(Cl), formation vol. of Frenkel defect 8-79606
 AgPO₃-AgI glass system, solution calorimetry, enthalpy of formation (*French*) 8-64527
 Al, vacancy formation enthalpy, positron annihilation spectroscopy 8-67707
 Au-Ni, liquid alloy system, determ. of thermodynamic props. using Knudson effusion method, phase diagram calc. (*German*) 8-51707
 CaO-MgO-SiO₂, melts, mixing enthalpy, 1700-1873K 8-79785
 ClNO₂, kinetics of thermal decomposition (*German*) 8-95924
 e-Cr₂N phase, analysis of expt. results of Mills and Schwerdtfeger to yield partial enthalpy and entropy 8-52783
 Fe, low temperature deform., strain-rate cycling and stress relaxation tests (*Japanese*) 8-52876
 Fe-Al (0.069 and 0.158 wt.%), internally oxidised, low temp. deform. (*Japanese*) 8-52876
 Fe-C solid solution, volume effects on enthalpy and internal energy 8-75839
 α-Fe-V, dilute alloy, Mossbauer diffusion line broadening, exponential fitting evaluation 8-52379
 FeS-Ni₃S₂-Cu₂S melt, enthalpy (*Russian*) 8-95730
 InSb-Pb(Bi), thermodynamic prop. (*German*) 8-75847
 KCl:Sr, Ca, simultaneous diffusion, coefficients meas. 8-79813
 K₂O-Al₂O₃ system, high temp. thermodynamics and phase equilibria 8-80521
 N₂, arc jet enthalpy meas. by fast miniature total calorimetric probe 8-67486
 N₂O₄, dissociated, enthalpy, 310-782K 8-73073
 N₂O₄ dissociating coolant, O₂ generation time constant, enthalpy change (*Russian*) 8-58345
 NaCl-graphite interface, elec. cond. 8-52060
 NaNO₂, enthalpy of soln. and dilution, obs. 8-80781
 Nb, enthalpy and heat capacity determ. 8-71866
 Pb-Ag, liquid alloy, exam. of thermodynamic props. using solid oxide galvanic cell 8-75851
 Pu-Ga (1-8.56 at.%) alloys, enthalpy sp. ht. determ. at elevated temp. 8-78458
 Ti-O system, O/Ti<1, high-temp. thermodynamics using Tian-Calvet microcalorimetry 8-85190
 TiO₂, slightly reduced rutile, diffusion of Ti 8-79799
 V, enthalpy and heat capacity determ. 8-71866
 V-Cr alloys, absorption of H₂, thermodynamic parameters 8-87862
 V₃S₄-V₂S₃ system, exam. of thermodynamic props. at temp. from 650 to 800°C 8-52784
 ZrI₄, thermodynamics of vaporisation and high temp. enthalpy 8-91432

entropy*see also entropy of substances*

- anisotropic solids with magnetic symm., unified dynamic theory 8-77713
 charged droplets metastable state (*Czech*) 8-86231
 chemical impurities, entropy and enthalpy of solution 8-51691
 collision processes, information theoretic maximal entropy theory, rel. to scatt. theory 8-81888
 density matrix calc. of entropy 8-62148
 discontinuous systems, time depend. of entropy prod., stationary states 8-61043
 efficiency and existence of entropy in classical thermodynamics 8-54324
 electrical circuit, slowly modulated dissipative steady state, dQ=TdS far from equil. 8-81934
 EM classical single-mode fields with given degrees of coherence, max. entropy 8-50697
 fission reactor neutron gas, nonequilibrium thermodynamics (*Japanese*) 8-62595
 Freidrichs model, Lyapunov function evaluation 8-73876
 gaseous diffusion in stressed thermoelastic solid, thermodynamic struct. 8-51065
 general props. review of implications in statistical mechanics 8-73955
 Gibbs mixing entropy paradox, quantum gases 8-49588
 gravothermal catastrophe and negative specific heat of self-gravitating systems 8-93593
 hard-sphere fluid, modified nonlinear Enskog eqn., entropy function 8-63526
 Kolmogorov entropy, quantum generalisation 8-86232
 lattice, gas, entropy and phase transitions in partially ordered sets 8-77808
 macrostructural nonequilibrium entropy (*Russian*) 8-77826
 magnetofluid, self-gravitating, local behaviour of congruences 8-89384

entropy continued

- maximum entropy principle anal., relative freq. reln. and appls. 8-73948
 plasma, ordered motion in ring, mag. field effect, decreasing entropy 8-59553
 plasma, prod. by anomalous drift wave transport 8-75263
 plasma-beam system, entropy theorem and plasma waves spontaneous emission 8-69677
 plastic deformation, steady-state, irreversible thermodynamic description 8-72831
 point mass in plane convex region, stochastic transition and entropy 8-54288
 polymer attached to surface, dynamics, bead and spring model 8-75931
 polymer solutions, conc., Adam-Gibbs theory, for viscoelasticity and glass transition 8-83353
 production deceleration, hydrodynamical eqns. 8-93094
 quantum dynamical semigroups, entropy prod. 8-57883
 quantum irreversible kinetic eqn. for strongly interacting system, increasing entropy 8-54300
 radioactive contamination in aquatic organisms, evaluation by statistical and information theory 8-53535
 Rayleigh gas, irreversible processes, generalisation to non-equil. systems (*Russian*) 8-54329
 reacting reversible small bimolecular systems, numerical anal. of statistical functions 8-64831
 stars, rotating Newtonian, specific entropy distrib. rel. to secular instability 8-53922
 stellar degenerate C core, entropy rel. to collapse triggering by thermonuclear burning 8-65608
 sticking condition for fluid at solid boundary, entropy change 8-83359
 thermal diffusion, entropy production minimum theorem, generalisation thermal cond. coeff. depend. (*French*) 8-73943
 thermomechanics, derivation of jump condition 8-87250
 Universe, weak interactions and isotropy 8-61947
 von Neumann entropy and entropies of meas. 8-54229
 Wehrli entropy conjecture proof, Bloch coherent spin states analogous problem 8-89418
 K₂O-Al₂O₃ system, high temp. thermodynamics and phase equilibria 8-80521
 La_{1-x}Ca_xNi₅, role of entropy change during H₂ sorption 8-91533
 La(Ni_{1-x}Cu_x)₅, role of entropy change during H₂ sorption 8-91533
 Li₃N, heat capacity 5 to 350K, thermochem. props. to 1086K 8-92500
 TaB₂, heat capacity thermodynamic properties from 5 to 350K 8-91446
 TiB₂, heat capacity thermodynamic properties from 5 to 350K 8-91446

entropy of substances

- aeroacoustic fluid dynamic equations, acoustic energy conservation, vibrational relaxation effects 8-90566
 alkali metal, thermodynamics of melting (*Russian*) 8-71840
 2,3-benzo-1,6-methano(10)-annulene, mol. geom. and gas phase thermodynamic props., minimisation scheme 8-78829
 computer generated phase diagrams 8-83928
 cresols, ideal gas thermodynamic props. 8-75250
 4,7-dioxaoctanal, equil. anionic polymerisation, -90 to -68°C, polar substituent effects 8-88631
 elasto-plastic metal-dislocation system, stress-activated dislocation motion, thermodynamic theory (*Chinese*) 8-83868
 homovalent disordered solid alloy, entropy-vol. correlation 8-63868
 hydrocarbon liquid, residual energy and entropy, rel. to liq. and mol. structs. 8-71869
 hydrocarbons, thermodynamic props., optimum incremental diagram calc. method (*German*) 8-51702
 impurity distribution on growing crystals. from melt 8-52656
 isotropic media, linear dynamical eqns. of state, general formalism 8-93639
 Lennard-Jones (100) crystal-liquid interface, structure 8-91284
 macromolecules, crystallisation thermodynamics, various degrees of coiling 8-51445
 mesomorphic mixtures, binary phase diagrams, thermodynamic props., diagm. anisotropy 8-95139
 metal, equation of state, isentropic expansion method 8-91414
 metal, formation entropy per vacancy, anal. of exptl. data 8-75657
 metallic glass, thermal stability, validity of energy and entropy interfacial tension models 8-91255
 metals, entropy of fusion and allotropic behaviour, exam. of correlation and modification of Richard's rule 8-71838
 1,5-methano(10)-annulene, mol. geom. and gas phase thermodynamic props., minimisation scheme 8-78829
 n-octanal, equil. anionic polymerisation, -90 to -68°C, polar substituent effects 8-88631
 PET, thermodynamic equil. melting parameters, effect of annealing 8-71837
 phenol, ideal gas thermodynamic props. 8-75250
 polydiethylsiloxane chains, dipole moments 8-78844
 polyethylene oxide, aq. salt soln., meas.-based thermodynamic quantities 8-75525
 polythene melts of high density, viscosity meas., entropy and compressibility (*German*) 8-67162
 propylene, computer generated phase diagrams 8-83928
 single metals, monovacancy formation parameters, temp. depend., pseudopot. theory 8-75658
 spin glass, mean field approx. 8-52280
 TBBA, liq. cryst., metastable phase, thermodynamic props., differential scanning calorimetry meas. 8-94985
 transition and noble metal dilute alloys, Einstein's temp. and vibrational entropy, rel. to electronic struct. 8-83900
 AgClO₄ benzene, complex, heat capacity 8-75843
 Ag₂Si, superionic conductor, ordered phase struct. 8-83792
 Ar-Kr, liq. mixture, excess thermodynamic props. 8-75836
 ClNO₂, kinetics of thermal decomposition (*German*) 8-95924
 CrAs, heat capacity, enthalpy increments, thermodynamic props., 5 to 1280K 8-91450
 e-Cr₂N phase, analysis of expt. results of Mills and Schwerdtfeger to yield partial enthalpy and entropy 8-52783
 Cu, entropy factors for vacancy formation and migration 8-75866
 DyCo₂, field induced vol. magnetostriction 8-91920
 ErCo₂, field induced vol. magnetostriction 8-91920

entropy of substances continued

- Fe, BCC, computer simulation of entropy of $\frac{1}{2}\{111\}\{110\}$ edge dislocation 8-67716
 Fe, BCC, vib. entropy of $\frac{1}{2}\{111\}\{110\}$ edge dislocations 8-63768
 Fe₂Mo, standard Gibbs energies, enthalpies, entropies of formation 8-61042
 Fe₃Mo₂, standard Gibbs energies, enthalpies, entropies of formation 8-61042
 FeMoO₃, standard Gibbs energies, enthalpies, entropies of formation 8-61042
 Ga₂V₂O₇, resistivity, EPR, enthalpy and entropy meas., rel. to semiconductor-metal transition 8-88004
 GeH₄, heat capacity, dielectric const., thermodynamic props. 8-83967
³He, significant structure theory, thermodynamic props. 8-51774
⁴He, HCP→FCC transition, temp. hysteresis 8-56021
⁴He, liq., entropy meas. under press. between 0.7 and 1.35K 8-56004
 HoCo₂, field induced vol. magnetostriction 8-91920
 K, thermodynamics of melting at high pressures 8-91426
 KCl, entropy change associated with substitutional anion defects calc. 8-79782
 KCl:Sr, Ca, simultaneous diffusion, coefficients meas. 8-79813
 KNO₃, polymorphism, calorimetric investigation 8-75827
 LaF₃, heat capacity of 350K, enthalpy to 1477K, calorimetric determ. 8-79781
 Li, entropy and enthalpy of solution of H 8-51692
 Li, thermodynamics of melting at high pressures 8-91426
 Mg, phonon spectrum and thermodynamic functions, inelastic coherent cold neutron scatt. (Russian) 8-55917
 MgIn₂O₄, free energy, entropy of form. 8-91433
 Mg(NH₄)₂(ClO₄)₂, phase exam. by adiabatic calorimetry and X-ray diff. methods 8-63854
 Na entropy and enthalpy of solution of O(N)(C)(H) 8-51692
 NaAsO₂, aq. solns., O exchange between AsO₂(OH)₂⁺ and water 8-92459
 NaNH₂SO₄·2H₂O, ferroelec. and thermal props. 8-83968
 Na₂UBr₆, phase transformations, elec. cond. and entropy meas., synthesis (French) 8-79763
 Ni(H₂O)₆(ClO₄)₂, specific heat meas., 90 to 376K, phase transitions 8-83970
 NiS₂, high press. effect on mag. transition temps. 8-91866
 Pb-Ag, liquid alloy, exam. of thermodynamic props. using solid oxide galvanic cell 8-75851
 Pb-In (40-60 at.%), type II superconducting Ettingshausen effect, transport entropy of vortices 8-56272
 Pb₅Ge₃O₁₁, dynamic central peaks and phonon interactions near structural phase transitions 8-83903
 Pb(Zr,Ti,Ge)O₃, antiferro-ferroelectric transition 8-95565
 Pt, chemisorption of H, entropy, temp. and press. effects 8-84059
 Rb, thermodynamics of melting at high pressures 8-91426
 S₇, Raman and IR spectra, vibr. anal., force consts., thermodynamic functions 8-50545
 α-Se, monoclinic, heat capacities and thermodynamic properties, 3-300K 8-95162
 SnCl₂·2H₂O, high temp. entropy of ionic model for phase transition 8-55949
 SrTiO₃, dynamic central peaks and phonon interactions near structural phase transitions 8-83903
 TbPO₄, sp. ht., 0.5-10K 8-52298
 ThH₂, ThH_{3.75}, heat capacity and thermodynamic props. to 1000K 8-91451
 UAs₂(Sb₂), heat capacities, antiferromag.-paramag. transitions 8-76253
 V-Cr alloys, absorption of H₂, thermodynamic parameters 8-87862
 V₃S₄-V₅S₈ system, exam. of thermodynamic props. at temp. from 650 to 800°C 8-52784
 VSi₂, thermodynamic props. determ. using ternary phase equilibria 8-91449
 V₂Si, thermodynamic props. determ. using ternary phase equilibria 8-91449
 V₂Si₃, thermodynamic props. determ. using ternary phase equilibria 8-91449
 ZnX₂, ZnXY, X and Y=halogen, matrix isolation IR and Raman spectra 8-55171
 ZrI₄, thermodynamics of vaporisation and high temp. enthalpy 8-91432

environmental engineering

- see also air conditioning; cooling; ergonomics; lighting; safety; space heating; temperature control; ventilation
 control equipment noise reduction, steam power, chemical, petrochemical industries appl. 8-51002
 curricula for undergraduate courses 8-77644
 laser fusion generating stations, safety, environmental effects 8-50337
 laser fusion reactor, environment and safety features 8-50333

environmental requirements see environmental engineering**environmental testing**

- see also corrosion testing
 air pollution monitoring networks, automatic systems 8-93009
 coatings in space environment 8-85827
 optics in adverse environments, conf., San Diego, USA (Aug. 1977) 8-82976
 SAW device production and test programme progress report 8-59206
 space qualification of optical instruments, using long duration exposure facility 8-85826
 Space Shuttle, environmental effects during launch and reentry 8-85681
 Space Shuttle payload verification requirements 8-85812
 thermal meas. using digital systems 8-81966
 CO₂ conc. regulation in climatic cabinets for corrosion testing (German) 8-53069

epitaxial growth

- see also liquid phase epitaxial growth; vapour phase epitaxial growth
 nucleation theory 8-75961
 polyoxymethylene, epitaxial growth on KBr single crystal (Japanese) 8-56054
 CdS, epitaxial layers on Cd single crystal, direct synthesis and struct. 8-68628
 Si, amorphous, epitaxial regrowth by pulsed laser beam 8-91554
 Si, amorphous, Si implanted, substrate-orientation depend. of epitaxial regrowth rate 8-79900
 Si, amorphous layer, epitaxial growth by laser annealing 8-79899

epitaxial growth continued

- Si, crystal defects in integrated circuits, review 8-88547
 Si, defects, solid-phase epitaxy process, rel. to Si dissolution into Al 8-95188
 Si electron beam deposited film, epitaxy by pulsed laser annealing 8-56055
 Te-Se-CdO struct., fabrication and characts. 8-76106

epitaxial layers

- see also magnetic epitaxial layers; metallic epitaxial layers; semiconductor epitaxial layers
 periodic misfit-dislocation networks, electron diff. 8-59815
 polyethylene crystal, preferred orientation relationship, epitaxy 8-67923
 steel, magnetite film formation at metal scale interface, during cooling 8-88575
 TGS-d, TGSe-d, IR transmission spectra (French) 8-72742
 Bi film, elec. cond., obs. of epitaxial growth mechanism (French) 8-84329
 Cu₂S, epitaxial overgrowths on Cu films, characts., TEM and RHEED obs. 8-84101
 Fe-Cr, oxidation, in H₂/H₂O vapour mixtures, epitaxial oxide phase formation, effect on oxidation 8-88568
 Ge, epitaxial layer deposition by vacuum pyrolysis 8-52676

epitaxy see epitaxial growth**EPR line breadth**

- computation, fast, EPR (ST-EPR) spectra, master supermatrix eqn. soln. 8-62213
 cyclodextrin, trapped electrons in cryst. matrices, ESR, optical absorption spectra 8-80768
 directional field dependence of ESR and relaxation 8-91931
 ESR spectroscopy, spectra collection and anal. using KRS-4200 mini-computer (German) 8-57998
 free radicals in soln., spin exchange and EPR broadening 8-52357
 guanidinium aluminium sulphate hexahydrate:Mn²⁺, NMR 8-91939
 lipid bilayers, spin-labelled, pure, EPR lineshape evidence of phase transitions 8-69004
 lipids, from rat liver and hepatoma mitochondria, stochastic EPR anal. 8-76984
 liver tissue, mouse, appearance of free radical centres on low temp. oxidation 8-69013
 magnets, EPR line shape 8-91926
 metal, CESR line shape, strong surface relax. case (Russian) 8-56378
 metallic mononitrides:Gd, coupling between 4f electrons and conduction electrons, EPR linewidth 8-52347
 molecular aggregates, triplet, ESR line shape in solid matrix, fine and HFS 8-58878
 molecular crystal, triplet exciton excess EPR linewidth, orientational order effect 8-72389
 naphthalene, triplet pairs in naphthalene-d₈, ESR, nonreson. 8-64257
 naphthalene-d₈:naphthalene-h₈ cryst., triplet excitons in A-B pairs, origin of inhomogen. broadened ESR lines 8-91623
 paramagnets, conc., ESR line shift, phonon relax. influence 8-88171
 polystyrene, spin-labelled, EPR, end group mobility, temp. and solvent depend. 8-56368
 pulse shape of second harmonic generated by two level system 8-60327
 quasi-one dimensional organic systems, ESR 8-52358
 rare earth alloys, dil., ESR linewidth of rare-earth ions 8-68373
 rare-earth magnets, low-frequency modes 8-88087
 spin system with weak exchange couplings, EPR spectrum 8-64258
 spin systems, longit. paramag. suscept. inhomog. broadening conditions 8-88169
 TCNE⁻, anionic spin probe for ESR of amphiphilic liq. cryst. 8-75548
 TCNE, electron donor-acceptor complexes, EPR (German) 8-55187
 TCNQ, electron donor-acceptor complexes, EPR (German) 8-55187
 TCNQ salt, 1-ethyl-3'-methyl-2,2'-quinosenelacyanine-(TCNQ)₂, EPR linewidth, angular and temp. depend. 8-76313
 TCNQ salt, 3,3'-diethyl-6,6'-dimethyl-2,2'-thiacyanine-(TCNQ)₂, EPR linewidth, angular and temp. depend. 8-76313
 TMMC, exchange-narrowed EPR linewidth, temp. depend. 8-52292
 TMMC, one-dimens. Heisenberg magnet, EPR sidebands 8-88163
 transient ESR line profiles, S=I=1/2 system, calcs. 8-88170
 TTF-TCNQ type salt, trimethylene-TTF-TCNQ, unsymmetric cation, phys. props. 8-76059
 AgBr_{1-x}Cl_x, self-trapped holes, Jahn-Teller and reorientation effects in ESR 8-64273
 β-Al₂O₃-Na₂O, EPR and optical absorpt. studies of X-ray produced defects 8-95517
 β-Al₂O₃-Na₂O:Ag²⁺, EPR measurements 8-95515
 As₂Se₃ and As₄Se₃Ge glasses, struct. changes, Mn²⁺ EPR expts. 8-79534
 As₂Te₃Ge(Si) glass, struct. changes, Mn²⁺ EPR expts. 8-79534
 C-C composites, existence diagram and properties (French) 8-64517
 CaF₂:Gd³⁺-M⁺, (M=Li, Na, K, Rb, Cs, Ag), electric field effect expts., EPR line breadths, lattice distortions 8-80210
 CePd₃-Gd, EPR of Gd³⁺ impurities in host with interconfig. fluctuations 8-56377
 CrB₃, crit. spin-relax. in hard mag. direction 8-72390
 Cu, surface spin-flip probability from TESR 8-91953
 Cu(ethylenediamine)₂²⁺, electron tunnelling probability as function of distance for chem. reactions 8-80759
 GaAs:Co²⁺, EPR expts., y-factor determ. 8-76301
 Gd, EPR linewidth and spin-spin relax. near T_c 8-68369
 Ge, amorphous, EPR 8-88167
 Ge-Al film, amorphous, EPR meas. 8-80212
 Ge-Cu film, amorphous, EPR meas. 8-80212
 KHSO₄:SO₃⁻, X-irradiated, ESR saturation 8-80220
 La_{3-x}V_xS₄:Gd³⁺ localised moment-conduction electron interact., ESR obs. 8-88183
 Lu₂V₂O₇, pyrochlore struct., mag. props. 8-72335
 Mg₂MnO₈, EPR in magnesium-manganese spinel (Russian) 8-91936
 Mn complexes in solution, hyperfine linewidth in EPR spectra 8-91937
 MnCl₂-KCl system, molten, EPR spectra, linewidth study 8-88173
 MnTe, magnetic resonance at high hydrostatic pressure 8-76247
 NH₄H₂AsO₄-NH₄H₂PO₄, EPR spectra of central peak fluctuations 8-91932
 NiSiF₆·6H₂O, ESR spectra at low temperatures and high pressures 8-52339

EPR line breadth continued

- O₂, diffusion coeff. in liqs. determ. by ESR line widths 8-91929
 SCH₃, Pt, Gd, effect of Pt on Gd³⁺ ESR lineshape 8-68371
 Si, amorphous, EPR 8-88167
 Si:P, ion implanted, resist. changes induced by ESR 8-68377
 Tm₂V₂O₇, pyrochlore struct., mag. props. 8-72335
 YAG:M³⁺, ESR absorption spectra, line broadening of Fe³⁺, Cr³⁺, Gd³⁺ 8-91940
 Yb₂V₂O₇, pyrochlore struct., mag. props. 8-72335
 ZnO:Li, optically detected ESR, donor-acceptor pairs, line broadening 8-80256

epsilon meson resonances *see eta meson resonances*

equations

- see also Bethe-Salpeter equation; differential equations; equations of state; functional equations; integral equations; nonlinear equations*
 geodesy, telluroid definition and three-dimensional mapping eqns. 8-65171
 geodesy, three-dimensional mapping eqns. for non-rigid Earth models (German) 8-73304
 pure harmonic tide in canal, eqns. of motion quadratic resistance term linearisation 8-69369

equations of state

- see also equations of state of gases; equations of state of liquids; equations of state of solids; phase transformations; thermodynamics*
 1/n expansion up to 1/n², eqn. of state and correlation function 8-89412
 adsorbed phase, virial expansion, eqn. of state and isotherms (German) 8-95235
 computer generated phase diagrams 8-83928
 condensed phase, lattice gas model 8-73931
 crystals with three particle interactions, state eqns. with account of collective oscillations (Russian) 8-70086
 dense matter, U(1) symm. gauge model, eqn. of state 8-62500
 differential renormalisation-group generators, exact and approx. 8-77825
 Earth, eqn. of state fits to lower mantle and outer core 8-85522
 electron gas, classical diamagnetism, Gibbs method (Russian) 8-73918
 fluid, equation of state and Euler's turbine eqn. (Rumanian) 8-79400
 fluid of rigid spherocylinders, virial eqn. of state 8-63836
 freezing, molecular theory, eqn. of state, free energy, from 1st BBGKY eqn. 8-67804
 gas-liquid interface, irreversible thermodynamics, eqn. of state 8-51800
 hard disc fluid, sixth and seventh virial coeffs. 8-91047
 hard spherocylinders, Monte Carlo simulation 8-91046
 Heisenberg system, parametric representation in crit. region 8-79741
 insoluble monolayers, thermodynamic eqn. of state for uncharged films 8-85195
 isotropic media, linear dynamical eqns. of state, general formalism 8-93639
 Lennard-Jones fluid, hypernetted-chain eqn. of state 8-67800
 lipid monolayer, statistical mech. theory 8-73141
 liquid-vapour equilibrium, Van der Waals' eqn. of state, heat of evaporation 8-51640
 liquid-vapour phase equilb., modified Redlich-Kwong eqn. of state 8-83908
 microemulsions of micelles, interpretation of second virial coeff. of osmotic press. (French) 8-64891
 Mie-Grüneisen eqn. of state, generalisation 8-96194
 neutrons, relativistic, ultra-degenerate, non-interacting gas, Fermi energy and eqn. of state in intense mag. field 8-89401
 nuclear matter with neutrinos retention, eqn. of state and chemical comp. 8-96390
 nuclear reactor mats., crit. constns., review 8-59931
 N Pacific Ocean waters, densities rel. to comp. and eqn. of state 8-73391
 plasma, nonideal 8-75261
 plasma, quantum statistical theory 8-91627
 plasma, superdense, compression, role of eqn. of state and boundary press. profile, simulation 8-83589
 polydisperse hard-disc systems, equations of state, particle size effects 8-73947
 polydisperse hard-sphere systems, equations of state, particle size effects 8-73947
 propylene, computer generated phase diagrams 8-83928
 quark stars with 'realistic' equations of state 8-73725
 random spin system, 1/n expansion 8-62173
 tensor virial theorem, quantum mechanical generalisation for Born-Oppenheimer approx., atoms, mols. 8-86182
 theories rel. to high-compression data (German) 8-81148
 Thomas-Fermi shell model, at high press. and temp. 8-79738
 two-dimensional fluid, with 12-6 pot., fourth virial coeff. 8-59723
 vapour-liquid equilibria, generalised method for calc. and prediction at high press. 8-87780
 virial equation, truncation errors 8-87764
 water-entrained gas flow, force on moving body 8-63480
 weakly random system, limit $n \rightarrow \infty$, scaling function for eqn. of state 8-73953
³He, equations of state, 3.3 to 14K (Russian) 8-83912
⁴He, equations of state, 3.3 to 14K (Russian) 8-83912
 Xe+CO(N₂), ¹²⁹Xe chem. shielding, second virial coeff. 8-66563

equations of state of gases

- benzene, vapour-flow calorimetry 8-91058
 binary gas mixtures, nonspherical mols., second virial coeffs. calc. 8-75247
 chemical potential, near crit. density, Thom's catastrophe theory 8-91063
 gas mixtures, third virial coeffs., nonadditive dispersion interactions effects 8-67299
 ideal gases, solns., basic props. kinetic derivation from elastic collision processes 8-91048
 Lennard-Jones gas, third virial coeffs., empirical eqns. 8-94876
 metal, equation of state, isentropic expansion method 8-91414
 polyatomic molecules, quadrupolar and dipolar, numerical evaluation of second virial coeff. 8-91050
 polyatomic substances, thermal eqns. of states (French) 8-91413
 real gases, new eqn. of state (Ukrainian) 8-67297
 thermophysical props. tabulated for mixture composition certification 8-80818

equations of state of gases continued

- Wigner-Kirkwood expansion of second virial coeff., convergence accel. 8-91052
 n-D₂, fluid, eqn. of state from P-V-T and US vel. meas. up to 20 kbar 8-63837
 D₂O, saturated and superheated steam, eqn. of state up to 500°C 8-79401
 HCl, acid vapour, eqn. of state 8-79402
 He, second virial coeff., 0-500°C, two-temp. gas-expansion method 8-55711
 He, third virial coeffs. calcs. using realistic Beck pair potential 8-94880
⁴He, Wigner-Kirkwood expansion of second virial coeff., convergence accel. 8-91052
 N₂, cryogenic, shock wave-boundary layer interaction (German) 8-71370
 N₂, thermodynamic and transport props., consistent correlation using Lennard-Jones (12-6) and Buckingham (exp-6) pots. 8-91045

equations of state of liquids

- Alfven wave system, eqn. of state, thermodynamic props., Bose-Einstein statistics 8-87397
 Clausius eqn. of state, thermodynamic props. calc. 8-83909
 Clausius modified eqn. (French) 8-91412
 EBBA, pVT data and viscosity-press. behaviour 8-94989
 fluid-solid surface interaction, two-particle correlation function 8-79880
 Gibbs-Duhem equation, appl. to water/magma systems 8-57205
 hard spheres, partition functions, Miller's method 8-71828
 heavy water dynamic viscosity coefficient in supercritical region of parameters of state, experimental investigation 8-67845
 hydrocarbon+CO₂(H₂S) mixtures, vapour-liq. equilibrium, crit. locus curve, Soave eqn. 8-83913
 hydrocarbon liquid, residual energy and entropy, rel. to liq. and mol. structs. 8-71869
 light scattering, ratio of Brillouin to total scatt. intensity 8-52515
 MBBA, pVT data and viscosity-press. behaviour 8-94989
 methane-propane(pentane)(n-heptane)(n-decane)(H₂S) mixtures, densities calc., van der Waals model 8-79740
 molecular liquid, thermodynamic functions, interaction site model calc. 8-71661
 nematic liquid crystals, equation of state, anisotropic props., perturbation theory 8-67645
 nematic-isotropic transition, Onsager's orientational order theory 8-79750
 PAA, nematic, equation of state, anisotropic props., perturbation theory 8-67645
 n-paraffins, generalised eqn. of state from acoustical meas. 8-51642
 polymer, isotropically swollen networks, vol. depend. of elastic eqn. of state 8-67832
 polymer branched chains, chain length, mol. architecture rel. to second virial coeff. 8-94964
 polymeric liquid, entropic elasticity and time temp. superposition principle, thermodynamic eqn. of state 8-63406
 simple liquid intermolecular interaction, extremal values 8-87602
 ternary liquid-liquid equilibria, associated soln. theory capabilities 8-83910
 water, saline and pure max. density points meas. 8-57900
 Cu, equation of state, isentropic expansion method 8-91414
 n-D₂, fluid, eqn. of state from P-V-T and US vel. meas. up to 20 kbar 8-63837
 Pb, equation of state, isentropic expansion method 8-91414

equations of state of solids

- bulk moduli, Wachtman's eqn., and temp. depend. 8-75799
 dynamic, shock wave expts. (German) 8-59858
 graphitised C black, adsorption of inert gases, gas-solid virial coeffs. 8-75928
 high pressure, appl. to alkali halides 8-55935
 isothermal equations of state, P-V relation, elements and selected compounds (Chinese) 8-79739
 lattice-attice scaling, reln. to scaled eqn. of state, appl. to Ising model 8-70067
 metal plastic deformation, influence of mech. vibrations 8-60722
 nonuniformly stressed crystal, statics and kinetics of vacancies (Russian) 8-55863
 nuclear reactor core mats., constitutive eqn. 8-80598
 poly(alkyl methacrylate), vitreous state, thermal cond., hole theory of liqs., press. 8-84013
 polymer, flexible chain collapse 8-87628
 statistical mech. treatment of phase transitions impurity states 8-64004
 superionic crystals, phase transitions 8-75826
 transition metal, eqn. of state, s- and d-contribs. 8-91633
 transition metal alloy, ground state properties, self-consistent calc. 8-91587
 Al, under very high dynamic load (German) 8-59858
 Ar, solid, density at melting and isochoric equations of state 8-83915
 CrBr₃, parametric representation of the equation of state of a Heisenberg system in the critical region 8-79741
 Fe, P-V-T data for Lennard-Jones potential, computer expt. 8-75800
 Ge, eqn. of state, under press. 8-75801
 p-H₂, solid, anisotropic contribs. to ground state props. 8-83914
 H₂, solid, equation of state, intramol. zero pt. energy contrib., total sublimation energy 8-71829
 Kr, solid, density at melting and isochoric equations of state 8-83915
 Ne, P-V-T data for Morse pot., computer expt. 8-75800
 PbS, thermomech. props., SCF X α scatt. wave theory 8-71704
 Pd:II, elastic props. of dilute solid solutions 8-75706
 Si, eqn. of state, under press. 8-75801

equilibrium, chemical *see chemical equilibrium*

equilibrium, phase *see phase equilibrium*

equilibrium constants *see chemical equilibrium*

equilibrium diagrams *see phase diagrams*

equivalence classes

visual stimuli equivalence classes, model neural network 8-69064

equivalent circuits

see also network analysis

angular spectrum of EM field, elec. network equivalent 8-78867

cell electric circuit model, alternating signal interaction 8-77011

cell electric circuit model, alternating signal interaction 8-77012

equivalent circuits continued

- complex US vibratory systems, equiv. circuit anal. 8-50997
 electrochemical converters, conc. type, for elec. signals, diffusion theory of conc. networks 8-61026
 electroretinographic response rel. to vars. of visual performance during day 8-77051
 equatorial electrojet, equivalent circuit anal. of neutral wind effects 8-57392
 glottal sound source, self-oscillating model (*Japanese*) 8-92654
 glow discharge, transversely inhomogeneous, stability, equiv. cct. theory 8-51373
 gravimeter, LaCoste and Romberg, equivalent ccts. rel. to vibr. charact. (*Japanese*) 8-65400
 gravitational wave antennas, with and without piezoelectric ceramics, elec. equivalent circuits 8-73915
 IR detectors, microwave-biased extrinsic photoconductors, performance anal. 8-49898
 Jupiter ionosphere, current cct. rel. to decametric radiation modulation by Io 8-89110
 local tract area function, estimation by adaptive deconvolution and adaptive speech anal. system (*Japanese*) 8-92658
 MHD generator, diagonal type, end effects anal. by means of equivalent cct. (*Japanese*) 8-87505
 modular chirp Z transform equivalent to two-lens optical Fourier transform 8-78943
 one-port SAW resonators, config. and cct. anal. 8-63258
 piezoelectric modulation transducers for alternating pressures 8-77891
 piezoelectric transducers, acoustically loaded, expt. method for equivalent circuit parameter determination 8-51036
 resistance and capacitance determ., lecture demonstration 8-69938
 rod outer segment adaptation anal. based on a simple equiv. cct. 8-73157
 Schottky-barrier metal-semiconductor junction carrier migration and equivalent cct. analysis (*Russian*) 8-84294
 skeletal muscle fibre with helicoidal T system, linear elec. props. 8-80852
 spectrum analyser for radar signal processing 8-78942
 strip-coupled varactor SAW convolvers, parametric cct. anal. 8-71245
 Ag(α -AgI) interface, impedance meas., equivalent circuit parameters, calc., electrolyte defect struct. 8-59975
 Si reverse-biased p-n junction DC characteristics interpretation (*Polish*) 8-91761

erbium

- see also nuclei with
 film, elec. resist. results 8-84326
 Hall constant and elec. resist., 80-700K (*Russian*) 8-60110
 optical absorption in paramagnetic and antiferromagnetic states (*Russian*) 8-56497
 spin wave exam. 8-56306
 Ag:Er, orbit-lattice coupling, nonuniform strain effects 8-88182
 Al:Er, orbit-lattice coupling, nonuniform strain effects 8-88182
 BaF₂:Er³⁺, single-site multiphonon and energy transfer relax. 8-52547
 CaWO₄:Er³⁺, phase relaxation, spin echo meas. 8-68375
 Er³⁺, luminesc. sensitisation by Yb³⁺, in liq., efficiency (*Russian*) 8-90116
 LaBe₁₃:Er, ESR, crystalline field single ion effects 8-84481
 LaF₃:Er³⁺, ZZ 8-80381
 LiYF₄:Er³⁺, ZZ 8-80381
 LuBe₁₃:Er, ESR, crystalline field single ion effects 8-84481
 LuF₃:Er³⁺, ZZ 8-80381
 POCl₃-ZrCl₄:Yb³⁺, Er³⁺, energy transfer from Yb³⁺ to Er³⁺, agglomeration formation 8-64405
 Tb(OH)₃:Er³⁺, ferromag., anisotropic exchange effects in optical spectra 8-80141
 TbBe₁₃:Er, ESR, crystalline field single ion effects 8-84481
 YAG:Er³⁺(Er³⁺, Ga³⁺), LPE and luminesc. 8-64408
 YF₃:Er³⁺, ZZ 8-80381

erbium alloys

- dilute, ESR linewidth of rare-earth ions 8-68373
 Er-Au, dil., Mossbauer exam. of mag. hyperfine field at ¹⁹⁷Au impurity 8-88244
 ErAl₂, conduction electron spin and orbital polarisation effects 8-80228
 ErCo₂, field induced vol. magnetostriction 8-91920
 ErCo_{5.6}, easy magnetisation direction 8-84415
 Er₄Co₃, cryst. field effect on mag. moment direction, neutron diffr. meas. 8-80132
 Er₆Co₃₅, amorphous, amg. ordering, susceptibility, magnetisation and hysteresis meas. 8-68190
 (ErCo₂)₁(ErAl₂)_{1-x}, mag. and struct. investigations of intermetallic systems 8-95440
 ErCo₅-Ni₂, ferrimagnetic series, magnetisation, coercive field meas. 8-91896
 ErCu, cubic antiferromag., mag. excitations inelastic neutron scatt. meas. 8-72341
 ErFe₂, excited state spin waves inelastic scatt. meas. 8-76234
 ErFe₂, Laves phase, cryst. field effects on spin wave dispersion relations 8-84408
 Er_{1-x}Fe_x, amorphous film, cosputtered, struct. and mag. props. 8-60323
 ErFe₂Al₆, mag. props. 8-52250
 ErGa₂, mag. susceptibility, 1.5-300K and Neel temp. 8-68184
 Er_{1-x}Sm_xCo₂Ni₃, giant intrinsic magnetic hardness 8-56347
 ErZn, magnetoelastic and quadrupolar couplings 8-52328
 Sc-Er, dil., high field magnetisation 8-56292
 Sm₂Er_{1-x}Co₅, temp. compensated magnetic material, mag. and struct. characterisation 8-68177

erbium compounds

- see also erbium alloys
 CeEr₂S₄, spinel, crystal struct. (*French*) 8-91326
 CaF₂:ErF₃, clustering, defect struct., NMR study 8-80229
 ErAG, facet formation 8-63687
 ErAl₂, crystal field study rel. to La_{0.9}Er_{0.1}Al₂ 8-76036
 ErB₄, theory of metamagnetic transitions (*Russian*) 8-95436
 ErBi, thermal expansion, thermal cond., 300-900K 8-91453
 ErCl₃(AlCl₃)_x, vap. complexes, absorpt. spectra, 6000-44000 cm⁻¹, relax. props. 8-62799
 ErF₃, crystal growth by Bridgman-Stockbarger method 8-52660
 ErFeO₃, far IR spectra 8-88303

erbium compounds continued

- ErFeO₃, sound velocity meas. at high press., spin-reorientation transition 8-76254
 ErH₃, cryst. fields and mag. props. 8-68181
 Er_{1-x}Ho_xRh₄B₄, re-entrant supercond. and mag. ordering 8-60240
 ErMo₅S₈(Se₈), ternary superconductor, paramagnetic relax. effects 8-68112
 ErMo₅Se₈, mag. ordering and supercond., neutron diffr. 8-68125
 Er₂O₃, 300 to 900K, mag. susceptibility and Curie temp. meas. 8-56288
 Er₂O₃, solid, photoacoustic spectra 8-58044
 ErOHCO₃, synthesis of rare earth carbonates under hydrothermal conditions 8-72714
 ErPO₄-Pb₂F₂O₇, solubility curves for high temp.-melts for growth of single crystals. 8-95687
 ErRh₄B₄, supercond., re-entrant magnetism, energy band calcs. 8-52140
 ErRh₄B₄, ternary superconductor, paramagnetic relax. effects 8-68112
 ErSb, cryst. field effects on transport props. 8-72133
 Er₂Se₃, elec. resist., thermoelectromotive force, temp. depend., 300 to 1400K (*Russian*) 8-84243
 Gd₂Er_{1-x}Rh_xB₄, mag. and supercond. transitions 8-68127
 GdF₃-ErF₃, stabilisation of rhombic β-YF₃ type struct. 8-67700
 Ho_{0.7}Er_{0.3}FeO₃, crystn. on seeds, layer morphology 8-72041
 β-KEr₂F₁₀, cryst. struct. (*French*) 8-51500
 (Sm,Er)(Ga,Fe)₅O₁₂, LPE, non-grooved film, thermomag. writing 8-76278

erection

- LWR power station construction in France, standardisation advantages (*French*) 8-58397

ergodic theorem see statistical mechanics**ergonomics**

- see also human factors; man machine systems
 repetitive muscular contraction, localised fatigue evaluation from EMG power spectrum 8-57103

erosion

- beach sedimentology of Mustang and Padre Islands, time series approach 8-77211
 cultivated loamy soils, Belgium, splash and wash 8-73410
 Cumberland Peninsula, Baffin Is., tors, felsenmeer and glaciation 8-61442
 fixed dunes, Sahel, central Niger, erosion 8-81225
 Grote Nete basin, Belgium, geomorphology (*Flemish*) 8-61452
 Hurricane Agnes storm and flood, geomorphic effects, SE.Pennsylvania 8-77280
 icy permafrost in NE.British Columbia, distrib. and sensitivity to erosion 8-77277
 impact erosion and meteorite bombardment 8-57476
 Lake Eyre North, S.Australia, bottom profile rel. to inshore scouring 8-69376
 landscapes, soils and erosion, Wither Hills, New Zealand 8-88864
 landscapes, relationship to rainfall, Kitakyushu City, Japan (*Japanese*) 8-88848
 Mahone Bay, Nova Scotia, Late Quaternary glacial erosion history 8-77232
 Mantaro landslide, Peru, seismological and geological aspects 8-96248
 Mars, chaotic terrain erosion rel. to fossil H₂O liquid-ice interfaces 8-65539
 Mars, CO₂ permafrost as erosive agent rel. to topography 8-65535
 Mars, erosion rel. to crater streaks form. in Chryse Planitia, early Viking results 8-65534
 Mars fretted terrain, erosional debris flow 8-65537
 Mars polar regions, stepped topography origin 8-65536
 montmorillonite neoformation by post-depositional subsurface weathering in slope deposit 8-73367
 New England submarine canyons, bedrock geology 8-73356
 Point Pelee, SW.Ontario, erosion rel. to geomorphology and landscape elements origin 8-92857
 raffle formation model 8-63482
 Rotoehu Ash weathering in Bay of Plenty district, New Zealand 8-85558
 salts, dissolving and outwashing from soil and rock, hydromechanical treatment (*Russian*) 8-77279
 sedimentary organic matter, subaerial weathering effects 8-57206
 sedimentation and erosion, problems rel. to water supply, research needs 8-61444
 shore platform formation on SE. coast of Izu peninsula, Japan 8-81147
 silicate rocks, chem. denudation rates in tropical catchments 8-73414
 solute loading and chem. denudation rate mapping in Devon, England 8-69375
 stone movement through snow creep, 1963-75 period, Mt. Twynam, Australia 8-69374
 tholeiitic basalts, rare earth elements behaviour during submarine weathering 8-73369
 topsoil mineralogy, Ngunguru Basin, New Zealand 8-85557
 volcanosedimentary levels, S.Pacific, neoformation and weathering (*French*) 8-73353
 water erosion characteristics in Siberia, Russian plains and central Asia 8-61449
 watershed geomorphology, relative scales of time and effectiveness of climate 8-81229
 weathering model in palaeomag. field intensity meas. on ancient fired clays 8-61328

error analysis

- see also error correction
 acetylene-d₀, (-d₂), IR intensities, relative error anal. 8-58686
 approximation method for solution of nonlinear integral equation with error estimation for problems in heat or mass transfer (*Russian*) 8-57879
 artificial satellites, effective isotropic radiated power, error anal. using calibrated radio star 8-93070
 astrometric observations, systematic errors, spectral anal. of obs. series (*Russian*) 8-73614
 atomic frequency standard prediction error analysis 8-57906
 bell type volume dynamic systems for gas flow meas. 8-75239
 chemical reaction kinetics, temp. integral approximating eqns. accuracy 8-92445
 cinerointerferometry, quantitative biplane method, error propag. 8-73224

error analysis continued

- coherent Doppler anemometer for turbulent vel. meas., potential accuracy anal. (*Russian*) 8-71406
 crystallography, electron densities, thermal smearing, limited resolution effects 8-71635
 digitising error from period and freq. counting techniques 8-61570
 directional-hemispheric reflectance factor scale establishment, Van den Akker method 8-77967
 Earth tide observations processing, errors combination rel. to monthly data sets weighting (*Russian*) 8-88789
 education, least squares fit, uncertainty calc. 8-86068
 EEG slope descriptor computation, time and frequency domain comparison 8-57115
 experimental data interpretation, chemical analysis appl. 8-77827
 gas absorption analyser, mean risk criterion (*Russian*) 8-70088
 geodesy, props. of Gauss-Helmert least-squares adjustment model (*German*) 8-61309
 gyrohorizon with harmonic and random swinging (*Russian*) 8-62194
 high precision voltage meas. automatic error correction using iterative method (*Russian*) 8-70089
 hot-wire anemometer temp. compensation errors estimation (*Russian*) 8-57345
 hysteresis-free magnetic (*Russian*) 8-86305
 image correlation with geometric distortion effect on local accuracy 8-71040
 indicating measuring instruments, error estimation (*Croatian*) 8-57886
 Information Measuring System error computation considering communication channel characts. 8-73957
 information-meas. system accuracy, influence of residual voltages 8-77828
 light spot location photocathode of quantum detect. accuracy estimation 8-77832
 low-loss dielectric microwave measurement in the E_{010} resonator, numerical error analysis (*Polish*) 8-70153
 measurement errors, random, simulation (Monte Carlo) method, teaching appl. 8-86062
 measurement instruments, rack and pinion types, indication error reduction (*Polish*) 8-49818
 nonlinear variation eqns., convergence of finite element solns. 8-86127
 pendulum accelerometers vibration errors (*Russian*) 8-77874
 rain-rate estimates from attenuating radar, error analysis 8-73540
 reservoir storage size sampling error 8-61466
 RMS digital voltmeter calibrator for VLF 8-86293
 satellite-to-satellite statistical orbit determ. error analysis 8-65486
 Stokes problem with conforming Lagrangian finite elements, soln. error estimates (*French*) 8-62085
 strain gauge with screw tenso-resistor, linearity anal. (*Russian*) 8-89475
 Sturm-Liouville, error estimation 8-81818
 tenso-resistive strain gauge output error (*Russian*) 8-89474
 thermal conductivity measurement method, normal to thin film, error anal. 8-90682
 thermal converter AC-DC transfer errors determ., absolute method 8-93643
 tolerated errors in determining transfer-function parameters of temperature transducers 8-73959
 UV backscatter expt., airborne, for O_3 distrib. determ., error anal. 8-92985
 Weibull wind speed distrib. parameters, vertical extrapolation formulae, errors 8-92916
 wire strain gauge in heat cycling condition, method (*Russian*) 8-65916
 X-ray crystallography, struct. factors, accuracy assessment 8-71636
 Pt resistance thermometer calibration characts. linearisation methods (*Russian*) 8-70123

error compensation

- see also error correction
 fluxmeter measurement range extension 8-57993

error correction

- astrometric observations with transit instrument, elimination of systematic errors (*Russian*) 8-73615
 clock synchronisation cct., error monitoring correction appl. 8-73970
 eccentricity of rotating cylinder, error calc. in viscosity meas. (*German*) 8-67291
 flow curve correction by FORTRAN program (*German*) 8-79394
 flowmeters, correction factor appls. for blunting of diaphragm input rim 8-75240
 hygrometer, Meteorological Office Mk3, frostpoint meas. systematic error 8-73538
 imaging system shading effects and countermeasures 8-78922
 instrument operation speed increase, additive-iterative correction method (*Russian*) 8-89423
 measuring instrument inspection, optimal error correction signal 8-77829
 meteorology, surface synoptic obs., automatic real-time quality control 8-92920
 ocean microwave radiometry, correction for external sources and intervening atmosphere 8-81416
 passive value parameter transducer (*Russian*) 8-49819
 space research, spacecraft mag. field correction via dual magnetometer method 8-77459
 thermocouple dynamic error correction cct. 8-77909
 X-ray fluoresc. anal. using matrix correctional procedure, appls. to alloys, Al_2O_3 -supported catalysts 8-80817
 X-ray spectral anal., theoretical correction parameters rel. to chem. composition of steels 8-61108

error recovery (computers) see system failure and recovery**error statistics**

- chemical anal. by counting meas. calibration determs., statistical uncertainties of anal. 8-92533
 dynamic emission computed tomography, quantitative pots. 8-77105
 error prediction in meas. of probability densities (*French*) 8-57885
 holographic interferometry, errors in small vector displacements meas., statistical anal. 8-78953
 instrument mechanism analysis, linear (*Hungarian*) 8-49823
 inverse filter which is optimum in error-distrib. sense, stability characts. 8-81424
 measurement errors, random, simulation (Monte Carlo) method, teaching appl. 8-86062

error statistics continued

- optical communication using two-photon laser, optimum control of quantum noise 8-71049
 optical signal receivers, optimal and nonoptimal, logical structs. efficiency comparison, simulation (*Russian*) 8-71041
 photoelectric transducers with astatic characteristics, statistical error determ. 8-93760

errors

- see also coding errors; measurement errors
 atmospheric transmittance, profile depend., line parameter vars. 8-77322
 chemical analysis, instrumental, minicomputer appls., errors 8-92543
 flow, of liq., thermal markers for vel. field meas., error reduction 8-91036
 Fourier transform spectroscopy, minicomputer appls., errors 8-92543
 geomagnetic declination field near Earth surface, error in analytic representation 8-73307
 nuclear reactor in-core 8-82476
 open channel acoustic flowmeters, design, calibration and errors 8-55701
 virial equation, truncation errors 8-87764
 H II regions radio emission analysis, consequences of improper analytic methods 8-54000

Esaki diodes see tunnel diodes**Esaki effect** see tunnelling**ESCA** see electron spectroscopy; spectrochemical analysis; X-ray photoelectron spectra**estimation theory**

- see also information theory
 film-grain noise degraded image estimation 8-54479
 hail-prevention operations, cost effectiveness estimation methods anal. 8-93013
 nuclear reaction rate Monte Carlo estimators, unified definition 8-58334
 statistical thermodynamics from statistical theory of estimation 8-54328
 underwater sound, Confidence bounds for magnitude-squared coherence estimates 8-66979

eta meson resonances

- η , η' and η_c mixing and decays in nonrelativistic quark model for QCD idea 8-82166

eta mesons

- charmonium photoprod., gluon-exchange model 8-74214
 free η^+ meson gas, creation in nuclear matter with neutrinos retention 8-96390
 mass formulae and mixing in SU(8) and $SU_w(8)$ symmetries (*Russian*) 8-66097
 $ep \rightarrow e\eta$, meas. in $S_{11}(1535)$ reson. region 8-50038
 $ep \rightarrow e\eta$ at $S_{11}(1535)$ resonance, longit. to transverse cross sections ratio 8-78194
 η , η' and η_c mixing and decays in nonrelativistic quark model for QCD idea 8-82166
 $\eta(549)$, $\eta'(958)$ with inert component, gluon bound state 8-74226
 $\eta \rightarrow \gamma e^+ e^-$, form factor slope calc., VDM 8-58181
 $\eta \rightarrow \pi^+ \pi^- \pi^0$, decay width 8-70362
 η_c predictions of existence by extrapolation methods 8-93863
 $\eta_c \rightarrow \gamma + \text{anything}$, OZI rule violating decay in QCD 8-89709
 η_c mass determ. from QCD sum rules 8-74223
 η_c mass from dispersion sum rules in QCD, identification with $X(2.83)$ (*Russian*) 8-89681
 $\eta_c \rightarrow \pi^0$, effects of EM mixing on pn mass difference (*Russian*) 8-74255
 $\pi^+ p \rightarrow \eta X$, pseudoscalar meson prod. in triple Regge region, absorpt. corrections 8-78228
 $\pi^+ p \rightarrow \eta \eta \pi$, 40 GeV/c, production cross sections and $\eta \eta$ angular distrib. (*Russian*) 8-78223
 $\psi \rightarrow \psi + \eta$, two gluon mechanism, Y dynamics test 8-89665
 $Y \rightarrow \eta \gamma$ or $\eta' \gamma$, other hadronic and two body charmed and strange modes 8-78175
 $Y' \rightarrow Y + \eta$, two gluon mechanism, Y dynamics test 8-89665

etalons see interferometers**etchants** see etching**etching**

- see also crystal defects; dislocation etching
 cellulose nitrate, proton, H_2^+ mol. ion, and heavy ion irradi., track prod., etching obs. 8-86757
 cellulose nitrate (CN) detectors, effect of pre-irrad. thermal treatment on track revealing props. 8-94168
 ceramics, archaeological, dating by alpha-recoil tracks in mica 8-70237
 CR-39 polymeric nuclear track detector, props. and appls. 8-94170
 CR-39 thermoset plastic nuclear track recorder, etching in hot NaOH 8-74535
 electrochemical etching, of neutron-induced tracks in plastic detectors using HV 50 Hz supply 8-86738
 fission fragment track registration in crystals., development efficiencies, etchant (etching conditions) depend. 8-66454
 holographic grating, fine, made of positive photoresist AZ2400, anal. of two-dimensional etching effect on profile 8-82928
 intaglio imaging with nuclear particles 8-65993
 Kapton, optical, elec. props., struct., ion textured surface 8-72904
 metallographic ion etching, adaption of simple sputtering apparatus 8-56849
 nuclear filters, prep. from polymers using Ar ions 8-86714
 Permalloy sputtered film, bevelling by chemical etching, for this film mag. header 8-92375
 plasma etching, flow rate effects 8-72906
 plasma etching, mass spectroscopic exam. 8-72909
 plasma etching for IC processing, chemically selective anisotropic 8-64755
 plasma etching mechanisms 8-72905
 plasma stream transport method 8-52684
 polycarbonate foil electrochemical etching for dosimetry, bulk etching rate evaluation 8-78506
 polypropylene film and fibre, plasma etching 8-95871
 quartz, dissolution of grown synthetic quartz inside the autoclaves 8-63911
 quartz, ion-etching of grooves for SAW devices 8-95822

etching continued

quartz inclusion morphology for thermolum. dating, effect of HF etching 8-70240
 quartz SAW resonator deep etching 8-59248
 quartz surface, chemical polishing by etching 8-60858
 reactive sputter etching, plasma gas temp. determ. 8-63586
 RF plasma etching for IC processing, mechanistic considerations for selective etching 8-64754
 RF plasma utilisation in sputtering and surface reactions 8-84714
 steel, high alloy, potentiostatic development of structures 8-95887
 steel, high speed, tempered, etching reagents for austenite grain boundaries 8-80704
 steel, high-speed, eutectic carbide structure, determ. by SEM 8-85075
 steel, mild, etching method for revealing plastic deformation 8-72825
 steel, stainless, Cr-Ni-Mo, surface, scraping, mech. (electrolytic) polishing, ion etching, effects on ESCA 8-53037
 steel, stainless, determ. of fracture surface orientation, due to stress corrosion cracking (*Japanese*) 8-53025
 steel, stainless, ground surface ion bombardment, in DC glow discharge 8-95098
 steel, stainless, surface cleaning by H⁺ bombard., AES study 8-53022
 steel, X5CrNiTi26.6, ferrite-austenitic struct., optical and electron microscopy 8-84848
 surface relief gratings, 3200 Å period fabrication, effect on film growth 8-84089
 surface treatment by gas plasma (*Japanese*) 8-92386
 technique for revealing plastic zone in Al 8-72955
 Teflon, optical, elec. props., struct., ion textured surface 8-72904
 tetrafluoromethane plasma, etching of Si, SiO₂, O₂ addition effects 8-75363
 wear study, analytical surface tool, review 8-64718
 wire, device for uniform electrolytic removal of surface layers for residual stress determ. 8-60918
 Al, and its alloys, reactive etching in RF plasma containing halogen species 8-72923
 Al, plasma etching in CCl₄, end point determ. by spectroscopy 8-76786
 α-Al₂O₃, thermal etching (*German, English*) 8-60934
 β-Al₂O₃-Na₂O, thermal etching (*German, English*) 8-60934
 Al plasma bridge neutraliser operation with 10 cm beam diameter ion etching source 8-74102
 As₂S₃ film, effect of light exposure and heat cycling 8-94417
 BaSO₄, single cryst., neutron bombard. effect on struct. 8-63793
 C and low-alloy steel inherent austenitic grain size determ., exam. of methods used 8-85071
 Ca₃(PO₄)₂F, dislocation struct. exam. (*Russian*) 8-63770
 CaTiSiO₅, sphere, effects of thermal annealing on track etching rate 8-65435
 CdS-Cu₂S heterojunction, elec. and photoelec. characts., effect of etching of CdS 8-80048
 CdS-InP(GaAs) heterojunction prep. by CdS CVD and etching 8-52062
 Cu surface, surface cleaning by H⁺ bombard., AES study 8-53022
 CuO surface, contaminated, cleaning treatments, ion scatt. anal. 8-53307
 Cu₂O, creep substruct. under compression, X-ray diffr. study 8-95785
 GaAs, chem. etching and ion-bombardment effects, during ESCA 8-92171
 GaAs, chemical etching processes, review 8-95832
 GaAs, epitaxy using TMG and AsH₃, chloride etching effect 8-76606
 GaAs, etchant, universal, multipurpose 8-53008
 GaAs, heavy metal migration, ESCA and ion etching study (*French*) 8-75885
 GaAs, ion etching, effects on optical props. and lattice disorder 8-83122
 GaAs LPE layers, dopant tracing of terrace growth 8-75948
 GaP, chemical etching processes, review 8-95832
 GaP, etching in aqua regia and bromine-methanol-water solns. 8-68833
 Ge, chemical etching processes, review 8-95832
 Ge, rough surface, polarisation angles, ellipsometric meas. 8-56449
 Ge-metal Schottky barrier junction, surface electron states spectrum (*Russian*) 8-84297
 InP substrates, HCl etching speed and polarity obs., with aid of laser beams (*Slovak*) 8-56575
 InP substrates preparation, etching and polishing in Br-methyl alcohol solution (*Slovak*) 8-56576
 InSb, surface analysis, X-ray photoelectron spectra, surface oxidation-etchant correlation 8-56029
 LiNbO₃, microfabrication by ion-bombardment enhanced etching 8-76779
 LiO₂ pellets, sintered, exam. of microstructure 8-72749
 MgO, etching in acids, kinetics and mechanism of dissolution 8-85014
 MgO, etching on {100} faces by H₃PO₄ acid 8-67714
 Na₂O-CaO-SiO₂, plates, exam. of Hertz crack branching 8-72887
 PbNb₂O₆, ferroelectric thick crystals, domain formation and dislocation loops 8-60410
 Se₉₀-Te₁₀ alloy crystals, growth and cleavage 8-88421
 Si, chemical etching processes, review 8-95832
 Si, etching by CF₄ plasma, mechanisms 8-72907
 Si, HCl oxidation conditions for stacking fault nuclei gettering and undesirable etching 8-68830
 n-Si high-temp. vacuum etching, p-n junction photodetectivity 8-95355
 Si, plasma etching, effect of O₂ additions to CF₄ plasmas 8-72908
 Si, rough surface, polarisation angles, ellipsometric meas. 8-56449
 Si wafers, etched in HCl, exam. of bunch formation 8-68831
 Si:P, polycryst. etching characts. in CF₄ plasma 8-76777
 Si₃N₄, enhanced etching by ion beam, localised substrate heating effects 8-51573
 Si₃N₄, low temp. deposition using microwave-excited active N₂ 8-84718
 Si₃N₄ on Si, optical monitoring of etching using grating 8-76775
 Si₃N₄, ion-implanted, enhanced etching in buffered HF solns. 8-72903
 SiO₂ layers, passivating, deposition by plasma decomp. in planar reactor, etching rate 8-88430
 SiO₂ on Si, optical monitoring of etching using grating 8-76775
 SiO₂, plasma etching, effect of O₂ additions to CF₄ plasmas 8-72908

etching continued

SiO₂-Na₂O-CaO, electrochemically coloured, chemical composition and structure of surface layers 8-84758
 Sn-Ni metastable alloy, surface film comp., time depend., XPS 8-60870
 ether drift *see special relativity*
 Ettingshausen effect *see thermomagnetic effects*
 europium
 see also nuclei with
 -- (*Russian*) 8-72403
 atom, Kα line widths, precise meas. 8-62761
 calibo glass:Eu³⁺, Ho³⁺, energy transfer 8-76510
 film, optical cond. meas. 8-76112
 Mossbauer isomer shift and magnetic hyperfine field, press. effect 8-52386
 Al₂O₃:Eu, surface luminesc. centres excitation characts. 8-52560
 Ba aluminate:Eu, effect of non-stoichiometry on luminesc. 8-68550
 CaEO₂:Eu³⁺, energy transfer after red edge excitation 8-52552
 CaF₂:Eu²⁺, nuclear spin diffusion barrier, ¹⁹F NMR Obs. 8-64282
 CaO, Eu, Eu²⁺ to Eu³⁺ charge transformation (*Russian*) 8-72403
 Eu⁺, electron impact, resonant line excitation 8-82847
 Eu²⁺ in aqueous solution, multiphoton excitation and emission 8-94222
 Eu³⁺ fluoresc. lineshape in glass, temp., time and conc. depend., two-phonon Raman scatt. 8-64406
 Eu³⁺, intracavity enhancement of absorpt. in nanosecond regime 8-78839
 Eu⁺+Sr, light-induced collisional energy transfer 8-50614
 Eu⁺+Sr+hν→Eu+Sr^{**}, photon assisted collisional energy transfer 8-90285
 KBr:Eu(Yb), electron-irrad., photostimulated luminesc., ionic processes 8-52561
 KCl:Eu²⁺, radiationless processes 8-80391
 KCl(Br):Eu, Eu²⁺ ESR meas. 8-80209
 KI:Er²⁺, elec. field effect on mech. of recomb. 8-80397
 KI:Eu, electron-irrad., photostimulated luminesc., ionic processes 8-52561
 KY₃F₁₀:Eu³⁺, fluoresc. intensity, 77 to 4K, cryst. field parameters of Eu³⁺ 8-72580
 KY₃F₁₀:Eu³⁺, fluoresc. decay, radiative and nonradiative transition probabilities 8-72581
 LaAl₂:Gd³⁺(Eu²⁺), cryst. field parameters, relax. rates 8-84482
 NaCl(Br):Eu, Eu²⁺ ESR meas. 8-80209
 PbFCl:Eu²⁺, crystal field splitting, parametrisation of temperature dependence 8-91652
 RbCl:Eu, electron-irrad., photostimulated luminesc., ionic processes 8-52561
 RbCl:Eu, γ-irrad., thermoluminesc., EPR meas. 8-84670
 RbCl(Br):Eu, Eu²⁺ ESR meas. 8-80209
 SmS:Eu, excited-state exchange interactions, EPR meas. 8-68374
 Sm₂S₃:Eu, excited-state exchange interactions, EPR meas. 8-68374
 SmSe:Eu, excited-state exchange interactions, EPR meas. 8-68374
 SnO₂:Eu³⁺, luminesc. and charge compensation 8-76532
 SrF₂:Eu²⁺, spectral, spatial and temporal phonon spectroscopy, new spectrometer 8-83892
 Y₂O₃:Eu, surface luminesc. centres excitation characts. 8-52560
 Y₂O₃:Eu³⁺, absorpt. spectra, fluoresc., electron beam excitation 8-92093
 YVO₄:Eu³⁺, absorpt. spectra, fluoresc., electron beam excitation 8-92093
 YVO₄:Eu³⁺, laser site-selection spectroscopy investigation 8-68556
 Y₂WO₁₂:Eu³⁺, crystal struct., fluorescence spectra, exam. 8-52558
 europium alloys
 valence fluctuations, role of charge screening 8-51944
 valence fluctuations, thermal occupation effects 8-72118
 Ba-Eu, phase diag. (*Russian*) 8-80514
 Bi₂Sr_{1-x}Eu_x, supercond. and mag. ordering 8-56252
 Eu-transition metal intermetallics, valence fluctuations 8-91649
 EuAs₃, cryst. struct. of high and low temp. phases 8-75626
 Eu(Ni_{1-x}Cu_x)₅, mixed valency, isomer shift temp. depend. 8-84511
 EuNi₂Cu_{2-x}, mixed valency of Eu, Mossbauer expts. 8-52407
 EuNi₂Zn_{2-x}, mixed valency of Eu, Mossbauer expts. 8-52407
 La_{1-x}Eu_xAl₂, cryst. field splitting and spin-spin interaction of Eu²⁺, ESR meas. 8-68370
 europium compounds
 see also europium alloys
 monochalcogenides, anti-stokes luminesc. 8-60515
 tetrahedral complexes, ligand struct., rel. to luminesc. spectra satellite intensity (*Russian*) 8-72603
 (YSmEuCa)₃(FeGe)₃O₁₂, garnet film, ion implanted, bubble domain props. 8-88152
 β-Al₂O₃-EuO, X-ray diffuse scatt. 8-71725
 Ba₂EuFaO₆, luminescence Raman spectra, means for localisation of binding energy levels (*German*) 8-88304
 Ba₂EuNbO₆, luminescence Raman spectra, means for localisation of binding energy levels (*German*) 8-88304
 Ca_{1-x}Eu_xSi₂, solid solns., α-ThSi₂ struct. type, comp. and press depend. 8-91322
 Cs₂NaEuCl₆, luminescence Raman spectra, means for localisation of binding energy levels (*German*) 8-88304
 (Eu₂Lu₂)Fe₂O₁₂, submicron bubble films on rare earth-Ga garnet substrates, prep. and mag. props. 8-91909
 Eu complex, (Et₄N)₃[Eu(NCS)₆], Eu³⁺ ion site symm. 8-84656
 Eu complex, benzoylacetate, energy transfer at high pressures 8-52541
 Eu₂As₄, cryst. struct. determ., symmetrical version of Sm₂Ge₄-type struct. 8-63710
 EuB₆, (La,Eu)B₆, (Eu,Y)B₆, (Eu,Ba)B₆, single crystal growth for thermionic emission 8-92183
 EuB₆, valence mixed state, Kondo lattice, Anderson localisation models (*Japanese*) 8-51945
 EuB_{6-x}C_x, magnetic and elec. props. 8-91842
 Eu_{0.5}Ba_{0.5}TiO₃, ferromag., ferroelec., ceramic, Curie temps. determ. 8-68230
 EuCl₂, EuCl₂-EuCl₃, EuCl₂.HCl, mag. props., 77-292K 8-52197
 EuCo₂Ge₂, magnetism and hyperfine interactions 8-76228
 EuCu₂Ge₂, magnetism and hyperfine interactions 8-76228
 EuFe₂Ge₂, magnetism and hyperfine interactions 8-76228
 Eu(III) complexes with gluconate ions, reduction, polarographic behaviour 8-92568

euroium compounds continued

- (EuLu)₃Fe₂O₁₂, Ga, Al or (Ca,Ge) substituted, mag. props. and growth of 2 μ m bubbles 8-91910
 EuMn₂Ge₂, magnetism and hyperfine interactions 8-76228
 EuNi₂Ge₂, magnetism and hyperfine interactions 8-76228
 EuO, dynamic dipolar cross over 8-76339
 EuO, electron correls., defects, metal-insulator transition 8-63960
 EuO, ferromag. semicond., electronic spectrum, influence of finite carrier conc. 8-76220
 EuO, ferromagnetic, mag. field effect on optical absorpt. edge, piezotransmission spectra 8-95578
 EuO, mag. struct. and transition temp., indirect exchange 8-91860
 EuO, quadrupole coupling due to lattice imperfections 8-76347
 EuO, rotation of polarisation plane in very high mag. field 8-92054
 EuO, spin wave damping, theory compared with expt. 8-52237
 EuO, spin-disorder induced phonon Raman scatt. 8-60457
 EuO, transport properties at ferromag. reson. 8-68387
 EuO:Gd, electron mobility below Curie temp. 8-91696
 EuO:La, phototreshold reduction by mag. induced space charge layer 8-72692
 Eu₂O₃, appl. to LMFBR control 8-50261
 Eu₂O₃, sintering kinetics 8-52731
 Eu₂O₃-Ta₂O₅, microcracking, elastic props., internal friction 8-92326
 Eu_{1-x}N_x, ferromag. semicond., elec. and mag. props. (French) 8-79993
 Eu(ReO₄)₃·4H₂O, (ReO₄)⁻ ion vibrs. rel. to static field, Raman investigation (Russian) 8-76470
 EuS, conduction band density of states, redistrib. near ferromag. saturation 8-67939
 EuS, mag. struct. and transition temp., indirect exchange 8-91860
 EuS, pure and Gd doped, electronic struct., mag. exchange and elec. transport props. 8-87974
 EuS, spin relax. in crit. region 8-52270
 EuS, spin relaxation crit. behaviour 8-76251
 EuS, spin-disorder induced phonon Raman scatt. 8-60457
 EuS-metal contact, electrical switching exam. 8-68085
 EuS_x film, vacuum deposited, composition depend. on substrate temp. and deposition rate 8-84107
 EuSe, mag. struct. and transition temp., indirect exchange 8-91860
 EuSe, metamagnetic, magnetostriction ferromag. 8-88160
 EuSe, spin config. stabilisation by lattice distortion 8-52251
 EuSe, spin-disorder induced phonon Raman scatt. 8-60457
 EuSm₂S₄, mag. props. 8-68237
 Eu₃Sn_{1-x}Mo_xSn₈ (Se₈), ternary superconductor, paramagnetic relax. effects 8-68112
 Eu_{1-x}Sr_xSi₂, solid solns., α -ThSi₂ struct. type, comp. and press depend. 8-91322
 EuTe, field depend. correl. function theory of Raman scatt. near antiferromag.-paramag. transition 8-68490
 EuTe, mag. struct. and transition temp., indirect exchange 8-91860
 EuTe, spin-disorder induced phonon Raman scatt. 8-60457
 (EuX₂)₃²⁺ (X=Br, Cl), spectral hypersensitive intensity, ligand polarisability contrib. 8-51946
 Eu_{1-x}Yb_xO, solid soln., ferromag. semicond., increase of exchange interaction 8-88109
 Eu_{1-x}Yb_xS, solid soln., ferromag. semicond., increase of exchange interaction 8-88109
 K₂Eu(MoO₄)₄, electric dipole transition cross section and effective site symmetry of Eu³⁺ 8-52556
 (Y,Eu,Lu,Ca)₃(Fe,Ge)₅O₁₂, bubble memory chip, dynamic conversion comparison with (Y,Sm,Lu,Ca)₃(Fe,Ge)₅O₁₂ 8-68319
 (Y,Eu,Tm,Ca)₃(Fe,Ge)₅O₁₂, Ca, Ge substituted garnet LPE films, elec. props., charge imbalance, Seebeck effect 8-68101
 (Y,Eu,Tm,Ca)₃(Fe,Ge)₅O₁₂ garnet film coercivity, new annealing method 8-84459
 (Y,Eu)₃(Fe,Ga)₅O₁₂, LPE growth from molybdate fluxes, bubble props. 8-68322
 (YCaEuYb)₃(FeGe)₅O₁₂, LPE, stripe end motion, effect of in-plane field 8-68330
 (YEu)₃(FeGa)₅O₁₂ rigid magnetic bubble transition to normal behaviour 8-95501
 Y_{2.35}Eu_{0.65}Ga_{1.3}Fe_{3.8}O₁₂, bubble translation vel., ion-implantation effects 8-68327
 (YEuLuCa)₃(FeGe)₅O₁₂ film, stable state of bubbles containing Bloch lines 8-76281
 Y_{1.52}Eu_{0.5}Tm_{0.3}Ca_{0.88}Gd_{0.88}Fe_{4.12}O₁₂, bubble translation vel., ion-implantation effects 8-68327
 (YEuYbCa)₃(FeGe)₅O₁₂ film, mag. α -bubbles, automation props. 8-88150
 (YEuYb)₃(FeGa)₅O₁₂, LPE, stripe end motion, effect of in-plane field 8-68330

eutectic alloys

- directional solidification, effect of thermal parameters, two-dimens. heat transfer model 8-88456
 multiphase solidification theory 8-95740
 nontransition element/alkali metal systems, direct calorimetric exam. 8-84775
 phase volume fraction determ. using manual point count practice 8-53052
 solidification mechanisms, contribution of microgravity expts. 8-88457
 steel, 12Kh18N9T-TiB₂, high temp. props. 8-84931
 steel, high-speed, eutectic carbide structure, determ. by SEM 8-85075
 Al-Ag₂Al, eutectic alloy, exam. of terminal solid solubility limits 8-76633
 Al-Al₃ eutectic, abrasive fragmentation (Czech) 8-64715
 Al-Al₃Ni, effect of some thermal parameters on the directional solidification process 8-88456
 Al-Al₃Ca, eutectic alloy, unidirectionally solidified, exam. of growth and crystallography 8-72771
 Al-CuAl₂ eutectic, thermal instability in temp. gradient 8-52851
 Al-Fe, plastically deformed, influence of microstruct. on energy stored 8-84894
 Al-Fe-Si, eutectic alloy growth, by twinning plane propagation (French) 8-60667
 Al-Ge, directionally solidified lamellar eutectics, specimen prep. for TEM (German, English) 8-95885
 Al-Mn alloys, study of solidification by rapid cooling (Japanese) 8-88459
 Al-Si, hypereutectic silumins, P and Na modification 8-84792
 Al-Si eutectic, directionally solidified, tensile props. 8-64531

eutectic alloys continued

- Al-Si eutectic, Na, Sb and Sr alloying addition effects on microstructure (French) 8-64548
 AuSn₄-Sn, unidirectionally solidified, X-ray diff. anal. of crystal struct. 8-91308
 Cd-Zn, directionally solidified lamellar eutectics, specimen prep. for TEM (German, English) 8-95885
 Co-Al-Cr(Nb)(Ta), eutectic alloys, charact. by melting, oxidation resistance and composition 8-52768
 Co-Al-Nb, monovariant directionally solidified eutectics, struct. and mech. props. (Russian) 8-92254
 Co-Cr-Mo (Zr)(Nb)(Ta), eutectic alloys, charact. by melting, oxidation resistance and composition 8-52768
 Co-Cr-Ni-TaC, directionally solidified eutectic, mech. props. and struct., thermal cycling effects (Russian) 8-92282
 Co-Cr(VC)((Ti,V)C)-(Al), eutectic alloy, unidirectional solidification, oxidation and tensile tests 8-52790
 Co-Si-Nb(Zr), eutectic alloys, charact. by melting, oxidation resistance and composition 8-52768
 Cu-Al, eutectic composition, exam. of high temp. mechanical behaviour (French) 8-72818
 Cu-Al hypoeutectic alloy, water-quenched, tensile fatigue strength at high temp. in vacuo (Japanese) 8-72837
 Cu-Al(In), lamellar eutectoids, calorimetric determ. of interfacial enthalpy 8-60668
 β -Cu-In, directionally transformed eutectoid, morphology exam. by metallography (German) 8-92257
 β -Cu-In, unidirectionally transformed eutectoid, lamellar microstructure, influence of grain boundaries on thermal stability 8-72795
 Fe-Al eutectic alloy, duplex crystals, unit cell parameters, appl. of Weissenberg technique 8-67684
 Fe-C, lamellar eutectoid, calorimetric determ. of interfacial enthalpy 8-60668
 Fe-C, pearlite, eutectoid alloy, efficiency of directional transformation on orientated growth 8-76642
 Fe-Cr-Ta, eutectic alloy, exam. of eutectic temp., composition, and oxidation resistance 8-52767
 Fe-Si-Ti(Zr)(V)(Nb), eutectic alloy, exam. of eutectic temp., composition, and oxidation resistance 8-52767
 Fe₂Ti-Fe eutectic alloy, directional solidification singularities (Russian) 8-68678
 Ga/rare earth systems, direct calorimetric exam. 8-84775
 In-Bi alloy system at high press. and temp. 8-92238
 In-Ga alloy, electrode metal-solvent interaction rel. to elec. double layer struct., adsorpt. 8-61023
 Mn-Bi eutectic alloy, mag. anisotropy 8-68220
 Mn-Pt (<29 at.%), eutectoid transform., antiferromag. struct. transform. (French) 8-92259
 Mo-TiN (3.5 vol.%), failure characts. exam. 8-68788
 Nb-Nb₂C, directional crystn. using plasma heating 8-60569
 Nd-Tl phase diagram, intermediate phases 8-60653
 Ni-Al-Ti, eutectic alloy charact. by melting temp., composition and oxidation resistance 8-52771
 Ni-Co-Cr-Ta-Al-W-Mo-Ti, cast, phase volume fraction determ. using manual point count practice 8-53052
 Ni-Cr-Nb-Al eutectic alloys, sulphidation/oxidation at high temps., corrosion mechanism 8-72934
 Ni-Cr-Ti(Nb)(Zr), eutectic alloy charact. by melting temp., composition and oxidation resistance 8-52771
 Ni-W directionally solidified eutectic composite, foil prep. for TEM 8-53072
 Ni₃Ti-Ni eutectic alloy, directional solidification singularities (Russian) 8-68678
 Pb-Sn, eutectic alloy, plastic deform., work hardening (German) 8-92279
 Pb-Sn, superplastic eutectic, roll load and torque necessary for rolling (French) 8-95761
 Pb-Sn eutectic, cavitation during superplastic flow, affecting factors 8-60728
 Sb-Ge, unidirectionally solidified, exam. of compressive props. and struct. 8-68730
 Sn-Pb eutectic, struct. and plasticity, thermomech. treatment effects (Russian) 8-60686
 W-W₂C, directional crystn. using plasma heating 8-60569
 Zn-Al (22 wt.%), superplastic, eutectoid alloy, ductility and fracture 8-60819

eutectic structure

- borophosphate glasses, effect of F on props. 8-67657
 ferrous eutectic liquids, exam. of structures 8-71668
 Bi_{0.52}Sb_{1.48}Te₃ thermoelec. solid soln., homogeneity, effects of prep. method 8-52698
 Co-Al-Nb, monovariant directionally solidified eutectics, struct. and mech. props. (Russian) 8-92254
 Pb-Sn, unidirectionally solidified eutectic, lamellar microstructure, influence of grain boundaries on thermal stability 8-72795
 Sc-Fe system phase diag. (Ukrainian) 8-84773
 Te-Bi₂Te₃ oriented eutectic, microhardness, influence of size of phases (Russian) 8-92322
 Te-Sb₂Te₃ oriented eutectic, microhardness, influence of size of phases (Russian) 8-92322
 Ti-C-Ni, reaction kinetics under simulated liq.-phase sintering 8-52746

eutectoid steel see carbon steel**evaluation**

- see also function evaluation
 abdominal and pelvic diagnosis, US and computed tomography evaluation 8-61228
 clinical ECG real-time telephone transmission usefulness and reliability 8-57108
 flat solar collector, energy and economic analyses 8-83236

evaporated layer production see vapour deposition**evaporation**

- see also drying; field evaporation
 accommodation coefficients, effects on evaporation and condensation (Japanese) 8-81933
 adsorbed monolayers, permeation and evaporation resistance, attractive forces effects 8-67892
 alkali halide, morphology of growth and evaporation surface 8-79544
 bubble, of vap., with microlayer, universal growth relations 8-71266
 capillary and porous surfaces, liquid boiling and evap. heat transfer 8-94526

evaporation continued

- capillary pore; evaporation from digital surface, mass transfer kinetics 8-51233
- cathode spots on Ag, Ni, Cu, and W vac. arc discharge electrodes, model 8-91179
- cloud, warm cumulus, three-dimens. numerical model with microphysical processes (*Russian*) 8-88884
- cooling pond, heat transfer processes evaluation 8-61458
- crystal, Langmuir torsion effusion meas., recoil force correction factors 8-75929
- detonation of unmixed liq.-gas mixture with surface evap., fluid dynamical characts. (*Russian*) 8-55630
- dielectric surface, nonlinearly-absorbing, laser-induced evap. 8-80438
- drop electrification by evaporation or vapour condensation (*French*) 8-61511
- drop evaporation rate in forced convective flow with transverse sound fields 8-51224
- droplet evaporation, modelled by wet porous sphere, heat-transfer meas. 8-59268
- droplet evaporation on heated surfaces, theory 8-87785
- droplets of soln. dispersed in gas flow, heat and mass transfer during evaporation 8-90998
- extended liquid masses, film boiling heat transfer, partial evaporation method 8-90668
- ferrous metallurgy, surface purification using laser and N₂ jet 8-92392
- fogs formation theory and prediction 8-61522
- heat conduction, unsteady, in quarter plane, appl. to bubble growth 8-75045
- hypersonic gas flow, radiant heat and evaporative cooling 8-91028
- kinetic theory, disequilibrium conditions 8-79755
- kinetic theory, evaporation, condensation, linear, nonlinear problems 8-75802
- kinetic theory, hydrodynamic eqn. and slip boundary condition 8-63903
- kinetic theory of one-dimensional evaporation and condensation problem (*Japanese*) 8-81932
- Leidenfrost effect, demonstrations 8-81744
- liquid, spontaneously evaporating, critical discharge from channel 8-59456
- liquid droplet, idealised models for preheat stage 8-94586
- liquid film, evaporating, interline heat sink capability, optical and thermophysical props. depend. 8-71276
- liquid film, falling, laminar, transport augmentation by surface waves 8-71343
- metal, evaporation under laser irradiation (*German*) 8-52599
- metals and alloys, thermodynamic props., evaporation, optical spectral method appls., review (*Russian*) 8-75822
- nucleation, microscopic theory (*Russian*) 8-67801
- organic solvent evaporation, internal heating by IR irradi. 8-87237
- pine forest wet canopy evap. meas. 8-61460
- refractory carbides, thermodynamic evap. characts., cluster-component calcs. 8-51704
- river/atmosphere time dependent, single dimensional heat exchange, analysis (*Bulgarian*) 8-57221
- sea-atmosphere heat-transfer expts. (*Russian*) 8-81206
- semifinite porous media, heat cond., phase transitions effects 8-94523
- simultaneous melting and evaporation due to area heat source (*German*) 8-59282
- soil water, evaporation rel. to ground surface temp. and moisture content, vegetation layer effects 8-73373
- spherical liquid droplets, nonlinear condensation and evaporation 8-63902
- subarctic and tundra surfaces, evap. equilib. model 8-61459
- Tokamak, Diva, metal impurities origin, arcing ion sputtering, evap. 8-59691
- turbulent exchange coefficients for sensible heat and H₂O vapour under advection conditions 8-92907
- two-phase flow, dryout region of forced convection evaporation, heat transfer coeff. 8-90988
- vegetation-atmosphere interaction, simplified one-dimens. theory 8-61479
- vortex filament form. from ascending flows over evap. liquid 8-63440
- water, bulk evaporation coeffs. depend. on air-water interfacial conditions, isotopic method determ. 8-85576
- water, deep evaporation characterisation, from homogeneous porous medium (*French*) 8-59468
- water, evaporation coefficient, reply to comments 8-75912
- water, evaporation coefficient, variation with observation conditions 8-75909
- water, evaporation coefficients, comments 8-75911
- water, saturated (subcooled), crit. discharge through differently shaped channels 8-55681
- water droplet evaporation, heat transfer characts., on heated surfaces 8-59269
- water evaporation coefficients, comments 8-75910
- Ag, ultrafine powder, role of evap. during sintering 8-64505
- AgBr, thin layers, evaporation conditions, photoresponse (*Bulgarian*) 8-78017
- Al, vapour deposition on substrates, splash-free, using modified W helix 8-52689
- Cd, influence of source material and shape on sublimation props. 8-80474
- CdCr₂Se₄, evap., mass spectra 8-53238
- CdSe, influence of source material and shape on sublimation props. 8-80474
- KBr, rot. of vacuum thermal etch pits 8-87674
- Ni-W (2%), Mg diffusion meas., 970-1330K, appl. of vapour collect and AES method 8-75876
- Se_{5,6}, influence of source material and shape on sublimation props. 8-80474

Evershed effect see sunspots

evolution (biological)

- asteroidal terrestrial cratering, plate tectonics and evolution of life 8-96421
- chance and origin of life 8-69269
- dynamic processes on Earth, extraterrestrial causes, rel. to extinction of life 8-92820
- early Earth regolith formation and origin of life 8-85698

evolution (biological) continued

- ecological disasters and ice ages, prod. by Earth-comet close approach 8-53714
- optical asymmetry correl. with parity violating weak interaction 8-69000
- origin of life, astrochemistry and organic mols. form. 8-73660
- origin of life, from origin of universe to earliest geological times 8-69923
- origin of life, monomers to polymers 8-69461
- origin of life, pre-biotic era 8-69460

EXAPT see problem oriented languages

exchange forces in nucleus see nuclear forces

exchange interactions (electron)

- see also antiferromagnetism; ferromagnetism; RKKY interaction; superexchange interactions
- alkali halide, exchange charge polarisation, dielectric const., Dick and Overhauser model 8-55832
- alloy, binary, with mixed ferro- and antiferromag. exchange, magnetisation, phenomenological theory (*German*) 8-56297
- amorphous ferromagnets, ferromag. saturation, spatially random magnetostatic, magnetocrystalline, magnetostrictive and exchange fluctuations 8-60277
- amorphous magnet, finite temperature calculations, random anisotropy model 8-80112
- anisotropic linear spin chain, two-magnon problem with arbitrary interaction radius 8-72320
- antiferromagnetic metal, with paramag. impurities, Neel temp., impurity conc. depend calc. 8-68232
- Berthollides, chaotic mag. states 8-56330
- bipolarons, localised, in ionic crystals 8-67957
- bis(diethylammonium) copper tetrachloride, mag. susceptibility, EPR spectra 8-68193
- bisgalvinoxyl biradical, cryst., spin-spin dipolar and exchange interactions 8-52356
- charge transfer allowance in effective Hamiltonian method, technique 8-68001
- Chichibabin's hydrocarbon, ESR spectra, electron exchange integral 8-50562
- covalent elements, cohesion in condensed phases, corrections to simple Huckel approx. 8-59779
- density matrix formalism for coupled dynamical systems 8-95522
- diagrammatic Green function technique appl. to cryst. field systems with exchange 8-68130
- diamond, ESR studies, review 8-95521
- domain wall micromagnetic dynamics, numerical model 8-72381
- DPPH-benzene complex, ht. capacity, 0.55-20K, mag. susceptibility, 0.4-300K 8-56317
- electron gas, interacting, elec. cond. 8-95276
- EPR of heteropairs with strong exchange coupling, hyperfine struct. 8-72395
- ferroelectric antiferromagnets, exchange enhancement of the magnetoelectric coupling 8-88159
- ferromagnet, magnetisation at low temp., disorder induced behaviour 8-52234
- ferromagnet, one-dimensional, with biquadratic exchange, solitary excitations 8-76232
- ferromagnet, surface magnetoelastic waves in the presence of exchange interactions and pinning of surface spins 8-80186
- ferromagnet, uniaxial, with random exchange bonds of different signs, spin waves 8-76233
- ferromagnet, uniaxial with single-ion and exchange anisotropies, magnetisation in transverse mag. field 8-56277
- ferromagnet film, spin wave propagation near surface 8-68308
- ferromagnetic semiconductor, autolocalised electron states 8-51924
- ferromagnetic semiconductor, spectrum of quantum spin waves in field of strong EM wave 8-91857
- ferromagnets, metallic, spin wave damping, magnetisation relax. 8-88106
- ferromagnets and antiferromagnets, transverse dynamical susceptibility within the local exchange approx. 8-76229
- ferromagnetic conductor, electric field response and electrofluctuation instability (*Russian*) 8-56083
- film, rel. to micromagnetic dynamics in domain walls, numerical model 8-72382
- free radicals in soln., spin exchange and EPR broadening 8-52357
- Frenkel excitons, optical resonance 8-91621
- heat magnetization in the singlet-triplet model 8-64211
- Heisenberg antiferromagnet, dil., CPA calc. 8-68263
- Heisenberg antiferromagnet, dil. with random first- and second-neighbour exchange bonds, CPA theory 8-52187
- Heisenberg ferromag. localised magnons around surface impurity (*Russian*) 8-84376
- Heisenberg film, spin-one isotropic, quadratic interactions, quadrupolar-paramag. T. 8-64210
- Heisenberg paramagnet, dil., uniaxial anisotropy, frequency moments of spin correlation function 8-84377
- Hubbard antiferromag. semiconductor, electron correlations, weak coupling 8-67969
- Hubbard model, two band, magnetic behaviour 8-80119
- impurity centres, exchange interaction due to phonons (*Russian*) 8-79678
- interatomic interactions between electrons 8-64017
- Ising S=1, 1/2 mixture, one-dimens., random, mag. props., spin distrib. 8-95407
- Ising site model, random mixtures, Monte Carlo simulation 8-73935
- Ising system, finite, statistically layered, crit. phenomena 8-95446
- layered compounds, effect of exchange on CDWs 8-60078
- Lorentz-Lorenz formula, microscopical derivation 8-92014
- magnetic 3d impurity in non-magnetic metal, effective ion Hamiltonian 8-64016
- magnetic insulators, indirect exchange interactions, polar model study 8-88110
- magnetic resonance line, exchange narrowing at low temp. (*Russian*) 8-56366
- magnetic semiconductor, multispin indirect exchange (*Russian*) 8-56311
- magnetic susceptibility of cryst. with strong s-d exchange (*Russian*) 8-56283
- metal, conduction electron coupling with moments of 3d and 4f ions 8-60090

exchange interactions (electron) continued

- metal, inhomogeneous electron system, nonlocal exchange and correlation 8-56097
- metal, magnetic impurity, model of resonance level in Kondo problem (*Russian*) 8-80129
- metal, pressure equation derived, Hartree-Fock approx. 8-72103
- metal surface, exchange-correlation hole 8-80037
- metal surface, step potential model, static semiclassical response of bounded electron gas 8-72221
- metallic mononitrides:Gd, coupling between 4f electrons and conduction electrons, EPR linewidth 8-52347
- one-dimensional systems, exchange effects in plasmon dispersion 8-91628
- orbital interaction and chemical bonds. Exchange repulsion and rehybridization in chemical reactions 8-85142
- polaritons, multi-component, reflectance spectrum 8-87921
- pseudospins, $S=1/2$, simple cubic array, with anisotropic exchange between nearest neighbours, ground state configs. 8-72340
- random, and 'frustration effect' 8-68212
- rare earth alloys, amorphous, magnetoresistivity, exchange scatt. model 8-95287
- rare earth alloys, amorphous, random anisotropy antiferromag. model 8-95428
- rare earth alloys, dil., ESR linewidth of rare-earth ions 8-68373
- rare earth amorphous alloys, antiferromagnetism, mol. field approx. 8-80142
- rare earth and rare earth intermetallic hydrides, magnetic properties, effect of hydrogenation 8-68210
- rare earth impurities in s-band metals, Kondo anomaly 8-52208
- rare earth ions, energy transfer rates, unified method using standard tensor calc. (*French*) 8-79965
- rare earth-cobalt intermetallics, R_4Co_3 , cryst. field effect on mag. moment direction, neutron diffr. meas. 8-80132
- rare earths, spin waves and excitations 8-84407
- ruby:Cr³⁺, exchange integral, pressure depend., test of theory 8-87741
- semiconductor, metamagnetic, magnetostriction ferrous 8-88160
- semiconductor, spin relax., in quantising mag. field, effect of carriers 8-72388
- soft magnetic metals, ideal, AC response 8-64223
- spin deviation states in spin-1 system with Heisenberg and biquadratic exchange 8-84378
- spin glass, local exchange invariance concept 8-60288
- spin systems with three-atom exchange, elementary excitations 8-84404
- spin waves in strongly anisotropic magnets, canonical transform theory 8-68197
- spin-Hamiltonian formalism for exchange-coupled pairs of paramag. ions, second-order corrections 8-68133
- spinel structures, electroconductivity and electron exchange 8-84207
- standing spinwave resonance in film with nearest and next-nearest neighbour exchange 8-68390
- TMMC:M, impurity (M) effects on Neel temp. and low temp. mag. susceptibility 8-88113
- TMMC, antiferromag. coupling in linear chains, molecular orbital approach 8-52239
- TMMC, exchange-narrowed EPR linewidth, temp. depend. 8-52292
- transition metal surface, spin fluctuations 8-95451
- transition metal vanadates 8-51991
- TTF.PtS₄.C₆(CF₃)₄, quasi-one-dimensional cpd., exchange, thermal and mag. study 8-68209
- two-sublattice system, with strong antisymm. exchange and fourth order anisotropy, mag. configs. 8-68167
- uniaxial magnet, free energy of system with weak exchange interactions and high mag. anisotropy (*Russian*) 8-68213
- wavevector-dependent spin susceptibility, variational principle 8-91586
- Wolff model, effective mag. interactions between impurity and conduction electrons 8-68143
- Ag-Mn alloys, dilute, low temp. elec. resist. (*Russian*) 8-68024
- Au-Cr Kondo alloy, effect of press. on resistivity 8-79978
- Ba₂Fe₁₆O₂₇, hexagonal ferrite, W-struct., Mossbauer spectra of Fe³⁺ and Fe²⁺ 8-88242
- CO catalytic oxidation on spinel type ferrites, role of mag. exchange interactions 8-56916
- CdS, model $S=1/2$ amorphous antiferromagnet, spin polarisation 8-52288
- CeCl₃(Br₃), interaction parameters, high freq. meas. of adiabatic differential susceptibility 8-68211
- Co-Fe alloys, FCC structure, average mag. moment, conc. depend. 8-88099
- CoU₂S₃, mag. struct., exchange energy, magnetisation and neutron diffr. expts. 8-68170
- Cr complex, trimeric clusters, low temp. mag. props. 8-76261
- CsNiCl₃, antiferromag. coupling in linear chains, molecular orbital approach 8-52239
- CsVCl₃, antiferromag. coupling in linear chains, molecular orbital approach 8-52239
- CuCl₂.2H₂O, antiferromag. to paramag. transition, high field magnetisation meas. 8-64204
- Cu₂Zn_{1-x}ZrF₆.6H₂O, distortions of nearest Jahn-Teller [Cu(H₂O)₆]²⁺ centres 8-68000
- Dy, spin wave exam. 8-56306
- Er, paramagnetic and antiferromagnetic states, optical absorption (*Russian*) 8-56497
- Er, spin wave exam. 8-56306
- ErB₄, theory of metamagnetic transitions (*Russian*) 8-95436
- ErCu, cubic antiferromag., mag. excitations inelastic neutron scatt. meas. 8-72341
- ErZn, magnetoelastic and quadrupolar couplings 8-52328
- EuO, mag. struct. and transition temp., indirect exchange 8-91860
- EuS, conduction band density of states, redistrib. near ferromag. saturation 8-67939
- EuS, mag. struct. and transition temp., indirect exchange 8-91860
- EuS, pure and Gd doped, electronic struct., mag. exchange and elec. transport props. 8-87974
- EuSe, mag. struct. and transition temp., indirect exchange 8-91860
- EuTe, mag. struct. and transition temp., indirect exchange 8-91860
- Eu_{1-x}Yb_xO, solid soln., ferromag. semicond., increase of exchange interaction 8-88109
- Eu_{1-x}Yb_xS, solid soln., ferromag. semicond., increase of exchange interaction 8-88109

exchange interactions (electron) continued

- Fe based ternary alloys, Coulomb and exchange scatt. amplitudes, spin dependent residual resistivities 8-64033
- Fe, de Haas-van Alphen effect and exchange splitting, effect of pressure (*Russian*) 8-95252
- Fe, ferromagnetic, cluster method, environmental effects 8-95405
- Fe-Cr, Invar alloy, explanation of phys. anomalies (*Russian*) 8-88112
- Fe-Cr-Ni, mag. state at low temps. (*Russian*) 8-56298
- Fe-Gd film, amorphous, mag. props., mean field analysis 8-64236
- Fe-Ni, Invar alloy, explanation of phys. anomalies (*Russian*) 8-88112
- Fe-Ni/pure Fe exchange coupled films, mag. reversals, hard layer thickness effects (*Russian*) 8-56359
- Fe₈₀B₂₀, amorphous ferromag., hyperfine field distrib., Mossbauer effect 8-60371
- Fe₂Cu_{1-x}Rh₂S₄, mag. tetrahedral intrasublattice interaction, X-ray, magnetisation and Mossbauer expts. 8-52241
- Fe_{3-x}Ni_xO₄, low temp. Mossbauer spectra, electron transfer and spin density distribution 8-52404
- Fe₃O_{4-x}F_x, low temp. Mossbauer spectra, electron transfer and spin density distribution 8-52404
- FeS, zinc blende type, crystallographic and Mossbauer obs. 8-87650
- FeS, zinc blende type, mag. struct. (*French*) 8-91846
- FeU₂S₃, mag. struct., exchange energy, magnetisation and neutron diffr. expts. 8-68170
- Fe₂Zn_{1-x}F₂, Neel temp. mag. cone depend., CPA calcs. 8-88122
- Fe_{3-x}Zn_xO₄, low temp. Mossbauer spectra, electron transfer and spin density distribution 8-52404
- Gd compounds, NaCl type, exchange striction 8-84409
- Gd, spin wave exam. 8-56306
- Gd, spin wave temp. depend., exchange coupling role 8-68199
- Gd-Co, and Gd-Co-Mo films, amorphous, mag. props., annealing effects 8-64235
- Gd-Co-Fe film, amorphous, bias-sputtered, uniaxial perpendicular anisotropy 8-64234
- Gd-Fe film, amorphous, mag. props., annealing effects 8-64235
- GdAg_{1-x}In_x, magnetic transition temp., effect of hydrostatic press. 8-76244
- GdCl₃, interaction parameters, high freq. meas. of adiabatic differential susceptibility 8-68211
- GdLa_{1-x}Pd_x, ESR linewidths, g-shifts, effective electron interaction, spin-lattice relax., spin-flip scatt. 8-68372
- GdP, electronic struct., mag. exchange and elec. transport props. 8-87974
- GdS, electronic struct., mag. exchange and elec. transport props. 8-87974
- Gd₂Y_{1-x}Fe₃, s-d exchange interaction integral, change due to hydrostatic compression 8-88199
- Gd₂Y_{1-x}Fe₃, saturation magnetisation, magnetostriction, Curie temp., ferrimag. ordering, exchange field (*Russian*) 8-68343
- ³He with C particles, pulsed NMR, mag. susceptibility surface induced ferromagnetism, antiferromagnetic exchange interaction 8-79844
- n-Hg_{1-x}Mn_xTe, quantum transport phenomena, exchange interaction influence 8-76093
- Ho₂Tb_{1-x}Fe₃, single cryst., spin orientations 8-84425
- Ho₂Y_{1-x}F₃, calc. of Ho³⁺→Ho³⁺ energy transfer rates (*French*) 8-79966
- HoZn, magnetoelastic and quadrupolar couplings 8-52328
- KClO₄, X-irrad., ESR spectra of O₃⁻ and ClO₃ exchange-coupled to K₂O 8-64856
- KCuF₃, chain-like antiferromag., parallel susceptibility 8-80137
- K₂Cu_{1-x}Mn_xF₄, Cu-Mn exchange interaction, optical determ. 8-72551
- K₂Cu_{1-x}Zn_xF₄, two-dimens., ferromag., spin wave excitations 8-80140
- KMn_{0.18}Zn_{0.82}F₃, excitation of Mn²⁺ clusters, neutron scatt. 8-68200
- LaBe₁₃-Er(Dy), dil., ESR, crystalline elec. field splitting, exchange parameters 8-52348
- (La_{1-x}Gd_x)Al₂, dil., reverse resistance anomaly 8-76054
- Lu-Gd, dil., positive exchange Kondo system, magnetisation and resist. 8-68158
- Lu₂V₂O₇, pyrochlore struct., mag. props. 8-72335
- Mg-Mn, dil. alloy, de Haas-van Alphen effect, exchange interaction, Kondo effect 8-88093
- MgEr₂S₄, magnetisation and susceptibility, exchange interactions obs. 8-52242
- Mg₈MnO₈, EPR in magnesium-manganese spinel (*Russian*) 8-91936
- Mn complex, manganese (II)(1,2,4-triazole)₂(NCS)₂, 2-dimens. Heisenberg antiferromag., mag. props. 8-72336
- MnCl₂-KCl system, molten, EPR spectra, linewidth study 8-88173
- Mn₃Cr₂Ge₃O₁₂ garnet, antiferromag. ordering (*Russian*) 8-80146
- MnEr₂S₄, magnetisation and susceptibility, exchange interactions obs. 8-52242
- MnF₂:Ni²⁺, IR fluoresc., field depend., exchange energy 8-68543
- Mn_{1-x}Fe_xAs, mag. props. in ground state (*Russian*) 8-56294
- MnFe₂O₄, exchange splitting of ionic S-state, neutron scatt. 8-52240
- Mn₂Mg_{1-x}S solid solution, mag. props. 8-60269
- Mn₂Mg_{1-x}Y₂S₄, magnetisation and susceptibility, exchange interactions obs. 8-52242
- Mn₂Pd_{8-x}Ged₁₈, amorphous alloys, mag. props. 8-91906
- MnY₂S₄, magnetisation and susceptibility, exchange interactions obs. 8-52242
- Mo, nuclear indirect interaction, NMR line shape anal. 8-52360
- NaF, ab-initio calc. of cohesion energy, compressibility and density 8-71782
- Nd₂Co_{1-x} film, amorphous, mag. props. meas. 8-68312
- Nd₂Fe_{1-x} film, amorphous, mag. props. meas. 8-68312
- Ni (111), band struct. and temp.-depend. mag. exchange splitting, angle resolved photoemission obs. 8-60546
- Ni based ternary alloys, Coulomb and exchange scatt. amplitudes, spin dependent residual resistivities 8-64033
- Ni, ferro- to paramag. transition, angular resolved photoemission 8-68603
- Ni-Co, ferromagnetic resonance, surface anisotropy 8-95526
- Ni-Fe film, unidirectional anisotropy by exchange coupling, appl. to biasing of magnetoresist. read head 8-91907
- Ni-Mn alloy, disordered, exchange-anisotropy field, magnetisation curves 8-72365
- Ni-Mn alloy, disordered, mag. struct., high field twist deform. 8-68166
- NiO, exchange striction 8-56309
- NiSnCl₆.6H₂O, ESR line shift at very low temps. 8-56375
- Pd, CESR expts. using transmission technique 8-91954

exchange interactions (electron) continued

- Pd, electronic struct., effects of press. and alloying with Ru, Rh, Ag, and Rh+Ag 8-91581
 Pr₂Tl, induced ferromag., mag. props. under hydrostatic press. 8-56315
 Rb₂FeF₅, 1D antiferromagnetic system, Mossbauer investigation 8-95533
 Si MOS inversion layer, subband struct., many body effects 8-64131
 Si, phonon-mediated intervalley electron-electron interaction 8-95125
 Sm₂(Co_{1-x}Al_x)₁₇ (Russian) 8-64202
 Sm₂(Co_{1-x}Fe_x)₁₇, anisotropy consts., conc. and temp. depend. (Russian) 8-64202
 SmCo₅Ni_{5-5x}, exchange fluctuations and giant intrinsic mag. hardness 8-56310
 Sm₂Co_{17-x}Ni_x, effect of Ni on mag. props. 8-68296
 Sm_{1-x}La_xS, mag. suscept., moment, impurity effects, indirect exchange interaction 8-68147
 SmNi_{5-x}Cu_x, giant intrinsic mag. hardness due to randomised cryst. field interactions 8-68208
 SmS:Eu, excited-state exchange interactions, EPR meas. 8-68374
 Sm₂S₄:Eu, excited-state exchange interactions, EPR meas. 8-68374
 SmSe:Eu, excited-state exchange interactions, EPR meas. 8-68374
 Tb(OH)₃:E³⁺, ferromag., anisotropic exchange effects in optical spectra 8-80141
 Tm, from anisotropy meas. on Gd-Tm alloys 8-68216
 Tm₂V₂O₇, pyrochlore struct., mag. props. 8-72335
 TmZn, cooperative Jahn-Teller effect 8-67998
 US, electronic struct. calc. 8-91615
 Y-Co, amorphous alloy film, spin reson. meas., exchange stiffness 8-68389
 YCo₅, amorphous ferromagnet, exchange dominated surface modes 8-52359
 Y₂Co_{17-x}Ni_x, effect of Ni or mag. props. 8-68296
 Y₆(Mn_{0.75}Fe_{0.25})₂₃, mag. scatter state, hysteresis loops 8-56350
 Yb₂V₂O₇, pyrochlore struct., mag. props. 8-72335
 Zn-Cr, dil., mag. anisotropy, 0.001 to 2K 8-68157
 ZnSiF₆:Cu²⁺, spin-spin interactions of impurity pairs (Russian) 8-72397
 ZnTe:Mn, mag. field splitting α n=2 exciton state (Russian) 8-79940

exchange models see peripheral models**exchanges (chemical)** see chemical exchanges**excimer lasers**

- CW lasers, homogeneously broadened, with uniform distribution loss, exam. of output power 8-55332
 electronic transition lasers, conf., Snowmass Village, USA (Sept. 1976) 8-63076
 energy storage and nonstoring advanced lasers for fusion appls. 8-79027
 Group VIA photolytic laser systems, for fusion research 8-59002
 inert gas, stimulated emission kinetics in nonself-sustained elec. discharge 8-50753
 inert gas fluoride, discharge and electron beam pumped, review 8-71083
 inert gas fluoride exciplex laser pumping efficiency 8-74892
 inert gas fluoride laser, using NF₃-inert gas mixture, long pulse UV emission (French) 8-58982
 inert gas fluorides, covalent and ionic states, ab initio CI calcs. 8-78634
 inert gas halides, kinetic processes 8-63098
 inert gas halogen excimer laser principles, performance and applications 8-55342
 inert gas oxide amplifiers, appl. and performance 8-63085
 inert gases, electron beam excited, absorpt. characts. 8-82948
 inert halide lasers, emission spectra, efficiencies, pulse energy, appls. 8-58993
 intense lasing with HCl halogen donor 8-90411
 mercuric halide dissociation lasers, discharge pumping 8-79009
 metal atom oxidation reactions, kinetics of chemilum. emitter form. and quenching 8-63107
 metal oxide, temp. depend. of chemilum. reactions, activation energies for excited state form. 8-66818
 metal vapour laser discharges, stability criteria 8-66802
 oscillation and amplification, high output and efficiency 8-66807
 pulsed and CW optically pumped lasers for novel applications in spectroscopy and kinetics 8-90413
 radioactive source preionisation of visible and UV discharge lasers 8-63096
 rare gas halide lasers, high repetition rate, multiple cct. pulse generator 8-94399
 tunable UV and visible lasers 8-59029
 Ar-F₂, proton excited mixtures, energy transfer processes 8-66647
 Ar-Kr-F₂, proton excited mixtures, energy transfer processes 8-66647
 Ar-Kr-F₂ mixture, electron beam pumped, spectroscopy and kinetics of 248, 414 nm bands 8-63081
 Ar-N₂, intense proton beam pumping 8-78998
 Ar-N₂ electron beam pumped laser characts. at 25-350°C 8-58984
 Ar-Xe-F₂, proton excited mixtures, energy transfer processes 8-66647
 Ar-Xe-NF₃ mixture, fluorescence from e-beam excitation at low temp. and high press. (French) 8-58727
 Ar₂, electron beam excited, absorpt. characts. 8-82948
 ArF, 50 mJ double discharge excimer laser, spectroscopy and characts. 8-63082
 ArF, laser emission, ab initio config. interaction calcs. on electronic states 8-63083
 ArF, laser expts. on $^2\Sigma^+ \rightarrow ^2\Sigma$ transitions 8-63080
 ArO, lasing, low-lying electronic states, ab initio config. interaction calcs. 8-63084
 ArXeF*, gain meas. at 4416 Å 8-50758
 Bi₂, vap., optically pumped, laser action 8-71081
 Br₂, optically pumped at 532 nm, lasing obs. in visible and near IR 8-63094
 BrCl, time-resolved fluoresc. of a²I_{1/2}⁺ state 8-63093
 CN (A²Π), chem. prod., CN number densities for gain, emission and absorpt. meas. 8-63112
 CN radicals, electronic transition laser, using C₃F₄CN and (CN)₂C₄F₈ photodissociation 8-50769
 CdHg, positive gain measurements or 470 nm continuum band 8-66805
 CdHg* excimer, kinetic model of sustained discharge excitation 8-66804

excimer lasers continued

- CdHg*, metal vapour exciplex laser, stability criteria 8-66802
 F₂, VUV high-power laser, laser-induced fusion 8-58996
 GeO, produced in Ge+N₂O reaction, kinetics of chemilum. emitter form. and quenching 8-63107
 Hg₂ excimer states, energy transfer kinetics 8-63090
 Hg₂ excimers in constricted positive column, radial intensity distrib. meas. 8-63091
 Hg₂, high press. transverse discharge for high efficiency, elec. and optical props. 8-63092
 HgBr dissociation laser is elec. discharge 8-50768
 HgCl discharge laser, electron beam sustained, operation, appls. 8-59043
 HgCl(B→X) laser, photolytic pumping, HgCl(B) state radiative lifetime meas. 8-94390
 HgCl*, metal vapour excimer laser, stability criteria 8-66802
 HgCl*(B1/2), fluoresc., collisional quenching kinetics 8-94269
 HgX (X=F, Cl, Br, I), three-body ion-ion recombination rates 8-63068
 I₂, optically pumped, lasing obs. on 342 nm band 8-79008
 Kr₂, kinetics of optically excited electronic states 8-63059
 KrCl, laser expts. on $^2\Sigma^+ \rightarrow ^2\Sigma$ transitions 8-63080
 KrF, 0.8 J multi-atm. laser, glow discharge characts. 8-58992
 KrF, 1/4J discharge pumped laser 8-74927
 KrF, absorpt. spectra of ArKr⁺, ab initio calc. of potential energy curves 8-74568
 KrF, discharge and electron beam pumped, review 8-71083
 KrF, discharge pumped laser, efficient amplification 8-78997
 KrF, electron beam sustained discharge excitation, threshold power density meas. 8-63078
 KrF, fluoresc. spectrum, theoretical modelling using electronic potential curves 8-63086
 KrF, Kr₂F, in electron beam pumped Ar-Kr-F₂ mixture, spectroscopy and kinetics of 248, 414 nm bands 8-63081
 KrF laser action in return-current discharge-excited F₂/Kr/He mixtures 8-94920
 KrF laser beam, Raman pulse compression, for fusion expts. 8-59086
 KrF, laser emission, ab initio config. interaction calcs. on electronic states 8-63083
 KrF, laser performance, collisional quenching rates 8-63066
 KrF, laser spectrum, discharge-pumped, absorption bands and lines, assignment 8-79004
 KrF, radiative lifetime and quenching 8-63063
 KrF, small signal gain meas. and kinetic modelling 8-63077
 KrF* laser, influence of F₂ dissociation and degree of ionisation 8-50756
 KrF* laser discharges, electron beam sustained, instability onset 8-63065
 KrF*, waveguide laser excited by capacitively coupled discharge 8-94391
 KrF*, gain meas. at 4416 Å 8-50758
 KrF*, radiative lifetime and quenching rate consts. 8-63056
 KrO, lasing, low-lying electronic states, ab initio config. interaction calcs. 8-63084
 Kr₂, radiative lifetime and quenching rate consts. 8-63056
 Kr₂, stimulated emission kinetics in nonself-sustained elec. discharge 8-50753
 La-F₂(ClF)(Cl₂)(SF₆), visible chem. laser development from reactions yielding visible chemilum. 8-63111
 Li₂, laser, continuous, optically pumped 8-87046
 Mg₂, A²Σ⁺+X²Σ⁺ system, discrete and continuous Franck Condon factors, J-depend. 8-66811
 N₂ electron impact excitation, rate coeffs., momentum transfer cross-section 8-78819
 N₂, first positive system, for optical fibre meas. 8-59020
 N₂, high-press., UV (Japanese) 8-55346
 N₂ laser, electrode configuration for high peak powers and high repetition rates 8-55379
 N₂, TE, anal. of time variation of discharge channel voltage by Pockels effect 8-90412
 N₂, TEA laser, compact high power, modification 8-90427
 N₂, UV laser, long pulse from N₂-CF₄ mixture 8-63067
 N₂⁺, gain and saturation 8-79001
 NF, b¹Σ⁺ state, enhancement by I laser pumping, lasing potential 8-79012
 NF, chem. pumped electronic transition laser system, chem. and scale-up 8-63103
 NF, excited, lasing potential, prod. by N+O₂F reaction 8-63106
 NF(a⁴Δ)+I(²P_{1/2}) system, electronic angular momentum transfer, chem. kinetic model 8-63104
 NF(b⁴Σ⁺) enhancement by I laser pumping 8-63105
 Na-Xe vapour, high power discharge, potential excimer laser 8-82957
 Na₂, gain optimisation on A→X transitions, Na-Xe discharge kinetic model 8-63088
 Na₂, laser, continuous, optically pumped 8-87046
 Na₂, laser excited broadband violet emission, 420 to 457 nm 8-79006
 NaXe, gain optimisation on A→X transitions, Na-Xe discharge kinetic model 8-63088
 Ne-NF₃, long pulse UV laser emission in electron beam excited supersonic flow 8-66801
 O₂, high energy pulsed laser feasibility at 1.27 μm, O₃ photolysis 8-63117
 S₂ laser, optically pumped, lasing obs. 470 to 480 nm 8-63095
 Sc-F₂(ClF)(Cl₂)(SF₆)(Br₂), visible chem. laser development from reactions yielding visible chemilum. 8-63111
 ScF supersonic mixing flame, spontaneous emission, electronic transition chem. laser pot. 8-66817
 SiF, chemilum. obs. of A²Σ⁺ and a⁴Σ⁻ states 8-66816
 SnO, produced in Sn+N₂O(O₂)(O) reactions, kinetics of chemilum. emitter form. and quenching 8-63107
 SrF, temp. depend. of chemilum. reactions, activation energies for excited state form. 8-66818
 Xe₂, efficient vac. UV laser, 172 nm at 6 atm 8-50793
 Xe₂, large-scale laser, gas purity 8-87063
 XeBr, high-energy lasing in elec. discharge 8-55340
 XeCl, efficient Raman conversion of radiation in Ba vapour 8-79069
 XeCl excimer laser, electron beam controlled discharge, construction and operation 8-63125
 XeCl excimer laser, high power, discharge pumped 8-55375
 XeCl, intense lasing with HCl halogen donor 8-90411
 XeCl, using chlorinated hydrocarbons as Cl donors 8-79007

excimer lasers continued

- XeF, 1 μ sec pulse lasing, cold cathode electron beam initiation 8-63079
 XeF, discharge and electron beam pumped, review 8-71083
 XeF, double pulse fast discharge driven laser, optimal timing and power enhancement 8-63132
 XeF, electron beam controlled, output power, efficiency 8-82951
 XeF, electron beam excited, long pulse operation 8-50794
 XeF, electron beam excitation, kinetics scheme 8-78999
 XeF, electron beam sustained discharge excitation, threshold power density meas. 8-63078
 XeF, energy ordering of excited states, rel. to fluoresc. and laser action 8-74887
 XeF, from photodissoc. of XeF₂, B(1/2)-X² Σ^+ transition, stimulated emission 8-71097
 XeF, high pulse repetition freq. laser action, appl. of multiple-circuit pulse generator 8-94399
 XeF, laser emission, ab initio config. interaction calcs. on electronic states 8-63083
 XeF, long pulse UV laser emission in electron beam excited supersonic flow 8-66801
 XeF, optically excited by incoherent Xe₂^{*} radiation, B \rightarrow X band emission 8-87044
 XeF, self-sustained discharge laser, kinetic processes 8-74888
 XeF, superradiant laser, gain saturation effects 8-66808
 XeF(Cl)(Br), covalent and ionic states, spectroscopic props., ab initio CI calc., laser emission 8-90092
 XeF^{*} (C_{1/2}), radiative lifetime meas. 8-63087
 XeF^{*} laser mixture, Ne- and Ar-rich, absorption 8-63062
 XeF^{*}, waveguide laser excited by capacitively coupled discharge 8-94391
 XeO, lasing, low-lying electronic states, ab initio config. interaction calcs. 8-63084
 Y-F₂(ClF)(Cl₂)(SF₆)(Br₂)(IBr), visible chem. laser development from reactions yielding visible chemilum. 8-63111
 YCl supersonic mixing flame, spontaneous emission, electronic transition chem. laser pot. 8-66817
 YO, temp. depend. of chemilum. reactions, activation energies for excited state form. 8-66818
 ZnHg, optical pumping of Zn reson. line, optical and kinetic props. 8-58991

excimers

see also excimer lasers

- m-aminoacetophenone+t-amyl alcohol, in soln., fluoresc. and absorpt. spectra, excimer form. 8-78737
 anthracene, γ -irradiated, temp. depend. of photolum. (Russian) 8-56511
 anthracene-tetracene amorphous films, host-guest energy transfer 8-60505
 aromatic hydrocarbons, excimer decay dynamics, rate const. rel. to solvent 8-58729
 1,2-benzanthracene, monomer and excimer fluoresc. in soln., triplet-triplet annihilation and mag. field depend. 8-78738
 3,4-benzopyrene, monomer and excimer fluoresc. in soln., triplet-triplet annihilation and mag. field depend. 8-78738
 N-carbazolyl-(CH₂)_n-tetrachlorophthalimide, (n=2,3,4,7) intramol. electron donor-acceptor system, photophys. 8-82763
 9-cyano anthracene-dimethyl aniline, exciplex, fluoresc. of vap., 185-231°C 8-74693
 9-cyano anthracene-tributyl amine, exciplex, fluoresc. of vap., 185-231°C 8-74693
 9-cyano anthracene-triethyl amine, exciplex, fluoresc. of vap., 185-231°C 8-74693
 9-cyanoanthracene:perylene, exciplex emission 8-60513
 9-cyanoanthracene, luminesc., excimeric species 8-84637
 9-cyanoanthracene, quenching of solid state photodimerisation reaction by cryst. doping 8-68547
 di(1-pyrenylmethyleneoxycarbonyl) alkanes, intramol. excimer emission 8-70862
 α,α -dinaphthylalkanes, absorpt. spectra and phosphoresc. in soln., triplet excimers 8-62816
 dinaphthylalkanes, triplet-triplet annihilation of excimers in soln. 8-86904
 dinaphthylamine, fluoresc. in soln., intramol. excimer and exciplex form. 8-62836
 donor excimers, effect on resonant energy transfer (Russian) 8-76530
 lepidopterene exciplex, luminesc. intramolecular anthracene-ethylene exciplex, mol. geometry-fluoresc. relationship 8-58728
 1-naphthyl methacrylate-9-vinylanthracene copolymer, time-resolved fluoresc. spectra 8-80401
 α -perylene, excitation spectra of exciton fission in organic crystals 8-92116
 phthalocyanine, metal-free, solid, fluoresc., lifetimes temp. depend., polymorphic modification 8-80388
 poly-1-naphthyl methacrylate, time-resolved fluoresc. spectra 8-80401
 poly-9-vinyl carbazole, fluoresc. props. 8-84647
 polymers containing carbazole units, optically active, fluoresc. props. 8-84647
 pyrene:rubicen(coronen), exciton migration and energy transfer, temp. depend., model 8-79932
 pyrene, monomer and excimer fluoresc. in soln., triplet-triplet annihilation and mag. field depend. 8-78738
 pyrene+N,N-dimethylaniline (deuterate)(3,5 dimethoxy-N,N-dimethylaniline), geminate recomb., solvent, isotope, mag. field effects 8-56888
 pyrene excimer formation in micellar surfactant solns., distributional effects 8-64855
 sodium dodecyl sulphate micelles, diarylalkane intramolecular excimer formation, microfluidity and fluoresc. meas. 8-80791
 styrene-method methacrylate copolymer glassy soln., excimer form., energy migration, fluoresc. depolarisation meas. 8-70986
 thionine-mono-haloaniline triplet exciplex, quenching position dependent heavy atom effect, intersystem crossing 8-53197
 2-vinylanthracene-methyl methacrylate copolymer glassy soln., excimer form., energy migration, fluoresc. depolarisation meas. 8-70986
 Ag, matrix isolated, fluoresc. spectra, excimeric bond effects 8-50498
 Ar:O₂(N₂), long-wave UV luminesc. (Russian) 8-88347
 Ar₂⁺ Σ_u^+ excimer state, photoion. cross section 8-70882
 Ar₂, excited state pot. curves, ab initio CI calc. 8-78643
 ArF, proton excited mixtures, energy transfer processes 8-66647

excimers continued

- Cd₂^{*} excimer, fluoresc. band shape, decay rates 8-70866
 CsXe excimer, laser-excited fluoresc. in Cs-Xe mixture, pumping, level scheme 8-86909
 HgXe, fluoresc. spectra, pot. curves and binding energy 8-66581
 KXe, exciplexes (n=1-4), visible emission bands 8-78746
 K(5S)₂Xe, K(5S)Kr, excimer, visible emission band, exptl. results relative to theory 8-82779
 Kr:N₂O, photoluminesc. from KrO (¹S) excimers 8-68544
 KrF, laser spectrum, discharge-pumped, absorption bands and lines, assignment 8-79004
 KrF(B), excimer, collisional quenching rates, photolysis meas. 8-63066
 Na+Kr(Xe), excimer bands, multiperturber interactions 8-66497
 Na(4S)Xe, Na(4S)Kr, excimer, visible emission band, exptl. results relative to theory 8-82779
 Ne:O₂ (N₂), long-wave UV luminesc. (Russian) 8-88347
 Xe:N₂O, photoluminesc. from XeO (¹D) excimers 8-68544
 XeF^{*}, in enhanced quenching of Xe+F by intense laser light, computer modelling 8-55232
 Xe₂^{*}, Xe₂⁺, Xe₂, pot. energy curves, relativistic ab initio effective core pots. 8-86800

exciplexes see excimers

excitonic molecules

- change of binding type and dissoc. in strong mag. field 8-62744
 polar crystals, biexciton stability 8-76002
 CdS, reson. Raman Scatt. under two-photon excitation of excitonic mol. 8-52486
 CuCl, exciton mol. creation by pure and phonon-assisted two-photon transitions 8-63987
 CuCl, excitonic mol. luminesc. spectra, picosecond time anal. 8-52548
 CuCl, reson. two-photon excitation of excitonic mol. using circ. polarised light 8-84566
 CuCl, resonantly excited excitonic molecules, time resolved spectroscopy 8-92109
 GaAs, biexciton stability, appl. of theory for polar crystals. 8-76002
 Ge, exciton mol. creation by pure and phonon-assisted two-photon transitions 8-63987
 MnF₂, biexciton decay, time resolved laser spectra 8-75999
 ZnO, optical gain and induced absorption from excitonic mol. 8-84609

excitons

see also excitonic molecules; phonon-exciton interactions

- absorption band, integrated intensity 8-72084
 alkali halide, defect formation, model of excitonic mech. 8-91337
 alkali halides, self trapped exciton, optical detection of spin relax. processes 8-60358
 alkali metal halides, irradiated, annealing 8-92494
 anthracene, cryst., triplet exciton pair kinematics, diffusion model 8-79931
 anthracene, electron irradi., creation and evolution of excited states, scintillation obs. 8-92128
 anthracene, excitation spectra of exciton fission in organic crystals 8-92116
 anthracene, nonlinear fluorescence quenching 8-52562
 anthracene, polarised reflection spectra, surface and vol. exciton coupling, vibronic states 8-72543
 anthracene, single cryst., X-radiation damage recovery, using triplet state exciton probe 8-75694
 anthracene, singlet exciton fission, prompt and delayed fluoresc. mag. field depend., temp. effects 8-52540
 anthracene, triplet exciton trapping, structural imperfections and delayed fluorescence 8-68551
 anthracene, triplet excitons, phosphoresc. and delayed fluoresc. excitation spectra 8-63986
 anthracene crystals, resonance Raman spectra sensitivity to exciting light intensity (Russian) 8-52504
 anthracene-d₁₀-s-tetracyanobenzene, rotational mode coupling in phase transition 8-71827
 anthracene-pyromellitic dianhydride, cryst., charge transfer exciton transitions, refl. spectra obs. 8-72540
 anthracene-tetracene amorphous films, host-guest energy transfer 8-60505
 benzophenone, charge carrier generation and mobility 8-84231
 biexcitons, many exciton effects, appl. to CuBr(Cl) 8-51901
 binding energy to neutral acceptor, calcs. using atomic-like variable wave function 8-79937
 biomembrane active transport and energy transformation, quantum mechanism 8-53364
 biphenyl, cryst., electronic absorpt. and refl. spectra 8-64377
 bounded crystals, auxiliary boundary conditions in theory of additional light waves and excitons (Russian) 8-56080
 Brillouin scattering, resonant, analogy to modulation spectroscopy (Japanese) 8-68526
 carbazolyl substituted diacetylene monomer cryst., ODMR and triplet state kinetics 8-76355
 chalcogenide glass, mech. for electron-hole recomb. 8-72196
 complex particle emission, pre-equilibrium exciton model anal. 8-66280
 condensation and liquefaction in strong mag. field, RPA and variational calcs. 8-63984
 cryst. with defects 8-60478
 diamond structure, energy levels of direct exciton formed by split-off valence band 8-91624
 1,4-dibromonaphthalene, optical props., struct. disorder effects 8-52525
 p-dichlorobenzene-p-dibromobenzene, solid soln., local struct. and triplet energy migration 8-60489
 diphenyl:naphthalene, benzophenone, phosphoresc., triplet diffusion excitons 8-63985
 electron hole plasma, excitons, influence of dynamical effects 8-76004
 electron-hole system, phase transition during formation of exciton condensate (Russian) 8-60060
 elementary excitations in crystals, dielectric theory 8-60076
 exact derivation of a generalized master equation for the motion of excitons 8-87911
 exciton, insulator, differential thermo EMF, temp. depend. (Russian) 8-72182
 exciton-ionised donor complex, binding energy, effective electron-hole interaction pot. 8-67949

excitons continued

- excitonic insulators, study of coherence factors 8-76338
ferromagnetic dielectric, crit. behaviour of exciton relaxation consts. 8-84442
fluorene, exciton band struct., two-photon fluoresc. excitation 8-64402
fluorene, lowest singlet state, exciton band struct. calc. 8-63983
fluorene, near 6K, two-photon excitation spectrum, g-exciton states location 8-64393
Frenkel excitons, optical resonance 8-91621
GaP, reevaluation of bandgap and free exciton binding energy 8-60061
ground state of two- and three-dimens. excitonic molecule 8-72076
HF characteristics at low temps., multiphoton absorpt., tunnelling under dimensional quantisation effect (*Russian*) 8-68073
inert gas, solid, dead layer effects in UV reflectance of excitons 8-72553
inert gas crystals, excitons exam. 8-51898
inert gas solids, core excitons, nonstructural theory 8-84148
inert gas solids, exciton states, nonstructural theory using effective mass approx. 8-84147
inert gases, solid, electronic excitations, nonstructural theory 8-79942
inert gases, solid, exciton states, intermediate coupling interaction 8-67952
inhomogeneous state of exciton ferromagnet (*Russian*) 8-88132
interband transitions and currents in systems with electron-hole pairing 8-72302
layered crystal, light absorption by excitons, interlayer hoppings (*Russian*) 8-68532
light scattering by excitons localised at dislocations 8-60479
magneto-optical crystals, spectra of hybrid excitations from transverse photons, excitons, magnons interactions 8-80320
metal, damping of excited molecules located above surface 8-92160
methyl substituted ammonium halides, UV exciton absorpt. bands 8-72547
molecular crystal, dipole plasma oscillations, Bose-Einstein condensation of excitons (*Russian*) 8-84155
molecular crystal, Frenkel excitons, effect on charge carrier transfer 8-79936
molecular crystal, LEED differential cross-section, Frenkel excitons effects 8-51398
molecular crystal, LEED specular beam intensity, bulk Frenkel exciton effects 8-51399
molecular crystal, triplet exciton excess EPR linewidth, orientational order effect 8-72389
molecular crystal/electrolyte interface, illuminated, space charge behaviour 8-84290
molecular crystals, effects of impurity scatt. and transport topology on trapping 8-95263
molecular crystals, energy transport dynamics, picosec. transient-grating method 8-72079
molecular crystals, exciton propagation and memory effect at low temp. 8-67947
molecular crystals, neutron scattering and exciton spectrum due to impurities 8-91622
molecular crystals, optical props., struct. disorder effects 8-52525
molecular crystals, spectroscopy, bibliography for 1976 8-72585
molecular solid, electronic polaris. energy, quantum dynamic rel. to classical microelectrostatic approach 8-52427
molecular solid, triplet exciton system, motional correlation effects, model 8-75997
MTPA(TCNO), radical salt, triplet exciton system, motional correlation effects, model 8-75997
Nakajima Zwanig's generalised master equation, integro-differential eqn. kernel evaluation, exciton motion appl. 8-86123
naphthalene: β -chloronaphthalene, reaction rate constants of triplet excitons 8-80407
naphthalene, 2-methylnaphthalene and anthracene doped, single cryst., sensitised fluoresc. 8-68548
naphthalene, a-exciton temp. depend. scatt., optical absorpt. profile 8-72088
naphthalene, cryst., singlet exciton interactions, prompt fluoresc. decay 8-60500
naphthalene, crystalline, singlet exciton diffusion coeff. meas., fluorescence quenching anal. 8-67945
naphthalene, nonlinear fluorescence quenching 8-52562
naphthalene, triplet excitons, phosphoresc. and delayed fluoresc. excitation spectra 8-63986
naphthalene cryst., anthracene doped, fluoresc., two-photon excited 8-68560
naphthalene- d_8 :naphthalene- h_8 cryst., triplet excitons in A-B pairs, origin of inhomogen. broadened ESR lines 8-91623
nuclear matter, particle-particle collision probability, vol. integral using preequilibrium exciton model 8-70477
nuclear preequilibrium decay, exciton model formulation, reply to comments 8-78354
one-dimensional molecular crystal, soliton-like solns. of eqns. for excitations 8-84149
one-dimensional substitutionally disordered system, energy transfer, coherence, tunnelling, thermal promotion 8-56078
organic crystals, kinetic model of triplet exciton dynamics 8-67948
organic mixed crystals, energy transfer 8-76515
organic molecular crystals, optical spin alignment, phosphoresc. (*Russian*) 8-84652
pentacene, in p-terphenyl, electronic excitation transport, acousto-optical effects 8-72079
percolation model, one-dimens., spectral diffusion 8-80411
perylene, excitation spectra of exciton fission in organic crystals 8-92116
polar semiconductor, impurity levels, influence of electron-phonon coupling 8-64007
poly-1,6-di-N-carbazolyl-2,4-hexadiyne, synthesis, thermal expansion, photocond., optical transition 8-76858
poly-2,4-hexadiyne-1,6-diol bis (p-toluene sulphonate), cryst., exciton surface polaritons, reflectivity of (100) face, 295K 8-80372
polydiacetylenes, excited singlet state electronic struct., band and excitonic models 8-91620
polymer:trimethylamine, field-depend. UV photogeneration of holes, polymer composition depend. 8-76104
polymers and molecular crystals, vibronic spectra exam. 8-67778
preequilibrium decay, differences of alternate formulations, possible exciton formulation errors 8-70507

excitons continued

- pyrene:rubicon(coronen), exciton migration and energy transfer, temp. depend., model 8-79932
quantum defect theory, analogy to Rydberg states 8-51902
Raman scattering, reson., second-order, theory for case of strong excitonic effects 8-76460
reflectance spectrum, calc., multi-component polaritons 8-87921
semiconductor, collective magnetoexciton transition under action of light (*Russian*) 8-79939
semiconductor, excitonic surface potential 8-76000
semiconductor, optical absorpt., Coulomb screening influence, exciton ionisation energy 8-72568
semiconductor, reson. in fundamental absorpt. region, quasi-mol. model interpretation 8-76490
semiconductor, tetravalent, fundamental absorpt. spectra, direct interband transitions 8-63972
semiconductor film, Wannier-Mott exciton states (*Russian*) 8-79943
semiconductor multiple bound excitons, binding energy calc. 8-51900
semiconductor with nonspherical bands, diamag. excitons and Franz-Keldysh effect 8-72554
semiconductor-metal, surface exciton modes for plane and spherical interfaces 8-64113
semimetals, exciton phase, transport effect in strong mag. fields 8-7977
short-range ordered mag. cluster pinning by localised optical excitation 8-68279
trans-stilbene, cryst., triplet excitons, $S_0 \rightarrow T_1$ transition 8-76518
stilbene, single cryst., free charges and excitons generated by electron pulses 8-63988
surface channel, quasitwo dimens. excitons and plasmons at different carrier conc. 8-60063
surface-exciton polaritons, dispersion theory 8-72089
TCNQ compounds, dimensionality of triplet excitons 8-91974
TCNQ- M_2P charge transfer complex, triplet spin excitons, EPR spectra 8-80192
tetracene, cryst., singlet exciton fission rate const. RYDMR spectra meas. 8-91619
tetracene, cryst., triplet exciton pair kinematics, diffusion model, prompt fluoresc. decay 8-79931
tetracene, singlet exciton fission, kinematic theory 8-87913
1,2,4,5-tetrachlorobenzene, impurity induced states, spin dephasing, spin coherence expts. 8-84498
1,2,4,5-tetrachlorobenzene, linear chain triplet excitons, electron spin-echo and ODMR 8-76357
1,2,4,5-tetrachlorobenzene, localised excitations thermal promotion to exciton band, impurity states effect 8-52539
transfer rates, effect of nucl. degrees of freedom 8-60057
transition into excitonic phase, boundary effects 8-76003
transition metal dichalcogenides, modulation spectroscopy obs. 8-80377
tunnel self-trapping of electrons or Frenkel excitons, theory (*Russian*) 8-60192
zincblend structure, energy levels of direct exciton formed by split-off valence band 8-91624
AgBr, optical absorpt. of indirect exciton in high mag. field 8-60486
AgCl, AgCl:AgBr, X-ray and ultraviolet effects, ODMR 8-79933
AgCl, cryst. luminesc. and photovoltaic effect kinetics 8-64391
AgCl, optical absorpt. of indirect exciton in high mag. field 8-60486
 β -AgI, exciton refl. spectra, optical activity (*Russian*) 8-64380
AlAs-GaAs monolayer crystal, two-photon absorpt. spectrum 8-52589
Ar, liquid, triplet state of self-trapped exciton states, evidence of existence, luminescence meas. 8-72608
Au-Ge Schottky diode, phonon energies, barrier heights, photovoltage spectra 8-64112
CdS, A-exciton-polariton, time depend. optical spectrosc. obs. 8-80376
CdS, exciton cathodoluminesc. of semicond. with surface pot. barriers 8-88366
CdS, exciton luminescence, surface recombination, space-charge-layer effects 8-80410
CdS, excitonic region, nonlinear optical meas., 4.2K 8-68531
CdS, induced absorption and gain from high density excitons 8-68533
CdS, induced absorption in energy ranges of exciton and exciton-biexciton transitions 8-72548
CdS, ODMR, bound excitons 8-80253
CdS, photorefl. in exciton region, surface layer influence 8-76489
CdS, reson. Raman scatt., second-order, theory for case of strong excitonic effects 8-76460
CdS, spatial dispersion effects, exciton decay const. depend. (*Russian*) 8-72086
CdS, two-phonon resonant Brillouin scatt. 8-84597
CdS:Cl, extrinsic, exciton absorption 8-72569
CdS:Ni, exciton reflection spectra 8-72557
Cd₂Se_{1-x} mixed crystals, exciton spectra 8-92131
CsI, correl. between UV emission band at 300 nm and self-trapped excitons, 4.2K 8-75998
CsMnF₃, mag. field- and temp.-depend. of light absorption spectra 8-52528
CuBr, evaporated film, magneto-optical effects on exciton bands 8-72624
CuBr-Ag system, spectral distrib. of photosensitivity (*Russian*) 8-56535
CuBr(Cl), biexcitons, many exciton effects 8-51901
CuCl, biexciton luminescence and two photon Raman emission, polarisation props. 8-80406
CuCl, evaporated film, magneto-optical effects on exciton bands 8-72624
CuCl, existence of charged excitons 8-76496
CuCl, reson. two-photon Raman scatt., excitonic polariton dispersion 8-72509
CuCl, resonantly excited excitonic molecules, time resolved spectroscopy 8-92109
CuCl, Z_2 -exciton, temp. dependent TPA linewidth 8-67946
Cu₂O, is yellow exciton, lineshape studies by reson. Raman scatt. 8-76465
Cu₂O, exciton spectrum, effect of isotopic substitution 8-67955
Cu₂O, excitons and structural defects at low temp. 8-84255
Cu₂O, reson. Raman scatt., yellow and green excitonic series 8-72511
Cu₂O, yellow exciton series, silver impurity influence on spectrum 8-64388
Cu₂O:Ag⁺, yellow series line width, exciton-impurity scatt. 8-64386

excitons continued

- Cu₂O: Cd, dipolar and quadrupolar bound excitons, absorption spectrum (*Russian*) 8-92099
 FeBr₂, metamagnetic, optical study of mag. phase diagram 8-56312
 n-GaAs, exciton luminescence, excitation intensity depend. 8-52554
 GaAs, excitonic polariton reson. interaction with LA phonons 8-60481
 GaAs, excitons, diamond like semiconductor, variational calculation of binding energies 8-79938
 GaAs FET structure, sharp line photolum. spectra 8-72248
 GaAs_{1-x}P_xN, 0.6 < x < 1, photoluminesc., comp. depend. 8-52546
 GaN epitaxial layers, exciton cathodolum. (*Russian*) 8-76543
 GaP (110), surface excitonic binding energy for relaxed cleavage surface 8-91744
 GaP, first order Mott transition of exciton gas 8-76535
 GaP, MCD of phonon-assisted exciton transitions 8-92053
 GaP, shallow impurity states, free exciton binding energy 8-79960
 GaP:N, photoluminesc., temp. depend., exciton recombination mechanism 8-88355
 GaSe, exciton, excitation-induced absorption and luminesc. 8-60516
 GaSe exciton absorpt., change under a pulsed dye laser 8-92088
 GaSe_{0.9}Te_{0.1}, undulation spectra associated with acceptor complexes 8-80392
 Ge, elec. cond., optically injected carrier density and temp. depend. 8-68046
 Ge, electron-hole droplets, transient photoluminesc. intensities 8-88353
 Ge, far IR magnetoabsorption of free and bound excitons 8-52474
 Ge, influence of dislocations on free-exciton lifetime 8-60064
 Ge, interband Faraday ellipticity 8-92052
 GeS, exciton luminescence 8-52555
 HgI₂, electrons and holes cyclotron reson. 8-72061
 HgI₂, red, reson. Raman scatt. and luminesc. 8-84579
 HgI₂, stimulated emission at high exciton density, temp. depend. 8-84608
 InSe, excitonic absorpt. edge 8-88352
 KBr, heavy ion irradi., σ and π exciton emission spectra, 4.2K 8-76534
 KBr:Li, radiative recomb. of localised excitons 8-72605
 KBr:Li⁺(Na⁺), electronic struct. of (V_{Li})₂ 8-95269
 KBr:NO₂, Na effect of Na⁺ impurity on self-trapped hole (*Japanese*) 8-67982
 KCN, ionic mol. cryst., exciton struct. 8-79935
 KCl crystal, F-H centre formation by opt. conversion of self-trapped excitons 8-91335
 KMnF₃, antiferromag., multi-magnon luminesc. sidebands 8-76525
 KNiF₃, electronic UV laser excited Raman, scatt. by mag. excitons 8-68492
 K₂NiF₄, electronic UV laser excited Raman, scatt. by mag. excitons 8-68492
 Kr, film, absorpt. in exciton region 8-52529
 Kr, liquid, triplet state of self-trapped exciton states, evidence of existence, luminescence meas. 8-72608
 Kr:N₂O, photoluminesc. from KrO (¹S) excimers 8-68544
 LiH (D), single crystals, electronic excitations, review (*Russian*) 8-72574
 LiI crystal, emission spectra under UV-light excitation at 77K 8-92110
 MgF₂, cryst., Roentgenoluminesc., exciton emission (*Russian*) 8-95609
 MgO, electronic excitations and luminescence, review (*Russian*) 8-72575
 MnF₂, antiferromag., multi-magnon luminesc. sidebands 8-76525
 MnF₂, one-magnon luminesc. sidebands of excitonic transition 8-60517
 MnF₂, two-exciton many photon absorption, effect of statistical props. of light on intensity (*Russian*) 8-95589
 MoS₂(Se₂), effect of uniaxial stress on excitonic optical spectra 8-84606
 NaCl, search for IR absorption by triplet self-trapped excitons 8-56473
 NaI, exciton luminesc., characteristics near absorption edge 8-88363
 NaNiF₃, electronic UV laser excited Raman, scatt. by mag. excitons 8-68492
 Ne:O₂(N₂), long-wave UV luminesc. (*Russian*) 8-88347
 NiF₂, electronic UV laser excited Raman, scatt. by mag. excitons 8-68492
 α -O₂, elementary excitations, effect of mag. anisotropy (*Russian*) 8-76317
 PbF₂(Cl₂)(Br₂), lowest exciton states 8-72082
 PbI₂, film, highly excited, oscillator strength of excitons, absorpt. and emission spectra 8-76001
 PbI₂-Ag system, effect of bound and free exciton states on light sensitivity (*Russian*) 8-71169
 Pr, magnetic ordering due uniaxial stress, mag. excitons by neutron scatt. 8-84467
 RbMnF₃, antiferromag., multi-magnon luminesc. sidebands 8-76525
 Si, amorphous, electron-hole recombination, mech. 8-72196
 Si, exciton and deformation pot. fine struct. 8-88301
 Si, exciton-impurity complexes, emission spectra, Zeeman splitting (*Russian*) 8-64413
 Si, plastically deformed, hot-exciton luminesc. as function of strain 8-88361
 Si, pure and heavily doped, 2p core levels and core exciton binding energy, photoemission obs. 8-76583
 Si, recombination luminescence, electron-hole drop, excitons orientation in mag. field 8-88362
 n-Si, surface space-charge layer, intersubband-cyclotron combined reson. 8-68063
 Si:Al, bound-exciton absorption 8-56507
 Si:Al(B)(P), bound multiexciton complexes, work function thermodynamic determ. 8-72078
 Si:Ga, bound-exciton absorption 8-56507
 Si:Ga(Al), edge luminesc. spectra of acceptors, multiexciton complexes 8-56517
 Si:In, bound exciton photolum. obs. 8-95607
 Si:In, bound-exciton absorption 8-56507
 Si:P, excitation density depend. of cathodoluminesc. from bound multiexciton complexes 8-72609
 Si:P, luminesc. lines, multiexciton complexes and uniaxial stress 8-92114

excitons continued

- Si:Ti, optical absorption and photolum. of bound exciton 8-88359
 p-SiC:B (4H), absorption spectra of bound excitons 8-88338
 SiO₂, vitreous, exam. of electron excitations and intrinsic defects 8-87905
 Tb₂Y_{1-x}PO₄, H₂ VUV laser excitation, fluoresc. decay characts. 8-60510
 ThF₄, 5d X-ray spectra 8-88382
 ThO₂, 5d X-ray spectra 8-88382
 TiSe₂, UPS, excitonic instability indicated from study of band struct. 8-56069
 TiBr, piezoreflectance of first exciton band obs. 8-64347
 TiCl, piezoreflectance of first exciton band obs. 8-64347
 UO₂ complexes, cubic cryst., low temp. optical spectra (*Russian*) 8-92083
 WS₂(Se₂), effect of uniaxial stress on excitonic optical spectra 8-84606
 Xe, liquid, triplet state of self-trapped exciton states, evidence of existence, luminescence meas. 8-72608
 Xe:N₂O, photoluminesc. from XeO (¹D) excimers 8-68544
 Zn₂Cd_{1-x}Te, relaxation processes, emission spectra (*Russian*) 8-72598
 ZnO, optical gain spectra, direct recording using laser modulation 8-66834
 ZnO phosphors, origin of UV emission 8-64400
 ZnO, Zeeman splitting of A1-exciton emission lines, k-linear term effects 8-52563
 ZnS₂Se_{1-x}, band gap, comp. depend., exciton refl. spectrum obs. 8-56071
 ZnSe, cubic, magnetoreflexion of s-excitons 8-60426
 ZnSe, cubic, valence band parameters, magnetoreflexion of Γ_6 - Γ_8 exciton 8-60056
 ZnTe, band parameters from bound exciton, donor-acceptor pair excitation luminescence 8-92111
 ZnTe, free exciton refl., surface layer effects 8-76493
 ZnTe, high quality p-type cryst., predominant acceptors 8-60504
 ZnTe, relaxation processes, emission spectra (*Russian*) 8-72598
 ZnTe:Mn, exciton refl. band, giant mag. splitting (*Russian*) 8-56079
 ZnTe:Mn, mag. field splitting α n=2 exciton state (*Russian*) 8-79940

exhibitions

- Michigan Space Center and model solar system 8-69653

exobiology *see extraterrestrial life***exoelectron emission**

- attenuation length, escape depth and probability for excited electrons in solids 8-76593
 exoelectron emission defectoscopy, metal fatigue strength prediction 8-76807
 exoemission defectoscopy in initial stages of fatigue fracture 8-53126
 fatigue damage early prediction by acoustic and exoelectron emission 8-53170
 ionic crystals, photostimulated electron emission after photoexcitation, diffusion approach 8-52641
 technological strength and nondestructive methods of testing during heat treatment 8-85090
 Al alloys, oxide-covered, characteristic emission of negatively charged particles during tensile deform. 8-92179
 Al, anodised, photostimulated exoelectron emission, effect of oxide thickness 8-80461
 Al, polycrystalline, abrasion, deform., fatigue, study by exoelectron microscope (*Japanese*) 8-74108
 Al₂O₃, exoelectron emission, energy and ang. distrib. anal. (*German*) 8-92180
 NaCl, deform. process, exoemission and desorption meas. (*Russian*) 8-75708
 SiO₂-Si structure P⁺ bombardment damage, exoelectron emission obs. 8-95383
¹⁸²Ta-containing Ta sheet, radioactive electron emission spectrum (exoelectrons), surface elec. field and Auger effects 8-72705

exosphere

- H global density distrib. vars., escape fluxes 8-93023
 H latitude vars., rel. to polar wind, heating and charge exchange processes 8-93024
 temperature, models seasonal vars. at solar max. and low geomag. activity 8-57376
 H atoms vel. distrib. from OGO-5 meas. of Lyman α emission 8-61642
 H escape flux, charge exchange induced, diurnal and solar cycle vars. 8-93022
 H⁺ loss during solar cycle, charge exchange processes 8-93021

exotic atoms

- see also hadronic atoms; muonic atoms*
 atomic spectral line shifts for heavy quark atoms 8-62965
 hyperfine splitting, recoil corrections calcs. 8-50667
 light nuclei, with unequal numbers of protons and neutrons, radioactive decay 8-89831
 monopole H atom, spectra, energy levels, transition probabilities (*Chinese*) 8-90322
 nuclear electric moment determ. from exotic atom X-ray meas., review 8-50061
 H-like atoms, quadrupole moments 8-90072
 H-positron bound state, effective one-body pot. to prove absence 8-82871
 He mesoatoms, π^- , μ^- , K^- , p^- atoms, energy spectra, wave functions (*Russian*) 8-55264
 Li, mesoatoms, π^- , μ^- , K^- , p^- atoms, energy spectra, wave functions (*Russian*) 8-55264

expanding universe *see cosmology***expansion, thermal** *see thermal expansion***expansion chambers** *see cloud chambers***exploding foils** *see exploding wires and foils***exploding wires and foils**

- continuum radiation, spectral radiant intensity meas. 8-91134
 fusion reactor high-voltage production using underwater exploding foil fuse 8-54948
 fusion reactor inductive storage technology, new applications, review 8-55019
 nonlinear evolution of exploded wire plasma, numerical simulation 8-83605
 plasma, convective instability in inhomogeneous mag. field 8-67340
 potential drop across exploded foil, theory of expt. determ. 8-71515

exploding wires and foils continued

- Al foil, elec. explosion, dielec. breakdown 8-67388
- Al, foil, elec. explosion, immersion medium effects 8-67389
- Cs, plasma diagnostics by wire explosion 8-71516
- Cu exploding foils, rapid mag. energy transfer, conductivity law (*French*) 8-91135
- Cu foil, elec. explosion, dielec. breakdown 8-67388
- Fe exploded wire, X-ray line emission and plasma conditions 8-59670
- Li, ionisation and radiation dynamics simulation 8-83606
- W exploding wire, peripheral arc initiation 8-87559

explosion bubbles *see bubbles***explosions**

- see also accidents; detonation; exploding wires and foils; nuclear explosions; safety; shock waves*
- blast propagation, statistics of amplitude and spectrum 8-63224
- cratering explosion, pulsed hydrodynamic model 8-51180
- craters, coherently overturned flaps produced by hydrodynamic type wave motion 8-57209
- dense plasma generation by ionised gaseous filament explosion 8-71507
- dielectric constants and losses of explosive mixtures below 100 kHz 8-56422
- electron explosive emission regime, quasiplane cathode processes 8-75460
- explosion-induced accel. of cylindrical metal liners, form stability anal. 8-83425
- fragmentation of asteroids and artificial satellites in orbit 8-53858
- in galaxies, source and nature of explosions in nuclei 8-96546
- hyperdetonation eccentric shock wave, approx. soln. 8-67070
- hyperdetonation shock wave passage through jump like nonhomogeneity 8-67069
- impulsive discharge noise, balloon burst and engine exhaust systems, acoustic pulse parameters determ. 8-90588
- interfacial waves launched by an explosive line-source in a submerged elastic half-space 8-75088
- late stage equivalence of near-surface explosions 8-61353
- Leidenfrost effect, demonstrations 8-81744
- liquid with ring shaped explosive, toroidal gaseous cavity one-dimens. pulsation 8-83423
- LMFBR thermal explosion hazards, review of present understanding and simulation expts. 8-82464
- metal powder explosive compaction 8-64501
- methyl isocyanide, laser initiated thermal isomerisation, thermal explosion 8-80725
- neutron generation by implosion of D₂ gas target 8-54869
- off-centre point explosion in spheroid 8-63450
- plane hyperdetonation wave generation, optimum conditions 8-67068
- point explosion in arbitrary atmosphere with radiative heat transfer 8-53708
- ray parameter-epicentral distance curves for point source on boundary 8-61336
- reflection of explosion waves from plane surface (*Russian*) 8-87361
- S-wave propag. from explosion in transversely isotropic medium 8-81110
- seismic radiation from a finite cylindrical explosive source 8-61340
- seismic wave reflection at wide angles, travea times 8-65202
- shock waves, explosive charges of finite radius, energy hypothesis 8-55658
- solid-liquid model for explosion in ground 8-96158
- spark generator for dust explosion hazard assessment and gas ignition 8-57983
- thermal explosion, critical condits., step function reaction rate approx. 8-92480
- thermal explosions, fragmentation requirements for detonation 8-71368
- thermal homogeneous, influence of reactant consumption on critical conditions 8-92483
- thermal instability of vibr.-excited mol. gas, appl. to surface ignition (*Russian*) 8-56895
- Tunguska event, thermal explosion of porous meteoroid, model 8-61813
- ultrahigh vacuum discharge cathode erosion minimum conditions 8-75461
- H₂-F₂-O₂, chem. laser mixture, multiatm., spontaneous explosions 8-73044
- Hg+water systems, drop fragmentation rel. to thermal explosion detonation requirements 8-71368

exposure meters *see photometers***extended Huckel theory calculations** *see EHT calculations***extensive air showers** *see cosmic ray showers and bursts***extensometers**

- bricks, extensometer for meas. of linear expansion due to freezing 8-53062
- capacitance-torsion balance for measuring small stresses and strains 8-73988
- dilatometer for small linear expansion temp. coeffs. 8-77957
- dilatometry and its versatility in metallurgical studies. I (*French*) 8-65919
- dilatometry with pressure transducing instrumentation, apparent molar vol. of NaOH in water 8-75702
- fatigue tests with axial and diametral extensometers 8-85062
- laser extensometer with scanning beam modulation, improved gauging precision 8-57896
- pneumatic extensometer for large deformations (*Russian*) 8-77901
- polymers, hygrospecific, lateral extensometer, appl. to creep testing of nylon-6,6 8-95883
- volumetric dilatometer, design, exam. of petroleum asphalts 8-57939

external flows

- cylinder wake, external turbulence effects 8-94665
- free surface gravity flow, finite element anal. with variable domain 8-79294
- heat transfer bibliography 8-63425
- jet flow, viscous, with surface tension, finite element soln. 8-79349
- non-Newtonian flow along thin needle, vel. profile, skin friction 8-67229
- turbulence, book 8-90839
- unsteady transitional and turbulent boundary layers, expt. and calc. methods (*French*) 8-75125

extraordinary ray *see birefringence***extrapolation**

- Langmuir probe characteristics at low plasma densities, numerical analysis 8-63592
- orbital amplitudes of nuclei, extrapolation procedure, gaussian basis set and nucl. cusp eqn. 8-74560
- periodic solns., numerical extrapolation 8-69663
- SCF calculations, simplified extrapolation procedure 8-82604
- time scale realisation models and predictions 8-57907

extraterrestrial atmospheres

- see also comets; planetary atmospheres; stellar atmospheres*
- Moon, atmosphere and meteoritic flux transformation 8-61768
- Titan, Kuiper bands detect. in spectrum 8-85898

extraterrestrial life

- alien probe flux density calc. 8-81563
- CETI from Earth satellite orbit 8-61758
- civilisations possible self-annihilation through thermonuclear war 8-81562
- Dyson spheres, mass and energy requirements rel. to IR emission 8-69710
- exotic life and exobiology, characts. 8-69708
- interstellar colonisation 8-61756
- interstellar communication, signalling strategy 8-61757
- interstellar human civilisation likelihood 8-81561
- interstellar travel and communication, bibliography 8-81564
- Mars, Viking biological expts. findings 8-65542
- microwave observational approach 8-61759
- radio contact problems 8-69707
- radio emission leakage in interstellar communication, Earth model 8-57474
- signal processing equipment in SETI programme 8-69709

extraterrestrial radiofrequency radiation *see radiofrequency cosmic radiation***extremum control** *see optimal control***extrusion** *see forming processes***eye***see also vision*

- accommodation response, effects of colour 8-69042
- astigmatism of central and peripheral cornea, asymm. meas. by photokeratoscopy 8-64981
- barnacle photoreceptor visual response rel. to metarhodopsin transitions 8-69050
- binocular eye movements during accommodation vergence 8-61186
- binocular summation, eye accommodative-vergence state rel. to binocular instrument collimation 8-53417
- blink response to startle evoking stimuli in humans, excitatory and inhibitory components 8-77050
- cataractous lens, NMR study of state of water (*Hungarian*) 8-64986
- chromatic stereopsis, opposition of photometric and dioptric factors (*Italian*) 8-56986
- chromoretinoscopy, longit. chromatic aberration meas. 8-56967
- cone and rod involvement in grating detection and resolution 8-92626
- cone pigment ecology in teleost fish 8-69041
- cone specific c-wave in turtle retina 8-69060
- crustacea with scotopic eyes, screening pigment effects on spectral sensitivity 8-65009
- cyclofusional response, human, effect of stimulus size 8-61187
- cyclorotatory trained voluntary eye movements, influence on egocentric orientation 8-92633
- detective quantum efficiency of human eye 8-56976
- education, cornea, radius of curvature, quantitative geometric optics expt. 8-62004
- education, human eye, artificial model, physics laboratory for medical students 8-62003
- elasticity of sclera and choroid in humans, rel. to scleral rigidity and accommodation 8-80907
- electro-oculographic response, recording and interpretation review (*Italian*) 8-73156
- electro-oculographic response interocular comparison, unpredictability of residual long-term effects 8-53392
- electroretinogram, automatic meas. of b-wave amplitude and peak latency (*German*) 8-80993
- electroretinographic response rel. to vars. of visual performance during day 8-77051
- electroretinography, clinical, use of Mingograph ink-jet recorder 8-92731
- extrinsic muscle nerve terminals 8-56970
- eyeblink, human, dynamics model 8-61167
- falconiform eye, depression in deep fovea acting as telephoto lens system 8-88705
- fish, chromatic aberration and effect on refr. state 8-64985
- fixation changes in transverse plane at eye level, Hering's law of equal innervation 8-61184
- glaucoma diagnosis by digital processing of optic nerve head images 8-81043
- gonioscopy, foot-operated camera trip for Nikon photo slit lamp 8-80986
- horseshoe crab, anal. of adapting bump model 8-73160
- human retina model for props. of vision 8-77655
- hydrodynamic model of aqueous flow in posterior chamber 8-69122
- insect compound eye, internal desynchronisation of bilaterally organised circadian oscillators 8-80875
- insect eye slow cell resonances, colour adaptation 8-64988
- intraocular lens implant evaluation 8-81061
- intraocular pressure measurement, applanation tonometer correls. 8-77047
- isorhodopsin chromophore conform. and orientation in frog disc membrane 8-64980
- kitten, optical quality development 8-64982
- kitten, optical surface development 8-64983
- kitten cornea optical development 8-64984
- laser trabeculotomy in glaucoma treatment 8-53470
- lens, normal and senile cataractous, PMR study of state of water 8-64987
- lens hazards from high-energy beta-rays 8-65131
- lens opacification in mice exposed to 14 MeV neutrons 8-65097
- lens pigmentation in humans rel. to UV light exposure 8-65100
- Limulus ventral nerve photoreceptor response height vs. stimulus intensity curve 8-69058

eye continued

- mathematical model for eye tracking movements of acoustic targets 8-80870
- microtremor clinical recording, using piezoelec. strain gauge transducer 8-96109
- microvilli membrane fragment protonic and ionic processes, of cephalopod visual cell 8-73159
- microwave induced hazardous thermal stresses in ocular lens of human eye 8-80914
- movements, nonadditivity of vergence and saccadic components 8-69095
- movements during learning-set form., monkey 8-77057
- movements of African chameleons, spontaneous saccade timing 8-69053
- movements while reading, annotated bibliography 8-53394
- movements while reading, interocular comparison for normal and amblyopic subjects 8-53393
- oculomotor control system, expt. set-up for clinical investigation, visual, acoustic, vestibular stimulations 8-80990
- ophthalmological tissue differentiation, digitisation of HF US signals 8-80935
- ophthalmology diagnosis, computer assisted 8-92739
- optokinetic movement inversion in anterior visual field, albino rabbit 8-77052
- pattern induced flicker colours, sensory process sensitivity to short time delays 8-96048
- photocoagulation using ruby laser, colour discrimination time variability 8-53401
- photoreceptor cells, daily rhythms and vision research 8-61176
- photoreceptor form dichroism in vertebrates 8-56969
- photoreceptor membrane, lipid free radical oxidation kinetics rel. to lipid composition 8-80872
- photoreceptors, light propag. in twisted anisotropic media 8-63004
- photosensory membrane of Limulus ventral nerve photoreceptor, effect of extracellular Ca/Na ratio 8-69067
- pigment reactions, coupling of charge stabilisation, torsion and bond alternation 8-64999
- pigment responses to prolactin in trout, effect of thiourea 8-69065
- pigment system kinetics, bistable system meas. appl. 8-92624
- pigment system kinetics, mathematical anal. 8-92623
- pineal eye rel. to swimming behaviour in *Xenopus* tadpoles 8-64978
- pupil noise amplitude control, interaction of sensory and motor mechanisms 8-64998
- pupillary sphincter, light-induced Ca release in photosensitive vertebrate smooth muscle 8-64994
- pupillometer, objective device using counter-rot. perspex blocks 8-81000
- pursuit movements in absence of target, perceptual effect 8-73162
- pursuit movements of disappearing moving target 8-61174
- refractive error measurement using Humphrey Vision Analyser, reliability and validity 8-61265
- refractor, automatic, optical system 8-61274
- retina, dark-adapted, time integrative props. 8-53399
- retina, toad, evidence for passive electrotonic interactions in red rods 8-92627
- retina of cat, neural path real time simulation (Spanish) 8-96046
- retina of Limulus, spatially synchronised oscillatory response theory 8-73158
- retina of turtle, horizontal cells influence on bipolar cells' membrane pot. 8-88708
- retina structure in whistling ducks rel. to feeding habits 8-53391
- retina thermal injury following laser irradi., asymptotic rate process calcs. 8-80916
- retinal bipolar cells, frog, Golgi study 8-56968
- retinal blood flow, laser Doppler meas. 8-69174
- retinal cells of cat, spatio-temporal model 8-92621
- retinal damage by 325 nm He-Cd laser radiation 8-69136
- retinal ganglion cell of cat, refractoriness in maintained discharge 8-64991
- retinal ganglion cells of cat, response patterns for moving contours 8-69059
- retinal internal circulation visualisation using Purkinje's methods 8-69043
- retinal light responses, simultaneous recording by extra- and intracellular electrodes in crayfish 8-69055
- retinal on-centre bipolar cell, ionic mechanisms of rod and cone signals 8-61177
- retinal responsivity compression, V-log I functions and increment thresholds 8-61181
- retinal rod outer segments, birefr. analysis 8-56954
- retinal tissue damage, by single ultrashort laser light pulses 8-96065
- retinals, catalysed cis-trans isomerisation by crude tissue extracts 8-64925
- retinoscopy, theory including aperture stops 8-85308
- retinoscopy of infants at distance, limits of normal and anomalous reflexes 8-61170
- retinula peripheral cells within *Drosophila* visual mutants, response to monochromatic white-noise 8-69078
- rhabdom spectral absorption, crayfish visual pigment, photoproduct and pH sensitivity 8-65008
- rhabdomere transmittance decrease due to blue light, rel. to desensitisation of peripheral photoreceptors 8-64993
- rhodopsin, bovine, kinetics of NaBH₄CN reduction 8-64926
- rhodopsin flash photolysis, rabbit retina 8-76996
- rhodopsin formation, opsin recognition of longit. length of retinal isomer 8-61137
- rhodopsin photoproduct kinetics in frog retinas, rapid scanning microspectrophotometer meas. 8-92763
- rhodopsins of oceanic decapods, absorpt. spectra 8-61182
- rod early receptor potential isolation from frog retina 8-69066
- rod ERG, human, rel. to psychophysical responses in light and dark adaptation 8-69063
- rod ERG of mudpuppy, effect of dim red backgrounds 8-69062
- rod network in turtle retina, elec. spread 8-80874
- rod outer segment, *Rana pipiens*, birefringence meas. of struct. inhomogeneities 8-77048
- rod outer segment adaptation anal. based on a simple equiv. cct. 8-73157
- rod outer segment shedding, intraocular initiation 8-85309
- rod threshold, human, influence of cones stimulated by contrast flashes 8-69074

eye continued

- saccades, large, error-correcting mechanisms 8-61175
- Stiles-Crawford function peak shift with wavelength 8-92631
- superior colliculus in rat, plasticity of developing visual system, sensory deprivation effects 8-88706
- synaptic projections formation mechanism in arthropod visual system 8-88707
- torsional movements, rapid phase, in humans 8-69045
- US ophthalmological signal acquisition and image enhancement 8-57045
- UV effects, review 8-80917
- UV effects 300 to 400 nm, literature review 8-57042
- vergence eye movement role in stereoscopic perception of space 8-85315
- vertebrate cornea, transparent layered structure thickness monitor 8-92737
- vestibular nystagmus, computer anal. of irregularities indicating central vestibular disorders 8-81036
- vestibuloocular reflex of cat, quick phase generation model 8-56971
- visual stimulator for flicker fusion expt. 8-96053
- vitreous surgery via pars plana, instrument design 8-81056

F-centres

see also A-centres; M-centres; R-centres; Z-centres

- alkali halide, binding energies of positron to F and F' colour centres 8-87667
- alkali halide, defect formation, model of excitonic mech. 8-91337
- alkali halide, with oppositely charged defect centres, autoionisation-tunnel relax. of electron excitation 8-72112
- alkali halide crystal, irradi., chemiluminesc. process during dissolution (Russian) 8-92133
- alkali halide host cryst. F-centre lasers, tunable IR emission 8-59030
- alkali halides, bound polarons, vibronic theory, appl. to F-centre excited states 8-84150
- alkali halides, F'-centres, thermal and photolytic decay processes 8-95053
- alkali halides, F-centre, cluster-Bethe lattice treatment 8-63762
- alkali halides, F-centre trapping of conduction electrons, photocond. study 8-56179
- alkali halides, influence of purity of crystals on stability of F-centres and interstitials 8-91336
- alkali halides, photodichroic, as optical processing elements 8-83056
- alkali halides, resonance Raman scattering, electron-phonon interaction for F centres 8-68519
- alkali metal halides, irradiated, annealing 8-92494
- alkaline earth fluoride crystals, colour centre thermal stability 8-83811
- halides, form. photochem., review 8-63763
- ionic crystals, surface F centres, electronic struct., numerical soln. of one electron Schrodinger eqn. 8-64091
- laser design, tunable CW for spectroscopy and photochemistry 8-94397
- oxides, excited states of F-centres 8-64006
- relaxed excited states, vibronic model of stress effects 8-95118
- sapphire, F-type centre induction, 6.1 eV optical absorpt. band 8-88332
- tunable IR lasers with F₁(II) and F₂(II) colour centres 8-90420
- Zeeman interaction, relativistic corrections and very small g-shifts, contrib. to EPR 8-72393
- β -Al₂O₃-Na₂O, EPR and optical absorpt. studies of X-ray produced defects 8-95517
- BaClF, two types of F-centres, identification by ENDOR 8-60355
- BaF₂, F-centres, muffin-tin approx. inadequacy 8-63761
- CSi:Na cryst., V_k-Na⁰ centre pairs, tunnelling recomb. 8-91952
- CaF₂, F-centres, muffin-tin approx. inadequacy 8-63761
- CaO, F-centres, ³T_{1u} relaxed excited state, uniaxial stress effect and spin-lattice coupling 8-72405
- CaO, random intrinsic strain effect on ODMR, PMDR, of F-centre in Jahn Teller states 8-84499
- Cs halides, F-centres, first excited degenerate states, props. of electron-phonon interaction 8-63824
- CsBr, electron-phonon interactions of F-centres, first-order Raman scatt. 8-64370
- CsBr, first-order Raman off- and on-reson. scatt. induced by F-centres 8-92073
- CsCl, electron-phonon interactions of F-centres, first-order Raman scatt. 8-64370
- CsCl, first-order Raman off- and on-reson. scatt. induced by F-centres 8-92073
- CsF, doped with F-centres, first order Raman scatt. 8-52492
- CsF, electron-phonon interactions of F-centres, first-order Raman scatt. 8-64370
- CsI, correl. between UV emission band at 300 nm and self-trapped excitons, 4.2K 8-75998
- GeO₂, radiation damaged, paramag. point defects, F-centres, ESR, absorpt. spectra 8-80213
- HfO₂, stabilised, low temp. induced centres, ESR meas. 8-72409
- KBr, efficiency of creation of X₃⁻ centres in X-rayed alkali halides (Russian) 8-71731
- KBr, electron irradi. at 4K, role of V_k centres in equilib. among centres 8-67712
- KBr, kinetic eqns. of formation of F-centres and V_k-centres 8-67713
- KBr, transient infrared absorption of bound polarons 8-92071
- KBr whisker, X-irrad., defect form., thermolum. and ionic cond. obs. (Russian) 8-84666
- KBr, X-irrad., thermally stimulated and tunnelling luminescence 8-72606
- KBr:Eu(Yb), electron-irrad., photostimulated luminesc., ionic processes 8-52561
- KCN, optical F centres and phase transitions 8-56504
- KCl crystal, F-H centre formation by opt. conversion of self-trapped excitons 8-91335
- KCl, distant F-centre pairs, ODNMR 8-68414
- KCl, efficiency of creation of X₃⁻ centres in X-rayed alkali halides (Russian) 8-71731
- KCl, electron injection, F-centre formation efficiency 8-63790
- KCl, F-F' conversion at room temp. 8-51539
- KCl, F-center pairs, light excitation, mag. field and resonance effects on absorption bands 8-92094
- KCl, irradiated, determ. of molar extinction coeff. and oscillator strength of V₂-centre (Russian) 8-80384

F-centres continued

- KCl, press. shifts of F-centre hyperfine interaction parameters 8-79957
 KCl, radiation damaged, proton and $^4\text{He}^+$ channelling, F-centre production, optical absorpt. meas. 8-79656
 KCl, room temp. X-irrad., first stage F-centre form. 8-67709
 KCl surface, vacuum UV radiation damage, spectroscopic study 8-71758
 KCl, X-irrad., thermally stimulated and tunnelling luminescence 8-72606
 KCl:Eu, luminescence and absorption of color centres in RbCl:Cu and KCl:Eu crystals 8-92118
 KCl:I(Br), colouration under two-photon excitation, absorption spectra 8-84618
 KCl:Sr $^{2+}$, X-irrad., thermolum., impurity aggregation, trapping centre form. 8-88367
 KCl(Br), coloured, irrad. damage during positron bombardment 8-63791
 KF:Hg $^{2+}$, electrolytic colouration 8-75665
 KF(Cl)(Br), mag. props. of relaxed excited state of F-centre, vibronic theory 8-60502
 KI, efficiency of creation of X_3^- centres in X-rayed alkali halides (*Russian*) 8-71731
 KI, recomb. luminesc. of H-centre and F-centre electrons (*Russian*) 8-80402
 KI:Eu, electron-irrad., photostimulated luminesc., ionic processes 8-52561
 KI:S $^{2-}$, photochemical reaction, F-centre production 8-64861
 KI(Br), irradiated at room temp., thermolum. and F-centre thermal stability 8-84669
 Li halides, F-band energies press. effect 8-60086
 LiCl, electron irrad., F-centre emission 8-60501
 LiCl, press. shifts of F-centre hyperfine interaction parameters 8-79957
 LiF, coherent radiation generation in F $_2$ -centres 8-50782
 LiF, influence of neutron irrad. temp. on F-aggregate centre form. 8-72561
 LiF, radiation damaged, proton and $^4\text{He}^+$ channelling, F-centre production, optical absorpt. meas. 8-79656
 LiF:Hg $^{2+}$, electrolytic colouration 8-75665
 MgO, radiation induced O interstitials, EPR meas. 8-55866
 Na $_2\text{Al}_6\text{Si}_6\text{O}_{24}$, zeolite, luminescence and coloration (*Russian*) 8-72578
 Na $_2\text{Al}_6\text{Si}_6\text{O}_{24}\cdot\text{F}_2(\text{Cl})(\text{Br})(\text{I})$, sodalite, luminescence and coloration (*Russian*) 8-72578
 NaBr, lifetime of colour centres 8-92115
 NaCN, optical F centres and phase transitions 8-56504
 NaCl, efficiency of creation of X_3^- centres in X-rayed alkali halides (*Russian*) 8-71731
 NaCl, filamentary crystal, vacancy-enriched surface layers 8-51536
 NaCl, irradiated, determ. of molar extinction coeff. and oscillator strength of V $_2$ -centre (*Russian*) 8-80384
 NaCl, press. shifts of F-centre hyperfine interaction parameters 8-79957
 NaCl, radiation damaged, proton and $^4\text{He}^+$ channelling, F-centre production, optical absorpt. meas. 8-79656
 NaCl, transient infrared absorption of bound polarons 8-91642
 NaCl, X-ray irrad., F-centre accumulation and rad. hardening (*Russian*) 8-51538
 NaCl:Cu $^+$, X-ray irrad., role of Cu $^+$ in thermoluminesc. 8-56526
 NaCl(F), irradiated at room temp., thermolum. and F-centre thermal stability 8-84669
 NaF, radiation damaged, proton and $^4\text{He}^+$ channelling, F-centre production, optical absorpt. meas. 8-79656
 NaF:Hg $^{2+}$, electrolytic colouration 8-75665
 RbCl:Eu, electron-irrad., photostimulated luminesc., ionic processes 8-52561
 RbCl:Eu, luminescence and absorption of color centres in RbCl:Cu and KCl:Eu crystals 8-92118
 SrF $_2$, F-centres, muffin-tin approx. inadequacy 8-63761
 SrF $_2$, Q-switching of ruby laser by saturated absorption 8-71157
 SrF $_2$:CeF $_3$ (GdF $_3$)(TbF $_3$), absorpt. spectra of γ -irrad. cryst., 77K, 200-700 nm 8-84615
 ZrO $_2$, stabilised, low temp. induced centres, ESR meas. 8-72409

F $_2$ -centres *see* M-centresF $_3$ -centres *see* R-centresF $_n$ -centres *see* A-centresF-layer *see* F-region**F-region**

- artificially-injected gases dispersal in night-time atm. 8-65460
 convective electric field determ. from rocket meas. of thermal ion spectra 8-57386
 cosmic radio noise absorpt. rel. to mag. storms at Delhi 8-69589
 diffusion inhomogeneities, small-scale, dissipative parametric generation 8-69580
 disappearance, due to Earth encounter with interstellar cloud 8-57292
 electric field oscills. meas. near auroral arc, assoc. with MHD wave 8-65457
 electric fields, poleward-directed, at subauroral latits. 8-88970
 electron density and ion vel. during isolated substorm incoherent scatter radar meas. 8-65452
 electron density max., harmonic analysis and periodicities 8-57383
 electron heat conduction importance in energy balance 8-61649
 equatorial, neutral winds determ. from O I 6300 Å nightglow Doppler shifts 8-81473
 equatorial F-region irregularity patches, localised origin 8-77404
 equatorial ionosphere spread-F echoes in HF and VHF bands, theoretical model 8-85764
 equatorial spread-F, artificial control technique 8-69602
 equatorial spread-F, artificially created, initial report on ionosphere modification 8-88972
 equatorial spread-F, high freq. drift waves with wavelengths below ion gyroradius 8-88973
 equatorial spread-F, solar cycle effects at Huancaayo 8-61647
 equatorial spread-F, VHF scattering 8-61661
 equatorial spread-F and ionospheric holes, ion chemistry and transport 8-88982
 equatorial spread-F onset characts. 8-69562
 f $_o\text{F}_2$, correl. with riometer meas. of ionospheric radio wave absorpt. 8-85763
 f $_o\text{F}_2$, median values obs. over S.Atlantic Ocean 8-81505

F-region continued

- F $_2$ layer of quiet night ionosphere, calculated and measured decay rates comparison 8-81493
 F $_2$ -layer, plasma continuity eqn., comparative anal. of numerical soln. methods 8-69578
 F $_2$ -layer, scintillation of signals from extraterrestrial radio noise sources in mid-latit. trough 8-73574
 F $_2$ -layer, zonal and meridional elec. fields effects in evening sector 8-69571
 F $_2$ -layer at middle latitudes, electron density oscills. rel. to lunar tide 8-61655
 F $_2$ -layer at middle latitudes, ion and neutral gas vel. oscills. rel. to lunar tide 8-61656
 F $_2$ -layer critical frequency, forenoon bite-out characts. 8-65453
 F $_2$ -layer field-aligned and field-perpendicular vels. theory 8-85760
 F $_2$ -layer thermal plasma interhemispheric flow in closed mag. flux tube, sunspot min. conditions 8-93035
 F $_2$ -layer variations, hemispherical differences rel. to neutral atmosphere 8-69603
 F $_2$ -layer vertical sounding, radio signal Doppler spectrum and arrival angle meas. (*Russian*) 8-61651
 F-lacuna events rel. to state of ionosphere 8-93036
 field-aligned irregularity excitation and thermal parametric instability 8-77419
 general circulation at altitudes >100 km, empirical model 8-61664
 gradient drift instability, high-altitude limit 8-88984
 gravity waves, obs. during tornado outbreak (1974 April 3) 8-85753
 ion cloud releases, E-region induced disturbances 8-61657
 irregularities, drift vels. from ATS-6 140 MHz Faraday rot. records 8-69599
 LF sound waves relax. absorpt. (*Russian*) 8-65356
 midlatitude convection electric fields, occurrence rel. to ring current development 8-57395
 morphological studies of rising equatorial spread F bubbles 8-77410
 motions in equatorial F-region, deduction from Sq currents 8-96344
 n $_2\text{F}_2$ annual vars. with latit. and solar activity level 8-69577
 neutral winds, determ. from ionosonde meas. of hmF $_2$ at low latit. mag. conjugate regions 8-81477
 nighttime dynamics from airglow features mapping 8-88980
 nighttime seasonal electron density anomaly 8-69566
 nonstationary nighttime disturbances produced by internal gravity waves 8-73565
 peak electron densities of F $_2$ -layer, comparison of CCIR predictions with in situ meas. 8-57394
 polar cap and auroral zone, math. model 8-65458
 protonosphere-F-region nighttime proton fluxes 8-93034
 radiowave absorption separation from cosmic radio noise absorpt. 8-85769
 radiowave scintillation studies using ATS-6 radio beacons at Delhi 8-69600
 Rayleigh-Taylor gravitation-induced instability, rel. to equatorial spread-F 8-69595
 spatial resonance effect in nighttime equatorial F-region 8-96341
 spread-F bubbles, nonlinear Rayleigh-Taylor mode theory in two dimensions 8-88986
 spread-F in equatorial ionograms assoc. with horizontal elec. field reversal 8-69560
 spread-F recurrence, relationship to ionospheric height rises and polar mag. substorms 8-81494
 stationary nighttime F-layer, analytical model 8-73564
 structure variations rel. to thermospheric diurnal tide seasonal-latitudinal struct. 8-77377
 sudden frequency deviations and phase anomalies due to solar flares (*Italian*) 8-96345
 travelling disturbances, possible correl. with jet stream activity 8-69601
 travelling disturbances characts. over Thumba 8-69590
 travelling disturbances study using multistation rapid-run ionosondes 8-93041
 VLF electrostatic emissions form. mechanism at high latits. 8-93037
 Ba striated clouds, electron density struct. meas. 8-88974
 N $_2^+$, electron impact dissociative recomb. coeffs. inferred from Atmosphere Explorer meas., objections 8-86957

faces (crystal) *see* crystal faces**facsimile***see also* video signals

random halftone contact screens, transmittance control of tone reproduction 8-66775

facsimile communication *see* facsimilefacsimile document reproduction *see* photocopying**facsimile equipment**

X-ray picture laser scanning system for digital image transmission over telephone channel 8-80953

facsimile signals *see* video signalsfacsimile transmission *see* facsimilefaculae *see* Sun**fading***see also* radiowave propagation

atmosphere, turbulent, conditional fading statistics of scintillation 8-66757

Earth-satellite paths, 11.5 GHz, annual and annual-worst-month statistics of fading 8-57238

HF sky-wave received signal level determination for communication link 8-85758

ionosphere sounding, filtering effect on drift parameters determined by full correl. anal. 8-65450

radiowave scintillation studies using ATS-6 radio beacons at Delhi 8-69600

satellite links, ionospheric wave disturbances effect on polarisation fading freq., simulation 8-69572

turbulence and wavelength effect on scintillation fading at mm. wavelengths 8-85623

failure, electrical *see* electrical faults**failure (mechanical)***see also* fracture; mechanical strength; plastic deformation

adhesive joint failure, adhesive/electronically conducting substrate, exam. of electrochemical aspects 8-60979

asymptotic time to failure of a mechanical system of parallel members 8-83240

failure (mechanical) continued

- fibre reinforced metals, fatigue limit (*German*) 8-72859
 glass fabric reinforced polyester, biaxial stress failure surface under static and fatigue loading 8-72836
 graphite fibre reinforced epoxy, laminated plate under tension, stacking sequence and lay up angle effect on free edge stresses round hole 8-88524
 ice shelves, floating, tidal flexure cracks, fracture mechanics 8-69368
 laminated plate under tension, stacking sequence and lay up angle effect on free edge stresses round hole 8-88524
 polyhedral sandwich domes, elastic behaviour, failure, practical investigation and numerical simulation 8-59309
 polymer, deformation, failure, kinetic model (*Russian*) 8-72832
 PTFE/graphite bond in H_3PO_4 environment, electrochemical exam. of joint failure 8-60979
 ring shaped bodies, collapse (*German*) 8-87258
 rock failure precursors during anelastic deformation 8-61405
 steel, low-alloy sheet, welded hydraulic turbine volute chamber, strength and toughness 8-68820
 SiC, hot pressed, brittle fracture and subcritical crack growth 8-72885
 Si_3N_4 , hot pressed, flawed plate under combined stresses, failure prediction 8-72884
 SiO_2 fibres, fused, failure predictions based on fatigue strength 8-71293

failure analysis

- see also electrical faults; wear
 fault tree technique and electron fractography 8-53071
 fibre reinforced composite failure analysis by acoustic emission 8-80691
 graphite reinforced epoxy steel scarf joint, adhesively bonded, exam. of failure 8-92350
 nuclear reactor emergency core cooling system motor operated valves, failure criteria 8-70592
 nuclear steam supply, emergency core cooling system motor operated valves, failure mode anal. 8-54866
 PWRs, auxiliary feedwater system, fault tree anal. 8-54867
 W, filament, incandescent lamps, creep, failure, life prediction 8-84927

fallout

- see also air pollution
 Bikini lagoon, coral alpha emitters, solid-state track detection 8-53661
 Chinese nuclear test explosion, September 1976, hot particle anal. from γ -spectra (*Japanese*) 8-82519
 damping coefficients 8-92961
 education, nuclear fallout radioactivity γ -ray detection and anal., Chinese fission bomb anal. 8-49596
 magnetic particle fallout recorded in recent ombrotrophic peat sections 8-61519
 Nagasaki atomic bomb fallout effects 8-85393
 nuclides determ., 19th Chinese test 8-82520
 radioactive fallout in air and rain, results to end of 1977 8-82535
 radioactive fallout on Milan 1976-7, influence of Chinese nuclear expts. (*Italian*) 8-58501
 reactor airborne plume deposition estimation model evaluation 8-94148
 soil and vegetation, surface β -activity caused by nuclear explosion products, depend. on isotope vertical migration 8-86700
²⁴¹Am, conc. in thermonuclear test debris, collected near Bikini Atoll 8-96103
²⁴²Cm and ²⁴⁴Cm in global fallout, lichen sample results 8-57263
¹³⁷Cs, dating of salt marsh sedimentation rates 8-96247
¹³⁷Cs fallout in arid watersheds, phys. and chem. parameters affecting transport 8-61461
¹³⁷Cs levels in soils and vegetation of W.Malaysia 8-73263
¹³¹I population thyroid dose in USA after Chinese atm. nucl. weapons tests 8-77116
²¹⁰Pb tropospheric residence time 8-85396
^{239,240}Pu, conc. in thermonuclear test debris, collected near Bikini Atoll 8-96103
⁹⁰Sr and T conc. and distrib. in N.Atlantic surface water 8-65345
⁹⁰Sr tropospheric residence time 8-85396

Faraday effect

- atomic forward reson. scatt. spectrometry using magneto-optical effect (*Japanese*) 8-76956
 atomic system, magnetoelc. susceptibility in static mag. field 8-55143
 atomic systems, nonlinear magnetoelc. susceptibility, Faraday effect, laser intensity depend. 8-59076
 chalcogenide spinels, Faraday effect optical isolators for CO₂ laser system 8-50816
 compact extragalactic radio sources, electron-positron pair prod. rel. to Faraday rot. 8-73770
 Dirac-spinor form of Maxwell's eqns., polarised light beams in gravitational fields 8-50696
 fusion reactor, Shiva Faraday rot. coils, circuit and mag. anal. 8-54951
 garnet epitaxial film, Faraday effect and magnetometrical meas. 8-52317
 garnet optical waveguide, with high Faraday rotation, mode degeneracy 8-94454
 geostationary satellite VHF Faraday rotation mea. for ionospheric electron content 8-61599
 glass, photochromic, types FkhS-3, S-4, S-4a and FkhPP, exam. of magneto-optical rotation 8-88284
 ionosphere, irregularities drift vels. from ATS-6 140 MHz Faraday rot. records 8-69599
 ionosphere, total electron content meas. at Gauhati, using ATS-6 140 MHz transmissions 8-69598
 ionosphere, total electron content obs. at Kurukshetra, using ATS-6 140 MHz transmissions 8-69597
 ionosphere, VHF scintillation rel. to peculiar Faraday rotation fluctuations 8-61663
 modulation of polarisation, small ang., beam in diamag. glass (*Korean*) 8-50918
 optical instrumentation, atomic and mol. structure determ. 8-54466
 optically active material, nonreciprocal Faraday effect (*Russian*) 8-55298
 polarisation propagator calculations of frequency-dependent polarisabilities, Verdet constants, and energy weighted sum rules 8-58647
 polyethylene glycol, mol. polarisability from Faraday effect 8-58726

Faraday effect continued

- rare earth compounds, paramagnetic, Faraday and Cotton-Mouton effects for acoustic phonons 8-52476
 rare earth systems, crystal field effects 8-67987
 resonance medium, high power radiation polarisation ellipse, mag. rot. (*Russian*) 8-70794
 satellite links, ionospheric wave disturbances effect on polarisation fading freq., simulation 8-69572
 semiconductor, Faraday rotation in presence of attractive traps 8-76081
 stimulated Brillouin backscattering in laser heated solenoid 8-71511
 tarotien, effects of pulsewidth 8-71540
 AgBr, optical absorpt. of indirect exciton in high mag. field 8-60486
 AgCl, optical absorpt. of indirect exciton in high mag. field 8-60486
 Be, freq.-depend. polarisabilities and Verdet consts., calcs. 8-62781
 Bi₂, vap. phase Faraday effect, P-invariance in M1 transitions, calc. 8-82805
 CO, freq.-depend. polarisabilities and Verdet consts., calcs. 8-62781
 CdCr₂S₄, ferromag. semicond. film, props. 8-76175
 CdCr₂S₄(Se₄), spin depend. phonon Raman scatt., band struct. 8-68491
 CdS crystal, magnetic field intensity meas. by obs. of Faraday effect 8-93739
 CdS, model $S=1/2$ amorphous antiferromagnet, spin polarisation 8-52288
 CdS:In, spin flip Raman scatt., electron dynamics 8-80342
 CoCr₂S₄, Faraday effect, appl. to CO₂ laser systems, radiation damage resist. 8-95579
 Co₂Fe₃₋₄Cr₂O₄, epitaxial, magneto-optical props., effect of Cr³⁺ 8-52590
 Co₂Fe₃₋₄O₄, single cryst. mag. films, holograms recording and thermomagnetic writing 8-55324
 CuBr, evaporated film, magneto-optical effects on exciton bands 8-72624
 CuCl, evaporated film, magneto-optical effects on exciton bands 8-72624
 DyAG, crit., tricrit., and crossover phenomena, light scatt. 8-68251
 DyFeO₃, spin reorientation near Morin temp., magnetooptical exam. 8-68284
 EuO, rotation of polarisation plane in very high mag. field 8-92054
 FH, freq.-depend. polarisabilities and Verdet consts., calcs. 8-62781
 FePd epitaxial film, vacuum-deposited, for thermomag. recording, mag. and magneto-optical props. (*Russian*) 8-60319
 FePt epitaxial film, vacuum-deposited, for thermomag. recording, mag. and magneto-optical props. (*Russian*) 8-60319
 n-GaAs, Verdet const., free carrier density depend. 8-56462
 (GdPrBi)₃(FeGaIn)₂O₁₂, pure and In³⁺ doped, near IR absorpt. and Faraday rot. 8-95580
 Ge, interband Faraday ellipticity 8-92052
 He, freq.-depend. polarisabilities and Verdet consts., calcs. 8-62781
 Hg_{1-x}Cd_xTe, Faraday effect at CO₂ laser freq. 8-64348
 HoIG, Faraday rotation, mag. field depend., 4.2 to 300K, magneto-optical coeffs. 8-95577
 I₂, use as test mol. in modern spectroscopy, review 8-90317
 KTB₃F₁₀, mag., optical, magneto-optical behaviour 8-68484
 KTB₃F₁₀, temp., field and wavelength depend. 8-72542
 LiTbF₄, LiTb_{0.5}Y_{0.5}F₄, and LiTb_{0.25}Gd_{0.75}F₄, temp., field and wavelength depend. 8-72542
 LiTbF₄, mag., optical, magneto-optical behaviour 8-68484
 Na₂O-SiO₂ glass, magnetooptical props. 8-80318
 TbGa garnet, Verdet const. meas. with pulsed mag. field 8-68486
 TbIG, anisotropic garnet, mag. struct., magnetisation and Faraday rotation obs. 8-68169
 YFeO₃, monocrystalline, mag. field depend. of magnetic domain (*Korean*) 8-68337
 YIG, computer optical isolator for near IR region 8-83104
 YIG, single cryst., Neel lines, Faraday effect obs. 8-64216
 (YLaBi)₃(FeGa)₂O₁₂, pure and In³⁺ doped, near IR absorpt. and Faraday rot. 8-95580
 ZnP₂, tetragonal, interband Faraday effect (*Russian*) 8-72490

fast amplifiers see pulse amplifiers**fast Fourier transforms**

- computerised tomography image reconstruction, interpolation effect 8-77110
 Dirichlet problem, response function method for fast soln. of Laplace eqn. 8-86119
 EEG frequency analyser, real-time, microprocessor monitored 8-57092
 faradaic admittance, rapid drop time on-line FFT meas. 8-92544
 fluctuations generation with arbitrary power spectrum, algorithm 8-73927
 fluid dynamics, pseudo-spectral FFT technique, non-periodic problems 8-59359
 fluorescence, and laser Raman decay times, evaluation water pollution detect. appl. 8-81444
 Fourier hologram machine synthesis (*Czech*) 8-66784
 gamma-ray spectral anal. (*Japanese*) 8-90047
 geomagnetic field microstructure separation, digital filtering methods 8-69480
 linear time dependent partial differential eqns., solns. by Laplace transform and FFT 8-57763
 modal anal., formulations for numerical calcs. 8-57767
 SAW chirp filter FFT processor 8-87209
 solar type IV radio events, FFT anal. rel. to pulsating structs. 8-96455
 spectral analysis for teachers 8-81750
 symmetrised neutron transport eqn., fast Fourier transform method solns. 8-78435
 tomograph noise filtering, lung boundaries determ. using neuristic search 8-73240
 voltammetry, cyclic, AC, on-line digital FFT faradaic admittance data acquisition 8-61118

fast-response computer systems

- X-ray cylindrical scanning multiaxial computerised tomography unit 8-80956

fastening *see* joining processes

fatigue

for corrosion fatigue *see* stress corrosion cracking; for thermal fatigue *see* thermal stress cracking
see also fatigue cracks; fatigue testing
 aircraft parts, microfractographic fracture analysis exam., SEM exam. (*Japanese*) 8-52950
 Al alloy, type AK4-IT1, effect of high temp. ageing, on endurance of thin walled joints 8-80570
 alloy, thermal cycling fracture 8-60839
 amorphous polymers, intrinsic time to fracture criterion 8-92320
 amplitude transformation procedure, for fatigue life prediction 8-68796
 body force method, to calculate stress intensity factors, for crack, in arbitrarily shaped plate 8-90775
 composite material, fracture and fatigue, review 8-68781
 concrete, unreinforced, fatigue strength under cyclic loads obs. (*Dutch*) 8-52945
 cumulative damage rule, exam. of new model 8-92358
 cumulative damage theory for fatigue failure 8-75101
 cup and cone fatigue fracture, electron fractographic obs. (*Japanese*) 8-72838
 cylinder under pulsating internal press., limit and life prediction 8-55595
 design elements, reliability rating during fatigue failure 8-79275
 design fatigue analysis, use of fracture mechanics, exam. 8-90794
 engineering materials at elev. temp. 8-80646
 epoxy resin, low temp. fatigue, tensile strength, Young's modulus (*German*) 8-76748
 exoelectron emission defectoscopy, metal fatigue strength prediction 8-76807
 exoelectron emission defectoscopy in initial stages of fatigue fracture 8-53126
 failure characts. of steel 15G2AFDps, effect of loading freq. and temp., SEM exam. of failure surface 8-84995
 fatigue strength, low cycle steels and welds, relationship to static tensile props. 8-64684
 fibre bundles, stochastic strength and fatigue 8-79262
 fibre reinforced composites 8-68767
 fibre reinforced ionomer composites, fatigue strength, dynamic viscoelastic props. and fracture surface exam. (*Japanese*) 8-92339
 fibre reinforced metals, fatigue limit (*German*) 8-72859
 float glass, exam. of dynamic fatigue 8-80631
 fusion reactor blanket, thermal stresses and cyclic creep-fatigue 8-62655
 fusion reactor first wall/blanket system, thermal-hydraulics and fatigue life modelling 8-58453
 fusion reactor materials, material requirements exam., review 8-50257
 geometry effects 8-67132
 glass fabric reinforced polyester, biaxial stress failure surface under static and fatigue loading 8-72836
 glass fibre reinforced epoxy, as electrical insulation for Tokamak toroidal field coils, mech. props. 8-64610
 glass fibre reinforced plastic tube under cyclic pressurisation 8-68761
 glass fibre reinforced vinyl ester matrix, axial fatigue failure sequence and mechanism 8-68773
 graphite fibre reinforced polyester, pultruded fibres, interlaminar shear fatigue 8-56742
 graphite/epoxy laminates fatigue characts. under compression loading 8-84971
 high cycle fatigue diagram based on dynamic severity criterion 8-60759
 high strength structural mats., microstruct. influences on fatigue and fracture resist. 8-56728
 high temp., hold time effects, cavitation nucleation, creep interaction 8-60734
 high temp. fatigue, review 8-56773
 Incoloy 800, 600 and 718, press. vessel, fatigue design criteria 8-60758
 Incoloy 800, austenitic, creep fatigue interaction at 600°C 8-64672
 life dispersion in rolling contact, new model 8-59349
 material with heterogeneous struct., fracture mechanism 8-67127
 metal structures, inelastic anal. 8-70586
 metals, fatigue failure, book 8-76747
 metals and alloys, cyclic strength in nonisothermal loading, exam. of method and equipment 8-85096
 micro plastic strain energy criterion applied to reversed biaxial fatigue 8-63391
 notch and size effect, new method for calc. 8-63389
 notch fatigue life predictions, using smooth bar fatigue data 8-63387
 notched bodies, exam. of fatigue limit 8-71291
 notched components, generalised design procedure for estimating fatigue life 8-63388
 notched plates, monotonic and cyclic loaded, exam. of elastic-plastic stress-strain behaviour 8-63390
 nuclear reactor structural materials assessment, AISI 316 and 9Cr-1Mo steels, for UK LMFBR 8-86581
 optical fibres, UV curable epoxy acrylate coated, long-term mech. behaviour 8-95802
 PMMA, fracture toughness under biaxial stress 8-76760
 polymers, fracture and fatigue, review 8-68781
 polystyrene, fatigue behaviour, cyclically loaded, mean stress effect 8-52968
 polystyrenes, monodisperse, static and dynamic props., mol. wt. effect 8-84938
 residual strength based on strength life equal rank assumption 8-67094
 stainless steel, 304, tensile stress effects on high-cycle fatigue 8-86603
 steel, 14G2AFD and 15G2AFDps, fatigue resistance when strengthened by nitrides and welded joints 8-95790
 steel, alloy, carburized case parameters, effect on props. of 20Kh3MVFA and 12Kh2N4A 8-52989
 steel, alloy, Cr-Mo-V, fatigue, failure probability based on residual strength 8-68797
 steel, alloy, Ni-Cr-Mo, SNCM8, mech. strength under combined alternating strength 8-64690
 steel, alloy, static and fatigue strength, tension and compression test results 8-95810
 steel, alloy, type 25G, increasing fatigue resistance by surface plastic deformation 8-88530

fatigue continued

steel, alloy cyclic strength after strain hardening and tempering, precip. hardened 40FT, and 40 8-52988
 steel, ASTM A588, fatigue test of fillet weld, practical aspects of anal. 8-64682
 steel, austenitic, precipitation of Cr₂₃C₆ at grain boundaries 8-84846
 steel, austenitic stainless, 316, surgical implant ion beam textured, stress/strain relations, fatigue characts. 8-73297
 steel, austenitic stainless, equivalent alternating stress from two-level multiple-step wave (*Japanese*) 8-92333
 steel, austenitic stainless, fast neutron irradi., effect on mech. props. 8-92309
 steel, austenitic stainless, fatigue damage, under sawtooth wave strain cycling at elevated temp. (*Japanese*) 8-84977
 steel, austenitic stainless, stressing conditions, influence on fatigue behaviour (*French*) 8-68776
 steel, austenitic stainless, type 316, effect of hold times on fatigue life, explanation in terms of grain boundary sliding damage 8-72851
 steel, ball bearing with modified chem. comp., improved rolling contact fatigue 8-64732
 steel, C, cumulative damage rule, based on reduction in fatigue limit, experimental confirmation 8-92358
 steel, C, EN8, Mo coated, fretting wear and fatigue strength assessment 8-88583
 steel, C, fretting fatigue damage, SEM exam. 8-88541
 steel, C, type S15CK, tufttrided, fatigue strength at elevated temp., under reversed axial strength (*Japanese*) 8-84980
 steel, C (0.1 to 1.15 wt.%), fatigue, mean stress effects (*German*) 8-56721
 steel, case hardened, MnCr, shot peening effect on bending fatigue strength (*German*) 8-56777
 steel, CC Cr-Mo-V, creep fatigue interaction 8-60841
 steel, CC Cr-Mo-V, creep/fatigue interaction 8-64632
 steel, CC Cr-Mo-V, low alloy, creep fatigue interaction 8-64673
 steel, constructional, fracture toughness in cyclic loading 8-72860
 steel, Cr-Mo-V (0.5, 0.5, 0.25 wt.%), heat treated, microstructure effect on threshold region fatigue 8-56757
 steel, creep and fatigue fracture prevention 8-60837
 steel, fatigue life prediction for fillet welded attachments, under service loadings 8-64683
 steel, ferrite-pearlite, cyclic behaviour, fatigue, chem. comp. and microstruct. effects 8-60833
 steel, fibre reinforced Al, fracture mechanics under fatigue (*Czech*) 8-64629
 steel, fracture toughness, influence of low-cycle damage 8-72873
 steel, fracture toughness and dynamic strength, surface active agent effects (*Russian*) 8-56812
 steel, heat treatment with induction heating, 8-92285
 steel, high-strength, endurance in air and NaCl soln., loading freq. effects (*Russian*) 8-56810
 steel, influence on positron annihilation 8-76551
 steel, low, C, rimmed and killed, exam. of impact fatigue behaviour (*Japanese*) 8-88528
 steel, low alloy, fatigue fractographs (*Japanese*) 8-92335
 steel, low alloy, St 52-3, structural, fracture toughness, fatigue precracking and grain size effect 8-60782
 steel, low alloy, type 4340, quenched and tempered, effect of plastic strain followed by ageing, on torsion fatigue resistance 8-92360
 steel, low C, fatigue damage, under sawtooth wave strain cycling at elevated temp. (*Japanese*) 8-84977
 steel, low C, fatigue fractographs (*Japanese*) 8-92335
 steel, low C, grain size effect on fatigue strength, high temps. 8-68759
 steel, low C, push-pull fatigue strength, effect of tensile preload on plastic strain range (*Japanese*) 8-64625
 steel, low C, thermomechanically processed, martensitic fibre development, fatigue fracture 8-64572
 steel, low C, type AISI 1010, effect of Se, Te additions on fatigue props. 8-92359
 steel, low C and mild, fatigue deformation, phenomenological exam. 8-64691
 steel, maraging, (18 wt.% Ni), solution annealed, exam. of cryogenic tensile, fatigue, and fracture props. 8-92311
 steel, medium C, fatigue behaviour of NiAl precipitation hardening 8-84983
 steel, medium C, fretting fatigue, microstructural and environment effects 8-64734
 steel, mild, high temp. fatigue, effect of temp. variation 8-64685
 steel, MnCr (16, 5 wt.%), bending fatigue behaviour improvement by surface treatment (*German*) 8-84957
 steel, Ni, cross girder connections, fatigue strength, design stress 8-64700
 steel, notch sensitivity in fatigue 8-60757
 steel, pearlitic, fatigue, metallographic aspects 8-60828
 steel, pressure vessel, fatigue design criteria 8-60758
 steel, short-cycle, fatigue, stress concentration effect 8-95859
 steel, stainless, 316, creep fatigue interaction failure 8-80652
 steel, stainless, fatigue, high temp. under isothermal and thermal cycling conditions 8-60836
 steel, stainless, martensitic SUS 403-B, high temp. rotating bending fatigue 8-60756
 steel, stainless, prestrained, heat treatment effect on fatigue strength (*Czech*) 8-60747
 steel, stainless, type 304, grain boundary sliding in isothermal and thermal fatigue (*Japanese*) 8-84979
 steel, stainless 304, stress crack initiation in chloride soln., role of corrosion pits (*Japanese*) 8-92397
 steel, stainless type 316, monotonic and cyclic biaxial loading at room temp. 8-52928
 steel, structured, fatigue life distrib., statistical anal., mixed Weibull distrib. (*Japanese*) 8-72841
 steel, thermal cycling fracture 8-60839
 steel, type 20, fatigue, low cycle, exam. of damage accumulation rule, for loading in air and H impregnating medium 8-64649
 steel, water accelerated fatigue, lubricant additive effects 8-64710
 steel 1Kh18N9T, physico-mech. props. after boring in metallic melts (*Russian*) 8-56736
 steel C, fatigued, strengthening by surface plastic deformation 8-88505
 steel C, high tensile load, during stress cycling on push-pull fatigue strength (*Japanese*) 8-92332
 steel fibre reinforced Al, fatigue strength (*Czech*) 8-60748

fatigue continued

- steel plate, high tensile strength, fatigue props. of butt welded joint 8-80649
- steel structures, appl. of risk analysis to brittle fracture and fatigue 8-56768
- stress intensity factor crack opening displacement relationship for compact tension specimen 8-90778
- structure components, damage sum 8-55589
- US atomizer, construction, fatigue strength, elec. characts. 8-81959
- Al, adhesively bonded and weld bonded aircraft struct. subjected to acoustic excitation, determ. of sonic fatigue life 8-92351
- Al alloy, fatigue endurance scatter in transitional region of fatigue curve (*Russian*) 8-56738
- Al alloy, fatigue life distrib., statistical anal., mixed Weibull distrib. (*Japanese*) 8-72841
- Al alloy, yield surface of material subjected to combined cyclic loadings 8-84905
- Al alloy 2024, loading sequence, normal and reversed sequence effect 8-68791
- Al alloy JIS A5083-O, notch sensitivity in fatigue 8-60757
- Al alloys, preliminary forging effects on struct. and mech. props. of extruded sections (*Russian*) 8-80564
- Al, cold rolled, X-ray diffr. and optical microscope exam. of fatigue damage (*Japanese*) 8-84976
- Al, fatigue induced dislocation struct. and hardening, exam. (*Japanese*) 8-64624
- Al foil, modification of texture by fatigue, X-ray diffr. exam. 8-88477
- Al, mechanical deformation with superimposed insonation, volume effects 8-60723
- Al, polycrystalline, abrasion, deform., fatigue, study by exoelectron microscope (*Japanese*) 8-74108
- Al/polyethylene/Al sandwich construction, flexural fatigue props. (*Japanese*) 8-56751
- Al-Cu alloy RR58, high strain fatigue life, prior treatment effect 8-60835
- Al-Cu-Mg alloy, influence of plastic deformation on fatigue limits, for prestrained components 8-68799
- Al-Cu(Zn-Mg), age hardening, conditions leading to localised plastic deform. and fracture in slip bands during fatigue 8-64670
- Al-Zn-Mg-Cu, alloy 7075, fatigue, loading sequence, normal and reversed sequence effect 8-68791
- Al₂O₃, cyclic fatigue in direct push-pull, exam. 8-56746
- Al₂O₃, porous, sintered, delayed failure, static fatigue in distilled water 8-64750
- Al₂O₃, vitreous-bonded, eval. of proof testing to assure against delayed failure 8-84954
- C fibre reinforced Cu composite, fatigue strength under constant strain (*Russian*) 8-95796
- C fibre reinforced plastic, $\pm 45^\circ$ orientation, creep, fatigue, repeated loading and crack growth 8-68729
- C, isotropic pyrolytic, for biomedical devices, mech. props. 8-65150
- Co alloy, X-40, creep-fatigue interaction at high-temp. 8-84958
- Co base superalloy, rupture life, prior temperature cycling effect 8-60840
- Co-W-Cr (15,20 wt.%), surgical implant ion beam textured, stress/strain relations, fatigue characts. 8-73297
- Cu, fatigue behaviour effect of Zn, Au diffused coatings 8-72850
- Cu-Al (10 wt.%) alloy, water-quenched, tensile fatigue strength at high temp. in vacuo (*Japanese*) 8-72837
- Cu-Cr (1 wt.%), exam. of low cycle fatigue props. at elevated temp. 8-64674
- Cu-Cr-Zr-Mg (0.5, 0.1, 0.03 wt.%), exam. of low cycle fatigue props. at elevated temp. 8-64674
- Cu-Zn-Al, pseudoelastic alloy, exam. of fatigue props. 8-76744
- Fe alloys, universal diags. of cohesive strength (*Russian*) 8-56733
- Fe, cast, fatigue strength, effect of notches and effective sectional area, for cast Fe with various graphite sizes (*Japanese*) 8-64626
- Fe, cast, pearlitic, residual compressive stress distrib. effect on resultant stress conc. in notched samples 8-92336
- Fe, cast, rare-earth-Mg nodular, fracture toughness and fatigue (*Chinese*) 8-95791
- Fe, fatigue fracture strength and failure, at 77K after cyclic loading at room temp. 8-84996
- Fe, sintered, fatigue, metallographic obs. 8-64646
- Fe waisted cylinders, fatigue, exam. of Miner's rule 8-64689
- Fe-Ni, brittle transgranular and intergranular fatigue crack growth rate, yield strength effect 8-68786
- Fe-Si (3.72 wt.%) fatigue failure in vacuum and air 8-68789
- α -Ge, Se_{1-y}, photoluminescence and fatigue effects 8-84648
- Mg, cyclic hardening of single crystal 8-64552
- Mo single crystals, substruct. variation during fatigue, kinetics (*Russian*) 8-60742
- Ni base superalloy, rupture life, prior temperature cycling effect 8-60840
- Ni base superalloy IN 100, corrosion resistant intermetallic coating, microstruct. effect on mech. props. 8-85058
- Ni-Al, CC Ni-Al (42 at.%), Al₂O₃ growth, morphology and spalling model 8-53030
- Si₃N₄, static fatigue, fitting of data to iterative trivariate analysis 8-76732
- SiO₂ fibres, fused, failure predictions based on fatigue strength 8-71293
- Ti alloys, β -annealing and controlled rate quenching effects 8-80568
- Ti alloys, universal diags. of cohesive strength (*Russian*) 8-56733
- Ti, fatigue fracture surface microstruct., electron microscope obs. 8-60834
- Ti, mechanical deformation with superimposed insonation, volume effects 8-60723
- Ti-Al-Cr-Mo-Fe(V)(Zr), effect of structure and heat treatment on tensile strength, ductility, fatigue limit and notch sensitivity 8-56711
- Ti-Al-V (Mo-Sn)(Zr), environmental effects in alloy fretting, effect on fatigue props. 8-56787
- Ti-Al-V (6.4 wt.%), surgical implant ion beam textured, stress/strain relations, fatigue characts. 8-73297
- α Ti-Al(Zr), embrittlement due to ageing 8-56673
- β -Ti-Mn, exam. of reloading yield points 8-72822
- U-Mo (10 wt.%), commercial alloys, influence of metallurgical factors on fracture processes (*French*) 8-60751

fatigue cracks

2056 MW nuclear reactor pressure tubes cracking 8-82463

fatigue cracks continued

- adhesively bonded metallic panels, 2-ply, finite element and integral eqns. anal. of fatigue crack growth 8-92347
- AE detection in aircraft wing test 8-60925
- Al alloy 2024-T3, fatigue crack closure with negative stress ratio, following single tensile overloads 8-64687
- alloy steels, delayed retardation phenomena of fatigue crack growth, exam. 8-56745
- blunting and growth, prediction of threshold stress intensity using dislocation model 8-79662
- α -brass, dislocation structure around crack tips in early stage of fatigue 8-60830
- brittle fracture, stability problem, three-dimensional linearised theory (*Russian*) 8-55606
- closure, influence of mech. factors 8-67100
- complex structure fatigue life prediction using critical location concept 8-59348
- computer simulation of crack propagation, based on crack closure concept 8-68793
- crack closure related to crack propag., prediction method for crack growth 8-67099
- crack propagation, brittle amorphous solids 8-75721
- cup and cone fatigue fracture, electron fractographic obs. (*Japanese*) 8-72838
- damage parameter, energy based, for fatigue and creep-fatigue appl. 8-59347
- development in real structures, appl. to aircraft design 8-56769
- dislocation diffusion mech. of form. 8-60829
- Dugdale crack model, continuous damage approach, to fatigue process 8-90780
- early stage problems 8-56758
- energy criteria in rupture and fatigue (*French*) 8-90771
- energy-balance approach to fatigue crack growth 8-90773
- epoxy resin, low temp. fatigue, tensile strength, Young's modulus (*German*) 8-76748
- fatigue crack growth, model prediction, two coupled differential equations 8-67103
- fracture mechanics parameters, applicability to creep, fatigue crack propag., at evaluated temp., exam. using various materials (*Japanese*) 8-52962
- graphite reinforced epoxy steel scarf joint, adhesively bonded, exam. of failure 8-92350
- growth, assessment of threshold 8-63392
- growth, mechanisms, crack geometry 8-64703
- growth, model prediction, two coupled differential equations 8-67103
- growth model, notch anal. of fracture approach 8-52984
- growth propagation, delayed retardation phenomenon, from single overload 8-92317
- growth rate prediction, using phenomenological approach 8-67101
- hybrid bodies, propagation of multiple ended fatigue crack 8-68801
- impact test, finite element analysis 8-68806
- internal fatigue crack growth in vacuum 8-56729
- metal propagation and initiation, high frequency, US meas. 8-60978
- metal structural part, fatigue crack propag., new approach 8-56752
- metallic alloys, fracture toughness and fatigue crack growth data, compendium of sources 8-84963
- metals, fatigue failure, book 8-76747
- metals, US device for determining growth rate 8-60917
- micro and macro fracture mechanics, exam. of brittle fracture and fatigue crack growth 8-60774
- notched beam, fatigue crack emanates from notch root, fracture strength 8-72866
- notched components, fatigue crack growth 8-83329
- nuclear components, struct. integrity assessment mat. prop. variations 8-89953
- optical fibres, plastic coated fused silica, dynamic fatigue data reliability 8-87166
- Paris differential eqn., numerical calculation of parameters 8-63384
- plastics, fatigue fracture props. correl. with viscoelastic damping 8-52993
- PMMA, effect of temp. on freq. sensitivity of fatigue crack propag. 8-76762
- polycarbonate, cyclic deformation and craze growth 8-76759
- polycarbonate, effect of temp. on freq. sensitivity of fatigue crack propag. 8-76762
- polymeric fibres, cyclic tension endurance, Prevorsek-Lyons theory 8-52967
- polypropylene, crystalline, morphological aspects of crack growth 8-76761
- polysulphone, effect of temp. on freq. sensitivity of fatigue crack propag. 8-76762
- propagation, in deformable media with nonlinear characteristics, model 8-63393
- propagation, theoretical expl. of delaying effects of overloads 8-67093
- propagation behaviour, under stress amplitude, below fatigue limit on fatigue life (*Japanese*) 8-92331
- propagation rate, mechanical property effects of materials 8-90776
- propagation theory, threshold derivation, Paris regime crack growth rate 8-83338
- propagation theory, threshold derivation 8-83337
- quasibrittle body with internal determ. of crack growth kinetics and life expectancy 8-63383
- Rene 95, Ni based superalloy, effect of grain size and gamma prime size, on fatigue crack propag. 8-64686
- SAW, harmonic generation at unbonded interfaces and fatigue cracks 8-90562
- shaft or axle type components, crack propagation and residual strength, problems specification 8-51120
- spectrum growth under cyclic compressive-compressive loads 8-79267
- steel, 0.40/0.50 C, crack growth, Weibull analysis 8-92319
- steel, 1045, fatigue crack growth testing, decreasing stress intensity technique, computer-controlled 8-72949
- steel, A533 B, fatigue crack propagation, grain size and temp. effects 8-56727
- steel, alloy, HY140, fatigue crack initiation and propag. at notch tip 8-80647
- steel, alloy, HY180, fatigue crack initiation and propag. at notch tip 8-80647
- steel, alloy, Ni (5.5 wt.%), fatigue fracture toughness, crack propag., at low temp. 8-68823

fatigue cracks continued

steel, alloy, Ni-Co-Mo, fatigue crack growth, during impact tests exam. of kinetics 8-88525

steel, alloy, Ni-Cr-Mo, alloys SNCM8, SAE 4161, heat treated, residual stress at fatigue fracture surface (*Japanese*) 8-64622

steel, alloy, Si-Mn(Mn-Cr), heat treated, exam. of microfractographic aspects of fatigue cracks (*Japanese*) 8-52959

steel, anisotropic rolled plate, fatigue crack growth, rel. to laminated struct. and inclusions 8-92313

steel, austenitic, precipitation hardening, effect on fatigue strength 8-84829

steel, austenitic stainless, fatigue crack growth rates in type 316, effects of overloads on growth rate 8-64688

steel, austenitic stainless, type 07Kh25N12G2T, US monitoring of fatigue crack growth 8-60917

steel, C, fatigue crack features, in S 35 C and SK 5, anal. by precision matching method (*Japanese*) 8-52955

steel, C, fatigue crack growth in air and seawater, under constant amplitude and random loading 8-64679

steel, C, fatigue crack propag. and crack closure, of part through cracks (*Japanese*) 8-72842

steel, C, fatigue crack propag. and fractography under periodic over-stressing, exam. (*Japanese*) 8-52958

steel, C, heat treated, exam. of microfractographic aspects of fatigue cracks (*Japanese*) 8-52959

steel, C, transition from initiation to propagation of fatigue cracks 8-68802

steel, C and alloy, notched beam, fatigue crack emanates from notch root, fracture strength 8-72866

steel, Cr, cast, fracture toughness and fatigue crack propagation, structural components of hydro-turbines, in water and air 8-68822

steel, Cr-Mo-V, brittle failure, heat treatment and influence of cold plastic deform. 8-72858

steel, fatigue crack growth, exam. of some aspects 8-56772

steel, fatigue crack propag. under random loading 8-76726

steel, fatigue crack propagation rate in types 15KP, ST3, 15G and 10G251 with different yield strengths 8-52987

steel, fracture micromechanisms, fracture toughness, exam. 8-56766

steel, high strength, fatigue crack growth 8-64697

steel, high strength, fatigue crack propag. and fractography under periodic over-stressing, exam. (*Japanese*) 8-52958

steel, high strength, low alloy, fatigue crack growth from a surface flaw 8-68803

steel, high strength, WT 80C, fatigue crack propag. and crack closure behaviour, under various loading conditions 8-68795

steel, high tensile strength, base plate and welded joints, exam. of fatigue crack growth rate (*Japanese*) 8-52956

steel, HT80, fatigue crack closure over stress ratio range, stress intensity threshold 8-80619

steel, hybrid bodies, propagation of multiple ended fatigue crack 8-68801

steel, kinetics of fatigue crack propagation 8-68804

steel, low alloy, constructional, fatigue cracking in corrosive media 8-85081

steel, low alloy, exam. of fatigue crack growth, and Paris Law parameter relationship 8-92343

steel, low alloy, thermally fatigued, fracture toughness 8-72872

steel, low C, fatigue crack plasticity, effect of water vapour 8-64678

steel, low C, fatigue crack propag. and crack closure behaviour, under various loading conditions 8-68795

steel, low C, fatigue crack tip, observation of crack closure phenomena, by electron microscopy 8-68794

steel, low C, prior austenite grain size, effect on near threshold fatigue crack growth 8-92341

steel, low C, prior austenite grain size, effect on near threshold fatigue crack growth 8-92342

steel, maraging, fatigue crack growth, during impact tests, exam. of kinetics 8-88525

steel, maraging, type 200, effect of freq. on cyclic crack growth in salt water environment 8-64680

steel, martensitic, fatigue crack form. associated with cyclic slip deform. along prior austenite grain boundaries 8-60831

steel, martensitic, low tempered, high strength, fatigue crack, propag. rate (*Czech*) 8-64770

steel, metastable austenitic stainless, fatigue damage, static and dynamic simultaneous obs. (*French*) 8-88516

steel, mild, exam. of fatigue damage, using thermography 8-92356

steel, mild, fatigue crack growth from a surface flaw 8-68803

steel, mild, fatigue crack initiation, fractographic exam. (*Japanese*) 8-52957

steel, mild, mode II fatigue crack growth threshold 8-92362

steel, mild, stress history effect on fatigue crack retardation 8-64627

steel, Ni, microstruct., plastic zone size and crack propag. 8-60790

steel, NiCr, random load fatigue crack propag. 8-64692

steel, rail and structural, fatigue crack growth 8-64695

steel, rolled, effect of inclusions on torsional fatigue 8-92314

steel, SNCM8, HT80, A553, fatigue crack growth, delayed retardation phenomenon, from single overload 8-92317

steel, stainless, 316, crack propag. in low cycle fatigue below 600°C, SEM obs. 8-64631

steel, stainless, crack propag. at high temp. under low cycle loading 8-60838

steel, stainless, fatigue crack morphology of type 304 cycled at const. stress amplitude at elev. temps. 8-64671

steel, stainless, growth, plastic zone form. 8-64702

steel, stainless, low fatigue crack growth rate 8-64701

steel, stainless, orthopaedic fixation devices, failure, SEM exam. of fatigue crack surfaces and microstructure 8-77156

steel, stainless, SUS304, fatigue crack closure over stress ratio range, stress intensity threshold 8-80619

steel, steam turbogenerator rotors, fatigue crack initiation and growth, from macroscopic slag inclusions 8-64681

steel, temp. effect on fatigue failure (*Russian*) 8-88517

steel, TRIP, fatigue crack propagation 8-64696

steel, trifurcated, observation of fatigue fracture surface (*Japanese*) 8-52951

steel, ultrahigh strength, effects of strength and grain size on near-threshold fatigue crack growth 8-64704

steel component strengthened by surface plastic deformation anal. 8-88529

fatigue cracks continued

steel rollers, case-hardened, nitrided, surface failure, durability 8-84959

steel U8, hydrogenation effects on fatigue crack propag. (*Russian*) 8-56800

structural bonded joints, fatigue crack growth of adhesive bond line cracks 8-92346

subcritical development, effect of stress state on rate of development 8-79276

surface crack shape change in bending fatigue, resonant fatiguing apparatus 8-72950

thermal detection 8-92423

threshold stress intensity for crack growth, prediction using dislocation model 8-83870

type HT80, delayed retardation phenomena of fatigue crack growth, exam. 8-56745

weakest link model, for prediction of crack growth rate 8-90797

X-ray microbeam meas. of local stress, appl. to fatigue crack growth (*Japanese*) 8-64793

Al alloy, 2024-T3, crack closure 8-72833

Al alloy, A2017, A5083, fatigue crack growth, delayed retardation phenomenon, from single overload 8-92317

Al alloy, crack opening displacement, expt. and FEM study 8-68811

Al alloy, effect of frequency changes on fatigue crack growth 8-64693

Al alloy, fatigue crack growth, crack closure 8-80650

Al alloy, fatigue crack propag. and fractography under periodic over-stressing, exam. (*Japanese*) 8-52958

Al alloy, loading freq. effect on fatigue growth rate 8-83873

Al alloy, low fatigue crack growth rate 8-64701

Al alloy, plastic zone form. and fatigue crack growth 8-64702

Al alloy 2024-T3, effect of stress level on fatigue crack delay behaviour 8-68790

Al alloy BS 2L71, crack closure during fatigue crack growth, for two thicknesses 8-68792

Al alloy fatigue cracked alloy 7075 T6, repair machining and inspection of components 8-80689

Al alloys, A356 T6 and 2219-T851, fatigue crack growth testing, decreasing stress intensity technique, computer-controlled 8-72949

Al alloys, delayed retardation phenomena of fatigue crack growth, exam. 8-56745

Al alloys, fatigue crack arrest, corrosive environment, at low stress intensities 8-92415

Al alloys, fatigue crack growth, exam. of some aspects 8-56772

Al alloys, fatigue crack propag., mechanism of overload effect 8-56730

Al alloys, fracture micromechanisms, fracture toughness, exam. 8-56766

Al alloys selection using fracture mechanics 8-56725

Al, bicrystal, fatigue crack initiation, crystal boundary effects (*Japanese*) 8-92328

Al, cold rolled and annealed, substruct. near fatigue crack tip, X-ray microbeam technique exam. (*Japanese*) 8-64621

Al, fatigue crack initiation, model using probabilistic technique 8-68800

Al-Cu, O transport during fatigue crack growth 8-52981

Al-Cu (4 wt.%), aged to contain Guinier Preston zones, crystallographic fatigue crack growth 8-60832

Al-Cu-Mg, alloys A-U4, A-U4G1, A-U2GN, effect of environment on fatigue crack growth 8-64677

Al-Cu-Mg-Mn (4.5, 1.5, 0.6, wt.%), alloy 2024-T81, plates, adhesively bonded, exam. of fatigue crack growth 8-92349

Al-Zn-Mg, O transport during fatigue crack growth 8-52981

Al-Zn-Mg-Cu, alloy 7075-T6, fatigue crack closure with negative stress ratio, following single tensile overloads 8-64687

Al-Zn-Mg-Cu alloy, laminated, adhesively bonded alloy 7075-T6, exam. of fracture resistance 8-76754

Al-Zn-Mg-Cu-Cr, (5.6, 2.5, 1.6, 0.3 wt.%), laminates, 8 and 22 layers, adhesively bonded exam. of fatigue crack propag. 8-92345

Al-Zn-Mg-Cu-Cr, (5.6, 2.5, 1.6, 0.3 wt.%), alloy 7075, plates, adhesively bonded, exam. of fatigue crack growths 8-92348

Al₂O₃, vitreous-bonded, eval. of proof testing to assure against delayed failure 8-84954

C fibre reinforced plastic, $\pm 45^\circ$ orientation, creep, fatigue, repeated loading and crack growth 8-68729

Cu, crack nucleation and stage I propag. in high strain fatigue, microscopic and interferometric obs. 8-52936

Cu, crack nucleation and stage I propag. in high strain fatigue, mechanism 8-52937

Cu, cyclic hardening rôle in crack nucleation at high strain amplitude 8-64633

Cu, fatigue crack initiation, model using probabilistic technique 8-68800

Cu single crystal film, electrodeposited, fatigue cracks (*Japanese*) 8-84975

Fe, Armo, crack and slip band form. during US fatigue 8-56723

Fe, Armo, fatigue cracking under 23 kHz loading at 23°, 60° and 100°C 8-60763

Fe, dislocation struct. around fatigue cracks, exam. (*Japanese*) 8-64623

Fe, low-temperature fatigue crack propagation 8-72876

Fe-Si, low-temperature fatigue crack propagation 8-72876

Ni alloy, kinetics of fatigue crack propagation 8-68804

Ni alloy 718, fatigue crack growth at 298 and 823K, frequency and wave form effects 8-64636

Ni, fatigue cracks, use of SEM in quantitative stereofractographic anal. 8-80645

Ni superalloy Mar-M200, slow fatigue crack propagation rate meas. using high freq. resonant technique 8-52983

Ni-Co-Cr-Mo-Ti-Al Nimonic 105, loading frequency and environmental effects on high temp. fatigue crack growth 8-64675

Ni-Cr, O transport, during fatigue crack growth, exam. 8-52981

Ni-Cr-Co-Al-Ti-W-Ta-Mo, IN 738 LC, loading frequency and environmental effects on high temp. fatigue crack growth 8-64675

Ti alloy, kinetics of fatigue crack propagation 8-68804

Ti alloys, fatigue crack growth, exam. of some aspects 8-56772

Ti fatigue crack growth, exam. of O transport 8-52981

Ti-11, fatigue crack propag. under dwell time conditions 8-80639

Ti-11, unstable shear modes in fatigued β -annealed specimens 8-84984

Ti-Al-V (6, 4, wt.%), delayed retardation phenomena of fatigue crack growth, exam. 8-56745

fatigue cracks continued

- Ti-Al-V (6, 4 wt.%), fatigue crack propag. under dwell time conditions 8-80639
- Ti-Al-Zr (6,5 wt.%), alloy IMI 685, SEM exam. of crack growth 8-72849
- Ti-alloy, IMI-685, unstable shear modes in fatigued β -annealed specimens 8-84984
- Ti-V (40 at.%), microcracks intersecting fatigue crack, exam of origin 8-80638
- Zr-Nb, pressure tube alloy, initiation COD as fracture criterion 8-72862

fatigue failure *see fatigue***fatigue fracture** *see fatigue***fatigue life** *see fatigue***fatigue testing**

- for corrosion fatigue testing, see corrosion testing*
- acetal homopolymer, exam. of bending strength, using new method 8-53056
- C-shaped fatigue specimen 8-68867
- constructional material fatigue resistance test under asymmetric loading 8-85083
- crack growth testing, decreasing stress intensity technique, computer-controlled 8-72949
- crack propagation in shaft or axle type components, problems specification 8-51120
- cycle ductility determ. in low cycle tests 8-56835
- data analysis for lifetime predictions for ceramics 8-95870
- endurance determ. method over wide range of load asymmetry 8-56836
- equivalent alternating stress from two-level multiple-step wave (*Japanese*) 8-92333
- equivalent alternating stress from two-level multiple-step wave or multiple-level multiple-step wave (*Japanese*) 8-92334
- impact fatigue testing machine 8-56838
- low-cycle fatigue tests with axial and diametral extensometers 8-85062
- machine for long fatigue tests under varying load conditions 8-60909
- machines, crank driven, electromech. system for stabilisation and programming static load 8-64801
- metal fatigue monitoring by US velocity and attenuation meas. 8-60970
- NDT for early prediction by acoustic and exoelectron emission 8-53170
- plastics, bending fatigue, exam. of new method of testing 8-53056
- polymer cyclic deformation amplitude, automatic meas., apparatus design 8-85082
- resonant electromagnetic fatigue tester, features (*French*) 8-56870
- smooth test pieces, method of estimating scale relationship of endurance limit 8-60914
- steel, fatigue crack propag. under random loading 8-76726
- steel, fatigue testing, exam. of scale relationship of endurance limit 8-60914
- steel weld fatigue life estimation, multichannel NDT monitor 8-56846
- stiffened plates, tests on interactive buckling 8-71286
- stress concentrator effects (*Russian*) 8-56831
- thermal detection of cracks 8-92423
- vibrating bench, automated design, exam. of gas turbine blades 8-64800
- Al alloy, fatigue testing, exam. of scale relationship of endurance limit 8-60914
- Al alloy 2024-T3, Alclad, dimpled loaded-hole fatigue strength, effect of interf. 8-72948
- Al alloy V95T1, endurance determ. method over wide range of load asymmetry 8-56836
- Nb₃Sn, filamentary, fatigue tests on small coils 8-64652

fault currents

- see also flashover; leakage currents; short-circuit currents*
- flameproof coating for PVC insulated cables, composition, tests (*Russian*) 8-68828

fault location

- 600 MW pulsed energy converters for toroidal field coil, design philosophy 8-58496
- electrical thermometers, functional fault detect. using electronic devices, report (*German*) 8-81972
- optical fibre cables for field trials, meas. methods (*German*) 8-50922
- remote diagnostic techniques used in Viking lander operations 8-57426
- SiO₂ film, local defects detection by electrolytic decoration (*Bulgarian*) 8-60896

faults, electrical *see electrical faults***f.d.m.** *see frequency division multiplexing***feature extraction** *see pattern recognition***feedback**

- see also control systems; control theory*
- afferent nerve stimulation in below-elbow amputees 8-57125
- arm movements controlled by peripheral feedback, in humans, simulation 8-80891
- at-power reactor noise, second-order coherent functions 8-94070
- auditory feedback, effect on guitar playing intensity and speech prod. 8-85322
- biochemical multiple-loop negative feedback control networks, oscills., periodic metabolic systems 8-85285
- cell growth regulation, effects of cell density and metabolite flux on dynamics 8-85296
- cell growth regulation, effects of cell density and metabolite flux on dynamics 8-88701
- cell population auto-activation, math. model 8-77017
- cognitron, feedback-type, self-organising neural network with associative memory 8-56962
- driven-sweep generator scan velocity transducer 8-57925
- electrostatic generator terminal voltage on-line feedback stabilisation using digital computer 8-82004
- feedback stabilization of an $I=0,1,2$ high-beta stellarator 8-75404
- fixed-frequency laser beam scanning device 8-59135
- hybrid image processing system, space and time picture oscillation, by active incoherent feedback 8-58924
- incoherent feedback optical system 8-66924
- membrane potentials tracing system, using amplifier for voltage clamping (*German*) 8-61285

feedback continued

- motoneurons excited by phasic muscle stretches, discharge pattern shaping, recurrent inhibitory feedback effects 8-85303
- MW impulse generator system, for ion cyclotron heating, fusion reactor 8-70635
- neutral beam power supply, series switch/regulator system, 40 kV, 80 A, 10 ms, for fusion reactor 8-66366
- noise analysis of power reactor, simulation using nucleate boiling noise generator 8-54840
- nuclear reactor core 8-54860
- optical systems, noisy image restoration 8-63020
- plasma, in multiple mag. mirror, axial feedback stabilisation of flute mode instability 8-75408
- plasma instability, suppression by feedback method automatic control, stabilisation methods 8-63564
- portable easy-operation long-period seismometer, peripheral stabilising device 8-65399
- RF charged-particle separator power recovery, for synchrotron 8-66440
- rotor vibration control appl. (*Russian*) 8-70116
- Scyllac fusion reactor, feedback stabilisation system 8-54887
- sensory feedback code comparison using electrocutaneous tracking, for prosthetics 8-69255
- tilt meters, photoelectric, with negative feedback, block diagrams anal. (*Russian*) 8-88948
- Tokamak, ISX, dynamics and feedback control 8-71528
- Tokamak plasma equilibrium, feedback control 8-55738
- trapped electron instability, feedback diagnostic 8-51350
- X-ray spectrometer, Si(Li) detector, preamplifier with drain feedback 8-66448

feeds, antenna *see antenna feeders***Fermi-Dirac statistics** *see quantum statistical mechanics***Fermi gas** *see fermion systems***Fermi level**

- chalcogenide lone-pair semicond. charged impurities, effect on carrier concs., Street-Mott model 8-67984
- FCC clusters, size and shape depend., tight binding approximation 8-79920
- graphite, electronic props., self-consistent LCAO calc. 8-51887
- III-V semiconductor Schottky barrier formation, Fermi-level pinning, defect mech. 8-95358
- insulators, noncryst., electron density captured at traps, liberated to conduction band 8-87946
- lamellar graphite acceptor intercalation cpds., charge distrib. in c direction 8-87935
- metal surface, inert gas bombard., 1.05 keV, electron yields, Fermi energy estimate 8-52611
- metal-semiconductor interface, Schottky barrier formation, microscopic model 8-52087
- semiconductor, polaronic hopping conduction at low temp. 8-51906
- semiconductor-electrolyte contact, electrolytic decomposition and photodecomposition 8-95357
- semiconductor-metal interfaces, intrinsic surface states and Fermi-level pinning 8-95319
- Al_{0.5}Ga_{0.5}As, analytic approx. for Fermi energy 8-63973
- Bi electron properties, carrier spectrum 8-84137
- CaSb, resist., susceptibility and thermopower rel. to electronic struct. 8-67935
- Co, liq., density of states of d-band, heat of vaporisation 8-95253
- Eu-transition metal intermetallics, valence fluctuations 8-91649
- Fe, UPS, density of states determ. 8-52623
- Fe_{0.65}Ni_{0.35}, UPS, density of states determ. 8-52623
- Fe_{1-x}O, wustite phase, surface elec. props. 8-76133
- GaAs surfaces (110) and (111)As, UPS and LEED 8-91514
- n-GaSb:Te(Se), forbidden optical band gap, Moss-Burstein effect 8-88335
- N-Ge, pressure influence on photoconductivity temp. dependence 8-76109
- p-HgTe, experimental and theoretical study of the dynamic dielectric function 8-92069
- Li₂Ag_{2-x}In_x, optical props., struct., energy bands, interband transitions 8-72539
- Li₂Cd_{2-x}In_x, optical props., struct., energy bands, interband transitions 8-72539
- MnSb, resist., susceptibility and thermopower rel. to electronic struct. 8-67935
- Nb₃Au, BCC, density of states, comparison with A-15 8-80095
- NbSe₃, chemical bonding and dimensionality 8-75992
- Ni, UPS, density of states determ. 8-52623
- NiSb, resist., susceptibility and thermopower rel. to electronic struct. 8-67935
- Pb_{1-x}Ge_xTe, Fermi level stabilization, transport props. meas., 77-400K 8-56065
- Pd, hydride and alloys, electronic band struct., comparative study of electric and mag. props. 8-95259
- Pd-Al alloys, Fermi level position rel. to mixing behaviour, Al activity, thermodynamic props. (*German*) 8-75835
- Pd_{1-x}Ag_xH_x, superconducting transition temp., APW band struct. calcs. 8-95393
- Sb, de Haas-van Alphen effect, effective mass, Fermi levels 8-75982
- Sb:Te, de Haas-van Alphen effect, effective mass, Fermi levels 8-75982
- Sb-Sn, dil., de Haas-van Alphen effect, effective mass, Fermi levels 8-75982
- Si (111) surface, Al overlayers, theoretical study 8-95366
- Si film, amorphous, effects of annealing of gap states 8-72115
- p-Si, neutron irradiated, elec. props. 8-51939
- Si:Ni(Co)(Mn), influence of neutron irradiation as elec. props. 8-55895
- Si:O, O rich polycryst. film, carrier transport 8-80076
- Ti, liq., density of states of d-band, heat of vaporisation 8-95253
- V₃Si, neutron irradiat., sound velocity, magnetic susceptibility and upper critical field 8-88074
- V₃Si, neutron irradiat., ht. capacity and resistivity 8-88075

Fermi liquid *see fermion systems***Fermi resonance**

- ethylene carbonate, Fermi reson., isotopic substitution meas. 8-86870
- phase transitions soft modes and dipole relaxations 8-91409
- polymethylene chain, vibr. spectra, CH stretching region, struct. and assignments 8-70991

Fermi resonance continued

- $C^{18}O_2$, Raman spectra in Fermi reson. region 8-74664
 ClCN, and isotopic derivatives, rot. depend. 8-94227
 H-bonds, IR spectra, ν band interpretation 8-58653
 HCN, and isotopic derivatives, rot. depend. 8-94227
 H_2O , electronic ground state, SCF HF and CI calcs, pot. energy hyper-surface, spectroscopic consts. 8-50473
 $KB_3O_8 \cdot 4H_2O$, polariton Fermi reson., spontaneous parametric light scatt. 8-87923

Fermi surface

- actinide metals and compounds, nearly magnetic, thermoelec. power 8-84197
 actinides, band structure Fermi surface, magnetisation density 8-84140
 α -brass, electronic momentum densities by two-dimensional angular correlation of annihilation radiation 8-91605
 disordered alloys, short range order diffuse electron scatt. 8-87595
 double magic nuclei, self consistent description of low lying collective states (Russian) 8-89783
 electron liquid, cyclotron reson. at skipping orbits (Russian) 8-72240
 electronically driven phonon anomalies and phase transforms. 8-63834
 graphite, galvanomagnetic effects, trigonal warping of constant energy surfaces 8-87987
 graphite intercalation compounds, props. and appls. 8-71711
 graphite- Br_2 , intercalation process 8-63965
 HMTSF-TCNQ, obs. of the de Haas-Shubnikov oscills. 8-84201
 Hume-Rothery alloys, magnetism 8-95417
 intermediate state, thermal cond., Fermi surface shape and topology effects (Russian) 8-72314
 isotropic metals, CDW, Fermi-surface instability 8-79947
 metal, charge screening and Friedel oscillations of electron density (Russian) 8-79951
 metal, Lifshitz transitions and tunnelling effect 8-91591
 metal, phonon spectra, singularities caused by local geometry of Fermi surface 8-91401
 metal, surface impedance in magnetic field, Azbel-Kaner cyclotron resonance 8-87901
 metal spherical Fermi surface, cyclotron reson. line shape and cyclotron waves 8-95251
 metals, sound absorpt. and dispersion, Fermi surface flattening 8-91596
 phase transition with valency change, sound vel. renormalisation (Russian) 8-79963
 phonon anomaly near Fermi surface topological transition 8-95120
 rare earths, band structure Fermi surface, magnetisation density 8-84140
 superconductors with dielectric gap in Fermi surface, exceeding of paramag. limit (Russian) 8-95402
 transition metal, 3d, paramag., energy band calcs. 8-91608
 transition metal, Fermi surface, stress depend., from quantum oscill. effects 8-91597
 transition metal alloys, elastic properties, vol. depend. 8-95103
 TTF-TCNQ, band struct., Fermi surface and density of states, LCAO calc. 8-60048
 Ag, Fermi velocity from proximity effect tunnelling 8-51875
 β' -AgMg, de Haas-van Alphen effect, LMTO band struct. and Fermi surface 8-75984
 Al alloy, dil., Hall coeff., calc. by 4-OPW approx. 8-76052
 Al, cryst. and polycryst., inhomogeneity effects on galvanomagnetic props. 8-60109
 Al, EM generation of ultrasound, obs. of anomalies 8-84131
 Al, electron-phonon scattering rates, anisotropic, meas. on Fermi surface 8-87753
 Al, electronic momentum densities by two-dimensional angular correlation of annihilation radiation 8-91605
 Al, Fermi surface, scattering anisotropy of conduction electrons on dislocations (Russian) 8-60051
 Bi, $2\frac{1}{2}$ order electron phase transition under extension (Russian) 8-75981
 Bi, band structure model parameters, deformation theory (Russian) 8-56067
 Bi, diffusion thermoelectric power in mag. field, calcs. 8-56167
 Bi, electron isoenergetic surface, variation of connectivity under press. (Russian) 8-60050
 Bi electron properties, carrier spectrum 8-84137
 Bi, single crystal, drift velocity of charge carriers (Russian) 8-84208
 Bi, whiskers, hardness, elec. props. (Russian) 8-51874
 Bi-Sb narrow gap semiconductor, EM wave propagation in direction parallel to mag. field 8-80014
 Bi-Te, electron isoenergetic surface, variation of connectivity under press. (Russian) 8-60050
 BiSb, hybrid resonance in a quantising magnetic field, spin splitting parameter 8-67933
 $C_{12n}(SbCl_3)$, magnetothermal oscill. and electronic struct. 8-84129
 Cd, Fermi surface changes under uniaxial compression 8-51876
 Cd, inversion of cyclotron resonance data 8-91593
 Cd, strain depend., from US vel. oscills. 8-84133
 Cd, US attenuation of conduction electrons calc. 8-91588
 Cd, US attenuation of conduction electrons, shear waves calc. 8-91589
 Co, de Haas van Alphen oscill., effective mass 8-87900
 Cu, elec. resist., electron-electron scatt., Fermi surface calc. 8-64023
 $Cu_2Mo_6S_8$, normal state and superconducting property measurements 8-91660
 Cu_2Ni_{1-x} , Fermi surface of concentrated paramag. alloys 8-95257
 Ga, de Haas-van Alphen effect, expt. and interpretation 8-84132
 GaAs-Ga $_{1-x}$ Al $_x$ As superlattice, sub-band dimensionality 8-63981
 Gd, de Haas-van Alphen effect 8-84138
 In, US absorption and dispersion, lineshape studies of quantum oscills., anomalous behaviour 8-63966
 In $_2$ Bi, de Haas-van Alphen effect 8-91594
 K-Na, dil., dynamical props. of quasiparticle excitations, de Haas-van Alphen effect meas. 8-84128
 metals, model pseudopotential calcs., elastic consts., spin susceptibility, Fermi surface distortions 8-79922
 Mg, Fermi surface changes under uniaxial compression 8-51876
 Mg, US attenuation of conduction electrons calc. 8-91588
 Mg, US attenuation of conduction electrons, shear waves calc. 8-91589
 Mo, magnetoacoustic studies, to 500 MHz 8-91604
 MoO_2 , Fermi surface calcs. 8-67934

Fermi surface continued

- Nb, electronic and optical properties 8-91612
 NbSe $_3$, non-ohmic transport props. near phase transitions 8-72213
 NbSe $_3$, oscillatory magnetotransport, Fermi surface anisotropy, Hall effect, g-factor, Dingle temp. 8-51975
 NbSe $_3$, quantum oscillation, Fermi surface exam. 8-60049
 NbSe $_3$, satellite electron diff. below 59K, Fermi surface features 8-84136
 Nb $_3$ Sn, A-15 superconductor, dHvA effect 8-75985
 Ni $_3$ (Fe,M), M=Cu, Cr, Mo, W, kinetic phenomena rel. to ordering and electron struct. (Russian) 8-76043
 Pb, effective cyclotron masses of central and noncentral ξ orbits, de Haas-van Alphen effect 8-63968
 PbMo $_6$ S $_8$, normal state and superconducting property measurements 8-91660
 Pb $_{1-x}$ Sn $_x$ Se, determ. of anisotropy coeff. of Fermi surface, magnetoresist. meas. 8-51878
 Pd, stress depend., oscillatory magnetostriction and de Haas-van Alphen torque obs. 8-91602
 PdH, electronic struct. and proton spin-lattice relax. calc. 8-67937
 PdSb, electronic struct., optical transitions, Fermi surface 8-51885
 Pt, de Haas van Alphen obs. 8-91601
 Rb-K, dil., dynamical props. of quasiparticle excitations, de Haas-van Alphen effect meas. 8-84128
 Re, RF size effect, Fermi surface dimensions determ. 8-91598
 Re, single crystal, size effect in elec. resistivity (Russian) 8-87961
 Re, strain depend., from US vel. oscills. 8-84133
 Re, stress depend., quantum oscills. obs. 8-91599
 Ru, electronic structure and mag. breakdown, galvanomag. props. obs., 1.3-20.4K 8-91600
 Ru, single crystal, size effect in elec. resistivity (Russian) 8-87961
 Sb, carrier energy spectrum, effect of hydrostatic pressure 8-87903
 Sb, de Haas-van Alphen effect, effective mass, Fermi levels 8-75982
 Sb, tension effect (Russian) 8-75980
 Sb $_2$ Te, de Haas-van Alphen effect, effective mass, Fermi levels 8-75982
 Sb-Sn, dil., de Haas-van Alphen effect, effective mass, Fermi levels 8-75982
 Si, inversion layer, interacting electron system, cyclotron reson. 8-87902
 4Hb-TaS $_2$, charge transfer and charge density waves 8-79926
 UGe $_3$, de Haas-van Alphen effect, band struct. calc. 8-72068
 V, amorphous film, supercond. props., gaseous impurities effect (Russian) 8-72301
 V, energy bands, calcs. using LCGO method 8-91608
 V $_3$ Si, A-15 superconductor, dHvA effect 8-75985
 W, magnetoacoustic studies, to 500 MHz 8-91604
 WO $_2$, Fermi surface calcs. 8-67934
 Y, Fermi surface and de Haas-van Alphen effect 8-75983
 YAl $_2$, de Haas-van Alphen effect 8-91590
 Zn, Fermi surface changes under uniaxial compression 8-51876
 Zn, superconducting, ultrasonic attenuation 8-88071
 Zn, US attenuation of conduction electrons calc. 8-91588
 Zn, US attenuation of conduction electrons, shear waves calc. 8-91589
 ZrB $_2$, Fermi surface, de Haas-van Alphen effect meas. 8-84134

Fermi-Thomas model *see Thomas-Fermi model***fermion systems**

- see also electron gas; liquid helium-3*
 asymmetric nuclear matter, isospin and density waves, Landau theory 8-66235
 configuration interaction and coupled cluster solns., analytic continuation 8-62147
 confinement and bosonisation, quantum sine-Gordon field theory, quark confinement 8-86442
 cyclotron wave measurements, Fermi-liquid parameter determ. 8-60069
 delta function fermion gas, solitons and HF solns. 8-49755
 disordered system, elementary excitation exam. 8-56086
 dressed fermions in Abelian gauge theories 8-82093
 electron liquid, density response function 8-67961
 electron liquid, two dimensional, lattice model 8-67964
 electron-hole liquid, microscopic theory (Russian) 8-51905
 extended system, energy expectation value per particle, lack of $O(A^{-1})$ contribution in Iwamoto-Yamada expansion 8-60081
 Fermi gas, slightly non-ideal one-dimens., spectral ground state, energy determ. method (Russian) 8-62149
 fermion clusters, many particle correlations, method of transition density operators 8-49763
 fermions on the hypertorus 8-74149
 free-fermion condition for generalised vertices 8-93622
 Hartree-Fock states in thermodynamic limit, low-density clustering 8-54296
 Heisenberg eqns. on C^* algebra of quasilocal observables, boson and fermion systems 8-57854
 infinite nuclear matter, response function, quantum field theory of fermion systems 8-70480
 interacting particles, Tomonaga model, 3-D analogue (Russian) 8-71900
 kinetic theory of normal Fermi liquids 8-87841
 lattice gauge theories with fermions, phase transitions and renormalised struct. 8-82105
 low density Fermi liquids in mag. field, theory (Russian) 8-59959
 magnetic susceptibility quantum oscillations, low temp., mag. instabilities in electron liq. (Russian) 8-87928
 many fermion energy calculations 8-66238
 massive neutron star, fermionic matter, coupled Dirac-Einstein eqns., self consistent soln. 8-73731
 N-fermion problem, improved lower bounds 8-54292
 N-fermion problem, incorrect lower bounds 8-65865
 N-fermion translation invariant systems, derivation of energy lower bound models 8-65866
 N-particle Schrodinger eqn., macroscopic behaviour, superconductor and fermion systems 8-60242
 neutrino-antineutrino mixture, transport props. 8-93625
 neutrinos+antineutrinos gas, transport coeff., thermal diffusion (French) 8-86217
 neutrons, relativistic, ultra-degenerate, non-interacting gas, Fermi energy and eqn. of state in intense mag. field 8-89401
 normal quantum fluid, kinetic theory, transport props. 8-77799

fermion systems continued

- nuclear dynamics, adiabatic TDHF limit versus TDHF, in soluble model 8-50113
 nuclear field theory, path integral techniques, Fermi systems with two body force interactions 8-50096
 nuclear field theory of Fermi systems in an external field, path integrals 8-93954
 nuclear many body problem, boson-fermion descript. (Chinese) 8-82297
 nuclear matter, thermodynamic model, shear viscosity temp. dependence 8-62499
 one dimensional continuous quantum systems, limit Gibbs state 8-93599
 one-body dissipation of nuclear deformation collective energy, semiclassical approx. (Russian) 8-86502
 one-dimensional, and plane xy model, behaviour of correlation functions 8-56091
 one-dimensional backward-scattering model with generalised coupling const., variational soln. 8-66036
 orthonormalisation method, appl. to j-j coupling of fermions in single j-shell 8-81922
 para-Fermi algebra representation 8-65867
 plasma long-wave oscillation damping calc. (Russian) 8-75302
 QCD of highly condensed matter 8-70267
 radiation gauge static pot. between fermion and antifermion, non Abelian gauge fields 8-89621
 Schrodinger fluid velocity field, fermion system moments of inertia 8-65868
 self consistent RPA for three body forces in Fermi systems 8-89810
 semiclassical density matrix, fermion system in one body pot. 8-65872
 solution of the Dirac equation with anomalous magnetic moment 8-82133
 star with neutron core, gravitational equilib. relativistic treatment 8-57570
 superfluid Fermi liquids, stability conditions, small-gap spin excitations 8-87839
 time dependent Hartree Fock approx., fermion system appl. 8-49780
 two-dimensional quantum systems at zero temp., liquid to gas phase transitions 8-77798
 variational wave function, three-body correlations 8-87834
 Yang-Mills pseudoparticles, fermion Green's functions 8-54548
 (e,e'), deep inelastic, meson exchange currents from Fermi gas model 8-66268
 Ge, electron-hole drop phase separation, due to uniaxial stressing 8-84145
³He, specific heat second layer adsorbed on Grafoil 8-87843

fermions

- see also baryons; fermion systems; leptons
 bound states from instantons 8-78087
 dual fermion model, inclusive single particle distrib., $\pi N \rightarrow \pi X$ appl. 8-86446
 expectation values using program SCHOONSCHIP 8-74555
 fermion-antifermion eqn., appl. to positronium, Breit eqn. 8-62963
 Friedmann cosmological models, fermion pair creation by gravit. field and singularity (Russian) 8-93493
 relativistic bound state of fermion and antifermion, fermion fields, quark model 8-82151
 spinor Bethe Salpeter and Goldstein eqns., fermion-boson coupling, numerical soln. 8-86400
 strong external fields, fermion and boson interactions 8-49987
 SU(2)⊗U(1) gauge model of EM and weak interactions, fermion mass restriction (Russian) 8-89650
 ultra heavy, weak interactions, high energy scattering, low energy renormalisation corrections 8-93838
 Universe, isotropic models, regularisation of fermion stress-energy tensor 8-81725
 Young's double beam interference experiment with spinor and vector waves 8-89363

fermium

- see also nuclei with
 No entries

fermium compounds

- No entries

ferrimagnetic properties of substances

- see also ferrimagnetism; ferrites; garnets; magnetic semiconductors
 Mn_{1.98-x}Cr_xFe_{0.02}Sb, Mossbauer effect exam. 8-68432
 oxides with perovskite struct., neutron diff., ferri- and ferromag. props. 8-52214
 rare earth iron alloy, amorphous film, cosputtered, struct. and mag. props. 8-60323
 rare earth-Co amorphous film, sputtered, in-plane anisotropy induced by rare gas annealing 8-84458
 rare earth-Fe alloy, RFe₂ (R=Tb, Dy, Ho and Y) crit. phenomena, Mossbauer exam. 8-52403
 rare earth-transition metal alloy amorphous film, magnetostriction, dipolar mechanism 8-95502
 rare earth-transition metal alloys amorphous thin films, anisotropic mag. and microstruct. props. 8-95487
 rare earth-transition metal film, amorphous, microstruct., TEM obs. 8-72018
 rare earth-transition metal film, amorphous, microstruct. and magnetism 8-64230
 titanomagnetites, domain struct. var. with temp. 8-65272
 Co-Gd-Mo-Ar film, amorphous, mag. props. 8-80182
 CoCr₂S₄, Faraday effect, appl. to CO₂ laser systems, radiation damage resist. 8-95579
 Co_{2-x}Ni_xO₄, 0<x≤1.1, struct., semicond.-semimetal transition, Seebeck coeff. 8-87972
 CrO₂, single particle material for tape and disc manufacture, prep., props., and appls. 8-52308
 D₁₂Fe₃O₂, anomalous magnetisation, compensated to uncompensated mag. arrangement transition 8-52254
 Dy(Fe,Ni_{1-x})₂, mag. behaviour, susceptibility and Mossbauer expts., 4.2-1300K 8-52235
 Dy_{0.7}Tb_{0.3}Fe₂, magnetostrictive material, liq. phase sintering 8-64493
 ErCo_{5.6}, easy magnetisation direction 8-84415
 Er₂Co₃, cryst. field effect on mag. moment direction, neutron diff. meas. 8-80132
 ErCo_{5-x}Ni_x series, magnetisation, coercive field meas. 8-91896
 ErFe₂, excited state spin waves inelastic scatt. meas. 8-76234

ferrimagnetic properties of substances continued

- Fe-Gd amorphous films with comp. gradient, volume and surface hysteresis (Russian) 8-88148
 Fe-Gd film, amorphous, mag. props., mean field analysis 8-64236
 Fe-Gd film, amorphous, O₂ contamination effects on mag. props. 8-64231
 Fe-R alloys, mag. elastic properties 8-52331
 Fe_{1-x}Cr_xBO₃, magnetisation, 4.2-600K 8-68187
 γ-Fe₂O₃ powders, influence of densification on mag. props. 8-95481
 γ-Fe₂O₃, single mag. particle, remanent coercive force and remanent loop meas. 8-95480
 α-Fe₂O₃, single particle material for tape and disc manufacture, prep., props., and appls. 8-52308
 Fe₃O₄ film, prep. by reactive condensation and mag. props. 8-64241
 Fe₃O₄, hyperfine fields and spin densities below 20K 8-52405
 Fe₃O₄, magnetite, electronic struct. at low temps., NMR anal. 8-67686
 Fe₃O₄, magnetite, ferrimag. reson. at 9.3 GHz near Verwey temp., g-factors (French) 8-91959
 Fe₃O₄, NMR exam. of low temp. phase 8-56401
 Fe₃O₄, NMR of low temp. phase, electron ordering anal. 8-56402
 Fe₃O₄:Zn, and pure, influence of mag. order on charge delocalisation, Mossbauer spectra 8-68423
 Fe_{1-x}Zn_x/O₂, solid soln. prep., struct. and mag. moment 8-52228
 Gd-Co, and Gd-Co-Mo films, amorphous, mag. props., annealing effects 8-64235
 Gd-Co amorphous sputtered films, magnetoelastic contrib. to perpendicular anisotropy, internal stress meas. 8-95490
 Gd-Co film, amorphous, Ar sputtered, struct. 8-63946
 Gd-Co film, amorphous, phase separation as source of perpendicular anisotropy 8-64244
 Gd-Co film, amorphous, preferential resputtering effect induced anisotropic distrib. of atomic pairs 8-63950
 Gd-Co film, amorphous, selective resputtering-induced anisotropy 8-72376
 Gd-Co film, bias-sputtered, dipolar mechanisms for mag. anisotropy 8-64233
 Gd-Co film, sputtered, inert gas incorporation effect on uniaxial anisotropy 8-64232
 Gd-Co-Fe film, amorphous, bias-sputtered, uniaxial perpendicular anisotropy 8-64234
 Gd-Co-Mo film, amorphous, Ar sputtered, struct. 8-63946
 Gd-Co-Mo film, amorphous, in-plane susceptibility near compensation point 8-64238
 Gd-Fe amorphous sputtered films, magnetoelastic contrib. to perpendicular anisotropy, internal stress meas. 8-95490
 Gd-Fe film, amorphous, in-situ ion beam sputtered, microstruct. and Lorentz mag. struct. 8-63947
 Gd-Fe film, amorphous, mag. props., annealing effects 8-64235
 Gd-Fe film, amorphous, preferential resputtering effect induced anisotropic distrib. of atomic pairs 8-63950
 Gd_{1-x}Co_x film, resistivity, Hall effect, domain wall density 8-76169
 Gd₆₅Co₃₅, amorphous, amg. ordering, susceptibility, magnetisation and hysteresis meas. 8-68190
 GdCoMo film, amorphous, sputtered, ferrimag., in-plane susceptibility near compensation point 8-64240
 Gd(Fe_{1-x}Co_x)₂, ferromag. reson. of pseudobinary cubic compounds 8-91961
 Gd_{1-x}Ni_x sputtered amorphous films, mag. props. and Hall meas. 8-95488
 (GdPrBi)₃(FeGaIn)₅O₁₂, pure and In³⁺ doped, near IR absorpt. and Faraday rot. 8-95580
 Gd₂Y_{1-x}Fe₃, saturation magnetisation, magnetostriction, Curie temp., ferrimag. ordering, exchange field (Russian) 8-68343
 Ho₄Co₃, cryst. field effect on mag. moment direction, neutron diff. meas. 8-80132
 HoFe₂, spin wave and cryst. field excitations, neutron scatt. 8-68196
 Ho(Fe,Ni_{1-x})₂, mag. behaviour, susceptibility and Mossbauer expts., 4.2-1300K 8-52235
 HoIG, Faraday rotation, mag. field depend., 4.2 to 300K, magneto-optical coeffs. 8-95577
 Mn₂As₂Sb_{1-x}, 0<x<0.25, specific magnetisation, temp. dependence, 300 to 600K 8-76248
 Mn_{2-x}Fe_xSb, Mossbauer effect exam. 8-68432
 Tb_{0.22}Dy_{0.78}Fe₂, domain configurations, obs. by Kerr effect and synchrotron radiation topographs 8-64215
 Tb_{0.27}Dy_{0.73}Fe₂, LF magnetoelastic effects 8-68348
 TbFe₂, domain configurations, obs. by Kerr effect and synchrotron radiation topographs 8-64215
 Tb₂Fe_{1-x} film, amorphous, magnetostriction and magnetisation 8-68305
 ThCu₂Mn₂O₁₂, mag. struct. of new perovskite-type ferrimag. 8-52222
 TmCo₅, easy magnetisation direction 8-84415
 TmFe₂, low temp. magnetisation and magnetostriction 8-64249
 YFe₂ film, (x=2), magnetoelastic excitations obs. 8-68307
 YFeO₃:Co, NMR of ⁵⁷Fe, spin echo 8-91987
 YIG epitaxial film and cryst., bound magnetostatic waves controlled by field gradients 8-95425
 (YLaBi)₃(FeGa)₅O₁₂, pure and In³⁺ doped, near IR absorpt. and Faraday rot. 8-95580

ferrimagnetic resonance

- ferrites, LPE growth and characterisation 8-68640
 ferrites, soft and microwave, grain-size effects on mag. props., review 8-64222
 magnetic bubble films, spin wave and magnetoelastic resonance meas. 8-91913
 Fe₃O₄, magnetite, ferrimag. reson. at 9.3 GHz near Verwey temp., g-factors (French) 8-91959
 Li_{0.5}Fe_{2.5}O₄, LPE growth on spinel substrate crystals, ferrimagnetic resonance exam. 8-76613
 Mg₂Fe_{3-x}O_{4-y} precipitates, g-factor, ferrimag. reson. meas. 8-60337
 Y_{1-x}Ca_{2x}Fe_{2-y}In_{1-x}V_yO₁₂, first magnetocryst. anisotropy const., ferrimag. reson. obs. 8-68218
 Y_{3-y}Ca_{2y}Fe_{2-z}Zr_yFe₂O₁₂, first magnetocryst. anisotropy const., ferrimag. reson. obs. 8-68218

ferrimagnetism

- see also ferrimagnetic properties of substances
 amorphous alloy, dipolar mechanisms for mag. anisotropy 8-64233
 uniaxial two-sublattice ferrimagnet, magnetisation intensity, crit. fields in applied fields (Russian) 8-68285

ferrite applications

see also ferrite devices

ferrite/steel composite bar magnet, large size, for mobile appls. 8-93740

ferrite devices

see also ferrite applications; magnetostatic wave devices

microstructural depend. of operating characts. 8-88548

synchrotron miniature pulse deflector construction 8-82545

Li, fine particle, for arc plasma spraying mm-wave phase shifter 8-64469

ferrites

see also ferrimagnetic properties of substances; ferrimagnetism; ferrite applications; ferrite devices

ceramic, microstructure and physical props. 8-72756

composition determination, interelement effects by X-ray fluorescence analysis 8-85259

fast firing in kilns with jet burners 8-64496

flux quantisation 8-80136

hysteresis loop rectangularity, inverse domain vol. depend. (Russian) 8-76270

limiting hysteresis loop and number of easy magnetisation axes connection (Russian) 8-72364

LPE growth and characterisation 8-68640

magnetic permeability, meas. method, UHF waves total internal reflect. 8-57994

magnetised, nonreciprocal refl. of EM waves 8-71006

magnetostrictive, relationship between static parameters and piezoactivity 8-95507

microstructure role in characteristics, review 8-88548

microwave and soft, grain-size effects on mag. props. 8-64222

microwave flaw detection 8-53122

orthoferrite garnet, mag. bubble lattice nucleation obs. 8-76283

permanent magnet ferrites, forming. 8-64495

powder, grain size meas. by electron microscopy, sample prep. (German) 8-56833

rare earth orthoferrites and orthochromites, exchange interactions 8-60279

rod with domain structure, magnetostatic waves and internal field (Russian) 8-76236

semiconductor-ferrite structure, nonlinearity and conditions of existence of convective instability 8-72241

semiconductor-ferrite structure, reson. galvanomagnetic phenomena in semicond. 8-87989

semiconductor-ferrite structure, surface magnetostatic wave instability 8-76235

semiconductor-ferrite-semiconductor structure, absolute instability of magnetostatic surface waves interacting with drifting carriers 8-95486

slab, transversely magnetised, adjacent to semicond., mag. surface wave amplification 8-72339

spin wave instability on approaching FMR (Russian) 8-76318

spinel type, catalytic oxidation of CO, role of mag. exchange interactions 8-56916

steel, alloy, Cr-C (12, 0.2 wt.%) growth of grain boundary ferrite allotriomorphs, photoemission electron microscope exam. 8-88468

unmagnetised polycrystalline, gyrotropic susceptibility and effective anisotropy 8-64224

US testing 8-53084

β -Al₂O₃-K₂O/K ferrite, interfaces and solid soln., thermal expansion and lattice parameter variations 8-55959

(Ba,Sr)Fe₁₂O₁₉, Ferroxidure, developments and research 8-84455

BaCo_{1.5}Fe_{16.5}O₂₇, type W ferrite, spin reorientation 8-60301

BaFe₂O₄-Fe₂O₃-ZnFe₂O₄ system, phase relations at 1200°C 8-72767

Ba₂Fe₁₈O₂₇, hexagonal ferrite, W-struct., Mossbauer spectra of Fe³⁺ and Fe²⁺ 8-88242

BaFe₂Ti₂O₁₁, R-type hexaferrite, spin struct. and mag. props. 8-52216

BaZn_{1.35}Co_{0.65}Fe₁₆O₂₇, W-type hexaferrite cryst., first order magnetisation processes 8-95472

Ba₂Zn₂Fe₁₂O₂₂, anisotropic magnetisation and susceptibility 8-84411

BiBi₄Ti₃FeO₁₅, perovskite-like layer-type ferroelec. magnetic cpd., Mossbauer expts., 80-1200K 8-64329

CaV ferrite garnet, large grained, mag. props. 8-64222

Cd₂Ni_{1-x}Fe_xO₄, mag. behaviour, Mossbauer meas. 8-52390

Co₂Fe_{3-x}Cr_xO₄, epitaxial, magneto-optical props., effect of Cr³⁺ 8-52590

Co_x²⁺Fe_{1-x}²⁺Fe₂³⁺O₄ ferrites, effect of Fe²⁺ on Mossbauer parameters 8-76360

CoFe₂O₄ formation rate consts. meas. by Mossbauer effect 8-68875

Co_{1-x}Fe_{2+x}O₄, prep. by wet and ceramic methods, struct., mag. and surface props. 8-52307

Co₂Fe_{3-x}O₄, single cryst. mag. films, holograms recording and thermomagnetic writing 8-55324

Cu ferrites, crystallisation of monocrystals from high temp. soln. 8-60561

CuFe₂O₄, LPE grown, domain struct. rel. to tetragonal distortion 8-92205

Cu_{1-x}Fe_{2+x}O₄, cation distrib. and valence state 8-63732

DyFeO₃, spin reorientation near Morin temp., magneto-optical exam. 8-68284

ErFeO₃, sound velocity meas. at high press., spin-reorientation transition 8-76254

Fe_{3-x}Ni_xO₄, low temp. Mossbauer spectra, electron transfer and spin density distribution 8-52404

Fe₃O₄, hyperfine fields and spin densities below 20K 8-52405

Fe₃O₄ particles, entrapped in drug carrying microsphere, intravascular mag. guidance method 8-73188

Fe₃O₄, photocond. 70-130K, temp. range including metal-semicond. transition (Russian) 8-56178

Fe₃O₄, single cryst., surface magnetism, spin polarized photoemission 8-52622

Fe₃O₄, spherulitic film growth, elec. and mag. props. 8-68627

Fe₃O_{4-x}F_x, low temp. Mossbauer spectra, electron transfer and spin density distribution 8-52404

Fe_{3-x}Zn_xO₄, low temp. Mossbauer spectra, electron transfer and spin density distribution 8-52404

β -Ga₂O₃-K₂O/K ferrite, interfaces and solid soln., thermal expansion and lattice parameter variations 8-55959

Ho_{0.7}Er_{0.3}FeO₃, crystn. on seeds, layer morphology 8-72041

Li_{0.5}Fe_{2.5}Al_{0.3}O₄:Co, single cryst., domain struct., mag. annealing effect depend. on induced anisotropy 8-68290

LiFe₂O₈, material loss and high-temp. phase transition 8-64534

ferrites continued

Li_{0.5}Fe_{2.5}O₄, LPE growth on spinel substrate crystals, ferrimagnetic resonance exam. 8-76613

Li_{0.5}Fe_{2.5}O₄, uniaxial anisotropy energy, elec. field depend. 8-68346

Li_{0.5}Fe_{2.5}O₄-CuFe₂O₄-ZnFe₂O₄, order-disorder transition, quadratic transformation (French) 8-76447

Li_{1-x}Fe_{3-x}O₈:Co, single cryst., domain struct., mag. annealing effect depend. on induced anisotropy 8-68290

LiTiZn ferrites, elec. resist., mag. props., effect of Bi addition 8-95474

Li_{0.5(1-x)}Zn_xFe_{2.5-0.5x}O₄, canted spin struct., neutron diffr. study 8-68175

Mg_{0.5}Fe_{2.5}O₄, ferrimag. epilayer, superparamag. interface, mag. props., FMR 8-95492

Mg₂Fe_{3-x}O₄, magnetostriction consts., 80 to 320K 8-95503

MgM³⁺Fe_{2-x}O₄, M=In,Al,Cr,Sc, comp. effects on ferrite characts. 8-52305

MnFe ferrites, reson., effect of EM propagation 8-64277

MnFe_{2-x}In_xO₄, magnetic props., In substitution effects (Russian) 8-91849

MnFe₂O₄, exchange splitting of ionic S-state, neutron spectra 8-52240

MnFe₂O₄, valence states, NMR investig. (Czech) 8-72420

Mn_{0.82}Fe_{2.18}O₄, anelasticity, 280 to 730K, 125 kHz vibr. study 8-87740

MnZn ferrite, appreciable SiO₂ content, origin of core losses, microstructure and mag. props. 8-64225

MnZn ferrite, mag. susceptibility freq. spectrum, effect of pressure 8-95420

MnZn ferrite, nonstoichiometric, neutronographic determ. of cation distrib. (Bulgarian) 8-83656

MnZn ferrites, impurity induced exaggerated grain growth 8-92222

MnZn ferrites, Ti substituted, mag. permeab. meas., grain boundary comp. AES obs. 8-95473

MnZn, gas phase fluorination for improved props. 8-52306

Mn_{1.18}Zn_{0.06}Co_{0.01}Fe_{1.75}O₄, transport props. near Curie points 8-88100

Ni, gas phase fluorination for improved props. 8-52306

NiCo ferrite, induced mag. anisotropy, hysteresis loops, Barkhausen effect (Russian) 8-64203

NiZn ferrite, mag. susceptibility freq. spectrum, effect of pressure 8-95420

NiZn ferrites, Mossbauer effect and IR spectra 8-64300

NiZn ferrites under high press., grain growth (Chinese) 8-52825

Ni_{0.36}Zn_{0.64}Fe₂O₄, normal grain growth 8-72796

SrFe₁₂O₁₉, ceramic compact, sublattice magnetisation and textures 8-68426

Sr₂Fe₁₀O₂₂-Fe₂O₃-ZnFe₂O₄ system, phase relations at 1100°C 8-68676

Sr₂Fe₁₀O₂₂, mag. props. and spin order 8-52232

TmFeO₃, orthoferrite, vel. of planar domain wall 8-72363

(Y,Sm,Ca)₃(Fe,Ge,Si)₂O₁₂ single-crystal films, props. 8-64247

Y orthoferrite, magneto-optical controlled transparencies, paper compositors 8-50932

Y_{1-x}Bi_xFe₂O₁₂, ferrite-garnet formation 8-52737

YFeO₃, Bloch, Neel and head to head wall vels. 8-68287

YFeO₃, mag. domain walls, photomagnetic effects, ⁵⁷Fe NMR obs. 8-95464

YFeO₃ monocrystalline, mag. field depend. of magnetic domain (Korean) 8-68337

YFeO₃, orthoferrite, vel. of planar domain wall 8-72363

YFeO₃ platelets, domain wall mobility, dynamic coercivity 8-91884

YFeO₃:Co, NMR of ⁵⁷Fe, spin echo 8-91987

Y₃GaFe₄O₁₂, mag. props. meas. in high mag. fields, review (Japanese) 8-52303

ferritic steel see stainless steel**ferroacoustic resonance**

No entries

ferroelasticity

see also shape memory effects

alkali metal double molybdates, M^{III}(MoO₄)₂, M^{III}=Al,Sc,Fe,In, struct. transitions phenomenological approach 8-51674

alkali metal double tungstates, M^{III}(WO₄)₂, M^{III}=Sc,In, struct. transitions, phenomenological approach 8-51674

dicalcium strontium propionate, ferroelasticity and opt. activity rel. to transition 8-76420

gyrotropic phase transitions 8-71852

lithium ammonium tartrate monohydrate, in paraelec. phase, Brillouin scatt. 8-64373

lithium ammonium tartrate monohydrate, spontaneous shear strain, X-ray obs. 8-56433

prototype temperature setting rel. to soft modes 8-63833

quartz ferroelastic twinning coercive stress obs. 8-59854

tanane, crit. behaviour near ferroelec.-ferroelastic transition 8-52459

BaCl₂·2H₂O, cryst. struct. determ. by neutron diffr. 8-75639

BiVO₄, linear coupling between soft optical and ferroelastic acoustic modes 8-79716

Hg₂Cl₂ prototype phase, soft mode, inelastic neutron scattering, Raman effect 8-91411

KCN, dipolar impurity tunnelling model, elastic interaction and const. 8-71826

KCN, optical F centres and phase transitions 8-56504

KCl_{1-x}CN_x, dipolar impurity tunnelling model, elastic interaction and const. 8-71826

KH₂(SeO₃)₂, KD₃(SeO₃)₂, second-order ferroelastic phase transitions, piezo-opt. props. obs. 8-95558

KH₂(SeO₃)₂, slightly deuterated, central peak obs. in Brillouin spectra 8-64374

KH₂(SeO₃)₂:Cr³⁺, ferroelastic material, EPR, 77-300K 8-60331

K₂Pt(CN)₄Br_{0.3}H₂O, specific heat and ferroelastic behaviour 8-91447

NaCN, optical F centres and phase transitions 8-56504

NdP₂O₁₄, sp. hts. near ferroelastic phase transitions 8-63863

Pb₃O₄, IR and Raman study of structural phase transitions (French) 8-84582

Pb₃(PO₄)₂, ferroelastic, switching processes, in pulse mech. field 8-59853

Pb₃(PO₄)₂, nonintrinsic ferroelastic properties 8-91374

Pb₂(PO₄)₂:Mn²⁺, EPR study around ferroelastic transition point of Pb₃(PO₄)₂ 8-76303

PrP₂O₁₄, sp. hts. near ferroelastic phase transitions 8-63863

ferroelasticity continued

- RbCaF₃, thermal props. near phase transition 8-75850
 TiCdF₃, thermal props. near phase transition 8-75850

ferroelectric Curie temperature

- liquid crystals, temp. depend. of elec. susceptibility and spontaneous polarisation (*Japanese*) 8-68467
 TGS, neutron diffraction enhancement near Curie point with DC field appl. (*Chinese*) 8-68462
 Ba_{0.92}Ca_{0.08}TiO₃ ceramic, uniaxial stress effects, US dilatometric and dielec. meas. 8-52454
 BaTiO₃, cubic-tetragonal phase transition, birefringence meas., surface distortion effects 8-95564
 BaTiO₃-Ni(Co, Mn)Fe₂O₄, ceramic, exam. of prep. and physical props. 8-68655
 BiBi₄Ti₃FeO₁₅, perovskite-like layer-type ferroelec. magnetic cpd., Mossbauer expts., 80-1200K 8-64329
 Bi₂Sb_{1-x}SI, atomic substitution and ferroelec. phase transition 8-68464
 Cs₂KMO₃F₃, (M=Mo, W), low temp. phase transitions (*French*) 8-92036
 Cs₂RbMO₃F₃, (M=Mo, W), low temp. phase transitions (*French*) 8-92036
 Eu_{0.5}Ba_{0.5}TiO₃, ferromag., ferroelec., ceramic, Curie temps. determ. 8-68230
 KH₂AsO₄, ferroelec., temp. broadening of hard mode Raman lines near T_c 8-88296
 KH₂PO₄, ferroelec., temp. broadening of hard mode Raman lines near T_c 8-88296
 KH₂PO₄-KD₂PO₄ mixed crystals, static and dynamic props., proton-lattice coupled mode model 8-64328
 LiTaO₃-CaZrO₃, struct. and dielec. props. 8-80298
 PbBi₄Ti₃O₁₅ ceramic, dielec. props., temp. depend. 8-95561
 Pb(Mg_{0.5}W_{0.5})O₃-BiFeO₃, dielec. props., cryst. struct. 8-84534
 Rb₂KMO₃F₃, (M=MO, W), low temp. phase transitions (*French*) 8-92036
 SbSI, free energy function, temp. depend. and anisotropy of dielec. const., ferro- and paraelec. phases 8-64330
 SbSI materials, piezoelectric props. rel. to use as electroacoustic transducers 8-52445

ferroelectric devices

- ceramic films, resonant autothermostabilisation (*Russian*) 8-52451
 PLZT ceramics, optical information storage and spatial light modulation 8-83097

ferroelectric domains *see electric domains***ferroelectric materials**

- see also antiferroelectric materials; electric domain walls; ferroelectric semiconductors; ferroelectric thin films; ferroelectric transitions; lattice dynamics of ferroelectric crystals*
 alkali trihydrogen selenite: Mn²⁺ single crystal, EPR 8-72396
 bibliography (Oct. 1976 to May 1977) 8-95557
 ceramic, axially loaded, nature of elec. field and resulting voltage 8-72468
 ceramic, microstructure and physical props. 8-72756
 ceramic blocks, TsTS-23, TBk-3, TsTSNV-1, longit. piezoelec. effect and moduli 8-56430
 ceramics, ferroelec., dielec. losses due to domain wall oscill. 8-84541
 chemical reactions in plasma generated near ferroelectric surface, obs. 8-68931
 chiral smectic C, ferroelec. props., dielec. meas. 8-52463
 conference, Novosibirsk, USSR (Sep. 1976) 8-76393
 copper formate tetrahydrate, model two-dimensional ferroelec., short-range order, neutron scatt. 8-68458
 Debye temperature, tabulation of calorimetric values 8-51639
 dialkylxyazoxybenzenes, synthesis of ferroelec. smectic B, smectic C, and nematic phases 8-94969
 diazoxycinnamates, synthesis of ferroelec. smectic C and smectic A phases 8-94969
 dicalcium lead propionate, ferroelec., piezoelec. and elastic props. 8-84528
 dielectric props. meas. in vicinity of phase transition, microwave method 8-74022
 DOBAMBC, and DOBAMBCC, chiral smectic C liq. cryst., dielec. const., electroclinic effect 8-94980
 electroacoustic echo 8-95549
 electrogyration in ferroelec. crystals, appls. 8-76394
 guanidinium aluminium sulphate, domain wall energies and domain structures 8-92039
 guanidinium aluminium sulphate hexahydrate: Mn²⁺, NMR 8-91939
 HOBAPC, chiral smectic C liq. cryst., dielec. const., electroclinic effect 8-94980
 improper, electro-opt. props. 8-76426
 liquid crystals, temp. depend. of elec. susceptibility and spontaneous polarisation (*Japanese*) 8-68467
 lithium ammonium tartrate monohydrate, in paraelec. phase, Brillouin scatt. 8-64373
 lithium ammonium tartrate monohydrate, spontaneous shear strain, X-ray obs. 8-56433
 (NH₄)₂SO₄:Mn²⁺, ferroelec. phonon driven phase transform., reduction of spin Hamiltonian const. 8-92033
 noncentrally symmetric phase identification using SHG 8-74947
 optical recording media, review 8-71172
 P- and T-nonconserving interactions, macroscopic effects 8-84532
 perovskite crystals, static and dynamic aspects of PAC meas. 8-88241
 photorefractive effect, mechanisms 8-92045
 photorefractive materials for optical data storage 8-79086
 polyvinylidene fluoride, X-ray diff. evidence for ferroelectricity 8-60399
 Raman scattering, near phase transition point 8-76466
 Rochelle salt, ²H NMR spectrum, correl. effects 8-76324
 Rochelle salt, depend. on mechanoluminescence on charge prod. during fracture 8-88370
 Rochelle salt, polarisation echo, near ferroelec. transition 8-88266
 SHG determ. of ferroelec. and antiferroelec. props. 8-74947
 siegnette magnets with hexagonal barium titanate structure 8-76397
 smectic liquid crystal, new ordered smectic phases 8-51407
 specific heat calc., soft mode contrib. near T_c 8-64338
 squaric acid, hydrostatic press. effect on phase transition, dielec. and dilatometric meas. 8-55941
 squaric acid and deuterated derivative, vibrational study, IR and Raman spectra 8-92076

ferroelectric materials continued

- SrTiO₃, second harmonic generation, bond charge theory 8-76395
 submillimetre monochromatic spectroscopic determination of dielec. props. of electro-opt. materials 8-76428
 surface sound waves on domain boundaries, low temp. sp. ht. 8-71937
 tanane, crit. behaviour near ferroelec.-ferroelastic transition 8-52459
 TBK-3, ferroelectric ceramic, 90° electric domain processes, mech. stress, X-ray diff. 8-72478
 TDOBAMBCC, chiral smectic C liq. cryst., dielec. const., electroclinic effect 8-94980
 tetramethylammonium tetrachlorocobaltate, ferroelectricity 8-76408
 TGS, domain boundaries, X-ray topography 8-60409
 TGS, electrooptic switching anomalies 8-52473
 TGS, ferroelec. transition, struct. changes, ¹³C NMR obs. 8-60344
 TGS, gamma irradi. effects on heat capacity, Curie temp., permittivity 8-67737
 TGS, large scale inhomogeneity effect on ferroelectric transition (*Russian*) 8-76411
 TGS, neutron diffraction enhancement near Curie point with DC field appl. (*Chinese*) 8-68462
 TGS, sound group vel. vector direction, temp. depend. 8-67774
 TGS, temp. depend. and effect of Cr and α-alanine impurities 8-91448
 TGS, US vel. and absorpt. anisotropy and crit. anomalies, acousto-opt. obs. 8-95574
 TGS, vacuum-cleaved cryst., charge compensation, ferroelec. field effect obs. 8-95556
 TGS family, change of order of phase transition under hydrostatic pressure 8-52452
 TGSe, dielectric const. near ferroelec. transition temp., effect of surface capacitance 8-56438
 TGSe, US vel. and absorpt. anisotropy and crit. anomalies, acousto-opt. obs. 8-95574
 thiourea, expansion coeffs. in phase transition range 8-76407
 thiourea single cryst., γ-irrad. effect on elec. permittivity 8-64311
 tris sarcosine calcium chloride:VO²⁺, EPR and absorpt. spectra 8-60330
 trissarcosine calcium chloride:Mn²⁺, ferroelec., electron spin-lattice relax. 8-80208
 TsTS-23, ferroelectric ceramic, 90° electric domain processes, mech. stress, X-ray diff. 8-72478
 volume phase holographic storage in ferroelec. crystals 8-82929
 AgNa(NO₂)₂, ultraslow crit. dynamics of order parameter, ²³Na spin relax. times obs. 8-76410
 Ag₂SbS₄, dielec. and acoustic props. (*German*) 8-64335
 Ba_{0.92}Ca_{0.08}TiO₃ ceramic, uniaxial stress effects, US dilatometric and dielec. meas. 8-52454
 Ba₃Fe₂BO₉ (B=Re, Te, W, Mo), siegnette magnets with hexagonal barium titanate structure 8-76397
 Ba₂FeSbO₆, siegnette magnets with hexagonal barium titanate structure 8-76397
 Ba₂Na(Nb,Ti)₂O₁₀, prep. and electro-opt. props. 8-76432
 Ba₂NaNb₂O₁₅, cathodlum. spectral and temp. depend. 8-84665
 Ba₂NaNb₂O₁₅, ferroelec. conversion to single domain, elec. and photoelec. props. 8-88271
 Ba_{0.25}Sr_{0.75}Nb₂O₆, thermal and spectral variations in the photovoltaic current in ferroelectrics 8-91719
 Ba_{0.5}Sr_{0.5}Nb₂O₆, temp. depend. of Raman spectra 8-72524
 Ba_{0.54}Sr_{0.46}Nb₂O₆:Y(La)(Tm), dielectric and electrooptic props. 8-68466
 Ba₂Sr_{1-x}Nb₂O₆, ferroelec., cathodlum. spectral and temp. depend. 8-84665
 BaTiO₃, 90° electric domain processes, mech. stress, X-ray diff. 8-72478
 BaTiO₃, A₁(TO) phonon spectrum, ferroelectric phase transition, Raman scatt. meas. 8-56478
 BaTiO₃, automatic anomalous noise meas. for ferroelectric capacitor parameters, not in equilib. (*French*) 8-74029
 BaTiO₃, c-domain cryst., HF dispersion of permittivity 8-60379
 BaTiO₃ ceramic, mech. strength 8-64332
 BaTiO₃, dielec. and elastic const., temp. depend. (*Russian*) 8-64307
 BaTiO₃, doped, loss mechanism and domain stabilisation 8-84542
 BaTiO₃, Doppler-broadened positron annihilation 8-64428
 BaTiO₃, dynamic Rayleigh light scatt. in region of ferroelectric-paraelectric transition 8-64371
 BaTiO₃, ferroelectric ceramic, dielec., piezoelec. and elastic props., orientational contrib. 8-68468
 BaTiO₃, LF relaxational polarisation 8-68460
 BaTiO₃, logarithmic velocity variations for longitudinal US waves near ferroelec. transition 8-72472
 BaTiO₃, magnetochemical exam. of phase transition, mag. suscept. meas. 8-88265
 BaTiO₃, martensite type phase transition 8-64326
 BaTiO₃, monocrystalline, dielectric loss after superposition of unidirectional electric field time depend. (*Slovak*) 8-52435
 BaTiO₃, para ferroelec. transition, strong Rayleigh scatt. 8-76486
 BaTiO₃, photo-ferroelectric noise effect (*Russian*) 8-52450
 BaTiO₃, polariton freq. meas. by Raman scattering and permittivity 8-76006
 BaTiO₃, struct. changes due to cubic-tetragonal phase transition 8-60407
 BaTiO₃ type crystals, determ. of phase transitions using symmetry breaking theory (*French*) 8-83950
 BaTiO₃ type perovskite ferroelectric, neutron irradiated, amplification of freq. dispersion of permittivity (*Russian*) 8-52419
 BaTiO₃, vibronic ferroelec., spontaneous birefringence calc. 8-68473
 BaTiO₃:Co, charact. behaviour of spontaneous polarisation and dielec. const. 8-60382
 BaTiO₃:Cu, photoferroelec. props., Jahn-Teller effect, laser irradi. effect on pyroelec. props. 8-60400
 Bi₂Bi₄Fe₂Ti₃O₈, dielec. and magnetoelec. props. 8-95562
 BiBi₄Ti₃FeO₁₅, perovskite-like layer-type ferroelec. magnetic cpd., Mossbauer expts., 80-1200K 8-64329
 Bi₂Sb_{1-x}SI, atomic substitution and ferroelec. phase transition 8-68464
 Bi₂WO₆ single crystal, growth from flux in Bi₂WO₆-Na₂WO₄, below transformation temperature 8-72713
 Co₃B₂O₁₁I, intermediate phase between paraelectric and ferroelectric phase (*Russian*) 8-68465

ferroelectric materials continued

- CsH₂PO₄, neutron-diffraction study of cryst. struct. in paraelectric phase 8-79592
- Cs₃MoO₃F₃, ferroelec. and order-disorder phase transitions 8-92037
- Cs₃WO₃F₃, ferroelec. and order-disorder phase transitions 8-92037
- dicalcium strontium propionate, electro-opt. props. 8-76426
- Eu_{0.5}Ba_{0.5}TiO₃, ferromag., ferroelec., ceramic, Curie temps. determ. 8-68230
- Fe₃B₂O₇I₃, electro-opt. props. 8-76426
- Fe₃B₂O₇I₃, ferroelec., mag. ordering, neutron diff. meas. 8-72331
- Gd₂(MoO₄)₃, and isotypes exam. of crystal growth, and defect generation 8-68617
- Gd₂(MoO₄)₃, domain structure obs. by GdF₃ decoration 8-84544
- Gd₂(MoO₄)₃, electro-opt. props. 8-76426
- Gd₂(MoO₄)₃, prismatic domain exam. 8-56441
- Gd₂(MoO₄)₃, spontaneous electrooptic effect, role of induced birefringence 8-68480
- KD₂PO₄, polarisation echo, near ferroelec. transition 8-88266
- KD₂AsO₄, phase transition and Raman scattering 8-84540
- K(D₂H₂₁)PO₄, ferroelectric, photovoltaic and photorefractive effects 8-72187
- KD₂PO₄, ferroelec. transition, ³¹P chem. shift obs. 8-76414
- KD₂PO₄, H-bonded phase transitions, SCF approach 8-92030
- KD₂PO₄, IR and Raman polarised spectra, rel. to crystal struct. 8-56489
- KD₂PO₄ type ferroelects., distrib. functions and thermodynamic props. 8-76409
- KD₂(SeO₃)₂, D NMR above and below ferroelec. transition, H-bond behaviour 8-52460
- K₂Fe(CN)₆·3H₂O, internal field and ferroelec. ordering 8-76406
- K₂Fe(CN)₆·3H₂O, sp.ht. and spontaneous polarisation, -65 to 0 degrees C, mol. field model 8-64333
- K(H,D)₂PO₄ crystals, effect of isotopic replacement on growth kinetics 8-95006
- KH₂AsO₄, above T_c, ⁷⁵As NMR spectrum, correl. effects 8-76324
- KH₂AsO₄, ferroelec., temp. broadening of hard mode Raman lines near T_c 8-88296
- KH₂AsO₄, phase transition and Raman scattering 8-84540
- KH₂PO₄, Bloch equations 8-64324
- KH₂PO₄, central components in ferroelec. phase 8-56436
- KH₂PO₄, dynamic central peak in ferroelectric phase 8-84538
- KH₂PO₄, ferroelec., temp. broadening of hard mode Raman lines near T_c 8-88296
- KH₂PO₄, ferroelectric, photovoltaic and photorefractive effects 8-72187
- KH₂PO₄, ferroelectric transition, press. induced tricrit. point 8-80301
- KH₂PO₄, H-bonded phase transitions, SCF approach 8-92030
- KH₂PO₄, internal friction, torsion pendulum technique 8-72474
- KH₂PO₄, KD₂PO₄, high-press. struct. rel. to dynamical models 8-80307
- KH₂PO₄, optical activity meas. 8-52466
- KH₂PO₄ type crystals, low lying ferroelec. modes, cluster dynamical theory 8-80305
- KH₂PO₄, variational treatment of proton-photon system 8-88261
- KH₂PO₄:SeO₄³⁻, slowing down of fluctuations near T_c, EPR obs. 8-60403
- KH₃(SeO₃)₂, slightly deuterated, central peak obs. in Brillouin spectra 8-64374
- K₂MoO₃F₃, ferroelec. and order-disorder phase transitions 8-92037
- KNbO₃, single domain crystal growth, SHG with Nd:YAG laser 8-74954
- KNbO₃, orthorhombic, anharmonic effects 8-79721
- KNbO₃, photoferroelectric effects 8-92029
- KNbO₃ single crystals, preparation of pure, Fe doped, and reduced crystals 8-60564
- KNbO₃:Fe, thermal and spectral variations in the photovoltaic current in ferroelects 8-91719
- KNbWO₆, crystallography, polymorphism and phys. props. 8-79599
- KTa_{0.65}Nb_{0.35}O₃, ferroelectric devices for optical systems 8-90473
- KTa_{1-x}Nb_xO₃ film, RF sputtering, structural and electrical properties obs. 8-88426
- KTa_{1-x}Nb_xO₃, local polarisability in quantum paraelec. and quantum ferroelec. phases 8-64325
- KTaO₃, complex refr. index meas. in far IR, by dispersive Fourier transform spectroscopy 8-92042
- KTaO₃, incipient ferroelectric, mode-mode coupling 8-79717
- KTaO₃, photoconduction in ferroelects 8-91720
- KTaO₃, second harmonic generation, bond charge theory 8-76395
- K₂WO₃F₃, ferroelec. and order-disorder phase transitions 8-92037
- La_{0.5}Pb_{0.5}Zr_{0.5}Ta_{0.5}O₃, ferroelec. with diffuse phase transition, electrostriction-optical props. 8-68457
- LiNH₄SO₄, LiNH₄SeO₄, nonlinear opt. props. including SHG 8-76396
- Li(N₂H₅)SO₄, thermal diffusivity exam. 8-63886
- LiNbO₃, band struct. and spontaneous polarisation calcs. 8-95261
- LiNbO₃, cathodlum. spectral and temp. depend. 8-84665
- LiNbO₃, ferroelec., phonon dispersion relations, neutron inelastic scatt. meas. 8-56435
- LiNbO₃, ferroelectric devices for optical systems 8-90473
- LiNbO₃, induced refl. and transparency increase (*Russian*) 8-59094
- LiNbO₃, LF sound attenuation, internal friction 8-63804
- LiNbO₃, LiNbO₃:Fe, amplification of laser beams by ferroelectrics 8-90393
- LiNbO₃, LiNbO₃:Fe, holography in ferroelectrics 8-90394
- LiNbO₃, LiNbO₃:Fe, photorefraction in ferroelectrics rel. to electro-opt. effects 8-92048
- LiNbO₃, light emission from surface on heating or cooling 8-64416
- LiNbO₃, microfabrication by ion-bombardment enhanced etching 8-76779
- LiNbO₃, optical damage in doped and undoped ferroelectric, mechanism 8-95570
- LiNbO₃, optical phonon modes and anharmonic couplings 8-60466
- LiNbO₃, photovoltaic effect, latent-image formation kinetics, electrophotography appl. 8-84246
- LiNbO₃, pyroelectric induced optical damage 8-52446
- LiNbO₃, thermal and spectral variations in the photovoltaic current in ferroelectrics 8-91719
- LiNbO₃:Fe, calc. of photorefraction (*Russian*) 8-92032
- LiNbO₃:Fe, laser induced optical damage 8-95572
- LiNbO₃:Fe, photorefractive effect in a ferroelectric 8-92047
- LiNbO₃:Fe, treated in Li₂CO₃, formation of Fe²⁺ state, Mossbauer effect 8-92003

ferroelectric materials continued

- LiNbO₃:Fe holographic information storage material 8-55321
- LiNbO₄, dispersion of vibrational excitations, Raman scatt. 8-84588
- LiTaO₃, near ferroelec. transition, elasticity, photoelasticity 8-88268
- LiTaO₃, optical phonon modes and anharmonic couplings 8-60466
- LiTaO₃:M, optical damage of transition-metal-doped ferroelectric 8-95571
- LiTaO₃-CaZrO₃, struct. and dielec. props. 8-80298
- LiTaO₃, light scatt. from ferroelec. domains 8-80310
- ND₄D₂PO₄ type ferroelects., distrib. functions and thermodynamic props. 8-76409
- (NH₄)₂BeF₄, paraelec. phase, cryst. struct. 8-95025
- (NH₄)₂BeF₄, improper ferroelec., incommensurate-commensurate transitions 8-60404
- (NH₄)₂BeF₄, powder, IR spectra, assignments, mol. libration, in paraelec. and ferroelec. phases 8-88299
- NH₄H₂AsO₄:Cr³⁺, ENDOR spectra 8-88224
- (NH₄)₂H₂PO₄:Cr³⁺, EPR exam. above and below T_c 8-68363
- NH₄LiSO₄, ferroelec., PMR line shape and spin-lattice relax. 8-88205
- NH₄LiSO₄, I-II phase transition in improper ferroelec., hydrostatic press. effects 8-84533
- (NH₄)₂SO₄, Brillouin scatt. from room temp. to -70°C 8-52517
- (NH₄)₂SO₄, ferroelec., dielec. behaviour and nature of phase transition 8-88262
- (NH₄)₂SO₄ ferroelectric, X-ray anal. of sub-lattice order parameters 8-92035
- (NH₄)₂SO₄, ferroelec., ion group reorientation temp. and press. depend., PMR obs. 8-72470
- (NH₄)₂SO₄:Cd²⁺, ferroelec. transition, soft mode contrib., EPR obs. 8-72469
- Na(D₂H₂₁)₃(SeO₃)₂, Raman spectra and nature of phase transitions 8-80341
- NaNd₂C₄H₂D₂O₆·4D₂O, ferroelec. phase, incommensurate satellite refls. 8-84531
- NaNH₄SO₄·2H₂O, NaNH₄SeO₄·2H₂O, nonlinear opt. props. including SHG 8-76396
- NaNH₄SO₄·2H₂O, ferroelec. and thermal props. 8-83968
- NaNO₂, 163°C phase transition, thermal history effects on range of modulated struct. 8-95563
- NaNO₂, band struct., polarisation and piezoelec. consts. calc. 8-52448
- NaNO₂, ferroelectric transitions, based on model thermodynamic pot. 8-80295
- NaNO₂, phonon side bands of triplet absorption 8-76488
- NaNO₂, X-ray crit. scatt. 8-52461
- NaNO₂:Mn²⁺, ferroelectric phase metastable struct., EPR obs. 8-60328
- NaNO₃, press. induced ferroelec. transition, soft mode dynamics, Raman scatt. meas. 8-72475
- NaNbO₃, birefr., temp. depend., behaviour at P≠N struct. transition 8-64331
- PLZT ceramic, ferroelec., cathodlum. spectral and temp. depend. 8-84665
- PLZT ceramic birefringence props., transverse electro-optical meas. 8-72487
- PLZT, deposition of transparent electrodes, opt. storage device applic. 8-74848
- PLZT, electro-optical, physical elec. and optical props. and fabrication (*Polish*) 8-56458
- PLZT, ferroelectric devices for optical systems 8-90473
- PLZT, opt. spectra and luminesc. 8-76508
- PLZT, photorefractive effect and photoconductivity 8-92046
- PLZT, transparent ferroelec., RF sputtering and film characterisation 8-72727
- Pb₂-Sr_{1-x}(Zr_{1-x}Ti_x)O₃:Cr₂O₃, ferroelec. ceramic, reversible characts. and dielectric losses (*Russian*) 8-84517
- (Pb_{0.715}Ba_{0.285})_{0.991}(Zr_{0.707}Ti_{0.293})_{0.981}Bi_{0.019}O₃, slim loop ferroelec. ceramic, shock wave compressed, elec. response 8-80293
- PbBi₄Ti₄O₁₅ ceramic, dielec. props., temp. depend. 8-95561
- Pb₂Ge₂O₁₁ acoustic relax. assoc. with phase transition at hypersonic freq. 8-88267
- Pb₂Ge₂O₁₁, dynamic central peaks and phonon interactions near structural phase transitions 8-83903
- Pb₂Ge₂O₁₁, ferroelectric transition exam. by Raman scatt. 8-56439
- Pb₂(Ge_{1-x}Si_x)₂O₁₁, dielec. spectra, ferroelec. behaviour 8-60406
- Pb₂Ge_{2-x}Si_xO₁₁, ferroelec. soft mode, temp., press. and comp. depend. 8-80304
- Pb₂Ge_{2-x}Si_xO₁₁, ferroelec., switching vel. and spontaneous polarisation 8-84543
- PbHfO₃, elec. field gradient, crit. behaviour, DPAC meas. 8-80303
- PbMg_{1/3}Nb_{2/3}O₃, cathodlum. spectral and temp. depend. 8-84665
- PbMg_{1/3}Nb_{2/3}O₃, PMN, electro-opt., elasto-opt., opt. and photo-induced props. 8-95560
- PbMg_{1-x}Nb_xO₃, ferroelec. with diffuse phase transition, electrostriction-optical props. 8-68457
- Pb₂MgNb₂O₉, crystal growth procedure, meas. electro-optic and dielectric props. 8-88418
- Pb₂Mg₂Ta₂O₉, crystal growth procedure, meas. electro-optic and dielectric props. 8-88418
- PbNb₂O₆, ferroelectric thick crystals, domain formation and dislocation loops 8-60410
- PbNb₂O₆, ferroelectric single crystals, domain struct., cryst. planes, twinning 8-64340
- Pb₃O₄, IR and Raman study of structural phase transitions (*French*) 8-84582
- Pb(Ti_{1-x}[Fe_{1/2}Ta_{1/2}])O₃, pyroelec. props. at transition between ferroelec. phases 8-52447
- PbTiO₃ ceramic, mech. strength 8-64332
- PbTiO₃, cryst., polarisation and resistivity, elec. field effects 8-64313
- PbTiO₃, damping of soft E-symmetry phonon, Raman scatt. meas. 8-67799
- PbTiO₃, domain struct. formation during jump motion of phase front 8-64339
- PbTiO₃, ferroelectric ceramic, dielec., piezoelec. and elastic props., orientational contrib. 8-68468
- PbTiO₃, neutron powder profile refinement, temp. depend. 8-51476
- PbTiO₃ single crystals, electroluminesc., elec. field, freq. and temp. depend. 8-80422
- PbZn_{1/3}Nb_{2/3}O₃, PZN, electro-opt., elasto-opt., opt. and photo-induced props. 8-95560
- Pb(Zr,Ti,Ge)O₃, antiferro-ferroelectric transition 8-95565
- Pb(Zr,Ti)O₃ ceramic, mech. strength 8-64332

ferroelectric materials continued

- Pb(Zr,Ti)O₃, ceramic, axially loaded, nature of elec. field and resulting voltage 8-72468
 Pb(Zr,Ti)O₃, photovoltaic ferroelectric as optical memory storage medium 8-50877
 Pb(Zr,Ti)O₃ thin layers, tan δ temp. dependence obs. (*Bulgarian*) 8-88259
 PbZrO₃-monocryst., elec. cond., permittivity, polarisation, para- and ferro- to antiferroelec. phase transitions 8-60402
 PbZr_{0.9}Ti_{0.1}O₃, neutron powder profile refinement, temp. depend. 8-51475
 PbZr_{0.95}Ti_{0.05}O₃, impact loading, mech. and elec. response, elec. state effect 8-64317
 Pb(Zr_{0.47}Ti_{0.43}Sn_{0.10})O₃:Cr₂O₃, ferroelec. ceramic, reversible characts. and dielectric losses (*Russian*) 8-84517
 RbH₂AsO₄, internal friction, torsion pendulum technique 8-72474
 RbH₂PO₄, internal friction, torsion pendulum technique 8-72474
 RbH₂PO₄, longit. US wave propag. near ferroelectric phase transition temp. 8-84536
 RbHSO₄, anisotropy of US anomaly near ferroelec. phase transition 8-72473
 RbHSO₄, compressed powder, dielectric const. and particle size, 77-355K 8-76371
 RbH₂(SeO₃)₂, improper ferroelectric phase transformation, neutron scattering study 8-80302
 Rb₃MoO₃F₃, ferroelec. and order-disorder phase transitions 8-92037
 RbNH₄SO₄, ferroelec., ion group reorientation temp. and press. depend., PMR obs. 8-72470
 Rb₃WO₃F₃, ferroelec. and order-disorder phase transitions 8-92037
 Rb₂ZnBr₄, dielectric const. and ferroelectric hysteresis 8-84535
 SC(NH₄)₂, ferroelectric transitions, based on model thermodynamic pot. 8-80295
 SbSI, abrupt polarisation changes under influence of external forces 8-68459
 SbSI, birefr. and phase transitions 8-60405
 SbSI, ferroelec., phase transitions, birefringence meas. 8-56440
 SbSI, max. vel. of domain boundaries in polarisation reversal, Barkhausen effect meas. 8-60411
 SbSI, tricrit. point at 1.4 kbar and 235K 8-68463
 SbTaO₄, X-ray and ESR study of phase changes 8-72476
 Sn₂P₂S₆, ferroelec., IR and Raman spectra, photocond., edge absorpt. spectra, spontaneous polarisation, forbidden gap 8-68514
 Sr_{0.5}Ba_{0.5}Nb₂O₆, ferroelec., dielec. behaviour 8-80309
 Sr_{0.75}Ba_{0.25}Nb₂O₆, ferroelectric devices for optical systems 8-90473
 Sr_{0.75}Ba_{0.25}Nb₂O₆, large cryst. growth, control of opt. defects 8-76595
 SrBa_{1-x}Nb₂O₆, neutron and light scatt. in phase transition region 8-64336
 SrTiO₃, cathodlum. spectral and temp. depend. 8-84665
 SrTiO₃, complex refr. index meas. in far IR, by dispersive Fourier transform spectroscopy 8-92042
 SrTiO₃, dielectric loss at microwave frequencies (*Russian*) 8-52440
 SrTiO₃, dynamic central peaks and phonon interactions near structural phase transitions 8-83903
 SrTiO₃, forced thermal Rayleigh scattering 8-80371
 SrTiO₃, incipient ferroelectric, mode-mode coupling 8-79717
 SrTiO₃, photoluminesc., thermoluminesc. and thermally stimulated currents 8-92121
 SrTiO₃, structural phase transition at 110K, theory 8-80300
 SrTiO₃, surface defects, electronic struct., LEED, AES, UPS study 8-84273
 SrTiO₃, X-ray and Mossbauer γ -ray scatt., near phase transition, energy width of central peak 8-79724
 TGS, ferroelec., temp. autostabilisation, impedance var. with DC bias 8-72467
 TiO₂, rutile, ferroelectric ceramic, dielec., piezoelec. and elastic props., orientational contrib. 8-68468

ferroelectric phenomena *see ferroelectricity***ferroelectric semiconductor materials** *see ferroelectric semiconductors***ferroelectric semiconductors**

- perovskite structure, semiconductor props., review (*Polish*) 8-56437
 n-SrTiO₃, surface electronic struct. calc. 8-88011
 vibronic, interband light absorption 8-72555
 Ba₂Sr_{1-x}Nb₂O₆, anomalous photovoltaic effect and photocond. 8-52449
 BaTiO₃, anomalous photovoltaic effect and photocond. 8-52449
 BaTiO₃, donor doped, elec. props., effect of kinetic processes 8-64042
 n-BaTiO₃, elec. transport props., theoretical discussion and expt. 8-84215
 BaTiO₃, perovskite structure, semiconductor props. (*Polish*) 8-56437
 GeTe:Fe, ferroelectric transition exam. 8-88264
 KNbO₃, perovskite structure, semiconductor props. (*Polish*) 8-56437
 KNbO₃:Fe, anomalous photovoltaic effect and photocond. 8-52449
 LiNbO₃, anomalous photovoltaic effect and photocond. 8-52449
 NaNbO₃, perovskite structure, semiconductor props. (*Polish*) 8-56437
 Pb_{1-x}Ge_xTe, dielec. const. determ. near ferroelec. transition 8-88269
 Pb_{1-x}Ge_xTe, electron-phonon interaction effect on ferroelec. transition 8-76416
 PbTiO₃, ferroelec. phase, photocond. and photovoltaic effect, temp. depend. 8-95309
 PbTiO₃, perovskite structure, semiconductor props. (*Polish*) 8-56437
 PbZrO₃, perovskite structure, semiconductor props. (*Polish*) 8-56437
 SbNbO₄, anomalous photovoltaic effect and photocond. 8-52449
 Sb₂S₃, effect of screening by conduction electrons on phase transitions 8-84537
 SbSI, effect of screening by conduction electrons on phase transitions 8-84537
 SbSI, ferroelec. semicond., laser-modulated reflectance near T_c 8-72552
 SbSI, free energy function, temp. depend. and anisotropy of dielec. const., ferro- and paraelec. phases 8-64330
 SbSI materials, piezoelectric props. rel. to use as electroacoustic transducers 8-52445
 SbSI, paraelectric phase, jump-like switching processes, ferroelec. surface layer 8-92038
 Sn₂P₂S₆, soft mode, temp. depend. of Raman spectra near phase transition 8-88263
 SnTe, electron-phonon interaction effect on ferroelec. transition 8-76416

ferroelectric switching

- TGS, electrooptic switching anomalies 8-52473
 Ba_{0.92}Ca_{0.08}TiO₃ ceramic, uniaxial stress effects, US dilatometric and dielec. meas. 8-52454
 Pb₂Ge_{1-x}Si_xO₁₁, ferroelec., switching vel. and spontaneous polarisation 8-84543
 Pb(Zr,Ti)O₃, photovoltaic ferroelectric as optical memory storage medium 8-50877
 SbSI, paraelectric phase, jump-like switching processes, ferroelec. surface layer 8-92038

ferroelectric thin films

- ceramic, resonant autothermostabilisation (*Russian*) 8-52451
 electrical hysteresis investigation, electronic system for loops display on CRO 8-89496
 phase transitions, second order, thermodynamics (*Russian*) 8-52458
 polyvinylidene fluoride, X-ray diffr. evidence for ferroelectricity 8-60399
 pyroelectric effects, origin 8-88258
 vacuum deposition method using RF sputtering technique 8-84712
 KTa_{1-x}Nb_xO₃, preparation by RF sputtering, structural and electrical properties obs. 8-88426
 PLZT, transparent ferroelec., RF sputtering and film characterisation 8-72727
 PZT, ferroelec. film, elec. props., composition anal., AES 8-84530
 Pb(Zr,Ti)O₃ thin layers, tan δ temp. dependence obs. (*Bulgarian*) 8-88259

ferroelectric transitions

- see also critical fluctuations; displacive transformations; ferroelectric Curie temperature; order-disorder transformations*
 alkali trihydrogen selenite: Mn²⁺ single crystal, EPR 8-72396
 ammonium Rochelle salt, incommensurate phases and ferroelectricity 8-52455
 critical dynamics at phase transitions and nuclear relaxation 8-75805
 crystal classification by transition mechanisms (*Russian*) 8-60401
 dicalcium lead propionate, ferroelec., piezoelec. and elastic props. 8-84528
 dielectric props. meas. in vicinity of phase transition 8-74022
 displacive, unified theory, quantum limit, zero point energy 8-68461
 displacive type ferroelectric, thermal expansion and effect of press. on transition temp. 8-72471
 electrogyration in ferroelec. crystals, appls. 8-76394
 electron spin echo investigations 8-84476
 electron subsystem, steady-state statistical equilb. conditions, adiabatic approx. 8-87754
 equilibrium configuration of ferroelectric domains near Curie temp. 8-88270
 films, ferroelec., phase transitions, second order, thermodynamics (*Russian*) 8-52458
 gyrotropic phase transitions 8-71852
 high pressure studies, rel. to Earth and planetary interiors 8-69334
 incommensurate-commensurate transitions in ferroelec., general approach 8-60404
 light scattering on central peaks (*Japanese*) 8-52522
 liquid crystals, temp. depend. of elec. susceptibility and spontaneous polarisation (*Japanese*) 8-68467
 (NH₄)₂SO₄:Mn²⁺, ferroelec. phonon driven phase transform., reduction of spin Hamiltonian consts. 8-92033
 NMR, and soft collective lattice modes, spins and pseudospins, study 8-88208
 nonconducting linear chain systems, 3D Coulomb coupling and charge ordering 8-60075
 order-disorder ferroelec., crit. dynamics, NMR data compared with dielec. data 8-76415
 orthorhombic base centred lattices, Fourier transform of dipole-dipole interaction 8-76404
 orthorhombic lattices, Fourier transform. of dipole-dipole interaction 8-64334
 perovskite crystals, static and dynamic aspects of PAC meas. 8-88241
 polaron density of states near low temp. ferroelec. transition 8-60065
 prototype temperature setting rel. to soft modes 8-63833
 pyroxene, ferroelectric-like phase transformation in mantle 8-61362
 Rochelle salt, optical characteristics in UV region (*Russian*) 8-84550
 Rochelle salt, polarisation echo, near ferroelec. transition 8-88266
 Rochelle salt, structural phase transitions 8-83938
 semiconductor, vibronic, interband light absorption 8-72555
 sodium ammonium tartrate, polarisation, improper ferroelec. transition 8-72477
 specific heat calc., soft mode contrib., near T_c 8-64338
 squaric acid, ¹³C chemical shift tensor study of antiferroelec. second order phase transition 8-52462
 squaric acid and deuterated derivative, vibrational study, IR and Raman spectra 8-92076
 structural phase transitions in crystals, effect of high-power visible and IR laser radiation 8-71825
 tanane, crit. behaviour near ferroelec.-ferroelastic transition 8-52459
 tetramethylammonium tetrachlorocobaltate, ferroelectricity 8-76408
 TGS, ferroelec. transition, struct. changes, ¹³C NMR obs. 8-60344
 TGS, gamma irradi. effects on heat capacity, Curie temp., permittivity 8-67737
 TGS, large scale inhomogeneity effect on ferroelectric transition (*Russian*) 8-76411
 TGS family, change of order of phase transition under hydrostatic pressure 8-52452
 TGSe, dielectric const. near ferroelec. transition temp., effect of surface capacitance 8-56438
 thermodynamic potential of systems with size effects (*Russian*) 8-80297
 thermoelectric conversion in ferroelectric ceramics during phase transitions (*French*) 8-76412
 thiourea, expansion coeffs. in phase transition range 8-76407
 trisarcosine calcium chloride:Mn²⁺, ferroelec., electron spin-lattice relax. 8-80208
 uniaxial ferroelectric, static and dynamic crit. phenomena, Larkin-Khmelnitzkii theory 8-64327
 uniaxial ferroelectric, US vel. and absorpt. anisotropy and crit. anomalies, acousto-opt. obs. 8-95574
 vibrational modes, crit. behaviour of uniaxial materials 8-84539
 vibronic theory of antiferroelec. and struct. modulated transitions, soft modes 8-79719

ferroelectric transitions continued

- AgNa(NO₃)₂, ultraslow crit. dynamics of order parameter, ²³Na spin relax. times obs. 8-76410
- Ag₅SbS₄, dielec. and acoustic props. (*German*) 8-64335
- Ba₂NaNb₅O₁₅, ferroelec. conversion to single domain, elec. and photoelec. props. 8-88271
- Ba_{0.5}Sr_{0.5}Nb₂O₆, temp. depend. of Raman spectra 8-72524
- Ba_{0.5}Sr_{0.45}Nb₂O₆·Y(La)(Tm), dielectric and electrooptic props. 8-68466
- Ba_{1-x}Sr_xNb₂O₆, ferroelec., cathodlum. spectral and temp. depend. 8-84665
- BaTiO₃, A₁(TO) phonon spectrum, ferroelectric phase transition, Raman scatt. meas. 8-56478
- BaTiO₃, cubic-tetragonal phase transition, birefringence meas., surface distortion effects 8-95564
- BaTiO₃, doped, loss mechanism and domain stabilisation 8-84542
- BaTiO₃, dynamic Rayleigh light scatt. in region of ferroelectric-paraelectric transition 8-64371
- BaTiO₃, logarithmic velocity variations for longitudinal US waves near ferroelec. transition 8-72472
- BaTiO₃, magnetochemical exam. of phase transition, mag. suscept. meas. 8-88265
- BaTiO₃, martensite type phase transition 8-64326
- BaTiO₃, para to ferroelec. transition, strong Rayleigh scatt. 8-76486
- BaTiO₃, perovskite structure, semiconductor props. (*Polish*) 8-56437
- BaTiO₃, polariton and central mode softening 8-76006
- BaTiO₃, struct. changes due to cubic-tetragonal phase transition 8-60407
- BaTiO₃ type crystals, determ. of phase transitions using symmetry breaking theory (*French*) 8-83950
- BaTiO₃·Co, charact. behaviour of spontaneous polarisation and dielec. const. 8-60382
- Bi₂Bi₂Fe₂Ti₂O₈, dielec. and magnetoelec. props. 8-95562
- BiBi₂Ti₂FeO₁₅, perovskite-like layer-type ferroelec. magnetic cpd., Mossbauer expts., 80-1200K 8-64329
- Bi₂Sb_{1-x}Si_x, atomic substitution and ferroelec. phase transition 8-68464
- BiTaO₄, X-ray and ESR study of phase changes 8-72476
- Cd₂Nb₂O₇, Raman-scattering investigation of vibrational structure 8-76441
- Co₂B₂O₇, intermediate phase between paraelectric and ferroelectric phase (*Russian*) 8-68465
- CsH₂PO₄, high press. phase diagram 8-52457
- CsH₂PO₄, single cryst. growth, struct. and elec. props. 8-71693
- Cs₂KMO₃F₃, (M=Mo, W), low temp. phase transitions (*French*) 8-92036
- Cs₂MoO₃F₃, ferroelec. and order-disorder phase transitions 8-92037
- Cs₂RbMO₃F₃, (M=Mo, W), low temp. phase transitions (*French*) 8-92036
- Cs₂WO₃F₃, ferroelec. and order-disorder phase transitions 8-92037
- Gd₂(MoO₄)₃, electro-optical properties 8-88281
- Gd₂(MoO₄)₃, uniaxial stress effect on ferroelec. transition, Raman scatt. 8-80360
- GeTe: I, ferroelectric transition exam. 8-88264
- KCN, optical F centres and phase transitions 8-56504
- KD₂PO₄, polarisation echo, near ferroelec. transition 8-88266
- KD₂AsO₄, phase transition and Raman scattering 8-84540
- KDP-type cryst., Raman scattering and phase transitions, deuteration effects 8-76400
- KDP-type crystals, phase transitions, quadratic electrooptic coeff., electrostriction 8-76430
- KD₂PO₄, ³¹P chem. shift obs. 8-76414
- KD₂PO₄, H-bonded phase transitions, SCF approach 8-92030
- KD₂PO₄, high press. phase diagram 8-52457
- KD₂PO₄ type ferroelects., distrib. functions and thermodynamic props. 8-76409
- KD₃(SeO₃)₂, D NMR above and below ferroelec. transition, H-bond behaviour 8-52460
- K₄Fe(CN)₆·3H₂O, internal field and ferroelec. ordering 8-76406
- K₄Fe(CN)₆·3H₂O, sp.ht. and spontaneous polarisation, -65 to 0 degrees C, mol. field model 8-64333
- KH₂AsO₄, fast and slow dynamic reorientation 8-80306
- KH₂AsO₄, phase transition and Raman scattering 8-84540
- K(H_{1-x}D_x)₂PO₄, single cryst., .77K, γ-radiation damage centres, and EPR obs. 8-68379
- KH₂PO₄, central components in ferroelec. phase 8-56436
- KH₂PO₄, dynamic central peak in ferroelectric phase 8-84538
- KH₂PO₄, ferroelec. cryst., internal friction, torsion pendulum obs. 8-72474
- KH₂PO₄, ferroelectric transition, press. induced tricrit. point 8-80301
- KH₂PO₄, H-bonded phase transitions, SCF approach 8-92030
- KH₂PO₄, KD₂PO₄, high-press. struct. rel. to dynamical models 8-80307
- KH₂PO₄ type crystals, low lying ferroelec. modes, cluster dynamical theory 8-80305
- KH₂PO₄, variational treatment of proton-photon system 8-88261
- KH₂PO₄·SeO₄³⁻, slowing down of fluctuations near T_c, EPR obs. 8-60403
- KH₂PO₄·KD₂PO₄ mixed crystals, static and dynamic props., proton-lattice coupled mode model 8-64328
- KH₂(SeO₃)₂, slightly deuterated, central peak obs. in Brillouin spectra 8-64374
- K₃MoO₃F₃, ferroelec. and order-disorder phase transitions 8-92037
- KNbO₃, perovskite structure, semiconductor props. (*Polish*) 8-56437
- K₂SeO₄, Raman scattering spectra and discovery of soft mode 8-76442
- K₂WO₃F₃, ferroelec. and order-disorder phase transitions 8-92037
- La₂Pb_{1-x}Zr_xTa_{1-y}O₃, ferroelec. with diffuse phase transition, electrostriction-optical props. 8-68457
- LiNH₄SO₄, phase transitions and phys. props. 8-76399
- LiNbO₃, ferroelec., phonon dispersion relations, neutron inelastic scatt. meas. 8-56435
- LiNbO₃:Fe, calc. of photorefractive (*Russian*) 8-92032
- LiTaO₃, near ferroelec. transition, elasticity, photoelasticity 8-88268
- ND₄D₂PO₄ type ferroelects., distrib. functions and thermodynamic props. 8-76409
- (NH₄)₂BeF₄, incommensurate-commensurate transitions 8-60404
- NH₄H₂AsO₄·Cr³⁺, fast and slow dynamic reorientation 8-80306
- NH₄IO₃, phase transitions, SHG obs. 8-76398
- NH₄LiSO₄, I-II phase transition in improper ferroelec., hydrostatic press. effects 8-84533

ferroelectric transitions continued

- NH₄LiSO₄, phase transforms., SHG obs. 8-76398
- (NH₄)₂SO₄, Brillouin scatt. from room temp. to -70°C 8-52517
- (NH₄)₂SO₄, ferroelectric, X-ray anal. of sub-lattice order parameters 8-92035
- (NH₄)₂SO₄, ferroelec., ion group reorientation temp. and press. depend., PMR obs. 8-72470
- (NH₄)₂SO₄·Cd²⁺, ferroelec. transition, soft mode contrib., EPR obs. 8-72469
- (NH₄)₂SO₄·Cr³⁺, EPR study of ferroelec. phase transition 8-64337
- NaCN, optical F centres and phase transitions 8-56504
- Na(D_xH_{1-x})₂(SeO₃)₂, Raman spectra and nature of phase transitions 8-80341
- Na_{1-x}Li_xNbO₃, dielec. const. and X-ray diff., for Curie temp. and phase diagrams 8-72768
- NaNd₂C₂H₂D₂O₆·4D₂O, ferroelec. phase, incommensurate satellite refls. 8-84531
- NaNH₂SeO₄·2H₂O, ferroelectric crystal, effect of hydrostatic pressure on phase transition 8-52453
- NaNO₂, 163°C phase transition, thermal history effects on range of modulated struct. 8-95563
- NaNO₂, adiabatic and isothermal elastic compliances, critical behaviour 8-92031
- NaNO₂, compressed powder, dielec. props., surface layer effects 8-76413
- NaNO₂, crit. dynamics, nuclear relax. 8-75805
- NaNO₂, elastic constants and US attenuation coeffs., anisotropic charact. 8-63809
- NaNO₂, ferroelectric transitions, based on model thermodynamic pot. 8-80295
- NaNO₂, mechanism of ordering type ferroelec. transition, vibr. spectroscopy 8-76402
- NaNO₂, mechanism of order-disorder transition, opt. spectra 8-76403
- NaNO₂, X-ray crit. scatt. 8-52461
- NaNO₂:Mn²⁺, ferroelectric phase metastable struct., EPR obs. 8-60328
- NaNO₂, press. induced ferroelec. transition, soft mode dynamics, Raman scatt. meas. 8-72475
- NaNO₂, soft mode dynamics at ferroelec. transition 8-80308
- NaNbO₃, birefr., temp. depend., behaviour at P≠N struct. transition 8-64331
- NaNbO₃, perovskite structure, semiconductor props. (*Polish*) 8-56437
- Ni₂B₂O₇, Raman spectra in paraelec. phase 8-60434
- PbF₂, phonon energy dispersion relations 8-79697
- Pb₂Ge₂O₁₁, acoustic relax. assoc. with phase transition at hypersonic freq. 8-88267
- Pb₂Ge₂O₁₁, dynamic central peaks and phonon interactions near structural phase transitions 8-83903
- Pb₂Ge₂O₁₁, ferroelectric transition exam. by Raman scatt. 8-56439
- Pb₂(Ge_{1-x}Si_x)₂O₁₁, dielec. spectra, ferroelec. behaviour 8-60406
- Pb₂Ge_{2-x}Si_xO₁₁, ferroelec. soft mode, temp., press. and comp. depend. 8-80304
- Pb_{1-x}Ge_xTe, dielec. const. determ. near ferroelec. transition 8-88269
- Pb_{1-x}Ge_xTe, electron-phonon interaction effect on ferroelec. transition 8-76416
- Pb_{1-x}Ge_xTe, phase transitions 8-60408
- PbHfO₃, elec. field gradient, crit. behaviour, DPAC meas. 8-80303
- PbMg_{1/3}Nb_{2/3}O₃, cathodlum. spectral and temp. depend. 8-84665
- PbMg₂Nb_{1-x}O₃, ferroelec. with diffuse phase transition, electrostriction-optical props. 8-68457
- Pb₂MgNb₂O₃, diffuse phase transition, Brillouin scatt. and acoustic phonons 8-76401
- Pb₂O₃, IR and Raman study of structural phase transitions (*French*) 8-84582
- Pb(Ti₂Zr_{1-x}(Fe_{1/2}Ta_{1/2}))O₃, pyroelec. props. at transition between ferroelec. phases 8-52447
- PbTiO₃, damping of soft E-symmetry phonon, Raman scatt. meas. 8-67799
- PbTiO₃, domain struct. formation during jump motion of phase front 8-64339
- PbTiO₃, perovskite structure, semiconductor props. (*Polish*) 8-56437
- Pb(Zr_{1-x}Ti_x)O₃, antiferro-ferroelectric transition 8-95565
- PbZrO₃, perovskite structure, semiconductor props. (*Polish*) 8-56437
- PbZrO₃-monocryst., elec. cond., permittivity, polarisation, para- and ferro- to antiferroelec. phase transitions 8-60402
- PbZr_{1-x}Ti_xO₃ solid solutions, tricritical behaviour 8-80296
- RbH₂AsO₄, ferroelec. cryst., internal friction, torsion pendulum obs. 8-72474
- RbH₂PO₄, ferroelec. cryst., internal friction, torsion pendulum obs. 8-72474
- RbH₂PO₄, high press. phase diagram 8-52457
- RbH₂PO₄, longit. US wave propag. near ferroelectric phase transition temp. 8-84536
- RbHSO₄, anisotropy of US anomaly near ferroelec. phase transition 8-72473
- Rb₂H(SO₄)₂, phase transitions at 56°C and 126°C, dielec. const. meas. 8-76405
- RbH₂(SeO₃)₂, improper ferroelectric phase transformation, neutron scattering study 8-80302
- Rb₂KMO₃F₃, (M=MO, W), low temp. phase transitions (*French*) 8-92036
- Rb₂MoO₃F₃, ferroelec. and order-disorder phase transitions 8-92037
- RbNH₄SO₄, ferroelec., ion group reorientation temp. and press. depend., PMR obs. 8-72470
- Rb₂WO₃F₃, ferroelec. and order-disorder phase transitions 8-92037
- SC(NH₂)₂, ferroelectric transitions, based on model thermodynamic pot. 8-80295
- Sb₂S₃, ferroelectric semiconductor, effect of screening by conduction electrons on phase transitions 8-84537
- SbSI, birefr. and phase transitions 8-60405
- SbSI, ferroelec., phase transitions, birefringence meas. 8-56440
- SbSI, ferroelec. semicond., laser-modulated reflectance near T_c 8-72552
- SbSI, ferroelectric semiconductor, effect of screening by conduction electrons on phase transitions 8-84537
- SbSI, free energy function, temp. depend. and anisotropy of dielec. const., ferro- and paraelec. phases 8-64330
- SbSI, tricrit. point at 1.4 kbar and 235K 8-68463
- SbTaO₄, X-ray and ESR study of phase changes 8-72476
- SnCl₂·2H₂O, crit. dynamics, nuclear relax. 8-75805

ferroelectric transitions continued

- SnCl₂·2H₂O-type layer cpds., two dimens. ferroelec. ordering sp. ht. obs. 8-92034
 Sn₂P₂S₆, soft mode, temp. depend. of Raman spectra near phase transition 8-88263
 SnTe, electron-phonon interaction effect on ferroelec. transition 8-76416
 Sr₂Ba_{1-x}Nb₂O₆, neutron and light scatt. in phase transition region 8-64336
 SrTiO₃, dynamic central peaks and phonon interactions near structural phase transitions 8-83903
 SrTiO₃, forced thermal Rayleigh scattering 8-80371
 SrTiO₃, X-ray and Mossbauer γ -ray scatt., near phase transition, energy width of central peak 8-79724
 TGSe, anomalous sound velocity near ferroelec. phase transition at high pressure 8-52456

ferroelectricity

- see also antiferroelectricity; ferroelectric devices; ferroelectric materials; ferroelectric switching; ferroelectric transitions
 antiferromagnet, energy gap in spin wave spectrum 8-91858
 antiferromagnet, ferroelec., exchange enhancement of magnetoelec. coupling 8-88159
 automatic anomalous noise meas. for ferroelectric capacitor parameters, not in equil. (French) 8-74029
 critical parameters of ferroelec. cryst. meas. (Polish) 8-88272
 de Gennes' model sum rules, decoupling procedure in Green's function method (Russian) 8-56434
 electret effects in ferroelectrics, phenomenological theory 8-88260
 ferromagnet, energy gap in spin wave spectrum 8-91858
 glass, dielectric instabilities in high permittivity glass 8-52433
 nematic and smectic liquid crystals, ferroelectricity explanation (French) 8-83729
 photo-Hall effect in ferroelectric crystal without centre of symmetry (Russian) 8-60152
 photostimulated processes in inorganic materials and optical information storage, review 8-82926
 photovoltaic current, bulk, in ferroelectrics, model calc. 8-84256
 KTaO₃, SHG and quadratic electrooptic effect 8-76429
 SrTiO₃, SHG and quadratic electrooptic effect 8-76429

ferrofluids see magnetic fluids**ferromagnetic-antiferromagnetic transitions**

- see also metamagnetism; Morin temperature
 Ising ferromagnet, 3-D critical behaviour in random mag. field 8-68250
 magnetic material, fluctuational breakdown of metastable states at phase transitions (Russian) 8-52245
 metamagnetic dielectrics, at finite temp. (Russian) 8-88118
 semiconductor, metamagnetic, magnetostriction ferrons 8-88160
 Fe-Cr-Ni, mag. state at low temps. (Russian) 8-56298
 Fe₂Mn_{1-x}Pt₃, ferro-antiferromag. transform. at 4.2K (Russian) 8-88117
 Fe₂O₃, haematite, optical indicatrix deform. and rot. during field induced phase transition 8-68482
 GdMg₃, mag. props. 8-72346
 MnPt, disordered film produced by RF sputtering, ferromag. behaviour 8-68310
 NdFeTiO₃, magnetic props. and crystal growth 8-92185
 NiS₂, high press. effect on mag. transition temps. 8-91866
 TbMg₃, mag. props. 8-72346
 TbNi_{2-x}Cu_x, elec. resist. and mag. props. 8-72348

ferromagnetic Curie temperature see Curie temperature**ferromagnetic-paramagnetic transitions**

- see also Curie temperature
 anisotropic system, libron interactions, transition temp. depend. (German) 8-76237
 critical dynamics above crit. temp., dipolar coupling 8-52286
 education, renormalisation group theory, second order phase transitions, undergraduate statistical physics 8-62012
 ferromagnet, triple dynamic magnetisation fluctuation correl. and feasibility of polarised neutron exam. (Russian) 8-88133
 Heisenberg film, spin-one isotropic, quadratic interactions, quadrupolar-paramag. T_c 8-64210
 magnetic material, fluctuational breakdown of metastable states at phase transitions (Russian) 8-52245
 rare earth cobalt intermetallics, RCo₂, elastic moduli, 4.2-300K 8-52332
 rare earth-transition metal alloys, H₂ absorption, effect on mag. props. 8-68231
 Dy, rel. to longitudinal galvanomag. effect in single crystals. (Russian) 8-56132
 DyCo₂, field induced vol. magnetostriction 8-91920
 ErCo₂, field induced vol. magnetostriction 8-91920
 EuS, spin relaxation crit. behaviour 8-76251
 Fe, Mossbauer energy shift near Curie temp. 8-52388
 Gd-Dy alloy, rel. to longitudinal galvanomag. effect in single crystals. (Russian) 8-56132
³He in Grafoil, ultralow temp. NMR mag. susceptibility, surface magnetisation and transition 8-79843
³He with C particles, pulsed NMR, mag. susceptibility surface induced ferromagnetism, antiferromagnetic exchange interaction 8-79844
 (Ho,Y)Co₂, first order phase transitions 8-84426
 HoCo₂, field induced vol. magnetostriction 8-91920
 Ni, angular resolved photoemission 8-68603
 Ni, atomic layers, Pauli paramagnetism to band ferromagnetism transition thickness depend. 8-72377
 Ni, oxidation kinetics near Curie temperature 8-88578
 Ni-Fe solid soln., precip. hardened, paramag.-ferromag. transition on ageing 8-52255
 Pd based 3d metal alloys, mag. phase diagram calc. 8-80144
 TbG₃, uniaxial ferromagnet, logarithmic corrections to crit. behaviour 8-60294
 UMn₂-UCo₂, mag. props., ferromag. transition (Russian) 8-68148
 UMn₂-UF₂, mag. props., ferromag. transition (Russian) 8-68148

ferromagnetic properties of substances

- see also ferromagnetic relaxation; ferromagnetic resonance; ferromagnetism; magnetic semiconductors
 Alnico, interaction domains after heat treatment in mag. field (Russian) 8-68286
 Alnico 5, thermal treatment in mag. field, mag. props. 8-91905

ferromagnetic properties of substances continued

- Alnico 8 permanent magnet, magnetic props. rel. with crystallographic texture 8-95483
 amorphous ferromagnets, itinerant electron model, Invar anomalies, review 8-95413
 biotite, thermal decomposition, stability of ferromag. products 8-57195
 blast furnace magnetic structure of ferromagnetic metals and alloys, metallographic study (Bulgarian) 8-73008
 chromindur, origin of coercivity, Lorentz microscopy, magnetisation and Mossbauer effect 8-64219
 chromindur, phase separation, Mossbauer obs. 8-88116
 demagnetisability of grain-oriented materials 8-84449
 electromagnetic props. inspection by electromagnetic transducer with frequency output signal 8-53131
 ferromagnetic, EMF generation by pulsed laser irradi. 8-68021
 fine particle systems, physical basis and applications 8-84457
 Invar, hysteresis loop displacement 8-52312
 Invar, magnetisation reversal, fast, forced by external RF mag. field, Mossbauer obs. 8-52311
 Invar, specific heat, temp. depend. (Russian) 8-56341
 Invar-type alloys, review of magnetomechanical effects and state of art of materials 8-52330
 magnetisation and hysteresis losses, math. model (Russian) 8-88140
 magnetocrystalline anisotropy meas., capacitance torque meter 8-93743
 metallic glass, isotropic and anisotropic magnetoelastic effects, review 8-68352
 metallic glass, magnetostrictive film, overlay for variable SAW delay line 8-63240
 metallic glasses, Mossbauer investigation of electronic struct. 8-92009
 oxides with perovskite struct., neutron diff., ferri- and ferromag. props. 8-52214
 palaeomagnetic record carriers synthetic analogues, preparation, characterisation and mag. props. 8-65276
 pearlite in C steels (0.08 to 1.6 wt.%), exam. of temp. depend. of mag. coercivity 8-52304
 Permalloy, electrodeposition, mag. props. (French) 8-64488
 Permalloy, magnetisation improvement through solid state refining 8-91893
 Permalloy, magnetisation reversal, fast, forced by external RF mag. field, Mossbauer obs. 8-52311
 Permalloy 51N, powder metallurgy product. and props. 8-60603
 Permalloy film, galvanomag. rotation characts., under uniaxial stress 8-84466
 random binary alloys, elastic neutron scatt. cross section 8-91845
 rare earth allys, amorphous, magnetoresistivity, exchange scatt. model 8-95287
 rare earth alloys, R₂Co₁₇, formation of mag. anisotropy role of rare earth ions (Russian) 8-76238
 rare earth cobalt intermetallics, RCo₂, elastic moduli, 4.2-300K 8-52332
 rare earth ferromagnets, spin polarised electron tunnelling 8-68094
 rare earth intermetallics, RFe_{3-x}Ni_x, giant intrinsic mag. hardness 8-56354
 rare earth intermetallics, RMg₂, cryst. and mag. props., ordering 8-68185
 rare earth metals, ferromag. ordering (Russian) 8-60262
 rare earth metals, RKKY interaction and conduction electron polarisation 8-91859
 rare earth orthotitanites, unusual mag. props., role of mag. moments 8-84400
 rare earth systems with singlet ground states, low freq. modes 8-68131
 rare earth ternary borides, RRh₄B₄, supercond., re-entrant magnetism, energy band calcs. 8-52140
 rare earth-Co₂-Al, dil., nonmag. impurities effect on ordering temp. 8-84427
 rare earth-Co permanent magnets, microstruct., TEM obs., magnetisation 8-91901
 rare earth-cobalt intermetallics, permanent magnet production and props. 8-52309
 rare earth-Fe₂, magnetomech. coupling and Young's modulus 8-84472
 rare earth-Fe, intermetallic compounds, mag. props. (Rumanian) 8-92007
 rare earth-Fe alloys, highly magnetostrictive, isotropy breaking magnetoelastic behaviour 8-72386
 rare earth-iron alloys, elastic vs. magnetoelastic anisotropy 8-68347
 rare earths, heavy, mag., electronic struct., book 8-60259
 Recalloy, Fe-Nb, semihard magnetic alloy, magnetic props., hardness, microstruct. 8-56660
 semiconductor, optical transparency, photoferromag. effect, Curie temp. shift (Russian) 8-72387
 siegnette magnets with hexagonal barium titanate structure 8-76397
 steel, C, resistivity, thermal and elec., spin disorder scatt. anal. 8-76063
 steel, C, rotational hysteresis 8-91889
 steel, low alloy and C, hardened and tempered parts, nondestructive magnetic inspection 8-95889
 steel, magnetisation transitions, Barkhausen noise 8-91894
 steel, mild, rotational hysteresis 8-91889
 stress determ. by portable magnetic equipment 8-53172
 Ticonal, interaction domains after heat treatment in mag. field (Russian) 8-68286
 transformer, EM losses, effect of degree of perfection of crystallographic texture (Russian) 8-60309
 transition metal alloy, electronic structure, mag. props. 8-95254
 transition metal alloy, H-impurity complex obs. by mag. aftereffect 8-72373
 transition metal alloy ferromagnetic thin films, fabrication by sputtering, and mag. props. 8-91881
 transition metal alloys, electronic specific heat, near and weak ferromagnetics 8-80158
 transition metal alloys, ferromag., with atomic short range order, local environment effects on electronic struct., Fe-V appl. 8-67936
 transition metal alloys, ferromagnetic, BCC, spin wave stiffness constant 8-91851
 transition metal alloys, magnetically ordered, effect of magnetic field on P-T diagram 8-52246
 transition metal silicides, NMR and μ SR, microscopic mag. props. (Japanese) 8-52368

ferromagnetic properties of substances continued

- transition metal-metalloid amorphous alloys, mag. props. review 8-52300
- transition metals, electronic structure and ordering of sp defects 8-91639
- $[(CH_3)_3NH]CoCl_3 \cdot 2H_2O$, chain ferromag. two magnon bound state, nuclear spin-lattice relax. 8-88206
- Ag-Ni, composite, fibre and layer structs., anomalous props. caused by internal phase boundaries 8-72754
- $Al_2Mn_3Si_2O_{12}$, spin correlations and phase transitions, neutron diffraction. 8-84390
- Au-Fe, competing interactions in FCC alloys 8-95453
- Au-Fe, finite mag. clusters near percolation conc. 8-72371
- Au-Ni, heat capacity, 1.5 to 15K 8-95452
- AuFe, spin glass freezing above ferromag. percolation limit 8-52264
- Au_2MnAl , Heusler alloy, ferromag., NMR meas. 8-76320
- Au_2MnIn , Heusler alloy, ferromag., NMR meas. 8-76320
- $(Au,Pb)_{1-x}$, Fe_x , ferromag. and spin glass ordering 8-56335
- $Ba_2Fe_2BO_6$, (B=Re, Te, W, Mo), siegnette magnets with hexagonal barium titanate structure 8-76397
- Ba_2FeSbO_6 , siegnette magnets with hexagonal barium titanate structure 8-76397
- $BaVS_3$, exam. of ferromagnetic, antiferromagnetic behaviour, depending on stoichiometry 8-52233
- $Bi_2Bi_4Fe_2Ti_3O_{18}$, dielec. and magnetoelec. props. 8-95562
- $Cd_{1-x}Ag_xCr_2Se_4$, ferromag., magneto-resistance exam. (Russian) 8-84238
- $CdCr_2S_4$, ferromag. semicond. film, props. 8-76175
- $CdCr_2Se_4$, ferromag. semiconductor, light scatt. from magnons under strong fields 8-84554
- $CdCr_2Se_4$, mag. semicond., photoinduced binding of domain walls (Russian) 8-80174
- $CdCr_2Se_4$, Ag, ferromag. reson. field and linewidth anisotropy, Se vacancy effects 8-60338
- $CdCr_2Se_4$, In, ferromag. semicond., carrier mobility, electron-two magnon scatt. Hall effect 8-51992
- $CdCr_2Se_4(S_4)$, ESR line intensity near Curie point 8-64269
- $Cd_{1-x}Fe_xCr_2S_4$, Cu, effect of doping on elec. props. and Curie temp. 8-84214
- $Ce_{1-x}Gd_xRu_2$, superconductivity and ferromagnetism coexistence, 60 mK-4.2K, spin echo NMR 8-84349
- (Co, Cu, Fe)₂Ce, sintered permanent magnets, magnetic charact. 8-60608
- (Co,Cu,Fe)₂Ce, sintered, mag. props. 8-68302
- Co, atomic layers, Pauli paramagnetism to band ferromagnetism transition thickness depend. 8-72377
- Co, atomic magnetic moments comparison to values of ferromagnetic metal 8-52244
- Co based alloys, resistivity magnetoresistance, s,p impurities in ferromag. host 8-68008
- Co based amorphous alloy, mag. ordered, hyperfine field distrib., NMR meas. 8-68409
- Co, electrical resistivity, effect of domain wall orientation at 4K 8-91662
- Co, ferromagnetic, EMF generation by pulsed laser irradi. 8-68021
- Co, HCP to FCC transition, mag. domain nucleation 8-64218
- Co, internal fields, positive muon investigation 8-68438
- Co, modulus defect due to internal strain 8-76286
- Co, NMR spectra temp. depend. 8-52364
- Co surface, electron spin polarisation, electron capture spectroscopy 8-95645
- Co-Al, mag. struct. of Co rich intermetallic cpd., neutron scatt., cluster model 8-80130
- Co-Cd, dil. alloy, impurity hyperfine interactions 8-84416
- Co-Cr recording films, perpendicular mag. anisotropy, hysteresis loop, microstruct., TEM obs. 8-95491
- Co-Fe alloy, HCP and DHCP, magnetostriction consts. determ. 8-80184
- Co-Fe alloys, FCC structure, average mag. moment, conc. depend. 8-88099
- Co-Fe-Mn, dil. ferromag. alloy, mag. moment, saturation magnetisation meas. 8-64195
- Co-Fe-Nb-Mo, semihard magnetic alloy, magnetic props. 8-95469
- Co-Fe-Ti (12.6 wt.%), semihard permanent magnet, magnetic precipitation hardening 8-52830
- Co-H, solid soln., magnetisation curve 8-84452
- Co-Mn alloys, FCC, mag. moments of Mn atoms 8-76226
- Co-Ni, electrodeposition, mag. props. (French) 8-64488
- Co-P, amorphous alloy, domain struct., effect of annealing 8-60304
- Co-P, cryst. and amorphous mag. films, ferromag. resonance line width (Russian) 8-88192
- Co-P, electrodeposited amorphous alloy, mag. permeability 8-52310
- Co-P electroless film on Al base disc substrate, microstruct. rel. to mag. props. 8-68304
- Co-P film, amorphous, spin wave dispersion law, spin wave reson. obs. (Russian) 8-88196
- Co-Pt, struct. and mag. props. rel. to degree of order 8-72368
- $Co_{1-x}Au_x$, amorphous, elec. resist., temp. depend., spin wave contrib. and resist. minimum 8-51961
- $Co_2Ga_{2-x}Cu_x$, mag. and struct. phases from magnetisation, neutron, X-ray diff. techniques 8-52253
- $Co_2Ga_{2-x}Ni_x$, mag. and struct. phases from magnetisation, neutron, X-ray diff. techniques 8-52253
- $Co_2HfSn-Fe$, dil., Heusler alloy, Fe hyperfine fields, Mossbauer obs. 8-68424
- Co_4P , amorphous, mag. excitations and static struct., neutron scatt. obs. 8-68204
- $Co_{74}Si_{16}B_{16}$, amorphous toroidal core, switching characts. and domain structs. 8-95477
- $Co_2TiSn-Fe$, dil., Heusler alloy, Fe hyperfine fields, Mossbauer obs. 8-68424
- CoU_2S_5 , mag. struct., exchange energy, magnetisation and neutron diffraction. expts. 8-68170
- $Co_2ZrSn-Fe$, dil., Heusler alloy, Fe hyperfine fields, Mossbauer obs. 8-68424
- CrB₃, crit. spin-relax. in hard mag. direction 8-72390
- CrI₃, ferromagnetic, origin of magnetic hyperfine field transferred at iodine 8-92000
- CrO₂, single mag. particle, remanent coercive force and remanent loop meas. 8-95480
- CrTe, effect of high pressures on magnetic properties 8-52238

ferromagnetic properties of substances continued

- $CsNiF_3$, ^{19}F NMR, spin fluctuation suppression 8-91970
- $CsNiF_3$, NMR and relax. exam. 8-52371
- Cu-Fe, composite, fibre and layer structs., anomalous props. caused by internal phase boundaries 8-72754
- $CuCl_2 \cdot TMSO$, ferromag. spin $1/2$ linear chain, mag. susceptibility 8-68180
- $CuCr_2Se_4$, experimental obs. 8-76227
- $Cu_2Cr_2Se_4 \cdot Br_x$, ferromag. magneto-resistance exam. (Russian) 8-84238
- Cu_2MnAl , ferromag. Heusler alloy, polarised neutron study of mag. moment density 8-84391
- Dy, field induced transitions of helical state 8-72349
- Dy film, magnetoelastic waves, GHz, excitation, field depend. 8-72378
- Dy, internal fields, positive muon investigation 8-68438
- Dy, longitudinal galvanomag. effect in single crystals. (Russian) 8-56132
- Dy, spin wave exam. 8-56306
- Dy-Fe, amorphous, random anisotropy effects 8-68223
- $DyCo_2$, field induced vol. magnetostriction 8-91920
- DyF_3 , transferred hyperfine interaction, NMR study 8-68393
- $DyFe_2$, high field magnetostriction and magnetisation 8-84471
- $DyFe_2$, magnetisation and magnetic anisotropy 8-91862
- $Dy,Tb_{1-x}Fe_2$, and $Ho,Tb,Dy_{1-x-y}Fe_2$, high magnetostriction cpd., mag. anisotropy origins 8-68217
- Er, spin wave exam. 8-56306
- $ErCo_2$, field induced vol. magnetostriction 8-91920
- $(ErCo_2)_x(ErAl_2)_{1-x}$, mag. and struct. investigations of intermetallic systems 8-95440
- $ErFe_2$, Laves phase, cryst. field effects on spin wave dispersion relations 8-84408
- $Eu_{0.5}Ba_{0.5}TiO_3$, ferromag., ferroelec., ceramic, Curie temps. determ. 8-68230
- $EuNi_2Cu_{3-x}$, mixed valency of Eu, Mossbauer expts. 8-52407
- $EuNi_2Zn_{3-x}$, mixed valency of Eu, Mossbauer expts. 8-52407
- EuO, dynamic dipolar cross over 8-76339
- EuO, ferromag. semicond., electronic spectrum, influence of finite carrier conc. 8-76220
- EuO, ferromagnetic, mag. field effect on optical absorpt. edge, piezotransmission spectra 8-95578
- EuO, mag. struct. and transition temp., indirect exchange 8-91860
- EuO, quadrupole coupling due to lattice imperfections 8-76347
- EuO, spin wave damping, theory compared with expt. 8-52237
- EuO, transport properties at ferromag. reson. 8-68387
- EuO:Gd, electron mobility below Curie temp. 8-91696
- EuO:La, phototreshold reduction by mag. induced space charge layer 8-72692
- $EuO_{1-x}N_x$, ferromag. semicond., elec. and mag. props. (French) 8-79993
- EuS, conduction band density of states, redistrib. near ferromag. saturation 8-67939
- EuS, mag. struct. and transition temp., indirect exchange 8-91860
- EuS, pure and Gd doped, electronic struct., mag. exchange and elec. transport props. 8-87974
- EuS, spin relax. in crit. region 8-52270
- EuS, spin relaxation crit. behaviour 8-76251
- EuSe, mag. struct. and transition temp., indirect exchange 8-91860
- $EuSm_2S_4$, mag. props. 8-68237
- $Eu_{1-x}Yb_xO$, solid soln., ferromag. semicond., increase of exchange interaction 8-88109
- $Eu_{1-x}Yb_xS$, solid soln., ferromag. semicond., increase of exchange interaction 8-88109
- $(Fe,Mo)_{80}B_{20}$, glassy alloy, Curie temp. and crystn. temp., Mo additions effect, Mossbauer spectra 8-68428
- Fe alloys, amorphous, room-temp. saturation induction 8-95476
- Fe alloys, anisotropic precipitation struct. in external mag. field (German) 8-72785
- Fe alloys, ferromagnetic, EMF generation by pulsed laser irradi. 8-68021
- Fe alloys, temperature-time instability of initial susceptibility meas., using bridge instrument with electronic demagnetiser (Slovak) 8-57989
- Fe, atomic layers, Pauli paramagnetism to band ferromagnetism transition thickness depend. 8-72377
- Fe, atomic magnetic moments comparison to values of ferromagnetic metal 8-52244
- Fe, atomized powder compacts for mag. cores, mag. props. (Japanese) 8-72751
- Fe based alloys, amorphous toroidal core, switching characts. and domain structs. 8-95477
- Fe based alloys, resistivity magnetoresistance, s,p impurities in ferromag. host 8-68008
- Fe based amorphous alloy, mag. ordered, hyperfine field distrib., NMR meas. 8-68409
- Fe based ternary alloys, Coulomb and exchange scatt. amplitudes, spin dependent residual resistivities 8-64033
- Fe, cast, grey, pearlitic relationship of magnetic props. to condition of C 8-56353
- Fe, cluster method, environmental effects 8-95405
- Fe, cold work stored energy effects on mag. moment vs. temp. curve 8-95419
- Fe, compression deformed single cryst., induced uniaxial anisotropy 8-52336
- Fe, de Haas-van Alphen effect and exchange splitting, effect of pressure (Russian) 8-95252
- Fe, deformed, dislocation structure determ. from magnetic props. 8-55874
- Fe, elastoresistivity effect, meas. of resistance at 4.2K and 300K, using mag. field method 8-72132
- Fe film, amorphous and polycrystalline, Hall effect, resistivity and mag. moment 8-91786
- Fe film, effect of tensile stress on mag. domain struct. 8-68332
- Fe film, Hall resist., effect of N impurity codeposition 8-64146
- Fe film, nuclear magnetisation relax. at 77 to 500K 8-60352
- Fe film, single crystal, less than 1000 Å thick, inclined 90° walls 8-72384
- Fe, film mag. structures and stresses, ferromagnetic resonance 8-72375
- Fe, first order shock induced mag. transitions characts. and discrimination from TRM 8-64205

ferromagnetic properties of substances continued

- Fe, hyperfine fields at impurities in ferromag. metal 8-52244
 Fe, internal fields, positive muon investigation 8-68438
 Fe, itinerant model of spin polarised field emission 8-95685
 Fe, lattice vibrations, temp. depend. 8-95124
 Fe, magnetic aftereffect of interstitial O 8-91903
 Fe, Mossbauer energy shift near Curie temp. 8-52388
 Fe, μ^+ hyperfine field and relaxation, temp. depend. 8-95538
 Fe particles, lunar matter, FMR study, effective linewidth method 8-95523
 Fe, photoelectron spin polarisation and itinerant magnetism 8-68602
 Fe, plastically deformed, dislocation arrangement exam. by ferromag. techniques 8-63774
 Fe, rotational hysteresis 8-91889
 Fe sheet, surface magnetisation, ferromag. nucl. reson. meas. 8-60348
 Fe, spin polarisation in electron field emission, surface magnetism 8-68607
 Fe, thermal acoustic magnons, Brillouin scatt. meas. 8-95424
 Fe, transient mag. field, vel. and atomic number depend. 8-91999
 Fe, UPS, density of states determ. 8-52623
 Fe, whisker, mag. crit. phenomena, size effects 8-68258
 Fe:Xe, isotope ion implantation control (*Flemish*) 8-79623
 Fe-Al (16 wt.%), improvement of certain props. discussion (*Chinese*) 8-84826
 Fe-Al-Ni-Co-Cu alloys, Ti alloying and deoxidising addition (*Russian*) 8-80181
 Fe-B, amorphous metallic glasses, high-temp. mag. anal. 8-91258
 Fe-B alloys, rapidly quenched metastable solid solns., prop. and mag. props. 8-92218
 Fe-B metallic glass, role of Fe₃B in crystn., mag. and Mossbauer expts. 8-94997
 Fe-Co, BCC, ferromag., spin wave stiffness constant 8-91851
 Fe-Co, partially ordered, elec. cond. 8-91663
 Fe-Co alloy, diffusion of H₂, diffusion coefficient and permeability (*Russian*) 8-79819
 Fe-Co alloy, local environment effect on atomic moments, itinerant model 8-68188
 Fe-Co alloy particles for mag. tapes, mag. props. 8-95479
 Fe-Co-Cd(Sn), mag. hyperfine fields at Fe, Cd and Sn sites, Mossbauer and TDPAC meas. 8-60363
 Fe-Cr, BCC, ferromag., spin wave stiffness constant 8-91851
 Fe-Cr, Invar alloy, explanation of phys. anomalies (*Russian*) 8-88112
 Fe-Cr alloy, mag. moments and Fe site hyperfine fields, magnetis. obs. 8-76276
 Fe-Cr-Al alloys, low temp. sp. ht., resistivity and coercive force 8-63866
 Fe-Cr-Ce, decomposition of solid soln. in mag. field, neutron and X-ray diff. study (*Russian*) 8-68694
 Fe-Cr-Co (31 wt.%, 23 wt.%), microstruct. and mag. props., ageing and thermomag. treatment effects 8-76769
 Fe-Cr-Co-Al (27.5, 17.5, 0.5) alloy, magnetic props. and microstructure 8-72367
 Fe-Cr-Co-Al (27.5, 17.5, 0.5 wt.%) alloy, induced anisotropy 8-76239
 Fe-Cr-Co-Si alloy, interaction domains after heat treatment in mag. fields (*Russian*) 8-68286
 Fe-Cr-Co-V alloy, microstruct. and mag. props. 8-68221
 Fe-Cr-(Co), decomposition of solid soln. in mag. field, neutron and X-ray diff. study (*Russian*) 8-68694
 Fe-Cu metastable dil. alloy film, hyperfine interactions 8-52398
 Fe-Mn, BCC, ferromag., spin wave stiffness constant 8-91851
 Fe-Mn alloy, magnetovolumetric anomaly (*Russian*) 8-64248
 Fe-Ni, (35 wt.%), transport props. and Invar features (*Russian*) 8-51973
 Fe-Ni, BCC, ferromag., spin wave stiffness constant 8-91851
 Fe-Ni, dil., point defect relax. after low temp. neutron irradi. 8-52316
 Fe-Ni, electrodeposition, mag. props. (*French*) 8-64488
 Fe-Ni, FCC, anomalous props. at high temp. and new phase (*Japanese*) 8-80520
 Fe-Ni, Invar alloy, explanation of phys. anomalies (*Russian*) 8-88112
 Fe-Ni, low frequency power losses 8-95466
 Fe-Ni alloy, cold work stored energy effect on mag. moment vs. temp. curve 8-95419
 Fe-Ni alloy, surface decarburisation rate in dry H₂, soft mag. material manufacture 8-60882
 Fe-Ni alloy toroidal core, magnetic noise (*Russian*) 8-60308
 Fe-Ni alloys, anomalous thermal expansion, Gruneisen eqn. 8-83980
 Fe-Ni/pure Fe exchange coupled films, mag. reversals, hard layer thickness effects (*Russian*) 8-56359
 Fe-Ni-Al alloys, phase diagram, miscibility gap, mag. props. 8-92237
 Fe-Ni-Mn-H, ferromag., magnetisation curves 8-88144
 Fe-Pd, FCC, ferromag., spin wave stiffness constant 8-91851
 Fe-Pt, Invar type, strong ferromagnetism, mag. props. 8-64197
 Fe-Si, grain oriented, core losses (*Japanese*) 8-60303
 Fe-Si, grain oriented, effect of tensile stress on domain struct. 8-95462
 Fe-Si, low frequency power losses 8-95466
 Fe-Si, stress and plastic deform. effect on Barkhausen effect, instrumentation 8-52313
 Fe-Si, thermally activated motion of 180° Bloch wall 8-95457
 Fe-Si (3 wt.%), domain wall spacing and losses, orientation depend. 8-56343
 Fe-Si (3 wt.%), effect of heating rate during primary recrystn. on props. after secondary recrystn. 8-84837
 Fe-Si (3 wt.%), Goss oriented, stress effects 8-91916
 Fe-Si (3 wt.%), grain oriented, lowest core loss 8-91887
 Fe-Si (3 wt.%), grain orientated, negative magnetostriction, theory 8-91917
 Fe-Si (3 wt.%), grain oriented, domain wall variation throughout magnetisation cycle 8-95459
 Fe-Si (3 wt.%), grain oriented, power loss depend. on domain wall bowing 8-95460
 Fe-Si (3 wt.%), orientation development during secondary recrystallisation, primary matrix effect, magnetic props. (*Czech*) 8-60679
 Fe-Si (3 wt.%), rotational power losses, freq. depend. 8-91888
 Fe-Si (3 wt.%), total losses under tensile stress, rel. to orientation near (110)[001] 8-76272
 Fe-Si (3 wt.%), transformer laminations, processing and props. 8-52325
 Fe-Si (3 wt.%) steel, high permeability, grain oriented 8-91886
 Fe-Si (3.5 wt.%), magnetisation reversal and domain walls 8-84451

ferromagnetic properties of substances continued

- Fe-Si (3.5 wt.%) picture frame cryst., domain wall bowing dynamic neutron depolarisation 8-56344
 Fe-Si (3.5 wt.%) picture frame, domain wall bowing, time-depend. neutron depolarisation 8-95458
 Fe-Si (6.5 wt.%), ductility and mag. props., Ni and Mn addition effects 8-76704
 Fe-Si-Al (6.4 wt.%), Sendust alloy, effect of Ni content on mag. props. 8-72897
 Fe-Si-B magnetic powder, amorphous, prep. by atomisation technique 8-92213
 Fe-Si-Mn, effect of Mn addition on mag. props. and elec. resist. 8-91890
 Fe-Si (6.5 wt.%) steel, core mat. development (*Korean*) 8-60852
 Fe-V alloy, local environment effect on atomic moments, itinerant model 8-68188
 Fe-W-Cr-Mo-Co with austenitic phase, magnetic and mech. props., cold working and ageing effects (*Japanese*) 8-60678
 Fe₃Al, magnetic form factor 8-76222
 Fe₃Al, partly disordered B2 struct., spin wave dispersion relation 8-64201
 Fe_{1-x}Al_x, amorphous, elec. resist., temp. depend., spin wave contrib. and resist. minimum 8-51961
 Fe₂Al_{1-x}, amorphous ferromagnetic, resistivity, anisotropic, field dependence 8-87960
 Fe_{100-x}B_x, mag. and struct. props., comp. depend. 8-60314
 Fe_{100-x}B_x, metallic glass, magnetisation meas. 8-80134
 Fe₈₀B₂₀, evaluation of complex Mossbauer spectra 8-60370
 Fe₈₀B₂₀, ferromagnetic metallic glasses, Brillouin scattering 8-92085
 Fe₈₀B₂₀, metallic glass, Mossbauer spectroscopy 8-60365
 Fe₈₀B₂₀ Metglass, Mossbauer spectra line broadening 8-52400
 Fe₈₀B₂₀, sputter deposited amorphous, low field mag. props. 8-68335
 Fe₂C_{1-x}, amorphous sputtered film, mag. props. 8-68311
 Fe_{0.65}Co_{0.35}B, crystalline disordered, evaluation of complex Mossbauer spectra 8-60370
 (Fe_{0.9}Co_{0.1})₇₅Si₂₅, (Fe_{1-x}Co_x)₇₅Si₂₅ amorphous ribbons, magnetomech. coupling and saturation magnetostriction 8-68353
 (Fe_{0.9}Co_{0.1})_{100-(y+z)}Si_yB_z amorphous ribbon, mag. moment and Curie temp., comp. depend. 8-95421
 Fe₂Mn_{1-x}Pt_x, ferro-antiferromag. transform. at 4.2K (*Russian*) 8-88117
 Fe_{3-x}Mn_xSi, evidence for the ang. depend. of the hyperfine interactions 8-76241
 FeNi-Cu, composite fibre and layer structs., anomalous props. caused by internal phase boundaries 8-72754
 Fe_{0.65}Ni_{0.35}, UPS, density of states determ. 8-52623
 Fe₆₅Ni₃₅, ferromagnetic Invar alloy, lattice vibrations 8-91403
 Fe₆₅Ni₃₅, quasi-localised spin system, neutron scatt. 8-68194
 Fe₆₅Ni₃₅, electron irradiated, small angle neutron scatt. 8-52218
 Fe₇₀Ni₃₀, short range order, diffuse elastic neutron scatt. study 8-52219
 Fe₇₀Ni₃₀, small angle neutron scatt., magnetisation inhomogeneity 8-52218
 Fe₆₅(Ni_{1-x}Cr_x)₃₅, remanent magnetisation, temp. depend., anomalies near Curie temp. (*Russian*) 8-60310
 Fe₃₂Ni₃₆Cr₁₄P₁₂B₆, Metglas 2826A, Hall resistivity, effect of thermal cycling and annealing 8-56125
 Fe₄₀Ni₃₀Mo₁₀B₁₈ glassy alloy, high permeability, low field mag. characts. 8-68301
 (Fe_{1-x}Ni_x)₈₀P₁₀B₁₀, amorphous microwires, magnetisation reversal and anisotropy 8-91885
 Fe₄₀Ni₄₀P₁₄B₆, (Metglas 2826), ferromag. Curie temp. determ. 8-64206
 Fe₄₀Ni₄₀P₁₄B₆ amorphous ribbon, mag. anisotropy distrib. near surface 8-95430
 Fe₄₀Ni₄₀P₁₄B₆, ferromagnetic metallic glasses, Brillouin scattering 8-92085
 Fe₄₀Ni₄₀P₁₄B₆, Metglas 2826, amorphous ribbon core, appl. in force transducer 8-93669
 Fe_{80-x}P₁₄B₆ metallic glasses, low temp. resistivities 8-91659
 (Fe_{0.5}Ni_{0.5})₇₅P₁₅B₁₀Al₃ glass, struct. relax. as origin of Curie temp. ageing 8-84418
 (Fe_{1-x}Ni_x)₈₀P₁₀B₁₀Al₃, amorphous alloy, low temp. elec. resist. saturation 8-68005
 Fe₂₉Ni₄₉P₁₄B₆Si₂, Metglas 2826B, Hall, elec. resist., magnetisation and heat capacity meas. 8-68019
 α -Fe₂O₃, analysis of car exhaust by Mossbauer spectroscopy 8-92963
 γ -Fe₂O₃, elongated particles, mag. struct. 8-88096
 Fe₇₅P_{0.15}C_{0.10}, amorphous, mag. excitations and static struct., neutron scatt. obs. 8-68204
 Fe₇₅P₁₅C₁₀ amorphous foil, ferromag. domain orientation, Mossbauer exam. 8-52402
 FePd epitaxial film, vacuum-deposited, for thermomag. recording, mag. and magneto-optical props. (*Russian*) 8-60319
 Fe₃Pd₄₆P₂₀, amorphous, sp. ht. and resist. near ferromag. phase transition 8-56333
 FePt epitaxial film, vacuum-deposited, for thermomag. recording, mag. and magneto-optical props. (*Russian*) 8-60319
 Fe₃Pt, Invar alloy, theory of elastic anomalies 8-95505
 Fe₃Pt, quasi-localised spin system, neutron scatt. 8-68194
 Fe₇₅Pt₂₅, ferromagnetic Invar alloy, lattice vibrations 8-91403
 Fe₄₈Rh₅₂, hyperfine mag. field at ⁵⁷Fe and ¹¹⁹Sn nuclei, press. depend. (*Russian*) 8-80266
 Fe₃Si-based alloy, dil., cond. electron polarisation and moment perturbations 8-68224
 Fe_{3+2x}Si_{1-2x}, electron transport 8-91669
 Fe₃Si_{1-x}, amorphous, struct. and mag. props., giant moment form. at mag. ordering 8-68192
 Fe₃SiB₂, Mossbauer spectra, 140-784K, spin rotation 8-52409
 Fe₇₅(Si_{0.5}B_{0.5})₂₅ film, amorphous, sputtered, thermal stability 8-76280
 Fe₂Sn_{1-x}, amorphous, mag. behaviour 8-95478
 Fe₂Sn_{1-x} amorphous alloy films, magnetisation meas. and Mossbauer spectra 8-95489
 Fe_{2.4-x}Ti_{0.4}Al_xO₄, Fe_{2.4-x}Ti_{0.4}Al_xO₄, titanomagnetite, monodomain, mag. props. 8-56346
 Fe₂TiO₄-Fe₂O₄, titanomagnetite, prepared at different oxidation conditions, hysteresis props. 8-56352
 Fe₂TiO₆O₄, titanomagnetite, single-crystal, mag. props. of multidomain TRM 8-56345
 FeU₂S₃, mag. struct., exchange energy, magnetisation and neutron diff. expts. 8-68170

ferromagnetic properties of substances continued

- Gd, high quality single cryst., mag. anisotropy 8-84413
 Gd, internal fields, positive muon investigation 8-68438
 Gd, longitudinal galvanomag. effect in single crystals. (Russian) 8-56132
 Gd, mag. domain struct., 77K 8-84447
 Gd, mag. domains, Lorentz microscopy obs. 8-84448
 Gd, self consistent relativistic ferromag. band struct. 8-91609
 Gd, spin wave exam. 8-56306
 Gd, spin wave temp. depend., exchange coupling role 8-68199
 Gd, working medium in mag. Stirling cycle wheel, refrigerator and heat engine modes of operation 8-57964
 Gd-Ag, vap. quenched alloys, struct. and mag. props. 8-84461
 Gd-Ag(Cu) alloy film, amorphous, struct. and mag. props. 8-52318
 Gd-Al(Cu), amorphous alloy films, mag. phase diagram, spin glass and ferromag. regions 8-68234
 Gd-Al(Cu)(Ga)(Rh)(Pd), amorphous alloys, mag. coupling of rare earth moments 8-88108
 Gd-Dy alloy, longitudinal galvanomag. effect in single crystals. (Russian) 8-56132
 Gd-Ir, dil., hyperfine interaction of ^{193}Ir , Mossbauer effect meas. 8-52413
 Gd-Mo-Mo amorphous film, domain drag effect obs. 8-91911
 Gd-Tm alloy, mag. anisotropy, from magnetisation meas. at 4.2K 8-68216
 Gd_{0.9}La_{0.1}Al₂, ferromag., NMR of ^{139}La 8-52377
 Gd_{1-x}La_xZn, magnetisation and paramag. suscept. 8-88101
 GdMg₃, mag. props., Mg conc. depend. 8-84392
 GdMn₂-GdAl₂ intermetallics, mag. props., 80-650K 8-60282
 (GdMn₂)_x(GdAl₂)_{1-x}, mag. and struct. investigations of intermetallic systems 8-95440
 (Gd_{0.5}Y_{0.5})Ni, FeB struct., cryst. field effects on mag. struct. 8-52226
 Ge-Se-Fe films, metallic and semicond., amorphous, mag. and elec. props. 8-52319
 GeTe:Mn, thermoelec. power, 2.5-25K, magnon drag effect 8-56169
³He, vacancy relaxational phenomena (Russian) 8-95203
³He with C particles, pulsed NMR, mag. susceptibility surface induced ferromagnetism, antiferromagnetic exchange interaction 8-79844
 HgCr₂Se₄, ESR line intensity near Curie point 8-64269
 HgCr₂Se₄, ferromag. semicond., Raman spectra 8-52496
 HgCr₂Se₄, ferromag. semicond., transport props. 8-68039
 Hg_xZn_{1-x}Cr₂Se₄, absorption spectra near the absorption edge 8-80340
 Ho-Sn, dil. alloy, hyperfine interaction of ^{119}Sn , Mossbauer meas. 8-91998
 HoAl₂, heat capacity, 1.5-12K, magnetocryst. anisotropy effects 8-68236
 HoCo₃, field induced vol. magnetostriction 8-91920
 HoMo₅S₈, reentrant supercond., direct. obs. of long range ferromag. order 8-76190
 Ho_{0.7}Tb_{0.3}Fe₂, and Ho_xTb_{1-x}Dy_{1-x}Fe₂, high magnetostriction cpd., mag. anisotropy origins 8-68217
 Ho_{0.7}Tb_{0.3}Fe₂, Laves phase, mag. anisotropy meas., cubic harmonic anal. 8-84410
 Ho_{0.7}Tb_{0.3}Fe₂, single cryst., spin orientations 8-84425
 Ho_xTb_{1-x}Fe₂, single crystals, continuous spin orientations, magnetisation easy direction 8-84453
 K₂CuF₄, ferromag., orbital ordering, review (Japanese) 8-76224
 K₂CuF₄, spin wave meas. in low energy range, inelastic neutron scatt. 8-88105
 K₂Cu_{1-x}Ni_xF₄, two-dimens., ferromag., spin wave excitations 8-80140
 KFeS₂, magnetic reson. meas. 8-95524
 KTB₃F₁₀, mag., optical, magneto-optical behaviour 8-68484
 La-Fe, amorphous alloy film, spin reson. meas. 8-68389
 (La_{1-x}Gd_x)Al₂, dil., reverse resistance anomaly 8-76054
 LiTbF₄, Faraday rotation, optical absorpt. spectra and refr. index 8-72542
 LiTbF₄, mag., optical, magneto-optical behaviour 8-68484
 Lu-Fe, amorphous alloy film, spin reson. meas. 8-68389
 Lu₂V₂O₇, pyrochlore struct., mag. props. 8-72335
 Mn-Al permanent magnets, defect structure, mag. props. TEM obs. 8-91902
 Mn-Bi eutectic alloy, mag. anisotropy 8-68220
 Mn-H(D), ferromag., thermal, struct. mag. props. 8-88145
 Mn₅₅Al₄₅ alloy, permanent mag. props., depend. on particle size 8-91899
 MnAu, domain struct. exam. by powder method (German) 8-91883
 MnBi film, magnetic reversal mechanism, hysteresis loops for polycryst. and single cryst. specimens (Russian) 8-60318
 MnBi films, stability of magneto-optical props. on pulse heating (Russian) 8-88282
 Mn_{1-x}Fe_xAs, high-pressure phase, magnetic properties 8-52247
 MnPt, disordered film produced by RF sputtering, ferromag. behaviour 8-68310
 MnSb, electronic state, neutron diffr. study 8-87906
 Mn_{1+x}Sb_{1-x}Sn_x, magnetisation and Curie temp., prep. and comp. depends. 8-64200
 MnSi, μ^+ Knight shift, temp. depend. 8-80270
 Mo ternary chalcogenide, MMo₂X₈ (M=metal, X=chalcogen) Chevrel phase, supercond. and normal state props. 8-56267
 Nb₅₀Ni_{50-x}Fe_x, amorphous alloy, mag. interactions 8-95432
 NdCo₅, single ion anisotropy consts. temp. depend. effect of spatial variation of mag. moment 8-91864
 Ni (110) surface, positive spin polarisation in field emission and demagnetisation by H₂ adsorption 8-52646
 Ni (111), band struct. and temp.-depend. mag. exchange splitting, angle resolved photoemission obs. 8-60546
 Ni, amorphous film, getter sputtered at 25K, resistivity, Curie temp. 8-52673
 Ni, anomalous resistivity near Curie temp., band theoretical calc. 8-56127
 Ni, atomic layers, Pauli paramagnetism to band ferromagnetism transition thickness depend. 8-72377
 Ni, atomic magnetic moments comparison to values of ferromagnetic metal 8-52244
 Ni based alloys, resistivity magnetoresistance, s,p impurities in ferromag. host 8-68008
 Ni based ternary alloys, Coulomb and exchange scatt. amplitudes, spin dependent residual resistivities 8-64033
 Ni, chemisorption of H, surface magnetism 8-95510
 Ni, electrodeposited film, saturation magnetisation and perpendicular anisotropy meas. 8-76277

ferromagnetic properties of substances continued

- Ni, ferromagnetic, EMF generation by pulsed laser irradi. 8-68021
 Ni, ferromagnetic, electron-magnon interactions 8-68205
 Ni film, mag. structures and stresses, ferromag. resonance 8-72375
 Ni film, strained and strain-free, ferromag. reson. meas. 8-95525
 Ni foil, saturation magnetisation, during cathodic charging with H 8-71860
 Ni, internal fields, positive muon investigation 8-68438
 Ni, magnetocryst. anisotropy consts., determ. from magnetisation perpendicular to applied field 8-68219
 Ni, magnetoelastic effects, ΔE -effect and macroeddy current damping, internal friction meas. 8-64253
 Ni, modulus defect due to internal strain 8-76286
 Ni, photoelectric effect in paramag. and ferromag. states, Auger spectra 8-95649
 Ni, pure and doped, mech., mag. relax. meas. dumb-bell self-interstitial reorientation (German) 8-52879
 Ni, resistivity, thermal and elec., spin disorder scatt. anal. 8-76063
 Ni, single cryst., domain patterns in cyclically deform. cryst., behaviour during annealing 8-71740
 Ni, specific heat, temp. depend. (Russian) 8-56341
 Ni, spin polarisation in electron field emission, surface magnetism 8-68607
 Ni surface, electron spin polarisation, electron capture spectroscopy 8-95645
 Ni, surface decarburisation rate in dry H₂, soft mag. material manufacture 8-60882
 Ni, thermal acoustic magnons, Brillouin scatt. meas. 8-95424
 Ni, UPS, density of states determ. 8-52623
 Ni-alloys, spin polarised tunnelling 8-95494
 Ni-B alloy film, magnetisation-temp. characts., order-disorder transform. (Japanese) 8-76279
 Ni-Cd, dil., ferromagnetic dynamic crit. exponent, hyperfine interaction vs. neutron scatt. expts. 8-84437
 Ni-Co, ferromag. films, magnetoresistance effect, crystal struct. 8-68017
 Ni-Co, ferromagnetic resonance, surface anisotropy 8-95526
 Ni-Co-Mn, dil. ferromag. alloy, mag. moment, saturation magnetisation meas. 8-64195
 Ni-Cu, low field magnetisation meas., mag. props. comp. depend. 8-91879
 Ni-Fe, epitaxial thin film, mag. structures and stresses, ferromag. resonance 8-72375
 Ni-Fe, film, anomalous Hall and Nernst-Ettingshausen effect, contribution of phonon and impurity scatt. (Russian) 8-64145
 Ni-Fe, film, domain struct., effect of biaxial stresses 8-88153
 Ni-Fe alloy, extraordinary viscous magnetic wall motion 8-84465
 Ni-Fe film, effect of tensile stress on mag. domain struct. 8-68332
 Ni-Fe films, US generation by ferromag. reson. 8-88155
 Ni-Fe solid soln., precip. hardened, paramag.-ferromag. transition on ageing 8-52255
 Ni-Fe-Co film, magnetoelastic vibr. generation during high freq. mag. reversals (Russian) 8-60320
 Ni-Fe-Mn, ferromag. reson. linewidth and saturation magnetisation 8-72418
 Ni-Fe-Nb alloys, mag. permeability and struct. (Chinese) 8-84450
 Ni-Fe-Nb-Al alloys, mag. permeability and struct. (Chinese) 8-84450
 Ni-Mn alloy, disordered, exchange-anisotropy field, magnetisation curves 8-72365
 Ni-Mn alloy, disordered, mag. struct., high field twist deform. 8-68166
 Ni-P electrodeposit, magnetisation coercivity and magnetostriction 8-68338
 Ni-Pd, FCC disordered polycryst. alloy, magnetisation, band ferromag. 8-80180
 Ni-Pd alloy, disordered, local environment effects, neutron scatt. expts. 8-68172
 Ni-Pd-P, Ni-Pt-P, amorphous and electronic structs., NMR Knight shifts and linewidths meas. 8-68400
 Ni-Rh alloy, disordered, local environment effects, neutron scatt. expts. 8-68172
 Ni_{1-x}Au_x, amorphous, elec. resist., temp. depend., spin wave contrib. and resist. minimum 8-51961
 Ni₃(Fe,M), M=Cu, Cr, Mo, W, kinetic phenomena rel. to ordering and electron struct. (Russian) 8-76043
 NiFe soft magnetic alloys, magnetic props., effect of annealing and fabrication (German) 8-53004
 Ni₂Mn_{0.9}Fe_{0.1}Sn, Fe site hyperfine field and mag. moment, Mossbauer effect meas. 8-76365
 Ni₄Pt_{1-x} disordered alloy, itinerant system, induced magnetism 8-52191
 Ni_{0.97}Ru_{0.03}, mag. form factor and moment distrib., obs. using polarised neutrons 8-68171
 NiTiF₆·6H₂O, mag. and struct. transitions 8-68257
 NiZrF₆·6H₂O, uniaxial ferromagnetism 8-80143
 O single layer on Au, ferromag. props., thermomag. effect (Russian) 8-64256
 Pd based alloys, extraordinary Hall effect 8-76053
 Pd-Fe, Mossbauer spectra, scatt. and transmission geometries, differences in crit. behaviour near T_c 8-76367
 Pd-Fe alloy, IR absorpt. characts., 0.9 to 19 μm , mag. order effect 8-84577
 Pd-Fe(Co)(Ni) dilute alloys, ferromag., magnetoresist. 8-91665
 Pd-Ni, local susceptibilities, ^{61}Ni Mossbauer spectroscopy 8-95536
 Pd-Ni alloy, dil., ferromagnetism, local moments, susceptibility, magnetisation and Curie temp. (Russian) 8-88115
 PrCo₅, heat treated, coercive force exam. 8-68298
 Pr₃Se₄, induced ferromagnet, effect of press. on magnetisation 8-95422
 Pr₂Sm_{1-x}Co₂, magnetisation and magnetocryst. anisotropy 8-68215
 Pr₂Ti, induced ferromag., mag. props. under hydrostatic press. 8-56315
 Pt-Co alloys, crit. neutron scatt. in crit. conc. region for onset of ferromagnetism 8-72347
 Pt-Fe, competing interactions in FCC alloys 8-95453
 Rh-Fe, competing interactions in FCC alloys 8-95453
 Rh₂CoSn, crit. exponent of ^{119}Sn hyperfine field, Mossbauer obs. 8-92008
 Rh₂CoSn, metallic ferromagnet, hyperfine mag. field temp. depend. (Russian) 8-80265

ferromagnetic properties of substances continued

- Rh₂FeSn, metallic ferromagnet, hyperfine mag. field temp. depend. (*Russian*) 8-80265
 Sm-Co, alloy powders and sintered magnets, effect of chem. treatment on mag. props. 8-60311
 Sm-Co, decomp. kinetics when aged, X-ray mag. props. and metallography study (*Russian*) 8-56644
 Sm-Pr-Co, added Fe₂Sn, permanent magnets, demagnetisation curves, X-ray obs. 8-91900
 SmCo₅, heat treated, coercive force exam. 8-68298
 SmCo₅ hydride films, mag. props. 8-68306
 SmCo₅, intrinsic coercivity losses, temp. depend. 8-95468
 SmCo₅ isotropic plasma sprayed magnet, high coercivity 8-68295
 SmCo₅ sintered alloy magnetic properties (*Russian*) 8-72369
 SmCo₅, substituted alloy, low reversible temp. coeff. 8-68178
 SmCo₅, mag. and struct. investigations of intermetallic systems 8-95440
 Sm₂(Co_{1-x}Al_x)₁₇ (*Russian*) 8-64202
 Sm(Co_{1-x}Cu_x)₈ alloys, coercive fields, domain wall energies, mag. and metallographic exam. 8-91897
 SmCo_{3.5}Cu_{1.5}, time dependent magnetisation 8-80176
 SmCo_{5-y}Cu_y, giant intrinsic magnetic hardness, high field meas. 8-68289
 Sm₂(Co_{1-x}Fe_x)₁₇, anisotropy consts., conc. and temp. depend. (*Russian*) 8-64202
 Sm(CoFeCuMn)₇, coercive force and anisotropy temp. depend. 8-68297
 SmCo₂Ni₃-Y(Pr)(Gd)(Tb)(Er), giant intrinsic magnetic hardness 8-56347
 SmCo_{5-x}Ni_x, giant intrinsic magnetic hardness, high field meas. 8-68289
 SmCo_{5-x}Ni_x, giant intrinsic magnetic hardness analysis 8-88146
 SmCo_{5-x}Ni_x, exchange fluctuations and giant intrinsic mag. hardness 8-56310
 Sm_{1-x}Nd_xCo₅ alloys, magnetisation, magnetocrystalline anisotropy, 4.2 to 280K 8-91863
 SmNi_{1-x}Cu_x, giant intrinsic mag. hardness due to randomised cryst. field interactions 8-68208
 Tb, conduction electron polarisation and high field magnetisation 8-72332
 Tb film, GHz magnetoelastic wave excitation, field depend. 8-52334
 Tb, mag. domains, Lorentz microscopy obs. 8-84448
 Tb, spin wave exam. 8-56306
 Tb-Fe, amorphous, random anisotropy effects 8-68223
 TbB₂, mag. props. and neutron diff. 8-84401
 Tb_{0.27}Dy_{0.73}Fe₂, magnetisation and magnetic anisotropy 8-91862
 Tb_{0.27}Dy_{0.73}Fe₂, perpendicular suscept., magnetomechanical coupling and shear modulus 8-91918
 Tb_{0.3}Dy_{0.7}Fe₂, elastic vs. magnetoelastic anisotropy 8-68347
 Tb₂Dy_{1-x}Fe₂, Laves phase alloy, magnetostriction depend. on powder orientation before sintering 8-76284
 TbFe₃, transferred hyperfine interaction, NMR study 8-68393
 TbFe₂, high field magnetostriction and magnetisation 8-84471
 TbFe₂, magnetisation and magnetic anisotropy 8-91862
 TbG₃, uniaxial ferromagnet, logarithmic corrections to crit. behaviour 8-60294
 Tb₂Gd_{1-x}Al_x, magnetic anisotropy, magnetostriction 8-56364
 TbMg₃, mag. props., Mg conc. depend. 8-84392
 Tb(OH)₃:Er³⁺, ferromag., anisotropic exchange effects in optical spectra 8-80141
 Tb_{0.75}Y_{0.25}, spin waves rel. to cond. electron susceptibility 8-68195
 Ti-Permalloy thin film diffusion couples, low temp. interdiffusion interdiffusion 8-71889
 TiFe_{1-x}Co_x, mag. props., under high press. and in high mag. fields 8-95423
 TmFe₂, magnetisation and magnetic anisotropy 8-91862
 Tm₂V₂O₇, pyrochlore struct., mag. props. 8-72335
 U₂N₂Bi(Sb)(Te), mag. props. 8-72333
 V-Fe, ferromagnetism to micromagnetism at low Fe conc. 8-91878
 Y-Co, amorphous alloy film, spin reson. meas., exchange stiffness 8-68389
 YCo₃, amorphous ferromagnet, exchange dominated surface modes 8-52359
 Y(Fe₂Co_{1-x})₂, ferromag. reson. of pseudobinary cubic compounds 8-91961
 YFeO₃, monocrystalline, mag. field depend. of magnetic domain (*Korean*) 8-68337
 (Y_{1-x}Co_x)Co₅, anisotropy fields, coercivities, annealing effects 8-91898
 Yb₂V₂O₇, pyrochlore struct., mag. props. 8-72335
 Zr-Co(Fe), amorphous alloy film, spin reson. meas. 8-68389
 Zr₄₀Cu_{60-x}M_x (M=Gd, Tb, Fe or Mn), amorphous alloy, mag. interactions 8-95432

ferromagnetic relaxation

see also *ferromagnetic resonance*

- dynamics of ferromagnet in strong alternating mag. field (*Russian*) 8-88097

ferromagnetic resonance

see also *ferromagnetic relaxation*

- chemisorption on metal films, use of external mag. field, review 8-72003
 elliptical spin precession in microscopic spin-wave resonance theory, validity 8-80224
 ferrite, formulation of resonance, principal types of devices 8-88548
 ferroelectrics, ferromag. reson., press. influence 8-88193
 ferromagnet, easy-axis, higher order corrections to spectrum 8-80222
 film, with internal isotropically coupled impurity layer, spin wave reson. spectrum 8-80223
 garnet bubble film, high g, two resonant peaks 8-68388
 line broadening by dislocations 8-64275
 magnetostriction, meas. by means of strain modulated ferromag. reson. 8-76285
 magnon coherent generation by optical technique using mag. Raman nonlinearity 8-68201
 magnon splitting, photon effects 8-64276
 multidomain magnetic disc, ferromagnetic reson. 8-68386
 multilayer thin films, spin wave resonance, model 8-76316
 phonon propagation 8-88194
 polariton linewidths in ferromagnets, theory 8-87918

ferromagnetic resonance continued

- rare earth-Co amorphous film, sputtered, in-plane anisotropy induced by rare gas annealing 8-84458
 spin wave instability on approaching FMR (*Russian*) 8-76318
 standing spinwave resonance in film with nearest and next-nearest neighbour exchange 8-68390
 stationary and transition processes in region of identical nucl. and electron mag. reson. freqs. (*Russian*) 8-80225
 stripe domain structure, magnetostatic modes 8-68333
 tensorial permeability and conductivity medium, EM wave propag., ferromag. resonance, spin waves (*French*) 8-74820
 CdCr₂Se₄:Ag, ferromag. reson. field and linewidth anisotropy, Se vacancy effects 8-60338
 Co, NMR spectra temp. depend. 8-52364
 Co-P, cryst. and amorphous mag. films, ferromag. resonance line width (*Russian*) 8-88192
 Co-P film, amorphous, spin wave dispersion law, spin wave reson. obs. (*Russian*) 8-88196
 Cu-Ni, film, compositionally modulated, enhanced magnetisation density 8-84460
 CuCr₂Se₄, experimental obs. 8-76227
 EuO, transport properties at ferromag. reson. 8-68387
 Fe film, mag. structures and stresses 8-72375
 Fe particles, lunar matter, FMR study, effective linewidth method 8-95523
 (Fe_{1-x}Ni_x)₈₀P₁₀B₁₀, amorphous microwires, magnetisation reversal and anisotropy 8-91885
 Gd(Fe₂Co_{1-x})₂, ferromag. reson. of pseudobinary cubic compounds 8-91961
 Gd_{0.5}Y_{0.5}Tm_{1.1}Ga_{0.44}Fe_{4.56}O₁₂, ion implanted, ferromag. reson. meas. 8-68385
 KFeS₂, magnetic reson. meas. 8-95524
 La-Fe, amorphous alloy film, spin reson. meas. 8-68389
 Lu-Fe, amorphous alloy film, spin reson. meas. 8-68389
 Mg_{0.5}Fe_{2.5}O₄, ferrimag. epilayer, superparamag. interface, mag. props., FMR 8-95492
 MnFe ferrites, reson., effect of EM propagation 8-64277
 Ni film, mag. structures and stresses 8-72375
 Ni film, strained and strain-free, ferromag. reson. meas. 8-95525
 Ni-Co, ferromagnetic resonance, surface anisotropy 8-95526
 Ni-Fe, epitaxial thin film, mag. structures and stresses, ferromag. resonance 8-72375
 Ni-Fe films, US generation by ferromag. reson. 8-88155
 Ni-Fe-Mn, ferromag. reson. linewidth and saturation magnetisation 8-72418
 Y-Co, amorphous alloy film, spin reson. meas., exchange stiffness 8-68389
 YCo₃, amorphous ferromagnet, exchange dominated surface modes 8-52359
 YCo₃ film, amorphous, DC sputtered, easy axis and easy plane magnetisation 8-64237
 YFe_x film, (x=2), magnetoelastic excitations obs. 8-68307
 Y(Fe₂Co_{1-x})₂, ferromag. reson. of pseudobinary cubic compounds 8-91961
 YIG, parallel microwave pumping threshold, RF modulation of mag. field 8-88195
 YIG:Ca, epilayer, reversible oxidation, ferromag. reson. 8-76781
 Zr-Co(Fe), amorphous alloy film, spin reson. meas. 8-68389

ferromagnetism

see also *ferromagnetic properties of substances*; *ferromagnetic relaxation*; *ferromagnetic resonance*; *Ising model*; *spin waves*

- alloy, binary, with mixed ferro- and antiferromag. exchange, magnetisation, phenomenological theory (*German*) 8-56297
 alloy, binary random Heisenberg ferromagnet transition temp., crit. conc. RKKY model 8-52266
 alloy, ferromag., temp. depend. of mag. props. and sp. ht., mag. phase transition region 8-64207
 alloys, crystalline and amorphous mag. props. from Rhodes-Wohlfarth plot 8-52190
 alloys, ferromag., hyperfine field systematics of nonmag. ions 8-60093
 alloys, Lifshitz point occurrence, review 8-52265
 amorphous and crystalline ferromagnets, evaluation of complex Mossbauer spectra 8-60370
 amorphous and fine-crystalline ferromagnets, with dipole-dipole interaction, spin waves (*Russian*) 8-56308
 amorphous ferromag., law of approach to magnetic saturation, effect of precipitates 8-72334
 amorphous ferromagnet, mag. excitations 8-68204
 amorphous ferromagnet, random anisotropy effects 8-68223
 amorphous ferromagnet, resist. 8-64021
 amorphous ferromagnets, ferromag. saturation, spatially random magnetostatic, magnetocrystalline, magnetostrictive and exchange fluctuations 8-60277
 amorphous Heisenberg ferromagnet, spin waves, effective medium approx. 8-68203
 amorphous magnet, Bethe-Peierls-Weiss approx. 8-76263
 amorphous system, directional order and induced anisotropy energy, theory 8-95431
 anisotropic critical freq. depend. of spin correlation functions 8-56321
 basic models, classification of theories (*Rumanian*) 8-91840
 Berthollides, chaotic mag. states 8-56330
 Bloch wall steady-state motion in ferromag. 8-68291
 Blume-Capel model for plane-triangular and FCC lattices 8-80114
 chain, isotropic, solitary waves 8-64180
 chiral connection with axisymmetric gravitational problem and SU(2) vacuum gauge field 8-70258
 coexistence of phases, equiv. of different order parameter 8-49772
 concentrated alloys, ferromag., spin fluctuations 8-64290
 conductor, electric field response and electrofluctuation instability (*Russian*) 8-56083
 constitutive eqns. of ferromagnetic bodies (*Italian*) 8-72317
 constitutive equations for ferromagnetic bodies (*Italian*) 8-84372
 continuous-spin Ising ferromagnets phase transitions 8-60260
 critical dynamics above crit. temp., dipolar coupling 8-52286
 cubic ferromagnet, magnetoelastic interaction energy, arbitrary coordinate system 8-52335
 Curie point determ. from saturation magnetisation-temp. charact. 8-60281
 Curie temperature of ferromag. with random anisotropy, constant coupling approx. 8-76264

ferromagnetism continued

- dense neutron matter, ferromag. transition, pure hard core gas model 8-70478
 dielectric, crit. behaviour of exciton relaxation const. 8-84442
 dilute ferromagnet, spin wave excitations, multicomponent CPA theory 8-68135
 dislocation motion, mag. moments around screw dislocations, spin waves retarding dislocations 8-87670
 disordered itinerant-electron ferromagnet, spin waves 8-95427
 domain structure, effect of defects, electron microscopy 8-64214
 domain structure, Landau-Lifshitz, in appl. mag. field (Russian) 8-60305
 domain structure, multiaxial ferromag. applied stress effect (Russian) 8-76267
 domain wall motion, effect of transverse mag. field 8-68292
 domain wall motion, limiting velocity (Russian) 8-56342
 domain wall pinning effect and intrinsic coercivity, computer simulation 8-64217
 domains, dynamic behaviour, struct., rel. to ferromag., teaching appl. 8-86080
 domains, ferromagnetic and antiferromagnetic, neutron techniques for obs., review 8-64213
 double transition spin glass-ferromagnetic systems, differential susceptibility 8-88131
 dynamical critical exponent crossover, hyperfine interaction vs. neutron scatt. expts. 8-84437
 dynamics of ferromagnet in strong alternating mag. field (Russian) 8-88097
 eddy-current problems, including moving Fe parts, numerical soln. 8-90340
 elastic ferromagnets, higher order surface couplings 8-79212
 electron gas, two dims. 8-60258
 electron gas, two dimensional, mag. props. 8-56095
 EM wave penetration, plane, penetration depth calc. (Bulgarian) 8-50679
 EM wave propagation, nonlinear waves and strong discontinuities (Russian) 8-74819
 EMF in ferromag. material under torsion (Rumanian) 8-86986
 exciton ferromagnet, inhomogeneous state (Russian) 8-88132
 FCC Ising ferromagnet., cluster variation approx. 8-68278
 ferroelectric ferro- and antiferromagnet, energy gap in spin wave spectrum 8-91858
 ferromagnet, Bloch walls correlation and magnetic loss 8-95456
 ferromagnet, easy-axis, higher order corrections to spectrum 8-80222
 film, φ^4 domain walls, magnetisation, occurrence of crit. point 8-95500
 film, Bloch wall struct. and anisotropy, analytical representation 8-88151
 film, phenomenology of domain walls, review (Rumanian) 8-60324
 film, spin wave propagation near surface 8-68308
 fine particle systems, physical basis and applications 8-84457
 flux quantisation in ordered ferromagnetic substances 8-80136
 Gaussian random field, ferromagnets in $4+\epsilon$ space dims. 8-73954
 Hall conductivity, scattering-independent contribs. 8-51957
 hard magnetic materials, demagnetisation curve, single function approx. using computer (Hungarian) 8-60307
 harmonic rotator, Coulomb plasma and related model, two dims. case 8-88137
 harmonic rotator, Coulomb plasma and related models, case of dimensions $D < 2$ and $D > 2$ 8-88136
 harmonic rotator, Coulomb plasma and related models, renormalisation group treatment 8-88135
 Heisenberg ferromag. localised magnons around surface impurity (Russian) 8-84376
 Heisenberg ferromagnet, anharmonic, renormalised magnons and phonons 8-91837
 Heisenberg ferromagnet, crit. dynamics in $2+\epsilon$ dims., low temp. phase 8-76262
 Heisenberg ferromagnet, diagram techniques for Greens functions with spin operators 8-91836
 Heisenberg ferromagnet, dil., mag. excitations, localisation, wavefunctions 8-60275
 Heisenberg ferromagnet, instanton contrib. to correlation function (Russian) 8-95412
 Heisenberg ferromagnet, longitudinal dynamic susceptibility 8-64181
 Heisenberg ferromagnet, spin coherent state representation, spin waves excitation spectrum 8-80117
 Heisenberg ferromagnet, structurally disordered, variational method for cluster model 8-91839
 Heisenberg ferromagnet, three-dims., two magnon states, effect of next nearest neighbour interactions 8-64178
 Heisenberg ferromagnetic alloy, critical behaviour (Russian) 8-88127
 Heisenberg model, quasilow dimensional, small dilution perturbation theory at OK 8-56281
 Heisenberg spin- $1/2$ ferromagnets, 1st order Green's function theory 8-72323
 Hume-Rothery alloys, magnetism 8-95417
 hysteresis, swallow tail catastrophe anal. 8-56349
 infinite ferromagnetic medium, energy and mobility of Bloch point singularities 8-68331
 insulating systems, magnetic, review of expts. 8-68240
 interaction between localised moments in system with electron hole pairing (Russian) 8-88111
 intermediate valence compounds, phonon produced instabilities, periodic Anderson model 8-79964
 internal fields, positive muon investigation 8-68438
 ion implantation in ferromagnets (Flemish) 8-79623
 Ising ferromagnet, 2-D, with quenched bond disorder, critical temp. 8-56328
 Ising ferromagnet, crit. correlation-function approxs. 8-56324
 Ising ferromagnet, crit. exponents in integral representation 8-56325
 Ising ferromagnet, disordered, approximate treatment 8-52262
 Ising ferromagnet, $S=1$, single-ion type uniaxial anisotropy, cluster-variation method appl. in pair approx. 8-68281
 Ising ferromagnet, site diluted, crit. props. 8-72351
 Ising ferromagnet, spin-operator reduction relations, representation 8-95443
 Ising ferromagnet, rectangular, n-point functions 8-76250
 Ising model, bond-diluted, first and second neighbour interactions 8-91870
 Ising model, Curie point in quenched bond model 8-56318

ferromagnetism continued

- Ising model, ferromag. and antiferromag. in mag. field, new perturbation approach 8-56336
 Ising model, renormalised crit. behaviour 8-52272
 Ising model, three-dimensional, two-spin correlation function, method for phase diagram 8-56323
 Ising $S=1$, $1/2$ mixture, one-dimens., random, mag. props., spin distrib. 8-95407
 Ising site model, random mixtures, Monte Carlo simulation 8-73935
 Ising site model, random mixtures, Monte Carlo simulation 8-73936
 isotropic two-dimensional magnetism, long range forces effect 8-52291
 itinerant electron ferromagnet, effective Lorentz force and Landau level 8-80120
 itinerant electron ferromagnet with domain struct., spin waves 8-64182
 itinerant electron ferromagnetism, spin fluctuation theory 8-80151
 itinerant electron ferromagnetism at zero temp. 8-56285
 itinerant ferromagnet in disordered phase, energy band struct. 8-68141
 Krieger-James approx. of short range order effects, antiferro- and ferro-mag. 8-56276
 lattice diffusion, Heisenberg ferromagnet 8-88090
 linear Ising-Heisenberg ferromagnet, spin waves vs. bound states, exact soln. 8-68202
 liquid ferromagnet, model calculation 8-88088
 local field at positive muon 8-92010
 magnetic anisotropy, local variations due to linear defects (Russian) 8-68214
 magnetic bubbles as tilted cylindrical magnetic domains 8-64246
 magnetisation at low temp., disorder induced behaviour 8-52234
 magnetisation of large ferromagnetic parts, by use of applied electromagnets 8-72999
 magnetisation of uniaxial ferromagnet with single-ion and exchange anisotropies in transverse mag. field 8-56277
 magnon density of states for ferromag. with screw dislocation 8-84402
 magnons and lattice deformations, solitary bound states, Dyson-Maleev representation 8-91838
 material inspection by method of two harmonics 8-88608
 Maxwell's equations in ferromagnetic materials, asymptotic solns. (Italian) 8-78860
 mean spherical model, Langevin approach 8-72350
 metal, amorphous ferromagnetic, paramagnetic Curie temp. determ. 8-76242
 metal, anisotropic, spin-fluctuation resist. 8-56137
 metal, asymmetric electron scatt., anomalous Hall effect in ferromags. (Slovak) 8-79986
 metal, dynamic scatt. effects on crit. transport props. 8-84239
 metal, hyperfine fields at rare earth impurity 8-87947
 metal, itinerant electron model, for US propagation and structural instabilities 8-95508
 metal, with domain struct., resistivity 8-95285
 metamagnetic dielectrics, at finite temp. (Russian) 8-88118
 Migdal's recursion relation, generalisation, appl. to $O(n)$ symmetric spin systems, $n > 2$ 8-91834
 modulus defect due to internal strain 8-76286
 moving conducting ribbon, interaction with ferromag. inductor field (Russian) 8-94359
 neutron depolarisation on passage through ferromag., statistical theory 8-87593
 nondestructive inspection of ferromagnets, using magnetic noise method 8-72997
 nonuniform ferromagnet, spontaneous magnetisation, mean field theory (Chinese) 8-91865
 one-dimensional, with biquadratic exchange, solitary excitations 8-76232
 one-dimensional dilute Heisenberg system, mag. props. 8-64179
 order parameter for exactly soluble model 8-76207
 parametric excitation on spin waves in the induced magnetoelastic crystals (Russian) 8-60272
 Peierls condition and number of ground states 8-80150
 phenomenological theory 8-52184
 planar cyclic remagnetisation of ferromagnet under sinusoidal induction (Russian) 8-80177
 plate, domain struct. during spin reorientation, phase diagram (Russian) 8-52320
 polydomain magnetic struct., excitation of sound 8-88162
 quantum mechanical theories of magnetism, review of properties and explanations 8-76215
 random exchange interactions, and 'frustration effect' 8-68212
 random impurity effects on long range order 8-95061
 randomly anisotropic ferromagnet, long wavelength mag. excitations 8-84406
 remanent magnetisation during thermal demagnetisation near a phase transition 8-88142
 resistivity anomalies of ferromag. metals near Curie temp., itinerant mag. electron theory 8-95292
 resistivity of magnetic systems, critical behaviour 8-87955
 resonance excitation of ultrasound in ferromagnetic fluids 8-95112
 retarded EM modes in ferromag. slab 8-84405
 semiconductor, autolocalised electron states 8-51924
 semiconductor, electronic quasiparticle spectrum in sf-model 8-52188
 semiconductor, electronic spectrum, influence of finite carrier conc. 8-76220
 semiconductor, ferromag., electron mobility below Curie temp. calc. 8-51992
 semiconductor, spectrum of quantum spin waves in field of strong EM wave 8-91857
 semiconductor-ferromagnetic structure, thermal fluctuations during amplification of magnetoacoustic surface waves 8-88158
 semiconductors, nondegenerate, magnon drag thermoelec. power calcs. 8-80012
 single ion anisotropy const. temp. depend., effect of spatial variation of mag. moment 8-91864
 spin deviation states in spin-1 system with Heisenberg and biquadratic exchange 8-84378
 spin glass model, stability of Sherrington-Kirkpatrick soln. 8-56319
 spin systems with three-atom exchange, elementary excitations 8-84404
 spin wave damping, magnetisation relax. 8-88106

ferromagnetism continued

- spin wave damping, theory, and comparison with expt. for EuO 8-52237
 spin wave excitation, with moving domain wall (*Russian*) 8-88103
 spin wave stiffness coefficient, spin density functional theory 8-76230
 spin waves above Curie temp., Fisher's droplet model 8-56307
 spin-one Ising system, phase diagram 8-95441
 Stoner ferromagnetism, criteria in doped semimetals, uncompensated metals, derivation 8-68145
 substrate, ferromagnetic transition, anomalies in adsorption equilib. near crit. point 8-79895
 surface magnetoelastic waves in the presence of exchange interactions and pinning of surface spins 8-80186
 thermal conductivity of ferromagnets, crit. anomalies (*Russian*) 8-80159
 transition metal, 3d and 4d, local density theory, mech. and mag. props. evaluation 8-91630
 transition metal alloy, ferromag., local environment effect on atomic moments, itinerant model 8-68188
 transition metals, conf., Toronto, Canada (Aug. 1977) 8-91577
 transition metals, electron spin polarisation, review 8-76591
 transition metals, electron spin polarisation, review 8-76592
 transverse dynamical susceptibility within the local exchange approx. 8-76229
 triangular Ising lattice with small second neighbour interaction crit. temps. 8-56331
 triple dynamic magnetisation fluctuation correl. and feasibility of polarised neutron exam. near T_c (*Russian*) 8-88133
 twisted domain wall dynamics in ferromag. plate 8-68340
 two-dimensional spin model, Wilson renormalisation group theory appl. (*Norwegian*) 8-56275
 uniaxial ferromagnet, arbitrary spin and single-ion anisotropy of second order, Green's function 8-84379
 uniaxial ferromagnet, dynamical behaviour near mag. transition point (*Russian*) 8-84431
 uniaxial ferromagnet, neutron depolarisation calc. 8-64192
 uniaxial ferromagnet, with flat-parallel domain struct., classical phenomenological description 8-56316
 uniaxial ferromagnet with random exchange bonds of different signs, spin waves 8-76233
 US spectrum, RF field in multidomain struct. 8-68056
 wavevector-dependent spin susceptibility, variational principle 8-91586
 wire, circular magnetisation meas. 8-70167
 Yang-Lee edge singularity and ϕ^2 field theory 8-65882

ferromagnets see *ferromagnetic properties of substances; ferromagnetism*

ferrous alloys see *iron alloys*

Feshbach resonances see *atomic resonant states; molecular resonant states*

f.e.t. see *field effect transistors*

few-nucleon reactions see *nuclear reactions involving few nucleon systems*

few-nucleon scattering see *nuclear scattering involving few nucleon systems*

few-nucleon systems see *nuclei with mass number 1 to 5*

Feynman diagrams

- $\lambda\phi^4$ theory, dual string theory from Feynman graph expansion 8-54544
 $\lambda\phi^4$ theory, renormalised perturbation theory, Feynman graphs 8-54570
 Φ^3 field theory, Regge pole behaviour 8-66053
 asymptotic expansion, Feynman amplitudes, theorem 8-93790
 Feynman integrals, singularity struct. study using micro differential eqns. 8-74123
 Feynman maps and the Wiener integral 8-77758
 high energy behaviour of a double discontinuity and the bare Pomeron 8-82179
 high-energy behaviour of renormalised Feynman amplitudes 8-58114
 inverse bremsstrahlung, high energy, nucl. mag. contribs. 8-74350
 IR divergences in Yang-Mills theories, Feynman diagram labelling 8-54547
 large order expansions in perturbation theory 8-54525
 perturbation expansion of quantised composite field theory, gauge invariance (*Chinese*) 8-82156
 points splitting and dimensional renormalisation for Feynman amplitudes 8-86402
 QCD, gauge independence of IR cancellation, fermion-fermion scatt. 8-50006
 regularised diagrams without Feynman parameters 8-49970
 sine-Gordon S-matrix, origin of double poles 8-70292
 ep deep inelast. scatt., QCD perturbative corrections 8-74263

fiber optics see *fibre optics*

fibres see *fibres*

fibre optics

- boroscope 8-50938
 catheter transducer, side hole type, for intracardiac press. meas. (*Japanese*) 8-73272
 catheter-tip micromanometer as intracardiac press. transducer (*Japanese*) 8-73270
 coupling loss investigations, scanning automatised optical bench 8-83124
 dark field magnification microphotographic illumination system 8-58025
 dermatological photobiology, fibre optic light guides for phototesting 8-53472
 endoscope, image quality improvement 8-71219
 endoscope one-component objective dimensional design (*Russian*) 8-69228
 endoscopic laser photocoagulation, use of gas jet appositional pressurisation 8-53468
 endoscopic manometry in gastroenterology 8-92730
 fusion reactor, fibre optic telemetering for high voltage test stand 8-54939
 fusion reactor, pulser system, air-driven fibre-optic coupled for Los Alamos ZT-40 expt. 8-54943
 heterodyne interferometer for vibr. meas. in biological systems 8-77101
 image tube with fibre optics, cooling effect 8-96401
 incoherent optical power launching limits, fibre endoscopic inspection appl. 8-63193
 interferometer, laser single-mode fibre 8-49892
 intravascular O_2 saturation continuous meas. using fibre optic catheter (*German*) 8-85411

fibre optics continued

- Kohler illumination using fibre optics and quartz-halogen lamp 8-58027
 light shield, fibre selector with absorbing cladding, Fraunhofer diffr. 8-90521
 light source for curved platen illumination 8-63163
 medical applications, review (*Italian*) 8-53540
 microinterferometer transducer, air-bearing, for use with universal inspection machines 8-57899
 monolithic component glasses and rigid sintered fibre-optic elements, microcrack form. during grinding 8-87175
 multimode fibre bussing, active fail-safe terminal 8-55438
 oil detection, in water, using combined GaAlAs laser and fibre optic bundles 8-96301
 parametric oscillator, Brillouin, mode-locked optical fibre, bandwidth-limited operation 8-50851
 pinhole light source, bright and inexpensive 8-83058
 quality of fibre optic glass pairs, effective aperture and light scatt. analysis 8-90522
 ring interferometer gyroscope, Fresnel drag effect 8-79142
 ruby fibre laser, room temp. continuous operation without cooling, crystal growth, heating effects 8-66833
 sonar, computerised system, geological and hydrographic survey applications 8-88947
 spectroscopic cooled and intensified array detectors 8-65983
 strain gauge, arbitrarily shaped path length meas. 8-70112
 strain gauge 8-94426
 visible IR spin-scan radiometer 8-59160
 vitreous surgery via pars plana, instrument design 8-81056
 Nd:glass conical fibre optics quantum amplifier parameters 8-59024
 Nd:Y₂O₃ single crystal fibre laser, room temp. CW operation at 1.07 and 1.35 μm 8-63121
 SiO₂, fused, fibre Raman laser emitting over very large spectral region (*French*) 8-55405

fibre reinforced composites

- see also *carbon fibre reinforced composites; glass fibre reinforced plastics*
 adhesive debonding, exam. 8-60773
 angle ply laminate, fibre reinforced, interlaminar strength test for delamination 8-88523
 apparent fibre spacing 8-79222
 asbestos fibre reinforced Portland cement analytical fracture resistance curve expression 8-76756
 biaxially fibre reinforced composites, two dimens. mixture theory, dynamic crack appl. 8-87301
 borsic fibre reinforced Ti, unidirectional, K-calibration and compliance curves 8-88518
 brittle fibre reinforced alloys, anal. of fracture process and fibre strength, by Monte Carlo simulation (*Japanese*) 8-80634
 calculation of stress distrib. and X-ray elastic consts. (*German*) 8-52883
 chain of bundles probability model for fibrous material strength 8-67095
 chain of bundles probability model for strength, numerical study of convergence 8-88496
 Cotac 74, directionally solidified composite, creep behaviour prediction (*French*) 8-68754
 cracking and fracture, review 8-60772
 creep behaviour of fibre reinforced metals (*German*) 8-52931
 dispersive waves, phase and group vels. determ. 8-81848
 elastic characteristics (*Russian*) 8-59304
 elastic fibre reinforced composites, wave guide-type propag., microstruct. theory 8-83279
 elastic modulus, estimate for composites isotropic on the average 8-51077
 failure analysis by acoustic emission 8-80691
 fatigue 8-68767
 fibre reinforced plastic, fracture mechanism study, cumulative failure model 8-92315
 fiberglass composite, oriented, model, conditions of monolithicity, exam. 8-67044
 FRC, reinforcement parameter 8-79223
 ideal, finite plane deformation and energy dissipation 8-79274
 imperfections, piezo- and elasto-optical effects under longitudinal shear (*Russian*) 8-56457
 ionomer composites, fatigue strength, dynamic viscoelastic props. and fracture surface exam. (*Japanese*) 8-92339
 laminated plate under tension, stacking sequence and lay up angle effect on free edge stresses round hole 8-88524
 layered, harmonic elastic waves, dispersion 8-63223
 mechanical characterisation at low temps. 8-64611
 mechanical model 8-51105
 metal gauze reinforced porous permeable mats. with prearranged struct., prep. 8-68652
 metal matrix composites, thermal expansion effects, fibre length depend. 8-51708
 metals, fibre reinforced, fatigue limit (*German*) 8-72859
 modulus of brittleness, crit. tensile span 8-92318
 mullite fibre reinforced mullite, in vitro degradation, bending strength, Young's modulus, density meas. 8-85011
 notched fibre reinforced composites, tensile fracture 8-52991
 orthotropic materials design for stress optimisation 8-63291
 plastic matrix, fracture mechanism study, cumulative failure model 8-92315
 plastic matrix, oriented fibre wear mechanism against mild steel 8-56782
 polypropylene fibrillated film reinforced cement, loading capacity, cracking 8-72759
 porous composite anal. by US wave velocity meas. of fibre vol. and matrix porosity 8-95902
 prestressed elastic circular cylinder, stability 8-79234
 radiographically opaque fibres, inspection aid by B fibre addition 8-95880
 refractory composites, fibre reinforced, directionally solidified tensile tests, in HVEM, deform. and fracture (*French*) 8-68785
 secondary stresses associated with structures, exam. 8-67043
 shell under external press., max. stability 8-94597
 short fibre reinforced polymers, expressions governing stress-strain curves 8-80592
 short steel wire reinforced (polymer impregnated) concretes, cracking and toughening 8-80626

fibre reinforced composites continued

- steel, fibre reinforced Al, fracture mechanics under fatigue (*Czech*) 8-64629
- steel fibre reinforced Ag, exam. of recrystallisation behaviour (*German*) 8-84849
- steel fibre reinforced Al, fatigue strength (*Czech*) 8-60748
- steel fibre reinforced cementitious material, radiographic anal. of fibre distrib. 8-52747
- steel fibre reinforced Cu, exam. of creep behaviour, comparison with theory (*German*) 8-52931
- steel wire reinforced Portland cement mortar, wire pull out, inelastic behaviour 8-56681
- strength props., US method for evaluating 8-76796
- thermal diffusion, quasi-one-dimens., mixture theory 8-71271
- thermal expansion coeff. 8-67836
- thermal stress fracture in compound materials, exam. 8-75103
- thick laminar reinforced plastics, deformation fixing in polarisation optics (*Ukrainian*) 8-90802
- ultrasonic scanning, C-scan technique for fibre misorientations, delaminations, bond failures 8-95882
- unidirectional model for longit. tensile strength prediction 8-95778
- uniform plane stress states, method for prod. 8-85064
- Ag composite, SiC whisker-reinforced, prep. aboard Skylab. 8-84741
- Ag-Cu, anomalous props. caused by internal phase boundaries 8-72754
- Ag-Ni, composite, fibre and layer structs., anomalous props. caused by internal phase boundaries 8-72754
- Al-matrix, composites preparation by Na-process, interface reactions 8-84742
- Al₂O₃ fibre reinforced Al-Mg(Mg-Cu)(Cu) exam. of interface interactions during fabrication 8-76616
- B fibre reinforced Al, fracture mechanical study, unidirectional composites 8-88520
- B fibre reinforced Al, strength determ. procedure in annular specimens (*Russian*) 8-95864
- B fibre reinforced Al, unidirectional, K-calibration and compliance curves 8-88518
- B fibre reinforced epoxy, fracture mechanical study, unidirectional composites 8-88520
- B reinforced Al, double lapped composite joints, efficiency in bending with steel hub 8-68870
- B reinforced epoxy, double lapped composite joints, efficiency in bending with steel hub 8-68870
- B-Al cast braid, crystallisation and structuring of Al matrix (*Russian*) 8-52725
- C fibre reinforced epoxy phenol plastic, resistance to interlayer shear and elec. resistivity 8-68752
- Cu-Fe, composite, fibre and layer structs., anomalous props. caused by internal phase boundaries 8-72754
- FeNi-Cu, composite fibre and layer structs., anomalous props. caused by internal phase boundaries 8-72754
- Mo fibre reinforced Al and Al alloys, SEM study (*Slovenian*) 8-84923
- Mo fibre reinforced Ni-Cr, effect of fibre coatings on composite strength 8-56710
- SiC fibre reinforced Ni-Cr, alumina coated fibres, hot pressed, annealed, IR study 8-60623
- SiC fibres reinforced Ni complex alloy, influence of TiN coating on fibre matrix interaction (*Russian*) 8-95820
- W fibre reinforced epoxy resin, strength of metal-polymer adhesive contact, time-temp. depend. 8-68753
- W fibre reinforced Ni-Cr alloys, Ni, Co, Co alloys, and Ni alloys, effect of alloying on structural stability, mech. props. 8-56600
- W-ThO₂ fibre reinforced Ni base alloys, powdered matrices, fibre/matrix interaction above 1300°C, alloying effects (*Russian*) 8-95755

fibres

- see also carbon fibres; composite materials; fibre reinforced composites; glass fibres; optical fibres
- aliphatic polymer fibres, supermol. struct., X-ray diffr. and acoustic methods 8-75570
- amphibole fibre conc. in water, interlaboratory meas. by TEM 8-88590
- aromatic polymer fibres, supermol. struct., X-ray diffr. and acoustic methods 8-75570
- bundles, stochastic strength and fatigue 8-79262
- cellulose, surface aggregation of dispersed resin particles in elec. field 8-53262
- cellulose fibre, moist, dielec. props. 8-76380
- chrysothile fibre conc. in water, interlaboratory meas. by TEM 8-88590
- cotton, water drainage, by capillary flow (*Japanese*) 8-95208
- cotton fibre fineness and maturity comparison on air flow instruments 8-88591
- crystallite shear deforms. rel. to small-angle X-ray scatt. pattern (*Russian*) 8-71690
- degummed silk fibres, mol. motion and fine struct., X-ray, thermal, mech., dynamic loss tangent meas. (*Japanese*) 8-59765
- equipment for testing elongation of high strength and high tensile fibres 8-56844
- fatigue properties, biaxial rotation over a pin 8-64699
- haemoglobin S, fibres, discs having six-fold symmetry, electron microscopy 8-76989
- Kevlar 49 high modulus polyaromatic fibre, supramolecular struct. 8-55819
- Kevlar-49, chemical characterisation 8-95725
- metal fibre mats., porous, struct., hydraulic characts., liq. permeability 8-67848
- nylon 6,6, drawn fibre, selective degradation, cryst. morphology 8-71683
- nylon-6 fibre, chain rupture and tensile deform. viscosity-av. mol. wt. obs. 8-76714
- nylon-quartz fibre support for low temp. mag. suscept. meas. 8-65947
- PA-6, polymer fibre, orientation changes during stretching, IR spectra 8-75568
- PET, filament form. from gels 8-80508
- poly(L-alanine) fibres, mol. motion and fine struct., X-ray, thermal, mech., dynamic loss tangent meas. (*Japanese*) 8-59765
- poly(p-phenylene terephthalamide) fibres, chain orientation distrib., and elastic props. 8-75566
- poly-p-benzamide fibre, supermol. struct., X-ray diffr. and acoustic methods 8-75570

fibres continued

- poly-p-phenylene terephthalate, high modulus fibre, struct. obs. 8-75564
- polyacrylonitrile, struct. of heat treated fibres, X-ray diffr. 8-83752
- polyamide fibre, chain-segment orientation, US vel. meas., humidity effects (*German*) 8-75590
- polycarbonate fibre, highly-oriented, drawing behaviour and mech. props. 8-76708
- polyethylene, hard elastic fibres, deform. and struct., -196 to 80°C 8-51437
- polyethylene melt, drawing filaments, surface instabilities 8-71305
- polyethylene melt spinning, extensional flow induced crystallisation 8-55818
- polyethylene terephthalate, chain rupture and tensile deform., viscosity-av. mol. wt. obs. 8-76714
- polyethylene terephthalate fabric, surface struct., props. rel. to plasma surface treatment 8-95831
- polyethylene terephthalate fibres, high freq. US effects on physical and chem. structs. (*Polish*) 8-51446
- polyethylene terephthalate fibres, interdependence between struct. and thermal contraction (*Rumanian*) 8-91259
- polyethylenes, linear, ultra-high modulus, tensile creep, recovery 8-95784
- polymer fibre, highly oriented, struct. and mech. props. 8-75563
- polymer fibre formation, fibrous crystallisation and chain extension 8-75573
- polymer solution elongational flow, wet spinning process for fibres 8-72760
- polymeric fibres, cyclic tension endurance, Prevorsek-Lyons theory 8-52967
- polypropylene, film and fibre, chain rupture and tensile deform., viscosity-av. mol. wt. obs. 8-76714
- polypropylene, monofilaments, drawing behaviour, melt-induced orientation effects 8-84922
- polypropylene fibre, melt-spun with twist, helical orientation and mech. props. 8-75569
- polypropylene fibres, homologue mixtures, props. 8-76709
- polypropylene film and fibre, plasma etching 8-95871
- polypropylene-nylon 11 fibres, bimodal cryst. texture, X-ray diffr. and electron microscopy 8-75567
- polystyrene fibre, ageing effects on elongation to fracture (*German*) 8-76750
- PTE, polymer fibre, orientation changes during stretching, IR spectra 8-75568
- PTFE fibres, US effects on structure (*Polish*) 8-68702
- steel wire reinforced Portland cement mortar, wire pull out, inelastic behaviour 8-56681
- B, reinforced Al, strength determ. procedure in annular specimens (*Russian*) 8-95864
- B, to graphite reinforced epoxy, radiographic inspection aid 8-95880
- K₂O.3MoO₃.3H₂O, fibrillar crystals, morphology and struct. 8-63959
- Li₂O.3MoO₃.5.7H₂O, fibrillar crystals, morphology and struct. 8-63959
- Nb₃Sn, filamentary conductors, type-II, low temp. 30 GeV proton effects on critical props. 8-52178
- NbTi, filamentary conductors, type-II, low temp. 30 GeV proton effects on critical props. 8-52178
- NiCr-AlY sintered fibre metal struct. abrasable seal material, friction and wear 8-56785
- Pb, filament production, ejection of molten metal through nozzle, jet stability (*Japanese*) 8-52719
- SiC fibre development using organosilicon polymer precursor 8-60627
- SiC fibres with protective Al₂O₃ coatings in Ni-Cr alloy based composites, IR investigation 8-60623
- V₃Ga, filamentary conductors, type-II, low temp. 30 GeV proton effects on critical props. 8-52178
- W, KAl, KSi, KSiAl and KSiGa, addition effects on workability (*German*) 8-64557
- W, KSiAl doped, recrystallisation, Li diffusion effects, hardness, strength, microstructure meas. (*German*) 8-64644
- field, crystal internal** see crystal field interactions
- field effect devices**
- see also field effect integrated circuits; field effect transistors; metal-insulator-semiconductor devices
- junction field effect structures, 2-D subbanding 8-64125
- MOS, generation lifetimes from C-t transients 8-88036
- GaAs, epitaxial layers, low freq. current noise between 4.4 and 300K 8-95388
- field effect integrated circuits**
- see also charge-coupled device circuits
- MIS integrated stepped-sawtooth waveform generator 8-86376
- MOS LSI passivation using reactive plasma deposited Si-N films 8-56584
- MS²IS structure free carrier redistribution control 8-95384
- Schottky-barrier metal-thin oxide-semicond. structures, physical processes and microelectronics applications (*Russian*) 8-84307
- SOS film, electron mobility 8-91792
- Si, polycryst. barrier layer formation, investigation (*Slovak*) 8-92196
- field effect transistor circuits**
- Used for general papers and papers where the use of field effect transistors is significant
- charge-sensitive preamplifier, universal, using FET, cct. 8-77932
- oscillator, for quartz thermometer 8-81967
- six-channel MOSFET commutator, monopolar mass spectrometer appls. (*Russian*) 8-74099
- field effect transistors**
- see also field effect integrated circuits; insulated gate field effect transistors; junction gate field effect transistors; Schottky gate field effect transistors
- probes for improving CRO meas. 8-93667
- GaAs, continuous growth of LPE double layers 8-64487
- GaAs, sharp line photolum. spectra 8-72248
- SiO₂ in FET, electron trapping due to electron beam deposited Al 8-80060
- WSi₂ film, FET gate electrode, oxidation mechanism, SiO₂ overlayer formation 8-76773
- field emission, electron** see electron field emission
- field emission electron microscopes**
- see also field emission electron microscopy
- STEM, microanal. by energy loss spectrometry 8-53286

field emission electron microscopy

see also *field emission electron microscopes*

haemoglobin S, fibres, discs having six-fold symmetry, electron microscopy 8-76989

p-Ge, adsorption of Au, effect on I-V characteristics field emission study 8-67925

Pt, Cs adsorption 8-51822

U, emissive props. 8-88409

field emission ion microscopes

see also *field emission ion microscopy*

No entries

field emission ion microscopy

see also *atom probe field ion microscopy; field emission ion microscopes*

atom-probe FIM data, quantification appl. to surface segregation of alloys 8-62263

detects in materials, direct observation and characterisation 8-88617

electrical contacts surface damage caused by closing voltages 8-64098

Faraday cup for simultaneous ion-beam current obs. and meas. 8-49865

gnomonic method for indexing of micrographs 8-82078

grain boundary migration obs. using FIM 8-79617

image contrast, gas distrib., hypothesis reexamined 8-60552

projection geometry of field-ion image 8-66011

Al, atomistic images of field ion microscopy at high temps. 8-55792

Au, atomistic images of field ion microscopy at high temps. 8-55792

Cu, atomistic images of field ion microscopy at high temps. 8-55792

Fe deposited W tip, FIM obs., epitaxial growth 8-79904

Fe whisker, polycryst., FIM obs. of struct. 8-84111

GaAs, atom probe field ion microscopy 8-80460

GaP, atom probe field ion microscopy 8-80460

In, epitaxial layer on imperfect FEM/FIM W emitter 8-60037

Mo wire, laser shock induced microstructural changes, rel. to explosive shock induced phenomena 8-67768

Re₂, adsorbed on W (211) surface, dissoc., thermodynamics 8-87861

W, FIM study of lattice damage caused by low-energy He ion bombardment 8-95090

W surface, atom zigzag chains obs. by field ion microscopy 8-84036

W wire, laser shock induced microstructural changes, rel. to explosive shock induced phenomena 8-67768

field evaporation

atom probe FIM evaporation pulse generator 8-78041

transition metals, field evaporation rate meas. 8-76590

vacuum arc cathode spot dynamic models 8-75481

GaAs, atom probe field ion microscopy 8-80460

GaP, atom probe field ion microscopy 8-80460

field intensity patterns (antenna) see *antenna radiation patterns***field interactions (condensed matter)**

see also *crystal field interactions; hyperfine field interactions (condensed matter)*

No entries

field ion emission

fine focus beams, field ionisation source appl. for microprobe 8-76589

image contrast, gas distrib., hypothesis reexamined 8-60552

organic liquids, electrohydrodynamic ionisation, solvated ion mass spectroscopy, anal. appl. 8-73102

W, multiple field ion emitters, props., ionisation efficiency improvement 8-76588

field ion microscopy, atom-probe see *atom probe field ion microscopy***field ionisation**

atoms, ionisation of Rydberg states, depend. on $|m_l|$ 8-58856

excited atoms, field ionisation mechanisms 8-70761

halogen intense negative ion source 8-66001

1-hexene-water-(D₂O), field-induced surface reactions, field ionis. mass spectra obs. 8-95949

inert gas, field ionis. and proton capture, critical energy deficits 8-82853

Rydberg states, fine struct. splitting, quantum beat and double reson. spectroscopy 8-86979

NH₃, field ionis., critical energy deficits, field depend. 8-82852

Na, Rydberg states, millimeter spectra, quantum defect, fine struct., polarisability, field ionis. obs. 8-82672

Xe(nf)+NH₃, at. Rydberg state further excitation by rot. transfer, field ionis. obs. 8-58795

field measurement, electric see *electric field measurement***field measurement, magnetic** see *magnetic field measurement***field plotting**

see also *field strength measurement*

echo sounder transducer field plotter 8-59238

LF and MF ground waves in realistic terrain, elec./mag. field ratios 8-88795

field strength measurement

see also *electric field measurement; magnetic field measurement*

No entries

field theories, unified see *unified field theories***field theory, classical** see *classical field theory***field theory, crystal** see *crystal field interactions***field theory, electromagnetic** see *electromagnetic field theory***field theory, meson** see *meson field theory***field theory, quantum** see *quantum field theory***fields, electric** see *electric fields***fields, magnetic** see *magnetic fields***filament lamps**

chromatic adaptation effects and colour appearance at various illum. levels (*Japanese*) 8-92628

W, filament, incandescent lamps, creep, failure, life prediction 8-84927

W filament lamp, Stefan's law demonstration, student expt. 8-54125

file management see *file organisation***file organisation**

see also *data handling; database management systems*

geodetic data base, basic entities definition 8-65392

mass storage directory entry repair for lost data retrieval 8-77954

filled polymers

blends, viscoelastic props. (*Russian*) 8-72808

elastic moduli, interfacial slippage effect anal. 8-76688

epoxy, Al₂O₃-filled, shock-wave compression, 0.4-3.7 GPa 8-59856

epoxy material, filled, US props. for sonar transducers 8-59867

filled polymers continued

epoxy resin, glass bead filled, particle size effect on Young's modulus (*Japanese*) 8-60694

furan resin, effect of silica fillers on compressive strength (*Polish*) 8-68740

maleate-acrylate polyester resin, with phenol and glass microspheres, rheological behaviour 8-53267

mathematical model of strengthening (*German*) 8-63279

metal-filled epoxy resin, temp. variation, current interruption appl. 8-76124

phenol formaldehyde resin, (Novolak) with filler, mech. props. determ. (*German*) 8-84933

phenol formaldehyde resin (Novolak), with and without feldspar filler, mech. and thermal props. determ. (*German*) 8-84828

phenol resin (Resol), with and without feldspar filler, mech. and thermal props. determ. (*German*) 8-84828

phenolphoromaledehyde resin moulding compounds, dynamic testing (*German*) 8-76699

phenolic resin, linen impregnated, abrasion, SEM obs. 8-64742

PMMA-filled with SiO₂, degrading effect of filler on polymer fracture energy 8-52939

polyamide-Cu(Ni) oxalate, oxalate decomposition kinetics, in polymeric medium, thermogravimetry and DTA 8-52749

polyester, unsaturated, glass bead filled, particle size effect on Young's modulus (*Japanese*) 8-60694

polyethylene, filled with glass particles, uniaxially drawn, elastic constants, filler addition effect (*Japanese*) 8-95780

polyethylene, filled with SiO₂, degrading effect of filler on polymer fracture energy 8-52939

polyethylene, high-density, effect of fillers and moulding process parameters on strength (*Russian*) 8-60640

polyethylene, model, effect of stiff fillers on elastic modulus 8-68720

polyphenylquinoxaline cyclotriphosphazine hexaisothiocyanate networks, dynamic mech. props. (*Russian*) 8-72809

polystyrene, microcryst. cellulose filled, glass transition temp. shifts 8-95144

PTFE-Al, adhesion joints, effect of Cu and CuO 8-53183

PVA, microcryst. cellulose filled, glass transition temp. shifts 8-95144

rubber, filled, birefringence 8-68472

spherical inclusions, slope discontinuity prediction in stress/strain behaviour 8-94596

thermosetting, anisotropic structure on injection moulding (*German*) 8-76625

Al₂O₃-loaded epoxy, shock-wave compressed, dielectric props. 8-80281

PVC-Cu, particulate composite, mech. props. effect of particle size 8-95799

SiO₂ powder filled epoxy resin, flow props. during curing (*Japanese*) 8-59355

films

see also *adsorbed layers; coatings; foils; Langmuir films; liquid films;*

monolayers; optical films; polymer films; replicas; thick films; thin films

heat flux density and unsteady state temp. of surface film 8-75036

multilayer orthotropic films, calc. of stability (*Russian*) 8-63281

particle size measurement by monoparticulate film method (*Japanese*) 8-95874

water cryofilm, on specular and diffusing surfaces, bidirectional reflectance 8-88274

filtering and prediction theory

see also *information theory; Kalman filters; random processes; Walsh*

functions

acoustics, speech and signal processing, conf., Tulsa, USA, 1978, April 8-63242

adaptive matched filters for the measurement of acoustically evoked potentials in the EEG (*German*) 8-88755

airborne radiometric data inversion, radioactive elements conc. mapping 8-77347

average evoked potentials, a posteriori Wiener filtering theory and practice 8-96038

average visual evoked response estimation, predictor-subtractor-restorer filter 8-65143

biomedical signals, development of common struct. for filters, correlators and Fourier analysers (*German*) 8-88748

C-CD transversal filter anal. in pattern recognition 8-71052

composite signal anal., by cepstral inverse filtering, biomedical appl. 8-69243

digital signal modelling and classification with the teleseismic data 8-73325

EEG epileptic transient detect., pattern recognition techniques 8-53542

European air temperature change patterns 8-92957

geomagnetic field microstructure separation, digital filtering methods 8-69480

geopotential fields, filtering and transform. theory using information on input data noise 8-61584

heat conduction, inverse nonlinear problems, simulation methods 8-94513

image processing, two-dimensional recursive digital filtering method, problems 8-58933

image processing, two-dimensional recursive filtering, system theory concept 8-58934

image processing and eigen representation 8-55312

Infinite dimensional filtering problems in optical communication systems 8-66779

inverse filter which is optimum in error-distrib. sense, stability characts. 8-81424

ionosphere sounding, filtering effect on drift parameters determined by full correl. anal. 8-65450

Kalman for nuclear reactor control system design (*Japanese*) 8-50278

Kolmogorov-Wiener least-squares filters appl. to geophys. anomalies separation 8-61580

optical differential operator processor, filter fabrication feasibility studies 8-58925

optimal numerical filters fitted for noise damping, atm. circulation simulation appl. 8-92997

seismic data, optimum mixed delay spiking filters appls. 8-77346

seismic data, single-channel white-noise estimators for deconvolution 8-77345

seismic spectra, least-squares inverse filtering and wavelet deconvolution 8-61339

filtering and prediction theory continued

- seismic wavelet estimation using short-time homomorphic signal 8-88930
- seismology, multidimensional polarization analysis 8-73528
- short-time homomorphic signal analysis, appls. to seismic wavelet estimation 8-81426
- statistical error prediction in meas. of probability densities (*French*) 8-57885
- time-domain wave-shaping filter weights computation 8-77351
- US image reconstruction processing limitations 8-73184

filters

- see also band-pass filters; crystal filters; digital filters; electromechanical filters; Kalman filters; low-pass filters; microwave filters; optical filters; passive filters; spatial filters; switched filters*
- 31st Annual Frequency Control Symposium, Atlantic City (1977) 8-57905
- acoustic lens-filter plate, log-periodic, variation of props. with freq. 8-63256
- acoustic signal processing equipment for ANSI standard psychoacoustic testing 8-83198
- DVMs measurement errors reduced by user-controllable filtering 8-77931
- magnetic separation, particle capture and axial filters, theory 8-92516
- magnetic separation, particle capture in axial filters, theory and performance 8-92515
- momentum filter for separation of electrons and negative ions 8-78034
- nuclear filters, prep. from polymers using Ar ions 8-86714
- nucleopore filters, amosite fibres collection efficiency 8-81341
- SAW filter appl. to TV receiver (*Japanese*) 8-71247
- SAW filters with weighting of electrode overlap without beam integration (*German*) 8-51011
- sleep EEG automatic K-complex detector 8-53557
- speech formant extraction, tracking loop filters 8-65051
- whistler detection, multichannel filter and shift register obs. system 8-93031

filters, optical *see optical filters***filtration**

- disperse systems, polymer-modified, filtration coeffs. 8-67264
- dynamics, free boundary enclosure 8-55687
- efficiency, comparing particle-size distribution, in feed stream to filtrate 8-92417
- grid filters, collection efficiency, effect of Stokes and Reynolds numbers 8-61592
- heat pipe, heat transfer agent flowrate through porous wick, approx. calc. method 8-75197
- multiway sorption filters, development and use for radioactive iodine removal from air 8-61543
- non-Newtonian liquid filtration eqn. 8-55690
- nucleopore filter, collection efficiency for asbestos fibres 8-57351
- oil, slurries, ultrasonic effects 8-94504
- PWR, in-reactor loop expts. on corrosion product transport and water chemistry 8-58335

FIM, atom-probe *see atom probe field ion microscopy***fine structure, atomic** *see atomic fine structure***fine structure, molecular** *see molecular fine structure***finite element analysis**

- adhesively bonded metallic panels, 2-ply, finite element and integral eqns. anal. of fatigue crack growth 8-92347
- aerofoil in unsteady viscous flow, numerical soln. procedures 8-75165
- anisotropic solid fluid flow with free or artesian surface, GROW1 program 8-92872
- automatic subdivision of 2-d region into finite elements, use of computer algorithm 8-81819
- axial-flow compressor cascade flows computer simulation 8-79333
- axisymmetric elements, numerical comparison 8-89313
- axisymmetric large elastoplastic strain problems, natural finite element anal. 8-83259
- beam, large displacement-small strain anal., finite elements with rot. degrees of freedom 8-86161
- beams with elastically restrained ends, large-amplitude vibrations 8-90747
- blood pulsative flow digital simulation 8-92670
- boundary element method for partial differential eqns. soln. 8-94634
- boundary layer flows, finite difference method 8-51155
- Boussinesq equation of fluid dynamics 8-79292
- buckling of simply supported skew plates 8-59319
- building two-dimensional heat load anal. 8-71336
- C¹-class on tetrahedron 8-57759
- cantilever cones, buckling under external pressure, exptl. and numerical solns. 8-71287
- cantilever cylindrical shells, seismic design, appl. to nuclear steam system 8-58339
- cascade flow, varying flow rate 8-90910
- cascade flow in large distorted periodic flow, finite element soln. 8-87348
- cat eardrum model as thin shell 8-65036
- circumferentially notched tensile specimen 8-67150
- collocation for groundwater flow digital simulation 8-93018
- combined bend mode specimens, calc. of stress intensity factors 8-79284
- complex part stress anal., photoelasticity and finite element methods 8-71279
- compliant bearing lubrication, finite element model minimisation algorithm 8-63400
- composite electrostrictive resonators, finite element simulation 8-59237
- composite materials, bimaterial plate, cracked, finite element anal. of stress distribution 8-75104
- computational methods, book 8-81820
- conducting slab response to source fields, EM analogue model and finite difference calcs. 8-61329
- conjugate gradient solutions, finite element elastic problem with high Poisson ratio 8-90707
- connectivity theory for formally symmetric operators 8-49651
- constrained finite element solns., convergence proof 8-54168
- convection-diffusion partial differential eqn. soln. 8-90889
- cooling towers with column supports, free vibration analysis 8-83292
- coupled solid/fluid/surface wave dynamic interaction problem, improved fluid superelement 8-81108

finite element analysis continued

- crack, elastodynamic anal. by finite element method using singular element 8-55603
- crack, virtual extension method for combined tensile and shear loading 8-67149
- crack anal., three-dimens., finite element method 8-83332
- crack propag. simulation, using moving grid based finite difference scheme 8-83334
- crack propagation under compression, finite element analysis 8-67148
- crack tip opening displacement by finite element anal. (*Czech*) 8-59343
- crack-tip problems and quarter-point triangular elements 8-83333
- cracked lug, test and analysis 8-67153
- cracked thick walled cylinder, elastic plastic fracture anal. under displacement controlled loading 8-67119
- creep, rapid cycling problems 8-63317
- cylinder-to-cylinder structure, analytical and exptl. stress anal. 8-59308
- dam porous media unsteady flow calc. 8-91012
- dam unsteady compressible fluid flow digital simulation 8-90820
- diffusion-convection eqn. soln. 8-90888
- duct, nonuniform, finite element method for acoustic transmission 8-83140
- Dugdale model solution, of cracked bodies 8-67116
- dynamic crack propagation and arrest 8-68758
- dynamic destinations, removal of redundant operations in front algorithm 8-62064
- edge dislocation climb, numerical anal. 8-71736
- elastic contact problem with friction, solution using nodal parameters (*French*) 8-63401
- elastic contact problems, in fracture mech., friction effects 8-67142
- elastic material, finite element anal. of crack problems 8-67146
- elastic mechanical systems, design sensitivity analysis, adjoint variable methods 8-90706
- elastic sandwich plates, finite element anal. 8-67046
- elastic solid, cracked or notched, general numerical method for three dimensional singularities 8-67137
- elastic-plastic crack problem, comparison of finite element soln. 8-79263
- elastic-plastic finite element analysis, interpolation vs. iterative soln. for Tresca yield condition 8-59312
- elastic-plastic materials, finite deformation anal. of crack-tip opening 8-51126
- elastic-plastic solid containing holes in vicinity of crack tip, finite element anal. 8-67147
- elasticity, finite element method, reduced integration 8-75066
- elasticity, one-dimens. problems, diagonal mass matrices and finite element eqns. 8-73857
- elasticity theory, finite element formulation 8-69985
- elasto-plastic anal. of shallow shells (*Japanese*) 8-63323
- elasto-viscoplastic analysis of large deform. problems, natural finite element formalism 8-83258
- elastoplastic thermal stresses in axisymm. problems (*Japanese*) 8-51096
- electric and magnetic fields, 2D open boundary problems 8-94354
- elliptic boundary value problem, second order, hybrid finite element methods, Dirichlet problem 8-73835
- EM instruments for use in liquid sodium, theoretical anal. 8-54857
- EM scattering calculations, boundary element method 8-90347
- engineering applications of finite-element and finite-difference methods 8-57765
- environmental release prediction digital simulation 8-92880
- equilibrium equations soln. for rapidly rot. stars 8-65601
- estuary water quality models, finite difference and finite element methods 8-77375
- F₂-layer, plasma continuity eqn., comparative anal. of numerical soln. methods 8-69578
- fatigue crack closure, influence of mech. factors 8-67100
- fatigue crack propag., in deformable media with nonlinear characteristics, model 8-63393
- field problem inference-finite element model 8-81923
- finite difference calc., campylotropic coords. for boundary value problems 8-65757
- flames, premixed, laminar, time-depend. soln. determ. 8-67282
- flow due to gravity, free surface, variable domain method 8-79294
- fracture, appl. of continuum theory of dislocations fracture mechanics 8-67767
- fracture mechanics, calc. of integral J_I 8-67129
- fracture toughness parameters J and G^A, effect of load biaxiality 8-67128
- free surface flow digital simulation 8-90819
- frictionless tidal channel behaviour 8-92876
- fusion reactor, three-dimens. solid finite element anal. for simulating composite windings 8-55003
- fusion reactor, Tokamak constant tension D-shaped coils, lateral support struct. 8-55013
- fusion reactor anisotropic B_z-coil two-dimens. finite element anal. of laminate sliding 8-50382
- fusion reactor B_z-coil stress anal., constraint finite element anal. for contact problem 8-55004
- fusion reactor eddy current analysis, finite element circuit method 8-66373
- fusion reactor solenoid, orthotropic, finite element stress anal. 8-55010
- fusion reactor superconducting magnet magnetoelectric energy calcs., finite element anal. 8-55002
- fusion reactor TESPE coil, finite element method calc., winding package modelling 8-50376
- fusion reactor vacuum vessel, magnetic stress induced by plasma motion, 3-dimens. anal. 8-66370
- fusion reactor vacuum vessel, stress anal. 8-66371
- Galerkin for lakes or bays landslide wave generation simulation 8-92879
- Galerkin-finite element simulation of the effects of artificial recharge on flow and chemical quality in an alluvial aquifer 8-81263
- general shell finite elements development 8-87274
- geometrically similar elements 8-57760
- glass, ion-exchanged, anomalous stress profile, photoelastic meas. 8-90803
- glass, narrow sandwich seals, shape factor, finite element anal. 8-75111

finite element analysis continued

graphite fibre reinforced epoxy, epoxy matrix, effect of material variability on predicted environmental behaviour, numerical anal. 8-90733

gravitational collapse, finite-particle scheme for three-dimens. gas dynamics 8-67218

groundwater, unsteady flow through tunnel opening, reductive finite element/Crank-Nicolson anal. 8-92861

groundwater discrete kernel generator model 8-92873

groundwater flow anal. 8-92875

groundwater flow calc. 8-89320

groundwater flow model 8-92874

groundwater unsteady flow from tunnel opening (*Japanese*) 8-96251

heat conduction, transient problems, finite element and matrix methods calcs. 8-94515

heat conduction in reactor solids 8-62593

heat conduction numerical soln. oscillations, nonlinearity allowance scheme effect (*Ukrainian*) 8-90625

heat conduction transient, two-dimens., crit. time step for finite element solns. 8-71260

heat transfer, calc. (*Japanese*) 8-89414

heat transfer, nonlinear, iterative-variational method 8-94511

hierarchical elements and precomputed arrays 8-62063

high precision triangular laminated anisotropic cylindrical shell finite element 8-79206

HTGR, annular fuel rod, contact viscoelastic stress anal. (*Japanese*) 8-54817

HTGR fuel and graphite structure stress analysis methods and programs (*Japanese*) 8-74434

hybrid displacement method, simplified, appl. of line integrals 8-89314

hybrid elements, historical note and definition 8-57761

hydrodynamics models, nonstationary gas flow, two dimens., variational approach to finite difference scheme 8-51147

hydrological system tracer digital simulation 8-92881

impact test, fracture toughness 8-68806

impacted pretensioned plate, dynamic finite element and photoelastic analyses 8-67111

implicit finite element algorithm for geometrically nonlinear problems of struct. dynamics, stability anal. 8-86157

implicit finite element algorithms for geometrically nonlinear problems of struct. dynamics, accuracy anal. 8-86158

insulating and semiconducting media, electric field numerical soln. (*Slovak*) 8-66710

intensive finite element grading for stress concs. 8-55587

intervertebral joint, systems identification for material props. 8-69125

isoparametric quadrilaterals, integration formulas 8-89317

iterative procedures for penalty function solns. of algebraic systems 8-57770

J-integral evaluation for CT specimen 8-67131

jet, buoyant, turbulent in cross flow, finite difference method 8-90907

jet flow with surface tension, viscous flow 8-79349

Klein Gordon equation, equivalent variational integral, numerical soln. by finite element method 8-78064

lake, wind-induced circulation and water level changes, two-dimensional finite difference model 8-77287

laminar flows of viscoelastic fluids in concentric annuli with axially moving boundaries 8-79295

laminar incompressible boundary layer eqns. finite element soln. 8-79304

large amplitude water wave digital simulation 8-92851

large deflection anal. of tail-wheel struct. of light aircraft 8-83272

large deformation elastoplastic analysis of arbitrary shells, triangular finite element 8-83257

lateral tibial plateau, axisymm. finite element anal. 8-69127

leaky aquifer anal. 8-93017

linear accelerator cavity anal., evaluation of LACC program 8-90000

linear elastic half-space, frictional unloading problem, variational soln. for stress analysis 8-59350

linear strain triangular element solns. 8-90719

linear viscoelastic bodies, approx. anal. using Legendre polynomials, finite element soln. (*Japanese*) 8-83266

LMFBR, finite element formulation for thin reactor struct. thermal stress anal. 8-70613

LMFBR cores, numerical method for predicting subassembly seismic induced impact 8-74447

LMFBR subassembly ducts dynamic response, comparison of finite element code with expts. 8-70614

LMFBR subassembly simulation, finite element computer model, safety anal. 8-70612

machine vibrations anal. and obs. block deformability influence (*Italian*) 8-51108

magnetic field calc. from current distrib., finite element techniques 8-94358

magnetic fields, boundary-value problems, finite element and finite difference anal. 8-94353

magnetic fields, quasi-stationary 8-94356

magnetic problems, grid and metric optimisation, finite difference and finite element methods 8-94352

mechanical dished supports, oscillation and stability conditions based on mixed finite elements (*German*) 8-87299

medullary implants with porous coating, stress distrib. 8-69256

metal bicrystal, mech. behaviour, continuous theory of dislocations appl. 8-67717

metal structures, inelastic anal. 8-70586

metals, residual stress and deformation, due to quenching, elastic-plastic anal. (*Japanese*) 8-83268

MHD, nonsimilar incompressible laminar boundary layers, finite-difference scheme 8-79386

MHD generator, Faraday type, current profile optimisation, electrode cond. profile 8-94939

Navier-Stokes equation solution, smoothing techniques 8-90823

Navier-Stokes equations, theory and numerical analysis, book 8-77721

nearshore circulations finite element modelling 8-77270

neutron flux computation, finite element code 8-50449

non-Newtonian flow in pipe, finite difference methods 8-94770

nonlinear elastic stability problems using a finite difference perturbation method 8-83273

nonlinear heat cond. problem with phase change, finite element anal. 8-75030

finite element analysis continued

nonlinear hyperbolic conservation laws, finite difference methods 8-49649

nonlinear post-buckling anal., perturbation approach to imperfect structs. and snap-buckling 8-79244

nonlinear variation eqns., convergence of finite element solns. 8-86127

nonlinear wave propagation and unsteady transonic flow, variational formulations 8-55660

nonrectangular reverberation chamber design and construction 8-83196

notched flat tensile specimens, deform. zone (*German, English*) 8-64603

nuclear fuel pellets, cracked, thermal stress anal. 8-82462

nuclear fuel-cladding interaction between cracked surfaces, mechanical and temp. contact 8-66341

optical fibre connector, using resilient alignment method 8-71230

optical waveguide, trapezoidal cross-section ridge design, propag. characts. 8-55436

optimal choice of finite element grids 8-77698

partial differential eqns. reduction by Galerkin, collocation, and method of lines 8-77693

partial differential equations, time depend., Method of Lines compared to finite difference scheme 8-79291

patch test for nonconforming finite elements, conditions for piecewise polynomial functions 8-77697

Petrov-Galerkin finite element method, boundary layer problem 8-69989

plane notch and crack problems, appl. of displacement and hybrid stress methods 8-63375

PLASTE code, numerical simulation of thermoelastoplastic behaviour using finite element method 8-90731

plasticity and viscoplasticity problems (*French*) 8-63334

plate, obliquely stiffened, subjected to uniform compression, buckling strength (*Japanese*) 8-67067

plate, rib stiffened, studies on vibrations 8-83297

plate bending elements, quadrilateral, finite element anal. with reduced integration 8-75071

plate bending elements, quintic triangle 8-77716

plate structures, two-dimensional cracks, computer program based on superposition method (*Japanese*) 8-51123

Poisson equation over complex domain, finite difference method, Neumann boundary conditions 8-79189

polyhedral sandwich domes, elastic behaviour, failure, practical investigation and numerical simulation 8-59309

porous media one-dimensional unsteady drainage digital simulation 8-91011

potential energy with iterative correction or deterioration 8-89315

pressure vessel and nozzle junction, optimum shape design 8-89941

pulsating turbulent flow onto elastic surface, finite difference method (*Russian*) 8-75153

quarter elliptical cracks in irregular bodies, exam. using finite element alternating method 8-90796

quasi static crack growth, in sheet materials 8-67106

radial rotating beams, natural freqs. 8-59326

radiation problem simplified boundary elements 8-86226

radio meteor wind data, anal. using finite element approximation 8-81475

reactive scattering, anal. methods 8-92453

rocks asymmetric folding, finite-element simulation 8-77222

shallow thin shell finite element, stiffness matrix development 8-90705

shallow water with moving boundaries digital simulation 8-92847

shell structures, thin, curved finite element 8-79205

shells, paraboloid, elliptic, computerised stress analysis 8-59294

shells of revolution with variable geometry, optimisation of mass 8-67030

shock wave ionisation in transverse magnetic field, finite-difference methods 8-51249

skew conditions, specification 8-62057

slab with temp. depend. thermal cond., convective boundary, transient cond., finite difference method 8-75031

soil, unsaturated, coupled heat and water movement prediction, math. model 8-61446

soil-struct., interaction initial stress finite element method 8-59313

solar energy compound parabolic concentrator, natural convection, finite element soln. 8-90634

spherically symmetric elasticity problems, finite element soln. 8-63293

spring, complex arch type, movable, snap-through action characts., appl. to microswitches 8-63339

spring, complex arch type, movable, snap-through action characts., microswitch appls. 8-63340

stability analysis of skew orthotropic plates by the finite strip method 8-79235

stable crack-growth, fracture criteria, numerical approach 8-67104

state determinants method (*Russian*) 8-77695

stationary heat cond. using successive overrelaxation and conjugate gradients 8-83206

steel, CrMoV, compact tension specimen, thickness effect 8-68764

steel, Ni, cross girder connections, fatigue strength, design stress 8-64700

steel, stainless, 316, nuclear fuel cladding, crack nucleation 8-72864

steel, stainless, type 304, elastoplastic fracture mechanics for reactor piping 8-68777

Stoke's problem in velocity pressure formulation, mixed finite element approx. (*French*) 8-86164

Stokes problem with conforming Lagrangian finite elements, soln. error estimates (*French*) 8-62085

stratified turbulent flow digital simulation 8-90964

strength of axisymmetric body, optimum shape calc., finite element technique 8-51060

stress analysis, improved equilibrium finite elements 8-75067

stress analysis of cracks, elastoplastic range 8-67144

stress intensity factors, UNCLE finite element system calcs., appls. in fracture mechanics 8-67098

structural anal., underlying concepts 8-66337

structural analysis of toroidal field coil struct. response 8-50396

structural stiffness matrix eqn., algorithms for direct access Gaussian soln. 8-57766

structures of discontinuous shape, finite element analysis of bending behaviour (*Japanese*) 8-83238

finite element analysis continued

- structures with rotational degrees of freedom, large displacement-small strain anal. 8-89310
 Sturm-Liouville, error estimation 8-81818
 supersonic three-dimens. flow, finite difference method 8-51190
 synthetic seismograms using finite difference techniques 8-73326
 thermal stresses in rectangular plates, variational and finite element solns. 8-51082
 thick-walled shells of revolution, axisymmetric problems soln. by design and exptl. methods (*Russian*) 8-73853
 thin film eddy current integro-differential eqns. soln. 8-90343
 tidal estuary two-dimensional hydrodynamic digital simulation 8-92846
 tidal flow, finite element analysis model, flow in rectangular channel example (*German*) 8-96233
 tidal waves in estuaries, explicit finite-element formulation (*German*) 8-94755
 tides, spectral modelling, finite element method, appl. to M_2 tide in English Channel 8-61579
 time-dependent Navier-Stokes eqn. soln. 8-92956
 Timoshenko beams, finite element eigenvalue anal. 8-59327
 Tokamak, Texas exptl., homopolar generator, eddy currents, EM forces (torques), due to misalignment 8-54953
 transient and unconfined groundwater flow analysis 8-92871
 transient diffusion with n-order irreversible chem. reaction, finite element method 8-85122
 transitions elements for use with quarter point crack-tip elements 8-63376
 Tresca yield condition usage in finite element plane strain anal. 8-83263
 tsunami long wave propagation anal. at Hawaiian Islands and Long Beach and Los Angeles harbours 8-92849
 tsunami wave propagation anal. 8-92848
 tsunamis interaction with Hawaiian Islands, finite element numerical model 8-69361
 turbulent channel flow, secondary current numerical simulation 8-94828
 two dimensional flow with singularities formulation 8-90822
 two-dimens. structs., finite dynamic element for free vibr. anal. 8-83287
 two-dimensional hydrodynamics and water quality digital simulation 8-92877
 two-dimensional potential fields in complex media (*Slovak*) 8-94351
 two-phase flow soln. technique 8-79366
 unsaturated porous media flow 8-92869
 unsaturated soil simultaneous heat and moisture transport anal. 8-92868
 unstable crack propag., in 2-dimensional geometries, transient finite element analysis 8-67151
 unsteady heat cond. in domains of irregular boundary, numerical expts. 8-51039
 upwind finite elements development 8-89312
 US exponential solid horn 8-94496
 vertebral model, computer-aided technique for 3-D finite element model generation 8-92591
 vibration anal. by combined holographic interferometry and finite element anal. (*German*) 8-90806
 viscosity by capillary rheometer, end correction for power-law fluids 8-91037
 water pollution prediction 8-93019
 water resources, conf. at London, England 1978 8-92867
 water wave propag., long-period, finite difference-element integration scheme 8-75157
 wells, large diameter bottom entry flow anal. 8-92870
 yield zone form., fracture resistance, influence of specimen configuration 8-68817
 yielding of plates with hardening and large deformations 8-59311
 Al alloy, crack opening displacement, expt. and FEM study 8-68811
 Fe, cast, spherical, mech. behaviour, continuous theory of dislocations appl. 8-67717
 NaCl, rock salt, progressively mined soln. cavities, struct. behaviour 8-61409
 O silent discharge, numerical simulation 8-63629
 α - β Ti-Mn (8 wt.%), calc. of stress-strain curves by finite element method, comparison with expt. curve 8-84924

Finlay-Freundlich red-shift hypothesis see *gravitational red shift*

fireproofing see *flameproofing*

fires

- see also *accidents; combustion; flames; safety*
 convection plume over fire in polytropic atmosphere (*Russian*) 8-96262
 enclosure fire, static pressure meas. 8-90871
 flameproof coating for PVC insulated cables, composition, tests (*Russian*) 8-68828
 nuclear power plant, fire hazard 8-50269
 nuclear safety exercises carried out in French industrial facilities (*French*) 8-55051
 United States, synoptic weather situations assoc. with major wildland fires 8-61499
 wood burning, atm. CO_2 input 8-81368

fission

- see also *fission of plutonium; fission of uranium; photofission; spontaneous fission*
 asymmetric, statistical theory explanation, association with higher quantum state density 8-70509
 double humped fission barrier using biharmonic oscillator pot., penetrability calcs. 8-86524
 EAS, atomic nuclei fragmentation, analytical method (*Russian*) 8-65472
 excitation during collective deformation, time depend. Hartree Fock Bogolyubov method, fission process 8-58229
 explosive r process cooling process 8-69791
 fission, ATDHF validity 8-50149
 fission barrier determ. in region $Z=82$, $N=126$, using polycarbonate thin film and electron linac 8-55104
 frictional effects in nuclear reactions with large scale collective motion, review 8-78336
 heavy ion collision induced fission, fragment ang. distrib., reaction mech. 8-74412

fission continued

- heavy ion reactions, fission fragment angular distrib., shape of saddle point of compound nucleus (*Chinese*) 8-78427
 heavy ion reactions, potential energy surfaces, binary fission, fusion, liquid drop model (*Rumanian*) 8-86547
 heavy ion reacts., cross-sections for fusion, quasifission and deep inelastic collisions (*Russian*) 8-54801
 heavy ions collision, liquid drop model generalisation (*Rumanian*) 8-58260
 heavy-ion induced fusion reaction products, statistical and liquid drop model anal. 8-66312
 modified one body nuclear dissipation 8-50071
 nucleon exchange between fission fragments in two centre oscillatory pot. below threshold (*Russian*) 8-89847
 one body dissipation and super viscosity of nuclei, nuclear fission, collisions and deformation 8-86501
 r-process, astrophysical, implications of fission mass distrib. 8-93204
 Sommerfeld-Watson transformation (*Rumanian*) 8-86526
 spontaneously fissioning isomers, probabilities of α -, β - and γ -transitions accompanied by changes in nuclear shape (*Russian*) 8-89820
 statistical fission parameters, ang. momentum depend. in statistical/rotating liquid drop model 8-89846
 statistical model de-excitation calcs. of compound nuclei 8-50146
 statistical theory, critical evaluation 8-70508
 superdense nuclei production (*Russian*) 8-58310
 superheavy region, neutron drip line, energy density mass formula extrapolation 8-93932
 time-dependent variational approach to heavy ion reaction, appl. to fission 8-50193
 (n,f), integral data meas. in $\Sigma\Sigma$ neutron field 8-70537
 (n,f), near thermal, effects of phonon transfer on cross sections 8-50221
 p induced reactions at intermediate energy, nuclear fissility anal. 8-70579
 (π^- ,f), at rest, exciton model 8-94042
¹⁹⁶Au, proton induced, 1 GeV, cross section (*Russian*) 8-94041
¹⁹⁷Au(⁴⁰Ar,X) 259 MeV, differential recoil range distributions, large contrib. of deep inelastic processes 8-70565
¹⁹⁷Au(⁸⁶Kr, Z,f), 618 MeV, ang. momentum depolarisation, sequential fission 8-62585
¹⁹⁷Au(d,f), 2.1 GeV, binary and ternary fission kinetics (*French*) 8-70577
²⁰⁸Bi(d,f), 2.1 GeV, binary and ternary fission kinetics (*French*) 8-70577
²⁴⁹Cf(n,f), separation, identification of Ru, Rh isotopes 8-89924
²⁵²Cf fission, n angular distrib., 0 to 30° (*Russian*) 8-86564
 Fe assembly, meas. of absolute fission rates/source neutron using solid state track detectors 8-58559
 (⁴He,xnf)²³⁹Am, statistical model anal. of fission isomer production 8-66326
¹⁹⁴Hg compound nucleus, fission, ³H and ⁴He emission 8-50220
²⁴⁶Mg+e, 21 to 32 MeV, E0 and E2 excitations, fission into two ¹²Cg.s. nuclei 8-54744
^aPa, A=236, 238, β strength function struct., influence on β -delayed fission 8-89826
²³¹Pa(n,f), fission spectrum averaged cross section 8-70576
 Pb, A=206, 208, proton induced, 1 GeV, cross section (*Russian*) 8-94041
 Pb(α ,f), 0.65, 1.74, 4.12 GeV, fission fragment recoil characts. 8-89925
²⁰⁷Pd(d,f), 2.1 GeV, binary and ternary fission kinetics (*French*) 8-70577
²¹²Po, fission excitation functions anal., shell effects at saddle point, nuclear shape 8-54737
 Sm, proton induced, 1 GeV, cross section (*Russian*) 8-94041
¹⁸¹Ta, proton induced, 1 GeV, cross section (*Russian*) 8-94041
¹⁴⁹Tb compound nucleus, statistical model de-excitation calcs. 8-50146
²³²Th fuel, conversion and fission yield, irradiation expt. 8-86609
²³²Th, muonic, μ induced prompt fission, fate of the μ . 8-86557
²³²Th muonic atom, n emission, bound μ influence on fission barrier 8-89845
²³²Th, μ capture rate in the fission mode, μ lifetime 8-89827
²³²Th, proton induced, 1 GeV, cross section (*Russian*) 8-94041
²³²Th(d,f), 2.1 GeV, binary and ternary fission kinetics (*French*) 8-70577
²³²Th(n,f), Kr and Xe isotope yields 8-74410
²³²Th(n,f), yields of ¹³¹,¹³²Sn, ¹³¹,¹³³Sb isotopes determ. 8-89923
 Th(α ,f), 0.65, 1.74, 4.12 GeV, fission fragment recoil characts. 8-89925
²³⁶U fission path, zero point energies in two centre shell model 8-93952
²³⁸U+⁴⁰Ar, cross-sections for fusion, quasifission and deep inelastic collisions (*Russian*) 8-54801
¹⁸⁶W+⁸⁶Kr, cross-sections for fusion, quasifission and deep inelastic collisions (*Russian*) 8-54801
 Yb, proton induced, 1 GeV, cross section (*Russian*) 8-94041

fission counters

- activation detector ave. cross sections in ²⁵²Cf benchmark field 8-82598
 ionisation chamber with intrinsic suppression of α -background, for fission fragment detection 8-78581
 miniature, for neutron field meas. in critical assemblies 8-82422
 neutron self-powered detector with fissile emitter, theoretical evaluation 8-74533
²³⁷Np dosimeter and spark counting system, for routine personnel monitoring 8-89984

fission of plutonium

- fine structure of yields of Xe isotopes, A=131-135 8-86560
 laser induced fission, Monte Carlo anal., critical mass and radius for bare spheres 8-62583
 (n,f), integral data meas. in $\Sigma\Sigma$ neutron field 8-70537
 (⁴He,2nf), statistical model anal. of fission isomer production Pu, A=235, 237 8-66326
^aPu(n,f), A=240, 242, 244, 0.1 to 30 MeV, cross-sections rel. to ²³⁵U 8-50217
²³⁹Pu muonic atom, n emission, bound μ influence on fission barrier 8-89845
²³⁹Pu, thermal neutron-induced fission, ⁹⁶Nb and ⁹⁸Nb yields 8-54807
²³⁹Pu+n, 13.9, 14.6 MeV, absolute neutron fission cross sections, associated particle method 8-89926

fission of plutonium continued

- ²³⁹Pu+n, ratio between capture and fission cross sections up to 30 keV 8-70538
²³⁹Pu(n,f), 0.3 eV resonance energy, mass distrib. of products 8-70578
²³⁹Pu(n,f), separation, identification of Ru, Rh isotopes 8-89924
²³⁹Pu(n,f), thermal, correlation for independent fission prod. yield uncertainties 8-50216
²⁴⁰Pu, moments of inertia of fissioning isomers, cranking model 8-74299
²⁴⁰Pu, P-odd neutron emission asymmetry (*Russian*) 8-74413
²⁴⁰Pu, reson. in isomeric and prompt fission probabilities 8-74429
²⁴¹Pu compound nucleus lifetime by the shadow effect in ²³⁸U(³He,f) (*Russian*) 8-86562
²⁴¹Pu(n,f) thermal, correlation for independent fission prod. yield uncertainties 8-50216

fission of uranium

- absolute fission rate distrib. in standard U shell, comparison with ANISN code 8-62584
 fine structure of yields of Xe isotopes, A=131-135 8-86560
 fission track annealing characteristics of epidote, appls. to geochronology, geol. 8-94038
 fission track dating and estimation of U in garnets 8-94039
 laser induced fission, Monte Carlo anal., critical mass and radius for bare spheres 8-62583
 ores, estimation of ratio of induced to spontaneous fission 8-53234
 quasistatic scission configurations obtained from long range particle accompanied fission distributions 8-74411
 (n,f), integral data meas. in $\Sigma\Sigma$ neutron field 8-70537
²⁴⁰Pu, moments of inertia of fissioning isomers, cranking model 8-74299
²⁴⁰Pu, thermal neutron induced, average angular momenta of even-even fragments 8-86525
 U anal. of natural waters by fission tracks 8-82587
^aU(³He,xn) A=233-235, x=1-4, cross sections, fission evaporation competition in Pu isotopes 8-66325
^aU(d,f), A=235, 238, 2.1 GeV, binary and ternary fission kinetics (*French*) 8-70577
²³⁸U solution, criticality anal. using KENO and SU-HAMMER codes 8-89949
²³⁸U, thermal neutron-induced fission, ⁹⁶Nb and ⁹⁸Nb yields 8-54807
²³⁸U(n,f), thermal, correlation for independent fission prod. yield uncertainties 8-50216
²³⁸U, thermal neutron induced, average angular momenta of even-even fragments 8-86525
²³⁸U, fission recoils, chem. effects, energy deposition efficiencies, surface conditions depend. 8-80776
²³⁸U, internal conversion cascading fission fragments 8-94036
²³⁸U, proton induced, 1 GeV, cross section (*Russian*) 8-94041
²³⁸U solution, criticality anal. using KENO and SU-HAMMER codes 8-89949
²³⁸U, subthreshold photofission 8-66323
²³⁸U, thermal neutron-induced fission, ⁹⁶Nb and ⁹⁸Nb yields 8-54807
²³⁸U, thermal-neutron-induced microscopic approach to statistical theory (*Chinese*) 8-86559
²³⁸U+n, 13.9, 14.6 MeV, absolute neutron fission cross sections, associated particle method 8-89926
²³⁸U(d,pf), 23 MeV, total KE release 8-78426
²³⁸U(γ ,f), ang. distrib. of fragments (*Russian*) 8-54808
²³⁸U(n,f), 6-9 MeV, fission product yields 8-66324
²³⁸U(n,f), separation, identification of Ru, Rh isotopes 8-89924
²³⁸U(n,f), thermal, α -particle spectra 8-78425
²³⁸U(n,f), thermal, correlation for independent fission prod. yield uncertainties 8-50216
²³⁸U(n_{th},f), fission fragment yield distrib., excitation energy depend. 8-50218
²³⁸U(n_{th},f), fragment-mass depend. of fission neutron spectrum, TOF method 8-82398
²³⁸U(n_{th},f) ionic charge distrib., effect of internal conversion 8-78428
²³⁸U, induced fission dynamics 8-66261
²³⁸U, thermal neutron induced, average angular momenta of even-even fragments 8-86525
²³⁸U(α , α'), 50 MeV, total KE release 8-78426
²³⁸U, muonic, μ induced prompt fission, fate of the μ 8-86557
²³⁸U, μ capture rate in the fission mode, μ lifetime 8-89827
²³⁸U, natural spontaneous fission, Xe prod., determ., extraction from granite 8-96216
²³⁸U, proton induced, 1 GeV, cross section (*Russian*) 8-94041
²³⁸U, spontaneous fission, half life and fragment kinetic energy meas. using cylindrical ionisation chamber 8-86555
²³⁸U+²³⁸U, 1785 MeV, cross sections, charge and mass distrib. of products 8-78408
²³⁸U+n, 13.9, 14.6 MeV, absolute neutron fission cross sections, associated particle method 8-89926
²³⁸U(¹²C,f), mass distrib. of fission fragments determ. (*Chinese*) 8-86558
²³⁸U(²⁷Al,f) 169, 190, 227 MeV, Z=105 compound nucleus lifetime using shadow effect (*Russian*) 8-86563
²³⁸U(³He,f), ²⁴¹Pu compound nucleus lifetime by the shadow effect (*Russian*) 8-86562
²³⁸U(⁴⁰Ar,X), 237, 250 MeV, differential recoil range distributions, large contrib. of deep inelastic processes 8-70565
²³⁸U(⁴⁸Ca,X), 276 MeV, differential recoil range distributions, large contrib. of deep inelastic processes 8-70565
²³⁸U(n,f), 1.8-16.8 MeV, fission fragment energy spectra using glass sandwich detectors 8-82399
²³⁸U(n,f), 6-9 MeV, fission product yields 8-66324
²³⁸U(n,f), separation, identification of Ru, Rh isotopes 8-89924
 U(α ,f), 0.65, 1.74, 4.12 GeV, fission fragment recoil characts. 8-89925
 U(γ ,f), 5.2-6.4 MeV, A=234, 236, 238, doubly even isotopes, ang. distrib., fragment yields 8-50219
 U(μ ,f), emission of conversion μ in radiation free fission (*Russian*) 8-62587

fission products

- alpha-particle energy spectrum, fission-emitted, fission-fragment shape and orientation depends. 8-74346
 delayed-n precursors in various mass chains half lives and P_n values 8-70497

fission products continued

- density distribution of fission traces, meas. by tracer's method in dielectrics, fuel meas. appl. (*Rumanian*) 8-90033
 desorption fission fragment induced, method for correlated events in TOF mass spectrometry 8-58089
 EBR II, fission product source identification using Xe tag 8-70588
 fast reactor whole core accidents, fission products rule 8-54854
 fission gas bubble distrib. in mixed oxide fast reactor fuel pin, anal. of TEM obs. 8-58358
 fission gas re-solution, comparison of single knock on and complete bubble destruction models 8-82455
 fuel reprocessing waste ¹³⁷Cs, ⁹⁰Sr and rare earth radioisotope separation by cation exchange 8-78486
 gamma peaks, appl. to burn up determ. of irradi. fuel samples (*Hungarian*) 8-82458
 gamma-ray and half life data tables 8-50134
 gamma-spectra, estimation using nucl. systematics 8-70587
 gas release from ThO₂ and ThO₂-UO₂ fuel 8-86651
 heavy ion reactions, fission fragment angular distrib., shape of saddle point of compound nucleus (*Chinese*) 8-78427
 HTGR coated fuel particles, behaviour of fission products (*Japanese*) 8-54830
 HTGR core during transient temp. excursion, fission product release, computerised analysis (*Japanese*) 8-82467
 HTR, expt. JAERI, safety anal. of fission product behaviour and hypothetical accident (*Japanese*) 8-66330
 LMFBR, fuel and fission gas response to simulated thermal transients 8-74453
 LMFBR, yield characts. of short-lived fission products in Na heat-transfer agent 8-66338
 muonic atom fission, distribution of muons among fragments (*Russian*) 8-94040
 nonequilibrium fission gas behaviour 8-86626
 nuclear energy, nonconventional conversion systems (*Rumanian*) 8-86705
 nucleon exchange between fission fragments in two centre oscillatory pot. below threshold (*Russian*) 8-89847
 radioactive fallout in air and rain, results to end of 1977 8-82535
 radioisotopes in cooling system, prod., transfer, life cycle, radiation calcs. using program system TIBSO 8-54821
 recoil characteristics, fission fragments due to high-energy α bombardment of U, Th, Pb 8-89925
 release and distrib. in coated particles, development and testing of laser system (*German*) 8-82403
 scattering kinematics of fission fragments, multiparametric anal. TDF instrument with semiconductor detectors 8-78550
 scattering kinematics of fission fragments, multiparametric anal., electronic meas. system, semiconducting detectors 8-78551
 spin distrib., statistical theory predictions, asymmetric fission explanation 8-70509
 track registration in crystals, development efficiencies, etchant (etching conditions) depend. 8-66454
 whitlockite from Bjurböle chondrite, origin of fission fragment tracks 8-81595
¹⁴⁵Ba, fission product, β -decay anal. 8-78323
²⁰⁹Bi(¹²C,f), mass distrib. of fission fragments determ. (*Chinese*) 8-86558
 Br series isotopes, sensitivities to various parameters, analytical evaluation 8-82424
¹⁴⁵Ce, fission product, β -decay anal. 8-78323
²⁵²Cf fission source, ionisation characts. of electron oscillating ion source coupled to He-jet skimmer system 8-70661
²⁵²Cf, spontaneous fission, fragment ranges and kinetic energies in Al 8-94037
^aCs, A=139-144, beta endpoint energy measurements 8-93975
 Kr, A=90, 91, ²³²Th fission products, yields, γ -ray spectra 8-74410
 Kr series isotopes, sensitivities to various parameters, analytical evaluation 8-82424
¹⁴⁵La, fission product, β -decay anal. 8-78323
²⁰⁸Pb(¹³⁶Xe,X)^Y, 470 MeV, search for delayed fission products from superheavy nuclei 8-70562
¹⁰⁷Pd(n, γ) and transmission meas., level parameters 8-58277
 Pt alloy, fission-fragment-induced He blistering 8-86601
²³⁹Pu(n,f), 0.3 eV resonance energy, mass distrib. of products 8-70578
^aRb, A=88-94, beta endpoint energy measurements 8-93975
 Rh, A=108-111, prod. by fission of ²³⁵U, ²³⁸U, ²³⁹Pu, ²⁴⁹Cf, separation, identification 8-89924
 Ru isotopes, A=107-113, prod. by fission of ²³⁵U, ²³⁸U, ²³⁹Pu, ²⁴⁹Cf, separation, identification 8-89924
 Sb, A=131, 133 prod. by ²³²Th reactor induced fission, yield, radiochem. separation, anal. 8-89923
 Sb isotopes, fission product conc., sensitivity anal. of various key parameter effects 8-82428
 Se series isotopes, sensitivities to various parameters, analytical evaluation 8-82424
¹⁴⁹Sm poisoning calc., of KS-150 reactor, using spatial models (*Slovak*) 8-54850
 Sn, A=131, 132 prod. by ²³²Th reactor induced fission, yield, radiochem. separation, anal. 8-89923
 Sn isotopes, fission product conc., sensitivity anal. of various key parameter effects 8-82428
 Te isotopes, fission product conc., sensitivity anal. of various key parameter effects 8-82428
 U anal. of natural waters by fission tracks 8-82587
²³⁵U fission fragments, internal conversion cascading 8-94036
²³⁵U, fission recoils, chem. effects, energy deposition efficiencies, surface conditions depend. 8-80776
²³⁵U(n,f), 6-9 MeV, fission product yields 8-66324
²³⁵U(n_{th},f), fission fragment yield distrib., excitation energy depend. 8-50218
²³⁵U(n_{th},f), fragment-mass depend. of fission neutron spectrum, TOF method 8-82398
²³⁵U(n_{th},f) ionic charge distrib., effect of internal conversion 8-78428
²³⁸U+²³⁸U, 1785 MeV, cross sections, charge and mass distrib. of products 8-78408
²³⁸U(¹²C,f), mass distrib. of fission fragments determ. (*Chinese*) 8-86558
²³⁸U(n,f), 1.8-16.8 MeV, fission fragment energy spectra using glass sandwich detectors 8-82399
²³⁸U(n,f), 6-9 MeV, fission product yields 8-66324

fission products continued

- U(γ ,f), 5.2-6.4 MeV, A=234, 236, 238, doubly even isotopes, ang. distrib., fragment yields 8-50219
 Xe, A=131-135, fine structure of yields for heavy nuclei fission 8-86560
 Xe, A=139, 140, ²³²Th fission products, yields, γ -ray spectra 8-74410
 Xe ions measurement, Si surface-barrier detectors for fission fragments 8-78571
¹³⁵Xe poisoning calc., of KS-150 reactor, using spatial models (Slovak) 8-54850
¹³⁵Xe-induced core instabilities, extended λ -mode linear anal., CANDU appl. 8-82494

fission reactor cooling and heat recovery

- see also cooling; fission reactor core control and monitoring
 AGR, heat transfer to accel. gas flows, expt. and calcs. 8-54823
 AGR boiler tube, serpentine geometry at high press., two phase heat transfer 8-94077
 AGR line development status and performance (German) 8-86568
 annular flow model, critical heat flux 8-94090
 blowdown from horiz. pipe 8-94093
 BWR, simulation of cooling system conditions, stress corrosion cracking test 8-80696
 BWR, transition boiling under forced convective conditions, reactor accident condition 8-89961
 BWR boiling noise, local and global component obs. and calc. 8-94066
 BWR core flow fluctuation and neutron noise obs. 8-94060
 BWR critical heat flux density, heat transfer with boiling and burnout phenomenon (German, English) 8-58330
 BWR neutron noise local component meas., two phase flow study 8-94059
 BWR stochastic neutron flux fluctuation obs. and modelling, thermo-hydraulic parameters 8-94065
 BWR void effects, stochastic point model and zero-power reactor simulation 8-94061
 BWR-4 neutron noise analysis spectra, instrument tube flow-induced vibr. 8-94063
 CANDU secondary coolant circuit chemistry control, automated system development 8-66359
 circular channel with rod clusters, heat transfer characts. 8-75140
 circular rods with regular polygonal concentric inner bore, heat flow shape factors 8-51048
 cladding temp. fields in critical regions of rod bundles with Na flow 8-94084
 combined convection heat transfer in rod arrays, numerical anal., FBR cooling appl. 8-90898
 condensation heat transfer of steam flow on ice surface 8-94099
 conduction centrifugal EM pump for nuclear reactor coolants, characts., operation 8-86246
 containment negative pressure evaluation 8-50275
 containment tightness, integral leakage rate tests 8-89956
 coolant boiling crisis in rod assemblies 8-94087
 critical energy in heat transfer channels of complex shape, fuel rod assembly 8-78453
 direct contact condensation of flowing steam onto injected water 8-94097
 DISTAV calc. code for temp. determ. of Na and pile cladding (French) 8-94085
 dryout, premature in conventional and nuclear power station evaporators, model 8-94120
 ducts and pipes intricately shaped cross section, heat transfer, Laplace and structural method 8-83477
 electrochemical O₂ meter for meas. in liquid Na 8-58337
 EM instruments for use in liquid sodium, theoretical anal. 8-54857
 EM pumps for liquid metal fast breeder reactor, review 8-94074
 emergency core cooling system motor operated valves, failure mode anal. 8-54866
 emergency core cooling system motor operated valves, failure criteria 8-70592
 falling film rewetting 8-75906
 film boiling and rewetting heat transfer during bottom flooding of a hot tube 8-94094
 forced convection in annuli and rod bundles with variable heat flux distribution 8-94082
 fuel element bundles at coolant boiling, fuel exchange enhancement 8-94086
 fuel element modeling rod bundle in longit. air flow, heat transfer expt. 8-82415
 fuel elements, cracked, gas-filled, temp. distrib. calc. 8-78446
 fuel pins, eccentrically placed pellets, finite difference method for heat transfer 8-82419
 fuel rod arrays, radiative heat transfer, Monte Carlo method, temp. distrib. 8-78447
 fuel rod vibration induced by coolant water and air/water flow (Japanese) 8-74429
 gas-cooled porous fuel elements, thermal design 8-94100
 GCFR, borax (Na₂B₄O₇) internal core catcher 8-58372
 heat exchange component vibrations in liquid and two-phase cross-flow 8-90770
 heat exchanger tube banks, crossflow induced vibr. 8-50245
 hermetically sealed valve for the safety systems of a nuclear power station (Russian) 8-89952
 HGTR core, multiregional coupled conduction-convection model 8-94083
 homogeneous nuclear reactor, water pool boiling, produced by distrib. internal heat sources 8-90685
 hot water leakage from first loop, 22.8 MPa initial pressure, flow characts. 8-66357
 HTGR, consequence anal. of hypothetical accidents, core heatup and afterheat removal 8-58381
 HTGR, heated vertical pipe, gas buoyancy effect on downward flow and heat transfer 8-74427
 HTGR hypothetical accidents, consequences following breach of primary circuit and safeguard failure (German) 8-58390
 hydrodynamic oscillations in Gentilly-1 reactor steam mains, GISMO program 8-54824
 interchannel heat and mass transfer, wire-spaced fuel pins effect 8-94080
 lattice cell meas. in 36 element natural UO₂ fuel, stopping effect of coolant 8-58347

fission reactor cooling and heat recovery continued

- liquid metal heat transfer in regular fuel element arrays, Nusselt no. calc. 8-89932
 liquid-vapour critical flow, two-fluid model 8-90973
 LMFBR, accident anal., radiative transfer treatment 8-94573
 LMFBR, coolant start of boiling detection by acoustic method 8-86646
 LMFBR, dynamic response of containment vessel and coolant wave propag., REXCO-EUR code manual 8-58349
 LMFBR, leak detection in steam generator, by acoustic spectra meas. (Czech) 8-54849
 LMFBR, primary cooling circuits, Na loop system, anal. of radioactive corrosion product transfer 8-78464
 LMFBR, squeeze flow between two adjacent subassemblies, discrete model 8-86634
 LMFBR, US flowmeter (Japanese) 8-78455
 LMFBR, wastage effects in small leak Na+water reactions, safety considerations 8-82418
 LMFBR, water leaks in secondary cooling circuit boilers 8-86572
 LMFBR, yield characts. of short-lived fission products in Na heat-transfer agent 8-66338
 LMFBR cooling channels blockages, simulation testing (German) 8-94044
 LMFBR outlet plenum, air flow model, interferometric meas. of fluctuating temp. using FFTF 8-89943
 LMFBR overpower excursions, mechanistic model of fuel freezing, channel plugging and continued coolability 8-58371
 LMFBR steam generator, dryout characts. 8-90990
 LMFBR subassemblies, coolant boiling calc., using Claymore code 8-82473
 LOCA in water reactors, reversal of laminar flow in circular pipe 8-50271
 LWR anal., pressure-crossflow soln. method, COBRA-III codes 8-82417
 marine reactor systems, Monte Carlo reliability anal. of power and heat removal systems (Japanese) 8-58396
 molten fuel-coolant interaction studies, simulated reactor accident, wind-scale shock tube rig 8-58363
 neutronic noise, relations with coolant temp. fluctuation and control rod vibr. at KUR 8-58327
 nuclear power station with HTR and He turbine, dry closed circuit cooling, principles and advantages (German) 8-74426
 pin bundle, two-phase flow, eqns. of motion 8-86570
 pressure-suppression systems, direct heat transfer 8-94096
 propagating physical quantity transit time estimation, improved correl. method, coolant bubbles appl. 8-94067
 pump coolant tests, computerised monitoring 8-70585
 PWR, 450 MWe, noise obs., analysis and interpretation 8-94072
 PWR, crit. and transient heat flux exam. (Hungarian) 8-86580
 PWR, data acquisition system for high press. water loop (Hungarian) 8-82432
 PWR, in-reactor loop expts. on corrosion product transport and water chemistry 8-58335
 PWR, modification of subcooled boiling calc. in COBRA-3/KFKI program (Russian) 8-82434
 PWR, MULTIFLEX code, anal. of hydraulic force with hydro-structural interactions during LOCA 8-58373
 PWR, peak cladding temp. sensitivity to LOCA reflood parameters 8-86639
 PWR, sensitivity of LOCA heat transfer anal. 8-50246
 PWR, thermohydraulic processes in high press. water loop, constructional details of loop (Hungarian) 8-82431
 PWR, thermohydraulic processes study, models and expt. instrumentation (Hungarian) 8-82433
 PWR depressurisation, hydraulic analogy 8-50243
 PWR natural circulation U-tube steam generator, digital code UTSG 8-50242
 PWR steady state thermal anal., single-pass procedure using simplified nodal layout 8-50244
 PWR surface boiling, heat transfer with boiling and burnout phenomenon (German, English) 8-58330
 radiochemical control of reactor cooling water (Korean) 8-54820
 radioisotopes in cooling system, prod., transfer, life cycle, radiation calcs. using program system TIBSO 8-54821
 rewetting of very hot vertical and horizontal channels by flooding 8-94095
 rod bundles, transient critical heat flux 8-94089
 rod cluster assembly, forced convection heat transfer, Poisson eqn. by finite difference scheme 8-79189
 spray cooling, heat and mass atmospheric transfer 8-94078
 steam generator tube survey, causes of failures, repair procedure 8-54826
 subcooled film boiling heat transfer from spheres 8-51047
 Superphenix internal shells, vibr. anal. (French) 8-50247
 thermal hydraulic anal., of rod bundle fuel elements, COBRA-3C/KFKI digital computer program 8-54822
 transient 1-D two-phase flow eqns., finite difference approx. 8-51229
 transient two phase thermal hydraulics in channel, model 8-94091
 tubes with nonuniform axial heat distrib., heat transfer burnout 8-94088
 turbulent heat transfer in annulus, transient, heating element, reactor cooling theory 8-86569
 turbulent interchange in triangular array bare rod bundles 8-94081
 two-fluid thermohydraulics computer program, RELAP/SLIP 8-94092
 two-phase annular flow, flooding and flow reversal 8-51230
 two-phase flow characterisation by neutron noise techniques 8-94058
 two-phase flow instability, programme for heat removal expt. at low power 8-54814
 two-phase flow patterns, high pressure water in heated four rod bundle 8-89938
 vent clearing in pressure suppression pools 8-94098
 vibration analysis of heat exchanger and steam generator designs 8-66333
 water droplets react. with molten Na 8-71263
 water radiolysis, mathematical modelling for kinetics in operating reactors 8-61036
 Zircaloy heated surface, FeO deposition in boiling water 8-58353
 Ar loaded K heat pipe performance characteristics 8-89934
 Co radioactive release from reactor cooling water, fixation by sandy soil (Japanese) 8-74443

fission reactor cooling and heat recovery continued

- ⁶⁰Co, shutdown dose rate prediction in BWR primary coolant circuit 8-74445
- N₂O₄ coolant, dissociating system, dynamic sorption of ¹³¹I from gas phase (*Russian*) 8-58356
- N₂O₄ coolant action on stainless steel, TEM study of intergranular corrosion (*Russian*) 8-58357
- N₂O₄ dissociating coolant, chemical reaction kinetics in transient regimes (*Russian*) 8-58344
- N₂O₄ dissociating coolant, O₂ generation time constant, enthalpy change (*Russian*) 8-58345
- Na, fission reactor coolant, meas. accuracy of plugging indicators 8-54813
- Na, liquid, heat transfer characteristics of flow field (*Japanese*) 8-54815
- Na, liquid, local boiling behind local flow blockage, simulated LMFBR fuel subassembly 8-54842
- Na, plugging indicator measuring accuracy, impurity conc. 8-54813
- Na, pool boiling heat transfer, liq. head effects 8-89951
- Na temperature fluctuation in single-pin-heated blocked annular channel 8-78439
- Na transient boiling in single-pin annular channel under loss of flow 8-89933
- Na vapour condensation from rising bubble, effects of internal circulation velocity and noncondensable gas 8-50258
- Na-H₂O reaction testing in large leak test rig 8-86577
- ³⁵S content of coolant gas in Windscale AGR, gas chromatographic and radiochemical anal. 8-73125
- Th-U alloy fuel behaviour in organic-cooled reactor 8-86605
- UO₂, thermal cond. meas. under simulated in-reactor conditions 8-94079
- UO₂ vapour condensation from rising bubble, effects of internal circulation velocity and noncondensable gas 8-50258
- UO₂/Na, fuel/coolant thermal interaction in FBR, out of pile preliminary tests (*Italian*) 8-54828

fission reactor core control and monitoring

- see also fission reactor safety; fission research reactors; nuclear engineering; nuclear reactor instrumentation*
- Bruce core, ZED-2 mockup, responses of Pt, V and Co self powered flux detectors 8-58391
- BWR, appl. of warm water injection method to in-core wet sipping for leak detection 8-78450
- BWR, Dodewaard reactor, power control using Gd absorbers (*Dutch*) 8-50277
- BWR, spent fuel γ -ray spectrometry and chemical analysis 8-54841
- BWR core, moderator temp. coeff. and neutron leakage, DIFFUSION-ACE calc. 8-54844
- BWR in-core instrument tube vibration obs. by reactor noise techniques 8-94064
- BWR load following plant, low sensitivity design for controller 8-78473
- BWR neutron noise local component meas., two phase flow study 8-94059
- BWR neutron noise source identification, stochastic model data anal. 8-94106
- BWR power fluctuations, noise source estimation by autoregression 8-78476
- BWR power plant, neutron noise meas. and analysis 8-94105
- BWR simulation diagnosis by noise analysis 8-94062
- BWR stochastic neutron flux fluctuation obs. and modelling, thermo-hydraulic parameters 8-94065
- BWR-4 neutron noise analysis spectra, instrument tube flow-induced vibr. 8-94063
- CANDU, development of irradi. fuel bundle counters for reactor safeguards systems 8-94119
- CANDU fuels, nondestructive determ. of burnup by gamma scanning, fission monitor appl. 8-94076
- CANDU pressurised HWR fuel, bundle end neutron flux peaking effects, plenum use 8-58385
- CANDU secondary coolant circuit chemistry control, automated system development 8-66359
- CANDU simulated core in ZED-2, transient meas. anal., CERKIN code exam. 8-58386
- CANDU simulated cores, transient expts., validation of computer codes 8-54825
- CANDU-BLW reactor spatial power control 8-89962
- channel reactors, automatic control system design for energy distrib. 8-82475
- control rod drive system penetration assemblies for Caorso Mark 2 primary containment 8-58368
- data acquisition program for research reactor 8-86679
- data sheets for Stade Nuclear Power Station, West Germany (*German*) 8-58366
- digital computer control in Canadian nuclear plants, past performance and future outlook 8-58383
- distributed parameter optimal control methods 8-54858
- distributed parameter reactor system pointwise control and observation problems 8-54859
- Dragon reactor zero energy expts., further n energy group and transport calcs. 8-78445
- EM instruments for use in liquid sodium, theoretical anal. 8-54857
- energy distrib., discrete monitoring error 8-82476
- fast reactor, effects of reactivity of materials 8-86575
- fast reactor integral expt. anal., appl. of uncertainty and sensitivity theory 8-50239
- first power emergence, pressure excursion in fuel elements with compact UO₂ 8-82477
- fission products, solubility rules based on lattice parameter differences 8-59953
- fuel burnup determ., irradi. samples, from γ -peak analysis of fission products (*Hungarian*) 8-82458
- fuel rod pellet-clad gap thermal conductances, exptl. results, anal. correl. 8-70606
- fuel rods, defect detection 8-86640
- HTGR, consequence anal. of hypothetical accidents, core heatup and afterheat removal 8-58381
- HTGR hypothetical accidents, consequences following breach of primary circuit and safeguard failure (*German*) 8-58390
- in-core meas. of energy release, computerised (*Czech*) 8-86637
- integration method for reactor systems analysis 8-78438

fission reactor core control and monitoring continued

- IRT 2000 reactor in Sofia, neutron spectra and doses in exptl. canals (*Bulgarian*) 8-82489
- Kalman filtering theory appl. (*Japanese*) 8-50278
- lattice cell meas. in 36 element natural UO₂ fuel, stopping effect of coolant 8-58347
- leakage neutron spectrum meas. in light water using time of flight technique 8-62592
- LMFBR, compact Na cooled reactor, KNK-1, total and fast neutron flux meas. (*German*) 8-62591
- LMFBR, props. of Eu₂O₃ as control material 8-50261
- LMFBR, yield characts. of short-lived fission products in Na heat-transfer agent 8-66338
- LMFBR (SNR 300), design of core catcher system 8-89937
- LOCA, spray cooling of hollow rod cladding 8-50262
- LWR, power modulation testing of pre-irradiated fuel pins 8-70607
- LWR core meltdown, activity release and aerosol characts. 8-82469
- LWR hydrogen formation during core melt accident 8-50267
- melting pool surfaces, temp. meas. by ratio pyrometers 8-82471
- MSBR, transient Xe anal. 8-54843
- neutron beta-emission cable-type detector with Ag emitter, sensitivity during long service in reactor 8-86644
- neutron detector efficiency estimation, variational techniques 8-62601
- neutron flux distrib., optimal allocation of in-core detectors 8-54839
- neutron flux peaking anal., nuclear fuel bundle ends, program PEAKAN 8-82493
- neutron self-powered detector with fissile emitter, theoretical evaluation 8-74533
- neutronic noise, relations with coolant temp. fluctuation and control rod vibr. at KUR 8-58327
- noise analysis of power reactor, simulation using nucleate boiling noise generator 8-54840
- nonlinear coupled core reactor, computer simulation of decoupling theory appl. to power control 8-54845
- nuclear fuel, radial distribution of nuclides, exam. during irradi. by gamma spectrometry (*French*) 8-78467
- nuclear reactor, two-phase flow characterisation by neutron noise techniques 8-94058
- optimal conditions for reactor shutdown for known period 8-86642
- PBHTR, out-of-core instrum. for detection of spatial flux irreg. (*German*) 8-82430
- PBR, simulated THTR, spline anal. of dynamic transit reactivity meas. for pebbles (*German*) 8-66339
- Phenix reactor, characts. and operating behaviour of fuel element (*French*) 8-66349
- PHWR valve bellows, effect of service parameters on fatigue life and fracture 8-58348
- power reactor noise anal. (*Bulgarian*) 8-82488
- propagating physical quantity transit time estimation, improved correl. method, coolant bubbles appl. 8-94067
- PURNIMA 1 fast reactor, k_e variation during core insertion into reflector 8-74438
- PWR, 450 MWe, noise obs., analysis and interpretation 8-94072
- PWR, data acquisition system for high press. water loop (*Hungarian*) 8-82432
- PWR, optimal fuel loading and operation planning 8-50276
- PWR, oxide fuel rods, computer program for mechanical and thermal anal. (*Korean*) 8-86571
- PWR CANDU, thermal neutron flux distribution, meas. and simulation 8-82492
- PWR core barrel motion from neutron noise spectral density using scale factor 8-74450
- PWR core barrel motion quantification using scale factor and statistical noise parameters 8-74451
- PWR steam supply control system optimisation 8-50251
- R-A reactor fuel burnup, gamma-spectrometric determ. 8-50265
- RA fuel burnup determ. from γ -ray spectrometry of ¹⁰⁶Ru, ¹³⁴Cs, ¹³⁷Cs 8-54848
- reactivity insertion, unexpected, rapid detection 8-58370
- research reactor, IRT-2000, algorithms for direct digital control of neutron field 8-86643
- rod worth meas., improved rod drop method (*Japanese*) 8-54846
- SGHWR fuel pins, fuel cladding ratchetting study 8-54855
- spatial control optimisation methods 8-54860
- temperature monitoring, can thermocouple distribution procedure 8-54856
- thermal conduct. of gas mixture under fuel element jacket during burn-up 8-82478
- THTR, core rod drive (*German*) 8-54837
- TR-1 reactor, thermal spectrum using neutron radiography of wedge shaped absorber 8-74439
- two phase control absorber, results from out-reactor static tests 8-58389
- two-phase flow instability, programme for heat removal expt. at low power 8-54814
- water-moderated water-cooled reactor, local control of loop channel energy release profile and magnitude 8-86645
- CaSO₄:Dy TLD meas. of reactor thermal neutrons 8-78441
- Pu(NO₃)₄ in light water, reactivity predictions using discrete ordinates transport theory 8-89957
- UO₂-PuO₂ fuelled lattice, reactivity predictions using multigroup transport theory 8-89957
- ¹³⁵Xe-induced core instabilities, extended λ -mode linear anal., CANDU appl. 8-82494

fission reactor fuel

- see also claddings; fission of plutonium; fission of uranium; fission reactor fuel preparation and reprocessing; isotope separation; radioactive waste*
- ²⁵²Cf based nondestructive assay system for fissile material 8-73119
- advanced reactors, materials and design 8-78452
- analytical modeling of fuel rod ramp experiment 8-86590
- assembly design features 8-89939
- automatic evaluation of isotope anal. of nuclear fuels, isotope dilution, mass and a spectrometry 8-55120
- autoradiograph techniques for rapid inventory of reactor fuel 8-82066
- burnup determ., irradi. samples, from γ -peak analysis of fission products (*Hungarian*) 8-82458
- BWR, spent fuel γ -ray spectrometry and chemical analysis 8-54841
- CANDU fuel bundles, outline of Canadian R and D programme on fuel behaviour in transients 8-94102

fission reactor fuel continued

CANDU fuel performance in NPD reactor with two-phase coolant 8-89950
 CANDU fuels, nondestructive determ. of burnup by gamma scanning, fission monitor appl. 8-94076
 CANDU PHWR, Wolsung nuclear power plant, fuel cost anal. 8-54832
 CANDU pressurised HWR fuel, bundle end neutron flux peaking effects, plenum use 8-58385
 CANDU Th cycle fuels, review of potential for actinide redistrib. 8-66347
 carbide fuel element testing in fast reactor BOR-60 8-86582
 cladding performance during power changes on fuel element model, strain defects 8-58359
 cladding tensile testing, diametral meas. by precision laser extensometer 8-57896
 Colgate fission plasma reactor, high temp., gaseous fissionable material, design, technical problems (*Dutch*) 8-50249
 computer modelling of fuel element behaviour 8-86617
 computerized axial tomography for neutron radiography of nuclear fuel 8-82529
 conference, nuclear power plant construction, operation and development, Tokyo, Japan (Sept. 78) 8-86672
 critical const., review 8-59931
 density distribution of fission traces, meas. by tracer's method in dielectrics, fuel meas. appl. (*Rumanian*) 8-90033
 depletion chain eqns., FORTRAN program for solns. using analytical methods 8-74423
 disposal safety in Switzerland (*German*) 8-74455
 FBR, neutron/physical behaviour of thorium, expt. (*German*) 8-94109
 fission gas, steady state behaviour in carbide fuels, modelling 8-78469
 fission gas bubble distrib. in mixed oxide fast reactor fuel pin, anal. of TEM obs. 8-58358
 fission gas re-solution, comparison of single knock on and complete bubble destruction models 8-82455
 fission product release and distrib. in coated particles, laser system (*German*) 8-82403
 fuel cycle, national and international aspects (*German*) 8-86665
 fuel cycle industry development, limiting factors (*French*) 8-66430
 fuel defect test loop, design of remote handling system 8-82436
 fuel management calc. procedures, applicability 8-58341
 fuel pins, eccentrically placed pellets, finite difference method for heat transfer 8-82419
 fuel rod pellet clad interaction failures, I stress corrosion cracking tests 8-58351
 fuel rod structural anal. criticism 8-82441
 fuel-cladding chem. interactions at high burnup 8-86584
 fuel-cladding interaction between cracked surfaces, mechanical and temp. contact 8-66341
 Go-r nuclear power plant, fuel cycle schemes, economic comparison 8-54831
 HTGR coated fuel particles, behaviour of fission products (*Japanese*) 8-54830
 HTGR fuel and graphite structure stress analysis methods and programs (*Japanese*) 8-74434
 HTR fuel, high neutron flux, high temp., post irradiation exam. 8-58360
 HTR fuel specimens, neutron irradiated, post irradiation exam., microradiography, metallography, burn-up determ. 8-58361
 inspection by neutron radiography, review 8-60890
 irradiated, α -autoradiography, effect of β -radiation (*German*) 8-78466
 irradiation expt. 8-86587
 laser boring for material sampling of coated fission fuel particles 8-55399
 lattice cell meas., natural UO_2 fuel in ZED-2 hot loop facilities 8-58347
 LMFBR, fuel and fission gas response to simulated thermal transients 8-74453
 LMFBR, SNR-300, fuel rod performance and modelling at high burnup 8-58336
 LMFBR assembly, fuel pin deformations, analytical method, computational code (SHADOW) 8-54829
 LMFBR fuel subassembly, pin bundle deflection anal. 8-78449
 LMFBR single component and mixed oxide fuel solidification anal. 8-74435
 LMFBR type mixed oxide fuel pins, composition of corrosion product oxide phases in pin gaps 8-70599
 LWR fuel-cladding gap, Cs-U-Zr-H-I-O system, chemical thermodynamics 8-82440
 mixed oxide, in Phenix reactor, characts. and operating behaviour of fuel element (*French*) 8-66349
 mixed oxide fast reactor fuel pin, fission gas bubble distrib. 8-78459
 mixed-oxide fuel, cladding breaches 8-82450
 mixed-oxide fuel, in-pile homogenisation 8-86576
 mixed-oxide fuel, irradiation expt. 8-86586
 mixed-oxide fuel, performance in EBR-II anal. 8-86585
 mixed-oxide fuel pin, cladding breaches 8-82451
 molten fuel-coolant interaction studies, simulated reactor accident, wind-scale shock tube rig 8-58363
 MX type nuclear fuels, self diffusion in- and out-of-pile 8-82457
 MX type reactor fuels, microscopic swelling meas., effects of grain boundary migration 8-66348
 MX-type fuel, porosity and stability obs. 8-86629
 neutron flux peaking anal., nuclear fuel bundle ends, program PEAKAN 8-82493
 neutron radiography, reson. energy techniques 8-82528
 nuclear fuel cycle, core design optimisation 8-82420
 nuclear fuel processing plant operation, critical safety criteria (*German*) 8-74440
 PBHTR, 'once through' cycles for enriched fuels, breeding variations 8-58382
 pellet-cladding interaction, irradiation tests 8-86588
 pin gaps, probabilistic distrib. within wire-spaced fuel subassembly 8-78448
 pin-cell burnup code BETTY 8-89946
 production process, fuel rods for HTGR 8-86614
 PWR, oxide fuel rods, computer program for mechanical and thermal anal. (*Korean*) 8-86571
 PWR neutron noise interpretation by vibration analysis 8-94073
 pyrocarbon fuel coating, irradiation tests 8-86594
 R-A reactor fuel burnup, gamma-spectrometric determ. 8-50265

fission reactor fuel continued

RA fuel burnup determ. from γ -ray spectrometry of ^{106}Ru , ^{134}Cs , ^{137}Cs 8-54848
 radial distribution of nuclides, during irradi., gamma spectrometry exam. (*French*) 8-78467
 review, worldwide variation of energy production, future Hungarian energy requirements (*Hungarian*) 8-70580
 review of nuclear fuel cycles and waste management 8-54863
 rod vibration induced by coolant water and air/water flow (*Japanese*) 8-74429
 rods, defect detection 8-86640
 safeguards control, integrated fuel cycles 8-82446
 safeguards planning in plant design process 8-82423
 safety aspects of solvent nitration in HTGR fuel reprocessing 8-86650
 SGHWR fuel pins, fuel cladding ratchetting study 8-54855
 solvent extraction in HTGB fuel reprocessing 8-86667
 stainless steel, 316, mechanical behaviour, 760 to 1204C 8-86604
 stoichiometry effects on cladding attack on mixed oxide fuel 8-86583
 stresses in fuel rod cladding, effect of fuel-pellet chips 8-86589
 thermal reactor, reuse of power Pu and U, neutron regeneration 8-82421
 thermal stress calc., cracked fuel pellets 8-82462
 transport by air, feasibility and economics 8-94154
 transportation of irradiated nuclear fuel, in Canada, emergency planning 8-50411
 tribology study reactor fuel element, PEC type, in Na at high temps. (*Italian*) 8-58362
 US thermometers, nuclear fuel temp. profile meas., TRESON expts. 8-57955
 YN-UN, solid soln., decomp. press.-temp. relations 8-52780
 Zircaloy/ UO_2 fuel design, LOWI 8-70600
 BeO- UO_2 fuel testing, annular core pulse reactor 8-86593
 Cs concentrations, mixed-oxide fuel 8-82452
 Cs transport and isotopic fractional in fuel rods 8-82453
 $^{134}\text{Cs}/^{137}\text{Cs}$ activity ratio, spent fuel assembly 8-82487
 O_2 getters for LMFBR fuel pins 8-74437
 Pu, large samples, thermal-neutron coincidence counting 8-82444
 α -Pu, production difficulties 8-50252
 Pu proliferation, comparison thermal, FBR reactors, nuclear power stations appl. 8-86641
 Pu-Ga (1-8.56 at.%) alloys, enthalpy sp. ht. determ. at elevated temp. 8-78458
 Pu(C,N), lattice parameter variation, 50 to 300K 8-51709
 PuC(N), lattice parameter variation, 50 to 300K 8-51709
 Pu(IV) oxide polymer, potential pollutant from fuel reprocessing, IR spectrum 8-76456
 Pu(NO_3) $_4$ in light water, reactivity predictions using discrete ordinates transport theory 8-89957
 ^{239}Pu , anal. by cyclic activation of delayed neutrons 8-53296
 (Th, U) fuel, burnup determ., using ^{148}Nd 8-82459
 Th alloys, irradiation effects 8-86606
 Th blanket pellets, grain growth kinetics 8-86613
 Th, CANDU-PWR, comparison of three axial fuel management strategies 8-94075
 Th, fast neutron total cross section, 0.1 to 5.0 MeV 8-58278
 Th fuel cycle, CANDU reactors 8-86620
 Th fuel cycle, feasibility study, CANDU system 8-86619
 Th fuel cycle, nucl. strategy and recycle technology 8-86662
 Th fuel cycles in CANDU 8-86661
 Th metal, diffusion and electrotransport of Th metal 8-86611
 Th, selective separation from lanthanides on sulphonic ion exchangers 8-58860
 Th solid fuel utilisation in power reactors (*Japanese*) 8-74433
 Th-based fuel for LWR and LMFBR 8-86624
 Th-based fuel pellets, fabrication 8-86669
 Th-U alloy fuel behaviour in organic-cooled reactor 8-86605
 Th-U metallic fuel, irradiation performance 8-86608
 Th-U Na-bonded metal fuel, transient heating test 8-86607
 Th-U non-oxide compounds, use as refractory breeder fuels 8-86612
 Th-U-C-O system, HTGR fuel system, thermodynamic assessment 8-70598
 Th(IV), selective separation from rare earth elements on chelate ion exchangers 8-58861
 ThO $_2$ and ThO $_2$ - UO_2 fuel, fission gas release 8-86651
 ThO $_2$, Gruneisen coeff., lattice vibrational frequencies in range 298-2300K 8-79712
 ThO $_2$ in HTGR fuel design 8-86622
 ThO $_2$ - UO_2 fuel performance after irradiation 8-86621
 ThO $_2$ - UO_2 in PWR fuel rod, LIFE-THERMAL computer code anal. 8-86623
 ^{232}Th fuel, conversion and fission yield, irradiation expt. 8-86609
 (U,Pu)C fuel, interaction with molten stainless-steel shroud 8-86592
 (U,Pu)CNO irradiated fuel, electron microprobe anal. 8-70601
 (U,Pu) O_2 fuels, O distrib. during irradiation, calc. using CODIF program 8-70604
 (U,Pu) O_2 , mixed oxide fuel elements, lenticular pore movement 8-78460
 (U,Pu) O_2 , mixed oxide fuel elements, Pu redistribution 8-78463
 U assay by passive gamma-ray spectrometry 8-92576
 U blanket management, effects of power and irradiation behaviour 8-86595
 U exploration and international cooperation 8-86628
 U, field emission microscopy, emissive props. 8-88409
 U fuel, burnup determ., using ^{148}Nd 8-82459
 U, γ - and β -hardened, recrystallisation, effect of impurity distrib. 8-70602
 U ore detection, using trace detection sensitive to ^{222}Rn α -particles (*Hungarian*) 8-77339
 U resources, consumption and 30 year fuel commitments for Canada and the world, 1975-2025 8-82456
 U, selective separation from lanthanides on sulphonic ion exchangers 8-58860
 U supply, Canada's role 8-86627
 U-C-N system, high temp. X-ray diffr. exam. of structure (*French*) 8-72765
 U-Cr-Al (0.2, 0.1 at.%) fuel elements with high swelling resistance for KS-ISO reactor 8-78471
 U-Pu mixed oxides, impurities, emission spectrometric anal., single carrier method 8-68944
 U-Si-Al fuel rods, Zr-Nb cladding, irradiation behaviour with peripheral voidage 8-54835

fission reactor fuel continued

- UAl₂-Al dispersion fuel, effect of reactions on Young's modulus and rupture strength (*German*) 8-62596
 UC, MX-type LMFBF fuels, TEM exam. of microscopic swelling 8-70596
 UC, computer simulation of C activity and transport 8-86618
 U₂C₃+UC, MX-type LMFBF fuels, TEM exam. of microscopic swelling 8-70596
 UC₂N_{1-x}, self diffusion processes 8-50259
 UO₂, commercial fuel pin, irradiation induced volume changes, comparison with model 8-78465
 UO₂ compact, first power emergence, pressure excursion in fuel elements 8-82477
 UO₂, compressed, dislocation substructure obs. (*French*) 8-78461
 UO₂ film, vacuum evaporated, He⁺ ion energy loss parameter 8-50253
 UO₂, Gruneisen coeff., lattice vibrational frequencies in range 298-2300K 8-79712
 UO₂, γ attenuation coeffs. meas. for burn-up determ. correction (*Russian*) 8-82597
 UO₂, interaction with Na, dropping experiments and subassembly test 8-82460
 UO₂, irradiated, spacing of intergranular fission gas bubbles 8-66340
 UO₂, irradiated sample, 1000 to 2100K, swelling and fission gas obs. 8-78462
 UO₂, irradiation induced vol. change 8-67740
 UO₂, liquid, pressure generated by encapsulated Na (*Italian*) 8-82454
 UO₂, neutron irradiated, diffusion of fission product T 8-67866
 UO₂, sintered pellets, relationship between intercept length and grain diameter 8-52743
 UO₂, thermal and in-reactor densification 8-66364
 UO₂, thermal cond. meas. under simulated in-reactor conditions 8-94079
 UO₂, transfer of fission gas between grain faces and edges 8-79815
 UO₂, vapour condensation from rising bubble, effects of internal circulation velocity and noncondensable gas 8-50258
 UO₂/Na, fuel/coolant thermal interaction in FBR, out of pile preliminary tests (*Italian*) 8-54828
 UO₂-(Ni), surface, grain boundary and interfacial energies 8-71905
 UO₂-PuO₂, mixed oxide fast reactor-fuel pin, fission gas bubble distrib. 8-78459
 UO₂-PuO₂, fuelled lattice, reactivity predictions using multigroup transport theory 8-89957
 UO₂-Zr fuel pins, ramp testing 8-86591
 UO_{2+x}, elect. cond. and thermoelectric power 8-52020
 UO_{2.2x}, O self and chem. diff. coeff. 8-71879
 UO₂(II), selective separation from rare earth elements on chelate ion exchangers 8-58861
 (U_{1-x}Pu_x)O_{2-x}, thermodynamics 8-70594
 U_{0.8}Pu_{0.2}C₂N_{1-x} (0 ≤ x ≤ 1), MX-type LMFBF fuels, TEM exam. of microscopic swelling 8-70596
 U_{0.8}Pu_{0.2}N, self diffusion of ²³⁸Pu 8-78457
 (U_{0.8}Pu_{0.2})N, self diffusion of ²³⁸Pu 8-82461
 U_{0.75}Pu_{0.25}O_{2-x}, variation in O₂ potential with simulated burnup 8-70597
 (U_{1-x}Pu_x)O_{2-x}, thermodynamics 8-70593
 U_{1-x}Th_xO₂, solid solution, single crystal growth by chemical transport reactions 8-72708
²³³U and Pu fuels, relative occupational hazards 8-94101
²³³U/²³²Th metal fuel, irradiation expt. 8-86610
²³⁵U, ²³⁵U systems, criticality anal. using KENO and SU-HAMMER codes 8-89949
²³⁵U, anal. by cyclic activation of delayed neutrons 8-53296

fission reactor fuel preparation and reprocessing

see also *isotope separation; radioactive waste*

- actinide nuclear transmutation, photon and neutron surface dose rates for actinide containing fuel 8-66428
 actinides, chemical separation from PUREX raffinates using organic solvents 8-66676
 alkaline radioactive waste decontamination by ion exchange 8-50263
 American Nucl. Soc. winter meeting 1977 8-58315
 American Nucl. Soc. Winter Meeting 1977 8-82408
 anion-exchange refinement of Pu and Np separated during extraction refinement of spent fuel elements 8-70624
 British Nuclear Fuels' thermal oxide, reprocessing plant at Windscale, Development programme 8-82497
 CANDU fuel storage in pods and air-cooled concrete canisters 8-89963
 CANDU irradiated fuel, monitoring for sheath defects in shipments 8-54864
 CANDU irradiated fuel storage, concrete canister programme, heat transfer and shielding effectiveness 8-58388
 CANDU-PHW, advanced fuel cycles 8-89968
 chemical reprocessing, H₂NNH₂, HNO₃, NaNO₂, Fe(NH₄)SO₃ 8-78487
 criticality accidents at facilities processing fissile material, characts., detect. and action procedures (*French*) 8-55054
 decontamination and waste management at shutdown reprocessing plant, experience 8-66354
 dodecane-tributylphosphate solns. radiolysis 8-74459
 energy-dispersive X-ray fluorescence analysis of highly radioactive samples with small tubes and pyrographite crystals 8-92578
 fast reactor, advanced fuel cycles 8-89968
 fissionable isotopes in aq. soln., assay by pulsed neutron interrogation 8-68966
 fuel cycle, national and international aspects (*German*) 8-86665
 fuel cycle environmental assessment methodology 8-94112
 fuel reprocessing technology, development up to current status 8-58393
 fusion-fission reactor symbiotic design, simple fuel reprocessing 8-66365
 gas centrifuge, effect of compressible flow on max. separating power 8-70644
 German Government responsibility w.r.t. storage facility, legal aspects (*German*) 8-86701
 hot cell for reprocessing of spent nuclear fuel samples 8-58364
 input analysis, verification (*German*) 8-70623
 isotope centrifuge, effect of thermal convection on separative power, numerical anal. 8-58500

fission reactor fuel preparation and reprocessing continued

- isotope separation, ideal cascades, 2-up 1-down, separative power and interstage flow anal. 8-58499
 Japanese nucl. fuel cycle for LWRs 8-86670
 liquid waste from nuclear reprocessing, vitrification, durability 8-54852
 liquid-liquid extraction column online control by modal control techniques 8-54865
 LMFBF spent fuel shipping cask designs, subcriticality guidelines, Monte Carlo calcs. 8-82470
 LWR, Tokai reprocessing plant in Japan, experience 8-89967
 LWR, use of recycle Pu in mixed oxide fuel, generic environmental statement (*Japanese*) 8-54862
 LWR fuel cycle effluent model for ENFORM system 8-94111
 LWR stowaway fuel cycle effluent projections 8-94110
 nondestructive assay of irradiated nuclear fuel for safeguards, review 8-82495
 nuclear energy, technical economic and safety aspects (*Hungarian*) 8-82465
 nuclear fuel centre, fuel and waste facilities, safety, protection and socioeconomic aspects 8-58395
 nuclear fuel processing plant operation, critical safety criteria (*German*) 8-74440
 on-line control (*Russian*) 8-74460
 production process, fuel rods for HTGR 8-86614
 pyrocarbon deposition in fluidised bed, qualitative model, investigation with Stromungsrohr 8-56595
 radioactive waste, vitrification, industrial scale plant, under construction in France 8-78478
 reprocessing fast reactor fuel in Britain 8-89966
 review of nuclear fuel cycles and waste management 8-54863
 safety aspects of solvent nitration in HTGR fuel reprocessing 8-86650
 safety exercises carried out in French industrial facilities (*French*) 8-55051
 separation technologies, review 8-89965
 solvent extraction in HTGB fuel reprocessing 8-86667
 spent fuel reprocessing facilities continuous criticality control, dynamic approach 8-50291
 spent nuclear fuel, storage alternatives 8-74456
 technical safety rules, catalogue and classification for reactors and fuel cycle plants 8-58384
 Tokai reprocessing facility start-up (*Japanese*) 8-74457
 Trombay nuclear facilities, effluent release monitoring procedures 8-89993
 waste ¹³⁷Cs, ⁹⁰Sr and rare earth radioisotope separation by cation exchange 8-78486
 Zircaloy/UO₂ fuel design, LOWI 8-70600
⁹⁹Mo, separation regeneration of breeder reactor fuel (*Czech*) 8-82496
 Pu ecological export from reprocessing waste pond 8-53533
 Pu, LWR recycling in the European Communities 8-58394
 α -Pu, production difficulties 8-50252
 Pu radiation protection device based on neutron detection (*French*) 8-66362
 Pu recycling by chemical process 8-58367
 Pu, recycling in LWRs and environmental impact 8-89969
²²²Rn release from U ore crushing, grinding and leaching 8-89970
 Tc, radiochemical characts. and role in nuclear fuel reprocessing, review (*Czech*) 8-82496
⁹⁹Tc separation regeneration of breeder reactor fuel (*Czech*) 8-82496
 (Th,U)O₂ reactor fuel, dissolution in HNO₃-HF mixtures, fuel reprocessing study 8-59951
 Th fuel cycle, CANDU reactors 8-86620
 Th sulphito complex ion precipitation with hexamine Co(III) chloride cation 8-92495
 Th-based fuel pellets, fabrication 8-86669
 ThO₂ and (Th,U)O₂ fuel kernels, simplified preparation 8-86668
 U and Pa decontamination, sorption and distillation methods, review (*Czech*) 8-82496
 U enrichment, centrifuge, URENCO facilities at UK and Netherlands (*German*) 8-86666
 U enrichment by gaseous diffusion process (*French*) 8-70622
 U isotope separation, influence of flow field struct. in the separation nozzle 8-82498
 U isotope separation processes development (*French*) 8-66361
 U mill radiological effluent and environmental monitoring guidelines 8-94153
 U nuclear fuel particle prep. by ion exchange resin loading (*German*) 8-82499
 UC-(PuC), ceramic fission reactor fuels, fabrication and performance, review 8-58392
 UF₆, temp. and density profiles in freely expanding gas for laser enrichment 8-74458
 UN-(PuN), ceramic fission reactor fuels, fabrication and performance, review 8-58392
 UO₂ powder prep., effect of ammonium uranate props. 8-66363
 UO₂, sintered, fuel manufacturing technology (*Czech*) 8-50290
 UO₂, sintered pellets, relationship between intercept length and grain diameter 8-52743
 UO₂, thermal and in-reactor densification 8-66364
 UO₂-(PuO₂)(BeO), ceramic fission reactor fuels, fabrication and performance, review 8-58392
 UO₂(II), Th(IV), Cu(II), Ni(II), Fe(III), selective separation from rare earth elements on chelate ion exchangers 8-58861
 U(VI), extraction from sea water using polyacrylamide gel containing metal hydroxides 8-54861
 U(VI) peroxo complex ion precipitation with Co(III) complex cation 8-80728
²³⁵U isotope separation, efficiency improvement by nuclear excitation by electron transition 8-55039

fission reactor instrumentation see *nuclear reactor instrumentation*

fission reactor materials

- see also *claddings; fission reactor fuel; fusion reactor materials; materials handling; moderators; radioactive waste*
 advanced reactors, materials and design 8-78452
 AGR, fuel cladding performance obs., biaxial creep meas. of 20/25/Nb stainless steel 8-82442
 biaxial creep behaviour, ribbed GCFR cladding at 650C 8-86597
 α -brass, electron irradiated, defect production and interdiffusion 8-67739

fission reactor materials continued

bubble nucleation, He-assisted, computer simulation 8-86625
 BWR, Dodewaard reactor, power control using Gd absorbers (*Dutch*) 8-50277
 cladding, stainless steel, cold-worked Type 316, transient mechanical behaviour 8-86598
 cladding performance during power changes on fuel element model, strain defects 8-58359
 containment liner seismic reliability under statistical uncertainty, cracking 8-89948
 control with VACOSS variable coding seal system 8-82491
 controllable unit approach to material control 8-82445
 core reactivity and space-domain noise effects of randomly dispersed materials 8-94071
 corrosion research in FBR and PWR nuclear power plants, review of problems (*Czech*) 8-62598
 decision analysis in safeguarding special nuclear material 8-82485
 dimensional instability of CF8 stainless-steel castings at elevated temperatures 8-82448
 fission product release and distrib. in coated particles, laser system (*German*) 8-82403
 fission products, solubility rules based on lattice parameter differences 8-59953
 fracture mechanics of reactor primary system under operating and accident conditions 8-66342
 fracture problems in reactor technology 8-78472
 fuel cladding, slightly oval cylindrical shells, creep anal. 8-78468
 fusion and fast breeder reactors, a comparison, book 8-78430
 graphite, failure criterion, J-integral critical value 8-84999
 graphite, fracture toughness up to 2600°C 8-68760
 graphite, pyrolytic, ion bombard., flaking, stress fields around penny-shaped cracks 8-52946
 graphite, pyrolytic, numerical discussion of flaking mechanism from ion bombard. 8-52947
 graphite, thermal shock fracture toughness eval. by arc discharge heating 8-72835
 heavy water dynamic viscosity coefficient in supercritical region of parameters of state, experimental investigation 8-67845
 Incoloy 800, 600 and 718, press. vessel, fatigue design criteria 8-60758
 intrareactor facility for physicomaterial props. investig. by pulsed US spectroscopic method 8-70591
 irradiation effects, precipitation in pile, rel. to void swelling 8-70595
 kohlestein insulation for use in HTR systems, further investigations (*German*) 8-66346
 laser fusion driven actinide waste burner, neutronics anal. 8-58459
 liquid-metal valves, materials selection 8-82449
 LMFBR, exam. of material requirement 8-50255
 LMFBR, H burden from steam side corrosion in Na heated steam generators 8-58355
 LMFBR, HCDA conditions, PuO₂-UO₂-Na aerosol formation, aerodynamic and chem. behaviour 8-94104
 LMFBR, UK, AISI 316 and 9Cr-1Mo steels assessment 8-86581
 LMFBR components, materials anal. 8-82447
 LMFBR materials, exam. of material requirement 8-50256
 LMFBR performance, effects of irradiation creep and swelling 8-78482
 LWR, stress conc. in cladding produced by cracked fuel pellets 8-50260
 LWR, structural integrity of pressure boundary 8-66334
 LWR fuel-cladding gap, Cs-U-Zr-H-I-O system, chemical thermodynamics 8-82440
 material irradiation facility in the WR-1 research reactor, structural material development 8-54868
 metal, anisotropic, inelastic deform. under complex loading conditions and high neutron flux, equation 8-80598
 metal surface, He implantation lateral stress, role in bluster form. mech. 8-95068
 NDT of special nucl. materials 8-82443
 neutron capture cross sections, expt. determ., fast reactor materials (*Italian*) 8-82355
 nonequilibrium fission gas behaviour 8-86626
 nuclear fuel processing plant operation, critical safety criteria (*German*) 8-74440
 performance of safeguards technology 8-82484
 physical protection safeguards for nuclear materials and facilities 8-82483
 pressure vessel, A508 C1 2 steel, microcrack formation during stress-relief annealing of a weldment 8-80629
 pressure vessel material, radiation embrittlement, current regulation assessment 8-52966
 pressure vessels, brittle fracture probability using reactor surveillance capsule data 8-80641
 pressure vessels, exam. for compliance with safety regulations 8-89954
 PWR, in-reactor loop expts. on corrosion product transport and water chemistry 8-58335
 PWR-type, pressure component manufacture, new materials, technologies and equipment development 8-74436
 radioactive effluent gases from nuclear power industry, ambient contamination (*Spanish*) 8-61540
 radiographic testing, sensitivity using 10 MeV microtron 8-70603
 radioisotopes in cooling system, prod., transfer, life cycle, radiation calcs. using program system TIBSO 8-54821
 radiolytically formed chelating agents, corrosion prevention appls. 8-64745
 reactor cladding waste, spent fuel contamination, composition and amounts arising in EC 8-66360
 reactor safety, materials science contribution (*German*) 8-58352
 refractories, swelling on proton, deuteron and He ion bombardment 8-67750
 sieve tray froths occurring in heavy water plants, expt. and anal. 8-82438
 sieve trays for heavy water plants, development 8-82437
 silicate glasses, swelling on proton, deuteron and He ion bombardment 8-67750
 stainless steel, 304, tensile stress effects on high-cycle fatigue 8-86603
 stainless steel, 316, simulation of radiation damage and phase stability 8-86602
 stainless steel oxides, absorption of Cs, meas. of contamination using washing test 8-62597
 steam generators, Na-heated, material consideration 8-82503

fission reactor materials continued

steam generators, Na-heated, material selection 8-82504
 steel, 6 MeV γ penetration, bremsstrahlung in reactor shielding calcs. 8-58350
 steel, A533 B, fatigue crack propagation, grain size and temp. effects 8-56727
 steel, A-533 B, J_{IC}-testing, statistical eval. of different techniques 8-56828
 steel, austenitic, neutron irradi., He release kinetics 8-79638
 steel, austenitic, X6CrNi1811 and X6CrNiMo1713, crack growth under Na cooled fast breeder reactor conditions (*German*) 8-56798
 steel, austenitic stainless, influence of steel comp. on corrosion in high temp. Na 8-80675
 steel, austenitic stainless, irradiation induced creep, AISI 316, 20% cold worked effect of temp. change 8-72816
 steel, austenitic stainless, irradiation induced creep by alpha particles, in type 316 steels (*French*) 8-72791
 steel, austenitic stainless, type 304 with He distrib., foil, effect of momentum transfer, damage energy gradient, on He distrib. 8-71773
 steel, corrosion, Na loop system, analysis of radioactive corrosion product transfer 8-78464
 steel, Cr-Mo, constitutive eqn. model for high temp. behaviour of fast reactor structural alloys 8-66343
 steel, Cr-Mo-Nb-Ni, low alloy, material selection for LMFBR steam generator tubes 8-54834
 steel, Cr-Mo-Nb-Ti low alloy, material selection for nuclear steam generator tubes 8-54834
 steel, ferritic, FV607, void swelling, theory 8-71763
 steel, ferritic, FV607, void swelling in 1 MeV electron irradiation 8-71762
 steel, martensitic, delayed fractures suppression, by neutron irradiation (*Czech*) 8-67743
 steel, mild, bolt thread strain meas. 8-60972
 steel, nuclear pressure vessel, type A533B-1, three point bending, yield stress, exam., Charpy V-notch and precracked specimens 8-92310
 steel, reactor vessel, neutron irradi. effect on brittle fracture characts. (*Slovak*) 8-50254
 steel, stainless, 304, void form., effect of sequential and simultaneous He implantation 8-71719
 steel, stainless, 304L, T grainboundary diffusion and trapping, autoradiographic exam. 8-51738
 steel, stainless, 316, nuclear fuel cladding, crack nucleation 8-72864
 steel, stainless, attack by liquid and vaporised CsOH 8-68840
 steel, stainless, Cr-Ni-Nb-Ti, effect of I₂ vapour on creep fracture props. 8-72814
 steel, stainless, D implanted, thermal desorption 8-71750
 steel, stainless, oxidised, adsorption and absorption of Cs 8-84061
 steel, stainless, radiation-thermal treatment, N₂O₄ coolant action, intergranular corrosion (*Russian*) 8-58357
 steel, stainless, sintered Kh18N10T, friction and corrosion props. for frictional units of nuclear plants 8-60845
 steel, stainless, Ti modified 316, uniaxial tensile behaviour, Na environment effect 8-52916
 steel, stainless, type 304, elastoplastic fracture mechanics for reactor piping 8-68777
 steel, stainless, type 316, cold worked effect of prior neutron induced creep on burst strength 8-62599
 steel, stainless, type 316, electron irradiated, void swelling 8-55891
 steel, stainless, type 316, neutron flux and irradi. temp. dependence of swelling 8-79636
 steel, stainless, type AISI 316, carburisation of crevices by impure liquid Na 8-80680
 steel, stainless austenitic, neutron irradi., swelling due to gamma prime and M₂₃(C₁Si)₆ form. 8-51590
 steel, stainless type 316, monotonic and cyclic biaxial loading at room temp. 8-52928
 steel, trace element anal., spectra of laser plasma 8-88691
 steel Cr-Mo low-alloy, material selection for nuclear steam generator 8-54834
 steel for nucl. reactors, trace element anal., implications for decommissioning 8-54833
 steel pearlitic, statistical anal. of joint effect of Ni, Cu, P on irradiation embrittlement 8-71770
 steels, dynamic material props. for FBR safety anal., testing devices 8-60966
 tube flaw detection by annular US transducers 8-60971
 water, transition boiling under forced convective conditions, reactor accident condition 8-89961
 water droplets react. with molten Na 8-71263
 water-moderated-water-cooled reactor VVER-1000, power plant technology 8-82501
 Zircaloy-4 fuel sheathing, inverted primary creep 8-86615
 Zircaloy, steam oxidised, partitioning behaviour of O₂ 8-68839
 Zircaloy 2/I₂ system, stress corrosion crack growth for short cracks 8-80685
 Zircaloy 4, stress relaxation in bending 8-68719
 Zircaloy creep collapse, hot cell examination 8-86596
 Zircaloy fuel cladding, O embrittlement obs. 8-89947
 Zircaloy heated surface, FeO deposition in boiling water 8-58353
 Zircaloy-2, exposed to I₂ vapour, stress corrosion crack initiation sites 8-92324
 Zircaloy-2, pressure tube, fragmentation on failure 8-72863
 β -Zircaloy-2, tensile creep and creep rupture props. under vacuum 8-52915
 Zircaloy-4, Poisson's ratio determ. at several temp. levels 8-52874
 Zircaloy-4, quenched, strain ageing behaviour, ageing time and temp. effects 8-56657
 Zircaloys, fractographic distinction between hydride cracking and stress corrosion cracking 8-92363
 Ag, Doppler factor, comparison between calculated values and measured results 8-54811
 Al-Ge alloy, Ge precip., ion irradi., dose rate and temp. depend. 8-79642
 Au, Doppler factor, comparison between calculated values and measured results 8-54811
 B₄C rings, Al bonded, exam. of fabrication techniques 8-72748
 B₄C, used as control rods in FBR, irradiation effects 8-67742
¹⁰B separation using anion exchange resin, isotopic plateau holding displacement chromatography (*Japanese*) 8-56886
 Be, two group calcs. for neutron wave propagation across an absorption discontinuity 8-89931

fission reactor materials continued

- C, activated adsorption of 0.98 mol.% Ar, vol. adsorption capacity 8-75933
- ⁶⁰Co, shutdown dose rate prediction in BWR primary coolant circuit 8-74445
- Cu, He conc. profile meas. rel. to blistering 8-95089
- Cu-Ag (Au), dil., dose depend. of impurity detrapping stages after electron irradiation 8-51582
- Cu(II), selective separation from rare earth elements on chelate ion exchangers 8-58861
- D₂O leak detection, on-line infrared analyzers, CANDU report 8-82038
- Eu₂O₃, appl. to LMFBR control 8-50261
- Eu₂O₃-Ta₂O₅, microcracking, elastic props., internal friction 8-92326
- Fe, gamma fields induced by ²⁵²Cf neutrons 8-50240
- Fe, ns. slowing down time, expt. obs. 8-58319
- Fe-(Mo)-CaF₂, sintered, friction and corrosion props. for frictional units of nuclear plants 8-60845
- Fe-Cu (0.21, 0.2 wt.%), neutron irradiated, torsional props. effect of Cu additions and annealing temp. 8-56699
- Fe-Cr-Ni alloy, dual-ion-irradiated, swelling anal. 8-86600
- Fe(III), selective separation from rare earth elements on chelate ion exchangers 8-58861
- H₂(D₂) pumping by Ti film, pumping speed comparison 8-51819
- Hf, calciothermic, electrorefining 8-68647
- I, PWR core, nonlinear balance eqns. and distrib. 8-58322
- I partition equilibrium between air and NaOH aq. effect of CO₂ conc. 8-78474
- LiF tile and sheet for thermal neutron shielding (*Japanese*) 8-74510
- Mg alloy scales, F conc. profiles determ. using ¹⁹F(p,αγ) 8-88678
- Mo, irradiation temp. determ. by electrical resistivity meas. 8-58354
- Mo, sputtering yield meas. by AES 8-95633
- N₂O₄ coolant, dissociating system, dynamic sorption of ¹³¹I from gas phase (*Russian*) 8-58356
- N₂O₄ dissociating coolant, chemical reaction kinetics in transient regimes (*Russian*) 8-58344
- Na, neutron flux integral meas., interactive graphic techniques 8-62590
- Na, plugging indicator measuring accuracy, impurity conc. 8-54813
- Na, pool boiling heat transfer, liq. head effects 8-89951
- Na temperature fluctuation in single-pin-heated blocked annular channel 8-78439
- Na vapour condensation from rising bubble, effects of internal circulation velocity and noncondensable gas 8-50258
- Na₂B₄O₇, borax, internal core catcher for GCFR 8-58372
- Nb, neutron irradi. effects on mech. props. 8-91361
- Nb, O₂ getters for LMFBR fuel pins 8-74437
- Nb₃Sn, filamentary conductors, type-II, low temp. 30 GeV proton effects on critical props. 8-52178
- NbTi, filamentary conductors, type-II, low temp. 30 GeV proton effects on critical props. 8-52178
- Ni, permeability and diffusivity of hydrogen (*Japanese*) 8-66345
- Ni-Mo-Cr steel, elastic-plastic material characterisation 8-72854
- Ni-ThO₂, irradiated with 5 MeV Ni⁺⁺, ThO₂ redistrib. 8-71771
- Ni(II), selective separation from rare earth elements on chelate ion exchangers 8-58861
- Pb, 6 MeV γ penetration, bremsstrahlung in reactor shielding calc. 8-58350
- Pt alloy, fission-fragment-induced He blistering 8-86601
- ²²²Rn in biologically produced gas from reactor cooling pond 8-80976
- Si compounds in Na system, deposition and effects 8-86599
- SiC, diffusion behaviour of fission products, 1650 to 1850°C 8-79814
- SiC, energetic H and Ar ion sputtering, AES-SIMS-FDS combined obs. 8-80444
- T, release from CTR, radiological dose calc. 8-78511
- ThBC, crystal struct. 8-55853
- Ti, O₂ getters for LMFBR fuel pins 8-74437
- TiB₂, low-temp. neutron irradi., electrical resistance and stored energy 8-67744
- UO₂-(Zr-Nb) system, high-temp. reaction 8-66344
- V, O₂ getters for LMFBR fuel pins 8-74437
- V₃Ga, filamentary conductors, type-II, low temp. 30 GeV proton effects on critical props. 8-52178
- W, irradiation temp. determ. by electrical resistivity meas. 8-58354
- W, thermal neutron irradiated, radiation damage and stage III defect annealing 8-51586
- Xe oscillation model for PWRs, neutron diffusion eqn., nonlinear system 8-58322
- YN, decomp. press.-temp. relations 8-52780
- α-Zr and Zircaloy-4, O stabilized, O diffusion using ¹⁸O tracer 8-51737
- Zr base alloys, irradiation growth, dislocation model 8-51595
- Zr, dissolution of γ-ZrH₂ in situ study, HVEM obs. 8-55951
- Zr, γ attenuation coeffs. meas. for burn-up determ. correction (*Russian*) 8-82597
- Zr-Al (8.6 wt.%), effect of fast neutron irradiation on irradiation growth of Zr₃Al 8-55896
- Zr-Al(8.6 wt.%), mech. props., corrosion and fast neutron irradi. influence 8-84948
- Zr-Nb, pressure tube alloy, initiation COD as fracture criterion 8-72862
- Zr-Nb (1 wt.%) exam. of creep behaviour, 373 to 773K 8-80599
- Zr-Nb (2.5 wt.%), cold worked, press. tubes, secondary cracking obs. 8-80630
- Zr-Sn alloys, mathematical models for transient deform. 8-86616
- Zr₃Al, disordering by 1 MeV electron irradiation 8-51583
- Zr₃Al, ordered, exam. of Young's modulus and thermal expansion coeff. 8-72805
- ZrC, solubility, diffusion and permeation of Cs 8-51684
- ZrNb, pressure tube, fragmentation on failure 8-72863

fission reactor operation

- see also fission reactor cooling and heat recovery; fission reactor core control and monitoring; fission reactor safety*
- advanced reactor development in Japan 8-86663
- AGR line development status and performance (*German*) 8-86568
- at-power reactor noise, second-order coherent functions 8-94070
- burnup determ., accuracy requirements for fuel cycle design, reactor operation and safety 8-58342
- BWR dynamics, multivariable autoregressive identification 8-94107
- BWR power plant, routine checks and radiation protection 8-74462

fission reactor operation continued

- BWR power plant turbine building, radiation protection, calc. and obs. 8-74461
- CANDU, nuclear quality high pressure valve bellows, development, report 8-82490
- CANDU, Th fuel cycles 8-86661
- CANDU fuel performance in NPD reactor with two-phase coolant 8-89950
- CANDU PHW commercial nucl. elec. stations, commissioning and operating experience 8-86656
- CANDU PHWR, Wolsung nuclear power plant, fuel cost anal. 8-54832
- CANDU-PHW, advanced fuel cycles 8-89968
- DC power failure following AC power failure 8-78483
- dynamic simulation of the Gentilly-1 reboiler system 8-82439
- electric heaters for nucl. applic. 8-86649
- fast reactor, advanced fuel cycles 8-89968
- FBR, neutron/physical behaviour of thorium, expt. (*German*) 8-94109
- fuel savings by 'stretch out' operation (*German*) 8-86632
- fusion and fast breeder reactors, a comparison, book 8-78430
- Genkai PWR plant operating experience 8-86655
- Go-ri nuclear power plant, fuel cycle schemes, economic comparison 8-54831
- Hamaoka BWR plant, operational experience 8-86654
- LMFBR performance, effects of irradiation creep and swelling 8-78482
- LWR diversion resistant processes and cycles 8-86677
- LWR operation and maintenance 8-86653
- PBHTR, 'once through' cycles for enriched fuels, breeding variations 8-58382
- PBHTR, Julich, 10 year operation (*German*) 8-54838
- PHWR, CANDU reactor system, appropriate technology 8-58338
- poisoning with fission products, ¹³⁵Xe and ¹⁴⁹Sm, spatial calc. (*Slovak*) 8-54850
- power plant control appls., problems and trends 8-70609
- power plants, diagnostic system using noise anal. 8-50279
- PWR, CANDU, operation, status and prospects of nuclear power in Canada 8-86664
- PWR, pressure tubes cracking, Zr-Nb alloy, Pickering power station experience 8-82472
- PWR neutron noise interpretation by vibration analysis 8-94073
- PWR neutron noise sources 8-94108
- PWR operation, statistical analysis (*French*) 8-58374
- PWRs, auxiliary feedwater system, fault tree anal. 8-54867
- radioactivity release, air monitoring, emergency procedures 8-70610
- water-moderated-water-cooled reactor VVER-1000, power plant technology 8-82501
- Th fuel cycle, nucl. strategy and recycle technology 8-86662

fission reactor safety

- see also fission reactor cooling and heat recovery; fission reactor core control and monitoring*
- 2056 MW nuclear reactor pressure tubes cracking 8-82463
- accident features affecting emergency measures 8-55055
- accident handling, conf., Vienna, Austria (Feb.-Mar., 1977) 8-53518
- accidents, effects on public, casualty management 8-53519
- accidents, meas. of crit. environmental exposure by I radioisotopes 8-57081
- accidents due to loss of coolant, multiple-element model and computer solution 8-66358
- accidents in power stations of Electricite de France, protection organisation (*French*) 8-55049
- atmospheric emissions from nuclear plants, applications related concept for radiation exposure calc. (*German*) 8-82531
- automated approach to nuclear facility safeguards effectiveness evaluation 8-82486
- Berger coeffs. for Eisenhauer-Simmons γ-ray buildup factors in concrete 8-78510
- biological shield wall for Caorso nuclear plant, design, construction and erection 8-86694
- Bruce core, ZED-2 mockup, responses of Pt, V and Co self powered flux detectors 8-58391
- burnup determ., accuracy requirements for fuel cycle design, reactor operation and safety 8-58342
- BWR, appl. of warm water injection method to in-core wet sipping for leak detection 8-78450
- BWR, simulation of cooling system conditions, stress corrosion cracking test 8-80696
- BWR plants in Japan, seismic design and tests 8-86652
- BWR power plant, neutron noise meas. and analysis 8-94105
- CANDU, development of irradi. fuel bundle counters for reactor safeguards systems 8-94119
- CANDU simulated core in ZED-2, transient meas. anal., CERKIN code exam. 8-58386
- CEGB nuclear power station emergency arrangements 8-55050
- CEGB nuclear power station emergency monitoring procedures 8-55053
- channel-type reactors, γ-ray dose rate spatial distrib. over entire thickness of side shield 8-86697
- computer appl. to reactor scram system (*German*) 8-86635
- containment air contamination, sampling and measurement techniques (*French*) 8-89997
- containment liner seismic reliability under statistical uncertainty, cracking 8-89948
- containment negative pressure evaluation 8-50275
- containment tightness, integral leakage rate tests 8-89956
- core temp. monitoring, can thermocouple distribution procedure 8-54856
- CRBR, primary pipe rupture accident anal. with DEMO code 8-70621
- critical const., review 8-59931
- DC power failure following AC power failure 8-78483
- decision analysis in safeguarding special nuclear material 8-82485
- district heating, safety study for BWR heating and power station 8-62600
- downtime distrib. in reliability theory for single repairable component, time structs. 8-89959
- dryout, premature in conventional and nuclear power station evaporators, model 8-94120
- dynamic simulation of the Gentilly-1 reboiler system 8-82439
- EBR-II, Na-water, leak detection system 8-78484

fission reactor safety continued

education at Northwestern Univ. 8-58376
 educational courses at UCLA 8-58377
 educational programme at Purdue 8-58380
 electrical and mechanical equipment, improved seismic tests, research needs 8-94053
 EM instruments for use in liquid sodium, theoretical anal. 8-54857
 emergency core cooling system motor operated valves, failure mode anal. 8-54866
 emergency core cooling system motor operated valves, failure criteria 8-70592
 emergency medical assistance programmes for nucl. power reactors 8-53532
 emergency protection drive, optimum ratio between operational component times 8-82474
 Emergency Response Planning and Preparedness Training Programmes, USA 8-57079
 fast reactor whole core accidents, fission products role 8-54854
 fault tree anal., modular representation 8-78480
 fault tree anal. code SUPKIT (*Japanese*) 8-54847
 FBR, modelling molten fuel-coolant interaction, INTER and CEFRA (*Czech*) 8-66352
 FBR, US development, safety aspects 8-86671
 fire hazard assessment 8-50269
 fission gas re-solution, comparison of single knock on and complete bubble destruction models 8-82455
 fracture mechanics of reactor primary system under operating and accident conditions 8-66342
 fuel cycles, safeguards 8-82446
 fuel elements, cracked, gas-filled, temp. distrib. calc. 8-78446
 fuel reprocessing in HTGR, safety aspects of solvent nitration 8-86650
 fuel rod arrays, radiative heat transfer, Monte Carlo method, temp. distrib. 8-78447
 fuel rods, defect detection 8-86640
 fusion and fast breeder reactors, a comparison, book 8-78430
 GCFR, 1000 MW, calc. of depressurisation and flow coast down accidents 8-50274
 GCFR, borax ($\text{Na}_2\text{B}_4\text{O}_7$) internal core catcher 8-58372
 GCFR core support structural assembly, seismic response via modal synthesis 8-89942
 globe main steam isolation valve unbalanced forces and novel actuator design 8-50288
 Go-ri nuclear power plant, containment integrated leak rate test (*Korean*) 8-54851
 graphite, failure criterion, J-integral critical value 8-84999
 HCDA, REXCO code, comparison with flexible vessel expts. 8-70618
 HCDA, vapour condensation from rising bubble, effects of internal circulation velocity and noncondensable gas 8-50258
 hermetically sealed valve for the safety systems of a nuclear power station (*Russian*) 8-89952
 hot water leakage from first loop, 22.8 MPa initial pressure, flow characteristics 8-66357
 HTGR, consequence anal. of hypothetical accidents, core heatup and afterheat removal 8-58381
 HTGR core, 2-D vibr. test and simulation anal. for vertical slice model (*Japanese*) 8-58328
 HTGR core during transient temp. excursion, fission product release, computerised analysis (*Japanese*) 8-82467
 HTGR hypothetical accidents, consequences following breach of primary circuit and safeguard failure (*German*) 8-58390
 HTR, expt. JAERI, safety anal. of fission product behaviour and hypothetical accident (*Japanese*) 8-66330
 HWR, explosive rupture of power channel pressure tube 8-70605
 infinite cylinders, critical and subcritical, n multiplication factor, nuclear criticality safety 8-78442
 inservice inspection, power plant design and fabrication 8-78451
 instructional programs at RPI, LWR and FBR appl. 8-58375
 international safeguards, research 8-82482
 isolation and relief valve/piping transient force anal. program 8-50287
 laser system for determ. of fission product release and distrib. in coated particles (*German*) 8-82403
 LMFBFR, computer modelling of piping components for transient hydrodynamic structural response 8-74449
 LMFBFR, coolant start of boiling detection by acoustic method 8-86646
 LMFBFR, effect of cracks in fast neutron embrittled hexagonal subassembly ducts 8-74446
 LMFBFR, finite element formulation for thin reactor struct. thermal stress anal. 8-70613
 LMFBFR, fuel and fission gas response to simulated thermal transients 8-74453
 LMFBFR, fuel freezing and drainage in shield plug following HCDA 8-50270
 LMFBFR, HCDA conditions, $\text{PuO}_2\text{-UO}_2\text{-Na}$ aerosol formation, aerodynamic and chem. behaviour 8-94104
 LMFBFR, leak detection in steam generator, by acoustic spectra meas. (*Czech*) 8-54849
 LMFBFR, modelling in prompt burst HCDA calcs. 8-74454
 LMFBFR, primary cooling circuits, Na loop system, anal. of radioactive corrosion product transfer 8-78464
 LMFBFR, response to abnormal events, applied mechanics in design and safety review 8-70611
 LMFBFR, squeeze flow between two adjacent subassemblies, discrete model 8-86634
 LMFBFR, wastage effects in small leak Na+water reactions, safety considerations 8-82418
 LMFBFR, water leaks in secondary cooling circuit boilers 8-86572
 LMFBFR (SNR 300), design of core catcher system 8-89937
 LMFBFR assembly, fuel pin deformations, analytical method, computational code (SHADOW) 8-54829
 LMFBFR containment, anal. of nonlinear fluid-struct. interaction, improved ICECO code 8-70615
 LMFBFR containment response anal., Eulerian computer code MICE for multifield fluids 8-70616
 LMFBFR cooling channels blockages, simulation testing (*German*) 8-94044
 LMFBFR cores, numerical method for predicting-subassembly seismic induced impact 8-74447
 LMFBFR head closures, dynamic struct. response to HCDA 8-70617

fission reactor safety continued

LMFBFR overpower excursions, mechanistic model of fuel freezing, channel plugging and continued coolability 8-58371
 LMFBFR prestressed concrete reactor vessels, analytical model and code applications 8-74448
 LMFBFR safety, comparison of ICECO code with flexible vessel expts. 8-70619
 LMFBFR safety, comparison of ICEPEL code with straight flexible pipe expts. 8-70620
 LMFBFR safety analysis, computational techniques 8-66355
 LMFBFR simulated fuel subassembly, local Na boiling behind flow blockage 8-54842
 LMFBFR single component and mixed oxide fuel solidification anal. 8-74435
 LMFBFR subassemblies, coolant boiling calc., using Claymore code 8-82473
 LMFBFR subassembly ducts dynamic response, comparison of finite element code with expts. 8-70614
 LMFBFR subassembly simulation, finite element computer model, safety anal. 8-70612
 LMFBFR thermal explosion hazards, review of present understanding and simulation expts. 8-82464
 LOCA, spray cooling of hollow rod cladding 8-50262
 LOCA conditions, transient two-phase flow reversal prediction 8-94811
 LOCA in water reactors, reversal of laminar flow in circular pipe 8-50271
 Lucens reactor accident, alarm and surveillance 8-50283
 LWR, plutonium fuelled, control and safety investigations 8-89969
 LWR, seawater levels of radioactive ^{54}Mn , ^{59}Fe , $^{58,60}\text{Co}$ 8-85608
 LWR, stress conc. in cladding produced by cracked fuel pellets 8-50260
 LWR, structural integrity of pressure boundary 8-66334
 LWR, technical safety rules, catalogue and classification for reactors and fuel cycle plants 8-58384
 LWR 1300 MWe system, design of containment to withstand core melt 8-66335
 LWR core meltdown, activity release and aerosol characts. 8-82469
 LWR hydrogen formation during core melt accident 8-50267
 LWR operation and maintenance 8-86653
 LWR power station radioactive unplanned discharge meas. 8-89995
 LWRs, accident prevention study 8-66356
 materials control with VACOSS variable coding seal system 8-82491
 materials science contribution to safety, components failure probabilities (*German*) 8-58352
 melting pool surfaces, temp. meas. by ratio pyrometers 8-82471
 molten fuel-coolant interaction studies, simulated reactor accident, wind-scale shock tube rig 8-58363
 NDT of special nucl. materials 8-82443
 near-stack dose calc., diffusion model applicability 8-94147
 neutron leakage spectra from critical assemblies, depth dose, dose equiv. and quality factor 8-58504
 nondestructive assay of irradiated nuclear fuel for safeguards, review 8-82495
 nuclear energy, technical economic and safety aspects (*Hungarian*) 8-82465
 Nuclear Energy Research Centre, Mol, Belgium, emergency plan organisation in event of major accident (*French*) 8-53527
 nuclear fuel cycle, safeguards implementation technology 8-86660
 nuclear power plant, aircraft impact, simplified derivation of reaction-time history 8-89958
 nuclear power station, seismic anal., slab modelling 8-50414
 nuclear structures, probabilistic design, state of art, research needs 8-94055
 performance of safeguards technology 8-82484
 physical protection safeguards for nuclear materials and facilities 8-82483
 pollutant release assessment, JEREMIAH computational system environmental transport and dose calcs. 8-94150
 pool heated volumetrically, reactor accident condition, phase change, free surface, thermal instability 8-89960
 power plant control appls., problems and trends 8-70609
 power plant emergencies, prevention of excessive irradiation of staff and population (*Russian*) 8-50286
 power reactor noise anal. (*Bulgarian*) 8-82488
 power stations in Italy, district emergency exercises 8-55052
 pressure vessel, ZR-6M rupture test using scaled simulation (*Hungarian*) 8-89964
 pressure vessels, exam. for compliance with safety regulations 8-89954
 pressure vessels, remote controlled US pre-service and in-service inspections 8-89955
 pressure vessels, unconditioned probability of brittle fracture 8-78479
 probabilistic anal., 1978 American Nuclear Society meeting, overview 8-82468
 probabilistic assessment of risks, of accidents and normal operation 8-50281
 probabilistic structural design, component level, Monte Carlo simulation approach 8-94056
 PWR, determ. of typical accidents and consequences, rel. to emergency planning (*French*) 8-50285
 PWR, MULTIFLEX code, anal. of hydraulic force with hydro-structural interactions during LOCA 8-58373
 PWR, peak cladding temp. sensitivity to LOCA reflood parameters 8-86639
 PWR, reliability assessment of containment 8-78481
 PWR, sensitivity of LOCA heat transfer anal. 8-50246
 PWR, St. Lucie 850 MWe, neutron streaming meas. and shielding recommendations 8-70608
 PWR depressurisation, hydraulic analogy 8-50243
 PWR plant, cut-and-cover construction, feasibility and safety (*German*) 8-82429
 PWR power plant, development trends (*German*) 8-50282
 PWR power plant, radiation protection (*French*) 8-82521
 PWR power plant steam dump valve stability anal. 8-50289
 PWR pressure vessel safety, term paper from course at Georgia Tech 8-58379
 PWRs, auxiliary feedwater system, fault tree anal. 8-54867
 radioactive aerosol dispersiveness in main ventilation system 8-70650
 radiochemical control of reactor cooling water (*Korean*) 8-54820
 Reactor Safety Study (Wash-1400) and implications for radiological emergency response planning 8-50284

fission reactor safety continued

- reinforced concrete, nonlinear dynamic response under loading, research status and needs 8-94054
- reinforced concrete containment structures, improved design, research requirements 8-94049
- research needs, standards improvement, nuclear power plant design 8-94046
- risk-benefit evaluation of nuclear power plant siting, comparison with coal-fired power station (*Czech*) 8-50266
- safeguards planning in plant design process 8-82423
- seismic areas, nucl. power plant siting 8-82481
- seismic effects in secondary containments: research needs 8-94050
- seismic load effects on structures, R and D requirements 8-94051
- seismic load studies on nuclear power plants, research needs 8-94052
- seismic response spectrum normalisation 8-50415
- seismic testing for class 1E equipment 8-78475
- siting of power plant, geological and seismology surveys of US midcontinent 8-85501
- steam generating system, seismic design, math. model 8-58339
- steam generator, modular, liquid Na heated, pressure and temp. loading in breakdown situation (*Czech*) 8-50264
- steam generator, multiple tube rupture, radiological consequences 8-74452
- steels, dynamic material props. for FBR safety anal., testing devices 8-60966
- structural design and analysis, research survey, nuclear power plants 8-94048
- structural design and analysis research programme for nuclear power stations 8-94047
- structural integrity assessment, mat. prop. variations 8-89953
- structural protection measures, against disruptive accidents (*German*) 8-94118
- Superphenix internal shells, vibr. anal. (*French*) 8-50247
- Swedish State Power Board nuclear power stations, training of emergency organisation 8-50412
- Swiss Federal Institute for Reactor Research emergency organisation 8-55047
- teaching, MIT nucl. engineering dept. courses, USA 8-58378
- test gauge, operation at low multiplication 8-82526
- transient fluid and structural dynamics problems, flow singularity methods 8-86633
- vibration analysis of heat exchanger and steam generator designs 8-66333
- water, transition boiling under forced convective conditions, reactor accident condition 8-89961
- Zircaloy fuel cladding, O embrittlement obs. 8-89947
- Zircaloy-2 cladding, reactor accident conditions, creep and creep rupture props., 1000 to 1500°C 8-78470
- Co radioactive release from reactor cooling water, fixation by sandy soil (*Japanese*) 8-74443
- ⁶⁰Co, shutdown dose rate prediction in BWR primary coolant circuit 8-74445
- D₂O leak detection, on-line infrared analyzers, CANDU report 8-82038
- I partition equilibrium between air and NaOH aq, effect of CO₂ conc. 8-78474
- I radioisotopes, high efficiency mixed species air sampling, readout and dose assessment system 8-57074
- Na transient boiling in single-pin annular channel under loss of flow 8-89933
- UO₂, interaction with Na, dropping experiments and subassembly test 8-82460
- UO₂, liquid, pressure generated by encapsulated Na (*Italian*) 8-82454

fission reactor theory and design

- see also fission reactors; fission research reactors; neutron transport theory
- absolute fission rate distrib. in standard U shell, comparison with ANISN code 8-62584
- advanced reactors, materials and design 8-78452
- AGR, advantages of downward flow config. over conventional design 8-70584
- at-power reactor noise, second-order coherent functions 8-94070
- basic nuclear engineering, book 8-54810
- burnup, anal. of sources of errors in calculational and experimental methods 8-58343
- burnup determ., accuracy requirements for fuel cycle design, reactor operation and safety 8-58342
- burnup equations, determination of neutron flux and isotopic changes in reactor cell 8-58340
- BWR, noise anal. model 8-50237
- BWR boiling noise, local and global component obs. and calc. 8-94066
- BWR core, moderator temp. coeff. and neutron leakage, DIFFUSION-ACE calc. 8-54844
- BWR dynamics, multivariable autoregressive identification 8-94107
- BWR load following plant, low sensitivity design fo controller 8-78473
- BWR plants in Japan, seismic design and tests 8-86652
- BWR power fluctuations, noise source estimation by autoregression 8-78476
- BWR simulation diagnosis by noise analysis 8-94062
- BWR stochastic neutron flux fluctuation obs. and modelling, thermo-hydraulic parameters 8-94065
- BWR void effects, stochastic point model and zero-power reactor simulation 8-94061
- CANDU fuel bundles, outline of Canadian R and D programme on fuel behaviour in transients 8-94102
- CANDU pressurised HWR fuel, bundle end neutron flux peaking effects, plenum use 8-58385
- CANDU simulated core in ZED-2, transient meas. anal., CERKIN code exam. 8-58386
- CANDU-PWR, comparison of three axial fuel management strategies 8-94075
- checkerboard pool core, series of two group calcs. 8-74424
- Colgate fission plasma reactor, high temp., gaseous fissionable material, design, technical problems (*Dutch*) 8-50249
- control rod drive system penetration assemblies for Caorso Mark 2 primary containment 8-58368
- cooling system, flow around obstacles determ. (*Czech*) 8-66331
- core and shield calc., radiation transport program benchmark tests 8-78440

fission reactor theory and design continued

- core reactivity and space-domain noise effects of randomly dispersed materials 8-94071
- coupled cores, calc. of buckling variation and neutron flux, Green's function method 8-74421
- coupled-core reactors anal. with method of moderator region response function 8-58331
- critical energy in heat transfer channels of complex shape, fuel rod assembly 8-78453
- cylindrical source shielding eqns. including buildup, lateral dose rate, compact function use 8-89982
- depletion chain eqns., FORTRAN program for solns. using analytical methods 8-74423
- ducts and pipes intricately shaped cross section, heat transfer, Laplace and structural method 8-83477
- electrical and mechanical equipment, improved seismic tests, research needs 8-94053
- energy distrib., discrete monitoring error 8-82476
- fast critical expts., effective delayed neutron fractions and central reactivity worths 8-62602
- fast reactor integral expt. anal., appl. of uncertainty and sensitivity theory 8-50239
- FBR, methods of condensing efficient cross sections (*Spanish*) 8-58325
- FBR, multigroup 1-D diffusion program MED 8-78456
- FBR, neutron-physical calc., multi-group diffusion equation solution (*Czech*) 8-66332
- finite element heat cond. in reactor solids, review and TEMPEL computer program 8-62593
- fission gas, steady state behaviour in carbide fuels, modelling 8-78469
- fission product sensitivities, analytic evaluation 8-82424
- flux calculation in complex heterogeneous reactor cells by imbedding element method (*Russian*) 8-58321
- fuel assembly design features 8-89939
- fuel element modeling rod bundle in longit. air flow, heat transfer expt. 8-82415
- fuel element spacers, structural anisotropic plates composed of cylindrical shells 8-89940
- fuel elements, cracked, gas-filled, temp. distrib. calc. 8-78446
- fuel pin gaps, probabilistic distrib. within wire-spaced fuel subassembly 8-78448
- fuel pin-cell burnup code BETTY 8-89946
- fuel rod arrays, radiative heat transfer, Monte Carlo method, temp. distrib. 8-78447
- fuel rod structural anal. criticism 8-82441
- functional anal. of multigram neutron diffusion problem 8-58317
- fusion and fast breeder reactors, a comparison, book 8-78430
- fusion-fission breeder reactor, supercond. poloidal field coil design 8-70640
- fusion-fission reactor symbiotic design, simple fuel reprocessing 8-66365
- gamma spectra of fission products, estimation using nucl. systematics 8-70587
- GCFR core support structural assembly, seismic response via modal synthesis 8-89942
- global reactor calcs. review, practical calc. for reactor burnup 8-58341
- HCDA, REXCO code, comparison with flexible vessel expts. 8-70618
- heterogeneous computer program for square fuel rod lattices in cylindrical tank 8-58346
- higher order perturbation methods, implicit and explicit, for reactor anal. 8-78444
- HTGR, annular fuel rod, contact viscoelastic stress anal. (*Japanese*) 8-54817
- HTGR steam power plant, nonlinear dynamic model, digital simulation 8-78437
- HTR, expt. multipurpose, status of core design studies at JAERI (*Japanese*) 8-66330
- HWR, Wolsung power reactor, D₂O moderated, temp. coeff. of reactivity, numerical calcs. 8-54818
- infinite cylinders, critical and subcritical, n multiplication factor, nuclear criticality safety 8-78442
- inservice inspection, power plant design and fabrication 8-78451
- integral and integro-differential transport theory 8-50228
- integration method for reactor systems analysis 8-78438
- irradiation effects, precipitation in pile, rel. to void swelling 8-70595
- Japanese Evaluated Nuclear Data Library, first version evaluation (*Japanese*) 8-74428
- Kalman filtering theory appl. (*Japanese*) 8-50278
- kinetics, higher order prompt jump approx. 8-50238
- lattice cell diffusion coefficients, unified derivation of definitions 8-58332
- LMFBR, computer modelling of piping components for transient hydrodynamic structural response 8-74449
- LMFBR, dynamic response of containment vessel and coolant wave propag., REXCO-EUR code manual 8-58349
- LMFBR, effect of cracks in fast neutron embrittled hexagonal subassembly ducts 8-74446
- LMFBR, finite element formulation for thin reactor struct. thermal stress anal. 8-70613
- LMFBR, modelling in prompt burst HCDA calcs. 8-74454
- LMFBR, pool-type, dried hot concrete vessel design 8-50248
- LMFBR, response to abnormal events, applied mechanics in design and safety review 8-70611
- LMFBR, SNR-300, fuel rod performance and modelling at high burnup 8-58336
- LMFBR, water leaks in secondary cooling circuit boilers 8-86572
- LMFBR (SNR 300), design of core catcher system 8-89937
- LMFBR assembly, fuel pin deformations, analytical method, computational code (SHADOW) 8-54829
- LMFBR benchmark calcs. by 2 and 3 dimens. diffusion methods 8-74432
- LMFBR burnup calc., allowance for ²³⁹Np 8-89936
- LMFBR containment, anal. of nonlinear fluid-struct. interaction, improved ICECO code 8-70615
- LMFBR containment response anal., Eulerian computer code MICE for multifield fluids 8-70616
- LMFBR cores, numerical method for predicting subassembly seismic induced impact 8-74447
- LMFBR fuel subassembly, pin bundle deflection anal. 8-78449
- LMFBR head closures, dynamic struct. response to HCDA 8-70617

fission reactor theory and design continued

- LMFBR power reactor, objective function optimisation (*Russian*) 8-70590
- LMFBR prestressed concrete reactor vessels, analytical model and code applications 8-74448
- LMFBR safety, comparison of ICECO code with flexible vessel expts. 8-70619
- LMFBR safety, comparison of ICEPEL code with straight flexible pipe expts. 8-70620
- LMFBR single component and mixed oxide fuel solidification anal. 8-74435
- LMFBR subassembly ducts dynamic response, comparison of finite element code with expts. 8-70614
- LMFBR subassembly simulation, finite element computer model, safety anal. 8-70612
- Los Alamos density exponent formula, integral version, comparisons using multigroup theory 8-74425
- LWR, structural integrity of pressure boundary 8-66334
- LWR 1300 MWe system, design of containment to withstand core melt 8-66335
- LWR anal., pressure-crossflow soln. method, COBRA-III codes 8-82417
- LWR plant, economic effect of increased seismic load on design and construction costs 8-66432
- LWR power plant, general design philosophy (*Japanese*) 8-54816
- LWRs in Japan, design improvement and standardisation 8-86579
- metal structures, inelastic anal. 8-70586
- multigroup-multipoint diffusion operator spectrum with delayed n 8-74430
- neutron diffusion, linear eqns., soln. by method of implicit non-stationary iteration 8-70581
- neutron diffusion and transport, GGTC-ENEL computer code for multigroup cross sections 8-58323
- neutron flux distrib., optimal allocation of in-core detectors 8-54839
- neutron gas, nonequilibrium thermodynamics (*Japanese*) 8-62595
- neutron pulse behaviour in multizone breeder system, two-zone system pulse method 8-86574
- neutron transport, eigenvalue eqns., appl. to fast and thermal neutron systems 8-50231
- noise analysis, irreversible circulation parameter 8-94069
- noise analysis of power reactor, simulation using nucleate boiling noise generator 8-54840
- noise theory, fluctuation coarse-graining and normality preservation 8-94068
- nonanalogue Monte Carlo games, conditions concerning nonanalogue transition kernels and estimators 8-62594
- nonlinear coupled core reactor, computer simulation of decoupling theory appl. to power control 8-54845
- nuclear data files of UK Chemical Committee, summary of data, available in ENDF/B format 8-82425
- nuclear fuel cycle, core design optimisation 8-82420
- nuclear structures, probabilistic design, state of art, research needs 8-94055
- offshore floating plants, design and anal. methodologies 8-66336
- particle collision method in spherical geometry by escape probabilities, flux transport eqn. 8-78433
- PBR, fast power excursions, DYN and COSTANZA programs 8-50241
- PBR, simulated THTR, spline anal. of dynamic transit reactivity meas. for pebbles (*German*) 8-66339
- perturbation higher order time depend. theory, appl. to nuclear reactors 8-58333
- PHWR valve bellows, effect of service parameters on fatigue life and fracture 8-58348
- pin bundle, two-phase flow, eqns. of motion 8-86570
- planning and construction of nuclear power plant (*Korean*) 8-54819
- point-like nuclear reactor neutron kinetics solns. using numerical method (*Italian*) 8-58324
- polynomial solns. to tensorial differential eqns. for monoenergetic neutrons in slab and sphere geom. 8-50232
- pool heated volumetrically, reactor accident condition, phase change, free surface, thermal instability 8-89960
- power reactor, neutron density fluctuations, stochastic nonlinear model, Fokker-Planck eqn. 8-58316
- pressure vessel and nozzle junction, optimum shape design 8-89941
- pressure vessels, exam. for compliance with safety regulations 8-89954
- probabilistic structural design, component level, Monte Carlo simulation approach 8-94056
- pulsed neutron source, use of perturbation theory for exptl. study 8-66328
- PURNIMA 1 fast reactor, k_e variation during core insertion into reflector 8-74438
- PWR, modification of subcooled boiling calc. in COBRA-3/KFKI program (*Russian*) 8-82434
- PWR, oxide fuel rods, computer program for mechanical and thermal anal. (*Korean*) 8-86571
- PWR, reliability assessment of containment 8-78481
- PWR, thermohydraulic processes study, models and expt. instrumentation (*Hungarian*) 8-82433
- PWR core, Xe oscillation model, neutron diffusion eqn., nonlinear system 8-58322
- PWR core barrel motion from neutron noise spectral density using scale factor 8-74450
- PWR core barrel motion quantification using scale factor and statistical noise parameters 8-74451
- PWR neutron noise interpretation by vibration analysis 8-94073
- PWR neutron noise sources 8-94108
- PWR plant, cut-and-cover construction, feasibility and safety (*German*) 8-82429
- PWR reliability prediction in design, empirical and Monte Carlo techniques 8-54827
- PWR steady state thermal anal., single-pass procedure using simplified nodal layout 8-50244
- PWR steam supply control system optimisation 8-50251
- PWR three unit 1300 MW(e) plant, engineering and design 8-86578
- radioactive nuclide decay data for reactor calcs., activation products and related isotopes 8-82426
- radioisotopes in cooling system, prod., transfer, life cycle, radiation calcs. using program system TIBSO 8-54821
- reaction rate Monte Carlo estimators, unified definition 8-58334

fission reactor theory and design continued

- reactivity increase due to compaction of unmoderated fissile materials 8-70589
- reactivity insertion, unexpected, rapid detection 8-58370
- reactor kinetics eqns., appl. of higher order prompt-jump approx. 8-74422
- reactor noise theory as a Markov process 8-74420
- reflected cylindrical reactor, eigenfunction and numerical solns. to critical problem 8-58326
- reinforced concrete, nonlinear dynamic response under loading, research status and needs 8-94054
- reinforced concrete containment structures, improved design, research requirements 8-94049
- reliability and maintainability symposium, Los Angeles (1978) 8-50250
- removal-diffusion shielding code SHREDI, bidimensional, fundamentals and results 8-70645
- research criteria, economical nuclear power plant structs. and components 8-94045
- research needs, standards improvement, nuclear power plant design 8-94046
- safeguards planning in plant design process 8-82423
- seismic effects in secondary containments: research needs 8-94050
- seismic load effects on structures, R and D requirements 8-94051
- seismic load studies on nuclear power plants, research needs 8-94052
- seismic response anal. of structures, new discrete models 8-67081
- standard variance reduction techniques in Monte Carlo transport problems, leakage estimator 8-78443
- steam system, seismic design study using cantilever cylindrical shells 8-58339
- stressed state in reactor pressure vessels, model studies by polarised optics 8-78454
- structural anal., underlying concepts of finite element analysis 8-66337
- structural design and analysis, research survey, nuclear power plants 8-94048
- structural design and analysis research programme for nuclear power stations 8-94047
- Superphenix internal shells, vibr. anal. (*French*) 8-50247
- symmetric SOR and SIP methods, numerical soln. of multigroup diffusion eqn. 8-74431
- symmetrised neutron transport eqn., fast Fourier transform method solns. 8-78435
- thermal hydraulic anal., of rod bundle fuel elements, COBRA-3C@KFKI digital computer program 8-84222
- thermal reactor, reuse of power Pu and U, neutron regeneration 8-82421
- turbulent heat transfer in annulus, transient, heating element, reactor cooling theory 8-86569
- two-dimensional fast reactor model, space-time synthesis 8-89935
- two-phase flow patterns, high pressure water in heated four rod bundle 8-89938
- U isotopes, sensitivities to cross sections, decay constants flux and time, analytical evaluation 8-82427
- vibration analysis of heat exchanger and steam generator designs 8-66333
- water shield, neutron transport, 2-D benchmark expt. 8-58318
- Am isotopes, sensitivities to cross sections, decay constants flux and time, analytical evaluation 8-82427
- Br series fission product isotopes, sensitivities to various parameters, analytical evaluation 8-82424
- Kr series isotopes, sensitivities to various parameters, analytical evaluation 8-82424
- Np isotopes, sensitivities to cross sections, decay constants flux and time, analytical evaluation 8-82427
- O cross section data test using n spatial distrib. in water 8-74417
- Pu isotopes, sensitivities to cross sections, decay constants flux and time, analytical evaluation 8-82427
- Pu(NO₃)₄ in light water, reactivity predictions using discrete ordinates transport theory 8-89957
- Sb isotopes, fission product conc., sensitivity anal. of cross section effects 8-82428
- Se series fission product isotopes, sensitivities to various parameters, analytical evaluation 8-82424
- Sn isotopes, fission product conc., sensitivity anal. of cross section effects 8-82428
- UO₂/Na, fuel/coolant thermal interaction in FBR, out of pile preliminary tests (*Italian*) 8-54828
- UO₂-PuO₂ mixed lattice, reactivity predictions using multigroup transport theory 8-89957

fission reactors

- see also fission reactor materials; fission reactor operation; fission reactor theory and design; fission research reactors; nuclear engineering; nuclear physics; nuclear power stations
- American Nucl. Soc. winter meeting 1977 8-58315
- American Nucl. Soc. Winter Meeting 1977 8-82408
- BWR dynamics, multivariable autoregressive identification 8-94107
- catalysed D fusion-fusion hybrid reactors 8-58436
- Colgate fission plasma reactor, high temp., gaseous fissionable material, design, technical problems (*Dutch*) 8-50249
- current status, USA, as of 31/12/1977 8-58398
- FBR, US development, safety aspects 8-86671
- FBR power stations, plutonium waste treatment, comparison with thermal reactors 8-86641
- fusion and fast breeder reactors, a comparison, book 8-78430
- fusion-fission Tokamak, T breeding, optimisation with geom. program 8-74477
- HTR process steam for coal gasification 8-78488
- important types used in West, survey (*German*) 8-74463
- LMFBR, energy investment 8-78512
- NBS reactor, summary of activities, (July 1976 to June 1977) 8-82435
- noise, specialists' meeting, Gatlinburg, USA, Sept. 1977 8-94057
- PHWR, CANDU reactor system, appropriate technology 8-58338
- pressure vessel, stress intensities for nozzle cracks 8-70583
- PWR, St. Lucie 850 MWe, neutron streaming meas. and shielding recommendations 8-70608
- PWR with straight tube steam generator, 1300 MW, characts. (*German*) 8-50292
- systems reliability, computer programs (*Slovak*) 8-82416

fission reactors continued

- Tokamak hybrid breeder blanket, liq. metal coolant, MHD effects 8-74481
 two-component Torus hybrid system, pressure tube convertor for hybrid blanket 8-74478
- fission research reactors**
see also fission reactor core control and monitoring; fission reactor theory and design; nuclear reactor instrumentation
 advanced reactor development in Japan 8-86663
 AGR, heat transfer to accel. gas flows, expt. and calcs. 8-54823
 Bruce core, ZED-2 mockup, responses of Pt, V and Co self powered flux detectors 8-58391
 carbide fuel element testing in fast reactor BOR-60 8-86582
 Czechoslovak Rez Nuclear Research Institute airborne radioactive release monitoring 8-89991
 data acquisition program for reactor control 8-86679
 Dragon reactor zero energy expts., further n energy group and transport calcs. 8-78445
 EBR II, fission product source identification using Xe tag 8-70588
 EBR-II, Na-water, leak detection system 8-78484
 epithermal neutron radiation field development for cerebral tumour therapy (*Japanese*) 8-88742
 fast critical expts., effective delayed neutron fractions and central reactivity worths 8-62602
 IRT 2000 reactor in Sofia, neutron spectra and doses in exptl. canals (*Bulgarian*) 8-82489
 LMFBR outlet plenum, air flow model, interferometric meas. of fluctuating temp. using FFTF 8-89943
 Lucens reactor accident, alarm and surveillance 8-50283
 neutron irradiation facility in WR-1 organic-cooled research reactor, corrosion testing 8-89945
 noise analysis of power reactor, simulation using nucleate boiling noise generator 8-54840
 PBHTR, Julich, 10 year operation (*German*) 8-54838
 PBHTR, out-of-core instrum. for detection of spatial flux irreg. (*German*) 8-82430
 research reactor, IRT-2000, algorithms for direct digital control of neutron field 8-86643
 thermal neutron flux density, working standard based on F-1 reactor 8-82410
 TR-1 reactor, thermal spectrum using neutron radiography of wedge shaped absorber 8-74439
 Trombay nuclear facilities, effluent release monitoring procedures 8-89993
 two-component torus hybrid reactor, double wall for first wall, struct. anal. 8-66409
 West German nuclear plant airborne radioactive effluent monitoring 8-89990
 WR-1 organic reactor, material irradiation facility 8-54868
 YAYOI core absorbed dose meas. by chemical dosimeters (*Japanese*) 8-86695
 ZED-2, simulated CANDU cores, transient meas. anal. 8-58386
 ZED-2 hot loop, lattice cell meas. in 36 element natural UO₂ fuel, stopping effect of coolant 8-58347
 zero power reactor simulation of BWR void effects 8-94061

fissures *see cracks***flame sprayed coatings**

No entries

flame spraying

No entries

flameproofing*see also fires*

- flameproof coating for PVC insulated cables, composition, tests (*Russian*) 8-68828
 plastics, materials testing, application-oriented test standardisation (*French*) 8-85061

flames*see also chemically reactive flow; combustion; fires*

- acoustic radiation rel. to flame loudspeakers 8-59227
 atom distribution, in flame spectrometry, moving point source model 8-61084
 axisymmetric confined flame, aerodynamic and heat transfer, finite difference scheme, program 8-94689
 axisymmetric laminar jet diffusion flame, split operator finite difference solns. 8-51252
 coaxial burner flame, struct., holographic interferometry determ. (*Russian*) 8-94851
 combustion diagnostics, laser Raman and fluoresc. techniques 8-88635
 confined burning jet, droplet vaporisation, expt. and theory 8-94855
 diffusion flame, oppositely directed jets, elec. props. 8-56896
 diffusion flames; laminar and planar, large activation energies, asymptotic development (*German*) 8-91035
 electric field effect on propagation rate, precombustion Joule heating 8-53207
 flow velocity field induced by flame spreading over fuel, laser velocimeter meas. 8-59529
 fuel droplet, deflagration and extinction in weakly reactive atoms. 8-64840
 gas jets, laminar homogeneous, combustion process (*Russian*) 8-94850
 n-hexane, tank flame, turbulence, holographic interferometric synchronous photography (*German*) 8-51255
 hydrocarbon diffusional combustion in air, finite activation energy anal. 8-95930
 industrial flare flames, smoke detection and control by electric fields 8-81360
 jet flame, props. and mixing process in recirculation zone 8-91025
 laminar, rise velocity meas., spectroscopic method 8-74064
 laminar flame, front, hydrodynamic instability, numerical solns. 8-51254
 laminar flame front, hydrodynamic instability, nonlinear integro-differential eqn. 8-51253
 laminar mixed-mode forced-free diffusion type, on vert. burning fuel slab 8-91033
 laser induced fluoresc. spectroscopy in flames, detectability limit 8-73096
 methane-air, OH conc., temp. and rot. temp., laser absorption spectroscopy 8-76862
 optical properties and temp. measurement of light scatt. particles containing flame (*Russian*) 8-56894

flames continued

- photometers with automatic dilutor 8-49878
 pool flames, heat and mass transfer (*German*) 8-94677
 premixed laminar flame, time-depend. soln. determ. 8-67282
 premixed turbulent flame combustion, heat transfer obs. and calc. (*French*) 8-94688
 propane-air flame, chem. anal. of reaction zone by Raman spectra 8-64837
 radiation measurement techniques 8-94506
 reaction rate coefficients, for flame calcs. 8-85160
 saturated fluorescence excitation, transition probabilities and particle density determ. 8-58871
 soot-gas mixture, in luminous flames and smoke, IR mean absorption coeffs. calc. procedure 8-91061
 stabilisation behind bluff-body flame holder (*Japanese*) 8-67284
 temperature determ. by laser Raman optical multichannel analyser 8-73098
 turbulent diffusion flame, analytic incorporation of probability density functions 8-75232
 turbulent diffusion flame, visible length of vertical free flames 8-85163
 turbulent premixed flame, theoretical predictions (*French*) 8-94853
 C particles in flame, laser heating and sublimation 8-61012
 CH, in low pressure flame, laser-excited fluoresc. 8-90199
 H₂-O₂-N₂ flame, photochem. reactions involving Na⁺, laser saturated conditions 8-80762
 H₂-O₂-N₂ flames, diffusion coeff. meas. for CO, Br, I and Ti 8-51272
 HCl, dissociation, electron attachment kinetics in flame, mass spectra obs. 8-68872
 NO₂ laser fluoresc. meas. in flames 8-56923
 Na, two-photon excitation in flame, saturation broadening, fluoresc. obs., broad-band excitation 8-74625
 NaCO₃+ZrC, flame, optical and temp. characts. meas. method, light scatt. ZrO₂ particles (*Russian*) 8-56894
 O₃, decomposition flame, flat, laminar, vel., struct. 8-51256
 S containing aerosols, continuous meas. and speciation by flame photometry 8-95974
 S₂ in flames, laser induced fluoresc. meas. 8-61132
 SH, in flames, laser induced fluoresc. meas. 8-61132
 SO, SO₂ in flames, laser induced fluoresc. meas. 8-61132

flare stars *see stars***flares, solar *see solar flares*****flash lamps**

- alkali metal vapour flash lamp, absolute spectral distrib. and radiant output 8-66510
 inert gas flash lamp, absolute spectral distrib. and radiant output 8-66510
 laser pumping, discharge development effects on pumping efficiency 8-71114
 laser pumping, optimal lamp filling, review (*Russian*) 8-63123
 prepulsed, anomalous plasma resistivity in discharges 8-87508
 pulsed Xe spectrophotometer with parallel wavelength sensing 8-54427
 Nd³⁺:YAlO₃ laser double-pulse flashlamp trigger cct. 8-55378

flash photolysis *see photolysis***flashover**

- arc quenching system for transient and statistical flashover, fusion reactor systems 8-75455
 back discharge, flashover meas., streamer or steady glow mode, dust layer effects 8-59708
 breakdown voltage of air, effect of sand particle pollution 8-81363
 dielectric surface creep discharge flash intensity and time distrib. obs. 8-67562
 probability dependence and Weibull distribution (*Czech*) 8-67449
 rod-to-plane air gap breakdown under negative impulse voltage 8-67563
 solid insulator surface flashover in vacuum streak photography 8-59700

flaw detection *see crack detection***flexural strength *see bending strength*****flicker noise *see random noise*****flip-chip devices***see also thin film circuits*

No entries

floating zone method (crystal growth) *see zone melting***floating zone refining *see zone refining*****flocculation***see also colloids; sedimentation*

- agglomeration, computer simulation (*Japanese*) 8-95706
 book, scientific basis of flocculation 8-92520
 disperse systems, coagulation, slow, turbulent 8-53259
 polystyrene latex dispersions, aqueous, in presence of poly(vinyl alcohol), stability, crit. flocculation temp. 8-85207
 polystyrene particles flocculation, light scatt. for close range struct. determ. 8-53273
 sterically stabilised dispersions, critical flocculation temperature, effect of dipolar substituent groups 8-61061

flow

- see also chemically reactive flow; compressible flow; Couette flow; external flows; flow instability; flow measurement; flow through porous media; Knudsen flow; laminar flow; magnetohydrodynamics; multiphase flow; non-Newtonian flow; plasma flow; Poiseuille flow; pulsatile flow; rotational flow; shear flow; stratified flow; supersonic flow; transonic flow*
 advection processes, finite difference method, balanced expansion technique 8-77719
 bifurcation and nonequilibrium phase transitions of limit cycles and multiperiodic flows in continuous media 8-81937
 book, for undergraduates 8-59358
 boundary elements method appl. 8-90821
 boundary-value problems three-dimensional region elliptic transformation 8-55624
 Boussinesq equation, finite element anal. 8-79292
 channel, straight (buckled), two-dimens. flow, stability anal. 8-59490
 collapsible tubes, oscils. 8-59488
 containment dyke, flow over wall 8-71412
 dense liquid flow around deforming contour (*Russian*) 8-67178
 distorting duct, restoration of turbulent energy, evidence (*French*) 8-90841

flow continued

drop, spherical or cylindrical, flow produced by uniform translation along cylinder vertical axis (*French*) 8-90967
 electrosag refining, mathematical formulation for EMF, fluid flow, and heat transfer 8-52722
 enclosure fire, static pressure meas. 8-90871
 expansion process, initial value problem, two step difference method (*German*) 8-57877
 fluid flow equations, solns. 8-90817
 fluids with memory, simple, thermodynamics of linear flows 8-90812
 free surface, digital simulation by finite element method 8-90819
 gas flow, Monte Carlo simulation, book contrib. 8-59365
 gas flow in smooth and rough channels, heat transfer efficiency comparison 8-51243
 gas motion in channel with cryogenic walls 8-59487
 groundwater, calc. by boundary element method 8-94634
 groundwater, unsteady flow from tunnel opening, reductive finite element anal. (*Japanese*) 8-96251
 groundwater calc. by finite element Galerkin method 8-89320
 groundwater migration during soil freezing, obs. (*Japanese*) 8-88862
 groundwater two-dimensional flow digital simulation using finite element method 8-93018
 heat exchanger check calculations with parallel/mixed flow, standard expressions 8-67199
 heat transfer, separated flow over triangular prisms 8-87339
 homogeneous mixtures, flow, theory (*Russian*) 8-87326
 hydraulic equivalent of generalized one-dimensional flow 8-94627
 hyperbaric Fano flow of Newtonian fluids, device 8-94863
 incompressible irrotational axisymmetric flow about body of revolution and the inverse problem 8-94630
 instationary, in incompressible micropolar fluids, existence theorems 8-63465
 linear viscoelastic fluids in channel and pipe, unsteady flow 8-75375
 liquid flow blockage in circular tube below freezing point, theory and expt. 8-94830
 Mars fretted terrain, erosional debris flow 8-65537
 narrow channels, effect of surface induced gradual viscosity increase 8-83488
 Navier-Stokes equation solution, smoothing techniques 8-90823
 Navier-Stokes initial value problem approx. soln., incompressible boundary-free flow 8-57788
 nonlinear fluid motion, order and disorder 8-94629
 nonlinear free surface, anal. by boundary integral eqn. method 8-92850
 nonlinear singular perturbation problem on a semi-infinite interval 8-94631
 nonsteady flow through the ports of a hydrodynamic siren 8-94824
 numerical modelling appls., conf., Southampton, England (July 1977) 8-77285
 one-dimens. unsteady non-equilib. flows, method of characts., exponential fitting 8-49648
 open channel flow with side discharge, recirculation zone, depth-averaged model 8-63499
 oscillatory flow through axisymmetric pipes and two dimens. channels 8-94823
 Oseen, unsteady three dimens., applied conc. force 8-67167
 paraboloid wholly immersed in infinite inviscid, thrust due to source at point on axis 8-59360
 pipe flow, thermal entry length problem, numerical soln. (*German*) 8-83494
 pipe mode characteristics determination, pipe flow conditions effects (*French*) 8-79246
 piped fluids in motion, turbulent flow, direct analytical soln. 8-87393
 pipes, variable cross-section, potential axisymmetrical motion 8-59489
 potential flow, approx. numerical solns. 8-79293
 potential flow, transient state, Liesegang rings demonstration 8-63408
 rarefied gas flow induced by thermal stress, imperfect accommodation at boundary 8-87362
 rectangular catchment basin downflow and infiltration, kinematic wave models 8-81235
 sound generation and transmission in flow ducts with axial temperature gradients 8-90551
 steady and non-steady flow through IC engines inlet valve with heat transfer 8-59390
 steady flows, fully stalled, flow computation in two dimens. passages 8-94826
 steady plane isochoric flows, acceleration and pressures 8-81845
 steam condensation in annular duct flow, heat transfer to condensate film 8-94709
 Stefan and dam problems, free boundary convexity 8-83356
 Stoke's problem in velocity pressure formulation, mixed finite element approx. (*French*) 8-86164
 Stokes flow due to a Stokeslet in a pipe 8-67268
 Stokes flow edge and biharmonic problems, convergence of biorthogonal series 8-81847
 tidal flow, finite element analysis model, flow in rectangular channel example (*German*) 8-96233
 transient and unconfined groundwater flow analysis by finite element method 8-92871
 two-dimensional gas flow model, comparison of two methods of computation (*Russian*) 8-59413
 two-dimensional torus, first order quasilinear partial differential eqns. (*French*) 8-89345
 two-dimensional with singularities, anal. by finite element method 8-90822
 valve connected to pipe, acoustic oscills. from flow 8-59491
 viscous incompressible flow, integral eqn., soln. by function-theoretic method 8-69990
 Al alloy, sheets, type 7004, asymmetrical solidification structures, fluid flow, in W arc welds 8-84794
 U isotope separation, influence of flow field struct. in the separation nozzle 8-82498

flow birefringence

aqueous solution charact. relations, transmitted radiation 8-56453
 atmosphere, boundary layer turbulence, birefringence, ellipsometric meas. 8-69453
 macromolecular solution, local flow birefr. in double roller mill (*French*) 8-80315
 Maxwell stress, deformable surface, general case 8-59501

flow birefringence continued

polyethylene glycol, conformation in liq. state from flow birefringence 8-76423
 polymer melt in intermittent shear flow, transient birefringence 8-63457
 scattered radiation charact. 8-60418

flow control

axial flowmeter aperture ratio calc. method (*Dutch*) 8-67285
 drip feed unit microprocessor control development 8-53563
 drying, heat and mass transfer, optimal control 8-67006
 jet, axisymmetric, modelling of large eddies, harmonic forcing effect 8-90957
 liquid metal systems, mechanical or MHD flow rate regulators (*Russian*) 8-75229
 molecular flow measurement, precision, and control for single and multigas systems 8-70135
 PWR power plant steam dump valve stability anal. 8-50289
 thermal regenerator, with variable mass flow rate, computer model 8-75047
 transducer for automated gas flow control 8-59508

flow instability

aerofoil, dynamic forces acting, subsonic instabilities (*French*) 8-67213
 aerosol impactors, fluid jet impinging upon void 8-63472
 aircraft dynamics, unsteady airloads prediction, aeroelastic anal. 8-71346
 annular flow, linear stability 8-63497
 arc, axial flow stability, cathode emission mechanism change effect 8-83638
 atmosphere, exchange stabilities principle (*French*) 8-88871
 atmosphere, finite amplitude Kelvin-Helmholtz billows, evolution 8-81293
 atmosphere, turbulent shearing layers, growth, limiting thickness, dominant eddy scale 8-92955
 axial flow in annuli, instability 8-55631
 axial flow in annulus, numerical stability anal. 8-83363
 baroclinic instabilities of deep fluid 8-79307
 Benard convection, in heat conducting media (*German*) 8-79308
 Benard Karman street of vortices generated in asymmetric fluid field (*Italian*) 8-83406
 boiling, sustained and transient, inlet subcooling effect on flow instabilities 8-94809
 boiling in channel, thermally induced two-phase flow instabilities, thermal nonequib. 8-51240
 cantilever pipes, internal flow induced instabilities 8-63496
 cascade static stability and critical velocity (*German*) 8-79306
 cavitation bubble, dynamic instability phenomenon, governing eqn. 8-59434
 cavitation bubbles, linear stability of growth or collapse, slightly viscous liquid 8-90947
 cavity type geometries, self sustaining cavity oscills., review 8-94645
 concentric spheres, unstable motion of viscous fluid (*Russian*) 8-55649
 convection of vertical layer, flow stability, boundary thermal props. effect 8-55644
 convection onset, natural, in heated water-saturated porous cylinder 8-59478
 Cosserat fluid, flow stability 8-51203
 counter-current two-phase flow, annuli, rod bundles, liq. film behaviour, flooding 8-59452
 critical Reynolds number in pipe Poiseuille flow 8-94644
 dam porous media unsteady flow calculation, combined finite element/characteristics methods appl. 8-91012
 double injection with recombination, EHD linear and nonlinear stability 8-87412
 double row of moving vortices near a wall, stability condition (*Italian*) 8-83407
 dry ice sublimation, Taylor instability 8-90689
 electrically conducting rarefied gas, oscill. flow, past vertical porous plate, free convection 8-90830
 electrohydrodynamic stability in rigid cylinder, dielectric viscous fluids, eigen wavenumbers 8-59497
 ethanol-water mixture, saturated, min. film boiling temp. on horiz. stainless steel and Cu surfaces 8-90692
 film boiling destabilisation, liq. drop falling onto hot liq. surface 8-94588
 flame front, laminar, hydrodynamic instability, nonlinear integro-differential eqn. 8-51253
 flame front, laminar, hydrodynamic instability, numerical solns. 8-51254
 fluid layer, under general convective boundary conditions 8-94683
 fluid motion within ellipsoidal cavity, Coriolis force field rel. to instability regions (*Russian*) 8-81296
 free convection mass transfer from horizontal surface, electrochemical and holographic interferometric obs. 8-87344
 free convective flow in porous medium, longit. vortices, onset, linear stability anal. 8-94813
 free shear layer tone phenomenon, probe interface 8-71324
 fully developed laminar flow with internal heat generation between horizontal parallel plates, thermal instability 8-90899
 gas-liquid film interface stability behind slipping shock wave front (*Russian*) 8-55630
 generalised biharmonic eqn., appl. to hydrodynamic stability using homogeneous boundary conditions 8-90834
 heat exchange component vibrations in liquid and two-phase cross-flow 8-90770
 heat transfer and flow instability of natural convection over upward-facing horizontal surfaces 8-94698
 helical velocity and magnetic fields, stability 8-73624
 hydrodynamic instabilities, transition to turbulence, Couette flow, vertex streets, Rayleigh-Benard instability 8-83362
 hydrodynamic stability, open disc theorem, upper bound of eigenvalues 8-59370
 insulating liquid subject to unipolar injection, EHD stability, nonlinear phenomena 8-87411
 interfacial stability with heat and mass transfer, appl. to Rayleigh-Taylor and Kelvin-Helmholtz cases 8-67253
 ionosphere turbulent polar cusp, Kelvin-Helmholtz instability in low-energy proton flow 8-96343
 jet, horizontal five-layer, instability 8-79348

flow instability continued

jet, liq. cylindrical, flowing into pulsating stream of immiscible liq., stability 8-83444
 jet exhaust noise, shear layer instability effect 8-94791
 jet flame, props. and mixing process in recirculation zone 8-91025
 jets, quasi-parallel, MHD instability 8-83495
 Kutta condition, unsteady 8-90917
 laminar jet, axisymmetrical, with and without buoyancy (*German*) 8-83450
 laminar vapour flow in film boiling, stability limits 8-90832
 linear induction MHD machines, instability (*Russian*) 8-94841
 liquid jet, capillary instability, effect of harmonics 8-71378
 liquid mixture, binary, oscillatory convective instability, thermodynamic anal. 8-94753
 liquid-liquid disperse systems, Taylor instabilities rel. to drop fragmentation and thermal explosions 8-71368
 liquid-liquid interface, with temp. discontinuity, shock wave generation 8-51197
 local mass-transfer coeffs. meas. by holographic interferometry, vortex instability effect 8-75234
 lower critical Reynolds number, pipes and annuli, Newtonian and non-Newtonian flow, stability parameter anal. 8-87363
 magnetic fluid, thermoconvective instability, with mag. field perturbations 8-94847
 magnetised fluids, surface instability in nonisothermal layer (*Russian*) 8-94834
 Magnus method appl. to nonlinear eqns. near stability boundaries (*Russian*) 8-87331
 main-sequence stars envelopes, hydrodynamical instabilities constraints from Li, Be and B obs. 8-93202
 melting, of substrate into different miscible liq. layer, hydrodynamic instability, heat transfer 8-90695
 MHD channel flow, thermally radiative, stability 8-55695
 MHD sausage instability growth time, current-carrying liq. cond. 8-67279
 MHD shear flow stability 8-51244
 micropolar fluid with stretch, convection, appl. to Earth mantle 8-51202
 nematic liq. cryst., nonlinearities and fluctuations at hydrodynamic instability threshold 8-87614
 nematic liquid crystals, homogeneous instabilities 8-63674
 non-Newtonian fluid, hydrodynamic stability of free convection in vertical layer 8-59430
 non-Newtonian plane jet, stability to infinitely small perturbations 8-51211
 nonlinear wave propagation and unsteady transonic flow, variational formulations 8-55660
 oblique instability of periodic waves in shallow water 8-63418
 ocean, hydrodynamic friction layer instability rel. to Langmuir circulation 8-92840
 ocean near-surface mixing layer, Kelvin-Helmholtz instability in stable heating conditions 8-85568
 open channel thermally stratified flow, eddy diffusivity buoyancy effects, obs. 8-90904
 Orr-Sommerfeld eqn., continuous spectrum and eigenfunctions 8-67176
 partially ionised fluid, thermal instability, compressibility and collisional effects 8-55693
 permeable surface, injection, laminar to turbulent transition, heat and mass transfer 8-83361
 pipe flow, finite amplitude stability theory 8-63498
 plane plate with roughness element, nonsteady flow, numerical calc. (*German*) 8-94663
 plastic non-Newtonian fluids in circular pipes, laminar flow stability loss 8-79342
 Poiseuille flow, plane, horiz., rot., stability, effect of Coriolis force 8-67203
 Poiseuille flow in elastic channel 8-90835
 Poiseuille flow in elliptic pipe 8-71397
 Poiseuille pipe flow of incompressible second order fluid (*German*) 8-87395
 polymer solns., unstable flow, reservoir to capillary, jet instability onset and flow patterns, obs. 8-87364
 polymer solution, flow singularities, polymer chain extension and hydrodynamic instabilities 8-71376
 Rayleigh-Benard convection, crit. effects 8-71328
 Rayleigh-Taylor instability, method of generalised coords. 8-65771
 Rayleigh-Taylor instability, two superposed cond. fluids, with suspended particles 8-87399
 rectangular pipe with large aspect ratio, plane Poiseuille flow nonlinear instability 8-59492
 relaxation autooscillations of granular bed 8-59472
 Rossby waves, barotropic, instabilities 8-55654
 rotating horizontal fluid layer, thermal instability 8-63438
 rotating stratified flow, in horizontal mag. field, stability 8-67246
 rotating stratified fluid, hydromagnetic stability 8-55692
 shear flow instability problem, Howard's semi-circle reduction 8-90833
 shear instability, vortex nutation, amplitude oscill. 8-51171
 shear layer, instability and edgetone 8-94672
 small inviscid disturbance, evolution to marginally unstable stratified shear flow 8-83453
 spherically symmetric flow stability 8-83456
 spray nozzles, stability of thin, radially moving liquid sheets 8-71381
 stagnation flow, nonlinear stability 8-90831
 stagnation flow, two-dimens., stability, longit. vortices, perturbation method 8-75146
 steam jet condensation, dynamical pressure pulse effects 8-94549
 steam-generating tube, bubble/plug flow boiling regimes, elevated press., drift vel. and void fraction determs. 8-87379
 stratified fluid layer, heated from below, thermal instability 8-63476
 suspension of slender fibres, Poiseuille flow stability 8-71388
 Taylor instability in flow between rot. cylinders (*German*) 8-79308
 Taylor-Görtler instability in turbulent shear flows and boundary layer transitions 8-90836
 thermal instability anal. for horizontal liq. layers with a density max. 8-67193
 thermally driven shear flow heated from below, stability 8-67177
 thin cylindrical shell, compression dynamics, nonlinear evolution of Rayleigh-Taylor instability 8-79243
 time dependent flows, stability criteria 8-79305

flow instability continued

transient boundary layer on porous plate, coolant injection, laminar flow stability and heat transfer 8-83389
 transient convective turbulent heat transfer in tubes, thermal and hydrodynamic instability 8-83485
 transportation flows in pipes, energy comparison for steady, unsteady flow 8-91017
 tube array, whirling instability, phase relationships 8-51175
 turbulence transition, predictability 8-87332
 two dimensional flows stability, Eckhaus and Benjamin-Feir resonance mechs. 8-55632
 two-phase, programme for nucl. reactor heat removal expt. at low power 8-54814
 two-phase flow instability in parallel channels 8-94810
 vapour generator, two-phase flow dynamics 8-94808
 viscoplastic liquid film on vertical vibr. wall, with slip, shaking loose 8-59371
 viscous fluid drop, induced flow field in oscillating fluid 8-90980
 viscous liquid unsteady flow in annular channel 8-75205
 vortex sheet, plane, in ideal fluid 8-63437
 vortices, body-centred polygonal configs. 8-71341
³He-A, hydrodynamic stability of ³He-A uniform superflow, truncated variational approx. 8-67881

flow measurement

see also *anemometers*; *flow visualisation*; *flowmeters*; *laser velocimeters*
 aerosol measurement, particle deposition in sampling lines 8-81472
 anemometer, constant resistance hot wire, flow average temp. variations effect on reading (*Russian*) 8-88925
 anemometer, hot-wire, computerised, for vel.-and temp.-meas. in heat turbulent flow 8-91040
 anemometer, inside-out type, constructional details 8-59516
 arterial pulse wave vel. meas. by Doppler shifted US and EM flowmetry 8-69229
 bell type volume dynamic systems for gas flow meas., error anal. 8-75239
 blood flow measurement by US Doppler method, computer-aided determ. of angles (*German*) 8-80931
 blood flow speed and quantity determ. from digital angiograms (*German*) 8-92690
 blood flow vel. meas. in microvessels using video correl. system 8-53543
 blood velocity, catheter meas., cross correl. technique 8-80943
 blood velocity noninvasive meas. in large vessels, broadband pulsed Doppler US system 8-61224
 bubbly flows, simultaneous meas. of local liquid vel. and void fraction by gas laser, accuracy (*Japanese*) 8-67295
 BWR core flow fluctuation and neutron noise obs. 8-94060
 capillary rheometer, viscous heating from power law fluid, perturbation expansion anal. 8-63519
 cardiac output measurement, in vitro comparison of six commercially available thermodilution systems 8-77135
 cardiocirculatory computer-aided monitoring after open-heart surgery, appl. to adrenaline effects meas. 8-81059
 cavitation tunnel, for high-temp. operation 8-63521
 cerebral blood flow computer for use in angiogram theatres 8-73227
 cerebral regional blood flow meas. with ¹³³Xe, functional landscapes in brain 8-85356
 curve correction by FORTRAN program (*German*) 8-79394
 cylindrical, convergent flowmeter, medium expansion correction factor determination 8-67296
 differential pressure, inductive, ultrasonic methods, charact., appls. 8-83507
 Doppler sonographic flow meas. over small cross-sections in vitro and in vivo (*German*) 8-88729
 drag sphere velocity probe, miniature, development and testing 8-55705
 electroconductivity technique for holdups meas. in fluidised beds 8-67286
 flames, laminar, rise velocity meas., spectroscopic method 8-74064
 flow over cone, dual-plate holographic interferometry 8-63512
 flowmeter selection guidelines 8-71404
 fluorescence polarimeter for flow cytometry 8-73191
 four wire probe for turbulent flow temp. and vel. meas. 8-67290
 free shear layer tone phenomenon, probe interface 8-71324
 fundamentals and techniques, book 8-81941
 gas, standard methods review 8-94864
 gas dynamics diagnostics by glow discharge-generated high-power pulsed electron beam 8-63515
 holographic interferometry appl. in turbulence effects on optical wavefront 8-82936
 hot wire and hot film temperature compensating circuits, temp. probe appl. 8-59510
 hot-wire sensor, effect of centrifugal and Coriolis forces on rotating probe 8-94862
 impedance plethysmography, influence of erythrocyte vel. 8-61238
 integrating float, lag effects on water flow vels. integration 8-93012
 jet, nonisothermal axisymmetric turbulent transfer, vel. and temp. fluctuations, correl. coeffs. 8-83445
 laser anemometer Doppler system, optics and signal processor for turbulent low speed flows (*French*) 8-59521
 laser Doppler velocimeter direction-sensitive simultaneous multivelocity component 8-94857
 laser Doppler velocimeter two-dimens. meas. of flow induced by flames 8-59529
 laser Doppler velocimeter with variable frequency shift for combustion flow meas. (*Japanese*) 8-67294
 laser scattered light intensity, recurrence rate correl. 8-66760
 laser velocimeter for wind tunnel measurements, principles 8-71405
 laser velocimetry, flow velocity at olfactory organ nares of fishes (*German*) 8-69262
 laser velocimetry principles and aerodynamic appls. (*French*) 8-63518
 light scattering techniques, digital correlation appl. 8-57916
 LMFBR, US flowmeter (*Japanese*) 8-78455
 LMFBR outlet plenum, air flow model, interferometric meas. of fluctuating temp. using FFTF 8-89943
 local circulatory system characterisation by CW Doppler US flow meas. 8-57109
 low and high turbulence flows, hot wire measurement based analysis 8-59511

flow measurement continued

microcirculation semiquantitative demonstration using US noninvasive meas. method (*German*) 8-85348
 microkymography, flow vel. meas. in microvascular bed after exdotoxin administration (*German*) 8-77173
 mixing length determination, from turbulence characts. meas., in tubes and boundary layers (*Russian*) 8-83371
 molecular flow measurement, precision, and control for single and multigas systems 8-70135
 Newtonian liquid between coaxial cylinders, end-effect correction of Margules eqn. 8-79399
 NMR with nonuniform RF field, appl. to self diffusion and liq. flow meas. 8-60343
 non-Newtonian tube flow, small internal press. meas. 8-51260
 nonisothermal flow, two-wire probe, simultaneous vel. and temp. meas. 8-91042
 nuclear reactor, two-phase flow characterisation by neutron noise techniques 8-94058
 ocean, mobile sand grains underwater detect. 8-96192
 open channel acoustic flowmeters, design, calibration and errors 8-55701
 open channel acoustic flowmeters, design, meas. errors and operation 8-63516
 optical instrument for measuring fluctuating velocities in highly turbulent flows 8-83500
 orifice meters, relative error in nonstandard approach conditions 8-79398
 oscillatory boundary layer, on bed beneath gravity waves, laser Doppler anemometry 8-90929
 particulate materials, dynamic shear strength and flow behaviour, shear cell meas. 8-53048
 pipeline networks, flow rates distrib. (*Japanese*) 8-91015
 plasma flow, meas. method for solid particles (*Russian*) 8-94903
 Preston tube calibration in transpired turbulent boundary layer 8-79397
 pulsed-neutron activation anal., asymmetry effects 8-83508
 radionuclide mean clearance time transverse section imaging 8-73222
 reciprocating pumps, control system, high performance liquid chromatographic detectors appl. 8-92559
 rheometer, rot., inertial normal force correction 8-63520
 rotary gas flowmeter error anal. (*Russian*) 8-71407
 schlieren instruments threshold sensitivity to turbulent inhomogenities 8-79134
 sea water, current vel. determ. via neutron-activation method (*Russian*) 8-77358
 shear force instrument, force-balance 8-51263
 spatial flow field determination, hot wire anemometry based analysis 8-59512
 spatial vorticity distrib. meas. technique 8-67289
 speckle photography, flow velocity distrib. meas. 8-67288
 static pressure probe, yaw insensitive, development and testing 8-94869
 supersonic stream flow in vacuum, by electron diff. instrument 8-75235
 thin film shear-stress gauge for three dimensional flow 8-55702
 thrombophlebitis diagnosis, reliability of Doppler and impedance techniques 8-77144
 total, using auxiliary pipe line (*Japanese*) 8-79395
 tubes with ball seatings, basic groups, appl. in flowmeters (*Russian*) 8-67287
 turbulent, optical Doppler instrument, small flow velocities appl. 8-90838
 turbulent flow measurement by laser Doppler anemometry, concentration and size of tracer particles, theoretical limits 8-59514
 two phase diffuse flow, investigation 8-59513
 US blood flow spectral anal. using coherent optics 8-53459
 US Doppler velocimetry for 3D blood flow meas. 8-88730
 US flowmeter metrological properties (*Polish*) 8-51265
 velocity meas. in capillary using pulsed NMR 8-83506
 velocity vector and temp. fields, three-dimens. reconstruction from acoustic transmission meas. 8-51261
 void fraction and phase distrib. meas. in transient flow boiling by neutron scatt. 8-94870
 vortex shedding flowmeter characts. improvement in low Reynolds number (*Japanese*) 8-79396
 Weissenberg rheogoniometer, computerised calib. and meas. of Newtonian fluids 8-87323
 x-array hot wire probe, prong config. 8-75243
 NO₂, real time method using tapered variable area flowmeter 8-71410

flow resistance see viscosity**flow through porous media**

annular region, steady flow 8-75201
 blood, red cell flexibility, whole blood filtration technique using 5 μm pores (*German*) 8-57030
 boiling and evaporating liq. heat transfer, on capillary and porous surfaces 8-94526
 capillary porous body, drying, X-ray absorption obs., radiometry, temp. control 8-67023
 capillary-porous bodies, heat and moisture transfer, analytical formulae 8-67013
 cascade wake pattern with trailing-edge slot or surface suction 8-90909
 channel with periodically varying diameter, model for randomly packed beds 8-63493
 column drainage, moving boundary problems, theory and numerical analysis 8-81252
 condensable rarefied gas flow through porous media, heat and mass transfer 8-59473
 convection, natural, in horizontal porous medium subjected to end-to-end temp. difference 8-91010
 convection in porous cavity, Darcy medium, 2-dimens. solns. 8-91007
 convection in rectangular box containing saturated porous material 8-71393
 convection onset, natural, in heated water-saturated porous cylinder 8-59478
 coolant flow rates through porous media, heat and mass transfer (*Russian*) 8-59479
 Couette flow, permeable wall layer, heat transfer and temp. distrib. 8-51165

flow through porous media continued

dam porous media unsteady flow calculation, combined finite element/characteristics methods appl. 8-91012
 Darcy flow, chilled pipe freezing zone, finite difference method 8-94734
 diffusers, 2-dimens., with suction through porous parallel side walls, characts. (*Japanese*) 8-83492
 disc packed column with falling liquid film, gas phase mass transfer involving vap. diffusion 8-94815
 ducts with porous walls, Navier-Stokes exact eqns. 8-67266
 elastic porous media, transient compressible liq. flow, linearisation of nonlinear partial differential eqn. 8-63490
 electrically conducting rarefied gas, oscill. flow, past vertical porous plate, free convection 8-90830
 evaporation from capillary pore, mass transfer kinetics 8-51233
 fibre bundle, centrifugal flow, fluid vel. and press. distrib. (*Polish*) 8-51236
 filtration problem, free boundary enclosure 8-55687
 fixed and fluidised beds, heat transfer from particle to fluid, stochastic model 8-51234
 fixed swarm of permeable spheres, appl. of self-consistent model 8-67260
 flat plate boundary layer in porous medium, free convection, similarity solns. 8-75199
 flow normal to perforated plates, heat transfer and friction loss 8-94733
 fluid saturated porous solid, eqns. of motion 8-79208
 liquid-infiltrated elastic materials, deformation of cavities and inclusions 8-51073
 fluidised bed reactor, gas flow anal. 8-83468
 free convective flow, longit. vortices, onset, linear stability anal. 8-94813
 free molecular vapour flow, mass transfer during condensation in channel 8-51198
 friction factor for isothermal and nonisothermal flow 8-91008
 gas flow, diffusion eqn., continuity of soln. in n space dimensions 8-95130
 gels for extended wear contact lenses, water flow cond. 8-81062
 glasses, porous, thermosmotic flow, filtration, of water 8-53248
 groundwater, unsteady flow through tunnel opening, reductive finite element/Crank-Nicolson anal. 8-92861
 heat pipe, heat transfer agent flowrate through porous wick, approx. calc. method 8-75197
 heat transfer, capillary porous media with variable parameters 8-83471
 heat transfer, forced convection in low-porosity media 8-83472
 heat transfer, Nusselt no., temp. distrib. permeable bed boundary layer flow 8-51166
 heat transfer bibliography 8-63425
 heat transfer from porous sphere in low Reynolds number flow 8-59482
 heat transfer in channel with permeable wall 8-63426
 heat transfer to porous cylinder with intense injection 8-79370
 Hele-Shaw cell, permeability determ., geothermal modelling appl. 8-59466
 heterogeneous flows of multi-component mixtures in porous media-review 8-59471
 hydraulic characts. of liqs. flowing through porous metal fibre mats., permeability laws 8-67848
 hydromagnetic flow near oscillating porous flat plate 8-51250
 inductively-heated particle bed, water-cooled, natural convection heat transfer 8-71396
 infiltration, parameter estimation of Green and Ampt eqn. 8-61473
 isobutane-air, in packed bed, heat and mass transfer, axial mass dispersion 8-75200
 isotope separation by gaseous diffusion, aerodynamic effects 8-59469
 Knudsen to Poiseuille flow transition, capillary model 8-55689
 laminar boundary layer, on permeable surface, in crossed elec. and mag. fields (*Russian*) 8-75118
 laminar film condensation from moving vapour, with suction 8-59459
 laminar flow along porous vertical wall 8-90825
 laminar flow through porous tube or channel, nonunique solns. 8-94816
 law of the wall, appl. to turbulent boundary layer calc. with injection or suction 8-67187
 liquid filtration US enhancement 8-59526
 membrane, passive transport through open membrane, multicomponent system, statistical-mech. theory 8-67261
 methane-H₂, in packed bed, heat and mass transfer, axial mass dispersion 8-75200
 MHD convective viscous flow past porous plate with suction, mass transfer effects 8-87398
 MHD Ekman layer on porous flat plate, heat transfer, steady asymptotic soln. 8-79385
 MHD flow around porous plate with time-varying motion 8-51251
 MHD flow over porous plate, Hall effect 8-51246
 MHD of elec. cond., incompressible, viscous fluid, unsteady flow 8-59496
 migration of salts in a porous medium allowing for their crystallisation (*Russian*) 8-87388
 miscible or immiscible displacements, identification and modelling 8-69392
 moist material, external heat transfer, calc. methods, drying kinetics 8-59467
 natural convection mass transfer along porous vertical plate 8-90876
 natural thermoconvective filtration in circular porous interlayers 8-94817
 non-Newtonian liquid filtration eqn. 8-55690
 non-steady flow problem in two-layer porous medium 8-81260
 nonlinear heat/mass transfer problem, soln. using invariant groups 8-55688
 nonlinear laminar flow of fluid into fully penetrating cylindrical well 8-75198
 nonsteady multiphase flow through porous media, struct. determ. 8-51237
 Oldroyd liquid, unsteady flow between two porous walls 8-63452
 oscillatory convection, in porous medium heated from below 8-79320
 packed beds, low Peclet number particle-to-fluid heat and mass transfer 8-94799
 packed beds, thermal response at low Reynolds number 8-87386

flow through porous media continued

- partial differential eqn., strong soln. existence and uniqueness (*French*) 8-62084
- percolation theory, bond problem, critical probabilities, bond clusters 8-86224
- percolation threshold, asymptotic method—diagram technique calcs. 8-79374
- permeable plate, numerical anal. of turbulent boundary layers 8-67186
- permeable spheres in incompressible fluid, hydrodynamic interaction, mobility tensors 8-71395
- permeable spheres in incompressible fluid, hydrodynamic interaction vel. fluid, friction consts. 8-75202
- permeable surface, injection, laminar to turbulent transition, heat and mass transfer 8-83361
- permeable tube with wall injection, transient turbulent boundary layer 8-83486
- plate, with suction, three-dimens. fluctuating flow, heat transfer, skin friction 8-87389
- plate with simultaneous injection and suction, turbulent layer friction and vel. profile 8-83469
- polymer membrane gas permeation, pore size distrib. (*Japanese*) 8-79372
- polymer solution, semidilute, hydrodynamic interaction of two permeable spheres, method of reflections 8-71394
- polymer solutions, flow behaviour in porous media (*German*) 8-55666
- Preston tube calibration in transpired turbulent boundary layer 8-79397
- radioactive gas adsorpt. in porous medium, convective diffusion (*Russian*) 8-87387
- rectangular cavity packed with porous media, heat transfer 8-71392
- rock, subjected to water jet, drag force on grains in permeable medium 8-55691
- saturated medium, macroscopic behaviour (*French*) 8-51235
- saturated porous medium, completely confined, onset of thermal convection 8-83387
- saturated-unsaturated media, hysteresis effect influence on transient flows 8-59481
- screens, book contrib. 8-59483
- sintered composite-liq. metal, interaction, mass transfer eqn. approx. soln. 8-67262
- slip flow, MHD, over porous plate, with variable suction, heat transfer 8-79337
- smectic-A liquid crystal, permeative flow around obstacle, extended boundary layers 8-67644
- soil, blocked air pore volume meas. based on volume-weight relns. 8-57231
- solute dispersion in porous medium in MHD flow between parallel plates, homo- and heterogeneous reaction effects 8-55697
- steady flow between a rotating and a porous stationary disc in the presence of transverse magnetic field 8-79382
- steady flow prod. by rot. disc, series soln. anal. 8-71308
- surface suction effect on condensation in presence of noncondensable gas 8-90691
- surfaces covered with capillary-porous structures, heat transfer with boiling, approximate theory 8-94537
- three dimensional free convection flow and heat transfer along a porous vertical plate 8-90866
- transient boundary layer on porous plate, coolant injection, laminar flow stability and heat transfer 8-83389
- tube of elliptic cross-section, steady viscous flow, generalised momentum eqn. 8-75203
- turbulent axisymmetric boundary layer, weak and strong disturbances effect 8-90857
- turbulent boundary layer, at permeable surface, in crossed elec. and mag. fields (*Russian*) 8-94836
- turbulent boundary layer on porous plate, suction (*French*) 8-51156
- turbulent boundary layer on rough surface with blowing, heat transfer behaviour 8-71334
- turbulent flow in channel with porous walls 8-67179
- twisted air flow in permeable tube, local heat transfer 8-71338
- two-phase flow, fingero-imbibition, composite expansion soln. 8-79373
- two-phase flow through porous media, perturbation soln. due to differential wettability 8-59470
- two-phase porous cooling system development 8-59477
- underground cable system, convectively cooled, temp. distrib., heat transfer correlations 8-71262
- underground cable system, convectively cooled, vel. distrib., press. drop correlations 8-71330
- underground nuclear explosion, gas flow in permeable Earth formation with crack 8-61372
- unsaturated porous media flow anal. by finite element method 8-92869
- unsteady drainage, one-dimens., digital simulation, finite element method appl. 8-91011
- vapour dynamic diffusion batcher with porous partition 8-79404
- visco-elastic liquid, flow past hot porous circular cylinder, free and forced convection 8-83386
- viscoelastic free convection boundary layer flow past infinite plate with constant suction 8-90936
- viscous flow in a rotating channel bounded below by a permeable bed 8-91013
- viscous flow in porous solid, relaxation phenomena (*French*) 8-87385
- viscous flow of variable viscosity between porous bed and moving impermeable plate 8-90962
- water, deep evaporation characterisation (*French*) 8-59468
- waves, travelling, gravity-capillary, on liq. film surface falling past permeable bed 8-87351
- wetting, capillary rise, contact angle effect (*German*) 8-84033
- wind tunnel, wall interference, two-dimens., correction method, examples (*French*) 8-67293
- He II, flow through porous plugs, space cooling system appl., plug characts. 8-49842
- N₂, flow, cold gas, through porous-tube, heat-transfer, suction effect 8-59474
- Na, vaporisation from capillary-porous structs. (heat tubes, vap. chambers) crit. heat flux 8-90631

flow visualisation

- bluff bodies, cylindrical, flow visualisation investig. of wakes at low Reynolds number 8-83405
- bounded turbulent shear flow mechanism obs. 8-90854
- bursting, spanwise struct. obs., in turbulent channel wall region 8-90855
- cathodic diffusion boundary layer, free convective flow obs. with shadow Schlieren method 8-68894
- convection, free, laminar, three-dimens., about surface, numerical anal., visualisation (*French*) 8-87343
- convection measurement, differential interferometer with achromatic $\lambda/2$ compensation 8-87419
- corrugated wall, exptl. study of flow (*French*) 8-90844
- cylinder, circular, with slit, flow characts., control, patterns, wake flow, vortices 8-83404
- free convection mass transfer from horizontal surface, electrochemical and holographic interferometric obs. 8-87344
- gas flow application of shearing interferometers 8-55706
- glycerine-water drops, collision dynamics, ang. of incidence influence (*Russian*) 8-83461
- Helmholtz resonators with grazing flow, dye streamlines 8-63511
- jet, circ., controlled perturbation, smoke visualisation 8-90956
- jet, circ., free shear layer transition wave development 8-94643
- jet, subsonic, of gas, vortices, flow visualisation patterns 8-63471
- jets, radial turbulent, flow, attachment to disc plate, flow patterns, nozzle dimension effects 8-83443
- laminar and turbulent flow around free and surface-mounted obstacles, topology, flow visualization 8-51157
- liquid crop falling into still liq., vortex ring formation 8-90946
- local mass-transfer coeffs. meas. by holographic interferometry, vortex instability effect 8-75234
- PMMA latex particles, laser light scatt. for visualisation in EHD 8-75236
- pool barbotage, heat transfer coeffs., high-speed cine-photography and oscillography 8-90982
- potential flow, transient state, Liesegang rings demonstration 8-63408
- shear flow, stratified, free-turbulent, buoyancy effects on large scale struct. 8-90849
- smoke flow visualisation combined with hot-wire anemometry, technique, appl. to turbulent boundary layer 8-91044
- supersonic flow over hemisphere-cylinder at incidence up to 19° 8-59419
- thermal markers for liq. vel. field meas., error reduction 8-91036
- turbulence separation, subsonic and supersonic, ultra-short duration visualisation (*French*) 8-75128
- turbulent flow relaminarisation, flow visualisation 8-75244
- venous blood flow visualisation using dynamic leg scintigraphy with large field-of-view scintillation camera 8-73215
- He hypersonic flow, Na vapour seeded, velocity profile visualisation 8-59530

flowmeters

- see also anemometers; flow measurement; laser velocimeters
- 4 MHz range-gated US Doppler flowmeter design and application 8-59527
- analogue output device for Rotameter flow rate measurements, photoelectric cells appl. 8-75237
- arterial haemodynamic transfer function calc. from Doppler US flowmeter waveforms 8-61235
- axial, aperture ratio calc. method (*Dutch*) 8-67285
- calibration by electronic weighing 8-55700
- constricting device for flowmeters of viscous liquids and gases 8-75241
- constriction meter orifice, swirling flow component effect on discharge coeffs. 8-63514
- correction factor appls. for blunting of diaphragm input rim 8-75240
- corrosive liquid flowmeter with UHF heater (*Russian*) 8-59523
- cylindrical, convergent flowmeter, medium expansion correction factor determination 8-67296
- digital 2D full range Doppler velocity meter for cardiovascular diagnosis 8-88731
- Doppler US blood velocity meas., phase-locked loop technique 8-61234
- drag sphere velocity probe, miniature, development and testing 8-55705
- elbow, wall curvature inaccuracies rel. to discharge coeffs. 8-83501
- electromagnetic, anal. in ducts and open channels 8-59524
- low and high turbulence flows, hot wire measurement based analysis 8-59511
- magnetic, bubble noise effects on output signal, Na loop test 8-91038
- open channel acoustic flowmeters, design, calibration and errors 8-55701
- open channel acoustic flowmeters, design, meas. errors and operation 8-63516
- orifice meters, influence of bends (*Italian*) 8-94859
- respirometer, flowmeter-polarographic electrode sensor, for respiratory function telemetering 8-80995
- rotary gas flowmeter error anal. (*Russian*) 8-71407
- selection guidelines for fluid flow meas. 8-71404
- total flow meas. using auxiliary pipe line (*Japanese*) 8-79395
- tubes with ball seatings, basic groups, appl. in flowmeters (*Russian*) 8-67287
- turbine, historical development 8-51262
- turbine and vortex, comparison 8-55699
- turbulent flow measurement by laser Doppler anemometry, concentration and size of tracer particles, theoretical limits 8-59514
- types and usage 8-55698
- US, for measuring rapidly changing gas flows, freq. range, excitation and signal processing (*German*) 8-83502
- US, for Na cooled FBR coolant flow meas. (*Japanese*) 8-78455
- US, metrological properties (*Polish*) 8-51265
- US flowmeter cell unconventional designs 8-59528
- US flowmeter data processing, transfer function modelling of arteries 8-61225
- US implantable CW Doppler blood flowmeter, optimal system design 8-53460
- vortex shedding, characts. improvement in low Reynolds number (*Japanese*) 8-79396

fluctuations

see also *Brownian motion*; *critical fluctuations*; *current fluctuations*; *noise*; *random processes*
 albumin, bovine serum, solutions, fluctuation transport theory 8-70057
 arc plasma, thermal density fluctuations, light scatt. using CW CO₂ laser and heterodyne detection 8-59677
 atmosphere, synoptic object localisation, long-period tidal fluctuations (*Russian*) 8-81321
 atmospheric optical intensity fluctuations, frozen turbulence hypothesis expt. (*Russian*) 8-61557
 atmospheric pressure fluctuations, influence on Earth surface tidal tilts (*Russian*) 8-88790
 autocatalytic reaction system, sustained oscills., deterministic and stochastic theories 8-95922
 BBGKY hierarchy, scaling method of kinetic eqn. derivation 8-54286
 biological membranes, single-file diffusion, for teaching 8-54127
 black hole, quantum gravitational fluctuations, energy dissipation mechanism 8-57572
 boiling, pool saturated, subcooled, in narrow spaces, interferometry obs. 8-94527
 boiling, two-phase boundary layer, temp. fluctuations 8-51222
 BWR boiling noise, local and global component obs. and calc. 8-94066
 BWR core flow fluctuation and neutron noise obs. 8-94060
 BWR dynamics, multivariable autoregressive identification 8-94107
 cell population auto-activation, math. model 8-77017
 climate, temp. and precip. temporal fluctuations averaged for Europe and N.America 8-92958
 climate fluctuations, relation of moistening to thermal regime 8-92937
 collimated laser beam propag. in turbulent atm., phase fluctuations spectrum 8-78914
 cosmology, primaeval fluctuation spectrum rel. to covariance function 9 Mpc break 8-65688
 cyano-biphenyl, nematic liq. crystals, director fluctuation quenching by mag. field (*French*) 8-87613
 deep ocean, low freq. press. fluctuations prod. by surface waves 8-81184
 disordered system, residual resistivity 8-87954
 dissipation theorem for excess noise 8-70059
 dissipative dynamical system, iterative transitions between periodic and turbulent 8-62159
 Earth rotation, harmonic fluctuations correl. with secular geomag. field vars. 8-73302
 electronic transport coeff., soln. between Mori-Green-Kubo formulae and Boltzmann approx. 8-79971
 ethanol, aq. soln., conc. fluctuations, shear and longit. relax., Brillouin scatt. and pulse techniques 8-71792
 expanding universe, density fluctuations rel. to struct. development 8-93489
 expanding universe, density perturbations three-point correl. function and higher order functions prediction 8-65730
 F₂-layer vertical sounding, radio signal Doppler spectrum and arrival angle meas. (*Russian*) 8-61651
 flow, combined visualisation-anemometry technique, appl. to turbulent boundary layer 8-91044
 flow boundary layer, stochastic model of fluctuations 8-90818
 flow over plate with suction, heat transfer, skin friction 8-87389
 fluctuating plasma, Trivelpiece-Gould mode parametric decay 8-75321
 fluctuation-dissipation theorem for classical systems 8-49764
 gases, chem. reacting, kinetic fluctuations (*Russian*) 8-59552
 generation of fluctuations which arbitrary power spectrum, algorithm 8-73927
 geomagnetic field fluctuations at synchronous orbit, power spectra 8-96358
 hydrodynamic fluctuation theories 8-87327
 intensity fluctuation linewidth, Jakeman-Pike approx., black-body and laser models 8-58960
 interference pattern fluctuation statistics in turbulent atmospheric layer 8-53727
 ionic conductor, charge fluctuations, collective dynamics 8-67841
 jet, axisymmetric, turbulent bulge struct. 8-90955
 jet, circ., controlled perturbation, smoke visualisation 8-90956
 jet, free, turbulent flow, large scale struct., discrete values meas. 8-90840
 Landau-Lifshitz hydrodynamic fluctuations in nonequilib. systems, Boltzmann eqn. reduction 8-81929
 Langevin-equation approach, generalised phase space method 8-54303
 laser beam intensity fluctuations in turbulent atm. over water surface (*Russian*) 8-69449
 laser propagation in turbulent atm., detector nonlinearity effects on statistics of fluctuating signal 8-55301
 laser scattered light intensity, recurrence rate correl. 8-66760
 linear dynamic system with many fluctuating parameters, single group approx. (*Russian*) 8-62154
 linear response theory, many-body van Hove limit 8-62156
 local fluctuations in chemical reactions, nonlinear master eqn., dimensionality expansions, augmented mean field theory 8-73019
 magnetic fluid, thermoconvective instability, with mag. field perturbations 8-94847
 many particle spectra, statistical props., two point correlations and fluctuations 8-86216
 matrix theory of small oscillations, for teachers 8-61986
 metastable states, relax. and fluctuation theory 8-49769
 meteor trails, causes of fluctuations in effective linear electron density 8-73687
 molecular reorientation, dielec. friction theory 8-87599
 nematic liq. cryst., nonlinearities and fluctuations at hydrodynamic instability threshold 8-87614
 nematic liquid crystals, hydrodynamic correlation functions, propagating modes 8-94988
 neurosecretory structure particle motion, effect of increased K⁺ concs. 8-77046
 non-Markovian equilibrium dynamics and fluctuation-dissipation theorem 8-62157
 nonequilibrium critical phenomena, probability density functions, fluctuations 8-54327
 nonequilibrium phase transition, dynamical features (*Chinese*) 8-83030
 nuclear reactor noise analysis, irreversible circulation parameter 8-94069

fluctuations continued

nuclear reactor noise theory, fluctuation coarse-graining and normality preservation 8-94068
 one-dimensional chain, thermal fluctuation induced rupture, computer simulation 8-91378
 open binary mixtures, fluctuation theory, entropy prod. and energy dissipation (*German*) 8-64879
 optical bistability, scatt. light spectrum atomic fluctuations 8-94383
 optical bistability and spectrum of fluctuations, quantum anal. 8-71067
 optical goniometer accuracy effect of atm. turbulence 8-55461
 optical image processing, noise fluctuations and coherence 8-66771
 N Pacific Ocean, wind stress fluctuations rel. to water temp. anomalies vertical struct. 8-73394
 particle motion in stochastic force fields 8-73928
 plasma, fluctuation-dissipative relation in nonlinear electrodynamics (*Russian*) 8-79410
 plasma, kinetic fluctuations (*Russian*) 8-59552
 plasma density fluctuation evaluation by microwave interferometry 8-67437
 plasma ion temp. meas. by 10.6 μ scatt. from thermal fluctuations 8-67431
 polyethylene, uniaxially stretched, density fluctuations 8-75587
 power reactor, neutron density fluctuations, stochastic nonlinear model, Fokker-Planck eqn. 8-58316
 primordial background radiation, temp. fluctuations due to gravit. waves 8-65728
 proportional counter, energy loss of relativistic electrons and its fluctuation 8-94171
 quantum fluctuations of instantons 8-54530
 quenched critical fluid, time evolution of fluctuation spectrum 8-65893
 random impurity system, density of states tails, fluctuations and mobility edges 8-67983
 random medium with finite inhomogeneity correl. range, EM wave fluctuations (*Russian*) 8-78870
 Rayleigh scattering, reson. enhancement in absorbing media, fluctuation theory 8-72533
 resin slab, stress response, fluctuating external moisture (temp.) effects 8-55620
 sea level fluctuations along west coast of N.America, alongshore correl vars. 8-73381
 sea upper layer, wind waves components of temp. fluctuations spectrum (*Russian*) 8-53655
 second-order radiometry, fluctuating sources 8-50879
 self turbulence in free particle motion 8-86177
 single-impurity Kondo system, fluctuation conductivity 8-76064
 Smoluchowski process, number fluctuation anal. of random locomotion 8-54318
 solidification and crystal nucleation 8-83761
 solutions, fluctuation transport theory 8-70057
 squid joint axon membrane potential fluctuations, cross-correlations 8-92616
 stationary Markov systems, generalised fluctuation theorems 8-62153
 stellar Balmer-index photometry, bandpass fluctuations as noise source 8-96404
 streamwise velocity fluctuations spectrum, following channel wall roughness step 8-90861
 structurally incommensurate systems, fluctuation spectrum, incommensurate phases 8-91419
 thermocouple temperature transfer functions, theoretical and expt. determ. (*German*) 8-49827
 thermodynamic density fluctuations effect on low of mass action and kinetics (*Russian*) 8-60990
 thermopile, harmonic temp. variations generation, analytic method 8-79193
 time averaged magnitude fluctuations during measuring process (*Russian*) 8-73923
 TMMC, field-suppression of spin fluctuations, NMR obs. 8-91971
 traffic current fluctuation on expressway, observance of Burgers eqn. 8-49765
 turbulence, intermittency model in three-dimensions 8-59376
 turbulent boundary layer, large-scale modes obs. 8-90859
 turbulent flow, press. fluctuation spectrum, elastic boundary compliance effect 8-63422
 turbulent flow, temp. and conc. fluctuations (*German*) 8-59372
 underwater light-field fluctuations, experimental studies of spatial struct. (*Russian*) 8-53656
 unstable states, relax. and fluctuation theory 8-49769
 Wiener-Khinchin theorem 8-57851
 wind velocity gust factors, analytical approach 8-88897
 CsNiF₃, ¹⁹F NMR, spin fluctuation suppression 8-91970
 He-Ne lasers, discharge reson. props. effect on radiation fluctuations, expt. 8-74883
⁴He, liq., dynamic scaling, possible breakdown at lambda point 8-91498
³²S(d, α)³⁰P, statistical fluctuations at 135°, 2.0-2.5 MeV 8-89882
³²S(d,p)³³S, statistical fluctuations, at 135°, 2.0-2.5 MeV 8-89882

fluctuations in superconductors

used only for thermal (thermodynamic) fluctuations around the order parameter near the critical point
 crossover near fluctuation induced phase transitions, appl. to nematic-smectic A liq. cryst. transition 8-80098
 incommensurate 1-D Peierls system, fluctuation conductivity 8-91817
 Josephson tunnelling junctions, supercond. fluctuations, below transition temp. 8-84354
 three-dimensional organic chain conductors, one-dimensionalisation by impurities 8-91681
 type II superconductors, fluctuation induced diamagnetism above H_{c2} 8-80097
 Al, film in presence of Formvar, excess elec. cond. above T_c 8-60250
 Al, small particles, Josephson-coupled, local fluctuation effects 8-72308
 Al, superconducting particles, nucl. relax. and supercond. fluctuations 8-60251
 La_{1.8}Au_{0.2}, amorphous, evidence for short wavelength cutoff in fluctuation spectrum 8-68113
 Nb₃Al, quasi-one-dimensional supercond., giant enhancement of nucl. relax. rate near T_c 8-56257

fluctuations in superconductors continued

- Nb₃Sn, quasi-one-dimensional supercond., giant enhancement of nucl. relax. rate near T_c 8-56257
 Sn, small particles, Josephson-coupled, local fluctuation effects 8-72308
 Zr₇₅Rh₂₅, amorphous, evidence for short wavelength cutoff in fluctuation spectrum 8-68113

fluctuations of cross sections *see statistical theory of nuclear reactions and scattering***fluid composition control** *see chemical variables control***fluid composition measurement** *see chemical variables measurement***fluid dynamics**

- see also aerodynamics; biological fluid dynamics; drag reduction; electrohydrodynamics; flow; hydrodynamics; Navier-Stokes equations; rarefied fluid dynamics; relativistic fluid dynamics; surface waves (fluid); turbulence; wakes*
 boundary element methods versus finite elements 8-73860
 Burger's equation, coupled stream function-vorticity eqns., Method of Lines compared to finite difference scheme 8-79291
 classical unidimensional model of fluid motion, Burgers eqn., absence of turbulence 8-87328
 disc-halo galaxies gaseous components, boundary layer circulation 8-57627
 discrete equations of fluid flow and elasticity 8-65781
 elliptic systems and numerical transforms. 8-65780
 energy-momentum tensor, effect of motions, meson field and perfect fluid 8-73903
 Euler equations, solid-body boundary conditions, numerical implementation 8-90814
 FFT pseudo-spectral technique for non-periodic problems 8-59359
 first-order Cosserat fluid kinetic energy decay with heat and mass transfer 8-94524
 flow in irregular geometries, numerical method calcs. 8-94522
 fluid interaction with obstacles, method of deformable coords. (*Ukrainian*) 8-65776
 glycerine-water drops, collision dynamics, ang. of incidence influence (*Russian*) 8-83461
 helical axisymmetrical motion, of perfect fluid through diffuser, function series soln. 8-49669
 Howard's formula applicability 8-55622
 immersed body with active flexible skin in perfect incompressible fluid (*French*) 8-59362
 Jupiter atmosphere, equatorial light and dark spots obs. rel. to fluid dynamics 8-57493
 Lax-Wendroff difference scheme, appl. in fluid dynamics 8-65758
 linear viscoelastic fluids, Stokes' problems 8-51142
 LMFBF, squeeze flow between two adjacent subassemblies, discrete model 8-86634
 Magnus method appl. to nonlinear eqns. near stability boundaries (*Russian*) 8-87331
 Mars rampart craters, impact in viscous-liq. targets rel. to fluidised material ejecta deposits 8-65530
 mean residence times in steady-flow and non-flow systems 8-83357
 multisoliton solutions in two-layer finite depth fluid 8-55621
 nonstationary motion in one-dimens. continuous medium, partial analytic solns. (*Russian*) 8-73859
 nuclear engineering transient fluid and structural dynamics problems, flow singularity methods 8-86633
 Petrov-Galerkin finite element method, boundary layer behaviour 8-69989
 pipes carrying fluid flow, oscillation stability (*German*) 8-87298
 potential flow, elliptic PDE with discontinuous coeff., finite difference soln. 8-89347
 potential flow problems, partition technique integral eqn. method 8-49652
 prismatic plate struts. submerged in liquid, natural freq. and vibr. modes 8-79256
 review of progress in last thirty years 8-89290
 Rossby wave, critical layer evolution 8-79329
 selfgravitating liquid ring with inner flow (*Russian*) 8-65783
 semiconvection in stars, semitheory 8-69787
 Stokes law, Reynolds no., erythrocyte sedimentation rate, for teaching 8-49610
 Stokes problem with conforming Lagrangian finite elements, soln. error estimates (*French*) 8-62085
 three dimensional layer theory, using shell geometrical concepts 8-90815
 two dimensional fluid transient analysis, nearcharacteristics method 8-89349
 two-dimensional nonstationary Euler eqn. solution in time-dependent bounded domain (*Italian*) 8-69986
 Na, liquid, heat transfer characteristics of flow field (*Japanese*) 8-54815

fluid flow *see flow***fluid instability** *see flow instability***fluid mechanics**

- see also capillarity; cavitation; compressibility of gases; compressibility of liquids; fluid dynamics; hydrostatics; Mach number*
 Bernoulli and Lagrange-Cauchy integrals, p/γ term 8-65779
 book, annual review (1978) 8-59357
 book, for undergraduates 8-59358
 computational aspects, book contrib. 8-59366
 extensible string motion in nonviscous fluid (*Russian*) 8-77718
 flotation of solid body on liquid surface, equilib. state (*Russian*) 8-67029
 helical curve motion and soliton eqns., scaling invariance 8-49667
 history of fluid mechanics at Cambridge, book contrib. 8-57726
 nonlinear interaction of deformable body with liquid pressure wave (*Ukrainian*) 8-65777
 viscometric flows of general fluids (*Japanese*) 8-87425
 viscous fluid cosmological model in general relativity 8-61944

fluid theory, dense *see liquid theory***fluid valves** *see valves***fluidic amplifiers**

- pneumatic amplifier pump, for supercritical fluid chromatography, control and programming 8-88665

fluidic devices

- intra-aortic balloon heart assist device fluidic drive system 8-53566

fluidic logic

- nonstationary flow meas. by laser Doppler velocimeter with frequency tracker (*Japanese*) 8-55707

fluidised beds

- bed to surface heat transfer, fluidised bed of large particles 8-63269
 bubble raise rate in nonuniform fluidised bed 8-67263
 bubbling electrofluidised bed, heat transfer rates 8-87242
 cylinder array, convective mass transfer with surface reaction 8-79369
 expansion of air fluidised sand and silica gel beds, high porosity packings (*Russian*) 8-59480
 expansion of an inhomogeneous fluidised bed 8-63492
 fluid-solid flow, holdup, expt. 8-79361
 gas flow in reactor 8-83468
 gas-solid, particle temp. meas. 8-83464
 gas-solid, solid circulation 8-79359
 grid design using orifice eqn. 8-91006
 grid effect on bed inhomogeneity 8-79367
 heat and mass transfer for low Peclet numbers 8-94799
 heat transfer from immersed heater 8-71391
 heat transfer from particle to fluid, stochastic model 8-51234
 heat transfer from surface of fixed body 8-79368
 heat transfer parameters, in packed beds, estimation from radial temp. profiles 8-83467
 heat transfer to horizontal tube (*German*) 8-59387
 interparticle electrical forces, meas. 8-63491
 jets issuing into bed, quasisteady axisymmetric jet 8-83470
 liquid fluidisation, study of mass transfer between a liquid and a mobile object in a bed (*French*) 8-83465
 minimum fluidisation vel. of spherical particles by liq. (*French*) 8-75196
 minimum fluidisation velocities in beds of mixed solids 8-91005
 nonuniform, force on fixed sphere, rising gas bubble force field 8-59476
 object immersed in shallow fluidised bed 8-91004
 packed bed thermal storage systems, single- and two-phase models 8-91009
 plasma jet cooling mechanism 8-79371
 porosity measurement device, exam. 8-60911
 pressure drop through fixed beds of spherical particles 8-83466
 pyrocarbon deposition in fluidised bed, qualitative model, investigation with Stromungsrohr 8-56595
 reaction near grid in fluidised beds, two-phase model 8-67280
 regimes of fluidization for large particles 8-83463
 relaxation autooscillations of granular bed 8-59472
 Richardson-Zaki eqn. for spherical particle in bed 8-59465
 semifluidised liquid beds, residence time expts. 8-94814
 solid aerosol collection in spouted bed, electric field effect 8-91019
 solid-liquid bed, particle distrib., particle dynamics 8-59464
 three-phase, electrocond. technique for meas. of axial var. of holdups 8-67286
 viscosity, of water-fluidised bed, by oscills. damping meas. 8-59475

fluidised powders *see powders***fluidity** *see viscosity***fluids**

- see also bubbles; classical theories of fluid structure; disperse systems; fluid mechanics; fluidised beds; gases; gravity waves; liquids; non-Newtonian fluids; quantum fluids; quantum theories of fluid structure*
 No entries

fluorescence

- see also atomic fluorescence; fluorescent lamps; fluorescent screens; molecular fluorescence; nonradiative transitions; X-ray fluorescence analysis*
 air pollution detection, optical methods (*Czech*) 8-69444
 amorphous solids, electron-phonon interactions, fluoresc. line broadening and spectral diffusion 8-84655
 anisotropy decay determ. by single photoelectron counting 8-84635
 anthracene:2-hydroxyanthracene, site-selective photochem., fluoresc. spectra at 3K 8-80756
 anthracene:tetracene, upper excited vibronic states optically pumped energy transfer matrix fluoresc. 8-76512
 anthracene:tetracene (pentacene), effect of elec. field on fluoresc. (*Russian*) 8-56521
 anthracene, excitation spectra of exciton fission in organic crystals 8-92116
 anthracene, fluoresc. spectra and decay curves, 4-300K, reabsorpt. in cryst. (*German*) 8-68561
 anthracene, nonlinear fluorescence quenching 8-52562
 anthracene, singlet exciton fission, prompt and delayed fluoresc. mag. field depend., temp. effects 8-52540
 anthracene, triplet excitons, phosphoresc. and delayed fluoresc. excitation spectra 8-63986
 anthracene crystals, structural imperfections and delayed fluorescence 8-68551
 anthracene in 2 methyl-THF glass, low temp. fluoresc. bandshape, excess energy effects 8-76509
 anthracene-dimethylpyromellite-imide, CT complex, reaction yield detect. double reson., delayed fluoresc. quenching (*Russian*) 8-88230
 anthracene-tetracene amorphous films, host-guest energy transfer 8-60505
 aqueous solution fluorescence spectra, refr. correction 8-93766
 azomethines, photochromic, intramol. proton phototransfer sensitisation, organic cation energy transfer 8-53230
 cell analysis in flow systems, geometry for orienting flat cells 8-77161
 combustion diagnostics, laser Raman and fluoresc. techniques 8-88635
 condensed phase, reson. Raman and reson. fluoresc. spectra, density matrix approach 8-80323
 contour plotter, automated, 3-dimens., for fluoresc. meas. 8-58046
 correlation spectroscopy, effect of clipping 8-55198
 9-cyanoanthracene:perylene, exciplex emission 8-60513
 9-cyanoanthracene, quenching of solid state photodimerisation reaction by cryst. doping 8-68547
 cytochrome-c, coherent reson. Raman scatt. and incoherently broadened reson. fluoresc., condensed phase 8-60429
 cytofluorometer, imaging system for correlating fluoresc. cell meas. in flow 8-61240
 cytometry, hydrodynamic orientation of sperm heads in flow systems 8-77162
 3,5-di-tert-butyl-4-hydroxybenzylidenemalononitrile, excited-state proton transfer, cryst. and mol. struct. 8-84630
 disordered systems spectral transfer, time development models 8-84643

fluorescence continued

- dye adsorption by cells, permeab. polarity and control by phytochrome 8-77025
 Ehrlich ascites carcinoma cell fluoresc. after X-irrad. 8-69143
 Ehrlich ascites vital cell UV primary fluoresc. rel. to ^{60}Co γ -ray dose 8-69142
 elastic scintillation, fluoresc. meas. 8-86747
 electron optical picosecond chronoscopy, 140 MHz repetition rate, fluoresc. lifetime meas. 8-78019
 eye lens fluorescence due to UV stimulation, appl. to pupillary response meas. 8-64977
 fluorene, exciton band struct., two-photon fluoresc. excitation 8-64402
 fluorene, lowest singlet state, exciton band struct. calc. 8-63983
 fluorene, near 6K, two-photon excitation spectrum, g-exciton states location 8-64393
 gated constant-fraction discriminator for use with fast-focused photo-multiplier tubes 8-58063
 indole, in PMMA matrix, high press. luminesc. 8-84629
 inner filter effects in front face and total refl. fluoresc. 8-88357
 IR laser induced fluorescence cell for multiple photon processes 8-54475
 laser spectroscopy, high-resolution, using fast ion beams 8-86975
 life time decay curve meas. and anal. 8-54465
 Mars surface materials, chemistry, anal. of Viking X-ray fluoresc. spectrometer data (*German*) 8-85884
 5-methylindole, in PMMA matrix, high press. luminesc. 8-84629
 3-methylpentane, γ -irradiated, isothermal luminescence in presence of aromatic solutes at 77K 8-76519
 microspectrofluorimetry, low temp., design of cold chamber 8-57144
 minerals, physical theories for origin of colour 8-69323
 multicomponent systems, video fluorometer anal., rank annihilation method appls. 8-92546
 naphthalene: β -chloronaphthalene, reaction rate constants of triplet excitons 8-80407
 naphthalene, 2-methylnaphthalene and anthracene doped, single cryst., sensitised fluoresc. 8-68548
 naphthalene, cryst., singlet exciton interactions, prompt fluoresc. decay 8-60500
 naphthalene, crystalline, singlet exciton diffusion coeff. meas., fluorescence quenching anal. 8-67945
 naphthalene, nonlinear fluorescence quenching 8-52562
 naphthalene, triplet excitons, phosphoresc. and delayed fluoresc. excitation spectra 8-63986
 naphthalene cryst., anthracene doped, fluoresc., two-photon excited 8-68560
 opaque samples, proposed indices of degree of fluoresc. 8-54425
 organic crystals, kinetic model of triplet exciton dynamics 8-67948
 organic mixed crystals, energy transfer 8-76515
 percolation model, one-dimens., spectral diffusion 8-80411
 perylene, excitation spectra of exciton fission in organic crystals 8-92116
 phase fluorometer for measurement of picosecond processes 8-66691
 phthalocyanine, metal-free, solid, fluoresc., lifetimes temp. depend., polymorphic modification 8-80388
 picosecond fluorescence spectroscopy, competing events 8-58051
 plastic scintillator props. meas., streak camera technique 8-66450
 PMMA crosslinked by dimethacryloxymethylanthracene, radiothermoluminesc. (*Russian*) 8-73068
 polarisation apparatus, for simultaneous meas. of orientation and mobility in uniaxial media 8-86320
 polymer, uniaxial, fluoresc. polarisation, orientation and mol. dynamics effects 8-76516
 polymer orientation measurement, in solid, by spectroscopic techniques, mech. anisotropy 8-75558
 radiation problems, semiclassical theory 8-74684
 resonance fluorescence of thin crystal films, superradiance 8-68573
 resonant, air pollution detection appl. (*Czech*) 8-81359
 ruby, fluorescence line narrowing, energy transfer studies 8-84642
 ruby, phonon bottleneck effect, 29 cm^{-1} phonons 8-68562
 Smoluchowski equation, with Coulomb pot., appl. to fluoresc. quenching 8-73051
 sodium dodecyl sulphate micelles, diarylalkane intramolecular excimer formation, microfluidity and fluoresc. meas. 8-80791
 sodium fluorescein dil. soln., luminesc. absolute quantum yields, thermal blooming method 8-72582
 solar EUV spectrum, CO fluoresc. obs. 8-93184
 solar transition region, Bowen fluoresc. rel. to electron density determ. 8-93179
 solid solutions, inhomogeneity and site selective impurity-phonon coupling effects 8-84625
 solution, multicomponent, excitation energy transfer 8-84621
 specific volume meas., for ruby R_1 fluoresc. press. gauge calibration, 0.06-1 Mbar 8-70150
 spectrofluorimetric system, multifunctional, for luminesc. meas. 8-80811
 spectrometry, anal. appls., historical review 8-93507
 trans-stilbene, cryst., triplet excitons, $S_0 \rightarrow T_1$ transition 8-76518
 synchrotron radiation, appls. 8-74825
 tetracene, cryst., triplet exciton pair kinematics, diffusion model, prompt fluoresc. decay 8-79931
 tetracene, fluorescence, effect of weak external electric field (*Russian*) 8-80416
 tetracene, singlet exciton fission, kinematic theory 8-87913
 N,N,N',N'-tetramethylparaphenylenediamine, recomb. fluoresc., elec. field quenching 8-92107
 thin layer chromatography, luminesc. meas. methods 8-53305
 UV laser possible pumping by synchrotron radiation, NaCl:I(Br) luminesc. 8-66835
 virus size measurement using optical microscope, Virometer design 8-61296
 Al_2O_3 , sintered, residual stress meas., piezospectroscopic technique 8-52704
 BaClF:Sm $^{2+}$, energy levels, optical props. 8-84631
 BaF $_2$:Er $^{3+}$, single-site multiphonon and energy transfer relax. 8-52547
 BaO-B $_2$ O $_3$ -UO $_2^{2+}$, Nd $^{3+}$ glass, radiative and nonradiative energy transfer 8-60508
 BaS:Cu, thermoluminesc. and decay 8-80426
 Bi $_2$ Al(Ga) $_2$ O $_9$, fluoresc. and X-ray data 8-80403
 CaF $_2$:Dy $^{3+}$, high temp. fluorescence using Ar $^+$ and N $_2$ lasers 8-56514
 CaF $_2$:Pr $^{3+}$, multisite system, laser selective excitation and energy transfer 8-84634
 fluorescence continued
 CaO-Li $_2$ O-Al $_2$ O $_3$ -SiO $_2$:Nd $^{3+}$, CaO enriched, laser-type glasses, spectroscopic behaviour 8-60497
 Ca $_3$ (PO $_4$) $_2$ F:Nd $^{3+}$, optical fluorescence intensity and cryst. field parameters 8-52570
 CaS-Pb,Mn, phosphors, thermoluminesc. and fluoresc. spectra 8-64396
 CdS:Cl, heavily doped, fluoresc. spectrum upper threshold calculated 8-52568
 Cs $_2$ NaBiCl $_6$, optical props. 8-68549
 Cs $_2$ NaYCl $_6$:Re,Tm, fluorescence, two-step blue up-convertors 8-95603
 Eu $^{3+}$ fluoresc. lineshape in glass, temp., time and conc. depend., two-phonon Raman scatt. 8-64406
 KCl:Eu $^{2+}$, radiationless processes 8-80391
 K $_2$ Eu(MoO $_4$) $_4$, electric dipole transition cross section and effective site symmetry of Eu $^{3+}$ 8-52556
 KY $_3$ F $_{10}$:Eu $^{3+}$, fluoresc. intensity, 77 to 4K, cryst. field parameters of Eu $^{3+}$ 8-72580
 LaF $_3$:Ho $^{3+}$, laser excited fluorescence absorption spectra, symmetry groups 8-60514
 Mn complexes, verification of laws of luminesc. of solids 8-60506
 MnF $_2$, biexciton decay, time resolved laser spectra 8-75999
 MnF $_2$:Ni $^{2+}$, IR fluoresc., field depend., exchange energy 8-68543
 Nd $_2$ O $_3$ -Y $_2$ O $_3$ -As $_2$ O $_5$ glass, spectroscopic props., rel. to possible appl. in lasers 8-84624
 NdP $_2$ O $_4$, laser site-selection time-resolved spectroscopy 8-76524
 Nd $_2$ Y $_2$ -P $_2$ O $_5$, fluoresc. conc. quenching, decay rate consts. 8-64404
 P $_2$ O $_5$ -glass, diffusion of Cu $^+$, fluoresc. meas. 8-59980
 POCl $_3$ -ZrCl $_4$:Yb $^{3+}$, Er $^{3+}$, energy transfer from Yb $^{3+}$ to Er $^{3+}$, agglomeration formation 8-64405
 PrVO $_4$, energy levels, opt. and NMR measurements 8-80226
 Tb $_2$ Y $_2$ -PO $_4$, H $_2$ VUV laser excitation, fluoresc. decay characts. 8-60510
 YAG:Ce $^{3+}$, excited state absorpt. loss, 5d \rightarrow 4f rare earth lasers 8-90417
 Y $_2$ O $_3$:Eu $^{3+}$, absorpt. spectra, fluoresc., electron beam excitation 8-92093
 YVO $_4$:Eu $^{3+}$, absorpt. spectra, fluoresc., electron beam excitation 8-92093
 YVO $_4$:Eu $^{3+}$ laser site-selection spectroscopy investigation 8-68556
 Y $_2$ WO $_6$:Eu $^{3+}$, crystal struct., fluorescence spectra, exam. 8-52558
 ZnS:Mn $^{2+}$, Jahn-Teller effect in fluorescent level 8-52566
 ZnSe:Mn $^{3+}$, Jahn-Teller effect in fluorescent level 8-52566
 fluorescence of atoms *see atomic fluorescence*
 fluorescence of molecules *see molecular fluorescence*
 fluorescent lamps
 chromatic adaptation effects and colour appearance at various illum. levels (*Japanese*) 8-92628
 fluorescent screens
see also electroluminescence
 electroluminescent memory screens, evaluation of X-ray defectoscopic parameters 8-72992
 glass, uranyl-doped, appl. in planar solar energy convertor and concentrator 8-71213
 insulating material monitoring by electroluminescent screens, defect imaging 8-53083
 CsI:Na phosphor screen, absolute efficiency under fluoroscopy conditions 8-82084
 fluorimetry *see spectrochemical analysis*
 fluorine
see also nuclei with
 alkali metal chloride: F $^-(\text{Br}^-)(\text{I}^-)$, anion impurities substitution, energies of soln., association and migration 8-83831
 atom, and isoelectronic series, Z=10-100, L-shell energy struct. and level classification 8-55129
 atom, electron affinity, modified variational approx. 8-66679
 atom, ground state energy, HF calc., second-order correction 8-86784
 chemical laser, combustion driven nozzle, F $_2$ absorption meas. 8-79011
 concentration profiles determ. in Mg alloy scales using $^{19}\text{F}(\text{p},\gamma)$ 8-88678
 determination, in atm. samples by $^{19}\text{F}(\text{p},\alpha)^{16}\text{O}$ react. using low energy accelerator 8-85239
 F ions recoiling in gases, hyperfine interactions 8-74735
 ion addition to $\beta\text{-Al}_2\text{O}_3$, effect on structural state 8-76620
 molecule, Compton scatt. profile, SCF MO theory calcs. 8-58577
 molecule, dissoc. attachment by 0-8 eV electrons 8-74776
 molecule, dissociation, weak bias and anharmonicity effects 8-82661
 molecule, effective core potentials, all-electron calcs. 8-62704
 molecule, electron impact dissoc., influence on KrF* laser props. 8-50756
 molecule, statistical correlation energies 8-78637
 muonic K-shell X-ray transitions, nuclear charge radius 8-66195
 VUV high-power laser, laser-induced fusion 8-58996
 Ar-Kr-F $_2$ mixture, electron beam pumped, spectroscopy and kinetics of 248, 414 nm bands 8-63081
 Ar+Xe(F $_2$), proton excited mixtures, energy transfer processes 8-66647
 CaO:F, X-ray and UV luminesc., electron-hole recombination processes (*Russian*) 8-76528
 F I, reson. transitions, radiative lifetimes, astrophys. appls. 8-62767
 F III, IV, beam-foil spectra, mean lives, 2150-3200 angstrom 8-55224
 F K α , 676 eV X-ray source for ESCA 8-53301
 F $^+$, photodetachment cross section, Stieltjes imaging method 8-55149
 F $^+$, X α method predicting unstable state 8-82640
 F+Al, molecular K X-ray transitions, mol. radiative electron capture effect 8-58802
 F+D $_2$, electronic-to-rot. energy transfer cross sections 8-86935
 F+DX, (X=I, Br, Cl), H abstraction, absolute reaction rate, H/D isotope effect 8-80721
 F+formic acid (formaldehyde), microscopic reaction dynamics, branching ratio, IR chemiluminesc. 8-73021
 F+H $_2$, collinear quasiclassical trajectory study 8-80718
 F+H $_2$, transition states, trapped trajectories, and classical bound states in continuum 8-88630
 F+H $_2$, ZZ 8-80729
 F+H $_2 \rightarrow \text{FH}+\text{H}$, collinear probability, quantum calc. using pot. energy surface 8-64829
 F+H $_2 \rightarrow \text{FH}+\text{H}$, vibr.-rot. energy distrib. of HF, DWBA calc. 8-80722

fluorine continued

- F+H₂→HF+H energy profile, minimal basis ab initio VB calcs. 8-50477
 F+HD→HF+D(DF+H), branching ratios, information theory test by classical trajectory calcs. 8-64822
 F+HX, (X=I, Br, Cl), H abstraction, absolute reaction rate, H/D isotope effect 8-80721
 F+Xe, collision in laser field, ang. momentum anal., quantum mech. theory 8-74733
 F+Xe, enhanced quenching in intense KrF laser light, computer modelling 8-55232
 F+methane, MINDO/3-FORCES study, reactant energy, products and paths 8-95926
 F₂ absorption diagnostic, sensitive technique, for chem. laser flow 8-74896
 F₂, mag. dipole terms evaluation, internucl. distance depend. 8-82864
 F₂-inert gas mixtures, transport and attachment processes 8-59542
 F₂+H(D), exothermic triatomic exchange reactions, prod. energy distrib., statistical dynamic model 8-92455
 F₂+H(D)(T)(Mu), impulsive triatomic reaction, vibr. state distrib., impulsive energy release model 8-92456
 F₂+Li, electron transfer reactions, semiempirical pot. energy surfaces calcs. 8-73022
 F₂+XeF*, quenching rates for XeF in (B) state 8-58730
¹⁹F recovery during transport from reactor 8-78821
¹⁹F, chem. shielding in isolated haloalkanes, temp. depend. 8-86888
¹⁹F NMR in one-dimensional ferromagnet CsNiF₃ 8-91970
 H+F₂, vibr. prod. distrib., Einstein coeffs. 8-92448
 H₂-F₂-He chemical CW laser, flows (*Russian*) 8-74895
 H₂-F₂-O₂, chem. laser mixture, multiatm., spontaneous explosions 8-73044
 He-F, doublet series laser lines near 700 μm, hyperfine splitting and broadening meas. 8-63070
 He-F gas mixture, electron drift velocities, laser modelling 8-63061
 Si+F₂, fast flow reactor, second order rate coeff. determ. 8-80723
 SiO₂:F layers, deposition from SiCl₄-SiF₄-O₂ gas mixture by plasma CVD method 8-95699
 ZnSe:F, signal enhancement by field modulation, ODMR expts. 8-56406

fluorine compounds

- diatomic fluorides, exact force field calcs. using at. force consts. 8-62739
 fluxing material, effect on oxidation of graphite crucibles (*Japanese*) 8-84755
 FCN, general quartic force field, Machina-Overend parameters 8-50532
 FCN+N₂, rot. spectra and geom. struct. of FCN 8-82725
 FH₂⁺, reactive processes, ab initio MCSCF-CI and diatomics in mols. calc. 8-56881
 FHCl⁻, deuteron quadrupole coupling const., nuclear mag. shielding, geometry depend. 8-58586
 FHF⁺, deuteron quadrupole coupling const., nuclear mag. shielding, geometry depend. 8-58586
 FHe⁺, fragmentation and potential energy curves from FT β-decay 8-56910
 FNO, electronic transitions, limited GSMO and ESMO CI calcs., oscillator strengths, spectra 8-70750
 F₂O₂, geometry, SCF CI calcs. 8-55126
 FSO₄, electrolytic polishing of Ta and Ta alloys 8-85094
 F₂SiOSiF₃, vibr. bands, normal coord. calcs. (*Russian*) 8-70814
 HF, variation-perturbation minimal Gaussian geminal basis sets correl. energy calc. 8-78629
 SF₆ insulated switching installations and devices, gas chromatography appl. (*German*) 8-88668

flux (magnetic) *see magnetic flux*

flux (neutron) *see neutron flux*

flux creep

- see also flux pinning*
 vortex array, pinning of flux lines by randomly-spaced pinning centres 8-52172

flux crystal growth *see crystal growth from solution*

flux flow

- see also flux pinning*
 Josephson junction, flux flow characteristics 8-84351
 nearly pure superconductor, flux line motion, semiphenomenological theory 8-52171
 superconductor, flux flow curves as function of temp. 8-84344
 Nb, neutron irradiation, low temp., 15 MeV, effect on superconducting props. 8-52179
 Pb-In (40-60 at.%), type II superconducting Ettingshausen effect, transport entropy of vortices 8-56272
 Pb_{0.87}Sn_{0.129}, supercond., hysteresis in flux flow characts., normal metal precipitates 8-80107

flux-line lattice

- continuum approach of physical line structs., appl. to flux line lattice of supercond. 8-81859
 dielastic interaction with internal stresses of cryst. imperfections 8-56270
 film, inversion temp. in pinning of vortices by periodic struct. 8-56274
 flux pinning force, derivation from a potential 8-68128
 Josephson contact, vortex pinning and energy (*Russian*) 8-68117
 phase transition between triangular and square lattices 8-76202
 stress tensor theory of AC permeability 8-56271
 Nb, supercond., field history effect of flux gradient 8-91828
 Pb-Tl alloys, pinning parameters 8-52173
 Pb_{0.87}Sn_{0.129}, supercond., hysteresis in flux flow characts., normal metal precipitates 8-80107

flux line motion *see flux flow*

flux pinning

- see also flux creep; flux flow*
 film, vortices, static and dynamic interaction with periodic pinning potential 8-52170
 flux pinning force, derivation from a potential 8-68128
 Josephson contact, vortex pinning and energy (*Russian*) 8-68117
 one-dimensional analogue model, for pinning study in type II supercond. 8-88086
 summation curves from TEM data 8-52165

flux pinning continued

- vortex array, pinning of flux lines by randomly-spaced pinning centres 8-52172
 Cu₂MoS₈, evaporated two-phase, crit. current and scaling laws 8-91831
 Nb and Nb alloys, superconductor, flux pinning under heavy ion irradiation 8-52167
 Nb, irradiated superconductor, fluxoid defect interactions 8-52166
 Nb, neutron irradiation, low temp., 15 MeV, effect on superconducting props. 8-52179
 Nb, supercond., dielastic interaction of flux line lattice with internal stresses of cryst. imperfections 8-56270
 Nb:O, type II supercond., radiation-induced flux pinning 8-80106
 Nb-Zr, type II supercond., radiation-induced flux pinning 8-80106
 Nb₃Ge, CVD, impurity doping effect on supercond. crit. props. 8-52174
 Nb₃Sn, filamentary segments, flux pinning, proximity effects, percolation thresholds 8-56269
 Nb₃Sn, critical current density 8-52176
 Nb₃Sn, critical current enhancement by low temp. fast neutron induced flux pinning centres 8-52177
 Nb₃Sn multifilament conductors, strain effect on crit. props. 8-80108
 Nb₃Sn, neutron irradi., crit. current change rel. to temp. and metallurgy 8-80109
 Nb₃Sn, radiation damage effect on superconducting props. 8-52127
 Nb₃Sn, superconducting props., effect of radiation induced atomic disorder 8-52133
 Nb₃Sn superconductor, low temp. deuteron irradiation 8-52182
 Pb-Na, peak-effect supercond., flux pinning 8-95403
 Pb-Tl alloys, pinning parameters 8-52173
 PbMoS₈, sputtered film, critical current density meas. 8-84369
 Pb_{0.87}Sn_{0.129}, supercond., hysteresis in flux flow characts., normal metal precipitates 8-80107
 V, superconducting, fluxoid pinning by VC_x precipitates 8-52169
 V, superconducting props., effect of voids 8-52168
 V₃Ga, high current density multifilament wire, neutron effects on equilibrium and transport props. 8-52126
 V₃Ga, pinning characteristics (*Japanese*) 8-91829

flux vortex flow *see flux flow*

flux vortex lattice *see flux-line lattice*

fluxmeters

- see also magnetic field measurement; magnetic flux*
 magnetic saturation measuring coil and fluxmeter system 8-93738
 measurement range extension 8-57993
 micro, MHD motion in water 8-79384

fluxoid array *see flux-line lattice*

foams

- see also bubbles*
 bubble size distribution, changes due to interbubble gas diffusion 8-85204
 education, bubble cohesion in foam, binding energy calc. 8-61978
 ocean surface simulation, spectral characts. of microwave thermal emission from foams (*Russian*) 8-69353
 polymer, foamed, rigidity 8-95769
 polyurethane foam, X-ray exam. (*German*) 8-75596
 polyurethane foam layers, open-cell, refl. characts. for ultrasound in air 8-83139
 polyurethane foam solar concentrator, thermal and thermohydrolytic ageing 8-92281
 PVC, density rel. to rheological, surface props. of PVC pastes (*Polish*) 8-85212
 stability, interfacial phenomena interpretation using schematic density profiles 8-60012

focused collision sequences *see sputtering*

focusing

- see also self-focusing*
 attenuated total reflection with focused light, appl. to guided waves on grating 8-74992
 automatic camera lens focusing, using optolinear chip 8-54480
 automatic focusing of cameras using self-contained IC 8-82069
 camera, Polaroid Sonar One-Step, US automatic focusing 8-78011
 charged-particle beam, axisymmetric, focusing in hyperbolic electrostatic field 8-50688
 collimated light beam, focus and alignment sensing 8-59065
 cylindrical particle analyser, fringing field 8-94165
 double focusing bending magnet, meas. of optical props. with thin alpha source 8-55073
 dye laser fast light deflection, ultrahigh resolution 8-63178
 dynamically focused US diagnostic phased array 8-61232
 electron beam distrib. function in focusing mag. field (*Russian*) 8-82898
 electron micrograph optical and digital spatial freq. filtering 8-70231
 electron-beam focusing optimisation with specified image parameters 8-86385
 EM field, in focal region of wide-angular annular lens and mirror systems 8-90485
 energy-focused atom probe design and performance 8-85276
 Faraday double transmitting cup, ion optical control device 8-82556
 fibre-optic integral data source/receiver package 8-63179
 fibre-optic light source for curved platen illumination 8-63163
 focal plane design and optimal processing for scattered optical fields 8-78935
 four-point field coherence function meas. in laser random focusing region (*Russian*) 8-58910
 gross surgical specimen photography, centimetre rule/elevator rod technique 8-61287
 heavy ion beam focusing, accelerated, decelerated beam, electrostatic lenses 8-89588
 heavy-ion intense beam, periodic focusing, mag. channels 8-55079
 ion beam focusing and neutralised transport 8-50323
 ion beam focusing by means of mag. insulated diodes 8-50324
 ion beams, prod. and focusing for fusion 8-50322
 ions, trajectory in const. mag. field plus orthogonal sinusoidal elec. field 8-50687
 laser, multiple-beam pellet irradiance, diffraction analysis 8-50845
 laser beam, far-field profile, focal plane technique 8-87087
 laser beam distrib. in focal region, transmission monitoring through pinhole 8-90441
 laser fusion reactors, optical design, focusing optics 8-82518

focusing continued

- laser linear, annular and radial focusing with axicons, laser machining machining appl. 8-66856
 lens centring monitors design, using variable parameter system (*Russian*) 8-50883
 lens system design with extended depth of focus, Version 14 optimisation program 8-90489
 lens-axicon doublet illuminated by Gaussian beam, ring focal pattern 8-55421
 light concentration using inversion of wave front technique (*Russian*) 8-63154
 magnetic lens, wide-angle focusing device for low energy π collection 8-70664
 magnetic vector man analyser, stigmatic focusing condition 8-70215
 mass spectrometer electrostatic analyser attachment 8-86377
 mass spectrum, second order image aberration correction by electrostatic hexapole lens 8-70216
 miniature slow proton source for focusing efficiency obs. 8-78538
 multi-lens focusing systems for energy Nd:glass lasers 8-50848
 neutron spin echo, matrix anal. 8-86715
 neutrons, ultracold, zone mirrors for high resolution image form. 8-87003
 optical waveguides, deflection and focusing of radiation by stepwise inhomogeneities 8-83093
 pinched beam diode, geometrical focusing of intense ion beams 8-58898
 proton synchrotrons, non-linearities 8-78897
 radiative damping effect for ultrarelativistic channelled particles 8-67758
 radiowave gravitational focusing in interstellar medium, model (*Russian*) 8-81905
 Rayleigh-Debye scattering with focused laser beams 8-71030
 ring-type state selector and space focuser for mols. with positive induced dipole moment, appl. to mol. beam maser 8-54503
 Shiva optical system 8-59039
 Solar Thermal Test Facility, 5 MW, heliostat focus and alignment system 8-50894
 space charge lens for high current ion beams 8-55075
 synchrotron radiation, separated function focusing monochromator system 8-62278
 tester for focusing adjuster, optimal parameters anal. 8-8307e
 thermo-gasdynamic control in laser beam guidance, review of developments 8-74942
 whistler-mode waves focusing and interference in spatially varying mag. field 8-65465
 H^+ beam, pure, production by four-lens Hall accelerator, focusing 8-66441
 I laser, high-power, beam quality, gain saturation effect, for fusion ignition 8-63149

focusing, particle see focusing; particle optics**fog**

- acoustic sounding of radiation fog 8-69419
 California coastal fog and stratus microstruct. 8-61505
 Cheddar Gorge, England, oblique false-colour photograph 8-57290
 clearance, by laser-beam induced heat and mass transfer 8-93635
 cloud condensation nuclei from paper mill effluents, induced fog (*French*) 8-96270
 evaporation fogs formation theory and prediction 8-61522
 holography through fog, coherence requirements for light source 8-58949
 IR wavelengths extinction by aerosols in coastal fog 8-81400
 laser beam broadening and depolarization in dense water-droplet fogs 8-92981
 laser beam transmission, heating, ion emission 8-59063
 laser radiation transmission meas. at 10.6 μm 8-92977
 lidar probing of fogs and clouds, double scatt. approx. 8-73512
 lidar returns from fog, doubly scatt. radiation contrib. 8-77326
 liquid water content, organic aerosol effects 8-73465
 liquid water content rel. to atm. visibility 8-81404
 organic material impact on fog and cloud processes 8-73467
 radiation fog, relationship to dew 8-73446
 radiative transfer through fog, 2D numerical soln. algorithm 8-71032
 turbulent and radiative transport interaction in development of fog and low-level stratus 8-81313

foils

- electropolishing technique for transmission electron microscope specimen preparation 8-57919
 electrothinning, laser-monitored, for preparing ultrathin metal foils 8-53074
 flux-distortion factor for a foil in an exponentially varying flux 8-89930
 membrane waves excit. 8-90578
 metal, thickness, X-ray fluoresc. meas. method, appls. (*Russian*) 8-56582
 polyester foil, static polarisation depend. on heat ageing 8-60688
 thin metal films, for electron microscopy, production by jet polishing apparatus 8-86247
 transition metal foil-electrolyte interface, optical and elec. expts. 8-88644
 Al foil, sputtering with ^{252}Cf fission products, desorbed secondary ions 8-68596
 Al, thin foil, adhesion and friction, rel. to observed dislocation density 8-64706
 Al-Be, two-layer foils, mech. props. (*Russian*) 8-51858
 C foil+ $\text{H}_2^+(\text{H}^+)$, 0.5-2.5 MeV, forward electron vel. distrib., peak shape 8-78794
 Cu foil, sputtering with ^{252}Cf fission products, desorbed secondary ions 8-68596
 Cu, role of grain-boundary porosity in superplasticity (*Russian*) 8-56690
 Cu-polymer composite foils, fracture surface exam. by XPS (*German*) 8-84592
 CuO surface, contaminated, cleaning treatments, ion scatt. anal. 8-53307
 Cu₂O polycrystalline and single cryst. mech. behaviour 8-95777
 Fe- ^{133}Xe , heavy ion implantation, recovery, Mossbauer effect meas. 8-52393
 Ge-Si alloy foils, prep. by improved jet thinning 8-88589
 Nb-Sn, supercond. foils, phase anal. by Mossbauer spectra 8-64305
 Ni foil, sputtering with ^{252}Cf fission products, desorbed secondary ions 8-68596

foils continued

- Pt, quenched, 1.2 MeV electron irradi., subthreshold irradi. effects 8-51585
 ^{235}U foil, sputtered, energy spectrum, fission track technique 8-68593

Fokker-Planck equation

- aerosol particles diffusion and gravitational settling in tube 8-90976
 boundary-value problem, two-point, statistical variant using Einstein-Fokker-Planck eqn. (*Russian*) 8-81924
 Brownian motion of revolving particles, solution (*Russian*) 8-77802
 Brownian particle, Fokker-Planck equation, systematic soln. for high-friction case 8-49767
 Brownian rotation in external fields, relaxation times 8-62160
 Chapman-Enskog procedure, complete 8-65860
 damped harmonic oscillator, eqns. of motion in quantum statistical theory (*French*) 8-89399
 dense fluids, translational motion, modified Fokker-Planck eqn. 8-75517
 diffusion process modelling, equivalence of different methods 8-57818
 Feynman path integrals, white noise approx., inertialess Brownian system 8-57859
 fission reactor neutron gas, nonequilibrium thermodynamics (*Japanese*) 8-62595
 gas kinetics, integro-differential eqn. approx. by Fokker-Planck type 8-91049
 integration method, plasma appl. 8-91067
 Langevin equations, stochastic integrals, removal of ambiguity, invariance postulate 8-70061
 laser, containing saturable absorber, bistability, semiclassical and quantum theories 8-82943
 many-particle system, generalised diffusion processes 8-73942
 master equation, path integral solns., stationary Markov process 8-86233
 Navier-Stokes fluid, Fokker-Planck description 8-94632
 nonlinear diffusion process, path integral evaluation, by Fourier series 8-70075
 nonspherical molecules, rot. and translational motion, modified Fokker-Planck equation 8-75518
 optical fibres, randomly bent, ray theory 8-66921
 particle motion in stochastic force fields 8-73928
 particle number conservation in charged particles diffusive transport 8-75266
 path integrals for inertial classical particles, rapid stochastic processes 8-57858
 plasma heating, ion-cyclotron, Tokamaks and mirrors, quasilinear model 8-59626
 power reactor, neutron density fluctuations, stochastic nonlinear model, Fokker-Planck eqn. 8-58316
 quasideterministic Fokker-Planck dynamics 8-93627
 reactive and translational dynamics coupling 8-60988
 ring laser, coherence theory, counter-rotating laser modes 8-55387
 spherical stellar system, distrib. of stars around massive central black hole 8-65660
 steady states of weakly dissipative systems 8-81918
 stochastic quantisation, path integral formulation of Fokker-Planck equation 8-86228
 string, nonlinear stretched, randomly excited, anal. 8-83312
 variational techniques application 8-89415
 void nucleation, continuum description 8-87707
 X-rays transfer through optically thick shell 8-65488

food processing industry

- baking, EHD augmented, corona wind impingement effects 8-87235
 radiation and isotopes appl., development trends 8-55041

forbidden gap see energy gap**Forbush decreases** see cosmic ray variations**force**

- see also atomic forces; coercive force; Coriolis force; force measurement; molecular force constants; nuclear forces
 biomechanics using a crane boom 8-81759

force constants see lattice dynamics; molecular force constants**force measurement**

- see also dynamometers
 aircraft rudder-bar, strain-gauge dynamometer appl. (*French*) 8-49825
 distribution under human foot, online meas. system 8-96110
 foot vertical force during walking, continuous meas. device (*Japanese*) 8-73273
 impact force vs. displacement curves, expt. determ. 8-83344
 piezoelectric dynamometer for dynamic force meas. (*Hungarian*) 8-65918
 ponderomatic meas. for fluid detection in chem. anal. 8-68953
 pressure-force transducer using 32.768 kHz X-Y flexure watch crystal 8-57934
 sensitivity limitations on force and weight meas. in vac. 8-65908
 shear force instrument, force-balance 8-51263
 strain gauge with screw tenso-resistor, linearity anal. (*Russian*) 8-89475
 tenso-resistive strain gauge output error anal. (*Russian*) 8-89474
 tensometer with one-piece sensitive element, electric circuit analysis (*Russian*) 8-49824
 transducer using amorphous ribbon core 8-93669

force meters see force measurement**forecasting, technological** see technological forecasting**forging**

- disk and strip forging for the determination of friction and flow strength values 8-85004
 steel, alloy, type 25G5, increasing fatigue resistance by surface plastic deformation 8-88530
 steel, CC Cr-Ni, soaking at forging temp., effect on struct. and mech. props. (*Czech*) 8-64628
 steel, Cr-Mn, powder forged, fracture processes and fracture toughness 8-72870
 steel, Ni-Mo, powder forged, fracture processes and fracture toughness 8-72870
 Al alloys, 6061, A356, forging of liquid and partially solid alloys 8-80569
 Sn-Pb (15 wt.%), forging of liquid and partially solid alloys 8-80569

form factors

- ϕ^4 model, Pade approximants, EM form factor, pseudoscalar particles 8-74122
 baryon decay, semi-leptonic weak interactions, book contrib. 8-78162

form factors continued

- bi-local field in external source, scatt. amplitude 8-74182
 bi-local field interaction with external field 8-66030
 bound state, relation to binding potential using nonrelativistic Schrödinger eqn. 8-58187
 charmed meson semileptonic decay, effective chiral Lagrangian method 8-74254
 collective props. of nuclei deduced from electron scatt., deformed nuclei, review 8-50064
 Compton scatt. polarisability, use of Ward identity on off-shell form factors 8-66120
 deformed nuclei, single nucleon form factor for knockout and pick-up reactions, (p,2p) calcs. 8-93999
 deuteron, EM quadrupole form factor peak value, determination of percentage D-state 8-93950
 E₇ exceptional group, calc. of 6, symbols 8-57800
 exact from factors in field theoretic models with soliton behaviour 8-82211
 hadron electroprod., $\Delta(3,3)$ region, low hadronic mass, Δ , τ , and nucleon axial vector form factors 8-74259
 hadrons, axiomatic local constraints (*Russian*) 8-58190
 heavy-ion deeply inelastic collisions, form factors determ. within statistical model 8-50205
 imaginary inelastic transition form factor, microscopic theory 8-50175
 IR singularities in gauge theories, renormalisation group method, coupled massless field theories 8-54538
 isovector M6 excitations, open shell RPA calcs., appl. to electron scatt. form factors 8-50112
 lattice Schwinger model, form factors of dipole states 8-66029
 light atoms, large-q form factors, calcs. for ³Li to ¹⁹K, ²²Ti 8-58589
 light atoms, large-q form factors for momentum transfer 8-70734
 nuclear bag states containing quarks, detection 8-70465
 nuclear currents, microscopic anal. of elementary particle description 8-82304
 nucleon, inelastic, form factors, spectral representation (*Russian*) 8-93881
 nucleon charge form factor, quark model 8-62352
 nucleon EM structure, $\psi(3.1)$ in VDM of nucleon form factors 8-50034
 nucleon in time domain, EM form factor (*Russian*) 8-78183
 nucleon structure functions from quark distrib. functions anal. of μp and μd interactions 8-50035
 nucleus+ γ , electron pair production, screening corrections for intermediate, high energies, using relativistic form factors 8-93986
 progenitor sum rules, nuclear theory appl., meson+nucleon interaction, inelastic form factors 8-54690
 pseudoscalar Dalitz decays, form factor slopes, VDM with subtracted dispersion relation 8-58181
 quark double logarithmic form factor derivation, QCD, hard semi-inclusive processes 8-93862
 quark form factor, asymptotic behaviour 8-89660
 quark magnetic form factor, significance of instantons 8-70339
 radiative corrections, fourth order, book contrib. 8-82213
 relativistic harmonic oscillator quark model, N and $\Delta(1236)$ form factors 8-93852
 Sturm-Liouville expansion method, one- and two-particle transfer form (*Russian*) 8-89844
 trinucleon bound state using Paris pot., binding energy and form factors 8-89803
 two pion exchange charge density in static approx. ³He, ³H form factors 8-66222
 (α,α), antisymmetrisation effects, α pot. form factor, optical model anal. 8-82366
 d, 6 quark system, wave function, elastic form factor, NN forces, spectroscopy (*Russian*) 8-50015
 d, form factors relation to wave functions 8-70462
 d charge form factor accompanying high imparted momentums (*Russian*) 8-58189
 d EM form factors at large transferred momentum, six-quark state (*Russian*) 8-89715
 ed, elastic and deep inelastic scatt. at large momentum transfer, quark model (*Russian*) 8-86529
 $e^+e^- \rightarrow \pi^+\pi^-$, vector meson dominance anal. for π form factor 8-70370
 $eN \rightarrow eN\Delta$, low energy, ΔN axial form factors soft-pion theory 8-70380
 $eN \rightarrow eN\pi$, π form factor determ. 8-66128
 $ep \rightarrow ep\pi^0$ or $en\pi^+$, threshold cross section slope, form factors, π axial mass and radius 8-62411
 $ep \rightarrow e\pi^+n$, longitudinal and transverse contribs., π^+ EM form factor 8-66126
 $F^+ \rightarrow \pi^+e^+e^-$, enhancement due to π^+ EM form factor, generalised PCAC applicability 8-82164
 $\gamma^*n\Delta_{1236}$ transitional form factors, review (*Russian*) 8-54636
 $\gamma^*p\Delta_{1236}$ transitional form factors, review (*Russian*) 8-54636
 $\gamma p \rightarrow \gamma^*p$, one-pion exchange contrib., vertex corrections 8-50039
 k, quark-antiquark systems combined by Coulomb type attractive force 8-89677
 K decay, semi-leptonic weak interactions, book contrib. 8-78162
 $K^0 \rightarrow \pi^+e^-v$, vector form factor meas. in large H bubble chamber 8-93875
 K₄ decay in relativistic quark model, axial vector form factors and decay rate 8-66109
 μ magnetic moment, pionic contrib., using exact soln. of Meiman problem concerning form factors 8-78182
 n, elec. form factor from ed quasi-elastic scatt. 8-82210
 N, Mandelstam representation, double dispersion relation 8-74256
 N EM form factors, EM effects in precision anal. of low-energy np interaction data 8-93896
 NN nonrelativistic 1-boson exchange potentials based on generalised meson field theory 8-70459
 νN , deep inelastic scatt., structure functions, form factors, negative scaling violation 8-74241
 (π,π) elastic scatt. on light nuclei, optical pot. and scatt. amplitude model (*Russian*) 8-89918
 π , analytic and unitary representation at all Q² accommodating higher vector meson states 8-58188
 $\pi \rightarrow e\nu\gamma$, branching ratio, axial vector form factor determ. 8-74247
 πN S-matrix, inelastic effects in sidewise dispersion relations for nucleon EM form factors 8-82212
 πNN form factors, influence on two nucleon data, one particle exchange 8-70369

form factors continued

- $\pi^+p \rightarrow e^+e^-n$, induced pseudoscalar nucleon form factor, current algebra appl. (*Russian*) 8-78212
 ρ form factors ratio, high momentum transfer behaviour in QCD 8-70340
 t+nucleus, form factors for two-nucleon stripping process with Skyrme potentials, DWBA 8-58287
 B(e,e), A=10, 11, form factors, Hartree Fock calcs. 8-58263
¹²C, electron elastic and inelastic scatt., form factor calc. 8-50108
¹²C, weak hadronic form factor and recoil polarisation in muon capture 8-62508
¹²C(γ,π^-)¹²N_g, threshold prod., 15.11 MeV M1 form factor 8-62519
⁴⁰Ca(n,n')⁴⁰Ca, imaginary inelastic transition form factor, microscopic theory 8-50175
⁴⁰Ca(t,p)⁴²Ca, form factors for two-nucleon stripping process with Skyrme potentials, DWBA 8-58287
⁵²Cr(α,α), 15-19 MeV, inelastic scatt. form factors, Coulomb-nuclear interference region 8-66288
⁵²Cr(e,e'), 90-226 MeV, excitation of low-lying states (*Russian*) 8-54746
⁵³Cr(e,e'), 90-226 MeV, excitation of low-lying states (*Russian*) 8-54746
⁵⁶Fe(α,α), 15-19 MeV, inelastic scatt. form factors, Coulomb-nuclear interference region 8-66288
³He(e,e), form factors and dimensional scaling quark model 8-93991
⁴He, binding energy and form factor calcs., Reid interaction 8-54678
⁴He(e,e), form factors and dimensional scaling quark model 8-93991
 He(e,e), A=3 and 4, high momentum transfer, elastic struct. functions 8-62521
⁶Li, (anp) 3 body model using hyperspherical harmonics, bound states 8-70469
⁶Li, charge form factor, short range Jastrow corrls. in harmonic oscillator shell model 8-70467
²⁰Ne quadrupole transitions, electron scatt. form factors, shell model calcs. 8-62523
 Ni(¹⁶O,¹⁸O), surface transparent pots., and CCBA anal. of diffractive behaviour 8-50206
⁶⁰Ni(α,α), 15-19 MeV, inelastic scatt. form factors, Coulomb-nuclear interference region 8-66288
¹⁶O, 0⁺ states, appl. of K-harmonics method 8-54685
¹⁶O, weak hadronic form factor and recoil polarisation in muon capture 8-62508
¹⁶O(γ,p)¹⁵N and ¹⁶O(γ,n)¹⁵O, 60-300 MeV, absorpt. mech., residual nucleus form factor 8-70511
¹⁷O(n,n')¹⁷O, imaginary inelastic transition form factor, microscopic theory 8-50175
²⁰⁷Pb+e, high resolution inelastic scatt. cross sections, induced charge of neutron, form factors 8-78366
²⁰⁸Pb+⁴⁰Ar, deeply inelastic collisions, form factors determ. within statistical model 8-50205
¹⁰⁸Pd, vibr. states study, elastic and inelastic electron scatt., anharmonic vibrator model 8-62520
¹²⁰Sn+⁴⁰Ar, deeply inelastic collisions, form factors determ. within statistical model 8-50205
⁶⁴Zn(α,α), 15-19 MeV, inelastic scatt. form factors, Coulomb-nuclear interference region 8-66288
⁹⁰Zr(α,α), E=26.2-166 MeV, antisymmetrisation effects, α pot., form factor, optical model anal. 8-82366

form factors, atomic see *atomic structure***formal languages**

- contrastive linguistics, P-struct. C-struct. grammar 8-69959

formal logic

- axiomatisation of set of formulae of intuitionistic logic 8-57730
 Herbrand theorem for ω^* -valued logic 8-57731
 history of mathematics, causal and formal logic unification 8-77639

formation, heat of see *heat of formation***forming processes**

- see also *casting*; *electroforming*
 butadiene rubber, polymer melt, extrusion at constant deformation rate 8-68744
 composite discs, fibre-reinforced, rotating strength, stress distrib., failure criterion rel. to mould process 8-76701
 ingot formed in EM crystalliser, control of metal melt circulation (*Russian*) 8-84790
 metallic glass, moulding process 8-80536
 polyethylene, high-density, effect of fillers and moulding process parameters on strength (*Russian*) 8-60640
 polyisobutylene, polymer melt, extrusion at constant deformation rate 8-68744
 polymer, filled, thermosetting, anisotropic structure on injection moulding (*German*) 8-76625
 sheet metal forming, material behaviour 8-95787
 solar concentrator facet quality evaluation for deformational forming 8-90483
 steel, C and alloy, cold formability (*French*) 8-60681
 steel, creep-resistant influence of temp., holding time, cooling rate on formability (*German*) 8-84901
 steel, creep-resistant pipe steel, influence of chemical comp. on formability (*German*) 8-84900
 steel, low C, forming limit diagram, eval. of applicability of theoretical anal. 8-60682
 thin shell forming processes, geom. props. (*Russian*) 8-51061

FORTAN

- least-squares approximation program, lateral absorbed dose distrib. for 25 MeV electrons appl. (*Japanese*) 8-74505

Foucault currents see *eddy currents***fountain effect** see *liquid helium-4*; *superfluidity***Fourier analysis**

- see also *Fourier transforms*; *harmonic analysis*; *waveform analysis*

- beat Cepheids, Fourier anal. 8-69811
 biomedical signals, development of common struct. for filters, correlators and Fourier analysers (*German*) 8-88748
 cuboid surrounded by infinite elastic space, stress field due to initial strains 8-55565
 CVD, interface morphology on profiled substrates, calc. of development 8-60040
 data with closely spaced frequencies, erroneous results 8-89298
 difference schemes for Laplace eqn. in rot. symm. system, Fourier anal. 8-77677

Fourier analysis continued

- diffusion process, nonlinear, path integral evaluation by Fourier series 8-70075
- early-type stars photospheric expansion, meas. via. Fourier anal. technique 8-93224
- eclipsing binary stars, Fourier anal. of light curves 8-69830
- eclipsing binary stars, Fourier anal. of light curves for transit eclipses 8-96506
- eclipsing variable stars, Fourier anal. of light curves 8-93311
- eclipsing variables, Fourier anal. of light curves, photometric perturb. 8-96507
- eigenfunction expansions assoc. with vector-matrix differential eqn., convergence 8-69965
- Einzel-type electrostatic field with rot. symmetry, Fourier-Bessel soln. 8-82878
- evoked potential optimal filtering in sequential range (*German*) 8-85401
- gamma-ray, 3-dimens. image processing appl. to coded aperture imaging (*French*) 8-57067
- grain size and strain determ. by Fourier anal. of X-ray diff. profiles 8-88588
- human vision, Fourier anal. and texture discrimination 8-96051
- integral determ. from derivative of given function (*German*) 8-49644
- meteorological fields, objective analysis method (*Russian*) 8-81272
- multidielectric stack control using chromatic maximeter, Fourier series anal. of signal (*French*) 8-83111
- multipurpose Fourier spectral analysis program for analytical chemistry 8-64896
- muscle, skeletal, deriving viscoelastic modulus from transient pulse propag. 8-77077
- noise, Fourier transform as perturbation criterion, appl. to NMR intensity 8-65948
- potential field transformation from relief to single reference plane, Fourier anal. appl. (*Russian*) 8-53759
- Riesz summability of Fourier series and its conjugate 8-54155
- scattering density variance minimisation criteria for Fourier synthesis 8-55774
- signature analysis systems with Fourier analyzer 8-87195
- stars, eclipsing variables, light curve Fourier analysis, eclipse parameters, geometrical determinacy 8-96503
- stress analysis of plastic zone during rolling under plane strain condition, Fourier calcs. (*Russian*) 8-80555
- US image feature enhancement via digital processing 8-73183
- visual physiology and psychophysics polar coordinate data 8-56988
- X-ray diff. line profile analysis, on-line computer routine 8-79498

Fourier series see series (mathematics)**Fourier transform optics**

- see also *Fourier transform spectroscopy*
- acoustooptic snapshot PROM, real-time optical, signal spectrum analyzer 8-90494
- astigmatic coherent processor analysis 8-78927
- biological cell diff. pattern, Fourier optical extraction of morphological parameters 8-92749
- blood cell smear pathology differentiation by optical transform method 8-69248
- coherent light valve optical processor for GHz bandwidth signals 8-78937
- coherent optical data processing fundamentals 8-78923
- coherent optics fundamentals 8-78910
- compact real-time matched-filter optical processor 8-74869
- conjugate Fourier series approach to optical data analysis 8-90378
- diffraction and causality principle 8-55295
- exact spatial frequency plane of Fourier transforming lens 8-63012
- filter function, circularly symm. positive, realisation by transparent rings 8-94448
- Fresnel images, form. of 2-D transparencies with extended periodic struct., theory 8-82920
- graphological elements meas. using optical Fourier transform (*Italian*) 8-50707
- hologram memory using one dimensional Fourier transform image hologram 8-87032
- hologram recording and reconstruction, using materials with low resolving power (*Czech*) 8-90399
- holograms, long-wavelength, recording and reconstructing schemes 8-87029
- holographic interference correlators, theory 8-78969
- holography, maximum recordable number of particles 8-58946
- holography method, fast Fourier transform 8-71064
- image formation in scanning microscopes with partially coherent source and detector 8-58923
- imaging, significance of Fourier transform (*German*) 8-50709
- imaging system using intensity triple correlator 8-74846
- inverse radon transform by optical convolution 8-66777
- lenses, simple, as Fourier transform elements, performance meas. techniques 8-94374
- metaxial optics, centred refracting systems, undiaphragmed and without aberration (*French*) 8-94369
- microprocessor-based optical/digital processor 8-63027
- microscope, with optical spatial filtering 8-58028
- modular chirp Z transform equivalent to two-lens optical Fourier transform 8-78943
- Mueller matrix photopolarimetric meas., Fourier analysis of single detected signal 8-74048
- multidielectric spectral filters, synthesis and realisation (*French*) 8-74998
- multiple image form. by addition of optical signals 8-66776
- object reconstruction from Fourier transform modulus 8-74852
- optical data processing, appls., book 8-90388
- optical imaging, systems theory appl. (*German*) 8-74851
- pattern recognition, Mellin transform method 8-63021
- phase accuracy of Fourier processor, coherence effects 8-90377
- phase computation from intensity meas. 8-66768
- phase error model for simple Fourier transform lenses 8-71037
- phase problems, image recovery from Fourier transform modulus 8-82918
- phase retrieval and polarisation identity 8-71042
- Photoelectric recording of optical fields by correlation processing 8-71048
- photoelectric registration of Fourier transform of optical field distrib. 8-82925

Fourier transform optics continued

- photopolarimeter with rot. polariser and analyser for meas. Jones and Mueller matrices 8-54435
 - pockels readout optical modulator, for optical/digital processing systems 8-79125
 - Pockels readout optical modulator, image and signal processing appls. 8-79123
 - power spectrum determination of random pattern, comparison between numerical and analogic processing methods (*French*) 8-58922
 - pseudocolour encoding, of holographic imaging, new technique 8-78963
 - radar ambiguity function, optical processing techniques 8-78938
 - radar ambiguity function display and one-dimensional correlation/convolution by coherent optical processors 8-78950
 - radioastronomical aperture synthesis imagery data optical reconstruction 8-69702
 - restoration, of optical objects using regularisation 8-78929
 - satellite derived cloud imagery, optical Fourier transform anal. 8-85749
 - signal detection methods, optical/digital components evaluation in hybrid processor 8-63026
 - signal processing in integrated optical format 8-50950
 - sky image coherent-optical processor for moving object location 8-78944
 - spatial convolution and correlation of optical fields via degenerate four-wave mixing 8-71044
 - speckle patterns, photographic recordings, fringes generated in Fresnel plane 8-66763
 - spectrum analyser, energy spectrum smoothing using multimode laser radiation 8-55311
 - spectrum analyser for radar signal processing 8-78942
 - spherically symmetric objects, reconstruction from slit-imaged emission, appl. to spatially resolved spectroscopy 8-78930
 - stack of dielectric layers, Fourier description of analysis and synthesis operations 8-94449
 - surface acousto-optic lens, Fourier and Mellin transform props. 8-78926
 - surface scattering rel. to microroughness, surface transfer function 8-58917
 - thermoplastic-photoconductor films for optical data processing 8-50875
 - transaxial topography, optical method, optical fibre, refr. index meas. (*French*) 8-66778
 - two dimensional unitary transforms for image processing 8-58928
 - two-dimensional, props., image sampling/scanning appl. 8-58929
 - underwater US video system (*German*) 8-94471
 - US blood flow spectral anal. using coherent optics 8-53459
 - virtual Fourier transform as analytical tool, appl. to single lens processing system 8-71036
 - wave field three-dimensional energy distrib. 8-71009
 - Wiener image filtering, object fast restoration after PSF degradation 8-90379
 - Wigner distribution function applied to optical signals and systems 8-50713
 - Zernike's three-slit interferometer, Fourier optical synthesis 8-65960
- Fourier transform spectroscopy**
- air pollution measurement 8-61564
 - airborne IR astronomical obs. 8-61747
 - analytical chemistry, IR spectroscopy appls. 8-61092
 - benzyl alcohol, C-C spin coupling, two-dimens. Fourier transformation 8-90194
 - cholesterol, proton-coupled ¹³C NMR spectrum, double Fourier transform 8-78725
 - complex biological systems, Fourier transform. IR obs. 8-68945
 - conference, Columbia, USA (June 1977) 8-58067
 - correcting errors in optical path difference, computational method 8-70192
 - data handling, minicomputer appls., errors 8-92543
 - demonstration for students 8-57722
 - dispersive, mode of operation of polarising interferometer 8-78003
 - dispersive reflectivity meas. on highly absorbing solids, using modular interferometer 8-89568
 - double resonance NMR, two- and three-spin systems 8-80249
 - far IR, appls. in laboratory, industry and environment 8-58069
 - far IR, meas. techniques and data reduction methods 8-62240
 - far IR dispersive Fourier transform spectroscopy, complex refr. index determ. of solids 8-92042
 - far IR Fourier spectroscopy, attainment of high resolution 8-86361
 - Fourier transform ion cyclotron double resonance, complicated ion-molecule reactions 8-80808
 - Fourier transform spectroscopy, Doppler-limited high-accuracy, 10⁶ samples 8-58068
 - gamma-ray spectral anal. using FFT (*Japanese*) 8-90047
 - gas chromatographic effluents, FT IR spectrometric identification 8-73091
 - gas dispersive Fourier transform spectrometry, using modular interferometer 8-89567
 - high resolution spectrometer, 0.005 cm⁻¹, for 0.6 to 100 μm spectral range 8-70204
 - industrial IR analysis using Fourier transform spectrometer 8-61091
 - interferometer, two beam, comparison of refl. and refr. optics in condensing element 8-77968
 - iodomethane, liq. (liq. mixtures), vibr. relax. and reorientation, symmetric C-H bending mode 1st overtone 8-62884
 - IR, absorbance compensation technique, anal. appls. 8-74083
 - IR, dynamic range improvement 8-89565
 - IR, focal shift photometric errors 8-86358
 - IR, real-time, for liq. chromatography detect. system 8-86357
 - IR, scatter eliminated spectrometry 8-89564
 - IR absorption technique for airborne atm. comp. meas. 8-61604
 - IR detector with gas chromatograph collects, stores spectral data, monitors functional groups 8-92560
 - IR spectrometer, dual beam 8-70201
 - IR spectrometer, for satellite, optical design problems (*German*) 8-86360
 - IR spectrometer, sensitivity 8-74082
 - IR spectrometers history, current status and commercial future 8-58072
 - lamellar-grating spectrometer, high resolution, for submm. region 8-70203

Fourier transform spectroscopy continued

- light divider phase distortion compensation improvement 8-58073
 liquid dielec. permittivity meas., sub-mm wave, using laser- and Fourier transform-spectrometry 8-95568
 Martin-Puplett interferometer, use as Fourier spectrometer and for OTF meas. 8-70179
 Michelson interferometer, all-refl., for far IR Fourier spectroscopy 8-70205
 Michelson interferometer for Fourier transform. IR spectroscopy 8-49914
 NMR, line-broadening mechanisms, dispersion-absorption plots 8-89512
 NMR, selective excitation, theory and appls. 8-77953
 NMR, two-dimens., sensitivity, comparison with one-dimens. FT NMR 8-78724
 nonlinear processing of interferogram 8-89553
 optical pulse Fourier transform spectroscopy, coherent transients 8-86974
 planetary atmosphere, remote sensor, high resolution Fourier transform spectropolarimetry 8-57469
 polarising submillimetric Fourier interferometer with achromatic internal modulation 8-65959
 polyacrylonitrile, thermal degradation, Fourier transform IR obs. 8-92474
 polymer system, Fourier transform IR spectroscopy appl. 8-58870
 potassium palmitate-d₃₁, spin-lattice relax., chain position and temp. depends. 8-68405
 Raman, signal modulation within elec. bandpass 8-82041
 rapid scan, use of opto-acoustic effect 8-78004
 resolution of Fourier spectrometer, determ. using solid-state Fabry-Perot etalon 8-89569
 secondary interferograms, effect on reconstituted spectra (*French*) 8-82043
 selective modulation interferometric spectrometer, theory, design 8-58054
 silane, coupling agent on E-glass fibre, structure, Fourier transform infrared spectroscopy 8-60643
 silane, coupling agent on porous silica, Fourier transform infrared spectroscopy 8-60642
 solid mixture charact. discrete Fourier transform, spectroscopy, computer simulation 8-63859
 spin echo, rot., in solids, anisotropic interaction recovery 8-68410
 student laboratory experiment using inexpensive interferometers 8-49609
 subtractive dispersion monochromator for Fourier transform spectroscopy (*French*) 8-83079
 surface analysis using FT-IR spectroscopy 8-76943
 time resolved, improvements 8-58070
 transient system, IR spectroscopic techniques 8-58071
 visible and UV range 8-58060
 CO₂, 30°1₁₁←00°0 band, meas. at different temps. of absolute intensities, line half-widths and broadening by Ar and N₂ 8-86865
 CO₂, 30°1₁←00°0 and 30°1_{1v}←00°0 bands, absolute intensity meas. at different temps. 8-86864
⁶³Cu, ⁶⁵Cu, Fourier transform NMR studies 8-94262
 H₂¹⁸O, line positions and intensities, $\nu_1 + \nu_2$ and $\nu_2 + \nu_3$ bands 8-74656
 NO₂+ROO→ROONO₂, (R=C_nH_{2n+1}), Fourier transform IR spectroscopic meas. 8-53194
 P₂, b²Π_g-w²Δ_u and A¹Π_g-W¹Δ_u systems, IR emission spectrum 8-94244

Fourier transforms

- see also fast Fourier transforms; Fourier analysis; Fourier transform optics*
 acoustic holography, numerical image reconstruct., applicability conditions for Fourier transform (*Japanese*) 8-59208
 acoustic system identification, from multiple input/output data, comment and reply 8-83179
 action functional in distrib. spaces 8-54207
 astronomical observations, transforms of data sampled at unequal intervals 8-69697
 cepstrum performance, improvement through windowing of log spectrum 8-89303
 coagulating dispersions, light scatt. data, Fourier inversion anal. 8-76932
 contrast profile method of vector mag. field meas., Fourier transforms appl., for solar meas. 8-53839
 cosmic ray spectra, leakage error 8-89023
 crystal structure least squares refinement technique based on fast Fourier transform algorithm 8-91197
 crystallography, electron distributions, aspherical-at. least squares refinements combined with Fourier methods 8-71633
 cylinder, composite circular, transient thermal stresses 8-79217
 drag on sphere accelerating rectilinearly in elastico-viscous fluid, Fourier transform technique 8-51145
 electron image formation, partial coherence and inelastic scatt. 8-58897
 EM radiation scattering by dielectric spheroids and ellipsoids, integral eqn. soln. 8-85622
 EM wideband freq. response conversion to transient response using segmented transform. 8-77349
 Euler-Lagrange eqns., generalised solns. 8-54206
 finite length theoretical gravity anomaly interp. 8-61299
 generalised Fourier transforms 8-54205
 generalised X-ray scattering factors, two-centre case with Slater type orbitals 8-79491
 geodesy, altitude obs. Fourier transform. (*German*) 8-61312
 geomagnetic anomalies, interpretation with end-corrected Fourier transforms 8-65418
 gravity anomalies due to faults, general expression for Fourier transform 8-61300
 heteronuclear double-resonance spectra, modulations 8-86897
 image reconstruction, Fourier techniques evaluation in relation to number of X-ray sums 8-77112
 infinite strip, with elliptical hole, definition of stress (*Russian*) 8-55562
 liquid structure factor, pair correlation function errors, dilute hard sphere approx. 8-79514
 maximum likelihood spatial filtering examples 8-63038
 Maxwell fluid, unsteady flow past flat plate, transform technique 8-59428

Fourier transforms continued

- molecular structure, forces acting upon nuclei, Fourier transform calcs. 8-86774
 nonlinear, evolution equations soln. using spectral transform method 8-57745
 nonlinear evolution equation with linearly x-depend. coeffs., spectral transform, single soliton soln. 8-57746
 numerical, singularity expansions and product integration 8-89316
 Oldroyd liquid, unsteady flow between two porous walls 8-63452
 optical imaging, Fourier transform, using SAW memory-correlator 8-83090
 optical systems, correlation coeffs. of planar sources and their far fields 8-66750
 orthorhombic base centred lattices, Fourier transform of dipole-dipole interaction 8-76404
 orthorhombic lattices, Fourier transform. of dipole-dipole interaction 8-64334
 polystyrene, sol, light scatt. data, Fourier inversion anal. 8-76932
 radio astronomy, direct transform hardware processing of rot. synthesis data 8-85856
 radio astronomy, direct transform hardware processing of rot. synthesis data 8-85857
 scalar wave diffraction by two parallel slits in plane 8-49671
 scattering experiments, deconvolution of thermal averaging using integral transform methods 8-92442
 seismic data migration by Fourier transform 8-77341
 shallow water wave propagation, Pekeris operator resolvent 8-90575
 strings, stretched, vibr. control by an external distributed force 8-83308
 two-dimensional neutron diffusion eqn. for triangular region 8-78432
 US image reconstruction processing limitations 8-73184
 wave function determ. by position and momentum distributions 8-93548
 2-zinc insulin, rhombohedral, cryst. struct. refinement, experience with fast Fourier least squares 8-92595

fractionation *see* distillation**fracture**

- see also brittle fracture; crack-edge stress field analysis; cracks; creep fracture; ductile-brittle transition; ductile fracture; embrittlement; fatigue; fracture toughness; stress corrosion cracking*
 acoustic emission, phenomenological model, calc. of intensity 8-85110
 activation of fracture mechanisms 8-63380
 adhesive fracture mechanics, review 8-60773
 adhesive fracture specimen, DCB, crack tip stress field anal. 8-55602
 alite paste, mature, microstructure study by SEM, TG and X-ray diffr., corrosion 8-92381
 amylose, micromech. fracture anal. 8-68784
 arbitrary criterion, weakest link theory reformulated 8-90786
 arteriograph opening characts. as fracture phenomena 8-92746
 biaxially fibre reinforced composites, two dimens. mixture theory, dynamic crack appl. 8-87301
 biological material freeze-fracture preparation for SEM 8-61290
 bonded plate or membrane strips, exam. of adhesive fracture 8-59342
 bone morphology and fracture, exam. 8-57036
 brass, textured thin specimens, fracture 8-60816
 α-β brass, two-phase bicrystals, plastic deform. and fracture mechanism 8-84898
 bulk cold working processes, fracture criterion 8-56775
 case hardened components, exam. of fracture surface by TEM. (*Japanese*) 8-52949
 ceramics, microstructure dependence of mechanical behaviour, fracture energy and path 8-88533
 combined bend mode specimens, calc. of stress intensity factors 8-79284
 combined mode cracks, fracture criteria 8-79285
 composite discs, fibre-reinforced, rotating strength, stress distrib., failure criterion rel. to mould process 8-76701
 composite material, fracture and fatigue, review 8-68781
 composite materials, physical nature of fracture 8-80653
 compression failure anal., glassy materials investigation 8-55608
 concrete, crack growth, computer simulation using Monte Carlo method 8-76764
 concrete plates, cracked, and beams existence of critical strain energy release rate 8-76765
 crack, stress intensity factor, near doubly riveted stiffeners 8-67152
 crack growth, quasistatic, nonlocal model, thermodynamics of irreversible processes basis 8-83324
 crack growth determination, in mixed mode loading system 8-67105
 cracked holes and rings, loaded with polynomial crack face pressure distrib., stress intensity factor solution 8-83335
 cracked lug, test and analysis 8-67153
 cracked thick walled cylinder, elastic plastic fracture anal. under displacement controlled loading 8-67119
 criteria, integral eqn. 8-79279
 crystal cleavage due to dislocation tilt wall splitting 8-91377
 debond dynamics for elastic strip, Timoshenko beam props. and steady motion 8-55604
 dielectric materials, electromagnetic radiation in crack formation process, exam. 8-76771
 Earth upper mantle, micromechanisms of flow and fracture 8-69331
 elastic media, longit. shear fracture, dynamical problem for region with curvilinear cuts 8-81842
 elastic-perfectly plastic material, theory of stable crack growth 8-79272
 elastic-plastic crack tip characterisation, relation to R-curves 8-56767
 elastic-plastic materials, finite deformation anal. of crack-tip opening 8-51126
 epoxy resin, fracture energy under plane strain conditions 8-80624
 epoxy resin-Al alloy 5086, scarf joint test specimen, mixed mode adhesive fracture, bond angle effect 8-68768
 ferrous material fractured surface exam., oxide scale removal 8-95886
 fibre reinforced composite failure analysis by acoustic emission 8-80691
 fibre reinforced plastic, fracture mechanism study, cumulative failure model 8-92315
 fibre reinforced plastics, exam. of strength criteria 8-75105
 film, stability and rupture using perturbation analysis 8-79911
 flow of solute atoms near crack tip, time dependent, exam. 8-75722
 generalised three dimensional work of fracture specimen, stability considerations 8-67140

fracture continued

geological faults, fracture, creep and strain 8-69345
 glass bead, impact fracture (*Japanese*) 8-92338
 glass fibre reinforced epoxy, short aligned fibres, mech. charact., SEM and optical obs. 8-72761
 glass plates, biaxially stressed, anal. of localised impact damage 8-68772
 glass/C reinforced epoxy resin, hybrid effects, conditions for positive or negative effects vs. rule of mixtures, mech. props. 8-68769
 graphite, fracture, stress gradient effect 8-92321
 hydrogen embrittlement, role of plastic fracture processes, exam. 8-60810
 ice shelves, floating, tidal flexure cracks, fracture mechanics 8-69368
 ideal fibre reinforced composites, finite plane deformation and energy dissipation 8-79274
 impacted pretensioned plate, dynamic finite element and photoelastic analyses 8-67111
 Indiana limestone fracture toughness, confining pressure effect 8-57197
 initiation under metal working conditions 8-64662
 integral I and elastic-plastic fracture criteria (*Chinese*) 8-75100
 integral J₁, calculation by finite element analysis 8-67129
 intensity factor, single edge V-notched plates in tension 8-90782
 intergranular, low temp. mechanism 8-60795
 internal heat source action in material 8-67025
 ionic crystals, in mag. field 8-59855
 J-integral evaluation for CT specimen 8-67131
 kinetics, static, dynamic loading, comparison 8-87738
 lens, Schott S-1005, static fracture resist. rel. to thickness 8-81063
 limiter materials, for Doublet III fusion research machine, selection 8-55026
 matched asymptotic expansions, in nonlinear fracture mechanisms 8-51127
 material divagation, appl. to fracture 8-67109
 material minimum lifetimes, failure probability after proof testing, exam. using Monte Carlo method 8-79273
 of materials, conf., Waterloo, Canada (June 1977) 8-56763
 mechanics, linear elastic, appl. to crack stability in brittle struct., elastic-plastic conditions 8-90800
 mechanics, variational bounds, qualitative method. 8-67134
 mechanics, variational bounds and qualitative methods 8-79283
 mechanism maps, exam. of development 8-56764
 metal, plasticity under hydrostatic pressure (*Russian*) 8-68726
 metal, stress-induced EM effect, phys. model 8-55909
 metal failure, due to hydrostatic pressure, exam. of kinetics 8-52944
 metals, effect of hydrostatic pressure and stress on plasticity 8-52907
 methodological questions in determ. of failure criteria in complex stressed states and complex loading (*Russian*) 8-67089
 nonlinear fracture mechanics, exam. of J-integral criterion for crack growth initiation 8-60775
 nonlinear mechanics 8-79261
 notched fibre reinforced composites, tensile fracture 8-52991
 nuclear reactor pressure vessel ZR-6M rupture test using scaled simulation (*Hungarian*) 8-89964
 nuclear reactor technology, fracture problems 8-78472
 nuclear reactor valve bellows, effect of service parameters on fatigue life and fracture 8-58348
 pacemaker, lead wire fracture 8-57134
 pearlite, SEM obs. of tensile deform. and fracture 8-84897
 photoelastic determination, of mode I stress intensity factors 8-90781
 pin loaded single edge notched tension specimens, K-COD relationship 8-67133
 plastic deformation, appl. of continuum theory of dislocations fracture mechanics 8-67767
 and plastic deformation 8-88497
 plastic materials, crack resistance (*Russian*) 8-63377
 PMMA, critical stress-intensity factor, determ. under mixed mode loading conditions by shadow optics 8-68868
 PMMA, fracture surface parabola markings, temp. 8-52969
 PMMA, struct.-prop. relationship between mol. wt. and fracture surface energy 8-80633
 political and social decision making rel. to fracture, failure, risk anal. and safe design 8-77661
 polybutadiene, elastic fracture, polymer chain entanglement criterion 8-79290
 polycarbonate, plane strain fracture energy instability and mixed mode crack prop. 8-68775
 polymer, drawing properties, role of interfibrillar tie mols. 8-76706
 polymer, failure, book 8-92361
 polymer, fracture time variability, endochronic prediction 8-76734
 polymer crystals, deform. and fracture, submicrocrack nucleation and supermod. struct. 8-52918
 polymers, solid-liquid state transitions, state before breakdown 8-63842
 polypropylene fibrillated film reinforced cement, loading capacity, cracking 8-72759
 polystyrene, elastic fracture, polymer chain entanglement criterion 8-79290
 polystyrenes, monodisperse, static and dynamic props., mol. wt. effect 8-84938
 portland cement paste, microstructure study by SEM, TG and X-ray diff., corrosion 8-92381
 precipitative processes and intercrystalline failure, quantitative methods (*Czech*) 8-60672
 pressure diecast automatic components, processing condition effect on performance 8-88623
 pressure vessels, thin-walled, containing surface flaws, fracture mechanics and acoustic emission exam. of failure 8-84981
 profilometric anal. 8-88600
 propagating rectangular fracture in semi-infinite elastic medium 8-57168
 quasi static crack growth, in sheet materials 8-67106
 reactor containment liner seismic reliability under statistical uncertainty, cracking 8-89948
 reactor primary system under operating and accident conditions 8-66342
 recognition from stereo photographs 8-54140
 refractory composites, fibre reinforced, directionally solidified tensile tests, in HVEM, deform. and fracture (*French*) 8-68785
 Rochelle salt, depend. on mechanoluminescence on charge prod. during fracture 8-88370

fracture continued

rock, fracture mechanics approach to in situ stress field determ. via hydrofracturing 8-81435
 rock, symmetrically extending plane crack, self-similar pressure profiles 8-69340
 rocks, fracture regularities with internal friction and dilatancy 8-85537
 rollers, steel casting installation, effect of thermal stresses on fracture characts. 8-64650
 sea ice, failure by compression (*Japanese*) 8-88841
 separation energy rate for crack advance 8-56765
 sheet metal forming, material behaviour 8-95787
 singular crack borders, constitutive preps. 8-67108
 slitlike crack arrays, plastic and strain hardened materials, fracture characts. 8-90798
 snow, uniaxial tension, strain rate and fracture (*Japanese*) 8-88855
 solid composite propellants, fracture criterion, fracture time computation 8-75106
 spheres at high pressure, contact stresses and spreading resistance 8-71296
 stable crack-growth, fracture criteria, numerical approach 8-67104
 steel, austenitic heat-resisting, deformation and fracture rel. to grain-boundary reaction nodules 8-80591
 steel, austenitic stainless, tensile fracture, phase transform. effect, comparison of stable and metastable phases 8-60798
 steel, Ck 45, alternating bending, fracture surface appearance (*German*) 8-52995
 steel, Cr-Mo-V, press. vessel, fracture, effect of tempering 8-60799
 steel, delayed fracture, hydrogen and impurities 8-84988
 steel, forged axle spindle, fractographic anal. of shear fracture 8-68821
 steel, high speed, matt-facet fractures (*Chinese*) 8-95793
 steel, notched bar, plastic zone determ. near rupture (*French*) 8-88515
 steel, stainless, 316, nuclear fuel cladding, crack nucleation 8-72864
 steel, stainless, duplex, hot ductility and fracture mechanism 8-60731
 steel, stainless, type 304, elastoplastic fracture mechanics for reactor piping 8-68777
 steel, structural, influence of deform. heat on the mech. props. (*German*) 8-84904
 steel 81B45, chevron fracture in tube reduction by spinning 8-64664
 steel shot, cast, impact fracture (*Japanese*) 8-92338
 steel welding, development and results of an instrumented restrained cracking (IRC) test (*German*) 8-85060
 stress intensity factor, of simplified geometries of structural parts, experimental determ. 8-68866
 stress intensity factors, UNCLE finite element system calcs., appls. in fracture mechanics 8-67098
 stress intensity factors by enriched finite elements 8-90774
 structural materials in complex stress state, criterion for strength at low temp. 8-71292
 teaching, description of Open University course 'Materials under Stress' 8-57720
 teaching in universities 8-77645
 theory, future trends and appl. 8-90799
 thermoplastics, homogeneous, fracture under plane strain and plane stress conditions 8-52941
 viscoelastic bodies, adhesion and fracture mechanics, review 8-83336
 Weibull statistical theory 8-51132
 Ag-MgO, laws of plasticity of dispersion strengthened materials 8-84832
 Al alloy, laminates, fracture of bonded 2024-T3/7075-T6 8-56722
 Al alloy 7075, fracture props., effect of thermomechanical treatment 8-60793
 Al alloys, 7075-T6, H₂ effects and Cd segregation to grain boundaries 8-84764
 Al alloys, deformation processes in sheet materials, application of failure maps 8-56718
 Al alloys, limiting plastic props. (*Russian*) 8-88504
 Al alloys 7178 and M580, chevron fracture in tube reduction by spinning 8-64664
 Al, anodised, photostimulated exoelectron emission, effect of oxide thickness 8-80461
 Al, fracture due to shock waves leaving surface, shear stresses 8-51128
 Al-Al₂ eutectic, abrasive fragmentation (*Czech*) 8-64715
 Al-Cu-Mg-Mn (4.5, 1.5, 0.6 wt.%), alloy 2024-T3, exam. of residual strength of plate containing crack, fracture anal. 8-90792
 Al-Cu(Mg), age-hardenable, US cavitation erosion mechanisms, effects of comp. and heat treatment 8-53002
 Al₂O₃, dense, surface segregation of Ca under exposure to steam and steam-CO 8-85013
 C fibre reinforced composites, kinking as structural degradation mode 8-52893
 C stripper foils, lifetime enhancement, heavy ion bombardment 8-94156
 β-CaSiO₃ fibre, continuous unidirectional crystallisation from melt 8-95739
 Cu, fracture due to shock waves leaving surface, shear stresses 8-51128
 Cu-polymer composite foils, fracture surface exam. by XPS (*German*) 8-84992
 Fe, cast, heated in CO atm., obs. cracks around graphite flakes (*Japanese*) 8-84974
 Fe, fatigue fracture strength and failure, at 77K after cyclic loading at room temp. 8-84996
 α-Fe, grain boundary segregation of C, N₂ and C Auger spectroscopy 8-72778
 Fe, grey cast, deform. and fracture regions in microzones (*Russian*) 8-80585
 Fe, powder, consolidated, exam. of mech. and electrical props. 8-56599
 Fe, whisker, H₂ effect on deform. 8-68755
 Ir-W (0.3 wt.%), P segregation to grain boundaries, effect on high temp. ductility 8-95754
 Mo fibre reinforced Al and Al alloys, SEM study (*Slovenian*) 8-84923
 Ni-Al-Cr, precipitation-strengthened, mechanical props. 8-84968
 Ni-B, hydrogen embrittlement, effect of B additions (*Japanese*) 8-84973
 SiN film, on Si substrate, thermal stresses and cracking resist. 8-63958

fracture continued

- Si₃N₄ film, on Si substrate, thermal stresses and cracking resist. 8-63958
 SiO₂ film, on Si substrate, thermal stresses and cracking resist. 8-63958
 Sn-Pb (38 wt.%), graphite fibre reinforced, effect of interface on fracture characts. 8-76723
 Ti alloy, VT23, ht. treatment effects on fracture (*Russian*) 8-80623
 $\alpha + \beta$ Ti alloys, fracture, influence of phase comp. in VT16 and VT9, quenching effects (*Russian*) 8-56665
 Ti-Al-Sn-Zr-Mo (6,2,45 wt.%), surface cracking under unidirectional loading 8-56753
 Ti-Al-V (6,4 wt.%), surface cracking under unidirectional loading 8-56753
 Ti-Mo, fracture behaviour and tensile props. at elev. temp. 8-60822
 V-Mo, effect of ion plated Mo on corrosion in liquid Na, mech. props. 8-53020
 WC-Co, various combinations, fracture characts. in bending, compression, and toughness tests 8-60808
 Zr-Nb (2.5 wt.%), cold worked, press. tubes, secondary cracking obs. 8-80630

fracture strength *see fracture toughness***fracture strength testing** *see fracture toughness testing***fracture toughness**

- see also notch brittleness; notch ductility; notch strength*
 alloy, high temperature, mechanical, thermal and corrosion props. 8-95763
 alumina, grain size and fracture toughness, effect of fracture toughness test methods 8-72883
 alumina, multiaxial fracture, general approach to statistical anal. 8-90785
 amylose, micromech. fracture anal. 8-68784
 Araldite B, crack arrest toughness determination 8-72867
 asbestos fibre reinforced Portland cement analytical fracture resistance curve expression 8-76756
 borsic fibre reinforced Ti, unidirectional, K-calibration and compliance curves 8-88518
 brass, crack opening displacement, rel. to flow stress 8-68810
 brittle circular disc under impact loading, fracture mech. 8-88514
 brittle cracks, stability, propagation, fracture mech. (*Czech*) 8-79257
 brittle fracture, structure design, method of calculation 8-72869
 carboxyl terminated butadiene nitride-diglycidyl ether of bisphenol A epoxy resin, struct. and mech. props. 8-52901
 cemented carbides, indentation fracture, surface fracture toughness nature 8-60849
 ceramics, fracture toughness, exam. of methods of enhancing, merits and limitations 8-60771
 concrete cylinders, fracture, fluid pressure testing using H₂O and N₂ gas 8-60750
 constitutive equations of continuum creep damage mechanics 8-67054
 crack extension criterion of maximum shear or principal stress 8-79278
 crack length dependence 8-67120
 dental restorative materials, empirical eqn. including fracture toughness for friction 8-61283
 elastic-plastic solid containing holes in vicinity of crack tip, finite element anal. 8-67147
 engineering structures, welded exam. of fracture processes, review 8-60777
 epoxy resin, low temp. irradiation effects on mechanical props., use in superconducting magnets 8-60737
 evaluation method (*Japanese*) 8-92330
 fibre reinforced composites, cracking and fracture, review 8-60772
 fibrous composite, short steel wire reinforced (polymer impregnated) concretes, cracking and toughening 8-80626
 float glass, toughening by ion exchange, selection of technology parameters 8-84757
 fracture mechanics, recent theoretical and experimental developments, review 8-60776
 fusion reactor materials, fracture resistance 8-82515
 glass bead, impact fracture (*Japanese*) 8-92338
 graphite, failure criterion, J-integral critical value 8-84999
 graphite fibre reinforced panels, low energy impact testing 8-72845
 graphite reinforced epoxy resin, average stress failure criterion appl. 8-88519
 high strength materials, exam. of flow localisation and fracture toughness 8-60764
 high strength structural mats., microstruct. influences on fatigue and fracture resist. 8-56728
 Homalite 100, dynamic fracture toughness 8-60740
 hydrostatic pressure effects on fracture, exam. 8-60779
 impact damage in elastic response regime 8-71785
 impact test, finite element analysis 8-68806
 Inconel alloy 718, exam. of struct., properties and continuum synthesis of ductile fracture 8-76736
 LMFBR, effect of cracks in fast neutron embrittled hexagonal subassembly ducts 8-74446
 metallic alloys, fracture toughness and fatigue crack growth data, compendium of sources 8-84963
 multiaxial, general approach to statistical anal. 8-90785
 notched beam, fatigue crack emanates from notch root, fracture strength 8-72866
 parameters J and G^A, effect of load biaxiality 8-67128
 PFE, impact fracture toughness, rate effect 8-56741
 plastic material, material scale length as meas. of fracture toughness in fracture mechanics 8-68763
 plate, thin, fracture toughness from plastic deform. induced thickness contraction 8-75109
 PMMA, effect of mol. orientation on fracture toughness 8-52992
 PMMA, fracture toughness under biaxial stress 8-76760
 PMMA based composite (acrylic bone cement), effect of BaSO₄ and glass particle dispersions, on fracture behaviour 8-76753
 PMMA-filled with SiO₂, degrading effect of filler on polymer fracture energy 8-52939
 polycarbonate, dielec. relax. and ductile brittle transition 8-52438
 polyethylene, filled with SiO₂, degrading effect of filler on polymer fracture energy 8-52939
 polyethylene, impact fracture toughness, rate effect 8-56741
 polypropylene, crystalline, morphological aspects of crack growth 8-76761

fracture toughness continued

- polypropylene, homopolymer, effect of mol. orientation on fracture toughness 8-52992
 pressure vessel, strength analysis, by thermal shock 8-68819
 reactor graphite, thermal shock fracture toughness eval. by arc discharge heating 8-72835
 reactor graphite, up to 2600°C 8-68760
 refractories, role of fracture toughness in thermal shock resistance (*French*) 8-80618
 rock, deformation and fracture under general triaxial stress states, anisotropic dilatancy (*Japanese*) 8-56750
 S glass-Ni sphere composite, exam. of crack shape and fracture toughness 8-72886
 small crystals, fracture strength and triboluminesc. 8-64420
 β -spodumene-mica glass ceramic, thermal expansion thermal shock and moduli of rupture and elasticity 8-60736
 steel, alloy, C-Cr-Mo-V, exam. of fracture toughness and critical flow anal. 8-72848
 steel, alloy, crack arrest toughness determination 8-72867
 steel, alloy, cyclic strength after strain hardening and tempering, precip. hardened 40FT and 40 8-52988
 steel, alloy, Fe-Cr-Mo-Si-V, various steels, short rod stress intensity factor tests up to 700K, exam. 8-60815
 steel, alloy, Fe-Cr-Ni-Mo-Al, (13, 8, 2, 1, wt.%), H₂ effects on fracture, exam. 8-60809
 steel, alloy, maraging, 18% Ni, effect of solution and ageing treatments, on microstruct., tensile props., fracture toughness 8-80648
 steel, alloy, maraging, 250-grade, ductility and toughness of hot isostatically pressed powder 8-52925
 steel, alloy, Mn-Si-C, exam. of fracture toughness for sheets, using linear elastic fracture mechanics 8-56762
 steel, alloy, Ni (5.5 wt.%), fatigue fracture toughness, crack propag., at low temp. 8-68823
 steel, alloy, toughness evaluation inconsistency of AISI 4340 austenitised at increasing temp. 8-52982
 steel, alloy, type 4340, fracture toughness, effect of partially dissociated N₂ 8-80642
 steel, alloy 4340, fracture and high temp. props., 533K to 1255K 8-60821
 steel, austenitic, AISI 4340, effect of step quenching on microstruct. and fracture toughness 8-84834
 steel, austenitic, fracture toughness props. of A533B, prior austenite grain size effect 8-60780
 steel, austenitic stainless, fracture toughness and transition temp., T₅₀, effect of cooling rate and supercooling temp. 8-84987
 steel, C, crack opening displacement, rel. to flow stress 8-68810
 steel, C, crack resistance, preliminary loading condition effects in crack appl. 8-56739
 steel, C, spheroidised, fracture toughness, cementite particle effects, optic and electron obs. 8-60785
 steel, C, tempered martensite embrittlement, and retained austenite, exam. 8-56754
 steel, C and alloy, notched beam, fatigue crack emanates from notch root, fracture strength 8-72866
 steel, cast, effect of non-uniform struct. on props. 8-84850
 steel, CC Cr-Ni, soaking at forging temp., effect on struct. and mech. props. (*Czech*) 8-64628
 steel, CC Ni-maraging weld metal, increasing fracture toughness by heat treatment 8-72871
 steel, constructional, fracture toughness in cyclic loading 8-72860
 steel, Cr, cast, fracture toughness and fatigue crack propagation, structural components of hydro-turbines, in water and air 8-68822
 steel, Cr-Mn, powder forged, fracture processes and fracture toughness 8-72870
 steel, Cr-Mo-V, medium strength, correlation between crack initiation, propag. and microstruct. 8-60787
 steel, CrMoV, compact tension specimen, thickness effect 8-68764
 steel, CrMoV, failure in post yield regime using single edge notched tension specimens 8-68765
 steel, die, with high heat resist. and toughness 8-84989
 steel, fracture micromechanisms, fracture toughness, exam. 8-56766
 steel, fracture toughness and dynamic strength, surface active agent effects (*Russian*) 8-56812
 steel, fracture toughness testing, obs. of crack initiation and stable growth processes (*Japanese*) 8-52954
 steel, high strength, alloy, initiation of cracks at delayed fracture, AE study 8-72868
 steel, high strength, low alloy, mech. props. 8-60739
 steel, high strength, low alloy, rare earth treated, ductile fracture mech. 8-64658
 steel, high-speed, fracture toughness of powder metallurgy vs. conventionally produced steels 8-64647
 steel, hydrogen embrittlement, experimental test of Petch-Stables theory 8-60738
 steel, low alloy, exam. of fatigue crack growth, and Paris Law parameter relationship 8-92343
 steel, low alloy, high strength, correlation between fracture toughness, tensile props., fracture morphology 8-60789
 steel, low alloy, naval, stretch zone width meas., COD for ductile crack initiation 8-68813
 steel, low alloy, St 52-3, structural, fracture toughness, fatigue precracking and grain size effect 8-60782
 steel, low alloy, thermally fatigued, fracture toughness 8-72872
 steel, low alloy, type SNCM 8, rotor disc, exam. of fracture, using a J integral approach 8-92352
 steel, low C, martensitic, fracture toughness variations during tempering 8-60812
 steel, low S, ESR, overheating effect on toughness 8-52860
 steel, low strength, blunting effects on fracture toughness 8-68814
 steel, low-alloy sheet, welded hydraulic turbine volute chamber, strength and toughness 8-68820
 steel, maraging, (18 wt.% Ni), solution annealed, exam. of cryogenic tensile, fatigue, and fracture props. 8-92311
 steel, maraging, fracture toughness data, comparison with equivalent energy and energy per unit area data 8-52965
 steel, martensite-ferrite combined microstructure, two-phase, tensile fracture strength 8-60783
 steel, martensitic, delayed fractures suppression, by neutron irradiation (*Czech*) 8-67743
 steel, material scale length as a measure of fracture toughness in fracture mechanics of plastic materials 8-68763

fracture toughness continued

steel, medium strength, fracture toughness eval. of small specimens 8-60762
 steel, mild, plate, effect of striking velocity on perforation energy 8-68818
 steel, Mn, as rolled bainitic, tensile, impact and machinability props., transport appl. 8-88503
 steel, Mo-V, creep rupture strength, heat treatment effects (*German*) 8-72834
 steel, Ni, cross girder connections, fatigue strength, design stress 8-64700
 steel, Ni-Cr-Mo-V, turbine rotor shaft, fracture toughness, validity criterion for K_{Ic} 8-72861
 steel, Ni-Mo, powder forged, fracture processes and fracture toughness 8-72870
 steel, nuclear pressure vessel, type A533B-1, three point bending, yield stress, exam., Charpy V-notch and precracked specimens 8-92310
 steel, prestrained pressure vessel, correl. between dynamical toughness characteristics 8-68816
 steel, reactor vessel, neutron irradiation effect on brittle fracture characts. (*Slovak*) 8-50254
 steel, stainless, austenitic, CC Ni-Al, γ -phase, fracture mechanical aspects of abrasive friction, wear, chip formation 8-72865
 steel, stainless, ferritic, subjected to 475°C embrittlement, exam. of fracture toughness 8-84982
 steel, structural, rel. between static and dynamic fracture toughness 8-68815
 steel, structural 8-68808
 steel, thermal shock cracking, fracture mechanics and fractographic exam. (*Japanese*) 8-52964
 steel 40Kh, surface working effects on crack resist. (*Russian*) 8-56734
 steel plates, C and alloy steels, comparison of dynamic tear and Charpy V notch impact props. 8-92357
 steel shot, cast, impact fracture (*Japanese*) 8-92338
 stress intensity factor calc., infinite similar element method 8-79277
 structural alloys, fracture at temps. approaching absolute zero 8-72877
 thermoplastics, effect of mol. orientation on fracture toughness 8-52992
 thin skin structures, residual strength prediction, using crack resistance curves 8-90795
 $\alpha+\beta$ Ti alloys, prior β grains and α platelet morphology, exam. 8-76679
 toughness-porosity phenomena 8-72874
 wear resistance rel. to specific fracture energy for various materials (*Russian*) 8-85005
 yield zone form., fracture resistance, influence of specimen configuration 8-68817
 Al alloy, D16, Fe and Si impurity effects on K_{Ic} 8-84990
 Al alloys, fracture micromechanisms, fracture toughness, exam. 8-56766
 Al alloys, fracture toughness under plane stress 8-92316
 Al alloys, quenching rate rel. to mech. props., residual stresses, optimum quench coolings (*French*) 8-64562
 Al-Cu-Mg-Mn (4.5, 1.5, 0.6 wt.%), thin sheet, exam. of fracture toughness, and fatigue crack growth 8-92353
 Al-epoxy adhesive systems, opening and edge-sliding fracture toughness 8-95805
 Al-Mg alloy AMg6, mech. props. of welded joints, impurity effects 8-95789
 Al-Mg-Si-Mn, Mn addition effects on fracture 8-60791
 Al-Zn-Mg, effect of microstruct. on localised shear failure 8-52996
 Al-Zn-Mg-Cu, alloy 7075, effect of purity level, dispersoid type, heat treatment, on fracture toughness 8-80636
 Al-Zn-Mg-Cu alloy, laminated, adhesively bonded alloy 7075-T6, exam. of fracture resistance 8-76754
 Al_2O_3 , fracture toughness specimen, appl. of wedge indentation technique for precracking 8-85087
 B fibre reinforced Al, fracture mechanical study, unidirectional composites 8-88520
 B fibre reinforced Al, unidirectional, K-calibration and compliance curves 8-88518
 B fibre reinforced epoxy, fracture mechanical study, unidirectional composites 8-88520
 BN, toughening by stress-induced phase transforms. 8-80635
 Fe alloy, fracture toughness of cryogenic temp. 8-72878
 Fe, cast, ferritic SG ductile fracture initiation and propagation 8-64661
 Fe, cast, rare-earth-Mg nodular, fracture toughness and fatigue (*Chinese*) 8-95791
 Fe, porous, density, elec. cond., Young's modulus, toughness 8-64645
 Fe-Cr (26 wt.%) effect of Ni content and austenite phase, on low temp. toughness and embrittlement 8-60754
 Fe-Mn-Ni, fracture toughness, thermomechanical treatment effects 8-60794
 Fe-Ni, fracture toughness at cryogenic temp. 8-72878
 Fe-Ni-C (9, 0.1 wt.%), effect of intercritical tempering on impact energy, exam. of mech. props. 8-52861
 Fe-Ni-Cr-Ti-Mn-Mo, (25.8, 14.04, 2.17, 1.27, 1.30 wt.%), superalloy A-286, precipitation hardening, exam. of fracture toughness and mech. props. 8-92355
 $K_2O-Al_2O_3-SiO_2$ system, crystallisation of glasses in primary phase field of leucite 8-67658
 Na_2O-SiO_2 glass, coated with SnO coeff. of friction and fracture toughness 8-80657
 Ni-Fe solid soln., precip. hardened, paramag.-ferromag. transition on ageing 8-52255
 Ni(Cr)-Mo-V, fracture toughness data, comparison with equivalent energy and energy per unit area data 8-52965
 SiC, fracture toughness specimen, appl. of wedge indentation technique for precracking 8-85087
 Sn-Pb (38 wt.%), graphite fibre reinforced, effect of interface on fracture characts. 8-76723
 steel, Cr-Mo-V, charact. investigation 8-72857
 Ti alloy, VT23, ht. treatment effects on fracture (*Russian*) 8-80623
 Ti-Al-Mo-Cr (4.5, 5, 1.5 wt.%), CORONA-5, effect of microstructure and heat treatment on fracture 8-60805
 Ti-Al-Sn (5, 2.5 wt.%), fracture mechanism at cryogenic temps. 8-64642
 Ti-Al-V (6.4 wt.%), strongly textured, influence of cryst. orientation on fracture toughness 8-84951

fracture toughness continued

UAl_2 -Al dispersion fuel, effect of reactions on Young's modulus and rupture strength (*German*) 8-62596
 WC-Co, comparison of indentation crack resistance, and fracture toughness 8-76739
 WC-Co, various combinations, fracture characts. in bending, compression, and toughness tests 8-60808
 WC-Co alloys, single edge notched beams, exam. of fracture toughness 8-52975
 WC-Co cemented carbide, fracture toughness meas., model for variation with microstruct. 8-60806
 WC-Co cemented carbides, high temp. transverse rupture strength, effect of domain size of binder phase (*Japanese*) 8-92329
 WC-Co hard alloy-steel welds, effect of intermediate layer composition on structural changes and mechanical properties 8-60616
 WC-Ta-C, cemented carbide, strength improvement by hot isostatic pressing 8-84969
 ZrO_2 , containing metastable tetragonal phase, stress induced phase transform. effect on props. 8-68683

fracture toughness testing
 see also notch testing
 acoustic emission, inspection technique 8-68860
 alloys, influence of test piece geometry 8-84951
 alumina, grain size and fracture toughness, effect of fracture toughness test methods 8-72883
 amplifier to record heat pulse during material fracture 8-60921
 brittle materials, diametral compressive stress considering Hertzian contact, fracture and tensile strength meas. (*Japanese*) 8-72946
 castings, fracture toughness characteristics, using double torsion method 8-68863
 ceramics, wedge indentation technique for precracking, appl. to Al_2O_3 and SiO_2 8-85087
 crack growth gauge for assessing flaw growth potential in structural components 8-68859
 diametral compress test using circular anvils (*Japanese*) 8-72947
 diamond surface soldered to metal film, contact strength determ. device 8-60910
 disc test measurement of combined mode fracture toughness stress analysis 8-92432
 dynamic, by instrumented impact tests 8-68861
 exoemission defectoscopy in initial stages of fatigue fracture 8-53126
 film, diamond indentation and draw tester for meas. of ultra-adherence 8-72944
 fractographic study on evaluation of fracture toughness 8-68865
 graphite, fracture toughness measurement, by disc test comparison with stress analysis of disc test 8-92432
 graphite, structural, impact toughness, reln. to compressive strength 8-88605
 impact three point bend testing for notched and precracked specimens, testing and data analysis procedures 8-53053
 J_{Ic} -testing, statistical eval. of different techniques, applic. to A-533 B steel 8-56828
 J integral estimation procedure, summary and comparison 8-85088
 K_{Ic} determ. for reduced size specimens (*Russian*) 8-56830
 Kassem method 8-92412
 marble, fracture toughness measurement, by disc test comparison with stress analysis of disc test 8-92432
 metal, US propag. factor rel. to fracture toughness props. 8-80698
 method of unloading in experimental fracture mechanics (*Russian*) 8-56829
 NDT, role in fracture mechanics evaluation 8-68862
 notch production with small root radius on test samples (*German*) 8-64795
 nuclear components, struct. integrity assessment mat. prop. variations 8-89953
 plane strain, testing with C-shaped specimens 8-92414
 plaster, fracture toughness measurement, by disc test comparison with stress analysis of disc test 8-92432
 plastic zone, direct meas. in side grooved fracture toughness specimens 8-68864
 pressure vessels, brittle fracture probability using reactor surveillance capsule data 8-80641
 ring segments, radially cracked, displacement coeffs. from boundary collocation anal. 8-71298
 steel transition temp. determ. from fibrous structure in fracture, exam. of method 8-85080
 stress rupture test using photoelectronic monitoring of tube deform. 8-78470
 surface crack shape change in bending fatigue, resonant fatiguing apparatus 8-72950
 thermal shock fracture toughness eval. by arc discharge heating 8-72835
 Al alloy, fracture toughness testing, acoustic emission, inspection technique 8-68860

fractum
 see also nuclei with
 atom, evidence for optical transition (*French*) 8-86829
 Fr I, wavelength estimate of first and second resonance lines 8-58617

francium compounds
 No entries

Franck-Condon factors
 C_{3v} -type mols., doubly degenerate electronic states, Jahn-Teller interaction 8-50536
 electron and exciton transfer rates, effect of nucl. degrees of freedom 8-60057
 interference structure in Franck-Condon overlap functions 8-94287
 large molecule, novel ultrafast two-pulse excitation spectroscopy 8-94331
 molecule, diatomic, Franck-Condon factors calc. using Rydberg-Klein-Rees pot. 8-70878
 molecule dissociation, transition amplitudes, semiclassical evaluations 8-62860
 nonadiabatic collisions, Franck-Condon approach for electronic state quenching 8-66640
 photovoltaic effect mechanism, expt. obs. of thermal and spectral variations in the photovoltaic current in ferroelectrics 8-91719
 Al, continuous UV emission under inert gas ion bombard. 8-84664
 Al, electronic spectrum, Franck-Condon factors, r-centroids 8-62817
 AlO , A-X transition, Franck-Condon factors computation, iterative method compared with Langer's method 8-86762

Franck-Condon factors continued

- AlO_2 , $\text{D}^2\Sigma-\text{X}^2\Sigma$, Franck-Condon factors and V-centroids (*Russian*) 8-74642
 C_2 , Swan, Phillips, Deslandres-d'Azhambuja and Fox-Herzberg systems, rotational dependence 8-74701
 CH A-X , B-X and C-X systems, rotational dependence 8-74701
 CN , red and violet band systems, rotational dependence 8-74701
 CO A-X system, rotational dependence 8-74701
 CO , high resolution lifetime meas., perturbation and collisional transfer correl. 8-78699
 CO_2 , Franck-Condon transition amplitudes for mol. dissoc., semiclassical evaluations 8-62860
 H-bond complex formation, enthalpy change due to electronic excitation, spectroscopic determ. 8-92496
 HCN , Franck-Condon transition amplitudes for mol. dissoc., semiclassical evaluations 8-62860
 $\text{HI+D} \rightarrow \text{H+DI}$, Franck-Condon theory 8-60984
 ICN , Franck-Condon transition amplitudes for mol. dissoc., semiclassical evaluations 8-62860
 $\text{I}(\text{S}^2\text{P}_{1/2}) + \text{benzene-d}_6(\text{-d}_8)$, fluoresc. quenching, spin-orbit interaction, isotope effect obs. 8-62763
 LaF_3 , Franck-Condon factors and R-centroids, rot.-vibr. effects 8-50596
 $\text{Mg}_2 \text{A}^1\Sigma_g^+ - \text{X}^1\Sigma_g^+$ system, discrete and continuous Franck Condon factors, J-depend. 8-66811
 MgD , emission spectra, 600 to 850 nm, rot. anal., dissoc. energies 8-62815
 MgH , emission spectra, 600 to 850 nm, rot. anal., dissoc. energies 8-62815
 NO , UV photoelectron spectrum, autoionisation from Rydberg state, vibr. progressions, Franck-Condon factors 8-50583
 NO_2 , 8920 Å band temp. depend., location of 000-000 band of $\text{A}^2\text{B}_2 - \text{X}^2\text{A}_1$ transition 8-70826
 Na_2 , two-photon transition, velocity tuned, polarisation depend. and Franck-Condon factors 8-90250
 O_2^+ , Franck-Condon factors calc. using Rydberg-Klein-Rees pot. 8-70878
 $\text{SO}_3(\text{SO}_3^-)$, Jahn-Teller interaction, Franck-Condon factors and vibronic energy level calc. 8-50536
 ScF_3 , Franck-Condon factors and R-centroids, rot.-vibr. effects 8-50596
 SiO , vibr. wavefunctions, Franck-Condon factors, at low quantum numbers 8-55203
 XeF , 3500 Å band, vibr. anal. 8-70843
 XeF , X, B, and D-states, spectra, vibr. and rot. consts. 8-70844
 YF , Franck-Condon factors and R-centroids, rot.-vibr. effects 8-50596
 YO , spectra, 4500-6900 Å, mol. consts. 8-50551

Frank-Read sources

- grain boundary dislocations, Burgers vectors, grain boundary dislocations 8-87680
screw dislocation control of plastic deformation in crystals 8-51605

Fraunhofer lines see solar spectra

free-electron approximation

- transition metals and their alloys, amorphous, elec. resist. 8-60103

free electron lasers

- collective and single-electron interactions of electron beams with EM waves and free-electron lasers 8-55330
feasibility of design without external inducing source (*Russian*) 8-50746
free electron laser, enhanced gain 8-63050
laser fusion applications 8-58974
momentum distribution function, classical single particle theory 8-58973
nonlinear phase equation, numerical solns. 8-87035
relativistic Compton laser, power potentiality (*Russian*) 8-90405
relativistic electron beam Raman laser 8-74877
research status 8-82940
review 8-90406
stimulated emission and absorption in classical systems 8-63047

free energy

- aging media, thermodynamic pots. in creep theory (*Russian*) 8-63318
Alfven wave system, eqn. of state, thermodynamic props., Bose-Einstein statistics 8-87397
alkali halides, premelting elec. cond., heat capacity 8-91445
alloy, binary, atomic misfit effect on coexistence and spinodal transform. boundary 8-60644
alloy, role of phase boundaries in phase transformations 8-72772
alloys, determ. by X-ray and neutron scatt. expts. 8-83974
amorphous insulator, phase diagram and statistical mechanics 8-52268
anharmonic crystals, unsymmetrised SCF approx. 8-63830
benzene-cyclohexane system, vap. press., excess free energies, isotope effects 8-59939
2,3-benzo-1,6-methano(10)-annulene, mol. geom. and gas phase thermodynamic props., minimisation scheme 8-78829
binary alloy, quenched, time evolution of struct. function free energy 8-55937
binary liquid mixture, surface tension, free energy density expansion 8-91509
 β -brass, cryst. struct., elastic consts., central force model 8-51637
cresols, ideal gas thermodynamic props. 8-75250
crystal, statistical thermodynamics with collective vibrations 8-54289
cubic margules solution model, miscibility gap and crit. point behaviour 8-59925
defect energy of formation, Gibbs free energy 8-91332
deformation kinetics, Gibbs eqn. and nonequilibrium thermodynamic models (*Ukrainian*) 8-90720
dilute systems of dipoles and dipolar charged particles, Mayer resummation method 8-83710
double Ising chain, model in zero external field (*Russian*) 8-84430
elasto-plastic metal-dislocation system, stress-activated dislocation motion, thermodynamic theory (*Chinese*) 8-83868
electron gas, two dimensional, classical, hypernetted chain solns. 8-67963
enzyme catalysis, electron pairing as source of cyclic instabilities 8-95953
ferroelectric, incommensurate-commensurate transitions 8-60404
ferroelectric crystal classification by transition mechanisms (*Russian*) 8-60401

free energy continued

- ferromagnetic film, ϕ^4 domain walls, magnetisation, occurrence of crit. point 8-95500
fluid, randomly-stirred, vel. correlations, variational principle for path-integral functionals 8-81846
fluid-solid type phase transition, one dimens. model 8-63838
freezing, molecular theory, eqn. of state, free energy, from 1st BBGKY eqn. 8-67804
gaseous diffusion in stressed thermoelastic solid, thermodynamic struct. 8-51065
Heisenberg model, long-range interaction, free energy 8-56282
heterogeneous nucleation systems, crit. conditions characterising formation 8-56023
heteropolymer in random mag. field, Ising chains, statistical mechanics, free energy, numerical calcs. 8-77803
ideal type II superconductor, thermodynamics of inhomogeneous mixed phase 8-84365
ion solvation, in polar media, continuous charge distrib. model, quantum mech. calcs. 8-68913
Ising ferromagnet, 2-D, with quenched bond disorder, critical temp. 8-56328
Ising model, free energy, recursion method calcs. 8-52186
Ising model, two-dimens., interface free energy 8-60261
Lennard-Jones liq., press. and temp. consistent, approx. theory, Helmholtz free energy 8-63647
liquid crystal with slowly varying orientational order parameters (*Russian*) 8-75533
liquid mixtures, local mole fractions consistency 8-83702
macromolecules, crystallisation thermodynamics, various degrees of coiling 8-51445
metal, mag. susceptibility, effects of impurities and temp. (*Russian*) 8-84429
metal to ceramic reaction welding, interfacial free energy rel. to noble metal corrosion 8-53035
1,6-methano(10)-annulene, mol. geom. and gas phase thermodynamic props., minimisation scheme 8-78829
microemulsions, thermodynamic stability, theory 8-85203
molecular fluid perturbation theory, Pople expansion third order term, anisotropic pot. 8-79510
molecular liquid, thermodynamic functions, interaction site model calc. 8-71661
molecular solvation, in polar media, continuous charge distrib. model, quantum mech. calcs. 8-68913
one dimensional continuous quantum systems, limit Gibbs state 8-93599
phenol, ideal gas thermodynamic props. 8-75250
polyethylene, oxidation rel. to spherulitic crystn. (*Russian*) 8-71689
polymer, isotropically swollen networks, vol. depend. of elastic eqn. of state 8-67832
polymer chain, elasticity for different vibr. modes, algorithm 8-66696
polymer flexible lattice chain in limited vol., behaviour (*Russian*) 8-70992
polymers, heterophase mixtures, excess energy 8-53264
porous solid with below-freezing pt. adsorbate, isothermal adsorption and dimensional changes obs. 8-75925
pseudocritical phenomena near the spinodal point 8-65894
renormalisation theory, variational principles 8-73951
roughening models, step free energies, and correlation functions in X-Y models 8-67675
simple metals, monovacancy formation parameters, temp. depend. 8-75658
solid-on-solid model, screw dislocations, rel. to correl. in X-Y model 8-63691
solutions, dilute, Monte Carlo free energy calcs. in isothermal-isobaric ensemble 8-92498
spin glass, random molecular fields, Edwards-Anderson theory 8-80164
spin glass model, stability of Sherrington-Kirkpatrick soln. 8-56319
spin-glass model, stability of Sherrington Kirkpatrick soln. 8-80152
square lattice finite thickness slabs, long self-avoiding walks, steric stabilisation model 8-54309
steel, alloy with additions of Mn, Si, Ni, Cr, Mo, Cu, thermodynamic prediction of Ae_3 temp. 8-64524
superionic crystals, phase transitions 8-75826
ternary dil. soln., free energy of transfer determ. by vapour press. method 8-64871
type II superconductor, ideal, wire, macroscopic current in longitudinal field 8-84366
uncorrelated-pairs approximation for anharmonic free energy, tests 8-59920
uniaxial magnet, free energy of system with weak exchange interactions and high mag. anisotropy (*Russian*) 8-68213
univalent gaseous ions, free energy of solvation, 1-layer continuum model 8-95944
Ag film, on mica, microstruct. changes 8-72013
 $\text{AgNO}_3\text{-TiNO}_3\text{-Cd(NO}_3)_2\text{-H}_2\text{O}$ mixtures, Henry's law, excess free energy 8-68908
 Ag_2S , α - β transform., heterogeneous solid state reactions, role of phase boundaries, dynamic equilib. at interfaces 8-71848
 Ag_2S , α - β transform., role of phase boundaries in heterogeneous solid state reactions 8-71849
Al-Ag, discontinuous decomposition (*Polish*) 8-52808
Al-Ga-In, liq. alloys, excess Gibbs functions 633 to 1173K 8-60655
Al-Zn, discontinuous decomposition (*Polish*) 8-52808
Ar-Kr, liq. mixture, excess thermodynamic props. 8-75836
Au-Ni, liquid alloy system, determ. of thermodynamic props. using Knudsen effusion method, phase diagram calc. (*German*) 8-51707
Au-Ni-Co phase diagrams, thermodynamic calc. (*Korean*) 8-68672
Ca-Ag(In), liquid alloy, thermodynamic exam 8-75848
 CsPbCl_3 , $\text{O}_h - \text{D}_{4h}$ transition, US and thermodynamic props. 8-67826
Cu-O system, liq., thermodynamic study (*Japanese*) 8-64529
Cu-Sn liquid alloys, thermodynamic meas. 8-52765
p-D₂, order-disorder phase transition 8-79726
Fe-Mn-C system, Gibbs energy, high temp. phase relations 8-80779
Fe-Ni, FCC and BCC lattices, X-ray characteristic temp. (*Russian*) 8-67797
Fe, Mo, standard Gibbs energies, enthalpies, entropies of formation 8-61042
Fe₂Mo₂, standard Gibbs energies, enthalpies, entropies of formation 8-61042

free energy continued

- FeMoO₃, standard Gibbs energies, enthalpies, entropies of formation 8-61042
 o-H₂, order-disorder phase transition 8-79726
 HBr-HCl, thermodynamics of binary liquid mixtures 8-64876
 HBr-Xe, thermodynamics of binary liquid mixtures 8-64876
 H₂O, free energy of liq. water, ab initio Monte Carlo calc. 8-83975
³He, superfluid A phase, planar textures 8-79837
³He, superfluid A-phase, composite solitons, mag. reson. 8-51779
⁴He, liq., lambda transition free energy in Feynman's model (French) 8-71895
 KCl:Sr, Ca, simultaneous diffusion, coefficients meas. 8-79813
 KH₂PO₄, variational treatment of proton-photon system 8-88261
 Li-Pb, quasi-ionic, thermodynamic props. using EMF meas. 8-51705
 Li₃N, heat capacity 5 to 350K, thermochem. props. to 1086K 8-92500
 Mg, phonon spectrum and thermodynamic functions, inelastic coherent cold neutron scatt. (Russian) 8-55917
 MgIn₂O₄, free energy, entropy of form. 8-91433
 NH₃, ND₃, crystals, rotation mol. motion (Russian) 8-87762
 NH₄H₂PO₄, improper antiferroelec. phase transition, elastic props., free energy, thermodynamic theory 8-80299
 Na₂SO₄, liq., standard free energy of formation from 1160 to 1220K 8-56911
 Ni-S system, Knudsen effusion and thermodynamics 8-79759
 NiO-NiAl₂O₄-Al₂O₃, heterogeneous solid state reactions, role of phase boundaries, dynamic equilib. at interfaces 8-71848
 Pb-Ag, liquid alloy, exam. of thermodynamic props. using solid oxide galvanic cell 8-75851
 PbO-PbSO₄, melts, thermodynamics, determination of free energies of mixing at 1253K 8-83976
 SbSI, free energy function, temp. depend. and anisotropy of dielec. const., ferro- and paraelec. phases 8-64330
 α-Se, monoclinic, heat capacities and thermodynamic properties, 3-300K 8-95162
 UAs₂(Sb₂), heat capacities, antiferromag.-paramag. transitions 8-76253
 V₂S₅-V₂S₈ system, exam. of thermodynamic props. at temp. from 650 to 800°C 8-52784
 VSi₂, thermodynamic props. determ. using ternary phase equilibria 8-91449
 V₂Si, thermodynamic props. determ. using ternary phase equilibria 8-91449
 V₃Si₂, thermodynamic props. determ. using ternary phase equilibria 8-91449

free field rooms see *anechoic chambers***free radical reactions**

- N-acetylglucosamide, substrate-inhibitor of lysozyme, localisation of unpaired electrons 8-68992
 allyl chain free radical, decay kinetics in γ-irrad. polyethylene state depend. 8-76855
 CIDEP, examples of S-T₂₁ polarisation 8-86891
 DNA, single-stranded, alkali-labile sites and post-irrad. effects induced by H radicals 8-68994
 ferricytochrome, photoreduction in presence and absence of electron donor 8-53337
 indole, aq. solns., flash photolysis, transient absorpts., 600 to 800 nm 8-53228
 lipid free radical oxidation kinetics rel. to lipid composition, photoreceptor membrane 8-80872
 methyl radical+O₂ (NO), mass spectra, absence of reaction in combustion system 8-53195
 naphthalene anion radical+H₂O, react., H₂ prod. 8-92460
 nitroxyl radical reduction kinetics, modelling non-enzymatic influence of membranes 8-64945
 peptide aqueous solution, EPR of spin-trapped radicals, OH radical reactions 8-68993
 pyrene+N,N-dimethylaniline (deuterate)(3,5 dimethoxy-N,N-dimethylaniline), geminate recomb., solvent, isotope, mag. field effects 8-56888
 submitochondrial particle succinic dehydrogenase, interaction of ubiquinone with Fe-S centre, EPR 8-69016
 CH₂+H₂→CH₄, MINDO/3-FORCES calc., activation energy and enthalpy of reaction 8-66472
 H+NH₃→NH₄, react., force, density anal. 8-60997
 HO₂+Cl react. rate const. determ. at 298K (French) 8-64817
 ND⁺+DN₃→ND₃⁺+N₂, chemiluminesc. reaction of electronically excited species, rate const. 8-80771
 NO₂+ROO→ROONO₂, (R=C₈H_{2n+1}), Fourier transform IR spectroscopic meas. 8-53194
 OH+2-methyl-2-butene, reaction rate const. meas. 8-61001
 OH+dimethyl sulphide, flash photolysis reson. fluoresc. rate const. determ., pollution aspects 8-95913
 OH+formaldehyde (acetaldehyde), rate const., 299-426K, UV flash photolysis, reson. fluoresc. obs. 8-68873
 OH+HCN, reaction rate, press. depend. 8-85135
 OH+OCS(CS₂), flash photolysis reson. fluoresc. rate const. determ., global S cycle 8-95914

free radicals

- see also *free radical reactions; paramagnetic resonance of free radicals*
 acid amide+H₂O₂, aq. solns., photolysis, EPR study of spin-trapped radicals formed during photolysis 8-68996
 acyloxy radical ion, in irrad. Rochelle salt, decarboxylation, pulse radiolysis and EPR obs. 8-70854
 albumin, human serum, kinetics of eosin-sensitised photochemilum. of solns. 8-68991
 alkanes, electron localisation and solvation, radical ion theory 8-87936
 alkoxy free radicals, produced by X-irrad. of hydroxy containing cpds., characterisation by ESR and ENDOR 8-95938
 N-alkyl free radicals, ESR study, conformational anal. of N-alkyl group 8-62831
 allyl radicals, in irrad. polyethylene, distrib., trapping regions 8-91957
 amino acid, in polycryst., γ-irrad. induced radical pair form., 77K, EPR obs. 8-85292
 atmospheric meas. by matrix isolation and EPR 8-73535
 bacteriophage T7, radiation inactivation 8-65083
 benzene, cation radical, charge exchange reagent appls. 8-70929
 benzene, substituted cations, spectroscopy, substituent effects 8-58709

free radicals continued

- benzophenone in isopropanol, submicrosecond time resolved EPR, laser photolysis, CIDEP polarisation mech. 8-80764
 p-benzosemiquinone monoprotonated radical, submicrosecond time resolved EPR, laser photolysis, CIDEP polarisation mech. 8-80764
 benzyl radical, MINDO/3-FORCES, geom. of heat of formation 8-66472
 binaphthyl anion radicals, photoisomerisation, local heating effects 8-85179
 binary complex, quinone-phenol radical pair EPR, geometry calc. 8-90101
 butadienyl radical, interstellar, detect. towards (IRC+10216) 8-93374
 t-butyl radical, VUV photoelectron spectrum, geometry, vibr. struct. and ionisation pots. 8-50577
 carbonyl oxide, config. interaction calc., using DODS natural orbit approach 8-66476
 carboxylic esters, γ-irrad. glass, trapped radical photolysis, ESR 8-85178
 carbyne and interstellar grains 8-69859
 chloroethane diradical, MINDO/3 for optimised geometry and heat of form. 8-78830
 chloromethylene radical, MINDO/3 for optimised geometry and heat of form. 8-78830
 chlorophyll a, photo-oxidation by p-benzoquinone, nature of electron-excited state 8-76991
 chlorophyll-a radical cations, in disordered systems, electron spin echo envelope modulation, isotope effects 8-61141
 CIDEP, examples of S-T₂₁ polarisation 8-86891
 condensed media, electron localisation and solvation, radical ion theory 8-87936
 cytidine-5'-monophosphate, γ-irrad. aq. soln., spin-trapped radicals, liq. chromatography and EPR spectroscopy 8-53340
 di-t-butyl nitroxide radical, solid, nucl. and electron spin relax. times meas. 8-60350
 diatomic radicals, wavefunctions, populations and orbital energies, Roothaan calcs. 8-86773
 1,3- and 1,4-dichlorobenzene radical cation, emission and photoelectron spectra, lifetimes meas. 8-86905
 dichloromethylene radical, MINDO/3 for optimised geometry and heat of form. 8-78830
 difluoromethane, triplet state emission spectra, phosphoresc. and energy transfer 8-53196
 9,10-diphenylanthracene, electrogenerated chemiluminescence, T₂ state emission 8-60524
 DNA, transforming, X-ray sensitivity rel. to presence of free radicals 8-68995
 DPPH, mag. susceptibility of solvent-free and DPPH-benzene complex 8-70963
 DPPH-benzene, organic radical, pressure induced mag. ordering (Russian) 8-88120
 duro-semiquinone monoprotonated radical, submicrosecond time resolved EPR, laser photolysis, CIDEP polarisation mech. 8-80764
 ethenoxy, config. interaction calc., using DODS natural orbit approach 8-66476
 ethyl radical, geom. struct., Hartree-Fock calcs. 8-62722
 ethynyl radical, interstellar abundance and distrib. 8-65664
 glyceraldehyde-3-phosphate dehydrogenase radiolysis, active-site and SH loss 8-77000
 heat capacities, molar, correlation coeffs., data collection 8-85188
 hexafluoride radicals, prep. and EPR spectra comparison, hyperfine splitting 8-68381
 hydrocarbon radicals, planar and nonplanar, g-factors, π-σ delocalisation 8-58580
 1-hydronaphthyl radical, in naphthalene single cryst., anisotropic oscill. strength 8-50591
 hydroxymethylene intermediacy in low-temp. matrix photolysis of formaldehyde, IR obs. 8-76877
 iminoxyl radicals, influence on elec. cond. of MBBA, EBBA liq. crystals (Russian) 8-67641
 methyl isocyanide photodissoc., cyanide radical energy partitioning chemical laser determ. 8-73063
 methyl radical, ab initio projected unrestricted Hartree-Fock calcs. 8-58582
 methyl radical in glassy organic matrices, electron spin-lattice relax. 8-76312
 methylbenzene cations, photodissoc. spectra, substituent effects 8-58710
 methylchloride, CH₃Cl⁺, photofragmentation at 366 nm 8-58752
 muonium-substituted transient radicals observed by muon spin rotation 8-74678
 naphthalene, C₁₀H₈ and C₁₀D₈, optical absorpt. spectra of hydronaphthyl radicals, isotope effects 8-60487
 naphthalene radical anion, ethereal soln., far IR spectra 8-62796
 naphthalene radical cation, in organic glass, 77K, reson. Raman spectra 8-78704
 neutral free radicals, in Ar matrix, IR spectrosc. evidence 8-66546
 nitron, config. interaction calc., using DODS natural orbit approach 8-66476
 phenoxyl type radical, ¹H and ¹³C ENDOR studies in soln. 8-94266
 pheophytin-a, photochem. generation of cation-radical, spectral-kinetic characts. 8-96008
 polyethylene, elec. trees free radical ESR study 8-60393
 pyrene-DMA-methanol solution, photoinduced radical ion pair geminate recombination, triplet yield 8-76879
 pyrometallic dianhydride radical anion, MTHF glass, 77K, reson. Raman spectra 8-78704
 radical ion pair formation, ESR spectroscopic obs. 8-73038
 spin relaxation, Heisenberg exchange interaction between unlike free radicals 8-84490
 p-terphenyl anion radicals, photoisomerisation, local heating effects 8-85179
 thymidine, frozen aq. solns., final products of gamma radiolysis 8-77001
 thymidine-5-monophosphate, γ-irrad. aq. soln., spin-trapped radicals, liq. chromatography and EPR spectroscopy 8-53340
 thymine+muonium, radical form. in aq. soln., spin reson. obs. 8-74679
 1,3,5-trichlorobenzene radical cation, emission and photoelectron spectra, lifetimes meas. 8-86905
 L-tryptophan-HCl radical form. after X-irrad. 8-64940

free radicals continued

- vinyl radical, MINDO/3-FORCES, geom. of heat of formation 8-66472
- BH⁺, spin-extended Hartree-Fock ab initio calculations for small radicals 8-70746
- BH₃F⁺, B-F bond, interference density and kinetic energy 8-74566
- BO₂, gas, optically detected mag. reson. spectrum, X²II rovibronic sublevels 8-82756
- BeH, spin-extended Hartree-Fock ab initio calculations for small radicals 8-70746
- C₃, electron spectrum, ab initio MRD CI calcs. 8-90089
- CCN radical in solid Ar, emission and excitation spectra 8-70868
- CF₂, absolute IR intensity of fundamental vibrs. 8-58743
- CF₂, in Ar matrix, conc. determ. by intensity calcs. 8-68941
- CF₂, X¹A₁ radical, form. in chlorofluoromethane collision-free multiphoton dissociation, translational energy meas. 8-92491
- CF₃, absolute IR intensity of fundamental vibrs. 8-58743
- CF₃, in Ar matrix, conc. determ. by intensity calcs. 8-68941
- CF₃Cl⁺, and parent cations, IR spectra in matrix radiolysis and photoionization of Freons 8-80767
- CH, chemiluminescence in flowing afterglow of Ar+methane 8-64839
- CH, photoionization and photodissociation near ionization threshold, SCF MO CI and Stieltjes imaging 8-58749
- CH, radiative lifetimes, electron-photon delayed coincidence meas. 8-50594
- CH radical, sputtered from acetone chemisorption layer on Si, rot. and vibr. population distrib. 8-64436
- CH⁺, continuum electron wavefunction, electron capture width 8-78805
- CH₃, experimental determ. of the geometry and electron affinity 8-82860
- CN (A²II), chem. prod., CN number densities for gain, emission and absorption meas. 8-63112
- CN, A- and B-state lifetimes, collisional transfers and perturbations 8-78756
- CN, form. by photodissociation of parent molecules, possible detection in comets 8-61798
- CN, radical, nonradiative transition rates, matrix isolated molecule 8-78740
- CN, radical fluorescence excitation spectrum and laser emission from ICN photolysis 8-76892
- CN radicals, electronic transition laser, using C₃F₇CN and (CN)₂C₄F₈ photodissociation 8-50769
- CN, solar lines in 7100-7600 Å range, table 8-77495
- CNC radical vibr. and electronic spectra, in VUV photolysis of matrix-isolated cyanomethane 8-85180
- CNN, matrix isolation spectrum, 2600-1900 Å 8-86880
- CS, heat of formation from electron impact dissociation of CS₂ and OCS 8-73074
- CS₂, electron impact dissociation, CS heat of formation. determ. 8-73074
- ¹³C-labelled organic radicals, ¹³C- and proton-ENDOR in soln. 8-55190
- ClO, A²II-X²II, UV absorption spectrum 8-74673
- ClO, bond strength determ. of fundamental vibr.-rot. spectrum 8-70872
- ClO, laser spectroscopy relevant to stratospheric photochemistry 8-88951
- ClO radical, IR vibr.-rot. spectra, background data for atm. meas. 8-58679
- ClO₂ radical, laser mag. reson., ν₁ band 8-94263
- ClO₃ radical, in KClO₄ EPR obs., X-irradiation creation 8-76311
- CrO₃ radical in K₂CrO₄ and KCrO₃Cl, g-factor anisotropy 8-67994
- HC₂ radical, electron affinity, ab initio SCF and CI calcs. 8-50468
- HCN⁺, SCF ab initio ground state potential energy surface, geometry, rel. to HCN 8-78646
- HCO, UV matrix isolation spectra, 14K, 210-260 nm, C-X transition 8-62819
- HF₂, neutral free radicals, in Ar matrix, IR spectroscopic evidence 8-66546
- HNC⁺, radical cation, charge exchange mass spectrometry, HNC⁺ ion recombination and ionization potential 8-76838
- HO₂ radical, EPR spectrum, ground state parameters 8-90193
- HO₂ radical, ν₃ fundamental band, laser mag. reson. 8-66566
- HPO₄⁻, in γ-irradiated K(H_{1-x}D_x)₂PO₄, 77K, optical and EPR obs., form. mechanism 8-68379
- H₂PO₄⁻, in γ-irradiated K(H_{1-x}D_x)₂PO₄, 77K, optical and EPR obs., form. mechanism 8-68379
- HS₂, ground and first excited states, geometry, ab initio SCF calcs. 8-50657
- HSO, ground and first excited states, geometry, ab initio SCF calcs. 8-50657
- LiH⁺, spin-extended Hartree-Fock ab initio calculations for small radicals 8-70746
- ND, b¹Σ⁺ state, radiative lifetime, Einstein coeff. 8-90217
- ND, dissociation energy, calc. from c¹ II state predissociation. (German) 8-90237
- NF, b¹Σ⁺ state, enhancement by I laser pumping, lasing potential 8-79012
- NF, chem. pumped electronic transition laser system, chem. and scale-up 8-63103
- NF, excited, lasing potential, prod. by N+O₂F reaction 8-63106
- NF(a⁴Δ)+I(P_{1/2}) system, electronic angular momentum transfer, chem. kinetic model 8-63104
- NF(b¹Σ⁺) enhancement by I laser pumping 8-63105
- NH, b¹Σ⁺ state, radiative lifetime, Einstein coeff. 8-90217
- NH, dissociation energy, calc. from c¹ II state predissociation. (German) 8-90237
- NH, radiative lifetimes, electron-photon delayed coincidence meas. 8-50594
- NH₂, vibronic levels, excited by blue CW dye laser 8-86907
- NO (v=1), vibr. fluorescence detection of trifluoroformamide photodissociation. 8-74712
- NO, hyperfine splitting constant, H-bond contribution 8-74799
- NO, biradicals, conform., spin probe appls. 8-86895
- O₂⁻, superoxide radical role in lipid photoperoxidation in isolated chloroplasts 8-77016
- O₂F+N→N₂(NF), lasing potential of excited fluorides 8-63106
- O₂F(Cl)(Br) radicals, matrix IR spectra, bonding 8-90160
- OH, A²Σ state, predissociation rates, high freq. deflection meas. 8-62864
- OH, excitation in interstellar clouds 8-65669
- OH, excited free radicals, form. by ion-mol. reactions 8-56890

free radicals continued

- OH inactivated papain, optical density, amino acid composition and fluorescence. 8-53344
- OH, J=9/2 Λ-doublet line detection in W3(OH) 8-65670
- OH Meinel bands intensity distribution in airglow, OH^{*} quenching mechanisms 8-65447
- OH radical, gas phase EPR, rot. states electronic structure and Zeeman parameters 8-86896
- OH radicals, microwave spectra data tables 8-50542
- OH, spin-extended Hartree-Fock ab initio calculations for small radicals 8-70746
- OH, vibrationally excited, high-resolution hyperfine Λ-doubling spectrum 8-90153
- OH^{*}, proton affinity, integral Hellmann-Feynman theorem 8-70767
- OH+2-methyl-2-butene, reaction rate constants. meas. 8-61001
- OH(OD), A²Σ⁺ state, vibrational energy transfer in collisions, rot. resolved fluorescence. 8-74742
- PH, (b¹Σ⁺) state, radiative lifetime, time resolved spectra 8-78750
- PH₂ radical, laser-induced fluorescence. 8-94277
- PS, electronic transition B²II-X²II, vibr. and rot. anal. (French) 8-78716
- SF₆, equilib. electron-transfer reactions in gas phase involving long-lived neg. ion radicals 8-58807
- SF₆BF₄:SF₆, cryst., γ-irradiation, radical form., EPR 8-91955
- SOH, ground and first excited states, geometry, ab initio SCF calcs. 8-50657
- SeH(X²π_{3/2}), far IR LMR spectrum 8-66564
- SiH, rot. transition freqs. calc., rel. to search in interstellar space 8-93100
- SiH⁺, rot. transition freqs. calc., rel. to search in interstellar space 8-93100

freezing

see also refrigeration

- annular region, perturbation soln. for melting/freezing interface 8-59286
- bifurcation of crystalline solutions and freezing 8-67814
- biological material, prep. for X-ray microanal. of diffusible elements, methods of drying ultrathin cryosections 8-77166
- biological material freeze-fracture preparation for SEM 8-61290
- biological material prep. for X-ray microanal. of diffusible elements, rapid freezing and ultrathin section prep. 8-77165
- biological specimen rapid freezing under controlled and reproducible conditions 8-57139
- biological tissue prep. without chem. fixation, freeze-drying for electron microscopy 8-65164
- bricks, extensometer for meas. of linear expansion due to freezing 8-53062
- cell structure and function, freezing patterns and post-thaw survival 8-64960
- charged fluids near freezing point, static dielectric behaviour 8-56417
- Darcy flow, chilled pipe freezing zone, finite difference method 8-94734
- dendritic ice form. in pipe, cooling rate effect 8-90690
- erythrocyte survival after slow freezing in glycerol, temp. depend., human cells 8-77019
- erythrocytes, slowly frozen human cells, phys.-chem. basis of protection by glycerol 8-77020
- ethanol-water system, metastable states, hydrates existence and props., low temp. 8-71835
- freeze-fracture electron microscopy freezing method evaluation by low temp. X-ray diff. 8-57145
- freeze-fracture specimen temp. changes during rapid quenching in liq. coolants 8-57140
- frost formation, struct. model of frost layer growth 8-79200
- Heisenberg spin-glass, crit. dynamics 8-60295
- ice, on CuS aerosol prepared by burning pyrotechnic mixture, freezing temps. 8-96279
- ice phase formation in natural and seeded storms 8-61509
- ice-water interface struct., fluctuations during solidification 8-59935
- liquid flow blockage in circular tube below freezing point, theory and expt. 8-94830
- metastable liquid, nonlinear diffusion eqn., multi-mode one dimension. anal. 8-87771
- molecular dynamics simulation, Gaussian core model 8-67811
- molecular theory, eqn. of state, free energy, from 1st BBGKY eqn. 8-67804
- multidimensional problems in arbitrary domains, numerical method 8-90693
- noble gas fluids, press. induced transition in neighbourhood of alkaline earth impurity 8-51770
- porous solid with below-freezing pt. adsorbate, isothermal adsorption and dimensional changes obs. 8-75925
- reference standards for radiation pyrometry, silver and copper freezing points 8-57888
- sea water freezing, induced haline convection expts. (Japanese) 8-88843
- soil, frost heave in Tomakomai, Hokkaido, 1976 to 1977 (Japanese) 8-92860
- soil freezing, water migration obs. (Japanese) 8-88862
- stability of solid freezing front 8-63844
- steam condensation heat transfer on below-freezing pt. surface 8-75042
- thermal problems, one-dimens., with phase change, efficient numerical technique 8-59270
- tissue molecular dynamics and freezing phase transition studied by proton spin relax. 8-68983
- tube flow, heat transfer problem of flowing liquid solidification onto a melting wall 8-94585
- ultrathin cryo-section stabilization by freeze-drying 8-54349
- Van der Waalsian theory, 3D Ornstein-Zernike equation 8-91424
- water, forced laminar convection in horizontal pipe, density inversion effects, numerical anal. 8-90900
- water drops, ice splinter production during rimeing 8-85662
- water in capillary, freezing and melting behaviour, dilatometry, elec. cond. meas. 8-75908
- water-ice transition, production of stimulated coherent radiation 8-83920
- H₂, on inner surface of spherical polymer shell, cryogenic targets for laser-driven fusion 8-86688

Frenkel defects

- alkali perchlorates, elec. transport during struct. transforms. 8-59971
 graphite, point defects and self diffusion 8-63758
 metal, BCC, neutron irradiated, spontaneous recombination volumes of
 Frenkel defects, rel. to compressibility 8-71765
 metal, irradiated, containing self-interstitials and vacancies, electronic transport props. 8-60105
 semiconductor, collective magnetoexciton transition under action of light (*Russian*) 8-79939
 AgBr, self-diffusion of Br^- by both single vacancies and vacancy pairs 8-55978
 AgBr(Cl), formation vol. of Frenkel defect 8-79606
 $\alpha\text{-Ag}_2\text{S}$, electronic and electrogalvanic props., completely ionised Frenkel defects (*French*) 8-84237
 $\beta\text{-Al}_2\text{O}_3\text{-M}_2\text{O}$, $\text{M}=\text{Ag, K, Rb, Na, Eu}$, X-ray diffuse scatt. 8-71725
 $\beta\text{-AgI}$, ionic cond. and dielec. meas., Frenkel defect formation energy 8-87814
 Cu, Frenkel pair production threshold energy, temp. depend., exam. 8-51530
 Cu, thermal vibr. and zero-point motion effects on low-energy collision cascades 8-87705
 He, solid, ion current modulation by thermal waves 8-91506
 KBr, defect recombination, 4.2 to 77K 8-72606
 KCl, defect recombination, 4.2 to 77K 8-72606
 KCl, X-irradiated, formation of cation defects 8-91359
 Pt, electron and deuteron irradiated, close Frenkel pair recomb. during annealing 8-87716
 Si, ion-implanted, secondary defects development, three-stage model 8-87725

frequency allocation

- IEEE International EMC Symposium, Atlanta (1978) 8-82876

frequency changers *see frequency converters***frequency control**

see also automatic frequency control

- 31st Annual Frequency Control Symposium, Atlantic City (1977) 8-57905
 digital clocks, 1 min. interval signal from standard freq. transmitter (*German*) 8-57902
 field-frequency lock, for a superconducting spectrometer 8-86312
 telescope drive, controlled 300 Hz freq. supply 8-61746

frequency converters *see frequency convertors***frequency convertors**

see also mixers (circuits); optical frequency conversion

- cyclotron-resonance maser amplifier with freq. conversion 8-55329
 differential frequency convertor cct. (*Russian*) 8-77872
 high resolution IR mol. spectroscopy with difference frequency generation, refinements 8-90321
 intermittent sinusoidal voltage phase difference meas. device 8-77941
 sideband upconversion in injection lasers 8-79047

frequency division multiplexing

- holocinematography, high speed, acousto-optic beam deflection for spatial freq. multiplexing 8-74860
 SAW digital FM compression system (*Russian*) 8-55541

frequency-domain analysis

- EEG slope descriptor computation, time and frequency domain comparison 8-57115

frequency measurement

see also atomic clocks

- absolute wavelength measurement, ^{127}I stabilised He-Ne laser, pressure scanning Fabry-Perot interferometer appl. 8-73971
 acoustic signal mean frequency meas. (*Russian*) 8-81441
 differential frequency convertor cct. (*Russian*) 8-77872
 gastrointestinal electrical rhythm frequency estimation by autoregressive modelling 8-56948
 hearing aid measurement system comparison 8-65151
 induction motors, piezoelectric pick-up appl. (*Russian*) 8-65911
 International time and freq. comparison using Loran-C radio waves (*Japanese*) 8-81951
 ionosphere HF radiowave propag., freq. standard utilisation 8-93027
 ionospheric EM wave propagation in HF and MF bands, Doppler meas. accuracy 8-77417
 laser freq. meas., review and extension to 197 THz 8-81952
 laser spectroscopy conf., Jackson Lake Lodge, WY, USA, 1977 July 8-82666
 laser wavelength measurements, why? how? and how accurate? 8-89446
 laser-Doppler-velocimeter, digital, signal processor accuracy testing (*German*) 8-86242
 optical frequency standard, Doppler-free stimulated-emission technique 8-93765
 reinforced concrete structural integrity assessment, NDT method 8-56847
 small frequency shifts meas. using two open resonators at mm wavelengths 8-81949
 three-phase frequency meas. transducers with saturating transformers 8-77893
 Ag beam mag. resonance apparatus as freq. standard, features 8-89458
 CO_2 laser transition absolute freqs. by multiplication of difference-freqs. 8-90445
 Cs beam deflection system for time and freq. primary standard 8-89453
 Cs beam freq. standards, freq. offset due to spectral impurities 8-89455
 Rb freq. standard, Measurement Standards Laboratory, capability improvement 8-54332

frequency meters

see also wavemeters

- 5 MHz digital frequency meter (*German*) 8-62206
 digital, for LF meas., using TTL ICs 8-86296
 digital, using variable measuring times and automatic scale conversion (*Spanish*) 8-49862
 high precision laser freq. meas., sigmameter, motionless two-channel Michelson interferometer 8-89449

frequency modulation

- cardiac valve motion obs. CW FM sonar 8-61230
 CW FM sonar with aural displays, improvements 8-87221
 dye laser jet stream, thickness meas. in real time, by optical technique 8-82975

frequency modulation continued

- Fabry-Perot resonator, laser mode sweeping dynamics, optical length effects 8-83001
 far IR lasers, optically pumped, frequency modulated noise measurements 8-55392
 fluoromethane far IR laser FM and stabilisation by Stark effect 8-59056
 laser, double heterostruct. junction type, US wave freq. modulation anal. 8-83009
 low-distortion FM demodulator using SAW delay device 8-51014
 microwave backscatter modulation by shoaling ocean waves 8-57212
 microwave spectrometer baseline suppression using FM and harmonic detection 8-82866
 non-redundant scanning, high efficiency freq. modulation, of light beam in half space 8-78907
 photoelectronic phase and frequency modulation 8-79131
 ring laser gyroscopes, multioscillator approach to locking problem 8-79042
 SAW digital FM compression system (*Russian*) 8-55541
 surface roughness estimation using linear FM signal (*Russian*) 8-77353

frequency regulation *see frequency control***frequency response**

- aerosol layer depth remote meas. by microwave-modulated laser (*Russian*) 8-57338
 Earth strain-tides, spectroscopy 8-73301
 hearing aid measurement system comparison 8-65151
 imaging system, maximum likelihood spatial filtering examples 8-63038
 IR charge transfer device imaging arrays 8-77990
 piezoelectric modulation transducers for alternating pressures 8-77891
 seismic sensors, mechanical, influencing factors (*Japanese*) 8-85722
 sound level meter meas. accuracy 8-59211
 vibrator, flexural piezoelectric, split-electrode, suppression of spurious responses (*Japanese*) 8-83204
 GaAs CW DH laser, inherent oscillations and subharmonic resonances obs. in light output 8-74910

frequency stability

see also frequency control; laser frequency stability

- 1.2 GHz temperature stable SAW oscillator 8-59226
 atomic frequency standard prediction error analysis 8-57906
 field-frequency lock, for a superconducting spectrometer 8-86312
 quartz SAW resonator deep etching 8-59248
 α -quartz SAW temp. depend. 8-51813
 quartz-LZT wide-range instrument transducer, practical feasibility 8-51035
 radio time signal coding and clocks for private and industrial use (*German*) 8-89445
 sapphire single-crystal clocks and frequency standards 8-57915
 SAW narrow pass band filter (*Japanese*) 8-90603
 SAW oscillator frequency stability developments 8-59253
 stable frequency standards comparison by TV carrier beat note transmission 8-57909
 Cs beam frequency standard design for satellites 8-57911
 Cs beam frequency standard drift and noise performance rel. to velocity distributions 8-57912
 Cs frequency standard, NRLM-I, improvement of freq. stability 8-62184
 H generator, freq. shift due to atomic collisions with storage flask walls 8-77870
 H maser design for NAVSTAR Global Positioning System satellite clock 8-58969
 H maser improvements at Smithsonian Astrophysical Observatory 8-58971
 $^{199}\text{Hg}^+$ trapped ion frequency standard 8-57914
 NH_3 special-purpose frequency standard and clock 8-57913
 ^{87}Rb maser and related oscillators, time- and frequency-domain stability 8-58968
 Si single-crystal clocks and frequency standards 8-57915

friction

see also internal friction; lubrication

- acrylic resin wear and cutting surface against brass (*Japanese*) 8-56779
 aerosol, solid phase motion, large Reynolds no., carrying agent drag 8-79363
 air flow, urban area effect on frictional convergence and convective precip. 8-81338
 alloy testing for use in heat treatment furnace, disc tribometer with high temp. pin 8-95900
 angle detector for meas. (*French*) 8-92434
 atmosphere, role of horizontal friction forces in tropical circulation (*Russian*) 8-65360
 biharmonic equation, analogue technique, cylinders falling between parallel walls 8-55628
 bluff body, two-dimens., drag and wake (*Japanese*) 8-55647
 brittle fracture, transition from plastic to brittle contact (*Russian*) 8-53000
 Brownian particle, freq.-depend. friction coeff. in fluid near crit. pt. 8-73929
 car tyre, friction and traction, for teachers 8-81751
 coefficient, effect of surface curvature 8-87310
 condensation in channel, local (total) heat transfer coeffs., friction factors 8-51045
 cone/plate system in fluid, friction heating and convection 8-87238
 convection, natural, over uniform heat flux vertical surface, higher-order approx. 8-59388
 Couette flow, striated boundary effect on viscous drag 8-59367
 crossblow, by cone over thread, numerical solution (*Russian*) 8-55612
 cylinder in cross flow, skin friction and vortex shedding freqs. 8-94758
 dental restorative materials; empirical eqn. including fracture toughness for friction 8-61283
 disk and strip forging for the determination of friction and flow strength values 8-85004
 drag force on sphere moving in medium with variable viscosity 8-67173
 dynamic rigid indentation induced by sliding frictionless contact 8-75107
 elastic contact and friction mechanisms, for rough surfaces 8-87309

friction continued

elastic contact problem with friction, solution using nodal parameters (*French*) 8-63401
 elastic contact problems, in fracture mech., friction effects 8-67142
 epoxy resin wear and cutting surface against brass (*Japanese*) 8-56779
 experimental device for measuring friction between ski and snow 8-92410
 extrusion, benefit of vibrations 8-51135
 flow, creeping, about sphere, general soln. of linear Navier-Stokes eqn. 8-71307
 flow, Reynolds analogy extension for fully rough surface 8-51159
 flow, rot., between rot. and static discs, with radial flow, numerical method 8-59403
 flow, Stokes law, Reynolds no., for teaching, erythrocyte sedimentation rate 8-49610
 flow between rot. disc and fixed wall, friction coeffs. 8-63439
 flow between rotating spheres, frictional moment 8-79301
 flow in annular channel with vortex generators, crit. heat flux, hydraulic resistance (*Russian*) 8-83397
 flow instability, two-phase, in parallel channels 8-94810
 flow normal to perforated plates, heat transfer and friction loss 8-94733
 flow over plate with simultaneous injection and suction, turbulent layer friction and vel. profile 8-83469
 flow through porous media, friction factor 8-91008
 fluidised bed, nonuniform, force on fixed sphere, rising gas bubble force field 8-59476
 fluoro epoxy resins, surface props., appls., wear resistance and friction 8-64713
 friction machine, residual stresses meas., appl. to wear resist., surface wear 8-60906
 gas, with variable physical props., pipe flow, turbulent momentum and heat transfer calc. 8-90869
 gas-liquid annular two-phase flow, wave and interfacial friction characts. 8-67249
 glass fibre reinforced PTFE and polyacetal, friction and wear against glass and steel 8-56783
 heat exchanger, with lamellar surfaces and smooth ribs, gas flow resistance, heat exchange (*Russian*) 8-83218
 heat pipe, with header and single or two-phase artery systems 8-90981
 heat transfer and friction factors for laminar flow through finned tube 8-94730
 high contact speed, sliding friction coeff. determ. 8-87308
 hydraulic machines, liquid and dry power losses calc. method 8-85009
 hydrodynamic, sticking and slipping boundary conditions, friction of rot. bumpy cylinder 8-63410
 hydrodynamic thermal breakdown in viscous fluid, Couette flow between cylinders 8-83391
 hydroplaning of a rotating cylinder on water 8-63522
 hydroplaning plate, lift, drag 8-63523
 ice single crystal, friction of steel ball load, velocity and temp. depend. (*Japanese*) 8-88537
 ice single crystal, friction of WC ball, anisotropy (*Japanese*) 8-88539
 ice single crystal, friction of WC ball, slider size effect (*Japanese*) 8-88538
 interface of two solids, sliding mechanism without slipping 8-51136
 jet impact system with unilateral outlet, air flow, heat exchange (*Russian*) 8-83449
 laminar film condensation from moving vapour, with suction 8-59459
 linear elastic half-space, frictional unloading problem, variational soln. for stress analysis 8-59350
 liquid pipe flow, heat exchange and resistance calc. 8-94819
 macroscopic Van der Waals interactions, contrib. to frictional force 8-55613
 metal, friction and slip during cold rolling 8-64707
 metal surface, AES anal. in adhesion, friction and wear 8-53179
 metal transfer in frictional contact of rough hard surface 8-64739
 metal wear energy balance under abrasive and boundary friction, expt. 8-85006
 MHD convective viscous flow past porous plate with suction, mass transfer effects 8-87398
 MHD turbulent heat and momentum transfer in 2-dimens. channel with transverse mag. field 8-94848
 Ni, friction props. of surface films in air and high vacuum 8-60850
 non-Newtonian flow along thin needle, vel. profile, skin friction 8-67229
 nonspherical particle, friction coeffs. in incompressible fluid with spin 8-87350
 numerical integration of eqn. system for nonadiabatic compressible gas flow in tube (*Russian*) 8-83427
 nylons, exam. of frictional behaviour (*Japanese*) 8-64714
 permeable spheres in incompressible fluid, hydrodynamic interaction, mobility tensors 8-71395
 permeable spheres in incompressible fluid, hydrodynamic interaction vel. fluid, friction consts. 8-75202
 pipe, heated, vertical, gas buoyancy effect on downward flow and heat transfer 8-74427
 pipe flow, turbulent, temp.-depend. viscosity effect on convective heat transfer 8-90884
 plastic flow round crack under friction and combined stress 8-79280
 plate tectonics, roles of boundary friction, basal shear stress and deep mantle convection 8-57188
 plume, turbulent, thermal, along vert. wall, struct. and heat transfer 8-90880
 polyamide resin wear and cutting surface against brass (*Japanese*) 8-56779
 polyethylene, branched, frictional props., true area of contact 8-64735
 polyethylene pellets, falling in air in pipe, equilb. region press. drop, friction factor 8-63479
 polyimide films, effect of atm. and temp. on wear, friction and transfer 8-85003
 polymer, calc. of coeff. for isotropic surface contact 8-64716
 polymer additives in pseudo-turbulent flow, nonlinear dumbbell model 8-51206
 polymer films, between contacting surfaces, effect of contact pressure and temp. 8-60842
 polymer solution, semidilute, hydrodynamic interaction of two permeable spheres, method of reflections 8-71394
 polymer solutions, viscosity, intrinsic, friction coeff., porous sphere model 8-71301

friction continued

polymers, friction and wear, role of mech. props. 8-52998
 press forming of sheet metal, frictional surface damage 8-76768
 PTFE, sliding charact., friction and wear (*Japanese*) 8-56778
 PTFE impregnated porous bronze, coeff. of friction, temp. effect 8-64737
 pulsating laminar-boundary layer, heat transfer and skin friction 8-94711
 pyrex, plates, exam. of friction, wear and elastic constant mechanisms 8-87309
 rib-roughened surface, friction factor and heat transfer correlations with rib characts. 8-87233
 shallow water basin, wind-driven current, eddy viscosity, bottom friction 8-65319
 skin friction, Reynolds number depend. of bulk flow variables in duct flow 8-94827
 skin friction coefficient, correl. with momentum thickness Reynolds number and free stream press. gradient 8-94640
 slip flow, MHD, over porous plate, with variable suction, heat transfer 8-79337
 sphere in unsteady motion in liq., drag, calc. 8-67170
 spiral vibration of rotating shaft rubbing against interference element (*German*) 8-87252
 stagnation point boundary layer on subliming surface with roughness elements 8-94635
 steady flow in collapsible tubes 8-57033
 steam-generating tube, bubble/plug flow boiling regimes, elevated press., drift vel. and void fraction determs. 8-87379
 steam-water, flow characts. at high press. 8-94805
 steel, 40Kh, heat-treated, wear during friction under extreme conditions 8-85007
 steel, case-hardened cast, contact endurance rel. to austenizing (*Russian*) 8-56805
 steel, hypoeutectic, texture development from frictional stress (*German*) 8-53003
 steel, mild, conical rider on Cu surface plastic deform. and wear at friction junction, SEM exam. 8-88542
 steel, sheet galling, development of quantitative test 8-92433
 steel, sheet structural changes during rolling influence of lubricants on friction and wear 8-95815
 steel, stainless, austenitic, CC Ni-Al, γ -phase, fracture mechanical aspects of abrasive friction, wear, chip formation 8-72865
 steel, stainless, sintered Kh18Ni10T, friction and corrosion props. for frictional units of nuclear plants 8-60845
 steel wire reinforced Portland cement mortar, wire pull out, inelastic behaviour 8-56681
 superionic wave drag of planar singularity distributions 8-83430
 terrestrial gyrocompass dry friction anal. (*Russian*) 8-77899
 test machine, SMTs-2, broadening of test capabilities by modification 8-60919
 testing equipment for use at high temp. in air 8-56839
 thermal desorption with large variable friction constant 8-71974
 top rising by friction, exact mathematical soln. 8-83343
 translational friction, for arbitrary shaped objects, modified Oseen tensor calcs. 8-71311
 transonic vel. profiles, local skin friction coeff. 8-67214
 tribology study reactor fuel element, PEC type, in Na at high temps. (*Italian*) 8-58362
 tube, horizontal, laminar combined convection, circumferentially nonuniform heating effect 8-71331
 tube wall heating during steady state tube drawing (*German*) 8-84899
 turbulent air flow in round tube, high-temp., friction resistance, cooling (*Russian*) 8-75135
 turbulent axisymmetric boundary layer, skin friction, weak and strong disturbances effect 8-90857
 turbulent boundary layer, compressible, extended mixing length appls. 8-94655
 turbulent boundary layer, large eddy destruction effect on skin friction 8-90860
 turbulent boundary layer, separation region, oscillatory flow effects 8-75127
 turbulent boundary layer, supersonic, wall temp. effect 8-94765
 turbulent boundary layer on rough surface with blowing, heat transfer behaviour 8-71334
 turbulent boundary layer with surface roughness and injection 8-94654
 turbulent water film, with different initial flow conditions and high temp. gradients, heat transfer 8-90862
 two-phase channel flow with friction 8-59458
 two-phase flow, compressibility effect on hydrodynamics, resistance coeff. 8-55684
 US inspection of friction materials 8-60931
 variational method of investigating contact problems with slip and cohesion 8-63398
 viscoplastic liquid film on vertical vibr. wall, with slip, shaking loose 8-59371
 water surface, free, roughness determ., from air flow struct. anal. 8-63441
 water-entrained gas flow, force on moving body 8-63480
 wear mechanism review 8-72891
 wear resistance, surface treatments, selection procedure, review 8-72892
 Westerly granite, high temp. frictional sliding mechanisms 8-73357
 wing, rectangular, with tip clearance in channel, aerodynamic characts. 8-59415
 Ag, sliding charact., friction and wear (*Japanese*) 8-56778
 Al, thin foil, adhesion and friction, rel. to observed dislocation density 8-64706
 Al-graphite particulate composite, exam. of friction, wear and tensile props. 8-72890
 Al-Si-Cu-Ni alloy casting, thermal props. 8-95814
 Al_2O_3 - (TiO_2) coatings, detonation deposited on steel, prep., wear resist., antifriction props. 8-60877
 Au, friction props. of surface films in air and high vacuum 8-60850
 Au, sliding charact., friction and wear (*Japanese*) 8-56778
 BC, sintered and hot pressed, friction and wear, 20 to 1500°C 8-60844
 BN, pyrolytic, in contact with various metals, friction and transfer behaviour 8-88535
 C fibre reinforced PTFE and polyacetal, friction and wear against glass and steel 8-56783

friction continued

- Cr, sliding charact., friction and wear (*Japanese*) 8-56778
 Cu, friction props. of surface films in air and high vacuum 8-60850
 Cu, friction under electrolyte immersion condition 8-64738
 Cu single crystals, influence of friction and geometry of deformation, on texture inhomogeneities during rolling 8-72792
 Cu, sliding charact., friction and wear (*Japanese*) 8-56778
 Cu-graphite starter brushes, effect of high velocities, current densities on wear, friction 8-88544
 Cu-M alloys (M=Zn,Al,Sn,Mn,Pb), diffusive redistrib. during friction (*Russian*) 8-52999
 Fe, friction props. of surface films in air and high vacuum 8-60850
 Fe-(Mo)-CaF₂, sintered, friction and corrosion props. for frictional units of nuclear plants 8-60845
 Fe-based materials, wear resistance, surface hardening processes, review 8-72894
 Fe-Cr-Mo-C, X-ray investigation after friction and oxidation 8-52997
 Ge, supercond, friction layer formed during friction between Ge and Pb (*Russian*) 8-52143
 He, flow, of liq.-vap. mixture, frictional press. drop, adiabatic and heated conditions 8-90983
 He, near-critical, friction factors for flow in curved tubes 8-83367
 MoS₂, sliding charact., friction and wear (*Japanese*) 8-56778
 N₂O₄, dissoc. flow in tube, heat transfer and drag 8-71402
 N₂O₄, dissociating, turbulent pipe flow, heat transfer, resistance 8-91026
 Na, liq., in vert. pipe, hydraulic resistance under boiling conditions 8-90968
 Na₂O-SiO₂ glass, coated with SnO coeff. of friction and fracture toughness 8-80657
 Ni, sliding charact., friction and wear (*Japanese*) 8-56778
 NiCr-AlY sintered fibre metal struct. abradable seal material, friction and wear 8-56785
 Se, amorphous, friction and wear under lightly loaded contact 8-64740
 Ti alloy, VT3-1, vacuum-chromized, fretting-corrosion in couple with unprotected BT3-1 and steel 40KhNMA (*Russian*) 8-56804
 Ti-Cr, sintered, friction and wear, structural factors 8-60843
 Ti-Cr-TiC, sintered, friction and wear, structural factors 8-60843
 Ti-Ti system, sintered, friction and wear, structural factors 8-60843
 TiC-Ni-Mo hard alloy, wear resistance under end face friction cond. 8-60846
 WC-Co sputter deposited film, friction and wear 8-72918

friction, internal see *internal friction*

frictional electricity see *triboelectricity*

fuel

- see also *coal; fission reactor fuel*
 natural gas tunnel burner, heat transfer, computer model predictions test 8-59504
 rocket propellants, thermodynamic evolution, extension of Huff's method 8-75054
 H₂, synthetic fuel production, Tokamak high-temp. blanket 8-74479

fuel batteries see *fuel cells*

fuel cells

- LiAlO₃, fuel cell electrolyte matrix, prep. and struct. characts. 8-80488

fugacity

- see also *kinetic theory of gases*
 vapour-liquid equilibria, generalised method for calc. and prediction at high press. 8-87780
 O₂ fugacity of basaltic magmas, role of gas forming elements 8-77218

full wave rectification see *rectification*

function approximation

- see also *Chebyshev approximation; interpolation*
 bordering functions based interpolation method 8-81816
 bordering functions based numerical method 8-81815
 chemical composition centre waves, periodic chaotic, Pade approximant scheme 8-80716
 elastic shells, two-dimensional eqn. system (*Ukrainian*) 8-89342
 minimum norm, numerical methods convergence 8-54166
 multidimensional integrals, numerical calc. 8-89323
 multivariate approximants with branch points, off diagonal approximants 8-54160
 multivariate approximants with branch points, practical evaluation 8-54161
 orthogonal polynomials expansions, summation procedure 8-81805
 Pade approximants, variational approach to NN dynamics 8-62427
 Pade approximants via continued fraction approach 8-61972
 power series, class of algorithms for obtaining rational approximants 8-54169
 Rayleigh-Schrodinger, appl. of Pade approximants 8-65806
 stochastic approx. procedures in continuous time 8-69969

function evaluation

- asymptotic series coefficient, generalised calculus using steepest descent method (*Rumanian*) 8-89304
 atomic struct., numerical HF radial function during SCF iteration, convergence 8-58574
 Earth gravity field spherical functions, numerical development (*German*) 8-61311
 fibre-optic digital transmission, shot noise probability distribution function 8-50717
 fluid dynamics, pseudo-spectral FFT technique, non-periodic problems 8-59359
 Ursell functions, group functions and derivatives 8-70049

function generators

- see also *pulse generators; signal generators; square-wave generators; time bases*
 analogue-digital function generator, for pulsed AAS (*Russian*) 8-70199
 digital based triangular wave generator for Mossbauer spectroscopy 8-55113
 digitally controlled, and storage instrum., electronic modelling appls. 8-77937
 optical wideband ambiguity function generator with Doppler compensation 8-78936

functional analysis

- see also *harmonic analysis*
 ϕ^3 interaction, four-dimensional Green's function model (*Russian*) 8-77775

functional analysis continued

- Airy functions, stress problem solns., teaching appl. 8-86063
 algebra of pseudodifferential operators and the asymptotics of quantum mechanics 8-93547
 analytic continuation of the Fourier Series on connected compact Lie groups 8-93511
 dimensional base selection in expt. design and planning 8-49636
 dusty gas, unsteady flow in cylinders, numerical soln. 8-51231
 field quantisation, number operators for distinguishing Bose, Fermi and parastatistics 8-93562
 fission reactor, functional anal. of multigroup neutron diffusion problem 8-58317
 fracture mechanics, appl. of method of pots. 8-51121
 H-functions of radiative transfer problems, representation for multiplying media 8-53808
 induced potential problem in 3-D, functional analytic approach 8-58880
 linear functionals in nonlinear problems, general estimates 8-49643
 Minkowski spaces, estimates for constants of local unconditional struct. 8-89299
 mixed continuous mechanics problems, orthogonal functions (*Russian*) 8-49659
 nonlinear oscillator, stroboscopic phase portrait and strange attractors 8-54177
 optical system with annular pupil, orthogonal polynomials, appl. to Fraunhofer diff. 8-50714
 optimal control of 1-D linear distributed parameter systems with cost functionals 8-59257
 Schrodinger operator, scatt. and local absorpt. 8-93546
 shells of revolution, thin-walled, heated, temp. field, thermostatic control 8-67003
 spherical delta functions, multipole expansions for fields, using Cartesian Taylor series 8-86118
 spheroids, harmonically oscillating, unsteady airload prediction, analytical soln. 8-51184
 turbulent boundary layer on a moving surface, integral and numerical methods 8-63421
 viscoelasticity, Il'yushin kernels, analytical representation 8-67055

functional equations

- approximation functionals, simplification in elastoplasticity theory (*Russian*) 8-63328
 bifurcation of stable stationary solns. from symmetric modes 8-57752
 continuum mechanics, macroscopic determinancy principle corollaries (*Russian*) 8-77714
 fission reactor, functional anal. of multigroup neutron diffusion problem 8-58317
 quasiclassical asymptotic behaviour of functional integrals, scatt. amplitude 8-62325
 random heat conduction in solids, functional eqns. 8-83210
 Saint-Venant torsion problem, classical, integral and functional eqns. 8-57780
 strong Markov process time change (*French*) 8-62151
 superposition of numerical graphs, functional changes (*Ukrainian*) 8-89293

functionals see *functional equations*

functions

- see also *Bessel functions; Boolean functions; describing functions; Green's function methods; random functions; recursive functions; transfer functions; vertex functions; Walsh functions*
 diffusion, non-stationary one-dimensional, psi-functions 8-54322
 distribution function $y=ax^b \exp[-c(\ln x)^2]$, props. (*German*) 8-77686
 Gaussian distribution, unconventional calc. of moments 8-49647
 gravity disturbance covariance functions, upward continuation integrals 8-85468
 Hamiltonian, quantification of geodesic flow of sphere Sⁿ (*French*) 8-54151
 kernel functions in EM closed region problems, singularity extraction 8-66728
 Mathieu modified functions, second kind, integer order for small values of parameter, limiting form (*French*) 8-86113
 mechanical systems with non-holonomic constraints, existence of potential function (*French*) 8-86128
 Neumann's operator in potential theory, contractivity 8-69966
 nonstationary one-dimensional diffusion under forced convection, Omega functions as auxiliary functions 8-93631
 ocean remote sounding instruments, quasi-optimum operating functions (*Russian*) 8-77362
 parabolic cylinder functions, asymptotic approximations 8-89301
 parabolic cylinder functions, asymptotic expansions, comment on previous letter 8-89302
 Payne-Rayner isoperimetric inequality, extension to N dimensions (*French*) 8-54323
 radiative transfer, exit function for unified treatment of reflected and transmitted intensities 8-85838
 Sheffer, one variable, main diagonal necessary and sufficient conditions 8-54152
 stellar spectral line shapes, convolution function for combined expansion and rot. effects 8-53920
 Voigt functions, partial derivatives 8-89052

fundamental constants see *constants*

fundamental law tests

- Eotvos expts. and weak interactions, anal. 8-78129

fundamental particles see *elementary particles*

fundamental physics concepts see *physics fundamentals*

fundamentals of physics see *physics fundamentals*

furnaces

- see also *electric furnaces; refractories*
 burner with diffusive control, intermixing of gas streams with transverse swirled air flow 8-87418
 carbon furnace for IR source, practical consideration 8-81976
 control, Nicrosil-Nisil alloy thermocouple appl. 8-49831
 horizontal epitaxial reactor having multiple elongated-inclined susceptors 8-80475
 Mossbauer furnace, high-precision for use up to 1100K 8-66021
 optical vacuum furnace for Raman and Brillouin spectroscopy 8-58062
 radiation flux model 8-93689
 tunnel furnace, natural gas fired, heat transfer, 3-dimens. computer model predictions test 8-59504

furnaces continued

- ultra-high extraction furnace for inert gas analysis 8-77918
- vacuum melting furnaces and casting techniques 8-84727
- Ta foil lining of graphite furnace, at. spectrosc. 8-74078
- WC vacuum sintering furnace systems 8-84737

Furry theorem *see quantum electrodynamics***fuses, electric** *see electric fuses***fusion** *see melting***fusion, nuclear** *see nuclear fusion***fusion reactor ignition**

- see also fusion reactor materials; plasma heating; plasma production*
- accelerator grid assemblies, 120 keV, fabrication and brazing 8-66379
- advanced lasers for fusion, modelling and anal. 8-50819
- ANTARES device, target-induced parasitic oscils. 8-59072
- ASDEX fusion experiment, toroidal field coil construction features (*German*) 8-54877
- Asterix III and German laser fusion programme 8-63136
- Baseball II-T experiment, microcomputer-based pellet trajectory guidance system 8-62623
- beam injection, ripple-assisted, magnetics design for ISX-B and TFTR Tokamaks 8-62643
- beat heating, system, using double-barrelled laser 8-67386
- Berkeley type ion source, long life cathode 8-66375
- coil design, cost anal., for neutral beam magnets 8-55005
- concentric shock wave, const. speed, in nonhomogeneous medium, thermonuclear microfusion 8-83281
- cryogenic laser fusion targets, fabrication 8-58485
- cryogenic laser fusion targets, irradi. systems 8-58486
- cryopumps for high power neutral injectors, design and performance 8-74494
- cryopumps for PLT neutral beam injectors 8-58439
- CTR neutral beam source, SCR series switch and impulse crowbar 8-66395
- deuterium-tritium thermonuclear ignition, high current density approach, expt. 8-54874
- double shell targets, low aspect ratio, for high density and high gain 8-58479
- Doublet III noncircular Tokamak, neutral beam injection system 8-54970
- duopigatron ion source, modified, ion composition 8-54914
- duopigatron ion source for PLT injectors 8-54913
- E-beam sustained large amplitude CO₂ laser discharge, for fusion appls. 8-55382
- eight-beam CO₂ laser system, high-voltage engineering 8-58492
- eight-beam CO₂ laser system, minicomputer-CAMAC control system 8-58493
- electron accelerators, pulsed power technology for fusion expts. 8-50321
- electron beam focusing and target irradi. in Angara-I accelerator 8-54911
- electron beam pinching from discrete cathodes 8-50318
- exploding pusher target, performance of fixed laser power theory 8-58481
- exploding pusher targets, expts. of Lawrence Livermore Lab 8-58482
- explosive implosion of polyethylene shell in D₂-filled cone, fusion neutron prod. 8-82510
- Fabry-Perot interferometer transients, for ultrashort laser pulse generation 8-58019
- fast ion beam, in Tokamak plasma, quasilinear relax. (*Russian*) 8-87457
- feedback laser fusion using direct nucl. pumped laser 8-58445
- free electron laser, fusion appls. 8-58974
- fuelling profile sensitivities of trapped particle mode transport for TNS 8-58421
- fusion reactor neutral beam transport system 8-54968
- Group IV photolytic laser expts., for fusion research 8-63101
- Group VIA photolytic laser systems, for fusion research 8-59002
- gyrotrons and gyrokystrons, small signal theory, fusion reactor appl. 8-70633
- gyrotrons for high power millimeter wave generation 8-62611
- heavy ion fusion, linear accelerator facilities at Argonne 8-50327
- high current switch, fast closing, for fast discharge expt. 8-74483
- high current switch, fast-closing, for Doublet III poloidal field circuit 8-74484
- high n flux fusion heating, ⁶Li(n,t)⁴He use 8-89975
- high-power pulsed laser requirements and performances 8-83592
- hollow-cathode multipole boundary ion source, IBIS, plasma prod. and containment system 8-74521
- hyperdetonation eccentric shock wave, approx. soln. 8-67070
- hyperdetonation shock wave passage through jump like nonhomogeneity 8-67069
- ICF targets, material response and implosion dynamics obs. 8-58477
- ignition Tokamak, neutral beam system 8-54973
- implosion heating coil, radially fed, design, fabrication 8-55006
- inductor for high power impulse production, Joint European Torus appl. (*German*) 8-50293
- inert gas hydride laser, use two-step nucl. fusion dissipative confinement of doubly isotopic boron hydrides 8-82506
- inertial confinement, reaction gains, reheat calcs., collective model 8-59664
- inertial confinement, temporally shaped laser pulse generation 8-50831
- inertial confinement fusion, electric power generation 8-50314
- inertial confinement fusion, LASNEX code simulation 8-58478
- inertial confinement fusion, requirements for commercialization 8-50330
- inertial confinement fusion targets 8-50299
- inertially confined fusion with heavy ion beams 8-50313
- inverse bremsstrahlung absorption intensity depend., in inhomogeneous standing wave, laser fusion appls. 8-67382
- ion beam, low ang. momentum, for pellet fusion 8-50326
- ion beam accelerator, multimewatt, high-voltage power system, design philosophy 8-62613
- ion beam accelerators, high voltage protection, using floating deck modulators 8-66392
- ion beam direct conversion 8-54920
- ion beam focusing and neutralised transport 8-50323
- ion beam focusing by means of mag. insulated diodes 8-50324
- ion beam periodic transport system, K-V distrib. stability 8-50329
- ion beams, prod. and focusing for fusion 8-50322

fusion reactor ignition continued

- ion beams, transport, space charge effects, computer simulation 8-50328
- ion beams from pulsed linear accelerator for inertial fusion 8-50325
- ion cyclotron heating, Tokamaks and mirrors, quasilinear model 8-59626
- ion extractor electrode CAD (*Japanese*) 8-86680
- ion source, Periplasmatron, for neutral beam injection systems 8-54915
- ion source for JT-60 neutral beam injector 8-54912
- ion-ring igniter for inertial fusion 8-78497
- JAERI experimental fusion reactor, neutral injection system 8-54972
- laminated coatings, for fuel confinement, strength optimisation 8-60883
- laser, alignment system for large high-power pulsed CO₂ laser fusion system 8-59075
- laser, fusion experiment alignment accuracy meas. 8-55731
- laser, multiple-beam pellet irradiance, diffraction analysis 8-50845
- laser acceleration of reactor-fuel pellets 8-86687
- laser beam alignment, accuracy, Snout test 8-59073
- laser beam steering, investig. using hole grating attenuator 8-59071
- laser design for inertially confined fusion reactor 8-58423
- laser driven implosion, expts. using the Shiva target irradi. facility 8-58483
- laser driven implosion of gas-filled microballoons 8-50317
- laser fusion, 4 TW system 8-74471
- laser fusion, beam transport optics 8-83017
- laser fusion, CO₂ single beam irradi., diagnostics 8-51329
- laser fusion, electric power generation 8-50315
- laser fusion, fast optical shutters for Nova 8-66854
- laser fusion, truncated Maxwellian electron vel. distrib., ion expts. 8-51326
- laser fusion, wavelength scaling 8-51328
- laser fusion diagnostics with axisymmetric grazing incidence X-ray microscope 8-75422
- laser fusion experiments, performance of Argus Nd:glass laser system 8-55361
- laser fusion expts., tamper temp. and compression, simultaneous proton and α -particle meas. 8-83607
- laser fusion expts. at Osaka, pellet compression 8-50300
- laser fusion implosion, X-ray diagnostics 8-51362
- laser fusion reactor concepts 8-58422
- laser fusion reactor engineering design aspects of SOLASE 8-58425
- laser fusion reactor study, SOLASE, laser, optics and pellet design 8-58426
- laser fusion reactor study, SOLASE 8-58424
- laser fusion reactor targets, energy partition and neutron spectra 8-58451
- laser fusion reactors, optical design, focusing optics 8-82518
- laser fusion target, fast ions 8-51327
- laser fusion target, loading and kinematic positioning 8-58487
- laser fusion targets, automated prod. system 8-62608
- laser fusion the Japanese way (*German*) 8-66838
- laser high energy systems, conference, Reston, VA, USA (Apr. 1977) 8-50783
- laser imploded targets, compressed core density and radius, X-ray spectroscopy meas. calcs. 8-59685
- laser inertial confinement fusion research, 100 kJ CO₂ laser optical design 8-82990
- laser irradiated target, mag. field transport, nonlocal cond. effects, simulation 8-59637
- laser irradiation facility, OMEGA fusion system 8-50811
- laser plasma density profile modification by ponderomotive force 8-59634
- laser plasma simulation code, PHD-IV 8-59640
- laser saturable absorber cells for CO₂ fusion, parasitic oscils. suppression 8-87066
- laser system, high energy Nd:glass, multi-lens focusing systems 8-50848
- laser system, multibeam, OMEGA-10, automatic alignment system 8-50847
- laser system, Shiva Nd:glass, for fusion expts. 8-50812
- laser thermonuclear fusion problems and progress 8-74500
- laser-driven implosion, Rayleigh-Taylor instability, nonlinear development, calcs. 8-58475
- laser-driven implosion experiments 8-58490
- lasers for fusion appls., energy storage and nonstoring laser media 8-79027
- magnetic cusp, relativistic electron beam driven inertial fusion, transport calcs. 8-75268
- magnetic field generation by Rayleigh-Taylor instability 8-58476
- microexplosion of pellet, debris energy deposition in wall 8-54890
- microwave start-up of Tokamak plasmas near electron cyclotron and upper hybrid resonances 8-94137
- Mirror Fusion Test Facility, neutral beam injection, optimisation by computer graphics 8-66376
- mirror-damage thresholds for laser-fusion pulse shapes 8-74467
- multichannel configuration, relativistic electron beam driven inertial fusion, transport calcs. 8-75268
- multiple shell ICF capsules, stability 8-58474
- MW impulse generator system, for ion cyclotron heating 8-70635
- Naval Research Laboratory, USA, inertial confinement fusion programme 8-59042
- negative ion beam, generation, transport and accel. 8-66378
- negative ion beam, intense 150 kV test stand electronics system 8-54934
- negative ion beam acceleration to energies up to 120 keV 8-54918
- neutral atomic beam source, power supply system 8-66393
- neutral beam, 120 keV, calorimetric and optical diagnostics 8-54933
- neutral beam, pulsed, arc (arc filament) power supplies 8-70637
- neutral beam accelerator electrodes, spark discharge protection 8-62609
- neutral beam filament supply, 15 V 10³ A, programmable, regulated 8-70630
- neutral beam high-voltage test stand 8-70632
- neutral beam injection scenarios for TNS 8-58464
- neutral beam injection vac. components 8-74493
- neutral beam injector, beam line studies 8-54969
- neutral beam injector, monoenergetic, power flow and gas flow models 8-66398

fusion reactor ignition continued

neutral beam injector system, for 2XIIB expt., automated control 8-62620
 neutral beam injectors, electrostatic energy recovery system 8-66400
 neutral beam module, 80 keV 8-54917
 neutral beam power supply, series switch/regulator system, 40 kV, 80 A, 10 ms 8-66366
 neutral beam power system, for Princeton TFTR fusion reactor 8-70639
 neutral beam source 8 MW voltage series regulator 8-70631
 neutral beam system, 120 keV 8-66377
 neutral beam test facility, 150 keV 8-62660
 neutral beam test stand, 120 keV, computer based diagnostic and control system 8-66389
 neutral beams, continuously operating, mech. design criteria 8-66380
 neutral injection beam line, parameter studies, computer programme 8-66390
 neutral injection beam line, Ti getter pump, corrugated surface and pumping speed 8-74491
 neutral injection beam power monitor system 8-54944
 neutral injection power supply system, for Princeton large torus fusion reactor 8-70638
 neutral injection system, cold gas flow pattern evaluation 8-66397
 neutral-beam divergence due to imperfect magnetic shielding 8-78489
 neutron generation by implosion of D₂ gas target 8-54869
 non-self-sustaining thermonuclear reaction in Tokamak 8-94138
 Nova: the laser fusion scientific feasibility experiment 8-59040
 nuclear pumped lasers, 'next step' expt., inertial confinement fusion appls. 8-58997
 ohmic heating energy storage for power reactor, costing 8-58495
 ohmic heating system for TFTR Tokamak 8-55017
 Omega laser system for fusion studies, Rochester Univ. 8-59041
 optics in adverse environments, conf., San Diego, USA (Aug. 1977) 8-82976
 particle accelerators, power flow studies 8-50320
 particle beam target, for inertial confinement fusion, mag. field prod. and heating in fuel 8-58480
 pellet ablation layer, Rayleigh-Taylor stability 8-58473
 pellet fusion targets, fast protons energy deposition 8-58404
 pellet heated by multi-GeV heavy ions, filamentation instability 8-89976
 pellet implosion reactor engineering, use of advanced fuels 8-58444
 planar streak tube, for X-ray and optical cameras, laser fusion appls. 8-59686
 plane hyperdetonation wave generation, optimum conditions 8-67068
 plasma polymerised films on glass, as laser fusion targets, deposition method 8-60860
 plasma source for Tokamak fusion test reactor beam lines 8-54916
 PLT, neutral beam injectors, component design 8-54966
 PLT, neutral beam lines, development and testing 8-54967
 PLT, neutral beam test stand, data acquisition system 8-62622
 PLT neutral beam injection, impurity studies expt. ORMAK 8-58438
 PLT neutral beam injection system cryopump, liq. He-cooled 8-74495
 PLT neutral particle injectors 8-58437
 polyethylene microspheres, deuterated, variable density, laser fusion targets, prep. 8-74468
 pulsed laser, electronic instrumentation systems 8-78498
 rare earth halide vapour, discharge, potential fusion laser systems 8-63074
 reflectionless shock-waves used to homogenise a jump-inhomogeneous medium 8-83568
 relativistic electron beam pinching and combination for inertial confinement fusion 8-50319
 relativistic electron beams, transport in laser prod. plasma channel 8-71568
 saturable absorber gases, for CO₂ laser gain isolation 8-59095
 Shiva, laser-target and laser isolation 8-59035
 Shiva alignment systems 8-59033
 Shiva high-radiance nd-doped disc laser amplifiers 8-59036
 Shiva laser, 25 MJ energy storage and delivery system 8-55015
 Shiva laser, 25 MJ energy storage and delivery system 8-59038
 Shiva laser beam diagnostics 8-59037
 Shiva laser computer control system 8-59034
 Shiva laser fusion facility construction, optical engineering problems 8-82989
 Shiva laser performance, nominal interstage beam energy, power 8-59032
 Shiva laser system for laser fusion 8-50820
 Shiva mechanical systems 8-63135
 Shiva optical system 8-59039
 Shiva pulse power conditioning, isolation and control system 8-54935
 Solase laser fusion reactor, wall protection scheme. 8-58491
 target fabrication of CVD of Mo₂C 8-60861
 target production, for inertial confinement fusion power plants, costs. 8-58488
 TFTR, neutral beam injection system 8-54971
 TFTR neutral beam injector, calorimeter and beam dump design 8-66382
 TFTR neutral beam source, power supply system 8-66394
 TFTR prototype neutral beam injector, test facility 8-62659
 TFTR type neutral beam system, ion accelerator design and fabrication 8-66381
 thermonuclear neutron pulse, electron beam generated, scintillator-photomultiplier response 8-51357
 TMX injector system, mech. design 8-66403
 TMX neutral beam power supply, 40 kV, 25 ms 8-62610
 Tnr criterion for fusion plasmas, fusion-fission analogy 8-74469
 TNS, ignition test reactor, decision modelling 8-50362
 TNS Tokamak plasma, small radius start-up, moving limiter effects 8-50360
 tokamak, decision model for near term (TNS) ignition reactor 8-58415
 Tokamak, experimental power reactor, plasma studies 8-66418
 Tokamak, heating by accelerated neutralised charge carriers (German) 8-67377
 Tokamak, Petula, vac. vessel and RF coils for compressional transit time mag. pumping heating 8-70634
 Tokamak, reactor size, diffusive losses and scaling law 8-87478
 Tokamak fusion ignition, lower hybrid heating system 8-70636
 Tokamak high field ignition test reactor using Bitter magnets 8-58417

fusion reactor ignition continued

Tokamak ignition test reactor, TNS, consideration of bundle divertors 8-58440
 Tokamak plasma, fueling profiles and radial transport 8-66421
 Tokamak plasma startup system 8-62612
 Tokamak power reactors, initiation pulse prod. methods in ohmic heating circuits 8-55730
 toroidal plasma, D-T to catalysed-D operation, trapped ion scaling law 8-66419
 twin beam mirrors, effect of hot beam injection angle 8-58466
 ultraintense heavy ion beam generation, by radiation cooling in long drift tube 8-58489
 Wendelstein VII A, injector design 8-54965
 Z-pinch for CO₂ laser pellet simulation expts. 8-55742
 D-T pellet, ideal gas treatment, implosion and shock waves 8-55735
 CF₃I, I laser medium, UV absorption profile modification by vibr. excitation, for fusion ignition 8-58717
 CO-O₂-SF₆, efficient CO₂ laser radiation 3rd harmonic generation, for fusion ignition 8-59087
 CO₂ laser, nsec pulse amplification at efficiencies greater than 20% 8-50818
 CO₂ laser, optical isolation by flowing gaseous saturable absorbers 8-59096
 CO₂ laser amplifier, short pulse amplification calcs. 8-58979
 CO₂ laser systems for laser fusion appls. 8-50817
 D plasma neutron generation by CO₂ laser implosion of polyethylene shell into conical region 8-87468
 D-T ball, compressive plasma fusion using CO₂ lasers 8-82507
 D-T charges, explosion-induced compression for thermonuclear microfusion, power station parameters 8-82508
 D-T filled glass shells, plasma polymerisation coating method 8-60859
 D-T plasma, kinetics of compression induced fusion chain reaction 8-50297
 D-T plasma ball, critical continuously shaped concentric explosive compression, approx. estimate 8-87473
 D₂ filled glass microspheres for multibeam laser-target expts. 8-82509
 D₂-³He, filled microspheres, implosion expts. 8-59672
 F₂, VUV high-power laser, laser-induced fusion 8-58996
 H ion source, hollow cathode device 8-54921
 H⁺, production by Hall accelerator in Cs vapour, space-charge effects 8-67375
 H⁺ source, for neutral beam injection 8-54919
 HF, high-energy laser, energy extraction, beam quality, for fusion ignition 8-63102
 H₂O, dielectric insulation for electron accelerators and impulse current generators (Russian) 8-75430
 HgCl discharge laser, electron beam sustained, operation, appls. 8-59043
 I laser, high-power, beam quality, gain saturation effect, for fusion ignition 8-63149
 KrF laser beam, Raman pulse compression, for fusion expts. 8-59086
 Nd:YAG short-pulse oscillator, for Shiva 8-63134
 Ne plasma, compression, spectra, temp. and density calc. model 8-59663
 OCS laser, two-quantum excitation, photolysis, energy transfer, for fusion expts. 8-59003
 Pd alloy membrane pump, for thermonuclear fusion devices 8-89980
 Se photolytic fluorescence pumped gas laser system 8-62606
 SiO₂, laser-fusion microballoon, expansion density profile, 10.6 μm irradiation 8-86686
 T low inventory for inertially confined fusion, high thermonuclear gains 8-50339
 Tb-Al-Cl vapour complex, fusion laser gain medium 8-63073
 TbCl₃-AlCl₃ vap., high-energy laser medium props., for fusion ignition 8-63075
 U, profiled explosion-induced compression 8-50296

fusion reactor materials

see also fission reactor materials; radioactive waste
 A15 superconductors, radiation induced Tc, gap anisotropy effects 8-52125
 austenitic stainless steel 316, trapping up to 7 eV D, depth profiles 8-71751
 blanket designs, near term, thermal-hydraulic and mechanical anal. 8-58452
 blanket designs for catalysed D-D and D-³He Tokamak reactors 8-74480
 bubble nucleation, He-assisted, computer simulation 8-86625
 C and graphite cloths and fibres, neutron irradiation effects 8-78496
 catalysed D fusion reactor blanket, gas-suspended, B₄C cooled, nuclear characts. 8-58400
 compound superconductors, radiation effects on critical currents 8-52175
 cryogenic targets for laser-driven fusion, H₂ freezing on inner surface of spherical polymer shells 8-86688
 damage energy functions for compounds and alloys 8-86692
 dielectric target fabrication for electron beam fusion 8-50302
 discrete ordinates method, sputtering calc. 8-86689
 Doublet III, limiters, materials selection 8-55026
 electrical contacts, for homopolar generators, tests at high surface vels. and current densities 8-54964
 electrical insulators, radiation effects on organic polymers and ceramics 8-95082
 first wall and divertor plate material selection 8-94129
 first wall radiation damage, H and He gas prod. from stainless steel 8-82512
 first wall structural materials, prediction of life limiting props. 8-62605
 first-wall material, computer model, design lifetimes determ. 8-82513
 first-wall materials, sputtering model 8-82514
 fracture resistance determ. 8-82515
 fusion and fast breeder reactors, a comparison, book 8-78430
 fusion reactor first walls, temp. and displacement transients 8-58427
 glass and polymer shells fabrication for inertial confinement fusion 8-50316
 glass fibre reinforced epoxy, as electrical insulation for Tokamak toroidal field coils, mech. props. 8-64610
 glass fibre reinforced epoxy prepreg, PDX TF coil insulation 8-62656
 glass fibre reinforced epoxy resin, mech. props. 8-64582
 glass fibre reinforced polymer matrix laminates, compressive strength 8-64609

fusion reactor materials continued

glass microbubbles, method for polishing bubbles into hemispheres 8-95869
 glass shells fabrication 8-50301
 graphite, energetic deuteron irradiated surface struct. quantitative meas. 8-95210
 graphite, energetic ion sputtering, appl. of AES-SIMS (IMA)-FDS combined systems to physical and chemical processes 8-95636
 graphite, energy deposition from pellet microexplosion 8-54890
 graphite, pyrolytic, behaviour of implanted D and He 8-95071
 graphite, sputtering yield, use as first wall material 8-95629
 graphite, Tokamak mag. limiter plate, electron irradi. and thermal shock 8-66416
 graphite sputtering by low energy H and D 8-95630
 graphite structure Li₂O cooled blanket, thermal, mech. and neutronic design 8-62652
 Hastelloy X, H permeability using permeation method (*Japanese*) 8-51740
 Hastelloy B, equilibrium surface bombarded with high dose He⁺ ions 8-95091
 Inconel, sputtering and blistering from H⁺ and He⁺ bombardment 8-79649
 Inconel 600, equilibrium surface bombarded with high dose He⁺ ions 8-95091
 Inconel 600, fusion reactor vac. vessel, air, N, adsorpt., thermal desorpt., heat treatment effects 8-54880
 Inconel 718 gas-cooled blanket, mech. and thermal design 8-66387
 laser fusion target, 4 π interferometric meas. of defects 8-50307
 laser fusion target, gas content anal. 8-50306
 laser fusion target, microradiographic meas. of microspheres 8-50308
 laser fusion target, microradiography using monochromatic X-rays 8-50310
 laser fusion target, semiautomated anal. of radiographs 8-50309
 material requirements exam., review 8-50257
 material requirements for fusion reactors, exam. 8-50255
 metal, clean surface, H release rate 8-95187
 metal atoms sputtered by light and heavy particles, velocity distrib. meas. by fluorescence spectroscopy 8-95626
 microballoons, batch processing technique 8-50312
 microparticle array preparation device 8-94139
 microspheres, computer modelling, image analysis of X-ray radiographs 8-50311
 Nimonic PE-16, equilibrium surface bombarded with high dose He⁺ ions 8-95091
 organic materials, adhesives and bulk materials, mechanical characterisation at low temps. 8-64611
 pellet implosion reactor engineering, use of advanced fuels 8-58444
 physical sputtering model for fusion reactor first-wall materials 8-80445
 plasma cooling by metal snow, expt. evidence 8-71495
 plasma cooling by metal snow, origin of effect and elimination 8-71494
 plasma-wall interactions in controlled fusion devices conf., Abingdon, England (April 1978) 8-94917
 polyethylene microspheres, deuterated, variable density, laser fusion targets, prep. 8-74468
 quartz, forming machine for helical or toroidal tubes 8-54886
 radiation effects in superconductors conf., Argonne, IL, USA (June 77) 8-52120
 radiation induced exchange reaction kinetics of H₂, D₂ and T₂, review 8-61005
 stainless steel, energy deposition from pellet microexplosion 8-54890
 stainless steel, type 316, first wall structural materials, prediction of life limiting props. 8-62605
 stainless steel panel with graphite liner, first wall thermal response during cyclic operation 8-62651
 steel, austenitic stainless, stressed state blistering 8-95085
 steel, stainless, 304L, T grainboundary diffusion and trapping, autoradiographic exam. 8-51738
 steel, stainless, 316 and 304, equilibrium surface bombarded with high dose He⁺ ions 8-95091
 steel, stainless, 321 and 304, D implanted, thermal desorption and bombardment induced release 8-95072
 steel, stainless, embrittlement by low energy ionic and atomic H particles 8-95809
 steel, stainless, first wall/blanket system, thermal-hydraulics and fatigue life modelling 8-58453
 steel, stainless, H recycle from Tokamak walls using plasma-wall interaction simulator 8-94131
 steel, stainless, ion induced release of trapped D 8-95095
 steel, stainless, Li compatibility, H₂ influence 8-68844
 steel, stainless, low energy D implanted, microstruct. 8-95073
 steel, stainless, neutron activation of struct. components 8-74476
 steel, stainless, sputtering and chem. attack by H ions of 100 eV energy 8-95635
 steel, stainless, sputtering by low energy H and D 8-95630
 steel, stainless, surface damage under high dose ⁴He⁺ ion irradiation 8-95092
 steel, stainless, trapping and replacement of 1 to 14 keV H and D 8-95070
 steel, stainless, type 304, electron stimulated desorption rel. to CTR first wall appl. 8-51818
 steel, stainless 316, blanket struct. for JAERI fusion reactor 8-62654
 steel, stainless 316, ion sputtered, surface anal. by Auger effect and SEM 8-95632
 steel, stainless 316, irradiated, D trapping 8-95069
 superconducting compounds, neutron effects 8-52121
 superconducting fusion magnets, radiation effects 8-50294
 superconducting magnet materials, irradiation damage (*Japanese*) 8-54873
 T₂ release, air detritiation operation, computer model and scale expt. 8-66413
 TETR Tokamak hybrid blanket design, breeding and power capabilities 8-62615
 Tokamak, blanket and shield of high-field compact reactor 8-74475
 Tokamak, mag. limiter plate, electron irradi. and thermal shock, Mo, SiC and graphite 8-66416
 Tokamak devices, blistering and flaking by He atoms 8-86690
 Tokamak plants, neutron wall loading and structural lifetime goals 8-58408
 Tokamak reactor, resistive requirements of vacuum wall 8-66410

fusion reactor materials continued

toroidal fusion magnet systems, radiation damage effect on max. attainable magnetic field 8-50295
 void nucleation, continuum description 8-87707
 water, decomposition by fusion energy, H₂ prod., synthetic fuel 8-50335
 water splitting thermochemical cycle for synthetic fuel prod. 8-58458
 Ag, energy reflection coefficient for 5 to 10 keV He ions 8-95639
 Ag, sputtered, angular distrib. during He⁺ and Ar⁺ ion bombardment 8-95624
 Al blanket/shield design, high field ignition test reactor 8-54899
 Al conduction cooled blanket, thermal analysis 8-62653
 Al min. activity blanket design for TFTR upgrade 8-58460
 Al, sputtering and chem. attack by H ions of 100 eV energy 8-95635
 Al₂O₃, D plasma interaction, surface structure, chemistry and resistivity changes 8-53010
 α -Al₂O₃, rapid firing, XPS study of cryst. struct. 8-68663
 Al₂O₃, void formation by fast neutron irradiation, TEM exam. 8-51591
 Au, energy reflection coefficient for 5 to 10 keV He ions 8-95639
 Au, sputtered with 15 or 30 keV H⁺, He⁺ and Ar⁺ ions, energy and angular distrib. 8-95625
 Au, sputtering and chem. attack by H ions of 100 eV energy 8-95635
 BC, ion bombarded, chemical effects on secondary photon and ion emission 8-95637
 B₄C, sputtering yield, use as first wall material 8-95629
 Be, blistering model, correlation between blister diameter and skin thickness 8-95067
 Be, ion bombarded, chemical effects on secondary photon and ion emission 8-95637
 Be, plasma-sprayed, response to He⁺ bombardment determ. 8-86691
 BeO, sputtering by low energy H and D 8-95630
 C coating on Pt temp. depend. of H₂⁺ sputtering 8-95634
 C, interaction with D⁺ ions, 5-30 keV, temp. depend. of methane formation 8-79645
 C, ion bombarded, chemical effects on secondary photon and ion emission 8-95637
 C pyroceramic, sputtering and blistering from H⁺ and He⁺ bombardment 8-79649
 C, pyrolytic, energy depend. of methane prod. during deuteron bombardment 8-95939
 C, reflection of H, D and He ions 8-95640
 Ce binary alloys, absorpt. of D, T-getters for CTR evaluation 8-51683
 Cu, energy reflection coefficient for 5 to 10 keV He ions 8-95639
 Cu, Frenkel pair production threshold energy, temp. depend., exam. 8-51530
 Cu, He conc. profile meas. rel. to blistering 8-95089
 Cu, isochronal recovery of high energy d-Be neutron damage 8-51592
 Cu, sputtered with 15 or 30 keV H⁺, He⁺ and Ar⁺ ions, energy and angular distrib. 8-95625
 Cu, X-ray studies of fusion energy neutron damage 8-51593
 D₂-DT-T₂ mixture, solid and liq., props. for fusion reactor applications 8-66415
 D(⁶Li)-T₂, inertially-confined, high thermonucl. gain with low T inventory 8-58403
 DT fill system for laser fusion targets 8-50303
 DT filled microballoon, gaseous content anal. 8-50305
 DT filled microballoons, fuel content characterisation 8-50304
 DT, solid and liq., fusion reactor applications 8-66415
 Fe, Armo, corrosion and mechanical behaviour in liquid Li 8-53036
 H isotopes, techniques for uniform charged particle generation, fusion reactor fuel 8-86682
²H-³H molten-salt-cooled fusion reactor blankets, nuclear heating and radiation leakage 8-78490
 He cooled molten salt hybrid blanket for TCT-hybrid reactor 8-62614
 He, hydraulic resistance to forced two-phase flow in narrow channels 8-87383
 He, liq. and vap., dielectric breakdown across epoxy insulation 8-62658
 He unit requirements, for superconductive energy appl. in USA 8-89999
 He⁺ implanted stainless steel, microstructure anal. 8-82516
 In, amorphization by ion implantation 8-52135
 In, film, embedded with He particles, superconductor ion implantation study of inhomogeneities 8-52181
 Li, blanket coolant for Tokamak reactor, flow resist., MHD effects 8-66423
 Li cooled first wall/blanket system, thermal-hydraulics and fatigue life modelling 8-58453
 Li, energy deposition from pellet microexplosion 8-54890
 Li, liq., first wall/blanket concepts, thermal hydraulic anal. 8-62650
 Li metal sphere, T prod. meas. using new methods of neutron source strength determ. 8-74470
 Li-Al alloys, T recovery 8-58455
 Li-SAP alloys, T recovery 8-58455
 LiF, ns. slowing down time, expt. obs. 8-58319
 LiF-LiCl-LiBr, molten, H electrochemical extraction, appl. to fusion reactor blanket processing 8-53217
 LiO₂, Monte Carlo anal. of asymmetric effects 8-74464
 Li₂O, Ar⁺ implantation, depth distrib. by proton backscatt. 8-51577
 Li₂O, lattice energy calc. 8-79556
 Li₂O, fund. optical absorpt. edge, number of displaced atoms from ⁶Li(n, α)³H reaction 8-51594
⁶Li(n, α)³H, 3-800 keV, cross section meas. 8-89865
 Mo, blister erosion reduction by multi-groove surface microstruct. 8-95211
 Mo, D⁺ impact, surface blistering, SEM study 8-71774
 Mo, energetic deuteron irradiated surface struct. quantitative meas. 8-95210
 Mo, energy deposition from pellet microexplosion 8-54890
 Mo, reflection of H, D and He ions 8-95640
 Mo single crystal 8-52136
 Mo, sputtered, angular distrib. during He⁺ and Ar⁺ ion bombardment 8-95624
 Mo, Tokamak mag. limiter plate, electron irradi. and thermal shock 8-66416
 NaCl Polytan laser windows, for CO₂ lasers, fusion appls. 8-59067
 Nb and Nb alloys, superconductor, flux pinning under heavy ion irradiation 8-52167

fusion reactor materials continued

- Nb, blister form. on single crystal under Ne^+ ion bombardment 8-71772
- Nb, effect of O ion irradiation on supercond. 8-52131
- Nb, energy deposition from pellet microexplosion 8-54890
- Nb, fusion neutron damage effects on mech. props., simulation by 16 MeV protons 8-71768
- Nb, irradiated superconductor, fluxoid defect interactions 8-52166
- Nb, isochronal recovery of high energy d-Be neutron damage 8-51592
- Nb, neutron irradi. effects on mech. props. 8-91361
- Nb, neutron irradiation, low temp., 15 MeV, effect on superconducting props. 8-52179
- Nb, superconductor, neutron irradiation, low temp., effect on critical current 8-52180
- Nb-Sn(Ge), A-15 compound formation by ion implantation 8-51572
- Nb-Ti, radiation effects on critical currents 8-52175
- Nb-Zr (1 wt.%), He bubble growth, α -particle effects 8-67749
- Nb-Zr (1%), He bubbles and voids with ringed images SEM and TEM exam. 8-51529
- Nb₃Al, multifilamentary wires, supercond. props. 8-64175
- Nb₃Ge, neutron irradiated, A15 compound, recovery of T_c by annealing 8-52132
- Nb₃Ge(Sn), electron irradiation at cryogenic temps., effect on T_c and transport props. 8-52122
- Nb₃Sn, critical current density 8-52176
- Nb₃Sn, critical current enhancement by low temp. fast neutron induced flux pinning centres 8-52177
- Nb₃Sn, degradation mechanism of superconducting transition temp. under high energy neutron irradiation 8-52124
- Nb₃Sn, effect of O ion irradiation on supercond. 8-52131
- Nb₃Sn, filamentary, fatigue tests on small coils 8-64652
- Nb₃Sn, multifilament conductors, strain-crit. current meas. 8-64174
- Nb₃Sn, neutron irradi. effect on supercond. fusion magnet props. 8-52128
- Nb₃Sn, radiation damage effect on superconducting props. 8-52127
- Nb₃Sn, superconducting props., effect of radiation induced atomic disorder 8-52133
- Nb₃Sn superconductor, low temp. deuteron irradiation 8-52182
- Nb₃Sn, X-ray study of fission fragment induced structural damage 8-51589
- Nb₃Sn(Al), neutron irradiated, A15 compound, recovery of T_c by annealing 8-52132
- Nb₃Sn(Ge), resistivity and T_c measurement after low temp. neutron irradiation 8-52123
- NbTi, neutron irradi. effect on supercond. fusion magnet props. 8-52128
- Ni, blistering model, correlation between blister diameter and skin thickness 8-95067
- Ni, fusion neutron damage effects on mech. props., simulation by 16 MeV protons 8-71768
- Ni, H permeability using permeation method (*Japanese*) 8-51740
- Ni, irradiated, with He^+ bubble depth distrib. meas. by TEM and blister form. mech. 8-95088
- Ni, permeability and diffusivity of hydrogen (*Japanese*) 8-66345
- Ni, reflection of H, D and He ions 8-95640
- Ni, transient irradi.-induced creep under D bombardment, mechanism 8-80597
- Ni-ThO₂, irradiated with 5 MeV Ni^{++} , ThO₂ redistrib. 8-71771
- Pb, effect of O ion irradiation on supercond. 8-52131
- Pt, isochronal recovery of high energy d-Be neutron damage 8-51592
- SiC, energetic deuteron irradiated surface struct. quantitative meas. 8-95210
- SiC, energetic ion sputtering, appl. of AES-SIMS (IMA)-FDS combined systems to physical and chemical processes 8-95636
- SiC, exam. of T_2 diffusion coeffs. and D_2 solubility 8-79816
- SiC on graphite substrate, Tokamak mag. limiter plate, electron irradi. and thermal shock 8-66416
- SiC, sputtering yield, use as first wall material 8-95629
- SiC surface, H^+ , D^+ and Ar^+ bombardment, 5 to 15 keV, meas. of erosion yield 8-79647
- SiC-C, sputtering and blistering from H^+ and He^+ bombardment 8-79649
- SiO₂, laser-fusion microballoon, expansion density profile, 10.6 μm irradi. 8-86686
- Sn, effect of O ion irradiation on supercond. 8-52131
- T breeding costs in critical fission reactor 8-58456
- T breeding in fusion-fission Tokamak, optimisation with geom. program 8-74477
- T fuel handling, safety and control systems for TFTR 8-50364
- T, fuel handling systems, for TNS Tokamak 8-50363
- T processing systems for inertial confinement fusion facilities 8-50338
- T prod. meas. in Li metal sphere using new methods of neutron source strength determ. 8-74470
- T recovery from solid Li-Al and sintered Al product blanket materials 8-58455
- T, removal from liq. K and Li by sorption onto Y 8-66411
- T transport in fusion reactors, limitations 8-70628
- T₂, cryocondensation pumping, smooth surface at 4.2K, fusion reactor application 8-74492
- T₂ valve, pulsed gas feed into Tokamak reactor 8-66412
- TZM, D^+ impact, surface blistering, SEM study 8-71774
- TaC-C fibre composite, neutral beam target appls. 8-66399
- Ti alloy, radioactive structures, recycle time 8-58457
- Ti, blister form. by He and H ion bombardment, target struct. effect 8-95087
- Ti coated Nb, reduction of void number density and size by ion irradiation 8-51600
- Ti, getter pump, corrugated surface and pumping speed, fusion reactor application 8-74491
- Ti, reflection of H, D and He ions 8-95640
- Ti, sputter-erosion and impurity emission under low energy ion bombardment 8-95628
- TiC, sputtering yield, use as first wall material 8-95629
- V alloys, first wall/blanket system, thermal-hydraulics and fatigue life modelling 8-58453
- V, annealing after irradiation with 210 keV He at 625°C at high fluences 8-67751
- V, blister form and stress build-up, under the bombardment, surface prep. effects 8-95094
- V, blister form. by He and H ion bombardment, target struct. effect 8-95087

fusion reactor materials continued

- V, effect of O ion irradiation on supercond. 8-52131
- V, evap. layer, ion bombardment effect on superconducting transition temp. 8-52136
- V, first wall material, irradi. with 40 keV ^4He ions, blistering 8-55897
- V, irradiation with 2 MeV He ions, low cycle at elev. temp. 8-95086
- V, sputter-erosion and impurity emission under low energy ion bombardment 8-95628
- V, superconducting props., effect of voids 8-52168
- V, superconductor, neutron irradiation, low temp., effect on critical current 8-52180
- V-Cr-Ti, fusion reactor first wall structural materials, prediction of life limiting props. 8-62605
- V-Mo, effect of ion plated Mo on corrosion in liquid Na, mech. props. 8-53020
- V₂Ga, high current density multifilament wire, neutron effects on equilibrium and transport props. 8-52126
- V₂Ga, neutron irradiation and annealing 8-52130
- V₂HfZr, C-15 cryst. struct. supercond. props. 8-64173
- V₃Si, neutron irradiated, A15 compound, recovery of T_c by annealing 8-52132
- V₃Si single crystal, radiation damage and superconductivity 8-52129
- W, FIM study of lattice damage caused by low-energy He ion bombardment 8-95090
- W, reflection of H, D and He ions 8-95640
- Zr, deuteron implanted, temp. depend. depth profiles of deuterons 8-95076
- Zr₃Al, ordered, exam. of Young's modulus and thermal expansion coeff. 8-72805
- Zu, reflection of H, D and He ions 8-95640

fusion reactors

- see also fusion reactor ignition; fusion reactor materials; plasma heating
- 2XIIB, liq. N₂ cooled liners 8-50406
- 475 MVA pulsed motor generators for TFTR 8-58498
- 600 MW pulsed energy convertors for toroidal field coil, design philosophy 8-58496
- advanced fuel bumpy tori studies 8-58430
- advanced fuel fusion reactor, SURMAC, employing axisymmetric surface mag. confinement 8-58431
- advanced fuel Tokamak, ILB systems, bundle divertor designs and appls. 8-62618
- Alcator-C, mag. coil systems 8-50355
- alpha particle transport in thermonuclear Tokamak plasma 8-94895
- alpha particles, fusion-generated, producing plasma transport 8-83533
- alternative magnetic confinement systems 8-58428
- American Nucl. Soc. winter meeting 1977 8-58315
- American Nucl. Soc. Winter Meeting 1977 8-82408
- analogue safety data link, for Princeton Large Torus control room 8-54938
- anisotropic B_z-coil two-dimens. finite element anal. of laminate sliding 8-50382
- arc quenching system for transient and statistical flashover 8-75455
- Argonne experimental power reactor, equilib. field coil system design 8-50367
- Argonne National Laboratory energy storage and transfer program 8-55031
- Argonne National Laboratory Experimental Power Reactor, superconducting magnet system 8-50372
- ASDEX circuit breaker system, design, calcs. and tests 8-55032
- ASDEX divertor Tokamak, toroidal and poloidal mag. field coils 8-50352
- ATC machine, lower hybrid heating using pulsed UHF TV klystron 8-66404
- B-coil stress anal., constraint finite element anal. for contact problem 8-55004
- bellows valve, large rectangular for mirror fusion reactors 8-50404
- blanket, gas-cooled, mech. and thermal design 8-66387
- blanket, graphite struct., Li₂O cooled, thermal, mech. and neutronic design 8-62652
- blanket, thermal stresses and cyclic creep-fatigue 8-62655
- blanket design for toroidal fusion reactor 8-62649
- blanket designs, near term, thermal-hydraulic and mechanical anal. 8-58452
- blanket structure design for JAERI experimental fusion reactor 8-62654
- blanket temp. variation with slab geometry 8-78495
- blankets, conduction cooled, thermal analysis 8-62653
- blankets, redundant coolant capability 8-58454
- capacitor banks, optimum design rules, neutral beam power supply 8-74487
- capacitor energy storage, propylene film-paper-phthalate ester capacitors 8-74486
- capacitors, 10 kV foil-and-paper, low-cost energy storage 8-74485
- catalysed D fusion-fusion hybrid reactors 8-58436
- catalysed D-D noncircular Tokamak, graphite blanket design 8-74480
- cavity wall loads and stresses, scaling 8-58446
- chaotic motion theories with appl. to controlled fusion research, review 8-93605
- circuit breaker, liquid metal plasma valve, tokamak and stellarator heating circuit 8-74488
- coil, multilayer structs., laminated beam theory anal. 8-55011
- coil design codes 8-66367
- composite superconductor continuous resistive transition self-field instability depend. 8-50369
- confinement, alternative approaches, literature survey 8-87477
- control valve, low-noise, rolling closure 8-54888
- cryo-pumps, nucl. heat deposition, Monte-Carlo method 8-66414
- cryogenic laser fusion targets, fabrication and characterisation 8-58484
- cryosorption pumping, D₂-He (5 at.%), on mol. sieve, 5A, 4.2K 8-74499
- cryosorption pumping of D at 6 to 20K, fusion reactor appl. 8-70626
- DC superconducting magnets, pot. damage due to HF EM wave propagation. 8-50371
- dense plasma focus, capacitor bank system design and safety 8-54889
- design and economics, confinement physics effects 8-50358
- design and performance requirements, cost and systems anal. 8-50357
- diagnostics, mech. techniques in fluctuating mag. fields 8-54946
- diagnostics, visible spectrum monochromator, scanning drive 8-54940
- dielectric joints, effect on struct. behaviour of Tokamak 8-62657

fusion reactors continued

direct current accelerator for 14 MeV neutron prod., thermal-mech. design 8-66383
 direct energy conversion from fusion plasma exhaust of divertor 8-54898
 Doublet III indented vac. vessel, mech. design 8-74490
 doublet reactor, neutron wall loading, two-dimens. calc. 8-66407
 electrical output power profiles, utility interface 8-54906
 electromagnetic insulation systems, features 8-89506
 electrostatic end plugging, open-ended mag. confinement system 8-55743
 electrotechnical component practicalities, operational safety and economics (*German*) 8-94140
 Elmo bumpy torus, physics and engineering aspects 8-54981
 ELMO bumpy torus design 8-58429
 Elmo bumpy torus reactor, economics 8-54994
 energy storage, 10 MJ homopolar machine, superconducting magnet design 8-54927
 energy storage, inductive, appl. of homopolar generator 8-54948
 energy storage for Tokamak reactor cycles 8-62661
 engineering problems, conf., Knoxville, USA, (1977) 8-50342
 engineering problems, TFTR experience 8-54974
 experimental power reactor, energy storage and transfer system 8-54955
 Faraday MHD generator with thermonuclear reactor, efficiency 8-75432
 fibre optic telemetering for high voltage test stand, Lawrence Livermore lab. 8-54939
 field reversed mirror reactor, 2nd generation design calcs. 8-58465
 first wall/blanket concepts using liq. Li, thermal hydraulic anal. 8-62650
 Fiseatron fusion reactor principle, Z-pinch device using ^6LiD 8-78492
 flywheel energy storage system for JT-60 toroidal field coil 8-62662
 force cooled superconductor cryostability expt. 8-50378
 Frascati high field Tokamak, technological aspects 8-50351
 fuel feed and removal systems, plasma heating and vacuum technology problems (*German*) 8-50298
 fuel handling system for TNS, and cost model 8-58441
 fusion and fast breeder reactors, a comparison, book 8-78430
 fusion design team, undergraduate education 8-58469
 fusion power commercialisation 8-58405
 fusion reactor, beam-profile fast scan monitor 8-54941
 fusion reactor, diagnostics of radial plasma transport rate, data acquisition and handling system 8-54937
 fusion technology progress 8-62607
 fusion-fission breeder reactor, supercond. poloidal field coil design 8-70640
 fusion-fission reactor symbiotic design, simple fuel reprocessing 8-66365
 fusion-fission Tokamak, T breeding, optimisation with geom. program 8-74477
 fusion-MHD power plant, exhaust plasma pulsed accel. 8-62644
 HEGLF, Antares power amplifier 8-54958
 high energy gas laser facility, energy storage system design 8-55030
 high field ignition test reactor, Al blanket/shield design 8-54899
 homopolar generator, fast discharge machine, design, fabrication, testing 8-54952
 homopolar machine, 10 MJ, fast-discharging 8-54950
 homopolar pulse power machine, current collection system 8-54949
 HVDC interrupter test facility, dual 30 kA systems 8-55035
 ICF reactor design considerations 8-50331
 ignition test reactor, design features 8-54978
 ignition TNS Tokamak reactor, engineering parameters 8-50359
 ignitrons, high current, for plasma physics expt. equipment (*German*) 8-75435
 imploding liner fusion system 8-54979
 imploding liners for LINUS-O, high press. gas generator 8-54904
 impurity and gas throughput control 8-54907
 impurity radiation loss, for corona equilib. 8-91074
 Impurity Study Experiment, mag. field calcs. using GFUN-3D programme 8-66368
 inductive storage technology, new applications, review 8-55019
 inertial confinement fusion, commercialisation anal. 8-58410
 inertially confined DT plasma, nucl. fusion yield due to reheat 8-82517
 integrated composite conductor for LCS program 8-62631
 interferometric phase detection system, using high speed digital techniques 8-62629
 ISX, coil design and fabrication 8-50353
 ISX, Tokamak, assembly details 8-54883
 ISX-B, differentially pumped bellows 8-55025
 ITR vacuum vessel, free standing, structural design 8-54900
 JET, control and data acquisition system, CODAS 8-62619
 JET, cryopumps 8-50399
 JET, high voltage network to load AC/DC pulse power conversion 8-58497
 JET, inner poloidal field coil mechanical design 8-50387
 JET, synchronous generator, bridge convertor and ohmic heating systems, digital simulation 8-54960
 JET, toroidal field coil design and manufacture 8-50349
 JET, vacuum vessel construction 8-55024
 JET additional heating power supply and protection 8-66391
 JET project, project description and proposed expt. programme 8-89977
 JET project, technical developments, administrative and managerial aspects 8-54986
 JET project description 8-58399
 jet target intense neutron source 8-66384
 JT-60, poloidal field coil internal voltage oscils. 8-50386
 JT-60 large Tokamak device, position and cross-section control 8-50366
 JT-60 Tokamak vacuum vessel, stress anal. 8-66371
 Large Coil Program, cryostabilised conductor cooling system 8-50393
 Large Coil Program, General Dynamics Convair conceptual design test coil 8-50389
 Large Coil Program, General Electric test coil conceptual design 8-50390
 Large Coil Program, He liquefier-refrigerator and distrib. system 8-50398
 Large Coil Program, Nb₃Sn forced flow superconductor design considerations 8-50394

fusion reactors continued

Large Coil Program, pulse coil concepts 8-50397
 Large Coil Program, struct. response of toroidal field coils, finite element anal. 8-50396
 Large Coil Program, superconducting toroidal field coils for Tokamaks 8-50388
 Large Coil Program, support struct. conceptual design 8-50395
 Large Coil Program, Westinghouse Electric conceptual design for test coil 8-50392
 Large Coil Segment test, struct. anal., mag. force loadings 8-50373
 laser driven, Monte Carlo study of asymmetric effects of LiO₂ blanket 8-74464
 laser fusion 8-59635
 laser fusion breeder, impact on nuclear economy 8-50336
 laser fusion deployment scenario 8-58411
 laser fusion driven actinide waste burner, neutronics anal. 8-58459
 laser fusion generating stations, safety, environmental effects 8-50337
 laser fusion power plants, final optics 8-50334
 laser fusion reactor, environment and safety features 8-50333
 laser fusion reactor, wetted-first-wall, falling liq. film 8-66408
 laser fusion reactor design 8-50332
 laser fusion system using Shiva 8-54990
 laser fusion targets, plating methods 8-60862
 laser fusion targets, vapour deposited coatings, surface finish obs. 8-60863
 laser induced magnetically enhanced reactor, LIME 8-58434
 laser reactor Li₂O blanket, Monte Carlo and discrete ordinate scoping models 8-62603
 laser solenoid concept, fusion reactor development 8-54980
 laser solenoid fusion concept 8-58435
 laser thermonuclear synthesis for future energy production (*Russian*) 8-89978
 laser-fusion reactor, surface heating of 1st wall by pulsed photon and ion irradi. 8-89979
 light ion sputtering in fusion reactors, discrete ordinates method calcs., ANISN code 8-92158
 linear reactor, impurity seeded multiple-mirror end plug 8-63580
 linear reactor system with impurity-seeded multiple-mirror end plug 8-78493
 LINUS conceptual reactor 8-58432
 LINUS-O prototype liner implosion system 8-54902
 liquid He cryopump, for fusion machines, degassing 8-54382
 liquid liners with annular piston drive, hydrodynamic model expts. 8-54903
 magnet coil, 125 kG, 1 m, design, fabrication 8-55008
 magnetic coil systems, EM field, force and inductance calc. by EFFI code 8-62648
 magnetic confinement near term designs, overview 8-58413
 magnetic confinement of plasmas 8-94928
 magnetic mirror fusion experiments 8-50343
 maintenance, cassette blanket and vacuum building concepts 8-66386
 Marshall coil, epoxy-insulated, fabrication 8-66388
 microexplosion containment vessel, structural design 8-50341
 Migmacell, low gain driven fusion power amplifier as interim energy source 8-54875
 mirror fusion hybrid reactor, T handling systems 8-62617
 mirror fusion reactors, remote servicing features 8-58448
 mirror hybrid reactor power plant, mechanical struct. 8-58449
 mirror plasma, electron heating using external power 8-87482
 molten salt hybrid blanket, He-cooled, theory 8-62614
 motor generator set, for inductive energy storage systems, voltage protection scheme 8-55037
 multiple mirror reactor with depressed ion temp., power balance 8-67393
 neutral beam diagnostics of ion temp., Princeton large torus 8-54942
 neutral beam targets, water-cooled swirl tubes, heat transfer calcs. 8-67018
 neutral-beam requirements for compression-boosted ignited Tokamak plasmas 8-78494
 neutron induced activity and biological dose rates in and around JAERI reactor 8-54872
 Oak Ridge National Laboratory superconducting coil fabrication development 8-50370
 Oak Ridge TNS program (1976/1977) 8-54975
 ohmic heating coil, fast ramp superconductor 8-62638
 ohmic heating pulsed superconducting coil 8-62640
 ohmic heating superconducting solenoid, Tokamak TNS appl. 8-54928
 ohmic heating system, superconducting 8-62634
 ORNL Tokamak, hybrid equilib. field coils, power supply 8-54895
 ORPUS-3, pulsed superconducting solenoid for poloidal field coils 8-62641
 parametric anal. of utility operations 8-58409
 PCX facility, intense laser radiation effects on mag. confined plasma 8-66405
 PDX, mech. design and assembly 8-50350
 PDX canned poloidal coils, design, fabrication and mag. alignment 8-50385
 PDX device, overview and status report 8-54985
 PDX machine, poloidal field power supplies, performance 8-54956
 PDX magnetic islands anal. 8-62646
 PDX poloidal field coil power tests 8-50384
 PDX toroidal field coil mag. force distrib. anal. 8-50380
 plasma confinement and heating, basic problems rel. to extraterrestrial plasmas 8-69672
 plasma divertor experiment, management techniques and procedure 8-54891
 plasma-wall interaction, permissible degree criterion 8-89981
 plasma-wall interactions in controlled fusion devices conf., Abingdon, England (April 1978) 8-94917
 PLT, coil stress and deflection analysis, ANSYS computer code appls. 8-50356
 PLT, ohmic heating system operation 8-66401
 PLT machine, multi-channel TV-Thomson scatt., apparatus, mech. aspects 8-54932
 PLT toroidal field coils, operational deflection meas. 8-62627
 pollution hazards assessment (*Czech*) 8-86681
 power conversion system, (PULSAR), with inductive storage 8-55029
 power plants, engineering limitations 8-74473
 power supply, three-phase system, computer aided cct. design 8-54959
 Princeton large torus 3-coil test 8-54945

fusion reactors continued

pulsed fusion experiments, computer-based control systems 8-62624
 pulser system, air-driven fibre-optic coupled for Los Alamos ZT-40 expt. 8-54943
 Q-enhanced mirror fusion system, plasma-surface interaction 8-94130
 radiological hazards, reliability requirements 8-58447
 reactant distribution functions in fusion reactors, fast computing method using Legendre polynomials expansion 8-78491
 relativistic electron beam fusion reactor, parametric anal. 8-50340
 relativistic electron beam hybrid reactor, economic model 8-58412
 remote leak detection for Tokamak Fusion Test Reactor 8-50403
 remotely operable large vacuum seals for fusion reactors 8-50405
 reversed field mirror, alpha-particle effects 8-58468
 reversed field pinch, burn stability 8-58467
 reversed field pinch reactor, choice of parameters for 600 MW net electrical output 8-58471
 reversed field pinch reactor, physical principles, design, operation and plasma stability 8-58470
 reversed field pinch reactor, preliminary engineering design 8-58472
 reversed field pinch reactor 8-58433
 reversed-field pinch burn dynamics, global computer code 8-63579
 RFC-XX, coil system, design, fabrication, testing 8-55007
 RFX field system design 8-54884
 Scylla IV-P, computer-based control and data acquisition system for CTR 8-62621
 Scylla IV-P linear theta-pinch, material end plugging 8-55744
 Scyllac reactor, feedback stabilisation system 8-54887
 Shiva Faraday rot. coils, circuit and mag. anal. 8-54951
 solenoid, orthotropic, finite element stress anal. 8-55010
 Sorb-ac wafer pumps, behaviour in plasma machines, review 8-70627
 spark gap overpressure, 0.2 MA, design and appl. 8-75456
 stellarator, with 3 mag. axes, Doublestar, numerical study 8-91140
 structure neutron activation, experimental power reactor 8-74476
 superconducting 7.5 Tesla segment test facility 8-54929
 superconducting cables for PF and TF coils, losses and transient field effect 8-62635
 superconducting coil, multifilamentary composite losses 8-62637
 superconducting composite, eddy current losses 8-62636
 superconducting energy storage coil 8-54924
 superconducting energy storage coils, conductor design 8-62639
 superconducting magnet for mirror fusion test facility, conductor fabrication 8-62642
 superconducting magnet magentoelastic energy calcs., finite element anal. 8-55002
 superconducting magnet system, appl. to Tokamak 8-54925
 superconducting magnets, composite superconductors, stability anal. by thermal analyser digital computer program 8-54995
 superconducting magnets, cooling system using liquid He 8-54998
 superconducting magnets, force-cooled conductors design 8-54999
 superconducting magnets, hollow conductors, cooled by supercritical He 8-54997
 superconducting magnets, toroidal field coil thermal design and anal. 8-50368
 superconducting magnets cryostabilisation using superfluid He 8-54996
 superconducting Tokamak TF coil system, protective control features 8-62625
 superconducting Ying-Yang magnet system for mirror fusion test facility 8-54922
 superconductor strain and mag. system design parameters, closed-form anal. 8-50377
 superconductors, built-up, current transfer 8-62633
 switches, supercond., high specific breaking power 8-55020
 T-10 M tokamak toroidal field coil shape struct. anal. 8-50374
 T-10M Tokamak, normal and supercond. inductive energy storage and switching 8-55018
 tandem mirror device, operation, Q-factor calcs. (Russian) 8-74466
 tandem mirror experiment, mag. field requirements 8-54988
 tandem mirror experiment, system design 8-54987
 Tandem Mirror Experiment, vacuum system 8-55023
 tandem mirror experiment 8-54885
 temperature distrib. in first wall systems 8-58450
 TESPE coil, finite element method calc., winding package modelling 8-50376
 Texas experimental Tokama, homopolar generator, eddy currents, EM forces (torques), due to misalignment 8-54953
 TEXT, poloidal coil systems power supplies 8-54957
 TEXT, pulsed homopolar generator power supply, engineering and design 8-55016
 TEXT, regulating resistors and interrupters 8-55038
 TEXT, Tokamak structural system 8-54882
 TEXT, toroidal and poloidal field coil design 8-50354
 TEXT data acquisition, multichannel AD subsystem 8-54936
 TEXT fusion plasma research facility 8-54984
 TEXT poloidal field coils 8-62645
 TEXT toroidal field coil stress anal. 8-50381
 TEXTOR, toroidal field magnet design 8-50348
 TFR, high power neutral beam injection and ion power balance, anomalous heat conduction 8-82511
 TFTR, AC distrib. system for pulsed loads 8-54963
 TFTR, ceramic insulator rings 8-55022
 TFTR, diagnostic interface systems, problems 8-62626
 TFTR, HV switch tube development 8-66385
 TFTR, neutral beam line cryopanel, cryogenic supply systems 8-55027
 TFTR, neutral beam line injectors, cryopumping system 8-55028
 TFTR, plasma position control, linear feedback optimal method 8-50365
 TFTR, T fuel handling, safety and control systems 8-50364
 TFTR, three-dimens. solid finite element anal. for simulating composite windings 8-55003
 TFTR, vacuum chamber for neutral beam injection system 8-55021
 TFTR, vacuum system design, performance curves 8-70625
 TFTR auxiliaries, power distrib. system 8-54962
 TFTR poloidal field coils design details 8-50383
 TFTR technology and Tokamak engineering 8-50344
 TFTR toroidal field coil case design 8-50347
 TFTR toroidal field coil design 8-50346
 TFTR vacuum system, description, operation, safety 8-74497
 TFTR vacuum system transient simulator 8-74496

fusion reactors continued

thermonuclear power station based on microexplosion-induced D-T initiation 8-82508
 theta-pinch device for modelling fusion reactor operation 8-89972
 time depend. diffusion eqn. for neutronic calcs., use of exterior differential forms 8-54871
 TMX, magnets, mech. design 8-58494
 TNS, air core and Fe core ohmic heating systems 8-66402
 TNS, design related RD&D assessment 8-54976
 TNS, electrical design costing 8-55014
 TNS, T handling system design 8-62616
 TNS conceptual design, parametric anal. 8-54991
 TNS Tokamak, T fuel handling system design 8-50363
 TNS Tokamaks, costing and sizing, computer code 8-50361
 TNS Tokamaks, trade study anal. 8-54992
 Tokamak, axisymm. MHD instability, feedback stabilisation 8-87484
 Tokamak, blanket and shield of high-field compact reactor 8-74475
 Tokamak, diffusion of runaway electrons across mag. field 8-87480
 Tokamak, DITE, recycling in gettered and diverted discharges 8-94132
 Tokamak, DITE H conc. meas. in walls and limiters 8-94136
 Tokamak, DIVA, impurity shielding and sweeping out, axisymm. divertor 8-86685
 Tokamak, DIVA, radiation loss and power balance, pyroelectric detection 8-86684
 Tokamak, divertor expts. for controlling plasma-wall interactions 8-94125
 Tokamak, doublet reactor, parallel connected ohmic heating coil 8-54930
 Tokamak, eddy current analysis, finite element circuit method 8-66373
 Tokamak, eddy currents, 3-dimens., perturbation-polynomial expansion calcs. 8-66372
 Tokamak, energy balance, computing method 8-54982
 Tokamak, experimental power reactor, plasma studies 8-66418
 Tokamak, expt. power reactor, first wall/blanket/shield system, mech. design 8-74482
 Tokamak, fusion reactor, axisymmetric, slowing-down alpha particle loss, Monte-Carlo calc. 8-59653
 Tokamak, heat transfer in wall region (Russian) 8-87501
 Tokamak, high-beta, with force-free currents, MHD stability 8-87481
 Tokamak, high-temp. blanket, generating efficiency and H₂ synthetic fuel prod. 8-74479
 Tokamak, ISX-B, design improvements for neutral particle heating 8-54881
 Tokamak, LT-3, disruptive instability, spectroscopic observations 8-87483
 Tokamak, magnet conceptual design 8-54983
 Tokamak, nonaxisymmetric, reduced fusion neutron production 8-63577
 Tokamak, ohmic heating coil arrangement 8-54896
 Tokamak, ohmic heating solenoids, engineering design solns. 8-54893
 Tokamak, optimum conceptual scaling 8-54908
 Tokamak, plasma limiter design 8-54910
 Tokamak, plasma-wall interactions, review 8-94123
 tokamak, plasma-wall-divertor model 8-58462
 Tokamak, PLT, disruptive instabilities, X-ray study 8-89974
 Tokamak, recycling processes 8-94126
 Tokamak, surface effects and impurity production 8-94127
 Tokamak, surface interactions and conditioning techniques 8-94124
 Tokamak, surface processes in plasma-wall interactions 8-94121
 Tokamak, TFR, variable-radius Mo and graphite limiters 8-63600
 Tokamak, TNS, equil. field coils and free boundary equil. considerations 8-58420
 Tokamak and stellarator, progress in experiments 8-94122
 tokamak confinement, next step beyond TFTR 8-58414
 Tokamak constant tension D-shaped coils; lateral support struct. 8-55013
 Tokamak construction criteria (Norwegian) 8-74474
 Tokamak contamination, comparison of different refuelling methods 8-94133
 tokamak demonstration hybrid reactor 8-58418
 Tokamak divertor, toroidal field mag., vacuum system 8-54909
 Tokamak energy storage superconducting solenoids 8-66369
 Tokamak experimental power reactor, plasma position control and sensor requirements 8-62628
 Tokamak Fe cores, design advantages 8-54897
 tokamak first wall, 3.5 MeV alpha bombardment 8-58463
 Tokamak fusion power generation 8-74472
 tokamak fusion power plants, major cost drivers 8-58443
 tokamak fusion reactor, generic PSAR for TF coil system 8-58407
 Tokamak fusion reactors, commercial feasibility 8-58406
 Tokamak Fusion Test Reactor, elec. resistance bellows for vacuum vessel 8-50407
 Tokamak hybrid blanket, neutronics and thermal hydraulics 8-66406
 Tokamak hybrid blanket design, breeding and power capabilities 8-62615
 Tokamak hybrid breeder blanket, liq. metal coolant, MHD effects 8-74481
 Tokamak machines, eddy currents, numerical and exptl. anal. 8-66374
 Tokamak magnets, EM forces, TORMAC computer program 8-62647
 tokamak medium field ignition test reactor, plasma engineering 8-58419
 tokamak next step designs, system size and cost trends 8-58416
 Tokamak plants, neutron wall loading and structural lifetime goals 8-58408
 Tokamak plasma, ISX, plasma position dynamics 8-66420
 Tokamak plasma, real and simulated, impurity behaviour 8-94128
 Tokamak plasma, RF driven electron currents for confining poloidal field 8-91145
 Tokamak plasma, superthermal fusion products, α -particle transport theory 8-66417
 Tokamak poloidal divertor, compact, reference design 8-54894
 tokamak power reactors, design approaches for engineering feasibility 8-58442
 Tokamak power systems, economics 8-54993
 Tokamak power systems technology 8-50345
 Tokamak reactor, commercial, plasma driving system requirements 8-54954
 tokamak reactor, impurity effects on α -particle loss 8-58461
 Tokamak reactor, overhaul procedure 8-54905

fusion reactors continued

- Tokamak reactor, resistive requirements of vacuum wall 8-66410
 Tokamak reactor first walls, thermal response during cyclic operation 8-62651
 tokamak reactor superconducting toroidal field magnet computational model, technical and economic 8-50375
 Tokamak TNS reactor, plasma engineering innovations 8-66422
 Tokamak toroidal field coils, superconducting 8-62632
 Tokamaks, elongated, axisymm. MHD stability 8-86683
 Tokamaks, gas breakers for ohmic heating circuits 8-66396
 Tormac DT fusion reactor, power gain and net output 8-58402
 toroidal device with nonplanar mag. axis, magnet and coil engineering 8-55009
 toroidal discharge, dynamic stabilisation in weak longit. mag. field (*Russian*) 8-87476
 toroidal field coil stress anal., cost effective procedures for TFTR 8-50379
 toroidal field coils, bending-free, for Tokamak reactor 8-55012
 toroidal field magnet system utilizing normal metal trimming coils 8-54931
 toroidal field magnets conceptual design for expt. fusion reactor 8-50391
 toroidal field ripple effects, computer simulation 8-54892
 toroidal plasma, 2-D neutral H transport 8-59661
 toroidal Z-pinch, ZT-40 8-54989
 torus with superconducting toroidal coils, TESPE 8-54926
 transient gas feed in Tokamak discharges, numerical investigation of buildup phase of neutral H layer near wall 8-94135
 transient neutral gas interactions with plasmas and walls 8-94134
 turbomolecular pump in pulsed mag. field, operational effects 8-50402
 turbomolecular pump with mag. bearings, fusion expt. device appl. 8-50400
 two-component torus hybrid reactor, double wall for first wall, struct. anal. 8-66409
 two-component Torus hybrid system, pressure tube convertor for hybrid blanket 8-74478
 two-stage opening switch technique, for high inductive voltage generation 8-55034
 ultra high vacuum technology developments (*Japanese*) 8-49845
 upgradable ignition test reactor, engineering features 8-54977
 vacuum engineering for fusion reactors (*Japanese*) 8-58401
 vacuum interrupter, for high voltage DC current 8-74489
 vacuum outer containment, safety, T control and monitoring 8-74498
 vacuum vessel, magnetic stress induced by plasma motion, 3-dimens. anal. 8-66370
 vacuum vessel, of General Atomic TNS, toroidal resist. and low Z armour/limiter 8-54901
 vacuum vessel, performance of silver-coated metal seals, 20 to 450C (*German*) 8-81996
 wall problem, reactor modular set up (*German*) 8-54879
 X-rays to electricity conversion scheme for advanced fusion reactors 8-70641
 ZT-40, power crowbar system design 8-55033
 ZT-40, switching components development 8-55036
 ZT-40, toroidal Z-pinch, circuit design and plasma simulation 8-54961
 D-³He satellite fusion reactor, field-reversed mirror confinement 8-70643
 D-³He Tokamak, blanket design, Al layers with organic coolant 8-74480
 D-D fusion reactor, heliotron (*Japanese*) 8-54878
 D-D fusion reactor blanket, nucl. characts., summary 8-89973
 DT plasma, free expansion hydrodynamics 8-70629
 H₂, synthetic fuel production, Tokamak high-temp. blanket 8-74479
 He distrib. system for Large Coil Test Facility 8-55001
 He, liq., narrow channel flow and heat transfer characts., void fraction in steady and transient states 8-55000
 Li, liq. cooled pulsed fusion reactor blanket heat transfer, numerical calc. 8-94141
 Li sphere, neutron spectra and T prod. meas. 8-62604
 Nb-Ti superconductor, for fusion facility, cold-pressure-welded joints 8-62630
 NbTi superconducting magnet, 0.8 m free bore toroidal magnet module 8-54923
 Ni-Cr foil strain gauge, for cryogenic anal. of supercond. structs. in high mag. fields 8-54947
⁹⁰Sr fission reactor waste management, by fusion reactor transmutation 8-70642
 T₂ valve, pulsed gas feed into Tokamak reactor 8-66412

g-factor

see also gyromagnetic ratio; Zeeman effect

- alkali metal-hexamethylphosphoramide, low temp. glass, EPR of solvated K, Cs and Rb 8-91927
 alkoxy free radicals, produced by X-irrad. of hydroxy containing cpds., characterisation by ESR and ENDOR 8-95938
 arbitrary spin particles in EM field, mag. dipole g-factor 8-93829
 biological systems, containing Fe, electronic and mag. struct., semiempirical MO cluster calcs. 8-62733
 bis(diethylammonium) copper tetrachloride, mag. susceptibility, EPR spectra 8-68193
 chloroacetamide, X-irrad., ESR of CH₂ClCO radical 8-76882
 diamond, magnetic field and stress splitting of GR1 line 8-60095
 garnets, mag. props. of V⁴⁺ ion, effect of covalency 8-64010
 glass:Mn²⁺, EPR, low-field hyperfine struct. 8-95513
 haemoglobin, human, EPR spectrum, g-value during oxygenation-deoxygenation reaction 8-53333
 heavy atoms, g-factor anomalies and strongly forbidden M1 transitions 8-78825
 heavy atoms, strongly forbidden M₁ transitions, g-factor anomalies (*Russian*) 8-78648
 hydrocarbon radicals, planar and nonplanar, g-factors, π - σ delocalisation 8-58580
 iron porphyrin in triphenylene, ESR 8-60329
 liver tissue, mouse, appearance of free radical centres on low temp. oxidation 8-69013
 molecules, electronic transitions, g-factor determ. by polarisation plane mag. reson. rot. (*Russian*) 8-70954
 quasi-one dimensional organic systems, ESR 8-52358

g-factor continued

- shape isomers, spontaneous fission, static and decay props. and excitations, review, book contrib. 8-82402
 shell-model, mag. dipole moments 8-82280
 transient ESR line profiles, $S=1/2$ system, calcs. 8-88170
 TTF-TCNQ type salt, trimethylene-TTF-TCNQ, unsymmetric cation, phys. props. 8-76059
 vinyl formate, rot. Zeeman study, g-factors, mag. susceptibility, quadrupole moments 8-50572
 Zeeman interaction, relativistic corrections and very small g-shifts, contrib. to EPR 8-72393
 e, meas. at low energy and 110 keV 8-57777
 μ , (g-2) value, second order weak correction in arbitrary gauge models 8-62301
⁴He(3P), fine struct., level crossing obs. 8-82686
 Ag:Er(Dy), orbit-lattice coupling, nonuniform strain effects 8-88182
 AgBr, optical absorpt. of indirect exciton in high mag. field 8-60486
 AgCl, optical absorpt. of indirect exciton in high mag. field 8-60486
 AgCl: Cd²⁺, Pb²⁺, Br⁻, EPR anal., mechanism for photoinduced decomposition 8-80219
 AgClO₃, ClO₂ spin Hamiltonian 8-60326
¹¹⁰Ag^m, oriented, T-reversal test and struct. study 8-86505
 Al:Er(Dy), orbit-lattice coupling, nonuniform strain effects 8-88182
 Al₂SiO₅, EPR of Fe³⁺ at V-band and the pair spectra 8-80204
²⁰⁷At, g-factor of 25/2⁺ isomeric state, evidence for neutron excitation 8-70447
 BO₂, gas, optically detected mag. reson. spectrum, X² Π rovibronic sublevels 8-82756
 BaTbO₃:Tb³⁺, perovskite struct., EPR, cryst. field parameters determ. (*Italian*) 8-52350
 Be₂SiO₄:P, EPR and ENDOR 8-76295
 CaF₂, low symmetry U³⁺ centres 8-76307
 CaF₂:Ce, Stark struct., phototransitions, g-factors 8-67995
 CaF₂:U³⁺, cubic site substituent, EPR spectra obs. 8-72392
 p-CdTe, ESR optical detect., Overhauser shift, g-factor 8-80252
 ClO₂, gas-phase electron g-tensor, magic doublet rot. Zeeman spectra 8-90212
 Cr complex, dimer di- μ -diphenylphosphinatoacetylacetonatochromium(III), EPR of exchange coupled Cr³⁺ pairs 8-88172
 CrO₃ radical in K₂CrO₄ and KCrO₄Cl, g-factor anisotropy 8-67994
 Cu complex, with acetylene, Ar matrix-isolated EPR obs., bonding 8-50564
 Cu²⁺, dopant, ground state wavefunctions and Δg 8-64012
 Cu-Fe, dil., transmission ESR meas. 2 to 40K 8-68364
 Fe complexes, electronic and mag. struct., semiempirical MO cluster calcs. 8-62733
 Fe₈₀B₂₀, ferromagnetic metallic glasses, Brillouin scattering 8-92085
 Fe₄₀Ni₆₀P₁₄B₆, ferromagnetic metallic glasses, Brillouin scattering 8-92085
 Fe₃O₄, magnetite, ferrimag. reson. at 9.3 GHz near Verwey temp., g-factors (*French*) 8-91959
⁵⁴Fe^m, static moments, perturbed ang. distrib. with combined dipole and quadrupole interactions 8-62482
 GaAs:Co²⁺, EPR expts., y-factor determ. 8-76301
 GaP, MCD of phonon-assisted exciton transitions, g-value of hole forming free exciton 8-92053
 Gd-Al, amorphous film, microwave mag. reson. 8-91948
 Gd₂La_{1-x}Pd₃, ESR linewidths, g-shifts, effective electron interaction, spin-lattice relax., spin-flip scatt. 8-68372
 Ge, amorphous, EPR 8-88167
 Ge-Al film, amorphous, EPR meas. 8-80212
 Ge-Cu film, amorphous, EPR meas. 8-80212
 H₂, Zeeman effect in 3d singlet states, g-values 8-50571
 HO₂ radical, EPR spectrum, ground state parameters 8-90193
 H₂, 3d complex, radiative lifetimes, hyperfine constants 8-70873
 n-InSb, effective g-value of electrons determ. by spin flip Raman scatt. and electric-dipole-excited ESR 8-52494
 Ir, A=191, 193, hyperfine struct. of low lying fine struct. levels, hyperfine anomaly, electronic g-factor 8-66214
 KF(Cl)(Br), mag. props. of relaxed excited state of F-centre, vibronic theory 8-60502
 KFeS₂, magnetic reson. meas. 8-95524
 LuR₂-Nd³⁺, dil., ESR, hyperfine crysts. of ^{143,145}Nd, g-factor, crystalline field splitting 8-52349
 LuRh₂-Nd³⁺, dil., ESR, hyperfine crysts. of ^{143,145}Nd, g-factor, crystalline field splitting 8-52349
 Mg₂Fe_{3-x}O_{4-y} precipitates, g-factor, ferrimag. reson. meas. 8-60337
 MgO:Cr³⁺, strain modulated ESR 8-88175
 MnF, MnF₂, EPR, in inert gas matrices, high spin mag. parameters, level diagrams 8-66565
¹⁴N₂, ¹⁶O, elec. and mag. props., hyperfine struct., mol. beam elec. reson. obs. 8-62792
¹⁴N, g-factor, lifetime meas. of 5.106 MeV 2⁻ state of ¹⁴N 8-93965
 NbSe₃, oscillatory magnetotransport, Fermi surface anisotropy, Hall effect, g-factor, Dingle temp. 8-51975
 NdF₃, Zeeman splitting in mag. fields up to 100 kG 8-52483
 Ni(ClO₄)₂·6H₂O, EPR and IR spectra, 98-298K, phase transition at 224K 8-84477
 OH radical, gas phase EPR, rot. states electronic struct. and Zeeman parameters 8-86896
 Pd-Mn, ESR meas., evidences of bottlenecked relax. for Mn²⁺ ion 8-72401
 Sb, nucl. spin-lattice relax., 4.2K 8-91984
 Sb, spin splitting meas. from de Haas-van Alphen effect, g-factors 8-51881
 Si, amorphous, EPR expts. 8-88167
 n-Si inversion layer, resist. minima in surface quantum oscils. 8-60215
 SiO amorphous thin film capacitor, EPR, elec. cond. 8-68358
 SmS:Eu, excited-state exchange interactions, EPR meas. 8-68374
 Sm₂S₃:Eu, excited-state exchange interactions, EPR meas. 8-68374
 SmSe:Eu, excited-state exchange interactions, EPR meas. 8-68374
 SrCl₂:Fe²⁺(Co²⁺) electronic absorption spectra in far and middle infrared 8-68537
 SrF₂:Yb³⁺, trigonal centres, superhyperfine interaction, model 8-88114
 TaSe₃, oscillatory magnetotransport, Fermi surface anisotropy, Hall effect, g-factor, Dingle temp. 8-51975
 Tm₃Al₅O₁₂:Yb³⁺, g-shift meas., EPR 8-56376

g-factor continued

- mV_2O_5 (100-m) P_2O_5 , ($m=100-2$), V(IV) complexes conc., absorpt. and ESR spectra 8-64266
 YbF(Σ^+), matrix isolated ESR spectra 8-86890
 ZnSe, cubic, valence band parameters, magnetorefectance of Γ_6 - Γ_8 exciton 8-60056
 ZnTe:As(P), spin flip acceptor scatt. 8-92072

gadolinium

see also nuclei with

- atom, long-lived autoionisation state (*Russian*) 8-94216
 cover, effective energy cut-off determ., rel. to neutron flux meas. in high-temp. reactor 8-86573
 crystal structure, P-T phase diagram 8-84776
 cubic metal:Gd, influence of cryst. field on EPR 8-52346
 de Haas-van Alphen effect, Fermi surface determ. 8-84138
 EPR linewidth and spin-spin relax. near T_c 8-68369
 ferromagnetic, self-consistent relativistic band struct. calc. 8-91609
 film, elec. resist. results 8-84326
 film, vacuum deposition, using liq. He cooled cryopumping panel 8-56581
 fused salt electrorefining, evaluation of electrolytes 8-92215
 galvanomagnetic effect, longit., in single crystals (*Russian*) 8-56132
 internal fields, positive muon investigation 8-68438
 magnetic domain struct., 77K 8-84447
 magnetic domains, Lorentz microscopy obs. 8-84448
 magnetocrystalline anisotropy, high quality single cryst. 8-84413
 metallic mononitrides:Gd, coupling between 4f electrons and conduction electrons, EPR linewidth 8-52347
 purification by electrorefining, exam. 8-52721
 rare earth sulphate:Gd³⁺, hydrated, EPR spectra, host lattice effects 8-95516
 small ion-getter pump 8-89487
 spin wave exam. 8-56306
 spin wave temp. depend., exchange coupling role 8-68199
 surface, O₂ layer thickness, reson. α -scatt. from ¹⁶O 8-64778
 texture formation during cold rolling (*Russian*) 8-92275
 working medium in mag. Stirling cycle wheel, refrigerator and heat engine modes of operation 8-57964
 CaF₂:Gd³⁺, ITC spectra of impurity aggregate 8-71883
 CaF₂:Gd³⁺, ligand ENDOR cubic centres, elec. field effect (*Russian*) 8-60357
 CaF₂:Gd³⁺, S-state splitting, investigation by ESR and ENDOR at high pressure 8-52345
 CaF₂:Gd³⁺-M⁺, (M=Li, Na, K, Rb, Cs, Ag), electric field effect expts., EPR line breadths, lattice distortions 8-80210
 CaF₂:SrF₂-BaF₂:Gd³⁺, luminescence spectrum of Gd³⁺ ion and solid solution region obs. 8-84638
 CdF₂:Gd³⁺, hydrostatic press. and temp. effects on EPR spectrum 8-76304
 EuO:Gd, electron mobility below Curie temp. 8-91696
 EuS:Gd, electronic struct., mag. exchange and elec. transport props. 8-87974
 Gd³⁺, hyperfine interactions, relativistic CI using many-body calcs. 8-78638
 Gd³⁺, Zeeman interaction, relativistic corrections and very small g-shifts, contrib. to EPR 8-72393
 Gd³⁺-doped crystals, mag. susceptibility, cryst. field calc. 8-76035
 Gd+H⁺, K-shell ionisation, 7-15 MeV, relativistic effects 8-82830
 LaAl₃:Gd³⁺(Eu²⁺), cryst. field parameters, relax. rates 8-84482
 LaBe₁₃:Gd, ESR, crystalline field single ion effects 8-84481
 La_{3-x}V_xS₂:Gd³⁺ localised moment-conduction electron interact., ESR obs. 8-88183
 LuBe₁₃:Gd, ESR, crystalline field single ion effects 8-84481
 Na₂S:Gd³⁺, PbFCl:Gd³⁺, crystal field splitting, parametrisation of temperature dependence 8-91652
 Nd₂(SO₄)₃.8H₂O:Gd³⁺, EPR, zero field splittings, spin-Hamiltonian parameters 8-91949
 Pr₂Zn₃(NO₃)₁₂.24H₂O:Gd³⁺, EPR 8-64270
 SCH_{1.9}:Pt, Gd, effect of Pt on Gd³⁺ ESR lineshape 8-68371
 Si:Gd, radiation defect form., effect of Gd impurities, elec. and optical meas. 8-71764
 Sm₂(SO₄)₃.8H₂O:Gd³⁺, EPR, zero field splittings, spin-Hamiltonian parameters 8-91949
 SF₆:Gd³⁺, spin-lattice relax. of Gd³⁺, EPR line shifts meas. 8-72404
 ThBe₁₃:Gd, ESR, crystalline field single ion effects 8-84481
 YAG:Gd³⁺, EPR absorpt. spectrum 8-76305
 YAG:Gd³⁺, ESR absorption spectra, line broadening 8-91940

gadolinium alloys

- La_{1-x}Gd_xRu₂, mag. ordered superconductor, re-entrant superconductivity 8-88059
 Ce_{1-x}Gd_xRu₂, superconductivity and ferromagnetism coexistence, 60 mK-4.2K, spin echo NMR 8-84349
 CePd₂-Gd, EPR of Gd³⁺ impurities in host with interconfig. fluctuations 8-56377
 Co-Gd-Mo-Ar film, amorphous, mag. props. 8-80182
 Co₂Ga_{2-x}Cu_x, mag. and struct. phases from magnetisation, neutron, X-ray diff. techniques 8-52253
 Co₂Ga_{2-x}Ni_x, mag. and struct. phases from magnetisation, neutron, X-ray diff. techniques 8-52253
 Fe-Gd amorphous films with comp. gradient, volume and surface hysteresis (*Russian*) 8-88148
 Fe-Gd film, amorphous, mag. props., mean field analysis 8-64236
 Fe-Gd film, amorphous, O₂ contamination effects on mag. props. 8-64231
 Gd-Ag, vap. quenched alloys, struct. and mag. props. 8-84461
 Gd-Ag(Cu) alloy film, amorphous, struct. and mag. props. 8-52318
 Gd-Al, amorphous alloy films, mag. phase diagram, spin glass and ferromag. regions 8-68234
 Gd-Al, amorphous film, microwave mag. reson. 8-91948
 Gd-Al(Cu)(Ga)(Rh)(Pd), amorphous alloys, mag. coupling of rare earth moments 8-88108
 Gd-Au, dil., Mossbauer exam. of mag. hyperfine field at ¹⁹⁷Au impurity 8-88244
 Gd-Co, and Gd-Co-Mo films, amorphous, mag. props., annealing effects 8-64235
 Gd-Co, CPA calcs., moments and transition temps. 8-52252
 Gd-Co alloy amorphous thin films, anisotropic mag. and microstruct. props. 8-95487
 Gd-Co amorphous films, model calculations for anisotropy formation induced by resputtering processes 8-64242

gadolinium alloys continued

- Gd-Co amorphous sputtered films, magnetoelastic contrib. to perpendicular anisotropy, internal stress meas. 8-95490
 Gd-Co film, amorphous, Ar sputtered, struct. 8-63946
 Gd-Co film, amorphous, microstruct. and magnetism 8-64230
 Gd-Co film, amorphous, phase separation as source of perpendicular anisotropy 8-64244
 Gd-Co film, amorphous, preferential resputtering effect induced anisotropic distrib. of atomic pairs 8-63950
 Gd-Co film, amorphous, selective resputtering-induced anisotropy 8-72376
 Gd-Co film, amorphous, stability of small bits to temp. and mag. field changes 8-68314
 Gd-Co film, bias-sputtered, dipolar mechanisms for mag. anisotropy 8-64233
 Gd-Co film, homogeneity of films prepared by bias sputtering 8-72379
 Gd-Co film, sputtered, inert gas incorporation effect on uniaxial anisotropy 8-64232
 Gd-Co-Fe film, amorphous, bias-sputtered, uniaxial perpendicular anisotropy 8-64234
 Gd-Co-Mo film, amorphous, Ar sputtered, struct. 8-63946
 Gd-Co-Mo film, amorphous, in-plane susceptibility near compensation point 8-64238
 Gd-Cu, amorphous alloy films, mag. phase diagram, spin glass and ferromag. regions 8-68234
 Gd-Dy, galvanomag. effect, longit., in single crystals (*Russian*) 8-56132
 Gd-Fe, amorphous film, thermomagnetic writing 8-84428
 Gd-Fe, CPA calcs., moments and transition temps. 8-52252
 Gd-Fe alloy, amorphous thin films, anisotropic mag. and microstruct. props. 8-95487
 Gd-Fe amorphous sputtered films, magnetoelastic contrib. to perpendicular anisotropy, internal stress meas. 8-95490
 Gd-Fe film, amorphous, in-situ ion beam sputtered, microstruct. and Lorentz mag. struct. 8-63947
 Gd-Fe film, amorphous, mag. props., annealing effects 8-64235
 Gd-Fe film, amorphous, microstruct. and magnetism 8-64230
 Gd-Fe film, amorphous, preferential resputtering effect induced anisotropic distrib. of atomic pairs 8-63950
 Gd-Fe-Y, amorphous film, thermomagnetic writing 8-84428
 Gd-Hg, dil., mag. hyperfine field, TDPAC meas. 8-52414
 Gd-Ir, dil., hyperfine interaction of ¹⁹³Ir, Mossbauer effect meas. 8-52413
 Gd-Mo-Mo amorphous film, domain drag effect obs. 8-91911
 Gd-Ni, CPA calcs., moments and transition temps. 8-52252
 Gd-Tm, mag. anisotropy, from magnetisation meas. at 4.2K 8-68216
 Gd-Y alloy, anomalous thermal expansion, interferometric meas. 8-52333
 Gd-Y alloy, metal sphere prod. by spark erosion technique 8-81956
 GdAg_{1-x}In_x, magnetic transition temp., effect of hydrostatic press. 8-76244
 GdAu_{3.6}, ordering temps. and effective moments 8-60283
 GdCo film, amorphous, sputtered, in-plane anisotropy induced by rare gas annealing 8-84458
 Gd_{1-x}Co_x film, resistivity, Hall effect, domain wall density 8-76169
 Gd₂Co₇, amorphous film, ZZ 8-68014
 Gd₂Co₃₅, amorphous, amg. ordering, susceptibility, magnetisation and hysteresis meas. 8-68190
 GdCoMo film, amorphous, sputtered, ferrimag., in-plane susceptibility near compensation point 8-64240
 Gd₂Cu_{1-x}, amorphous film, magnetisation meas., fully aligned moment 8-68309
 Gd_{1-x}Fe_x amorphous film, cosputtered, struct. and mag. props. 8-60323
 GdFe₄Al₈, mag. props. 8-52250
 Gd(Fe₂Co_{1-x})₂, ferromag. reson. of pseudobinary cubic compounds 8-91961
 GdGa₂, mag susceptibility, 1.5-300K and Neel temp. 8-68184
 Gd_{0.9}La_{0.1}Al₂, ferromag., NMR of ¹³⁹La 8-52377
 Gd_{1-x}La_xZn, magnetisation and paramag. suscept. 8-88101
 GdMg₃, mag. props., Mg conc. depend. 8-84392
 GdMg₃, mag. props. 8-72346
 GdMn₂-GdAl₂ intermetallics, mag. props., 80-650K 8-60282
 (GdMn₂)(GdAl₂)_{1-x}, mag. and struct. investigations of intermetallic systems 8-95440
 GdNi₃, anomalous behaviour near Curie point 8-91880
 GdNi_{1-x}, sputtered amorphous films, mag. props. and Hall meas. 8-95488
 Gd_{1-x}Sm_xCo₂Ni₃, giant intrinsic magnetic hardness 8-56347
 Gd₂Y_{1-x}Fe_x, s-d exchange interaction integral, change due to hydrostatic compression 8-88199
 Gd₂Y_{1-x}Fe_x, saturation magnetisation, magnetostriction, Curie temp., ferrimag. ordering, exchange field (*Russian*) 8-68343
 (Gd_{0.5}Y_{0.5})Ni, FeB struct., cryst. field effects on mag. struct. 8-52226
 (La_{0.5}Gd_{0.5})Al₂, mag. props. 8-52299
 (La_{1-x}Gd_x)Al₂, dil., reverse resistance anomaly 8-76054
 La_{1-x}Gd_xAl₂, Gd³⁺, ESR meas. 8-68370
 Lu-Gd, dil., positive exchange Kondo system, magnetisation and resist. 8-68158
 Tb₂Gd_{1-x}Al₂, magnetic anisotropy, magnetostriction 8-56364
 TbMg₃, mag. props. 8-72346
 Y_{1-x}Gd_xCo₂, NMR of ⁵⁹Co 8-52376
 Zr₄₀Cu_{60-x}Gd_x, amorphous, mag. ordering and local random anisotropy 8-68273
 Zr₄₀Cu_{60-x}Gd_x, amorphous alloy, mag. interactions 8-95432

gadolinium compounds

see also gadolinium alloys

- and UO₂-Gd₂O₃ solid soln., high temp. thermal expansion, 298-1700K 8-83979
 exchange striction in NaCl type compounds 8-84409
 (Gd,Bi)₃(Fe,Ga)₂O₁₂ magneto-optic film, ion irradiation effect on storage props. 8-52324
 (Gd,Lu)₃(Fe,Mn,Al)₂O₁₂ epilayer with orthorhombic anisotropy, domain wall vel. 8-52322
 Gd complex, benzoylacetate, energy transfer at high pressures 8-52541
 GdAlO₃, crossover effects near spin-flop multicritical point 8-68245
 Gd₂Al₂O₇, phase obtained by crystallisation of amorphous Gd₂O₃.5/3Al₂O₃ by quenching 8-92224

gadolinium compounds continued

- GdBi, thermal expansion, thermal cond., 300-900K 8-91453
 GdCl₃, interaction parameters, high freq. meas. of adiabatic differential susceptibility 8-68211
 GdCo₂Ge₂, magnetism and hyperfine interactions 8-76228
 GdCu₂Ge₂, magnetism and hyperfine interactions 8-76228
 GdEr_{1-x}Rh_xB₄, mag. and supercond. transitions 8-68127
 GdF₃, crystal growth by Bridgman-Stockbarger method 8-52660
 GdF₃-RF₃, R=Tb, Ho, Er, Yb, stabilisation of rhombic β-YF₃ type struct. 8-67700
 GdFe₂Ge₂, magnetism and hyperfine interactions 8-76228
 GdGa garnet, Czochralski grown, substrate material dislocation propagation 8-59771
 Gd₃Ga₅O₁₂, brilliance, sparkliness and fire of diamond simulants 8-90363
 Gd₃Ga₅O₁₂, Ca, Zr and Mg substituted artificial garnets, track registration props. 8-62679
 Gd₃Ga₅O₁₂, Czochralski grown, effect of melt flow phenomena on perfection 8-88419
 Gd₃Ga₅O₁₂, growth of 3" diameter crystals 8-68616
 Gd₃Ga₅O₁₂, opt. dispersion 8-64343
 Gd₃Ga₅O₁₂, substrate, electron examination of microstruct. and microsegregation 8-67919
 Gd₃Ga₅O₁₂:Nd³⁺, cryst. field anal. 8-64013
 Gd₃Ga₅O₁₂:Nd³⁺, growth, stimulated emission, spectral props. 8-95593
 Gd₂Ge₂O₇, polymorphism under pressure (*French*) 8-95150
 Gd₂Ge₂O₇(OH)₂, cryst. struct. 8-71714
 GdIG, mag. props. meas. in high mag. fields, review (*Japanese*) 8-52303
 Gd_{0.4}La_{0.3}P_{0.3}O₁₄, photoemission spectra, 4f, 5p and 5s giant reson. enhancement 8-95660
 Gd₂La_{1-x}Pd_x, ESR linewidths, g-shifts, effective electron interaction, spin-lattice relax., spin-flip scatt. 8-68372
 GdMn₂Ge₂, magnetism and hyperfine interactions 8-76228
 Gd₂(MoO₄)₃, and isotypes exam. of crystal growth, and defect generation 8-68617
 Gd₂(MoO₄)₃, domain structure obs. by GdF₃ decoration 8-84544
 Gd₂(MoO₄)₃, electro-optical properties 8-88281
 Gd₂(MoO₄)₃, improper ferroelectric, electro-opt. props. 8-76426
 Gd₂(MoO₄)₃, prismatic domain exam. 8-56441
 Gd₂(MoO₄)₃, spontaneous electrooptic effect, role of induced birefringence 8-68480
 Gd₂(MoO₄)₃, uniaxial stress effect on ferroelec. transition, Raman scatt. 8-80360
 Gd₂Mo₆Se₈, Gd³⁺ ESR meas., 1.4-290K 8-88184
 GdNi₂Ge₂, magnetism and hyperfine interactions 8-76228
 Gd₂O₃ coatings, neutron collimators, comparison with enriched ¹⁰B coatings 8-82564
 Gd₂O₃ film on CaF₂ substrate, computational algorithm for optical consts. determ. 8-72617
 GdOHCO₃, Gd₂O₃CO₃, synthesis of rare earth carbonates under hydrothermal conditions 8-72714
 GdP, electronic struct., mag. exchange and elec. transport props. 8-87974
 GdP-GdS systems, mag. exchange interactions, free carrier conc. 8-60278
 GdPO₄, rotating Carnot-cycle magnetic refrigerators for use near 2K 8-57965
 (GdPrBi)₃(FeGaIn)₅O₁₂, pure and In³⁺ doped, near IR absorpt. and Faraday rot. 8-95580
 Gd(ReO₄)₃.4H₂O, (ReO₄)⁻ ion vibr. rel. to static field, Raman investig. (*Russian*) 8-76470
 GdS, electronic struct., mag. exchange and elec. transport props. 8-87974
 GdS, metallic FCC antiferromag., phonon Raman scatt. 8-60458
 GdS, vaporisation thermodynamics and dissociation energy obs. 8-67822
 Gd₂(SO₄)₃.8H₂O, rotating Carnot-cycle magnetic refrigerators for use near 2K 8-57965
 Gd₂Y_{1-x}Rh_xB₄, mag. and supercond. transitions 8-68127
 Gd_{0.5}Y_{1.1}Gd_{0.44}Fe_{4.56}O₁₂, ion implanted, ferromag. reson. meas. 8-68385
 HfO₂-Gd₂O₃, phase relations 8-72769
 MnGd₂S₄, mag., struct. and Mossbauer effect study 8-51507
 Nd-Gd-Te alloys of R₂Te₃-T₃Te₄ region, physicochem. props. 8-52017
 Sm_{1-x}Gd_xS, press. induced electronic transitions 8-68058
 SrCl₂-GdCl₃, prep. and purification 8-88420
 SrF₂:GdF₃, absorpt. spectra of γ-irrad. cryst., 77K, 200-700 nm 8-84615
 Y_{3-x}Gd_xFe₅O₁₂, field depend. of susceptibility (*Russian*) 8-68176
 (Y₂GdYbBi)₃(FeAl)₅O₁₂, epitaxial garnet film, with mag. compensation point, behaviour of 'compromise' phase boundary 8-60321
 Y₂O₃-Gd₂O₃-Nd₂O₃ solution phase diagrams and thermal conductivity (*Russian*) 8-88448
 ZrO₂-GdO_{1.5} (80 mol.%), X-ray diff. exam. of continuous transition 8-68684

gain (amplification) see *amplification*

gain measurement

communications satellite system measurements 8-61712

galactic cosmic rays

- antimatter model for galactic nuclei and quasars (*Chinese*) 8-73771
 antiprotons and antihelium, relative abundance in primary cosmic radiation 8-73594
 cosmic rays propagation and distribution in Galaxy 8-69621
 discrete gamma-ray sources rel. to galactic cosmic ray distrib. (*Russian*) 8-65719
 energy loss in expanding areas of Galaxy (*Russian*) 8-93055
 gamma radiation, possible origin, data from COS-B and SAS-2 satellites (*French*) 8-85776
 gamma ray bursts, size spectrum, idealised galactic distrib. of sources 8-65716
 gamma-ray bursts and cosmic fireballs 8-54087
 gradient in 1971-4 period derived from Gorlovka meteorite 8-61695
 halo, relativistic electrons spectrum from radio obs. 8-96544
 highest energy nuclei and EAS records 8-57413
 injection into dense supernova shells by pulsars 8-65638
 intercloud cosmic ray ionisation rate 8-85989
 interplanetary anisotropies, quiet time obs. from Pioneer 10 and 11 8-77442
 galactic cosmic rays continued
 interplanetary flux, Mars spacecraft meas. (1971-74) 8-96365
 interstellar local electron spectrum determ. from galactic radio background 8-93056
 isotopes composition rel. to origin and containment time 8-53781
 isotopic composition, meas. with isotope spectrometer on International Sun-Earth Explorer C spacecraft 8-85797
 isotopic composition of Fe-group elements, balloon meas. 8-89024
 north-south gradient rel. to solar polar coronal holes 8-89019
 nuclei from 3000 MeV to 50 GeV per nucleon, charge comp. and energy spectra 8-93059
 particle radiation satellite obs. (*Danish*) 8-69631
 propagation, leaky-box model 8-57409
 propagation in dynamical halo, retrodictive probability approach 8-65467
 propagation in finite solar cavity, theoretical model 8-69623
 proton/electron ratio 8-69633
 protons, as extraterrestrial source of atmospheric water vapour 8-69416
 solar equator vicinity, daily cosmic ray flows during solar cycle 8-69622
 stellar daily variation, semiannual modulation 8-69626
 subcosmic rays rel. to active solar processes 8-61693
 super-high energy cosmic rays, anisotropy in galactic disc direction (*Russian*) 8-57410
 transient cosmic ray intensity vars., solar flare origin 8-89021
 transient cosmic ray intensity vars., solar source 8-89022
 velocity diffusion, turbulent mag. field, Monte Carlo calc. 8-53777
⁷Be, cosmic ray accel. probe 8-81512
galactic radio waves see *radiofrequency cosmic radiation*
galaxies
 see also *BL Lacertae-type objects; clusters of galaxies; H I regions; H II regions; intergalactic matter; nebulae; The Galaxy*
 0915+320, wide-angle-tail radio source in group of galaxies, 4.9 GHz map 8-93441
 active galactic nuclei, H emission-line spectra 8-96557
 active galaxies, forbidden lines theory 8-93408
 active nuclei, black hole gravity power model 8-57667
 active nuclei, continuous optical spectra 8-57644
 active nuclei, high energy neutron beams 8-69881
 active nuclei, IR obs., future prospects 8-57651
 active nuclei, local space density 8-57676
 active nuclei, physical props. from emission-line spectra 8-57650
 active nuclei, radio obs., future prospects 8-57652
 active nuclei in spiral and Seyfert galaxies 8-57653
 angular momentum in Local Group 8-93400
 apparent distribution, intragalactic factor due to interstellar clouds 8-96552
 apparent magnitudes estimation rel. to zodiacal light brightness (*Russian*) 8-93389
 Australian Astronomical Society, conf. Melbourne, Australia (May-June '77) 8-69655
 B2 1506+34, peculiar radiogalaxy, H I absorption detection 8-54048
 bidimensional stellar systems in uniform rot., stability for nonaxisymm. modes 8-85980
 binary stellar systems, tidal disruption and coalescence 8-93330
 black hole in galactic nucleus, sustenance 8-57632
 bright galaxies, Arecibo 2380 MHz, survey 8-57470
 3C273, spectroscopic obs. and redshift of associated galaxy 8-77606
 5C2 survey revised distances of optical objects from radiosources 8-57472
 3C 123, radio struct. at 2.7 and 15 GHz 8-54050
 3C 285, 3C 265, 3C 390.3, optical emission in radio lobes 8-57630
 3C 293, radio galaxy, radio and optical obs. 8-93418
 3C 33, optical emission detect. in SW radio lobe 8-57665
 3C 33 and 327, double radiogalaxies, spectrophotometry 8-54066
 3C 382, 3C 386, radio galaxies, two-freq. high resolution obs. 8-86031
 3C 48, 3C 295, radio galaxies, scintillation at 25 MHz rel. to ang. struct. 8-65711
 catalogue of galaxies and clusters of galaxies in SMC direction 8-96410
 Cepheid variables in different galaxies, progression in period-amplitude diagrams characts. 8-53956
 chains of galaxies, stabilisation by continuous background (*Russian*) 8-73765
 Circinus Sb galaxy, Mt. Stromlo Schmidt red plates (*Swedish*) 8-69877
 close pairs, excess radio emission 8-57658
 cluster galaxies, gas ejection rel. to intracluster Fe-enriched gas origin 8-93390
 cluster galaxies, luminosity function 8-54058
 cluster galaxies, luminosity function rel. to clusters Bautz-Morgan classes 8-54057
 clustering spectrum, low mass portion anal. 8-81695
 clustering spectrum, rel. to cosmic luminosity 8-81696
 compact, distrib. in compact groups of galaxies (*Russian*) 8-61926
 compact, mean surface brightness and integral brightness relation 8-93412
 compact, spectroscopic and photometric obs. 8-77603
 compact galaxies in compact cluster Shakhbazian 1, photometry (*Russian*) 8-93428
 compact objects on UK Schmidt plates 8-81687
 compact radio sources, struct. and time vars. 8-57669
 cool stellar discs, equilib. 8-54037
 cool stellar discs, radial modes of oscill. 8-57628
 correlation functions, for density perturbations in expanding universe 8-65730
 covariance function, explanation for 9 Mpc break 8-65688
 3CR radio sources counterparts, optical field investigations to faint limiting magnitudes 8-54067
 Cygnus A model, radio source powered by M87 type knots 8-57661
 dense nuclei, disruptive stellar collisions 8-65621
 density oscillations in uniformly rotating disc galaxy 8-57635
 density waves excitation and evolution 8-65684
 density waves in self-gravitating disc, accretion-induced overinstability 8-73752
 development in expanding Universe (*Danish*) 8-86019
 differentially rotating spiral system, density wave-star interaction 8-69871

galaxies continued

- disc-halo galaxies, boundary layer circulation 8-57627
 disclike galaxies, stability, numerical expts. 8-89251
 disclike galaxies in massive halos, stability, models 8-93403
 dwarf spheroidal galaxies, H I content upper limits 8-57633
 E and S0 galaxies, new colours, magnitudes and types 8-89246
 early-type, metallicity effects on integrated colours, calibration 8-89227
 early-type galaxies, rot. curves meas. 8-54034
 elliptical, in Abell 426 and 1367 clusters, surface brightness and colour distrib. 8-81681
 elliptical, search for H I emission 8-65681
 elliptical galaxies, surface photometry 8-57625
 elliptical galaxies stellar population, evolutionary synthesis for late M giants, comp. effects 8-57626
 ellipticals, formation, analytical model 8-69868
 ellipticals, polarisation by interstellar matter 8-93399
 ellipticals, rotation 8-54052
 emission-line galaxies in dense clusters 8-65703
 emission-line objects, Univ. of Michigan List IV 8-77494
 ESO 103-G35, type I Seyfert, optical counterpart of H 1834-653 X-ray source 8-96547
 ESO 140-G43 (Fairall-51), new southern Seyfert 1 galaxy discovery 8-54044
 ESO 290-G50, spectral obs. of type I supernova 8-96496
 ESO/Uppsala galaxies, second catalogue 8-77497
 evolution, three-dimens. computer simulation 8-81551
 evolution and stellar populations, Yale conference (May 1977), report 8-69879
 evolution rel. to quasar evolution 8-57693
 explosions, source and nature in galactic nuclei 8-96546
 extended radio galaxies (>1 arcsecond), large-scale struct. 8-57668
 extended radiosources and elliptical galaxies, search for radio cores using Very Large Array 8-81700
 extended radiosources and elliptical galaxies, small-diameter components in extended structs. 8-81699
 extragalactic distance scale, review of distance indicators 8-93396
 extragalactic objects clustering in Universe (*Polish*) 8-96580
 formation, free collapse of stars rotating sphere 8-93325
 formation, violet gas dynamics 8-86018
 formation and clustering rel. to core condensation in heavy haloes 8-54051
 formation from primordial material and dissipative processes 8-57654
 formation theories rel. to enriched gas in clusters and dynamics 8-77596
 Fornax cluster bright galaxies, surface photometry 8-96548
 Fourcade-Figueroa galaxy near NGC 5128, resolution, redshift and distance 8-73758
 gaseous protoclusters spatial struct. and galaxy form. 8-93415
 giant galaxies in clusters, radioactive accretion flow 8-93433
 Haro 15, spectrophotometry and morphology of galaxy with UV excess (*Russian*) 8-93387
 head-tail radio galaxies, galaxy counts in surrounding region rel. to tail orientation 8-54060
 head-tail radio galaxies in poor clusters, radio and optical obs. 8-96530
 heavy halos, resulting twisted and warped discs 8-65694
 Hubble diagram for type I and II objects supernovae 8-53967
 IC 1613, structure and content of Local Group dwarf galaxy 8-86006
 IC 342, CO emission from late-type galaxy 8-89250
 II Zw 70/II Zw 71, compact galaxies, H I maps, tidal interactions 8-96531
 integrated Brandt masses 8-93398
 interacting galaxies, numerical models appl. (*Russian*) 8-93421
 interstellar gas self-gravity effects on galactic shock waves 8-73761
 Irregular II galaxies origin 8-77601
 isolated pairs, radio continuum survey 8-57657
 large-scale distribution and motion, in adiabatic theory of form. 8-54056
 late-type galaxies, integral props. derived from H I obs. 8-86015
 Leo A, H I 21 cm. line survey of dwarf irregular galaxy 8-81688
 Leo I dwarf galaxy, 23 new variables discovered 8-53953
 LMC, colour magnitude diagram and metal abundances of Hodge 11 cluster 8-69850
 LMC, emission line objects (*French*) 8-69875
 LMC, far IR obs. of H II regions 8-81671
 LMC, four super-giant H II shells obs. 8-86012
 LMC, giant H II ring obs. rel. to energetic stellar winds 8-77593
 LMC, integrated photometric props. 8-54054
 LMC, interstellar extinction and stellar population in 30 Doradus region 8-96517
 LMC, obs. of A0538-66 recurrent X-ray transient source 8-54085
 LMC, radio model of 30 Doradus region 8-96523
 LMC, radiosources at 3.4 cm, catalogue and spectral indices 8-65695
 LMC, spectrophotometric study of Henize S22, emission line star 8-69803
 LMC, UV reddening law in 30 Doradus complex 8-96516
 LMC, yellow stars UBV photometry and LMC members number 8-93417
 LMC stellar population structure, count-brightness ratios for central regions 8-89245
 LMC supergiant stars, comments on catalogue of Stock et al. (*French*) 8-53941
 LMC X-4, identification with eclipsing binary system, review (*German*) 8-81713
 Local Group, distances for six nearest galaxies 8-89247
 low surface brightness galaxies, luminosity function, props. 8-96532
 luminosity function models, observational test 8-77605
 M101, chemical comp. of H II regions 8-93359
 M101, gas and stellar mass determ. in NGC 5471 H II region (*Russian*) 8-93426
 M101, spectra of H II regions, comp. gradient across spiral galaxy 8-65683
 M31, inner nuclear regions, spectral features and dwarf content 8-86005
 M31, polarised radio emission detect. 8-86017
 M32 is in front of M31, evidence from planetary nebula (M32-1) 8-93394
 M33, far IR obs. of H II regions 8-61923
 M33, H I large-scale struct. 8-96539
 M33, new variable star discovery 8-73717

galaxies continued

- M49, globular clusters space distrib. 8-93393
 M51, spiral arm struct. and star form. 8-73762
 M51 system, extended H I obs. 8-89253
 M82, compact radio source 41.9+58 in nucleus 8-93442
 M82 as exploding radiogalaxy, image tube spectrogram evidence 8-69880
 M84, M86, positional coincidence with extended X-ray emission 8-54090
 M87, halo globular clusters metallicity 8-89244
 M87, nature of jet 8-54055
 M87, photographic surface BV photometry of giant elliptical 8-69867
 M87 jet, internal shocks in plasma beam 8-93416
 M 31 spiral structure, morphological approach 8-65690
 Magellanic Clouds, chem. comp. of H II regions, photoelec. spectrophotometry 8-77607
 Magellanic Clouds, H II regions chem. comps. 8-93381
 Magellanic Stream, turbulent wake of Magellanic Clouds in galactic halo 8-69884
 magnetic fields from light polarisation obs. 8-69872
 Markarian 132, spectrum and redshift systems 8-89248
 Markarian 298 (=IC 1182-4), multicolour photometry (*Russian*) 8-57641
 Markarian 374, Seyfert galaxy, spectra of double nucleus components 8-69882
 Markarian II, spectra of stellar population 8-54047
 massive halos, contrib. of heavy stable neutral leptons 8-93091
 MCG 10-16-117, supernova classification and spectrum 8-69818
 MCG 10-16-117, supernova discovery 8-69817
 MCG 43223, spectrum of Type V supernova 8-93288
 MCG-4-32-23, possible supernova discovery 8-53968
 MCG-5-9-22, supernova discovery 8-81643
 MCG-5-9-22, supernova obs. and red shift 8-81644
 merging of galaxy pairs, N-body simulation 8-77600
 missing mass, role of brown dwarfs and black holes 8-61879
 morphological evolution and galactic cannibalism 8-93404
 NGC 1052, active elliptical, radio and optical study 8-65693
 NGC 1052, elliptical galaxy, H I obs. 8-69873
 NGC 1068, light polarisation in Seyfert galaxy 8-54046
 NGC 1068, Seyfert, 2-2.5 μ m spectrum, H₂ detect. 8-57636
 NGC 1068, Seyfert galaxy, IR photometry and polarimetry 8-54035
 NGC 1097, jets on image-processed plates of galaxy 8-61922
 NGC 1275, Perseus A, refutation of colliding elliptical and spiral galaxies theory 8-57639
 NGC 1275, vel. field mapping 8-81680
 NGC 1510, tidal interaction with NGC 1512 companion galaxy 8-81682
 NGC 2742, spiral galaxy, rot. and mass. (*French*) 8-89255
 NGC 315, NGC 6251, very large radio galaxies, 11.1 cm obs. 8-86014
 NGC 3256, peculiar galaxy, kinematics 8-96537
 NGC 3312, in Hydra I cluster, ram-pressure sweeping of interstellar medium 8-93429
 NGC 3379, luminosity profile of elliptical rel. to formation model 8-69868
 NGC 3620, southern emission-line galaxy at low galactic latitude 8-86022
 NGC 3628, detection of emerging H I plume at 21 cm wavelength 8-54038
 NGC 3898 and 4036, B photographic photometry 8-54045
 NGC 4151, Seyfert, optical polarimetry, circumnuclear dust envelope 8-61916
 NGC 4151, UV photometry and extended spectrum of Seyfert galaxy 8-89249
 NGC 4151, X-ray flares in Seyfert, thermal model and central black hole 8-93407
 NGC 4472, very weak radio galaxy, struct. and radio power 8-65708
 NGC 4473, flattened elliptical, spectroscopic obs., dynamics 8-57631
 NGC 4565, spiral galaxy, minor axis brightness profile rel. to massive halos problem 8-93409
 NGC 4631 group, tidal interactions model 8-54059
 NGC 4631/NGC 4656, neutral H aperture synthesis obs. 8-54043
 NGC 4945, water vapour emission obs. 8-93427
 NGC 5236 (M83), Sc galaxy, CO obs. 8-65689
 NGC 5296/7 and nearby quasar, radio obs. 8-93419
 NGC 5383, barred spiral, radio continuum emission obs. at 1415 MHz 8-73753
 NGC 5506, IR obs. of X-ray Seyfert-like galaxy 8-65696
 NGC 5506, X-ray Seyfert, spectra 8-93411
 NGC 5907, rotation and mass of edge-on galaxy from spectra (*French*) 8-77595
 NGC 6251, extended radio galaxy, polarisation at 610 MHz 8-61918
 NGC 6946, CO emission from late-type galaxy 8-89250
 NGC 6946, spiral, N overabundance in nucleus (*French*) 8-89257
 NGC 7213, IR photometry of lenticular Seyfert X-ray galaxy 8-89262
 NGC 7213, S0 galaxy with Seyfert nucleus, spectra and direct obs. 8-86024
 NGC 7479, barred spiral, surface photometry, struct. 8-81690
 NGC 7743, barred spiral, surface photometry, struct. 8-81690
 NGC 891, radio halo, Westerbork obs., electron propag. and magnetic fields 8-61920
 nuclei of massive galaxies, recurrent activity 8-89261
 optical identifications for 2A X-ray sources 8-89273
 optical redshifts, of 719 bright galaxies 8-89252
 origins, galactic angular momenta and magnetic fields 8-93405
 pairs, axis ratios and posn. angles 8-93430
 pairs containing one Markarian and one normal galaxy, morphology 8-96535
 paradoxical redshifts compatibility with gravitation theory 8-73757
 parallaxes, meas. via radio interferometric techniques 8-53796
 peculiar nuclei, relation to galaxy type 8-73759
 photometry, standard total magnitudes of 139 bright galaxies in Virgo cluster area 8-65685
 PKS 0211-47 and 0634-20, giant radiogalaxies, optical and radio obs. 8-81702
 PKS 1402+044, dissector scanner obs. of red object with 3.20 redshift 8-65710
 PKS 1934-63, spectrophotometry of radiogalaxy 8-54066
 primaeval giant elliptical galaxies, observable props. 8-89260
 primordial heavy leptons halos, annihilation contrib. to cosmic gamma-ray background 8-93479

galaxies continued

- QSO redshifts and field galaxies 8-89271
 QSOs disorientations, intervening galaxies rel. to absorpt. line regions physics 8-57680
 quasar absorption lines, intervening galaxies hypothesis and $z=1.95$ peak in redshifts 8-57685
 quasars and galaxies active nuclei, conference, Copenhagen, Denmark, (1977 June 27 to July 2) 8-57675
 radiation-driven outflow models of nonthermal energy source 8-57687
 radio and CD galaxies, optical props. 8-93413
 radio emission of active and normal nuclei, review 8-57646
 radio galaxies, bivariate size-luminosity function determ. 8-65687
 radio galaxies, interpretation and theory of extended and compact components 8-57670
 radio galaxies, narrow-lined, spectrophotometry 8-93391
 radio galaxies, optical emission in radio lobes 8-57630
 radio galaxies, optical emission-line spectra 8-57643
 radio galaxies, radio brightness distrib. obs. with RATAN-600 telescope 8-65698
 radio galaxies, relativistic jets and beams 8-96541
 radio galaxies, -variable, ten-year study at centimetre wavelengths 8-89267
 radio galaxies in Abell clusters fields, Westerborg obs. 8-96549
 radio galaxies search for variability at 18 cm wavelength, complete sample obs. 8-89268
 radio galaxies with short wave radio emission excess, flux densities and variability at 1.35 cm (Russian) 8-57666
 radio recombination line studies of nearby galaxies 8-93397
 radio recombination lines, stimulated emission 8-86030
 radio sources, rapidly varying, relativistic plasmoids dynamics 8-93438
 radiogalaxies, hot spots in outer lobes 8-69899
 radiogalaxies, linear polarisation meas. at 99 GHz 8-93439
 radiogalaxies and supermassive black holes 8-61882
 radiosources optical identifications, statistical anal., data selection 8-61928
 reddening determ. method 8-54039
 redshift-distance square law statistical scrutiny 8-81683
 redshift-magnitude bands and galactic evolution, obs. of Perseus and A1367 clusters 8-54033
 redshift-magnitude bands and galaxies evolution, data anal. 8-57629
 redshifts, Doppler shifts distrib. for relativistic gas 8-65492
 redshifts of radio tail galaxies in clusters 8-69889
 relaxation from aspherical initial conditions 8-96538
 ring structures form. by collisions with intergalactic gas clouds (Russian) 8-93425
 rotating gravitating disc of stars, Jeans' instability self-suppression (Russian) 8-93422
 rotating stellar systems, two-dimensional, nonlinear nonradial oscill. stability 8-53992
 rotation in turbulent layers with proto-galactic eddies 8-54040
 secondary distance indicators 8-93402
 Seyfert, classification, jets and spirals existence (Chinese) 8-69878
 Seyfert, contrib. to low-energy γ -ray background 8-86007
 Seyfert, list of 33 objects 8-77602
 Seyfert, source of diffuse cosmic γ -ray background 8-57700
 Seyfert 2 galaxies, spectrophotometry 8-93391
 Seyfert and radio-galaxy nuclei, optical spectra of ionis. gas region, model 8-93420
 Seyfert galaxies, accretion discs thermal continuum as optical emission source 8-54075
 Seyfert galaxies, accurate optical positions 8-89254
 Seyfert galaxies, broad H lines prod. by suprathermal protons passing through neutral gas (Russian) 8-57642
 Seyfert galaxies, IR energy distrib. obs. 8-57645
 Seyfert galaxies, optical emission-line spectra 8-57643
 Seyfert galaxies nuclei, optical variability from U, B, V and H α photometry 8-96543
 Seyfert galaxies X-ray emission, Uhuru obs. 8-93392
 Seyfert galaxies X-ray emission detectability in deep X-ray surveys 8-96567
 Seyfert nuclei, black flash model 8-57673
 Seyfert nuclei, emissive regions, self-consistent models 8-57686
 Seyfert-like galaxies, medium-redshift, redshift-magnitude-ang. dia. data statistical anal. 8-86016
 Seyferts, obs. at 1.3 and 2.8 cm wavelength, spectra 8-69866
 SMC, C stars in NGC 419 globular cluster 8-53962
 SMC, photometric study of wing and eastern halo 8-86011
 SMC, radial vels. of supergiant stars 8-93237
 SMC, red variable in NGC 371 OB association 8-53961
 SMC, stellar content of NE outer arm and halo 8-86013
 SMC, struct. and kinematic behaviour (French) 8-89258
 SMC, surface brightness meas. with UV Sky Survey Telescope 8-93414
 SMC, UVB photoelectric photometry (German) 8-77594
 SMC, Wolf-Rayet stars spectral classification 8-73716
 SMC star clusters catalogues, identifications and coordinates 8-89086
 SMC wing, photoelectric UVB sequence 8-69874
 SMC X-2, SMC X-3 optical counterparts, spectra 8-93469
 southern Molonglo radio galaxies, optical spectra 8-96555
 spherical, gravit. stability of rotating embedded gas discs (Russian) 8-61915
 spherical stellar systems, potential (Russian) 8-93386
 spiral, density wave evolution (Chinese) 8-86020
 spiral, gamma-ray luminosity, contrib. to diffuse background above 100 MeV 8-93481
 spiral, nearly edge-on illusionary warps in H I discs 8-65682
 spiral, ring structs., nonlinear density wave theory (Russian) 8-93423
 spiral, ring-like structs., H II regions and OB associations distrib. (Russian) 8-93424
 spiral density wave caused by orbiting retrograde companion, props. 8-96533
 spiral galactic potential, planar stellar orbits 8-69845
 spiral galaxies, interstellar gas hydrodynamic flows in regions of Lindblad resons. 8-96527
 spiral galaxies pair at low galactic lat., discovery 8-96536
 spiral modes in disc galaxies, density wave theory 8-54053
 spiral structure, rel. to stochastic star formation 8-93395
 spiral systems, Lin's density-wave theory, observational possibilities (German) 8-73756
 spirals, primordial star generation rel. to heavy haloes 8-61946
 spirals, radio haloes 8-89263

galaxies continued

- stellar H-R diagrams, appl. to studies of galaxies 8-81619
 stellar orbits in growing spiral field in galaxy near corotation resonance 8-61891
 stellar space density derivation methods, systematic comparison 8-61917
 supernova discovery in anon. galaxy in Grus, position 8-93289
 Sz 80, southern emission-line galaxy at low galactic latitude 8-86022
 tidal disruption by a massive black hole and collisions in galactic nuclei 8-77597
 tidally interacting galaxies, evolution of mass and tidal radius 8-65699
 UKS 1927-177 and 2323-326, 21 cm. obs. of new dwarf irregulars 8-65697
 unidentified high latitude radiosources 8-57672
 universe model, computer simulation of galaxy distrib. in Lick catalogue 8-81718
 UV galaxies with double and multiple nuclei (Russian) 8-61914
 UV spectra, International Ultraviolet Explorer (IUE) obs. 8-96540
 variable galactic nuclei, props. and observing techniques 8-81691
 warping of galactic plane and ellipticity changes 8-69847
 X-ray emitting galactic nuclei, luminosity function and variability time scale 8-57701
 X-ray sources correl. with radiosources from 26.3 MHz survey 8-65707
 III Zw 2, X-ray and radio emission from compact galaxy 8-65691
 I Zw 92, III Zw 77, compact galaxies with broad emission lines, spectra 8-73760
 H I surface density distrib. at periphery of galaxies, effects of ionising background radiation 8-65729

gallium

see also nuclei with

- 1/f noise, meas. in solid and liq. phases 8-64073
 3d and $L_2M_{4,5}$ binding energy, Ga, GaAs and Ga_2O_3 , ESCA absolute energy calibr. 8-92171
 alkali halides: Ga^+ , optically detected EPR in relaxed excited states of Ga^+ 8-72437
 atomic electron impact excitation cross sections calc. (Russian) 8-55240
 atoms and ions, regularities within Stark widths of reson. lines 8-78662
 Auger spectrum, effect of $L_1L_{2,3}M$ Coster-Kronig processes 8-72681
 complexation by amino acids, with basic or heterocyclic groups (French) 8-53318
 concentration determ. in atm. and rainwater in Vizcaya, Spain (Spanish) 8-57264
 contact angle meas. between melt and crystal during Czochralski growth 8-64461
 de Haas-van Alphen effect, expt. and interpretation 8-84132
 desorption, from W oxidised polycryst. surface, kinetics 8-75939
 determination, in flux-grown magnetic garnets, by AAS 8-92585
 diffusion into Si through SiO_2 layer, junction depth 8-51574
 gaseous reduction and extraction from mica 8-92216
 liquid, elec. resist. calc., 19 and 35°C, using calc. and expt. struct. factors (Russian) 8-56124
 liquid, electrode metal-solvent interaction rel. to elec. double layer struct., adsorpt. 8-61023
 liquid, embrittlement of Al 8-64653
 liquid, neutron diff. room temp. to 1303K, struct. model 8-51405
 liquid struct. factor, short range repulsive forces 8-75528
 liquid-solid phase transition, photoacoustic detection 8-75810
 melting-point apparatus for thermometer calibration, enzymologic appl. 8-85460
 melting-point standard, near 30°C, clinical chemistry appl. 8-80997
 plastic deform. and fracture obs. by acoustic emission of Zn single crystals in metal melt (Russian) 8-56737
 superconducting thin film, tunnelling meas. in high mag. field 8-68120
 surface props. rel. to adsorbed O_2 , H_2O vapour, work function determ. 8-60187
 $CdCr_2Se_4$:Ca, temp. driven metal-semiconductor transition, temp. and mag. field depend. (Russian) 8-88003
 CdS :Cu, In, Ga, spray deposited film, struct., X-ray obs. 8-71713
 Ga I, relativistic and cancellation effects in line strength ratios 8-62689
 Ga I, Rydberg series, discrete levels and continua of finite bandwidth 8-74603
 Ga-GaAs interface immersed in electrolytic solns., elec. props. 8-95368
 Ga-GaAs(110) structure, interface states, photoemission study 8-95359
 Ga-NaX zeolite system, press. depend. of metal-insulator transition 8-88005
 GaAs: C^+ , Ga^+ , dual implantation of C^+ and Ga^+ , sheet resist. and Hall effect meas. 8-67728
 GaAs-Ga, (110) interface electron states, photoemission study, chemical shift, surface charge redistrib. 8-72259
 ^{73}Ga , β -decay rate for estimation of ultra-high pressure 8-77927
 p-Ge:Ga, carrier heating by weak elec. field, hole-hole collision influence 8-72161
 Ge:Ga, effects of destabilising vertical thermal gradients on cryst. growth and segregation 8-52659
 Ge:Ga, photoconductivity oscillation with respect to applied mag. field (Russian) 8-80026
 $Pb_{1-x}Ge_xTe$:Ga, Fermi level stabilization, transport props. meas., 77-400K 8-56065
 Si, diffusion of Ga in closed capsule, surface damage elimination 8-87691
 Si:Ga, bound-exciton absorption 8-56507
 Si:Ga, edge luminesc. spectra of acceptors, multiexciton complexes 8-56517
 Si:Ga, gettering of Au and Cu during Ga diffusion 8-91350
 Si:Ga, LPE growth on Si substrate, melt-back approach 8-80481
 α -SiC:Ga, piezoresist. rel. to acceptor levels 8-60129
 TiO_2 : Ga^{3+} , EPR spectra of trapped hole centre 8-80214
 VO_2 :Ga, Mo, conductivity transitions 8-76121
 YAG:Er $^{3+}$, Ga^{3+} , LPE and luminesc. 8-64408
 Zn-Ga, metal/liquid metal, exam. of crack propag. in liquid metal environment 8-60766
 ZnSiP $_2$:Ga, effect of doping conc. on elec. cond. and Hall coeff. 8-76077

gallium alloys

see also **gallium compounds**

- rare earth intermetallics, RGa_2 , AlB_2 -type struct., electron transfer, bonding, heat of form. theory 8-92499
 rare earth intermetallics, RGa_2 , mag susceptibility, 1.5-300K and Neel temp. 8-68184
 rare earth- Ga_2 intermetallics, mag. structs. 8-84394
 Ag-Ga, α -phase alloy, thermopower at low temps. 8-84196
 Ag-Ga solid soln., internally oxidised, hardness (*Japanese*) 8-60744
 Ag-Nb-Ga, phase relations, A15 phase diffusion layer formation 8-52764
 Al-Ga (10 wt.%), exam. of ^{27}Al diffusion by NMR technique 8-87813
 Al-Ga-In, liq. alloys, excess Gibbs functions 633 to 1173K 8-60655
 $\text{Al}_{10.4}\text{Ga}_{90.6}\text{V}$, low temp. thermal expansion 8-95167
 Co-Ga system, exam. of thermodynamics of α and β' phases 8-71870
 Co-Ga-B, phase diagram, metallographic, X-ray and electron probe anal. 8-92241
 Cr-Co(Ni)-Ga, phase equilibria diagrams at 800 and 600°C (*Ukrainian*) 8-92236
 Cu-Ga, dil. alloy, thermopower and resistivities, validity of Nordheim-Gorter relation 8-91671
 Cu-Ga, liq., mag. susceptibility, diamag. 8-72326
 Cu-Ga, magnetic susceptibility, comp. and temp. depend., melting effects 8-52202
 Fe-Ga, Mossbauer effect for phase transitions, 20-720°C, 25.7-28.3 at.% Ga (*German*) 8-68437
 Fe-Ga, volume change during solid state transformation (*German*) 8-84802
 Fe-Ge (10 to 50 at.%), phase diagram rel. to heat treatment, supercooling diagram (*German*) 8-92240
 Ga/rare earth systems, direct calorimetric exam. 8-84775
 Ga-Al, effect of Al on solidification kinetics, and morphology of Ga 8-56628
 Ga-Al alloys, solubility of GaAs, in multilayer LPE of $\text{Ga}_x\text{Al}_{1-x}\text{As}$ 8-52690
 Ga-In, dil., elec. resist., temp. and impurity depend., deviation from Matthiessen's b-axis crystals 8-51970
 Ga-In-Sn, thermal analysis, determination of liquidus and reactions 8-88446
 Ga-Sn, dil., elec. resist., temp. and impurity depend., deviation from Matthiessen's b-axis crystals 8-51970
 Ga-T alloys, relationship between struct. and thermodynamic props. (*German*) 8-91307
 Ga-Zn, dil., elec. resist., temp. and impurity depend., deviation from Matthiessen's b-axis crystals 8-51970
 Gd-Ga, amorphous alloy, mag. coupling 8-88108
 Ge-Ga alloys, amorphous, far IR absorption 8-88306
 Hf-Co-Ga system, crystal atomic struct. and phase equilibria (*Ukrainian*) 8-84772
 In-Ga alloy, electrode metal-solvent interaction rel. to elec. double layer struct., adsorpt. 8-61023
 Mn-Ga, DO_{22} type alloys, magnetic props., crystal struct. (*Japanese*) 8-59784
 Mn-Ga (19.0 to 31.2 at.%), exam. of phase diagram, using X-ray diffr., thermal expansion and mag. meas. 8-76634
 Mn_3GaC , mag. symmetry of ordered phases 8-71698
 Nb-Ga-Cu, phase diagram, metallographic and X-ray study, annealed and as-cast supercond. crit. temp. (*Russian*) 8-56617
 Nb-Ga-Ir, phase equilib. at 1000°C, cryst. data for intermediate phases 8-52763
 Nb_3Ga , supercond. transition temp., rel. to A15 phase stability 8-52137
 Nb_3Ga , ZZ 8-91613
 Pu-Ga (1-8.56 at.%) alloys, enthalpy sp. ht. determ. at elevated temp. 8-78458
 Sn-Mn(Fe)-Ga, isothermal sections of phase diagram (*Ukrainian*) 8-92235
 Ti_3Ga , lattice period and crystallographic struct., temp. depend. (*Russian*) 8-55835
 (V,Fe) $_3\text{Ga}$, solid soln. form. and supercond. T_c (*Russian*) 8-80512
 V-Ga-Sc, phase diagram, metallographic and X-ray meas., solubility boundaries (*Russian*) 8-56618
 V_3Ga , filamentary conductors, type-II, low temp. 30 GeV proton effects on critical props. 8-52178
 V_3Ga , high current density multifilament wire, neutron effects on equilibrium and transport props. 8-52126
 V_3Ga , neutron irradiation and annealing 8-52130
 V_3Ga , supercond., pinning characteristics (*Japanese*) 8-91829
 V_3Ga , ZZ 8-91613
 Yb-Ga, phase diagram, differential thermal and X-ray analysis (*Russian*) 8-56615

gallium arsenide

- absorption coefficients, method of meas. 8-83048
 acoustic phonon disturbances, effect on conductivity 8-91697
 amorphous layer formation, ion implantation, IR spectra 8-95063
 annealed, surface cond. change, n-p double layer 8-64095
 anodic oxidation using O plasma, and oxide layer evaluation 8-85015
 anodic oxide, refl. and transmission, 0.01-6 eV 8-95613
 anodic oxide film, optical props. 8-72626
 anodic oxide film, self drifting of ionic charges, detection by surface potential decay method 8-72295
 avalanche breakdown voltage for p-n junction, calc. 8-88020
 band structure, modulation spectroscopy, two-ray methods (*Russian*) 8-54469
 biexciton stability, appl. of theory for polar crystals 8-76002
 boundary scattering and phonon conductivity, 2-10K 8-63888
 bulk acoustic phonons, light scatt. from phonon-induced surface ripples 8-75924
 carrier lifetime profile, depth depend. 8-68036
 carrier mobility profiles meas. at room temp. by Corbino effect 8-60128
 cascade capture of carriers by attractive impurity centres, cross section 8-56157
 CESR, optical detect. by spin orientation techniques, anal. 8-80251
 chemical etching processes, review 8-95832
 creep and dislocation velocities 8-95783
 crystal structure stability, P-T diagrams 8-51886
 CVD in $\text{Ga-AsCl}_3\text{-H}_2$ system with different input supersaturations (*Russian*) 8-68098

gallium arsenide continued

- CVD of SiO_2 on GaAs, using tetraethoxysilane oxidation 8-60582
 Debye temperature, atomic mean square displacement 8-87757
 deep level trap emission identification by indirect conduction minima technique 8-84163
 DH laser, planar stripe geometry and channelled substrate, lateral current confinement 8-66823
 disordered, ion implanted, elec. props. 8-84212
 doping structures production and appl. (*German*) 8-95064
 double-cavity laser with branching output waveguides 8-63128
 dual implantation of C^+ and Ga^+ , sheet resist. and Hall effect meas. 8-67728
 electroabsorption avalanche photodiode waveguide detector 8-65965
 electrode liq. junction solar cells, photocurrent spectra, carrier recombination 8-76142
 electrodeposition from molten soln. 8-64486
 electrolytic decomposition and photodecomposition at GaAs-electrolyte contacts 8-95357
 electron effective mass, temp. depend. for various degrees of doping and compensation (*Russian*) 8-79923
 electron momentum distribution, anisotropy, positron annihilation (*Russian*) 8-84676
 electron transient vel. characts., Γ -L-X cond. band ordering 8-79997
 electron-hole liquid theory, generalised RPA 8-87914
 electron-hole plasma, ground state energy 8-84244
 electronic surface structure, Cs(Rb)(Na) adsorpt. processes, AES, LEED, EELS, study 8-68068
 electrooptic switches and directional couplers, wavelength depend. 8-79143
 epilayer structures, patterned, MBE writing 8-56590
 epitaxial unintentionally doped layer growth using MBE 8-72741
 epitaxial film on GaAs substrate, two-interface surface polariton modes 8-60180
 epitaxial growth in Ga- $\text{AsCl}_3\text{-He}_2$ system, expt.-statistical analysis (*Bulgarian*) 8-60580
 epitaxial layer, AuGe ohmic contact production by laser alloying 8-88026
 epitaxial layers, characterisation Hall effect and Schottky diode profile meas. 8-91791
 epitaxial layers, low freq. current noise between 4.4 and 300K 8-95388
 epitaxial layers on conductive substrate, elec. characterisation 8-91790
 epitaxial n-n $^+$ structure, for CW microwave electroacoustic amplifier 8-59235
 epitaxial tunnel diode pressure sensors 8-57975
 epitaxy using TMG and AsH_3 , chloride etching effect 8-76606
 ESCA absolute energy calibr., Ga 3d and $\text{L}_{2,3}\text{M}_{4,5}\text{M}_{4,5}$ and As 3d binding energies 8-92171
 etchant, universal, multipurpose 8-53008
 exciton luminescence, excitation intensity depend. 8-52554
 exciton to neutral acceptor binding energy, calcs. using atomic-like variable wave function 8-79937
 excitonic polariton reson. interaction with LA phonons 8-60481
 excitons, diamond like semiconductor, variational calculation of binding energies 8-79938
 FET, continuous growth of LPE double layers 8-64487
 FET structure, sharp line photolum. spectra 8-72248
 field evaporation, atom probe field ion microscopy 8-80460
 film, differential mobility anisotropy effect on wave propag. 8-88050
 film, plasma oxidation and oxide props. 8-95825
 film, radiative relax. time, nonequilibrium carriers 8-84657
 forbidden Raman scatt. by LO phonons 8-64367
 Ga(AsP) on GaAs, LPE, growth with Ge and Sn solvents, phase diags. 8-88434
 n-GaAs:O, press. depend. of deep level associated with O, transient capacitance meas. 8-64000
 GaAs- $\text{Ga}_{1-x}\text{Al}_x\text{As}$, ultrathin layer heterostruct., pseudopot. calcs. 8-95343
 GaInAsP quaternary alloys, orientation effects in LPE growth 8-92203
 gas-solid interface, EPR centres induced by microwave gas plasma 8-80215
 grown-in dislocation density, impurity effect 8-51543
 heavy metal migration, ESCA study (*French*) 8-75885
 hole effective mass, press. depend., theory and tunnelling expts. 8-75986
 hot carrier distribution, optically excited, picosec. time resolved reflectivity obs. 8-76495
 impact ionisation initiated by acoustoelectric effect 8-52038
 impact ionisation rates for electrons and holes, photocarrier multiplication obs. 8-87995
 implantation of Si, Al, Hf, Ta into InP and GaAs, form. of protective oxide 8-79622
 impurities, conc. of C, O, Si 8-59832
 impurity scattering of current carriers in quantizing mag. field 8-51954
 indirect band edge, determ. by quantum-well bandfilling 8-92120
 injection laser, intensified luminesc. (*Russian*) 8-90416
 injection laser integration with Gunn oscillator on semi-insulating GaAs 8-71232
 injection lasers, longitudinal mode spectrum, effect of carrier diffusion 8-71099
 interface with anodic and thermal oxides, comparison of AES and ESCA 8-95980
 ion bombardment, composition changes, AES 8-72662
 ion etching, effects on optical props. and lattice disorder 8-83122
 ion implantation damage, TEM exam. of variation with ion species and stoichiometry 8-59827
 ion implantation disorder, flux and fluence depend., electrorefl. expts. 8-83833
 ion implantation of S and Se 8-55884
 ion irradiation damage, strain effect contrib., channelling meas. 8-67752
 IR transparent materials, forward and backward scatt. data 8-59099
 IR vibrational absorption, effect of fast neutron irradi. 8-75776
 junction field effect structures, 2-D subbanding 8-64125
 k-linear coupling, E_1' transitions 8-91583
 laser, DH, inherent oscillations and subharmonic resonances obs. in light output 8-74910
 laser, operation characteristics (*Rumanian*) 8-87053
 laser, surface temp. distrib. (*Russian*) 8-74909

gallium arsenide continued

laser diodes, coupling light efficiency into parabolic-index fibres 8-94435
 laser irradiated, origin of periodic surface struct. 8-91513
 laser material, secondary dislocation climb during optical excitation 8-75672
 lasers, at room temp., modulation at X-band frequencies 8-87079
 lattice thermal cond. from three phonon scatt. relax. rate 8-51755
 lightly doped, movement of dissociated dislocations in diamond cubic struct. 8-59806
 liquid-solid equilibrium of Ga-As system, Krupkowski model (*German*) 8-95132
 LPE, charge carrier conc. distrib. (*Russian*) 8-52694
 LPE, transient-mode, on InP 8-72746
 LPE film, thickness comparison with $\text{Ga}_{1-x}\text{Al}_x\text{As}$, for layers grown by linear cooling 8-87892
 LPE growth of high purity layers by sliding boat method 8-76610
 LPE layers, dopant tracing of terrace growth 8-75948
 LPE with AsCl_3 -saturated Ga/As solns. 8-63953
 magnetic circular dichroism at E_i edges 8-92051
 magnetic freezeout in ultraquantum limit 8-76017
 maximum electric field in high-field domain in Gunn devices 8-79996
 MESFET, deep trapping effects at GaAs-GaAs:Cr interface 8-72245
 metal-insulator transition in impurity band induced by mag. field and loss of dimens. 8-52042
 metallisation, anodic oxidation anal. 8-80673
 microwave diode chips, elec. characterisation 8-91791
 minority carrier diffusion length, Schottky barriers, electron bombard. investigation 8-68037
 minority carrier diffusion lengths, contact metal effects 8-72260
 minority carrier diffusion lengths in semicond. SEM meas. interpretation 8-80002
 MIS capacitor, transient capacitance and C-V characts. 8-95374
 MIS dynamic optically controlled transparencies 8-90523
 MIS structure, elec. props., effect of interface As domains 8-88032
 MIS structures, review 8-95372
 MOS structure, white light emission obs. 8-76148
 multiphonon IR absorpt. expt. 8-60461
 multiphonon nonradiative transition rate for electrons in semicond. and insulators 8-60503
 n-type, coupled plasmon-LO phonon modes, Raman scatt. meas. 8-60472
 n-type, diffusion coeff., Monte Carlo calc., rel. to trapped domain behaviour 8-56152
 n-type, electron and gamma ray irradiated, introduction and annealing of defects 8-67736
 n-type, heat treated, origin of 1.41 eV emission band, photolum. expt. 8-72579
 n-type, hybrid-hybrid mode interaction in crossed elec. and mag. fields 8-51997
 n-type, influence of uniaxial stress on low field resist. 8-87976
 n-type, ion implanted, compensation 8-75680
 n-type, lattice scatt. identified as cause of 1/f noise 8-64074
 n-type, melt-grown, stoichiometry, photolum. obs. 8-72583
 n-type, model describing removal and scattering of charge carriers by defect clusters 8-76069
 n-type, photo-Hall effect meas. of ionised impurity scatt. 8-56182
 n-type, proton irradi., $E_p=30$ MeV, defect form., orientation depend. 8-55898
 n-type, smooth and continuous ohmic contacts using epitaxial Ge films alloyed with Ni 8-68086
 n-type, two-valleyed semicond., hot electron diffusion coeff., random walk calc. 8-68033
 n-type, Verdet const., free carrier density depend. 8-56462
 n-type epitaxial, film, potential barrier height, temp. depend. (*Russian*) 8-68070
 n-type interface with insulator, elec. props. 8-95370
 nitriding, GaN formation, preparation variables rel. to dielectric data 8-60591
 nonlinear extrinsic luminescence 8-84645
 ohmic contacts using epitaxial Ge films 8-88027
 one-sided abrupt junctions, distinction between avalanche and tunnelling breakdown 8-56211
 optical modulation spectra, proton damage effect 8-76487
 optical waveguides, exam. of GaAs as cladding materials, for cutoff polariser 8-55474
 optoelectronic devices, conf., Berlin, DDR 8-91755
 optoelectronic devices, thin-film optical waveguide periodic structures appls. (*Polish*) 8-50947
 oxide, passivated layers, quantitative in-depth profile, AES-SIMS, thermal, anodic and plasma oxidations 8-84087
 oxide film, thermal and anodic, in-depth profiles, XPS expts. 8-84086
 oxide layer, plasma grown, semiquantitative chemical depth profiles, Auger spectroscopy and neutron activation anal. 8-53284
 p-n junction, Zn^{2+} implanted, residual radiation defect influence on characts. (*Russian*) 8-84287
 p-n junctions, planar, Be ion implantation, fabrication and characts. 8-88022
 p-type, electronic props. 8-68040
 p-type, IR plasma reflectivity spectra calc. 8-52511
 p-type circular polarisation of hot luminesc. 8-52572
 p-type epitaxial layer, electron-hole plasma, quantum effects in magnetoluminesc. 8-72591
 p-type epitaxial layer, thermalisation of electron-hole plasma, photolum. meas. 8-80408
 Peltier induced growth kinetics of LPE 8-64485
 periodic surface corrugation generation by holography 8-55469
 phonon surface density, Brillouin elasto-optic cross section 8-72536
 photocathodes, photoelectron emission, energy levels, influence of dimens. quantisation (*Russian*) 8-64447
 photoconductivity spectra with deep traps, interpretation 8-52030
 photodetectors, pin- and avalanche diodes, characts. (*Swedish*) 8-89545
 photoluminescence intensity of cleaved surface, ambient gas influence 8-88345
 piezoresistance and conduction band minima 8-51993
 plasma anodisation in DC discharge, AES and MIS diode expts. 8-95826
 positron annihilation 8-72636
 positronium-like states, low temp., ang. correl. of annihilation photons 8-76549

gallium arsenide continued

radiation defects, Schottky diode characts. obs. 8-76024
 Raman scattering, electron-phonon deformation potential coupling 8-52502
 reactor-irradiated, anisotropy in diffuse small angle neutron scatt. 8-51598
 Schottky barrier diodes, electron processes at metal-semicond. interface (*Russian*) 8-84301
 Schottky barrier diodes, freq. and voltage depend. of impedance 8-64114
 Schottky barrier formation, Fermi-level pinning, defect mech. 8-95358
 Schottky diode, trap refilling, depth and capture cross section determ. 8-80052
 Schottky diode, use in acoustic memory correlator 8-66989
 Schottky gate FET struct., obs. of localisation in two-dimens. systems 8-60213
 solid solubility of Se, SIMS 8-67830
 solubility in Ga-Al alloys in multilayer LPE of $\text{Ga}_x\text{Al}_{1-x}\text{As}$ 8-52690
 spin polarised electron source for LEED 8-83693
 sputtered neutral mass spectrometry using post-ionisation in microwave plasma 8-92579
 structural defects, detection by electrochemical etching 8-55872
 substrate, evidence for insulator film growth-induced damage from photolum. expts. 8-75953
 substrate for AlAs epilayers, MBE growth, self-terminating thermal oxidation 8-92374
 subsurface atomic displacements, LEED exam. 8-71912
 surface, {001} layer, dislocation etch pits revealed by molten KOH 8-63772
 surface, (110), atomic and electronic struct. 8-72223
 surface, (110), bond angle and lengths of rearranged As and Ga atoms 8-71918
 surface, (110), pseudocharge density calcs. 8-84275
 surface, Ar ion bombardment induced photon emission, rel. to target temp. 8-72612
 surface, cluster model approach for electronic struct. 8-56205
 surface, $\text{CO}(\text{O}_2)$ interactions, surface electronic struct. (surface chem.) using synchrotron radiation 8-53254
 surface, energy-minimisation approach to atomic geometry 8-95213
 surface, thermally oxidised, TEM obs. 8-72036
 surface (100), comp. and struct. of differently prepared surfaces, LEED and AES 8-91524
 surface (110), chemisorbed O_2 , extrinsic surface states 8-91535
 surface (110), electron states from transfer matrix method 8-56203
 surface (110), electronic states and initial steps in oxidation 8-91534
 surface (110), electronic struct., ang. resolved photoemission expts. and tight binding calcs. 8-91743
 surface (110), surface and near-surface atomic struct., LEED 8-91515
 surface (110), surface states and matrix elements in angle-resolved photoemission 8-91741
 surface (110), valence band Auger spectra, from Ga and As CCV transitions 8-92149
 surface (110), wave functions and surface struct. 8-91519
 surface (111), (111), (110), XPS, photo-Auger ionisation cross section, electron mean free paths 8-56558
 surface final-state effects on core electron transition energies 8-91745
 surface impurities, struct. and comp. of compounds using IR spectroscopy 8-63918
 surface segregation of implanted alkali metals, photoemitter prep. and props. (*French*) 8-60544
 surface states in bond orbital model 8-91749
 surface states symmetry determ. using polarisation-depend. ang. resolved photoemission, for GaAs (110) 8-91742
 surface structure and orbital symmetries of (110) surface state 8-72229
 surfaces (110) and (111)As, UPS and LEED 8-91514
 thermal oxidation, 450 to 760°C, Rutherford back scattering obs. 8-76780
 thermal oxidation in As_2O_3 vapour 8-56792
 time of flight atom-probe mass spectra 8-92584
 transferred electron devices, ohmic contacts 8-52082
 transmutation doped, shallow donors, magneto-optical study, photocond. meas. 8-87996
 two-photon absorption of Nd:glass laser radiation 8-87107
 valence band structure, CPA, bond orbital calcs. 8-87909
 VPE growth, growth rate anal. 8-52680
 VPE layers, role of diffused Ga vacancy in degradation 8-95050
 VPE on Ge substrate, and characterisation 8-72736
 (Al,Ga)As DH injection lasers, internal quantum efficiency, algorithm for meas. 8-66822
 (Al,Ga)As long-lived DH injection lasers for fibre optic communication, degradation exam. 8-50778
 (Al,Ga)As/GaAs, LPE grown heterostructures, X-ray diffr. exam. of interfacial elastic strains 8-72019
 (Al,Ga)As-GaAs laser, transverse junction stripe, high temp. single mode CW operation 8-74918
 Al-GaAs heterostruct. with confined current flow, fabrication 8-68081
 Al-GaAs-Al sandwich-type sputtered film, elec. props. 8-91780
 AlAs-GaAs (110) interface, self-consistent calc. of interface states and electronic struct. 8-52066
 AlAs-GaAs heterojunctions, on graphite substrate, props., solar cell appls. 8-91760
 AlAs-GaAs monolayer crystal, two-photon absorpt. spectrum 8-52589
 AlGaAs CW oxide defined stripe laser, optical feedback effects 8-79045
 AlGaAs constricted DH diodes, stable single filament laser action obs. 8-55358
 (AlGa)As DH laser, insulating C film deposition to prevent facet deterioration 8-87049
 (AlGa)As, transverse junction stripe single mode oscillating laser, gain spectra 8-55356
 AlGaAs-GaAs DH laser, carrier leakage, physical mechanisms 8-66824
 AlGaAs-GaAs DH lasers, accelerated life test 8-66830
 $\text{Al}_{0.3}\text{Ga}_{0.7}\text{As}:\text{Te}(\text{SN})$, impurity effects on interface morphology of LPE films on corrugated GaAs substrates 8-88435
 $\text{Al}_{0.5}\text{Ga}_{0.5}\text{As}$, first order phonon spectrum replicas 8-60467
 $\text{Al}_{1-x}\text{Ga}_x\text{As}$ laser, transverse junction stripe, with low threshold current and high efficiency 8-82985
 $\text{Al}_{1-x}\text{Ga}_x\text{As}$, transient-mode LPE on GaP 8-72746

gallium arsenide continued

- Al_{1-x}Ga_xAs, analytic approx. for Fermi energy 8-63973
 Al_{1-x}Ga_xAs DH p-n junction, surface recomb. effects on current, luminesc. expts. 8-72246
 n-Al_{1-x}Ga_xAs, epitaxial, photolum. emission and excitation spectra 8-76526
 Al_{1-x}Ga_xAs heterojunction LED, fabrication by negative profiling of substrate and characts. 8-56523
 Al_{1-x}Ga_xAs, LPE, cathodoluminesc. obs. 8-68565
 Al_{1-x}Ga_xAs layer, LPE, graded band gap solar cell, composition profile, Rutherford backscatt. 8-76612
 Al_{1-x}Ga_xAs native oxide, low leakage, MOS characterisation 8-91795
 Al_{1-x}Ga_xAs, p-n homojunction, hot carrier recomb., overheating luminesc. 8-92122
 Al_{1-x}Ga_xAs p-n junction, photolum. and current, interface recomb. effects 8-95346
 Al_{1-x}Ga_xAs, Raman spectroscopy, characterisation of thin films and heterostructures 8-76439
 Al_{1-x}Ga_xAs:Cr, high resist. film, photolum. and photocond. meas. 8-72596
 Al_{1-x}Ga_xAs:O, appl. as insulating layer in MIS struct. 8-64115
 Al_{1-x}Ga_xAs-GaAs heterojunction photodiodes, high-efficiency fast-response 8-52073
 Al_{1-x}Ga_xAs-GaAs multilayer heterostructures, optical birefringence 8-64422
 Al_{1-x}Ga_xAs-GaAs n-n heterojunction, LPE, Auger profiling and absence of rectification 8-95349
 Al_{1-x}Ga_xAs-GaAs-Al_{1-x}Ga_xAs photopumped quantum-well laser, room temp. CW operation 8-74908
 AlGaAsP/GaAs heterojunction, X-ray characterisation of defects 8-95239
 Al_{1-x}Ga_{1-y}As_{1-x}Sb_x-Ga_{1-y}Sb_z buried heterojunction electroabsorption modulation 8-55439
 Al_{1-x}Ga_{1-y}In_zAs, LPE on InP, solid-liq. equilib. calcs. 8-84083
 As₂Te₃-GaAs, amorphous-monocrystalline heterojunctions, space charge limited conduction 8-64099
 AuGe/n-GaAs, SIMS study Au behaviour during annealing 8-75947
 Ga-GaAs interface immersed in electrolytic solns., elec. props. 8-95368
 Ga_{1-x}Al_xAs, metal-gap channel waveguides, intensity modulation 8-66899
 GaAlAs, DH CW diode laser, picosecond pulse generation 8-83002
 (GaAl)As DH laser, low-current, proton-bombarded, design and characts. 8-87059
 GaAlAs DH laser diode, deep level associated with slow degradation 8-87050
 (GaAl)As, DH lasers, degradation mechanisms, temp. depend. 8-66825
 GaAlAs DH pump laser for photoluminescence lifetime meas. 8-74085
 GaAlAs embedded DH stripe laser with GaAsP strip-waveguide modulator 8-66957
 (GaAl)As high performance diode laser, high-reflectivity cavity mirrors 8-82994
 (GaAl)As injection lasers, self-pulsations, Q-switching and mode-locking effects 8-66827
 GaAlAs laser transmitter for optical fibre communication, features 8-90423
 (GaAl)As lasers, low threshold proton isolated, spectral and transient response 8-87052
 GaAlAs novel DH lasers fabrication 8-50803
 GaAlAs-GaAs double heterostructure, interfacial recomb. velocity, photolum. meas. 8-68075
 GaAlAs-GaAs epitaxial heterostructures for integrated optics functional elements 8-50948
 Ga_{0.5}Al_{0.5}As-GaAs, DH, interfacial recomb., photolum. time decay meas. 8-95347
 Ga_{1-x}Al_xAs DH injection laser diode, long-term-degraded, TEM obs. 8-71102
 Ga_{1-x}Al_xAs-GaAs DH lasers, very low threshold, grown by metalorganic CVD 8-55365
 Ga_{1-x}Al_xAs, channelled substrate, planar struct. and DFB lasers 8-79032
 Ga_{1-x}Al_xAs LPE film, with x=0.23 and 0.37, grown by linear cooling, thickness comparison with GaAs 8-87892
 Ga_{1-x}Al_xAs p-i-n structure photoelectric props. 8-95353
 Ga_{1-x}Al_xAs Schottky barrier, oxide free, surface composition and fabrication 8-68084
 Ga_{1-x}Al_xAs, VPE, on-time comp. depend. 8-67915
 Ga_{1-x}Al_xAs, Zn diffusion, depend. on Al content 8-59981
 Ga_{1-x}Al_xAs-GaAs injection laser, branching waveguide coupler fabrication by LPE 8-63202
 Ga_{1-x}Al_xAs-GaAs laser, distributed Bragg confinement, room temp. operation 8-74907
 Ga_{1-x}Al_xAs-GaAs low threshold room temp. DH lasers grown by metalorganic CVD 8-50804
 Ga_{1-x}Al_xAs embedded stripe DH laser monolithically integrated with strip waveguide 8-59025
 Ga_{1-x}Al_xAs, LPE, charge carrier conc. distrib. (Russian) 8-52694
 Ga_{1-x}Al_xAs, LPE, GaAs solubility in Ga-Al alloys investig. 8-52690
 Ga_{1-x}Al_xAs-GaAs DH laser, continuous room temp. operation 8-55363
 Ga_{1-x}Al_xAs_{1-y}P_y-GaAs quaternary heterojunction, misfit dislocation charact. by synchrotron radiation white beam topography 8-63771
 Ga(As,P)/(In,Ga)P DH laser, red-emitting, optical and elec. characts. 8-66826
 GaAs (001)-Ag contact, surface stoichiometry and struct., and electronic surface states 8-95361
 GaAs (110)-Al(Ga) interface, interface states, photoemission study 8-95359
 GaAs (110)-Au Schottky barriers on ordered and disordered GaAs surfaces, props. 8-95360
 n-GaAs, absorption tails in surface depletion layer and bulk 8-64379
 GaAs, anodic oxide film, annealing effect on carrier density profile 8-88040
 GaAs, chemical shift and effective atomic charges 8-88201
 GaAs optical modulator for coupled-waveguides 8-71235
 GaAs, optically pumped laser with acoustic distributed feedback 8-82977
 GaAs, polyethylene mixture, optical props., IR bandpass filter appls. (Russian) 8-90468

gallium arsenide continued

- GaAs, Raman spectroscopy, characterisation of thin films and heterostructures 8-76439
 GaAs substrate, epitaxial growth of single crystal layers of Cd_{1-x}Sn_xS, close-spaced geometry 8-92198
 GaAs:B, electron or neutron irradiated, low symmetry interstitial B centre 8-79605
 GaAs:Be, annealing effect during MBE 8-79898
 GaAs:Co²⁺, EPR expts., y-factor determ. 8-76301
 GaAs:Cr, fine structure in cathodoluminescence spectrum 8-56524
 GaAs:Cr, IR spectral detectivity 8-70184
 GaAs:Cr, luminesc. stress splitting, 4.2K 8-84627
 GaAs:Cr, semi-insulating, characterisation by photoelectronic data 8-68051
 GaAs:Cr, semiinsulating solid-state inductance, theory and expt. 8-56138
 GaAs:Cr, Si, deep centre photoluminescence spectra 8-95601
 GaAs:Cr, site symmetry of Cr ions, ground-state splitting, ballistic phonon expts. 8-95273
 GaAs:Cr, VPE grown, exam. of doping GaAs using Cr(CO)₆ 8-72737
 n-GaAs:Cu, contaminated single cryst., deep level photoluminesc. model 8-68554
 GaAs:Cu, in MSM struct., phototrigger effect 8-56238
 GaAs:Cu, supersaturated solid solns., decomp., surface impurity content 8-51681
 GaAs:Fe, profile of impurity optical absorption bands 8-56509
 GaAs:Ge, LPE, on semi-insulating GaAs, film-substrate interface characterisation 8-72017
 GaAs:Ge, vap. grown, diatomic complex donor and acceptor model 8-80003
 GaAs:Mn, p-type semiconductors, internal strain on bound hole-phonon interaction 8-91492
 GaAs:O, photocapacitance quenching effect 8-91727
 GaAs:O, photocond., electron traps, level-broadening, 90 to 150K 8-60158
 GaAs:O, slow domains, origin 8-60132
 n-GaAs:O carrier removal profiles meas. 8-56154
 GaAs:P⁺, defect form. on P⁺ implantation at various temp., He⁺ backscatt. obs. 8-59828
 GaAs:Se, implanted, annealing with O-free CVD Si₃N₄ encapsulant 8-83834
 GaAs:Si, Cr, carrier concs. from Hall effect, microscopy, localised vibrational modes absorption meas. 8-56104
 GaAs:Si p-n structure, radiative recombination region 8-52071
 GaAs:Si(Ge) LPE layers, luminesc. props. rel. to substrate quality 8-52583
 GaAs:Sn, LPE layers, electronic props., depend. on Sn incorporation 8-87883
 GaAs:Sn, surface segregation of Sn during MBE, SIMS and AES 8-72031
 n-GaAs:Te, heavily doped, interband luminesc. intensity, heat treatment effect 8-72593
 GaAs:Te, heavily-doped, annealing-induced prismatic dislocation loops and elec. changes 8-51546
 p-GaAs:Zn, Mn, degenerate, tunnel p-n junction and semicond.-metal struct., I-V characts. 8-72252
 GaAs:Zn diffused, meas. of depth profiles, photoluminescence technique, LED applic. 8-72587
 GaAs-(Ga,Al)As heterostructure transmission photocathodes, characts. and epitaxial growth (French, English) 8-52616
 GaAs-(Ga,Al)As light modulators and distributed Bragg reflector laser, monolithic integration 8-50944
 GaAs-(Ga,Al)As epitaxial layers and DH lasers, deep centre 1.02 eV luminesc. 8-80387
 GaAs-(Ga,Al)As LOC-DBR laser, high differential quantum efficiency 8-79031
 GaAs-Al Schottky barrier diode, prep. by MBE on GaAs, and characts. 8-72257
 GaAs-Al_{0.5}Ga_{0.5}As-Cr/Au MIS capacitors, characts. meas. 8-95371
 GaAs-Al_{1-x}Ga_xAs lar, PbO-SiO₂ glass optical coating 8-71113
 GaAs-Al_{1-x}Ga_xAs, optically pumped taper coupled laser, second order Bragg reflector 8-50788
 GaAs-Al_{1-x}Ga_xAs, DH laser, effect of bulk nonradiative recombination 8-82967
 GaAs-Al_{1-x}Ga_xAs, monolithic integrated optics, rib waveguide switches with MOS electrooptic control 8-87168
 GaAs-Al_{1-x}Ga_xAs DH laser structures, high-resolution composition profiling with photolum. 8-71101
 GaAs-Al_{1-x}Ga_xAs DH laser, room temp. threshold current 8-79019
 GaAs-Al_{1-x}Ga_xAs optical modulator for coupled-waveguides 8-71235
 GaAs-Al_{1-x}Ga_xAs stripe geometry DH laser, threshold current density, effect of optical mode losses 8-59008
 GaAs-Al_{1-x}Ga_xAs superlattice, mag. field induced dimensionality change 8-64381
 GaAs-AlAs, pseudobinary alloy, phase diagram calc. 8-52786
 GaAs-AlAs (100) interface, tight binding calc. of electronic struct. 8-95342
 GaAs-AlAs abrupt (110) interface, electronic struct. 8-95339
 GaAs-AlAs alternating monolayers, zone folding effects on phonons 8-72510
 GaAs-AlAs and related monolayer heterostructures, pseudopot. calc. 8-60198
 GaAs-AlAs layered superlattices, deposited by MBE, exam. of crystal growth kinetics 8-72739
 GaAs-AlGaAs DH laser with buried facet 8-55373
 GaAs-AlGaAs distributed Bragg reflector integrated twin-guide laser, temp. characts. 8-87064
 GaAs-AlGaAs double heterostructure, optically induced dislocation glide, cooperative phenomena 8-74911
 GaAs-AlGaAs transverse junction stripe laser, single mode behaviour after 12000 hr ageing test 8-66831
 GaAs-Br₂(-Zn) system, filamentary cryst. prep. 8-52650
 GaAs-CdS heterojunction, prep. by CdS CVD and etching 8-52062
 GaAs-Ga_{1-x}Al_x (110) interface electron states, photoemission study, chemical shift, surface charge redistrib. 8-72259
 GaAs-Ga_{1-x}Al_xAs, superlattice unklapp processes in resonant Raman scattering 8-64362
 GaAs-Ga_{1-x}Al_xAs n⁺-v-n junction, avalanche carrier multiplication (Russian) 8-76140
 GaAs-Ga_{1-x}Al_xAs superlattice, sub-band dimensionality 8-63981

gallium arsenide continued

- GaAs-Ga_{1-x}Al_xAs thin film structs., LEDs, deep levels (*French*) 8-56218
 GaAs-GaAlAs, DH laser material, LPE grown, obs. of melt carryover 8-91553
 GaAs-GaAlAs, transverse Bragg-reflector injection lasers 8-74926
 GaAs-GaAlAs DH internally striped planar laser with flat freq. response up to 2 GHz 8-66829
 GaAs-GaAlAs DH LED, transient current trap spectroscopy 8-80049
 GaAs-GaAlAs DH laser diode, lateral modes 8-59009
 GaAs-GaAlAs DH material, dislocation glide and climb, electron diff. 8-83824
 GaAs-GaAlAs injection lasers on semi-insulating substrates using laterally diffused junctions 8-55364
 GaAs-GaAlAs optically pumped DFB laser, wavelength tuning effect 8-82979
 GaAs-GaP(Sb), pseudobinary alloy, phase diagram calc. 8-52786
 GaAs-Ge, n-n isotype heterojunctions, fixed-interface-charge model 8-56215
 GaAs-Ge (100) interface, electronic struct., scattering-theoretic approach 8-95340
 GaAs-Ge (110), heterojunction chemistry, photoemission expts. 8-95244
 GaAs-Ge abrupt (110) interface, electronic struct. 8-95339
 GaAs-Ge interface, XPS obs. of electronic struct. 8-95341
 GaAs-In_{1-x}Ga_xP heterojunction, VPE, energy band gap and lattice parameter, lattice mismatch effects 8-95345
 GaAs-InAs, pseudobinary alloy, phase diagrams calc. 8-52786
 GaAs-InSe p-n junctions, 'optical' contacts, elec. props. 8-56222
 n-GaAs-YIG layered structure, magnetostatic surface wave amplification 8-88107
 GaAs-ZnS p-n heterojunction, epitaxial, elec. props. (*Russian*) 8-88023
 GaAsP, composition dependence of phonon frequencies 8-75764
 GaAsP, negative-electron-affinity, photoemission transmission coeff. 8-56560
 GaAsP strip-waveguide modulator with GaAlAs embedded DH stripe laser 8-66957
 GaAs_{0.6}P_{0.4}Be, implanted annealing studies, elec. resist., Hall effect meas. 8-84213
 GaAs_{1-x}P_x based structs., carrier conc., mobility calcs. from Hall effect meas. 8-60138
 GaAs_{1-x}P_x, continuously tunable electron beam pumped laser 8-50802
 GaAs_{1-x}P_x, diffusion of implanted Zn ions, ion microbe analysis 8-95190
 GaAs_{1-x}P_x films, use in recording phase relief holograms (*Russian*) 8-50741
 GaAs_{1-x}P_x, heterogeneous struct. obs. by anodisation-electrorefl. technique 8-84088
 GaAs_{1-x}P_x, VPE, on-time comp. determ. 8-67915
 GaAs_{1-x}P_x, VPE on Ge substrate, and LED characts. 8-72736
 GaAs_{1-x}P_x:N, 0.6 < x < 1, photoluminesc., comp. depend. 8-52546
 GaAs_{1-x}P_x:N, film, optical absorpt. from photoluminesc. meas. 8-92134
 GaAs_{1-x}P_x:Zn, diffusion profile determ., ³²P/⁶⁵Zn double tracer technique 8-55888
 GaAsP_{1-x}, luminous intensity ang. distrib. and total light flux meas. device (*Chinese*) 8-82018
 GaAs_{1-x}Sb_x, MBE grown, surface struct. exam. by MEED 8-87847
 GaAs_{1-x}Sb_x-Ga_{1-x}In_xP_{1-y}As_y, multilayer structure, continuously tunable electron beam pumped laser 8-50802
 GaAsSb_{1-x}, epitaxial layer, struct. defects rel. to luminesc. 8-72040
 Ga_{0.47}In_{0.53}As, MBE, InP/Ga_{0.47}In_{0.53}As/InP DH laser fabrication and room temp. operation 8-74906
 Ga_{1-x}In_xAs, photocathode, work function depend. of photoelectric emission 8-68071
 Ga_{1-x}In_xAs, alloy film surface processes controlling growth by MBE RHEED and AES exam. 8-84084
 p-Ga_{1-x}In_xAs, Auger recomb., theory and luminesc. expts. 8-56518
 Ga_{1-x}In_xAs, cryst. growth on (100) InP by LPE 8-56591
 Ga_{1-x}In_xAs on InP, lattice matched LPE film growth and characts. 8-72033
 GaInAsP-InP avalanche photodiode, fabrication and characts. 8-54454
 Ga_{1-x}In_xAsP_{1-y}, anodisation, effect of pH, current density and illumination 8-95823
 Ga_{1-x}In_xAsP_{1-y}, LPE layers matched to InP, comp. and lasing wavelengths 8-71103
 Ga_{1-x}In_xAsP_{1-y}-InP injection laser, partially loaded with distributed Bragg reflector 8-82986
 GaInPAs-InP DH lasers, misplaced p-n junctions due to Zn contamination 8-87051
 Ga_{1-x}In_xPyAs_{1-y}, In rich bulk single crystals, growth from melt via gradient freeze method, and characterisation 8-68618
 GaP on GaAs, LPE, growth with Ge and Sn solvents, phase diag. 8-88434
 Ge-GaAs (110) interface, self-consistent calc. of interface states and electronic struct. 8-52066
 Ge-GaAs superlattice and interface, electronic struct. 8-52065
 IR spectra, manifestation of local vibr. 8-88339
 InGaAs, transferred electron photoemission to 1.65 μm 8-68600
 InGaAs-InP heterojunction detector for 1.0-1.7 μm wavelength range 8-49895
 InGaAs-InP p-p heterojunction, field-assisted minority carrier electron transport, in photocathode struct. 8-95651
 In_{0.53}Ga_{0.47}As, incorporation of Ga during LPE growth on (111)B and (100)InP substrates 8-91557
 In_{1-x}Ga_xAs-GaSb_{1-y}As_y, new heterostruct. characts. 8-72247
 In_{1-x}Ga_xAs-GaSb_{1-y}As_y, superlattice heterostruct., MBE 8-95348
 In_{1-x}Ga_xAs, heteroepitaxial, MBE grown, props. 8-84328
 In_{1-x}Ga_xAs, thick LPE growth, electrolum. obs. 8-60589
 InGaAsP, lattice matched, LPE growth on (100) InP, for 1.15-1.31 μm spectral region 8-64483
 InGaAsP/InP heterojunction, X-ray characterisation of defects 8-95239
 InGaAsP-InP 1.27 μm CW DH injection lasers, 1.1 Gb/s pseudorandom PCM 8-55390
 InGaAsP-InP DH lasers, carrier lifetimes meas. 8-66828
 In_{1-x}Ga_xAsP_{1-y}, LPE growth on InP (100), lattice matched composition 8-87881

gallium arsenide continued

- In_{1-x}Ga_xAsP_{1-y}, lattice vibr., Raman study 8-91391
 In_{1-x}Ga_xAsP_{1-y}-InP photodetectors, construction and performance 8-65966
 In_{1-x}Ga_xP_{1-y}As_y, single thin active layer visible spectrum heterostruct. lasers 8-63120
 LED, luminous intensity ang. distrib. and total light flux meas. device (*Chinese*) 8-82018
 ZnSe-GaAs thin film DE electroluminescent cell with 20 V threshold voltage 8-76141
- gallium compounds**
 see also gallium alloys; gallium arsenide
 Ga₂S₃-Ga₂Te₃ phase diag. (*French*) 8-76635
 Ga(AsP) on GaAs, LPE, growth with Ge and Sn solvents, phase diag. 8-88434
 GaInAsP quaternary alloys, orientation effects in LPE growth 8-92203
 n-GaP, quasidirect radiative recombination of free holes at neutral shallow donors 8-64410
 GaP, reevaluation of bandgap and free exciton binding energy 8-60061
 AgGaSe₂ and Ag₃GaSe₆, XPS, Auger and direct electron spectra 8-52620
 AgGaSe₂(Te₂), phonons, far IR refl. obs. 8-60459
 AlGaAsP/GaAs heterojunction, X-ray characterisation of defects 8-95239
 Al_{1-x}Ga_xAs_{1-y}Sb₂-Ga_{1-x}Sb₂ buried heterojunction electroabsorption modulation 8-55439
 Al_{1-x}Ga_xP, IR phonons, lattice reflection spectra 8-51626
 Al_{1-x}Ge_xSb, photolum. spectra 8-95602
 Ca₃Ga₂Ge₃O₁₂, substrate, electron examination of microstruct. and microsegregation 8-67919
 CdGa₂S₄, photoluminesc. and photocond. meas. 8-60159
 CdGa₂S₄:Ag(In), photoluminesc. and photocond. meas. 8-60159
 CuGa₂In_{1-x}S₂ solid soln., IR refl. spectra, comp. depend. 8-52498
 CuGaSe₂, temp. depend. of fundamental absorpt. edge 8-92090
 Ga complex, photoluminesc. spectra, π→π* and charge transfer L→M transitions, Stokes shift 8-64407
 Ga-In-Sb, solidus isotherms and isoconcentration lines 8-56624
 Ga-Te, liq., reflectance, 0.65-3 eV, comp. depend. 8-72549
 Ga_{1-x}Al_xP, two-phonon optical absorpt. 8-88341
 Ga_{1-x}Al_xSb p-n homojunction LPE and photovoltaic effect obs. (*French*) 8-64108
 Ga_{1-x}Al_xSb p-n structure, variable-gap, electroluminescence 8-52582
 Ga_{1-x}Al_xSb, small wave vector modes 8-75785
 n-Ga_{1-x}Al_xSb, transport phenomena in low and high mag. fields 8-80007
 Ga(As,P)(In,Ga)P DH laser, red-emitting, optical and elec. characts. 8-66826
 GaAs-GaP(Sb), pseudobinary alloy, phase diagram calc. 8-52786
 GaAsP, composition dependence of phonon frequencies 8-75764
 GaAsP, negative-electron-affinity, photoemission transmission coeff. 8-56560
 GaAs_{0.6}P_{0.4}Be, implanted annealing studies, elec. resist., Hall effect meas. 8-84213
 GaAs_{1-x}P_x based structs., carrier conc., mobility calcs. from Hall effect meas. 8-60138
 GaAs_{1-x}P_x, continuously tunable electron beam pumped laser 8-50802
 GaAs_{1-x}P_x, diffusion of implanted Zn ions, ion microbe analysis 8-95190
 GaAs_{1-x}P_x, heterogeneous struct. obs. by anodisation-electrorefl. technique 8-84088
 GaAs_{1-x}P_x, VPE, on-time comp. determ. 8-67915
 GaAs_{1-x}P_x, VPE on Ge substrate, and LED characts. 8-72736
 GaAs_{1-x}P_x:N, 0.6 < x < 1, photoluminesc., comp. depend. 8-52546
 GaAs_{1-x}P_x:N, film, optical absorpt. from photoluminesc. meas. 8-92134
 GaAs_{1-x}P_x:Zn, diffusion profile determ., ³²P/⁶⁵Zn double tracer technique 8-55888
 GaAs_{1-x}Sb_x, MBE grown, surface struct. exam. by MEED 8-87847
 GaAs_{1-x}Sb_x-Ga_{1-x}In_xP_{1-y}As_y, multilayer structure, continuously tunable electron beam pumped laser 8-50802
 GaAsSb_{1-x}, epitaxial layer, struct. defects rel. to luminesc. 8-72040
 GaCl₃, force and compliance const., OVFF, UBFF and GVFF models 8-50663
 Ga₃, molten, electrical cond., press. effect, 0-1 kbar 8-55963
 GaInAsP-InP avalanche photodiode, fabrication and characts. 8-54454
 Ga_{1-x}In_xAsP_{1-y}, LPE layers matched to InP, comp. and lasing wavelengths 8-71103
 Ga_{1-x}In_xAsP_{1-y}-InP injection laser, partially loaded with distributed Bragg reflector 8-82986
 GaInPAs-InP DH lasers, misplaced p-n junctions due to Zn contamination 8-87051
 Ga_{1-x}In_xPyAs_{1-y}, In rich bulk single crystals, growth from melt via gradient freeze method, and characterisation 8-68618
 Ga_{1-x}In_xSb, LPE on GaSb by stepwise grading, and characterisation 8-72745
 Ga_{1-x}In_xSb, vapour phase epitaxial growth by open tube method 8-84109
 Ga_{1-x}In_xSb:Zn(Te), photolum. and stimulated emission obs. 8-72595
 Ga_{1-x}In_xSe, layered, luminescence and photocond. obs., two-photon excitation 8-76521
 Ga_{1-x}Mn_xSb alloys, mag. phase transition obs. 8-52248
 GaN, elastic constant calc., elastic wave propag. vel. 8-87734
 GaN epitaxial layers, exciton cathodolum. (*Russian*) 8-76543
 GaN, plasma deposition and elec. cond. 8-60585

gallium compounds continued

- GaN, preparation variables rel. to dielectric data, GaAs conversion 8-60591
- GaN:As(P), implanted single cryst. film, cathodolum. 8-60523
- GaNbO₄, diffuse refl. and luminesc. spectra 8-56516
- Ga₂Nb₂O₇ and Ga₂Nb₂O_{7.25}, new phase of mixed oxide 8-59787
- β-Ga₂O₃, doped, photolum., emission centres struct. 8-52557
- Ga₂O₃, Ga 3d and L₂M_{4,5}M_{4,5} and O 1s binding energies, ESCA absolute energy calibr. 8-92171
- Ga₂O₃ in vitreous silica, effects on viscosity of impurity alkali oxide, OH, Al₂O₃ and Ga₂O₃ 8-64580
- β-Ga₂O₃, pure and doped samples, UV luminesc. obs., 5 to 300K 8-80396
- Ga₂O₃-Fe₂O₃ system, anomalous Mossbauer line shapes, incomplete annealing 8-92006
- β-Ga₂O₃-K₂O/K ferrite, interfaces and solid soln., thermal expansion and lattice parameter variations 8-55959
- Ga₂O₃-PbO, phase diag. 8-80524
- Ga₂O₃.6Bi₂O₃, IR and Raman spectra, vibr. anal. 8-76464
- GaP (III) B surface, negative-electron-affinity, photoemission transmission coeff., comparison with GaAsP 8-56560
- GaP, (001), adsorpt. of Cs, photoemission meas. 8-87874
- GaP (110), surface bands in relaxed cleavage surface, tight binding model 8-91744
- GaP (110), wave functions and surface struct., EPR expts. 8-91519
- GaP, anodically grown insulating layers, prep. and props. (German) 8-64158
- GaP, atom probe field ion microscopy 8-80460
- GaP, chemical etching processes, review 8-95832
- n-GaP, cryst. growth, synthesis solute diffusion method, elec. characts. (Korean) 8-52653
- GaP, Debye temperature, atomic mean square displacement 8-87757
- GaP, diffusivity and solubility of Cu 8-51743
- GaP, dislocation loops and bipolar obs. by chemical etching 8-55873
- GaP, dispersion of vibrational excitations, Raman scatt. 8-84588
- GaP, dopant dislocations, scanning electron micrographs, cathodoluminesc. 8-91340
- p-GaP electrode, for solar cell, differential capacitance meas. for flat-band potential determ. 8-72256
- GaP, electron hole droplet, motion damping, impurity and piezoelec. scatt. 8-67951
- GaP, electron-hole plasma photolum. obs. 8-52559
- p-GaP, epitaxial layers grown from liq., overcompensated, doping levels 8-91353
- GaP, etching in aqua regia and bromine-methanol-water solns. 8-68833
- GaP film, deposited by RF sputtering, struct. and elec. props. obs. (Czech) 8-52667
- GaP film, polycrystalline, with negative affinity, secondary emission (Czech) 8-52604
- GaP, first order Mott transition of exciton gas 8-76535
- GaP, heteroepitaxial growth on Si substrate by MBE 8-64481
- GaP, high-order Raman spectra, polariton scatt. 8-56483
- GaP, ion irradi. damage, strain effect contrib., channelling meas. 8-67752
- GaP, ion-implanted, form. and annealing of radiation damage 8-91363
- GaP, LEC, SSD and CVD samples, Zn tracer diffusion profiles in solids 8-95189
- GaP, LEC crystal, cathodolum. and photolum. around dislocations 8-84663
- GaP, LPE at 650°C from In solvent, low Si contamination 8-80480
- p-GaP, LPE layers, Hall effect 8-91704
- GaP, MCD of phonon-assisted exciton transitions 8-92053
- GaP, manifestation of local vibr. of dislocations in IR spectra 8-88339
- GaP, momentum distrib. of electrons, anisotropy, positron annihilation (Russian) 8-84676
- GaP, obs. of Raman scatt. by Cu vapour laser 8-95586
- GaP on GaAs, LPE, growth with Ge and Sn solvents, phase diags. 8-88434
- GaP, one-sided abrupt junction, distinction between avalanche and tunnelling breakdown 8-56211
- GaP, optoelectronic devices, conf., Berlin, DDR 8-91755
- GaP, p⁺-n diode junction, admittance meas. and carrier traps 8-91757
- GaP p-n junction, capacitance-freq. dispersion and electroluminescence efficiency 8-64101
- GaP, plasma deposition and elec. cond. 8-60585
- GaP, positron annihilation 8-72636
- GaP, Raman scattering selection rules for surface polaritons 8-72091
- GaP, rare earth doped, photolum. and elec. props. (Russian) 8-52545
- GaP, SEM, cathodoluminesc., impurity and defect detect. 8-83695
- GaP second order Raman spectrum, polarisation meas. 8-64368
- GaP, shallow impurity states, free exciton binding energy 8-79960
- GaP, single cryst., Raman scatt., effective cross-section rel. to nonlinear coeffs. (Russian) 8-71152
- GaP, single-crystal, anodically oxidised layers, AES measurements 8-91556
- GaP, soln. growth of bulk crystals, luminesc. and elec. props. 8-92181
- GaP substrate, transient-mode LPE of Al_{1-x}Ga_xAs 8-72746
- GaP, surface, chem. anal., low energy ISS compared with SIMS 8-64908
- GaP surface, quantitative XPS meas. 8-56559
- GaP, surface sensitivity, low energy electron transmission optical modulation 8-76567
- GaP, two photon absorption relative to Raman cross sections 8-87098
- GaP, upper polariton branch obs. by ATR 8-68510
- GaP, valence band structure, CPA, bond orbital calcs. 8-87909
- GaP: Au, diffusion, solubility, and electrotransport of Au 8-91489
- GaP:Cr, ESR of doubly ionised Cr acceptor and IR luminesc. 8-56374
- GaP:Cu, thermally and optical excited cond., deep level centres 8-72190
- GaP:Cu p⁺-n junction, deep level parameters, TSC meas., rel. to photo-current techniques 8-72249
- GaP:Cu-Ni, Schottky barrier, TSC meas., trap levels 8-91709
- GaP:Fe, profile of impurity optical absorption bands 8-56509
- GaP:N, appl. of temp. modulated photolum. induced by photoexcitation technique 8-95605

gallium compounds continued

- GaP:N, photoluminesc., temp. depend., exciton recombination mechanism 8-88355
- GaP:N LED, acoustic emission, NDT of dislocation motion 8-91759
- GaP:N(Te), ion implanted at 40 keV, refl. spectra, 210-2000 nm, annealing (Russian) 8-80386
- GaP:O, optical transitions via deep levels, phonon interaction 8-87939
- GaP:O, optical transitions via deep levels, cross section temp. depend. 8-87940
- GaP:S, ENDOR meas., symmetries, hyperfine parameters 8-72435
- GaP:s, elec. props. following 1.7 MeV electron irradiation 8-80005
- n-GaP:Te, doping parameters calc., by means of Hall data analysis 8-51925
- GaP:Te, Hall effect and elec. cond., 80-400K 8-91705
- n-GaP:Te, LPE layers, Hall effect 8-91704
- GaP:Zn, diffusion profile determ., ³²P/⁶⁵Zn double tracer technique 8-55888
- GaP:Zn, Hall effect and elec. cond., 80-400K 8-91705
- GaP:Zn, isolated Ga vacancy due to electron irradi., EPR study 8-95519
- GaP:Zn, thermodynamics of Zn doping by liquid phase epitaxy 8-83832
- GaP-anodic oxide devices, optoelectronic device, processing appl. 8-84304
- p-GaP-aqueous CO₂ liq. junction solar cells, CO₂ photoelectrochemical reduction 8-88649
- GaP-electrolyte contact, electrolytic decomposition and photodecomposition 8-95357
- GaP-InP, pseudobinary alloy, phase diagram calc. 8-52786
- GaP(Sb), avalanche breakdown voltage for p-n junction, calc. 8-88020
- GaS, optical phonons, IR and Raman scatt. meas. 8-59903
- GaS, optimisation of crystal growth conditions by I₂ vapour transport 8-68611
- GaS, refr. index in far IR, permitt. meas. 8-64360
- GaS, sp. ht., vibr. spectra and Debye temp. 8-87796
- GaS, XPS and valence band density of states, tight binding approx. 8-63974
- Ga₂Se_{1-x}, optical phonons, IR and Raman scatt. meas. 8-59903
- Ga₂Se_{1-x} solid solns., electrical props. meas. 8-84216
- Ga₂S₂Te, peritectic decomp., Ga₂S₃-Ga₂Te₃ phase diag. (French) 8-76635
- GaSb, CESR, optical detect. by spin orientation techniques, anal. 8-80251
- GaSb, chemical shift and effective atomic charges 8-88201
- GaSb crystal, phonon dispersion curves, valence force field 8-95121
- GaSb, Debye temperature, atomic mean square displacement 8-87757
- GaSb, electron-hole plasma, ground state energy 8-84244
- n-GaSb, galvanomagnetic effects 8-72172
- p-GaSb, heavy and light holes scattering 8-91692
- n-GaSb, local resist. near dislocations, eqns. 8-60123
- GaSb, manifestation of local vibr. of dislocations in IR spectra 8-88339
- GaSb, photolum., electrolum. meas. in p-n junction, temp. influence 8-72594
- GaSb, pulled crystal, microfacet obs. near irregularly remelted surfaces 8-91278
- GaSb, reson. two phonon Raman scatt. near E₁ and E₁+Δ₁ gaps 8-60470
- GaSb Schottky barrier formation, Fermi-level pinning, defect mech. 8-95358
- GaSb surface, quantitative XPS meas. 8-56559
- n-GaSb, temp. distrib. around dislocations, due to Joule heating, calc. 8-71734
- GaSb, valence band structure, CPA, bond orbital calcs. 8-87909
- n-GaSb:S, thermal quenching of residual cond. 8-56188
- n-GaSb:S-metal surface barrier struct., elec. and photoelec. props. 8-56229
- n-GaSb:Te, heavily doped, electron-hole recomb., photoluminesc. spectra 8-84644
- n-GaSb:Te(Se), forbidden optical band gap, Moss-Burstein effect 8-88335
- GaSb/InSb superlattice thin films, sputtered, ion-bombardment-enhanced diffusion during growth 8-87882
- GaSb-Au structure, metal-semicond. interaction, soft XPS meas. 8-60203
- GaSb-InAs (001) superlattice, electronic struct., tight binding calcs. 8-95350
- GaSb-InAs superlattices, two-dim. electronic structure 8-75995
- GaSe, 4 to 12 μm tunable down-conversion from LiNbO₃ parametric oscillator 8-66865
- GaSe, additional IR electrolum. band obs. at 77K 8-72607
- GaSe, electron spectroscopy, energy loss and photoemission 8-72682
- GaSe, exciton, excitation-induced absorption and luminesc. 8-60516
- GaSe exciton absorpt., change under a pulsed dye laser 8-92088
- GaSe film, amorphous, I-V characts. in strong elec. fields, 173-373K 8-56248
- GaSe film, charge transport models (Russian) 8-60233
- GaSe, Hall mobility anisotropy 8-68041
- GaSe, one-carrier SCL currents in solid with two sets of traps distributed in energy 8-72158
- GaSe, optical phonons, IR and Raman scatt. meas. 8-59903
- GaSe, optimisation of crystal growth conditions by I₂ vapour transport 8-68611
- GaSe, photocond. at high excitation rates 8-52036
- GaSe, sp. ht., vibr. spectra and Debye temp. 8-87796
- GaSe-SnO₂ spray heterojunction, electro-optical props. 8-64102
- Ga₂Se, semiconductor, basis of ionising radiation detectors 8-86743
- GaSe(S), layer dynamics of high-symmetry crystals with atom-atom interactions 8-71799
- GaSe_{0.9}Te_{0.1}, undulation spectra associated with acceptor complexes 8-80392
- GaTe, sp. ht., vibr. spectra and Debye temp. 8-87796
- GaTe-SnO₂ spray heterojunction, electro-optical props. 8-64102
- Ga₂Te, semiconductor, basis of ionising radiation detectors 8-86743
- Ga₂Te₃-Cu system solid solns., elec. cond. 8-51988
- Ga₂V_{1-x}O₂, resistivity, EPR, enthalpy and entropy meas., rel. to semicond.-metal transition 8-88004
- GdGa garnet, Czochralski grown, substrate material dislocation propagation 8-59771

gallium compounds continued

- (In, Ga)Sb, sputter deposited amorphous film, impulse stimulated explosive crystallisation 8-84098
InGaAsP, lattice matched, LPE growth on (100) InP, for 1.15-1.31 μm spectral region 8-64483
InGaAsP/InP heterojunction, X-ray characterisation of defects 8-95239
In_{1-x}Ga_xAs_{1-y}P_{1-y}, LPE growth on InP (100), lattice matched composition 8-87881
In_{1-x}Ga_xAs_{1-y}P_{1-y}, lattice vibr., Raman study 8-91391
In_{1-x}Ga_{1-x}As_{1-x}P_{1-x}-InP photodetectors, construction and performance 8-65966
In_{1-x}Ga_xP, epitaxial film, cathodolum. obs., recomb. mechanisms 8-72613
In_{1-x}Ga_xP, two-phonon IR absorpt. 8-52493
In_{1-y}Ga_{1-y}P-GaAs heterojunction, VPE, energy band gap and lattice parameter, lattice mismatch effects 8-95345
In_{1-x}Ga_xP_{1-x}As_{1-x} single thin active layer visible spectrum heterostruct. lasers 8-63120
In_{1-x}Ga_{1-x}Sb, influence of annealing on microstruct., exam. 8-56669
In_{1-x}Ga_{1-x}Sb, vertical Bridgman Stockbarger growth, magnetic field effect 8-60565
InSb-GaSb, directionally solidified, determination of non-constant distrib. coeffs. 8-76641
K₂O₅-Ga₂O₃.xFe₂O₃, K ion cond. 8-83998
LaGaO₃, cryst. struct. determ. (French) 8-79575
La₂O₂S-AgS-Ga₂S₃, ionic conducting glasses (French) 8-79804
Mn_{0.75}Ga_{2.17}S₄, twinning and cryst. struct. determ. (French) 8-83798
SrF₂-Ga₂O₃, carrier for impurity anal. of U-Pu oxides by emission spectrography 8-68944
TbGa garnet, Verdet const. meas. with pulsed mag. field 8-68486
TiGaS₂(Se₂) film, elec. and photoelec. props. (Russian) 8-52109
TiGaSe₂, Raman and IR spectra, zone centre optical phonons 8-76462
Y_{2.35}Eu_{0.65}Ga₂Fe_{3.8}O₁₂, bubble translation vel., ion-implantation effects 8-68327
Y₂GaFe₄O₁₂, mag. props. meas. in high mag. fields, review (Japanese) 8-52303

gallium phosphide light emitting diodes see light emitting diodes

galvanomagnetic effects

- see also Hall effect; magnetoresistance; Suhl effect; thermomagnetic effects
anisotropic solid with macroscopic inclusions, elec. consts. (Russian) 8-68002
graphite, grain boundary scattering effect on temp. depend. of electroresistivity, galvanomagnetic effect (Russian) 8-56148
graphite, low field data and free carrier densities 8-87986
graphite, trigonal warping of constant energy surfaces 8-87987
impurity scattering of current carriers in quantizing mag. field 8-51954
magnetoconcentration effect in variband struct. (Russian) 8-60143
narrow band-gap semiconductor, energy depend. relax. time, EM response of electrons 8-60142
Permalloy film, galvanomag. rotation characts., under uniaxial stress 8-84466
semiconductor, model, transport phenomena in presence of medium range disorder (French) 8-56162
semiconductor crystal surface, nonequilib. electron effects due to chem. excitation 8-72239
semiconductor in mag. and US wave fields, electronic density of states (Russian) 8-72056
semiconductor voltage and current transducers, Gauss effect compensation 8-77892
semimetals, exciton phase, transport effect in strong mag. fields 8-87977
thermoelectric materials, meas. under isothermal conditions (Russian) 8-56160
 α -Ag₂S, electronic and electrogalvanic props. (French) 8-84237
Bi, polycryst., grain boundary scattering effect on temp. depend. of electroresistivity, galvanomagnetic effect (Russian) 8-56148
Bi_{1-x}Sb_x, semiconductor, anomalous conductance in strong electric and longit. quantised mag. field (Russian) 8-76084
Bi₈₈Sb₁₂-Sn, current carrier energy spectrum (Russian) 8-60139
n-Cd_{1-x}Hg_x-Te, in strong mag. field, current-voltage characts., current instabilities 8-87980
Dy, longitudinal galvanomag. effect in single crysts. (Russian) 8-56132
n-GaSb, galvanomagnetic effects 8-72172
Gd, longitudinal galvanomag. effect in single crysts. (Russian) 8-56132
Gd-Dy alloy, longitudinal galvanomag. effect in single crysts. (Russian) 8-56132
Ge:Ga, photoconductivity oscillation with respect to applied mag. field (Russian) 8-80026
HgCr₂Se₄, ferromag. semicond., transport props. 8-68039
InAs surface accumulation layers, magneto-transconductance meas. 8-64137
n-InSb, degenerate, acoustomagneto-elec. effect obs. 8-72207
InSb, impact-ionisation magneto-elec. effect 8-52016
Si, amorphous, photoconductivity, mag. field depend. 8-80023
Si, powdered, microwave propag. 8-56175
Si surface doped channels, gate controlled, quantum galvanomagnetic effects 8-64134
YIG-Ge structure, profile and position of reson. galvanomag. effect curve 8-72242

galvanomagnetism see electromagnetism

galvanometers

- Low-inertia mirrors for galvanometers 8-71191
picture taking parameters display in amateur cameras, review 8-89578

galvanothermodynamic effects see thermomagnetic effects

game theory

- see also information theory
information distance and extent, knowledge distance, concepts evaluation 8-77687
nonanalogue Monte Carlo games, conditions concerning nonanalogue transition kernels and estimators 8-62594
nonlinear mechanical system with time optimal condition, synthesis 8-54176
stochastic search game 8-77689

gamma fission reaction see photofission

gamma radiation see gamma-rays

gamma-ray absorption

- dosimetry, restricted energy absorption coefficients 8-80971
heavy element analysis through absorption jump in interfering element 8-85263
reactor shielding materials, Pb and steel, 6 MeV γ penetration bremsstrahlung 8-58350
water as source medium, calc. of absolute photopeak efficiency 8-78558

gamma-ray angular distribution

- see also gamma-ray spectra
computer program for coeffs. for X-rays of mixed multiplicities from partially-aligned nuclei 8-86503
continuum γ rays, multipolarity, enhanced ang. correlation meas., heavy ion-compound nucleus reactions 8-93963
E1-E2 direct-semidirect model for fast nucleon radiative capture, γ ang.-distrib. 8-62536
heavy ion induced reactions, γ -ray multiplicity, ang. momentum and struct. depend. (Rumanian) 8-89906
ions, deceleration in polarised ferromag. media, transient field phenomena 8-72445
neutron radiative capture, DSD capture model 8-89861
nucleon radiative capture model, through collective M1 excitation, photon angular distrib. 8-58276
 $e^+e^- \rightarrow 2\gamma$, ang. correl. meas. device (German) 8-86726
⁷⁵As(n,n' γ)⁷⁵As, deexcitation gammas, energy levels, branching ratios, spins, parities, excitation function meas. 8-89869
⁹Be(d,p γ)¹⁰Be, 1.5 MeV, angular correlation meas. 8-94015
⁴⁰Ca(n, γ)⁴¹Ca, 8,12 MeV γ -ray ang. distrib. 8-66279
⁴¹Ca, highly stripped ions, recoiling in vacuo, γ -decays of isomeric states obs. 8-50119
Cd, A=104 and 105, populated in α +Pd reactions, high spin states 8-62484
⁵⁶Fe isobaric analogue resonances, γ ang. distrib., spin assignments, decay characts. 8-78342
⁶⁷Gd, γ -spectroscopy of high-spin levels via ⁶⁴Zn(α ,p γ), ⁵³Cr(¹⁶O,pn γ) 8-93960
¹⁶⁵Ho(p,xny γ), 60 MeV, n and γ energies and ang. distrib. 8-89872
¹¹¹In band structure and hole-core coupling, ¹⁰⁹Ag(α ,2n γ), branching and mixing ratios 8-58249
⁴¹K, highly stripped ions, recoiling in vacuo, γ -decays of isomeric states obs. 8-50119
⁴¹K, populated by ³⁸Ar(α ,p γ), levels props., shell model calc. 8-62588
²⁶Mg+¹⁸O, 34 MeV, yrast states in ⁴¹K, ⁴¹Ca, spins, parities from γ meas. 8-85250
²¹Ne(p, γ)²²Na, γ -ray ang. distrib. and mixing ratios, analogue resons. 8-62504
⁶²Ni(α , n γ), 8-14 MeV, γ ray study of ⁶²Zn odd-parity states, energies, transitions 8-50120
¹⁸O(p,p' γ), 3-3.5 MeV, γ -ray ang. distrib., for ¹⁹F reson. and bound levels 8-89790
²⁰⁸Pb(N, γ), 6 to 40 MeV, dipole/quadrupole interference, direct-semidirect model, γ ang. distrib. 8-93994
²⁰⁸Pb(p, γ) fast capture, direct-semidirect model excitation function calcs. 8-94004
²⁸Si, prolate and oblate intrinsic states (French) 8-70482
²⁸Si(¹⁶O, α p γ) or (¹⁶O,2p γ), high spin states, in ³⁹K and ⁴²Ca from γ meas. 8-89787
¹⁴⁴Sm+⁸⁶Kr, 490 MeV, γ -ray multiplicity moments 8-54798
Sn, single closed shell even mass nuclei, collective bands, spin, parity, from Cd(α ,2n γ), γ meas. 8-54719
⁸⁸Sr(n, γ), 7-11 MeV ang. distrib. from fast capture 8-54758
¹⁸W, A=173, 175, high-spin states, single-particle structure 8-93922
⁸⁹Y high spin states from γ -ang. distrib. in ⁸⁷Rb(α ,2n γ), 30-55 MeV 8-93941
⁹⁹Y(n, γ), 7-11 MeV ang. distrib. from fast capture 8-54758
⁶⁷Zn, populated in ⁶⁴Ni(α ,n), level struct. below 2.0 MeV, γ -ray studies 8-62483
Zn(p, γ)^{67,69}Ga, 3 MeV, γ -ray ang. distrib. 8-74353
⁹⁶Zr(¹⁸O, 4n γ), 56 MeV, γ yields, polarisations, ang. distrib., ¹⁰⁸Cd decay scheme 8-66301

gamma-ray applications

- see also radiation therapy
fast diffusion meas., nondestructive, using positron emitter as tracer 8-54519
qualitative assessment, field assessment 8-85444
radiography, use of Se electroradiography plates 8-72978
rate meter-type flaw detector, measuring circuits 8-60963
thickness meas. of spacecraft equipment 8-66013

gamma-ray astronomical observations

- burst obs. at altitude of possible Cygnus source (Japanese) 8-61933
burst source on 1976 August 16, balloon-borne obs. 8-54078
3C273, COS B high-energy gamma-ray obs. 8-93454
cosmic gamma-ray bursts, obs. and new limits on distrib. 8-93465
diffuse gamma-ray radiation, MeV excess in energy spectrum 8-73777
galactic plane, search for 1.2 MeV γ -ray line 8-93475
primordial black holes, search for high energy gamma ray bursts 8-54084
PSR 0833-45, Vela pulsar, radio and γ -ray pulses, relative phases 8-85966
pulsar NP 0532, COS-B satellite obs., appl. of X- γ synchronisation to non-parametric anal. 8-73729
Scorpius X-1, low-energy γ -rays, Dec. 1974 balloon obs. in 0.2-5 MeV range (Portuguese) 8-57702
spiral galaxies, gamma-ray luminosity, contrib. to diffuse background above 100 MeV 8-93481

gamma-ray astronomy

- see also gamma-ray sources (astronomical)
cosmic ray primaries meas., 10 to 100 GeV, using air showers Cherenkov light distrib., detector system 8-73597
experimental basis, review (Polish) 8-96394
large scale telescopes for high resolution obs. 8-93114
origin of gamma-rays in cosmic ray interactions with matter (Polish) 8-96571
Ge(Li) spectrom., balloon-borne, recent meas. 8-93107

gamma-ray detection and measurement

- see also gamma-ray spectrometers; radioactivity measurement
astronomical Compton telescope, high ang. resolution, for 0.3-10.0 MeV gamma-rays (Portuguese) 8-85847

gamma-ray detection and measurement continued

- Bayesian deconvolution, appl. and algorithm implementation 8-70103
 beam time saving technique for measuring excitation functions in heavy ion reactions 8-70721
 cellulose nitrate solid state nucl. track detector, gamma dose meas. 8-73247
 channel-type reactors, γ -ray dose rate spatial distrib. over entire thickness of side shield 8-86697
 Cherenkov counter, liq.-filled, for gamma-ray counting of large samples 8-53491
 coincidence and sum method, appl. to ^{110}Cd spectra (French) 8-62675
 coincidence method for Coulomb excitation studies of weakly populated vibr. like levels 8-70716
 cryogenically pumped gas target for γ -ray ang. distrib. meas. 8-55076
 defectoscope, multichannel, spectrometric method of recording γ -radiation in scintillation counter 8-53099
 delayed coincidence summing, nucl. half life meas. 8-55088
 diffractometer using ^{198}Au source at FRM reactor 8-54514
 digital multidiscriminator for use in gamma-gamma coincidence experiments 8-70707
 dosimeter, differential microcalorimeter, 0.01-10 W (Russian) 8-85385
 dosimeter, KG21, features 8-74509
 Double Compton Telescope, background sensitivity to atmospheric neutrons 8-53827
 dust samples, neutron activation anal. using high-rate loss-free gamma spectroscopy system 8-61129
 education, nuclear fallout radioactivity γ -ray detection and anal., Chinese fission bomb anal. 8-49596
 electron-photon cascades separation by scintillation counter system 8-78563
 EM shower sampling counters, characteristics of plastic scintillator and radiator layers 8-58530
 Geiger-Mueller counter γ dosimeters, fast neutron sensitivities, mixed field dosimetry 8-92705
 graphite ionisation chamber with CO_2 filling, Monte Carlo anal. of fast neutron irradiation 8-82583
 hodoscopic spectrometer, gamma-quanta coordinate meas. in NITsE scintillation spectrometer 8-78549
 intense proton beam current measurement via prompt γ rays from nuclear reactions 8-93784
 liquid scintillator determ. of dose rates from homogeneously distrib. β , γ - and EC , γ -emitters in phantom organs 8-53501
 mixed field, of fast neutrons and γ -rays, Fricke and $\text{Ce}_2(\text{SO}_4)_3$ dosimeter appls. 8-74514
 mobile gamma camera with remote image processing computer system, for nuclear medicine 8-92700
 multiplicity meas., fast converging bootstrap method for data anal. 8-70730
 multiwire proportional gamma camera for imaging $^{99}\text{Tc}^m$ radionuclide distrib. 8-53493
 NE 213 liquid scintillator, decay under neutron and gamma excitation (German) 8-55097
 NE 213 liquid scintillator, deuterated, decay mode (German) 8-55096
 NE 238 fast liquid scintillator, scintillation decay and n- γ discrimination (German) 8-55101
 nondestructive assay of irradiated nuclear fuel for safeguards, review 8-82495
 nonhydrogenous organic liquid scintillator gamma-ray detector, sensitivity function calc. 8-78572
 nuclear imaging of tumour, optimum detector spatial resolution performance study 8-73223
 nuclear picosecond lifetime meas., appl. to ^{207}Pb 8-55090
 ocean sedimentation rates determ. by nondestructive gamma-gamma coincidence spectrometry 8-85709
 on-line data acquisition system for monitoring high resolution multidimensional spectra 8-58567
 peak areas and detection limits, digital calc. methods 8-50433
 phoswich detector, field monitoring of alpha-emitting contaminants in environment 8-70646
 p photon collimation problems, Monte Carlo anal. 8-70724
 positron annihilation, 2-D Doppler broadened technique 8-70722
 positron annihilation, Doppler broadened spectra, deconvolution using solid state detector 8-72631
 positron annihilation, Doppler broadened spectra, parameters 8-72630
 positron annihilation in rare gases, Doppler broadening meas., electron mom. distrib. 8-55131
 positron two-photon annihilation coincidence technique, difference mode 8-54516
 proportional counter, spherical, with isotropic sensitivity, for soft γ -radiation 8-61732
 pulse shape discrimination cct. for n and γ multidetector meas. 8-70709
 real-time environmental α - β - γ radiation monitoring system 8-94152
 REM ratemeter for direct reading of dose equivalent rate 8-53502
 resonance gamma-ray absorpt. method 8-55089
 scintillation counter multidetector arrangement for on-line meas. of neutron and γ -ray multiplicities 8-50440
 scintillator detector, toluene based, Pb-foil radiator (Japanese) 8-90032
 self-powered flux detectors, response characts. in CANDU reactors 8-82594
 semiconductor detector for ionising radiation dosimetry, anisotropy of dose sensitivity 8-70705
 spacecraft instrumentation, induced background radiation 8-85821
 spark chamber, electron-photon shower recording, single-particle background suppressing method 8-78573
 spectral meas. of secondary neutrons and photons from 52 MeV proton irradi. of thick targets of C, Fe, Cu, and Pb 8-58282
 sum-coincidence spectra, pairs of extraneous peaks 8-70718
 thermoluminescence dosimeter, low dose meas. (Japanese) 8-86696
 TLD, use in high level photon dosimetry 8-74503
 walk-free centroid method for lifetime meas. with pulsed beams 8-70715
 whole body counter, portable chair type for in vivo internal contamination monitoring 8-61260
 X-ray pellicle stack, γ -ray family from cosmic-ray hadron reactions, accelerated scanning method 8-78546
 $e^+e^- \rightarrow 2\gamma$, ang. correl. meas. device (German) 8-86726
 $^{110}\text{Ag}^m$ decay, precise γ -ray spectroscopy 8-58251

gamma-ray detection and measurement continued

- Al_2O_3 TLD for dosimetry after accidental gamma radiation release 8-57076
 ^{41}Ar release from TRIGA reactor, comparison of γ -ray detectors 8-57309
 $\text{CaSO}_4:\text{Dy}$ TLD, fading in high γ -dose region 8-90027
 CdTe , growth by travelling heater method, high resistivity charact., γ -ray detector appl. 8-84707
 ^{60}Co , absorbed-dose standards comparison 8-74512
 $\text{CsI}(\text{TI})$ well-detector for low background γ -spectrometry, comparison with $\text{NaI}(\text{TI})$ 8-86724
 ^{152}Eu , intercomparison of gamma ray emission rate meas., using Ge spectrometers 8-82568
 Ge detector, delayed coincidence summing, nucl. half life meas. 8-55088
 Ge(Li) detector, use in activity determ. of gamma source with flat surface (German) 8-58528
 Ge(Li) detectors, anal. of monochromatic γ -ray and annihilation spectra 8-50429
 Ge(Li) spectrom., precision energy meas. of gamma rays of ^{51}Cr , ^{103}Ru , ^{109}Cd , ^{144}Ce , and ^{203}Hg 8-58533
 Ge(Li)- $\text{NaI}(\text{TI})$, Compton suppression spectrometer for in-beam expts., design and performance 8-78553
 In_2Te_3 type semiconductors, basis of ionising radiation detectors 8-86743
 ^{43}K evaluation for rectilinear scanner imaging using performance index technique 8-73226
 ^{140}La γ -ray intensities, meas. with coaxial Ge(Li) detector (French) 8-58534
 LiF thin layers, effect of LET on thermolum. props. 8-73255
 NaI detectors, synthesis of response functions to gamma-rays 8-94158
 NaI spectrometer, response matrix for 6 MeV γ -ray penetration meas., benchmark data 8-50432
 NaI, through well, well type detectors, comparison 8-90020
 NaI:TI scintillator response, γ -ray, (X-ray) rel. $1/2$ -width energy depend., undergrad. expt. 8-49600
 NaI(Tl) scintillator, specific sensitivity in γ -ray recording from radioactive ores 8-81449
 Pb glass EM shower detector, test results 8-70689
 Pt self-powered detectors, neutron/gamma sensitivity 8-78557
 ^{81}Rb evaluation for rectilinear scanner imaging using performance index technique 8-73226
 ^{222}Rn concentration in water, meas. by gamma counting 8-53733
 Si(Li) detectors, efficiency for 0.05-1.25 MeV γ -rays 8-86744
 ThBr_3 , inorganic scintillator, use in nucl. and accelerated particle detection 8-58540
 U-bearing rocks, radioactive disequilib. determ., isotopes relative abundance meas. 8-57330
 UO_2 , γ attenuation coeffs. meas. for burn-up determ. correction (Russian) 8-82597
 Zr, γ attenuation coeffs. meas. for burn-up determ. correction (Russian) 8-82597

gamma-ray diffraction

- channelled charged particles, diffr. of emitted radiation 8-75699
 pentaerythritol, Bragg reflection, thermal diffuse scatt. meas. (German) 8-75509
 $\alpha\text{-NbD}_3$, under hydrostatic press., γ ray diffr., Bragg refls. 8-75726
 TbVO_4 , Jahn-Teller phase transition, γ -ray diffractometry 8-91205

gamma-ray effects

- see also biological effects of gamma-rays; radiolysis
 anthracene, γ -irradiated, temp. depend. of photolum. (Russian) 8-56511
 anthracene, irradiated, optical absorption and EPR meas., low temps. 8-68538
 aromatic ethers, comparative study of X-ray and γ -induced photolysis and radiolysis (German) 8-64854
 aromatic polycrystals, γ -irrad., radical pair form., EPR meas. 8-80757
 chromatographic support materials decomposition by ionising radiation (German) 8-92587
 epoxy resin, low temp. irradiation effects on mechanical props., use in superconducting magnets 8-60737
 ferroelectric ceramic, defect effects on mech. strength 8-64332
 fusion reactor electrical insulators 8-95082
 glasses, aqueous soln., stabilising excess electrons, DTA at cryogenic temps. 8-76889
 light flash excited by γ -quantum pulse without direct visibility of source 8-69457
 metallic elements, gamma-ray irradiated, energy spectra of secondary electrons 8-84683
 organic crysts., γ -irrad., positron lifetime rel. to free radical conc. 8-72635
 organic insulating materials, dielect. parameters changes (Hungarian) 8-59836
 plastic fibre-optic waveguide, effect of ionising radiation on optical attenuation 8-63170
 PMMA, thermoelectrets, γ -irrad., heterocharge stability, TSC spectra 8-72453
 PMMA, viscoelastic props., γ -irrad. influence (Russian) 8-88492
 poly-1,6-di-N-carbazolyl-2,4-hexadiene, synthesis, thermal expansion, photocond., optical transition 8-76858
 polyethylene, γ -irrad., alkyl radicals ESR and hindered oscill. 8-85182
 polyethylene microspheres, deuterated, variable density, laser fusion targets, prep. 8-74468
 polymethylpentene, viscoelastic props., γ -irrad. influence (Russian) 8-88492
 polyvinyl alcohol, γ -irrad., ESR of trapped free radicals 8-85183
 polyvinylidene fluoride, γ -irradiated, low temp. internal friction 8-83874
 pyrene, single cryst., γ -irradiated, EPR and optical absorption meas. 8-72412
 quartz, smoky, HF US relax. 8-71796
 quartz, smoky, sp. ht. 8-71867
 quartz, thermoluminesc., γ -irrad. sample, heat treatment 8-64418
 radial clearance determ. for engine crankshafts by γ -ray method 8-53147
 square cut irradiated rod-rod gap sparkover under nonstandard impulse voltage 8-67564
 superconducting fusion magnets, radiation effects 8-50294
 teflon, positron lifetime spectra, low dose range 8-76550

gamma-ray effects continued

- TGS, gamma irradi. effects on heat capacity, Curie temp., permittivity 8-67737
thiourea single cryst., γ -irrad. effect on elec. permittivity 8-64311
vitamins, B group, γ -irrad. resist. 8-76890
Al-Li alloy, dil., quenched and irradi., recovery, resist. and internal friction obs. 8-52848
Ba(ClO₃)₂·H₂O, Γ -irrad. defects, ³⁵Cl NQR, 77 and 300K 8-91981
BaGeF₆, Group IV hexafluoride anion radical γ -irrad., EPR spectra 8-72411
BaPbF₆, Group IV hexafluoride anion radical γ -irrad., EPR spectra 8-72411
CaF₂, low symmetry U⁵⁺ centres 8-76307
CaF₂:RF₃, colour centre prod. by γ -irrad., absorpt. spectra obs. 8-72565
CaSO₄:Dy, TLD phosphor, gamma-ray induced sensitisation 8-74542
D-D fusion reactor blanket, nucl. characts., summary 8-89973
FeSO₄·7H₂O, γ -ray irradiated, Fe³⁺ formation, Mossbauer study (*Russian*) 8-84509
n-GaAs, electron and gamma ray irradiated, introduction and annealing of defects 8-67736
GaAs, radiation defect obs. using Schottky diode characts. 8-76024
GaP LED degradation, effect of γ -irradiation 8-95610
n-Ge, group V doped, point defect form. due to γ -ray irradi., carrier density, mobility meas. 8-71759
n-Ge:Sb, γ -irrad. effects on donor conc. and compensation by acceptors 8-56106
p-Ge-nn⁺-Si, heterojunction, γ -radiation effect on forward I-V characteristics (*Russian*) 8-72255
HfO₂, stabilised, low temp. induced centres, ESR meas. 8-72409
InSb, gamma irradiated, changes in energy spectrum of impurity spectrum 8-51937
KCl, F-F' conversion at room temp. 8-51539
KCl, irradiated, determ. of molar extinction coeff. and oscillator strength of V₂-centre (*Russian*) 8-80384
KClO₃, Γ -irrad. defects, ³⁵Cl NQR, 77 and 300K 8-91981
K₂CrO₄, K₂CrO₄Cl, γ -irrad. single crystals, identification of paramag. centres 8-67994
K(H₁-D₂)₂PO₄, single cryst., 77K, γ -radiation damage centres, and EPR obs. 8-68379
KI(Br), irradiated at room temp., thermolum. and F-centre thermal stability 8-84669
K₂SnF₆, Group IV hexafluoride anion radical γ -irrad., EPR spectra 8-72411
LiF, γ -irradiated, chemilum. during dissolution (*Russian*) 8-80427
NaCl, irradiated, determ. of molar extinction coeff. and oscillator strength of V₂-centre (*Russian*) 8-80384
NaCl(F), irradiated at room temp., thermolum. and F-centre thermal stability 8-84669
NaClO₃, Γ -irrad. defects, ³⁵Cl NQR, 77 and 300K 8-91981
NaClO₃, reson. Raman scatt. from metastable O₂ produced by γ -irrad. 8-60432
NaClO₃, single crystals, change of elastic constants by gamma radiation 8-63800
NaClO₃:O₃⁻, form. by γ -irrad., reson. Raman scatt., temp. depend. 8-92062
RbCl:Eu, γ -irrad., thermoluminesc., EPR meas. 8-84670
n-Si, γ -irrad. (E_{max}=100 MeV), carrier recomb. 8-56158
Si-SiO₂ interface, γ -ray irradiated thin oxide, MOS struct. (*Russian*) 8-84302
SiO₂, doped, fibre-optic waveguide, effect of ionising radiation on optical attenuation 8-63170
SiO₂, vitreous, grown from vapour, gamma ray irradiated, ESR and thermoluminescence exam. 8-88189
SrF₂:CeF₃(GdF₃)(TbF₃), absorpt. spectra of γ -irrad. cryst., 77K, 200-700 nm 8-84615
TiCl₃(TiCl)₃, labelled, exchange of Ti atoms rel. to γ -irrad., heat treatment, grinding 8-92470
ZrO₂, stabilised, low temp. induced centres, ESR meas. 8-72409

gamma-ray interactions

see also gamma-ray scattering

No entries

gamma-ray lasers

No entries

gamma-ray polarisation

- Ag+⁴⁰Ar(⁸⁶Kr), γ -ray circular polarisation meas. 8-54788
¹²⁹Ba, γ -ray linear polarisation meas. from ¹²⁰Sn(¹²C,3n) 8-50121
Ca(n, γ), A=42, 44, γ circular polarisation meas. 8-62533
¹⁹F(p,p'), 5.5 MeV; time differential obs. of perturbed γ linear polarisation distrib., Hanle effect 8-78360
Fe(n, γ), A=56, 58, γ circular polarisation meas. 8-62533
²H photodisintegration and electrodisintegration, weak interaction and P nonconservation 8-89849
⁴¹K, populated by ³⁸Ar(α ,py), levels props., shell model calc. 8-62588
⁶⁴N(n, γ), γ circular polarisation meas. 8-62533
²¹Ne, γ -ray circular polarisation, parity mixing 8-70443
⁵⁸Ni+¹⁶O, 100 MeV, γ -ray circular polarisation meas. 8-54788
⁴⁶Ti(n, γ), γ circular polarisation meas. 8-62533
⁶⁷Zn, populated in ⁶⁴Ni(α ,n), level struct. below 2.0 MeV, γ -ray studies 8-62483

gamma-ray production

- 4.43 MeV source, Am-Be or Pu-Be surrounded by hydrocarbon, for undergraduate laboratory 8-77648
autonomous γ -irradiator, construction (*Bulgarian*) 8-78053
dosimeter, thermoluminesc., calibration, γ -ray irradiator (*Japanese*) 8-66452
gamma source with flat surface, activity determ. using Ge(Li) detector (*German*) 8-58528
heavy ion induced reactions, γ -ray multiplicity, ang. momentum and struct. depend. (*Rumanian*) 8-89906
high-energy cosmic-ray components in atmosphere, scaling features 8-93062
ion induced γ -rays, thick sample reaction yields, energies, appl. in prompt nuclear anal. 8-62502
radiation protection at γ -irradiation installation, GOU-1 (*Bulgarian*) 8-82530
solid angle, self-absorption factors, evaluation by Monte Carlo method (*Rumanian*) 8-58526
steel, stainless, fusion reactor shield, neutron induced activity and γ -ray source investigation 8-54872

gamma-ray production continued

- e⁺e⁻ $\rightarrow\gamma\pi^0$, inclusive production, 4.9 to 7.4 GeV, cross sections 8-89723
NN system, single γ and π emission rates, meson quantum number assignments 8-78208
Al(n,x γ)Al, E_n=5.3 MeV, γ prod. cross-section obs. 8-89863
⁶⁰Co-charging of γ -irradiation installation (*Bulgarian*) 8-82558
Cu, fusion reactor shield, neutron induced activity and γ -ray source investigation 8-54872
Cu(n,x γ)Cu, E_n=5.3 MeV, γ prod. cross-section obs. 8-89863
¹⁵²Eu, intercomparison of gamma ray emission rate meas., using Ge spectrometers 8-82568
Mo, fusion reactor shield, neutron induced activity and γ -ray source investigation 8-54872
¹⁵³Sm, reactor prod. of curie strength photon beam 8-86709

gamma-ray scattering

- see also Compton effect; gamma-ray interactions
media interface, calc. of gamma-ray backscattering 8-85106
memointerference or vibointerference phenomenon and application 8-55313
steel, subsurface defect detection using gamma rays 8-85104
CaO, coherent/incoherent scatt. cross-sections of 136-278 keV γ -rays 8-70881
Th, L-shell electrons, incoherent γ -photon scatt. cross-sections 8-62768

gamma-ray sources see gamma-ray production

gamma-ray sources (astronomical)

- binary stars, short period, X- and γ -ray bursts from mag. reconnection 8-81654
burst source in Cygnus, high altitude obs. (*Japanese*) 8-61933
burst source on 1976 August 16, balloon-borne obs. 8-54078
burst sources, optical counterpart identification using proper motion data 8-93457
bursts and cosmic fireballs 8-54087
3C273, COS B high-energy gamma-ray obs. 8-93454
CG 135+1, new highly variable radio source as possible counterpart 8-54095
CG 135+1, possible X-ray counterpart identification 8-54092
CG 195+4, pulsating γ -ray source, no pulsed ratio emission at 325 MHz 8-65717
CG 312-1, possible X-ray counterpart identification 8-54092
CG 327-0, possible X-ray counterpart identification 8-54092
COS B catalogue and identifications 8-73775
COS B sources, 26-1200 keV hard X-ray obs. of error boxes 8-73774
COS-B γ -ray sources, nearby faint X-ray sources detect. 8-54093
cosmic gamma ray bursts, size spectrum, idealised galactic distrib. of sources 8-65716
cosmic gamma-ray background, prod. by annihilation of primordial stable neutral heavy leptons 8-93479
cosmic gamma-ray burst sources, new limits on distrib. 8-93465
cosmic X-ray sources, multiple Compton scatts. effects on X-ray emission spectrum 8-96389
Crab pulsar, high-energy photon spectrum rel. to energetic particles momentum distrib. 8-73727
dense clouds and diffuse production of gamma-rays 8-54011
diffuse gamma radiation, galactic and isotropic components 8-65725
diffuse gamma-ray radiation, MeV excess in energy spectrum 8-73777
discrete gamma-ray sources rel. to galactic cosmic ray distrib. (*Russian*) 8-65719
galactic gamma radiation, possible origin, data from COS-B and SAS-2 satellites (*French*) 8-85776
galactic gamma-ray emission, discrete source contrib. 8-69907
pulsars, gamma ray emission model 8-65641
pulsars, gamma-ray emission theory 8-53975
pulsars, observability 8-81646
Scorpius X-1, low-energy γ -rays, Dec. 1974 balloon obs. in 0.2-5 MeV range (*Portuguese*) 8-57702
Seyfert galaxies, source of diffuse cosmic γ -ray background 8-57700
Seyfert galaxies contrib. to low-energy γ -ray background 8-86007
spiral galaxies, gamma-ray luminosity, contrib. to diffuse background above 100 MeV 8-93481

gamma-ray spectra

see also gamma-ray angular distribution; gamma-ray spectra of liquids and solids; nuclear decay theory

- ¹⁸¹Ta(n, γ), γ -ray spectral shape depend. on n energy diverging interval size 8-78373
Ce, A=136, 137, 138, from (α ,xn) reactions, high spin states and isomers obs. using in-beam γ -spectroscopy 8-82309
Chinese nuclear test explosion, September 1976, hot particle anal. from γ -spectra (*Japanese*) 8-82519
cosmic ray electrons, detect. by synchrotron radiation in geomag. and interstellar mag. fields 8-57412
diffusion model of heavy ion induced reacts. 8-54789
doubly odd deformed nuclei, EM transitions, nanosec. lifetimes 8-62505
even-even nuclei, 58≤A≤150, E2, M1 multipole mixing ratio, data survey 8-50118
exciton model of γ -emission in (N, γ) reactions 8-62539
fission product gamma-ray and half-life 29≤A≤69, data collection 8-50134
fission products, estimation using nucl. systematics 8-70587
fission reactor spent fuel γ -ray spectrometry and chemical analysis 8-54841
heavy ion induced reactions, information from γ -spectroscopy (*Rumanian*) 8-58300
high-spin states, means and methods of investig. 8-86722
intense proton beam current measurement via prompt γ rays from nuclear reactions 8-93784
ion induced γ -rays, thick sample reaction yields, energies, appl. in prompt nuclear anal. 8-62502
least squares peak fitting with very low statistics 8-74529
liquid air, transport of neutron and secondary γ -rays from 14 MeV source 8-50234
massive transfer in heavy ion reactions on rare-earth targets, α - γ coincidence 8-70556
Mossbauer effect probability determ. using resonance detectors 8-94160
multiplicity distribution, shape, and low-fold coincidence probabilities 8-54779

gamma-ray spectra continued

- nanosecond isomers, in-beam gamma spectroscopic investigation, Ge(Li) detector 8-86506
- neutron activation anal., computer simulated γ -ray spectra 8-92577
- prod. cross sections from shell model theory 8-62501
- R-A reactor fuel burnup, gamma-spectrometric determ. 8-50265
- RA fuel burnup determ. from γ -ray spectrometry of ^{106}Ru , ^{134}Cs , ^{137}Cs 8-54848
- reactor shielding materials, Pb and steel, Γ leakage spectra, computer calcs. 8-58350
- resonance gamma-ray absorpt. method 8-55089
- single full energy peaks, automatic examination program 8-82571
- spectral analysis using FFT (*Japanese*) 8-90047
- p+nucleus, 303 GeV/c, in emulsion chambers, high energy γ -rays 8-70521
- pp annihilation, γ spectra, evidence for quasinuclear bound states 8-54642
- $\pi^-d \rightarrow 2n + \gamma$, n-n scatt. length from γ spectrum 8-62576
- ^2Ag , $A=97$, 98 and 99^{m} decay spectral meas. 8-93976
- ^{108}Ag , low-lying states and state distrib. following $^{107}\text{Ag}(n,\gamma)$ 8-50084
- $^{27}\text{Al} + ^{12}\text{C}$, 107, 155, 197 MeV, evaporation residue ^{39}K , prompt γ deexcitation 8-74395
- $^{27}\text{Al} + ^{20}\text{Ne}$, 120 MeV, prompt γ emission, reaction products deexcitation 8-74396
- $^{27}\text{Al} + \pi^-$, $\gamma\pi^-$ coincidence spectra, 190 MeV 8-89913
- $\text{Al}(n,\gamma)$, γ -ray energies and intensities 8-89876
- ^{232}Am α -decay, absolute γ yields 8-86516
- ^{241}Am , α -decay low-energy γ -radiation (*French*) 8-74342
- ^{41}Ar states from $^{40}\text{Ar}(d,p)$, lifetimes meas. by DSA method 8-78308
- ^{44}Ar β decay into ^{44}K , neutron rich isotopes, weak coupling predictions, γ -ray meas. 8-74336
- $^{75}\text{As}(n,n'\gamma)^{75}\text{As}$, deexcitation gammas, energy levels, branching ratios, spins, parities, excitation function meas. 8-89869
- ^{209}At , gamma-ray spectra, produced by $^{209}\text{Bi}(\text{He}, 3n\gamma)^{209}\text{At}$, 28 and 26 MeV 8-74377
- ^{129}Ba , γ -ray linear polarisation meas. from $^{120}\text{Sn}(^{12}\text{C}, 3n)$ 8-50121
- ^{204}Bi , decay scheme 8-50122
- ^{207}Bi , spin and parity of states with $J \leq 21/2$, $^{205}\text{Tl}(\alpha, 2n)^{207}\text{Bi}$ and $^{205}\text{Tl}(\alpha, 2n)^{207}\text{Bi}$ 8-89788
- ^{209}Bi , pion $^-$ capture, high spin states and neutron multiplicities meas. 8-54806
- ^{76}Br , populated by $^{76}\text{Se}(p, n\gamma)$, level scheme 8-50091
- C+p, 52 MeV, spectral meas. of secondary neutrons and photons from thick targets 8-58282
- $^{12}\text{C}(^{12}\text{C}, \gamma)^{24}\text{Mg}$, 5 to 11 MeV, γ yields, resonance features 8-54799
- Cd, $A=104$ and 105, populated in α +Pd reactions, high spin states 8-62484
- ^{109}Cd , gamma-ray precision energy meas. 8-58533
- ^{110}Cd , γ -ray spectra using coincidence and sum method (*French*) 8-62675
- ^{144}Ce , gamma-ray precision energy meas. 8-58533
- $^{37}\text{Cl}(n,\gamma)^{38}\text{Cl}$, recoil energy spectrum calcs. 8-86531
- $\text{Cl}(n,\gamma)$, γ -ray energies and intensities 8-89876
- ^{56}Co standard source, relative γ -ray intensities 8-55069
- $^{\text{a}}\text{Cr}(n,n'\gamma)$, $A=50-54$, 0.84-3.97 MeV, neutron inelast. scatt. cross-sections determ. 8-62529
- ^{51}Cr , gamma-ray precision energy meas. 8-58533
- ^{52}Cr studied via $(\alpha, 2n\gamma)$, high spin states, shell model calcs. 8-54675
- $\text{Cr}(\pi^-, \pi^0)$, 200 MeV, deexcitation γ spectra, transitions in ^{52}Mn 8-89912
- Cs, $A=114-118$, neutron deficient isotopes, half lives, β^+ , γ , delayed p and α meas. 8-70489
- $^{133}\text{Cs}(N,\gamma)^{134}\text{Cs}$, exciton model, γ spectra calc. 8-62539
- ^{134}Cs , half-life, gamma-spectrometric determ. 8-93972
- Cu+p, 52 MeV, spectral meas. of secondary neutrons and photons from thick targets 8-58282
- ^{63}Cu , level struct. from $^{63}\text{Cu}(p,p'\gamma)$ react. 8-78378
- $^{148}\text{Dy}_{32}$ 10^+ isomer, $\pi h_{11/2}$ effective E2 charge 8-93964
- $\text{Dy}(\alpha, xn \gamma)\text{Er}$, 90 MeV, preequilibrium and equilibrium de-excitation processes 8-50185
- $^{160}\text{Er} + ^{86}\text{Kr}$, 5.99 MeV/N, are γ -ray multiplicity 8-82375
- $^{143}\text{Eu}^{\text{m}}$, decay obs., struct. determ. 8-50130
- ^{152}Eu , level scheme, low energy transitions, reaction data, Nilsson model interpretation 8-66215
- Fe, gamma fields induced by ^{252}Cf neutrons 8-50240
- Fe+p, 52 MeV, spectral meas. of secondary neutrons and photons from thick targets 8-58282
- ^{20}Fe , β - γ directional correlation, second class current 8-50127
- ^{54}Fe , studied via $(\alpha, 2n\gamma)$, high spin states, shell model calcs. 8-54675
- $\text{Fe}(n,\gamma)$, γ -ray energies and intensities 8-89876
- $^{72}\text{Ga} + ^{72}\text{Ge}$, gamma and beta-ray spectra, intensities, branching ratios, spin and parity assignments (*Korean*) 8-50128
- ^{67}Gd , γ -spectroscopy of high-spin levels via $^{64}\text{Zn}(\alpha, p\gamma)$, $^{53}\text{Cr}(^{16}\text{O}, p\gamma)$ 8-93960
- ^{146}Gd , lowest 2^+ state and energy gap at $Z=64$ 8-82310
- $^{157}\text{Gd}(n,\gamma)$, γ and conversion electron spectra, ^{158}Gd collective bands 8-89819
- Ge(Li) detectors, anal. of monochromatic γ -ray and annihilation spectra 8-50429
- Ge(Li) γ -ray spectra, NUKLID program for automatic line identification (*German*) 8-58536
- ^{72}Ge , gamma-ray spectra, energy levels, spin and parity assignments, from ^{72}Ga beta-decay (*Korean*) 8-50128
- $^{74}\text{Ge}(^{12}\text{C}, 3n)^{83}\text{Sr}$, high spin states and spin ordering, γ -ray excitation functions 8-66199
- $^{76}\text{Ge}(^{12}\text{C}, 3n)^{85}\text{Sr}$, high spin states and spin ordering, γ -ray excitation functions 8-66199
- $^{\text{a}}\text{He}$, prod. cross section calc., γ decay spectrum, shell model theory 8-62501
- Hg, $A=191, 2, 3, 5, 7, 9$, rot. aligned bands, high spin states, energy levels $B(E2)$ values 8-70483
- $^{198}\text{Hg}(\alpha, 2n)$, 30 MeV, levels of ^{200}Pb and isomers 8-66192
- ^{203}Hg , gamma-ray precision energy meas. 8-58533
- $^{165}\text{Ho}(p, xn\gamma)$, 60 MeV, preequilibrium and equilibrium de-excitation processes 8-50185
- $^{165}\text{Ho}(p, xn\gamma)$, 60 MeV, n and γ energies and ang. distrib. 8-89872
- $^{\text{a}}\text{In}$, $A=104$, 106, β -decay half lives and decay schemes 8-74333
- ^{106}In level scheme via ^{106}Sn decay 8-93971
- ^{111}In band structure and hole-core coupling, $^{109}\text{Ag}(\alpha, 2n\gamma)$, branching and mixing ratios 8-58249
- K, $A=48, 49, 50$, half lives, γ meas. 8-74341

gamma-ray spectra continued

- ^{41}K states from $^{40}\text{Ar}(d,n)$, lifetimes meas. by DSA method 8-78308
- Kr, $A=90, 91$, ^{232}Th fission products, yields, γ -ray spectra 8-74410
- Lu, $A=162, 4, 5$, from $\text{Eu}(^{16}\text{O}, xn)$, gamma transitions, half-lives anal. 8-62509
- ^{24}Mg , 11.86 MeV level, confirmation of $J^\pi=8^+$ assignment from $^{12}\text{C}(^{16}\text{O}, \alpha\gamma) 42 \text{ MeV}$ 8-70445
- $^{26}\text{Mg} + ^{18}\text{O}$, 34 MeV, yrast states in ^{41}K , ^{41}Ca , spins, parities from γ meas. 8-58250
- $^{55}\text{Mn}(\alpha, \alpha')$, 4.5 to 7 MeV, Coulomb excitation, search for 1.29 MeV $1/2^-$ level 8-82360
- $^{14}\text{N}(\alpha, \gamma)^{15}\text{N}$, hadronic nuclear-parity violation with change of isospin, γ spectrum search 8-94018
- $^{93}\text{Nb}(n,\gamma)^{94}\text{Nb}$, exciton model, γ spectra calc. 8-62539
- $^{144}\text{Nd}(^{12}\text{C}, 6n)^{150}\text{Dy}$, 112 MeV, high spin isomers of ^{150}Dy , gamma-ray spectra 8-50075
- $^{146}\text{Nd}(^{12}\text{C}, 8n)^{150}\text{Dy}$, 118 MeV, high spin isomers of ^{150}Dy , gamma-ray spectra 8-50075
- $^{150}\text{Nd}(^{20}\text{Ne}, xn\gamma)$, multipolarities of yrast and statistical cascades, total γ conversion coeff. 8-70484
- $\text{Ni} + ^{12}\text{C}$, 107, 155, 197 MeV, evaporation residue Se, prompt γ deexcitation 8-74395
- ^{58}Ni spallation by 1 GeV protons, reaction channels (*Russian*) 8-74370
- $^{58}\text{Ni}(^{16}\text{O}, 2p\gamma)$, 54.5, 59.5, 64.5 MeV high spin and excitation energy regions in ^{72}Se , γ cascade 8-54795
- $^{62}\text{Ni}(\alpha, n\gamma)$, 8-14 MeV, γ ray study of ^{65}Zn odd-parity states, energies, transitions 8-50120
- $\text{Ni}(\pi^-, \pi^-)$, 200 MeV, deexcitation γ spectra, transitions in $^{58,60}\text{Cu}$ 8-89912
- $(^{16}\text{O}, xn)$, population of $^{174,175}\text{W}$, ^{161}Yb , γ continuum spectra, yrast cascades, dipole component 8-54794
- $^{16}\text{O} + ^{12}\text{C}$, 15-72 MeV, gross struct. in γ -ray yields 8-78405
- $^{16}\text{O}(\pi^-, \gamma n)$, γ -spectrum and γ -n ang. correlation function from continuum shell model 8-86551
- $^{16}\text{O}(\pi^-, \gamma n)^{15}\text{N}$, information from radiative π capture coincidence spectra 8-86550
- $^{192}\text{Os}(2n,\gamma)^{194}\text{Os}$, level transitions, prolate-oblate transition 8-62540
- P, $A=30, 32$, high spin states from $^{16}\text{O} + ^{16,18}\text{O}$ reactions and $^{27}\text{Al}(\alpha, n)$, γ -ray meas. 8-74386
- ^{234}Pa isomers from $^{234}\text{Th} \beta^-$ decay, low energy γ -spectrum 8-70493
- Pb+p, 52 MeV, spectral meas. of secondary neutrons and photons from thick targets 8-58282
- ^{204}Pb populated by ^{204}Bi decay, isomeric transitions, J^π assignments 8-50122
- $^{207}\text{Pb}(n,\gamma)$, primary E2 transitions to ^{208}Pb ground state 8-58284
- ^{208}Pb compound nucleus, γ -decay spectral function depend. on ang. momentum (*Russian*) 8-86467
- $^{149}\text{Pm} \rightarrow ^{149}\text{Sm}$, beta decay matrix elements 8-70488
- $^{207}\text{Po}^{\text{a}}$ decay, spin from conversion electron meas., γ intensities 8-58252
- ^{208}Po , yrast two proton-two neutron hole states 8-78307
- ^{150}Pr decay into ^{150}Nd vibr. levels 8-89817
- ^{228}Ra levels from ^{230}Th α decay, search for $K^\pi=0^+$ excited states 8-86504
- ^{109}Rh level scheme from fast n scatt., γ transitions, spins, parities, cross sections 8-78374
- ^{103}Ru , gamma-ray precision energy meas. 8-58533
- ^{150}Ru , level and γ -decay scheme determ. 8-82312
- $^{121}\text{Sb}(n,\gamma)$, γ and conversion electron spectra, ^{122}Sb energy level scheme 8-54721
- $^{45}\text{Sc}(\alpha, p\gamma)$, ^{48}T excited states, level struct., lifetimes, from DSA and $\pi\gamma$ coincidence meas. 8-74326
- $^{28}\text{Si}(^{16}\text{O}, \alpha p\gamma)$ or $(^{16}\text{O}, 2p\gamma)$, high spin states, in ^{39}K and ^{42}Ca from γ meas. 8-89787
- Sm, ion recoiling into gas and vac., hyperfine field and correl. time meas. 8-66240
- $^{144}\text{Sm} + ^{86}\text{Kr}$, 490 MeV, γ -ray multiplicity moments 8-54798
- $^{149}\text{Sm}(n,\gamma)^{150}\text{Sm}$, neutron capture γ -ray spectra calcs. 8-94006
- Sn, single closed shell even mass nuclei, collective bands, spin, parity, from $\text{Cd}(\alpha, 2n\gamma)$, γ meas. 8-54719
- ^{106}Sn decay, ^{106}In level scheme determ. 8-93971
- $^{120}\text{Sn} + ^{86}\text{Kr}$, 5.99 MeV/N, are γ -ray multiplicity 8-82375
- ^{48}T excited states from $^{45}\text{Sc}(\alpha, p\gamma)$, level struct., lifetimes, from DSA and $\pi\gamma$ coincidence meas. 8-74326
- ^{176}Ta , isomeric states and rot. struct. anal., in-beam γ -ray spectroscopy 8-78312
- ^{181}Ta , pion $^-$ capture, high spin states and neutron multiplicities meas. 8-54806
- ^{153}Tb excited states from $\text{Eu}(\alpha, xn)$, rot. bands, spin, parity, γ spectra 8-62552
- ^{104}Tc , β^- decay, γ -spectra, ^{104}Ru level scheme determ. 8-82313
- ^{49}Ti , polarised, T violation test, γ -ray directional correlation 8-62330
- ^{57}Ti , studied via $(\alpha, 2n\gamma)$, high spin states, shell model calcs. 8-54675
- Tl, $A=195, 197$, rot. bands, high spin states 8-62476
- $^{205}\text{Tl}(\alpha, 3n)$, 35-51 MeV, ^{206}Bi high-spin states anal. 8-82368
- ^{165}Tm , levels excited by β -decay of ^{165}Yb 8-74334
- ^{169}Tm , γ -ray transitions for level struct., obs. in ^{169}Yb electron capture decay 8-82307
- $^{238}\text{U}(\alpha, \alpha\gamma)^{234}\text{Th}$, cross section, α -spectra, γ -spectra of ^{234}Th decay 8-58262
- $^{\text{a}}\text{W}$, $A=173, 175$, high-spin states, single-particle structure 8-93922
- Xe , $A=139, 140$, ^{232}Th fission products, yields, γ -ray spectra 8-74410
- $^{176}\text{Yb}(d, n\gamma)$, 14 MeV, gamma-ray spectra (*Russian*) 8-54720
- $^{176}\text{Yb}(p, xn\gamma)$, 6.6 MeV gamma-ray spectra (*Russian*) 8-54720
- ^{67}Zn , γ spectroscopy of low spin states from $^{64}\text{Ni}(\alpha, n\gamma)$, 8.2 MeV 8-78303
- ^{67}Zn , populated in $^{64}\text{Ni}(\alpha, n)$, level struct. below 2.0 MeV, γ -ray studies 8-62483
- Zr, $A=86, 87, 88$, high spin states 8-74383
- $^{96}\text{Zr}(^{16}\text{O}, 4n\gamma)$, 56 MeV, γ yields, polarisations, ang. distrib., ^{108}Cd decay scheme 8-66301

gamma-ray spectra of liquids and solids

see also Mossbauer effect

- allowed β - γ angular correlations induced by mag. interactions 8-68419
- antiferroelectric structures, gamma-ray generation by fast electrons 8-76545
- antiferromagnetic structures, gamma-ray generation by fast electrons 8-76545

gamma-ray spectra of liquids and solids continued

- metal, positron annihilation, ang. correl. data analysis 8-52592
 neutron activation analysis, gamma-ray spectra prediction, detection limits, computational procedure 8-85242
 perovskite crystals, static and dynamic aspects of PAC meas. 8-88241
 polyglutamic acid, helix-random coil transition observed by gamma-ray ang. correlation 8-80828
 polyglutamic acid molecular dynamics in soln., γ -ray perturbed angular correl. 8-94960
 quantum beats from nuclei excited by synchrotron pulses 8-88239
 sea water, gamma-radiation from neutrons radiative capture rel. to chlorinity determ. (*Russian*) 8-77360
 Ag-Pd, dil., elec. field gradient, conc. and temp. effects 8-68416
 Al:¹¹¹In, electron irradi., defect trapping at impurities 8-55892
 Be-Ru, dil., quadrupole interactions at ⁹⁹Ru, TDPAC meas. 8-91996
 Cd-Hg, dil., anomalously high elec. field gradients below 0.05K 8-72442
 Cr, spin density waves detected by Ta mag hyperfine field meas. 8-60364
 Cs₄Hf(C₂O₄)₄.nH₂O, electric field gradient at metal site, γ -ray perturbed ang. correlation meas. 8-52380
 Cu-Mn Kondo system, ⁵⁴Mn nucl. orientation 8-68421
 Fe, gamma fields induced by ²⁵²Cf neutrons 8-50240
 Fe, mag. hyperfine field of K, Ca and Ti, TDPAC meas. 8-52389
 Fe, transient mag. field, vel. and atomic number depend. 8-91999
 Fe:¹⁷²Yb, hyperfine mag. field, TDPAC meas. 8-52394
 Fe:K(Ar), mag. hyperfine interaction, temp. depend. 8-68420
 Fe-Co-Cd(Sn), mag. hyperfine fields at Fe, Cd and Sn sites, Mossbauer and TDPAC meas. 8-60363
 Fe₃C, cementite, modified by rare earth metal and alloying additions, thermal stability (*Russian*) 8-56663
 Gd-Hg, dil., mag. hyperfine field, TDPAC meas. 8-52414
 HfO₂, chem. induced elec. field gradient, perturbed ang. correl. obs. 8-80257
 HfO(H₂PO₄)₂.H₂O, chem. induced elec. field gradient, perturbed ang. correl. obs. 8-80257
 HfP₂O₇, chem. induced elec. field gradient, perturbed ang. correl. obs. 8-80257
 Hf₂Zr_{1-x}, elec. quadrupole interactions at ¹⁸¹Ta impurities, TDPAC meas. 8-76364
¹⁸¹Ho:¹⁸¹Ta, dil., elec. field gradient at impurity, anomalous temp. depend., host 4f levels, γ - γ correls. 8-95272
 In-Cd, dil., elec. field gradient at Cd impurities, press. depend., TDPAC meas. 8-64302
 K content in natural samples, γ spectrometric determ. (*Russian*) 8-92562
 KCl, delocalised positronium, 4.2K, direct obs. γ -spectra 8-88235
 K₄Hf(C₂O₄)₄.nH₂O, electric field gradient at metal site, γ -ray perturbed ang. correlation meas. 8-52380
 Lu, electric field gradient, at ¹⁸¹Ta substitutional atoms, pressure dependence 8-52385
 (NH₄)₄Hf(C₂O₄)₄.nH₂O, electric field gradient at metal site, γ -ray perturbed ang. correlation meas. 8-52380
 Na₄Hf(C₂O₄)₄.nH₂O, electric field gradient at metal site, γ -ray perturbed ang. correlation meas. 8-52380
 NaNO₃, N atom velocity, NO₃⁻ vib. and orientation, nucl. reson. photon scatt. 8-68433
 Ni:¹⁷²Yb, hyperfine mag. field, TDPAC meas. 8-52394
 NiO:⁶⁷Zn, perturbed ang. correl. 8-95535
 Pb, energy of form. of monovacancies, positron annihilation obs. (*German*) 8-71721
 PbHfO₃, elec. field gradient, crit. behaviour, DPAC meas. 8-80303
 Ra content in natural samples, γ spectrometric determ. (*Russian*) 8-92562
 Rb₄Hf(C₂O₄)₄.nH₂O, electric field gradient at metal site, γ -ray perturbed ang. correlation meas. 8-52380
 Re-Hg, dil., anomalously high elec. field gradients below 0.05K 8-72442
 Se, electric field gradient of ¹⁸¹Ta substitutional atoms, press. depend. 8-52385
 TaS₂ intercalated with NH₃, charge transfer, PAC meas. 8-76366
 Te, elec. field gradient and lattice locati8n of Sn, TDPAC and Mossbauer effect meas. 8-52395
 Th content in natural samples, γ spectrometric determ. (*Russian*) 8-92562
 U, assay in fuel rods, by passive gamma-ray spectrometry 8-92576
 U content in natural samples, γ spectrometric determ. (*Russian*) 8-92562
 U, electric field gradient, of ¹⁸¹Ta substitutional atoms, press. depend. 8-52385
 Zn, quadrupole interaction at ¹⁸¹Ta, TDPAC meas. 8-52392
 Zn-Hg, dil., anomalously high elec. field gradients below 0.05K 8-72442
 ω -Zr, electric field gradients at substitutional Ta atoms, TDPAC high-pressure study 8-52384

gamma-ray spectrometers

see also *gamma-ray spectra*

- automated complex, Mossbauer spectra information retrieval and processing (*Russian*) 8-82091
 automated correlation spectrometer with two Ge(Li) detectors 8-82562
 body radioactivity measurement, SABRE 3 computer system 8-85425
 collimator system, for high intensity, accurate Compton profile meas., construction 8-90013
 cosmic gamma-ray telescope in 10-30 MeV range 8-73638
 digital based triangular wave generator for Mossbauer spectroscopy 8-55113
 double Compton gamma-ray telescope, calibration in neutron beam 8-53827
 double Mossbauer spectrometer for small resonance line shift meas. 8-82560
 EM shower sampling counters, characteristics of plastic scintillator and radiator layers 8-58530
 gamma-ray spectrometric logging and surface exploration equipment calibration 8-85706
 hodoscopic spectrometer, gamma-quanta coordinate meas. in NITsE scintillation spectrometer 8-78549
 Mossbauer apparatus for resonance studies at high press. and low temps. 8-49943

gamma-ray spectrometers continued

- Mossbauer spectrometer, high field, with Bitter magnets, arrangements, problems 8-89608
 NE 213 liquid scintillator, decay under neutron and gamma excitation (*German*) 8-55097
 NE 213 liquid scintillator, deuterated, decay mode (*German*) 8-55096
 NE 238 fast liquid scintillator, scintillation decay and n- γ discrimination (*German*) 8-55101
 peak areas and detection limits, digital calc. methods 8-50433
 response function interpolation by splines 8-82561
 river water pollution detection, multielement anal. 8-69511
 scintillation counter multidetector arrangement for on-line meas. of neutron and γ -ray multiplicities 8-50440
 scintillation time-of-flight telescope for cosmic γ -ray preselection 8-82572
 scintillator response, pulse height spectra unscrambling, computer program 8-55092
 CsI(Tl) well-detector for low background γ -spectrometry, comparison with NaI(Tl) 8-86724
 Ge detectors appl., high-purity, preparation and properties 8-86723
 Ge spectrom., intercomparison of ¹⁵²Eu gamma-ray emission rate meas. 8-82568
 Ge-Li spectrom., re-evaluation of precise γ -ray energies for calibration 8-90015
 Ge(Li) coaxial detector, triple const. fraction discriminator evaluation 8-70708
 Ge(Li) detector, use in activity determ. of gamma source with flat surface (*German*) 8-58528
 Ge(Li) detectors, anal. of monochromatic γ -ray and annihilation spectra 8-50429
 Ge(Li) γ -ray spectra, NUKLID program for automatic line identification 8-58536
 Ge(Li) spectrom., balloon-borne, recent meas. 8-93107
 Ge(Li) spectrom., precision energy meas. of gamma rays of ⁵¹Cr, ¹⁰³Ru, ¹⁰⁹Cd, ¹⁴⁴Ce, and ²⁰³Hg 8-58533
 Ge(Li), spectrometer efficiency, dead time and pulse pile-up correction 8-50442
 Ge(Li)-NaI(Tl), Compton suppression spectrometer for in-beam expts., design and performance 8-78553
 NaI detector absolute photopeak efficiency calc. for water as source medium 8-78558
 NaI detectors, synthesis of response functions to gamma-rays 8-94158
 NaI gamma spectrometer with ⁶LiH shielding for neutron background reduction 8-90012
 NaI, meas. of fast neutron capture cross sections 8-74530
 NaI spectrometer, response matrix for 6 MeV γ -ray penetration meas., benchmark data 8-50432
 NaI:Tl scintillator response, γ -ray, (X-ray) rel. 1/2-width energy depend., undergrad. expt. 8-49600
 NaI(Tl) well type detector, efficiency determ. 8-55087
 ThBr₃, inorganic scintillator, use in nucl. and accelerated particle detection 8-58540

gamma-ray transport see *photon transport theory***gamma-rays**

- extended sources, energy distrib. calc., rel. to remote spectroscopy, of Earth surface 8-61586

gamma transition see *glass transition***Gamow-Teller transitions** see *beta-decay***garnets**

- includes *ferrimagnetic insulators, M₂Fe₅O₁₂, for rock-type garnets, MM'(SiO₄), see minerals*
 see also *ferrimagnetic properties of substances*
 bubble domain, empirical relation for saturation vel. 8-95496
 bubble film, high g, two resonant peaks 8-68388
 charged wall behavior in 1- μ m bubble implanted structures 8-91892
 doped, site symm. exam., ang. variation of induced linear dichroism 8-95429
 epilayers, domain structure, technique for observation 8-91914
 epitaxial film, Faraday effect and magnetometrical meas. 8-52317
 epitaxial thin films, for mag. bubble memories (*Czech*) 8-88147
 Faraday element fabrication for intracavity laser appls. 8-66852
 film, dynamic behaviour of domain walls and bubbles 8-52321
 film, dynamic charges in bubble domain lattice 8-60325
 film, ion-implanted, domain wall mobility 8-95495
 film, magnetic rag-domains, appl. to magneto-optical displays 8-91912
 film, magnetoelastic energy of stripe domain patterns 8-68334
 film, numerical display element exploiting rag domains 8-68339
 film preparation, single crystal, for magnetic bubble domain appl. 8-60588
 films, bubble statics, dynamics (*Japanese*) 8-52326
 flux-grown magnetic garnets, comp. anal. by AAS 8-92585
 garnet:Nd³⁺, spectral, structural regularities, anal. 8-51948
 garnet bubble films, 111 orientated, mag. anisotropy predictions, model 8-68326
 LPE film growth thermally induced substrate fracture 8-68639
 LPE garnet bubble films, capping layer upper cap-switch field, model 8-95498
 LPE growth, using horizontal dipping, exam. of growth kinetics 8-60039
 LPE layers, bubble collapse field meas., new method 8-56356
 magnetic bubble dynamic props. rel. to bias-field-determined bubble size 8-91915
 magnetic bubble stability in ion implanted channels, model 8-68320
 magnetic bubble state stability in rot. field 8-68317
 magnetic properties of V⁴⁺ ion, effect of covalency 8-64010
 magnetoelastic symmetry, growth-induced lowering 8-64255
 optical waveguide with high Faraday rotation, mode degeneracy 8-94454
 orthoferrite garnet, mag. bubble lattice nucleation obs. 8-76283
 rare earth garnets, appl. of superposition model to cryst. field 8-68132
 stripe head vel. meas. using magnetoresist. signal 8-68316
 structural parameters, appl. of Poix formula 8-67701
 (YSmEuCa)₃(FeGe)₂O₁₂, garnet film, ion implanted, bubble domain props. 8-88152
 Ca₃Fe₂(Mn₂)Ge₂O₁₂, single magnetic sublattice antiferromagnetic garnets 8-52652
 Ca₃Ga₂Ge₃O₁₂, substrate, electron examination of microstruct. and microsegregation 8-67919

garnets continued

- Ca₃Mn₂Ge₂O₁₂, highly anisotropic garnet, neutron diffr. obs. of mag. struct. 8-68168
 CaV ferrite garnet, large grained, mag. props. 8-64222
 CaY₂Mg₂Ge₂O₁₂:Nd, CW room temp. laser operation, 0.941 and 1.059 μm 8-66842
 DyAG, adiabatic magnetisation, optical obs. 8-88283
 DyAG, crit., tricrit., and crossover phenomena, light scatt. 8-68251
 DyAG, forced magnetostriction meas. 8-68349
 DyAG, single cryst. growth by Czochralski method 8-95690
 DyIG, mol. field coeffs., magnetisation and mag. susceptibility anal. 8-95406
 ErAG, facet formation 8-63687
 (Eu,Lu)₃Fe₂O₁₂, submicron bubble films on rare earth-Ga garnet substrates, prep. and mag. props. 8-91909
 (Eu,Lu)₃Fe₂O₁₂, Ga, Al or (Ca,Ge) substituted, mag. props. and growth of 2 μm bubbles 8-91910
 Fe garnet, Bi substituted, epitaxial film, magneto-optical controlled transparencies 8-50932
 Ga substituted garnet films, mag. prop. control during LPE growth and processing 8-68638
 (Gd,Bi)₃(Fe,Ga)₂O₁₂ magneto-optic film, ion irradi. effect on storage props. 8-52324
 (Gd,Lu)₃(Fe,Mn,Al)₂O₁₂ epilayer with orthorhombic anisotropy, domain wall vel. 8-52322
 Gd₃Al₂O₁₂ phase obtained by crystallisation of amorphous Gd₂O₃-5/3Al₂O₃ by quenching 8-92224
 GdGa garnet, Czochralski grown, substrate material dislocation propagation 8-59771
 Gd₃Ga₂O₁₂, brilliance, sparkliness and fire of diamond simulants 8-90363
 Gd₃Ga₂O₁₂, Ca, Zr and Mg substituted artificial garnets, track registration props. 8-62679
 Gd₃Ga₂O₁₂, Czochralski grown, effect of melt flow phenomena on perfection 8-88419
 Gd₃Ga₂O₁₂, growth of 3" diameter crystals 8-68616
 Gd₃Ga₂O₁₂, opt. dispersion 8-64343
 Gd₃Ga₂O₁₂, substrate, electron examination of microstruct. and microsegregation 8-67919
 Gd₃Ga₂O₁₂:Nd³⁺, cryst. field anal. 8-64013
 GdIG, mag. props. meas. in high mag. fields, review (*Japanese*) 8-52303
 (GdPrBi)₃(FeGaIn)₂O₁₂, pure and In³⁺ doped, near IR absorpt. and Faraday rot. 8-95580
 Gd_{0.9}Y_{0.1}Tm_{0.1}Ga_{0.44}Fe_{0.56}O₁₂, ion implanted, ferromag. reson. meas. 8-68385
 Ge substituted garnet films, mag. prop. control during LPE growth and processing 8-68638
 HoIG, Faraday rotation, mag. field depend., 4.2 to 300K, magneto-optical coeffs. 8-95577
 HoIG, mol. field coeffs., magnetisation and mag. susceptibility anal. 8-95406
 LuAG:Nd³⁺, cryst. field anal. 8-64013
 Lu₃Ga₂O₁₂:Nd³⁺, cryst. field anal. 8-64013
 Mn₂Cr₂Ge₂O₁₂, garnet, antiferromag. ordering (*Russian*) 8-80146
 NdGa₂O₁₂ wafer, dislocations, etch pits and birefr. obs. 8-83818
 (Sm,Er)₃(Ga,Fe)₂O₁₂, LPE, non-grooved film, thermomag. writing 8-76278
 (Sm,Lu)₃Fe₂O₁₂, submicron bubble films on rare earth-Ga garnet substrates, prep. and mag. props. 8-91909
 (Sm,Y)₃(Fe,Ga)₂O₁₂, epitaxial mag. layer, LPE, growth rotation rate, effect on props. 8-56053
 SmCaGe garnet LPE bubble film, coercivity, thickness depend. 8-68324
 Sm_{0.2}Lu_{0.2}Tm_{0.2}Y_{1.45}Ca_{0.85}Fe_{4.15}Ge_{0.85}O₁₂, LPE growth, saturation magnetisation, collapse field, bubble diameter 8-95703
 Sm_{0.1}Y_{1.9}CaFe₂GeO₁₂, LPE growth, saturation magnetisation, collapse field, bubble diameter 8-95703
 Sm_{0.4}Y_{0.6}Fe_{3.8}Ga_{1.2}O₁₂, LPE, improved method of stirring 8-68641
 Sm_{0.4}Y_{0.6}Ga_{1.1}Fe_{3.9}O₁₂, LPE, growth rate anisotropy and kinetic coeffs. of vicinal faces 8-51846
 TbGa garnet, Verdet const. meas. with pulsed mag. field 8-68486
 TbIG, anisotropic forced magnetostriction meas. 8-64251
 TbIG, anisotropic garnet, mag. struct., magnetisation and Faraday rotation obs. 8-68169
 TbIG, appl. of superposition model to cryst. field 8-68132
 TbIG, mol. field coeffs., magnetisation and mag. susceptibility anal. 8-95406
 Tb₂Lu₂Fe₂O₁₂ film, magnetostriction meas. using double cryst. X-ray diffractometry 8-84468
 Tb_{0.2}Y_{0.8}Fe₂O₁₂, Mossbauer investigation of spin-reorientation transition 8-88243
 (Y,Eu,Lu,Ca)₃(Fe,Ge)₂O₁₂, bubble memory chip, dynamic conversion comparison with (Y,Sm,Lu,Ca)₃(Fe,Ge)₂O₁₂ 8-68319
 (Y,Eu,Tm,Ca)₃(Fe,Ge)₂O₁₂, Ca, Ge substituted garnet LPE films, elec. props., charge imbalance, Seebeck effect 8-68101
 (Y,Eu,Tm,Ca)₃(Fe,Ge)₂O₁₂ garnet film coercivity, new annealing method 8-84459
 (Y,Er)₃(Fe,Ga)₂O₁₂, LPE growth from molybdate fluxes, bubble props. 8-68322
 (Y,Sm,Ca)₃(Fe,Ge,Si)₂O₁₂ single-crystal films, props. 8-64247
 (Y,Sm,Lu,Ca)₃(Fe,Ge)₂O₁₂, bubble memory chip, dynamic conversion comparison with (Y,Eu,Lu,Ca)₃(Fe,Ge)₂O₁₂ 8-68319
 (Y,Sm,Lu,Ca)₃(Fe,Ge)₂O₁₂ garnet film coercivity, new annealing method 8-84459
 (Y,Sm,Lu)₃(Fe,Ga)₂O₁₂, LPE mag. film, suitability for 1 to 3 micron bubble devices 8-68323
 (Y,Sm)₃(Fe,Ge)₂O₁₂, Ca, Ge substituted garnet LPE films, elec. props., charge imbalance, Seebeck effect 8-68101
 YAG, brilliance, sparkliness and fire of diamond simulants 8-90363
 YAG, colour centres conceived as bound polarons 8-63990
 YAG, Czochralski grown crystals, interface shape change 8-83760
 YAG, facet formation 8-63687
 YAG laser, resonator length effects on loss coeffs. and output energy (*German*) 8-66849
 YAG, solubility in solvent PbO-PbF₂, phase form. in system Y₂O₃-Fe₂O₃-PbO-PbF₂-B₂O₃ 8-95247
 YAG:Ce³⁺, new fast scintillator for SEM 8-86394
 YAG:Cr³⁺, electronic states interactions with crystal odd vibr., R-lines vibr. recurrences 8-84639
 YAG:Gd³⁺, EPR absorpt. spectrum 8-76305

garnets continued

- YAG:Ge³⁺, excited state absorpt. loss, 5d→4f rare earth lasers 8-90417
 YAG:M³⁺, ESR absorption spectra, line broadening of Fe³⁺, Cr³⁺, Gd³⁺ 8-91940
 YAG:Nd laser, crystal defects influence on energetic effectiveness obs. (*Czech*) 8-79022
 YAG:Nd³⁺, cryst. field anal. 8-64013
 YAG:R³⁺, R=Nd, Er, (Er, Ga), LPE and luminesc. 8-64408
 YAG: rare earth, phonon impurity scatt., lattice thermal cond. and US attenuation meas. 8-87748
 Y₃₋₂Bi₂Fe₂O₁₂, ferrite-garnet formation 8-52737
 (YCaEuYb)₃(FeGe)₂O₁₂, LPE, stripe end motion, effect of in-plane field 8-68330
 Y₃₋₂Ca₂Fe₂₋₂In₂Fe₃₋₂V₂O₁₂, first magnetocryst. anisotropy const., ferri-mag. reson obs. 8-68218
 Y₃₋₂Ca₂Fe₂₋₂Zr₂Fe₂O₁₂, first magnetocryst. anisotropy const., ferrimag. reson obs. 8-68218
 (YEuErCa)₃(GeFe)₂O₁₂: H, Ne, Ar ion-implanted, threefold symmetrical bubble properties 8-64243
 (YEu)₃(FeGa)₂O₁₂ rigid magnetic bubble transition to normal behaviour 8-95501
 Y_{2.35}Eu_{0.65}Ga_{1.2}Fe_{3.8}O₁₂, bubble translation vel., ion-implantation effects 8-68327
 (YEuLuCa)₃(FeGe)₂O₁₂ film, stable state of bubbles containing Bloch lines 8-76281
 Y_{1.55}Eu_{0.3}Tm_{0.3}Ca_{0.88}Ge_{0.88}Fe_{4.12}O₁₂, bubble translation vel., ion-implantation effects 8-68327
 (YEuYbCa)₃(FeGe)₂O₁₂ film, mag. σ-bubbles, automation props. 8-88150
 (YEuYbCa)₃(GeFe)₂O₁₂: H, Ne, Ar ion-implanted, threefold symmetrical bubble properties 8-64243
 (YEuYb)₃(FeGa)₂O₁₂, LPE, stripe end motion, effect of in-plane field 8-68330
 Y(Fe, Ga)₂O₁₂, garnet film, strip domain struct. behaviour in applied field 8-68341
 Y₂Fe₃₋₂Ga₂O₁₂ epitaxial layers grown from soln., prep. and props. (*German*) 8-52691
 Y₂GaFe₂O₁₂, mag. props. meas. in high mag. fields, review (*Japanese*) 8-52303
 Y₃Ga₂O₁₂:Nd³⁺, cryst. field anal. 8-64013
 Y₃₋₂Gd₂Fe₂O₁₂, field depend. of susceptibility (*Russian*) 8-68176
 (YGdYbBi)₃(FeAl)₂O₁₂, epitaxial garnet film, with mag. compensation point, behaviour of 'compromise' phase boundary 8-60321
 YIG, bulk, low mag. domain wall mobility 8-95463
 YIG, computer optical isolator for near IR region 8-83104
 YIG, diamagnetic substituted, anal. of polar Kerr rot. spectra 8-68485
 YIG epitaxial film and cryst., bound magnetostatic waves controlled by field gradients 8-95425
 YIG epitaxial layers grown from soln., prep. and props. (*German*) 8-52691
 YIG film, calc. of magnetostatic mode freq. 8-68313
 YIG film, dielec. layered struct., magnetostatic volume wave propag. 8-95426
 YIG film, shallow groove effect on magnetostatic forward volume wave reflection 8-84473
 YIG, Hf response and thermodynamic props. (*Russian*) 8-72338
 YIG, LPE film, non-Ohmic currents 8-68099
 YIG, magnetisation density, polarized neutron expts. 8-52215
 YIG, magnetoresistance of bulk and epitaxial films 8-91706
 YIG, parallel microwave pumping threshold, RF modulation of mag. field 8-88195
 YIG, precipitation of Fe₂O₄ 8-84815
 YIG, press. depend. of effective mag. fields on ⁵⁷Fe nuclei 8-52383
 YIG, single cryst., Neel lines, Faraday effect obs. 8-64216
 YIG substituted film waveguides, TE→TM mode conversions 8-66904
 YIG: Ca²⁺ epitaxial films, Fe⁴⁺ centres, MCD, optical absorpt., and thermoelectric power meas. 8-95595
 YIG:Ca, epilayer, reversible oxidation, ferromag. reson. 8-76781
 YIG:Ca, O diffusion depend. on defect conc. 8-67857
 YIG:Co²⁺, mag. permeability, illumination and impurity depend. (*Russian*) 8-64220
 YIG:Si⁴⁺, mag. permeability, illumination and impurity depend. (*Russian*) 8-64220
 YIG/n-GaAs layered structure, magnetostatic surface wave amplification 8-88107
 YIG-Ge structure, profile and position of reson. galvanomag. effect curve 8-72242
 (YLaBi)₃(FeGa)₂O₁₂, pure and In³⁺ doped, near IR absorpt. and Faraday rot. 8-95580
 Y_{2.8}Pr_{0.2}Fe₂O₁₂, magneto-optical props. 8-72489
 (YSmCa)₃(FeGe)₂O₁₂ LPE films, optimum growth conditions for low coercivity 8-95499
 Y_{2.2}Sm_{0.4}(Fe,Ga)₂O₁₂, garnet film, strip domain struct. behaviour in applied field 8-68341
 (YSm)₃(FeGa)₂O₁₂, growth rate anisotropy and kinetic coefficients of vicinal faces 8-63954
 Y₃₋₂Sm₂Fe₂₋₂Ga₂O₁₂ epitaxial layers grown from soln., prep. and props. (*German*) 8-52691
 (YSm)₃(GeFe)₂O₁₂: H, Ne, Ar ion-implanted, threefold symmetrical bubble properties 8-64243
 (YSmLuCa)₃(FeGaGe)₂O₁₂, reproducibility in bubble garnet LPE growth 8-92204
 YSmLuCaFeGe garnets, growth and temp. characts. of small bubbles 8-80183
 (YSmLuCa)₃(FeGe)₂O₁₂, mag. props. and growth of 2 μm bubbles 8-91910
 (YSmLuCa)₃(FeGe)₂O₁₂, LPE growth, growth reproducibility of bubble props. 8-92208
 (YSmLuCa)₃(GeFe)₂O₁₂, garnet film, refractive index dispersion 8-88273
 (YSmLuCa)₃(GeFe)₂O₁₂: H, Ne, Ar ion-implanted, threefold symmetrical bubble properties 8-64243
 YSmLuCaGeIG, mag. props. and defects, depend. on B₂O₃ conc. on growth in PbO-B₂O₃ solvents 8-68321
 (YSmTmCa)₃(GeFe)₂O₁₂ film, YY pattern racetrack discrimination and state stability of S=1 and 0 bubbles 8-91908
 YiG-Bi layer struct., Landau electron absorpt. mechanism, spin wave amplification 8-72344

gas *see gases*gas analysis *see chemical analysis*

gas blast circuit breakers

see also air blast circuit breakers

arc boundary in nozzle throat section, arc diameter, RF technique 8-87528

arc model, current zero period, boundary layer integral method 8-87522

conference, Liverpool, England, Sep. 1978 8-87521

hot gas surrounding arc core, thermal disturbances 8-87529

Tokamaks, gas breakers for ohmic heating circuits 8-66396

SF₆, 20 kA arc, electrode vap. contamination, time depend. energy balance 8-87525SF₆ arc model, convection-loss dominated 8-87519SF₆, clogging transition 8-87530SF₆, electron temp. at current zero, 3 kA arc 8-87526SF₆, energy clogging, current and voltage meas. at different press. 8-87531SF₆ high-current arc props., influence of electrode material 8-71592SF₆, particle densities in decaying plasma 8-75442SF₆, very high current arcs, elec. conductance of arc gap 8-87524gas breakdown *see electric breakdown of gases*gas bubbles *see bubbles*gas discharge lamps *see discharge lamps*

gas-discharge tubes

see also ion sources; mercury arc rectifiers; thyatrons

AC plasma display panel wall charge magnitude and distribution probe 8-67487

cathode region transfer process simulation, Monte Carlo method 8-71600

cold-cathode controlled gas discharge switch 8-86300

colour display panels, comparison of light output (*Japanese*) 8-62191

gas-filled diode, rarefied gas breakdown time delay statistics 8-87571

glow discharge, detector for millimeter rad., cyclotron reson. effect on sensitivity 8-62222

glow discharge, tube impedance with and without metal cover 8-67508

inert gas ion laser discharge, energy balance 8-74884

inert gas ion laser ion-acoustic wave excitation 8-74885

phototube, gas-filled, rise time spectral depend., appl. to EM radiation detector miniaturisation 8-86318

H atomic source, for electron scatt. expts. 8-94332

gas discharges *see discharges (electric)*gas dynamics *see aerodynamics*gas ionisation *see ionisation of gases*

gas lasers

*see also chemical lasers; excimer lasers; gasdynamic lasers; ion lasers*acetonitrile sub mm laser, generation lines identification (*Russian*) 8-82952

amplification of incoherent radiation 8-55334

amplifier, quasi-Gaussian pulse propagation, effect on line-shape parameter anal. 8-55333

anisotropy due to saturating fields 8-55337

Antares laser, for laser fusion expts., energy storage system design 8-55030

atomic constants and collision cross sections determ. by level crossing 8-50763

capacitive mesh output couplers for optically pumped far IR mol. lasers 8-74916

carbon tetrafluoride 16 μ m laser, radiance enhancement 8-87045cavity unit for radiation lead-out (*Russian*) 8-90433CO₂ lasers, CW, high-power appl. of photoinitiated impulse-enhanced electrically excited discharge 8-50785

computer model for CW optically-pumped submm laser performance prediction 8-87041

conical laser plasma tube, electron density distrib. 8-58981

coupling modulated, mode coupling distortions minimisation anal. 8-55384

CW lasers, homogeneously broadened, with uniform distribution loss, exam. of output power 8-55332

direct nucl. pumped laser for feedback laser fusion 8-58445

discharge pumped generic wavelength system for fusion reactor ignition 8-58423

electrically excited preionisation unit with electron beam energy recuperation 8-59013

electroionisation lasers, closed gas-flow cycle without mech. elements 8-94401

electron beam stabilised discharge in flowing medium, numerical calc. 8-94943

electron beam sustained discharge, electron neutral inverse bremsstrahlung, rel. to high-press. IR lasers 8-63604

electronic transition lasers, conf., Snowmass Village, USA (Sept. 1976) 8-63076

energy storage and nonstoring advanced lasers for fusion appls. 8-79027

far IR laser, optically pumped, electronic tuning and phase-locking 8-59055

far IR laser, pump radiation self-focusing and defocusing 8-79003

far IR lasers, optically pumped, frequency modulated noise measurements 8-55392

fluoromethane, far IR laser, electronic tuning and phase-locking 8-59055

fluoromethane, far IR laser, pump radiation self-focusing and defocusing 8-79003

fluoromethane, laser submillimetre with optical pumping energy yield, emission pulse delay time depend. on pumping pulse (*Russian*) 8-71088

fluoromethane far IR laser FM and stabilisation by Stark effect 8-59056

fluoromethane waveguide laser, tunable, for far IR freq. synthesis in 500-70 μ m region 8-90439

foilless anode electron-beam laser with chopper-wheel gas pulser 8-63122

formaldehyde-d₂ vapour, far IR laser emissions 8-63072formic acid, laser transitions near 5.6 μ m, HF laser optical pump 8-58995

frequency stability measurement techniques, mass-production appl. 8-90444

fusion reactor study, SOLASE, laser, optics and pellet design 8-58426

gas lasers continued

fusion reactor study, SOLASE 8-58424

high energy gas laser facility, energy storage system design 8-55030

high power lasers and their applications 8-87092

high-pressure metal-vapour/inert-gas mixture discharge peculiarities 8-71620

holographic method for laser radiation divergence reduction (*Russian*) 8-63147

homogeneously broadened laser, two mode operation, analytical string signal analysis 8-55331

inert gas, electron beam pumped, visible absorpt. rel. to visible laser development 8-63057

inert gas hydride laser, use two-step nucl. fusion dissipative confinement of doubly isotopic boron hydrides 8-82506

iodomethane, laser submillimetre with optical pumping energy yield, emission pulse delay time depend. on pumping pulse (*Russian*) 8-71088

longitudinal flow, effect of flow on output power 8-58975

metal vapour, explosively formed, apparatus for stimulated emission obs. 8-50764

metal vapour laser, upper and lower laser states population densities, simultaneous determ. method 8-87042

methane stabilised laser, stability evaluation (*Japanese*) 8-90437methanol, CH₃OH and CD₃OH, far IR laser lines, optically pumped by CO₂ laser 8-90415methanol, far IR laser resonator for TEM₀₀ mode operation 8-66847methanol-d₃, CO₂ laser pumped, CW far IR laser lines obs., 34.5 to 287 μ m 8-71082methanol-d₃, optically pumped, CW far IR laser lines obs. 8-79005

methyl alcohol-d, optically-pumped laser line freqs. 8-55345

methyl bromide sub mm laser, generation lines identification (*Russian*) 8-82952

methyl fluoride, CW optically pumped far IR laser with variable output Michelson coupler 8-55372

methylfluoride laser, CW, 496 microns, rate equation model, review 8-55343

multigas electron beam pumped lasers 8-94396

multimode, active medium polarisation with excitation modulation 8-82942

non-self-sustained discharge plasma, thermal instability development, laser appls. 8-71611

 α -NPO-Ar mixture, vapour phase laser, electron beam pumping 8-63097operation, fast electron beam irradi. effects (*Russian*) 8-74878

organic vapour phase laser, electron beam pumping of inert gas-organic vapour mixture 8-63097

oscillations in gas laser discharge, review 8-55339

pulsed plasma laser, falloff rate of field 8-82944

radioactive source preionisation of visible and UV discharge lasers 8-63096

rare earth halide vapour, discharge, potential fusion laser systems 8-63074

resonating structure loss reduction, wave propag. in hollow rectangular anisotropic guide 8-83084

ring, nonlinear interaction of opposing beam waves with arbitrary polarisation, anal. (*Russian*) 8-82993

ring laser, multimode, high-Q power resonances 8-82997

ring laser, nonlinear Zeeman effect 8-71123

ring laser, resonance phenomena with saturated absorpt. (*Russian*) 8-59048

sub-mm CW optically pumped laser, scaling 8-55341

unstable resonator properties, small-scale phase inhomogeneity influence 8-59050

waveguide laser, construction and operation characteristics (*Rumanian*) 8-59049Zeeman linearly polarised laser, Izsing atom susceptibilities, first and third order approx. (*Japanese*) 8-71071Zeeman linearly polarised laser, mag. field reson. on laser output, freq. stabilisation (*Japanese*) 8-66798Ar I, high press. tunable laser emitting at 0.91 μ m 8-50755

Ar*(4p), (5p) states, lifetimes and two-body rate consts. meas. 8-63058

Ba vapour laser, pulse repetition frequency scaling law 8-82954

Br₂, optically pumped at 532 nm, lasing obs. in visible and near IR 8-63094

CO, acetone decomposition, near IR laser action 8-63055

CO, CO₂ lasers, appl. to atmospheric pollutants selective quantitative meas. 8-69526

CO CW electric discharge laser, saturation parameter expt. determ. 8-50762

CO discharge, low-pressure laser striation obs. 8-66814

CO, efficient self-sustained pulsed laser 8-55377

CO electric discharge unstable resonator laser, computer model 8-58988

CO sealed laser, approximate analytic theory 8-58994

CO-He low press. mixture, CO vibr. distrib. to high level 8-58985

CO₂, 1 mJ line tunable optically pumped laser 8-66840CO₂, 100 kJ laser, optical design and components 8-82990CO₂, 10.6, 9.4 μ m laser bands high-press. absorpt.-spectra 8-66543CO₂, 200 J TEA laser, injection mode locking 8-79049CO₂, ANTARES device, target-induced parasitic oscills. 8-59072CO₂, absolute transition freqs. by multiplication of difference-freqs. 8-90445CO₂, acetone decomposition, near IR laser action 8-63055CO₂, adaptive resonator expt. config. 8-55386CO₂, beam steering, using hole grating attenuator 8-59071CO₂, CW high power lasers, appls. for metal working 8-79026CO₂ CW laser, sealed-off design, NaCl Brewster angle mirrors 8-55370CO₂, CW waveguide laser, anodised Al waveguide construction 8-55376CO₂, CW waveguide laser, nearly atm. press., using plasma injection technique 8-74925CO₂, compact flowing gas system for waveguide lasers 8-87067CO₂ convection laser discharge, negative ion effects 8-55335CO₂, E-beam sustained large amplitude discharge, for fusion appls. 8-55382CO₂, electric discharge convection laser, saturation characts. (*Chinese*) 8-90408CO₂, electron beam controlled laser with plasma mirror, stimulated emission dynamics 8-50799

gas lasers continued

- CO₂ electron beam controlled laser, plasma mirror refl. characts. 8-70104
- CO₂ electron-beam-controlled laser, operation characts., 1 to 10 atm range 8-70118
- CO₂ electron-beam-controlled laser, pulse forming network power source 8-74928
- CO₂ fast flow laser, combined pulse and DC discharge as pump 8-71017
- CO₂ fast-flow laser, pumping efficiency by AC discharge 8-50801
- CO₂ for optically pumped CW FIR lines from ¹⁵NH₃, CD₃OH and CH₃OH 8-90405
- CO₂ freq. stabilised laser with OsO₄ absorber, output freq. reproducibility 8-50800
- CO₂ frequency control by spectrally depleted destructive two-beam method 8-74441
- CO₂ gaseous saturable absorber cell to suppress parasitic oscillations 8-87066
- CO₂ He recovery system 8-82974
- CO₂ high power, CW, electron beam sustained, performance, theory and expt. 8-71074
- CO₂ high power, transmissive optical components 8-79057
- CO₂ high power elec. discharge laser, multielement cathode design and operational characts. 8-82983
- CO₂ high power laser beam monitor 8-74943
- CO₂ high stability CW waveguide laser, for high resolution saturation spectroscopy 8-71112
- CO₂ high-power high-energy, using an absolute calorimeter 8-93686
- CO₂ high-press. tunable IR lasers 8-59050
- CO₂ IR laser, transients obs. by modulation of intracavity absorber 8-74953
- CO₂ KCl laser windows at 10.6 μ m, optical distortion parameter 8-79056
- CO₂ laser, 16 GHz tunable sideband generation 8-90428
- CO₂ laser, double transverse pulsed discharge characteristics 8-71617
- CO₂ laser, Faraday effect optical isolation at 10.6 μ m using chalcogenide spinels 8-50816
- CO₂ laser, glow discharges at high press., voltage-current characts. 8-87056
- CO₂ laser, high repetition rate-pulsed, weak shock wave effect 8-90409
- CO₂ laser, high-power photopreionisation stabilised, operation at press. up to 13 atm. 8-83151
- CO₂ laser, intracavity IR absorpt. of vinyl chloride, ethylene, and propylene 8-78835
- CO₂ laser, long and short pulse formation, optimum conditions 8-87057
- CO₂ laser, nsec pulse amplification at efficiencies greater than 20% 8-50815
- CO₂ laser, optical isolation by flowing gaseous saturable absorbers 8-59096
- CO₂ laser, pulse flow stretching (Chinese) 8-90435
- CO₂ laser amplifier, double-discharge at 1800 torr 8-50815
- CO₂ laser amplifier, high power large aperture electron beam controlled, development (Japanese) 8-80840
- CO₂ laser amplifier, short pulse amplification calcs. 8-58979
- CO₂ laser amplifier design, IR laser: optical pumping appl. 8-63133
- CO₂ laser beam alignment, accuracy, Snout test 8-59073
- CO₂ laser beam meas. using pyroelectric vidicons 8-49907
- CO₂ laser discharge, special case of effect of initial conditions on homogeneous discharge development 8-63613
- CO₂ laser discharges, determ. of recombination coeff. 8-90407
- CO₂ laser discharges, electrode surface field and preionisation effects on spatial distrib. of arcs 8-83054
- CO₂ laser electron beam pulsed, sealed electron guns 8-71119
- CO₂ laser frequency measurements: a review, limitations, extension to 197 THz (1.5 μ m) 8-81952
- CO₂ laser gain isolation by saturable absorber gases 8-59095
- CO₂ laser generation by pulsed microwave excitation 8-74879
- CO₂ laser implosion of polyethylene shell into D-filled conical region, neutron generation 8-87468
- CO₂ laser intensity distrib., hot spot detect. using Ag halide film 8-82945
- CO₂ laser line selection using metal film reflection filter 8-55368
- CO₂ laser long-path absorption system, computer automation, air pollution monitoring 8-82971
- CO₂ laser pulse mode quality, effect on multiple photon absorpt. 8-86615
- CO₂ laser resonator, intracavity deformable mirror adaptive optical system 8-87078
- CO₂ laser self-sustained discharge, effect of low-ionisation-potential additives 8-71616
- CO₂ laser stability and heterodyne frequency calibration 8-59031
- CO₂ laser system, eight beam, optical anal. 8-50814
- CO₂ laser systems, Faraday rotator technology using CoCr₂S₄ 8-95579
- CO₂ laser systems for laser fusion appls. 8-50817
- CO₂ lasers used in compressive plasma fusion of D-T macrosamples 8-82507
- CO₂ line-selectable waveguide laser, optoacoustic detect. of ethylene 8-56947
- CO₂ low energy output meas. with absolute calorimeter 8-55396
- CO₂ multiatmospheric UV-preionised lasers 8-50805
- CO₂ PRF control by BCl₃ gaseous phototropic shutter 8-50833
- CO₂ periodically operated laser, pulse repetition freq. limits 8-50750
- CO₂ pulsed, laser induced medium perturbation 8-58977
- CO₂ pulsed electron-beam-controlled laser, parameters optimisation 8-71116
- CO₂ pulsed laser, high power, oscill. spectrum expansion (Russian) 8-74882
- CO₂ pulsed laser beam, thermal coupling 8-63145
- CO₂ saturation parameter from gain meas. 8-66797
- CO₂ sealed photoionisation TEA laser, limiting processes 8-82946
- CO₂ small-gap multiatm. press. system 8-74921
- CO₂ Stark cell noise reduction 8-59059
- CO₂ TE laser, passive mode locking using p-Ge saturable absorber 8-71127
- CO₂ TE laser, performance improvement with tripropylamine additives 8-78991
- CO₂ TEA amplifier, gain meas. on sequence bands 8-78990
- CO₂ TEA laser, compact sealed single mode operation 8-50810

gas lasers continued

- CO₂ TEA laser, energy extraction improvement in multiline double band mode 8-63129
- CO₂ TEA laser, pulse shape and duration, excitation method (German) 8-83010
- CO₂ TEA laser design and construction (Italian) 8-55360
- CO₂ TEA laser discharge, influence of additives and contaminants evaluated by electrical meas. 8-94388
- CO₂ TEA laser electrical excitation rates, theory and expt. 8-71078
- CO₂ TEA laser emission on sequence bands 8-71075
- CO₂ TEA laser with long optical resonator, mode-locked operation 8-79041
- CO₂ TEA lasers, SF₆ dissociation processes 8-74713
- CO₂ TEA oscillator, simultaneous freq. stabilisation and injection 8-55362
- CO₂ TEA sealed laser, seed gas compatible system with unheated oxide catalyst 8-63130
- CO₂ versatile high-power industrial system 8-55380
- CO₂ vibr. distribs., O₂ addition effect 8-50757
- CO₂ waveguide high press. laser, line selection and tunability 8-59026
- CO₂ waveguide laser, small signal gain, saturation intensity and volumetric output power 8-74880
- CO₂ waveguide laser, transversely RF excited 8-63127
- CO₂-N₂-H₂ electron beam controlled laser, efficiency and output energy depend. on H₂ 8-58978
- CO₂-N₂-He, fluorescent IR radiation from glow discharge 8-94386
- CO₂-N₂-He flowing gas mixture, glow discharge produced population inversion 8-78992
- ¹³CS₂ laser emission at 6.9 μ m, HF laser optical pump 8-58995
- Cd vapour laser LG-70, specification 8-74889
- Cs vapour heat pipe discharge tube pumping for 823 cm⁻¹ tunable IR laser 8-63069
- Cu, CuBr laser, continuously pulsed, long duration, high efficiency operation 8-79029
- Cu halide, transverse excitation, large active volume 8-59021
- Cu, using Cu acetylacetonate as Cu atom donor 8-82956
- Cu vapour, discharge heated longit., scaling 8-50790
- Cu vapour, explosively formed, apparatus for stimulated emission obs. 8-50764
- Cu, vapour electron energy distrib. function computation 8-71091
- Cu, vapour laser emission, pulse characteristics rel. to plasma parameters 8-71090
- Cu, vapour production method, hollow cathode arc, Ar buffer gas 8-86981
- Cu-Ne mixture, 3-20 kHz pulse discharge obs. 8-71092
- CuBr, continuously pulsed laser, cable-capacitor Blumlein discharge circuit, expt. characts. 8-82981
- CuBr laser, bubble gas effects on ground and metastable populations 8-82955
- CuCl, continuously pulsed laser, cable-capacitor Blumlein discharge circuit, expt. characts. 8-82981
- CuCl, potential, high-energy large vol. device 8-50807
- CuCl pulsed laser, time depend. of Cu-atom conc. in ground and metastable states 8-66806
- D₂O FIR lasers, reststrahlen laser resonator for 66 μ m line 8-55385
- D₂O, heterodyne meas. of IR absorpt. freqs. 8-55175
- D₂O, laser submillimetre with optical pumping energy yield, emission pulse delay time depend. on pumping pulse (Russian) 8-71088
- D₂O, pulsed laser-pumped submm amplifier, gain spectrum 8-79000
- Fe, pumping using KrF laser, vap. form. by flash and discharge decomp. of Fe(CO)₅ 8-74890
- Fe(CO)₅, photodissociation laser 8-74886
- H₂, Lyman system nonsaturated laser line intensity obs. 8-71089
- HCN compact CW laser optimisation 8-59022
- H₂O, IR ellipsometer for Si epitaxial layers meas., expt. 8-62219
- H₂O, pulsed oscill., elongation by admixture of He 8-87039
- H₂O vapour, 118.6 mm radiation absorption by H₂O vapour, temp. and press. effects meas. 8-75255
- He-Cd(Zn) hollow cathode laser, upper level decay rate, mag. field tuning dip meas. 8-87043
- He-F, doublet series laser lines near 700 μ m, hyperfine splitting and broadening meas. 8-63070
- He-F gas mixture, electron drift velocities, laser modelling 8-63061
- He-Ne, ¹²⁷I, frequency stabilisation, 612 nm and 640 nm 8-66871
- He-Ne, ¹²⁷I, stabilised, absolute wavelength measurements 8-73971
- He-Ne, ¹²⁷I, stabilised, freq. shifts, limitations 8-90440
- He-Ne, 6328 Å, single-mode collapse 8-94404
- He-Ne, anisotropy due to saturating fields 8-55337
- He-Ne, discharge reson. props. effect on radiation fluctuations, expt. 8-74883
- He-Ne, factors affecting service life (German) 8-90424
- He-Ne, fluctuation spectra of freq. and amplitude 8-82950
- He-Ne, high stability, single freq., 3.39 μ m 8-71121
- He-Ne, I₂, hyperfine component classification, suitability for laser wavelength stabilisation 8-86965
- He-Ne, I₂ stabilised laser, wavelengths comparison by two-beam interferometer 8-86326
- He-Ne, I₂ stabilised lasers, conf., Germany (Feb. 1977) 8-87069
- He-Ne, I₂ stabilised laser design, freq. reproducibility 8-87070
- He-Ne, I₂ stabilised laser research 8-87071
- He-Ne, I₂ stabilised laser with hot wall I₂ cell 8-87073
- He-Ne, I₂ stabilised lasers, length metrology (French) 8-87074
- He-Ne, I₂ stabilised laser, spectral profile modulation broadening 8-87083
- He-Ne, I₂ stabilised laser, instrumental freq. offsets 8-87084
- He-Ne, I₂ stabilised lasers, international intercomparison meas., hyperfine struct. spacings 8-87088
- He-Ne, I₂ stabilised lasers, beat frequency, international comparisons (French) 8-87090
- He-Ne, intensity fluctuations meas., comparison with He-Cd laser 8-71087
- He-Ne, laser frequency measurements: a review, limitations, extension to 197 THz (1.5 μ m) 8-81952
- He-Ne, laser transfer printing, microfilm 8-65994
- He-Ne, low noise manufacturing 8-79038
- He-Ne, manufacturing problems with low noise specification 8-59047
- He-Ne, methane and I₂ stabilised lasers, wavelength intercomparison using Michelson interferometer 8-87089
- He-Ne, microwave pumping advantages 8-50754
- He-Ne, mode selection and mode locking, effect on two-photon absorption efficiency 8-83023

gas lasers continued

- He-Ne, oscills. in laser discharge 8-55339
 He-Ne, population inversion radial distrib. in active element, excitation conditions effect 8-71079
 He-Ne, stabilised by I_2 saturated absorpt., technological principles (*French*) 8-87075
 He-Ne, standard wavelength sources 8-74957
 He-Ne, with methane absorpt. cell, hyperfine struct. influence on freq. reproducibility 8-50864
 He-Ne complex resonator laser, stabilisation 8-55374
 He-Ne internal mirror laser, degeneration of longitudinal modes and freq. stabilisation (*Japanese*) 8-90426
 He-Ne laser, 60 mW, perturbation spectroscopy (*Rumanian*) 8-50752
 He-Ne laser, I_2 stabilised, realisation of length unit 8-87068
 He-Ne laser, in axial mag. field, output power dependence of mode locking phenomena 8-71129
 He-Ne laser, output power, unsaturated gain distrib. 8-50751
 He-Ne laser freq. determ., interferometric comparison with upconverted CO_2 laser radiation 8-55395
 He-Ne laser plasma, line profiles meas. by optogalvanic spectroscopy 8-62233
 He-Ne laser status, I_2 vapour stabilised 8-87072
 He-Ne laser wavelength stabilisation on I_2 (*Czech*) 8-87061
 He-Ne lasers, I_2 stabilised, 633 nm line, performance improvement 8-90429
 He-Ne ring laser, nonlinear polarisation interaction of opposite waves 8-50828
 He-Ne ring laser, nonlinear Zeeman effect 8-71123
 He-Ne two-mode travelling-wave laser, Zeeman beats 8-50827
 He-Ne laser tube, using coaxial glass technique, LGR 7627 8-90410
 3He direct nucl. pumped laser, power density 8-58980
 3He -Ne stabilised by saturated absorption ^{127}I , laser wavelength standard development appl. (*German*) 8-79034
 Hg vapour laser, optically pumped, gain and output power 8-66843
 Hg- N_2 , optical pumping, vibr. excitation, laser theory 8-66517
 HgCl(B \rightarrow X) laser, photolytic pumping, HgCl(B) state radiative lifetime meas. 8-94390
 I, dye laser pumped to dissociation point of I_2 , laser action 8-63064
 Kr, laser, tunable, Lyman alpha radiation, nonlinear generation 8-87038
 KrF $^+$, waveguide laser excited by capacitively coupled discharge 8-94391
 N I, laser transition obs. at 9064 Å in He- N_2 afterglow 8-74891
 N_2 electron-beam-sustained discharge stability model 8-71608
 N_2 laser discharge emission model and meas. 8-71093
 N_2 , TEA, pump for dye laser amplifier system 8-82984
 NH_3 , high power, 12.08 μm , optically pumped, for appl. to UF_6 isotope separation 8-74923
 NH_3 , laser submillimetre with optical pumping energy yield, emission pulse delay time depend. on pumping pulse (*Russian*) 8-71088
 NH_3 , two photon excited 16 μm laser 8-58986
 NH_3 , two-photon-excited, 16 μm emission, wavelength meas. technique 8-71085
 N_2O IR laser, transients obs. by modulation of intracavity absorber 8-74933
 N_2O isotopes, laser transitions near 4.6 μm , HF laser optical pump 8-58995
 $^{14}NH_3$, two-photon pumping for 12.16 μm radiation for isotope separation 8-90414
 $^{15}NH_3$, far IR laser lines, optically pumped by CO_2 laser 8-90415
 Na, in shock heated salt vapour, anomalous emission from atomic lines 8-63089
 NaI, inversion and superfluoresce. emission of Na reson. line by selective photodissoc. 8-87040
 Ne 6328 Å laser transition, homogeneous saturation due to collisions, weak collision model 8-78995
 PH $_3$, laser emission 83 to 223 μm region, laser line assignments 8-71084
 Pb, long life operation at 7229 Å 8-79037
 Pb vapour, long-lived sealed-off laser design, 7229 Å emission 8-50808
 Rb, in shock heated salt vapour, anomalous emission from atomic lines 8-63089
 Rb vapour, dynamic Stark tuned far IR laser 8-63126
 Se photolytic fluorescence pumped gas laser system 8-62606
 Tb-Al-Cl vapour complex, fusion laser gain medium 8-63073
 $TbCl_3$ -AlCl $_3$, vap., high-energy laser medium props., for fusion ignition 8-63075
 UF_6 -He fission pumped nucl. laser, power deposition 8-58987
 Xe, 3.5 μm transition, quasi-Gaussian pulse propagation, effect on line-shape parameter anal. 8-55333
 Xe, 3.51 μm laser transition, phase-changing broadening, inert gas perturbers 8-82949
 XeF $^+$, waveguide laser excited by capacitively coupled discharge 8-94391

gas permeability *see permeability***gas phase electron diffraction**

- benzene, electron diffraction cross-section, finite scatt. geom. in mol. beam expt. 8-74803
 bicyclo [4.4.0] decane, cis and trans forms, mol. struct., electron diff., mol. mechanics 8-50658
 channel electron multiplier appl. for fast expts. 8-83684
 metal cluster generator for gas-phase electron diff., variation of microcryst. with size 8-63645
 molecular beam scattering, effect of finite scatt. geom. 8-74802
 partial wave electron scatt. factors evaluation 8-86963
 tetrafluoromethane, electron diffraction cross-section, finite scatt. geom. in mol. beam expt. 8-74803
 CO_2 , electron diffraction cross-section, finite scatt. geom. in mol. beam expt. 8-74803
 I_2 , electron diffraction parameters, spectrosc. calc. 8-70932
 O_2 , electron diffraction parameters, spectrosc. calc. 8-70932
 Pb microclusters, mol. beam electron diff., amorphous struct. 8-66703
 TaF_5 , gas phase electron diff. patterns, mol. struct., three-at. scatt. 8-66662

gas-surface interactions *see sorption***gas technology, natural** *see natural gas technology***gas turbines**

- Ar isotope separation by axial flow turbomachine model 8-78500
 NiAl, gas turbine material, oxidation, effect of gaseous NaCl 8-95853

gasdynamic lasers

- convective cooled fast flow high repetition rate CO_2 laser, pulse discharge stability 8-94389
 high energy laser system, optical distortion sources 8-83018
 MHD laser, admixture atom conc., automatic meas. system (*Russian*) 8-73123
 multipass CW gasdynamic laser cavity, simplified theory 8-63140
 CO_2 CW burning CO in air for pump energy, saturation parameters 8-71077
 CO_2 CW gasdynamic mixing lasers, pumped by N_2 or air, low stagnation temp. characts. 8-63053
 CO_2 , electric discharge gasdynamic 16 μm laser, high average power, high repetition rate 8-55381
 CO_2 gasdynamic laser, gain supersonic flow heating effect, condition optimisation 8-82947
 CO_2 laser, thermally pumped, output power enhancement by Ar gas addition 8-55336
 CO_2 mixing gasdynamic laser 8-71073
 CO_2 , rapid wavelength switching probe laser, J-line scan gasdynamic laser diagnostic 8-59044
 CO_2 , two-stage expansion of N_2 , supersonic nozzle 8-71076
 CO_2 - N_2 , gasdynamic laser mixture, vibr.-nonequilib. nozzle flows, numerical and approx. solns. 8-74881
 HCl- D_2 -He mixture 8-50761
 Li plasma dynamic laser, using supersonic nozzle, population inversion, excitation cross section 8-50760
 N_2O CW gasdynamic mixing lasers, pumped by N_2 or air, low stagnation temp. characts. 8-63053

gases

- see also aerodynamics; compressibility of gases; density of gases; dielectric properties of gases; diffusion in gases; electric breakdown of gases; electrical conductivity of gases; equations of state of gases; ionisation of gases; kinetic theory of gases; liquefaction of gases; luminescence of gases; Scott effect; Senfuleben-Beenakker effect; specific heat of gases; thermal conductivity of gases; thermal diffusion in gases; viscosity of gases*
 No entries

gauge field theory

- see also Weinberg model*
 8-vacua energy depend., P and T conservation in the presence of instantons 8-89628
 Abelian gauge field, $A_0=0$ gauge, canonical and path-integral quantisation 8-70277
 Abelian Higgs Kibble model, generalised Slavnov invariance, supersymm. struct. 8-78070
 Abelian Higgs model, two dims., multiple vacs. in lattice formulation 8-54543
 Abelian Higgs-Kibble model on lattice, spontaneous magnetisation 8-57870
 Abelian lattice gauge theory, quark confinement 8-66040
 anomalous currents in curved space 8-62336
 asymptotic behaviour of classical Yang-Mills fields in Minkowski space, Gribov ambiguities 8-93800
 Atiyah-Singer index theorem, local version for vector fields 8-58128
 axial gauge, canonical quantisation of non-Abelian gauge theories 8-70279
 axion emission in decay of excited nucl. states 8-49975
 axion mass in extended $SU(2)\times U(1)$ colour gauge theory 8-78080
 baryon-lepton symmetry model, μ -number and flavour nonconserving neutral currents 8-66069
 Becchi-Rouet-Stora transform. for gravitational field 8-93590
 Bethe-Salpeter eqn. for two fermion EM bound state systems 8-78058
 Bianchi identities for supersymmetric gauge theories 8-62299
 Bianchi IX metrics, self-dual asymptotically Euclidean, quantum gravity 8-65857
 bound states from instantons 8-78087
 broken $SU(3)$ gauge model of strong and EM interactions, scatt. lengths, baryon mag. moments 8-74133
 Cabibbo current and CP violation in a six quark gauge model 8-70329
 canonical Yang-Mills theory with invariant gauge families 8-74140
 charge-monopole composites, system of identical particles, statistics 8-93796
 charmonium, rel. to gluons, quantum chromodynamics theory 8-62362
 charmonium spectrum, relativistic and nonrelativistic theory 8-50010
 chiral $U(1)$ symmetry and CP invariance in presence of instantons 8-78075
 chirally extended supergravity, Maxwell-Einstein supergravity, auxiliary field struct. 8-78126
 classical interactions of 't Hooft monopoles 8-78233
 classical particle in Yang-Mills field, eqns. of motion and general covariance 8-74125
 classical Yang-Mills theory, screening solns., state external source 8-62302
 colour screening, $SU(3)$ gauge fields 8-82102
 complex structure of monopoles, instanton techniques, classical monopole eqns. 8-54537
 conformal relativity, kinematic theory of mass 8-77706
 conformal relativity, special, theory of mass 8-77707
 conformal supergravity, props., gauge theory 8-78085
 Coulomb scattering, Lee-Nauenberg theorem analysis 8-54595
 coupled Einstein-Higgs field, mag. monopole and dipole soln. (*Chinese*) 8-82112
 currents in $Su(5)$ and E_7 unified gauge theories 8-54600
 deep inelastic lepton-hadron scatt. in massive vector gauge models 8-74262
 deep-inelastic neutral-current cross-sections 8-66074
 dense matter, $U(1)$ symm. gauge model, eqn. of state 8-62500
 dipole ghost gauge theory as gluon model, confinement 8-66079
 disconnected gauge groups and the global violation of charge conservation 8-78086
 discrete finite nilpotent Lie algebras: new models for unified gauge field theory 8-66025

gauge field theory continued

discrete symmetries, Cabibbo universality, flavour mixing angles, in gauge model with six quarks 8-62346
 dressed fermions in Abelian gauge theories 8-82093
 dressed quark-gluon vertices, instantaneous approx. 8-78091
 dual charges, U_1 gauge field in SU_n gauge field (Chinese) 8-86417
 E6 unified gauge model, breaking patterns, quark-lepton symmetry and mass scales 8-86434
 education, EM wave interaction with matter, gauge invariant formulation 8-62006
 education, gauge invariance, analogy with relativity, particle internal symmetry 8-49595
 embeddings of gauge groups in Yang-Mills theory, $SU(3)$ case 8-93802
 Euclidean field theory, nonclassical configs. as minima of constrained systems 8-70256
 exceptional gauge theories in 3×3 matrix formalism 8-70248
 extended hadrons and quark confinement, description using nonlinear De Sitter symmetry 8-58140
 extended supergravity, eqns. of motion in terms of geometrical quantities in superspace 8-65856
 extended supergravity, three loop counterterms, nonrenormalisability 8-65854
 Fermi quantisation of Landau gauge 8-54591
 fermion and boson fields interacting with gravitational fields 8-86208
 fermion fields, spin $1/2$, $3/2$, accelerated states, stress-energy tensor vac. expectation value 8-70313
 fermion fields, vanishing theorem, harmonic spinors 8-62314
 fermions on the hypertorus 8-74149
 Feynman rules for lattice gauge theory of quark confinement, Green's functions, review 8-93850
 fibre bundle techniques in gauge theories 8-54573
 fibre bundles, gauge theory of strong and EM interactions 8-54574
 fibre-bundle approach to gauge field theory 8-58130
 four dimensional gauge theories, classical mass spectrum quantum corrections using supersymmetry algebra 8-89630
 fundamental length hypothesis, concept in gauge vector field theory 8-93836
 G_1 , spin depend. struct. function, scaling violations 8-93880
 gauge invariance, minimal coupling, and torsion 8-78084
 gauge theories, an introduction for experimental particle physicists 8-82119
 gauge variables and singular Lagrangians 8-78063
 general relativity, superspace, local supersymmetry, superfibre bundle theory 8-77782
 general-relativistic and gauge field theories 8-86212
 geometric gravity Lagrangian, $SP(4)$ and general coord. transforms. 8-70039
 geometrical gauge theory of gravit., strong interactions, EM interactions 8-70041
 gravitation, appl. of Palatini-type variational principle to $SL(2, C)$ gauge invariant Lagrangian density 8-78059
 gravitational field quantised using Feynman path integral 8-73914
 gravitational instanton, CP^2 props. compared with $SU(2)$ Yang-Mills instanton 8-81909
 gravitational instantons and universal spin structs. 8-78128
 Gribov ambiguity, gauge transform. on set of all connections of principle bundle 8-58108
 Gribov ambiguity, same origin as spin $3/2$ field problem 8-93808
 gauge fixing problem around classical solns. of Yang-Mills theory 8-70260
 hadron mass, instanton effects on light quark spectroscopy, MIT bag model 8-62372
 hadron mass spectrum in lattice gauge theory 8-74139
 hamiltonian formulation of non-Abelian gauge fields and nonrelativistic bound states 8-70280
 heavy stable neutral lepton, astrophysical consequences of existence 8-93091
 Higgs boson, spontaneously broken gauge theory phenomenon, possible weak interaction model 8-74200
 Higgs mechanism in temporal gauge 8-70278
 Higgs meson prod., possible signals in high energy collisions, gauge groups 8-89649
 Higgs-Kibble mechanism, superfield theoretical treatment 8-89616
 Higgs-Kibble mechanism and electron-muon mass ratio 8-66065
 indefinite metric quantum field theory of general relativity 8-65853
 indefiniteness of gravitational action, path integrals convergence, one-loop approx. 8-70318
 instanton effective size estimate from gluon field strength tensor vacuum expectation value 8-70326
 instanton effects on axion mass 8-58127
 instanton soln., Dirac eqn. 8-82100
 instantons, numerical significance at short distances 8-70339
 instantons and infrared divergences 8-70284
 instantons and restoration of symmetries 8-66033
 instantons on line, gauge equivalence to fields 8-62310
 IR singularities in gauge theories, renormalisation group method, coupled massless field theories 8-54538
 jet processes in QCD 8-82104
 Lagrangian formalisms with CPT violation, causal Lagrangian, gauge theories 8-62303
 Landau gauge, commutators for integer spin fields 8-93807
 lattice Coulomb gas representations of two-dimensional problems 8-70068
 lattice gauge theories with fermions, cluster expansion 8-58119
 lattice gauge theories with fermions, phase transitions and renormalised struct. 8-82105
 lattice Schwinger model, form factors of dipole states 8-66029
 left-right symm. gauge theories, CP violation, absolutely stable hadrons 8-74155
 left-right symmetric $SU(2)_L \times SU(2)_R \times U(1)$ gauge theory, atomic P violation 8-74144
 lepton pair prod., hard-scatt. expansion 8-66091
 lepton-hadron deep inelastic scatt., massive vector gauge model (Russian) 8-89720
 Lie algebras, BRS transform. 8-93591
 linearised $GL(4)$ gravities, dynamical structure 8-65846
 local covariant gauge quantum field theories, cluster property 8-70265
 locally supersymmetric theories with model-independent transformation laws 8-93819

gauge field theory continued

loop phase factor approach, equivalence problem, space-time symm. (Chinese) 8-82110
 lorentz transformations of observable and ghost particle states in quantum electrodynamics and in a massive gauge theory 8-66061
 macroscopic gauge theory of gravity, uniform gravitational collapse, lepton pair creation 8-81724
 magnetic monopoles in broken SO_3 and SU_2 gauge theories (Chinese) 8-86459
 magnetically extended Lagrangian theory, $O(3)$ gauge theories with spontaneous symm. breaking, shared photon sector 8-62306
 Mandelstam-'t Hooft duality in Abelian lattice models 8-78057
 massive gauge fields, complete spontaneous symm. breaking, asymptotic freedom, symplectic and G_2 groups 8-62305
 massive Schwinger model, asymptotic completeness and confinement 8-66028
 massive Schwinger model, consistency and Lorentz invariance 8-89613
 massive Schwinger model, vacuum degeneracy and confinement 8-78090
 massive supergravity, from spontaneous breaking orthosymplectic gauge symmetry 8-77787
 massless QCD 8-78093
 massless spin two field, covariant quantisation in general covariant gauge 8-66027
 meson wave functions in $1+1$ dimens. QCD 8-54559
 mixing of leptons with different quantum numbers in gauge theories of weak and EM interactions (Russian) 8-54601
 monopole, accelerated, field strength determ. (Chinese) 8-77740
 monopole solns. in spontaneously broken $SU(n)$ gauge theory 8-82103
 mutually interacting charge fields, gauge theoretical formulations of elementary particle processes 8-58122
 $N=2$ supergravity with gauged central charge 8-62349
 $n=4$ supergravity theory with local $SU(2) \times SU(2)$ invariance 8-66067
 N-O model, quantum expansion around vertex type soln., energy eigenvalue (Chinese) 8-82111
 Nambu-Jona-Lasinio type unified model for gravitational and EM forces 8-65850
 neutrinos, gauge theories, EM props., forbidden processes and currents with anomalous Lorentz struct. 8-54599
 non-Abelian gauge theories, constraints on finite energy solns. 8-58117
 non-Abelian group $SU(2)$ mag. monopole (Chinese) 8-78096
 non-Riemannian generalised super-gauge formalism, corresponding invariant physical theory 8-82122
 nonAbelian gauge model, Becchi-Rouet-Stora invariant, superfield struct. 8-74121
 nonabelian gauge theories, coherent state approach to IR behaviour 8-82107
 nonAbelian gauge theories, gauge fixing degeneracies, confinement 8-54545
 nonAbelian gauge theories, path depend. phase factors, point splitting 8-49959
 nonAbelian gauge theories, quantisation 8-78066
 noncompletely reducible representations of the Poincare group associated with the generalised Lorentz gauge 8-70249
 nonlinear gauge fields and the structure of gravity and supergravity theories 8-77791
 nonlinear Lagrangians and spontaneous symm. breaking 8-70303
 nonperturbative gauge technique soln. for Schwinger model of 2-dimens. electrodynamics 8-78120
 nonrelativistic algebraic models, gauge invariance, causality props. 8-62319
 nucleon structure function, asymptotically free gauge theory 8-50036
 null gravodynamics, initial value problem and Dirac-bracket relations 8-77781
 $O(3)$ σ -model, nonlinear, quantum fluctuations of instanton solns. (Russian) 8-74161
 observable phase factors and symmetry of electric and magnetic charges 8-86428
 one loop finiteness of quantum gravity off mass shell 8-62142
 order-disorder transitions in gauge and spin systems 8-70072
 particles in curved space-time, group of parallel transports 8-54602
 partition function of degenerate quadratic functional and Ray-Singer invariants 8-54531
 perturbation expansion of quantised composite field theory, gauge invariance (Chinese) 8-82156
 perturbative QCD and exptl. signatures of weak bosons 8-93916
 phase transition in nonAbelian quantised gauge field theories, permanent quark confinement 8-70322
 potential scatt., amplitude, quasiclassical asymptotic behaviour, quantum correction 8-62325
 preon model for hadron and lepton struct. 8-78124
 proceedings of the 1977 CERN-JINR School of Physics, Nafplion, Greece (May-June 1977) 8-81726
 projective invariance in general space times with spinor, torsion and Yang-Mills fields 8-57832
 pseudoparticle fields, propagation functions 8-54556
 pseudoparticle fields, role of fermionic zero modes 8-74159
 QCD, μ pair transverse momentum distrib. in Drell-Yan processes 8-62374
 QCD, axial gauge, mass shell behaviour 8-49966
 QCD, dynamical props. 8-70332
 QCD, e^+e^- annihilation energy, asymptotically free perturbation theory 8-66045
 QCD, electric field representation without gauge field constraints 8-93846
 QCD, field strength and action copies in any axial-like gauge 8-82143
 QCD, gauge independence of IR cancellation, fermion-fermion scatt. 8-50006
 QCD, gluon colour screening by Higgs mechanism 8-93861
 QCD, hard processes, universality of mass singularities 8-82101
 QCD, infinite-mass limit determ. 8-66039
 QCD, lattice-gauge theory calc. of π and ρ -meson decay consts. 8-74154
 QCD, strong interaction gauge theory, $SU(3)$ colour gauge vector mesons, confinement 8-78136
 QCD, two-dimens. extrapolation to four-dimens. 8-78081
 QCD and polarised quarks (Russian) 8-74217
 QCD effects, parton transverse momenta, large- p_t hadron prod. 8-66083

gauge field theory continued

- QCD estimates for heavy-particle prod. 8-82108
 QCD invariant charge, study of gauge theory by Lipatov's method (*Russian*) 8-74220
 QCD of highly condensed matter 8-70267
 quadratic Poincare gauge theory of gravitation, short range confining component 8-89388
 quantisation, using path integral procedure, physical state Hilbert space construction 8-82106
 quantum fluctuations of instantons 8-54530
 quark confinement in condensate of non-Abelian vortices 8-70328
 quark electric dipole moment from CP noninvariant gauge theory, left handed currents (*Russian*) 8-74218
 quark-antiquark pot., charmonium model modifications, spin forces and instantons 8-93842
 quarks and leptons, fermion physics in terms of $SU(2) \times SU(1)$ gauge theory 8-74197
 quasiperiodic boundary conditions, vac. struct., in gauge theories, quantum mech. analogue 8-70255
 quaternion model, gauge theory for leptons and quarks (*Russian*) 8-62315
 radiation gauge static pot. between fermion and antifermion, non Abelian gauge fields 8-89621
 radiative corrections in gauge theories, QCD current algebra formulation, weak interaction universality 8-93883
 radiative corrections to parity violation in atoms in $SU(3) \times U(1)$ gauge theory 8-62402
 real-time approach to instanton phenomena, multidimensional pots. with degenerate absolute minima 8-78067
 recursion eqns. for renormalisation group transforms. in lattice gauge theories including fermion variables 8-62298
 Regge behaviour of spontaneously broken non-Abelian gauge theory 8-70287
 relativistically invariant two-dimens. models, classification method (*Russian*) 8-70291
 renormalizable interactions in two dimensions and sharp-time fields 8-81882
 scalar and $SO(3,1)$ gauge Minkowskian field theory, instanton solns. 8-49956
 scalar-vector instantons in n-dimens., surface terms 8-49958
 scaling violation in infinite-momentum frame 8-70286
 Schwinger model, $A=0$ gauge, breaking of chiral symm. 8-62307
 Schwinger model, chiral symm. breaking and vac. struct. 8-89615
 self-dual gauge field, Green function 8-82099
 self-dual $SU(2)$ gauge field, Pontryagin density 8-66044
 semisimple unified gauge theories 8-70282
 seven lepton model, quantum flavour dynamics, mixing angle, masses, spontaneous symmetry breaking 8-89652
 singular gauge transformations, monopole vortex line systems, Nielsen Olsen $SU(2)$ Higgs model, Nambu model 8-66034
 $SL_{2,c}$ gauge theory of gravit., Lagrangian approach 8-77777
 SO_4 , $SL_{2,c}$ classical gauge field eqns., isotropic and solitary-wave solns. 8-93795
 $SO(3, 1)$ gauge field, Einstein-Weyl-Yang system, strong gravity model 8-86201
 soft CP violation, renormalisable gauge model for strong, weak and EM interactions 8-74196
 soft graviton emission in scatt. processes, linearised gauge theory 8-49746
 sourceless, gauge fields, natural connections on Stiefel bundles 8-58118
 space translation, gauge invariant, spinor field-electromag. pot. (quantised or unquantised) interaction 8-62296
 spinor monopole soln. (*Chinese*) 8-78097
 spontaneously broken symmetry restoration in mag. field, massive charged vector meson effects (*Russian*) 8-74178
 stability and supersymmetry, models with local gauge symmetry, renormalisation group anal. 8-70296
 string tape solns., in classical gauge field theories, broken gauge symmetry 8-62317
 strong gravity, supersymmetric theory for f- and g-gravitons and massive gravitinos 8-62141
 SU_2 gauge model, light neutral gauge boson, consequences for e^+e^- and $pp(\bar{p})$ reactions 8-58154
 $SU_2 \times U(1)$ gauge models and neutral current reacts. 8-89648
 $SU(4) \times U(1)$ as gauge symm. for quark, lepton quartets, weak and EM interactions, weak currents 8-74174
 $SU(2)_c \times SU(2)_L \times U(1)$ gauge symm., Higgs particles, parity conservation 8-70305
 $SU(2)_c \times U(1) \times SU(2)_L$, model for lepton decay and neutrino lifetime 8-62331
 $SU(2) \times U(1)$ gauge theories of weak and EM interactions, neutral current constraints 8-70272
 $SU(2) \times U(1)$ unified gauge theory threshold effects 8-82098
 $SU(2) \otimes U(1) \otimes U(1)$ gauge model without parity violation in heavy atoms 8-82097
 $SU(2) \otimes U(1)$ gauge model of EM and weak interactions, fermion mass restriction (*Russian*) 8-89650
 $SU(2)$ gauge field, ground state wave functionals 8-74142
 $SU(2)$ gauge fields, classification 8-70281
 $SU(2)$ gauge fields, eigenspinor-eigenvalue eqn. 8-78076
 $SU(2)$ gauge fields, sourceless solns. of static monopole systems (*Chinese*) 8-86418
 $SU(2)$ gauge fields in Minkowski space-time reparametrisation invariant formulation 8-70257
 $SU(2)$ gauge group, magnetic monopole as finite energy smooth soliton soln., review 8-89625
 $SU(2)$ gauge model, classical soln. instability 8-93806
 $SU(2)$ gauge theory, polarised eN scatt. anal. 8-58193
 $SU(2)$ group potentials (*Chinese*) 8-78098
 $SU(2)$ instanton, physical interpretation of degrees of freedom 8-62312
 $SU(2)$ vacuum gauge field, chiral connection with ferromagnetism and axisymmetric gravitational problem 8-70258
 $SU(2)$ Yang-Mills theory in Coulomb gauge, quantisation 8-54546
 $SU(3)_c \times SU(3)_L$, as gauge groups of weak and associated charges, symm. breaking 8-74175
 $SU(3) \times U(1)$ gauge theory of weak and EM interactions 8-70317
 $SU(3) \times U(1)$ modified model, quark and lepton mass hierarchy 8-89653
 $SU(4)$ gauge fields, pseudoparticle solns. (*Chinese*) 8-74128

gauge field theory continued

- $SU(6)$ based renormalisable unified gauge model with calculable masses 8-89647
 $SU(6)$ unified gauge group, neutral current coupling to ν_μ and ν_τ 8-54626
 super-gauge symmetry in general relativity, Einstein's A transformation (*German*) 8-86199
 supergravity, auxiliary fields for closed algebra using S-matrix 8-81911
 supergravity, geometry of superspace, vector-spinor matter 8-49744
 supergravity, ghost counting on one-loop level of Rarita-Schwinger field, gauge fixing 8-93589
 supergravity, locally invariant supersymmetric gauge field theory 8-49742
 supergravity, minimal set of auxiliary fields, gauge algebra closure 8-49743
 supergravity, Poincare and conformal, multiplication rule and supersymmetric densities for multiplets 8-70037
 supergravity, Poincare and conformal models with closed algebra 8-74198
 supergravity, Weyl and Einstein, unified approach to matter coupling 8-54275
 supergravity in 11 dimens., action and transform. laws 8-70038
 superspace, generally covariant theories of gauge fields 8-54568
 supersymmetric gauge models of weak and EM interactions 8-58106
 supersymmetric nonlinear σ -model in 4-D, coupling to supergravity 8-49981
 supersymmetry algebras with central charges, $SU(4)$ invariance, gauge theory 8-70301
 symmetry breaking and space-time geometry 8-54533
 taming of the dipole ghost in relativistic quantum field theory 8-66035
 tetrad gravitational field, weak principle of equivalence and gauge theory (*Russian*) 8-62135
 topological excitations in Abelian Higgs model 8-70275
 transverse pure gauge fields and nonlinear chiral solitons, Coulomb condition 8-78068
 trimuon production by neutrinos, heavy lepton cascade mechanism using $SU(2) \times U(1)$ gauge model 8-58180
 two loop calculation about quantum mech. instanton, test of tunnelling 8-58126
 two-dimens. $U(1)$ -Goldstone model, QFT on lattice 8-74158
 $U(2)$ invariant solutions to Yang-Mills equations in compactified Minkowski space 8-70262
 unified field theory bounds on number and masses of quarks and leptons 8-58151
 unified gauge field theory with torsion, symmetries 8-89386
 unified gauge theories and the baryon number of the universe 8-85842
 unified $SU(3) \times U(1)$ gauge theory with different muon and electron neutral currents 8-58152
 unified theory of direct interaction between particles, strings and membranes 8-86433
 unified theory of gauge fields and supersymmetry 8-58150
 unified weak and EM interactions, semi simple $SU(3)_L$ gauge groups for hadrons 8-74195
 unitarising high energy scatt. amplitudes in field theory QED 8-62341
 unitary gauge, ambiguities and breakdown configs. 8-93798
 universal CP noninvariant superweak interaction and baryon asymmetry of the universe 8-66072
 vacuum gauge field for Yang Mills theory in Landau gauge 8-70259
 vacuum polarisation induced by intense gauge field, renormalisation group method 8-49994
 vacuum structure of $SU(3)$ gauge field theory in Coulomb gauge 8-62311
 vector meson masses, possible bounds on their ratios in gauge hierarchies 8-93791
 vortex strings, mag. monopoles in gauge field theory 8-70283
 VV+AA type gauge models, effective ν interactions 8-66038
 weak and EM interactions with $SU(3) \times U(1)$ symmetry 8-58153
 weak external gauge fields, energy levels, modified functional measure 8-49973
 weak interactions of ultra heavy fermions 8-93838
 Weinberg model, universality and weak isospin leptons, nucleons, quarks 8-70273
 Yang's R gauge for self-dual $SU(3)$ gauge fields 8-78088
 Yang-Mills fields, quark confinement and Gribov ambiguities in Coulomb gauge 8-62297
 Yang-Mills self-dual solns. and a superposition principle 8-82096
 Yang-Mills-Higgs $SO(3,1)$ gauge theory, classical solns. 8-54550
 e^+ -nucleus parity violating neutral current interaction, gauge theory predictions, radiative corrections 8-86436
 $e^+p \rightarrow e^+\nu + X$, deep-inelastic bremsstrahlung, quark charges, colour gluon mass 8-74216
 $\gamma\nu$ weak interaction, spontaneous breakdown of γ and gauge symm. at finite temp. 8-70299
 μ , (g-2) value, second order weak correction in arbitrary gauge models 8-62301
 $\mu \rightarrow \bar{\nu}_\mu \pi^+$, hypothetical, search for scalar charged boson, apparatus and theoretical aspects 8-58177
 μ pair prod., QCD ang. correl. 8-49976
 μN deep inelastic scatt., asymm., quark proton model evaluation, gauge theories test 8-62408
 $np \rightarrow d\gamma$, γ -polarisation, NN weak pot. in simple gauge model 8-54644
 ν oscills., weak-interaction-induced, gauge models 8-70359
 ν_μ transition magnetic moment 8-78168
 $\nu_\mu(\bar{\nu}_\mu)p \rightarrow \nu_\mu(\bar{\nu}_\mu)p$ hadronic neutral current, final-proton polarisation 8-82200
 π prod. by weak neutral current, comparison of gauge theory models 8-82139
 Y(9.4) family, gauge theory mass anal., harmonic oscillator pot. 8-82186
 Y(9.5) hadronic prod., parton distrib. and QCD 8-78142
 Y(9.5), implications of Y for ν interactions in weak gauge theories 8-70271

Gaussian noise see random noise

Gaussian orbital calculations see GO calculations

Gaussian-type orbital calculations see GTO calculations

Ge-Si alloys

dilute, impurity concentration effects 8-75777

Ge-Si alloys continued

- jet thinning apparatus for foil prep. 8-88589
 lattice thermal conductivity rel. to grain size and carrier conc. 8-91495
 n-type, phonon thermal cond. of hot pressed alloy, 300-1100K 8-91494
 phonon boundary scatt., reduction of lattice thermal cond. 8-55921
 Si-Ge (22 at.%) alloy, thermoelec. props., time and temp. dependence 8-91712
 Si-Ge:Al, B, P, hot-pressed alloy, thermoelec. props. 8-91711

gegensehein *see zodiacal light***Geiger counters**

- CANDU, development of irradi. fuel bundle counters for reactor safeguards systems 8-94119
 counting loss correction using anticoincidence gated scaler and a live timer 8-86737
 fast neutron sensitivities of Geiger-Mueller counter γ dosimeters, mixed field dosimetry 8-92705
 ^{41}Ar release from TRIGA reactor, comparison of γ -ray detectors 8-57309

Geiger Muller counters *see Geiger counters***gelatin***see also gels*

- films with Fe, Cu, Ag and S containing compounds, IR spectra (*Russian*) 8-49928
 hardened layer structuralisation, kinetic anal. using swelling 8-62255
 holographic optical element fabrication using dye-sensitised dichromated gelatin 8-63043
 IR spectroscopic study of effects of impurities and other actions, fine struct. (*Russian*) 8-58083
 Fe, corrosion pitting in acid, alkaline solution, gelatin effect 8-95838

gels

- biopolymer negative resistance, rel. to living cell props. 8-64923
 branched polymers near gelation threshold, field theory statistics 8-91220
 cement paste, hardened, physics and chemistry 8-73013
 contact lens gel materials for extended wear, water flow cond. 8-81062
 critical concentration fluctuation dynamics, near phase separation 8-56921
 defibrillator electrode gel testing, meas. of impedance to transthoracic DC discharge 8-57056
 dynamic light scattering theory 8-60475
 gels, dynamic light scattering in poor solvent 8-88318
 graph-like state of matter, electrical cond. of random networks, gelation and elasticity 8-65875
 lipid phase transition, cluster model, appl. to bilayer mol. passive permeation and struct. relax. 8-53346
 PET, filament form. from gels 8-80508
 polyacrylamide-water gels, copolymerised with N,N-methylene bisacrylamide, dynamic light scatt. 8-60477
 polymer gelation, crit. percolation probabilities, appl. to hard sphere packing expt. 8-61063
 polymer solutions, microgel-containing, physico-chem. and rheological props., light scatt. obs., review (*Polish*) 8-50704
 polysaccharide gels and sols, PMR relax. times rel. to temp., pH and conc. 8-56952
 polystyrene, porous gel, solute elution behaviour in high performance liq. chromatography 8-92524
 precipitation, spontaneous pattern formation, symmetry breaking instabilities 8-80792
 rheological properties, Weiler-Rhebinder method, polymer conc. (*Russian*) 8-53274
 sickle haemoglobin gelation, reaction order and crit. nucleus size 8-76983
 silica, ion exchanger, isotope separation appls. 8-86961
 silica (metallised) gels, thermal cond., 10-200K, cryogenic appls. 8-79828
 silica gel, fixed substance identification using Raman spectroscopy (*French*) 8-88664
 silica gel, polymer adsorption into surface pores, computer simulation, phase transition (*Russian*) 8-51824
 silica gel, skeletal struct. modification with alcohols and water vap., thermal analysis obs. 8-88659
 silica gels, surface treatment, adsorption properties (*Japanese*) 8-95855
 silicic acid sol., gel formation, characteristics of light scattering 8-53269
 sol-gel transition, sol viscosity, Rouse approx. (*French*) 8-61054
 soya protein gels and sols, PMR relax. times rel. to temp., pH and conc. 8-56952
 Al_2O_3 hydrated gel synthesis by homogeneous precip. method using NaAlO_2 , phase change by heating (*Japanese*) 8-68937
 SiO_2 gel. struct., IR spectra obs. 8-88297
 SiO_2 - ZrO_2 adsorbents, coprecipitated, porous struct. rel. to form. conditions 8-53263

general relativity

- see also cosmology; gravitation; gravitational red shift; Schwarzschild metric; space-time configurations; unified field theories*
 algebraic type of space-times possessing a nonsingular killing horizon 8-62126
 anisotropic uniform model universes with cosmical const., flat space 8-73788
 anisotropy damping through quantum effects in early universe 8-57708
 anomalous currents in curved space 8-62336
 Barotropic fluid in semi-Riemannian manifold, classical and relativistic vorticity 8-65842
 Bel-Petrov field classification, algorithm 8-93566
 Bianchi VIII/IX cosmological models, anisotropic, with matter and EM fields 8-73784
 binary stars, gravit. waves interaction, tidal reson. 8-93089
 binary system with compact objects, static two-body problem and attraction law 8-93574
 black holes, Robinson's identity, EM generalisation 8-81649
 black holes, stationary, uniqueness theorems 8-96500
 Bonnor electrovac counterparts of Tomimatsu-Sato solns. of Einstein eqn. 8-57835
 book, relativistic theories of materials 8-81907
 bound states of nonlinear scalar field in general relativity 8-77778

general relativity continued

- bounded system of extended bodies, relativistic eqns. of motion 8-73898
 Brans Dicke's scalar field, geometrisation 8-54258
 Brans-Dicke theory, EM solns. 8-57841
 C-metric black hole solution to vac. Einstein field eqns. 8-89216
 Cauchy problem for general relativistic perfect magnetofluid 8-70024
 Cauchy surfaces, determ. from intrinsic props. 8-70023
 charge in cosmological models, effect on curvature parameter 8-69921
 charged body free fall motion in gravit. field, field energies and equivalence principles 8-49740
 charged fluid, orthonormal tetrads in general relativity 8-54269
 charged fluid sphere, exact interior solns. of Einstein-Maxwell field equations 8-62122
 charged Kerr-Tomimatsu-Sato family of solns. 8-62130
 charged particle motion, charged Robinson Trautman soln. 8-62124
 charged rotating bodies, generation of metrics 8-49735
 charged stationary axially-symm. metric 8-62131
 chirally extended supergravity, Maxwell-Einstein supergravity, auxiliary field struct. 8-78126
 Christoffel symbol, generalized, extension to projective quaternion space (*Rumanian*) 8-81892
 chronogeometry and dyadic method (*Russian*) 8-65826
 classical pseudoparticle solutions in general relativity 8-89390
 classical quark confinement from general relativity 8-58162
 collapsing relativistic stars, linearised odd-parity radiation 8-93297
 complex line bundles 8-49732
 conformal invariant model of localised spinning test particles 8-49729
 conformal relativity, classification of metric bosons 8-93803
 conformal relativity, particle species classification, symms., space time origin of isospin 8-93815
 constitutive theory of general relativistic EM fluids 8-57843
 continuous media with spin 8-57845
 coordinate identification in line elements, isometries, Killing solns. 8-54252
 cosmological models with Hoyle's hypothesis 8-86045
 cosmological principle, new look 8-86042
 cosmology, general relativity, big bang model, nucleosynthesis, scale covariant theory, review 8-73789
 covariant eqns. of relativistic electrodynamics of continua 8-57842
 cylindrical general relativistic collapse, numerical study results 8-93585
 decomposable differential operators in cosmological context 8-57825
 deformations of the embedded Einstein spaces 8-54254
 differential geometry, math. model 8-69968
 differential geometry in infinite dims., dynamical formulation of general relativity 8-93582
 discontinuity surface, local interior-exterior distinction 8-70030
 early Universe, EM and gravit. Green's functions 8-73786
 Einstein's eqn., exact vac. solns. from linearised solns. 8-65833
 Einstein's eqns., characterisation of Tomimatsu-Sato stationary solns. 8-65835
 Einstein's field equations, exact solns., nonstatic charged fluid spheres 8-89370
 Einstein's field equations, homogeneous solns. 8-65824
 Einstein's field equations for charged static spheres of fluid, exact interior solns. 8-73892
 Einstein's field equations with zero-rest-mass scalar fields, wave solns. 8-89373
 Einstein's matter free theory of gravit. construction using Yang Mills theories 8-70026
 Einstein's theory of gravitation generalised using tetrad field to avoid singularities 8-57833
 Einstein's vacuum equations, class of self-dual solns. 8-81900
 Einstein eqns., classification system for one Killing vector solns. 8-93579
 Einstein eqns., plane wave solutions 8-70022
 Einstein equation, exact solns. (*Russian*) 8-65825
 Einstein equations with zero-rest-mass scalar meson field 8-70021
 Einstein Maxwell space-times with symms., nonnull EM fields 8-65823
 Einstein-Cartan, Friedmann-like cosmological models without singularities 8-77632
 Einstein-Cartan theory, bounce of spheres 8-93572
 Einstein-Cartan theory of gravitation in a Hamiltonian form 8-93581
 Einstein-Maxwell eqns., axially symmetric stationary solns. 8-93576
 Einstein-Maxwell equations, family of solns. 8-89375
 Einstein-Maxwell equations, some Robinson-Trautman solns. 8-89374
 Einstein-Maxwell field, stationary, axisymmetric generation method 8-86202
 Einstein-Maxwell field eqns., new solns. from electrovac space times with isometries 8-62128
 Einstein-Maxwell fields, with null Killing vector 8-65821
 Einstein-Maxwell homogeneous fields 8-65829
 Einstein-Maxwell stationary axisymmetric eqns., exact solns. 8-93578
 elastic solids, constitutive theory 8-57844
 elasticity and electro-magneto-elasticity 8-70025
 elastomechanics, compatibility relations (*German*) 8-81902
 electrodynamic and gravitational effects of Proca stresses in astrophys. 8-93098
 EM null point source intensity in stationary spherically symmetric space-time 8-57839
 energy loss in scattering problems, Einstein quadrupole formulae 8-89379
 energy momentum tensor symmetries, concomitant conservation laws, Einstein massless scalar meson field appl. 8-86205
 energy tensor definition for system of charged particles and EM fields 8-77734
 energy-momentum in general relativity 8-54263
 energy-momentum tensor, effect of motions, meson field and perfect fluid 8-73903
 expanding universe effect on quantum mechanics of electromag. bounded spin 1/2 particles 8-54271
 field theory approach to gravitation 8-81910
 five-dimensional theory, conditions of existence of horizons 8-73907
 formalism of external forms and non-inertial reference systems (*Russian*) 8-81894
 Friedmann cosmological models, relativity of space finiteness-infiniteness 8-96582
 galaxies and quasars paradoxical redshifts compatibility with gravitation theory 8-73757

general relativity continued

gauge conditions anal. 8-70031
 Gauss-Hertz principle continuum form, derivation of general relativity in time domain 8-73851
 generalised Peres space-time plane wave-like solns. of weakened field eqns. 8-57827
 generalised Takeno space-time, coupled EM and zero-rest-mass scalar meson fields 8-70020
 Godel universe, scalar perturbations 8-57709
 gravitation theories derived from nonlinear Lagrangian with limiting curvature 8-81897
 gravitation wave propagation in expanding universe 8-73787
 gravitational analogue of mag. monopole, Mandelstam path-dependent formalism 8-81898
 gravitational collapse, Einstein's gravitational equations, local and global modifications 8-61719
 gravitational constant variation with time, Dirac's extension of general relativity (*Norwegian*) 8-69674
 gravitational field energy localisation, logic 8-49728
 gravitational inertial field and critical systems, free motion 8-93484
 gravitational inertial field eqns., Lagrangian density, Hubble law 8-93483
 gravitational radiation and invariants of curvature tensor in general relativity 8-57836
 gravitational waves detector, appl. of photon-graviton resonance, technical problems, expt. possibilities 8-73905
 gravitational-inertial field of Universe, generalised metric tensor theory 8-89275
 gravitationally nondegenerate Bianchi type I cosmological model 8-93490
 H-space, metric and curvature props. 8-89376
 Hamilton-Jacobi equation for free particle in Riemann space (*Russian*) 8-73901
 Hawking effect and Euclidean QFT 8-73732
 hierarchical cosmology, exact model 8-69917
 ideal liquid, general theory of relativity, introduction of canonical variables in hydrodynamic eqns. 8-63510
 indefinite metric quantum field theory of general relativity 8-65853
 indefinite-metric QFT of general relativity 8-89391
 inhomogeneous cosmological models containing spacelike and timelike singularities alternately 8-69925
 interstellar flyby missions, relativistic effects 8-61729
 isolated gravit. systems, energy-momentum and ang. momentum 8-73900
 isometry Lie algebras, new technique for struct. anal. 8-65831
 isotropic models of Universe, regularisation of fermion stress-energy tensor 8-81725
 Kasner type solns. to field eqns. generated by square of secular curvature 8-54256
 Kerr and Tomimatsu-Sato metrics from group transformation, rot. vacuum soln. 8-65838
 Kerr metric, vector solns. to generalised almost Killing eqn. 8-65830
 Kerr metric, vortical type geodesics, causality non-violation 8-54251
 Kerr metric sources, ellipsoidal space-times 8-54249
 Kerr naked singularity, classical instability 8-57834
 Kerr-Newman background space, nonstatic nuclear forces, meson field at black hole event horizon 8-61880
 Kerr-Schild generalised metric and Einstein-Maxwell fields 8-77783
 Kerr-Taub-NUT soln. generalisation 8-49734
 Kerr-Tomimatsu-Sato family of solns. with nonintegral distortion parameter 8-86204
 Killing tensors, symmetric and skew symmetric 8-93573
 Killing vectors in plane HH spaces 8-54104
 Lie algebras, BRS transform. 8-93591
 light deflection by Sun, principle of equivalence calcs. 8-81729
 Lorentz transformation, generalised, and behaviour of physical quantities at R- and T-region boundary (*Russian*) 8-49725
 magnetofluid, self-gravitating, local behaviour of congruences 8-89384
 mass splitting in high dims. extensions 8-89371
 massless vector particles in general background metric, stress energy tensor trace anomaly 8-86200
 matter-filled universe, relativity of space and time finiteness-infiniteness 8-96581
 measurement theory, interrelation of quantum theory and gravitation 8-54235
 mesonic test fields and spacetime cohomology 8-78065
 metric tensor and energy-impulse tensor, components at boundary between R- and T-regions (*Russian*) 8-49726
 metric tensor components interpretation, astrophys. implications 8-93097
 metrical connection in space-time, Newton's and Hubble's laws 8-57435
 microwave background radiation polarisation, anisotropic cosmological expansion 8-73778
 miniphantom geometrodynamics for 2+2 resolution of space-time 8-62132
 N twisting gravitational field soln. to Einstein eqn., integrability conditions 8-86203
 neutrino radiation soln. 8-54261
 neutron stars mass upper limit for stability against black hole form. 8-96498
 non-linear wave equations in a curved background space 8-65827
 noninertial reference system, electrodynamics eqns. (*Russian*) 8-81895
 nonlinear electrodynamics, Birkhoff's theorem analogue (*Russian*) 8-54273
 NUT metric in background of Einstein's static universe 8-93565
 optical coordinates in general relativity, axiomatic approach 8-86207
 particle creation by singularities in asymptotically flat spacetime 8-54260
 particle models, and effective radius (*German*) 8-86198
 perihelion precession rate in system of two charged masses 8-73897
 Petrov type {3,1} vacuum solns. with twist, Killing struct. of family 8-54253
 photon emission from gravitationally intense cylindrical bodies 8-57840
 physical singularities and big bang theory (*Russian*) 8-81893
 plane-symmetric cosmological model, Einstein eqn. solns. for dust 8-49733
 planet, internal structure is general relativity 8-57477
 polarisation dynamics, fully relativistic kinetic model 8-62134

general relativity continued

positivity of energy 8-57830
 principle of equivalence, expt. test (*Russian*) 8-77795
 projective invariance in general space times with spinor, torsion and Yang-Mills fields 8-57832
 quantum field theory, symmetry aspects 8-62139
 quantum spinors and singularity theorems 8-70027
 quantum theory, gauge fields 8-86212
 quark confinement, event horizons around a particle surrounded by a static confinement potential 8-66075
 radiative transfer for polarized light, eqn. soln. method in relativistic cosmology 8-73781
 Reissner Nordstrom metric, static sources 8-93575
 Riemannian manifold, harmonic forms of curvature type (*French*) 8-86124
 Robinson's theorem, shear free condition 8-93586
 rotating body metrics, Einstein vacuum field eqns. solns. using local symm. 8-54257
 rotating charged dust, Newtonian and general relativistic treatments 8-73908
 rotating pressure-free space-time, thin self-similar disc config. 8-96387
 rotating relativistic stars, generic instability 8-93567
 rotating stars stability and gravit. radiation 8-93210
 rotating steady-state configurations 8-73899
 rotating system of observers, covariant decomposition (*German*) 8-49724
 Schwarzschild black hole in ext. mag. field, radiation emitted by relativistic particles 8-96501
 self-similar space-times, perturbation scheme 8-54099
 self-similar space-times, solutions to general relativity eqns. 8-54098
 semiclassical theory of scalar field in globally hyperbolic universe 8-54250
 separable coords. in four-dims. Riemannian spaces 8-57826
 singularities, in static axially symm. coupled fields 8-65822
 singularity-free extended particle model in general relativity 8-54255
 $SL_{2,c}$ gauge theory of gravit., Lagrangian approach 8-77777
 $SO(3, 1)$ gauge field, Einstein-Weyl-Yang system, strong gravity model 8-86201
 space-time properties, local and global, Einstein's eqns., Universe matter density 8-61942
 spatial conformal flatness in homogeneous and inhomogeneous cosmologies 8-69924
 spatial tensor anal. 8-93571
 spherical stars, reformulations of Einstein eqn. solns. 8-49731
 spontaneous particle creation in strong gravitational field, semiclassical theory 8-54281
 standard hot big bang model of Universe, dynamics 8-69922
 star, spherical, emitting neutrinos, relativistic model 8-73705
 star with neutron core, gravitational equilib. relativistic treatment 8-57570
 stars, rotating Newtonian, secular instability to gravit. radiation and viscosity 8-53922
 static field, Einstein vacuum field eqns. 8-65836
 static Universe model with two centres, red shift explanation 8-57706
 stationary axially symmetric Einstein eqns., linear eigenvalue problem, complete integrability 8-77780
 stationary axially symmetric vacuum solns. (*German*) 8-81903
 stationary Einstein Maxwell field equations, pots., nonlinear symm. transforms. 8-86206
 stellar equilibrium statistical mechanics of relativistic systems with energy cutoff 8-93327
 $SU(2,1)$ symmetry of the Einstein-Maxwell fields. II 8-93577
 super-gauge symmetry in general relativity, Einstein's A transformation (*German*) 8-86199
 supergauge extensions, geometric backgrounds, supermanifolds 8-73891
 supergravity, geometry of superspace, vector-spinor matter 8-49744
 superspace, local supersymmetry, superfibre bundle theory 8-77782
 symmetries of energy momentum tensor, concomitant conservation laws 8-57831
 symmetry breaking and space-time geometry 8-54533
 symmetry of charged rotating body metrics 8-77776
 syntopic spacetime meas., time dilatation and Lorentz contraction meas. 8-73896
 Taub-NUT instanton with an horizon 8-89392
 tetrad formalism of Maxwell equations with effect of gravitation. II 8-77784
 tetrad gravitational field, weak principle of equivalence and gauge theory (*Russian*) 8-62135
 tetrad potentials gauge, reference systems with Newtonian time (*Russian*) 8-89378
 thermodynamic equilib. of gravitating sphere in Lyra's geom. 8-65840
 Tomimatsu-Sato family, exact soln. 8-89377
 transport processes, relativistic generalisation in continuum (*Hungarian*) 8-89383
 trichromatic theory and time vector in relativity theory (*French*) 8-57006
 twisted quantum fields in a curved space-time 8-73913
 twisted scalar field, vacuum solns. 8-93804
 unified gauge field theory with torsion, symmetries 8-89386
 unified treatment of null and spatial infinity 8-65848
 viscous fluid cosmological model in general relativity 8-61944
 Weyl solns. of Einstein vac. field eqns. 8-93580
 white dwarfs, degenerate magnetic, critical parameters estimation, general relativistic corrections 8-65622
 ν radiation, Einstein-Dirac eqns. (*Russian*) 8-49727

generator coordinate method

see also nuclear structure theory
 adiabatic time-depend. Hartree Fock, relation to generator coordinate method, conjugate parameters 8-86498
 Brueckner-generator-coord. method, α - α scatt. 8-62487
 collective subspace of many-body Hilbert space, generator coord. approach, kinematics 8-70055
 even parity states in ^{19}F , ^{21}Ne , ^{23}Na , generator coord. method, projected Hartree-Fock, and complete diagonalisation calcs. comparison 8-89796
 giant resonance description, RPA, GCM, and semiclassical theories unification 8-54671
 heavy ion interactions, generator coordinate method, microscopic treatment 8-66304

generator coordinate method continued

- pairing vibrational and isospin rot. states in particle number and isospin projected GCM 8-54696
 pf-shell nuclei, Hermitian operator method calcs., energy levels, transitions 8-54702
 quartic anharmonic oscillator, symmetry properties in generator coord. method 8-49699
⁵⁴Fe(p,p'), testing self consistent models of collective and single particle struct. 8-82300

generators, acoustic see *acoustic generators***generators, electric** see *electric generators***geochemistry**see also *Earth structure; geology*

- Alpine meltwaters, ion exchange influence on dissolved load 8-81228
 anorthosite gneisses, trace element comp. rel. to petrogenesis 8-65224
 Archaean plutonic rocks, Pb isotope comp. 8-65223
 Archaean continental crust, magma genesis by crustal anatexis, garnet-pyroxene thermometry and barometry 8-65236
 Central Atlantic Ocean, phosphate content rel. to underwater irradiance meas. (*Russian*) 8-77257
 basalt, oceanic, Pb isotope comp., rel. to mantle evolution 8-65217
 basaltic and gabbroic rocks from W. Mariana basin and Mariana trench 8-65254
 basalts, deep sea, statistical anal. of clinopyroxenes 8-88828
 basalts, from Pacific Ocean Basin, Sr isotope comp. rel. to mantle comp. 8-65218
 basalts, oceanic, noble gas abundance patterns controlling factors 8-65220
 biotite+apatite system, thermochemical data rel. to use as geothermometer 8-85704
 bytownite megacrysts., study of trapped basaltic melts, petrogenetic process study 8-95688
 calcite dissolution by fossil fuel CO₂, effect of sediment mixing 8-81212
 calcrete deposits from Europe, Africa and India, isotopic comp. 8-73368
 carbonate, (Si, Cl)-bearing from limestone-granite contact zone near Ikizdere, Turkey (*French*) 8-69339
 classification of radiolarian cherts and siliceous sediments (*French*) 8-96319
 continental crust, evolution age and isotope evidence 8-65233
 continental crust, heat-producing radioactive elements distrib. and redistribution. 8-65232
 core formation effects, model 8-61368
 crust and mantle chemical evolution from Early Archaean rocks comp. 8-65222
 crustal geological-geophysical zoning possibility 8-57342
 data management and processing 8-57324
 enstatite, low solubility of Al₂O₃, palaeogeotherm uncertainties 8-65283
 feldspar/water O isotope exchange, effect of fluid press. 8-57204
 fractionation of Co and Sc versus Fe content for crystalline phases of ultramafic nodules 8-65306
 geological samples, trace element characterisation, by instrumental neutron activation anal. 8-73116
 geothermal resources, nucl. techniques in geochemical studies 8-85746
 Gulf of St. Lawrence and estuary, geochem. of Zn, Cu and Pb in sediments 8-92855
 haematite, reduction to magnetite under natural and laboratory conditions 8-65277
 Harp dikes rel. to Helikian geological record in central Labrador 8-61411
 heavy metals, distrib. and speciation in aquatic systems, analytical techniques 8-69390
 hydrometeorology, atmospheric contrib. to water systems chemical budget 8-96240
 Iceland, Skagi and western neovolcanic zones, geochemical vars. 8-96171
 Iceland high-temperature geothermal systems, aquifer chemistry 8-96245
 Icelandic basalts, general mixing eqn. appl. 8-53625
 igneous rocks, granitic comp., trace elements appl. to petrogenesis 8-65215
 intrusive granitoids chem. comp. influence on mag. props. (*Russian*) 8-85535
 ionic diffusion in naturally-occurring aqueous solns., use of activity coeffs. in transition-state models 8-57224
 isotopic equilibrium, regional and local, in mantle, from volcanic rocks comp. 8-65216
 Izu Peninsula, Japan, groundwater geochem. in crustal uplift area, rel. to earthquake prediction (*Japanese*) 8-96242
 komatiites and high-MgO lavas, origin, crystallisation 8-65312
 lacustrine sediments, selective chem. extraction of CO₃²⁻ associated metals 8-65406
 Lake Assal (FTAI), geothermal zone, geochemical and expt. studies 8-69314
 Larderello field, secondary changes in composition of geothermal fluids 8-69387
 late Precambrian mafic dykes, Montana, geochemistry and Rb-Sr geochronology rel. to Belt tectonics 8-77196
 Loc Uisg granophyre, Isle of Mull, isotopic and chem. evidence for origin 8-65303
 Mackenzie, N.W.T., Canada, Devonian-Cambrian stratigraphic differentiation by S isotopes in gypsum 8-61413
 magma mixing at mid-ocean ridges, DSDP data 8-77209
 magmas, thermal history, low press. reference point 8-65244
 Manicouagan impact melt, Quebec, chemical interrelationships with basement rel. to form. processes 8-81165
 marine mineral suspensates and geochemical exploration 8-88936
 metamorphism, bathozones and bathograds as measure of regional scale post-metamorphic uplift 8-81113
 minerals, magnetic trends on alkali-Fe-Mg diagrams 8-85551
 minerals, metal-rich deposits in oceanic lithosphere, origin 8-53634
 mixing models for geothermal systems and chemical geothermometers 8-69503
 natural waters, U content meas. technique 8-85705
 neutron activation anal. technique for Na/K ratios in fluid inclusions determ. 8-61568
 Norwegian Sea pycnocline, T vertical distrib. rel. to apparent vertical eddy diffusion rates 8-81185

geochemistry continued

- ocean floor basalts and ferromanganese deposits, Pb, Nd and Sr isotope comp. 8-61395
 ocean floor spilites, seawater/basalt ratio effects on chem. and mineralogy 8-92819
 ocean ridge basalts, trace elements, rel. to mantle comp. 8-65219
 oceanic basalts, differential Sm/Nd evolution 8-61391
 oceanic basalts, hydrothermal alteration by seawater at high temp. 8-69327
 oceanic basalts, trace element mobility during hydrothermal alteration 8-69328
 oceans, origin of Cl and Br 8-65342
 oilfield brines from Kansas and Colorado, Sr isotopic comp. 8-57225
 Omo River project (Ethiopia) data management system appraisal 8-57326
 Ontario Precambrian diabase dike, trace element geochemistry 8-61414
 ore-deposition through geological time, review 8-77235
 N Pacific Ocean waters, densities rel. to comp. and eqn. of state 8-73391
 Palaeozoic granitoid plutons from contrasting tectonic zones, NE. Newfoundland, geochem. 8-57201
 Peru-Chile Trench basalts, fractionation and mantle heterogeneity 8-53626
 PETPAK, computing package for petrologists 8-57323
 phosphorites from Spanish continental margin, geochemistry and mineralogy (*French*) 8-65258
 plutonic granitic rocks, O and H isotope comps. 8-65221
 pyroxene geotherms, thermodynamics 8-65282
 Red Sea brines origin, new isotopic evidence 8-96236
 rock samples, Sn determ. by neutron activation method 8-85258
 Saguenay Fjord, suspended particulate matter geochemistry 8-92852
 Scandinavian rocks, giant and dwarf haloes geochemistry rel. to unknown radioactivity 8-81157
 seawater, organic chemistry of particulate matter 8-65344
 seawater, radioactivity, and salinity changes with advection of water masses (*Russian*) 8-77275
 sedimentary organic matter, subaerial weathering effects 8-57206
 serpentinisation, modern low temp., in New Caledonia, Oman and Yugoslavia 8-69344
 silicate content of anoxic pore waters, effects of oxidation during sampling 8-61394
 silicate rock, chem. denudation rates in tropical catchments 8-73414
 E. Sivash waters, ⁹⁰Sr content and salinity vars. (*Russian*) 8-77282
 sphalerite, FeS content as geobarometer, experimental extension to 10 kbar 8-85703
 spinel ilherzolite nodules from Pleistocene cinder cone, upper mantle origin 8-65299
 subsurface water chemistry study, coring and squeezing technique 8-57332
 tholeiitic basalts, rare earth elements behaviour during submarine weathering 8-73369
 tholeiitic basalts from Japan, geochemical types 8-96206
 Tilting Harbour igneous complex, Fogo Island, Newfoundland, petrology 8-77230
 trace element behaviour in magmatic processes, quantitative models 8-65214
 ultramafic inclusions, petrogenesis, geochem. and petrologic data 8-65301
 volcanic rocks, altered, at Matagami, Quebec, geochemistry and geothermal model for massive sulphide genesis 8-77231
 volcanic rocks, Tetagouche Group, Canada, geochem. rel. to origin 8-65298
 volcanic rocks classification using Irvine and Baragar classification scheme, FORTRAN IV program 8-57203
 volcanosedimentary levels, S. Pacific, neof ormation and weathering (*French*) 8-73353
 water and magmas, appl. of Gibbs-Duhem eqn. 8-57205
 B abundance determ. in rocks, soils, plants, waters and fertilisers 8-85559
 B, inorganic, in St. Lawrence Estuary, determ. (*French*) 8-77274
 Ca₂HPO₄SO₄·4H₂O, synthetic, cryst. struct. and relation to brushite and gypsum 8-83785
 Cu, inorganic speciation in estuarine environments 8-69371
 H isotope exchange between clay minerals and seawater 8-69329
 Hq, abundance in Greenland Ice Sheet 8-65349
 Mn deposition and nodule growth in Jervis Inlet, British Columbia, effect of sediment-water exchange 8-96187
 O isotope fractionation in decarbonation metamorphism, Mottled Zone Event 8-65307
 O isotopes in dissolved sulphate and water from hot springs and drill holes, reservoir temp. indicators 8-69382
¹⁸O scales, proportional vars., interlaboratory comparison 8-69326
 O₂ self-diffusion in feldspars, ion microprobe determ. 8-69325
¹⁸O composition of metamorphosed chert and Fe formation from W. Greenland 8-81155
⁸⁷Rb/⁸⁷Sr studies of waters in geothermal area, Cantal, France 8-61443
 S isotope exchange between sulphate and sulphide in acid solns., expt. determ. at 300°C and 1000 bars 8-62937
³⁴S/³²S ratio meas. using SO₂ and SF₆ methods, discrepancies 8-65405
 Sr evolution in W. Greenland-Labrador craton, early Rb depletion in mantle 8-69304
 Sr isotope comp. of Alpine tectonite ilherzolites, evidence for mantle origin 8-65302
 Sr, Pb, isotope geochemistry rel. to catastrophic or continuous core form. 8-57178
 U resource evaluation by neutron activation anal. 8-85741

geochronologysee also *radioactive dating*

- Aiyansh Volcano, British Columbia, ages of eruptions 8-92811
 Alcaparrosa Formation (Upper Ordovician), Argentina, palaeomagnetism and K-Ar age 8-96135
 N. American Cordillera near Fortieth Parallel, tectonics and chronology 8-81138
 apatite fission track ages, from Himachal Himalaya, India, tectonic interpretation 8-57182
 Archaean layered greenstone from Pilbara Block, age of volcanics 8-53627
 Archaean lithospheric/crustal thickness from volcano spacings 8-65225

geochronology continued

- Arran dykes of British Tertiary igneous province, palaeomagnetism and ages 8-73306
- S. Atlantic Ocean, opening chronology from equatorial fracture zone trends 8-85527
- basalt, erupted at Reykjanes Ridge crest, vesicularity 8-73351
- basalts, Lower Silesian, K-Ar ages, Tertiary polarity events 8-53614
- Black Sea, mantle material intrusion age rel. to mag. anomalies: nature (*Russian*) 8-85473
- Brezovica peridotite base, Jurassic metamorphism 8-96169
- British Columbia, S central, late Pleistocene stratigraphy 8-92804
- Central Alps, structural zones history and continental collision 8-81124
- cirque glaciations, Holocene and latest Pleistocene, in Shuswap Highland, British Columbia, ages 8-92856
- continental crust, evolution age and isotope evidence 8-65233
- core formation, chronology from Sr and Pb isotope geochemistry constraints 8-57178
- dating techniques, effects of thermal annealing on track etching rate of sphene, CaTiSiO_5 8-65435
- deep sea sediment core from E. Mediterranean, chronology and palaeoclimatic record 8-57294
- Denali fault system, geological history rel. to S. Alaska tectonic development 8-81137
- diabase pebbles of val d'Illez conglomerates (Haute-Savoie), geochronology (*French*) 8-92810
- Duncansby volcanic neck, NE. Scotland, palaeomag., K/Ar ages, tectonic implications 8-61369
- NE Ellesmere Island, NWT, Canada, glacial geology and chronology 8-77233
- Elsonian magmatism in Labrador, age, characts. and tectonic setting 8-73365
- fission track annealing characteristics of epidote, appls. to geochronology, geol. 8-94038
- fission track dating and estimation of U in garnets 8-94039
- E. Greenland, Jurassic basin evolution, chronology and sedimentation 8-73344
- Hebridean continental margin, seismic evidence for Mesozoic age sedimentary troughs 8-53643
- W. Hellenic Trench, high sedimentation rates and variable dispersal patterns 8-57193
- ice-wedge casts in NE county Wicklow, distrib., struct. and age 8-69379
- Iceland-Faeroe Ridge, subsidence history rel. to Lower Tertiary laterite and Thulean land bridge 8-85514
- Imataca Series, Venezuela, total-rock U-Pb and Rb-Sr systematics 8-96168
- inclined seismic zones rel. to age-length depend. of subducting margin 8-57175
- insular phosphorite from Ebon atoll, Micronesia, U series dating 8-81121
- Ionian Sea, sapropels distrib. and ages E. Mediterranean Sea late Quaternary palaeoceanography 8-73350
- King Island, Australia, fission track ages rel. to continental rifting 8-53628
- Lake Ontario, Late Wisconsin sediments, aspartic acid racemisation and ^{14}C dating 8-73415
- Lake Ontario, sedimentation rates determ., ^{210}Pb dating method 8-73408
- lake sediments, radionuclide geochronology and pollution history 8-61451
- Laschamp geomagnetic polarity reversal, K-Ar and $^{40}\text{Ar}/^{39}\text{Ar}$ age 8-81105
- Late Palaeozoic slate belt, deform. chronology and plate tectonic significance 8-81140
- late Precambrian mafic dykes, Montana, geochemistry and Rb-Sr geochronology rel. to Belt tectonics 8-77196
- Late Tertiary Verde Formation, Arizona, magnetostratigraphy 8-65179
- Loch Lomond, Scotland, palynology, palaeomag. and ^{14}C dating of Flandrian marine and freshwater sediments 8-81234
- Loyalty Islands uplift rates, $^{230}\text{Th}/^{234}\text{U}$ dating of raised coral terraces 8-73347
- Manicouagan melt sheet, Rb-Sr isochron age 8-81168
- Massif Central, upper mantle regional struct. and geodynamics chronology 8-81120
- Mehone Bay, Nova Scotia, Late Quaternary geological history 8-77232
- metamorphic rocks, thermal overprinting of NMR and K/Ar ages 8-65278
- metasomatic anhydrite in Mississippian reservoir carbonates, age determ. 8-73328
- New England submarine canyons, bedrock geology 8-73356
- oceanic basalts, differential Sm/Nd evolution 8-61391
- Oligocene unconformities, oceanic and continental, in Australian region, chronologies 8-73370
- ore mineralisation in Erma River Area, Bulgaria, age, genesis, Pb isotope and K-Ar investigs. 8-81115
- ore-deposition through geological time, review 8-77235
- Pacific plate absolute motion, early Cainozoic change prod. by change in boundaries 8-85529
- Pacific Pleistocenes palaeoclimatic stratigraphies, comparative anal. of results 8-57295
- Palaeogene revised polarity time scale 8-77201
- Pearson Formation (Great Slave Supergroup, NWT), palaeomagnetism age and Coronation polar loop 8-77179
- plate tectonics in Phanerozoic 8-92812
- Pliocene and Pleistocene glaciations chronology, evidence from bottom of Barents Sea 8-57227
- Precambrian-Cambrian boundary, from Jbel Boho volcano zircons (*French*) 8-61359
- Quaternary deposits of Corsica (France), props. and chronological conclusions 8-57234
- rock glaciers in Jasper National Park, Alberta distrib. and ages 8-77276
- Sao Miguel, Azores, quantitative study of volcanism, tephrochronology 8-61382
- sedimentation rates determ. in rapidly accreting salt marsh by ^{137}Cs dating 8-96247
- silicic igneous rocks, Burlington Peninsula, Newfoundland, Rb-Sr ages, deform. 8-65212

geochronology continued

- South Fork Mountain Schist (N Coast Ranges, California), early Cretaceous metamorphic age 8-81114
- speleothems, in N. America, late Pleistocene palaeoclimates chronology 8-57297
- stalactite, from Akiyoshi cave, thermoluminescence and ESR dating comparison 8-88807
- structural characts. and tectonisms around microcontinent Japan Paleozoic-Mesozoic geosyncline 8-81139
- thermoluminescence dating of sediments baked by Chaine des Puys lava flows 8-92808
- Troodos ophiolitic sheeted complex 8-61365
- Upper Cretaceous palaeomagnetic stratigraphy at Moria (Umbrian Apennines), verification of Gubbio section 8-96132
- upper Mesozoic subduction complexes along N. America west coast, distrib. and character 8-81136
- volcanosedimentary levels, S. Pacific, neof ormation and weathering (*French*) 8-73353
- ^{14}C dating, thermal diffusion enrichment, N. American glacial history extended to 75000 yrs ago 8-77284
- ^{14}C dating, time scale extension by thermal diffusion enrichment, appl. to NW. Europe climatology 8-77314
- ^{14}C dating of geological and archaeological samples 8-92993
- ^{14}C dating rel. to magnetic and other dating methods 8-57359
- O isotope palaeotemperatures, from Tertiary period in North Sea area 8-88903
- Pb sulphides, isotopic composition, mineralisation time determ. 8-73372
- ^{210}Pb chronologies of lake and marine sediments, problems 8-81122
- Rb/Sr whole-rock systems and chemical control 8-61366

geodesy

- see also gravity*
- altitude observations, Fourier transform. (*German*) 8-61312
- approximate ellipsoidal-Earth equations for mapping and fix-taking calculations 8-73303
- array algebra for multilinear least squares prediction and filtering 8-69470
- astronomical azimuth determ., accuracy, geodetic networks orientation control appl. 8-92774
- astronomical azimuths of terrestrial objects, as indicators of continental blocks rot. 8-53613
- cavity effect in tunnels of various cross-sections, theory (*Russian*) 8-88784
- contributions to geodynamics (*German*) 8-81101
- coordinate systems, time and reference frames 8-69272
- data base, basic entities definition 8-65392
- data inversion and model of 1927 Tango earthquake conjugate fault system 8-88779
- direct gravity formula for 1967 Geodetic Reference System 8-92775
- Earth surface tidal tilts, influence of atmospheric press. fluctuations (*Russian*) 8-88790
- Earth tide observations processing, individual monthly sets weightings (*Russian*) 8-88789
- Gauss-Helmert model for least-squares adjustment, props. (*German*) 8-61309
- generalised Laplace condition 8-69271
- geopotential, 15th-order resonance effects of Nimbus 1 rocket (1964-52B) 8-65168
- Lageos for crustal movement meas. 8-65441
- Lake Lugano, bathymetric map 8-96252
- levelling data, time-space domain representation, computer program 8-88932
- local vectors connection in actual gravity field of Earth; model field, disturbing pot. 8-61297
- Molodensky's problem in gravity space, review of results 8-65173
- Nova Scotia, gravity and tilt obs. rel. to improved ocean tide models 8-92821
- ocean, geoid and topography via Seasat-A experimental oceanographic satellite 8-77455
- ocean topography, computations and obs. comparison 8-77250
- oceanic loading on European laser-ranging sites 8-85462
- odd zonal harmonics determ. using modified equations 8-92773
- pole secular motion, global plate tectonics effects on Earth axis of figure 8-65172
- reference and coordinate system for global geodetic methods, subdecimetric precision range (*German*) 8-81102
- satellite altimeter data analysis, role of orbit determ. 8-77177
- satellite geodesy, geometrical and dynamic methods, development (*Polish*) 8-88780
- sea surface topography, four dimensional reference system realisation for ocean dynamics 8-77176
- sequential solutions, with bandtype system of obs. eqns. 8-65169
- spherical triangles, numerically stable computation (*German*) 8-88793
- Starlette satellite, precision orbit computation 8-65478
- statistical geodesy, engineering perspective 8-81099
- stereoplotter, TOPOCART B, accuracy and performance study 8-81436
- telluroid, definition 8-65171
- three dimensional geodesy, datum problem 8-61310
- three-dimensional geodesic mapping eqns., rel. to Earth best-known figure determ. (*German*) 8-73304
- tidal tilts, parallel recording through digital print-out and photorecording channels (*Russian*) 8-88785
- tilt meter observations at Berezovaya Rudka station, results (*Russian*) 8-88783
- tilt meter observations harmonic anal., influence of S_1 diurnal meteorological wave (*Russian*) 8-88788
- TRANSIT satellites' contribution to navigation and geodesy 8-57161
- variational formulation of geodetic boundary-value problem 8-92772
- VLBI appl. to geodesy, Earth rot. and network geometry optimisation 8-92996
- water levels, obs. via electrooptical distance meas. (*German*) 8-69280

geodetics *see geodesy***geolectricity** *see terrestrial electricity***geography**

- ISO FORTRAN IV program for generating isopleth maps on small computers 8-57157
- north magnetic pole, 1975 position analytical determ. 8-92778

geography continued

- Sulawesi, Indonesia, palaeomag. data rel. to palaeogeographic reconstructions 8-61330
surface patterns in theoretical geography 8-57156

geology

see also rocks

- NE Africa, geologic evolution and Pan-African belt plutonism 8-65305
Alabama Piedmont, structural development 8-65290
albritonite, new mineral from Llano County, Texas 8-65286
Alpine tectonite lherzolites, Sr isotope comp., evidence for mantle origin 8-65302
N.America west coast, upper Mesozoic subduction complexes distrib. and character 8-81136
Archaean peridotitic komatiites in La Motte Township, Quebec, emplacement 8-77234
Archaean continental crust, magma genesis by crustal anatexis, garnet-pyroxene thermometry and barometry 8-65236
Arctic seafloor studies with Tethered Remote Operated Vehicle 8-61576
arfvedsonite, sodic amphibole occurrence in basalt dykes, Newfoundland 8-65287
Arran dyke swarms, British Tertiary igneous province, palaeomagnetism 8-73306
Australia continental slope and shelf, sedimentary basins evolution from Mesozoic times 8-96175
Australian region, contrasts between oceanic and continental Oligocene unconformities 8-73370
basic intrusions emplacement mechanism 8-61374
Bay of Islands Ophiolite Suite, evidence for oceanic crust hypothesis 8-81117
Benue Trough, Nigeria, early Cretaceous basalt volcanism and initial continental rifting 8-61417
Black Sea depression basin as young trough (*Russian*) 8-88830
borehole temp. gradient logs and lithology correlation 8-61416
Boston Bay Group, Massachusetts, origin and significance of cylindrical sandstone struts. 8-69343
Botswana, dyke swarm interpretation as failed Gondwana spreading axis 8-57180
Brevard ductile deformation zone, N.Carolina, struct. and seismic refl. study 8-65289
N.Britain, crustal struct. from Lithospheric Seismic Profile in Britain (LISPB) 8-73329
British Columbia, S central, late Pleistocene stratigraphy 8-92804
British Isles, 1978 guide to information sources 8-88922
calc-alkaline rocks from the East Carpathians, K, Rb and Sr distrib. 8-85555
calcrete deposits from Europe, Africa and India, isotopic comp. 8-73368
Canadian Shield, structure of Archean basin-craton complexes 8-61412
Cape Breton Is., Canada, post-Mississippian thrust faulting 8-61360
Cerro Galan Caldera, NW.Argentina, volcanic history rel. to plate tectonics setting 8-85523
charnockites from Visakhapatnam, India, allanite occurrence 8-65285
CLAIR data system overview 8-57325
Clyde Foreland, Baffin Is., last interglacial-glacial cycle, stratigraphy, biostratigraphy and chronology 8-61536
coal banding-plane indicator, magnetic susceptibility anisotropy meas. 8-77221
Coosa Valley, Alabama, struct., folding and thrust faulting 8-65291
Cornwallis Pb-Zn district, deposits controlled by stratigraphy and tectonics, discussion 8-73366
crustal geological-geophysical zoning possibility 8-57342
cylindrical shell, thin, instability rel. to mechanical anal. of geologic struts. (*Chinese*) 8-73364
data management and processing 8-57324
Denali fault system, geological history rel. to S.Alaska tectonic development 8-81137
Devonian alkalic basalt dykes, NE.Newfoundland, tensional environment 8-88826
Devonian metamorphism, in the Bas-Limousin areas (Massif Central, France) 8-96204
Devonian Millboro Shale, Appalachian Plateau, slip planes, discfold anal. 8-65293
Deweras Group sedimentary environment, Rhodesia, palaeorift system 8-53650
Dinarides, Yugoslavia, middle Triassic volcanism rel. to peri-Mediterranean tectonics 8-77238
Dnieper-Donets depression, sedimentary cover struct. along Jagotin-Baturin profile (*Russian*) 8-92806
Early Archaean rocks comp. rel. to crust and mantle chem. evolution 8-65222
NE Ellesmere Island, NWT, Canada, glacial geology and chronology 8-77233
Elsonian magmatism in Labrador, age, characts. and tectonic setting 8-73365
SW.Ethiopia, magnetostratigraphy of Shungura and Usno Formations 8-85470
faulting analysis in three dimens., strain field 8-77225
Franciscan melanges, comparison with olistostromes of Taiwan and Italy 8-81159
Frankische Alb, slope forms in Al(1) clay, statistical investigation (*German*) 8-57211
garnet-cordierite gneisses, geothermometry of granulite facies rocks from Rogaland, Norway 8-96193
GEOSAT, geological industry recommendations on remote sensing from space 8-69495
geothermal research in Netherlands (*Dutch*) 8-61415
glossary 8-88833
Gorringe Bank, oceanic mantle and crust, geological survey 8-53632
granodiorite, late Precambrian, strain anal. of shear zone 8-77223
gravel, ice-thrusting, shear deform. 8-65347
gravity vertical gradient meas. for detect. of small geological and anthropogenic forms, discussion 8-61575
W.Greenland, ¹⁸O composition of rocks 8-81155
E.Greenland, Jurassic basin evolution 8-73344
greenstone belts, ancient marginal basins or ensialic rift zones 8-61418
halokinesis and thermal convection 8-65308

geology continued

- Haramosh-Nanga Parbat structure and Karakorum range junction, geological notes 8-85553
Harp dikes rel. to Helikian geological record in central Labrador 8-61411
harzburgite xenolith, evidence for upper mantle multiple spinel-garnet peridotite transitions 8-65309
Haute-Savoie, France, metamorphic events ages from conglomerate diabase pebbles geochronology (*French*) 8-92810
W. Hellenic Trench, high sedimentation rates and variable dispersal patterns 8-57193
Higashi-Izu monogenetic volcano group, Japan, geology (*Japanese*) 8-96176
Hinterland Belt, Canadian Cordillera, deformation episodes 8-88825
Iceland, geothermal activity rel. to geological struct. 8-61376
intraplate volcanism, geological and geophysical parameters 8-65243
Ionian Sea, sapropel distrib. and E.Mediterranean Sea late Quaternary palaeoceanography 8-73350
Jan Mayen Ridge, Cepan 1 1975 survey 8-96184
Japan, granitic rocks rel. to country rocks 8-81119
Job's Hill, Jamaica, geology rel. to dickite ordered and disordered varieties 8-83786
karst landscapes, origin of labyrinth and tower styles, necessary climatic conditions 8-96208
kimberlite nodules, upper mantle petrology and geotherms 8-65310
komatiites and high-MgO lavas, origin, crystallisation 8-65312
Krivoi Rog basin (Krivbas), geological bodies rel. to gravity anomalies interpretation (*Russian*) 8-85466
Labrador Trough, Canada, early recumbent folds in northeastern part 8-65300
Lachlan Fold Belt in New South Wales, description, tectonic history 8-96211
landslides on Ryuohzan Mountain, Japan, geology, model (*Japanese*) 8-96217
large impact craters, meteoritic material detect. and chemistry 8-57208
Late Palaeozoic slate belt, structural succession and tectonic significance 8-81140
late Precambrian mafic dykes, Montana, geochemistry and Rb-Sr geochronology rel. to Belt tectonics 8-77196
Loc Uisg granophyre, Isle of Mull, isotopic and chem. evidence for origin 8-65303
loess geological environments, China (*Chinese*) 8-81156
Lower Palaeozoic black shales rel. to geologic-oceanographic model 8-61436
Mackenzie, N.W.T., Canada, Devonian-Cambrian stratigraphic differentiation by S isotopes in gypsum 8-61413
Manicouagan structure, Quebec, central mag. anomaly rel. to mafic rock uplift 8-81169
Mantaro landslide, Peru, seismological and geological aspects 8-96248
Mehone Bay, Nova Scotia, Late Quaternary geological history 8-77232
Mentese region, SW Turkey, LANDSAT imagery appls. 8-77236
metabasites, geothermometry of granulite facies rocks from Rogaland, Norway 8-96193
metadolerite dykes and assoc. folds, Caledonides of Finnmark, Norway 8-61375
meteorite craters, form., props. and catalogue 8-96411
Middle Jurassic magnetic polarity, from Summerville and Curtis Formations, Utah 8-65180
Middle Ordovician formations, E.Tennessee, tectonic significance of distal turbidites 8-65296
Miramichi Bay, New Brunswick, Canada, echo sounder and seismic profiling survey 8-61390
Mole (Haute-Savoie, France), geological profile of south flank rel. to struct. and tectonics (*French*) 8-69348
montmorillonite neof ormation by post-depositional subsurface weathering in slope deposit 8-73367
SW New Brunswick and SE Maine, stratigraphy and tectonic setting of Palaeozoic sedimentary rocks 8-57199
New Caledonia, Oman and Yugoslavia, modern low temp. serpentinisation 8-69344
New England submarine canyons, bedrock geology 8-73356
E. Newfoundland, aborted Proterozoic rifting 8-57200
nuclear power plant siting, US midcontinent 8-85501
oceanography, geological, book 8-92845
Omo River project (Ethiopia) data management system appraisal 8-57326
ophiolite complexes, effects of alteration on NRM and implications for oceanic crust 8-65280
ophiolite suites, upper mantle origin rel. to oceanic lithosphere generation 8-65311
ophiolites, seismic vels. and oceanic crustal struct. 8-77226
ore mineralisation in Erma River Area, Bulgaria, age, genesis, Pb isotope and K-Ar investigs. 8-81115
Otago schist megaculmination, origins and tectonic significance in New Zealand Rangitata Orogen 8-81142
Palaeozoic granitoid plutons from contrasting tectonic zones, NE. Newfoundland, geochem. 8-57201
palaeozoic sequences palaeobathymetric anal., rel. to basin tectonics 8-69341
parallel metamorphic belts in NW Himalaya 8-57207
PETPAK, computing package for petrologists 8-57323
Phanerozoic sedimentary basins, Australia, tectonic implications 8-96174
Precambrian development rel. to geophysical evolution 8-53651
Precambrian dykes, preferred orientation of intrusion 8-88829
Precambrian high grade metamorphic terrains, interplate deform. rel. to SE Asian neotectonics 8-65250
prospecting data processing system, Poland (*Polish*) 8-88929
Pyrenees, central southern region, gravity gliding and compressive nappes 8-69342
quartzites, microscopic deform. and flow laws, South Mountain Anticline 8-77220
radioactive waste disposal into salt deposits, fault tree anal. appl. to safety assessment 8-55046
salt dome evolution, fluid dynamics model 8-77237
Scandinavian Caledonides, nappe displacement 8-81143
seismic waves interference effects in thin layers 8-92780
seismite, occurrence in Precambrian rocks, Rajasthan, India 8-77227
seismoacoustic activity distrib. near coal bed face 8-73320

geology continued

- sequential deformation in central Appalachians 8-65294
- shore platform formation on SE. coast of Izu peninsula, Japan 8-81147
- silicic igneous rocks, Burlington Peninsula, Newfoundland, Rb-Sr ages, deform. 8-65212
- Slate belt, volcanic evolution, possible primitive oceanic island arc 8-81125
- soil resistance meter, geological and archaeological applications (*German*) 8-57361
- Sokoman Iron Formation near Ardua Lake, Quebec, mineralogy and petrology 8-77228
- Somerset Island Formation, intertidal/supratidal succession 8-65297
- southern continents, geology rel. to revised reconstruction 8-92805
- Spain, residual gravity anomalies rel. to geology (*Spanish*) 8-88781
- sphalerite geobarometry in Balmat-Edwards district, New York 8-65261
- spinel ilmenite nodules from Pleistocene cinder cone, upper mantle origin 8-65299
- Strandja Mountain, Bulgaria, new facial type of Triassic 8-81154
- sulphate evaporites, Middle Proterozoic, at Mount Isa mine, Australia 8-73371
- Tasman Fold Belt System in New South Wales, description 8-96210
- Tasman Fold Belt System in Tasmania, description 8-96209
- Tasman Fold Belt System in Victoria, evolution, tectonics, deform. 8-96212
- Tasman Orogenic Zone, description of eastern part 8-96214
- Tasman Orogenic Zone, Thomson Orogen, tectonically active area 8-96213
- E.Tennessee, palinspastic map 8-65295
- Tennessee Valley and Ridge, folding 8-65292
- S. central Texas, effect of Balcones Faults on groundwater movement 8-53672
- Tilting Harbour igneous complex, Fogo Island, Newfoundland, petrology 8-77230
- TRIPLLOT, APL program for plotting triangular diagrams 8-57335
- ultramafic bodies in S.Appalachians, review 8-65288
- ultramafic inclusions, petrogenesis, geochem. and petrologic data 8-65301
- Upper Cretaceous palaeomagnetic stratigraphy at Moria (Umbrian Apennines), verification of Gubbio section 8-96132
- US, Missouri and S.Carolina seismic areas 8-85505
- volcanic rocks, Tetagouche Group, Canada, geochem. rel. to origin 8-65298
- Vredefort Dome, S.Africa, coesite and stishovite discovery 8-53653
- late Wisconsinian till sheets, Brantford-Woodstock area, S.Ontario, trend surface anal. 8-92858
- zones of influence of linear geological structures, computation program 8-57202
- U ore systems, morphogenetic grouping 8-81158

geomagnetic storms *see magnetic storms***geomagnetic variations***see also micropulsations*

- aa annual index, appl. to solar cycle 21 max. intensity and date prediction 8-73696
- antisymmetric S_{α} -variations, appl. of plasmasphere dynamo electric field-aligned currents theory 8-81499
- ap indices, daily vars., determ. of interplanetary mag. field sector struct. 8-93066
- archaeomagnetic data compared with analytical representation of geomag. field for last 2000 years 8-73305
- archaeomagnetic field determ. and secular var. in Caucasus 8-73309
- Arizona, Curie point isotherm from magnetic total intensity anomalies 8-61315
- auroral particle instantaneous energy deposition rate, var. with mag. activity 8-81491
- auroral zone magnetic indices, correl. with dayside magnetosphere mag. flux transfer 8-96355
- bays observed at coastal observatory, effect of induced currents in sea 8-65462
- Butkin anomaly of secular var. in Urals 8-69288
- Canada, secular change for 1975 8-65177
- crochet associated solar microwave bursts, nature 8-69772
- D_{α} index, annual and daily vars. 8-96351
- daily variation of geomag. vertical intensity at Marion Island, phase shifts 8-81107
- disturbances, rel. to occurrence of forenoon bite-out in F_2 -layer critical freq. 8-65453
- Dst time derivative, rel. to ring current development and midlatit. convection elec. fields 8-57395
- E-region, electron density variations during geomag. disturbances 8-69567
- E-region, mag. disturbances rel. to cross polar cap horizontal currents and elec. fields 8-77405
- earthquake precursors, rocks stress cycling and inelastic volumetric strain rel. to remanent magnetisation 8-88820
- effects on cancer deaths, glaciers and incident cosmic radiation 8-53615
- equatorial ionosphere, mag. vars. rel. to interplanetary mag. field vars. 8-77413
- equivalent linear amplitude geomagnetic indices, evidence for strong artificial components 8-89008
- field disturbances produced by interplanetary mag. field B_z -component pulses 8-73583
- high-latitude variations, coupling to ionosphere equatorial elec. field 8-93029
- induction vectors, local time var. 8-85477
- Izu Peninsula, Japan, geomag. force intensity vars. in crustal uplift area (*Japanese*) 8-96128
- K_p -index during August 1972, correl. with cosmic rays north-south anisotropies 8-89018
- Laschamp geomagnetic polarity reversal, K-Ar and $^{40}\text{Ar}/^{39}\text{Ar}$ age 8-81105
- local variations assoc. with earthquakes dilatancy-magnetic effect (*Chinese*) 8-61333
- lunar daily geomagnetic variations at Tucson, anal. for M_2 -tide 8-96136
- magnetic tail, field vars. rel. to plasma flow pulsations 8-77436
- magnetosphere, geomag. field fluctuations power spectra at synchronous orbit 8-96358

geomagnetic variations continued

- magnetosphere, geomagnetic field fluctuations at synchronous orbit rel. to particles radial diffusion 8-96359
- meteor radar rates correl. with geomag. activity and solar wind sector struct. 8-65553
- north magnetic pole, 1975 position and secular and diurnal vars. 8-92778
- palaeomagnetosphere, third type of planetary magnetosphere during polarity reversals and geomag. excursions 8-61683
- Pc 5 micropulsations, mag. vars. prediction from ionospheric reson. region radar obs. 8-65454
- polar regions, small-scale transverse magnetic disturbances 8-77423
- pole-tide signal at low-latitude coastal station 8-61322
- pulsations before solar proton flares (*Russian*) 8-69291
- quiet time field at successive universal times 8-61325
- quiet time var. rel. to interplanetary mag. field, autocorrel. effects 8-61697
- quiet time vertical magnetic field component over India 8-61326
- reversal during Wisconsinian Ice Age, evidence from Iceland 8-61327
- reversals, transitional field configs. 8-65182
- reversals and climatic change, statistical correl. 8-61537
- S_{α} variation at mag. conjugate points and interplanetary mag. field var. 8-69287
- secular changes effects on cosmic ray variational coeffs. 8-93058
- secular var. anomalies around Sverdrlovsk magnetic observatory 8-61319
- secular variation for 1965, definitive model derivation and comparison with IGRF 8-96133
- secular variations, correl. with Earth daily rot. vars. 8-73302
- short period variations in EM field, anal. for wave type and propag. direction determ. (*Russian*) 8-85474
- simultaneous high and low-latitude vars., polar elec. fields transmission to Equator 8-65456
- small bay disturbances, possible correl. with VLF hiss emissions 8-81509
- solar eclipse, 1976, October 23, mag. obs. in Australia 8-81498
- spectral analysis, rel. to correl. with solar oscills. 8-89013
- terrain induced aeromagnetic anomalies, reduction by parallel surface continuation 8-61316
- ^{14}C concentration in Earth's atmosphere, corrections with astrophysical and geophysical phenomena 8-61477
- ^{14}C concentration in Earth's atm. with variations of geomag. field, spectral anal. 8-61478
- ^{14}C in atmosphere content variation, past geomagnetic and cosmic ray intensity variations 8-61691

geomagnetism*see also geomagnetic variations; magnetic storms*

- anisotropic inhomogeneities oriented along geomagnetic field, radiowave scattering 8-53771
- anomalies, interpretation, Kolmogorov-Wiener least-squares filters appl. 8-61580
- anomalies, interpretation with end-corrected Fourier-transforms 8-65418
- anomalies, linear anal. (*Russian*) 8-53755
- anomalies calc. for regular homogeneous perturbing bodies (*German*) 8-69478
- anomalies caused by two-dimens. vertical faults, direct interpretation method 8-77181
- anomaly due to vertical right circular cylinder with arbitrary polarisation 8-77180
- apparent source depth of mag. field, appl. to planetary fields and internal struct. 8-57478
- N. Atlantic, sea floor spreading and early opening, mag. and gravity data 8-65247
- Atlantic bottom topography and magnetic field of elevated area (*Russian*) 8-85531
- atmosphere electrodynamic state, horizontal mag. field component influence (*Russian*) 8-73556
- Black Sea, nature of mag. anomalies (*Russian*) 8-85473
- Canada, 1975 annual report for magnetic observatories 8-61323
- central Canada, 3-component aeromagnetic survey 8-96138
- charged particles motion in one-dimens. mag. current sheets 8-65464
- coal banding-plane indicator, magnetic susceptibility anisotropy meas. 8-77221
- coal seam thickness meas. using resonant loop as EM sensor 8-57366
- cooling orogen, magnetic and isotopic blocking temps. 8-65226
- cooling orogen, magnetic blocking temp. 8-65227
- core-mantle boundary irregularities, effect on fluid speed and geomag. field 8-73333
- cosmic ray electrons, detect. by synchrotron radiation in geomag. and interstellar mag. fields 8-57412
- crustal magnetic model under Ukrainian Shield 8-61313
- Cuddapah basin, India, regional mag. profiles 8-85476
- damping of satellite rotation, magnetic field effects 8-69645
- damping of satellite rotation, shielding effects 8-69646
- data reduction on arbitrary surface in regions of high topographic relief 8-61298
- declination field near Earth surface, error in analytic representation 8-73307
- Dnieper-Donets depression, magnetotelluric sounding data rel. to deep struct. (*Russian*) 8-96170
- dual-spin satellite magnetic attitude control system, geomag. field effects 8-65484
- dynamo theory, MHD, book contrib. 8-61331
- E-layer crit. freq., geomagnetic east component, and sunspot number relationships 8-65461
- E-polarisation, numerical soln., improved geomagnetic boundary conditions 8-77182
- eddy current torques, air torques, and spin decay of orbiting cylindrical rocket bodies 8-93074
- EM field short period variations, anal. for wave type and propag. direction determ. (*Russian*) 8-85474
- EM fields of vertical mag. dipole over thin conductive overburden 8-65183
- EM ground waves, elec./mag. field ratios in realistic terrain 8-88795
- EM inverse interpretation, trend influence 8-81103
- English Channel, deep structs. and mag. anomalies, possible hidden suture NW of Brittany 8-61397
- equivalent linear amplitude geomagnetic indices, evidence for strong artificial components 8-89008

geomagnetism continued

- F₂-layer field-aligned and field-perpendicular vels. theory 8-85760
 field definitive model and secular variation for 1965, derivation and comparison with IGRF 8-96133
 field intensity vector components, determ. from magnitude, error estimate 8-73308
 field line merging and slippage in auroral arcs 8-77393
 field meas., magnetotelluric sounding technique using SQUID devices 8-96322
 field reversals, relaxation model 8-85480
 folds, magnetic fabric 8-85481
 frequency EM sounding, anomalous high cond. bands discovery in crystalline foundation (*Russian*) 8-96137
 ground magnetic perturbations rel. to interplanetary magnetic field vars. 8-77431
 ground subsurface, EM transient response 8-57166
 horizontal component of field, absolute value determ. method 8-81420
 hydromagnetic dynamo of atmosphere 8-96335
 induced polarisation technique for prospecting 8-69473
 induction in arbitrarily shaped infinitely conducting oceans 8-61318
 induction vectors, local time var. 8-85477
 ionosphere, evidence for closed field lines in dayside auroral region 8-77391
 ionosphere, mag. field orientation rel. to intersatellite whistler-mode pulses propag. 8-69605
 ionosphere plasma stream propag., geomag. field effects in controlled rocket-borne expt. 8-57424
 Italy, anomalies from regional magnetic survey 8-65175
 kinematic dynamo of three spherical eddies, model 8-69286
 magnetosphere, adiabatic modulation of equatorial pitch angle anisotropy by mag. field 8-89003
 magnetosphere, assoc. elec. field, mag. field and electron precip. fluctuations 8-81507
 magnetosphere, dayside mag. flux transfer assoc. with expansions and contractions 8-96355
 magnetosphere, elec. currents and mag. field in hot adiabatic plasma 8-89002
 magnetosphere, equilib. mag. flux distrib. in moving force tube 8-69618
 magnetosphere, field-line reconnection, static-state model 8-61677
 magnetosphere, frontside boundary layer obs. and reconnection problem 8-89010
 magnetosphere, geomagnetic diagnosis, book 8-89015
 magnetosphere, mag. field models rel. to drifting energetic protons pitch angle dispersion 8-77428
 magnetosphere, mag. field tension rel. to plasma sheet press. anisotropies 8-89009
 magnetosphere, plasma mantle and ionospheric plasmas, field aligned distrib. 8-57406
 magnetosphere boundary, mag. field from laboratory simulation data 8-57396
 magnetosphere tail, explosive tearing mode reconnection 8-88992
 magnetotail, adiabatic particle motion in nearly drift-free mag. field 8-57399
 magnetotail, expected reconnection signatures 8-96361
 magnetotail, unsteady mag. reconnection rel. to plasma flow pulsations 8-77436
 magnetotail boundary layers, mag. merging, hot tenuous plasmas and fireballs 8-77438
 magnetotail configuration near midnight during quiet and weakly disturbed periods, mag. field modelling 8-96354
 magnetotail neutral sheet wavy profile, Imp 5 meas. 8-61665
 magnetotelluric field in homogeneous layer with cylindrical inclusion (*Russian*) 8-53617
 magnetotelluric impedance function estimation 8-85731
 magnetotelluric measurements, using lock-in signal detect. 8-81104
 magnetotelluric sounding, high-resistance horizons in laminated medium (*Russian*) 8-69290
 magnetotelluric sounding localization and accuracy improvement (*Russian*) 8-53754
 magnetovariational sounding curves, effect of relief of high-impedance basic horizon 8-85475
 Manicouagan structure, Quebec, central mag. anomaly 8-81169
 meteor plasma diffusion, geomagnetic field effect expt. (*Russian*) 8-61814
 Mezen' Bay (White Sea), marine tides EM fields 8-73378
 microstructure separation, digital filtering methods 8-69480
 Newfoundland, geomag. sounding near northern termination of Appalachian System 8-61314
 normal and observed mag. field, separation method 8-69479
 north magnetic pole, 1975 position analytical determ. 8-92778
 ocean-coast model, EM response to E-polarisation induction 8-61321
 E-Pacific Rise-Galapagos Rise system, magd mag. anomalies and rock magnetism 8-73331
 plasma sheet, near-Earth, search for mag. neutral line from Imp 6 mag. field obs. 8-89007
 plasma sheet, plasma flows and mag. field vectors during substorms 8-96357
 plasma sheet outer boundary, satellite meas. and field-line mapping during substorms 8-88990
 quasi-static EM fields of horizontal electric dipole on polarisable half-space surfaces 8-69283
 SI units (*German*) 8-65391
 singular points in mag. field models 8-69289
 static potential fields data inversion, generalised inverse appl. 8-77350
 thermosphere, polar airglow mag. ordering 8-57378
 transient EM response from irregular surface models 8-57165
 Trivandrum, crust-mantle structure from Indian geomagnetic data 8-85520
 underground quarries, EM transmission meas. 8-57365

geometric programming

- T breeding in fusion-fission Tokamak, optimisation with geom. program 8-74477

geometrical optics

- beam wave, propag. through weak turbulence, frequency spectra 8-78911
 Cherenkov radiation, in inhomogeneous medium, geometric optics description 8-66766

geometrical optics continued

- circular symmetrical reflector with laterally defocused light source, axial ray trace equations (*Russian*) 8-90365
 education, cornea, radius of curvature, quantitative geometric optics expt. 8-62004
 EM wave diff. on convex, smooth, ideally conducting and electrically large surface 8-94363
 EM wave reflection from nonhomogeneous plane stratified plasma 8-87453
 fibre, spherical-ended, efficient coupling to LED, geometrical optics anal. 8-83086
 fibre light propagation (*Czech*) 8-74997
 fibres, randomly bent, ray theory 8-66921
 flux concentrators, approach to ideality 8-66885
 funnel concentrator optics, ray tracing 8-58900
 graded index waveguide problem soln., comparison of wave and ray techniques 8-59140
 holography, two-dimensional volume, coupled wave differential eqns. derivation 8-55317
 Huygens-Fresnel integral in circular coords., asymptotic soln. 8-87013
 illuminator using laser light source, geometrical optical anal. (*Russian*) 8-79094
 inhomogeneous plane wave shadowing by an edge 8-90356
 laser beam, far-field profile, focal plane technique 8-87087
 laser beams, spatial structure 8-83014
 laser cavities with two foci, stability conditions 8-66850
 lens, multi-element, defective surfaces, tilt meas. 8-66886
 light ray reflection at dielectric-vacuum interface, exam. using Fermat's principle and evanescent waves 8-58902
 Maxwell fish-eye theory, formal equivalence with Kepler problem 8-81733
 MHD wave propagation in inhomogeneous media, calc. allowing for finite cond. (*Russian*) 8-63553
 microcapillary gas-dielectric filled waveguide with azimuthally asymmetrical cross-section, attenuation calcs. 8-83105
 paraxial approximation to scalar Helmholtz eqn., discrete eikonal and ray eqns. 8-90360
 randomly bent multimode fibres, ray theory 8-79129
 ray statistics of multimodal optical fibres 8-94450
 reduced wave eqn., parabolic approx., asymptotic solns. 8-78908
 source dimension estimation from diffraction image using Chebyshev approx. (*Russian*) 8-82903
 square law medium, incident Gaussian beam field distrib. 8-74840
 stray light phenomena, GUERAP III Monte Carlo simulation 8-58907
 stray light simulation with advanced Monte Carlo techniques 8-58906
 stray radiation analysis using first-order deterministic APART program 8-59116
 surface representation in cartesian coordinates, optical path calc. appl. (*German*) 8-78902
 teaching, paraxial and nonparaxial approx., matrix methods 8-77638
 trajectories of reflected and transmitted beams in oblique tunnel effect 8-78903
 tunnelling ray attenuation in fibres, generalised parameters 8-66908
 uniaxial crystals interface, EM wave refl. and refr. laws, tensor derivation 8-71029
 unstable resonators with rounded edges, mode losses 8-79039
 wide aperture optical systems, irradiance field formation, comparative analysis 8-90479
 Wigner distribution function applied to optical signals and systems 8-50713

geometry*see also space time configurations*

- angular structure of unique spherical shells, appl. to ang. momentum quantisation 8-73873
 area of intersection of n equal circular discs, appl. to hard-disc fluid model 8-57755
 boundary-value problems, variational principles and hypercircle 8-57749
 complex space-times, real geom. 8-77684
 conharmonic curvature tensor, Kahler space 8-54146
 coordinate transformation of Laplace operator in 2-D, for teachers 8-61999
 differential, appl. to mechanics, math. model of general relativity 8-69968
 differential forms in mathematical physics, book 8-81810
 dimensionality of physical space, assumption of three-dimensionality 8-93515
 faceless linear cones, orders, gauge, and distance, appl. to continuum mechanics and special relativity 8-57753
 fibre bundle techniques in gauge theories 8-54573
 fibre bundles, gauge theory of strong and EM interactions 8-54574
 fibre-bundle approach to gauge field theory 8-58130
 field theory in Finsler spaces, nonlocalisation, internal variable 8-49963
 general relativity, dynamical formulation using infinite dimensional differential geometry 8-93582
 general relativity, superspace, local supersymmetry, superfibre bundle theory 8-77782
 inverse power law potentials about polygonal prisms and in polygonal cavities 8-95232
 isometric folding of Riemannian manifold 8-77685
 Kerr metric, vortical type geodesics, causality non-violation 8-54251
 Lagrangian field theory, vector bundles, rth order Noether invariants and canonical symmetries 8-86409
 Lane-Emden eqn. of index 5, geometric technique for M-solns. 8-61851
 Lie group, path integral and quasiclassical asymptotic behaviour 8-54230
 Lobachevskii space vector and relativistic kinematics 8-62076
 Lorentz manifolds, potentially umbilical, structured by parallel spatial connection (*French*) 8-49646
 Nelson's stochastic mechanics on Riemannian manifolds, classical dynamical system 8-57860
 nonholonomic mech. systems of second order, geometrisation of motion 8-57771
 orbital motion of three bodies, Hill's curves, geometric prop. 8-77474
 Poincare's conventionalism of applied geometry 8-86110
 Riemann curvature of conservative systems in classical mechanics 8-89332

geometry continued

- Riemannian manifold, harmonic forms of curvature type (*French*) 8-86124
- Rosen's bimetric theory of gravity, orbital topoography and other astro-physical consequences 8-54274
- semiclassical theory of scalar field in globally hyperbolic universe 8-54250
- Sine-Gordon eqns., differential geometry appls., soluble relativistic field theories (*Russian*) 8-74162
- single elastic body point, geom. of motion 8-49662
- smooth vector fields, geometrical generalization of relation between limit cycles and symms. 8-54163
- solar hour angle, formula rel. to latit.-independ. sundial construction 8-81549
- some thermodynamical remarks on the theory of gravitational field 8-81899
- spinor Lie derivative, geometric significance 8-73826
- supergeometry mathematics, supersymmetries 8-73891
- supergravity, geometry of superspace, vector-spinor matter 8-49744
- superspace, generally covariant theories of gauge fields 8-54568
- supersymmetry, geometric model 8-54579
- variational principles on rth order jets of fibre bundles in field theory 8-86168

geons see *gravitons*

geophones see *seismometers*

geophysical aspects of cosmic rays

- 1972, August cosmic ray storm, north-south anisotropies and related phenomena 8-89018
- altitude differences and geomag. field secular changes effects on variational coeffs. 8-93058
- atmosphere, ion-pair production rate above 18 km altitude, parametrisation 8-65469
- atmospheric Cherenkov pulse duration, depend. on cosmic ray shower parameters 8-89025
- cosmic rays, velocity diffusion, turbulent mag. field, Monte Carlo calc. 8-53777
- dynamic processes on Earth, extraterrestrial causes, rel. to extinction of life 8-92820
- equator-pole symmetrical anisotropy during unusual cosmic ray storm 8-89020
- geomagnetic effects on incident cosmic radiation 8-53615
- hard X-rays, cosmic ray and electron-induced background, HXX results from ANS in Earth orbit 8-81716
- high-energy cosmic-ray components in atmosphere, scaling features 8-93062
- inclined muon monitors, muon spectra, generating functions, rel. to diurnal variation at Kiruna 8-85783
- intensity var. from tree ring stable isotope conc. 8-61692
- ionisation events in stratosphere, effects on NO₂, O₃ and climate, rel. to life extinction 8-96273
- meteorological conditions determ. from cosmic ray obs., spectrographic method 8-69627
- muons, sea-level spectrum, Dao scaling model for pp→π⁺X 8-61694
- muons and neutrinos detect. in deep sea using manned submersibles 8-81510
- neutrons at aircraft altitudes, Ames collaborative study on mid-latitude flights 8-53538
- nucleon spectrum meas. at GSFC, vertical sea-level meson-neutrino spectrum determ. 8-85782
- pion spectrum, at top of atmosphere 8-53780
- polar cap absorption intensity and solar cosmic rays north-south asymm., riometer data 8-69629
- protons, as extraterrestrial source of atmospheric water vapour, Sun-weather relationships appls. 8-69416
- recurrent Forbush decreases and solar active regions rel. to M-regions 8-96367
- sea-level muon spectra, model using kaon-pion ratio 8-93064
- snow gauge, cosmic ray, construction, characts., snow-water equivalent meas. (*Japanese*) 8-69498
- splash and re-entrant albedo electrons, energy spectra 8-69630
- temperature variations, spectrographic obs. of secondary cosmic rays 8-69628
- turbulent diffusion, partially averaged field approach 8-53776
- ⁷Be production in troposphere, mean residence time calc. 8-85633
- ¹⁴C in atmosphere content variation, past geomagnetic and cosmic ray intensity variations 8-61691

geophysical equipment

- see also *atmospheric measuring apparatus; geophysical prospecting; geophysical techniques; meteorological instruments; oceanographic equipment; seismometers*
- AC demagnetisation apparatus, palaeomagnetic research appl. 8-85733
- airborne multicoil EM survey system for resistivity mapping 8-77348
- airguns, linear arrays, signature and amplitude 8-69297
- deep ocean seamount detection using reconnaissance sonar 8-69551
- discharge transient recorder for induced polarisation meas. 8-65398
- distance measurement device, electro-optical, appl. to water levels obs. (*German*) 8-69280
- Fourier transform IR spectrometer, for satellite, optical design problems (*German*) 8-86360
- gamma-ray spectrometric logging and surface exploration equipment calibration 8-85706
- geothermal field station GS-1 with thermoquartz resonators, description (*Russian*) 8-93000
- gravimeter, LaCoste and Romberg, vibr. characts. (*Japanese*) 8-65400
- gravimeters, sensitivity determ. rel. to gravity tidal changes at Poltava (*Russian*) 8-88782
- gravity gradiometer, moving-base, surveys and interpretation 8-77344
- high temperature MOSFET characteristics for geothermal instrumentation, up to 300°C 8-73553
- hot water drill, open circuit, for hole drilling in cold glaciers 8-65402
- IR system performance in airborne environment 8-82039
- laser interferometer with path difference up to 1 km, geophysical appl. 8-61616
- Laterolog 7 resistivity logging, field tests 8-61574
- measuring equipment, metrological provisions, oil, natural gas reserves appl. 8-93002
- Mini-Sosie high resolution seismic reflection system, operational principles 8-85707
- optical reimaging system, out-of-field radiation analysis 8-59117

geophysical equipment continued

- optical-mechanical scanners for Earth observation (*Russian*) 8-96321
- pore pressure transducer, appl. to Kayenta sandstone mechanical props. meas. 8-81150
- probes with semiconductor temp. sensors for sediments thermal cond. meas. (*Russian*) 8-65431
- profilograph, for rock joints roughness determ. 8-96315
- radar systems, space based, development, appl. 8-81525
- resistivity surveying, apparatus, interpretation, underground. fieldwork 8-49623
- rocks hardness and abrasiveness meas. apparatus, suggested methods of use 8-9631
- shear wave transducer for use in marine sediment studies 8-63257
- snow gauge, cosmic ray, construction, characts., snow-water equivalent meas. (*Japanese*) 8-69498
- snow melt calorimeter (*Japanese*) 8-88934
- soil freq. shift dielectric 8-53739
- soil moisture meter, development (*Japanese*) 8-88935
- soil resistance meter, geological and archaeological applications (*German*) 8-57361
- sonar, fibre optic system, geological and hydrographic survey applications 8-88947
- Spectral Infrared Experiment equipment and objectives 8-81456
- spectroradiometer for airborne remote sensing 8-88943
- spindle stage, turning point for optical crystallography 8-85702
- strong motion accelerographs, characts. of EM starters 8-65396
- superconducting magnets, appl. to minerals mag. separation (*Czech*) 8-88923
- temperature and pressure transducers with ground-level tape recorder, hydrodynamic logging in boreholes (*Russian*) 8-53761
- temperature wave generator for diurnal temp. wave propag. simulation 8-85735
- theodolite standardised series, specification 8-73543
- theodolites, electrooptical and microprocessor-based (*Czech*) 8-77860
- thermomagnetometers, for rocks remanent mag. meas. 8-85719
- tide-recording equipment, phototransducers emission source light output ratio stabilisation (*Russian*) 8-88949
- tilt gauge, based on Hg pool 8-88931
- tilt meter at Berezovaya Rudka station, obs. and sensitivity vars. (*Russian*) 8-88783
- tilt meters, photoelectric, with negative feedback, block diagrams anal. (*Russian*) 8-88948
- tiltmeter for long-baseline operation 8-81440
- trace elements in rocks, analysis by direct-reading spectrometer 8-85738
- vector magnetometer stabilisation using independent servo system 8-77355
- Rn-Th monitor for earthquake prediction research 8-73532

geophysical prospecting

see also *minerals*

- airborne radiometric data inversion, radioactive elements conc. mapping 8-77347
- airguns, linear arrays, signature and amplitude 8-69297
- borehole casing perforation by liquid metal jet, nozzle design, theory (*Russian*) 8-51216
- borehole-layer system, neutrons elastic and nonelastic scatt. on nuclei of rock-forming elements 8-61582
- Canadian deposits, reconnaissance programme (*French*) 8-88827
- coal, seismic respons. of carboniferous rock, synthetic seismograms 8-69293
- coal banding-plane indicator, magnetic susceptibility anisotropy meas. 8-77221
- coal seams with discontinuities, SH channel wave attenuation 8-69292
- common depth point survey data, vel. characts. determ., refl. interfaces inclination angles (*Russian*) 8-53753
- common depth point survey technique appl. in permafrost conditions (*Russian*) 8-53751
- continental basement exploration by seismic reflection profiling 8-96172
- continental shelf, possibility of geoelec. mapping 8-57341
- deep water surveying, new techniques 8-85730
- depth determ. from seismic refraction data, iterative method 8-96302
- direct current regimes, theorem proof 8-96131
- Dnieper-Donets depression, magnetotelluric sounding data rel. to deep struct. (*Russian*) 8-96170
- Dnieper-Donets depression, sedimentary cover struct. along Jagotin-Baturin profile (*Russian*) 8-92806
- drill-rod telemetry, calcs. for toroidal coil source 8-85710
- electrical resistivities overlaid Earth, transformation using digital filters 8-96304
- EM field properties reproduction, spherical, by real meas. devices (*Russian*) 8-85729
- EM fields of horizontal electric dipole on polarisable half-space surface 8-69283
- EM fields of vertical mag. dipole over thin conductive overburden 8-65183
- EM inverse interpretation, trend influence 8-81103
- EM prospecting, wave type and direction from EM field short-period vars. anal. (*Russian*) 8-85474
- EM wideband freq. response conversion to transient response using segmented transform. 8-77349
- exploratory drilling exhaustion sequence plot program 8-57334
- frequency EM sounding, anomalous high cond. bands discovery in crystalline foundation (*Russian*) 8-96137
- gamma-ray spectrometric logging and surface exploration equipment calibration 8-85706
- gamma-rays from extended sources, energy distrib. calc., rel. to remote spectroscopy 8-61586
- geochemical exploration using marine mineral suspensates 8-88936
- geoelectrical prospecting in marine areas, resistivity methods 8-65417
- geological prospecting data processing system, Poland (*Polish*) 8-88929
- geothermal energy exploration using chemical geothermometers and mixing models 8-69503
- geothermal prospecting, via field station GS-1 with thermoquartz resonators (*Russian*) 8-93000
- geothermal reservoirs, downhole meas. of thermal conductivity 8-61618
- gravity profile inversion by method 8-69476
- induced polarisation technique for prospecting 8-69473

geophysical prospecting continued

- inductive dipole sounding anomaly, low-impedance overburden screening (*Russian*) 8-81106
- inverse gravity problem, infinite polygonal cylinders 8-53607
- inverse problems, max. entropy method, extreme models 8-65230
- lateral logging three-electrode probe, effective field model (*Russian*) 8-53762
- lateal resistivity logging, effectiveness increase (*Russian*) 8-53760
- Laterolog 7 resistivity logging, field tests 8-61574
- magnetotelluric field in homogeneous layer with cylindrical inclusion (*Russian*) 8-53617
- magnetotelluric sounding, multiple-reflection method appl. to inverse problem soln. 8-61581
- magnetotelluric sounding localization and accuracy improvement (*Russian*) 8-53754
- magnetovariational sounding curves, effect of relief of high-impedance basic horizon 8-85475
- Mini-Sosie high resolution seismic reflection system, operational principles 8-85707
- offshore seismic refraction surveying, nonexplosive energy sources (*Russian*) 8-53752
- oil, new seismic reflection techniques 8-73541
- oil exploration, seismic appls. 8-96151
- oil well productivity rel. to seismic reflection amplitude 8-69295
- petroleum, digital recording of ultrasonic signals [petroleum prospecting] 8-73552
- petroleum exploration, marine seismic data for detrital sediments 8-96303
- polarisable half-space, current pulses, transient EM field 8-96130
- radiation and isotopes appl., development trends 8-55041
- radioactive ores, specific sensitivity of NaI(Tl) scintillator in γ -ray meas. 8-81449
- radiometry diagrams, statistical standardisation check (*Russian*) 8-69483
- reflection seismic exploration, data processing requirements 8-96325
- reflection seismic recordings, minimum entropy deconvolution 8-81423
- reflection seismology, tool for energy resource exploration, book 8-96162
- reflection seismology, use of kepsrum in signal anal. 8-81425
- resistivity logging, direct problem soln. using graphic display (*Russian*) 8-69481
- resistivity mapping using airborne multicoil EM survey system 8-77348
- resistivity sounding on multilayered Earth with transitional layers, examples 8-69282
- resistivity surveying, apparatus, interpretation, undergrad. fieldwork 8-49623
- salt mines, radar propag. in rock salt 8-96215
- seismic cross sounding, data interpretation via reflected wave method (*Russian*) 8-92796
- seismic data deconvolution 8-53736
- seismic exploration, iterative identification of non-invertible autoregressive moving-average systems 8-81422
- seismic holography, kinematic mutuality of reflected and refracted waves (*Russian*) 8-69298
- seismic Rayleigh channel waves for reflection method, dipping coal seam discontinuity obs. 8-69471
- seismic reflection data inversion 8-96307
- seismic signals, adaptive deconvolution 8-53737
- seismic waves interference effects in thin layers 8-92780
- seismic sounding, screening in media with inclined boundaries (*Russian*) 8-92794
- telluric profiling technique for apparent pseudo-resistivity mapping (*French*) 8-69285
- temperature and pressure transducers with ground-level tape recorder, hydrodynamic logging in boreholes (*Russian*) 8-53761
- two-fold resistivity mapping of lateral inhomogeneities 8-61573
- underground quarries, EM detection (*French*) 8-96306
- vertical frequency effect sounding in induced polarization and galvanic resistivity methods 8-69284
- VLF scattering by perfectly conducting half plane below stratified overburden 8-57167
- wire loop laid on ground, radiation resistance calc., antenna for parametric depth sounding (*Chinese*) 8-61565
- U content determ. using liquid scintillation spectroms. (*Czech*) 8-69487
- U exploration and international cooperation 8-86628
- U in natural waters, field meas. technique 8-85705
- U in rock samples, meas. by track registration in plastic detectors 8-73533
- U ore detection, using trace detection sensitive to ^{222}Rn α -particles (*Hungarian*) 8-77339
- U ores, integrated Rn emanation mapping for gases long-distance migration detect. 8-85560
- U resource evaluation by neutron activation anal. 8-85741
- U-bearing rocks, radioactive disequilib. determ., isotopes relative abundance meas. 8-57330

geophysical techniques

see also *atmospheric techniques*; *geophysics*; *ionospheric techniques*; *oceanographic techniques*

- acoustic signal mean frequency meas. (*Russian*) 8-81441
- active faults, aerial photographs interpretation (*Japanese*) 8-96124
- adaptive deconvolution of seismic signals 8-53737
- aerial photography, multispectral, soil survey in New Zealand 8-85728
- airborne radiometric data inversion, radioactive elements conc. mapping 8-77347
- altimetric data file acquisition automatic digital correlation method 8-61633
- anisotropic seismic surface-wave dispersion, isotropic inversion significance 8-96156
- array algebra for multilinear least squares prediction and filtering 8-69470
- asbestos fibres identification, electron microscope techniques comparison 8-66012
- ATS-6 electron content data presentation 8-61593
- automated shipboard acquisition and processing of offshore geophys. data (*Russian*) 8-53750
- binary seismic holography, kinematic principle (*Russian*) 8-92795
- biotite-apatite geothermometer, re-examination 8-85704

geophysical techniques continued

- body-wave seismograms synthesis, modified first motion approximation 8-73315
- Bremmer series decomposition of solns. to lossless wave eqn. in layered media 8-53738
- cartography stereomapping processes 8-61631
- coal layer thickness meas., EM technique 8-53740
- coal research, appl. of neutron activation anal. 8-85740
- common depth point survey data, vel. characts. determ., refl. interfaces inclination angles (*Russian*) 8-53753
- common depth point survey technique appl. in permafrost conditions (*Russian*) 8-53751
- contact surface parameters determ., regularisation method (*Russian*) 8-53756
- continental shelf, possibility of geoelec. mapping 8-57341
- coring and squeezing technique for study of subsurface water chem. 8-57332
- coupled solid/fluid/surface wave dynamic interaction problem, improved fluid superelement 8-81108
- crop classification from Landsat data, pattern recognition, temporal trend analysis 8-65440
- crustal motions detect. using spaceborne laser ranging systems 8-92995
- data processing, underground mapping reflection seismic method 8-96325
- dating techniques, effects of thermal annealing on track etching rate of sphene, CaTiSiO_5 8-65435
- deconvolution in freq. domain using self-matching filter 8-69477
- deep sea cores sedimentation rates determ. by fission/alpha track counting 8-61392
- depth determ. from seismic refraction data, iterative method 8-96302
- digital image anal. for natural resources inventories 8-96326
- digital image processing for resources monitoring 8-96328
- digital image processing techniques for planetary program and Earth resources information 8-96408
- digital seismic data processing, struct. anal. of graphs (*Russian*) 8-53749
- digital signal modelling and classification with the teleseismic data 8-73325
- diving waves in multilayered medium, time-distance curve transformation 8-69472
- Dnieper-Donets depression, sedimentary cover struct. determ. by seismic common depth point method (*Russian*) 8-92806
- Earth crust in situ stress field, determ. via hydrofracturing, fracture mechanics approach 8-81435
- Earth interior density distrib., determ. from gravity logging data (*Russian*) 8-92999
- Earth resource thermal imaging by airborne system, possible LED use 8-93010
- Earth resources sensing, LANDSAT system features 8-96330
- Earth tide observations processing, individual monthly sets weightings (*Russian*) 8-88789
- Earth tides measurement, cavity effect in tunnels of various cross-sections (*Russian*) 8-88784
- Earth tides observations, monthly data set anal. (*Russian*) 8-88786
- earthquake focal depth determ. using Rayleigh surface waves, principal mode and harmonics obs. 8-61351
- earthquake foci motion, typification technique, seismotectonic problems soln. 8-61350
- earthquake prediction, using He/Ar and N_2/Ar ratio vars. in fault zone groundwater air bubbles 8-88803
- earthquakes, automatic identification from microearthquake network data 8-81412
- earthquakes, centrifuge modelling 8-81429
- electrical resistivities overlaid Earth, transformation using digital filters 8-96304
- electron microprobe, automated, evolution of quantitative elementary point anal. in geosciences (*French*) 8-78046
- elemental concentration of geological samples 8-85268
- EM field properties reproduction, spherical, by real meas. devices (*Russian*) 8-85729
- EM prospecting, wave type and direction from EM field short-period vars. anal. (*Russian*) 8-85474
- explosion seismology primary signal form., effect of partial multiple refl. (*Russian*) 8-85484
- fibre optics appl., IR LED and optical cables improvements 8-59123
- frequency EM sounding, anomalous high cond. bands discovery in crystalline foundation (*Russian*) 8-96137
- geochemical exploration using marine mineral suspensates 8-88936
- geodesy, geometrical and dynamic methods, development (*Polish*) 8-88780
- geolectrical prospecting in marine areas, resistivity methods 8-65417
- geological materials mechanical behaviour, studies via stress relaxation testing method 8-96309
- geological-geophysical zoning possibility 8-57342
- geomagnetic field horizontal component, absolute value determ. method 8-81420
- geomagnetic field intensity vector components, determ. from magnitude, error estimate 8-73308
- geomagnetic field microstructure separation, digital filtering methods 8-69480
- geopotential fields, filtering and transform. theory using information on input data noise 8-61584
- geothermal areas in Iceland, H-water isotope thermometer appl. 8-69384
- geothermal energy, heat extraction from hot dry rock masses 8-61378
- geothermal prospecting, via field station GS-1 with thermoquartz resonators (*Russian*) 8-93000
- geothermal reservoirs, downhole meas. of thermal conductivity 8-61618
- geothermal resources, nucl. techniques in geochemical studies 8-85746
- geothermal systems, sulphate-water O isotope thermometry 8-69383
- geothermal tracing with atmospheric and radiogenic noble gases 8-69502
- geothermometry, chemical and isotopic techniques 8-69501
- glacier thickness meas. using dielectric permeability characts. 8-89500
- glaciology of Columbia Icefield, surveying techniques 8-61445
- gravity, anomalies separation from background field, FON computer program (*Russian*) 8-53757
- gravity and magnetic, anomalies, linear anal. (*Russian*) 8-53755

geophysical techniques continued

- gravity anomalies interpretation, algorithm for calc. gravit. attraction of models of structural features (*Russian*) 8-53758
- gravity anomalies measured in Krivoi Rog basin (Krivbas) underground workings, interpretation (*Russian*) 8-85466
- gravity disturbance covariance functions, upward continuation integrals 8-85468
- gravity profile inversion by method 8-69476
- Greenland ice sheet topography from satellite radar altimetry 8-81233
- groundwater flow calc. by finite element method 8-89320
- groundwater flow digital simulation, finite element method 8-93018
- holographic terrain displays in 3D 8-78979
- hydraulic fractures mapping using elec. potential technique 8-69543
- ice sheets in polar regions, radio obs. appls. 8-81419
- ice-cover thickness on rivers and lakes, pulsed radar meas. method 8-92862
- induced polarisation meas. using discharge transient recorder 8-65398
- induced polarisation technique for prospecting 8-69473
- inverse problems soln. by method of dynamic models (*Russian*) 8-85714
- ISO FORTRAN IV program for generating isopleth maps on small computers 8-57157
- isotope geothermometry in the Larderello geothermal field 8-69312
- isotope techniques, appls. to geothermal systems in New Zealand 8-69313
- Kolmogorov-Wiener least-squares filters appl. to geophys. anomalies separation 8-61580
- LANDSAT data high-level computer processing 8-69546
- LANDSAT image, digital anal. and appls. 8-65404
- LANDSAT image processing, pipelined systems, design 8-96329
- LANDSAT imagery processing and enhancement 8-69545
- LANDSAT multispectral data classification algorithms 8-61629
- LANDSAT ratio image dynamic range reduction technique 8-69547
- LANDSAT spectral data classifications, atmospheric correction 8-69548
- leaky aquifer analysis, finite element method soln. 8-93017
- limestone diagenesis simulation, computer model based on Sr depletion 8-73358
- local gravity anomalies interpretation, integral ratios (*Russian*) 8-85463
- macroseismic data processing and interpretation 8-61583
- magnetic anomalies, interpretation with end-corrected Fourier transforms. 8-65418
- magnetic field meas., magnetotelluric sounding technique using SQUID devices 8-96322
- magnetotelluric impedance function estimation 8-85731
- magnetotelluric measurements, using lock-in signal detect. 8-81104
- magnetotelluric sounding, multiple-reflection method appl. to inverse problem soln. 8-61581
- Mahalanobis' D^2 distance for sediment distinction (*Portuguese*) 8-61388
- marine gravimetry, cross-coupling effect compensation by intersection point method 8-57340
- metal species, pollutants, identification and determ. by chromatographic-at. spectrosc. method 8-68972
- metamorphic bathozones and bathograds, meas. of regional scale post-metamorphic uplift and erosion 8-81113
- meteorological real-time data acquisition and anal. 8-69466
- microwave scanning radiometry, appls. 8-73551
- minerals, anal. of small samples using X-ray quantometer 8-61112
- minerals, mag. separation using supercond. mags. (*Czech*) 8-88923
- modelling techniques, statistical tests for goodness of fit 8-57333
- multiple covering problem for large scale seismic network modelling 8-69540
- multiple water reflections recorded at ocean bottom 8-57331
- multispectral remote sensing ratio image digital processing and interpretation 8-81461
- multispectral scanner image rectification, practical experience 8-88940
- multispectral scanner imagery rectification 8-88939
- natural resource digital image anal. development in USA 8-96327
- natural surface polarisation imagery, remote sensing appl. 8-61625
- neutron activation anal., using standard reference materials as multielement irradiated standards 8-80815
- neutron activation anal. technique for Na/K ratios in fluid inclusions determ. 8-61568
- neutron activation analysis, gamma-ray spectra prediction, detection limits, computational procedure 8-85242
- ocean bottom geology, underwater robot/manipulator development 8-77356
- oil prospecting, new seismic reflection techniques 8-73541
- palaeointensity methods using AF demagnetisation and anhysteretic remanence, reliability 8-77352
- palaeomagnetic analysis, effects of haematite reduction to magnetite 8-65277
- parameter sensitivity analysis method for differential eqn. models 8-81453
- petroleum exploration, marine seismic data for detrital sediments 8-96303
- photogrammetry, real-time, instrumentation for analytical video stereoscopy of extended images 8-88926
- polarography, amalgam, film, with accumulation, appl. to micro-, macro-object anal., review 8-61098
- polymetamorphic terrain primary age determ. 8-96168
- potential field transformation from relief to single reference plane, Fourier anal. appl. (*Russian*) 8-53759
- radar probing for rock salt 8-96215
- radioactive tracer detection techniques, flow problems appl. (*Japanese*) 8-96320
- radiometry diagrams, statistical standardisation check (*Russian*) 8-69483
- recrystallised grain size geopiezometer, applicability limits 8-85715
- recursive derivation of reflection coefficients from noisy seismic data 8-73324
- recursive multichannel max. entropy spectral estimation 8-53735
- reflection seismic recordings, minimum entropy deconvolution 8-81423
- reflection seismology, tool for energy resource exploration, book 8-96162
- reflection seismology, use of kepsrum in signal anal. 8-81425
- remote sensing, survey of methods and appls. 8-77364
- remote sensing image data processing/acquisition techniques 8-61627

geophysical techniques continued

- remote sensing of atmosphere, land and sea props. 8-93015
- remote-sensed data texture anal. in computerised picture processing 8-61628
- resistivity mapping using combined telluric profiling technique (*French*) 8-69285
- RESMAC seismic array, interactive epicentre location procedure 8-65395
- resource management, conf., Alamogordo, NM, USA, 1978 8-69541
- river ice break-up, satellite monitoring 8-65350
- river quality modelling by sequential extended Kalman filters 8-81248
- rivers/open channels level and vel. meas. by surface wave signal anal. 8-57328
- rock dynamic strength determ., reflected shear wave technique 8-57344
- rock joints roughness determination, new laboratory method 8-96315
- rock materials, strength determ. in triaxial compression, suggested methods 8-81432
- rock materials tensile strength determination, suggested methods 8-96314
- rock mechanics, appl. of AE (*Japanese*) 8-56845
- rock samples, Sn determ. by neutron activation method 8-85258
- rocks, anal. of small samples using X-ray quantometer 8-61112
- rocks, petrographic description, suggested method 8-81431
- rocks elastic properties determination, modified borehole jack method 8-81448
- rocks hardness and abrasiveness determ., suggested methods 8-96313
- rocks magnetic susceptibility anisotropy meas. using inductive magnetometers 8-85541
- rocks sound velocity determination, suggested methods 8-81433
- rocks texture heterogeneity, study via dielectric const. and elec. resistance (*Russian*) 8-96195
- satellite geodesy, role of orbit determ. in altimeter data anal. 8-77177
- satellite on-board processing for Earth resources data 8-61626
- satellite range measurements, formula for refr. effects computation 8-73609
- sediment and nutrient loadings to Lake Ontario calc., methodological arguments 8-77278
- sedimentation rates determ. in rapidly accreting salt marsh by ^{137}Cs dating 8-96247
- sediments thermal cond. meas. using probes with semiconductor temp. sensors (*Russian*) 8-65431
- seismic cross sounding, data interpretation via reflected wave method (*Russian*) 8-92796
- seismic data, optimum mixed delay spiking filters appls. 8-77346
- seismic data, single-channel white-noise estimators for deconvolution 8-77345
- seismic data deconvolution, review 8-53736
- seismic data migration by Fourier transform 8-77341
- seismic data migration in two and three dims., integral formulation 8-77342
- seismic exploration, iterative identification of non-invertible autoregressive moving-average systems 8-81422
- seismic holography, integral representations of space time functions (*Russian*) 8-85483
- seismic holography, kinematic mutuality of reflected and refracted waves (*Russian*) 8-69298
- seismic pattern recognition, fundamental problems 8-81428
- seismic Rayleigh channel waves for reflection method, dipping coal seam discontinuity obs. 8-69471
- seismic reflection data inversion 8-96307
- seismic refraction surveying, offshore, nonexplosive energy sources (*Russian*) 8-53752
- seismic source props. determ. by seismograms linear inversion 8-65394
- seismic surface waves, anal. using PDP-15 interactive graphics 8-81427
- seismic velocity determination in formations with curved interfaces (*Russian*) 8-53748
- seismic wave reflection at wide angles, travel times, interpretation method 8-65202
- seismic wave vel. calc. using reflection amplitude 8-69296
- seismic wavelet estimation, short-time homomorphic signal anal. appls. 8-81426
- seismic wavelet estimation using short-time homomorphic signal 8-88930
- seismic waves group velocity, high resolution anal. appl. to explosion and earthquake 8-81111
- seismology, multidimensional polarization analysis 8-73528
- seismology, ray approx. for laminated heterogeneous media (*Russian*) 8-69482
- separation method for normal and observed geomag. field 8-69479
- seismic facies analysis 8-96151
- seismic profiles, two-dimens., dip-domain migration 8-77343
- seismic sounding, screening in media with inclined boundaries (*Russian*) 8-92794
- silicate measurement in anoxic pore waters, effects of oxidation during sampling 8-61394
- snowfield assessment from Landsat 8-88941
- soil, thermal conduction flux in situ meas., methods (*French*) 8-96331
- soil and winter wheat yield on Great Plains, Landsat data evaluation 8-65351
- soil moisture, microwave remote sensing, sampling techniques for ground truth data 8-65439
- soil moisture content, microwave radiometer meas. over bare and vegetated surfaces, comparison 8-88851
- soil water flow modelling, finite difference and Galerkin techniques 8-81249
- soils, thermal props., transient measuring method (*German*) 8-61619
- solute loading and chem. denudation rate mapping in Devon, England 8-69375
- spatial filtering of higher Rayleigh mode phase vels. 8-77187
- spatial spectrum of random field, use of reference sensor in autoregression evaluations (*Russian*) 8-61578
- spectral estimation techniques for discrete time series 8-53734
- sphalerite geobarometer, experimental extension to 10 kbar 8-85703
- sphalerite geobarometry in Balmat-Edwards district, New York 8-65261
- stable operational processes appl. to inverse geophys. problems 8-85718
- static potential fields data inversion, generalised inverse appl. 8-77350

geophysical techniques continued

- statistical algorithms for scaling geophysical fields 8-73527
- stereophotogrammetry, automatic, using structural pattern recognition techniques 8-61632
- stream temp. modelling, 'dishonest' method 8-81454
- streamflow, empirical data, multivariate gamma distrib. fitting 8-81240
- subsidence and ground movement, holographic interferometry 8-57343
- surface waves, phase vel. and attenuation simultaneous inversion, Love waves in W North America 8-85491
- synthetic aperture radar imaging in geosynchronous orbit 8-65442
- synthetic seismogram computation, new method 8-85711
- thermal radiation from randomly inhomogeneous stratified media, calc. methods (*Russian*) 8-96312
- thermoluminescence dating of sediments baked by Chaine des Puys lava flows 8-92808
- tidal tilts, parallel recording through digital print-out and photorecording channels (*Russian*) 8-88785
- time-domain wave-shaping filter weights computation 8-77351
- track registration of U in rock samples 8-73533
- transient thermal conductivity meas., thermal contact resistance 8-53744
- underground quarries, EM detection (*French*) 8-96306
- variational inequality method, ditch seepage appl. 8-81251
- vertical frequency effect sounding in induced polarization and galvanic resistivity methods 8-69284
- Vibroseis system, encoding techniques 8-69474
- VlBI appl. to geodesy, Earth rot. and network geometry optimisation 8-92996
- volcanic rocks classification using Irvine and Baragar classification scheme, FORTRAN IV program 8-57203
- water levels, obs. via electrooptical distance meas. (*German*) 8-69280
- water pollution prediction, finite element method appls. 8-93019
- water resource system, Monte Carlo simulation, variance reduction techniques 8-81244
- wind stress on sea ice, meas. techniques and results (*Japanese*) 8-88842
- X-ray fluorescence analysis of natural water, precon. technique 8-61620
- As determ. in ores of reduced heteropoly acids, photometric method 8-61103
- ¹⁴C dating rel. to magnetic and other dating methods 8-57359
- Ca, determ. in lake sediments, by atomic absorption spectroscopy 8-95970
- Fe, determ. in waters, colorimetric-acid digestion method 8-61088
- Na determ. in rock, mineral samples, X-ray fluoresc. quantometer modification 8-61589
- P determ. in ores of reduced heteropoly acids, photometric method 8-61103
- ²¹⁰Pb dating method for determ. of Lake Ontario sedimentation rates 8-73408
- Rn integrated emanation, mapping for gases long-distance migration detect. 8-85560
- Rn measurement in groundwater and springs for earthquake prediction 8-88924
- ³⁴S/³²S ratio meas. using SO₂ and SF₆ methods, discrepancies 8-65405
- U in natural waters, field meas. technique 8-85705

geophysics

- see also *Earth; erosion; geochronology; geodesy; geology; geomagnetism; geophysical aspects of cosmic rays; geophysical techniques; groundwater; lakes; meteorology; oceanography; radiation belts; rivers; rocks; seismology; solar-terrestrial relationships; space research; terrestrial atmosphere; time and latitude; upper atmosphere*
- Mid-Atlantic Ridge, geophysical and petrological constraints 8-85508
- data storage by metallic carrier electroerosion via liquid pulsed discharge (*Russian*) 8-61563
- Geos satellite, first six months' obs. 8-61705
- global problems of fluid dynamics 8-96173
- MHD induction, simplest physical model of generator 8-71548
- natural resource digital image anal. development in USA 8-96327
- oceanography, geological, book 8-92845
- pressure solution thermodynamics, interaction between chemical and mechanical forces 8-57194
- Quetelet, A.L.J., life and spread of science in Belgium during 19th century (*French*) 8-65742
- thermodynamical Gruneisen gamma formulation 8-65264
- time series, nonstationarity of mean and Hurst phenomenon 8-81253
- upper atmosphere, ionosphere and magnetosphere, handbook 8-73557
- Weddell Sea, geophysical studies (1978 Jan./Feb.) (*German, English*) 8-96188

geophysics computing

- see also *computerised instrumentation*
- air pollution density distrib., flow pattern in Tanabe area, Japan, numerical anal. (*Japanese*) 8-96289
- algorithm for processing of observational series, ocean currents appl. (*Russian*) 8-65421
- atmosphere, molecular absorption, Lowtran 3B model 8-85690
- atmosphere photon transport problems, modified Monte Carlo procedure 8-61560
- atmospheric boundary layer turbulence, multi-component linear digital simulation 8-61513
- atmospheric infrasound waves recording method and computer anal. (*Russian*) 8-65407
- atmospheric pollution monitoring, centralised supervision system in Fos-Etang de Berre region 8-81410
- atmospheric transmission LOWTRAN 3B predictions, long-path high-resolution 8-92972
- atmospheric transmittance profiles calc. method 8-85696
- CLAIR data system overview 8-57325
- climate simulation, geophysical fluid system 8-81353
- climatic model experiments, simulated changes in albedo, surface roughness, surface hydrology, solar energy conversion effects 8-81354
- cloud droplet coalescence growth, fast computational method for Telford's theory 8-69486
- data processing, underground mapping reflection seismic method 8-96325
- digital radar data computer processing for High Plains Coop. Program (HIPLEX) 8-92989

geophysics computing continued

- digital seismic data processing, struct. anal. of graphs (*Russian*) 8-53749
- direct gravity formula for 1967 Geodetic Reference System 8-92775
- earthquake wave analysis program WAVE, DEMOS-E library program 8-92800
- electron microprobe, automated, evolution of quantitative elementary point anal. in geosciences (*French*) 8-78046
- EM wideband freq. response conversion to transient response using segmented transform. 8-77349
- estuary models of Tampa Bay, Florida, comparison 8-77269
- exploratory drilling exhaustion sequence plot program 8-57334
- F-region, polar cap and auroral zone, math. model 8-65458
- filtration simulation, hybrid, use of electrically conducting paper with discretely distributed capacitance (*Russian*) 8-88850
- fluctuations generation with arbitrary power spectrum, algorithm 8-73927
- geodesy, props. of Gauss-Helmert least-squares adjustment model (*German*) 8-61309
- geodetic data base, basic entities definition 8-65392
- geological and geochemical data management and processing 8-57324
- gravity, anomalies separation from background field, FON computer program (*Russian*) 8-53757
- gravity anomalies interpretation, algorithm for calc. gravit. attraction of models of structural features (*Russian*) 8-53758
- gravity studies using the facilities of UMRCC and the Computer Graphics Unit 8-77878
- gridded data convolution and padding algorithm 8-69475
- inverse filter which is optimum in error-distrib. sense, stability characts. 8-81424
- ionosphere incoherent scatter data, analytic partial derivatives for least-squares fitting 8-73581
- ionospheric data processing, improvement of convergence of least squares method (*Russian*) 8-85700
- Kolmogorov-Wiener least-squares filters appl. to geophys. anomalies separation 8-61580
- LANDSAT, Earth resource information 8-96330
- LANDSAT data high-level computer processing 8-69546
- LANDSAT imagery processing and enhancement 8-69545
- levelling data, time-space domain representation, computer program 8-88932
- limestone diagenesis simulation, computer model based on Sr depletion 8-73358
- macroseismic data processing and interpretation 8-61583
- mass consistent atmospheric flux model (MASCON) for complex terrain regions 8-92964
- meteorological real-time data acquisition and anal. 8-69466
- meteorology, data editing and validation using interactive graphics 8-77330
- meteorology, surface synoptic obs., automatic real-time quality control 8-92920
- microearthquake network data, automatic anal. 8-81412
- Mississippi River computerized data bank 8-73520
- nightglow multislit spectrometer design, computer simulation 8-73542
- oil spill simulation in Florida Gulf outer continental shelf 8-73406
- Omo River project (Ethiopia) data management system appraisal 8-57326
- optical crystallography computer anal. of spindle stage data 8-85702
- optimal numerical filters fitted for noise damping, atm. circulation simulation appl. 8-92997
- optimal sampling and anal. method 8-73530
- PETPAK, computing package for petrologists 8-57323
- potential field transformation from relief to single reference plane, Fourier anal. appl. (*Russian*) 8-53759
- power curve regression equations for Ohio River, statistical computer program 8-61472
- reflection seismic recordings, minimum entropy deconvolution 8-81423
- reflection seismograms signal anal., use of kepstrum 8-81425
- resistivity, magnetic and IP data interpretation techniques 8-85708
- resistivity logging, direct problem soln. using graphic display (*Russian*) 8-69481
- rocks asymmetric folding, finite-element simulation 8-77222
- safety assessment of radioactive waste disposal into salt deposits, fault tree anal. appl. 8-55046
- seismic data migration by Fourier transform 8-77341
- seismic data migration in two and three dims., integral formulation 8-77342
- seismic pattern recognition, fundamental problems 8-81428
- seismic risk analysis of lifeline networks 8-65192
- seismic surface waves, anal. using PDP-15 interactive graphics 8-81427
- seismic wavelet estimation, short-time homomorphic signal anal. appls. 8-81426
- seismic waves group velocity, high resolution anal. appl. to explosion and earthquake 8-81111
- seismic profiles, two-dimens., dip-domain migration 8-77343
- soil, unsaturated, coupled heat and water movement prediction, math. model 8-61446
- statistical algorithms for scaling geophysical fields 8-73527
- surface patterns in theoretical geophysics 8-57156
- synthetic seismograms using finite difference techniques 8-73326
- theodolites, electrooptical and microprocessor-based (*Czech*) 8-77860
- tides, spectral modelling, finite element method, appl. to M₂ tide in English Channel 8-61579
- time-domain wave-shaping filter weights computation 8-77351
- triggering digital seismograph with microprocessor 8-96308
- TRIPLLOT, APL program for plotting triangular diagrams 8-57335
- troposphere, radio propag. characts. prediction using FORTRAN computer programs (*Italian*) 8-85666
- tropospheric range correction algorithm 8-61591
- turbulent atmospheric transport, Monte Carlo simulation, radioactive pollution appl. 8-61550
- Vela seismological network, use of datacomputer 8-81411
- volcanic rocks classification using Irvine and Baragar classification scheme, FORTRAN IV program 8-57203
- weather, numerical prediction review 8-69393
- wind-wave interaction, two-layer flow, numerical simulation 8-92823

geophysics computing continued

zones of influence of linear geological structures, computation program 8-57202
NaCl, rock salt, progressively mined soln. cavities, struct. behaviour 8-61409

geopotential see *geodesy*

geothermal power stations

American Nucl. Soc. winter meeting 1977 8-58315
American Nucl. Soc. Winter Meeting 1977 8-82408
Iceland, geothermal energy exploitation 8-57181

germanate glasses

film, SiO₂ rich, prepared by modified CVD, refr. index behaviour 8-60526
BaO-La₂O₃-GeO₂, exam. of glass forming region, properties and crystallisation 8-88454
Cs₂O-SiO₂(-GeO₂) system glasses, X-ray diffr. anal., electron radial distrib. curves 8-87622
GeO₂, thermal expansion at low temperatures 8-83982
K₂O-GeO₂:tb³⁺, Yb³⁺ glass, luminesc. cooperative sensitization correlated with Rayleigh scatt. intensity 8-52573
K₂O-SiO₂(-GeO₂) system glasses, X-ray diffr. anal., electron radial distrib. curves 8-87622
Na₂O-GeO₂ glasses, struct. changes, X-ray diffr. study (*Japanese*) 8-91254
Na₂O-GeO₂-Yb₂O₃, glass struct., Yb³⁺ ion segregation 8-87620
Na₂O-GeO₂(SiO₂), thermal expansion at low temperatures 8-83982
PbO-Bi₂O₃-GeO₂, exam. of glass forming and liquid phase separation regions, and optical props. 8-88453
SiO₂-GeO₂-B₂O₃, prepared by modified CVD, refr. index behaviour 8-60526
ZnO-La₂O₃-GeO₂, exam. of glass forming region, properties and crystallisation 8-88454

germanium

see also *nuclei with*

α-irrad., stopping power for fast channelled α-particles 8-79654
amorphous, effects of ion implantation on structure 8-55881
amorphous, EPR 8-88167
amorphous, far IR absorption 8-88306
amorphous, thermoelec. power in phonon-assisted hopping regime, Coulomb effects 8-76097
amorphous film, DC cond., Meyer-Neldel rule 8-64152
amorphous film, variable range hopping 8-76176
amorphous layer, epitaxial recrystn. by electron irrad., solar cell appl. 8-84079
amorphous overlayer on ultrathin Pt film, effect on cond. 8-72284
antireflection coating, two given wavelength design method 8-59102
atom, excited states, quadrupole moments, Sternheimer shielding factors 8-82630
bicrystal cleavage plane, Shubnikov-de Haas oscills. (*Russian*) 8-64094
bolometer, cryogenic, for 20 to 500 μm spectral region 8-70187
charge carrier diffusion coeff. 8-84218
chemical etching processes, review 8-95832
chemisorption of CO(Cl), surface photoemission, adsorption gate geometry 8-73079
coadsorption of K and O₂, rel. to work function, K thermodesorpt. spectra 8-79874
cold semiconductor, Mott transition 8-91616
complex with vacancy in Si, electron state calcs. 8-67980
compressed electron hole plasma, luminesc. 8-72592
concentration determ. in atm. and rainwater in Vizcaya, Spain (*Spanish*) 8-57264
contact angle meas. between melt and crystal during Czochralski growth 8-64461
CVD, vapour transport rate, Ge-I₂ equilib. 700 to 1300K (*French*) 8-64476
cyclotron resonance, irradiation effects 8-72416
deformation, annealing characts., X-ray study 8-75713
detector for X-ray and gamma-ray spectroscopy, high-purity, preparation and properties 8-86723
diamond, P-T diagram, cryst. struct. stability 8-51886
dielectric properties, mean point value calc. 8-87930
donor-acceptor electron transfer at low temps., photocond. tail 8-84249
electrical conductivity, optically injected carrier density and temp. depend. 8-68046
electron MFP determ. by depth and ang. depend. of inelastically scatt. electron spectra 8-92154
electron momentum distribution, anisotropy, positron annihilation (*Russian*) 8-84676
electron scattering, inelastic, 70-1400 eV, mean free path 8-84696
electron-hole drop, interaction with crystal surface 8-79941
electron-hole drop magnetostriction 8-87912
electron-hole drop phase separation, due to uniaxial stressing 8-84145
electron-hole drop velocities, excitation wavelength depend. 8-88358
electron-hole drop velocities as probe of phonons 8-68517
electron-hole droplet, attachment to donor 8-87916
electron-hole droplet, motion damping, impurity and piezoelec. scatt. 8-67951
electron-hole droplets, surface props., SCF calc. 8-51904
electron-hole droplets, transient photoluminesc. intensities 8-88353
electron-hole drops, accel. by IR radiation field 8-95264
electron-hole drops, far IR absorption 8-56467
electron-hole drops, far IR magneto-optical effects 8-84565
electron-hole drops, magnetoplasma resonance (*Russian*) 8-79944
electron-hole drops, spatial distrib., time and spatially resolved absorption at 3.4 μm 8-92075
electron-hole drops, surface struct. 8-60058
electron-hole liquid, luminesc. under infinite uniaxial compression 8-87915
electron-hole liquid, pinch effect 8-87993
electron-hole liquid theory, generalised RPA 8-87914
electron-hole plasma, high density, IR absorpt. at low temps. 8-92078
electron-hole-droplet cloud, photoluminesc. of laser excited surface, phonon wind 8-84146
electronic energy bands of diamond-type crysts., appl. of EHT method 8-87907
electronic struct. from SCF calc. using intersecting spheres model 8-51888
electroreflectance, effect of surface and nonuniform fields 8-68511

germanium continued

epitaxial, on n-GaAs, with Ni overlayer, smooth and continuous ohmic contact form. by solid-state diffusion 8-68086
epitaxial film on Si, influence of fragmentary struct. on galvanomag. effects (*Ukrainian*) 8-84327
epitaxial films, ohmic contacts for GaAs devices 8-88027
epitaxial growth from monogermene at 685°C 8-51833
epitaxial layer deposition by vacuum pyrolysis 8-52676
epitaxial layer on GaAs tetragonal distortion in heteroepitaxial layer, X-ray diffr. exam. 8-67922
epitaxial layers, on GaAs substrate, misfit dislocation multiplication mechanism 8-87673
equation of state, under press. 8-75801
evaporated film, lattice parameters and phase transition temp., surface influence of glass substrates 8-94996
exciton mol. creation by pure and phonon-assisted two-photon transitions 8-63987
film, amorphous, ⁷⁴Ge ion implanted, defect struct. obs. 8-51848
film, polycrystalline, structural and elec. props. 8-76173
film, vacuum deposited, O⁺ bombardment sputtering rates 8-88390
foil, traversed by H⁺(He⁺), energy loss and straggling meas. 8-95100
free-exciton lifetime, influence of dislocations 8-60064
Hall effect in finite specimens of arbitrary lifetime and trap content 8-72175
hole drift velocity, effect of impurity scatt. 8-60127
hot electrons, intervalley diffusion 8-84227
hot-electron diffusion coefficient 8-87982
impurity photoconductivity, temp. elec. field and impurity centre conc. effects 8-56190
interband Faraday ellipticity 8-92052
interface structural model between amorphous and crystalline phase 8-63941
interfacial tension, crystal-liquid determ. 8-75809
ionised impurity scatt. limited mobility in semiconductors with spatially variable dielec. function 8-51986
IR absorption and scatt. by electron-hole drops 8-51903
IR magnetoabsorption of free and bound excitons 8-52474
IR optical material, prod. techniques and characts. 8-50873
IR transparent materials, forward and backward scatt. data 8-59099
lattice dynamical calc. using extended Born-von Karman scheme 8-59889
lattice dynamics, inversion matrix, approx. inversion 8-71797
lattice dynamics of diamond type crysts., Keating's valence force field 8-79687
lattice dynamics of group IV elements with the local Heine-Abarenkov model potential 8-63821
lightly doped, movement of dissociated dislocations in diamond cubic struct. 8-59806
magnetic circular dichroism at E_i edges 8-92051
magnetoacoustic effects in the drag of electron-hole drops by phonons 8-68057
magnetoresistance of thin n-type plate, size effect 8-72179
Mossbauer effect, ⁵⁷Fe isomer shift, quadrupole coupling and interat. distance correl. 8-52408
n-type, dislocated, temp. dependence of photoconductivity, pressure influence 8-76109
n-type, elec. cond., effect of shock waves (*Russian*) 8-87979
n-type, H-linear planar Hall effects of hot electrons 8-76082
n-type, heavily doped, extrinsic sp. ht. in metallic regime 8-59956
n-type, longit. piezoresist., in strong elec. field 8-56147
n-type, Mott transition, dielec. enhancement and conduction electron screening 8-72073
n-type, noise spectra of hot carriers 8-76083
negative differential cond., ambipolar size effect due to hot carriers 8-72185
negative electron affinity surface, with Cs and Cs+O₂ overlayers, thermal stability of work function 8-92167
one-sided abrupt junctions, distinction between avalanche and tunnelling breakdown 8-56211
optical pulse transmission, pulse-width depend. 8-55403
optical saturable absorber, passive mode locking of TE CO₂ lasers 8-71127
p-type, 2 mm wave radiation interaction with charge carriers (*Russian*) 8-87991
p-type, lattice scatt. identified as cause of 1/f noise 8-64074
p-type, odd magnetoresist., ionised impurity scatt., theory 8-72178
p-type adsorption of Au, effect on I-V characteristics, field emission study 8-67925
p-type film, transverse magnetoresist. meas. 8-72293
phase conjugate reflection, pulsed 10.6 μm, via intracavity degenerate four-wave mixing 8-87097
phonon boundary scatt., reduction of lattice thermal cond. 8-55921
phonon dispersion curves, appl. of deformable-ion model 8-59887
phonon drag of electron-hole drops in longit. quantizing mag. field (*Russian*) 8-64070
phonon scattering and dislocation effect on low temp. phonon cond. 8-51754
photodetectors, pin- and avalanche diodes, characts. (*Swedish*) 8-89545
photoelastic consts. determ. 8-68474
photoluminescence, role of intrinsic surface states 8-52571
photoresistor, Cu doped, liquid N₂ cooled, detectability 8-80019
point defect form. due to γ-ray irrad., carrier density, mobility meas. 8-71759
positron thermalisation, theory (*Russian*) 8-84170
proton impact X-ray emission, ang. distrib. and polarisation fraction 8-56546
quartz:Ge, α-β phase transition, refr. index meas. 8-83945
Raman shift, effect of pressure 8-92064
refractive index meas. of single cryst. prism, interlaboratory comparison 8-54443
resistance thermometer appls. below 0.1K 8-73999
resistance thermometers, characts. from 1 to 35K, ISU mag. temp. scale 8-81970
resistance thermometers, stability test at 20K 8-81971
rough surface, polarisation angles, ellipsometric meas. 8-56449
Schottky barrier, electronic struct., pseudopot. calc. 8-95364
Schottky barrier junction, surface electron states spectrum (*Russian*) 8-84297
slow surface, states, optical excitation investigation 8-76129
solvent, LPE growth of GaP-GaS and Ga(AsP)-GaAs 8-88434

germanium continued

- spectrally selective EM wave absorber, solar energy collector material, props. (*Dutch*) 8-50872
 stacking fault width determ. from 224 reflections with $g \cdot b = 0$ 8-59722
 STEM, bright field single atom images with half plane detectors 8-66010
 structure of annealed (111) surface 8-75916
 superconducting friction layer formed during friction between Ge and Pb (*Russian*) 8-52143
 surface, (100), Ar ion bombarded, determ. of atomic steps, LEED 8-63913
 surface, (111) 2×1 , surface electron states detected by external reflectivity 8-80036
 surface, (111), chemisorption of H_2 , effect of surface states 8-51823
 surface, (111), Sn monolayer, induced 7×7 superlattice struct. 8-91521
 surface, cluster model approach for electronic struct. 8-56205
 surface (111), 500 eV Ar^+ bombard., high temp. annealing, recovery, RHEED obs. 8-87723
 surface reconstruction-induced subsurface strain, theory 8-91516
 surface states, Tamm-like and field sustained, model studies, localisation props. 8-64092
 surface subjected to chem. excitation, nonequilib. electron effects 8-72239
 thermal expansion coeffs. meas., room temp. to 250°C 8-55416
 two-phonon difference absorption spectra 8-76452
 ultrafine multiply twinned particles, form. by gas-evaporation technique 8-63685
 ultrafine particle, positron annihilation exam. 8-56542
 uniformly stressed, density and binding energy of electron-hole droplets, photolum. meas. 8-60062
 vacancy paradox 8-59804
 X-ray diffraction, three and four wave, comparison of diamond type crystals 8-67608
 X-ray monochromatisation by Ge crystal diffraction 8-62277
 X-ray transmission, anomalous, in presence of four-wave diffr. 8-79494
 zincblende structure group IVA covalent crystals, Murnaghan parameter estimates from Morse pot. 8-95014
 zz 8-91367
 Al-Si₃N₄-SiO₂-Ge structure, small signal HF photo EMF meas. 8-52097
 Au-Ge Schottky diode, phonon energies, barrier heights, photovoltage spectra 8-64112
 Au-Ge-Au, room temp. interdiffusion 8-76161
 CdTe:Ge, mag. props. 8-56289
 GaAs:Ge, LPE, on semi-insulating GaAs, film-substrate interface characterisation 8-72017
 GaAs:Ge, vap. grown, diatomic complex donor and acceptor model 8-80003
 GaAs:Ge LPE layers, luminesc. props. rel. to substrate quality 8-52583
 Ge I, transition probabilities, $4p^2-4p4d$ and $4p^2-4p5s$, 1900-4700 Å (*French*) 8-74600
 Ge III, effect of pressure on the Raman shift 8-92064
 Ge, valence band effective mass strain depend. 8-51880
 Ge:⁵⁷Fe, quadrupole interac. 8-92005
 Ge:Al(Sb) film, amorphous, ion implantation, effect on cond. 8-83839
 Ge:As(Ga), photoconductivity oscillation with respect to applied mag. field (*Russian*) 8-80026
 Ge:Cu, IR detector, impurity photoconductivity (*German*) 8-82036
 Ge:Ba, Ca, recomb. props. 8-56156
 n-Ge:Cu, characts. of radiation defects 8-55893
 Ge:Cu, IR detector, impurity photoconductivity (*German*) 8-82036
 Ge:Cu, quenched, interaction between shallow-level defects and Cu atoms, Hall effect meas. 8-64002
 p-Ge:Ga, carrier heating by weak elec. field, hole-hole collision influence 8-72161
 Ge:Ga, effects of destabilising vertical thermal gradients on cryst. growth and segregation 8-52659
 Ge:Hg photoconductive detector, laser damage thresholds calc. 8-90443
 Ge:inert gas, ion implantation, UV photoemission exam. 8-80457
 Ge:Li, supersaturated solid solns., decomp., surface impurity content 8-51681
 Ge:Mn, amorphous, cond. increase by Mn doping 8-72155
 Ge:Na (111) surface, O₂ adsorpt., work function, surface cond. changes meas. 8-79875
 Ge:P, conc. depend. of diffusion coeff. at P diffusion 8-95185
 Ge:P, lattice thermal cond., role of electron-phonon interactions and peripheral phonons 8-79702
 Ge:P, lattice thermal resistivity due to electrons 8-51756
 Ge:S, photoionisation cross section of deep impurity centres 8-56510
 Ge:Sb, acoustic attenuation, uniaxial stress effects 8-59863
 n-Ge:Sb, fast neutron irradi. effects on donor conc., and annealing 8-56107
 n-Ge:Sb, γ -irrad. effects on donor conc. and compensation by acceptors 8-56106
 Ge:Sb, impurity conductivities 8-91691
 Ge:Sb, neutron irradi., carrier mobility theory and expt. 8-56166
 Ge:Sb, phonon thermal cond. calc. 8-71893
 Ge:Sb,Cu, exactly compensated, impurity absorpt. and photocond. spectra 8-56189
 Ge:Sb(In), film, electronic props. 8-84330
 Ge:Si, impurity lattice modes due to single and paired defects 8-75780
 Ge:Si, impurity modes and IR absorption 8-76506
 Ge-CdSe heterojunctions, epitaxial, azimuthal rotation 8-84085
 Ge-electrolyte contact, current-voltage characts., effect of mechanical deform. 8-68082
 Ge-GaAs, n-n isotype heterojunctions, fixed-interface-charge model 8-56215
 Ge-GaAs (100) interface, electronic struct., scattering-theoretic approach 8-95340
 Ge-GaAs (110), heterojunction chemistry, photoemission expts. 8-95244
 Ge-GaAs (110) interface, self-consistent calc. of interface states and electronic struct. 8-52066
 Ge-GaAs abrupt (110) interface, electronic struct. 8-95339
 Ge-GaAs interface, XPS obs. of electronic struct. 8-95341
 Ge-GaAs superlattice and interface, electronic struct. 8-52065

germanium continued

- Ge-N₂O, rate coeff. meas. for $Ge + N_2O \rightarrow GeO + N_2$ reaction 8-63110
 p-Ge- nn^+ -Si, heterojunction, γ -radiation effect on forward I-V characteristics (*Russian*) 8-72255
 Ge-pyrolytic SiO₂ system, carrier trapping, GeO₂ sublayer effect 8-91775
 Ge-Sb, D⁻ complexes and band form., photocond. 8-84251
 Ge-SiO multilayer edge filter design, 3.2 to 4.9 μ m range 8-87131
 Ge-SiO₂-Al, vacuum heating effect on stability 8-64143
 Ge-ZnS p-n heterojunction, epitaxial, elec. props. (*Russian*) 8-88023
 Ge-ZnSe abrupt (110) interface, electronic struct. 8-95339
 Ge-ZnSe interface, electronic struct., self-consistent pseudopot. calc. 8-91747
 Ge+Ge, symmetric collisions, MO-2p σ radiation anisotropy, quasimolecular nature 8-70924
 Ge+O₂(NO)(N₂O), reaction rate consts. at 350K 8-53186
 Ge(3²P_{3/2}) + O₂(Cl₂)(COS)(N₂O)(NO₂)(NO+Ar) oxidation reacts., gas phase, kinetics 8-92468
 In-Ge:As, Schottky barrier tunnel junction, zero bias resistance, temp. depend. 8-72258
 Kr²⁴⁺+Ge, K X-ray prod., impact parameter depend. 8-58800
 N₂⁺+Group IV elements and oxides, XPS and UPS prod. determ. 8-73084
 Si:Ge, P(B), impurity-pair diffusion, influence of elastic stresses 8-87824
 YIG-Ge structure, profile and position of reson. galvanomag. effect curve 8-72242

germanium alloys

see also *Ge-Si alloys*

- Ge-Sn barrier Josephson tunnel junctions 8-68114
 Nb₃Ge, supercond., single phase, sp. ht. meas., 4-29K 8-72307
 rare earth intermetallics, RMn₂Ge₂, cryst. struct. 8-59782
 rare earth-Fe(Co)-Ge, ThCu₂Si₂ type, lattice parameters 8-51469
 Ag-Ge, α -phase alloy, thermopower at low temps. 8-84196
 Ag-Ge, liq., viscosity, temp. depend. (*French*) 8-59964
 Ag-Ge (4.5 at.%), FCC, vapour-deposited, lattice imperfections, X-ray diffr. 8-72032
 Al-Ge, dil., deviation from Matthiessen's rule at high temps. 8-64025
 Al-Ge, directionally solidified lamellar eutectics, specimen prep. for TEM (*German, English*) 8-95885
 Al-Ge (2 wt.%), quenched and aged, deform. slip line obs. 8-51544
 Al-Ge alloy, Ge precip., ion irradi., dose rate and temp. depend. 8-79642
 Au-Ge (27 at.%), metastable phase struct. determ. by electron diffr. 8-83780
 AuGe, ohmic contact to epitaxial GaAs, production by laser alloying 8-88026
 AuGe/n-GaAs, SIMS study Au behaviour during annealing 8-75947
 Co-Si-Ge system, X-ray diffr. exam., band struct. (*Russian*) 8-56623
 Cr₁₁Ge₈, CrGe₈, and Cr₁₁Ge₁₀ amorphous films, short-range order, electron diffr. obs. (*Russian*) 8-56050
 Cr_xPd_{82-x}Ge₁₈, amorphous, RF sputtered, elec. resist. and magnetoresist., Kondo type behaviour 8-76066
 Cr_xPd_{82-x}Ge₁₈ amorphous alloys, magnetoresist., mag. susceptibility, magnetisation 8-80148
 Cu-Ge, dil. alloy, thermopower and resistivities, validity of Nordheim-Gorter relation 8-91671
 Cu-Ge, dilute solid soln., exam. of recrystallisation and stored energy 8-52836
 Cu-Ge, liq., mag. susceptibility, diamag. 8-72326
 Cu-Ge (8.7 wt.%) pulse duration effects on shock hardening 8-80561
 Cu-Ge (8.7 wt.%) shock hardening behaviour at very short pulse durations 8-80560
 Cu-Ge film, thermoelec. power, 80-350K 8-68096
 FeGe, hexagonal, low-temp. mag. struct., neutron diffr. meas. 8-95418
 FeGe₂, mag. struct., Mossbauer method 8-60268
 FeGe_{2-x}, amorphous, mag. behaviour, rel. to Fe_xSi_{1-x} and Fe_xSn_{1-x} amorphous alloys 8-95478
 Fe_xGe_{1-x} amorphous alloys, conversion electron Mossbauer spectroscopy 8-84504
 Ge-Al film, amorphous, EPR meas. 8-80212
 Ge-Al film, elec. resist. and IR transmission, comp. and substrate temp. depend. 8-52112
 Ge-Cu (0, 23, 40 at.%), amorphous film struct. (*German*) 8-95391
 Ge-Cu film, amorphous, EPR meas. 8-80212
 Ge-Ga alloys, amorphous, far IR absorption 8-88306
 Ge-Ni, smooth and continuous ohmic contact to n-GaAs 8-68086
 Ge-Se-Fe films, metallic and semicond., amorphous, mag. and elec. props. 8-52319
 Mn_xPd_{82-x}Ged₁₈, amorphous alloys, mag. props. 8-91906
 Nb₃Ge, A-15 compound formation by ion implantation 8-51572
 Nb₃Ge, amorphous and crystalline A-15 phases 8-83896
 Nb₃Ge amorphous films, X-ray diffr. analysis of microstruct. 8-72035
 Nb₃Ge, anomalous resistivity, insight from band theory 8-60106
 Nb₃Ge, CVD, impurity doping effect on supercond. crit. props. 8-52174
 Nb₃Ge, electron irradiation at cryogenic temps., effect on T_c and transport props. 8-52122
 Nb₃Ge film, CVD fabrication of supercond. tape for high-field magnets 8-95698
 Nb₃Ge film, nucleation of high-T_c phase in presence of impurities 8-88054
 Nb₃Ge film, prep. by coevaporation, supercond. props. 8-91830
 Nb₃Ge film, supercond., epitaxial growth on Nb₃Ir and Nb₃Rh substrates 8-80473
 Nb₃Ge film, superconducting, A-15 type, getter-sputtering with controlled additions of O 8-88427
 Nb₃Ge, granular supercond., simple model for resistive-nonresistive transition 8-72298
 Nb₃Ge, metallic bonding, electronic states calcs. 8-79916
 Nb₃Ge, metallic glass, internal friction peak obs. 8-79666
 Nb₃Ge, neutron irradiated, A15 compound, recovery of T_c by annealing 8-52132
 Nb₃Ge, plasma energies, tight-binding energy-band model 8-84159
 Nb₃Ge, RF and DC sputtered films comparison, O content effect 8-72022
 Nb₃Ge, resistivity and T_c measurement after low temp. neutron irradiation 8-52123

germanium alloys continued

- Nb₃Ge, supercond. film, CVD, crit. temp., crit. current density 8-76204
 Nb₃Ge, supercond. film, electron beam codeposition, synthesis and props. 8-72296
 Nb₃Ge, supercond. tape, growth technique via amorphous state 8-84708
 Nb₃Ge, supercond. transition temp., rel. to A15 phase stability 8-52137
 Nb₃Ge tape, prepared continuously by CVD, props. 8-60257
 Nb₃Ge, ZZ 8-91613
 Nb₃Ge, film deposition by ion beam methods 8-72728
 Ni-Ge (1 to 9 at.%), twinning stress used to eval. stacking fault energy of pure Ni (*Japanese*) 8-59820
 Pd-Ge glass, short range order obs. for Pd₈₀Ge₂₀ and Pd₇₈Ge₂₂, EXAFS expts. 8-55815
 Sb-Ge, unidirectionally solidified, exam. of compressive props. and struct. 8-68730
 Sn-Ge, liquid alloy, exam. of activity and heat of mixing, using mass spectrometry 8-51706
 UGe₃, de Haas-van Alphen effect, band struct. calc. 8-72068
 (V,Fe)₃Ge, solid soln. form. and supercond. T_c (*Russian*) 8-80512
 V-Al/Cu-Ge composite tape, transition temp., upper crit. field 8-68126
 V₃Ge, A-15 compounds, interlattice displacements, elastic const. 8-55906
 V₃Ge, A-15 struct. supercond., microhardness, bonding 8-76199
 V₃Ge, bronze-processed, stress-induced enhancement of supercond. T_c 8-64159
 V₃Ge, plasma energies, tight-binding energy-band model 8-84159
 V₃Ge, resist. characts. in normal state 8-51963
 V₃Ge, third order elastic const. 8-88490
 V₃Ge, ZZ 8-91613
 V₃Si, supercond. tape, growth technique via amorphous state 8-84708
 V₃Si-Ge, cryst. struct., supercond. T_c comp. depend. 8-51494
 Zr-Nb-Ge, singularities of $\beta \rightarrow \omega$ transform. in alloy, with high content of β -stabiliser (*Russian*) 8-76644

germanium compounds

see also *germanium alloys*

- GeO₂, hexagonal needle crystals, vapour growth 8-52651
 LPE growth, saturation magnetisation, collapse field, bubble diameter 8-95703
 SnTe-PbTe-GeTe, alloy semiconductor, phase transition (*Japanese*) 8-91443
 As-Se-Ge, amorphous film, relief-type hologram mode, hologram replication (*Japanese*) 8-78959
 As₂Se₃Ge glass, struct. changes, Mn²⁺ EPR expts. 8-79534
 As₄₀Se₆₀₋₇₀S₁₀Ge₁₀ film strip-loaded waveguide formed in graded-index LiNbO₃ planar waveguide 8-74965
 As₄Te₆Ge glass, struct. changes, Mn²⁺ EPR expts. 8-79534
 As₂₀Te₄₈Ge₁₀Si_{0.12}, amorphous film, transient switching processes 8-84232
 BaGeF₆, Group IV hexafluoride anion radical γ -irrad., EPR spectra 8-72411
 Ca₃Ga₂Ge₃O₁₂, substrate, electron examination of microstruct. and microsegregation 8-67919
 Cd₆Ge₃As₁₁, band gap, DC cond., elastic const., and glass transition temp., pressure depend. 8-72064
 Ge-As-Te system, glasses, magnetochemical exam. 8-88092
 Ge-I₂, equilibrium study 700 to 1300K, vapour transport rate of Ge (*French*) 8-64476
 Ge-S film, amorphous, photo-induced ESR and optical absorption edge shift 8-88374
 Ge-Se, glassy, photoinduced photolum. fatigue (*Russian*) 8-60520
 Ge-Se glass, elastic props. under press., US interferometry. 8-79658
 Ge-Se glass system, effect of changes in local surrounding of atoms on optical props. (*Russian*) 8-80414
 Ge-Se-Fe films, metallic and semicond., amorphous, mag. and elec. props. 8-52319
 GeF, A² Σ^+ state, time-resolved fluoresc. 8-58732
 GeH₄, abundance in Jupiter atm. from IR spectrum anal. 8-61791
 GeH₄, heat capacity, dielectric const., thermodynamic props. 8-83967
 GeH₄, IR spectra, Jovian atm. absorpt. profile, computer simulation 8-81584
 GeH₄, Lorenz-Lorentz coeff., refr. index, crit. const. and density depend. 8-92041
 GeH₄, ν_3 fundamental, theoretical absolute J-manifold intensities 8-74707
 Ge₂H₆, valence electronic struct., model pot. in floating spherical GO formalism 8-74563
 GeO, produced in Ge+N₂O reaction, kinetics of chemilum. emitter form. and quenching 8-63107
 GeO₂, new high-pressure modification 8-75825
 GeO₂, radiation damaged, paramag. point defects, F-centres, ESR, absorpt. spectra 8-80213
 GeO₂, tetrahedral glass, Raman studies 8-71823
 GeO₂:Si, optical props. IR absorpt., UV reflection spectra 8-84619
 GeO₂:6Bi₂O₃, IR and Raman spectra, vibr. anal. 8-76464
 GeS, (001) surface struct., LEED expt. 8-84034
 GeS, cryst. struct. (*German*) 8-51484
 GeS, exciton luminescence 8-52555
 GeS₈ glass, activation energies after neutron irradiation, elec. cond. and transmission coeff. 8-83850
 GeS₂(O₂), thermal expansion at low temperatures 8-83982
 GeS₂Se₁₋₂₀, IR spectra, differential calorimetry, phase diagram (*Russian*) 8-52513
 GeSe amorphous films, photoconductivity measurements, recombination model 8-64061
 GeSe₂ film, chalcogenide glasses band gap variation 8-90461
 GeSe₂ film, glassy, self-controlled laser-beam chopping effect 8-60528
 GeSe₂, IR and Raman spectra 8-95585
 Ge₂Se₁₋₂₀, 0<x<0.2, crystallisation in amorphous bulk and thin films 8-55813
 Ge₂Se₁₋₂₀, amorphous semicond., elec. props. 8-84219
 Ge₂Se_{1-y}, glass, bulk and film, IR transmission and reflectivity meas., struct. model assignments 8-79537
 α -Ge₂Se_{1-y}, photoluminescence and fatigue effects 8-84648
 Zr-Te film, amorphous, evaporated and annealed, variable range hopping cond. 8-80077

germanium compounds continued

- GeTe, X-ray emission spectra, amorphous and cryst. struct. (*Russian*) 8-88385
 GeTe:I, ferroelectric transition exam. 8-88264
 GeTe:Mn, thermoelec. power, 2.5-25K, magnon drag effect 8-56169
 (GeTe)_x(AgSbTe₂)_{1-x}, thermoelectric props. of monolithic and pressed samples at 300K 8-80009
 IrGe_{1.5}S_{1.5}(Se_{1-x}), new skutterudite relation compounds, prep. and charact. 8-52700
 Na₂O-GeO₂, thermal expansion at low temperatures 8-83982
 Pb_{1-x}Ge_xTe, dielec. const. determ. near ferroelec. transition 8-88269
 Pb_{1-x}Ge_xTe, electron-phonon interaction effect on ferroelec. transition 8-76416
 Pb_{1-x}Ge_xTe, phase transitions 8-60408
 Pb_{1-x}Ge_xTe:Ga, Fermi level stabilization, transport props. meas., 77-400K 8-56065
 RhGe_{1.5}S_{1.5}, new skutterudite relation compounds, prep. and charact. 8-52700
 Se-Ge glass, lattice vibr. spectra, photostruct. change, far IR absorpt. 8-72494
 Si₁₂Te₄₈As₃₀Ge₁₀, amorphous film, elec. cond. mechanisms, temp. depend. (*Japanese*) 8-80078
 SmCaGe garnet LPE bubble film, coercivity, thickness depend. 8-68324
 Sm_{0.3}Lu_{0.2}Tm_{0.2}Y_{1.45}Ca_{0.85}Fe_{4.15}Ge_{0.85}O₁₂, LPE growth, saturation magnetisation, collapse field, bubble diameter 8-95703
 Te₈₀Ge₁₂Pb_{7.5}, phase-separated system, overlapping effects of glass transition and crystaln., DSC results 8-83739
 Y_{1.52}Eu_{0.3}Tm_{0.3}Ca_{0.88}Ge_{0.88}Fe_{4.12}O₁₂, bubble translation vel., ion-implantation effects 8-68327

getters

see also *electron tube manufacture; vacuum techniques*

- Sorb-ac wafer pumps, behaviour in plasma machines, review 8-70627
 vacuum outgassing material selection and treatment 8-81994
 Gd small ion-getter pump 8-89487
 Si, solubility of Au, gettering by P 8-83961
 Si:P, Au gettering by P diffusion and P-induced dislocations 8-91346
 Ti, getter pump, corrugated surface and pumping speed, fusion reactor application 8-74491
 Zr-Al getter pumping in beam driven Tokamaks 8-50401

GFRP see *glass fibre reinforced plastics***giant pulsations (earth)** see *micropulsations***giant resonances** see *nuclear collective states and giant resonances***giant stars**

see also *supergiant stars*

- abundances in M3 and 13 globular clusters 8-93334
 atmospheres, microturbulence rel. to evolution 8-81625
 α Aurigae, UV spectrum obs. by International Ultraviolet Explorer 8-96475
 α Aurigae (Capella), intense line emission in soft X-ray spectrum 8-93228
 α Bootis (Arcturus), UV obs. of chromospheric emission line profiles 8-81620
 α Canis Majoris B (Sirius B) as historical red giant, search for surrounding nebulosity 8-93242
 R Cassiopeiae, late-type giant, possible H₂O thermal emission identification 8-81628
 CD-38°245, metal-deficient halo red giant, spectrum, photometry and Ca/H ratio 8-69797
 β Cephei stars, search south of declination -20°, B-type giants and subgiants 8-61863
 R Coronae Borealis stars, long-term IR behaviour 8-96490
 V460 Cygni, cool C star, atmospheric ¹²C/¹³C ratio 8-93223
 CH Cygni, linear polarisation vars. rel. to circumstellar dust grains form. 8-69808
 F-, G- and K-type, in solar neighbourhood, absolute magnitudes 8-81632
 halo giant in north galactic cap, photometry and spectra 8-85942
 HD 147508, spectroscopic binary, orbit from photoelectric radial vels. 8-69839
 HD 76932, subgiant halo star, chem. comp. rel. to nucleosynthesis 8-81626
 Henyey-type evolution code, appl. to stars with shell energy sources 8-61848
 α Herculis, location of α^2 Herculis along line of sight 8-73739
 HR 6766, weak G-band star, light-element abundances 8-57548
 internal mixing, rel. to strong CN phenomenon 8-53921
 IRC+10216, C star, possibility of detecting cyanoacetylene-d₁ (DC₃N) 8-69901
 IRC+10°216, circumstellar methane in IR spectrum 8-57694
 K-type giant stars, Population I, CN strengths and ¹²C/¹³C ratios 8-93229
 late M-type giants in elliptical galaxies, evolutionary synthesis of stellar population 8-57626
 late-type, space distrib. in nuclear bulge of Galaxy, ellipsoidal density model 8-86009
 late-type, sphericity effects in extended atms., models 8-81617
 late-type giants, near IR photometry with balloon-borne telescope 8-73713
 late-type stars, Ca II emission V/R ratio rel. to mass loss 8-93208
 LMC central regions, stellar count-brightness ratios rel. to population struct. 8-89245
 long-period variable stars, OH maser lines struct. and saturation 8-93264
 M3, M13, M92, M67, giant stars IR photometry, bolometric magnitudes and effective temps. 8-57595
 M-type, circumstellar envelopes, observational study 8-53939
 M-type, in solar neighbourhood, absolute magnitudes 8-81631
 molecular spectra of pure S stars 8-77554
 MWC 342, emission line spectrum in 1974-75 period 8-57558
 optical emission from stars with IR excesses, intrinsic linear polarisation origin 8-96481
 β Pegasi, M-type giant star, Mg II h and k emission obs. 8-53945
 red giant stars, evolutionary sequences 8-65611
 red giants, spectra, TiO bands obs. and theory 8-96480
 red giants in Galaxy nuclear bulge, areal density vars. from UBV photometry 8-53926
 red giants in globular clusters, mass loss 8-93238
 red giants with neutron cores, energy sources (*Russian*) 8-93197

giant stars continued

- red variable star, possible optical candidate of 2S 1702-363, spectroscopic obs. 8-77566
 S-type stars in Southern Milky Way, objective prism survey and BVI photometry 8-61754
 α Tauri, grazing occultations during 1979 visible from Scandinavia (Swedish) 8-69656
 weak-G band stars, Li abundance determ. 8-53948
 C stars, 3.9 micron absorpt. band identification 8-93231
 C stars, Li line formation 8-65615
 CO in giants in globular cluster, IR obs. 8-93339
 He content of envelope, zero age horizontal branch loci 8-77551
 He flash in stars with shell energy sources 8-89169
 OH/IR stars, new SiO transition detect. 8-53954

Gibbs free energy *see free energy***Gibbs function** *see free energy***Ginzburg-Landau theory**

- antiferromagnet, superfluid flow states, existence from Ginzburg-Landau theory (Russian) 8-72085
 chain conductors, CDW ordering 8-79731
 disordered systems, electron localisation and classical solns. in Ginzburg-Landau field theory 8-56108
 effective potentials, Ginzburg-Landau model 8-52287
 flux pinning force, derivation from a potential 8-68128
 localised defects, one-dimens. model, nearly ferromag. system, solids near displacive phase transitions 8-71820
 metallic chain, weakly coupled, Ginzburg-Landau theory 8-91626
 N-particle Schrodinger eqn., alternative derivation of Ginzburg-Landau eqn. 8-60242
 proximity effect sandwiches, bifurcation theory and order of phase transition 8-84353
 superconducting junction proximity sandwich, mag.-supercond.-mag., phase diagram 8-95399
 type II superconductor, dielastic interaction of flux line lattice with internal stresses of cryst. imperfections 8-56270
 Al, small particles, Josephson-coupled, local fluctuation effects 8-72308
³He, superfluid A-phase, slab, nonplanar textures 8-51777
³He, superfluid B-phase, domain struct., derived from Ginzburg-Landau eqns. 8-63896
 Sn, small particles, Josephson-coupled, local fluctuation effects 8-72308

glaciology

- Alpine meltwaters, ion exchange influence on dissolved load 8-81228
 N.America, depth contours of last ice age glacier, rel. to geomagnetism 8-53615
 N. American glacial history extended to 75000 years ago 8-77284
 American Southwest, cryogenic deposits rel. to cold, dry full-glacial climate 8-57296
 Antarctic iceberg melting 8-88863
 Atlantic Eurafican continental margin, glacial eastern boundary current 8-81179
 Berendon Glacier, BC, Canada, movement, ice structures and medial moraine at confluence 8-61441
 Bermuda, Late Pleistocene sea level vars. 8-73400
 British Columbia, S central, late Pleistocene glacial and nonglacial stratigraphy 8-92804
 coastal California, late Quaternary climate and evidence for Ice Age refugium 8-57293
 Canadian high Arctic, past glacial activity 8-81236
 Canadian High Arctic ice caps, ice thickness meas. 8-61439
 climate model, sensitivity and role of cloudiness (Russian) 8-88902
 Clyde Foreland, Baffin Is., last interglacial-glacial cycle, stratigraphy, biostratigraphy and chronology 8-61536
 Columbia Icefield, surveying techniques 8-61445
 Corsica (France), Quaternary glacial deposits props. and chronology 8-57234
 Cumberland Peninsula, Baffin Is., tors, felsenmeer and glaciation 8-61442
 NE Ellesmere Island, NWT, Canada, glacial geology and chronology 8-77233
 NW.Europe, appl. of extended ¹⁴C time scale by isotope enrichment 8-77314
 glacier structure and flow rel. to elongated air bubbles in ice (Japanese) 8-88861
 glacier thickness meas. using dielectric permeability characts. 8-89500
 global mass and energy requirements for glacial oscills. rel. to mean ocean temp. oscills. 8-81351
 Greenland Ice Sheet, Hg contents 8-65349
 Holocene and latest Pleistocene cirque glaciations in Shuswap Highland, British Columbia, ages 8-92856
 hot water drill, open circuit, for hole drilling in cold glaciers 8-65402
 ice ages, prod. by Earth encounter with interstellar cloud 8-57292
 ice ages and ecological catastrophes, prod. by Earth-comet close approach 8-53714
 ice sheets in polar regions, radio obs. appls. 8-81419
 ice-wedge casts in NE county Wicklow, distrib. and struct. 8-69379
 icebergs, calving from floating glaciers by vibrating mechanism 8-81197
 Infracambrian glaciogenic sediments from Sierra Leone 8-69378
 interglacial episode termination and Wilson Antarctic surge hypothesis 8-53669
 Lake Ontario, Late Wisconsin sediments, aspartic acid racemisation and ¹⁴C dating 8-73415
 Late Quaternary climatic changes, W.Africa, from deep sea sedimentation 8-73355
 Late Quaternary sea levels, central British Columbia coastal area 8-73377
 late-Wisconsin glaciation extent in NW.Greenland and N.Ellesmere Island, glaciological and geological evidence 8-57232
 Lys glacier, conditions of front in 1971, 1975 and 1976 (Italian) 8-85610
 Mahone Bay, Nova Scotia, Late Quaternary glacial erosion and sedimentation 8-77232
 Mizuho Plateau, ice sheet thinning, possible causes 8-57229
 Mount Elgon (Kenya/Uganda border), deglaciation date determ. 8-53670
 Newfoundland, Late Wisconsinian glaciectonic struct. and post glacial permafrost 8-61440

glaciology continued

- Pelee-Lorain moraine, SW.Ontario, influence on Point Pelee geomorphology 8-92857
 Pleistocene, ice fluctuations rel. to southern trade winds and oceanic upwelling during last 75000 years 8-57217
 Pleistocene drift, ice-marginal sedimentary, glaciectonic and morphologic features, Newfoundland example 8-57233
 Pleistocene glacial cycles, Pacific palaeoclimatic stratigraphies comparative anal. 8-57295
 Pleistocene-Holocene transition, W.Pacific, from stable isotopes anal. in deep sea carbonates 8-73354
 Pliocene and Pleistocene glaciations rel. to Barents Ice Sheet, evidence from Barents Sea 8-57227
 polythermal glaciers flow, detailed continuum model, preliminary anal. 8-85617
 pressure melting within glacier, indicated by regelation ice chem. comp. 8-61447
 rock glaciers in southern part of Jasper National Park, Alberta, distrib. and characts. 8-77276
 sedimentation processes and patterns in glacier-fed lake with low sediment input 8-88849
 thermal radiation polarisation, of permanent snow fields, from meas. obtained from the 'Meteor' satellite 8-88870
 upper ocean layer, global freshening during deglaciation 8-53658
 late Wisconsinian till sheets, Brantford-Woodstock area, S.Ontario, trend surface anal. 8-92858
¹⁸O stratigraphy in deep-sea sediments, evidence for deglacial meltwater effect 8-85530

glass

- for semiconductor glasses *see amorphous semiconductors and chalcogenide glasses*
see also aluminosilicate glasses; amorphous semiconductors; borate glasses; b rosilicate glasses; chalcogenide glasses; germanate glasses; glass fibre reinforced plastics; glass fibres; glass-metal seals; optical glass; phosphate glasses; phosphosilicate glasses; vitreous state; vitrification
 adherence, of polyurethane 8-83336
 air cooled, flat, duration of inelastic deformation 8-84908
 alkali silicate glass, CuO doped, ESR spectra of Cu⁺, quadrupole effects 8-64265
 alkali-alkaline earth silicate glasses, IR refl. spectra (Japanese) 8-52505
 aqueous soln., stabilising excess electrons, DTA at cryogenic temps. 8-76889
 band structure and forbidden gap in glasses and amorphous semiconductors, review 8-75987
 basaltic, expt. study of cationic diffusion of alkali and alkali-earth ions 8-95180
 bead, impact fracture (Japanese) 8-92338
 bead-filled epoxy resin, elastic moduli, interfacial slippage effect anal. 8-76688
 beam, rectangular, flexurally vibrating Timoshenko's shear coeff. 8-83866
 bottles, qualitative method for monitoring chemical corrosion 8-85068
 cabal glass:SiO₂(TiO₂), microheterogeneity, and elec. cond. 8-83997
 ceramic, machinable, machining techniques 8-77881
 crack propagation, by mech. and thermal stresses 8-75721
 crystallisation and opacity, exam. by high temp. viscometry and X-ray diffr. (Polish) 8-84875
 density fluctuations from elastic dipoles at low temps. 8-79709
 dielectric instabilities in high permittivity glass 8-52433
 electron microscopy using electrostatic field (German) 8-82081
 engineering materials, nature and props., book 8-72707
 equilibrium thermodynamics, sp. ht., refr. index and glass transition (German) 8-83745
 erosion impact of annealed 310 stainless steel, SEM and TEM study 8-64725
 film, Brillouin scatt. from surface phonons, SAW vel. and attenuation 8-95587
 film deposition by vac. evap. struct. mech. and optical props. (Czech) 8-80469
 flat, dependence of microbrittleness on SO₃ conc. 8-84960
 flat glass in vacuum, exam. of temp. dependence of microhardness and microstrength 8-88532
 float, exam. of dynamic fatigue 8-80631
 float glass, toughening by ion exchange, selection of technology parameters 8-84757
 friction and wear against C and glass fibre reinforced PTFE and polyacetal 8-56783
 Gaussian size distrib. of rigid particles, AE anal. 8-62181
 glass:Mn²⁺, EPR, low-field hyperfine struct. 8-95513
 hydrophilic protective coatings 8-85019
 ion-exchanged, anomalous stress profile, photoelastic meas. 8-90803
 laser fusion targets, plating methods 8-60862
 laser fusion targets, vapour deposited coatings, surface finish obs. 8-60863
 laser irradiation, nondirectional glow prod. 8-52575
 liquid quenching equipment 8-84854
 Mars surface, glass alteration as source of clay minerals 8-89097
 melt, thermal inhomogeneity, method of determining 8-84756
 melting related to chemical composition, for glass manufacturing industry (Czech) 8-80505
 metal-glass mats, alloyed with Cu, powder prep. and props. 8-72912
 microbeads, binary, inhomogeneity-packing density relations 8-92211
 microbubbles, method for polishing bubbles into hemispheres 8-95869
 microsphere reinforced, composite, mech. charact. calc. 8-64578
 microstructure of glass and oxide glasses 8-88442
 mixed alkali silicate glasses, heat capacity (Japanese) 8-55954
 mould heat transfer during pressing 8-80500
 narrow sandwich seal, correction factor for thermal expansion mismatch 8-75110
 narrow sandwich seals, shape factor, finite element anal. 8-75111
 nonequilibrium thermodynamics, diffusion and relax. processes (German) 8-83746
 optical small angle polarisation modulation, by Faraday rot. in diamag. glass (Korean) 8-50918
 optimal polynomials in calcs. of complex glass's properties 8-68026
 Ostwald ripening and its application to precipitates and colloids in ionic crystals and glasses [Review] 8-80548
 oxide, elec. cond. and dielec. relax., correl. 8-79801

glass continued

oxide glasses, multivariant system of oxides and partial props. prediction from V-phenomenon 8-79540
oxide-electrolyte interface, transition layer model 8-68895
particles impacting on metal barriers, piercing, stony meteorite simulation 8-89043
peeling of rubber film, spontaneous creation of interfacial dislocations 8-73011
phase separating, interpretation of temp. dependence of transport process 8-87806
phase transform. in steep thermal gradients, apparatus 8-84767
phonon avalanches, exptl. conditions for obs. 8-71822
phonon echoes and self-induced transparency 8-79710
phototropic, kinetic investig. (*German*) 8-64868
plastic, engineering, nondestructive structural identification 8-92422
plate, flexure crack propag., expt. and anal. 8-80620
plates, biaxially stressed, anal. of localised impact damage 8-68772
plates, effect of localized damage on energy losses, during impact by glass spheres 8-52973
plates, fast crack propagation meas. continuous stress meas., new method 8-73009
polymer, thermodynamics of densification process 8-95723
polymer coated, exam. using ion scattering spectroscopy and scattered ion mass spectrometry 8-60641
porous, adsorbed water, proton spin-lattice relax. meas. by pulse NMR 8-84053
porous, thermosmotic flow, filtration, of water 8-53248
powder, coupled with silane, Fourier transform infrared spectroscopy 8-60642
protective glassy layers at 500°C for Cu passivation 8-76785
pyrex, plates, exam. of friction, wear and elastic constant mechanisms 8-87309
pyroelectric, low-temp. behaviour 8-56432
rare earth glasses, R_2O_3 -S-Ga₂S₃, (R=La to Nd), exam. of preparation and props. (*French*) 8-80504
rare earth oxide (R_2O_3)-M₂O_y glassy systems (M=Ti,Nb,Ta), rapid quenching by laser beam, exam. of composition and crystallization 8-52856
reflectivity, quantitative meas., undergrad. lab. expt. 8-49624
relaxation of props. during isothermal swell period, method of calc. 8-67654
shell, for laser fusion targets, plasma polymerisation coating method 8-60859
silica glass, ball mill grinding, rate constant determination (*Japanese*) 8-95828
silica glass, ball mill grinding, wet, dry, rate constant determination (*Japanese*) 8-95827
silicate, glasses corrosion by aq. solns. 8-64752
silicate, neutron diffr. determ. of struct. 8-79533
silicate, surface and near surface struct. 8-87850
silicate glass, IR reflection spectra relation to corrosion state of surface (*Japanese*) 8-88554
silicate glass corroded by moisture, IR refl. spectra change (*Japanese*) 8-53013
silicate glass darkening due to UV radiation from laser produced plasma jet 8-52598
silicate glasses, elastic moduli calc. 8-60696
silicate glasses, exam. of chemical stability, in alkali solns. 8-88557
silicate glasses, ion-microprobe determ. of Li diffusion 8-53649
silicate glasses, low temp. synthesis, exam. of formation conditions, structure, and props. 8-88441
silicate glasses, stabilised, exam. of stress relaxation and deformation 8-92292
silicate glasses, struct. and phase transform. 8-64538
silicate glasses, swelling on proton, deuteron and He ion bombardment 8-67750
silicate glasses with high oxide modifier concs., property-comp. relns. 8-67655
sital coatings in Li₂O-Na₂O-CaO-SiO₂ system, heat treatment effects on tech. characts. 8-84853
soda-lime, surface, damage due to impact of small glass and steel spheres 8-52994
soda-lime glass, depth profiles of Na and Ca by SIMS and AES 8-51805
specific heat time depend., rel. to US props., at low temps. 8-59957
spectral diffusion 8-59914
sphere mixture, polydisperse system, AE anal. 8-62180
 β -spodumene-mica glass ceramic, thermal expansion thermal shock and moduli of rupture and elasticity 8-60736
steel antioxidation protective glass enamel cladding exam. of development 8-85031
strain intensity criterion for crack branching in brittle mats. 8-55592
strength test, biaxial, use of Weibull statistics 8-68798
structural relaxation, order parameter model 8-83740
substrate, glow discharge effects on surface props. and struct. 8-85201
substrate, subbing for AgBr layers, effect on photographic characts. (*Bulgarian*) 8-78016
surface, physical chemistry 8-60854
surface, sputtering with inert gas ions 8-64438
surface anal. by AES 8-60013
surface treatment effect, on chemical polishing time of crystal products 8-92436
tempered, density and refractive index variation 8-64564
tempered, spontaneous fracture due to NiS inclusions, exam. of behaviour mechanics 8-71294
tempered discs, meas. of nonuniform distribution of residual stresses 8-95865
tempered plate, stress state model and heat transfer rate determ. 8-60684
tempering, stress and structural relaxation 8-64574
ternary oxide systems, metastable two liquid tie line calc. 8-92246
toughened, stress corrosion characts., exam. 8-71295
toughened glass, 200 to 600°C stress relax., anal. (*Czech*) 8-79661
transparent glass-ceramics, microstruct. and props. 8-59960
transparent materials, defective surface layer formation during abrasion, laser-induced breakdown (*Russian*) 8-53007
ultrasonic NDT techniques, low-frequency 8-80690
viscous flow, examination of mechanism 8-87805
Vycor, porous, adsorption of carbonium ions, reson. Raman spectra 8-84571

glass continued

Vycor, preferential adsorption of ⁴He from ³He-⁴He mixtures 8-84023
white Cl-containing slag glass-ceramic, synthesis with nonsulphide catalyst 8-52748
window glass, temp. depend. of coeff. of thermal expansion rel. to const. fictive temp. 8-67839
X-ray transmission, circular waveguides of curved Pb glass capillaries 8-86395
Young's modulus determination, using static compression, tension, and dynamic loading 8-83867
BaO-Fe₂O₃-Na₂O glass, mag. props. 8-88123
BaO-SiO₂ glass ceramic, nucleation, effect of electric fields 8-83742
C fibre reinforced glass, SiC fibre coating, hot pressing production method (*German*) 8-95724
CaO-SiO₂-ZnO continuous unidirectional crystn. of fibrous metasilicates from melt 8-95739
Cs₂O-SiO₂-(GeO₂) system glasses, X-ray diffr. anal., electron radial distrib. curves 8-87622
Eu³⁺ fluoresce. lineshape in glass, temp., time and conc. depend., two-phonon Raman scatt. 8-64406
Fe-C(C-B)(C-Si), splat cooled, formation of metastable crystalline phases and glasses 8-88461
K₂CO₃-SiO₂ glass forming batch, Raman spectroscopy 8-64519
K₂O-BaO-SiO₂ glass, rare earth ion activated, spectral intensity, effect of number of 4f electrons 8-84602
K₂O-SiO₂ glass, improvement in water resist. by ion exchange 8-85012
K₂O-SiO₂-(GeO₂) system glasses, X-ray diffr. anal., electron radial distrib. curves 8-87622
K₂O.3CaO.BaO.xSiO₂, property-comp. relns. 8-67655
Li₂O-2SiO₂, glass, devitrification with ageing 8-79536
Li₂O-CaO-SiO₂ phase equilibria 8-64528
Li₂O-SiO₂ glass, improvement in water resist. by ion exchange 8-85012
Li₂O-Fe₂O₃-SiO₂ glass, struct. and crystallisation behaviour 8-83738
Li₂O-TeO₂ glasses, struct., IR reflection spectra 8-68516
Li₂O.2SiO₂ glass, kinetics of crystal nucleation, effect of Pt and other impurities 8-88440
Na conductive glass-Na amalgam interface, electrochem. obs. 8-76870
Na₂-SiO₂ glass, prep. by metallic-organic derived method, phase separation 8-56610
Na₂O-CaO glass tube, fracture by field assisted ion exchange 8-68771
Na₂O-CaO-SiO₂, crack nucleation around plastic indents 8-92327
Na₂O-CaO-SiO₂, evaluation of crack resistance and crack velocity, using controlled fracture experiments 8-72881
Na₂O-CaO-SiO₂, foil, exam. of surface plasticity, and cracks, by electron microscopy 8-68733
Na₂O-CaO-SiO₂, glass, light scatt. rel. to heat treatment (*German*) 8-84598
Na₂O-CaO-SiO₂, lifetime predictions, dependence on crack propag. eqns. 8-72882
Na₂O-CaO-SiO₂, origins of acoustic emission in fracture 8-72889
Na₂O-CaO-SiO₂, particle track detector appl., for neutron dosimetry (*Czech*) 8-66425
Na₂O-CaO-SiO₂, plates, exam. of Hertz crack branching 8-72887
Na₂O-CaO-SiO₂ glass, soln. of commercial refractories, 1200-1350°C 8-95821
Na₂O-CaO-SiO₂ glass rods, prediction of thermal fatigue resist. 8-84955
2Na₂O-CaO-XSiO₂ glass, He mobility, interconnectivity, miscibility limits, effect of morphology 8-67864
Na₂O-FeO-Fe₂O₃-SiO₂, chemical durability at different pH values 8-72902
Na₂O-SiO₂, effect of annealing on absorbed H₂O action on temp. spectra of internal friction 8-88487
Na₂O-SiO₂, glass, devitrification with ageing 8-79536
Na₂O-SiO₂ glass, coated with SnO coeff. of friction and fracture toughness 8-80657
Na₂O-SiO₂ glass, magneto-optical props. 8-80318
Na₂O-SiO₂ glass, pulsed EPR study of Cu 8-84479
Na₂O-SiO₂ glass, stability at high press., X-ray diffraction obs. (*German*) 8-92251
Na₂O-SiO₂ vitreous system with relaxing structure, spinodal decomposition 8-75553
Na₂O-SiO₂-MgO melt, elec. cond. meas., MgO behaviour (*Japanese*) 8-75857
Na₂O-SiO₂-SnO₂ (TiO₂) glass, exam. of Na⁺ self diffusion, elec. conductivity, and viscosity 8-87819
Nd₂O₃-SiO₂ glass, exam. of spectroscopic and luminescent props. 8-88364
PbO-K₂O-SiO₂-(Al₂O₃), corrosion in acid, leaching kinetics 8-92378
PbO-SiO₂, corrosion in acid, conc. profile meas. 8-92379
PbO-SiO₂, optical coating for GaAs-Al_{0.5}Ga_{0.5}AS laser 8-71113
PbO-SiO₂-(Al₂O₃), corrosion in acid, leaching kinetics 8-92378
Sb₂O₃ glass, X-ray diffr. anal. of struct. 8-87621
SiO₂ glass, crystallinity positron annihilation study 8-72629
SiO₂ glass, heat treatment study by positron annihilation 8-55812
SiO₂ glass, porous, below-freezing pt. adsorbed layer, isothermal adsorption and dimensional changes obs. 8-75925
SiO₂, molten, struct., X-ray radial distrib. anal. 8-67651
SiO₂, planarised sputter deposition 8-75959
SiO₂.OH⁻, vitreous, elec. dipolar echoes 8-52430
SiO₂-Na₂O glass, Na⁺ diffusion 8-91478
SiO₂-Na₂O-CaO, electrochemically coloured, chemical composition and structure of surface layers 8-84758
SiO₂-Na₂O(Li₂O) glasses, bonding of Si-O exam. by X-ray emission spectra 8-52594
SiO₂-PbO-K₂O glass, reflection spectra 8-88325
(SiO₂)₄₅(CaO)₅₅(Fe₂O₃)₃₅ glass, effect of melt atmosphere on mag. props. 8-68299
Si₂O₆(OH)₂⁴⁻ group, electronic struct. calcs. 8-67971
SnO-SiO₂ glass, exam. of immiscibility 8-75837
TeO₂-Fe₂O₃ system, atomic arrangement, neutron diffr. data 8-83743
TeO₂-MoO₃-M₂O_m, glass formation range 8-71680
TeO₂-WO₃-R₂O_m glass formation range 8-71680
TiO₂-SiO₂, semicond. glass, small polaron hopping cond. 8-60126
TiO₂-SiO₂, semicond. glass, optical props. 8-60412
ZrF₄ glasses, elec. props. (*French*) 8-75868

glass fibre reinforced plastics

- dome, anal. and expt. stress anal. 8-72813
 elastic moduli meas., effect of deform. rate (*German*) 8-64796
 electric connector moulding compound, low press. diallyl phthalate, props. 8-52750
 epoxide resin, light polarisation exam. of stress 8-68857
 epoxy cross-ply laminates, multiple transverse cracking 8-95800
 epoxy matrix, room temp. curable, mech. props. and thermal conductivity 8-68669
 epoxy matrix, short aligned fibres, mech. charact., SEM and optical obs. 8-72761
 epoxy matrix, unidirectional, strength distrib. 8-68735
 epoxy resin matrix, mech. props. 8-64582
 exam. using ion scattering spectroscopy and scattered ion mass spectrometry 8-60641
 fabric reinforced polyester, biaxial stress failure surface under static and fatigue loading 8-72836
 fibreglass, mechanoluminescence during monoaxial stretching 8-68742
 glass fibre reinforced epoxy, as electrical insulation for Tokamak toroidal field coils, mech. props. 8-64610
 glass textolite cylindrical shells, parallel wound, feasibility of diagnosing strength 8-67157
 hybrid C and glass fibre, fracture energy 8-95801
 mechanical characts. under compressive load (*Japanese*) 8-92301
 polyacetal matrix, friction and wear against glass and steel 8-56783
 polyester resin/glass fibre discs, rotating strength, stress distrib., failure criterion rel. to mould process 8-76701
 polymer matrix, compressive strength 8-64609
 PTFE matrix, friction and wear against glass and steel 8-56783
 semifinished product nonlinearity model, force anal. of winding 8-63325
 silane, coupling agent on E-glass fibre, structure, Fourier transform infrared spectroscopy 8-60643
 silane, coupling agent on porous silica, Fourier transform infrared spectroscopy 8-60642
 tube under cyclic pressurisation 8-68761
 vinyl ester matrix, axial fatigue failure sequence and mechanism 8-68773
 VMP fibre reinforced epoxide binder, structure and strength, effect of fibrous filler tension 8-68751
 Al/polyurethane foam/glass fibre reinforced plastic (*Japanese*) 8-56707
 C/glass reinforced epoxy resin, hybrid effects, conditions for positive or negative effects vs. rule of mixtures, mech. props. 8-68769

glass fibres

- see also fibre optics; optical fibres*
 E-glass fibre, coupled with silane, structure, Fourier transform infrared spectroscopy 8-60643
 E-glass fibre strength, effect of forming and ageing atmos. 8-92283
 fibreglass, mechanoluminescence during monoaxial stretching 8-68742
 homogeneous, large aperture bundle tied by helix of metal or glass filament, light propag. anal. 8-87154
 optical, tensile strength testing, Weibull statistics 8-59128
 optical fibres, production for fibre optics, exam (*Polish*) 8-83130
 optical fibres with high tensile strength prep. 8-63211
 performance specification for optical communication (*Dutch*) 8-83112
 phosphate glass optical fibres, transparent in UV region, manufacturing 8-87113
 Al₂O₃-SiO₂, clad with B₂O₃-SiO₂ effect of drawing tension on residual stresses 8-64554
 β-CaSiO₃ fibre, continuous unidirectional crystallisation from melt 8-95739
 Na₂O-SiO₂ fibre, reactivity to atmospheric moisture below annealing range, internal friction measurement 8-92288
 SiO₂ fibres, fused, failure predictions based on fatigue strength 8-71293
 SiO₂ glass fibres, exam. of phase separation effect on internal friction 8-88455

glass-metal seals

- see also electron tube manufacture*
 fibreguide to metal hermetic seal, using Cu tube component 8-83120
 hermetic seal, optical fibre-to-metal, construction 8-83078
 vacuum seals for MgF₂ windows 8-94457

glass transition

- Adam-Gibbs theory, for conc. polymer soln. 8-83353
 alkali halide aq. solns., homogeneous nucleation glass form., press. depend. 8-51649
 composition dependence 8-59936
 dichloromethane-decalin glass, mol. dynamics, from dielec. loss meas., 107-148K, 293K 8-76379
 epoxide network polymers, glass-transition and chem. struct. (*Russian*) 8-51653
 equilibrium thermodynamics, sp. ht., refr. index and glass transition (*German*) 8-83745
 ethanol-water system, metastable states, hydrates existence and props., low temp. 8-71835
 glass-forming liquids, relax. times, temp. depend. 8-83924
 kinetics, linear nonequib. thermodynamic theory 8-67815
 multipolymers, glass transition rel. to phase separation 8-91270
 phenolformaldehyde resin, sp. ht. obs. (*German*) 8-75845
 polyalkyleneoxide polymer, proton nuclear mag. relaxation (*Rumanian*) 8-91977
 polyethylene, relax. phenomena, -30 to 200°C, premelting and glass transition 8-51440
 polyethylene oxide, relax. phenomena, -30 to 200°C, premelting and glass transition 8-51440
 polyethylene terephthalate, glass-rubber transition determ., small-angle X-ray scatt. 8-95145
 polymer, glass transition elevation by entanglements 8-83926
 polymer, glass transition under high-press., dielec. loss method obs. (*Russian*) 8-71841
 polymer glass, isothermal struct. relax., in high elasticity transition region, mol. model (*Russian*) 8-87629
 polymer glass transition, dynamic props., mol. model (*Russian*) 8-87777
 polymer glass transition, temp., conform. effects 8-83925
 polymer glass transition T_g rel. to ESR parameter T_{50g}, mol. interpretation 8-67817
 polymer glass-transition point meas. apparatus using vibration meas. of immersed plate (*Russian*) 8-71842

glass transition continued

- polymer glasses, thermodynamics of densification process 8-95723
 polymer reactions, two phase, below glass transition temp., limiting conversions 8-88632
 polymeric cryoprotectants in preservation of biological ultrastruct., aq. soln. low temp. states 8-65157
 polymers, crosslinked, specific characts. (*German*) 8-75585
 polymers, glass transition, positron annihilation studies, review 8-95614
 polymers, transient current nature 8-80278
 polyoxymethylene, relax. phenomena, -30 to 200°C, premelting and glass transition 8-51440
 polystyrene, microcryst. cellulose filled, glass transition temp. shifts 8-95144
 polystyrene glasses, transition temp. and thermodynamic state 8-75819
 polyurethanes based on toluene di-isocyanate, struct.-prop. relns. 8-80509
 polyvinyl fluoride, relax. phenomena, -30 to 200°C, premelting and glass transitions 8-51439
 polyvinylidene fluoride, γ-irradiated, low temp. internal friction 8-83874
 polyvinylidene fluoride, relax. phenomena, -30 to 200°C, premelting and glass transitions 8-51439
 PVA, microcryst. cellulose filled, glass transition temp. shifts 8-95144
 PVC, glass-rubber transition determ., small-angle X-ray scatt. 8-95145
 PVC, heat capacity and thermodynamic props., 6 to 375K obs. 8-79779
 rubber, natural, stretching effects on glass transition, sp. ht. obs. (*German*) 8-79753
 soft core model of simple liquids self diffusion, glass transition 8-67634
 styrene-acrylonitrile copolymer swelling, glass transition and crazing, polar group incorporation 8-85017
 Cd(NO₃)₂·4H₂O-CoCl₂, melt viscosity, equivalent conductivity, glass transition temp. 8-75855
 Cd(NO₃)₂·4H₂O-NiCl₂, melt viscosity, equivalent conductivity, glass transition temp. 8-75855
 (Fe,Co)PBAI, metallic glass, viscous flow, alloying effect 8-79793
 NiPBAI, metallic glass, viscous flow, alloying effect 8-79793
 Pd-Ni-P, metallic glass, viscous flow, alloying effect 8-79793
 Pd₇₇Cu₆Si_{16.5} metallic glass, diffusion of Au 8-55983
 Pt-Ni-P, metallic glass, viscous flow, alloying effect 8-79793
 Te₈₀Ge_{12.5}Pb_{7.5}, phase-separated system, overlapping effects of glass transition and crystn., DSC results 8-83739

glasses *see glass***glassy state** *see vitreous state***glide, dislocation** *see slip***globular star clusters**

- age and chemical comp. determ., review (*Polish*) 8-61751
 binary stellar systems, tidal disruption and coalescence 8-93330
 ω Centauri, cluster membership determ. for V65 and V78 8-73743
 ω Centauri, search for new variables 8-61895
 ω Centauri, UBV photometry of RR Lyrae stars 8-73719
 dust patches, UBV photometric obs. 8-81662
 dynamic evolution, review of obs. and numerical theories 8-77585
 equilibrium statistical mechanics of gravitating systems with energy cutoff 8-93326
 equilibrium statistical mechanics of relativistic systems with energy cutoff 8-93327
 gas outflow models including photoionisation 8-93338
 Hodge 11, in LMC, colour-magnitude diagram, metal abundances 8-69850
 M10 and M12, obs. star distrib. rel. to gravitational disturbance 8-69849
 M15, BVR area photometry 8-85983
 M15, nucleus brightness profiles of X-ray globular cluster 8-69848
 M15, surface brightness distrib. from electronographic obs. 8-85981
 M22, blue variable obs. 8-85945
 M3, inner structure, photoelec. scanning method (*Italian*) 8-93343
 M3, M13, M15, UBVR photometric obs., dust patches 8-81662
 M3 and 13, abundances in cluster red giants 8-93334
 in M49, giant elliptical galaxy, globular clusters space distrib. 8-93393
 mass loss from stars 8-93238
 metal abundances, rel. to galactic populations and Galaxy evolution 8-96545
 metal-poor-stars, spectral energy distrib. and Fe/H ratio 8-53937
 metallicity effects on integrated colours, calibration 8-89227
 NGC 1851, Hα absorption of UV5 and core 8-61896
 NGC 1851, periods and light curves for 19 RR Lyrae variables 8-73714
 NGC 419 in SMC, C star content 8-53962
 NGC 6256, probable galactic globular cluster, BV photometry 8-77583
 NGC 6266, colour magnitude diagram, distance and metallicity 8-61894
 NGC 6624, optical studies of X-ray source 8-93335
 NGC 6624, UBV photometry of X-ray globular cluster 8-93337
 NGC 6752, evidence for white dwarfs 8-93233
 NGC 7099, metal-poor globular cluster, UBV photoelectric photometry 8-77584
 pre-horizontal branch evolution and Oosterhoff dichotomy in globular clusters 8-69784
 spherical stellar system, distrib. of stars around massive central black hole 8-65660
 steepest descent technique and stellar equilibrium statistical mechanics, stability 8-65659
 stellar evolution in horizontal and asymptotic branches 8-81613
 stellar systems with continuous mass spectrum, necessary condition for equilib. 8-93328
 strip photometry application, multicolour obs. 8-89229
 47 Tucanae, colour-magnitude diagrams for inner regions 8-57598
 47 Tucanae, spectral inhomogeneities in faint stars 8-93340
 variable stars in clusters, problems 8-81641
 winds, nova-driven, rel. to intracluster gas Hα emission 8-57596
 X-ray source, evolution of 100 M_⊙ black hole in binary 8-61932
 X-ray sources, models 8-81706
 zero age horizontal branch stars, expected location 8-77551
 CO in giants in globular cluster, IR obs. 8-93339

glossaries

geology 8-88833
solar and solar-terrestrial physics, illustrated glossary 8-57537

glow discharge lamps see *discharge lamps*

glow discharge microphones see *microphones*

glow discharges

air, non-self-sustained discharge plasma ionisation instability obs. 8-71609
air flow with transverse mag. field 8-71562
anomalous glow discharge transition to nozzle hollow cathode discharge 8-67531
atomic and ionic spectral line excitation in cathodic region (*Russian*) 8-63611
atomic fluorescence spectrometry, hollow cathode lamp, pulsing conditions optimisation 8-65972
back discharge, flashover meas., streamer or steady glow mode, dust layer effects 8-59708
cathode region microscopic model 8-67524
cathode surface heating by high pressure glow discharge, catastrophic bridging 8-87574
characteristics meas. for sputtering appl. 8-72726
cylindrical hollow cathode negative glow, fast electron angular distrib. obs. 8-67529
DC and UHF field energy transfer to glow discharge plasma electrons 8-67539
detector for millimeter rad., cyclotron reson. effect on sensitivity 8-62222
diagnostics with electric probes, sputtering appl. 8-71537
dielectric surface creep discharge photon intensity rel. to charge transport 8-67561
electron beam generation, pulsed, high power, gas dynamics appl. 8-63515
emission spectrometry, current developments (*Japanese*) 8-86356
forward ionisation waves rel. to acoustic phenomena 8-75282
gas gap subject to pulsed ionising radiation, volt-amp characts. 8-51377
gas temp. meas. in glow discharge in capillary using thermocouples (*Russian*) 8-59694
gaseous inclusions in insulating solid, elec. strength and degradation 8-83631
glass substrate, glow discharge effect on surface props. and struct. 8-85201
glow discharge detection, gas breakdown theory 8-58035
hollow cathode discharge, electron temp meas. 8-67445
hollow cathode discharge, H₂ prod. in H₂O vap. plasma 8-75441
hollow-cathode glow discharge with static stepped V-I characteristic (*Russian*) 8-75443
ion source using HF glow discharge, temp. and electron density profile meas. (*German*) 8-70221
ionisation instability, stabilising effect of turbulent transport processes (*Russian*) 8-59698
ionisation overheat instability in alternating fields, h.v. pulse stabilisation (*Russian*) 8-91175
Langmuir probe characteristics at low plasma densities, numerical analysis 8-63592
mass spectroscopic source combination with quadrupole mass filter for solids anal. 8-61075
methane, ion-molecule reactions in glow discharge, mass spectrometric obs. 8-63627
negative glow plasma, contact electrode charging time meas. 8-67525
nitrided steel surface wear-related topography 8-60847
non self-sustained, detachment process effects 8-59713
nonequilibrium plasma chemical reaction kinetics 8-76863
phototube, gas-filled, rise time spectral depend., appl. to EM radiation detector miniaturisation 8-86318
plasma diagnostic techniques appl. to glow discharge characterisation 8-71536
plasma line emission intensity calc. and meas. 8-67526
polyhexamethyldisiloxane thin film form. in glow-discharge flow system 8-68631
polymer layer, glow deposition rate obs. in DC discharges 8-68633
polymer thin film growth by glow discharge polymerisation, temp. depend. 8-68632
population inversion in transverse flowing gas, discharge struct., from optical meas. 8-78992
pulsed DC glow discharge, cataphoresis eqns. 8-67506
pulsed glow discharge, externally maintained, by electron beam 8-79490
spectrochemical analysis with glow-discharge lamp (*Japanese*) 8-85262
spectroscopic light source, characts. using Ar(He) carrier gas, Al(graphite) cathodes 8-82047
sputtering and reactive effects in a stainless steel tube during glow discharge treatment 8-70141
sputtering diagnostics, optical spectroscopy 8-72666
stationary, contraction dynamics in air flow (*Russian*) 8-87511
steel, surface cleaning in glow discharge, ion bombardment effect (*Russian*) 8-95848
TE glow discharge, influence of fluid-dynamic phenomena 8-71619
temperature measurement, using electronic rot.-vibr. mol. spectra (*Russian*) 8-71575
transversely inhomogeneous, stability, equiv. cct. theory 8-51373
tube impedance with and without metal cover 8-67508
VUV source, laser induced two photon blackbody radiation from He atoms in glow discharge 8-58102
Al storage ring vacuum chambers, glow discharge processing versus bakeout 8-70658
Ar, Ar+O₂, ground surface ion bombardment of stainless steel in DC glow discharge 8-95098
Ar, cylindrical hollow cathode, ignition and breakdown expts. 8-91169
Ar, imprisonment of reson. rad. in cold cathode region 8-59703
Ar negative glow fast electron density rel. to discharge pressure and current 8-67528
C oxides, glow discharge, excitation and ionisation mech., elec. and optical obs. (*Russian*) 8-59695
C steel joints, with interference, increasing supporting capacity, by electrophysical methods, exam. 8-85055
CO₂ dissociation obs. in flow system with cylindrical hollow cathode 8-66674
CO₂ dissociation obs. in hollow-cathode glow discharge 8-70946

glow discharges continued

CO₂ glow discharge, acoustic wave influence on F⁻ forward ionisation wave 8-67521
CO₂ glow discharge chemical processes and rate coefficients 8-63626
CO₂ laser, convective-cooled, fast-flow, pulse discharge stability 8-94389
CO₂ laser, glow discharges at high press., voltage-current characts. 8-87036
CO₂-N₂-H₂, non-self-maintained glow discharges at atm. pressure, elec. characteristics and energy exchange 8-71606
CO₂-N₂-He gas mixtures, fluorescent IR radiation from glow discharge 8-94386
CO₂-N₂-He gas mixtures, time-of-flight meas. of electron transport parameters 8-94387
CO₂-N₂-He mixture volumetric glow discharge formation at atm. pressure 8-71615
Cd-Ar low-pressure discharge column, energy balance obs. 8-67504
H-isotope enrichment using low-temp. glow discharge technique 8-66675
HCl, dissoci. excitation in flowing afterglow, Cl form., light emission 8-90115
He, 2³P level population relax., laser absorpt.-perturbation meas. 8-59706
He constricted glow discharge, space charge double layer influence obs. 8-67492
He flowing discharge, glow/arc transition and cathode-zone wave structure obs. 8-75475
He hollow-cathode discharge, Ba⁺ and Sr⁺ formation 8-67527
He low-current discharge, metastable atoms, radial density distrib. obs. and calc. 8-67495
He-Na mixture, low-pressure discharge, radial cataphoresis obs. 8-67507
Hg low-pressure pulse-modulated discharge optical and electrical parameters 8-67491
Hg-TlI, lamp, chem. comp., temporal and spatial evolution 8-87532
K, discharge plasma, anomalous bright 5730 Å band excitation mechanism 8-67475
Kr, DC glow discharge excited atoms, radial conc. distrib. obs. 8-67494
Kr, hollow-cathode glow discharge with gas flow 8-67532
KrF, 0.8 J multi-atm. laser, glow discharge characts. 8-58992
N cooled discharge plasma electron energy distrib. function 8-63633
N₂, flowing discharge, characts. depend. on initial conditions 8-51378
N₂, glow discharge, decay instability and contraction, interferometric and photographic obs. (*Russian*) 8-59696
N₂, mol. excitation, in glow discharge and afterglow 8-63623
N₂, molecular plasmas, electron kinetics (*German*) 8-91171
N₂-H₂ mixture, glow discharge, ionisation and excitation obs. 8-67505
Ne discharge, ionisation wave, phase instability and disintegration obs. 8-67518
Ne, glow discharge, turbulent ionisation waves, correlation meas. 8-67519
Ne medium-pressure discharge, electron temp. radial profile meas. by electron-atom bremsstrahlung continuum 8-67497
Ne, reson. absorpt. plasma of glow discharge positive column, Ne super-radiation pulse variation 8-71489
Ne stationary discharge with diffuse recombination, limit current and multiple states 8-67498
Ne, voltage change due to laser irradi., 572-654 nm 8-63605
Ne-Cu hollow-cathode laser discharge sputtering obs. 8-66800
Ne-He DC glow discharge electron density decay, microwave cavity obs. 8-91167
Ne-O₂, DC glow discharge, Ne I spectral line intensities 8-74610
O atom concentration, in O₂, (CO)(CO₂) glow discharge, mass spectrometric determ. (*Russian*) 8-87512
O glow discharge atomic radial distribution obs. 8-67501
O₂ gas-discharge plasma, interaction with Si surface 8-83840
O₂, low press. and current, theory 8-87560
SF₆ glow discharge, non-linear effects on self-exciting wave 8-83633
SiO₂, substrate, glow discharge effect on surface props. and struct. 8-85201
SiO₂, surface reactivity modification by Ar/O₂ plasma treatment 8-64890

GO calculations
acetylene, ground and triplet states, electronic and geom. struct. 8-94184
benzene, electronic struct., mag. susceptibilities, ab initio calcs. 8-74571
bis(fluoroxy)difluoromethane, ab initio MO calcs. of geometry, torsional barriers 8-90313
chloromethane+Cl⁻, S₂ reaction, local orbital description, ab initio FSGO method 8-76842
electron repulsion integrals, computation involving Gaussian basis functions 8-58572
ethane, valence electronic struct., model pot. in floating spherical GO formalism 8-74563
ethylene, ab initio GO calc. 8-94187
floating spherical GO open-shell calculations, double gaussians, first row atoms and ions 8-94182
fluoroxyperoxytrifluoromethane, ab initio MO calcs. of geometry, torsional barriers 8-90313
Gaussian-70 MO program, LCAO-SCF eqn. soln., population anal., appl. 8-70742
glyoxal, ³nm* states, ab initio STO-3G CI calcs., ΔE_{ex} transition energies 8-94194
homonuclear diatomics, equilib. geometries, Gaussian-based model pot. calcs. 8-94183
methane, localisability in MO calcs., measured by absolute overlap and 2nd moment dispersions 8-74557
methyl glyoxal, ³nm* states, ab initio STO-3G CI calcs., ΔE_{ex} transition energies 8-94194
methylene+H₂→CH₃+H, triplet methylene abstraction, partial open shell FSGO calc. 8-80719
molecular polarisability, selection of Gaussian basis sets 8-58865
orbital amplitudes of nuclei, extrapolation procedure, gaussian basis set and nucl. cusp eqn. 8-74560
partial at. charges calc. from ab initio mol. electrostatic pots., appls. 8-70739
trifluoroacetic acid, ab initio MO calcs. of geometry, torsional barriers 8-90313

GO calculations continued

- ArHCl, ab initio FGO calc. 8-50467
 BH, localisability in MO calcs., measured by absolute overlap and 2nd moment dispersions 8-74557
 BH₃, localisability in MO calcs., measured by absolute overlap and 2nd moment dispersions 8-74557
 BN, cubic, energy band and piezoelec. calcs. 8-72071
 B₂N₂H₆, electronic struct., mag. susceptibilities, ab initio calcs. 8-74571
 BeH₂, localisability in MO calcs., measured by absolute overlap and 2nd moment dispersions 8-74557
 CH₃SiH₂, ab initio GO calc. 8-94187
 Ge₂H₆, valence electronic struct., model pot. in floating spherical GO formalism 8-74563
 H₂, D₂, photoionisation, body-frame Hund's case b description 8-94295
 HCN⁺, photoelectron spectra of third electronic state, ab initio calc. of pot. energy surface 8-70871
 H₂O, localisability in MO calcs., measured by absolute overlap and 2nd moment dispersions 8-74557
 HPO, mol. struct. and props., ab initio, calc., Gaussian lobe orbital 8-62713
 HS₂, rotamers, electronic and geometrical structs., ab initio floating GO basis calcs. 8-74572
 LiH₂O⁺, geom., electronic struct. FSGO model calcs. 8-82614
 LiN₂, geom., electronic struct. FSGO model calcs. 8-82614
 LiNH₂⁺, geom., electronic struct. FSGO model calcs. 8-82614
 NH₃, LCAO-MO-SCF calcs., analysis of Gaussian basis sets rel. to one-electron props. 8-55122
 NH₃, localisability in MO calcs., measured by absolute overlap and 2nd moment dispersions 8-74557
 Si₂H₆, valence electronic struct., model pot. in floating spherical GO formalism 8-74563
 V(CN)₆NO³⁻, struct., FSGO calcs. 8-70736
 V(CN)₆NO⁴⁻, struct., FSGO calcs. 8-70736

gold

- see also nuclei with
 adsorption, of Pb, formation of AuPb₂ epitaxial layer, LEED, AES study of Au/AuPb₂ interface 8-71988
 adsorption of O₂, Auger spectra 8-87879
 adsorption on Ge, effect on I-V characteristics, field emission study 8-67925
 adsorption on platinised Pt electrodes in aq. HCl 8-56914
 AES, valence band spectra, solid-state and atomic features 8-72646
 angular-dependent studies on some prototype vertically and laterally inhomogeneous samples 8-95655
 atom, excitation by FKα and AlKα ESCA sources 8-53301
 atom, oscillator strengths, relativistic HF, core-polarisation model pot. 8-86818
 atom, relativistic effective core pots., appl. to AuH and AuCl ab initio calcs. 8-86767
 atom, transition probability of valence shells, relativistic pseudopot. calc. 8-86803
 atomistic images of field ion microscopy at high temps. 8-55792
 Au, ultra-microhardness testing for vacuum deposited film and bulk specimen 8-79910
 bicrystal, dislocation networks in twin boundaries in TEM obs. 8-51556
 bicrystalline film, lattice imaging of low angle tilt boundaries by TEM 8-79620
 bicrystals, interaction of lattice dislocations with grain boundaries, electron microscope obs. 8-51579
 black film, structural composition and its influence on optical props. 8-56530
 capture cross section in n-type Si, MOS struct. expts. 8-91772
 chemisorption, of H(O), on electrode, volume of adsorbed species, temp. and press. effects 8-84060
 coated diffraction gratings, UV light polarisation at grazing incidence 8-87129
 coating on Cu crystals, effect of coating on Cu fatigue behaviour 8-72850
 condensation of Pb on Au (100) 8-91569
 convoy electrons from solids, ion vel. and Z and target material depend. 8-84692
 crystallites, formation in flowing Ar system, density, size distrib. and size dispersion 8-88415
 Debye temperature var. at high temp. (French) 8-63831
 Debye Waller determ. from modified Cheveau model 8-59918
 decoration, obs. of graphite surface behaviour under various vacuum conditions 8-75915
 deformed bars, cold rolled, exam. of microstruct. by thin foil TEM 8-88502
 diffusion in Ga_{0.5}In_{0.5}P, epitaxial film, effect of intrinsic impurities 8-87825
 diffusion of Pd and Pt, 700-1000°C (Russian) 8-91484
 diffusion on atomically clean Si (111) surface 8-72037
 discontinuous film, elec. cond. and current noise, temp. depend. meas. 8-56245
 discontinuous film, optical transmittance 8-56529
 Doppler factor, comparison between calculated values and measured results 8-54811
 electrical resistivity, press. variation 8-84193
 electrical resistivity of dislocations, calc. (Russian) 8-60117
 electrode, adsorption of metal ions, kinetics, surface struct. 8-79873
 electrodeposit, struct., texture, influence of As on brightness (Bulgarian) 8-79862
 electrodeposit, struct., texture, influence of substrate (Bulgarian) 8-79863
 electrodeposited coating, Cu diffusion under high temperature, influence on contacts performance (Czech) 8-91486
 electrodes, partially covered with photoresists. layer, ferricyanide reduction 8-85236
 electromigration and residual resistivity of ⁵⁷Co 8-71881
 electron beam energy losses 8-91368
 electronic props., pseudopotential calc. 8-51960
 energy reflection coefficient for 5 to 10 keV He ions 8-95639
 epitaxial growth in NaCl with continuous C-intermediate film 8-84102
 epitaxy on W (001) 8-60041
 film, aggregated, absorpt. peaks, collective oscills. of electrons 8-80428
 gold continued
 film, beam splitter phase coatings, for producing phase quadrature interferometer outputs 8-77974
 film, discontinuous, optical transmittance, effect of island morphology 8-84673
 film, electron inelastic scatt. mean free paths, synchrotron radiation photoelectron spectra meas. 8-76587
 film, energy losses of 20-40 keV electrons 8-92153
 film, epitaxial growth, characterisation of [001] tilt boundaries 8-84097
 film, ionic sputtering and AES anal. (French) 8-76959
 film, on Si, coincidence site phase boundaries 8-67927
 film, on ZnS crystal for composition control, calc. of defect conc. 8-95052
 film, refr. index, obs. using automated Fourier-Stokes analyser ellipsometer system 8-49886
 film, transmission sputtering 8-52613
 film, vacuum deposited, O⁺ bombardment sputtering rates 8-88390
 film bicrystals, exam. of low energy planes for tilt grain boundaries 8-51551
 film continuity, observations by Auger spectroscopy 8-64433
 film on Si substrate, solid-solid reactions 8-95369
 fine particles, adhesion, role of twinning and surface energy, TEM obs. 8-72009
 foil, average thermal neutron flux determ. method 8-73112
 foil, electrodeposition of alpha activity, use in Si surface barrier detector 8-82565
 foil, neutron activation cross sections meas. for generalised intermittent irradiation, fusion machines appl. 8-58283
 friction props. of surface films in air and high vacuum 8-60850
 getting, of Au in Si by P diffusion and P-induced dislocations 8-91346
 HEED, band theory, zone axis crit. voltage effect 8-83659
 high current density plated, Co diffusing out, oxidation kinetics 8-92393
 implanted ion detection by X-ray emission anal. in TEM 8-51575
 interatomic potentials from experimental phonon spectra 8-75621
 IR absorption coefficient, temp. depend., 3 to 30 μm 8-74953
 lattice vibration and electron press., central pair pot. model calc. 8-75749
 migration in GaAs, ESCA study (French) 8-75885
 monolayer, on W(001), elec. struct. 8-72236
 multiphoton photoeffect, new effect due to ps laser pulses 8-80452
 neutron yield calcs., electron beam incidence 8-95622
 nucleation on organic substrates, ion bombard. effects 8-75965
 ore, leaching, effects of ultrasonics and their appls. 8-92214
 phonon dispersion relations, screened shell model 8-83894
 phonon dispersion relations and Debye-Waller factor calcs. 8-51630
 phonon resistivity, low temp. 8-79978
 photoelectron count rates, using VUV He reson. line radiation source in UHV apparatus 8-89602
 piezoelectric modulator for 10.6 μm radiation using Au clad amorphous Se optical waveguide 8-66956
 planar channelling of α-particles, stopping power of solids 8-51602
 polycrystalline film, RF bias-diode and triode sputtered, resist. and microstruct. 8-80072
 polycrystalline wire, internal oxidation of impurities 8-83842
 positron annihilation characteristics, effect of temp. 8-64427
 positron annihilation rates, electron-electron and electron-positron correl. effects 8-76548
 positron-vacancy interactions, equilib. temp. depend. of positron annihilation 8-76547
 pseudopotential, fitted to elastic data 8-75705
 radioactive waste disposal method including encapsulation in thick gold layer 8-74441
 reflection of H, D and He ions 8-95640
 SEM, electron channelling patterns 8-83697
 semiempirical, relativistic oscillator strengths including core polarisation for p-, s-, d-series 8-74609
 sliding charact., friction and wear (Japanese) 8-56778
 sol, grain boundary struct. obs. and boundary diffusion 8-51552
 solubility in Si, gettering by P 8-83961
 spectral distrib. of X-ray braking radiation, due to electrons, calc. using Monte Carlo method 8-56538
 sputtered with 15 or 30 keV H⁺, He⁺ and Ar⁺ ions, energy and angular distrib. 8-95625
 sputtering and chem. attack by H ions of 100 eV energy 8-95635
 stopping power for 28 MeV α-particles, re-evaluation 8-79651
 stopping power meas. for 4-5 MeV/N ¹⁶O, ⁴⁰Ar, ⁶⁵Cu, and ⁸⁴Kr 8-70720
 stopping powers, projectile range for Z=8-20, 0.0125-12.0 MeV/nucleon 8-83856
 substrate, periodic arrays of misfit dislocations during epitaxial growth of Cu and Pd, electron diffr. 8-51857
 surface, (110), electron spin polarisation in LEED 8-83692
 surface, cadmium arachidate monolayer, reson. surface plasmon reflection 8-56536
 surface, O single layer, ferromag. props. (Russian) 8-64256
 surface, resonant absorpt. of sound (Russian) 8-95216
 surface plasma waves, dispersion curves, attenuated total reflection spectra 8-88015
 surface plasmon obs. using X-ray emission 8-92146
 surface state on (111), E(k) relation, ang. resolved photoemission 8-76582
 TEM exam. of ion damage in FCC metals 8-87727
 thermal conductivity at high press. meas. 8-95283
 thin disc prep. and electropolishing for TEM 8-88601
 twinned crystals, epitaxial growth on KCl crystals, electron microscopic study of microstructure 8-91566
 UPS examination, temp. effects 8-68604
 vacancy clusters, quenching and ageing, electron microscopy study 8-76671
 vacuum deposition, on (100) surfaces of KBr, KCl and NaCl substrates with colloidal centres (Rumanian) 8-60579
 valence band Auger spectra 8-76563
 VPE, nucleation on NaCl, role of surface steps 8-79902
 X-ray photoelectron spectra ang. depend. (German) 8-72679
 XPS, achromatic X-ray source, spectrum iterative deconvolution, doublet and valence band 8-72689
 XPS, of polycryst., appl. of monochromated spectroscopic UV discharge lamp 8-89601

gold continued

- Ag+H⁺, L-shell ionisation at large scatt. angles 8-90283
 Al-AlN-Au, voltage controlled negative resist., O₂ press. effect 8-72281
 Al-Au bimetal thin film interdiffusion zone, intermetallic phase form kinetics, 70-160°C 8-75891
 Al-SiO₂-Au, thin layer struct., electrolumesc. (*French*) 8-76531
 Al-SiO₂-Au cathode, emitted electron energy distrib. 8-52645
 Al₂O₃ to Au solid state reaction bond, effect of ambient atmosphere 8-67914
 Au I, absorpt. spectrum obs., 1300 to 1900 Å 8-62751
 Au, ZZ 8-75883
 Au-Ag bilayers, conc. profile by AES, interdiffusion coefficient determ. (*French*) 8-84077
 Au-As₂Se₃ contact, model of charge injection 8-68088
 Au-CdIn₂S₄ surface-barrier diodes, mech. of current flow 8-56228
 Au-dielectric cermets, optical constants, incl. proximity effects 8-56446
 Au-GaAs (110) Schottky barriers on ordered and disordered GaAs surface, props. 8-95360
 Au-GaSb structure, metal-semicond. interaction, soft XPS meas. 8-60203
 Au-GaSb surface barrier struct., elec. and photoelec. props. 8-56229
 Au-Ge Schottky diode, phonon energies, barrier heights, photovoltage spectra 8-64112
 Au-Ge-Au, room temp. interdiffusion 8-76161
 Au-InP Schottky diodes, barrier height study 8-52088
 Au-Pb₃Sn₁-Te-Au structure, third harmonic variations at 77K and 300K 8-84313
 Au-Si, spatial origin of electrons in internal photoemission struct. (*French*) 8-91770
 Au-Si Schottky-barrier, formation process anal., V-I characts. (*French*) 8-91768
 Au-Si-Al structure electrode mass transfer and switching with memory 8-95389
 Au-tetrathiotetrahene-Al systems, dark cond., photocond. mechanisms rel. to contact phenomena (*Russian*) 8-52103
 Au-zinc phthalocyanine-Au junction, microstruct. characterisation by TEM method 8-95241
 Au+H⁺, K-shell ionisation, 7-15 MeV, relativistic effects 8-82830
 Au⁺+X, X=H, H₂, He, C, N, O, cross-section, closure-Born approx. 8-66630
 Br⁻ adsorpt. on Au electrode, specular reflect. investig. 8-61047
 Cu/Au+0.03 at.% Fe, thermocouple characteristics, in mag. field at low temps. (*Russian*) 8-54365
 Cu-Au alloy, ZZ 8-75883
 GaP-Au, diffusion, solubility, and electrotransport of Au 8-91489
 GaP-Au, Schottky barrier, layer formation, elec. and optical props. 8-91766
 Ge:Au, IR detector, impurity photoconductivity (*German*) 8-82036
 He-Au UV laser, spectral range, threshold, power output 8-66809
 KCl:Au⁺, Jahn-Teller effect 8-64015
 Ni/Au film on silicon vacuum deposited, electron impact mass spectrometric exam. of surface contaminants 8-75957
 Pd_{77.5}Cu₆Si_{16.5}-Au metallic glass, diffusion of implanted Au 8-55983
 Si:Au, (111) surface impurity, ESCA obs. 8-52640
 Si:Au, degeneracy factor of acceptor level 8-51927
 Si:Au, electron capture cross section, energy level of Au acceptor centre 8-51926
 Si:Au, neutron irradiated, penetration of Au into Si 8-59984
 Si:Au, nonequilib. population of electron states and photomemory of surface pot. 8-56206
 Si:Au, recoil implantation from thin surface films, backscatt. obs. 8-63783
 Si:Ga, Cu, Au, gettering of Cu and Au during Ga diffusion 8-91350
 Si:P, Au, neutron irradiated, distrib. of P and Au determ. 8-79627
 Si-SiO₂ interface, Au conc., effective impurity doping 8-52094
 Ta-Ta₂O₅-ZnS:TaF₃-Au thin films, MIS struct., DC electrolum. obs., Poole-Frenkel effect 8-88038

gold alloys

- see also gold compounds*
 alkali metal-Au alloys, elec. props. 8-84187
 Cr-Au alloys, dil., elec. resist., 77-700K 8-64035
 dilute, containing rare earth impurities, magneto-transport props. 8-68015
 electrical resistivity, deviations from Matthiessen rule and scattering anisotropy 8-76051
 electrodeposits for electronics industry, characts. 8-52695
 mutual alloying behaviour of the elements straddling the line Li-Mg-Cu-Au in the long periodic table 8-84769
 rare earth intermetallics, RAu₃, ordering temps. and effective moments 8-60283
 rare earth-Au, dil., Mossbauer exam. of mag. hyperfine field at ¹⁹⁷Au impurity 8-88244
 rare earth-Au alloys sputtering, negative ions origin and effects 8-60574
 Ag-Au, dil., low temp. elec. resist. 8-51964
 Ag-Au (50 at.%), thermal expansion and lattice parameters, temp. depend. 8-91456
 Ag-Au-Pd, liquidus and solidus surfaces 8-60649
 Ag-Cu-Au, effect of additions on eutectic and peritectic temp., of binary alloys 8-84801
 AgAu, sputtered neutral mass spectrometry using post-ionisation in microwave plasma 8-92579
 Al-Au bimetal thin film interdiffusion zone, intermetallic phase form kinetics, 70-160°C 8-75891
 Au-Ag, thermal conductivity, data anal. and synthesis 8-95284
 Au-Ag-Cd, martensitic transformation, preceding struct. anomaly 8-68692
 Au-Ag-Cu, chem. surface anal., low energy ISS compared with SIMS 8-64908
 Au-Al system, influence of current on phase form. in diffusion layer (*Russian*) 8-52826
 Au-Cd (47.5 at.%), effect of cooling rates on stress-strain behaviour 8-76721
 Au-Co, dil., local moments, third harmonic de Haas-van Alphen wave shape anal. 8-84127
 Au-Cr, dil., spin glass, elec. resist., press. and conc. effects 8-52278
 Au-Cr alloy pressure gauges, annealing effects 8-49854
 Au-Cr Kondo alloy, effect of press. on resistivity 8-79978

gold alloys continued

- Au-Cu, refr. index and absorpt. coeff., 1-5 eV (*Russian*) 8-60484
 Au-Cu, surface comp. as function of temp., AES expts. 8-95212
 Au-Cu, thermal conductivity, data anal. and synthesis 8-95284
 Au-Cu-Ag dental alloy, age-hardened, struct. and morphology 8-92272
 Au-Fe, competing interactions in FCC alloys 8-95453
 Au-Fe, dil., approach to saturation of magnetisation 8-56293
 Au-Fe, dil., local moments, third harmonic de Haas-van Alphen wave shape anal. 8-84127
 Au-Fe, finite mag. clusters near percolation conc. 8-72371
 Au-Fe, impurity spin dynamics in magnetic glasses at low frequencies (*French*) 8-88126
 Au-Fe, micromagnet, freq. depend. of susceptibility max. 8-95445
 Au-Fe, spin glass in low DC field, mag. viscosity, time decays of remanences 8-64209
 Au-Fe, very dil. alloy, Kondo temp. 8-91688
 Au-Fe alloy, spin glass, neutron scatt. 8-68265
 Au-Fe film spin glass, low temp. resistivity, mean free path effects 8-80163
 Au-Ge (27 at.%), metastable phase struct. determ. by electron diffr. 8-83780
 Au-In, electrodeposited from acid cyanide electrolyte, exam. of wear and corrosion resistance 8-80482
 Au-Mg (18 at.%), superstruct. determ., electron microscope obs. 8-75630
 Au-Mn, dil. spin glass, thermopower, rel. to spin glass freezing temp. 8-79983
 Au-Mn alloys, equiatomic region of phase diagrams crystallographic and mag. exam. 8-52755
 Au-Mn system, AABBB struct., experimental evidence for occurrence 8-63698
 Au-Ni, heat capacity, 1.5 to 15K 8-95452
 Au-Ni, liquid alloy system, determ. of thermodynamic props. using Knudsen effusion method, phase diagram calc. (*German*) 8-51707
 Au-Ni (15 at.%) film, evidence of modulated struct., TEM exam. 8-87887
 Au-Ni-Cu phase diagrams, thermodynamic calc. (*Korean*) 8-68672
 Au-Pd, thermal conductivity, data anal. and synthesis 8-95284
 Au-Si, amorphous sputtered film, elec. props. 8-68006
 Au-Sn (100 ppm Sn), vacancy clusters, quenching and ageing, electron microscopy study 8-76671
 Au-Tl (29 to 100 at.%), thermal analysis, exam. of phase diagram 8-88445
 Au-V, dil., Kondo alloy, spin dynamics, nuclear spin relax obs. 8-68155
 Au-Zn(Cu), electrolytic thinning for use in transmission electron microscopy 8-57918
 Au₃Cd, sputtered epitaxial films, order-disorder reaction obs. 8-84092
 Au₃Cd, ht. of order-disorder transform., differential microcalorimetry (*French*) 8-57950
 AuFe, spin glass freezing above ferromag. percolation limit 8-52264
 AuGe, ohmic contact to epitaxial GaAs, production by laser alloying 8-88026
 AuGe/n-GaAs, SIMS study Au behaviour during annealing 8-75947
 Au₁₁Mn₄, electron diffraction and microscopy obs. 8-75512
 Au₁₁Mn₄, ordering, electron diffr. and high resolution TEM obs. 8-71707
 Au₂Mn ordered alloy, coincidence sites in domain boundaries, high resolution TEM obs. 8-71708
 Au₂Mn, ordered, coincidence sites in domain boundaries, high resolution TEM obs. 8-71708
 Au₂Mn₂, electron microscope exam. of ordering 8-63697
 Au₂MnAl, Heusler alloy, ferromag., NMR meas. 8-76320
 Au₂MnIn, Heusler alloy, ferromag., NMR meas. 8-76320
 AuPb₂, epitaxial layer, formation during Pb absorpt. on Au, LEED, AES study of Au/AuPb₂ interface 8-71988
 (Au,Pb)_{1-x}Fe_x, ferromag. and spin glass ordering 8-56335
 Au(Pd)-Zn, martensitic transformation, Hall coeff., specific elec. resistivity and X-ray powder diffraction 8-72774
 Au_{1-x}Si_x, amorphous film, spectra 0.01-6.2 eV, 0.13≤x≤0.5 8-68574
 AuSn₄-Sn, unidirectionally solidified, X-ray diffr. anal. of crystal struct. 8-91308
 Ce₃₀Au₂₀, amorphous, cryst. field effects and mag. interactions, magnetisation and transport props. meas. 8-68191
 Co_{1-x}Au_x, amorphous, elec. resist., temp. depend., spin wave contrib. and resist. minimum 8-51961
 CsAu, NMR line shape, Knight shift, X-ray diffr. study, struct. props. 8-68402
 CsAu, photoelectron spectroscopy and energy bands calc. 8-76581
 Cs_{1-x}Au_x, liq., metal-nonmetal transition, electronic theory 8-79930
 Cu-Au, critical voltage effect (*Japanese*) 8-91206
 Cu-Au, dil., dose depend. of impurity detrapping stages after electron irradiation 8-51582
 Cu-Au, dil., enhanced lattice sp.ht. 8-51699
 Cu-Au, dil., O₂ solubility, thermodynamic and residual resist. study 8-59952
 Cu-Au, order-disorder transform, influence of strain energy 8-84796
 Cu-Au (50 at.%), ordered, influence of elastic stresses on mech. props. (*Russian*) 8-92298
 Cu-Au alloy, ZZ 8-75883
 Cu-Au dilute alloys, thermopower and resistivities, validity of Nordheim-Gorter relation 8-91671
 CuAu, calc. of elastic interaction between locally transformed regions with screw and edge dislocations 8-83844
 CuAu-type superstructure, interaction of reacting dislocations (*Russian*) 8-83814
 Cu₃Au, fast neutron irradiation, displacement cascades 8-83852
 Cu₃Au, mechanical damping in terms of Granato-Lucke theory, comparison with leaded and unleaded brass 8-95772
 Fe_{1-x}Au_x, amorphous, elec. resist., temp. depend., spin wave contrib. and resist. minimum 8-51961
 Hg-Au, liquid dilute amalgams, elec. cond. and thermoelec. power 8-51976
 La₁₈Au₂₂, amorphous, evidence for short wavelength cutoff in fluctuation spectrum 8-68113
 MnAu₄, domain struct. exam. by powder method (*German*) 8-91883
 Nb₃Au, A-15 struct. supercond., microhardness, bonding 8-76199
 Nb₃Au, BCC, density of states, comparison with A-15 8-80095
 Ni-Au, dil., orientation depend. of surface segregation, AES and SEM obs. 8-71908

gold alloys continued

- Ni_{1-x}Au_x, amorphous, elec. resist., temp. depend., spin wave contrib. and resist. minimum 8-51961
 Pb-In-Au, film, supercond. penetration depth 8-72306
 Pd-Ag-Au, temp. effect on lattice parameters and thermal expansion 8-51473
 (Pd_{0.8}Au_{0.2})D_{0.04}, lattice location of D, ion channelling obs. 8-67708
 Pt-Au (4.0 at.%), ion irradiated, direct obs. of vacancy struct. of (220) platelet 8-51534
 PtMnSn, ¹⁹⁷Au and ¹¹⁹Sn hyperfine fields, Mossbauer expt. 8-72439
 RbAu, NMR line shape, Knight shift, X-ray diffr. study, struct. props. 8-68402
 RbAu, photoelectron spectroscopy and energy bands calc. 8-76581
 Sb-Au, amorphous film, elect. resist. 8-95390
 SmAu, diode sputtering, negative ion MFP 8-95641
 SmAu, significance of negative ion formation in sputtering and SIMS anal. 8-72663
 Sn-Au, liquid alloy, exam. of activity and heat of mixing, using mass spectrometry 8-51706
 Te-Au, dil. liq. alloy, elec. cond. at high temp. and press. 8-87959
 Ti-Au, thermodynamics and kinetics of β to α_m transformation 8-84795
 V₂Au, supercond., electronic density of states and T_c changes with atomic ordering 8-91800
 YbAu₂, surface effects on valence 8-91746

gold compounds

see also gold alloys

- AgI-AuI, pseudo-binary phase diagram 8-76637
 Au(CN)₂⁻, electrochemical reduction kinetics 8-73052
 AuF₃, ¹⁹F NMR chemical shift, crystal chemistry 8-87645
 AuH, AuCl, ZZ 8-86767
 AuTeI, cryst. struct. 8-51504
 Cs₂Au₂Cl₆, ¹⁹⁷Au Mossbauer high press. study of mixed valence compound 8-52387

goniometers

- bakable UHV, precision three-axis goniometer 8-70673
 crystal mounting on ends of fibres using a controlled method 8-93663
 GUR-5, for small-angle X-ray scattering meas. 8-74115
 interferometric, mes. of angles (Czech) 8-49794
 interpolating indexing instrument for UDP-025 goniometer 8-74119
 optical goniometer accuracy effect of atm. turbulence 8-55461
 spectral reflectometry of 0.1 mm surface elements appl. (Japanese) 8-89527
 topography settings, white beam X-ray, for cryst. defects, synchrotron radiation 2-axis spectrometer 8-67619
 Weissenberg rheogoniometer, computerised calib. and meas. of Newtonian fluids 8-87323
 X-ray, for fine metal fibre stress/strain curves determ. (German) 8-92413
 X-ray diffractometer, double-crystal, design features, appl. 8-49948

GP zones see Guinier-Preston zones**grain boundaries**

- for grain boundary diffusion, see diffusion in solids; for grain boundary segregation, see segregation
 see also bicrystals; subboundary structure; twin boundaries
 alloy, drag 8-51550
 bronze-steel, phase composition and struct. of diffusional interlayer in fusion zone, X-ray analysis 8-56821
 cavity nucleation at second phase particles in grain boundaries 8-59819
 ceramic, ferrimag. or ferroelec., microstructure and physical props. 8-72756
 coupled grain boundary sliding and migration, computer modeling 8-87687
 crack growth, estimation of creep rupture time (Chinese) 8-83325
 creep crack growth, model based on vacancy diffusion along grain boundaries 8-75716
 defect diffusion, radiation effects 8-87827
 dislocation elimination by recrystallisation (German) 8-51559
 Earth mantle peridotites, stress estimates from structural studies 8-69330
 edge dislocation interactions in infinite array, elastic energy 8-55871
 electromigration, general anal., composition profiles from steepest descent methods 8-67849
 electron dynamical diffraction from periodic arrays of dislocations 8-83669
 F 8-84820
 ferrites, soft and microwave, grain-size effects on mag. props., review 8-64222
 film, rel. to effect of surface condition on diffusion at low temp. 8-91469
 fracture, intergranular, low temp. mechanism 8-60795
 glide dislocation interaction with intrinsic boundary structure 8-87686
 grain and phase boundaries between crystals, conf., Konigstein, Germany (Oct. 1977) 8-72762
 grain rearrangement, solids with hexagonal grain struct. 8-84896
 graphite, grain boundary scattering effect on temp. depend. of electrorresistivity, galvanomagnetic effect (Russian) 8-56148
 hot-pressed with crystn. grain boundary phases 8-95716
 leucosapphire crystals, block boundary energies 8-55877
 liquid phase sintering, role of grain and phase boundaries 8-72747
 metal, grain boundary diffusion, temp. depend. and activation energy 8-95191
 metal, grain boundary groove migration at solid-liquid interface, simulation and with camphene 8-52789
 metal, hardening due to increased subgrain boundary stability 8-52934
 metal, migration obs. using FIM 8-79617
 metal, polycryst., Bauschinger effect and mutual restriction between grains 8-52895
 metal, resistometric studies of lattice defects review (Japanese) 8-59799
 metal, stress conc. caused by grain boundary sliding under power law creep 8-60732
 metal film, elec. cond., size effect 8-76162
 metal film, with grain boundary scatt., thermoelec. power, Fuchs-Sondheimer eqns. 8-52108
 metal wire, influence of grain boundaries on high temp. creep (German) 8-72812

grain boundaries continued

- metallic film, grain boundary electron scattering by effective mean free path 8-84320
 metallic films, monocrystalline, size and grain boundary effects in elec. cond. 8-76164
 MX type reactor fuels, microscopic swelling meas., effects of grain boundary migration 8-66348
 piezoelectric semiconductor, piezoresist. of grain boundaries 8-51995
 polycrystalline heterostructure solar cells, grain boundary effects 8-52063
 polystyrene latex, grain boundary struct. obs. and boundary diffusion 8-51552
 random close packing based model 8-95058
 refractory metal, generalised model for prediction of periodic trends in sintering activation 8-64498
 scanning optical microscopy examination of grain boundaries of polycryst. solar cells 8-79618
 semiconductor structures, grain boundary barriers, sudden change in current 8-56246
 sliding, stresses and deform. 8-68739
 steel, alloy, Cr-C (12, 0.2 wt.%) growth of grain boundary ferrite allotriomorphs, photoemission electron microscope exam. 8-88468
 steel, austenitic, grain boundary sliding, exam. by tensile creep tests 8-76715
 steel, austenitic, precipitation hardened, ductility of grain boundaries and crack propag. (German) 8-52834
 steel, austenitic Cr-Ni (18,12 wt.%), containing coarse irregular carbide precipitates along grain boundaries, ductility 8-60718
 steel, austenitic heat-resisting, deformation and fracture rel. to grain-boundary reaction nodules 8-80591
 steel, austenitic stainless, grain boundary migration during high temp. creep, TEM exam. 8-88509
 steel, austenitic stainless, structural inhomogeneity, electron and optical microscope exam. 8-72827
 steel, austenitic stainless, temper embrittled, type 304, Auger spectroscopic exam. of grain boundary surface phases 8-76741
 steel, austenitic stainless, type 316, effect of hold times on fatigue life, explanation in terms of grain boundary sliding damage 8-72851
 steel, cast high-strength, local intergranular fractures, formation mechanism (Russian) 8-95795
 steel, high speed, tempered, etching reagents for austenite grain boundaries 8-80704
 steel, low alloy ferritic, sub-micron cavity nucleation, SEM obs. 8-95753
 steel, low C, C content effects in corrosion fatigue in nitrate solns. (Russian) 8-56811
 steel, martensitic, fatigue crack form. associated with cyclic slip deform. along prior austenite grain boundaries 8-60831
 steel, Mn-Ti-B-rare earth, distrib. of B (Chinese) 8-84811
 steel, Ni-Cr, intergranular segregation of P in austenite, grain boundary coherency depend. 8-84761
 steel, stainless, grain boundary ledges, contrast phenomena identification 8-51555
 steel, stainless, radiation-thermal treatment, N₂O₄ coolant action, intergranular corrosion (Russian) 8-58357
 steel, stainless, type 304, grain boundary sliding in isothermal and thermal fatigue (Japanese) 8-84979
 steel, type A508, C1 2, microcrack formation during stress-relief annealing of a weldment 8-80629
 steel low C, γ - α transform. kinetic rel. with self-diffusion characts. (Russian) 8-67850
 stress induced drift diffusion, appl. to creep and growth of grain boundary voids 8-72811
 superplastic deformation, grain rearrangements 8-83828
 surface-moving grain boundary interaction, anal. (Russian) 8-67721
 TEM determ. of Burgers vectors for grain boundary dislocations 8-87680
 Ag film, epitaxial growth, characterisation of [001] tilt boundaries 8-84097
 Ag, implanted grain boundary cavities effect on cavity growth kinetics and creep fracture 8-52935
 Ag, large grain boundary cavity coalescence during tension creep 8-52894
 Ag particles, lattice defect influence on size effect 8-88329
 Ag, surface self diffusion coefficient, O₂ pot. effect (Japanese) 8-60014
 Ag-Cu (6.2 at.%), tricrystalline specimens, fine lamellar discontinuous precipitation (German) 8-52822
 Al alloys, 7075-T6, H₂ effects and Cd segregation to grain boundaries 8-84764
 Al, bicrystal, fatigue crack initiation, crystal boundary effects (Japanese) 8-92328
 Al, dislocation generation from grain boundary, in situ obs. 8-51547
 Al, film, photoelectron-grain boundary scatt. in Al-SiO₂-Si struct. 8-64120
 Al-Mn-Si, recrystallisation and precipitation 8-52824
 Al-Sn, (<0.28 wt.%) corrosion behaviour in 16% HCl 8-85054
 Al-Zn, dil., grain boundary diffusion 8-91475
 Al-Zn-Mg, grain boundary segregation, AES meas. 8-72781
 Al-Zn-Mg, plastic instability rel. to grain boundary failure at low temps. 8-56702
 Al₂O₃, sintered, containing MgAl₂O₄ precipitates, Mg distribution at grain boundaries 8-80498
 Al₂O₃, sintered, MgO-enhanced densification, test of second phase and impurity segregation models 8-64511
 Au bicrystalline film, lattice imaging of low angle tilt boundaries by TEM 8-79620
 Au bicrystals, interaction of lattice dislocations with grain boundaries, electron microscope obs. 8-51579
 Au electrodeposited coating properties obs., Cu diffusion under high temperature (Czech) 8-91486
 Au film, epitaxial growth, characterisation of [001] tilt boundaries 8-84097
 Au film bicrystals, exam. of low energy planes for tilt grain boundaries 8-51551
 Au, polycryst. film, RF bias-diode and triode sputtered, resist. and microstruct. 8-80072
 Au sol, grain boundary struct. obs. and boundary diffusion 8-51552
 BaTiO₃, donor doped, elec. props., effect of kinetic processes 8-64042

grain boundaries continued

- Bi, polycryst., grain boundary scattering effect on temp. depend. of electroresistivity, galvanomagnetic effect (*Russian*) 8-56148
 Ca_2SiO_4 , bredigite-larnite rock from Sawt Hill, electron microprobe anal. 8-68952
 Cu annealed and cold rolled, with bamboo structure, exam. of grain boundaries as vacancy sources in diffusional creep 8-88508
 Cu bicrystals, effect of grain boundary on tensile deformation (*Japanese*) 8-88495
 Cu bicrystals, grain boundary sliding and intergranular fracture studies 8-75717
 Cu, crack nucleation and stage I propag. in high strain fatigue, microscopic and interferometric obs. 8-52936
 Cu, crack nucleation and stage I propag. in high strain fatigue, mechanism 8-52937
 Cu foil, role of grain-boundary porosity in superplasticity (*Russian*) 8-56690
 Cu, lattice and grain boundary diffusion of P, exam. of diffusion rates by tracer sectioning technique 8-79817
 Cu wire, residual elec. resist., size effect and grain boundary contribs., heat treatment effects (*Russian*) 8-56126
 β -Cu-In, unidirectionally transformed eutectoid, lamellar microstructure, influence of grain boundaries on thermal stability 8-72795
 Cu-Ni-Fe (26.8 wt.%), microduplex struct. form., recrystn. annealing (*Japanese*) 8-76659
 Cu_2O , film, thermoelec. power, activation energy variation with electrode spacing in DC sputtering 8-76099
 Fe, Armco, corrosion and mechanical behaviour in liquid Li 8-53036
 Fe based alloys, solute segregation to grain boundaries 8-72780
 Fe, diffusion and solid solubility of Sb, 773-873K, ion backscatt. anal., rel. to intergranular embrittlement 8-71880
 α -Fe, grain boundary segregation of C, N_2 and C Auger spectroscopy 8-72778
 Fe-Ni (3 wt.%), grain boundary segregation microanal. using X-ray (STEM) and AES 8-87685
 Fe-Ni-C, role of strain in deform. induced martensitic transform. (*Japanese*) 8-92263
 Fe-Si (2.35 wt.%), misorientation dependence of grain boundary segregation, Auger spectroscopy exam. 8-76629
 Fe_3O_4 , finely dispersed, electronic phase transition, cond. and DTA meas. 8-91736
 GaP, SEM, cathodoluminesc., impurity and defect detect. 8-83695
 Ge film, polycrystalline, structural and elec. props. 8-76173
 Ir, brittle fracture, impurity segregation to grain boundary effects 8-64637
 Ir-W (0.3 wt.%), P segregation to grain boundaries, effect on high temp. ductility 8-95754
 KCl-KBr, dislocation rosettes, diffusion origin 8-83820
 KCl-KBr mixed crystals, microhardness studies, nonlinear depend. on composition 8-83872
 KCl-NaCl, dislocation rosettes, diffusion origin 8-83820
 LiF, thermal phonon scatt. by low angle grain boundaries 8-67795
 Mg-Mn-Ce alloy, MA8, dislocations at grain boundaries and grain-boundary glide 8-64605
 Mn-Al permanent magnets, defect structure, mag. props. TEM obs. 8-91902
 MnZn ferrites, Ti substituted, mag. permeab. meas., grain boundary comp. AES obs. 8-95473
 NaCl, thermal phonon scatt. by low angle grain boundaries 8-67795
 NaNbO_3 , crystallite boundary structural instability during solidification (*Russian*) 8-95738
 Nb, high purity, faceting of boundaries 8-83826
 NdGa_2O_2 wafer, dislocations, etch pits and birefr. obs. 8-83818
 Ni, grain boundary ledges, contrast phenomena identification 8-51555
 Ni, vol. and grain-boundary diffusion of Ag (*Russian*) 8-67863
 Ni/Pt double layers on Si substrate, silicide formation 8-84010
 α -Ni-In, solid solution, lamellar microstructure, influence of grain boundaries on thermal stability 8-72795
 Ni_2O , film, thermoelec. power, activation energy variation with electrode spacing in DC sputtering 8-76099
 Pb-Sn, unidirectionally solidified eutectic, lamellar microstructure, influence of grain boundaries on thermal stability 8-72795
 Si CVD grown polycrystal recrystallisation 8-64560
 Si, epitaxial regrowth and grain struct. of Al metallisation on (100)Si 8-79901
 Si, neutron transmutation doped, zero-bias resist. of grain boundaries 8-76072
 Si, polycrystalline, grain growth study 8-92188
 Si_2O , O rich polycryst. film, carrier transport 8-80076
 Si_3N_4 , hot-pressed with crystn. grain boundary phases, prep. 8-95715
 Si_3N_4 - Al_2O_3 , hot-pressed with crystn. grain boundary phases, prep. 8-95715
 Si_3N_4 - Al_2O_3 , hot-pressed with crystn. grain boundary phases 8-95716
 Ti, metallographic specimen prep. for chem., mech. electrolytic polishing 8-80705
 α -Ti, S, C and Cl diffusion, AES meas. 8-51735
 UO_2 , transfer of fission gas between grain faces and edges 8-79815
 UO_2 -(Ni), surface, grain boundary and interfacial energies 8-71905
 W, grain boundary migration initiated by high hydrostatic press. 8-51554
 W, wire, doped, high temp. creep behaviour 8-88499
 W, wire, exam. of grain boundary segregation, using Auger spectroscopy, new technique 8-80551
 Zn, hot rolled, grain boundary fine structures, TEM exam. 8-76680
 Zn-Al alloys, dislocations obs. in superplastic deformation 8-51549
 ZnO, segregation of Li_2O at grain boundaries 8-64513
 Zr base alloys, irradiation growth, dislocation model 8-51595
 Zr-Ru(Pd), heat treated, mech. props. and struct. 8-80571
 β -Zr-Sn, zircaloy-2, exam. of grain boundary sliding 8-79616
 Zr_3Al , ordered polycrystals, ductile fracture 8-64641

grain boundary diffusion see *diffusion in solids***grain growth**

- nucleation, criterion for dynamic recrystallisation during hot working 8-52852
 powdered compact, densification model with simultaneous grain growth 8-80486
 single crystal growth during massive transformations 8-56629
 sintering, packing fraction effects (*German*) 8-64494
 steel, alloy, Cr-C (12, 0.2 wt.%) growth of grain boundary ferrite allotriomorphs, photoemission electron microscope exam. 8-88468

grain growth continued

- steel, austenitic stainless, estimation of grain growth time dependence, activation energy 8-72787
 steel fibre reinforced Ag, exam. of recrystallisation behaviour (*German*) 8-84849
 Ag, sintering and grain growth, effect of Sb solute addition 8-84730
 Al and Al-Mn (1 wt.%), subgrain growth during annealing after cold work 8-56656
 Al_2O_3 , sintered, MgO-enhanced densification, test of second phase and impurity segregation models 8-64511
 α -brass, defect removal, obs. by positron annihilation 8-84677
 Cu, defect removal, obs. by positron annihilation 8-84677
 β -Cu-In, unidirectionally transformed eutectoid, lamellar microstructure, influence of grain boundaries on thermal stability 8-72795
 Fe, zone refined, strained, substructural changes during annealing (*Slovenian*) 8-84845
 Fe-Cr-Al, elec. heating alloy, effect of rare earth additives on quality (*Chinese*) 8-84825
 Mg, recrystallisation after cold rolling 8-72790
 MnZn ferrites, impurity induced exaggerated grain growth 8-92222
 Ni, defect removal, obs. by positron annihilation 8-84677
 Ni-based alloys, binary, ternary, complex, TiC additions, effects 8-92305
 Ni-based-Ta(C,N) hard metals, isostatic hot pressing influence on mechanical properties 8-92219
 α -Ni-In, solid solution, lamellar microstructure, influence of grain boundaries on thermal stability 8-72795
 NiZn ferrites under high press., grain growth (*Chinese*) 8-52825
 $\text{Ni}_{0.36}\text{Zn}_{0.64}\text{Fe}_2\text{O}_4$, normal grain growth 8-72796
 Pb-Sn, unidirectionally solidified eutectic, lamellar microstructure, influence of grain boundaries on thermal stability 8-72795
 Si, polycryst. manufacturing methods for photovoltaic energy prod., solar cells, grain growth from melt (*Dutch*) 8-52661
 Si, polycrystalline, grain growth study 8-92188
 Th blanket pellets, grain growth kinetics 8-86613
 W-Ni liquid alloys, sintered, coarsening of W grains, exam. 8-56598
 ZnO, additives effects on sintering and grain growth 8-80497

grain refinement

- steel, austenitic, 16H2NMB, struct., texture and mech. props. of product of transform. 8-92273
 steel, maraging, grain refinement due to cyclic heat treatment 8-52971
 Al, effect of Al_3Ti , TiC and B 8-52828
 Al-Ti-Si phase diagram, calc., interpretation of grain refinement results 8-84781
 α -U, pseudo-single cryst. and polycryst., low temp. sp. ht. 8-83972

grain size

- see also *grain growth*; *grain refinement*
 alloy, cold-worked, particle size and strain determ. from X-ray diffr. profiles 8-88588
 alumina, grain size and fracture toughness, effect of fracture toughness test methods 8-72883
 beaches, SE Rio de Janeiro state, sediment textural characts., grain size (*Portuguese*) 8-81144
 brittle fracture relationship 8-80651
 ceramic, ferrimag, or ferroelec., microstructure and physical props. 8-72756
 ceramics, effects on room temperature fracture energy and on tensile strength 8-88533
 deposited film thickness and grain size determ. on non-conductive SEM specimens 8-77170
 electrophotographic two-component developer discharge and contact interaction (*German*) 8-62258
 ferrite powder, grain size meas. by electron microscopy, sample prep. (*German*) 8-56833
 ferrites, soft and microwave, grain-size effects on mag. props., review 8-64222
 Manicouagan impact melt, Quebec, stratigraphy, chemistry and grain size var. 8-81164
 measurement, NDT deep-drawing steel sheet and band, method and instrum. (*German*) 8-85059
 metal, cold-worked, particle size and strain determ. from X-ray diffr. profiles 8-88588
 metal film, vacuum deposited, grain struct., influence of impurities and alloying elements (*Russian*) 8-56048
 metal growth in space, theoretical models, comparison with ground expts. 8-84786
 metallic films, size effects, resistivity derivation 8-76163
 Rene 95, Ni based superalloy, effect of grain size and gamma prime size, on fatigue crack prop. 8-64686
 sediments of Point Pelee, SW. Ontario, grain size rel. to geomorphology and origin 8-92857
 single-phase structure, nonuniform, grain size quantitative rating, exam. of system used 8-85072
 soil, Martian, fine-grained component model based on Viking lander data 8-85882
 steel, A533 B, fatigue crack propagation, grain size and temp. effects 8-56727
 steel, alloy, Cr-Cu-Mn-C, HT80, effect of grain size on sensitivity to reheat cracking (*German*) 8-72856
 steel, alloy, maraging, 18% Ni, effect of solution and ageing treatments, on microstruct., tensile props., fracture toughness 8-80648
 steel, austenitic, fracture toughness props. of A533B, prior austenite grain size effect 8-60780
 steel, austenitic, grain boundary sliding, exam. by tensile creep tests 8-76715
 steel, austenitic grain size rating methods, comparison 8-85074
 steel, Cr-Ni-Mo-V, quenched, morphology, structural constitution after austenite form. by heating (*Russian*) 8-68709
 steel, low alloy, St 52-3, structural, fracture toughness, fatigue precracking and grain size effect 8-60782
 steel, low C, dual phase structures (martensite and ferrite), effect of martensite composition on content, mech. props. 8-76717
 steel, low C, ductile-brittle transition behaviour, grain size effects 8-52942
 steel, low C, grain size effect on fatigue strength, high temps. 8-68759
 steel, low C, prior austenite grain size, effect on near threshold fatigue crack growth 8-92341
 steel, low C, prior austenite grain size, effect on near threshold fatigue crack growth 8-92342

grain size continued

- steel, maraging, 18% Ni content, exam. of age hardening-grain size relationships 8-84833
- steel, Mn-Ti-B-rare earth, distrib. of B (*Chinese*) 8-84811
- steel, pearlitic eutectoid, cleavage fracture, grain size effect 8-60784
- steel, stainless, type 316, 20% cold worked, exam. of creep 8-72817
- steel, structural, C10, C15 and St52-3, grain size dependence of low yield point (*German*) 8-56689
- steel, structural, unalloyed, brittle fracture, grain size and precipitate thickness effect 8-60786
- steel, transformer, formation of perfect cubic texture in thin sheets (*Russian*) 8-80557
- steel, ultrahigh strength, effects of strength and grain size on near-threshold fatigue crack growth 8-64704
- steel, yield point charact., grain size effect (*German*) 8-72810
- steel grain size spread, quantitative rating method 8-85073
- steel Ni-Cr, Sb doped, temper embrittlement susceptibility, intercritical heat treatment effect 8-64570
- superplastic deformation, grain arrangements 8-83828
- superplasticity, mechanism rel. to hyperfine grain struct. 8-84930
- α Ti, work hardened in tension, developed of internal strain (*French*) 8-76716
- two phase polycrystals, grain size stability and switching, dislocation climb and glide, computer model 8-75715
- water-sediment interface US reflection with bidirectional displacement 8-60017
- Al alloys, fracture, grain size effect 8-60781
- Al alloys, preliminary forging effects on struct. and mech. props. of extruded sections (*Russian*) 8-80564
- Al-Fe, cast, influence of Zr on precipitation, solidification and grain size (*Rumanian*) 8-84813
- Al-Zn, precipitation struct. and phys. props. effect of miscibility gap (*German*) 8-92265
- Al-Zn-Mg, plastic instability rel. to grain boundary failure at low temps. 8-56702
- $\text{Al}_2\text{O}_3\text{-Na}_2\text{O-Li}_2\text{O}$ (8.8, 0.75 wt.%) exam. of Na^+ resistivity as function of temp. grain size model 8-80654
- C and low-alloy steel inherent austenitic grain size determ., exam. of methods used 8-85071
- Cd, grain size effect on acoustic emission generated during plastic deformation 8-80609
- CdS, chem. sprayed film, struct. and morphology 8-72020
- CdS, film for solar cells, struct. and elec. props., thickness depend. 8-72289
- Cr, evap. film, refl. and struct. 8-72021
- Cu and Cu-Al alloys, polycryst., effect of grain size, specimen thickness, on mech. props. 8-84945
- Cu, cold worked, grain size effects on short-term strength (*Russian*) 8-56693
- Cu film, annealing effect on grain size 8-72015
- Cu, grain size effect on acoustic emission generated during plastic deformation 8-80609
- Cu-Ni-Cr system, coarsening in the $(\gamma_1 + \gamma_2)$ region, metallographic study 8-84762
- α -Fe-Fe₃C alloys, ground surface layer exam. of props. 8-84840
- Fe-Ni-C austenite, effects of strain rate grain size, temp., on yield stress 8-72821
- Fe-Ni-Cr coating, electrodeposited, exam. of passivity 8-80655
- Fe-Si (3 wt.%), effect of heating rate during primary recrystn. on props. after secondary recrystn. 8-84837
- Ge film, polycrystalline, structural and elec. props. 8-76173
- Mo, evap. film, refl. and struct. 8-72021
- Nb₃Ge, RF and DC sputtered films comparison, O content effect 8-72022
- Ne, solid, lattice thermal cond. 0.5 to 10K, dislocation densities, average grain sizes 8-79830
- Ni, powder, correlation between specific surface area and technological props. 8-64503
- Ni-based alloys, binary, ternary, complex, TiC additions, effects 8-92305
- $\text{Ni}_{0.36}\text{Zn}_{0.64}\text{Fe}_2\text{O}_4$, normal grain growth 8-72796
- Si continuous polycrystalline films on C substrates 8-64490
- Si, film, polycryst., for photovoltaic appl., grain size effects 8-72034
- Si, self-implanted layer, grain size, laser irradi. energy density depend. 8-72012
- Si:O, O rich polycryst. film, carrier transport 8-80076
- Si-Ge alloy, thermoelec. material, lattice thermal conductivity rel. to grain size and carrier conc. 8-91495
- Ti, grain size effect on acoustic emission generated during plastic deformation 8-80609
- Ti, grain size effect on yield stress and work hardening at 295 and 575K 8-64593
- Ti, vacuum deposited, cryst. struct. and elec. props. 8-79908
- UO_2 , sintered pellets, relationship between intercept length and grain diameter 8-52743
- W alloy, determ. by acoustic method 8-72961
- W-ThO₂ composite, struct., lamination tendency, effects of method of manuf. 8-68653
- WC-Co cemented carbides, high temp. transverse rupture strength, effect of domain size of binder phase (*Japanese*) 8-92329
- Zn, ductile-brittle transition pressure, grain size effect (*Japanese*) 8-60745
- Zn-Al (0.4 wt.%), grain size effect on acoustic emission generated during plastic deformation 8-80609
- ZrO_2 , containing metastable tetragonal phase, stress induced phase transform. effect on props. 8-68683

grain structure see crystal microstructure**grain subboundaries** see subboundary structure**grammars**

- contrastive linguistics, P-struct. C-struct. grammar 8-69959

gramophones

- No entries

Granato-Lucke theory see dislocation damping**granular materials**

see also granular structure

- body submerged in granular layer, heat and mass transfer 8-94536
- capacitive dispersion field transducers for granular material exam. 8-85078
- cohesionless granular materials, flow at high deformation rates and low stress levels 8-90810

granular materials continued

- ferrite powder, grain size meas. by electron microscopy, sample prep. (*German*) 8-56833
- heat transport coefficients, contacting particles in noncond. medium 8-59261
- inhomogeneous granular solid, one dims. accel. waves, speed, amplitude 8-87288
- metal, selective solar energy absorption, particle shape depend. 8-71162
- modelling by steel spheres, packing density coeff. 8-84916
- polyethylene pellets, falling in air in pipe, equilb. region press. drop, friction factor 8-63479
- separation of minerals using supercond. mags. (*Czech*) 8-88923
- shock waves, 1-dimens. in uniformly distributed granular material, porosity discontinuity 8-83285
- spheres at high pressure, contact stresses and spreading resistance 8-71296
- thermal conductivity prediction of heterogeneous mixture, digital simulation technique 8-87247
- vibration test rig for wear meas. of granules 8-56840
- void compaction and material nonuniformity, influence on acceleration waves, addendum 8-83280
- Al alloy AK5M2 granules, rolling speed effects 8-60604

granular metallic thin films see discontinuous metallic thin films**granular structure**

see also granular materials

- single-phase structure, nonuniform, grain size quantitative rating, exam. of system used 8-85072

graph theory

see also trees (mathematics)

- classical fluids, graph theoretic techniques 8-71662
- diffraction pattern of selected area, indexing, graphical technique, for teaching 8-54132
- dimer config. enumeration, n-dimensional theory, graph paths 8-54315
- electron gas, interacting, elec. cond. 8-95276
- graph-like state of matter, electrical cond. of random networks, gelation and elasticity 8-65875
- hypernetted chained equation, series soln., simple chain recursion method 8-65861
- master eqns., discrete, struct. of exact solns. 8-77821
- Penrose graphs, scatt. process representation 8-49983
- Percus-Yevick equation, series soln., simple chain recursion method 8-65861
- polymer chains, Forsman's equations, graph theory appls. 8-55265
- relativistic field equations for half odd integer spin and unique mass, graph theoretical methods 8-62290
- superposition of numerical graphs, functional changes (*Ukrainian*) 8-89293

graphic equipment, computer see computer graphic equipment**graphics, computer** see computer graphics**graphite**

- adsorbed butane, struct. and dynamics, neutron scatt. study 8-87870
- adsorbed dense monolayer on graphite cleavage face, phase transition 8-56034
- adsorbed Kr, X-ray diffr. from 2-D solid 8-75498
- adsorption of Ar, orientational ordering of incommensurate monolayers, LEED obs. 8-95233
- adsorption of Kr submonolayer, melting, X-ray scatt. obs. 8-95234
- adsorption of NO, crit. and triple point temps. of first adsorbed layer 8-91548
- adsorption of NO, monolayer melting and polymorphism 8-84063
- adsorption of o-H₂ (p-D₂), NMR, orientational behaviour, weak crystal field 8-75935
- AES, obtaining density of states information from self-deconvolution of Auger band-type spectra 8-92150
- atomiser for flameless atomic absorption spectrophotometer, disc form, exam. 8-54463
- cathodes for glow discharge and hollow cathode spectroscopic light sources 8-82047
- cellular method calc. for nonspherical potential 8-56063
- chemisorption, of O, CO-NDO calcs. 8-75937
- chromatographic columns, efficiency rel. to particle size 8-92536
- composite materials, survey 8-56609
- crack propag., temp. and environment effects 8-56794
- desorption of surface oxides, kinetics 8-60025
- diametral compressive strength, comparison with uniaxial tensile strength (*Japanese*) 8-72947
- double plasma arc, rotation in graphite tube 8-71599
- E₂ mode splitting, two-phonon spectrum 8-92077
- electrode breakdown voltage dependence on adsorbed gases 8-75465
- electron microscopy, controlled-atmosphere, specimen temp. meas. using opt. pyrometry 8-93690
- electronic props., self consistent LCAO calc., point vacancy in 2-dimens. cryst. 8-51932
- electronic props., self-consistent LCAO calc. 8-51887
- energetic deuteron irradiated surface struct. quantitative meas. 8-95210
- energetic ion sputtering, appl. of AES-SIMS (IMA)-FDS combined systems to physical and chemical processes 8-95636
- enthalpy of solution at 1320K, heat of transformation from diamond 8-59945
- extraction of N₂ from Ta powder, by vacuum hot extraction method, effect of graphite (*Japanese*) 8-84729
- failure criterion, J-integral critical value 8-84999
- fibre reinforced Al, temp. and press. effect on interface chemistry, mech. prop. meas. 8-64595
- film for solar selective surfaces, effect of Cu, Ag or Ni substrate 8-74952
- fracture, stress gradient effect 8-92321
- fracture toughness measurement, by disc test comparison with stress analysis of disc test 8-92432
- fusion reactor wall, microexplosion of pellet, energy deposition 8-54890
- galvanomagnetic effects, low field data and free carrier densities 8-87986
- galvanomagnetic effects, temp. and field dependencies 8-64050
- galvanomagnetic effects, trigonal warping of constant energy surfaces 8-87987

graphite continued

- grain boundary scattering effect on temp. depend. of electroresistivity, galvanomagnetic effect (*Russian*) 8-56148
 graphite monofluoride, surface alteration by interaction with Ar⁺ and Xe⁺ beams 8-91347
 HTGR fuel and graphite structure stress analysis methods and programs (*Japanese*) 8-74434
 intercalated with nitrate, galvanomagnetic props. 8-76092
 intercalation compounds, props. and appls. 8-71711
 intercalation compounds; struct. and order-disorder transforms. 8-71710
 intercalation compounds with K and Cs, low temp. sp. ht. 8-71868
 intercalation process with Br₂ 8-63965
 ionisation chamber with CO₂ filling, Monte Carlo anal. of fast neutron irradiation 8-82583
 lattice atom displacements near end of implanted μ^+ tracks 8-55890
 lattice dynamics of adsorbed Ar and N₂ monolayers 8-75946
 lattice vibrations, long wavelength, Raman and IR reflectivity spectra 8-75746
 low field Hall coefficient, effect of warped energy surfaces 8-68043
 neutron irradiated, effect on quantum limit Shubnikov-de Haas oscils. 8-95304
 oxidation, corrosion resistance, bend strength, assessment for rotary glass fibre making apparatus 8-64753
 oxidation loss and wettability of inorganic fluxing materials for crucible manuf. (*Japanese*) 8-84755
 phonon dispersion, temp. depend., 4K-1500°C, neutron spectroscopy 8-59906
 point defects and self diffusion 8-63758
 powder mixture with 30 wt.% Si, reaction hot pressing 8-60592
 powder-cushion gripping to promote good alignment in tensile testing 8-92418
 precipitates in quenched Ni-C alloy, TEM structural examination (*Russian*) 8-68695
 PTFE/graphite bond in H₃PO₄ environment, electrochemical exam. of joint failure 8-60979
 pyrolytic, Ar⁺, N⁺ and He⁺ ion bombardment numerical discussion of flaking 8-52947
 pyrolytic, oriented ellipsoidal voids, small-angle X-ray scatt. 8-64429
 pyrolytic, behaviour of implanted D and He 8-95071
 pyrolytic, ion bombard., flaking, stress fields around penny-shaped cracks 8-52946
 pyrolytic, irregular end-plane sections for rot. ring-disc electrode 8-92488
 quartz-graphite junction, thermal cond., 6 to 95K, junction rectification 8-63890
 reactor, fracture toughness up to 2600°C 8-68760
 reactor, thermal shock fracture toughness eval. by arc discharge heating 8-72835
 reinforced epoxy, laminated plate under tension, stacking sequence and lay up angle effect on free edge stresses round hole 8-88524
 RF plasma utilisation in sputtering and surface reactions 8-84714
 ribbon, interlayer interaction effects on diamagnetism London theory 8-52201
 spatial distribution of particles in cast Fe, metallographic study 8-92419
 spheroidization, effect on fatigue strength of cast Fe (*Japanese*) 8-64626
 sputtering by low energy H and D 8-95630
 sputtering yield, use as first wall material 8-95629
 strain measurement, 298 to 3000K, new optical technique 8-85063
 stress/strain behaviour, exam. with high temp. short time testing facility 8-53051
 structural, impact toughness, reln. to compressive strength 8-88605
 surface, adsorbed inert gas at. excitation spectrum 8-71943
 surface, adsorbed Kr, Potts lattice gas, renormalisation-group treatment 8-67908
 surface alteration by interaction with Ar⁺ and Xe⁺ beams 8-91347
 surface behaviour under various vacuum conditions, Au decoration obs. 8-75915
 surface cleaning, air cleavage and UHV cleavage, obs. using Au decoration 8-80665
 surface interaction and band struct. effects for He derived from scatt. data 8-92162
 thermal vib. amplitudes from integrated intensities corrected for TDS 8-67780
 Tokamak, TFR, variable-radius Mo and graphite limiters 8-63600
 Tokamak fusion reactor, mag. limiter plate, electron irradi. and thermal shock 8-66416
 vacuum gap electrode surface sorption, mass spectroscopic obs. 8-75466
 wear, thin layer activation meas. technique, assessment 8-92366
 X-ray K-absorpt. edge, EELS meas. 8-56551
 Al-graphite adhesion and contact angle, effects of metal additives (*Japanese*) 8-60008
 Br₂-graphite systems, adsorbed and intercalated, EXAFS 8-72638
 C₆AsF₆ intercalation compound, NMR and static mag. susceptibility meas. 8-88214
 Cr₂C₃, form. from Cr₂O₃/graphite mixture in H₂ atmos. (*Japanese*) 8-92225
 Cu-graphite starter brushes, effect of high velocities, current densities on wear, friction 8-88544
 Fe, cast, heated in CO atm., obs. cracks around graphite flakes (*Japanese*) 8-84974
 Fe, cast, Mg, despheroidising effect of Bi, Sn on graphite in alloy 8-56670
 Fe-S-C (1.3 wt.%), sulphidised Fe-graphite bearing materials, sintering, struct. form. 8-60601
 FeCl₂-graphite, intercalation compound, formation by reduction of Fe(III) compounds with Fe(CO)₅ 8-63721
 N₂⁺+Group IV elements and oxides, XPS and UPS prod. determ. 8-73084
 NaCl-graphite interface, elec. cond. 8-52060

graphitisation

- catalytic, three-phase, of phenolic resin C by Ni particles 8-68922
 diamond tools on steel, graphitisation due to clean surface reactions 8-85008
 film, work function, heat treatment 8-64563
 pyrolysis mechanism, electron microscopy, DTA, IR, ESR obs. 8-56593

graphitisation continued

- steel, alloy, low C, effects of pre-treatment on graphitisation behaviour (*Japanese*) 8-84860
 texture change on ht. treatment under press. 8-60687
 C fibres struct. and physical props. effects of B additions and heat treatment temp. 8-68715
 C-C composites, existence diagram and properties (*French*) 8-64517

graphitising

- Fe, cast, rare earth-Mg, metallurgical and technological features, appl. in China (*Chinese*) 8-84851
 Fe-C system, liq.-solid equil. at high press., influence of graphitising elements (*Russian*) 8-56613
 Fe₃C, cementite, modified by rare earth metal and alloying additions, thermal stability (*Russian*) 8-56663

graphs

- see also *nomograms*
 computer programs for high-school expts. 8-86094
 digital seismic data processing, struct. anal. of graphs (*Russian*) 8-53749
 equilibrium constants determination, projection map technique 8-53240
 histogram plotting, FORTRAN program 'HIST' 8-77876
 hydrocarbons, saturated, topological orbitals, graph theory and ionis. pots. 8-82615
 optical system design, multi-layer, using equivalent films (*Czech*) 8-90486

gratings (diffraction) see diffraction gratings**gratings (optical) see diffraction gratings****gratings (spectra) see diffraction gratings****gravimeters**

- see also *geodesy*
 Askania type gravimeters, sensitivity determ. rel. to gravity tidal changes at Poltava (*Russian*) 8-88782
 cross-coupling effect compensation, by intersection point method, marine gravimetry 8-57340
 gas gravimeter use for variable linear acceleration meas. 8-77875
 gradiometer, moving-base, surveys and interpretation 8-77344
 La Coste and Romberg model D, scale factor determ. 8-85724
 LaCoste and Romberg gravimeter, vibration characts. (*Japanese*) 8-65400

gravimetric instruments see gravimeters**gravimetry see density measurement; weighing****gravitation**

- see also *general relativity; gravitational collapse; gravitational red shift; gravitational waves; quantum field theory of gravitation; Schwarzschild metric; unified field theories*
 absolute space time theory, criticism 8-86210
 absolute space time theory, reply to criticism 8-86211
 acceleration of two massive bodies, for teachers 8-81766
 axisymmetric gravitational fields, nonlinear differential eqn. giving exact eigenfunction solns. 8-77779
 Bel-Petrov field classification, algorithm 8-93566
 bimetric gravitation theory, cosmological basis, closed universe 8-65844
 black-hole evaporation unified gravit. and electromag. field theory 8-53979
 Brans-Dicke theory, charged particle field 8-65849
 Brans-Dicke theory, cosmological solns. for homogeneous isotropic universe 8-96579
 Brans-Dicke theory, cylindrically dust distrib. in rigid rotation 8-62136
 causality and relativity 8-81901
 central field, interstellar flyby missions, relativistic effects 8-61729
 charged body free fall motion in gravit. field, field energies and equivalence principles 8-49740
 charged tachyon, gravitational field 8-54282
 classical gravity with higher derivatives, massive excitations 8-65845
 conformal supergravity, props., gauge theory 8-78085
 cosmology, general relativity, big bang model, nucleosynthesis, scale covariant theory, review 8-73789
 decoupled eqn. solns., EM and gravitational perturbation eqn. soln. construction 8-70029
 Dirac particles in Minkowski space with torsion 8-57824
 Dirac-spinor form of Maxwell's eqns., polarised light beams in gravitational fields 8-50696
 dynamical space and gravitation within a purely geometrical framework including Machian ideas 8-93587
 Einstein's theory of gravitation generalised using tetrad field to avoid singularities 8-57833
 Einstein-Cartan theory, static spherically symmetric solns. 8-89387
 Einstein-Cartan theory of gravitation, generalized 8-73895
 Einstein-Cartan theory of gravitation in a Hamiltonian form 8-93581
 Einstein-Maxwell fields, Kerr-NUT metric 8-89382
 electrodynamic and gravitational effects of Proca stresses in astrophys. 8-93098
 embedding classical fields in QFT, electrodynamics, Yang-Mills theories, gravit. appls. 8-54223
 formalism, using vector field 8-89385
 freely falling object in reference frame of accelerated rotating observer 8-54259
 Friedmann cosmological models, fermion pair creation by gravit. field and singularity (*Russian*) 8-93493
 gaseous rotating cylinders, thermodynamic stability anal. by linear series 8-81618
 geometric gravity Lagrangian, SP(4) and general coord. transforms. 8-70039
 gravitational-inertial field of Universe, generalised metric tensor theory 8-89275
 gravity mass invariance 8-57778
 gravothermal catastrophe 8-81536
 gyroscopic precession, starlight aberration, calcs. in stationary metrics 8-54284
 isotropic Universe, kinetics of small perturbations (*Russian*) 8-54102
 isotropic Universe, kinetics of small perturbations (*Russian*) 8-54103
 isotropic universe, kinetics of small perturbations (*Russian*) 8-65731
 light deflection by gravit. field, work of Johann Georg Soldner (1776-1834) 8-81787
 light deflection by Sun, principle of equivalence calcs. 8-81729

gravitation continued

- light deflection in gravit. fields, rel. to meas. of parallaxes of objects at cosmological distances 8-53796
 linearised GL(4) gravities, dynamical structure 8-65846
 liquid metal tube flow, turbulence, heat transfer, thermogravitation effect 8-71315
 lunar tidal acceleration determ. from laser range meas. 8-69718
 Mach's principle equivalence principle, violation, for teachers 8-61998
 magnetism analogy 8-65851
 massive vector fields and black holes 8-96499
 measurement theory, interrelation of quantum theory and gravitation 8-54235
 metrical connection in space-time, Newton's and Hubble's laws 8-57435
 Newton's law, introduction of a repulsive force 8-73839
 null gravodynamics, initial value problem and Dirac-bracket relations 8-77781
 NUT metric in background of Einstein's static universe 8-93565
 parametrised post-Newtonian parameters, results from strain-tide spectroscopy 8-73301
 particle dynamics in special relativity 8-93529
 particles and fields conference, Argonne, IL, USA (Oct. 1977) 8-78130
 perihelion precession rate in system of two charged masses 8-73897
 plane waves in the bimetric gravitation theory 8-93583
 planetary gravitational fields, inform. theory appl. 8-53835
 polar g-values 8-81727
 QED in an external gravitational field, S-matrix evaluation, pair prod. 8-82131
 QED in external gravitational field, S-matrix construction 8-78116
 QED with scalar gravitational field interactions, nonelimination of divergences 8-93834
 quadratic Poincare gauge theory of gravitation, short range confining component 8-89388
 quadratic theory, Fridman's problem (Russian) 8-65847
 radiowave focusing in interstellar medium, model (Russian) 8-81905
 relativistic gravitating particles with cylindrical symmetry, calc. of averages in equil. system (Russian) 8-73904
 Rosen's bimetric theory of gravity, orbital topography and other astrophysical consequences 8-54274
 scalar-tensor theory, plane-symmetry solns. 8-70035
 scale covariant gravitation theory, rel. to stellar vel. dispersion age depend. 8-65661
 screening effect rel. to Earth tides obs., assessment (Russian) 8-88787
 soft graviton emission in scatt. processes, linearised gauge theory 8-49746
 solid bodies in solar system, gravitational potential 8-77550
 some thermodynamical remarks on the theory of gravitational field 8-81899
 spin strings theory, EM waves propag. (Russian) 8-81906
 spin-3/2 axial anomaly, Feynman graph, point splitting, topological and zeta function methods 8-93588
 spinor field and gravitational field interactions, classical theory 8-93569
 spontaneous particle creation in strong gravitational field, semiclassical theory 8-54281
 star with neutron core, gravitational equil. relativistic treatment 8-57570
 supergravity, geometry of superspace, vector-spinor matter 8-49744
 supergravity, local supersymmetry in (2+1) dimens., differential forms. 8-49980
 supergravity, locally invariant supersymmetric gauge field theory 8-49742
 supergravity, minimal set of auxiliary fields, gauge algebra closure 8-49743
 supersymmetric nonlinear σ -model in 4-D, coupling to supergravity 8-49981
 tetrad gravitational field, weak principle of equivalence and gauge theory (Russian) 8-62135
 tetrad potentials gauge, reference systems with Newtonian time (Russian) 8-89378
 three body problem, Lagrange equilateral triangle, Euler collinear solns., generalisation to nongrav. forces 8-54178
 torsion enables metric to allow gravit. field 8-73902
 trace anomalies in a two-dimensional de Sitter metric and black-body radiation 8-65841
 translatory-rotary motion of gravitating spheroids (Russian) 8-73841
 vacuum, particle-free state and group representations, stratification and C^* -algebra (Russian) 8-81896
 vacuum state, influence of gravitation and cosmological effects on symmetry breaking (Chinese) 8-65858
 viscous fluid cosmological model in general relativity 8-61944
 Weyl's geometry appl. 8-65843

gravitational acceleration *see gravitation***gravitational collapse**

- see also black holes; cosmology*
 black flash model of QSOs and Seyfert nuclei 8-57673
 black holes, accretion disc as quasar and galactic nuclei power source 8-57667
 Bonnor electrovac counterparts of Tomimatsu-Sato solns. of Einstein eqn. 8-57835
 classical and quantum, problems (Russian) 8-53815
 classical problem, nonlinear differential eqns., solns. 8-93099
 collapsing relativistic stars, linearised odd-parity radiation 8-93297
 cylindrical general relativistic collapse, numerical study results 8-93585
 dust, thin spherical shell, around black hole, dynamics, Russner-Nordstrom geometry 8-77481
 Einstein's gravitational equations, local and global modifications 8-61719
 Einstein-Cartan theory, bounce of spheres 8-93572
 finite-particle scheme for three-dimens. gas dynamics 8-67218
 galactic chemical evolution at initial rapid-collapse phase 8-69870
 galaxies and galaxy clusters, relaxation from aspherical initial conditions 8-96538
 gas cloud, three-dimens. collapse and fragmentation 8-77552
 gravothermal catastrophe and negative specific heat of self-gravitating systems 8-93593
 gravothermal instability in two dimensions 8-89395

gravitational collapse continued

- horizon instability in perturbed scalar field (Russian) 8-53816
 interstellar clouds, structure and evolution under external pressure 8-61898
 interstellar gas clouds gravit. collapse, caustic and critical times for one-dimens. model 8-93367
 interstellar grain cloud, gravit. collapse rel. to star form. 8-69788
 Kerr and Tomimatsu-Sato metrics from group transformation, rot. vacuum soln. 8-65838
 magnetofluid, self-gravitating, local behaviour of congruences 8-89384
 massive neutron star, fermionic matter, coupled Dirac-Einstein eqns., self consistent soln. 8-73731
 mathematical physics, success and failure viz. Kolmogorov-Arnold-Moser theorem, gravit. collapse, singularities, matter stability (German) 8-65744
 neutrino viscosity in collapsing stellar cores 8-61875
 neutron stars mass upper limit for stability against black hole form. 8-96498
 nonlinear electrodynamics, Birkhoff's theorem analogue (Russian) 8-54273
 particle creation by singularities in asymptotically flat spacetime 8-54260
 photon emission from gravitationally intense cylindrical bodies 8-57840
 rotating gas cloud, binary system form., three-dimens. hydrodynamical anal. 8-65494
 star, collapse triggering by thermonuclear burning in degenerate C core 8-65608
 stars, neutrino bursts and gravit. waves, proposed search for correl. 8-77567
 stars, slowly rotating, gravit. collapse, supernova explosion, neutron star or pulsar remnant 8-96472
 stars rotating sphere, free collapse 8-93325
 stellar N-body systems, two-body tidal dissipation rel. to core collapse 8-93329
 stellar systems with continuous mass spectrum, necessary condition 8-93328
 thermodynamic equil. of gravitating sphere in Lyra's geom. 8-65840
 uniform gravitational collapse, lepton pair creation, macroscopic gauge theory of gravity 8-81724
 weak neutral current, effects in stellar collapse, review, book contrib. 8-85964
 ν emission in gravitational collapse, Liouville line element 8-57437

gravitational constant

- binary pulsars, relation between speed ups and variation of gravitational constant 8-73728
 Brans-Dicke closed space cosmology, exact soln. for radiation-filled era 8-93488
 cosmological limit on possible var. 8-93492
 cosmologies with varying gravit. const., theory 8-57705
 geophysical determ. of Newtonian gravit. const. 8-81098
 measurement, balance appl., thermal noise effect 8-65906
 Newtonian cosmology with diminishing gravitational constant 8-54100
 Newtonian cosmology with time-vary ng constant 8-65733
 Newtonian cosmology with varying gravitational constant, alternative approach 8-54101
 time variation, rel. to form. times of rich clusters of galaxies 8-69892
 time varying Newtonian gravity, Q in cosmology 8-77634
 time-varying force law in Newtonian theory, rel. to Earth thermal history 8-93592
 variation, impossibility in Newtonian physics 8-69675
 variation with time (Norwegian) 8-69674
 varying to cosmology with primordial star generation 8-61946

gravitational experiments

- cooled gravitational wave antennas, explanation of expt. obs. 8-54280
 correlation techniques, poss. detect. of gravit. waves 8-89393
 detector of gravitational waves, appl. of photon-graviton resonance, technical problems, expt. possibilities 8-73905
 Earth stain-tides, spectroscopy rel. to parametrised post-Newtonian parameters 8-73301
 Earth tides observations, gravity screening effect assessment (Russian) 8-88787
 gravitational radiation detection (Japanese) 8-77792
 gravitational wave detection by compact EM systems (Russian) 8-49747
 laser detector of gravitational waves (Russian) 8-77794
 Maxwell's eqns. in matter, covariant formulation 8-57798
 radiation detector, limits to meas. of displacement 8-86215
 stars, neutrino bursts and gravit. waves, proposed search for correl. 8-77567
 velocity of gravitational effects, meas. by Roll-Krotkov torsion balances (German) 8-81912
 wave antennas, gravitational, with and without piezoelectric ceramics, elec. equivalent circuits 8-73915
 Al alloy disc, quality factor of vibr. rel. to gravit. radiation detector 8-75093

gravitational radiation *see gravitational waves***gravitational red shift**

- see also cosmology*
 cosmological red shift, Doppler and gravitational components using Birkhoff's theorem 8-86041
 light velocity and gravitational potential, Laplace's deduction of differential aberration (German) 8-57838
 solar spectrum, convective correction to measured wavelengths 8-93181
 static Universe model with two centres, red shift explanation 8-57706
 thermodynamic equil. of gravitating sphere in Lyra's geom. 8-65840
 white dwarfs, visual surface brightness relation appl. 8-81624

gravitational waves*see also gravitons*

- Bel-Petrov field classification, algorithm 8-93566
 binary stars, gravit. waves interaction, tidal reson. 8-93089
 boundary coupling of gravitational wave and EM radiation in cavity 8-54267
 classical gravitational bremsstrahlung, wave generation 8-93093
 collapsing relativistic stars, linearised odd-parity radiation 8-93297
 conversion of gravitational waves into electromagnetic waves by a moving charge 8-93584
 cosmic coherent avalanche catastrophies, gamma-freq. graviton radiation 8-85844

gravitational waves continued

- cosmological field of high press. gravit. radiation, energy 8-57837
- cosmological gravitational waves, prod. of temp. fluctuations in primordial background radiation 8-65728
- Crab pulsar, upper limit for gravit. radiation energy flux 8-73730
- cylindrical general relativistic collapse, numerical study results 8-93585
- detection by compact EM systems (*Russian*) 8-49747
- detector of gravitational waves, appl. of photon-graviton resonance, technical problems, expt. possibilities 8-73905
- effect on fine-scale anisotropy of cosmic microwave background 8-81535
- Einstein eqns., plane wave solutions 8-70022
- elastic solid, effect of gravitational waves, oscills. (*German*) 8-81904
- elastic spacetime rel. to black holes and gravitational waves 8-73625
- elliptically polarized, interaction with field of mag. dipole (*Russian*) 8-49738
- EM spherical cavity resonator, amplitude of standing gravitational waves (*Russian*) 8-73906
- energy loss in scattering problems, Einstein quadrupole formulae 8-89379
- exponential amplification in gravitational field of ultrarelativistic rotating body 8-93594
- fields of identical tensor dimensions, correspondence (*Russian*) 8-65839
- general relativity, gravitational radiation and invariants of curvature tensor 8-57836
- generalised Perses space-time plane wave-like solns. of weakened field eqns. 8-5827
- intrinsic coupling between gravitational wave and quantised EM radiation 8-54268
- Kerr-Schild generalised metric and Einstein-Maxwell fields 8-77783
- laser detector (*Russian*) 8-77794
- neutron hot perfect fluid relativistic stars, asymptotic eigenfrequency distrib. for even parity perturbations 8-49668
- neutron stars, rapidly rotating, gravit. radiation 8-65646
- plane waves in the bimetric gravitation theory 8-93583
- plane-fronted, integrals of wave equations in space time (*Russian*) 8-89380
- possible detection using correlation techniques 8-89393
- propagation of gravitational waves in expanding universe 8-73787
- quasi-stellar objects, gravitationally pumped masers model 8-54071
- radiation, detection, review (*Japanese*) 8-77792
- radiation detector, limits to meas. of displacement 8-86215
- relativistic theories of gravitation, expt. testing using spacecraft-Doppler detection 8-77793
- Robinson's theorem, shear free condition 8-93586
- rotating stars stability and gravit. radiation 8-93210
- scattering, from vacuum black holes 8-65648
- Schwarzschild black hole in ext. mag. field, radiation emitted by relativistic particles 8-96501
- spinning rod, gravitational radiation 8-62137
- stars, neutrino bursts and gravit. waves, proposed search for correl. 8-77567
- stars, rotating Newtonian, secular instability to gravit. radiation and viscosity 8-53922
- supernova neutrino bursts, gravit. radiation generation 8-81642
- supernovae, gravit. radiation generation by escaping neutrinos 8-93092
- weak plane, radiation of freely gravitating charge (*Russian*) 8-89381
- white dwarfs, rapidly rotating, gravit. 8-65646
- Al alloy disc, quality factor of vibr. rel. to gravit. radiation detector 8-75093

gravitons

- cosmic coherent avalanche catastrophies, gamma-freq. graviton radiation 8-85844
- pairing model, dynamical method for generating gravit. 8-70042
- photoproduction, static mag. dipole field due to steady currents, radiative corrections 8-62138
- quantum field theory of electrostatic potential in gravitational field 8-54270
- quasi-stellar objects, graviton to photon conversion model 8-54071
- soft graviton emission in scatt. processes, linearised gauge theory 8-49746
- spinning rod, gravitational radiation 8-62137
- strong gravity, supersymmetric theory for f- and g-gravitons and massive gravitinos 8-62141

gravity

see also gravitation

- absolute meas. at Potsdam (*Russian*) 8-69274
- anomalies, approx. design for modelling, algorithms (*Russian*) 8-85464
- anomalies, interpretation, Kolmogorov-Wiener least-squares filters appl. 8-61580
- anomalies, linear anal. (*Russian*) 8-53755
- anomalies calc. for regular homogeneous perturbing bodies (*German*) 8-69478
- anomalies due to faults, general expression for Fourier transform 8-61300
- anomalies interpretation, algorithm for calc. gravit. attraction of models of structural features (*Russian*) 8-53758
- anomalies rel. to intraplate seismicity 8-53606
- anomalies separation from background field, FON computer program (*Russian*) 8-53757
- N. Atlantic, sea floor spreading and early opening, mag. and gravity data 8-65247
- Australia, isostasy and evolution of compensation mechanism 8-65252
- Bouguer anomaly theory and misconceptions 8-61302
- cavity effect in tunnels of various cross-sections, theory (*Russian*) 8-88784
- data reduction on arbitrary surface in regions of high topographic relief 8-61298
- direct gravity formula for 1967 Geodetic Reference System 8-92775
- disturbance covariance functions, upward continuation integrals 8-85468
- Earth, coordinates of gravit. field stationary points 8-53805
- Earth, precision orbit computations for Starlette satellite 8-65478
- Earth tides observations, monthly data set anal. (*Russian*) 8-88786
- earthquake sources exhibiting anelastic vol. changes, gravity effects 8-57176

gravity continued

- Europe, absolute meas. 8-85469
- finite length theoretical anomalies, Fourier transforms 8-61299
- geopotential, 15th-order resonance effects of Nimbus 1 rocket (1964-52B) 8-65168
- geopotential second derivative var. sign, variometer meas. (*Russian*) 8-69278
- global gravity anomalies rel. to two-scale mantle convection 8-85528
- gravimetric density formula for Earth of spherical shells 8-61303
- Haicheng earthquake, 1975 February 2, associated gravity field vars. (*Chinese*) 8-61332
- inertialless charged particles, collection on elliptical and irregular cylinders by elec. forces and gravitation 8-68924
- infinite polygonal cylinders, inverse gravity problem 8-53607
- Izu Peninsula, Japan, crustal uplift, Mogi model, related gravity change (*Japanese*) 8-96165
- Izu Peninsula, Japan, earthquake swarm epicentres distrib. rel. to Bouguer anomaly (*Japanese*) 8-96144
- Izu Peninsula, Japan, gravity change assoc. with earthquake swarm (*Japanese*) 8-96123
- Jupiter, figure parameters and gravit. moments 8-65547
- Krivoj Rog basin (Krivbas) underground workings, gravity anomalies interpretation (*Russian*) 8-85466
- Kupjansk-Novozovskoe profile quasiperiodic gravity anomalies and structural confinement (*Russian*) 8-85465
- Kuril Trench, gravity profiles rel. to lithosphere elastic-perfectly plastic bending 8-73341
- Ligurian Sea area, crustal and upper mantle structure from seismic and gravity data 8-65209
- loading of large reflector antenna, structural design 8-57448
- local anomalies interpretation, integral ratios (*Russian*) 8-85463
- local vectors connection in actual gravity field of Earth, model field, disturbing pot. 8-61297
- logging data, appl. to interior density distrib. determ. (*Russian*) 8-92999
- lunar Apennines and regional surroundings, gravity data rel. to isostatic state 8-77503
- Manicouagan impact crater, gravity study and upper crust density contrasts 8-81170
- Mars, coordinates of gravit. field stationary points 8-53805
- Mars, global topography harmonics and Bouguer gravity anomaly map 8-85880
- E.Mediterranean, crustal struct., sedimentary layers 8-69311
- E.Mediterranean gravity anomalies, volcanic activity rel. to tectonic development 8-69318
- Moon, coordinates of gravit. field stationary points 8-53805
- normal gravity minus radial component, accurate formula 8-65170
- normal potential and gravity of levelled ellipsoid (*Russian*) 8-69276
- Nova Scotia, gravity and tilt obs. rel. to improved ocean tide models 8-92821
- odd zonal harmonics determ. using modified equations 8-92773
- odd zonal harmonics from Cosmos 248 eccentricity oscill. analysis 8-81100
- Peking-Tientsin area, China, crustal struct. from gravity data, rel. to seismicity (*Chinese*) 8-61357
- Poltava, tidal changes in force of gravity (1973 to 1976) (*Russian*) 8-88782
- potential coeffs, to degree 52 from 5° equal area gravity anomalies 8-69273
- potential derivatives evaluation using Bernstein multidimens. inequality (*German*) 8-93081
- potential field transformation from relief to single reference plane, Fourier anal. appl. (*Russian*) 8-53759
- Potsdam plumb-line, hydrologic influence on long-period motions (*Germany*) 8-57222
- profile inversion by polynomial method 8-69476
- Pyrenees, central southern region, gravity gliding and compressive nappes 8-69342
- quasi-periodic vars. rel. to earthquakes and crustal structure (*Russian*) 8-69275
- Saturn, figure parameters and gravit. moments 8-65547
- Saturn, gravit. quadrupole moment rel. to maintenance of rings 8-53869
- secular variations, correl. with anomalous local atm. press., USSR (*Russian*) 8-53612
- secular variations, due to water quantity vars. in lithosphere (*Russian*) 8-53609
- secular variations, in Caucasus, correl. with geological struct. and seasonal hydrogeologic vars. (*Russian*) 8-53611
- Spain, residual anomalies rel. to geology (*Spanish*) 8-88781
- spherical functions analysis, contrib. to numerical development (*German*) 8-61311
- spherical harmonics expansion of potential, convergence 8-81097
- static potential fields data inversion, generalised inverse appl. 8-77350
- statistical algorithms for scaling geophysical fields 8-73527
- statistical gravity disturbance model, three-dimensional, algebraic errors correction 8-96125
- statistical model from gravity anomalies and HB, model 8-61306
- subduction zone, gravity regime of descending lithosphere, effect of subduction angle 8-77206
- Tashkent Palaeozoic crystalline basement, tectonic struct., gravity survey (*Russian*) 8-53610
- telluroid, definition 8-65171
- tidal gravity measurements, comparison with self-consistent equilib. ocean tides 8-96218
- transworld tidal gravity profile 8-57160
- two dimensional vertical fault, gravity approx. and interp. 8-61301
- two-dimensional gravimetry problem with variable mass density, equivalence theorems 8-85467
- two-dimensional masses, field calc. using analytical continuation (*Russian*) 8-69277
- vertical gradient meas. for detect. of small geological and anthropogenic forms, discussion 8-61575

gravity meters see gravimeters

gravity waves

- acoustic gravity waves, atmospheric, harmonic generation 8-88956
- acoustic-gravity waves, dispersive eqns. obtained by kinetic eqn. method (*Russian*) 8-85620
- atmosphere, acoustic-gravity waves generation by ionosphere press. oscills. 8-77296

gravity waves continued

- atmosphere, gravity waves generated during solar eclipse 8-88887
 atmosphere, layer structs. response to gravity waves 8-81290
 atmosphere, marginally unstable interfacial gravity waves in boundary layer (*French*) 8-92888
 atmosphere, ray tracing, tornadic storms and hurricanes warning system 8-73448
 atmosphere, squall line formation, nonlinear process 8-81323
 atmosphere, turbulence and internal waves spectra in stably stratified boundary layer (*Russian*) 8-81297
 atmosphere, wave generation and frontal collapse 8-77300
 atmosphere gravity wave-meanflow interaction, indication in radar obs. 8-81282
 atmosphere Na layer, gravity waves and tidal oscills., lidar obs. 8-88955
 atmospheric internal wave component identification on airglow charts, multiple-point method 8-73526
 capillary wave form, on gravity water waves, model eqn., surface tension, viscosity 8-83421
 capillary waves generated by steep gravity waves, meas. 8-59409
 capillary-gravity waves, linear problems 8-51178
 capillary-gravity waves in viscous fluid 8-51177
 creeping waves, on shallow water, numerical investigation 8-90928
 critical point hydrodynamics 8-59361
 deep ocean, fine struct., internal gravity waves and wave breaking meas. and models 8-85578
 directional gravity wave spectra and surface currents, remote sensing with dual freq. radar 8-96323
 ducting in thermosphere 8-77378
 E_z-layer, h-type at Uppsala, downward generation by internal gravity waves 8-81497
 F-region, nonstationary nighttime disturbances produced by internal gravity waves 8-73565
 gravity waves, long period, on beach, generalised KdV-eqn., soln. 8-92844
 internal, buoyant-parcel motion 8-55655
 internal nonlinear waves in stratified fluid in closed basin 8-75159
 ionosphere, travelling disturbances, possible correl. with jet stream activity 8-69601
 ionosphere, travelling disturbances characts. over Thumba 8-69590
 ionosphere F-region, gravity waves, obs. during tornado outbreak (1974, April 3) 8-85753
 ionospheric, lower, layer structs. response to gravity waves 8-81290
 ionospheric effects of sudden commencement assoc. gravity wave 8-57385
 liquid with superficial film and diffusion effect (*French*) 8-75156
 MHD gravity waves, dispersion on running stream of inviscid elec. cond. liq. 8-59502
 MHD gravity-capillary waves in liq. film falling by permeable bed 8-67277
 nonlinear free surface flow digital simulation by boundary integral eqn. method 8-92850
 nonstationary effects of gravity waves on ion formation in lower ionosphere 8-73567
 ocean, monomolecular slicks drift response to wind and wave action 8-69364
 ocean, surface and internal gravity waves generated by baric disturbances (*Russian*) 8-77252
 ocean internal tidal oscills. spatial characts. from temp. meas. 8-61434
 ocean internal waves, shear instability (*Russian*) 8-69352
 ocean surface waves, low freq. noise prod. in deep ocean 8-81184
 ocean wave detection by microwave radar, gravity-capillary wave modulation 8-77333
 ocean wave groups, vels. and refr. laws verification 8-85575
 ocean waves, directional spectra, remote sensing by microwave radar 8-57364
 oscillations of two liquids separated by membrane (*French*) 8-87355
 oscillatory boundary layer, on bed beneath gravity waves, laser Doppler anemometry 8-90929
 permanent wave structs. on an open two layer fluid 8-59411
 solar atmosphere, MHD-gravity wave critical levels 8-77531
 standing waves, finite amplitude, on finite-depth perfect liq. surface (*Russian*) 8-75155
 stratification effects in boundary layer flow over hills 8-53707
 stratosphere, lower, radar meas. of gravity waves 8-81292
 surface waves, tsunami wavelength, wave equation soln. 8-90927
 terrestrial atmosphere acoustic-gravity waves, generation mechanisms (*Russian*) 8-85621
 thermosphere, lower, gravity waves detect. by French incoherent scatter facility 8-81478
 thermosphere, lower, tides and gravity waves interaction rel. to thin shear turbulent layers 8-65444
 thermosphere, source in tropospheric jet stream (*French*) 8-69554
 thermosphere, vertical energy flux from medium scale gravity waves generated by jet stream 8-81479
 thermosphere, wave-induced diffusion effects on acoustic-gravity waves 8-61637
 travelling gravity-capillarity surface waves, on liq. film falling past permeable bed 8-87351
 troposphere, ground level gravity waves occurrence in SE.Australia, microbarographs obs. 8-73439
 two-dimensional, created against vertical cliff, uniform asymptotic soln. 8-67210
 two-layer fluid, weakly nonlinear solitary long gravity waves 8-83419
 water, surface gravity water propag., wave action and set-down on shear current 8-90920
 water-wave diffr. by semi-infinite vertical barrier on rotating Earth 8-83417

greasing see lubrication**Green's function methods**

- see also CPA calculations; KKR calculations
 $\lambda\phi^4$ theory, renormalised perturbation theory, Green's function calc. by R operation 8-54570
 Σ perturbation method using Green's functions for mol. calcs. 8-55123
 ϕ^3 interaction, four-dimensional Green's function model (*Russian*) 8-77775
 acoustic radiators, directivity pattern calc. from near-field sound meas. 8-83149

Green's function methods continued

- amorphous semiconductor superconductivity feasibility model (*Russian*) 8-80092
 antiferromagnetic metal, with paramag. impurities, Neel temp., impurity conc. depend calc. 8-68232
 arbitrarily shaped dielectric body inside waveguide, three-dimensional anal. 8-71005
 asymptotic behaviour in renormalisable QFT, Green's functions 8-70254
 atom, with two internal vacancies, characts. calc. by Green function method (*Russian*) 8-50450
 atom, with two internal vacancies, chem. shift of characts. (*Russian*) 8-50451
 atoms, multiphoton ionisation, reson. cross-section, very-narrow-bandwidth source 8-55150
 axially symmetric Helmholtz eqn., fundamental solution 8-77722
 bilocal fields, ϕ^3 vertex, unitary S-matrix 8-62323
 Brillouin scattering, resonant, analogy to modulation spectroscopy (*Japanese*) 8-68526
 Brillouin scattering by oblique-incidence acoustic phonons, lineshapes 8-72534
 chemisorption on metal, intra-adsorbate Coulomb correl. and surface struct. roles 8-71979
 chemisorption on metal, intra-adsorbate Coulomb correl. and surface struct. roles 8-71980
 chemisorption site determ., by angle-resolved UPS 8-71970
 chemisorption substrates with complex band struct., new technique 8-71961
 classical EM wave diffraction by a thin periodic slab, rigorous approach 8-82890
 composite media, generalised Fourier expansions, homog. equations 8-77712
 Coulomb problem, zero-energy 8-62097
 coupled channel multiparticle scattering theories, Green function eqns., factorisation props., spurious solns. 8-82323
 cracks, emanating from fastener holes 8-67118
 cubic lattice, Green's function determ. 8-62162
 cylindrical light beam diffr. on wideband US signal 8-50698
 decoupling procedure in Green's function method, sum rules for de Gennes' model (*Russian*) 8-56434
 density matrix, asymptotic high temperature expansion 8-54115
 diagrammatic Green function technique appl. to cryst. field systems with exchange 8-68130
 dilute binary alloys, formation energy, lattice relax. and zero-point vibrations 8-83771
 dilute binary alloys, formation energy, lattice relax. and zero-point vibrations 8-87646
 disordered system, orbital mag. susceptibility of conduction electrons 8-76217
 disordered systems, coarse-grained quantities and short-range order 8-75787
 disordered systems, short-range order and off-diagonal randomness 8-75782
 distribution functions and Green functions (*Russian*) 8-65890
 dynamical properties of solid surfaces, analytic approach 8-71929
 early Universe, EM and gravit. Green's functions 8-73786
 electromagnetic scatt., time depend., boundary value formulation, integro-differential eqns. 8-66726
 electron-hole system spectrum, in one-dimens. infinitely deep pot. well (*Russian*) 8-67944
 EM field calculation using integral eqn. method (*Russian*) 8-82887
 empirical parametrisation of electronic structure 8-91585
 energy level calcs. for cryst. with vacancies or substitutional impurities (*Russian*) 8-56101
 ethylene mol. Green's function Σ perturbation method for mol. calcs. 8-55123
 Fabry-Perot, and confocal resonators, comparison of diffraction formulas 8-87077
 FCC metals, dynamics of multiple interstitials and interstitial impurity complexes 8-75775
 Feller eqn., generalised, boundary condition solns. 8-62167
 Fermi weak interaction theory, consistent renormalisation scheme, Yang-Mills theory parallel 8-66071
 Fermion contribution to instantons 8-78079
 ferromagnet, randomly anisotropic, long wavelength mag. excitations 8-84406
 ferromagnet, uniaxial with arbitrary spin and second order single ion anisotropy 8-84379
 ferromagnet, uniaxial with single-ion and exchange anisotropies, magnetisation in transverse mag. field 8-56277
 ferromagnetic polariton linewidths, theory 8-87918
 Feynman rules for lattice gauge theory of quark confinement, Green's functions, review 8-93850
 formic acid, ionis. and photoelectron spectra, inner valence electrons 8-82784
 ϕ^4 theory, strong coupling limit of Green functions, anharmonic oscillator appl. 8-78071
 generalised Wilson expansions in dimensional renormalisation 8-86403
 heat conductivity eqns., soln. of boundary value problems by Green's function method (*Russian*) 8-63267
 Heisenberg ferromagnet, diagram techniques for Greens functions with spin operators 8-91836
 Heisenberg ferromagnet, higher order corrections to spectrum 8-80222
 Heisenberg ferromagnet, longitudinal dynamic susceptibility 8-64181
 Heisenberg film, spin-one isotropic, quadratic interactions, quadrupolar-paramag. T_c 8-64210
 Heisenberg spin-1/2 ferromagnets, 1st order Green's function theory 8-72323
 Heisenberg-biquadratic and Blume-Emery-Griffiths interactions dipolar and quadrupolar susceptibility 8-76257
 Helmholtz and Green's theorems, integral eqn. methods, static equivalence principle 8-57090
 Higgs-Kibble mechanism, superfield theoretical treatment 8-89616
 Hubbard antiferromag. semiconductor, electron correlations, weak coupling 8-67969
 Hubbard model, electrical conductivity calculation, dielectric function and plasma oscillations 8-64020
 Hubbard model, Ward identities, particle number conservation, analytical structure of self energy 8-79913

Green's function methods continued

integral characteristics of the electron structure of crystalline surfaces 8-64078
 Ising model with transverse field, commutator and anticommutator Green functions 8-76211
 Ising model with transverse field in paramagnet 8-68138
 Jost function and S-matrix for pot. of general form., Schrodinger eqn. soln. in hypergeometrical functions (*Russian*) 8-81870
 Klauder augmented quantum field theory, ϕ^4 model 8-78094
 light-cone finite normal products 8-86408
 linear crystal with thermal gradient, electronic Green's function 8-64019
 linear hemitropic micropolar isotropic elastostatics 8-49661
 liquid metal, electron momentum density, perturbed Green's function method 8-60052
 loaded thin circular plate stability criterion 8-77700
 local impurity states, existence, levels, Green function, tight-binding calcs. 8-67981
 many body problems, real time Green's function 8-57855
 many fermion energy calculations 8-66238
 many-particle system, generalised diffusion processes 8-73942
 mass spectrometer sample line diffusion processes 8-64907
 maximal variational principle for transport theory 8-62166
 metal, quasimagnetic impurity, exact solution of Wolff's model 8-56105
 metal, surface relaxation, lattice statics calc. 8-63925
 metal surface, narrow band, self consistent model calc. of electronic states 8-95333
 metal-metal interface, simple, electronic props. 8-72234
 microstrip anisotropic electrostatic field problems, Green's function technique 8-70998
 molecular crystal, dipole plasma oscillations, Bose-Einstein condensation of excitons (*Russian*) 8-84155
 moment method for solution of two Pocklington type integral equations 8-55279
 momentum autocorrelation functions from classical Green's functions. [Teaching] 8-61976
 multiple scattering of classical EM waves by fixed dielectric obstacles, Fredholm's method 8-71008
 non-homogeneous elastic medium, sudden twisting of penny shaped flow 8-87302
 nonlinear singular perturbation problem on a semi-infinite interval 8-94631
 nuclear matter, dispersion relations, HF method for hard core interactions (*German*) 8-54713
 nuclear reactor, coupled cores, calc. of buckling variation and neutron flux, Green's function method 8-74421
 off shell scattering amplitude, S-matrix, pot. scatt., Mittag-Leffler expansions of Green's function, convergence 8-73874
 optical waveguide, scattering from arbitrarily located inhomogeneity 8-87161
 path integral formalism, barrier penetration effects on wave functions and energy spectrum 8-62117
 phonon dynamics 8-79704
 photoemission, external, many-body aspects 8-72703
 piezoelectric surface waves on semifinite crystal, asymptotic expressions 8-51812
 plasma, cyclotron harmonic absorption via the Green's function for the mode conversion-tunneling equation 8-75296
 plasma, inhomogeneity spreading in weakly ionised current-carrying plasma 8-71445
 polycrystalline material, scatt., lattice representation 8-65774
 pseudoparticle fields, propagation functions 8-54556
 quadrupolar systems, excitation spectra from Green's function methods 8-56278
 quantum field theory, relativistic, reconstruction of local observable algebras from Euclidean Green's functions 8-54522
 radiative transfer in noncoherent anisotropically scatt. plane-parallel slab (*Russian*) 8-61723
 random dielectric, mean pot. and field 8-55271
 relativistic two-body problem, 3-D formulation in terms of rapidities 8-49985
 renormalised perturbation theory, model of 3-D nonlinear field, free of UV divergences 8-54567
 RKKY interaction and conduction electron polarisation, Green's function and multiple scatt. formalism 8-91859
 rough surface, dispersion relation for surface plasmons, quantum mechanical approach 8-72099
 Saint-Venant torsion problem, classical, integral and functional eqns. 8-57780
 Schwinger-DeWitt expansion, boundary terms, flat space results 8-77815
 screw dislocations, inelastic neutron scatt. 8-75774
 self consistent RPA for three body forces in Fermi systems 8-89810
 self-dual gauge field, Green function 8-82099
 semi-infinite array of identical potentials, surface effects and electronic density of states 8-54110
 semiconductor film, Wannier-Mott exciton states (*Russian*) 8-79943
 singularity at corner of wedge shaped punch or crack 8-83252
 solid sheet with selective optical props., combined radiative and conductive heat transfer 8-90672
 spinor and scalar particles in mag. field (*Russian*) 8-49997
 stress intensity factors FOR X-formed arrays of cracks 8-67121
 strong-coupling limit of renormalisable interacting quantum fields 8-49968
 subsonic and supersonic aerodynamics, SOUSSA computer code 8-71352
 superconductive tunnelling, extension of Feuchtwang method 8-68121
 surface, effects of roughness on dynamical props. 8-75923
 surface, Green function method for electronic struct. and vibr. modes calc. 8-88012
 surface, lattice force constant determination 8-71933
 surface electronic structure from matching Green function method 8-88013
 transition metal (001) surface, model, chemisorption, coverage depend. of adsorption behaviour 8-71976
 transition metal impurities in transition and noble metal hosts, electronic struct. 8-75990
 two body scatt., non-relativistic, variational matrix Pade approximants (*German*) 8-54247
 two-particle bound state, lifetimes and level shifts 8-75265

Green's function methods continued

two-particle-hole Tamm-Dancoff approximation (2ph-TDA) equations for closed-shell atoms and molecules 8-70937
 unidirectional wave motions, book 8-77730
 valence electron photoionisation, ionisation pot. and spectral intensities 8-70883
 velocity dependent pot. uncoupled Schrodinger eqn. soln. using Green's technique 8-69998
 Ward identity, conformally invariant form, Green's function and two conserved currents 8-86421
 wave propagation in inhomogeneous media, backscatter folding series (*Russian*) 8-73862
 XPS, angle-resolved, role of electron diffraction 8-64446
 XY₃ pyramidal molecules, change in mean square amplitude values, calc. 8-55158
 Yang-Mills pseudoparticles, fermion Green's functions 8-54548
 Al, liquid, electron momentum density, correlations and ionic potentials 8-60052
 CsI, isotope diffusion 8-75875
 Cu, entropy factors for vacancy formation and migration 8-75866
 Cu-Al, change in force constant due to volume effects 8-75778
 Cu-Al, impurity concentration effects 8-75777
 Cu-Be, impurity concentration effects 8-75777
 Cu-Si, change in force constant due to volume effects 8-75778
 Cu-Si, impurity concentration effects 8-75777
 p-D₂, order-disorder phase transition 8-79726
 Ge-Si, impurity lattice modes due to single and paired defects 8-75780
 Ge-Si, impurity concentration effects 8-75777
 H₂ mol., Green's function Σ perturbation method for mol. calcs. 8-55123
 o-H₂, order-disorder phase transition 8-79726
 H₃⁺, dynamic polarisability, electronic states two centre Coulombic Green's function, continuous spectrum exclusion 8-82626
 HCN, ionis. and photoelectron spectra, inner valence electrons 8-82784
 H₂S, gas-phase, states in valence photoelectron spectrum 8-94284
 H₂S, inner valence electron ionisation calcs., photoelectron spectra obs. 8-82619
 K halides, surface lattice dynamics, by Green's function method 8-71936
 KBr, electronic states at (100) surface, accounting for spin-orbit interaction (*Russian*) 8-91750
 KCl, electronic states at (100) surface, accounting for spin-orbit interaction (*Russian*) 8-91750
 KCl:Pb²⁺ (0.005% Pb), A band fine structure, electron-phonon interaction 8-60491
 KI, electronic states at (100) surface, accounting for spin-orbit interaction (*Russian*) 8-91750
 KI, gapmode calc. using Green's function technique, effect of uncertainty in eigendata 8-79708
 Mg, single crystal, Green's function method of lattice statics, monovacancy 8-55865
 MgO, intrinsic surface states at (100) and (110) surfaces 8-91740
 Mo(001), surface electron struct., matching Green function method calcs. 8-88014
 N₂, shake-up peak positions and intensities calcs. using eqns. of motion Green's function method 8-86910
 α -N₂, solid, anharmonic lattice vibrations calcs. 8-71812
 NH₃⁺, ionisation pot. of ²E state, Jahn-Teller effect 8-62948
 Ni (001), chemisorption site determ. for S and CO, angle-resolved UPS 8-71970
 Ni(001), surface electron struct., matching Green function method calcs. 8-88014
 PH₃, inner valence electron ionisation calcs., photoelectron spectra obs. 8-82619
 Si, ideal vacancy, self consistent Green's function calc. 8-91640

grinding

ball mill grinding, rate constant determination (*Japanese*) 8-95828
 ball mill grinding, wet, dry, rate constant determination (*Japanese*) 8-95827
 breakage distribution, in batch grinding, mathematical model determination 8-92416
 comminution of solids under hydrostatic pressure, technique 8-52702
 microchannel plate surface finishing using liquid 8-90544
 monolithic component glasses and rigid sintered fibre-optic elements, microcrack form. during grinding 8-87175
 optical blank grinding and polishing, for LAT primary mirror 8-90541
 optical component manufacturing of low stiffness plates 8-71236
 optical glass, semiautomatic machines kinematics (*Czech*) 8-63208
 optical workshop machines, kinematic relationships (*Czech*) 8-50953
 particle size measurement techniques, rapid response, online methods, continuous industrial processes appl. 8-89429
 particles, small, impossibility of comminution by compression 8-52709
 pellet precision grinding and high-speed polishing using synthetic material 8-50958
 polycarbonate, decomposition by H₂SO₄ and grinding by ball mill, exam. of molecular chain scission (*Japanese*) 8-64827
 powder, moist, granulation on vibrated chute (*Japanese*) 8-95710
 powder, ultra fine, surface roughness effect on formation by rotating friction mill (*Japanese*) 8-95709
 Reciprocating motion for fine diamond grinding 8-71237
 semiautomatic machines, kinematic ratios calc. (*Czech*) 8-79146
 steel, martensitic cracks form. mechanism obs., impingement cracks and strain influence (*Japanese*) 8-56747
 steel 40Kh, surface working effects on crack resist. (*Russian*) 8-56734
 steel stainless, solar energy collector optical props. rel. to heat treatment 8-94455
 vibratory mill, prod. of small amounts of finely divided unoxidised mat. 8-68646
 vibratory tools, hand-arm energy dissipation and accel. levels 8-96116
 Al₂O₃, abrasive, wear in simulated hot grinding 8-56784
 Cr-Fe (30 wt.%) alloys, refined fine comminution 8-60598
 InP substrates, HCl etching speed and polarity obs., with aid of laser beams (*Slovak*) 8-56575
 K₂O-Al₂O₃-B₂O₃-SiO₂, glass, ESR exam. of paramagnetic centres formed during mech. destruction by grinding 8-88188
 SiC, abrasive, wear in simulated hot grinding 8-56784
 TiCl₃(TiCl₃), labelled, exchange of Ti atoms rel. to γ -irrad., heat treatment, grinding 8-92470

grinding continued

- U ore, ^{222}Rn release 8-89970
 ZnO, adsorpt. of H_2O vapour, annealing and grinding effects 8-68656
 $\text{ZnO-B}_2\text{O}_3$, glass, ESR exam. of paramagnetic centres formed during mech. destruction by grinding 8-88188
 ZrSiO_4 , mechanochemical effect by mechanical grinding (*Japanese*) 8-84754

grinding mills see grinding**ground services, aerospace** see ground support systems**ground support systems**

- see also *aircraft communication; navigation; telemetering systems*
 aeronautical meteorology, progress and challenges 8-53692
 communications satellite system measurements 8-61712
 International Ultraviolet Explorer (IUE), ground data processing system performance 8-96383
 International Ultraviolet Explorer (IUE) spacecraft, instrumentation and ground control 8-96382
 weather service, future trends 8-53694

grounding see earthing**groundwater**

- alluvial aquifer, Galerkin-finite element simulation of recharge 8-81263
 aquifer response to tidal forcing and 1964 March 28 Alaskan earthquake 8-73407
 aquifers, effects of drought in England and Wales, 1975-6 period 8-88866
 aquifers, transport model parameters determ. 8-61463
 N.Baja California, groundwater rel. to submarine hydrothermal activity 8-61431
 Broadlands geothermal field, New Zealand, boiling curves 8-85516
 column drainage through porous media, moving boundary problems, theory and numerical analysis 8-81252
 distributed parameter system identification using doubly cubic spline, underground aquifer appl. 8-69391
 England, decreasing wetness in 1969-77 period 8-65377
 finite element Galerkin method for groundwater flow calc. 8-89320
 flow anal. by finite element method 8-92871
 flow anal. by finite element method 8-92875
 flow digital simulation, finite element method 8-93018
 flow model using finite element method 8-92874
 frost heave in Tomakomai, Hokkaido, 1976 to 1977 (*Japanese*) 8-92860
 geopressured geothermal wells production characts. 8-81223
 geothermal areas in Iceland, H-water isotope thermometer appl. 8-69384
 geothermal systems, sulphate-water O isotope thermometry 8-69383
 geothermal tracing with atmospheric and radiogenic noble gases 8-69502
 geothermometry, chemical and isotopic techniques 8-69501
 geysers, lab. models rel. to natural phenomena 8-69373
 gravity secular variations, due to water quantity vars. in lithosphere (*Russian*) 8-53609
 hot spring and drill hole water, geothermal reservoir temp. determ. using O isotopes 8-69382
 hot springs, Japan, heat output vars. rel. to earthquakes (*Japanese*) 8-96241
 hydrologic cycle, rel. to nuclear waste disposal 8-94103
 hydrologic influence on long-period motions of Potsdam plumb-line (*Germany*) 8-57222
 hydrothermal alteration of volcanic rocks at Matagami, geochemistry rel. to massive sulphide genesis 8-77231
 Iceland, D tracing in hydrothermal systems 8-69386
 Iceland high-temperature geothermal systems, aquifer chemistry 8-96245
 ionic diffusion in naturally-occurring aqueous solns., use of activity coeffs. in transition-state models 8-57224
 Izu Peninsula, Japan, groundwater geochem. in crustal uplift area, rel. to earthquake prediction (*Japanese*) 8-96242
 Lake Assal (FTAI), geothermal zone, geochemical and expt. studies 8-69314
 Larderello field, secondary changes in composition of geothermal fluids 8-69387
 leaky aquifer, approx. differential eqn. 8-81242
 leaky aquifer analysis, finite element method soln. 8-93017
 limestone diagenesis simulation, computer model based on Sr depletion 8-73358
 management, finite element discrete kernel generator 8-92873
 migration during soil freezing, obs. (*Japanese*) 8-88862
 modified Richards' eqn., oscill. of numerical soln. 8-81243
 non-steady flow problem in two-layer porous medium 8-81260
 nonsteady flow through tunnel opening, reductive finite element/Crank-Nicolson anal. 8-92861
 oilfield brines from Kansas and Colorado, Sr isotopic comp. 8-57225
 pollutants from underground coal gasification 8-92865
 pollution below Dharwar, India 8-69380
 porous media, miscible or immiscible displacements, identification and modelling 8-69392
 radioactivity in Arizona water, baseline values 8-81230
 radionuclide chain migration 8-85616
 saturation rel. to dissolved carbonates in Edwards artesian aquifer, Texas 8-73416
 seepage from free surface of triangular channel, variational inequality method 8-81251
 soil fluid flow with free or artesian surface 8-92872
 soil hydraulic conductivity var. of Wisconsin soil series 8-81250
 soil moisture movement and groundwater recharge by T tagging technique 8-61438
 soil water flow modelling, finite difference and Galerkin techniques 8-81249
 stability of solid freezing front 8-63844
 stream-connected aquifer system, lumped parameter stochastic model 8-81241
 stream-well-aquifer system groundwater flow anal., linear system models 8-77289
 subsurface water chemistry study, coring and squeezing technique 8-57332
 Tarmanskii Marsh, influence of human activity on hydrological and thermal regimes 8-92864
 Tehran groundwater pollution by detergents 8-61453

groundwater continued

- S. central Texas, effect of Balcones Faults on groundwater movement 8-53672
 transient aquifers, modified optimisation method for parameters estimation 8-61462
 Tuwa spring water, activity ratio and separation of $^{223}\text{Rn}/^{226}\text{Ra}$ 8-86962
 two-dimensional unconfined saturated flow, boundary integral solns. 8-77291
 unsaturated zone hydrology, United States educational effort 8-81224
 unsteady flow from tunnel opening, reductive finite element anal. (*Japanese*) 8-96251
 water resource finite element anal., conf. at London, England 1978 8-92867
 water table movement modelling using dynamic filtration (*Russian*) 8-88850
 well water levels at Funabara and Kakigi, Japan, rel. to earthquakes (*Japanese*) 8-96241
 wells, flow anal. by finite element method 8-92870
 wetland mapping in New Jersey and New York 8-77265
 Cl^- content, appl. to Miocene aquifer isopermeability map 8-81256
 He/Ar and N_2/Ar ratio vars. in fault zone groundwater air bubbles for earthquake prediction 8-88803
 $^{87}\text{Rb}/^{87}\text{Sr}$ studies of waters in geothermal area, Cantal, France 8-61443
 Rn in geothermal reservoirs 8-69381
 Rn measurement in groundwater and springs for earthquake prediction 8-88924
 ^{222}Rn concentration in N.Carolina groundwater supplies rel. to stomach dose and conc. standards 8-85612
 S isotope exchange between sulphate and sulphide in acid solns., expt. determ. at 300°C and 1000 bars 8-62937
 U in natural waters, field meas. technique 8-85705

group theoretical schemes

- hadron mass, instanton effects on light quark spectroscopy, MIT bag model 8-62372
 symmetries of 6j coefficients 8-86423

group theory

- see also *Clebsch-Gordan coefficients; crystal symmetry; elementary particle theory; group theoretical schemes; Lie groups; renormalisation; SU_n theory*
 anisotropic constitutive equations and Schur's lemma 8-89337
 asymptotic reduction products of representations of covering group of $\text{SU}(1,1)$ 8-58137
 atom, unitary group generators representation matrices calcs. 8-78610
 autonomous dynamic systems, limit cycles and one parameter transformation groups 8-49641
 bi-local model, Poincare group and position operator 8-93844
 bifurcation from rotationally invariant states 8-77671
 capillary-porous body, nonlinear heat/mass transfer problem, soln. using invariant groups 8-55688
 commutation relation $[A, B] = -iC$ for one parameter unitary groups 8-65811
 conformal invariant 2- and 3-point functions for tensor fields with arbitrary spin 8-49977
 conformal transformations in superspace 8-70295
 covariant coherent states for quantized systems with nilpotent symmetry group (*German*) 8-73865
 double group theory, half-shell and two-level system, optical polarisation 8-49594
 dual current vertex, group theoretical struct. 8-74229
 dynamic critical phenomena closed-form differential renormalisation group generator 8-86413
 education, group theory of covariant harmonic oscillators, interacting quarks 8-61970
 education, renormalisation group theory, second order phase transitions, undergraduate statistical physics 8-62012
 entropy prod. for quantum dynamical semigroups 8-57883
 EPR, symmetry adaptation and operator equivalents (*French*) 8-91924
 ergodic properties of an operator obtained from a continuous representation 8-89305
 flexible Jordan admissible algebra, dims. seven, hadron physics appl. 8-93792
 fluid layer, selection mechanisms for convective motion pattern form. 8-54316
 G_2 , weight multiplicities 8-78105
 Galilean semi-group for more general theory of symmetries, isolated quantum system 8-49718
 Galilean formulation of spin, Clifford algebras and spin groups 8-57736
 gauge equivalence of representations of symmetry groups in quantum mechanics 8-77752
 gradient formula for the $\text{O}(5) \supset \text{O}(3)$ chain of groups 8-78285
 hadron gravitational interaction, band spinor representation of $\text{GL}(N, \mathbb{R})$ 8-50000
 homogeneous Lorentz group, chirality, Weyl spinors 8-93810
 homotopy groups of condensed matter physics 8-63752
 hyperboloids, wave eqn., $\text{O}(2,2)$ symm., separation of variables 8-77679
 intelligent states, computation of Clebsch Gordan coeff. 8-62101
 intelligent states, group-theoretic study and computation of matrix elements 8-62100
 intrinsic $\text{SO}(2,1) \times \text{GL}(1, \mathbb{R})$ invariance of Dirac eqn. 8-93826
 invariance groups for class of countable systems of first-order partial differential eqns. 8-49635
 irreducible representations of groups with subgroup of index 2 8-57733
 Ising lattices, position-space renormalisation-group transformations, problems and proofs 8-93619
 $\text{IU}(n)$ group, matrix elements of irreducible representations (*Russian*) 8-54149
 K-harmonics method, group of canonical transformations 8-50106
 linear Jahn-Teller systems, continuous group invariances 8-60092
 Lorentz group in oscillator realisation 8-77755
 Lorentz type internal symmetry 8-50005
 magnetic resonance, symmetry adaptation and operator equivalents (*French*) 8-51924
 massive gauge fields, complete spontaneous symm. breaking, asymptotic freedom, symplectic and G_2 groups 8-62305

group theory continued

- methane, hyperfine struct., Racah finite group algebra appls. 8-78617
 minimal EM coupling in elementary quantum mechs., group theoretical derivation 8-54590
 molecular, symmetry coordinates construction, arbitrariness limitation 8-55252
 molecular electronic struct., group function model 8-62700
 molecular point groups, infinite, complete reduction of representations, mol. vibrs., electronic states appls. 8-94206
 multispinor Lagrangian, symm. group 8-58115
 Nambu-Goldstone realisations of dynamical groups and nonlinear eqns. (Russian) 8-89632
 nematic-isotropic transition, nature, field renormalisation group formalism study 8-87775
 Neumann, completely positive maps, semigroup generators 8-93545
 noncompact groups, equiv. problem to 2-centre integrals in quantum mechanics (Russian) 8-89367
 nonrelativistic algebraic models, gauge invariance, causality props. 8-62319
 nuclear 3-cluster systems, resonating group method 8-50108
 $O(n)$ shift operators, normalisation coeffs. 8-57738
 orbital correspondence anal. in max. symm., appl. to spin-forbidden processes 8-78631
 orthogonal groups, raising, lowering weight operators 8-57737
 permutation group outer-product reduction coeffs., rel. to SU_n group CG coeffs. (Chinese) 8-49631
 Poincare and Galilei groups, quantum mechanics 8-49701
 Poincare and Galilei groups in arbitrary dimensional spaces 8-77672
 Poincare group representations in the free quantum field framework (German) 8-77772
 Poincare-like groups, Kronecker product decomposition, appl. to Weyl group 8-49632
 polynomial irreducible tensors, generating functions 8-49633
 projected basis set for the irreducible representation $\{2^{n/2-1}, 1^{2n}\}$ of $U(n)$ 8-77668
 pseudo-Riemannian curvature spaces, group struct. 8-57829
 quantum dynamical semigroups, approach to equilibrium 8-49710
 quantum dynamical semigroups and spin multipole relaxation in isotropic surroundings 8-86813
 quasisymmetry (P-symmetry) groups in crystallography, semidirect products method 8-51457
 real-space renormalisation giving differential renormalisation-group eqns., two-dimens. triangular Ising lattice 8-65881
 recoupling coefficients of the general linear group in bases adapted to shell theories 8-77670
 recoupling coefficients of the symmetric group involving outer plethysms 8-77669
 relativistic quantum mechanics, Galilean limit, group contraction, probabilistic interpretation 8-77760
 renormalisation group approach to scaling, phys. appl. 8-49634
 semi-group for vision lateral inhibition process modelling 8-65010
 semigroup generation by second-order hypoelliptic differential operators 8-65755
 sine-Gordon equation, one dimens., group of invariance, dimens. anal. method 8-54528
 $SL(2, R)$ and solitons 8-57748
 $SO(n)$ groups, ($n > 5$), representation theorem 8-86407
 solution of the Dirac equation with anomalous magnetic moment 8-82133
 space-time conformal group, metric tensors 8-93816
 spin system, isotropic, N-component, with long- and short-range interactions, crit. behaviour 8-76256
 spinor norm, new formula 8-62048
 symmetries of 6j coefficients 8-86423
 triangular Ising model percolation props., renormalisation group anal. 8-93620
 twisted products for cotangent bundles of classical groups and Stiefel manifolds 8-49680
 Wigner-Weyl isomorphism, group theoretical aspects and basic props., $E^{(2)}$ symmetry group 8-62089
 H atoms, two-photon transition matrix elements, group theory calc. 8-62776
 3He , superfluid, topology of non-singular textures using relative homotopy groups 8-84021
 ^6Li+n , 12 and 20 MeV, resonating group method exam., effective inter-nuclear potential 8-50159
 ^{16}O , band system generation by infinitesimal operators of subgroup $Sp(2, R)$ 8-50109

Gruneisen coefficient

- acetone-chloroform (-iodomethane) ($-CS_2$), liq. mixture, excess Gruneisen parameter, intermol. interaction 8-67635
 alkali hydrides, bulk props. prediction from molecular behaviour 8-51468
 alkali metal, lattice vibr. and Gruneisen parameter 8-59917
 alkali metals, thermal properties and Gruneisen parameters, employing model pot. 8-71815
 alkali halide, optic mode Gruneisen parameters and strain derivatives, Born-Mayer and Szigeti model 8-55929
 Anderson-Gruneisen parameter, heavy metal halides 8-79715
 Anderson-Gruneisen parameter effect of anharmonicity 8-79714
 Anderson-Gruneisen parameter for cryst. of cubic symmetry, determ. using elastic moduli 8-79713
 Anderson-Gruneisen parameter for cubic crystals 8-79672
 benzene-ethylene dichloride ($-CCl_4$), liq. mixture, excess Gruneisen parameter, intermol. interaction 8-67635
 bulk moduli, Wachtman's eqn., and temp. depend. 8-75799
 carbon tetrachloride-benzene, liq. mixture, excess Gruneisen parameter, intermol. interaction 8-67635
 chloroform-acetone, liq. mixture, excess Gruneisen parameter, intermol. interaction 8-67635
 Earth interior, Gruneisen parameter rel. to generalised eqn. of state 8-96194
 ethylene dichloride-benzene, liq. mixture, excess Gruneisen parameter, intermol. interaction 8-67635
 geophysical appl. 8-65264
 harmonic approx., theoretical evaluation by Legendre polynomial expansion 8-59916
 homovalent disordered solid alloy, entropy-vol. correlation 8-63868
 iodomethane-acetone, liq. mixture, excess Gruneisen parameter, intermol. interaction 8-67635

Gruneisen coefficient continued

- noble metal, Gruneisen parameter temp. variation calc. 8-51638
 US parameter for nonconducting cubic crystals 8-87744
 Ag-Mn, dil., anomalous thermal expansion below 50K 8-51710
 AgBr, dielectric behaviour under hydrostatic press. 8-52420
 AgCl, dielectric behaviour under hydrostatic press. 8-52420
 Al, Gruneisen parameter behaviour at high press. 8-83899
 $Al_{10.4}Ga_{0.08}V$, low temp. thermal expansion 8-95167
 $Al_{10}V$, low temp. thermal expansion 8-95167
 alkali halides, interatomic forces, Born model anal. on US data 8-55833
 $As_2S_3(Se_2)$, thermal expansion at low temperatures 8-83982
 BF, sp. ht., Debye temp., compressibility and Gruneisen coeff. meas. 8-63865
 $Ba(NO_3)_2$, press. derivatives of elastic-moduli, ultrasonic velocity meas. 8-95102
 CS_2 -acetone, liq. mixture, excess Gruneisen parameter, intermol. interaction 8-67635
 $CdCr_2S_4$, thermodyn. props. 8-51703
 Cr, linear expansion coefficient, at low temp. 8-83977
 Cu, Gruneisen parameter behaviour at high press. 8-83899
 Cu-Mn, dil., anomalous thermal expansion below 50K 8-51710
 Cu_2O , thermal expansion at low temp. 8-59959
 Fe, Gruneisen parameter behaviour at high press. 8-83899
 Fe, highly pure, phonon contrib. to elec. resist., 1.6-298K 8-84194
 Fe in Earth's core 8-61361
 Fe-Ni alloys, anomalous thermal expansion, Gruneisen eqn. 8-83980
 Ge, effect of pressure on the Raman shift 8-92064
 GeO_2 , thermal expansion at low temperatures 8-83982
 GeS_2 , thermal expansion at low temperatures 8-83982
 In, Gruneisen parameter behaviour at high press. 8-83899
 KCN, crystal props., log potential model calc. 8-63829
 KCN, polymorphism, high pressure, Raman spectra 8-88302
 $^6LiH(D)$, cryst., cohesive energy, force const., lattice freq., Debye temp., Gruneisen parameters, calc. 8-91293
 Mo, linear expansion coefficient, at low temp. 8-83977
 NH_3 , ND_3 , crystals, rotation mol. motion (Russian) 8-87762
 NaCN, crystal props., log potential model calc. 8-63829
 $Na_2O-GeO_2(SiO_2)$, thermal expansion at low temperatures 8-83982
 NiS_2 , high press. effect on mag. transition temps. 8-91866
 Pb, Gruneisen parameter behaviour at high press. 8-83899
 $Pb(NO_3)_2$, press. derivatives of elastic-moduli, ultrasonic velocity meas. 8-95102
 $(PbSe)_{1-x}(SnTe)_x$, lattice dynamic props., Gruneisen parameters (Russian) 8-83984
 RbBr, phonon freqs. at 80, 290, 370K, neutron inelastic scatt. study, comparison to Gruneisen parameters 8-51631
 RbCN, crystal props., log potential model calc. 8-63829
 Se-Ge glass, rel. to photostruct. change of lattice vibr. spectra 8-72494
 SiO_2 , fused, US study by harmonic generation, elastic const., Gruneisen parameters 8-83735
 SnI_4 , Raman spectra, temp. and press. meas. and lattice dynamical calcs. 8-56472
 $Sr(NO_3)_2$, press. derivatives of elastic-moduli, ultrasonic velocity meas. 8-95102
 ThO_2 , temp. depend., lattice vibrational frequencies in range 298-2300K 8-79712
 TiBr, dielectric behaviour under hydrostatic press. 8-52420
 TiCl, dielectric behaviour under hydrostatic press. 8-52420
 UO_2 , temp. depend., lattice vibrational frequencies in range 298-2300K 8-79712
 W, linear expansion coefficient, at low temp. 8-83977
- GTO calculations**
 alkanes, ab initio calcs. using FSGO, internal rot. 8-82639
 diatomic molecules, electric polarisabilities, EFV GTO basis set 8-50661
 heat of reaction, basis set of effect and approx. natural orbitals in SCF CI GTO calcs. 8-76904
 HEED, many beam problem, use of Gauss-type orbitals and plane waves 8-83661
 methylene ion, pot. energy surfaces of excited states, ab initio GTO SCF CI calcs. 8-58602
 molecular geometry, basis set effect and approx. natural orbitals in SCF CI GTO calcs. 8-76904
 silanes, ab initio calcs. using FSGO, internal rot. 8-82639
 BH, variation-perturbation minimal Gaussian geminal basis sets correl. energy calc. 8-78629
 HCN, dipole moment derivative, sign anomaly, CGTO ab initio calc. 8-74795
 HCN, SCF ab initio ground state pot. energy surface, geometry, rel. to HCN^- 8-78646
 HCN^- , SCF ab initio ground state pot. energy surface, geometry, rel. to HCN 8-78646
 HF, nuclear spin-spin coupling const., finite perturbation calcs. 8-78616
 HF, variation-perturbation minimal Gaussian geminal basis sets correl. energy calc. 8-78629
 H_2O+Li^+ , ab initio GTO calc. of vibr. intensity changes of spectroscopic parameters 8-58583
 He_2 , pair polarisability correl. effects, SCF-CI-GTO-SO calc. 8-82651
 LiH , variation-perturbation minimal Gaussian geminal basis sets correl. energy calc. 8-78629
 Si (111), chemisorbed Cl layer, SCF LCAO band struct. calcs. 8-88010
 SiO_2 , mol., ab initio SCF calcs., ground state stability, struct., vibr. freqs. 8-86781
- Gudden-Pohl effect** see electroluminescence
- guided electromagnetic wave propagation**
 see also guided light propagation; waveguides
 atmosphere, radio refractive index structure in transitional boundary layer 8-57268
 dielectric three-ply system with space heterogeneity, surface EM waves (Russian) 8-55288
 evaporation ducts, polarisation depend. of transient signals 8-57269
 HF peculiar lunar echoes, guided wave propag. in ionosphere and magnetosphere 8-93032
 ionosphere, diffraction trapping of HF waves by waveguide 8-53772
 rectangular waveguides, EM field calc. (Russian) 8-82884
 selflocalised EM fields in dense plasma 8-75350

guided electromagnetic wave propagation continued

- SHF beyond-the-horizon signals, evaporation duct influences 8-92935
 troposphere, radio refr. index struct. parameter height distrib. and duct thickness 8-73491
 whistler-mode waves guidance through plasmasphere 8-93054

guided light propagation

see also *optical waveguides*

- amplitude modulated laser beam prog. in random inhomogeneous medium, phase fluctuation anal. 8-87017
 exponentially decaying gain medium, waveguiding 8-50774
 field wave front correction, emitted from fibre lightguide (Ukrainian) 8-83081
 film, refr. index and thickness determ. using guided optical waves 8-74049
 focused light ATR method, appl. to guided waves on grating 8-74992
 glass fibres, light propag. in a large aperture bundle, tied together by a helix metal or glass filament 8-87154
 optical fibres, phase modulation of coherent light using HF sound 8-87142
 by single curved surface 8-71196
 stochastic wave propagation, ambiguity function 8-69993
 LiNbO₃, leaky SAW and guided light Bragg interaction, theoretical anal. 8-72484

Guinier-Preston zones

- Al alloys, age-hardening, resistivity charge by low temp. deform., GP zone cutting (Japanese) 8-84831
 Al-Cu (3.71 wt.%), stress oriented precipitation of Guinier-Preston zones and θ' 8-52809
 Al-Cu (4 wt.%), AE during deform., effect of ageing at 170°C 8-64597
 Al-Cu (4 wt.%), aged to contain Guinier Preston zones, crystallographic fatigue crack growth 8-60832
 Al-Cu (4 wt.%), enhanced precipitation under electron irradiation in HVEM 8-52818
 Al-Mg-Ag, age effect on age hardening (Japanese) 8-52831
 Al-Zn, dil. alloy, ageing and reversion, annealing curves, X-ray obs. 8-88485
 Al-Zn, formation of Guinier-Preston zones, and their limit temp. (Japanese) 8-84861
 Al-Zn (7 at.%), liquid quenched, early stage phase separation, exam. 8-68698
 Al-Zn alloys, relation between microhardness and average radius of Guinier-Preston zones 8-95811
 Al-Zn alloys, room temp. decomp. of metastable phases precipitated at 200°C 8-84814
 Al-Zn-Mg, plastic instability rel. to grain boundary failure at low temps. 8-56702
 Al-Zn-Mg alloys, decomp. kinetics from Young's modulus obs., microprocesses (German) 8-64522
 Al-Zn-Mg alloys, decomposition kinetics, resistivity meas., extended jump model 8-84766
 Al-Zn-Mg-Ti, Ti effect on microstructure during ageing 8-64568
 Cu-Be (0.99 wt.%), direct obs. of small Guinier-Preston zones 8-72776

Gunn devices

see also *Gunn diodes*

- GaAs, epitaxial layers on conductive substrate, elec. characterisation 8-91790
 GaAs, maximum electric field in high-field domain 8-79996
 GaAs transferred electron devices, ohmic contacts 8-52082
 InP, maximum electric field in high-field domain 8-79996

Gunn diodes

- n-GaAs, AuGe contact, total resist. meas., temp. dependence 8-76146

Gunn effect

see also *limited space charge accumulation; negative resistance effects*

- two-dimensional semiconductor, Gunn instability 8-84305
 n-GaAs, diffusion coeff., Monte Carlo calc., rel. to trapped domain behaviour 8-56152
 GaAs:O, slow domains, origin 8-60132

Gunn effect devices see *Gunn devices***Gunn oscillators**

- injection laser integration with Gunn oscillator on semi-insulating GaAs 8-71232

guns, plasma see *plasma guns***gyration** see *rotation***gyromagnetic effect**

see also *gyromagnetic ratio; magnetic resonance*

- gyroscope, coupled to rotating ring, Barnett effect 8-86260

gyromagnetic ratio

see also *g-factor; magnetic resonance*

- even-even nuclei, backbending mechanism anal. (Chinese) 8-78247
 proton, in weak field, review of results of last 15 years 8-57887

gyroscopes

see also *navigation*

- angle velocity meas., precision increase, using structural redundancy (Russian) 8-49804
 astatic, natural frequencies, elastic cardan suspension (Russian) 8-51056
 astatic gyroscope with elastic cardan suspension, dynamics (Russian) 8-63273
 Barnett effect, in gyroscope, coupled to rotating ring 8-86260
 body dither laser gyro, scale factor nonlinearity 8-79062
 cardan suspension, geometric interpretation of condition for regular precession (Russian) 8-86148
 dynamically tuned precession, linear acceleration effect on stability (Russian) 8-62193
 electrostatic, geometry of suspension, max. rigidity case 8-62072
 fibre optic ring interferometer gyroscope, Fresnel drag effect 8-79142
 gyrodamper, passive satellite attitude control system appl. 8-96379
 gyrohorizon with harmonic and random swinging, error anal. (Russian) 8-62194
 gyrostabilizer, nonlinear suspension bearing, dynamic error (Russian) 8-75063
 gyrostat, nonregular precessions in a Newtonian central field (Italian) 8-81825
 gyrostat inertial motion, ang. velocity hodographs (Russian) 8-86137
 gyrostat inertial motions, hodograph eqns., dividing motion (Russian) 8-86138
 gyrostat motion, analytic props. of soln. (Russian) 8-86132

gyroscopes continued

- Lagrange, system of n, stability of uniform rotation (Russian) 8-86136
 Lagrange gyroscope type body, periodic solns. to eqns. of motion (Russian) 8-86142
 Lagrangian hodographs of ang. velocity (Russian) 8-86133
 Lagrangian moving ang. velocity hodograph (Russian) 8-86134
 laser vibratory gyroscope, steepness characts. and S/N ratio anal. (Russian) 8-59070
 motion in cardan suspension, investigation (Russian) 8-73985
 motion in Newtonian gravitational field, averaging method (Russian) 8-65766
 nonholonomic error (Russian) 8-63272
 nonrigid cardan suspension, shock absorber parameters choice (Russian) 8-89473
 pendulum-gyroscopic platform stabilised in inertial space, autonomous determ. of coords. (Ukrainian) 8-65760
 precession, starlight aberration, calcs. in stationary metrics 8-54284
 Raytheon laser gyroscope using MnBi magnetic mirror 8-79064
 Raytheon multioscillator ring laser gyroscope 8-79063
 resonant motion of gyroscope with contactless suspension on vibr. support (Russian) 8-51054
 ring laser gyroscope for missile guidance using magneto-optic bias mirror 8-79061
 ring laser gyroscopes, multioscillator approach to locking problem 8-79042
 superconducting, trapped-flux spin-down torques 8-57941
 terrestrial gyrocompass, dry friction anal. (Russian) 8-77899
 two-axes indicating gyrotilastabiliser stability anal. (Russian) 8-54360
 vertical gyroscope theory, nonlinear problem (Russian) 8-51053

H-centres

- alkali metal halides, irradiated, annealing 8-92494
 diamond, type Ib, electron irradiated, migration of N, optical absorption meas. 8-56505
 KBr, efficiency of creation of X₃⁻ centres in X-rayed alkali halides (Russian) 8-71731
 KBr, H-centre struct., hyperfine interactions 8-79611
 KBr, X-irrad., activation energy and thermal diffusion 8-72606
 KBr:Rb, H-centre interaction with Rb⁺ ion 8-75662
 KCl crystal, F-H centre formation by opt. conversion of self-trapped excitons 8-91335
 KCl, efficiency of creation of X₃⁻ centres in X-rayed alkali halides (Russian) 8-71731
 KCl, H-centre struct., hyperfine interactions 8-79611
 KCl, X-irrad., activation energy and thermal diffusion 8-72606
 KCl:Ca,H, ENDOR studies of localised vibrations of substitutional atomic H 8-80248
 KCl:I(Br), colouration under two-photon excitation, absorption spectra 8-84618
 KI, recomb. luminesc. of H-centre and F-centre electrons (Russian) 8-80402
 LiF:Na⁺ H₂-centre struct., hyperfine interaction 8-79611
 MgO, radiation induced O interstitials, EPR meas. 8-55866
 NaCl, efficiency of creation of X₃⁻ centres in X-rayed alkali halides (Russian) 8-71731
 RbCl:Ca,H, ENDOR studies of localised vibrations of substitutional atomic H 8-80248

H I regions

- 21 cm line, profiles and brightness temps. rel. to galactic shocks 8-54042
 absorption lines high-resolution mapping in direction of NGC 2024, M17, W49 and Orion A 8-81667
 cloud model, intragalactic factor in external objects apparent distrib. 8-96552
 in dwarf spheroidal galaxies, upper limits to H I content 8-57633
 elliptical galaxies, search for H I emission 8-65681
 G48.6+0.0 direction, H I absorpt. 8-85996
 galactic centre, expanding H I features rel. to nuclear eruptive phenomena 8-57647
 galactic H I 21 cm line survey, low latits. 20-42° galactic longit. 8-57637
 galactic H I regions, emission-absorpt. obs. from Arecibo 8-57610
 galactic longitude-velocity map 8-86023
 galactic rotation curve from H I maps, mass distrib. 8-96529
 in galaxies peripheral regions, ionising background radiation effects on H I density 8-65729
 HVC 132+23-211, small high-velocity cloud, detailed struct. 8-89241
 IC 443, supernova remnant, negative vel. H I condensations obs. 8-54016
 II Zw 70/II Zw 71, compact galaxies, H I maps, tidal interactions 8-96531
 intercloud winds, theory from two-phase interstellar medium model 8-85991
 in late-type galaxies, H I obs. rel. to integral props. derivation 8-86015
 in LMC, super-giant H I+H II shells obs. 8-86012
 M33, H I large-scale struct. 8-96539
 M51 system, extended H I obs. 8-89253
 in M 31, H I density distrib. rel. to spiral struct. morphology 8-65690
 NGC 1052, elliptical galaxy, H I obs. 8-69873
 NGC 3628, detection of emerging H I plume at 21 cm wavelength 8-54038
 NGC 4631 group of galaxies, intergalactic neutral H rel. to tidal interactions model 8-54059
 NGC 4631/NGC 4656, interacting pair of galaxies, neutral H aperture synthesis obs. 8-54043
 Orion A, C recomb. lines and H I clouds obs. 8-57605
 PHL 938, quasar, continuum spectrum reddening and dust/gas ratio 8-96561
 spiral galaxies, nearly edge-on illusionary warps in H I discs 8-65682

H II regions

- anisotropic H II regions with axial symmetry, models 8-85993
 chemical composition of galactic and extragalactic H II regions 8-93359
 Crab Nebula, magnetoparametric instabilities 8-61727
 30 Doradus complex, in LMC, UV reddening law 8-96516
 30 Doradus region, in LMC, interstellar extinction and stellar population 8-96517
 30 Doradus region, in LMC, radio model 8-96523

H II regions continued

DR 21, ethynyl radical abundance and distrib. 8-65664
 dusty H II regions, non on-the-spot (OTS) models 8-85995
 element abundances, model anal. of ionisation correction formulae 8-57623
 elemental abundances, empirical determ. method test 8-61908
 emission line objects in LMC (*French*) 8-69875
 expanding gas shells in Canis Major-R1 and OB1 associations 8-93336
 G12.2-0.1, radio and IR obs. of OH/H₂O source 8-57620
 G333.6-0.2, 2 μ m line emission detect. 8-54017
 G333.6-0.2, G298.2-0.3, southern compact H II regions, IR emission lines obs. 8-96522
 G37.7+0.1, double recombination line galactic thermal source, obs. at 1400 and 2371 MHz 8-69897
 G45.1+0.1, 8-13 μ m spectrophotometry of compact H II region 8-65672
 G48.6+0.0, galactic H II region, direction, H I, OH and H₂CO absorpt. line meas. 8-85996
 G49.5-0.4 (W51), high resolution obs. at 5 and 15 GHz 8-54065
 galactic and in spiral galaxies, ring-like distrib. (*Russian*) 8-93424
 galactic centre, expanding H II arc and nuclear turbulent ionised gas 8-57647
 galactic centre, extended thermal component, broad-line H9 α emission 8-77598
 galactic new H II regions and exciting stars, obs., rel. to spiral struct. 8-61900
 galactic nucleus, 6 cm recomb. line emission vels. 8-69885
 giant H II regions, radio maps interpretation 8-85994
 HD 153919, X-ray source, IUE UV spectrum obs. rel. to circumstellar H II region 8-96569
 IC 1318, giant H II region, large-scale line splitting discovery 8-96521
 IC 1795/1805, H II regions IR luminosity compared with exciting star total luminosity 8-96519
 IC 1805, radio identification of IR object assoc. with passage of shock front 8-93369
 inhomogeneities in high excitation H II regions, effects on spectra 8-54007
 ionisation and temperature structure, influence of star, gas density and chemical comp. 8-61911
 ionization front, oblique refraction 8-54025
 IR line emission, airborne obs. 8-93353
 IR obs. of H II regions in M33 galaxy 8-61923
 in LMC, far IR obs. 8-81671
 in LMC, four super-giant H II shells obs. 8-86012
 LMC, giant H II ring obs. rel. to energetic stellar winds 8-77593
 M101, spectra of H II regions, comp. gradient across spiral galaxy 8-65683
 M17, large-scale vel. components, insect-eye Fabry-Perot obs. 8-93380
 M43, emission nebula around NU Orionis, radio and IR obs. 8-54012
 in M 31, distrib. rel. to spiral struct. morphology 8-65690
 Magellanic Clouds, chem. comp. of H II regions, photoelec. spectrophotometry 8-77607
 Magellanic Clouds, H II regions chem. comps. 8-93381
 NGC 2024, interstellar ¹⁶OH/¹⁸OH abundance ratio obs. 8-54024
 NGC 2237, Rosette Nebula, decametric obs., brightness temp. contours 8-57615
 NGC 2359, radial vels. and internal motions in ring-type nebula 8-81678
 NGC 5471, in galaxy M101, gas and stellar mass determ. (*Russian*) 8-93426
 NGC 6334 and 6357, distances from early type star photometry 8-85998
 NGC 7822 (W1) optical studies of kinematics rel. to supernova remnant struct. 8-54028
 Orion A, C recomb. lines and H I clouds obs. 8-57605
 Orion A, H I absorpt. lines high resolution mapping 8-81667
 Orion Nebula, C I IR forbidden emission lines obs. 8-85987
 Orion Nebula, ethynyl radical abundance and distrib. 8-65664
 Orion Nebula, IR obs. by Fourier transform spectroscopy 8-61747
 Orion Nebula, photographic obs. in H α , H β and He I 10830 Å lines 8-81669
 Orion Nebula, search for vibrationally excited H₂ emission 8-93346
 λ Orionis, absorption shell and core 8-77590
 λ Orionis A, far UV flux, emission line obs. of surrounding H II region 8-93303
 radio recombination line obs., of C and H from 10 regions 8-93360
 RCW 36, H₂CO and OH obs. in nearby mol. cloud 8-69862
 RCW 38, RCW 57, interstellar ¹⁶OH/¹⁸OH abundance ratio obs. 8-54024
 S104, 609 MHz aperture synthesis obs. 8-57618
 S106, radio obs. of assoc. mol. cloud, CO, HCO⁺, HCN, OH and formaldehyde lines 8-61906
 Sharpless 155 nebula and Cepheus OB3 association, thermal radio emission obs. 8-96514
 Sharpless H II regions, small-scale struct. at 4.995 GHz, high-resolution catalogue 8-61755
 southern H II regions, NH₃ obs. 8-69863
 W12 (NGC 2024), H I absorpt. lines high resolution mapping 8-81667
 W33, H II complex, high resolution obs. at 2.8, 6, 18 and 21 cm wavelength 8-57619
 W3(OH) and surrounding diffuse ionised gas, radio recomb. line obs. 8-93371
 W3 (OH), non-metastable NH₃ absorption at 23.1 GHz, first obs. 8-65677
 W40 and W48, near IR and CO mm wavelength obs. 8-65667
 W51, first optical detection, rel. to galactic spiral struct. 8-61900
 W75-DR 21 region, structure of CO in molecular cloud complexes 8-89232
 weak shocks, properties 8-93348
 CH, obs. of 3.3 GHz ground state transitions 8-77592
 Fe abundances in gaseous nebulae, from forbidden Fe III and Fe VI lines intensities 8-53806
 H₂O maser lines very-high-velocity satellite features generation by stimulated Raman scatt. 8-73746
 H₂O sources, spectra and autocorrel. anal. 8-65713
 He II abundance and IR excess 8-86000

H II regions continued

OH and H₂O masers assoc. with compact H II regions, model 8-81666
 OH, radio lines absorpt. obs. in galactic radio sources 8-54068
 S abundance from S III 6312 Å forbidden line, using ionization correction scheme 8-54018

hadron classification schemes
 SU(4) 20-plet of vector mesons (*Russian*) 8-58220
 topological expansion for baryons and mesons, Veneziano scheme 8-70335

hadron current
see also current algebra
 nuclear currents, microscopic anal. of elementary particle description 8-82304
 semi-leptonic weak interactions, book contrib. 8-78162
 three triplet quark model with observable colour, hadron weak current, $\Delta T=1/2$ rule (*Russian*) 8-74219
 weak charged V-A current 8-74179
 μ radiative capture, appl. to nuclear spin and isospin doublets 8-82320
 νp high energy interactions, vector meson diff. prod., charged and neutral current 8-54625
¹²C(μ^- , ν_μ)¹²B, appl. of μ^- radiative capture to nucl. spin and isospin transitions 8-86511

hadron decay
see also baryon decay; meson decay
 cascade generation, 100-10000 GeV, anomalous effects (*Russian*) 8-70366
 hadrons as compounds of bradyons and tachyons, ground state and decay anal. 8-58156
 multiparticle decay theoretical models for heavy hadrons containing charmed quarks 8-70344
 quark model and SU(4) 8-62366

hadron-deuteron interactions
see also hadron-deuteron scattering; hyperon-deuteron interactions; meson-deuteron interactions; proton-deuteron interactions
 polarised deuteron, h+D \rightarrow p+X, S and D wave functions, nuclear core hypothesis 8-62417
 d breakup, exotic final state interaction, intermediate Δ , ΔN threshold parameters 8-50043
 nd \rightarrow pnn, 800 MeV, quasielastic charge exchange, p spectra meas. 8-70389
 D+hadron, inclusive π , N spectra in high energy hadronic reactions, d fragmentation region (*Russian*) 8-54809

hadron-deuteron scattering
see also hadron-deuteron interactions; hyperon-deuteron scattering; meson-deuteron scattering; proton-deuteron scattering
 inelastic shadow correction for hadron+deuteron elastic scatt., complex cut integral 8-70347
 dd collisions, 4.3, 6.3, 8.9 GeV/c, d spectra high momentum struct., multiple NN scatt. model 8-89727
²H(n,n)²H, polarised n, 12 MeV, analysing power, similarity with (p,p) scatt. 8-70514

hadron electroproduction
 charmed particle prod. in e⁺e⁻ annihilation 8-78199
 cumulative π , electroproduction from d, effect of rescatt., scaling effects (*Russian*) 8-74265
 deep inelastic processes book contrib. 8-82222
 impulse approximation in QCD, partons p_i distrib., appl. to deep inelastic electron scatt. 8-62368
 inclusive electroproduction of hadrons, virtual photon prod., quark fragmentation region 8-54634
 Landau's hydrodynamic model, further aspects 8-82173
 nucleus-electron hadron electroproduction 8-66267
 QCD, charm contrib. to electroprod. struct. functions 8-58170
 QCD, transverse momentum of jets in electroprod. of hadrons 8-62367
 resonance states below 2.2 GeV observed in e⁺e⁻ annihilations 8-78197
 rising hadronic cross section effects on EM processes, generalised vector dominance formulation 8-93868
 scale breaking parton model for electron and neutrino deep inelastic scatt. 8-66122
 vector meson electroprod. in deep inelastic e and μ scatt. 8-78184
 $\Delta(3,3)$ region, low hadronic mass, Δ , τ , and nucleon axial vector form factors 8-74259
 e⁺e⁻ \rightarrow HX, associated production of gluonic jets and heavy mesons 8-93892
 e⁺e⁻ \rightarrow hadrons, azimuthal correlations, quantum chromodynamics anal. 8-70382
 e⁺e⁻ \rightarrow hadrons, jet struct. in the energy range 3.1-9.5 GeV 8-89725
 e⁺e⁻ \rightarrow hadrons, multiplicity, scaling, inclusive spectrum, simple hadron cascade model 8-66135
 e⁺e⁻ \rightarrow hadrons, search for narrow resonances in 1.45-1.92 GeV mass region 8-89724
 e⁺e⁻ inclusive hadron prod., neutral weak currents 8-50041
 eN \rightarrow e π^{\pm} X, sum rules for polarised N 8-89718
 eN \rightarrow e π N, π form factor determ. 8-66128
 ep \rightarrow ep π^0 , elastic π^0 electroprod. above resonance region, cross section, direction 8-62412

hadron-hadron interactions
see also baryon-baryon interactions; hadron-hadron scattering; meson-baryon interactions; meson-meson interactions
 asymptotic behavior of multiplicities in theories with Koba-Nielsen-Olesen scaling 8-78083
 baryonium interactions, string model, dual amplitudes (*Russian*) 8-54620
 charm prod. cross section and particle lifetimes, Monte Carlo anal. 8-89679
 complex momenta eikonal approx., hadron-nucleus collisions at asymptotically high energies (*Russian*) 8-74294
 cosmic rays, models of hadronic collisions rel. to EAS computer simulation 8-57415
 Drell-Yan contrib. to lepton pair prod., incident hadron qq correlation function 8-89668
 Drell-Yan dynamics, lepton pair from qq collision, energy scaling breakdown 8-54610
 elastic quark-quark scatt. model, relations for hadron pairs 8-66092
 gluon fusion model, hadronic charm prod. 8-66081

hadron-hadron interactions continued

- hadronic atom, HN interactions, multiple scatt. expansion for level shifts 8-70978
 hadronic massive lepton pair prod., theory review, Drell-Yan model 8-89752
 high energy inelastic hadron reactions, π prod., scaling law, fireball model 8-74287
 high-energy hadronic collisions, classical space-time concepts 8-70420
 high-energy inclusive spectra near phase-space boundary using quark fragmentation model 8-89658
 inclusive $3\pi^-$ correlation functions, Mueller scheme with Bose-Einstein statistics 8-93915
 inclusive production of hadrons in particle-particle collisions at high energies, scaling low 8-54656
 large p_t jet prod. in hadronic collisions, QCD calc. for inclusive cross section 8-86439
 lepton pair prod. in hadron-hadron collision 8-66138
 Lepton pair production cross section using Drell Yan formula, sum rules, moments 8-54611
 lepton pair production in hadronic collisions, parton model and scaling approach 8-82150
 lepton prod. with large transverse momentum, SU(6) parton model 8-89673
 multiplicity, semi-empirical formula 8-58210
 pomeron building mechanism, in fragmentation region 8-89687
 QCD quark-gluon plasma, hadronic prod. of leptons, photons and ψ (Russian) 8-89672
 QCD quark-gluon plasma, hadronic prod. of leptons, photons charm and ψ 8-89669
 quantum chromodynamics, hadroprod. of lepton pairs and real photons 8-50056
 quantum number distrib. and fluctuations in multiparticle prod., quark-parton model 8-82249
 scale invariant variable (Russian) 8-82227
 structure function relations, lepton pair processes at large transverse momenta 8-82214
 two-particle correlations involving neutral strange particles, at 250 GeV/c 8-82242
 μ pair prod., QCD ang. correl. 8-49976
 μ pair production in hadron-hadron collisions, gluon effects, QCD predictions 8-78148

hadron-hadron scattering

- see also *baryon-baryon scattering; hadron-hadron interactions; meson-baryon scattering; meson-meson scattering*
 correlational anal. of inelastic hadronic processes, multicluster mechanism (Russian) 8-89684
 iteration models, elastic reactions beyond diffraction peaks 8-93839

hadron interactions see *hadron-deuteron interactions; hadron-hadron interactions; lepton-hadron interactions; photon-hadron interactions***hadron leptonproduction**

- see also *baryon production; hadron electroproduction; meson production*
 deep inelastic hadron leptonproduction on nuclei, inclusive hadron final states 8-54741
 diquark jets in leptonprod. and large p_t reactions, fragmentation functions 8-82149
 quark fragmentation into mesons, statistical model, vector meson contrib. 8-54639
 scale breaking parton model for electron and neutrino deep inelastic scatt. 8-66122
 $lp \rightarrow l'hX$, azimuthal depend., parton model calc. 8-93887
 $v(\bar{v})N$, hadronic system charged particle multiplicities and transverse momentum distrib. 8-78165
 $Ne + \nu_\mu(\bar{\nu}_\mu)$, inclusive prod. of hadrons, preliminary data 8-89853

hadron photoproduction

- see also *baryon photoproduction; meson photoproduction*
 jet struct. at large transverse momentum 8-82225
 rising hadronic cross section effects on EM processes, generalised vector dominance formulation 8-93868
 total cross sections for $E > 4$ GeV, review 8-78186

hadron production

- see also *baryon production; hadron leptonproduction; hadron photoproduction; meson production*
 asymptotic behavior of multiplicities in theories with Koba-Nielsen-Olesen scaling 8-78083
 $C Ne + \nu_\mu(\bar{\nu}_\mu)$, inclusive distrib. of produced hadrons 8-89854
 cluster concept in multiple hadron prod. 8-66177
 composite model of quarks, large P_t hadron prod. 8-62472
 elastic quark-quark scatt. model, relations for hadron pairs 8-66092
 Feynman scaling, multihadron prod. through intermediate reson. 8-78152
 fragmentation in quark combinatorics, hadron prod. processes (Russian) 8-89671
 high-energy cosmic-ray components in atmosphere, scaling features 8-93062
 long-range correl., overlapping independent emission 8-82141
 multiparticle production of nuclei, intranuclear cascading of secondaries 8-66262
 nonperturbative QCD effects at large momentum transfers, e^+e^- annihilation to hadrons 8-82226
 polarisation in hadron cumulative prod. and large transverse momentum processes (Russian) 8-74293
 QCD perturbation theory, quark decay functions, heavy hadron prod. 8-62364
 QCD predictions for large p_t hadron prod. by polarised hadrons 8-82148
 quantum number distrib. and fluctuations in multiparticle prod., quark-parton model 8-82249
 quarkonium decay, gluon jets and gluonic resonances, QCD test 8-93841
 s -dependence of proton fragmentation by hadrons, 30-250 GeV/c 8-74291
 s -dependence of proton fragmentation by hadrons 4-24 GeV/c 8-74290
 string junction model, large p_t hadron prod. 8-62380
 $e^+e^- \rightarrow$ hadrons, 53 GeV², π^- and K^- cross sections, scaling 8-78201
 μN scattering, 2.8-4.5 GeV, struct. functions and charge ratios 8-74264
 pp interactions, hadron prod. 23.4 to 63.4 GeV, charged multiplicity density for various p_t 8-70414

hadron scattering see *hadron-deuteron scattering; hadron-hadron scattering; lepton-hadron scattering; photon-hadron scattering***hadronic atoms**

- see also *mesic atoms*
 antiprotonic H atoms, first obs. of L X-rays 8-90111
 level shifts, multiple scat. expansion 8-70978
 low-energy hadron-nucleus interaction theory 8-70977
 nuclear interactions of strange particles and resonances, conf. Warsaw, Poland (Ict. 1976) 8-70406
 ponium, isospin anal. of energy shifts 8-62961
 pp , isospin anal. of energy shifts 8-62961
 $p\bar{p}$ system, possible evidence for narrow bound states below threshold, mesonic struct. 8-62443
 Σ^- hyperonic atom, nuclear capture rate calcs. using $\Sigma^- p \rightarrow \Gamma n$ amplitude 8-62962
 H , isospin anal. of energy shifts 8-62961
 3He , isospin anal. of energy shifts 8-62961
 ^4He-p , X-ray spectrum, energies and relative intensities for 3d and 2p levels 8-70979

hadrons

- see also *baryon resonances; baryons; hadron classification schemes; hadron current; hadron decay; meson resonances; mesons*
 form factors, axiomatic local constraints (Russian) 8-58190
 gravitational interaction, band spinor representation of GL(n,R) 8-50000
 relativistic harmonic oscillators and hadronic struct., 1st year graduate quantum mechs. 8-61971

haemodynamics

- see also *blood*
 aorta entrance, flow anal. 8-69124
 aorta model, two chambered, viscoelastic, press. estimation in ascending and descending aorta 8-77076
 aortic dynamics in man, analogue simulation model 8-80903
 aortic valve prosthesis, wall shear stress in Bjork-Shiley and Starr-Edwards types in vitro (German) 8-81067
 arterial haemodynamic transfer function calc. from Doppler US flowmeter waveforms 8-61235
 arterial pressure automatic determ., using microprocessor based instrument, Dinamap 8-96108
 arterial pressure modulator for perfusion circuit of isolated organ (French) 8-81004
 arterial pressure-flow relationships in anaesthetised dog 8-69120
 arterial pulse wave vel. meas. by Doppler shifted US and EM flowmetry 8-69229
 arterial system least energy regulation 8-53434
 arterial system math. model, press.-flow relationships 8-53435
 artificial mitral valves, insufficiency, press. and work losses (German) 8-88764
 artificial ventricle, all-pneumatic system, cardiovascular dynamics simulation 8-81082
 atrial pacing stress test quantification, normal, abnormal values, coronary artery disease in man 8-85449
 atrio-aortal left ventricular bypass, haemodynamics in calf (German) 8-88763
 Baylor left ventricular bypass pump, calf expts. 8-73295
 blood flow measurement by US Doppler method, computer-aided determ. of angles (German) 8-80931
 blood pressure instruments, direct systolic/diastolic meas., review 8-69234
 blood pressure instruments, noninvasive arterial meas. using US Doppler effect 8-69167
 blood pump implantations in animals, regulation mechanisms in circulation and fluid balance (German) 8-81064
 blood velocity noninvasive meas. in large vessels, broadband pulsed Doppler US system 8-61224
 capacitoplethysmography for heart and lung meas. (Japanese) 8-53465
 capillary blood flow, long-term effects of ^{60}Co gamma and fission spectrum neutrons, mouse 8-80927
 cardiac output and shunt calc. from dye dilution curves using automated catheterisation system 8-81023
 cardiac output control mechanism modelling (Japanese) 8-69133
 cardiac output measurement, in vitro comparison of six commercially available thermodilution systems 8-77135
 carotid thrombosis, canine model, ^{131}I fibrinogen for clot detect. 8-85363
 cerebral blood flow computer for use in angiogram theatres 8-73227
 cerebral regional blood flow meas. with ^{133}Xe , functional landscapes in brain 8-85356
 cerebral regional O_2 distrib. model during continuous inhalation of $^{15}O_2$, $C^{15}O$ and $C^{15}O_2$ 8-65108
 computer system SYSCORMORAM for haemodynamic and cineangiographic data treatment 8-81030
 computer-aided monitoring after open-heart surgery, appl. to adrenaline effects meas. 8-81059
 coronary sinus blood flow on-line computerised assessment by thermodilution 8-81024
 dielectrography methods and apparatus, recording capacitance changes due to blood vol. fluctuations 8-57046
 Doppler sonographic flow meas. over small cross-sections in vitro and in vivo (German) 8-88729
 Doppler US blood velocity meas., phase-locked loop technique 8-61234
 drug-carrying microspheres, intravascular mag. guidance 8-73188
 erythrocyte sedimentation rate, for teaching 8-49610
 flow imaging with nucl. mag. reson. spin echoes 8-85330
 flow speed and quantity determ. from digital angiograms (German) 8-92690
 flowmeters, digital 2D full range Doppler velocity meter for cardiovascular diagnosis 8-88731
 forced oscillations in large vessels of circulatory system, dog's arterial blood flow anal. 8-85329
 impedance plethysmography, influence of erythrocyte vel. 8-61238
 indicator-dilution meas. of flows and vols. in patients with transposition of great vessels 8-61209
 intra-aortic balloon heart assist device fluidic drive system 8-53566
 laminar blood flow, gas and heat transport, platelet and protein diffusion 8-92669
 left ventricular assist device testing using calf model 8-73296

haemodynamics continued

- left ventricular function, normal and abnormal, vel.-strain relationship 8-69119
- left-heart haemodynamics, mathematical model 8-65074
- local circulatory system characterisation by CW Doppler US flow meas. 8-57109
- lung numerical modelling, human 8-80911
- lung perfusion determination by dilution principle with expiration detection of indicator (*German*) 8-85326
- lung perfusion determination using O isotopes and dilution principle (*German*) 8-85327
- microcirculation semiquantitative demonstration using US noninvasive meas. method (*German*) 8-85348
- microkymography, flow vel. meas. in microvascular bed after exdotoxin administration (*German*) 8-77173
- microwave heating of tissue, effect of surface cooling and blood flow 8-57038
- models, numerical integration method for improving soln. stability 8-69118
- monitoring of blood vol. change in menstruation, vaginal photoplethysmographic transducer 8-92733
- non-Newtonian fluids, particle movement, appl. to dyeing and haematology (*German*) 8-87369
- oxygenator using microchannel membrane, transport and flow phenomena 8-69253
- physical principles, comparison of meas. methods (*German*) 8-92735
- pressure for extracorporeal circulations, elec. sensor (*German*) 8-92721
- pressure measurement, blood gas anal., silicone rubber catheter operating mechanism (*Japanese*) 8-61273
- prosthetic heart and mock circulatory system, math. model 8-81080
- prosthetic heart valves, disc, ball and tilting disc types, fluid stresses in vitro 8-81078
- prosthetic heart valves, rigid leaflet and caged-ball types, diastolic ventricular mechs. 8-81079
- pulmonary blood flow, spatial distribution in dogs in increased force environments 8-92664
- pulsative flow, digital simulation by finite element method 8-92670
- pulsed Doppler blood velocity meter readout 8-69158
- pump, experiences with miniaturised press.-controlled servo (*German*) 8-88762
- radionuclide mean clearance time transverse section imaging 8-73222
- red cell flexibility, whole blood filtration technique using 5 μm pores (*German*) 8-57030
- reduced hydrodynamic drag of normal human blood 8-61210
- renal artery with deformed vascular wall, blood flow 8-65063
- retinal blood flow, laser Doppler meas. 8-69174
- retinal internal circulation visualisation using Purkinje's methods 8-69043
- RF EM noninvasive transcutaneous measurement technique (*Italian*) 8-85352
- rheological and thermophysical fluid props., physicochem. composition depend. 8-80902
- shear flow, thixotropic fluid appl. (*Russian*) 8-87365
- thrombophlebitis diagnosis, reliability of Doppler and impedance techniques 8-77144
- US blood flow spectral anal. using coherent optics 8-53459
- US Doppler velocimetry for 3D blood flow meas. 8-88730
- US flowmeter data processing, transfer function modelling of arteries 8-61225
- US implantable CW Doppler blood flowmeter, optimal system design 8-53460
- valveless elastic tube, pumping effect, model (*German*) 8-59493
- vascular interface system for automation of haemodynamic monitoring and therapy 8-81054
- velocity meas. in microvessels using video correl. system 8-53543
- velocity measurement using catheter, cross correl. technique 8-80943
- venous blood flow visualisation using dynamic leg scintigraphy with large field-of-view scintillation camera 8-73215
- ventilation-perfusion ratio distrib. determ. from inert gas data with enforced smoothing algorithm 8-61208
- ventricular function computer simulation, development of model and parameter estimation 8-53439
- ventricular wall dynamics and obs. on blood flow 8-80896
- video-tracking of micro-circulation, appl. of bit-slice processors (*German*) 8-88749
- viscosity factors in severe nondiabetic and diabetic retinopathy 8-65069
- viscosity variations associated with hyperlipoproteinaemia, rel. to cardiovascular risk factors (*German*) 8-57031

haemoglobin see *proteins***hafnium**see also *nuclei with*

- atom, even config., parametric calcs. 8-82631
- atom, partial level density, statistical props. of atomic energy levels 8-70732
- calciothermic, electrorefining 8-68647
- high temperature thermophysical properties 8-91404
- implantation of Si, Al, Hf, Ta into InP and GaAs, form. of protective oxide 8-79622
- solid state phase transformation $\alpha \rightarrow \omega$, exam. of phase transformation kinetics under static, and dynamic pressures 8-80541
- solvent extraction and complex formation with tridentate organophosphorous compounds 8-76853
- thermotransport and thermopower of O₂ 8-76055
- β -Hf, electrotransport and diffusion of Ta impurities (*German*) 8-87826
- α -Hf, electrotransport of O impurities (*German*) 8-87826

hafnium alloyssee also *hafnium compounds*

- Co₂HfSn-Fe, dil., Heusler alloy, Fe hyperfine fields, Mossbauer obs. 8-68424
- Cr-M, optimum alloying with rare earth metals, Ti, Zr, Hf, Nb, Ta 8-68651
- Hf-Co, phase diagram, X-ray diffr., thermal anal. and metallography obs. 8-60652
- Hf-Co-Ga system, crystal atomic struct. and phase equilibria (*Ukrainian*) 8-84772
- Hf-Mo-C system, isothermal section of phase diag. at 1700°C 8-68674

hafnium alloys continued

- Hf-Nb (30 to 50 at.%) exam. of beta phase decomposition processes 8-76674
- HfP₂, corrosion resist. and elec. cond., bulk and film samples 8-72285
- HfV₂, supercond., dielec. phase transition (*Russian*) 8-64168
- HfV₂, supercond. compound, thermal expansion at low temp. 8-76189
- Hf₂Zr_{1-x}, elec. quadrupole interactions at ¹⁸¹Ta impurities, TDPAC meas. 8-76364
- Hf_{1-x}Zr_xV₂, lattice const. at 4K and room temp., phase division at $x=0.4$ 8-51474
- Hf_{0.5}Zr_{0.5}V₂H₂(D₀), enhanced supercond. transition temp. on H(D) additions 8-80083
- Nb-Hf, single cryst. elastic const. 77-298K 8-84879
- Ni-Hf, wetting of AlN, effect of alloys exam. 8-80710
- Ta-W-Hf (8.2 wt.%), T-111, O₂ absorption, effect on lattice parameter and specimen dilation 8-83958
- V₂(Hf,Zr), Laves phase compounds, electrical resistivity, temperature dependence 8-76047
- V₂Hf_{1-x}Ta_x, C15 supercond., electronic and lattice props. 8-68110
- V₂HfZr, C-15 cryst. struct. supercond. props. 8-64173

hafnium compoundssee also *hafnium alloys*

- tetrahallides, struct., force field and Coriolis const. calcs. 8-86843
- HFSe₂, optical phonon modes and localised effective charges, reflection spectra 8-76453
- HfC, single crystal growth by plasma heating 8-60569
- HfO₂, chem. induced elec. field gradient, perturbed ang. correl. obs. 8-80257
- HfO₂ protected Al mirror, high refl. 8 to 12 μm , normal to high incident angles 8-79090
- HfO₂, stabilised, low temp. induced centres, ESR meas. 8-72409
- HfO₂, Y₂O₃-stabilised, solid soln., Raman scatt. anal. of struct. transform. 8-88312
- HfO₂-Gd₂O₃, phase relations 8-72769
- HfO₂-Y₂O₃, solid soln., diffuse X-ray scatt. by vacancies 8-71728
- HfO(H₂PO₄)₂·H₂O, chem. induced elec. field gradient, perturbed ang. correl. obs. 8-80257
- HfP₂O₇, chem. induced elec. field gradient, perturbed ang. correl. obs. 8-80257
- HfS, equilibria, nonstoichiometry and elec. props. temp. depend. (*French*) 8-64053
- HfSiO₄·U⁴⁺(U⁵⁺), opt. spectra 8-88334
- Hf₂Ta_{1-x}C, thermal cond. and diffusivity, 1000-2200°C, elec. cond. 8-91491
- K₈Hf(MoO₄)₆, X-ray structural investigation 8-79597
- La₂Zr₂O₇-La₂Hf₂O₇ system, cryst. struct., phase diagram 8-83806

half-lives (radioactive) see *radioactive decay periods***half wave rectification** see *rectification***halides**see also *compounds of individual elements, e.g. "tungsten compounds" and "organic compounds"*see also *alkali metal halides; halogens*

- Anderson-Gruneisen parameter, heavy metal halides 8-79715
- F-centre form. photochem., review 8-63763
- fluorides, muon Coulomb capture ratio 8-62959
- hexahalides, shapes and other props. 8-82647
- inert gas halides, triatomic, optical emission 8-66558
- inert gas monohalides, hyperfine interactions, struct., valence bond calcs. 8-66473
- ion transport 8-63878
- mixed metal chloride acousto-optical props. (*Russian*) 8-60419
- NMR spectra of halogen nuclei, shielding and quadrupole coupling const. 8-84487
- perovskite systems, ABX₃, cryst. chem., X-ray diffr. 8-95042
- XeF(CI)(Br)(I), covalent and ionic states, spectroscopic props., ab initio CI calc. 8-90092

Hall constant see *Hall effect***Hall effect**

- alkali metal-NH₃ solutions, metal-nonmetal transition Hall mobility, electrodeless meas. 8-56194
- carrier conc., temp. depend., computer data anal., effect of band parameter errors (*Russian*) 8-52006
- chemisorption on metal films, use of external mag. field, review 8-72003
- contactless Hall coeff. meas. in materials of small Hall angle in skin depth regime 8-86303
- disordered system, phononless HF Hall effect 8-87953
- education, Hall effect, positive voltage interpretation by electron motion 8-69945
- ferrite-semiconductor structure, resonance galvanometric phenomena in semicond. 8-87989
- ferroelectric crystal without centre of symmetry, photo-Hall effect (*Russian*) 8-60152
- ferromagnet, scattering-independent contribs. to Hall cond. 8-51957
- ferromagnetic metal, atomic layers, Pauli paramagnetism to band ferromagnetism transition thickness depend. 8-72377
- ferromagnetic semiconductors, carrier mobility, electron-two magnon scatt. Hall effect 8-51992
- film with unlike surfaces, magnetomorphic oscills., generalised Sondheimer model 8-56243
- graphite, low field Hall coefficient, effect of warped energy surfaces 8-68043
- graphite intercalated with nitrate, galvanomagnetic props. 8-76092
- impurities, conc. of C, O, Si 8-59832
- metal, asymmetric electron scatt., anomalous Hall effect in ferromags. (*Slovak*) 8-79986
- metal, irradi., containing self-interstitials and vacancies, electronic transport props. 8-60105
- metal, kinetic effects at high anisotropic strains, elec. transport props. meas. 8-54384
- metal, liq., tight binding theory of transport props., Ishida-Yonezawa approx. for single-band model 8-84190
- metallic thin films, size effect conductivity in transverse mag. field, Hall coeff. (*French*) 8-91787
- MHD, thermodiffusive mixture flows, Hall and ion-slip effects, uniqueness theorem 8-87415
- MHD flow over porous plate, Hall effect 8-51246
- MHD generator, Faraday type, current profile optimisation, electrode cond. profile 8-94939

Hall effect continued

MHD Poiseuille flow in annular channel with radial mag. field, Hall effect 8-67276
 MHD wave propagation in anisotropic media, electrical dissipation effects (*Japanese*) 8-87445
 mixed powder materials, mixing rule of Hall carrier mobility (*German*) 8-52008
 α -MnS, elec. props. meas. 8-87971
 noble metals containing rare earth impurities, magneto-transport props. 8-68015
 partially ionised plasma, thermal instability, Hall currents 8-63551
 powder combinations, compressed, mixing rules concerning Hall effect and Hall mobility (*German*) 8-84234
 semiconductor, galvanomagnetic-effects in strong elec. field 8-56163
 semiconductor, Hall effect in finite specimens of arbitrary lifetime and trap content 8-72175
 semiconductor, resolution of transport equation, by linearisation (*French*) 8-79989
 semiconductor with disordered regions, carrier mobility, theory and expt. 8-56166
 semiconductors, even dynamic photoelectric Hall effect 8-91708
 semiconductors, kinetic effects at high anisotropic strains, elec. transport props. meas. 8-54384
 SOS MOS devices, hole mobility under residual stress, Hall meas., valence band struct. 8-88039
 spatially inhomogeneous system, galvanomagnetic effects (*Russian*) 8-72129
 spin glass, Hall effect anomaly conditions 8-68267
 Ti-Te melt system, semicond., Hall effect 8-56164
 transition metals and alloys, noncrystalline 8-95280
 two-component layered system, with interpenetrating components, thermolec. and galvanomag. props. 8-79982
 Al alloy, dil., Hall coeff., calc. by 4-OPW approx. 8-76052
 $As_2(S,Se,Te)_3$ glasses, Hall mobility composition depend. 8-68042
 Au(Pd)-Zn, martensitic transformation, Hall coeff., specific elec. resistivity and X-ray powder diffraction 8-72774
 Bi film, carrier conc. and mobility, resist., galvanomag. and thermolec. meas. 8-52111
 $Bi_{1-x}Sb_x$, semicond.-semimetal transition, temp. and press. depend. of transport props. 8-76120
 C, amorphous, elec. cond. and Hall effect, temp. depend. 8-60141
 Cd, Hall effect and elec. resist., temp. depend. 8-64030
 Cd-Sb thin film prep. by vacuum deposition, elec. props. 8-92194
 $CdCr_2Se_4$:Cu, elec. props., temp. depend. (*Russian*) 8-72181
 $CdCr_2Se_4$:In, ferromag. semicond., carrier mobility, electron-two magnon scatt. Hall effect 8-51992
 $Cd_{1-x}Hg_xSe$ mixed cryst., electron mobility and electron scatt. 8-95296
 $Cd_{1-x}Hg_xTe$, fine-graded gap struct., electrophysical props. (*Russia*) 8-60144
 $Cd_{1-x}Hg_xTe$, IR detector appls., prep., elec. props. (*German*) 8-86332
 p-CdSe, Hall density and mobility, in Se vapour atm., 600-1100K 8-52014
 $CdSnP_2$, Hall mobility of holes 8-52015
 $CdSnP_2$:Cu, deep centres, emission transitions, polarisation (*Russian*) 8-84650
 CdTe:Cl, single cryst., photo Hall effect obs. 8-76094
 $Ce_{1-x}La_xAl_3$, extraordinary Hall effects, 4.2-300K, cryst. field interaction 8-79980
 Co, ZZ 8-68014
 $Cr_{1-x}Mn_xSi_2$, semicond. props. 8-79992
 $CrSi_2$, semicond. props. 8-79992
 $Cu_2Mo_8S_8$, normal state and superconducting property measurements 8-91660
 $Cu_xMo_6S_8$, Hall effect and magnetoresistivity 8-95400
 Er, Hall const. and elec. resist., 80-700K (*Russian*) 8-60110
 Fe film, amorphous and polycrystalline, Hall effect, resistivity and mag. moment 8-91786
 Fe film, Hall resist., effect of N impurity codeposition 8-64146
 Fe, ZZ 8-68014
 Fe-N alloy, dil., galvanomag. effects, 4.2-250K 8-87964
 Fe-Ni, (35 wt.%), transport props. and Invar features (*Russian*) 8-51973
 Fe-Si amorphous film, Hall const. and magnetoresistive effect 8-52105
 $Fe_{32}Ni_{36}Cr_{14}P_{12}B_6$, Metglas 2826A, Hall resistivity, effect of thermal cycling and annealing 8-56125
 $Fe_{29}Ni_{49}P_{14}B_6Si_2$, Metglas 2826B, Hall, elec. resist., magnetisation and heat capacity meas. 8-68019
 $Fe_{3+x}Si_{1-x}$, electron transport 8-91669
 $n-Ga_{1-x}Al_xSb$, transport phenomena in low and high mag. fields 8-80007
 GaAs, dual implantation of C^+ and Ga^+ , sheet resist. and Hall effect meas. 8-67728
 p-GaAs, electronic props. 8-68040
 GaAs, epitaxial layers, elec. characterisation 8-91791
 n-GaAs, photo-Hall effect meas. of ionised impurity scatt. 8-56182
 n-GaAs, proton irradi., $E_p=30$ MeV, defect form., orientation depend. 8-55898
 GaAs:Be, annealing effect during MBE 8-79898
 GaAs:Cr, semi-insulating, characterisation by photoelectric data 8-68051
 GaAs:Ge, LPE, on semi-insulating GaAs, film-substrate interface characterisation 8-72017
 GaAs:Se, implanted, annealing with O-free CVD Si_3N_4 encapsulant 8-83834
 GaAs:Si, Cr, carrier concs. from Hall effect, microscopy, localised vibrational modes absorption meas. 8-56104
 $GaAs_{0.6}P_{0.4}$:Be, implanted annealing studies, elec. resist., Hall effect meas. 8-84213
 $GaAs_{1-x}P_x$ based structs., carrier conc., mobility calcs. from Hall effect meas. 8-60138
 $Ga_{1-x}Mn_xSb$ alloys, mag. phase transition obs. 8-52248
 p-GaP, LPE layers, Hall effect 8-91704
 GaP:s, elec. props. following 1.7 MeV electron irradiation 8-80005
 n-GaP:Te, doping parameters calc., by means of Hall data analysis 8-51925
 GaP:Te, Hall effect and elec. cond., 80-400K 8-91705
 n-GaP:Te, LPE layers, Hall effect 8-91704
 GaP:Zn, Hall effect and elec. cond., 80-400K 8-91705

Hall effect continued

$GaS, Se_{(1-x)}$, Bridgman-grown, electrical props. meas. 8-84216
 n-GaSb, galvanomagnetic effects 8-72172
 GaSe, Hall mobility anisotropy 8-68041
 $Gd_{1-x}Co_x$ film, resistivity, Hall effect, domain wall density 8-76169
 $Gd_{1-x}Ni_{1-x}$ sputtered amorphous films, mag. props. and Hall meas. 8-95488
 Ge epitaxial film on Si, influence of fragmentary struct. on galvanomag. effects (*Ukrainian*) 8-84327
 Ge film, polycrystalline, structural and elec. props. 8-76173
 n-Ge, H-linear planar Hall effects of hot electrons 8-76082
 Ge:Cu, quenched, interaction between shallow-level defects and Cu atoms, Hall effect meas. 8-64002
 n-Ge:Sb, γ -irrad. effects on donor conc. and compensation by acceptors 8-56106
 $HgCr_2Se_4$, ferromag. semicond., transport props. 8-68039
 HgTe, vacancy doping by off-stoichiometry, influence on transport props. 8-55862
 Ho, Hall const. and elec. resist., 80-700K (*Russian*) 8-60110
 In, Hall field, reversal, 6-280K 8-72135
 InAs, intrinsic point defects, nature and influence on electrophys. props. 8-79609
 InAs surface layers, oscillatory transport coeffs. 8-64136
 In_2O_3 :Sn, film, HF sputtered, cond., Hall mobility, oxidation, charge carrier density 8-72287
 n-InP, 10-300K, thermal activation energy and influence of compensation 8-72171
 n-InP, epitaxial, Hall effect, electron mobility and density, temp. depend. 8-72288
 p-InSb, deformed, giant negative magnetoresistance 8-87990
 p-InSb film, elec. transport props. 8-72291
 InSb, gamma irradiated, changes in energy spectrum of impurity spectrum 8-51937
 InSb, high-purity specimen irradiated at 80K, transport prop. and defect annealing 8-95307
 InSb:Cr, press. effects on transport props. 8-56146
 $InSb_{1-x}Bi_x$, disordered solid solns, ionisation energy of fluctuation levels 8-72116
 K, Hall effect, temp. depend. 8-64029
 K, magnetoresistance anomalies due to inhomogeneities, examination 8-56130
 $KTaO_3$, photoconduction in ferroelectrics 8-91720
 LaB₆ film, structure, stoichiometry, elec. properties 8-60043
 $La_{0.65}Pb_{0.35}MnO_3$, transport props. near Curie points 8-88100
 Mg, Hall effect and elec. resist., temp. depend. 8-64030
 $Mn_{1-x}Zn_{0.06}Co_{0.01}Fe_{1.75}O_4$, transport props. near Curie points 8-88100
 $Na_xVS_2(Se_2)$, mag. and elec. props. rel. to struct. transitions 8-91848
 NbSe₃, linear-chain metal, Hall effect meas. 8-76058
 NbSe₃, oscillatory magnetotransport, Fermi surface anisotropy, Hall effect, g-factor, Dingle temp. 8-51975
 nbSe₂ (2H) single crystal, elec. resistivity, effect of hydrogen intercalation (*Russian*) 8-84338
 $Nd_{1-x}Co_x$ film, amorphous, mag. props. meas. 8-68312
 $Nd_{1-x}Fe_{1-x}$ film, amorphous, mag. props. meas. 8-68312
 Ni, ZZ 8-68014
 Ni-Fe, film, anomalous Hall and Nernst-Ettingshausen effect, contribution of phonon and impurity scatt. (*Russian*) 8-64145
 $Ni_3(Fe,M)$, $M=Cu, Cr, Mo, W$, kinetic phenomena rel. to ordering and electron struct. (*Russian*) 8-76043
 $Pb_{1-x}Cd_x$, epitaxial, resist. and Hall coeff., substrate temp., thickness and comp. depend. 8-72290
 $Pb_{1-x}Ge_xTe$:Ga, Fermi level stabilization, transport props. meas., 77-400K 8-56065
 $PbMo_6S_8$, Hall effect and magnetoresistivity 8-95400
 $PbMo_6S_8$, normal state and superconducting property measurements 8-91660
 PbO₂ and pyrolusite compressed powder mixtures, mixing rules concerning Hall effect and Hall mobility (*German*) 8-84234
 PbS film, polycryst., chem. deposition from soln. and characterisation 8-72743
 PbS, nonstoichiometric, increase of rest pot. with p-type semicond. character 8-56170
 $Pb_{0.59}Sn_{0.41}Se$, struct. phase transition, temp and hydrostatic press. influence, Hall effect, resistivity (*Russian*) 8-51675
 p-Pb_{0.82}Sn_{0.18}Te, Hall coeff. sign-inversion temp. 8-52010
 $Pb_{1-x}Sn_xTe$, Cd-In diffusion, changes in elec. props. 8-91348
 PbTe, ion-implanted, doping profile evaluation by Hall effect and sheet resist. meas. 8-59831
 Pd based alloys, extraordinary Hall effect 8-76053
 Ru, electronic structure and mag. breakdown, galvanomag. props. obs., 1.3-20.4K 8-91600
 (SN)_x film, Hall effect, elec. cond. and magnetoresist. meas. 8-84314
 n-Si, A-centre ionisation energy change due to uniaxial deform. 8-71733
 Si epitaxial film, correlation between electrooptical and electrical props., IR absorpt. spectra (*Russian*) 8-60453
 p-Si, fast electron irradi., Hall mobility, temp. depend. 8-56165
 n-Si, γ -irrad. ($E_{max}=100$ MeV), carrier recomb. 8-56158
 Si, inversion layer, Hall effect meas. 8-56199
 Si inversion layers, stress and intersubband correlation 8-60227
 Si, MOS inversion layers, Hall effect 8-64118
 p-Si polycrystalline films on graphite substrates (*French*) 8-64154
 Si:Al, acceptor levels, IR spectra 8-67972
 Si:As, elec. activation of implanted As during low temp. anneal, Hall effect meas. 8-51571
 Si:Gd, radiation defect form., effect of Gd impurities, elec. and optical meas. 8-71764
 Si:P, annealing characteristics at low temp., elec. props. 8-63781
 Si:P, carrier mobility and distrib. rel. to annealing, 400-910°C 8-79995
 Si:P, Hall effect 8-72176
 Si:P, neutron transmutation doped, radiation damage exam., elec. props. 8-95080
 β -SiC, cubic, elec. props. 8-51996
 $Sn_{1-x}Pb_xTe$, elec. and struct. props. of epitaxial layers (*Russian*) 8-64147
 SnSse, electron mobility, elec. cond. and Hall effect meas. 8-80004
 SnTe, Hall coeff., temp. depend., interpretation 8-87988
 SnTe, isothermal meas. of galvanomag. and thermomag. effects (*Russian*) 8-56160

Hall effect continued

- Ta-Ti-N, reactive sputtered film, elec. props. 8-84336
 TaS_{2-x}Se_x layer compound, Hall coeff., 4-200K 8-95305
 TaSe₃, oscillatory magnetotransport, Fermi surface anisotropy, Hall effect, g-factor, Dingle temp. 8-51975
 Te, lightly doped, galvanomagnetic props. in fields up to 140 kOe 8-91707
 Te, warm hole conductivity 8-72160
 Te:Sb, 96 to 500K, cond. Hall const., hole mobility, conc., dislocation effects (*Russian*) 8-64039
 Ti, vacuum deposited, cryst. struct. and elec. props. 8-79908
 TiS₂, resistivity, Hall effect and mag. suscept. 8-79991
 Ti_{1-x}V_xS₂, resistivity, Hall effect and mag. suscept. 8-79991
 VO₂, metallic phase, electronic props., plasma freq., Hall coeff. 8-84195
 VSe₂, press. depend. of CDW transitions, role of Coulomb correlations, elec. props. 8-87927
 W, alternating sign Hall effect and doppleron spectrum 8-79981
 W, temperature dependence 8-91666
 Zn, Hall effect and elec. resist., temp. depend. 8-64030
 ZnGeP₂, synthesis, characts., applic. to laser windows (*French*) 8-80467
 ZnO accumulation layers, Hall mobility and work function, correl. 8-60185
 ZnO, surface phenomena, interpretation by compensation model 8-95323
 ZnSe:In, heavily doped, Hall effect and DC cond. expts., compensating acceptors 8-52013
 ZnSe:In, heavily doped, impurity band cond., Hall coeff. and cond. expts. 8-72147
 ZnSiP₂:Ga, effect of doping conc. on elec. cond. and Hall coeff. 8-76077

Hall effect devices

- plasma accelerator, using Cd vap. 8-71553
 plasma accelerator, with extended accel. zone, ion stream modulation at exit 8-79480

Hall effect transducers

- compensation-point Hall effect temperature sensor 8-93679
 probes for defect field meas. 8-53155
 remote meas. of axial/radial components of magnetic fields in conducting coils 8-93659

Hall generators *see* Hall effect devices**halogens**

- see also* astatine; bromine; chlorine; fluorine; halides; iodine
 alkene-halogen, matrix isolation vibr. spectroscopy, complex form. studies 8-62952
 exothermic trihalogen Borne-Bunker reaction, long lived intermediates, comment 8-92464
 exothermic trihalogen Borne-Bunker reaction, long lived intermediates, reply 8-92465
 inert gas halogen excimer laser principles, performance and applications 8-55342
 leak detector, reduction of background effects by means of chromatographic columns 8-70110
 metal vapour lamp, additive partial pressure determ. from self-reversed spectral line maxima 8-67476
 surface ionisation, on LaB₆, using ion source 8-60538

Hamidashi effect *see* ferroelectricity**hand tools**

- IC wiring tools for laboratory use 8-86073

handling, materials *see* materials handling**Hanle effect**

- atomic collisions, relaxation coefficients, meas. method (*French*) 8-58771
 compact non-LTE radiative transfer theory 8-61728
 gas laser, atomic constants and collision cross sections determ. by level crossing 8-50763
 magnetometer, one-component Hanle effect, with feedback, stability and operating range 8-82011
 Ar, 3p²5p config. aligned in discharge, interf. signals, lifetimes and collision cross sections 8-70796
 Ar, collisional depolarisation of selectively excited 2p levels (*French*) 8-86830
 Cd, 6³P₁, level, relax. of alignment and population 8-70795
 He I 1s3d levels, cascade-free lifetime meas., using He⁺+He 35 keV collisions 8-58607
 He I D₃ line, Stokes parameters for quiescent prominences, Hanle effect quantum theory 8-85924
 Hg+He(Xe), collisionally induced coherence, orientation and alignment, transfer among 6s6d levels 8-74747
 H₂, 3d complex, radiative lifetimes, hyperfine constants 8-70873
 In I, 6²S_{1/2} state lifetime meas. by Hanle effect method 8-90097
 K₂, B¹II, state lifetimes, Hanle effect 8-90218
 Rb 5²P_{3/2} state, Hanle effect intensities 8-66521

hard soldering *see* brazing**hard-sphere fluids** *see* classical theories of fluid structure; liquid theory; quantum theories of fluid structure; statistical mechanics**hardening**

- see also* dispersion hardening; quench hardening; radiation hardening; solid solution hardening; surface hardening; work hardening
 elastoplastic anal. using ASKA program system, bending, isotropic/kinematic hardening 8-63312
 elastoplastic material, variational inequality 8-63320
 ferroelectric ceramic, defect effects on mech. strength 8-64332
 gelatin hardened layer structuralisation, kinetic anal. using swelling 8-62255
 hydride forming, metals and alloys, phase hardening 8-52833
 metal, hardening due to increased subgrain boundary stability 8-52934
 plane strain problem of hardening and softening plastic materials, theory 8-83869
 polymer solns., shear and normal stress behaviour, flow hardening (*German*) 8-67165
 steel, alloy, type 52100, exam. of microstruct. and fracture, as function of austenitising in temp. range 800 to 1100°C 8-76673
 steel, heat treatment with induction heating, 8-92285
 steel, high hardenability carburising, accelerated annealing technique 8-84857

hardening continued

- steel, low alloy and C, hardened and tempered parts, nondestructive magnetic inspection 8-95889
 steel, low S, ESR, overheating effect on toughness 8-52860
 steel, stainless, Cr-Ni, maraging, effect of Mo, Co additions on hardening 8-84835
 steel, statistical distrib. of mech. props., and life characts. exam. 8-64606
 thin walled bearing races eddy current inspection of hardening and tempering quality 8-95892
 CdO-WO₃-H₂O, interconnection between kinetics of structure formation and chem. reactions 8-53198
 Cr-Mn-Si steel, heat-treatment quality, higher harmonics of EMF obs. 8-60941
 U, γ - and β -hardened, recrystallisation, effect of impurity distrib. 8-70602

hardness*see also* abrasion; hardness testing

- brittle abrasive material, rating capability for elastic deformation 8-56680
 ceramics, microstructure dependence of mechanical behaviour 8-88533
 covalent crystal, resistance to microindentation 8-60753
 diamond, synthetic, carbonado type, struct. and microhardness 8-84994
 die steels for cold plastic working, powder metallurgy, characts. 8-68649
 dislocation interaction, force between dislocation, and misfitting ordered particle, calc. 8-83815
 flat glass, in vacuum, exam. of temp. dependence of microhardness and microstrength 8-88532
 glass-ceramics, transparent, microstruct. and props. 8-59960
 hardness, elastic moduli, density, cryst. temp., mech. props., for flywheel appl. (*Dutch*) 8-52878
 ice single crystal, rel. to friction of steel ball (*Japanese*) 8-88537
 indentation hardness, the effect of mechanical stresses (*German*) 8-95794
 melt-spread coating, microhardness of transition layers formed on Fe-group metals by Al alloy melt 8-60879
 metallic glass, hardness, elastic moduli, density, cryst. temp., mech. props., for flywheel appl. (*Dutch*) 8-52878
 metals, surface sliding damage, no lubrication, materials depend. (*Japanese*) 8-56780
 mutual alloying behaviour of the elements straddling the line Li-Mg-Cu-Au in the long periodic table 8-84769
 plastic zone, direct meas. in side grooved fracture toughness specimens 8-68864
 plexiglass, red, gamma dose meas. by optical absorpt., elec. conductivity, and mechanical hardness 8-55045
 polyethylene, chain-extended, oriented, microindentation hardness 8-76728
 rare earth glasses, R₂O₂-S-Ga₂S₃, (R=La to Nd), exam. of preparation and props. (*French*) 8-80504
 Recalloy, Fe-Nb, semihard magnetic alloy, magnetic props., hardness, microstruct. 8-56660
 refractory materials, group IVa and Va, slip, microhardness comments 8-84967
 rocks hardness and abrasiveness determ., suggested methods 8-96313
 sand, resin-coated, curing effects on physico-mech. props. (*Korean*) 8-60855
 snow, hardness and particle shape effects on drifting phenomena (*Japanese*) 8-88856
 steel, alloy, high C, amorphous, produced by rapid quenching from melt, hardness and strength 8-59764
 steel, alloy, maraging, 18% Ni, effect of solution and ageing treatments, on microstruct., tensile props., fracture toughness 8-80648
 steel, alloy, U20Kh6T2D, structural transformations during heat treatment, and wear resistance 8-88484
 steel, ball bearing with modified chem. comp., improved rolling contact fatigue 8-64732
 steel, C, fretting fatigue damage, SEM exam. 8-88541
 steel, C, prestrain effect on non ductile transition temp. and bending speed relationship (*Japanese*) 8-84919
 steel, C, type S15CK, tuffrided, fatigue strength at elevated temp., under reversed axial strength (*Japanese*) 8-84980
 steel, hypoeutectoid Widmanstatten struct. form., contrib. to the laws (*Slovenian*) 8-84817
 steel, low alloy, type 3sp, effect of temp. at end of rolling on mech. props., and coercive force 8-72799
 steel, low alloy, type 4340, quenched and tempered, effect of plastic strain followed by ageing, on torsion fatigue resistance 8-92360
 steel, mild, high temp. fatigue, effect of temp. variation 8-64685
 steel, Mn-Cr-V, structural changes during solution annealing (*Czech*) 8-84864
 steel, quenched, verification of change of props. in mag. field 8-52985
 steel, tempered StE70, water quenched, residual stress field in centrally welded plates (*German*) 8-72794
 steel, tool, thermal treatment effect on abrasive wear resistance 8-92369
 steel, type 55SM5FA, formation of hardened layer during burnishing 8-85046
 steel 1Kh18N9T, physico-mech. props. after boring in metallic melts (*Russian*) 8-56736
 steel bearing parts, magnetic inspection of heat treatment quality 8-73007
 steel rollers, case-hardened, nitrided, surface failure, durability 8-84959
 strengthening by modified ausforming 8-76665
 vacuum deposited films, mech. props. 8-75968
 wear mechanism review 8-72891
 Ag composite, SiC whisker-reinforced, prep. aboard Skylab. 8-84741
 Ag, ultra-microhardness testing for vacuum deposited film and bulk specimen 8-79910
 Ag-Ga solid soln., internally oxidised, hardness (*Japanese*) 8-60744
 Ag-Ni, two ductile phase alloy, exam. of softening behaviour after cold rolling 8-72847
 Al alloy 7001, ageing effect on hardness and tensile props. rel. to delay time till quenching 8-92286
 Al, fatigue induced dislocation struct. and hardening, exam. (*Japanese*) 8-64624

hardness continued

- Al-Ag (up to 40 at.%), exam. of anelastic phenomena and structural state 8-76693
 Al-Li solid soln., decomposition exam. by secondary ion ion emission (*Russian*) 8-68696
 Al-Mg-Ag, age effect on age hardening (*Japanese*) 8-52831
 Al-Mg-Li alloy, 01420, surface layer props. (*Russian*) 8-80674
 Al-Mn alloys, study of solidification by rapid cooling (*Japanese*) 8-88459
 Al-Zn, precipitation struct. and phys. props. effect of miscibility gap (*German*) 8-92265
 Al-Zn alloys, relation between microhardness and average radius of Guinier-Preston zones 8-95811
 Al₂O₃-B₂O₃-P₂O₅ glasses, formation and props. 8-83737
 AsSe_{1.5-x}Te_x glasses, physical props. 8-68028
 Au, ultra-microhardness testing for vacuum deposited film and bulk specimen 8-79910
 Au-Cu-Ag dental alloy, age-hardened, struct. and morphology 8-92272
 B-C system, region of existence of B₄C phase 8-76636
 B,C, metallography and Knoop microhardness (*French*) 8-76730
 BN, hardness rel. to temp., phase compositions 8-60752
 BaSO₄, single cryst., neutron bombard. effect on struct. 8-63793
 Be bronze BrB2, quenched deformed, substruct. and props., effect of prerecrystallisation annealing (*Russian*) 8-60677
 Bi, recrystn., effect of Sb, Sn and Pb 8-52841
 Bi, whiskers, hardness, elec. props. (*Russian*) 8-51874
 α-brass, defect removal, obs. by positron annihilation 8-84677
 Cd-Zn (Ag), annealed, work softened, exam. of crystallographic texture, hardness 8-80559
 Co-Al-Nb, monovariant directionally solidified eutectics, struct. and mech. props. (*Russian*) 8-92254
 CrC, plasma sprayed coating 8-68835
 Cu, defect removal, obs. by positron annihilation 8-84677
 Cu, electrodeposited coating, annealing effect on struct. and microhardness (*Russian*) 8-76668
 Cu, ultra-microhardness testing for vacuum deposited film and bulk specimen 8-79910
 Cu-Al, internally oxidised, structural, elec. and mech. characts. 8-60761
 Cu-Al (11.6 wt.%), mech. props., tempering temps. effects 8-76669
 Cu-Ni-Fe (26.8 wt.%), microduplex struct. form., hardness meas., optical and electron microscopy (*Japanese*) 8-76659
 Fe, Armco, microstruct., effect of strain rate on change, due to tension-compression 8-80614
 Fe, cast, white Cr alloyed, wear resistance, effect on abrasive hardness 8-64722
 Fe-Al(Cr)(V)(Ti), hardness after nitriding, metallographic, electron microscopic and microprobe anal. 8-51608
 Fe-B metallic glass, hardness, elastic moduli, density, cryst. temp., mech. props., for flywheel appl. (*Dutch*) 8-52878
 Fe-C, softening of high purity Fe, by C, due to double kink nucleation (*French*) 8-84949
 Fe-C-Ni-Cr(Cu), dynamically hot pressed, mech. props., additives effect 8-60620
 Fe-Cr, role of C in transform. by heating in (α+γ) phase (*French*) 8-52798
 Fe-Cr-Al-Y (Y-Al₂O₃)(Y₂O₃), preparation and exam. of mech. props. 8-52720
 Fe-Fe₂O₃ composite films, structural props., microhardness, 250 to 700K 8-84095
 α-Fe-Fe₂C alloys, ground surface layer exam. of props. 8-84840
 Fe-Si (3.72 wt.%) fatigue failure in vacuum and air 8-68789
 Fe-Si(Cr)(Ni)(Mn)(C), alloy layers formed by reaction with molten Al, X-ray, EPMA anal., hardness meas. (*Japanese*) 8-72926
 Fe-W-Cr-Mo-Co with austenitic phase, magnetic and mech. props., cold working and ageing effects (*Japanese*) 8-60678
 InP, microstructs. assoc. with hardness indentations 8-80627
 KCl-KBr mixed crystals, microhardness studies, nonlinear depend. on composition 8-83872
 LiF, ultra-microhardness testing for vacuum deposited film and bulk specimen 8-79910
 Mg-Zn metallic glass, hardness, elastic moduli, density, cryst. temp., mech. props., for flywheel appl. (*Dutch*) 8-52878
 MgF₂, ultra-microhardness testing for vacuum deposited film and bulk specimen 8-79910
 MgO, lattice misorientation and displaced vol. for microhardness indentation 8-64617
 Mn-Pt, exam. of Elinvar props., from -150 to 500°C 8-76684
 Mn₂As-Mn₂Sb, structural and magnetic props. determ. 8-76248
 Nb-Ni metallic glass, hardness, elastic moduli, density, cryst. temp., mech. props., for flywheel appl. (*Dutch*) 8-52878
 Nb₃Au, A-15 struct. supercond., microhardness, bonding 8-76199
 Nb₃Ir, A-15 struct. supercond., microhardness, bonding 8-76199
 Nb₃Sn, A-15 struct. supercond., microhardness, bonding 8-76199
 Nd-Gd-Te alloys of R₂Te₃-T₃Te₄ region, physicochem. props. 8-52017
 Ni coating hardness rel. to sulphamate electrolyte selection (*Bulgarian*) 8-88552
 Ni, defect removal, obs. by positron annihilation 8-84677
 Ni-based-Ta(Cn,N) hard metals, isostatic hot pressing influence on mechanical properties 8-92219
 Ni-Cr-Fe-Mo-Co (21.41, 19.28, 8.64, 2.16 wt.%), Hastelloy alloy X, exam. of thermal stability 8-84865
 Ni-Cr-W-C(Si) hardness, corrosion resistance, wear resistance tests in 10% HCl (*German*) 8-92368
 Ni-Fe-Nb alloys, mag. permeability and struct. (*Chinese*) 8-84450
 Ni-Fe-Nb-Al alloys, mag. permeability and struct. (*Chinese*) 8-84450
 Ni-ZrO₂, thin layers, vapour deposited, dispersion strengthened, exam. of struct., mech. props. 8-80554
 PVC-Cu, particulate composite, mech. props. effect of particle size 8-95799
 Pb-Al₂O₃ composites, mech. alloyed, hot hardness meas. (*Japanese*) 8-84830
 Re coating on cemented carbides, CVD, hardness (*German*) 8-64777
 SiC fibre reinforced Ni-Cr alumina coated fibres, hot pressed, annealed, IR study 8-60623
 α-Si₃N₄, hardness anisotropy 8-95804
 Ta-O solid soln., interstitial ordering and precipitation at 100 to 270°C, exam. 8-52813

hardness continued

- Ta₁₆W₁₈O₄₄, characterisation, of thermally contracting tungstates 8-63869
 Ta₂WO₆, characterisation of thermally contracting tungstates 8-63869
 Ta₂₂W₆O₆₇, characterisation of thermally contracting tungstates 8-63869
 Te-Bi₂Te₃ oriented eutectic, microhardness, influence of size of phases (*Russian*) 8-92322
 Te-Sb₂Te₃ oriented eutectic, microhardness, influence of size of phases (*Russian*) 8-92322
 Ti alloy, VT16, decomposition of metastable β-phase (*Russian*) 8-68710
 Ti alloys, β-annealing and controlled rate quenching effects 8-80568
 Ti-Be-Si glass ribbons, physical and mech. props. 8-95767
 Ti-Ni-Si metallic glass, prep., thermal and mech. props. 8-64497
 TiB₂, hardness of sintered material 8-60636
 TiC-Cr₃C₂(Cr₃C₂-WC), powder mixture, steel bonded, exam. of sintering behaviour 8-52712
 TiO₂, sintering, hardness, density, elec. cond. and colour (*Japanese*) 8-68659
 US,N₂O₂, neutron diffraction exam. of structure 8-79777
 V-Mo, effect of ion plated Mo on corrosion in liquid Na, mech. props. 8-53020
 V₃Ge, A-15 struct. supercond., microhardness, bonding 8-76199
 V₃Si, A-15 struct. supercond., microhardness, bonding 8-76199
 W fibre, KSiAl doped, recrystallisation, Li diffusion effects, hardness, strength, microstructure meas. (*German*) 8-64644
 W-WC, activated sintering, mech. props. (*Korean*) 8-60622
 WC, plasma sprayed coating 8-68835
 WC-Co, exam. of effect of continuous carbide phase, on hardness, and deformation 8-52974
 WC-TaC-Co, cemented carbide, strength improvement by hot isostatic pressing 8-84969
 WCuB prep. by infiltration of W skeleton by CuB, hardness meas. (*German*) 8-64508
 ZnO (1010) surface bias voltage effect on hardness, charge exchange near dislocations 8-52078
 ZnO-Al₂O₃SiO₂, transparent glass-ceramic, microstruct., physical props., crystallisation ht. treatment depend. 8-80506
 ZnS, ultra-microhardness testing for vacuum deposited film and bulk specimen 8-79910
 α-Zr, polycrystalline, cyclic deformation (*Japanese*) 8-68757
 β-Zr-Mo-(Al)(Ti)(La), metastable, deform. induced transform. 8-52805
 Zr-Ru(Pd), heat treated, mech. props. and struct. 8-80571

hardness testing

- ball insertion curves, effect of load appl. on indices 8-60903
 Brinell press attachment for testing at 250 to 300°C 8-56842
 deadweight standard Rockwell hardness testing machine, design and performance 8-88592
 film, diamond indentation and draw tester for meas. of ultra-adherence 8-72944
 indentation testing, mech. characts. calcs. inc. elastic strains (*Russian*) 8-95863
 metal, hardening temp. determ. using pulsed laser 8-72942
 metal, stress/strain diagram determ. by spherical punch (*German*) 8-76803
 microhardness, Knoop numbers, correction factors, elastic recovery 8-72952
 plastics, penetration hardness testing, exam. of thermal effects (*German*) 8-76801
 steel, crankshaft forgings, by type NChG instrument 8-53133
 steel 8-53114
 steel SS-41, plastic working with vibr., US hardness tester 8-53044
 tempered glass discs, meas. of nonuniform distribution of residual stresses 8-95865
 ultra-microhardness tester, for expts. on vacuum deposited films 8-53161
 Vickers hardness meas. of curved-surface components 8-80699
 Cr-Mn-Si steel, heat-treatment quality, higher harmonics of EMF obs. 8-60941
 Y₂O₃, plasticity, microhardness testing, indentation, plastic deform. temp. depend. (*French*) 8-56713

harmonic analysis

- see also waveform analysis
 atmospheric O₃ total amount at Belsk, Poland, harmonic anal. 8-92883
 aurora, southern oval, spherical harmonic analysis 8-81487
 Earth's gravity potential, convergence of spherical harmonics expansion 8-81097
 Earth gravity field, numerical development of spherical functions (*German*) 8-61311
 Earth surface tidal tilts, harmonic anal. and atmospheric press. fluctuations influence (*Russian*) 8-88790
 geomagnetic field, definitive spherical harmonic model and secular var. for 1965 8-96133
 gravitational fields of Earth, Moon and Mars, harmonics rel. to stationary points coordinates 8-53805
 gravity, tidal changes at Poltava, 1973 to 1976, harmonic anal. (*Russian*) 8-88782
 Mars global topography, harmonics and geophysical implications 8-85880
 plate, elastic, under tension stress conc. due to surface pit 8-83243
 plate, thick, containing eccentric spherical cavity, transverse bending stresses 8-63288
 seismic Rayleigh waves of period 50 seconds, group vel. distrib. in Pacific Ocean 8-65197
 thermal-motion correction for bond angles, harmonic approx. 8-55777
 tilt meter observations harmonic anal., influence of S₁ diurnal meteorological wave (*Russian*) 8-88788

harmonic generation

- see also optical harmonic generation
 acoustic gravity waves, atmospheric, harmonic generation 8-88956
 electron cyclotron instabilities, multi-harmonic, theory 8-87442
 magnetoelastic crystal, cubic, acoustic SHG, static magnetisation effects (*Russian*) 8-56362
 magnetoplasma, third harmonic generation by Gaussian EM beam 8-83572
 plasma, SHG by Gaussian beam 8-91112

harmonic generation continued

- power line harmonic VLF radiation, transmitter-induced amplification in magnetosphere 8-96360
- pulse shape of second harmonic generated by two level system 8-60327
- SAW, harmonic generation at unbonded interfaces and fatigue cracks 8-90562
- second harmonic generation, nonequilib. media 8-77726
- thin conductors, SHG and size cyclotron reson. 8-72186
- two-photon resonant up-conversion, third harmonic generation 8-90453
- $\text{Al}_2\text{O}_3\text{:Cr}_2\text{O}_3$, saturation effects by double-quantum transitions 8-80197
- SiO_2 , fused, US study by harmonic generation, elastic consts., Gruneisen parameters 8-83735

harmonic oscillators

- anharmonic oscillator, energy level asymptotic behaviour by coherent states method 8-81873
- anharmonic oscillator, quantum mechanical, eigenvalues of secular eqns. 8-49698
- anharmonic oscillators, quantum theory, independent to spherically coupled, level crossing 8-77747
- asymptotic series expansion and complex classical trajectories 8-93557
- atom+diatom collinear collision, refined Born approx. 8-74724
- coherent states for general pots. with harmonic oscillator props. 8-73883
- covariant generalisation, two-body relativistic systems 8-69977
- damped, eqns. of motion in quantum statistical theory, Fokker-Planck eqn. (French) 8-89399
- diffusion process modelling, equivalence of different methods 8-57818
- distorted wave Glauber approximation, Pauli eqn. soln. 8-57809
- double humped fission barrier using biharmonic oscillator pot., penetrability calcs. 8-86524
- double well anharmonic oscillator, no horn of singularities 8-73884
- driven oscillator motion with nondecreasing input vels., use in inertia actuated fuse 8-59293
- education, group theory of covariant harmonic oscillators, interacting quarks 8-61970
- education, quantum mechanics, spherically symmetric pots., ladder operators, energy levels and degeneracy 8-62013
- education, thermodynamic work and harmonic oscill. 8-49598
- Feynman's variational principle for real path integrals, generalisation 8-89365
- four nucleon wave functions, Taylor series method 8-66223
- g_0^4 theory, strong coupling limit of Green functions, anharmonic oscillator appl. 8-78071
- graphical method for matrix determinant and inverse, generating functions for harmonic oscillator integrals 8-57732
- inverse matrix diagonal and off diagonal elements, self energy perturbation theory 8-82607
- IR interaction with mols., classical/semiclassical theory 8-90164
- isotopic molecules, reduced partition function ratio, generalised finite polynomial approx. 8-66529
- linear harmonic oscillator on lattice, wave functions, energy eigenvalues, Pade approximant method 8-57817
- molecular predissociation model, level widths, shifts and curve crossing 8-90239
- molecule-molecule reaction, ergodic energy transfer, vibr. quantisation effects 8-85137
- momentum autocorrelation functions from classical Green's functions. [Teaching] 8-61976
- nonlinear oscillator in harmonic force field, averaged quantum eqn. of motion 8-54232
- oscillating Hermite-Gaussian wave functions for harmonic oscillator Schrodinger eqn. 8-70004
- oscillator basis for octupole collective motion in nuclei 8-70470
- periodic Hamiltonian flows, generalised Bertrand's problem, isotropic harmonic oscillator 8-86131
- perturbation theory, anharmonic oscillator, strong coupling regime, appl. to Φ_4^4 model 8-89622
- phase space, creation, annihilation operators 8-73871
- q-equivalent particle Hamiltonians 8-93525
- quadratic Hamiltonians, exact propagators 8-49709
- quadratic Lagrangian exact propagator 8-77762
- quantum harmonic damping oscillator, loss energy states 8-49719
- quantum harmonic oscillator, driven and stochastically modulated, reduced eq. of motion 8-77764
- quantum nondemolition meas., oscillator in coherent state 8-54228
- quantum oscillator interacting with massless modes, correlation function long time limit 8-65814
- quartic anharmonic oscillator, symmetry properties in generator coord. method 8-49699
- random excitation of harmonic oscillations of single degree of freedom systems 8-54175
- relativistic harmonic oscillator quark model, N and $\Delta(1236)$ form factors 8-93852
- relativistic harmonic oscillators and hadronic struct., 1st year graduate quantum mechs. 8-61971
- resonant scattering of laser pulses by a system of N atoms 8-74617
- rotating nuclei, selfconsistency conditions in cranked harmonic oscillator model, HF calcs. 8-58239
- Schrodinger eqn., discrete-time, linear harmonic oscill. 8-49717
- solitons, weakly damped, mechanical model, anharmonic oscillator in pot. well 8-86192
- spin-oscillator coupled system, stochastic model for dynamics, projection operator approach 8-77813
- time dependent, Noether's theorem 8-93554
- time-dependent harmonic oscillator, Lewis invariant generalisation 8-93560
- translation invariant harmonic matter, exact Schrodinger eqn. soln. 8-65802
- two particle system, interaction through action-at-a-distance force, relativistic mechs. 8-66055
- YAG, colour centres conceived as bound polarons 8-63990

harmonics

see also harmonic analysis

No entries

Hartmann lines see Luder's bands

Hartree calculations see SCF calculations

Hartree-Fock approximation see HF calculations

Hartree-Fock calculations see HF calculations

Hasiguti relaxation see anelastic relaxation; dislocation damping

He see helium

headphones

see also earphones

No entries

health effects of radiation see biological effects of radiation

health hazards

see also biological effects of radiation

- actinide element movement through food chain 8-61264
- actinide industrial dusts, lung clearance studies at NRPPB 8-65137
- aquatic life, protocols for evaluating effects of chemical substances 8-53604
- benzo(a)pyrene and C black combined aerosol form., rel. to air pollution and health hazards 8-80796
- beta-rays, high-energy, hazards to eye lens and gonads 8-65131
- bronchial cancer induction by α -emitting warm particles 8-96078
- cancer, geomagnetism, weather and cosmic radiation 8-53615
- Chalk River Nuclear Laboratories research in radiation biology, environment and radiation protection 8-61222
- CO dose meter for working places exposed to extreme peaks of CO contamination 8-81096
- combustion aerosols, particle size distrib., health hazards 8-81394
- EM radiation protection, in transmission stations, Polish and international regulations (Polish) 8-61263
- energy, environment and health, Failla Memorial Lecture, learning from nucl. experience 8-80982
- fusion reactors hazards assessment (Czech) 8-86681
- gamma sources in walls of dwelling rooms, exposure rate calc. 8-73260
- HV transmission line elec. and mag. field exposure effects and hazards 8-77083
- industrial deafness risk, British Government code of practice 8-55513
- microwave induced thermal stresses in ocular lens of human eye 8-80914
- microwave potentially hazardous radiation sources, review 8-73173
- microwave radiation hazard assessment methodology for USA Army Radiation Protection Program 8-85389
- neutron yield calcs., electron beam incidence, radiation protection implications for accelerators 8-95622
- noise, statistical estimation of percentage of overexposed noise-impacted workers 8-92671
- nonionising electromagnetic radiation bioeffects research and related occupational health aspects 8-73172
- nuclear power plant siting evaluation, comparison with coal-fired power station (Czech) 8-50266
- organic micropollutants, adsorpt. on chrysotile and crocidolite, rel. to carcinogenic props. 8-80790
- radiation, low-level, current estimates of hazards to human populations, review 8-57043
- radiation low level link with cancer deaths in atomic plant employees 8-85339
- radioactive fallout effects of Nagasaki atomic bomb 8-85393
- respirable fraction of airborne dust, performance characs. of samplers 8-53438
- retinal damage by 325 nm He-Cd laser radiation 8-69136
- retinal tissue damage, by single ultrashort laser light pulses 8-96065
- static and low frequency magnetic fields, biological effects review (Slovak) 8-88722
- transport vibration prevention approaches 8-55506
- UV radiation standards for health and safety 8-74056
- HTO potential radiation dose to man, HT gas escape into forest ecosystem 8-96101
- ^{131}I population thyroid dose in USA after Chinese atm. nucl. weapons tests 8-77116
- Pu translocation from simulated wound sites in rat 8-77117
- $\text{PuO}_2\text{-UO}_2\text{-Na}$ aerosol, from LMFBF HCDA conditions, characterisation 8-94104
- ^{237}Pu , ^{239}Pu , citrate, early retention in mature beagles 8-96095
- ^{239}Pu acute inhalation, early mortality and morbidity estimate 8-96079
- Rn, concentration of ^{222}Rn , ^{220}Rn and decay products in room air, exhalation, ventilation and deposition effects 8-73261
- Rn daughter concentrations in air of dwellings in Great Britain 8-77118
- U, miners Rn daughter inhalation and pulmonary cancer incidence 8-96080
- UO_2 inhaled particle distrib. and clearance on first bifurcation and trachea of rats 8-73267
- ^{233}U and Pu fuels, relative occupational hazards 8-94101

hearing

see also bioacoustics; ear; hearing aids; speech

- absolute thresholds and kanamycin-induced hearing loss in guinea pig 8-57017
- acoustic filter components for ANSI standard psychoacoustic testing 8-83198
- acoustic fluctuation strength models comparison 8-65033
- acoustic reflex, in animals, influence on loudness of pulsed pure tones 8-92647
- active noise reduction system for ear defenders 8-92748
- additive masking effects of noise bands of different levels 8-57021
- AM noise, rate and modulation thresholds detect. by mass 8-85320
- articulation status and improvement for /r/ and /s/, delayed judgment speech-sound discrimination 8-65060
- asymptotic threshold shift in chinchillas exposed to impulse noise 8-57019
- audiometer, screening, and real-time computer techniques 8-81009
- audiometric testing, A-weighted equivalents of permissible ambient noise 8-69107
- auditory nerve response from cats raised in low-noise chamber 8-53420
- auditory nerve responses and cochlear microphonics in cats using pulsed US 8-61200
- averaged electroencephalic response to tone pips in normal-hearing and hearing-impaired subjects 8-65049
- backward masking, detection versus recognition 8-61201
- band-limiting experiments, suppression and critical bands study 8-92641
- bat, moustache, aural representation in Doppler-shifted-CF-processing area 8-80892

hearing continued

- bats, binaural perception and resolving power, correlation interferometer model (*French*) 8-80883
- behavioural, unit and AP thresholds, relationship in normal and abnormal ears 8-92642
- binaural detection at high frequencies with time-delayed waveforms 8-61196
- binaural interaction, depend. on interaural line and amplitude differences in discrimination and detect. 8-92637
- binaural interaction, model for subjective lateral position 8-92640
- binaural processing of information on short sounds, neuronal model 8-80885
- binaural summation of the loudness of pure tones 8-92638
- binaural system, monaural information processing on short sounds, neuronal model 8-65031
- bone conduction vibrators, calibration force levels 8-65046
- brain stem evoked responses, acoustically depend. wave V latencies 8-85318
- brain-stem auditory evoked response in young and old adults, normal variability 8-77064
- California sea lion, upper limit of underwater auditory freq. discrimination 8-69106
- cat, response of collicular auditory neuron to human speech 8-92646
- categorical perception, melodic musical intervals 8-53421
- central optimal processing for pitch of complex tones, general template 8-57016
- chinchilla, freq. discrimination study 8-92639
- chinchilla, identification functions for synthetic VOT stimuli 8-57022
- chinchilla, threshold shifts following 3 days noise exposure 8-88712
- click-evoked brainstem potentials in man using high pass noise masking 8-61193
- cochlea freq. selectivity sharpening models comparison 8-53418
- cochlear nucleus neurone response, model of phase struct. of binaural stimulus 8-80887
- combination tones, compatibility between psychophysical and physiological meas. 8-57014
- comfortable loudness levels for pure tones and speech 8-65050
- comparison with vision, broadcasting appl. (*Japanese*) 8-73155
- consonant confusion patterns, effects of filtering and sensorineural hearing loss 8-73163
- cricket, directional information coding by descending interneuron 8-77066
- dichotic listening as diagnostic tool, computerised dichotic tape generation 8-92740
- dichotic listening audio tapes preparation 8-57010
- dichotic two-response paradigm, random guessing model 8-61206
- distance perception in binaural hearing 8-61202
- earplugs, real-ear noise attenuation and effectiveness 8-87199
- evoked potential development in early childhood, longit. study 8-77061
- evoked potentials in EEG, meas. by adaptive matched filters (*German*) 8-88755
- evoked potentials in normal human subjects, age-related vars. 8-77063
- evoked response audiometry, on-line statistical detect. of average pots. 8-69245
- evoked responses, computer driven bipolar stimulator 8-57011
- feedback, effect on guitar playing intensity and speech prod. 8-85322
- formant frequencies of steady-state and consonant-bound vowels, difference limens 8-53426
- frequency discrimination, effects of leading tone (*Japanese*) 8-85324
- frequency discrimination capacities in goldfish, phase-locking in saccular nerve fibres 8-88720
- frequency-following potential components in man 8-77062
- gerbil, LF neural and cochlear-microphonic tuning curves 8-88718
- green tree frog, female discrimination of intermediate sounds in synthetic cat continuum 8-69109
- group delay distortions in electroacoustical systems 8-69105
- handicap of hearing impairment and limited benefit of hearing aids 8-53424
- head-related stereophonic recording techniques, dummy head method 8-61286
- human equivalent audibility thresholds for bone cond., age variation 8-96054
- industrial deafness risk, British Government code of practice 8-55513
- industrial hearing protection, types and limitations 8-55509
- infants, discrimination of voiced stop consonants 8-61207
- intensity difference detect. between brief adjacent tonal stimuli 8-53427
- intensity perception, effect of fixed standard on resolution in identification 8-88719
- lateralisation thresholds based on interaural time differences for three tone harmonic complexes 8-57008
- localisation acuity in horizontal plane 8-85323
- loudness and power series transformation, preliminary model and meas. 8-57012
- loudness growth depend. on excitation pattern skirts 8-61195
- loudness perception, for short-duration tones in masking noise 8-65047
- low-level pure tone masking, tuning curves obtained with simultaneous and forward masking 8-65042
- magnetic auditory evoked response using SQUID 8-80889
- masking effects on lip movements during speech 8-65061
- masking-level difference for repeated filtered transients 8-85321
- mastoid, human, model of mech. system imitating acoustic props. 8-80886
- microwave induced auditory responses in mammals, using 3 GHz pulses 8-53444
- middle-ear muscle contraction, influence on auditory threshold 8-85319
- moving stimulus, detectability of varying interaural temporal diffs. 8-53422
- music, acoustic component of Western consonance and dissonance perception 8-90607
- noise-induced threshold shift and cochlear pathology in the Mongolian gerbil 8-65035
- occupational noise exposure, permanent threshold shift, from an A-weighted Leq of 89 dB 8-92644
- Old World monkeys, localisation of pure tones 8-65038
- optimal processor theory of aural processing in pitch of complex tones 8-57015

hearing continued

- parakeet, auditory duration discrimination 8-65045
- perceptibility of phonetic features, in fluent speech 8-92635
- perception of uniform rhythm in sound impulse sequences, functional model 8-65032
- perceptual effects of spectral modifications on musical timbres 8-65039
- periodicity measures for repeated random auditory patterns 8-61197
- peripheral auditory system, anal., noise appls. 8-80888
- phase locking in monaural and binaural neurons 8-88717
- phoneme boundaries, effects of adaptation 8-80884
- phoneme recognition system based on human audition, psychophysical expts. 8-69115
- pitch and pitch discrimination of broadband signals with rippled power spectra 8-61199
- pitch strength meas. associated with ripple noise 8-88716
- psychoacoustical aspects of synthesized vertical local cues, computer synthesis 8-61198
- psychophysical tuning curves for simultaneous and forward masking 8-53423
- range effect in the perception of voicing 8-65044
- residue pitch adaptation, monaural perceptibility meas. 8-57020
- resolving capacity of human auditory analyser 8-69104
- ripple noise pitch detection by human, adaptive model 8-73166
- simultaneous notes perception in polyphonic music 8-61191
- simultaneous pure-tone masking, masking asymmetry depend. on intensity 8-65041
- sine wave tones, effect of amplitude envelope on pitch 8-65034
- sound differences in sensory space for sound reproduction engineering (*Russian*) 8-55521
- speech comprehension ability of hard-of-hearing, calc. model (*Dutch*) 8-73165
- speech discrimination in infants, developmental changes 8-65048
- speech interference level as predictor of face-to-face communication in noise 8-57018
- speech-pattern learning in French and English children 8-57025
- squirrel monkey, temporary threshold shift from noise exposure 8-88715
- subjective hearing event, directivity of loudspeaker (*German*) 8-79174
- subjective noise characts. comp. using PL/I program 8-59192
- syllable perception with alternate formants presented to opposite ears 8-65043
- syncopated auditory polyrhythms, discontinuous reversals in meter interp. 8-55528
- temporal order perception for vowels and consonant-vowel syllables 8-69108
- temporal switching between binaural information sources 8-53425
- thresholds, auditory and acoustic reflex, effects of stimulus duration and stimulus off time 8-73164
- timbre discrimination in musical patterns 8-88713
- timbre perception, review 8-77068
- timbre-classification of complex tones. (The relation between subjective and physical parameters) 8-77060
- tone glides, temporal integration 8-57013
- tracking procedures for training and evaluating speech reception 8-61204
- transition length, effects on perception of stop consonants 8-92636
- trombones, trombonist's perception 8-90611
- two-tone suppression, stimulus freq. effect, physiological and psychophysical obs. 8-85317
- two-tone suppression in cat auditory nerve, rate-intensity and temporal anal. 8-61194
- tympanic membrane perforation in cats, LF hearing loss 8-53419
- vertex short latency acoustic responses in cat, factors affecting amplitudes and latencies 8-61192
- visual field displacements evoked by intense sound exposure, humans 8-85332
- voice qualities, multidimensional classification 8-92651
- vowel perceived duration, temporal course 8-77065
- wind noise, expts. on human beings 8-92648
- Zwicker's masking period patterns, computational model 8-88714

hearing aids

- handicap of hearing impairment and limited benefit of hearing aids 8-53424
- measurement system comparison 8-65151
- sound pressure in insert earphone couplers and real ears 8-65152
- speech comprehension ability of hard-of-hearing, calc. model (*Dutch*) 8-73165

heat

- see also *heat transfer; heating; latent heat; specific heat; temperature; terrestrial heat; thermal variables control; thermal variables measurement; thermodynamic properties; thermodynamics*
- thermodynamic principles of heat-work transfer (*German*) 8-62171

heat capacity see *specific heat***heat conduction**

- see also *thermal conductivity*
- ablation, multidimens., embedding in inverse heat cond. problem, finite difference method 8-94508
- absorbing-scattering infinite slab, combined conductive and radiative heat transfer 8-71269
- absorbing-scattering semitransparent planar layer, flat temp. waves 8-90683
- anisotropic to isotropic transformation 8-87231
- approximation analytic solutions, heat cond. in adjacent regions (*Russian*) 8-83212
- bibliography of heat transfer 8-63425
- binary mixture theory for thermal diffusion in unidirectional fibrous composites 8-87230
- boundary value problems, soln. for heat conductivity eqns. by Green's function method (*Russian*) 8-63267
- boundary-value problems, numerical solutions (*Russian*) 8-55545
- boundary-value problems for nonuniform media 8-63266
- bubble-liq. mixture with nonsteady interphase heat transfer, shock struct. 8-83424
- building two-dimensional heat load, anal. by finite element method 8-71336
- closed cylindrical shell with insulated cross crack (*Ukrainian*) 8-90638
- coaxial cylindrical discs, radial heat flow 8-75032
- complex domain heat exchange, new soln. techniques 8-94509
- composite materials, numerical method calcs. 8-94522

heat conduction continued

composite wall, constant props., transient heat cond. problem (*French*) 8-87229

cone/plate system in fluid, friction heating and convection 8-87238

convergent and divergent flows, turbulent boundary layer with press. gradient, Reynolds analogy 8-83382

coupled conduction-turbulent convection in a circular tube 8-94691

critical radius effect with a variable heat transfer coefficient 8-83205

cross flow heat exchanger, longit. wall heat conduction, numerical calcs. 8-90645

diffusivity measurement, using wave packet soln. and microprocessor-controller 8-73989

droplet evaporation on heated surfaces, theory 8-87785

drops, noncirculating, direct contact condensation 8-94548

dust laden gas in channel, combined heat transfer 8-91031

dynamical thermoplasticity, appl. of mathematical system theory 8-83271

education, homogeneous ellipsoidal inclusions, general theorems, Poisson theorem, dielectric polarisation, conduction and elasticity 8-61979

electrical circuit, slowly modulated dissipative steady state, $dQ=TdS$ far from equilb. 8-81934

electrode units in MHD channel, temp. distrib. 8-59258

energy transfer in a heat-conducting medium with arbitrary scattering of thermal radiation 8-94507

fibre-reinforced composite, quasi-one-dimens. thermal diffusion, mixture theory 8-71271

finite element discretisation, two-dimens. stationary heat cond. using successive overrelaxation and conjugate gradients 8-83206

finite element heat cond. in reactor solids, review and TEMPEL computer program 8-62593

flat plate, in forced flow, approx. method for heat transfer calc. 8-94682

flow, of liq., thermal markers for vel. field meas., error reduction 8-91036

fluid thermal conductivity meas., transient hot-wire technique, theory 8-65933

fluidised beds, packed or quiescent, heat transfer from immersed heater 8-71391

frost growth rate prediction eqn. for cooled surfaces 8-87248

fusion reactor, blanket temp. variation with slab geometry 8-78495

generalised Legendre transforms, operational props. and appl. to heat transfer 8-59256

giant heat pulse, temp. distrib., classical Fourier and wave heat cond. eqns. 8-94518

harmonic thermal flux monitoring quasistationary temp. distrib. 8-51040

heat and electrical transfer differential eqns. 8-67004

heat flow eqn., different schemes 8-90627

heat transfer on layered composites 8-71264

HGTR core, multiregional coupled conduction-convection model 8-94083

hyperbolic equation, integral variational principle (*Russian*) 8-83213

ingot, temp. field calc. approx. by equiv. cylinder (*German*) 8-84788

inhomogeneous thermal conduction equations 8-70074

inverse boundary-value problems, finite difference method 8-63263

inverse nonlinear problems, simulation methods 8-94513

inverse problem, Fourier eqn. Runge-Kutta integration 8-89417

Lagrangian, for heat cond. with finite wave speed 8-94519

laminate, 3-phase, longitudinal heat propag. at high exciting freqs. 8-90684

laser light with time-varying intensity in optical medium, temp. field kinetics 8-59098

liquid droplet evaporation, idealised models for preheat stage 8-94586

materials with memory, linear theory of heat cond., final value problem, existence, uniqueness theorems 8-59266

media with volumetric heat absorpt., thermal disturbances propag. 8-59259

melting and solidification, formulated as heat conduction problem 8-91420

metallic joints, electrolytic tank appl. 8-83207

minimum final distance and fuel problem of 1-D heat cond. system 8-59257

modified equations for wave number dependent relax. time 8-71259

molecular-kinetic generalisation of the heat-transfer equation 8-67219

multilayer rectangular fins, conduction efficiency 8-63262

multilayered cylinders, nonstationary temp. fields with rotational symmetry (*German*) 8-79190

nonlinear, direct and reverse processes, mathematical modelling 8-94514

nonlinear equations, class of solns. 8-63264

nonlinear heat cond. problem with phase change, finite element anal. 8-75030

nonlinear heat conduction problems, soln. construction procedure, Kantorovich method 8-59264

nonlinear heat eqn. soln. by Picar's method (*Russian*) 8-51041

nonlinear heat transfer in solids, direct and inverse problems, approx. soln. method 8-94510

nonlinear thermal diffusion equation, parameter calcs., numerical calcs. (*French*) 8-94584

nonstationary heat transfer phenomena, variational description 8-89416

nonsteady nonlinear thermal cond. of complex bodies, numerical method 8-59263

numerical soln. oscillations, nonlinearity allowance scheme effect (*Ukrainian*) 8-90625

numerical soln. to heat cond. eqn., Laplace transform and FFT 8-57763

periodic system of narrow inclusions, effect on steady temp. field 8-63265

photomultiplier cooling by semiconductor microrefrigerators 8-57942

pipe, of variable thermal and elec. conds., elec.-heated, flow-cooled, temp. distrib. 8-90626

planar body, with circ. boundary and thermally insulated cracks, temp. distrib. 8-67002

plate, heated surface, transient thermal process calc. for symmetrical heating (*Russian*) 8-83211

porous medium, deep evaporation characterisation, of water (*French*) 8-59468

porous reactors, with temp. depend. heat generation rate, element geom. effects 8-94738

heat conduction continued

quasisteady mode with asymmetric boundary conditions 8-83208

radial heat transfer, conduction, convection and heat of phase change 8-90700

random heat conduction in solids, functional eqns. 8-83210

random medium, method of time ordered cumulants 8-54320

rigid wall-hot gas stream interaction, heat cond. eqns. soln. 8-79194

rod, expanding, conductive heat transfer computation, fast numerical technique 8-75029

rod, finite, insulated, unsteady heat cond. and temp. distrib., non-equilib. theory 8-67000

semi-transparent irradiated plate, combined conduction-radiation heat transfer, anal. soln. 8-75051

semiinfinite porous media, heat cond., phase transitions effects 8-94523

semiinfinite solid, with spherical inclusion, temp. field 8-94520

shells of revolution, thin-walled, heated, temp. field, thermostatic control 8-67003

simple materials, restrictions on heat conduction 8-63260

slab with temp. depend. thermal cond., convective boundary, transient cond., finite difference method 8-75031

snow, frost, heat transfer, cond., radiation and water vapour diffusion model 8-94563

solar collector tube, bore heat flux and outside surface temp. variations 8-90629

solid sheet with selective optical props., combined radiative and conductive heat transfer 8-90672

solid surface response to high-power incident flux, with temperature dependent absorptivity 8-51038

stochastic theory of atomic chain coupled to two reservoirs 8-54319

superconducting composite media, effect of axial conduction and metal-helium heat transfer on local stability 8-91832

surface film, heat flux density and unsteady state temp. 8-75036

synthesis of optimum boundary control (*Ukrainian*) 8-55544

thermoelastic periodic problems for infinite solid with disc shaped cracks, integral eqn. solns. (*Ukrainian*) 8-55559

thermoelectric element, arbitrary shape, cooling efficiency 8-67010

transient, accuracy, stability and oscills., calc. methods 8-94516

transient, two-dimens., crit. time step for finite element solns. 8-71260

transient convective turbulent heat transfer in tubes, thermal and hydrodynamic instability 8-83485

transient heat conduction, residual method with Lagrange multipliers 8-90630

transient nonlinear problems, optimal reference temp. for thermophys. props. 8-94517

transient problem, generalised model of inhomogeneous system 8-94521

transient problems, finite element and matrix methods calcs. 8-94515

transient radiation-conduction heat transfer in selectively absorbing media 8-90670

transient radiation-conductive heat transfer in selectively-absorbing media 8-94572

two-layer thermal shielding, pulsed heat flow, temp. field 8-59260

two-point boundary-value problems with eigenvalue parameter in boundary conditions 8-73830

underground pipeline, unsteady heat loss, analytic expressions 8-83223

unsteady heat cond. in domains of irregular boundary, numerical expts. 8-51039

unsteady heat conduction equation, numerical soln. characts. at early times 8-79185

unsteady heat conduction in quarter plane, appl. to bubble growth 8-75045

variable relaxation heat propag., exact hyperbolic eqn. soln. 8-79184

viscoelastic media, deform. theory with account of thermodiffusion (*Ukrainian*) 8-67052

viscous fluid, smooth transition to convection 8-83396

wall temperature distributions, in regions of deteriorated heat transfer 8-83377

Na vapour, heat cond., temp. discontinuity for dissociating gas 8-94887

heat content *see* **enthalpy****heat convection** *see* **convection****heat dissipation** *see* **cooling****heat engines**

book, concepts and logic of classical thermodynamics, theory of heat engines 8-81938

education, heat engines and external work, thermodynamics, conceptual expts. 8-49586

magnetic Stirling cycle wheel, refrigerator and heat engine modes of operation 8-57964

pistonless engine capable of utilising solar energy, dynamics 8-71277

solid-state engine with Nitinol memory material 8-59288

LaNi₅, appl. as H storage system for heat engines (*Ukrainian*) 8-67022

heat exchange *see* **heat transfer****heat exchangers**

see also **cooling towers**

blood heating/cooling, thermal design, equipment and blood props. considerations, appls. 8-92744

boiling crisis and press. drop, heat transfer enhancement devices 8-55638

check calculations with parallel/mixed flow, standard expressions 8-67199

condensate film flow on finned surfaces, heat transfer, heat exchanger design 8-75038

condensation augmentation, horizontal tube, using twisted tape inserts and internal fins 8-71265

counterflow heat exchangers for gas to gas appls., irreversibility concept 8-90699

cross flow heat exchanger, longit. wall heat conduction, numerical calcs. 8-90645

crossflow induced vibr. of tube banks 8-50245

electric heaters for nucl. applic. 8-86649

flow field computations in distributing collectors, MHD heat exchanger (*Russian*) 8-75227

fluid heating mantle using heat-exchanger principles 8-93665

fluidelastic vibration of tube arrays 8-94615

heat exchangers continued

- gas, in channels with lamellar surfaces and smooth ribs, flow resistance, heat exchange (*Russian*) 8-83218
 gas mixture turbulent concurrent double pipe heat exchanger equilib. and nonequilib. reaction 8-94856
 heat transfer conference, Aug. 78, Toronto, Canada 8-90624
 high capacity, inexpensive construction 8-49826
 high temp. heat exchangers, heat transfer improvements, radiation between walls, effects (*Japanese*) 8-87244
 interrupted plates type, Nusselt no. plate thickness depend. 8-87232
 longitudinal and cross flow around heat exchanger tube bundles comparison, heat transfer efficiency aspects 8-94687
 mechanically-produced unsteady boundary layer flow effect on convective heat transfer augmentation 8-71261
 models, approx. of dynamics of method of weighted residuals (*Japanese*) 8-67024
 nuclear steam generator, Cr-Mo low alloy steels suitability comparison 8-54834
 ocean thermal energy conversion plant, 100 MW, systems aspects 8-96235
 oil-cooling baffled shell-and-tube heat exchanger expt. 8-83395
 periodic flow thermal regenerator, transient performance 8-59389
 Rapadie and Phenix plants intermediate heat exchangers experience 8-82502
 small flow-through cryostat for polarization microscope 8-86327
 thermal regenerator, with variable mass flow rate, computer model 8-75047
 true vibrations numerical soln. 8-75094
 tube bank duct acoustic resonances 8-90550
 tube bundle transient heat transfer and hydrodynamics with large flow and heat flux perturbations 8-83484
 vibrations of components in liquid and two-phase cross-flow 8-90770
 wire-packed step heat exchanger for dilution refrigerators 8-54363

heat flow *see* **heat transfer****heat insulation** *see* **thermal insulation****heat losses***see also* **thermal insulation**

- high vacuum, HV bushings, for cryogenic appl. 8-81977
 plasmatron with interelectrode insert, output electrode turbulent heat transfer 8-71555
 radiation shield, for cryogenic apparatus, thermodynamic optimisation 8-81982

heat measurement *see* **thermal variables measurement****heat of adsorption**

- activated chemisorption kinetics, differential heat of adsorption meas. 8-84062
 macromolecular layer, energy of interaction between two spherical particles 8-53271
 pyridine, ethyl pyridine, heat of adsorpt. on sponge Fe, Fe₂O₃, CuO, adhesive wear, flow calorimetry 8-85193
 simple metals, atomic chemisorption, atom-jellium model 8-84066
 stearic acid, heat of adsorpt. on Fe₂O₃ powder, surface area meas. by flow calorimetry 8-81974
 transition metal (001) surface, model, chemisorption, coverage depend. of adsorption behaviour 8-71976
 Al₂O₃, adsorption of H₂O, energetics, effects of adsorption temperature on surface processes 8-60028
 Fe film, polycryst., heat of adsorpt. of H₂ and D₂ 8-91530
 Ni films, CO-covered of H₂, isotherms, resist., work function changes 8-75926
 Pt, of Cs field-emission microscopy 8-51822
 TiO₂, differential heat of chemisorption of H₂O 8-84052
 W (100), adsorbed La, depend. of work function, heat of adsorpt. on surface coverage, contact potential study 8-67912
 ZnO 1010 surface, reaction of O₂, AES, LEED, EPR, desorpt., surface cond. and work function expts. 8-95950
 ZnO, differential heat of chemisorption of H₂O 8-84052

heat of combustion

- inorganic solids, high energy irradiation, energy storage meas. 8-51581
 polymers, correlation between flammability and heat of combustion (*Polish*) 8-53246

heat of crystallisation

- Fe, glassy, heat of crystn., and bulk modulus, calc. using struct. model 8-51428
 Si, web dendritic ribbon growth, thermal analysis of solidification 8-72770

heat of dissociation

- struct. and props. exam. 8-92245
 As₄, gaseous, atomisation enthalpy and enthalpy of form., mass-spectroscopic Knudsen cell method 8-80780
 As₂Sb, As₂Sb₂, AsSb₃, and AsSb, gaseous, atomisation enthalpy and enthalpy of form., mass-spectroscopic Knudsen cell method 8-80780
 As₂Sb₂O₆, AsSb₃O₆, and As₂SbO₆, gaseous, atomisation enthalpy and enthalpy of form., mass-spectroscopic Knudsen cell method 8-80780
 BaPd, BaRh, gaseous, dissoci. energies, obs. and calc. values 8-58864
 GdS, vaporisation thermodynamics and dissoci. energy obs. 8-67822
 HgCl₂+metallic Cu+neutral salt, heat of dissociation of complex salts 8-64887
 NO, adsorbed on MgO, dimer form., heat of dissoci., EPR obs. 8-82755
 O₂-N₂, O₄ and O₂N₂ form., influence on N₂-induced O₂ absorption in Herzberg continuum 8-87429
 S_n, properties of small aggregates rel. to metallic character of Te_n 8-86985
 Sb₄, gaseous, atomisation enthalpy and enthalpy of form., mass-spectroscopic Knudsen cell method 8-80780
 Se_n, properties of small aggregates rel. to metallic character of Te_n 8-86985
 Te_n, small aggregate, metallic character 8-86985

heat of formation

- alkali metal nitrates, standard heat of formation, electron affinity 8-91295
 alkali metals, dil. binary solns., heat of formation 8-75840
 benzyl radical, MINDO/3-FORCES, geom. of heat of formation 8-66472
 cresols, ideal gas thermodynamic props. 8-75250
 haloalkanes, max. overlap approx., heat of form. and dipole moment 8-94198

heat of formation continued

- nontransition element/alkali metal systems, direct calorimetric exam. 8-84775
 phenol, ideal gas thermodynamic props. 8-75250
 quantum-defect theory of heats of formation and struct. transition energies 8-55830
 rare earth and actinide halides and oxides, stability study, energy difference between trivalent and tetravalent metal states 8-79553
 rare earth carbonates, carbonates, standard ht. of formation determ. 8-53239
 rare earth intermetallics, RGa₂, AlB₂-type struct., electron transfer, bonding, heat of form. theory 8-92499
 transition metal hydrides, electronic struct., heat of formation, single particle lifetimes, Dingle temp. meas. 8-51923
 transition metal-group IIIB alloys, relationship between struct. and thermodynamic props. (*German*) 8-91307
 vinyl radical, MINDO/3-FORCES, geom. of heat of formation 8-66472
 yttrium carbonates, standard ht. of formation determ. 8-53239
 AgPO₃-AgI glass system, solution calorimetry, enthalpy of formation (*French*) 8-64527
 α-Al₂O₃, atomic disorder, dominant type 8-63757
 As₄, gaseous, atomisation enthalpy and enthalpy of form., mass-spectroscopic Knudsen cell method 8-80780
 As₂Sb, As₂Sb₂, AsSb₃, and AsSb, gaseous, atomisation enthalpy and enthalpy of form., mass-spectroscopic Knudsen cell method 8-80780
 As₂Sb₂O₆, AsSb₃O₆, and As₂SbO₆, gaseous, atomisation enthalpy and enthalpy of form., mass-spectroscopic Knudsen cell method 8-80780
 C/H containing species, MINDO calc. (*German*) 8-82646
 CS, heat of formation from electron impact dissociation of CS₂ and OCS 8-73074
 CdCr₂Se₄, evap., mass spectra 8-53238
 ClNO₃, standard enthalpies of form. determ. (*German*) 8-53235
 ClO₂, standard enthalpies of form. determ. (*German*) 8-53235
 ClO₄⁻, single ion props. by lattice energy minimisation 8-83769
 Cl₂O, standard enthalpies of form. determ. (*German*) 8-53235
 Co-Ga system, exam. of thermodynamics of α and β' phases 8-71870
 Co₃S₄, Cu_{0.5}Co_{2.5}S₄, CuCo₂S₄, spinels, ht. of formation 8-53237
 CuCo₂S₄, Cu_{0.5}Co_{2.5}S₄, spinels, ht. of formation 8-53237
 CuH, electronic struct., heat of formation, single particle lifetimes, Dingle temp. meas. 8-51923
 Fe-Mn-C system, Gibbs energy, high temp. phase relations 8-80779
 Fe₂Mo, standard Gibbs energies, enthalpies, entropies of formation 8-61042
 Fe₃Mo₂, standard Gibbs energies, enthalpies, entropies of formation 8-61042
 FeMoO₃, standard Gibbs energies, enthalpies, entropies of formation 8-61042
 Ga/rare earth systems, direct calorimetric exam. 8-84775
 H-bond complex formation, enthalpy change due to electronic excitation, spectroscopic determ. 8-92496
 K₂CrO₄, enthalpy of form. 8-53236
 Li₃N, heat capacity 5 to 350K, thermochem. props. to 1086K 8-92500
 Li₂ZrO₃, thermal decomposition, enthalpy of formation 298.15K 8-61003
 Li₂ZrO₄, thermal decomposition, enthalpy of formation 298.15K 8-61003
 Li₂ZrO₆, thermal decomposition, enthalpy of formation 298.15K 8-61003
 Mn₃C₂, enthalpy of formation at 1320K, from enthalpy of soln. expts. 8-59945
 N₂H₄, heat of form. determ. by electron impact dissociation. 8-61040
 (NO)₂, heat of form., UV spectrum temp. depend. 8-64872
 NaBrO₃, lattice parameters, thermal expansion, defect formation energy 8-79786
 Na₂SO₄, liq., standard free energy of formation from 1160 to 1220K 8-56911
 PdH, electronic struct., heat of formation, single particle lifetimes, Dingle temp. meas. 8-51923
 Sb₄, gaseous, atomisation enthalpy and enthalpy of form., mass-spectroscopic Knudsen cell method 8-80780
 SeBr₄, enthalpy of formation determ. 8-80777
 SeCl₄, enthalpy of formation determ. 8-80777
 SiF, heat of form. mass spectrometric determ. 8-76900
 SiF₂, heat of form. mass spectrometric determ. 8-76900
 SiF₃, heat of form. mass spectrometric determ. 8-76900
 SrO, enthalpy of solution, enthalpy of formation, 298.15K, from heat of soln. meas. 8-61041
 ThH₂, ThH_{3.75}, heat capacity and thermodynamic props. to 1000K 8-91451
 U-C-N system, high temp. X-ray diffr. exam. of structure (*French*) 8-72765
 γ-VO₃, standard enthalpy of formation 8-88654
 VSi₂, thermodynamic props. determ. using ternary phase equilibria 8-91449
 V₃Si, thermodynamic props. determ. using ternary phase equilibria 8-91449
 V₃Si₃, thermodynamic props. determ. using ternary phase equilibria 8-91449

heat of fusion

- binary solid-liquid equilibria, student experiment, phase diagram computer program 8-89285
 2,6-dioxadadamantane, plastic phase, transition and fusion thermodynamics, DSC meas. 8-75603
 ethane, solid, thermodynamic props. between double solid-to-solid transition and triple point temp. 8-75828
 2-oxa-6-thiaadamantane, plastic phase, transition and fusion thermodynamics, DSC meas. 8-75603
 2-oxadadamantane, plastic phase, transition and fusion thermodynamics, DSC meas. 8-75603
 PET, thermodynamic equilib. melting parameters, effect of annealing 8-71837
 polycarbonate fibre, highly-oriented, drawing behaviour and mech. props. 8-76708
 rare earth metals, thermodynamic props. determ. form US vel. meas. 8-55912
 2-thiaadamantane, plastic phase, transition and fusion thermodynamics, DSC meas. 8-75603
³He, melting, specific heat, entropy, latent heat 8-75904

heat of fusion continued

Mo, liquid and solid, thermophysical props. 8-75808
 Pd, liq. and solid, thermophysical props. 8-75808
 TiNO₃, boiling and melting pts., heats of transformation, solid-solid transformation 8-91441

heat of mixing

cubic margules solution model, miscibility gap and crit. point behaviour 8-59925
 cyclohexane+toluene, binary liq., viscosity and excess free energy of mixing 8-51680
 cyclooctane+toluene, binary liq., viscosity and excess free energy of mixing 8-51680
 dilute binary alloys, formation energy, lattice relax. and zero-point vibrations 8-83771
 dilute binary alloys, formation energy, lattice relax. and zero-point vibrations 8-87646
 ethylbenzene+toluene, binary liq., viscosity and excess free energy of mixing 8-51680
 ethylene + N₂, gaseous, excess enthalpy, determ. by flow calorimetry 8-91057
 III-V semiconductor solid solutions, interaction parameters 8-51688
 toluene+ethylbenzene (cyclohexane) (cyclooctane), binary liq., viscosity and excess free energy of mixing 8-51680
 transition metal-group IIIB alloys, relationship between struct. and thermodynamic props. (*German*) 8-91307
 Ag-Li, solid and liquid alloys, calorimetric investigation of mixing enthalpy (*German*) 8-52773
 Ar-Kr, liq. mixture, excess thermodynamic props. 8-75836
 Au-Ni, liquid alloy system, determ. of thermodynamic props. using Knudsen effusion method, phase diagram calc. (*German*) 8-51707
 Cu-Sn liquid alloys, thermodynamic meas. 8-52765
 HNO₃ cycle process for ocean thermal energy extraction 8-53660
 K₂O-SiO₂, vap. press., thermodynamic props. and phase diagram at high temps. 8-83932
 PbO-PbSO₄ melts, thermodynamics, determination of free energies of mixing at 1253K 8-83976
 Sn-Ge(Au), liquid alloy, exam. of activity and heat of mixing, using mass spectrometry 8-51706
 Ti-O system, O/Ti<1, high-temp. thermodynamics using Tian-Calvet microcalorimetry 8-85190

heat of reaction

see also heat of combustion; heat of dissociation; heat of formation
 automatic heat flow calorimeter for heats of reaction meas. 8-54373
 basis set effect, and approx. natural orbitals, SCF CI GTO calcs. 8-76904
 4,7-dioxaoctanal, equilib. anionic polymerisation, -90 to -68°C, polar substituent effects 8-88631
 enthalpimetry, direct injection, inverse technique 8-92569
 n-octanal, equilib. anionic polymerisation, -90 to -68°C, polar substituent effects 8-88631
 polycaprolactam characteristics dependence, at equilibrium state, on polymerisation conditions, in closed system (*Japanese*) 8-95928
 CH₂+H₂→CH₄, MINDO/3-FORCES calc., activation energy and enthalpy of reaction 8-66472
 CH₃+→CH₃+H, MINDO/3-FORCES calc., activation energy and reaction enthalpy 8-66472
 NaOBr, solns., as reagents in enthalpimetric determs. 8-68954
 PbS-CdSe, phase boundary processes 8-71857

heat of solution

BCC transition metals, solubility of C 8-71861
 chemical impurities, entropy and enthalpy of solution 8-51691
 Compton scattering determ. method 8-83974
 diamond, enthalpy of solution at 1320K, enthalpy of diamond-graphite transform. 8-59945
 graphite, enthalpy of solution at 1320K, enthalpy of diamond-graphite transform. 8-59945
 polyconjugate system, interrelation between physicochem. props. and microstruct. 8-55816
 polyethylene oxide, aq. salt soln., meas.-based thermodynamic quantities 8-75525
 rare earth carbonates and chlorides in standard ht. of formation determ. 8-53239
 transition metals, solubility of H₂ and bulk modulus 8-55950
 yttrium carbonates and chlorides in standard ht. of formation determ. 8-53239
 Al, heat of soln. of H, electron charge distrib. calc. 8-51689
 Li, of H, entropy and enthalpy of solution 8-51692
 Mg, heat of soln. of H, electron charge distrib. calc. 8-51689
 Mn, enthalpy of solution at 1320K, enthalpy of form. of Mn₃C₂ 8-59945
 Mn_{0.6}Ni_{0.4}, liq., soln. enthalpies of C and Mn, enthalpy determ. for graphite-diamond transform. and Mn₃C₂ form. 8-59945
 Na, of O(N)(C)(H), entropy and enthalpy of solution 8-51692
 NaNO₂, enthalpy of soln. and dilution, obs. 8-80781
 Pd, solubility of S, 600-1000°C, H₂-H₂S gas phase composition depend. (*French*) 8-87791
 Sr, enthalpy of solution, 298.15K, rel. to SrO heat of formation determ. 8-61041
 SrO, enthalpy of solution, enthalpy of formation, 298.15K, from heat of soln. meas. 8-61041
 Ti-O system, O/Ti<1, high-temp. thermodynamics using Tian-Calvet microcalorimetry 8-85190

heat of sublimation

Ar, solid, internal energy, determ. from vapour pressure 8-91435
 GdS, vaporisation thermodynamics and dissoc. energy obs. 8-67822
 Kr, solid, internal energy, determ. from vapour pressure 8-91435
 Xe, solid, internal energy, determ. from vapour pressure 8-91435

heat of transformation

see also heat of crystallisation; heat of fusion; heat of sublimation; heat of vaporisation
 aragonite-calcite, effect of impurities, DTA 8-51662
 EBBA, phase transition enthalpies, 1 bar to 2.5 kbar 8-75814
 ethane, solid, thermodynamic props. between double solid-to-solid transition and triple point temp. 8-75828
 graphite to diamond transformation, 1320K, from enthalpy of soln. expts. 8-59945
 liquid crystal mixture phase equilibria and transition temperatures 8-63845
 mesomorphic mixtures, binary phase diagrams, thermodynamic props., diimag. anisotropy 8-95139

heat of transformation continued

metamagnetic phase diagram, determ. method 8-68254
 nematic-isotropic phase transition at high press., thermodynamics (*Russian*) 8-87778
 N-pentanol-Na-N-octanoate-water system, partial molar enthalpies 8-75543
 radial heat transfer, conduction, convection and heat of phase change 8-90700
 rare earth dicarbides, solid solns., phase transformation, strain energy 8-51672
 Ag₃SI, superionic conductor, ordered phase struct. 8-83792
 Au₃Cu, ht. of order-disorder transform., differential microcalorimetry (*French*) 8-57950
 CrAs, heat capacity, enthalpy increments, thermodynamic props., 5 to 1280K 8-91450
 Cu-Al(In), lamellar eutectoids, calorimetric determ. of interfacial enthalpy 8-60668
 Fe-C, lamellar eutectoid, calorimetric determ. of interfacial enthalpy 8-60668
 Ga₂V_{1-x}O₂, resistivity, EPR, enthalpy and entropy meas., rel. to semicond.-metal transition 8-88004
 IF₃, vapour press., phase transform. enthalpy (*German*) 8-51654
 IF₅, vapour press., phase transform. enthalpy (*German*) 8-51654
 InSb, heats of transformation for high pressure, orthorhombic modification, exam. 8-56627
 KNO₃, polymorphism, calorimetric investigation 8-75827
 MoF₆, vapour press., phase transform. enthalpy (*German*) 8-51654
 NaNO₂, enthalpy of soln. and dilution, obs. 8-80781
 α-Se, monoclinic, heat capacities and thermodynamic properties, 3-300K 8-95162
 SrAl₂O₄-BaAl₂O₄ system, solid solubility, α-β transition 8-63860
 Ti-Ag(Au)(Si), thermodynamics and kinetics of β to α_m transformation 8-84795
 TiNO₃, boiling and melting pts., heats of transformation, solid-solid transformation 8-91441
 α-U, pseudo-single cryst. and polycryst., low temp. sp. ht. 8-83972
 UF₆, vapour press., phase transform. enthalpy (*German*) 8-51654
 V₂Si, neutron irradiat., sound velocity, magnetic susceptibility and upper critical field 8-88074
 V₂Si, neutron irradiat., ht. capacity and resistivity 8-88075
 WF₆, vapour press., phase transform. enthalpy (*German*) 8-51654

heat of vapourisation

benzene, vapour-flow calorimetry 8-91058
 binary mixtures, latent heat of vapourisation, prediction 8-83930
 liquid metal, pure, surface tension and electron density 8-51803
 liquid-vapour equilibrium, Van der Waals' eqn. of state, heat of evaporation 8-51640
 low-temperature heat pipe wick evaporation (*Ukrainian*) 8-90639
 rare earth metals, theor. determ. from valence band model 8-91431
 transition metal, 3d, liq., density of states of d-band, heat of vaporisation 8-95253
 Co, liq., density of states of d-band, heat of vaporisation 8-95253
³He film adsorbed on graphite 8-87842
 MoF₆-Al₂O₃-Cr₂O₃, vacuum vaporisation, Langmuir method 8-95149
 MgO-Cr₂O₃, vacuum vaporisation 8-91434
 Ti, liq., density of states of d-band, heat of vaporisation 8-95253

heat of wetting *see wetting***heat pipes**

artery and header system, for single or two-phase operation 8-90981
 capillary struct., amount of coolant effect on operation 8-75037
 centrifugal, cylindrical, heat transfer, heat flux density and vap. press. effects 8-79188
 coloration apparatus for laser-quality alkali halide crystals 8-74917
 cryogenic heat pipe/radiator dynamic testing 8-94532
 EHD heat pipe designs, performance characts. 8-87241
 gas-controlled cryogenic heat pipe, performance anal. 8-75034
 header and artery systems, theory and design 8-94679
 low temp. heat pipe, metal-fibre wick thermal cond., heat transfer coeffs. 8-83217
 low-temperature heat pipe wick evaporation (*Ukrainian*) 8-90639
 metal-screen wick low temp. heat pipe, internal heat transfer visualisation 8-94533
 porous wick, heat transfer agent flowrate, conformal mapping approx. calc. method 8-75197
 rotating heat pipes, condensation heat transfer, noncondensable gas effects 8-51167
 surfaces covered with capillary-porous structures, heat transfer with boiling, approximate theory 8-94537
 water heat pipe, evaporator heat transfer, obs. 8-83216
 wickless tank, gas-controlled, steady-state and starting characts. 8-79187
 Ar loaded K heat pipe performance characteristics 8-89934
 Cs vapour heat pipe discharge tube pumping for 823 cm⁻¹ tunable IR laser 8-63069
 Na vapour heat pipe performance rel. to nozzle discharge theory 8-75033

heat pumps

see also heat sinks
 operating principles and performance 8-71274
 rectangular monolithic infinite cascade thermojunctions 8-57944

heat radiation

atmosphere outgoing thermal radiation, meas. rel. to O₃ profile determ. 8-92945
 atmosphere thermal radiation, particulate pollution effects rel. to climatology 8-85678
 cryogenic vessel, thermal load by radiation from the neck (*German*) 8-86276
 early universe, thermal radiation during quantum era rel. to relic radiation origin (*Russian*) 8-81717
 Earth IR emission, Lambertian, of spherical surface, radiation press. on satellite (*French*) 8-81529
 emissivities for halfspace geometry, variational procedure 8-87245
 emitter, radiant heat exchange with heated body, appl. to vapour deposition (*Russian*) 8-95701
 fluid thermal cond. meas. by transient line source method, radiation effects 8-94889
 furnace radiation flux model 8-93689
 high temp. heat exchangers, heat transfer improvements, radiation between walls, effects (*Japanese*) 8-87244

heat radiation continued

- multidimensional body, radiative-convective heating, unsteady temp. calc. method 8-90640
- multiple-plate glass systems, spectral directional radiation characts. prediction 8-74956
- nuclear reactor, fuel rod arrays, radiative heat transfer, Monte Carlo method 8-78447
- ocean thermal radiation, critical phenomena for periodically rough water surface (*Russian*) 8-81188
- parabolic boundary value problem optimal control, heating process 8-67021
- photon-scalar boson scatt., impact on Planck's radiation law and Hubble effect 8-54212
- polarisation, permanent snow fields from meas. obtained from the 'Meteor' satellite 8-88870
- radial heat transfer, conduction, convection and heat of phase change 8-90700
- radiant plate, diametrical Ar gas flow (*Russian*) 8-94565
- radiative transfer in planar medium, anisotropic scatt. and directional boundaries 8-90679
- randomly inhomogeneous stratified media, thermal radiation calc., appl. to Earth surface (*Russian*) 8-96312
- semi-transparent irradiated plate, combined conduction-radiation heat transfer, anal. soln. 8-75051
- shape factors in space thermodynamics, determ. using shape factor-meter (*German*) 8-73610
- shield, for cryogenic apparatus, thermodynamic optimisation 8-81982
- snow, frost, heat transfer, cond., radiation and water vapour diffusion model 8-94563
- steam generator, radiant heat flux distrib., light model simulation 8-94567
- Stephan's constant determ., student expt. 8-69948
- thermal conductivity prediction of heterogeneous mixture, digital simulation technique 8-87247
- vector field, electroconductive, analogy 8-90681

heat sinks

- temperature sensor with temp. sink chip on flexible dielectric cable 8-86264

heat systems

- see also boilers; heating
- No entries

heat transfer

- see also condensation; convection; cooling; evaporation; heat conduction; heat radiation; radiative transfer; thermal diffusivity
- ⁴He, superfluid, heat transfer at wall, healing and relax. 8-75899
- ablating blunt body, heat transfer near stagnation point 8-94736
- ablating body shape, numerical soln. method (*Russian*) 8-75134
- ablation of elastic solid, variational principle 8-90698
- aerodynamic heating problems with 1st order shape change, reentry vehicle, review 8-94735
- aerodynamically heated body, stable shape during ablation (*Russian*) 8-75162
- AGR, heat transfer to accel. gas flows, expt. and calcs. 8-54823
- air-steam mixtures, heat transfer to moving droplets 8-90997
- air-water interface, energy transfers at high wind speeds, effect of spray 8-85574
- air-water two-phase flow in concentric annulus, heat transfer 8-91002
- Alad'ev wall superheat correl., expt. validity test 8-83393
- alkali metal vapour condensation from gas flow (He,Ar,N₂) heat and mass transfer 8-75192
- annular turbulent flows with heat transfer 8-94718
- annulus, rot. inner cylinder, outer cylinder heat transfer to enclosed flowing liq. 8-83478
- annulus turbulent air flow heat transfer, physical prop. variability depend., expt. 8-83482
- approximation method for solution of nonlinear integral equation with error estimation for problems in heat or mass transfer (*Russian*) 8-57879
- N.Atlantic central water, vertical mixing due to salt fingers 8-85571
- axisymmetric field flow around obstacle, effect of turbulence (*Russian*) 8-83385
- bed to surface heat transfer, fluidised bed of large particles 8-63269
- bibliography 8-63425
- bibliography 8-75141
- bibliography of Soviet works on heat and mass transfer 8-75027
- Blasius flow, horizontal, heated from below, longitudinal vortices onset 8-71342
- blunt body moving in atmosphere, heat protective coating destruction (*Russian*) 8-87251
- body submerged in granular layer, heat and mass transfer 8-94536
- boiler tube, serpentine geometry at high press., two phase heat transfer 8-94077
- boiling, critical heat flux variation, very nonuniform annular heat release 8-51043
- boiling, nucleate, heat transfer model 8-75056
- boiling, nucleate, subcooled, latent heat transport contrib. 8-75046
- boiling, pool saturated, subcooled, in narrow spaces, interferometry obs. 8-94527
- boiling, pool-type, heat transfer stability prediction, finite disturbances 8-75044
- boiling and evaporating liq. heat transfer, on capillary and porous surfaces 8-94526
- boiling crisis at concentric (eccentric) annuli with turbulence promoters 8-55639
- boiling heat transfer in two-phase thermosyphons 8-90686
- boiling liquid thin film rupture, heat-transfer surface state effect 8-55552
- boiling on circumferential fins 8-59272
- boundary layer flow, laminar, thermal response behaviour 8-75136
- boundary layer on conical body with gas injection (*Japanese*) 8-59417
- boundary layer turbulence, heat transfer coeff. meas. by dilatometry 8-83388
- bubble, of vap., with microlayer, universal growth relations 8-71266
- bubble collapse, heat transfer controlled, in isothermal tube 8-90979
- bubble growth, noncondensing gas-vap. injected into liquid 8-55553
- bubbling electrofluidised bed, heat transfer rates 8-87242
- building, fundamentals in reln. to heating and cooling load calcs. 8-90628
- buried cylindrical heat source, transient temp. distrib., upper and lower bounds 8-75048

heat transfer continued

- capillary porous media with variable parameters 8-83471
- capillary-porous bodies, heat and moisture transfer, analytical formulae 8-67013
- capillary-porous body, nonlinear heat/mass transfer problem, soln. using invariant groups 8-55688
- carbon tetrachloride-I₂-water system, mass transfer in pulsed perforated plate column 8-71385
- channel, annular, with vortex generators, and uniform (nonuniform) heat injection length, crit. heat flux (*Russian*) 8-83397
- channel, rectangular, forced flow boiling and burnout 8-94530
- channel flows of high temp. gases, heat transfer 8-94722
- channel turbulent gas flow with HF press. fluctuations, heat transfer rate depend. 8-83487
- channels with single- or two-phase heat transfer fluid, computer simulation of transients 8-90969
- circular channel with laminar flow, convective heat transfer (*French*) 8-63424
- circular rods with regular polygonal concentric inner bore, heat flow shape factors 8-51048
- complex heat exchange in scatt. laminar flow in cylindrical channel 8-83490
- composite cylinder, nonstationary temp. field 8-67014
- compound unbounded cones, temp. fields (*Ukrainian*) 8-54317
- compressible gas, turbulent boundary layer, surface roughness 8-90931
- compressible nonadiabatic gas flow in tube, eqns. system numerical integration (*Russian*) 8-83427
- compressible turbulent tube flow, heat transfer 8-71314
- condensable rarefied gas flow through porous media, heat and mass transfer 8-59473
- condensate film flow on finned surfaces, heat transfer, heat exchanger design 8-75038
- condensate pattern for condensation of immiscible liquid binary vapour 8-94558
- condensation, filmwise, onto vertical fluted plate, numerical anal. 8-94552
- condensation, gas-vap. mixture, in high-press. pipe 8-94589
- condensation, laminar, intermittent charact. 8-94555
- condensation, superheated vapour in vertical tube 8-87783
- condensation augmentation, horizontal tube, using twisted tape inserts and internal fins 8-71265
- condensation in channel, local (total) heat transfer coeffs., friction factors 8-51045
- condensation in tubes with in-line static mixers, surface renewal model 8-75060
- condensation of steam in tubes, augmented internal geom., and press. drop 8-94556
- condensation of water vapour in rectangular channel, partially cooled perimeter 8-94557
- condensing turbulent annular-mist flow, wall and interfacial shear stress 8-94812
- conducting fluid, flow and heat transfer in channel in mag. field (*Russian*) 8-75218
- conference, Aug. 78, Toronto, Canada 8-90624
- conjugate, numerical method calcs. 8-94522
- conjugated heat transfer in plate in flow, integral eqn. 8-87345
- contact angle hysteresis, dropwise condensation heat transfer 8-71273
- contact heat transfer between heat-liberating element and surface of subliming solid cryoagent 8-81987
- cooling pond, heat transfer processes evaluation 8-61458
- Couette flow, permeable wall layer, heat transfer and temp. distrib. 8-51165
- critical energy in heat transfer channels of complex shape, fuel rod assembly 8-78453
- cryogenic electrical cables, heat influx problem, calc. 8-81988
- cryogenic liquids, boiling, crit. heat flux, heating surface props. effects 8-90662
- crystal growth by vertical directional crystallisation device, heat transfer, analytical investig. (*Russian*) 8-52654
- curved duct laminar flow and heat transfer 8-75144
- cylinder in cross flow in turbulent pipe flow, heat transfer 8-90874
- Darcy flow, chilled pipe freezing zone, finite difference method 8-94734
- deteriorated, in vertical steam generating tube at low pressures and moderate mass velocities of flow 8-67257
- dielectric liquid, film condensation, heat transfer enhancement in elec. field 8-55551
- diesel engine composite pistons, heat transfer calc. method (*French*) 8-63424
- dimensionless equations for heat transfer in laminar flow with variable physical properties 8-83384
- dimers, dissociating, in nonisothermal ideal gas phase, stationary state anal. 8-76848
- disc with cut-out opening, temp. gradient 8-83222
- dispersed flow, heat and mass transfer, phase transition effect 8-67252
- dispersed phase flow, heat transfer 8-90996
- drop, heat transfer, electric field effect 8-59276
- droplet evaporation, modelled by wet porous sphere, heat-transfer meas. 8-59268
- droplet evaporation on heated surfaces, theory 8-87785
- droplet vapourisation in two-phase, gas+solid particle, flow 8-55677
- droplets of soln. dispersed in gas flow, heat and mass transfer during evaporation 8-90998
- drops and films, heat and mass transfer during vapour absorpt. 8-63427
- drops in continuous flow, effect of pulsation on mass and heat transfer (*French*) 8-55686
- drops in immiscible liquid, intermittent elec. field heat transfer augmentation 8-94872
- dropwise condensation, max. drop size rel. to heat transfer coeff. 8-94559
- dropwise condensation of Hg, heat transfer meas. 8-94560
- drying, heat and mass transfer, optimal control 8-67006
- drying, temperature coeff. depend. on heat and mass transfer similarity criteria 8-83214
- dual extremum principles for heat eqn. 8-70077
- dual extremum principles for heat transfer problems with variable thermal props. 8-66999

heat transfer continued

duct, narrow, plane, temp. distrib., heat flow to dense blown layer (*Russian*) 8-83402
 duct flow, with transverse plate blockage, surface heat and mass transfer coeffs. 8-75138
 duct rotating around perpendicular axis, flow and heat transfer, finite difference method 8-94752
 Earth global heat balance, annual var. 8-73300
 eddy turbulent heat transfer in stabilised pipe flow, calc. 8-83474
 Eells-Sampson heat eqn., lifetime (*French*) 8-86227
 EHV transmission cable, in backfill, heat and mass transfer, physical props. effects 8-94543
 elastic viscoplastic body, differential rheological eqn. (*Ukrainian*) 8-55617
 electrolytic cell, nonaqueous medium, heat transfer through diaphragm 8-73049
 electronic components cooling tube, calc. method (*Russian*) 8-59271
 electroslog refining, mathematical formulation for EMF, fluid flow, and heat transfer 8-52722
 ethanol, boiling, crit. heat flux in low press. region 8-90663
 ethanol-water mixture, saturated, min. film boiling temp. on horiz. stainless steel and Cu surfaces 8-90692
 evaporation of organic solvents, internal heating by IR irradi. 8-87237
 extended liquid masses, film boiling heat transfer, partial evaporation method 8-90668
 extended surface heat transfer with condensation on to fin 8-94551
 ferromagnetic suspension, mag. field effect on heat transfer, thermal cond. 8-59500
 film boiling, minimum heat flux anal. 8-90665
 film condensation enhanced by surface forces, optimum condenser tube fin geometry 8-75039
 film condensation of steam in vertical Cu tube, heat transfer coeff. 8-94553
 finite element method of calculation (*Japanese*) 8-89414
 finned tubes with longitudinal flow 8-94731
 fins, extended surface array, heat flow evaluation, efficient algorithm 8-90635
 first-order Cosserrat fluid kinetic energy decay with heat and mass transfer 8-94524
 fixed and fluidised beds, heat transfer from particle to fluid, stochastic model 8-51234
 flat duct, inlet turbulence, local heat transfer, expt. 8-83480
 flat duct, inlet zone turbulence under differing boundary layers, heat transfer, expt. 8-83481
 flow, in tube, of air, local heat exchange meas. using heat flux transducers (*Russian*) 8-83509
 flow, nonequilib., two-phase, relation between thermal and flow characts. 8-55694
 flow, periodic thermally developed regime in ducts with streamwise periodic wall temperature or heat flux 8-59484
 flow, steam-generating tubes, rough (smooth), post-dryout, heat transfer 8-55678
 flow and heat transfer in the thermogravitational generation mode 8-94684
 flow normal to perforated plates, heat transfer and friction loss 8-94733
 fluid film, laminar, convective coupled heat transfer, Nusselt no. computation 8-59398
 fluidised bed, heat transfer from surface of fixed body 8-79368
 fluidised bed, plasma jet cooling mechanism 8-79371
 fluidised beds, heat transfer to horizontal tube (*German*) 8-59387
 fluidised beds, packed or quiescent, heat transfer from immersed heater 8-71391
 fluted tube, condensation heat transfer, Gregorig model 8-87236
 Fourier-Bessel series summation (*Polish*) 8-77818
 freezing, multidimensional problems in arbitrary domains, numerical method 8-90693
 Freon-114, Leidenfrost phenomena, crit. press. obs. 8-90667
 Freon-11, pool-boiling, heat transfer from inclined plate 8-51046
 frost, snow, heat transfer, cond., radiation and water vapour diffusion model 8-94563
 fuel element modeling rod bundle in longitud. air flow, heat transfer expt. 8-82415
 furnace heat transfer, 3-dimens, computer model predictions test 8-59504
 gas, with variable physical props., pipe flow, turbulent momentum and heat transfer calc. 8-90869
 gas flow in smooth and rough channels, heat transfer efficiency comparison 8-51243
 gas-cooled annuli, turbulent heat transfer 8-94723
 gas-liquid flow in vertical tubes, Graetz problem 8-91001
 gas-solid flow, nonreacting, heat and mass transfer, thermodynamic approach 8-51223
 gas-solid fluidised bed, particle temp. meas. 8-83464
 gas-solid particle suspension, turbulent flow in curvilinear channel, local heat exchange 8-63484
 gas-vapour droplets, nonuniform mixture, acoustic wave attenuation 8-83154
 general, anal. using CSMP package 8-75145
 generalised thermomechanics, principle of least constraint (*Russian*) 8-59295
 geothermal energy, heat extraction from hot dry rock masses 8-61378
 glass to mould heat transfer during pressing 8-80500
 granular materials pneumatically transported, heat transfer and lateral mixing 8-87378
 granulate-fluid heat exchange, analogy with calorimetry problem 8-90644
 heat flux equation, turbulent boundary layer, local similarity model 8-75142
 heat pipe, centrifugal, cylindrical, heat transfer, heat flux density and vap. press. effects 8-79188
 n-heptane, self-excited thermoacoustic oscills. in heat transfer 8-79186
 high-speed rotating anode disc, spot motion and erosion calc. 8-71498
 horizontal cylinder, local boiling heat flux density, saturated, subcooled conditions 8-90659
 horizontal heated surface, post-nucleate boiling and crit. heat flux models 8-90664
 hot film transmitter, simulation, Beuken method (*German*) 8-55546
 hot wall with impinging liq. droplet, transient temp. profile 8-75050
 human skin and subcutaneous tissue, unsteady state heat transfer, similarity transformations 8-95990

heat transfer continued

hydrodynamic thermal breakdown in viscous fluid, Couette flow between cylinders 8-83391
 hyperthermia in dogs, rel. to post surgical rewarming by thoracic flush 8-80834
 ice, heated water jet impingement melting, cavity formation, expt. and simulation 8-95133
 incompressible laminar limit layer, heat transfer with phase transition (*French*) 8-94561
 inorganic solid, interfacial endothermic reaction, abnormal thermal decomp. rate 8-76852
 insulated plate thermometer, incompressible boundary layer flow 8-55626
 insulating element, laminated, vac. drying in inert heat-transfer vap. 8-56875
 interfacial stability with heat and mass transfer, appl. to Rayleigh-Taylor and Kelvin-Helmholtz cases 8-67253
 interline region heat transfer, London-Van der Waals dispersion force effect 8-71276
 isobutane-air, in packed bed, heat and mass transfer, axial mass dispersion 8-75200
 isotropic porous media, heat and mass transfer, physical props. effects 8-94543
 Japanese literature (1975-1976) 8-79314
 jet, axisymmetric, turbulent bulge struct. 8-90955
 jet, nonisothermal axisymmetric turbulent transfer, vel. and temp. fluctuations, correl. coeffs. 8-83445
 jet, turbulent and heated, temp. and vel. meas. 8-94784
 jet heat transfer, impact model, hydrodynamic conditions 8-83447
 jet impact system with unilateral outlet, air flow, heat exchange (*Russian*) 8-83449
 jet row impinging on concave semi-cylinder surface, heat transfer, theory and expt. 8-94794
 Jupiter, solar heating and internal heat flow 8-85888
 lake vertical temp. profile determ. by one-dimensional heat transfer eqn. soln. 8-77290
 laminar boundary layer flow, heat transfer, rel. to vel. fluctuations 8-94710
 laminar boundary layer, heated, with nonuniform surface temp. distrib., stability 8-67175
 laminar boundary layer flow along vaporising liq. layer (*German*) 8-83403
 laminar compressible boundary layer swirling flow in nozzle, flow and heat transfer 8-94795
 laminar cyclone, free and forced convection 8-55548
 laminar film condensation, non-condensing gas in tube 8-94554
 laminar flow, circular channel with rod clusters, heat transfer characts. 8-75140
 laminar flow in internally finned tubes 8-94725
 laminar flow through finned tube, friction factors 8-94730
 laminar heat transfer, downstream of sudden duct enlargement 8-67196
 laminar impinging jets, heat and mass transfer 8-94777
 laminar jet, dynamic and heat problems 8-67241
 laminar-vacuum insulation, nonstationary heat and mass transfer 8-59279
 laminar-vacuum insulation, nonstationary heat and mass transfer 8-59280
 land basin with snow, radiative cooling 8-88872
 laser-fusion reactor, surface heating of 1st wall by pulsed photon and ion irradi. 8-89979
 law of metastability, appl. to effect of mag. field on boiling liqs. 8-79199
 linear heat equation from kinetic theory of gases 8-94877
 liquid, dielectrophoretic heat transfer 8-94874
 liquid droplet, direct contact with high temp. surface, Leidenfrost temp. model 8-90666
 liquid film, falling, laminar, transport augmentation by surface waves 8-71343
 liquid films, boiling, heat transfer peculiarities 8-90656
 liquid flow blockage in circular tube below freezing point, theory and expt. 8-94830
 liquid fuel droplets, transient heat flow in combustion gases, models 8-63507
 liquid fuel film, combustion behind shock wave, heat and mass transfer in turbulent boundary layer (*Russian*) 8-71401
 liquid jet, burnout in nucleate boiling 8-90991
 liquid metal film, turbulent flow down vertical wall under gravity, heat transfer 8-59396
 liquid metal heat transfer in regular fuel element arrays, Nusselt no. calc. 8-89932
 liquid metal tube flow, turbulence, heat transfer, thermogravitation effect 8-71315
 liquid metals, flow in tube in mag. field, turbulent transfer coeff. (*Russian*) 8-75220
 liquid pipe flow, heat exchange and resistance calc. 8-94819
 liquid-vapour flow, heat transfer crisis, wall shear stress 8-90986
 liquid-vapour flow, wave pattern and liq. film burnout 8-90985
 liquid-vapour flow in heat transfer crisis, liq. film limiting flow rate 8-90987
 longitudinal and cross flow around heat exchanger tube bundles comparison, heat transfer efficiency aspects 8-94687
 low temp. heat pipe, internal heat transfer visualisation 8-94533
 low temp. heat pipe, metal-fibre wick thermal cond., heat transfer coeffs. 8-83217
 magnetofluid, self-gravitating, local behaviour of congruences 8-89384
 Manicouagan impact melt sheet, Quebec, clast-melt heat transfer rel. to thermal history 8-81167
 Mars, thermal history and evolution and surface heat flux 8-65533
 mathematical model, stochastic perturbation effect 8-94546
 melting, of substrate into different miscible liq. layer, hydrodynamic instability, heat transfer 8-90695
 melting and evaporation simultaneously due to area heat source (*German*) 8-59282
 melting solid, role of natural convection 8-71275
 melting/freezing interface, annular region, perturbation soln. 8-59286
 l-menthol, vap., homogeneous nucleation, high-temp. Becker-Doering theory predictions 8-67820
 metal-liquid He interface, electron-phonon interaction, thermal boundary resistance 8-67899
 meter dynamic properties (*Russian*) 8-86265

heat transfer continued

MHD, nonsimilar incompressible laminar boundary layers, finite-difference scheme 8-79386
 MHD channel, ion slippage 8-75431
 MHD Ekman layer on porous flat plate, heat transfer, steady asymptotic soln. 8-79385
 MHD flow in rot. channel, wall conductances effect on heat transfer 8-51245
 MHD power generation problems, overview 8-87503
 MHD turbulent heat and momentum transfer in 2-dimens. channel with transverse mag. field 8-94848
 micropolar fluid on circular cylinder, thermal boundary layer 8-75174
 mixture, binary, nucleate boiling heat transfer, conc. depend. 8-87249
 moist material, external heat transfer, calc. methods, drying kinetics 8-59467
 moist materials, drying kinetics calc. method, heat (moisture) transfer 8-55555
 molecular-kinetic generalisation of the heat-transfer equation 8-67219
 multilayer antisolar glazing heat throughput calc. 8-94415
 multiphase flow, spherical particles, thermal conductivity determ. 8-71390
 muscle contraction, simulation of thermophysical processes 8-96063
 non-Newtonian fluids in jacketed agitated vessel, heat transfer, viscosity correl. 8-75143
 nonlinear, iterative-variational method 8-94511
 nonstationary heat exchange with phase transformations, delayed boiling influence (Russian) 8-83235
 nonstationary heat fluxes meas. by heat meters using auxiliary wall method 8-59275
 nuclear fuel pins, eccentrically placed pellets, finite difference method for heat transfer 8-82419
 nuclear fuel-cladding interaction between cracked surfaces, mechanical and temp. contact 8-66341
 nuclear power station spray cooling, heat and mass atmospheric transfer 8-94078
 nuclear reactor, fuel rod arrays, radiative heat transfer, Monte Carlo method 8-78447
 nuclear reactor accidents, molten fuel-coolant interaction modelling, INTER and CEFRA (Czech) 8-66352
 nucleate boiling of liq. Ar, N_2 , in centrifugal accel. field, heat transfer and flux 8-94538
 ocean heat and salt mixing, double-diffusive intrusions into density gradient 8-85569
 oil-cooling baffled shell-and-tube heat exchanger expt. 8-83395
 open cavity, modelling 8-55640
 organic heat carriers, charact. (German) 8-79198
 packed bed thermal storage systems, single- and two-phase models 8-91009
 packed beds, estimation of parameters from radial temp. profiles 8-83467
 packed beds, low Peclet number particle-to-fluid heat and mass transfer 8-94799
 packed beds, thermal response at low Reynolds number 8-87386
 partially buried buildings, heat flux through soil, calc. (German) 8-55554
 peak heat flux in pool boiling, hydrodynamic and surface effects 8-90661
 n-pentane, liquid, containing suspended particles, superheating expt. 8-90642
 pentane/chloroform mixture, liquid, containing suspended particles, superheating expt. 8-90642
 perforated plane, thermoelastic-plastic problem (Russian) 8-55571
 permeable bed boundary layer flow, temp. distrib. and Nusselt no. 8-51166
 permeable surface, injection, laminar to turbulent transition, heat and mass transfer 8-83361
 permeable tube with wall injection, transient turbulent boundary layer 8-83486
 phase boundary, moving, analytic heat eqn. soln. 8-90694
 phase transformation-involving one-dimens. thermal problems, efficient numerical technique 8-59270
 pipe, heated, vertical, gas buoyancy effect on downward flow and heat transfer 8-74427
 pipe, local heat transfer to turbulent flow, superposition principle, expt. 8-83479
 pipe flow, thermal entry length problem, numerical soln. (German) 8-83494
 pipe flow of anomalously viscous liqs. 8-59485
 pipe flow with coolant temp. depend. thermophysical props., heat transfer 8-94821
 pipe flow with thermal load variation, heat transfer 8-94820
 pipes, header and artery systems, theory and design 8-94679
 plate, downward-facing, flat, heat transfer augmentation by nonuniform elec. field corona 8-94873
 plate, thin, in gradient current flow, coupled heat exchange (Russian) 8-83398
 plate, with suction, three-dimens. fluctuating flow, heat transfer, skin friction 8-87389
 plate at angle to flow, heat loss meas. for boundary turbulence and separation 8-90846
 plate condenser with grid pattern slotlike channels, low-press. steam condensation, heat transfer 8-75040
 plate with cylindrical heat generating inclusion, temp. field (Ukrainian) 8-55549
 plates, collinear, interrupted, flow-aligned, heat transfer and press. drop 8-87232
 plates floating on air cushion, heat transfer 8-83220
 plume, turbulent, thermal, along vert. wall, struct. and heat transfer 8-90880
 PMMA, spreading of two-phase film of melt, heat and mass exchange, ignition and combustion (Russian) 8-76861
 pneumatic gauging appl. to mass and heat transfer coeff. meas. 8-58329
 polynary mixtures, natural convection boiling, heat transfer 8-90658
 pool barbotage, heat transfer coeffs., high-speed cine-photography and oscillography 8-90982
 pool flames, heat and mass transfer (German) 8-94677
 porous cylinder with intense injection, heat transfer 8-79370
 porous media, simultaneous heat and mass transfer governing eqns., soil heating appl. 8-94562

heat transfer continued

porous reactors, with temp. depend. heat generation rate, element geom. effects 8-94738
 porous sphere in low Reynolds number flow, heat transfer 8-59482
 power law fluids laminar pipe flow, heat transfer 8-59425
 premixed turbulent flame combustion, heat transfer obs. and calc. (French) 8-94688
 primary fluid heated by solar energy in linear collector, thermal regimes and appl. 8-75061
 pseudoplastic fluid, flowing upward in vert. heated tube, variable physical props. 8-90945
 pulsating laminar-boundary layer, heat transfer and skin friction 8-94711
 quenching temperature, 0.03-1.3 MPa, base material thermal props. depend. 8-94587
 radiometer optical head thermostabilisation structure 8-86316
 Rankine-Hugoniot jump conditions, viscous and thermal effects 8-59418
 re-entry vehicle heat transfer meas. in separated laminar base flow 8-61708
 refrigerant R-113 upflow in heated tube, liq. film dryout 8-90989
 regenerative refrigerators, closed-cycle, for cooling small supercond. devices, concept 8-93698
 Reynolds analogy for boiling, heat transfer 8-59277
 rib-roughened surface, friction factor and heat transfer correlations with rib characts. 8-87233
 ribbed plate, local heat transfer characts. in flow 8-83381
 rigid wall-hot gas stream interaction, heat cond. eqns. soln. 8-79194
 river to atmosphere heat and mass transfer data 8-96253
 rod bundles, boiling crisis and press. drop, heat transfer enhancement devices 8-55638
 rod bundles longitudinally bathed by gas, heat exchange intensification 8-79191
 roped tubes, helix angle effect on performance 8-94729
 rotary kiln, direct fired, exam. of heat flow processes 8-83224
 rotary kilns, direct fired, exam. of heat flow processes 8-83225
 rotating body, axisymmetric, arbitrary surface temp. distrib., thermal boundary layer, exact solns. 8-75133
 rotating cylindrical body, local heating and cooling on peripheral surface, temp. distrib. 8-67001
 rotating cylindrical pipe turbulent nonisothermal flow, temp. fluctuation and pulsatile heat flux calc. 8-83475
 rotating heat pipes, condensation heat transfer, noncondensable gas effects 8-51167
 rotating radial convergent duct, air flow heat transfer boundary conditions, turbulent and transition flow 8-83476
 rough surface heat transfer in turbulent boundary layer, mixing length hypothesis 8-83378
 rough surface turbulent flow heat and mass transfer, Reynolds analogy deviations 8-83380
 saturated liquid, boiling onset, film boiling transition, crit. heat flux densities (Russian) 8-83234
 Schrodinger invariant generalised heat eqns., similarity methods and tri- vial solns. 8-62164
 sea-atmosphere heat-transfer expts. (Russian) 8-81206
 seawater, optical anisotropy coeff., temp. fluctuation, optical meas. method 8-69488
 separated flow, theoretical anal. 8-79315
 separated flow over triangular prisms 8-87339
 separated flow with laminar mixing region, heat and mass transfer, math. simulation 8-59397
 shape of drop on inclined plane, solar still aspects 8-79856
 shearing flow over wavy boundary, heat, mass, momentum transfer, turbulence model 8-87335
 shock heat exchange, effect on shock curves (Russian) 8-75170
 shock layer, hypersonic, vibr. nonequilib., near stagnation streamline, low Reynolds no. flow 8-87417
 shuttle heat transfer in plastic displacers at low speeds 8-93700
 slip flow, MHD, over porous plate, with variable suction, heat transfer 8-79337
 snow cover energy budget, energy flux meas. 8-92859
 soils, freezing, heat flux, meas. (Japanese) 8-88835
 solar collector tube, bore heat flux and outside surface temp. variations 8-90629
 solar power plant, transient temp. vars. in primary network 8-75062
 solid transported by gas in pipe, heat output 8-63486
 solid-liquid slug flow, radial heat transfer characts. 8-63495
 colloidal solution droplets, solid, particle form., heat and mass transfer 8-95967
 solution droplets vaporisation, in high-temp. gas flow, heat and mass transfer 8-75191
 spheres in vertical flow, transient transition boiling heat fluxes 8-90994
 spray drying, of highly viscous conc. solns., heat and mass transport (Russian) 8-83230
 stagnating thermal turbulent boundary layer mean and fluctuating characts., divergent flow heat transfer 8-83370
 stationary boundary layer flow, plane heat balance eqn. asymptotic soln. (German) 8-63430
 steady and non-steady flow through IC engines inlet valve with heat transfer 8-59390
 steam, dropwise condensation, effect of condenser tube material on heat transfer 8-75059
 steam, film condensation in tube, heat transfer, vibr. effect 8-51044
 steam, horizontal flow on cylinder, condensation 8-94550
 steam condensation heat transfer on below-freezing pt. surface 8-75042
 steam condensation in annular duct flow, heat transfer to condensate film 8-94709
 steam generating tubes, burnout mechanism 8-90984
 steam jet condensation, dynamical pressure pulse effects 8-94549
 steam turbine turbulent flat jet condenser, nozzle hydraulic and heat transfer characts. 8-94793
 steam-inert gas, uncondensable gas content effect on steam condensation heat transfer in vert. tube 8-75041
 steam-water, flow characts. at high press. 8-94805
 steam-water mixture, with high vap. content, annular flow, heat transfer, press. loss 8-75193
 steel, quenched, verification of change of props. in mag. field 8-52985
 Stefan and dam problems, free boundary convexity 8-83356
 streaming, of vel. and temp., in oscill. boundary layers 8-83358

heat transfer continued

strip in shear flow, heat and mass transfer 8-51163
 subcooled film boiling heat transfer from spheres 8-51047
 superheated binary liquid mixtures, homogeneous nucleation of bubbles 8-67818
 superheated droplets, flash boiling, undergraduate student expt. 8-81748
 surfaces covered with capillary-porous structures, heat transfer with boiling, approximate theory 8-94537
 temperature drop parameter when testing with const. thermal flux 8-51049
 temperature field, heat transfer problems, linear algebraic soln. method 8-59281
 temperature fluctuation production in airstream, small scale 8-94686
 thermal instability of layer heated from below 8-63476
 thermal regenerator, with variable mass flow rate, computer model 8-75047
 thermally developed duct flow, boundary conditions rel. to Nusselt numbers 8-91016
 thermoelasticity theory with appl., book 8-79219
 thermosiphon, evaporative, heat transfer intensity in boiling section 8-67017
 thermosiphon, inverse, thermo-hydraulic design 8-94534
 three dimensional free convection flow and heat transfer along a porous vertical plate 8-90866
 Tokamak, time resolved heat flux to wall meas., sheath model with secondary electron emission 8-79468
 transformer, oil-cooled, heat exchange anal., network method (*Russian*) 8-83399
 transient boiling, bubble nucleation and growth instabilities 8-90649
 transient boundary layer on porous plate, coolant injection, laminar flow stability and heat transfer 8-83389
 transient effects, leading up to nucleate boiling 8-90650
 transient flow boiling in duct, dynamics 8-94528
 transient thermal process calculation method, approx. polynomial representation (*Russian*) 8-83211
 tube, annular high Prandtl no. flow, turbulent heat transfer, surface rejuvenation model 8-71333
 tube, horizontal, laminar combined convection, circumferentially nonuniform heating effect 8-71331
 tube, transversely finned, in air flow, metal thermal cond. effect 8-75043
 tube, vertical, laminar and turbulent heat transfer, air and Ar 8-71332
 tube, vertical, steam generating annular flow, dry-out position prediction, computer model 8-59447
 tube bundle transient heat transfer and hydrodynamics with large flow and heat flux perturbations 8-83484
 tube flow, heat transfer problem of flowing liquid solidification onto a melting wall 8-94585
 tube in convergent channel oblique flow heat transfer 8-55643
 tube inlet region, high temp. gas turbulent heat transfer, temp. factor, expt. 8-83483
 tube wall heating during steady state tube drawing (*German*) 8-84899
 tube with turbulence promoter 8-94728
 tubes with nonuniform axial heat distrib., heat transfer burnout 8-94088
 tubeside laminar flow heat transfer augmentation 8-94726
 tubular reactor, model calc. with longitudinal transfer and heat losses through sides (*Russian*) 8-73043
 turbine blade and nozzle guide vane, transient cascade, heat transfer meas., wind tunnel 8-94768
 turbulence, book 8-90839
 turbulence, grid-generated, heat transfer 8-59393
 turbulence, isotropic, spectral space, comparison between kinematic and scalar fields (*French*) 8-87334
 turbulence generated by grid, temp. fluctuations and heat flux 8-94651
 turbulence structure and mechanisms, conference, Berlin, Germany (Aug. 1977) 8-94647
 turbulent boundary layer, diffusion model and rel. to mass transfer 8-94544
 turbulent boundary layer, external flow turbulence effect 8-94713
 turbulent boundary layer, free-stream turbulence effects 8-94714
 turbulent boundary layer, Hassid-Poreh energy model anal., inc. accel. and surface heat transfer step change 8-51158
 turbulent boundary layer, periodic intermittent model for wall region 8-87336
 turbulent boundary layer, supersonic, wall temp. effect 8-94765
 turbulent boundary layer, temperature profile and Reynolds analogy expressions 8-87337
 turbulent boundary layer flow over flat plate 8-94715
 turbulent boundary layer on rough surface with blowing 8-71334
 turbulent boundary layers near separation point, numerical prediction, heat transfer (*French*) 8-94657
 turbulent duct flow, heat transfer, mixing length model 8-94720
 turbulent entry region of pipe, temp. and vel. fluctuations 8-94717
 turbulent filmwise condensation heat transfer coeffs. 8-63429
 turbulent flow at tube entry region, high Prandtl number 8-94716
 turbulent flow in channel with permeable wall 8-63426
 turbulent gas, heat transfer and heat production (*German*) 8-90867
 turbulent gas flow, acoustic oscils. effect 8-59394
 turbulent gas flow in tube, temp. fluctuations 8-94721
 turbulent heat and mass transfer in abruptly changing wall boundary conditions 8-94545
 turbulent heat and mass transfer rates at high Pr, electrochemical modelling 8-83383
 turbulent heat transfer in annulus, transient, heating element, reactor cooling theory 8-86569
 turbulent jet, structure functions of temp. fluctuations 8-71380
 turbulent jets, heat, mass and momentum transport, into ambient air 8-51210
 turbulent liquid flow in heated tube at supercritical press., heat transfer 8-71316
 turbulent non-isothermal flow, temp. pulsations 8-94712
 turbulent pipe flow with heat transfer and chem. reaction 8-51257
 turbulent water film, with different initial flow conditions and high temp. gradients, heat transfer 8-90862
 twisted air flow in permeable tube, local heat transfer 8-71338
 two-component fluid, laminar boundary layer, temp. and conc. field calcs. (*German*) 8-71386

heat transfer continued

two-phase countercurrent flow in tube, max. heat flux 8-90992
 two-phase flow, hydrodynamics and heat exchange in film flow 8-91000
 two-phase flow in pipe, effect of mass transfer on heat transfer 8-91003
 two-phase laminar flow, in circular pipe, heat transfer, inlet temp. effects 8-67265
 underground boilers; 3-D heat transfer (*Ukrainian*) 8-55550
 underground cable system, convectively cooled, temp. distrib., heat transfer correlations 8-71262
 underground pipeline, unsteady heat loss, analytic expressions 8-83223
 unsaturated porous media, heat and mass transfer, expt. and simulation (*French*) 8-94542
 upstream adiabatic zone, subsonic, supersonic downstream boundary layer heat transfer effects 8-83379
 vapour bubble, in immiscible liquid, collapse 8-94547
 vapour condensation on vertical surface, laminar flow in film condensate 8-75057
 viscomagnetic heat flux, in a Burnett regime, gas kinetic theory 8-71400
 viscometer, high pressure, non-isothermal flow, thermal boundary conditions (*German*) 8-67292
 viscous dissipation effect on heat transfer, circ. cylinder axisymmetric stagnation flow 8-51164
 water, pool boiling, produced by distrib. internal heat sources, in homogeneous nucl. reactor 8-90685
 water droplet evaporation, heat transfer characts., on heated surfaces 8-59269
 water heat pipe, evaporator heat transfer, obs. 8-83216
 water jet impinging on hot surface, boiling heat transfer 8-90993
 water-cooled swirl tubes, for neutral beam targets, heat transfer calcs. 8-67018
 wire, in longitudinal laminar air stream, heat exchange (*Russian*) 8-83401
 Al alloys, 6061, A356, forging of liquid and partially solid alloys 8-80569
 Al, rapid melting and solidification of surface layer, exam. using computer heat flow model 8-83228
 Al₂O₃, temperature drop parameter when testing with const. thermal flux 8-51049
 BF₃, boiling/condensation heat transfer props., cryogenic appls. 8-79192
 CO, boiling/condensation heat transfer props., cryogenic appls. 8-79192
 Cu, horizontal plate, pool-boiling heat transfer, nucleation centre size, surface roughness 8-90652
 Fe, rapid melting and solidification of surface layer, exam. using computer heat flow model 8-83228
 H₂-N₂-Ar, two-phase flow film boiling, in vap. generator, heat transfer 8-75190
 H₂O, boiling, crit. heat flux in low press. region 8-90663
 H₂O, sessile drop impinging on heated surface, heat and mass transfer mechanism 8-90908
 He, liq., narrow channel flow and heat transfer characts., void fraction in steady and transient states 8-55000
 He, liq., transient heat transfer, temp. meas. with μ s response time 8-71270
 He liquid, transient heat transfer, static coolant 8-75049
 He, liquid film, transient heat transfer, film boiling regime 8-83219
 He vapour column, solid vapour heat transfer, at low temps. 8-83376
 *He, superfluid, combined axial mass and heat transport 8-63894
 *He, superfluid, superheating and bubble formation 8-56000
 hydrocarbon-water, emulsions, superheated, bubble nucleation 8-61056
 Li, liq. cooled pulsed fusion reactor blanket heat transfer, numerical calc. 8-94141
 N₂, flow, cold gas, through porous-tube, heat-transfer, suction effect 8-59474
 N₂, liquid, pool boiling heat transfer from horizontal plates (*Japanese*) 8-67016
 NO, boiling/condensation heat transfer props., cryogenic appls. 8-79192
 N₂O₄, dissoc. flow in tube, heat transfer and drag 8-71402
 N₂O₄, dissociating, turbulent pipe flow, heat transfer, resistance 8-91026
 Na, liq., in vert. pipe, hydraulic resistance under boiling conditions 8-90968
 Na, liquid, heat transfer characteristics of flow field (*Japanese*) 8-54815
 Na, pool boiling heat transfer, liq. head effects 8-89951
 Na, vapourisation from capillary-porous structs. (heat tubes, vap. chambers) crit. heat flux 8-90631
 Na vapour heat pipe performance rel. to nozzle discharge theory 8-75033
 Ni, rapid melting and solidification of surface layer, exam. using computer heat flow model 8-83228
 Sn- α brass interface, heat flux rectification, rectification coefficient 8-76048
 Sn-Pb (15 wt. %), forging of liquid and partially solid alloys 8-80569

heat treatment

see also annealing; normalising; quenching (thermal); spheroidizing; tempering; thermomagnetic treatment; thermomechanical treatment
 alloy, heat-resistant, alloying and heat treatment effects on struct. and strength 8-95758
 alloy, high temperature, mechanical, thermal and corrosion props. 8-95763
 automatic induction hardening equipment 8-92284
 cellulose nitrate (CN) detectors, effect of pre-irrad. thermal treatment on track revealing props. 8-94168
 chamotte glazed masses, deformation occurring during heat treatment 8-84747
 component checking after heat treatment, steady magnetising field 8-60958
 creep rupture like improvement mechanism, reheate treatment 8-64666
 fibre lens, plastic focusing, change of ref. index profile during heat treatment process in fabricating 8-83091
 fracture mech. during creep, interference microscopy exam. of 12Kh18N9, 08Kh18N10T 8-56756

heat treatment continued

- grain and phase boundaries between crystals, conf., Konigstein, Germany (Oct. 1977) 8-72762
- granite, extraction of fission Xe, anomalous fission yields 8-96216
- Hastelloy X, relations between weld heat affected zone cracking and microstruct., Gleeble test (*Japanese*) 8-52858
- Hastelloy X, H permeability using permeation method (*Japanese*) 8-51740
- ice, floating sheet, viscoelastic response under prolonged loading 8-51093
- Inconel 706 and 718, relations between weld heat affected zone cracking and microstruct., Gleeble test (*Japanese*) 8-52858
- metal sheet strength improvement by localised thermal shock 8-88483
- optimisation, simplex method 8-84869
- polyacrylonitrile, struct. of heat treated fibres, X-ray diff. 8-83752
- polyethylene terephthalate, effects of preliminary ht. treatment on crystallisation (*German*) 8-75593
- polypropylene, crystalline, morphological aspects of crack growth 8-76761
- porcelain, conventional and rapid fired, comparison of texture and props. (*German*) 8-64510
- quartz, synthetic hydrostatic pressure effect on precip. of structure bound water in microinclusions 8-75838
- quartz, thermoluminesc., γ -irrad. sample, heat treatment 8-64418
- quartz porcelain fast fired, development of microstruct. (*German*) 8-60625
- rapid electrothermal treatment of wire 8-84871
- sitall coatings in $\text{Li}_2\text{O}-\text{Na}_2\text{O}-\text{CaO}-\text{SiO}_2$ system, heat treatment effects on tech. chars. 8-84853
- steel, abrasive wear resistance, effects of microstruct. 8-92367
- steel, alloy, HY140, fatigue crack initiation and propag. at notch tip 8-80647
- steel, alloy, HY180, fatigue crack initiation and propag. at notch tip 8-80647
- steel, alloy, Mn-Si-C, exam. of fracture toughness for sheets, using linear elastic fracture mechanics 8-56762
- steel, alloy, softening process in deformed type 15GYuT, metallographs (*Russian*) 8-52840
- steel, case-hardened cast, contact endurance rel. to austenizing (*Russian*) 8-56805
- steel, cast, effect of non-uniform struct. on props. 8-84850
- steel, Cr-Mn, powder forged, fracture processes and fracture toughness 8-72870
- steel, Cr-Mo-V, brittle failure influence of cold plastic deform. 8-72858
- steel, Cr-Mo-V, steamline bends, restorative heat treatment effects 8-68716
- steel, Cr-Mo-V (0.5, 0.5, 0.25 wt.%), heat treated, microstructure effect on threshold region fatigue 8-56757
- steel, ferrite-pearlite, cyclic behaviour, fatigue, chem. comp. and microstruct. effects 8-60833
- steel, heat treatment achievements and prospects in USSR 8-95765
- steel, heat treatment with induction heating, 8-92285
- steel, low alloy, exam. of fatigue crack growth, and Paris Law parameter relationship 8-92343
- steel, low C, $V(\text{C}, \text{N})$ precipitation and twinning in $\gamma \rightarrow \alpha$ transform. (*Polish*) 8-52807
- steel, maraging, heating of thin samples with brief ageing, N6G4M, ON18KMST 8-52866
- steel, martensite-ferrite combined microstructure, two-phase, tensile fracture strength 8-60783
- steel, Mo-V, creep rupture strength, heat treatment effects (*German*) 8-72834
- steel, Ni, microstruct., plastic zone size and crack propag. 8-60790
- steel, Ni-Mo, powder forged, fracture processes and fracture toughness 8-72870
- steel, reheat cracking in weld zone, method for evaluating sensitivity to cracking 8-72855
- steel, stainless, corrosion protection by heat treatment method 8-68836
- steel, stainless, ferritic and duplex, Mossbauer effect study of 475°C embrittlement 8-52933
- steel, stainless, maraging, type 03Kh11N10M2T2, exam. of thermal embrittlement 8-84986
- steel, stainless, maraging, type 03Kh11N10M2T, exam. of thermal brittleness 8-88526
- steel, stainless, radiation-thermal treatment, N_2O_4 coolant action, intergranular corrosion (*Russian*) 8-58357
- steel, stainless, stabilised, knife line attack phenomenon, dissoln. of carbides in thermal cycles (*Japanese*) 8-68701
- steel, stainless stabilised, knife line attack phenomenon, dissoln. of carbide during isothermal heat treatment (*Japanese*) 8-72784
- steel, strengthening by rapid electrothermal treatment 8-84870
- steel, structural mechanism of recrystallisation during ht. treatment 8-84847
- steel, tool, thermal treatment effect on abrasive wear resistance 8-92369
- steel, transformer, formation of perfect cubic texture in thin sheets (*Russian*) 8-80557
- steel, wear resistance of broaching bits in relation to boriding and heat treatment 8-85051
- steel 40Kh, thermally strengthened, influence of loading rate and sea water on K_{IC} value (*Russian*) 8-56799
- steel antioxidation protective glass enamel cladding exam. of development 8-85031
- steel bearing parts, magnetic inspection of heat treatment quality 8-73007
- steels, alloy, surface plastic deform., effect of heating conditions, types 45, 40 Kh 8-53033
- technological strength and nondestructive methods of testing during heat treatment 8-85090
- thermoplastics, post manufacture high temp. heat treatment, controlled geometry loss technique 8-52853
- Ag and Ag alloys, yield stress temp. variation hysteresis (*Russian*) 8-52905
- Al-Cu (4 wt.%), aged to contain Guinier Preston zones, crystallographic fatigue crack growth 8-60832
- Al-Cu(Mg), age-hardenable, US cavitation erosion mechanisms, effects of comp. and heat treatment 8-53002
- Al-Mg-Li alloy, 01420, surface layer props. (*Russian*) 8-80674

heat treatment continued

- Al-Zn, solid soln., exam. of evolution by thermo EMF meas. (*French*) 8-52862
- Al-Zn-Mg-Cu, alloy 7075, effect of purity level, dispersoid type, heat treatment, on fracture toughness 8-80636
- $\gamma\text{-Al}_2\text{O}_3$, heat treatment rel. to texture 8-72789
- C, anthracene char, density fluctuations effect on physical properties 8-51420
- C fibres struct. and physical props. effects of B additions and heat treatment temp. 8-68715
- C, film, work function, heat treatment 8-64563
- C, phenolic resin-derived, oxidation, ht. treatment effects 8-56790
- C steel, strain hardening parameters, determination from stress-strain curves 8-80562
- C, texture change on ht. treatment under press. 8-60687
- C-C composites, existence diagram and properties (*French*) 8-64517
- $\text{CaB}_6\text{-SmB}_6$ system complex borides, prep. and props. 8-52703
- $\text{CaF}_2\text{:U}^{5+}$, rhombic centre EPR spectrum, heat treatment effects 8-72407
- CdS layers from $\text{CdS+Cr}_2\text{O}_3$ system, effect of heat treatment on spectral distrib. of photosensitivity 8-80017
- CdS, pure and Al doped, vacuum deposited film, heat treatment effect on photoelectric props. 8-60162
- CdS, surface props., photorefectance spectra in the exciton region 8-95324
- Co-Cr-Ni-TaC, directionally solidified eutectic, mech. props. and struct., thermal cycling effects (*Russian*) 8-92282
- Co-Pt, struct. and mag. props. rel. to degree of order 8-72368
- Cr-Mn-Si steel, heat-treatment quality, higher harmonics of EMF obs. 8-60941
- $\text{Cr}_2\text{O}_3\text{-Al}_2\text{O}_3$, solid soln., effect of Cr on point of zero charge 8-61021
- Cu, high-cond., high spt. ht., for cryogenic appl., prep. 8-76670
- Cu surfaces, O_2 adsorbed, exam. of structure by LEED, O_2 pressure-temp. diagram (*Japanese*) 8-79884
- Cu-Al-Ni-Fe, (10, 5, 5 wt.%), cast microstruct. 8-80535
- $\beta\text{-Cu-In}$, unidirectionally transformed eutectoid, lamellar microstructure, influence of grain boundaries on thermal stability 8-72795
- Cu-Ni dil. paramagnetic alloys, sp. elec. resist., effect of Ni clusters (*German*) 8-95293
- Fe, atomised powder compacts for mag. cores, oxidation, compressibility, heat treatment (*Japanese*) 8-72752
- Fe, cast, heated in CO atm., obs. cracks around graphite flakes (*Japanese*) 8-84974
- Fe, cast, Mg treated, graphite modularisation by Mg gas bubbles 8-52867
- Fe, cast, nodular graphite, welded, struct. exam., heat treatment effects 8-80703
- Fe-Al (12 wt.%) alloy 23 kHz US transducer piezomagnetic props. 8-59240
- Fe-Cr, role of C in transform. by heating in $(\alpha+\gamma)$ phase (*French*) 8-52798
- Fe-Ni (20 to 100 wt.%), exam. of C diffusion coeff., in temp. range 950 to 1100°C 8-51747
- Fe-Ni (3 wt.%), grain boundary segregation microanal. using X-ray (STEM) and AES 8-87685
- Fe-Ni alloy, surface decarburisation rate in dry H_2 , soft mag. material manufacture 8-60882
- Fe-Ni-C (24, 0.45 wt.%), martensites, TEM observation of double twinning 8-76651
- Fe-Si (3 wt.%), effect of heating rate during primary recrystn. on props. after secondary recrystn. 8-84837
- $\gamma\text{-Fe}_2\text{O}_3$, prep. from thermal decomp. of $[\text{Fe}_2(\text{HCOO})_6(\text{OH})_2]\text{HCOO} \cdot 4\text{H}_2\text{O}$ and characterisation 8-80741
- $\text{Fe}_2\text{O}_3\text{-Al}_2\text{O}_3$, solid solns., effect on Fe on point of zero charge 8-61021
- n-GaAs, heat treated, origin of 1.41 eV emission band, photolum. expt. 8-72579
- n-GaAs:Te, heavily doped, interband luminesc. intensity, heat treatment effect 8-72593
- $\text{Ga}_{0.9}\text{In}_{0.1}\text{P}$, undoped liquid epitaxial layers, effect of heat treatment on photoluminescence 8-60512
- $\text{K}_2\text{O-Al}_2\text{O}_3\text{-SiO}_2$ system, crystallisation of glasses in primary phase field of leucite 8-67658
- $\text{Li}_2\text{O-Na}_2\text{O-B}_2\text{O}_3\text{-SiO}_3$, exam. of metastable phase separation region 8-88450
- $\text{LiTaO}_3\text{-SiO}_2\text{-Al}_2\text{O}_3$, transparency in relation to microstruct. 8-53005
- $\text{MgO-Al}_2\text{O}_3\text{-SiO}_2$, metastable liq. phase separation region, electron microscope exam. 8-88451
- Mo, RF sputtered, diffusion barrier props. 8-71887
- NaNO_2 , 163°C phase transition, thermal history effects on range of modulated struct. 8-95563
- $\text{Na}_2\text{O-Al}_2\text{O}_3\text{-SiO}_2\text{-TiO}_2$, effect of Cr_2O_3 , NiO, and MgO additions on crystallisation 8-87626
- $\text{Na}_2\text{O-CaO-SiO}_2$, glass, light scatt. rel. to heat treatment (*German*) 8-84598
- Ni, surface decarburisation rate in dry H_2 , soft mag. material manufacture 8-60882
- Ni/Pt double layers on Si substrate, silicide formation 8-84010
- Ni-Cr, solid soln., exam. of back stress role in creep behaviour of particle strengthened alloys 8-52889
- Ni-Cr-Al-Ti (Ti-Co), exam. of back stress role in creep behaviour of particle strengthened alloys 8-52889
- Ni-Cr-Co-Mo-Al-Ti alloys, Waspaloy, Astroloy, exam. of microstruct. effect on crack growth 8-52977
- Ni-Fe-Nb alloys, mag. permeability and struct. (*Chinese*) 8-84450
- Ni-Fe-Nb-Al alloys, mag. permeability and struct. (*Chinese*) 8-84450
- $\alpha\text{-Ni-In}$, solid solution, lamellar microstructure, influence of grain boundaries on thermal stability 8-72795
- Ni-maraging weld metal, increasing fracture toughness by heat treatment 8-72871
- Ni-Si interface, NiSi formation from Ni_2Si , Pt marker study 8-87830
- Pb-Sn, unidirectionally solidified eutectic, lamellar microstructure, influence of grain boundaries on thermal stability 8-72795
- Si:Fe, EPR and neutron activation anal. of thermal defects 8-91355
- SiC, reaction sintered, TEM exam. of recrystallisation, phase transformation 8-80567
- SiO_2 films, dehydroxylation, sintering, IR investig. (*Russian*) 8-75967
- SiO_2 glass, heat treatment study by positron annihilation 8-55812
- SiO_2 , optical fibre, phys. behaviour of neck-down region during furnace drawing 8-83127

heat treatment continued

- SiO₂, vitreous, low temp. sp. ht., effect of heat treatment 8-59955
 Si₂Te₃, passivated single cryst., elec. conductivity 8-95299
 Sn-Ni metastable alloy, surface film comp., time depend., XPS 8-60870
 Ta₂O₅, plane optical waveguide, fabrication by reactive sputtering 8-71221
 Ta₂O₅-SiO₂, plane optical waveguide, fabrication by reactive sputtering 8-71221
 α,α+β Ti alloys, structural instability during prolonged periods of heating (*Russian*) 8-56664
 Ti-Al-Mo-Cr (4.5, 5, 1.5 wt.%), CORONA-5, effect of microstructure and heat treatment on fracture 8-60805
 Ti-Al-Mo-Zr (Cr-Fe), effect of heating on thermal stability of phases, lattice constants and chem. comp. 8-56672
 Ti-Al-Sn-Cu-Zn, (5, 2.5, 3, 1.5 wt.%), embrittlement after high temperature long-time exposure (*Chinese*) 8-95792
 Ti-Mo alloys, elasticity moduli, 80-300°C (*Russian*) 8-80574
 β-Ti-Mo-V-Fe-Al (8, 8, 2, 3, wt.%), exam. of stress induced H₂ migration 8-87823
 TiC base hard metals, N₂-containing surface wear resistant layers, struct. anal. (*German*) 8-92405
 TiC-Kh6V3M steel alloy, reaction during sintering and heat treatment 8-60617
 α-U, pseudo-single cryst. and polycryst., low temp. sp. ht. 8-83972
 ZnO-Al₂O₃-SiO₂, transparent glass ceramics, heat treatment effect on microstruct. 8-56667
 ZnO-Al₂O₃-SiO₂, transparent glass-ceramic, microstruct., physical props., crystallisation ht. treatment depend. 8-80506
 p-ZnSe:As, ion implantation and heat treatment 8-87700
 Zr(HPO₄)₂, cryst., heat treated, acid strength distrib. 8-92377

heated cathodes see thermionic cathodes**heating**

- see also electric heating; induction heating; ovens; plasma heating; refractories; space heating*
 AC thermometry and DC heating circuitry in thermal props. meas. 8-74000
 atmosphere, inhomogeneous 9.6 μm O₃ band heating, new approx. method 8-88918
 chromosphere heating by solar flares, charged particles beam collisional interaction with H target 8-93095
 clusters of galaxies, intracluster gas heating by relativistic electrons rel. to X-ray and radio emission 8-57655
 composite materials, bearing capacity of designs, subject to intense surface heating 8-67057
 cone/plate system in fluid, friction heating and convection 8-87238
 dissipative heating of medium during disk rot. in bounded space 8-67012
 hollow cylinder, internal one sided heating, nomogram construction, for computing temp. state 8-63271
 hypervelocity particle impact, heating and vaporisation, temp. estimation 8-59290
 interstellar medium, heating due to weak shock waves dissipation 8-81674
 Jupiter, solar heating and internal heat flow 8-85888
 Mars, thermal history and evolution model 8-65533
 Mars dusty atmosphere, solar heating rates 8-85878
 mass-spectrometric leak detector, ion source heating up to 550°C, sensitivity improvement 8-78028
 ocean near-surface mixing layer, microstruct. in stable heating conditions 8-85568
 optimal control of heating of body with thermoelastic stress restrictions (*Ukrainian*) 8-83245
 photoelectric heating of interstellar gas 8-77587
 planetoids in early solar system, ²⁶Al as heat source 8-65511
 plasma rail accelerator, ambient medium heating expt. 8-75439
 semiconductors, temp. rise due to nonlinear heat generation 8-87983
 solar atmosphere upper layers, heating by convective noise waves dissipation in mag. struct. 8-65600
 solar chromosphere heating, acoustic shock waves dissipation and H⁺ radiation 8-96454
 solar chromosphere models, short period acoustic heating theory appl. (*Italian*) 8-85926
 solar corona, plasma heating by anomalous current dissipation 8-53895
 solar impulsive flares, adiabatic heating 8-93176
 solar wind heating and acceleration, implications of coronal fast waves evanescence 8-89147
 spacecraft atmospheric entry, body shape for minimal radiative heat inflow (*Russian*) 8-77457
 surface waves, parametric excitation, heating effect 8-67209
 urban heating patterns, satellite temp. meas. appls. 8-65393
²H-²H molten-salt-cooled fusion reactor blankets, nuclear heating and radiation leakage 8-78490

heating, buildings see space heating**heating elements**

- see also electric heating*
 C-CD based control system for Si cryst. growth 8-68623
 double helix vacuum resistance heater element design and construction details 8-49839
 implosion heating coil, radially fed, design, fabrication and appl. 8-55006
 parallel connected ohmic heating coil for double Tokamak fusion reactor 8-54930
 single crystal diffraction, heating device construction 8-74116

heavily doped semiconductor materials see heavily doped semiconductors**heavily doped semiconductors**

- see also degenerate semiconductors; superconducting semiconductors*
 density of eigenvalues, localisation, general disordered system 8-56109
 G (*Russian*) 8-56083
 impurity bands, overlapping electronic orbitals, theory 8-56102
 n-type, in MOS structs., gate biasing elec. field rel. to charge carriers 8-52092
 n-type, Mott transition, dielec. enhancement and conduction electron screening, unified treatment 8-72073
 transparent heat reflectors (*German*) 8-79197
 CdS:Cl, heavily doped, fluoresc. spectrum upper threshold calculated 8-52568
 CdTe:In, lightly- and heavily-doped, cathodoluminesc., temp., injection level and freq. depend. 8-52584

heavily doped semiconductors continued

- n-GaAs, absorption tails in surface depletion layer and bulk 8-64379
 n-GaAs, coupled plasmon-LO phonon modes, Raman scatt. meas. 8-60472
 GaAs:Te, heavily-doped, annealing-induced prismatic dislocation loops and elec. changes 8-51546
 n-GaAs:Te, interband luminesc. intensity, heat treatment effect 8-72593
 n-GaSb:Te, heavily doped, electron-hole recomb., photoluminesc. spectra 8-84644
 n-Ge, heavily doped, extrinsic sp. ht. in metallic regime 8-59956
 α-HgS, natural, yellow emission 8-68567
 N-InAs, Moss-Burstein effect, S, Sn, Te dopants 8-64389
 InN film, refl. and transmission spectra, band struct. 8-72625
 Si, 2p core levels and core exciton binding energy, photoemission obs. 8-76583
 n-Si, Debye temp., electronic effect 8-83901
 n-Si, heavily doped, extrinsic sp. ht. in metallic regime 8-59956
 n-Si, heavily doped, Raman phonons, interband excitation effects 8-52501
 n-Si, heavily doped, self energy of phonons interacting with free electrons, Raman scatt. 8-64366
 Si, polarisation dependent electrorefl. spectra, surface phenomena 8-68479
 Si:B(P), heavily diffusion-doped layers, Co diffusion 8-59982
 Si:P, characterisation by IR reflectivity 8-56501
 Si:P, electrostatic field on impurity atoms, heavy doping effects 8-51570
 Si:P, heavily doped, thermal oxidation 8-56793
 Si:P, high dose implantation, outside dislocation generation 8-87672
 Si:P, polycrystalline, thermal oxidation in wet O₂ 8-92376
 Si:P heavily-doped, photoluminescence 8-72572
 n-Si-Ge, phonon thermal cond. of hot-pressed alloy, 300-1100K 8-91494
 Si-Ge:Al, B, P, hot-pressed alloy, thermoelec. props. 8-91711
 ZnSe:In, heavily doped, Hall effect and DC cond. expts., compensating acceptors 8-52013
 ZnSe:In, impurity band cond., Hall coeff. and cond. expts. 8-72147

Heaviside layer see E-region**heavy ion excited X-ray emission see ion microprobe analysis****heavy ion-nucleus reactions**

- for inelastic heavy ion-nucleus scattering, see "heavy ion-nucleus scattering"*
 charge distribution in heavy ion-reactions 8-74304
 classical many-body model for heavy ion collisions nuclear binding energy and density 8-66302
 cohesion of nuclear matter in heavy ion collisions 8-66314
 collective transition average lifetimes, spin (30-50) region in heavy ion-nucleus reactions 8-89822
 complex nuclei interaction, generator coordinate method, microscopic treatment 8-66304
 compound nuclei, Z=98, 100, 102, statistical description of (heavy ion, xn) cross section (*Russian*) 8-86549
 continuum γ rays, multipolarity, enhanced ang. correlation meas., heavy ion-compound nucleus reactions 8-93963
 Coulomb interactions, heaviest nucleon systems, heavy ion experiments at UNILAC (*German*) 8-66435
 coupled channel Born approximation code, OUKID, finite range heavy ion direct reactions, appls. 8-89832
 cross-sections for fusion, quasifission and deep inelastic collisions (*Russian*) 8-54801
 damped-heavy-ion collisions, book contrib., review 8-82388
 deep inelastic collisions, evolution within ang. distrib. 8-86544
 deep inelastic heavy ion collisions, light particle emission, dissipation mechanism 8-50191
 deep inelastic heavy ion collisions, statistical fluctuations, quantal effects, l-window 8-89895
 deep inelastic heavy ion collisions, unified model, collectivity and statistics, coupled channel eqns. 8-66320
 deep inelastic heavy ion scatt., one body dissipation mech. 8-62567
 deep inelastic reactions, Coulomb and nuclear forces effects on double differential cross section pattern 8-70560
 deep inelastic reactions, particle transfer, excitation of collective surface vibr., in damping processes 8-70555
 deep inelastic scattering, fragment nuclides distrib., neutron rich nuclei prod., diffusion model 8-58297
 deep inelastic transfer reactions, between complex nuclei, review 8-74400
 deep-inelastic reactions, zero-point motion of surface vibr. 8-82372
 deeply inelastic collisions, form factors determ. within statistical model 8-50205
 diffusion model, KE, mass, angular distrib. and γ-ray multiplicities 8-54789
 direct reactions and scatt., multi-step processes, asymptotic and peripheral regions 8-50190
 DWBA computer program for heavy-ion transfer reactions 8-50145
 excitation function meas. using beam time saving technique 8-70721
 fireballs in high energy heavy ion collisions, hydrodynamical description 8-58294
 fission fragment angular distrib., shape of saddle point of compound nucleus (*Chinese*) 8-78427
 fission induced by heavy ion-collisions, fragment ang. distrib., reaction mech. 8-74412
 friction model for fusion and deep inelastic reactions, review 8-86546
 frictional effects in nuclear reactions with large scale collective motion, review 8-78336
 fusion, heavy ion induced, yrast lines versus entrance channel limitation 8-89929
 fusion, schematic classification of nuclear processes (*Rumanian*) 8-58313
 fusion cross section at sub-Coulomb energies, effective pot. barrier 8-58314
 fusion excitation functions, dynamical model, one-body friction 8-50224
 fusion reactions, statistical and liquid drop model anal. 8-66312
 gamma spectroscopy, in heavy ion induced reactions (*Rumanian*) 8-58300
 ground-state correlations observable in hard heavy-ion reactions 8-78406
 hadron chemistry, heavy ion collisions 8-82389

heavy ion-nucleus reactions continued

- heavy relativistic nuclei, interaction cross section and scatt. phase shift (*Russian*) 8-89908
 high energy heavy ion collisions, hydrodynamic and classical microscopic descriptions 8-54791
 high energy internuclear reactions, multiple collision theory (*Russian*) 8-94028
 high energy nuclear collisions, isobaric-gas model, shock waves, temp., density, pionisation 8-94022
 high-spin states, means and methods of investig. 8-86722
 idealized, one-body dissipation, general classical theory, quantal corrections 8-86494
 inclusive production of hadrons in particle-particle collisions at high energies, scaling low 8-54656
 influence functionals in heavy ion deep inelastic scatt. 8-62565
 interaction potential between magic nuclei, Skyrme interaction energy functional, microscopic and proximity pots. 8-62556
 K-shell ionization in heavy-ion collisions, book contrib. 8-82834
 liquid drop model generalisation (*Rumanian*) 8-58260
 mass transport theory, transport coeffs. including ang. momentum 8-58302
 massive transfer in heavy ion reactions on rare-earth targets, α - γ coincidence 8-70556
 microscopic transport theory, fragment shell struct. effects on mass transfer 8-58301
 molecular reson. in heavy-ion scatt. 8-62561
 multiple collision model anal., at high and relativistic energies 8-86542
 multiplicity distribution, shape, and low-fold coincidence probabilities 8-54779
 multiplicity distributions of charged π in 2 GeV/nucleon ^{12}C , ^{16}O induced reactions in nuclear emulsions 8-66297
 nuclear structure, conf. 8-50059
 nucleon transfer in light+heavy ion reactions, classical statistical model 8-58304
 nucleon tunnelling model of mass diffusion in deep inelastic heavy ion collisions 8-78409
 nucleus-nucleus collisions, fragmentation velocity, source vel. mass independ. correlation 8-93979
 one body dissipation and super viscosity of nuclei, nuclear fission, collisions and deformation 8-86501
 optical potential, real part, effective pot. using folding models 8-70499
 optical potentials, real part calc. by classical inversion procedure 8-89892
 parameter free model of strongly damped collisions, mass and charge variance 8-62568
 Pauli principle and absorption in heavy ion reacts. 8-50188
 polarisation in heavy ion reactions, Strutinsky model, asymptotic Clebsch-Gordan coeffs. 8-74391
 potential energy surfaces, binary fission, fusion, liquid drop model (*Rumanian*) 8-86547
 primary cosmic ray interactions with photoemulsion nuclei using satellite Intercosmos-6 (*Russian*) 8-93063
 proximity treatment of the interaction between deformed nuclei 8-78338
 QED in strong and supercritical fields 8-74193
 rarefaction of oblate shaped nuclear matter, hydrodynamics calcs. of heavy ion collisions. 8-89894
 recoil effect, kinematics of mol. states approach to heavy ion transfer reactions 8-62557
 relativistic, π^- multiplicity distrib., collective tube model 8-89902
 relativistic, composite particle formation in explosive nucleosynthesis 8-69678
 relativistic heavy ion accelerator description and applications (*German*) 8-78522
 relativistic heavy ion reactions, central collisions, review 8-50195
 retardation effects, Coulomb gauge calcs. 8-50211
 review of heavy ion physics undertaken with UNILAC 8-50194
 review of heavy ion reactions, reaction types, reaction theories 8-74401
 rotating nuclei, from heavy ion collision, high spin states instability against fission (*Rumanian*) 8-50150
 saturation effects in interactive region, microscopic anal. of $^{16}\text{O}+^{16}\text{O}$ 8-89899
 semiclassical approxs. for heavy-ion transfer reactions 8-94021
 sensitivity of real part of nucleus-nucleus potential to nuclear densities 8-82291
 separable approx. to TDHF calcs. in 3-D 8-74320
 static model of complete fission 8-86543
 statistical model for nuclei at high excitation and angular momenta 8-86523
 statistical model of deeply inelastic heavy-ion reactions 8-50192
 stellar interior, C burning products at const. temp. (*Russian*) 8-61722
 superheavy elements, search and synthesis, review 8-50117
 target nucleon+ ^6Li potential, microscopic model with antisymmetrisation effects 8-62516
 time dependent Hartree Fock solns. for heavy ion scatt., wave packets to stationary waves 8-62558
 time-dependent variational approach to heavy ion reactions 8-50193
 transfer reacts., nuclear wave function polarisability 8-54785
 viscosity, quantum phenomenology 8-54298
 α -transfer reacts. between light nuclei 8-54787
 γ -ray multiplicity, reaction mech., ang. momentum and struct. depend. (*Rumanian*) 8-89906
 Ag+ ^{40}Ar , 340 MeV, binary aspects, particle multiplicities of fragments 8-70554
 Ag+ ^9Be , breakup of ^9Be in Coulomb field 8-50203
 Ag+C, rarefaction of oblate shaped nuclear matter, hydrodynamics calcs. 8-89894
 Ag+O, rarefaction of oblate shaped nuclear matter, hydrodynamics calcs. 8-89894
 AgBr($^{40}\text{Ar},\text{X}$), 1.8 GeV, central collisions, Maxwell-Boltzmann distrib. anal. 8-66315
 AgBr($^{16}\text{O},\text{X}$), 2.1 GeV, central collisions, Maxwell-Boltzmann distrib. anal. 8-66315
 $^a\text{Ag}(^{63}\text{Cu},\text{X})\text{Y}$, A=107, 109, new Ir, Os and Re isotopes 8-70563
 $^{109}\text{Ag}+^{40}\text{Ar}$, 197 MeV, evaporation residue cross section calc. 8-50146
 $^{109}\text{Ag}+^{40}\text{Ar}$, fusion excitation functions, dynamical model calc. 8-50224

heavy ion-nucleus reactions continued

- $^{27}\text{Al}+^{12}\text{C}$, 107, 155, 197 MeV, evaporation residue ^{39}K , prompt γ deexcitation 8-74395
 $^{27}\text{Al}+^{12}\text{C}$, complete fusion cross sections, excitation functions (*Chinese*) 8-82406
 $^{27}\text{Al}+^{16}\text{O}$, fusion excitation functions, dynamical model calc. 8-50224
 $^{27}\text{Al}+^{20}\text{Ne}$, 120 MeV, prompt γ emission, reaction products deexcitation 8-74396
 $^{27}\text{Al}(^{12}\text{C},\alpha\text{n})$, 27-45 MeV, obs. of ^{34}Cl high spin states 8-82289
 $^{27}\text{Al}(^{12}\text{C},\alpha\text{n})$, high spin negative parity states in ^{34}Cl , lifetime meas. 8-74327
 $^{27}\text{Al}(^{24}\text{Mg},\alpha\text{pn})^{45}\text{Ti}$, ^{45}Ti ZZ 8-62560
 $^{36}\text{Ar}(^6\text{Li},\text{d})^{40}\text{Ca}$, 0^+ levels of ^{40}Ca , DWBA calcs. with optical model parameters 8-62571
 $^{38}\text{Ar}(^6\text{Li},\text{d})$, wave functions of 0^+ states in ^{42}Ca 8-74308
 $^{40}\text{Ar}+^{58}\text{Ni}$, triple differential cross-section, dynamical model calcs. 8-50212
 $^{197}\text{Au}+^{136}\text{Xe}$, recoil range distrib. of heavy mass products in deep inelastic reacts. 8-66309
 $^{197}\text{Au}+^{16}\text{O}$, 140 and 315 MeV, energy depend. of heavy ion peripheral reactions 8-74399
 $^{197}\text{Au}+^6\text{Li}$, 75 MeV, γ -rays form α and d fragment transfer 8-86545
 $^{197}\text{Au}+^9\text{Be}$, breakup of ^9Be in Coulomb field 8-50203
 $^{197}\text{Au}+\text{Kr}$, recoil range distrib. of heavy mass products in deep inelastic reacts. 8-66309
 $^{197}\text{Au}(^{40}\text{Ar},\text{X})$ 259 MeV, differential recoil range distributions, large contrib. of deep inelastic processes 8-70565
 $^{197}\text{Au}(^{86}\text{Kr},\text{Z},\text{f})$, 618 MeV, ang. momentum depolarisation, sequential fission 8-62585
 α -particle transfer spectroscopic factors using interacting boson approx., A=44 to 68 8-78258
 $^{10}\text{B}(^{14}\text{N},\alpha)^{20}\text{Ne}$, 10 MeV, search for resonances 8-82385
 $^{10}\text{B}(^{16}\text{O},\text{d})$, 60 MeV, ^{24}Mg yrast states up to 24 MeV excitation energy 8-89781
 ^9Be elastic scatt., 14-26 MeV, universal optical pot. determ. (*German*) 8-70552
 $^9\text{Be}+^7\text{Li}$, 2 MeV neutron energy spectrum meas. using nuclear emulsion technique 8-62574
 Bi+Xe, 1130 MeV, parameter free model of strongly damped collisions 8-62568
 $^{209}\text{Bi}+^{12}\text{C}$, complete fusion cross sections, excitation functions (*Chinese*) 8-82406
 $^{209}\text{Bi}+^{136}\text{Xe}$, 1130 MeV, differential cross section calc., statistical model 8-50192
 $^{209}\text{Bi}+^{136}\text{Xe}$, stochastic model for strongly damped collisions with liquid drop driving forces 8-89834
 $^{209}\text{Bi}+^{84}\text{Kr}$, 600 MeV, differential cross section calc., statistical model 8-50192
 $^{209}\text{Bi}+^{84}\text{Kr}$, 600 MeV, strongly damped collisions, time-depend. mean field theory 8-82374
 $^{209}\text{Bi}+^{12}\text{C}$, 60-72 MeV, excitation functions for Fr and At isotope prod. (*Chinese*) 8-82387
 $^{209}\text{Bi}(^{12}\text{C},\text{f})$, mass distrib. of fission fragments determ. (*Chinese*) 8-86558
 C+C 800 MeV/N, p and π inclusive spectra, energy and ang. distrib. 8-54790
 $^{12}\text{C}-^{12}\text{C}$ quasimolecular resonance, coupled channel anal. 8-78402
 $^{12}\text{C}+^{14}\text{B}$, 100 MeV, 2n and 2p transfer reacts., DWBA anal. 8-50207
 $^{12}\text{C}+^{12}\text{C}$, molecular config., ^{24}Mg high spin props., Strutinsky method 8-50201
 $^{12}\text{C}+^{17,18}\text{O}$ one- and many-nucleon transfer reactions at 12.6 to 14 MeV c.m. energies 8-82371
 $^{12}\text{C}+\text{ZZ}$ 8-70561
 ^{12}C -photoemulsion nucleus, 50 GeV/c, low energy particles in stars produced (*Russian*) 8-89907
 $^{12}\text{C}(^{12}\text{C},^8\text{Be})^{16}\text{O}^*$, 78 MeV, spectroscopy of high spin states in ^{16}O 8-50066
 $^{12}\text{C}(^{12}\text{C},^8\text{Be})^{16}\text{O}(\text{GS})$, excitation functions and Legendre anal. for resonance J^π assignments 8-78347
 $^{12}\text{C}(^{12}\text{C},\alpha)^{20}\text{Ne}$, populates 8p-4h 0^+ level, α -decay 8-50132
 $^{12}\text{C}(^{12}\text{C},\gamma)^{24}\text{Mg}$, 5 to 11 MeV, γ yields, resonance features 8-54799
 $^{12}\text{C}(^{13}\text{C},\text{n})$, 13.4-15.3 MeV, nonstatistical population of ^{24}Mg high spin states 8-74385
 $^{12}\text{C}(^{14}\text{N},\alpha)$, 30.3-45.5 MeV, ^{22}Na deduced levels 8-93944
 $^{12}\text{C}(^{15}\text{N},\alpha)$, 36-39 MeV, population of ^{23}Na levels 8-50070
 $^{12}\text{C}(^{16}\text{O},\alpha)^{24}\text{Mg}$, population of resonant $^{12}\text{C}+^{12}\text{C}$ states 8-62563
 $^{12}\text{C}(^{16}\text{O},^{12}\text{C})^{16}\text{O}$, 22.7 to 33.0 MeV, excitation function enhancement for 0^+ , 6.049 MeV ^{16}O state 8-58299
 $^{12}\text{C}(^{16}\text{O},^{16}\text{O})^{12}\text{C}^*$ (2^+ , 4.44 MeV) mol. reson., band crossing model 8-62562
 $^{12}\text{C}(^{16}\text{O},\alpha)^{24}\text{Mg}$, 10.9 MeV ^{28}Si resonance, spin, parity 8-74384
 $^{12}\text{C}(^{16}\text{O},\alpha\gamma)$ 42 MeV, ^{24}Mg , 11.86 MeV level, confirmation of $J^\pi=8^+$ assignment 8-70445
 $^{12}\text{C}(^{18}\text{O},^{16}\text{O})^{14}\text{C}$, two nucleon transfer reactions, one and two step transfer process anal. 8-82370
 $^{12}\text{C}(^6\text{Li},\alpha)^{14}\text{N}$, E(^6Li)=20 MeV, using polarised ^6Li source, exact finite range DWBA anal. 8-58293
 $^{12}\text{C}(^6\text{Li},\text{d})^{16}\text{O}$, 42 MeV, α spectroscopic factors, reduced widths, stellar He burning 8-89897
 $^{12}\text{C}(^7\text{Li},^1\text{H})^{16}\text{O}$, 34 MeV, α spectroscopic factors and reduced widths, stellar fusion 8-89896
 $^{13}\text{C}+^{17,18}\text{O}$ one- and many-nucleon transfer reactions at 12.6 to 14 MeV c.m. energies 8-82371
 $^{13}\text{C}(^6\text{Li},\text{d})$ 26, 29, 34 MeV, ^{17}O α -cluster states, α -decay orbital momenta and parities (*Russian*) 8-86486
 $^{14}\text{C}(^{16}\text{O},^{18}\text{O})^{12}\text{C}$, full recoil one and two step DWBA anal. 8-70564
 $^{14}\text{C}(^7\text{Li},^1\text{H})^{18}\text{O}$, 20.4 MeV, FRDWBA anal. 8-82381
 Ca+ ^{40}Ar , A=42, 48, 236 MeV, fragments mass and charge distrib. in deep inelastic reactions 8-58296
 $^{40}\text{Ca}+^{16}\text{O}$, 3-D TDHF calcs. 8-54781
 $^{40}\text{Ca}+^{16}\text{O}$, 45-63 MeV, excitation function determ. 8-82404
 $^{40}\text{Ca}+^{16}\text{O}$, inelastic scatt., exit channel distorting pot., DWBA calc. 8-94025
 $^{40}\text{Ca}+^{40}\text{Ca}$, 278 MeV, comparison of 2-D and 3-D TDHF 8-82386
 $^{40}\text{Ca}+^{40}\text{Ca}$, 278 MeV, particle transfer width, 3. dims. TDHF calcs. 8-74389
 $^{40}\text{Ca}+^{40}\text{Ca}$, 3-D TDHF calcs. 8-54781
 $^{40}\text{Ca}+^{40}\text{Ca}$, 3-dimens., time depend. HF calcs. for fusion cross sections 8-66318
 $^{40}\text{Ca}(^{12}\text{C},3\text{p})^{49}\text{V}$, ^{49}V ZZ 8-62560

heavy ion-nucleus reactions continued

- ⁴⁰Ca(¹³C, ¹⁴N)³⁹K and ⁴⁰Ca (¹³C, ¹²C)⁴¹Ca, 60, 68 MeV, spin depend. effects 8-66300
- ⁴⁰Ca(¹⁴N, 2p)⁵¹Mn, ⁵¹Mn ZZ 8-62560
- ⁴⁰Ca(⁶Li, d)⁴⁴Ti, higher-order process, coupled channels calcs. 8-82327
- ⁴⁴Ca(⁷Li, 3np)⁴⁷Ti, ⁴⁷Ti ZZ 8-62560
- ⁴⁸Ca(¹¹B, pn), 21 MeV 8-70436
- ⁴⁸Ca+heavy ion fusion evaporation reacts., yrast decay schemes 8-66308
- ⁴⁸Ca(¹⁶O, ¹⁴C)⁵⁰Ti, full recoil one and two step DWBA anal. 8-70564
- ⁴⁸Ca(¹⁶O, ¹⁴C)⁵⁰Ti, two nucleon transfer reactions, one and two step transfer process anal. 8-82370
- ⁴⁸Ca(¹⁸O, ¹⁵B)⁵¹V, mass of ¹⁵B determ. 8-70433
- ⁴⁸Ca(¹⁸O, ¹⁶O)⁵⁰Ca, two nucleon transfer reactions, one and two step transfer process anal. 8-82370
- ⁴⁸Ca(¹⁸O, α p) 70 MeV, ⁶⁰Mn, mass and β -decay half life 8-78317
- ⁴⁸Ca(⁶³Cu, X)Y, A=106, 108, 110, new Ir, Os and Re isotopes 8-70563
- ³⁵Cl(¹⁶O, α p)⁴⁵Ti, ⁴⁵Ti ZZ 8-62560
- ²⁴⁸Cm+⁴⁸Ca, search for volatile superheavy elements 8-94027
- ²⁴⁸Cm+⁴⁸Ca superheavy element prod., radiochem. separation 8-74390
- ⁵⁰Cr+⁴⁰Ar, 236 MeV, fragments mass and charge distrib. in deep inelastic reactions 8-58296
- ⁵²Cr+¹²C, 56 MeV, heavy ion fusion, evaporation model breakdown, preequilibrium α emission from ⁶⁴Zn 8-89927
- ⁵³Cr(¹⁶O, pny), 35-51 MeV, γ -spectroscopy of ⁶⁷Ga high spin levels 8-93960
- Cu+⁴⁰Ar spallation, 80 GeV, 35 radioactive nuclide prod. cross sections 8-66260
- Cu+Ne, 800 MeV/N, p and π inclusive spectra, energy and ang. distrib. 8-54790
- ⁶³Cu+¹⁴⁷Au, triple differential cross-section, dynamical model calcs. 8-50212
- ⁶³Cu+²⁰Ne, deep inelastic reaction, evaporation, energy thermalisation 8-94024
- ⁶⁵Cu(¹⁶O, p2n), 42-58 MeV, high spin states in ⁷⁸Kr, band struct. 8-74387
- ⁶⁵Cu(³²S, 2n2p), 120 MeV, ⁹³Tc ¹⁷/₂ isomer, parity mixing search, partial γ -decay widths 8-93936
- Dy(¹⁶O, xn), 70-110 MeV, high spin states in ^{172,174,176}W, decoupled quasiparticle bands, backbending 8-50199
- ⁸⁰Dy(¹⁶O, 4n), A=161, 163, 83-89 MeV, study of CC α W, A=173, 175, high-spin states, single-particle structure 8-93922
- ¹⁶⁶Er+⁸⁶Kr, 5.99 MeV/N, are γ -ray multiplicity 8-82375
- ¹⁶⁶Er+⁸⁶Kr, 5.99 MeV/N, angular-momentum dissipation in heavy-ion collisions 8-82376
- ¹⁶⁶Er+⁸⁶Kr, 602 MeV, neutron emission in strongly damped collisions 8-82373
- Eu(¹⁶O, xn), ^{162,164,165}Lu prod., γ transitions, half-lives determ. 8-62509
- ¹⁹F(⁶Li, d), 16.0 MeV, DWBA anal. of α -spectroscopic factors 8-82383
- ⁵⁴Fe(¹⁸O, 2pn), ⁶⁹As, recoil distance level lifetime meas. 8-78311
- ⁵⁶Fe+¹²C, 192 MeV, energy spectra and yields of p,d and t 8-66306
- ⁵⁶Fe+⁴⁰Ar, 236 MeV, fragments mass and charge distrib. in deep inelastic reactions 8-58296
- ⁵⁶Fe(¹⁶O, p2n), ⁶⁹As, recoil distance level lifetime meas. 8-78311
- ¹⁶⁰Gd(⁷Be, 5n), 59 MeV, multiple high spin band struct. in ¹⁶⁴Er, backbending 8-70429
- ⁷⁴Ge(¹²C, 3n)⁸³Sr, high spin states and spin ordering, γ -ray excitation functions 8-66199
- ⁷⁶Ge(¹²C, 3n)⁸⁵Sr, high spin states and spin ordering, γ -ray excitation functions 8-66199
- ¹H(¹⁵N, α), use for H depth profiling in materials (French) 8-91357
- ¹H(¹⁵N, α)¹²C, energy loss of ¹⁵N in solids, use in ¹H profiling 8-59845
- ²H(⁴⁰Ca, p), 60 MeV, ⁴¹Ca, lifetimes of excited 3/2⁻ states 8-70487
- ²⁰⁴Hg(¹³C, 5n), ²¹²Rn high spin isomers with core excited neutron configs. 8-54792
- Kr induced deeply inelastic collisions, transport eqn. appl. 8-82380
- ⁶Li+⁶Li→³He, 0.5-2.75 MeV, meas. of cross sections and fusion parameters 8-50223
- ⁷Li+⁷Li reaction, 2 MeV, neutron energy spectrum meas. using nuclear emulsion technique 8-62573
- ¹⁷⁵Lu+¹⁹F, 142 MeV fission ¹H and ⁴He emission from ¹⁹⁴Hg compound nucleus 8-50220
- ²⁴Mg(¹⁶O, ¹²C)²⁸Si, excitation functions for O⁺ and 2⁺ states of ²⁸Si 8-54800
- ²⁴Mg(³²S, 2 α p)⁴⁷V, ⁴⁷V ZZ 8-62560
- ²⁴Mg(³²S, α 3p)⁴⁹V, ⁴⁹V ZZ 8-62560
- ²⁶Mg+¹⁸O, 34 MeV, yrast states in ⁴¹K, ⁴¹Ca, spins, parities from γ meas. 8-58250
- ²⁶Mg(¹¹B, ¹⁰B)²⁷Mg, semiclassical approxs. for heavy-ion transfer reactions 8-94021
- ²⁶Mg(¹¹B, ¹⁰Be)²⁷Al, semiclassical approxs. for heavy-ion transfer reactions 8-94021
- ²⁶Mg(¹³⁶Xe, 4n), prod. of ¹⁵⁸Dy Yrast states, lifetimes 8-54793
- ²⁶Mg(¹⁴N, ^{10,11}B), 60-95 MeV, ^{29,30}Si states, reaction mech., spectroscopic factors 8-66299
- ²⁶Mg(¹⁶O, ¹⁴C)²⁸Si, full recoil one and two step DWBA anal. 8-70564
- ⁵⁵Mn(¹⁶O, 2n), ⁶⁹As, recoil distance level lifetime meas. 8-78311
- ¹⁰⁶Mo(¹⁴N, ¹²B)¹⁰²Ru, 90 and 125 MeV, spin polarisation of ¹²B 8-50196
- ¹⁴N+¹⁰B, 100 MeV, 2n and 2p transfer reacts., DWBA anal. 8-50207
- ¹⁴N+¹²C, TDHF appl. 8-54709
- ¹⁴N+ZZ 8-70561
- ¹⁴N(¹²C, α), 39.3 MeV, ²²Na deduced levels 8-93944
- NaF+Ne, 800 MeV/N, p and π inclusive spectra, energy and ang. distrib. 8-54790
- Nd+¹²C, 70.4 MeV, excitation of 3⁻ states in ^{148,150}Nd deformed nuclei 8-62559
- ⁹⁰Nd(⁶Li, xnp), A=142, 146, 150, 54-99 MeV, determ. of cross sections 8-66307
- ¹⁴⁴Nd(¹²C, 6n)¹⁵⁰Dy, 112 MeV, high spin isomers of ¹⁵⁰Dy, gamma-ray spectra 8-50075
- ¹⁴⁶Nd(¹²C, 8n)¹⁵⁰Dy, 118 MeV, high spin isomers of ¹⁵⁰Dy, gamma-ray spectra 8-50075
- ¹⁵⁰Nd(²⁰Ne, xny), multipolarities of yrast and statistical cascades, total γ conversion coeff. 8-70484

heavy ion-nucleus reactions continued

- ¹⁵⁰Nd(²⁰Ne, xny), angular momentum effects in pre-equilibrium processes 8-50208
- ¹⁵⁰Nd(²⁰Ne, xny), angular momentum effects in pre-equilibrium processes 8-50208
- Ne, 800 MeV interactions, inclusive proton spectra 8-70557
- Ni+¹²C, 107, 155, 197 MeV, evaporation residue Se, prompt γ deexcitation 8-74395
- Ni(⁶Li, d)^{62,64}Zn, multipole pairing states, correspondence between 2 and 4 particle transfer reactions 8-62569
- Ni(¹⁶O, ¹⁸O), surface transparent pots., and CCBA anal. of diffractive behaviour 8-50206
- ⁵⁸Ni+¹⁶O, 100 MeV, γ -ray circular polarisation meas. 8-54788
- ⁵⁸Ni+¹⁶O, deep-inelastic collisions, light particle pre-equilibrium emission 8-54786
- ⁵⁸Ni+²³Na, deformed aligned projectile ions, elastic scatt., fusion, polarisation effects 8-58303
- ⁵⁸Ni(¹⁶O, 2py), 54.5, 59.5, 64.5 MeV high spin and excitation energy regions in ⁷²Se, γ cascade 8-54795
- ⁵⁸Ni(¹⁶O, 2p), ⁷²Se recoil distance level lifetime meas. 8-78311
- ⁵⁸Ni(¹⁶O, α p), ⁶⁹As, recoil distance level lifetime meas. 8-78311
- ⁶⁰Ni+⁴⁰Ar, 236 MeV, fragments mass and charge distrib. in deep inelastic reactions 8-58296
- ⁶²Ni+³⁵Cl, fusion excitation functions, dynamical model calc. 8-50224
- (¹⁶O, xn), population of ^{174,175}W, ¹⁶¹Yb, γ continuum spectra, yrast cascades, dipole component 8-54794
- ¹⁶O+¹⁰B, 100 MeV, 2n and 2p transfer reacts., DWBA anal. 8-50207
- ¹⁶O+¹²C, 15-72 MeV, gross struct. in γ -ray yields 8-78405
- ¹⁶O+¹²C, 45-80 MeV, fusion cross sections using time-of-flight technique, TDMF calcs. 8-94043
- ¹⁶O+¹²C, fine struct. in fusion cross section 8-89928
- ¹⁶O+¹⁶O, high spin states of ^{30,32}P, γ -ray meas. 8-74386
- ¹⁶O+¹⁶O, 3-D TDHF calcs. 8-54781
- ¹⁶O+¹⁶O, 3-dimens., time depend. HF calcs. for fusion cross sections 8-66318
- ¹⁶O+¹⁶O, 35-80 MeV, fusion cross sections using time-of-flight technique, TDMF calcs. 8-94043
- ¹⁶O+¹⁶O, microscopic anal. of saturation effects in interactive region 8-89899
- ¹⁶O+¹⁶O, mol. config., ³⁶S high spin props., Strutinsky method 8-50201
- ¹⁶O+¹⁶O collisions, 105 MeV, appl. of 3-dimens. time-depend. HF calcs. 8-66317
- ¹⁶O+¹⁶O heavy ion folding potential, antisymmetrisation effects 8-94023
- ¹⁶O+ZZ 8-70561
- ¹⁶O(¹²C, ¹²Co)¹²C, 68 to 80 MeV, sequential decay via excited states in ¹⁶O 8-50189
- ¹⁶O(¹²C, ⁸Be)²⁰Ne*, 78 MeV, spectroscopy of high spin states in ²⁰Ne 8-50066
- ¹⁶O(⁶Li, d)²⁰Ne, 43 MeV, α spectroscopic factors, reduced widths, stellar He burning 8-89897
- ¹⁶O(⁷Li, ³He)²⁰F, 24 MeV, ang. distrib. of states below 6.25 MeV, gas target 8-82369
- ¹⁶O(α , α)¹⁶O*, resonance observation of 8p-4h state in ²⁰Ne 8-50132
- ¹⁸O+^{12,13}C fusion evaporation reactions, 100 MeV, comparison of residues with statistical calcs. 8-66311
- ¹⁸O+¹⁷O, one and two neutron transfer reacts., 18.52 MeV 8-54783
- ¹⁸O+¹⁸O, mol. config., ³⁶S high spin props., Strutinsky method 8-50201
- (¹⁸O, ¹⁵O)²¹O, 91 MeV, determ. of ²¹O mass 8-50078
- Pb, xn reactions, prod. of ¹⁵⁸Dy Yrast states, lifetimes 8-54793
- Pb targets, possibilities for producing super-heavy elements Z>102, new projectiles (Russian) 8-86548
- Pb+¹⁴N, complete fusion cross sections, excitation functions (Chinese) 8-82406
- Pb+⁴C, Pb+Ne, 800 MeV/N, p and π inclusive spectra, energy and ang. distrib. 8-54790
- Pb+Pb, positron emission, evidence for strong field QED processes 8-93833
- Pb+U, positron emission, evidence for strong field QED processes 8-93833
- ²⁰⁸Pb+¹⁶O, 140 and 315 MeV, energy depend. of heavy ion peripheral reactions 8-74399
- ²⁰⁸Pb+²⁰⁸Pb, 1600 MeV, axially symmetric TDHF 8-74398
- ²⁰⁸Pb+²⁰⁸Pb, positron form. 8-62873
- ²⁰⁸Pb+⁴⁰Ar, deeply inelastic collisions, form factors determ. within statistical model 8-50205
- ²⁰⁸Pb+⁸⁴Kr, 494 MeV, strongly damped collisions, time-depend. mean field theory 8-82374
- ²⁰⁸Pb+⁸⁴Kr, 500 and 700 MeV, differential cross section calc., statistical model 8-50192
- ²⁰⁸Pb(¹³⁶Xe, X)Y, 470 MeV, search for delayed fission products from superheavy nuclei 8-70562
- ²⁰⁸Pb(¹⁶O, ¹⁵N) 104, 138.5, 216.6 MeV, DWBA and optical model anal., energy dependence 8-82378
- ²⁰⁸Pb(¹⁶O, ¹⁵N) 312.6 MeV, optical model and DWBA anal., energy depend., lower energy comparison 8-82379
- ²⁰⁸Pb(¹⁶O, ¹⁵O), 312.6 MeV, optical model and DWBA anal., energy depend., lower energy comparison 8-82379
- ²⁰⁸Pb(¹⁶O, ¹⁷O) 104, 138.5, 216.6 MeV, DWBA and optical model anal., energy dependence 8-82378
- ²⁰⁸Pb(¹⁶O, ¹⁸O)²⁰⁶Pb, 69-73 MeV, 2 neutron transfer mechanism 8-89900
- ²⁰⁸Pb(⁴He, 2ny), ²⁰⁹Bi EM props. of particle vibration coupling states 8-70485
- ¹¹⁰Pd(⁶³Cu, X)Y, new Ir, Os and Re isotopes 8-70563
- ¹⁹²Pt+⁸⁴Kr, 370 MeV, Pt transition probabilities determ. 8-62506
- ²⁸Si(¹⁶O, α p) or (¹⁶O, 2py), high spin states, in ³⁹K and ⁴²Ca from γ meas. 8-89787
- ²⁸Si(⁷Be, α), 20 MeV, localisation of direct reaction processes, fusion and total cross sections 8-78353
- ²⁸Si(⁷Be, p), 20 MeV, localisation of direct reaction processes, fusion and total cross sections 8-78353
- Sm+O¹⁶ fusion, cross sections for spherical and deformed Sm isotopes, shape effects 8-78407
- ¹⁴⁴Sm+⁸⁶Kr, 490 MeV, γ -ray multiplicity moments 8-54798
- ¹⁵⁰Sm(⁶Li, xnp), 54-99 MeV, determ. of cross sections 8-66307
- Sn(³²S, 4ny), yrast traps and very high spin yrast states in ¹⁵²Dy 8-89778

heavy ion-nucleus reactions continued

- $^{112}\text{Sn}+^{32}\text{S}$ fusion, 160 MeV, mass, velocity, angular and charge state distribts. 8-82405
 $^{116}\text{Sn}+^{35}\text{Cl}$, fusion excitation functions, dynamical model calc. 8-50224
 $^{118}\text{Sn}(^{18}\text{O},^{16}\text{O})^{120}\text{Sn}$, 53 to 62 MeV, optimum Q value at the Coulomb barrier 8-78413
 $^{120}\text{Sn}+^{40}\text{Ar}$, deeply inelastic collisions, form factors determ. within statistical model 8-50205
 $^{120}\text{Sn}+^{86}\text{Kr}$, 5.99 MeV/N, are γ -ray multiplicity 8-82375
 $^{120}\text{Sn}(^{12}\text{C},3n)$, 52 MeV, obs. of ^{129}Ba γ -ray linear polarisation 8-50121
 $^{124}\text{Sn}+^{86}\text{Kr}$, 440 and 720 MeV, energy division versus mass of strongly damped products 8-54797
 $^{159}\text{Tb}+^{86}\text{Kr}$, 620 MeV, energy spectra, charge and ang. distribts., diffusion model 8-50202
 $^{128}\text{Te}(^{16}\text{O},5n\gamma)$, prolate-oblate transitions in Nd isotopes 8-70438
 $^{130}\text{Te}+^{28}\text{Si}$, 140 MeV, diffusion model 8-82382
 $^{130}\text{Te}(^{40}\text{Ar},n\gamma\gamma)$, angular momentum effects in pre-equilibrium processes 8-50208
 $^{232}\text{Th}+^{16}\text{O}$, 140 and 315 MeV, energy depend. of heavy ion peripheral reactions 8-74399
 $^{232}\text{Th}+^{40}\text{Ar}$, 388 MeV, differential cross section calc., statistical model 8-50192
 $^{232}\text{Th}+^{40}\text{Ar}$, 390 MeV, $Z\leq 38$ products energy spectra, reaction mechanism, dynamic deformation (*Russian*) 8-89909
 $^{48}\text{Ti}+^{16}\text{O}$, 120 MeV, deep inelastic collisions, charged particle+gamma coincidences 8-74388
 $^{48}\text{Ti}+^{16}\text{O}$, 57.74 MeV, heavy ion fusion, evaporation model breakdown, preequilibrium α emission from ^{64}Zn 8-89927
 $^{56}\text{Ti}+^{40}\text{Ar}$, 236 MeV, fragments mass and charge distribts. in deep inelastic reactions 8-58296
U+U high energy nuclear collisions, large baryon densities prod. 8-86540
 $^{238}\text{U}+^{20}\text{Ne}$, expt. and relativistic two fluid model energy spectra 8-78298
 $^{238}\text{U}+^{238}\text{U}$, 1785 MeV, cross sections, charge and mass distribts. of products 8-78408
 $^{238}\text{U}+^{40}\text{Ar}$, cross-sections for fusion, quasifission and deep inelastic collisions (*Russian*) 8-54801
 $^{238}\text{U}+^{86}\text{Kr}$, recoil range distribts. of heavy mass products in deep inelastic reacs. 8-66309
 $^{238}\text{U}(^{12}\text{C},f)$, mass distrib. of fission fragments determ. (*Chinese*) 8-86558
 $^{238}\text{U}(^{27}\text{Al},f)$ 169, 190, 227 MeV, $Z=105$ compound nucleus lifetime using shadow effect (*Russian*) 8-86563
 $^{238}\text{U}(^{40}\text{Ar},X)$, 237, 250 MeV, differential recoil range distributions, large contrib. of deep inelastic processes 8-70565
 $^{238}\text{U}(^{48}\text{Ca},X)$, 276 MeV, differential recoil range distributions, large contrib. of deep inelastic processes 8-70565
 $^{182}\text{W}+^{12}\text{C}$, 98 MeV, fission, ^1H and ^4He emission from ^{194}Hg compound nucleus 8-50220
 $^{186}\text{W}+^{86}\text{Kr}$, cross-sections for fusion, quasifission and deep inelastic collisions (*Russian*) 8-54801
Xe induced deeply inelastic collisions, transport eqn. appl. 8-82380
 $^{136}\text{Xe}+^{209}\text{Bi}$, 1130 MeV, very heavy-ion collision mechanisms 8-89905
 $^{64}\text{Zn}(^{7}\text{Li},^4\text{He})^{65}\text{Ga}$, 36 MeV, CC ^{65}Ga , spin assignments of levels by forward-angle j dependence 8-93935
 $^{64}\text{Zn}(\alpha,py)$, 13-15 MeV, γ -spectroscopy of ^{67}Ga high-spin levels 8-93960
 $^{94}\text{Zr}+^{16}\text{O}$, 140 and 315 MeV, energy depend. of heavy ion peripheral reactions 8-74399
 $^{96}\text{Zr}(^{16}\text{O},4n\gamma)$, 56 MeV, γ yields, polarisations, ang. distribts., ^{108}Cd decay scheme 8-66301

heavy ion-nucleus scattering

- band crossing model, appl. to $^{12}\text{C}+^{16}\text{O}$ scatt. 8-89898
charged particle scatt., optical pot. in approx. of strong absorption (*Russian*) 8-89839
classical microscopic model of heavy ion reactions 8-66298
Coulomb-nuclear interference, implications for reorientation effect meas. 8-70559
deeply inelastic collisions, mass transport 8-86541
direct reactions and scatt., multi-step processes, asymptotic and peripheral regions 8-50190
elastic scatt. pots., spin-orbit terms, appl. to ($^6\text{Li},^6\text{Li}$) 8-66313
generalised Fresnel model for very heavy ion elastic scatt., rel. to optical model 8-74393
generalised Fresnel model for very heavy ion elastic scatt., dynamic polarisation effects 8-74394
generalised Fresnel model for very heavy ion elastic scatt. 8-74392
microscopic anal. 8-54780
momentum projection methods in nucleus-nucleus scatt., optical pot. 1-channel problem 8-78403
nucleus-nucleus potential from liquid drop model 8-50204
optical model code A-THREE, appl. to heavy ion scatt. 8-89837
positron prod. in heavy ion collisions 8-50198
projected proton method for heavy ion energy meas., device for 3-6 MeV beams (*French*) 8-82567
QED in strong and supercritical fields 8-74193
reflected and refracted trajectories in elastic scatt. 8-50200
review of heavy ion reactions, reaction types, reaction theories 8-74401
short range correlations in nucleus-nucleus scatt. amplitude, optical phase shift expansion 8-70502
subCoulomb elastic heavy ion scatt., influence of low lying collective states 8-78414
two-proton azimuthal angle correlations, in 2 GeV/N interactions 8-62572
 $^{197}\text{Au}+^{14}\text{N}$, 161 MeV, giant resonances in inelastic scatt. 8-62564
 $^{11}\text{B}+^{12}\text{C}$ elastic scatt., resonances 8-89901
 $^{209}\text{Bi}+^{14}\text{N}$, 161 MeV, giant resonances in inelastic scatt. 8-62564
 ^{12}C , vector polarised ^6Li elastic scatt., full optical model anal. 8-70553
 $^{12}\text{C},^{12}\text{C}$ scattering, fusion cross-section, folding model study, coupled channel effects 8-89893
 $^{12}\text{C}+^{12}\text{C}$, sub-Coulomb total cross section, simple pot. model of resonances 8-66303
 $^{12}\text{C}+^{12}\text{C}$ elastic scatt., induced rot., energy depend. of optical pot. real part 8-89903

heavy ion-nucleus scattering continued

- $^{12}\text{C}+^{12}\text{C}$ in elastic scatt., high energy, resonances obs., evidence for band crossing model 8-66305
 $^{12}\text{C}+^{12}\text{C}$, rotational band fragmentation rotation-vibr. model 8-54665
 $^{12}\text{C}+^{16}\text{O}$ scatt., band crossing model of resonances 8-89898
 $^{12}\text{C}+^6\text{Li}(^7\text{Li})$, 9 MeV, isotopic shape effects in elastic scatt. of aligned ions 8-89904
 $^{12}\text{C}(^{16}\text{O},^{16}\text{O}')$ 46 to 56 MeV, $^{16}\text{O}(0^+,6.05\text{ MeV})$ intermediate struct. resonances 8-78410
 $^{12}\text{C}(^{16}\text{O},^{16}\text{O}^*)^{12}\text{C}$, 33-54 MeV, intermediate struct. resonances, ang. distribts., statistical anal. 8-82330
 $^{12}\text{C}(^{16}\text{O},^{16}\text{O})^{12}\text{C}$, 15.4 to 30.9 MeV, correlation between fusion and inelastic scatt. 8-66310
 $^{13}\text{C}+^{13}\text{C}$, appl. of molecular particle core model 8-82384
 $^{13}\text{C}+^6\text{Li}(^7\text{Li})$, 9 MeV, isotopic shape effects in elastic scatt. of aligned ions 8-89904
 $^{40}\text{Ca}+^{14}\text{N}$, 161 MeV, giant resonances in inelastic scatt. 8-62564
 $^{40}\text{Ca}+^{20}\text{Ne}$, 36-95 MeV, Coulomb-nuclear interference 8-50210
 $^{40}\text{Ca}(^{16}\text{O},^{16}\text{O}')$, 60 MeV, direct reaction calcs., ang. distribts. 8-58298
 $^{59}\text{Co}(^{16}\text{O},^{16}\text{O})$, 142 MeV, optical model anal. of ang. distrib. meas. 8-58295
 $\text{Cu}(^{16}\text{O},^{16}\text{O})$, $A=63,65$, 40 to 46 MeV, differential cross sections, G-matrix and adiabatic pot. models 8-78411
 $^{162}\text{Dy}(^{40}\text{Ar},^{40}\text{Ar}'\gamma)$, 148.6 MeV, ^{162}Dy rotational states lifetime meas. 8-50123
 $^{139}\text{La}(^{86}\text{Kr},X)$, 505, 610 and 710 MeV, elastic and deeply inelastic reactions, optical model anal. 8-66316
 $(^6\text{Li},^6\text{Li})$ elastic scatt., failure of double folded pot. model 8-62566
 ^6Li , Coulomb disintegration in field of heavy target nucleus, perturbation theory 8-66319
 $^{24}\text{Mg}+^{16}\text{O}$, 30-81 MeV, fusion cross section, elastic scatt. ang. distrib., optical model anal. 8-78412
 $^{24}\text{Mg}+^{18}\text{O}$, 32-72 MeV, fusion cross section, elastic scatt. ang. distrib., optical model anal. 8-78412
 $^{24}\text{Mg}(^{18}\text{O},^{18}\text{O})$, 29, 35 MeV, coupled channel, first order DWBA, optical pot. calcs. 8-54796
 $^{26}\text{Mg}+^{16}\text{O}$, 29-81 MeV 8-78412
 $^{150}\text{Nd}(^{40}\text{Ar},^{40}\text{Ar}'\gamma)$, 149 MeV, Doppler shift meas. of ground state bands lifetimes 8-50124
 $^{20}\text{Ne}+^{208}\text{Pb}$, elastic and inelastic, 131 MeV, ^{20}Ne nuclear moments from inelastic data 8-66204
 $^a\text{Ni}(^{32}\text{S},^{32}\text{S}')$, 72 MeV, $A=58-64$ even, magnetic mom. of 2_1^+ states 8-66202
 ^{58}Ni vector polarised ^6Li elastic scatt., full optical model anal. 8-70553
 $^{58}\text{Ni}+^{23}\text{Na}$, deformed aligned projectile ions, elastic scatt., fusion, polarisation effects 8-58303
 $^{58}\text{Ni}+^6\text{Li}(^7\text{Li})$, 12.7 MeV, isotopic shape effects in elastic scatt. of aligned ions 8-89904
 $^{60}\text{Ni}(^{16}\text{O},^{16}\text{O})$, 142 MeV, optical model anal. of ang. distrib. meas. 8-58295
 $^{60}\text{Ni}(^{18}\text{O},^{18}\text{O}')$, stripping-pick-up mechanism, coupled channel theory 8-54784
 ^{16}O , vector polarised ^6Li elastic scatt., full optical model anal. 8-70553
 $^{16}\text{O}+^{12}\text{C}$ scattering, l -depend. absorptive pot., long life pot. resonances 8-62570
 $^{16}\text{O}+\text{CNO}$, $^{16}\text{O}+\text{AgBr}$, 2 GeV/nucleon, two-proton azimuthal angle correlations 8-62572
 $^{17}\text{O}(^{16}\text{O},^{16}\text{O})$, repeated neutron transfer, coupled channels anal. 8-54782
Pb+Pb(U), positron prod. 8-50197
Pb+Pb(U), positron prod. in heavy ion collisions 8-50198
 $^{208}\text{Pb}+^{12}\text{C}(^{14}\text{N})$, giant resonances, ang. distrib., inelastic scatt. 8-62564
 $^{208}\text{Pb}(^{16}\text{O},^{16}\text{O})$ 104, 138.5, 216.6 MeV, DWBA and optical model anal., energy dependence 8-82378
 $^{208}\text{Pb}(^{16}\text{O},^{16}\text{O})$ 312.6 MeV, optical model and DWBA anal., energy depend., lower energy comparison 8-82379
 $^{208}\text{Pb}(^{40,48}\text{Ca},^{40,48}\text{Ca})$, dist. of closest approach for classical Rutherford scatt. 8-78404
 $^{208}\text{Pb}(^{40}\text{Ar},^{40}\text{Ar})$, 302 MeV 8-78404
 $^{208}\text{Pb}(^{48}\text{Ti},^{48}\text{Ti})$, 252 MeV 8-78404
 $^{194}\text{Pt}(^{16}\text{O},^{16}\text{O}')$, 7-17.5 MeV, Coulomb excitation, low lying collective state reduced matrix elements, triaxiality 8-82269
 ^{28}Si , vector polarised ^6Li elastic scatt., full optical model anal. 8-70553
 $^{28}\text{Si}(^{12}\text{C},^{12}\text{C})$, 24, 29 MeV, coupled channel, first order DWBA, optical pot. calcs. 8-54796
 $^{28}\text{Si}(^{16,18}\text{O},^{16,18}\text{O})$, near Coulomb barrier, coupled channel, first order DWBA, optical pot. calcs. 8-54796
 $^{28}\text{Si}(^{16}\text{O},^{16}\text{O})$, 142 MeV, optical model anal. of ang. distrib. meas. 8-58295
 $^{28}\text{Si}(^{16}\text{O},^{16}\text{O})$, parity depend. of heavy-ion optical pot. 8-74397
 $^{28}\text{Si}(^9\text{Be},^9\text{Be})$, 20 MeV, localisation of direct reaction processes, fusion and total cross sections 8-78353
 $^{30}\text{Si}(^{16}\text{O},^{16}\text{O})$, elastic and inelastic, 60 MeV, to 1st excited 2^+ state, coupled channels anal. 8-82377
 $^{54}\text{Sm}+^{20}\text{Ne}$, $A=148$, 150, 152, 70 MeV, Coulomb absorpt. obs. 8-70558
 ^{122}Te , backscatt. of ^4He , ^{14}N , ^{16}O , and ^{18}O , reorientation effect meas. 8-50209
 ^{128}Te backscatt. of ^4He , ^{14}N , ^{16}O , and ^{18}O , reorientation effect meas. 8-50209
U+U, positron prod. 8-50197
U+U, positron prod. in heavy ion collisions 8-50198
 $^{238}\text{U}+^{238}\text{U}$ (^{136}Xe), nuclear Coulomb excitation, inner shell ionisation and internal conversion, quasimol. formation 8-94026
 $^{136}\text{Xe}+^{209}\text{Bi}$, 1130 MeV, very heavy-ion collision mechanisms 8-89905
 $^{90}\text{Zr}+^{12}\text{C}(^{14}\text{N})$, giant resonances in inelastic scatt. 8-62564

heavy leptons

- Big Bang model, galaxy cluster missing mass from massive leptons, additional ν species 8-81719
charmonium photoprod., gluon-exchange model 8-74214
chronon in quantum theory of electron, existence of heavy leptons, neutrino spectrum 8-70008
cosmic radiation underground, search using scintillation+Cherenkov detectors 8-65470

heavy leptons continued

- dilepton and trilepton production in neutrino experiments (*Polish*) 8-89704
 discovery, props., prod. in e^+e^- collision, review 8-89694
 four-element lepton models, non-diagonal neutral currents (*Chinese*) 8-78132
 hadronic massive lepton pair prod., theory review, Drell-Yan model 8-89752
 helicity calculations for prod. in ν interactions and cascade decay 8-93870
 Higgs-Kibble mechanism and electron-muon mass ratio 8-66065
 inclusive anomalous lepton signals from leptonic and semileptonic decay modes 8-78198
 lepton mixing and neutrino oscillations, cosmic neutrinos, heavy leptons, μ decay 8-82193
 massive lepton pairs, transverse momentum distrib. from inclusive hadron prod. 8-89760
 neutral effectively stable leptons, test for existence using beam-dump expt. 8-66185
 neutral heavy lepton signatures in ν induced dilepton events, $SU(2) \times U(1)$ model 8-70353
 neutrino induced dilepton events, extraction of heavy quark and heavy lepton signals 8-74243
 neutrino oscills. and heavy lepton mixing review 8-66182
 neutrinos, limits on props. from primordial nucleosynthesis 8-57438
 primordial stable neutral heavy leptons, annihilation as source of cosmic gamma-ray background 8-93479
 QCD, hard semi-inclusive processes 8-93862
 quark model anal. of τ prod. and decay 8-54605
 stable neutral lepton, astrophysical consequences of existence 8-93091
 superheavy, review of exptl. results and theoretical advances (*German*) 8-66184
 tau, discovery and antiparticle antitau 8-58222
 trimuon prod., heavy-lepton cascade decay, energy ratios 8-66103
 trimuon prod. mechanism, $\nu(\bar{\nu})$ interactions 8-82199
 trimuon production by neutrinos, heavy lepton cascade mechanism using $SU(2) \times U(1)$ gauge model 8-58180
 $D^- \rightarrow \tau^- \bar{\nu}_\tau$, charmed mesons, heavy lepton decays, ν_τ neutrino mass depend. (*Russian*) 8-62394
 E^0 , neutral electron-type heavy lepton, and W-boson mass 8-66100
 e^+e^- annihilation, above 6 GeV, inference of τ decay 8-50042
 e^+e^- annihilation, anomalous lepton prod., charmed mesons and heavy leptons 8-66134
 $e^+e^- \rightarrow e^+e^-$ or $\mu^+\mu^-$, decay products from new charged heavy lepton pair prod. 8-74238
 $e^+e^- \rightarrow e^+X^\pm$, 3.1 to 7.4 GeV, threshold behaviour of $\tau^+\tau^-$ prod. 8-70351
 $e^+e^- \rightarrow eX$, τ branching ratio and e momentum spectrum, D decay 8-89693
 $e^+e^- \rightarrow \tau^+\tau^-$, neutral-current effects on ψ -like resonance 8-74239
 $F^- \rightarrow \tau^- \bar{\nu}_\tau$, charmed mesons, heavy lepton decays, ν_τ neutrino mass depend. (*Russian*) 8-62394
 $\mu \rightarrow e \gamma$ in Weinberg Salam model, spontaneously broken μ -like charge symm., heavy leptons (*Chinese*) 8-82191
 μ -e events, alternative heavy-lepton model 8-66102
 $\mu^+\mu^-$ anomalous prod. from e^+e^- annihilation, heavy lepton prod. and decay 8-82190
 ν associated with heavy leptons, stability, cosmological He production 8-73783
 ν high energy experimental physics at Fermilab, review 8-50028
 $\nu N \rightarrow \mu^- \mu^+ N$, 350, 400 GeV, event origin, heavy lepton or quark cascade upper limit 8-89698
 νN tetramuon prod. sources, heavy quark and lepton cascades, charm prod. 8-70356
 $\nu_e N \rightarrow \mu^- e^+$, obs. in BEBC 8-78170
 τ decay, large timelike Q^2 , conservation of vector current and current algebra 8-78155
 τ decay involving hadronic vector current 8-66101
 τ lepton, search in neutrino expts., neutrino mixing (*Russian*) 8-54604
 τ mass, from $e^+e^- \rightarrow e^+(\mu^+)+1$ charged track, cross section energy depend. 8-89695
 $\tau \rightarrow \pi \pi \pi$, π invariant mass distrib. predictions, hadronic decay rates 8-70352
 $\tau \rightarrow \pi \nu$, decay observation, branching ratio 8-89766
 $\tau \rightarrow \pi \nu$, spin 3/2 heavy leptons, decay suppression, weak current (*Chinese*) 8-82192
 $\tau \rightarrow \pi \pi \pi \pi$, π invariant mass distrib. predictions, hadronic decay rates 8-70352
 $\tau \rightarrow \mu \pi \nu$, halflife and mass determination from e^+e^- interactions 8-89765
 τ -neutrinos, in beam dump expts. 8-50004
 τ^+ as a paraelectron, positron and muon decay modes 8-50024

heavy water

- density in capillaries, temperature of maximum 8-51801
 dielectric effects, high field, Piekara factor meas. 8-68441
 dynamic simulation of the Gentilly-1 reboiler system 8-82439
 dynamic viscosity coefficient in supercritical region of parameters of state, experimental investigation 8-67845
 FIR lasers, reststrahlen laser resonator for 66 μ m line 8-55385
 gaseous, viscosity, 200-400°C, up to 300 bar 8-63527
 IR spectra, $\nu_2 + \nu_3$ band shape 8-62855
 IR spectral refl. and complex index of refr. of D_2O 8-68501
 laser, pulsed laser-pumped submm amplifier, gain spectrum 8-79000
 laser induced breakdown, comparison with H_2O 8-68453
 laser submillimetre with optical pumping energy yield, emission pulse delay time depend. on pumping pulse (*Russian*) 8-71088
 leak detection, on-line infrared analyzers, CANDU report 8-82038
 molecule, heterodyne meas. of IR absorpt. freqs. 8-55175
 molecule, vibr. freq. shifts in polyatomic solutes 8-58654
 partition function ratio, reduced, generalised finite polynomial approx. H_2O rel. to D_2O 8-66529
 sieve tray froths occurring in heavy water plants, expt. and anal. 8-82438
 sieve trays for heavy water plants, development 8-82437
 solvated electron, in D_2O , IR and vis. spectra, 292 to 445K 8-74672
 structure and motion at high pressure 8-87606
 US attenuation, for vol. viscosity, 0-60°C 8-63871
 $Cs + D_2O$, ion-pair form., energy, angle and mass anal. of products 8-70970

heavy water continued

- $D_2O + Ar(Kr)$, $(^3P_{0,2})$ state quenching cross sections 8-70912
 $D_2O + methanol-d_0(-d_2)(-d_4)$, D exchange reaction, thermodynamics 8-94328
 $NiCl_2$ -heavy water solution, inelastic neutron scattering 8-91203
- HEED** see high energy electron diffraction
- height measurement**
 No entries
- Heisenberg model**
 alloy, binary random Heisenberg ferromagnet transition temp., crit. conc. RKKY model 8-52266
 amorphisation (*Russian*) 8-80118
 amorphous ferromagnet, spin waves, effective medium approx. 8-68203
 amorphous systems, excitations and critical phenomena within framework of phenomenological models 8-52267
 anisotropic lattice spin systems, phase transitions 8-73930
 anisotropic pseudo one-dimensional Heisenberg systems, phase diagrams 8-52289
 antiferromagnet, dil., CPA calc. 8-68263
 antiferromagnet, dil. with random first- and second-neighbour exchange bonds, CPA theory 8-52187
 antiferromagnet, disordered, magnetic atom-conc. near percolation threshold, mag. props. (*Russian*) 8-80171
 antiferromagnet, ground state energy, pair correl. 8-72321
 antiferromagnet, phase diagram and multicrit. behaviour 8-56337
 antiferromagnet, phase transitions in quantum spin systems 8-84434
 antiferromagnetic, second order self-energy 8-56279
 antiferromagnetic alloy, critical behaviour (*Russian*) 8-88128
 antiferromagnetic insulator, one-dimens., Friedel type oscills. 8-60296
 asymptotic behaviour of Heisenberg model with long-range interaction 8-56282
 C^* algebra of quasiloc observables, Heisenberg eqns., boson and fermion systems 8-57854
 classical Heisenberg chains, low temp. spin dynamics 8-68243
 constant coupling approx., derivation 8-76213
 copper formate. $4D_2O$, field-induced antiferromag. order above T_c 8-84389
 coupled phonon-linear Heisenberg chain system, phase transition 8-64208
 diethylammonium-manganese chloride, spin diffusion, quasi-two-dimensional Heisenberg paramagnet 8-88129
 dilute Heisenberg antiferromagnet, mean spin on finite clusters 8-68139
 diluted, spin dynamics at elevated temp. 8-84433
 diluted Heisenberg magnet, spin diffusion const., conc. depend. 8-88089
 dimethyl ammonium manganese chloride, sp. ht., quasi-one dimens. behaviour 8-52293
 DPPH-benzene complex, ht. capacity, 0.55-20K, mag. susceptibility, 0.4-300K 8-56317
 equations of state, parametric representation in crit. region 8-79741
 ferromagnet, anharmonic, renormalised magnons and phonons 8-91837
 ferromagnet, crit. dynamics in 2+ ϵ dimens., low temp. phase 8-76262
 ferromagnet, diagram techniques for Greens functions with spin operators 8-91836
 ferromagnet, dil., mag. excitations, localisation, wavefunctions 8-60275
 ferromagnet, easy-axis, higher order corrections to spectrum 8-80222
 ferromagnet, instanton contrib. to correlation function (*Russian*) 8-95412
 ferromagnet, linear Ising-Heisenberg, spin waves vs. bound states, exact soln. 8-68202
 ferromagnet, localised magnons around surface impurity (*Russian*) 8-84376
 ferromagnet, longitudinal dynamic susceptibility 8-64181
 ferromagnet, phonon thermal cond., crit. anomalies (*Russian*) 8-80159
 ferromagnet, spin coherent state representation, spin waves excitation spectrum 8-80117
 ferromagnet, three-dimens., two magnon states, effect of next nearest neighbour interactions 8-64178
 ferromagnet, variational method for the cluster model of the structurally disordered Heisenberg ferromagnet 8-91839
 ferromagnet with random anisotropy, Curie temp., constant coupling approx. 8-76264
 ferromagnetic alloy, critical behaviour (*Russian*) 8-88127
 ferromagnetic systems, solitary bound states of magnons and lattice deformations, Dyson-Maleev representation 8-91838
 ferromagnetism, basic models, classification of theories (*Rumanian*) 8-91840
 film, spin-one isotropic, quadratic interactions, quadrupolar-paramag. T_c 8-64210
 ground state representation of infinite 1-D ferromagnet, scatt. theory 8-77807
 Heisenberg-Ising bonds, randomly mixed three dimens. system, critical props. 8-76249
 insulating systems, magnetic, review of expts. 8-68240
 lattice diffusion, Heisenberg ferromagnet 8-88090
 layered magnet, phase transition 8-76252
 linear chain, spin dynamics, theory vs. computer simulation 8-80155
 longitudinal correlation functions, for system with single-ion anisotropy 8-76214
 magnon relaxation, Heisenberg chain, in external field (*Russian*) 8-91854
 nitroxide free radical mag. interaction with lanthanides or Cu^{2+} in liqs., ESR 8-68380
 one-dimensional dilute Heisenberg system, mag. props. 8-64179
 one-dimensional disordered spin system with isotropic antiferromag. interaction, susceptibility and Knight shift (*Russian*) 8-88202
 paramagnet, electronic spin dynamics, NMR 8-76266
 paramagnet, randomly diluted, high temp. series expansion 8-56280
 paramagnet, uniaxial anisotropy, frequency moments of spin correlation function 8-84377
 planar classical Heisenberg model, quadrupole phase transition 8-95447
 pseudo-one-dimensional Heisenberg system, Neel temp. field depend. 8-68277
 quantum-classical model, high-temp. series 8-80116

Heisenberg model continued

- quasi-one-dimensional electron gas with strong on-site interaction 8-67966
- quasilow dimensional, small dilution perturbation theory at 0K 8-56281
- random magnetic bonds, phys. props. near crit. point 8-84440
- rutile structure Heisenberg paramagnets, two-spin light scatt. 8-80336
- short-range ordered mag. cluster pinning by localised optical excitation 8-68279
- spin deviation states in spin-1 system with Heisenberg and biquadratic exchange 8-84378
- spin glass, crit. dynamics 8-60295
- spin glass, random site, phase diagrams and dimensionality shift 8-52282
- spin glasses, recent developments 8-68264
- spin relaxation, Heisenberg exchange interaction between unlike free radicals 8-84490
- spin systems with three-atom exchange, elementary excitations 8-84404
- spin-1/2 ferromagnets, 1st order Green's function theory 8-72323
- spin-Peierls transition in Heisenberg Hubbard models 8-68242
- spontaneous magnetisation in d-dimensional models for $d \geq 2$ 8-72319
- susceptibility, dipolar and quadrupolar, Heisenberg-biquadratic and Blume-Emery-Griffiths interactions 8-76257
- susceptibility, dipolar and quadrupolar, Heisenberg-biquadratic and Blume-Emery-Griffiths interaction 8-76258
- TMMC, exchange-narrowed EPR linewidth, temp. depend. 8-52292
- TMMC, linear Heisenberg antiferromag., effect of mag. field on 3d ordering and spin correlations. 8-68229
- TMMC, one-dimens. Heisenberg magnet, EPR sidebands 8-88163
- transformation methods in anal. of crit. prop. 8-49771
- triangular antiferromagnetic lattice, ground state energy, upper bound determ. using renormalisation 8-76212
- two-dimensional systems, phase transitions 8-68241
- uniaxial ferromagnet, arbitrary spin and single-ion anisotropy of second order, Green's function 8-84379
- Cr complex, trimeric clusters, low temp. mag. props. 8-76261
- CrBr_3 , parametric representation of the equation of state of a Heisenberg system in the critical region 8-79741
- $\text{Cs}_2\text{FeCl}_5\text{H}_2\text{O}$, mag. phase boundaries, susceptibility, 3D Heisenberg antiferromag. behaviour 8-84420
- KCuF_3 , one-dimensional $S=1/2$ Heisenberg antiferromag., mag. energy, optical birefringence meas. 8-52467
- Mn complex, manganese (II)(1,2,4-triazole) $_2$ (NCS) $_2$, 2-dimens. Heisenberg antiferromag., mag. props. 8-72336
- MnF_2 , uniaxial antiferromag. anisotropy in paramag. susceptibility, cluster variation theory 8-52200

Heising modulation see *amplitude modulation***helical dislocations** see *screw dislocations***helicity (elementary particles)**

- dispersion sum rules for Reggeon-particle scatt. 8-54583
- dual-resonance model, M-loop amplitudes for excited states 8-50019
- G_1 , spin depend. struct. function, scaling violations 8-93880
- heavy lepton, helicity calculations for prod. in ν interactions and cascade decay 8-93870
- pomeron flip-nonflip interference term in elastic polarisation, s-channel helicity 8-50021
- pseudoscalar transition between spin-J and spin 5/2 baryon 8-50032
- QCD of large-p, hadron prod., helicity of quarks and gluons 8-50057
- Zweig suppressed decay of heavy 1^{--} vector mesons, helicity amplitudes 8-54616
- γ -Pomeron-Regge vertex function, spin depend. calc., multiperipheral model 8-82223
- $K^+p \rightarrow \pi^+Y^*(1385)$, 11.5 GeV/c, confirmation of exchange degeneracy predictions in line reversed reac. 8-82247
- Λ helicity meas. in $\Xi^0 \rightarrow \Lambda \pi^0$ 8-93878
- NN $I=1$ amplitudes struct. at 6 GeV/c 8-70395
- pp helicity amplitudes at $t=0$, dispersion theoretic anal. 8-62340
- pp inelastic scatt., cross sections for opposite helicities, parity violation 8-62435
- pp total cross-section difference of pure helicity states, 2100 to 2500 MeV, obs. of structs. 8-78206
- $\pi^+p \rightarrow K^+Y^*(1385)$, 11.5 GeV/c confirmation of exchange degeneracy predictions in line reversed reac. 8-82247
- τ^+ as a paraelectron, daughter lepton helicities 8-50024

heliconssee also *solid-state plasma*

- metal, helicon-phonon interaction for parallel wave propagation 8-64054
- n-InSb powder, microwave propag., 90-300K, magnetoplasma and helicon wave excitations 8-72183

helicopters

- icing problems, role of meteorology 8-85657
- rotor noise, simplified Mach number scaling law 8-83167

heliotron see *plasma devices***heliports** see *airports***helium**

- see also *nuclei with*
- see also *helium atoms; liquid helium; solid helium*
- abundance enhancement in planetary nebulae 8-93376
- adsorbed ^3He on graphite, sp. ht. 8-87842
- adsorption on metal, interaction energy, quantum mech. density functional formalism calc., comp. with expt. 8-67911
- afterglow, electron energy distrib., radial variation 8-71570
- afterglow, electron energy distrib. and collisions during decay, peculiarities 8-63621
- afterglow plasma, $\text{He}(2^3\text{S}_1)+e \rightarrow \text{He}(1^1\text{S}_0)+e+\text{KE}$, rate const., electron energy distrib. 8-71571
- beam-plasma discharge, optical radiation polarisation 8-67478
- blister formation in irradi. Mo, vacancy mutation to divacancies by He trapping 8-51601
- bubbles, and voids, with ringed images in Nb-Zr (1%), TEM and SEM 8-51529
- bubbles growth in Nb-Zr (1 wt.%), α -particle effects 8-67749
- chemisorption on Pd(111) surface, mol. beam scatt. expts. 8-79878
- Clausius-Mossotti function, exam. of variation with gas density 8-52418
- condensation forevacuum pump 8-86282

helium continued

- constricted glow discharge, space charge double layer influence obs. 8-67492
- continuum radiation emission obs. to near vacuum UV 8-71582
- cooling system, for fusion reactor molten salt hybrid blanket 8-62614
- cryogenic discharge, current oscills. 8-67463
- DC discharge electron free streaming wave propagation obs. 8-75314
- dielectric breakdown across epoxy insulation 8-62658
- discharge, hollow-cathode, radiation signals in weak mag. field 8-70789
- discharge, positive column, axial electric field in transverse mag. field 8-55766
- discharge lamp, UV, monochromated, addition to XPS spectrometer 8-89601
- electric breakdown voltage, 300-2100K (*Russian*) 8-51370
- electron mobility, anomalous density and temp. depend. at low temp. 8-75253
- energetic radiation belt ions obs. at geomag. equator during quiet conditions 8-88999
- equations of state, 3.3 to 14K (*Russian*) 8-83912
- F ions recoiling in gases, hyperfine interactions 8-74735
- field-theory renormalization and critical dynamics above T_c : helium, antiferromagnets, and liquid-gas systems 8-87767
- flow, alkali metal vap. condensation, heat and mass transfer 8-75192
- flow, of liq.-vap. mixture, frictional press. drop, adiabatic and heated conditions 8-90983
- flowing discharge, glow/arc transition and cathode-zone wave structure obs. 8-75475
- fusion reactor, cryosorption pumping, $\text{D}_2\text{-He}$ (5 at.%), on mol. sieve, 5A, 4.2K 8-74499
- fusion reactor first wall radiation damage, H and He gas prod. from stainless steel 8-82512
- gas, breakdown by alternating electric field near ion cyclotron freq. 8-55765
- gas discharge, high voltage, low current, anal. of cathode fall 8-51375
- glow discharge, 2^3P level population relax., laser absorpt.-perturbation meas. 8-59706
- HF discharge double-probe meas. 8-67541
- high-current pulse discharge plasma kinetic and dynamic processes 8-67601
- high-current pulse discharge plasma partial LTE disturbances 8-67600
- hollow-cathode discharge, Ba^+ and Sr^+ formation 8-67527
- hydraulic resistance to forced two-phase flow in narrow channels 8-87383
- hypersonic flow, Na vapour seeded, velocity profile visualisation 8-59530
- implanted in pyrolytic graphite, depth profiles 8-95071
- ions, uniform concentration implantation, simulated neutron irradiation damage 8-79648
- isotropic plasma, metastable atoms, equilib. distrib. function 8-91068
- laser, direct nucl. pumped, power density 8-58980
- leak detection in large cryogenic vessels 8-93694
- liquid film, transient heat transfer, film boiling regime 8-83219
- low-current discharge, metastable atoms, radial density distrib. obs. and calc. 8-67495
- Mercury, He exosphere model based on Mariner 10 UV spectrometer data 8-77509
- metal:He, ion implanted, statistical model of low temp. blister formation 8-67754
- multicomponent inhomogeneous plasma, spectroscopic analysis 8-67425
- near-critical, friction factors for flow in curved tubes 8-83367
- noise source, gas jet, absolute calibr. 8-59228
- permeability in $2\text{Na}_2\text{O-CaO-XSiO}_2$ glass, interconnectivity, miscibility limits, effect of morphology 8-67864
- plasma, electron beam generated, recomb. decay, Ne. addition effects 8-59545
- plasma, EM waves, parametric decay near upper hybrid freq. 8-59590
- plasma, moderately dense, electron density and ion temp. meas. using He II lines 8-67407
- plasma, relaxation time determ. for establishing quasisteady state population 8-59639
- plasma, strongly ionised, impact radiative recomb. rate 8-59546
- plasma, Z-pinch, ionisation and radiation dynamics simulation 8-83606
- positive column, magnetised, exptl. study on moving striations 8-83634
- positive column, moving striations in longitudinal homogeneous mag. field 8-67523
- positive column ion-acoustic waves, obs. 8-75312
- positive column ionisation waves, influence of longitudinal mag. field 8-67522
- positron annihilation decay consts., temp., elec., and mag. field depend., computer anal. 8-78809
- positron annihilation in rare gases, Doppler broadening meas., electron mom. distrib. 8-55131
- positron in condensing He, Monte Carlo lifetime spectra, temp. and elec. field effects 8-55263
- positronium annihilation rate in dense gas 8-55258
- pressure, in vacuum chamber in cryogenic environment, meas. technique 8-77925
- pulsed discharge, He_2 mol. formation in early afterglow, time-resolved spectra 8-63585
- quantum magnetometer, impurities influence on signal parameters (*Russian*) 8-82010
- radiation source, VUV He reson. line, for UHV photoelectron spectroscopy 8-89602
- relativistic electron beam transport at low pressures 8-75373
- scintillation detectors appl. (*Czech*) 8-86727
- second virial coeff., 0-500°C, two-temp. gas-expansion method 8-55711
- selective adsorption induced intensity maxima, scattering from LiF surface 8-72667
- solar wind, He abundance long-term vars., Imp 6, 7 and 8 results 8-77452
- solid surfaces, reflection of slow H^+ and He^+ ions 8-76572
- specific heat of ^3He film adsorbed on graphite 8-87842
- spectroscopic light source carrier gas glow discharge and hollow cathode types 8-82047
- steel, austenitic, neutron irradi., He release kinetics 8-79638
- stony meteorites, light noble gases anal. compilation 8-65574

helium continued

- stopping powers and ranges in all elements 8-58565
 submonolayer physisorbed, rel. to liquid to gas phase transitions in two-dimensional quantum systems 8-77798
 thermal conductivity, near 300K, density depend., 0.8-35 MPa 8-67304
 thermal conductivity, temp. depend. 8-59534
 third virial coeffs. calcs. using realistic Beck pair potential 8-94880
 Townsend discharge field emission by higher-order ion clusters 8-67550
 twin-hollow-cathode interferometer-spectrometer, discharge characts. (*German*) 8-67461
 twin-hollow-cathode of interferometer-spectrometer, radial electron temp. (*German*) 8-67462
 two dimensional quantum crystal on graphite (*Russian*) 8-60001
 unit requirements, for superconductive energy appl. in USA 8-89999
 upper atmosphere He dynamics, use of Jacchia (1977) empirical model 8-77381
 vapour, thermal cond. as function of density 8-55712
 vapour column, solid vapour heat transfer, at low temps. 8-83376
 Wigner-Kirkwood expansion of second virial coeff., convergence accel. 8-91052
 Al:He, pseudopotential calc. of screening of He atom 8-51917
 CO-He low press. mixture, CO vibr. distrib. to high level. 8-58985
 CO₂-N₂-He gas mixtures, fluorescent IR radiation from glow discharge 8-94386
 CO₂-N₂-He gas mixtures, time-of-flight meas. of electron transport parameters 8-94387
 CO₂-N₂-He mixture volumetric glow discharge formation at atm. pressure 8-71615
 Cl, in Ar and He gas, diffusion const. of atom 8-71417
 Cs⁺ in He and Ne gas, ion mobility and longit. diffusion coeff. 8-67308
 D-³He satellite fusion reactor, field-reversed mirror confinement 8-70643
 D₂-³He, filled microspheres, implosion expts. 8-59672
 desorption from solid Ar(Kr)(Xe) surface, appl. of simplified continuum model 8-87860
 α-Fe:He, impurity clustering in vacancies bound to edge dislocations 8-91358
 H⁺, calc. of mobility in He, 10 to 700K 8-66629
 H-He, H hyperfine struct. shift, commutator computational method 8-78608
 H-He arc lamp, 60-360 nm, calibration 8-87117
 H₂-F₂-He chemical CW laser, flows (*Russian*) 8-74895
 H₂-He mixture, collision integrals, modelling of spacecraft entry into Jupiter atmosphere 8-71413
 HCl-D₂-He mixture, gasdynamic laser theory, gain depend. on parameters 8-50761
 H₂O-He laser, pulsed oscill., elongation by admixture of He 8-87039
 H₂(³Σ_u⁺)-He(2³S), discharge ionisation growth, diffusion coeffs. 8-83636
 Hd-Cd hollow cathode laser in mag. field, Cd II stimulated emission 8-79002
 He I, II excited state population densities in non-LTE plasmas 8-67328
 He I plasma arc, spectral line profiles, λλ=4471 Å and 4922 Å (*French*) 8-83625
 He, microwave breakdown of nanosecond duration, calc. of threshold fields 8-94948
 He/Ar ratio vars. in fault zone groundwater air bubbles for earthquake prediction 8-88803
 He-air, thermal cond. meas., conc. depend., 315K, 330K (*Russian*) 8-71421
 He-Ar, collision-induced absorption, exact line shapes 8-66512
 He-Ar gas mixture, velocity slip in free jet expansions 8-90951
 He-Au UV laser, spectral range, threshold, power output 8-66809
 He-burning in core of massive stars 8-93207
 He-Cd hollow cathode laser, laterally emitted light 8-66810
 He-Cd II lasers, positive column, hollow cathode types, 4416 Å oscill. characts. (*Japanese*) 8-94392
 He-Cd laser, intensity fluctuations meas., comparison with 8-71087
 He-Cd⁺ laser, population densities of He excited states in positive column discharge 8-58989
 He-Cd⁺ laser, upper and lower laser states population densities, simultaneous determ. 8-87042
 He-Cd(Zn) hollow cathode laser, upper level decay rate, mag. field tuning dip meas. 8-87043
 He-Cs mixture discharge, B-invariant transformation theory 8-67503
 He-Cs plasma, HF instability in crossed fields, obs. 8-75305
 He-F, doublet series laser lines near 700 μm, hyperfine splitting and broadening meas. 8-63070
 He-F gas mixture, electron drift velocities, laser modelling 8-63061
 He-like ions, spectral line intensity, density depend., plasma diagnostic appls. 8-83617
 He-N₂, discharge ionisation growth, diffusion coeffs. 8-83636
 He-N₂-CO₂, discharge ionisation growth, diffusion coeffs. 8-83636
 He-Na mixture, low-pressure discharge, radial cataphoresis obs. 8-67507
 He-Ne, 6328 Å, single-mode collapse 8-94404
 He-Ne, I₂ stabilised lasers, conf., Germany (Feb. 1977) 8-87069
 He-Ne, I₂ stabilised laser design, freq. reproducibility 8-87070
 He-Ne, I₂ stabilised laser research 8-87071
 He-Ne, I₂ stabilised laser with hot wall I₂ cell 8-87073
 He-Ne, I₂ stabilised laser, instrumental freq. offsets 8-87084
 He-Ne, I₂ stabilised lasers, international-intercomparison meas., hyperfine struct. spacings 8-87088
 He-Ne, I₂ stabilised lasers, beat frequency, international comparisons (*French*) 8-87090
 He-Ne, laser frequency measurements: a review, limitations, extension to 197 THz (1.5 μm) 8-81952
 He-Ne, methane and I₂ stabilised lasers, wavelength intercomparison using Michelson interferometer 8-87089
 He-Ne, oscills. in laser discharge 8-55339
 He-Ne, plasma He I 4471 Å line profile obs. at high electron density 8-67472
 He-Ne, thermal diffusion factor, 65 to 300K 8-71418
 He-Ne complex resonator laser, stabilisation 8-55374
 He-Ne internal mirror laser, degeneration of longitudinal modes and freq. stabilisation (*Japanese*) 8-90426
 He-Ne laser, ¹²⁷I₂ stabilised, freq. shifts, limitations 8-90440

helium continued

- He-Ne laser, 60 mW, perturbation spectroscopy (*Rumanian*) 8-50752
 He-Ne laser, anisotropy due to saturating fields 8-55337
 He-Ne laser, high stability, single freq., 3.39 μm 8-71121
 He-Ne laser, I₂ stabilised, realisation of length unit 8-87068
 He-Ne laser, in axial mag. field, output power dependence of mode locking phenomena 8-71129
 He-Ne laser, intensity fluctuations meas., comparison with He-Cd laser 8-71087
 He-Ne laser, low noise manufacturing 8-79038
 He-Ne laser, manufacturing problems with low noise specification 8-59047
 He-Ne laser, microwave pumping advantages 8-50754
 He-Ne laser, mode selection and mode locking, effect on two-photon absorpt. efficiency 8-83023
 He-Ne laser, output power, unsaturated gain distrib. 8-50751
 He-Ne laser, population inversion radial distrib. in active element, excitation conditions effect 8-71079
 He-Ne laser, stabilised by I₂ saturated absorpt., technological principles (*French*) 8-87075
 He-Ne laser fluctuation spectra of freq. and amplitude 8-82950
 He-Ne laser plasma, line profiles meas. by optogalvanic spectroscopy 8-62233
 He-Ne laser status, I₂ vapour stabilised 8-87072
 He-Ne laser unit, factors affecting service life (*German*) 8-90424
 He-Ne laser wavelength stabilisation on I₂ (*Czech*) 8-87061
 He-Ne laser with methane absorpt. cell, hyperfine struct. influence on freq. reproducibility 8-50864
 He-Ne lasers, discharge reson. props. effect on radiation fluctuations, expt. 8-74883
 He-Ne lasers, I₂ stabilised, 633 nm line, performance improvement 8-90429
 He-Ne lasers, standard wavelength sources 8-74957
 He-Ne ring laser, nonlinear polarisation interaction of opposite waves 8-50828
 He-Ne ring laser, nonlinear Zeeman effect 8-71123
 He-Ne two-mode travelling-wave laser, Zeeman beats 8-50827
 He-Ne(Ar), thermal cond., composition dependence 8-51276
 He-O₂ corona discharge CV characteristics 8-91168
 He-SF₆, AC particle initiated breakdown, compressed gas mixture 8-87556
 He-UF₆ gas mixture, velocity slip in free jet expansions 8-90951
 He-Zn hollow cathode laser, 7588 Å in ZnII, operating characts. and upper level operating mech. 8-63071
 He+H₂, collision-induced dipole, ab initio VB calc. 8-94202
 He+H₂ microwave plasma, pulsed high current heating at atm. press., MHD instability 8-55728
 He+H₂⁺, 10 keV dissoci. charge exchange collisions 8-94319
 He+N²⁺(O²⁺)(Ne²⁺)(Ar²⁺)(Ar³⁺), electron transfer cross-section, <100 eV 8-66654
 He⁺+Ar(N₂)(He), up to 70 keV, symmetric (antisymmetric) reson. charge transfer cross sections (*Korean*) 8-50636
 He⁺+O, charge exchange laser 8-50759
³He, selective adsorption on NaF and LiF, atomic beam scatt. meas., binding energies 8-63935
³He, specific heat second layer adsorbed on Grafoil 8-87843
³He-Ne stabilised by saturated absorption ¹²⁷I₂ laser wavelength standard development appl. (*German*) 8-79034
⁴He excess in Teggau Lake, NW Ontario, rel. to U ore body 8-65353
⁴He, selective adsorption and NaF and LiF, atomic beam scatt. meas., binding energies 8-63935
⁴He stopping cross sections, 1-8.5 MeV 8-58558
 Kr²⁺, mobility in He gas, drift-tube meas. 8-66657
 N₂-He mixture, film condensation, appls. to condensers for cryogenic installations 8-59941
 Ne-He DC glow discharge electron density decay, microwave cavity obs. 8-91167
 Pb-He discharge, excitation process, Pb⁺ emission lines 8-66803
 UF₆-He fission pumped nucl. laser, power deposition 8-58987
 Xe²⁺, mobility in He gas, drift-tube meas. 8-66657

helium, liquid see liquid helium

helium, solid see solid helium

helium-3 interactions see helium 3-nucleus reactions

helium 3-nucleus reactions

for inelastic helium 3-nucleus scattering, see "helium 3-nucleus scattering"

⁹Be(²He, αα)⁴He, 2.5, 2.7 MeV, energy depend., quasifree reaction near Coulomb barrier 8-74381⁹Be(²He, α)⁸Be(O), reaction mechanism and isoscalar giant resonances in C¹² (*French*) 8-78341²⁰⁹Bi(³He, 3nγ)²⁰⁹At, gamma-ray spectra of ²⁰⁹At, 26 and 28 MeV 8-74377¹²C(²He, α), 35.6 MeV, ¹²C energy levels, ang. distrib., DWBA calcs. comparison 8-78396¹²C(²He, γ₀)¹⁵O, differential cross section in giant dipole reson. region 8-78395¹²C(²He, n), 12-24 MeV, ¹⁴O low lying states, exact finite and zero range DWBA anal. 8-82286¹²C(²He, p)¹⁴N, g-factor, lifetime meas. of 5.106 MeV 2⁻ state of ¹⁴N 8-93965¹³C(²He, p), 3.6-6.6 MeV, ¹⁵N level excitation functions, resonance, p ang. distrib. 8-93942⁴⁸Ca(²He, α), 25 MeV, ⁴⁷Ca high spin states through double step processes, CCBA calcs. 8-89797⁵⁰Cr(²He, pn)⁵¹Mn, ⁵¹Mn ZZ 8-62560⁵²Cr(²He, dy), 18 MeV, ⁵³Mn γ decay and splitting of analogue states 8-70505⁵⁴Fe(²He, dy), 18 MeV, ⁵⁵Co γ decay and splitting of analogue states 8-70505⁵⁷Fe(τ, d)⁵⁷Co, 18 MeV, level props. study DWBA calcs. 8-93946²(He, H), charge exchange reaction, mean energy regions, diffraction model (*Russian*) 8-82352³He(²He, dd)pp, 50, 78 MeV, cross sections, two-spectator quasifree process 8-86539²⁵Mg(³He, d)²⁶Al, 18 MeV, l-assignments for ang. distrib., level J^π information, spectroscopic strengths 8-62554¹⁴N(²He, p), 15 MeV, ¹⁶O excited states from ang. distrib. meas. 8-89891¹⁴N(²He, p), 15 MeV, obs. of T=0 pairing vibr. 8-70422²⁰Ne(³He, ⁸Li), ¹⁵F mass excess and T=3/2 levels 8-78264

helium 3-nucleus reactions continued

- $^{20}\text{Ne}(^3\text{He},^3\text{Li})$, 88 and 75 MeV, ^{19}F mass excess 8-78245
 $^{21}\text{Ne}(^3\text{He},\text{p})$, 18 MeV, ^{23}Na positive parity states ang. distrib., DWBA anal. 8-82284
 $^{22}\text{Ne}(^3\text{He},\text{p})$, 18 MeV ^{24}Na , level struct. and spin assignments, DWBA anal. 8-86477
 $^{58}\text{Ni}(^3\text{He},\text{d}\gamma)$, 18 MeV, ^{59}Co γ decay and splitting of analogue states 8-70505
 $^{31}\text{P}(^3\text{He},\text{d})$, 25 MeV, ^{32}S energy levels and ang. distrib., DWBA anal. 8-78265
 $^{208}\text{Pb}(^3\text{He},\alpha)^{207}\text{Pb}$, 70 MeV, deephole states, $T_{1/2}=45/2$ components 8-82362
 $^{208}\text{Pb}(^3\text{He},\alpha)^{207}\text{Pb}$, $T=45/2$ isobaric analogue state obs. 8-93928
 $^{208}\text{Pb}(^3\text{He},t)^{208}\text{Bi}$, 80 MeV, Gamow-Teller M1 state excitation 8-50184
 $\text{Pt}(^3\text{He},4\text{n})$, Hg isotopes, level energies, $B(E2)$ values, rot. aligned bands 8-70483
 $\text{Pt}(^3\text{He},\text{d})$, $A=194$, 196, 198, 41.2 MeV, stripping strength, Au excitation energies, high spin states 8-78398
 $^{76}\text{Se}(^3\text{He},\text{d})$, 41 MeV, ^{77}Br level struct., l-transfers, spectroscopic factors, DWBA anal. 8-86479
 $^{78}\text{Se}(^3\text{He},\text{d})$, 41 MeV, ^{79}Br level struct., l-transfers, spectroscopic factors, DWBA anal. 8-86479
 $^{28}\text{Si}(^3\text{He},\text{d})$, 25 MeV, spectroscopic factors 8-66294
 $^{29}\text{Si}(^3\text{He},\text{p})$, 15 MeV, excitation energies and ang. distrib. below 7.2 MeV, in ^{31}P 8-82361
 $^{144}\text{Sm}(^3\text{He},\text{ap})^{142}\text{Pm}$, 39 MeV, proton decay of hole analogue states 8-70451
 $\text{Sn}(^3\text{He},\text{n})$, 25.4 MeV, ang. distrib., $^{114,118,120,122,126}\text{Te}$ deduced levels 8-89890
 $^{17}\text{Sn}(^3\text{He},\alpha)\text{Sn}$, $A=114, 116, 118, 120$, deeply bound hole state struct. 8-93930
 $^{115}\text{Sn}(^3\text{He},\text{d})$, 28.4 MeV, ^{116}Sn state excitation energies, and partial half lives, spectroscopic factors 8-66295
 $\text{Te}(^3\text{He},\text{d})$ 35 MeV, ^{121}I , $A=121, 123, 125$, mass excesses, ^{121}I energy levels 8-78246
 $^{120}\text{Te}(^3\text{He},\text{d})$, ^{121}I single particle strength distrib. 8-70423
 $^{234}\text{U}(^3\text{He},\alpha)$, 30 MeV, states in ^{233}U 8-66208
 $^{238}\text{U}(^3\text{He},\text{f})$, ^{241}Pu compound nucleus lifetime by the shadow effect (Russian) 8-86562
 $^{70}\text{Zn}(^3\text{He},\text{B})^{68}\text{Co}$, mass excess of ^{65}Co 8-93931
 $^{90}\text{Zr}(^3\text{He},t)^{90}\text{Nb}$, 80 MeV, Gamow-Teller M1 state excitation 8-50184
 $^{96}\text{Zr}(^3\text{He},\text{ap})$ 39 MeV, ^{94}Y deduced levels spectroscopic factors, spin and parity 8-70451

helium 3-nucleus scattering

- eikonal approx. and distortions in heavy particle stripping mechanism (Russian) 8-78337
monopole excitations in heavy nuclei, hadron induced 8-86471
 $^{40}\text{Ca}+^3\text{He}$ inelastic scatt., isoscalar multipole reson. 8-66190
 $(^3\text{He},^3\text{He})$, 18-33 MeV polarised ^3He , ^6Be excitation 8-78400
 $^4\text{He}(^3\text{He},^3\text{He})$, $^7\text{Be}+^3\text{He}$ coupling, dispersion anal. 8-89889
 $^{24}\text{Mg}(^3\text{He},^3\text{He})$, 130 MeV, elastic scatt. ang. distrib., optical model anal. 8-94020
 $^{208}\text{Pb}(^3\text{He},^3\text{He})$, 130 MeV, elastic scatt. ang. distrib., optical model anal. 8-94020
 $^{120}\text{Sn}(^3\text{He},^3\text{He})$, 130 MeV, elastic scatt. ang. distrib., optical model anal. 8-94020
 $^{90}\text{Zr}(^3\text{He},^3\text{He})$, 130 MeV, elastic scatt. ang. distrib., optical model anal. 8-94020

helium-3 scattering see helium 3-nucleus scattering**helium atoms**

- $2^3\text{S}-3^3\text{S}$ electron impact excitation, first Born and Glauber cross sections 8-55243
CI wavefunctions, ang. correl. of electrons 8-62730
clustering of atoms around positron and positive ions 8-55270
correlation energy of ground state, pair approx. 8-90065
double excited states, lifetime meas. by beam-foil technique 8-74590
dynamic multipole polarisability, functional calcs. 8-74595
dynamic polarisability, CHF method 8-50472
(e,2e) coplanar symmetry reaction, factorised distorted-wave approx., 200-1200 eV 8-55246
electron and positron total scatt. cross sections, positronium form. 8-62916
electron correlation and Coulomb hole in momentum space 8-86793
electron elastic scattering, modified Glauber approx. 8-74764
electron impact, $^3\text{P}_g$ and $^{13}\text{D}_u$ states excitation, electron correlation influence, Rudge-type approx. 8-74771
electron impact excitation, $^3\text{P}_g$ and $^{13}\text{D}_u$ states, electron correlation influence, Born-Oppenheimer approx. 8-74770
electron impact excitation, cross-sections, modified Oppenheimer approx. 8-82843
electron impact excitation, high Rydberg state, dipole transitions, impact parameter method 8-62922
electron impact fluorescence, polarisation of 5876 line 8-82848
electron impact ionis., triple differential cross section 8-62924
electron impact ionisation, 7-1000 eV, cross-section 8-86956
electron impact ionisation, cross section ratios 8-94326
electron impact ionisation, distorted wave approx., 80-250 eV 8-86955
electron impact ionisation, emitted electron ang. distrib. 8-55241
electron impact ionisation, generalised differential oscillator strengths 8-55239
electron impact ionisation, reaction mechanism 8-62926
electron impact spectroscopy for Compton profile meas. 8-90299
electron scatt., 2^3S and 2^1S excitation cross sections, partial wave anal. 8-90301
electron scatt., absolute total scatt. cross sections, 0.5 to 50 eV 8-74765
electron scattering, elastic, at low-energy, polarised orbital calc. 8-82840
electron scattering, elastic, differential cross section, 3-50 eV, 20-130°, rel. to HCN 8-90291
excitation and ionisation, by instationary shock fronts 8-59540
excitation transfer between excited states, neutral atoms in transient plasma 8-70914
excited S, D and F state radiative lifetimes, electron impact method 8-94325
excited states, Galerkin-Petrov method, nonlinear parameters 8-78619
excited states, relativistic corrections 8-62734

helium atoms continued

- fine structure, triplet P state splittings, higher order corrections of theoretical calc., book contrib. 8-82632
formaldehyde+ $\text{He}(\text{H}_2)$, collisional relax. times and lineshape distortion, Stark absorpt. linewidth obs. 8-74744
generalised oscillator strength, variational determ., extremum principle appls. 8-94213
ground state wavefunction, SCF HF calc. 8-90070
Hartree-Fock energy, perturbative corrections, incomplete basis set problem 8-70744
high-flux fast neutral beam source 8-54507
imaginary frequency multipole polarisability and long-range dispersion consts, functional calcs. 8-74596
isoelectronic sequences, screening constants, ground and excited states 8-62701
isoelectronic series, dipole oscillator strength distrib. moments, systematics 8-86821
isoelectronic series, energy level and classifications of doubly-excited states 8-62736
isoelectronic series, excitation regimes, nucl. orientation due to hyperfine interaction 8-70928
laser induced level shift 8-58627
magnetic interactions of electrons (German) 8-82610
mesic and muonic mol. ion formation in liq. He, X-ray intensities, Auger and Stark transitions 8-94338
mesoatoms, π^- , μ^- , K^- , p^- atoms, energy spectra, wave functions (Russian) 8-55264
metastable, impact on $\text{Mo}[110]$ surface 8-95642
metastable $1s2s$ S state, photoionisation, perturbation theory calcs. 8-78759
muonic, atomic spectra, QED, strong and supercritical fields, book contrib. 8-74193
optical excitation function of 5876 Å line near threshold 8-70797
oscillator strength, sums, one-term approx. 8-66509
Penning collisions, orientation transfer for ion excited state lifetime meas. (French) 8-50621
photoionisation, frozen-core HF perturbation theory, oscillator strength, dipole length and vel. calc. 8-78672
photoionisation cross sections of excited states 8-66523
plasma, non-equilib., of strong current pulse discharge, diagnostics (Russian) 8-75271
polarisability and Verdet consts., freq.-depend., calcs. 8-62781
positron scatt., total cross section 8-70933
pseudospectral dipole oscillator strength distrib. 8-50503
quantum static multipole polarisabilities 8-82859
scattering of 63 meV He atoms from LiF, single Rayleigh phonon interaction 8-80447
spontaneous decay probability of 3^3P level, expt. and theoretical values 8-50501
Stark effect on optically excited plasma atoms in static mag. field 8-66505
Stark shift and line broadening in 3-D stochastic laser field, He plasma 8-50502
synchrotron radiation scattering cross sections 8-55213
two-electron excited states 8-58605
variational energies for highly excited states 8-62737
Voigt profile, line absorpt. calcs. of 388.9 nm triplet, 501.6 nm singlet lines 8-90123
VUV source, laser induced two photon blackbody radiation from He atoms in glow discharge 8-58102
X-ray scatt., total, two-electron density functions 8-70889
 $^4\text{He}(3^3\text{P})$, fine struct., level crossing obs. 8-82686
Ar+He* Penning ionisation, semiclassical discretisation procedure 8-90275
Ar+He, $\text{X}^2\Sigma$ and $\text{A}^2\Pi$ states, CI pots. 8-74727
 $\text{CH}_4+\text{H}^+(\text{He}^+)(\text{O}^+)$, 1 MeV dissociation, kinetic energy spectra 8-94302
CO+He, rot. excitation, infinite order sudden approx. 8-74740
 $\text{CS}_2+\text{He}(\text{Ar})(\text{N}_2)$, perturbed rot. diffusion of CS_2 , IR spectra 8-75245
Cs-He, new absorption/emission bands perturbed Cs transitions assignment, pot. energy curves 8-66486
 $\text{H}^++\text{H}(\text{He})$, electron detachment cross sections 8-90265
 $\text{H}^++\text{He}(\text{Ar})$, electron detachment cross sections 8-58810
 H^++He^+ , charge transfer and ionis. cross sections, coincidence meas. 8-50634
 $\text{H}^++\text{He}(\text{Ar})$ electron transfer cross sections 8-58809
HCN+He, rot. excitation, infinite order sudden approx. 8-74740
HCl+Ar(He), rot. excitation, infinite order sudden approx. 8-74740
HD+He collisions, rotational transitions 8-70909
 $\text{H}_2(\Sigma_g^+)-\text{He}(2^3\text{S})$, discharge ionisation growth, diffusion coeffs. 8-83636
He (2^3P)+Ca(Sr), collisional quenching of metastable states, excitation transfer cross sections 8-66653
He I, 4471 Å line profile in various plasmas, ion perturbation effects 8-94214
He I, interf. beat period determ. of nondegenerate states 8-70807
He I, transfer excitation energy between $n=5$ levels 8-70942
He I $1s3d$ levels, cascade-free lifetime meas., using He^++He 35 keV collisions 8-58607
He I D_3 line, Stokes parameters for quiescent prominences, Hanle effect quantum theory 8-85924
He II, Stark broadening of VUV transitions at 304, 1215, 1640 Å 8-66506
He II abundance and IR excess in H II regions 8-86000
He II recombination lines, calc. intensities in UV 8-94212
He, scatt. from LiF (001) surface, sudden decoupling approx. 8-64437
He*, form. by $\text{He}^{2+}+\text{H}_2$ collisions 8-58811
He*, wave function structure, complex coord. method 8-94190
He*, dynamic multipole polarisability, functional calcs. 8-74595
He*, electron impact excitation to S states exchange effects 8-58835
He*, electron impact ionisation, electron ang. momentum exchange 8-78820
He*, electron inelastic scatt., effective exchange potentials 8-90300
He*, electron scatt., elastic, modified Coulomb-Glauber approx. 8-86949
He*, electron scatt., Glauber exchange amplitudes 8-74772
He*, imaginary frequency multipole polarisability and long-range dispersion consts, functional calcs. 8-74596
He* ions, electron impact ionisation 8-66666
He*, lifetime of metastable state, ion beam meas. 8-55141

helium atoms continued

- He-Ar(Kr)(Xe), intermol. forces, combining rules 8-66622
 He-CH₃⁺ interaction energy, nonempirical calc. 8-86799
 He-like ions, electron impact, collision strengths for fine-struct. transitions 8-62925
 He-like ions, line intensities results 8-89051
 He-like ions, P₁⁰⁻¹S₀ and ³P₁⁰⁻¹S₀ intercombination-line transitions 8-70771
 He-like multiply charged ion, superdense plasmas, line intensity ratio 8-63538
 He+Ar(Kr), translation band spectral moments, induced dipole moments 8-55218
 He+B(Be)(C), target atom K-shell binding energy by Auger spectra 8-50525
 He+CO, nuclear mag. shielding consts., interaction geometry depend., chemical shift, gauge invariant method 8-62866
 He+H, low energy elastic scatt. cross section MCSCF calc., van der Waals forces 8-70897
 He+H, stripping cross-section, 0.3 to 3 keV 8-78807
 He+H (inert gas atom), long range interactions for (2¹S) and (2³S) states 8-70895
 He+H₂, collision dynamics, generalised Langevin eqn. approach 8-70900
 He+H₂, final quantum state assignment, improved quasiclassical histogram method 8-66617
 He+H₂, Van der Waals pot., ab initio SCF model 8-74728
 He+H₂⁻⁴¹, 200-850 eV, attenuation and fragmentation 8-62968
 He+H₂⁺, collision in laser field, vibr. excitation 8-86937
 He+H₂⁺, reactive and dissociative scatt., crossed-beam and trajectory obs. 8-64833
 He+H₂(D₂), vibr. deexcitation, cross sections, rate consts., vibr. rot. model 8-62879
 He+H₂(D₂)(T₂), vibr.-rot. transitions, optical potential approach 8-62885
 He+H₂(HD) potential, asymmetric, isotope substitution effect, Legendre expansion coord. transformation 8-70894
 He+H₂(He)(Ar)(N₂), fast metastable at. collisional destruction cross section 8-74760
 He+H⁺, determ. of He excited state populations by two-photon reson. ionisation spectroscopy 8-82707
 He+H⁺, excitation, ang. differential cross-sections for 25, 50 and 100 keV protons 8-82832
 He+H⁺(H₂⁺)(H₃⁺)(He⁺) collisions, polarisation degree of prominent H lines 8-70916
 He+HCl(CO), energy sudden approx., beam scatt. meas. mol. anisotropy effects 8-78802
 He+HD, thermal energy scatt., distorted-wave and close coupling calcs. 8-86938
 He+He, metastable atoms, collisional ionisation cross-sections 8-70911
 He+He⁺, excitation cross-section calcs. 8-90273
 He+He⁺, resonant charge transfer cross sections, 2 to 100 eV 8-66655
 He+He²⁺, electron capture collisions, spin conservation 8-82837
 He+Hg, metastable He, collision rate consts. in pulsed discharge after-flow 8-50627
 He+K, 93 eV, excitation of K atom, photon-scatt.-atom coincidence study 8-82829
 He+Li⁺(Co⁺)(Au⁺), cross-section, closure-Born approx. 8-66630
 He+N₂⁺, (A²Π_g) Meinel band deactivation cross sections above thermal energies 8-66635
 He+NH₃, rot. relax., double and triple reson. obs. 8-90196
 He+NH₃, rot. relax. double and triple reson. obs. 8-66570
 He+Na₂, rot. transitions, state-resolved differential cross-sections 8-62887
 He+Ne pot., differential cross section, quantum mechanical inversion 8-70896
 He+O₂, collisional energy transfer in unimol. reaction, classical trajectory calcs. 8-62882
 He+XeF⁺, quenching rates for XeF in (B) state 8-58730
 He⁺+1,3-butadienes, singlet-triplet transitions, energies, relative cross sections 8-86942
 He⁺+acetylene-d₀(-d₂), CH⁺(CD⁺), A-X luminesc., in near-thermal charge exchange 8-50632
 He⁺+alkali metal atom, ionisation cross sections, binary encounter approx. with HF electron vel. distrib. 8-55225
 He⁺+Ar, low energy charge transfer collisions, kinetic energy depend. 8-86947
 He⁺+C, beam-foil spectra, He atom orientation, ang. variation 8-86944
 He⁺+C, K-shell ionisation, impact parameter depend. 8-62891
 He⁺+CO, dissociation, charge transfer, energy transfer processes 8-74759
 He⁺+H, unpolarised and spin-change collision, low energy 8-86943
 He⁺+H₂, charge transfer at 1.5 and 3 keV, He(³P) excitation 8-66658
 He⁺+H₂O, 50 to 250 keV, OH radical form. 8-56890
 He⁺+He, 2¹P level, direct and charge-exchange excitation, 150-1000 keV 8-70913
 He⁺+He, elastic scatt. and charge exchange, differential cross-section, 0.4-30 eV 8-66659
 He⁺+He(Ne), model pot. for low energy scatt. 8-66642
 He⁺+Mg, inner-shell ionisation by H⁺, He⁺ impact, target atom ionic alignment, Born approx. 8-78789
 He⁺+Mg(Zn), inelastic collisions, 2-800 eV, excited state form. 8-94312
 He⁺+N₂, charge exchange, time-resolved emission probe 8-86946
 He⁺+Na(K), excited state form. by inelastic processes, energy partitioning 8-82833
 He⁺+Na(K)(Cs), 5-100 keV, electron capture form. of fast metastable He 8-74760
 He⁺+Pb, at. beam and surface interaction, scatt. ion yield oscils. 8-55221
 He⁺+Si(Al), X-ray spectra, two-electron one-photon transition in solid target, 2 MeV 8-94209
 He²⁺+H₂(O₂), electron capture collisions, spin conservation 8-82837
 He²⁺+H₂→He⁺H⁺+H⁺, two-electron capture 8-58811
 He²⁺+He, 5 to 100 keV, elastic and double charge exchange, mol. treatment 8-82813
 He²⁺+He, He⁺ form. in various electron states (Russian) 8-58815
 He²⁺+He(Ne), electron capture collisions, spin conservation 8-82837

helium atoms continued

- He²⁺+Hg, autoionisation, 5-20 eV, electron and ion ang. distrib. 8-78795
 He²⁺+N₂, 200-600 eV, 0-20°, comparison with He²⁺+Ne(Ar) 8-74732
 He²⁺+Ne(He), electron transfer cross-section, <100 eV 8-66654
 He₂, a³Σ_u⁺ metastable state, fine struct., mol. beam mag. reson. obs. 8-78720
 He₂, ground state, generalised dipole polarisability, bivariational calcs. 8-58611
 He₂, pair polarisability correl. effects, SCF-CI-GTO-SO calc. 8-82651
 He₂, photoion. cross sections of excited states 8-66523
 He₂, polarisability, generalised London formula for dispersion coeff. 8-82662
 He₂⁺, rate coeffs. for bimol. and termol. ion-mol. reactions 8-53188
 He₂, bound state at small and large separations, variational calcs. 8-50609
 He₂+Mg(Zn), inelastic collisions, 2-800 eV, excited state form. 8-94312
 He₃, dipole moment, large separation, perturbation theory 8-62946
 HeH, neutral and negative ion states SCF pot. energy curves 8-62745
 He₂(²Σ⁺)+Ar, press. depend. reactions, rate coeffs. 8-64823
 He, ¹S₀ ground state, NMR obs. by transverse modulation of mag. field 8-82671
 He, optical pumping signal, special features 8-82700
 He⁴He ratio in josephinite 8-65313
 He²⁺+H(H₂), electron capture at impact energies below 10 keV 8-50633
 He+π⁻, strong interaction shift, multiple scatt. and absorptive effects, calc. 8-62958
 He, muonic, Lamb shift calcs. 8-94199
 He trimer and tetramer, binding energy, appl. of ATMS 8-94349
 He-p, X-ray spectrum, energies and relative intensities for 3d and 2p levels 8-70979
 He⁺+Ar, Penning ionisation, laser modified collisional effects in electron energy spectrum 8-90278
 He⁺+H(H₂)(Ar), metastable state, ionis. processes 8-62907
 He⁺, doubly excited, spatial correl. of at. electrons 8-70760
 He(2³S) collisions, elastic scatt., Penning ionisation, polarisations (Russian) 8-70922
 He(2³S)+H₂O(H₂S), energy transfer processes, reaction products, UV and visible obs. in flowing afterglow 8-85138
 He(2³S)+e→He(1¹S₀)+e+KE, in afterglow, rate const., electron energy distrib. 8-71571
 Hg+He, laser excitation of Hg 6s6d³D₁ level, transition probabilities and collisional excitation transfer 8-55146
 Hg+He(Xe), collisionally induced coherence, orientation and alignment, transfer among 6s6d levels 8-74747
 Kr⁺+He, persistence of velocity following elastic collisions 8-78779
 Kr⁺+He(Ar), vel. changing collisions studied by saturated absorpt. 8-62892
 Li+He, direct excitation of Li I (nl) levels in keV collisions 8-90280
 Mg+H⁺(He⁺) and electron impact ionis., Auger study of collisionally induced alignment 8-90279
 NH₃+He(Ar), ammonia inversion spectrum press. broadening 8-86915
 Ne+Ne(He), 7d' states, isotope shift, press. shift, press. broadening, two-photon spectra obs. 8-55155
 Si³⁺+He, q=2-11, K-shell fluoresc. yields, charge-state depend. 8-55231
 Xe+He, saturated absorpt. of 3.51 μm line, vel. changing collisions by line width 8-86819

helium compounds

- He⁺+Ar, charge transfer cross section, kinetic energy dependence in low energy region (Japanese) 8-90100
 HeH, HeH⁺, variable screening model calcs. 8-74587
 HeH, neutral and negative ion states SCF pot. energy curves 8-62745
 HeH⁺, (HeD⁺), rot. predissoc., nucl. motion effects on rovibr. energies and widths 8-70885
 HeH⁺ in planetary nebula NGC 7027, search for near IR emission lines 8-73748
 HeH⁺, photodissoc. by electronic and vibr. transitions 8-90244
 HeH⁺, triplet Σ, Π and Δ states, config. interactions 8-78633
 HeH⁺+Ne, collinear reaction, pot. energy surface SCF-LCAO-MO and DIM calc. 8-92467
 HeNO₂, molecular geometry and stability, ab initio calcs. 8-90075
 HeNO₂, vibr. predissoc., rel. to van der Waals triatomic mol. theory 8-55208
 HeNO₂, vibr. predissoc. rel. to van der Waals mol. theory, anharmonicity effects 8-55209

helium nuclei see nuclei with mass number 1 to 5; nuclei with mass number 6 to 19

Hellman-Feynman theorem see quantum theory

Helmholtz free energy see free energy

Hertzsprung-Russell diagram see stellar evolution

heterodyne detection see demodulation

heterodyne wavemeters see wavemeters

heuristic programming

see also artificial intelligence

nuclear facility, optimisation of radiation detector position and number 8-55043

HF calculations

see also Xalpha calculations

(J²) quantum number calcs. 8-90059

A=42 nuclei, T=1, J=0 states, Coulomb displacement energies, Hartree-Fock wave functions, charge depend. 8-89773

acridine C-radical, polarised absorpt. and ESR spectra, dichroism and HF-CI calc. 8-50563

anharmonic collective motion, adiabatic TDHF as consistent theory 8-78291

anions, struct. and energetic predictions, modified HF procedure evaluation 8-62720

ATDHF theory 8-54710

atom, Slater transition-state calculations of multi-electron X-ray transition energies 8-90110

atomic effective charge distrib. in cpds., chem. shift of electron levels 8-86785

atomic electron elastic scatt., perturbation theory calc., computer program 8-50637

HF calculations continued

- atomic struct., numerical HF radial function during SCF iteration, convergence 8-58574
back bending, Hartree-Fock Bogolyubov approach, cranking method 8-58228
back bending effect, Hartree-Fock-Bogolyubov treatment of cranking method, yrast states 8-82264
basis states generation by variational methods 8-78295
bound neutral polynuclear systems, existence anal. 8-70475
carbonyl oxide, config. interaction calc., using DODS natural orbit approach 8-66476
CDW instability of electron gas in a strong magnetic field 8-79950
chemisorption, embedding problem, SCFMO formalism 8-71977
Choquard nonlinear eqn. minimising soln. existence and uniqueness 8-67315
cluster calculations, unrestricted HF approach, cluster-environment interaction 8-84117
coreless pseudopot. for atoms K through Zn 8-55121
correlation energy calculation, from CHF method 8-90087
Coulomb ionisation of inner shell electrons, screening effects 8-74749
cranked Hartree-Fock-Bogoliubov wave functions, ang. momentum distrib. at band crossings 8-93956
cumulative type infinite chain cryst., energy bands, ab initio Hartree-Fock orbital calc. 8-60066
deformations of rare earth nuclei, Skyrme-HF calcs. 8-62480
deformed nuclei, collective props., HF calcs., review 8-50064
delta function fermion gas, solitons and HF solns. 8-49755
dense plasma, atomic energy level deform. and eqn. of state 8-71435
diatomic molecules, electric polarisabilities, EFV GTO basis set 8-50661
diatomic radicals, wavefunctions, populations and orbital energies, Roothaan calcs. 8-86773
dynamic polarisability, TDHF theory and RPA sum rules 8-78292
effective interaction constraints imposed by antisymm. and charge independ. 8-86500
EHF theory in chem. reactions, wave functions symmetry props. 8-92447
ESCA photoionisation cross section, relative intensities calcs., comparisons 8-50464
ethenoxy, config. interaction calc., using DODS natural orbit approach 8-66476
ethyl radical, geom. struct., Hartree-Fock calcs. 8-62722
even parity states in ^{19}F , ^{21}Ne , ^{23}Na , generator coord. method, projected Hartree-Fock, and complete diagonalisation calcs. comparison 8-89796
excitation during collective deformation, time depend. Hartree Fock Bogolyubov method, fission process 8-58229
expansion of MO wave functions into VB work functions 8-74580
 $f_{7/2}$ shell nuclei, odd-A, collective bands of positive parity states 8-54677
fermion system, Hartree-Fock states in thermodynamic limit, low-density clustering 8-54296
fission, ATDHF validity 8-50149
formaldehyde, first hyperpolarisability, Hartree-Fock-Slater calc. (French) 8-78625
formaldehyde, orbital contribs. to relax. energies accompanying core ionis., ASCF HF calcs. 8-82642
free lattice electron gas with nearest and second nearest neighbour hopping 8-51873
generator coordinate method with conjugate parameters, adiabatic time depend. HF relation 8-86498
giant resonance description, RPA, GCM, and semiclassical theories unification 8-54671
Group IVA elements, excited states, quadrupole moments, Sternheimer shielding factors 8-82630
hard-core interactions, Hartree-Fock calcs. possibility due to overlapping orbitals 8-89811
Hartree Fock Bogoliubov method, high nuclear spins, quadrupole pairing, moment of inertia, yrast traps 8-54712
He, Hartree-Fock energy, perturbative corrections, incomplete basis set problem 8-70744
heavy ion reactions, Hartree-Fock approx., statistical aspects 8-50193
heavy-ion react., separable approx. to TDHF calcs. in 3-D 8-74320
highly ionised atoms, relativistic effects, book contrib. 8-74588
Hubbard antiferromag. semiconductor, electron correlations, weak coupling 8-67969
Hubbard model, local moments 8-95414
Hubbard model with nearest and next nearest neighbour hopping in Hartree Fock approx. 8-52189
hybridization effect on phase transitions in the Falicov-Kimball model 8-91617
hydrocarbons, α -substituent effects in ^{13}C NMR, quantum chem. calcs. 8-74680
infinite nuclear matter, response function, quantum field theory of fermion systems 8-70480
ionisation, Alpha transition state and transition operator method calcs. 8-70743
ions, radial density functions, expectation values 8-62718
ions with partly filled L-shells, relativistic Hartree-Fock energy calcs. 8-82656
Koopmans atomic valence electron ionisation energy, $1/Z$ expansion method, reorganisation corrections 8-78623
magnetic solutions of Hubbard model, Hartree-Fock approx. 8-52195
metals, press. eqn., Hartree-Fock approx. 8-72103
methane, first hyperpolarisability, Hartree-Fock-Slater calc. (French) 8-78625
methane, force consts., equil. geom., Hartree-Fock and CEPA calcs. 8-70753
methyl radical, ab initio projected unrestricted Hartree-Fock calcs. 8-58582
molecular electron density contour diagram, polarisability anisotropy 8-66681
molecular total energy and orbital energy, semiempirical calcs. 8-78614
monofluoromethane, X-ray photoelectron spectral linewidth of F core, ab initio HF calc. 8-62841
multi-configuration Hartree-Fock program 8-50471
N-electron atomic Hamiltonian first eigenvalue; Hartree-Fock approx. method 8-90062
nitrene, config. interaction calc., using DODS natural orbit approach 8-66476

HF calculations continued

- nuclear collective motion, consistent microscopic theory in an ATDHF approach framework 8-70472
nuclear collective motion, damping, time depend. Hartree model study 8-54711
nuclear collective motion, generalised Schwinger representation, time depend. Hartree Bogoliubov theory quantisation, anharmonic vibr. 8-54673
nuclear collisions, conf. 8-50136
nuclear collisions, TDHF calcs. using separable three dims. wavefunctions, $^4\text{He}+\alpha$ appl. 8-50111
nuclear drop model, mass formula, higher-order vol. symm. terms, Hartree-Fock effective interactions 8-89808
nuclear dynamics, adiabatic TDHF limit versus TDHF, in soluble model 8-50113
nuclear matter, dispersion relations, HF method for hard core interactions (German) 8-54713
nuclear matter, N-N separable non-local interaction, single particle potential 8-58245
nuclear matter props., charge dependent N-N potential, HF calcs. 8-50115
nuclei with $A=4n$, energy levels, BE(2) transition rates, HF approx. using Skyrme force 8-82315
open shell excited states, perturbation effects, restricted Hartree-Fock calcs. 8-86770
orbital amplitudes of nuclei, extrapolation procedure, gaussian basis set and nucl. cusp eqn. 8-74560
outer atomic electrons, corrected by statistical correl. pots. (German) 8-90083
particle collision inclusion in extended time dependent HF approx. 8-49780
Peierls-Hubbard model, quasione dims., antiferromagnetism and Peierls distortion 8-67931
polarisation propagator calculations of frequency-dependent polarisabilities, Verdet constants, and energy weighted sum rules 8-58647
polyacetylene type infinite chain cryst., energy bands, ab initio Hartree-Fock orbital calc. 8-60066
polyatomic closed-shell systems, ab initio Hartree-Fock instabilities 8-78628
polydiacetylene backbone sequence, electronic structs., unrestricted HF approach 8-63975
pseudopotentials, ang. momentum projector, 1st principles HF and local density functional schemes comparison 8-62702
reality conditions for classical motions along collective paths 8-66234
rotating nuclei, selfconsistency conditions in cranked harmonic oscillator model, HF calcs. 8-58239
semi-infinite nuclear matter with complete forces (finite range and spin-orbit term) 8-86499
silathylene, triplet carbenoid isomers, thermodynamic stability 8-90076
single particle width in nuclei, deviations of mass operator from HF values 8-62477
solvent effects, virtual charge model representation of solvent polaris. 8-74593
spherical nuclei, small amplitude vibrs., giant resonances, TDHF, fluid dynamics comparison 8-66233
spherical shell model, collective features, review 8-50098
spherical shell model, renormalisation for collective model within truncated space 8-54697
spin density waves, nearly commensurate, effect of harmonics, Hartree-Fock calcs. 8-88104
stationary nonlinear Hartree eqn., asymptotic soln. 8-49723
TDHF and functional approaches, Lipkin model 8-93957
TDHF eqns. for quantum mechanical many body systems 8-78296
tetrafluoromethane, X-ray photoelectron spectral linewidth of F core, ab initio HF calc. 8-62841
time dependent Hartree Fock solns. for heavy ion scatt., wave packets to stationary waves 8-62558
transition metal alloy, electronic structure, mag. props. 8-95254
transition metal nitrosyls, ab initio HF calcs. 8-90082
transition metals, electronic structure and ordering of sp defects 8-91639
triaxial shapes in nuclei, projected HF and Hartree-Fock-Bogoliubov overlap integrals 8-78293
UHF wavefunctions, spin densities improvement 8-62688
universal atomic basis sets, light atom HF ground state energies 8-78605
yrast traps at very high angular momenta, microscopic description 8-70426
 α - α scatt., 75.2 MeV, TDHF calcs. in 2 and 3 dimensions 8-78401
Ag, oscillator strengths, relativistic HF, core-polarisation model pot. 8-86818
 ^{27}Al , shape mixing using ang. momentum projection from Hartree-Fock intrinsic states 8-86472
Ar IX, Ne I like reson. and Na I-like satellite lines, relativistic HF calc., beam-foil spectra 8-94210
 Ar^{2+} , levels of $2p^3 3p^5$ 8-74574
 ^{37}Ar , M/L capture ratio, multiconfig. Hartree-Fock calc. atomic electron correlations 8-762510
Au, oscillator strengths, relativistic HF, core-polarisation model pot. 8-86818
B, ground state energy, HF calc., second-order correction 8-86784
B, ground state wavefunction, SCF HF calc. 8-90070
 B^+ , dynamic multipole polarisability, coupled Hartree-Fock 8-82858
BH, electron density, basis set, electron correl. effects 8-74581
 BH^+ , spin-extended Hartree-Fock ab initio calculations for small radicals 8-70746
 B(e,e) , $A=10, 11$, form factors, Hartree Fock calcs. 8-58263
Be, dynamic multipole polarisability, coupled Hartree-Fock 8-82858
Be, freq.-depend. polarisabilities and Verdet consts., calcs. 8-62781
Be, ground state wavefunction, SCF HF calc. 8-90070
 BeH , spin-extended Hartree-Fock ab initio calculations for small radicals 8-70746
 ^7Be , L/K capture ratio, multiconfig. Hartree-Fock calc. atomic electron correlations 8-62510
C, ground state energy, HF calc., second-order correction 8-86784
C, ground state wavefunction, SCF HF calc. 8-90070
C, theoretical ionis. energies and oscill. strengths, excited s-, p- and d-levels 8-86823
 C^{2+} , dynamic multipole polarisability, coupled Hartree-Fock 8-82858

HF calculations continued

- CN⁻, first hyperpolarisability, Hartree-Fock-Slater calc. (French) 8-78625
- CO, first hyperpolarisability, Hartree-Fock-Slater calc. (French) 8-78625
- CO, freq.-depend. polarisabilities and Verdet consts., calcs. 8-62781
- CO, orbital contribs. to relax. energies accompanying core ionis., ΔSCF HF calcs. 8-82642
- CO, X-ray K-absorpt. spectra, vibr. fine struct., ab initio restricted HF calc. 8-86883
- COH⁺, orbital contribs. to relax. energies accompanying core ionis., ΔSCF HF calcs. 8-82642
- ¹²C(π⁻, NN), bound π absorpt., HF wave functions, branching ratios, ang. distrib. 8-54803
- Ca, isotopes 40, 42, 44, 48, charge distrib., Hartree-Fock anal. (Russian) 8-70747
- Ca XV, transition probabilities, energy spectra calcs. 8-70791
- ⁴⁰Ca+¹⁶O, 3-D TDHF calcs. 8-54781
- ⁴⁰Ca+⁴⁰Ca, 278 MeV, comparison of 2-D and 3-D TDHF 8-82386
- ⁴⁰Ca+⁴⁰Ca, 278 MeV, particle transfer width, 3 dims. TDHF calcs. 8-74389
- ⁴⁰Ca+⁴⁰Ca, 3-D TDHF calcs. 8-54781
- ⁴⁰Ca+⁴⁰Ca, 3-dimens., time depend. HF calcs. for fusion cross sections 8-66318
- Cd, quadrupole antishielding factors, Hartree-Fock perturbation theory 8-62723
- Ce II, isotope shift and screening, pseudo-relativistic HF calc. 8-90096
- Cl VIII, Ne I like reson. and Na I-like satellite lines, relativistic HF calc., beam-foil spectra 8-94210
- Cs, discrete level raising into far continuum, oscillator strength to shape reson. transfer 8-78624
- Cs I, atomic wavefunctions collapse 8-70733
- Cu, oscillator strengths, relativistic HF, core-polarisation model pot. 8-86818
- ¹⁵⁸Er, moment of inertia anomaly at ang. momentum of 26 to 30 8-62496
- ¹⁶⁶Er, Skyrme-HF calcs., deformation, electric moments, spin-orbit potentials 8-62480
- F, ground state energy, HF calc., second-order correction 8-86784
- FH, freq.-depend. polarisabilities and Verdet consts., calcs. 8-62781
- Fe, hyperfine interaction parameters, effect of local exchange, Xα and HF calcs. 8-78622
- Fe XXI, transition probabilities, energy spectra calcs. 8-70791
- Fe³⁺, quadrupole antishielding factors, Hartree-Fock perturbation theory 8-62723
- ⁵⁴Fe(p,p'), testing self consistent models of collective and single particle struct. 8-82300
- Ga I, Rydberg series, discrete levels and continua of finite bandwidth 8-74603
- GaAs (110), electronic states and initial steps in oxidation 8-91534
- H₂, ¹π_u and ³π_u states, singlet-triplet energy difference, Hund's rule, inequality formulation 8-66482
- H₂, mag. field depend. orbitals for mag. screening and susceptibility of mol. 8-78611
- HCN, dipole moment derivative, sign anomaly, CGTO ab initio calc. 8-74795
- HCO⁺, orbital contribs. to relax. energies accompanying core ionis., ΔSCF HF calcs. 8-82642
- HCl, bond dependence of dipole polarisabilities 8-74573
- HF, bond dependence of dipole polarisabilities 8-74573
- HF, mag. field depend. orbitals for mag. screening and susceptibility of mol. 8-78611
- H₂O, elec. and mag. props. in static fields, perturbed Hartree-Fock calcs. 8-50462
- H₂O, electron density, basis set, electron correl. effects 8-74581
- H₂O, electronic ground state, SCF HF and CI calcs, pot. energy hypersurface, spectroscopic consts. 8-50473
- H₂S, electron density, basis set, electron correl. effects 8-74581
- He, dynamic polarisability, CHF method 8-50472
- He, freq.-depend. polarisabilities and Verdet consts., calcs. 8-62781
- He, ground state wavefunction, SCF HF calc. 8-90070
- He, photoionisation, frozen-core HF perturbation theory, oscillator strength, dipole length and vel. calc. 8-78672
- He-CH₃⁺ interaction energy, nonempirical calc. 8-86799
- He+CO, nuclear mag. shielding consts., interaction geometry depend., chemical shift, gauge invariant method 8-62866
- He⁺+alkali metal atom, ionisation cross sections, binary encounter approx. with HF electron vel. distrib. 8-55225
- In I, Rydberg series, discrete levels and continua of finite bandwidth 8-74603
- In, quadrupole antishielding factors, Hartree-Fock perturbation theory 8-62723
- Ir, hyperfine interaction parameters, effect of local exchange, Xα and HF calcs. 8-78622
- KOH, MHD plasma mol., pot. energy curves and dipole moment, bond lengths 8-71462
- La, ground state, two band Hubbard model, for almost mixed valence system 8-84171
- Li (100), O adsorption, cluster models, ab initio HF LCAO theory 8-71978
- Li-like ions, fine struct. in 1s2p² ⁴P and 1s2s2p ⁴P⁰ states 8-66471
- Li+He, direct excitation of Li I (n) levels in keV collisions 8-90280
- Li₂, and anion, electronic struct., spin-unrestricted, spin-restricted SCF HF calc. 8-90331
- LiH⁺, spin-extended Hartree-Fock ab initio calculations for small radicals 8-70746
- LiNa, and anion, electronic struct., spin-unrestricted, spin-restricted SCF HF calc. 8-90331
- ²⁴Mg, HF microscopic anal. of core struct. for deformed nucleus 8-78294
- Mo even isotopes, HFB calc. of deform. due to isoscalar n-p interaction 8-74302
- N, ground state energy, HF calc., second-order correction 8-86784
- N₂, core ionisation, single orbital relax. energy contrib. calcs. 8-82637
- N₂, X-ray K-absorpt. spectra, vibr. fine struct., ab initio restricted HF calc. 8-86883
- NH₃⁺, ionisation pot. of ²E state, Jahn-Teller effect 8-62948
- ¹⁴N+¹²C, TDHF appl. 8-54709
- Na core polarisation effect on oscillator strengths and energy level locations 8-82688

HF calculations continued

- Na-like ions, transition probabilities for reson. transitions 8-66494
- Na₂, and anion, electronic struct., spin-unrestricted, spin-restricted SCF HF calc. 8-90331
- NaF, ab-initio calc. of cohesion energy, compressibility and density 8-71782
- Ne, converged E⁽²⁾ values 8-66479
- Ne, ground state wavefunction, SCF HF calc. 8-90070
- Ne⁺, converged E⁽²⁾ values 8-66479
- ²⁰Ne, basis states generation by variational methods 8-78295
- ²⁰Ne, HF microscopic anal. of core struct. for deformed nucleus 8-78294
- Ni, chemisorption of H, Xα cluster calcs. (Japanese) 8-72002
- NiCO, and core ionised, binding and relax. energy ab initio LCAO MO SCF calc. 8-62712
- O, ground state energy, HF calc., second-order correction 8-86784
- O₂ molecule, UHF description of ground and lowest singlet states 8-90056
- O₃, ab initio projected unrestricted Hartree-Fock calcs. 8-58582
- O₃, approximate spin extended HF calcs., singlet and triplet states 8-78621
- OH, spin-extended Hartree-Fock ab initio calculations for small radicals 8-70746
- ¹⁶O energy states, HF calcs. using cartesian basis wave functions 8-74319
- ¹⁶O+¹²C, 45-80 MeV, fusion cross sections using time-of-flight technique, TDMF calcs. 8-94043
- ¹⁶O+¹⁶O, 3-d TDHF calcs. 8-54781
- ¹⁶O+¹⁶O, 3-dimens., time depend. HF calcs. for fusion cross sections 8-66318
- ¹⁶O+¹⁶O, 35-80 MeV, fusion cross sections using time-of-flight technique, TDMF calcs. 8-94043
- ¹⁶O+¹⁶O collisions, 105 MeV, appl. of 3-dimens. time-depend. HF calcs. 8-66317
- ¹⁶O+⁴He, 3-D TDHF calcs. 8-54781
- PN, valence state interactions, ab initio and semiempirical estimates 8-74567
- PbO, appl. of effective pots. to relativistic HF calcs. of mol. props. 8-74559
- ²⁰⁸Pb+²⁰⁸Pb, 1600 MeV, axially symmetric TDHF 8-74398
- ²⁰⁸Pb(e,e'), 50 to 335 MeV, mag. spin state excitation cross section 8-50155
- Ru complex, HF calc., electron densities and Mossbauer isomer shift, chemical binding 8-50470
- Ru, hyperfine interaction parameters, effect of local exchange, Xα and HF calcs. 8-78622
- SF₆, ionisation pot., discrete variational Xα calc., Slater-type orbitals in Hartree-Fock basis 8-78837
- Si (111), electronic states and initial steps in oxidation 8-91534
- Si₂, charge density and pseudo charge density, pseudopot. and SCF calcs. 8-70740
- SiH₄, ab initio Hartree-Fock SCF-LCAO-MO method 8-94195
- SiH₄, barrier to internal rotation 8-66680
- SiH₄F₂, ab initio Hartree-Fock SCF-LCAO-MO method 8-94195
- SiH₃F, ab initio Hartree-Fock SCF-LCAO-MO method 8-94195
- ²⁷Si, shape mixing using ang. momentum projection from Hartree-Fock intrinsic states 8-86472
- ²⁸Si HF microscopic anal. of core struct. for deformed nucleus 8-78294
- ¹⁵²Sm, HF one body density for core and valence nucleons 8-78294
- ¹⁵⁴Sm, Skyrme-HF calcs., deformation, electric moments, spin-orbit potentials 8-62480
- Tl I, Rydberg series, discrete levels and continua of finite bandwidth 8-74603
- UF₆, electronic struct., non-relativistic Hartree-Fock-Slater method 8-50469
- V, electron distribution 8-75979
- Zn I isoelectronic series, theoretical oscillator strengths for resonance transitions 8-74616
- Zn, Zn²⁺, quadrupole antishielding factors, Hartree-Fock perturbation theory 8-62723
- ⁶²Zn, band mixing HF model, struct. and electromag. transitions 8-54676

h.f. transmission lines see high-frequency transmission lines

hierarchical systems

see also multivariable systems
dissipative systems, dynamical field theory, hierarchical struct. of field thermodynamics 8-73132

high-energy cosmic ray interactions

- γ-rays ultra-high energy, emulsion chamber anal. (Chinese) 8-89028
- fireball coplanar decay, 24 GeV/c proton-nucleus interaction 8-50157
- hadronic collisions, models rel. to computer simulation of large cosmic ray showers 8-57415
- muons and muon pairs, EM interactions, 5-1200 GeV (Russian) 8-73598
- primary cosmic ray interactions with photoemulsion nuclei using satellite Intercomos-6 (Russian) 8-93063
- scaling features of high-energy cosmic-ray components in atmosphere 8-93062
- secondary particle correl., N-nucleus interactions, 10¹² eV 8-66178
- space radiation, high-energy astronomy expt. 8-85780

high energy electron diffraction

- see also reflection high energy electron diffraction
band theory, zone axis crit. voltage effect 8-83659
- Bloch functions rel. to at. or mol. orbitals 8-83662
- convergent beam diffraction in HV electron microscope 8-83674
- Convergent beam diffraction of 300 keV electrons (German) 8-63646
- HCP metals, critical voltages, using n-beam dynamical theory 8-71644
- many beam problem, use of Gauss-type orbitals and plane waves 8-83661
- metal, electron wave flux distrib. fine struct. near Bragg refl. 8-83670
- SEM, ultra-high, vac., diffr. unit 8-83699
- Al film, room temp. oxidation, scanning HEED expts. 8-91567
- Cu, cryst. pot. in electron diffr. and band theory 8-83677
- Ge film, amorphous, ⁷⁴Ge ion implanted, defect struct. obs. 8-51848
- In_{1-x}Ga_xAs-GaSb_{1-x}As, superlattice heterostruct., MBE 8-95348
- Si, electron transmission at 15 MeV 8-83671
- Xe, adsorbed monolayer, THEED intensity meas. 8-84075

high-energy nuclear reactions and scattering *see nuclear reactions and scattering*

high field effects

see also Gunn effect; hot carriers; impact ionisation; limited space charge accumulation; Poole-Frenkel effect; Schottky effect; Zener effect
amorphous semiconductor, computer simulation 8-88002
carrier distribution function, high energy asymptote (Russian) 8-72163
energy-focused atom probe design and performance 8-85276
noninteracting electrons, in strong elec. field, distrib. function, mean values (Russian) 8-87984
nonlinear dielectric relaxation 8-60389
polar semiconductor, transient high-field conductivity, theory 8-79998
semiconductor, amorphous or disordered, cond. mechanisms, model of medium-range comp. disorder 8-79994
semiconductor, nonlinear current density, theory 8-56149
semiconductor with quasirelativistic band struct., hot electron kinetic equation 8-84222
Stark-Ladder current theory 8-68035
strong elec. field, pulsed V-I characteristics (Russian) 8-64156
weakly conducting layer, elec. field transient penetration 8-84525
As₂Se₃Te_{3-x} chalcogenide glasses, cond. meas., field strength and temp. depend. 8-84225
B₁₄Si₃ switching and high field effects, cond. mechanism 8-64048
Bi, electron gas heating at low temp. 8-60133
Bi_{1-x}Sb_x semiconductor, anomalous conductance in strong electric and longit. quantised mag. field (Russian) 8-76084
Bi₂Te₃-Sb₂Te₃ film, residual cond. 8-52110
CdCr₂Se₄, ferromag. semicond., high field effects, magnon carrier scatt. 8-87981
CdCr₂Se₄, velocity-field characts., above T_c 8-64049
GaAs, electron transient vel. characts., Γ -L-X cond. band ordering 8-79997
n- GaAs, hybrid-hybrid mode interaction in crossed elec. and mag. fields 8-51997
GaSe film, amorphous, I-V characts. in strong elec. fields, 173-373K 8-56248
Ge, hot-electron diffusion coefficient 8-87982
n-Ge, longit. piezoresist., in strong elec. field 8-56147
n-Ge, noise spectra of hot carriers 8-76083
n-Si, current-voltage characts., static high field domains 8-84223
Si inversion layer, negative differential resist. 8-60225
Si MOSFET, electron and hole drift velocities in high elec. field, Monte Carlo calc. 8-60224
Si pin diode, current filament temp. and Au acceptor level capture cross section temp. depend. 8-95351
Si-thermal SiO₂-electrolyte system, cond. in superhigh elec. field 8-52080
Si₃N₄, unsteady cond. in high elec. fields 8-76152
SiO₂, thermal, elec. stressed film, dielec. breakdown 8-64322
V₂O₅, elec. cond. in strong fields, tunnelling mechanism 8-91699
ZnO, surface phenomena, interpretation by compensation model 8-95323
ZnS, single crystal, effect of elec. field on cond. 8-84228

high-frequency discharges

AF glow discharge positive column, stratification obs. 8-67509
air, RF discharge, electron temp. and density 8-51371
air breakdown in superimposed DC and HF electric fields 8-67571
air HF corona discharge ignition characteristics 8-67589
arc, high current, burning in channel 8-63614
arc column helical instability in axial mag. field, damping and RF-DC discharge 8-71595
beam-plasma discharge, microwave field spatial distrib., visible emission polaris. 8-67372
crossed-field discharge plasma instabilities, obs., 10 kHz to 2 GHz 8-75306
DC and UHF field energy transfer to glow discharge plasma electrons 8-67539
EM wave ionisation instability model 8-67512
free plasma column in gas at high pressure 8-75477
gasdynamic parameters meas. and calc. 8-94934
ion source using HF glow discharge, temp. and electron density profile meas. (German) 8-70221
low-pressure discharge in mag. field, alternating voltage distrib. obs. 8-67546
low-pressure discharge rectifying props., expt. 8-67545
low-pressure RF discharge electron temp. probes 8-67542
microwave plasma discharge, appl. to passivation of metals by polymerisation 8-64762
microwave plasma generation at atm. pressure, departure from LTE 8-67597
multicomponent inhomogeneous plasma, spectroscopic analysis 8-67425
partially ionised inert gases in travelling HF mag. field 8-75474
plasma anomalous skin effect conditions 8-67544
point discharge formation, photoelectric obs. 8-67581
polymer breakdown plasma analysis, mass-spectrometric installation 8-88670
quiet plasma, in mag. field, produced by transverse diffusion from RF discharge 8-79448
RF, for sputter deposition and sputter etching, RFI/EM 8-71566
RF discharge in mag. field, plasma rate equation 8-67455
RF discharge plasma skin effect counteraction by external mag. field 8-67543
RF ion source 15 cm stable working region determ. 8-75381
stationary stratified HF discharge in plane wave fields 8-67513
streamers, primary-secondary sequence in short point to plane air gaps 8-87569
surfatron low-pressure RF plasma source 8-67548
Tesla coil, effect on plastic track detectors 8-86742
UHF discharge plasma parameter meas., three-probe method 8-63630
UHF nonequilibrium plasma diagnostics by atomic bremsstrahlung continuum 8-67483
Ar breakdown in superimposed DC and HF electric fields 8-67571
Ar RF discharge plasma, magnetically stabilised, electron temp. using optical spectroscopy (German) 8-63582
CO₂, laser generation by pulsed microwave excitation 8-74879
H₂-Ne, hollow-cathode discharge, electron energy distrib. 8-71573
He HF discharge double-probe meas. 8-67541
He I beam-plasma discharge, optical radiation polarisation 8-67478

high-frequency discharges continued

Hg 40.8 MHz discharge electrode space-charge sheath thickness obs. 8-67547
Kr, high-frequency discharges, at sub. atm. press. 8-67460
N₂ breakdown in superimposed DC and HF electric fields 8-67571
Ne HF discharge plasma electron energy distrib. 8-67540
Ne microwave breakdown field calc., Monte Carlo method 8-67551
Ne-Ar mixtures, glazed electrode AC discharge mode transition obs. 8-67558

high-frequency effects

see also helicons; hot carriers; skin effect; solid-state plasma
degenerate semiconductor, EM wave absorption 8-95308
dimensional quantisation effect, HF characteristics at low temps., multi-photon absorpt., tunnelling (Russian) 8-68073
disordered system with two level atom, low temp. zero photon high freq. conductivity 8-91718
ferrite-semiconductor structure, resonance galvanometric phenomena in semicond. 8-87989
p-Ge, 2 mm wave radiation, interaction with charge carriers (Russian) 8-87991
inhomogeneous semiconductor with nonequilibrium carriers, EM wave propag. 8-52024
intrinsic semiconductor, nonlinear theory of EM wave propagation (Russian) 8-60150
Josephson tunnel junctions, high frequency losses 8-88083
metal, surface charges waves (Russian) 8-64077
metal film, transverse E-type quantum waves (Russian) 8-91785
metal surface, semiclassical infinite barrier model 8-64079
metallic crystal, RF size effect, electron scatt. by impurities diffuse layer boundary (Russian) 8-91717
semiconductor, amorphous or disordered, cond. mechanisms, model of medium-range comp. disorder 8-79994
semiconductor, hopping conduction influence of HF elec. field 8-52025
semiconductor, Kane, thermoelec. power and thermomag. effects of hot electrons 8-56174
semiconductor, many-valley, conductivity in RF heating field (Russian) 8-76085
semiconductor with quasirelativistic band struct., hot electron kinetic equation 8-84222
semiconductor with superlattice, EM wave absorpt. by free carriers, high freq. quantum transport eqn. 8-60148
semiconductor-insulator boundary, space charge layers, HF magnetoconductivity 8-60231
superconducting contact, crit. current, effect of UHF field (Russian) 8-72313
thin conductors, SHG and size cyclotron reson. 8-72186
transition metal oxides, 3d-, microwave cond. at high temp. (Japanese) 8-91715
Bi-Sb narrow gap semiconductor, EM wave propagation in direction parallel to mag. field 8-80014
Fe₃O₄, dielec. props. of low temp. phase, at microwave freq. 8-64309
n- GaAs, hybrid-hybrid mode interaction in crossed elec. and mag. fields 8-51997
Ge, near intrinsic, negative differential cond., ambipolar size effect due to hot carriers 8-72185
n-InSb, 2 mm wave radiation interaction with charge carriers (Russian) 8-87991
n-InSb, microwave displacement effect in longit. elec. and transverse mag. fields 8-87992
n-InSb, millimetre rare modulation in semicond. plasma, use of effects of high elec. field. 8-60149
n-InSb powder, microwave propag., 90-300K, magnetoplasma and helicon wave excitations 8-72183
n-InSb, subjected to mag. field normal to current, coherent HF oscills. 8-52026
Na_{0.33}V₂O₅, dielec. const. and microwave cond. 8-60378
Si inversion layer, high freq. cond., Drude relax., 2D plasmons and minigaps in surface lattice 8-60230
n-Si, microwave and far IR hot carrier mobility, Monte Carlo calc. appl. to mm. transit time oscill. efficiency 8-72184
p-Si, millimetric and far IR cond., evidence for interband transitions 8-52022
Si, powdered, microwave propag. 8-56175
Si, two-dimensional electrons in superlattice, HF cond. 8-64055

high-frequency electronic transport *see high-frequency effects*
high-frequency heating *see radiofrequency heating*
high-frequency transmission lines
linear accelerators, HF struct. with standing waves (German) 8-50420
high power amplifiers *see power amplifiers*
high-pressure effects in solids
see also high-pressure solid-state phase transformations; piezo-optical effects
Adirondack anorthosite, deform. characts. 8-61399
alkali halides, exchange charge shell model analysis of strain derivatives of static polarisability, effective charge parameter 8-91296
alkali halide, optic mode Gruneisen parameters and strain derivatives, Born-Mayer and Szigeti model 8-55929
anion exchange, in tablet pressure for IR spectroscopy (Russian) 8-95927
chalcogenide glasses, elec. cond., press. effects 8-56142
comminution of solids under hydrostatic pressure, technique 8-52702
crystal under high pressure, dislocation theory 8-55870
diamond polycrystal, sintering under high press., binary inclusion-diamond interaction (Chinese) 8-80484
dislocation mobility at high hydrostatic pressure 8-55869
dislocations and point defects in hydrostatically compressed crystals (Russian) 8-75666
ductile-brittle transition pressure, grain size effect (Japanese) 8-60745
dunite, elec. cond during shock compression from 12.5 to 45 GPa 8-85536
effect of pressurisation on acoustic emission characts. during tensile testing 8-92304
elastic wave transit time meas., 100 kbar apparatus 8-79176
equations of state, shock wave expts. (German) 8-59858
ferroelectric phases, rel. to Earth and planetary interiors 8-69334
n-GaAs:O, press. depend. of deep level associated with O, transient capacitance meas. 8-64000
glass fibre reinforced plastic tube under cyclic pressurisation 8-68761

high-pressure effects in solids continued

- ice VI, high-pressure Raman spectra, bending and librational bands 8-68499
- ice VII, melting curve up to 150 kbar 8-67812
- Indiana limestone fracture toughness, confining pressure effect 8-57197
- lanthanum ethyl sulphate nonahydrate: Tb³⁺, ESR spectrum, spin lattice relax., effect of hydrostatic compression 8-88185
- metal, kinetic effects at high anisotropic strains, elec. transport props. meas. 8-54384
- metal, plasticity under hydrostatic pressure (*Russian*) 8-68726
- metal, specific volume meas., for ruby R₁ fluoresc. press. gauge calibration, 0.06-1 Mbar 8-70150
- metal failure, due to hydrostatic pressure, exam. of kinetics 8-52944
- metals, effect of hydrostatic pressure and stress on plasticity 8-52907
- metals, high press. expts., review (*Japanese*) 8-71790
- Mossbauer apparatus for resonance studies at high press. and low temps. 8-49943
- parametrisation for solids under hydrostatic press. 8-72120
- perovskite-like oxides, high-pressure series, rel. between structure and physical properties 8-51493
- PMMA, X-ray absorption, shock wave compression meas. (*German*) 8-95618
- poly(alkyl methacrylate), vitreous state, thermal cond., hole theory of liqs., press. 8-84013
- polycarbonate, yielding and crazing behaviour in torsion under superimposed hydrostatic press. 8-52898
- polyethylene, polyethylene-D₄, migration and copolymerisation at high press. with shearing stress 8-51678
- polymer, partially crystalline, sp. vol. press. depend. (*German*) 8-75852
- polymethylpentene, press. effects on melting 8-56625
- press. depend. of effective mag. fields on ⁵⁷Fe nuclei 8-52383
- PVC, X-ray absorption shock wave compression meas. (*German*) 8-95618
- quartz, synthetic hydrostatic pressure effect on precip. of structure bound water in microinclusions 8-75838
- rocks, elastic props. experimental studies rel. to Earth crust press.-temp. conditions modelling (*Russian*) 8-96207
- rocks physical props. under mantle conditions, conf., Durham, England (Aug. 77) 8-69333
- ruby:Cr³⁺, exchange integral, pressure depend., test of theory 8-87741
- ruby, single cryst. struct. determ. for press. up to 90 kbar 8-83875
- semiconductors, kinetic effects at high anisotropic strains, elec. transport props. meas. 8-54384
- spin glasses under high press., resist. meas. 8-52277
- steel, alloy, ductility, hydrostatic press. effects 8-80615
- steel, high speed, powder, cold isostatic compaction effect on thermophysical props. 8-52717
- transition metal alloys, magnetically ordered, effect of magnetic field on P-T diagram 8-52246
- transition metal oxides, pressure-induced high-spin-low-spin transitions 8-85549
- TTF-TCNQ, const. vol. resist., linear temp. depend. 8-51977
- twinning and linear compressibility anisotropy under hydrostatic press. 8-51553
- Ag, elec. resist., press. variation 8-84193
- Ag, isothermal compression curves to 120 kbar, X-ray diff. study 8-83876
- Ag, thermal conductivity at high press. meas. 8-95283
- Ag₄I₅, ionic cond., effect of press. 8-51733
- Al, cast, strength and plasticity under hydrostatic pressure 8-56694
- Al, Gruneisen parameter behaviour at high press. 8-83899
- Al, isothermal compression curves to 120 kbar, X-ray diff. study 8-83876
- Al, X-ray absorption, shock wave compression meas. (*German*) 8-95618
- Al₂O₃, elec. props. under isentropic compression up to 500 GPa 8-71789
- Ar:NO₂, Raman spectra, high press., low temp. effects 8-52479
- As, zone centre phonons and elastic const., hydrostatic press. depend. 8-59905
- As₂Se₃, and As₄Se₃Ge glasses, struct. changes, Mn²⁺ EPR expts. 8-79534
- As₄Te₃Ge(Si) glass, struct. changes, Mn²⁺ EPR expts. 8-79534
- As₅₀Te₄₅I₅, glass, semicond., elec. switching, high press. effects 8-72212
- Au, elec. resist., press. variation 8-84193
- Au-Cr, dil., spin glass, elec. resist., press. and conc. effects 8-52278
- Ba, superconductivity, pressure dependence, ion core 8-91805
- Ba_{0.92}Ca_{0.08}TiO₃ ceramic, uniaxial stress effects, US dilatometric and dielec. meas. 8-52454
- Bi, US propagation anomalies, under hydrostatic press. (*Russian*) 8-83884
- Bi, zone centre phonons and elastic const., hydrostatic press. depend. 8-59905
- Bi_{1-x}Sb_x, semicond.-semimetal transition, temp. and press. depend. of transport props. 8-76120
- CaF₂:Gd³⁺, S-state splitting, investigation by ESR and ENDOR at high pressure 8-52345
- CdF₂:Gd³⁺, hydrostatic press. and temp. effects on EPR spectrum 8-76304
- CdS-CaS, solid soln., rock salt struct., high press. phase equilibrium study 8-52777
- CdS-MgS, solid soln., rock salt struct., high press. phase equilibrium study 8-52777
- CdS-SrS, solid soln., rock salt struct., high press. phase equilibrium study 8-52777
- Ce, sp. ht. and temp. coeff. of resist., 20 kbar at 300K 8-83973
- Cr-Al, disordered alloy, effect of high press. on resistivity 8-95286
- CrTe, effect of high pressures on magnetic properties 8-52238
- Cs₂Au₂Cl₆, ¹⁹⁷Au Mossbauer high press. study of mixed valence compound 8-52387
- CsCdF₃, nonlinear elastic behaviour, US velocity, 1 bar-3 kbar 8-59851
- CsCl, thermal expansivity determ. at high press. 8-79787
- Cu, elec. resist., press. variation 8-84193
- Cu, Gruneisen parameter behaviour at high press. 8-83899
- Cu, interdiffusion with sintered Al powder, struct. effect at high press. 8-60606

high-pressure effects in solids continued

- Cu-Cr, dil., spin glass, elec. resist., press. and conc. effects 8-52278
- CuCl, zincblende struct., high press. Raman scatt., 77K 8-60463
- Cu₂O polycrystalline and single cryst. mech. behaviour 8-95777
- ErFeO₃, sound velocity meas. at high press., spin-reorientation transition 8-76254
- Eu complex, benzoylacetate, energy transfer at high pressures 8-52541
- Eu, Mossbauer isomer shift and magnetic hyperfine field, press. effect 8-52386
- Fe based porous metals, exam. of volume change under high pressure 8-52906
- Fe, cast strength and plasticity under hydrostatic pressure 8-56694
- Fe effect of repressing and double sintering on impact strength (*Japanese*) 8-92217
- Fe, equation of state determ., high temp. and pressure, computer expt. 8-75800
- Fe, Gruneisen parameter behaviour at high press. 8-83899
- α-Fe, hydrostatic pressure effect on creep rate and failure time 8-92306
- Fe: ¹¹⁹Sn, pressure dependence of effective magnetic fields 8-52382
- Fe-Al-Si, bending test, mech. props. under high press. and temp. (*Japanese*) 8-76711
- Fe-H system, influence of H press. on Fe crit. points and H solubility 8-52758
- Fe-Si (3 wt.%), exam. of plastic deformation, slip band dislocation, under hydrostatic pressure 8-56695
- GaAs, hole effective mass, press. depend., theory and tunnelling expts. 8-75986
- Gd complex, benzoylacetate, energy transfer at high pressures 8-52541
- Gd₂(MoO₄)₃, uniaxial stress effect on ferroelec. transition, Raman scatt. 8-80360
- Gd₂Y_{1-x}Fe_x, s-d exchange interaction integral, change due to hydrostatic compression 8-88199
- Ge, effect of pressure on the Raman shift 8-92064
- Ge, eqn. of state, under press. 8-75801
- Ge-Se glass, elastic props. under press., US interferometry 8-79658
- H₂, isentropically compressed, elec. cond. at Mbar press. 8-95315
- HBr, far IR Ar matrix isolated spectra, 4.2K, press. and conc. effects 8-62801
- HCl, far IR Ar matrix isolated spectra, 4.2K, press. and conc. effects 8-62801
- In, Gruneisen parameter behaviour at high press. 8-83899
- K, device for press. variation of yield stress, elastic constants 8-53047
- KCl absorption and emission of F₁(Li) centres under hydrostatic pressure 8-92117
- KCl, press. shifts of F-centre hyperfine interaction parameters 8-79957
- KH₂PO₄, ferroelectric transition, press. induced tricrit. point 8-80301
- KH₂PO₄, KD₂PO₄, high-press. struct. rel. to dynamical models 8-80307
- KI:NO₂, Raman spectra, high press., low temp. effects 8-52479
- (La, Ce)Sn₃, dil. alloys, supercond. and normal state props. 8-76184
- LaCuO₃, struct. rel. to phys. props., high-pressure series of perovskite-like oxides 8-51493
- Li halides, F-band energies press. effect 8-60086
- LiCl, press. shifts of F-centre hyperfine interaction parameters 8-79957
- LiF, thermal expansivity determ. at high press. 8-79787
- LiH, zero temp. phases, high density props. 8-75725
- Li₂O-Al₂O₃-SiO₂, glass ceramic, elastic props. at high press., US meas. 8-83863
- Lu, electric field gradient, at ¹⁸¹Ta substitutional atoms, pressure dependence 8-52385
- MgIn, X-ray diff. exam. of compressibility 8-51610
- Mn_{1-x}Fe_xAs, high-pressure phase, magnetic properties 8-52247
- MnZn ferrites, mag. susceptibility freq. spectrum, effect of pressure 8-95420
- Mo, polycrystalline, fracture and ductile-brittle transition, hydrostatic press. effects 8-60735
- Mo, powder, cold isostatic compaction effect on thermophysical props. 8-52717
- NH₄Cl(Br)(I), NMR under high press. 8-84485
- NaCl, press. shifts of F-centre hyperfine interaction parameters 8-79957
- NaF, thermal expansivity determ. at high press. 8-79787
- Na₂O-SiO₂ glass, stability at high press., X-ray diffraction obs. (*German*) 8-92251
- Nb, plastically deformed, hydrostatic pressure effect on dislocation relaxation, US exam. 8-76696
- Ne, P-V-T data for Morse pot., computer expt. 8-75800
- Ne, solid, elec. cond. obs., insulating up to 500 GPa 8-95315
- Ni based porous metals, exam. of volume change under high pressure 8-52906
- Ni:¹¹⁹Sn, 8-52382
- NiSiF₆·6H₂O, ESR spectra at low temperatures and high pressures 8-52339
- NiZn ferrites, mag. susceptibility freq. spectrum, effect of pressure 8-95420
- NiZn ferrites under high press., grain growth (*Chinese*) 8-52825
- Pb, Gruneisen parameter behaviour at high press. 8-83899
- Pb, phonon softening, neutron scatt. at high press. 8-80091
- Pb, superconducting, press. depend. of supercond. transition temp. 8-84340
- Pb-Sb, crystal struct., supercond. after subjection to high press. 8-88064
- PbS, epitaxial layer on rock salt substrate, stresses, hydrostatic press. effects 8-51831
- Pr pnictides and chalcogenides, press. depend. of cryst. field splitting 8-68392
- Pr₃Se₄, induced ferromagnet, effect of press. on magnetisation 8-95422
- RbAg₄I₅, ionic cond., effect of press. 8-51733
- RbCaF₃, nonlinear elastic behaviour, US velocity, 1 bar-3 kbar 8-59851
- RbCdF₃, nonlinear elastic behaviour, US velocity, 1 bar-3 kbar 8-59851
- (SN)₂ and S₈N₄, high press. study 8-52782
- (SN)₂, supercond. props., press. depend., up to 9.5 kbar 8-68106
- Sb, carrier energy spectrum, effect of hydrostatic pressure 8-87903

high-pressure effects in solids continued

- Sb, thermoelectric figure of merit, 1-12 kbar, 100K 8-80013
 Sb, zone centre phonons and elastic consts., hydrostatic press. depend. 8-59905
 Sc, electric field gradient of ^{181}Ta substitutional atoms, press. depend. 8-52385
 Si eqn. of state, under press. 8-75801
 $\text{Sm}_{1-x}\text{Gd}_x\text{S}$, press. induced electronic transitions 8-68058
 SmS , first-order transition from semiconducting to metallic state 8-52040
 SrTiO_3 under [111] uniaxial stress, neutron scatt. 8-67798
 $\text{TiFe}_{1-x}\text{Co}_x$, mag. props., under high press. and in high mag. fields 8-95423
 TlCdF_3 , nonlinear elastic behaviour, US velocity, 1 bar-3 kbar 8-59851
 U, electric field gradient, of ^{181}Ta substitutional atoms, press. depend. 8-52385
 W, grain boundary migration initiated by high hydrostatic press. 8-51554
 W, powder, cold isostatic compaction effect on thermophysical props. 8-52717
 YIG, press. depend. of effective mag. fields on ^{57}Fe nuclei 8-52383
 YbO , Yb_2O_3 , form. at high press. from $\text{Yb} + \text{Yb}_2\text{O}_3$ 8-85192
 $\text{ZnS}:\text{Cl}^-$, $\text{Cu}^+(\text{Ag}^+)$, phosphor, thermoluminesc. 8-64419
 ω -Zr, electric field gradients at substitutional Ta atoms, TDPAC high-pressure study 8-52384

high-pressure phenomena and effects

- see also *high-pressure effects in solids*
 AGR boiler tube, serpentine geometry at high press., two phase heat transfer 8-94077
 carbon tetrachloride, thermal cond. and phase diagram under pressure 8-75893
 cast Fe, spheroidal graphite, hydrostatic pressure effects on ductile fracture 8-60779
 conference on high pressure physics and technology, Moscow, Russia (May 1975) 8-51611
 EBBA, pVT data and viscosity-press. behaviour 8-94989
 equations of state, Thomas-Fermi shell model, and high temps. 8-79738
 feldspar/water O isotope exchange, effect of fluid press. 8-57204
 fluid binary mixtures, phase equilibria and critical phenomena at high press. 8-51648
 hydrostatic pressure effects on fracture, exam. 8-60779
 ice, press. effects on Raman spectrum 8-95582
 ice, pressure melting within glacier, indicated by regelation ice chem. comp. 8-61447
 MBBA, pVT data and viscosity-press. behaviour 8-94989
 metal- H_2 systems, determ. of absorption/desorption isotherms, high press. 8-51679
 metal-vapour/inert-gas mixture discharge peculiarities 8-71620
 molecular electronic spectra, high press. effects 8-78754
 polyethyl siloxane, liqs., thermal cond. at high press., 20-200°C 8-79825
 polyethylene, effect of pressure and environment on fracture and yield 8-76757
 polyoxymethylene, effect of pressure and environment on fracture and yield 8-76757
 polypropylene, effect of pressure and environment on fracture and yield 8-76757
 polystyrene, effect of pressure and environment on fracture and yield 8-76757
 polyvinylidene fluoride, high-press. melting and crystallisation 8-91422
 pressed powder bed, determ. of side pressure distrib. 8-84734
 reverse-buckling safety discs, release pressure 8-89489
 surface viscosities at high pressure gas-liquid interfaces 8-75907
 Teflon, creep under joint action of tension, hydrostatic pressure 8-68750
 vapour-liquid equilibria, generalised method for calc. and prediction at high press. 8-87780
 vapour-liquid equilibrium, phenomenological description 8-91415
 water, high-pressure Raman spectra, bending and librational bands 8-68499
 water, molar heat capacity under high press. near solidification point 8-51695
 water, viscosity, 10-150°C, press. effects 8-51715
 water structure and motion at high pressure 8-87606
 Al-Zn-Mg-Cu, alloy 7075, hydrostatic pressure effects on ductile fracture 8-60779
 Ar, dense gas, thermal cond. and viscosity coeffs., irreversibility and Kirkwood superposition hypothesis (French) 8-94881
 CO_2 , liq., 100 to 3000 atm., depolarised Rayleigh spectra, orientation dynamics, wings 8-92084
 Cd_2P_2 , high press. phase relns. and cryst. structs. 8-59792
 Cs , liq., specific heat meas., at temp. up to 1700K under pressure 8-51696
 $n\text{-D}_2$, fluid, eqn. of state from P-V-T and US vel. meas. up to 20 kbar 8-63837
 D_2O , gaseous, viscosity, 200-400°C, up to 300 bar 8-63527
 Fe-C system, liq.-solid equilib. at high press., influence of graphitising elements (Russian) 8-56613
 H_2 , diffusion through Pt membranes at high press. and temps. 8-55984
 K, thermodynamics of melting at high pressures 8-91426
 Li, thermodynamics of melting at high pressures 8-91426
 N_2 , density up to 2000K and 6 kbar by displacement method 8-51266
 NaNO_3 , aq. soln., Raman spectra, vibr., orient. relaxation (French) 8-62808
 Rb, thermodynamics of melting at high pressures 8-91426
 S , liq., optical absorption spectrum, up to supercrit. conditions 8-88320
 SCN^- , associated with metallic cations in aq. soln., press. effect, Raman spectra (French) 8-80333
 $\text{WC-Co}(\text{TiC-Co})$, powder compacts, effect of additional pressing at hydrostatic pressures on props. 8-56596

high-pressure solid-state phase transformations

- actinides, struct. props. rel. to F electrons 8-83951
 albite, phase behaviour between 100 and 280 kbar at 1000°C 8-53644
 alkali halides, sudden jump transitions, transformed fraction and reaction rate meas. 8-51667

high-pressure solid-state phase transformations continued

- calcite rock, phase transitions rel. to compression wave studies 8-81151
 conference on high pressure physics and technology, Moscow, Russia (May 1975) 8-51611
 crystal classification by transition mechanisms (Russian) 8-60401
 cyclohexane, differential thermal anal. under high press. 8-51669
 2,2'-dimethylbutane, differential thermal anal. under high press. 8-51669
 n-heptacosane, differential thermal anal. under high press. 8-51669
 hexamethyl benzene, high press., variable temp. Raman spectra 8-56488
 high press. transforms., kinetics and hysteresis 8-51668
 II-V semiconductor, electronic theory, covalent-metallic or covalent-ionic phase transition under pressure 8-72105
 III-V semiconductor, electronic theory, covalent-metallic or covalent-ionic phase transition under pressure 8-72105
 jadeite, phase behaviour between 100 and 280 kbar at 1000°C 8-53644
 nematic-isotropic phase transition at high press., thermodynamics (Russian) 8-87778
 nepheline, phase behaviour between 100 and 280 kbar at 1000°C 8-53644
 octafluoronaphthalene, high press. struct., neutron powder diff. 8-63743
 n-octatriacontane 8-51669
 olivine, partial phase transition from 12.5 to 45 GPa, evidence from dunitic elec. cond. 8-85536
 polymer, glass transition under high-press., dielec. loss method obs. (Russian) 8-71841
 rare earths, struct. props. rel. to f electrons 8-83951
 silicate glasses, struct. and phase transform. 8-64538
 squaric acid, hydrostatic press. effect on phase transition, dielec. and dilatometric meas. 8-55941
 stacking faults, plasticity and transform. kinetics under high press. 8-51560
 tetramethylsilane, phase rels. under press., DTA obs. 8-71850
 TGS family, change of order of phase transition under hydrostatic pressure 8-52452
 AgI, elastic behaviour near phase transitions with negative dP/dT 8-83885
 BN, toughening by stress-induced phase transforms. 8-80635
 BN, wurtzite type, effect of TiB_2 and B additions, on transformation to zinc blende type 8-80542
 Ba, elastic properties, Debye temp., 20°C, 20 to 70 kbar, US wave velocity meas. 8-87735
 C, film, work function, heat treatment 8-64563
 C, texture change on ht. treatment under press. 8-60687
 CF, cryst. struct. from X-ray diff. 8-83766
 $\text{Ca}_{1-x}\text{Eu}_x\text{Si}_2$, solid solns., $\alpha\text{-ThSi}_2$ struct. type, comp. and press. depend. 8-91322
 CaF_2 , fluorite, phase relations, to 60 kbar and 1800°C 8-84785
 $\text{Ca}_3(\text{PO}_4)_2$, new cryst. phase prep. and struct. (French) 8-83789
 $\text{Ca}_{1-x}\text{Sr}_x\text{Si}_2$, solid solns., $\alpha\text{-ThSi}_2$ struct. type, comp. and press. depend. 8-91322
 Ce, $\alpha \rightarrow \alpha'$ high press. transition, volumetric study 8-83940
 Ce, sp. ht. and temp. coeff. of resist., 20 kbar at 300K 8-83973
 Cs, electronic transition from self consistent APW X α calcs. 8-51884
 CsCdCl_3 , phase transition under pressure 8-51664
 CsH_2PO_4 , high press. phase diagram 8-52457
 CsPbCl_3 , phase transition under pressure 8-51664
 $\text{Eu}_{1-x}\text{Sr}_x\text{Si}_2$, solid solns., $\alpha\text{-ThSi}_2$ struct. type, comp. and press. depend. 8-91322
 Fe-Mn, γ to ϵ phase transform. induced by high press. and plastic deform. 8-68686
 FeF_2 (rutile), high press. phase transform. 8-79761
 FeOOH , high-pressure phase, neutron diffraction study 8-52212
 $\text{Gd}_2\text{Ge}_2\text{O}_7$, polymorphism under pressure (French) 8-95150
 GeO_2 , new high-pressure modification 8-75825
 I, metallic solid, high press. struct., phase transition, X-ray diff. study 8-87647
 In-Bi alloy system at high press. and temp. 8-92238
 InSb, polymorphism and cryst. struct. at high temp. and press. 8-95026
 KCN, disordered ordinary and metastable phases, light scatt., press. depend. 8-95151
 KCN, polymorphism, high pressure, Raman spectra 8-88302
 KD_2PO_4 , high press. phase diagram 8-52457
 La, superconducting, electron-phonon coupling, hydrostatic press. depend. 8-80087
 Mg_2Sn , phase transition under hydrostatic pressure, Mossbauer effect and electric resistance 8-51665
 ND_4Cl , order-disorder transformation, elasticity and heat capacity temp. depend., US obs. 8-71851
 NH_4Br , phase diagrams, from Raman meas. under high press. 8-52776
 NH_4Cl , molar heat capacity near order-disorder transform. under high press. 8-51697
 NH_4Cl , order parameter, electro-optic measurement 8-88280
 NH_4I , phase diagram from Raman meas. under high press. 8-52776
 NH_4LiSO_4 , I-II phase transition in improper ferroelec., hydrostatic press. effects 8-84533
 $(\text{NH}_4)_2\text{SO}_4$, ferroelec., ion group reorientation temp. and press. depend., PMR obs. 8-72470
 $\text{NaNH}_4\text{SeO}_4 \cdot 2\text{H}_2\text{O}$, ferroelectric crystal, effect of hydrostatic pressure on phase transition 8-52453
 NaNO_3 , soft mode dynamics at ferroelec. transition 8-80308
 NaPF_6 , high press. phase diagram, vibr. spectra 8-60446
 NbS_2 , high pressure polymorphs 8-51459
 NbSe_2 , high pressure polymorphs 8-51459
 Nb_3Si , high press. phase, prod. by recrystn. of metastable sputter deposits, struct. and supercond. props. 8-60571
 NbTe_2 , high pressure polymorphs 8-51459
 Ni-Co-H system, phase transform. under high H_2 press., Co additive effects (Russian) 8-60645
 NiF_2 , press. induced strain transition obs., neutron powder diff. meas. 8-55948
 $\text{Pb}_{0.59}\text{Sn}_{0.41}\text{Se}$, struct. phase transition, temp and hydrostatic press. influence, Hall effect, resistivity (Russian) 8-51675
 $\text{Pd}_{50}\text{Si}_{50}$, amorphous alloy crystn., high press. effect 8-95001
 RbH_2PO_4 , high press. phase diagram 8-52457

high-pressure solid-state phase transformations continued

- RbI, phase transition, diffuse neutron scatt. in metastable press. region 8-67825
 RbI, single cryst., press.-induced B1-B2 phase transition, X-ray diffr. meas. 8-63852
 RbNH₄SO₄, ferroelec., ion group reorientation temp. and press. depend., PMR obs. 8-72470
 Se-H system 8-63853
 Si, polymorphism under high press. (*Russian*) 8-59947
 SiO₂, new high-pressure modification 8-75825
 Sm₂Bi₃, press. induced valence instability, elec. resist. transition 8-95317
 SmS, vol. changes at press. up to 20 kbar 8-71791
 TGSe, anomalous sound velocity near ferroelec. phase transition at high pressure 8-52456
 TeO₂, paratellurite, phase transition at high-press., Raman and far IR spectra 8-80328
 TeO₂, zone centre optical phonons under uniaxial stress 8-79700
 TiAsS₄, struct. and soft mode behaviour 8-91327
 TiN₃, press. induced transition dynamics, light scatt. 8-80362
 Ti₃PSe₄, struct. and soft mode behaviour 8-91327
 V₃Si, nontransforming, press.-induced phase transformation 8-80084
 Yb-H system 8-63853
 Zn₃P₂, high press. phase relns. and cryst. structs. 8-59792
 ZrO₂, containing metastable tetragonal phase, stress induced phase transform. effect on props. 8-68683

high-pressure techniques

- anvil, truncated, compressive strength, high press. apparatus appl. 8-84906
 apparatus with shaped Bridgman anvils, calibration 8-49856
 bending test apparatus under high press. and high temp. (*Japanese*) 8-76795
 cell for Raman spectroscopy, appl. to hexamethyl benzene 8-56488
 chamber calibration using ruby R₁ luminescence line shift, 80 to 550K 8-86284
 chamber for pulsed NQR spectrometer 8-86308
 chamber thermocouple lead-ins for highly compressible media 8-86285
 comminution of solids under hydrostatic pressure, technique 8-52702
 conference on high pressure physics and technology, Moscow, Russia (May 1975) 8-51611
 conical plug seals, plastic flow under pressure, tightness mechanism 8-54386
 contacting surfaces, optimisation of elastic strain distrib., anvil shape 8-49847
 continuous flow helium cryostat for optical studies at fixed high pressure 8-81984
 diamond anvil cell adaption to automatic for circle X-ray diffractometer 8-75501
 diamond cell, single cryst., revised operating method, NaCl struct. refinement at 32 kbar 8-67610
 diamond-anvil high pressure cell used in automatic diffractometer up to 90-kilobars 8-54387
 EPR cavity sensitivity improvement 8-54419
 ESR meas. at hydrostatic pressures to 60 kilobars 8-54418
 free piston gauge 8-54385
 gas high pressure cell for optical studies at low temp. and hydrostatic pressure 8-82016
 generation in large volume, up to 77 kbar and 2000°C 8-57972
 glass capillary for high resolution NMR measurements at pressures up to 400 MPa 8-65950
 heat capacity measurement, low temp., of metals under press. 8-81979
 inlet for elec. conductor into high-pressure chamber 8-74016
 ion-molecule reactions, gas-phase, and high-press. mass spectrometer, review (*Japanese*) 8-64830
 low-temperature single crystal strong uniaxial compression apparatus 8-57973
 mechanical pressure generators, anal. 8-86287
 metals, high press. expts., review (*Japanese*) 8-71790
 microwave cavity for EPR at high hydrostatic pressures 8-89518
 miniature toroid high press. cell with superhard pistons 8-49858
 molecular fluorescence polarisation meas. at high press. 8-66576
 Mossbauer apparatus for resonance studies at high press. and low temps. 8-49943
 neutron spectrometer appls. 8-49852
 NMR high-pressure probe, high-resolution proton NMR 8-89517
 NMR spin-echo high-pressure system 8-58002
 NQR, apparatus for study under high hydrostatic pressure 8-74038
 piston-cylinder device for H₂ compression to 30 kbar 8-49853
 plasma cutting at elevated press., underwater appl. 8-87507
 pressure calibration by resistance-jump transitions up to 500 kilobars 8-54388
 primary high-pressure standard, USSR 8-49855
 quasihydrostatic pressures, up to 300 kbar at 0.1 to 200K, production method 8-49848
 resistivity meas. method for up to 50 kbar and 1000°C 8-57978
 reverse-buckling safety discs, release pressure 8-89489
 sliding anvil device for high press. generation 8-49849
 solid-press. cell, generation of uniform press. and temp. distrib. 8-49857
 specific heat meas., at temp. up to 1700K under pressure, expt. on liq. Cs 8-51696
 specimen cross section during low temp. compression, apparatus design 8-57940
 standard gas mixture preparation at high pressures certification 8-93718
 surface structure analysis, at high press. by electron spectroscopy 8-73103
 temperature field distrib. determ. for high press. chamber 8-82001
 viscometer, applic. up to 4 kbar and 300°C 8-59515
 X-ray diffractometer, high-pressure-low-temp. type, appl. 8-82089
 X-ray diffractometer with high pressure cell, data collection measuring procedure 8-75495
 CO₂, compression to 34 kbar, apparatus and technique, diamond anvil cell 8-74017
 N₂, density measurement up to 1800K and 8 kbar, procedure 8-81947
 Pb(Zn_{1/3}Nb_{2/3})O₃, perovskite type, high-press. high temp. synthesis (*Chinese*) 8-68654

high-temperature phenomena and effects

see also *refractories*

- ablation, statistical characteristics of mass lost in thermal destruction, zero gas dynamic press. 8-83429
 corrosion at high temp., review (*Japanese*) 8-72911
 socks, elastic props. experimental studies rel. to Earth crust press.-temp. conditions modelling (*Russian*) 8-96207
 Al, atomistic images of field ion microscopy at high temps. 8-55792
 Au, atomistic images of field ion microscopy at high temps. 8-55792
 CaF₂, fluorite, phase relations, to 60 kbar and 1800°C 8-84785
 Cu, atomistic images of field ion microscopy at high temps. 8-55792
 Ni-Cr-Nb-Al eutectic alloys, sulphidation/oxidation at high temps., corrosion mechanism 8-72934
 SF₆ high-temp. electrical breakdown parameters 8-67567

high-temperature techniques

see also *pyrometers; refractories*

- absorption spectroscopy for temp. meas., principle 8-54375
 adsorbed species, catalytic reaction, high temp. IR obs. 8-88655
 bending test apparatus under high press. and high temp. (*Japanese*) 8-76795
 centrifuge construction 8-57938
 contactless testing by EM acoustics 8-85095
 crystal growth from high-temp. melt, reaction cell for microscopic obs. 8-64457
 dynamic testing of metals, alloys over wide temp. range, unit 8-60908
 gas diagnostics by spectral remote sensing 8-74002
 high pressure chamber, temp. field distrib. determ. 8-82001
 HTGR fuel and graphite structure stress analysis methods and programs (*Japanese*) 8-74434
 IR tunable diode laser technique, temp. meas. of high-temp. gases 8-86268
 microsamples, high-temp. mech. testing, unit 8-60904
 MOSFET characts. for geothermal instrumentation, up to 300°C 8-73553
 Nichrome, Kh20N80, varying porosity, effective thermal cond., 373-1400K, meas. method 8-75053
 porous cylindrical specimens, effective thermal cond. meas. method, 373-1400K 8-75053
 pressure generation in large volume, up to 77 kbar and 2000°C 8-57972
 reference standards for radiation pyrometry, silver and copper freezing points 8-57888
 resistivity meas. method for up to 50 kbar and 1000°C 8-57978
 rheonometer, Weissenberg-type, sample temp. meas. procedure 8-75113
 specific heat meas., at temp. up to 1700K under pressure, expt. on liq. Cs 8-51696
 US thermometers, nuclear fuel temp. profile meas., TRESON expts. 8-57955
 X-ray thermographic installation, for temp. recording up to 1500°C 8-74003
 Ga, gaseous reduction and extraction from mica 8-92216
 N₂, arc jet enthalpy meas. by fast miniature total calorimetric probe 8-67486
 N₂, density measurement up to 1800K and 8 kbar, procedure 8-81947
 Pb(Zn_{1/3}Nb_{2/3})O₃, perovskite type, high-press. high temp. synthesis (*Chinese*) 8-68654
 Pt, resistance thermometers for high temperatures (*Russian*) 8-57958
 Ta treated, graphite atomiser tubes, for high temp. AAS 8-73093

high vacuum gauges see *vacuum gauges***high-voltage engineering**

see also *high-voltage techniques*

- air insulation, predischage-stabilised breakdown voltage (*German*) 8-63608
 arc quenching system for transient and statistical flashover, fusion reactor systems 8-75455
 fusion reactor implosion heating coil, radially fed, design, fabrication 8-55006
 laboratory ion density due to repetitive impulse generation 8-65913
 laser fusion, eight-beam system, high-voltage engineering 8-58492
 neutral beam accelerator electrodes, spark discharge protection, for fusion reactor 8-62609
 ohmic heating system for TFTR Tokamak 8-55017
 polyethylene, elec. trees free radical ESR study 8-60393
 Shiva laser, 25 MJ energy storage and delivery system 8-55015
 transmission line elec. and mag. field exposure effects and hazards 8-77083
 SF₆ insulated switching installations and devices, gas chromatography appl. (*German*) 8-88668
 SF₆ insulation, predischage-stabilised breakdown voltage (*German*) 8-63608

high-voltage techniques

- 600 kV repetitive stacked line transformer pulse generator 8-77935
 AC Penning discharge, vacuum pumping characts. 8-93713
 analogue safety data link, for Princeton Large Torus control room 8-54938
 electrostatic inflector and extractor for cyclic accelerators, HV expts. 8-50421
 fusion reactor, fibre optic telemetering for high voltage test stand 8-54939
 fusion reactor, JET, high voltage network to load AC/DC pulse power conversion 8-58497
 fusion reactor, pulser system, air-driven fibre-optic coupled for Los Alamos ZT-40 expt. 8-54943
 fusion reactor, use of homopolar generator for inductive energy storage 8-54948
 heavy-current arc gap 8-87514
 HF high voltage meas. by electro-optical effect 8-86301
 HV nanosecond transient meas. from pulsed low inductance gas discharge, Kerr effect 8-51380
 ion beam accelerator, multimegawatt, high-voltage power system, design philosophy, for fusion reactor 8-62613
 neutral beam high-voltage test stand, for fusion reactor 8-70632
 neutral beam source 8 MW voltage series regulator, for fusion reactor 8-70631
 pulse generator for modulation spectroscopy 8-77995
 Kr, hollow-cathode glow discharge with gas flow 8-67532
 SF₆ breakdown distributions, low-value fractile determ. 8-67578

history

- acoustics, Kircher's 'Phonurgia nova' (*German*) 8-81788
 agriculture, expansion in late 19th century rel. to CO₂ levels in atmosphere 8-53717
 Aristotle's theory of falling bodies, pre-sixteenth century objections, for teachers 8-62026
 Aryabhata, 5th century Indian astronomer and mathematician, life and works 8-65741
 astronomical ephemerides of the early seventeenth century 8-77659
 astronomical events and Gospel records rel. to Christ's birth date 8-93127
 astronomy and civilisation in time of Aryabhata I, 5th century AD 8-89289
 astrophysics, America, E.C. Pickering and Henry Draper Memorial 8-86102
 biophysics in USSR 8-93506
 Brownian motion, account of discovery, for teachers 8-86090
 Chamberlin-Moulton cosmogony 8-86104
 chemical formulae, historical development, review 8-73822
 Christmas Star, identification as supernova in Aquila 8-81781
 cinematography, colour film processes and cameras, review, 1894 to date (*German*) 8-93773
 climate correl. with wheat prices and wages 8-81346
 comets, obs. in Greek and Roman sources before 410 AD 8-77658
 Compton currents, historical aspects and recollections 8-80018
 course in liberal arts technology 8-86061
 Crab supernova explosion of 1054, sighting in Near East 8-62028
 earthquake in Odawara City, Japan, 1853 March 11, intensity, damage and magnitude from old documents (*Japanese*) 8-96146
 earthquakes, Japanese, records in 'Diary of Librarians of Edo Bakufu (Feudal Government)' 8-65200
 elementary particles discovered during 1974-7 (*Czech*) 8-86103
 Evans, Thomas Simpson, 1777-1818, mathematician and astronomer 8-89287
 exponential law, concepts prior to 1900, review 8-86052
 fluid dynamics, turbulence, statistical mechanics, progress in last thirty years 8-89290
 fluid mechanics at Cambridge, book contrib. 8-57726
 fluorescence spectrometry, anal. appls., historical review 8-93507
 Fulton's orrery, 19th century instrument to demonstrate planetary system motions 8-69695
 Galileo and Tower of Pisa expt., discussion 8-49582
 gas transport, in synthetic polymer membranes, history 8-76912
 great year in Greek, Persian and Hindu astronomy 8-81790
 Hamiltonian dynamics, integrable and nearly integrable systems historical review 8-93521
 Harriot's lunar maps drawn in 1609 and 1610 8-81783
 Heisenberg's work on anomalous Zeeman effect and multiple spectra of atoms 8-70784
 Henry Norris Russell, and Hertzprung-Russell (H-R) diagram 8-69957
 inelastic electron tunnelling spectroscopy, past and future 8-90255
 inertia, concept development from Aristotle to Newton 8-81786
 inorganic micro and trace analysis, historical perspectives 8-81784
 instrumentation, History of Sciences Collections, Royal Swedish Academy of Sciences, catalogue 8-81789
 interstellar molecules, pioneering investigations 1935-42 period 8-69855
 ion selective electrodes, review 8-85165
 Johann Georg Soldner (1776-1834), forgotten bicentenary 8-81787
 Kepler and Mars, construction and rejection of first oval orbit 8-62027
 Laplace, P.S., chronology and citations of early work, 1770-1773 period 8-93505
 magnetopause, development of understanding 8-61667
 Mars satellites, history of discovery 8-89099
 Martian satellites, history of discovery and positional obs. (1877 to 1977) 8-89101
 mass spectroscopy, history of development 8-56928
 mathematical physics, success and failure viz. Kolmogorov-Arnold-Moser theorem, gravit. collapse, singularities, matter stability (*German*) 8-65744
 of mathematics, causal and formal logic unification 8-77639
 Max Born, biography, review of contributions to physics 8-86100
 Maxwellian electrodynamic theory, history from eqn. discovery to mag. monopoles (*German*) 8-65791
 Mercury craters, discovery from Earth (in 1901) 8-53847
 Mesoamerican calendrical systems chronology reconstruction 8-81782
 meteors, meteor showers and meteorites in Middle Ages, from European mediaeval sources 8-86105
 microchemistry (*German*) 8-81785
 micromagnetics and domain theory, developments from 1930 8-68288
 N-rays, work of Blondlot and assistant (1903) 8-49626
 Neptune ring, history of obs. 8-69745
 neutrinos, historical review 8-89288
 Newcomb, Simon, American astronomer, 1835-1909, life and works 8-93504
 H.C. Oersted, first spark of electrotechnology, biography (*French*) 8-69955
 partons, similar concepts in ancient Greek, Hindu and Chinese philosophy, for teaching 8-54143
 photographic nucleonics history, record of lost opportunities 8-65986
 Pierre Gassendi, 17th century, early mechanics and philosophy 8-62025
 Poincaré's conventionalism, origin and significance 8-86109
 Poincaré's conventionalism of applied geometry 8-86110
 Polish Physical Society, 1920 to 1939 (*Polish*) 8-54145
 Pulkovo Observatory, astronomical activities 8-81538
 quantum mechanical tunnelling, historical survey 8-54141
 quantum mechanics, development and Heisenberg's role (*Polish*) 8-89291
 Quetelet, A.L.J., life and spread of science in Belgium during 19th century (*French*) 8-65742
 Raman effect, its discovery 8-73819
 Raman effect discovery 8-49627
 Raman spectra, recent developments and historical review 8-73821
 rare earth research developments since 1950 8-84116
 Royal Astronomical Society, catalogue of archives and manuscripts 8-69705
 semiconductor physics and technology, history and development in USSR, brief survey 8-54142

history continued

- solar activity, long-period vars. from historical records (*French*) 8-73695
 solar energy concentrators, design methods, historical aspects 8-83063
 special relativity, secondary-school course not relying on historical approach 8-86096
 stellar convection theory (1930-1945) 8-89177
 sunspot cycle before Maunder minimum, evidence for 11-year periodicity 8-61825
 Tien-Kuan guest star of 1054, Crab supernova, historical records (*Chinese*) 8-65743
 tsunamis, in Japan Sea, behaviour and source areas 8-65198
 tsunamis of 1707 and 1854 along Shizuoko coast, Japan, field surveys (*Japanese*) 8-96149
 Ulugh Beg observatory, meridian instrument axis azimuth rel. to continental blocks rot. 8-53613
 unusual weather frequency variability over last century 8-73479
 Se, semiconducting, and related materials, historical study, 1833-1919 8-57727

HIXE see ion microprobe analysis**HMO calculations**

- alkanes, electron density, bond order, hydrogen suppressed graphs, extended Huckel theory 8-90088
 covalent elements, cohesion in condensed phases, corrections to simple Huckel approx. 8-59779
 covalent elements, cohesion of σ and π bonds in condensed phases, simple Huckel approx. 8-59778
 student use, computerised visual aids 8-77649
 TMMC, antiferromag. coupling in linear chains, molecular orbital approach 8-52239
 CsNiCl₃, antiferromag. coupling in linear chains, molecular orbital approach 8-52239
 CsVCl₃, antiferromag. coupling in linear chains, molecular orbital approach 8-52239
 Na particle, consisting of ats., metallic Na, model, electronic levels 8-50673

H₃O⁺ see hydroxonium ion**hodoscopes see cosmic ray apparatus****hole mobility see carrier mobility****hole theory of liquids see liquid theory****hole traps**

- see also electron traps
 anthracene, prep. and growth of single cryst. 8-64463
 degenerate semiconductor, recombination-generation currents derivation 8-52007
 MOS capacitor, threshold voltage instability due to defect states produced during e-beam metallisation 8-72264
 semiconductor, Faraday rotation in presence of attractive traps 8-76081
 semiconductor containing traps, minority, carrier lifetime 8-60137
 sisal wax, electronic conduction and persistent internal polarisation 8-80277
 tetracene, noncryst., localised valence states in forbidden gap 8-72113
 AgBr, doped, neutralisation of trapped photoholes 8-76108
 Au-tetrathiotetracene-Al systems, dark cond., photocond. mechanisms rel. to contact phenomena (*Russian*) 8-52103
 GaAs MESFET, deep trapping effects at GaAs-GaAs:Cr interface 8-72245
 GaP, p⁺-n diode junction, admittance meas. and carrier traps 8-91757
 Ge, donor-acceptor electron transfer at low temps., photocond. tail 8-84249
 KBr:NO₂, Na effect of Na⁺ impurity on self-trapped hole (*Japanese*) 8-67982
 KClO₄, ClO₃⁻ detection by EPR of ClO₃ radicals created by X-irrad. 8-76311
 PbS oxide, optical excitation meas. of trap charging surface film (*Russian*) 8-76180
 Si pin diode, current filament temp. and Au acceptor level capture cross section temp. depend. 8-95351
 Si:Co, study of impurity states 8-76020
 Si/SiO₂ interface, slow-trapping instability, kinetics 8-76151
 SiO₂ film on Si, negative bias instability 8-91773
 SiO₂, vitreous, exam. of electron excitations and intrinsic defects 8-87905
 TiCl-TiBr mixed cryst., impurity-induced self-trapping of holes and minority-ion percolation 8-64398
 ZnSe, laser induced modulation of opt. absorpt. 8-88324

hollow cathodes see cathodes**holmium****see also nuclei with**

- atom, X-ray emission, K shell, energy shifts, role of atomic struct. 8-70777
 calibo glass:Eu³⁺, Ho³⁺, energy transfer 8-76510
 Hall constant and elec. resist., 80-700K (*Russian*) 8-60110
 magnetoelastic interactions 8-64252
 particles, effect of size on paramag. Curie temp. 8-60317
 Ho+N₂O→HoO⁺+N₂ chemiluminesc. reaction, cross-section 8-76847
 LaF₃:Ho³⁺, laser excited fluorescence absorption spectra, symmetry groups 8-60514
 NaYF₄:Ho, Yb, two photon anti-Stokes effect, excited by 2 μ m radiation 8-50852
 SnO₂:Ho³⁺, luminesc. and charge compensation 8-76532
 Y₂O₃:S:Ho, Yb, two photon anti-Stokes effect excited by 2 μ m radiation 8-50852

holmium alloys

- (Ho,Y)Co₂, first order phase transitions 8-84426
 (Ho,Y)Co₂, mag. props., elec. resist. and thermal expansion 8-76246
 Ho-Au, dil., Mossbauer exam. of mag. hyperfine field at ¹⁹⁷Au impurity 8-88244
 Ho-Co alloy amorphous thin films, anisotropic mag. and microstruct. props. 8-95487
 Ho-Co film, amorphous, microstruct. and magnetism 8-64230
 Ho-Sn, dil. alloy, hyperfine interaction of ¹¹⁹Sn, Mossbauer meas. 8-91998
 HoAl₂, heat capacity, 1.5-12K, magnetocryst. anisotropy effects 8-68236
 HoAl₂, magnetoelastic effects on elastic consts., 4.2-280K 8-72385
 HoAu_{3.6}, ordering temps. and effective moments 8-60283

holmium alloys continued

- HoCo film, amorphous, sputtered, in-plane anisotropy induced by rare gas annealing 8-84458
 HoCo₂, field induced vol. magnetostriction 8-91920
 Ho₂Co₃, cryst. field effect on mag. moment direction, neutron diffr. meas. 8-80132
 Ho₂Cu_{1-x}, amorphous film, magnetisation meas., local anisotropy effects 8-68309
 HoFe₂, amorphous, struct. determ., EXAFS exam. 8-51421
 HoFe₂, crit. phenomena, Mossbauer effect 8-52403
 HoFe₂, spin wave and cryst. field excitations, neutron scatt. 8-68196
 Ho_{1-x}Fe_x, amorphous film, cosputtered, struct. and mag. props. 8-60323
 HoFe₄Al₈, mag. props. 8-52250
 Ho(Fe_{0.9}Ni_{0.1})₂, mag. behaviour, susceptibility and Mossbauer expts., 4.2-1300K 8-52235
 HoGa₂, mag susceptibility, 1.5-300K and Neel temp. 8-68184
 HoSb, quadrupole scatt. anisotropy, magnetically ordered material 8-64034
 Ho_xTb_{1-x}Fe₂, and Ho_xTb_{1-x}Dy_{1-x-y}Fe₂, high magnetostriction cpd., mag. anisotropy origins 8-68217
 Ho₂Tb_{1-x}Fe₂, Laves phase, mag. anisotropy meas., cubic harmonic anal. 8-84410
 Ho₂Tb_{1-x}Fe₂, single cryst., spin orientations 8-84425
 Ho_xTb_{1-x}Fe₂, single crystals, continuous spin orientations, magnetisation easy direction 8-84453
 HoZn, magnetoelastic and quadrupolar couplings 8-52328
¹⁸¹Ho-¹⁸¹Ta, dil., elec. field gradient at impurity, anomalous temp. depend., host 4f levels, γ-γ correls. 8-95272

holmium compounds

see also holmium alloys

- Er_{1-x}Ho_xRh₄B₄, re-entrant supercond. and mag. ordering 8-60240
 GdF₃-HoF₃, stabilisation of rhombic β-YF₃ type struct. 8-67700
 HoBi, thermal expansion, thermal cond., 300-900K 8-91453
 HoCrO₃, Ho³⁺ mag. form factor meas. by inelastic neutron scatt. 8-52221
 Ho_{0.7}Er_{0.3}FeO₃, crystn. on seeds, layer morphology 8-72041
 HoF₃, crystal growth by Bridgman-Stockbarger method and Czochralski method 8-52660
 HoIG, Faraday rotation, mag. field depend., 4.2 to 300K, magneto-optical coeffs. 8-95577
 HoIG, mol. field coeffs., magnetisation and mag. susceptibility anal. 8-95406
 HoMo₈S₈, reentrant supercond., direct. obs. of long range ferromag. order 8-76190
 Ho₂O₃, 300 to 900K, mag. susceptibility and Curie temp. meas. 8-56288
 Ho₂O₃, solid, photoacoustic spectra 8-58044
 HoPo₄-Pb₂P₂O₇, solubility curves for high temp.-melts for growth of single crystals. 8-95687
 HoRh₄B₄, supercond., re-entrant magnetism, energy band calcs. 8-52140
 HoSe₃, elec. resist., thermoelectromotive force, temp. depend., 300 to 1400K (Russian) 8-84243
 HoVO₄, NMR, parameters in nuclear Hamiltonian 8-72422
 Ho₂Y_{1-x}F₃, calc. of Ho³⁺→Ho³⁺ energy transfer rates (French) 8-79966

holographic gratings

- aberration balancing for grating mountings with large aberrations 8-66906
 beam expansion with diffr. grating in dye laser cavity 8-66858
 binary information image reconstruction, aberrations, shrinkage effects 8-78967
 blazed holographic gratings, suitable for use on synchrotrons 8-63187
 Bragg and Raman-Nath diffr. regimes rel. to grating thickness 8-71028
 colour separation phase gratings 8-83072
 computer-generated, prod. of two-dimens. laser beam deflections 8-58956
 concave and plane gratings, achromatic imaging of distant objects, in selective wavelength bands 8-94372
 dye CW laser, tuning and spectral narrowing using low-loss diffr. grating 8-71109
 fine, made of positive photoresist AZ2400, anal. of two-dimensional etching effect on profile 8-82928
 focused light ATR method, appl. to guided waves on grating 8-74992
 Fourier hologram machine synthesis (Czech) 8-66784
 high flux grazing incidence monochromator based on holographic grating for synchrotron radiation 8-62271
 integrated optics, grating lens fabrication 8-75004
 laminar holographic gratings, efficiency, synchrotron radiation monochromisation 8-63189
 matched filtering system adjustment by diffraction gratings 8-87027
 multislit spectrometer for the night airglow observation 8-73542
 normal incidence monochromator for synchrotron radiation, charact. modification using holographic concave gratings 8-62236
 periodic surface corrugation generation by holography 8-55469
 photopolymer imaging systems, for laser recording 8-71173
 polarisation effects on thin transmittance grating fabrication and diffr. efficiency (Korean) 8-50731
 scattered light, specification and meas. from diffr. gratings 8-78905
 spectrophotometer, single-beam, holographically recorded concave diffraction grating appl. 8-54468
 torical grating calc. for very wide field camera (French) 8-81547
 transmission, appl. to UV and X-ray synchrotron radiation monochromators 8-63186
 UV region, 300 to 2000 Å, simple selection rules 8-55435
 LiNbO₃, LiNbO₃:Fe, amplification of laser beams by ferroelectrics 8-90393
 LiNbO₃, LiNbO₃:Fe, holography in ferroelectrics 8-90394
 Nd:glass ring laser, holographic dispersion element (Russian) 8-59051

holographic instruments

see also holography

- applications and theory review, background and current status 8-74866
 compact real-time matched-filter optical processor 8-74869
 corneal wound holographic stress testing in postoperative patients, specular illum. arrangement 8-65102
 electronic speckle pattern interferometry of surface shapes 8-94380
 interferometer, for optical glass homogeneity determ. 8-90401

holographic instruments continued

- interferometer, three-dimens. optical inhomogeneity quantitative evaluation 8-87030
 IR tracking receiver with holographic information processing 8-78970
 laser beam deflector quality factor N/r, comparison of holographic and acousto-optical deflectors (French) 8-55318
 scanner, computer produced hologram, with auxiliary reflector 8-71054
 scanning system, lens design for hologram generation 8-50742
 thick, holographic optical element design and construction 8-55315

holographic interferometry

- acoustic field holograms, moire processing 8-55539
 acoustic field visualisation by optical holography 8-59216
 applications and theory review, background and current status 8-74866
 biological specimen 3-dimens. imaging using vibro-interference and holography 8-53584
 boundary diffr. wave, holographic anal. (German) 8-63041
 circular hole, normal surface displacement, reflection holographic interferometry 8-57893
 computer-aided interferograms evaluation, of thermal boundary layers (Czech) 8-62220
 concrete to steel rod chemical bond 8-88593
 continuously scanning reconstruction beam, strain and displacement determ. 8-71055
 crack initiation determ. 8-60933
 diffuse objects, fringe loci and visibility in holographic interferometry 8-58951
 dipropylammonium manganese chloride, layer perovskite, step bunching obs. by compound holographic microscopy 8-63682
 direction-sensitive displacement analysis by multiple freq. holographic interferometry 8-54338
 displacement, deformation and vibration meas. (Italian) 8-54337
 displacement components and derivatives, holographic-moire technique 8-51140
 displacement measurement techniques, expt. comparison 8-71057
 double exposure method, partial coherence and interference pattern visibility (German) 8-82932
 electronic speckle pattern interferometry of surface shapes 8-94380
 errors in small vector displacements meas., statistical anal. 8-78953
 film, stress measurement method using real-time holographic interferometry 8-84099
 film adhesion testing, simple real-time holographic interferometry method 8-92411
 flame structure determ. method (Russian) 8-94851
 flow, local mass-transfer coeffs. meas. method 8-75234
 flow over cone, dual-plate holographic interferometry 8-63512
 Fourier lensless technique, hologram recording and reconstruction, using materials with low resolving power (Czech) 8-90399
 free convection mass transfer from horizontal surface, electrochemical and holographic interferometric obs. 8-87344
 frozen-fringe method, using thermoplastic recording media 8-90402
 n-hexane, tank flame, turbulence, holographic interferometric synchronous photography (German) 8-51255
 holographic length comparator using phase heterodyne, appl. to gauge blocks 8-58953
 length meas. device appl. (Rumanian) 8-49796
 magnetic domain walls, off-axis electron microholography 8-82080
 measuring techniques, significance of holography (German) 8-90395
 memointerference or vibrointerference phenomenon and application 8-55313
 mining applications, subsidence and ground movement meas. 8-57343
 NDT appl. 8-53164
 object geometries comparison, speckle pattern interferometry, holographic illum. elements 8-66785
 optical glass homogeneity determ. using holographic interferometer 8-90401
 particle vel. distrib. meas. (Japanese) 8-95873
 phase objects with scatterer, fringe visibility and localisation 8-50736
 photoelasticity, holographic determination of absolute retardation fringes by vectorial reconstruction 8-87315
 plasma flow phenomena, Ba II ion density meas. 8-55751
 plate, rib stiffened, studies on vibrations 8-83297
 PMMA, methanol crazes, craze-strain profile from holographic interferometry meas. 8-72844
 polarised light impulse response matrix formalism, appl. to holography 8-63045
 pulsed, for nondestructive evaluation and anal. of structs. 8-60977
 Pulsed lasers in electronic speckle pattern interferometry 8-65961
 rainbow process, double exposure and time-average interferograms 8-55320
 real-time fringe obs., interferometry without reference beam 8-71063
 rotating object, vibration anal., image detector in hologram interferometry and speckle photography 8-59351
 speckle holography measurements of stars ξ Cancri and ADS 3358 8-93120
 steel bar deformation meas. by holographic interferometry using four point bending machine 8-60721
 stellar observations, mutual coherence function 8-53838
 stellar spectra recording by interferometric method in thick photographic emulsions 8-73651
 stress analysis using holographic interferometry and speckle photography 8-70095
 stroboscopic analysis of asymmetric membrane vibrs. 8-66786
 surface contour and inhomogeneity testing, interf. fringe distortion with imprecise focusing 8-89531
 surface contouring by displacing object and illum. beam 8-74864
 thermoplastic recording with homogeneous mixture of thermoplastic and organic photoconductors 8-63161
 three-dimensional optical inhomogeneity quantitative evaluation 8-87030
 time-averaged holography theory, for three dimens. vibrs. at single freq. 8-90397
 turbulence effects on optical wavefront, holographic appl. 8-82936
 vibration anal. by combined holographic interferometry and finite element anal. (German) 8-90806
 vibration analysis, computer-aided, for vectorial displacements of bladed discs 8-71056
 zero order fringe identification, direction of motion detection, in holographic displacement meas. 8-63044

holographic interferometry continued

- CO₂, thermal diffusivity and cond. in crit. region (*German*) 8-59942
³He-⁴He mixtures, dynamic behaviour, appl. of holographic interferometry technique 8-51781
 N₂+H₂O 8-66631

holographic storage

- binary information image reconstruction, aberrations, shrinkage effects 8-78967
 bleached holograms with binary data, parameters under physical development 8-50735
 electrophotographic recording media, high resolution, expt. characts. 8-70208
 ferroelectric devices for optical systems 8-90473
 Fourier transform image hologram for ROM 8-87032
 materials and methods, conf., San Diego, USA (Aug. 1977) 8-71171
 microfilms, expts. to improve recording density 8-82931
 photorefractive materials for optical data storage 8-79086
 photorefractive memory materials, elec. field and photocurrent meas. 8-71066
 reflection phase hologram storage system 8-78966
 review of recording media 8-71172
 thermoplastic photoconductor technology for optical recording and storage 8-71175
 thermoplastic recording, IR laser heating 8-71065
 volume phase holographic storage in ferroelec. crystals. 8-82929
 LiNbO₃, phase hologram, dynamic holography 8-95572
 LiNbO₃:Fe holographic information storage material 8-55321
 MnBi magnetic film, method for recording holograms of diffusely scattering objects 8-74862

holography

- see also *acoustic holography; computer-generated holography; holographic gratings; holographic instruments; holographic interferometry; holographic storage; microwave holography*
 aberration elimination, holographic microscopy 8-74861
 alkali halides, photodichroic, as optical processing elements 8-83056
 amplitude transmittance expansion in Taylor series (*Spanish*) 8-50732
 applications and theory review, background and current status 8-74866
 aspheric surface quality assurance 8-50962
 binary seismic holography, kinematic principle (*Russian*) 8-92795
 bleached holograms with binary data, parameters under physical development 8-50735
 bleached single (multiple) exposure holograms, diff. efficiency, SNR and resolution 8-71059
 bubble chamber event recognition by optical correl. (*German*) 8-70704
 chromogen developed photography emulsions 8-55319
 cinematography in USSR 8-78976
 coded reference beam use, theory 8-50739
 coherence relaxation methods 8-78977
 colour image generation with one-step rainbow holograms 8-66781
 continuous random phase mask 8-66788
 contour mapping of moving object, using injection locked flash pumped dye laser 8-50737
 deep-image rainbow holograms 8-71061
 diffraction efficiency, depend. on size of developed Ag particles 8-78965
 digital, joint meas. of ang. coords. and range on basis of optical phase fronts 8-78933
 dynamic correction scheme for disturbed laser wavefront (*Russian*) 8-55326
 dynamic holograms, amplification (*Russian*) 8-82934
 educational course, liberal arts-physics 8-73798
 electro-optical crystal recording medium, set-up for hologram parameters meas. 8-87031
 emulsion thickness change effects, in 3-dimens. holograms 8-78968
 evanescent waves, diff. efficiency, TE polarisation 8-66782
 evanescent waves, diff. efficiency, TM polarisation 8-66783
 fog, coherence requirements for light source 8-58949
 Fourier colour holograms, archival characts. 8-55314
 Fourier hologram recording using pulse semiconductor laser radiation 8-50738
 Fourier holograms, enhancement of diffraction efficiency (*German*) 8-78954
 Fourier holograms, long-wavelength, recording and reconstructing schemes 8-87029
 Fourier holography, double exposure method, intermodulation noise (*German*) 8-82932
 Fourier holography, two-point resolution (*German*) 8-82933
 Fourier spectroscopy, nonlinear processing of interferogram 8-89553
 frequency swept imaging principle 8-78964
 gated viewing by holographic range-gating 8-71060
 holo cinematography, high speed, acousto-optic beam deflection for spatial freq. multiplexing 8-74860
 holographically stored X-ray images, grey-tone reproduction 8-65120
 hydrocarbons, heavy, self-holograms of laser-induced surface depressions 8-82927
 image coding with far-field holograms 8-90389
 image degradation due to reflected light depolarisation 8-90398
 image luminance, depend. on hologram recording geometry 8-63042
 image phase compensation and real-time holography by four-wave mixing in optical fibres 8-63039
 image plane holograms, for students 8-77647
 image plane holograms for holographic microscopy 8-58944
 in-line holograms, elimination of DC in reconstructed wavefronts 8-55323
 industrial applications, review (*Japanese*) 8-78958
 interference correlators, theory 8-78969
 inverse radon transform by optical convolution 8-66777
 large scale holographic display, in photographic emulsion, image reconstruction 8-78974
 large-scale reflection and transmission, for displays 8-78975
 laser nonstationary generation induced interference pattern phase distortion, holographic meas. 8-58945
 laser radiation divergence reduction, holographic method (*Russian*) 8-63147
 light-in-flight recording 8-94379
 magnetic domain walls, off-axis electron microholography 8-82080
 maximum recordable number of particles 8-58946
 measuring techniques, significance of holography (*German*) 8-90395

holography continued

- molecular spectroscopy, holographic recording 8-62954
 multicolour image from superposition of rainbow holograms 8-58957
 NMR determination of phys. and biological struct. (*Rumanian*) 8-49874
 nonlinear optical four-wave mixing as real time holography 8-50853
 object beam depolarisation effect on holographic image light flux (*Spanish*) 8-50733
 objective, hemispherical, concentric, in holographic memory, spherical aberration calc. method (*Russian*) 8-71184
 on-axis hologram, student experiment 8-86084
 optical data processing, appls., book 8-90388
 optical element design using analogous lens model 8-58955
 optical element fabrication using dye-sensitised dichromated gelatin 8-63043
 optical image and signal processing, United States Air Force programmes 8-74854
 optical signal and image processing, conference, San Diego (1977) 8-74853
 optical storage materials and methods, conf., San Diego, USA (Aug. 1977) 8-71171
 phase conjugate optics and real-time holography 8-83034
 phase determination of amplitude modulated complex wavefront 8-55305
 phase distributions, linear and nonlinear, determ. using electro-optical system 8-58954
 phase relief hologram recording on semiconductor films (*Russian*) 8-50741
 phase retrieval and polarisation identity 8-71042
 photomaterials with mirror layer for newly developed holographic process (*Russian*) 8-55325
 photopolymer imaging systems, for laser recording 8-71173
 photoresist, Shipley AZ-1375, sensitivity and nonlinearity at 441.6 and 457.9 nm 8-90475
 principles developed on Fresnel eqn. basis, Jones vector representation of images 8-90400
 projection-type holographic displays 8-78972
 pseudocolour encoding, of holographic imaging, new technique 8-78963
 pseudocolour encoding of holographic images using single wavelength 8-87025
 radioastronomical aperture synthesis imagery data optical reconstruction 8-69702
 rainbow hologram by one-step process 8-71062
 rainbow holograms using large-aperture condensing lenses 8-78962
 real image of point source in idealised holographic system 8-63040
 real-time coherent object edge reconstruction with Bi₁₂SiO₂₀ crystals 8-90372
 recording, and reconstruction in spatially incoherent white light 8-78955
 refractive index changes, holographic meas. 8-74865
 review (*Japanese*) 8-78957
 SAW holographic visualisation, improved S/N ratio (*French*) 8-75023
 SAW observable amplitude limitation in freq. shift holography 8-71058
 scalar diffusor autocorrelation (*French*) 8-90369
 screens production with third order spheric aberration compensation (*Russian*) 8-90404
 seismic holography, integral representations of space time functions (*Russian*) 8-85483
 sensitised film preparation methods (*Italian*) 8-50730
 solid rocket propellant combustion, holographic recording 8-82935
 space-variant holographic systems using phase-coded reference beams 8-74868
 Speckle noise of redundant Fourier holograms for one class of diffusers 8-50734
 stereogram imagery 8-78978
 synthesized holograms, information visualisation 8-82930
 T-E curve classification, appl. in spectrum analysis and holography 8-82916
 terrain displays in 3D 8-78979
 thermoplastic media for hologram recording (*Russian*) 8-58948
 thermoplastic photoconductor media, review (*Japanese*) 8-78956
 thermoplastic photoconductor technology for optical recording and storage 8-71175
 thermoplastic recording, IR laser heating 8-71065
 thermoplastic recording 8-78961
 thermoplastic-photoconductor films for optical data processing 8-50875
 thermoplastic-photoconductor plate, exam. of microscopic response in holographic recording 8-58947
 thermoplastic-photoconductor tape for holographic recording, spatial filter prod. 8-90391
 thick, holographic optical element design and construction 8-55315
 thick film phase holograms recorded using coded reference waves 8-50740
 thin unbleached holograms, diffraction efficiency, relief phase modulation 8-66789
 three dimensional imaging, conf., San Diego, USA (Aug. 1977) 8-78971
 three-beam polarisation holography, influence of photographic material nonlinearity 8-58952
 three-dimensional image prod., reversal method using reflective and lenticular screens 8-90403
 three-dimensional information 8-78973
 three-dimensional measurement on image reconstructed by holographic process 8-58958
 two-dimensional volume, coupled wave differential eqns. derivation 8-55317
 volume hologram two-dimens. theory, incl. varying average dielec. const. effect 8-78960
 volume holograms as colour-sensitive spatial filters 8-87150
 volume holograms constructed from computer-generated masks 8-87026
 volume phase holograms operation, model 8-55316
 wavefront conversion by volume holograms between cylindrical and plane waves 8-90396
 waveguide hologram using optical thin films high-efficiency relief-type hologram 8-66958
 wide-angle holography, step by step multi-sided recording technique (*Chinese*) 8-90392

holography continued

- X-ray crystallography, holographic computing step for image display 8-91199
 X-ray laser holography, pumping by synchrotron radiation from storage rings 8-55322
 As-Se-Ge, amorphous film, relief-type hologram mode, hologram replication (*Japanese*) 8-78959
 Bi₁₂SiO₂₀, volume hologram polarisation props. and appls. 8-74859
 Co₃Fe_{3-x}O₃, single cryst. mag. films, holograms recording and thermo-magnetic writing 8-55324
 Cu-As-Se glasses, recording and erasure by laser beam (*Russian*) 8-71170
 KCl:Na, photoinduced reorientation of A-centres near room temp. 8-64344
 LiNbO₃, holograms stored by photorefractive effect, reading and optical erasure 8-90390
 LiNbO₃ photorefractive reversible optical memory (*Russian*) 8-58943
 LiNbO₃ SAW device, holographic obs. of bulk waves and surface waves through side planes of several cuts 8-71238
 MnBi film for recording optical information, analogue characts. (*Russian*) 8-50716
 NaCl crystal, radiation coloured by electron beam, holographic lattice recorded by He-Ne laser 8-58950

homopolar generators

- electrical contacts, for homopolar generators, tests at high surface vels. and current densities 8-54964
 fast discharging 10 MJ machine design, for fusion reactor 8-54950
 fusion reactor, fast discharge machine, design, fabrication, testing 8-54952
 fusion reactor, Shiva Faraday rot. coils, circuit and mag. anal. 8-54951
 fusion reactor, TEXT, pulsed homopolar generator power supply, engineering and design 8-55016
 fusion reactor, Tokamak, commercial, plasma driving system requirements 8-54954
 fusion reactor, use of homopolar generator for inductive energy storage 8-54948
 pulse power machine current collection system, for fusion research 8-54949
 superconducting field coils, design and appl. 8-54927
 Tokamak, Texas exptl., homopolar generator, eddy currents, EM forces (torques), due to misalignment 8-54953

homopolar machines

see also homopolar generators

- fusion reactor, ohmic heating energy storage for power reactor, costing 8-58495

homopolymers *see polymers***hopping conduction**

- amorphous semiconductor, DC hopping cond., pre-exponential factor 8-76074
 amorphous semiconductor, macroscopic theory of carrier pulse propagation 8-72154
 anisotropy of hopping conduction, percolation theory 8-72156
 chalcogenide glass, AC conductivity, temp. depend. 8-72153
 chlorophyll-a, microcryst., trapped-electron doping in photovoltaic sandwich cells 8-53334
 compensated semicond. film, jump-over cond., control by external field 8-80080
 DC hopping conductivity, r-percolation in 3D 8-51958
 diamond:B hopping conductivity in range 12 to 1300K 8-51994
 diamond, synthetic, elec. cond. 8-56144
 Hubbard model, Ward identities, particle number conservation, analytical structure of self energy 8-79913
 kinetic equations, effect of strong EM wave 8-76107
 localised electron states, establishment of transport eqn. (*French*) 8-56141
 one-dimensional hopping, moment expansions and occupancy (site) correlation functions 8-55972
 polaron, small hopping, reaction rate treatment, role of vibrational relaxation 8-72092
 polaronic hopping conduction at low temp. 8-51906
 polyacrylonitrile, pyrolyzed, elec. cond. and dielec. const. in AC regime 8-60173
 power law frequency dependent dielectric function and nonanalyticity properties 8-60387
 quasi-one-dimensional lattice gas with three-dimensional ordering, hopping conductivity 8-91473
 semiconductor, hopping conduction influence of HF elec. field 8-52025
 semiconductors, multicharged defects, screening of electrostatic fields 8-79959
 superionic conductor, thermoelec. power calc., nature of hopping process 8-51727
 transition metal vanadates, elec. and mag. props., stoichiometry 8-51991
 two sublattice structure 8-56140
 Al, granular, hopping cond., supercond., magnetoresist., Zeeman splitting 8-60243
 BaO-B₂O₃-SiO₂:Ti³⁺, elec. cond., struct. 8-72148
 Cd-palmitate (arachidate) multilayer struct., hopping rate, direct evaluation 8-88045
 FeO-P₂O₅ glasses, electrical and mechanical losses 8-80283
 GaP film, deposited by RF sputtering (*Czech*) 8-52667
 GaSe film, amorphous, I-V characts. in strong elec. fields, 173-373K 8-56248
 Ge, amorphous, thermoelec. power in phonon-assisted hopping regime, Coulomb effects 8-76097
 Ge, amorphous film, variable range hopping 8-76176
 Ge:Mn, amorphous, cond. increase by Mn doping 8-72155
 n-Ge:Sb, fast neutron irradiat. effects on donor conc., and annealing 8-56107
 n-Ge:Sb, γ -irrad. effects on donor conc. and compensation by acceptors 8-56106
 Ge-Se-Fe films, metallic and semicond., amorphous, mag. and elec. props. 8-52319
 GeTe film, amorphous, evaporated and annealed, variable range hopping cond. 8-80077
 Ni-SiO₂, granular film, hopping cond., magnetoresist. 8-56240
 NiO, localised charge carrier transport, Seebeck, resistivity meas. 8-72152

hopping conduction continued

- Sb amorphous film, elect. resist. 8-95390
 Sb-Au amorphous film, elec. resist. 8-95390
 Se, amorphous, carrier lifetime and drift mobilities 8-87985
 Si, amorphous, thermoelec. power in phonon-assisted hopping regime, Coulomb effects 8-76097
 Si, amorphous film, variable range hopping 8-76176
 Si:Mn, amorphous, cond. increase by Mn doping 8-72155
 SiO₂, thermally grown films, LF conductance 8-80081
 SiO₂ film, MIM struct., DC bias dependent dielectric dispersion props. 8-76178
 SnTe film, amorphous, evaporated and annealed, variable range hopping cond. 8-80077
 TiO₂-SiO₂, semicond. glass, small polaron hopping cond. 8-60126
 WO₃ amorphous film, elec. cond. and dielec. const. 8-60238

horology *see time measurement***hospital administration** *see medical administrative data processing***hot carrier conduction** *see hot carriers***hot carriers**

- degenerate quasi-two-dimensional semiconductor, warm electrons 8-60222
 drift solutions, discontinuities, hot carriers injection and accumulation 8-51999
 energy relaxation of photoexcited hot electrons at very low temperatures 8-91724
 III-V semiconductor, low temperature, high mobility transistor materials 8-87970
 inhomogeneous semiconductor with nonequilibrium carriers, EM wave propag. 8-52024
 many-valley semiconductor, conductivity in RF heating field (*Russian*) 8-76085
 MOS structure hot electron transport, review 8-60221
 p-n junction, planar, junction breakdown walkout exam. 8-60199
 piezoelectric semiconductor film, mobility of hot electrons 8-56247
 semiconductor, electron trap, positively charged, hot electron capture coeff. 8-52003
 semiconductor, Faraday rotation in presence of attractive traps 8-76081
 semiconductor, galvanomagnetic-effects in strong elec. field 8-56163
 semiconductor, hot plasma, wave instability 8-84245
 semiconductor, Kane, thermoelec. power and thermomag. effects of hot electrons 8-56174
 semiconductor, optical props. under intense laser fields 8-72513
 semiconductor, quasi-two-dimens., transient response under hot electron conditions 8-60223
 semiconductor, spreading and noise diffusion coeffs., identity 8-64047
 semiconductor negative conductivity due to hot electrons transfer in geometric space (*German*) 8-56150
 semiconductor with quasirelativistic band struct., hot electron kinetic equation 8-84222
 Al_{0.5}Ga_{0.5}As, p-n homojunction, hot carrier recomb., overheating luminesc. 8-92122
 Bi, electron gas heating at low temp. 8-60133
 CdSe, direct gap, picosec. time resolved reflectivity obs. 8-76495
 CdTe negative dielectric relax. of hot electrons 8-52001
 GaAs, direct gap, picosec. time resolved reflectivity obs. 8-76495
 n-GaAs, two-valleyed semicond., hot electron diffusion coeff., random walk calc. 8-68033
 n-Ge, H-linear planar Hall effects of hot electrons 8-76082
 Ge, hot-electron diffusion coefficient 8-87982
 Ge, intervalley diffusion of hot electrons 8-84227
 Ge, near intrinsic, negative differential cond., ambipolar size effect due to hot carriers 8-72185
 n-Ge, noise spectra of hot carriers 8-76083
 p-Ge:Ga, carrier heating by weak elec. field, hole-hole collision influence 8-72161
 He, liq., hot electrons on surface (*Russian*) 8-87832
⁴He liquid surface, hot carrier mobility 8-59988
 Hg_{1-x}Cd_xTe, zero-gap semicond. with nonparabolic band struct., hot electron mobility and conc. 8-76080
 n-InSb, directional temp. of hot electrons under elec. and mag. fields 8-84135
 n-InSb, hot electron magnetophonon effect, 77K, mag. field modulation method 8-60140
 InSb, nonlinear optical properties, hot electron effects 8-71139
 n-InSb, photo-induced magnetophonon reson., 4.2K, peak shifts 8-84250
 n-InSb, photoconductivity, 1.8K, hot-carrier and free-carrier absorption. effects 8-84254
 Si (100) inversion layer, hot electron drift velocity, Monte Carlo calcs. inc. 3 subbands 8-91752
 n-Si, anisotropy of differential conductivity and transverse diffusion coefficient 8-76078
 n-Si, hot-electron diffusion, effect of ionised impurity scatt. 8-56151
 n-Si, microwave and far IR hot carrier mobility, Monte Carlo calc. appl. to mm. transit time oscill. efficiency 8-72184
 Ta-Ta₂O₅-ZnS:TbF₃-Au thin films, MIS struct., DC electrolum. obs., Poole-Frenkel effect 8-88038
 Te, warm hole conductivity 8-72160

hot cathode tubes *see thermionic tubes***hot cathodes** *see thermionic cathodes***hot electrons** *see hot carriers***hot pressing**

- glass to mould heat transfer during pressing 8-80500
 graphite-Si powder mixture, reaction hot pressing 8-60592
 high level radioactive waste disposal, incorporation of 3CaO-Al₂O₃ cement 8-78485
 hot-pressed with crystn. grain boundary phases 8-95716
 S glass-Ni sphere composite, exam. of crack shape and fracture toughness 8-72886
 steel, alloy, maraging, 250-grade, ductility and toughness of hot isostatically pressed powder 8-52925
 steel, high speed, atomised powder, defects in parts produced by hot isotactic pressing 8-60612
 AlN-Al₂O₃, powders, crystalline phase obs. 8-95720
 Al₂O₃, pressing method, for the telecommunication industry (*Hungarian*) 8-52728
 Al₂O₃, reactive hot pressing, exam. of pressing characteristics 8-80499

hot pressing continued

- β - Al_2O_3 - K_2O /K ferrite, interfaces and solid soln., thermal expansion and lattice parameter variations 8-55959
 β - Al_2O_3 - Na_2O , vacuum hot pressed, densification kinetics 8-72758
 Al_2O_3 - SiO_2 glass powder, mullite crystallisation during hot pressing 8-60639
 BC, sintered and hot pressed, friction and wear, 20 to 1500°C 8-60844
 B_4C rings, Al bonded, exam. of fabrication techniques 8-72748
 BaF_2 , optical ceramic, hot pressing in vacuum, rel. to spectral transmission 8-52730
 $\text{Bi}_2\text{Te}_{3-x}\text{Se}_x$, thermoelec. mat., prep. effects on inhomogeneities 8-51576
 C fibre reinforced glass, SiC fibre coating, hot pressing production method (German) 8-95724
 CaB_2 - SmB_6 system complex borides, prep. and props. 8-52703
 CaO - CaF_2 , effects of CaF_2 addition, sintering behaviours and microstructs. investig. (Japanese) 8-95721
 Fe compacts, porous, dynamic hot pressing, press. rel. to density, time 8-60599
 Fe effect of repressing and double sintering on impact strength (Japanese) 8-92217
 Fe-C-Ni-Cr(Cu), dynamically hot pressed, mech. props., additives effect 8-60620
 Fe-Ni-Cr-Ti, superalloy A286, powder, exam. of microstruct. and mech. properties 8-52979
 $\gamma\text{Fe}_2\text{O}_3$, transform. to α -phase, effect of preliminary pressing or vibromilling 8-84798
 β - Ga_2O_3 - K_2O /K ferrite, interfaces and solid soln., thermal expansion and lattice parameter variations 8-55959
 LiF, ceramic, characts. on pressing in vacuum and in air 8-52734
 LiF compact, particle size rel. to pore characts. 8-60631
 LiF tile and sheet for thermal neutron shielding (Japanese) 8-74510
 Ni-based-Ta(Cu,N) hard metals, isostatic hot pressing influence on mechanical properties 8-92219
 Ni-Cr (20 wt.%), powdered, prod. of Mo fibre reinforced composite by hot pressing exam. of strength 8-56710
 Si-Al-O-N system, TEM exam. of X phase structure 8-56606
 n-Si-Ge, phonon thermal cond. of hot-pressed alloy, 300-1100K 8-91494
 Si-Ge:Al, B, P, hot-pressed alloy, thermoelec. props. 8-91711
 SiC fibre reinforced Ni-Cr alumina coated fibres, hot pressed, annealed, IR study 8-60623
 SiC fibres reinforced Ni complex alloy, influence of TiN coating on fibre matrix interaction (Russian) 8-95820
 SiC, hot pressed, brittle fracture and subcritical crack growth 8-72885
 SiC, meas. of critical stress intensity factor and subcritical crack propag. rates 8-72880
 SiC, polytypic transform. during hot pressing 8-52739
 Si_3N_4 , hot pressed, flawed plate under combined stresses, failure prediction 8-72884
 Si_3N_4 , hot pressed, high temp. compressive cracking, optical and electron microscopy exam. 8-76733
 Si_3N_4 , hot pressed, slow crack growth from controlled surface flaws 8-80632
 Si_3N_4 , hot pressed, Y_2O_3 fluxed, microstruct. 8-64512
 Si_3N_4 , hot pressing with Y_2O_3 and Li_2O additives 8-92220
 Si_3N_4 , hot-pressed with crystn. grain boundary phases, prep. 8-95715
 Si_3N_4 , meas. of critical stress intensity factor and subcritical crack propag. rates 8-72880
 Si_3N_4 , reaction bonded and hot pressed. exam. of thermal shock behaviour (German) 8-64561
 Si_3N_4 - Al_2O_3 , hot-pressed with crystn. grain boundary phases, prep. 8-95715
 Si_3N_4 - Al_2O_3 , hot-pressed with crystn. grain boundary phases 8-95716
 Si_3N_4 + MgO , reaction during hot pressing 8-68658
 (Ti,V)C carbides, prep. and mech. props. 8-64518
 $\text{TiC-Cr}_3\text{C}_2(\text{Cr}_3\text{C}_2\text{-WC})$, powder mixture, steel bonded, exam. of sintering behaviour 8-52712
 WC-TaC-Co, cemented carbide, strength improvement by hot isostatic pressing 8-84969
 ZnO, segregation of Li_2O at grain boundaries 8-64513
 ZnS, hot pressed, water drop impact damage, SEM exam., IR transmission 8-88543
 ZrO_2 , cubic, nitride stabilised 8-92223

hot shortness see brittleness**hot strength** see tensile strength**hot working**

- α - β brass, exam. of creep fracture by tensile tests 8-88531
 hot twisting, shearing stresses, anal. determ. 8-60900
 metals, recrystallisation during hot deform. 8-68714
 nucleation, criterion for dynamic recrystallisation during hot working 8-52852
 steel, alloy, cluster formation susceptibility in 40 KhN, influence of isothermal working in H_2 (Russian) 8-56643
 steel, alloy 4340, fracture and high temp. props., 533K to 1255K 8-60821
 steel, Cr-Ni(-Mo) austenitic, strengthening by modified ausforming 8-76665
 steel, stainless, duplex, hot ductility and fracture mechanism 8-60731
 steel, stainless, hot rolling resist., multistage mode of deform. effects (Russian) 8-80583
 steel plates, hot rolled, anisotropic texture, exam. of elastic deformation behaviour (Japanese) 8-64586
 steel spheroidised type AISI 1090, hot rolled H_2 promotion of plastic instability 8-60725
 Al alloys, preliminary forging effects on struct. and mech. props. of extruded sections (Russian) 8-80564
 Cu, wires, effect of heat treatment during drawing 8-56659
 Fe-Si (3 wt.%), orientation development during secondary recrystallisation, primary matrix effect, magnetic props. (Czech) 8-60679
 Ni-based alloys, binary, ternary, complex, TiC additions, effects 8-92305
 Ti-Al (6.1 wt.%), hot rolled sheet, ductile fracture nuclei, SEM obs. 8-64654
 Y_2O_3 - TiB_2 , ceramic, production by sintering in vacuo, or hot moulding at 1500°C 8-60629
 Zn, hot rolled, grain boundary fine structures, TEM exam. 8-76680

household appliances see domestic appliances**hovercraft**

- ship hydrodynamics, drag on displacement ships, hydrofoils, hovercrafts 8-63423

Hubbard model

- antiferromagnet, electron struct. in mag. field (Russian) 8-60287
 antiferromagnetic semiconductor, electron correlations, weak coupling 8-67969
 arbitrary electron density case, functional integral approach 8-76219
 dielectric function, strong correlation limit 8-87929
 disordered local moment state 8-95414
 disordered quasi-one-dimensional systems with electron correlation, electronic properties 8-87966
 electrical conductivity calculation, dielectric function and plasma oscillations 8-64020
 electrostatic interaction Hamiltonian, tensor struct. (Russian) 8-76216
 FCC lattice, mag. and elec. props. 8-56334
 ferromagnet, disordered itinerant-electron, spin waves 8-95427
 ferromagnetism, basic models, classification of theories (Rumanian) 8-91840
 free lattice electron gas with nearest and second nearest neighbour hopping 8-51873
 half-filled, mag. couplings 8-52192
 itinerant antiferromagnetism 8-91841
 magnetic phase diagram 8-80119
 magnetic phases, nearest and next nearest neighbour hopping in Hartree Fock approx. 8-52189
 magnetic solutions of Hubbard model, Hartree-Fock approx. 8-52195
 metal-insulator interface, Hubbard model, possibility of insulator-metal transition 8-52084
 metal-insulator transition, anharmonism effects 8-56072
 metamagnetic dielectrics, at finite temp. (Russian) 8-88118
 Mott metal-insulator transition, ten-fold spin-orbital degeneracy 8-52285
 narrow band systems, momentum distrib., cluster var. method 8-72060
 optical conductivity, strongly attractive chain model 8-79915
 partly filled narrow band, electron correlation and mag. props. 8-67968
 phase transitions, low-temp. 8-72359
 quasideimensional Peierls-Hubbard model, antiferromagnetism and Peierls distortion 8-67931
 solitons in a one-dimensional modified Hubbard model 8-87895
 spin-Peierls transition in Heisenberg Hubbard models 8-68242
 TCNQ, dimer gas model 8-87926
 TCNQ salt, NMP-TCNQ, realisation of disordered Hubbard model, dielec. props. 8-79917
 transition metal, chemisorpt. of H_2 , Hubbard-type surface mol. model binding energy calcs. 8-71990
 transition metal alloys, spin glass behaviour, simple itinerant model 8-84436
 transition metal oxides, sulphides, and selenides, Mott transition electronic and mag. phase diagrams 8-51894
 transition metal surface, spin fluctuations 8-95451
 TTF-TCNQ, spin waves, scatt. at 4k, spin-Peierls fluctuations 8-72093
 TTT-(I_3) $_{0.5}$, one-dimens. metal, mag. susceptibility, elec. resist., thermopower meas. 8-87967
 two-dimensional systems, phase transitions 8-68241
 Ward identities, particle number conservation, analytical structure of self energy 8-79913
 La, ground state, two band Hubbard model, for almost mixed valence system 8-84171
 VO_2 , discontinuous metal insulator and spin dimerisation transition, Hubbard model 8-51893

Hubble model see cosmology**Huckel molecular orbital calculations** see HMO calculations**hue** see colour**Hugoniot diagrams** see equations of state**human engineering** see ergonomics**human factors**

- see also biocybernetics; ergonomics; man-machine systems
 image transformations, picture processing algorithm 8-58939
 nuclear accident phenomena, human elements (French) 8-57084
 reliability and maintainability symposium, Los Angeles (1978) 8-50250
 visual prosthesis design, human factors and electrophysiological considerations 8-53583

human-machine systems see man-machine systems**human relations** see social and behavioural sciences**humidity**

- see also atmospheric humidity; hygrometers
 optical fibres, UV curable epoxy acrylate coated, long-term mech. behaviour effect on stress-free ageing 8-95802
 polyamide fibre, chain-segment orientation, US vel. meas., humidity effects (German) 8-75590
 HNO_3 -water, homogeneous nucleation, relative humidity depend. 8-71846
 H_2SO_4 -water, homogeneous nucleation, relative humidity depend. 8-71846

humidity control

- creep testing, at const. temp., humidity, appl. to nylon-6,6 8-95883
 test chamber, convectively mixed, calibration appl. 8-54379

humidity measurement

- see also hygrometers
 capacitive dew-point sensor 8-81421
 electronic thermometer appl., dual 8-65925
 microwave moisture content-attenuation-voltage convertor with time-domain attenuation comparisons (Polish) 8-70131

h.v. engineering see high-voltage engineering**hybrid computer methods** see hybrid simulation**hybrid computers**

- filtration simulation, use of electrically conducting paper with discretely distributed capacitance (Russian) 8-88850

hybrid integrated circuits

- see also flip-chip devices; microwave integrated circuits
 No entries

hybrid simulation

- digestive tract electrical rhythms simulation 8-64970
- filtration, dynamic, use of electrically conducting paper with discretely distributed capacitance (*Russian*) 8-88850

hydrated electrons *see solvated electrons***hydraulic control equipment**

- see also hydraulic motors*
- pressure regulator device, behaviour anal. 8-93668

hydraulic motors

- liquid and dry friction power losses calc. method 8-85009
- paraplegic human leg orthosis, hydraulic power control system 8-53577

hydraulic systems

- linear hyperbolic mixed boundary value problem, soln. existence, uniqueness, hydraulics appl. (*German*) 8-93514
- materials-testing system with 10 nm positional accuracy 8-85065

hydroacoustics *see underwater sound***hydrodynamics**

- see also jets; liquid oscillations; liquid waves; viscosity of liquids*
- Aegean basin, hydrodynamic eqns., numerical solns. 8-65317
- Archaeon peridotite komatites in La Motte Township, Quebec, emplacement hydrodynamics 8-77234
- asthenosphere, flow rel. to plate motions 8-96180
- E Atlantic Ocean, equatorial adjustment 8-88836
- Bay of Fundy, Canada, tidal flow vels. rel. to bedforms hydraulic stability relationships 8-88814
- bodies in non-planar stream, 3D motion, finite difference method soln. (*Russian*) 8-75116
- book, liquids and their props., mol. and macroscopic treatise 8-87604
- carbon tetrachloride, generalised transport coeffs., hydrodynamic eqn. 8-87803
- cell analysis in flow systems, geometry for orienting flat cells 8-77161
- cell hydrodynamics, information-conserving theory 8-55623
- cell membrane nuclear hydrodynamic shear, non-equil. Ising model, master eqn. 8-61146
- Cepheid variables, double-mode and bump, rot. and convection effects on period ratios 8-93249
- circumferentially ground rough disc, elastohydrodynamic lubrication 8-64708
- cochlear fluid mechanics, kinetic theory 8-53440
- coupled solid/fluid/surface wave dynamic interaction problem, improved fluid superelement 8-81108
- Crab Nebula filaments, shock waves hydrodynamics effects on spectra 8-85997
- cratering explosion, pulsed hydrodynamic model 8-51180
- critical point hydrodynamics 8-59361
- cytometry, hydrodynamic orientation of sperm heads in flow systems 8-77162
- debris dent effect on elastohydrodynamic lubrication 8-64709
- deep ocean, currents fine struct. rel. to internal gravity waves and wave breaking 8-85578
- Earth core, effect of boundary irregularities on fluid speed and geomag. field 8-73333
- elastohydrodynamic contact optimisation 8-79288
- entropy production deceleration 8-93094
- evaporation and condensation, kinetic theory, hydrodynamic eqn. and slip boundary condition 8-63903
- eye, hydrodynamic model of aqueous flow in posterior chamber 8-69122
- fluctuation theories 8-87327
- Fokker-Planck approach to Brownian rotation 8-62160
- globular star clusters, gas outflow models including photoionisation 8-93338
- gravitational collapse of rot. gas cloud, binary systems form. 8-65494
- Gulf of Guinea, simple upwelling model 8-88837
- heat transfer equation, mol.-kinetic generalisation 8-67219
- horizontal heated surface, post-nucleate boiling and crit. heat flux models 8-90664
- hydraulic equivalent of generalized one-dimensional flow 8-94627
- hydrodynamic oscillations in Gentilly-1 reactor steam mains, GISMO program 8-54824
- hydrodynamics, drag on displacement ships, hydrofoils, hovercrafts 8-63423
- hydrofoils, tail-loaded, fully cavitating, avoidance of turbulent separation 8-94659
- hydroplaning of a rotating cylinder on water 8-63522
- hydroplaning plate, lift, drag 8-63523
- incompressible irrotational axisymmetric flow about body of revolution and the inverse problem 8-94630
- initial, periodic and travelling disturbances, unsteady waves development, asymptotic anal. (*Russian*) 8-77254
- Kuroshio jet current system region, density field calc. 8-92843
- large Reynolds number, 2-D hydrodynamic lubricating theory (*Russian*) 8-59368
- liquid, laser breakdown, photoacoustic and photohydrodynamic parameters 8-52597
- liquid crystals, instabilities generated by US field, review 8-91235
- 2,6-lutidine-H₂O, phase separation, hydrodynamic effects 8-83960
- main-sequence stars envelopes, hydrodynamical instabilities constraints from Li, Be and B obs. 8-93202
- MBBA, nematic liq. cryst., ultrasound produced rolls, spatial coherence props. of scatt. light 8-75534
- meteorology, vertical eqn. of motion and wind eqns. 8-69428
- Mezen' Bay (White Sea), marine tides EM fields, rel. to hydrodynamics 8-73378
- moments of multiple distrib. functions 8-49750
- mooring cable in nonuniform stream, equilib. shape and tension (*French*) 8-63277
- nematic liquid crystals, hydrodynamic correlation functions, propagating modes 8-94988
- non-Newtonian lubricant hydrodynamic theory (*German*) 8-79341
- nonlinear free surface flow problems, divergent low Froude number series expansion 8-51146
- nonstationary gas flow, two dimens., variational approach to finite difference scheme 8-51147
- ocean, artificial upwelling induced by ocean currents theory and expt. 8-81217
- ocean, currents rel. to computed and observed surface topography 8-77250

hydrodynamics continued

- ocean, development of spatial internal waves generated by moving disturbances (*Russian*) 8-77251
- ocean, hydrodynamic friction layer instability rel. to Langmuir circulation 8-92840
- ocean, mobile sand grains underwater detect. 8-96192
- ocean, normal Rossby modes of closed basin with topography 8-73385
- ocean, rel. shear microstructure and energy dissipation meas. adjacent to island 8-85573
- ocean, upwelling circulation meas. during Hurricane Eloise (1975) 8-77302
- ocean continental shelf circulation, diagnostic model 8-85581
- ocean dynamics investigation, realisation of four dimensional topographic reference system 8-77176
- ocean mesoscale eddies, influence on sea surface temp. (*Russian*) 8-81191
- ocean near-surface mixing layer, microstruct. in stable heating conditions 8-85568
- ocean synoptical eddies, numerical scheme (*Russian*) 8-81190
- ocean water masses advection, radioactivity and salinity changes (*Russian*) 8-77275
- ocean waters mixing, effects of eddies and islands 8-85572
- Okhotsk Sea, currents, rel. to pack ice drift radar meas. (*Japanese*) 8-96224
- Okhotsk Sea coast of Hokkaido currents rel. to ice field divergence and rot. meas. (*Japanese*) 8-96223
- open disk theorem, hydrodynamic stability, upper bound of eigenvalues 8-59370
- polymer liq. flow, hydrodynamic eqns., centre of mass model, friction approx. 8-55664
- polymer solution, mean field theory 8-67227
- porous media, moving boundary problems, theory and numerical analysis 8-81252
- prestellar gas clouds, hydrodynamics rel. to relic radiation spectral lines (*Russian*) 8-77628
- pure harmonic tide in canal, eqns. of motion quadratic resistance term linearisation 8-69369
- PWR, MULTIFLEX code, anal. of hydraulic force with hydro-structural interactions during LOCA 8-58373
- quantum liquids, hydrodynamics, canonical eqns. 8-91497
- relative diffusion, meas. at small scales and oceanic appls. 8-88838
- self-gravitating disc, density waves accretion-induced overstability 8-73752
- ship model, hydrodynamic resistance, analytic calc. (*Russian*) 8-75123
- ships, drag on displacement ships, hydrofoils, hovercrafts 8-63423
- Southern Ocean, large-scale relative dynamic topography and current flow 8-85580
- spherically symmetric polymers, in soln., Faxen theorems 8-94342
- spherically symmetric polymers, in soln., hydrodynamic interaction 8-94343
- spheroids, in streaming suspension, dynamics, dielectric consts. 8-76374
- spiral galaxies, interstellar gas hydrodynamic flows in regions of Lindblad reson. 8-96527
- stars, self-gravitating systems, fluctuating hydrodynamics and thermodynamics 8-77485
- steam mains, Gentilly-I generating station, inertial analysis of hydrodynamic oscils. 8-89944
- stellar convection, hydrodynamics rel. to solar obs. 8-89182
- sticking and slipping boundary conditions, friction of rot. bumpy cylinder 8-63410
- Stokes equations, Galerkin-type representations 8-51143ic
- Stokes problem for a suspension of spheres at finite concentrations 8-55967
- Taylor vortices above higher instability points 8-75150
- thermal breakdown in viscous fluid, Couette flow between cylinders 8-83391
- traction prediction in elastohydrodynamic contacts 8-63394
- transport processes, relativistic generalisation in continuum (*Hungarian*) 8-89383
- tsunamis, transform. in coastal zone 8-77192
- tube bundle transient heat transfer and hydrodynamics with large flow and heat flux perturbations 8-83484
- turbulent noise suppression investigations using hydrodynamic press. meas. and cross-correlation techniques 8-79157
- two-dimensional hydrodynamics and water quality by finite element method 8-92877
- two-phase flow, compressibility effect on hydrodynamics, resistance coeff. 8-55684
- two-phase flow, hydrodynamics and heat exchange in film flow 8-91000
- Venus thermosphere, H global circulation and distrib. 8-89093
- vibratory liquid-gas mixture, nonlinear resonance expt. (*Ukrainian*) 8-90811
- waves development from periodic disturbances in non-uniform fluid, surface tension effect (*Russian*) 8-77253
- H₂O, cavitation nuclei conc., holographic and hydrodynamic obs. 8-83440
- ⁴He, superfluid, canonical hydrodynamic equations (*Russian*) 8-79835
- Rb, liquid, longitudinal modes, transverse modes and velocity correlations 8-94954

hydroelectric power stations

- see also dams; pumped-storage power stations; water supply; wave power generation*
- Tornio River plans, review 8-57236

hydrogen

- see also nuclei with*
- see also deuterium; hydrogen ions; hydrogen neutral atoms; hydrogen neutral molecules; protons; solid hydrogen; tritium*
- absorption, in Pd, electronic band struct., comparative study of electric and mag. props. 8-95259
- absorption by V-Cr alloys, thermodynamic parameters 8-87862
- absorption in FeTi, surface segregation and catalytic effect on hydrogenation 8-84819
- absorption/desorption isotherms, metal-H₂ system at high press. 8-51679
- adsorbed layer, inelastic low energy electron scatt. 8-72653
- adsorbed layer on Si {100}(1×1) surface, LEED study 8-67910

hydrogen continued

adsorbed monolayer on Cu surface, UV-visible polarised modulation spectra obs. 8-72619
 adsorbed on Cu, adsorbate induced photoemission 8-95668
 adsorbed on microcrystalline WC, mol. dynamics 8-71941
 adsorbed on Pd black, vibr. spectrum assignments, inelastic neutron scatt. obs. 8-71942
 adsorbed on Si (100) surface, LEED and AES meas. 8-60016
 adsorbed on W surface, energy spectra for electron stimulated desorption of H⁺ calc. 8-79892
 adsorption of CO on Al₂O₃-Ni catalyst in H₂-He, effect of H₂S on IR spectrum 8-71945
 adsorption on CO covered Ni films, resist., work function changes, isotherms 8-75926
 adsorption on graphite of O-H₂, NMR, orientational behaviour, weak crystal field 8-75935
 adsorption on LiF (001) surface, molecular orbital calc. 8-87878
 adsorption on Ni(111) surface at low temps., LEED meas. 8-56045
 adsorption on W, surface reflectance spectroscopy on low index planes 8-71965
 adsorption on W(100), nondipole electron impact vibr. excitations obs. 8-63922
 adsorption on ZnO powder, light irradiation effects (Japanese) 8-95230
 arc axial ground state population meas. 8-67598
 arc plasma Balmer spectrum decay and two-fluid model 8-67603
 bond dynamics in soln. 8-84573
 charging of Fe, lattice distortions, X-ray diffraction obs. 8-79629
 chemisorbed, on Ni foil, surface states and thermo EMF 8-91674
 chemisorbed on metal surface, electron correlation, friction coefficient 8-60026
 chemisorbed on Si and Ge surface, cluster model approach for electronic structure 8-56205
 chemisorption, on Au(Pt) electrode, volume of adsorbed species, temp. and pressure effects 8-84060
 chemisorption, on Pt electrode, entropy, temp. and pressure effects 8-84059
 chemisorption, on transition metals, Hubbard-type surface mol. model binding energy calcs. 8-71990
 chemisorption by Ni (110) surface, demagnetisation, positive spin polarisation in electron field emission 8-52646
 chemisorption of Ni, surface magnetism 8-95510
 chemisorption on CeO₂, kinetics and characters 8-51821
 chemisorption on clean Fe (100) and (111) surfaces, LEED and thermal desorption 8-71996
 chemisorption on metal surfaces, linear response theory 8-91543
 chemisorption on metal surfaces, relaxation energies in UPS 8-91544
 chemisorption on narrow d-band metals, semiempirical theory 8-75927
 chemisorption on Ni film, effect on ferromagnetic resonance 8-72375
 chemisorption on Ni surfaces, X_α cluster calcs. (Japanese) 8-72002
 chemisorption on Pt(100), (111), polycryst. electrode surfaces, electrochemical activity, comparison 8-61015
 chemisorption on semiconductor, effect of surface states 8-51823
 chemisorption on Si, atom-probe FIM obs. 8-71968
 chemisorption on Si(111), conduction-band surface resonance 8-52051
 chemisorption on W (001), angle-resolved photoemission, symmetry-related polarisation effects 8-56566
 chemisorption on ZnO, electrical conductivity examination. adsorption centres 8-67913
 concentration in Nb and V, neutron scattering meas. 8-67735
 condensed on surfaces, spin aligned, obs. 8-63929
 dense plasma, H_β line red shift expt. 8-67473
 dense plasma, ionisation, master equation analytical solution. 8-59544
 depth profiling in materials, use of ¹H(¹⁵N,αγ) resonant reaction (French) 8-91357
 desorption from metals by light ion bombardment, cross sections 8-95096
 determination, in H₂O after photolysis, gas chromatography 8-61089
 determination by simultaneous heavy-ion induced nuclear reactions. and at X-ray emission 8-85240
 diffusion and permeability in Fe at 49 to 506°C 8-59977
 diffusion and solubility in PTFE, activation enthalpy 8-79775
 diffusion coefficients calculation for H isotopes in FCC metals (Russian) 8-91483
 diffusion in α-Pd, by galvanostatic charging 8-84001
 diffusion in α-Pd, next-neighbour jumps of H in quasi-elastic neutron scattering 8-91487
 diffusion in alloy steels (Japanese) 8-52857
 diffusion in annealed and cold worked Ni (Japanese) 8-51739
 diffusion in Fe, 230-300K (Japanese) 8-84004
 diffusion in high strength steels HT80, HY130, effect of quenching and tempering (Japanese) 8-64565
 diffusion in Mo, 900-1100°C (Russian) 8-79811
 diffusion in Nb, influence of H-H pairing, jump model 8-75878
 diffusion in Ni, Pd, V, quantum rate theory for symmetric double well potential. 8-55970
 diffusion through Pt membranes at high pressure and temperature. 8-55984
 dissolved in Pd-Ag alloy, dil. solution, H-H interaction 8-71862
 distribution in Cr-plated steel, laser-mass spectrometer investigation. 8-61113
 electric breakdown, Paschen's law violations 8-87570
 electron beam sustained discharge, electron neutral inverse bremsstrahlung 8-63604
 electron surface barriers for dense phases 8-91754
 ethylene, surface reaction on Pt (111), EELS of radical vibrations. 8-71947
 extraction from LiF-LiCl-LiBr melt, applications. to fusion reactor blanket processing 8-53217
 freezing on inner surface of spherical polymer shell, cryogenic targets for laser-driven fusion 8-86688
 fusion reactor first wall radiation damage, H and He gas production from stainless steel 8-82512
 gas, 16 μm, generation by CO₂, pumped rotational Raman scattering. 8-94410
 gas, electron swarms, anisotropic scattering model 8-91059
 gas, light scattering, approximate line shapes 8-90221
 gas, Rayleigh-Brillouin spectrum at high densities 8-90189
 gas, stimulated rotational Raman scattering. pumped by CO₂ TEA laser 8-94411
 gas, thermal condensation, thermistor detector, ortho/para H₂ composition, temperature-jump region, 1-30 Torr 8-86263
 heat of adsorption on polycryst. Fe film 8-91530
 heat of solution in Al, electron charge distribution calculation. 8-51689
 heat of solution in Mg, electron charge distribution calculation. 8-51689

hydrogen continued

impurity in simple metal, electronic structure. 8-67978
 internal friction, influence of H₂ on Ti (French) 8-75723
 interstitials, random walk diffusion models, generalisation to correlations over two jumps 8-79794
 isotope diffusion in BCC metals, self-capture effect and activation energy (Russian) 8-75879
 isotope enrichment using low-temperature glow discharge technique 8-66675
 liquid, US vel., 18.25-32.38K (Russian) 8-75731
 LMFB, H burden from steam side corrosion in Na heated steam generators 8-58355
 LWR fuel-cladding gap, Cs-U-Zr-H-I-O system, chemical thermodynamics 8-82440
 magnetic relaxation study in Fe 8-64228
 maser, time-dependent frequency shift obs. 8-89457
 maser, wall shift, comparison between TFE 42, FEP 120 Teflon coatings 8-78984
 maser design for NAVSTAR Global Positioning System satellite clock 8-58969
 maser dissociator, H beam production performance characters. 8-87034
 maser improvements at Smithsonian Astrophysical Observatory 8-58971
 maser response to coherent Zeeman perturbations 8-58972
 maser with double configuration bulb for wall shift meas. 8-58970
 metal-H system, bond energy calcs. 8-51940
 metallic, Coulomb crystal energy, analysis of the tail of the density series 8-91300
 methane-H₂, in packed bed, heat and mass transfer, axial mass dispersion 8-75200
 monolayer, on triangular lattice, orientational phases 8-75934
 nuclear reactor, LWR hydrogen formation during core melt accident 8-50267
 permeability, diffusivity and solubility in pure Fe at 10 to 60°C 8-75887
 permeability and diffusivity in nickel (Japanese) 8-66345
 permeability of Fe membranes with electrodeposited metal coatings, proposed catalytic mechanism 8-53252
 permeation, in Pd, comparison to D₂ (Russian) 8-75881
 permeation through metal barrier, adsorption processes 8-63879
 permeation through Ni and Hastelloy X (Japanese) 8-51740
 plasma, at fluorescence, collisional depopulation rate of n=2 level 8-79463
 plasma, electron kinetic coefficients. interpolation calcs. (Russian) 8-71429
 plasma, H_β line profile for plasma microfield distribution. function reconstruction 8-71539
 plasma, H line curvilinear trajectories and Stark broadening 8-67324
 plasma, inertial confinement, reaction gains, reheat calcs., collective model 8-59664
 plasma, Lyman system nonsaturated laser line intensity obs. 8-71089
 plasma collision-dominated electron distribution. function with turbulent heating 8-71509
 plasma diagnostics, laser-induced parametric instabilities 8-51345
 plasma distribution function inference from optical spectra 8-67406
 pressure, in vacuum chamber in cryogenic environment, measurement technique 8-77925
 production in decomposition of water by fusion energy, synthetic fuel 8-50335
 pumping by Ti film, pumping speed comparison between H₂ and D₂ 8-51819
 release rate from clean metal surface 8-95187
 solid p-H₂, very low O-H₂ concentration, order-disorder transition, NMR 8-56384
 solubility and bulk modulus in transition metals, examination. 8-55950
 solubility in Fe in 600-1500°C temperature and 0.1000 atm. pressure ranges (Russian) 8-59948
 solubility in Zr, optical metallography, internal friction meas. 8-83962
 sorption by rare earth-transition metal alloys, effect on magnetic properties. 8-68231
 sorption on polar ZnO surfaces, EELS 8-64434
 spin aligned, relative to liquid to gas phase transitions in two-dimensional quantum systems 8-77798
 stabilised arc as vacuum UV radiation standard for 600 to 900 Å 8-66879
 sticking coefficient, initial, on polycryst., O₂ and S covered Ni surface 8-63937
 stimulated Raman scattering, tunable UV radiation obs. 8-55408
 storage, in La-Ni, Ce-Ni, hydriding characters. 8-83955
 superpure, storage and production, use of FeTi crystals (German) 8-53184
 synthetic fuel production, Tokamak high-temperature blanket 8-74479
 threshold for pore formation during solidification in Al-Si (8 wt.%) alloys 8-52794
 Tokamak plasma, Doppler temperature and particle confinement time from H_α-line meas. 8-55737
 transition metal alloy, ferromagnetic, H-impurity complex obs. by magnetic aftereffect 8-72373
 transport in various liquids and metals, neutron radiography study, results review 8-59961
 trapping and replacement of 1 to 14 keV H and D in stainless steel 8-95070
 Ar plasma, H impurity, equilibrium state of highly ionised plasma 8-83597
 Ar-H₂ plasma, thermodynamic properties 8-63542
 Ar-N₂-H₂ plasma equilibrium compositions and thermodynamic properties. 8-71433
 CO₂-N₂-H₂ electron beam controlled laser, efficiency and output energy depend. on H₂ 8-58978
 Cu-H, interaction of H and vacancies, positron annihilation, Doppler broadening 8-80434
 H/D ratio in planetary atmospheres, determined from CH₃D 9613 Å band 8-86861
 H-C, thermal desorption, one-phonon antiscatter, 3-dimensions, continuum model 8-87860
 H-He arc lamp, 60-360 nm, calibration 8-87117
 H-like ion, relativistic acceleration, quasi-Stark effect (German) 8-58621
 H₂ electron swarms transport parameters meas., nonuniformities effect 8-83613
 H₂/CO surface complex, in W (100), flash desorption and AES obs. 8-73083
 H₂-Ar(Kr)(Xe) mixtures, intermolecular forces 8-62867

hydrogen continued

- H₂-CO₂, turbulent flow heat transfer, expt. and numerical anal. 8-94690
 H₂-F₂-He chemical CW laser, flows (*Russian*) 8-74895
 H₂-F₂-O₂, chem. laser mixture, multiatm., spontaneous explosions 8-73044
 H₂-He mixture, collision integrals, modelling of spacecraft entry into Jupiter atmosphere 8-71413
 H₂-N₂-Ar, two-phase flow film boiling, in vap. generator, heat transfer 8-75190
 H₂-Ne, hollow-cathode discharge, electron energy distrib. 8-71573
 H₂-O₂-N₂ flame, photochem. reactions involving Na*, laser saturated conditions 8-80762
 H₂-O₂-N₂ flames, diffusion coeff. meas. for CO, Br, I and TI 8-51272
 H₂+NO+CO interaction over Pt, Rh, Ru and Os, NH₄OCN formation 8-73082
 H₂+O*→OH*+H, rate const. and vibr. energy distrib. in OH*, for $\dot{O}(^3P)$ 8-60998
 HD, isotopic effects in predissociations 8-86924
 HD, viscomagnetic heat flux, in a Burnett regime 8-71400
 He+H₂, microwave plasma, pulsed high current heating at atm. press., MHD instability 8-55728
⁴He stopping cross sections, 1-8.5 MeV 8-58558
 KCl:Ca,H, ENDOR studies of localised vibrations of substitutional atomic H 8-80248
 Mg:H, solid soln. produced by ion implantation 8-67733
 N₂-H₂ mixture, glow discharge, ionisation and excitation obs. 8-67505
 N₂+H₂, reaction rate determ. 8-60985
 Ni:H, energy and electron density of states 8-51929
 O₂-H₂, gas mixture, mag. field effect on thermal conductivity 8-59533
 Pd:H, elastic props. of dilute solid solutions 8-75706
 Pd:H, energy and electron density of states 8-51929
 Pd-H, dil. soln., partial molar props., temp. depend. 8-68910
 RbCl:Ca,H, ENDOR studies of localised vibrations of substitutional atomic H 8-80248
 Rh:H, energy and electron density of states 8-51929
 Si:H, amorphous, rehydrogenation, photoluminesc. recovery 8-72571
 Si:H, ion implanted Monte Carlo calcs. of profiles of H ions 8-55889
 Si:H film, amorphous, elec. cond., effect of adsorbed gases and illumination 8-88048
 Si-Fe-H₂-N₂, combined effect of Fe and H₂ 8-95722
 ZnO:Cu,H, motional effects in EPR spectra 8-80207

hydrogen bonds

- acetic acid dimer, gas phase, H-bonded complex struct. from elec. dipole moment obs. 8-74791
 acetonitrile-phenol(-d₁), in CCl₄ (CDCl₃) solns., H-bonds vibr. relax. bands anal. 8-84560
 adipic acid, monoclinic crystals, IR absorption and dichroism 8-88293
 L-alanine, solid, H bonding, wide line NMR obs. 8-52362
 amide group in soln., interactions, IR, Raman spectral investigs., peptide, protein struct., review 8-90330
 associated solutions, H bonding and anomalous saturation 8-52426
 1-aziridineethanol, mol. spectrum and hydrogen bonding 8-70820
 biomembranes, proton transport, mol. mechanisms 8-96035
 block copolymers, IR spectroscopy for struct.-props. relations 8-91268
 o-chlorobenzoic acid, solid, H bonding, wide line NMR obs. 8-52362
 cholesterol+water, interaction in organic media, dielec. and NMR spectroscopy 8-76979
 chymotrypsin, charge relay system, H-bond models, IR spectra 8-64935
 complex formation, enthalpy change due to electronic excitation, spectroscopic determ. 8-92496
 complexes, H-bonded, microwave spectra, assignments, mol. consts. 8-62794
 crystal, IR absorpt. spectra band shape, X-H stretching vibr. temp. depend., isotope effect 8-76445
 dicarboxylic acids, D quadrupole coupling constants, ENDOR study 8-90195
 dioxan-phenol(-d₁), in CCl₄ solns., H-bonds vibr. relax. bands anal. 8-84560
 DNA, molecular electrostatic pots. of complementary base pairs 8-92597
 electrolyte aq. solns., IR librational bands, struct. making and breaking 8-56476
 ethylene methacrylic acid polymer and Na salt, ionic aggregation and melt rheology, H₂ bonding effect 8-67159
 ferroelectrics, H-bonded, NMR and soft modes study 8-88208
 formamide, partly deuterated, in electrolytic soln., IR spectra, anion-solvent H-bonding 8-84558
 formamide dimer, hydrogen bond, ab initio MO calcs. 8-58588
 formic acid dimer, gas phase, H-bonded complex struct. from elec. dipole moment obs. 8-74791
 formic acid dimer, hydrogen bond, ab initio MO calcs. 8-58588
 formic acid-acetic acid, gas phase, H-bonded complex struct. from elec. dipole moment obs. 8-74791
 formic acid-water polymers, gas phase, H-bonded complex struct. from elec. dipole moment obs. 8-74791
 ice, press. effects on Raman spectrum 8-95582
 IR absorption of H-bonded species, intramol. interactions effect 8-50595
 IR spectra, ν , band interpretation 8-58653
 isoquinoline semiperchlorate, H-bonding, strong, stochastic model and IR spectra temp. effects 8-62805
 lysozyme, aq., Raman intensities, interac. 8-58704
 methanol, H-bonded struct., IR spectra, assignments 8-62800
 methyamine-t₁-NH₃, β -decay effect on H-bond, ab initio LCAO SCF MO calc. 8-76894
 3-methylisoquinoline, semiperchlorate, H-bonding, strong, stochastic model and IR spectra temp. effects 8-62805
 β -naphthol, IR dichroic ratio, oriented gas and effective charge models calcs. 8-60437
 o-nitrophenol, cryst. and mol. struct., H bond distance 8-51523
 NMR high resolution of solids method, appl. to H-bonded systems 8-76323
 organic ortho compounds, solid, H bonding, wide line NMR obs. 8-52362
 phenol(-d₁)-dioxan-(acetonitrile), in carbon tetrachloride (CDCl₃) solns., H-bonds vibr. relax. bands anal. 8-84560
 polyacids, unsaturated carboxylic, in organic solvents, hydrogen bonding, structurisation (*Russian*) 8-71666

hydrogen bonds continued

- polyurethanes based on toluene di-isocyanate, struct.-prop. relns. 8-80509
 Raman spectra of liq. phase weak H-bonds, short range order and anharmonicity effects 8-64357
 solid, H-bonded, NMR chem. shift tensors (*German*) 8-84489
 solution, H-bonded species, vibr. relax. model 8-84559
 solutions with closed loop coexistence curves, directionality depend. of lattice models 8-95158
 stochastic model, strong H-bonds, IR spectra temp. effects 8-62805
 strong H bonded systems, vibr., Raman, IR spectra, biology appls. 8-82735
 symmetric AHA([±]), A-H stretching vibr., liq. IR band shape, strong coupling phonon model 8-64358
 tertiary phosphine oxide+aliphatic alcohol, $\pi\pi$ - $\pi\pi$ conjugation, electronegativity and H-bond energy 8-82863
 tetramethylammonium hexachloroplatinate, ZZ 8-92060
 tetramethylammonium hexachlorostannate, ZZ 8-92060
 urea, single crystal Compton profiles, H-bonding and dimer config. effects, calc. and meas. 8-80431
 van der Waals criterion for H bonding 8-91292
 water, and ionic dissoc. products, polarisation model 8-91216
 water, H-bonded struct. IR spectra, assignments 8-62800
 water-anion H-bonds, nature, from IR and Raman OH(OD) splittings 8-62811
 water-HF(HBr)(HCl) complex, in supersat. soln., Raman spectra assignments 8-70840
 zinc malonate dihydrate, cryst. struct., X-ray refl. obs. 8-75652
 γ -AIOOD, boehmite, hydrogen bond, neutron profile refinement of struct. 8-71701
 (B(OH)₃)₂, hydrogen bond, ab initio MO calcs. 8-58588
 Ca₁₀(PO₄)₆(OH)₂ halogenated derivatives, IR absorpt. spectra (*Spanish*) 8-52489
 CaZn(SiO₄)₂H₂O, clinohedrite, cryst. struct., H bonds 8-79593
 Co complex, bisdimethylglyoxime (thiosemicarbazide)-cobalt (III) nitrate, mol. and cryst. struct. of dihydrate 8-83803
 Cu²⁺ complex, in water-ethanol soln., struct., EPR 8-50565
 D₂O₂⁺, isotope effects, easily polarisable H and D bonds 8-94231
 FeOOH, H-bonding, strong, stochastic model and IR spectra temp. effects 8-62805
 H-bonded complexes, OH stretching vibr. band, temp. effect 8-90158
 HCN, self-assoc., matrix isolation vibr. spectroscopy, complex form. studies 8-62952
 HCl, anhydrous conc. solns. in methanol, Raman and IR spectra 8-82724
 HCl-dimethylether complex, gaseous, H-bond IR spectra, temp. depend. theory 8-62804
 HCl-X, matrix isolation vibr. spectroscopy, complex form. studies 8-62952
 HCl.6H₂O, cryst. struct., H bonds, X-ray determ. 8-83783
 HF, H-bonded chains, vibr. modes in liq. and solids 8-59873
 HNO₃, aq. soln., H bonds, IR spectra 8-94243
 (HNO₃)₂, gas phase, H-bonded complex struct. from elec. dipole moment obs. 8-74791
 H₂O+Li⁺, ab initio GTO calc. of vibr. intensity changes of spectroscopic parameters 8-58583
 KD₂AsO₄, ferroelec., phase transition and Raman scattering 8-84540
 KD₂PO₄, IR and Raman polarised spectra, rel. to crystal struct. 8-56489
 KD₂(SeO₄)₂, D NMR above and below ferroelec. transition, H-bond behaviour 8-52460
 KH₂AsO₄, ferroelec., phase transition and Raman scattering 8-84540
 (NH₄)₂M(SO₄)₂.6H₂O, Tutton's salts, IR spectra, correl. of vibr. freq. and N...O distance for NH₃D⁺ 8-92066
 NH₃.TNH₃, β -decay effect on H-bond, ab initio LCAO SCF MO calc. 8-76894
 NO, hyperfine splitting const., H-bond contrib. 8-74799
 Na₂ZnCl₄.3H₂O, NQR of ²³Na and ³⁵Cl, single-cryst. study 8-91983

hydrogen compounds

- see also deuterium compounds; hydroxonium ion; ice; steam; tritium compounds; water
 aqua regia, etching of GaP 8-68833
 diatomic hydrides, variation-perturbation minimal Gaussian geminal basis sets correl. energy calc. 8-78629
 H₂O:HF ice, single crystal, velocity of individual dislocations by X-ray topography (*French*) 8-87677
 H₂O₂, propan-1,3-dioic acid, KIO₃, MnSO₄, HClO₄, I₂, periodic chem. reactions, bi- and tristability, rel. to biological mech. (*French*) 8-80726
 halides, I*(⁵P_{1/2}) quenching, electronic-vibr. energy transfer 8-63114
 HCl-NOCl gas mixture, vibr. relaxation, collisional de-excitation (*French*) 8-86934
 neutral free radicals, in Ar matrix, IR spectrosc. evidence 8-66546
 polysilicic acid, IR spectra, struct., crystallisation effects (*Russian*) 8-72528
 silicic acid sol., gel formation, characteristics of light scattering 8-53269
 silicic and aluminosilicic acids, effect of increased size of scattering centres in sols 8-53270
 β -Al₂O₃-H₂O, H⁺ and H₃O⁺ conduction, dehydration effect 8-51726
 β -Al₂O₃-H₂O, stability and dehydration 8-51693
 Ar-HCl, Van der Waals mol., far IR spectrum, anisotropic intermol. force effects 8-62869
 Cl+HNO(H₂O₂)(HO₂), rate consts., stratospheric appl. 8-85125
 D+HCl(HBr)(HI), abstraction and exchange reactions 8-73025
 DF-HF CW lasers, performance, computer modelling 8-71094
 HBr, dissociative attachment of electrons 8-62931
 HBr, electron scatt., elastic rot. scatt. and vibr. excitation 8-58822
 HBr, electronic to vibr. energy transfer from excited halogen atoms, IR fluoresc. 8-63113
 HBr, far IR Ar matrix isolated spectra, 4.2K, press. and conc. effects 8-62801
 HBr, isotopic struct. and spectral characts. of vibr. band, using liq. N₂ Raman laser source 8-50859
 HBr, liq., transient stimulated vibr. Raman scatt. 8-71144
 HBr, precession magnetic shielding of proton, semiempirical functions 8-82654
 HBr, vibr. energy transfer, laser selective isotope excitation 8-82790
 HBr, vibr.-rot. absorpt. spectra at very high foreign gas densities 8-78687

hydrogen compounds continued

- HBr-HCl, thermodynamics of binary liquid mixtures 8-64876
 HBr-water complex, in supersat. soln., Raman spectra assignments 8-70840
 HBr-Xe, thermodynamics of binary liquid mixtures 8-64876
 HBr+($5^2P_{1/2}$), electronic-vibrational energy transfer, fluoresc. obs. 8-66579
 HBr+H⁺, ZZ 8-80729
 HCN, (001)→(000) fluorescence following dye laser photolysis of s-tetrazine 8-88652
 HCN and HNC, analytic functions from pot. energy surfaces 8-62743
 HCN, and isotopic derivatives, rot. depend. of Fermi resonance 8-94227
 HCN compact CW laser optimisation 8-59022
 HCN dimer, interstellar abundance, upper limit 8-54004
 HCN, dipole moment derivative, sign anomaly, CGTO ab initio calc. 8-74795
 HCN, dipole moment derivatives and force consts., CI calcs. 8-90091
 HCN, elastic electron scatt. differential cross section, 3-50 eV, 20-130°, rel. to He 8-90291
 HCN, electron impact, dissociation cross-sections, fragment obs. 8-62936
 HCN, electronically excited states, SCF CI calc. using Slater type orbitals 8-78645
 HCN emission detect. in Sagittarius A mol. cloud 8-73750
 HCN, finite field method calc., moments, polarisability, field-induced shifts in mol. props. 8-74561
 HCN, Franck-Condon transition amplitudes for mol. dissoci., semiclassical evaluations 8-62860
 HCN, HNC, electronic reorganisation, with core ionisation 8-94196
 HCN, HNC, interstellar, form., role of H₂ CN⁺ isomers 8-81672
 HCN, HNC, molecular electronic struct., unlinked cluster effects 8-94185
 HCN, ionis. and photoelectron spectra, inner valence electrons 8-82784
 HCN, nuclear quadrupole coupling and mol. deformations 8-90191
 HCN, photodissoc., vibr. energy states population meas. 8-58751
 HCN, relative signs of CH/CN dipole moment derivatives 8-74796
 HCN, SCF ab initio ground state pot. energy surface, geometry, rel. to HCN⁻ 8-78646
 HCN, self-assoc., matrix isolation vibr. spectroscopy, complex form. studies 8-62952
 HCN, self-assoc. in matrices, IR vibr. spectra of multimers 8-86858
 HCN, vibr. fine struct. accompanying core ionis., STO calcs. 8-62844
 HCN⁻, SCF ab initio ground state pot. energy surface, geometry, rel. to HCN 8-78646
 HCN⁺, photoelectron spectra of third electronic state, ab initio calc. of pot. energy surface 8-70871
 HCN-HF, elect. dipole moment, Stark effect of linear mol. 8-70818
 HCN+He, rot. excitation, infinite order sudden approx. 8-74740
 HCN+OH, reaction rate, press. depend. 8-85135
 (HCN)₂, and isotopic forms, microwave spectroscopic investigations of hydrogen-bonded complexes 8-62794
 HCNH⁺+e, dissociative recomb. reaction in interstellar clouds, products, statistical theory 8-57604
 HCO⁺, geom. struct., ab initio mol. orbital study 8-62939
 H₂CO⁺+H₂S→H₂S⁺+HCHO, chemical equilib. consts., proton affinity of HCHO and H₂S 8-85189
 H₂CO⁺+HCN→H₂CN⁺+HCHO, chemical equilib. consts., proton affinity of HCHO and HCN 8-85189
 HCl, acid vapour, eqn. of state 8-79402
 HCl, anhydrous conc. solns. in methanol, Raman and IR spectra 8-82724
 HCl, bond dependence of dipole polarisabilities 8-74573
 HCl, corrosion behaviour of Al-Sn alloys 8-85054
 HCl cryosorption-pumped CW chemical laser 8-74894
 HCl, dissociation electron attachment kinetics in flame, mass spectra obs. 8-68872
 HCl, dissociation excitation in flowing afterglow, Cl form., light emission 8-90115
 HCl, effective core potentials, all-electron calcs. 8-62704
 HCl, electronic to vibr. energy transfer from excited halogen atoms, IR fluoresc. 8-63113
 HCl, far IR Ar matrix isolated spectra, 4.2K, press. and conc. effects 8-62801
 HCl gas in ambient air, detection using coated piezoelec. quartz cryst. 8-92532
 HCl, interaction with evaporated metal films, adsorpt. 8-75945
 HCl, isotope exchange reactions, equilib. consts., adiabatic correction, electron correl. effects 8-88626
 HCl laser, V=3 to V=2 band process, computer simulation 8-71095
 HCl, liq., transient stimulated vibr. Raman scatt. 8-71144
 HCl, nuclear quadrupole coupling and mol. deformations 8-90191
 HCl, photodissoc. cross section, from high vibr. levels, Poschl-Teller oscill. model 8-55210
 HCl, polymer degradation products, chem. anal. by UV photoelectron spectroscopy 8-53300
 HCl, precession magnetic shielding of proton, semiempirical functions 8-82654
 HCl, solid, incoherent neutron scatt. of proton motions 8-75600
 HCl, spectral data analysis using graphics display terminal 8-54473
 HCl, vapour, etching behaviour of CaF₂ crystals 8-59812
 HCl, vibr. energy transfer, laser selective isotope excitation 8-82790
 HCl, vibr.-rot. absorpt. spectra at very high foreign gas densities 8-78687
 H³⁵Cl, H³⁷Cl, IR Fourier absorption spectra, press. induced shifts 8-74706
 HCl-D₂-He mixture, gasdynamic laser theory, gain depend. on parameters 8-50761
 HCl-dimethylether complex, gaseous, H-bond IR spectra, temp. depend. theory 8-62804
 HCl-N₂ mixture, electron swarm, Cl⁻-HCl cluster formation, dissociation, attachment, drift tube mass spectra 8-68884
 HCl-water complex, in supersat. soln., Raman spectra assignments 8-70840
 HCl-X, matrix isolation vibr. spectroscopy, complex form. studies 8-62952
 HCl+Ar, rot. linewidth calcs., using different pots. 8-66602
 HCl+Ar, rotationally inelastic collision, planar trajectory, classical centrifugal decoupling calcs. 8-58788
 HCl+Ar(He), rot. excitation, infinite order sudden approx. 8-74740

hydrogen compounds continued

- HCl+Br, quenching of 4P_{1/2} state, vibr. excitation, temp. depend. 8-58792
 HCl+Cl, vibr. energy transfer to oscillatory, restricted rot. and translational motion 8-70908
 HCl+HCl, rot. transitions, 0.025 eV, semiclassical exponential approx. 8-62883
 HCl+HCl(Ar), pure rot. Raman lines, press. broadening cross sections 8-74702
 HCl+He, energy sudden approx., beam scatt. meas. mol. anisotropy effects 8-78802
 HCl+I($5^2P_{1/2}$), electronic-vibrational energy transfer, fluoresc. obs. 8-66579
 HCl+NH*, rate const., time resolved chemiluminesc. 8-60982
 HCl+O⁻(O₂⁻)(NO₂⁻)(CO₃⁻)(CO₄⁻), rate consts. at 300K 8-76829
 HCl+Sr*(3P_1), laser-excited atom reaction, energy deposition 8-85134
 HCl(DCl)+Ar potential, asymmetric, isotope substitution effect, Legendre expansion coord. transformation 8-70894
 HCl(J;v)+Na→H+NaCl, reaction rate, rot. excitation depend. 8-64818
 HClO₄, aq. soln., thermal capacity at 25°C 8-83965
 HClO₄, propan-1,3-dioic acid, H₂O₂, KIO₃, MnSO₄, I₂, periodic chem. reactions, bi- and tristability, rel. to biological mech. (French) 8-80726
 HCl.2ZnCl₂.2H₂O, struct. refinement 8-51488
 HCl.6H₂O, cryst. struct., H bonds, X-ray determ. 8-83783
 HD, in interstellar diffuse clouds, column densities rel. to temps. determ. 8-93385
 HD+D₂, rot. inelastic differential cross sections, diffr. oscils. in elastic and inelastic scatt. 8-74743
 HD+inert gas, isotropic Raman Q branch, vibr. dephasing effects and motional narrowing 8-74738
 H(D)I+Cl, exothermic triatomic exchange reactions, prod. energy distrib., statistical dynamic model 8-92455
 HF, bond dependence of dipole polarisabilities 8-74573
 HF CW chemical laser with cylindrical telescopic resonator, flame front model 8-59001
 HF chemical laser, laminar flow pattern (Russian) 8-87048
 HF, chemical laser, rot. population transfer effect obs. 8-79013
 HF chemical laser, spherical telescopic resonator, design 8-71120
 HF chemical laser, stable discharges, with large electrode separation 8-55371
 HF chemical laser mixture, H₂-F₂-O₂, spontaneous explosions 8-73044
 HF cryosorption-pumped CW chemical laser 8-74894
 HF, cw chem. diffusion laser, amplifier operation 8-79015
 HF, effective core potentials, all-electron calcs. 8-62704
 HF, electron impact excitation, dissociation, emission spectrum 8-90305
 HF, etchant for fission fragment track visualisation in crystals. 8-66454
 HF, force consts., ab initio CI calcs. (French) 8-90093
 HF, H-bonded chains, vibr. modes in liq. and solids 8-59873
 HF, high-energy laser, energy extraction, beam quality, for fusion ignition 8-63102
 HF, highly excited, ionis. pot., mass spectrometric meas. 8-58603
 HF, IR Fourier absorption spectra, press. induced shifts 8-74706
 HF laser, pulsed unstable resonator, mode control and performance studies 8-82995
 HF, laser action by pulsed microwave discharge 8-58998
 HF, linear response function, diagonal ARPA calcs. 8-74594
 HF, mag. field depend. orbitals for mag. screening and susceptibility of mol. 8-78611
 HF, mol. props. internucl. separation depend., MCSCF calc. 8-70965
 HF, nonequilibrium dissociation in electric discharge, vibrational excitation 8-94306
 HF, nuclear spin-spin coupling const., finite perturbation calcs. 8-78616
 HF, pot. curve, one-config. Hartree-Fock-Roothaan calc. for force consts. 8-82627
 HF, pot. energy curve, minimal basis ab initio VB calcs. 8-50477
 HF, precession magnetic shielding of proton, semiempirical functions 8-82654
 HF, pulsed H₂+F₂ chain reaction laser, rot. nonequilibrium mechanisms effect on performance 8-82958
 HF, vibr. relax. rates, ν=3, 4 8-82817
 HF-cyanomethane, microwave spectroscopic investigations of hydrogen-bonded complexes 8-62794
 HF-H₂O, microwave spectroscopic investigations of hydrogen-bonded complexes 8-62794
 HF-HCN, microwave spectroscopic investigations of hydrogen-bonded complexes 8-62794
 HF-water complex, in supersat. soln., Raman spectra assignments 8-70840
 HF+Ca(Sr), beam reaction, vibr. excitation 8-68877
 HF+D, vibr. threshold energies, reagent energy effects 8-85145
 HF+HF, momentum exchange rate, Boltzmann eqn. predictions 8-78781
 HF+HF, rotationally inelastic scattering, classical trajectory study 8-82819
 HF+HF, vibr. relax., temp. depend. calcs. 8-70906
 HF+HF, vibr.-vibr., vibr.-rot., and vibr.-translational energy transfer calcs. 8-70907
 HF+H(D), kinetic isotope effect and temp. depend. 8-53202
 HF+Li, electron transfer reactions, semiempirical pot. energy surfaces calcs. 8-73022
 HF+Sr*(3P_1), laser-excited atom reaction, energy deposition 8-85134
 HF⁺, A-type doubling and spin-doubling 8-74633
 (HF)₂, intermol. force model, rel. to liq. struct. 8-78773
 HF₂, neutral free radicals, in Ar matrix, IR spectrosc. evidence 8-66546
 HF₂⁻, dipole derivatives, rel. to refl. spectra of Na and K salts 8-80324
 HF₂⁻, matrix isolated, IR spectra and struct. 8-74655
 HF(J;v)+Na→H+NaF, reaction rate, rot. excitation depend. 8-64818
 HF*+ethylene (fluoroethylenes), vibr. deactivation rate constant 8-50615
 HI, 1→0 IR absorpt. band 8-86863
 HI, H abstraction by thermal H, 10-30K, ESR evidence 8-76839
 HI, line strength meas., 0→4 and 0→5 absorpt. bands, dipole moment (French) 8-62847
 HI, precession magnetic shielding of proton, semiempirical functions 8-82654

hydrogen compounds continued

- HI+Cl, chem. laser, energy distrib., spectrosc. obs. 8-71096
 HI+D→H+DI, Franck-Condon theory 8-60984
 HI+O₃, HOI formation, matrix reaction, IR spectra, isotope shifts and band assignments 8-80737
 HIO₃, ¹H/²H quadrupole reson. freqs. detected by double reson. with level crossing 8-84497
 α-HIO₃, dispersion anal. of IR reflection spectrum (*Russian*) 8-56493
 HIO₃, single crystal, ang. depend. of Raman spectra 8-72518
 HI₃O₈, NQR freqs. of ¹²⁷I 8-72433
 H₂MoO₃, (0<x≤2.0), phase relationships, X-ray diffr. exam. of microstruct. 8-76639
 HN₃, IR multiphoton dissociation 8-80771
 HN₃→N₂⁺+NH⁺, laser photolysis, primary products, energy distrib., intermediate reactions 8-61037
 HN₃+NH⁺→NH₂⁺+N₃⁺, rate const., time resolved chemiluminesc. 8-60982
 HNC, anharmonic force field, equilib. struct., rot. consts. and bond lengths 8-90147
 HNC, finite field method calc., moments, polarisability, field-induced shifts in mol. props. 8-74561
 HNC⁺, radical cation, charge exchange mass spectrometry, HNC⁺ ion recombination and ionisation pot. 8-76838
 H₂NNH₂, nuclear fuel processing solutions 8-78487
 HNO, HON, electronic reorganisation, with core ionisation 8-94196
 HNO₂, and protonated forms, electrostatic pot. predictions, basis set depend. 8-74786
 HNO₃, aq. soln., H bonds, IR spectra 8-94243
 HNO₃ cycle process for ocean thermal energy extraction 8-53660
 HNO₃, in stratosphere, obs. in N.hemisphere for three seasons 8-81288
 HNO₃, vapour, global tropospheric meas. 8-88904
 HNO₃, vibr.-rot. spectrum, 855-915 cm⁻¹ (*French*) 8-50543
 HNO₃/NO₂ conc. ratio in daytime stratosphere 8-73460
 HNO₃-HF mixtures, dissolution of (Th,U)O₂ reactor fuel, fuel reprocessing study 8-59951
 HNO₃-water, homogeneous nucleation, relative humidity depend. 8-71846
 (HNO₃)₂, gas phase, H-bonded complex struct. from elec. dipole moment obs. 8-74791
 HO+methane, H abstraction, rate consts. calcs. 8-95921
 HO₂ radical, EPR spectrum, ground state parameters 8-90193
 HO₂ radical, ν₃ fundamental band, laser mag. reson. 8-66566
 HO₂⁺, ab initio calc. of three lowest states 8-62711
 HO₂+Cl react. rate const. determ. at 298K (*French*) 8-64817
 HO₂+NO reaction rate constant effects on O₃ perturbations, model of stratosphere 8-73474
 HO₂+O₃→OH+2O₂, rate coeff., effects on stratospheric O₃ 8-96275
 H₂O 22 GHz maser emission from W3(OH), 49N and 51, spatial distrib. 8-93355
 H₂O⁺, electron affinity, mol. geom. effects calcs. 8-82618
 H₂O⁺, vibronic A²A₁ states, lifetimes, delayed coincidence meas. 8-70874
 H₂O+He(2³S), energy transfer processes, reaction products, UV and visible obs. in flowing afterglow 8-85138
 H₂O₂ aq. solns., struct. and dielec. props. 8-63659
 H₂O₂, geometry, internal rot. barriers, electron correl. calcs. 8-70751
 H₂O₂, inactivated papain, optical density, amino acid composition and fluoresc. 8-53344
 H₂O₂, UV prod. of OH radicals, reactions with peptides in aq. soln., EPR 8-68993
 H₂O₂, Zeeman effect and mol. quadrupole moment, beam maser spectrosc. 8-90152
 H₂O₂+acid amide, aq. solns., photolysis, EPR study of spin-trapped radicals 8-68996
 H₃O⁺+e, dissociative recomb. reaction in interstellar clouds, products, statistical theory 8-57604
 HOCl, chloramine, isoelectronic mol., vap. phase UV photoelectron spectra, struct. 8-66600
 HOCl, photodissoc., ab initio SCF CI calcs. 8-50604
 HOI, O₂(O)+HI matrix reaction, IR spectra, isotope shifts and band assignments 8-80737
 HO₂NO₂, unimol. decomp., press. and temp. depend. 8-68887
 HO₂NO₂+N₂⇌HO₂+NO₂+N₂ react., kinetics, RRKM theory appl. 8-73032
 HPO, mol. struct. and props., ab initio, calc., Gaussian lobe orbital 8-62713
 HPO₄³⁻, in γ-irrad. K(H_{1-x}D_x)₂PO₄, 77K, optical and EPR obs., form. mechanism 8-68379
 H₂PO₄⁻, in γ-irrad. K(H_{1-x}D_x)₂PO₄, 77K, optical and EPR obs., form. mechanism 8-68379
 H₃PO₄, welding of MgO single crystals, to form bicrystals 8-56796
 HS₂, ground and first excited states, geometry, ab initio SCF calcs. 8-50657
 HS₂, rotamers, electronic and geometrical structs., ab initio floating GO basis calcs. 8-74572
 H₂S absorpt. on zeolites with varied Si/Al ratios 8-60029
 H₂S, adsorption on Pt (100), intermolecular forces and kinetics of adsorption 8-75930
 H₂S contrib. to atmospheric S cycle 8-73473
 H₂S, double hole states POCI calc., Auger spectrum 8-78630
 H₂S, effect on IR spectrum of CO adsorbed on Al₂O₃-Ni catalyst in H₂-He 8-71945
 H₂S, electron density, basis set, electron correl. effects 8-74581
 H₂S, excitation energy, one-centre approx. calcs. 8-70737
 H₂S, gas-phase, states in valence photoelectron spectrum 8-94284
 H₂S in air, preconc., determ. by flame photometric detection 8-92535
 H₂S, inner valence electron ionisation calcs., photoelectron spectra obs. 8-82619
 H₂S, KLL Auger spectrum, obs. and ab initio SCF CI calc. 8-50654
 H₂S, stress corrosion cracking of Ni-Cr-Mo-V alloy steel, exam. of overload effects 8-60886
 H₂S-methane mixture, densities calc., van der Waals model 8-79740
 H₂S+Ar⁺, emission spectra obs. 8-50622
 H₂S+Cl→HCl+HS, laser-initiated chain reactions, rate consts., product energy distrib. 8-85144
 H₂S+hydrocarbon mixtures, vapour-liq. equilibrium, crit. locus curve, Soave eqn. 8-83913
 H₂S+O⁺, chemiluminesc. matrix reaction, diffusion controlled, 8-20K, O(³P) 8-61013

hydrogen compounds continued

- H₃S⁺+HCN⇌H₃CN⁺+H₂S, equilib., rate coeffs. and proton affinity, flowing afterglow 8-56885
 HSO, ground and first excited states, geometry, ab initio SCF calcs. 8-50657
 H₂SO₄ aerosol medium of Venus clouds, IR optical props. 8-65526
 H₂SO₄, aerosols characts. in Venus atm. from isophotes, spacecraft obs. 8-81575
 H₂SO₄, aerosols form., expt. and theory 8-96256
 H₂SO₄, air pollution, new detector, aerosol mobility chromatograph 8-96297
 H₂SO₄ and SO₃.H₂O, CNDO/2 calc. of thermal stability 8-76840
 H₂SO₄, dissociation and absorpt. consts., ultrahigh resolution obs. of 8.2, 11.3 μm bands 8-70825
 H₂SO₄, gaseous, IR absorpt. coeffs., partial press. variations 8-56922
 H₂SO₄ in S hemisphere stratospheric aerosol, impactor and in situ single-particle meas. 8-73437
 H₂SO₄, solns., static permittivity, kinetic depolarisation, time-domain spectroscopy 8-68440
 H₂SO₄-poly-1,4-phenylene terephthalamide, dilute soln., viscosity 8-75524
 H₂SO₄-water, homogeneous nucleation, relative humidity depend. 8-71846
 H₂SO₄+gallic acid+BrO₃⁻ system, uncatalysed oscillatory chemical reactions 8-61004
 H₂SeO₃, ¹H/²H quadrupole reson. freqs. detected by double reson. with level crossing 8-84497
 H₂SeO₃, ⁷⁷Se Fourier transform NMR 8-95528
 H₂SeO₄, NMR of ⁷⁷Se, chemical shift and screening tensors (*Russian*) 8-64285
 HSiCl₃, Raman and IR spectra, mol. motion 8-64353
 HSiN and HNSi, analytic functions from pot. energy surfaces 8-62743
 HSiN-HNSi isomers, MRD-CI calcs. of struct. and stability 8-82635
 H₃SiNCO, low freq. bending mode, pot. function 8-82728
 H₃SiNCS, far IR and Raman spectra, vibr. mode and quasilinear config. 8-62940
 H(UO₂P(AsO₄)₄)₄H₂O, H motion, PMR obs. 8-80239
 H₂WO₃, atom motion 8-75874
 H₂WO₃ film, effect of struct. on optical and electrical props. 8-84671
 HX+F, (X=I, Br, Cl), H abstraction, absolute reaction rate, H/D isotope effect 8-80721
 K_{1-x}Rb_xCl.HF₂⁻, dynamic inhomogeneous broadening of bands of local vibr. 8-92102
 MCN+Ar, CN quartet state production, fluoresc. anal. 8-68888
 Ne-HCl mixture breakdown obs. 8-67553
 O+HCl, vibr. excited, laser enhanced reaction rate, OH vibr. distrib. obs. 8-95912
 SOH, ground and first excited states, geometry, ab initio SCF calcs. 8-50657
 Si-H, amorphous, energy gap negative-U states, Si-H-Si three centre bond model 8-91606

hydrogen embrittlement

- cracking at notches, due to H embrittlement, model 8-84985
 fracture of materials, conf., Waterloo, Canada (June 1977) 8-56763
 lattice hardening due to dissolved H₂ in Fe, and ferritic steel 8-76656
 limiter materials, for Doublet III fusion research machine, selection 8-55026
 Petch-Stables theory, review of objections 8-60738
 plastic fracture processes, exam. of role in hydrogen embrittlement 8-60810
 steel, alloy, Cr-Mo, alloy SCM3, hydrogen embrittlement, delayed fracture, exam. (*Japanese*) 8-64620
 steel, alloy, Fe-Ni, effect of metallurgy on stress corrosion cracking, and hydrogen embrittlement 8-60885
 steel, alloy, Fe-Ni-Cr-Mo-V-C, HY130, effect of H₂ and impurities on brittle fracture, review 8-60765
 steel, alloy, Fe-Ni-Mn-Si-Cr-Ni-Mo, effect of metallurgy on stress corrosion cracking, and hydrogen embrittlement 8-60885
 steel, austenitic stainless, type 304, intergranular H₂ assisted fracture, exam. of mechanism 8-80644
 steel, C, diffusion of H₂, SCC via martensite form. cooling rate changes on Mn and Ni addition (*Russian*) 8-56813
 steel, C, hydrogen embrittlement, elastic interaction of H₂ with precipitates 8-92340
 steel, cracking due to H₂S, exam. of fracture surface by SEM (*Japanese*) 8-53024
 steel, delayed fracture, hydrogen and impurities 8-84988
 steel, high strength, alloy, initiation of cracks at delayed fracture, AE study 8-72868
 steel, high strength, weld cold cracking, anal. of fracture morphology, using SEM (*Japanese*) 8-52960
 steel, Mn, H₂ embrittlement mechanism (*Korean*) 8-68774
 steel, stainless, embrittlement by low energy ionic and atomic H particles 8-95809
 steel, stainless, type 304, exam. of H₂ induced cracking 8-76738
 steel, type 4340, effect of H₂ and impurities on brittle fracture, review 8-60765
 steel U8, hydrogenation effects on fatigue crack propag. (*Russian*) 8-56800
 Zircaloy-2, pressure tube, fragmentation on failure 8-72863
 Zircalloys, fractographic distinction between hydride cracking and stress corrosion cracking 8-92363
 Al alloy 7075-T6, embrittlement by cathodic H₂, surface film effect 8-64643
 Al-Mg (7 wt.%), corrosion cracking, exam. of slip dissolution and hydrogen embrittlement mechanisms 8-72852
 Fe alloys, review of hydrogen embrittlement mechanisms 8-72853
 Fe-Ni-C, martensitic, H₂ effect on fracture charact. (*Czech*) 8-60746
 Nb-H, behaviour of H in Nb, relation to mech. props. 8-80572
 Ni-B, hydrogen embrittlement, effect of B additions (*Japanese*) 8-84973
 U-Mo (10 wt.%), gaseous O₂ and hydrogen embrittlement, exam. 8-60811
 Zr and Zr alloys, cracking, H₂ induced delay, strain energy effect on H₂ solubility 8-92364
 ZrNb, pressure tube, fragmentation on failure 8-72863

hydrogen ion activity see pH**hydrogen ion concentration see pH****hydrogen ions**

- education, H₂⁺ bonding and virial theorem 8-49599

hydrogen ions continued

electron excitation of H and hydrogenic ions, cross-sections and rates 8-50649
 emission spectrum, last observable line, rel. to solar obs. through Earth atm. 8-77536
 $H^+ + Mg$ collisions double electron capture 8-58777
 isoelectronic series, excitation regimes, nucl. orientation due to hyperfine interaction 8-70928
 Lyman- α line wings, contribution of proton perturbers 8-67325
 magnetic interactions of electrons (*German*) 8-82610
 plasma, H lines, electron width and shift (*Russian*) 8-67421
 plasma, proton behaviour in JFT-2 Tokamak, charged-exchanged fast ion anal. 8-51341
 plasmopause location and H^+ density decreases, correl. 8-81500
 polarimeter designs for high energy p and d beams, polarised beam spin anal. 8-58516
 polarised ion sources and low energy collector rings, H^- , D^- beams 8-58515
 Seyfert galaxies, broad H lines prod. by suprathermal protons passing through neutral gas (*Russian*) 8-57642
 solar chromosphere, H^- radiation and acoustic dissipation 8-96454
 solar wind H^+ , implantation in interplanetary dust grains rel. to upper atmosphere H chemistry 8-65445
 solid surfaces, reflection of slow H^+ and He^+ ions 8-76572
 E United States precipitation, H^+ ions concs. behaviour 8-92962
 $Ar + H^-$, collisional electron detachment, complete ang. distrib. 8-66650
 $CH_4 + H^+(He^+)(O^+)$, 1 MeV dissociation, kinetic energy spectra 8-94302
 $F + Xe(H)(H_2)$, ($^2P_{3/2}$) state quenching, Franck-Condon approach 8-66640
 H^- and H electron loss in plasma target 8-67371
 H^- , autoionising states, electric field effect 8-50528
 H^- , dipole oscillator strength sum, in He isoelectronic series calcs. 8-86821
 H^- , electron detachment by electron impact, 1s state product, Born approx. 8-78816
 H^- , fluoresc. in γ - and UV-irrad. solvent matrices at 77K 8-70779
 H^- , grazing incidence collision with surface, Balmer radiation, elliptical polarisation 8-86804
 H^- , ground state energy, post-adiabatic approx. calcs. 8-58827
 H^- ion yield from duoplasmatron discharge 8-75382
 H^- , polarised prod. in $H^+ + Cs$ atomic collision at 40 keV, 2.9 μA 8-55078
 H^- , production by Hall accelerator in Cs vapour, space-charge effects 8-67375
 H^- , S autoionising states, time stability theory 8-90130
 H^- , surface plasma source, ion form. and secondary electrons (*Russian*) 8-71503
 H^- vac. UV spectra, narrow reson. at 1129.5 Å, H-arc spectra 8-66490
 H^+ beam, pure, production by four-lens Hall accelerator, focusing 8-66441
 H^+ , calc. of mobility in He, 10 to 700K 8-66629
 H^+ , electron capture from Si foil, cross-section calcs. 8-95623
 H^+ , grazing incidence collision with surface, Balmer radiation, elliptical polarisation 8-86804
 H^+ , impact on Al(Cu)(Mo)(stainless steel) surface, energy refl. coeffs. 8-54969
 H^+ , ion-surface collision with Mo, optical radiation emission 8-95644
 H^+ , removal, using Itaya-zeolite (*Japanese*) 8-95951
 H-like atom or ion, electron-electron interaction operator, dipole approx. 8-58821
 H-like ions, electron impact excitation to S states exchange effects 8-58835
 H-like ions, electron impact excitation to s state 8-58836
 H-like ions, electron impact excitation, Coulomb Born approx. 8-58840
 H-like ions, electron impact ionis. from 3s sub-level 8-90297
 H-like ions, fluoresc. polarisation of Stark quenched spin-polarised beam 8-66501
 H-like ions, Glauber exchange amplitudes for electron scatt. 8-74772
 H-like ions, spectral line intensity, density depend., plasma diagnostic appls. 8-83617
 H-like multiply charged ion, superdense plasmas, line intensity ratio 8-63538
 H^- -like ions, electron correlation and Coulomb hole in momentum space 8-86793
 $H + H^+$, excitation ang. differential cross section, 25, 50 and 100 keV incident 8-66651
 $H + H^+$, electron capture, continuum distorted wave calcs. 8-50635
 $H + H(He)$, electron detachment cross sections 8-90265
 $H + He(Ar)$, electron detachment cross sections 8-58810
 $H + M^+$ ($M = \text{alkali metal atom}$), ion-ion recombination 8-58779
 $H + \text{methane} \rightarrow \text{methane} + H^-$, nucleophilic substitution, ab initio pot. energy classical trajectory anal. 8-68886
 $H^+ + Ag$, L-shell ionisation at large scatt. angles 8-90283
 $H^+ + Ag(Cu)$, X-ray emission, optical transition radn. 8-58618
 $H^+ + Ag(Gd)(Yb)(Ta)(Au)(Pb)(Th)$, K-shell ionisation, 7-15 MeV, relativistic effects 8-82830
 H^+ atom, electron capture, two-state atomic expansion 8-62912
 $H^+ + C$, K-shell ionisation, impact parameter depend. 8-62891
 $H^+ + C$ foil, 0.5-2.5 MeV, forward electron vel. distrib., peak shape 8-78794
 $H^+ + CN$, perturbed rotational state approach 8-92469
 $H^+ + C(N)(O)(Ne)(Ar)$, electron capture cross sections 8-62912
 $H^+ + Cs$, elastic and charge exchange collisions, projected valence bond method 8-78804
 $H^+ + Cs(6s)$, elastic scatt., pot. determ. from differential cross-sections meas. 8-78778
 $H^+ + D_2$, differential inelastic and reactive scatt., low energies 8-62911
 $H^+ + D \rightarrow H + D^+$ near threshold rel. to HD molecule formation in interstellar medium 8-89239
 $H^+ + H$, charge transfer cross section calc., up to 100 keV 8-55235
 $H^+ + H_2$, ZZ 8-80729
 $H^+ + H_2(O)$, inelastic scatt., 4-6 eV energy loss region 8-90277
 $H^+ + H(D)$, elastic scatt. and charge exchange, resonances 8-78777
 $H^+ + H(O)$, in upper atm., rel. to H^+ loss during solar cycle 8-93021
 $H^+ + H(1s)$, radiative charge exchange, 1-50 MeV 8-55234
 $H^+ + He$, determ. of He excited state populations by two-photon reson. ionisation spectroscopy 8-82707

hydrogen ions continued

$H^+ + He$, excitation, ang. differential cross-sections for 25, 50 and 100 keV protons 8-82832
 $H^+ + He^+$, charge transfer and ionis. cross sections, coincidence meas. 8-50634
 $H^+ + He(Ar)$ electron transfer cross sections 8-58809
 H^+ inert gas, 4s-state electron capture cross-section meas. 8-82836
 $H^+ + Mg$, inner-shell ionisation by H^+ , He^+ impact, target atom ionic alignment, Born approx. 8-78789
 H^+ multi-electron atom, fast collision, electron capture, differential cross section calcs. 8-94318
 $H^+ + N_2$ collision, binary encounter calcs. of proton energy deposition 8-74746
 $H^+ + N_2^+$, fluoresc. efficiency, 3914 Å band of N_2^+ (1N), 100 eV-10 MeV 8-74697
 $H^+ + Na(K)$, excited state form. by inelastic processes, energy partitioning 8-82833
 $H^+ + Na(Mg)(Al)(Si)(Ti)$, K-shell ionisation cross sections for 15-65 keV protons 8-90284
 $H^+ + O_2$, energy transfer, vibronic excitation, emission spectra 8-66578
 $H^+ + Rb$, single photon emission following double K-shell ionisation, contrib. to superheavy element search data 8-50625
 H_2^- , collision induced dissociation, positive and negative ions form. 8-50612
 H_2^- , free free absorpt. rel. to opacity in stellar atms. 8-81610
 H_2^- , dissociation following beam-foil interaction 8-70920
 H_2^+ , dynamic dipole polarisability, variational perturbation theory 8-94330
 H_2^+ , dynamic polarisability, electronic states two centre Coulombic Green's function, continuous spectrum exclusion 8-82626
 H_2^+ , electron scatt. eqns. convergence, H_2 continuum states, appl. to photoionis. 8-66663
 H_2^+ , energy spectrum, variational cellular method calcs. 8-94192
 H_2^+ , grazing incidence collision with surface, Balmer radiation, elliptical polarisation 8-86804
 H_2^+ , impact on Al(Cu)(Mo)(stainless steel) surface, energy refl. coeffs. 8-54969
 H_2^+ , in mag. field, LCAO calcs. 8-82628
 H_2^+ , ion-surface collision with Mo, optical radiation emission 8-95644
 H_2^+ , moment functions calcs. and radiative corrections 8-90141
 H_2^+ , nonadiabatic vibrational energies, ab initio calcs. 8-90142
 H_2^+ , repulsive states in dissociative ionis. of H_2 at 304 Å 8-82792
 $H_2 + He$, 200-850 eV, attenuation and fragmentation 8-62968
 $H_2 + H^+$, combined rot. sudden and vibr. exact quantum treatment 8-74739
 $H_2 + H^+$, electron capture probability 8-58808
 $H_2 + H^+$ differential inelastic and reactive scatt., low energies 8-62911
 $H_2 + 1,3$ -butadienes, singlet-triplet transitions energies, relative cross sections 8-86942
 $H_2 + Ar(He)(H_2)$, 10 keV dissociation charge exchange collisions 8-94319
 $H_2 + C$ foil, 0.5-2.5 MeV, forward electron vel. distrib., peak shape 8-78794
 $H_2 + CO$, dissociation, charge transfer, energy transfer processes 8-74759
 $H_2 + H_2O$, inelastic scatt., 4-6 eV energy loss region 8-90277
 $H_2 + He$, collision in laser field, vibr. excitation 8-86937
 $H_2 + He$, reactive and dissociative scatt., crossed-beam and trajectory obs. 8-64833
 H_2^- , collision induced dissociation, positive and negative ions form. 8-50612
 H_2^+ , dipole polarisabilities, variational perturbation theory calcs. 8-70765
 H_2^+ , dissociation following beam-foil interaction 8-70920
 H^+ expt. determ. struct., foil-induced dissociation fast mol-ion beam 8-74752
 H_2^+ , grazing incidence collision with surface, Balmer radiation, elliptical polarisation 8-86804
 H_2^+ , ion-surface collision with Mo, optical radiation emission 8-95644
 H_2^+ , uncoupled symmetric stretching freq. calcs. 8-66532
 $H_2^+ + Ar(H_2)(air)$, dissociation, 400-800 keV, product charge state distrib. model 8-82838
 H_4^+ , ground and excited state pot. energy surfaces and geom. struct., SCF and CI calcs. 8-78769
 H^+ ($n=3,5,7,9,11$), stability, struct., ab initio MO calcs. 8-74810
 $H^+ + e$, electron-ion dissociation recomb., rate const., electron beam sustained discharge 8-50652
 HD^- , collision induced dissociation, positive and negative ions form. 8-50612
 HD^+ , ground state vibr.-rot. spectrum, high resolution laser-ion beam reson. expt. 8-82733
 HD^+ , nonadiabatic vibrational energies, ab initio calcs. 8-90142
 HD^+ , spontaneous IR rot.-vibr. emission probability 8-50535
 $HD^+ + He$ collisions, rotational transitions 8-70909
 HD_2^- , collision induced dissociation, positive and negative ions form. 8-50612
 $H_2^+(HD^+)$, expectation values, Born-Oppenheimer, adiabatic and non-adiabatic results 8-82624
 $H_2O + H^+ \rightleftharpoons H_3O^+$, equilib., H_2O proton affinity calc. 8-92497
 $H(1s) + p \rightarrow p + H(1s)$, 15-200 keV, ang. distrib., differential cross sections calc. 8-82839
 $He + H^+(H_2^+)(H_3^+)(He^+)$ collisions, polarisation degree of prominent He lines 8-70916
 $Mg + H^+(He^+)$ and electron impact ionis., Auger study of collisionally induced alignment 8-90279
 $N + H_2^+$, triplet state ab initio CI pot. energy surfaces 8-74729
 $N_2 + H^+$, spatial distrib. of excited moles. induced by 100 and 150 keV proton beams 8-58793
 $Xe + H^+$, M-subshell ionisation cross section, binary encounter approx. 8-62890

hydrogen neutral atoms

$3P_{3/2} - 3D_{3/2}$ Lamb shift, double quantum saturation spectrosc. obs. 8-94223
 absorption in B2 1506+34, peculiar radiogalaxy, 21 cm line obs. 8-54048
 adsorption, on Cu, potential energy curves, pairwise, additive model calcs. 8-73087
 adsorption, on MgO , ($\alpha-Al_2O_3$), ($\alpha-SiO_2$), microweighing and X-ray obs. (*German*) 8-51825
 antiprotonic H atoms, first obs. of L X-rays 8-90111
 atomic electron impact excitation, 2s state, differential cross section 8-86953

hydrogen neutral atoms continued

atomic spectral line shifts for heavy quark atoms 8-62965
 Balmer α line fine struct., Stark effect (*German*) 8-82673
 beam, $2^3S_{1/2}$ metastable at., nonadiabatic transition in mag. field 8-55157
 coherent excitation of $n=3$ level by electron impact, density matrix anal. 8-78817
 detection by resonant three photon ionisation 8-74624
 dipole transitions, asymptotic expansion of radial-dipole integral 8-82667
 dynamic multipole polarisability, functional calcs. 8-74595
 eigenvalue resonances in Stark effect and perturbation theory 8-90118
 elastic electron scattering, static exchange amplitude, dispersion rels. 8-66664
 electron and positron scattering, elastic, 100 and 500 eV, second-order eikonal approx. 8-78814
 electron elastic scatt., differential cross sections calc. 8-90293
 electron elastic scatt., logarithmic ang. depend. for excited ats. 8-50638
 electron impact excitation, Born and classical cross-sections (*German*) 8-86952
 electron impact excitation, simplified model, low and medium energy 8-86954
 electron impact ionisation, electron-photon coincidence meas. 8-55242
 electron inelastic scatt., dynamic polaris. pot. 8-78818
 electron inelastic scatt., effective exchange potentials 8-90300
 electron scatt., forward elastic exchange amplitudes and forward dispersion relations, anal. props. 8-78812
 electron scatt. in presence of a laser field, theory 8-74767
 electron-photon excitation, high-energy resonant cross sections 8-70938
 energy levels, influence of the expanding universe 8-54271
 energy levels in strong mag. field 8-90071
 energy spectrum in expanding Robertson-Walker universe 8-73869
 excited state interaction with photon field, simultaneous eqns. 8-66481
 excited states, in elec. field, semi-classical approx. (*Russian*) 8-86797
 exosphere, H global density distrib. vars., escape fluxes 8-93023
 exosphere, H latitude vars., rel. to polar wind, heating and charge exchange processes 8-93024
 exponential decay law for $2P_{1/2} \rightarrow 1S_{1/2}$ transition 8-78649
 formaldehyde, UV photolytic separation of D from H in cryogenic solns. 8-95937
 galaxies active nuclei, H emission-line spectra 8-96557
 gas, two-photon absorpt. of ultrashort pulses, reson. intensities 8-59077
 gas discharge H atomic source for electron scatt. expts. 8-94332
 generator, freq. shift due to atomic collisions with storage flask walls 8-77870
 ground state props., polynomial perturbation problem 8-73878
 highly excited resonant states, Stark effect, nonperturbative regime 8-70786
 hyperfine frequency meas. of ground state 8-78984
 imaginary frequency multipole polarisability and long-range dispersion consts, functional calcs. 8-74596
 inelastic exchange kernels, semiclassical exchange approximation theory 8-50642
 interstellar gas, dust and molecules, review 8-54006
 interstellar H I survey from Lyman α absorption meas. towards 100 stars 8-93357
 ionisation by laser radiation, as polarised proton source 8-78541
 isoelectronic series 8-78820
 isotope composition of plutonic granitic rocks 8-65221
 $La/H\alpha$ ratio for solar flares, quasars and prominences 8-61826
 Ly α radiation reson. scatt. as a neutral density diagnostic for fusion plasmas 8-83612
 Lyman α 1216 Å solar line, temporal var. 8-93186
 Lyman α and β , interplanetary Voyager UV spectrometer obs. 8-81673
 molecular internal stresses, stress tensor, one electron system 8-62686
 multipole moments, elec. field-induced, polarisability density concept limitations 8-70964
 multipole polarisability, dynamic, for S state, closed-form expression 8-82857
 multipole polarisability and shielding factors, hydrodynamic analogy to quantum mech. 8-66677
 oscillator strength, sums, one-term approx. 8-66509
 oscillator strengths, 2s-3p transition, Glauber approx. 8-74613
 positron elastic scattering, low-energy S-wave phase shifts calcs. 8-78813
 proton spreading in strong mag. field 8-70769
 pseudospectral dipole oscillator strength distrib. 8-50503
 quantum static multipole polarisabilities 8-82859
 quasars, H emission-line spectra 8-96557
 radiative magnetic energy shift, H in 2p state 8-58601
 relativistic, in superstrong mag. fields 8-90095
 relativistic Dirac equation, for teachers 8-62019
 relativistic model of spin 1/2 particles interacting with external EM field 8-70756
 relativistic spin 1/2 particle dynamics 8-70001
 self-interaction of excited at. with radiation field 8-86794
 solar chromosphere, H α seven components rel. to 9873 MHz line appearance 8-89151
 spin aligned, condensed on surfaces 8-63929
 spin flipping, quantum mech. eqns. of change 8-70003
 Stark effect, asymptotic expansion for level width 8-70783
 Stark shift, classical adiabatic theory of Stark ionis. threshold 8-82687
 strongly magnetised, quantum number assignments, semi-classical approach 8-90055
 terrestrial H escape flux, charge exchange induced, diurnal and solar cycle vars. 8-93022
 toroidal plasma, 2-D neutral H transport 8-59661
 two-photon transition matrix elements, group theory calc. 8-62776
 Venus thermosphere, H global circulation and distrib. 8-89093
 H (2s) metastable state elastic electron scatt. 8-55238
 H isotope exchange between clay minerals and seawater 8-69329
 H⁻ and H electron loss in plasma target 8-67371
 H-He, H hyperfine struct. shift, commutator computational method 8-78608
 H-like atom or ion, electron-electron interaction operator, dipole approx. 8-58821

hydrogen neutral atoms continued

H-like atom+bare ion, electron capture to continuum, cross-section cusp 8-90289
 H-like atoms, quadrupole moments 8-90072
 H-like atoms, relativistic acceleration, quasi-Stark effect (*German*) 8-58621
 H⁺He²⁺, electron capture at impact energies below 10 keV 8-50633
 H+Br₂(Cl₂), nonreactive scatt., long range anisotropic pot. determ. 8-66626
 H+Br₂→HBr+Br, pot. energy surface, ab initio generalised valence bond calc. 8-73026
 H+Cl₂, impulsive triatomic reaction, vibr. state distrib., impulsive energy release model 8-92456
 H+Cl₂(H₂), activation energy and trajectory calcs., temp. and isotope effects 8-76835
 H+Cl₂(SOCl₂)(S₂Cl₂)(SOCl₂)(SO₂Cl₂), energy disposal, HCl IR chemiluminesc. obs. 8-92484
 H+F₂, impulsive triatomic reaction, vibr. state distrib., impulsive energy release model 8-92456
 H+F₂, vibr. prod. distrib., Einstein coeffs. 8-92448
 H+F₂(Cl₂), exothermic triatomic exchange reactions, prod. energy distrib., statistical dynamic model 8-92455
 H+H, pair polarisabilities, continuum electrostatic theory 8-86769
 H+H₂, CI calc. of three dimens. pot. energy surface 8-56882
 H+H₂, collinear, quantum mech. reactive scatt., exchange kernels calcs. 8-68880
 H+H₂, elastic differential cross section high resolution meas. 8-50610
 H+H₂, finite element methods for reactive scattering 8-92453
 H+H₂, least squares fit to ab initio pot. energy function 8-56883
 H+H₂, reactive scatt., sudden approx. calcs. 8-68878
 H+H₂, transition states, trapped trajectories and classical bound states in continuum 8-88630
 H+H₂($v=1$)→H₂+H, exchange reaction, classical trajectory method, vibr. excitation, partial rate consts. 8-60993
 H+H₂→H₂+H, IR laser induced reaction 8-80761
 H+H₂→H+H+H, two path dissociation 8-62875
 H+H⁺, excitation ang. differential cross section, 25, 50 and 100 keV incident 8-66651
 H+HF, kinetic isotope effect and temp. depend. 8-53202
 H+H(H₂), atom-atom pots., Hilbert Schmidt expansion, transition operators 8-66621
 H+He⁺, unpolarised and spin-change collision, low energy 8-86943
 H+He(N₂), stripping cross-section, 0.3 to 3 keV 8-78807
 H+He(Ne)(Ar)(Kr)(Xe), low energy elastic scatt. cross section MCSCF calc., van der Waals forces 8-70897
 H+heavy charged ion, total electron capture cross section charge depend. oscill. behaviour 8-66656
 H+heavy ion (highly stripped), electron loss, charge state depend. 8-70921
 H+Li⁺(Co⁺)(Au⁺), cross-section, closure-Born approx. 8-66630
 H+Li(Li₂), superthermal collisions, photon and positive ion prod. 8-78788
 H+methane, H abstraction, rate consts. calcs. 8-95921
 H+N, stripping cross-sections, binary encounter approx. theory 8-50618
 H+N₂O→N₂+OH, rate const., 2000-2850K, combustion of H₂/N₂O/CO/Ar 8-85162
 H+N₂(O₂), charge prod. cross sections and differential scatt. calcs. 8-94313
 H+N^{q+}(O^{q+})(C^{q+}), q=1-5, single electron capture cross sections 8-55233
 H+NH₃→NH₃ react., force, density anal. 8-60997
 H+Na(K), covalent and ionic states interaction, config. mixing 8-50613
 H+O₂, singlet state O₂ form., reaction mechanism, mass spectrometric obs. 8-53204
 H+O₂→OH+O, combustion, quasiclassical trajectory calcs. 8-53201
 H+O₃, absolute reaction rate const., 219-360K 8-80734
 H+O⁺, in upper atm., rel. to H⁺ loss during solar cycle 8-93021
 H+Pb(³P₁), spin-orbit relax., fluoresc. intensity meas. 8-82681
 H+positron, charge exchange, excited positronium states form. 8-58873
 H⁺+H(He), electron detachment cross sections 8-90265
 H⁺+H, charge transfer cross section calc., up to 100 keV 8-55235
 H⁺+H(D), elastic scatt. and charge exchange, resonances 8-78777
 H⁺+H(1s), radiative charge exchange, 1-50 MeV 8-55234
 H₂-H mixture positive column, static electric charact. 8-67500
 H₂+NH₃, rot. relax., double and triple reson. obs. 8-90196
 H α line shape, plasma broadened, fine struct. effects at low electron densities 8-62765
 H(D), ground state Lamb shift, isotope shift and relativistic nuclear recoil correction 8-82696
 H₂(HD)+He potential, asymmetric, isotope substitution effect, Legendre expansion coord. transformation 8-70894
 H(1s), electron impact, elastic phase shift, post-adiabatic approx. calcs. 8-58827
 H(1s)-H(1s)(³ Σ_u^+) isotropic intermol. force, model for approx. method, crit. test 8-78771
 H(1s)+p→p+H(1s), 15-200 keV, ang. distrib., differential cross sections calc. 8-82839
 He+H (inert gas atom), long range interactions for (2¹S) and (2³S) states 8-70895
²⁸Si+H(H₂), single electron capture cross sections 8-58812

hydrogen neutral molecules

3d complex, radiative lifetimes, hyperfine constants 8-70873
 Λ doubling, C¹ Π_u states, calc. methods 8-90227
 adsorption, on MgO, (Al₂O₃), (α -SiO₂), microweighing and X-ray obs. (*German*) 8-51825
 adsorption on W(100), effect on NVV Auger spectra, comp. to band struct. calcs. 8-72643
 atmosphere H₂, production from oxidation of vegetation hydrocarbon emissions 8-88881
 binding type change, and dissociation for H₂-like mols. in strong mag. field 8-62744
 coherent anti-Stokes Raman scatt. integrated power, press. depend. 8-59081
 collisional excitation of interstellar molecules 8-77586
 concentration in primitive prebiological atmosphere 8-73514
 coupled states approximation for scattering of two diatoms 8-62872

hydrogen neutral molecules continued

- dissociation, on Cu surface, effect of surface roughness, classical trajectory calcs. 8-76925
 dissociation, weak bias and anharmonicity effects 8-82661
 dissociative chemisorption on Fe(Ni) (*German*) 8-53257
 dissociative electron attachment, Faddeev calcs. of cross sections (*Russian*) 8-70945
 electron elastic scatt., free-electron-gas model exchange pot. 8-58824
 electron elastic scatt., modified Glauber theory 8-94320
 electron impact excitation and dissoc., close-coupling method appl. 8-74778
 electron impact spectroscopy for Compton profile meas. 8-90299
 electron scatt., ab initio theory, elastic scatt. and rot. excitation 8-50640
 electron scatt., elastic, incident-energies, 100-2000 eV calcs. 8-55237
 electronic and vibrational structure, theoretical developments 8-62707
 expectation values, Born-Oppenheimer, adiabatic and non-adiabatic results 8-82624
 formaldehyde+He(H₂), collisional relax. times and lineshape distortion, Stark absorpt. linewidth obs. 8-74744
 gas phase transverse NMR low density spectrum 8-74681
 interstellar, form., catalytic prod. on transition metal grains 8-57616
 interstellar dark clouds, CO/H₂ ratio meas. 8-96513
 interstellar H₂, form. by catalysis process 8-54005
 interstellar H₂, vibrationally excited, search for 8150 Å emission line 8-93346
 liquid n-H₂, n-D₂, Ne mixtures, deviation from Rao-Wada rule 8-75729
 magnetic interactions of electrons (*German*) 8-82610
 metastable state, Doppler-free linear single-photon spectroscopy 8-50487
 molecule, electron impact ionis., differential cross sections 8-58839
 naphthalene anion radical+H₂O, react., H₂ prod. 8-92460
 orbital calculation, using mag. field depend. orbitals, mag. shielding and mag. susceptibility 8-78611
 oriented molecules, vibrationally inelastic electron scatt. 8-67907
 ortho, high rot. states, inter- and intramol. effects, mol. beam mag. reson. obs. 8-70852
 ortho-para conversion, equilibration, appl. in vapour press. thermometry 8-62198
 ortho-para conversion on paramagnetic crystal impurity, mag. field effects, theory 8-61050
 ortho-para ratio in dense interstellar clouds, protoplanets and planetary atmospheres 8-89233
 photoionisation, body-frame Hund's case b description 8-94295
 photoionisation, dissociative, at 304 Å, photoion ang. distrib. photoelectron channels 8-82792
 polarisability, generalised London formula for dispersion coeff. 8-82662
 polarisability anisotropy derivative determ. from relative Raman intensities 8-55177
 positron scatt., rot. excitation 8-50653
 precession magnetic shielding of proton, semiempirical functions 8-82654
 pseudospectral dipole oscillator strength distrib. 8-50503
 quadrupole lines detect. in spectrum of Uranus 8-93149
 quadrupole mass filter sensitivities and β -particle induced exchange kinetics 8-58090
 quadrupole moment, adiabatic approx. calcs. 8-62742
 radiation induced exchange reaction kinetics of H₂, D₂ and T₂, review 8-61005
 Raman spectra, appl. of high resolution CW stimulated Raman technique 8-70973
 Raman spectra, vibr. freq. press. shifts 8-78703
 S₀(3) pure rot. quadrupole transition, obs. using tunable diode laser 8-82723
 singlet-triplet anticrossings, doubly excited 3¹K-g(3d)³Σ_g⁺ states 8-50598
 spectral line shapes, for radiative light scatt. in gas 8-90221
 synchrotron radiation scattering cross sections 8-55213
 T Tauri stars, H₂ emission obs. 8-93230
 thermal dissociation at heated filament at low press. 8-85156
 X²Σ_g⁺ state, vibr. energy levels, radiative corrections calcs. 8-90094
 X-ray scatt., total, two-electron density functions 8-70889
 Zeeman effect in 3d singlet states, g-values 8-50571
 Ar laminar plasma jet, H₂ diffusion obs. 8-71557
 Ar⁺+H₂(v=0)→ArH⁺+H, electronic nonadiabatic transitions, two-state model calc. 8-73035
 BrCl₃+H₂ laser induced chemistry, theory 8-76884
 Br+H₂ laser field interacting with collision dynamics, model system 8-62876
 CO⁺+H₂, ion-molecule reaction detection of laser-induced ion spectrum, rot. components 8-74671
 Cs+H₂, rot. excitation, infinite order sudden approx. 8-74740
 F+H₂→HF+H energy profile, minimal basis ab initio VB calcs. 8-50477
 F+Xe(H⁺(H₂), (²P_{3/2}) state quenching, Franck-Condon approach 8-66640
 H+H₂, CI calc. of three dims. pot. energy surface 8-56882
 H+H₂, elastic differential cross section high resolution meas. 8-50610
 H+H₂, finite element methods for reactive scattering 8-92453
 H+H₂, least squares fit to ab initio pot. energy function 8-56883
 H+H₂(v=1)→H₂+H, exchange reaction, classical trajectory method, vibr. excitation, partial rate consts. 8-60993
 H₂, ¹π_u and ³π_u states, singlet-triplet energy difference, Hund's rule, inequality formulation 8-66482
 H₂, (4,0) S(1) quadrupole line intensity and pressure shift 8-90178
 H₂, isotope exchange reactions, equil. consts., adiabatic correction, electron correl. effects 8-88626
 H₂, metastable c³Π_u state, population densities and quenching times meas. 8-94296
 H₂ mol., Green's function Σ perturbation method for mol. calcs. 8-55123
 H₂-BCl₃, photochem. with Ti, Pb catalysts, isotopic excitation by laser 8-64882
 H₂-H mixture positive column, static electric charact. 8-67500
 H₂-H₂S, solubility of S in Pd, 600-1000°C, gas mixture composition depend. (*French*) 8-87791
 H₂-³⁸Cl, reactions, characterisation, effect of ethylene-I₂ scavenger 8-73071

hydrogen neutral molecules continued

- H₂+³He²⁺, electron capture at impact energies below 10 keV 8-50633
 H₂+Ar, vibr. energy transfer rate, ab initio calcs. 8-82821
 H₂+Ar⁺, charge transfer reactions, excited products, Ar initially metastable 8-68879
 H₂+C⁺, charge transfer cross-sections, 0.7-2.4 keV, C⁺(²P) and C⁺(⁴P) 8-58806
 H₂+C⁺→CH⁺+H, classical trajectory anal. 8-53192
 H₂+D₂, exchange reaction, steady-state, surface reaction effects (*French*) 8-85148
 H₂+D₂, exchange reaction, gas phase, heterogeneous initiation (*French*) 8-85149
 H₂+D₂, reactive and inelastic scatt. using repulsive model pot. energy surface 8-66620
 H₂+D₂→2HD, transition state, study of Jahn-Teller instability of H₄ 8-60995
 H₂+F, collinear quasiclassical trajectory study 8-80718
 H₂+F(H⁺), ZZ 8-80729
 H₂+F→FH+H, collinear probability, quantum calc. using pot. energy surface 8-64829
 H₂+F→FH+H, vibr.-rot. energy distrib. of HF, DWBA calc. 8-80722
 H₂+Fe(001), gas-surface reactions, semiempirical generalised LEPS pot. 8-68923
 H₂+H, atom-atom pots., Hilbert Schmidt expansion, transition operators 8-66621
 H₂+H, collinear, quantum mech. reactive scatt., exchange kernels calcs. 8-68880
 H₂+H, reactive scatt., sudden approx. calcs. 8-68878
 H₂+H₂⁺, 10 keV dissoc. charge exchange collisions 8-94319
 H₂+H₂⁺, dissoc., 400-800 keV, product charge state distrib. model 8-82838
 H₂+H⁺, combined rot. sudden and vibr. exact quantum treatment 8-74739
 H₂+H⁺, electron capture probability 8-58808
 H₂+H⁺ differential inelastic and reactive scatt., low energies 8-62911
 H₂+H(F), transition states, trapped trajectories and classical bound states in continuum 8-88630
 H₂+H(I), activation energy and trajectory calcs., temp. and isotope effects 8-76835
 H₂+H→H+H₂, IR laser induced reaction 8-80761
 H₂+H→H+H+H, two path dissoc. 8-62875
 H₂+He, collision dynamics, generalised Langevin eqn. approach 8-70900
 H₂+He, vibr. deexcitation, cross sections, rate consts., vibr. rot. model 8-62879
 H₂+He, vibr.-rot. transition, optical potential approach 8-62885
 H₂+He⁺, charge transfer at 1.5 and 3 keV, He(²P) excitation 8-66658
 H₂+He²⁺, electron capture collisions, spin conservation 8-82837
 H₂+He(Ne), Van der Waals pot., ab initio SCF model 8-74728
 H₂+inert gas, cross section meas. with state selected beams 8-62910
 H₂+Kr, elastic total cross section, orbiting effects, Regge theory 8-82814
 H₂+Li⁺(Co⁺)(Au⁺), cross-section, closure-Born approx. 8-66630
 H₂+methylene*→CH₃+H, barrier height, CI with double zeta polarisation basis 8-64812
 H₂+methylene→CH₃+H, triplet methylene abstraction, partial open shell FSGO calc. 8-80719
 H₂+N³⁺(O^{q+})(C^{q+}), q=1-5, single electron capture cross sections 8-55233
 H₂+NH₃, rot. relax. double and triple reson. obs. 8-66570
 H₂+O⁺(⁴S)(²D), charge transfer reactions, cross-sections meas. 8-92462
 H₃, CI calc. of three dims. pot. energy surface 8-56882
 H₃, three atom ab initio energy surface calc. 8-82663
 HD, detect. in Saturn and Uranus atms., D/H abundance ratio calc. 8-57495
 HD, dissociative electron attachment, Faddeev calcs. of cross sections (*Russian*) 8-70945
 HD, ground state props., nonadiabatic var. calcs. 8-58576
 HD, isotope exchange reactions, equil. consts., adiabatic correction, electron correl. effects 8-88626
 HD molecules, rate coeff. for H⁺+D→H+D⁺ near threshold 8-89239
 HD search at 6045 Å, D/H ratio upper limits for Jupiter and Saturn 8-85892
 HD+F→HF+D(DF+H), branching ratios, information theory test by classical trajectory calcs. 8-64822
 HD+He, thermal energy scatt., distorted-wave and close coupling calcs. 8-86938
 H₂O maser line evidence for circumstellar ring systems in supergiant stars 8-89195
 H₂O⁺+H₂, ion-molecule reaction detection of laser-induced ion spectrum, rot. components 8-74671
 He+H₂, collision-induced dipole, ab initio VB calc. 8-94202
 He+H₂, final quantum state assignment, improved quasiclassical histogram method 8-66617
 He+H₂(He)(Ar)(N₂), fast metastable at. collisional destruction cross section 8-74660
 He²⁺+H₂→He⁺H⁺+H⁺, two-electron capture 8-58811
 N⁺+H₂, triplet state ab initio CI pot. energy surfaces 8-74729
 N₂+H₂, (A³Σ_u⁺, v=0,1) metastable state quenching rate coeffs. 8-90206
 N₂⁺+O₂(H₂)(He), (A²Π_u) Meinel band deactivation cross sections above thermal energies 8-66635
 OCS+H₂, rot. excitation, infinite order sudden approx. 8-74740
 S+inert gas (N₂)(H₂), rare gas sulphide S(¹S) emissions 8-82828
 SF₆-H₂ mixture photolysis, S atom nucleation particulate formation 8-76836
²⁸Si+H(H₂), single electron capture cross sections 8-58812
 T+HT→TH+T, collinear reactivity bands 8-85143
hydromagnetic waves see magnetohydrodynamic waves
hydromagnetics see magnetohydrodynamics
hydrometers
 see also density measurement
 crude-oil hydrometers calibration 8-73969
hydrophones
 see also sonar
 array response calc. errors due to two dimensional beam pattern assumption 8-66972

hydrophones continued
bottom reverberations picked up by hydroacoustic dipoles, spatial correlation functions (*Russian*) 8-53659
C-mode US imaging by electronically scanned coaxial circular spherical receiving array 8-59222
calibration using complex exponential signal representation 8-79183
Lorentz force hydrophone for low MHz frequencies 8-59243
parametric acoustic receiving array vibration sensitivity anal. 8-66971
passive bearing estimation in unequal S/N ratio, optimum element placement 8-87210
piezoelectric polymer flexural disk hydrophone 8-63254
undersea acoustic holographic transducer array development 8-59209
underwater sound arrival angle estimation by multiple cross-correlation meas. 8-66978

hydrophotometers *see* photometers

hydrostatics
nematic nonpolar liquid crystals, hydrostatics, universal soln. 8-83722

hydrothermal crystal growth *see* crystal growth from solution

hydroxonium ion
 $H^+(H_2O)_3$, $H^+(H_2O)_4$, $H^+(H_2O)_5$ in stratosphere, abundance meas. 8-88877
 $H_3O^+(H_2O)_n$, electron recomb., electron temp. depend. 8-82854
 $H_2O \cdot 2H_2O$, in 2,5-dichlorobenzenesulphonic acid trihydrate, neutron diff. obs. 8-58855

hydroxyl group *see* oxygen compounds

hygiene
see also medicine
No entries

hygrometers
see also humidity measurement
elongation hygrometer, relative performance of squid skin, egg-shell membrane, bamboo film as hygroscopic body (*Japanese*) 8-57968
IR fluctuation hygrometer, design, calibration, field trial results 8-77368
Meteorological Office Mk3, frost point meas. systematic error 8-73538
UV fluorescence hygrometer, stratospheric M_2O vapour meas. (*French*) 8-65401

hyperfine field interactions (condensed matter)
see also crystal hyperfine field interactions; nuclear screening
ferromagnet, amorphous and crystalline, evaluation of complex Mossbauer spectra 8-60370
glass: Mn^{2+} , EPR, low-field hyperfine struct. 8-95513
 As_2Se_3 , and As_4Se_3 -Ge glasses, struct. changes, Mn^{2+} EPR expts. 8-79534
 As_2Te_3 -Ge(Si) glass, struct. changes, Mn^{2+} EPR expts. 8-79534
 $As_2Te_{3-x}Se_x$ amorphous and cryst. phases, ^{125}Te Mossbauer expts. 8-88232
 $Fe_{80}B_{20}$, amorphous ferromag., hyperfine field distrib., Mossbauer effect 8-60371
 $Fe_{50}Sn_{50-x}$ amorphous alloy films, magnetisation meas. and Mossbauer spectra 8-95489
Ge, amorphous, EPR 8-88167
 $PbO \cdot 2B_2O_3 \cdot Fe_2O_3$ glass, Mossbauer study, struct., crystallite formation, broadened quadrupole doublet 8-59761
Si, amorphous, EPR expts. 8-88167

hyperfine field interactions in crystals *see* crystal hyperfine field interactions

hyperfine structure, atomic *see* atomic hyperfine structure

hyperfine structure, molecular *see* molecular hyperfine structure

hyperfragments *see* hypernuclei

hypernuclei
Friedel sum rule, hadron phys. meaning, nuclear matter density, binding energy 8-82305
p-shell hypernuclei, shell model anal. of Λ binding energies 8-78300
recoilless Λ prod. in (K^- , π^-) on light nuclei, hypernuclear spectroscopy 8-50116
stable charmed hyperfragments containing charmed baryon+nucleons, binding energies, lifetimes 8-89815
(K^- , π^-), 390 MeV/c, formation of hypernuclear excited states in ^{12}C , ^{16}O , ^{27}Al 8-74402
(K^- , π^-) reactions, 900 MeV/c, sum rule for hypernuclear formation, distorted wave impulse approx. 8-70572
 Λ -N two term separable pots., comparison 8-66239
 $^9Be_\Lambda$, hypernuclear excited states in 1p shell (*Chinese*) 8-82306
 C_Λ , $A=12,13$, hypernuclear excited states in 1p shell (*Chinese*) 8-82306
 ^{12}C hypernucleus detection in p+emulsion nucleus, 250 GeV, Λ binding energy (*Russian*) 8-89816
 3H , binding energy, role of spin forces in Λ -N interactions (*Russian*) 8-54718
 7He , prod. cross section calc., γ decay spectrum, shell model theory 8-62501
 7Li , prod. cross section calc., γ decay spectrum, shell model theory 8-62501

hyperon absorption
No entries

hyperon capture
see also hypernuclei
No entries

hyperon decay
constituent rearrangement model, nonleptonic hyperon decay 8-62357
lightlike chiral structure of hadrons, nonleptonic hyperon decays 8-74253
non-leptonic weak interactions, book contrib. 8-78163
nonleptonic, $SU(3) \times U(1)$ symmetry, gauge theory 8-58153
nonleptonic hyperon decays, CP violation, deviations from $\Delta I = 1/2$ rule 8-70367
polarised proton beam production in high energy hyperon decay 8-58517
 $\Delta^+ \rightarrow p + \gamma$, radiative decay in the MIT bag model 8-66110
 $\Lambda(1520) \rightarrow \Lambda(1115) + \gamma$, Melosh transform, $[70.1^-] \rightarrow [56.0^+] + \gamma$ (*Russian*) 8-66116
 $\Omega^- \rightarrow \Lambda K^-$, Ω^- lifetime, spin from $K^- p \rightarrow \Omega^- + X$, 8.25 GeV/c 8-93877
 $\Omega^- \rightarrow \Xi^0 \pi^-$, $\Xi^- \pi^0$, or $\Lambda^0 k^-$, nonleptonic decay rates, $\Delta I = 1/2$ contrib. 8-62399
 $\Xi^- \rightarrow \Lambda e^- \nu$, branching ratio meas., Monte Carlo prediction 8-54631
 $\Xi^- \rightarrow \Lambda e^- \nu$ branching ratio meas., Monte Carlo prediction 8-54631
 $\Xi^0 \rightarrow \Lambda \pi^0$, meas. of Λ helicity 8-93878

hyperon detection and measurement
No entries

hyperon-deuteron interactions
see also hyperon-deuteron scattering
No entries

hyperon-deuteron scattering
see also hyperon-deuteron interactions
No entries

hyperon effects
No entries

hyperon interactions *see* hyperon-nucleon interactions; hyperon-nucleus reactions; kaon-hyperon interactions; lepton-hadron interactions; photon-hadron interactions; pion-hyperon interactions

hyperon magnetic moment
 Σ^- mag. moment calc. from dispersion relations in t 8-82257

hyperon mass
 Λ , instanton effects on light quark spectroscopy, MIT bag model, hadron mass 8-62372

hyperon-nucleon interactions
see also hyperon-nucleon scattering
p-shell hypernuclei, shell model anal. of Λ binding energies 8-78300
 Σ^- hyperonic atom, nuclear capture rate calcs. using $\Sigma^- p \rightarrow \Gamma n$ amplitude 8-62962

hyperon-nucleon scattering
see also hyperon-nucleon interactions
No entries

hyperon-nucleus reactions
for inelastic hyperon-nucleus scattering, *see* "hyperon-nucleus scattering"
see also hyperon capture; hyperon-nucleon interactions
hadron-nucleus collisions at high energies, simple collective effects model (*Russian*) 8-89809
 Σ^- hyperonic atom, nuclear capture rate calcs. using $\Sigma^- p \rightarrow \Gamma n$ amplitude 8-62962

hyperon-nucleus scattering
see also hyperon-nucleon scattering
hadron-nucleus scatt., optical treatment in terms of scatt. amplitudes 8-89838
hadronic atoms, low-energy hadron-nucleus interaction theory 8-70977

hyperon production
nuclear matter with neutrinos retention, hyperon creation order 8-96390
pp annihilation, 3.0 GeV/c, differential cross sections and polarisation of Λ^0 and K_s^0 8-58197
recoilless Λ prod. in (K^- , π^-) on light nuclei, hypernuclear spectroscopy 8-50116
ep deep inelastic inclusive K_s^0 and Λ electroproduction, quark fragmentation 8-66123
ep $\rightarrow e \Delta^+$ scatt. asymmetry predictions, $SU(2)$ gauge theory 8-58193
 $\gamma p \rightarrow K^+ \Lambda^0$, resonance region, Λ^0 polarisation 8-66131
 $K^- n \rightarrow \Sigma^- \pi^+ \pi^- (\pi^0)$, 2.87 GeV/c, search for exotic $I=2$ hyperons 8-82234
 $K^- p$, neutral channel cross section meas., 1470 to 1560 MeV CM energy 8-82237
 $K^- p$ inclusive interactions, 10, 16 GeV/c, polarisation of forward produced Λ 8-62466
 $K^- p \rightarrow \Lambda^0 +$ pions, 8.25 GeV/c, resonance prod., fluctuations cluster emission model 8-93904
 $K^- p \rightarrow \Lambda(\Sigma) K^0$, $K^+ \pi^-$, 4.2 GeV/c, 1550 MeV, $I=1$ enhancement in ($\Lambda \pi$) and ($\Sigma \pi$) systems 8-89735
 $K^- p \rightarrow \Omega^- + X$, 8.25 GeV/c, Ω^- lifetime, spin 8-93877
 $K^- p \rightarrow \pi^- Y^*(1385)$, 11.5 GeV/c, confirmation of exchange degeneracy predictions in line reversed reacts. 8-82247
 $K^- p \rightarrow \Sigma^- \pi^+$ or $\Sigma^+ \pi^-$ at rest, interaction ratio for charged Σ prod. 8-78213
 $K^- p \rightarrow \Sigma^- \pi^+ \omega$, 4.2 GeV/c, B (1235) backward prod., $\pi^+ \omega$ mass enhancement 8-89736
 $K^- p \rightarrow \Sigma^- \pi^+$, threshold and below, ratio of $\Sigma^- \pi^+$ to $\Sigma^+ \pi^-$ production 8-70407
 $K^+ p \rightarrow \Lambda p n \pi^+$, 12 GeV/c, narrow resonant state in $\Lambda \Delta^{++}(1232)$ and $\Sigma^+(1385)p$ combinations 8-89744
 $K^+ p \rightarrow$ hyperon + X, 4-16 GeV/c, unified descript. of $\Lambda, \Lambda, \Sigma^+, \Xi^-$ prod., urbaryon model 8-66173
 Λ^0 , cumulative, production cross section from $\pi^- \pi^-$ meson-nucleus reactions (*Russian*) 8-78419
 Λ^0 , Λ^0 prod. by p+Be at 400 GeV, polarisation determ. 8-82253
 $\bar{\nu} p$, strange particle prod. at CERN PS 8-82195
 $\bar{p} p \rightarrow \Lambda \Lambda$, 1.50-2.06 GeV/c, polarisations, cross sections, spin correl. coeffs. 8-74271
 $pp \rightarrow nX$ or ΛX , 12, 24 GeV/c, n/ Λ ratio, cross sections 8-58213
 $pp \rightarrow \Sigma^+(1385)X$, $\Sigma^-(1385)X$, 12 GeV/c prod. cross sections 8-93911
 $\pi \pi^-$ interaction, K^+ hyperon prod., mass quantisation anal. (*French*) 8-70401
 $\pi^+ d$ interactions, strange-particle cross-sections at 4 GeV/c 8-89734
 $\pi^- p$ 5 GeV/c interactions, inclusive distrib. of I^0 and K^0_1 (*Russian*) 8-54652
 $\pi^- p \rightarrow K^0 \Lambda^0$, 1400 to 2380 MeV/c, differential cross sections and polarisations, partial wave anal. 8-70405
 $\pi^- p \rightarrow K^0 \Lambda^0$, up to 1334 MeV/c, cross sections and polarisation, energy depend. phase shift anal. 8-70404
 $\pi^- p \rightarrow K^0 \Sigma^0$, threshold to 1334 MeV/c, differential cross-section and polarisation 8-89733
 $\pi^+ p \rightarrow K^+ Y^*(1385)$, 11.5 GeV/c confirmation of exchange degeneracy predictions in line reversed reacts. 8-82247
 $\pi^- p \rightarrow \Lambda K \pi$, 10.3 GeV/c, threshold enhancements in ΛK mass spectra 8-74284
 $\pi^- p \rightarrow \Sigma K \pi$, 10.3 GeV/c, threshold enhancements in ΛK mass spectra 8-74284
 $Be + p(p)(K^-)(\pi^-)$, 200 GeV/c, forward inclusive prod. spectra, of K_s^0 , Λ^0 , Λ^0 , n 8-82393

hyperon resonances
 $SU(4)$ symmetry breaking pattern and baryon masses 8-89690
 Δ excitation, contrib. to pp bremsstrahlung field theoretic calc. 8-62451
 $\Delta^+ \rightarrow p + \gamma$, radiative decay in the MIT bag model 8-66110
 $\Gamma(1405)$, dynamical nature is low energy KN interactions 8-70408
 $K^- n \rightarrow \Sigma^- \pi^+ \pi^- (\pi^0)$, 2.87 GeV/c, search for exotic $I=2$ hyperons 8-82234

hyperon resonances continued

- K⁺p→Λ⁰+pions, 8.25 GeV/c, resonance prod., fluctuations cluster emission model 8-93904
 K⁺p→Λ(Σ)K⁰, K⁺π[±], 4.2 GeV/c, 1550 MeV, I=1 enhancement in (Λπ) and (Σπ) systems 8-89735
 Λ5/2⁻(1830) inversion relative to Λ1/2⁺(1115), symmetry breaking mechanism 8-50013
 pp→Σ[±](1385)X, Σ[±](1385)X, 12 GeV/c prod. cross sections 8-93911
 Σ⁻→Λe⁻ν, branching ratio meas., Monte Carlo prediction 8-54631
 Σ5/2⁻(1765) inversion relative to Σ1/2⁺(1190), symmetry breaking mechanism 8-50013
 Θ*(1820) reson., Minnaert spin test 8-89767
 Ξ⁻→Λe⁻ν branching ratio meas., Monte Carlo prediction 8-54631

hyperon scattering see hyperon-nucleon scattering; hyperon-nucleus scattering; kaon-hyperon scattering; lepton-hadron scattering; photon-hadron scattering; pion-hyperon scattering

hyperon spin and parity

- Λ polarisation, forward produced particles in K⁺p inclusive interactions 8-62466
 Λ⁰, Λ⁰ prod. by p+Be at 400 GeV, polarisation determ. 8-82253
 Θ*(1820) reson., Minnaert spin test 8-89767

hyperons

see also hyperon resonances

- nuclear interactions of strange particles and resonances, conf. Warsaw, Poland (Ict. 1976) 8-70406
 quark gluon model of hadronic structure functions at x→1 (Russian) 8-54617
 Λ helicity meas. in Ξ⁰→Λπ⁰ 8-93878
 Λ⁰, Λ⁰, differential cross section and polarisation from p \bar{p} annihilation 8-58197
 Λ=Σ⁰ effects of EM mixing on pn mass difference (Russian) 8-74255
 Ω⁻ lifetime, spin from K⁺p→Ω⁻+X, 8.25 GeV/c 8-93877

hypersonic flow

- ablating blunt body, heat transfer near stagnation point 8-94736
 ablation, statistical characteristics of mass lost in thermal destruction, zero gas dynamic press. 8-83429
 blunted sphere cones, viscous shock layer solns. 8-51186
 body shape for minimal radiative heat inflow, spacecraft atmospheric entry (Russian) 8-77457
 gas flow, radiant heat and evaporative cooling 8-91028
 hypersonic viscous shock-layer equation, method for successive approximations for integration (Russian) 8-59421
 laminar hypersonic wake of a lifting body, Navier-Stokes solns. (Russian) 8-87359
 secondary shock waves in mag. field (Russian) 8-87401
 shock layer, hypersonic, vibr. nonequilib., near stagnation streamline, low Reynolds no. flow 8-87417
 slender vehicle dynamics, viscous interaction or support interference 8-71363
 solar wind flow past planets, axisymm. implicit blunt body computation technique 8-96370
 turbine blade and nozzle guide vane, transient cascade, heat transfer meas., wind tunnel 8-94768
 viscous shock layer flow over highly cooled sphere, coupled eqns. anal. 8-51189
 He, Na vapour seeded, velocity profile visualisation 8-59530

hypersorption see sorption

hypertritons see hypernuclei; tritons

hypervirial theorem see quantum theory

hypochromism see light absorption

hypothesis formation see heuristic programming

hypothetical particles

- see also charm particles; heavy leptons; intermediate bosons; magnetic monopoles; quarks; tachyons
 axion, astrophysical limitations on mass (Russian) 8-61835
 axion mass in extended SU(2)×U(1) colour gauge theory 8-78080
 axion production in νp interactions, 26 GeV, cross sections, decay rate 8-62387
 axions, review of research 8-66183
 dyons, supersymmetric Yang-Mills theory 8-62334
 energy-range relations for heavy protons and heavy quarks, use in detection 8-58566
 hadrons as compounds of bradyons and tachyons, ground state and decay anal. 8-58156
 orthopositronium decay into axions 8-78125
 superluminal particles motion in gravit. field of nonrot. black hole (Russian) 8-93103
 supersymmetric new hadronic states, production, decay and detection 8-70302
 Cu+p, 400 GeV, dimuon and trimuon prod., prompt ν source, DD prod., axions 8-89860
 Cu+p, 400 GeV, prompt ν prod., axion prod. upper limit 8-89859

hysteresis

- see also coercive force; dielectric hysteresis; elastic hysteresis; magnetic hysteresis; remanence
 contact angle, at homogeneous surfaces 8-51793
 electric breakdown voltage hysteresis, electrode coating effects in air and SF₆ 8-87553
 electrotechnical steel, hysteresis curves, plotting (Russian) 8-76269
 inhomogeneous systems, hysteresis of phase transitions, general soln. 8-59926
 vibration damping, continuum description 8-67078
 H₂O, contact angle on polystyrene, cause of hysteresis 8-95206

I-II-VI₂ semiconductors see ternary semiconductors

I-III-VI₂ semiconductors see ternary semiconductors

IC see integrated circuits

IC engines see internal combustion engines

ice

see also glaciology; snow

- AES, chemical-state effects 8-92566
 Antarctic deep core ice, X-ray diffr. topographic studies 8-63803
 Antarctic ice sheet, thermal radiation calc. from randomly inhomogeneous stratified medium (Russian) 8-96312
 Antarctic iceberg melting 8-88863
 Arctic Basin, sea-ice conc. and multiyear ice fraction time depend. 8-81174
 Arctic seas, ice forecasts and practical appls. 8-96230

ice continued

- biological sample electron probe microanal., charging effect in electron-irrad. ice 8-57141
 Camp Century core ice, O isotope ratios rel. to late-Wisconsin glaciation in NW.Greenland and N.Ellesmere Island 8-57232
 Canadian high Arctic, past glacial activity 8-81236
 climate model, sensitivity and role of cloudiness (Russian) 8-88902
 cloud model, shallow convective, precip. mechanisms 8-81311
 clouds, directional light scatt. coeffs. in droplet and cryst. clouds (Russian) 8-96292
 clouds, ice and water content from Nimbus 6 IR sounder data 8-92925
 clouds, ice splinter production during riming 8-85662
 clouds, lidar backscatter from horizontal ice crystal plates 8-92984
 clouds, phase discrimination with polarisation diversity lidar 8-96269
 condensation and phase transitions, electrical effects 8-67821
 corona discharges from ice points on metal electrodes 8-67587
 crystal structure of ice accretions rel. to hailstones 8-85668
 crystallisation on CuS aerosol prepared by burning pyrotechnic mixture, freezing temps. 8-96279
 cumulus congestus clouds, NE Colorado, graupel particles characts. 8-81312
 dendritic ice form. in pipe, cooling rate effect 8-90690
 dielectric anisotropy in Ih phase 8-64310
 dislocation velocity, quantum mechanical approach 8-91339
 floating ice layer thickness meas. using nanosecond impulse X-band radar 8-62178
 floating ice shelves, tidal flexure cracks, fracture mechanics 8-69368
 floating sheet, viscoelastic response under prolonged loading 8-51093
 formation in natural and accelerated storms 8-61509
 friction between steel ball and ice single cryst., load, velocity and temp. depend. (Japanese) 8-88537
 friction between WC ball and ice single cryst., anisotropy (Japanese) 8-88539
 friction between WC ball and ice single cryst., slider size effect (Japanese) 8-88538
 frost mounds, Bear Rock, NW Territories, Canada, obs. during 1975-76 period 8-65346
 Galilean satellites, icy crater model to explain radar scatt. results 8-61789
 glacier structure and flow rel. to elongated air bubbles in ice (Japanese) 8-88861
 glaze ice and rime deposition, effects of hills relief and geographical location 8-61525
 glaze storms and wire icing in Ukraine 8-81329
 Grand Banks, icebergs drift model 8-81200
 gravel, ice-thrusting, shear deform. 8-65347
 Greenland ice sheet topography from satellite radar altimetry 8-81233
 Greenland Sea, LF sound propag. in marginal ice zone 8-85567
 ground, perennially frozen, under cold store, struct. (Japanese) 8-88834
 growth beneath water film, air bubble precipitation 8-83922
 Gulf of Bothnia, sea ice flexural waves meas. (Japanese) 8-96225
 H₂O:HF ice, single crystal, velocity of individual dislocations by X-ray topography (French) 8-87677
 hail, Doppler radar spectra at vertical incidence 8-65368
 hail, during thunderstorm of 1976 June 27 at Heatree, Devon, England 8-57288
 hail suppression seeding, Ag analysis 8-65367
 hail suppression seeding, crop response anal., Nelspruit project, South Africa 8-57257
 hail-prevention operations, cost effectiveness estimation methods anal. 8-93013
 hailfalls kinetic energy, hailstone spectra anal. 8-92924
 hailpads calibration 8-93001
 hailstone samples, Project DUSTORM, microprobe anal., element abundances 8-73453
 hailstone trajectories determ. from crystallography, D content and radar backscatt. 8-61614
 hailstones, foreign material obs. and derivation 8-96260
 hailstorms variability on South African plateau 8-92911
 helicopter icing problems, role of meteorology 8-85657
 high-pressure Raman spectra, bending and librational bands 8-68499
 interglacial episode termination and Wilson Antarctic surge hypothesis 8-53669
 interstellar ice, evidence from refl. nebulae simplified models 8-96526
 lake ice-cover thickness, pulsed radar meas. method 8-92862
 liquid-solid phase transition, photoacoustic detection 8-75810
 localised excess electrons, semiconductor models 8-73129
 Mars, crust, possible fossil H₂O liquid-ice interfaces 8-65539
 Mars fretted terrain, rock glaciers flow 8-65537
 melting, heated water jet impingement melting, cavity formation, expt. and simulation 8-95133
 melting, one-phase Stefan problem, continuity of soln. in n space dimensions 8-95130
 microcrystal dispersions, dielec. props. (French) 8-60374
 microcrystals, NH₄Cl doped, activation energy of Debye's dipolar relax., influence of salt content (French) 8-56424
 North Sea, microwave meas. using SLAR 8-77245
 ocean, broken ice effects on ship waves (Russian) 8-65326
 pack ice, drift observed using radar buoys (Japanese) 8-96224
 particles, interpretation of foil impactor impressions, rel. to hail research 8-57356
 permafrost, common depth point survey technique appl. (Russian) 8-53751
 permafrost, icy, in NE.British Columbia, distrib. and thickness 8-77277
 pressure melting within glacier, indicated by regelation ice chem. comp. 8-61447
 Raman spectrum, press. effects 8-95582
 river ice, book contrib. 8-61476
 river ice break-up, satellite monitoring 8-65350
 river ice-cover thickness, pulsed radar meas. method 8-92862
 rivers, acoustic noise from breaking ice 8-53671
 rivers, ice jams form. conditions and forecasts 8-92863
 rupture mechanism exam. (German) 8-52976
 Saturn ring system, presence of H₂O ice from far UV spectrum obs. 8-53867
 sea, ice-covered, flow vel. and ice thickness effects on unsteady waves (Russian) 8-65324
 sea ice, complex dielec. const., 0.1-40 GHz 8-61430

ice continued

- sea ice, EM wave scattering from slightly rough boundary 8-77266
 sea ice, energy exchange in central Arctic 8-85584
 sea ice, failure by compression (*Japanese*) 8-88841
 sea ice, haline convection induced by sea water freezing (*Japanese*) 8-88843
 sea ice, low-salinity, radiometer studies 8-81175
 sea ice, microwave radiometric obs. appls. 8-81415
 sea ice, microwave remote sensing in AJDDEX main expt. 8-81173
 sea ice, sea floor scouring 8-92822
 sea ice, wind stress meas. (*Japanese*) 8-88842
 sea ice field of Okhotsk Sea coast of Hokkaido, divergence and rot. meas. (*Japanese*) 8-96223
 sea ice in polar regions, radio obs. appls. 8-81419
 sea ice near Showa Station, Antarctica, physical props. (*Japanese*) 8-96226
 sea ice structure, effects of artificial inclusion (*Japanese*) 8-88844
 semi-infinite plate subjected to increasing boundary force, dynamic response, ice sheets 8-83254
 soil, frost heave in Tomakomai, Hokkaido, 1976 to 1977 (*Japanese*) 8-92860
 soil freezing, water migration obs. (*Japanese*) 8-88862
 soils, freezing, heat flux, meas. (*Japanese*) 8-88835
 storms, principal component anal., hail index (*French*) 8-96267
 sublimation drying in UHF EM field 8-83936
 supercooled cloud, drop size distrib. influence on secondary ice particles prod. during graupel growth 8-73481
 Tarmanskii Marsh, permanently frozen layers form., influence of human activity 8-92864
 tidal energy dissipation by Antarctic ice shelf flexing 8-88845
 troposphere ice particles, depolarisation of 19 and 28 GHz Earth-space signals 8-73492
 VII, melting curve up to 150 kbar 8-67812
 water-ice interface struct., fluctuations during solidification 8-59935
 D₂O, thermal cond., H and D order effects 8-67871
 D₂O-H₂O ice, thermal cond., H and D order effects 8-67871
 Na montmorillonite, water vapour adsorption and ice form. at -5°C 8-65540

iconoscopes see television camera tubes**identification**

- see also control theory; correlation methods; frequency response; modelling; parameter estimation; simulation
 biological compartmental systems, multi-input and multi-output, controllability, observability and structural identifiability 8-76978
 BWR dynamics, multivariable autoregressive identification 8-94107
 crayfish stretch receptor repetitive firing behaviour nonlinear systems anal. 8-80853
 distributed parameter system identification using doubly cubic spline, underground aquifer appl. 8-69391
 ecological system model sampling/identification, input signal anal. 8-69267
 EEG nonstationary point automatic detect. (*French*) 8-57112
 external geniculate body receptive field of cat, space-time wt. function 8-64989
 external geniculate body receptive fields, neuronal network model 8-64990
 hydrological system statistical modelling (*German*) 8-96246
 image degradation, methods 8-58941
 intervertebral joint, systems identification for material props. 8-69125
 plasma physics problems 8-71532
 porous media, miscible or immiscible displacements, identification and modelling 8-69392
 probabilistic vector model for identification of intervocalic stop consonants 8-69114
 upper-limb prostheses multifunctional control microprocessor system, myoelectric signal identification method 8-88766

jets see tunnelling spectra; tunnelling spectroscopy**IEXE** see ion microprobe analysis**i.g.f.e.t.** see insulated gate field effect transistors**ignition**

- see also electric ignition
 laminar diffusion boundary layers, ignition and extinction 8-64838
 PMMA, spreading of two-phase film of melt, heat and mass exchange, ignition and combustion (*Russian*) 8-76861

ignitrons see mercury arc rectifiers**II-III₂-VI₂ semiconductors** see ternary semiconductors**II-IV-V₂ semiconductors** see ternary semiconductors**II-VI semiconductors**

- electron-hole liquid theory, generalised RPA 8-87914
 electronic theory, covalent-metallic or covalent-ionic phase transition under pressure 8-72105
 electronic theory, cryst. energy and bulk modulus 8-72104
 fundamental absorpt. spectra, direct interband transitions 8-63972
 heterojunctions, photovoltaic effects and solar efficiency 8-52076
 local force variations due to substitution impurities 8-51633
 p-n junction photovoltaic diode, appl. as IR detector 8-86330
 performance at large bias currents (*Russian*) 8-76105
 phosphors, ODMR, defect excited states 8-80254
 piezoelectric semiconductor, piezoresist. of grain boundaries 8-51995
 polar semiconductor, impurity levels, influence of electron-phonon coupling 8-64007
 zinc blende structured semiconductor surface analysis by X-ray photoelectron spectroscopy (*Japanese*) 8-88672
 zincblende compounds, (111) and (111) faces, surface electron states 8-80035
 zincblende structure p-type semiconductors, internal strain on bound hole-phonon interaction 8-91492
 Cd_{0.2}Hg_{0.8}Se, longitudinal Nernst-Ettingshausen effect, effect of disorder scatt. 8-84240
 Cd_{0.1}Hg_{0.9}Se mixed cryst., electron mobility and electron scatt. 8-95296
 Cd_{0.1}Hg_{0.9}Se type semiconductor, small-gap, electron scatt. and transport props. 8-95294
 Cd_{0.1}Hg_{0.9}Se type semiconductor, small-gap, electron scatt. and transport props. 8-95295
 (CdHg)Te photoconductive detector, thermal figure of merit limit 8-89540
 Cd_{0.25}Hg_{0.75}Te, p-n homojunction breakdown voltage for onesided abrupt junctions (*German*) 8-56210

II-VI semiconductors continued

- Cd_{0.1}Hg_{0.9}Te, fine-graded gap struct., electrophysical props. (*Russian*) 8-60144
 Cd_{0.1}Hg_{0.9}Te, gap width temp. depend., absorpt. band edge meas. 8-72521
 Cd_{0.1}Hg_{0.9}Te, IR detector appls., prep., elec. props. (*German*) 8-86332
 n-Cd_{0.1}Hg_{0.9}Te, in strong mag. field, current-voltage charact., current instabilities 8-87980
 Cd_{0.1}Hg_{0.9}Te, isothermal growth of epitaxial layers 8-60577
 n-Cd_{0.1}Hg_{0.9}Te, magnetophonon oscills. of transverse magnetoresist. 8-72177
 Cd_{0.1}Hg_{0.9}Te, temp. shift of energy gap, contrib. of lattice dilatation 8-51892
 CdO, magnetoresistance, temp. depend. of degenerate, narrow and broad samples 8-95306
 CdS, A-exciton-polariton, time depend. optical spectrosc. obs. 8-80376
 CdS, absorpt. spectra, 400-650 nm, electron irradi. defects and absorpt. edge shift 8-64382
 CdS, acoustic phonon intensity fluctuations after strong nonlinear amplification 8-59909
 CdS, chem. sprayed film, struct. and morphology 8-72020
 CdS, chem. sprayed film growth using centrifugal disc atomiser 8-92189
 CdS, collision controlled light scatt. by electrons, influence of elec. field (*Russian*) 8-64375
 CdS, cubic, ab initio band struct. calcs. within local density functional formalism 8-87910
 CdS cylindrical crystal, transverse SAW obs. 8-84042
 CdS, edge emission spectra alteration by uniaxial stress (*Russian*) 8-72486
 CdS, electrocrystallisation of films on Cd 8-72014
 CdS, epitaxial layers on Cd single crystal, direct synthesis and struct. 8-68628
 CdS, exciton cathodoluminesc. of semicond. with surface pot. barriers 8-88366
 CdS, exciton luminescence, surface recombination, space-charge-layer effects 8-80410
 CdS, excitonic region, nonlinear optical meas., 4.2K 8-68531
 CdS film, double-layered polycrystalline, on LiNbO₃ substrate, fabrication and props. rel. to SAW appl. 8-64480
 CdS film, influence of nonstoichiometric surface layer on props. 8-64148
 n-CdS film, transient photoconductivity effects (*French*) 8-87994
 CdS, film, X-ray diffr. and elec. cond. 8-64149
 CdS, film electrolytically deposited, surface and bulk photocond. props. 8-60154
 CdS, film for solar cells, struct. and elec. props., thickness depend. 8-72289
 CdS films, vac. evaporation from CdS.Cr₂O₃ system, photoelec. props. 8-80074
 CdS, flexural waves in resonator platelets, synchronous amplification and generation 8-84527
 CdS, gain spectroscopy and plasma recomb. 8-88327
 CdS, heterojunctions with InP and GaAs, prep. by CdS CVD and etching 8-52062
 CdS, induced absorption and gain from high density excitons 8-68533
 CdS, induced absorption in energy ranges of exciton and exciton-biexciton transitions 8-72548
 CdS, lattice attenuation meas. by US injection method 8-76480
 CdS layers from CdS+Cr₂O₃ system, effect of heat treatment on spectral distrib. of photosensitivity 8-80017
 CdS, luminesc. data, statistical anal. (*Russian*) 8-68559
 CdS, luminesc. from heavy ion tracks 8-88365
 CdS MIS devices surface states 8-72267
 CdS, mode corrected TA phonons, reson. Brillouin scatt. 8-72535
 CdS, model S=1/2 amorphous antiferromagnet, spin polarisation 8-52288
 CdS, neutron and fast electron irradi., local centre form., TSC and photoluminesc. meas. 8-87719
 CdS, neutron irradiated, intrinsic defects 8-51599
 CdS, nonlinear refr. index coeffs. meas. by nonlinear refraction method (*Russian*) 8-79066
 CdS, ODMR, bound excitons 8-80253
 CdS, photoanodes in sulphide-polysulphide electrolytes, instability 8-80755
 CdS, photoconducting, surface acoustic noise amplification by carrier drift 8-72208
 CdS, photoref. in exciton region, surface layer influence 8-76489
 CdS, pure and Al doped vacuum deposited film, photoelectric props. and optical absorption 8-60162
 CdS, reson. Raman scatt., second-order, theory for case of strong excitonic effects 8-76460
 CdS Schottky contact, photovoltage 8-95337
 CdS screen for laser CRT, stimulated emission with TV type operation 8-59028
 CdS, seeded growth from vapour of large single crystals 8-64449
 CdS, spatial dispersion effects, exciton decay const. depend. (*Russian*) 8-72086
 CdS, spin-flip line shape 8-88307
 CdS spray pyrolysis film prep. and characterisation 8-64492
 CdS surface, nonequilib. electron effects due to chem. excitation 8-72239
 CdS, surface energy levels, O(C) adsorpt., AES study (*Japanese*) 8-88008
 CdS, surface props., photorefectance spectra in the exciton region 8-95324
 CdS, thin films, deposition onto hot substances, vapour phase method 8-95694
 CdS, two-phonon resonant Brillouin scatt. 8-84597
 CdS, up-conversion and optical storage, spatially modulated band struct. 8-64397
 CdS:Bi film, implantation and post annealing, superlinearity 8-52028
 CdS:Cd(In), Cu- or defect-compensated, optical ageing rel. to storage cond. 8-84247
 CdS:Cl, extrinsic, exciton absorption 8-72569
 CdS:Cl, heavily doped, fluoresc. spectrum upper threshold calculated 8-52568
 CdS:Cu, In, Ga, spray deposited, struct., X-ray obs. 8-71713
 CdS:Cu, photocond. under high excitation intensity 8-52033

II-VI semiconductors continued

- CdS:Cu, spectral sensitisation by cyanine dyes 8-64064
 CdS:In, spin flip Raman scatt., electron dynamics 8-80342
 CdS:In whiskers, prep. by vapour deposition 8-75969
 CdS:Li, anisotropy of the absorption by impurity centers in hexagonal crystals 8-88343
 CdS:Ni, dark cond. and photoconductivity 8-76110
 CdS:Ni, elec., photoelec. and luminesc. props. (*Russian*) 8-84259
 CdS:Ni, exciton reflection spectra 8-72557
 CdS:P, implanted, photoluminesc. and electroluminescence spectra (*Russian*) 8-52544
 CdS-Cu₂S heterojunction, elec. and photoelec. charact., effect of etching of CdS 8-80048
 CdS-CuI film heterojunction photocells, prep., photoelec. props. 8-80044
 CdS-InP heterostructure formation and elec. evaluation 8-72738
 CdS-Si n-p heterojunction photodetector, fabrication and charact. 8-52068
 CdS-type semiconds., Dember effect, theory 8-72189
 CdS_{0.75}Se_{0.25}, linear electro-optic effect meas., light modulator appl. 8-76434
 CdS_{1-x}Se_x, mixed cryst., electron-hole drops and plasma, luminesc. obs. (*Russian*) 8-92119
 CdS_{1-x}Se_x, spatial distribution and lasing modes under one photon optical excitation (*Russian*) 8-59012
 CdS₂Se_{1-x}, laser damage, self-focusing influence 8-50844
 CdS₂Se_{1-x} mixed crystals, exciton spectra 8-92131
 n-CdS(Se)(Te) semicond. liq. junction solar cells, photocurrent spectra, carrier recombination 8-76142
 CdSe, charge transport 8-84233
 CdSe crystal, stimulated emission from electron-hole plasma, temp. depend. 8-88331
 CdSe, defect struct. in Se vapour 8-64043
 CdSe, direct gap, picosec. time resolved reflectivity obs. of optically excited hot carrier distrib. 8-76495
 CdSe, fundamental vibr., Raman scatt. and IR refl. obs. 8-60451
 p-CdSe, Hall density and mobility, in Se vapour atm., 600-1100K 8-52014
 CdSe, nonstoichiometry, Cd and Se press. meas., up to 1400K 8-87664
 CdSe, optical parametric devices, freq. tuning possibility by uniaxial press. 8-59084
 CdSe, optically pumped, dynamic polarisation of nucl. moments 8-68411
 CdSe, photoanodes in sulphide-polysulphide electrolytes, instability 8-80755
 CdSe, photosensitivity of elastic properties 8-92049
 CdSe:Cu, Cu, photo-induced changes in absorpt. spectra 8-80382
 CdSe:P, effect of P on edge luminesc. 8-64399
 CdSe-Ge (111) heterojunctions, epitaxial, azimuthal rotation 8-84085
 CdTe cathodic deposition from aqueous electrolytes 8-64484
 CdTe, creep activation energy and velocity (*Russian*) 8-56716
 p-CdTe, ESR optical detect., Overhauser shift, g-factor 8-80252
 CdTe film, cathode sputtered, chemical composition and struct. 8-84100
 CdTe film, excitation by H of anomalously high voltage (*Russian*) 8-60235
 CdTe, film grown in quasi-closed volume, struct. (*Russian*) 8-75952
 CdTe, growth by travelling heater method, high resistivity charact., γ -ray detector appl. 8-84707
 CdTe, lattice mode, dispersive refl. meas. using modular interferometer 8-89568
 CdTe negative dielectric relax. of hot electrons 8-52001
 CdTe, P-T diagram, cryst. struct. stability 8-51886
 CdTe, plastic deformation activation anal. below room temp. 8-84935
 CdTe, single cryst. IR laser window, low absorption at 10.6 μ m 8-79081
 CdTe single-crystal film, switching and memory effects 8-76174
 CdTe, temp.-depend. of root-mean-square dynamic displacements, characteristic temp., X-ray study 8-83895
 CdTe, tunable high efficiency microwave freq. shifting of IR laser 8-71126
 CdTe, use in X-ray detectors 8-86745
 CdTe:Be, impurity modes and IR absorption 8-76506
 CdTe:Cl, single cryst., photo Hall effect obs. 8-76094
 CdTe:Ge, mag. props. 8-56289
 CdTe:In, lightly- and heavily-doped, cathodoluminesc., temp., injection level and freq. depend. 8-52584
 CdTe:Zn, TSC, carrier traps, depth and quenching by IR radiation 8-56420
 CdTe-metal contact, surface barrier exam. 8-64111
 CdTe_{1-x}Se_x, long-wavelength optical phonons, composition depend., IR and Raman spectra 8-67788
 CdTe_{1-x}Se_x, Raman scatt. spectra, two-mode behaviour 8-60450
 CdZnS-CdS bifilm solar photocells, feasibility, study 8-76113
 (CdZn)S-Cu₂S solar cell, film form. and charact. 8-68080
 Cd_{1-x}Zn_xS 10 μ m film optical and electrical characterisation (*French*) 8-64153
 Cd_{1-x}Zn_xS, electro-optical multilayer film, for data storage and display 8-71176
 Cd_{1-x}Zn_xS, epitaxial growth of single crystal layers on (111) GaAs substrate, close-space geometry 8-92198
 Cd_{1-x}Zn_xS, RF sputtered electro-optical film for data storage and display 8-83047
 Cds, reson. Brillouin scatt. by piezoelectrically inactive TA phonon domains 8-84593
 Cr₂O₃ addition to CdS₂Se_{1-x} photoresistors, extension of cutoff freq. (*Russian*) 8-84248
 Cu₂S-CdS film junction formation by dry-barrier process 8-64109
 GaP, two photon absorption relative to Raman cross sections 8-87098
 HgCdTe IR photovoltaic detectors for 8-14 μ m range, review (*Italian*) 8-54451
 HgCdTe MIS structure, modelling and appl. to CCD IR imagery 8-80058
 Hg_{0.6}Cd_{0.4}Te, annealing temp. effect on carrier conc. 8-72167
 Hg_{0.7}Cd_{0.3}Te, 17 to 77K, photo- and cathodoluminesc. 8-52569
 Hg_{1-x}Cd_xTe, Faraday effect at CO₂ laser freq. 8-64348
 Hg_{1-x}Cd_xTe, high intensity IR transmission limit 8-79074
 Hg_{1-x}Cd_xTe, Hooke's flicker noise MIS expt. 8-56233
 Hg_{1-x}Cd_xTe IR detector technology 8-77989
 Hg_{1-x}Cd_xTe IR focal plane status and performance 8-77987

II-VI semiconductors continued

- n-Hg_{1-x}Cd_xTe, photoconductor, contact noise at 77K 8-88028
 Hg_{1-x}Cd_xTe, quasi-local acceptor levels and electron mobility 8-67974
 Hg_{1-x}Cd_xTe, zero-gap semicond. with nonparabolic band struct., hot electron mobility and conc. 8-76080
 Hg_{2-x}Cd_xTe, single-LO-phonon and -plasmon recombination channels narrow-bandgaps 8-91728
 HgS film, deposition from colloidal solns. 8-92209
 α -HgS, natural, yellow emission 8-68567
 HgSe-CdSe pseudobinary alloy, phase diagram and cryst. growth 8-68620
 HgSe(Te), dynamic dielectric function, IR absorpt. meas. 8-68508
 HgTe, creep activation energy and velocity (*Russian*) 8-56716
 HgTe type semiconductor, small-gap, electron scatt. and transport props. 8-95294
 HgTe type semiconductor, small-gap, electron scatt. and transport props. 8-95295
 HgTe, vacancy doping by off-stoichiometry, influence on transport props. 8-55862
 (InAs)_{1-x}(CdTe)_x, band gap and effective mass, IR spectra obs. 8-56491
 Mg₂Zn_{1-x}Te, high purity, luminesc. and band gap 8-68553
 Mg₂Zn_{1-x}Te, long wavelength optical phonon replica 8-60468
 PbS oxide, optical excitation meas. of trap charging surface film (*Russian*) 8-76180
 TiSe, vibr. props., Raman and far IR spectra meas. 8-71800
 ZnSe, surface, energy-minimisation approach to atomic geometry 8-95213
 (ZnCd)S:Ag phosphor, absolute efficiency under fluoroscopy conditions 8-73203
 Zn_{0.1}Cd_{0.9}S-CdTe p-n junction, prep. by spray pyrolysis, photovoltaic props. 8-60196
 Zn_{1-x}Cd_xS film, prep. by soln. spray method, and struct., optical and elec. props. 8-52666
 Zn_{1-x}Cd_xS, laser damage, self-focusing influence 8-50844
 Zn_{1-x}Cd_xS, lasing modes and spatial distrib. under one-photon excitation, cavity model 8-74913
 Zn_{1-x}Cd_xS:In, low resist. film for solar cell window 8-71200
 Zn_{1-x}Cd_xTe, reflection spectra, energy band struct. comp. depend. (*Russian*) 8-56500
 Zn_{1-x}Cd_xTe, relaxation processes, emission spectra (*Russian*) 8-72598
 ZnO 1010 surface, reaction of O₂, AES, LEED, EPR, desorpt., surface cond. and work function expts. 8-95950
 ZnO (0001), adsorption of alkali metal, anomalous behaviour of Na 8-79883
 ZnO (0001) and (0001) polar surfaces, 6-fold LEED patterns 8-71920
 ZnO (1010) surface bias voltage effect on hardness, charge exchange near dislocations 8-52078
 ZnO accumulation layers, Hall mobility and work function, correl. 8-60185
 ZnO, acoustic phonon intensity fluctuations after strong nonlinear amplification 8-59909
 ZnO, CVD films on sapphire substrates, use as optical waveguide 8-90500
 ZnO ceramics, non-Ohmic, cond. mech. 8-68034
 ZnO, change in exciton-phonon mechanism due to defects 8-71804
 ZnO epitaxial film with smooth surface from CVD onto a sputtered ZnO film on sapphire, waveguide appl. 8-56588
 ZnO film, chemisorption of H, electrical cond. exam. adsorption centres 8-67913
 ZnO, low energy cathodolum., surface effects 8-60522
 ZnO, optical gain and induced absorption from excitonic mols. 8-84609
 ZnO, optical gain spectra, direct recording using laser modulation 8-66834
 ZnO, particulate, Dember effect, rel. to electrography 8-95314
 ZnO pellets, and ZnO:Li single crystals, photo-induced AC impedance meas., photodielec. effect 8-52034
 ZnO phosphors, origin of UV emission 8-64400
 ZnO, polar surface, clean (O₂-H-exposed), reflection energy loss spectra, 2-30 eV 8-64434
 ZnO, rate of deposition and morphology 8-84719
 ZnO, single cryst. growth in ZnO-H₂O-O₂ vapour, morphology, electrophys. and opt. props. 8-52649
 ZnO, small crystal, optical surface phonon modes 8-71940
 ZnO, surface charge transfer in presence of photosensitising dyes 8-68049
 ZnO, surface phenomena, interpretation by compensation model 8-95323
 ZnO thin film SAW device manufacture, sputtering system and film characterisation 8-95692
 ZnO, varistor action, homojunction breakdown mechanism 8-60193
 ZnO, Zeeman splitting of A₁-exciton emission lines, k-linear term effects 8-52563
 ZnO, Zn 3d core-level transition in electron energy loss spectra, rel. to ZnSe (111) surface 8-68584
 ZnO:Dy(Nd)(Sm), phosphor, electroluminesc., photoluminesc. spectra 8-80421
 ZnO:La phosphor, electrolum. brightness waves, -168 to +85°C 8-52580
 ZnO:Li, optically detected ESR, donor-acceptor pairs, line broadening 8-80256
 n-ZnS based heterojunctions, epitaxial, elec. props. (*Russian*) 8-88023
 ZnS, chemisorption of O₂ after illumination and in presence of CO and O₂ 8-87877
 ZnS, cubic, gel growth, expt. conditions 8-68614
 ZnS, electroluminesc. and photoluminesc. spectra, fine struct. (*Russian*) 8-84661
 ZnS, electroluminesc., ageing rate, voltage effects (*Russian*) 8-84662
 ZnS film, photovoltaic effects under illum. from above and below 8-52031
 ZnS, film, vac. deposition onto NaCl cryst. in H₂S environment 8-63945
 ZnS, lattice dynamics, deformable-ion model 8-91396
 ZnS, low voltage cathodoluminescence 8-52585
 ZnS, luminesc. data, statistical anal. (*Russian*) 8-68559
 ZnS, plastically deformed, anisotropic cond. 8-56143

II-VI semiconductors continued

- ZnS, powder phosphor, IR-induced changes in emission spectra 8-80389
 ZnS, single crystal, effect of elec. field on cond. 8-84228
 ZnS, Stark-Ladder current theory 8-68035
 ZnS with Au film coating, calc. of defect conc. 8-95052
 ZnS:Ag,Al, computer calc. of band model for luminesc. and photocond. (*Russian*) 8-52542
 ZnS:Ag film, evaporated, IR quenching of photocapacitance, deep levels obs. 8-56180
 ZnS:Al, signal enhancement by field modulation, ODMR expts. 8-56406
 ZnS:Be, impurity modes and IR absorption 8-76506
 ZnS:Cr(Mn)(Fe)(CoXVI), vibr. modes of transition element impurities 8-76472
 ZnS:Cu, Br based electroluminesc. cells, light, const. field effects on electroluminesc. 8-84658
 ZnS:Cu, effect of elec. field on photoluminescence, model of luminogen centre 8-76522
 ZnS:Cu,Al, anisotropy of blue-Cu luminescence centres 8-64390
 ZnS:Cu(Cl), electroluminesc. and photoluminesc. spectra, fine struct. (*Russian*) 8-84661
 ZnS:Mn film, emission centres of DC electrolum. 8-68564
 ZnS:Mn film device, laser modulation of electrolum. 8-52576
 ZnS:Mn²⁺, Jahn-Teller effect in fluorescent level 8-52566
 ZnS:Pb phosphor mech. of elec. field liberation of electrons from traps 8-72616
 ZnS-Cu, comet shaped electroluminesc. lines 8-52578
 ZnS(Se), highly transparent semicond., multiphonon IR absorpt. 8-60461
 ZnS_{1-x}Se_{1-x} band gap, comp. depend., exciton refl. spectrum obs. 8-56071
 ZnS_{1-x}Se_{1-x} layer on ZnS, ZnSe, growth by solid-state diffusion technique 8-56578
 ZnS_{1-x}Se_{1-x}:Mn(Cu), luminesc. obs. 8-60519
 ZnS_{1-x}(Te), relative supersaturation, formula valid for different technological conditions (*Russian*) 8-84081
 ZnS(Se)(Te):Cr²⁺, Jahn-Teller coupling 8-67997
 ZnSe, absorpt. modulation of light, and its appl. to page composer (*Japanese*) 8-83083
 ZnSe, charged dislocation motion mechanism (*Russian*) 8-79820
 ZnSe, cubic, magnetoreflexion of s-excitons 8-60426
 ZnSe, elastic moduli, temp. depend., 293-973K, electrostatic reson. determ. 8-59850
 ZnSe, epitaxial growth by vapour flow method 8-64482
 ZnSe, high conductivity films appl. to p-n heterojunctions 8-68100
 ZnSe, laser induced modulation of opt. absorpt. 8-88324
 ZnSe, linear electro-optic coeff. dispersion, relation to reson. Raman scatt. 8-56459
 ZnSe, nonstoichiometry, Zn and Se press. meas., up to 1400K 8-87664
 ZnSe, ODMR expts., A and V-centres, origin of emission bands 8-80255
 ZnSe, optically pumped stimulated emission at 4580 Å, near band edge luminesc. 8-71105
 ZnSe, P-T diagram, cryst. struct. stability 8-51886
 ZnSe, single cryst., electron-hole drops, boundary luminesc. (*Russian*) 8-80412
 ZnSe surface, quantitative XPS meas. 8-56559
 ZnSe, thermolec. power meas. 8-52021
 ZnSe, transport props., effect of In-doping and Zn-annealing 8-76075
 ZnSe, twinning effect on electro-optical props. 8-68478
 ZnSe, two photon absorption relative to Raman cross sections 8-87098
 p-ZnSe:As, ion implantation and heat treatment 8-87700
 ZnSe:Cu, Al, single cryst., low-voltage red cathodolum. 8-80423
 ZnSe:F, signal enhancement by field modulation, ODMR expts. 8-56406
 ZnSe:In, heavily doped, Hall effect and DC cond. expts., compensating acceptors 8-52013
 ZnSe:In, heavily doped, impurity band cond., Hall coeff. and cond. expts. 8-72147
 ZnSe:Mn²⁺, Jahn-Teller effect in fluorescent level 8-52566
 ZnSe-GaAs thin film DE electroluminescent cell with 20 V threshold voltage 8-76141
 ZnSe-Ge (100) interface, electronic struct., self-consistent pseudopot. calc. 8-91747
 ZnSe-Ge abrupt (110) interface, electronic struct. 8-95339
 ZnSe-HgSe, solid soln., defect distrib., elec. props., Hagemark's theory 8-64040
 ZnSeCu, double comet shaped electroluminesc. 8-52577
 ZnTe, band parameters from bound exciton, donor-acceptor pair excitation luminescence 8-92111
 ZnTe, donor acceptance pairs, photoluminesc. excitation spectra (*Japanese*) 8-64409
 ZnTe, excited acceptor, donor states, luminesc. 8-72604
 ZnTe, free exciton refl., surface layer effects 8-76493
 ZnTe, high quality p-type cryst., predominant acceptors 8-60504
 ZnTe, relaxation processes, emission spectra (*Russian*) 8-72598
 ZnTe:As(P), spin flip acceptor scatt. 8-92072
 ZnTe:Mn, exciton refl. band, giant mag. splitting (*Russian*) 8-56079
 ZnTe:Mn, mag. field splitting α n=2 exciton state (*Russian*) 8-79940
 ZnTe:O,Zn, dual ion implantation, luminesc. spectra obs. 8-87697
 ZnTe:Sb film, electrical props. 8-76172
 ZnTe-metal structures, photosensitivity spectrum (*Russian*) 8-76147
 ZnTe-MgTe, long wavelength optical phonons, IR refl. and Raman obs. (*French*) 8-60433

III-V semiconductors

- anodic oxidation (*Japanese*) 8-92385
 avalanche breakdown voltage for p-n junction, calc. 8-88020
 carrier mobility anisotropy due to dislocations 8-60124
 CESR, optical detect. by spin orientation techniques, anal. 8-80251
 dislocations, local temp. distrib., due to Joule heating 8-71734
 doped, zinc blende type, electron-phonon interaction, reson. scatt. theory 8-64036
 electron-hole liquid theory, generalised RPA 8-87914
 electronic dielec. const., interionic separation d-core effect 8-60046
 electronic theory, covalent-metallic or covalent-ionic phase transition under pressure 8-72105
 electronic theory, cryst. energy and bulk modulus 8-72104

III-V semiconductors continued

- epitaxial growth by CVD 8-92195
 Ga(AsP) on GaAs, LPE, growth with Ge and Sn solvents, phase diag. 8-88434
 n-GaAs:O, press. depend. of deep level associated with O, transient capacitance meas. 8-64000
 GaAs-Ga_{1-x}Al_xAs, ultrathin layer heterostruct., pseudopot. calcs. 8-95343
 GaInAsP quaternary alloys, orientation effects in LPE growth 8-92203
 galvanomagnetic phenomena, model, transport phenomena in presence of medium range disorder (*French*) 8-56162
 n-GaP, quasidirect radiative recombination of free holes at neutral shallow donors 8-64410
 GaP, reevaluation of bandgap and free exciton binding energy 8-60061
 impurities, conc. of C, O, Si 8-59832
 n-InP, magneto-impurity resonances, obs. of central cell struct. 8-95303
 ion implantation, effect of implantation temp. 8-75683
 ion implanted layers, amorphisation, recrystallisation 8-63782
 ionic, tetrahedral, electrical susceptibility, chemical bond approach 8-87931
 local force variations due to substitution impurities 8-51633
 low temperature, high mobility transistor materials 8-87970
 MBE, review and appls. (*German*) 8-68630
 MIS structures, review 8-95372
 mixed, electron mobility theory 8-84210
 multilayer structures, contact resistance profiling method 8-56213
 negative electron affinity III-V photocathodes for soft X-ray detection 8-93110
 p-type epitaxial layer, thermalisation of electron-hole plasma, photolum. meas. 8-80408
 phonon frequencies, Brout sum rule and trace variable forces 8-59892
 piezoelectric semiconductor, piezoresist. of grain boundaries 8-51995
 piezoresistive, local resist. near dislocations, eqns. 8-60123
 point defects, internal friction meas. 8-71787
 positron annihilation 8-72636
 quaternary alloys, energy bandgap and lattice const. 8-67940
 quaternary-binary heterojunction, X-ray characterisation of defects 8-95239
 Schottky barrier formation, Fermi-level pinning, defect mech. 8-95358
 solid solutions, interaction parameters 8-51688
 sphaleritic structure, effective mass, forbidden band width and lattice constant relation (*Slovak*) 8-51879
 surface barrier structures with metals, production by chem. precipitation of metals, props. (*Russian*) 8-84298
 VPE of ternary layers, on-time comp. determ. 8-67915
 zinc blende structured semiconductor surface analysis by X-ray photoelectron spectroscopy (*Japanese*) 8-88672
 zinc-blende structure, plasmon line shape, local field effects 8-76011
 zincblende compounds, (111) and (111) faces, surface electron states 8-80035
 zincblende structure p-type semiconductors, internal strain on bound hole-phonon interaction 8-91492
 (Al,Ga)As DH injection lasers, internal quantum efficiency, algorithm for meas. 8-66822
 (Al,Ga)As long-lived DH injection lasers for fibre optic communication, degradation exam. 8-50778
 (Al,Ga)As/GaAs, LPE grown heterostructures, X-ray diffr. exam. of interfacial elastic strains 8-72019
 (Al,Ga)As-GaAs laser, transverse junction stripe, high temp. single mode CW operation 8-74918
 Al-Ga-As heterostruct. with confined current flow, fabrication 8-68081
 Al-GaAs-Al sandwich-type sputtered film, elec. props. 8-91780
 AlAs epilayers, MBE growth on GaAs, self-terminating thermal oxidation 8-92374
 AlAs-GaAs (100) interface, tight binding calc. of electronic struct. 8-95342
 AlAs-GaAs (110) interface, self-consistent calc. of interface states and electronic struct. 8-52066
 AlAs-GaAs abrupt (110) interface, electronic struct. 8-95339
 AlAs-GaAs heterojunctions, on graphite substrate, props., solar cell appls. 8-91760
 AlAs-GaAs monolayer crystal, two-photon absorpt. spectrum 8-52589
 AlGaAs CW oxide defined stripe laser, optical feedback effects 8-79045
 AlGaAs constricted DH diodes, stable single filament laser action obs. 8-55358
 (AlGa)As DH laser, insulating C film deposition to prevent facet deterioration 8-87049
 (AlGa)As, transverse junction stripe single mode oscillating laser, gain spectra 8-55356
 AlGaAs-GaAs DH lasers, accelerated life test 8-66830
 Al_{0.5}Ga_{0.5}As:Te(SN), impurity effects on interface morphology of LPE films on corrugated GaAs substrates 8-88435
 Al_{0.5}Ga_{0.5}As, first order phonon spectrum replicas 8-60467
 Al_{1-x}Ga_xAs laser, transverse junction stripe, with low threshold current and high efficiency 8-82985
 Al_{1-x}Ga_xAs, transient-mode LPE on GaP 8-72746
 Al_{1-x}Ga_{1-x}As, analytic approx. for Fermi energy 8-63973
 Al_{1-x}Ga_{1-x}As DH p-n junction, surface recomb. effects on current, luminesc. expts. 8-72246
 n-Al_{1-x}Ga_{1-x}As, epitaxial, photolum. emission and excitation spectra 8-76526
 Al_{1-x}Ga_{1-x}As heterojunction LED, fabrication by negative profiling of substrate and characts. 8-56523
 Al_{1-x}Ga_{1-x}As, LPE, cathodoluminesc. obs. 8-68565
 Al_{1-x}Ga_{1-x}As layer, LPE, graded band gap solar cell, composition profile, Rutherford backscatt. 8-76612
 Al_{1-x}Ga_{1-x}As native oxide, low leakage, MOS characterisation 8-91795
 Al_{1-x}Ga_{1-x}As, p-n homojunction, hot carrier recomb., overheating luminesc. 8-92122
 Al_{1-x}Ga_{1-x}As p-n junction, photolum. and current, interface recomb. effects 8-95346
 Al_{1-x}Ga_{1-x}As, Raman spectroscopy, characterisation of thin films and heterostructures 8-76439
 Al_{1-x}Ga_{1-x}As:Cr, high resist. film, photolum. and photocond. meas. 8-72596

III-V semiconductors continued

- Al_{1-x}Ga_xAs-GaAs heterojunction photodiodes, high-efficiency fast-response 8-52073
 Al_{1-x}Ga_xAs-GaAs multilayer heterostructures, optical birefringence 8-64422
 Al_{1-x}Ga_xAs-GaAs n-n heterojunction, LPE, Auger profiling and absence of rectification 8-95349
 Al_{1-x}Ga_xAs-GaAs-Al_{1-x}Ga_xAs photopumped quantum-well laser, room temp. CW operation 8-74908
 AlGaAsP/GaAs heterojunction, X-ray characterisation of defects 8-95239
 Al_{1-x}Ga_{1-x}As_{1-x}Sb_xGa_{1-x}Sb_x buried heterojunction electroabsorption modulation 8-55439
 Al_{1-x}Ga_{1-x}In_xAs, LPE on InP, solid-liq. equilib. calcs. 8-84083
 Al_{1-x}Ga_{1-x}P, IR phonons, lattice reflection spectra 8-51626
 Al_{1-x}Ge_{1-x}Sb, photolum. spectra 8-95602
 Al_{1-x}In_xSb, DC sputtering and struct. 8-52674
 AlN, VPE by closed space vapour process, and optical absorpt. edge 8-88371
 AlP(As)(Sb), avalanche breakdown voltage for p-n junction, calc. 8-88020
 AlSb (110), wave functions and surface struct. 8-91519
 As₂Te₃-GaAs, amorphous-monocrystalline heterojunctions, space charge limited conduction 8-64099
 BP, epitaxial growth on Si substrate, Si impurity profile, ion microanal. 8-87886
 BP, VPE, diffused layers formed in Si substrates, device appls. 8-56585
 CdS, vacuum epitaxial growth on CuInSe₂ 8-92193
 Ga-As system, phase equilib., Krupkowski model (*German*) 8-95132
 Ga-GaAs interface immersed in electrolytic solns., elec. props. 8-95368
 Ga-In-Sb, solidus isotherms and isoconcentration lines 8-56624
 GaAs (110), wave functions and surface struct. 8-91519
 Ga_{1-x}Al_xAs, metal-gap channel waveguides, intensity modulation 8-66899
 GaAlAs, DH CW diode laser, picosecond pulse generation 8-83002
 (GaAl)As, DH laser, low-current, proton-bombarded, design and characts. 8-87059
 GaAlAs DH laser diode, deep level associated with slow degradation 8-87050
 (GaAl)As, DH lasers, degradation mechanisms, temp. depend. 8-66825
 (GaAl)As high performance diode laser, high-reflectivity cavity mirrors 8-82994
 (GaAl)As injection lasers, self-pulsations, Q-switching and mode-locking effects 8-66827
 GaAlAs laser transmitter for optical fibre communication, features 8-90423
 (GaAl)As lasers, low threshold proton isolated, spectral and transient response 8-87052
 GaAlAs novel DH lasers fabrication 8-50803
 GaAlAs-GaAs double heterostructure, interfacial recomb. velocity, photolum. meas. 8-68075
 GaAlAs-GaAs epitaxial heterostructures for integrated optics functional elements 8-50948
 GaAlAs-GaAs optoelectronic devices, optical waveguide periodic structures appls. (*Polish*) 8-50947
 Ga_{0.5}Al_{0.5}As-GaAs, DH, interfacial recomb., photolum. time decay meas. 8-95347
 Ga_{1-x}Al_xAs DH injection laser diode, long-term-degraded, TEM obs. 8-71102
 Ga_{1-x}Al_xAs, channelled substrate, planar struct. and DFB lasers 8-79032
 Ga_{1-x}Al_xAs LPE film, with x=0.23 and 0.37, grown by linear cooling, thickness comparison with GaAs 8-87892
 Ga_{1-x}Al_xAs p-i-n structure photoelectric props. 8-95353
 Ga_{1-x}Al_xAs Schottky barrier, oxide free, surface composition and fabrication 8-68084
 Ga_{1-x}Al_xAs, Zn diffusion, depend. on Al content 8-59981
 Ga_{1-x}Al_xAs-GaAs injection laser, branching waveguide coupler fabrication by LPE 8-63202
 Ga_{1-x}Al_xAs-GaAs laser, distributed Bragg confinement, room temp. operation 8-74907
 Ga_{1-x}Al_xAs-GaAs low threshold room temp. DH lasers grown by metalorganic CVD 8-50804
 Ga_xAl_{1-x}As embedded stripe DH laser monolithically integrated with strip waveguide 8-59025
 Ga_xAl_{1-x}As, LPE, charge carrier conc. distrib. (*Russian*) 8-52694
 Ga_xAl_{1-x}As-GaAs DH laser, continuous room temp. operation 8-55363
 Ga_{1-x}Al_xAs_{1-x}P_x-GaAs quaternary heterojunction, misfit dislocation charact. by synchrotron radiation white beam topography 8-63771
 Ga_{1-x}Al_xP, two-phonon optical absorpt. 8-88341
 Ga_{1-x}Al_xSb p-n homojunction LPE and photovoltaic effect obs. (*French*) 8-64108
 Ga_{1-x}Al_xSb p-n structure, variable-gap, electroluminescence 8-52582
 n-Ga_{1-x}Al_xSb, transport phenomena in low and high mag. fields 8-80007
 Ga(As,P)/(In,Ga)P DH laser, red-emitting, optical and elec. characts. 8-66826
 GaAs (001)-Ag contact, surface stoichiometry and struct., and electronic surface states 8-95361
 GaAs, (100), comp. and struct. of differently prepared surfaces, LEED and AES 8-91524
 GaAs (110), chemisorbed O₂, extrinsic surface states 8-91535
 GaAs (110), electron states from transfer matrix method 8-56203
 GaAs (110), electronic states and initial steps in oxidation 8-91534
 GaAs (110), pseudocharge density calcs. 8-84275
 GaAs (110), subsurface atomic displacements, LEED exam. 8-71912
 GaAs (110), surface and near-surface atomic struct., LEED 8-91515
 GaAs (110), surface electronic struct., ang. resolved photoemission expts. and tight binding calcs. 8-91743
 GaAs (110), surface states and matrix elements in angle-resolved photoemission 8-91741
 GaAs (110), surface states symmetry determ. using polarisation-depend. ang. resolved photoemission 8-91742
 GaAs (110), unrelaxed, surface states in bond orbital model 8-91749
 GaAs (110), valence band Auger spectra, from Ga and As CCV transitions 8-92149
 GaAs (110) surface, atomic and electronic struct. 8-72223

III-V semiconductors continued

- GaAs, (110) surface, bond angle and lengths of rearranged As and Ga atoms 8-71918
 GaAs (110)-Al(Ga) interface, interface states, photoemission study 8-95359
 GaAs (110)-Au Schottky barriers on ordered and disordered GaAs surfaces, props. 8-95360
 GaAs {001} layer, LPE, dislocation etch pits revealed by molten KOH 8-63772
 GaAs, absorption coefficients, method of meas. 8-83048
 n-GaAs, absorption tails in surface depletion layer and bulk 8-64379
 GaAs, amorphous layer formation, ion implantation, IR spectra 8-95063
 GaAs, anodic oxidation using O plasma, and oxide layer evaluation 8-85015
 GaAs anodic oxide, refl. and transmission, 0.01-6 eV 8-95613
 GaAs anodic oxide film, optical props. 8-72626
 GaAs, anodic oxide film, annealing effect on carrier density profile 8-88040
 GaAs, atom probe field ion microscopy 8-80460
 GaAs, band struct., modulation spectroscopy, two-ray methods (*Russian*) 8-54469
 GaAs, biexciton stability, appl. of theory for polar crystals. 8-76002
 GaAs, binding of exciton to neutral acceptor 8-79937
 GaAs, CESR, optical detect. by spin orientation techniques, anal. 8-80251
 GaAs, CVD in Ga-AsCl₃-H₂ system with different input supersaturations (*Russian*) 8-68098
 GaAs CW DH laser, inherent oscillations and subharmonic resonances obs. in light output 8-74910
 GaAs, carrier mobility profiles meas. at room temp. by Corbino effect 8-60128
 GaAs, chemical etching processes, review 8-95832
 GaAs, chemical shift and effective atomic charges 8-88201
 p-GaAs, circular polarisation of hot luminesc. 8-52572
 GaAs cryst., creep and dislocation vel. at different doping and temps. 8-95783
 GaAs, Debye temperature, atomic mean square displacement 8-87757
 GaAs, deep trapped impurities, photocond. spectra, interpretation 8-52030
 GaAs devices, ohmic contacts using epitaxial Ge films 8-88027
 n-GaAs, diffusion coeff., Monte Carlo calc., rel. to trapped domain behaviour 8-56152
 GaAs, direct gap, picosec. time resolved reflectivity obs. of optically excited hot carrier distrib. 8-76495
 GaAs directional couplers and electrooptic switches, wavelength depend. 8-79143
 GaAs, disordered, ion implanted, elec. props. 8-84212
 GaAs doping structures, production and appl. (*German*) 8-95064
 GaAs double-cavity laser with branching output waveguides 8-63128
 GaAs, dual implantation of C⁺ and Ga⁺, sheet resist. and Hall effect meas. 8-67728
 GaAs, electroabsorpt. avalanche photodiode waveguide detectors 8-65965
 n-GaAs, electron and gamma ray irradiated, introduction and annealing of defects 8-67736
 GaAs, electron effective mass, temp. depend. for various degrees of doping and compensation (*Russian*) 8-79923
 GaAs, electron transient vel. characts., Γ-L-X cond. band ordering 8-79997
 GaAs, electron-hole plasma, ground state energy 8-84244
 p-GaAs, electronic props. 8-68040
 GaAs, electronic surface structure Cs(Rb)(Na) adsorpt. processes, AES, LEED, EELS, study 8-68068
 GaAs, epitaxial and metallic thin-films, anodic oxidation anal. 8-80673
 n-GaAs epitaxial film, potential barrier height, temp. depend. (*Russian*) 8-68070
 GaAs, epitaxial film on GaAs substrate, two-interface surface polariton modes 8-60180
 GaAs, epitaxial growth in Ga-AsCl₃-He₂ system, expt.-statistical analysis (*Bulgarian*) 8-60580
 GaAs epitaxial layer, AuGe ohmic contact production by laser alloying 8-88026
 p-GaAs epitaxial layers, electron-hole plasma, quantum effects in magnetoluminesc. 8-72591
 GaAs epitaxial layers, characterisation Hall effect and Schottky diode profile meas. 8-91791
 GaAs, epitaxial layers on conductive substrate, elec. characterisation 8-91790
 GaAs epitaxial tunnel diode pressure sensors 8-57975
 GaAs, epitaxy using TMG and AsH₃, chloride etching effect 8-76606
 GaAs, etchant, universal, multipurpose 8-53008
 GaAs, exam. as cladding material, for optical waveguides as cutoff polariser 8-55474
 n-GaAs, exciton luminescence, excitation intensity depend. 8-52554
 GaAs, excitonic polariton reson. interaction with LA phonons 8-60481
 GaAs, excitons, diamond like semiconductor, variational calculation of binding energies 8-79938
 GaAs FET, continuous growth of LPE double layers 8-64487
 GaAs FET structure, sharp line photolum. spectra 8-72248
 GaAs film, piezoelec. semicond., cascade capture of carriers by attractive impurity centres, cross sections 8-56157
 GaAs film, plasma oxidation and oxide props. 8-95825
 GaAs, film, radiative relax. time, nonequilibrium carriers 8-84657
 GaAs, forbidden Raman scatt. by LO phonons 8-64367
 GaAs, grown-in dislocation density, impurity effect 8-51543
 n-GaAs, heat treated, origin of 1.41 eV emission band, photolum. expt. 8-72579
 GaAs, heavy metal migration, ESCA study (*French*) 8-75885
 GaAs, highly transparent semicond., multiphonon IR absorpt. 8-60461
 GaAs, hole effective mass, press. depend., theory and tunnelling expts. 8-75986
 n-GaAs, hybrid-hybrid mode interaction in crossed elec. and mag. fields 8-51997
 p-GaAs IR plasma reflectivity spectra calc., rel. to carrier conc. 8-52511
 GaAs, illuminated, carrier lifetime profile, depth depend. 8-68036
 n-GaAs, impact ionisation initiated by acoustoelectric effect 8-52038

III-V semiconductors continued

GaAs, impact ionisation rates for electrons and holes, photocarrier multiplication obs. 8-87995
 GaAs, implantation disorder, flux and fluence depend., electrorefl. expts. 8-83833
 GaAs, implantation of Si, Al, Hf, Ta into InP and GaAs, form. of protective oxide 8-79622
 GaAs, impurity scattering of current carriers in quantizing mag. field 8-51954
 n-GaAs, influence of uniaxial stress on low field resist. 8-87976
 GaAs injection laser, intensified luminesc. (*Russian*) 8-90416
 GaAs injection lasers, longitudinal mode spectrum, effect of carrier diffusion 8-71099
 GaAs interface with anodic and thermal oxides, comparison of AES and ESCA 8-95980
 GaAs, ion etching, effects on optical props. and lattice disorder 8-83122
 GaAs, ion implantation damage, TEM exam. of variation with ion species and stoichiometry 8-59827
 GaAs, irradiated with fast neutrons, IR vibrational absorpt. 8-75776
 GaAs, k-linear coupling, E_1' transitions 8-91583
 GaAs, LPE, charge carrier conc. distrib. (*Russian*) 8-52694
 GaAs LPE film, thickness comparison with $Ga_{1-x}Al_xAs$ for layers grown by linear cooling 8-87892
 GaAs, LPE growth of high purity layers by sliding boat method 8-76610
 GaAs LPE layers, dopant tracing of terrace growth 8-75948
 GaAs, LPE with $AsCl_3$ -saturated Ga/As solns. 8-63953
 GaAs laser, surface temp. distrib. (*Russian*) 8-74909
 GaAs, laser irradiated, origin of periodic surface struct. 8-91513
 GaAs laser material, secondary dislocation climb during optical excitation 8-75672
 GaAs lasers, at room temp., modulation at X-band frequencies 8-87079
 n-GaAs, lattice scatt. identified as cause of 1/f noise 8-64074
 GaAs, lattice thermal cond. from three phonon scatt. relax. rate 8-51755
 GaAs MESFET, deep trapping effects at GaAs-GaAs:Cr interface 8-72245
 GaAs MIS capacitor, transient capacitance and C-V characts. 8-95374
 GaAs MIS dynamic optically controlled transparencies 8-90523
 GaAs MIS struct., appl. of $Al_xGa_{1-x}As$:O as insulating layer 8-64115
 GaAs MIS struct., elec. props., effect of interface As domains 8-88032
 GaAs MIS structs., review 8-95372
 GaAs, magnetic freezeout in ultraquantum limit 8-76017
 GaAs, manifestation of local vibr. of dislocations in IR spectra 8-88339
 GaAs, maximum electric field in high-field domain in Gunn devices 8-79996
 n-GaAs, melt-grown, stoichiometry, photolum. obs. 8-72583
 n-GaAs, metal-insulator transition in impurity band induced by mag. field and loss of dims. 8-52042
 GaAs, minority carrier diffusion length, Schottky barriers, electron bombard. investigation 8-68037
 GaAs, minority carrier diffusion lengths, contact metal effects 8-72260
 GaAs minority carrier diffusion lengths in semicond. SEM meas. interpretation 8-80002
 n-GaAs, model describing removal and scattering of charge carriers by defect clusters 8-76069
 GaAs, multiphonon nonradiative transition rate for electrons in semicond. and insulators 8-60503
 GaAs n-n⁺ epitaxial structure for CW microwave electroacoustic amplifier 8-59235
 GaAs, nonlinear extrinsic luminescence 8-84645
 GaAs, operation characteristics (*Rumanian*) 8-87053
 GaAs, optical modulation spectra, proton damage effect 8-76487
 GaAs optical modulator for coupled waveguides 8-71235
 GaAs, optically pumped laser with acoustic distributed feedback 8-82977
 GaAs, optoelectronic devices, conf., Berlin, DDR 8-91755
 GaAs oxide, passivated layers, quantitative in-depth profile, AES-SIMS thermal, anodic and plasma oxidations 8-84087
 GaAs oxide, plasma grown, semiquantitative chemical depth profiles Auger spectroscopy and neutron activation anal. 8-53284
 GaAs oxide film, thermal and anodic, in-depth profiles, XPS expts. 8-84086
 GaAs, P-T diagram, cryst. struct. stability 8-51886
 GaAs, p-n homojunction breakdown voltage for onesided abrupt junctions (*German*) 8-56210
 GaAs, p-n junction, Zn⁺ implanted, residual radiation defect influence on characts. (*Russian*) 8-84287
 GaAs patterned epilayer structures, MBE writing 8-56590
 GaAs, Peltier induced growth kinetics of LPE 8-64485
 GaAs, periodic surface corrugation generation by holography 8-55469
 GaAs, phonon surface density, Brillouin elasto-optic cross section 8-72536
 n-GaAs, photo-Hall effect meas. of ionised impurity scatt. 8-56182
 GaAs, photocathodes, photoelectron emission, energy levels, influence of dims. quantisation (*Russian*) 8-64447
 GaAs, photoluminescence intensity of cleaved surface, ambient gas influence 8-88345
 n-GaAs, piezoelectric semiconductor, influence of acoustic phonon disturbances on conductivity 8-91697
 GaAs, piezoresistance and conduction band minima 8-51993
 GaAs planar p-n junctions, Be ion implantation, fabrication and characts. 8-88022
 GaAs planar stripe geometry and channelled substrate DH laser, lateral current confinement 8-66823
 GaAs, plasma anodisation in DC discharge, AES and MIS diode expts. 8-95826
 GaAs, positronium-like states, low temp., ang. correl. of annihilation photons 8-76549
 GaAs, radiation defect obs. using Schottky diode characts. 8-76024
 GaAs, Raman scatt., electron-phonon deformation potential coupling 8-52502
 GaAs, Raman spectroscopy, characterisation of thin films and heterostructures 8-76439
 GaAs, reactor-irradiated, anisotropy in diffuse small angle neutron scatt. 8-51598

III-V semiconductors continued

GaAs, S and Se ion implantation 8-55884
 n-GaAs Schottky barrier diode, electron processes at interface (*Russian*) 8-84301
 GaAs Schottky diode, use in acoustic memory correlator 8-66989
 GaAs Schottky gate FET struct., obs. of localisation in two-dims. systems 8-60213
 n-GaAs semicond. liq. junction solar cells, photocurrent spectra, carrier recombination 8-76142
 n-GaAs, smooth and continuous ohmic contacts using epitaxial Ge films alloyed with Ni 8-68086
 GaAs, solid solubility of Se, SIMS 8-67830
 GaAs, solubility in Ga-Al alloys in multilayer LPE of $Ga_xAl_{1-x}As$ 8-52690
 GaAs, structural defects, detection by electrochemical etching 8-55872
 GaAs substrate, epitaxial growth of single crystal layers of $Cd_{1-x}Sn_xS$, close-spaced geometry 8-92198
 n-GaAs substrates, ion implanted, compensation 8-75680
 GaAs surface, Ar ion bombardment induced photon emission, rel. to target temp. 8-72612
 GaAs surface, cluster model approach for electronic struct. 8-56205
 GaAs surface, energy-minimisation approach to atomic geometry 8-95213
 GaAs, surface (111), (111), (110), XPS, photo-Auger ionisation cross section, electron mean free paths 8-56558
 GaAs, surface final-state effects on core electron transition energies 8-91745
 GaAs surface impurities, struct. and comp. of compounds using IR spectroscopy 8-63918
 GaAs, surface segregation of implanted alkali metals, photoemitter prep. and characts. (*French*) 8-60544
 GaAs, surface structure and orbital symmetries of (110) surface state 8-72229
 GaAs surfaces (110) and (111)As, UPS and LEED 8-91514
 GaAs, synthesis by molten salt electrolysis 8-64486
 GaAs, thermal oxidation, 450 to 760°C, Rutherford back scattering obs. 8-76780
 GaAs, thermal oxidation in As_2O_3 vapour 8-56792
 GaAs, thermally oxidised, TEM obs. 8-72036
 GaAs thin films, differential mobility anisotropy effect on wave propagation 8-88050
 GaAs, time of flight atom-probe mass spectra 8-92584
 GaAs transferred electron devices, ohmic contacts 8-52082
 GaAs, transient-mode LPE on InP 8-72746
 GaAs, transmutation doped, shallow donors, magneto-optical study, photocond. meas. 8-87996
 GaAs, two-photon absorpt. of Nd:glass laser radiation 8-87107
 n-GaAs, two-valleyed semicond., hole electron diffusion coeff., random walk calc. 8-68033
 GaAs unintentionally doped layer growth using MBE 8-72741
 GaAs VPE growth, growth rate anal. 8-52680
 GaAs VPE layers, role of diffused Ga vacancy in degradation 8-95050
 GaAs, VPE on Ge substrate, and characterisation 8-72736
 GaAs, valence band structure, CPA, bond orbital calcs. 8-87909
 n-GaAs, Verdet const., free carrier density depend. 8-56462
 GaAs:B, electron or neutron irradiated, low symmetry interstitial B centre 8-79605
 GaAs:Be, annealing effect during MBE 8-79898
 GaAs:Co²⁺, EPR expts., y-factor determ. 8-76301
 GaAs:Cr, fine structure in cathodoluminescence spectrum 8-56524
 GaAs:Cr, IR spectral detectivity 8-70184
 GaAs:Cr, luminesc. stress splitting, 4.2K 8-84627
 GaAs:Cr, semi-insulating, characterisation by photoelectronic data 8-86051
 GaAs:Cr, semiinsulating solid-state inductance, theory and expt. 8-56138
 GaAs:Cr, Si, deep centre photoluminescence spectra 8-95601
 GaAs:Cr, site symmetry of Cr ions, ground-state splitting, ballistic phonon expts. 8-95273
 GaAs:Cr, VPE grown, exam. of doping GaAs using Cr(CO)₆ 8-72737
 n-GaAs:Cu, contaminated single cryst., deep level photoluminesc. model 8-68554
 GaAs:Cu, in MSM struct., phototriger effect 8-56238
 GaAs:Cu, supersaturated solid solns., decomp., surface impurity content 8-51681
 GaAs:Fe, profile of impurity optical absorption bands 8-56509
 GaAs:Ge, LPE, on semi-insulating GaAs, film-substrate interface characterisation 8-72017
 GaAs:Ge, vap. grown, diatomic complex donor and acceptor model 8-80003
 GaAs:O, photocapacitance quenching effect 8-91727
 GaAs:O, photocond., electron traps, level-broadening, 90 to 150K 8-60158
 GaAs:O, slow domains, origin 8-60132
 n-GaAs:O carrier removal profiles meas. 8-56154
 GaAs:P⁺, defect form. on P⁺ implantation at various temp., He⁺ backscatt. obs. 8-59828
 GaAs:Se, and undoped sample, annealed, surface cond. change, n-p double layer 8-64095
 GaAs:Se, implanted, annealing with O-free CVD Si₃N₄ encapsulant 8-83834
 GaAs:Si, Cr, carrier concs. from Hall effect, microscopy, localised vibrational modes absorption meas. 8-56104
 GaAs:Si p-n structure, radiative recombination region 8-52071
 GaAs:Si(Ge) LPE layers, luminesc. props. rel. to substrate quality 8-52583
 GaAs:Sn, LPE layers, electronic props., depend. on Sn incorporation 8-87883
 GaAs:Sn, surface segregation of Sn during MBE, SIMS and AES 8-72031
 n-GaAs:Te, heavily doped, interband luminesc. intensity, heat treatment effect 8-72593
 GaAs:Te, heavily-doped, annealing-induced prismatic dislocation loops and elec. changes 8-51546
 GaAs:Zn, diffused, depth profile by photoluminesc., LED applic. 8-72587
 p-GaAs:Zn, Mn, degenerate, tunnel p-n junction and semicond.-metal struct., I-V characts. 8-72252

III-V semiconductors continued

GaAs-(Ga,Al)As heterostructure transmission photocathodes, characts., and epitaxial growth (*French, English*) 8-52616
 GaAs-(Ga,Al)As light modulators and distributed Bragg reflector laser, monolithic integration 8-50944
 GaAs-(GaAl)As epitaxial layers and DH lasers, deep centre 1.02 eV luminesc. 8-80387
 GaAs-(GaAl)As LOC-DBR laser, high differential quantum efficiency 8-79031
 GaAs-Al Schottky barrier diode, prep. by MBE on GaAs, and characts. 8-72257
 GaAs-Al_{0.5}Ga_{0.5}As-Cr/Au MIS capacitors, characts. meas. 8-95371
 GaAs-Al_{1-x}Ga_xAs lar, PbO-SiO₂ glass optical coating 8-71113
 GaAs-Al_{1-x}Ga_xAs, optically pumped taper coupled laser, second order Bragg reflector 8-50788
 GaAs-Al_{1-x}Ga_xAs, DH laser, effect of bulk nonradiative recombination 8-82967
 GaAs-Al_{1-x}Ga_xAs, monolithic integrated optics, rib waveguide switches with MOS electrooptic control 8-87168
 GaAs-Al_{1-x}Ga_xAs DH laser structures, high-resolution composition profiling with photolum. 8-71101
 GaAs-Al_{1-x}Ga_xAs DH laser, room temp. threshold current 8-79019
 GaAs-Al_{1-x}Ga_xAs optical modulator for coupled waveguides 8-71235
 GaAs-Al_{1-x}Ga_xAs stripe geometry DH laser, threshold current density, effect of optical mode losses 8-59008
 GaAs-Al_{1-x}Ga_xAs superlattice, mag. field induced dimensionality change 8-64381
 GaAs-AlAs, pseudobinary alloy, phase diagram calc. 8-52786
 GaAs-AlAs (100) interface, tight binding calc. of electronic struct. 8-95342
 GaAs-AlAs alternating monolayers, zone folding effects on phonons 8-72510
 GaAs-AlAs and related monolayer heterostructures, pseudopot. calc. 8-60198
 GaAs-AlAs layered superlattices, deposited by MBE, exam. of crystal growth kinetics 8-72739
 GaAs-AlGaAs DH laser with buried facet 8-55373
 GaAs-AlGaAs distributed Bragg reflector integrated twin-guide laser, temp. characts. 8-87064
 GaAs-AlGaAs double heterostructure, optically induced dislocation glide, cooperative phenomena 8-74911
 GaAs-AlGaAs transverse junction stripe laser, single mode behaviour after 12000 hr ageing test 8-66831
 GaAs-Br₂(-Zn) system, filamentary cryst. prep. 8-52650
 GaAs-Ga, (110) interface electron states, photoemission study, chemical shift, surface charge redistrib. 8-72259
 GaAs-Ga_{1-x}Al_xAs, superlattice umklapp processes in resonant Raman scattering 8-64362
 GaAs-Ga_{1-x}Al_xAs n⁺-v-n junction, avalanche carrier multiplication (*Russian*) 8-76140
 GaAs-Ga_{1-x}Al_xAs superlattice, sub-band dimensionality 8-63981
 GaAs-GaAlAs, DH laser material, LPE grown, obs. of melt carryover 8-91553
 GaAs-GaAlAs, transverse Bragg-reflector injection lasers 8-74926
 GaAs-GaAlAs DH internally striped planar laser with flat freq. response up to 2 GHz 8-66829
 GaAs-GaAlAs DH LED, transient current trap spectroscopy 8-80049
 GaAs-GaAlAs DH laser diode, lateral modes 8-59009
 GaAs-GaAlAs DH material, dislocation glide and climb, electron diffr. 8-83824
 GaAs-GaAlAs injection lasers on semi-insulating substrates using laterally diffused junctions 8-55364
 GaAs-GaAlAs optically pumped DFB laser, wavelength tuning effect 8-82979
 GaAs-GaP(Sb), pseudobinary alloy, phase diagram calc. 8-52786
 GaAs-Ge, n-n isotype heterojunctions, fixed-interface-charge model 8-56215
 GaAs-Ge (100) interface, electronic struct., scattering-theoretic approach 8-95340
 GaAs-Ge (110), heterojunction chemistry, photoemission expts. 8-95244
 GaAs-Ge abrupt (110) interface, electronic struct. 8-95339
 GaAs-Ge interface, XPS obs. of electronic struct. 8-95341
 GaAs-InAs, pseudobinary alloy, phase diagrams calc. 8-52786
 GaAs-InSe p-n junctions, 'optical' contacts, elec. props. 8-56222
 GaAs-insulator film interface, evidence for growth-induced damage from photolum. expts. 8-75953
 GaAs-insulator interface, elec. props. 8-95370
 GaAs-metal Schottky barrier diodes, impedance, freq. and voltage depend. 8-64114
 n-GaAs-YIG layered structure, magnetostatic surface wave amplification 8-88107
 GaAs-ZZ (*Russian*) 8-90468
 GaAs-ZnS p-n heterojunction, epitaxial, elec. props. (*Russian*) 8-88023
 GaAs(P), ion irradi. damage, strain effect contrib., channelling meas. 8-67752
 GaAs(P), momentum distrib. of electrons, anisotropy, positron annihilation (*Russian*) 8-84676
 GaAsP, negative-electron-affinity, photoemission transmission coeff. 8-56560
 GaAs_{0.6}P_{0.4}Be, implanted annealing studies, elec. resist., Hall effect meas. 8-84213
 GaAs_{1-x}P_x based structs., carrier conc., mobility calcs. from Hall effect meas. 8-60138
 GaAs_{1-x}P_x, continuously tunable electron beam pumped laser 8-50802
 GaAs_{1-x}P_x, diffusion of implanted Zn ions, ion microbe analysis 8-95190
 GaAs_{1-x}P_x, heterogeneous struct. obs. by anodisation-electrorefl. technique 8-84088
 GaAs_{1-x}P_x, VPE on Ge substrate, and LED characts. 8-72736
 GaAs_{1-x}P_xN, 0.6 < x < 1, photoluminesc., comp. depend. 8-52546
 GaAs_{1-x}P_xN, film, optical absorpt. from photoluminesc. meas. 8-92134
 GaAs_{1-x}P_xZn, diffusion profile determ., ³²P/⁶⁵Zn double tracer technique 8-55888
 GaAs_{1-x}Sb_x, MBE grown, surface struct. exam. by MEED 8-87847
 GaAs_{1-x}Sb_x-Ga_{1-x}In_{1-x}P_{1-x}As_x, multilayer structure, continuously tunable electron beam pumped laser 8-50802
 GaAsSb_{1-x} epitaxial layer, struct. defects rel. to luminesc. 8-72040

III-V semiconductors continued

Ga_{0.47}In_{0.53}As, MBE, InP/Ga_{0.47}In_{0.53}As/InP DH laser fabrication and room temp. operation 8-74906
 Ga_{1-x}In_xAs, alloy film surface processes controlling growth by MBE RHEED and AES exam. 8-84084
 p-Ga_{1-x}In_xAs, Auger recomb., theory and luminesc. expts. 8-56518
 Ga_{1-x}In_xAs, cryst. growth on (100) InP by LPE 8-56591
 Ga_{1-x}In_xAs on InP, lattice matched LPE film growth and characts. 8-72033
 GaInAsP-InP avalanche photodiode, fabrication and characts. 8-54454
 Ga_{1-x}In_xAsP_{1-y}, anodisation, effect of pH, current density and illumination 8-95823
 Ga_{1-x}In_xAsP_{1-y} LPE layers matched to InP, comp. and lasing wavelengths 8-71103
 Ga_{1-x}In_xAsP_{1-y}InP injection laser, partially loaded with distributed Bragg reflector 8-82986
 Ga_{1-x}In_xP alloy films, surface processes controlling growth by MBE, RHEED and AES exam. 8-84084
 Ga_{1-x}In_xP, epitaxial film, diffusion of Cu(Au)(Zn), intrinsic impurity effects 8-87825
 n-Ga_{1-x}In_xP, optical props. and energy spectrum of donors 8-72567
 Ga_{1-x}In_xP, undoped liquid epitaxial layers, effect of heat treatment on photoluminescence 8-60512
 Ga_{1-x}In_xP:N, Delta lattice parameter model, correl. with electronic props. 8-91560
 GaIn_{4-x}PyAs_{1-y}, In rich bulk single crystals, growth from melt via gradient freeze method, and characterisation 8-68618
 Ga_{1-x}In_xSb, LPE on GaSb by stepwise grading, and characterisation 8-72745
 Ga_{1-x}In_xSb, vapour phase epitaxial growth by open tube method 8-84109
 Ga_{1-x}In_xSb:Zn(Te), photolum. and stimulated emission obs. 8-72595
 GaN, elastic constant calc., elastic wave propag. vel. 8-87734
 GaN epitaxial layers, exciton cathodolum. (*Russian*) 8-76543
 GaN, plasma deposition and elec. cond. 8-60585
 GaN, preparation variables rel. to dielectric data, GaAs conversion 8-60591
 GaN:As(P), implanted single cryst. film, cathodolum. 8-60523
 GaP (III) B surface, negative-electron-affinity, photoemission transmission coeff., comparison with GaAsP 8-56560
 GaP (110), surface bands in relaxed cleavage surface, tight binding model 8-91744
 GaP (110), wave functions and surface struct., EPR expts. 8-91519
 GaP, anodically grown insulating layers, prep. and props. (*German*) 8-64158
 GaP, atom probe field ion microscopy 8-80460
 GaP, chemical etching processes, review 8-95832
 n-GaP, cryst. growth, synthesis solute diffusion method, elec. characts. (*Korean*) 8-52653
 GaP, Debye temperature, atomic mean square displacement 8-87757
 GaP, diffusivity and solubility of Cu 8-51743
 GaP, dislocation loops and bipolar obs. by chemical etching 8-55873
 GaP, dispersion of vibrational excitations, Raman scatt. 8-84588
 GaP, dopant dislocations, scanning electron micrographs, cathodoluminesc. 8-91340
 p-GaP electrode, for solar cell, differential capacitance meas. for flat-band potential determ. 8-72256
 GaP, electron hole droplet, motion damping, impurity and piezoelec. scatt. 8-67951
 GaP, electron-hole plasma photolum. obs. 8-52559
 p-GaP, epitaxial layers grown from liq., overcompensated, doping levels 8-91353
 GaP, etching in aqua regia and bromine-methanol-water solns. 8-68833
 GaP film, deposited by RF sputtering, struct. and elec. props. obs. (*Czech*) 8-52667
 GaP film, polycrystalline, with negative affinity, secondary emission (*Czech*) 8-52604
 GaP, first order Mott transition of exciton gas 8-76535
 GaP, heteroepitaxial growth on Si substrate by MBE 8-64481
 GaP, high-order Raman spectra, polariton scatt. 8-56483
 GaP, ion-implanted, form. and annealing of radiation damage 8-91363
 GaP, LEC, SSD and CVD samples, Zn tracer diffusion profiles in solids 8-95189
 GaP, LEC crystal, cathodolum. and photolum. around dislocations 8-84663
 GaP, LPE at 650°C from In solvent, low Si contamination 8-80480
 p-GaP, LPE layers, Hall effect 8-91704
 GaP, MCD of phonon-assisted exciton transitions 8-92053
 GaP, manifestation of local vibr. of dislocations in IR spectra 8-88339
 GaP, obs. of Raman scatt. by Cu vapour laser 8-95586
 GaP on GaAs, LPE, growth with Ge and Sn solvents, phase diag. 8-88434
 GaP, optoelectronic devices, conf., Berlin, DDR 8-91755
 GaP, p⁺-n diode junction, admittance meas. and carrier traps 8-91757
 GaP, p-n homojunction breakdown voltage for onesided abrupt junctions (*German*) 8-56210
 GaP p-n junction, capacitance-freq. dispersion and electroluminescence efficiency 8-64101
 GaP, plasma deposition and elec. cond. 8-60585
 GaP, Raman scattering selection rules for surface polaritons 8-72091
 GaP, rare earth doped, photolum. and elec. props. (*Russian*) 8-52545
 GaP, SEM, cathodoluminesc., impurity and defect detect. 8-83695
 GaP second order Raman spectrum, polarisation meas. 8-64368
 GaP, shallow impurity states, free exciton binding energy 8-79960
 GaP, single cryst., Raman scatt., effective cross-section rel. to nonlinear coeffs. (*Russian*) 8-71152
 GaP, single-crystal, anodically oxidised layers, AES measurements 8-91556
 GaP, soln. growth of bulk crystals., luminesc. and elec. props. 8-92181
 GaP substrate, transient-mode LPE of Al_{1-x}Ga_xAs 8-72746
 GaP surface, quantitative XPS meas. 8-56559
 GaP, surface sensitivity, low energy electron transmission optical modulation 8-76567
 GaP, upper polariton branch obs. by ATR 8-68510
 GaP, valence band structure, CPA, bond orbital calcs. 8-87909
 GaP:Cu, diffusion, solubility, and electrotransport of Au 8-91489

III-V semiconductors continued

GaP:Cr, ESR of doubly ionised Cr acceptor and IR luminesc. 8-56374
 GaP:Cu, thermally and optical excited cond., deep level centres 8-72190
 GaP:Cu p⁺-n junction, deep level parameters, TSC meas., rel. to photo-current techniques 8-72249
 GaP:Cu-Ni, Schottky barrier, TSC meas., trap levels 8-91709
 GaP:Fe, profile of impurity optical absorption bands 8-56509
 GaP:N, appl. of temp. modulated photolum. induced by photoexcitation technique 8-95605
 GaP:N, photoluminesc., temp. depend., exciton recombination mechanism 8-88355
 GaP:N LED, acoustic emission, NDT of dislocation motion 8-91759
 GaP:N(Te), ion implanted at 40 keV, refl. spectra, 210-2000 nm, annealing (*Russian*) 8-80386
 GaP:O, optical transitions via deep levels, phonon interaction 8-87939
 GaP:O, optical transitions via deep levels, cross section temp. depend. 8-87940
 GaP:S, ENDOR meas., symmetries, hyperfine parameters 8-72435
 GaP:s, elec. props. following 1.7 MeV electron irradiation 8-80005
 n-GaP:Te, doping parameters calc., by means of Hall data analysis 8-51925
 GaP:Te, Hall effect and elec. cond., 80-400K 8-91705
 n-GaP:Te, LPE layers, Hall effect 8-91704
 GaP:Zn, diffusion profile determ., ³²P/⁶⁵Zn double tracer technique 8-55888
 GaP:Zn, Hall effect and elec. cond., 80-400K 8-91705
 GaP:Zn, isolated Ga vacancy due to electron irradi., EPR study 8-95519
 GaP:Zn, thermodynamics of Zn doping by liquid phase epitaxy 8-83832
 GaP-anodic oxide devices, optoelectronic device, processing appl. 8-84304
 GaP-Au, Schottky barrier, layer formation, elec. and optical props. 8-91766
 GaP-InP, pseudobinary alloy, phase diagram calc. 8-52786
 GaP(As)(Sb), avalanche breakdown voltage for p-n junction, calc. 8-88020
 GaSb, CESR, optical detect. by spin orientation techniques, anal. 8-80251
 GaSb, chemical shift and effective atomic charges 8-88201
 GaSb crystal, phonon dispersion curves, valence force field 8-95121
 GaSb, Debye temperature, atomic mean square displacement 8-87757
 GaSb, electron-hole plasma, ground state energy 8-84244
 n-GaSb, galvanomagnetic effects 8-72172
 p-GaSb, heavy and light holes scattering 8-91692
 n-GaSb, local resist. near dislocations, eqns. 8-60123
 GaSb, manifestation of local vibrs. of dislocations in IR spectra 8-88339
 GaSb, p-n homojunction breakdown voltage for onesided abrupt junctions (*German*) 8-56210
 GaSb, photolum., electrolum. meas. in p-n junction, temp. influence 8-72594
 GaSb, pulled crystal, microfacet obs. near irregularly remelted surfaces 8-91278
 GaSb, reson. two phonon Raman scatt. near E₁ and E₁+Δ₁ gaps 8-60470
 GaSb surface, quantitative XPS meas. 8-56559
 n-GaSb, temp. distrib. around dislocations, due to Joule heating, calc. 8-71734
 GaSb, valence band structure, CPA, bond orbital calcs. 8-87909
 n-GaSb:S, thermal quenching of residual cond. 8-56188
 n-GaSb:S-metal surface barrier struct., elec. and photoelec. props. 8-56229
 n-GaSb:Te, heavily doped, electron-hole recomb., photoluminesc. spectra 8-84644
 n-GaSb:Te(Se), forbidden optical band gap, Moss-Burstein effect 8-88335
 GaSb-Au structure, metal-semicond. interaction, soft XPS meas. 8-60203
 GaSb-InAs (001) superlattice, electronic struct., tight binding calcs. 8-95350
 Ge-GaAs, n-n isotype heterojunctions, fixed-interface-charge model 8-56215
 Ge-GaAs (110) interface, self-consistent calc. of interface states and electronic struct. 8-52066
 Ge-GaAs superlattice and interface, electronic struct. 8-52065
 (In, Ga)Sb, sputter deposited amorphous film, impulse stimulated explosive crystallisation 8-84098
 In-Te system, IR spectra (*Russian*) 8-84589
 p-InAs, Auger recomb., theory and luminesc. expts. 8-56518
 InAs, intrinsic point defects, nature and influence on electrophys. props. 8-79609
 n-InAs, negative magnetoresist. in extreme quantum limit 8-64051
 InAs, p-n homojunction breakdown voltage for onesided abrupt junctions (*German*) 8-56210
 InAs, second order Raman scatt., electron-two phonon deform. pots. determ. 8-60473
 InAs surface accumulation layers, magneto-transconductance meas. 8-64137
 InAs surface layers, oscillatory transport coeffs. 8-64136
 InAs, valence band structure, CPA, bond orbital calcs. 8-87909
 p-InAs-Au contacts, influence of free surface on elec. behaviour 8-95362
 InAs-GaSb (001) superlattice, electronic struct., tight binding calc. 8-95350
 InAs-GaSb superlattices, two-dim. electronic structure 8-75995
 (InAs)_{1-x}(CdTe)_x, band gap and effective mass, IR spectra obs. 8-56491
 InAs_{1-x}P_x, continuously tunable electron beam pumped laser 8-50802
 InAs(P)(Sb) MIS structs., review 8-95372
 InGaAs, transferred electron photoemission to 1.65 μm 8-68600
 InGaAs-InP heterojunction detector for 1.0-1.7 μm wavelength range 8-49895
 In_{0.53}Ga_{0.47}As, incorporation of Ga during LPE growth on (111)B and (100)InP substrates 8-91557
 In_{1-x}Ga_xAs-GaSb_{1-y}As_y, new heterostruct. characts. 8-72247
 In_{1-x}Ga_xAs-GaSb_{1-y}As_y, superfine heterostruct., MBE 8-95348
 In_{1-x}Ga_{1-x}As, heteroepitaxial, MBE grown, props. 8-84328

III-V semiconductors continued

In_{1-x}Ga_{1-x}As, thick LPE growth, electrolum. obs. 8-60589
 InGaAsP, lattice matched, LPE growth on (100) InP, for 1.15-1.31 μm spectral region 8-64483
 InGaAsP/InP heterojunction, X-ray characterisation of defects 8-95239
 InGaAsP-InP 1.27 μm CW DH injection lasers, 1.1 Gb/s pseudorandom PCM 8-55390
 InGaAsP-InP DH lasers, carrier lifetimes meas. 8-66828
 In_{1-x}Ga_xAs_{1-y}P_{1-y}, LPE growth on InP (100), lattice matched composition 8-87881
 In_{1-x}Ga_xAs_{1-y}P_{1-y}, lattice vibrs., Raman study 8-91391
 In_{1-x}Ga_{1-x}As_{1-x}P_{1-x}-InP photodetectors, construction and performance 8-65966
 In_{1-x}Ga_xP, epitaxial film, cathodolum. obs., recomb. mechanisms 8-72613
 In_{1-x}Ga_xP, two-phonon IR absorpt. 8-52493
 In_{1-y}Ga_{1-y}P-GaAs heterojunction, VPE, energy band gap and lattice parameter, lattice mismatch effects 8-95345
 In_{1-x}Ga_xP_{1-x}As, single thin active layer visible spectrum heterostruct. lasers 8-63120
 In_{1-x}Ga_{1-x}Sb, influence of annealing on microstruct., exam. 8-56669
 In_{1-x}Ga_{1-x}Sb, vertical Bridgman Stockbarger growth, magnetic field effect 8-60565
 InN film, refl. and transmission spectra, band struct. 8-72625
 InP (001)-Ag, contact, surface stoichiometry and struct., and electronic surface states 8-95361
 InP, anodisation, effect of pH, current density and illumination 8-95823
 InP, CESR, optical detect. by spin orientation techniques, anal. 8-80251
 InP carrier profiling using liq. barrier contact 8-76087
 InP, crystal growth by synthesis solute diffusion method 8-64454
 InP electrode-electrolyte interface, Schottky barrier obs. 8-52079
 InP, electron-hole plasma, ground state energy 8-84244
 n-InP, epitaxial, Hall effect, electron mobility and density, temp. depend. 8-72288
 n-InP, epitaxial, subthreshold velocity-field charact., 77K 8-64038
 InP film, CVD on preferentially etched Mo, initial growth behaviour 8-51855
 InP, grown-in dislocation density, impurity effect 8-51543
 n-InP, Hall effect, 10-300K, thermal activation energy and influence of compensation 8-72171
 InP, implantation of Si, Al, Hf, Ta into InP and GaAs, form. of protective oxide 8-79622
 InP interface with anodic and thermal oxides, comparison of AES and ESCA 8-95980
 InP, LPE, high purity, use of baking to reduce Si contamination 8-72744
 InP, low temp. diffusion of radioactive Ag 8-75884
 InP, MIS capacitor, transient capacitance and C-V characts. 8-95374
 InP, manifestation of local vibrs. of dislocations in IR spectra 8-88339
 InP, maximum electric field in high-field domain in Gunn devices 8-79996
 InP, n-type doping by ion-implantation of S and Si, expt. 8-91351
 InP, photoluminescence intensity of cleaved surface, ambient gas influence 8-88345
 InP, planar reactive deposition on CdS, heterostruct. formation and elec. evaluation 8-72738
 InP, pure and S doped, VPE, exam. of molar fraction controlled impurity in In-PCl₃-H₂ 8-56587
 InP, reson. Raman scatt., deformation pots. 8-52495
 InP substrate, transient-mode LPE of GaAs 8-72746
 InP substrates HCl etching speed and polarity obs., with aid of laser beams (*Slovak*) 8-56575
 InP substrates preparation, etching and polishing in Br-methyl alcohol solution (*Slovak*) 8-56576
 InP surface, interaction with Cl, electron spectroscopic obs. 8-56036
 InP, valence band structure, CPA, bond orbital calcs. 8-87909
 InP:Si, vibr. modes of Si, IR absorpt. bands 8-55922
 InP/Ga_{0.47}In_{0.53}As/InP DH laser, lattice matched, MBE and room temp. operation 8-74906
 InP/InGaAs/InP field assisted photocathode, minority carrier electron transport across p-p heterojunction 8-95651
 InP-Au Schottky diodes, barrier height study 8-52088
 InP-GaInPAs DH lasers, misplaced p-n junctions due to Zn contamination 8-87051
 InP(As)(Sb), avalanche breakdown voltage for p-n junction, calc. 8-88020
 InS, layer single cryst., Raman scatt. meas. 8-76478
 n-InSb, 2 mm wave radiation interaction with charge carriers (*Russian*) 8-87991
 InSb, acoustic NMR, role of incoherent phonons (*Russian*) 8-80230
 InSb, acoustoelectric effect at 77K 8-72209
 n-InSb, acoustoelectric gain coeff., nonlinear elec. field depend. 8-76115
 InSb, amplification and vel. change of acoustic waves due to external temp. gradient 8-84260
 InSb, Auger recombination, calc. for diamond-like narrow-gap semiconductor, compared with expt. 8-63978
 InSb, crystal structure stability, P-T diagrams 8-51886
 InSb, cyclotron harmonic transitions, warping and inversion asymm. effects 8-68383
 p-InSb, cyclotron reson. of nonequilib. photoelectrons, distrib. function and line profile 8-60336
 InSb, Debye temperature, atomic mean square displacement 8-87757
 p-InSb, deformed, giant negative magnetoresistance 8-87990
 n-InSb, degenerate, acoustomagnetoelec. effect obs. 8-72207
 n-InSb, directional temp. of hot electrons under elec. and mag. fields 8-84135
 InSb, donor excitation spectra in high mag. field 8-80027
 n-InSb, effective g-value of electrons determ. by spin flip Raman scatt. and electric-dipole-excited ESR 8-52494
 InSb, electronic surface struct., Cs(Rb)(Na) absorpt., AES, LEED, EELS study 8-68068
 InSb fast response submm. detector 8-89541
 p-InSb, film, elec. transport props. 8-72291
 InSb film, quantum size effects, transport props. 8-76171
 InSb film, synthesis by 2-source mol. beam technique and AES characterisation 8-72729
 InSb film, threshold singularity on quantising mag. fields 8-87904

III-V semiconductors continued

- InSb, gamma irradiated, changes in energy spectrum of impurity spectrum 8-51937
 n-InSb, HF EM and acoustic oscill. generation in LF electric field 8-64068
 InSb, heats of transformation for high pressure, orthorhombic modification, exam. 8-56627
 InSb, high-purity specimen irradiated at 80K, transport prop. and defect annealing 8-95307
 n-InSb, hot electron magnetophonon effect, 77K, mag. field modulation method 8-60140
 InSb, impact-ionisation magnetoelec. effect 8-52016
 InSb inversion layer, electromagnet mode 8-60080
 p-InSb inversion layer, magnetotransport 8-64138
 InSb inversion layer, spectroscopy of electron subband levels 8-64364
 InSb laser detector, dynamic range increase 8-49899
 InSb, lattice thermal cond. from three phonon scatt. relax. rate 8-51755
 n-InSb, low temp. mag. and electric resonances meas., model (*Russian*) 8-56159
 n-InSb, MCD due to free carriers 8-56462
 InSb, magneto-optical anomalies of impurity electrons, two-LO-phonon region 8-72415
 n-InSb, magnetoacoustic effects using two-band model 8-60170
 n-InSb, microwave displacement effect in longit. elec. and transverse mag. fields 8-87992
 n-InSb, millimetre rare modulation in semicond. plasma, use of effects of high elec. field. 8-60149
 InSb, momentum distrib. of electrons, anisotropy, positron annihilation (*Russian*) 8-84676
 InSb n^+ -p and p^+ -n photodetectors fabrication by S and Be ion implantation 8-49906
 InSb, nonlinear absorption and pulse shaping for 10.6, 9.6 μ m laser radiation 8-79077
 InSb, nonlinear optical properties, hot electron effects 8-71139
 InSb, p-n homojunction breakdown voltage for onesided abrupt junctions (*German*) 8-56210
 n-InSb, parametric excitation 8-52023
 InSb, phonon dispersion curves, appl. of deformable-ion model 8-59887
 n-InSb, photo-induced magnetophonon reson., 4.2K, peak shifts 8-84250
 n-InSb, photoconductivity, 1.8K, hot-carrier and free-carrier absorption. effects 8-84254
 n-InSb, photomagnetic effect anomalies, 90 to 300K (*Russian*) 8-84257
 n-InSb photoresistors of Carbinio disc shape in mag. field, enhancement of responsivity 8-56186
 n-InSb, plasma filament form. under impact ionisation conditions 8-60147
 InSb, plastically bent single crystals, dislocation struct. obs. 8-59816
 InSb, polymorphism and cryst. struct. at high temp. and press. 8-95026
 n-InSb powder, microwave propag., 90-300K, magnetoplasma and helicon wave excitations 8-72183
 InSb, resonance effects in mag. field, effect of additional laser illumination 8-72417
 InSb spin-flip Raman laser external-cavity system, oscill. characts. 8-55383
 n-InSb, stimulated recomb. radiation 8-90456
 n-InSb, subjected to mag. field normal to current, coherent HF oscills. 8-52026
 InSb, superconducting phases at high press. 8-88063
 InSb, surface analysis, X-ray photoelectron spectra, surface oxidation-etchant correlation 8-56029
 n-InSb, threshold field dependence on sample length, 77K 8-76116
 InSb type semiconductor, small-gap, electron scatt. and transport props. 8-95294
 InSb type semiconductor, small-gap, electron scatt. and transport props. 8-95295
 InSb, valence band structure, CPA, bond orbital calcs. 8-87909
 InSb, volume plasmon dispersion, anisotropy 8-56090
 InSb:Cr, press. effects on transport props. 8-56146
 InSb/GaSb superlattice thin films, sputtered, ion-bombardment-enhanced diffusion during growth 8-87882
 InSb/LiNbO₃ acoustoelectric convolver, gap-coupled, for IR imaging device 8-94492
 InSb-type semiconductor, spatial dispersion of permittivity 8-67967
 InSb-type semiconductor, inelastic scatt. of electrons by optical phonons 8-76073
 InSb_{1-x}Bi_x, disordered solid solns, ionisation energy of fluctuation levels 8-72116
 InSb_{1-x}Bi_x, film, multitarget sputtering growth technique 8-84711
 ZnSe-GaAs thin film DE electroluminescent cell with 20 V threshold voltage 8-76141

III-VI semiconductors

- electrical characterisation, review 8-60120
 Ga_{1-x}In_xSe, layered, luminescence and photocond. obs., two-photon excitation 8-76521
 GaS, optimisation of crystal growth conditions by I₂ vapour transport 8-68611
 GaS, refr. index in far IR, permitt. meas. 8-64360
 GaS, sp. ht., vibr. spectra and Debye temp. 8-87796
 GaS, XPS and valence band density of states, tight binding approx. 8-63974
 GaS(Se), layered, optical phonons, IR and Raman scatt. meas. 8-59903
 GaS₂(Se_{1-x}) solid solns., electrical props. meas. 8-84216
 GaSe, 4 to 12 μ m tunable down-conversion from LiNbO₃ parametric oscillator 8-66865
 GaSe, additional IR electrolum. band obs. at 77K 8-72607
 GaSe, exciton, excitation-induced absorption and luminesc. 8-60516
 GaSe exciton absorpt., change under a pulsed dye laser 8-92088
 GaSe film, amorphous, I-V characts. in strong elec. fields, 173-373K 8-56248
 GaSe, Hall mobility anisotropy 8-68041
 GaSe, one-carrier SCL currents in solid with two sets of traps distributed in energy 8-72158
 GaSe, optimisation of crystal growth conditions by I₂ vapour transport 8-68611

III-VI semiconductors continued

- GaSe, photocond. at high excitation rates 8-52036
 GaSe, sp. ht., vibr. spectra and Debye temp. 8-87796
 GaSe-SnO₂ spray heterojunction, electro-optical props. 8-64102
 GaSe(S), layer dynamics of high-symmetry crystals with atom-atom interactions 8-71799
 GaSe_{0.9}Te_{0.1}, undulation spectra associated with acceptor complexes 8-80392
 GaTe, sp. ht., vibr. spectra and Debye temp. 8-87796
 GaTe-SnO₂ spray heterojunction, electro-optical props. 8-64102
 InSe, excitonic absorpt. edge 8-88352
 InSe, LF oscills. of current 8-56187
 InSe, layer single cryst., Raman scatt. meas. 8-76478
 InSe, layered crystalline slabs, growth by Czochralski method 8-68619
 n-InSe, optical spectra, photocond. and resistivity 8-88321
 InSe, Raman spectra, inter-, intra-layer interaction estimates 8-88313
 InSe-GaAs p-n junctions, 'optical' contacts, elec. props. 8-56222
 InTe-InSe p-n junctions, 'optical' contacts, elec. props. 8-56222
 In₂Te₃ type semiconductors, basis of ionising radiation detectors 8-86743

illumination *see lighting***image amplifiers** *see image intensifiers***image convertors***see also fluorescent screens; image intensifiers*

- alkali halides, photodichroic, as optical processing elements 8-83056
 cholesteric liquid crystal visualisation of microwave fields 8-58031
 crossed grid anode and its image partitioning 8-71217
 electron-optical photography, pico-femtosecond 8-82064
 fibre optic image tube, cooling effect 8-96401
 framing camera tube for <100 ps range 8-70207
 ion beam visual image produced by electron interaction on surface 8-58091
 liquid crystal light valve, appl. to real-time optical data processing 8-83102
 PCB, nematic liq. cryst., US imaging, convertor, acousto-optical effect 8-59218
 gamma-Ruticon image buffer, imaging props. 8-66915
 scanning photoelectric, optical inhomogeneities obs. by spectral modulator 8-59144
 state of art, vacuum- and nonvacuum-types survey (*Czech*) 8-63185
 streak camera 8-54484
 thermoplastic-photoconductor image transducer, input to coherent optical processor 8-83098
 Cs₂Te, photocathode for proximity focused image convertor, field enhancement of photoemission 8-72677

image iconoscopes *see television camera tubes***image intensifiers**

- astronomical spectrograph appl. of image intensifier 8-73647
 electron image deflection system, crossed elec. and mag. field, intensity modulation 8-89592
 enlarged photofluorography using 12 inch image intensifier (*Japanese*) 8-96087
 fluorescent X-ray intensifying screen efficiency determ., standard method 8-69198
 fluoroscopic spot film system image quality evaluation and optimisation 8-69205
 imaging process efficiency and quality, electrophotographic process, electronographic cameras and image intensifiers 8-78932
 industrial hard X-ray channel-plate image intensifier 8-54517
 medical imaging, sensitometry 8-69193
 neutron radiography with ²⁵²Cf, use of TV imaging techniques 8-60922
 radiographic imaging, digital video acquisition system for extraction of subvisual information 8-69208
 radiographic intensifying screen equivalent blur 8-69197
 radiographic intensifying screen information content and contrast, comparison of rare earth with CaWO₄ 8-73232
 radiographic proximity X-ray image intensifier tube 8-69206
 radiographic X-ray image intensifier video system, design characts. 8-69209
 radiographic X-ray image intensifier video system, psychophys. evaluation rel. to system measures 8-73234
 rapid filming appl., microchannel proximity tubes characts. (*French*) 8-49917
 SIT camera sensitivity expt. (*Japanese*) 8-89085
 spectroscopic cooled and intensified array detectors 8-65983
 state of art, single-stage and multi-stage types (*Czech*) 8-63185
 stigmatic spectrograph image intensifier system, appl. to plasma diagnostic work at low light levels 8-93767
 subpicosecond proximity-focused visible streak camera, evaluation and appl. 8-59155
 TV X-ray detector, high sensitivity, biological structure diff. study appl. 8-89609
 visual task prediction from image quality data 8-53415
 X-ray, for digestive tract radiography 8-92694
 X-ray, MTF, empirical eqn. 8-65123
 X-ray, relationship between resolution and speed 8-65124
 X-ray microchannel plate image intensifier, noise characts. 8-53483
 X-ray screen-film processing sensitometry standard developed by ANSI 8-69196
 X-rays, pulsed and continuous, motion picture filming of moving objects 8-57057

image orthicons *see television camera tubes***image processing** *see picture processing***image sensors***see also television camera tubes*

- BLIP systems, effect of f-number and other parameters on FLIR performance 8-77981
 body motion computer-aided tracking using CCD image sensor 8-61269
 C-CD, modelling and appl. of HgCdTe MIS struct. 8-80058
 C-CD based control system for Si cryst. growth 8-68623
 crossed grid anode and its image partitioning 8-71217
 fixed-frequency laser beam scanning device 8-59135
 imaging system shading effects and countermeasures 8-78922
 IR CCDC image sensors, operation (*German*) 8-63190
 laser line scanning sensor, spatial filtering design considerations 8-85752
 line scan sensor, spatial and temporal coding of GaAs laser 8-83022

image sensors continued

- multichannel photon counting image detector arrays 8-65970
- patterned optical filters for solid-state imager spectral encoding 8-66945
- photodiode array, simultaneous determination of diameters, velocity of moving solid particles (*Japanese*) 8-95872
- picture colour component detection in SAW scanning 8-59149
- solid state image sensors, devices and appl. (*Japanese*) 8-59142
- solid-state image sensor resolution evaluation by aperture sampling response 8-50939
- solid-state imaging devices, conference, San Diego (1977) 8-66944
- TV-microprocessor system, for high speed image counting and sizing 8-94377
- water penetration imagery, surface/depth data separation by multispectral scanning 8-69539
- X-ray picture laser scanning system for digital image transmission over telephone channel 8-80953

image storage tubes

- echocardiogram on-line computer anal. 8-80941
- scintigraphy, medical, digital image processing methods 8-80947

images, optical *see* optical images**imaging, acoustic** *see* acoustic imaging**imaging, infrared** *see* infrared imaging**IMMA** *see* ion microprobe analysis**impact (mechanical)**

- see also* ballistics; *impact strength*
- abrasion, wear, review (*German*) 8-88536
- acoustic emission simulation by SiC grain brittle fracture and elastic sphere impact, freq. anal. 8-55504
- bar, impact excitation, longitudinal vibr. 8-94606
- bar, nonuniform elastic, longit. vibr. dynamics of impact excitation 8-75086
- Bencubbin polymict meteoritic breccia, form. by impact on carbonaceous chondrite regolith 8-96443
- borosilicate glass surface, damage due to impact of small glass and steel spheres 8-52994
- BWR-4 neutron noise analysis spectra, instrument tube flow-induced vibr. 8-94063
- Caloris Basin (Mercury), age rel. to global tectonic features 8-85874
- Chenier Crater, on Moon, impacts rel. to lava-like material origin 8-81569
- comet on Earth, as cause of ice ages and ecological disasters 8-53714
- craters, coherently overturned flaps produced by hydrodynamic type wave motion 8-57209
- craters formed in viscous-liquid targets, expts. rel. to Martian rampart craters 8-65530
- dynamic finite element and photoelastic analyses, of impacted pretensioned plate 8-67111
- ejecta parameters depend. on primary vel. 8-59291
- elastically deformable striker and solid obstacle, impact phenomena 8-77703
- elliptic infinite bar, impulsive loads, three dims. elastic stress-strain anal. 8-87259
- erosion by impact on moon and planets 8-57476
- extensible string motion in nonviscous fluid (*Russian*) 8-77718
- glass bead, impact fracture (*Japanese*) 8-92338
- glass particles impacting on metal barriers, piercing, stony meteorite simulation 8-89043
- glass plates, effect of localized damage on energy losses, during impact by glass spheres 8-52973
- hailpads calibration 8-93001
- head-neck impact response using realistic human model 8-80909
- hypervelocity particle impact, heating and vaporisation, temp. estimation 8-59290
- interplanetary microparticle studies by space-borne instrumentation 8-57460
- interplanetary particles, impact collectors on spacecraft 8-57459
- lunar crater Giordano Bruno, AD 1778 impact obs. consistent with laser ranging results 8-69717
- Manicouagan impact crater, gravity study and upper crust density contrasts 8-81170
- Manicouagan impact crater, Quebec, investigation 8-81163
- Manicouagan impact melt, Quebec, chemical interrelationships with basement rel. to form. processes 8-81165
- Manicouagan impact melt, Quebec, stratigraphy, petrology and chemistry 8-81164
- Manicouagan impact melt sheet, Quebec, thermal history 8-81167
- Manicouagan impact structure, Quebec, melt rocks petrogenesis 8-81166
- Manicouagan melt sheet, Rb-Sr isochron age 8-81168
- Manicouagan structure, Quebec, central mag. anomaly 8-81169
- Mars, 4 to 10 km dia. craters distrib. and relations to global geologic units 8-65528
- Mars, rampart craters morphology 8-53854
- meteorite craters on Earth, form., props. and catalogue 8-96411
- meteorite impact and ejecta deposition on airless planetary bodies, topographic effects 8-65523
- meteoritic material at large impact craters, chemistry 8-57208
- meteoroid impact effect on spacecraft attitude 8-73608
- meteoroid impact on small solar system bodies, seismic effects, rel. to Phobos (*Russian*) 8-69754
- meteoroid shield for spacecraft, destructive effect and meteoroid vel. 8-53788
- micrometeoroid impact, laboratory simulation 8-57510
- nuclear plant, impact load for tornado generated missiles 8-51103
- nuclear plant equipment response to aircraft impact 8-50416
- penny-shaped crack, sudden twisting in a finite elastic cylinder, stress calcs. 8-67110
- Phobos, dynamical evolution and time to collision with Mars 8-89104
- Phobos, Stickney crater impact rel. to groove form. 8-89103
- plate, elastic deform. due to axisymmetric punch 8-75065
- plug formation in plates, cylindrical projectile impact, nonlocal viscous fluid model 8-49653
- PTFE, impact testing, elastic analysis of conventional test, reassessment of testing 8-60770
- punch-elastic body dynamic contact, superseismic stage, exact soln. 8-55614
- PVC rigid plate specimens, Charpy impacted, SEM exam. of fracture surface (*Japanese*) 8-52953

impact (mechanical) continued

- rectangular bar, semi-infinite, longitudinal impact, elasticity eqns. anal. 8-90703
- sea ice in Gulf of Bothnia, flexural waves meas. (*Japanese*) 8-96225
- single inclined plate impact expt., technique for determ. in-material longitudinal and shear particle velocity histories 8-79289
- soda-lime glass surface, damage due to impact of small glass and steel spheres 8-52994
- stability analysis, impact vibration, steady, body with impact hysteresis characts. 8-51099
- steel, alloy, Ni-Co-Mo, fatigue crack growth, during impact tests exam. of kinetics 8-88525
- steel, maraging, fatigue crack growth, during impact tests, exam. of kinetics 8-88525
- steel shot, cast, impact fracture (*Japanese*) 8-92338
- string vibrating against rigid wall, partially elastic or anelastic impact, energy calcs. 8-67028
- terrestrial rocks, impact shock effects on magnetism 8-85538
- three point bend testing for notched and precracked specimens, testing and data analysis procedures 8-53053
- trace metal aerosol dry deposition, inertial impaction and filtration model 8-73441
- Tunguska, 1908, catastrophe, cosmochemical anomaly in silicate microspherules comp. 8-96430
- Tunguska cosmic body, chemical comp. and nature 8-61810
- Vredefort Dome, S.Africa, coesite and stishovite discovery 8-53653
- Zhamanshin meteor crater, tektites-irgizites form. conditions from Fe ions states 8-61420
- Al₂O₃, biaxially stressed, exam. of localised impact damage 8-72846
- Fe-Mn (8 wt.%), quenched, exam. of intergranular embrittlement 8-76745
- Na₂O-CaO-SiO₂ plates, exam. of Hertz crack branching 8-72887
- Ni-Cr-Fe-Mo-Co (21.41, 19.28, 8.64, 2.16 wt.%), Hastelloy alloy X, exam. of thermal stability 8-84865
- PbZr_{0.95}Ti_{0.05}O₃, impact loading, mech. and elec. response, elec. state effect 8-64317
- Si₃N₄, biaxially stressed, exam. of localised impact damage 8-72846
- ZnS, hot pressed, water drop impact damage, SEM exam., IR transmission 8-88543

impact ionisation

- donors with excited states, non-equilibrium phenomena, theory of kinetics of electron transitions 8-79961
- film, breakdown mechanisms 8-76385
- maximum electric field in high-field domain in Gunn devices 8-79996
- MOS structure, n-channel, evidence for impact ionised electron injection in substrate 8-88031
- p-n junction, avalanche multiplication 8-84289
- plasmon mechanism for secondary breakdown 8-95352
- Schottky barrier, avalanche multiplication 8-84289
- Schottky layers, homogeneous avalanche breakdown instability mechanism, microplasma form. 8-72262
- semiconductor, switching under impact ionisation 8-72215
- n-GaAs, impact ionisation initiated by acoustoelectric effect 8-52038
- GaAs, impact ionisation rates for electrons and holes, photocarrier multiplication obs. 8-87995
- GaAs-Ga_{1-x}Al_xAs n⁺-v-n junction, avalanche carrier multiplication (*Russian*) 8-76140
- n-InSb, millimetre rare modulation in semicond. plasma, use of effects of high elec. field. 8-60149
- n-InSb, plasma filament form. under impact ionisation conditions 8-60147
- Si reverse-biased p-n junction DC characteristics interpretation (*Polish*) 8-91761
- Si:B, impurity excited state lifetimes 8-60083
- V₂O₅, switching mech. 8-60175

impact phenomena *see* collision processes**impact strength**

- see also* fracture toughness; *notch strength*
- armour material, selection criterion 8-53063
- boride coating on stainless steel, elec., mech. props., boronising sintering method investig. 8-60594
- brittle circular disc under impact loading, fracture mech. 8-88514
- brittle target, impact damage in elastic response regime 8-71785
- dynamic fracture toughness determination, by instrumented impact tests 8-68861
- epoxy, Al₂O₃-filled, shock-wave compression, 0.4-3.7 GPa 8-59856
- epoxy resin, mech. and thermal props., amine hardeners, added softeners and filler effects (*Polish*) 8-68741
- epoxy-anhydride-polycaprolactone, cross-linked block copolymer, morphology and impact strength 8-91265
- fracture in elastoplastic regime 8-51133
- glass plates, biaxially stressed, anal. of localised impact damage 8-68772
- granite plate, crack propagation by projectile impact load 8-60c41
- graphite, structural, impact toughness, reln. to compressive strength 8-88605
- graphite fibre reinforced panels, low energy impact testing 8-72845
- limestone plate, crack propagation by projectile impact load 8-60741
- metals, BCC, effect of screw dislocations, on mech. props. (*Russian*) 8-60704
- nuclear plant, impact load for tornado generated missiles 8-51103
- percussive impact wear, development of theory 8-94623
- PFFE, impact fracture toughness, rate effect 8-56741
- PMMA, impact strength, exam. with pulsed drop impact loading 8-84944
- PMMA, impact testing, elastic analysis of conventional test, reassessment of testing 8-60770
- polycarbonate, dielec. relax. and ductile brittle transition 8-52438
- polyethylene, impact fracture toughness, rate effect 8-56741
- polyethylene, medium density, impact testing, elastic analysis of conventional test, reassessment of testing 8-60770
- polymer, failure, book 8-92361
- polymer films and sheets 8-80590
- polymers, impact testing, elastic analysis of conventional test, reassessment of testing 8-60770
- polystyrene, polyisoprene modified, impact strength improvement 8-84993
- polystyrene-ethylene propylene copolymer, strength and impact props. 8-52899

impact strength continued

- polysulphone-polydimethylsiloxane, linear block copolymer, morphology and impact strength 8-91265
 PVC, impact strength, exam. with pulsed drop impact loading 8-84944
 PVC cases for Pb-acid batteries, pneumatic shock test (*German*) 8-85093
 PVC composite, MBS type multifunctional impact modifier effect on mech. and rheological props. (*Polish*) 8-52751
 steel, 12X2H4A, nonmetallic inclusion effect on plasticity and impact strength (*Ukrainian*) 8-92296
 steel, alloy, corrosion-impact-cyclic strength of boring bars, effective hardening treatment 8-53034
 steel, alloy, high-temp. combined ht. treatment and mech. working, C content effects (*Russian*) 8-52854
 steel, austenitic, fracture toughness props. of A533B, prior austenite grain size effect 8-60780
 steel, cast, effect of non-uniform struct. on props. 8-84850
 steel, constructional, impact strength/brittle fracture relationship in ductile-brittle transition zone 8-56740
 steel, Cr-Mo-V, brittle failure, heat treatment and influence of cold plastic deform. 8-72858
 steel, Cr-Mo-V, medium strength, correlation between crack initiation, propag. and microstruct. 8-60787
 steel, Cr-Mo-V, press. vessel, fracture, effect of tempering 8-60799
 steel, Cr-Ni-(Mo), austenitic, strengthening by modified ausforming 8-76665
 steel, high strength, low alloy, mech. props. 8-60739
 steel, high strength, low alloy, rare earth treated, ductile fracture mech. 8-64658
 steel, impact strength, exam. with pulsed drop impact loading 8-84944
 steel, low, C, rimmed and killed, exam. of impact fatigue behaviour (*Japanese*) 8-88528
 steel, low alloy, type 3sp, effect of temp. at end of rolling on mech. props., and coercive force 8-72799
 steel, low S, ESR, overheating effect on toughness 8-52860
 steel, low S, ESR and electric arc, notch toughness, interaction between overheating and tempering temp. effects 8-52970
 steel, medium strength, fracture toughness eval. of small specimens 8-60762
 steel, mild, plate, effect of striking velocity on perforation energy 8-68818
 steel, Mn, as rolled bainitic, tensile, impact and machinability props., transport appl. 8-88503
 steel, nuclear pressure vessel, type A533B-1, three point bending, yield stress, exam., Charpy V-notch and precracked specimens 8-92310
 steel, stainless, annealed 310, deform. at erosion sites, TEM and SEM studies 8-64725
 steel, stainless, ferritic, anisotropic lamellar fracture mechanism 8-64639
 steel, stainless, ferritic, subjected to 475°C embrittlement, exam. of fracture toughness 8-84982
 steel 1Kh18N9T, physico-mech. props. after boring in metallic melts (*Russian*) 8-56736
 steel cylindrical bar loaded by longitudinal impact, dislocation struct. and plastic deform. (*Czech*) 8-60713
 steel SS-41, plastic working with vibr., US hardness tester 8-53044
 test, finite element analysis 8-68806
 wear resistance, hardfacing, review 8-72937
 Al alloys, preliminary forging effects on struct. and mech. props. of extruded sections (*Russian*) 8-80564
 Al, annealed, subjected to torsional impact loading strain-rate effects 8-92303
 Al, impact strength, exam. with pulsed drop impact loading 8-84944
 Al-Mg alloy AMg6, mech. props. of welded joints, impurity effects 8-95789
 Al-Pb(Bi)(Cd), containing low melting point inclusions, impact props., temp. depend. 8-60792
 Cu, fracture criterion, expt. verification 8-64648
 Cu-Al (11.6 wt.%), mech. props., tempering temps. effects 8-76669
 Fe, Armco, impact strength, exam. with pulsed drop impact loading 8-84944
 Fe, sintered, effect of repressing and double sintering on impact strength (*Japanese*) 8-92217
 Fe-Cr alloy, impact strength, rel. to '475°C brittleness' (*Russian*) 8-92323
 Fe-Ni-C (9, 0.1 wt.%), effect of intercritical tempering on impact energy, exam. of mech. props. 8-52861
 Ir-W (0.3 wt.%), P segregation to grain boundaries, effect on high temp. ductility 8-95754
 PVC-Cu, particulate composite, mech. props. effect of particle size 8-95799
 Ti alloy, impact strength, exam. with pulsed drop impact loading 8-84944
 Zn, impact strength, exam. with pulsed drop impact loading 8-84944

impedance, acoustic *see acoustic impedance***impedance, electric** *see electric impedance***impedance, electric, measurement** *see electric impedance measurement***impedance, measurement, electric** *see electric impedance measurement***impedance matching**

- radiotelescope transmission lines, antenna arrays and impedance transformation 8-96399
 shock wave impedance match at low pressures 8-51264
 single-transducer coupler for diagnostic pulsed Doppler or pulse-echo US instrumentation 8-61236
 tunable variable bandwidth/frequency SAW resonator 8-59247
 wave impedance matching interface layer synthesis (*Russian*) 8-77728

imperfections, crystal *see crystal defects***impermeability** *see permeability***impulse amplifiers** *see pulse amplifiers***impulse generators** *see pulse generators***impulse testing**

- HV laboratory ion density due to repetitive impulse generation 8-65913
 Marx type fast rise impulse generator using laser triggered gap switches (*Japanese*) 8-94940

impulse voltages *see transients***impulse welding** *see resistance welding***impurities**

- for impurity vibrations *see* "lattice localised modes" or "molecular vibrations in solids"
see also chemical analysis; crystal inclusions; crystal purification; diffusion in solids; impurity-defect interactions; impurity distribution; impurity electron states; interstitials; magnetic impurity interactions; phonon-impurity interactions; segregation; semiconductor doping
 AES, depth profile analysis, influence of impurity gases in UHV systems 8-76958
 AES quantitative anal. of impurities (*Japanese*) 8-91356
 alkali halides, influence of purity of crystals on stability of F-centres and interstitials 8-91336
 alkali metal chloride: F(Br⁻)(I⁻), anion impurities substitution, energies of soln., association and migration 8-83831
 chemical impurities, entropy and enthalpy of solution 8-51691
 crystal growth from melt, macroparticle capture by growing cryst., influence of particle thermal cond. 8-79543
 diamond, Fresnel diffraction at platelets, defect struct. anal. by 3 Å phase-contrast microscopy 8-87701
 diffusion in solid, Kramer's rate formula 8-83992
 dipolar impurity tunnelling model, elastic interaction and const. 8-71826
 displacive transformations, single defect behaviour models 8-83904
 emulsions, long wave photosensitivity rel. to impurity centres (*Russian*) 8-49925
 metal film, vacuum deposited, grain struct., influence of impurities and alloying elements (*Russian*) 8-56048
 metal surfaces, clean, AES anal., contamination effects obs. 8-53293
 metals, atomic displacements, three-body interactions around impurity 8-87689
 methane, effects of impurities and annealing on triple point 8-83919
 molecular crystals, neutron scattering and exciton spectrum due to impurities 8-91622
 noble gas fluid, press. induced transition in neighbourhood of alkaline earth impurity 8-51770
 non-Newtonian fluid, effective diffusion of impurity in laminar flow of liquid 8-67228
 refractory refinement during prep. by self propagating high temp. synthesis 8-60634
 sapphire, vacuum UV spectra, Cr³⁺ impurity and anion vacancy conc. 8-84605
 silica, vitreous, effects on viscosity of impurity alkali oxide, OH, Al₂O₃ and Ga₂O₃ 8-64580
 steel, austenitic stainless, Mn-N interaction, internal friction obs. 8-84883
 superradiative transitions, acoustic and EM excitation 8-66872
 transition metal alloy, ferromag., H-impurity complex obs. by mag. aftereffect 8-72373
 vibrational energy transfer in solids, rot. mode participation 8-63815
 Ag film on Mo, epitaxial growth, exam. of S impurity segregation at interface 8-84076
 AgCl:Sr, effect of impurity doping on Sr²⁺ diffusion 8-84002
 Al alloy, D16, Fe and Si impurity effects on K_{IC} 8-84990
 Al-Al₂O₃-Al junctions, Dy doped at Al₂O₃-Al interface, electron transport mechanisms and barrier height 8-91778
 Al-Mg, dil., long-range solute-host interactions 8-95062
 Al-Mg alloy AMg6, mech. props. of welded joints, impurity effects 8-95789
 Al₂O₃:Ni²⁺, corundum, phaser production of transverse phonons by impurity centres (*Russian*) 8-91390
 Au polycrystalline wire, internal oxidation of impurities 8-83842
 B, purity evaluation by elec. meas. 8-59822
 BaO:Mn²⁺, impurity pot. well shape calcs. 8-87950
 CaCO₃, aragonite-calcite transformation, effect of impurities, DTA and IR studies 8-51662
 CaF₂:Ce, Stark struct., phototransitions, g-factors 8-67995
 CaFz crystals, grown from synthetic raw materials, quality, effect of impurities, composition 8-79083
 CaO:Mn²⁺, impurity pot. well shape calcs. 8-87950
 Cds, neutron and fast electron irradi., local centre form., TSC and photoluminesc. meas. 8-87719
 Cu film on Mo, epitaxial growth, exam. of S impurity segregation at interface 8-84076
 Fe based alloys, solute segregation to grain boundaries 8-72780
 Fe film, Hall resist., effect of N impurity codeposition 8-64146
 Fe, lattice distortions due to H, X-ray diff. exam. 8-79629
 Fe, molten, impurities effect on viscosity 8-95172
 Fe:I, ¹³¹I NMR, vacancy associated impurity sites 8-91964
 Fe-Gd film, amorphous, O₂ contamination effects on mag. props. 8-64231
 Gd-Co film, sputtered, inert gas incorporation effect on uniaxial anisotropy 8-64232
 Ir, brittle fracture, impurity segregation to grain boundary effects 8-64637
 KCl, entropy change associated with substitutional anion defects calc. 8-79782
 Li₂O.2SiO₂ glass, kinetics of crystal nucleation, effect of Pt and other impurities 8-88440
 MgO:Mn²⁺(Fe²⁺)(Cr²⁺), redox behaviour of ions, ESR and X-ray diff. 8-52341
 MnZn ferrites, impurity induced exaggerated grain growth 8-92222
 NH+CO, vibrational energy transfer in solids, rot. mode participation 8-63815
 (NH₄)₂SO₄, single crystal growth from aq. soln., effect of impurities on growth (*Japanese*) 8-92182
 Nb, sputter deposited film, O contamination, Auger anal. 8-52669
 Nb₃Ge, CVD, impurity doping effect on supercond. crit. props. 8-52174
 Nb₃Ge film, nucleation of high-T_c phase in presence of impurities 8-88054
 Ni superalloy powders, removal of interstitial contaminants 8-84735
 Pb₂Ge₂O₇:BaO, impurities, static central peak 8-92079
 Pb(Zr,Ti,Ge)O₃, antiferro-ferroelectric transition 8-95565
 RbAg₄I₃:AgI,Rb₂AgI₃, polycryst., ionic cond., impurity conc. effects 8-51734
 Se:Te, liq., viscosity, impurity effect, chain length role (*French*) 8-51717

impurities continued

- Si layer, neutron activation analysis, contamination and cross-contamination 8-83837
 Si wafers, Czochralski, gettering of surface and bulk impurities 8-64456
 Si:Ga, gettering of Au and Cu during Ga diffusion 8-91350
 SiO₂:Fe, vitreous and cryst., with or without Al₂O₃, Na₂O additions, exam. of Fe²⁺ coordination, IR spectroscopy 8-88344
 Sn, crystn., mechanism of influence of soluble impurities 8-71692
 Sn, liquid, electron transfer of rare earth impurities (*Russian*) 8-95278
 SrCl:Mn²⁺, shape of potential well, calc. 8-87951
 SrO:Mn²⁺, impurity pot. well shape calcs. 8-87950
 TiC-Mo₂C-Ni cermets, influence of anomalous phases on strength 8-92228
 TiD₂, clean and contaminated films, fabrication and AES 8-52600
 VO₂, doped, morphology, structure and props. (*German*) 8-59823

impurity and defect absorption spectra of inorganic solids

- adsorption rel. to dopant admixture 8-95596
 alkali aluminometaphosphate glass, MPO₃.Al(PO₃)₃:U (M=Li,Na,K), vibronic excitation, absorption and emission spectra 8-52524
 alkali bromide (chloride):V²⁺, electron spin transfer 8-87949
 alkali halide:Hg, EPR and optical props. 8-91933
 alkali halide:O₂⁻(NO₂⁻), effect of press. on vibronic spectra 8-52532
 alkali halide:Sn²⁺, V_c-centres, vacancy induced splitting of excited states, Sn²⁺ structure 8-51931
 alkali halides, bound polarons, vibronic theory, appl. to F-centre excited states 8-84150
 alkali halides, F-centres, thermal and photolytic decay processes 8-95053
 alkali halides, F-centre, cluster-Bethe lattice treatment 8-63762
 alkali halides, shift and broadening of local vibr. bands, temp. depend. 8-87755
 anthracene, irradiated, optical absorption and EPR meas., low temps. 8-68538
 calibo glass:Eu³⁺, Ho³⁺, energy transfer 8-76510
 chlorides, I⁻ or Br⁻ doped, optical investigation of atomic hydrogen centres 8-88351
 colour of imperfect crystals, lattice defects and impurities 8-72562
 diamond, GR 2-3 absorpt. line, uniaxial stress effects 8-72563
 diamond, GR defect, high resolution optical spectra after electron irradi. 8-56515
 diamond, synthetic and natural, neutron irradi., optical and elec. props. (*Russian*) 8-59841
 diamond, type Ib, electron irradiated, migration of N, optical absorption meas. 8-56505
 diamonds, artificially coloured, spectroscopic diagnostic technique 8-65281
 GaP, reevaluation of bandgap and free exciton binding energy 8-60061
 garnet:Nd³⁺, spectral, structural regularities, anal. 8-51948
 glass:Nd³⁺, multitype opt. centres 8-68558
 glass:Nd, stimulated emission cross section by absorpt. meas. from thermally populated ⁴I_{1/2} levels 8-71107
 impurities, conc. of C, O, Si 8-59832
 KBr, thermally processed cryst., optical absorption bands (*Russian*) 8-76513
 nonmetal, impurity optical absorption and emission, anharmonic effects 8-56503
 oxides, excited states of F-centres 8-64006
 phosphate glasses:Cu²⁺, EPR, optical spectra 8-72399
 phosphate glasses:V⁴⁺, EPR, optical spectra 8-72399
 plagioclase:Mn²⁺(Fe³⁺), ligand field bands of impurity luminesc. centres and their site occupancy 8-88350
 pyrene, single cryst., γ -irradiated, EPR and optical absorption meas. 8-72412
 quadratic Stark effect, Jahn-Teller effect in electroabsorption 8-68536
 quartz, electron irradiated, optical and anelastic absorptions and resonator freq. 8-64385
 quartz, rose, charge transfer mechanism for origin of colour, EPR and optical expts. 8-52537
 quartz, synthetic, lattice distortions, optical inhomogeneities by X-ray topography and optical birefringence meas. 8-55887
 ruby cryst. R-line absorpt. and dispersion spectra, mag. field effects (*Russian*) 8-92056
 sapphire, F-type centre induction, 6.1 eV optical absorpt. band 8-88332
 semiconductor, optical absorption by impurities, phonon-electron interaction 8-56502
 strontium tartrate tetrahydrate Co²⁺ electronic absorpt. spectrum 8-92098
 tellurite glass, Cu²⁺(Ni²⁺) coloured, band-pass filter characts. 550-616 nm 8-66919
 transition metal, impurities, as probes of critical points, in host band structure 8-91645
 vibrational spectra crystals with split configuration interstitial (*Russian*) 8-76450
 vibronic splitting and Zeeman effect for ⁴A_g→²E_g transition 8-60495
 Ag halide doped photochromic glass absorption spectra (*Russian*) 8-60490
 AgCl, colloid centres by heavy ion implantation 8-63780
 AgCl, colloid centres induced by reactor neutrons at 20K 8-72560
 AlH₃, photoelectric effect spectra and kinetics, photochem. mechanism colour centres 8-56506
 AlNbO₄, diffuse refl. and luminesc. spectra 8-56516
 Al₂O₃, corundum, doped, induced absorption spectra, low temp. irradi. effects (*Russian*) 8-72570
 Al₂O₃:V⁴⁺, dil. solution, stimulated phonon emission 8-63817
 β -Al₂O₃-Na₂O, EPR and optical absorpt. studies of X-ray produced defects 8-95517
 β -Al₂O₃-Na₂O:Fe, coordination site, oxidation state, Mossbauer, absorpt., emission spectra, mag. susceptibility meas. 8-68431
 As, amorphous, bonding coordination defects, Raman scatt. and IR absorption meas. 8-60498
 As₂S₃(Se₃), X-ray induced paramag. states and luminesc. 8-95520
 BaF₂:Mn²⁺, far IR absorption spectra 8-76507
 BaO-B₂O₃-SiO₂:Ti³⁺, optical absorpt. spectra 8-72564
 Ba₂(PO₄)₃, transition metal ion, optical and magnetic props. 8-64196
¹²C¹⁶O:¹²C¹⁸O isotopes, IR and Raman spectra, vibron band, vibron-phonon combination bands 8-68495

impurity and defect absorption spectra of inorganic solids continued

- CaF₂, bleaching characteristics of crystals coloured by low energy electrons 8-76497
 CaF₂:Ce, Stark struct., phototransitions, g-factors 8-67995
 CaF₂:PbO, UV absorption, impurity centres 8-68534
 CaF₂:Pr³⁺, multisite system, laser selective excitation and energy transfer 8-84634
 CaF₂:RF₃, colour centre prod. by γ -irrad., absorpt. spectra obs. 8-72565
 CaF₂:Sm, charge transitions, positron annihilation exam. 8-92143
 CaF₂.3Ca(PO₄)₂, apatite, fission damage detection, absorpt. spectra 8-84617
 CaO-Li₂O-Al₂O₃-SiO₂:Nd³⁺, CaO enriched, laser-type glasses, spectroscopic behaviour 8-60497
 CdIn₂S₄:Co, optical absorption meas. 8-64384
 CdS, absorpt. spectra, 400-650 nm, electron irradi. defects and absorpt. edge shift 8-64382
 CdS:Cl, extrinsic, exciton absorption 8-72569
 CdS:Li, anisotropy of the absorption by impurity centers in hexagonal crystals 8-88343
 CdSe:Cu, photo-induced changes in absorpt. spectra 8-80382
 CdTe:Be, impurity modes and IR absorption 8-76506
 Cr³⁺, electronic states interactions with crystal odd vibrs., R-lines vibr. recurrences 8-84639
 Cr³⁺ impurity spectra anal. with Trees' correction 8-68539
 CrO₂²⁻ in halide salt aqueous solution, absorpt. spectra, 4.2 to 290K (*Russian*) 8-60499
 Cs halides, F-centres, first excited degenerate states, props. of electron-phonon interaction 8-63824
 CsBr:Ti³⁺, perturbed lattice dynamics, breathing shell model calculation 8-75744
 CsSiF₆:Mn⁴⁺, splitting of vibronic levels 8-60496
 CsSrCl₃:Ti, absorpt. and luminesc. spectra 8-72586
 CuGaS₂, coloration, pure and Fe doped, EPR and optical absorpt. obs. 8-88336
 Cu₂O, yellow exciton series, silver impurity influence on spectrum 8-64388
 Cu₂O:Ag⁺, yellow series line width, exciton-impurity scatt. 8-64386
 Cu₂O:Cd, dipolar and quadrupolar bound excitons, absorption spectrum (*Russian*) 8-92099
 Ga_{1-x}Al_xP, two-phonon optical absorpt. 8-88341
 GaAs, amorphous layer formation, ion implantation 8-95063
 GaAs, irradiated with fast neutrons, IR vibrational absorpt. 8-75776
 GaAs:Fe, profile of impurity optical absorption bands 8-56509
 GaAs_{1-x}P_x:N, film, optical absorpt. from photoluminesc. meas. 8-92134
 n-Ga_{1-x}In_xP, optical props. and energy spectrum of donors 8-72567
 GaNbO₄, diffuse refl. and luminesc. spectra 8-56516
 GaP, shallow impurity states, free exciton binding energy 8-79960
 GaP:Fe, profile of impurity optical absorption bands 8-56509
 GaP:N(Te), ion implanted at 40 keV, refl. spectra, 210-2000 nm, annealing (*Russian*) 8-80386
 n-GaSb:Te(Se), forbidden optical band gap, Moss-Burstein effect 8-88335
 Gd₂Ca₂O₁₂:Nd³⁺, growth, stimulated emission, spectral props. 8-95593
 Ge:Sb,Cu, exactly compensated, impurity absorpt. and photocond. spectra 8-56189
 Ge:Si, impurity modes and IR absorption 8-76506
 Ge-S film, amorphous, photo-induced ESR and optical absorption edge shift 8-88374
 GeO₂, radiation damaged, paramag. point defects, F-centres, ESR, absorpt. spectra 8-80213
 GeO₂:Si, optical props. IR absorpt., UV reflection spectra 8-84619
 H₂WO₄, film, effect of struct. on optical and electrical props. 8-84671
 HfSiO₄:U⁴⁺(U⁵⁺), opt. spectra 8-88334
 N-InAs, Moss-Burstein effect, S, Sn, Te dopants 8-64389
 IrF₆, in mixed crystals., Jahn-Teller effect, $\Gamma_{8g}(t_{2g})^3$ state, 6800 Å 8-76032
 KBr, electron irradi. at 4K, role of V_k centres in equilb. among centres 8-67712
 KBr:Ca, X-ray re-irradiation effects on Z₁ centres 8-75664
 KBr:Li²⁺(Na⁺), electronic struct. of (V_k)_a 8-95269
 KBr:NO₂, Na effect of Na⁺ impurity on self-trapped hole (*Japanese*) 8-67982
 KBr:Rb, H-centre interaction with Rb⁺ ion 8-75662
 KBr-KI:Ti, spectral, polarisational and kinetic characts. 8-80385
 KCN, optical F centres and phase transitions 8-56504
 KCl absorption and emission of F_k(Li) centres under hydrostatic pressure 8-92117
 KCl, F-center pairs, light excitation, mag. field and resonance effects on absorption bands 8-92094
 KCl, H₂O-related centres 8-67711
 KCl, irradiated, determ. of molar extinction coeff. and oscillator strength of V₂-centre (*Russian*) 8-80384
 KCl, irradiated crystal, determ. of oscillator strength of V₃-centre (*Russian*) 8-92095
 KCl, radiation damaged, proton and ⁴He⁺ channelling, F-centre production, optical absorpt. meas. 8-79656
 KCl, room temp. X-irrad., first stage F-centre form. 8-67709
 KCl surface, vacuum UV radiation damage, spectroscopic study 8-71758
 KCl:Eu, luminescence and absorption of color centres in RbCl:Cu and KCl:Eu crystals 8-92118
 KCl:I crystals, V-band development using X-rays 8-88337
 KCl:I(Br), colouration under two-photon excitation, absorption spectra 8-84618
 KCl:KOH, influence of anion impurities on mech. props. of alkali halide crystals 8-87736
 KCl:Pb²⁺(0.005% Pb), A band fine structure, electron-phonon interaction 8-60491
 KCl:PbCl₂, tablet, 272 nm absorpt. band 8-84612
 KCl:S, influence of anion impurities on mech. props. of alkali halide crystals 8-87736
 KCl-KI:Ti, spectral, polarisational and kinetic characts. 8-80385
 KCl(Br), coloured, irradi. damage during positron bombardment 8-63791
 KCl_{1-x}Br_x:NCO⁻, absorpt. band defect broadening (*Russian*) 8-72526
 KCl_{1-x}I_x:NCO⁻, absorpt. band defect broadening (*Russian*) 8-72526
 K₂Cu_{1-x}Mn_xF₄, Cu-Mn exchange interaction, optical determ. 8-72551

impurity and defect absorption spectra of inorganic solids continued

- K(H_{1-x}D_x)₂PO₄, single cryst., 77K, γ -radiation damage centres, and EPR obs. 8-68379
- KI:S²⁻, photochemical reaction, F-centre production, optical absorption and ionic thermocurrent meas. 8-64861
- K₂O-BaO-SiO₂ glass, rare earth ion activated, spectral intensity, effect of number of 4f electrons 8-84602
- K_{1-x}Rb_xCl:HF₂⁻, dynamic inhomogeneous broadening of bands of local vibr. 8-92102
- LaF₃:Ho³⁺, laser excited fluorescence absorption spectra, symmetry groups 8-60514
- LiF, coherent radiation generation in F₂-centres 8-50782
- LiF, influence of neutron irradiation temp. on F-aggregate centre form. 8-72561
- LiF, radiation damaged, proton and ⁴He⁺ channelling, F-centre production, optical absorpt. meas. 8-79656
- LiF, Stark effect, M-centre absorpt. bands 8-84614
- LiNbO₃, two-photon and X-ray induced Nb⁴⁺ and O⁻ small polarons, ESR and optical absorpt. 8-76306
- LiNbO₃:Co, optical props. 8-64383
- Li₂O-Al₂O₃-P₂O₅:V⁴⁺, glass exam. of ESR spectrum of V⁴⁺, optical spectra, and structure 8-88180
- Li₂O, fund. optical absorpt. edge, number of displaced atoms from ⁶Li(n, α)³H reaction 8-51594
- MgO, Fe³⁺ and Cr³⁺ impurity ions valence conversion in single cryst. by UV irradiation (German) 8-84620
- MgO:K, implanted K aggregates, TEM and optical spectra obs. 8-83838
- MoO₃, film, colour centre studies, optical absorpt. spectra 8-71724
- MoO₄²⁻, in halide salt aqueous solution, absorpt. spectra, 4.2 to 290K (Russian) 8-60499
- N₂:CO, IR and Raman spectra, vibron band, vibron-phonon combination bands 8-68495
- NH₄Br:Cu²⁺, ESR and absorpt. spectra, 300-1500 nm 8-60492
- NaA zeolite:S, optical spectra 8-88342
- NaBr, thermally processed cryst., optical absorption bands (Russian) 8-76513
- NaCN, optical F centres and phase transitions 8-56504
- NaCl, irradiated, determ. of molar extinction coeff. and oscillator strength of V₂-centre (Russian) 8-80384
- NaCl, radiation damaged, proton and ⁴He⁺ channelling, F-centre production, optical absorpt. meas. 8-79656
- NaCl:Mg²⁺(Mn²⁺)(Ni²⁺)(Cd²⁺)(Pb²⁺), Zn-like centre, absorpt. spectra obs. 8-76498
- NaCl:Ni single crystals, VUV spectrum, ionic conductivity, X-ray diffraction 8-92097
- NaF, radiation damaged, proton and ⁴He⁺ channelling, F-centre production, optical absorpt. meas. 8-79656
- NaF, Stark effect, M-centre absorpt. bands 8-84614
- NaI:Cu⁺, luminesc. of isolated V_K-centres 8-84641
- Na₂O-B₂O₃ glass, covered with PbO film, deep penetration of Pb²⁺ ions 8-79535
- Na₂O-B₂O₃-SiO₂-Fe glass, near IR optical absorption of Fe (II) 8-84616
- Na₂O-P₂O₅, metaphosphate glass, active solute doped, absorpt. spectra of radiation products 8-64865
- Na₂O-SiO₂ glass, magnetooptical props. 8-80318
- Na₂S₉H₄O-NaOH-H₃BO₃ glass, IR and Raman spectra of boroultramarine, exam. of S₃⁻ presence 8-68502
- Na₂Zn(SO₄)₂·4H₂O:Ni, divalent state obs. 8-76501
- Nd:glass laser rod, piezoelectric detection of photoacoustic signals 8-54467
- Nd₂O₃-Al₂O₃-SiO₂ glass, exam. of spectroscopic and luminescent props. 8-88364
- Nd₂O₃-SiO₂ glass, exam. of spectroscopic and luminescent props. 8-88364
- RbCl:Eu, luminescence and absorption of color centres in RbCl:Cu and KCl:Eu crystals 8-92118
- RbCl:Sn crystals, Sn-centres, X-ray and coloration effects 8-76500
- ReO₄⁻, in halide salt aqueous solution, absorpt. spectra, 4.2 to 290K (Russian) 8-60499
- Si, far IR impurity spectra, effects of high uniaxial stress 8-56508
- Si, neutron irradiated, intrinsic defect exam. by IR spectra 8-52534
- Si, sputtered, cluster formation, influence of HF plasma interaction 8-64441
- Si:Al, absorpt. line broadening 8-95594
- Si:Al, bound-exciton absorption 8-56507
- Si:Al(In), acceptor levels, IR spectra 8-67972
- Si:Ga, bound-exciton absorption 8-56507
- Si:Gd, radiation defect form., effect of Gd impurities, elec. and optical meas. 8-71764
- Si:In, bound-exciton absorption 8-56507
- Si:O film, near IR absorption, O impurity states 8-88333
- Si:O film, near IR reflectivity at high temps. 8-56532
- Si:P, IR absorpt. and D⁻-band 8-52533
- p-SiC:B (4H), absorption spectra of bound excitons 8-88338
- n-SiC(6H), donor ground state splitting, IR spectra (Russian) 8-92104
- SiO₂, ion irradiation, H capture, absorpt. bands (Russian) 8-76505
- SiO₂, OH group interactions, IR and Raman spectra 8-80383
- SiO₂, vitreous, substrate for PbO film, interdiffusion reactions, UV spectroscopy obs. 8-51750
- SiO₂:Fe, vitreous and cryst., with or without Al₂O₃, Na₂O additions, exam. of Fe²⁺ coordination, IR spectroscopy 8-88344
- SrCl₂:Fe²⁺(Co²⁺) electronic absorption spectra in far and middle infrared 8-68537
- SrF₂, doped, far IR absorption spectra 8-76507
- SrF₂:CeF₃(GdF₃)(TbF₃), absorpt. spectra of γ -irradiated cryst., 77K, 200-700 nm 8-84615
- SrF₂:R³⁺, far IR vibr. spectra of F⁻ compensation ion 8-92059
- Tb(OH)₃:Er³⁺, ferromag., anisotropic exchange effects in optical spectra 8-80141
- ThSiO₄:U⁴⁺(U⁵⁺), opt. spectra 8-88334
- TiO₂, room temp. coloration by diffused Na and H from Na amalgam 8-84611
- TiO₂, rutile, deuteron and alpha-particle implantation, chemical effects, optical and cond. meas. 8-67755
- TiO₂-SiO₂, semicond. glass, optical props. 8-60412
- Xe, optical excitation of rotational transition of methane, 6K 8-60494
- YAG, colour centres conceived as bound polarons 8-63990

impurity and defect absorption spectra of inorganic solids continued

- YIG: Ca²⁺ epitaxial films, Fe⁴⁺ centres, MCD, optical absorpt., and thermoelectric power meas. 8-95595
- Y₂O₃:Eu³⁺, absorpt. spectra, fluoresc., electron beam excitation 8-92093
- YVO₄:Eu³⁺, absorpt. spectra, fluoresc., electron beam excitation 8-92093
- ZnGeP₂, P vacancies, lattice parameters, optical props. depend. on thermal treatment (Russian) 8-71729
- ZnS:Al-Cu, localised vibrational modes 8-63827
- ZnS:Be, impurity modes and IR absorption 8-76506
- ZnS:Mn²⁺, Jahn-Teller effect in fluorescent level 8-52566
- ZnSe:Mn²⁺, Jahn-Teller effect in fluorescent level 8-52566
- ZrSiO₄:U⁴⁺(U⁵⁺), opt. spectra 8-88334
- impurity and defect absorption spectra of solids**
see also *impurity and defect absorption spectra of inorganic solids*
- alcohols, trapped electron spectral relax., random-walk model 8-60493
- anthracene:cyclohexadienyl type radicals, charge transfer reactions 8-52535
- anthracene:tetracene, upper excited vibronic states optically pumped energy transfer matrix fluoresc. 8-76512
- anthracene, monocrysl., additional absorpt. spectrum at low temp. 8-92096
- 1, 12-benzperylene, in alkane matrices, zero-phonon lines, press. shifts (Russian) 8-76502
- calcium tartrate tetrahydrate:Ni²⁺, optical absorpt. spectrum 8-84610
- coronene, in alkane matrices, zero-phonon lines, press. shifts (Russian) 8-76502
- cyclodextrin, trapped electrons in cryst. matrices, ESR, optical absorption spectra 8-80768
- dielectric medium, impurity dispersion self energy calcs. 8-52536
- dispersive medium, QED and multiphoton processes at impurity centre (Russian) 8-71141
- ethylene, isotopically mixed, crystal, dilute guest probe orientational energy, IR, Raman spectra 8-68496
- 1-hydronaphthyl radical, in naphthalene single cryst., anisotropic oscill. strength 8-50591
- inhomogeneously broadened spectra, dip contour saturation (Russian) 8-76503
- intercombination transition intensities in strong crystal fields, symmetry reduction method 8-84175
- line shapes, quantum-mechanical moments 8-72566
- magnetic crystal, with impurity centre, anomaly of width and lineshape of light absorpt. 8-76499
- molecular crystals, spectroscopy, bibliography for 1976 8-72585
- organic compounds, inhomogeneously broadened absorption spectra, linear struct. detect. (Russian) 8-76504
- palladiumporphyrin, in n-alkane, S₁←S₀ absorpt. spectrum, vibronic coupling and avoided crossing, field splitting 8-84613
- quantum system interacting with nonequilibrium phonons, light absorption props. 8-88340
- Raman scattering by impurity centre pairs, possibility of cooperative effects 8-60449
- semiconductor, absorption line profile in static elec. field, effect of impurities 8-92101
- semiconductor, Coulomb screening influence 8-72568
- semiconductor, H⁻-H⁺ type impurity complexes, spectra, and pseudointeractions of mol. energy levels (Russian) 8-92100
- semiconductor with highly anisotropic bands, photoionisation cross section of deep impurity centres 8-56510
- solid solutions, impurity centres, internal mol. vibr., inhomogeneous band broadening 8-92103
- transition metal ions, in solid, nearly degenerate electronic levels, dynamical effects 8-68535
- tris sarcosine calcium chloride:VO²⁺, EPR and absorpt. spectra 8-60330
- V³⁺ in crystal field, intercombination transition intensities, symmetry reduction method 8-84175
- impurity clustering** see *segregation*
- impurity-defect interactions**
see also *impurity-dislocation interactions; impurity-vacancy interactions*
- diamond, type IIa, electron irradiation, EPR obs. of interstitial-impurity complexes 8-76310
- metal, solute atom displacement in mixed dumbbell interstitials for FCC lattice 8-79631
- thermal neutrons, inelastic scattering by one-dimens. defecton (Russian) 8-84169
- transition metals, electronic structure and ordering of sp defects 8-91639
- Al alloys, dil., size effect of impurity atoms rel. to trapping radii for migrating self-interstitials 8-75690
- Al:¹¹¹In, electron irradiation, defect trapping at impurities 8-55892
- Al-Cr(V)(Ti), dil., electron irradiation, interaction of self interstitials with undersized solute atoms 8-63789
- Al-Mn(Cu)(Ag), solute atom displacement in mixed dumbbell interstitials for FCC lattice 8-79631
- β -Al₂O₃, effect of halogen ion additions to structural state 8-76620
- Bi, quenching and annealing of defects, elec. resist. meas. 8-87973
- Bi:Sb(Te), quenching and annealing of defects, elec. resist. meas. 8-87973
- Cu alloys, dil., size effect of impurity atoms rel. to trapping radii for migrating self-interstitials 8-75690
- Cu-Be, solute atom displacement in mixed dumbbell interstitials for FCC lattice 8-79631
- Nb, neutron irradiation, effects on mech. props. 8-91361
- Si:Gd, radiation defect form., effect of Gd impurities, elec. and optical meas. 8-71764
- SiO₂, ion irradiation, H capture, absorpt. bands (Russian) 8-76505
- Ti, influence of H₂ on the internal friction (French) 8-75723
- impurity-dislocation interactions**
see also *dislocation locking; dislocation pinning*
- FCC crystal, elastic interaction of 60° and screw dislocations with point defects 8-63786
- microcreep, low temp., quantum effects (Russian) 8-71784
- semiconductor, containing screw dislocations, impurity centres 8-72111
- steel, cold-worked, state of cementite, nucl. gamma reson. meas., plastic deform. (Russian) 8-68706
- steel, delayed fracture, hydrogen and impurities 8-84988

impurity-dislocation interactions continued

- Al-Zn-Mg alloys, decomp. kinetics from Young's modulus obs., microprocesses (*German*) 8-64522
 Fe alloy, impurity-dislocation interaction and Snoek Koester relaxation (*Russian*) 8-59834
 α -Fe:He, impurity clustering in vacancies bound to edge dislocations 8-91358
 Fe-H system, cold work internal friction peak, appl. of Schoeck's model 8-95771
 Si, ion-implanted, disorders, nature and annealing behaviour, review 8-83836
 Si:Cu, interaction between vacancy emitting absorbing precipitates and dislocations, TEM obs. 8-71755
 Si:P, Au gettering by P diffusion and P-induced dislocations 8-91346

impurity distribution

- see also *doping profiles; segregation*
 alkali halides, divalent impurity dipole aggregation kinetics 8-79630
 crystal growth from melt, kinetic factor effects 8-52656
 durene-p-dibromobenzene system, phase diagram and X-ray diff. expts. 8-79774
 film sandwich structures Auger anal. 8-72030
 inclusion emersion in vertical zone refining 8-52663
 long-range order 8-95061
 nonconstant distribution coefficient, calc. from expt. data 8-75606
 optical inhomogeneities obs. by spectral modulator, using scanning image converter 8-59144
 plagioclase: $\text{Mn}^{2+}(\text{Fe}^{3+})$, ligand field bands of impurity luminesc. centres and their site occupancy 8-88350
 polypropylene, impurities redistribution during crystn. 8-75577
 quartz, synthetic, lattice distortions, optical inhomogeneities by X-ray topography and optical birefringence meas. 8-55887
 SEM cathodoluminescence analysis of impurities, localisation and sensitivity 8-95985
 semiconductor supersaturated solid solns., decomp., surface impurity content 8-51681
 solid, depth profiling of ^3He ion implantation 8-59830
 steel, Cr-plated, H_2 distrib., laser-mass spectrometer investig. 8-61113
 steel, mild, implantation of Cu(Cr), annealing and rolling behaviour of conc. profiles 8-75684
 wall and limiter materials for DITE Tokamak, H conc. meas. 8-94136
 X-ray diffraction line broadening from small subgrains containing gradients of spacing 8-67612
 Al: ^{12}B , relax. mechanism for polarised implant 8-87693
 Al_2O_3 , sintered, containing MgAl_2O_4 precipitates, Mg distribution at grain boundaries 8-80498
 $\text{Bi}_2\text{Te}_{3-x}\text{Se}_x$, thermoelec. mat., prep. effects on inhomogeneities 8-51576
 Fe, cast, Mg, despheroidising effect of Bi, Sn on graphite in alloy 8-56670
 Fe, diffusion and solid solubility of Sb, 773-873K, ion backscatt. anal., rel. to intergranular embrittlement 8-71880
 Fe, liq., of diffused alloying elements (*Russian*) 8-79791
 Fe-Ni, hydrogenated, Mossbauer effect meas. 8-92002
 GaAs:Cu, supersaturated solid solns., decomp., surface impurity content 8-51681
 GaP, LPE at 650°C from In solvent, low Si contamination 8-80480
 Ge:Li, supersaturated solid solns., decomp., surface impurity content 8-51681
 H depth profiling in materials, use of $^1\text{H}(^{15}\text{N},\alpha\gamma)$ resonant reaction (*French*) 8-91357
 H profiling, appl. of $^1\text{H}(^{15}\text{N},\alpha\gamma)^{12}\text{C}$, ^{15}N energy loss meas. 8-59845
 ^3He profiling, depth resolution using $^3\text{He}(\text{d},\alpha)^1\text{H}$ reaction 8-58557
 ^4He , solid, quantum diffusion of ^3He , tunnelling jumping approx. (*Russian*) 8-87844
 InSb-GaSb, directionally solidified, determination of non-constant distrib. coeffs. 8-76641
 $\text{MgSeO}_4 \cdot 6\text{H}_2\text{O}:\text{Mn}^{2+}$, EPR obs., rel. to Mn crystallographic sites 8-79628
 Na:O, evaluation of V wire equilibration method, for determining O content 8-79626
 Ni, trapping and release of inert gases, thermal evolution mass spectrometry 8-95077
 $(\text{Pd}_{0.8}\text{Au}_{0.2})\text{D}_{0.04}$, lattice location of D, ion channelling obs. 8-67708
 Si, ion implanted, laser-annealed, theoretical anal. of thermal and mass transport 8-91364
 Si, optical inhomogeneities obs. by spectral modulator 8-59144
 Si, ribbon, impurity distrib. in EFG 8-91280
 Si, sputtered, cluster formation, influence of HF plasma interaction 8-64441
 Si, swirl defects, gettering effects, obs. by photoluminesc. meas. 8-84623
 Si vacuum sublimated thin film structure impurity distrib. 8-95354
 Si: (B, P, Ge), impurity-pair diffusion, influence of elastic stresses 8-87824
 p-Si:Bi, high temp. treatment, effects on ion implanted impurity distrib. profile 8-79625
 Si:Bi, impurity conc. from photoluminesc. anal. 8-63785
 Si:Cu(Au), recoil implantation from thin surface films, backscatt. obs. 8-63783
 Si:Fe, EPR and neutron activation anal. of thermal defects 8-91355
 Si:P, Au, neutron irradiated, distrib. of P and Au determ. 8-79627
 Si:P, impurity conc. from photoluminesc. anal. 8-63785
 Si:Pb, implanted and annealed, impurity redistrib. 8-75689
 Si-SiO₂ interface morphology, P pileup effect, Auger sputter profiling 8-72006
 SiN_x, plasma deposited, H content meas. 8-63949
 Si₃N₄ film, diffusion of Al, AES and depth profiling 8-51744
 SiO₂ based optical fibre rod preform, optical meas. of OH ion distrib. 8-87130
 SiO₂, insulating films, neutron activation anal. and autoradiography 8-92574
 SiO₂:Na, film, depth profiling by SIMS 8-79624
 Ta film, determ. of thickness and O, N content 8-80824
 TaD_{0.10}, lattice location of D, ion channelling obs. 8-67708
 β -Ti-Mo-V-Fe-Al (8, 8, 2, 3, wt.%), exam. of stress induced H₂ migration 8-87823
 U, γ - and β -hardened, recrystallisation, effect of impurity distrib. 8-70602

impurity distribution continued

- W:K-Al-Si, state of bonding, distribution of impurities 8-92212
 Zr, deuterium implanted, temp. depend. depth profiles of deuterons 8-95076

impurity electron states

- see also *A-centres; Anderson model; charge compensation; deep levels; electron traps; heavily doped semiconductors; impurity scattering; OH-centres; U-centres; Z-centres*
 alkali halide: Sn^{2+} , V_c -centres, vacancy induced splitting of excited states, Sn^{2+} structure 8-51931
 alkali halides: Ga^+ , optically detected EPR in relaxed excited states of Ga^+ 8-72437
 alkali halides, F-centre, cluster-Bethe lattice treatment 8-63762
 carrier conc., temp. depend., computer data anal., effect of band parameter errors (*Russian*) 8-52006
 chalcogenide lone-pair semicond. charged impurities, effect on carrier concs., Street-Mott model 8-67984
 Cr-Au alloys, dil., elec. resist., 77-700K 8-64035
 crystal colour, lattice defects and impurities 8-72562
 d-band metals and alloys, s-d hybridisation 8-91644
 diamond, natural, N3 luminesc. decay time 8-76520
 donors with excited states, non-equilibrium phenomena, theory of kinetics of electron transitions 8-79961
 exciton to neutral acceptor binding energy, calcs. using atomic-like variable wave function 8-79937
 exciton-ionised donor complex, binding energy, effective electron-hole interaction pot. 8-67949
 ferromagnetic metal-rare earth, dil., hyperfine fields 8-87947
 n-GaP, quasidirect radiative recombination of free holes at neutral shallow donors 8-64410
 GaP, reevaluation of bandgap and free exciton binding energy 8-60061
 heavily doped semiconductor, n-type, Mott transition, dielec. enhancement and conduction electron screening, unified treatment 8-72073
 heavily doped semiconductor with overlapping electronic orbitals impurity bands, theory 8-56102
 impurities, conc. of C, O, Si 8-59832
 impurity centre-external elec. field interaction, charge transfer processes influence 8-87944
 indirect coupling between localised impurities, virtual bound state model 8-64001
 n-InP, magneto-impurity resonances, obs. of central cell struct. 8-95303
 insulators, improved effective mass for impurity levels 8-87941
 ionised impurity scatt. 8-51984
 layered piezoelectric-semiconductor surface state acoustic memory 8-90615
 local impurity states, existence, levels, Green function, tight-binding calcs. 8-67981
 magnetic alloys, dil., spin correlation 8-84385
 metal, quasimagnetic impurity, exact solution of Wolff's model 8-56105
 metal, simple, electronic struct. of H impurity 8-67978
 metal oxide surface, adsorption of electron acceptors, strength and distrib. of electron donor sites 8-84055
 metal-H system, bond energy calcs. 8-51940
 metal-nonmetal transition, universality aspects 8-56075
 molecular impurities in crystals, exclusion rules for librational-tunnelling states 8-84174
 naphthalene cryst., anthracene doped, fluoresc., two-photon excited 8-68560
 noncrystalline system, continuous and discontinuous metal insulator transitions 8-56076
 p-type semiconductors, internal strain on bound hole-phonon interaction 8-91492
 photovoltaic effect, impurity centre models (*Russian*) 8-60153
 piezoelectric semiconductor, cascade capture of carriers by attractive impurity centres, cross section 8-56157
 Poisson's equation for impurity ion in medium with spatially variable dielec. const., variational principle 8-60084
 polar semiconductor, impurity levels, influence of electron-phonon coupling 8-64007
 quartz, impurity microdefects. electron capture cross-sections (*Russian*) 8-76025
 random impurity system, density of states tails, fluctuations and mobility edges 8-67983
 semiconductor, absorption line profile in static elec. field, effect of impurities 8-92101
 semiconductor, containing screw dislocations, impurity centres 8-72111
 semiconductor, doped, zinc blende type, electron-phonon interaction, reson. scatt. theory 8-64036
 semiconductor, H^- - H^+ type impurity complexes, spectra, and pseudointeractions of mol. energy levels (*Russian*) 8-92100
 semiconductor, impurity band, molecular model 8-76018
 semiconductor, impurity ion pot., nonlinear Poisson eqn. soln., variational principles 8-67976
 semiconductor, impurity photocond., temp., elec. field and impurity centre conc. effects 8-56190
 semiconductor, lone-pair effect of electronegativity difference on defect chemistry 8-72063
 semiconductor, magnetic freezeout in ultraquantum limit, appl. to GaAs 8-76017
 semiconductor, nonlinear impurity screening 8-67977
 semiconductor, optical absorpt., Coulomb screening influence, shallow impurity centre photoionisation 8-72568
 semiconductor, quasilocal acceptor states, effects on band gap and electron mobility (*Russian*) 8-60082
 semiconductor, screened impurity in mag. field ground state energy of bound electron 8-72107
 semiconductor, spin relax., in quantising mag. field, effect of carriers 8-72388
 semiconductor, zincblende struct., phonon attenuation in presence of internal strains and mag. field 8-76118
 semiconductor gapless, with impurities, energy spectrum 8-67979
 semiconductor-insulator boundaries, impurity electron states near interface 8-95320
 shallow impurity centre conc. meas., junction capacitance technique, review (*Japanese*) 8-79958

impurity electron states continued

- statistical mech. treatment of phase transitions impurity states 8-64004
- statistical mechanics of impurity states 8-51930
- substitutional impurities, Green's function calc. (*Russian*) 8-56101
- 1,2,4,5-tetrachlorobenzene, impurity induced states, spin dephasing, spin coherence expts. 8-84498
- 1,2,4,5-tetrachlorobenzene, localised excitations thermal promotion to exciton band, impurity states effect 8-52539
- three-dimensional organic chain conductors, one-dimensionalisation by impurities 8-91681
- transition metal, impurities, as probes of critical points, in host band structure 8-91645
- transition metals, electronic structure and ordering of sp defects 8-91639
- triplet state population kinetics, of impurity molecules (*Russian*) 8-56519
- tunnelling of solitons and CDWs through impurities 8-51913
- two-dimensional electron impurity system, quantum theory of cyclotron reson. lineshape 8-64083
- two-dimensional electron-impurity system in strong mag. field, electron spectrum and cond. (*Russian*) 8-88016
- ultrathin doping levels as model for 2-dimens. systems 8-60182
- vacancy-impurity scattering, complex dispersion law 8-87957
- Al, adsorption of O₂, relation between energy-band and cluster model 8-52048
- Al:He, pseudopotential calc. of screening of He atom 8-51917
- Al-M, dil. alloy, electronic states of 3d-transition metal (M) impurities 8-64005
- BaS:Cu, thermoluminesc. and decay 8-80426
- CaF₂:Sm, charge transitions, positron annihilation exam. 8-92143
- CaF₂:SrF₂:BaF₂:Gd³⁺, luminescence spectrum of Gd³⁺ ion and solid solution region obs. 8-84638
- Ca₃(PO₄)₂:F:Nd³⁺, optical fluorescence intensity and cryst. field parameters 8-52570
- Cd_{1-x}Fe_xCr₂S₄:Cu, effect of doping on elec. props. and Curie temp. 8-84214
- CdS:Cd(In), Cu- or defect-compensated, optical ageing rel. to storage cond. 8-84247
- CdS:Cl, heavily doped, fluoresc. spectrum upper threshold calculated 8-52568
- CdS:Cu, spectral sensitisation by cyanine dyes 8-64064
- CdS:In, spin flip Raman scatt., electron dynamics 8-80342
- CdS:Ni, elec., photoelec. and luminesc. props. (*Russian*) 8-84259
- CsCl:Cr³⁺, ESR of Cr³⁺ centres, room temp. 8-91943
- Cu-Cr, dil. alloy, Knight shift temp. depend., electronic struct. 8-84488
- Cu-Cr(Mn)(Fe), dil., NMR satellite data, rel. to electronic struct. 8-68398
- Cu-Cr(Mn)(Fe), dil., NMR data, ionic model and Kondo temp. 8-68399
- Cu₂O, yellow exciton series, silver impurity influence on spectrum 8-64388
- EuO_{1-x}N_x, ferromag. semicond., elec. and mag. props. (*French*) 8-79993
- n-GaAs, electron and gamma ray irradiated, introduction and annealing of defects 8-67736
- n-GaAs, heat treated, origin of 1.41 eV emission band, photolum. expt. 8-72579
- GaAs, magnetic freezeout in ultraquantum limit 8-76017
- n-GaAs, metal-insulator transition in impurity band induced by mag. field and loss of dimens. 8-52042
- GaAs, transmutation doped, shallow donors, magneto-optical study, photocond. meas. 8-87996
- GaAs:Cr, site symmetry of Cr ions, ground-state splitting, ballistic phonon expts. 8-95273
- GaAs:Ge, LPE, on semi-insulating GaAs, film-substrate interface characterisation 8-72017
- GaAs:Mn, p-type semiconductors, internal strain on bound hole-phonon interaction 8-91492
- GaAs:O, photocapacitance quenching effect 8-91727
- GaAs:O, slow domains, origin 8-60132
- GaAs_{1-x}P_xN, film, optical absorpt. from photoluminesc. meas. 8-92134
- n-Ga_{1-x}In_xP, optical props. and energy spectrum of donors 8-72567
- Ga_{1-x}In_xP:N, Delta lattice parameter model, correl. with electronic props. 8-91560
- GaN:As(P), implanted single cryst. film, cathodolum. 8-60523
- GaP, shallow impurity states, free exciton binding energy 8-79960
- n-GaP:Te, doping parameters calc., by means of Hall data analysis 8-51925
- n-GaSb:Te, heavily doped, electron-hole recomb., photoluminesc. spectra 8-84644
- n-GaSb:Te(Se), forbidden optical band gap, Moss-Burstein effect 8-88335
- Ge, donor-acceptor electron transfer at low temps., photocond. tail 8-84249
- Ge, electron-hole droplet, attachment to donor 8-87916
- Ge film, polycrystalline, structural and elec. props. 8-76173
- N-Ge, pressure influence on photoconductivity temp. dependence 8-76109
- n-Ge, rel. to shock wave effects on elec. cond. (*Russian*) 8-87979
- Ge:Cu, quenched, interaction between shallow-level defects and Cu atoms, Hall effect meas. 8-64002
- n-Ge:Sb, fast neutron irradi. effects on donor conc., and annealing 8-56107
- n-Ge:Sb, γ -irrad. effects on donor conc. and compensation by acceptors 8-56106
- Ge:Sb, rel. to uniaxial stress effects on acoustic attenuation 8-59863
- Ge-Sb, D⁻ complexes and band form., photocond. 8-84251
- Hg_{1-x}Cd_xTe, quasi-local acceptor levels and electron mobility 8-67974
- α -HgS, natural, yellow emission 8-68567
- N-InAs, Moss-Burstein effect, S, Sn, Te dopants 8-64389
- n-InP, Hall effect, 10-300K, thermal activation energy and influence of compensation 8-72171
- InSb, donor excitation spectra in high mag. field 8-80027
- InSb, gamma irradiated, changes in energy spectrum of impurity spectrum 8-51937
- n-InSb, low temp., electric and mag. resonances, impurity level (*Russian*) 8-56159

impurity electron states continued

- InSb, magneto-optical anomalies of impurity electrons, two-LO-phonon region 8-72415
- Ir, chemisorption levels of CO and O on (100) and (110) faces 8-84704
- KBr:NO₂, Na effect of Na⁺ impurity on self-trapped hole (*Japanese*) 8-67982
- KI:Tl, (TI)₂ centre luminesc. 8-84632
- KLiSO₄:Cr, optical activity characts. cryst.-chem. exam. 8-95569
- LiCl:Cu⁺, luminescent centre, cluster MO calculation of energy levels 8-64411
- MgO, electronic excitations and luminescence, review (*Russian*) 8-72575
- NH₄Br:Cu²⁺, ESR and absorpt. spectra, 300-1500 nm 8-60492
- NH₄Cl:Cr³⁺, ESR of Cr³⁺ centres, room temp. 8-91943
- NaA zeolite:S, optical spectra 8-88342
- Ni:H, energy and electron density of states 8-51929
- Ni-Re, dil. alloys, two-band Mott conductivity (*Russian*) 8-60118
- Pb_{1-x}Ge_xTe:Ga, Fermi level stabilization, transport props. meas., 77-400K 8-56065
- Pd:H, energy and electron density of states 8-51929
- Poisson's equations for impurity ion in medium with spatially variable dielec. const., variational principle 8-60085
- Rh:H, energy and electron density of states 8-51929
- S:Si, implanted, defect signature by thermally stimulated meas. 8-91643
- Sc, sp. ht. data rel. to electronic props. 8-83971
- Se:As(Cl), trigonal, defect and impurity electron levels, surface photovoltage spectra 8-72108
- Si (111) surface, clean, ESCA obs., Ni(Au) surface impurities 8-52640
- Si, donor ground state wave functions 8-87937
- Si, exciton-impurity complexes, emission spectra, Zeeman splitting (*Russian*) 8-64413
- Si, far IR impurity spectra, effects of high uniaxial stress 8-56508
- n-Si inversion layer, electronic bound states, theory 8-60217
- Si, neutral undistorted vacancy 8-91638
- Si pin diode, current filament temp. and Au acceptor level capture cross section temp. depend. 8-95351
- Si, shallow donors, Zeeman interaction, relativistic corrections and very small g-shifts, contrib. to EPR 8-72393
- Si:Al(In), acceptor levels, IR spectra 8-67972
- Si:Au, degeneracy factor of acceptor level 8-51927
- Si:Au, electron capture cross section, energy level of Au acceptor centre 8-51926
- Si:Au, impurity capture cross section and generation lifetime determ., MOS expts. 8-91772
- Si:B, impurity excited state lifetimes 8-60083
- Si:B(P)(Sb), multiparticle impurity complexes (*Russian*) 8-72601
- Si:Co, study of impurity states 8-76020
- Si:Fe, EPR and neutron activation anal. of thermal defects 8-91355
- Si:Ga(Al), edge luminesc. spectra of acceptors, multiexciton complexes 8-56517
- Si:In, bound exciton photolum. obs. 8-95607
- Si:O film, near IR absorption, O impurity states 8-88333
- Si:P, heavily doped, thermal oxidation 8-56793
- Si:P, luminesc. lines, multiexciton complexes and uniaxial stress 8-92114
- Si:Sb(P)(As), shallow donor states with strong central cell perturbation theory 8-51933
- Si:Sb(P)(As), shallow donor electrons, hyperfine interactions, reply to Onffroy's calcs. 8-51934
- Si-SiO₂ interface, Na⁺ drifted, impurity bands in inversion layers 8-60211
- p-SiC:B (4H), absorption spectra of bound excitons 8-88338
- α -SiC:B(Be)(Ga), piezoresist. rel. to acceptor levels 8-60129
- SiC:Be, film donor impurity, diffusion influence on elec. and optical props. 8-87942
- SiO₂:Al, vitreous state, EPR of Al defects 8-91951
- p-Si(111) surface inversion layer, Cs covered, negative magnetoresist. in 2D impurity band 8-64135
- Sm-Fe, dil., valence impurity state, inference from mag. susceptibility 8-95270
- SrCl₂:Fe²⁺(Co²⁺) electronic absorption spectra in far and middle infrared 8-68537
- SrF₂:CeF₃(GdF₃)(TbF₃), absorpt. spectra of γ -irrad. cryst., 77K, 200-700 nm 8-84615
- Tb(OH)₃:Er³⁺, ferromag., anisotropic exchange effects in optical spectra 8-80141
- Te in MIS structure, impurity photocond. 8-72203
- Te, liquid, localized impurity states, paramag. susceptibilities 8-64185
- Te:I, semicond., elec. efficiency (*German*) 8-84166
- TlCl-TlBr mixed cryst., impurity-induced self-trapping of holes and minority-ion percolation 8-64398
- ZnP₂, pure and doped, carrier mobility and conc., donor and acceptor energy levels, 190 to 380K 8-84217
- ZnS:Al-Cu, localised vibrational modes 8-63827
- ZnSe, laser induced modulation of opt. absorpt. 8-88324
- p-ZnSiP₂, single cryst., recomb. processes, photoelec. props. (*Russian*) 8-68053
- ZnSiP₂:Ga, effect of doping conc. on elec. cond. and Hall effect 8-76077
- ZnTe, band parameters from bound exciton, donor-acceptor pair excitation luminescence 8-92111
- ZnTe, high quality p-type cryst., predominant acceptors 8-60504
- ZnTe:As(P), spin flip acceptor scatt. 8-92072
- ZnTe:Sb film, acceptor levels 8-76172

impurity scattering

- used for carrier scattering by impurities
- see also Kondo effect
- Boltzmann equation method, derived from Kubo formula 8-95277
- CDW drift velocity 8-56123
- DC electrical conductivity, microscopic fields and currents 8-56121
- degenerate semiconductor, EM wave absorption 8-95308
- electron gas, interacting, elec. cond. 8-95276
- electron-hole droplet, motion damping, impurity and piezoelec. scatt. 8-67951
- exciton insulator, differential thermo EMF, temp. depend. (*Russian*) 8-72182

impurity scattering continued

- ionised impurity scatt. limited mobility in semiconductors with spatially variable dielec. function 8-51986
 isotropic scattering of current carriers in quantizing mag. field 8-51954
 metallic crystal, RF size effect, electron scatt. by impurities diffuse layer boundary (*Russian*) 8-91717
 molecular crystals, effects of impurity scatt. and transport topology on trapping, Frenkel excitons 8-95263
 one-dimensional conductors, impurity scattering effect on electron pairing 8-60112
 quasi-one-dimensional conductor, impurity effects, interchain interaction 8-72138
 semiconductor, conduction electron scattering by vibrating impurities 8-95297
 semiconductor, doped, zinc blende type, electron-phonon interaction, reson. scatt. theory 8-64036
 semiconductor, ionised impurity scatt. 8-51984
 vacancy-impurity scattering, complex dispersion law 8-87957
 Al-Cu(Ag)(Ge), dil., deviation from Matthiessen's rule at high temps. 8-64025
 Al-M, dil. alloy, electronic states of 3d-transition metal (M) impurities 8-64005
 Au alloys, electrical resistivity, deviations from Matthiessen rule and scattering anisotropy 8-76051
 Cd_{0.2}Hg_{0.8}Se, longitudinal Nernst-Ettingshausen effect, effect of disorder scatt. 8-84240
 Cu-Al(Ge)(Sn) film, thermoelec. power, 80-350K 8-68096
 Cu-Ni dil. paramagnetic alloys, sp. elec. resist., effect of Ni clusters (*German*) 8-95293
 EuO:Gd, electron mobility below Curie temp. 8-91696
 Fe based ternary alloys, Coulomb and exchange scatt. amplitudes, spin dependent residual resistivities 8-64033
 p-GaAs, electronic props. 8-68040
 GaAs, impurity scattering of current carriers in quantizing mag. field 8-51954
 n-GaAs, photo-Hall effect meas. of ionised impurity scatt. 8-56182
 n-GaAs, piezoelectric semiconductor, influence of acoustic phonon disturbances on conductivity 8-91697
 n-GaSb, galvanomagnetic effects 8-72172
 p-GaSb, heavy and light holes scattering 8-91692
 Ge, hole drift velocity, effect of impurity scatt. 8-60127
 Ge, ionised impurity scatt. limited mobility in semiconductors with spatially variable dielec. function 8-51986
 p-Ge, odd magnetoresist., ionised impurity scatt., theory 8-72178
 Hg_{1-x}Cd_xTe, quasi-local acceptor levels and electron mobility 8-67974
 Ni based ternary alloys, Coulomb and exchange scatt. amplitudes, spin dependent residual resistivities 8-64033
 Ni-Fe, film, anomalous Hall and Nernst-Ettingshausen effect, contribution of phonon and impurity scatt. (*Russian*) 8-64145
 Ni-Re, dil. alloys, two-band Mott conductivity (*Russian*) 8-60118
 n-Si, hot-electron diffusion, effect of ionised impurity scatt. 8-56151
 Si, ionised impurity scatt. limited mobility in semiconductors with spatially variable dielec. function 8-51986
 Te:Sb, 96 to 500K, cond. Hall const., hole mobility, conc., dislocation effects (*Russian*) 8-64039

impurity-vacancy interactions

- β -AgI, valence state and impurity-vacancy dipole formation, Mossbauer effect meas. 8-68435
 alkali halide, impurity-vacancy dipole interaction with relaxed and non-relaxed holes (*Russian*) 8-75661
 alkali halides, impurity-vacancy complexes, association and orientation energies 8-51578
 alkali metal chloride: F⁻(Br⁻)(I⁻), anion impurities substitution, energies of soln., association and migration 8-83831
 AgBr, doped, neutralisation of trapped photoholes 8-76108
 AgCl:Sr, effect of impurity doping on Sr²⁺ diffusion 8-84002
 Al:¹¹¹In, electron irradi., defect trapping at impurities 8-55892
 Al-Mn (0.35 wt.%), quenched exam. of Mn-vacancy interaction 8-76676
 Al-Sn, dil. alloy, vacancy-impurity interaction, exam. by electrical resistivity meas. at 77K (*German*) 8-83846
 Al-Zn-Mg alloys, decomp. kinetics from Young's modulus obs., microprocesses (*German*) 8-64522
 CdF₂:NaF, formation and reorientation of Na⁺-anion vacancy complexes 8-84516
 Cu:H, interaction of H and vacancies, positron annihilation, Doppler broadening 8-80434
 CuGaSe₂ crystals, I₂ vapour transport grown, luminesc. spectra 8-88349
 α -Fe, He interaction with vacancies, computer simulation 8-79604
 α -Fe:He, impurity clustering in vacancies bound to edge dislocations 8-91358
 GaAs:Si(Ge) LPE layers, luminesc. props. rel. to substrate quality 8-52583
 GaAs:Te, heavily-doped, annealing-induced prismatic dislocation loops and elec. changes 8-51546
 KCl, pure and Sr doped crystals, strengthening effects rel. to IV-dipoles and aggregates 8-55907
 KCl:Sr²⁺, X-irrad., thermolum., impurity aggregation, trapping centre form. 8-88367
 KI:S²⁻, photochemical reaction, F-centre production 8-64861
 Mo, He interaction with vacancies, computer simulation 8-79604
 NaCl, pure and Sr doped crystals, strengthening effects rel. to IV-dipoles and aggregates 8-55907
 NaCl:Mn²⁺, dimer detection, EPR and ITC expts. 8-59833
 Si, carrier lifetime degradation at room temp. 8-95301
 Si, Sn or Ge complex with vacancy, many-electron approach 8-67980
 SrTiO₃:Fe, EPR, of Fe³⁺-rhombic, Fe²⁺-V₀ and Fe¹⁺-V₀ complexes 8-76302
 V, He interaction with vacancies, computer simulation 8-79604

incandescent lamps see filament lamps**inclusions in crystalline material see crystal inclusions****inclusive reactions, elementary particle see elementary particle inclusive interactions****incremental computers see digital differential analysers****independent particle model see nuclear optical model; nuclear shell model****indeterminacy**

- alkali halide, lattice energy, binding, indeterminacy principle theory 8-59777

indeterminacy continued

- commutation and uncertainty relations, deterministic interpretation, Planck's const. as coupling condition 8-73875
 demonstration of uncertainty principle using single-slit diffraction pattern 8-69953
 electrical conductivity and uncertainty principle 8-84182
 exclusion principle extended, particle classification anal. 8-49690
 Heisenberg's commutation rule, geometric interp., algebraic struct. of Pauli eqn. 8-93549
 minimum uncertainty states of angular momentum system 8-93559
 position-momentum, angle variable-momentum paradoxes in uncertainty principle boundary conditions 8-89280
 self turbulence in free particle motion 8-86177
 SU(1,1) non-compact group, existence of intelligent states 8-77753
 time-energy uncertainty relation, quantum-mechanical derivation 8-73894
 uncertainty relation for symmetric operators, extension using sesquilinear form methods 8-81872

indexing

- structural search codes for on-line compound registration 8-90319

indicating devices see indicators**indicating instruments see indicators****indicators****see also alarm systems**

- liquid crystal indicator of variable light-reading angle 8-57932
 thermogravimetric automatic temperature indicator 8-86257

indium**see also nuclei with**

- amorphization by ion implantation 8-52135
 atom, 451.1 nm transition, HFS and ¹¹³In-¹¹⁵In isotope shift 8-82674
 atom, integral K-shell Compton scattering, cross-section, for 1250 keV photons 8-90128
 atom, quadrupole antishielding factors, Hartree-Fock perturbation theory 8-62723
 atomic electron impact excitation cross sections calc. (*Russian*) 8-55240
 atoms and ions, regularities within Stark widths of reson. lines 8-78662
 conducting flat plate, electrostatic pot. distrib. transverse magnetoresistance, electrode effects 8-60108
 determination, in Sn or Cd by neutron activation analysis, stoichiometric method 8-76954
 diffusion, in Ni, temp. depend. (*Russian*) 8-75880
 diffusion coefficient of Pb, RF size effect meas. (*Russian*) 8-91717
 dislocation dynamic props., investigation by impact loading (*Russian*) 8-85069
 electrodeposition from acid sulphate solns., electrode reactions 8-88436
 electron density at nucleus, press. depend., Hartree SCF calcs. 8-56411
 epitaxial layer on imperfect FEM/FIM W emitter 8-60037
 film, embedded with He particles, superconductor ion implantation study of inhomogeneities 8-52181
 foil, neutron activation cross sections meas. for generalised intermittent irradiation, fusion machines appl. 8-58283
 gasification by atomic F, high temp. kinetics 8-53019
 Gruneisen parameter, behaviour at high press. 8-83899
 Hall field, reversal, 6-280K 8-72135
 k_{for}=for 8-80822
 liquid, struct. factor, Percus-Yevick equation perturb. treatment, square-well pot. approx. 8-75530
 metal cluster generator for gas-phase electron diff., variation of microcryst. with size 8-63645
 positron annihilation rates, electron-electron and electron-positron correl. effects 8-76548
 superconductivity, stimulation and enhancement by external micropower irradiation (*Russian*) 8-95394
 surface, (111), electron beam induced desorption and dissociation of chemisorbed CO 8-56043
 US absorption and dispersion, lineshape studies of quantum oscills., anomalous behaviour 8-63966
 vapour pressure over In+MgIn₂O₄+MgO mixture, 1095-1350K 8-91433
 wire, linear magnetoresist., effect of voids 8-51974
 Al:¹¹¹In, electron irradi., defect trapping at impurities 8-55892
 CdCr₂Se₄:In, temp. driven metal-semiconductor transition, temp. and mag. field depend. (*Russian*) 8-88003
 CdGa₂S₄:In, photoluminesc. and photocond. meas. 8-60159
 CdS:Cu, In, Ga, spray deposited film, struct., X-ray obs. 8-71713
 CdS:In, Cu- or defect-compensated, optical ageing rel. to storage cond. 8-84247
 CdS:In, spin flip Raman scatt., electron dynamics 8-80342
 CdS:In whiskers, prep. by vapour deposition 8-75969
 CdTe:In, lightly- and heavily-doped, cathodoluminesc., temp., injection level and freq. depend. 8-52584
 Cu-In solid/liquid interface, laws governing diffusive interaction (*Russian*) 8-95156
 Ge:In film, electronic props. 8-84330
 In I, 6²S_{1/2} state lifetime meas. by Hanle effect method 8-90097
 In I, relativistic and cancellation effects in line strength ratios 8-82689
 In I, Rydberg series, discrete levels and continua of finite bandwidth 8-74603
 In V, spectrum, levels in 4d⁶s and 4d⁵d configs. 8-62748
 In²⁺, emission spectrum, 340 to 6500 Å, ionisation pot. and dipole polarisability 8-78654
 In-CdS:In Josephson junction, exhibiting nonuniform max. current distrib. self-resonant modes 8-56263
 In-GaAs:Cu-In structure, phototrigger effect 8-56238
 In-Ge:As, Schottky barrier tunnel junction, zero bias resistance, temp. depend. 8-72258
 In-Mn, relative activity ratios in natural UO₂ reactor fuel 8-58347
^{115m}In, separation from ¹¹³Sn and ¹¹⁵Cd by chem. extraction 8-74783
 KCl(Br)(I):In⁺, Jahn-Teller split luminescence, high press. study 8-52565
 Pb-CdS:In Josephson junction, .. light-sensitive, .. structural fluctuations (*Russian*) 8-56265
 Si:In, acceptor levels, IR spectra 8-67972
 Si:In, bound exciton photolum. obs. 8-95607
 Si:In, bound-exciton absorption 8-56507

indium continued

- Zn_{1-x}Cd_xS:In, low resist. film for solar cell window 8-71200
 ZnSe:In, heavily doped, Hall effect and DC cond. expts., compensating acceptors 8-52013
 ZnSe:In, heavily doped, impurity band cond., Hall coeff. and cond. expts. 8-72147
 ZnSe:In elec. transport props., effect of Zn-annealing, 300 to 77K 8-76075

indium alloys

- see also *indium compounds*
 amalgam lamp, Hg vapour partial pressure meas. 8-67488
 liquid, concentration fluctuations, nucl. quadrupole spin relax. 8-91975
 Al-Ga-In, liq. alloys, excess Gibbs functions 633 to 1173K 8-60655
 Al-In (40, 70 wt.%), liq. phase immiscible system, solidification in microgravity 8-84770
 Al-In emulsion, solidification mechanisms at zero gravity, review 8-88458
 Au-In, electrodeposited from acid cyanide electrolyte, exam. of wear and corrosion resistance 8-80482
 Au₂MnIn, Heusler alloy, ferromag., NMR meas. 8-76320
 Ca-In liquid alloy, thermodynamic exam. 8-75848
 Cd-In diffusion into Pb_{1-x}Sn_xTe, changes in elec. props. 8-91348
 β-Cu-In, directionally transformed eutectoid, morphology exam. by metallography (*German*) 8-92257
 Cu-In, electron work function, contact pot. difference meas. 8-80041
 Cu-In, lamellar eutectoids, calorimetric determ. of interfacial enthalpy 8-60668
 Cu-In, magnetic susceptibility, comp. and temp. depend., melting effects 8-52202
 β-Cu-In, unidirectionally transformed eutectoid, lamellar microstructure, influence of grain boundaries on thermal stability 8-72795
 Cu₂Mn_{0.94}In_{1.0}, In-Heusler single crystal, elec. resist. 8-60107
 Ga-In, dil., elec. resist., temp. and impurity depend., deviation from Matthiessen's b-axis crystals 8-51970
 Ga-In-Sn, thermal analysis, determination of liquidus and reactions 8-88446
 Gd-Ir, dil., hyperfine interaction of ¹⁹³Ir, Mossbauer effect meas. 8-52413
 GdAg_{1-x}In_x, magnetic transition temp., effect of hydrostatic press. 8-76244
 In-Bi alloy system at high press. and temp. 8-92238
 In-Cd, dil., elec. field gradient at Cd impurities, press. depend., TDPAC meas. 8-64302
 In-Ga alloy, electrode metal-solvent interaction rel. to elec. double layer struct., adsorpt. 8-61023
 In-T alloys, relationship between struct. and thermodynamic props. (*German*) 8-91307
 In-Tl, electrodeposition from aq. sulphate soln., X-ray struct. 8-84722
 In₂Bi, de Haas-van Alphen effect 8-91594
 LaAg₂In_{1-x}, structural instability 8-79562
 Li₂Ag_{2-x}In_x, optical props., struct., energy bands, interband transitions 8-72539
 Li₂Cd_{2-x}In_x, optical props., struct., energy bands, interband transitions 8-72539
 LuIr:Gd influence of cryst. field on EPR 8-52346
 LuIr₂Nd³⁺, dil., ESR, hyperfine crystals of ^{143,145}Nd, g-factor, crystalline field splitting 8-52349
 Mg-In, catalytic effect of In on Mg/H₂ reaction, kinetics 8-76851
 Mg-In, complex energy band, l-depend. pseudopot. 8-84124
 MgIn, X-ray diffr. exam. of compressibility 8-51610
 Nb₂In, thin films with A-15 struct., prep. 8-80478
 Ni-In, FCC, cellular precipitation kinetics 8-52823
 α-Ni-In, solid solution, lamellar microstructure, influence of grain boundaries on thermal stability 8-72795
 Pb-In (40-60 at.%), type II superconducting Ettingshausen effect, transport entropy of vortices 8-56272
 Pb-In-Au, film, supercond. penetration depth 8-72306
 Pd₂Mn_{0.98}Sn_{1.02}, Heusler alloy, hyperfine fields at sp elements, spin echo NMR meas. 8-84496
 Pt₁₃In₉, exam. of crystal structure, and phase diagrams (*German*) 8-83779
 SeIr:Gd, influence of cryst. field on EPR 8-52346
 Sn-In dil. liq. alloy, electrodiffusion and electroconvection, effective diffusion coeff., apparent effective valence 8-87802
 Ta-Ir film, amorphous, temp. stability 8-63948

indium antimonide

- acoustic waves, amplification and vel. change due to external temp. gradient 8-84260
 acoustoelectric effect at 77K 8-72209
 acoustoelectric gain coeff., nonlinear elec. field depend. 8-76115
 adsorption rel. to dopant admixture 8-95596
 Auger recombination, calc. for diamond-like narrow-gap semicond., compared with expt. 8-63978
 avalanche breakdown voltage for p-n junction, calc. 8-88020
 crystal structure stability, P-T diagrams 8-51886
 cyclotron harmonic transitions, warping and inversion asymm. effects 8-68383
 Debye temperature, atomic mean square displacement 8-87757
 degenerate n-type, acoustomagnetolectric effect obs. 8-72207
 donor excitation spectra in high mag. field 8-80027
 effective g-value of electrons determ. by spin flip Raman scatt. and electric-dipole-excited ESR 8-52494
 electron momentum distribution, anisotropy, positron annihilation (*Russian*) 8-84676
 electronic surface structure, Cs(Rb)(Na) adsorpt. processes, AES, LEED, EELS, study 8-68068
 film, p-type, elec. transport props. 8-72291
 film, quantum size effects, transport props. 8-76171
 film, synthesis by 2-source mol. beam technique and AES characterisation 8-72729
 gamma irradiated, changes in energy spectrum of impurity spectrum 8-51937
 heats of transformation for high pressure, orthorhombic modification, exam. 8-56627
 impact-ionisation magnetolectric effect 8-52016
 inversion layer, electromagneto mode 8-60080
 inversion layer, spectroscopy of electron subband levels 8-64364
 ion implanted layers, amorphisation, recrystallisation 8-63782
 lattice thermal cond. from three phonon scatt. relax. rate 8-51755

indium antimonide continued

- magnetic circular dichroism at E₁ edges 8-92051
 magneto-optical anomalies of impurity electrons, two-LO-phonon region 8-72415
 MIS structures, review 8-95372
 n-type, 2 mm wave radiation interaction with charge carriers (*Russian*) 8-87991
 n-type, directional temp. of hot electrons under elec. and mag. fields 8-84135
 n-type, HF EM and acoustic oscill. generation in LF electric field 8-64068
 n-type, hot electron magnetophonon effect, 77K, mag. field modulation method 8-60140
 n-type, inelastic scatt. of electrons by optical phonons 8-76073
 n-type, magnetoacoustic effects using two-band model 8-60170
 n-type, MCD due to free carriers 8-56462
 n-type, microwave displacement effect in longit. elec. and transverse mag. fields 8-87992
 n-type, millimetre rare modulation in semicond. plasma, use of effects of high elec. field. 8-60149
 n-type, photo-induced magnetophonon reson., 4.2K, peak shifts 8-84250
 n-type, photomagnetic effect anomalies, 90 to 300K (*Russian*) 8-84257
 n-type, photoresistors of Corbino disc shape in mag. field, enhancement of responsivity 8-56186
 n-type, plasma filament form. under impact ionisation conditions 8-60147
 n-type, powder, microwave propag., 90-300K, magnetoplasma and helicon wave excitations 8-72183
 n-type, stimulated recomb. radiation 8-90456
 n-type, subjected to mag. field normal to current, coherent HF oscills. 8-52026
 n-type acoustoelec. current instabilities, threshold field dependence on sample length, 77K 8-76116
 nonlinear absorption and pulse shaping for 10.6, 9.6 μm laser radiation 8-79077
 nonlinear optical properties, hot electron effects 8-71139
 one-sided abrupt junctions, distinction between avalanche and tunnelling breakdown 8-56211
 p-type, cyclotron reson. of nonequilib. photoelectrons, distrib. function and line profile 8-60336
 p-type, deformed, giant negative magnetoresistance 8-87990
 p-type inversion layer, magnetotransport 8-64138
 parametric excitation in Kane's semiconductor 8-52023
 phonon dispersion curves, appl. of deformable-ion model 8-59887
 photoconductive laser detector, dynamic range increase 8-49899
 photoconductivity 1.8K, hot carrier and free carrier absorption effects 8-84254
 polymorphism and cryst. struct. at high temp. and press. 8-95026
 positron annihilation 8-72636
 Raman laser, spin-flip, oscill. characts. of external-cavity system 8-55383
 resonance effects in mag. field, effect of additional laser illumination 8-72417
 small-gap, electron scatt. and transport props. 8-95294
 small-gap, electron scatt. and transport props. 8-95295
 submillimetre detector, fast response 8-89541
 superconducting phases at high press. 8-88063
 surface analysis, X-ray photoelectron spectra, surface oxidation-etchant correlation 8-56029
 transistor mat. characterisation 8-87970
 valence band structure, CPA, bond orbital calcs. 8-87909
 volume plasmon dispersion, anisotropy 8-56090
 Al_{1-x}Sb_x, DC sputtering and struct. 8-52674
 Ga-In-Sb, solidus isotherms and isoconcentration lines 8-56624
 Ga_{1-x}In_xSb, LPE on GaSb by stepwise grading, and characterisation 8-72745
 Ga_{1-x}In_xSb, vapour phase epitaxial growth by open tube method 8-84109
 Ga_{1-x}In_xSb:Zn(Te), photolum. and stimulated emission obs. 8-72595
 (In, Ga)Sb, sputter deposited amorphous film, impulse stimulated explosive crystallisation 8-84098
 In₂Ga_{1-x}Sb, vertical Bridgman Stockbarger growth, magnetic field effect 8-60565
 InSb, acoustic NMR, role of incoherent phonons (*Russian*) 8-80230
 InSb film, threshold singularity on quantising mag. fields 8-87904
 InSb, irradi. real and clean surfaces, work function 8-95336
 InSb:Cr, press. effects on transport props. 8-56146
 InSb/GaSb superlattice thin films, sputtered, ion-bombardment-enhanced diffusion during growth 8-87882
 InSb/LiNbO₃ acoustoelectric convolver, gap-coupled, for IR imaging device 8-94492
 InSb-Pb(Bi), thermodynamic prop. (*German*) 8-75847
 InSb-SiO-Al MIS structure, prep. and characts. (*Italian*) 8-84715
 InSb_{1-x}Bi_x disordered solid solns, ionisation energy of fluctuation levels 8-72116
 InSb_{1-x}Bi_x, film, multitarget sputtering growth technique 8-84711
 LiNbO₃-InSb amplifier production, role of protective films 8-95220
 n-type, low temp. electric and mag. resonances meas., model (*Russian*) 8-56159
 plastically bent single crystals, dislocation struct. obs. 8-59816

indium compounds

- see also *indium alloys*; *indium antimonide*
 GaInAsP quaternary alloys, orientation effects in LPE growth 8-92203
 halides, UV photoelectron spectra of valence d shells, gas-phase 8-62845
 n-InP, magneto-impurity resonances, obs. of central cell struct. 8-95303
 maximum electric field in high-field domain in Gunn devices 8-79996
 AgInSe₂(Te₂), phonons, far IR refl. obs. 8-60459
 Al₂Ga_{1-x}In_xAs, LPE on InP, solid-liq. equilib. calcs. 8-84083
 As₂Se₃-In₂S₃, glass system, IR spectra 8-64365
 n-Cd_{1-x}In_xCr₂Se₄, effect of doping on elec. cond. and magnetoresist. 8-72174
 CuGa_{1-x}In_xS₂, solid soln., IR refl. spectra, comp. depend. 8-52498
 CuInS₂(Se₂)(Te₂), thin film, bulk polycryst. and single cryst. samples, AES 8-72648
 CuInSe₂ epitaxial growth on GaAs 8-84104

indium compounds continued

- CuInTe₂, grown from near stoichiometric comp., elec. and optical props. 8-68504
- GaAs-InAs, pseudobinary alloy, phase diagrams calc. 8-52786
- GaAs_{1-x}Sb_x-Ga_{1-x}In_xP_{1-y}As_y, multilayer structure, continuously tunable electron beam pumped laser 8-50802
- Ga_{0.4}In_{0.53}As, MBE, InP/Ga_{0.47}In_{0.53}As/InP DH laser fabrication and room temp. operation 8-74906
- Ga_{1-x}In_xAs, photocathode, work function depend. of photoelectric emission 8-68071
- Ga_{1-x}As, alloy film surface processes controlling growth by MBE RHEED and AES exam. 8-84084
- p-Ga_{1-x}In_xAs, Auger recomb., theory and luminesc. expts. 8-56518
- Ga_{1-x}In_xAs, cryst. growth on (100) InP by LPE 8-56591
- Ga_{1-x}In_xAs on InP, lattice matched LPE film growth and characts. 8-72033
- GaInAsP-InP avalanche photodiode, fabrication and characts. 8-54454
- Ga_{1-x}In_xAs_{1-y}P_{1-y}, anodisation, effect of pH, current density and illumination 8-95823
- Ga_{1-x}In_xAs_{1-y}P_{1-y}, LPE layers matched to InP, comp. and lasing wavelengths 8-71103
- Ga_{1-x}In_xAs_{1-y}P_{1-y}-InP injection laser, partially loaded with distributed Bragg reflector 8-82986
- GaInP, composition dependence of phonon frequencies 8-75764
- Ga_{1-x}In_xP alloy films, surface processes controlling growth by MBE, RHEED and AES exam. 8-84084
- Ga_{1-x}In_xP, epitaxial film, diffusion of Cu(Au)(Zn), intrinsic impurity effects 8-87825
- n-Ga_{1-x}In_xP, optical props. and energy spectrum of donors 8-72567
- Ga_{1-x}In_xP, undoped liquid epitaxial layers, effect of heat treatment on photoluminescence 8-60512
- Ga_{1-x}In_xP:N, Delta lattice parameter model, correl. with electronic props. 8-91560
- Ga_{1-x}In_xPyAs_{1-y}, In rich bulk single crystals. growth from melt via gradient freeze method, and characterisation 8-68618
- Ga_{1-x}In_xSe, layered, luminescence and photocond. obs., two-photon excitation 8-76521
- GaP-InP, pseudobinary alloy, phase diagram calc. 8-52786
- (In,Ga)P/Ga(As,P) DH laser, red-emitting, optical and elec. characts. 8-66826
- In complex, photoluminesc. spectra, $\pi \rightarrow \pi^*$ and charge transfer L \rightarrow M transitions, Stokes shift 8-64407
- In-Te, liq., reflectance, 0.65-3 eV, comp. depend. 8-72549
- In-Te system, IR spectra (Russian) 8-84589
- InAs, absorpt. rel. to dopant admixture 8-95596
- p-InAs, Auger recomb., theory and luminesc. expts. 8-56518
- InAs, intrinsic point defects, nature and influence on electrophys. props. 8-79609
- InAs MIS struct., review 8-95372
- n-InAs, negative magnetoresist. in extreme quantum limit 8-64051
- InAs, positron annihilation 8-72636
- InAs, second order Raman scatt., electron-two phonon deform. pots. determ. 8-60473
- InAs surface accumulation layers, magneto-transconductance meas. 8-64137
- InAs surface layers, oscillatory transport coeffs. 8-64136
- InAs, valence band structure, CPA, bond orbital calcs. 8-87909
- p-InAs-Au contacts, influence of free surface on elec. behaviour 8-95362
- InAs-GaSb (001) superlattice, electronic struct., tight binding calc. 8-95350
- InAs-GaSb superlattices, two-dim. electronic structure 8-75995
- (InAs)_x(CdTe)_{1-x}, band gap and effective mass, IR spectra obs. 8-56491
- InAs(P), avalanche breakdown voltage for p-n junction, calc. 8-88020
- InAs_{1-x}P_x, continuously tunable electron beam pumped laser 8-50802
- InCl₃, force and compliance consts., OVFF, UBFF and GVFF models 8-50663
- InF₃·3H₂O, cryst. struct. by X-ray diff. 8-63729
- InGaAs, transferred electron photoemission to 1.65 μ m 8-68600
- InGaAs-InP heterojunction detector for 1.0-1.7 μ m wavelength range 8-49895
- In_{0.53}Ga_{0.47}As, incorporation of Ga during LPE growth on (111)B and (100)InP substrates 8-91557
- In_{1-x}Ga_xAs-GaSb_{1-y}As_y, new heterostruct. characts. 8-72247
- In_{1-x}Ga_xAs-GaSb_{1-y}As_y, superfine heterostruct., MBE 8-95348
- In_{1-x}Ga_xAs, heteroepitaxial, MBE grown, props. 8-84328
- In_{1-x}Ga_xAs, thick LPE growth, electrolum. obs. 8-60589
- InGaAsP, lattice matched, LPE growth on (100) InP, for 1.15-1.31 μ m spectral region 8-64483
- InGaAsP/InP heterojunction, X-ray characterisation of defects 8-95239
- InGaAsP-InP 1.27 μ m CW DH injection lasers, 1.1 Gb/s pseudorandom PCM 8-55390
- InGaAsP-InP DH lasers, carrier lifetimes meas. 8-66828
- In_{1-x}Ga_xAs_{1-y}P_{1-y}, LPE growth on InP (100), lattice matched composition 8-87881
- In_{1-x}Ga_xAs_{1-y}P_{1-y}, lattice vibrs., Raman study 8-91391
- In_{1-x}Ga_{1-y}As_{1-z}P_{1-x-y-z}-InP photodetectors, construction and performance 8-65966
- In_{1-x}Ga_xP, epitaxial film, cathodolum. obs., recomb. mechanisms 8-72613
- In_{1-x}Ga_xP, two-phonon IR absorpt. 8-52493
- In_{1-y}Ga_{1-y}P-GaAs heterojunction, VPE, energy band gap and lattice parameter, lattice mismatch effects 8-95345
- In_{1-x}Ga_xP_{1-x}As, single thin active layer visible spectrum heterostruct. lasers 8-63120
- In_{1-x}Ga_{1-x}Sb, influence of annealing on microstruct., exam. 8-56669
- InI, vapour, excited by photodissociation, fluoresc. yields 8-55138
- InI₃, molten, electrical cond., press. effect, 0-1 kbar 8-55963
- In(III) complexes with gluconate ions, reduction, polarographic behaviour 8-92568
- InN film, refl. and transmission spectra, band struct. 8-72625
- InO species, vapour press. over In+MgIn₂O₄+MgO mixture, 1095 to 1350K 8-91433
- In₂O₃, elec. conducting film on glass substrate, measurement of optical constants and thickness 8-60525
- In₂O₃, entropy of transform. from rare-earth or corundum struct. 8-91433

indium compounds continued

- n-In₂O₃ film, RF sputter grown, substrate bias effect on elec. and optical props. 8-64150
- In₂O₃, optically selective coating, for multiple-plate glass system design 8-74956
- In₂O₃, Seebeck coeff., density of states effective mass 8-56171
- In₂O₃, transparent electrode deposition on PLZT ceramic, elec. and opt. props. 8-74848
- In₂O₃/Sn, film, HF sputtered, cond., Hall mobility, oxidation, charge carrier density 8-72287
- In₂O₃/Sn, HF sputtered films, temp. depend. studies of the elec. transport props. 8-76170
- In₂O₃/Sn, sputtered film, optical and elec. props. 8-76177
- In₂O₃-SnO₂, magnetron RF sputtered electro-optical film for data storage and display 8-83047
- In₂O₃-SnO₂ electro-optical film, for data storage and display 8-71176
- In₂O₃-SnO₂ film, reactive DC diode sputtering, using large scale system 8-72723
- In₂O₃-SnO₂ film, stress, and elec. and optical props. 8-51861
- In₂O₃-SnO₂-Si heterojunctions, elec. and photovoltaic characts. 8-52070
- InP (001)-Ag, contact, surface stoichiometry and struct., and electronic surface states 8-95361
- InP, anodisation, effect of pH, current density and illumination 8-95823
- InP, CESR, optical detect. by spin orientation techniques, anal. 8-80251
- InP carrier profiling using liq. barrier contact 8-76087
- InP, crystal growth by synthesis solute diffusion method 8-64454
- InP electrode-electrolyte interface, Schottky barrier obs. 8-52079
- InP, electron-hole plasma, ground state energy 8-84244
- n-InP, epitaxial, Hall effect, electron mobility and density, temp. depend. 8-72288
- n-InP, epitaxial, subthreshold velocity-field charact., 77K 8-64038
- InP film, CVD on preferentially etched Mo, initial growth behaviour 8-51855
- InP, grown-in dislocation density, impurity effect 8-51543
- n-InP, Hall effect, 10-300K, thermal activation energy and influence of compensation 8-72171
- InP, implantation of Si, Al, Hf, Ta into InP and GaAs, form. of protective oxide 8-79622
- InP interface with anodic and thermal oxides, comparison of AES and ESCA 8-95980
- InP, LPE, high purity, use of baking to reduce Si contamination 8-72744
- InP, low temp. diffusion of radioactive Ag 8-75884
- InP MIS capacitor, transient capacitance and C-V characts. 8-95374
- InP MIS struct., review 8-95372
- InP, manifestation of local vibrs. of dislocations in IR spectra 8-88339
- InP, microstructs. assoc. with hardness indentations 8-80627
- InP, n-type doping by ion-implantation of S and Si, expt. 8-91351
- InP, photoluminescence intensity of cleaved surface, ambient gas influence 8-88345
- InP, planar reactive deposition on CdS, heterostruct. formation and elec. evaluation 8-72738
- InP, pure and S doped, VPE, exam. of molar fraction controlled impurity in In-PCl₃-H₂ 8-56587
- InP, reson. Raman scatt., deformation pots. 8-52495
- InP Schottky barrier formation, Fermi-level pinning, defect mech. 8-95358
- InP substrate, LPE growth of GaInAsP on (100) and (111)B oriented crystal 8-92203
- InP substrate, transient-mode LPE of GaAs 8-72746
- InP substrates HCl etching speed and polarity obs., with aid of laser beams (Slovak) 8-56575
- InP substrates preparation, etching and polishing in Br-methyl alcohol solution (Slovak) 8-56576
- InP surface, interaction with Cl, electron spectroscopic obs. 8-56036
- InP, valence band structure, CPA, bond orbital calcs. 8-87909
- InP:Si, vibr. modes of Si, IR absorpt. bands 8-55922
- InP/Ga_{0.47}In_{0.53}As/InP DH laser, lattice matched, MBE and room temp. operation 8-74906
- InP/InGaAs/InP field assisted photocathode, minority carrier electron transport across p-p heterojunction 8-95651
- InP-Au Schottky diodes, barrier height study 8-52088
- InP-CdS heterojunction, prep. by CdS CVD and etching 8-52062
- InP-GaInPAs DH lasers, misplaced p-n junctions due to Zn contamination 8-87051
- InP₄, In₄(P₂S₆)₃, In₄(P₂Se₆)₃, struct. chem. 8-51482
- InS, layer single cryst., Raman scatt. meas. 8-76478
- In₂S₃ destabilisation of stabilised γ -phase, electron microscope obs. 8-71853
- In₂S₃-R₂S₃, intermediate combinations, cryst. types (French) 8-75648
- InSb-GaSb, directionally solidified, determination of non-constant distrib. coeffs. 8-76641
- InSb_{1-x}Bi_x, film, multitarget sputtering growth technique 8-84711
- InSe, excitonic absorpt. edge 8-88352
- InSe, LF oscills. of current 8-56187
- InSe, layer single cryst., Raman scatt. meas. 8-76478
- InSe, layer single crystal, infrared and Raman spectra 8-92070
- InSe, layered crystalline slabs, growth by Czochralski method 8-68619
- n-InSe, optical spectra, photocond. and resistivity 8-88321
- InSe, Raman spectra, inter-, intra-layer interaction estimates 8-88313
- InSe-GaAs p-n junctions, 'optical' contacts, elec. props. 8-56222
- InSe with p-n junctions produced by laser radiation, photoelec. characts. (Russian) 8-56226
- InSe-InSe p-n junctions, 'optical' contacts, elec. props. 8-56222
- α -In₂Se₃, far infrared optical study of ordered and disordered forms 8-84572
- In₂Se_{1-x}SnO₂ heterostructure, anomalous temp. depend. obs. on photo-voltage 8-56209
- In_{2-x}Sn_xO_{3-y} film, deposited from organometallic composition, transparent cond. appl. 8-91793
- In₂Ta₂O₇, new phase of mixed oxide 8-59787
- InTe-InSe p-n junctions, 'optical' contacts, elec. props. 8-56222
- In₂Te₃ type semiconductors, basis of ionising radiation detectors 8-86743
- In₂Te₃-type semicond. radiation-resistant fast-electron detectors 8-78559
- In_{0.30}WO₃, struct. anal. (French) 8-59786
- MgIn₂Fe_{2-x}O₄, comp. effects on ferrite characts. 8-52305

indium compounds continued

- MgIn₂O₄ free energy, entropy of form. 8-91433
 Si-In₂O₃:Sn heterojunctions for solar cells 8-64107
 TlBr, He II photoelectron spectra 8-94285
 TlCl, He II photoelectron spectra 8-94285
 TlI, He II photoelectron spectra 8-94285
 ZnIn₂S₄, and ZnIn₂S₄-In₂S₃ alloys, SCL currents, trap distrib. 8-52000
 ZnIn₂S₄ film, photoluminesc. and photocond. 8-52677
 Zn₂In₂S_{3+δ} residual cond. 8-56185

INDO calculations

- alkali borate glass networks, π -electron distrib. SCF INDO LCAO-MO calc., O basicity 8-79924
 biphenyl, INDO geometry optimisation 8-74575
 dicarboxylic acids, D quadrupole coupling constants, ENDOR study 8-90195
 force constants, semiempirical quantum mechanical method 8-62947
 methanol, charged fragments, structure and stability 8-90085
 PCILO method at INDO level, σ - π exchange phenomena 8-62725
 second-row molecular orbital calcs., INDO calc. for Na to Cl 8-82643
 L-tryptophan-HCl radical form. after X-irrad. 8-64940
 As₂S₃ glass, localised paramag. states, As₄S₆, As₄S₄ units, mol. analogue models 8-60087
 N₂O⁺, electronic ground state, INDO SCF MO calcs. 8-82644

INDOR

- see also nuclear Overhauser effect
 No entries

induced anisotropy (magnetic)

- caruba wax magneto-electret, Struve function 8-76287
 ferromagnetic amorphous system, directional order and induced anisotropy energy, theory 8-95431
 garnets, doped, site symm. exam., ang. variation of induced linear dichroism 8-95429
 rare earth-Fe alloys, highly magnetostrictive, isotropy breaking magnetoelastic behaviour 8-72386
 transition metal-metalloid amorphous alloys, mag. props. review 8-52300
 Fe, compression deformed single cryst., induced uniaxial anisotropy 8-52336
 Fe-Cr-Co-Al (27.5, 17.5, 0.5 wt.%) alloy, induced anisotropy 8-76239
 Fe-Ni-B-P amorphous alloys, mag. annealing mechanism, induced anisotropy 8-95484
 Fe-Ni-Co, rel. between induced uniaxial anisotropy and coercive force 8-91904
 Gd-Co film, amorphous, selective resputtering-induced anisotropy 8-72376
 GdCo film, amorphous, sputtered, in-plane anisotropy induced by rare gas annealing 8-84458
 HoCo film, amorphous, sputtered, in-plane anisotropy induced by rare gas annealing 8-84458
 Li_{0.5}Fe_{2.17}Al_{0.33}O₄:Co, single cryst., domain struct., mag. annealing effect depend. on induced anisotropy 8-68290
 Li_{1-x}Fe_{3-x}O₈:Co, single cryst., domain struct., mag. annealing effect depend. on induced anisotropy 8-68290
 NiCo ferrite, induced mag. anisotropy, hysteresis loops, Barkhausen effect (Russian) 8-64203
 YCo₃, amorphous ferromagnet, exchange dominated surface modes 8-52359
 YCo₃ film, amorphous, sputtered, in-plane anisotropy induced by rare gas annealing 8-84458

inductance

- amorphous semiconductor, solid-state inductance, theory and expt. 8-56138
 education, mechanical mutual inertia in spring coupled system, mutual inductance analogue 8-49590
 II-IV-V₂ semiconductor, glassy, solid-state inductance, theory and expt. 8-56138
 plane eddy current problems, calc. method (German) 8-58881
 semiconductor, compensated, solid-state inductance, theory and expt. 8-56138
 SQUID, with V-VO_x-Pb Josephson tunnel junctions, quantum interference, critical currents 8-91821
 GaAs:Cr, seminsulating solid-state inductance, theory and expt. 8-56138

inductance measurement

- defibrillator, damped sine wave, intact, evaluation of operating parameters 8-57120
 iron core inductor time invariance inductance meas. method 8-62207
 mutual inductance bridge using operational amplifiers 8-54407
 small active resistance and inductance meas. AC bridge 8-86299
 superconductor, accurate interferometric meas. technique 8-72306

induction, electromagnetic see electromagnetic induction**induction heating**

- see also electric furnaces; ovens
 arc furnaces, stabilisation methods (German) 8-75402
 automatic induction hardening equipment 8-92284
 education, eddy currents, levitation, metal detectors and induction heating 8-61967
 RF technique, for sample heating in surface science expts. 8-93691
 semiconductor, inductively heated, computer simulation of temperature and EM fields 8-55961
 steel, heat treatment with induction heating, 8-92285

induction motors

- see also squirrel cage motors
 475 MVA pulsed motor generators for TFTR 8-58498
 frequency and speed meas. using piezoelectric pick-ups (Russian) 8-65911

inductor microphones see microphones**inductors**

- see also coils; power inductors; transformers
 induction inspection unit with spaced windings, increasing sensitivity over magnetising and measuring length 8-56864
 iron core inductor time invariance inductance meas. method 8-62207
 simulated inductors, large voltage swing, used for oscillator and floating coupling cct. 8-69227
 steel, austenitic, intergranular defectiveness determ. using inductive instruments 8-53075
 Fe-Si(6.5 wt.%) steel, core mat. development (Korean) 8-60852

industrial atmospheres see air pollution**industrial control**

- cost-effective noise control 8-55515
 robots and manipulators, symposium, Warsaw (Sept., 1976) 8-53574

industrial economics see economics**industrial plants**

- chimney design with air pollution considerations (Dutch) 8-81364
 deafness risk, British Government code of practice 8-55513
 hard X-ray channel-plate image intensifier 8-54517
 hearing protection, types and limitations 8-55509
 industrialisation of space, introductory outline (French) 8-77454
 nuclear safety exercises carried out in French industrial facilities (French) 8-55051
 radioactive waste, vitrification, industrial scale plant, under construction in France 8-78478

industrial research management see research and development management**industrial standards** see standards**industries**

- this heading is restricted to those industries which are not covered by other specific headings
 see also automobile industry; cement industry; chemical industry; construction industry; electricity supply industry; food processing industry; metallurgical industries; paper industry; petroleum industry
 nuclear fuel cycle industry development, limiting factors (French) 8-66430
 thermography appls. in industry 8-79112

inelastic electron tunnelling spectra see tunnelling spectra**inelastic electron tunnelling spectroscopy** see tunnelling spectroscopy**inert anodes** see anodes**inert gas compounds**

- see also argon compounds; helium compounds; krypton compounds; neon compounds; radon compounds; xenon compounds
 fluoride exciplex laser pumping efficiency 8-74892
 fluoride laser, using NF₃-inert gas mixture, long pulse UV emission (French) 8-58982
 fluoride lasers, discharge and electron beam pumped, review 8-71083
 fluorides, covalent and ionic states, ab initio CI calcs. 8-78634
 halide lasers, emission spectra, efficiencies, pulse energy, appls. 8-58993
 halide lasers, kinetic processes 8-63098
 halides, triatomic, optical emission 8-66558
 halogen excimer laser principles, performance and applications 8-55342
 hydrides, laser active media, feasibility, energy storage 8-79014
 monohalides, hyperfine interactions, struct., valence bond calcs. 8-66473
 oxide amplifiers, appl. and performance 8-63085

inert gases

- see also argon; helium; krypton; neon; radon; xenon
 adsorbed on graphite surface, excitation spectrum 8-71943
 adsorption, on alkali halides, pot. energy calcs. 8-67902
 adsorption, on graphitised C black, gas-solid virial coeffs. 8-75928
 adsorption on Ag surface, physisorption energies 8-71944
 adsorption on metal, interaction energy, quantum mech. density functional formalism calc. 8-67911
 alkali metal atom+inert gas atom, hyperfine transition spectral line shift, quantum corrections 8-82655
 alkali metal-inert gas, inhomogeneous mixture, nonequilib. processes under conditions of T-layer form. 8-91079
 annealing atmosphere, inducing of in-plane anisotropy in rare earth-Co amorphous films 8-84458
 atom, electron impact double ionisation, binary encounter approx. calcs. 8-90294
 atom, field ionis. and proton capture, critical energy deficits 8-82853
 atom+diatomic molecule, collision in laser field, vibr. excitation 8-86937
 atom+H₂(NO), cross section meas. with state selected beams 8-62910
 atom-atom collision induced polarisabilities, perturbation treatment 8-86778
 atomic scattering, metastable states 8-62906
 basalts, oceanic, noble gas abundance patterns controlling factors 8-65220
 collision-induced absorption, exact line shapes, rare gas mixture, appl. to He-Ar 8-66512
 compressor for inert gas and mixtures 8-86286
 dense, positronium annihilation rate 8-55258
 diatomic ions, mobility in parent gas meas. 8-63532
 discharge, plasma electron ensemble, collision-dominated final periodic state and adjustment 8-71426
 discharge, positive column contraction, medium press., vol. recombination 8-51379
 discharge lamp, UV inert gas-type, monochromated, addition to XPS spectrometer 8-89601
 Earth mantle, noble gases, abundances and isotopic compositions 8-85521
 electron beam excited, absorpt. characts. 8-82948
 excimer lasers, stimulated emission kinetics in nonself-sustained elec. discharge 8-50753
 F ions recoiling in gases, hyperfine interactions 8-74735
 flash lamp, absolute spectral distrib. and radiant output 8-66510
 fluoromethane+Br, isotope selective photobromination, using c.w. CO₂ laser irrad. in excess inert gas 8-76843
 frequency conversion, fifth and seventh order, XUV coherent radiation generation 8-83033
 geothermal tracing with atmospheric and radiogenic noble gases 8-69502
 high-pressure metal-vapour/inert-gas mixture discharge peculiarities 8-71620
 inert gases, photoionisation cross sections of excited atoms and dimers 8-66523
 interactions, correl. and exchange energies, statistical methods calcs. 8-86931
 ion+oxides, energy loss spectra 8-58798
 ion laser, high repetition rate operation 195 to 225 nm 8-82980
 ion laser discharge, energy balance 8-74884
 ion laser ion-acoustic wave excitation 8-74885
 ion source, saddle-field type, gas depend. characts., at. spectroscopy appls. 8-78039

inert gases continued

- ions, in parent gas, transverse diffusion coeff., reson. charge exchange effects 8-63533
- ions, $X^+(^2P_{1/2})$, conversion into dimer ions 8-70903
- in Kakangari meteorite, unique chondrite, noble gases abundances and isotopic comps. 8-65570
- laser development, visible absorpt. in electron beam pumped gases 8-63057
- lasing, vacuum UV, from highly ionised inert gases 8-63060
- liberation in multiposition metallic reactor 8-59978
- liquid, compressibility, long wavelength limit of liquid struct. factor 8-67633
- metastable, at. collisions, intermediate energies 8-62904
- mixtures for particle detection high-pressure discharges in nonuniform elec. fields. 8-74545
- monolayer, physically adsorbed, many-body interactions 8-84068
- partially ionised inert gases in travelling HF mag. field 8-75474
- planetary-type rare gases in an upper mantle derived amphibole 8-96167
- rare gas concs. in Fe meteorites rel. to cosmic-ray-produced nuclides 8-65473
- rotating arc meas. in plasma centrifuge 8-75438
- solid, anharmonic crystals, unsymmetrised SCF approx. 8-63830
- solid, core excitons, nonstructural theory, appl. to core transitions 8-84148
- solid, dead layer effects in UV reflectance of excitons 8-72553
- solid, electronic excitations, nonstructural theory 8-79942
- solid, exciton states, intermediate coupling interaction 8-67952
- solid, exciton states, nonstructural theory using effective mass approx. 8-84147
- solid, unpaired elastic force model in lattice dynamical study 8-63820
- sputtering environment, contamination effects on uniaxial anisotropy of Gd-Co films 8-64232
- steam-inert gas, uncondensable gas content effect on steam condensation heat transfer in vert. tube 8-75041
- atom+H⁺, 4s-state electron capture cross-section meas. 8-82836
- B⁺+inert gas atom, pot. interactions 8-55219
- CO+inert gas, collision-induced intersystem crossing mechanism 8-74689
- D₃⁺+inert gas, ion decay, 1-40 eV (*Russian*) 8-90286
- F₂-inert gas mixtures, transport and attachment processes 8-59542
- Ge:inert gas, ion implantation, UV photoemission exam. 8-80457
- HD+inert gas, isotropic Raman Q branch, vibr. dephasing effects and motional narrowing 8-74738
- He-Ar(Kr)(Xe), intermol. forces, combining rules 8-66622
- He+H (inert gas atom), long range interactions for (²S) and (²S) states 8-70895
- Hg(6³P_{2,0})+inert gas, diffusion in low-current discharge 8-63618
- K(4²P)+He(Ne)(Ar)(Kr)(Xe), collisional excitation, differential cross-sections 8-66643
- Li+inert gas collisions, electron loss cross-section meas. (*French*) 8-86941
- Na+inert gas, 4D_{3/2} and 4D_{5/2} levels relax. 8-50526
- OCS, IR spectral moments and mean squared torques, rare gas effects 8-62944
- S+inert gas (N₂)(H₂), rare gas sulphide S(¹S) emissions 8-82828
- Se(³P₁)+inert gas, gas phase flash photolytic deexcitation obs., 1000K (*Russian*) 8-50626
- Te(³P₁)+inert gas, gas phase flash photolytic deexcitation obs., 1000K (*Russian*) 8-50626

inertial navigation

- aviation and astronautics, conference, Tel Aviv (1977) 8-81517

infinite series *see series (mathematics)***inflammability** *see combustion***information analysis**

- see also classification; indexing*
- atomic absorption spectroscopy, development in USSR, 1965-1975, science metrics investig. 8-61104

information retrieval

- see also information storage*
- crystallographic data, molecular geometry, computer retrieval and anal., general principles and methods 8-83643
- crystallographic data, molecular geometry, computer retrieval and anal., variance and interpretation 8-83644
- crystallographic data, molecular geometry, computer retrieval and anal., geometry of β -1'-aminofuranoside fragment 8-83645
- IR spectrometry, computer program LISE (Literature Search and Edit) 8-85223

information retrieval systems

- alloy, multicomponent phase diagram calc., NPL alloy data bank 8-92243
- X-ray phase analysis, information retrieval system 8-79501

information services

- British Isles, 1978 guide to information sources in geology 8-88922
- ocean data and information services, changes and challenges 8-69463

information storage

- see also information retrieval*
- geophysical data storage by metallic carrier electroerosion via liquid pulsed discharge (*Russian*) 8-61563
- Vela seismological network, information storage and retrieval by data-computer 8-81411

information storage systems *see information retrieval systems***information systems, management** *see management information systems***information theory**

- see also channel capacity; codes; correlation theory; decision theory and analysis; estimation theory; filtering and prediction theory; modulation; signal detection; signal processing; speech intelligibility*
- acoustic emission sources, localisation 8-87220
- chance and origin of life 8-69269
- chemical reactions, angular momentum disposal, information theory anal. 8-80730
- collision processes, information theoretic maximal entropy theory, rel. to scatt. theory 8-81888
- ECG lead system information content (*German*) 8-69226
- elementary particle interactions, statistical treatment of multiplicity data using information theory 8-89682
- irreversible energy conversion processes, information model (*Ukrainian*) 8-89419

information theory continued

- knowledge distance, information extent and information distance, concepts evaluation 8-77687
- liquids and amorphous solids, similarity and short range order parameters 8-83730
- measurement device information-theoretic characts. estimation via radiation absorption (*German*) 8-65900
- planetary gravitational fields, inform. theory appl. 8-53835
- radiation absorption measuring instrument characts. evaluation with reference to information theory (*German*) 8-86753
- radioactive contamination in aquatic organisms, evaluation by statistical and information theory 8-53535
- seagull effect in π semi-inclusive distrib. by information theory, p_1 - p_2 correlations 8-86458
- tachyon theory, information flow, causality 8-82261
- von Neumann entropy and entropies of meas. 8-54229

infrared astronomical observations

- 25 1702-363, IR candidate in error box, JHKL photometry 8-61934
- asteroids, photometry in 0.56-2.2 μ range for 30 objects 8-69725
- astronomical diffuse objects, strip photometry appl. to globular clusters multicolour obs. 8-89229
- Becklin-Neugebauer source in Orion, high resolution 1.5 to 5 micron spectroscopy 8-93368
- Canis Major R1, optical and IR props. of newly formed stars 8-93332
- 27 Canis Majoris, spectroscopic obs. in 0.14-4.7 μ range 8-85957
- α Canis Minoris (Procyon), CNO abundances from near IR spectrum 8-93222
- Y Canum Venaticorum, C₃ and IR spectrophotometry of C star 8-65619
- η Carinae, IR ang. diameter 8-93271
- γ Cassiopeiae, Be star, IR excess 8-93257
- CD -31°622 as metal-deficient subdwarf 8-65618
- UV Ceti, IR obs. of flares (*Russian*) 8-93278
- \circ Ceti (Mira), diameter apparent var. at 10.2 μ m 8-93267
- Circinus X-1, IR magnitude drop (1978 March-April) 8-54080
- Circinus X-1, JHKLM photometry and light curve 8-54086
- CNO abundances from near IR spectrum 8-93222
- Comet West (1976 VI), IR obs., results 8-81591
- compact galaxies, spectroscopic and photometric obs. 8-77603
- R Coronae Borealis stars, long-term IR behaviour 8-96490
- CRL 2104, CRL 2179, late WC stars, 2 to 4 μ m spectrophotometry and circumstellar dust 8-96491
- V460 Cygni, cool C star, atmospheric ¹²C/¹³C ratio 8-93223
- V1016 Cygni, IR spectrum 8-93266
- Cygnus OB2 No.12, high resolution 2 μ spectroscopy rel. to interstellar and stellar features 8-57613
- early-type stars, IR photometry, extinction ratio, 2200 Å interstellar absorpt. feature 8-53943
- equatorial IR catalogue (EIC), 2.7 μ high-precision sky survey results 8-81560
- extremely red stars at $l^{\text{II}}=113^\circ$, $-10^\circ \leq b^{\text{II}} \leq +90^\circ$, photometry and spectra 8-57554
- flare stars, photographic photometry of four new objects 8-89207
- G12.2-0.1, radio and IR obs. of OH/H₂O source 8-57620
- G333.6-0.2, G298.2-0.3, southern compact H II regions, IR emission lines obs. 8-96522
- G333.6-0.2, powerful H II region, 2 μ m line emission detect. 8-54017
- G45.1+0.1, 8-13 μ m spectrophotometry of compact H II region 8-65672
- G-type dwarfs, macroturbulence and age anticorrel. 8-93226
- Galactic central IR surface brightness obs. by balloon (*Japanese*) 8-61925
- galactic centre, linear polarisation in near IR 8-96534
- galactic centre, struct. from 2.4 μ m obs. 8-81689
- Galactic IR obs. at 2.4 μ m wavelength by balloon (*Japanese*) 8-61924
- galaxies, active nuclei, IR obs., future prospects 8-57651
- galaxies, metallicity on integrated colours, calibration of early-type objects 8-89227
- giant stars in M3, M13, M92 and M67, IR photometry, bolometric magnitudes and effective temps. 8-57595
- GL 915, 618, 2688, IR sources assoc. with double-lobed refl. nebulae, far IR obs. 8-54009
- globular clusters, metallicity effects on integrated colours, calibration 8-89227
- HDE 245770 (Ariel 0535+26), 1977 spectrum, objective prism study 8-61866
- Herbig Ae/Be stars, spectrophotometry 8-93258
- HR 6766, weak G-band star, light-element abundances 8-57548
- HR 8752, spectrum var. of superluminous supergiant, near IR obs. 8-81630
- Iapetus, normal reflectance from lunar occultation obs. 8-85897
- IC 5146 dark cloud complex and cluster 8-89234
- interstellar extinction law correl. with wavelength of max. polarisation 8-61902
- interstellar linear polarisation in 1-2.2 μ wavelength range 8-77588
- interstellar matter, far IR emission between $l=36^\circ$ and $l=55^\circ$ galactic longitudes 8-54014
- IR source assoc. with Sh 2-149, spectral type and luminosity class 8-73772
- IRC +10°216, circumstellar methane in IR spectrum 8-57694
- Jupiter, far IR spectrum showing NH₃ rotational bands 8-85891
- Jupiter, near IR polarisation studies 8-85899
- Jupiter, spectrophotometry in far IR 8-85890
- Jupiter atmosphere, GeH₄ abundance from IR spectrum anal. 8-61791
- Jupiter atmosphere, IR obs. by Fourier transform spectroscopy 8-61747
- Jupiter atmosphere, trace constituents upper limits from 5 μ m spectrum anal. 8-61790
- EV Lacertae, IR obs. of flares (*Russian*) 8-93278
- late-type stars, near IR photometry with balloon-borne telescope 8-73713
- LMC, far IR obs. of H II regions 8-81671
- α Lyrae, emission lines in IR spectrum, thin expanding extended atm. 8-53946
- M101, spectra of H II regions, comp. gradient across spiral galaxy 8-65683
- M43, emission nebula around NU Orionis, radio and IR obs. 8-54012

infrared astronomical observations continued

- M-type supergiants, photoelectric two-dimensional spectral classification 8-53936
 Mars, disc IR spectra compared with terrestrial analogues optical props. 8-85879
 Mars, occultation of ϵ Geminorum, obs. at Princeton 8-57482
 microwave background radiation polarisation, IR survey 8-73779
 Monoceros R2, obs. in 40-400 μ m range 8-69853
 Moon, regolith, IR spectra, Salyut 4 obs. in 3.5-7 μ m range 8-69716
 NGC 1068, Seyfert galaxy, 2-2.5 μ m spectrum, H α detect. 8-57636
 NGC 1068, Seyfert galaxy, IR photometry and polarimetry 8-54035
 NGC 2024, obs. in 40-400 μ m range 8-69853
 NGC 4151, Seyfert galaxy, optical polarimetry, circumnuclear dust envelope 8-61916
 NGC 5506, IR obs. of X-ray Seyfert-like galaxy 8-65696
 NGC 7027, 16-38 μ m spectral obs. and dust model of planetary nebula 8-93354
 NGC 7027, planetary nebula, near IR obs. 8-73748
 NGC 7027, search for vibrationally excited H $_2$ emission 8-93346
 NGC 7213, IR photometry of lenticular Seyfert X-ray galaxy 8-89262
 night sky background, 2.4 μ m meas. 8-81715
 Nova Cygni 1978, photometric obs., light vars., IR obs. showing dust form, phase 8-96494
 Nova Serpentis 1978, IR magnitudes and BVR photometry 8-65629
 ρ Ophiuchi cloud, search for vibrationally excited H $_2$ emission 8-93346
 Ophiuchus dark cloud complex, IR study 8-93363
 Orion molecular clouds, obs. in 40-400 μ m range 8-69853
 Orion Nebula, C I IR forbidden emission lines obs. 8-85987
 Orion Nebula, H $_2$ emission at 2 microns 8-93351
 Orion Nebula, IR obs. by Fourier transform spectroscopy 8-61747
 Orion Nebula, O III 51.8 μ m forbidden emission line obs. 8-65510
 Orion Nebula, photographic obs. in H α , H β and He I 10830 Å lines 8-81669
 Orion Nebula, S III 9096 Å forbidden line, Fabry-Perot obs., abundance determ. 8-96515
 Orion Nebula, search for vibrationally excited H $_2$ emission 8-93346
 V380 Orionis, near IR spectrum line identifications, equiv. widths (*Russian*) 8-61861
 FU Orionis stars, composite spectra rel. to three models 8-65617
 β Persei (Algol), light curve at 10 μ m near secondary min. 8-93315
 Q 0420-388, IR obs. of most luminous quasar 8-89272
 quasars, IR energy distrib. obs. 8-57645
 radio sources, coordinated photometric and spectroscopic observations of strong extragalactic 90 GHz sources 8-93440
 Rhea, normal reflectance from lunar occultation obs. 8-85897
 S140 IR, far IR spectrum 8-93372
 2S1728-337 vicinity, 5 IR sources detected by K-band photometry 8-54076
 2S 1702-363 field, IR object brightening and identification as Mira variable 8-81705
 S-type stars in Southern Milky Way, objective prism survey and BVI photometry 8-61754
 HM Sagittae, emission line variable, near IR spectrum (*Russian*) 8-81637
 HM Sagittae, IR spectrum 8-93266
 ν Sagittarii, absorpt. lines identification as Fe II high level transitions 8-93316
 SAO 158687, occultation of Uranus, 1977 March 10, rings discovery 8-69743
 Saturn, near IR polarisation studies 8-85899
 Saturn, spectrophotometry in far IR 8-85890
 V861 Scorpii, near IR meas. rel. to orbital phase 8-93324
 seeing, wavelength depend., atm. inhomogeneity effects 8-92979
 Seyfert galaxies, IR energy distrib. obs. 8-57645
 sky fluctuating emission in airborne astronomy, meas. and interpretation 8-81552
 sky noise at telescope focus, photometry of atmospheric IR emission, statistical props. (*French*) 8-53731
 solar brightness temperature near its minimum, meas. by balloon-borne lamellar-grating interferometer 8-85921
 solar coronal Fe XIII emission line polarisation, near IR polarimeter obs. 8-61740
 stars, near IR photometric obs. 8-69795
 stars IR colours, meas. rel. to diffuse interstellar bands strengths 8-93198
 stellar IR spectral obs. in 1-2.5 μ m range from balloon-borne telescope (*Japanese*) 8-61850
 stellar occultations by Uranus' rings, existence of rings confirmation and radii calc. 8-53872
 sunspots, umbral intensity rel. to phase in solar cycle 8-69773
 45 Tauri, Hyades cluster star, CNO abundances from near IR spectrum 8-93222
 SU Tauri, visible and IR photometry and polarimetry (*Russian*) 8-61860
 T Tauri star, extremely young, and assoc. nebula, fading 8-93236
 T Tauri stars, H $_2$ emission obs. 8-93230
 Titan, normal reflectance from lunar occultation obs. 8-85897
 Tycho's supernova remnant, filaments spectrum 8-73747
 Uranus rings, BD-15° 3969 occultation obs. 8-89118
 Venus, cloud properties from airborne obs. of near-IR reflectivity spectrum 8-53850
 Venus, thermal anomalies persistence and size 8-85876
 W40 and W48, near IR and CO mm wavelength obs. 8-65667
 Wolf-Rayet stars, 2 to 4 μ m spectrophotometry of late WC stars 8-96491
 zodiacal light IR radiance model and meas. 8-81588
 C stars, $^{12}\text{C}/^{13}\text{C}$ ratio determ. 8-73710
 C stars, 3.9 micron absorpt. band identification 8-93231
 CO in giant stars in globular clusters 8-93339
 H II regions, He II abundance and IR excess 8-86000
 H II regions, IR line emission, airborne obs. 8-93353
 H II regions in M33 galaxy 8-61923
 OH 0739-14, IR source assoc. with double-lobed refl. nebulae, far IR obs. 8-54009

infrared astronomy

see also *infrared sources (astronomical)*

- 3.8-m telescope on Mauna Kea, UK instrument 8-96397
 3-m telescope on Mauna Kea, NASA/Univ. of Hawaii instrument 8-96398

infrared astronomy continued

- accreting stars, model IR spectra for dusty circumstellar shells 8-85934
 airborne, fluctuating sky emission meas. and interpretation 8-81552
 airborne IR observations, methods and instruments 8-69688
 Australian Astronomical Society, conf. Melbourne, Australia (May-June '77) 8-69655
 bolometer, composite, for submm. wavelengths 8-65964
 British large IR telescope on Mauna Kea, construction 8-69686
 chopper for deep space IR interferometer/spectrometer 8-81545
 cryogenics appls., 1 mK to 10K temp. range, survey 8-93712
 flux collector on Tenerife 8-69684
 Fourier transform spectroscopy, airborne IR obs. 8-61747
 galaxies, active nuclei, IR obs., future prospects 8-57651
 heat trap field optics, compact lens-mirror system 8-55422
 heterodyne spectroscopy 8-85859
 instrumental developments review 8-61737
 interferometer, Michelson far IR 8-93118
 long wavelength IR telescope, ang. response meas., off-axis rejection performance 8-61739
 Mira phenomena, AIO IR bands 8-69801
 multiple mirror telescope, design, review 8-69687
 observation technique, space research appl. 8-61738
 orbiting astronomical telescopes, IR detector cryogenic cooling requirements 8-96400
 Pioneer Venus Orbiter cloud photopolarimeter 8-57429
 Pioneer-Venus large probe infrared radiometer optical system 8-81543
 polarimeter, near IR, for solar corona emission line obs. 8-61740
 sky noise at telescope focus, photometry of atmospheric IR emission, statistical props. (*French*) 8-53731
 sky noise correl. for IR telescope focal plane (*French*) 8-53725
 survey data processing techniques 8-81553
 TV detector, intensified-Si intensity target, near IR astronomy appls. 8-81544
 utilisation of IR technology, conf., San Diego (1977) 8-77984
 Viking IR thermal mapper, design 8-57440
 Wyoming Infrared Telescope (Jelm Mountain), IR universe exploration 8-85848
 Si extrinsic photoconductive IR detectors, VLF behaviour 8-81542
- infrared communication** see *optical communication*
- infrared detectors**
 see also *bolometers; photodetectors*
 airborne IR system performance 8-82039
 astronomical appl., current developments review 8-61737
 Balloon Altitude Mosaic Measurements Program 8-81455
 BLIP systems, effect of f-number and other parameters on FLIR performance 8-77981
 C-CD appl. for IR detection and imaging (*German*) 8-63190
 charge transfer device imaging arrays 8-77990
 cooling systems for space appls., He II flow through porous plugs 8-49842
 cryogenic, expt. using closed-cycle mech./adsorption refrigeration 8-93708
 development and characteristics 8-77986
 dimensions of IR detector, rapid meas. by Fresnel diffr. (*French*) 8-89435
 electric apparatus and power lines, temp. rise meas. by infrared radiometer (*Russian*) 8-89537
 epitaxial graded gap semiconductor layer appl. 8-74060
 film thermal device appl. 8-70189
 FT-IR detector with gas chromatograph (collects, stores spectral data, monitor functional groups) 8-92560
 glow discharge detection, gas breakdown theory 8-58035
 group specific detectors for gas chromatography 8-92557
 imaging, CCD, modelling and appl. of HgCdTe MIS struct. 8-80058
 intensified-Si intensity target vidicon application to IR astronomy 8-81544
 intrinsic semiconductor IR detector array data acquisition system 8-77991
 IR defectoscopy, optimum algorithm in case of noncontent temp. meas. 8-60947
 lag effect on thermal imaging system basic parameters 8-89544
 laser pulse recording, semicond. ionisation-type photographic system 8-49903
 laser radiation energy photoelectric meter, digital output 8-58040
 material exposure threshold meas. at 10.6 μ m 8-90471
 microwave-biased extrinsic photoconductors, equivalent circuit model 8-49898
 multiple pulse detection in atmospheric turbulence 8-92974
 near IR absorption analysis, differential compensation method 8-80819
 nondispersive analyser Infralyt 4 dynamic characts. (*German*) 8-88676
 optical fibre absolute power meas. thermistor sensor 8-65971
 optical system design (*Japanese*) 8-55428
 orbiting astronomical telescopes, IR detector cryogenic cooling requirements 8-96400
 p-n junction photovoltaic diode, appl. as IR detector 8-86330
 pyroelectric detector, temp. noise 8-89542
 pyroelectric detectors and materials 8-49901
 pyroelectric vidicon, CO $_2$ laser beam meas. 8-49907
 pyroelectric vidicons for instrum. with IR lasers 8-59150
 radiometer optical head thermostabilisation structure 8-86316
 RF and photodetection techniques at 10 μ m, comparison 8-89539
 rocketborne IR spectrometer 8-81460
 submillimetre wavelengths, techniques and devices for the detect. and sensing of radiation 8-93759
 surface temperature contactless meas. instrument 8-57946
 system limitations 8-77988
 TGS vidicon tube, used with optical multichannel analyser as IR detector 8-86329
 thin-film techniques appl. (*German*) 8-62226
 tracking receiver with holographic information processing 8-78970
 United States Air Force infrared reconnaissance set 8-81458
 utilisation of IR technology, conf., San Diego (1977) 8-77984
 Ba $_{0.25}$ Sr $_{0.75}$ Nb $_2$ O $_6$, fast-response pyroelec. cryst. detector 8-49904
 (CdHg)Te photoconductive detector, thermal figure of merit limit 8-89540
 Cd $_x$ Hg $_{1-x}$ Te, IR detector appls., prep., elec. props. (*German*) 8-86332

infrared detectors continued

- CuInSe₂ polycrystalline thin film anomalous photovoltaic effect (*German*) 8-68102
 D₂O leak detection, on-line infrared analyzers, CANDU report 8-82038
 GaAs, electroabsorpt. avalanche photodiode waveguide detectors 8-65965
 GaAs:Cr, IR spectral detectivity 8-70184
 GaInAsP-InP avalanche photodiode, fabrication and characts. 8-54454
 Ge cryogenic bolometer, for 20 to 500 μ m spectral region 8-70187
 Ge:As, based on Ga impurity photoconductivity, characts. (*German*) 8-82036
 Ge:Cu, based on Ga impurity photoconductivity, characts. (*German*) 8-82036
 Ge:Hg photoconductive detector, laser damage thresholds calc. 8-90443
 Ge-Pb_{1-x}Sn_xTe, amorphous/crystalline heterojunction, rectification props., IR detector appl. (*Japanese*) 8-60197
 HgCdTe, for 8-14 μ m range, review (*Italian*) 8-54451
 Hg_{1-x}Cd_xTe IR detector technology 8-77989
 Hg_{1-x}Cd_xTe IR focal plane status and performance 8-77987
 InSb fast response submm. detector 8-89541
 InSb n⁺-p and p⁺-n photodetectors fabrication by S and Be ion implantation 8-49906
 PbS-Si p-n heterojunction characts. and operation 8-52075
 PbSnTe, for 8-14 μ m range, review (*Italian*) 8-54451
 Pb_{1-x}Sn_xTe, impurity doped IR detector, spectral response depend. on impurity conc. (*Japanese*) 8-58036
 Pb_{1-x}Sn_xTe-PbTe, amorphous/crystalline heterojunction, rectification props., IR detector appl. (*Japanese*) 8-60197
 p-PbTe MIS capacitors 5 μ m IR detector appl. 8-52101
 Si extrinsic photoconductive IR detector, counterdoping scheme 8-49896
 Si extrinsic photoconductive IR detectors, VLF behaviour 8-81542
 Si, MIS photocapacitive IR detector 8-62223
 Si vidicon optical detector, laser data acquisition/analysis system 8-58041
 Zn₃P₂, photocond. and Demmer effect meas., 0.5 to 1.2 μ m, possible detector appl. 8-91721

infrared imaging

- airborne IR system performance 8-82039
 applications, conf., London, England, June (1977) 8-58042
 background suppression algorithm 8-77985
 basic parameters of thermal imaging system, effect of radiation detector lag 8-89544
 C-CD, modelling and appl. of HgCdTe MIS struct. 8-80058
 C-CDC image sensors, operation (*German*) 8-63190
 charge transfer device imaging arrays 8-77990
 composite thermal/visual display superposition technique 8-77992
 digital thermal field analysers 8-82034
 Earth resource thermal imaging by airborne system, possible LED use 8-93010
 ecosystem succession detection by aerial IR photography 8-81459
 fog in Cheddar Gorge, England, oblique false-colour photograph 8-57290
 infrathermograms properties and evaluation in nonblack radiators (*Hungarian*) 8-65922
 insulating material monitoring by electroluminescent screens, defect imaging 8-53083
 intrinsic semiconductor IR detector array data acquisition system 8-77991
 land and sea surface temp. fields, seasonal vars., NOAA 5 satellite IR obs. 8-85676
 laser pulse recording, semicond. ionisation-type photographic system 8-49903
 Limb Infrared Monitor of Stratosphere (LIMS) radiometer, design and performance, expt. goals 8-61601
 microwave-enhanced thermographic turnover detection, sweep-freq. illum. investigation 8-73194
 MTF equipment testing in IR using standard reference lens 8-50898
 nonlinear image upconverter systems 8-59091
 nonlinear optical upconversion, for IR imaging 8-79070
 photography, principles and appls., book 8-82068
 pyroelectric vidicon, CO₂ laser beam meas. 8-49907
 remote sensing of atmosphere, land and sea props. 8-93015
 reticulated sensing layers, thermal props., analytical solns. and design parameters 8-49897
 rheumatology, quantitative IR tele-thermography (*German*) 8-92684
 single-line scanning camera, portable, battery-operated 8-58029
 Spectral Infrared Experiment equipment and objectives 8-81456
 spinning cryogenic IR sensor, integrated thermal/structural/optical evaluations 8-82040
 steel, mild, exam. of fatigue damage, using thermography 8-92356
 temperature meas., thermograms anal. (*Hungarian*) 8-65923
 thermal imaging screens for visual display of infrared laser beams 8-66903
 thermal viewing system LF noise suppression 8-82035
 thermogrammetric temp. meas. method (*Hungarian*) 8-65924
 thermographic instrument, types 8-86266
 thermographic observability of tumours with microwave heating 8-73193
 thermography, biomedical appl. aspects 8-61279
 thermography, colour, environmental physiology appl. 8-58043
 thermography, skin temp. meas. appl. 8-61280
 thermography appls. in industry 8-79112
 thermography in clinical diagnosis and monitoring 8-57113
 United States Air Force infrared reconnaissance set 8-81458
 utilisation of IR technology, conf., San Diego (1977) 8-77984
 Viking IR thermal mapper, design 8-57440
 visible and infrared imaging radiometers for ocean observations 8-69536
 InSb/LiNbO₃ acoustoelectric convolver, gap-coupled, for IR imaging device 8-94492

infrared-infrared double resonance see *optical double resonance*

infrared radiometers see *radiometers*

infrared sources

- 'blackbody' IR sources 8-83059
 carbon furnace for IR source, practical consideration 8-81976
 LED, industrial appl. of fibre optics 8-59123

infrared sources continued

- Ar high-pressure arc plasma, IR continuum emission obs. 8-71604
 He-Ne lasers, standard wavelength sources 8-74957
 LiIO₃, 5.3 μ m down-conversion, IR source appls. (*German*) 8-90452
 LiIO₃, pulse-period parametric oscillator, tunable 0.63 to 3.4 μ m, for nonlinear spectroscopy 8-59083

infrared sources (astronomical)

- 5 GHz survey 8-69906
 accreting stars, model IR spectra for dusty circumstellar shells 8-85934
 Becklin-Neugebauer source in Orion, high resolution 1.5 to 5 micron spectroscopy 8-93368
 R Cassiopeiae, late-type giant, possible H₂O thermal emission identification 8-81628
 μ Cephei, late-type supergiant, possible H₂O thermal emission identification 8-81628
 circumstellar clouds, scattered stellar radiation circular polarisation theory 8-96428
 R Coronae Borealis stars, long-term IR behaviour 8-96490
 CRL 2104, CRL 2179, late WC stars, 2 to 4 μ m spectrophotometry and circumstellar dust 8-96491
 V1016 Cygni, IR spectrum 8-93266
 V1500 Cygni (Nova 1975), fine-struct. lines rel. to 10 micron excess 8-93269
 Cygnus OB2 No.12, high resolution 2 μ m spectroscopy rel. to interstellar and stellar features 8-57613
 dark globules, IR radiation theory 8-53999
 Dyson spheres, stellar energy requirements and IR emission 8-69710
 early-type stars, disc struct. in extended atms. 8-93206
 embedded sources, optical spectrophotometry 8-96520
 equatorial IR catalogue (EIC), 2.7 μ m high-precision sky survey results 8-81560
 field stars at North Galactic Pole, props. 8-81622
 G12.2-0.1, radio and IR obs. of OH/H₂O source 8-57620
 G333.6-0.2, G298.2-0.3, southern compact H II regions, IR emission lines obs. 8-96522
 G45.1+0.1, 8-13 μ m spectrophotometry of compact H II region 8-65672
 galactic centre, linear polarisation in near IR 8-96534
 galactic sources, IR fluxes calcs. for polysaccharide grain model 8-54008
 giant H II regions, radio and IR maps interpretation 8-85994
 GL 915, 618, 2688, IR sources assoc. with double-lobed refl. nebulae, far IR obs. 8-54009
 IC 1805, radio identification of IR object assoc. with passage of shock front 8-93369
 interstellar 10 μ m silicate absorpt. band equivalent widths and dust temps. 8-57614
 IRC+10216, C₂H (butadiynyl) radical detect. 8-93374
 IRC+10216, C star, possibility of detecting cyanoacetylene-d₁ (DC₃N) 8-69901
 IRC +10°216, circumstellar methane in IR spectrum 8-57694
 late-type stars, near IR photometry with balloon-borne telescope 8-73713
 M17, Platt particles and spatial temp. fluctuations 8-61907
 NGC 1068, Seyfert galaxy, IR photometry and polarimetry 8-54035
 NGC 7027, planetary nebula, near IR obs. 8-73748
 Nova Serpentis 1978, IR magnitudes and BVR photometry 8-65629
 Orion molecular clouds, obs. in 40-400 μ m range 8-69853
 planetary nebulae, molecular abundances and IR spectra 8-53998
 primaeval giant elliptical galaxies, observable props. 8-89260
 quasars, IR energy distribns. obs. 8-57645
 radiative transfer in nongray extended dust shell models, Eddington approx. generalization 8-73627
 S140 IR, far IR spectrum 8-93372
 2S1728-337 vicinity, 5 IR sources detected by K-band photometry 8-54076
 2S 1702-363 field, IR object identified as Mira variable 8-81705
 HM Sagittae, emission line variable, near IR spectrum (*Russian*) 8-81637
 HM Sagittae, IR spectrum 8-93266
 Seyfert galaxies, IR energy distribns. obs. 8-57645
 Sh 2-149 assoc. IR source, spectral type and luminosity class 8-73772
 stars with IR excesses, optical emission intrinsic linear polarisation origin 8-96481
 thermal emission spectrum from small interstellar grains with temp. fluctuation 8-69864
 variable stars, H₂O maser source in circumstellar envelope 8-73724
 W3(OH), production by moving compact object 8-54064
 W40 and W48, near IR and CO mm wavelength obs. 8-65667
 Wolf-Rayet stars, 2 to 4 μ m spectrophotometry of late WC stars 8-96491
 H II regions, anisotropic, with axial symmetry, models rel. to IR brightness distribns. 8-85993
 H II regions is IC 1795/1805, IR luminosity compared with exciting star total luminosity 8-96519
 OH 0739-14, IR source assoc. with double-lobed refl. nebulae, far IR obs. 8-54009
 OH/IR stars, new SiO transition detect. 8-53954

infrared spectra of diatomic inorganic molecules

- intensity prediction, at. polar tensor method, F containing mols. 8-62854
 intensity relation, IR to Raman intensity, matrix notation 8-62853
¹⁴N¹⁶O, 1-0 band at 1900 cm⁻¹, meas., interpret. 8-58651
 AIO stellar IR bands rel. to Mira phenomena 8-69801
 Ar₂, near IR absorpt. spectra 8-66547
 CO, absorpt. spectra around 2100 cm⁻¹, Fourier transform spectroscopy appl. 8-58068
 CO chemisorbed on Rh γ -Al₂O₃ disperse δ -phase, IR spectra, site distrib., mol. mobility 8-72496
 CO, ground-state, absorpt. oscillator strengths for vibr. rot. transitions 8-62846
 CO, high resolution lifetime meas., perturbation and collisional transfer correl. 8-78699
 CO, IR band nonrigid rot. absorption 8-91060
 CO in giant stars in globular clusters, IR obs. 8-93339
 CO, on Pt surface, IR spectrum obs. in presence of free CO 8-74654
 ClO, bandstrength determ. of fundamental vibr.-rot. spectrum 8-70872

infrared spectra of diatomic inorganic molecules continued

- ClO radical, IR vibr.-rot. spectra, background data for atm. meas. 8-58679
 CsBr, far IR spectra, matrix isolated, monomers, dimers, trimers 8-66545
 CsCl, far IR spectra, matrix isolated, monomers, dimers, trimers 8-66545
 CsF, far IR spectra, matrix isolated, monomers, dimers, trimers 8-66545
 CsI, far IR spectra, matrix isolated, monomers, dimers, trimers 8-66545
 H₂ emission at 2 microns from Orion Nebula 8-93351
 HBr, far IR Ar matrix isolated spectra, 4.2K, press. and conc. effects 8-62801
 HBr, isotopic struct. and spectral characts. of vibr. band, using liq. N₂ Raman laser source 8-50859
 HBr, vibr.-rot. absorpt. spectra at very high foreign gas densities 8-78687
 HCl, anhydrous conc. solns. in methanol, Raman and IR spectra 8-82724
 HCl, far IR Ar matrix isolated spectra, 4.2K, press. and conc. effects 8-62801
 HCl, spectral data analysis using graphics display terminal 8-54473
 HCl, vibr.-rot. absorpt. spectra at very high foreign gas densities 8-78687
 H³⁵Cl, H³⁷Cl, IR Fourier absorption spectra, press. induced shifts 8-74706
 HCl-dimethylether complex, gaseous, H-bond IR spectra, temp. depend. theory 8-62804
 HD⁺, ground state vibr.-rot. spectrum, high resolution laser-ion beam reson. expt. 8-82733
 HD⁺, spontaneous IR rot.-vibr. emission probability 8-50535
 HF, IR Fourier absorption spectra, press. induced shifts 8-74706
 HI, 1→0 IR absorpt. band 8-86863
 HI, line strength meas., 0→4 and 0→5 absorpt. bands, dipole moment (*French*) 8-62847
 H₂¹⁷O and H₂¹⁸O, centrifugal distortion anal. of ground vibr. states 8-70834
 Kr₂, near IR absorpt. spectra 8-66547
 MgO, from Mg+O₂ matrix reaction, IR spectra, isotope shifts and blue matrix shift 8-80736
 N₂, B³Σ_g⁻→B³Π_g (0,0) emission band 8-58690
 N₂, dispersive Fourier transform spectrometry using modular interferometer 8-89567
 N₂, energy levels, low lying triplet states, infrared emission analysis 8-58691
 N₂, high-resolution electronic emission spectrum, 15300 Å 8-66549
 NO, chemiexcited, form. in N(²D)+O₂, 90-180K, IR obs. 8-90163
 NO, IR band nonrigid rot. absorption 8-91060
 NO isotopes, spectrophone meas. at selected CO, CO₂ laser wavelengths 8-57310
 NO, press.-broadened linewidths of R(9.5)₂ transition 8-70824
 NO, sub-Doppler resolution IR spectra 8-86860
 NO+ClONO₂, react., gas phase, kinetics, mechanism, IR photometric investig. (*German*) 8-76834
 NaBr, far IR spectra, matrix isolated, monomers, dimers, trimers 8-66545
 NaCl, far IR spectra, matrix isolated, monomers, dimers, trimers 8-66545
 NaF, far IR spectra, matrix isolated, monomers, dimers, trimers 8-66545
 NaI, far IR spectra, matrix isolated, monomers, dimers, trimers 8-66545
 NaNe, laser spectroscopy, interat. pot. curves 8-86871
 Ne₂, near IR absorpt. spectra 8-66547
 O₂ 1.27 μ A-band intensity in lower atmosphere (*Japanese*) 8-61486
 O₂ 1.27 μ emission, auroral enhancement 8-81485
 O₂ 7594 Å telluric A-band on objective prism spectra of stars, radial vel. meas. appl. (*Japanese*) 8-89083
 O₂, dispersive Fourier transform spectrometry using modular interferometer 8-89567
 O₂, spectral line shape, Fourier representation of Voigt profile 8-90223
 P₂, b³Π_g-w³Δ_g and A¹Π_g-W¹Δ_g systems, IR emission spectrum 8-94244
 PuN, in Ar matrix, IR spectra, stretching freq. and isotope shifts 8-78690
 PuO, in Ar and Kr matrices, IR absorption spectra, normal coord. anal., assignments, force consts. 8-78681
 SbF₆ (f⁰, e⁰)-X₂ transition, rot. anal. 8-74657
 SeH(X²Π_{3/2}), far IR LMR spectrum 8-66564
 Xe₂, near IR absorpt. spectra 8-66547

infrared spectra of inorganic solids

- adsorbed species, catalytic reaction, high temp. IR obs. 8-88655
 alkali halides, absorpt. in molecules, clusters and microcrystals 8-80363
 alkali halides, shift and broadening of local vibr. bands, temp. depend. 8-87755
 alkali-alkaline earth silicate glasses, IR refl. spectra (*Japanese*) 8-52505
 aluminophosphate glass, multicomponent, 3.2 micron broad absorption band computer anal., residual H₂O vibr. 8-52478
 amorphous solid, very far IR props. 8-80344
 ceramic crystalline materials, IR transmission, review 8-55417
 chalcopyrite type ternary crystals, IR dispersion (*Russian*) 8-76451
 chemisorbed atoms and mols., vibrational motion dynamics, infrared absorpt. line shape 8-51814
 complex contours interpretation of IR refl. bands, dispersive analysis 8-72508
 diamond, synthetic and natural, neutron irradi., optical and elec. props. (*Russian*) 8-59841
 disordered solids, rel. between simple analytic models 8-76473
 frosts, Na and K doped, reflectance spectra and implications for Io surface 8-84561
 glass with hydrophilic protective coatings 8-85019
 highly absorbing solid, dispersive refl. meas. using modular interferometer 8-89568
 impurities, conc. of C, O, Si 8-59832
 ionic rectangular crystallites, IR absorpt. calcs. 8-95583
 Maxwell Garnett theory, validity range 8-68507

infrared spectra of inorganic solids continued

- metal, highly reflecting, determ. of IR optical constants by surface plasmon excitation 8-76418
 metal oxide metaphosphate glasses, vibr. study of metal cation reduction at surface 8-56797
 metal-insulator composite films, optical props., rel. to solar collector appls. 8-72622
 metallic particles, low-freq. EM absorption, particle size depend. 8-88311
 metallic particles, ultrafine, far IR absorpt. calc. 8-60454
 metallic powders, far IR absorption, self-consistent theory 8-56442
 methanation catalysts, nonreduced, IR spectra 8-88288
 minerals, IR spectra exam. 8-84567
 mixed alkali glasses, Raman and far IR spectra, vib. at cation site, struct. 8-60435
 molecular glass, density of states for IR active internal modes of tetrahedral mols. 8-75788
 oyster shell, IR and atomic mineral anal. 8-61116
 polysilicic acid, IR spectra, struct., crystallisation effects (*Russian*) 8-72528
 quartz, amorphous and crystalline, surface polaritons and splitting of optical frequencies 8-72090
 quartz, cryst. and melt, irradi., optical absorpt. spectra, computer calcs. (*Russian*) 8-92091
 quartz, electron irradiated, optical and anelastic absorptions and resonator freq. 8-64385
 quartz, hydrolytic weakening of natural and synthetic crystals, mech. and IR study 8-61410
 quartz, pure, fused, optical consts. in far IR, 20 to 120 cm⁻¹ 8-79080
 quartz, synthetic, lattice distortions, optical inhomogeneities by X-ray topography and optical birefringence meas. 8-55887
 quartz cylindrical fibres in regular struct., multiple frustrated total internal refl. calc. 8-83094
 rare earth oxide films, optical absorpt., refractive index, band gap and zone struct. (*Russian*) 8-76544
 rocks, IR spectra exam. 8-84567
 semiconductor, intervalley cyclotron-phonon reson., IR absorption in mag. field 8-60448
 semiconductor, IR plasma reflectivity spectra analysis 8-52480
 semiconductor, nonequilibrium optical phonons generated by electrons in laser radiation field 8-71802
 semiconductor film, quantised, one-phonon light absorption 8-60527
 semiconductor-insulator system, contact interaction mechanism, optical props. 8-88375
 silica gels, surface treatment, adsorption properties (*Japanese*) 8-95855
 silicate glass, IR reflection spectra relation to corrosion state of surface (*Japanese*) 8-88554
 silicate glass corroded by moisture, IR refl. spectra change (*Japanese*) 8-53013
 silicate glasses, struct. and phase transform. 8-64538
 space group refinement by vibr. spectroscopy methods, possibility 8-79507
 steel, stainless, hard, and mild, optical constant dispersion and emissivity, up to 900K 8-52464
 transition metal complex anion, vibr. spectra in solid and soln., struct. and fundamental mode assignment 8-62803
 transition metal dichalcogenides, optical phonon modes and localised effective charges, reflection spectra 8-76453
 uniaxial crystal, dispersion of bulk phonon polaritons meas. by IR refl. 8-59902
 vibrational spectra crystals with split configuration interstitial (*Russian*) 8-76450
 water cryofilm, on specular and diffusing surfaces, bidirectional reflectance 8-88274
 Ag, absorpt. coeff. temp. depend., IR, 3 to 30 μm 8-74953
 Ag sphere, ultrafine, with dielectric cores, optical absorpt. 8-60455
 Ag-SiO₂ film, elect. and struct. props., ion beam sputtering 8-80071
 AgGaSe₂(Te₂), phonons, far IR refl. obs. 8-60459
 AgI, superionic conductor, dynamical aspects 8-79695
 AgI type solid electrolytes, expt. props. 8-63877
 AgInSe₂(Te₂), phonons, far IR refl. obs. 8-60459
 Ag₂Si, superionic conductor, dynamical aspects 8-79695
 Al saponite, differential thermal anal., IR absorpt. spectra, chlorite-like mineral 8-88816
 Al_{1-x}Ga_xP, IR phonons, lattice reflection spectra 8-51626
 AlNbO₄, diffuse refl. and luminesc. spectra 8-56516
 Al₂O₃ anomalous absorpt., in far IR region 8-56464
 Al₂O₃, IR spectra, comparison to inelastic electron tunnelling spectra (*French*) 8-68489
 B-Al₂O₃-M₂O, M=Na, Ag, Rb, K, far IR absorption and ionic cond. 8-72512
 As, amorphous, bonding coordination defects, Raman scatt. and IR absorption meas. 8-60498
 As, amorphous and cryst., phonon density of states calc., comp. to IR absorpt. and neutron scatt. data 8-55924
 (As₂O₃)_n, claudette I, vibr. spectra, force field calc. (*French*) 8-60447
 As₂S₃ evaporated film, optical props., depend. on light exposure and heat cycling 8-68572
 As₂S₃ film, effect of light exposure and heat cycling 8-94417
 As₂S₃ glass, Raman and IR spectra, struct. model 8-80330
 As₂Se₃-InI₃, glass system, IR spectra 8-64365
 Au, absorpt. coeff. temp. depend., IR, 3 to 30 μm 8-74953
 Au discontinuous films, optical transmittance, effect of island morphology 8-84673
 Au_{1-x}Si_x, amorphous film, spectra 0.01-6.2 eV, 0.13≤x≤0.5 8-68574
 B, α-, β-rhombohedral and amorphous, struct. changes on Zn incorporation 8-79596
 BaF₂, optical ceramic, hot pressing in vacuum, rel. to spectral transmission 8-52730
 BaF₂:Mn²⁺, far IR absorption spectra 8-76507
 Ba₁₀(PO₄)₆(OH)₂, cryst., IR spectra, band assignments 8-60442
 BeF₂, vitreous, IR and reduced Raman spectra, weak Raman bands 8-68498
 Bi₂O₃ and sillenite struct. derivatives, MO_x.6Bi₂O₃, IR and Raman spectra, vibr. anal. 8-76464
 Bi₂O₃, transmission spectra of thin films 8-76440
 BiOI, synthesis, thermal decomposition in dry O₂ (*French*) 8-53205
 C film, amorphous, growth under ion impact in butane plasma, and IR transparency 8-52688

infrared spectra of inorganic solids continued

- C₁ pyrolysis mechanism, electron microscopy, DTA, IR, ESR obs. 8-56593
- CO, adsorbed on Pt (111), oxidation process, reflection-absorpt. IR study 8-76468
- α -CO, IR and Raman spectra, vibron band, vibron-phonon combination bands 8-68495
- ¹²C¹⁸O:CO isotopes, IR and Raman spectra, vibron band, vibron-phonon combination bands 8-68495
- CaCO₃, aragonite-calcite transformation, effect of impurities, DTA and IR studies 8-51662
- CaCO₃, IR reflectivity, oblique phonons 8-60440
- CaCO₃+SiO₂, in presence of NaF, thermal decomposition of Ca₂SiO₄ formation 8-68889
- CaF₂ trapezoid, ThF₄ and ZnSe coated, IR characterisation by internal-refl. spectra 8-71161
- CaF₂:D²⁺ submm. magnetospectroscopy, tunable far IR laser potential 8-52481
- CaFe₂·Fe³⁺(OH)O(Si₂O₇), ilvaite, IR spectrum and Mossbauer effect obs. (French) 8-80321
- Ca₁₀(PO₄)₆(OH)₂ halogenated derivatives, IR absorpt. spectra (Spanish) 8-52489
- Cd_{1-x}Hg_xTe, gap width temp. depend., absorpt. band edge meas. 8-72521
- CdIn₂S₄:Co, optical absorption meas. 8-64384
- CdR₂S₄ (R=Sc, Yb, Tm), IR and Raman spectra, force consts. 8-68503
- CdS_{1-x}Se_x, zone edge phonons 8-76475
- CdS, fundamental vibrs., Raman scatt. and IR refl. obs. 8-60451
- n-CdSnAs₂, optical absorption rel. to energy spectra (Russian) 8-75994
- CdTe, lattice mode, dispersive refl. meas. using modular interferometer 8-89568
- CdTe:Be, impurity modes and IR absorption 8-76506
- CdTe_{1-x}S_x, long-wavelength optical phonons, composition depend., IR and Raman spectra 8-67788
- Cd_{1-x}Zn_xS 10 μ m film optical and electrical characterisation (French) 8-64153
- CeN, optical props. and valence mixture 8-56450
- Co_{1-x}Fe_xSi, solid solution, optical props. 8-72556
- Co_{1-x}Ni_xSi, solid solution optical props. 8-72556
- CoSi, solid solution, optical props. 8-72556
- CoSi, thermoelectric and optical props. 8-91714
- CsBr:Ti⁴⁺, perturbed lattice dynamics, breathing shell model calculation 8-75744
- Cs₂SO₄, IR absorpt. spectra, polymorphism, site group approx. and SO₄ stretching mode 8-52510
- Cs₄(UO₂)₂F₈·2H₂O, IR absorpt. and Raman spectra, normal coordinate anal. (French) 8-52509
- CuBr, two-phonon optical absorpt. spectra 8-52485
- CuCl, two-phonon optical absorpt. spectra 8-52485
- CuCl(Br), multiphonon far IR absorpt., 2-80K 8-60462
- CuGa_{1-x}In_xS₂ solid soln., IR refl. spectra, comp. depend. 8-52498
- CuInTe₂, grown from near stoichiometric comp., elec. and optical props. 8-68504
- Cu₂O, refl.-absorpt. IR spectroscopy 8-84555
- D₂, solid, far IR absorption by phonons and librins in ordered state 8-80331
- D₃SiNCs, IR and Raman spectra, vibr. anal., LF bending mode 8-70842
- Er, paramagnetic and antiferromagnetic states, optical absorption (Russian) 8-56497
- ErFeO₃, far IR spectra 8-88303
- Eu complex, (Et₄N)₃ [Eu(NCS)₆], Eu³⁺ ion site symm. 8-84656
- EuS, conduction band density of states, redistrib. near ferromag. saturation 8-67939
- EuS, pure and Gd doped, electronic struct., mag. exchange and elec. transport props. 8-87974
- Fe, optical constant dispersion and emissivity, up to 900K 8-52464
- Fe-Co alloys, optical and spectrosc. props. (Russian) 8-72529
- Fe-Ni alloy, optical and electronic characts., 20-1750°C, comp. depend. (Russian) 8-84601
- FeF₂, magnon-acoustic phonon hybridisation in far IR absorpt. spectra 8-60271
- FeI₂, far IR magnetoabsorption, excitation of two spin deviations 8-80339
- FeO, Fe₂O₄, Fe₂O₃, absorption spectra, 0.1-6 eV, one electron energy level diagram 8-52487
- Fe₃O₄, O₂ annealed, optical absorpt., spin struct., polaronic absorpt., cryst. field transitions 8-68493
- Fe_xZrSe₂, intercalation compound, IR spectra 8-88300
- Ga_{1-x}Al_xP, two-phonon optical absorpt. 8-88341
- GaAs, amorphous layer formation, ion implantation 8-95063
- GaAs anodic oxide, refl. and transmission, 0.01-6 eV 8-95613
- GaAs, highly transparent semicond., multiphonon IR absorpt. 8-60461
- p-GaAs, IR plasma reflectivity spectra calc. 8-52511
- GaAs, irradiated with fast neutrons, IR vibrational absorpt. 8-75776
- GaAs, manifestation of local vibrs. of dislocations in IR spectra 8-88339
- GaAs surface impurities, struct. and comp. of compounds using IR spectroscopy 8-63918
- GaAs:Fe, profile of impurity optical absorption bands 8-56509
- GaAs-AlAs alternating monolayers, zone folding effects on phonons 8-72510
- GaAs-ZZ (Russian) 8-90468
- Ga_{1-x}In_xP, zone edge phonons 8-76475
- n-Ga_{1-x}In_xP, optical props. and energy spectrum of donors 8-72567
- GaNbO₄, diffuse refl. and luminesc. spectra 8-56516
- GaP, manifestation of local vibrs. of dislocations in IR spectra 8-88339
- GaP, upper polariton branch obs. by ATR 8-68510
- GaP:Fe, profile of impurity optical absorption bands 8-56509
- GaP:N(Te), ion implanted at 40 keV, refl. spectra, 210-2000 nm, annealing (Russian) 8-80386
- GaS(Se), layered, optical phonons, IR and Raman scatt. meas. 8-59903
- GaSb, manifestation of local vibrs. of dislocations in IR spectra 8-88339
- GdP, electronic struct., mag. exchange and elec. transport props. 8-87974

infrared spectra of inorganic solids continued

- (GdPrBi)₃(FeGaIn)₂O₁₂, pure and In³⁺ doped, near IR absorpt. and Faraday rot. 8-95580
- GdS, electronic struct., mag. exchange and elec. transport props. 8-87974
- Ge, amorphous, far IR absorption 8-88306
- Ge, electron-hole drop velocities as probe of phonons 8-68517
- Ge, electron-hole drops, far IR absorption 8-56467
- Ge, electron-hole drops, far IR magneto-optical effects 8-84565
- Ge, electron-hole drops, spatial distrib., time and spatially resolved absorption at 3.4 μ m 8-92075
- Ge, high density electron-hole plasma, infrared absorpt. at low temp. 8-92078
- Ge, IR absorption and scatt. by electron-hole drops 8-51903
- Ge, interband Faraday ellipticity 8-92052
- Ge, two-phonon difference absorption spectra 8-76452
- Ge:Si, impurity modes and IR absorption 8-76506
- Ge-Al film, elec. resist. and IR transmission, comp. and substrate temp. depend. 8-52112
- Ge-Ga alloys, amorphous, far IR absorption 8-88306
- Ge-Se glass system, effect of changes in local surrounding of atoms on optical props. (Russian) 8-80414
- GeS₂Se_{1-x} IR spectra, differential calorimetry, phase diagram (Russian) 8-52513
- GeSe₂, IR and Raman spectra 8-95585
- Ge,Se_{1-y}, glass, bulk and film, IR transmission and reflectivity meas., struct. mode assignments 8-79537
- Ge(111)2 \times 1, surface electron states detected by external reflectivity 8-80036
- H-bonded crystal, IR absorpt. spectra band shape, X-H stretching vibr. temp. depend., isotope effect 8-76445
- p-H₂, cryst., hexadecapolar induced absorption intensities 8-88290
- H₂, IR fundamental band, U-branch transitions 8-64361
- H₂, solid, far IR absorption by phonons and librins in ordered state 8-80331
- α -HIO₃, dispersion anal. of IR reflection spectrum (Russian) 8-56493
- H₃SiNCs, IR and Raman spectra, vibr. anal., LF bending mode 8-70842
- H₂WO₄, film, effect of struct. on optical and electrical props. 8-84671
- Hg-As-S-I system, glasses, optical and acousto-optical props. 8-83053
- Hg_{1-x}Cd_xTe, high intensity IR transmission limit 8-79074
- Hg₂I₂, large single crystal far IR spectra 8-92057
- HgSe(Te), dynamic dielectric function, IR absorpt. meas. 8-68508
- p-HgTe, far IR reflectivity spectra, experimental and theoretical study of the dynamic dielectric function 8-92069
- Hg_{1-x}Zn_xCr₂Se₄, absorption spectra near the absorption edge 8-80340
- In-Te system, IR spectra (Russian) 8-84589
- (InAs)_x(CdTe)_{1-x}, band gap and effective mass, IR spectra obs. 8-56491
- In_{1-x}Ga_xP, two-phonon IR absorpt. 8-52493
- InN film, refl. and transmission spectra, band struct. 8-72625
- n-In₂O₃ film, RF sputter grown, substrate bias effect on elec. and optical props. 8-64150
- InP, manifestation of local vibrs. of dislocations in IR spectra 8-88339
- InP:Si, vibr. modes of Si, IR absorpt. bands 8-55922
- InSb inversion layer, spectroscopy of electron subband levels 8-64364
- InSe, layer single crystal, infrared and Raman spectra 8-92070
- α -In₂Se₃, far infrared optical study of ordered and disordered forms 8-84572
- Ir complexes with adenosine, xanthosine, prep., elec. cond., IR spectra, characterisation 8-92065
- K salts, anion exchange, in tablet pressure for IR spectroscopy (Russian) 8-95927
- KB₃O₈·4H₂O, polariton Fermi reson., spontaneous parametric light scatt. 8-87923
- KBr, transient infrared absorption of bound polarons 8-92071
- KCN, optical F centres and phase transitions 8-56504
- KCl, bulk and surface absorpt., 2 to 10 μ m, calorimetric meas. 8-71160
- KCl, IR absorpt. calcs. in rectangular crystallites 8-95583
- KCl-Al(Pd) composite, far IR absorption 8-56466
- KCl_{1-x}Br_xNCO⁻, absorpt. band defect broadening (Russian) 8-72526
- KCl(Br)(I), far IR complex refr. indices, dispersive Fourier transform 8-80322
- KCl_{1-x}I_xNCO⁻, absorpt. band defect broadening (Russian) 8-72526
- KD₂PO₄, IR and Raman polarised spectra, rel. to crystal struct. 8-56489
- KDy(WO₄)₂, low temp. phase transitions (Russian) 8-87787
- K₂FeF₆, two dimensional planar antiferromag., mag. excitations, Raman and far IR spectra obs. 8-72343
- KHF₂, IR refl. spectra 8-80324
- KH₂PO₄ crystals, polarisation of unbound many particle states, IR spectra (Russian) 8-84556
- K₂Mg(S₂O₃)₂·6H₂O, isolation, struct., decomposition (French) 8-52506
- K₃N(SO₃)₃·2H₂O, cryst. binding of H₂O, IR spectra 8-75620
- K₂PtCl₆:Os⁴⁺, sharp line luminesc. band at 10K, vibr. assignment 8-95600
- K₂Rb_{1-x}Cl_{1-y}, IR reflection spectra 8-76474
- K₂SO₄, IR absorpt. spectra, polymorphism, site group approx. and SO₄ stretching mode 8-52510
- KTaO₃, complex refr. index meas. in far IR, by dispersive Fourier transform spectroscopy 8-92042
- KTbF₁₀, Faraday rotation, optical absorpt. spectra and refr. index 8-72542
- La(BrO₃)₃·9H₂O, IR and Raman spectra, vibr. assignments 8-84569
- γ -La₂S₃, indirect electron transitions, diffuse refl. and vibr. spectra 8-84576
- LiF, manifestation of local vibrs. of dislocations in IR spectra 8-88339
- LiF, Stark effect, M-centre absorpt. bands 8-84614
- Li_{0.5}Fe_{2.5}O₄-CuFe₂O₄-ZnFe₂O₄, order-disorder transition, quadratic transformation (French) 8-76447
- Li_{0.5}Ga_{2.5}O₄-CuCr₂O₄ system, phase diagrams, IR spectra, Cu²⁺ electronic spectra (French) 8-51461
- α -LiIO₃, attenuated total reflection spectra of anisotropic surface polaritons 8-87919
- LiN₃, evidence for N₃⁻ from static and dynamic props. 8-60465
- LiNbO₃, optical phonon modes and anharmonic couplings 8-60466
- Li₂O-TeO₂ glasses, struct., IR reflection spectra 8-68516

infrared spectra of inorganic solids continued

- Li₂SO₄, IR absorpt. spectra, polymorphism, site group approx. and SO₄ stretching mode 8-52510
- LiTaO₃, optical phonon modes and anharmonic couplings 8-60466
- LiTbF₄, LiTb_{0.5}Y_{0.5}F₄, and LiTb_{0.25}Gd_{0.75}F₄, Faraday rotation, optical absorpt. spectra and refr. index 8-72542
- LiTbF₄, Tb³⁺ absorption spectra, 4000 to 25000 cm⁻¹ 8-72550
- MgAl₂O₄, IR spectrum exam. 8-76454
- MgAl₂O₄, lattice dynamics, rel. to space group of spinel 8-59898
- MgO microcrystals, IR absorption 8-92074
- MgO-BaO-Al₂O₃-SiO₂, glass, IR absorpt. spectra and solid struct. exam. 8-88314
- MgR₂S₄, (R=Sc, Yb, Tm), IR and Raman spectra, force consts. 8-68503
- Mn₂Cd_{1-x}Te, far IR refl. spectra, phonon spectra 8-52497
- MnO, Jahn-Teller effect on optical absorption spectra 8-52484
- Mn_xRe_{1-x}(CO)₅X(X=Cl, Br), 0<x<5, vibr. spectra in the 2000 cm⁻¹ region of mixed and isotopic crystals 8-84585
- Mn₂Si_{2n-m}, thermoelectric and optical props. 8-91714
- MnTa₂O₆, columbite struct., X-ray diff., IR and Raman spectra (French) 8-63727
- Mo halides, [Mo₂X₈] cluster group identification in IR spectra of solids, normal vibrs. 8-64359
- N₂:CO, IR and Raman spectra, vibron band, vibron-phonon combination bands 8-68495
- NH₄AlCl₄, crystal struct., X-ray, Raman, IR and NMR 8-63720
- (NH₄)₂BeF₄, powder, IR spectra, assignments, mol. libration, in paraelec. and ferroelec. phases 8-88299
- NH₄Br:Cu²⁺, ESR and absorpt. spectra, 300-1500 nm 8-60492
- (NH₄)₂M(SO₄)₂·6H₂O, Tutton's salts, correl. of vibr. freq. and N...O distance for (NH₄)₂D⁺ 8-92066
- (NH₄)₂Mg(S₂O₃)₂·6H₂O, isolation, struct., decomposition (French) 8-52506
- Na polysilicates, IR spectra, struct., crystallisation effects (Russian) 8-72528
- NaCN, crystal props., log potential model calc. 8-63829
- NaCN, optical F centres and phase transitions 8-56504
- NaCl, bulk and surface absorpt., 2 to 10 μm, calorimetric meas. 8-71160
- NaCl, search for IR absorption by triplet self-trapped excitons 8-56473
- NaCl, transient infrared absorption of bound polarons 8-91642
- NaF, Stark effect, M-centre absorpt. bands 8-84614
- NaF(Cl), far IR complex refr. indices, dispersive Fourier transform 8-80322
- NaHF₂, IR refl. spectra 8-80324
- NaI, long wave phonon modes, IR absorpt. 8-79686
- NaNO₂, mechanism of ordering type ferroelec. transition, vibr. spectroscopy 8-76402
- NaNO₂, vibr. spectrum, interference effects 8-87752
- Na¹⁵NO₃, Na¹⁴NO₃, multiphonon transitions in microcryst. reflectivity 8-72499
- Na₂O-B₂O₃-SiO₂-Fe glass, near IR optical absorption of Fe (II) 8-84616
- Na₂SO₄, IR absorpt. spectra, polymorphism, site group approx. and SO₄ stretching mode 8-52510
- Na₂S·9H₂O-NaOH-H₃BO₃, glass, IR and Raman spectra of boron-ultramarine, exam. of S₃²⁻ presence 8-68502
- Na₄[M^{II}(NH₃)₄][M^I(S₂O₃)₂]₂·L, (M^I=Cu, Ni), (M^I=Cu, Ag), (L=H₂O, NH₃), IR spectra, vibr. anal. (French) 8-52477
- NbSe₂(2H)-hydrazine, intercalation compd., kinetic studies by transmittance meas. at 1600 nm 8-71981
- Nd(BrO₃)₃·9H₂O, IR and Raman spectra, vibr. assignments 8-84569
- NdF₃, Zeeman splitting in mag. fields up to 100 kG 8-52483
- Ni catalyst, Al₂O₃ supported, adsorpt. of CO in H₂-He, effect of H₂S on IR spectrum 8-71945
- Ni/Al₂O₃(SiO₂) methanation catalysts, nonreduced, IR spectra 8-88288
- Ni(ClO₄)₂·6H₂O, EPR and IR spectra, 98-298K, phase transition at 224K 8-84477
- NiI₂, far IR study of lattice dynamics 8-80359
- NiZn ferrites, Mossbauer effect and IR spectra 8-64300
- P-As-Se glasses, mag. susceptibility, dielec. const., opt. props. 8-64184
- P-Se glass system, IR spectra 8-64365
- Pb₃(AsO₄)₃Cl, mimetite, vibr. spectra, normal coord. anal. 8-88305
- PbGeS₃, vitreous and cryst., IR and Raman spectra (Russian) 8-72527
- Pb₃O₄, IR and Raman study of structural phase transitions (French) 8-84582
- Pb₃(PO₄)₂Cl, pyromorphite, vibr. spectra, normal coord. anal. 8-88305
- Pb₁₀(PO₄)₆(OH)₂, cryst., IR spectra, band assignments 8-60442
- PbS film, polycryst., chem. deposition from soln. and characterisation 8-72743
- Pb_{1-x}Sn_xTe, absorption edge shift, energy gap determ. 8-88308
- PbTe epitaxial film, stimulated emission, absorption spectra and recombination 8-80409
- PbTe surface space charge layers, far IR magnetoreflectance meas. 8-64349
- PbTe, TO phonon softening, free carriers and defects effects 8-79720
- Pb₃(VO₄)₃Cl, vanadinite, vibr. spectra, normal coord. anal. 8-88305
- Pd, optical properties, 0.1 to 6 eV 8-92092
- Pd-Fe alloy, IR absorpt. characs., 0.9 to 19 μm, mag. order effect 8-84577
- PrCl₃, one-dimensional X-Y system, far IR absorpt. spectra, cooperative spin excitations 8-95584
- PrVO₄, energy levels, opt. and NMR measurements 8-80226
- Pu(IV) oxide polymer, potential pollutant from fuel reprocessing, IR spectrum 8-76456
- RbCN, crystal props., log potential model calc. 8-63829
- RbCl(Br)I, far IR complex refr. indices, dispersive Fourier transform 8-80322
- RbDy(MoO₄)₂, low temp. phase transitions (Russian) 8-87787
- Rb₂FeF₄, two dimensional planar antiferromag., mag. excitations, Raman and far IR spectra obs. 8-72343
- RbO₂-Na₂O-P₂O₅ glasses, Raman and far IR spectra, vib. at cation site, struct. 8-60435
- Rb₂O-Li₂O-P₂O₅ glasses, Raman and far IR spectra, vib. at cation site, struct. 8-60435

infrared spectra of inorganic solids continued

- Rb₄(UO₂)₂F₈·2H₂O, IR absorpt. and Raman spectra, normal coordinate anal. (French) 8-52509
- Re(¹²CO)_{5-y}(¹³CO)_yX(X=Cl, Br), 0<y<5, vibr. spectra in the 2000 cm⁻¹ region of mixed and isotopic crystals 8-84585
- Rh complexes with adenosine, xanthosine, prep., elec. cond., IR spectra, characterisation 8-92065
- Ru complexes with adenosine, xanthosine, prep., elec. cond., IR spectra, characterisation 8-92065
- (SN)_x, phonon evolution during polymerisation of SN units 8-79711
- S₂N₄, solid and soln., IR and Raman spectra, vibr. assignment 8-74659
- S₂N₂Cl₂, solid and soln., IR and Raman spectra, vibr. assignment 8-74659
- S₂N₄H₄, and -d₄, solid and soln., IR and Raman spectra, vibr. assignment 8-74659
- Sb electrodeposit, amorphous explosive crystn., semicond-semimetal transition and IR absorpt. 8-51849
- Sb-Se-I system, exam. of glass formation, IR transmission spectra 8-88452
- SbF₃, IR spectra of solid and gas, rel. to struct. (French) 8-78692
- SbF₃(NH₂)₂CS and SbF₃[(NH₂)₂CS]₂, X-ray cryst. struct., IR spectrum (French) 8-87643
- Se, trigonal, model of lattice dynamics using long and short range interactions 8-59893
- Se-Ge glass, lattice vibr. spectra, photostruct. change, far IR absorpt. 8-72494
- SeMoOCl₄, prep., cryst. struct., characterisation (French) 8-63722
- Si epitaxial film, correlation between electrooptical and electrical props., IR absorpt. spectra (Russian) 8-60453
- Si, exciton and deformation pot. fine struct. 8-88301
- Si, far IR impurity spectra, effects of high uniaxial stress 8-56508
- Si, highly transparent semicond., multiphonon IR absorpt. 8-60461
- Si inversion layers, far IR reson. magnetotransmission, temp. and band gap light depend. 8-64363
- Si MOSFET inversion layers, IR photocond. and absorption 8-64123
- Si, neutron irradiated, intrinsic defect exam. by IR spectra 8-52534
- Si, sputtered, cluster formation, influence of HF plasma interaction 8-64441
- Si, vibrational properties of the (001) split interstitial 8-91405
- Si:Al, absorpt. line broadening 8-95594
- Si:Al(In), acceptor levels, IR spectra 8-67972
- Si:O film, near IR absorption, O impurity states 8-88333
- Si:O film, near IR reflectivity at high temps. 8-56532
- Si:P, characterisation by IR reflectivity 8-56501
- Si:P, IR absorpt. and D⁻ band 8-52533
- Si:Ti, IR excitation spectra 8-88289
- Si:Ti, optical absorption and photolum. of bound exciton 8-88359
- Si-H(-D), film, IR and Raman spectra, H bonding effects 8-72515
- SiC fibre reinforced Ni-Cr alumina coated fibres, hot pressed, annealed, IR study 8-60623
- β-SiC layer synthesized by C ion implantation in Si, IR absorpt. 8-56492
- n-SiC(6H), donor ground state splitting, IR spectra (Russian) 8-92104
- SiH₃PH₂BD₃, vibr. analysis, spectra and structure of P-B compounds 8-84586
- SiH₃PH₂BH₃, vibr. analysis, spectra and structure of P-B compounds 8-84586
- β-Si₃N₄, β'-Si₂Al₂N₄O₄, combined X-ray and IR analyses 8-79579
- SiO₂, amorphous and crystalline, surface polaritons and splitting of optical frequencies 8-72090
- SiO₂ films, dehydroxylation, sintering, IR investig. (Russian) 8-75967
- SiO₂ gel, struct., IR spectra obs. 8-88297
- SiO₂, ion irradi., H capture, absorpt. bands (Russian) 8-76505
- SiO₂, OH group interactions, IR and Raman spectra 8-80383
- SiO₂, powder, surface modes, IR spectra 8-92063
- SiO₂:Fe, vitreous and cryst., with or without Al₂O₃, Na₂O additions, exam. of Fe²⁺ coordination, IR spectroscopy 8-88344
- Si(111)2×1, surface electron states detected by external reflectivity 8-80036
- Sn borate glasses, IR and ¹¹⁹Sn Mossbauer spectra 8-60438
- Sn₂F₂S₆, ferroelec., IR and Raman spectra, photocond., edge absorpt. spectra, spontaneous polarisation, forbidden gap 8-68514
- Sr_{1-x}Cd_xF₂, lattice dynamics 8-75763
- SrCl₂:Fe²⁺(Co²⁺) electronic absorption spectra in far and middle infrared 8-68537
- SrF₂, doped, far IR absorption spectra 8-76507
- SrF₂:R³⁺, far IR vibr. spectra of F⁻ compensation ion 8-92059
- Sr₁₀(PO₄)₆(OH)₂, cryst., IR spectra, band assignments 8-60442
- SrSb₂O₃, SrSb₂O₉, SrSb₆O₁₀, mixed valence cpds., prep., IR and X-ray investigation (French) 8-88292
- SrTiO₃, complex refr. index meas. in far IR, by dispersive Fourier transform spectroscopy 8-92042
- SrTiO₃, plasmon-phonon reson., IR reflection spectra 8-56093
- Te intrinsic, intermediate IR optical absorpt., 5-20 μm 8-84562
- Te, trigonal, model of lattice dynamics using long and short range interactions 8-59893
- TeO₂, paratellurite, atomic motions corresponding to zone centre phonons 8-76461
- TeO₂, paratellurite, phase transition at high-press., Raman and far IR spectra 8-80328
- TiO₂, rutile, deuteron and alpha-particle implantation, chemical effects, optical and cond. meas. 8-67755
- (Ti₂O₃)_{1-x}(V₂O₃)_x, lattice polarisability, electronic contris. IR refl. obs. 8-59904
- TiBr₃, complex refr. index meas. in far IR, by dispersive Fourier transform spectroscopy 8-92042
- TiGaS₂, layer ternary semicond., polarised Raman, IR reflect. spectra 8-68513
- TiGaS₂(Se₂), optical phonons, IR and Raman scatt. meas. 8-59903
- TiGaSe₂, layer ternary semicond., polarised Raman, IR reflect. spectra 8-68513
- TiGaSe₂, Raman and IR spectra, zone centre optical phonons 8-76462
- β-TiInS₂, layer ternary semicond., polarised Raman, IR reflect. spectra 8-68513
- TlInS₂, optical phonons, IR and Raman scatt. meas. 8-59903
- Tl₂MoO₄, prep., characterisation 8-63731
- TlSe, optical phonons, IR and Raman scatt. meas. 8-59903
- TlSe, vibr. props., Raman and far IR spectra meas. 8-71800

infrared spectra of inorganic solids continued

- Tm, polycryst., optical props., temp. depend., photocond., relaxation parameters 8-84603
 UO₂, optical props. and electronic struct. 8-68527
 V₂O₅, optical characts., far IR transmission spectra 8-72525
 W_{1-x}Mo_xO₃, mixed cryst., structural phase transition, Raman and IR spectra 8-79766
 WSeF₆, cryst. struct., and preparation 8-63730
 Xe-MF₆, M=W, Mo, U, Re, Ir, charge transfer interactions, VUV and IR obs. 8-50664
 (YLaBi)₃(FeGa)₂O₁₂, pure and In³⁺ doped, near IR absorpt. and Faraday rot. 8-95580
 Zn_{1-x}Mg_xTe, long wavelength optical phonons, IR ref. and Raman obs. (French) 8-60433
 ZnO, small crystal, optical surface phonon modes 8-71940
 ZnS:Al-Cu, localised vibrational modes 8-63827
 ZnS:Be, impurity modes and IR absorption 8-76506
 ZnS(Se), highly transparent semicond., multiphonon IR absorpt. 8-60461
 ZnSeS₄, IR and Raman spectra, force consts. 8-68503
 ZrO₂, optimum sintering characts., density, X-ray diff., IR spectrum, UV spectrum obs. 8-76617
 ZrSiO₄, mechanochemical effect by mechanical grinding (Japanese) 8-84754

infrared spectra of organic molecules and substances

- see also molecular rotation; molecular vibration*
 2-chloronaphthalene, vibr. and calorimetric investigation of polymorphism 8-87641
 2-fluoronaphthalene, vibr. and calorimetric investigation of polymorphism 8-87641
 acenaphthene, vibr. spectra, mol. crystal dynamics, librational modes 8-64356
 acetaldehyde, torsional fundamental and combination bands, K-struct. anal. 8-78696
 acetaldehyde photolysis products, time resolved Fourier transform spectrum 8-58071
 acetic acid, protonated complexes, IR and Raman spectra (French) 8-78691
 acetone, solvent effects on oscillator integrated strength, IR absorpt. bands 8-84575
 acetonitrile, soln., IR perpendicular bands, profiles, rot. models 8-58695
 acetylene, and -d₂, integrated IR intensity, meas. and interpretation 8-66551
 acetylene-d₀, (-d₂), IR intensities, relative error anal. 8-58686
 acetylpyridines, vibr., IR and Raman spectra 8-74653
 adipic acid, monoclinic crystals, IR absorption and dichroism 8-88293
 adsorbed species, catalytic reaction, high temp. IR obs. 8-88655
 alicyclic ring compounds, vibrational spectra and structure, book 8-78700
 alicyclic ring cpds., vibr. spectra, conformational props., book contrib. 8-78702
 alkanes, overtone spectra, local mode anal., discrete excitation of nonequivalent CH oscills. 8-78688
 amide group in soln., interactions, IR, Raman spectral investigs., peptide, protein struct., review 8-90330
 amines, aliphatic and aromatic, H-bonding, strong, stochastic model and IR spectra temp. effects 8-62805
 amino acid block copolymers, morphology and mech. props. 8-91264
 4(6)-amino-uracil, IR absorpt. spectra, vibr. anal. 8-61143
 ammonium bioxalate monohydrate, refractive indices in IR region 8-52512
 ammonium uranyl formate, struct. determ. from X-ray diff. and IR spectrum (French) 8-75653
 analgesic group commercial tablet samples 8-74652
 aniline black, superconductivity at room temp. 8-80089
 band intensities, hybrid orbital rehybridisation model, mol. charge distrib. 8-74630
 benzene, 607- μ m line absorption curve 8-95581
 benzene, Ar and Kr matrix isolated, IR spectra, vibr. freqs. and intensities 8-50548
 benzene, in Br₂-carbon tetrachloride soln., complex form., IR spectra 8-70828
 benzene, p-disubstituted, MCD and absorpt. spectra, PPP calcs. 8-66574
 benzene, Raman and IR intensity anal. 8-70829
 benzene-d₀ (-d₆), polar tensors and at. effective charge, calculated from IR intensity 8-74703
 bicyclo(3.2.0)hept-6-ene, LF vib. spectra, conformations 8-58685
 bis(cyclopentadienyl)Ti(IV)chloride, reactions with oximes, IR spectra 8-92471
 block copolymers, IR spectroscopy for struct.-props. relations 8-91268
 1-bromo-2,2-dimethylpropane, Raman and IR spectra, vibr. anal. 8-90173
 5-bromo-uracil, IR absorpt. spectra, vibr. anal. 8-61143
 bromoacetic acid, cryst., films, polarised IR spectra, struct. 8-72502
 4-bromoquinoline, UV and IR spectra, f-values and ground state vibr. freqs. 8-58714
 butadiene elastomers, influence of intermol. interaction on durability (Russian) 8-76746
 camphor, optical isomers, separated, IR Lamb dip obs. 8-90197
 carbon tetrafluoride, intensities of binary overtones and combinations in IR spectrum 8-55172
 CF₃X⁺ cations, (X=Cl, Br, I, H), IR spectra in Ar matrix 8-74710
 p-chloraniline cryst., lattice vibr., IR and Raman spectra, lattice energy 8-56481
 3-chloro-1-butene, rot. isomerism, vibr. spectra assignments 8-58702
 chloroaluminium phthalocyanine, sublimed layer, IR absorption, vibr. assignments 8-55174
 p-chlorobromobenzene, single cryst., polarised Raman and IR spectra, assignments 8-60431
 4-chlorobutylchloride, Raman and vibr. IR spectra of solid and liq., rot. isomerism 8-62810
 2-chloroethanol, IR and Raman spectra, normal coord. anal., isomerism 8-74661
 chymotrypsin, charge relay system, H-bond models, IR spectra 8-64935
 complex biological systems, Fourier transform. IR obs. 8-68945
 conformers, dynamic interaction between ground states, effect on IR spectra 8-58767

infrared spectra of organic molecules and substances continued

- cyclooctanone, vibr., rot. spectra and conformations, pot. function 8-78707
 cyclopropane-d₀, d₆, absolute IR intensities, dipole moment derivatives and polar tensors 8-90165
 decomposition products of CO in corona discharge, qualitative anal. 8-60992
 dialkylammonium manganese chloride, order-disorder transition mechanism 8-79772
 2,5-dichloro-1,4-benzoquinone, mol. cryst., transition moment directions 8-64351
 4,4'-dichlorobenzophenone, cryst., T₁←S₀ singlet-triplet absorption profiles, temp. depend., phonon-exciton anal. 8-60436
 dichlorodifluoromethane, diode laser spectra near 10.8 μ m, air-broadening effects 8-61555
 1,3-dichloropropyne and -d₁, vibr. spectra, normal coord. anal. and centrifugal distortion constants 8-70832
 diene rubbers, highly filled, supermolecular struct. (Russian) 8-76627
 diethynylbenzenes, vibrational spectra, deuterated isomers 8-58705
 1,5-difluoronaphthalene, IR and Raman study of crystal dynamics 8-80346
 dihalobenzenes, IR and Raman spectra, phase transitions (French) 8-84557
 2-5-dihydrofuran, liq. phase far IR spectra, ring puckering (French) 8-92068
 p-diiodobenzene, far IR single cryst. transmission spectrum, temp. and polaris. depends., assignments 8-72498
 1,2-diiodotetrafluoroethane, Raman and far IR spectra, conformation 8-78715
 dimethyl aniline, IR spectra, 250-4000 cm⁻¹, vibr. anal. 8-62797
 dimethyl phosphine-d₄, isolated CH stretching frequencies, bond strength, bond lengths 8-90167
 dimethyl sulphide-d₄, isolated CH stretching frequencies, bond strengths, bond lengths 8-90167
 1,2-dimethyldiborane, IR and Raman spectra of cis and trans isomers 8-86868
 dimethyldihalostannanes, cryst., IR spectra bandwidth, CH₃ group internal rot. 8-52490
 2,4-dinitrotoluene, laser optoacoustic absorpt. spectra of explosive vapours 8-76941
 1,3-disilacyclobutane, ring-puckering combination band spectra in SiH₂ stretching region 8-70836
 disordered solids, rel. between simple analytic models 8-76473
 epoxy, Stycast 1266, very low temp. thermal conductivity and optical props. 8-55992
 ethane, in air, IR spectra, optical-acoustic investig. (Russian) 8-74663
 ethane, spectral parameters, Lamb dip method investig. 8-89560
 ethanol, solns., local struct. equilib., light scatt. and IR spectra obs. 8-84564
 ethanol mols. reorientation in ethanol-water mixtures, Raman and Rayleigh spectra 8-76449
 ethyldifluoroborane, microwave, Raman, IR spectra, conform., dipole moments, vibr. assignment 8-90155
 ethylene, in air, IR spectra, optical-acoustic investig. (Russian) 8-74663
 ethylene, isotopically mixed, crystal, dilute guest probe orientational energy, IR, Raman spectra 8-68496
 ethylene, liq., far IR absorption spectrum, quadrupole induced dipole interaction 8-86857
 ethylene carbonate, Fermi reson., isotopic substitution meas. 8-86870
 ethylene glycol dinitrate, laser optoacoustic absorpt. spectra of explosive vapours 8-76941
 explosive vapours, laser optoacoustic absorpt. spectra 8-76941
 2-fluoro-5-bromotoluene, IR and Raman spectra 8-70830
 m-fluoroaniline, vap. (liq.), Raman and IR spectra, vibr. assignments 8-58699
 formaldehyde, Doppler-limited spectra of C-H stretching fundamentals 8-70831
 formaldehyde, low-temp. matrix photolysis, hydroxymethylene intermediate, IR obs. 8-76877
 formaldehyde-d₁, absorpt. spectra, 9-11 μ m, ν_5 and ν_6 fundamental bands 8-70827
 formamide, partly deuterated, in electrolytic soln., IR spectra, anion-solvent H-bonding 8-84558
 formyl fluoride (-d₁), IR absorption intensity anal. 8-70813
 Fourier transform spectroscopy appl., far IR 8-58069
 Freon-12, absorpt. coeffs. for CO₂ laser radiation, press. and temp. depend. 8-55170
 gelatin, fine struct., IR spectroscopic study of effects of impurities and other actions (Russian) 8-58083
 gelatin films with Fe, Cu, Ag and S containing compounds, IR spectra (Russian) 8-49928
 haloanilines, far IR spectra, vibr. assignments 8-82726
 hexafluorobenzene, polar tensors and at. effective charge, calculated from IR intensity 8-74703
 hydrocarbons, high-temp. absorptivity of 3.39 μ m laser line 8-86856
 imidazole, vibr. spectra, mol. crystal dynamics, librational modes 8-64356
 intensity prediction, at. polar tensor method, F containing mols. 8-62854
 intensity relation, IR to Raman intensity, matrix notation 8-62853
 1-iodo-2-methylpropane, IR spectra, vibrational anal., stretching bands 8-90168
 1-iodo-3-methylbutane, IR spectra, vibrational anal., stretching bands 8-90168
 iodomethane, liq. (liq. mixtures), vibr. relax. and reorientation, symmetric C-H bending mode 1st overtone 8-62884
 isoquinoline semiperchlorate, H-bonding, strong, stochastic model and IR spectra temp. effects 8-62805
 K-vitamins, IR absorpt. spectra, vibr. anal., quinonoid struct. 8-61139
 ketene, IR spectra, rot.-vibr. anal. of Coriolis coupled bands 8-86859
 liquid, barrier to internal rot., IR spectral linewidths meas. 8-72507
 manganese stearate Langmuir-Blodgett layers on Ag, IR surface EM wave prism spectroscopy 8-52587
 methane, absorpt. meas. in 3.3 μ m band, temp. depend. 8-90159
 methane, absorpt. of 3.39 μ m He-Ne laser line, 300-2400K 8-90166
 methane, and methane-d₄, rotational transition in condensed Xe, 6K, optical excitation 8-60494
 methane, fluid, collision-induced light scatt. 8-68509
 methane, in air, IR spectra, optical-acoustic investig. (Russian) 8-74663

infrared spectra of organic molecules and substances continued

- methane, in liq. SF₆, ν_3 band IR profile, temp. depend. 8-58696
 methane, IR intensities, C and H atomic polar tensors 8-50592
 methane, IR line intensities 8-58687
 methane, liq., optical const. meas. in IR, possible planetary cloud cover component 8-64341
 methane-d₁, 9613 Å band rot. anal. 8-86861
 methanol, H-bonded struct., IR spectra, assignments 8-62800
 methoxytrimethylsilane-d₉(-d₃) 8-86853
 methyl 2-bromopropionate, IR and Raman liq. phase spectra, rot. isomerism 8-58680
 methyl 2-chloropropionate, IR and Raman liq. phase spectra, rot. isomerism 8-58680
 methyl anilines, IR spectra, 250-4000 cm⁻¹, vibr. anal. 8-62797
 methyl bromide, ν_6 band, CO₂ and N₂O laser Stark spectroscopy 8-78698
 methyl bromide, rot. absorption spectrum of ν_3 and 2 ν_3 excited vibr. states, mol. const. determ. 8-82732
 methyl chloride, absorption strength of perturbed ν_4 band 8-70833
 methyl indoles, UV and IR absorpt. spectra, f-values and ground state vibr. freqs. 8-58716
 3-methyl 1-butanethiol, Raman and vibr. IR spectra of solid and liq., rot. isomerism 8-62810
 methyl mercapto acetate, Raman and vibr. IR spectra of solid and liq., rot. isomerism 8-62810
 methyl phosphine-d₂, isolated CH stretching frequencies, bond strength, bond lengths 8-90167
 methyl symmetric stretching vibr. bandwidths, vibr. and reorientational effects, IR and Raman spectra 8-78686
 methyl vinyl ether, and -d₃, IR and Raman spectra, vibr., torsion and internal rot. 8-94250
 5-methyl-uracil, IR absorpt. spectra, vibr. anal. 8-61143
 3-methylisquinoline, semipchlorate, H-bonding, strong, stochastic model and IR spectra temp. effects 8-62805
 molecular crystals, IR absorpt. spectra, intermol. reson. interaction, temp. depend. 8-72506
 molecular glass, density of states for IR active internal modes of tetrahedral mols. 8-75788
 monofluoromethane, force const. and IR intensities, ab initio SCF finite difference method 8-86783
 MX₂ type molecules, IR intensity anal., dipole moment 8-62806
 naphthalene radical anion, ethereal soln., far IR spectra 8-62796
 β-naphthol, IR dichroic ratio, oriented gas and effective charge models calcs. 8-60437
 naphthols, IR spectra, assignments 8-58681
 naphthalene-d₈, fluoresc. and absorpt. Shpolskii spectra (Russian) 8-90208
 nematic liq. crystal, dielectric anisotropy, IR spectra, effect of AC elec. field 8-64355
 nematic liquid crystals, IR absorption, strong positive dielec. anisotropy, elastic const. 8-75545
 nitroglycerine, laser optoacoustic absorpt. spectra of explosive vapours 8-76941
 o-nitrophenol, solvent effects on oscillator integrated strength, IR absorpt. bands 8-84575
 p-nitrotoluene, low-freq. vibr. spectrum, Raman and IR spectra 8-56484
 one-dimensional conductor, IR and Raman activity 8-60441
 organonitrogen derivatives of Si, Ge and Sn, prep. and props. 8-60456
 1,3,4-oxadiazole derivatives, in soln., IR absorpt. and fluoresc. spectra, vibr. anal. 8-66597
 oxalic acid, monomeric, IR matrix-isolation spectra, vibr. anal. 8-66550
 2-oxybicyclo(3.2.0)hept-6-ene, LF vib. spectra, conformations 8-58685
 PA-6, polymer fibre, orientation changes during stretching, IR spectra 8-75568
 PAN, spectroscopic analysis of electrically polarised films 8-68443
 n-paraffins, IR spectra, -180°C, two-phonon absorpt. bands 8-72495
 pentachloro aniline, far IR spectra, mol. crystal orientational dynamics 8-60428
 pentachloronitro benzene, far IR spectra, mol. crystal orientational dynamics 8-60428
 phenanthrene, vibr. spectra, mol. crystal dynamics, librational modes 8-64356
 phenylsilanetriol-d₉(-d₃), cryst. and liq. vibr., IR and Raman spectra 8-86855
 phosgene, spectrophone meas. at selected CO, CO₂ laser wavelengths 8-57310
 poly-β-benzyl-L-aspartate films, conformational stability, effect of organic solvents, IR spectra 8-70988
 polyacids, unsaturated carboxylic, in organic solvents, hydrogen bonding, structuration (Russian) 8-71666
 polyacrylonitrile, thermal degradation, Fourier transform IR obs. 8-92474
 polyatomic molecules, dil. solns., IR spectral band shapes of fundamentals 8-66544
 polycarbonate, glassy, IR dichroism at small strains 8-56475
 polyether-amidourethane, segmented, polymer domain struct., IR spectra and optical microscope (Russian) 8-51453
 polyethylene, IR spectra, -180°C, two-phonon absorpt. bands 8-72495
 polyethylene, melt crystallized, amorphous phase, IR spectrum 8-76463
 polyethylene, polarised Raman studies of crystalline and amorphous orientation 8-67660
 polyethylene, single crystals, chain end location, IR spectra 8-71687
 polyethylene terephthalate, isotropic and oriented, refr. index meas. 40 to 300 cm⁻¹ 8-52482
 polyethylene terephthalate fabric, surface struct., props. rel. to plasma surface treatment 8-95831
 polymer film, supermolecular structure and mech. stress distrib. among chem. bonds 8-75562
 polymer orientation measurement, in solid, by spectroscopic techniques, mech. anisotropy 8-75558
 polymethylene chain, vibr. spectra, CH stretching region, struct. and assignments 8-70991
 polyperdeuteroethylene, IR and Raman spectra, 77K and room temp., vibr. anal. 8-72517

infrared spectra of organic molecules and substances continued

- polyurethanes under tension loads, spectral exam. (Ukrainian) 8-92058
 polyvinyl formate, far IR molecular vibrational spectroscopy by inelastic electron tunnelling 8-50546
 polyvinylidene fluoride film, cryst. dipole orientation in elec. field 8-80286
 porphin-d_n (n=2-14) electronic-vibr. interaction, quasi-line absorption (fluoresc.), mirror symmetry 8-55197
 potassium formate, IR absorpt. spectra, sampling effects, Davydov splitting and struct. 8-52508
 potassium hydrogen malonate single cryst., IR and Raman spectra 8-60444
 PTE, polymer fibre, orientation changes during stretching, IR spectra 8-75568
 purple membrane of halophil cells, homogeneity based on IR spectra 8-69003
 PVC:Fe(Cu) film, struct. and optical props., soln. growth technique 8-51837
 pyridine, IR spectra, adsorpt. on Zr(HPO₄)₂, acidity 8-92377
 pyridine-Ag₃I₄, superionic conductor, dynamical aspects 8-79695
 ring compounds, three-membered, vibr. spectra and struct., book control 8-78701
 saccharose, far IR absorpt. spectra, pyroelec. coeff. temp. depend. (French) 8-72503
 saccharose, far IR absorption, low temp. pyroelectricity 8-80348
 semitetrafluoroborates, H-bonding, strong, stochastic model and IR spectra temp. effects 8-62805
 solution, mol. vibr. spectral linewidth, conc. fluctuations effect 8-70880
 squaric acid and deuterated derivative, vibrational study, IR and Raman spectra 8-92076
 steel, rusted, exam. of tannin treatment action mode 8-88564
 strong H bonded systems, vibr., Raman, IR spectra, biology appls. 8-82735
 symmetric top mols., gas phase IR rot. velocity correl. functions, appls. to CH₃F, CHF₃ (French) 8-62778
 1,2,4,5-tetrabromobenzene, lattice vibr., Raman and far IR spectra 8-76444
 tetrachloro-p-benzoquinone, IR and Raman spectra of phase transition (French) 8-60445
 tetrafluoromethane, ν_4 fundamental of three isotopic species 8-70835
 tetrafluoromethane, pot. const., IR spectra 8-82808
 tetrafluoromethane, spherical top mol. vibr.-rot. spectrum with tunable diode laser 8-82734
 tetramethylammonium cation(-d₁₂) aqueous solution, Raman and IR spectra 8-82741
 tetramethylammonium hexachloroplatinate, order-disorder phase transition, IR and Raman spectra 8-92060
 TGS-d, TGS-e, single cryst. films, epitaxial growth method, IR transmission spectra (French) 8-72742
 thiosemicarbazide, mol. cryst., transition moment directions 8-64351
 thiourea, order-disorder transitions, soft modes 8-80361
 thiourea, soft mode and Debye relaxations 8-80347
 tribenzo [12] annulene, monovalent anion, MCD and absorpt. spectra 8-70859
 trimethyl phosphine-d₃, isolated CH stretching frequencies, bond strengths, bond lengths 8-90167
 trimethylsilyl azide, vibr. spectra, normal mode assignment 8-86867
 trimethylsilyl isocyanate, vibr. spectra, normal mode assignment 8-86867
 trimethylsilyl isothiocyanate 8-86867
 trimethoxybenzenes, liq. and solid, IR and Raman spectra, vibr. assignments 8-58701
 (TTT)₂I₃, optical, spin-reson., magnetoresist. study, nature of ground state 8-68023
 vanadyl phthalocyanine, sublimed layer, IR absorption, vibr. assignments 8-55174
 vinyl acetate, monomer and polymer, Raman and IR spectra, liq. and solid 8-58700
 vinylsilanetriol-d₉(-d₃), soln., vibr., IR and Raman spectra 8-86854
 water, H-bonded struct., IR spectra, assignments 8-62800
 BeF₂, aq. glass, 76K, solvated electron spectrum evolution, following ns radiolysis 8-88295
 CF₂, absolute IR intensity of fundamental vibrs. 8-58743
 CF₂, in Ar matrix, conc. determ. by intensity calcs. 8-68941
 CF₃, absolute IR intensity of fundamental vibrs. 8-58743
 CF₃, in Ar matrix, conc. determ. by intensity calcs. 8-68941
 CF₃⁺ cations, IR spectra in Ar matrix 8-74710
 CF₂Cl⁺, and parent cations, IR spectra in matrix radiolysis and photoionis. of Freons 8-80767
 CF₂Cl₂⁺, CF₂Cl⁺, IR spectra, in matrix radiolysis and photoionis. of Freons 8-80767
 CF₃X⁺ cations, (X=Cl, Br, I, H), IR spectra in Ar matrix 8-74710
 CF₃X⁺ cations, (X=Cl, Br, I, H), IR spectra in Ar matrix 8-74710
 CNC radical vibr. and electronic spectra, in VUV photolysis of matrix-isolated cyanomethane 8-85180
 H bond dynamics in soln. 8-84573
 H-bonded complexes, OH stretching vibr. band, temp. effect 8-90158
 H-bonded crystal, IR absorpt. spectra band shape, X-H stretching vibr. temp. depend., isotope effect 8-76445
 HCl-dimethylether complex, gaseous, H-bond IR spectra, temp. depend. theory 8-62804
 HCl-X, matrix isolation vibr. spectroscopy, complex form. studies 8-62952
 NO₂+ROO→ROONO₂, (R=C_nH_{2n+1}), Fourier transform IR spectroscopic meas. 8-53194
 Na-chlorofluoromethane, matrix radiolysis, photoionis., IR spectra of CF₂Cl⁺ and parent cations 8-80767
 Si₂O(Cl₂)₂, IR and Raman spectra, vibr. anal. 8-66552
 TCNQ salts, C₂(TCNQ)₃, quasi-one-dimens., IR spectra, electron-vibr. interaction 8-88309
 U complex, binding, by brown coal, from seawater, IR spectroscopic obs. 8-82855
 UO₂ complexes, cubic crystals., low temp. optical spectra (Russian) 8-92083

infrared spectra of polyatomic inorganic molecules

- alkali halides, IR absorpt. in molecules, clusters and microcrystals 8-80363
¹³C¹⁶O₂, ν_3 band, absorpt. spectrum 8-58693

infrared spectra of polyatomic inorganic molecules continued

conformers, dynamic interaction between ground states, effect on IR spectra 8-58767
 intensity prediction, at. polar tensor method, F containing mols. 8-62854
 intensity relation, IR to Raman intensity, matrix notation 8-62853
 metal surface, adsorbed molecule, IR spectra exam. by surface EM wave spectroscopy 8-71967
 (MX)_n (MX₂)_n ionic clusters, struct. and vibr. freqs. calcs. 8-94348
 MX₂ type molecules, IR intensity anal., dipole moment 8-62806
 polyatomic molecules, dil. solns., IR spectral band shapes of fundamentals 8-66544
 silane, coupling agent on E-glass fibre, structure, Fourier transform infrared spectroscopy 8-60643
 silane, coupling agent on porous silica, Fourier transform infrared spectroscopy 8-60642
 strong H bonded systems, vibr., Raman, IR spectra, biology appls. 8-82735
 transition metal complex anion, vibr. spectra in solid and soln., struct. and fundamental mode assignment 8-62803
 trifluoromethane, photodissoc., obs. of NO (v=1) 8-74712
 water, and isotropic forms, IR band intensities estimation 8-86916
 water vapour, atmospheric, IR continuum absorpt. calc. (Russian) 8-96293
 AlCl₃, soln., IR spectra 8-74649
 Al(OH)₃, soln., IR spectra 8-74649
 Ar-HCl, Van der Waals mol., far IR spectrum, anisotropic intermol. force effects 8-62869
 As₄O₆, IR and Raman spectra vibr. spectra, valence force field calc., pot. function (French) 8-50549
 BrONO₂, stratospheric photolysis, UV and IR spectra 8-53227
 CCN radical in solid Ar, emission and excitation spectra 8-70868
 CO₂, 10.6, 9.4 μm laser bands high-press. absorpt.-spectra 8-66543
 CO₂, 30¹₁-00⁰ band, meas. at different temps. of absolute intensities, line half-widths and broadening by Ar and N₂ 8-86865
 CO₂, 30¹₁-00⁰ and 30¹₁-00⁰ bands, absolute intensity meas. at different temps. 8-86864
 CO₂ atmospheric line freqs. in 4.3 μ region 8-88910
 CO₂, dispersive Fourier transform spectrometry using modular interferometer 8-89567
 CO₂, electron excitation-relax., time resolved Fourier spectra 8-58070
 CO₂, IR band nonrigid rot. absorption 8-91060
 CO₂, IR energy levels and line intensities 8-85691
 CO₂, press. broadening coeffs. at 4.2 μm, rot. quantum number 8-74704
 CO₂, transition calibration, rotational constants, absorption spectrum, 4.82-μm region 8-58868
 CO₂, transition moment of IR band near 7740 cm⁻¹ 8-90224
 CO₂, transition moment of IR band near 7740 cm⁻¹ 8-90225
 CO₂ vibr. luminesc., excited by DC discharge, rot. and vibr. mol. consts. 8-58867
¹²C¹⁶O₂, absorpt. spectrum at 4.3 microns 8-58692
¹³C¹⁶O₂, v₃ fundamental at 4.4 μm 8-86862
 CO₂+Ar(N₂), 301₁-000 band, intensities, press.- and self-broadening coeffs. meas. 8-78695
 C₃O₂, far IR and Raman spectra, vibr. mode and quasilinear config. 8-62940
 CS₂, v₃ band, dipole moment correl. function, isotope splitting and band contour 8-74650
 CS₂, vibr.-rot. bands at .46 μm, isotope effects 8-94245
 CS₂+He(Ar)(N₂), perturbed rot. diffusion of CS₂, IR spectra 8-75245
 CdFCl, CdFBr, existence and vibr. characterisation, IR and Raman matrix isolation obs. 8-78706
 CdFe(CO)₄, IR and Raman spectra, vibr. anal. 8-66553
 CdX₂, CdXY, (X,Y=Cl,Br,I), matrix isolated, far IR spectra, thermodynamic props. 8-86869
 ClONO₂+NO(ClNO) react., gas phase, kinetics, mechanism, IR photometric investig. (German) 8-76834
 CoSO₄.H₂O, IR spectra, H₂O external modes temp. depend. 8-58683
 Cs₂ReF₆, absorpt. spectra, splitting of I_g(⁴A_{2g}) ground state 8-74658
 Cs₂SO₄ molecules isolated in inert gas matrices, low freq. IR spectra 8-50547
 DCN, self-assoc. in matrices, IR vibr. spectra of multimers 8-86858
 D₂O, heterodyne meas. of IR absorpt. freqs. 8-55175
 D₂O, IR spectra, v₂+v₃ band shape 8-62855
 D₂SiNCs, low freq. bending mode, pot. function 8-82728
 D₂SiNCs, IR and Raman spectra, vibr. anal., LF bending mode 8-70842
 ErCl₃(AlCl₃)_x, vap. complexes, absorpt. spectra, 6000-44000 cm⁻¹, relax. props. 8-62799
 FCN+N₂, rot. spectra and geom. struct. of FCN 8-82725
 Fe complex, Fe (III) acetylacetonate, solvent effects on oscillator integrated strength, IR absorpt. bands 8-84575
 Fe(CO)₅, IR spectra and laser photochem., matrix isolated at 20K 8-74651
 FeCl₄⁻, effective charge, from IR and Raman scatt. intensity obs. 8-62809
 FeOOH, H-bonding, strong, stochastic model and IR spectra temp. effects 8-62805
 GeH₄, v₃ fundamental, Jovian atm. absorpt. profile, computer simulation 8-81584
 GeH₄, v₃ fundamental, theoretical absolute J-manifold intensities 8-74707
 HBr, far IR Ar matrix isolated spectra, 4.2K, press. and conc. effects 8-62801
 HCN, self-assoc., matrix isolation vibr. spectroscopy, complex form. studies 8-62952
 HCN, self-assoc. in matrices, IR vibr. spectra of multimers 8-86858
 HCl, far IR Ar matrix isolated spectra, 4.2K, press. and conc. effects 8-62801
 HCl-X, matrix isolation vibr. spectroscopy, complex form. studies 8-62952
 HClF, neutral free radicals, in Ar matrix, IR spectrosc. evidence 8-66546
 HF₂, neutral free radicals, in Ar matrix, IR spectrosc. evidence 8-66546
 HF₂⁻, matrix isolated, IR spectra and struct. 8-74655
 HNO₃, aq. soln., H bonds, IR spectra 8-94243
 HNO₃, vibr.-rot. spectrum, 855-915 cm⁻¹ (French) 8-50543
 H₂O, adsorbed in monolayer hydrate of halloysite, NMR obs. of mol. motion 8-95226

infrared spectra of polyatomic inorganic molecules continued

H₂O, computation of absorpt. near 4250 cm⁻¹ 8-82729
 H₂O, continuum IR absorpt. near 1200 cm⁻¹, temp. depend. 8-85687
 H₂O, dispersive Fourier transform spectrometry using modular interferometer 8-89567
 H₂O, IR continuum absorpt. due to librational mode of dimer 8-66542
 H₂O, IR spectrum, rot. anal., isotope effects 8-78694
 H₂O isotopes, spectrophone meas. at selected CO, CO₂ laser wavelengths 8-57310
 H₂O, linewidths and press. shifts, in N₂ and air, Anderson theory and quantum many-body theory 8-74708
 H₂O, v₁+v₂ combination band, evolution with temp. 8-66548
 H₂O vapour, absorption at 1 to 8 μm, rel. to atm. spectra 8-81402
 H₂¹⁷O, H₂¹⁸O, Stark spectra with CO laser, Lamb dip spectra of v₂ band 8-62840
 H₂¹⁸O, line positions and intensities, v₁+v₂ and v₂+v₃ bands 8-74656
 HOI, O₃(O₂)+HI matrix reaction, IR spectra, isotope shifts and band assignments 8-80737
 H₂S, absorbed on zeolites with varied Si/Al ratios 8-60029
 H₂SO₄, dissociation and absorpt. consts., ultrahigh resolution obs. of 8.2, 11.3 μm bands 8-70825
 HSiCl₃(DSiCl₃), Raman and IR spectra, mol. motion 8-64353
 H₂SiNCs, low freq. bending mode, pot. function 8-82728
 H₂SiNCs, IR and Raman spectra, vibr. anal., LF bending mode 8-70842
 HgFCl, HgFBr, HgFI, existence and vibr. characterisation, IR and Raman matrix isolation obs. 8-78706
 HgFe(CO)₄, IR and Raman spectra, vibr. anal. 8-66553
 K₂SO₄ molecules isolated in inert gas matrices, low freq. IR spectra 8-50547
 MgO₂(O₃), from Mg+O₃ matrix reaction, IR spectra, isotope shifts and blue matrix shift 8-80736
 MnSO₄.H₂O, IR spectra, H₂O external modes temp. depend. 8-58683
 NH₃, 10.6 μm region absorption lines, diode laser meas. 8-58689
 NH₃, 9.5 μm region diode laser spectra 8-58688
 NH₃, laser saturation time-delayed IR spectroscopy 8-86976
 NH₃, saturated absorpt. at 888 cm⁻¹ using tunable diode laser 8-94239
 N₂H₂(N₂D₂), ground and first excited state small vibr. coupling, ab initio CI calc. 8-62791
 NO₂, 8920 Å band temp. depend., location of 000-000 band of A²B₂-X²A₁ transition 8-70826
¹⁴N¹⁶O₂, v₁ band, high resolution IR spectra 8-55173
¹⁴N¹⁶O₂, v₁+v₃ band, IR absorpt. spectra 8-78693
 N₂O, IR band nonrigid rot. absorption 8-91060
 N₂O, IR bands, parametric deconvolution method 8-78697
 N₂O, in soln., Raman and IR v₁ and v₂ band shapes, mol. motion dynamics 8-64352
 N₂O, multiple reflection cell, laser spectroscopic meas. 8-86359
 NSF₃, IR spectra, matrix isolated, force const. calc. 8-62802
¹⁵NH₃, spectral parameters, Lamb dip method investig. 8-89560
 NiSO₄.H₂O, IR spectra, H₂O external modes temp. depend. 8-58683
 O₃, microwave and IR spectra, v₂ state, (v₃+v₂)-v₂ band, 10 micron lines 8-82718
 O₃ stratospheric 10 μ absorption line obs. with IR heterodyne spectrometer 8-61494
 OCS, IR spectral moments and mean squared torques, rare gas effects 8-62944
 O₂F(Cl)(Br) radicals, matrix IR spectra, bonding 8-90160
 ON¹⁹Br, anharmonic force field from IR and microwave data 8-82809
 ONCN, far IR spectra, pure rot. and vibr.-rot. bands 8-82731
 ON³⁵Cl, anharmonic force field from IR and microwave data 8-82809
 O₂O₂, 3v₁+v₂←2v₁ 4v₁+v₂←3v₁ Q-branches, diode laser analysis 8-74660
 OsO₄, and isotopic forms, stretching fundamental, 961 cm⁻¹, high resolution spectroscopy 8-90162
 OsO₄, tunable diode laser spectrosc. obs. 8-82061
 (PF₂)₂O, IR and Raman spectra, vibr. assignment 8-50544
 P₂O₆, IR and Raman spectra vibr. spectra, valence force field calc., pot. function (French) 8-50549
 PtCl₄⁻, effective charge, from IR and Raman scatt. intensity obs. 8-62809
 PuN₂, in Ar matrix, IR spectra, stretching freq. and isotope shifts 8-78690
 PuO₂, in Ar and Kr matrices, IR absorption spectra, normal coord. anal., assignments, force consts. 8-78681
 Rb₂SO₄ molecules isolated in inert gas matrices, low freq. IR spectra 8-50547
 S₇, Raman and IR spectra, vibr. anal., force consts., thermodynamic functions 8-50545
³²SF₂, ³⁴SF₂, matrix IR spectra, vibr. and force fields, bond angle (German) 8-74662
 SF₆, 10.5 μm spectrum, high-J assignments, identification of levels pumped by CO₂ P(12) and P(22) 8-70837
 SF₆, 3v₃ band anal., IR spectra 8-90161
 SF₆, emission spectrum of v₃ band, 1780K, dissociation effects 8-62795
 SF₆, IR laser isotopic enrichment in low temp. matrices 8-90318
 SF₆, IR spectra, v₄ vibr. band strength 8-94240
 SF₆, multiple reflection cell, laser spectroscopic meas. 8-86359
 SF₆, v₃ band, IR spectra, in supersonic mol. beam 8-66541
 SF₆, v₃ manifold, 3v₃ transition, 3-quantum transition probabilities, IR spectrum 8-86866
 SF₆, spectral parameters, Lamb dip method investig. 8-89560
 SF₆, spherical top mol. vibr.-rot. spectrum with tunable diode laser 8-82734
 SF₆, tunable diode laser spectrosc. obs. 8-82061
 SF₆, vibr. anharmonicity consts., v₄ region laser absorption obs. 8-94242
 S₂F₁₀, IR laser irradi., absorpt., reaction parameters 8-94241
 S₂N₄, solid and soln., IR and Raman spectra, vibr. assignment 8-74659
 S₂N₄Cl₂, solid and soln., IR and Raman spectra, vibr. assignment 8-74659
 S₂N₄H₄, and -d₄, solid and soln., IR and Raman spectra, vibr. assignment 8-74659
 SO₂, IR bands, emissivity, line shape and band model parameters 8-94246
 SPF₃, IR spectra, matrix isolated, force const. calc. 8-62802
 SSiCl₂, IR spectra, prod. in S₂Cl₂ photolysis 8-61033
 SnF₄, IR spectra of solid and gas, rel. to struct. (French) 8-78692

infrared spectra of polyatomic inorganic molecules continued

- Sb₂O₃, IR and Raman spectra vibr. spectra, valence force field calc., pot. function (*French*) 8-50549
 (SiCl₃)₂O, IR matrix isolation spectrum, Raman spectrum 8-82730
 Sm complex, mono-, di-, tri-glycolate, IR absorpt. spectra, vibr. freq. and co-ordination number 8-58684
 TiCl₄, IR absorpt. bands, absolute integrated intensities, obs. and calc. 8-78689
 U(BH₄)₄, IR and UV spectra of gas phase 8-62798
 UF₆, ν₃ manifold 3-quantum transition probabilities, spectral assignment 8-58648
 WO₃, IR spectra, normal coord. anal. 8-58682
 ZnFCl, existence and vibr. characterisation, IR and Raman matrix isolation obs. 8-78706
 ZnX₂, ZnXY, X and Y=halogen, matrix isolation IR and Raman spectra 8-55171

infrared telescopes *see telescopes***infrared transmitters** *see infrared sources***infrasonic waves** *see acoustic waves***initial value problems**

- α²-dynamios, finite amplitude, with large scale in compressible circulation, theory 8-81534
 artificial satellite motion, orbitally stable multistep methods 8-85834
 classical elastodynamics as linear symm. hyperbolic system, differentiability of solns. 8-57783
 Einstein-Cartan theory of gravitation, generalized 8-73895
 flames, premixed, laminar, time-depend. soln. determ. 8-67282
 flow depend. expansion process, initial value problem, two step difference method (*German*) 8-57877
 forced oscillations in rotating stratified liquid, initial value problem 8-63478
 gravity waves, created against vertical cliff, uniform asymptotic soln. 8-67210
 inertial waves and an initial-value problem for a thin spherical rotating fluid shell 8-55656
 Langmuir soliton formation with ion-acoustic density emission 8-75328
 line thermal numerical model, initial conditions influence 8-92932
 Navier-Stokes eqns., steady flow prod. by rot. disc, series soln., integral method 8-71308
 neural system model, excitation propagation 8-96044
 nonlinear reaction-diffusion models for interacting populations 8-65886
 null gravitodynamics, initial value problem and Dirac-bracket relations 8-77781
 numerical weather prediction, initialization with data assimilation method 8-57282
 Roberts, min. degree algorithm appl. 8-89311
 singular perturbations for initial value problems, hyperbolic nonlinear partial differential eqns. 8-58111
 thrown string problem 8-89331
 unconstrained variational statements 8-93518

injection lasers *see semiconductor junction lasers***injury by radiation** *see biological effects of radiation***inorganic insulators** *see insulating materials***inorganic molecule configurations***see also isomerism*

- AB₃, non-transition element complexes, shapes and other props. 8-82648
 AB₃, non-transition element complexes, shapes and other props. 8-86790
 AB₆, non-transition element complexes, shapes and other props. 8-82647
 alkali halide molecular clusters, equilib. geom., form. energy and vib. spectrum 8-55269
 chalcogen and pseudochalcogen mols., stereochem. using nonrigid mol. model 8-62788
 chloramine, HOCl, isoelectronic mols., vap. phase UV photoelectron spectra, struct. 8-66600
 diatomic molecules, equilibrium parameters and Morse anharmonic const., electron diff. determ. 8-58818
 homonuclear diatomics, equilib. geometries, Gaussian-based model pot. calcs. 8-94183
 MX₄ mole cules, distortion from T_d symm. appl. to PO₄, SO₄, AlCl₄ 8-63706
 MX₄ molecules, distortion from T_d symm. kernel, co-kernel and averaged configs. 8-63705
 (MX)_n, (MX₂)_n ionic clusters, struct. and vibr. freqs. calcs. 8-94348
 second-row molecular orbital calcs., INDO calc. for Na to Cl 8-82643
 1,2,5-selenadiazole, partially oriented in mesophase, r₂ struct. PMR obs. 8-58719
 transition metal complex anion, vibr. spectra in solid and soln., struct. and fundamental mode assignment 8-62803
 (AgCl)₃, photoelectron spectrum and valence shell struct. 8-62843
 Ar₂F, electronic states, ab initio POL CI calcs. 8-66474
 AsH₃, forbidden millimetre-wave transitions 8-55165
 BF₃OH, transient mol. form., microwave spectroscopic obs. 8-74643
 B₂H₆, mol., static electron densities 8-79552
 BH(OH)₂, transient mol. form., microwave spectroscopic obs. 8-74643
 CO₂, anomalous energy minima surfaces 8-86791
 CO₂ H⁺, geom. struct., ab initio mol. orbital study 8-62939
 C₂O₂, far IR and Raman spectra, vibr. mode and quasilinear config. 8-62940
 Cd complex, (Cd[SC(CH₃)₂CH₂NH₂]₂CdCl₂)₂·2H₂O cryst. and mol. struct. 8-74787
 CdFe(CO)₄, IR and Raman spectra, vibr. anal. 8-66553
 ClHCl⁺, deuteron quadrupole coupling const., nuclear mag. shielding, geometry depend. 8-58586
 Co complex, bisdimethylglyoxime (thiosemicarbazide)-cobalt (III) nitrate, mol. and cryst. struct. of dihydrate 8-83803
 Cu²⁺ complex, in water-ethanol soln., struct., EPR 8-50565
 CuAl₂Cl₆, Raman resonance spectra of vapour 8-94251
 (CuBr)₃, photoelectron spectrum and valence shell struct. 8-62843
 (CuCl)₃, photoelectron spectrum and valence shell struct. 8-62843
 (CuI)₃, photoelectron spectrum and valence shell struct. 8-62843
 Eu compounds tetrahedral, ligand struct., rel. to luminesc. spectra satellite intensity (*Russian*) 8-72603
 FCN+N₂, rot. spectra and geom. struct. of FCN 8-82725
 inorganic molecule configurations continued
 F₂CS, pot. surfaces, X¹A₁, a³A₂ and a³A₂(b₁) states, ab initio SCF calcs. 8-86795
 FHCli⁺, deuteron quadrupole coupling const., nuclear mag. shielding, geometry depend. 8-58586
 FHF⁺, deuteron quadrupole coupling const., nuclear mag. shielding, geometry depend. 8-58586
 F₂O₂, geometry, SCF CI calcs. 8-55126
 Fe(CO)₅, microwave dielec. relax., fluxional mechanism 8-94235
 Ge₂H₆, valence electronic struct., model pot. in floating spherical GO formalism 8-74563
 H₃⁺ expt. determ. struct. 8-74752
 H₄⁺, ground and excited state pot. energy surfaces and geom. struct., SCF and CI calcs. 8-78769
 H₃⁺ (n=3,5,7,9,11), stability, struct., ab initio MO calcs. 8-74810
 HCN, dipole moment derivative, sign anomaly, CGTO ab initio calc. 8-74795
 HCN, HNC, electronic reorganisation, with core ionisation 8-94196
 HCN, HNC, molecular electronic struct., unlinked cluster effects 8-94185
 HCN, nuclear quadrupole coupling and mol. deformations 8-90191
 HCO₂⁺, geom. struct., ab initio mol. orbital study 8-62939
 HCl, nuclear quadrupole coupling and mol. deformations 8-90191
 HNC (DNC), anharmonic force field, equilib. struct., rot. const. and bond lengths 8-90147
 HNO, HON, electronic reorganisation, with core ionisation 8-94196
 HNO₂, and protonated forms, electrostatic pot. predictions, basis set depend. 8-74786
 (HNO₃)₂, gas phase, H-bonded complex struct. from elec. dipole moment obs. 8-74791
 HO₂⁺, ab initio calc. of three lowest states 8-62711
 H₂O, electron affinity, mol. geom. effects calcs. 8-82618
 H₂O, electronic ground state, SCF HF and CI calcs, pot. energy hypersurface, spectroscopic const. 8-50473
 H₂O, geometry, SCF and CI calcs., basis set effects 8-62715
 H₂O, liq. surface, spreading vel., rel. to mol. struct. (*German*) 8-95209
 H₂O⁻, electron affinity, mol. geom. effects calcs. 8-82618
 H₂O₂, geometry, internal rot. barriers, electron correl. calcs. 8-70751
 HOCl, photodissoc., ab initio SCF CI calcs. 8-50604
 H₂O·2H₂O, in 2,5-dichlorobenzenesulphonic acid trihydrate, neutron diff. obs. 8-58855
 HPO, mol. struct. and props., ab initio, calc., Gaussian lobe orbital 8-62713
 HS₂, ground and first excited states, geometry, ab initio SCF calcs. 8-50657
 HSO, ground and first excited states, geometry, ab initio SCF calcs. 8-50657
 H₂SiNCS, far IR and Raman spectra, vibr. mode and quasilinear config. 8-62940
 HfBr₄(HfI₄), struct., force field and Coriolis const. calcs. 8-86843
 HgFe(CO)₄, IR and Raman spectra, vibr. anal. 8-66553
 I₂, equilibrium parameters and Morse anharmonic const., electron diff. determ. 8-58818
 I₃⁻, geom. and electronic struct., effective pot. calc. 8-74788
 I₅⁻, geom. and electronic struct., effective pot. calc. 8-74788
 ICN, microwave spectrum, vibr.-rot. const., equilib. struct. 8-58677
 IrF₆, in mixed crystals, Jahn-Teller effect, Γ_{8g}(t_{2g})³ state, 6800 Å 8-76032
 KrF, electronic states, ab initio POL CI calcs. 8-66474
 Li₃, geom. struct. and binding energy, diatomic-in-molecules 8-74785
 Li₄, geom. struct. and binding energy, diatomic-in-molecules 8-74785
 LiBH₄, pot. surface and geometry, ab initio calcs. 8-86771
 LiF oligomers, struct., stability SCF and CEPA-PNO calcs. 8-78640
 LiH oligomers, struct., stability SCF and CEPA-PNO calcs. 8-78640
 LiH₂O⁺, geom., electronic struct. FSGO model calcs. 8-82614
 LiN₂, geom., electronic struct. FSGO model calcs. 8-82614
 LiNC, metal atom motion, WKB calcs. 8-82623
 LiNC, struct. vibr. states and pot. energy calcs. 8-86776
 LiNH₂⁺, geom., electronic struct. FSGO model calcs. 8-82614
 MgF₂, ground state, nonempirical LCAO SCF calcs. 8-66469
 NH₂, geometry, SCF and CI calcs., basis set effects 8-62715
 NH₄⁺, nuclear quadrupole coupling and mol. deformations 8-90191
 NH₄I, (NH₄)_{0.16}K_{0.84}I and (NH₄)_{0.16}K_{0.84}Br, reorientation motion of NH₄⁺ 8-79542
 NO, biradicals, conform., spin probe appls. 8-86895
 NOCN, struct., dipole moment, quadrupole coupling, microwave spectra 8-94238
 Na₃, electronic struct., pot. energy surface, ab initio CI study 8-70996
 NaF oligomers, struct., stability SCF and CEPA-PNO calcs. 8-78640
 NaH oligomers, struct., stability SCF and CEPA-PNO calcs. 8-78640
 PdAl₂Cl₆, Raman resonance spectra of vapour 8-94251
 Pt(SeC(NH₂)₂)₄Cl₂, crystal and mol. struct. 8-59794
 S₂^x, x=2-, 0, 2+, struct. differences explained, SCF Xα scatt. wave MO calcs. 8-74784
 SN, struct., vibr. spectra, ab initio calcs. 8-66475
 SN⁺, struct., vibr. spectra, ab initio calcs. 8-66475
 S₂N₂, struct., vibr. spectra, ab initio calcs. 8-66475
 SOH, ground and first excited states, geometry, ab initio SCF calcs. 8-50657
 SbF₃, IR spectra of solid and gas, rel. to struct. (*French*) 8-78692
 Si₂H₄, ab initio GO calc., geom. optimisation 8-94187
 Si₂H₆, valence electronic struct., model pot. in floating spherical GO formalism 8-74563
 (SiH₃)₂O, and d₆, Raman spectra, vibr. mode and config. 8-62940
 SiO₂, mol., ab initio SCF calcs., ground state stability, struct., vibr. freqs. 8-86781
 Sr[Fe(CN)₅NO]·2H₂O, cryst. and mol. struct. 8-91311
 TeF₆, gas phase electron diff. patterns, mol. struct., three-at. scatt. 8-66662
 TiBr₄, (TiI₄), struct., force field and Coriolis const. calcs. 8-86843
 V(CN)₅NO⁺, struct., FSGO calcs. 8-70736
 V(CN)₆NO⁴⁻, struct., FSGO calcs. 8-70736
 X₂H⁺, X=Li, Na, K, equilib. geom. and dissoc. energy, pseudopot. calc. 8-94329
 X₂Y⁺, X,Y=Li, Na, K, equilib. geom. and dissoc. energy, pseudopot. calc. 8-94329
 ZrBr₄(ZrI₄), struct., force field and Coriolis const. calcs. 8-86843

inorganic molecule electronic structure *see molecular electronic states*

insolubility *see solubility*

inspection

see also quality control; reliability; testing

acoustic ranger for tube and pipe inspection 8-85092

automated US units for inspecting thin walled tubing 8-88606

automatic US inspection of heated objects by SGK-2Ts system 8-95894

BWR power plant, routine checks and radiation protection 8-74462

cold rolling rolls, magnetic inspection at heat treatment quality 8-88613

cold strip surface, flaw inspection with optoelectronic equipment 8-60967

defibrillators, review of instruments and maintenance 8-69251

dielectric material, electro-optical inspection of internal defects 8-56869

dielectric tube, electrospark inspection unit for defect obs. 8-92431

eddy current inspection, possibilities of phase generator circuits 8-88614

eddy current inspection of fastener holes, computer automation, exam. 8-53040

eddy current transducer part geometry effect on inspection 8-53078

electromagnetic NDT, digital method of edge effect suppression 8-56866

equipment, circuit for selecting signals in specified phase range 8-56863

failed steam accumulator anal., role of metallography and NDT 8-95877

ferromagnetic material, electromagnetic props. inspection by electromag-

netic transducer with frequency output singal 8-53131

ferromagnetic material, inspection by method of two harmonics 8-88608

ferromagnetic probe inspection unit for automatic inspection of welded

tubing 8-56860

ferromagnetic probe unit, MD-10F, automatic 8-56861

fracture toughness testing, acoustic emission, inspection technique 8-68860

friction material, US inspection 8-60931

gas turbine sand casting, US inspection 8-88594

glued members, low frequency acoustic flaw detector inspection 8-60954

high-temperature contactless testing by EM acoustics 8-85095

hot-rolled rods, surface defect detection without scale removal by NDT 8-95890

induction inspection unit with spaced windings, increasing sensitivity

over magnetising and measuring length 8-56864

large-scale angle inspection unit 8-77864

magnetic induction defectoscope with adjustment 8-53105

magnetizing flaw detection system for underground pipeline inspection 8-53103

measurement facility inspection, confidence and productivity improve-

ment 8-77840

measuring instrument inspection, optimal error correction signal 8-77829

metrology use in material inspection 8-95899

microinterferometer transducer, air-bearing, for use with universal

inspection machines 8-57899

multichannel US inspection unit, indicator of working order of elec-

tronic-acoustic circuits 8-92425

multilayer product, theory of laid-on shielded transducers for inspec-

tion 8-88610

multivariate inspection methods, theory 8-88609

nuclear fuel, inspection by neutron radiography, review 8-60890

nuclear fuel element assembly, X-ray technique appl. 8-72940

nuclear reactor pressure vessels, remote controlled US pre-service and

in-service inspections 8-89955

periodic inspection of meas. facilities, probabilistic confidence charac-

teristic selection 8-77839

piezoelectric transducer with oblique bottom immersion chamber inspec-

tion of plane parallel objects 8-53111

pressure vessels weld quality assessment, NDT methods and equipment 8-56871

radiographic inspection of welded joints, effectiveness investigation 8-56872

recording system, for automatic US flaw detection system 8-76815

reinforced plastics, low frequency acoustic flaw detector inspection 8-60954

specimen with varying thickness for US inspection 8-53137

stamped disc surface inspection by automated eddy current unit 8-92430

steel, castings for use at high temp., correlation between US and radio-

graphic inspection (German) 8-88599

steel, heat treated, electromagnetic device for quality inspection 8-53104

steel, hot, US inspection 8-88586

steel, low alloy and C, hardened and tempered parts, nondestructive

magnetic inspection 8-95889

steel, round bar inspection, EM-acoustic techniques 8-60973

steel, stainless, US methods for intergranular corrosion inspection 8-95898

thermal inspection of plates with internal defects, one and two sided,

heat transfer intensity effect 8-88616

thermal methods and apparatus for NDT of weld joints 8-88615

thin walled bearing races eddy current inspection of hardening and

tempering quality 8-95892

tube inspection, magnetic leakage flux method 8-95891

tubing, ferromagnetic probe coercive force meter, different heads 8-60943

US, nomogram for determ. of damping coeff. of transverse waves 8-56867

US, of seamless drill casting and linepipe, review 8-95879

US, online inspection, steel plate manufacture appl. 8-80702

US, with given reliability, optimal conditions 8-95895

US automatic inspection of tubing 8-56865

US inspection, automatic, thin walled large diameter pipes, flaw size

classification 8-60949

US inspection result reproducibility on welded joints of tubes in boiler

surfaces 8-60948

US inspection slanted probes, prism material choice 8-92428

inspection continued

US thickness gauge, Kvarts-6, design of automatic control block 8-73005

US wave damping in solid material, instruments for determ., review 8-92429

weld joint, furnace welded pipe inspection unit for above 1000°C 8-53134

weld joint, US inspection probe 8-92426

instability *see stability*

instrumentation

see also aerospace instrumentation; computerised instrumentation; digital

instrumentation; digital readout; display instrumentation; nuclear

instrumentation; physical instrumentation control; signal generators; signal

sources

calibration optimal interval determ., generalised method (Rumanian) 8-49787

EM precision meas., conf., Ottawa, Canada 1978 8-89462

experiment design (Japanese) 8-62190

experiments design (Japanese) 8-70087

instrument block optimal precision synthesis (Russian) 8-70092

mathematical models of instruments, fundamental principles 8-93641

probabilistic representation of quantities 8-49788

radiation chemistry, in Inst. Nuclear Res., Warsaw 8-76888

RF instrumentation based on superconducting quantum interference 8-57995

instruments

see also individual types of instruments, e.g. astronomical instruments,

bridge instruments, optical instruments

analytical instrument use and planned acquisitions 8-88684

History of Sciences Collections, Royal Swedish Academy of Sciences,

catalogue 8-81789

indicating measuring instruments, error estimation (Croatian) 8-57886

inductometer calibrator, U-738, description 8-74034

inspection, optimal error correction signal 8-77829

linear mechanism anal., error statistics (Hungarian) 8-49823

low-speed motion irregularity meas. equipment, portable 8-54346

measurement facility inspection, confidence and productivity improve-

ment 8-77840

operation speed increase, additive-iterative correction method (Rus-

sian) 8-89423

performance unified representation (Japanese) 8-70090

periodic inspection of meas. facilities, probabilistic confidence charac-

teristic selection 8-77839

rack and pinion type, indication error reduction (Polish) 8-49818

thermographic instrument, types 8-86266

O₂ meter, type 648, mains-free, features (German) 8-94858

insulated gate field effect transistors

electrometer, current noise meas. 8-54398

electron and hole drift vels. in high elec. field, Monte Carlo calc. 8-60224

high temperature MOSFET characteristics for geothermal instrumenta-

tion, up to 300°C 8-73553

inversion layer, two-dimens. semicond., Gunn instability 8-84305

inversion layers, (100) and (911), IR photocond. and absorption 8-64123

MAOS memory element, stored charge volatility 8-52100

MOSFET structures, photocond. rel. to intersubband transitions 8-64127

p-channel MOST, quantum galvanomagnetic effects in p-type accumula-

tion channels 8-64134

radiation dose measurement using radiation induced

changes (Japanese) 8-78504

SOS, cryst. perfection rel. to MOS transistor mobility 8-75956

surface states, spin orbit interaction and many-body effect 8-64132

insulated wires

corona impulse energy spectrum under high AC voltages 8-71621

insulating coatings

see also varnish; waxes

thermoregulative coatings, radiation effects on reflectivity, space vehicle

appl. (Russian) 8-76542

insulating materials

see also asbestos; ceramics; composite insulating materials; dielectric

materials; glass; insulating thin films; mica; organic insulating materials;

thermal insulating materials

air, predischARGE-stabilised breakdown voltage (German) 8-63608

electric field numerical soln. (Slovak) 8-66710

ESCA, X-ray type, C 1s contaminant buildup on conductors and insula-

tors 8-95981

SF₆ compressed, breakdown threshold, surface roughness and pressure

effects 8-75449

SF₆ avalanche breakdown as stochastic process 8-67574

SF₆ breakdown distributions, low-value fractile determ. 8-67578

SF₆ breakdown field strength, electrode surface roughness tolerance 8-67577

SF₆ breakdown mechanisms, review 8-59699

SF₆ coaxial gap breakdown probability determ., influence of meas.

procedure 8-67579

SF₆ electric strength, electrode surface roughness effects (German) 8-63609

SF₆ gas chromatography in design of switching installations and dev-

ices (German) 8-88668

SF₆ high-temp. electrical breakdown parameters 8-67567

SF₆ predischARGE-stabilised breakdown voltage (German) 8-63608

SF₆ rod-to-plate corona discharge characteristic obs. 8-67584

insulating materials, acoustic *see noise abatement*

insulating materials, thermal *see thermal insulating materials*

insulating oils

cable oil, EHD pumping 8-87414

electric strength for switching surges and long flash-over distances,

expt. (Czech) 8-56427

mineral oil, breakdown voltage, live electrode polarity depend. for

non-uniform field 8-75450

silicone oil, props. determ. by harmonical shear vibr. (German) 8-67164

insulating thin films

see also dielectric thin films; electronic conduction in insulating thin films

Auger depth profiling by angle lapping 8-53287

chlorophyll a film, charge injection and storage 8-53317

electrical breakdown mechanisms 8-76385

insulating thin films continued

- guided optical waves for refr. index and thickness determ. 8-74049
 poly(p-xylylene), electron MFP as function of kinetic energy, XPS 8-52114
 polyethylene terephthalate, between metal electrodes, electrochem. effects as source of EMF 8-72278
 polyferrocene film, plasma polymerised, dielec. props., 40 kHz to 50 MHz, 30-400°C 8-52439
 polyimide, dielectric breakdown in high-temperature region 8-84522
 PTFE film, reactive sputtering in Ar-CF₄ mixture, MSCA 8-92191
 self-drifting of ionic charges, detection by surface potential decay method 8-72295
 thermal conductivity normal to layer, meas. method, error anal. 8-90682
 thickness measurements determ. using ellipsometer with nonmonochromatic source (*Russian*) 8-51862
 Al-Al₂O₃-Al junctions, Dy doped at Al₂O₃-Al interface, electron transport mechanisms and barrier height 8-91778
 Al₂O₅23, amorphous film, non-thermal switching in Al-Al₂O₃-Al struct. (*Russian*) 8-80069
 Al₂O₃ amorphous layers in MIS structures, prep. and physical props. (*Slovak*) 8-64122
 Al₂O₃, composite film, barrier layer, ellipsometric meas. 8-67918
 Al₂O₃, electron beam deposition, heating of multiple layer structs. (*Russian*) 8-92192
 Al₂O₃ film, Al embedded, non-ohmic conduction behaviour 8-64157
 Al₂O₃, films, form., cross-sections, struct. obs. 8-67917
 Al₂O₃ on Al, anodic oxide film, effect of interface roughness on cracking 8-76755
 Al₂O₃, RF sputtered film, transient current meas. 8-52113
 Al₂O₃, self-drifting of ionic charges, detection by surface potential decay method 8-72295
 Al₂O₃, thick vacuum condensates, electron microscopy struct. investig. (*Russian*) 8-95242
 Bi₁₂GeO₂₀ vacuum-deposited film elec. and photoelec. props. (*Russian*) 8-60237
 Bi₁₂GeO₂₀ wide-zone dielectric injection contact characteristics (*Russian*) 8-60236
 C, amorphous, growth under ion impact in butane plasma, and IR transparency 8-56888
 Cu₂O film, thermoelec. power, activation energy variation with electrode spacing in DC sputtering 8-76099
 Fe₂O₃, prep. by reactive sputtering, struct. and props. (*Japanese*) 8-92190
 GaAs anodic oxide, refl. and transmission, 0.01-6 eV 8-95613
 GaAs anodic oxide, self drifting of ionic charges, detection by surface potential decay method 8-72295
 GaAs, anodic oxide film, annealing effect on carrier density profile 8-88040
 GaAs oxide, anodic, evidence for growth-induced damage from photolum. expts. 8-75953
 GaAs oxide, formation by plasma oxidation, and props. 8-95825
 GaAs oxide, passivated layers, quantitative in-depth profile, AES-SIMS thermal, anodic and plasma oxidations 8-84087
 GaAs oxide, thermal and anodic, in-depth profiles, XPS expts. 8-84086
 GaP, anodically grown insulating layers, prep. and props. (*German*) 8-64158
 LaB₆ film, structure, stoichiometry, elec. properties 8-60043
 MgO thin film, DC conduction 8-88051
 MoO₃, film, colour centre studies, optical absorpt. spectra 8-71724
 Ni₂O₃ film, thermoelec. power, activation energy variation with electrode spacing in DC sputtering 8-76099
 SiN film, on Si substrate, thermal stresses and cracking resist. 8-63958
 Si₃N₄, diffusion of Al, AES and depth profiling 8-51744
 Si₃N₄ film, grown by direct thermal reaction with N₂ 8-52665
 Si₃N₄ film, on Si substrate, thermal stresses and cracking resist. 8-63958
 Si₃N₄ film, thermal oxidation rate and masking effect against Si oxidation 8-64749
 Si₃N₄, on Si, implantation effects on substrate hardening and film stress reduction 8-71748
 Si₃N₄, self-drifting of ionic charges, detection by surface potential decay method 8-72295
 Si₃N₄, separation, effect of reactor geometry (*German*) 8-60583
 Si₃N₄, Si rich, CVD film prep. and props. 8-76607
 Si₃N₄, with varying refr. index, AES and XPS 8-72029
 Si₃N₄-SiO₂, interface, electron and hole cond. at moderate elec. fields 8-95376
 Si₃N₄, ion-implanted, enhanced etching in buffered HF solns. 8-72903
 Si₃N₄O₂ film, band diagram, optical props. and elec. cond. meas. 8-84333
 SiO₂, action of plasma in capacitive electrode HF discharge (*Russian*) 8-95818
 SiO₂, electric strength in MOS structures obs., under unidirectional, alternating and combined voltages (*Slovak*) 8-88034
 SiO₂, evaporated film, Debye-type dielec. dispersion props. 8-56421
 SiO₂ film, on Si, radiation damage structures, EPR obs. 8-95097
 SiO₂ film, on Si substrate, thermal stresses and cracking resist. 8-63958
 SiO₂ film on Si, negative bias instability 8-91773
 SiO₂, film thickness and field depend. of saturation defect density 8-56250
 SiO₂ films, dehydroxylation, sintering, IR investig. (*Russian*) 8-75967
 SiO₂, insulating films, neutron activation anal. and autoradiography 8-92574
 SiO₂ layers, passivating, deposition by plasma decomp. in planar reactor 8-88430
 SiO₂, on Si, thermal growth kinetics, oxidation profile meas. 8-88551
 SiO₂, self drifting of ionic charges, detection by surface potential decay method 8-72295
 SiO₂, Si rich, CVD film prep. and props. 8-76607
 SiO₂, thermal, elec. stressed film, dielec. breakdown 8-64322
 SiO₂, thermally grown film, optical absorption and photocond. 8-64421
 SiO₂, tunnelable film form. using vap. O₂ source at liq. N₂ temp. 8-76774
 SiO₂:Al film, ion-implanted, electron trapping behaviour 8-67729
 SiO₂:Na, film, depth profiling by SIMS 8-79624

insulating thin films continued

- SiO₂ film, vacuum evaporated, phase comp., electron spectroscopy obs. 8-60042
 SiO₂, on Si exposed to O₂, phase comp., electron spectroscopy obs. 8-60042
 Si₂O₃N₂, pyrolytic, on GaAs, evidence for growth-induced damage from photolum. expts. 8-75953
 (SiO₂)_x(Si₃N₄)_{1-x} on GaAs, deposition method and props. 8-91796
 Ta₂O₅ film, dielec. props. meas., two layer Maxwell-Wagner model 8-76373
 WO₃ amorphous film, elec. cond. and dielec. const. 8-60238
 Y₂O₃, struct. and elec. resist., electron diff. meas. 8-87888

insulation

- see also cable insulation; electric breakdown; insulating coatings; insulating materials; insulators
 electromagnets for nuclear fusion and high energy research, insulation systems, features 8-89506
 gases as electrical insulators, nature and practice 8-83632
 laminated insulating element, vac. drying in inert heat-transfer vap. 8-56875
 self-magnetic insulation in vacuum for coaxial geometry 8-78520
 solid, discharges, elec. strength and degradation 8-83631
 H₂O, as dielectric insulator, in plasma devices, electron accelerators and impulse current generators (*Russian*) 8-75430

insulation, thermal see thermal insulation**insulation testing**

- flameproof coating for PVC insulated cables, composition, tests (*Russian*) 8-68828
 insulating material monitoring by electroluminescent screens, defect imaging 8-53083
 N₂, compressed, insulation breakdown at cryogenic temp., obs. 8-51368

insulator-metal boundaries see metal-insulator boundaries**insulator-semiconductor boundaries** see semiconductor-insulator boundaries**insulators**

- ie. insulating devices. For materials see insulating materials
 see also bushings; insulation
 ceramic insulator rings, for Tokamak fusion test reactors 8-55022

integral equations

- see also integro-differential equations
 Abel integral eqn. solution by orthogonal polynomials 8-67436
 adhesively bonded metallic panels, 2-ply, finite element and integral eqns. anal. of fatigue crack growth 8-92347
 applications of integral equations in particle-size statistics 8-62050
 approximation method for solution of nonlinear integral equation with error estimation for problems in heat or mass transfer (*Russian*) 8-57879
 asymptotic behaviour of group integrals, infinite rank limit 8-62051
 asymptotic series coefficient, generalised calculus using steepest descent method (*Rumanian*) 8-89304
 atoms, molecules, pair energies, numerical soln. 8-90065
 Bernoulli and Lagrange-Cauchy integrals, p/γ term 8-65779
 bifurcation of crystalline solutions and freezing 8-67814
 boundary value problems, numerical soln. through integral eqns., review 8-81808
 Cauchy type singular integral eqns. with complex singularities, numerical soln., stress intensity factors 8-55611
 celestial mechanics, formal integrals for autonomous Hamiltonian system near equilib. point 8-89047
 Choquard nonlinear eqn. minimising soln. existence and uniqueness 8-67315
 circular disc, stress intensity factors and crack energy 8-79260
 clarinet, integral equation anal. of self sustained oscillations 8-94490
 collocation variational method for solving Fredholm integral eqns., convergence condition 8-57764
 composite particle scatt., integral eqns. taking Pauli principle into account 8-86496
 conjugated heat transfer in plate in flow, integral eqn. 8-87345
 connectivity theory for formally symmetric operators 8-49651
 constrained systems, quantum treatment using path integrals based on distrib. theory 8-65815
 continuum mechanics, suction force, interpretation of Rice integral 8-49658
 crack, in semiinfinite thermoelastic solid with heated boundary 8-55610
 crack branching, asymmetric, plane stressed and loaded plate 8-59344
 cracks, curvilinear, star-shaped array in infinite isotropic elastic medium 8-55609
 dense, quadrupolar, hard sphere fluid, integral eqn. approx. 8-63652
 dielectric coated gratings, general integral theory 8-66909
 diffraction gratings, Fredholm integral eqn. formalism 8-63192
 distribution functions and Green functions (*Russian*) 8-65890
 drop motion in immiscible liquid, integral eqn. for Stokes flow 8-71389
 duct, nonuniform, finite element method for acoustic transmission 8-83140
 ECG forward problem, relationships among Green's theorem, Helmholtz theorem and integral eqn. methods 8-57090
 edge dislocation interactions in infinite array, elastic energy 8-55871
 elastic, isotropic, incompressible solid, plane deform., integral eqn. formulation 8-51081
 elastic dissimilar semiinfinite strips, different widths, plane symmetric contact problem 8-55615
 elasticity, plane, inclusion problem, numerical soln. of Cauchy-type integral eqn. 8-54194
 elasticity, plane theory, singular integral eqn. for mixed problem soln. (*Ukrainian*) 8-89339
 EM field calculation using integral eqn. method (*Russian*) 8-82887
 EM field penetration into conductive spherical cavity 8-86990
 EM field penetration into thick, finitely conducting shell, anal. 8-62990
 EM field time domain reflection from inhomogeneous and dispersive slabs 8-62985
 EM radiation scattering by dielectric spheroids and ellipsoids, numerical soln. 8-85622
 EM scattering by multiple rectangular cylinders, numerical anal. 8-62992
 EM scattering by spherical shell with arbitrarily located circular aperture, anal. 8-62989

integral equations continued

- EM scattering from corrugated conducting surfaces with inhomogeneous surface impedance, anal. 8-62987
- EM wave impinging homogeneous layer transmission and refl. coeffs. (*German*) 8-82907
- energy resource usage, conservation effects 8-69941
- Fadeev integral eqns. for 3 particles in boundary condition model, wave function determ. 8-54248
- farfield scatt. from prolate spheroid, meas. and anal. 8-94459
- flow, viscous incompressible, integral eqn., soln. by function-theoretic method 8-69990
- flux calculation in complex heterogeneous reactor cells by imbedding element method (*Russian*) 8-58321
- Fredholm, first kind, appl. in electromag. field theory 8-94357
- Fredholm eqn. of the second kind for current distrib. in antenna theory (*Chinese*) 8-66708
- Fredholm eqns. soln. (*Russian*) 8-86120
- Fredholm integral first kind eqns., soln. via Riccati differential eqns. depending on parameter (*Russian*) 8-54153
- Fredholm-Poincare integral eqn., induced potential problem in 3-D 8-58880
- free convection laminar flow, viscous dissipation and pressure stress effects importance 8-63428
- freely gravitating charge, radiation, in field of weak plane gravitational wave (*Russian*) 8-89381
- groundwater two-dimensional unconfined saturated flow, boundary integral solns. 8-77291
- Helmholtz homogeneous equation, numerical soln. methods (*German*) 8-90337
- high temperature gas diagnostics by spectral remote sensing 8-74002
- interface penny-shaped crack, Fredholm integral eqn. soln. 8-90784
- inversionlike integral eqn. in multidimensional case 8-62054
- inversionlike integral equations generalisation, appl. to nonlinear partial differential equations soln. 8-86117
- Kepler motion, generalised, Lie groups of motor integrals 8-85831
- lifting surface integral eqn. solution (*Russian*) 8-73836
- Lippmann-Schwinger equation, numerical soln. 8-81802
- magnet immersed in ferrofluid, force on, surface integral calc. 8-94350
- magnetic field calc., two-dimens., boundary integral eqn. method 8-94355
- magnetostatic problems with thin plates or shells 8-50675
- mesometeorological stationary problem of flow around obstacle 8-81271
- meson bound state eqn. and solutions 8-78101
- mixed boundary value problems for Helmholtz eqn., integral eqn. method 8-57751
- mixed continuous mechanics problems, orthogonal functions (*Russian*) 8-49659
- mixtures of reacting gases, extension of Chapman Enskog method (*Russian*) 8-57878
- motion integral disappearance in multi-resonance conditions 8-77471
- multispectral radiance method for temp. distribution meas. (*Japanese*) 8-77912
- N particle systems, one-dimens., completely integrable, construction technique 8-57768
- N-particle quantum scattering theory, spurious solns. of integral eqns. 8-65812
- neutron hot perfect fluid relativistic stars, asymptotic eigenfrequency distrib. for even parity perturbations 8-49668
- non-Newtonian pulsatile laminar flow in tube 8-79346
- nonhomogeneous elastic layer bonded to nonhomogeneous half-space, torsion by circular die, Fredholm eqn. 8-87263
- nonsingular integral eqn. for three body scatt. problem 8-62106
- nuclear physics nonlinear integral eqn. solution (*Chinese*) 8-74324
- numerical inversion of Laplace transform and Fredholm integral eqns., eigenvalues and eigenfunctions 8-81800
- numerical soln. by boundary integral eqn. method 8-92850
- numerical soln. by multi-part mixed boundary value problems 8-62056
- numerical solution of a class of integral equations arising in two-dimensional aerodynamics 8-62086
- one group, integral transport eqn. for homogeneous sphere, neutron scatt., classical diffusion, anal. 8-62589
- optical waveguide, diffused, energy distribution determ. by rigorous solution 8-63200
- organ flue pipes, self-sustained oscillations, integral eqn. soln. 8-51015
- path integral representation for U- and S-matrix, scalar meson model renormalised S-matrix elements 8-78103
- penny-shaped crack, sudden twisting in a finite elastic cylinder, stress calcs. 8-67110
- periodic curvilinear cracks in isotropic medium, integral eqn. soln. 8-51118
- plane elastostatics, boundary value problems, spectra of integral operators 8-57782
- plane-fronted gravitational waves, integrals of wave equations in space time (*Russian*) 8-89380
- plasma cylinder short-wave probe, inverse diagnostics problem formation 8-67423
- plate, elastic, under uniform twisting, periodic collinear cracks (*Japanese*) 8-67097
- potential flow problems, partition technique integral eqn. method 8-49652
- radiation fields from polygonal sources, Fock method 8-83060
- radiation transport, multidimensional, in plane-parallel atmosphere, appl. to 4.3 μ m auroral arc 8-88917
- radiative transfer, unified treatment of reflected and transmitted intensities, integral eqn. 8-85838
- radiative transfer in expanding homogeneous sphere (*Russian*) 8-73945
- radiative transfer in fibrous media 8-94571
- radiative transfer in finite plane parallel media, linear Fredholm eqns., imbedding in infinite medium 8-81532
- radiative transfer in finite plane parallel media, linear Fredholm eqns., imbedding in semiinfinite medium 8-81533
- resolution method for second problem of elastic limits for plane (*French*) 8-57779
- retina of Limulus, spatially synchronised oscillatory response theory 8-73158

integral equations continued

- Saint-Venant torsion problem, classical, integral and functional eqns. 8-57780
- Schrodinger integral equation, soln. using El-Gendi approx. method 8-77749
- seismic data migration in two and three dimens., integral formulation 8-77342
- shallow water with moving boundaries digital simulation, finite element method appl. 8-92847
- singular, anal. of anisotropic discs (*German*) 8-87272
- spin lattice models, continuous-integral method 8-93615
- stability criteria, appl. to gas chromatography 8-62049
- stochastic Volterra eqn., existence and uniqueness of soln. 8-89405
- Stokes problem of motion of Cassinian cylinder in viscous fluid 8-71312
- stress intensity factors FOR X-formed arrays of cracks 8-67121
- surface lattice dynamics and density response 8-71930
- surface plasmon, eigenmodes, Fredholm integral eqns. (*French*) 8-56195
- thermoelastic periodic problems for infinite solid with disc shaped cracks, integral eqn. solns. (*Ukrainian*) 8-55559
- thermoelastoplasticity three-dimensional integral eqns. (*French*) 8-90718
- transition metal surface, electronic perturbations 8-95334
- turbulent boundary layer, compressible, extended mixing length appls. 8-94655
- uniform approximations to integral and integrodifferential equations 8-57742
- viscoelasticity, Il'yushin kernels, analytical representation 8-67055
- viscoplasticity anal., boundary integral eqn. method (*French*) 8-90728
- volume integrals of real part of nucleon optical pot. for A=10-238 8-78339
- water wave diffr. and radn., numerical methods, book contrib. 8-59412

integral transforms see transforms**integrated circuit manufacture**

- Used for commercial manufacture only
see also masks; photolithography
plasma etching, chemically selective anisotropic 8-64755

integrated circuit technology

- See also under specific integrated circuit headings
see also semiconductor technology
electron beam microfabrication, variable aperture projection and scanning system design 8-74836
MOS, dielectric breakdown in electrically stressed films of thermal SiO₂ 8-64322
MOS LSI passivation using reactive plasma deposited Si-N films 8-56584
NDT wire bonds on Si chips, IR microscopy 8-95867
photoprojection method of image formation of submicron patterns 8-71180
positive photoresist, formulation, photochem. props., teaching appls. 8-89284
reactive sputter etching, plasma gas temp. determ. 8-63586
RF plasma etching, mechanistic considerations for selective etching 8-64754
thin films in restricted geometry 8-72044
vector scan electron beam lithographic system, deflection distortion 8-74835
GaAs planar p-n junctions, Be ion implantation, fabrication and characts. 8-88022
Si epitaxy and oxidation, first-order process models 8-72049
SiN_x plasma deposited dielectric film, elec. props. 8-68103
Si₃N₄, low temp. deposition using microwave-excited active N₂ 8-84718

integrated circuit testing

- leak test, automatic, nondestructive, design, evaluation and implementation for IC assemblies 8-53180
NDT wire bonds on Si chips, IR microscopy 8-95867

integrated circuits

- see also digital integrated circuits; hybrid integrated circuits; large scale integration; linear integrated circuits; masks; microwave integrated circuits; monolithic integrated circuits; substrates; thick film circuits; thin film circuits
cardiac pacemaker, reliability technology conf., Gaithersburg, USA, (Jul. '76) 8-57129
strain measurement, in 10 μ m spots using X-ray microdiffractometer 8-86262

integrated logic circuits

- digital frequency meter, for LF meas., using TTL ICs 8-86296
digital logic using integrated circuit modules, for teachers 8-81755
CdTe single-crystal film, switching and memory effects 8-76174

integrated memory circuits

- layered piezoelectric-semiconductor surface state acoustic memory 8-90615
CdTe single-crystal film, switching and memory effects 8-76174

integrated optics

- see also fibre optics; optical films; optical modulation; optical waveguides; semiconductor junction lasers
anisotropic medium, optical wave reflectance, general formula (*Japanese*) 8-87012
anisotropic waveguide for integrated optics, monomolecular layered film 8-66954
application to branching, switching, modulation in light systems including multimode fibres 8-87169
bending losses of dielectric rectangular waveguides for integrated optics 8-63205
bibliography 8-66959
birefringent prism couplers, for thin film optical waveguides 8-55468
Bragg interactions in active medium, first and second order 8-50747
Bragg reflector statistical analysis 8-66882
Bragg switch for optical channel waveguides 8-75002
channel waveguide double-pole double-throw switch/coupler, using total internal refl. 8-71233
corrugated waveguides and lasers, improved coupled mode analysis for TM mode 8-83117
coupled waveguide modulator with p-n junction, multilayer planar waveguide config. 8-71235

integrated optics continued

- coupling methods in single mode fibre integrated optics systems, review 8-59162
- diffused waveguide tunnel excitation and emission 8-59146
- distributed Bragg deflector, multifunctional integrated optical device 8-83115
- distributed-feedback waveguide structure, dispersion characts. 8-66949
- electro-optic A/D conversion using channel waveguide modulators 8-66898
- electro-optic devices, guided wave, for logic and computation 8-66946
- Fabry-Perot nonlinear electro-optic device, using refl. light feedback 8-55457
- ferroelectric devices for optical systems 8-90473
- fibre optical coupling to film 8-87167
- fibre-optic integral data source/receiver package 8-63179
- film applications, review 8-71234
- filter with surface corrugated diff. grating, characts. for oblique incidence 8-50949
- Fourier transform signal processing in integrated optical format 8-50950
- Fresnel lens for thin-film waveguide 8-94452
- garnet optical waveguide, with high Faraday rotation, mode degeneracy 8-94454
- Gaussian beam propagation in thin film waveguides 8-79102
- geodesic lens, diffraction-limited, in polyurethane waveguide struct. 8-94453
- geodesic lenses, axially symmetric, design parameters 8-83114
- grating direct writing using SEM 8-83121
- grating lenses, fabrication by electron beam pattern generation, chem. etching and printing 8-75004
- grating reflector for thin film Fabry-Perot laser 8-55471
- injection laser integration with Gunn oscillator on semi-insulating GaAs 8-71232
- ion implanted integrated optic devices, fabrication parameters (*German*) 8-83119
- leaky-mode propagation in Ti-diffused LiNbO₃ and LiTaO₃ waveguides 8-87149
- lenses, thin-film waveguide, progress 8-66950
- lithographic focused laser system, integrated optical device fabrication appl. 8-55477
- modulator switch, balanced bridge, using Ti-diffused LiNbO₃ strip waveguides 8-63201
- modulator using electro-optic phase shifter pair with optical waveguide couplers 8-66952
- multilayer gyrotropic structures for nonreciprocal light propagation 8-90529
- multimode fibre bussing, active fail-safe terminal 8-55438
- optical communication appl. 8-87159
- optical communications, integrated optical circuits design (*Italian*) 8-55467
- optoacoustic deflector planar, expt. 8-74995
- optoacoustic device, planar, SAW loss meas. using light beam diffraction 8-74996
- periodic corrugated waveguides, grating coupled radiation and distrib. feedback 8-59161
- periodic surface corrugation generation by holography 8-55469
- plastic optics for optoelectronics, moulding techniques for single, multi-element systems 8-63210
- prism coupler for optical waveguides 8-94431
- review of integrated optics and optical waveguide devices 8-66948
- rib waveguide switches with MOS electrooptic control, monolithic integrated optics in GaAs-Al_xGa_{1-x}As 8-87168
- ridge waveguide, trapezoidal cross-section, propag. characts. 8-55436
- ring resonator, high-Q, asymmetric three-layered dielectrics, design 8-83118
- semiconductor heterostructures, elec. and optical phenomena, discrete devices, review 8-72250
- semiconductor-waveguide lasers in bent-guide structs., characts. (*Japanese*) 8-87062
- SHG, phase-matched, in four-layered optical waveguide struct. 8-74950
- single mode fibre network, coupling and integrated optical switches 8-59159
- soda lime glass, Ag⁺ ion exchanged, planar optical waveguide, manufacturing tolerances 8-71212
- spectrum analyzer dynamic range, waveguide scatt. effect 8-59163
- sputtered films, optical props. and appls. 8-72623
- strip waveguides, leakage and reson. effects, anal. 8-66953
- stripe geometry injection lasers, rigorous boundary value soln., for lateral modes 8-71100
- superconductor junction/optical waveguide combination 8-66955
- switch, 3×3, using single-mode waveguides in electrooptical material 8-55470
- switch, bistable, using LiNbO₃ phase modulator 8-79145
- switch, optically controlled two channel, based on directional coupler 8-83116
- tapered beam to film couplers, coupler eqns. 8-55472
- telecommunication appls., manufacturing technology (*French*) 8-50946
- thin-film periodic structures, optoelectronic devices appls. (*Polish*) 8-50947
- thin-film waveguides, propag. modes 8-71218
- tunable optical waveguide directional coupler filter 8-79144
- tunable switched directional couplers of two thin film waveguides using SAW 8-75003
- waveguide hologram using optical thin films high-efficiency relief-type hologram 8-66958
- waveguide props., mode anal., prism coupling method 8-66947
- wideband thin film modulators and switches, for optical communication 8-63206
- As₂S₃, thin film optical waveguide, for acoustooptic modulators 8-83051
- BaO crown and flint glasses, Ag and Cu diffusion for optical waveguide fabrication 8-59166
- GaAlAs embedded DH stripe laser with GaAsP strip-waveguide modulator 8-66957
- GaAlAs-GaAs epitaxial heterostructures for integrated optics functional elements 8-50948
- Ga_{1-x}Al_xAs-GaAs injection laser, branching waveguide coupler fabrication by LPE 8-63202
- Ga_{1-x}Al_xAs embedded stripe DH laser monolithically integrated with strip waveguide 8-59025

integrated optics continued

- GaAs directional couplers and electrooptic switches, wavelength depend. 8-79143
- GaAs double-cavity laser with branching output waveguides 8-63128
- GaAs, electroabsorpt. avalanche photodiode waveguide detectors 8-65965
- GaAs, exam. as cladding material, for optical waveguides as cutoff polariser 8-55474
- GaAs, ion etching, effects on optical props. and lattice disorder 8-83122
- GaAs patterned epilayer structures, MBE writing, for integrated optics 8-56590
- GaAs rib-waveguide directional-coupler switch with Schottky barriers 8-63204
- GaAs-(Ga,Al)As light modulators and distributed Bragg reflector laser, monolithic integration 8-50944
- GaAs-AlGaAs distributed Bragg reflector integrated twin-guide laser, temp. characts. 8-87064
- GaAs-GaAlAs, transverse Bragg-reflector injection lasers 8-74926
- LiNbO₃ graded-index planar waveguide, As₄₀Se_{50-x}S_xGe₁₀ film strip-loaded 8-74965
- LiNbO₃, high freq. plane acousto-optical light modulators (*Russian*) 8-79106
- LiNbO₃ optical waveguides, electrooptic modulation and switching, recent progress 8-50945
- LiNbO₃ waveguide, corrugated, electro-optic scanning of light diff. from grating output coupler 8-63172
- LiNbO₃:Ti, in-diffused waveguide, integrated bistable optical device development 8-75001
- LiNbO₃:Ti diffused strip waveguide, optical insertion losses 8-74985
- LiNbO₃:Ti waveguide, diffused, Mg diffusion effects on characts. 8-66905
- LiNbO₃:Ti waveguide directional coupler type modulator 8-66951
- LiTaO₃, multimode electro-optical 2×2 crossbar switch 8-55473
- Se amorphous Au clad waveguides piezoelectric modulator for 10.6 μm radiation 8-66956
- SiO₂-Ta₂O₅ film, refr.-index-adjustable, for integrated optical ccts., prep. and props. 8-63203
- YIG substituted film waveguides, TE→TM mode conversions 8-66904
- ZnO, CVD films on sapphire substrates, use as optical waveguide 8-90500

integrating circuits

- analogue, for dosimeter to meas. ion-beam current integrated flux 8-49865
- averaging meter for nonelectric periodic quantities, dual slope principle (*German*) 8-73983
- digital electronic integrator, for radioastronomical obs. processing (*Russian*) 8-57465
- multi-channel, for plasma magnetic-probe meas. 8-75413

integration

- anisotropic solid fluid flow with free or artesian surface analysis, finite element method soln. 8-92872
- Cauchy type singular integral eqns. with complex singularities, numerical soln., stress intensity factors 8-55611
- chemical reaction kinetics, temp. integral approximating eqns. accuracy 8-92445
- circular cylindrical shells, integral calc. involving characteristic beam functions 8-63359
- circulation models, numerical integration method for improving soln. stability 8-69118
- classical trajectory calcs., empirical testing of nonrandom integration method 8-50607
- complex variables method for soln. of large nonlinear differential eqns. systems 8-62062
- dam unsteady compressible fluid flow digital simulation, finite element method appl. 8-90820
- Earth gravity field, associated Legendre functions integration for spherical harmonics expansion (*German*) 8-61311
- elastic-perfectly plastic von Mises material, accuracies of numerical soln. constitutive eqns. 8-59315
- electron repulsion integrals, computation involving Gaussian basis functions 8-58572
- exact Slater integrals determ. for H wave functions, computer method 8-90074
- finite element isoparametric quadrilaterals, integration formulas 8-89317
- finite element method, reduced integration, appl. to elastostatics 8-75066
- finite geometry effects in scatt. expts., numerical integration method 8-82596
- Fokker-Planck eqn., integration method 8-91067
- Fourier transformation, singularity expansions and product integration 8-89316
- Gaussian plume model parameters determ. from diffusion-convection eqn. integration 8-81399
- grid points condensation in process of solving and using high order schemes in numerical integration of viscous gas flows (*Russian*) 8-59363
- groundwater flow analysis, finite element method soln. 8-92875
- hydrological system tracer digital simulation, finite element method soln. 8-92881
- hypersonic viscous shock-layer equation, method for successive approximations for integration (*Russian*) 8-59421
- IR radiation spectral absorbance and transmittance, accurate modelling technique 8-91062
- large amplitude water wave digital simulation, finite element method soln. 8-92851
- lifting wing calcs., spanwise integrations, computational economy improvement 8-71344
- magnetic film, micromagnetic dynamics in domain walls, numerical model 8-72382
- Monte Carlo iterative scheme for adaptive multidimensional integration 8-57762
- multidimensional integrals, numerical calc. 8-89323
- N twisting gravitational field soln. to Einstein eqn., integrability conditions 8-86203
- nonconservative systems, integration of motion eqns. (*Ukrainian*) 8-81827
- nuclear field theory of Fermi systems in an external field, path integrals 8-93954

integration continued

- numerical, of harmonic motion differential eqns., programmable calculator, teaching appl. 8-86083
 numerical integration of eqn. system for nonadiabatic compressible gas flow in tube (*Russian*) 8-83427
 path integral, canonical to covariant change 8-73877
 photoelectron spectra of cryst. solids, numerical integration within linear analytic approx. 8-60545
 plasma, rapidly changing, numerical integration of ionisation rate eqns. 8-55734
 plate bending elements, quadrilateral, finite element anal. with reduced integration 8-75071
 polaron theory, Bessel function integral, asymptotic evaluation 8-56082
 polyatomic molecules, quadrupolar and dipolar, numerical evaluation of second virial coeff. 8-91050
 radiation field of extended rectangular source, numerical integration 8-66424
 reactor shielding materials, Pb, and steel, γ leakage spectra, numerical integration of Boltzmann eqn. 8-58350
 rigid body with discrete symmetry, conditionally-linear integration of eqns. of motion (*Russian*) 8-86135
 Schrodinger eqn. with double-minimum potential, numerical integration 8-58573
 second order linear partial differential eqns. of math. phys., integration by separation of variables (*Italian*) 8-81798
 Sommerfeld integral in radiowave propag., numerical approximations for fast convergence 8-66727
 stationary satellite eqns. of motion numerical methods (*Japanese*) 8-85837
 time transformations and Cowell's method 8-77466

integro-differential equations

- see also Boltzmann equation; Fokker-Planck equation; Liouville equation; master equation; Vlasov equation
 aerofoil in unsteady viscous flow, numerical soln. procedures 8-75165
 Born-Green-Yvon eqn., two-dimensional, with anisotropic interac. 8-79882
 coagulation, with breakdowns, exact solution of integrodifferential equation 8-53272
 electromagnetic scatt., time depend., boundary value formulation, integro-differential eqns. 8-66726
 electron-atom collision theory, soln. of coupled integro-differential eqns. by computer program 8-86948
 EM wave two-dimensional transient scattering, new space-time integral eqn. 8-78861
 exact derivation of a generalized master equation for the motion of excitons 8-87911
 flame front, laminar, hydrodynamic instability, nonlinear integro-differential eqn. 8-51253
 flame front, laminar, hydrodynamic instability, numerical solns. 8-51254
 flow boundary layer, stochastic model of fluctuations 8-90818
 gas kinetics, integro-differential eqn. approx. by Fokker-Planck type 8-91049
 interacting systems, general theory of natural states, use for calc. of intermol. forces 8-82807
 interacting systems, natural states in the asymptotic $1/R$ expansion, use for calc. of intermol. forces 8-86930
 laser modelocking, soln. of 2nd order integro-differential eqns. 8-66796
 materials with memory, linear theory of heat cond., final value problem, existence, uniqueness theorems 8-59266
 modified Lane eqn. with integral term, exact soln. 8-63052
 Pocklington type, finite cylindrical scatterer near imperfectly conducting ground 8-71003
 radiating electron, stability of motion 8-65789
 resonance phenomena in systems described by eqns. with divergent arguments (*Russian*) 8-73832
 retarded Josephson equation, adiabatic and pendulum approx. 8-68119
 scattering, low-energy, by long-range pot. 8-74723
 thin film eddy current calc., finite element method solution 8-90343
 three-dimens. solitons 8-62053
 viscoelastic media, deform. theory with account of thermomodification (*Ukrainian*) 8-67052
 viscoelasticity, solns. for eqns. with small parameter (*Russian*) 8-62078
 H_2^+ , electron scatt. eqns. convergence, H_2 continuum states, appl. to photoionis. 8-66663

intelligence, artificial see artificial intelligence**intelligibility, speech** see speech intelligibility**intensification** see amplification**intensity measurement**

- see also acoustic intensity measurement
 absolute luminous intensity meas., apparatus (*Danish*) 8-62217
 laser beam diameter fluctuations meas. 8-87086
 liquid light scatt. coeff. absolute determ. apparatus 8-86319
 photoelectric radiation flux density meas. technique 8-89521
 photometric meas., digital meter, cct. and operation (*Polish*) 8-65943

interactive programming

- bioestereochemical modelling, interactive computer graphics, appl. to DNA-protein interaction 8-88693
 image processing software, structure and design philosophy 8-58940
 lake survey programme for water resource surveillance 8-81257
 particle track data in plastics, rapid anal. using interactive programming and graphic displays 8-66456

interactive terminals

- ECG data interactive display system 8-53550
 image analyser FAS II, scanning electron microscope appl. 8-89597
 thermogravimetric data acquisition and reduction program 8-64901

interatomic potentials see potential energy functions**intercalation compounds**

- drug-nucleic acid interactions, conformational flexibility at intercalation site 8-96005
 graphite intercalated with nitrate, galvanomagnetic props. 8-76092
 graphite intercalates, struct. and order-disorder transforms. 8-71710
 graphite intercalation compounds, props. and appls. 8-71711
 graphite with K and Cs, low temp.-sp. ht. 8-71868
 graphite- Br_2 , intercalation process 8-63965

intercalation compounds continued

- lamellar graphite acceptor type, charge distrib. and Fermi surface 8-87935
 Br_2 -graphite systems, adsorbed and intercalated, EXAFS 8-72638
 C_8K , superconductivity 8-91827
 $C_{12n}(SbCl_5)$, magnetothermal oscill. and electronic struct. 8-84129
 $FeCl_2$ -graphite, formation by reduction of $Fe(III)$ compounds with $Fe(CO)_5$ 8-63721
 $FeOCl$ intercalation cpds. with Li and amines, cryst. struct. 8-51512
 Fe_xZrSe_2 , intercalation compound, IR spectra 8-88300
 Li_2TiS_2 , Li ordering, electrochem. obs. 8-59795
 $NbSe_2(2H)$ -hydrazine, intercalation compd., kinetic studies by transmittance meas. at 1600 nm 8-71981
 $nbSe_2(2H)$ single crystal, elec. resistivity, effect of hydrogen intercalation (*Russian*) 8-84338
 PbI_2 intercalated with organic mols., energy band splitting (*Russian*) 8-76027
 $SnSe_2$, intercalated with cyclopropylamine, photoelectron spectra study of electronic struct. 8-84698
 TaS_2 intercalated with NH_3 , charge transfer, PAC meas. 8-76366
 TaS_2 intercalation complexes, superconductivity 8-91803
 Ta_2S_3 /pyridine intercalated, struct. and bonding 8-91323
 TaS_2 -copper tetra-4-dimethylaminophthalocyanine, dye intercalated layered cpd., struct. and superconductivity 8-84342
 Ta_2S_3 (pyridine) $_{1/2}$, superconducting intercalation complex, proton spin lattice relaxation time 8-80096
 WO_3M_x ($M=H, Li, Na, K, Ag$), bronzes, atom motion 8-75874

interdiffusion see diffusion**interface electron states**

- adsorption for noncoplanar geometry 8-79887
 compound semiconductor interfaces, conf., Los Angeles, USA (Jan. 1978) 8-91756
 deformed heterojunctions, one-dimens. model 8-64100
 desorption, time dependent escape rate from potential well 8-79888
 diamond Schottky barrier, electronic struct., pseudopot. calc. 8-95364
 double layer barrier, deform. of electron spectra (*Russian*) 8-84292
 effective mass approximation, interface effect 8-64082
 $GaAs-Ga_{1-x}Al_xAs$, ultrathin layer heterostruct., pseudopot. calcs. 8-95343
 heterojunction energy band lineups, orientation depend. 8-95344
 image potential near dielectric-dielectric interface 8-84274
 inversion layer, EM modes 8-80030
 junction field effect structures, 2-D subbanding 8-64125
 localisation in two-dimens. systems 8-60213
 metal surface or metal-metal interface, plasmon dispersion 8-52053
 metal-insulator interface, Hubbard model, possibility of insulator-metal transition 8-52084
 metal-metal interface, simple, electronic props. 8-72234
 metal-semiconductor interface, electronic structure 8-72261
 metal-semiconductor interface, Schottky barrier formation, microscopic model 8-52087
 metal-semiconductor junction photoelec. phenomena, effect of dielectric gap and surface states (*Russian*) 8-84299
 metal-semiconductor junctions, capacitance, temp.-depend., by space-charge methods 8-91758
 metal-semiconductor structure, quasitwo dims. excitons and plasmons at different carrier conc. 8-60063
 MIS dielectrics, charge centres, removal by RF annealing 8-88035
 MIS structure, Al_2O_3 insulating layer, electron gun evaporated, HF C-V characts. and surface state density 8-84310
 MIS structure, interface states, thermally stimulated surface pot. 8-68091
 MIS structure, quasitwo dims. excitons and plasmons at different carrier conc. 8-60063
 MIS structure surface characterisation by $C(V)$ curves 8-72276
 MIS structures, surface potential distributions (*Russian*) 8-80065
 MNOS system, interface states 8-84309
 MOS interface states, capture cross-sections 8-64129
 MOS structure, dynamic props. of interface states 8-95373
 MOSFET structure, artificial superlattice near carriers 8-64130
 p-n junctions, capacitance, temp.-depend., by space-charge methods 8-91758
 polariton modes at interface between two conducting or dielec. media, review 8-87922
 polyvinylcarbazole-Hg interface, contact electrification, internal photoemission study 8-60191
 rectifying barrier formation with metal-semiconductor junction (*Russian*) 8-84296
 Schottky barrier formation and shape determ. factors (*Russian*) 8-84295
 Schottky-barrier metal-semiconductor junction carrier migration and equivalent cct. analysis (*Russian*) 8-84294
 Schottky-barrier metal-thin oxide-semicond. structures, physical processes and microelectronics applications (*Russian*) 8-84307
 semiconductor, potential barrier height, temp. depend. (*Russian*) 8-68070
 semiconductor interface, scattering-theoretic approach and its appl. to Ge-GaAs 8-95340
 semiconductor metal interface, Schottky barrier, chemical reaction and charge redistrib. 8-95365
 semiconductor-insulator boundaries, impurity electron states near interface 8-95320
 semiconductor-metal, surface exciton modes for plane and spherical interfaces 8-64113
 semiconductor-metal interfaces, intrinsic surface states and Fermi-level pinning 8-95319
 semiconductor-metal Schottky barrier interfaces in pairing model, covalent-ionic trend 8-95367
 superconducting proximity effect, effect of non-mag. localised states at interface 8-64170
 two-dimensional system, electronic props., conf. Berchtesgaden, Germany (Sept., 1977) 8-60177
 two-dimensional system, random attractive electron-electron interactions 8-60183
 Ag, adsorbed on Si (111), electronic and cryst. struct., Schottky barrier form. obs. 8-84091
 $AlAs-GaAs$ (100) interface, tight binding calc. of electronic struct. 8-95342
 $AlAs-GaAs$ (110) interface, self-consistent calc. of interface states and electronic struct. 8-52066

interface electron states continued

- AlAs-GaAs abrupt (110) interface, electronic struct. 8-95339
 GaAs (001)-Ag contact, surface stoichiometry and struct., and electronic surface states 8-95361
 GaAs (110)-Al(Ga) interface, interface states, photoemission study 8-95359
 GaAs (110)-Au Schottky barriers on ordered and disordered GaAs surfaces, props. 8-95360
 GaAs, epitaxial film on GaAs substrate, two-interface surface polariton modes 8-60180
 GaAs, plasma anodisation in DC discharge, AES and MIS diode expts. 8-95826
 n-GaAs Schottky barrier diode, electron processes at interface (*Russian*) 8-84301
 GaAs-AlAs and related monolayer heterostructures, pseudopot. calc. 8-60198
 GaAs-Ga, (110) interface electron states, photoemission study, chemical shift, surface charge redistrib. 8-72259
 Ge, Schottky barrier, electronic struct., pseudopot. calc. 8-95364
 Ge-GaAs (100) interface, electronic struct., scattering-theoretic approach 8-95340
 Ge-GaAs (110) interface, self-consistent calc. of interface states and electronic struct. 8-52066
 Ge-GaAs abrupt (110) interface, electronic struct. 8-95339
 Ge-GaAs interface, XPS obs. of electronic struct. 8-95341
 Ge-GaAs superlattice and interface, electronic struct. 8-52065
 Ge-metal Schottky barrier junction, surface electron states spectrum (*Russian*) 8-84297
 Ge-ZnSe abrupt (110) interface, electronic struct. 8-95339
 He, liq., surface with trapped electron, parallel mag. field effect on interband transition 8-87835
 p-InAs-Au contacts, influence of free surface on elec. behaviour 8-95362
 InAs-GaSb (001) superlattice, electronic struct., tight binding calc. 8-95350
 InP (001)-Ag, contact, surface stoichiometry and struct., and electronic surface states 8-95361
 Ni-Se interface, reactive diffusion, electronic struct., UPS study 8-51748
 Pt-electrolyte interface, electron states, photoemission studies 8-85171
 Si (111), chemisorbed Cl layer, SCF LCAO band struct. calcs. 8-88010
 n-Si inversion layer, electronic bound states, theory 8-60217
 Si, inversion layer, Hall effect meas. 8-56199
 Si inversion layer, in strong mag. fields, electron localisation 8-60219
 n-Si inversion layer, resist. minima in surface quantum oscills. 8-60215
 n-Si inversion layers, in strong mag. field, quantum galvanomag. expts. 8-60214
 Si inversion layers, stress and intersubband correlation 8-60227
 Si, inversion layers, two-subband screening and transport 8-64126
 Si MOS (111) inversion layers, angular dependent negative magnetoresist. 8-80062
 Si MOS inversion layer, subband struct., many body effects 8-64131
 Si MOSFET inversion layers, IR photocond. and absorption 8-64123
 Si MOSFET structures, photocond. rel. to intersubband transitions 8-64127
 Si solar cells, interface states effects on performance 8-76153
 Si, two-dimensional electrons in superlattice, HF cond. 8-64055
 Si/SiO₂ interface, slow-trapping instability, kinetics 8-76151
 Si-Al₂O₃, inversion layer subbands, magnetocond. oscills. 8-64124
 Si-SiO₂, inversion layer, electronic ground state, stress, temp., mag. field and gate voltage depend. 8-60226
 Si-SiO₂ interface, in MOS struct., fast surface states density, electron irradi. effects 8-88042
 Si-SiO₂ interface, Na⁺ drifted, impurity bands in inversion layers 8-60211
 Si-SiO₂ interface in MIS struct., B⁺ ion implanted, elec. props. due to laser irradi. 8-72272
 Si-SiO₂ interface traps energy distribution meas., in MOS devices, under non-steady-state (*Korean*) 8-64119
 p-Si(111) surface inversion layer, Cs covered, negative magnetoresist. in 2D impurity band 8-64135
 ZnSe-Ge (100) interface, electronic struct., self-consistent pseudopot. calc. 8-91747

interface phenomena

- see also *adsorption; crystal surface and interface vibrations; interface structure; Kapitza resistance; semiconductor-electrolyte boundaries; surface phenomena*
 adsorbed monolayers, permeation and evaporation resistance, attractive forces effects 8-67892
 brass/water interface leaky Rayleigh wave reflectivity loss meas. 8-59187
 charged particle beam, influence of thin inhomogeneities 8-69219
 charged particle beam, influence of thin inhomogeneities 8-69220
 critical fluid interface, in gravit. field, renormalisation calc. in three-dimens. 8-83911
 dilute binary alloy monocrystal, thermodynamics of growth, model (*French*) 8-87635
 electric double layer capacitance meas., potentiostatic method 8-85169
 electrokinetic and surface potentials, for interfaces with two types of ionising groups 8-76136
 electrolyte-solid interface, electrochemistry of surface 8-80798
 electrolytic ion distribution near phase boundary (*German*) 8-56901
 fluid-solid surface interaction, two-particle correlation function 8-79880
 frictionless contact problem for elastic layer under axisymm. loading 8-83341
 gas-liquid annular two-phase flow, wave and interfacial friction charact. 8-67249
 gas-liquid interface, irreversible thermodynamics, eqn. of state 8-51800
 gas-liquid interface, mass transfer, ultramicroprobe method obs. 8-63901
 graphites, ARV, VPP, MPG-6, contact thermal resistance, surface finish and compression depends. 8-79829
 hydrocarbon layer, influence on laser-induced surface damage 8-60533

interface phenomena continued

- inorganic solid, interfacial endothermic reaction, abnormal thermal decomp. rate 8-76852
 interface of two phases or liquids, selective processes induced by resonance laser radiation 8-64867
 interfacial stability with heat and mass transfer, appl. to Rayleigh-Taylor and Kelvin-Helmholtz cases 8-67253
 Lennard-Jones fluid in contact with Lennard-Jones wall, interfacial density profile 8-67901
 Lennard-Jones system, molecular dynamics simulation of interfacial and co-existence props. at triple point 8-83916
 liquid dielectric-liquid conductor, separation surface equilib. and stability 8-91510
 liquid-air interface, dipole layer, electrolyte effect 8-51796
 liquid-liquid interface, adsorbed monolayer mol. orientation, electrolyte effects, reson. Raman obs. 8-60430
 metal surface struct. and initial stages of reactivity, review 8-68837
 metal-metal interface, EM wave propag., plasmon polaritons, computer simulation 8-84276
 metallic glass, thermal stability, validity of energy and entropy interfacial tension models 8-91255
 octane-water interface, water photo-oxidation in presence of adsorbed porphyrins 8-64933
 passivated semiconductor surface, net surface charge determ. using floating field ring devices 8-88037
 penny-shaped crack, Fredholm integral eqn. soln. 8-90784
 phase interfaces, balance eqns. and struct. models 8-59453
 Rayleigh-Taylor instability, method of generalised coords. 8-65771
 reflectivity of superconducting-normal metal interface and applications 8-91822
 SAW, harmonic generation at unbonded interfaces and fatigue cracks 8-90562
 shock wave generation, liq.-liq. interface with temp. discontinuity 8-51197
 sliding mechanism without slipping, interface of two solids 8-51136
 solidification interface in reduced gravity, bubble interactions 8-84787
 succinonitrile solid/liquid interface energy determ. by Abel-Cahn method 8-67909
 surface viscosities at high pressure gas-liquid interfaces 8-75907
 thermodynamics, nonequilib., of discontinuity surface, appl. to n-component viscoelastic mixture 8-93638
 thermoelectric phenomena, irreversible homogeneous materials, single (double) bimetallic junctions (*French*) 8-95291
 two-layer baths, dynamic rectification effect calcs. 8-95934
 viscoelastic interface, constitutive equation 8-84028
 water, supercooled emulsified droplets, relative permitt. and cond., Maxwell-Wagner interfacial polarisation 8-52423
 water-air interface, wind vel. profiles and drift current along wind-generated wave profile (*Russian*) 8-61429
 water-ice interface struct., fluctuations during solidification 8-59935
 water-sediment interface US reflection with bidirectional displacement 8-60017
 Ag/α-Ag₂S, interface, electrochemical transfer across phase boundaries 8-73046
 AgI, interfacial electrochem., review 8-80748
 Au-Ag bilayers, conc. profile by AES, interdiffusion coefficient determ. (*French*) 8-84077
 Cr₂O₃-Al₂O₃, solid soln., effect of Cr on point of zero charge 8-61021
 Cu-Al(In), lamellar eutectoids, calorimetric determ. of interfacial enthalpy 8-60668
 Fe-C, lamellar eutectoid, calorimetric determ. of interfacial enthalpy 8-60668
 Fe₂O₃-Al₂O₃, solid solns., effect on Fe on point of zero charge 8-61021
 Gd₃Ga₅O₁₂, Czochralski grown, effect of melt flow phenomena on perfection 8-88419
 Hg-aqueous electrolyte interface, double layer charge relax., thermal jump meas. 8-53216
 Na conductive glass-Na amalgam interface, electrochem. obs. 8-76870
 Ni-Al (42 at. %), Al₂O₃ growth, form. of voids at metal-oxide interface 8-53030
 Si-SiO₂-KCl_{aq}, interface, capacitance meas. 8-80051
 UO₂(Ni), surface, grain boundary and interfacial energies 8-71905

interface structure

- oxy interface, struct., thickness, intermediate phase effects 8-71831
 adsorption of liq. mixture on solid, equilib. thermodynamics 8-84045
 compound semiconductor interfaces, conf., Los Angeles, USA (Jan. 1978) 8-91756
 double-layer structure, electrohydrodynamical determination 8-95960
 electrode-electrolyte interface, orient. models for solvent 8-61017
 electrolyte-solid interface, electrochemistry of surface 8-80798
 film sandwich structures Auger anal. 8-72030
 gas-solid interfaces, topographic and thermodynamic aspects 8-68927
 glass/polymer, exam. using ion scattering spectroscopy and scattered ion mass spectrometry 8-60641
 graphite fibre reinforced Al, temp. and press. effect on interface chemistry, mech. prop. meas. 8-64595
 Lennard-Jones (100) crystal-liquid interface, structure 8-91284
 liquid-vapour interface, fluctuation theory 8-95204
 oxide layer-metal interface, ion-beam effects, ESCA obs. 8-52612
 oxide-electrolyte interface, transition layer model 8-68895
 periodic misfit-dislocation networks, electron diff. 8-59815
 random distributed steps at interfaces and surfaces, quantitative LEED evaluation 8-63912
 segregation, influence of cooling rate 8-72010
 semiconductor-metal interfaces, Schottky barriers, chemical trends 8-95363
 silane, coupling agent on E-glass fibre, structure, Fourier transform infrared spectroscopy 8-60643
 silane, coupling agent on porous silica, Fourier transform infrared spectroscopy 8-60642
 synchrotron radiation and sputter Auger techniques 8-61130
 zinc phthalocyanine film, between Au or Ag layers, microstruct. characterisation by TEM method 8-95241
 Al-SiO₂ film-substrate interface, obs. of Al₂O₃ and free Si 8-91571
 Al-SiO₂ interface, chem. struct., deposition conditions depend. 8-72007
 Co-Si film system, diffusion marker expts. 8-79824
 Co-Si film system, interaction kinetics 8-79823

interface structure continued

- Fe-Al interface, O₂ content, reson. α -scatt. from ¹⁶O 8-64778
 Fe-fluoro compounds, triboelectric charging, effects of fluorinated compounds 8-60188
 Ga_{1-x}Al_xAs_{1-y}P_y-GaAs quaternary heterojunction, misfit dislocation charact. by synchrotron radiation white beam topography 8-63771
 GaAs (001)-Ag contact, surface stoichiometry and struct., and electronic surface states 8-95361
 GaAs MIS struct., elec. props., effect of interface As domains 8-88032
 GaP, single-crystal, anodically oxidised layers, AES measurements 8-91556
 Ge, interface structural model between amorphous and crystalline phase 8-63941
 Hg, liq.-vap. interface, density profile near triple point, X-ray refl. 8-75821
 In_{1-y}Ga_yP-GaAs heterojunction, VPE, energy band gap and lattice parameter, lattice mismatch effects 8-95345
 InP (001)-Ag, contact, surface stoichiometry and struct., and electronic surface states 8-95361
 Mo-Mn-Fe-Si/Al₂O₃ ceramic seal, interfacial phases 8-72011
 Mo-SiO₂-Si, Mo-Si pelicular structures, struct. transitions during vacuum thermal treatment (*Russian*) 8-95238
 Ni, sputtered, on Si, annealing effects on transmission electron diffraction patterns, silicide form. 8-91562
 Ni-Ti, near equiatomic alloy, TEM exam. of austenite-martensite interface 8-51401
 Si, interface structural model between amorphous and crystalline phase 8-63941
 Si-SiO₂ interface, high-resolution electron microscopy study 8-56046
 Si-SiO₂ interface morphology, P pileup effect, Auger sputter profiling 8-72006
 Si-SiO₂-Si structures, P, As depth profiles, ion microanal. (*Japanese*) 8-85251
 Si-transition metal silicide interface, chemical state, AES expts. 8-91767
 SiC-SiO₂ interface, Auger anal. 8-95375
 Ti film, ultra-thin, AES and XPS anal. 8-91573

interface tension *see surface tension***interface vibrations** *see crystal surface and interface vibrations***interfaces, computer** *see computer interfaces***interfacial energy** *see surface energy***interfacial tension** *see surface tension***interference (signal)**

- see also crosstalk; electromagnetic interference*
 birth monitoring by cardiocography, interference effect by infusion pumps (*German*) 8-85416
 ECG, grounded, resistance to coherent mains interference, exptl. evaluation 8-85419
 film-grain noise, low-contrast image detection 8-94370
 foetal heart rate recording, interference due to infusion pump (*German*) 8-85414
 pacemaker interference simulation by models 8-81069
 plasma density IF phase meas. using three-mirror interferometer 8-75414

interference (wave)

- see also acoustic wave interference; electromagnetic wave interference*
 education, electron interference using standard electron microscope and electron biprism as interferometer 8-62005
 field emission electron beams, two beam interference 8-63002
 low intensity interference effects, hidden variable theories 8-70009
 phase evaluation by electron diffraction by electron interferences (*German*) 8-74112
 seismic waves interference effects in thin layers 8-92780
 Young's double beam interference experiment with spinor and vector waves 8-89363

interference spectrometers

- curved crystal spectrometer, geometrical aberrations analytical and numerical study 8-78002
 demonstration of Fourier transform spectroscopy for students 8-57722
 Fabry-Perot, signal noise limitations in data retrieval, winds, temp. and emission rate 8-93763
 Fabry-Perot laser spectrometer, for nonlinear superhigh-resolution spectroscopy 8-49912
 far IR spectrometer with interference selective AM 8-86362
 Fabry-Perot interferometer, with automated data acquisition and stabilisation system 8-70180
 Fourier spectrometer, amplitude-phase charact. of electrical channels 8-82058
 Fourier spectrometer, electrodynamic drive system 8-82059
 Fourier transform, Doppler-limited high-accuracy, 10⁶ samples 8-58068
 Fourier transform, history, current status and commercial future 8-58072
 Fourier transform spectrometer, simplified, for on-line anal. appl. 8-58074
 high resolution Fourier transform spectrometer, 0.005 cm⁻¹, for 0.6 to 100 μ m spectral range 8-70204
 high-resolution optical heterodyne spectrometer 8-82048
 holographic grating, calc., for very wide field camera (*French*) 8-81547
 interferometer-grating spectrograph for high resolution spectroscopy in middle UV 8-77490
 IR analyser, single-component, based on attenuated total reflection technique 8-58074
 lamellar-grating Fourier transform spectrometer, high resolution, for submm. region 8-70203
 large angle laser interferometer for 'curved' crystal spectrometer, precision 8-77973
 Martin-Puplett interferometer, use as Fourier spectrometer and for OTF meas. 8-70179
 Michelson interferometer, all-refl., for far IR Fourier spectroscopy 8-70205
 Michelson interferometer for Fourier transform. IR spectroscopy 8-49914
 microcomputer based scanning instrument controller, for Fabry-Perot interferometer 8-93764
 multislit spectrometer for the night airglow observation 8-73542

interference spectrometers continued

- resolution of Fourier spectrometer, determ. using solid-state Fabry-Perot etalon 8-89569
 scanning interferometric multiplex photometer, airglow appls. 8-62216
 selective modulation interferometric spectrometer, theory, design 8-58054
interference spectroscopy
see also Fourier transform spectroscopy
 dispersive Fourier transform spectroscopy, mode of operation of polarising interferometer 8-78003
 Fourier transform, comparison of refl. and refr. optics in condensing element of two-beam interferometer 8-77968
 multi-pulse spectroscopy with Ramsey fringes, resolution and signal strength 8-82869
 nonlinear processing of interferogram 8-89553
 optical Ramsey fringes in two-photon spectroscopy, time delayed pulsed Doppler free technique 8-82708
 optical screw, path difference meas. and control device, anal. of periodic errors 8-77972
 Ramsey fringes in saturation spectroscopy 8-82868
 saturation spectroscopy, improved S/N ratio 8-70193
 saturation spectroscopy using Jamin interferometer 8-74079

interference suppression

- see also echo suppression*
 60 Hz harmonic eliminator, for biomedical signals 8-77124
 adaptive filter based on SAW monolithic storage correlator, appl. to CW interf. suppression 8-87208
 amplifier, phase-sensitive, appl. to interference suppression and light detection (*Czech*) 8-86331
 demand pacemaker interference sensing functions 8-57123
 dental drill with noise, vibr. radiointerference reduction 8-85450
 ECG, grounded, standardisation of resist. to external cophasal power line interference for isolated patients 8-57085
 ECG fine structure analysis by noise reduction (*German*) 8-73268
 electron micrograph optical and digital spatial freq. filtering 8-70231
 evoked potential optimal filtering in sequential range (*German*) 8-85401
 extracellular action potential recording, interference suppression 8-61294
 finger tremor amplitude and freq. artefact reduced routine meas., portable equipment (*German*) 8-85407
 IR background suppression algorithm 8-77985
 LF noise suppression in thermal viewing system 8-82035
 Mollenstedt electron vel. analyser high-order energy loss lines removal 8-93786
 optical communication using two-photon laser, optimum control of quantum noise 8-71049
 random nucleated halftone screen 8-62192
 stimulus artifact suppression, sample and hold amplifier system 8-77163
 vertical ionosonde receivers (*Polish*) 8-88950

interferometers

- see also acoustic wave interferometers; electromagnetic wave interferometers; interferometry*
 double Josephson junction interferometer, dynamics 8-68118
 electron double crystal interferometer 8-83687
 fast interferometric chopper for neutrons and X-rays 8-82088
 Mollenstedt-Duker electron biprism, use of Wollaston wire 8-54512
 neutron interferometer, with two cryst. components, construction 8-83654

interferometry

- see also acoustic wave interferometry; electromagnetic wave interferometry; holographic interferometry; interferometers*
 calibration two-coordinate measuring devices (*German*) 8-89433
 phase detection using LSI-11 microcomputer and high-speed digital techniques 8-71545

intergalactic matter

- see also clusters of galaxies; galaxies*
 Abell 2118 cluster, extent of hot intergalactic gas 8-86021
 clusters of galaxies, gas content meas. by obs. of microwave background at 10.6 GHz 8-96551
 clusters of galaxies rel. to infalling intergalactic matter and X-ray luminosity 8-93487
 Coma cluster, intracluster mag. field from halo radio source meas. 8-86027
 Coma galaxy cluster, low energy X-ray absorpt. obs. 8-86025
 dust in galaxy clusters, evidence from Zel'dovich effect 8-54041
 enriched gas in clusters and dynamics of galaxies and clusters rel. to galaxy formation 8-77596
 galactic ring structs. form. by collisions with gas clouds (*Russian*) 8-93425
 H I associated with galaxies NGC 4631/NGC 4656, aperture synthesis obs. 8-54043
 head-tail radio galaxies in poor clusters, radio and optical obs. 8-96530
 Hydra I cluster, ram-pressure sweeping, optical evidence 8-93429
 II Zw 70/II Zw 71, compact galaxies, H I maps, tidal interactions 8-96531
 intracluster gas, heating by relativistic electrons rel. to cluster X-ray and radio emission 8-57655
 intracluster gas flow patterns and X-ray emission 8-65705
 Magellanic Stream, turbulent wake of Magellanic Clouds in galactic halo 8-69884
 matter-antimatter hydrodynamics, annihilation rate calc. 8-73780
 missing dark mass rel. to primordial star generation 8-61946
 NGC 315, NGC 6251, very large radio galaxies intergalactic mag. fields from 11.1 cm obs. 8-86014
 NGC 4631 group of galaxies, intergalactic neutral H rel. to tidal interactions model 8-54059
 Perseus galaxy cluster, low energy X-ray absorpt. obs. 8-86025
 prestellar gas clouds, spectral lines prediction (*Russian*) 8-77628
 QSOs directions, intervening primordial gas rel. to absorpt. line regions physics 8-57680
 quasar absorption line clouds, radiative accel. 8-57683
 quasars absorption lines origin, evidence for cosmological hypothesis 8-57684
 radiative accretion flow onto giant galaxies in clusters 8-93433
 reddening determ. method 8-54039
 star formation before galaxies, missing mass soln. 8-57654
 Virgo galaxy cluster, low energy X-ray absorpt. obs. 8-86025

intergalactic matter continued

- X-ray clusters of galaxies, radio limits on ionised gas 8-89243
 Fe-enriched gas in clusters of galaxies, origin and evolution 8-93390
 H I high velocity clouds, high sensitivity survey 8-65686

intermediate bosons

- colliding e^+e^- beams accelerator expts., 100 GeV, particle prod., weak currents, etc. (*Russian*) 8-58194
 Higgs boson, bremsstrahlung prod. with heavy fermion pair in e^+e^- collisions 8-86449
 Higgs boson, spontaneously broken gauge theory phenomenon, possible weak interaction model 8-74200
 Higgs new light boson, search 8-70319
 High energy behaviour of weak interactions and renormalisable theories, book contrib. 8-78164
 lepton-quark model, supermultiplet of weak bosons and Higgs scalar 8-62345
 light neutral gauge boson in SU(2) gauge model consequences for e^+e^- and $pp(\bar{p})$ reactions 8-58154
 massive Schwinger model, asymptotic completeness and confinement 8-66028
 perturbative QCD and exptl. signatures of weak bosons 8-93916
 universal CP noninvariant superweak interaction and baryon asymmetry of the universe 8-66072
 weak interaction theory review, Higgs bosons 8-78131
 weak interactions of ultra heavy fermions 8-93838
 e^+e^- inclusive hadron prod., neutral weak currents 8-50041
 Higgs meson prod., possible signals in high energy collisions, gauge groups 8-89649
 Y(9.5), nature of heavy particle anal. (*Chinese*) 8-86443
 W-boson mass and neutral electron-type heavy lepton 8-66100
 Z⁰ flux loops, more heavy particles in the Weinberg-Salam model 8-82136

intermediate state

- reflectivity of S-N interface, application for Rowell-Tomasch oscills. amps. and thermal cond. 8-91822
 thermal conductivity, Fermi surface shape and topology effects (*Russian*) 8-72314

intermetallic compounds *see alloys***intermodulation**

- ionospheric cross-modulation of radio signals between two nearby stations 8-93048
 laser diode characterisation, for multichannel applic. 8-87165
 optical communication, TDM pulse analogue modulation, diode laser nonlinearity 8-55455

intermodulation measurement

- No entries

intermolecular forces

- see also Van der Waals forces*
 atom+diatom potential, asymmetric, isotope substitution effect, Legendre expansion coord. transformation 8-70894
 benzene, $\pi\pi^*$ and Rydberg bands, cryogenic solvent effects 8-55182
 benzene, in Br₂-carbon tetrachloride soln., complex form., IR spectra 8-70828
 carbonyl groups, intermol. interactions in H₂CO-H₂CO system, quantum chem., classical calcs. 8-86932
 conformational props. rel. to spatial electron density determs., computer simulations 8-70763
 distance force consts., pseudocritical volumes 8-58765
 ethylene+Cl₂(Br₂) complex, intermolecular interaction and struct. SCF-MO-LCAO CNDO/2 calc. 8-58763
 fluid, intermolecular potentials, coulombic and multipolar, 2-dimens. mol. dynamics simulation 8-75520
 fluids with polar, quadrupolar, octupolar mols., thermodynamics, vapour-liq. equilibria 8-95127
 halogen molecular crystal, bond charge model, for lattice dynamics 8-79692
 interacting systems, general theory of natural states, use for calc. of intermol. forces 8-82807
 interacting systems, natural states in the asymptotic 1/R expansion, use for calc. of intermol. forces 8-86930
 iodomethane, liq. (liq. mixtures), vibr. relax. and reorientation, symmetric C-H bending mode 1st overtone 8-62884
 isotropic, approx. method, crit. test using H-H ($^3\Sigma_u^+$) as model 8-78771
 lipid bilayer membrane interaction forces in zone of contact 8-53345
 liquid metal, effective interionic potentials 8-91221
 liquids, long-range dipolar interactions in computer simulations of polar liquids, Monte Carlo calc. 8-87603
 polymer, liq., Brillouin scatt. and segmental motion, appl. to polypropylene glycol 8-91217
 Raman spectra of liq. phase weak H-bonds, short range order and anharmonicity effects 8-64357
 scattering, low-energy, by long-range pot. 8-74723
 simple liquid intermolecular interaction, extremal values 8-87602
 TCNE, K salt, in nematic liq. crystal solvent, ion pairing, EPR spectra 8-73020
 tertiary phosphine oxide+aliphatic alcohol, $\pi\pi$ - $d\pi$ conjugation, electronegativity and H-bond energy 8-82863
 tris-butadienyl metal D₃ complex pairwise chiral discriminations, stereochem. basis, extended transition monopole model 8-74725
 water, long range forces in mol. dynamics calcs. 8-79517
 Ar-N₂ interaction, electron gas pot. calc., Gordon-Kim model, ang. orientation depend. 8-70893
 CS₂, $\pi\pi^*$ and Rydberg bands, cryogenic solvent effects 8-55182
 DCN, self-assoc. in matrices, IR vibr. spectra of multimers 8-86858
 H+Br₂(Cl₂), nonreactive scatt., long range anisotropic pot. determ. 8-66626
 H₂-Ar(Kr)(Xe) mixtures, intermol. forces 8-62867
 HCN, self-assoc. in matrices, IR vibr. spectra of multimers 8-86858
 HCl-dimethylether complex, gaseous, H-bond IR spectra, temp. depend. theory 8-62804
 (HF)₂, intermol. force model, rel. to liq. struct. 8-78773
 H(1s)-H(1s)($^2\Sigma_u^+$) isotropic intermol. force, model for approx. method, crit. test 8-78771
 LiF oligomers, struct., stability SCF and CEPA-PNO calcs. 8-78640
 LiH oligomers, struct., stability SCF and CEPA-PNO calcs. 8-78640
 NH₃, ND₃, crystals, rotation mol. motion (*Russian*) 8-87762
 (NH₃)₂, dimer, intermol. pot. calc. 8-58764
 Na, liq., effective interionic potentials 8-91221
 NaF oligomers, struct. stability SCF and CEPA-PNO calcs. 8-78640

intermolecular forces continued

- NaH oligomers, struct., stability SCF and CEPA-PNO calcs. 8-78640
 Na⁺(3p)+Na₂, collisional and radiative processes, fluoresc. decay obs. 8-66638
 OCS, IR spectral moments and mean squared torques, rare gas effects 8-62944
 Pb, liq., effective interionic potentials 8-91221
 Rb, liq., effective interionic potentials 8-91221
 SBI₃, intermolecular bonding study using ¹²⁹I Mossbauer effect 8-72438

intermolecular mechanics

- see also association; intermolecular forces; kinetic theory of gases; liquid structure; liquid theory; Morse potential; potential energy functions*
 absorption profiles, relax. mechanisms effects 8-58664
 alkylammonium iodides, solns., MCD spectra of iodide ions 8-94268
 atom+symmetric harmonic oscillator, vibr. energy transfer, 1-D and 3-D rate consts. calcs. 8-50611
 bimolecular potentials, forces and torques, S- and V-function expansions 8-74730
 binary gas mixtures, force consts., intermol. pots. calcs. 8-66624
 carbon tetrachloride, isotropy, mol. interactions, effects, Raman scatt. obs. 8-58697
 chloroform-d₁, isotropy, mol. interactions, effects, Raman scatt. obs. 8-58697
 conformers, dynamic interaction between ground states, effect on IR spectra 8-58767
 differential cross sections, rainbow and diffr. oscills. damping, anisotropic pots. 8-50608
 dipolar molecules, IR absorpt. bands., temp. effects (*Russian*) 8-90228
 fluorinated hydrocarbons, mol. recognition and self-organisation, information storage appls. 8-82806
 inert gas interactions, correl. and exchange energies, statistical methods calcs. 8-86931
 liquids, solute-solvent interactions, moment anal. of IR absorpt. bands 8-58766
 microdrop, two-dimensional, on solid body surface, stability dynamics 8-51790
 molecular beam scattering experiments and techniques (*German*) 8-86971
 molecular fluid, pair correlation function, perturbation theory 8-55799
 polyatomic asymmetric top molecules, solns., IR spectra 8-58694
 TCNE, electron donor-acceptor complexes, EPR (*German*) 8-55187
 TCNQ, electron donor-acceptor complexes, EPR (*German*) 8-55187
 wetting, mechanism, mol. dynamics 8-51789
 ArKr, intermol. pots., differential cross-sections inversion calcs. 8-66619
 Cr³⁺ hydration model, external water interactions 8-78772
 H₂O, liq., intermol. coupling, isotope and salt effects, Raman spectra 8-90169
 Li⁺+H₂O, ab initio GTO calc. of vibr. intensity changes of spectroscopic parameters 8-58583
 NO, adsorbed on MgO, dimer form., heat of dissociation, EPR obs. 8-82755

intermolecular vibrations *see molecular rotational-vibrational energy transfer***intermolecular vibrations (molecular crystals)** *see lattice dynamics of molecular crystals***internal combustion engines**

- diesel engine composite pistons, heat transfer calc. method (*French*) 8-63424
 torsional vibr. dampers using silicone oil, props. of oil at various freqs. (*German*) 8-67164

internal conversion

- see also conversion electron spectra*
 K- and L₁-subshells internal conversion coeffs., relativistic effects 8-66245
 polarisation of conversion electrons, parity violating nuclear forces 8-50125
 radioactive nuclide decay data for reactor calcs., activation products and related isotopes 8-82426
¹³⁷Cs, 161 keV transition M1-E2 mixing ratio and nucl. struct. parameter 8-74332
⁶⁷Ge, from ⁶⁴Zn(α,n), coupling consts., M1, M2, E3 transitions 8-89823
⁶⁷Ge, mass excess and low lying states, comparison with ^{63,65}Ni, ^{65,67}Zn and ⁶⁹Ge, from ⁶⁵Zn($\alpha,n\gamma$) 8-66213
¹⁵⁸He^{g.m.} decay, obs. of ¹⁵⁸Dy collective excitations 8-82270
¹⁵⁸Nd(²⁰Ne, xny), multiplicities of yrast and statistical cascades, total γ conversion coeff. 8-70484
¹⁴⁷Pm, internal bremsstrahlung photon intensity and energy yield 8-86509
¹⁴⁸Sm levels from ¹⁴⁸Eu decay, struct. interpretation from boson expansion model (*Russian*) 8-78261
¹²¹Sn^m→¹²¹Sn^g→¹²¹Sb, branching fraction, K-shell IC coeff. 8-82319
⁹³Tc 17/2- isomer, internal conversion coeffs., parity mixing search from ⁹²Mo($\alpha,2np$) 43 MeV 8-78255
¹⁰⁶Tc internal conversion, isomeric level half life from ¹⁰⁰Mo(p,n), 3.7 MeV 8-78313
²³⁵U fission fragments, internal conversion cascading 8-94036
²³⁵U(n_{th},f) ionic charge distrib., effect of internal conversion 8-78428
²³⁸U, nuclear excitation rate in high-temp. environment 8-66244
²³⁸U+²³⁸U (¹³⁶Xe), nuclear Coulomb excitation, inner shell ionisation and internal conversion, quasimol. formation 8-94026

internal conversion in molecules *see nonradiative transitions***internal fields, crystal** *see crystal field interactions***internal friction**

- see also Bordoni effect; damping; Snoek effect; Zener relaxation*
 Bordoni relaxation, theoretical aspects, numerical calcs. from thermally activated double kink formation 8-63805
 Cotac 74, directionally solidified composite, creep behaviour prediction (*French*) 8-68754
 dislocation damping during electron irradiation, new model for peaking effect 8-87683
 elastic waves at frictional boundary, transmission (reflection), approx. anal. method 8-63371
 elasto-plastic metal-dislocation system, stress-activated dislocation motion, thermodynamic theory (*Chinese*) 8-83868

internal friction continued

- enstatite, elastic modulus and internal friction in single crystal 8-85550
 forsterite, elastic modulus and internal friction in synthetic polycrystal 8-85550
 III-V compounds, point defects, internal friction meas. 8-71787
 inelastic solids, anelastic relaxation anal., extended to creep at high temp., appl. to internal friction (*French*) 8-63806
 ionic single crystals, elec.-mech. coupling of dislocations 8-75676
 magnetostriuctive core dimens., influence on internal friction and shear modulus 'defect' 8-95506
 metals and alloys, polycrystalline, LF viscosity meas. 8-80576
 peridotite, elastic modulus and internal friction 8-85550
 polyvinylidene fluoride, γ -irradiated, low temp. internal friction 8-83874
 rocks, fracture regularities with internal friction and dilatancy 8-85537
 rocks, internal friction and resonant freqs. 8-65268
 shafts, noncircular cross section, effect of external forces and internal friction on rotary motion (*French*) 8-63274
 steel, austenitic stainless, Mn-N interaction, internal friction obs. 8-84883
 steel, C and Co, carbide transitions during post-strain ageing and tempering (*Russian*) 8-95741
 steel, Mn-Cr-Ni-N, N effect on relaxation behaviour, internal friction temp. depend. (*Russian*) 8-52872
 steel, Ni-Mn-C, austenitic, proof stress change meas. by internal friction with martensitic transform. 8-56638
 technological strength and nondestructive methods of testing during heat treatment 8-85090
 Ag, electron irradi., elastic moduli and internal function (*French*) 8-87703
 Al-Ag (up to 40 at.%), exam. of anelastic phenomena and structural state 8-76693
 Al-Fe, electron irradiated, interstitial-solute complexes, internal friction spectra 8-92289
 Al-Li alloy, dil., quenched and irradi., recovery, resist. and internal friction obs. 8-52848
 Al-Si, internal friction and Si precipitate nucleation 8-60690
 Cd, dislocation internal friction, orientation depend., for single crystals. 8-52882
 Cu, amplitude depend. modulus effect 8-64573
 Cu, cold worked, determ., of dislocation pinning and unpinning stages, using internal friction meas. 8-92278
 Cu, wire, polycryst., internal friction, ultrasonic vibrations effect (*Russian*) 8-76685
 Eu₂O₃-Ta₂O₅, microcracking, elastic props., internal friction 8-92326
 Fe-Co, damping capacity of Gentalloy, internal friction meas., mech. and mag. depend. (*Japanese*) 8-52875
 Fe-Co (5 to 25 wt.%), exam. of damping capacity of Gentalloy 8-72800
 Fe-H system, cold work internal friction peak, appl. of Schoeck's model 8-95771
 Fe-Ni alloy, N27T2 and N28, internal friction peaks after reverse martensitic transform. (*Russian*) 8-92287
 Fe-Ni base metallic glass, annealing embrittlement 8-64635
 FeO-P₂O₅ glasses, electrical and mechanical losses 8-80283
 KH₂PO₄, ferroelec. crystals, torsion pendulum technique 8-72474
 LiNbO₃, LF sound attenuation, internal friction 8-63804
 Mg, dislocation internal friction, orientation depend., for single crystals. 8-52882
 MgO, plastically deformed, recovery of internal friction at room temp. (*French*) 8-80577
 Mn_{0.82}Fe_{2.18}O₄, anelasticity, 280 to 730K, 125 kHz vibr. study 8-87740
 Na₂O-SiO₂, effect of annealing on absorbed H₂O action on temp. spectra of internal friction 8-88487
 Na₂O-SiO₂ fibre, reactivity to atmospheric moisture below annealing range, internal friction measurement 8-92288
 Nb, H₂ loaded, cold worked, plastic deformation, exam. of α internal friction peak 8-92307
 Nb, plastically deformed, hydrostatic pressure effect on dislocation relaxation, US exam. 8-76696
 Nb-H₂ behaviour of H in Nb, relation to mech. props. 8-80572
 Nb-H alloys, evidence of internal friction peak 8-52881
 Nb₂Ge, metallic glass, internal friction peak obs. 8-79666
 NbN_x, solid soln, strain ageing, internal friction, elec. cond. kinetics (*Russian*) 8-76667
 NbN_xO_y, solid soln, strain ageing, internal friction, elec. cond. kinetics (*Russian*) 8-76667
 NbO_x, solid soln, strain ageing, internal friction, elec. cond. kinetics (*Russian*) 8-76667
 Ni, magnetoelastic effects, ΔE -effect and macroeddy current damping, internal friction meas. 8-64253
 Ni, pure and doped, mech., mag. relax. meas. dumb-bell self-interstitial reorientation (*German*) 8-52879
 RbH₂AsO₄, ferroelec. crystals, torsion pendulum technique 8-72474
 RbH₂PO₄, ferroelec. crystals, torsion pendulum technique 8-72474
 Si, neutron irradi., internal friction obs. of defects 8-51597
 SiO₂ glass fibres, exam. of phase separation effect on internal friction 8-88455
 Ta, internal friction measurements, of O₂ and N₂ diffusion 8-75888
 Ti, influence of H₂ on the internal friction (*French*) 8-75723
 V, internal friction α -peak origin 8-95773
 Zn, dislocation internal friction, orientation depend., for single crystals. 8-52882
 Zr, terminal solid solubility of H, optical metallography, internal friction meas. 8-83962

internal friction of liquids see viscosity of liquids

internal mechanics, molecular see molecular vibration

internal mechanics of atoms see atomic structure

internal modes see molecular vibration in solids

internal stresses

- antiferromagnet, residual stress induced domains, specific heat meas. anal. 8-60286
 Bordoni relaxation, theoretical aspects, numerical calcs. from thermally activated double kink formation 8-63805
 ceramics, structural stress meas. using X-ray diff. meas. (*German*) 8-52744
 composite materials, density depend. of strength (*German*) 8-94592
 compressed crystals, dislocations and point defects (*Russian*) 8-75666

internal stresses continued

- cylinder, solid, residual tangential stress determ. from segment sections, appl. 8-60902
 diamond composite with Cu-Ti matrix, microstresses, X-ray diff. exam. 8-56679
 dispersion hardened alloy, calc. of back stress decrease, due to Orowan dislocation loop climb 8-83812
 electroplated coatings, theory and meas. review, effects in Ni and Zn (*German*) 8-56049
 fatigue crack growth in vacuum 8-56729
 fatigue crack propagation, in shaft or axle type components, problems specification 8-51120
 fibre reinforced composite, imperfections, piezo- and elasto-optical effects under longitudinal shear (*Russian*) 8-56457
 fibre reinforced materials, prod. of uniform plane stress states 8-85064
 film, stress measurement method using real-time holographic interferometry 8-84099
 film on single cryst. substrate, X-ray meas. method 8-51860
 friction machine, residual stresses meas., appl. to wear resist., surface wear 8-60906
 hardened components, residual stress, elastic characts. after surface plastic stress 8-60901
 incremental deformations of initially stressed media with couple stresses 8-62077
 ionic crystal, exposed to high-current electron beam pulses, min. size of excited region for crack initiation (*Russian*) 8-84961
 Lochseiten limestone, differential stress in Glarus overthrust 8-88822
 metal, internal stress meas. by decremental unloading technique 8-64576
 metal, oxide film growing by cation diffusion, stress generation 8-60865
 metal matrix composites, thermal expansion effects, fibre length depend. 8-51708
 metals, residual stress and deformation, due to quenching, elastic-plastic anal. (*Japanese*) 8-83268
 molecular internal stresses, stress tensor, one electron system 8-62686
 non-linear viscoelastic behaviour, numerical anal. 8-59318
 oblate spheroidal inclusion, internal stress, misfit, inhomogeneity and plastic deform. 8-60701
 oxide single crystals, Czochralski grown, thermoelastic stresses 8-55822
 plate, orthotropic multilayered, vibr. modes, acoustic transmission 8-83142
 polymer film, supermolecular structure and mech. stress distrib. among chem. bonds 8-75562
 polymer films and sheets 8-80590
 polystyrene conc. sols. in toluene, rheological behaviour (*German*) 8-55618
 portable X-ray analyser for residual stresses, design, operation and testing 8-53058
 Prandtl-Reuss plastic materials, with general work hardening, constitutive equations (*Japanese*) 8-92276
 α -quartz, Raman FTIR spectra, surface layer and vol. spectra comparison 8-52491
 rock bodies, cooling, residual stress development 8-88819
 sheet, cold rolled, texture form., model (*French*) 8-68705
 sintered granules, onset of stresses of first kind, mechanism (*Russian*) 8-80485
 solid solution, diffusion, influence of conc.-induced stresses (*Russian*) 8-55969
 steel, alloy, Ni-Cr-Mo, alloys SNCM8, SAE 4161, heat treated, residual stress at fatigue fracture surface (*Japanese*) 8-64622
 steel, deformed strain-aged St.3 and 09G2S, stress conc. susceptibility, H₂ effect 8-95774
 steel, free plate elastoplastic stress condition during phase transformation 8-95781
 steel, high strength, fine grained, quenched and tempered, residual welding stresses, stress relieving temp. (*German*) 8-72793
 steel, low-alloy sheet, welded hydraulic turbine volute chamber, strength and toughness 8-68820
 steel, low-C, sheet, thin, residual stresses determ. after bending 8-60708
 steel, nitrided EN41B, effect of residual stresses on fatigue failure 8-64698
 steel, notched bar, plastic zone determ. near rupture (*French*) 8-88515
 steel, spheroidized, Bauschinger effect and work hardening 8-64596
 steel, structural, brittle fracture, intermediate fracture stress, fracture initiation mode transition 8-60802
 steel, tempered StE70, water quenched, residual stress field in centrally welded plates (*German*) 8-72794
 steel shaft, residual tangential stress determ. after elastoplastic twisting 8-60902
 stress tensor in nematic liquid crystals, micropolar continuum mechanics 8-67647
 stress tensor in nematic liquid crystals, micropolar continuum theory 8-67648
 tempered glass discs, meas. of nonuniform distribution of residual stresses 8-95865
 theory, rel. to X-ray topography data 8-64254
 tube with hexagonal bore, crack formation during rolling (*Russian*) 8-80622
 type II superconductor, dielastic interaction of flux line lattice with internal stresses of cryst. imperfections 8-56270
 vacuum deposited films, mech. props. 8-75968
 wire, device for uniform electrolytic removal of surface layers for residual stress determ. 8-60918
 Ag ultra-thin film, deposited on MgF₂ and SiO substrates, struct. and internal stress 8-91572
 Al alloys, quenching rate rel. to mech. props., residual stresses, optimum quench coolings (*French*) 8-64562
 Al, orthogonal cut surface, effect of cutting condition on residual stress (*Japanese*) 8-85035
 Al-Cu-Mg alloy, influence of plastic deformation on fatigue limits, for prestrained components 8-68799
 Al₂O₃, sintered, residual stress meas., piezospectroscopic technique 8-52704
 Al₂O₃-SiO₂ clad with B₂O₃-SiO₂ effect of drawing tension on residual stresses 8-64554

internal stresses continued

- Bi₂-Sb₂Te₃, solid soln. film on mica substrate, effect of stresses on elec. cond. 8-51859
 Co-Ni alloys, electrodeposited, struct., internal stress, and mag. props. 8-95471
 Co₃B₂O₁₃, intermediate phase between paraelectric and ferroelectric phase (*Russian*) 8-68465
 Cu, internal stress meas. by decremental unloading technique 8-64576
 Cu, internal stresses in plastically deformed crystals (*Russian*) 8-79615
 Cu single crystals, in high temp. creep, meas. of internal stress 8-80608
 Cu-Au (50 at.%), ordered, influence of elastic stresses on mech. props. (*Russian*) 8-92298
 Dy, anomalous thermal expansion, interferometric meas. 8-52333
 Fe, internal stress meas. by decremental unloading technique 8-64576
 Fe, low temperature deform., strain-rate cycling and stress relaxation tests (*Japanese*) 8-52876
 Fe-Al (0.069 and 0.158 wt.%), internally oxidised, low temp. deform. (*Japanese*) 8-52876
 α -Fe-Fe₃C alloys, ground surface layer exam. of props. 8-84840
 Fe-Ti (0.056 at.%), mobile dislocations during stress relaxation 8-68722
 (Fe-Ni)_x-(SiO)_x, cermet film, internal stresses (*Russian*) 8-75951
 Gd-Co amorphous sputtered films, magnetoelastic contrib. to perpendicular anisotropy, internal stress meas. 8-95490
 Gd-Fe amorphous sputtered films, magnetoelastic contrib. to perpendicular anisotropy, internal stress meas. 8-95490
 Gd-Y alloy, anomalous thermal expansion, interferometric meas. 8-52333
 In₂O₃-SnO₂ film, stress, and elec. and optical props. 8-51861
 MgO, lattice misorientation and displaced vol. for microhardness indentation 8-64617
 Mo, film, vacuum deposited, elec. cond., internal stresses, surface corrosion, MOS gate appl. (*Japanese*) 8-80073
 NH₄Cl, order parameter, electro-optic measurement 8-88280
 NaCl, exposed to high-current electron beam pulses, min. size of excited region for crack initiation (*Russian*) 8-84961
 Si, deformed surface, defect struct. rel. to elec. props. 8-72231
 Si, epitaxial layer on sapphire, shear strain, TEM 8-51835
 Si, film, CVD, low press., struct. and stability, X-ray diff. and TEM obs. 8-91559
 Si, ion implantation damage, annealing, role of stresses 8-75679
 Si: (B, P, Ge), impurity-pair diffusion, influence of elastic stresses 8-87824
 Si:Sb, ion implanted, annealing behaviour of stress 8-63778
 Si-SiO₂ structure, mechanical stress at Si(111) surface 8-63921
 Si-SiO₂-Al structure, mechanical stress at Si(111) surface 8-63921
 SiN film, on Si substrate, thermal stresses and cracking resist. 8-63958
 Si₃N₄ film, on Si substrate, thermal stresses and cracking resist. 8-63958
 SiO₂ film, on Si substrate, thermal stresses and cracking resist. 8-63958
 SiO₂-Al₂O₃-B₂O₃-MgO-CaO-Na₂O, strengthened by ion exchange, exam. of internal stresses using polarising microscope 8-88549
 Ti, internal stress meas. by decremental unloading technique 8-64576
 Ti₂O₃, reduced rutile, elastic strain energy due to crystallographic shear plane arrays 8-55880
 V₂Ge, bronze-processed, stress-induced enhancement of supercond. T_c 8-64159

internuclear double resonance *see* INDOR**interplanetary magnetic fields**

- see also interplanetary matter*
 1972, August, field direction correl. with cosmic rays north-south anisotropies 8-89018
 B_z-component, magnetosphere response dusk-dawn asymmetry 8-89006
 B_z-component, pulses rel. to geomag. field disturbances 8-73583
 B_z-component, search for correl. with counter-electrojet 8-88983
 control of geomagnetic storm development 8-85771
 corotating regions, nucleon accel. and modulation of Jupiter electrons 8-61690
 cosmic ray intensity solar diurnal variation, interplanetary mag. field north-south component correl. 8-93057
 cosmic ray scatt. in stochastic mag. field, solar wind fluctuations, above 1 GeV 8-61689
 cosmic ray streaming perpendicular to mean mag. field, gyrophase distrib. function 8-53778
 cosmic rays, quiet-time anisotropies rel. to mag. field data 8-77442
 direction, rel. to mag. substorm phase and daytime ionospheric absorpt. surges 8-73575
 early field intensity determ. from remanent magnetisation of Kirin meteorite (*Chinese*) 8-89136
 fluctuations, power spectra rel. to geomag. field fluctuations at synchronous orbit 8-96358
 frequency spectra of fluctuations rel. to mean field direction 8-85905
 geomagnetic field quiet time var. rel. to interplanetary mag. field, autocorrel. effects 8-61697
 geomagnetic pulsations, connections with interplanetary mag. field 8-85773
 heliocentric distance dependence 8-73675
 HEOS-2 magnetometer data rel. to interplanetary diffusion coeff. for energetic particles 8-96364
 Imp-J of N-S component, auroral zone electric and geomagnetic responses 8-77431
 magnetosphere boundary, mag. field from laboratory simulation data 8-57396
 north to south component, correlated field and equatorial electrojet changes during mag. storm. 8-85766
 north-south component, vars. rel. to equatorial ionosphere EM state rel. to interplanetary mag. field vars. 8-77413
 orientation, rel. to zodiacal light circular polarisation 8-96428
 primeval field intensity determ. from Jilin chondrite (*Chinese*) 8-85917
 radio mapping expt. in International Sun-Earth Explorer C spacecraft 8-85796
 sector boundaries and comets, plasma tail disconnection due to mag. field line reconnection 8-93155

interplanetary magnetic fields continued

- sector boundaries rel. to Sun-weather relation, troposphere energetics anal. 8-81285
 sector structure, rel. to atmospheric electrification modulation and Sun-weather relationship 8-57261
 sector structure correl. with meteor radar rates and geomag. activity 8-65553
 sector structure inferred from geomag. ap indices daily vars. 8-93066
 solar corona, mag. field from Crab nebula polarised radioemission occultation obs. (*Russian*) 8-77527
 solar cosmic rays propag., diffusion in mag. fields, convection in solar wind, dimens. method soln. (*Chinese*) 8-81511
 solar magnetic sector crossings, lack of effects on troposphere 8-57244
 solar plasma regime, rel. to cosmic ray storm symmetrical equator-pole anisotropy obs. 8-89020
 solar wind, mag. field effect on MHD shock waves propag. speed 8-77449
 solar wind, mag. field parameters rel. to magnetospheric ring current plasma injection 8-96363
 solar wind pulsations rel. to Pc 3-4 pulsations 8-65476
 southward component, correl. with dayside magnetosphere mag. flux transfer 8-96355
 southward component, rel. to ring current development and midlatit. convection elec. fields 8-57395
 spiral field inhibition of thermal conduction in two-fluid solar wind models 8-96372
 variations rel. to geomag. S_q var. at mag. conjugate points 8-69287

interplanetary matter

- see also comets; cosmic dust; interplanetary magnetic fields*
 boulders, mass distrib. and sources 8-89119
 carbonaceous chondritic matrix material planet forming unit, occurrence, formation review 8-53892
 comets, origins, research and interplanetary relationships 8-57507
 comets and asteroids population in circumterrestrial space 8-73599
 comets plasma tails, disconnection rel. to mag. field line reconnection at interplanetary sector boundaries 8-93155
 comets plasma tails disruption, triggering by flute instability 8-93156
 cosmic dust, book 8-57498
 cosmic plasma properties from magnetospheric research, use in astrophys. 8-93051
 cosmic ray nuclei, low energy, ionisation states and origin 8-69634
 cosmic ray nuclei, low energy, props., Skylab expt. 8-69632
 cosmic ray propagation, Mars spacecraft meas. 8-53779
 cosmic ray streaming perpendicular to mean mag. field, gyrophase distrib. function 8-53778
 cosmic ray sunward flowing proton and alpha particle fluxes, characts. 8-89016
 cosmic rays, quiet time interplanetary anisotropies obs. from Pioneer 10 and 11 8-77442
 dust, causing dark patches in zodiacal light 8-93153
 dust, large fluffy particles as explanation of optical props. 8-57499
 dust, zodiacal light indications 8-57500
 dust cloud, large grains contrib. from Periodic Comet Encke 8-85908
 dust grains, H-implanted, role in upper atmosphere H chemistry 8-65445
 dust particles orbit distribution, Pioneer 8 and 9 obs. 8-89031
 electrons, meas. instrumentation on International Sun-Earth Explorer spacecraft 8-85786
 electrons, penetration into magnetosphere, satellite obs. 8-73587
 energetic particle flux meas. by International Sun-Earth Explorer A and B spacecraft 8-85799
 grain accretion in protoplanetary nebula, liquid drop effects 8-85862
 interstellar gas parameters change in stellar-wind-dominated environment, rel. to solar system 8-61904
 interstellar particles, optical detection during out-of-ecliptic mission 8-85906
 interstellar wind, Mariner 10 meas. of Lyman α and He I 584 Å interplanetary emissions 8-65474
 interstellar wind properties from Lyman α and He I 584 Å interplanetary emissions 8-65475
 irregular particle scattering, meas. results versus Mie theory 8-58918
 meteoroids from Periodic Comet d'Arrest, contrib. to interplanetary dust cloud 8-53876
 microparticle studies by space-borne instrumentation 8-57460
 nuclear and ionic charge distrib. particle expts. on International Sun-Earth Explorer spacecraft 8-85790
 particle dynamics 8-57501
 particles, sampling techniques 8-57459
 planetesimals scattered from Jupiter zone, bombardment of asteroid belt 8-53859
 plasma flow around planets, collisionless hydrodynamics rel. to Larmor freq. 8-69637
 plasma flow in curved mag. field 8-67329
 plasma physics basic problems 8-69672
 plasma wave expt. on International Sun-Earth Explorer C spacecraft 8-85794
 plasma-neutral gas interaction in cosmic physics 8-69669
 protons, low energy, expt. on International Sun-Earth Explorer C spacecraft 8-85791
 shock wave at 9.7 AU generated by solar flare, Pioneer 10 obs. 8-57422
 shock waves, flare generated, during second STIP interval (1976, March 15-May 15), obs. 8-81514
 shock waves, generated emission in 100-700 kHz range, Prognos obs. 8-69636
 shock waves during August 1972, directions rel. to cosmic rays N-S anisotropies 8-89018
 shock waves generation by solar flares (*Italian*) 8-96377
 silicates, optical props. in far UV 8-53875
 solar cosmic ray event, 1973 April 29, mean free paths near Earth 8-89017
 solar cosmic rays propag., diffusion in mag. fields, convection in solar wind, dimens. method soln. (*Chinese*) 8-81511
 solar equator vicinity, daily cosmic ray flows during solar cycle 8-69622
 solar flare electrons, peculiarity of ejection into interplanetary space (*Russian*) 8-77445
 solar flare energetic particles, interplanetary propag. model 8-65468

interplanetary matter continued

- solar plasma regime, rel. to cosmic ray storm symmetrical equator-pole anisotropy obs. 8-89020
- solar proton and electron events, scatt. mean free path 8-57421
- solar wind, Alfvén waves local instabilities in high speed streams 8-77546
- solar wind, ion cyclotron instability 8-77547
- solar wind, long-term vars. of selected props., Imp 6, 7 and 8 results 8-77452
- solar wind, nonlinear Langmuir waves during Type III radio bursts 8-93173
- solar wind, vel. estimation from multi-station interplanetary scintillation 8-73601
- solar wind, very low electron and proton temps., statistical anal., origin 8-65477
- solar wind 74 MHz interplanetary scintillation and IMP 7 obs. during 1973 8-89033
- solar wind flux depletion at high ecliptic latits., Mariner 10 UV obs. 8-96371
- solar wind pulsations rel. to Pc 3-4 pulsations 8-65476
- zodiacal light dust, orbits from Doppler shift meas. 8-85904
- H I Lyman α and β obs. by Voyager UV spectrometer 8-81673

interplanetary medium *see interplanetary matter***interpolation**

see also function approximation

- acoustic waves in solar atmosphere, efficiency of one-dimens. hydrodynamic codes 8-57520
- air pollution spatial distrib., objective interpolation formulae 8-65412
- bordering functions based interpolation method 8-81816
- computerised tomography image reconstruction, interpolation effect 8-77110
- distributed parameter system identification using doubly cubic spline, underground aquifer appl. 8-69391
- elastic-plastic finite element analysis, interpolation vs. iterative soln. for Tresca yield condition 8-59312
- gamma-ray detection, scintillator response, pulse height spectra unscrambling, computer program 8-55092
- Hermite, and convective difference schemes 8-63268
- Lagrange's interpolation formula program for Texas Instruments SR-56 8-77699
- spline interpolation of γ -ray spectrometer response function 8-82561
- three-dimensional interpolation method, appl. to phonon spectrum determ. for Pb 8-59890
- transaxial scanning X-ray tomography, oblique viewing plane reconstruction 8-77114
- two-dimensional wave propagation, method of characteristics 8-73863
- variational interpolation of linear functionals of inhomogeneous eqns. 8-49638

interstellar dust *see cosmic dust***interstellar magnetic fields**

see also interstellar matter

- cosmic ray electron spectrum determ. from galactic radio background 8-93056
- cosmic ray electrons, detect. by synchrotron radiation in geomag. and interstellar mag. fields 8-57412
- dark clouds, mag. compression rel. to star form. 8-73744
- electrodynmic and gravitational effects of Proca stresses in astrophys. 8-93098
- force free fields near Reissner-Nordstrom black hole 8-77572
- galactic dynamo model, appl. to mean mag. field calc. 8-81685
- galactic halo, mag. field strength from radio obs. 8-96544
- galaxies, mag. fields from light polarisation obs. 8-69872
- galaxy origins, galactic angular momenta and magnetic fields 8-93405
- M31, polarised radio emission detect. rel. to mag. field alignment 8-86017
- NGC 7822 (W1), supernova remnant with mag. field local enhancement 8-54028
- regular field structure and stellar polarisation 8-69869
- Zeeman effect in OH maser emission from W3 (OH) 8-93377

interstellar matter

see also cosmic dust; H I regions; H II regions; interstellar magnetic fields; nebulae

- absorption effects on Balmer discontinuity strengths 8-89238
- absorption lines in ξ Puppis spectrum 8-65665
- accretion onto star, gas pressure effect, stagnation point 8-53932
- atoms, reson. transitions, radiative lifetimes, lab. meas. 8-62767
- B, A and F stars in selected areas, intrinsic uvby β indices, distances and colour excesses 8-89171
- Becklin-Neugebauer source in Orion, high resolution 1.5 to 5 micron spectroscopy 8-93368
- α Canis Majoris (Sirius), search for surrounding nebulosity 8-93242
- carbyne and interstellar grains 8-69859
- α Carinae (Canopus) spectrum, effects of interstellar Compton scatt. 8-53938
- ω Centauri, cluster reddening from RR Lyrae stars UVB photometry 8-73719
- cloud model, intragalactic factor in external objects apparent distrib. 8-96552
- collapsing dust cloud, grain motions rel. to star form. 8-69788
- collapsing molecular clouds, line radiation transfer 8-73626
- contracting clouds, molecular evolution 8-85986
- cosmic dust, book 8-57498
- cosmic ray electron spectrum determ. from galactic radio background 8-93056
- cosmic ray scattering irregularities spectrum, evidence from nuclei charge comp. and energy spectra 8-93059
- Crab Nebula, interstellar shock waves hydrodynamics rel. to diffuse soft X-rays 8-85997
- cyanodiacetylene, microwave spectrum, mol. const. 8-74647
- cyanodiacetylene emission at 24 GHz assoc. with Heiles 2 cloud collision 8-65675
- cyanohexatriyne, detect. at 14.7 GHz in Heiles Cloud 2 and Sagittarius B2 8-73745
- Cygnus Loop, radio struct. at 25 MHz 8-54027
- Cygnus OB2 No.12, high resolution 2 μ spectroscopy rel. to interstellar and stellar features 8-57613
- dark globules, IR radiation theory 8-53999
- dark nebulae, visual extinctions determ. via star counts 8-57612
- dense cloud encounter with solar system, terrestrial consequences 8-57292

interstellar matter continued

- dense clouds and diffuse production of gamma-rays 8-54011
- dense clouds mol. cooling and thermal balance 8-65666
- density wave interaction in differential rotating spiral system 8-69871
- diffuse clouds temperatures, determ. from HD and OH column densities 8-93385
- diffuse interstellar band at 5780 Å, photoelectric meas. 8-93350
- diffuse interstellar bands, strengths rel. to stars IR colour excesses 8-93198
- 30 Doradus complex, in LMC, UV reddening law 8-96516
- 30 Doradus region, in LMC, interstellar extinction and stellar population 8-96517
- dust, Apollo 17 far UV search for starlight scatt. 8-65726
- dust, chemical composition 8-57624
- dust clouds rel. to diffuse galactic light and Milky Way brightness fluctuations 8-61921
- dust globules, microwave spectral lines obs. 8-57609
- dusty plasma clouds, physics rel. to star form. 8-73744
- dynamo model, appl. to galactic mean mag. field 8-81685
- early-type stars near Sun, space vels., ages and interstellar reddening 8-61858
- electrodynmic and gravitational effects of Proca stresses in astrophys. 8-93098
- electron transfer in ion-dust grain collisions 8-77591
- elliptical galaxies, search for H I emission 8-65681
- embedded IR sources, optical spectrophotometry 8-96520
- ethynyl radical abundance and distrib. 8-65664
- EUV spectrum of hot, optically-thin interstellar plasma 8-81665
- extinction and distrib. of stars in Galaxy (*Russian*) 8-73701
- extinction law correl. with wavelength of max. polarisation 8-61902
- extinction laws from 13-colour photometry 8-81676
- far IR emission between $l=36^\circ$ and $l=55^\circ$ galactic longitudes 8-54014
- formaldehyde, collisional excitation 8-89237
- formaldehyde polymer formation mechanism 8-54032
- G48.6+0.0, galactic H II region, direction, H I, OH and H₂CO absorpt. line meas. 8-85996
- galactic anticentre, space distrib. of stars and dust (*Russian*) 8-73754
- galactic centre, struct. from 2.4 μ m obs. 8-81689
- galactic centre direction, near IR polarisation due to aligned interstellar grains 8-96534
- galactic centre region, eruptive phenomena 8-57647
- galactic interstellar extinction law, vars. 8-85990
- galaxies, gas spiral density wave caused by orbiting retrograde companion 8-96533
- Galaxy, gas, dust and molecules review 8-54006
- gas clouds gravit. collapse, caustic and critical times for one-dimens. model 8-93367
- gas in disc-halo galaxies, boundary layer circulation 8-57627
- gas parameters change in stellar-wind-dominated environment, rel. to solar system 8-61904
- gas self-gravity effects on galactic shock waves 8-73761
- globular clusters, nova-driven winds 8-57596
- globular clusters, UBVR photometric obs., dust patches 8-81662
- grain destruction by chemical reactions, collisions and photodesorption 8-54021
- grain destruction by sputtering 8-54020
- grain mantle growth in UV-shielded dense clouds 8-54022
- grains in interplanetary space, optical detection during out-of-ecliptic mission 8-85906
- heating due to weak shock waves dissipation 8-81674
- heavy haloes in spiral galaxies rel. to primordial star generation 8-61946
- IC 361, open cluster, preliminary photometry and colour excess 8-89228
- intercloud cosmic ray ionisation rate 8-85989
- IR molecular line emission from grain surfaces in dense clouds 8-61905
- IR source in 2S 1702-363 field, identification and interstellar visual absorpt. 8-81705
- IR sources, 10 μ m silicate absorpt. band equivalent widths and dust temps. 8-57614
- IR sources, galactic, IR fluxes calcs. for polysaccharide grain model 8-54008
- isotope fractionation, expts. under simulated space conditions 8-73623
- isotopic composition, evidence from cosmic ray isotopes 8-53781
- Kirchoff's laws of spectral analysis, computer laboratory exercises 8-73790
- linear molecules CO, CS, OCS and cyanoacetylene, collisional excitation 8-81664
- linear polarisation in 1-2.2 μ wavelength range 8-77588
- Lo 807, open cluster, two-colour photographic photometry and interstellar reddening 8-96512
- β Lyrae, H emission profiles rel. to pattern of gaseous flow in system 8-57576
- maser emission by nebular regions and stellar atmospheres 8-89242
- methylidyne, obs. in Sagittarius B2 direction 8-65671
- molecular cloud near RCW 36, H₂CO and OH obs. 8-69862
- molecular clouds, radiation transport and kinematics 8-93347
- molecular lifetime in dark dust cloud model 8-85999
- molecules, pioneering investigations 1935-42 period 8-69855
- molecules, radio obs. of Taurus Molecular Cloud 1 condensation 8-69858
- molecules and chemical reactions, summary 8-93384
- molecules in planetary nebulae, abundances and IR spectra 8-53998
- nearby interstellar cloud, impending encounter with solar system 8-93352
- NGC 2264, young open cluster, differential reddening due to intra-cluster dust clouds 8-53996
- NGC 4151, Seyfert galaxy, optical polarimetry, circumnuclear dust envelope 8-61916
- in NGC 5236 (M83), Sc galaxy, CO obs. 8-65689
- NGV 6266, globular cluster, photometry, interstellar extinction and distance 8-61894
- Nova Cygni 1978, distance, colour excess and absolute magnitude 8-89212
- Nova Cygni 1978, interstellar polarisation obs. 8-89213
- ξ Ophiuchi, identification of interstellar lines in UV spectrum 8-93212
- ρ Ophiuchi cloud, search for vibrationally excited H₂ emission 8-93346
- optical interstellar lines towards stars of low reddening 8-57603
- organic molecules, astrochemistry and rel. to origin of life 8-73660

interstellar matter continued

- Orion A, C recomb. lines and H I clouds obs. 8-57605
 Orion A SiO maser intensity vars. 8-93256
 Orion Molecular Cloud, new dynamical model 8-93373
 photoelectric heating of interstellar gas 8-77587
 physical processes, book 8-65679
 planetary nebulae, interstellar reddening rel. to synthetic distance scale 8-89240
 plasma-neutral gas interaction in cosmic physics 8-69669
 polarisation by clouds in elliptical galaxies 8-93399
 polyatomic ion-electron dissociative recomb. reactions, neutral products, statistical theory 8-57604
 radiowave gravitational focusing in interstellar medium, model (Russian) 8-81905
 rotating cloud collapse, isothermal rings fragmentation, star form. 8-93205
 rotating clouds, multiple star system formation 8-93366
 rotating clouds, structure and evolution under external pressure 8-61898
 S106, H II region, radio obs. of assoc. mol. cloud, CO, HCO⁺ HCN, OH and formaldehyde lines 8-61906
 S140 IR, far IR spectrum 8-93372
 Sagittarius A, radio emission scattering from compact object 8-54049
 sedimentation of grains in interstellar clouds 8-93349
 Seyfert and radio-galaxy nuclei, optical spectra of ionis. gas region, model 8-93420
 Seyfert galaxies; suprathermal protons interaction with neutral gas rel. to broad H lines emission (Russian) 8-57642
 silicate grain condensation, laboratory expt. 8-54015
 silicates, optical props. in far UV 8-53875
 solar wind interaction with interstellar matter in heliosphere (Polish) 8-61696
 spherical galaxies, gravit. stability of rotating embedded gas discs (Russian) 8-61915
 in spiral galaxies, hydrodynamic flows in regions of Lindblad resons. 8-96527
 star formation, rel. to density waves accretion-induced overinstability in self-gravitating galactic disc 8-73752
 star formation and interstellar gas density in Galaxy 8-86008
 structure, pictorial analysis of radio signals 8-54026
 supernova remnants, H abundance rel. to H deficiency in Type I supernovae 8-53969
 thermal emission spectrum from small interstellar grains with temp. fluctuation 8-69864
 two-phase model, intercloud wind theory 8-85991
 UV absorption lines in HR 1099 direction, Copernicus obs. 8-93358
 UV extinction obs. in galactic plane from TD1 satellite 8-93382
 UV spectrum, comparison with spectra of organic compounds 8-61913
 velocity distrib. of interstellar gas, UV absorption line obs. 8-89235
 NQ Vulpeculae (Nova 1976), interstellar absorpt. and polarisation rel. to distance 8-89205
 W40 and W48, near IR and CO mm wavelength obs. 8-65667
 W51 H₂O source obs. with Crimea-Haystack interferometer (Russian) 8-69865
 X-ray burst propag. through interstellar dust, small-angle scatt. effects 8-57433
⁷Be, cosmic ray accel. probe 8-81512
 CH in diffuse interstellar medium, optical and radio obs. 8-93356
 CH, obs. of 3.3 GHz ground state transitions 8-77592
 CH⁺ formation in hot gas behind interstellar shock fronts 8-61910
 CH⁺ X ¹²C, dissoci. recomb. rate coeff., rel. to interstellar mol. form. 8-56884
 C₂H (butadiynyl) radical, detect. towards (IRC+10216) 8-93374
 CO, distrib. in Galaxy rel. to spiral pattern speed 8-54036
 CO emission from late-type galaxies 8-89250
 CO formation in contracting clouds, thermal instabilities 8-81675
 CO in molecular cloud complexes, structure of W75-DR 21 region 8-89232
 CO, reson. transitions, radiative lifetimes, lab. meas. 8-62767
 CO, time-dependent form. and chem. fractionation 8-57602
 CO/H₂ ratio in dark clouds, meas. 8-96513
 CS J=1-0 transition at 49 GHz in southern molecular clouds 8-65674
 D absorption line at 327 MHz, search towards galactic centre 8-77599
 D abundance in Galaxy rel. to cosmology 8-69883
 DCO⁺/HCO⁺ abundance ratio in cool interstellar clouds 8-65673
 H, as extraterrestrial source of atmospheric water vapour 8-69416
 H, at periphery of galaxies, effects of ionising background radiation 8-65729
 H I 21 cm absorption towards extragalactic radiosources, catalogues of 819 sources 8-57638
 H I absorption lines high-resolution mapping in direction of NGC 2024, M17, W49 and Orion A 8-81667
 H I Lyman α and β obs. by Voyager UV spectrometer 8-81673
 H I survey from Lyman α absorption meas. towards 100 stars 8-93357
 H-C, thermal desorption, one-phonon at. scatt., 3-dimens., continuum model 8-87860
 H₂ clouds, ionisation by supernovae 8-69856
 H₂ collisional excitation 8-77586
 H₂ emission at 2 microns from Orion Nebula 8-93351
 H₂, emission line obs. from vicinity of T Tauri 8-93230
 H₂, form., catalytic prod. on transition metal grains 8-57616
 H₂, form. by catalysis process 8-54005
 H₂ ortho-para ratio in dense clouds, protoplanets and planetary atmospheres 8-89233
 H₂, vibrationally excited, search for 8150 Å emission line 8-93346
 HCN dimer, interstellar abundance, upper limit 8-54004
 HCN emission detect. in Sagittarius A mol. cloud 8-73750
 HCN, HNC formation, role of H₂CN⁺ isomers 8-81672
 HC₃N, HC₇N, obs. in dark dust clouds 8-54023
 HC₃N, detect. in interstellar space 8-93370
 HD molecules, rate coeff. for H⁺+D→H+D⁺ near threshold 8-89239
 H₂O 22 GHz maser emission from W3(OH), 49N and 51, spatial distrib. 8-93355
 H₂O cosmic masers, influence of dust on collisional pumping 8-54030
 H₂O maser line evidence for circumstellar ring systems 8-89195
 H₂O maser source near NGC 2071, discovery 8-73768
 H₂O masers, in dense interstellar mol. clouds, high sensitivity survey 8-85988

interstellar matter continued

- H₂O, oscill. strengths of UV lines, rel. to abundance in interstellar clouds 8-90104
 H₂O sources, linear polarisation of 22 GHz line emission 8-77612
 H₂O sources, spectra and autocorrel. anal. 8-65713
 H₂O vapour sources struct. and kinematics in OB star form. regions 8-61901
 H₂O⁺, unsuccessful search and interstellar abundance 8-69860
 H₂¹⁸O, detect. in Orion mol. cloud and DR 21(OH), H₂O abundance estimate 8-57621
 LiH in diffuse clouds 8-93361
 N, overabundance in nucleus of NGC 6946 spiral galaxy (French) 8-89257
 NH₃, non-metastable absorption at 23.1 GHz, first obs. towards W3(OH) 8-65677
 NH₃, obs. in southern H II regions 8-69863
 NO, microwave detection in Sagittarius B2 direction 8-93378
 NS molecule, radio emission theory 8-54031
 NaH in diffuse clouds 8-93361
 O VI gas, circumstellar or interstellar origin 8-57528
 OH 1.6 GHz maser emission from W3(OH), 49N and 51, spatial distrib. 8-93355
 OH and H₂O masers, scintillation, solar wind vel. meas. (Russian) 8-69704
 OH and H₂O masers assoc. with compact H II regions, model 8-81666
 OH, excitation in molecular clouds 8-65669
 OH, J=9/2 Λ -doublet line detect. in W3(OH) 8-65670
 OH maser, temporal var. 8-53817
 OH maser emission from W3(OH), Zeeman effect 8-93377
 OH radicals, microwave spectra data tables 8-50542
 OH, radio lines absorpt. obs. in galactic radio sources 8-54068
 SiH, SiH⁺, line positions and oscill. strengths of rot.-vibr. bands, interstellar medium appl. 8-58644
 SiH, SiH⁺, rot. transition freqs. calc., rel. to search in interstellar space 8-93100
 SiO maser line evidence for circumstellar ring systems 8-89195
 Ti, obs. of interstellar Ti II 3384 Å line 8-57611

interstitials

- see also Cottrell atmospheres; crowdions; Snoek effect
 alkali halides, influence of purity of crystals on stability of F-centres and interstitials 8-91336
 alkali metal halides, irradiated, annealing 8-92494
 alloys, irradiated, segregation, inverse Kirkendall effect, effect of constitution on void swelling 8-91472
 α -brass, electron irradiated, defect production and interdiffusion 8-67739
 cluster nucleation at onset of irradiation 8-79635
 diamond, Fresnel diffraction platelets, defect struct. anal. by 3 Å phase-contrast microscopy 8-7701
 diamond, type IIa, electron irradi., EPR obs. of interstitial-impurity complexes 8-76310
 diffusion in crystals, nonadiabatic quantum theory 8-79818
 dilute alloy, ternary, substitutional solute element effect on diffusivity of interstitial solute element 8-59969
 distribution of dissimilar atoms among interstices of various types, appl. to isotopic ordering (Russian) 8-67706
 FCC metals, dynamics of multiple interstitials and interstitial impurity complexes 8-75775
 graphite, point defects and self diffusion 8-63758
 metal, HCP structure, interstitial ordering (Russian) 8-79610
 metal, irradi., containing self-interstitials and vacancies, electronic transport props. 8-60105
 metal, solute atom displacement in mixed dumbbell interstitials for FCC lattice 8-79631
 metals, irradiation creep strain, produced by vacancy loops, calc. of magnitude 8-72815
 metals and alloys, radiation damage prediction and measurement 8-75693
 metals irradiated, heavily, exam. of percolative mass transfer 8-79639
 selfinterstitials and He interstitials, interaction with vacancies and vacancy clusters, Monte Carlo simulation 8-71754
 solid solution, diffusion, influence of conc.-induced stresses (Russian) 8-55969
 steel, cold-worked, state of cementite, nucl. gamma reson. meas., plastic deform. (Russian) 8-68706
 strontium tartrate tetrahydrate Co²⁺ electronic absorpt. spectrum 8-92098
 superionics, with fluorite structure, Brillouin scattering and lattice defect energetics 8-80369
 tetrahedral semiconductor, interstitial type dislocation loop form. by vacancy precipitation 8-67715
 thermal neutrons, inelastic scattering by one-dimens. defecton (Russian) 8-84169
 vibrational spectra crystals with split configuration interstitial (Russian) 8-76450
 Zircaloy-4, quenched, strain ageing behaviour, ageing time and temp. effects 8-56657
 Ag, electron irradi., elastic moduli and internal function (French) 8-87703
 Ag, TEM exam. of ion damage in FCC metals 8-87727
 Al alloys, dil., size effect of impurity atoms rel. to trapping radii for migrating self-interstitials 8-75690
 Al, electron-irradi., NQR, EFG around vacancies and interstitials 8-88220
 Al, reactor irradiated, neutron inelastic scattering meas. of phonon dispersion curves 8-75758
 Al-¹¹¹In, electron irradi., defect trapping at impurities 8-55892
 Al-Cr(V)(Ti), dil., electron irradiated, interaction of self interstitials with undersized solute atoms 8-63789
 Al-Cu (up to 0.5 at.%), neutron damage rate, interpretation of results 8-63794
 Al-Fe, electron irradiated, interstitial-solute complexes, internal friction spectra 8-92289
 Al-Mn(Cu)(Ag), solute atom displacement in mixed dumbbell interstitials for FCC lattice 8-79631
 Al₂O₃, spinel, crystal struct. model 8-91333
 Au, TEM exam. of ion damage in FCC metals 8-87727
 Ba(N₃)₂, thermal decomp., role of defects 8-73033

interstitials continued

- β -AgI, ionic cond. and dielec. meas., Frenkel defect formation energy 8-87814
 CaF₂, (n, γ) induced point defects, struct. and annealing 8-59842
 CaF₂:Dy³⁺, Mossbauer obs. 8-64303
 CaF₂.3Ca(PO₃)₂, apatite, fission damage detection, absorpt. spectra 8-84617
 Cd, electron radiation damage in HVEM, nature of defect clusters 8-59838
 CdSe, defect struct. in Se vapour 8-64043
 Cu alloys, dil., size effect of impurity atoms rel. to trapping radii for migrating self-interstitials 8-75690
 Cu, electron irradi., rel. to stage III recovery kinetics 8-63792
 Cu irradiated, exam. of dislocation bias for interstitials to edge dislocations 8-79612
 Cu, TEM exam. of ion damage in FCC metals 8-87727
 Cu: μ^+ , lattice distortions, microscopic calc. 8-87665
 Cu-Be, solute atom displacement in mixed dumbbell interstitials for FCC lattice 8-79631
 Fe, magnetic aftereffect of interstitial O 8-91903
 Fe, μ^+ SR, theory of spin depolarisation rate 8-80271
 α -Fe, stress induced interaction of point defect pairs, in BCC solutions 8-79608
 Fe, vibrational spectrum with interstitial C atoms 8-67796
 Fe-Cu (0.21, 0.2 wt.%), neutron irradiated, torsional props. effect of Cu additions and annealing temp. 8-56699
 Fe-Ni, dil., point defect relax. after low temp. neutron irradi. 8-52316
 GaAs:B, electron or neutron irradiated, low symmetry interstitial B centre 8-79605
 n-Ge, group V doped, point defect form. due to γ -ray irradi., carrier density, mobility meas. 8-71759
 H₂, random walk diffusion models, generalisation to correlations over two jumps 8-79794
 KBr, X-irradiated, at 80K, interstitial K ions associated with interstitial Br ions (*Russian*) 8-75655
 KCl, X-irradiated, formation of cation defects 8-91359
 MgO, radiation induced O interstitials, EPR meas. 8-55866
 Mo:N, ion implanted proton-irradiated, annealing behaviour 8-91362
 Mo-C dilute alloy defect cluster nucleation and growth under 1250 keV electron microscope (*Japanese*) 8-87663
 NH₄Br:Cu²⁺, ESR and absorpt. spectra, 300-1500 nm 8-60492
 NaA zeolite:S, optical spectra 8-88342
 Na₂HAsO₄.7H₂O:Cu²⁺, ESR, Cu lattice location 8-52342
 NaPO₃, glass, Na diffusion 8-63875
 Nb, diffusion of H, influence of H-H pairing, jump model 8-75878
 Nb, lattice distortion due to di-interstitial clusters 8-71726
 Nb, stress induced interaction of point defect pairs, in BCC solutions 8-79608
 Nb-H, acoustic phonon anomaly at small wavevectors 8-59882
 NbH₂(D₂), cryst. struct., phase diagrams, order-disorder transition 8-55836
 NbO_x, interstitial O, diffuse neutron scatt. 8-83809
 Ni 200, C interstitial effect of yield point develop. during static strain ageing, model 8-88498
 Ni, pure and doped, mech., mag. relax. meas. dumb-bell self-interstitial reorientation (*German*) 8-52879
 Ni superalloy powders, removal of interstitial contaminants 8-84735
 Ni, TEM exam. of ion damage in FCC metals 8-87727
 Ni:H, energy and electron density of states 8-51929
 Ni_xO, electronic cond. at high temp., vacancies and interstitials effect (*French*) 8-79990
 Pd:H, energy and electron density of states 8-51929
 (Pd_{0.8}Au_{0.2})D_{0.04}, lattice location of D, ion channelling obs. 8-67708
 Pt, TEM exam. of ion damage in FCC metals 8-87727
 Rh:H, energy and electron density of states 8-51929
 Si, ion-implanted, secondary defects development, three-stage model 8-87725
 Si, neutron irradi., internal friction obs. of defects 8-51597
 Si, P diffused sample, stacking faults and dislocations formation from interstitials 8-95059
 Si, vibrational properties of the (001) split interstitial 8-91405
 Si:B, ion implanted, struct. of rod defects, TEM obs. 8-71744
 Si:Fe, EPR and neutron activation anal. of thermal defects 8-91355
 Si:Gd, radiation defect form., effect of Gd impurities, elec. and optical meas. 8-71764
 Ta, internal friction meas. of O, N diffusion 8-75888
 Ta, stress induced interaction of point defect pairs, in BCC solutions 8-79608
 Ta-O solid soln., interstitial ordering and precipitation at 100 to 270°C, exam. 8-52813
 TaD_{0.10}, lattice location of D, ion channelling obs. 8-67708
 TaH₂(D₂), cryst. struct., phase diagrams, order-disorder transition 8-55836
 Ti-Al-Sn (5, 2.5 wt.%), fracture mechanism at cryogenic temps. 8-64642
 TiO₂, slightly reduced rutile, diffusion of Ti 8-79799
 UO₂, irradiation induced vol. change 8-67740
 V, lattice distortion due to di-interstitial clusters 8-71726
 V, stress induced interaction of point defect pairs, in BCC solutions 8-79608
 VaH₂(D₂), cryst. struct., phase diagrams, order-disorder transition 8-55836
 W, single crystals, electron irradiated, recovery of resistivity, 4.5-380K (*German*) 8-87714
 W, split crowdon interstitial, (111), computer simulation of TEM imaging 8-71723
 W, thermal neutron irradiated, radiation damage and stage III defect annealing 8-51586
 Zn, electron radiation damage in HVEM, nature of defect clusters 8-59838
 ZrC, sintering shrinkage, effect of struct. vacancies in interstitial phases 8-60630

intersystem crossing see *nonradiative transitions*

intramolecular potentials see *potential energy functions*

intramolecular vibrations see *molecular vibration; molecular vibration in solids*

intrinsic magnetisation see *spontaneous magnetisation*

Invar

hysteresis loop displacement 8-52312

Invar continued

- magnetisation reversal, fast, forced by external RF mag. field, Mossbauer obs. 8-52311
 magnetomechanical effects of Invar-type alloys, review 8-52330
 specific heat, temp. depend. (*Russian*) 8-56341
 sputtered atoms, photon emissions, obs. of apparent local thermodynamic equil. in excitation 8-72672
 Fe-B, binary alloys, giant ΔE effect and Elinvar characts. 8-76291
 Fe-Cr, Invar alloy, explanation of phys. anomalies (*Russian*) 8-88112
 Fe-Ni, (35 wt.%), transport props. and Invar features (*Russian*) 8-51973
 Fe-Ni, Invar alloy, explanation of phys. anomalies (*Russian*) 8-88112
 Fe-Ni alloys, anomalous thermal expansion, Gruneisen eqn. 8-83980
 Fe₆₅Ni₃₅, UPS, density of states determ. 8-52623
 Fe₆₅Ni₃₅, ferromagnetic Invar alloy, lattice vibrations 8-91403
 Fe₆₅Ni₃₅, quasi-localised spin system, neutron scatt. 8-68194
 Fe₆₅Ni₃₅, electron irradiated, small angle neutron scatt. 8-52218
 Fe₇₀Ni₃₀, short range order, diffuse elastic neutron scatt. study 8-52219
 Fe₇₀Ni₃₀, small angle neutron scatt., magnetisation inhomogeneity 8-52218
 Fe₃Pt, Invar alloy, theory of elastic-anomalies 8-95505
 Fe₃Pt, quasi-localised spin system, neutron scatt. 8-68194
 Fe₇₂Pt₂₈, ferromagnetic Invar alloy, lattice vibrations 8-91403

invariance

see also *conservation laws*

- Hamiltonian continuum mechanics, differential geom. foundation 8-77708
 Lagrangian systems with one degree of freedom, invariance and conservation laws 8-62067
 Lie derivative of a differential form, invariance conditions and phys. laws 8-65748
 phase transitions, superradiant, gauge invariance theory 8-66795
 quantum field theory, conformal-invariant, composite field operators 8-81886
 space-time transformations leaving Einstein eqns. invariant (*French*) 8-62123

inverse Nyquist diagrams see *Nyquist diagrams*

iodine

see also *nuclei with*

- absorption site on Ag(111) EXAFS 8-84679
 adsorbed on Ag (111), geometry and bond length, surface EXAFS 8-71952
 alkali metal chloride: F⁻(Br⁻)(I⁻), anion impurities substitution, energies of soln., association and migration 8-83831
 atom, diffusion coeff. in laminar flames 8-51272
 atom, electronically excited, collisional release and photocomp. kinetics of I₂ 8-66819
 benzene-I₂, binary soln., charge transfer spectrum 8-90183
 carbon tetrachloride-I₂-water system, mass transfer in pulsed perforated plate column 8-71385
 chemical laser, electronic transition 8-55347
 filter, absorpt. lines removal from 514 nm excited Raman spectra 8-70200
 fission waste product, distrib. and concs. in reactor core 8-58322
 frequency stabilisation of He-Ne lasers 8-87070
 frequency stabilisation of He-Ne lasers 8-87071
 frequency stabilised He-Ne laser, instrumental freq. offsets 8-87084
 frequency stabilised He-Ne laser status 8-87072
 frequency stabilised He-Ne laser with hot wall I₂ cell 8-87073
 frequency stabilised He-Ne lasers, beat freq., international comparison (*French*) 8-87090
 frequency stabilised He-Ne lasers, conf., Germany (Feb. 1977) 8-87069
 frequency stabilised He-Ne lasers, length metrology (*French*) 8-87074
 frequency stabilised He-Ne lasers, technological principles (*French*) 8-87075
 gain measurements in chem. produced I system 8-63115
 I₂, air pollutant, spectroscopic analysis using scanning tunable dye laser 8-81362
 laser, 1.315 μ m transition line struct. 8-59000
 laser, Asterix III and German laser fusion programme 8-63136
 laser, continuously variable water filter for linearity testing of photore-sistors 8-55397
 laser, ICF, CN photodissociation 8-50769
 laser, photodissoc. dye laser pumped 8-63064
 laser, photodissociation, continuously pumped continuous flow 8-59027
 laser, pulsed photodissociation, based on methyl iodide 8-50767
 laser, smooth pulse oscillator for single mode operation 8-59057
 laser radiation wavelength stabilisation, He-Ne laser (*Czech*) 8-87061
 LWR fuel-cladding gap, Cs-U-Zr-H-I-O system, chemical thermodynamics 8-82440
 metallic solid, high press. struct., phase transition, X-ray diff. study 8-87647
 molecular crystal, bond charge model, for lattice dynamics 8-79692
 molecule, B² $\pi_{g^{-}}$ state deactivation efficiency, temp. depend. 8-70869
 molecule, B state, effective hyperfine Hamiltonian 8-58598
 molecule, band system, MC SCF pseudopot. calcs. 8-78632
 molecule, collisional release and photocomp. kinetics, I^{*} prod. 8-66819
 molecule, conc. profiles, shock tube unsteady expansion wave technique, applic. 8-61011
 molecule, dissociation by 0-8 eV electrons 8-74776
 molecule, electron diffraction parameters, spectrosc. calc. 8-70932
 molecule, equilibrium parameters and Morse anharmonic consts., electron diff. determ. 8-58818
 molecule, hyperfine component classification, suitability for laser wavelength stabilisation 8-86965
 molecule, hyperfine predissoc., Doppler-free spectrosc. obs. 8-89558
 molecule, hyperfine structure, 612 nm and 640 nm, saturated absorpt. expt. 8-66871
 molecule, hyperfine structure obs. in saturated fluoresc. 8-50569
 molecule, laser dissociation, in gas and soln. (*German*) 8-90240
 molecule, multiphoton reson. ionis. bands, 360-600 nm 8-90233
 molecule, photodissoc., theory of resonant Raman scattering (*Russian*) 8-55180
 molecule, picosecond relax., fluoresc. spectroscopy, solvent effects 8-58737
 molecule, props. as test mol. in modern spectroscopy, review 8-90317

iodine continued

- molecule, reson.-enhanced CARS, band contours, assignments 8-86980
 molecule, saturated absorpt. obs. using interferometric spectroscopy 8-74079
 molecule, visible absorpt. spectra, Fourier transform spectroscopy appl. 8-58060
 molecule photoluminesc. of matrix samples, laser spectroscopy, evidence for I_2 species 8-58735
 molten, electrical cond., press. effect, 0-1 kbar 8-55963
 partition equilibrium between air and NaOH aq. effect of CO_2 conc. 8-78474
 polyacetylene- I_2 , highly conducting, Raman, XPS and X-ray diffr. obs. 8-80454
 polyvinyl fluoride: I_2 , thermally stimulated currents 8-64315
 radioisotopes, high efficiency mixed species air sampling, readout and dose assessment system 8-57074
 radioisotopes, meas. of crit. environmental exposure for reactor accidents 8-57081
 stress corrosion cracking tests, nuclear fuel rod pellet clad interaction failures 8-58351
 UV laser possible pumping by synchrotron radiation, NaCl:I(Br) luminesc. 8-66835
 vapour cell as narrow band opt. filter 8-74993
 Ag+ I^- , impact parameter depend. of K X-rays 8-94308
 AgBr:I emulsion, photocond. and luminesc. at $-186^\circ C$, rel. to incident light intensity 8-64063
 atom, recombination, shock tube unsteady expansion wave technique, applic. 8-61011
 Fe:I, ^{131}I NMR, vacancy associated impurity sites 8-91964
 GeTe:I, ferroelectric transition exam. 8-88264
 I laser, high-power, beam quality, gain saturation effect, for fusion ignition 8-63149
 I laser medium, CF_3I , UV absorption modification, by vibr. excitation for fusion ignition 8-58717
 I, spectral transition probabilities, 500-1050 nm 8-82676
 I^- , in althylammonium iodides, in solns. of low parity, MCD spectra 8-94268
 I+ H_2 , activation energy and trajectory calcs., temp. and isotope effects 8-76835
 I_2 , angular momentum transfer, elastic, inelastic collisions, orientation and polarised fluoresc. 8-90271
 I_2 , dissociative attachment, thermal energy electrons 8-82850
 I_2 , frequency stabilised He-Ne laser 8-90429
 I_2 , gas phase flash photolysis, in ethane and propane, cage effect temp. depend. 8-80770
 I_2 , HFS using Doppler-free stimulated-emission technique 8-93765
 I_2 , optically pumped, lasing obs. on 342 nm band 8-79008
 I_2 , propan-1,3-dioic acid, H_2O_2 , KIO_3 , $MnSO_4$, $HClO_4$, periodic chem. reactions, bi- and tristability, rel. to biological mech. (French) 8-80726
 I_2 , stabilised He-Ne lasers, hyperfine struct. spacings, international inter-comparison meas. 8-87088
 I_2 vapour concentration monitoring, secondary laser cavity for weak absorptions 8-92551
 I_2 +Ar $^+$, ion-pair form. differential cross-section, 25-133 eV, metastable Ar 8-78787
 I_2 +CO, E-V energy transfer reactions, electronically excited I_2 8-64814
 $I_2^+ + N_2 \rightarrow I^+ + I + N_2$, 0.65-3.2 keV, dissoc. cross-section, internal excitation effects 8-64813
 I_2^- , geom. and electronic struct., effective pot. calc. 8-74788
 I_2^- , geom. and electronic struct., effective pot. calc. 8-74788
 $I(2P_{1/2}) + NF(a^1\Delta)$ system, electronic angular momentum transfer, chem. kinetic model 8-63104
 ^{51}I , $Ly_{2,3}$ X-ray emission spectra, line breadth 8-62760
 ^{127}I saturated absorpt. for He-Ne laser stabilisation, wavelength standard development (German) 8-79034
 $^{127}I_2$ absorption lines at 582 THz, Ar $^+$ laser freq. stabilisation 8-90430
 $^{127}I_2$ stabilised He-Ne laser, freq. shifts, limitations 8-90440
 ^{129}I in man, cow and deer 8-80975
 ^{131}I after surgery, thyroid carcinoma treatment 8-85373
 ^{131}I , dynamic sorption from gas phase of dissociating N_2O_4 (Russian) 8-58356
 ^{131}I measurement in human thyroid gland, use of NaI(Tl) scintillation survey meter 8-80970
 ^{131}I population thyroid dose in USA after Chinese atm. nucl. weapons tests 8-77116
 ^{131}I treatment of hyperthyroidism, carcinogenesis, comparison with surgery 8-85374
 $I^+ + I_2(Br_2)(Cl_2)(IBr)(ICl)(BrCl)$, collisional deactivation and reaction rate consts., obs. 8-80738
 $I(5^2P_{1/2})$ +benzene- d_0 (- d_6), fluoresc. quenching, spin-orbit interaction, isotope effect obs. 8-62763
 $I(5^2P_{1/2}) + Br_2$, deactivation kinetics, time-resolved spectrosc. obs. 8-95916
 $I(5^2P_{1/2}) + Br_2$, deactivation kinetics, $Br(4^2P_{1/2})$ prod., time-resolved spectrosc. obs. 8-95917
 $I(5^2P_{1/2}) + HCl(HBr)(NO)$, electronic-vibrational energy transfer, fluoresc. obs. 8-66579
KCl:I, colouration under two-photon excitation, absorption spectra 8-84618
KCl:I crystals, V-band development using X-rays 8-88337
NaCl:I, UV laser generation by optical pumping 8-82973
 $Na_2O \cdot P_2O_5 \cdot I_2$, metaphosphate glass, absorpt. spectra of radiation products 8-64865
 $O_2(^1\Delta_g) + I(^2P_{3/2})$, possible electronic transition chem. laser 8-63116
Te:I, semicond., elec. efficiency (German) 8-84166

iodine compounds

- Ge- I_2 , equilibrium study 700 to 1300K, vapour transport rate of Ge (French) 8-64476
 IBr, laser fluoresc. study of $B'O^+ \cdot X'^{\Sigma+}$ system 8-70867
 IBr, magnetic rot. spectrum, rot. and vibr. anal. 8-70861
 IBr, photodissoc., $Br^*(4^2P_{1/2})$ yield, wavelength depend., collisional release 8-64857
 IBr, photodissoc., curve crossing of $Br(2^3P_{1/2})$ and $Br(2^1P_{1/2})$ 8-62859
 ICN, Franck-Condon transition amplitudes for mol. dissoc., semiclassical evaluations 8-62860

iodine compounds continued

- ICN, general quartic force field, Machina-Overend parameters 8-50532
 ICN, microwave spectrum, vibr.-rot. const., equilib. struct. 8-58677
 ICN, photodissoc. and predissoc., cyanide radical fluoresc. excitation spectrum and laser emission 8-76892
 ICl, energy levels, near first dissoc. limit, 2-photon sequential absorption obs. 8-90246
 ICl, lifetimes of $A^3\Pi_1$ state vibr. levels, 6070-7300 Å 8-66605
 ICl+CO, E-V energy transfer reactions, electronically excited ICl 8-64814
 IF $_5$, microwave spectra obs., rot. assignments, mol. parameters (French) 8-55163
 IF $_5$, vapour press., phase transform. enthalpy (German) 8-51654
 $^{127}IF_6$, radical, prep. and EPR comparison with other hexafluoride radicals 8-68381
 IF $_7$, vapour press., phase transform. enthalpy (German) 8-51654
 IO $_3^-$, determ. in rainwater by neutron activation anal. 8-76953
 IO $_3^-$ in NaClO $_3$, Raman spectra, fundamental vibr. modes 8-78711
 I $_2O_5$, NQR freqs. of ^{127}I 8-72433
 KI, effect of addition on corrosion of Cu in seawater 8-80670
 Sb-Se-I system, exam. of glass formation, IR transmission spectra 8-88452

ion-atom collisions see atom-ion collisions

ion beam effects

see also ion-surface impact; plasma-beam interactions

- biological acute and late reactions, mice, comparison of heavy particles for therapy 8-85338
 cell survival, OER and RBE, comparison of heavy particles for therapy 8-85337
 cell survival vs. depth, comparison of heavy particles for radiotherapy 8-85336
 cellulose nitrate, proton, H_2^+ mol. ion, and heavy ion irradi., track prod., etching obs. 8-86757
 collision cascades, computer simulation, Monte Carlo code 8-67756
 disorder accumulation, saturation and sputter limitation 8-67753
 dual beam irradi. expts., used for void swelling simulation, theoretical exam. 8-79646
 graphite, energetic deuteron irradiated surface struct. quantitative meas. 8-95210
 graphite, energetic ion sputtering, appl. of AES-SIMS (IMA)-FDS combined systems to physical and chemical processes 8-95636
 graphite, pyrolytic, Ar $^+$, N $^+$ and He $^+$ ion bombardment numerical discussion of flaking 8-52947
 graphite, pyrolytic, ion bombard., flaking, stress fields around penny-shaped cracks 8-52946
 graphite, sputtering yield, use as first wall material 8-95629
 graphite, surface alteration by interaction with Ar $^+$ and Xe $^+$ beams 8-91347
 graphite monofluoride, surface alteration by interaction with Ar $^+$ and Xe $^+$ beams 8-91347
 graphite sputtering by low energy H and D 8-95630
 Hasteloy B, equilibrium surface bombarded with high dose He $^+$ ions 8-95091
 implanted ion detection by X-ray emission anal. in TEM 8-51575
 Inconel, sputtering and blistering from H $^+$ and He $^+$ bombardment 8-79649
 Inconel 600, equilibrium surface bombarded with high dose He $^+$ ions 8-95091
 Kapton, optical, elec. props., struct., ion textured surface 8-72904
 lamellar eutectic, specimen thinning for TEM (German, English) 8-95885
 laser-fusion reactor, surface heating of 1st wall by pulsed photon and ion irradi. 8-89979
 metal, He ion implanted, statistical model of low temp. blister formation 8-67754
 metal, ion and neutron irradi., low temp. defect prod. and stage 1 recovery 8-79637
 metal, ion impact desorption cross section of H and O by light in bombardment 8-95096
 metal atoms sputtered by light and heavy particles, velocity distrib. meas. by fluorescence spectroscopy 8-95626
 metals, irradiation creep strain, produced by vacancy loops, calc. of magnitude 8-72815
 metals irradiated, heavily, exam. of percolative mass transfer 8-79639
 molecular ions, interaction with thin solid targets 8-59844
 Nimonic PE-16, equilibrium surface bombarded with high dose He $^+$ ions 8-95091
 nuclear filters, prep. from polymers using Ar ions 8-86714
 plasma system, ion cyclotron harmonic instabilities (Japanese) 8-91124
 pyrolytic C, energy depend. of methane prod. during deuteron bombardment 8-95939
 quartz, radiation damage in birefringent samples, meas. using photoelastic modulator 8-87724
 recoil implantation from thin source, extension to recoil sputtering and moderately thick sources 8-95631
 refractories, swelling on proton, deuteron and He ion bombardment 8-67750
 saturation resistivity charges, ion and fission fragment irradi. induced 8-79643
 silicate glasses, swelling on proton, deuteron and He ion bombardment 8-67750
 stainless steel, 316, simulation of radiation damage and phase stability 8-86602
 steel, austenitic stainless, 316, surgical implant ion beam textured, stress/strain relations, fatigue chars. 8-73297
 steel, austenitic stainless, stressed state blistering 8-95085
 steel, austenitic stainless, type 304 with He distrib., foil, effect of momentum transfer, damage energy gradient, on He distrib. 8-71773
 steel, barding by ion bombardment with B_2H_6 (French) 8-60876
 steel, stainless, 316 and 304, equilibrium surface bombarded with high dose He $^+$ ions 8-95091
 steel, stainless, 321 and 304, D implanted, thermal desorption and bombardment induced release 8-95072
 steel, stainless, embrittlement by low energy ionic and atomic H particles 8-95809
 steel, stainless, ground surface ion bombardment, in DC glow discharge 8-95098
 steel, stainless, ion induced release of trapped D 8-95095

ion beam effects continued

- steel, stainless, sputtering and chem. attack by H ions of 100 eV energy 8-95635
- steel, stainless, sputtering by low energy H and D 8-95630
- steel, stainless, surface damage under high dose $^4\text{He}^+$ ion irradiation 8-95092
- steel, stainless, trapping and replacement of 1 to 14 keV H and D 8-95070
- steel, stainless 316, ion sputtered, surface anal. by Auger effect and SEM 8-95632
- steel, stainless 316, irradiated, D trapping 8-95069
- steel, surface cleaning in glow discharge, ion bombardment effect (*Russian*) 8-95848
- superlattice thin films, sputtered, ion-bombardment-enhanced diffusion during growth 8-87882
- surface barrier detector, pulse height defects, heavy-ion detection 8-55093
- surface layers, ESCA obs. 8-52612
- target assembly, ultra high vacuum, for charged particle irradiations in the materials research field 8-83841
- TCNQ-HMTSF, irradi. effects on resist. 21K 8-60113
- Teflon, optical, elec. props., struct., ion textured surface 8-72904
- Teflon, surface alteration by interaction with Ar^+ and Xe^+ beams 8-91347
- thin sample, structural change obs. by transmitted fission fragment energy 8-83853
- thin specimens, temp. control for mech. meas. under light ion irradi. 8-86278
- tissue-equivalent gas, energy loss of H, C, N and O ions for elastic nuclear collisions 8-86759
- whisker growth, new mechanism for the blistering of surfaces in complex radiation environments 8-95093
- Ag, TEM exam. of ion damage in FCC metals 8-87727
- Al, porous anodic film, ion beam thinned, electron microscopy 8-92390
- Al, sputtering and chem. attack by H ions of 100 eV energy 8-95635
- Al^{12}B , relax. mechanism for polarised implant 8-87693
- Al-Ge alloy, Ge precip., ion irradi., dose rate and temp. depend. 8-79642
- $\alpha\text{-Al}_2\text{O}_3$, ion bombard., vol. expansion, annealing compaction, surface props. 8-67748
- Au nucleation on organic substrates, ion bombard. effects 8-75965
- Au, sputtering and chem. attack by H ions of 100 eV energy 8-95635
- Au, TEM exam. of ion damage in FCC metals 8-87727
- BC, ion bombarded, chemical effects on secondary photon and ion emission 8-95637
- B_4C , sputtering yield, use as first wall material 8-95629
- Be, ion bombarded, chemical effects on secondary photon and ion emission 8-95637
- Be, plasma-sprayed, response to He^+ bombardment determ. 8-86691
- BeO , sputtering by low energy H and D 8-95630
- C, interaction with D^+ ions, 5-30 keV, temp. depend. of methane formation 8-79645
- C, ion bombarded, chemical effects on secondary photon and ion emission 8-95637
- C pyroceramic, sputtering and blistering from H^+ and He^+ bombardment 8-79649
- CdS, luminesc. from heavy ion tracks 8-88365
- Co-W-Cr (15,20 wt.%), surgical implant ion beam textured, stress/strain relations, fatigue characts. 8-73297
- Cu, He conc. profile meas. rel. to blistering 8-95089
- Cu, irradiation induced defects, electron microscope images 8-83854
- Cu surface, poly-cryst., Ar ion bombard., regular pyramid production 8-59843
- Cu, TEM exam. of ion damage in FCC metals 8-87727
- Fe, boriding by ion bombardment with B_2H_6 (*French*) 8-60876
- GaAs, disordered, ion implanted, elec. props. 8-84212
- GaAs, implantation disorder, flux and fluence depend., electrolum. expts. 8-83833
- GaAs, ion bombardment, composition changes, AES 8-72662
- GaAs, ion etching, effects on optical props. and lattice disorder 8-83122
- GaAs, p-n junction, Zn^+ implanted, residual radiation defect influence on characts. (*Russian*) 8-84287
- GaAs:F^+ , defect form. on P^+ implantation at various temp., He^+ backscatt. obs. 8-59828
- GaAs(P) , ion irradi. damage, strain effect contrib., channelling meas. 8-67752
- GaP , ion-implanted, form. and annealing of radiation damage 8-91363
- $(\text{Gd,Bi})_3(\text{Fe,Ga})_{12}$ magneto-optic film, ion irradi. effect on storage props. 8-52324
- $\text{Gd}_3\text{Ga}_5\text{O}_{12}$, Ca, Zr and Mg substituted artificial garnets, track registration props. 8-62679
- Ge (111) surface, 500 eV Ar^+ bombard., high temp. annealing, recovery, RHEED obs. 8-87723
- Ge film, amorphous, ^{74}Ge ion implanted, defect struct. obs. 8-51848
- Ge(100) surface, Ar ion bombarded, determ. of atomic steps, LEED 8-63913
- InSb/GaSb superlattice thin films, sputtered, ion-bombardment-enhanced diffusion during growth 8-87882
- KBr, heavy ion irradi., σ and π exciton emission spectra, 4.2K 8-76534
- LiF , N^+ and Ne^+ irradiation, MO X-ray intensity meas. 8-82831
- LiNbO_3 , microfabrication by ion-bombardment enhanced etching 8-76779
- Mo, blister erosion reduction by multi-groove surface microstruct. 8-95211
- Mo, energetic deuteron irradiated surface struct. quantitative meas. 8-95210
- Mo, irradiation induced defects, electron microscope images 8-83854
- Mo single crystal 8-52136
- Mo, surface blistering by 75 to 350 keV He ions, SEM study 8-72657
- Mo, vacancy mutation to divacancies by He trapping, percolation onset 8-51601
- NaCl(I) , acoustic radiation generated by ionising particles 8-87726
- NaI , Xe^+ ion bombard., sputtering processes, time of flight meas. 8-88392
- Nb and Nb alloys, superconductor, flux pinning under heavy ion irradiation 8-52167

ion beam effects continued

- Nb, blister form. on single crystal under Ne^+ ion bombardment 8-71772
- Nb, effect of O ion irradiation on supercond. 8-52131
- Nb film, ion bombardment with N_2^+ , Ar^+ , struct. changes, chemical compound formation (*Russian*) 8-95084
- Nb:O, type II supercond., radiation-induced flux pinning 8-80106
- Nb-Zr, type II supercond., radiation-induced flux pinning 8-80106
- $\text{Nb}_{40}\text{Ni}_{60}$, 3 MeV Ni^+ ion implantation, electron microscope exam. of ion damage 8-91365
- Nb_3Sn , effect of O ion irradiation on supercond. 8-52131
- Nb_3Sn , superconducting props., effect of radiation induced atomic disorder 8-52133
- Ni, irradiated, with He^+ bubble depth distrib. meas. by TEM and blister form. mech. 8-95088
- Ni, TEM exam. of ion damage in FCC metals 8-87727
- Ni-Al solid solns., N_2^+ irradi., void ordering 8-79644
- Ni-ThO₂, irradiated with 5 MeV Ni^{++} , ThO₂ redistrib. 8-71771
- Pb, effect of O ion irradiation on supercond. 8-52131
- Pt alloy, fission-fragment-induced He blistering 8-86601
- Pt, TEM exam. of ion damage in FCC metals 8-87727
- Pt-Au (4.0 at.%), ion irradiated, direct obs. of vacancy struct. of (220) plane 8-51534
- RbCl(Br)(I) , Xe^+ ion bombard., sputtering processes, time of flight meas. 8-88392
- Re, He ion irradi., blistering, SEM obs. 8-87722
- (SN)₂, neutron and heavy ion bombard., effect on elec. cond. along chain axis 8-56136
- Se, photoconductive film, field instability, Ar^+ ion irradi.-induced defects 8-87997
- Si (111) surface, 500 eV Ar^+ bombard., high temp. annealing, recovery, RHEED obs. 8-87723
- Si, Ar bombarded, blistering effects, SEM obs. 8-67745
- Si, diffusion of B,P and Sb, implantation damage effects 8-55988
- Si, ion implantation damage, annealing, role of stresses 8-75679
- Si, ion implanted, voids, electron microscopy 8-67757
- Si, ion implanted layers, laser annealing 8-67732
- Si, ion irradi. damage, strain effect contrib., channelling meas. 8-67752
- Si, ion-implanted, cryst. to amorphous transform., ESR expts. and composite model 8-59825
- Si, ion-implanted, secondary defects development, three-stage model 8-87725
- Si, ion-implanted layers, crystalline-to-amorphous transition, radiation defect prod. 8-87696
- Si, ion-implanted layers, residual defects after high temp. annealing 8-87695
- Si, sputtered, cluster formation, influence of HF plasma interaction 8-64441
- Si, strain meas. by Pendellosung effect after P ion bombard. 8-55773
- Si substrate, implantation effects on hardening and Si_3N_4 film stress reduction 8-71748
- Si surface, interaction of oxygen gas discharge plasma 8-83840
- Si wafer, colour-banded, sheet resist. variation following high dose implantation at high dose rates 8-95074
- Si:As , implanted, spatially varied activation during regrowth of amorphous layers, sheet resist. and backscatt. obs. 8-71749
- Si:As , ion implanted, anomaly of elec. activation by additional Ne irradiation 8-84211
- Si:Cu(Au) , recoil implantation from thin surface films, backscatt. obs. 8-63783
- Si:P , ion-implanted, optical refl. obs. of damage 8-55883
- Si-B, P diffusion and activity after Ar ion bombardment 8-95192
- SiC , energetic deuteron irradiated surface struct. quantitative meas. 8-95210
- SiC , energetic ion sputtering, appl. of AES-SIMS (IMA)-FDS combined systems to physical and chemical processes 8-95636
- SiC , sputtering yield, use as first wall material 8-95629
- SiC surface, H^+ , D^+ and Ar^+ bombardment, 5 to 15 keV, meas. of erosion yield 8-79647
- SiC-C , sputtering and blistering from H^+ and He^+ bombardment 8-79649
- Si_3N_4 , enhanced etching by ion beam, localised substrate heating effects 8-51573
- Si_3N_4 film, on Si, implantation effects on substrate hardening and film stress reduction 8-71748
- Si_3N_4 , ion-implanted, enhanced etching in buffered HF solns. 8-72903
- SiO_2 film, on Si, radiation damage structures, EPR obs. 8-95097
- SiO_2 , ion irradi., H capture, absorpt. bands (*Russian*) 8-76505
- $\text{SiO}_2\text{-Si}$ structure P^+ bombardment damage, exoelectron emission obs. 8-95383
- Sn, effect of O ion irradiation on supercond. 8-52131
- Ta film, ion bombardment with N_2^+ , Ar^+ , struct. changes, chemical compound formation (*Russian*) 8-95084
- Th, ion irradi., surface C and O, AES obs. 8-71775
- Ti, blister form. by He and H ion bombardment, target struct. effect 8-95087
- Ti coated Nb, reduction of void number density and size by ion irradiation 8-51600
- Ti film, ion bombardment with N_2^+ , Ar^+ , struct. changes, chemical compound formation (*Russian*) 8-95084
- Ti, sputter-erosion and impurity emission under low energy ion bombardment 8-95628
- Ti-Al-V (6.4 wt.%), surgical implant ion beam textured, stress/strain relations, fatigue characts. 8-73297
- TiC, sputtering yield, use as first wall material 8-95629
- TiO_2 , rutile, deuteron and alpha-particle implantation, chemical effects, optical and cond. meas. 8-67755
- V, annealing after irradiation with 210 keV He at 625°C at high fluences 8-67751
- V, blister form and stress build-up, under the bombardment, surface prep. effects 8-95094
- V, blister form. by He and H ion bombardment, target struct. effect 8-95087
- V, effect of O ion irradiation on supercond. 8-52131
- V, evap. layer, ion bombardment effect on superconducting transition temp. 8-52136
- V, first wall material, irradi. with 40 keV ^4He ions, blistering 8-55897
- V, H^+ ion bombardment, surface blistering, influence of temp. and crystallographic orientation (*Russian*) 8-95083
- V, irradiation with 2 MeV He ions, low cycle at elev. temp. 8-95086

ion beam effects continued

- V, oxidation during energetic particle irradiation, influence of reactive gases on sputtering and secondary ion emission 8-72656
 V, sputter-erosion and impurity emission under low energy ion bombardment 8-95628
 V-O (1 to 4 at.%), solid soln., void swelling, V ion beam irradiation, 550 to 905°C 8-63795
 V₂Si single crystal, radiation damage and superconductivity 8-52129
 W, FIM study of lattice damage caused by low-energy He ion bombardment 8-95090
 W, oxidation during energetic particle irradiation, influence of reactive gases on sputtering and secondary ion emission 8-72656
 Zr, irradiation induced defects, electron microscope images 8-83854

ion beams

- see also beam-foil spectra; beam-foil spectroscopy; energy loss of particles; ion beam effects; ion optics; ion-surface impact; mass spectrometers; particle accelerators; sputtering*
 coherent EM radiation intensity, produced by modulated electron/ion beams in gas 8-50686
 collective ion acceleration, by temporally modulated relativistic electron beam 8-50422
 conference on electron, ion and photon beam technology, Palo Alto, CA, USA (May 1978) 8-74827
 divergence, effect of preacceleration voltage 8-66743
 electron gas, energy loss of correlated charges 8-87729
 energy meas. of Van de Graaff accelerator using generating voltmeter 8-58508
 energy spectrum of beam from inductively coupled HF source, optical parameter meas. of gun 8-89590
 equilibrium negative charge state fractions 8-90288
 extraction from quiescent plasma, for pellet fusion 8-50326
 Faraday double transmitting cup, ion optical control device 8-82556
 focusing and transport in neutralising background, for fusion expt. 8-50323
 focusing by mag. insulated diodes, for inertial confinement fusion 8-50324
 Hall accelerator, four-lens, pure ion beam struct. 8-66441
 impurity anal. by backscatt. meas. 8-70223
 intense ion beams for implantation 8-66004
 intense negative ion beams from N₂ cluster ions, size specification 8-87006
 laser spectroscopy, high-resolution, using fast ion beams 8-86975
 light-ion beams, prod. and focusing for fusion expts. 8-50322
 light-ion beams for fusion programme at NRL 8-59042
 mass spectrometer electrostatic analyser attachment 8-86377
 negative ion beam, generation, transport and accel., fusion reactor appl. 8-66378
 neutralisation in free space 8-71027
 neutralisation in transverse mag. field 8-78513
 penetration switch, ion beam, for specimen thinning for TEM 8-70228
 periodic transport system, K-V distrib. stability 8-50329
 pinched beam diode, geometrical focusing of intense ion beams 8-58898
 polarised ion sources and low energy collector rings, H⁻, D⁻ beams 8-58515
 preacceleration effects on ion beam transmission effects 8-87005
 production in pulsed linear accelerator for inertial fusion 8-50325
 profile imaging by Ti tritide collector 8-78032
 profile monitor using holed sampling disc 8-54498
 pulsed charged beams, phase meas. and control 8-58523
 relativistic proton beam, energy monochromation using laser 8-90010
 saddle field ion source beam spectra, gas depend., at. spectroscopy appls. 8-78039
 scanning device for rapid meas. of emittance and brightness 8-58522
 slow proton beam spin polarisation meas. by Lamb shift 8-78031
 space charge effects in transport, computer simulation 8-50328
 steering by aperture displacement for tetrode accelerating structure 8-82075
 Tokamak-trapped 26 keV beam, RF wave heating 8-59627
 trajectories calc. in a 3-dimens. beam subjected to a space charge (French) 8-82902
 two-beam gain saturation in an electron-ion beam without capture of electrons 8-94919
 ultraintense heavy ion beam generation, by radiation cooling in long drift tube 8-58489
 visual image produced by electron interaction on surface 8-58091
 wedge type ion beam divergence profile calc. 8-82555
 C, energy loss of fast H₂⁺ ions 8-79653
 D⁻, polarised prod. in 'H+Cs atomic collision at 40 keV, 3.1 µA 8-55078
 H⁻, polarised prod. in 'H+Cs atomic collision at 40 keV, 2.9 µA 8-55078
 H₂⁺, energy loss of fast ions in solids 8-79652
 H₂⁺, fast ions, stopping power of C foil 8-79653
 Si surface-barrier detectors, characts. in Xe ion beam 8-78571
 U, 50 keV beam prod. by charge exchange in gas and metal vapour targets 8-70675

ion counters *see counters***ion cyclotron resonance heating** *see plasma heating***ion cyclotron resonance spectra** *see mass spectra***ion cyclotron resonance spectroscopy** *see mass spectroscopy***ion density**

- air corona discharge ion density and mobility obs. 8-67594
 air positive corona discharge between coaxial cylinders, critical density estimation 8-67595
 D-region, daytime solar proton event-disturbed model 8-93038
 flame, diffusion type, oppositely directed jets, elec. props. 8-56896
 holographic interferometry system for plasma flow phenomena, Ba II ion density meas. 8-55751
 HV laboratory ion density due to repetitive impulse generation 8-65913
 ionosphere effects of geomagnetic storms, OGO 6 obs. (Japanese) 8-85754
 liquid metal, surface ion density, nonmonotone, perturbative discrete ion introduction into jellium 8-72222
 Mars ionosphere, ion density and temps. in light of Viking obs. 8-96419
 mesosphere, ion bunches form. and concs. 8-73424

ion density continued

- negative impulse corona and sparkover, background ionisation effects 8-87540
 sporadic-E layer inhomogeneous structure influence of RF heating (Russian) 8-61653
 thermosphere, effects of geomagnetic storms, OGO 6 obs. (Japanese) 8-85754
 Z-pinch discharge, electron temp. and density variation obs. 8-75426
 H⁺, O⁺, conc. in upper atm., Aureole 2 satellite mass spectrometer obs. 8-53766

ion emission

- see also field ion emission; secondary ion emission; thermionic ion emission*
 electrolyte aqueous soln. drops, ion emission due to laser heating 8-59063
 Al alloys, oxide-covered, characteristic emission of negatively charged particles during tensile deform. 8-92179
 W (100), adsorbed O, electron stimulated desorption ion energy distrib. and surface struct. 8-75940

ion engines

- see also aerospace propulsion; rockets*
 No entries

ion exchange

- alkaline radioactive waste decontamination method 8-50263
 electrolytic ion separation, by ion exchange membranes 8-53247
 float glass, toughening by ion exchange, selection of technology parameters 8-84757
 fuel reprocessing waste ¹³⁷Cs, ⁹⁰Sr and rare earth radioisotope separation by cation exchange 8-78486
 Itaya zeolite, removal of H⁺, NH₄⁺, Cu²⁺, Cd²⁺ (Japanese) 8-95951
 lacustrine sediments, selective chem. extraction of CO₃²⁻ associated metals 8-65406
 liquid nuclear waste, simulated, ion exchange equilibration, radiotracer obs. 8-74444
 meltwater, from Alpine glaciers, ion exchange influence on dissolved load 8-81228
 membranes for ion exchange, ion and water transport eqns. 8-68930
 silica gel, ion exchanger, isotope separation appls. 8-86961
 sulphonic ion exchangers Ar selective separation of U and Th from lanthanides 8-58860
 5A-zeolites, cation distrib. and diffusion (German) 8-64828
¹⁰B enrichment by low-temp. exchange in BF₃.SO₂ system (Japanese) 8-55251
¹⁰B separation using anion exchange resin, isotopic plateau holding displacement chromatography (Japanese) 8-56886
 Cs selective resin, rapid determ. of Cs in seawater 8-85609
 Cu(II), selective separation from rare earth elements on chelate ion exchangers 8-58861
 Fe(III), selective separation from rare earth elements on chelate ion exchangers 8-58861
 KAlSiO₄ metastable polymorph, prep. by ion exchange with RbAlSiO₄, struct. 8-79585
 K₂O-SiO₂ glass, improvement in water resist. by ion exchange 8-85012
 KOH, aqueous solution, transport parameters for cation exchange membrane 8-64883
 LiO₂-SiO₂ glass, improvement in water resist. by ion exchange 8-85012
 Na₂O-CaO glass tube, fracture by field assisted ion exchange 8-68771
 Na₂O-SiO₂ glass, improvement in water resist. by ion exchange 8-85012
 Ni(II), selective separation from rare earth elements on chelate ion exchangers 8-58861
 SiO₂-Al₂O₃-B₂O₃-MgO-CaO-Na₂O, strengthened by ion exchange, exam. of internal stresses using polarising microscope 8-88549
⁹⁰Sr/⁹⁰Y radioisotope generator, educational aid 8-78535
 Th(IV), selective separation from rare earth elements on chelate ion exchangers 8-58861
 U nuclear fuel particle prep. by ion exchange resin loading (German) 8-82499
 U-Pu, isotope separation in HNO₃ by exchange resins 8-74782
 UO₂(II), selective separation from rare earth elements on chelate ion exchangers 8-58861
 Zn²⁺, transport in cation-exchange membranes 8-96033
 Zr(HPO₄)₂.H₂O-Kynar membranes, struct., ion mobility 8-76915

ion exchanging *see ion exchange***ion excited X-ray emission** *see ion microprobe analysis***ion implantation**

- see also semiconductor doping*
 AES quantitative anal. of impurities (Japanese) 8-91356
 austenitic stainless steel 316, by up to 7 eV D, depth profiles 8-71751
 conference on electron, ion and photon beam technology, Palo Alto, CA, USA (May 1978) 8-74827
 corrosion resistant surface alloy form. by ion implantation 8-88569
 diamond, review 8-87698
 doping of channelled ion implantations, apparatus for spatial uniformity 8-51569
 enhanced diffusion mechanisms, review 8-67847
 ESCA observation 8-52612
 films, props. and appls., review 8-71752
 free carrier profile measurement on thin-layers, fast current pulse MOS deep-depletion technique 8-80075
 Freeman type high current source for implantation appl. 8-66005
 garnet film preparation, single-crystal, for magnetic bubble domain appl. 8-60588
 graphite, pyrolytic, behaviour of implanted D and He 8-95071
 heterogeneous medium, ion implantation and energy deposition, path length approx. 8-87694
 III-V semiconductors, ion implantation, effect of implantation 8-75683
 integrated optic devices, fabrication parameters (German) 8-83119
 intense ion beams for implantation 8-66004
 magnetic bubble stability in ion implanted channels, model 8-68320
 metal, He ion implanted, statistical model of low temp. blister formation 8-67754
 metal surface, He implantation lateral stress, role in blister form. mech. 8-95068
 metalloid-transition metal amorphous surface alloys formed by ion implantation, TEM study 8-67730

ion implantation continued

microwave ion source for high-current implanter 8-70224
MOS structure, Ar ion effects on relax. of nonequilib. cap. 8-64140
p-n diode minority carrier storage effect reduction by F ion implantation damage 8-72243
quartz, ion-implanted, SAW velocity 0.9 to 6K 8-84040
quartz oscillator plate, surface treatment by 100 keV B ion implantation (*Japanese*) 8-59826
radionuclide, half-life meas. by ion implantation 8-70713
review, ion implantation, problems and perspectives 8-75687
secondary particle collection in ion implantation dose measurement 8-67731
semiconductor, surface, effects of ion sputtering, ion implantation 8-88395
semiconductor device fabrication appl. 8-87692
semiconductor doping by nuclear transmutation method (*German*) 8-95066
semiconductor layer, implanted, effectiveness of annealing by millisecond laser pulses 8-55885
solid, depth profiling of ³He ion implantation 8-59830
solid ion source by electron bombardment (*Japanese*) 8-78035
state of art, review (*Italian*) 8-59829
steel, mild, implantation of Cu(Cr), annealing and rolling behaviour of conc. profiles 8-75684
steel, stainless, 304, void form., effect of sequential and simultaneous He implantation 8-71719
steel, stainless, 321 and 304, D implanted, thermal desorption and bombardment induced release 8-95072
steel, stainless, D implanted, thermal desorption 8-71750
steel, stainless, low energy D implanted, microstruct. 8-95073
superconductivity applications 8-52134
target assembly, ultra high vacuum, for charged particle irradiations in the materials research field 8-83841
thin specimens, temp. control for mech. meas. under light ion irradiation 8-86278
X-ray emission analysis in TEM, implanted ion detection 8-51575
(YSmEuCa)₃(FeGe)₂O₁₂, garnet film, ion implanted, bubble domain props. 8-88152
Ag-Fe, implanted, Mossbauer conversion electrons spectroscopy, rel. to dose and annealing temp. 8-52397
AgCl, colloid centres by heavy ion implantation 8-63780
Al, hyperfine interactions of implanted Fe, conversion electron Mossbauer spectroscopy 8-52391
Al, ranges of implanted 10-30 keV D⁺ 8-83858
Al:¹²B, relax. mechanism for polarised implant 8-87693
Al-SiO₂-Si structures, implanted B⁺ ions, high-freq. CV characts. (*Russian*) 8-80056
Al-SiO₂-Si:B ions, annealing effect on energy spectrum of radiation defects (*Russian*) 8-88488
α-Al₂O₃, ion bombard., vol. expansion, annealing compaction, surface props. 8-67748
Be, blistering model, correlation between blister diameter and skin thickness 8-95067
C, amorphous, ranges of implanted 10-30 keV D⁺ 8-83858
Cd,Hg_{1-x}Te:Hg, p-n junction photovoltaic diode, appl. as IR detector 8-86330
CdS:Bi film, implantation and post annealing, superlinearity 8-52028
¹³⁷Cs T_{1/2} determ. using new specific activity meas. 8-70714
Cu, of Ag⁺ and Ta⁺, metastable alloy layer form. 8-71709
Cu, thermal oxidation, influence of ion implantation 8-64768
Fe:¹³³Xe, heavy ion implantation, recovery, Mossbauer effect meas. 8-52393
Fe:Xe, isotope ion implantation control (*Flemish*) 8-79623
Fe-Dy, dil., implanted impurity hyperfine interaction 8-68417
Fe-Ti-Sb-C alloys, Sb trapping effect on temper embrittlement, ion beam study 8-92312
GaAs, amorphous layer formation, IR spectra 8-95063
GaAs, disordered, ion implanted, elec. props. 8-84212
GaAs, dual implantation of C⁺ and Ga⁺, sheet resist. and Hall effect meas. 8-67728
GaAs, implantation disorder, flux and fluence depend., electrorefl. expts. 8-83833
GaAs, implantation of Si, Al, Hf, Ta into InP and GaAs, form. of protective oxide 8-79622
GaAs, ion implantation damage, TEM exam. of variation with ion species and stoichiometry 8-59827
GaAs, p-n junction, Zn⁺ implanted, residual radiation defect influence on characts. (*Russian*) 8-84287
GaAs planar p-n junctions, Be ion implantation, fabrication and characts. 8-88022
GaAs, S and Se ion implantation 8-55884
n-GaAs substrates, ion implanted, compensation 8-75680
GaAs, surface segregation of implanted alkali metals, photoemitter prep. and characts. (*French*) 8-60544
n-GaAs:O carrier removal profiles meas. 8-56154
GaAs:P⁺, defect form. on P⁺ implantation at various temp., He⁺ backscatt. obs. 8-59828
GaAs:Se, implanted, annealing with O-free CVD Si₃N₄ encapsulant 8-83834
GaAs_{0.6}P_{0.4}:Be, implanted annealing studies, elec. resist., Hall effect meas. 8-84213
GaAs_{1-x}P_x, diffusion of implanted Zn ions, ion microprobe analysis 8-95190
GaN:As(P), implanted single cryst. film, cathodolum. 8-60523
GaP, ion-implanted, form. and annealing of radiation damage 8-91363
GaP:N(Te), ion implanted at 40 keV, refl. spectra, 210-2000 nm, annealing (*Russian*) 8-80386
(Gd,Bi)₃(Fe,Ga)₂O₁₂ magneto-optic film, ion irradiation effect on storage props. 8-52324
Gd_{0.9}Y_{0.1}Tm_{0.1}Ga_{0.44}Fe_{0.56}O₁₂, ion implanted, ferromag. reson. meas. 8-68385
Ge amorphous film, effects of ion implantation on structure 8-55881
Ge:Al(Sb) film, amorphous, ion implantation, effect on cond. 8-83839
Ge:inert gas, ion implantation, UV photoemission exam. 8-80457
GeO₂:Si, optical props. IR absorpt., UV reflection spectra 8-84619
He, uniform concentration implantation, simulated neutron irradiation damage 8-79648
He⁺ implanted stainless steel, microstructure anal. 8-82516
In, amorphization by ion implantation 8-52135

ion implantation continued

In, film, embedded with He particles, superconductor ion implantation study of inhomogeneities 8-52181
InP by S and Si for n-type doping 8-91351
InP, implantation of Si, Al, Hf, Ta into InP and GaAs, form. of protective oxide 8-79622
InSb, ion implanted layers, amorphisation, recrystallisation 8-63782
InSb n⁺-p and p⁺-n photodetectors fabrication by S and Be ion implantation 8-49906
LiF:Mg, Ti, luminesc. increase by O implantation 8-64412
LiNbO₃, ion implanted, acoustic model of SAW delay lines (*French*) 8-55540
Li₂O, Ar⁺ implantation, depth distrib. by proton backscatt. 8-51577
Mg:H, solid soln. produced by ion implantation 8-67733
MgO, implanted K aggregates, TEM and optical spectra obs. 8-83838
Mo single crystal 8-52136
Nb-Sn(Ge), A-15 compound formation by ion implantation 8-51572
Nb₃Al_{0.2}Si_{0.8}, A-15 alloy synthesis by ion implantation 8-80489
Nb₄₀Ni₆₀, 3 MeV Ni⁺ ion implantation, electron microscope exam. of ion damage 8-91365
Ni, blistering model, correlation between blister diameter and skin thickness 8-95067
Ni, ranges of implanted 10-30 keV D⁺ 8-83858
Ni, trapping and release of inert gases, thermal evolution mass spectrometry 8-95077
Ni:K⁺(Ba⁺), ion implantation, effect on inelastic refl. and energy losses of fast primary electrons 8-55900
Ni-Dy, dil., implanted impurity hyperfine interaction 8-68417
Pb, ion implanted, diffusion of Co, exam. by activation analysis 8-91488
PbTe, ion-implanted, doping profile evaluation by Hall effect and sheet resist. meas. 8-59831
PtSi, Ar bubble formation after 20 to 160 keV sputtering, TEM and backscatt. spectrometry obs. 8-64435
Sb, combined with Si vacuum deposition (*Japanese*) 8-88428
Si, AES examination of Ar⁺ ion retention during Ar sputtering 8-56552
Si, amorphous, Si implanted, substrate-orientation depend. of epitaxial regrowth rate 8-79900
Si, amorphous layer, ion-implanted, spatially controlled cryst. regrowth by laser irradiation 8-55810
Si, Ar bombarded, blistering effects, SEM obs. 8-67745
Si, C ion implantation, IR absorpt. of synthesised β-SiC layer 8-56492
Si, channelled-ion implantation of group III and group IV ions 8-75682
Si, crystal defects in integrated circuits, review 8-88547
Si crystals, damage profiling after heavy ion implantation, MeV region 8-75686
Si dechanneling of MeV He ions by twinned regions 8-75700
Si, diffusion of B,P and Sb, implantation damage effects 8-55988
Si doping, atomic collision theory and range-energy relations 8-71753
Si, ion implantation damage, annealing, role of stresses 8-75679
Si, ion implanted, laser annealing, periodic regrowth phenomena 8-67724
Si, ion implanted, laser-annealed, theoretical anal. of thermal and mass transport 8-91364
Si, ion implanted, voids, electron microscopy 8-67757
Si, ion implanted layers, laser annealing 8-67732
Si ion implanted p-n junction, cryst. damage influence on elec. props. 8-56219
Si, ion-implanted, cryst. to amorphous transform., ESR expts. and composite model 8-59825
Si, ion-implanted, disorders, nature and annealing behaviour, review 8-83836
Si, ion-implanted, secondary defects development, three-stage model 8-87725
Si, ion-implanted layers, crystalline-to-amorphous transition, radiation defect prod. 8-87696
Si, ion-implanted layers, impurity profile meas. after laser annealing 8-87702
Si, ion-implanted layers, residual defects after high temp. annealing 8-87695
Si, ion-implanted surface, profiling method 8-95075
Si layer, neutron activation analysis, contamination and cross-contamination 8-83837
Si polycrystalline solar cells, ion implantation method and results 8-63784
Si, radiation damage, SEM electron beam absorpt. meas. 8-75696
Si, recrystallised amorphous layer, self-ion irradiated, defect structures, TEM obs. 8-75688
Si, self-implanted layer, grain size, laser irradiation energy density depend. 8-72012
Si, strain meas. by Pendellosung effect after P ion bombard. 8-55773
Si substrate, implantation effects on hardening and Si₃N₄ film stress reduction 8-71748
Si surface, interaction of oxygen gas discharge plasma 8-83840
Si, surface characterisation by Si-electrolyte interface impedance meas. 8-84291
Si wafer, colour-banded, sheet resist. variation following high dose implantation at high dose rates 8-95074
Si:Al(Sb) film, amorphous, ion implantation, effect on cond. 8-83839
Si:As, elec. activation of implanted As during low temp. anneal, Hall effect meas. 8-51571
Si:As, implanted, spatially varied activation during regrowth of amorphous layers, sheet resist. and backscatt. obs. 8-71749
Si:As, ion implanted, anomaly of elec. activation by additional Ne irradiation 8-84211
Si:As, time-resolved reflectivity during laser annealing 8-92086
Si:B, conc. profile of implanted cryst., by ¹¹B(p,α) chem. anal., annealing (*German*) 8-83843
p-Si:B, high temp. treatment, effects on ion implanted impurity distrib. profile 8-79625
Si:B, implemented laser annealed samples, unidirectional contraction 8-71747
Si:B, ion implanted, laser and thermal annealing compared, TEM obs. 8-75681
Si:B, ion implanted, localised defects, TEM study 8-87699
Si:B, ion implanted, struct. of rod defects, TEM obs. 8-71744
Si:B, polycrystalline, depth profiles of implanted B atoms, meas. by secondary ion mass spec. (*Japanese*) 8-67734

ion implantation continued

- Si:B, TEM study of stacking fault form. and annealing 8-51566
 Si:Cu(Au), recoil implantation from thin surface films, backscatt. obs. 8-63783
 Si:H, ion implanted Monte Carlo calcs. of profiles of H ions 8-55889
 Si:P, annealing characteristics at low temp., elec. props. 8-63781
 Si:P, Au gettering by P diffusion and P-induced dislocations 8-91346
 Si:P, high dose implantation, outside dislocation generation 8-87672
 Si:P, ion implantation, effects of high dose rate 8-83835
 Si:P, ion implanted, lattice damage and electrical activation correlation 8-67726
 Si:P, ion implanted, resist. changes induced by ESR 8-68377
 Si:P, ion-implanted, optical refl. obs. of damage 8-55883
 Si:Pb, implanted, laser annealing 8-75685
 Si:Pb, implanted and annealed, impurity redistrib. 8-75689
 Si:S, existence of isotope shift for S deep level, isothermal transient capacitance meas. 8-63999
 Si:Sb, ion implanted, annealing behaviour of stress 8-63778
 Si:Te, laser annealed, lattice location of Te 8-67725
 Si-B, diffusion-free annealing, use of scanning CW Kr laser 8-91345
 Si-SiO₂ interface in MIS struct., B⁺ ion implanted, elec. props. due to laser irradi. 8-72272
 Si₃N₄, enhanced etching by ion beam, localised substrate heating effects 8-51573
 Si₃N₄ film, on Si, implantation effects on substrate hardening and film stress reduction 8-71748
 Si₃N₄, ion-implanted, enhanced etching in buffered HF solns. 8-72903
 SiO₂:Al film, ion-implanted, electron trapping behaviour 8-67729
 Te, elec. field gradient and lattice location of Sn, TDPAC and Mossbauer effect meas. 8-52395
 TiO₂, rutile, deuteron and alpha-particle implantation, chemical effects, optical and cond. meas. 8-67755
 V, evap. layer, ion bombardment effect on superconducting transition temp. 8-52136
 V₃Si single crystal, radiation damage and superconductivity 8-52129
 (YEuErCa)₃(GeFe)₅O₁₂: H, Ne, Ar, threefold symmetrical mag. bubble props. 8-64243
 Y_{2.35}Eu_{0.65}Ga_{1.2}Fe_{3.8}O₁₂, bubble translation vel., ion-implantation effects 8-68327
 Y_{1.52}Eu_{0.3}Tm_{0.2}Ca_{0.88}Ge_{0.88}Fe_{4.12}O₁₂, bubble translation vel., ion-implantation effects 8-68327
 (YEuYbCa)₃(GeFe)₅O₁₂: H, Ne, Ar, threefold symmetrical mag. bubble props. 8-64243
 (YSm)₃(GeFe)₅O₁₂: H, Ne, Ar, threefold symmetrical mag. bubble props. 8-64243
 (YSmLuCa)₃(GeFe)₅O₁₂: H, Ne, Ar, threefold symmetrical mag. bubble prps. 8-64243
 Zn:Al, ion implantation of Al, defect flow induced outdiffusion 8-63779
 p-ZnSe:As, ion implantation and heat treatment 8-87700
 ZnTe:O,Zn, dual ion implantation, luminesc. spectra obs. 8-87697
 Zr, deuteron implanted, temp. depend. depth profiles of deuterons 8-95076
 Zr, ranges of implanted 10-30 keV D⁺ 8-83858

ion lasers

- commercial laser systems, design and manufacture 8-59046
 discharge, current limitation by electric double layer 8-66799
 inert gas, highly ionised, vacuum UV lasing 8-63060
 inert gas ion laser discharge, energy balance 8-74884
 inert gas ion laser ion-acoustic wave excitation 8-74885
 inert gas laser, high repetition rate operation 195 to 225 nm 8-82980
 longitudinal flow, effect of flow on output power 8-58975
 radioactive source preionisation of visible and UV discharge lasers 8-63096
 rare earth ion potential vapour laser systems, spectroscopic props. 8-66812
 UV metal ion lasers, spectral range 200-320 nm 8-66809
 XUV lasing, gain-verification problem 8-71086
 Ag II, 1 W multiline output power from 800.4, 825.5, 840.4 nm transitions 8-7953
 Ar, commercial laser systems, design and manufacture 8-59046
 Ar high power CW laser and its problems (*Japanese*) 8-59019
 Ar II, magnetically confined plasma, pulsating ion laser action 8-78994
 Ar ion laser, collisional radiative model and expt. 8-55338
 Ar ion system, collisional radiative model 8-71080
 Ar⁺, freq. stabilisation by ¹²⁷I₂ absorption lines at 582 THz 8-90430
 Ar⁺, radiation spectrum and influence of Fabry-Perot plate (*Polish*) 8-78993
 C ion, extended plasma source for short-wavelength amplifiers 8-79447
 Cd II, 441.6 nm, positive column He-Cd discharge, excitation mechanism 8-58983
 Cd⁺ in He-CdBr, He-CdCl₂ and He-CdI₂ discharges, CW laser oscill. 8-50765
 Cl II in CuCl and FeCl₂ vapours, pulse generation at 5218 Å, 5221 Å 8-58990
 Cu II, 1 W continuous output from 780.8 nm transition 8-82953
 Hd-Cd hollow cathode laser in mag. field, Cd II stimulated emission 8-79002
 He-Cd, intensity fluctuations meas., comparison with He-Ne laser 8-71087
 He-Cd hollow cathode laser, laterally emitted light 8-66810
 He-Cd II lasers, positive column, hollow cathode types, 4416 Å oscill. characts. (*Japanese*) 8-94392
 He-Cd⁺, population densities of He excited states in positive column discharge 8-58989
 He-Cd⁺ laser, exam. of Cd II 441.6 nm laser power increase by I addition 8-55344
 He-Cd⁺ laser, upper and lower laser states population densities, simultaneous determ. 8-87042
 He-Zn hollow cathode laser, 7588 Å in ZnII, operating characts. and upper level operating mech. 8-63071
 Kr, commercial laser systems, design and manufacture 8-59046
 Kr IV, very strong laser emission at 195.027, 175.641 nm 8-63060
 Kr, mode-locked, near UV, 50 ps pulse width 8-79030
 Li plasma dynamic laser, using supersonic nozzle, population inversion, excitation cross section 8-50760
 N₂⁺, gain and saturation 8-79001
 N₂⁺, pumping of coumarin derivative dye lasers 8-74903

ion lasers continued

- Nd³⁺ in Nd-Al-Cl complex, vapour phase laser expts. 8-66813
 Ne II, long pulse UV laser emission, electron beam excited Ne-NF₃ mixture 8-78996
 Ne-Cu hollow-cathode laser discharge sputtering obs. 8-66800
 O₂⁺, He₂⁺+O₂ charge exchange laser 8-50759
 Pb-He discharge, excitation process, Pb⁺ emission lines 8-66803
 Tb³⁺ in TbCl₃(AlCl₃)_x complex, potential vapour laser system, fluoresc. obs. 8-66812
 Zn⁺ in He-ZnB₂, He-ZnCl₂ and He-ZnI₂ discharges, CW laser oscill. 8-50765

ion lenses see lenses**ion microanalysis**

- see also ion microprobe analysis*
 implantation profiles meas. (*German*) 8-95978
 neutral particle beam separation, characts., anal. appl. (*Japanese*) 8-85248
 rare earth oxide mixtures, determ. of individual rare earths (*Japanese*) 8-88683
 BP, epitaxial growth on Si substrate, Si impurity profile, ion microanal. 8-87886
 Si, determ. of P, As by ion microanal. (*Japanese*) 8-85250
 Si-SiO₂-Si structures, P, As depth profiles, ion microanal. (*Japanese*) 8-85251

ion microprobe analysers see ion microprobe analysis**ion microprobe analysis**

- see also ion microanalysis*
 biological samples, thick, PIXE anal., elimination of charging 8-88775
 calibration using matrix ion species ratios, appls. 8-61070
 carbide-forming elements, K_α C line mass absorpt. coeffs. (*Czech*) 8-64905
 detector discrimination in SIMS: ion-to-electron converter yield factors for positive ions 8-73100
 element distributions obtained by ion microprobe, images quantification 8-73101
 energy-focused atom probe design and performance 8-85276
 environmental samples, using low energy particle accelerator 8-85239
 HIXE, metal vapour targets production 8-80822
 light element anal. by 2 MeV, 150 keV proton and photon induced X-rays 8-53295
 lubricating coating, solid, elemental anal. by proton-stimulated X-rays 8-88687
 monazite inclusions possessing pleochroic halos, PIXE anal. 8-69350
 multielement anal., proton-induced X-ray emission 8-85272
 PIXE, atmospheric aerosol; absolute element concs., PIXE and AAS, comparison 8-85237
 PIXE, synaptic vesicle ion content determ. 8-61166
 PIXE anal., conc. profile determ. using beam energy variation 8-76965
 PIXE anal. with 4 MeV protons, target chamber 8-56941
 PIXE trace element anal., new method to determ. concentrations 8-76966
 proton microprobe for nondestructive trace element analysis 8-64911
 quantitative trace analysis, using ion and proton induced X-rays (*German*) 8-64900
 SEM-AES-IMA combination with SIM spectrometer, Si device anal. appls. (*Japanese*) 8-85249
 trace element meas. in air water and organic materials by ion-induced X-ray fluoresc. (*Norwegian*) 8-53278
 ultrahigh depth resolution surface analysis, appls. 8-71917
 (pX,X) expt., partial sensitivity enhancement in trace element anal. 8-61128
 Al, Zn and Mg impurities PIXE anal., conc. profile determ. using beam energy variation 8-76965
 Co, (pX,X) expt., partial sensitivity enhancement in trace element anal. 8-61128
 CuO surface, contaminated, cleaning treatments, ion scatt. anal. 8-53307
 D, in Ti, Ti alloys, Zr, V, Nb, Ta, by ion microanalyser 8-56945
 GaAs_{1-x}P_x, diffusion of implanted Zn ions, ion microbe analysis 8-95190
 H, determ. by simultaneous heavy-ion induced nuclear reacts. and at X-ray emission 8-85240
 Ni, (pX,X) expt., partial sensitivity enhancement in trace element anal. 8-61128
 Pt₉₀Rh₁₀/Pt thermocouple, Inconel sheathed, MgO-insulated, decalibrations during 1200°C use, ion microprobe obs. 8-57957

ion microprobe mass analyzer see ion microprobe analysis**ion microscopes**

- see also field emission ion microscopes; ion microscopy*
 aberrations and image form., study by magnetic anal. of beam from HF source 8-55293

ion microscopy

- see also field emission ion microscopy; ion microscopes*

No entries**ion mobility**

- see also electrolytic ion mobility; ionic conduction in solids*
 aerosol, polydispersity, unipolar charging, charging mobility analysis 8-61059
 aerosol, size distrib. determ. from mobility distrib. of charged fraction 8-61065
 aerosol, unipolar diffusion charging, particle dielectric constant and ion mobility effects 8-61058
 air corona discharge ion density and mobility obs. 8-67594
 atmospheric, measurement of elec. cond. and small ion mobility, pollution aspects 8-92931
 benzene, liq., ion injection obs. 8-63870
 critical-velocity rotating plasma interaction with neutral gas, obs. 8-75344
 DC vacuum arc emitted particle flux 8-75470
 drift tube measurements, secondary electron effects 8-59538
 drift tubes, ion time of arrival spectra determ., using CAMAC crate interfaced to microcomputer 8-93661
 electrolyte solutions, dielec. dispersion and dielec. friction 8-52436
 inert gas, diatomic ions, mobility in parent gas meas. 8-63532
 inert gas ion, in parent gas, transverse diffusion coeff., reson. charge exchange effects 8-63533
 injected ion drift tube mass spectrometer ionic mobility data in non-parent gas 8-87428

ion mobility continued

- plasma ion velocity, distrib. diagnostics by neutral particle time-of-flight spectra 8-67439
 slags, application of activity concept to physical chemistry 8-53243
 water vapour, ion mobility, 20 to 70°C 8-75252
 Ar⁺, in Ar, transverse diffusion coeff., reson. charge exchange effects 8-63533
 CO⁺, CO, lateral diffusion in CO, mass spectra meas. 8-91055
 Cs⁺ in He and Ne gas, ion mobility and longit. diffusion coeff. 8-67308
 Cs⁺, ion mobility in Ar, Kr, Xe, diffusion, generalised Einstein relation 8-67298
 Cs⁺-Ar(Kr)(Xe), ion mobility and interaction pot., drift tube meas. at 300K 8-59537
 F₂-inert gas mixtures, transport and attachment processes 8-59542
 H⁺, calc. of mobility in He, 10 to 700K 8-66629
³He, liquid, normal and superfluid phases, NMR and ion mobility experiments 8-91505
³He, mobility of positive ions 8-51773
³He, normal liq., press. and temp. depend. of positive ionic mobility 8-91504
³He-⁴He, tricritical normal phase liq., ion mobility 8-79850
⁴He, liq., phase transitions, positive and negative ion mobilities meas. 8-87833
 Kr²⁺, mobility in He gas, drift-tube meas. 8-66657
 N₃⁺, N₄⁺, lateral diffusion in N₂, mass spectra meas. 8-91055
 N₄⁺ mobility in N₂ 8-60985
 O⁺ and O₂⁺ ion swarm in O₂, reactions and transport, Monte Carlo calc. 8-59539
 O₂⁺, lateral diffusion in O₂, mass spectra meas. 8-91055
 Xe²⁺, mobility in He gas, drift-tube meas. 8-66657
 Zr(HPO₄)₂·H₂O-Kynar membranes, struct., ion mobility 8-76915

ion-molecule reactions

- chemiluminescence, anal. of spectra 8-64832
 chloromethane+Cl⁺, S₂ reaction, local orbital description, ab initio FSGO method 8-76842
 drift tube with hollow cathode ion source, for reaction rate consts. meas. 8-64834
 endothermic reson. excited ats., optical excitation technique, radiation diffusion conditions 8-55227
 Fourier transform ion cyclotron double resonance, complicated ion-molecule reactions 8-80808
 gas phase reactions and high-press. mass spectrometer, review (*Japanese*) 8-64830
 infrared chemiluminescence detection, vibrational product states appl. 8-88625
 ion+polar molecule collisions, average dipole orientation theory, ang. momentum conservation 8-92466
 mesosphere, ion-neutral bunches charge exchange rel. to ion bunching 8-73424
 methane+O₂⁺, reaction rate const. kinetic energy depend., 300K, 0.125-0.450 torr 8-76850
 naphthalene anion radical+H₂O, react., H₂ prod. 8-92460
 perturbed rotational state approach to low energy ion+polar mol. collision 8-92469
 reactive and charge transfer collisions, between ions and molecules 8-62914
 transition state location from ang. momenta distrib. 8-64808
 Ar⁺+H₂, charge transfer reactions, excited products, Ar initially metastable 8-68879
 Ar⁺+H₂(v_i=0)→ArH⁺+H, electronic nonadiabatic transitions, two-state model calc. 8-73035
 C⁺+H₂→CH⁺+H, classical trajectory anal. 8-53192
 C⁺+NH₃, role in form. of interstellar HCN and HNC 8-81672
 CH₃+N⁺, role in form. of interstellar HCN and HNC 8-81672
 CH₃⁺+CH₄(CH₃D₂), dissoci. charge transfer reactions, H and D atoms elimination 8-85141
 CO⁺+H₂, ion-molecule reaction detection of laser-induced ion spectrum, rot. components 8-74671
 CO₂+OH⁺→HCO₃⁺ react., MO-LCAO-SCF calcs., energy barrier 8-76846
 ClO⁻+NO(NO₂)(SO₂)(CO₂), rate consts. at 300K 8-76829
 F+methane, MINDO/3-FORCES study, reactant energy, products and paths 8-95926
 H⁻+methane→methane+H⁻, nucleophilic substitution, ab initio pot. energy classical trajectory anal. 8-68886
 H⁺+CN, perturbed rotational state approach 8-92469
 H₃CO⁺+H₂S⇌H₃S⁺+HCHO, chemical equil. consts., proton affinity of HCHO and H₂S 8-85189
 H₃CO⁺+HCN⇌H₃CN⁺+HCHO, chemical equil. consts., proton affinity of HCHO and HCN 8-85189
 HCl-N₂ mixture, electron swarm, Cl⁻·HCl cluster formation, dissoci. attachment, drift tube mass spectra 8-68884
 HCl+O⁺(O₂⁻)(NO₂⁻)(CO₃⁻)(CO₄⁻), rate consts. at 300K 8-76829
 H₂O+H⁺⇌H₃O⁺, equil., H₂O proton affinity calc. 8-92497
 H₂O+He⁺(O⁺)(N₂⁺)(O₂⁺)(Ar⁺), 50 to 250 keV, OH radical form. 8-56890
 H₂O⁺+H₂, ion-molecule reaction detection of laser-induced ion spectrum, rot. components 8-74671
 H₃S⁺+HCN⇌H₃CN⁺+H₂S, equil., rate coeffs. and proton affinity, flowing afterglow 8-56885
 He⁺+acetylene-d₀(-d₂), CH⁺(CD⁺), A-X luminesc., in near-thermal charge exchange 8-50632
 He₂⁺, rate coeffs. for bimol. and termol. ion-mol. reactions 8-53188
 I₂⁺+N₂→I⁺+I+N₂, 0.65-3.2 keV, dissoci. cross-section, internal excitation effects 8-64813
 N⁺+H₂, triplet state ab initio CI pot. energy surfaces 8-74729
 N₃⁺+O₂(CO₂)(H₂)(D₂) reactions, flow-drift tube obs. 8-60985
 N₂⁺, (x=1 to 4) stratospheric chemistry, reaction rate coeffs. and product distrib. 8-81305
 NO⁺, stratospheric chemistry, reaction rate coeffs. and product distrib. 8-81305
 NO⁺+atmospheric gases, thermal energy reaction rates 8-92443
 N₂O₅+CO₃⁻(NO₂⁻)(F⁻)(Cl⁻)(Br⁻)(I⁻)=NO₃⁻+XNO₂, rate consts. 8-56879
 N₂O₅+H₂O⁺, rate consts. 8-56879
 N₂O₅+NO⁺=3NO₂⁺, N₂O₅+NO₂⁺, rate consts. 8-56879
 N₂O₅+O₂⁺=NO₂⁺+NO₃⁺, rate const. 8-56879
 O⁺, O₂⁺, stratospheric chemistry, reaction rate coeffs. and product distrib. 8-81305

ion-molecule reactions continued

- O⁺+D₂→OD⁺+D, crossed beam studies product ang. and energy distrib. 8-53203
 O⁺+atmospheric gases, thermal energy reaction rates 8-92443
 O⁺+N₂→N+NO⁺ react., mechanism, ab initio SCF calcs. 8-60996
 O₂⁺+atmospheric gases, thermal energy reaction rates 8-92443
 O⁺(²D)+N₂, charge exchange rate coefficient, effect of N₂⁺ recomb. on aeronom. determ. 8-88954
 SO₂XY, (X,Y=Cl,F), positive and negative ion chemistry 8-85140
- ion optics**
see also ion beams; ion microscopes; mass spectrometers
 beam deviation, plasma boundary neutralisation surface depend. (*Russian*) 8-59613
 beam-beam interactions in p-p storage rings 8-78900
 bicylinder mirrors for appl. in multichannel mag. mass spectrometer (*French*) 8-54494
 charged particle energy analyser, ang. focusing with cylindrical electrostatic field 8-78896
 double focusing bending magnet, meas. of optical props. with thin alpha source 8-55073
 energy spectrum of beam from inductively coupled HF source, optical parameter meas. of gun 8-89590
 field ionisation and desorption sources, for quadrupole and double focusing spectrometers 8-74092
 heavy ion beam focusing, accelerated, decelerated beam, electrostatic lenses 8-89588
 ion beam image transformation using magnetic quadrupole lenses 8-55071
 iteration scheme for optics of ion beams extracted from plasma 8-50693
 low energy ion beams, conference, Salford, Sept. 1977 8-66444
 magnetic vector man analyser, stigmatic focusing condition 8-70215
 mass spectrometer, quadrupole mass filter with flat electrodes, computer simulation 8-54492
 mass spectrometer, simultaneous ion detect. with variable mass dispersion 8-78027
 mass spectrum, second order image aberration correction by electrostatic hexapole lens 8-70216
 microscope aberrations and image form., study by magnetic anal. of beam from HF source 8-55293
 miniature slow proton source for focusing efficiency obs. 8-78538
 periodic focusing of mag. channels 8-55079
 pinched beam diode, geometrical focusing of intense ion beams 8-58898
 proton beams, coherent instabilities 8-78898
 proton synchrotrons, non-linearities 8-78897
 radial focusing, using magnetic analyser with inhomogeneous field and electrostatic lens 8-78895
 space charge ion optics, influence of chromatic aberrations 8-55294
 statistical phenomena in proton rings, expt. 8-78899
 trajectories in fields having straight main paths, calc. methods 8-90352
 two-sector system with two dims. H/r mag. field, ion optical characts. 8-66744
 two-stage ion beam optics for accelerator 8-50418
 wedge type ion beam divergence profile calc. 8-82555
 Kr⁺, and isotopes, trajectory in const. mag. field plus orthogonal sinusoidal elec. field 8-50687
⁸⁶Kr ions accelerated in UNILAC, energy meas. by recoil proton technique 8-58527
- ion plating**
 reactive ion plating (*Japanese*) 8-92202
 solid ion source by electron bombardment (*Japanese*) 8-78035
 thin film deposition, low energy in source modification 8-52687
 wear resistant surface, review 8-72938
 Al coating on steel, deposition conditions and props. (*Japanese*) 8-80477
 Al-Si, ion plated contacts (*Rumanian*) 8-88029
 Cu film, ion-plated, on stainless steel, porosity depend. on process parameters 8-84720
 V-Mo, effect of ion plated Mo on corrosion in liquid Na, mech. props. 8-53020
- ion probe analysers** *see ion microprobe analysis*
ion probe microanalysis *see ion microprobe analysis*
- ion pumps**
 cryopump-ion pump system, performance 8-70142
 ultrahigh vacuum pumps 8-89488
 Gd small ion-getter pump 8-89487
 Ti, getter pump, corrugated surface and pumping speed, fusion reactor application 8-74491
- ion recombination**
 cosmology, recomb. lines in primordial microwave radiation 8-54097
 dielectronic recombination and resonances in excitation cross sections 8-62915
 interstellar polyatomic ion-electron dissociative recomb. reactions, neutral products, statistical theory 8-57604
 ionisation, quiet nighttime, calculated and measured decay rates comparison 8-81493
 ionosphere, lower, shortcomings in understanding of recomb. coeffs. 8-81492
 pyrene+N,N-dimethylaniline (deuterate)(3,5 dimethoxy-N,N-dimethylaniline), geminate recomb., solvent, isotope, mag. field effects 8-56888
 pyrene-DMA-methanol solution, photoinduced radical ion pair geminate recombination, triplet yield 8-76879
 semi-self-maintained gas discharge, ionisation instability theory 8-67511
 solvated electron+ion, in ethanol, reactivity, ion pairing effects 8-85147
 X-ray spectra of impact excit. highly charged ions, dielectronic satellites 8-62762
 Ar arc deviation from Saha-Boltzmann equilibrium, heavy-particle effects 8-67596
 Ar plasma, recombination, kinetics of stimulated atomic populations (*Russian*) 8-87436
 Ar₂⁺, dissoci. recomb., total rate coeff. depend. on electron temp. 8-58817
 Be expanding laser-produced plasma, recombination effects 8-94935
 CH⁺X⁺Σ⁺, dissoci. recomb. rate coeff., rel. to interstellar mol. form. 8-56884

ion recombination continued

- $\text{CH}_3^+ + e$, dissociative recomb. reaction in interstellar clouds, products, statistical theory 8-57604
 $\text{H}^+ + \text{M}^+$ (M =alkali metal atom), ion-ion recombination 8-58779
 H_2 arc plasma Balmer spectrum decay and two-fluid model 8-67603
 H_2^+ , dissoc. following beam-foil interaction 8-70920
 H_2^+ , dissoc. following beam-foil interaction 8-70920
 $\text{H}_2^+ + e$, electron-ion dissoc. recomb., rate const., electron beam sustained discharge 8-50652
 H_2CN^+ , dissociative recomb., rel. to interstellar HCN and HNC form. 8-81672
 $\text{HCNH}^+ + e$, dissociative recomb. reaction in interstellar clouds, products, statistical theory 8-57604
 HNC^+ , radical cation, charge exchange mass spectrometry, HNC^+ ion recombination and ionisation pot. 8-76838
 $\text{H}_2\text{O} + \text{He}(2^3\text{S})$, energy transfer processes, reaction products, UV and visible obs. in flowing afterglow 8-85138
 $\text{H}_2\text{O}^+ + e$, dissociative recomb. reaction in interstellar clouds, products, statistical theory 8-57604
 $\text{H}_2\text{O}^+ (\text{H}_2\text{O})_n$, electron recomb., electron temp. depend. 8-82854
 He II recombination lines, calc. intensities in UV 8-94212
 HgX ($\text{X}=\text{F}, \text{Cl}, \text{Br}, \text{I}$), three-body ion-ion recombination rates 8-63068
 N plasma, ionis. and radiation characts. 8-71459
 N_2^+ , electron impact dissociative recomb. coeffs. inferred from Atmosphere Explorer meas., objections 8-86957
 N_2^+ recombination, effect on aeronomic determ. of $\text{O}^+(^2\text{D}) + \text{N}_2$ charge exchange rate coeff. 8-88954
 $\text{NH}_4^+ + e$, dissociative recomb. reaction in interstellar clouds, products, statistical theory 8-57604
 Ne stationary discharge with diffuse recombination, limit current and multiple states 8-67498
 Ne-He DC glow discharge electron density decay, microwave cavity obs. 8-91167
 SF_6 high-temp. electrical breakdown parameters 8-67567
 $\text{Se}(^3\text{P}_1) + \text{inert gas}$, gas phase flash photolytic deexcitation obs., 1000K (Russian) 8-50626
 $\text{Te}(^3\text{P}_1) + \text{inert gas}$, gas phase flash photolytic deexcitation obs., 1000K (Russian) 8-50626

ion solvation *see solvation***ion sources***see also ion emission*

- active sites, effect on mass spectral fragmentation patterns 8-89581
 beam plasma source, optimum discharge parameters 8-59617
 Berkeley type ion source, long life cathode 8-66375
 collective high-energy ion acceleration, by intense relativistic electron beam, localised pinch model 8-87460
 crossed-field arc discharge contraction ion source 8-86382
 design, for milling appl. 8-70222
 direct conversion of 120 kV beam 8-54920
 Doublet III noncircular Tokamak, neutral beam injection system 8-54970
 duopigatron, preacceleration effects on ion beam transmission effects 8-87005
 duopigatron gas discharge ion source, perform. characts. 8-54505
 duopigatron ion source, modified, ion composition 8-54914
 duoPIGatron ion source, optical telemetry and data transfer system 8-66443
 duopigatron ion source for JT-60 neutral beam injector 8-54912
 duopigatron ion source for PLT injectors 8-54913
 duoplasmatron gas discharge ion source, plasma expansion cup effects 8-58092
 duoplasmatron sputter source for multiply charged ions from solids 8-66446
 electron beam ion source, multiply charged heavy ion prod., charge exchange expts. 8-58816
 electron-bombardment ion source, cylindrically symmetric, low energy spread 8-89594
 electrostatic accelerator, multiply charged ion prod. at low energy 8-66437
 electrostatic electron oscillator design optimisation, ion source and vacuum gauge 8-74107
 energy spectrum of beam from inductively coupled HF source, optical parameter meas. of gun 8-89590
 extractor electrode CAD (Japanese) 8-86680
 FEBIAD source, plasma and beam characteristics 8-66002
 field ionisation and desorption sources, for quadrupole and double focusing spectrometers 8-74092
 Freeman type high current source for implantation appl. 8-66005
 Freeman type ion source in low press. arc operation, discharge characteristics and beam quality 8-66006
 fusion reactor, Wendelstein VII A, injector design 8-54965
 gas and vapour sources for low-energy accelerators 8-66445
 gas ion source, of mass spectrometer, ion extraction and energy discrimination 8-70226
 glow discharge source for nuclear thin film target prep. 8-55067
 Hall accelerator, four-lens, pure ion beam struct. 8-66441
 halogen intense negative ion source 8-66001
 heavy ion source with indirect heating 8-50427
 HF glow discharge source for chemical ionisation process studies (German) 8-70221
 hollow cathode discharge as negative ion source 8-82072
 hollow cathode discharge ion source, with drift tube, for reaction rate consts. meas. 8-64834
 hollow-cathode multipole boundary ion source, IBIS, plasma prod. and containment system 8-74521
 hot cavity, thermal ionisation 8-70677
 inert gas ion source, highly effective 8-66003
 intense ion beams for implantation 8-66004
 intense ion source discharge, delay of arc starvation saturation 8-79457
 ion beam accelerator, multimegawatt, high-voltage power system, design philosophy, for fusion reactor 8-62613
 ion prod. in hollow cathode source 8-74525
 Kyoto beam-plasma type ion source, ion extraction system 8-66007
 Lamb shift polarised ion source at FN tandem Van de Graaf at Univ. of Cologne 8-55065
 laser irradiated targets, limitations for GeV ion generation 8-55068
 laser plasma rel. ion yields (Russian) 8-59631
 ion sources continued
 low background cold cathode ion source for molecular beam detect. 8-54506
 low energy (100-500 eV) high efficiency ion source, for mass spectrometer 8-62261
 low energy ion beams, conference, Salford, Sept. 1977 8-66444
 mass spectrometer, measured- and estimated electrode voltage discrepancy 8-74098
 mass spectrometer ion source, LiF fragmentation 8-70944
 mass spectrometers for van der Waals dimers 8-89585
 mass spectrometric analysis, high-yield laser ion source with plasma focusing 8-61097
 mass-spectrometric leak detector, heating up to 550°C, sensitivity improvement 8-78028
 metal ion source using high power density electron impact 8-54497
 microwave ion source for high-current implanter 8-70224
 miniature slow proton source for focusing efficiency obs. 8-78538
 molten metal field ion sources 8-65999
 multichannel, with quadrupole HF beam filtering 8-74522
 multimode, plasma density and ion loss investigation 8-55080
 negative ion beam, intense, 150 kV test stand electronics system, for fusion reactor 8-54934
 negative ion beam acceleration to energies up to 120 keV 8-54918
 neutral beam injection system, for TFTR 8-54971
 neutral beam injector, beam line studies, for fusion reactor 8-54969
 neutral beam injectors, for Princeton Large Torus, component design 8-54966
 neutral beam lines, for Princeton Large Torus, development and testing 8-54967
 neutral beam system, 120 keV, for fusion reactor ignition 8-66377
 neutral beam system, for ignition Tokamak 8-54973
 neutral beam transport system, for fusion reactors 8-54968
 neutral injection system, for JAERI experimental fusion reactor 8-54972
 nonpolar molecules, ionis. by alkali ion attachment at electrolyte surface 8-65998
 Periplasmatron, ion source for neutral beam injection systems 8-54915
 pinched beam diode, geometrical focusing of intense ion beams 8-58898
 plasma electron-beam ion source 8-83584
 plasma emitter of ions, boundary conditions at surface 8-87432
 plasma source for Tokamak fusion test reactor beam lines 8-54916
 polarised ion sources and low energy collector rings, H^- , D^- beams 8-58515
 polarised proton beam production in high energy hyperon decay 8-58517
 polarised proton beams, higher energy, conf., Ann Arbor, MI, USA, Oct. 1977 8-58514
 relativistic self focusing from laser irradi. target, MeV and GeV ion prod. 8-51323
 review of sources for low energy accelerators 8-58521
 RF ion source, 15 cm diameter, stable working conditions calcs. 8-86388
 RF ion source, low energy component of extracted ions 8-55064
 RF ion source 15 cm stable working region determ. 8-75381
 saddle-field ion source behaviour, gas depend., at spectroscopy appls. 8-78039
 Scandinavian low output isotope separator, upgrading to 300 kV 8-66008
 self-accelerating microwave ion and plasma sources 8-66000
 single slit plasma source, consumption of fuel for singly charged ions 8-67379
 solid ion source by electron bombardment (Japanese) 8-78035
 space charge ion optics, influence of chromatic aberrations 8-55294
 sputter electrode preparation for multiply charged heavy ion sources 8-66009
 sputter negative ion sources, role of alkali metal 8-74526
 sputtering apparatus, review 8-72719
 thin film deposition, low energy in source modification 8-52687
 trajectory computation, computer simulation 8-71510
 two-grid accelerator systems, ion beam divergence characts. 8-82074
 Ar ion duoplasmatron source, new target ion source system for short lived nuclei meas. 8-66449
 Ar plasma bridge neutraliser operation with 10 cm beam diameter ion etching source 8-74102
 Ar, using duoplasmatron, props. 8-74523
 B^+ fraction from Freeman type high current source for implantation appl. 8-66005
 ^{14}C , beam production for Munich tandem 8-90008
 ^{252}Cf fission source, ionisation characts. of electron oscillating ion source coupled to He-jet skimmer system 8-70661
 Cs beam sputter ion source, T acceleration in FN tandem 8-55070
 D_2^+ , prep. by electrolysis of heavy water using self-controlled cell 8-80752
 H ion source, hollow cathode device 8-54921
 H^- ion yield from duoplasmatron discharge 8-75382
 H^- , production by Hall accelerator in Cs vapour, space-charge effects 8-67375
 H^- sources for neutral beam injection 8-54919
 ^{127}I ions, 20 MeV, emerging from gas stripper, absolute charge state yields 8-55066
 Ir(110), single cryst., fine focus beam with field ionisation 8-76589
 Mo, ion prod. in hollow cathode source 8-74525
 Nb, ion prod. in hollow cathode source 8-74525
 Re, ion prod. in hollow cathode source 8-74525
 Ta, ion prod. in hollow cathode source 8-74525
 ion-surface impact
see also particle backscattering; sputtering
 chemical surface analysis, low energy ISS compared with SIMS 8-64908
 convoy electrons from solids, ion vel. and Z and target material depend. 8-84692
 depth profiles, ion scatt. technique, digital data collection 8-56942
 drift tube measurement of ion mobility, secondary electron effects 8-59538
 electronic interactions, review 8-72674
 fusion reactor first-wall mat., physical sputtering model 8-80445
 glass/polymer interface exam. using ion scattering spectroscopy and scattered ion mass spectrometry 8-60641

ion-surface impact continued

- heavy ion+atom, radiative electron capture, target thickness depend. 8-58778
- ion sputtering process, model 8-88398
- light elements ($Z=15$ to 28), $s^{10}\text{B}$ ion bombardment, K-shell ionisation, X-ray obs. 8-95619
- light ion sputtering in fusion reactors, discrete ordinates method calcs., ANISN code 8-92158
- metal surface, clean, ion impact, mol. effects in electron emission 8-80446
- metal surface, inert gas bombard., 1.05 keV, electron yields, Fermi energy estimate 8-52611
- metallic targets, continuous emission spectra of particles ejected by ion beams (*Russian*) 8-55140
- molecular ions, interaction with thin solid targets 8-59844
- nitrided steel surface wear-related topography 8-60847
- polycrystalline materials, Ar and He ion scatt. spectra, multiple scatt. features 8-72671
- random solid, light ion backscattering energy spectra calcs. 8-72655
- single crystal surface, metal cluster form. by ion bombardment 8-92157
- slow protons, Auger neutralisation 8-72668
- solid surfaces, reflection of slow H^+ and He^+ ions 8-76572
- stainless steel, $\text{H}^+(\text{H}_2^+)$, energy refl. coeffs. 8-54969
- steel, stainless, surface cleaning by H^+ bombard., AES study 8-53022
- surface analysis, review of ion scattering spectroscopy 8-68948
- surface structure, energy spectra of scattered ions, new method of surface struct. determ. 8-87854
- surface structure determination, in scatt. methods, review 8-71907
- trajectory focusing in surface scatt. of channelled ions, surface struct. anal. 8-68594
- two-atomic scattering ions, refl. from single cryst. 8-68591
- Ag, energy reflection coefficient for 5 to 10 keV He ions 8-95639
- Ag, H_2^+ and $^3\text{He}^+$ ion bombardment, H^+ and He^+ yields at elastic scatt. energy 8-88394
- Ag, polycryst., energy spectrum of scattered Na^+ ions, double scatt. effect 8-92163
- Al alloy, 6061, vacuum material, desorpt. of neutral mols. by electron and ion bombardment 8-95229
- Al, continuous UV emission under inert gas ion bombard. 8-84664
- Al, $\text{H}^+(\text{H}_2^+)$, energy refl. coeffs. 8-54969
- Al, heavy ion ranges, He^+ backscatt. obs. 8-63796
- Au, energy reflection coefficient for 5 to 10 keV He ions 8-95639
- Be, oscillatory channelled $^3\text{He}^+$ ion scatt. yield 8-52610
- C, proton impact X-ray emission, ang. distrib. and polarisation fraction 8-56546
- C, reflection of H, D and He ions 8-95640
- CO_2^+ , thin foil impact, dissoci. struct. effects in ionic fragment energy spectra 8-50631
- Co surface, electron spin polarisation, electron capture spectroscopy 8-95645
- CrSi_2 formation on Pd₃Si and PtSi, Rutherford α -particle scatt. 8-60578
- Cu, chain effect for fast recoils, Ar^+ ion beam impact 8-56554
- Cu, ejected particle ang. distrib., classical dynamics model 8-95643
- Cu, energy reflection coefficient for 5 to 10 keV He ions 8-95639
- Cu, excited state formed by B^+ impact, light emission coeffs. 8-64417
- Cu, $\text{H}^+(\text{H}_2^+)$, energy refl. coeffs. 8-54969
- Cu, ion impact phenomena, computer simulation 8-88396
- Cu, polycryst., back sputtering of 100 to 500 eV Ne ions, computer simulation 8-60537
- Cu, polycrystalline, Ar ion double scatt. 8-88399
- Cu surface, surface cleaning by H^+ bombard., AES study 8-53022
- Cu-Ni, film, preferential sputtering due to altered layer struct., AES meas. 8-76573
- Cu_w , cluster formation, by ion bombardment of single cryst. surface 8-92157
- Fe, diffusion and solid solubility of Sb, 773-873K, ion backscatt. anal., rel. to intergranular embrittlement 8-71880
- GaAs surface, Ar ion bombardment induced photon emission, rel. to target temp. 8-72612
- $\text{Gd}_2(\text{MoO}_4)_3$, surface passivation by He ion irradi., domain struct. obs. 8-84544
- H_2^+ , dissoci. following beam-foil interaction 8-70920
- H_2^+ , dissoci. following beam-foil interaction 8-70920
- MgO-Ag porous layer, secondary electron emission from ion impact, gas discharge device appl. 8-68586
- Mo, D^+ impact, surface blistering, SEM study 8-71774
- Mo, excited state formed by B^+ impact, light emission coeffs. 8-64417
- Mo, $\text{H}^+(\text{H}_2^+)$ energy refl. coeffs., surface damage obs. 8-54969
- Mo, polycryst., $\text{H}^+(\text{H}_2^+)(\text{H}_3^+)$ impact, optical radiation emission 8-95644
- Mo, reflection of H, D and He ions 8-95640
- N_2^+ +Group IV elements and oxides, XPS and UPS prod. determ. 8-73084
- N_2O^+ , thin foil impact, dissoci. struct. effects in ionic fragment energy spectra 8-50631
- Ni, reflection of H, D and He ions 8-95640
- Ni surface, electron spin polarisation, electron capture spectroscopy 8-95645
- Pb, H^+ , H_2^+ and H_3^+ grazing incidence collision with surface, Balmer radiation, elliptical polarisation 8-86804
- Pb, He^+ scatt., oscillatory ion yields 8-55221
- Pd, H_2^+ and $^3\text{He}^+$ ion bombardment, H^+ and He^+ yields at elastic scatt. energy 8-88394
- Pt (111) and (100), surface struct. anal. by MeV ion backscatt. and channelling 8-71916
- Si (111) surface, anal. by ion-electron spectroscopy 8-72670
- Si, amorphous, heavy ion ranges, He^+ backscatt. obs. 8-63796
- Si, proton impact, electron capture cross-section calcs. 8-95623
- Si:As, implanted, spatially varied activation during regrowth of amorphous layers, sheet resist. and backscatt. obs. 8-71749
- SiC, energetic H and Ar ion sputtering, AES-SIMS-FDS combined obs. 8-80444
- SiO_2 covered Si surface, scattering of keV H and He ions and neutrals 8-95638
- TZM, D^+ impact, surface blistering, SEM study 8-71774
- Ta_2O_5 , XPS, low energy ion backscatt. spectra 8-72660
- Th, $\text{He}^+(\text{Ne}^+)(\text{Ar}^+)$ impact, appl. of double pass cylindrical mirror analyser 8-72658

ion-surface impact continued

- Ti, reflection of H, D and He ions 8-95640
- U, $\text{He}^+(\text{Ne}^+)(\text{Ar}^+)$ impact, appl. of double pass cylindrical mirror analyser 8-72658
- UO_2 (111), $\text{He}^+(\text{Ne}^+)(\text{Ar}^+)$ impact, appl. of double pass cylindrical mirror analyser 8-72658
- UO_2 , (111) and (553) surface struct., He^+ ion scatt. spectra 8-75917
- W, reflection of H, D and He ions 8-95640
- W, surface self-diffusion by ion impact, protrusion formation 8-75938
- WC-Co composite, surface anal. by quantitative AES 8-76622
- WC-Co composite chemical characterisation by AES and ISS 8-76621
- Zu, reflection of H, D and He ions 8-95640

ion thrusters see ion engines**ionic conduction in solids**

see also superionic conducting materials

- $\beta\text{-Al}_2\text{O}_3\text{-Na}_2\text{O}$, AE during breakdown under Na^+ transport 8-67860
- alkali perchlorates, elec. transport during struct. transforms. 8-59971
- cabal glass: $\text{SiO}_2(\text{TiO}_2)$, microheterogeneity, and elec. cond. 8-83997
- electrolyte, ionic conductivity, phenomenological theory 8-83994
- $(\text{H}_3\text{O})_{5-x}\text{Ta}_{11+x/2}\text{O}_{30}$, synthesis, non-stoichiometry, density and ionic cond. meas. (*French*) 8-52741
- hollandites, ionic cond., impedance, struct. 8-67856
- homogeneous solid, small signal AC response, mobile charge recomb., theory 8-52005
- hydroxyapatites, elec. cond., charge carrier identification 8-67855
- interface charge transfer, coupling to bulk transport props. of ionic crystals 8-95183
- ionic crystals, transport phenomena, appl. to solid state devices 8-55976
- oxide glasses, elec. cond. and dielec. relax., correl. 8-79801
- piperazinium $\text{Ag}_{10}\text{I}_{12}\cdot 4\text{-dimethylformamide}$, exam. of electrical cond. and crystal structure 8-5871
- polyimide film, dielectric breakdown in high-temperature region 8-84522
- Portland cement clinker, elec. props. 8-59976
- pyridine- Ag_2I_6 , superionic conductor, dynamical aspects 8-79695
- review (*German*) 8-79795
- simple ionic crystals, ion transport 8-63878
- statistical theory of relaxation current and low-freq. dielectric dispersion 8-60391
- superionic conductors, correlation functions theory 8-79674
- superionic conductors, microscopic theory 8-79809
- thermoelements in ionic crystals, review 8-60381
- $\text{Ti}_{1+x}(\text{Ta}_{1-x}\text{W}_{1-x})\text{O}_6$, exam. of ionic conductivity (*French*) 8-51729
- urea nitrate single cryst., elec. cond. anisotropy 8-79807
- AgBr , curvature of conductivity plots, consequence of anharmonicity 8-79800
- AgBr , phonons at elevated temp. 8-79810
- AgCl , curvature of conductivity plots, consequence of anharmonicity 8-79800
- $\alpha\text{-AgI}$, ionic motion, low freq. Raman scatt. 8-80354
- $\alpha\text{-AgI}$, molecular dynamics exam. of Ag diffusion 8-55981
- AgI , structural model for superionic conduction 8-79797
- AgI , superionic conductor, dynamical aspects 8-79695
- AgI type solid electrolytes, expt. props. 8-63877
- $\text{AgI-Ag}_2\text{O-B}_2\text{O}_3$ system, ionic cond., struct., electrochem. prop. in galvanic cell 8-95181
- AgI_3 , ionic cond., effect of press. 8-51733
- $\text{AgPO}_3\text{-AgX}$, $\text{X}=\text{I, Br, Cl}$, ionic conductivity (*French*) 8-79805
- $\text{AgPO}_3\text{-CdI}_2$ glasses, ionic conductivity and structure (*French*) 8-67854
- Ag_2SI , superionic conductor, dynamical aspects 8-79695
- $\beta\text{-Al}_2\text{O}_3\text{-H}_2\text{O}$, H^+ and H_3O^+ conduction, dehydration effect 8-51726
- $\text{B-Al}_2\text{O}_3\text{-M}_2\text{O}$, $\text{M}=\text{Na, Ag, Rb, K}$, far IR absorption and ionic cond. 8-72512
- $\text{Al}_2\text{O}_3\text{-MgO-H}_2\text{O}$ fast proton conductor 8-91480
- $\beta\text{-Al}_2\text{O}_3\text{-Na}_2\text{O:Mg}$, ionic cond., effect of microstruct. and phase composition 8-67859
- $\text{Al}_2\text{O}_3\text{-Na}_2\text{O-LiO}_2$ (8.8, 0.75 wt.%) exam. of Na^+ resistivity as function of temp. grain size model 8-80654
- $\beta''\text{-Al}_2\text{O}_3\text{-Na}_2\text{O-MgO}$ in Na-S batteries, blocking defects rel. to cond. loss 8-55879
- $\beta\text{-Al}_2\text{O}_3\text{-Na}_2\text{O-SiO}_2$, solid electrolytes, exam. of microstruct. ionic resistivity 8-80566
- $\text{BaF}_2\text{-UF}_6\text{-CeF}_3$ solid soln., surface degradation, complex admittance analysis 8-55980
- $\text{BaO-BaX}_2\text{-P}_2\text{O}_5$ glass, $\text{X}=\text{F, Cl}$, conductivity 8-67862
- CaF_2 , cond. meas. under controlled F_2 chem. pot. (*Japanese*) 8-59972
- CaF_2 film, ionic migration study by Rutherford scatt., defects, secondary emission (*French*) 8-55982
- $\text{CaF}_2\text{-Gd}^{3+}$, ITC spectra of impurity aggregate 8-71883
- $\text{CaF}_2\text{-UF}_6\text{-CeF}_3$ solid soln., surface degradation, complex admittance analysis 8-55980
- CaS, sintering method prep., ionic cond. meas., 650 to 900°C (*Japanese*) 8-75869
- CuCl-TlCl system, phase diagram and high ionic cond. obs. 8-79802
- $\text{H}(\text{UO}_2\text{P(AsO)}_4)_4\text{H}_2\text{O}$, H motion, PMR obs. 8-80239
- He, solid, ion current modulation by thermal waves 8-91506
- KBr whisker, X-irrad., defect form., thermolum. and ionic cond. obs. (*Russian*) 8-84666
- K_2CO_3 , study of elec. cond. and transition points 8-75873
- KCl, room temp. X-irrad., first stage F-centre form. 8-67709
- KCl, X-irradiated, formation of cation defects 8-91359
- KCl:BiCl₃, electrical cond. as a function of temp., charge transport mechanism 8-83996
- KI:S²⁻, photochemical reaction, F-centre production, optical absorption and ionic thermocurrent meas. 8-64861
- $\text{K}_{1.54}\text{Mg}_{0.77}\text{Ti}_{2.3}\text{O}_{16}$, one-dimens. superionic cond., ionic order, defect cond. 8-87815
- $\text{La}_2\text{O}_3\text{-Ag-S-Ga}_2\text{S}_3$, ionic conducting glasses (*French*) 8-79804
- $\alpha\text{-LiF}_3$, statistical theory of relaxation current and low-freq. dielectric dispersion 8-60391
- $\text{Li}_2\text{O-B}_2\text{O}_3$ glass, conductivity, permittivity, and dielectric loss obs., mixed isotope effect 8-95182
- $\text{Li}_4\text{Zn}(\text{GeO}_4)_4$, crystal struct. and ionic conductivity 8-51728
- NaCl:Mn^{2+} , dimer detection, EPR and ITC expts. 8-59833
- NaCl:Ni single crystals, VUV spectrum, ionic conductivity, X-ray diff. 8-92097
- NaCl-graphite interface, elec. cond. 8-52060

ionic conduction in solids continued

- NaCl-NaBr mixed crystals, ionic cond., 42-450°C, cation vacancy migration 8-59970
 $\text{Na}_2\text{Fe}_2(\text{PO}_4)_3$, polymorphism and ionic conduction (*French*) 8-67678
 $\text{Na}_2\text{O-Al}_2\text{O}_3\text{-SiO}_2$ glasses, elec. cond. and cation mobility 8-59973
 $\text{Na}_2\text{O-B}_2\text{O}_3\text{-Bi}_2\text{O}_3\text{-SiO}_2$, heterophase glass, diffusion and elec. cond. 8-67858
 $\text{Na}_2\text{O-NaF-B}_2\text{O}_3$ glass, nature of conductivity 8-63876
 $\text{Na}_2\text{O-SiO}_2\text{-SnO}_2$ (TiO_2) glass, exam. of Na^+ self diffusion, elec. conductivity, and viscosity 8-87819
 Na_3PO_4 , pure and doped ionic cond., doping effect 8-51725
 $\text{Na}_5\text{RSi}_4\text{O}_{12}$, superionic conductors, Na conductivity paths 8-91482
 $\text{Na}_2\text{SO}_4\text{-Y}_2(\text{SO}_4)_3$, solid solution, effect of defect concentration on ionic conductivity 8-75870
 $\text{Na}_{5-x}\text{Ta}_{11+x/5}\text{O}_{30}$, synthesis, non-stoichiometry, density and ionic cond. meas. (*French*) 8-52741
 $\text{Na}_{1+x}(\text{Ta}_{1-x}\text{W}_x)\text{O}_6$, exam. of ionic conductivity (*French*) 8-51729
 Na_2UBr_6 , phase transformations, elec. cond. and entropy meas., synthesis (*French*) 8-79763
 $\text{Na}_3\text{YSi}_4\text{O}_{12}$, high Na^+ ion conduct. 8-91479
 $\beta\text{-PbF}_2$, electrolytic props., AC cond. meas. 8-71878
 $\beta\text{-PbF}_2$ film, ionic migration study by Rutherford scatt., defects, secondary emission (*French*) 8-55982
 PbF_2 , NMR relax. and self diffusion 8-80236
 $\text{Pb}_{1-x}\text{ThF}_{2+2x}$, solid soln., anionic cond. (*French*) 8-91481
 RbAg_4I_5 , ionic cond., effect of press. 8-51733
 $\text{Rb}_{3-x}\text{Ga}_{11+x/5}\text{O}_{30}$, synthesis, non-stoichiometry, density and ionic cond. meas. (*French*) 8-52741
 SnF_2 , α and γ modifications, elec. cond., $\alpha\rightarrow\gamma$ phase transitions, structs. 8-75867
 SnF_2 , SnFCl , ionic conductivity (*French*) 8-79806
 $\text{SrF}_2\text{-UF}_6\text{-CeF}_3$ solid soln., surface degradation, complex admittance analysis 8-55980
 $\text{Ti}_{5-x}\text{Ta}_{1+x/5}\text{O}_{30}$, synthesis, non-stoichiometry, density and ionic cond. meas. (*French*) 8-52741
 Zn^{2+} , transport in cation-exchange membranes 8-96033
 ZrF_4 glasses, elec. props. (*French*) 8-75868

ionic conductivity in solids see ionic conduction in solids

ionic thermocurrents see thermally stimulated currents

ionisation

- see also associative ionisation; autoionisation; charge exchange; electron attachment; electron capture; field ionisation; ion recombination; ionisation of atoms; ionisation of gases; ionisation of liquids; ionisation of molecules; ionisation of solids; ionisation potential; Penning ionisation; photoionisation; surface ionisation
 aerosol fine particle charging by unipolar ions, review and expt. 8-88658
 hot cavity, thermal ionisation 8-70677
 H II regions ionisation structure, influence of star, gas density and chemical comp. 8-61911

ionisation chambers

- Andersson-Braun remmeter modifications for improved directional depend. and thermal neutron sensitivity 8-53499
 avalanche 2-D position sensitive parallel plate transmission counter 8-90023
 avalanche counters, Townsend coeffs. determ. 8-78582
 avalanche detector, position sensitive parallel plate with 2-D readout 8-55102
 C_A and C_e reevaluation using extended cavity ionisation theory, ferrous sulphate G-values appl. 8-92706
 cylindrical gridded, ^{238}U spontaneous fission half life and fragment kinetic energy meas. 8-86555
 dose mapping, automated system for TRIUMF biomedical pion beam 8-73254
 dosimeter, semiautomatic device for relative dose distrib. recording 8-85380
 dosimeters, individual controlled, using capacitor chambers 8-78509
 electrical resistance measurement for insulating materials (*French*) 8-77929
 electron transport in air and N_2 , Monte Carlo calcs. 8-90042
 fast particles, mean ionising cross-section and charge produced, meas. method 8-78577
 fission chamber with intrinsic suppression of α -background 8-78581
 free air ionisation chamber, mean level response for α -rays 8-90024
 free air parallel arid plate chambers, electrode emission effects on saturation current 8-74539
 gamma-ray dosimeter, KG21, features 8-74509
 graphite chamber with CO_2 filling, Monte Carlo anal. of fast neutron irradiation 8-82583
 ion collection efficiencies in pulsed and continuous radiation beams 8-53505
 Keithley diagnostic ion chambers, energy depend. of correction factors 8-53507
 multiwire proportional chamber, shift register read out system 8-86736
 parallel plate, saturation current determ. 8-55098
 Ramsauer chamber, positron scatt., optimisation study using Monte Carlo method 8-70706
 REM ratemeter, for mixed radiation, using two spherical ionisation chambers 8-96100
 REM ratemeter for direct reading of dose equivalent rate 8-53502
 smoke detector, ionisation type, model for response 8-88933
 Ar, liquid, drift of ionisation electrons 8-55100
 Fe-liquid scintillator multilayer calorimeter transition effects, muon burst rates 8-90019
 ^3He , calibration for use with filtered neutron beams (*German*) 8-58529
 Rn concentration measurement in groundwater and springs for earthquake prediction 8-88924

ionisation gauges

- In amalgam lamp, Hg vapour partial pressure meas. 8-67488

ionisation of atoms

- see also atomic electron impact ionisation
 AC Stark splitting in doubly reson, three-photon ionisation, nonmonochromatic field 8-94220
 alkaline earth atoms, multiphoton ionisation spectroscopy 8-82703
 atom, inner-shell photoionis., anisotropy of X-rays and Auger electrons 8-58633
 atom, two-photon resonant ionis. 8-58631
 atom+ H^+ , innershell ionisation 8-62930

ionisation of atoms continued

- atom+light ion, dipole transitions in K-shell ionisation 8-90281
 atom+metastable atom collision, associative ionisation 8-62907
 atom+metastable atom collision, Penning ionisation 8-62907
 atoms, multiphoton ionisation probability, laser pulse 8-86835
 atoms, two-photon photoelectron energy spectra, AC Stark splitting 8-86834
 C O, K-shell ionis., double and single, cross section meas. by ion bombardment 8-50629
 collisional inner-shell ionisation, semi-classical theory 8-62896
 collisions, improved impulse approx. 8-74754
 Compton scatt., bound and free electron Compton scatt. in coherent EM field 8-94225
 Coulomb ionisation of inner shell electrons, screening effects 8-74749
 Coulombic ionisation of inner shells 8-62898
 electron polarisation produced by reson. ionisation by intense EM field (*Russian*) 8-50518
 excited atomic states in EM field, ionisation by electron diffusion (*Russian*) 8-86798
 excited atoms, field ionisation mechanisms 8-70761
 fast heavy ion+atom, and solid targets, ionis. and excitation states 8-70927
 field-ionisation of Rydberg states, depend. on $|m_l|$ 8-58856
 gas discharge, photoionis. at low illumination intensity, nonlinearities, effective cross section 8-87517
 high-Z atom+ $\text{H}(\text{He})(\text{O})(\text{F})(\text{Cl})$ ions, $1s\sigma$ vacancy prod., relativistic and Coulomb deflection effects 8-58801
 inert gas, field ionis. and proton capture, critical energy deficits 8-82853
 inert gases, photoionisation cross sections of excited atoms and dimers 8-66523
 ion, positively charged, photoeffect theory 8-94219
 ion+atom collision, electron emission, book contrib. 8-74756
 ion induced inner shell vacancy formation 8-70926
 K-shell atomic ionisation by heavy particle, electronic relativistic effects, Dirac wavefunctions, semiclassical effects 8-78792
 K-shell ionisation probability by protons, $E_p=100$ keV-2 MeV, impact parameter depend. (*Japanese*) 8-86945
 K-shell ionization in heavy-ion collisions, book contrib. 8-82834
 K-shell vacancy production, by charged particles, relativistic effects calc. 8-58600
 Koopmans atomic valence electron ionisation energy, $1/Z$ expansion method, reorganisation corrections 8-78623
 lanthanides, Rydberg spectra and ionisation thresholds, time resolved resonant multistep technique 8-82701
 laser ionisation, modelling 8-90133
 laser-enhanced ionisation, appl. to anal. flame spectrometry 8-92528
 M-subshell ionisation cross section, by H^+ impact, binary encounter approx. 8-62890
 many electron effect on K-shell internal ionisation accompanying β -decay 8-86839
 model atom in electrostatic field, ionis. dynamics 8-90311
 multiphoton, laser temporal coherence and high laser intensity effects 8-66524
 multiphoton ionisation, reson. cross-section, very-narrow-bandwidth source 8-55150
 multiphoton resonant ionis., model calc. 8-62773
 non-Rydberg atomic spectroscopy, review 8-90127
 one-atom detection in individual ionisation tracks, heavy ion stopping in buffer gas 8-70802
 photoionisation, correlation effects 8-58842
 photoionisation, ion alignment, many electron correl. effect 8-74622
 photoionisation, post collision interactions in at. excitation processes 8-58803
 photoionisation, R-matrix method 8-58833
 photoionisation, R-matrix theory 8-58761
 photoionisation, radiative collision-induced 8-62858
 plasma, excited ats. population distrib., electron-density variation influence 8-87431
 PWBA for K shell ionisation cross sections 8-70923
 rare earth metals, photoionisation thresholds and Rydberg spectra 8-66522
 resonant two-photon ionisation in partially coherent radiation field 8-66525
 Rydberg atom+atom collision, expts. 8-62908
 Rydberg atom+ion, collision theory 8-62909
 Rydberg atoms, microwave ionisation and excitation 8-94217
 Rydberg states, fine struct. splitting, quantum beat and double reson. spectroscopy 8-86979
 second-row atom, photoemission energy, rel. to homonuclear diatomics 8-86832
 stripping cross sections, binary encounter approx. theory 8-50618
 three-electron atomic systems, autoionising states decay calcs. 8-78670
 two-photon ionis., incident light polaris. effect 8-62772
 Xalpha transition state and transition operator method calcs. 8-70743
 AR, population inversion, intershell transitions, photoionisation, from UV irradiation (*Russian*) 8-70803
 Ag, K-shell ionis., X-ray prod. cross section for incident H^+ , ^4He and ^{15}N ions 8-70923
 Ag+ H^+ , K-shell ionisation, 7-15 MeV, relativistic effects 8-82830
 Ag+ H^+ , L-shell ionisation at large scatt. angles 8-90283
 Al, ion beam bombardment, $(1s^{-1}2p^{-1})^1P_1$ state nonstatistical population, X-ray spectrum 8-62894
 Al+ $\text{H}(\text{D})(\text{He})(\text{Li})$ ions, K-shell ionis., universal cross sections 8-62895
 Ar, multiphoton ionisation, EM field gradient forces 8-66608
 Ar+ He^* Penning ionisation, semiclassical discretisation procedure 8-90275
 Ar+ I_2 , ion-pair form. differential cross-section, 25-133 eV, metastable Ar 8-78787
 Au+ H^+ , K-shell ionisation, 7-15 MeV, relativistic effects 8-82830
 B, K-shell ionis., double and single, cross section meas. by ion bombardment 8-50629
 Ba, diamag. quasi-Landau spectrum near ionis. threshold, two-photon ionis. spectra obs. 8-58642
 Ba I, absorption spectrum, 1560 to 1770 Å 8-66487
 Ba, multiphoton ionis. spectroscopy of even- and odd-parity states 8-86973
 Be isoelectronic series, inner-shell photoionis. cross sections 8-74623
 Be, K-shell ionis., double and single, cross section meas. by ion bombardment 8-50629

ionisation of atoms continued

- Br II levels, NF values meas. in Ne-Br₂ mixtures 8-62753
 Br, photoelectron spectra, photoionisation cross-sections 8-90131
 C, photoionisation of 2s shell, photoelectron ang. distrib. 8-86833
 C+H⁺(He⁺), K-shell ionisation, impact parameter depend. 8-62891
 Ca, multiphoton ionis. spectroscopy of even- and odd-parity states 8-86973
 Cd, photoionisation cross section, many-body perturbation theory, dipole length and vel. calc. 8-78674
 Cl I, photoionisation cross section, calc. by many-body perturbation theory 8-62771
 Cl, photoelectron spectra, photoionisation cross-sections 8-90131
 Cs, excited state, two-photon ionisation by ruby laser light 8-74621
 Cs, multiphoton ionisation, reson. peak amplitude, temporal effects 8-78760
 Cs, reson. multiphoton ionisation by ultrashort laser pulses, 1.06 μ m 8-58630
 Cs, resonant ionisation studies of proportional counter fluctuations 8-90025
 Cs+Ar, two-photon ionisation spectra, satellites, absorption line shape 8-82668
 CsI, four-photon ionisation near 6f resonance 8-70801
 Cu, γ -ray absorption cross-sections, 10-160 MeV 8-90136
 Cu, K-shell ionis., X-ray prod. cross section for incident H⁺, ⁴He and ¹⁴N ions 8-70923
 Cu, large angle K-shell ionisation probabilities, projectile charge and mass depend. 8-74750
 D, detection by resonant three photon ionisation 8-74624
 Gd atom, long-lived autoionisation state (Russian) 8-94216
 Gd+H⁺, K-shell ionisation, 7-15 MeV, relativistic effects 8-82830
 H, dense plasma, ionisation, master eqn. analytical soln. 8-59544
 H, detection by resonant three photon ionisation 8-74624
 H, resonant ionisation by laser radiation, as polarised proton source 8-78541
 H⁻ and H electron loss in plasma target 8-67371
 H⁻, S autoionising states, time stability theory 8-90130
 H+heavy ion (highly stripped), electron loss, charge state depend. 8-70921
 H+Li(Li₂), superthermal collisions, photon and positive ion prod. 8-78788
 H+N, stripping cross-sections, binary encounter approx. theory 8-50618
 H+N₂(O₂), charge prod. cross sections and differential scatt. calcs. 8-94313
 H⁺+He⁺, charge transfer and ionis. cross sections, coincidence meas. 8-50634
 H⁺+Na(Mg)(Al)(Si)(Ti), K-shell ionisation cross sections for 15-65 keV protons 8-90284
 He, excitation and ionisation, by instationary shock fronts 8-59540
 He, metastable, deexcitation process on Mo [110] impact 8-95642
 He, metastable 1s2s'S state, photoionisation, perturbation theory calcs. 8-78759
 He, photoionisation, frozen-core HF perturbation theory, oscillator strength, dipole length and vel. calc. 8-78672
 He+H⁺, determ. of He excited state populations by two-photon reson. ionisation spectroscopy 8-82707
 He+He, metastable atoms, collisional ionisation cross-sections 8-70911
 He⁺+alkali metal atom, ionisation cross sections, binary encounter approx. with HF electron vel. distrib. 8-55225
 He⁺+Ar, Penning ionisation, laser modified collisional effects in electron energy spectrum 8-90278
 He⁺+H(H₂)(Ar), metastable state, ionis. processes 8-62907
 Hg+He²⁺, autoionisation, 5-20 eV, electron and ion ang. distrib. 8-78795
 K, reson. three photon ionisation, saturation effects 8-90137
 K, two-step photoionisation, triple crossed beam obs. 8-66616
 K²⁺, photoionisation cross-section, R-matrix theory 8-82702
 Kr, population inversion, intershell transitions, photoionisation, from UV irradiation (Russian) 8-70803
 Li, photoionisation cross section meas. at 2P level 8-58637
 Li+inert gas collisions, electron loss cross-section meas. (French) 8-86941
 Mg, inner-shell ionisation by H⁺, He⁺ impact, target atom ionic alignment, Born approx. 8-78789
 Mg+H⁺(He⁺) and electron impact ionis., Auger study of collisionally induced alignment 8-90279
 N⁻, form., by double electron transfer, cross-section meas. 8-78806
 Na, multiphoton ionisation in third harmonic generation by mode locked Nd:YAG laser 8-94413
 Na, one and two-photon ionis. of 3s and 3p states 8-50512
 Na, reson. multiphoton ionisation, broadband laser AC Stark splitting 8-70808
 Na, resonant three-photon ionis., saturation effects 8-58632
 NaI isolectronic sequence, 3s-3p and 3p-3d transitions, ionisation energy 8-70773
 Ne, photoionisation, complex amplitudes at low energy singly and doubly excited reson. 8-78673
 Ne+Ne(Ne⁺)(Ne²⁺), 2s vacancy prod. 8-50623
 Ni+H(D)(He)(Li)(C)(O)(F) ions, K-shell ionis., universal cross sections 8-62895
 O, photoionisation absolute cross section 8-94218
 O⁺, electron loss, forward peak oscill. struct. 8-78796
 Pb, γ -ray absorption cross-sections, 10-160 MeV 8-90136
 Pb+H⁺, K-shell ionisation, 7-15 MeV, relativistic effects 8-82830
²⁰⁸Po, L-shell ionisation in α -decay 8-78324
 Rb+H⁺, single photon emission following double K-shell ionisation, contrib. to superheavy element search data 8-50625
 Si, K-shell ionis., X-ray prod. cross section for incident H⁺, ⁴He and ¹⁴N ions 8-70923
 Si⁹⁺ electron loss, forward peak oscill. struct. 8-78796
 Sn, γ -ray absorption cross-sections, 10-160 MeV 8-90136
 Sr, associative ionisation of laser-excited Rydberg states, mass spectrometry obs. 8-94303
 Sr, diamag. quasi-Landau spectrum near ionis. threshold, two-photon ionis. spectra obs. 8-58642
 Sr, multiphoton ionis. spectroscopy of even- and odd-parity states 8-86973
 Ta, γ -ray absorption cross-sections, 10-160 MeV 8-90136
 Ta+H⁺, K-shell ionisation, 7-15 MeV, relativistic effects 8-82830
 Th+H⁺, K-shell ionisation, 7-15 MeV, relativistic effects 8-82830

ionisation of atoms continued

- Th+X⁺, X=O, N, N₂, CO₂, charge transfer cross-section, 1-500 eV 8-82835
 Ti, K-shell ionis., X-ray prod. cross section for incident H⁺, ⁴He and ¹⁴N ions 8-70923
 Tl, two-photon laser spectroscopy and ionisation 8-55153
 U+X⁺, X=O, N, N₂, CO₂, charge transfer cross-section, 1-500 eV 8-82835
²³⁵U, hyperfine struct. and isotope shift meas., laser separation by two-step photoionisation 8-78822
²³⁸U+²³⁸U (¹³⁶Xe), nuclear Coulomb excitation, inner shell ionisation and internal conversion, quasil. formation 8-94026
 V, atomic energy levels in all stages of ionisation, data anal. 8-94207
 W, N-shell ionisation by proton impact 8-78800
 Xe, high Rydberg state, ionis. by collision with organic mols. 8-50620
 Xe, high Rydberg states, radiative lifetimes and transition probabilities 8-86817
 Xe, low-energy 5s-sp photoionization, relativistic effects 8-50515
 Xe, population inversion, intershell transitions, photoionisation, from UV irradiation (Russian) 8-70803
 Xe+H⁺, M-subshell ionisation cross section, binary encounter approx. 8-62890
 Xe(nf)+NH₃, at. Rydberg state further excitation by rot. transfer, field ionis. obs. 8-58795
 Yb+H⁺, K-shell ionisation, 7-15 MeV, relativistic effects 8-82830

ionisation of gases

- see also atmospheric ionisation; electron avalanches; Townsend discharge*
 critical ionisation velocity in gas mixtures, lab. expt. 8-67307
 electrical discharges, opto-galvanic effect with tunable gas lasers, spectroscopy appl. 8-95977
 electrically excited preionisation unit with electron beam energy recuperation 8-59013
 electrostatic instabilities role in critical ionisation vel. mechanism 8-67355
 gas in crossed electric and magnetic fields, elec. strength calcs. 8-87568
 HF discharge, EM wave ionisation instability model 8-67512
 high-power non-self-sustained discharge with ionisation by repetitive electrodeless pulses in closed-cycle laser 8-71514
 interstellar H II regions, ionization front, oblique refraction 8-54025
 moving gas, electric strength calcs., gas vel. effects 8-87568
 partially ionised inert gases in travelling HF mag. field 8-75474
 photons, monoenergetic, microdosimetric meas. of ionisation 8-65133
 plasma generation with multiply ionised species 8-75388
 power station plumes, ionisation effects on natural lightning 8-88909
 semi-stationary maintained gas discharge, ionisation instability theory 8-67511
 shock wave ionisation in transverse magnetic field, finite-difference methods 8-51249
 stack gas in coal-fired plants, in electrostatic precipitators, using electron beams 8-57346
 Ar, low voltage arc, ionisation waves, hydrodynamical model including inelastic interaction 8-87563
 Ar, UV photoion density meas. using high press. Langmuir probe 8-51340
 CO₂, ionisation current growth, Townsend swarm coeffs. 8-59541
 CO₂-N₂, ionisation current growth, Townsend swarm coeffs. 8-59541
 H II regions, high-excitation, effects of inhomogeneities on ionisation profiles 8-54007
 H₂ clouds, ionisation by supernovae 8-69856
 H₂(Σ_u^+)-He(2'S), discharge ionisation growth, diffusion coeffs. 8-83636
 He, excitation and ionisation, by instationary shock fronts 8-59540
 I₂, dissociative attachment, thermal energy electrons in equilib. with gas 8-82850
 Kr discharge, secondary ionisation processes 8-59711
 N₂, gas, in crossed elec. and mag. fields, elec. strength calcs. 8-87568
 N₂, ionisation current growth, Townsend swarm coeffs. 8-59541
 N₂-He-CO₂, discharge ionisation growth, diffusion coeffs. 8-83636
 N₂-NO(He), discharge ionisation growth, diffusion coeffs. 8-83636

ionisation of liquids

- high temperature boundary layer mass transfer, nonequilib. ionisation effects 8-93634
 organic, electrohydrodynamic ionisation, solvated ion mass spectroscopy, anal. appl. 8-73102
 Ba soln. in liq. ammonia, conductance at -62.37°C 8-91459
 Ba(ClO₄)₂, soln. in liq. ammonia, conductance at -62.37°C 8-91459
 KClO₄ soln. in liq. ammonia, conductance at -62.37°C 8-91459

ionisation of molecules

- see also molecular electron impact ionisation*
 acetylene, vibr. fine struct. accompanying core ionis., STO calcs. 8-62844
 alkali atom+methane derivative, collisional ionisation, nitromethane, perfluoromethyl bromide (iodide) electron affinities 8-66639
 aniline, photoemission for mol., polarised photoelectrons 8-66607
 atomic to molecular ion conversion, rate constant calc. 8-64835
 1-azo-bicyclo-2,2,2-octane, multiphoton ionis. spectra polaris. characts., two-photon symmetry assignment 8-74718
 benzene, multiphoton ionis. spectra polaris. characts., two-photon symmetry assignment 8-74718
 trans-1,3-butadiene, multiphoton ionis. spectra polaris. characts., two-photon symmetry assignment 8-74718
 chloramine, HOCl, isolectronic mols., vap. phase UV photoelectron spectra, struct. 8-66600
 cyclopropane-d₀, -d₆, multiphoton ionisation spectra, electronic struct. 8-82803
 cis-dibromoethylene, vac. UV spectrum, Rydberg transitions, ionisation limits 8-78718
 dichlorodifluoromethane, matrix radiolysis, photoionis., IR spectra of CF₂Cl⁺ and parent cations 8-80767
 dimethylanilines, photoemission for mol., polarised photoelectrons 8-66607
 ethylenimine, multiphoton ionisation spectra, electronic struct. 8-82803
 formaldehyde, orbital contribs. to relax. energies accompanying core ionis., ASCF HF calcs. 8-82642
 formamide, CI calc. of vertical ionisation and excitation energy 8-78836
 formic acid, ionis. and photoelectron spectra, inner valence electrons 8-82784

ionisation of molecules continued

- Freon, matrix radiolysis, photoionis., IR spectra of CF_3Cl^+ and parent cations 8-80767
- heavy ion collisions, $3d\sigma$ mol. orbital ionisation 8-94311
- hexafluorides, MF_6 , $\text{M}=\text{S}, \text{Se}, \text{Te}, \text{Mo}, \text{W}, \text{Re}, \text{Ir}, \text{Pt}$, ionisation 8-55226
- hydrocarbons, saturated and unsaturated, ionisation spectral intensities, correlation effects 8-90234
- 3-iodoaniline, photoemission for mol., polarised photoelectrons 8-66607
- ion induced inner shell vacancy formation 8-70926
- laser ionisation, modelling 8-90133
- 2-methylaniline, photoemission for mol., polarised photoelectrons 8-66607
- methylchloramines, CH_3NHCl , CH_3NCl_2 , $(\text{CH}_3)_2\text{NCl}$, UV photoelectron spectra, assignments 8-86911
- monohalobenzenes, inner shell excitation and ionis., electron energy loss spectra, XPS, assignments 8-62934
- multiphoton ionisation by spontaneous emission absorpt. 8-74721
- naphthalene, stepwise photoionisation process 8-82791
- nonpolar molecules, ionis. by alkali ion attachment at electrolyte surface 8-65998
- photoionisation ang. distrib. asymmetry, parity favouredness 8-50600
- polyatomic molecules, new method, laser photoionisation in a mass spectrometer 8-78840
- pyrazine, multiphoton ionisation spectra, circular to linear polarisation ratios, lowest ionisation pot. 8-74716
- pyrene, in alcohol solns., polar fluid electrons optical absorption coeffs., ns laser ionis. obs. 8-84600
- pyridine, multiphoton ionisation spectra, circular to linear polarisation ratios, lowest ionisation pot. 8-74716
- Rydberg transitions, term value-ionisation energy correl. 8-70738
- second-row homonuclear diatomics, photoemission energy, rel. to atoms 8-86832
- thiophosphoryl compounds, bond ionisation energies, mol. struct. from UV photoelectron spectra 8-82782
- trans-hexatriene, 6.2 eV Rydberg state symmetry, multiphoton ionis. spectrum polaris. assignment 8-70759
- trichlorofluoromethane, matrix radiolysis and photoionis. at 15K, IR spectrochem. anal. 8-76893
- tropomyosin, isotopic H exchange as function of state of ionisation of side groups 8-68979
- X-alpha transition state and transition operator method calcs. 8-70743
- Ar_2^+ , Σ_u^+ excimer state, photoionis. cross section 8-70882
- CH_3 , photoionis. and photodissoc. near ionis. threshold, SCF MO CI and Stieltjes imaging 8-58749
- CO , orbital contribs. to relax. energies accompanying core ionis., ΔSCF HF calcs. 8-82642
- COH^+ , orbital contribs. to relax. energies accompanying core ionis., ΔSCF HF calcs. 8-82642
- CS, valence electron photoionisation, ionisation pot. and spectral intensities 8-70883
- CS_2 , absorpt. spectra, Rydberg series converging to $\text{A}^2\Pi_u$ states of CS_2^+ 8-90182
- CoO , ionisation, electron density relax. effects. ab initio calcs. 8-50466
- CoO_6^{10-} , ionisation, electron density relax. effects. ab initio calcs. 8-50466
- Cs_2^+ , form. by Cs+Cs assoc. ionisation, dissociation energy 8-58804
- $\text{CsCl}(\text{Cs}_2\text{Cl}_2)+\text{Ar}(\text{Kr})(\text{Xe})$, collision-induced ion-pair form., absolute cross sections 8-73029
- $\text{H}+\text{Li}(\text{Li}_2)$, superthermal collisions, photon and positive ion prod. 8-78788
- $\text{H}+\text{N}_2(\text{O}_2)$, charge prod. cross sections and differential scatt. calcs. 8-94313
- H_2 , D_2 , photoionisation, body-frame Hund's case b description 8-94295
- H_2 , photoionisation, dissociative, at 304 Å, photoion ang. distrib. photoelectron channels 8-82792
- H_2 , photoionised continuum states, electron scatt. eqns. convergence 8-66663
- HCN , HNC , electronic reorganisation, with core ionisation 8-94196
- HCN , ionis. and photoelectron spectra, inner valence electrons 8-82784
- HCN , vibr. fine struct. accompanying core ionis., STO calcs. 8-62844
- HCO^+ , orbital contribs. to relax. energies accompanying core ionis., ΔSCF HF calcs. 8-82642
- HNO , HON , electronic reorganisation, with core ionisation 8-94196
- HOCl , chloramine, isoelectronic mols., vap. phase UV photoelectron spectra, struct. 8-66600
- H_2S , inner valence electron ionisation calcs., photoelectron spectra obs. 8-82619
- $\text{He}(2^3\text{S})+\text{H}_2\text{O}(\text{H}_2\text{S})$, energy transfer processes, reaction products, UV and visible obs. in flowing afterglow 8-85138
- I_2 , multiphoton reson. ionis. bands, 360-600 nm 8-90233
- I_2+Ar^+ , ion-pair form. differential cross-section, 25-133 eV, metastable Ar 8-78787
- Li_2 , isotope separation, by two-photon ionisation, ionisation pot. determ. 8-70950
- LiF , N^+ and Ne^+ irradiation, MO X-ray intensity meas. 8-82831
- N_2 , core ionisation, single orbital relax. energy contrib. calcs. 8-82637
- N_2 , K-shell photoabsorpt. spectra using synchrotron radiation 8-74711
- N_2 , multiphoton ionisation, EM field gradient forces 8-66608
- N_2 , photoionis., transition probabilities at threshold, to $\text{X}(2^2\Sigma_g^+)$, $\text{A}(2^1\Pi_u)$ and $\text{B}(2^2\Sigma_g^+)$ vibr. levels 8-94294
- $\text{N}_2+\text{CO}(\text{N}_2)(\text{O}_2)(\text{NO})(\text{CO}_2)$ (methane), ionis. at low energy 8-58791
- NH_3 , and ND_3 , new electronic state, multiphoton ionis. obs. 8-74717
- NH_3 , field ionis., critical energy deficits, field depend. 8-82852
- NH_3^+ , ionisation pot. of ^2E state, Jahn-Teller effect 8-62948
- NH_2Cl , NHCl_2 , NCl_3 , UV photoelectron spectra, assignments 8-86911
- NO , 4-photon ionis. spectrum 2- and 3-photon resons., low temp. assignments 8-70887
- NO , autoionisation struct. at first ionisation limit, photoionis. data 8-58748
- N_2O , K-shell photoabsorpt. spectra using synchrotron radiation 8-74711
- $\text{N}_3\text{P}_3\text{Cl}_6$, ionisation energy and electronic struct., UV photoelectron spectra and $\text{X}\alpha$ calcs. 8-94281
- Na_2 , 2-photon ionisation by Ar laser 8-55204
- O_2 , ab initio CI STO calc., photoelectron spectra 8-74585
- O_2 , photoionisation angular distribution of photoelectrons 8-90235

ionisation of molecules continued

- O_2^+ , symmetric charge transfer reactions, selected states, photo-ion, electron coincidence 8-73028
- P_2 , valence electron photoionisation, ionisation pot. and spectral intensities 8-70883
- PH_3 , inner valence electron ionisation calcs., photoelectron spectra obs. 8-82619
- PN , valence electron photoionisation, ionisation pot. and spectral intensities 8-70883
- SF_6 , ionisation pot., discrete variational $\text{X}\alpha$ calc., Slater-type orbitals in Hartree-Fock basis 8-78837
- UF_6 on C-coated Pt(Pt-W), mol. negative surface ionisation 8-56913
- ionisation of solids**
No entries
- ionisation potential**
see also work function
- acetylene, electron ionisation efficiency curves, fragment ion appearance pot. 8-86959
- acetylene, ionis. efficiency curves by electron impact, $\text{CH}_2^+(\text{C}_2\text{H}^+)$ form., ~ 10 eV 8-62935
- aldehydes, conjugated, ethylenic, UV photoelectron spectra (French) 8-90215
- alkali hydroxides, dissociation energies and bond lengths, ion props. depend. 8-86801
- alkali metaborates, dissociation energies and bond lengths, ion props. depend. 8-86801
- atom, s-electron binding energy regularities in $1s^m$ configs. 8-62731
- atomic electronegativity scale rel. to work function 8-64096
- binding energies, ionic, rel. to nonrelativistic neutral atom 8-90054
- t-butyl radical, VUV photoelectron spectrum, geometry, vibr. struct. and ionisation pots. 8-50577
- chloramine, HOCl , isoelectronic mols., vap. phase UV photoelectron spectra, struct. 8-66600
- 1,2-dibromoethane, gauche and trans conformers, photoelectron spectra 8-50574
- empirical calculation formula, new (Chinese) 8-70956
- ESCA chemical shift, indirect evaluation of Coulombic contribution to ionis. pots. for nonbonding electrons 8-92572
- ethane, electron ionisation efficiency curves, fragment ion appearance pot. 8-86959
- ethylene, electron ionisation efficiency curves, fragment ion appearance pot. 8-86959
- formamide, CI calc. of vertical ionisation and excitation energy 8-78836
- formic acid, ionis. and photoelectron spectra, inner valence electrons 8-82784
- hydrocarbons, ionisation pots. calc., PPP method 8-58592
- hydrocarbons, saturated, topological orbitals, graph theory and ionis. pots. 8-82615
- ketones, conjugated, ethylenic, UV photoelectron spectra (French) 8-90215
- methylchloramines, CH_3NHCl , CH_3NCl_2 , $(\text{CH}_3)_2\text{NCl}$, UV photoelectron spectra, assignments 8-86911
- molecules, MNDO semi-empirical SCF-MO calcs. 8-74578
- nitronaphthylamines, ESCA and UV photoelectron spectra, assignments 8-50588
- open shell systems, coupled cluster approach 8-58595
- propane, vertical electronic spectrum, ab initio MRD-CI calcs. 8-70810
- pyrazine, multiphoton ionisation spectra, circular to linear polarisation ratios, lowest ionisation pot. 8-74716
- pyridine, multiphoton ionisation spectra, circular to linear polarisation ratios, lowest ionisation pot. 8-74716
- rare earth elements, atomic energy levels, data tables 8-86805
- rare earth metals, photoionisation thresholds and Rydberg spectra 8-66522
- Rydberg transitions, term value-ionisation energy correl. 8-70738
- vertical ionisation potential, inner and valence shells, ab initio SCF MO CI perturbation calc. method 8-74800
- vinyl isocyanate, microwave and photoelectron study of cis- and trans-forms 8-70819
- zz 8-91367
- AlF_6^{3-} , octahedral complex, ionis. energy, SCF- $\text{X}\alpha$ study 8-70967
- C, theoretical ionis. energies and oscill. strengths, excited s-, p- and d-levels 8-86823
- CO_2 laser self-sustained discharge, effect of low-ionisation-potential additives 8-71616
- CS, valence electron photoionisation, ionisation pot. and spectral intensities 8-70883
- CS_2 , electronic struct., optical and photoelectron spectra 8-70745
- CS_2 , electronic struct., optical and photoelectron spectra 8-70982
- Cs, atom, XPS, free atom core binding energy 8-74699
- HCN , ionis. and photoelectron spectra, inner valence electrons 8-82784
- HF, highly excited, ionis. pot., mass spectrometric meas. 8-58603
- HNC^+ , radical cation, charge exchange mass spectrometry, HNC^+ ion recombination and ionisation pot. 8-76838
- H_2O , 8-82616
- HOCl , chloramine, isoelectronic mols., vap. phase UV photoelectron spectra, struct. 8-66600
- H_2S , gas-phase, states in valence photoelectron spectrum 8-94284
- HgCl_2 , ZZ 8-86767
- In^{2+} , emission spectrum, 340 to 6500 Å, ionisation pot. and dipole polarisability 8-78654
- InCl , InBr , InI , UV photoelectron spectra of valence d shells, gas-phase 8-62845
- InSb , Bi , disordered solid solns, ionisation energy of fluctuation levels 8-72116
- K, atom, XPS, free atom core binding energy 8-74699
- K_2 (KNa), prep. and photoionisation pots. 8-55268
- Li_2 , isotope separation, by two-photon ionisation, ionisation pot. determ. 8-70950
- Mg, atom, XPS, free atom core binding energy 8-74699
- NH_3^+ , ionisation pot. of ^2E state, Jahn-Teller effect 8-62948
- N_2H_2 , heat of form. determ. by electron impact dissociation 8-61040
- NH_2Cl , NHCl_2 , NCl_3 , UV photoelectron spectra, assignments 8-86911
- Na, atom, XPS, free atom core binding energy 8-74699
- Na particle, consisting of atoms, metallic Na, model, electronic levels 8-50673
- Na_3 , electronic struct., pot. energy surface, ab initio CI study 8-70996

ionisation potential continued

- Na_n, (NaK)_n, prep. and photoionisation pots. 8-55268
 Ne, atomic structure determ. by model pot. method 8-86777
 O₃, CI calc., ground and excited states, energy locations, transition probabilities 8-74584
 P₂, valence electron photoionisation, ionisation pot. and spectral intensities 8-70883
 PF₆⁻, octahedral complex, ionis. energy, SCF-X α study 8-70967
 PN, valence electron photoionisation, ionisation pot. and spectral intensities 8-70883
 PbCl₂, PbBr₂, PbI₂, UV photoelectron spectra of valence d shells, gas-phase 8-62845
 Rb, atom, XPS, free atom core binding energy 8-74699
 S_n, properties of small aggregates rel. to metallic character of Te_n 8-86985
 SF₆, ionisation pot., discrete variational X α calc., Slater-type orbitals in Hartree-Fock basis 8-78837
 SF₆, octahedral complex, ionis. energy, SCF-X α study 8-70967
 Se VI, 2400 to 90 Å spectrum anal. 8-58616
 Se_n, properties of small aggregates rel. to metallic character of Te_n 8-86985
 n-Si, A-centre ionisation energy change due to uniaxial deform. 8-71733
 SiF₆²⁻, octahedral complex, ionis. energy, SCF-X α study 8-70967
 SiH₄, ab initio Hartree-Fock SCF-LCAO-MO method 8-94195
 SiH₂F₂, ab initio Hartree-Fock SCF-LCAO-MO method 8-94195
 SiH₃F, ab initio Hartree-Fock SCF-LCAO-MO method 8-94195
 SnCl₂, SnBr₂, UV photoelectron spectra of valence d shells, gas-phase 8-62845
 Te_n, small aggregate, metallic character 8-86985
 TiCl, TiBr, TiI, UV photoelectron spectra of valence d shells, gas-phase 8-62845
 UF₆, electronic struct., non-relativistic Hartree-Fock-Slater method 8-50469

ionisation time see *ionisation*

ionogen see *electrolytes*

ionosondes see *ionospheric measuring apparatus*

ionosphere

see also *D-region; E-region; F-region; ionospheric electromagnetic wave propagation; ionospheric techniques; sporadic-E layer*

acoustic waves generation by LF radiowaves 8-69581
 antisymmetric S_c-variations, appl. of plasmasphere dynamo electric field-aligned currents theory 8-81499

S. Atlantic Ocean, shipborne ionosonde obs. 8-81505
 aurora, detached arcs in trough region 8-88965

auroral currents, magnetometer array and radar backscatt. joint obs., N.Scandinavia 8-85768

auroral electrojet region, elec. fields and mag. effects of solar flares 8-69576

auroral electron beam, electrostatic noise generation 8-85759

auroral energy input, effect on neutral and ion drifts 8-65446

auroral ionosphere, field-normal plasma-line scatt. detect. expt. 8-73580

auroral zone electric fields, conductivities and currents, latitudinal distrib. 8-77399

auroral zone electric fields rel. to interplanetary magnetic field vars. 8-77431

auroral zone energy dissipation due to ionospheric currents, high-resolution altitude profiles 8-88978

charged particles precip. by parallel elec. field, model 8-65459

Chatanika incoherent scatter radar obs. of field-aligned currents 8-57387

coherent parametric instabilities excited by two or more pump waves, theory 8-57381

counterelectrojet, search for correl. with interplanetary mag. field 8-88983

current distribution quantitative modelling 8-88988

current model rel. to quiet time vertical magnetic field component over India 8-61326

dayside aurora, rocket-borne meas. of particles and ion convection 8-77391

dayside auroral arcs and convection 8-81484

diffusion inhomogeneities, small-scale, dissipative parametric generation 8-69580

DP-2 current system, rel. to pulses in interplanetary mag. field B_z-component 8-73583

electric currents and fields due to field-aligned auroral currents 8-96339

electric currents variations during 23 October 1976 solar eclipse, mag. obs. in Australia 8-81498

electric fields, prod. by polar field-aligned currents 8-65455

electric fields at auroral latitudes, balloon meas. 8-57408

electron cyclotron harmonic waves excitation, lab. expt., rel. to topside ionosphere RF sounder expt. 8-93042

electron density rel. to whistler dispersion 8-93050

electron density spatial distrib. in nighttime polar ionosphere 8-73570
 electron kinetics in lower ionosphere (100 to 260 km) (Russian) 8-77395

electron precipitation daily vars., rocket meas. 8-69575

electrostatic double layers, review 8-67368

energetic ions and EM radiation in auroral regions 8-81490

equatorial, meridional currents detect. 8-85767

equatorial electrojet theory 8-69607

equatorial ionosphere, EM state rel. to interplanetary mag. field vars. 8-77413

equatorial ionosphere holes and spread-F, ion chemistry and transport 8-88982

field-aligned ionisation irregularities rel. to HF-induced plasma line 8-88979

general circulation above 100 km, empirical model 8-73558

general circulation at altitudes >100 km, empirical model 8-61664

geomagnetic storm effects, OGO 6 obs. (Japanese) 8-85754

gravity wave assoc. with sudden commencement, ionospheric effects 8-57385

gravity waves, density response of layer structs. 8-81290

handbook, of upper atmosphere, ionosphere and magnetosphere 8-73557

Harang discontinuity electric field, auroral radar and rocket double-probe obs. 8-88971

ionosphere continued

heating by radio waves, predictions for Arecibo and satellite power station 8-77403

height rises, relationship with polar mag. substorms and spread-F occurrence 8-81494

heterogeneous structure of the low-latitude ionosphere 8-96338

high-latitude electrostatic turbulence, polarisation, freq. and wavelengths 8-88981

horizontal electric currents, rel. to plasmasphere elec. fields and whistler ducts form. 8-57407

hydromagnetic dynamo 8-96335

ion convection, momentum sources obs. in thermosphere neutral comp. 8-77380

ion formation, nonstationary effects of gravity waves in lower ionosphere 8-73567

ion formation at high latits. during mag. quiet periods 8-69582

ion temp. troughs and interhemispheric plasma transport 8-96340

ionisation, effects of solar flares Fe XXV 1.87 Å line emission 8-65588

irregularities, drift vels. from ATS-6 140 MHz Faraday rot. records 8-69599

Langmuir envelope solitons in turbulent plasma 8-67334

LF sound waves relax. absorpt. (Russian) 8-65356

lower ionosphere, shortcomings in understanding revealed by radiowave absorpt. meas. 8-81492

lunar tides, theory 8-77382

magnetic field line merging and slippage in auroral arcs 8-77393

magnetic storm, Injun 5 low-energy plasma obs. 8-88987

magnetosphere interaction, elec. convection field at ionospheric heights 8-89004

metallic tethers in-ionospheric plasma, electrodynamics 8-69652

mid-latitude trough, scintillation of extraterrestrial radio noise sources signals 8-73574

mid-latitude trough location, noon and midnight obs. by Ariel 4 8-85765

midlatitude, dynamical model for 100-1000 km altitude range 8-53768

modification, initial report on artificially created equatorial spread-F 8-88972

multilayer model, electrodynamic state, horiz. mag. field component influence (Russian) 8-73556

nighttime ionospheric intermediate layer obs. by rocketborne impedance probe (Japanese) 8-61646

parallel electric field, signature in ion and electron distrib. in vel. space 8-89005

photoelectron daytime energy distrib. meas. by AE-E satellite 8-88953

photoelectron flux, low-altitude plasma line anisotropy theory 8-77414

photoelectron spectra allowing for Auger effect 8-69557

plasma, Debye screening and electron conc. nonuniformity effects on cylindrical antenna on satellite 8-69563

plasma, electrostatic cyclotron oscillation, photoionisation (Russian) 8-63552

plasma, HF radio wave-heated, with non-Maxwellian vel. distrib., electron oscils. (Portuguese) 8-83557

plasma, nonlinear mixing of EM waves 8-77406

plasma disturbances created by probes, impact on Spacelab proposed low-energy meas. 8-77458

plasma instabilities, obs. in multiple pump ionospheric heating expt., 8-57382

plasmopause, Kelvin-Helmholtz instability to hydromagnetic pulsations 8-73584

plasmopause location and H⁺ density decreases, correl. 8-81500

plasmopause signatures in ionosphere and magnetosphere 8-57391

plasmas, field aligned distrib. rel. to plasma mantle 8-57406

plasmasphere origin, dimensions and particle precip. 8-69584

polar cusp, turbulent, temps. and low-energy particles obs. rel. to Kelvin-Helmholtz instability 8-96343

polar electric fields, transmission to Equator 8-65456

polar regions, small-scale transverse magnetic disturbances 8-77423

polar wind profiles latit. var., Alouette II data 8-69588

polar-equatorial electrical coupling during magnetically active periods, theory 8-93029

pressure oscillations, generation of atmospheric acoustic-gravity waves 8-77296

protonosphere-F-region nighttime proton fluxes 8-93034

pulsed RF waves, proton cyclotron echoes, generating mechanism 8-77407

quasiperiodic disturbances, effect on guided MHD waves 8-73568

quiet auroral arcs, feedback instability in ionosphere-magnetosphere system 8-57379

quiet night ionosphere, calculated and measured decay rates comparison 8-81493

Rayleigh-Taylor bubbles in equatorial ionosphere 8-77409

Rayleigh-Taylor gravitation-induced instability, rel. to equatorial spread-F 8-69595

semidiurnal winds seasonal var. in dynamo region 8-93033

space sciences, conf., Trivandrum, India (Jan. 1977) 8-69586

substorms, role of ionosphere, field-aligned currents generation 8-88998

substorms, ULF mag. vars. assoc. with ionospheric cond. changes 8-88994

topside, low-energy plasma, Injun 5 Lepedeau obs. 8-77408

Tordo 1, polar cusp Ba plasma injection expt. obs. 8-77402

total electron content at Sagamore Hill, solar cycle var. 8-81496

total electron content diurnal and seasonal trends, obs. at Waltair 8-69596

total electron content meas. at Gauhati, using ATS-6 140 MHz transmissions 8-69598

total electron content numerical model, corrections for satellite tracking systems 8-69587

total electron content obs. at Kurukshetra, suing ATS-6 140 MHz transmissions 8-69597

total electron content obs. at low and mid latitude during mag. storms 8-77396

total electron density nighttime behaviour 8-69570

transverse electric fields rel. to field aligned currents, model 8-77397

travelling disturbances, electron density spectra 8-77398

travelling disturbances, possible correl. with jet stream activity 8-69601

ionosphere continued

- travelling disturbances characts. over Thumba 8-69590
 travelling disturbances study using multistation rapid-run ionosondes 8-93041
 whistlers, group vel. in two-ion plasma 8-87452
 winter polar ionosphere, Isis 1 and 2 meas. 8-77400
 zonal and meridional elec. fields effects in evening sector 8-69571
 H^+ , O^+ , conc. meas., Aureole 2 satellite mass spectrometer obs. 8-53766
 H_2O^+ density, contrib. from H-implemented interplanetary dust grains 8-65445
 N_2O^+ , pot. energy hypersurface characts. calc. in $O^+ + N_2 \rightarrow N + NO^+$ react. 8-60996
 O^+ reactions with N_2 , O_2 , and NO, nonthermal rate coeffs. 8-57375
 $O^+(^2D) + N_2$, charge exchange rate coefficient, effect of N_2^+ recomb. on aeronomic determ. 8-88954

ionospheric electromagnetic wave propagation

see also atmospheric

- airborne soundings over Kazakhstan, surface topography effects on electron density 8-69579
 ATS-6 140 MHz Faraday rot. records, irregularities drift vels. determ. 8-69599
 auroral absorption regions poleward expansion triggered by SSC 8-57403
 auroral ionosphere, field-normal plasma-line scatt. detect. expt. 8-73580
 auroral oval, VHF amplitude scintillation 8-61660
 backscatter radar data rel. to O I 6330 Å nightglow intensity 8-77401
 circumglobal signals in Atlantic equatorial zone (Russian) 8-69585
 cold lossless plasma half-space, transient response in presence of transverse static mag. field 8-67361
 condition forecasting and prediction, long- and short-terms 8-93046
 cosmic noise absorption, F-lacuna and slant-E condition rel. to E-region Farley-Buneman instability 8-73563
 cosmic radio wave absorpt. rel. to mag. storms at Delhi 8-69589
 cross-modulation of radio signals between two nearby stations 8-93048
 D-region, anomalous radiowave absorpt. during sudden disturbances, solar zenith angle depend., electron loss coeff. 8-69568
 D-region, diurnal vars. during storm after-effect 8-65451
 D-region, partial reflections, sensitivity to irregularity comp. 8-81495
 D-region absorption, effect on forward scatter radiometer amplitude distrib. index 8-65552
 D-region partial reflections, filtering effect on drift parameters determined by full correl. anal. 8-65450
 daytime absorption surges, as function of substorm phase and interplanetary mag. field direction 8-73575
 differential equation, generalised, inc. anisotropy, inhomogeneity and fluctuations 8-53770
 diffraction trapping of HF waves by ionospheric waveguide 8-53772
 dissipative parametric generation of small-scale diffusion inhomogeneities 8-69580
 Doppler fluctuations and angle-of-arrival var. caused by ionospheric scintillation 8-77411
 E_c -layer, behaviour in EM field during oblique irradiation by radio waves 8-73566
 E_c -layer, h-type, at Uppsala, features 8-81497
 E_c -layer, oblique incidence propag. and ionospheric attenuation 8-73578
 E_c -layer, temperate zone, maps of $f_0E_c > 7$ MHz 8-73579
 Earth-ionosphere channel excitation by LF sources in inhomogeneous ionosphere (Russian) 8-85757
 echo signals propag. characts., 10 and 15 MHz 8-69574
 electron density and recomb. coeff. profiles calc. rel. to absorpt. and rocket meas. 8-69559
 electron wave, transform. into ion wave in multicomponent plasma during quasilongit. propag. 8-73572
 ELF radiation flux during 1971 December 16 magnetic storm 8-69564
 ELF resonance mode splitting in Earth-ionosphere cavity during high solar activity 8-77416
 ELF transmission anomalies and energetic particle precip. 8-93040
 equatorial ionosphere spread-F echoes in HF and VHF bands, theoretical model 8-85764
 equatorial scintillation at 40, 140, 360 and 860 MHz simultaneous obs. 8-57393
 equatorial spread-F, artificial control technique 8-69602
 equatorial spread-F, VHF and UHF backscatter from high freq. drift waves 8-88973
 equatorial spread-F, VHF scattering 8-61661
 f_0F_2 , median values obs. over S. Atlantic Ocean 8-81505
 F_2 -layer, hemispherical f_0F_2 differences rel. to neutral atmosphere 8-69603
 F_2 -layer critical frequency, forenoon bite-out characts. 8-65453
 F_2 -layer vertical sounding, radio signal Doppler spectrum and arrival angle meas. (Russian) 8-61651
 F-lacuna events rel. to state of ionosphere 8-93036
 F-region, absorpt. separation from cosmic radio noise absorpt. 8-85769
 F-region, equatorial, irregularity patches obs. rel. to localised origin 8-77404
 F-region, n_F annual vars. with latit. and solar activity level 8-69577
 F-region field-aligned irregularity excitation and thermal parametric instability 8-77419
 Faraday rotation, effects of pulsewidth 8-71540
 geostationary satellite VHF Faraday rotation mea. for ionospheric electron content 8-61599
 heating experiment, coherent parametric instabilities excited by two or more pump waves 8-57381
 HF absorption at low latits., solar particle effects 8-69594
 HF and MF bands, Doppler meas. accuracy 8-77417
 HF Doppler method studies of high-latitude ionospheric dynamics 8-73569
 HF Doppler obs. over S.E. Australia during 1976 Oct. 23 total eclipse 8-61662
 HF oscillating echoes from polar E-region 8-57390
 HF peculiar lunar echoes, guided wave propag. in ionosphere and magnetosphere 8-93032
 HF propag., freq. standard utilisation 8-93027
 HF radiowave propag. at oblique incidence, anal. 8-93045

ionospheric electromagnetic wave propagation continued

- HF radiowaves, plasma heating, electron oscills. (Portuguese) 8-83557
 HF signals statistical characts. during auroral substorms 8-69583
 HF sky-wave received signal level determination for communication link 8-85758
 HF-induced plasma line rel. to field-aligned ionisation irregularities 8-88979
 incoherent scatter data, analytic partial derivatives for least-squares fitting 8-73581
 intersatellite wave propagation expts. at medium freqs., general results 8-69604
 intersatellite wave propagation expts. at medium freqs., whistler-mode pulses 8-69605
 ion cyclotron whistlers, topside ionosphere, complex ray tracing study 8-96346
 ionograms, multi-parameter, from universal digital ionosonde 8-73577
 LF broadcasting, sky-wave propag. in daytime 8-61648
 LF waves, acoustic waves generation 8-69581
 LF/VLF radiowave propag. characts. anal. 8-93049
 linear wave transformation in ionosphere and ion whistler formation (Russian) 8-65449
 low-latitude whistlers characts. observed at Okinawa, Japan 8-73576
 magnetic field effects 8-96332
 meteor burst data communication system 8-69608
 MF pulsed transmissions, method for separating D- and E-region contribs. to total absorpt. 8-69593
 mid-latitude trough, scintillation of extraterrestrial radio noise sources signals 8-73574
 multiple pump ionospheric heating expt. plasma instabilities obs. 8-57382
 plasma line, low-altitude anisotropy theory 8-77414
 polar cap absorption intensity and solar cosmic rays north-south asymm., riometer data 8-69629
 radio and optical, conf., Oslo, Norway (May 1978) 8-93044
 radio beacon expt., ATS-6, results 8-69592
 radio pulses, nonlinear phase distortion of partially refl. signal 8-69573
 radio time signals, Tokyo reception accuracy 8-69606
 radio wave absorption, riometer meas. 8-85763
 radio waves absorption in equatorial ionosphere, seasonal var. 8-85762
 radio waves interaction in plasma, nonstationary processes (Russian) 8-93028
 radiowave absorption measurements, anal. rel. to shortcomings in understanding of lower ionosphere 8-81492
 radiowave absorption rel. to solar activity 8-69591
 radiowave phase and amplitude meas. interpretation (Russian) 8-77394
 radiowave propag. studies by International Radio Consultative Committee 8-77311
 radiowave scintillation studies using ATS-6 radio beacons at Delhi 8-69600
 radiowave studies of ionosphere, incoherent scatter technique development, review 8-81503
 radiowave trajectories in horizontally inhomogeneous ionosphere 8-73571
 radiowaves, effects on communication systems 8-92954
 ray statistics in plane stratified isotropic medium with isomeric inhomogeneities (Russian) 8-53773
 reflection and transmission coeffs. determ., low freq., using 4×4 matrices 8-53769
 refractive index determ. using GEOS-3/ATS-6 satellite-to-satellite tracking data 8-93039
 round-the-world signal group delay, frequency dependence calc. (Russian) 8-61654
 satellite links, ionospheric wave disturbances effect on polarisation fading freq., simulation 8-69572
 scattering, appl. to ionospheric props. meas. at Arecibo Observatory 8-81488
 scattering by E-region anisotropic inhomogeneities oriented along geomag. field 8-53771
 scintillation, effects on received signal level 8-93047
 scintillation of solar bursts at 30 and 60 MHz, STEREO-5 obs. 8-81822
 sea: echo radar spectra resolution limitation inferred from ionospheric Doppler broadening 8-81489
 self-focusing of HF EM waves, striations 8-96347
 space sciences, conf., Trivandrum, India (Jan. 1977) 8-69586
 sporadic-E layer behaviour in EM field of strong decametric waves 8-69569
 sporadic-E layer inhomogeneous structure influence of RF heating (Russian) 8-61653
 stimulated Brillouin scattering, detect. by Jicamarca radar 8-77412
 stimulated resonance line scattering with Eiscat radar 8-57389
 sudden commencement absorption events at S. pole, rel. to lower cleft boundary 8-77437
 sudden frequency deviations, solar flare UV radiation spectral energy distrib. calc. 8-69771
 sudden frequency deviations and phase anomalies in F-region due to solar flares (Italian) 8-96345
 SW radio waves, polarisation on slant path 8-73573
 synchronisation by JJJ signal reception via the E-region 8-65910
 topside RF sounder expt. rel. to lab. excitation of electron cyclotron harmonic waves 8-93042
 VHF ionosphere forward scattering, effect of meteors (Japanese) 8-81504
 VHF scintillation rel. to peculiar Faraday rotation fluctuations 8-61663
 VHF SIRIO satellite link telemetry emission, use for ionospheric meas. 8-69553
 VLF hiss propag. characts. obs. at low latit. ground stations 8-69561
 VLF non-ducted whistler-mode signals at low latitudes 8-61658
 VLF propag. during sunrise 8-93030
 VLF sudden phase anomalies correl. with solar microwave burst energies 8-77418
 whistler detection, multichannel filter and shift register obs. system 8-93031
 whistler dispersion, group delay automatic meas., ionosphere and magnetosphere electron density 8-93050

ionospheric electromagnetic wave propagation continued

whistler mode signals, initial results from tracking receiver direction finder 8-77429
whistler propagation at low latits., review 8-73586

ionospheric measuring apparatus

Arecibo Observatory, ionospheric props. meas. without rockets 8-81488
Digisonde 128PS, universal digital ionosonde 8-73577
electric potential of rocket, and electron beam injection expts. (*Russian*) 8-93069
F₂-layer vertical sounding, radio signal Doppler spectrum and arrival angle meas. (*Russian*) 8-61651
geostationary satellite VHF Faraday rotation mea. for ionospheric electron content 8-61599
plasma gun, rocket-borne, use in controlled ionospheric experiment 8-57424
radar auragraph, for auroral radar echoes drift meas. 8-65436
rocket expt. high-power electron gun (*Japanese*) 8-61566
SIRIO VHF telemetry emission, use for ionospheric meas. 8-69553
vertical ionosonde receivers, interference suppression (*Polish*) 8-88950
whistler detection, multichannel filter and shift register obs. system 8-93031

ionospheric measuring instruments *see ionospheric measuring apparatus***ionospheric propagation** *see ionospheric electromagnetic wave propagation***ionospheric techniques**

see also electron density; ion density
auroral radar echoes drift meas. using radar auragraph 8-65436
automatic analysis of digital diurnal ionograms (*Italian*) 8-85699
D-region partial reflections technique, sensitivity to irregularity comp. 8-81495
drift parameters determination by full correl. anal., effect of filtering 8-65450
electric potential of rocket, and electron beam injection expts. (*Russian*) 8-93069
electron collision freq. profile determ., Volterra eqn. analytical method 8-73525
equatorial spread-F, artificial control technique 8-69602
exploration by radar 8-73663
F₂-layer, mid-latit. trough boundary determ. from radio sources signals scintillation 8-73574
F-region, absorpt. separation from cosmic radio noise absorpt. 8-85769
F-region, equatorial, motions deduction from Sq currents 8-96344
GEOS-3/ATS-6 satellite-to-satellite tracking data for ionospheric refr. index determ. 8-93039
heating by radio waves, predictions for Arecibo and satellite power station 8-77403
heating experiment, coherent parametric instabilities excited by two or more pump waves 8-57381
HF Doppler method studies of high-latitude ionospheric dynamics 8-73569
incoherent scatter data, analytic partial derivatives for least-squares fitting 8-73581
interference suppression for vertical ionosonde receivers (*Polish*) 8-88950
low-energy measurements by Spacelab, effects of probe-created plasma disturbances 8-77458
maximum entropy spectral anal. of radar auroral echoes 8-93006
meteor bursts, forward scatt. technique, obs. over India 8-89132
modification, initial report on artificially created equatorial spread-F 8-88972
multiple pump heating experiment, plasma instabilities obs. 8-57382
multistation rapid-run ionosondes for study of travelling disturbances 8-93041
peak electron densities of F₂-layer, comparison of CCIR predictions with in situ meas. 8-57394
radiowave phase and amplitude meas. interpretation (*Russian*) 8-77394
radiowave propag. condition forecasting and prediction, long- and short-terms 8-93046
radiowave studies of ionosphere, incoherent scatter technique development, review 8-81503
space science without rockets, ionospheric props. meas. at Arecibo Observatory 8-81488

ionotaphoresis *see electrophoresis***ions**

see also atoms; electrolytic ions; hydrogen ions; negative ions
No entries

I.R. astronomy *see infrared astronomy***I.R. detectors** *see infrared detectors***IR drop** *see electric potential***I.R. imaging** *see infrared imaging***I.R. sources** *see infrared sources***irasers** *see lasers***iridium**

see also nuclei with
atom, even config., parametric calcs. 8-82631
atom, hyperfine interaction parameters, effect of local exchange, X α and HF calcs. 8-78622
brittle fracture, impurity segregation to grain boundary effects 8-64637
chemisorption of CO, preexponential factor and desorption energy 8-71963
chemisorption of CO and O on (100) and (110) faces, electron states, electron field emission 8-84704
diffusion in liquid Cu (*Japanese*) 8-59962
filament for electron gun, ThO₂ coated poisoning resistant 8-54493
reconstructed surfaces, reorganisation of (100) 8-95214
recovery from laboratory residues 8-81957
spectrophotometric methods of determination, review 8-61115
surface electronic props. 8-95332
Si:Ir S-type diodes, characts. 8-56224

iridium alloys

see also iridium compounds
Cu-Ir, dil., impurity diffusion, temp. depend. (*Russian*) 8-67851
Fe-Ir, hyperfine field distrib., spin echo NMR meas. 8-76351
Ir-W (0.3 wt.%), P segregation to grain boundaries, effect on high temp. ductility 8-95754
LiIr, struct. and props. exam. 8-92245

iridium alloys continued

Nb-Ga-Ir, phase equilib. at 1000°C, cryst. data for intermediate phases 8-52763
Nb₃Ir, A-15 struct. supercond., microhardness, bonding 8-76199
ULr₃, (100) surface reconstruction, LEED, AES, electron energy loss spectra study 8-75918
Zr-Ir, $\alpha \rightleftharpoons \beta$ transform. (*Russian*) 8-80540

iridium compounds

see also iridium alloys
tetraethylene iridium chloride, ligand-ligand interactions; low freq. vibr. obs. 8-94255
tetraethylene iridium chloride dimer, ligand-ligand interactions, low freq. vibr. obs. 8-94255
Ir complexes with adenosine, xanthosine, prep., elec. cond., IR spectra, characterisation 8-92065
IrCl₆, reduction by BH₄⁻ 8-76854
IrF₆, electron affinities from collisional ionisation with alkali atoms 8-55226
IrF₆, in mixed crysts., Jahn-Teller effect, $\Gamma_{8g}(t_{2g})^3$ state, 6800 Å 8-76032
IrGe_{1.5}Si_{1.5}(Se_{1.5}), new skutterudite relation compounds, prep. and charact. 8-52700
IrO₂, electronic struct., XPS obs., rel. to TiO₂, RuO₂ 8-52632
IrO₃, anodic films, electrochem. characts., electrochromic system 8-80316
IrSn_{1.5}S_{1.5}, new skutterudite relation compounds, prep. and charact. 8-52700
Li₂IrH₆, and Li₂IrH₆, struct. and props. exam. 8-92245
Xe-MF₆, M=W, Mo, U, Re, Ir, charge transfer interactions, VUV and IR obs. 8-50664

iron

see also nuclei with

abundance in stars, Utrecht UV spectrophotometer obs. 8-69793
acoustic velocity, shock-compressed uniform solid, lateral discharge ang. semiempirical formula (*Russian*) 8-55910
adsorption of CO, random occupation of adsorption sites, LEED exam. 8-63930
adsorption on W, work function and field emission obs. (*Japanese*) 8-91536
amorphous, realistic structural model, search for Bernal holes 8-83734
anodic dissolution in acidic chloride solns., exam. 8-92389
antiferromagnetism of FCC Fe and its alloy 8-88124
Armco, corrosion and mechanical behaviour in liquid Li 8-53036
Armco, crack and slip band form. during US fatigue 8-56723
Armco, exam. of pore formation mechanism 8-85120
Armco, fatigue cracking under 23 kHz loading at 23°, 60° and 100°C 8-60763
Armco, impact strength, exam. with pulsed drop impact loading 8-84944
Armco, inelasticity when under cyclic strain, in active media 8-80613
Armco, kinetic singularities of plastic deform. during $\gamma \rightarrow \alpha$ transform. (*Russian*) 8-92262
Armco, microstruct., effect of strain rate on change, due to tension-compression 8-80614
Armco, screw dislocation effect on mech. props. (*Russian*) 8-60704
Armco, texture role in prestrain embrittlement 8-60796
atom, beam foil spectra, 20 to 350 nm wavelength, 16 to 110 MeV beam energy 8-78655
atom, double K-shell ionisation by electron impact, X-ray spectra 8-62928
atom, double K-shell ionisation by electron impact 8-62929
atom, hyperfine interaction parameters, effect of local exchange, X α and HF calcs. 8-78622
atom, X-ray production by protons by 0.5 to 2.0 MeV energy 8-66646
atom, X-ray spectra, chemical bonding and multiple ionis. effects 8-50630
atomic layers, Pauli paramagnetism to band ferromagnetism transition thickness depend. 8-72377
atomic magnetic moments comparison to values of ferromagnetic metal 8-52244
atomised powder compacts for mag. cores, oxidation, compressibility, heat treatment (*Japanese*) 8-72752
atomized powder compacts for mag. cores, mag. props. (*Japanese*) 8-72751
BCC, computer simulation of entropy of $\frac{1}{2}\{111\}\{110\}$ edge dislocation 8-67716
BCC, migration of vacancies near twin boundaries in α -phase 8-51535
BCC, one-dimens. Morse function cryst. stability anal., for teaching 8-54134
BCC, strain hardening and recovery by pure metal mode, high temp. deform. (*Japanese*) 8-52843
BCC and FCC struct., X-ray absorption spectra, Mossbauer spectra, comparison (*Russian*) 8-64299
boriding by ion bombardment with B₂H₆ (*French*) 8-60876
Bremsstrahlung distrib. from 22 MeV electron irradiation 8-59840
carbonyl, kinetic singularities of plastic deform. during $\gamma \rightarrow \alpha$ transform. (*Russian*) 8-92262
cast, ferritic, ductile fracture initiation and propag. 8-84966
chemisorption, dissociation of CO(H₂)(N₂), on cryst. surface (*German*) 8-53257
chemisorption of CO, CO₂, acetylene, ethylene, H₂ and NH₃ on clean (100) and (111) surfaces 8-71996
cold work stored energy effect on mag. moment vs. temp. curve 8-95419
compacts, porous, dynamic hot pressing, press. rel. to density, time 8-60599
compression deformed single cryst., induced uniaxial anisotropy 8-52336
concentration determ. in atm. and rainwater in Vizcaya, Spain (*Spanish*) 8-57264
contact reactions with Al base melt 8-60879
contact to GaAs, effect on minority carrier diffusion length 8-72260
in cores of planets rel. to formation from dust grains in early solar system 8-85869
corrosion and electrochem. behaviour in NaOH soln. containing ClO₃⁻ (*Japanese*) 8-72928
corrosion behaviour of borided and nitrided steels in aqueous media 8-95837

iron continued

corrosion pitting in acid, alkaline solution, gelatin effect 8-95838
 corrosion resistant surface alloys, form. by ion implantation 8-88569
 de Haas-van Alphen effect and exchange splitting, effect of pressure (Russian) 8-95252
 degree of charging of surfaces polished by TiC and synthetic diamond micropowders 8-60880
 determination, in flux-grown magnetic garnets, by AAS 8-92585
 determination, in radioactive soln., sub- and super-equivalence isotope dilution anal. 8-95984
 determination, in waters, colorimetric-acid digestion method 8-61088
 diffusion and permeability of H₂ and D₂ at 49 to 506°C 8-59977
 diffusion and solid solubility of Sb, 773-873K, ion backscatt. anal., rel. to intergranular embrittlement 8-71880
 diffusion coating by Cr and Pb melt bath, kinetics (Korean) 8-60873
 diffusion in Fe, Ni and Fe-Ni alloy, effect of plastic deform. and martensitic transformation (Ukrainian) 8-55974
 dislocation dynamics, HVEM in situ obs. 8-83822
 dislocation struct. around fatigue cracks, exam. (Japanese) 8-64623
 dislocation structure determ. from magnetic props. 8-55874
 dispersed particles, in lunar matter, FMR study, effective linewidth method 8-95523
 dissolution rate into molten Al, convection mass transfer (Japanese) 8-71858
 dissolved organic Fe, determ. in seawater 8-81208
 ductile fracture, effect of nonmetallic inclusions 8-64660
 edge dislocation modelling, flexible boundary conditions and nonlinear geometric effects in α -phase 8-75667
 elastoresistivity effect, meas. of resistance at 4.2K and 300K, using mag. field method 8-72132
 electrical resistivity of pure Fe, temp. depend., 1.6 to 298K 8-84194
 electron damage, appl. of KUR LINAC 8-71760
 electron spin polarisation in field emission, surface magnetism 8-68607
 epitaxial film on Sb, ultrahigh vac. deposition 8-56572
 epitaxial growth on W tip, FIM obs. 8-79904
 exploded wire, X-ray line emission and plasma conditions 8-59670
 explosive compaction of metal powders 8-64501
 fatigue crack propag., low temp. 8-72876
 fatigue fracture strength and failure, at 77K after cyclic loading at room temp. 8-84996
 ferromagnetic, cluster method, environmental effects 8-95405
 ferromagnetic, EMF generation by pulsed laser irradi. 8-68021
 film, amorphous and polycrystalline, Hall effect, resistivity and mag. moment 8-91786
 film, effect of tensile stress on mag. domain struct. 8-68332
 film, exchange coupled with Fe-Ni film, mag. reversals, hard layer thickness effects (Russian) 8-56359
 film, Hall resist., effect of N impurity codensation 8-64146
 film, nuclear magnetisation relax., at 77 to 500K 8-60352
 film, polycryst., heat of adsorpt. of H₂ and D₂ 8-91530
 film, single crystal, less than 1000 Å thick, inclined 90° walls 8-72384
 fine particulate Fe in lunar regolith (Russian) 8-89089
 friction props. of surface films in air and high vacuum 8-60850
 galactic cosmic rays, isotopic composition, balloon meas. 8-89024
 gamma fields induced by ²⁵²Cf neutrons 8-50240
 geochemistry of Fe in Puget Sound 8-69370
 glassy, heat of crystn., and bulk modulus, calc. using struct. model 8-51428
 Gruneisen parameter, behaviour at high press. 8-83899
 heart tissue, thalassaemic, Mossbauer spectra of Fe deposits 8-73202
 high C, interfacial tension in phase boundary with MnO-TiO₂-SiO₂(Al₂O₃) (Czech) 8-63907
 hydrostatic compression of Fe and related compounds, overview 8-83862
 hyperfine fields at impurities in ferromag. metal 8-52244
 implanted into Al, hyperfine interactions, conversion electron Mossbauer spectroscopy 8-52391
 internal fields, positive muon investigation 8-68438
 internal stress meas. by decremental unloading technique 8-64576
 La_{1,2} and L β X-ray emission spectrum, determ. using modified photoelectron spectrometer 8-50557
 laser, pumping using KrF laser, vap. form. by flash and discharge decomp. of Fe(CO)₅ 8-74890
 lattice atom displacements near end of implanted μ^+ tracks 8-55890
 lattice defects, relax. studies, computer simulation 8-79604
 lattice distortions due to H, X-ray diff. exam. 8-79629
 lattice hardening due to dissolved H₂ in Fe, and ferritic steel 8-76656
 lattice vibrations, temp. depend. 8-95124
 layers formed by reaction with molten Al, X-ray, EPMA and hardness meas. (Japanese) 8-72926
 liquid, absorption of gaseous O₂ 8-51686
 liquid, multiple scatt. calcs. of resist. 8-76039
 liquid, surface tension meas. with levitated metal droplets, influence of oscill. amplitude 8-51798
 low temperature deform., strain-rate cycling and stress relaxation tests (Japanese) 8-52876
 magnetic aftereffect of interstitial O 8-91903
 magnetic hyperfine field of K, Ca and Ti in Fe, TDPAD meas. 8-52389
 magnetic relaxation of H and D 8-64228
 magnetic transitions, first order, shock induced, characts. and discrimination from TRM 8-64205
 magnetoresistance, grain-oriented mag. steel sheet (German) 8-68020
 martensitic transformation at high temp., transform. temp., growth rate, stress relaxation 8-56636
 melt, treatment by high-temp. gas stream, math. model, applic. to nitriding (Russian) 8-53016
 membranes, effect of electrodeposited metals on H permeation, proposed catalytic mechanism 8-53252
 meteorite fusion crusts and ablation debris 8-61819
 mitochondria of bovine heart, EPR investigation of two forms of Fe-S centre N-2 8-69014
 molten, impurities effect on viscosity 8-95172
 Morse potential, equation of state determ., high temp. and pressure, computer expt. 8-75800
 Mossbauer energy shift near Curie temp. 8-52388
 muon⁺ hyperfine field and relaxation, temp. depend. 8-95538
 muon⁺SR, theory of spin depolarisation rate 8-80271
 neutron ns. slowing down time, expt. obs. 8-58319
 neutron yield calcs., electron beam incidence 8-95622

iron continued

nitriding, thermodynamic considerations (German) 8-60874
 noncrystalline, electronic density of states, multiple scatt. calcs. 8-91578
 nuclear inelastic channel suppression in ⁵⁷Fe, nuclear reson. and electronic scatt. of γ -quanta, hyperfine transitions 8-60361
 optical constant dispersion and emissivity, up to 900K 8-52464
 ore, leaching, effects of ultrasonics and their appls. 8-92214
 oxidation, combination anal. using ESCA, AES and SIMS 8-72924
 oxidation, conversion electron Mossbauer spectroscopy, appl. to surface props. and reactors 8-60359
 oxide film thickness determ. by electron backscatt. Mossbauer spectroscopy 8-72933
 oxide surface layer, TOF atom probe anal. 8-64766
 partial densities of states, electron-phonon interaction 8-51869
 permeability, diffusivity, and solubility, of H and D at 10 to 60°C 8-75887
 photoelectron spin polarisation and itinerant magnetism 8-68602
 pitting in Na₂SO₄-NaCl solns. (Japanese) 8-85042
 plagioclase:Fe²⁺, ligand field bands of impurity luminesc. centres and their site occupancy 8-88350
 plastic deformation mechanism, meas. of microplasticity 8-60720
 plastically deformed, dislocation arrangement exam. by ferromag. techniques 8-63774
 polishing in H₂SO₄+methanol, H₂PO₄ and HClO₄+methanol, polarisation curves 8-56851
 polycrystalline, exam. of Luders deformation 8-84893
 polyethylene-Fe, wear resistance on steel counterbody, exam. 8-68826
 porous, density, elec. cond., Young's modulus, toughness 8-64645
 porous, sintered, deform. diagram based on theory of plasticity (Russian) 8-88494
 positron annihilation, temp. depend. 8-56540
 powder, consolidated, exam. of mech. and electrical props. 8-56599
 powder, mag. susceptibility meas. by high frequency pulse technique 8-93739
 powder, Mossbauer spectra parameter calc. with aid of computer (Russian) 8-76361
 powder, reduction annealing, thermodynamic anal. 8-60597
 powder, supersonic vibration effect on pressing (German) 8-64500
 powders, rapidly solidified, nucleation, undercooling and homogeneous structs. 8-52708
 protective coating on Al powder (Russian) 8-60881
 PVC:Fe film, struct. and optical props., soln. growth technique 8-51837
 rapid melting and solidification of surface layer, exam. using computer heat flow model 8-83228
 rotational hysteresis 8-91889
 sheet, surface magnetisation, ferromag. nucl. reson. meas. 8-60348
 sheet metal, texture heterogeneity, numerical simulation (French) 8-92274
 Shockley surface states, three faces of BCC cryst. 8-76126
 sintered, effect of repressing and double sintering on impact strength (Japanese) 8-92217
 sintered, fatigue, metallographic obs. 8-64646
 sintered parts, struct. stabilisation with C potential control of protective atmosphere 8-60614
 solar central Fe-H plasma, limited solubility of Fe 8-89149
 solubility of H₂ in 600-1500°C temp. and 0.1000 atm. pressure ranges (Russian) 8-59948
 solute segregation to grain boundaries 8-72780
 spin polarisation of field emitted electrons, itinerant model 8-95685
 sponge, heat of adsorpt. of pyridine and ethyl pyridine, flow microcalorimetry 8-85193
 stopping power for 28 MeV α -particles, re-evaluation 8-79651
 stopping powers, projectile range for Z=8-20, 0.0125-12.0 MeV/nucleon 8-83856
 submitochondrial particle succinic dehydrogenase, interaction of ubiquinone with Fe-S centre, EPR 8-69016
 surface, Cl₂, CO₂, NH₃ and alkanes thermal accommodation coeffs., translational (internal) gas-solid energy exchange 8-92506
 surface, laser doping with V (Russian) 8-95065
 surface, magnetic order 8-95439
 surface, O₂ layer thickness, reson. α -scatt. from ¹⁶O 8-64778
 surface, purposeful modification by gas adsorption, charact. by photoemission 8-71955
 surface 8-60553
 surface catalyst for CO hydrogenation to methane and higher mol. wt. compounds 8-73034
 surface lattice dynamics 8-95224
 surface props. rel. to adsorbed O₂, H₂O vapour, work function determ. 8-60187
 surface relaxation, lattice statics calc. in α -phase 8-63925
 surface sliding damage, no lubrication, materials depend. (Japanese) 8-56780
 tektites-irgizites, Fe ions state rel. to form. conditions 8-61420
 thermal acoustic magnons, Brillouin scatt. meas. 8-95424
 thermodynamical Gruneisen function for pure Fe in Earth's core 8-61361
 transient mag. field, vel. and atomic number depend. 8-91999
 triboelectric charging, effects of fluorinated compounds 8-60188
 tribothermoluminescence of flakes in grinding wheel, rel. to solar coronal dust radiation 8-68570
 tunnelling electron spin polarisation rel. to band struct. 8-68095
 US velocity anomalies, at elevated temp., α - γ transition 8-75830
 vacancy formation energy by positron annihilation 8-51531
 vapour deposition, columnar struct. rel. to deposition conditions 8-52675
 vapour growth of small particles on Al₂O₃ substrate 8-75958
 vibrational spectrum with interstitial C atoms 8-67796
 waisted cylinders, fatigue, exam. of Miner's rule 8-64689
 wear measurement by thin layer activation technique 8-72945
 wear resistance, surface hardening processes, review 8-72894
 whisker, H₂ effect on deform. 8-68755
 whisker, polycryst., FIM obs. of struct. 8-84111
 whiskers, mag. crit. phenomena, size effects 8-68258
 whiskers, soft magnetic metals, ideal, AC response 8-64223
 work hardening, and behaviour and dislocation struct. in single crystals during simple shear tests 8-95762
 X-ray K absorpt. discontinuities 8-60532
 XPS obs. of Fe 2p states 8-52625
 yield stress, temp. depend. (Russian) 8-56691

iron continued

zone refined, strained, substructural changes during annealing (*Slovenian*) 8-84845
 $\text{Al}_2\text{O}_3\text{:Fe}^{2+}$, phonon spectroscopy using superconducting tunnel junctions 8-91389
 $\beta\text{-Al}_2\text{O}_3\text{-Na}_2\text{O:Fe}$, coordination site, oxidation state, Mossbauer, absorpt., emission spectra, mag. susceptibility meas. 8-68431
 $\text{CdBr}_2\text{:Fe}^{2+}$, charge transfer near UV spectra, 4.2K, mag. circular dichroism 8-80378
 $\text{CdCl}_2\text{:Fe}^{2+}$, charge transfer near UV spectra, 4.2K 8-80378
Co-Fe system, interdiffusion zone growths (*Czech*) 8-84009
Cu-Fe, composite, fibre and layer structs., anomalous props. caused by internal phase boundaries 8-72754
Cu-Fe (1 wt.%), stress induced martensitic transformation of spherical Fe particles, exam. 8-52803
 $\text{CuGaS}_2\text{:Fe}$, effect of Fe content and stoichiometry on coloration 8-88336
 $\gamma\text{-Fe}$, atomic mag. moment in FCC lattice of transition d-metals (*Russian*) 8-72337
Fe, BCC, vib. entropy of $\frac{1}{2}$ {111} {110} edge dislocations 8-63768
 $\alpha\text{-Fe}$, BCC metal, vacancy-edge dislocation interactions, computer simulation 8-83845
Fe based ternary solutions, liquid, exam. of thermochemistry 8-80782
 $\alpha\text{-Fe}$, chemisorption of acetylene, (ethylene) struct., bonding, dissoc., UPS obs., MO calcs. 8-84050
Fe, Compton profile from 662 keV γ -ray spectroscopy 8-56539
 $\alpha\text{-Fe}$, Debye-Waller factors, temp. variation, lattice dynamical calc. 8-55925
Fe, diffusion of alloying elements (*Russian*) 8-79791
 $\alpha\text{-Fe}$, distrib. of dislocations in intersecting pile-ups (*Russian*) 8-87668
 $\alpha\text{-Fe}$, grain boundary segregation of C, N_2 and C Auger spectroscopy 8-72778
 $\alpha\text{-Fe}$, hydrostatic pressure effect on creep rate and failure time 8-92306
Fe I line profiles and magnetic field in quiet network regions of solar photosphere 8-69758
Fe I lines limb shift in solar atmosphere, pressure shifts effect 8-89150
Fe III, Fe VI, electron impact excitation cross sections and gaseous nebulae Fe abundances 8-53806
Fe III, high-spin, in cancer, EPR 8-53466
Fe IV, spectrum, term anal., rel. to RR Telescopio 8-82677
Fe IX, Fe X, forbidden transitions, solar coronal spectrum appl. 8-77537
Fe IX, X, XI, dielectronic recomb. rates in θ -pinch plasma 8-71525
 $\gamma\text{-Fe}$, kinetics of carburisation in CO-He and CO- H_2 atmospheres at 920°C (*German*) 8-85024
 $\alpha\text{-Fe}$, plastic deform. in neck leading to fracture 8-64655
 $\alpha\text{-Fe}$ single crystal whiskers, controlled growth by H reduction of ferrous halides, X-ray and SEM exam. of crystals 8-60554
 $\alpha\text{-Fe}$, stress induced interaction of point defect pairs, in BCC solutions 8-79608
Fe, surface phonon spectra 8-71934
Fe, UPS, density of states determ. 8-52623
Fe whiskers grown from $\text{FeCl}_2\cdot 4\text{H}_2\text{O}$, exam. of growth morphology 8-72051
Fe X and XIV, solar line intensity ratio and coronal temp. determ. 8-73697
Fe XI, XII and XV solar line intensities, OSO-7 obs. of limb brightening 8-69759
Fe XIX, Fe XX, Fe XXI, forbidden lines obs. in solar flares 8-57519
Fe XXI, transition probabilities, energy spectra calcs. 8-70791
Fe XXII, XXIII, Be I and B I like spectra from laser-produced plasma, classification 8-67410
Fe XXIII and XXIV, reson. and intersystem transitions, oscill. strength, lifetime, beam-foil spectra 8-82685
 Fe^{14+} , Fe^{15+} , electron impact ionis. from 3s sub-level 8-90297
 Fe^{19+} , forbidden line in UV, Tokamak plasma diagnostics 8-83602
 Fe^{2+} electroactive species, electrolysis, conc. polarisation at electrode, interferometric investig. 8-68896
 Fe^{3+} ion compounds, effect on Mossbauer spectra of thermal vibrs. rel. to covalently populated 4S shell nucleus 8-72444
 Fe^{3+} , quadrupole antishielding factors, Hartree-Fock perturbation theory 8-62723
 Fe^{119}Sn , pressure dependence of effective magnetic fields 8-52382
 Fe^{133}Xe , heavy ion implantation, recovery, Mossbauer effect meas. 8-52393
 Fe^{172}Yb , hyperfine mag. field, TDPAC meas. 8-52394
Fe:C, decarburisation by H_2 , conversion electron Mossbauer obs. 8-85198
 $\alpha\text{-Fe:He}$, impurity clustering in vacancies bound to edge dislocations 8-91358
 Fe:I , ^{131}I NMR, vacancy associated impurity sites 8-91964
Fe:K(Ar), mag. hyperfine interaction, temp. depend. 8-68420
Fe:Xe, isotope ion implantation control (*Flemish*) 8-79623
 $\text{Fe/Al}_2\text{O}_3$ composite film, optical props., rel. to solar collector appls. 8-72622
 Fe/MgO composite film, optical props., rel. to solar collector appls. 8-72622
Fe-Al interface, O_2 content, reson. α -scatt. from ^{16}O 8-64778
Fe-Co(Ni)(Cu), bimetallic molecule, matrix isolated, Mossbauer spectrum 8-68425
Fe-Co(Ni)(Cu), bimetallic molecule, matrix isolated, Mossbauer spectrum 8-88233
Fe-Ni system, interdiffusion zone growths (*Czech*) 8-84009
Fe-SiO multilayer film, interface magnetisation, neutron Bragg refl. 8-56355
 Fe^{3+} -doped crystals, mag. susceptibility, cryst. field calc. 8-76035
Fe+Fe, symmetric collisions, MO-2pr radiation anisotropy, quasimolecular nature 8-70924
Fe(III), selective separation from rare earth elements on chelate ion exchangers 8-58861
 ^{55}Fe , appl. to determ. of Ti in laterite samples using energy dispersive XRF 8-76955
 ^{55}Fe uptake in marrow, rel. to ^{239}Pu deposition in bone, mouse 8-85395
GaAs:Fe, profile of impurity optical absorption bands 8-56509
GaP:Fe, profile of impurity optical absorption bands 8-56509
 $\text{Gd}_{25}\text{Co}_{75}$, amorphous film, ZZ 8-68014

iron continued

$\text{H}_2\text{+Fe(001)}$, gas-surface reactions, semiempirical generalised LEPS pot. 8-68923
 $\text{KMgF}_3\text{:Fe}$, EPR temp. depend. 8-80202
 $\text{KNbO}_3\text{:Fe}$, ferroelec., anomalous photovoltaic effect and photocond. 8-52449
 $\text{KNbO}_3\text{:Fe}$, single crystals, exam. of crystal preparation 8-60564
 $\text{LiGaO}_2\text{:Fe}$, phosphor, luminesc. 8-92108
 $\alpha\text{-LiIO}_3\text{:Fe}^{3+}$, EPR of impurity ion and radn. induced defects (*German*) 8-84480
 $\text{LiNbO}_3\text{:Fe}$, calc. of photorefractive (*Russian*) 8-90474
 $\text{LiNbO}_3\text{:Fe}$, ferroelectric, treated in Li_2CO_3 , formation of Fe^{2+} state, Mossbauer effect 8-92003
 $\text{LiNbO}_3\text{:Fe}$ crystal conductivity and photoinduced birefringence obs. (*Russian*) 8-60151
 MgO:Fe^{2+} , intrinsic spin-lattice relaxation rates, nonresonant US meas. 8-80203
 MgO:Fe^{2+} , redox behaviour, ESR and X-ray diffr. 8-52341
 MgO:Fe^{3+} , clustering, EPR meas. 8-56372
 MgO:Fe^{3+} , EPR, 94-600K, temp. depend. of cubic spin Hamiltonian parameter 8-60332
 MgO:Fe^{3+} , valence conversion in single crystals, by UV irradiation (*German*) 8-84620
 $\text{MgWO}_4\text{:Fe}^{3+}$, effect of electric field on ESR of Fe^{3+} ions 8-88176
Mo, arc, steady, vac., plasma ion mass and energy diagnostics 8-51385
 $\text{Na}_2\text{O-B}_2\text{O}_3\text{-SiO}_2\text{-Fe}$ glass, near IR optical absorption of Fe (II) 8-84616
NiO:Fe, estimation of 4s covalent bonding of Fe^{2+} and Fe^{3+} ions, Mossbauer spectra 8-72441
Si contaminant, effects on nitridation, mechanism 8-80496
Si:Fe, EPR and neutron activation anal. of thermal defects 8-91355
Si-Fe- H_2 - N_2 , combined effect of Fe and H_2 8-95722
 $\text{Si}_3\text{N}_4\text{-MgO}$, reaction with Fe to produce surface pitting 8-76778
 $\text{SiO}_2\text{:Fe}$, vitreous and cryst., with or without Al_2O_3 , Na_2O additions, exam. of Fe^{2+} coordination, IR spectroscopy 8-88344
 $\text{SrCl}_2\text{:Fe}^{2+}(\text{Co}^{2+})$ electronic absorption spectra in far and middle infrared 8-68537
 $\text{SrCl}_2\text{:Fe}^{3+}$, EPR spectra of $\text{Fe}^{3+}(\text{S}_2)$, 4-100K 8-95512
 $\text{SrO}_2\text{:Fe}^{2+}(\text{Fe}^{3+})$, EPR spectra, evidence for off-centre displacement of Fe^{2+} 8-72398
 $\text{SrTiO}_3\text{:Fe}$, EPR, of Fe^{3+} -rhombohedral, $\text{Fe}^{2+}\text{-V}_0$ and $\text{Fe}^{1+}\text{-V}_0$ complexes 8-76302
YAG:Fe $^{3+}$, ESR absorption spectra, line broadening 8-91940
ZnS:Fe, Raman spectra, impurity induced first order transitions 8-88310
ZnS:Fe, vibr. modes of transition element impurities 8-76472

iron alloys

see also Elinvar; Invar; iron compounds; Permalloy; steel
Alnico 5, thermal treatment in mag. field, mag. props. 8-91905
Alnico, interaction domains after heat treatment in mag. field (*Russian*) 8-68286
Alnico 8 permanent magnet, magnetic props. rel. with crystallographic texture 8-95483
anisotropic precipitation struct. in external mag. field (*German*) 8-72785
BCC and FCC struct., X-ray absorption spectra, Mossbauer spectra, comparison (*Russian*) 8-64299
cast, EM wave propagation, penetration depth calc. (*Bulgarian*) 8-50679
cast, grey, pearlitic Fe, relationship of magnetic props. to condition of C 8-56353
cast Fe, abrasive wear rel. to lamellar or spheroidal graphite content (*German*) 8-85000
cast Fe, Ce hypoeutectic, new phase formation sequence during crystallisation, X-ray obs. (*Russian*) 8-95731
cast Fe, dispersed with interdendritic graphite, eutectoid transformation of austenite during cooling 8-84800
cast Fe, fatigue strength, effect of notches and effective sectional area, for cast Fe with various graphite sizes (*Japanese*) 8-64626
cast Fe, ferritic SG ductile fracture initiation and propagation 8-64661
cast Fe, grey, density variation during slow crystallisation (*Russian*) 8-95737
cast Fe, grey, effect of quenching conditions, on elastic modulus 8-56675
cast Fe, heated in CO atm., obs. cracks around graphite flakes (*Japanese*) 8-84974
cast Fe, high Mg content (0.33%), exam. of phase composition characts. 8-84780
cast Fe, inoculated with Ce, exam. of phase composition 8-56620
cast Fe, Mg treated, graphite modularisation by Mg gas bubbles 8-52867
cast Fe, Mg-Sb, despheroidising composition and distribution of phases, X-ray obs. (*Russian*) 8-95732
cast Fe, Mo distribution 8-92269
cast Fe, nodular graphite, annealed, fracture behaviour at low temps. 8-72875
cast Fe, nodular graphite, welded, struct. exam., heat treatment effects 8-80703
cast Fe, noise reduction by electrolytic coating 8-80681
cast Fe, pearlitic, residual compressive stress distrib. effect on resultant stress conc. in notched samples 8-92336
cast Fe, photometric determ. of Ce (*German*) 8-68955
cast Fe, rare earth-Mg, metallurgical and technological features, appl. in China (*Chinese*) 8-84851
cast Fe, rare-earth-Mg nodular, fracture toughness and fatigue (*Chinese*) 8-95791
cast Fe, spatial dispersion of graphite particles, metallographic study 8-92419
cast Fe, spherical mech. behaviour, continuous theory of dislocations appl. 8-67717
cast Fe, spheroidal graphite, hydrostatic pressure effects on ductile fracture 8-60779
cast Fe, strength and plasticity under hydrostatic pressure 8-56694
cast Fe, white, Cr alloyed, wear resistance, effect on abrasive hardness 8-64722
cast Fe, with Mn, high S, exam. of sulphide phases, cocrystallisation during solidification 8-56646
chromindur, origin of coercivity, Lorentz microscopy, magnetisation and Mossbauer effect 8-64219

iron alloys continued

- chromiur, phase separation, Mossbauer obs. 8-88116
Coulomb and exchange scatt. amplitudes, spin dependent residual resistivities 8-64033
cyclic oxidation, static and dynamic, high temp. alloys 8-88576
 $\text{Fe}_2\text{Co}_{1-x}\text{Ti}_x$ ferromag., high field and high-pressure mag. behaviour 8-91919
ferromagnetic, EMF generation by pulsed laser irradiat. 8-68021
ferrous material fractured surface exam., oxide scale removal 8-95886
fracture toughness of cryogenic temp. 8-72878
grey cast, corrosion resist., Cu alloying additions effect (Russian) 8-56887
grey cast iron, deform. and fracture regions in microzones (Russian) 8-80585
Hastelloy N, Si additions, comp. of eta carbide after ageing 8-52816
Hastelloy B, equilibrium surface bombarded with high dose He^+ ions 8-95091
Haynes alloy 188, SEM exam. of fracture surface, due to low cycle fatigue at 700°C (Japanese) 8-52963
hydrogen embrittlement of Fe and alloys, review of embrittlement mechanisms 8-72853
Incoloy 800, 600 and 718, press. vessel, fatigue design criteria 8-60758
Incoloy 800, austenitic, creep fatigue interaction at 600°C 8-64672
Inconel 600, equilibrium surface bombarded with high dose He^+ ions 8-95091
Inconel 600, fusion reactor vac. vessel, air, N, adsorpt., thermal desorpt., heat treatment effects 8-54880
Inconel 718, superalloy, wear of superhard tool during cutting, SEM and metallographic obs. 8-64720
Inconel alloy 718, exam. of struct., properties and continuum synthesis of ductile fracture 8-76736
Inconel-sheathed MgO -insulated $\text{Pt}_{90}\text{Rh}_{10}/\text{Pt}$ thermocouple, decalibrations during 1200°C use, ion microprobe obs. 8-57957
Kh20N40 alloys, phase composition after quenching, tempering 8-60650
liquid, diffusion of N 8-75862
metalloid-transition metal amorphous surface alloys formed by ion implantation, TEM study 8-67730
 $\text{Mn}_{1.98-x}\text{Cr}_x\text{Fe}_{0.02}\text{Sb}$, Mossbauer effect exam. 8-68432
Monel, Ni-Cu-Fe-Mn, resistance spot weld quality evaluation, using stress wave emission technique 8-53066
Nilomag alloy 771 coloured, X-ray photoelectron spectroscopy of surface film 8-64899
p 8-68232
pig Fe, liquid gas bubble form. at nozzles, acoustic exam. 8-52723
rare earth alloys, RFe_2Al_6 , cryst. struct. mag. props. and hyperfine interactions 8-87648
rare earth intermetallic, amorphous film, cosputtered, struct. and mag. props. 8-60323
rare earth intermetallics, elastic vs. magnetoelastic anisotropy 8-68347
rare earth intermetallics, R_2Fe_7 , conc. depend. of Fe moments 8-56413
rare earth intermetallics, $\text{RFe}_5\text{-}_2\text{Ni}_x$, giant intrinsic mag. hardness 8-56354
rare earth- Fe_2 , magnetomech. coupling and Young's modulus 8-84472
rare earth-Fe, intermetallic compounds, mag. props. (Rumanian) 8-92007
rare earth-Fe alloys, highly magnetostrictive, isotropy breaking magnetoelastic behaviour 8-72386
rare earth-Fe alloys, magnetostrictive, elastic props. 8-84469
rare earth-Fe-Al alloys, RFe_2Al_6 , mag. props. 8-52250
rare earth-Fe-Si(Ge), ThCu_2Si_2 type, lattice parameters 8-51469
Recalloy, Fe-Nb, semihard magnetic alloy, magnetic props., hardness, microstruct. 8-56660
resistivity magnetoresistance, s.p. impurities in ferromag. host 8-68008
Snoek-Koester relaxation and impurity-dislocation interactions (Russian) 8-59834
solute segregation to grain boundaries 8-72780
steel, alloy, Fe-Ni-Mn-Si-Cr-Ni-Mo, effect of metallurgy on stress corrosion cracking, and hydrogen embrittlement 8-60885
steel, Ni-Cr, (4.1, wt.%), isothermal embrittlement, AES exam. of grain boundary segregation 8-60814
susceptibility meas., initial, temperature-time instability, using bridge instrument with electronic demagnetiser (Slovak) 8-57989
thermoelectric force caused by internal adsorption (Russian) 8-95288
Ticonal, interaction domains after heat treatment in mag. field (Russian) 8-68286
transition metal alloy, ferromag., H-impurity complex obs. by magnetic aftereffect 8-72373
twinned martensite structure, influence of plastic deform. (Russian) 8-88493
universal diags. of cohesive strength (Russian) 8-56733
wear resistance, surface hardening processes, review 8-72894
Ag-Fe, implanted, Mossbauer conversion electrons spectroscopy, rel. to dose and annealing temp. 8-52397
Al-Cu-Fe alloys, solid and liquid, exam. of constitution and mag. props. (German) 8-52206
Al-Cu-Mg-Mn-Fe-Si, alloy D16, effect of mechanisothermal treatment on mech. props. 8-56674
Al-Fe, cast, influence of Zr on precipitation, solidification and grain size (Rumanian) 8-84813
Al-Fe, electron irradiated, interstitial-solute complexes, internal friction spectra 8-92289
Al-Fe-Si, eutectic alloy growth, by twinning plane propagation (French) 8-60667
Al-Zn-Mg-Mn, correlation of microscopic features, with macroscopic crack propagation 8-60800
Au-Fe, competing interactions in FCC alloys 8-95453
Au-Fe, dil., approach to saturation of magnetisation 8-56293
Au-Fe, dil., local moments, third harmonic de Haas-van Alphen wave shape anal. 8-84127
Au-Fe, finite mag. clusters near percolation conc. 8-72371
Au-Fe, impurity spin dynamics in magnetic glasses at low frequencies (French) 8-88126
Au-Fe, micromagnet, freq. depend. of susceptibility max. 8-95445
Au-Fe, spin glass in low DC field, mag. viscosity, time decays of remanences 8-64209
Au-Fe, very dil. alloy, Kondo temp. 8-91688
Au-Fe alloy, spin glass, neutron scatt. 8-68265

iron alloys continued

- Au-Fe film spin glass, low temp. resistivity, mean free path effects 8-80163
AuFe, spin glass freezing above ferromag. percolation limit 8-52264
($\text{Au}_x\text{Pb}_{1-x}$) $_1\text{-}_x\text{Fe}_x$, ferromag. and spin glass ordering 8-56335
cast Fe, with Mg despheroidising effect of Bi, Sn on graphite in alloy 8-56670
cast Fe 8-53032
Ce-Fe-Si system, mag. props. in 77-300K range (Russian) 8-56290
 $\text{Ce}_{0.5}\text{Fe}$, absorpt. of D, heats of reaction and equilib. press., T-getters for CTR 8-51683
(Co, Cu, Fe) $_5\text{Ce}$, sintered permanent magnets, magnetic charact. 8-60608
(Co,Cu,Fe) $_5\text{Ce}$, sintered, mag. props. 8-68302
Co-Cu-Fe-Ce, mag. characteristics of sintered permanent magnets 8-60312
Co-Fe alloy, HCP and DHCP, magnetostriction consts. determ. 8-80184
Co-Fe alloys, FCC structure, average mag. moment, conc. depend. 8-88099
Co-Fe-Mn, dil. ferromag. alloy, mag. moment, saturation magnetisation meas. 8-64195
Co-Fe-Nb alloy, mag. precipitation-hardening and Bloch wall pinning 8-80173
Co-Fe-Nb-Mo, semihard magnetic alloy, magnetic props. 8-95469
Co-Fe-Ti (12.6 wt.%), semihard permanent magnet, magnetic precipitation hardening 8-52830
Co-Fe-Ti alloy, precipitation hardened, rel. between struct. and mag. props. 8-95470
 $\text{Co}_{1-x}\text{Fe}_x\text{Si}$, solid solution, optical props. 8-72556
 $\text{Co}_2\text{HfSn-Fe}$, dil., Heusler alloy, Fe hyperfine fields, Mossbauer obs. 8-68424
 $\text{Co}_2\text{TiSn-Fe}$, dil., Heusler alloy, Fe hyperfine fields, Mossbauer obs. 8-68424
 $\text{Co}_2\text{ZrSn-Fe}$, dil., Heusler alloy, Fe hyperfine fields, Mossbauer obs. 8-68424
Cr-Fe, antiferromag. phase boundary, neutron diff. meas. 8-95437
Cr-Fe, low conc. alloys, coexistence of itinerant antiferromagnetism with paramagnetism 8-84386
Cr-Fe (30 wt.%) alloys, refined fine comminution 8-60598
Cr-Fe-V, calc. of phase equilibria using thermodynamic values from different models 8-60646
Cr-Fe-V, dil., V effect on para- to incommensurate and commensurate transitions 8-68260
Cu-Al-Ni-Fe, (10, 5, 5 wt.%), cast microstruct. 8-80535
Cu-Fe, composite, simulation of tensile behaviour and fracture void initiation (Japanese) 8-52948
Cu-Fe, dil., Kondo system, host NMR exam. 8-80246
Cu-Fe, dil., NMR data, ionic model and Kondo temp. 8-68399
Cu-Fe, dil., NMR satellite data, rel. to electronic struct. 8-68398
Cu-Fe, dil., transmission ESR meas. 2 to 40K 8-68364
Cu-Fe, dilute solid soln., exam. of recrystallisation and stored energy 8-52836
Cu-Fe, mixed cryst., Debye-Waller factors, Mossbauer spectra obs. (German) 8-52412
Cu-Fe, supersaturated, spontaneous magnetisation region development, Mossbauer obs. (German) 8-64306
Cu-Fe (1 wt.%), stress induced martensitic transformation of spherical Fe particles, exam. 8-52803
Cu-Fe phase diagram, 650 to 1050°C (German) 8-60658
Cu-Fe-P alloy, CA 196, flat spring, mechanical props. in bending, stress relax. test, 23 to 232°C 8-72806
Cu-Ni-Fe (26.8 wt.%), microduplex struct. form., hardness meas., optical and electron microscopy (Japanese) 8-76659
 $\text{D}_{12}\text{Fe}_{32}\text{O}_2$, anomalous magnetisation, compensated to uncompensated mag. arrangement transition 8-52254
Dy-Fe, amorphous, random anisotropy effects 8-68223
 DyFe_2 , amorphous, struct. determ. EXAFS exam. 8-51421
 DyFe_2 , high field magnetostriction and magnetisation 8-84471
 DyFe_2 , magnetisation and magnetic anisotropy 8-91862
 $\text{Dy(Fe,Ni}_{1-x}\text{)}_2$, mag. behaviour, susceptibility and Mossbauer expts., 4.2-1300K 8-52235
 $\text{Dy}_{0.7}\text{Tb}_{0.3}\text{Fe}_2$, magnetostrictive material, liq. phase sintering 8-64493
 $\text{Dy,Tb}_{1-x}\text{Fe}_2$, and $\text{Ho,Tb}_{1-x}\text{Fe}_2$, high magnetostriction cpd., mag. anisotropy origins 8-68217
 ErFe_2 , excited state spin waves inelastic scatt. meas. 8-76234
 ErFe_2 , Laves phase, cryst. field effects on spin wave dispersion relations 8-84408
(Fe,Co)PBAI, metallic glass, viscous flow, alloying effect 8-79793
(Fe, $\text{Mo}_{0.3}\text{B}_{0.7}$) glassy alloy, Curie temp. and crystn. temp., Mo additions effect, Mossbauer spectra 8-68428
Fe based amorphous alloy, mag. ordered, hyperfine field distrib., NMR meas. 8-68409
Fe based porous metals, exam. of volume change under high pressure 8-52906
Fe-(Cu)-C, sintered parts, struct. stabilisation with C potential control of protective atmosphere 8-60614
Fe-(Mo)- CaF_2 , sintered, friction and corrosion props. for frictional units of nuclear plants 8-60845
Fe-Al, atom-probe field ion microscopy obs. (French) 8-86389
Fe-Al, local ordering, neutron scatt. study 8-64193
Fe-Al, paramag. props., T_c to 1500K 8-68153
Fe-Al (0.069 and 0.158 wt.%), internally oxidised, low temp. deform. (Japanese) 8-52876
Fe-Al (12 wt.%) alloy 23 kHz US transducer piezomagnetic props. 8-59240
Fe-Al (16 wt.%), improvement of certain props. discussion (Chinese) 8-84826
Fe-Al (40 at.%) B_2 type ordered alloy, C migration, resistivity meas. (French) 8-52868
Fe-Al (up to 7.2%), oxidation process 8-85022
Fe-Al eutectic alloy, duplex crystals, unit cell parameters, appl. of Weissenberg technique 8-67684
Fe-Al-C, low C, precip. of carbides and cementite after quenching and ageing 8-52814
Fe-Al-C, mag. permeability disaccommodation 8-88141
Fe-Al-Cr (10, 5 to 10, wt.%), corrosion by coal char, SEM and X-ray diff. exam. 8-88573
Fe-Al-Ni-Co-Cu alloys, Ti alloying and deoxidising addition (Russian) 8-80181

iron alloys continued

- Fe-Al-Si, bending test, mech. props. under high press. and temp. (*Japanese*) 8-76711
- Fe-Al(Cr)(V)(Ti), hardness after nitriding, metallographic, electron microscopic and microprobe anal. 8-51608
- Fe-B, amorphous metallic glasses, high-temp. mag. anal. 8-91258
- Fe-B, binary alloys, giant ΔE effect and Elinvar characts. 8-76291
- Fe-B, metallic glass, Mossbauer investigation of electronic struct. 8-92009
- Fe-B, rapidly quenched metastable solid solns., prop. and mag. props. 8-92218
- Fe-B amorphous alloy, crystallisation kinetics 8-83736
- Fe-B amorphous metallic glasses, low-temp. resistivity in mag. field 8-91667
- Fe-B glass, crystallisation kinetics, elec. resist. meas. 8-83741
- Fe-B metallic glass, hardness, elastic moduli, density, cryst. temp., mech. props., for flywheel appl. (*Dutch*) 8-52878
- Fe-B metallic glass, role of Fe_3B in crystn., mag. and Mossbauer expts. 8-94997
- Fe-B metallic glasses, crystn. kinetics by differential scanning calorimetry 8-91257
- α -Fe-based dil. solid solutions, electronic struct., hyperfine interactions 8-79968
- Fe-Be, formation of quasi-periodic distrib. of precipitates during ageing (*Russian*) 8-56642
- Fe-C, exam. of phase equilibria, at high temp. and pressure 8-52759
- Fe-C, lamellar eutectoid, calorimetric determ. of interfacial enthalpy 8-60668
- Fe-C, levitated drops, carburisation and decarburisation in CO-CO₂ gas mixture, exam. of reaction kinetics 8-85053
- Fe-C, pearlite, eutectoid alloy, efficiency of directional transformation on orientated growth 8-76642
- Fe-C, softening of high purity Fe, by C, due to double kink nucleation (*French*) 8-84949
- α -Fe-C (0.03 wt.%), structural singularities of transition from thermally activated to force-induced fracture (*Russian*) 8-56731
- Fe-C (0.52 wt.%), FCC structure, exam. of electromigration of C by steady state method 8-75865
- Fe-C (1.86 wt.%), exam. of C clustering in martensite, using Mossbauer spectroscopy 8-84821
- Fe-C alloys, thermodynamics of proeutectoid ferrite transform. re-exam. 8-84763
- Fe-C interstitial alloys, electronic structure and ordering of sp defects 8-91639
- Fe-C melt, mag. susceptibility and short range order, 900-1800°C 8-84382
- Fe-C melts, short-range order, neutron scatt. obs. (*German*) 8-71669
- Fe-C solid solution, volume effects on enthalpy and internal energy 8-75839
- Fe-C system, liq.-solid equilib. at high press., influence of graphitising elements (*Russian*) 8-56613
- Fe-C-B, amorphous, room-temp. saturation induction 8-95476
- Fe-C-Cr-Mo(Ni)(V), white cast, effect of abrasion on carbide microstructure (*German*) 8-88540
- Fe-C-Cu (0.21, 0.2 wt.%), neutron irradiated, torsional props. effect of Cu additions and annealing temp. 8-56699
- Fe-C-Fe₃O₄, cleavage initiation by ductile tearing 8-64656
- Fe-C-Ni-Cr, athermal alloy, exam. of martensite transformation kinetics 8-80545
- Fe-C-Ni-Cr(Cu), dynamically hot pressed, mech. props., additives effect 8-60620
- Fe-C-Si, effects of Si on matrix struct. of spheroidal graphite cast iron (*Korean*) 8-60666
- Fe-C(C-B)(C-Si), splat cooled, formation of metastable crystalline phases and glasses 8-88461
- Fe-Co, annealing of point defects produced by plastic deform. (*French*) 8-72829
- Fe-Co, BCC, ferromag., spin wave stiffness constant 8-91851
- Fe-Co, damping capacity of Gentalloy, internal friction meas., mech. and mag. depend. (*Japanese*) 8-52875
- Fe-Co, hyperfine field distrib., temp. and press. depend. 8-91651
- Fe-Co, local environment effect on atomic moments, itinerant model 8-68188
- Fe-Co, partially ordered, elec. cond. 8-91663
- Fe-Co (35 wt.% and 52 wt.%), heat treated, decrease in sensitivity of mag. props. to mech. stresses (*Russian*) 8-56363
- Fe-Co (5 to 25 wt.%), exam. of damping capacity of Gentalloy 8-72800
- Fe-Co alloy, diffusion of H₂, diffusion coefficient and permeability (*Russian*) 8-79819
- Fe-Co alloy particles for mag. tapes, mag. props. 8-95479
- Fe-Co alloys, optical and spectrosc. props. (*Russian*) 8-72529
- Fe-Co-B, metallic glass, Mossbauer investigation of electronic struct. 8-92009
- Fe-Co-C-B, amorphous, room-temp. saturation induction 8-95476
- Fe-Co-Cd(Sn), mag. hyperfine fields at Fe, Cd and Sn sites, Mossbauer and TDPAC meas. 8-60363
- Fe-Co-Mn, dil. alloys, NMR freq. temp. depend., spin echo meas. 8-64296
- Fe-Co-Ni-W alloy, 45KKhVN, plastic deform., electron microscope obs. (*Russian*) 8-80584
- Fe-Co-V, anelastic phenomena, related to atomic order, exam. of magnetostriction (*French*) 8-80579
- Fe-Co-V (2%), annealing of point defects produced by plastic deform. (*French*) 8-72829
- Fe-Co-V(2%) alloy, correl. of resistivity with microstructure 8-72896
- Fe-Cr, amorphous alloy, effect of metalloidal impurities on corrosion resistance and electrochem. behaviour 8-72925
- Fe-Cr, BCC, ferromag., spin wave stiffness constant 8-91851
- Fe-Cr, from ore reduction, metallographic investigation, optical microscopy and SEM (*French*) 8-68648
- Fe-Cr, high purity binary alloy, isothermal decomp. of austenite 8-64525
- Fe-Cr, impact strength, rel. to '475°C brittleness' (*Russian*) 8-92323
- Fe-Cr, Invar alloy, explanation of phys. anomalies (*Russian*) 8-88112
- Fe-Cr, mag. moments and Fe site hyperfine fields, magnetis. obs. 8-76276
- Fe-Cr, oxidation, in H₂/H₂O vapour mixtures, epitaxial oxide phase formation, effect on oxidation 8-88568
- Fe-Cr, role of C in transform. by heating in (α + γ) phase (*French*) 8-52798

iron alloys continued

- Fe-Cr (20 wt.%) high temp. oxidation behaviour with small La additions (0 to 1.3 wt.%) (*Japanese*) 8-85039
- Fe-Cr (26 wt.%) effect of Ni content and austenite phase, on low temp. toughness and embrittlement 8-60754
- Fe-Cr-Al, attenuation and vel. of acoustic shock waves, amplitude depend. 8-63810
- Fe-Cr-Al, elec. heating alloy, effect of rare earth additives on quality (*Chinese*) 8-84825
- Fe-Cr-Al (14, 0.1 to 2 wt.%), oxidation at high temps. (*Japanese*) 8-60872
- Fe-Cr-Al alloys, low temp. sp. ht., resistivity and coercive force 8-63866
- Fe-Cr-Al-Y (Y-Al₂O₃)(Y₂O₃), preparation and exam. of mech. props. 8-52720
- Fe-Cr-C, steel carbide formation during chromising, exam. in terms of ternary phase diagrams 8-56818
- Fe-Cr-Co, effect of heat treatment on strain gauge factor 8-72802
- Fe-Cr-Co (31 wt.%, 23 wt.%), microstruct. and mag. props., ageing and thermomag. treatment effects 8-76769
- Fe-Cr-Co alloys, permanent magnet material development 8-91895
- Fe-Cr-Co-Al (27.5, 17.5, 0.5) alloy, magnetic props. and microstructure 8-72367
- Fe-Cr-Co-Al (27.5, 17.5, 0.5 wt.%) alloy, induced anisotropy 8-76239
- Fe-Cr-Co-Si alloy, interaction domains after heat treatment in mag. fields (*Russian*) 8-68286
- Fe-Cr-Co-V alloy, microstruct. and mag. props. 8-68221
- Fe-Cr-Mo-C, X-ray investigation after friction and oxidation 8-52997
- Fe-Cr-Nb-C, X-ray microanal. of carbide phases rel. to Nb conc. (*Russian*) 8-88467
- Fe-Cr-Ni, electron irradiated, resistivity during annealing, 4.2-1300K 8-87962
- Fe-Cr-Ni, irradiated, Ni segregation to sinks 8-91472
- Fe-Cr-Ni, mag. state at low temps. (*Russian*) 8-56298
- Fe-Cr-Ni, textured (α + γ) alloy, α' lath martensite formation 8-95749
- Fe-Cr-Ni alloy, dual-ion-irradiated, swelling anal. 8-86600
- Fe-Cr-Ni alloys, oxidation-sulphidation in gas mixture, parabolic kinetics, thermochem. diagram 8-72932
- Fe-Cr-Ni-C (23.19, 4.91, 0.025 wt.%), two phase alloy, effect of prestrain above Md temp. on Ms temp. 8-80543
- Fe-Cr-Ni-Cu-Sn, Cu and Sn effect on Cr and Ni segregation (*German*) 8-72777
- Fe-Cr-P-C, amorphous, corrosion resist. in 1N HCl 8-80678
- Fe-Cr-SiC-B₄C powder mixture, compressibility and elec. cond. in cold pressing under low press. 8-60609
- Fe-Cr-Ta, eutectic alloy, exam. of eutectic temp., composition, and oxidation resistance 8-52767
- Fe-Cr-V-C, X-ray microanal. of carbide phases rel. to V conc. (*Russian*) 8-88467
- Fe-Cr-(Co), decomposition of solid soln. in mag. field, neutron and X-ray diffr. study (*Russian*) 8-68694
- Fe-Cu, protective coating on Al powder (*Russian*) 8-60881
- Fe-Cu (1.2 wt.%) effect of precipitation on recrystallisation, texture 8-88476
- Fe-Cu (30 wt.%) alloy, dendrite remelting during isothermal holding, microspin obs. (*Japanese*) 8-71836
- Fe-Cu metastable dil. alloy film, hyperfine interactions 8-52398
- Fe-Dy, dil., implanted impurity hyperfine interaction 8-68417
- α -Fe-Fe₃C alloys, ground surface layer exam. of props. 8-84840
- Fe-Ga, Mossbauer effect for phase transitions, 20-720°C, 25.7-28.3 at.% Ga (*German*) 8-68437
- Fe-Ga, volume change during solid state transformation (*German*) 8-84802
- Fe-Gd amorphous films with comp. gradient, volume and surface hysteresis (*Russian*) 8-88148
- Fe-Gd film, amorphous, mag. props., mean field analysis 8-64236
- Fe-Gd film, amorphous, O₂ contamination effects on mag. props. 8-64231
- Fe-Ge (10 to 50 at.%), phase diagram rel. to heat treatment, supercooling diagram (*German*) 8-92240
- Fe-H system, cold work internal friction peak, appl. of Schoeck's model 8-95771
- Fe-H system, influence of H press. on Fe crit. points and H solubility 8-52758
- Fe-Ir, hyperfine field distrib., spin echo NMR meas. 8-76351
- Fe-Mn, annealed, α - γ phase transformation obs. 8-75831
- Fe-Mn, BCC, ferromag., spin wave stiffness constant 8-91851
- Fe-Mn, effect of N on cryst. lattice parameter of austenite (*Russian*) 8-67683
- Fe-Mn, γ to ϵ phase transform. induced by high press. and plastic deform. 8-68686
- Fe-Mn, plastic deformation mechanism, meas. of microplasticity 8-60720
- Fe-Mn (8 wt.%), quenched, exam. of intergranular embrittlement 8-76745
- Fe-Mn alloy, magnetovolumetric anomaly (*Russian*) 8-64248
- Fe-Mn-As, crystal struct. and magnetic props. of intermetallic cmpds. with Cu₂Sb type struct. (*Japanese*) 8-59785
- Fe-Mn-C system, Gibbs energy, high temp. phase relations 8-80779
- Fe-Mn-C-Si alloy G20, effect of Si and Mn additions on phase composition in multiple γ - ϵ transitions (*Russian*) 8-95743
- Fe-Mn-Co-Ni-Cr, antiferromag. props., Neel temp. determ. 8-88124
- Fe-Mn-Ni, fracture toughness, thermomechanical treatment effects 8-60794
- Fe-Mn(Sb)(Sn), additive effect, on eutectoid transformation of Fe 8-52799
- Fe-Mo, hyperfine field distrib., spin echo NMR meas. 8-76351
- Fe-Mo (1.8%), creep, absence of instantaneous plastic strain upon stress changes 8-75718
- Fe-Mo systems, galvanic cell meas., 1160 to 1366K 8-61042
- Fe-Mo-C alloy, splat cooling, microstruct. changes 8-84855
- Fe-Mo-P-C, amorphous, corrosion resist. in 1N HCl 8-80678
- Fe-N alloy, dil., galvanomag. effects, 4.2-250K 8-87964
- Fe-N single crystals, solid soln. stress assisted nucleation of α' precipitates 8-52810
- Fe-Ni, BCC, ferromag., spin wave stiffness constant 8-91851
- Fe-Ni, brittle transgranular and intergranular fatigue crack growth rate, yield strength effect 8-68786
- Fe-Ni, dil., point defect relax. after low temp. neutron irradi. 8-52316

iron alloys continued

- Fe-Ni, effect of plastic deform. and martensitic transformation on Fe atom mobility (*Ukrainian*) 8-55974
- Fe-Ni, elect. phenomena rel. to martensitic avalanche (*French*) 8-68691
- Fe-Ni, electrodeposition, mag. props. (*French*) 8-64488
- Fe-Ni, FCC, anomalous props. at high temp. and new phase (*Japanese*) 8-80520
- Fe-Ni, FCC and BCC lattices, X-ray characteristic temp. (*Russian*) 8-67797
- Fe-Ni, fracture toughness of cryogenic temp. 8-72878
- Fe-Ni, hot shortness (*Japanese*) 8-84998
- Fe-Ni, hydrogenated, Mossbauer effect meas. 8-92002
- Fe-Ni, hyperfine field distrib., temp. and press. depend. 8-91651
- Fe-Ni, Invar alloy, explanation of phys. anomalies (*Russian*) 8-88112
- Fe-Ni, local ordering, neutron scatt. study 8-64193
- Fe-Ni, low frequency power losses 8-95466
- Fe-Ni, martensite burst transformation, supercooling 8-84806
- Fe-Ni, martensitic transform. dynamic, quasi-static atomic displacements, NGR, X-ray and electron scatt. meas. (*Russian*) 8-68688
- Fe-Ni, N27T2 and N28, internal friction peaks after reverse martensitic transform. (*Russian*) 8-92287
- Fe-Ni, optical and electronic characs., 20-1750°C, comp. depend. (*Russian*) 8-84601
- Fe-Ni, taenite, superstruct. in Fe meteorites 8-61820
- Fe-Ni, thermal conductivity, data anal. and synthesis 8-95284
- Fe-Ni, XPS obs. of Fe 2p states 8-52625
- Fe-Ni, yield stress, temp. depend. (*Russian*) 8-56691
- Fe-Ni (19wt.%), oxidation in CO₂, 700 to 1000°C, kinetics study 8-72931
- Fe-Ni (20 to 100 wt.%), exam. of C diffusion coeff., in temp. range 950 to 1100°C 8-51747
- Fe-Ni (29 at.%), calc. of elastic interaction between locally transformed regions with screw and edge dislocations 8-83844
- Fe-Ni (3 wt.%), grain boundary segregation of Sn and P embrittling additions, STEM microanal. 8-76654
- Fe-Ni (3 wt.%), grain boundary segregation microanal. using X-ray (STEM) and AES 8-87685
- Fe-Ni (3 wt.%), influence of temper embrittlement, on stress corrosion susceptibility 8-85023
- Fe-Ni (35 at.%), fine coherent effects, neutron diffr. study (*Russian*) 8-75502
- Fe-Ni (8 wt.%), monocrystal, thermodynamics of growth, model (*French*) 8-87635
- Fe-Ni alloy, cold work stored energy effect on mag. moment vs. temp. curve 8-95419
- Fe-Ni alloy, surface decarburisation rate in dry H₂, soft mag. material manufacture 8-60882
- Fe-Ni alloy toroidal core, magnetic noise (*Russian*) 8-60308
- Fe-Ni alloys, struct. of γ and α -phases near martensitic transform. point (*Russian*) 8-64541
- Fe-Ni base metallic glass, annealing embrittlement 8-64635
- Fe-Ni liquid alloy, physical and chemical props. deviations from Raoult's law (*Russian*) 8-95729
- Fe-Ni melt, short-range order, m.p. to 1750°C (*Russian*) 8-94966
- Fe-Ni mixed powders, effect of Ni particle size and unequal interdiffusion, on sintering process (*Japanese*) 8-84728
- Fe-Ni/pure Fe exchange coupled films, mag. reversals, hard layer thickness effects (*Russian*) 8-56359
- Fe-Ni-Al, correlation of microscopic features, with macroscopic crack propagation 8-60800
- Fe-Ni-Al alloys, phase diagram, miscibility gap, DTA meas. 8-92237
- Fe-Ni-Al-Ti, N27Yu2T2, aged austenite, diffuse electron scatt. distrib. during martensitic deform. (*Russian*) 8-60669
- Fe-Ni-B, metallic glass, Mossbauer investigation of electronic struct. 8-92009
- Fe-Ni-B-(P) amorphous alloys, mag. annealing mechanism, induced anisotropy 8-95484
- Fe-Ni-C, martensitic, H₂ effect on fracture charact. (*Czech*) 8-60746
- Fe-Ni-C, N31, austenite state in premartensitic temp. interval (*Russian*) 8-56634
- Fe-Ni-C, role of strain in deform. induced martensitic transform. (*Japanese*) 8-92263
- Fe-Ni-C, thin foil, high voltage TEM exam. of martensitic form. 8-92264
- Fe-Ni-C (24, 0.45 wt.%), martensites, TEM observation of double twinning 8-76651
- Fe-Ni-C (26.4, 0.24 wt.%) martensite, partially twinned, slip lines obs. 8-84913
- Fe-Ni-C (31.24, 0.21 wt.%) effect of deformation and ageing after deformation, on martensitic transformation temp. 8-76650
- Fe-Ni-C alloy, external stress effects on equilibrium morphology, thermodynamic model (*Russian*) 8-52804
- Fe-Ni-C austenite, effects of strain rate grain size, temp., on yield stress 8-72821
- Fe-Ni-C-B, and Fe-Ni-Co-B-C-Si, amorphous, room-temp. saturation induction 8-95476
- Fe-Ni-Co, rel. between induced uniaxial anisotropy and coercive force 8-91904
- Fe-Ni-Co-B-P soft magnetic metallic glasses, status report 8-64226
- γ -Fe-Ni-Cr, mag. struct., neutron scatt. study (*Russian*) 8-68160
- Fe-Ni-Cr (25, 15 wt.%), high temp. creep, dispersed γ -Ni₃(Al, Ti) effects (*Czech*) 8-64590
- Fe-Ni-Cr coating, electrodeposited, exam. of passivity 8-80655
- Fe-Ni-Cr-C, effect of austenite yield strength, stacking fault energy, on martensite morphology 8-80546
- Fe-Ni-Cr-Mn-Al-Ti Incoloy 800, exam. of scale morphology, alloying element distrib. after oxidation 8-80677
- Fe-Ni-Cr-P-B, Metglas 2826A, hardness, elastic moduli, density, cryst. temp., mech. props., for flywheel appl. (*Dutch*) 8-52878
- Fe-Ni-Cr-Ti, superalloy A286, powder, exam. of microstruct. and mech. properties 8-52979
- Fe-Ni-Cr-Ti-Mn-Mo, (25.8, 14.04, 2.17, 1.27, 1.30 wt.%), superalloy A-286, precipitation hardening, exam. of fracture toughness and mech. props. 8-92355
- Fe-Ni-Mn, dil. alloys, NMR freq. temp. depend., spin echo meas. 8-64296
- Fe-Ni-Mn, martensitic transforms., expt. investigation (*French*) 8-84803
- Fe-Ni-Mn-H, ferromag., magnetisation curves 8-88144

iron alloys continued

- Fe-Ni-Mo, ferrite plus martensite structures, exam. of mech. props. 8-56709
- Fe-Ni-Mo, inhomogeneous solid solns., annealed and work hardened states, X-ray K-absorption spectra (*Russian*) 8-56544
- Fe-Ni-Si, double spontaneous reversible deformation during thermal cycling 8-84942
- Fe-Ni-Te alloy system, first-order phase transformation obs. 8-64533
- Fe-Ni-V-Co, Co influence on age hardening (*Russian*) 8-68703
- Fe-Pd, FCC, ferromag., spin wave stiffness constant 8-91851
- Fe-Pd (50 at.%), ordering under load, nuclear gamma reson. obs. (*Russian*) 8-92258
- Fe-Pt, Invar type, strong ferromagnetism, mag. props. 8-64197
- Fe-Pt, nearly thermoelastic, irreversible lattice defects formed by martensitic transform. cycles 8-60671
- Fe-Pt, ordered, anisotropy of mag. props. (*Russian*) 8-60280
- Fe-Pt (23,24,25 at.%), effect of austenite ordering on some thermoelastic transform. factors 8-88466
- Fe-Pt (24 at.%), colour metallographic technique, for studying microstructural reproducibility, in martensitic transformations 8-72954
- Fe-R alloys, mag. elastic properties 8-52331
- Fe-Rh, hyperfine field distrib., spin echo NMR meas. 8-76351
- Fe-S-C (1.3 wt.%), sulphidised Fe-graphite bearing materials, sintering, struct. form. 8-60601
- Fe-Si, grain oriented, core losses (*Japanese*) 8-60303
- Fe-Si, grain oriented, effect of tensile stress on domain struct. 8-95462
- Fe-Si, liq. alloys, surface tension, sessile drop method meas. (*French*) 8-84029
- Fe-Si, low frequency power losses 8-95466
- Fe-Si, low-temperature fatigue crack propagation 8-72876
- Fe-Si, plastic deform., synchrotron X-ray topography dynamic expts. 8-67621
- Fe-Si, plastic deformation mechanism, meas. of microplasticity 8-60720
- Fe-Si, polycrystalline, exam. of stress-strain state of individual grains 8-80580
- Fe-Si, ribbon-form material, rapid quenching from melt (*Japanese*) 8-92210
- Fe-Si, stress and plastic deform. effect on Barkhausen effect, instrumentation 8-52313
- Fe-Si, thermally activated motion of 180° Bloch wall 8-95457
- Fe-Si, yield stress, temp. depend. (*Russian*) 8-56691
- Fe-Si (1%), LEED-Auger exam. of (110) surfaces 8-71915
- Fe-Si (10 wt.%), effect of short range order on yield stress (*German*) 8-52932
- Fe-Si (2.35 wt.%), misorientation dependence of grain boundary segregation, Auger spectroscopy exam. 8-76629
- Fe-Si (3 wt.%), degeneration of slip on (211) planes (*Russian*) 8-80587
- Fe-Si (3 wt.%), domain wall spacing and losses, orientation depend. 8-56343
- Fe-Si (3 wt.%), domain wall drift due to nucleation during cyclic magnetisation 8-95461
- Fe-Si (3 wt.%), effect of heating rate during primary recrystn. on props. after secondary recrystn. 8-84837
- Fe-Si (3 wt.%), exam. of plastic deformation, slip band dislocation, under hydrostatic pressure 8-56695
- Fe-Si (3 wt.%), Goss oriented, stress effects 8-91916
- Fe-Si (3 wt.%), grain oriented, lowest core loss 8-91887
- Fe-Si (3 wt.%), grain orientated, negative magnetostriction, theory 8-91917
- Fe-Si (3 wt.%), grain oriented, domain wall variation throughout magnetisation cycle 8-95459
- Fe-Si (3 wt.%), grain oriented, power loss depend. on domain wall bowing 8-95460
- Fe-Si (3 wt.%), grain oriented, MnS precipitate distribution, electron microscope observation (*Chinese*) 8-95751
- Fe-Si (3 wt.%), loss prediction, from distorted waveforms 8-76273
- Fe-Si (3 wt.%), orientation development during secondary recrystallisation, primary matrix effect, magnetic props. (*Czech*) 8-60679
- Fe-Si (3 wt.%), polycryst. (110), synchrotron radiation topographs and mag. domain obs. 8-67620
- Fe-Si (3 wt.%), rotational power losses, freq. depend. 8-91888
- Fe-Si (3 wt.%), secondary recrystallisation, effect of composition and original orientation 8-68707
- Fe-Si (3 wt.%), total losses under tensile stress, rel. to orientation near (110)[001] 8-76272
- Fe-Si (3 wt.%), transformer laminations, processing and props. 8-52325
- Fe-Si (3 wt.%) steel, high permeability, grain oriented 8-91886
- Fe-Si (3 wt.%) struct. and texture changes during repeated deform.-recrystn. (*Russian*) 8-88474
- Fe-Si (3.5 wt.%), cutting of bicrystal to compare mechanism for large crystals and polycrystals (*Japanese*) 8-60871
- Fe-Si (3.5 wt.%), magnetisation reversal and domain walls 8-84451
- Fe-Si (3.5 wt.%) picture frame cryst., domain wall bowing dynamic neutron depolarisation 8-56344
- Fe-Si (3.5 wt.%) picture frame, domain wall bowing, time-depend. neutron depolarisation 8-95458
- Fe-Si (3.72 wt.%) fatigue failure in vacuum and air 8-68789
- Fe-Si (6.5 wt.%), ductility and mag. props., Ni and Mn addition effects 8-76704
- Fe-Si amorphous film, conversion electron Mossbauer effect 8-72440
- Fe-Si amorphous film, Hall const. and magnetoresistive effect 8-52105
- Fe-Si film, amorphous, conversion electron Mossbauer study 8-84507
- Fe-Si layer, growth kinetics and morphology 8-95700
- Fe-Si-Al (6.4 wt.%), Sendust alloy, effect of Ni content on mag. props. 8-72897
- Fe-Si-B magnetic powder, amorphous, prep. by atomisation technique 8-92213
- Fe-Si-Mn, effect of Mn addition on mag. props. and elec. resist. 8-91890
- Fe-Si-Ti(Zr)(V)(Nb), eutectic alloy, exam. of eutectic temp., composition, and oxidation resistance 8-52767
- Fe-Si(Cr)(Ni)(Mn)(C), alloy layers formed by reaction with molten Al, X-ray, EPMA anal., hardness meas. (*Japanese*) 8-72926
- Fe-Si(Ni)(Cu)(Mn)(C), dissolution rate into molten Al, convection mass transfer (*Japanese*) 8-71858

iron alloys continued

- Fe-Ti (0.056 at.%), mobile dislocations during stress relaxation 8-68721
- Fe-Ti (0.056 at.%), mobile dislocations during stress relaxation 8-68722
- Fe-Ti-Sb-C alloys, Sb trapping effect on temper embrittlement, ion beam study 8-92312
- Fe-TiB₂, eutectic alloy, high temp. props. 8-84931
- γ-Fe-transition metal alloy, mag. moment in FCC d-metal lattices (*Russian*) 8-72337
- α-Fe-V, dilute alloy, Mossbauer diffusion line broadening, exponential fitting evaluation 8-52379
- Fe-V, local environment effect on atomic moments, itinerant model 8-68188
- Fe-V, with atomic short range order, local environment effects on electronic struct. 8-67936
- Fe-W-Cr-Mo-Co with austenitic phase, magnetic and mech. props., cold working and ageing effects (*Japanese*) 8-60678
- Fe-W-P-C, amorphous, corrosion resist. in 1N HCl 8-80678
- Fe-Y, amorphous, resist. and magnetoresist. meas., local moment system 8-68018
- Fe-Zn, liquid-solid reaction in Zn bath, effect of Fe concentration, alloy layer growth, exam. (*Japanese*) 8-85037
- Fe-Zn, multiphase diffusion 8-79822
- Fe-Zn, phase diagram, ferrite-austenite phase boundaries, X-ray diffr. exam. (*German*) 8-80510
- Fe-Zn, stable and metastable alloys, order-disorder, mag. interactions and corrosion behaviour 8-68422
- Fe₄₀Ni₄₀B₂₀, amorphous alloy, ductile-brittle transition temp., relation to composition 8-52972
- (Fe-Ni)_{1-x}(SiO)_x, cermet film, internal stresses (*Russian*) 8-75951
- FeAl B2 struct., band struct. and density of states, KKR calc. 8-63969
- FeAl, bonding, self-consistent energy bands 8-91610
- FeAl, isomer shift, electronic charge density 8-80264
- FeAl, positron localisation in metallic alloys 8-79962
- Fe₃Al, magnetic form factor 8-76222
- Fe₃Al, ordered alloys, atomic order parameters from topology of electron-microscope diffr. contrast from antiphase boundaries, quantitative determ. 8-95016
- Fe₃Al, ordered binary alloy, computer simulation of radiation effects 8-87709
- Fe₃Al, partly disordered B2 struct., spin wave dispersion relation 8-64201
- Fe₃Al, slip geometry and pseudoelastic behaviour, effect of crystal orientation (*French*) 8-87681
- Fe_{49.7}Al_{50.3}, Compton scatt., 59.54 keV γ-rays, charge transfer study 8-68578
- Fe_{1-x}Au_x, amorphous, elec. resist., temp. depend., spin wave contrib. and resist. minimum 8-51961
- Fe_{0.8}B_{0.2} alloy amorphous thin films, anisotropic mag. and microstruct. props. 8-95487
- Fe_{100-x}B_x (11.5 ≤ x ≤ 22), magneto-volume effect 8-91922
- Fe_{100-x}B_x, mag. and struct. props., comp. depend. 8-60314
- Fe_{100-x}B_x metallic glass, magnetisation meas. 8-80134
- Fe₈₀B₂₀, crystallisation of amorphous alloys, TEM and X-ray diffr. exam. of struct., growth characts. 8-79539
- Fe₈₀B₂₀, evaluation of complex Mossbauer spectra 8-60370
- Fe₈₀B₂₀, ferromagnetic metallic glasses, Brillouin scattering 8-92085
- Fe₈₀B₂₀, magnetostriction, temp. depend. 8-91921
- Fe₈₀B₂₀, metallic glass, Mossbauer spectroscopy 8-60365
- Fe₈₀B₂₀ Metglas, Mossbauer spectra line broadening 8-52400
- Fe₈₀B₂₀, sputter deposited amorphous, low field mag. props. 8-68335
- Fe₃C, cementite, modified by rare earth metal and alloying additions, thermal stability (*Russian*) 8-56663
- Fe_{1-x} amorphous sputtered film, mag. props. 8-68311
- FeCo, ordered alloy, 550°C change, study through elec. cond. and specific heat meas. 8-56633
- Fe_{0.65}Co_{0.35}B, crystalline disordered, evaluation of complex Mossbauer spectra 8-60370
- (FeCoNi)₈B₂₀, glass, evidence supporting split-band model from magnetostriction 8-95509
- (Fe_{0.9}Co_{0.1})_xSi_{1-x}B₂, (Fe_{1-x}Co_x)₇₈Si₈B₁₄ amorphous ribbons, magnetomech. coupling and saturation magnetostriction 8-68353
- Fe₃Co₇₀Si₁₃B₁₀, amorphous toroidal core, switching characts. and domain struts. 8-95477
- (Fe_xCo_{100-x})_{100-(y+z)}Si_yB_z amorphous ribbon, mag. moment and Curie temp., comp. depend. 8-95421
- FeGe, hexagonal, low-temp. mag. struct., neutron diffr. meas. 8-95418
- FeGe₂, mag. struct., Mossbauer method 8-60268
- Fe_xGe_{1-x}, amorphous, mag. behaviour, rel. to Fe_xSi_{1-x} and Fe_xSn_{1-x} amorphous alloys 8-95478
- Fe_xGe_{1-x} amorphous alloys, conversion electron Mossbauer spectroscopy 8-84504
- Fe₃Mn_{1-x}Pt_x, ferro-antiferromag. transform. at 4.2K (*Russian*) 8-88117
- Fe₃-Mn₅₁Si, evidence for the ang. depend. of the hyperfine interactions 8-76241
- Fe₂Mo, standard Gibbs energies, enthalpies, entropies of formation 8-61042
- Fe₃Mo₂, standard Gibbs energies, enthalpies, entropies of formation 8-61042
- Fe₇₈Mo₂B₂₀, exam. of mag. props. between 300 and 900K 8-85010
- FeNi-Cu, composite fibre and layer struts., anomalous props. caused by internal phase boundaries 8-72754
- Fe_{1-x}Ni_x (x < 29at.%), γ-phase dispersion, Mossbauer spectra 8-52399
- Fe₆₅Ni₃₅, quasi-localised spin system, neutron scatt. 8-68194
- Fe₄₀Ni₄₀B₂₀, metallic glass, embrittlement kinetics and crystn., quenching influence 8-68766
- Fe₅₀Ni₃₀B₂₀, crystallisation of amorphous alloys, TEM and X-ray diffr. exam. of struct., growth characts. 8-79539
- Fe₆₅(Ni_{1-x}Cr_x)₃₅, remanent magnetisation, temp. depend., anomalies near Curie temp. (*Russian*) 8-60310
- Fe₃₂Ni₃₆Cr₁₄P₁₂B₆, Metglas 2826A, Hall resistivity, effect of thermal cycling and annealing 8-56125
- Fe₃₂Ni₃₆Cr₁₄P₁₂B₆, shear band form. 8-68756
- Fe₄₀Ni₃₈Mo₂B₁₈ glassy alloy, high permeability, low field mag. characts. 8-68501
- Fe₄₀Ni₄₀P₂₀, amorphous alloy, ductile-brittle transition temp., relation to composition 8-52972

iron alloys continued

- (Fe_{1-x}Ni_x)₈₀P₁₀B₁₀, amorphous microwires, magnetisation reversal and anisotropy 8-91885
- Fe₄₀Ni₄₀P₁₄B₆, (Metglas 2826), ferromag. Curie temp. determ. 8-64206
- Fe₄₀Ni₄₀P₁₄B₆, amorphous alloy, ductile-brittle transition temp., relation to composition 8-52972
- Fe₄₀Ni₄₀P₁₄B₆ amorphous ribbon, mag. anisotropy distrib. near surface 8-95430
- Fe₄₀Ni₄₀P₁₄B₆, amorphous toroidal core, switching characts. and domain struts. 8-95477
- Fe₄₀Ni₄₀P₁₄B₆, ferromagnetic metallic glasses, Brillouin scattering 8-92085
- Fe₄₀Ni₄₀P₁₄B₆, Metglas 2826, amorphous ribbon core, appl. in force transducer 8-93669
- Fe₂Ni_{80-x}P₁₄B₆, amorphous, sp. ht. and susceptibility meas., spin glass and micromag. props. 8-68274
- Fe₂Ni_{80-x}P₁₄B₆ metallic glasses, low temp. resistivities 8-91659
- (Fe_{0.5}Ni_{0.5})₇₅P₁₅B₅Al₃ glass, struct. relax. as origin of Curie temp. ageing 8-84418
- (Fe_{1-x}Ni_x)₇₅P₁₅B₅Al₃, amorphous alloy, low temp. elec. resist. saturation 8-68005
- Fe₂₉Ni₄₉P₁₄B₆Si₂, Metglas 2826B, Hall, elec. resist., magnetisation and heat capacity meas. 8-68019
- Fe_{0.75}P_{0.15}Co_{0.10}, amorphous, mag. excitations and static struct., neutron scatt. obs. 8-68204
- Fe₇₅P₁₅C₁₀ amorphous foil, ferromag. domain orientation, Mossbauer exam. 8-52402
- Fe₇₅P₁₅C₁₀, temp. depend. of the ΔE-effect 8-80188
- Fe₈₀P₁₃C₇, amorphous toroidal core, switching characts. and domain struts. 8-95477
- FePd epitaxial film, vacuum-deposited, for thermomag. recording, mag. and magneto-optical props. (*Russian*) 8-60319
- Fe_{1-x}Pd_x film, air-exposed, comp. profiles by AES, ESCA and ion sputtering 8-95245
- Fe_{1-x}Pd_x film, UHV deposited, effects of applied stress on B-H loops 8-64239
- Fe₃₄Pd₄₆P₂₀, amorphous, sp. ht. and resist. near ferromag. phase transition 8-56333
- FePt epitaxial film, vacuum-deposited, for thermomag. recording, mag. and magneto-optical props. (*Russian*) 8-60319
- FePt₃, neutron scattering study of spin waves 8-91856
- Fe₃Pt, Invar alloy, theory of elastic-anomalies 8-95505
- Fe₃Pt, quasi-localised spin system, neutron scatt. 8-68194
- Fe₇₂Ti₂₈, ferromagnetic Invar alloy, lattice vibrations 8-91403
- Fe₄₈Rh₅₂, hyperfine mag. field at ⁵⁷Fe and ¹¹⁹Sn nuclei, press. depend. (*Russian*) 8-80266
- FeSb₂, phase structure, X-ray crystallography (*French*) 8-91305
- Fe_{1-x}Sb_x, phase structure, X-ray crystallography (*French*) 8-91305
- FeSi, NMR and μSR, microscopic mag. props. (*Japanese*) 8-52368
- FeSi-graphite-SiC refractory, oxidation loss and wettability of inorganic fluxing materials (*Japanese*) 8-84755
- Fe₃Si, etching of slip produced antiphase domain boundaries 8-63769
- Fe₃Si-based alloy, dil., cond. electron polarisation and moment perturbations 8-68224
- Fe₃Si-based dil. alloys, conduction electron polarisation, moment perturbations 8-68225
- Fe₃₄Si_{1-x}, electron transport 8-91669
- Fe₂Si_{1-x}, amorphous, mag. behaviour, rel. to Fe_xSn_{1-x} and Fe_xGe_{1-x} amorphous alloys 8-95478
- Fe_xSi_{1-x}, amorphous, struct. and mag. props., giant moment form. at mag. ordering 8-68192
- Fe₂SiB₂, Mossbauer spectra, 140-784K, spin rotation 8-52409
- Fe₇₅(Si_{0.8}B_{0.5})₂₅ film, amorphous, sputtered, ferromag., thermal stability 8-76280
- Fe₇₈Si₁₀B₁₂, amorphous toroidal core, switching characts. and domain struts. 8-95477
- Fe_xSn_{1-x}, amorphous, mag. behaviour 8-95478
- Fe_xSn_{1-x} amorphous alloy films, magnetisation meas. and Mossbauer spectra 8-95489
- FeTi crystals, use in storage and production of superpure H₂ (*German*) 8-53184
- FeTi, hydrogenation, effect of surface segregation on mag. props. 8-84819
- Fe₂Ti-Fe eutectic alloy, directional solidification singularities (*Russian*) 8-68678
- Fw-W(Co)(Ni)(Mo)(Nb)(Cr)(V), dil. system, high freq. induction melting and centrifugal casting, working curve sample prep. photoemission anal. (*Japanese*) 8-53050
- Gd-Co-Fe film, amorphous, bias-sputtered, uniaxial perpendicular anisotropy 8-64234
- Gd-Fe, amorphous film, thermomagnetic writing 8-84428
- Gd-Fe, CPA calcs., moments and transition temps. 8-52252
- Gd-Fe alloy amorphous thin films, anisotropic mag. and microstruct. props. 8-95487
- Gd-Fe amorphous sputtered films, magnetoelastic contrib. to perpendicular anisotropy, internal stress meas. 8-95490
- Gd-Fe film, amorphous, in-situ ion beam sputtered, microstruct. and Lorentz mag. struct. 8-63947
- Gd-Fe film, amorphous, mag. props., annealing effects 8-64235
- Gd-Fe film, amorphous, microstruct. and magnetism 8-64230
- Gd-Fe film, amorphous, preferential resputtering effect induced anisotropic distrib. of atomic pairs 8-63950
- Gd-Fe-Y, amorphous film, thermomagnetic writing 8-84428
- Gd(Fe_{1-x}Co_x)₂, ferromag. reson. of pseudobinary cubic compounds 8-91961
- Gd₂Y_{1-x}Fe_x, s-d exchange interaction integral, change due to hydrostatic compression 8-88199
- Gd₂Y_{1-x}Fe_x, saturation magnetisation, magnetostriction, Curie temp., ferrimag. ordering, exchange field (*Russian*) 8-68343
- Ge-Se-Fe films, metallic and semicond., amorphous, mag. and elec. props. 8-52319
- HoFe₂, amorphous, struct. determ., EXAFS exam. 8-51421
- HoFe₂, spin wave and cryst. field excitations, neutron scatt. 8-68196
- Ho(Fe_{1-x}Ni_x)₂, mag. behaviour, susceptibility and Mossbauer expts., 4.2-1300K 8-52235
- Ho₂Tb_{1-x}Fe_x, and Ho₂Tb_{1-x}Dy_{1-x-y}Fe_y, high magnetostriction cpd., mag. anisotropy origins 8-68217
- Ho₂Tb_{1-x}Fe_x, Laves phase, mag. anisotropy meas., cubic harmonic anal. 8-84410
- Ho₂Tb_{1-x}Fe_x, single cryst., spin orientations 8-84425

iron alloys continued

- Ho,Tb_{1-x}Fe₂, single crystals, continuous spin orientations, magnetisation easy direction 8-84453
 La-Fe, amorphous alloy film, spin reson. meas. 8-68389
 La-Fe, liquid quenched, X-ray diffr. and Mossbauer effect exam. of structure 8-76678
 Lu-Fe, amorphous alloy film, spin reson. meas. 8-68389
 γ -Mn-Fe, FCC \rightarrow FCT transform. temp. and Neel temp., X-ray and neutron diffr. expts. (*Russian*) 8-84797
 Mn_{1-x}Fe_xAs, high-pressure phase, magnetic properties 8-52247
 Mn_{1-x}Fe_xAs, mag. props. in ground state (*Russian*) 8-56294
 Mn_{2-x}Fe_xSb, Mossbauer effect exam. 8-68432
 Mo-Fe-O-H system, thermodynamic equilib. 8-60657
 Mo-Mn-Fe-Si/Al₂O₃ ceramic seal, interfacial phases 8-72011
 Nb-Mo-Fe, dil., local environment and mag. props. 8-64187
 Nb₅₀Ni_{50-x}Fe_x, amorphous, mag. ordering and local random anisotropy 8-68273
 Nb₅₀Ni_{50-x}Fe_x, amorphous alloy, mag. interactions 8-95432
 Nd,Fe_{1-x} film, amorphous, mag. props. meas. 8-68312
 Ni-Cr-Fe (15.7, 7.63 wt.%), Inconel 600, anal. of pit generation by 3.5% NaCl by stochastic theory (*Japanese*) 8-85038
 Ni-Cr-Fe-Mo-Co (21.41, 19.28, 8.64, 2.16 wt.%), Hastelloy alloy X, exam. of thermal stability 8-84865
 Ni-Cr-Ti-Al-Fe-Co (19.65, 2.40, 1.37, 0.78, 0.52 wt.%), strength of γ' hardened alloy, ageing exam. 8-88501
 Ni-Cr-Ti-Al-Mo-Nb-Fe (13-16, 2.35-2.75, 1.3-1.7, 2.8-3.2, 1.8-2.2, 2.0 wt.%), heat resistant props, mech props. struct., stepwise ageing effects (*Russian*) 8-76666
 Ni-Fe, epitaxial thin film, mag. structures and stresses, ferromag. resonance 8-72375
 Ni-Fe, film, anomalous Hall and Nernst-Ettingshausen effect, contribution of phonon and impurity scatt. (*Russian*) 8-64145
 Ni-Fe, film, domain struct., effect of biaxial stresses 8-88153
 Ni-Fe alloy, extraordinary viscous magnetic wall motion 8-84465
 Ni-Fe alloy, FCC, density, lattice parameters, X-ray diffr. and hydrostatic weighing 8-55904
 Ni-Fe film, effect of tensile stress on mag. domain struct. 8-68332
 Ni-Fe film, unidirectional anisotropy by exchange coupling, appl. to biasing of magnetoresist. read head 8-91907
 Ni-Fe films, US generation by ferromag. reson. 8-88155
 Ni-Fe protective coatings on Al powder (*Russian*) 8-60881
 Ni-Fe solid soln., precip. hardened, paramag.-ferromag. transition on ageing 8-52255
 Ni-Fe-Co film, magnetoelastic vibr. generation during high freq. mag. reversals (*Russian*) 8-60320
 Ni-Fe-Mn, ferromag. reson. linewidth and saturation magnetisation 8-72418
 Ni-Fe-Nb, Hardperm alloy, sheets, effect of sheet thickness, and annealing, on mag. props. 8-76772
 Ni-Fe-Nb, mag. props. and struct. (*Chinese*) 8-84450
 Ni-Fe-Nb-Al, mag. props. and struct. (*Chinese*) 8-84450
 Ni₃(Fe,M), M=Cu, Cr, Mo, W, kinetic phenomena rel. to ordering and electron struct. (*Russian*) 8-76043
 NiFe soft magnetic alloys, magnetic props., effect of annealing and fabrication (*German*) 8-53004
 Ni₃Fe, disordered single crystals., thermo-activated mechanism of plastic deform. (*Russian*) 8-84909
 Ni_{1-x}Fe_xAl, self-consistent embedded-cluster model for mag. impurities 8-67973
 Ni₄₀Fe₃₀B₁₀, magnetostriction, temp. depend. 8-91921
 Ni₃Mn₉₀Fe₁₀Sn, Fe site hyperfine field and mag. moment, Mossbauer effect meas. 8-76365
 Pd-Fe, dil., ferromag., magnetoresist. 8-91665
 Pd-Fe, Mossbauer spectra, scatt. and transmission geometries, differences in crit. behaviour near T_c 8-76367
 Pd-Fe alloy, IR absorpt. characts., 0.9 to 19 μ m, mag. order effect 8-84577
 Pd-Fe-Mn alloy, spin glass-ferromagnetic systems, differential susceptibility 8-88131
 Pd₃Fe, hyperfine interactions during atomic ordering, Mossbauer obs. (*Russian*) 8-56630
 Pd₇₀Fe₁₀Si₂₀ alloy, amorphous to cryst. transition, 350 to 450°C, Mossbauer spectra 8-59758
 Pt-Fe, competing interactions in FCC alloys 8-95453
 Rh-Fe, competing interactions in FCC alloys 8-95453
 Rh-Pd-Fe, dil., local environment and mag. props. 8-64187
 Rh-Pd-Fe, dil. alloy, mag. moment 8-95416
 Rh₂FeSn, metallic ferromagnet, hyperfine mag. field temp. depend. (*Russian*) 8-80265
 Ru-Fe, dil., localised spin fluctuation system, supercond. transition temp., conc. depend. 8-56253
 Sc-Fe system phase diag. (*Ukrainian*) 8-84773
 Sm-Fe, dil., valence impurity state, inference from mag. susceptibility 8-95270
 Sm₂(Co_{1-x}Fe_x)₁₇, anisotropy consts., conc. and temp. depend. (*Russian*) 8-64202
 Sm(CoFeCuMn)₇, coercive force and anisotropy temp. depend. 8-68297
 Tb-Fe, amorphous, random anisotropy effects 8-68223
 Tb_{0.27}Dy_{0.73}Fe₂, domain configurations, obs. by Kerr effect and synchrotron radiation topographs 8-64215
 Tb_{0.27}Dy_{0.73}Fe₂, LF magnetoelastic effects 8-68348
 Tb_{0.27}Dy_{0.73}Fe₂, magnetisation and magnetic anisotropy 8-91862
 Tb_{0.27}Dy_{0.73}Fe₂, perpendicular suscep., magnetomechanical coupling and shear modulus 8-91918
 Tb_{0.3}Dy_{0.7}Fe₂, elastic vs. magnetoelastic anisotropy 8-68347
 Tb₃Dy_{1-x}Fe₂, Laves phase alloy, magnetostriction depend. on powder orientation before sintering 8-76284
 TbFe₂, amorphous, struct. determ., EXAFS exam. 8-51421
 TbFe₂, domain configurations, obs. by Kerr effect and synchrotron radiation topographs 8-64215
 TbFe₂, high field magnetostriction and magnetisation 8-84471
 TbFe₂, magnetisation and magnetic anisotropy 8-91862
 TbFe₂, X-ray obs. of low temp. modifications of crystal struct. (*Russian*) 8-75632
 Tb,Fe_{1-x} film, amorphous, magnetostriction and magnetisation 8-68305
 Ti alloy VT3-1, large forgings, heat treatment, struct. and mech. props. 8-52864
 Ti-Al-Cr-Mo-Fe, effect of structure and heat treatment on tensile strength, ductility, fatigue limit and notch sensitivity 8-56711

iron alloys continued

- Ti-Al-Mo-Cr-Fe, effect of heating on thermal stability of phases, lattice constants and chem. comp. 8-56672
 β -Ti-Fe, (7.1 wt.%) exam. of ω phase formation, by X-ray diffr. and Mossbauer spectroscopy 8-52800
 β -Ti-Mo-V-Fe-Al (8, 8, 2, 3, wt.%), exam. of stress induced H₂ migration 8-87823
 β -Ti-Mo-V-Fe-Al (8,8,2,3 wt.%), metastable alloy, microstruct. and mech. props. ageing time and temp. effect 8-64569
 Ti(Fe_{1-x}Co_x), density of states estimation from magnetisation and resistivity meas. 8-84119
 TiFe_{1-x}Co_x, mag. props., under high press. and in high mag. fields 8-95423
 TmFe₂, amorphous, neutron scatt. at transition, spin diffusion, magnetisation meas. 8-68174
 TmFe₂, low temp. magnetisation and magnetostriction 8-64249
 TmFe₂, magnetisation and magnetic anisotropy 8-91862
 U₂Mn₂UFe₂, mag. props., ferromag. transition (*Russian*) 8-68148
 (V,Fe)₃M, M=Si, Ge, Ga, solid soln. form. and supercond. T_c (*Russian*) 8-80512
 V-Fe, ferromagnetism to micromagnetism at low Fe conc. 8-91878
 W-Fe, dil., excess resistivity, temp. depend. 8-68011
 W-Fe, dil., spin glass props., DC mag. susceptibility meas. 8-68283
 Y-Fe alloy amorphous thin films, anisotropic mag. and microstruct. props. 8-95487
 Y-Fe film, amorphous, microstruct. and magnetism 8-64230
 Y₂(Co,Fe_{1-x})₁₇, mag. anisotropy assoc. with Fe substitution 8-76240
 YFe, film, (x=2), magnetoelastic excitations obs. 8-68307
 Y_{1-x}Fe_x, amorphous, Mossbauer spectra, appearance of magnetism 8-52401
 Y(FeCo_{1-x})₂, ferromag. reson. of pseudobinary cubic compounds 8-91961
 YFe_{3-x}Ni_x, electronic sp. ht., saturation magnetisation and lattice parameter meas. 8-68261
 Y₂(Mn_{0.75}Fe_{0.25})₂₃, mag. scatter state, hysteresis loops 8-56350
 Zn-Fe, dil., ⁵⁷Fe Mossbauer effect meas. 8-95534
 Zn₁₃Fe, ⁵⁷Fe Mossbauer effect meas. 8-95534
 Zr-Fe, amorphous alloy film, spin reson. meas. 8-68389
 Zr(Al,Fe_{1-x})₂, Laves phase, H₂ absorption capacity meas. 8-87866
 Zr₃Co_{1-x}Fe_x, phase stability and supercond. T_c 8-80519
 Zr₄₀Cu_{60-x}Fe_x, amorphous, mag. ordering and local random anisotropy 8-68273
 Zr₄₀Cu_{60-x}Fe_x, amorphous alloy, mag. interactions 8-95432
 Zr(Fe_{1-x}Co_x)₂, density of states estimation from magnetisation and resistivity meas. 8-84119
- iron compounds**
see also ferrites; iron alloys
 biological systems, electronic and mag. struct., semiempirical MO cluster calc. 8-62733
 complexes, Mossbauer isomer shift and core electron binding energies of Fe 8-82620
 ferricyanides, reduction on Au electrodes partially covered with photoresist. layer 8-85236
 ferrite, spinel type catalytic oxidation of CO, role of mag. exchange interactions 8-56916
 ferritin, iron core particle size distrib., Mossbauer determ. 8-92696
 ferrocene, ordered, disordered phases, structs. (*French*) 8-63749
 garnet, Bi substituted, epitaxial film, magneto-optical controlled transparencies 8-50932
 haematite, neutron diffr. exam. of texture, comparison with magnetite 8-52849
 haematite, reduction to magnetite under natural and laboratory conditions 8-65277
 haematite, sintered granules, onset of stresses of first kind, mechanism (*Russian*) 8-80485
 hydrostatic compression of Fe and related compounds, overview 8-83862
 magnetite, neutron diffr. exam. of texture, comparison with haematite 8-52849
 nitrides, thermodynamic considerations of nitriding of Fe (*German*) 8-60874
 oxide reduction in V slag enrichment during plasma melting (*Russian*) 8-52716
 oxide surface layer, TOF atom probe anal. 8-64766
 oxides, disperse, reduction in electrical arc discharges (*Russian*) 8-95915
 pearlite in C steels (0.08 to 1.6 wt.%), exam. of temp. depend. of mag. coercivity 8-52304
 pentlandite, prep., H₂ reduction with lime, to yield Fe-Ni alloy 8-85018
 phosphites, polycryst. EPR and Mossbauer spectra 8-76369
 pyrrhotite (Fe_{1-x}S) in sulphide ores from Kambalda, W.Australia, sulphide fabrics 8-77229
 schorl tourmaline, elastic const. 8-68718
 sulphides, reduction by H₂ 8-61053
 tetramethylene bridged ferrocene derivatives, mol. struct., Mossbauer expt. 8-60372
 titanomaghemite, synthetic, cation distrib. 8-55856
 [Fe₂(HCOO)₄(OH)₂]HCOO.4H₂O, thermal decomp. 8-80741
 BaFe₂O₄-Fe₂O₃-ZnFe₂O₄ system, phase relations at 1200°C 8-72767
 BaO-Fe₂O₃, splat quenching struct. and crystn. mechanism (*French*) 8-51426
 BaO-Fe₂O₃-Na₂O glass, mag. props. 8-88123
 Ba[Fe(CN)₆NO]₂.2H₂O, NMR, H₂O orient. (*French*) 8-52366
 Cd_{1-x}Fe_xCr₂S₄:Cu, effect of doping on elec. props. and Curie temp. 8-84214
 Cr_{1-x}Fe_xS, metal-dielect. transition, X-ray, thermal anal., elec. cond. temp. depend. 8-67942
 Cu_{1-x}Fe_{2+x}O₄, cation distrib. and valence state 8-63732
 Cu_{1-x}Fe_x, chalcopyrite, electrode surface reduction kinetics 8-56897
 (Fe,Cr)₃C, reln. between bond energy and X-ray emission line shifts 8-50555
 Fe complex, electronic and mag. struct., semiempirical MO cluster calcs. 8-62733
 Fe complex, Fe (III) acetylacetonate, solvent effects on oscillator integrated strength, IR absorpt. bands 8-84575
 Fe complex, Fe II- and Fe III-porphyrins, metalloporphyrin triplet state quenching 8-76992
 Fe complex, FeCl₄⁻, effective charge, from IR and Raman scatt. intensity obs. 8-62809

iron compounds continued

- Fe complex, Fe(III) tris diseleno chelates, sextet doublet Boltzmann equilb. Mossbauer spectra 8-60366
- Fe complex, Fe(papt)₂, high spin $^5T_2 \rightleftharpoons$ low spin 1A_1 transition, Debye-Waller factors and magnetism 8-80259
- Fe complex, tris (1,10-phenanthroline) iron(II), transient bleaching, excitation wavelength absorpt. 8-73060
- Fe complex, ubiquinone-Fe, bacterial photosynthesis primary electron transfer processes, psec. dynamics 8-80841
- Fe complex Fe(NO)[S₂CN(C₆H₅)₂]₂ in frozen toluene, for dynamically proton polarised target 8-52378
- Fe-Fe₂O₃ composite films, structural props., microhardness, 250 to 700K 8-84095
- Fe-O noncrystalline RF sputtered film, vapour species control 8-60575
- Fe-S system, solubilities in aqueous H₂S and mass transport role in girdler-sulphide heavy water plants 8-83963
- Fe-SO₄-H₂O suspension system at 90°C, potential-pH diagram 8-61068
- Fe-thiamine solution, modified, photogalvanic effect 8-91722
- (Fe_{1-y}³⁺Al_y³⁺)₂O₃²⁻, γ to α transform. elec. cond. study, oxidation initial stage kinetics, lacunar spinel form. 8-92384
- FeBO₃, parametric effects in nucl. spin echo (*Russian*) 8-56404
- FeBO₃, photoinduced linear birefringence (*Russian*) 8-52469
- FeBO₆, critical indices splitting of sublattice magnetisation (*Russian*) 8-60299
- Fe₃B₂O₁₃I, ferroelec., mag. ordering, neutron diffr. meas. 8-72331
- Fe₃B₂O₁₃I, improper ferroelectric, electro-opt. props. 8-76426
- FeBr₂, dynamic Jahn-Teller system, Raman scatt. from electronic excitations and phonons 8-56474
- FeBr₂, metamagnetic, optical study of mag. phase diagram 8-56312
- FeBr₂, XPS, satellite of Br 4s line 8-56556
- FeCN₆⁴⁻, triplet state quenching agent, in ZnO electrode dye sensitisation obs. 8-76869
- Fe(CO)₃, bond angles, hybrid bond orbital calcs. 8-94188
- Fe(CO)₅, IR spectra and laser photochem., matrix isolated at 20K 8-74651
- Fe(CO)₅, microwave dielec. relax., fluxional mechanism 8-94235
- Fe(CO)₅, photodissociation laser 8-74886
- Fe(CO)₅+Ar*(³P), chemiluminesc. 8-61014
- FeCl₂, antiferromag. reson., temp. depend. 8-68384
- FeCl₂, dynamic Jahn-Teller system, Raman scatt. from electronic excitations and phonons 8-56474
- FeCl₂, magnetic phase diagram, optical studies 8-88121
- FeCl₂, metamagnet, optical determ. of thermodynamic phase diagram 8-60285
- FeCl₂, metamagnetic, phase diagram determ. 8-68254
- FeCl₂, pulse generation of Cl II at 5218 Å, 5221 Å 8-58990
- FeCl₂-graphite, intercalation compound, formation by reduction of Fe(III) compounds with Fe(CO)₅ 8-63721
- Fe_{1-x}Cl_{2-x}Cd_x, randomly disordered, tricrit. behaviour, light scatt. 8-68255
- FeCl₂2D₂O, magnon-phonon coupling 8-72530
- FeCl₂2H₂O, also deuterated, electronic transitions in Raman spectra 8-80337
- Fe_(1-x)Co_xCl₂2H₂O, random mixture of anisotropic antiferromags., isotropic state obs. 8-84396
- FeCoF₅7H₂O, Mossbauer spectra, thermal decomposition products 8-80258
- Fe_{1-x}Cr_xBO₃, magnetisation, 4.2-600K 8-68187
- (Fe_{1-y}³⁺Cr_y³⁺)₂O₃²⁻, γ to α transform. elec. cond. study, oxidation initial stage kinetics, lacunar spinel form. 8-92384
- FeCrS₄, vapour grown, growth mechanism of multisteps on surface 8-75605
- Fe₂Cu_{1-x}Rh_xS₄, mag. tetrahedral intrasublattice interaction, X-ray, magnetisation and Mossbauer expts. 8-52241
- FeF, electronic states, ab initio calcs., UV spectrum elucidation 8-74570
- FeF, electronic states, anal. of rot. struct. 8-74674
- FeF₂ (rutile), high press. phase transform. 8-79761
- FeF₂, absolute first order Raman polarisabilities 8-64369
- FeF₂, antiferromag. spin flop boundary 8-84419
- FeF₂, electronic and mag. struct., semiempirical MO cluster calcs. 8-62733
- FeF₂, magnon-acoustic phonon hybridisation in far IR absorpt. spectra 8-60271
- FeF₂, Raman spectra, cross section determ. 8-56471
- FeF₂, theory of Raman scattering, coupled phonon-magnon excitations 8-72531
- FeF₃, antiferromagnetic, press. depend. of effective mag. fields on ⁵⁷Fe nuclei 8-52383
- FeF₃ isomer shift, using LCAO form of molecular orbital method 8-62856
- FeF₃, muon Coulomb capture ratio 8-62959
- FeF₃, thin film prep. and charact. (*French*) 8-64470
- Fe₂F₅7H₂O, Mossbauer spectra, thermal decomp. products 8-80258
- FeI₂, far IR magnetoabsorption, excitation of two spin deviations 8-80339
- FeIn₂S₄, indite, thiospinel, cation ordering in tetrahedral sites, X-ray diffr. meas. 8-95028
- Fe_{1-x}Mg_xCl₂, magnetic excitations 8-91852
- Fe₂Mg_{1-x}SO₄7H₂O, EFG tensor evaluation, ⁵⁷Fe single crystal Mossbauer meas. 8-88237
- FeMnGaO₄, X-ray study of cryst. struct. and ionic config. 8-55851
- FeMoO₃, standard Gibbs energies, enthalpies, entropies of formation 8-61042
- FeMoS₄, Mossbauer spectra, 79-300K, Neel pt. determ. 8-60360
- Fe₂N₂, prep. by reactive sputtering, struct. and props. (*Japanese*) 8-92190
- Fe(NH₂)SO₃, nuclear fuel processing solutions 8-78487
- Fe₂Nb₂V_{2-2x}O₄, NMR analysis of semiconductor transitions 8-52367
- Fe_{2-x}Ni_xO₄, low temp. Mossbauer spectra, electron transfer and spin density distribution 8-52404
- FeO, absorption spectra, 0.1-6 eV, one electron energy level diagram 8-52487
- FeO inhibitor film on Fe, passivation and inhibitor props., X-ray photoemission spectroscopy exam. 8-88561
- FeO, lattice dynamics, coherent inelastic neutron scatt. 8-59899
- FeO-SiO₂, molten, viscosity and density 8-59965
- FeO₃, work function, high temp. meas. using dynamic condenser 8-64097

iron compounds continued

- Fe_{1-x}O, precipitation of Fe₂O₃ during decomposition 8-84823
- Fe_{1-x}O, thermodynamic props. of wustite phase of iron-oxygen system, review 8-79780
- Fe_{1-x}O, wustite, phonon and magnon props., inelastic neutron scatt. 8-52236
- Fe_{1-x}O, wustite disc reduction with CO, 573 to 845°C 8-53253
- Fe_{1-x}O, wustite phase, surface elec. props. 8-76133
- α -Fe₂O₃ (haematite), X-ray diffr. compression studies under hydrostatic isothermal conditions 8-85539
- Fe₂O₃, absorption spectra, 0.1-6 eV, one electron energy level diagram 8-52487
- Fe₂O₃, amorphous, temp. depend. of hyperfine field, Mossbauer spectroscopy 8-84508
- α -Fe₂O₃, analysis of car exhaust by Mossbauer spectroscopy 8-92963
- Fe₂O₃ crystallite formation in B₂O₃ and Na₂O.B₂O₃ glasses, Mossbauer obs. 8-68429
- Fe₂O₃, diffusion in gas phase during firing of MgO-Cr₂O₃ bricks (*French*) 8-80495
- γ -Fe₂O₃, elongated particles, mag. struct. 8-88096
- α -Fe₂O₃ film, prep. by reactive condensation and mag. props. 8-64241
- Fe₂O₃ film deposition, by reactive sputtering, increased capacity deposition system (*Bulgarian*) 8-60572
- α -Fe₂O₃, haematite, birefr. under uniaxial stress in mag. field (*Russian*) 8-88285
- Fe₂O₃, haematite, mag. domain distrib., appl. of mag. Laue neutron diffr. method 8-95455
- Fe₂O₃, haematite, optical indicatrix deform. and rot. during field induced phase transition 8-68482
- Fe₂O₃, heat of adsorpt. of pyridine and ethyl pyridine, flow microcalorimetry 8-85193
- Fe₂O₃, hematite, reduction, exam. of role of convective mass transfer 8-52724
- Fe₂O₃, PMMA-metal oxide composite powder, prep. and props. (*Japanese*) 8-95708
- α -Fe₂O₃, polycryst., pure and TiO₂ doped, flatband potentials, donor densities, photocurrent meas. 8-76089
- Fe₂O₃ powder, heat of adsorpt. of stearic acid, surface area meas., flow microcalorimetry 8-81974
- γ -Fe₂O₃ powders, influence of densification on mag. props. 8-95481
- γ -Fe₂O₃, prep. from thermal decomp. of [Fe₂(HCOO)₆(OH)₂]HCOO.4H₂O and characterisation 8-80741
- α -Fe₂O₃, pure and TiO₂ doped, electrode, photooxidation of H₂O appl. 8-76886
- Fe₂O₃, shocked hematite, Mossbauer exam. 8-64304
- γ -Fe₂O₃, single mag. particle, remanent coercive force and remanent loop meas. 8-95480
- α -Fe₂O₃, single particle material for tape and disc manufacture, prep., props., and appls. 8-52308
- γ -Fe₂O₃, small particle composite, preparation methods, superparamagnetism, optical transparency 8-60315
- γ -Fe₂O₃, transform. to α -phase, effect of preliminary pressing or vibromilling 8-84798
- γ -Fe₂O₃, vibro-milled, energy storage and liberation 8-83941
- α -Fe₂O₃:Al, hematite, spin reorientation, Mossbauer spectra obs. 8-72356
- Fe₂O₃-Al₂O₃, solid solns., effect on Fe on point of zero charge 8-61021
- Fe₂O₃-B₂O₃-PbO glass, semicond., elec. resist. meas. 8-95300
- Fe₂O₃-TiO₂ system, high temp. intergrowth struct., metal atom ordering in intergrowth boundaries 8-79573
- Fe₂O₃-WO₃, phase relations 8-92249
- α -Fe₂O₃+CaO, additive in ZrO₂ sintering 8-76617
- Fe₂O₃+MoO₃ coreduction kinetics, thermodynamic equilb. in Mo-Fe-O-H system 8-60657
- Fe₂O₃, absorption spectra, 0.1-6 eV, one electron energy level diagram 8-52487
- Fe₂O₃, adsorption of Cs, meas. of contamination using washing test 8-62597
- Fe₂O₃, dielec. props. of low temp. phase, at microwave freq. 8-64309
- Fe₂O₃ film, prep. by reactive condensation and mag. props. 8-64241
- Fe₂O₃, film, quantitative sputter rates, AES, ellipsometry determ. 8-72661
- Fe₂O₃, finely dispersed, electronic phase transition, cond. and DTA meas. 8-91736
- Fe₂O₃, hyperfine fields and spin densities below 20K 8-52405
- Fe₂O₃, low temp. sintering 8-92221
- Fe₂O₃, magnetite, electronic struct. at low temps., NMR anal. 8-67686
- Fe₂O₃, magnetite, ferrimag. reson. at 9.3 GHz near Verwey temp., g-factors (*French*) 8-91959
- Fe₂O₃, magnetite, oxidation kinetics, influence of cryst. size 8-79778
- Fe₂O₃, Mossbauer spectra above Verwey transition 8-68415
- Fe₂O₃, NMR exam. of low temp. phase 8-56401
- Fe₂O₃, NMR of low temp. phase, electron ordering anal. 8-56402
- Fe₂O₃ particles, entrapped in drug carrying microsphere, intravascular mag. guidance method 8-73188
- Fe₂O₃, photocond. 70-130K, temp. range including metal-semicond. transition (*Russian*) 8-56178
- Fe₂O₃, precipitation in YIG 8-84815
- Fe₂O₃, single cryst., surface magnetism, spin polarized photoemission 8-52622
- Fe₂O₃, spherulitic film growth, elec. and mag. props. 8-68627
- Fe₂O₃:Zn, and pure, influence of mag. order on charge delocalisation, Mossbauer spectra 8-68423
- Fe₂O₃-Fe₂S₃Ti_{0.2}O₄, interdiffusion expts. 8-55991
- Fe₂O₃, O₂ annealed, optical absorpt., spin struct., polaronic absorpt., cryst. field transitions 8-68493
- Fe₂O₃, prep. by reactive sputtering, struct. and props. (*Japanese*) 8-92190
- FeOI intercalation cpds. with Li and amines, cryst. struct. 8-51512
- Fe₂O₃-F₂, low temp. Mossbauer spectra, electron transfer and spin density distribution 8-52404
- Fe(OH)₃(SiF₆), phase transitions, spectrometric exam. (*French*) 8-88291
- FeOOH, H-bonding, strong, stochastic model and IR spectra temp. effects 8-62805
- FeOOH, high-pressure phase, neutron diffraction study 8-52212
- β -FeOOH, Mossbauer investigation of the quadrupole splitting 8-76370

iron compounds continued

- β -FeOOH, ultrafine particles, mag. struct., Mossbauer spectroscopy 8-72372
 FeS, thermal switching, resist.-temp. charact. 8-64071
 FeS, zinc blende type, crystallographic and Mossbauer obs. 8-87650
 FeS, zinc blende type, mag. struct. (French) 8-91846
 FeS-Ni₃S₂-Cu₂S melt, enthalpy (Russian) 8-95730
 FeS₂ (pyrite), glide elements study by electron microscopy and electron diff. 8-83817
 FeS₂, marcasite, Mossbauer elec. field gradient meas. 8-56407
 Fe_{0.996}S, Fe_{0.93}S, determination of quadrupole splitting sign, ground state appl. 8-76363
 Fe₂S₃, existence and thermal stability, Mossbauer study 8-83733
 α -FeSO₄, electronic and mag. struct., semiempirical MO cluster calcs. 8-62733
 FeSO₄, G-values, C₁ and C₂ reevaluation using extended cavity ionisation theory 8-92706
 FeSO₄·7H₂O, γ -ray irradiated, Fe³⁺ formation, Mossbauer study (Russian) 8-84509
 FeSb₂O₄, Mossbauer spectra, molecular field effects 8-91997
 FeSb₂O₄, defect struct. and mag. transition, elec. transport and Mossbauer expts. 8-59803
 FeSiF₆·6D₂O, ²H NMR spectrum, correl. effects 8-76324
 FeSiF₆·6H₂O, paramag., nucl. and electron spin lattice relax. 8-84494
 FeSiF₆·6H₂O, phase transform. exam. by X-ray and DSC methods 8-83948
 Fe₂SiO₄, fayalite, single crystal growth by floating zone method, exam. 8-60570
 Fe_{2-2x}SiO₄, fayalite, oxidation kinetics and growth of Fe₂O₃ whiskers 8-84113
 Fe_{0.5}Si_{0.5}(OH)₈, greenalite, metamag. clay mineral, mag. props. (French) 8-88817
 FeTh₂S(Se)₅, synthesis, cryst. characts. (French) 8-51517
 FeThSe₃, synthesis, cryst. characts. (French) 8-51517
 Fe_{2.6-x}Ti_{0.4}Al_{1-x}O₄, Fe_{2.4-x}Ti_{0.6}Al_{0.4}O₄, titanomagnetite, monodomain, mag. props. 8-56346
 Fe₂TiO₄, ulvöspinel, containing magnetized inclusions, mag. behaviour, cooling through Curie point 8-56314
 Fe₂TiO₄, ulvöspinel, mag. props. weak ferromag. in 4-200K temp. range 8-56351
 Fe₂TiO₄-Fe₂O₃, titanomagnetite, prepared at different oxidation conditions, hysteresis props. 8-56352
 Fe₂TiO₅, pseudobrookite, single cryst. growth by chem. transport 8-80464
 Fe_{2.4}Ti_{0.6}O₄, titanomagnetite, single-crystal, mag. props. of multidomain TRM 8-56345
 FeU₂O₈, mag. struct., exchange energy, magnetisation and neutron diff. expts. 8-68170
 Fe₂Zn_{1-x}F₂, Neel temp., CPA calc. 8-68233
 Fe₂Zn_{1-x}F₂, Neel temp. mag. cone depend., CPA calcs. 8-88122
 FeZnF₃·7H₂O, Mossbauer spectra, thermal decomp. products 8-80258
 Fe_{1-x}Zn_{3/2}O₃, solid soln. prep., struct. and mag. moment 8-52228
 Fe_{3-x}Zn_xO₄, low temp. Mossbauer spectra, electron transfer and spin density distribution 8-52404
 FeZrF₆, phase transition at 212.3K, Mossbauer, EPR study, quadrupole splitting, Jahn-Teller effect (German) 8-68430
 Fe₂ZrSe₂, intercalation compound, IR spectra 8-88300
 Ge-Se-Fe films, metallic and semicond., amorphous, mag. and elec. props. 8-52319
 K₂Fe(CN)₆·3H₂O, ferroelec., sp.ht. and spontaneous polarisation, -65 to 0 degrees C, mol. field model 8-64333
 K₂Fe₂Ti_{8-x}O₁₆, ionic cond. meas. 8-67856
 K₂O-B₂O₃-Fe₂O₃ glass, Mossbauer expts., 85-500K 8-80260
 K₂O-xGa₂O₃·xFe₂O₃, K ion cond. 8-83998
 La₂Fe_{1.76}S₅, cryst. struct. (French) 8-51499
 LaKFe(CN)₆·4H₂O, cryst. struct. determ. 8-55844
 Li₂O-B₂O₃-Fe₂O₃ glass, Mossbauer expts., 85-500K 8-80260
 Li₂O-Fe₂O₃-SiO₂ glass, struct. and crystallisation behaviour 8-83738
 (Mg,Fe)₂SiO₄, olivine, fayalite rich, single cryst., UV absorpt. spectra at high press. 8-85545
 Mg₂Fe_{3-x}O_{4-y} precipitates, g-factor, ferrimag. reson. meas. 8-60337
 MgO-CaO-SiO₂-Al₂O₃-Na₂O·P₂O₅, effect of NaPO₃ on phase composition rel. to basic refractories 8-80528
 Mg₂SiO₄-Fe₂SiO₄-CaAl₂Si₂O₈-SiO₂ system phase relations rel. to lunar basalts origin 8-65512
 MnFe ferrites, reson., effect of EM propagation 8-64277
 Mn_{1.18}Fe_{0.06}Co_{0.01}Fe_{1.75}O₄, transport props. near Curie points 8-88100
 Na₂(Fe(CN)₅NO)·2H₂O, powder, Mossbauer absorption in mag. field 8-68418
 Na₂Fe₃(PO₄)₃, synthetic alluaudite, cryst. struct. 8-83802
 Na₂O-B₂O₃-Fe₂O₃, and Na₂O-Al₂O₃-B₂O₃-Fe₂O₃ glass, Mossbauer expts., 85-500K 8-80260
 Na₂O-CaO-B₂O₃-Fe₂O₃ glass, Mossbauer expts., 85-500K 8-80260
 Na₂O-FeO-Fe₂O₃-SiO₂, chemical durability at different pH values 8-72902
 PbO-2B₂O₃-Fe₂O₃ glass, Mossbauer study, struct., crystallite formation, broadened quadrupole doublet 8-59761
 PbO·3B₂O₃·Fe₂O₃, EPR of Fe³⁺ ions 8-72400
 ScFe_{0.25}Si_{1.75}, X-ray determ. of struct., new representative of struct. type ZrSi₂ 8-79595
 ((SiO₂)₄₅(CaO)₅₅ (Fe₂O₃)₃₅ glass, effect of melt atmosphere on mag. props. 8-88299
 Sr₂Fe₁₀O₂₂-Fe₂O₃-ZnFe₂O₄ system, phase relations at 1100°C 8-68676
 SrO-Fe₂O₃, splat quenching struct. and crystn. mechanism (French) 8-51426
 Sr[Fe(CN)₅NO]·2H₂O, cryst. and mol. struct. 8-91311
 V₂O₅-Fe₂O₃-Li₂O ternary system, charge compensation of Fe ions, Mossbauer obs. 8-52410
 (Zn,Fe)S (sphalerite), FeS content as geobarometer, experimental extension to 10 kbar 8-85703
 Zn_{1-x}Fe_{0.85-x}O, prep. and struct., mag. and semicond. props. (French) 8-51506

iron phosphate semiconductor glasses see amorphous semiconductors

irradiation effects see radiation effects

irradiation induced creep

- fusion reactor materials, material requirements exam., review 8-50257
 LMFBR performance, effects of irradiation creep and swelling 8-78482

irradiation induced creep continued

- metals, irradiation creep strain, produced by vacancy loops, calc. of magnitude 8-72815
 metals and alloys, radiation damage prediction and measurement 8-75693
 nuclear fuel cladding, slightly oval cylindrical shells, creep anal. 8-78468
 ordered alloy, point defect annihilation kinetics and correlation creep, analysis 8-75659
 point defect trapping, effect on irradiation induced creep and swelling 8-71756
 point defect-dislocation interaction, radiation-induced creep, rate expression 8-87706
 SGHWR fuel pins, fuel cladding ratchetting study 8-54855
 steel, austenitic stainless, fast neutron irradi., effect on mech. props. 8-92309
 steel, austenitic stainless, irradiation induced creep, AISI 316, 20% cold worked effect of temp. change 8-72816
 steel, austenitic stainless, irradiation induced creep by alpha particles, in type 316 steels (French) 8-72791
 steel, stainless, neutron induced swelling, neutron flux and irradi. temp. depend. 8-79636
 steel, stainless, type 304, previously irradi. in fast neutron flux 8-80600
 steel, stainless, type 316, cold worked, effect of prior neutron irradiation on burst strength 8-62599
 Ni, D bombardment, 22 MeV at 224°C 8-80597

Ising lattices

see also Ising model

- correlation length, renormalisation group calc. (Russian) 8-77811
 correlation-function identities for general planar Ising systems 8-93616
 heteropolymer in random mag. field, Ising chains, statistical mechanics, free energy, numerical calcs. 8-77803
 lipid phase transition, cluster model, appl. to bilayer mol. passive permeation and struct. relax. 8-53346
 position-space renormalisation-group transformations, problems and proofs 8-93619
 random Ising model on cacti lattices 8-49773
 real-space renormalisation giving differential renormalisation-group eqns., two-dimens. triangular Ising lattice 8-65881
 rectangular ferromagnet, pair correlation function using spinor technique 8-70063
 renormalisation theory, variational principles 8-73951
 time dependent real-space renormalisation group for Ising system on triangular lattice, critical dynamics 8-60289
 triangular renormalisation group transformation, var. approximation 8-49776
 two dimensional spin s Ising system with lattice anisotropy, crit. props. 8-73932
 ND₄Cl, order-disorder transformation, elasticity and heat capacity temp. depend., US obs. 8-71851
 NH₄Cl, molar heat capacity near order-disorder transform. under high press. 8-51697

Ising model

see also Ising lattices

- anisotropic linear spin chain, two-magnon problem with arbitrary interaction radius 8-72320
 antiferromagnet, anisotropic, correction to scaling in specific heat 8-80168
 antiferromagnet, in mag. field, new perturbation approach 8-56336
 antiferromagnet, phase boundary determ. by real space renormalisation group methods 8-88134
 band-diluted random Ising model, criticality and crossover 8-56320
 Bethe lattice, Ising model with competing antiferromag. and ferromag. interactions, phase diagram 8-64177
 Blume-Capel model for plane-triangular and FCC lattices 8-80114
 bond-diluted ferromagnet with first and second neighbour interactions 8-91870
 Callan-Symanzik equation, perturbation analysis, crit. indices 8-52294
 cell membrane nuclear hydrodynamic shear, non-equil. Ising model, master eqn. 8-61146
 classical, crit. dynamics simulation in transverse field 8-59930
 classical, in transverse field, Monte Carlo simulation, statical props. 8-56326
 classical, molecular dynamics exam. in transverse field 8-80115
 cluster expansion of partition function of Ising model 8-49759
 coexistence of phases, equiv. of different order parameter 8-49772
 collinear metamagnets, two-sub-lattice Ising model 8-95410
 compressible random Ising model, crit. behaviour 8-80160
 continuous-spin Ising ferromagnets phase transitions 8-60260
 correlation function identities for models with general interactions 8-95409
 correlation functions of nondynamic interacting systems 8-57814
 correlation-function identities and inequalities for Ising models with pair interactions 8-84375
 critical behaviour, scaling functions for quantum crossover 8-68249
 critical temp. for 2-D Ising ferromagnet with quenched bond disorder. 8-56328
 cumulant approximation is crit. region 8-76255
 Curie point in quenched bond model 8-56318
 dilute ferromagnet, spin wave excitations, multicomponent CPA theory 8-68135
 disordered Ising spin chains in mag. field 8-57869
 double Ising chain, model in zero external field (Russian) 8-84430
 dynamic critical phenomena, real-space renormalisation group methods, appl. two-dimens. kinetic Ising model 8-77810
 FCC Ising ferromagnet, cluster variation approx. 8-68278
 ferromagnet, 3-D, critical behaviour in random mag. field 8-68250
 ferromagnet, crit. correlation-function approx. 8-56324
 ferromagnet, crit. exponents in integral representation 8-56325
 ferromagnet, disordered, approximate treatment 8-52262
 ferromagnet, in mag. field, new perturbation approach 8-56336
 ferromagnet, linear Ising-Heisenberg, spin waves vs. bound states, exact soln. 8-68202
 ferromagnet, phonon thermal cond., crit. anomalies (Russian) 8-80159
 ferromagnet, rectangular, n-point functions 8-76250
 ferromagnet, renormalised crit. behaviour 8-52272

Ising model continued

- ferromagnet, $S=1$, single-ion type uniaxial anisotropy, cluster-variation method appl. in pair approx. 8-68281
- ferromagnet, site diluted, crit. props. 8-72351
- ferromagnet, spin-operator reduction relations, representation 8-95443
- ferromagnetism, basic models, classification of theories (*Rumanian*) 8-91840
- four-dimensional Ising-like model, excitation spectrum, mol. dynamics 8-95411
- Fredholm determinant representation, Ising model two-point function 8-54314
- free energy, recursion method calcs. 8-52186
- Glauber-Ising model, 2-dimens., crit. dynamics, real-space renormalisation group theory 8-70070
- Glauber-Ising model, real space-time depend. renormalisation group 8-49774
- Green functions, commutator and anticommutator, in Ising model with transverse field 8-76211
- Heisenberg-Ising bonds, randomly mixed three dims. system, critical props. 8-76249
- insulating systems, magnetic, review of expts. 8-68240
- interface free energy 8-60261
- Ising system, two-state, crit. behaviour, Bragg-Williams approx. calcs. 8-86223
- Ising-system, two-state, crit. behaviour, Monte Carlo calcs. 8-86222
- kinetic, crit. dynamics, real-space renormalisation group study 8-49785
- kinetic model of ferromagnetism, simulation of equil. critical props. 8-89410
- Kramers-Wannier transform. for systems with $Z(n)$ symmetry (*Russian*) 8-77812
- lattice-lattice scaling, reln. to scaled eqn. of state, appl. to Ising model 8-70067
- Lee-Yang branch point and crit. behaviour 8-68253
- Lee-Yang theorem on generalised models with degeneracy 8-65879
- magnetic binary alloys, phase separation, double Ising system 8-91835
- magnetic specific heat, effect of spin-lattice coupling 8-80157
- metastability in two dimensional Ising model, dynamic Monte Carlo method, transfer matrix 8-72354
- mixture, one-dimens., random, of Ising $S=1$ and $1/2$ spins, mag. props., spin distrib. 8-95407
- nonequilibrium, intensive parameters and detailed balance, computer simulation calcs. 8-76208
- nonequilibrium, intensive parameters and detailed balance, theoretical estimate 8-76209
- one dimensional in skew mag. field, zero-temp. dynamical props. 8-80153
- one-dimensional disordered spin system with isotropic antiferromag. interaction, susceptibility and Knight shift (*Russian*) 8-88202
- order-disorder transitions in gauge and spin systems 8-70072
- paramagnet, transverse field model 8-68138
- particle struct. at low temps. 8-57865
- partition function for three dims. Ising model, closed form approx. (*Chinese*) 8-52185
- planar, higher order correl. functions calcs. 8-95408
- Potts model, spin anisotropy and crossover 8-56339
- quadrupolar systems of restricted dimensionality, absence of ordering 8-89411
- quantal and finite-sized, dimensional crossover 8-95444
- quasi-one-dimensional electron gas with strong on-site interaction 8-67966
- quenched mixture, spinodal decomposition theory, self-consistent method, structure function 8-68671
- quenched random magnets, thermodynamic behaviour from position-space renormalisation group 8-68244
- random magnetic alloys, mean field effective medium theory, Ising model appl., phases 8-84438
- random magnetic bonds, phys. props. near crit. point 8-84440
- random mixtures of three-dimens. Ising site model Monte Carlo simulation 8-73935
- random mixtures of three-dimens. Ising site model Monte Carlo simulation 8-73936
- random model, restricted annealing 8-80154
- random ordered phase, of Ising model, random quenched effective field approx. 8-84432
- relax. behaviour, Ising model with degeneracies 8-65880
- renormalisation group transform. of three-dimens. Ising models 8-62163
- renormalisation group transformations, cumulant expansion 8-70064
- sequential term prediction 8-57866
- short-range ordered mag. cluster pinning by localised optical excitation 8-68279
- spin glass, dil., low temp. phase diagram and crit. props. 8-60291
- spin glass, existence of phase transition 8-56327
- spin glass, infinite ranged models 8-80166
- spin glass, nature of ordering 8-80172
- spin glass near percolation threshold 8-72352
- spin glass phase, of Ising model, random quenched effective field approx. 8-84432
- spin glass transition in random bond Ising model in 2-D, and 3-D, renormalisation group approach 8-68275
- spin lattice models, continuous-integral method 8-93615
- spin systems on Cayley tree-like lattices, spontaneous magnetisation, correlation function far from boundary 8-68137
- spin-one Ising system, phase diagram 8-95441
- spin-one system, correlation functions with bilinear and biquadratic interactions 8-91876
- spontaneous magnetisation in d-dimensional models for $d \geq 2$ 8-72319
- statistically layered system, finite, crit. phenomena 8-95446
- structural stability theory, phase transition models, mean field theories, Ising model appls. (*German*) 8-77822
- thermodynamic limit in stochastic systems 8-73938
- three dimensional, crit. index. for correl. length 8-84444
- three-dimensional, two-spin correlation function, method for phase diagram 8-56323
- transformation methods in anal. of crit. prop. 8-49771
- transverse field, spin dynamics, mode coupling 8-56332
- triangular Ising lattice with small second neighbour interaction crit. temps. 8-56331
- triangular Ising model percolation props., renormalisation group anal. 8-93620

Ising model continued

- two-dimensional, renormalisation group approach 8-52261
- two-dimensional, with transverse field, phase diagram and crit. props., from real space renormalisation group 8-52295
- two-dimensional exponents, one-dimensional three-spin cell calc. 8-68280
- two-dimensional n-spin correl. functions 8-52296
- valency transition 8-60297
- Weiss Ising model, stability anal. C^* -algebra formalism 8-57868
- Yang-Lee edge singularity and ϕ^3 field theory 8-65882
- $[(CH_3)_3NH]CoCl_3 \cdot 2H_2O$, chain ferromag. two magnon bound state, nuclear spin-lattice relax. 8-88206
- KH_2PO_4 type ferroelectrics above T_c , soft mode and central-peak dynamics 8-87763
- KH_2PO_4 , variational treatment of proton-photon system 8-88261
- $NaNO_3$, order-disorder transition point, hyper-Rayleigh scatt. due to rotation of NO_3^- 8-52520
- Rb_2CoF_4 , two dims. Ising like antiferromag., spin wave excitations 8-72342
- $Rb_2CoMg_{1-x}F_4$, magnetic specific heat, dilution on a two-dimensional Ising-like antiferromagnet 8-91871

island-like metallic thin films *see discontinuous metallic thin films*

islet-like metallic thin films *see discontinuous metallic thin films*

isobaric analog states *see isobaric analogue states*

isobaric analogue resonances

- see also nuclear collective states and giant resonances*
- nuclear forces and isobar configs. in nuclei, review 8-50093
- reduced normalisation of isobaric analogue resonances from (p,p) reactions 8-86522
- strength functions for isobaric analogue resonances 8-50143
- ^{71}As , intermediate struct., props. 8-93948
- ^{207}Bi $3p_{1/2}$ isobaric analogue resonance from $^{206}Pb(p,p_0)$, polarised p, analysing power 8-78346
- ^{208}Bi $3p_{1/2}$ isobaric analogue resonance from $^{207}Pb(p,p_0)$ analysing power, polarised p 8-78346
- $^{12}C(\pi, \pi')$, collective resonances 8-78415
- ^{110}Cd , n spectra of isobaric analogue resonance decay from $^{115}In(p,n)^{115}Sn$ (*Russian*) 8-89841
- ^{55}Co , 1 $g_{9/2}$ analogue state fragmentation using analogue resonances from $^{54}Fe(p,\gamma)$, 3450 keV 8-70506
- ^{57}Co , $g_{9/2}$ IAR in $^{56}Fe(p,\gamma)$ 8-70504
- ^{57}Co obs. of $g_{9/2}$ IAR in $^{56}Fe(p,\gamma)$ 8-82332
- ^{52}Cr , γ -decay of analogue states obs. in $^{51}V(p,\gamma)$ 8-70503
- ^{137}Cs , anal. of $^{136}Xe(p,p_1)$, 11.82 MeV 8-66282
- ^{63}Cu , isobaric analogue reson. anal., from $^{64}Ni(p,p)$, (p,p') 8-78351
- ^{56}Fe isobaric analogue resonances corresponding to ^{56}Mn 335.5 and 340.9 keV states from $^{55}Mn(p,\gamma)$ 8-78342
- ^{69}Ga , IAR corresponding to $1/2^-$ and $9/2^+$ ^{69}Zn states from $^{68}Zn(p,\gamma)$, 3.8 MeV 8-66257
- $^{55}Mn(p,n)^{55}Fe$, neutron polarisation at isobaric analogue resonances 8-54759
- ^{22}Na , analogue resons., γ -ray ang. distrib. and mixing ratios in $^{21}Ne(p,\gamma)^{22}Na$ 8-62504
- ^{59}Ni , and $N=29$ nuclei f-p shell nuclei, unified model description 8-78343
- $^{208}Pb(^3He,t)^{208}Bi$, 80 MeV, Gamow-Teller M1 state excitation 8-50184
- $^{51}V(p,n)^{51}Cr$ neutron polarisation at isobaric analogue resonances 8-54759
- $^{90}Zr(^3He,t)^{90}Nb$, 80 MeV, Gamow-Teller M1 state excitation 8-50184

isobaric analogue states

- see also isobaric analogue resonances*
- Coulomb displacement energies of analogue states in mirror nuclei, review 8-78242
- high energy nuclear collisions, isobaric-gas model, shock waves, temp., density, pionisation 8-94022
- light nuclei, schematic model for isospin mixing 8-66198
- (d, 3He) on ^{12}C , ^{16}O , ^{24}Mg , ^{40}Ca , 29 MeV, polarised d, low lying analogue states, DWBA anal. 8-82285
- (d,t) on ^{12}C , ^{16}O , ^{24}Mg , ^{40}C , 29 MeV, polarised d, low lying analogue states, DWBA anal. 8-82285
- (p,n) scattering, charge exchange, isobaric analogue state, giant resonance effect, semimicroscopic model 8-89868
- $^{40}Ca+p$, fine struct. levels, spin meas., off-diagonal strength function, analogue state broadening theory test 8-78381
- ^{55}Co , γ decay and splitting of analogue states from $^{54}Fe(^3He,d\gamma)$ at 18 MeV 8-70505
- ^{58}Co , fine struct. of ground hole-state analogues 8-50065
- ^{58}Co , fragmentation of hole-state analogues 8-54731
- $^{59}Co(p,d)$, 50 MeV, fine struct. of ground hole-state analogues 8-50065
- ^{52}Cr , shell model study and gamma decay of isobaric analogue states 8-86492
- ^{59}Cu , γ decay and splitting of analogue states, from $^{58}Ni(^3He,d\gamma)$ at 18 MeV 8-70505
- $^3He(t,d)^4He$ asymmetry, cluster model anal., isobaric analogue states 8-78389
- ^{27}Mg excited analogue states high resolution study in $^{26}Mg(p,p)$ 8-78377
- ^{57}Mn , γ decay and splitting of analogue states from $^{52}Cr(^3He,d\gamma)$ at 18 MeV 8-70505
- ^{91}Mo , fine struct. of ground hole-state analogues 8-50065
- $^{91}Mo(p,d)$, 50 MeV, fine struct. of ground hole-state analogues 8-50065
- ^{22}Na bound and analogue state lifetimes, branching ratios, DSA method from $^{21}Ne(p,\gamma)$ 0.5-6.0 MeV 8-93967
- Ni , $A=57$, 59, 61 and 63, fine struct. of ground hole-state analogues 8-50065
- $^{58}Ni(p,d)$, 50 MeV, fine struct. of ground hole-state analogues 8-50065
- ^{59}Ni , fragmentation of hole-state analogues 8-54731
- $Ni(p,d)$, $A=60$, 62 and 64, 50 MeV, fine struct. of ground hole-state analogues 8-50065
- ^{207}Pb , $T=45/2$ isobaric analogue state obs. in $^{208}Pb(^3He,\alpha)^{207}Pb$ 8-93928
- ^{143}Sm , T_0 hole analogue states, p decay, deduced states and p branching ratio 8-70451
- ^{89}Zr , fine struct. of ground hole-state analogues 8-50065

isobaric analogue states continued

- $^{90}\text{Zr}(\text{p},\text{d})$, 50 MeV, fine struct. of ground hole-state analogues 8-50065
 ^{97}Zr , $T_{1/2}$ hole analogue states, p decay, deduced states and p branching ratio 8-70451

isobars see atmospheric pressure and density**isoelectronic series**

- acetylene, HCN, N_2 , vibr. fine struct. accompanying core ionis., STO calcs. 8-62844
 hexafluoride radicals, prep. and EPR spectra comparison, hyperfine splitting 8-68381
 ions with partly filled L-shells, relativistic Hartree-Fock energy calcs. 8-82656
 molecular, Compton profile, empirical correlation with energy 8-78758
 oxygen-type atoms, subdivision of 2p-shell 8-82609
 s^2xy , Koopmans atomic valence electron ionisation energy, 1/Z expansion method, reorganisation corrections 8-78623
 $skyz$, Koopmans atomic valence electron ionisation energy, 1/Z expansion method, reorganisation corrections 8-78623
 X-ray absorption edge-shifts, empirical relations, effective ionic charge for isoelectronic series 8-55136
 Al sequence, $4s^2\text{S}-4p^2\text{P}$ transition, f-values 8-78651
 BF_3 , BO_3^{2-} , CO_3^{2-} , NO_3^- , 8-86887
 Be, dynamic multipole polarisability, coupled Hartree-Fock 8-82858
 Be I, radiative props. determ. by model-pot. method 8-70788
 Be, inner-shell photoionis. cross sections 8-74623
 Be sequence, ($Z=4$ to 10, 14), $^3\text{P}_1 \rightarrow ^1\text{S}_0$ intercombination line, CI calc., Breit interaction 8-78641
 Cu I series, oscill. strengths, formula for cancellation disappearances 8-90124
 H-like atom+bare ion, electron capture to continuum, cross-section cusp 8-90289
 H-like atoms, dipole transitions, asymptotic expansion of radial-dipole integral 8-82667
 H-like atoms, multipole polarisability, dynamic, for S state, closed-form expression 8-82857
 H-like atoms, Stark shift, classical adiabatic theory of Stark ionis. threshold 8-82687
 H-like ion plasma, population inversion, soft X-ray transitions in cooling plasma 8-87437
 H-like ions, electron impact ionis. from 3s sub-level 8-90297
 H-like ions, electron impact excitation, Coulomb modified Glauber approx. calcs. 8-94324
 H-like ions, excitation regimes, nucl. orientation due to hyperfine interaction 8-70928
 H-like ions, fluoresc. polarisation of Stark quenched spin-polarised beam 8-66501
 H-like ions, Glauber exchange amplitudes for electron scatt. 8-74772
 H-like ions, spectral line intensity, density depend., plasma diagnostic appls. 8-83617
 H⁻-like ions, electron correlation and Coulomb hole in momentum space 8-86793
 HOCl, chloramine, isoelectronic mols., vap. phase UV photoelectron spectra, struct. 8-66600
 He isoelectronic series, dipole oscillator strength distrib. moments, systematics 8-86821
 He isoelectronic series, electron correlation and Coulomb hole in momentum space 8-86793
 He, screening constants, ground and excited states 8-62701
 He series, energy level and classifications of doubly-excited states 8-62736
 He-like ions, electron impact excitation, cross-sections, modified Oppenheimer approx. 8-82843
 He-like ions, excitation regimes, nucl. orientation due to hyperfine interaction 8-70928
 He-like ions, $\text{P}_1^0-1^1\text{S}_0$ and $^3\text{P}_1^0-1^1\text{S}_0$ intercombination-line transitions 8-70771
 He-like ions, spectral line intensity, density depend., plasma diagnostic appls. 8-83617
 Li I to F I, and isoelectronic series, $Z=10-100$, L-shell energy struct. and level classification 8-55129
 Li, screening constants, ground and excited states 8-62701
 Li⁺, isoelectronic series, electron correlation and Coulomb hole in momentum space 8-86793
 Li-like ions, fine struct. in $1s2p^2\text{P}$ and $1s2s2p^4\text{P}^0$ states 8-66471
 Mg XI-S XV ions, 2131-1s31 and 2121-1s21 radiative transitions and non-radiative decay probabilities 8-70781
 MnO_4^- , CrO_4^{2-} , VO_4^{3-} , electronic struct. determ. from X-ray spectra 8-86885
 Na isoelectronic sequence, Bethe excitation cross-sections 8-82657
 Na-like ions, transition probabilities for reson. transitions 8-66494
 NaI isoelectronic sequence, 3s-3p and 3p-3d transitions, ionisation energy 8-70773
 Ne I, reson. lines in Cl VIII and A IX beam foil spectra 8-94210
 Ne, one-electron and two-electron one-photon transitions 8-58775
 O II, III, IV, beam-foil spectra, mean lives, 270-490 angstrom 8-55223
 O-like ions, spectral line intensity, density depend., plasma diagnostic appls. 8-83617
 s^2x^2 , Koopmans atomic valence electron ionisation energy, 1/Z expansion method, reorganisation corrections 8-78623
 Zn I, theoretical oscillator strengths for resonance transitions 8-74616

isolators, microwave see microwave isolators**isomer shift**

- actinide ions, electronic props., Dirac-Fock studies 8-60094
 alkali borate glass, Mossbauer expts., 85-500K 8-80260
 ferromagnet, amorphous and crystalline, evaluation of complex Mossbauer spectra 8-60370
 group IV elements, ^{57}Fe isomer shift, quadrupole coupling and interat. distance correl. 8-52408
 mixed valence cpds. $\text{M}_2^{14}\text{SbO}_5\text{M}_3^{14}\text{Cl}_6$, ($\text{M}^{\text{I}}=\text{NH}_4$, Rb or Cs, $\text{M}^{\text{IV}}=\text{Se}$, Te or Sn), ^{121}Sb Mossbauer effect 8-84506
 rare earth-Fe-Al alloys, RFe_2Al_8 , mag. props. 8-52250
 transition metal impurities, volume-corrected Mossbauer isomer shifts 8-68434
 Al, hyperfine interactions of implanted Fe, conversion electron Mossbauer spectroscopy 8-52391
 Eu, Mossbauer isomer shift and magnetic hyperfine field, press. effect 8-52386

isomer shift continued

- $\text{Eu}(\text{Ni}_{1-x}\text{Cu}_x)_2$, mixed valency, isomer shift temp. depend. 8-84511
 $\text{EuNi}_2\text{Cu}_{2-x}$, comp. depend., Mossbauer obs. of mixed valency of Eu 8-52407
 $\text{EuNi}_2\text{Zn}_{2-x}$, comp. depend., Mossbauer obs. of mixed valency of Eu 8-52407
 Fe complexes, Mossbauer isomer shift and core electron binding energies of Fe 8-82620
 Fe, Mossbauer energy shift near Curie temp. 8-52388
 Fe powder, Mossbauer spectra parameter calc. with aid of computer (Russian) 8-76361
 Fe^{3+} ion compounds, effect on Mossbauer spectra of thermal vibr. rel. to covalently populated 4S shell nucleus 8-72444
 Fe-Cu metastable dil. alloy film, hyperfine interactions 8-52398
 Fe-Ni, hydrogenated, Mossbauer effect meas. 8-92002
 FeAl, isomer shift, electronic charge density 8-80264
 FeF_3 isomer shift, using LCAO form of molecular orbital method 8-62856
 $\text{Fe}_2\text{O}_3/\text{Zn}$, and pure, influence of mag. order on charge delocalisation, Mossbauer spectra 8-68423
 $\text{Fe}_{48}\text{Rh}_{32}$, hyperfine mag. field at ^{57}Fe and ^{119}Sn nuclei, press. depend. (Russian) 8-80266
 Ru complex, HF calc., electron densities and Mossbauer isomer shift, chemical binding 8-50470
 SnS_2/Se_x , ($0 \leq x \leq 2$), ^{119}Sn Mossbauer spectrum, lattice dynamics 8-71809
 ^{203}Tl , ^{205}Tl , core excitations to low-lying states, e.m. props., hyperfine splittings, isomer shifts 8-89794

isomerisation

- binaphthyl anion radicals, photoisomerisation, local heating effects 8-85179
 dicarbocyanine solns., photoisomerisation, fluoresc. and absorpt. spectra of photoisomer 8-85181
 1,5-dichloroanthracene, photodimerisation, orientational defects, lattice energy 8-80724
 trans-dichloroethylene, isomerisation by laser multiphoton vibr. and electron excitation radiation (Russian) 8-73041
 dynamics, in liquid solutions, statistical mechanics, transition state approx. 8-60999
 methyl isocyanide, laser initiated thermal isomerisation, thermal explosion 8-80725
 proteins, gel permeation chromatography of interacting multicomponent systems 8-68950
 proteins, kinetic consts. determ. by gel permeation chromatography of interacting multicomponent systems 8-68951
 retinals, catalysed cis-trans isomerisation by crude tissue extracts 8-64925
 rhodopsin, bovine, photochem. cis-trans isomerisation at liq. He temps. 8-64939
 stilbene, diphenylpolyenes, photoisomerisation, 'phantom' photochem. singlet state, PPP SCF CI calcs. 8-73058
 p-terphenyl anion radicals, photoisomerisation, local heating effects 8-85179
 tricarbocyanine solns., photoisomerisation, fluoresc. and absorpt. spectra of photoisomer 8-85181
 SSCl_2 , IR spectra, prod. in S_2Cl_2 photolysis 8-61033

isomerism

- see also isomerisation; nuclear isomerism; rotational isomerism
 bicyclo(3.2.0)hept-6-ene, LF vib. spectra, conformations 8-58685
 bicyclo [4.4.0] decane, cis and trans forms, mol. struct., electron diff., mol. mechanics 8-50658
 camphor, optical isomers, separated, IR Lamb dip obs. 8-90197
 N-5-chlorosalicylideneaniline, $\text{H}^+ \cdot ^{14}\text{N}$ double reson. NQR spectra temp. depend. thermochromism and tautomeric mech. 8-70849
 conformers, dynamic interaction between ground states, effect on IR spectra 8-58767
 1,2-dibromoethane, gauche and trans conformers, photoelectron spectra 8-50574
 2-5-dihydrofuran, liq. phase far IR spectra, ring puckering (French) 8-92068
 DNA, proton transfers between base pairs, LCAO SCF all-electron PRDO method 8-80829
 ethynol, ab initio calc., energy levels and geom. struct. of $\text{C}_2\text{H}_2\text{O}$ isomers 8-62716
 isopropylphosphine, gauche form, microwave spectrum, identification 8-58674
 ketene, ab initio calc., energy levels and geom. struct. of $\text{C}_2\text{H}_2\text{O}$ isomers 8-62716
 nitronaphthylamines, ESCA and UV photoelectron spectra, assignments 8-50588
 optical isomers, separated, IR Lamb dip obs. 8-90197
 oxirene, ab initio calc., energy levels and geom. struct. of $\text{C}_2\text{H}_2\text{O}$ isomers 8-62716
 2-oxybicyclo(3.2.0)hept-6-ene, LF vib. spectra, conformations 8-58685
 permutational isomers, enumeration by combinatorics, Polya's theorem 8-93501
 polyenes, twisting force consts., CNDO theory potential energy surface 8-50474
 porphyrins, isomers, enumeration by combinatorics, Polya's theorem 8-93501
 racemic liq. soln., mirror isomeric mol. separation by RF rot. polarisation elec. field 8-80317
 silaethylene, triplet carbenoid isomers, thermodynamic stability 8-90076
 terphenyl, ortho-, para-, meta-, total neutron cross sections for subthermal energies 8-74779
 s-tetrazine, pot. surface of low-freq. out-of-plane modes 8-62741
 vinyl isocyanate, microwave and photoelectron study of cis- and trans-forms 8-70819
 $\text{Fe}(\text{CO})_5$, microwave dielec. relax., fluxional mechanism 8-94235
 H_2CN^+ isomers, role in interstellar HCN and HNC form. 8-81672
 HSiN-HNSi isomers, MRD-CI calcs. of struct. and stability 8-82635
 $(\text{PF}_2)_2\text{O}$, IR and Raman spectra, vibr. assignment 8-50544
 SbH_3 , inversion barrier, ab initio SCF calcs. 8-78615

isomorphism

- organic compounds, crystallographic pedigree 8-91287
 $\text{K}_2\text{Hf}(\text{MoO}_4)_6$, and $\text{K}_2\text{Zr}(\text{MoO}_4)_6$, X-ray structural investigation 8-79597
 $\text{Ni}_7\text{I}_2\text{B}_{16}\text{O}_{30}$, isomorphous phase transition $\sim 120\text{K}$ 8-79764

isothermal transformations

- binary alloy, diffusion limited transform., planar phase interface stability 8-67809
 binary alloys, simple model to describe isothermic phase transform. 8-75832
 ethane, solid, thermodynamic props. between double solid-to-solid transition and triple point temp. 8-75828
 steel, alloy, transform. kinetics of supercooled austenite in 12Kh1MF, structural method 8-52801
 steel, Cr-Mo-V, creep fracture, microstruct. effects 8-64668
 steel, Si, upper bainite morphology (*Czech*) 8-64537
 $\gamma\text{Fe}_2\text{O}_3$, transform. to α -phase, effect of preliminary pressing or vibromilling 8-84798

isotope detection

- see also mass spectra
 automatic evaluation of isotope anal. of nuclear fuels, isotope dilution, mass and α spectrometry 8-55120
 radioactive spots on thin layer chromatograms, autoionographic detect. 8-86960
 radioisotope identification by coincidence methods (*German*) 8-90038
 ^{131}I in milk, extreme low level determ. 8-92703

isotope effects

- see also isotope shifts
 alkali halide solutions, ionic hydration, review 8-92501
 atom+diatom potential, asymmetric, isotope substitution effect, Legendre expansion coord. transformation 8-70894
 BCC metal, diffusion of H isotopes, self-capture effect and activation energy (*Russian*) 8-75879
 benzene, benzene- d_6 , vibrational anharmonicity, condensation effect, vap. press. isotope effect 8-58657
 benzene, vapour press., 5-80°C, isotope effects 8-59939
 benzene-cyclohexane system, vap. press., excess free energies, isotope effects 8-59939
 benzene-cyclohexane system, vap. press., isotope effects, theory 8-59940
 benzene- d_6 (- d_3)(- d_6), vibronic coupling, hot band absorpt. spectra 8-58708
 benzene- d_1 , (- d_2)(- d_3), oriented, order, D nucl. quadrupole coupling, mag. reson. spectra 8-74683
 benzophenone, triplet, optically detected EPR, ENDOR and ODMR, HFS, isotope and spin-orbit effects 8-86898
 chloroform, and d, polar soln., Raman line shape of ν , band 8-74705
 chlorophyll-a radical cations, in disordered systems, electron spin echo envelope modulation, isotope effects 8-61141
 cyclobutanol- d_0 , - d_1 , conformation, microwave spectrum 8-86852
 cyclohexane, vapour press., 5-80°C, isotope effects 8-59939
 1,1'-dicyanoethene(- d_2), microwave spectrum, Coriolis interaction, rot. assignments 8-82721
 O-, p-, m-diethynylbenzene, vibrational spectra, deuterated isomers 8-58705
 elimination reaction, D kinetic isotope effects, tunnelling, zero-point energy effects 8-56889
 ethyldifluoroborane, microwave, Raman, IR spectra, conform., dipole moments, vibr. assignment 8-90155
 ethylene, condensation, zero point energy shift, isotope effects 8-95147
 ethylene, isotopically mixed, crystal, dilute guest probe orientational energy, IR, Raman spectra 8-68496
 fluoroform., ^{13}C vap. press. isotope effect 8-59938
 fluoromethanes, condensation, zero point energy shift, isotope effects 8-95147
 formaldehyde, 4_0^1 band anal., isotope effects 8-86878
 formaldehyde(- d_1 , d_2), and isotopic forms, microwave spectrum, ν_4 - ν_6 vibr. states Coriolis reson. 8-82719
 fulminic acid- d_0 , - d_1 , rot. Zeeman effect and nucl. quadrupole coupling 8-78683
 1-hexene-water(- D_2O), field-induced surface reactions, field ionis. mass spectra obs. 8-95949
 IR spin flip laser, matrix isolated photochemistry, isotopic, stereochemical and lattice site selectivity 8-92492
 $\text{LiNO}_3 \cdot 3\text{H}_2\text{O}(3\text{D}_2\text{O})$, density, thermal expansion coeff., isotope effect 8-87733
 methane, condensation, zero point energy shift, isotope effects 8-95147
 methoxytrimethylsilane- d_0 (- d_1) 8-86853
 methyl bromide, ν_6 band, CO_2 and N_2O laser Stark spectroscopy 8-78698
 4-methyl-2,6-di-tert-butylphenol, γ -irrad. cryst., ENDOR transitions, ELDOR detect. 8-95531
 4-methyl-2,6-di-tert-butylphenol, methyl group rot. mechanisms, Raman effect 8-71691
 methylene fluoride, anharmonic pot. function and equilib. struct. 8-78774
 molecular ions, spontaneous IR rot.-vibr. emission probability 8-50535
 multiphoton absorption induced reactions, appl. of effective photon concept 8-88651
 muonium-substituted transient radicals observed by muon spin rotation 8-74678
 naphthalene-tetracyanobenzene, Raman spectra, phase transition and isotopic substitution 8-80364
 oxazole(- d_1), dipole moment, quadrupole coupling tensor, from microwave spectrum 8-55166
 PAA, quasielastic neutron scatt., isotope effects 8-83719
 partition function ratio, reduced, of isotopic mols., generalised finite polynomial approx. 8-66529
 phenol(- d_1)-dioxan(-acetone), in carbon tetrachloride (CDCl_3) solns., H-bonds vibr. relax. bands anal. 8-84560
 phenol (- d_1 , d_5 , d_6), excited A state, normal vibr. freqs, force consts., compliance coeffs. 8-50534
 polyatomic molecules, isotopic reduced partition function ratio approx., by polynomial perturbation method 8-66530
 porphind- d_n ($n=2-14$) electronic-vibr. interaction, quasi-line absorption (fluoresc.), mirror symmetry 8-55197
 PTFE, $\text{H}_2(\text{D}_2)$ solubility and diffusion, activation enthalpy 8-79775
 pyrene + N,N -dimethylaniline (deuterate)(3,5 dimethoxy-N,N-dimethylaniline), geminate recomb., solvent, isotope, mag. field effects 8-56888
 superconducting transition temperature, isotope effect, theory 8-91806

isotope effects continued

- tetracyanoethylene-benzene(-toluene), and isotopic forms, excited charge-transfer state nonrad. decay, vibr. role 8-82765
 tetrafluoromethane, pot. consts., IR spectra 8-82808
 tetramethylammonium hexachloroplatinate, ZZ 8-92060
 tetramethylammonium hexachlorotellurate, ZZ 8-92060
 s-tetrazine, cooled supersonic jet, Van der Waals complex, isotope effects, fluoresc. obs. 8-55194
 s-tetrazine(- d_1), and $^{15}\text{N}_2$ -substituted, rot. consts., ground and $^1\text{B}_{3u}$ excited states geometries 8-82862
 2-thiohydantoin- d_0 , (- d_1), mol. vibr. and force field calcs. 8-62779
 vibrational anharmonicity, condensation effect, vap. press. isotope effect 8-58657
 water, and isotropic forms, IR band intensities estimation 8-86916
 $\text{BCl}_3\text{-H}_2$, photochem. with Ti, Pb catalysts, isotopic excitation by laser 8-64882
 BHX_2 , X=F, Cl, Br, and isotopic forms, mol. pot. consts., amplitudes, Coriolis coupling, centrifugal distortion 8-50662
 ^{135}Ba , ^{137}Ba Fourier transform NMR, NQR studies 8-94261
 BrF , $\text{B}^3\Pi(0^+)$ states, collision-free lifetimes laser fluoresc. obs. 8-94278
 CF_2Cl^+ , and parent cations, IR spectra assignments, ^{13}C -forms verification 8-80767
 CNC radical vibr. and electronic spectra, in VUV photolysis of matrix-isolated cyanomethane 8-85180
 $\text{CO}+\text{Kr}(^3\text{P}_1)(^1\text{P}_1)$ $\text{A}^1\Pi\text{-X}^1\Sigma^+$ and $\text{b}^3\Sigma^+-\text{a}^3\Pi$ sensitised fluorescence, isotope effects 8-82761
 CO_2^+ , fluoresc. quantum yields, isotope effects, photon-photoion coincidence meas. 8-90200
 CS_2 , vibr.-rot. bands at 46 μm , isotope effects 8-94245
 $\text{Ca}+\text{HF}(\text{DF})$, beam reaction, vibr. excitation 8-68877
 CdFCl , CdFBr , existence and vibr. characterisation, IR and Raman matrix isolation obs. 8-78706
 CdX_2 , (X=Br, Cl), spectroscopic parameters of mols. from vibr. isotopic effects 8-74798
 CdXY , (X, Y=Cl, Br, I), spectroscopic parameters of mols. from vibr. isotopic effects 8-74798
 $\text{Cl}+\text{D}_2\rightarrow\text{DCl}+\text{Cl}$, LEPS pot. energy surface, rate consts., isotope effect, quasiclassical trajectory calc. 8-56887
 $^{38}\text{Cl}+\text{H}_2(\text{D}_2)$ reactions, characterisation, effect of ethylene- I_2 scavenger 8-73071
 CsI , isotope diffusion 8-75875
 Cu, diffusion in Al 8-84006
 ^{63}Cu , ^{65}Cu , Fourier transform NMR studies 8-94262
 DBr, vibr. energy transfer, laser selective isotope excitation 8-82790
 DCl, vibr. energy transfer, laser selective isotope excitation 8-82790
 D_2O ice, thermal cond., H and D order effects 8-67871
 $\text{D}_2\text{O-H}_2\text{O}$ ice, thermal cond., H and D order effects 8-67871
 D_2O_2^+ , isotope effects, easily polarisable H and D bonds 8-94231
 $\text{F}+\text{HX}$ or DX , (X=I, Br, Cl), H abstraction, absolute reaction rate, H/D isotope effect 8-80721
 Fe:Xe , isotope ion implantation contr'd (*Flemish*) 8-79623
 Fe-C melts, short-range order, neutron scatt. obs. (*German*) 8-71669
 H isotope diffusion coeffs. calc. for FCC metals (*Russian*) 8-91483
 H-bonded crystal, IR absorpt. spectra band shape, X-H stretching vibr. temp. depend., isotope effect 8-76445
 $\text{H}+\text{Cl}_2(\text{H}_2)$, activation energy and trajectory calcs., temp. and isotope effects 8-76835
 H_2 , D_2 , photoionisation, body-frame Hund's case b description 8-94295
 $\text{H}_2+\text{H}(\text{I})$, activation energy and trajectory calcs., temp. and isotope effects 8-76835
 HBr, isotopic struct. and spectral characts. of vibr. band, using liq. N_2 Raman laser source 8-50859
 HBr, vibr. energy transfer, laser selective isotope excitation 8-82790
 HCN, Franck-Condon transition amplitudes for mol. dissoci., semiclassical evaluations 8-62860
 $(\text{HCN})_2$, and isotopic forms, microwave spectroscopic investigations of hydrogen-bonded complexes 8-62794
 HCl, vibr. energy transfer, laser selective isotope excitation 8-82790
 HD, isotopic effects in predissociations 8-86924
 $\text{H}_2(\text{D}_2)$ permeation in Pd (*Russian*) 8-75881
 $\text{H}_2(\text{D}_2)$ pumping by Ti film, pumping speed comparison 8-51819
 $\text{HF}+\text{H}(\text{D})$, kinetic isotope effect and temp. depend. 8-53202
 H_2O isotopes, spectrophone meas. at selected CO , CO_2 laser wavelengths 8-57310
 $\text{He}^++\text{acetylene-}d_0$ (- d_1), $\text{CH}^+(\text{CD}^+)$, A-X luminesc., in near-thermal charge exchange 8-50632
 HeH^+ , (HeD^+), rot. predissoc., nucl. motion effects on rovibr. energies and widths 8-70885
 $\text{Hf}_{0.5}\text{Zr}_{0.5}\text{V}_2\text{H}_2(\text{D}_2)$, enhanced supercond. transition temp. on H(D) additions 8-80083
 HgFCl , HgFBr , HgFI , existence and vibr. characterisation, IR and Raman matrix isolation obs. 8-78706
 HgX_2 , (X=Cl, Br), spectroscopic parameters of mols. from vibr. isotopic effects 8-74798
 HgXY , (X, Y=Cl, Br, I), spectroscopic parameters of mols. from vibr. isotopic effects 8-74798
 $\text{I}(^5\text{P}_{1/2})+\text{benzene-}d_0$ (- d_6), fluoresc. quenching, spin-orbit interaction, isotope effect obs. 8-62763
 KD.AsO_4 , ferroelec., phase transition and Raman scattering 8-84540
 KDP-type cryst., Raman scattering and phase transitions, deuteration effects 8-76400
 $\text{KD}_3(\text{SeO}_3)_2$, central peak, soft acoustic shear mode, light scatt. study, isotope effects 8-52518
 $\text{K}(\text{H,D})_2\text{PO}_4$ crystals, effect of isotopic replacement on growth kinetics 8-95006
 KH-H_2 crystal-gas system, with D impurity, thermodynamic equilib. 8-59954
 KH.AsO_4 , ferroelec., phase transition and Raman scattering 8-84540
 KrF , laser spectrum, discharge-pumped, absorption bands and lines, assignment 8-79004
 $\text{Li}_2\text{O-B}_2\text{O}_3$ glass, conductivity, permittivity, and dielectric loss obs., mixed isotope effect 8-95182
 $\text{MnH}(\text{MnD})$, $^7\text{F}_2$ -state, mol. parameters, ESR and optical spectrosc. 8-94264
 $\text{MnH}_2(\text{MnD}_2)$, $^6\text{A}_1$ state, mol. parameters, ESR and optical spectrosc. 8-94264
 Mo_6Se_8 , Chevrel phase, isotope effect on supercond. T_c 8-52141
 Mo_6Se_8 , isotope effect, theory 8-91806

isotope effects continued

- (NH₄)₂CS₂Cl, negative isotope effect on II-III phase transition (*German*) 8-95155
 (NH₄)₂RbCl, negative isotope effect on II-III phase transition (*German*) 8-95155
 NH₄+CO, vibrational energy transfer in solids, rot. mode participation 8-63815
 NH₃, and ND₃, new electronic state, multiphoton ionis. obs. 8-74717
 NO (a⁴Π), condensed phase vibr. relax., isotope effect, time resolved obs. 8-94233
 NO isotopes, spectrophone meas. at selected CO, CO₂ laser wavelengths 8-57310
 NOCN, struct., dipole moment, quadrupole coupling, microwave spectra 8-94238
 Na(D₂H₁₋₃)₂(SeO₃)₂, Raman spectra and nature of phase transitions 8-80341
 Na¹⁵N, ¹⁴N₁₋₃O₃, reflection spectra, Kramers-Kronig anal. with preliminary dispersion anal. 8-49915
¹³O¹⁸O and ¹²C¹⁸O, emission bands of E¹Π-A¹Π transition 8-90177
 Pd-H(D), isotope effect, theory 8-91806
 PdH(D), stoichiometric, ¹H and ²D NMR, rel. to supercond. T_c 8-72430
 PdH₂(D₂), optical mode phonons, nonadiabaticity 8-55916
 Pt, catalysts, supported, characterisation, hydrogenation and H₂-D₁ equilib. 8-76910
⁸⁵Rb⁺(⁸⁷Rb⁺), hyperfine struct., in-flight saturated absorption laser spectrosc. 8-78650
 SO, a¹Δ state, laser mag. reson. spectrosc. 8-94265
 SeH(X^mπ_{3/2}), far IR LMR spectrum 8-66564
 Sr+HF(DF), beam reaction, vibr. excitation 8-68877
 V-D, exam. of phase diagram, using DTA and calorimetry, isotope effect 8-80527
 VO₂, semiconductor-metal transition, effect of ¹⁸O substitution 8-84268
 V₂O₃, semiconductor-metal transition, effect of ¹⁸O substitution 8-84268
 V₂O₅, semiconductor-metal transition, effect of ¹⁸O substitution 8-84268
 Zn, diffusion in Al 8-84006
 ZnFCl, existence and vibr. characterisation, IR and Raman matrix isolation obs. 8-78706
 ZnX₂, (X=Cl, Br, I), spectroscopic parameters of mols. from vibr. isotopic effects 8-74798
 ZnX₂, ZnXY, X and Y=halogen, matrix isolation IR and Raman spectra 8-55171
 ZnXY, (X, Y=Cl, Br, I), spectroscopic parameters of mols. from vibr. isotopic effects 8-74798

isotope exchanges

- chloro-1-propanol, ³⁸Cl for Cl substitution, optical enantiomers use 8-73031
 feldspar/water O isotope exchange, effect of fluid press. 8-57204
 propylene, chemisorbed on η-Al₂O₃, desorption and D exchange obs. 8-51827
 radiation induced exchange reaction kinetics of H₂, D₂ and T₂, review 8-61005
 reactions, equilib. const., adiabatic correction, electron correl. effects 8-88626
 tropomyosin, isotopic H exchange as function of state of ionisation of side groups 8-68979
 tryptophan, fluoresc. intensity increase due to deuteration 8-78739
¹⁰B enrichment by low-temp. exchange in BF₃.SO₂ system (*Japanese*) 8-55251
¹³C, ¹⁴C, substitution during catalytic oxidation of CO over NiO 8-80786
 D+HI→H+DI, Franck-Condon theory 8-60984
 D₂O+methanol-d₀(-d₁)(-d₄), D exchange reaction, thermodynamics 8-94328
 H isotope exchange between clay minerals and seawater 8-69329
 H⁺+D₂→D⁺+HD, low energies 8-62911
 H₂+D₂→2HD, transition state, study of Jahn-Teller instability of H₄ 8-60995
 H₂O+methanol-d₀(-d₁)(-d₄), D exchange reaction, thermodynamics 8-94328
 S isotope exchange between sulphate and sulphide in acid solns., expt. determ. at 300°C and 1000 bars 8-62937
 SrSO₄, mass transfer in precip. from mixed solvents (*German*) 8-67674
 T+HT→TH+T, collinear reactivity bands 8-85143

isotope relative abundance

see also *element relative abundance*

- Allende meteorite isotopic anomalies, rel. to He-driven r-process in supernovae 8-57567
 atmospheric pollutants, ¹⁴C/¹²C ratios rel. to origins and residence times 8-69445
 calcrete deposits from Europe, Africa and India, isotopic comp. 8-73368
 cosmic rays, isotopic comp. rel. to origin and containment time 8-53781
 cosmogenic concs. in lunar samples rel. to past solar activity 8-61828
 deep sea sediment core from E.Mediterranean, stable isotopes abundances and palaeoclimatic record 8-57294
 diabase pebbles of val d'Illeiez conglomerates (Haute-Savoie), ages and initial ⁴⁰Ar/³⁶Ar ratios (*French*) 8-92810
 distribution among the elements 8-74781
 Earth, Sr, Pb isotope geochemistry rel. to catastrophic or continuous core form. 8-57178
 Earth mantle melting, past and present, isotope and trace element evidence 8-65238
 eruptive gases, thermodynamic and isotopic studies 8-69316
 ethylene, laser-induced IR photolysis mechanism 8-56909
 explosive r process cooling process 8-69791
 feldspar/water O isotope exchange, effect of fluid press. 8-57204
 galactic cosmic rays, isotopic composition of Fe-group elements 8-89024
 geochemical δ¹⁸O scales, proportional vars., interlaboratory comparison 8-69326
 geothermometry, chemical and isotopic techniques 8-69501
 Greenland ice, O isotope ratios rel. to late-Wisconsin glaciation in NW.Greenland in N.Ellesmere Island 8-57232

isotope relative abundance continued

- HR 6766, weak G-band star, light-element abundances and ¹²C/¹³C ratio 8-57548
 Kakangari meteorite, unique chondrite, noble gases abundances and isotopic comps. 8-65570
 late Precambrian mafic dykes, Montana, initial ⁸⁷Sr/⁸⁶Sr ratios and Rb-Sr geochronology 8-77196
 light elements formation, thermal cycle, isotopic abundances problem (*French*) 8-96574
 lunar regolith, light element chemistry of Apollo 12 site 8-65515
 Manicouagan melt sheet, Rb-Sr isochron age and initial ⁸⁷Sr/⁸⁶Sr ratio 8-81168
 meteorites, polymict brecciated, O isotopic comp. rel. to multiple parent bodies 8-57513
 meteorites, rel. to supernova trigger for solar system formation 8-77499
 oceanic basalts, differential Sm/Nd evolution 8-61391
 p-nuclei, abundances produced by low-temp. photonuclear nucleosynthesis in degenerate H burning zones 8-57540
 p-process isotopes nucleosynthetic origin in supernova explosions 8-57541
 Red Sea brines, ¹⁸O/¹⁶O and D/H ratios rel. to origin 8-96236
 San Juan Capistrano meteorite, rare gas isotopic abundances rel. to cosmic ray record 8-57512
 in seawater, Ra and Th isotopes in Pacific surface waters 8-96234
 sedimentary organic matter, ¹³C enrichment prod. by subaerial weathering 8-57206
 solar system, local proton irradiation model for ¹⁶O and ²⁶Al isotopic anomalies 8-93128
 solid microvolume mass spectrometric isotopic analysis 8-58088
 speleothems in N.America, stable isotope studies rel. to late Pleistocene palaeoclimates 8-57297
 Tertiary sediments from North Sea area, ¹⁸O abundances and palaeotemps. 8-88903
 volcanic rocks from Aleutian Islands and Pribilof Islands, Alaska, Pb and Sr isotopes 8-57185
 water vapour in air-water interfacial layer, isotopic distrib. rel. to bulk evaporation coeffs. 8-85576
²⁶Al from meteorites, possible 'record' of solar wind action and luminosity variations 8-61830
³⁹Ar in meteorites, evidence for Maunder minimum in solar activity 8-57529
⁷Be, cosmic ray accel. probe 8-81512
 C at DSDP sites rel. to palaeoenvironment of NE.Atlantic during Cainozoic 8-96239
¹³C/¹²C, terrestrial, appl. to planetary nebulae CNO abundances and central stars masses 8-85992
 CNO isotopes, origin and evolution 8-93201
 CO₂, isotope ratios, optical anal. method 8-85228
¹²C/¹³C, ratio in atmospheric of cool C star V460 Cygni 8-93223
¹²C/¹³C determ. in C stars 8-73710
¹²C/¹³C ratios in Population I K-type giant stars, rel. to CN strengths 8-93229
¹³C/¹²C fractionation and isotope geothermometry in the Larderello geothermal field 8-69312
¹⁴C dating rel. to magnetic and other dating methods 8-57359
¹⁴C in atmosphere content variation, past geomagnetic and cosmic ray intensity variations 8-61691
¹⁴C variations in terrestrial atmosphere rel. to 11-year solar cycle 8-92885
¹⁴C/¹²C, in tree rings, rel. to solar activity long-period vars. (*French*) 8-73695
 Cd abundances in 28 meteorites and three terrestrial rocks 8-53891
²⁴²Cm and ²⁴⁴Cm in global fallout, lichen sample results 8-57263
 D/H ratio, interstellar, evidence for nearby interstellar cloud 8-93352
 D/H ratio in Saturn and Uranus atmos. 8-57495
 D/H ratio in Uranus atmosphere, meas. 8-57497
 D/H ratio upper limits for Jupiter and Saturn 8-85892
 DC₃NH/C₂N, ratio in IRC+10216 rel. to DC₃N detect. possibility 8-69901
 H, O, isotopic comp. in plutonic granitic rocks 8-65221
³He/⁴He ratio in josephinite 8-65313
⁴He excess in Teggau Lake, NW.Ontario, rel. to U ore body 8-65353
 Mn nodules, from sea-bed, isotopic and elemental composition, U, Pa, Th, radiochem. anal. 8-77215
 N abundance and isotopic comp. in stony meteorites 8-65558
 N isotope comp. in NH₄⁺ and NO₃⁻ in rain water collected at Julich, Germany 8-57284
¹⁵N, enrichment in Mars atm. due to cosmic ray interactions in early solar system 8-73669
¹⁵N rel. to atmospheric nitrogenous trace gases 8-73470
 Nd isotopes conc. in ocean floor basalts and ferromanganese deposits 8-61395
¹⁴³Nd/¹⁴⁴Nd ratio in Recent continental volcanic rocks 8-53635
 O at DSDP sites rel. to palaeoenvironment of NE.Atlantic during Cainozoic 8-96239
 O isotope fractionation in decarbonation metamorphism, Mottled Zone Event 8-65307
 O isotope records rel. to global freshening of upper ocean layer during deglaciation 8-53658
 O isotope thermometry for sulphate-water reaction in geothermal systems 8-69383
 O isotopes in dissolved sulphate and water from hot springs and drill holes, reservoir temp. indicators 8-69382
¹⁶OH/¹⁸OH, interstellar abundance ratio obs. 8-54024
¹⁸O composition of metamorphosed chert and Fe formation from W.Greenland 8-81155
¹⁸O/¹⁶O fractionation and isotope geothermometry in the Larderello geothermal field 8-69312
¹⁸O/¹⁶O ratio of dissolved O during FLEX 76 in North Sea 8-73404
 Pb, isotope comp. in oceanic basalts, rel. to mantle evolution 8-65217
 Pb, isotope comp. of Archaean plutonic rocks 8-65223
 Pb isotopes conc. in ocean floor basalts and ferromanganese deposits 8-61395
 Pb sulphides, isotopic composition, mineralisation time determ. 8-73372
⁸⁷Rb/⁸⁷Sr studies of waters in geothermal area, Cantal, France 8-61443
²²²Rn continuous meas. for air-sea gas exchange field determ. 8-73534

isotope relative abundance continued

- S in gypsum from Mackenzie, Canada rel. to Devonian-Cambrian stratigraphy 8-61413
 S isotope variations as pollution index in lakes near Sudbury, Ontario 8-57228
 S isotopic comp. in atm. precip. around Sudbury, Ontario 8-81361
³³S/³²S ratio in ocean water SO₄²⁻ 8-65340
³⁴S/³²S ratio meas. using SO₂ and SF₆ methods, discrepancies 8-65405
 Sm isotope anomalies in Allende meteorite 8-89134
 Sr and O isotope abundances of Loch Uisg granophyre, Isle of Mull, origin hypotheses 8-65303
 Sr anomalies and p-process odd-A abundances 8-93101
 Sr isotope anomalies in Allende meteorite 8-89133
 Sr isotope comp. of Alpine tectonite lherzolites, evidence for mantle origin 8-65302
 Sr isotopes conc. in ocean floor basalts and ferromanganese deposits 8-61395
 Sr, isotopic comp. of Pacific Ocean Basin basalts, rel. to mantle comp. 8-65218
⁸⁷Sr/⁸⁶Sr, ratios in oilfield brines from Kansas and Colorado 8-57225
⁸⁷Sr/⁸⁶Sr ratio in Recent continental volcanic rocks 8-53635
 Te isotopic composition in meteoritic and terrestrial materials 8-82856
 U, determ. in environmental samples, neutron activation, neutron assay and fluorometric methods 8-61087
 U-bearing rocks, radioactive disequilib. determ., isotopes relative abundance meas. 8-57330
 Xe, fissionogenic isotopes in CO₂ well gas 8-73374
 Zr in S-type stars R Cyg and V Cancri 8-53957

isotope separation

- see also isotope exchanges; laser isotope separation; radiochemistry*
 12.16 μm radiation, two-photon pumping of ¹⁴NH₃ 8-90414
 actinides, chemical separation from PUREX raffinates using organic solvents 8-66676
 anion-exchange refinement of Pu and Np separated during extraction refinement of spent fuel elements 8-70624
 computerized mass spectrometer for isotopic analyses of solids 8-78026
 dichlorodifluoromethane, laser photolysis for Cl isotope enrichment 8-58859
 EM isotope separators, appl. to extended Pt target preparation 8-70676
 enriched gaseous isotopes, recovery systems 8-58525
 enrichment by plasma centrifuge, rotational velocity meas. 8-74502
 formaldehyde, UV photolytic separation of D from H in cryogenic solns. 8-95937
 fuel reprocessing waste ¹³⁷Cs, ⁹⁰Sr and rare earth radioisotope separation by cation exchange 8-78486
 gas centrifuge, effect of compressible flow on max. separating power 8-70644
 gas jet recoil transport system, continuous separation of Se and Te from fission products 8-70674
 gaseous diffusion, aerodynamic effects 8-59469
 hexafluoride molecule selective excitation via Doppler free multiphoton process 8-55178
 ideal cascades, 2-up 1-down, separative power and interstage flow anal. 8-58499
 interstellar clouds, isotope fractionation expts. under simulated space conditions 8-73623
 ion space charge neutralisation, influence on mass separator transmission 8-82073
 isotope centrifuge, effect of thermal convection on separative power, numerical anal. 8-58500
 Leuven isotope separator on-line at CYCLONE cyclotron 8-70682
 liquid-liquid extraction column online control by modal control techniques 8-54865
 mass spectrograph type separators, throughput limit 8-65995
 metal, isotope enrichment by combined elec. migration and zone melting 8-76600
 meteorites, isotope fractionation expts. under simulated space conditions 8-73623
 molecules beam selection by quadratic Stark effect (Russian) 8-78823
 nuclear fuel, U and Pu decontamination, sorption and distillation methods, review (Czech) 8-82496
 plasma column, rot., in hollow cathode discharge 8-75454
 porous barrier fabrication for U isotope separation, powder metallurgy problems (Italian) 8-88439
 radioactive target production for use in charged particle reaction spectroscopy 8-70670
 rotating plasma technique, skewed mag. and elec. fields (Russian) 8-70969
 Scandinavian low output isotope separator, upgrading to 300 kV 8-66008
 sulphonic ion exchangers Ar selective separation of U and Th from lanthanides 8-58860
 superheavy element prod. in ⁴⁸Ca ion+²⁴⁸Cm, spontaneous fission 8-74390
 s-tetrazines, mol. crysts., laser-induced photochem., isotope separation and hole burning 8-85185
 wedge type ion beam divergence profile calc. 8-82555
 Ar isotope separation by axial flow turbomachine model 8-78500
³⁶Ar, separation, calc. of thermal diffusion cascade (Rumanian) 8-58862
³⁶Ar-⁴⁰Ar, thermal diffusion column transport coefficients (Rumanian) 8-51274
¹⁸B separation using anion exchange resin, isotopic plateau holding displacement chromatography (Japanese) 8-56886
²¹⁰Pb, separation from ²¹⁰Pb, using silica gel ion exchanger 8-86961
⁸⁷Br, prod. by radiochem. separation, for neutron decay obs. 8-70951
¹⁴C dating, thermal diffusion enrichment, N. American glacial history extended to 75000 yrs ago 8-77284
¹⁴C dating, time scale extension by thermal diffusion enrichment, appl. to NW. Europe climatology 8-77314
 Cl, isotope enrichment using laser photolysis of dichlorodifluoromethane 8-58859
 Cu(II), selective separation from rare earth elements on chelate ion exchangers 8-58861
¹⁸F recovery during transport from reactor 8-78821
 Fe(III), selective separation from rare earth elements on chelate ion exchangers 8-58861

isotope separation continued

- H-isotope enrichment using low-temp. glow discharge technique 8-66675
^{115m,113m}In, separation from ¹¹³Sn and ¹¹⁵Cd by chem. extraction 8-74783
 Li₂, isotope separation, by two-photon ionisation, ionisation pot. determ. 8-70950
⁹⁹Mo, separation regeneration of breeder reactor fuel (Czech) 8-82496
 N₂+N₂, isotopic variants, V-T and V-V exchanges 8-90270
 Ni(II), selective separation from rare earth elements on chelate ion exchangers 8-58861
²²³Ra, ²²⁶Ra, activity ratio and separation from Indian spring water 8-86962
 Rh, A=108-111, prod. by fission of ²³⁵U, ²³⁸U, ²³⁹Pu, ²⁴⁰Cf, separation, identification 8-89924
^{103m}Rh, separation from ¹⁰³Ru by solvent extraction 8-58857
 Ru isotopes, A=107-113, prod. by fission of ²³⁵U, ²³⁸U, ²³⁹Pu, ²⁴⁰Cf, separation, identification 8-89924
 S isotope exchange between sulphate and sulphide in acid solns., expt. determ. at 300°C and 1000 bars 8-62937
 Sn, A=131, 132 prod. by ²³²Th reactor induced fission, yield, radiochem. separation, anal. 8-89923
⁹⁹Tc separation regeneration of breeder reactor fuel (Czech) 8-82496
 Th(IV), selective separation from rare earth elements on chelate ion exchangers 8-58861
 U binding, by brown coal from seawater, IR spectroscopic obs. 8-82855
 U enrichment, centrifuge, URENCO facilities at UK and Netherlands (German) 8-86666
 U enrichment by gaseous diffusion process (French) 8-70622
 U enrichment by plasma centrifuge, partial pressure distrib. obs. 8-74501
 U enrichment processes development (French) 8-66361
 U, influence of flow field struct. in the separation nozzle 8-82498
 U-Pu, isotope separation in HNO₃ by exchange resins 8-74782
 U-Th, in natural waters, anal., separation and purification (German) 8-70952
 UO₂(II), selective separation from rare earth elements on chelate ion exchangers 8-58861
 UX₃, separation from U, using silica gel ion exchanger 8-86961
²³⁵U isotope separation, efficiency improvement by nuclear excitation by electron transition 8-55039

isotope shifts

- see also atomic spectra*
 atomic metastable states, Doppler-free linear single-photon spectroscopy 8-50487
 p-benzoquinone(-d₄), n-π* excited states, distant intramol. interaction between identical chromophores 8-90203
 chlorobenzene-d₅, and isotopic forms, microwave spectrum, rot. const. 8-88667
 cyanoacetylene, and deuterate, microwave spectrum, ground and excited vibr. states 8-90157
 cyanomethane, heavy nucleus isotope shift calcs. 8-86917
 cyclopropane-d₀, d₆, absolute IR intensities, dipole moment derivatives and polar tensors 8-90165
 cis-1,2-difluoroethylene oxide, substituent and isotope effects, microwave assignments 8-78682
 ethylene carbonate, Fermi reson., isotopic substitution meas. 8-86870
 fluoromethane ν₂, ν₃ rot.-vibr. Raman bands, anisotropic components, ¹³C shifts 8-74667
 formic acid(-d₁), dilute deuterated mixture, high-sensitivity NQR, double quadrupole reson. 8-68412
 cis-formic acid (-d₂,d₃), and isotopic forms, bond lengths and angs., microwave spectrum obs. 8-55169
 metalloporphins, deuterated, resonance Raman spectra, vibr. and vibronic levels 8-62812
 methane, heavy nucleus isotope shift calcs. 8-86917
 methyl bromide, rot. absorption spectrum of ν₃ and 2ν₃ excited vibr. states, mol. const. determ. 8-82732
 methyl bromide, rot. spectrum, microwave region (Russian) 8-70823
 methyl halides, harmonic force fields, high-low freq. separation calcs. 8-90067
 naphthalene, C₁₀H₈ and C₁₀D₈, optical absorpt. spectra of hydronaphthyl radicals, isotope effects 8-60487
 naphthalene-d₀₋₈, fluoresc. and absorpt. Shpolskii spectra (Russian) 8-90208
 polyatomic molecules, fundamental stretching freq. 8-50530
 pyridine-d₀, -d₅, vap. fluoresc. spectra 8-82771
 selenoacetaldehyde, microwave spectrum, struct. internal rot. barrier 8-74645
 vinylsilanetriol-d₀,(-d₃), soln., vibr., IR and Raman spectra 8-86854
 Ba II, even isotopes, optical isotope shifts, Lamb-dip spectrosc. obs. 8-78666
¹²C/¹⁶O isotopes, IR and Raman spectra, vibron band, vibron-phonon combination bands 8-68495
 CO₂ laser stability and heterodyne frequency calibration 8-59031
 CS₂, ν₃ band, dipole moment correl. function, isotope splitting and band contour 8-74650
 Ce II, isotope shift and screening, pseudo-relativistic HF calc. 8-90096
 Cs, HFS, isotope shift related to nucl. charge rad. 8-78826
 Cu₂O, exciton spectrum, effect of isotopic substitution 8-67955
 Dy II spark spectrum, isotope shift, config. mixing 8-58628
 H(D), ground state Lamb shift, isotope shift and relativistic nuclear recoil correction 8-82696
 H₂O, heavy nucleus isotope shift calcs. 8-86917
 H₂O, liq., intermol. coupling, isotope and salt effects, Raman spectra 8-90169
 HOI, O₃(O)+HI matrix reaction, IR spectra, isotope shifts and band assignments 8-80737
⁴Hg, A=198-202 and 204, nuclear charge radii variations from K X-ray isotope shifts 8-70441
 In, 451.1 nm transition, HFS and ¹¹³In-¹¹⁵In isotope shift 8-82674
 Li, A=6,7 two-photon intracavity dye laser spectroscopy 8-82706
 Li₂, and isotopic variants, low-lying X-B transition freq. calc. 8-90180
 Mg₂, Ar matrix isolated laser photoluminescence spectra, electronic absorpt., emission, vibronic and vibr. relax. 8-82744
 MgO(O₂), from Mg+O₂ matrix reaction, IR spectra, isotope shifts and blue matrix shift 8-80736

isotope shifts continued

- NH_3 , heavy nucleus isotope shift calcs. 8-86917
 $\text{N}_2\text{H}_2(\text{N}_2\text{D}_2)$, ground and first excited state small vibr. coupling, ab initio CI calc. 8-62791
 $^{14}\text{NH}^+(^{15}\text{NH}^+)(^{14}\text{ND}^+)$, ab initio CI calc. Λ type doubling in $\text{X}^2\Pi$ states 8-82714
 Ne, metastable state, Doppler-free linear single-photon spectroscopy 8-50487
 $\text{Ne}+\text{Ne}(\text{He})$, $7d'$ states, isotope shift, press. shift, press. broadening, two-photon spectra obs. 8-55155
 OsO_4 , and isotopic forms, stretching fundamental, 961 cm^{-1} , high resolution spectroscopy 8-90162
 OsO_4 , tunable diode laser spectrosc. obs. 8-82061
 $\text{PH}_3(\text{D}_3)$, ^{31}P NMR, chemical shielding, centrifugal distortion, anharmonic vibr., cubic force consts. 8-82752
 PuN , in Ar matrix, IR spectra, stretching freq. and isotope shifts 8-78690
 PuN_2 , in Ar matrix, IR spectra, stretching freq. and isotope shifts 8-78690
 PuO , in Ar and Kr matrices, IR absorption spectra, normal coord. anal., assignments, force consts. 8-78681
 PuO_2 , in Ar and Kr matrices, IR absorption spectra, normal coord. anal., assignments, force consts. 8-78681
 SF_6 , tunable diode laser spectrosc. obs. 8-82061
 SPF_3 , IR spectra, $^{32}\text{S}/^{34}\text{S}$ shift 8-62802
 Si:S , existence of isotope shift for S deep level, isothermal transient capacitance meas. 8-63999
 U I, relative isotope shifts, specific mass shifts 8-90122
 ^{235}U , hyperfine struct. and isotope shift meas., laser separation by two-step photoionisation 8-78822
 W, atomic spectra, isotope shifts in visible region and HFS 8-82694
 Xe, three level systems, obs. of isotope shifts 8-82670

isotopes

see also radioisotopes

- O, lung perfusion determination by dilution principle with expiration detection of indicator (*German*) 8-85326
 O, lung perfusion determination using O isotopes and dilution principle (*German*) 8-85327
 ^{238}U , natural spontaneous fission, Xe prod., determ., extraction from granite 8-96216

isotopic generators see radioactive sources**isotopic spin (elementary particles)**

- broken isospin symmetry in chiral $\text{SU}(4)\otimes\text{SU}(4)$ and D^+-D^0 mass difference 8-89691
 charmed baryons, nonleptonic decays 8-66118
 classical particle in external Yang-Mills field and $\text{SU}(2)$ coherent states 8-74150
 conformal relativity, particle species classification, symms., space time origin of isospin 8-93815
 exotic baryon resonance with isospins $\geq 5/2$, existence, sum rule in Reggeon field theory (*Russian*) 8-93824
 multiparticle production, quasi-classical description of isospin conservation 8-58134
 nonleptonic hyperon decays, CP violation, deviations from $\Delta I = 1/2$ rule 8-70367
 supersymmetry, superfield notation for supermultiplets spontaneous breaking, Lagrangians and internal symmetry incorporation (*German*) 8-74167
 Weinberg model, universality and weak isospin leptons, nucleons, quarks 8-70273
 Yang-Mills theory, conversion of isospin degree of freedom into spin degree of freedom 8-89617
 $\text{D}\rightarrow\text{K}^+\pi\pi$, branching ratios, isospin anal. 8-70363
 $\text{NN } I=1$ amplitudes struct. at 6 GeV/c 8-70395
 NN scatt., impact parameter representation, taking into account spin, isospin and Pauli principle 8-58198
 pp , isospin anal. of energy shifts 8-62961
 $\pi^-^3\text{He}$, isospin anal. of energy shifts 8-62961
 $\pi^+\text{p}$, isospin anal. of energy shifts 8-62961
 $\pi^+\pi^-$, isospin anal. of energy shifts 8-62961

iteration methods see iterative methods**iterative methods**

see also predictor-corrector methods

- atomic struct., numerical HF radial function during SCF iteration, convergence 8-58574
 Bayesian deconvolution, convergent props. 8-57861
 Boussinesq problem for material with different moduli in tension and compression 8-55564
 cell kinetic parameters estimation from flow microfluorometry 8-73143
 chemistry, method of successive approx., teaching 8-89281
 CLEAN method, iterative beam removal, mathematical-statistical description 8-57464
 coastal trapped ocean waves, anal. and numerical calc. by inverse iteration 8-69360
 compact storage for iterative soln. of large sparse linear systems of eqns. 8-57713
 complex alpha-spectra evaluation using program ALFUN 8-74552
 composite signal anal., by cepstral inverse filtering, biomedical appl. 8-69243
 compressible flow study, gas dynamics method based on iterative techniques (*Hungarian*) 8-94757
 computational methods, book 8-81820
 computerised tomography, iterative three dimensional reconstruct. from twin cone beam projections, simulation study 8-80949
 configuration interaction, iterative variational method calcs. 8-55127
 convex nonlinear boundary value problems, iterative bounds for stable solns. 8-54167
 depth determ. from seismic refraction data, iterative method 8-96302
 diatomic molecule, wave function computation, iterative method compared with Langer's method 8-86762
 dusty gas, two fluid model field eqn., time interval for soln., iteration method (*German*) 8-63489
 elastic-plastic finite element analysis, interpolation vs. iterative soln. for Tresca yield condition 8-59312
 electromagnetic wave scattering by inhomogeneous sphere, iterative soln. to p-tuple series eqns. 8-62976
 electron-hole transitions, nonstationary processes, numerical anal. (*Ukrainian*) 8-84229
 iterative methods continued
 finite element discretisation, two-dimens. stationary heat cond. using successive overrelaxation and conjugate gradients 8-83206
 flow, two-dimens. boundary layer, viscous-inviscid flow matching, transonic and supersonic flow (*French*) 8-79334
 foil bearing, deflection due to finite width bump 8-77691
 gamma-ray detection, scintillator response, pulse height spectra unscrambling, computer program 8-55092
 gas transport coeff. data inversion iterative procedure, pot. energy function determ. 8-91051
 Gauss-Seidel technique for Mississippi Pascagoula Estuary water quality planning 8-73402
 hard corrugated surface, wave scatt., iterative series 8-89355
 heat conduction, inverse nonlinear problems, simulation methods 8-94513
 heat conduction in solids, nonlinear, direct and inverse problems, approx. soln. method 8-94510
 heat transfer, nonlinear, iterative-variational method 8-94511
 high precision voltage meas. automatic error correction algorithm (*Russian*) 8-70089
 hydrometeorological data, Weibull distrib. appl. 8-65415
 image reconstruction principles, in X-ray computer tomography 8-88745
 image restoration, compare to singular value decomposition method 8-58930
 implicit fast iterative numerical method for solving multidimensional partial differential eqns. 8-93519
 instrument operation speed increase, additive-iterative correction method (*Russian*) 8-89423
 ion optics, high current beam extracted from plasma, iteration scheme 8-50693
 large scale general eigenvalue problem iterative method for soln. 8-89318
 magnetic fields, slot permeance ratio evaluation (*Italian*) 8-86987
 matrix Riccati eqn., quasi-linearisation, iterative approx. 8-57871
 membrane, rectangular under uniform pressure, large deflections 8-55560
 Monte Carlo iterative scheme for adaptive multidimensional integration 8-57762
 multispectral radiance method for temp. distribution meas. (*Japanese*) 8-77912
 nematic liquid crystal mixtures, extended range, iterative method for eutectic range 8-83728
 neutron diffusion, linear eqns., soln. by method of implicit non-stationary iteration 8-70581
 nonlinear elliptic problems for doubly connected domains, heuristic method (*Russian*) 8-86159
 nonlinear image restoration with signal-dependent noise, decomposed local algorithm 8-78951
 nonmetrical method for paired comparisons (*Japanese*) 8-77833
 nuclear reactor neutron-physical calc., FBR, multi-group diffusion equation solution (*Czech*) 8-66332
 organ flue pipes, self-sustained oscillations, integral eqn. soln. 8-51015
 particle tracks momentum determ. 8-70723
 particle velocity distrib. functions in nonuniform background, iterative calc. 8-71438
 penalty function solns. of algebraic systems 8-57770
 Percus-Yevick equation, numerical calc. of crit. exponents 8-91212
 polymer solution, semidilute, hydrodynamic interaction of two permeable spheres, method of reflections 8-71394
 potential energy with iterative correction or deterioration 8-89315
 radar attenuation in rain, iterative correction 8-92923
 radiative transfer in finite media, new technique for exact and unique soln. 8-77479
 radiotelescope with minimum noise, maximum gain by iterative relaxation 8-65498
 rectangular matrix pseudoinverse using column approx., inconsistency systems of linear eqns. solns. 8-62061
 rotating fluids, computation of velocity fields 8-59401
 SCF open shell orbitals, iterative process 8-90066
 seismic reflection data inversion 8-96307
 self-conjugate and positive definite operator, simultaneous calc. of eigenvalues (*Ukrainian*) 8-54154
 spectral estimation techniques for discrete time series 8-53734
 stable operational processes appl. to inverse geophys. problems 8-85718
 static fields in inhomogeneous anisotropic medium (*Ukrainian*) 8-81837
 steady-state response of difference eqns., digital computation schemes 8-57718
 stochastic constraints on iterative maximisation of system of differential eqns. 8-57757
 stream-well-aquifer system groundwater flow anal., linear system models 8-77289
 strength of axisymmetric body, optimum shape calc., finite element technique 8-51060
 tensile conc. optimisation using iterative method (*German*) 8-87271
 vibrational anal., iterative methods, accelerated automatic root search algorithm 8-59321
 water network anal. using sparse matrix and successive linearisation methods 8-85614
 X-ray fluoresc. element anal. in pulps, conc. calcs., iterative method 8-61109
 X-ray image reconstruction, iterative scheme 8-66014
 XPS, achromatic X-ray source, spectrum iterative deconvolution 8-72689
 itinerant model of magnetism see band model of magnetism
 IV-VI semiconductors
 properties and use for making devices, review 8-60131
 Au-Pb, Sn_{1-x}Te -Au structure, third harmonic variations at 77K and 300K 8-84313
 Ge-Pb $_{1-x}\text{Sn}_x\text{Te}$, amorphous/crystalline heterojunction, rectification props., IR detector appl. (*Japanese*) 8-60197
 GeS, (001) surface struct., LEED expt. 8-84034
 GeS, exciton luminescence 8-52555
 GeS, $\text{Se}_{1-x}\text{S}_x$ IR spectra, differential calorimetry, phase diagram (*Russian*) 8-52513
 GeTe, X-ray emission spectra, amorphous and cryst. struct. (*Russian*) 8-88385

IV-VI semiconductors continued

- GeTe: I, ferroelectric transition exam. 8-88264
 GeTe: Mn, thermoelec. power, 2.5-25K, magnon drag effect 8-56169
 (GeTe)_x-(AgSbTe₂)_{1-x}, thermoelectric props. of monolithic and pressed samples at 300K 8-80009
 Pb-Te, molten mag. susceptibility, conc. and temp. depend. 8-80121
 Pb_{1-x}Cd_xTe, epitaxial, resist. and Hall coeff., substrate temp., thickness and comp. depend. 8-72290
 Pb_{1-x}Ge_xTe, dielec. const. determ. near ferroelec. transition 8-88269
 Pb_{1-x}Ge_xTe, electron-phonon interaction effect on ferroelec. transition 8-76416
 Pb_{1-x}Ge_xTe, phase transitions 8-60408
 Pb_{1-x}Ge_xTe: Ga, Fermi level stabilization, transport props. meas., 77-400K 8-56065
 PbS, epitaxial layer on rock salt substrate, stresses, hydrostatic press. effects 8-51831
 PbS film, polycryst., chem. deposition from soln. and characterisation 8-72743
 PbS, nonstoichiometric, increase of rest pot. with p-type semicond. character 8-56170
 PbS, thermomech. props., SCF X α scatt. wave theory 8-71704
 PbS-Si p-n heterojunction, characts. and operation, IR detector appls. 8-52075
 PbS(Se), photoionisation cross section of atomic and final state effects on 5d core levels 8-84699
 PbS_xSe_{1-x} film, prep. by co-evaporation method (*Japanese*) 8-64477
 PbS_xSe_{1-x} film prep. by co-evap., elec. props. (*Japanese*) 8-80470
 PbS(Se)(Te), chemisorption of O₂, room temp., UPS and XPS obs. 8-91529
 PbSe, complex-composition film production method from vapour (*Russian*) 8-95702
 PbSe surface, clean and O₂-exposed, XPS (UPS) obs., electronic struct. 8-52637
 PbSe, valence band structure from angular resolved photoemission spectra 8-84143
 (PbSe)_{1-x}(SnTe)_x lattice dynamic props., Gruneisen parameters (*Russian*) 8-83984
 Pb_{0.2}Sn_{0.8}S, Mossbauer spectra, effect of optical emission (*Russian*) 8-60367
 Pb_{0.59}Sn_{0.41}Se, struct. phase transition, temp and hydrostatic press. influence, Hall effect, resistivity (*Russian*) 8-51675
 Pb_{0.975}Sn_{0.025}Se, film, acoustic wave modulation of electron current 8-64067
 Pb_{1-x}Sn_xSe, band inversion effect on phonon spectra 8-79699
 Pb_{1-x}Sn_xSe, determ. of anisotropy coeff. of Fermi surface, magnetoresist. meas. 8-51878
 Pb_{1-x}Sn_xSe-PbSe pulse laser diode, temp. tuning of modes 8-50777
 PbSnTe DH laser, anodic oxide film to avoid degradation by thermal cycling 8-50809
 PbSnTe IR photovoltaic detectors for 8-14 μ m range, review (*Italian*) 8-54451
 PbSnTe-PbTe heterostructs., effect of electrical grounding on electron irradi. 8-60194
 Pb_{0.8}Sn_{0.2}Te, hole conc. at 77K from room temp. thermoelec. meas. 8-56155
 Pb_{0.8}Sn_{0.2}Te, p-n homojunction breakdown voltage for onesided abrupt junctions (*German*) 8-56210
 Pb_{0.82}Sn_{0.18}Te, narrow band gap, relax. time for Shubnikov-de Haas effect 8-80006
 p-Pb_{0.82}Sn_{0.18}Te, Hall coeff. sign-inversion temp. 8-52010
 Pb_{0.82}Sn_{0.18}Te, carrier tunnelling through potential barrier in p-n junctions (*Russian*) 8-52074
 Pb_{1-x}Sn_xTe, absorption edge shift, energy gap determ. 8-88308
 Pb_{1-x}Sn_xTe, band struct. and phonon energies, tunnelling spectroscopy 8-72070
 Pb_{1-x}Sn_xTe, Cd-In diffusion, changes in elec. props. 8-91348
 Pb_{1-x}Sn_xTe, continuously tunable electron beam pumped laser 8-50802
 Pb_{1-x}Sn_xTe, electron-phonon interaction 8-71819
 Pb_{1-x}Sn_xTe, grown by LPE, solid-liquid tie line determ. 8-64526
 Pb_{1-x}Sn_xTe, impurity defused IR detector, spectral response depend. on impurity conc. (*Japanese*) 8-58036
 Pb_{1-x}Sn_xTe, lattice instability and phonon lifetimes, neutron scatt. 8-55932
 Pb_{1-x}Sn_xTe, MBE, O₂ uptake, AES, XPS and UPS expts. 8-95227
 Pb_{1-x}Sn_xTe monocrystal and sinter thermoelec. inhomogeneity 8-91713
 Pb_{1-x}Sn_xTe optically pumped lasers, power output and wavelength, 4 to 30K 8-79035
 Pb_{1-x}Sn_xTe-PbTe, amorphous/crystalline heterojunction, rectification props., IR detector appl. (*Japanese*) 8-60197
 Pb_{1-x}Sn_xTe-PbTe heterojunction, Sn diffusion profile, X-ray diffr. data interpretation 8-51832
 Pb_{1-x}Sn_xTe-PbTe pulse laser diode, temp. tuning of modes 8-50777
 Pb_{0.9}Sn_{0.1}Te-PbTe p-n junction, epitaxial, elec. props. and photore-sponse 8-56225
 Pb_{1-x}Sn_xY, Y=Te, Se, S, photocond. anisotropy rel. to lifetimes 8-52032
 PbTe (111), adsorption of O₂, UPS and XPS exam. 8-71962
 PbTe, carrier conc. inhomogeneity 8-52019
 PbTe, complex-composition film production method from vapour (*Russian*) 8-95702
 n-PbTe, epitaxial, time dependent negative weak field magnetoresist. 8-64151
 n-PbTe epitaxial film, magnetophonon and Shubnikov-de Haas oscills. 8-60234
 PbTe epitaxial film, stimulated emission, absorption spectra and recombination 8-80409
 PbTe epitaxial layers, orientation on different faces of LiNbO₃ 8-79907
 PbTe, ion-implanted, doping profile evaluation by Hall effect and sheet resist. meas. 8-59831
 p-PbTe MIS capacitors 5 μ m IR detector appl. 8-52101
 PbTe, magnetoreflexance of surface space charge layers 8-52475
 PbTe, solidus line anal., carrier conc. 8-75806
 PbTe surface space charge layers, far IR magnetoreflexance meas. 8-64349
 PbTe, TO phonon softening, free carriers and defects effects 8-79720
 p-PbTe, thermorefl., 1.0-4.6 eV 8-76492
 PbTe, thick epitaxial film, laser deposition technique 8-68629

IV-VI semiconductors continued

- PbTe-SnTe, solid soln. single crystals, TSM growth and elec. characts. 8-68625
 Pb_xTe_{1-x} film, highly absorbant, complex index of refr. determ. method 8-54445
 SnO₂, gas sensor, CO, H₂O vapour, surface temp. effect on cond. 8-76067
 Sn_{1-x}Pb_xTe, elec. and struct. props. of epitaxial layers (*Russian*) 8-64147
 Sn_xPb_{1-x}Te mixed cryst., cryst. growth and assessment 8-80463
 SnS₂, electron mobility, elec. cond. and Hall effect meas. 8-80004
 SnSe, electronic band struct. determ. 8-51890
 SnSe, Mossbauer spectra, effect of optical emission (*Russian*) 8-60367
 SnSe, sublimation growth, deviation from stoichiometry, elec. props. 8-76594
 SnTe, complex-composition film production method from vapour (*Russian*) 8-95702
 SnTe, electron-phonon interaction effect on ferroelec. transition 8-76416
 p-SnTe, film and bulk, weak-field magnetoresistance 8-84236
 SnTe, Hall coeff., temp. depend., interpretation 8-87988
 SnTe, isothermal meas. of galvanomag. and thermomag. effects (*Russian*) 8-56160
 SnTe, solidus line anal., carrier conc. 8-75806
 SnTe-PbTe-GeTe, alloy semiconductor, phase transition (*Japanese*) 8-91443
 ZnSe_xS_{1-x}, melt grown, 10K, band edge photoluminesc. 8-84628

J particles see *psi mesons***Jahn-Teller effect**

- alkali halides: Ga⁺, optically detected EPR in relaxed excited states of Ga⁺ 8-72437
 C_{3v}-type mols., double degenerate electronic states, Jahn-Teller and spin-orbit coupling 8-50537
 C_{3v}-type mols., doubly degenerate electronic states, Jahn-Teller interaction 8-50536
 cooperative Jahn-Teller effect and paramagnetic susceptibility of S=1 systems 8-68134
 cooperative Jahn-Teller systems of T nature, electron-phonon excitation branches 8-63823
 diamond, ESR studies, review 8-95521
 diamond, magnetic field and stress splitting of GR1 line 8-60095
 diamond, relaxation about the vacancy 8-71722
 EPR spectra, Jahn-Teller effect, multistate theory for ²E orbital states 8-56369
 fourfold symmetric systems, Jahn-Teller effects 8-58599
 halomethanes, vibronic struct. in electron spectra, Jahn-Teller and spin-orbit coupling 8-50537
 icosahedral molecules and complexes, Jahn-Teller effect, pot. surface 8-78642
 impurity centres in crystals, quadratic Stark effect, Jahn-Teller effect 8-68536
 ionic crystals, recent developments 8-64015
 iron porphrin, A_{2u} out of plane vibration, pseudo-Jahn-Teller effect 8-82712
 ligand trajectories, octahedral T₁ system 8-76028
 linear Jahn-Teller E-e effect, canonical transformation 8-67993
 linear Jahn-Teller systems, continuous group invariances 8-60092
 metalloporphyrins, Jahn-Teller effects 8-58599
 metalloporphyrins, Soret excited, reson. Raman excitation profiles, Jahn-Teller distortion and vibronic anal. 8-58698
 molecular shape, second-order Jahn-Teller effect, highest occupied mol. orbital postulate 8-86780
 molecule with fourfold symmetry axis, coexistence of two kinds of stable Jahn Teller distortions 8-84176
 monopyrazine zinc sulphate trihydrate: Cu²⁺, ESR meas. 8-84478
 polar crystal, vibronic levels for Jahn-Teller impurities 8-68520
 pyrazine, vibr. struct. and nonlinear vibronic coupling, pseudo Jahn-Teller effect 8-94234
 Rochelle salt, optical characteristics in UV region (*Russian*) 8-84550
 sandwich compounds, orbitally degenerate, EPR 8-86893
 tetragonal symmetry, dynamic Jahn-Teller vibronic coupling 8-60091
 trifluoriodomethane, X \rightarrow B Rydberg transition, Jahn-Teller coupling parameter, vibronic level calc. 8-50536
 triply degenerate singlet electronic states, reson. Raman scatt. 8-78714
 vibronic coupling model, for mol. spectra, rel. to pseudo Jahn-Teller effect 8-94234
 AgBr_{1-x}Cl_x, self-trapped holes, Jahn-Teller and reorientation effects in ESR 8-64273
 Al₂O₃:Cr²⁺, Jahn-Teller study, EPR data anal. 8-84172
 Al₂O₃:V³⁺, phonon scattering, comparison between theory and experiment 8-95116
 BaTiO₃:Cu, photoferroelec. props., Jahn-Teller effect, laser irradi. effect on pyroelec. props. 8-60400
 CaO, F-centres, ³T_{1g} relaxed excited state, uniaxial stress effect and spin-lattice coupling 8-72405
 CaO, random intrinsic strain effect on ODMR, PMDR, of F-centre in Jahn Teller states 8-84499
 Ca(OD)₂:Cu²⁺, ESR, secondary spectra 8-88174
 CsCrCl₃, co-operative Jahn-Teller distorted struct. determ. 8-63713
 CsI:Ti⁴⁺, Jahn-Teller split luminesc., high press. study 8-52565
 Cs₂PbCu(NO₂)₆, successive Jahn-Teller phase transitions, neutron and X-ray diffr. 8-95154
 Cu complex, Cu(en)₂Cl₂ 0.75 en, X-ray and ESR data, Jahn-Teller distortions 8-80206
 Cu₂Zn_{1-x}ZrF₆ 6H₂O, distortions of nearest Jahn-Teller [Cu(H₂O)₆]²⁺ centres 8-68000
 DyAsO₄, cooperative Jahn-Teller phase transitions, dielec. anomalies 8-64312
 DyVO₄, basal plane magnetisation anisotropy under Jahn-Teller distortion 8-68222
 DyVO₄, cooperative Jahn-Teller phase transitions, dielec. anomalies 8-64312
 DyVO₄, Jahn-Teller phase transition and improper antiferroelectricity (*Japanese*) 8-80294
 DyVO₄, mag. field depend. of cooperative distortion 8-79733
 FeBr₂, dynamic Jahn-Teller system, Raman scatt. from electronic excitations and phonons 8-56474

Jahn-Teller effect continued

- FeCl₂, dynamic Jahn-Teller system, Raman scatt. from electronic excitations and phonons 8-56474
 FeS, zinc blende type, crystallographic and Mossbauer obs. 8-87650
 FeZrF₆, phase transition at 212.3K, Mossbauer, EPR study, quadrupole splitting, Jahn-Teller effect (*German*) 8-68430
 IrF₆, in mixed crystals, Jahn-Teller effect, $\Gamma_{8g}(t_{2g})^3$ state, 6800 Å 8-76032
 KBr:Ti³⁺, Jahn-Teller split luminesc., high press. study 8-52565
 KCl-KI:Ti, spectral, polarisational and kinetic characts. 8-80385
 KCl(Br)(I):In³⁺, Jahn-Teller split luminescence, high press. study 8-52565
 K₂Cu_{1-x}Mn_xF₄, Cu-Mn exchange interaction, optical determ. 8-72551
 K₂Dy(WO₄)₂, low temp. phase transitions (*Russian*) 8-87787
 K₂PbCu(NO₂)₆, incommensurate Jahn-Teller phase transition 8-79730
 K₂PbCu(NO₂)₆, Jahn-Teller phase transitions, order-disorder model 8-79762
 K₂PbCu(NO₂)₆, Jahn-Teller phase transitions, X-ray and neutron measurements 8-91438
 K₂Zn(ZrF₆)₂·6H₂O, EPR of Cu²⁺, temp. depend. 8-80201
 Li₃, BO hypersurface and vibronic states, coupled electron pair approx. 8-94203
 MgO:Cr²⁺, critically coupled spin-phonon mode 8-67779
 MnO, Jahn-Teller effect on optical absorption spectra 8-52484
 Mn(PO₃)₃, cryst. struct. determ. (*French*) 8-55843
 NH₃⁺, ionisation pot. of ²E state, Jahn-Teller effect 8-62948
 Na₃, electronic struct., pot. energy surface, ab initio CI study 8-70996
 Na₂VS₂(Se₂), mag. and elec. props. rel. to struct. transitions 8-91848
 PrAlO₃, ²⁷Al NMR, electronic spin dynamics at Jahn-Teller phase transition 8-68403
 PrCl₃, one-dimensional X-Y system, far IR absorpt. spectra, cooperative spin excitations 8-95584
 PrCu₂, cryst. field transitions near cooperative Jahn-Teller transition 8-84178
 β-RbCrCl₃, co-operative Jahn-Teller distorted struct. determ. 8-63713
 RbDy(MoO₄)₂, low temp. phase transitions (*Russian*) 8-87787
 ReO₃Cl, near UV absorpt. spectra, dynamical Jahn-Teller effect 8-86881
 SO₃(SO₃)⁺, Jahn-Teller interaction, Franck-Condon factors and vibronic energy level calc. 8-50536
 Si, extended Huckel theory calculations for positive divacancy 8-87938
 Si:Cr, spin-lattice relax. of Jahn-Teller Cr⁰ centre (*Russian*) 8-72402
 Si:P, optically induced divacancy reorientation, EPR spectra 8-80216
 TbVO₄, Jahn-Teller phase transition, γ-ray diffractometry 8-91205
 TbVO₄, mag. field depend. of cooperative distortion 8-79733
 TcO₃Cl, near UV absorpt. spectra, dynamical Jahn-Teller effect 8-86881
 TmPO₄, Jahn-Teller induced elastic constant changes, 4.2 to 300K 8-79657
 TmZn, cooperative Jahn-Teller effect 8-67998
 UF₆, neat and mixed cryst. emission spectra, lowest charge transfer state, Jahn-Teller effect 8-67992
 U(OH)₂SO₄, cooperative Jahn-Teller effect, mag. susceptibility meas. 8-72121
 ZnS:Mn²⁺, Jahn-Teller effect in fluorescent level 8-52566
 ZnS(Se)(Te):Cr²⁺, Jahn-Teller coupling 8-67997
 ZnSe:Mn²⁺, Jahn-Teller effect in fluorescent level 8-52566

jellies see gels

jellium

- Al, one-electron calcs. of X-ray absorpt. and emission, jellium model 8-56543
 atom near metallic surface, resonant state, Schrodinger eqn. soln., jellium model 8-80033
 atomic chemisorption, chemical trends, core-hole relax. effects, jellium model 8-76909
 CDW system, attenuation of collective excitations 8-84157
 chemisorption of H on metal surface, relax. energies in UPS 8-91544
 chemisorption of H on metal surfaces, linear response theory 8-91543
 DC electrical conductivity, microscopic fields and currents 8-56121
 diamond Schottky barrier, electronic struct., pseudopot. calc. 8-95364
 liquid metal, surface ion density, nonmonotone, perturbative discrete ion introduction into jellium 8-72222
 metal surface, indirect long-range oscillatory interaction between adsorbed atoms 8-71997
 metal surface, step potential model, static semiclassical response of bounded electron gas 8-72221
 metal surface exposed to external radiation, solns. of Maxwell's eqns. 8-52054
 metals separated by dielectric, electronic component of metal-metal interaction force, calc. 8-52056
 simple metals, atomic chemisorption, atom-jellium model 8-84066
 surface energy of metals 8-91528
 Al, alkali metal adion-surface interaction energy, density formalism calcs. 8-68069
 Ge, Schottky barrier, electronic struct., pseudopot. calc. 8-95364
 Li, one-electron calcs. of X-ray absorpt. and emission, jellium model 8-56543
 Mg, one-electron calcs. of X-ray absorpt. and emission, jellium model 8-56543
 Na, one-electron calcs. of X-ray absorpt. and emission, jellium model 8-56543
 W, alkali metal adion-surface interaction energy, density formalism calcs. 8-68069

jet stream see atmospheric movements

jets

see also plasma jets; sprays

- acoustic noise, large-scale struct. importance 8-94792
 acoustic noise, shear layer instability effect 8-94791
 acoustic power distribution in a turbulent jet 8-67238
 aerofoil with jet flap, incompressible flow past 8-59414
 air jet, vertical axisymmetric buoyant, profile meas. 8-90906
 amorphous metal ribbon form. by cylindrical jet on flat moving substrate, uniformity 8-52718
 annular, conditions for self-excitation of oscills. 8-94782
 arc, plasma, of free jet laminar core, axial flow, strong localised disturbance effect 8-91178
 array of jets, thermal diffusion downstream meas. 8-94785
 array of jets impinging surface, convective heat transfer 8-90953
 atomisation of liquid by impinging jets, expt. and theory 8-87373

jets continued

- axisymmetric jets and wakes, calc. with turbulence model 8-67239
 axisymmetric laminar jet diffusion flame, split operator finite difference solns. 8-51252
 base flow at supersonic vel., rockets and re-entry vehicles appl. 8-67243
 buoyant, turbulent in cross flow, finite difference method 8-90907
 cantilever pipes, internal flow induced instabilities 8-63496
 capillary instability, determ. of dynamic surface tension of inks 8-84031
 circular air jet, zero entrainment, vel. field 8-51213
 circular jet turbulence under suction conditions (*Bulgarian*) 8-59437
 coaxial round, turbulent mixing, eddy Reynolds number var. 8-75179
 coaxial round jet turbulence characts., obs. 8-87372
 colliding supersonic coaxial underexpanded, investigation of flow 8-67237
 confined burning jet, droplet vaporisation, expt. and theory 8-94855
 controlled perturbation of circular jets, smoke visualisation 8-90956
 diffusion pump jet assembly and vaporiser design optimisation 8-81999
 dust laden jet, particle turbulent diffusion 8-83455
 dye laser jet stream, thickness meas. in real time, by optical technique 8-82975
 dynamic liquid surface tension determ. from drop oscillation frequency and capillary jet instability 8-56026
 dynamic surface tension, meas. by excited capillary jet axisymmetric disturbance growth rate 8-95205
 eddies, large, in axisymmetric jet, harmonic forcing, modelling 8-90957
 electrohydrodynamic convertor or nozzle for jet printer, output parameter exact solns. (*Russian*) 8-75230
 engine exhaust noise, orderly struct. as a source 8-94786
 engine exhaust noise, source coherence 8-94787
 entrainment in turbulent jets and plumes 8-94781
 fan jets with swirling, self-similar soln. 8-90950
 flame, diffusion type, oppositely directed jets, elec. props. 8-56896
 flow past airfoils with oscill. jet flaps, quasisteady theory 8-63467
 fluidised bed, plasma jet cooling mechanism 8-79371
 fluidised bed, quasisteady axisymmetric jet 8-83470
 free jet, homogeneous nucleation of clusters, noncryst. struct. (*French*) 8-79760
 free shear layer transition of circular jet, wave development 8-94643
 gas conc. profile determ. by laser Raman optical multichannel analyser 8-73098
 gas flow in duct, self-excited oscillations 8-55670
 gas injection technique, rapid response, design 8-94865
 gas jet injection into liq. in tank, math. model 8-63473
 gas jets, laminar homogeneous, combustion process (*Russian*) 8-94850
 gas mixtures, velocity slip in free jet expansions 8-90951
 gas-jet sound generator, Hartmann type, influence of jet temp. on characts. 8-51025
 heated water jet impingement melting, cavity formation, expt. and simulation 8-95133
 heavy laminar jet flowing into nonmixing medium 8-51212
 horizontal five-layer jet instability 8-79348
 hot surface quenching rate, countercurrent single- and two-phase flow effects 8-59451
 hydrodynamics conditions for jet heat transfer, impact model 8-83447
 hypermixing nozzle in thrust augmentor, three dimens. turbulent mixing 8-51214
 immersed nozzle, liq. gas discharge processes 8-83451
 impact system with unilateral outlet, air flow, heat exchange (*Russian*) 8-83449
 impinging jet cooling on heated plate, surrounding fluid effect 8-79350
 impinging on concave semi-cylinder surface, heat transfer, theory and expt. 8-94794
 injected into lifting wing-shed vortex, modification effect 8-63434
 isobaric turbulent reacting jet issuing into costream 8-63509
 laminar, axisymmetrical, with and without buoyancy (*German*) 8-83450
 laminar, dynamic and heat problems 8-67241
 laminar, uniform exit vel. profiles, developing region 8-79354
 laminar impinging jets, heat and mass transfer 8-94777
 liquid, cylindrical, flowing into pulsating stream of immiscible liq., stability 8-83444
 liquid jet, axisymmetric, impingement onto horizontal plane, hydrodynamics and mass transfer 8-94780
 liquid jet, burnout in nucleate boiling 8-90991
 liquid jet, capillary instability, effect of harmonics 8-71378
 liquid jet impingement, on disks, in zero gravity, free surface shape determ. 8-94783
 liquid jet penetration, rel. to drop breakup 8-94798
 liquid metal jet, borehole casing perforation feasibility, nozzle design, theory (*Russian*) 8-51216
 liquid vertical jet on horizontal plate, supercritical and subcritical flow, hydraulic jump (*French*) 8-59441
 MHD instability of quasi-parallel jets 8-83495
 micropolar fluid jet normal impingement on curved surface, flow near stagnation point 8-90949
 noise meas., source location, appl. of acoustic mirror, telescope and polar correl. techniques 8-83169
 noise source modification due to forward flight 8-63466
 noise spectrum, turbulent jet, approx. calc. 8-67236
 noise suppressors, lab. comparison 8-59193
 non-Newtonian plane jet, stability to infinitely small perturbations 8-51211
 nonisothermal axisymmetric turbulent transfer, vel. and temp. fluctuations, correl. coeffs. 8-83445
 nonuniform flow through propulsion nozzle 8-94796
 open channel flow with side discharge, recirculation zone, depth-averaged model 8-63499
 Orr-Sommerfeld eqn., continuous spectrum and eigenfunctions 8-67176
 pipes carrying fluid flow, oscillation stability (*German*) 8-87298
 polymer solns., unstable flow, reservoir to capillary, jet instability onset and flow patterns, obs. 8-87364
 power law liquid, comparison of 2-D and axisymmetric jet flows 8-79351

jets continued

- radial turbulent, flow, attachment to disc plate, flow patterns, nozzle dimension effects 8-83443
- resonance tube driven by subsonic jets, aerothermodynamic characts. vortex shedding 8-51208
- resonant oscils. in tube with jet inlet 8-59440
- round jet in cross flow, injection angle effect on vortex props. 8-94779
- shear flow, stratified, free-turbulent, buoyancy effects on large scale struct. 8-90849
- shear layer acoustic refraction theories, comparison, parameters for open jet wind tunnel shear layer correction 8-90556
- small air jet and quiet valve noise obs. 8-83165
- sound emitted by axisymmetric steady-state free gas jet, review (*French*) 8-67244
- sound power output, turbulent jet into gas with different sp. ht. 8-94789
- sound production in moving stream, Lighthill's acoustic analogy, jet noise 8-79313
- stability criteria for time-dependent flows 8-79305
- steam jet condensation, dynamical pressure pulse effects 8-94549
- steam turbine turbulent flat jet condenser, nozzle hydraulic and heat transfer characts. 8-94793
- stretching jet, convected Maxwell model 8-71379
- structure functions of temp. fluctuations, turbulent shear flows 8-71380
- submerged jet closed vessel recirculation flow, temp. distrib. and buoyancy 8-90958
- subsonic, of gas, vortices, flow visualisation patterns 8-63471
- subsonic, sound propagation due to a source near the duct exit 8-83446
- supersonic, flowing onto infinite perpendicular barrier, limiting expansion ratio 8-59439
- supersonic flow, self-induced oscils. 8-67215
- supersonic jet noise suppression by coaxial cold/heated jet flows 8-63468
- supersonic underexpanded jet, press. pulsations on flat plate 8-94778
- surface ages of water jets 8-83442
- surface buoyant jet, horizontal discharge into denser media, theory 8-90954
- swirling, radial, in free space, velocity components 8-55669
- swirling annular capillary jet flow (*Russian*) 8-75180
- turbojet noise suppression investigations using hydrodynamic press. meas. and cross-correlation techniques 8-79157
- turbulence, large scale struct., vortex rings, similarity region 8-90847
- turbulence of free coaxial jets with independent air supply to nozzles (*Bulgarian*) 8-59436
- turbulence of hot free jet, mixing zone coherent struct. 8-94788
- turbulent, axial momentum conservation 8-67240
- turbulent, chem. reaction at metal surface, modelling 8-64885
- turbulent, plane, impinging on plane surface, RMS boundary press. pulsations 8-59438
- turbulent, radiative transfer 8-94578
- turbulent, round jet/plane jet spreading rate anomaly 8-63469
- turbulent bulge structure in axisymmetric jet 8-90955
- turbulent flow in free jet, large scale struct., discrete values meas. 8-90840
- turbulent heated jet, temp. and vel. meas. 8-94784
- turbulent incident on plate, convective diffusion 8-67242
- turbulent jet, interaction with pure tone sound 8-94790
- turbulent jet noise, press. depend. for choked and subsonic jets (*Chinese*) 8-67235
- turbulent jets, heat, mass and momentum transport, into ambient air 8-51210
- turbulent shear flow, free, of plane jet, initial condition effect 8-90850
- turbulent two-dimens., parallel, mixing 8-51209
- turbulent vertical buoyant jet decay in uniform environment, unified scaling law 8-90905
- turbulent wall jets, self-preserving flow 8-79352
- two-dimensional jet flow in ideal compressible gas, calc. method 8-83448
- two-dimensional underexpanded jets, analysis (*Japanese*) 8-90952
- unsteady subsonic jets, entrainment characts. 8-63470
- US scatt. by submerged turbulent jet in liquid 8-50992
- viscous jet with surface tension, jet shape, finite element soln. 8-79349
- water, destruction of rock, theory based on drag force on grains in permeable medium 8-55691
- water, two-dimensional, effects of applied sound (*Japanese*) 8-79353
- water jet impinging on hot surface, boiling heat transfer 8-90993
- weakly conducting dielectric liquid, plane jet in strong nonuniform mag. field (*Russian*) 8-94838
- He gas jet noise source, absolute calibr. 8-59228
- Pb, filament production, ejection of molten metal through nozzle, jet stability (*Japanese*) 8-52719

j.f.e.t. see *junction gate field effect transistors*

Johnsen-Rahbek effect see *adhesion; electrostatics*

Johnson noise see *thermal noise*

joining processes

see also *brazing; cable jointing; soldering; welding*

No entries

jointing, cable see *cable jointing*

jointing (electric connectors) see *electric connectors*

Jordan-Thiry field see *cosmology; general relativity*

Josephson effect

- AC Josephson-Fiske effect, coherence 8-88082
- applications, recent developments (*Japanese*) 8-91819
- barrier inhomogeneities, effect on junction behaviour (*German*) 8-91818
- coherent tunable Josephson radiation generation, 2-18 GHz, with narrowed linewidth 8-88078
- contact microwave detector sensitivity and cutoff frequency rel. to capacitance 8-49902
- coupled Josephson weak links, phase locking 8-72309
- current-phase relation, Josephson contacts 8-76195
- double Josephson junction interferometer, dynamics 8-68118
- flux flow characteristics, large Josephson junction 8-84351
- Ge-Sn barrier Josephson tunnel junctions 8-68114

Josephson effect continued

- granular supercond. contact, Josephson-coupled, behaviour in microwave field (*Russian*) 8-52158
- granular superconductors with Josephson coupling, transition to coherent behaviour (*German*) 8-84362
- HF losses in tunnel junctions 8-88083
- Josephson-junction arrays, radiation props. (*German*) 8-88077
- junction, finite size, current distribution (*Russian*) 8-80103
- junction, in inhomogeneous field (*Russian*) 8-84350
- junction, quantum interference, determ. of characteristics (*Russian*) 8-88081
- junction threshold viewed as crit. point 8-56264
- long junction, oscils., exact solns. of sine-Gordon eqn. 8-68115
- motor, rotational solns. in BCS theory 8-72310
- nonlinear behaviour, qualitative theory 8-52159
- nonstationary nonlinear eqn., auto-oscills. (*Russian*) 8-60255
- optical waveguide controlled Josephson junction 8-66955
- quasi-autonomous contacts, props. 8-88084
- resistive junction, I-V characteristics 8-91820
- retarded Josephson equation, adiabatic and pendulum approx. 8-68119
- Riedel anomaly and nonlinear effects in Josephson point contacts 8-60253
- self-resonant modes in junction exhibiting nonuniform max. current distrib. 8-56263
- semiconductor-barrier, cavity resonances 8-84352
- shunted superconducting bridges, transition from relaxational to Josephson oscillations 8-72312
- SINIS junction proximity system, crit. Josephson current calcs. (*German*) 8-88079
- superconducting bridge, DC Josephson effect, microscopic theory (*Russian*) 8-56258
- superconductor-degenerate semiconductor-superconductor structures, critical Josephson current calc. 8-52162
- superconductor-insulator-superconductor contacts, critical Josephson current near T_c (*German*) 8-84361
- superconductor-insulator-superconductor contacts, Josephson tunnelling (*German*) 8-84359
- superconductor-semiconductor-superconductor system, semiconductor barriers (*German*) 8-84360
- thermometer, absolute noise, resolution of unmodelled errors 8-62196
- tunnel junctions, fabrication and four terminal resistance study (*Chinese*) 8-68116
- tunnel microwave coupling, influence resistance effects (*Chinese*) 8-80099
- tunnelling junctions, supercond. fluctuations, below transition temp. 8-84354
- undergraduate experiment, 3rd yr, Nb-Pb-Sn junction 8-54126
- voltage divider influence on Josephson voltage standard system 8-74027
- voltage measurement standard (*German*) 8-93722
- voltage-standard instrument, features 8-93729
- vortex motion in Josephson junction line (*Japanese*) 8-91824
- vortex pinning in Josephson contact (*Russian*) 8-68117
- weak link, model (*Russian*) 8-88080
- weak links, nonequilib. effects, Ginzburg-Landau model (*Chinese*) 8-95396
- weak links and films, scatt. model for Josephson behaviour 8-56261
- weakly coupled supercond.-insulator multilayer stack, crit. field calc. 8-52161
- Al, small particles, Josephson-coupled, local fluctuation effects 8-72308
- In-CdS-In Josephson junction, exhibiting nonuniform max. current distrib. self-resonant modes 8-56263
- Nb, point contact Josephson junctions, thermally recyclable, as low-noise mixers 8-62224
- Nb-Nb point contact junction, supercond. weak couplings, high-freq. props. 8-68122
- Nb-NbO_x-Pb Josephson junction, self-reson. modes 8-64169
- Nb₃Al, quantum interference and Josephson effect (*Russian*) 8-56259
- Pb, small junction, temp. and mag. field variations in resist. cos φ conductance and effective capacitance 8-84357
- Pb-CdS-In Josephson junction, light-sensitive, structural fluctuations (*Russian*) 8-56265
- Pb-Te-Pb Josephson junction, cavity resonances 8-84352
- Sn, small particles, Josephson-coupled, local fluctuation effects 8-72308
- Sn-SnO-Sn Josephson junction current-voltage characts., resonance detection cct. 8-54406
- TaS₂ intercalation complexes, superconductivity 8-91803

Joshi effect see *glow discharges*

Joule-Thomson effect

- gas mixtures, thermodynamic props. prediction 8-83512
- gas pipe flow, turbulent Graetz problem, Joule-Thomson effect 8-75204
- Cs, 768-1234K 8-71420
- Cs vapour, thermodynamic props. calc. from Joule-Thomson data 8-94886

junction gate field effect transistors

- radiation dose measurement using radiation induced changes (*Japanese*) 8-78504

junction lasers see *semiconductor junction lasers*

Jupiter

- asteroid, mean motion resonant with Jupiter, short-periodic perturbations 8-53803
- atmosphere, ¹²CH₄(¹³CH₄) ν_4 band, line parameters, 7.7 micron transmission 8-85894
- atmosphere, GeH₄, ν_3 fundamental, theoretical absolute J-manifold intensities 8-74707
- atmosphere, GeH₄ abundance from IR spectrum anal. 8-61791
- atmosphere, IR laser heterodyne spectroscopy for trace gases remote detect. 8-61606
- atmosphere, IR obs. by Fourier transform spectroscopy 8-61747
- atmosphere, microwave spectrum 8-85889
- atmosphere, NH₄OH aerosols existence, IR reflectivity spectra, Kramers-Kronig anal. 8-68500
- atmosphere, radiation-induced cooling 8-85885
- atmosphere, scavenging reactions of acetylene and ethylene for P containing radicals 8-81582
- atmosphere, spacecraft entry, modelling by H₂-He mixture 8-71413

Jupiter continued

- atmosphere, subliming boundary layer flow, simulation 8-65545
 atmosphere, trace constituents upper limits from 5 μm spectrum anal. 8-61790
 atmosphere, transport props. 8-57490
 atmosphere IR absorpt. profiles of GeH_4 , computer simulation 8-81584
 atmosphere simulation, synthesis of UV photoprod. organic solids, mol. anal. 8-69740
 corotating magnetosphere, self-consistent model 8-89109
 decametric emission features and vars. (*Russian*) 8-65546
 decametric radiation beaming, first direct meas. 8-89114
 decametric radiation modulation by Io, charged particles acceleration 8-89110
 decametric radio emission, freq. and time depend. 8-89113
 electron modulation, Pioneer 10 and 11 obs. 8-61690
 equatorial regions, light and dark spots lifetimes and motions 8-57493
 faint satellites (VI-XII), astrometric obs., (1974 to 1977) 8-89107
 fictitious satellites motion, long-period effects at 1/1 reson. 8-85830
 figure parameters and gravit. moments, fifth approximation calc. 8-65547
 formation of planet and satellites (*Chinese*) 8-69712
 Galilean satellites, diameters from Pioneer data 8-85893
 Galilean satellites, icy crater model to explain radar scatt. results 8-61789
 Galilean satellites, photometric eclipses anal. rel. to theory of motion 8-53864
 Galilean satellites, radar obs. during 1976, results 8-61788
 Galilean satellites atmospheres, existences and gas concs. upper limits 8-96415
 inflated magnetosphere, similarity model of rot. effects 8-57492
 inner magnetosphere, whistler mode noise 8-89112
 inner satellites mutual phenomena in 1979, ephemerides 8-53866
 Io, bright dawn terminator due to thermoluminesc. 8-96425
 Io, cometary ionosphere model 8-69738
 Io, long term light vars. (*Italian*) 8-93147
 Io, Na cloud direct images 8-61792
 Io, surface albedo rel. to laboratory samples 8-53865
 Io Na D-line emission, comparison of observed and theoretical line profiles 8-93145
 Io surface composition, implications of Na and K doped NH_3 frosts reflectance spectra 8-84561
 Io-Jupiter electrodynamic interaction, theory 8-81583
 L-bursts in decametric radio spectra 8-96424
 Leda (Jupiter XIII), continuation ephemeris (1978 Sept.-1979 May) 8-69739
 magnetic field apparent source depth, rel. to planet interior struct. 8-57478
 magnetosphere, energetic particles recirculation 8-89108
 magnetosphere, outer, protons accel. at 32 Jovian radii 8-57489
 near IR polarisation, obs. 8-85899
 outer magnetosphere, charged particles energisation 8-89111
 outer magnetosphere, temporal var. in heavy ion plasma 8-61787
 particle accel. near Jupiter, effect of solar activity on MHD oscills. 8-57526
 plasma sheet, self-consistent model 8-57494
 plasmasphere, thermal struct. 8-93148
 plasmasphere models 8-77517
 radiation belt, nucl. meas. techniques 8-85895
 radio emission, non-Io-related, solar wind effect 8-57491
 radio emission modulation below 8 MHz 8-81581
 regular satellite system, form. model rel. to masses 8-69714
 satellites icy interiors and surfaces evolution 8-61771
 satellites position meas. 8-81573
 solar heating and internal heat flow 8-85888
 spectrophotometry in far IR 8-85890
 spectrum in far IR showing NH_3 rotational bands 8-85891
 Voyager electrostatic discharge protection 8-89042
 CO in Jupiter upper atmosphere, extraplanetary source 8-93144
 H-He immiscibility, chemical differentiation rel. to excess luminosity 8-69798
 HD search at 6045 \AA , D/H ratio upper limits 8-85892
 S II forbidden line emission from thermal plasma 8-93146

K-capture see nuclear electron capture**K mesons** see kaons**K-N interactions** see kaon-nucleon interactions**Kalman filters**

- EEG sleep pattern feature extraction and recognition by real-time anal. (*Japanese*) 8-73271
 hydrology, river quality modelling by sequential extended Kalman filters 8-81248
 nuclear reactor reactivity insertion, unexpected, rapid detection 8-58370
 seismic data, single-channel white-noise estimators for deconvolution 8-77345
 star pattern sensors for real time spacecraft attitude determination 8-96380

kaon-baryon interactions

see also kaon-baryon scattering; kaon-hyperon interactions; kaon-nucleon interactions
 No entries

kaon-baryon scattering

see also kaon-baryon interactions; kaon-hyperon scattering; kaon-nucleon scattering
 No entries

kaon decay

- see also kaon hadronic decay; kaon leptonic decay
 form factors, semi-leptonic weak interactions, book contrib. 8-78162
 $K \rightarrow \text{ne}\nu$, radiative correction amplitudes from Ke_4 decay anal. 8-86451
 $K \rightarrow \pi\pi\nu$, Ke_4 decay, radiative correction amplitudes 8-86451
 $K^+ \rightarrow \pi^+ e^+ e^-$, pole contribs., test of theory by comparison with expt. 8-70360
 K^0, K_s^0 system, semi-leptonic decays, time depend., book contrib. 8-78173
 $K_f \rightarrow 2\gamma$ decay, contribution of Hamiltonian derived for weak two-photon decays (*Russian*) 8-66119
 $K_f^0 \rightarrow (\pi\mu)\bar{\nu}$, energies and intensities of $\pi\text{-}\mu$ atoms (*Russian*) 8-54629
 $K^0 \rightarrow \pi^+ e^- \nu$, vector form factor meas. in large H bubble chamber 8-93875

kaon decay continued

- K_{L} decay in relativistic quark model, axial vector form factors and decay rate 8-66109
 $K_s^0 \rightarrow 3\pi$, CP violation, book contrib. 8-78173

kaon hadronic decay

- non-leptonic weak interactions, book contrib. 8-78163
 $K \rightarrow 3\pi$, radiative correction amplitudes from Ke_4 decay anal. 8-86451
 $K \rightarrow \pi\pi\gamma\gamma$, scalar meson model for radiative decays involving $\delta(980)$ 8-82204
 $K \rightarrow \pi\pi\pi$, scalar meson model for radiative decays involving $\delta(980)$ 8-82204
 $K^+ \rightarrow \pi^+ + \text{axion}$, upper bound determ. 8-50031
 $K^+ \rightarrow \pi^+ \gamma\gamma$, scalar meson model for radiative decays involving $\delta(980)$ 8-82204
 $K_f \rightarrow \pi^0 \gamma\gamma, \pi^0 e^+ e^-$, decay rates calc. in baryon-loop model 8-70365
 $K_f^0 \rightarrow \pi^+ \gamma\gamma$, scalar meson model for radiative decays involving $\delta(980)$ 8-82204
 $K_f^0 \rightarrow \pi^+ \pi^- \pi^0$, matrix element expt. study (*Russian*) 8-78174
 $K^0(892) \rightarrow K\pi\pi$, decay width upper limit 8-78177
 $K^+ \rightarrow K + \gamma$, radiative decay in the MIT bag model 8-66110
 $K^*(1420) \rightarrow K^*(892)\pi^+ \pi^-$, partial width for decay mode 8-78177

kaon-hyperon interactions

see also kaon-hyperon scattering
 No entries

kaon-hyperon scattering

see also kaon-hyperon interactions
 No entries

kaon interactions see kaon-baryon interactions; kaon-nucleus reactions; lepton-hadron interactions; meson-meson interactions; photon-hadron interactions

kaon leptonic decay

- K_{L} weak radiative decays in chiral theory using virtual π^0 and η pole diagrams (*Russian*) 8-78172
 $K_f \rightarrow \mu\mu$, heavy particle decoupling effects in broken symmetry theory 8-82140
 $K_f - \mu^+ \mu^-$, $\text{SU}(3) \times \text{U}(1)$ symmetry, gauge theory 8-58153

kaon-nucleon interactions

- see also kaon-nucleon scattering; kaon-proton interactions
 100 GeV/c, multiplicities and pseudorapidity distrib. 8-82241
 cross-sections related by sum rules, pomeron hypothesis, heavy-quark channels and threshold predictions 8-89755
 inclusive hadroproduction of μ pairs, 39.5 GeV/c $\pi^\pm, K^\pm, p, \bar{p}$ beams on Cu target 8-62470
 nuclear interactions of strange particles and resonances, conf. Warsaw, Poland (Ict. 1976) 8-70406
 KN, 360-1320 MeV/c, partial-wave anal. 8-82235
 KN interactions, low energy, K matrix and dispersion relns., $\Gamma(1405)$ resonance 8-70408
 $K^- n \rightarrow \Sigma^- \pi^+ \pi^-(\pi^0)$, 2.87 GeV/c, search for exotic I=2 hyperons 8-82234
 $K^+ n \rightarrow K^+ \pi^- p(K^{*0}(890))$, comparative study of $\rho^0, \omega, K^{*0}(890)$ and $K^{*0}(890)$ production 8-58200
 $K^\pm n$, high-energy, react. differences and annihilations 8-74279
 $K^+ N, \psi$ hadronic production, gluon contrib. in QCD framework 8-78139

kaon-nucleon scattering

see also kaon-nucleon interactions; kaon-proton scattering
 No entries

kaon-nucleus reactions

- for inelastic kaon-nucleus scattering, see "kaon-nucleus scattering"
 see also kaon-nucleon interactions
 distorted waves, 100 to 200 MeV, difference between Schrodinger and Klein-Gordon wave functions 8-94033
 (K^-, π^-) , 390 MeV/c, formation of hypernuclear excited states in $^{12}\text{C}, ^{16}\text{O}, ^{27}\text{Al}$ 8-74402
 (K^-, π^-) on light nuclei, hypernuclear spectroscopy 8-50116
 (K^-, π^-) reactions, 900 MeV/c, sum rule for hypernuclear formation, distorted wave impulse approx. 8-70572
 K^- capture by emulsion nuclei, double charged particle yield (*Russian*) 8-78420
 K^- capture on emulsion nuclei, investig. of Σ^- to Σ^+ prod. ratio below K^-p threshold 8-70407
 K^- -nucleus reaction, in emulsion, ^8Li fragment energy, evaporation theory 8-62577
 $\text{Al} + K^-$, stopped kaon capture, Doppler shifted nuclear gamma rays 8-62578
 Be, 200 GeV/c, forward inclusive prod. spectra of $K_s^0, \Lambda^0, \Lambda^0, n$, 200 GeV/c 8-82393
 $^{12}\text{C}(K^-, \pi^-)$, 900 MeV/c, sum rule for hypernuclear formation, distorted wave impulse approx. 8-70572
 $^{40}\text{Ca}(K^-, \pi^-)$, 900 MeV/c, sum rule for hypernuclear formation, distorted wave impulse approx. 8-70572
 $^7\text{Li}(K^-, \pi^0)_\Lambda ^7\text{He}$, prod. cross sections from shell model theory 8-62501
 $^7\text{Li}(K^-, \pi^-)_\Lambda ^7\text{Li}$, prod. cross sections from shell model theory 8-62501

kaon-nucleus scattering

- see also kaon-nucleon scattering
 kaonic ^{12}C , coupled channel formalism, role of $\Lambda(1405)$, binding effect, Pauli blocking 8-55261
 K-nucleus optical pot. at low energy 8-94032
 $^{12}\text{C}(K^+, K^{*+})$, 300 MeV inclusive scatt., plane wave impulse approx. 8-50214

kaon production

- $p\bar{p}$ annihilation, 3.0 GeV/c, differential cross sections and polarisation of Λ^0 and K_s^0 8-58197
 ed, K^\pm/π^\pm ratio and symmetry props. of quark-parton model, fragmentation functions 8-93888
 $e^+e^- \rightarrow \text{hadrons}$, 53 GeV 2 , π^\pm and K^\pm cross sections, scaling 8-78201
 ep, K^\pm/π^\pm ratio and symmetry props. of quark-parton model, fragmentation functions 8-93888
 ep deep inelastic inclusive K_s^0 and Λ electroproduction, quark fragmentation 8-66123
 $\gamma \rightarrow KK$, EM radius, low-energy approx., comparison with pion 8-50033
 $\gamma p \rightarrow K^+ \Lambda^0$, 1.1 to 1.3 GeV, polarised proton target 8-66125
 K^0 meson production cross section (*Russian*) 8-82394
 $K^*(892)$ prod. in e^+e^- multihadron annihilation 8-66132
 $K^{*0} K^0$, production by charge exchange reactions, production cross section 8-58200

kaon production continued

- $K^{*+}(890)$ production in 205 GeV/c pp interactions 8-54659
 $K^-p \rightarrow \Lambda(\Sigma)K^0$, $K^+\pi^+$, 4.2 GeV/c, 1550 MeV, $I=1$ enhancement in ($\Lambda\pi$) and ($\Sigma\pi$) systems 8-89735
 $K^+p \rightarrow (K\pi)^+\pi$, 10 GeV/c, amplitude and natural parity exchange anal. 8-50053
 $K^+p \rightarrow K^0\pi^+\pi$, 10 GeV/c, $K\pi$ prod., two arm spectrometer studies 8-50052
 $\bar{p}p$, strange particle prod. at CERN PS 8-82195
 $\nu p \rightarrow \mu^+ K^+ p$, $E > 5$ GeV, cross-section meas. 8-93872
 $\bar{p}p$ 14.75 GeV/c, search for $K_s^0\pi^+\pi^-\pi^+$ resonance near 2.6 GeV/c 8-74289
 $\bar{p}p$ annihilations, 0.76 GeV/c, inclusive $K^{*+}(892)$ and K_s^0 prod. 8-62465
 $\bar{p}p$ annihilations, 0.76 GeV/c, KK correls., effect of resonance prod. 8-78205
 $\bar{p}p$ collisions, high momentum π^\pm and K^\pm prod., 45 GeV, cross sections 8-93910
 $\bar{p}p \rightarrow K^0 K_s^0 + \text{pions}$, 700-760 MeV/c, $K_s^0 K_s^0$, threshold enhancement in final states 8-82228
 $\bar{p}p \rightarrow K^+ K^- X$, search for narrow six quark resonance 8-89757
 $\bar{p}p \rightarrow K^\pm + \text{anything}$, 100-400 GeV expt. techniques and data analysis 8-58216
 $\bar{p}p \rightarrow K^*(890)X$, 12 GeV/c, prod. cross sections 8-93911
 π^- interaction, K +hyperon prod., mass quantisation anal. (French) 8-70401
 π^+d interactions, strange-particle cross-sections at 4 GeV/c 8-89734
 π^-p 5 GeV/c interactions, inclusive distrib. of Γ^0 and K^0_1 (Russian) 8-54652
 $\pi^-p \rightarrow K^0\Lambda^0$, 1400 to 2380 MeV/c, differential cross sections and polarisations, partial wave anal. 8-70405
 $\pi^-p \rightarrow K^0\Lambda^0$, up to 1334 MeV/c, cross sections and polarisation, energy depend. phase shift anal. 8-70404
 $\pi^-p \rightarrow K^0\Sigma^0$, threshold to 1334 MeV/c, differential cross-section and polarisation 8-89733
 $\pi^-p \rightarrow K^+K^-K^+K^-n$, 22.6 GeV/c, φ prod., Okubo-Zweig-Iizuka rule test 8-89743
 $\pi^+p \rightarrow$ four prong final states, 10.3 GeV/c, resonance prod. cross-sections 8-74276
 $\pi^+p \rightarrow K^+\Sigma^+$, exchange degeneracy in hypercharge exchange reacts. 8-82239
 $\pi^+p \rightarrow K^+Y^*(1385)$, 11.5 GeV/c confirmation of exchange degeneracy predictions in line reversed reacts. 8-82247
 $Al+p$, 200 GeV/c, relative yields of π^\pm , K^\pm , p , \bar{p} 8-93995
 $Be+p$, 200 GeV/c, relative yields of π^\pm , K^\pm , p , \bar{p} 8-93995
 $Be+(p)(K^-(\pi^-))$, 200 GeV/c, forward inclusive prod. spectra, of K_s , Λ^0 , Λ^0 , n 8-82393

kaon-proton interactions

see also *kaon-proton scattering*

- DC K^+p , 32 GeV/c, resonance inclusive prod. cross sections, quark model comparison 8-93913
quark fragmentation function universality, inclusive hadron interactions 8-66082
quasi two body processes extraction from three body final states: program EXTRA 8-82238
 K^+p , 32 GeV/c, 4 and 6 body final states, principal-axis variables anal. 8-58206
 $Kp \rightarrow K^+\pi^+n(K^{*0}(890))$, comparative study of ρ^0 , ω , $K^{*0}(890)$ and $K^{*0}(890)$ production 8-58200
 $Kp \rightarrow \pi X$, central region, Regge Mueller approach, inclusive cross sections (Russian) 8-58218
 K^-p , neutral channel cross section meas., 1470 to 1560 MeV CM energy 8-82237
 $K^-p \rightarrow \Delta^{++}(1232)+X$, 16 GeV/c, cross sections 8-66169
 K^-p inclusive interactions, 10, 16 GeV/c, polarisation of forward produced Λ 8-62466
 K^-p interactions, 14.3 GeV/c, two body diffraction dissociations, cross sections, mass spectra 8-62464
 K^-p interactions, 8.25 GeV/c, flow of strangeness and baryon number 8-74277
 $K^-p \rightarrow K^-\pi^-\pi^+p$, 10, 14.3 and 16 GeV/c, partial wave anal. of $\pi^+\pi^-\pi^+$ system 8-82251
 $K^-p \rightarrow K^0X$, pseudoscalar meson prod. in triple Regge region, absorpt. corrections 8-78228
 $K^-p \rightarrow K^0n$, 515 to 956 MeV/c, differential cross section 8-66153
 $K^-p \rightarrow K^0n$, 515-1065 MeV/c, total cross section meas. 8-66152
 $K^-p \rightarrow \Lambda^0 + \text{pions}$, 8.25 GeV/c, resonance prod., fluctuations cluster emission model 8-93904
 $K^-p \rightarrow \Lambda(\Sigma)K^0$, $K^+\pi^+$, 4.2 GeV/c, 1550 MeV, $I=1$ enhancement in ($\Lambda\pi$) and ($\Sigma\pi$) systems 8-89735
 $K^-p \rightarrow M^0 + \Lambda(\Sigma^0)(\Sigma^0-1385)$, 4.2 GeV/c, quark model relations 8-82233
 $K^-p \rightarrow \Omega^- + X$, Ω^- lifetime and spin 8-93877
 $K^-p \rightarrow \pi^-\Sigma^+(1385)$, 1775-2170 MeV, partial wave anal. 8-54653
 $K^-p \rightarrow \pi^-Y^*(1385)$, 11.5 GeV/c, confirmation of exchange degeneracy predictions in line reversed reacts. 8-82247
 $K^-p \rightarrow \pi^+\Sigma^+$ 8-82239
 $K^-p \rightarrow \rho^0 + \text{anything}$, or $f + \text{anything}$, 10, 16 GeV/c, central and fragmentation contribs., quark model predictions 8-62467
 $K^-p \rightarrow \Sigma^+\pi^+$ or $\Sigma^+\pi^-$ at rest, interaction ratio for charged Σ prod. 8-78213
 $K^-p \rightarrow \Sigma^+\pi^+\omega$, 4.2 GeV/c, B (1235) backward prod., $\pi^+\omega$ mass enhancement 8-89736
 $K^-p \rightarrow \Sigma^+\pi^+$, threshold and below, ratio of $\Sigma^-\pi^+$ to $\Sigma^+\pi^-$ production 8-70407
 $K^-p \rightarrow \Xi^-K^0\pi^+\pi^0$, Kp resonances, spin-parity 1^+ backward prod. at 1.28 GeV 8-70409
 K^+p , phase shift anal., exotic reson. Z_1^* 8-62456
 $K^+p \rightarrow K^0X$, pseudoscalar meson prod. in triple Regge region, absorpt. corrections 8-78228
 $K^+p \rightarrow \Lambda p \pi^+$, 12 GeV/c, narrow resonant state in $\Lambda\Delta^{++}(1232)$ and $\Sigma^+(1385)p$ combinations 8-89744
 K^+p , effective radius and total cross sections Pomeranchuk theorem confirmation (Russian) 8-89737
 K^+p , high-energy, react. differences and annihilations 8-74279
 $K^+p \rightarrow (K\pi)^+$, 10 GeV/c, amplitude and natural parity exchange anal. 8-50053

kaon-proton interactions continued

- $K^+p \rightarrow$ hyperon $+ X$, 4-16 GeV/c, unified descript. of $\Lambda, \Lambda, \Sigma^+, \Xi^-$ prod., urbaryon model 8-66173
 $K^+p \rightarrow K_s^0\pi^+\pi$, 10 GeV/c, $K\pi$ prod., two arm spectrometer studies 8-50052
kaon-proton scattering
see also *kaon-proton interactions*
 $Kp \rightarrow kp$, polarisation phenomena in hadron collisions at small momentum transfer (Russian) 8-58196
 $K^-p \rightarrow K^0\Delta^0$, 13 GeV/c⁻¹, sum rule in kaon-nucleon cross section meas. 8-82236
 $K^-p \rightarrow K^0n$, 13 GeV/c⁻¹, sum rule in kaon-nucleon cross section meas. 8-82236
 K^+p elastic scatt., dominant exchanges using Reggeon-photon coupling analogy 8-78204
 K^+p , 100 and 175 GeV/c, inclusive scatt. results from Fermilab single arm spectrometer 8-89746

kaon resonances see *meson resonances***kaon scattering** see *kaon-baryon scattering; kaon-nucleus scattering; lepton hadron scattering; meson-meson scattering; photon-hadron scattering***kaons**

- EM radius, low-energy approx., $\gamma \rightarrow KK$, $\pi\pi \rightarrow KK$ comparison with pion radius 8-50033
form factor, quark-antiquark systems combined by Coulomb type attractive force 8-89677
Klein Gordon equations superposition, meson model, φ , f' , F , K spectrum 8-58121
mass-sum rule, Veneziano-type amplitudes π and K mesons 8-74180
 K^+-K^0 , Coulomb and tadpole contributions to EM mass differences 8-89713
 K^0 , differential cross section from $\bar{p}p$ annihilation 8-58197

Kapitza-Dirac effect

see also *Schwarz-Hora effect*

- quantum modulation in field of opposite EM waves 8-74188

Kapitza resistance

- direct electronic contribution to Kapitza cond. 8-95221
metal-liquid He interface, electron-phonon interaction, thermal boundary resistance 8-67899
phonon mismatch theory comparison to computer expts., analogue of Khalatnikov theory 8-79834
surface roughness effects on heat exchange 8-75923
thermal boundary resistance, determ. in transport approach 8-51815
He, liq.-solid interface, heat transfer rel. to adsorbed monolayer (Russian) 8-51758
³He-magnetic salt boundary (Japanese) 8-51780
LiF-He interface, absence of anomalous Kapitza resistance 8-63923
NaF-He interface, absence of anomalous Kapitza resistance 8-63923
Pb, supercond., quasi-particle recomb. time, Kapitza resistance 8-68123

KDP see *potassium compounds***Kelvin-Helmholtz instability** see *flow instability***Kennelly-Heaviside layer** see *E-region; ionosphere***keratin** see *proteins***Kerr electro-optical effect**

- benzene, substituted benzenes, liq., Kerr effect in UV region, mol. optical anisotropy dispersion 8-72488
carbon tetrachloride, non-polar liq., microwave induced Kerr effect meas. 8-76435
conductive liquid Kerr constant meas. 8-88279
cyclohexane, non-polar liq., microwave induced Kerr effect meas. 8-76435
fluid, rarefied, symmetries of static elec. field induced opt. effects 8-55713
Freon-11, liq., elec. birefringence (French) 8-88278
n-hexane, non-polar liq., microwave induced Kerr effect meas. 8-76435
HV nanosecond transient meas. from pulsed low inductance gas discharge, Kerr cell appl. 8-51380
liquid motion induced by unipolar injection, solid spacer influence 8-87406
pentylxy-cyanobiphenyl, liq. cryst., laser and electrical Kerr effect 8-68477
piezoceramic articles, nonuniform polaris. investig. using microwave Kerr effect 8-72969
rod-like macromolecules in conc. soln., basic kinetic eqn. and appl. 8-67637
CS₂, liq., Kerr effect in UV region, mol. optical anisotropy dispersion 8-72488
CS₂, non-polar liq., microwave induced Kerr effect meas. 8-76435

Kerr magneto-optical effect

- amorphous toroidal core, switching characts. and domain structs. 8-95477
ferromagnetic transition metals, electron spin polarisation, review 8-76591
magnetic domains, demonstration expt. for teachers 8-69949
multiple-reflection-type light modulator using Kerr effect in mag. thin film 8-79110
Permalloy I-bars, Kerr magneto-optical effect meas., domain wall location determ., Kerr effect probe 8-68328
Co, film, Kerr magneto-optical const. 8-76541
Co-P, amorphous electrodeposited films, domain wall motion, Kerr effect 8-60322
Nd-Co film, amorphous, exam. of domain struct. 8-68336
Ni-Co-P, amorphous electrodeposited films, domain wall motion, Kerr effect 8-60322
Sm(Co_{1-x}Cu_x)_{7.8} alloys, coercive fields, domain wall energies, mag. and metallographic exam. 8-91897
Tb_{0.2}Dy_{0.8}Fe₂, domain configurations, obs. by Kerr effect and synchrotron radiation topographs 8-64215
TbFe₂, domain configurations, obs. by Kerr effect and synchrotron radiation topographs 8-64215
YIG, diamagnetic substituted, anal. of polar Kerr rot. spectra 8-68485
Y_{2.8}Pr_{0.2}Fe₃O₁₂, magneto-optical props. 8-72489

kicksorters *see counting circuits*

Kikuchi lines *see electron diffraction crystallography*

kinematic viscosity *see viscosity*

kinematics

see also acceleration; ballistics

axisymmetric rigid body in air, stability of unperturbed motion (*Russian*) 8-86146

bodies with binary material and kinematic-kinetic structure 8-73848

disclination, mathematical theory 8-63764

galaxies and clusters, large-scale distrib. and random motion 8-54056

Galaxy, stellar kinematics rel. to local struct. determ. (*Russian*) 8-77608

galaxy clusters, ratio of escape rel. to mean vel. (*German*) 8-53995

icebergs, drift in Grand Banks 8-81200

interstellar molecular clouds, radiation transport and kinematics 8-93347

Lagrangian gyroscope, hodographs of ang. velocity (*Russian*) 8-86133

Lagrangian gyroscopes, moving ang. velocity hodograph (*Russian*) 8-86134

linear systems, stability of motion rel. to part of variables (*Russian*) 8-86144

linked rigid body systems, nonlinear eqns. of motion (*German*) 8-87254

machine tools for optical glass grinding and polishing

semiautomatic (*Czech*) 8-63208

matrix differential equation, rotations as solns., for teachers 8-62021

NGC 3256, peculiar galaxy, kinematics 8-96537

NGC 7822 (W1) optical studies of kinematics rel. to supernova remnant struct. 8-54028

plastic shells, kinematics at large strains and displacements 8-79221

relativistic transformations, Newtonian force and EM field, for teaching 8-49601

star clusters, ratio of escape rel. to mean vel. (*German*) 8-53995

subduction zone, kinematic model for inter-arc basins 8-81127

sunspot groups, kinematic parameters rel. to convective zone cophasal regions 8-96469

thrown string problem 8-89331

Venus atmosphere, vertical extent of zonal winds 8-85875

kinematography *see cinematography*

kinetic theory

see also Boltzmann equation; collision processes; intermolecular mechanics; kinetic theory of gases

BBGKY hierarchy, scaling method of kinetic eqn. derivation 8-54286

Brownian motion in fluid, repeated-ring kinetic theory 8-59729

cloud drops stochastic coagulation, kinetic eqn. 8-92944

convex body aerodynamics in rarefied mol. flow, kinetic theory 8-59424

electron diffusion in gas, Maier-Leibnitz expt. reexamined 8-83516

evaporation, disequilibrium conditions 8-79755

Fermi liquids 8-87841

gas-liquid droplet system, phase transition kinetics and kinetic eqns. 8-83933

hard disc system, 4-point vel. correls., long time behaviour 8-93598

hard rods, in finite 1-D mixture, time displaced correlation functions 8-54287

liquid surface tension, kinetic tunnel model 8-56022

liquid viscosity, simple kinetic model 8-55793

liquid-gas bubbles system, phase transition kinetics and kinetic eqns. 8-83933

nonlinear oscillator interaction with discrete system of oscillators 8-70050

nonlinear viscous flow, in two and three dims., 8-71372

normal quantum fluid, kinetic theory, transport props. 8-77799

polarisation dynamics, fully relativistic kinetic model 8-62134

quantum kinetic equations, derivation, nonlocal Uehling Uhlenbeck eqn. 8-70054

quantum kinetic equations, derivation by collision expansions, three particle term 8-70053

simple classical liquids, kinetic theory, formal justification for memory function approx. 8-87598

teaching method for secondary schools 8-81767

kinetic theory of gases

see also Brownian motion; collision processes; equations of state; intermolecular mechanics; Joule-Thomson effect

biatomic molecular gas, quantum kinetic theory (*Rumanian*) 8-91053

Boltzmann kinetic equations, soln. methods 8-83511

Boltzmann-Lorentz kinetic equation, exptl. test 8-94875

diatomic gases, harmonic oscil. system, vibr. energy relax. 8-66632

dilute polyatomic gases, nonequilib. alignment phenomena in elec. and mag. fields 8-71414

distance force consts., pseudocritical volumes 8-58765

elastic cross-section analytical approximation (*Russian*) 8-75248

equilibrium correlation functions, turbulent flow kinetic theory (*German*) 8-90886

extended principle of corresponding states, rel. to pair interaction potential 8-51269

hard sphere gas interacting with hard wall, density profile, virial expansion 8-63928

ideal gases, solns., basic props. kinetic derivation from elastic collision processes 8-91048

linear heat equation from kinetic theory of gases 8-94877

mean free flight time of molecules, soln. of apparent concept inconsistency 8-63525

mixtures of reacting gases, extension of Chapman Enskog method (*Russian*) 8-57878

molecular flow in vacuum, kinetic method analysis, flux in elementary structs. 8-55663

molecular flow in vacuum, kinetic method for analysis basic formulation 8-51201

nonequilibrium processes, integro-differential eqn. approx. by Fokker-Planck type 8-91049

photodissociation, kinetic theory analysis 8-82795

polyatomic gas, in non-hydrodynamic domain, Rayleigh-Brillouin scatt. (*French*) 8-86872

shock tube boundary-value problem global soln. (*French*) 8-63449

temperature-jump problem with arbitrary accommodation 8-67221

transport coeff. data inversion iterative procedure, pot. energy function determ. 8-91051

transport coefficients density expansion, 1st logarithmic term, moderately dense gas 8-94878

kinetic theory of gases continued

viscomagnetic heat flux, in a Burnett regime, gas kinetic theory 8-71400

viscous gases, simplified transport coeffs. for vibr.-rotational relaxation (*Russian*) 8-51270

weakly ionised gases, in electrostatic field, Maxwell model, ion vel. distrib. and moments 8-94879

C, monatomic, transport properties, rel. to spacecraft entry into planetary atms. 8-87424

H₂-He mixture, collision integrals, modelling of spacecraft entry into Jupiter atmosphere 8-71413

kinetic theory of liquids *see kinetic theory; liquid theory*

kinetics of chemical reactions *see reaction kinetics*

kink bands

creep and dislocation velocities 8-95783

dislocation damping during electron irradiation, new model for peaking effect 8-87683

rocks, ultimate locking angles for conjugate and monoclinic kink bands 8-88821

kinoforms *see computer-generated holography*

Kirkendall effect *see diffusion in solids*

kitchen appliances *see domestic appliances*

KKR calculations

Cu₂Ni_{1-x} soft X-ray emission spectra 8-95620

disordered solid, l-depend. pseudopot. in theory of band struct. 8-84124

HEED, band theory, zone axis crit. voltage effect 8-83659

transition metal, model potential, generalised APW formulation 8-91579

transition metal, one-electron theory, atomic sphere approx. to KKR and LMTO methods 8-91584

CsAu, photoelectron spectroscopy and energy bands calc. 8-76581

Cu-Ni, alloys, electronic states, KKR-CPA calc. 8-84125

Cu₂Ni_{1-x} solutions of KKR-CPA equations for paramagnetic alloys 8-95256

FeAl B2 struct., band struct. and density of states, KKR calc. 8-63969

Mo ternary chalcogenides, supercond., band struct., muffin-tin orbitals and atomic-sphere approx. 8-51871

RbAu, photoelectron spectroscopy and energy bands calc. 8-76581

klystrons

see also reflex klystrons

Darmstadt linear accelerator high resolution scatt. facility 8-70653

EPR spectrometer, 2 mm band, with re-entrant resonator 8-86311

ETL linear electron accelerator, energy increased up to 40 MeV by improvement of klystron efficiency (*Japanese*) 8-78515

gyrotrons and gyroklystrons, small signal theory, fusion reactor appl. 8-70633

pulsar magnetosphere, vibrations generation by klystron mechanism 8-53971

UHF TV klystron, pulsed operation for lower hybrid heating in ATC machine 8-66404

Knight shift

see also nuclear magnetic resonance

ferromagnetic alloys, conc., spin fluctuations, SCR theory and CPA calcs. 8-64290

liquid metals, nonlocal pseudopot. calc. of Knight shifts 8-91965

one-dimensional disordered spin system with isotropic antiferromag. interaction, susceptibility and Knight shift (*Russian*) 8-88202

solid, hydrostatic pressure shifts, appl. of parametrisation 8-72120

superconductors, surface relax. time of conduction electron spins 8-91814

Al-Mn, dil., ⁵⁴Mn Knight shift meas. using nucl. orientation 8-68396

Al₂O₃ void formation by fast neutron irradiation, TEM exam., and Knight shift expts. 8-51591

CeAs, evidence for valence fluctuations, ⁷⁵As Knight shift data 8-91966

CsAu, semicond. and metallic, NMR line shape, Knight shift, X-ray diffr. study 8-68402

Cu-Cr, dil. alloy, Knight shift temp. depend., electronic struct. 8-84488

Cu-Cr(Mn)(Fe), dil., NMR satellite data, rel. to electronic struct. 8-68398

Cu-Cr(Mn)(Fe), dil., NMR data, ionic model and Kondo temp. 8-68399

Hg_{3-x}AsF₆, incommensurate chain compound, anisotropic Knight shift, spin-spin interactions 8-80233

Mg, electric field gradient and Knight shift, temp. depend., OPW calcs. 8-56387

α-Mn, NMR and susceptibility max., paramag. phase 8-56386

MnSi, μ⁺ Knight shift, temp. depend. 8-80270

Ni-Pd-P, Ni-Pt-P, amorphous and electronic structs., NMR Knight shifts and linewidths meas. 8-68400

⁶¹Ni, paramag. solid and liq. phases, nucl. spin relax. and Knight shift 8-76327

Pt, Knight shift and spin-lattice relax., up to 1358K 8-72425

RbAu, NMR line shape, Knight shift, X-ray diffr. study, struct. props. 8-68402

Te, NMR spectrum, electron paramagnetism and atomic self-diffusion mechanism 8-72426

VSe₂, CDW states, intrinsic mag. props., mag. susceptibility and NMR obs. 8-68397

Zn, liq. Knight shift, temp. depend. 8-80232

Zr_{0.9}Fe_{0.1}V₂, NMR and mag. susceptibility 8-95527

Zr_{0.99}Pt_{0.01}V₂, NMR and mag. susceptibility 8-95527

ZrV₂, NMR and mag. susceptibility 8-95527

Knudsen flow

evaporation from capillary pore, mass transfer kinetics 8-51233

gas creep along solid surface, half-space moments method calcs. 8-67222

multiple barriers 8-63451

polymer membrane gas permeation, pore size distrib. (*Japanese*) 8-79372

porous media, Knudsen to Poiseuille flow transition, capillary model 8-55689

steam, thermal cond. in large Knudsen range, theory and expt. 8-94888

thermodynamic activity meas., new appl. of the Knudsen method 8-79783

Knudsen flow continued

- vacuum valve, Monte Carlo method for conductance 8-71398
 Ni-S system, Knudsen effusion and thermodynamics 8-79759

Knudsen number *see* Knudsen flow**Kohn effect** *see* lattice dynamics**Kondo effect**

- alloy, dil., electrical resistivity, Kondo effect vs. spin glass behaviour 8-68269
 dilute and concentrated alloys, magnetism (*Rumanian*) 8-91843
 dilute Kondo alloys, calc. of host nucl. spin-lattice relax. 8-88215
 dispersion theory, in low mag. field, Hilbert problem, numerical investigation 8-84387
 impurity-impurity interaction effects on Kondo resist. 8-51981
 irradiated dilute alloy, containing self-interstitials and vacancies 8-60105
 magnetic alloys, dil., transition metal hosts, props. review 8-84417
 metal, magnetic impurity, model of resonance level in Kondo problem (*Russian*) 8-80129
 metal, quasimagnetic impurity, exact solution of Wolff's model 8-56105
 potential scattering, Wilson's numerical technique 8-79972
 rare earth compounds, valence mixed state, Kondo lattice, Anderson localisation models (*Japanese*) 8-51945
 rare earth impurities in s-band metals, Kondo anomaly 8-52208
 single-impurity Kondo system, fluctuation conductivity 8-76064
 spin 1/2 Kondo system, thermodynamical props. 8-52209
 spin glass to Kondo transition 8-68266
 spin glasses under high press., resist. meas. 8-52277
 superconductivity, magnetic impurity effects, Anderson model 8-52148
 superconductor, Kondo, nucl. spin-lattice relax. 8-52156
 transition metal impurities, Kondo problem exptl. advances and trends 8-84384
 Ag-Mn alloys, dilute, low temp. elec. resist. (*Russian*) 8-68024
 Al-Al₂O-Al tunnel junction, Fe doped, Kondo-type zero-bias conductance 8-56237
 Al-insulator-Au tunnel junction, conductance peaks produced by Kondo scatt. from O₂ 8-95387
 Au-Cr Kondo alloy, effect of press. on resistivity 8-79978
 Au-Fe, dil., approach to saturation of magnetisation 8-56293
 Au-Fe, very dil. alloy, Kondo temp. 8-91688
 Au-V, dil., Kondo alloy, spin dynamics, nuclear spin relax. obs. 8-68155
 CeAl₂, conf. Kondo system, sp. ht. meas. 8-52210
 CeAl₂, sp. ht. in high mag. fields, Kondo effect 8-52284
 CeAl₃, singlet ground state at T=0, mag. ordering 2.5-6K 8-84388
 Cr_xPd_{82-x}Ge₁₈, amorphous, RF sputtered, elec. resist. and magnetoresist., Kondo type behaviour 8-76066
 Cu-Cr(Mn)(Fe), dil., NMR satellite data, rel. to electronic struct. 8-68398
 Cu-Cr(Mn)(Fe), dil., NMR data, ionic model and Kondo temp. 8-68399
 Cu-Fe, dil., transmission ESR meas. 2 to 40K 8-68364
 Cu-Mn Kondo system, ⁵⁴Mn nucl. orientation 8-68421
 Cu-Mn(Fe)(Co), Kondo system, host NMR exam. 8-80246
 n-InSb, low temp. resonance excitation of Kondo effect (*Russian*) 8-56159
 (La,Ce)Al₃, conf. Kondo system, sp. ht. meas. 8-52210
 (La_{1-x}Gd_x)Al₂, dil., reverse resistance anomaly 8-76054
 Lu-Gd, dil., positive exchange Kondo system, magnetisation and resist. 8-68158
 Mg-Mn, dil. alloy, de Haas-van Alphen effect, exchange interaction, Kondo effect 8-88093
 Pd, hydride and alloys, electronic band struct., comparative study of electric and mag. props. 8-95259
 Pt-Cr(Nb)(Re)(Rh)(V), dil. alloy, 0.5 at.%, ¹⁹⁵Pt NMR for local mag. susceptibility 8-84484
 Sc, sp. ht. data rel. to electronic props. 8-83971
 W-Co, dil., excess resistivity, temp. depend., Kondo effect 8-68011
 Y-Ce, Kondo system, spatial extent of Ce moment, neutron diffr. meas. 8-68159
 Yb, FCC, nucl. orientation of 3d impurities and magnetisation meas. 8-64280

Korringa-Kohn-Rostoker calculations *see* KKR calculations**Koster effect** *see* dislocation damping**k.p calculations**

- Kane model, three-band, Auger recombination overlap integrals, kp approx. (*Russian*) 8-87897
 GaAs, k-linear coupling, E_i' transitions 8-91583
 Nb₃Sn, electronic struct. from three-dimens. k.p model 8-84139
 V₃Si electronic struct. from three-dimens. k.p model 8-84139

Kramers-Kronig relations

- complex reflection amplitudes of photons, sum rules 8-63006
 ionic conductive crystal, statistical theory of relaxation current and low-freq. dielectric dispersion 8-60391
 petrols, optical const. in 0.25 to 25 micron region, sea pollution detection appl. (*Russian*) 8-76976
 phenanthrene, cryst., refl. spectra of first singlet transition 8-88323
 reflection spectra, Kramers-Kronig anal. with preliminary dispersion anal. 8-49915
 transition metal oxides, energy loss spectra, ion polarisability 8-68585
 US attenuation and dispersion, appl. to haemoglobin 8-83135
 water, IR spectrum, influence of Cu²⁺ ions 8-72501
 CdIn₂S₄, fundamental optical constants 8-84549
 CeN, optical props. and valence mixture 8-56450
 Co_{1-x}Fe_xSi, solid solution, optical props. 8-72556
 Co_{1-x}Ni_xSi, solid solution optical props. 8-72556
 CoSi solid solution, optical props. 8-72556
 α-In₂Se₃, far infrared optical study of ordered and disordered forms 8-84572
 α-LiIO₃, statistical theory of relaxation current and low-freq. dielectric dispersion 8-60391
 NH₄X, X=OH, Cl, Br, aq. soln., IR reflectivity spectra, Kramers-Kronig anal. 8-68500
 NiI₂, far IR study of lattice dynamics 8-80359
 TiO, electronic excitations, electron energy loss spectra in 3 to 60 eV range (*French*) 8-80440
 TiO₂, electronic excitations, electron energy loss spectra in 3 to 60 eV range (*French*) 8-80440
 Ti₂O₃, optical const., polarisation dependent reflectivity 8-52531

Kramers systems *see* determinants**Kromayer lamps** *see* mercury vapour lamps**Kronig-Penney model**

- energy band structure, nearly-free and tightly-bound electron approx. 8-73792
 semiconductor-vacuum interface, phase rule 8-52049
 Stark ladder levels, width and spacing 8-72124
 surface states, transfer matrix approach 8-95321

krypton*see also* nuclei with

- adsorbed dense monolayer on graphite cleavage face, phase transition 8-56034
 adsorbed on graphite, Potts lattice gas, renormalisation-group treatment 8-67908
 adsorbed on graphite, X-ray diffr. from 2-D solid 8-75498
 adsorption potential energies on NaBr and KBr, calc. 8-71993
 afterglow spectra of pulsed discharge, levels populated by dissociative recombination 8-83640
 atom, 3p core hole spectrum, many electron description 8-50517
 atom, 3p X-ray photoelectron spectrum, many-electron effects 8-50513
 atom, 4p⁵5p and 4p⁵6p configs., level radiative lifetimes meas. 8-58625
 atom, Compton profile, local density approx., Kohn-Sham self consistent scheme 8-94193
 atom, electron impact excitation of autoionis. states 8-90302
 atom, electron impact ionis. of inner shells, coincidence expt. theory 8-58837
 atom, electron impact ionisation, cross section ratios 8-94326
 atom, electron scatt., threshold excitation spectra 8-70936
 atom, impulse Compton profiles, atomic optimised pot. model 8-74618
 atom, metastable, electron impact excitation cross-sections calcs. 8-94323
 atom, population inversion, intershell transitions, photoionisation, from UV irradiation (*Russian*) 8-70803
 Clausius-Mossotti function, exam. of variation with gas density 8-52418
 crystal, exciton exam. 8-51898
 DC glow discharge excited atoms, radial conc. distrib. obs. 8-67494
 diffusion in tetrafluoromethane, 243.15K, density depend., size effect 8-75859
 diffusion of ⁸⁵Kr in fluid Kr, apparatus and expt. results 8-54520
 discharge, secondary ionisation processes 8-59711
 excimer lasers, stimulated emission kinetics in nonself-sustained elec. discharge 8-50753
 film, absorpt. in exciton region 8-52529
 high-frequency discharges, at sub. atm. press. 8-67460
 hollow-cathode glow discharge with gas flow 8-67532
 ion impact on C foil, energy loss 8-55902
 ion laser, mode-locked, near UV, 50 ps pulse width 8-79030
 laser, tunable, Lyman alpha radiation, nonlinear generation 8-87038
 liquid, compressibility, long wavelength limit of liquid struct. factor 8-67633
 liquid, triplet state of self-trapped exciton states, evidence of existence, luminescence meas. 8-72608
 monolayer, adsorbed on Cu surface, many-body interactions 8-84068
 physisorbing on Ni, stay time meas. 8-56044
 radioactive effluent gases from nuclear power industry, ambient contamination (*Spanish*) 8-61540
 scintillation detectors appl. (*Czech*) 8-86727
 self-diffusion coeff. behaviour at low density, 293K 8-67302
 shear viscosity determination under high pressure, using capillary viscometer 8-55708
 solid, dead layer effects in UV reflectance of excitons 8-72553
 solid, density at melting and isochoric equations of state 8-83915
 solid, enthalpy of sublimation, internal energy, determ. from vapour pressure 8-91435
 solid, improved unsymmetrised SCF approx. for strongly anharmonic crystals. 8-75791
 solid, vibr. and thermal props., effect of polarisability 8-71807
 submonolayer, adsorbed on graphite, melting, X-ray scatt. obs. 8-95234
 surface, desorption of He, appl. of simplified continuum model 8-87860
 thermal conductivity, law of corresponding states (*Russian*) 8-87426
 thermal conductivity, near 300K, density depend., 1.1-16 MPa 8-67304
 triple point realisation, reference temperature appl. 8-73997
 viscosity, near solidification, 50°C, up to 6500 bar, meas. and simulation using Lennard-Jones pot. (*French*) 8-67301
 viscosity coeff., density expsn. 8-91054
 Ar-Kr, liq. mixture, excess thermodynamic props. 8-75836
 Ar-Kr, pair pot. function calcs. 8-74726
 Ar-Kr mixture, thermal cond., 120-273K 8-83514
 Ar-Kr-F₂ mixture, electron beam pumped, spectroscopy and kinetics of 248, 414 nm bands 8-63081
 Ar+Kr(³P₂), flowing afterglow metastable decay rates, diffusion, two- and three-body rate const. 8-73027
 CsCl(Cs₂Cl₂) + Ar(Kr)(Xe), collision-induced ion-pair form., absolute cross sections 8-73029
 Fe:K, mag. hyperfine interaction, temp. depend. 8-68420
 H₂-Ar(Kr)(Xe) mixtures, intermol. forces 8-62867
 H₂+Kr, elastic total cross section, orbiting effects, Regge theory 8-82814
 He+Ar(Kr), translation band spectral moments, induced dipole moments 8-55218
⁴He stopping cross sections, 1-8.5 MeV 8-58558
 Kr I, high resolution polarisation spectroscopy of 557 nm transition 8-74602
 Kr IV, very strong laser emission at 195.027, 175.641 nm 8-63060
 Kr VIII beam-foil decay curves for resonance transitions 8-74755
 Kr⁺, and isotopes, trajectory in const. mag. field plus orthogonal sinusoidal elec. field 8-50687
 Kr²⁺, mobility in He gas, drift-tube meas. 8-66657
 Kr:Mg, matrix isolated Raman spectra 8-90170
 Kr:N₂O, photolumesc. from KrO (¹S) excimers 8-68544
 Kr-Cs⁺, ion mobility and interaction pot., drift tube meas. at 300K 8-59537
 Kr-N₂O gas mixture, thermal diffusion const. 8-67300

krypton continued

- Kr+³⁵ClF(³⁷ClF) potential, asymmetric, isotope substitution effect, Legendre expansion coord. transformation 8-70894
 Kr+Ar⁺(Ar₂⁺)(Ne⁺)(Ne₂⁺), thermal energy charge transfer reaction rates, mass spectrometric obs. 8-61000
 Kr+Ar₂⁺, electron transfer cross-section, <100 eV 8-66654
 Kr+CO₂, collision dynamics, generalised Langevin eqn. approach 8-70900
 Kr+CO₂(001), deactivation pathways, quantal close-coupling calcs. 8-58787
 Kr+H, low energy elastic scatt. cross section MCSCF calc., van der Waals forces 8-70897
 Kr+H₂O(D₂O), (³P_{0,2}) state quenching cross sections 8-70912
 Kr+Na, excimer bands, multiperturber interactions 8-66497
 Kr+Na, reson. line broadening, press. depend. 8-66596
 Kr+Ne, elastic scatt. absolute total cross section, long range interaction 8-58768
 Kr+O(¹D), deactivation rate consts., 110-330K 8-88628
 Kr+Rb(Cs), metal atom spectral line breadth and shift, Van der Waals pot. calc. 8-90126
 Kr+U³⁶⁺, radiative charge exchange, 16, 64, 256 MeV/amu 8-55234
 Kr+Xe, excitation transferred populations, absorpt. profile analysis 8-74748
 Kr⁺+2Kr→Kr₂⁺+Kr, gas phase reaction rate const. calc. 8-92457
 Kr₂⁺+Kr, symm. reson. double charge transfer, 0.04-20 eV 8-66657
 Kr₂²⁴⁺+Ge, K X-ray prod., impact parameter depend. 8-58800
 Kr₂, kinetics of optically excited electronic states 8-63059
 Kr₂, near IR absorpt. spectra 8-66547
 Kr₂, photoelectron spectra 8-78748
 Kr₂⁺, photodissoc. cross sections at 3.0 and 3.5 eV 8-62861
 Kr₂⁺, photodissoc. cross-section, 6200-8600 Å 8-78761
 Kr₂⁺, photofragment energy spectra, pot. energy curves 8-55207
 Kr₂⁺, weakly bound excited states, dissoc. energies 8-78748
 Kr(³P₁)(³P₁)+CO, A'¹Π-X'¹Σ⁺ and b'³Σ⁺-a'¹Π sensitised fluorescence, isotope effects 8-82761
 Kr⁺+He, persistence of velocity following elastic collisions 8-78779
 Kr⁺+He(Ar₂), vel. changing collisions studied by saturated absorpt. 8-62892
 Kr^{*}, radiative lifetime and quenching rate consts. 8-63056
 Ne+Ar(Kr), translation band spectral moments, induced dipole moments 8-55218
 Ne⁺+Kr, low vel. collision, enhanced K-L vacancy sharing ratios, X-ray prod. cross section 8-78790
 Xe-Kr-Ar mixtures, VUV continuous spectrum prod. in low volt. lamp (Russian) 8-75451

krypton compounds

- K(5S)Xe, K(5S)Kr, excimer, visible emission band, exptl. results relative to theory 8-82779
 KrB, excimer, collisional quenching rates, photolysis meas. 8-63066
 KrCl, intense lasing with HCl halogen donor 8-90411
 KrCl, laser expts. on ²Σ⁺-²Σ transitions 8-63080
 KrF, 0.8 J multi-atm. laser, glow discharge characts. 8-58992
 KrF, 1/4J discharge pumped laser 8-74927
 KrF, covalent and ionic states, ab initio CI calcs. 8-78634
 KrF, discharge pumped laser, efficient amplification 8-78997
 KrF, electron beam sustained discharge excitation, threshold power density meas. 8-63078
 KrF, electronic states, ab initio POL CI calcs. 8-66474
 KrF excimer, collisional quenching rates, photolysis meas., rel. to laser performance 8-63066
 KrF, fluoresc. spectrum, theoretical modelling using electronic potential curves 8-63086
 KrF, Kr₂F, in electron beam pumped Ar-Kr-F₂ mixture, spectroscopy and kinetics of 248, 414 nm bands 8-63081
 KrF laser action in return-current discharge-excited F₂/Kr/He mixtures 8-94920
 KrF laser beam, Raman pulse compression, for fusion expts. 8-59086
 KrF, laser emission, ab initio config. interaction calcs. on electronic states 8-63083
 KrF, laser spectrum, discharge-pumped, absorption bands and lines, assignment 8-79004
 KrF lasers, discharge and electron beam pumped, review 8-71083
 KrF, radiative lifetime and quenching 8-63063
 KrF, small signal gain meas. and kinetic modelling 8-63077
 KrF* laser, influence of F₂ dissociation and degree of ionisation 8-50756
 KrF* laser discharges, electron beam sustained, instability onset 8-63065
 KrF*, waveguide laser excited by capacitively coupled discharge 8-94391
 Kr₂F*, gain meas. at 4416 Å 8-50758
 Kr₂F*, radiative lifetime and quenching rate consts. 8-63056
 KrO, lasing, low-lying electronic states, ab initio config. interaction calcs. 8-63084
 Na(4S)Xe, Na(4S)Kr, excimer, visible emission band, exptl. results relative to theory 8-82779

Kuhn-Thomas sum rule *see molecular energy levels*

Kurie plots *see beta-decay theory*

Kyropoulos method *see crystal growth from melt*

labelled atoms *see radioactive tracers*

labelled compounds *see radioactive tracers*

labelled molecules *see radioactive tracers*

laboratories

- see also acoustical laboratories*
 air-conditioned laboratories, automatic temp. control and meas. (Japanese) 8-86245
 cell cultures, equipment used in a modern laboratory 8-85457
 energy resource development role of Sandia Laboratories' photometrics division 8-58077
 forensic laboratory applications of combined chromatography/mass spectrometry techniques 8-92556
 frontiers in education, conference, Urbana-Champaign (1977) 8-81779
 hospital test instruments, scientific and medical instrumentation capability 8-69242
 HV laboratory ion density due to repetitive impulse generation 8-65913
 Naval Research Laboratory, USA, inertial confinement fusion programme 8-59042

laboratories continued

- Omega laser system for fusion studies, Rochester Univ. 8-59041
 photometric, facilities at National Measurement Laboratory, Australia 8-82019
 safety standards, realisation 8-77879
 Scripps Institution of Oceanography, research projects and education review 8-69464
 standards room, in factory air-raid bunker, general description 8-93646

laboratory apparatus and techniques

- see also specific instruments and techniques, e.g. balances, plasma probes, vacuum techniques*
see also instrumentation; instruments; measurement; student laboratory apparatus; test equipment; test facilities; testing
 air blowers, noise emission 8-61975
 annealing of electron field emitters and multiple multichannel analyser, precision temp. regulator 8-86384
 automated systems and digital techniques 8-57922
 automatic curve slope meter for physical or chemical quantities 8-49812
 automation in laboratories (Japanese) 8-93664
 calorimeter, dynamic differential types comparison, in linear macromol. heat capacity meas. 8-89482
 chemical monitoring, complete laboratory, installation 8-61123
 chemical reaction apparatus, automatic, for low temp. inert atmosphere system 8-93695
 chromatography, high performance radial 8-80802
 clinical electrophysiology laboratory automatic control system 8-57110
 collection device for capturing a spray sample 8-57920
 cryo-ultramicrotomy and myofibrillar fine struct., review 8-53592
 electric field probe, miniature 60 Hz 8-77930
 electrothinning, laser-monitored, for preparing ultrathin metal foils 8-53074
 experimental data interpretation, chemical analysis appl. 8-77827
 fluid heating mantle using heat-exchanger principles 8-93665
 humidity test chamber, convectively mixed, calibration appl. 8-54379
 ignitrons, high current, for plasma physics expt. equipment (German) 8-75435
 liquid chromatography, high performance low pressure equipment 8-80801
 magnetic stirrer with no external moving parts, digital cct. 8-93666
 manipulator for rotating spheres 8-73975
 Measurement Standards Laboratory, capability improvement 8-54332
 micromanipulator using microscope focus, appl. to yeast asci single spare isolation 8-61292
 piezoelectric displacement generator, annular, mathematical theory 8-62185
 plasterboard sound reduction indices and meas. 8-87196
 positioning equipment, hardware tradeoffs 8-62187
 real time data acquisition system for controlling and collecting data from laboratory instruments 8-54348
 sample orienting device with 2 degrees of freedom for galvanomagnetic meas. 8-81958
 semi-automatic grain size separation apparatus 8-54351
 short tube drawing from thin metal sheets 8-86248
 Spacelab passive atm. sounders, attitude control and stabilisation 8-65483
 spectrophotometric standards, glass filter SRM 930 by NBS, clinical laboratory appl. 8-54331
 stable frequency standards comparison by TV carrier beat note transmission 8-57909
 temperature wave generator for diurnal temp. wave propag. simulation 8-85735
 two plate capacitor with aerostatic electrode regulation for precise determination of capacitor loss factor (German) 8-74021
 vibratory polisher for semicond. single crystal, construction 8-80659
 water level short-term meas., systems 8-93654
 Ir, recovery from laboratory residues 8-81957
 (La_{0.8}Ca_{0.2})MnO_{3+y} sample preparation using O₂ partial pressure controller (Japanese) 8-73977
 Rb, portable clock for transcontinental and intercontinental time comparison 8-57908

labryrith speakers *see loudspeakers*

Lacertids *see BL Lacertae-type objects*

ladder filters *see filters*

lakes

see also rivers

- American Southwest, Pleistocene palaeolakes rel. to cold, dry full-glacial climate 8-57296
 Assal (FTAI), geothermal zone, geochemical and expt. studies 8-69314
 Balkhash, wind driven water level vars. 8-81237
 Caspian Sea, short internal waves in near-surface thermocline (Russian) 8-81231
 cooling pond, heat transfer processes evaluation 8-61458
 Erie, geomorphology and origin of Point Pelee, SW.Ontario 8-92857
 Eyre North, S.Australia, bottom profile 8-69376
 glacier-fed lake with low sediment input, sedimentation processes and patterns 8-88849
 Great Lakes, LANDSAT obs. of whittings and chlorophyll distribrs. 8-77283
 heavy metals, distrib. and speciation in aquatic systems, analytical techniques 8-69390
 ice-cover thickness, pulsed radar meas. method 8-92862
 interactive lake survey programme for water resource surveillance 8-81257
 internal long nonlinear waves, obs. in Babine Lake, Canada 8-69377
 internal surges, nonlinear internal wave model 8-63442
 Kamloops, fjord lake, internal Kelvin waves obs. 8-73411
 Lagoa dos Patos, Brazil, shallow water circulation modelling 8-77286
 lagoon sediments, 'Mahalanobis' D² distance appl. (Portuguese) 8-61388
 landslide wave generation digital simulation by Galerkin finite element method 8-92879
 Loch Lomond, Scotland, palynology, palaeomag. and ¹⁴C dating of Flandrian marine and freshwater sediments 8-81234
 Loch Ness, near surface mixing layer microstruct. in stable heating conditions 8-85568
 Lugano, bathymetric map 8-96252
 Michigan, Chicago Area Program, mesoscale meteorology 8-77294

lakes continued

- Michigan, pot. benefits from wave forecasting service for Port of Milwaukee 8-77357
 Michigan surface waters, N_2O concs. 8-57223
 numerical modelling appls., conf., Southampton, England (July 1977) 8-77285
 Ontario, Late Wisconsin sediments, aspartic acid racemisation and ^{14}C dating 8-73415
 Ontario, sediment and nutrient loadings, methodological arguments 8-77278
 Ontario, sedimentation rates determ., ^{210}Pb dating method 8-73408
 reservoirs, suspended load sedimentation, analysis and prediction method 8-53664
 Saroma (Hokkaido), wind stress meas. over ice (*Japanese*) 8-88842
 sediment leachates, trace element anal., multielement-direct reading method 8-69514
 sediments, radionuclide geochronology and pollution history 8-61451
 sediments, selective chem. extraction of CO_3^{2-} associated metals 8-65406
 shallow water basin, wind-driven current, eddy viscosity, bottom friction 8-65319
 E.Sivash waters, ^{90}Sr content (*Russian*) 8-77282
 stratified turbulent flow digital simulation using finite element method 8-90964
 subsurface water chemistry study, coring and squeezing technique 8-57332
 Superior, LANDSAT-1 obs. of internal standing wave pattern 8-96244
 Superior, remote determ. of chem. loading due to spring runoff 8-96243
 surface winds, small-scale, vars. over water surface, computation model 8-61480
 Tarmanskii Marsh, influence of human activity on hydrological and thermal regimes 8-92864
 Teggau, NW.Ontario, excess 4He rel. to U ore body 8-65353
 temperature distribution in deep and shallow lakes (*German*) 8-85618
 vertical temp. profile determ. by one-dimensional heat transfer eqn. soln. 8-77290
 water pollution control mathematical modelling, book 8-73418
 water surface, free, roughness determ., from air flow struct. anal. 8-63441
 wind-induced circulation and water level changes, two-dimensional finite difference model 8-77287
 B abundance determ. 8-85559
 Ca; determ. in lake sediments, by atomic absorption spectroscopy 8-95970
 Cd, determ. in sea and fresh waters, interlaboratory comparison 8-81209
 Fe, determ. in waters, colorimetric-acid digestion method 8-61088
 Hg determ. in sea and fresh waters, interlaboratory comparison 8-81209
 Hg determination, error anal. 8-69519
 P input, uncertainty analysis 8-81262
 Pu ecological export from reprocessing waste pond 8-53533
 S isotope variations as pollution index in lakes near Sudbury, Ontario 8-57228
 U in natural waters, field meas. technique 8-85705

Lamb shift

- atom between two perfectly conducting plates, effect on Lamb shift 8-78122
 high-Z electronic and muonic atoms, QED, strong and supercritical fields, book contrib. 8-74193
 muonic atom, heavy, $1s_{1/2}$ levels, self-energy corrections 8-55262
 muonic atoms, Dirac-Fock method 8-74805
 radiative corrections to electron form factors, book contrib. 8-82213
 radiative transitions, classical theory appl. 8-74597
 resonant scattering of laser pulses by a system of N atoms 8-74617
 slow proton beam spin polarisation meas. 8-78031
 two-level atom, EM radiation interaction, elec.- and mag.-dipole contri-
 butions, reaction field 8-94215
 Ba II, even isotopes, optical isotope shifts, Lamb-dip spectrosc. obs. 8-78666
 D, Lamb shift, from elec. field quenching radiation anisotropy 8-66502
 H, $3P_{1/2}$ - $3D_{3/2}$ Lamb shift, double quantum saturation spectrosc. obs. 8-94223
 H, self-interaction of excited at. with radiation field 8-86794
 H(D), ground state Lamb shift, isotope shift and relativistic nuclear recoil correction 8-82696
 H*, radiative magnetic energy shift, H in 2p state 8-58601
 4He , muonic, Lamb shift calcs. 8-94199
 SiH_4 , second-order stark effects, RF-IR double reson. 8-58739

lambda point see liquid helium-4; superfluidity**laminar flow**

- see also laminar to turbulent transitions
 aerodynamically heated body, stable shape during ablation (*Russian*) 8-75162
 aerofoil, dynamic forces acting, subsonic instabilities (*French*) 8-67213
 annular flow, linear stability 8-63497
 arc, plasma, of free jet laminar core, axial flow, strong localised disturbance effect 8-91178
 axisymmetric boundary layer flow between wall and paraboloid (*Russian*) 8-75121
 axisymmetric free shear layer, effects of initial momentum thickness 8-71325
 axisymmetric laminar jet diffusion flame, split operator finite difference solns. 8-51252
 axisymmetric stagnation flow on circ. cyl. 8-79298
 biharmonic equation, analogue technique, cylinders falling between parallel walls 8-55628
 binary mixture flow in vertical channel, film condensation 8-75139
 blood flow, gas and heat transport, platelet and protein diffusion 8-92669
 body of revolution, slender, nonlinear normal forces, Reynolds no. influence (*German*) 8-51191
 boundary alyer flow, heat transfer, rel. to vel. fluctuations 8-94710
 boundary flow, periodic wavy surface, nonlinear anal. 8-90826
 boundary flow over spinning blunt body of revolution, Magnus forces 8-94745

laminar flow continued

- boundary layer, convective diffusion due to incident turbulent jet 8-67242
 boundary layer, semiempirical calc. using arbitrary free stream press. gradient 8-94640
 boundary layer development under continuous incipient separation conditions 8-63415
 boundary layer flow, laminar, thermal response behaviour 8-75136
 boundary layer flow along vaporising liq. layer (*German*) 8-83403
 boundary layer of dilute suspension during application of elec. field (*Russian*) 8-63503
 boundary layer on conical body with gas injection (*Japanese*) 8-59417
 boundary layer separation at angular inflection on solid surface 8-67169
 boundary-layer flow over parabola, second approx. 8-63414
 channel, rectangular, laminar forced convective heat transfer for 3rd kind temp. boundary conditions 8-87341
 channel flow, heat transfer 8-79317
 channel flows of high temp. gases, heat transfer 8-94722
 chemically reacting gas, chemically reacting noncondensable components 8-51258
 circular channel, convective heat transfer (*French*) 8-63424
 circular channel with rod clusters, heat transfer characs. 8-75140
 circular slot, flow conditions and testing (*Hungarian*) 8-67267
 circulation flows near wall, ideal liq., two-dimens. anal. in Cartesian coords. 8-51173
 combined convection heat transfer in rod arrays, numerical anal. 8-90898
 combined convective laminar boundary flow, vertical cylinder in horizontal flow, finite difference approx. 8-90893
 complex heat exchange in scatt. laminar flow in cylindrical channel 8-83490
 compressible boundary layer swirling flow in nozzle, flow and heat transfer 8-94795
 compressible nonadiabatic gas flow in tube, eqns. system numerical integration (*Russian*) 8-83427
 condensate film flow on finned surfaces, heat transfer, heat exchanger design 8-75038
 conducting fluid, laminar rot. in cylindrical vessel, elec. and mag. field effects (*Russian*) 8-75222
 convection, free, laminar, three-dimens., about surface, numerical anal., visualisation (*French*) 8-87343
 convection, heated vertical surface, boundary-layer thickness and Prandtl number 8-51161
 convection, natural, laminar, enclosure with heat source and sink on horiz. boundary 8-90882
 convective coupled heat transfer, Nusselt no. computation 8-59398
 convective heat transfer from perforated surfaces 8-94727
 convective heat transfer in internally finned tubes 8-94724
 Couette flow, permeable wall layer, heat transfer and temp. distrib. 8-51165
 Couette-type channel flow, laminar equalising flow (*German*) 8-51239
 curved duct laminar flow and heat transfer 8-75144
 cylinder, circ., separated wake stagnation pt., 2nd order boundary-layer soln. 8-63432
 DHAB, nematic, ordering change due to external DC elec. field, permittivity obs. 8-94990
 dimensionless equations for heat transfer in laminar flow with variable physical properties 8-83384
 dispersion in rectangular conduits, side wall effects, convection 8-94636
 duct, circ., laminar convective MHD heat transfer for 3rd kind temp. boundary conditions 8-87342
 duct, narrow, plane, temp. distrib., heat flow to dense blown layer (*Russian*) 8-83402
 ducts, determ. of friction factors in hydrodynamic entry length region 8-94825
 ducts and pipes intricately shaped cross section, heat transfer, Laplace and structural method 8-83477
 dust-liquid channel flow, with varying inlet temp., transient forced convection soln. 8-87375
 dusty viscous fluid, unsteady flow through tube 8-59449
 dusty viscous fluid, unsteady flow through uniform pipe 8-59450
 electrohydrodynamic stability in rigid cylinder, dielectric viscous fluids, eigen wavenumbers 8-59497
 electrolyte, diffusion interactions between electrodes spaced on oscillating cylinder (*French*) 8-64849
 electrostatic image force charged particle deposition in rectangular and cylindrical channels with laminar flow 8-83491
 film, wavy, of fluid, instantaneous vel. profile meas. 8-79299
 film condensation from moving vapour, with suction 8-59459
 flame, laminar mixed-mode forced-free diffusion type, on vert. burning fuel slab 8-91033
 flames, premixed, laminar, time-depend. soln. determ. 8-67282
 flat plate, adiabatically densified fluid film, turbulent two-substance boundary layer (*German*) 8-90845
 flow between circ. tube and cylindrical eccentric capsule 8-79377
 flow round circular cylinder at low Reynolds number (*German*) 8-94641
 free and surface-mounted obstacles, topology, flow visualization 8-51157
 free convection boundary layers on cylinders of elliptic cross section 8-90877
 free convection laminar flow, viscous dissipation and pressure stress effects importance 8-63428
 free surface gravity flow, finite element anal. with variable domain 8-79294
 fully developed laminar flow with internal heat generation between horizontal parallel plates, thermal instability 8-90899
 heat convection, liq. flowing in annular channel with const. heat flux, numerical soln. 8-83392
 heat exchange in complex domains, new soln. techniques 8-94509
 heat transfer, downstream of sudden duct enlargement 8-67196
 heat transfer and flow instability of natural convection over upward-facing horizontal surfaces 8-64698
 heat transfer and friction factors for laminar flow through finned tube 8-94730
 heat transfer in internally finned tubes 8-94725
 heat transfer in laminar cyclone 8-55548
 heat transfer in laminar freely convecting boundary layer, series soln. predictive capability 8-71335

laminar flow continued

helical coiled tubes, laminar convective heat transfer 8-94678
 horizontal cylinder, laminar free convective heat transfer 8-75130
 horizontal cylindrical surface, free convection, local nonsimilarity anal. 8-75120
 horizontal tube, fully developed laminar flow, combined free and forced convection, expt. 8-87391
 hydrocarbons flowing through circular pipe, streaming currents developed in laminar and turbulent flows 8-87413
 hydrodynamic control of increase of diffusional boundary layer upon plate immersed in Ostwald fluid (*French*) 8-87329
 ideal liquid flow around spherical segment (*Russian*) 8-63411
 incompressible boundary layer eqns. finite element soln. 8-79304
 insulated plate thermometer, incompressible boundary layer flow 8-55626
 jet, dynamic and heat problems 8-67241
 jet, heavy, flowing into nonmixing medium 8-51212
 jet, surface age meas. 8-83442
 jet, uniform exit vel. profiles, developing region 8-79354
 jets, axisymmetrical, with and without buoyancy (*German*) 8-83450
 jets, impinging, heat and mass transfer 8-94777
 laminar convection in vertical tube, thermophysical prop. temp. depend., effects 8-90895
 laminar plume above a line heat source in a transverse magnetic field 8-67269
 large Reynolds number, 2-D hydrodynamic lubricating theory (*Russian*) 8-59368
 laser-Doppler technique, local size and vel. probability distrib., two-phase suspension flow 8-59517
 liquid film, falling, laminar, transport augmentation by surface waves 8-71343
 low speed flow up a step 8-79303
 magnetic fluid (cable coolant), natural convection heat transfer 8-94846
 mass transfer, linear wall resist. entrance region solns. 8-67168
 metal, liquid, fluid flow during blast furnace tapping, mathematical model 8-85117
 MHD, nonsimilar incompressible laminar boundary layers, finite-difference scheme 8-79386
 MHD axial flow in triangular pipe with transverse mag. field 8-59498
 MHD boundary layers, laminar, control problem (*German*) 8-91024
 MHD flow in rot. mag. field (*French*) 8-51248
 MHD induction pump channel press. loss, laminar liq. metal flow friction losses (*Russian*) 8-75224
 micropolar liquids, laminar plane channel flow, stability (*German*) 8-94773
 mixed convection on a horizontal plate with uniform surface heat flux 8-90903
 mixed-convection heat transfer around an isothermal flat surface of finite length 8-90891
 natural convection mass transfer along porous vertical plate 8-90876
 Newtonian vapour, with liquid droplets, throughflow between corotating disks, numerical anal. 8-94802
 non-Newtonian flow along thin needle, vel. profile, skin friction 8-67229
 non-Newtonian fluid, effective diffusion of impurity in laminar flow of liquid 8-67228
 non-Newtonian fluid film flow along vertical oscillating plate (*German*) 8-59431
 non-Newtonian fluid flow through helical coils, studies 8-51204
 non-Newtonian non-similar laminar boundary layers, rapid calc. procedure 8-90943
 non-Newtonian pulsatile laminar flow in tube 8-79346
 nonlinear laminar flow of fluid into fully penetrating cylindrical well 8-75198
 nonsimilar axisymmetric stagnation flow on a moving cylinder 8-79297
 nonsimilar laminar free convection flow along a nonisothermal vertical plate, finite difference method 8-75119
 nonsteady MHD thermal boundary layer, in incompressible laminar flow with variable elec. cond., approx. soln. 8-91022
 Orr-Sommerfeld eqn., continuous spectrum and eigenfunctions 8-67176
 parallel-plate channel wall solution in electrolyte laminar flow (*Russian*) 8-64848
 pipe, toroidal, extended Stokes series 8-51242
 pipe flow, developing, arbitrary curvature, Navier-Stokes eqn. 8-79378
 pipe flow, finite amplitude stability theory 8-63498
 pipe flow, numerical calc. 8-79376
 pipe flow of anomalously viscous liqs., heat transfer 8-59485
 plastic non-Newtonian fluids in circular pipes, laminar flow stability loss 8-79342
 plate, flat, optically thin boundary layer, of grey medium near leading edge, radiative-convective heat transfer 8-91027
 plate, thin, in gradient current flow, coupled heat exchange (*Russian*) 8-83398
 plate temp. oscillations, response of horizontal free convection boundary layer 8-59391
 point source of heat, laminar flow pattern, press., enthalpy, vel. 8-79316
 polymer melt, composite flow anal. in sandwich sheeting die 8-94637
 polymer solutions, laminar flow, effect of capillary entrance (*French*) 8-87330
 porous tube or channel, nonunique solns. 8-94816
 porous vertical wall, boundary layer and film thickness 8-90825
 power law fluids laminar pipe flow, heat transfer 8-59425
 pseudoplastic fluid, flowing upward in vert. heated tube, variable physical props. 8-90945
 pulsating laminar-boundary layer, heat transfer and skin friction 8-94711
 radial vane grids, numerical calcs. (*German*) 8-90824
 re-entry vehicle heat transfer meas. in separated laminar base flow 8-61708
 reversal in circular pipe, water reactor LOCA anal. 8-50271
 rotating annulus, stable stratification effect 8-94797
 rotating body, axisymmetric, arbitrary surface temp. distrib., thermal boundary layer, exact solns. 8-75133
 rotating discs, drag reduction in polymer soln., laminar to turbulent transition 8-75173
 rough subliming surface, laminar boundary layer, anal. 8-51148

laminar flow continued

sand, fluidised, determ. of flow parameters by simple model and new distributor design 8-83493
 separated flow with laminar mixing region, heat and mass transfer, math. simulation 8-59397
 separation due to curvilinear obstacle, successive approx. algorithm, convergence (*Russian*) 8-75117
 sintered composite-liq. metal interaction, mass transfer eqn. approx. soln. 8-67262
 sinusoidally curved pipe, pulsating laminar flow, anal. 8-87390
 skewed boundary layers in duct with streamwise press. grad. variation 8-79302
 smoke 8-90863
 stagnation flow, nonlinear stability 8-90831
 stagnation point boundary layer on subliming surface with roughness elements 8-94635
 steady flow prod. by rot. disc, series soln. anal. 8-71308
 steam-water mixture, with high vap. content, annular flow, heat transfer, press. loss 8-75193
 Stokes problem of motion of Cassinian cylinder in viscous fluid 8-71312
 streaming, of vel. and temp., in oscill. boundary layers 8-83358
 supersonic flow past slender cone at high incidence 8-90932
 supersonic separated flow changes, caused by throttling in round duct 8-63446
 thermal markers for liq. vel. field meas., error reduction 8-91036
 thermally developed duct flow, boundary conditions rel. to Nusselt numbers 8-91016
 throughflow between closely spaced rot. discs 8-51170
 transient boundary layer on porous plate, coolant injection, laminar flow stability and heat transfer 8-83389
 tube, horizontal, laminar combined convection, circumferentially nonuniform heating effect 8-71331
 tube, vertical, laminar and turbulent heat transfer, air and Ar 8-71332
 tubeflow laminar flow heat transfer augmentation 8-94726
 turbulent flow relaminarisation, flow visualisation 8-75244
 two-phase laminar flow, in circular pipe, heat transfer, inlet temp. effects 8-67265
 two-phase zero net flow in inclined pipe 8-83457
 underground cable system, convectively cooled, temp. distrib., heat transfer correlations 8-71262
 underground cable system, convectively cooled, vel. distrib., press. drop correlations 8-71330
 unsteady boundary layers, separated and attached, review 8-71313
 unsteady boundary layers with reversal and separation 8-75163
 vapour condensation on vertical surface, laminar flow in film condensate 8-75057
 vapour flow in film boiling, stability limits 8-90832
 vertical tube with laminar combined convection, water, finite difference anal. 8-90894
 viscoelastic fluid, natural convection heat transfer 8-83436
 viscoelastic fluids in concentric annuli with axially moving boundaries 8-79295
 viscous dissipation effect on heat transfer, circ. cylinder axisymmetric stagnation flow 8-51164
 viscous fluid, variable thermal conductivity, variational calc. of vel. profile and temp. in laminar boundary layer (*French*) 8-55625
 viscous fluid flow through slot between fixed and rotating surfaces of revolution (*Polish*) 8-79300
 water, forced laminar convection in horizontal pipe, density inversion effects, numerical anal. 8-90900
 wire, in longitudinal laminar air stream, heat exchange (*Russian*) 8-83401
 Ar, stabilised electric arc, laminar plasma flow section, length and characteristics. 8-91177
 Hg, liq., flow in transverse mag. field, laminar and transition, channel wall effects 8-63500
 N₂, cryogenic, shock wave-boundary layer interaction (*German*) 8-71370
 N₂O₄, dissociation flow in tube, heat transfer and drag 8-71402

laminar to turbulent transitions

accelerated flow past rough surface, unsteady, turbulent boundary layer generation 8-90828
 aerosol precipitation from laminar gas stream, free convection effect 8-83459
 Blasius flow, horizontal, heated from below, longitudinal vortices onset 8-71342
 boundary layer, heated, with nonuniform surface temp. distrib., stability 8-67175
 boundary layer, semiempirical calc. using arbitrary free stream press. gradient 8-94640
 boundary layer, temp. factor effect 8-63417
 convection, natural, from vert. DC current-heated plate, linear stability anal. 8-90873
 flame front, laminar, hydrodynamic instability, nonlinear integro-differential eqn. 8-51253
 flame front, laminar, hydrodynamic instability, numerical solns. 8-51254
 flow, unsteady, transitional and turbulent boundary layers, expt. and calc. methods (*French*) 8-75125
 gas-liquid film interface stability behind slipping shock wave front (*Russian*) 8-55630
 heat transfer behaviour, turbulent boundary layer on rough surface with blowing 8-71334
 hydrodynamic instabilities, transition to turbulence, Couette flow, vertex streets, Rayleigh-Benard instability 8-83362
 instability, transition to turbulence and predictability 8-87332
 jet, circ., free shear layer transition wave development 8-94643
 jet, subsonic, of gas, vortices, flow visualisation patterns 8-63471
 laminar vapour flow in film boiling, stability limits 8-90832
 non-steady boundary layer, turbulence development 8-90829
 nonlinear theory, perturbation amplitude threshold 8-63416
 permeable surface, injection, laminar to turbulent transition, heat and mass transfer 8-83361
 rotating discs, drag reduction in polymer soln., laminar to turbulent transition 8-75173
 rotating radial convergent duct, air flow heat transfer boundary conditions, turbulent and transition flow 8-83476

laminar to turbulent transitions continued

- structures and mechanisms of turbulence, conference, Berlin, Germany (Aug. 1977) 8-94647
- Taylor-Gortler instability in turbulent shear flows and boundary layer transitions 8-90836
- turbulence separation, subsonic and supersonic, ultra-short duration visualisation (*French*) 8-75128
- turbulent boundary layer, compressible, extended mixing length appls. 8-94655
- underground cable system, convectively cooled, temp. distrib., heat transfer correlations 8-71262
- viscous fluid flow down inclined plane, development of roll waves 8-75160
- wakes, transition to turbulence 8-94739
- Hg, liq., flow in transverse mag. field, laminar and transition, channel wall effects 8-63500

laminates

- I-shaped crack elastic energy evolution rate in laminate determ. by pliability vibr. meas. 8-83348
- adhesively bonded metallic panels, 2-ply, finite element and integral eqns. anal. of fatigue crack growth 8-92347
- angle ply laminate, fibre reinforced, interlaminar strength test for delamination 8-88523
- biaxially fibre reinforced composites, two dimens. mixture theory, dynamic crack appl. 8-87301
- bonded dissimilar materials, crack along bond, stress intensity factors 8-55607
- calculation of stress distrib. and X-ray elastic consts. (*German*) 8-52883
- dynamic response under large deformation, nonlinear mixture theory 8-56717
- elastic dissimilar semiinfinite strips, different widths, plane symmetric contact problem 8-55615
- fracture, effect of adhesive layers 8-90791
- free edge stress fields, in composite laminates 8-67039
- fusion reactor anisotropic B-coil two-dimens. finite element anal. of laminate sliding 8-50382
- fusion reactor coil, multilayer struts., laminated beam theory anal. 8-55011
- fusion targets, laminated coatings, strength optimisation 8-60883
- glass, narrow sandwich seals, shape factor, finite element anal. 8-75111
- glass fibre epoxy cross-ply laminates, multiple transverse cracking 8-95800
- glass fibre reinforced diallyl polymer, thermally stable, prep. (*Japanese*) 8-92232
- glass fibre reinforced plastic/polyurethane foam/Al sandwich, flexural props. (*Japanese*) 8-56707
- glass fibre reinforced polymer matrix laminates, compressive strength 8-64609
- glass narrow sandwich seal, correction factor for thermal expansion mismatch 8-75110
- glass textolite cylindrical shells, parallel wound, feasibility of diagnosing strength 8-67157
- graphite fibre reinforced epoxy, laminated plate under tension, stacking sequence and lay up angle effect on free edge stresses round hole 8-88524
- graphite fibre reinforced epoxy laminates, expt. investigation of tensile moduli and strength 8-52870
- graphite fibre reinforced panels, low energy impact testing 8-72845
- graphite/epoxy laminates fatigue characts. under compression loading 8-84971
- heat propagation, longitudinal, in 3-phase laminate, at high exciting freqs. 8-90684
- insulating element, laminated, vac. drying in inert heat-transfer vap. 8-56875
- layered cylinder, axisymmetric delaminations 8-79269
- layered rod on sagging elastic supports, aeroelastic stability, vibr. modes 8-51115
- metal panels, adhesively bonded, cracked, fracture anal., crack tip stress intensity factors 8-90792
- multilayer cylinder, exam. of stresses, considering layer contact characts. 8-63399
- multilayer object, layer separation detection by thermal method using thermal visualizer 8-53127
- multilayer plates, viscoelastic, equations of forced vibrs. 8-67084
- multilayer product, theory of laid-on shielded transducers for inspection 8-88610
- nonlinear transient pulse propag., interface reflection effect 8-63222
- plate, laminated, high-order deformation theory 8-63309
- plate under tension, stacking sequence and lay up angle effect on free edge stresses round hole 8-88524
- rectangular antisymmetric angle ply plates, shear deform. effects on vibr. 8-63356
- resonance splitting in ultrasonic spectroscopy 8-87214
- sandwich plate, modified Berger method, large thermal bending anal. 8-63297
- steel-aluminium plates, exam. of adhesion strength by impulse loading 8-84943
- strength anal. and distribution, failure prediction 8-88522
- stress field in composite laminates, theory based on Reissner's variational principle 8-67038
- thermal diffusivity for multimaterial composite laminate 8-90643
- thermal monitoring by near surface thermoelectric receivers 8-53107
- Al alloy, laminates, fracture of bonded 2024-T3/7075-T6 8-56722
- Al/polyethylene/Al sandwich construction, flexural fatigue props. (*Japanese*) 8-56751
- Al-Cu-Mg-Mn (4.5, 1.5, 0.6 wt.%), alloy 2024-T3, exam. of residual strength of plate containing crack, fracture anal. 8-90792
- Al-Cu-Mg-Mn (4.5, 1.5, 0.6, wt.%), alloy 2024-T81, plates, adhesively bonded, exam. of fatigue crack growth 8-92349
- Al-Zn-Mg-Cu alloy, laminated, adhesively bonded alloy 7075-T6, exam. of fracture resistance 8-76754
- Al-Zn-Mg-Cu-Cr, (5.6, 2.5, 1.6, 0.3 wt.%), laminates, 8 and 22 layers, adhesively bonded exam. of fatigue crack prop. 8-92345
- Al-Zn-Mg-Cu-Cr, (5.6, 2.5, 1.6, 0.3 wt.%), alloy 7075, plates, adhesively bonded, exam. of fatigue crack growths 8-92348
- B-epoxy-Al sandwich laminate. influence of residual stresses on tensile strength 8-60703
- C fibre reinforced plastics, ply multidirectional effects 8-95165

laminates continued

- Cr/Cu/Cr layer composite, influence of phase boundary on flow stress 8-60717
- Cu-polymer composite foils, fracture surface exam. by XPS (*German*) 8-84992
- Fe-B alloy reinforced polysulphone exam. of tensile and flexure props. 8-72823

laminations

- minor loop hysteresis loss in thin laminations calc. 8-90342
- Fe-Si (3 wt.%), grain orientated, negative magnetostriction, theory 8-91917

lamps

- see also discharge lamps; filament lamps; light sources
- gonioscopy, foot-operated camera trip for Nikon photo slit lamp 8-80986
- illuminants which give prescribed tristimulus values to given object colours, design technique (*Japanese*) 8-94420
- UV high energy photoionisation detector in gas chromatography appl. 8-92561
- UV sources for curing 8-88443

Landau levels

- Anderson localisation, transport props. of 2D disordered electron systems in strong mag. fields 8-95318
- CDW instability of electron gas in a strong magnetic field 8-79950
- film, electron states in longitudinal mag. field 8-91784
- inversion layers, mag. field depend. of reson. line width 8-56380
- itinerant electron ferromagnet, effective Lorentz force and Landau level 8-80120
- magnetoresistance, longitudinal, in weak mag. fields, Landau level depend. (*Russian*) 8-87965
- semiconductor, excitation spectrum and optical props. in field of standing EM wave and homogeneous field 8-91625
- semiconductor in quantized mag. field, multiphoton Stark effect (*Russian*) 8-72541
- semiconductor with nonspherical bands, diamag. excitons and Franz-Keldysh effect 8-72554
- two-dimensional electron impurity system, quantum theory of cyclotron reson. lineshape 8-64083
- wave function for crystalline electrons in mag. field 8-51918
- Wigner crystal, two-dimens., in strong mag. field, classical and quantum theory 8-79948
- Al, Fermi surface, scattering anisotropy of conduction electrons on dislocations (*Russian*) 8-60051
- Bi electron properties, carrier spectrum 8-84137
- GaAs-Al_{1-x}Ga_xAs superlattice, mag. field induced dimensionality change 8-64381
- InAs surface accumulation layers, magne o-transconductance meas. 8-64137
- InSb film, threshold singularity on quantising mag. fields 8-87904
- p-InSb inversion layer, magnetotransport 8-64138
- Pb_{0.82}Sn_{0.18}Te, narrow band gap, relax. time for Shubnikov-de Haas effect 8-80006
- Si inversion layers, cyclotron and subband emission 8-64128
- V₃Si, CDW instability and anharmonicity 8-79734

Lande g-factor see g-factor**Lande splitting factor** see g-factor**landing fields** see airports**Langmuir films**

- acetate, aq. soln. current-potential curve, influence of NO₃⁻, SO₄²⁻, PO₄³⁻ and Cl⁻, obs. (*Japanese*) 8-85172
- cadmium arachidate monolayer, Ag(Au) substrate, reson. surface plasmon reflection 8-56536
- carboxylate, aq. soln. current-potential curve, influence of NO₃⁻ and SO₄²⁻, obs. (*Japanese*) 8-85173
- dielectric relaxation, dark and photo-stimulated relaxation similarity 8-92021
- fatty acid, AC and DC cond. 8-56239
- manganese stearate Langmuir-Blodgett layers on Ag, IR surface EM wave prism spectroscopy 8-52587
- monomolecular and multimolecular built-up film, present status and future potential 8-71906
- optical anisotropic waveguide for integrated optics, monomolecular layered film 8-66954
- stearic acid layers, charge transport processes 8-84316
- surface balance, monolayer parameters meas. in radiation field 8-82092

Langmuir probes

- see also plasma diagnostics
- absolute wave amplitude determ., Langmuir probe RF coupling 8-75425
- characteristics at low plasma densities, numerical analysis 8-63592
- electron distrib., Langmuir probe effect on meas. 8-83609
- hollow cathode arc, Langmuir probe meas. for discharge model 8-87533
- ion temperature of low density plasmas by two-probe method 8-55749
- ionospheric rocket expt. high-power electron gun (*Japanese*) 8-61566
- pulsed DC discharge afterglow, electron conc. and temp., double-probe technique 8-63632

languages, formal see formal languages**lanthanides** see rare earth metals**lanthanons** see rare earth metals**lanthanum**

- see also nuclei with
- adsorption on W (100), depend. of work function, heat of adsorpt. on surface coverage, contact potential study 8-67912
- adsorption on W and Mo (011) face, influence of substrate electronic struct. on props. 8-60032
- atom, La I, lifetimes of ²F_{3/2}, ²D_{3/2}, ⁴G_{5/2} and ³D_{3/2} states 8-66489
- determination by X-ray fluorescence 8-61127
- FCC, ground-state props. 8-75989
- ground state properties of f band metals 8-91607
- Hubbard model, two band, almost mixed valence system, new ground state 8-84171
- phonon density of states, in DHCP and FCC phases 8-67791
- soft phonons, f-band induced instability 8-83907
- superconducting, electron-phonon coupling, hydrostatic press. depend. 8-80087

lanthanum continued

- Ba_{0.5} Sr_{0.46} Nb₂ O₆:La, dielectric and electrooptic props. 8-68466
 CaF₂:La, dielec. relax. spectrum, ion size trends 8-72460
 EuO:La, phototreshold reduction by mag. induced space charge layer 8-72692
 La²⁺, XPS in oxide and chromite, multicomponent struct. of 4d orbital 8-74620
 La-F₂(ClF)(Cl₂)(SF₆), visible chem. laser development from reactions yielding visible chemilum. 8-63111
 O₂+La(Y)(Sc), crossed beam chemiluminescence reaction, spectral simulation, hyperthermal energy meas. 8-80732
 ZnO:La phosphor, electrolum. brightness waves, -168 to +85°C 8-52580

lanthanum alloys

- see also *lanthanum compounds*
 La_{1-x}Gd_xRu₂, mag. ordered superconductor, re-entrant superconductivity 8-88059
 Ce-La, mag. ordering, sp. ht., susceptibility and resist. 8-68238
 Ce_{1-x}La_xAl₂, extraordinary Hall effects, 4.2-300K, cryst. field interaction 8-79980
 Cr-M, optimum alloying with rare earth metals, Ti, Zr, Hf, Nb, Ta 8-68651
 Fe-Cr (20 wt.%) high temp. oxidation behaviour with small La additions (0 to 1.3 wt.%) (*Japanese*) 8-85039
 Gd_{0.9}La_{0.1}Al₂, ferromag., NMR of ¹³⁹La 8-52377
 Gd_{1-x}La_xZn, magnetisation and paramag. suscept. 8-88101
 (La,Ce)Al₂, conf. Kondo system, sp. ht. meas. 8-52210
 (La, Ce)Sn₃, dil. alloys, supercond. and normal state props. 8-76184
 (La,Gd)Al₂, mag. props. 8-52299
 La-B, phase and thermodynamic props., vaporisation 8-51660
 La-Fe, amorphous alloy film, spin reson. meas. 8-68389
 La-Fe, liquid quenched, X-ray diffr. and Mossbauer effect exam. of structure 8-76678
 La-Ni, hydriding characts., applicability for H₂ storage material 8-83955
 La-Pr, superconductive tunnelling, cryst. field effects 8-88085
 La_{1-x}Ca_xNi₅, H₂ sorption props. 8-91533
 LaAgIn_{1-x}, structural instability 8-79562
 LaAl₂, cryst. field splitting and spin-spin interaction of Eu²⁺ and Gd³⁺, ESR meas. 8-68370
 LaAl₂:Gd³⁺(Eu²⁺), cryst. field parameters, relax. rates 8-84482
 LaAl₂-Ce, dil., linewidth of cryst. field excitations 8-67988
 La₁₈Au₂₂, amorphous, evidence for short wavelength cutoff in fluctuation spectrum 8-68113
 LaBe₁₃-Er(Dy), dil., ESR, crystalline elec. field splitting, exchange parameters 8-52348
 La_{1-x}Co_x, amorphous, conc. depend. of Co moment 8-56300
 LaCu₂Si₂, resistivity, thermal conductivity and thermopower between 1.5 and 300K 8-87963
 LaFe₄Al₈, mag. props. 8-52250
 (La_{1-x}Gd_x)Al₂, dil., reverse resistance anomaly 8-76054
 La(Ni_{1-x}Cu_x)₅, H₂ sorption props. 8-91533
 La₂Ni₅D₂, storage material, neutron, X-ray diffr. study 8-83954
 La_{1-x}Pr_xSn₃, supercond., 0.6 meV cryst. field transitions, neutron spectroscopy 8-67991
 LaPt₃, cryst. field effects on transport props. 8-72133
 La_{1-x}Tb_xAg, supercond., 0.6 meV cryst. field transitions, neutron spectroscopy 8-67991
 La_{1-x}Tb_xAl₂, supercond., 0.6 meV cryst. field transitions, neutron spectroscopy 8-67991
 La_{1-x}Tb_xSn₃, supercond., 0.6 meV cryst. field transitions, neutron spectroscopy 8-67991
 Nd-La, mag. ordering, sp. ht., susceptibility and resist. 8-68238
 Pr_{1-x}La_xSn₃, anomalous resistivity maxima in metallic magnetic system 8-79977
 Zr-Mo-Al-La, metastable deform. induced transform. 8-52805

lanthanum compounds

- see also *lanthanum alloys*
 ethyl sulphate nonahydrate: Tb³⁺, ESR spectrum, spin lattice relax., effect of hydrostatic compression 8-88185
 Al₂O₃-Y₂O₃-SiO₂ containing TiO₂, La₂O₃, exam. of elastic moduli and refractive indices 8-80502
 BaO-La₂O₃-GeO₂, exam. of glass forming region, properties and crystallisation 8-88454
 CaTiO₃-LaAlO₃ solid soln., phase redistrib. during roasting in H₂ 8-52735
 Ce₂La_{1-x}F₃, paramag. mixed crystal, scattering of optical phonons by rare earth ions 8-68518
 Gd_{0.67}La_{0.33}P₂O₁₄, photoemission spectra, 4f, 5p and 5s giant reson. enhancement 8-95660
 Gd₂La_{1-x}Pd₃, ESR linewidths, g-shifts, effective electron interaction, spin-lattice relax., spin-flip scatt. 8-68372
 LaB₆, (La,Eu)₆, (La,Y)B₆, (La,Ba)B₆, (La,Cs)B₆, single crystal growth for thermionic emission 8-92183
 LaB₆, (001) surface struct., XPS, LEED meas. 8-63909
 LaB₆, and related cpds., thermionic props. (*French*) 8-60541
 LaB₆ cathode, directly heated, for electron beam instruments, design and optimisation 8-93783
 LaB₆, chemical vapour growth of whiskers, and single crystals 8-72710
 LaB₆, clean and oxidised (100) surface, LEED, AES, work function, evaporation meas. 8-71989
 LaB₆ film, structure, stoichiometry, elec. properties 8-60043
 LaB₆ highly stable single cryst. cathode for conventional electron microprobe instruments 8-78043
 LaB₆ hollow cathode for dense plasma production 8-55729
 LaB₆, surface ionisation of halogens, using ion source 8-60538
 LaB₆ three-electrode 250 A pulsed electron gun 8-82553
 LaB₆, UPS and XPS of valence band 8-84703
 LaB₆:Y, Sc effects of impurities thermionic emission 8-60542
 LaB₆, x=4.24 to 29.2, thermoelectric electron emission, work function, 1400-2100K 8-60539
 LaBe₁₃:Er(Dy)(Gd), ESR, crystalline field single ion effects 8-84481
 La(BrO₃)₃·9H₂O, IR and Raman spectra, vibr. assignments 8-84569
 (La_{0.8}Ca_{0.2})MnO_{3+y}, sample preparation using O₂ partial pressure controller (*Japanese*) 8-73977
 LaCl₃:Pr³⁺, crystal field parameters using multiple-scatt.-X_α method 8-95271
 LaCoO₃, spin states, XPS meas. 8-68599

lanthanum compounds continued

- LaCoO₃, structural phase transition involving changes in spin and valency 8-79765
 LaCoO₃, synthesis and characterisation by powder X-ray diffr. 8-79580
 La₂CoO₄, synthesis and characterisation by powder X-ray diffr. 8-79580
 La₄Co₃O₁₀, synthesis and characterisation by powder X-ray diffr. 8-79580
 LaCrO₃, spin states, XPS meas. 8-68599
 LaCuO₃, struct. rel. to phys. props., high-pressure series of perovskite-like oxides 8-51493
 La_{0.5}Er_{0.1}Al₂, crystal field study rel. to ErAl₂ 8-76036
 LaF, Franck-Condon factors and R-centroids, rot.-vibr. effects 8-50596
 LaF₃, heat capacity of 350K, enthalpy to 1477K, calorimetric determ. 8-79781
 LaF₃, quantum yield, photoelectron spectra, density of states struct. 8-68601
 LaF₃, UV visible absorpt. by laser calorimetry, wavelength modulation spectroscopy 8-66876
 LaF₃:Ho³⁺, laser excited fluorescence absorption spectra, symmetry groups 8-60514
 LaF₃:Nd³⁺, vacuum UV luminesc. (*Russian*) 8-64414
 LaF₃:Nd³⁺(Er³⁺)(Tm³⁺) ZZ 8-80381
 LaF₃:Pr³⁺, photon echo lifetimes, conc. independ. 8-74951
 LaF₃:Pr³⁺, photon echo decay as modulation process 8-79078
 La₂Fe_{1.76}S₅, cryst. struct. (*French*) 8-51499
 LaGaO₃, cryst. struct. determ. (*French*) 8-79575
 LaH_{2.08}, proton mag. relax. by pulse NMR 8-88217
 LaH_{2.08}, proton mag. relax. by pulse NMR 8-88217
 LaKFe(CN)₆·4H₂O, cryst. struct. determ. 8-55844
 La₂Mg₃(NO₃)₁₂·24H₂O:Mn²⁺, linear electric field effect on ground state splitting, EPR 8-80198
 La₂Mg₃(NO₃)₁₂·24H₂O:Co²⁺, Ce³⁺, relax. and ESR in magnetically cooled systems 8-88225
 LaNi₅, appl. as H storage system for heat engines (*Ukrainian*) 8-67022
 La₆Ni₆P₁₇, synthesis and cryst. struct. 8-75634
 La₂O₃, aerosol, controlled production technique 8-76929
 LaOHCO₃, La₂Cl(CO₃)₄, synthesis of rare earth carbonates under hydrothermal conditions 8-72714
 La₂O₂S-Ag₂S-Ga₂S₃, ionic conducting glasses (*French*) 8-79804
 La₂O₂S-Ga₂S₃, exam. of preparation and props. (*French*) 8-80504
 LaP(As)(Sb)(Bi), coupling between Gd 4f electrons and conduction electrons, EPR linewidth 8-52347
 La_{0.65}Pb_{0.35}MnO₃, transport props. near Curie points 8-88100
 La₂Pb_{1-x}Zr_xTa_{1-x}O₃, ferroelec. with diffuse phase transition, electrostriction-optical props. 8-68457
 La₂RuO₁₁, prep. and struct. study, metal-metal bonding (*French*) 8-91325
 La₂Ru₂O₁₁, crystal struct., X-ray diffr. study 8-67688
 La₂Ru₂O₁₁, mixed valence oxide of new hexagonal struct. type 8-51503
 γ-La₂S₃, indirect electron transitions, diffuse refl. and vibr. spectra 8-84576
 LaSb, cryst. field effects on transport props. 8-72133
 LaTiO₃, spin states, XPS meas. 8-68599
 La₂-V₂S₄:Gd³⁺ localised moment-conduction electron interact., ESR obs. 8-88183
 La₂Zr₂O₇-La₂Hf₂O₇, system, cryst. struct., phase diagram 8-83806
 Na₂La(AsO₄)₂, allotropes, prep. and cryst. struct. (*French*) 8-63724
 Nd_{0.75}La_{0.25}P₂O₁₄, miniature laser system bonded mirrors, side pumped by LEDs 8-87058
 PLZT ceramic, ferroelec., cathodlum. spectral and temp. depend. 8-84665
 PLZT ceramic, possible construction of matrix-addressable controlled transparency 8-71222
 PLZT ceramic birefringence props., transverse electro-optical meas. 8-72487
 PLZT ceramics, optical information storage and spatial light modulation 8-83097
 PLZT, electro-optical, physical elec. and optical props. and fabrication (*Polish*) 8-56458
 PLZT, transparent ferroelec., RF sputtering and film characterisation 8-72727
 Sm_{1-x}La_xS₃, mag. suscept., moment, impurity effects, indirect exchange interaction 8-68147
 (YLaBi)₃(FeGa)₅O₁₂, pure and In³⁺ doped, near IR absorpt. and Faraday rot. 8-95580
 ZnO-La₂O₃-GeO₂, exam. of glass forming region, properties and crystallisation 8-88454

Laplace transforms

- compound unbounded cones, temp. fields (*Ukrainian*) 8-54317
 coordinate transformation of Laplace operator in 2-D, for teachers 8-61999
 cylinder, composite circular, transient thermal stresses 8-79217
 ducts and pipes intricately shaped cross section, heat transfer, Laplace and structural method 8-83477
 electrocoating, cell design, Fourier transform soln. of Laplace eqn. 8-76609
 EM wave diffr. by unidirectionally cond. strip, transform and Wiener-Hopf techniques 8-58883
 forced oscillations in rotating stratified liquid 8-63478
 kidney model transient behaviour 8-65065
 linear differential equations with variable algebraic coeffs. (*Czech*) 8-86115
 linear time dependent partial differential eqns., solns. by Laplace transform and FFT 8-57763
 Maxwell fluid, unsteady flow past flat plate, transform technique 8-59428
 modal anal., formulations for numerical calcs. 8-57767
 numerical inversion, Mellin transform expressed as two sided Laplace transform 8-77694
 numerical inversion of Laplace transform and Fredholm integral eqns., eigenvalues and eigenfunctions 8-81800
 penny-shaped crack, sudden twisting in a finite elastic cylinder, stress calcs. 8-67110
 renal medulla single loop solute cycling model, transient behaviour 8-73167

Laplace transforms continued

- resistance thermometer transmission function approximation (*Russian*) 8-62197
- scattering experiments, deconvolution of thermal averaging using integral transform methods 8-92442
- Schrodinger equation, scatt. theory 8-57806
- specific equilib. recombination rate coeffs., Laplace transform calcs. of temp. depend. 8-60989
- spray drying, of highly viscous conc. solns., heat and mass transport (*Russian*) 8-83230
- thermal desorption model analysis (*German*) 8-63940
- third-order nonlinear systems with aperiodic excitations 8-81830
- Timoshenko beams, effect of rotary inertia and shear deform. on freq. eqns. 8-83296

large scale integration

- MOS LSI passivation using reactive plasma deposited Si-N films 8-56584

large-scale systems

- see also *hierarchical systems*
- interconnected dynamical systems on Banach spaces, well posedness, instability, Lagrange stability 8-69976

laser accessories

- acousto-optical modulator, standing wave, thermal detuning effects 8-71197
- acousto-optical modulators, for laser freq. changes 8-74932
- alignment system for large high-power pulsed CO₂ laser fusion system 8-59075
- automatic alignment system, for OMEGA-10 multibeam laser system 8-50847
- automatic bias control cct. for injection lasers 8-71110
- beam expander, Galilean or Keplerian form telescope 8-50839
- beam transport optics for laser fusion 8-83017
- birefringent filters for tuning flashlamp-pumped dye lasers 8-74914
- bolometric laser power meter, sensitive meas. IR to vacuum UV spectral range 8-82031
- capacitive mesh output couplers for optically pumped far IR mol. lasers 8-74916
- chalcogenide spinels, Faraday effect optical isolators for CO₂ laser system 8-50816
- chopper-wheel gas pulsar for foilless anode electron-beam laser 8-63122
- coaxial relay current pulse generator for laser pumping 8-59014
- coupling reflector, involute-related, for flash lamp pumped laser systems 8-90425
- diffraction grating as beam expander in dye laser cavity 8-66858
- discharge power source for CO₂ laser, pulse forming network 8-74928
- electro-optical gate for nonpolarised emission (*Russian*) 8-59132
- Faraday element fabrication for intracavity laser appls. 8-66852
- fibre waveguide photosensitivity, appl. to refr. filter fabrication 8-63171
- filter, bleachable 8-50937
- flash lamp pumping of lasers, optimal lamp filling, review (*Russian*) 8-63123
- flash lamps, discharge development effects on pumping efficiency 8-71114
- flashlamp pumping and triggering cct., for Nd³⁺:YAlO₃ laser 8-55378
- focus alignment sensor, for collimated light beam 8-59065
- gas laser cavity unit for radiation lead-out (*Russian*) 8-90433
- graphite electrode open channel config. for N₂ laser 8-55379
- grating reflector for thin film Fabry-Perot laser 8-55471
- heat exchanger, high capacity, inexpensive construction 8-49826
- high-power laser luminance contrast meas. 8-87055
- hole grating attenuator, for beam steering investig. 8-59071
- holograms, computer-generated, prod. of two-dimens. laser beam deflections 8-58956
- holographic grating, for spectral narrowing and tuning of CW dye laser 8-71109
- injection laser/optical waveguide connection module 8-59023
- interference polarisers for lasers, development 8-83108
- lens, aspheric, stigmatic, for ruby or He-Ne laser, CAD (*Czech*) 8-55427
- metal film reflection filter for CO₂ laser line selection 8-55368
- metal mirrors, diamond turned, evaporated and sputtered, surface and optical studies 8-79098
- metallic wired grids as far IR semitransparent mirrors, use in HCN laser cavity 8-71188
- methane absorption cell for He-Ne laser, hyperfine struct. influence on freq. reproducibility 8-50864
- Michelson coupler with variable output for far IR methyl fluoride CW laser 8-55372
- modulation circuit, with 1 ns pseudo-random impulses 8-50836
- modulator using rotary diffraction grating 8-87080
- multi-lens focusing systems for energy Nd:glass lasers 8-50848
- multilayer dielectric mirrors, exam. of reflectance, optical thickness and refractive index 8-59106
- multilayer mirrors, high refl. at fundamental, second and third harmonic laser wavelengths 8-90490
- nonlinear interferometers for laser pulse shaping 8-59097
- nonlinear interferometers for laser pulse shaping 8-79051
- optical component laser damage mechanisms 8-83016
- optical path electronic simulator in GaAlAs laser power control loop (*German*) 8-82987
- optical power meters for laser photometry 8-65953
- optical shutters, fast acting, for Nova laser fusion reactor 8-66854
- passive nonresonant technique for pulse contrast enhancement and gain isolation 8-63142
- plasma diode, prevention of laser damage by back-reflected light 8-87057
- plasma mirror refl. characts., in electron beam controlled CO₂ laser 8-59064
- Pockels cell, variable length subnanosecond laser pulse prod. 8-94405
- prism used as beam expander in N₂ laser pumped dye laser, dispersion 8-74924
- pulse energy monitor 8-66839
- pulse generator, multiple-cct. for high repetition rate rare gas halide lasers 8-94399
- pulse generator for semiconductor laser pumping, cct. parameters 8-74919
- pulsed acousto-optical modulator RF driver for laser mode locking 8-90438

laser accessories continued

- ruby, one-freq. tunable one-pulse, selector parameter optimisation 8-74935
- saturable absorber gases, for CO₂ laser gain isolation 8-59095
- saturable absorbers, large scale flowing gas, for CO₂ lasers 8-59096
- scanning electro-optical deflectors 8-79060
- self-focusing suppression through low-pass spatial filtering and relay imaging 8-74938
- semiconductor laser pumping thyristor current pulse generator 8-79024
- semiconductor laser pumping thyristor nanosecond current pulse generator 8-79025
- Shiva, laser-target and laser isolation 8-59035
- Shiva laser, 25 MJ energy storage and delivery system 8-59038
- Shiva mechanical systems 8-63135
- Shiva optical system 8-59039
- shock isolator for closed-cycle refrigerator of diode laser 8-50796
- shutter, differential electro-optic with ns pulse operation 8-74994
- smooth pulse oscillator for single mode operation in I laser 8-59057
- solid-state laser miniature power pack 8-59015
- Stark cell noise reduction for CO₂ laser beam 8-59059
- surface cleaning, liquid spraying technique, appl. to laser glass, metal surfaces 8-72921
- thermal compensator for diode laser closed-cycle refrigerator stabilisation 8-50797
- thermal length control, for lasers and etalons 8-87056
- thermo-gasdynamical control in laser beam guidance, review of developments 8-74942
- transmissive optics for high power CO₂ lasers 8-79057
- transparent solids, absorpt. coeffs. by laser calorimetry, wavelength modulation spectroscopy 8-66876
- travelling wave lens, optically excited soft X-ray laser technique development 8-59016
- water continuously variable filter for I laser 8-55397
- Al₂O₃ coated Al mirrors, highly efficient refl. type polarisers for 10.6 μ m laser radiation 8-71177
- Al₂O₃-Si, alternating layers, dielec. facet reflector for semiconductor lasers 8-66841
- BCl₃ gaseous phototropic shutter control of CO₂ laser PRF 8-50833
- CO₂, 100 kJ laser, optical design and components 8-82990
- CO₂ high power laser beam monitor 8-74943
- CaF₂ trapezoid, ThF₄ and ZnSe coated, IR characterisation by internal-refl. spectra 8-71161
- CdTe, single cryst. IR laser window, low absorption at 10.6 μ m 8-79081
- CoCr₂S₄, Faraday effect, appl. to CO₂ laser systems, radiation damage resist. 8-95579
- GaAs, absorption coefficients, method of meas. 8-83048
- p-Ge saturable absorber, passive mode locking of TE CO₂ lasers 8-71127
- He recovery and recycling system, for CO₂ lasers 8-82974
- Hg_{1-x}Cd_xTe, Faraday effect at CO₂ laser freq. 8-64348
- KCl, bulk and surface absorpt., 2 to 10 μ m, calorimetric meas. 8-71160
- KCl IR window material, polish layer effect, ellipsometric meas. 8-55419
- KCl laser windows at 10.6 μ m, optical distortion parameter 8-79036
- KN₉O₃, single domain crystal growth, SHG with Nd:YAG laser 8-74954
- LiNbO₃ electrooptic phase modulator, axial mode locking of CW Nd³⁺:YAG ring laser 8-50835
- LiNbO₃ electrooptic phase modulator, freq. shift device for optical range 8-59147
- NaCl, bulk and surface absorpt., 2 to 10 μ m, calorimetric meas. 8-71160
- NaCl Polytran laser windows, for CO₂ lasers, fusion appls. 8-59067
- OsO₄ absorber for freq. stabilised CO₂ laser, output freq. reproducibility 8-50800
- PbO-SiO₂ glass, optical coating for GaAs-Al_{1-x}Ga_xAs laser 8-71113
- ZnGeP₂, synthesis, characts., applic. to laser windows (*French*) 8-80467

laser beam applications

- see also *holography; integrated optics; laser beam machining; laser beam welding; laser isotope separation; matrix isolation spectroscopy; measurement by laser beam; modulation spectroscopy; optical communication; optical radar; patient treatment; plasma production and heating by laser beam; Raman spectra; Raman spectroscopy; remote sensing by laser beam; spectroscopy; surgery; two-photon spectroscopy*
- air pollution, ambient sulphate aerosols laser-Raman monitoring 8-69532
- atmospheric pollutants, selective quantitative meas. using CO and CO₂ lasers 8-69526
- atmospheric science, conf., San Diego, USA (Aug. 77) 8-85748
- body dither laser gyro, scale factor nonlinearity 8-79062
- Bragg diffraction imaging for medical use 8-53462
- bubbly flows, simultaneous meas. of local liquid vel. and void fraction by gas laser, accuracy (*Japanese*) 8-67295
- buried-heterostructure laser packaging for wideband optical transmission systems 8-74920
- clinical rhinology, Ar⁺ laser instrument (*German*) 8-69177
- cold atoms, trapping and storage in laser field 8-86826
- colliding beam arrangement using laser linac, feasibility study, laser accelerator problems 8-78521
- communication, gigabit link development 8-66860
- computer printer using laser (*Japanese*) 8-90446
- deflector quality factor N/r, comparison of holographic and acousto-optical deflectors (*French*) 8-55318
- diffraction pattern approximation by laser simulation 8-55287
- discharger, fast response, sealed triggered by laser radiation 8-51391
- electron beam focusing by laser beam fields 8-74833
- electron gun cathode heating using focused laser beam (*German*) 8-89591
- electrothinning, laser-monitored, for preparing ultrathin metal foils 8-53074
- endoscopic laser photocoagulation, use of gas jet appositional pressurisation 8-53468
- engineering advances, conf., San Diego, CA, USA (Aug. 1977) 8-59017
- Fabry-Perot laser spectrometer, for nonlinear superhigh-resolution spectroscopy 8-49912

laser beam applications continued

ferrous metallurgy, surface purification using laser and N_2 jet 8-92392
 fibre drawing, tension rel. to drawing vel. and ultimate strength 8-74986
 fission fuel coated particles, laser boring for material sampling 8-55399
 fission products, release and distrib. in coated particles (*German*) 8-82403
 fixed-frequency laser beam scanning device 8-59135
 fluorescence life time decay curve meas. and anal. 8-54465
 gyroscope, vibratory laser, steepness characts. and S/N ratio anal. (*Russian*) 8-59070
 hardening temperature determ. using pulsed laser 8-72942
 high power lasers and their applications 8-87092
 hole melting in metal films, for real-time, high density digital data storage 8-71135
 imagery transmission, appl. of 3M and Kodak dry silver recording materials 8-70209
 industrial CO_2 high-power laser system, for welding, cutting, heat treating and irradi. 8-55380
 interferometer, acoustic vibration meas. 8-71253
 interferometer for angular measurement, autocollimating telescope calibration (*German*) 8-77853
 ion prod. in GeV range from laser irradiated targets, limitations 8-55068
 large angle laser interferometer for 'curved' crystal spectrometer, precision 8-77973
 laser spectroscopy conf., Jackson Lake Lodge, WY, USA, 1977 July 8-82666
 lithographic focused laser system, integrated optical device fabrication appl. 8-55477
 marksmanship training, moving target screen system with laser beam firing 8-54488
 material processing, overview 8-56826
 material processing, welding, cutting, drilling and surface hardening 8-80663
 medicine, diagnosis and treatment (*German*) 8-73192
 metal, evaporation under laser irradiation (*German*) 8-52599
 metal working, surface hardening and alloying using high power CW CO_2 lasers 8-79026
 metal working with high power lasers 8-80682
 micro-Raman spectrometer, for individual aerosol microparticles identification 8-68970
 microfilm, laser transfer printing 8-65994
 nondestructive testing of steel, using laser speckle photography 8-76797
 optical fibre, end preparation using CO_2 laser 8-55478
 optical illuminator light source, geometrical optical anal. (*Russian*) 8-79094
 optical mechanical scanning system, phase relations, grating screen quality (*Russian*) 8-94451
 optical surface figuring by laser controlled chem. reactions 8-63209
 patient-positioning laser alignment instrument 8-53471
 picture colour component detection in SAW scanning 8-59149
 point transfer machine, TRANSMARK, performance testing 8-81438
 PROBE, profile resolution obtained by excitation 8-76938
 proportion counter pulse height fluctuations, resonant ionisation studies 8-90025
 proton beam, relativistic, energy monochromation using laser 8-90010
 pulse laser appls., figure of merit 8-59069
 radiation press cooling of ions in Penning EM trap 8-66527
 Raytheon laser gyroscope using MnBi magnetic mirror 8-79064
 Raytheon multioscillator ring laser gyroscope 8-79063
 recorder of video signals, on dry-developed photosensitive paper (*French*) 8-92998
 ring laser gyroscope for missile guidance using magneto-optic bias mirror 8-79061
 ring laser gyroscopes, multioscillator approach to locking problem 8-79042
 rotor vibration control and meas. appl. (*Russian*) 8-70115
 scanner, augmented resolution eqns. 8-55398
 scanning, electro-optical deflectors 8-79060
 scanning, two-dimens. using computer-generated holographic grating 8-58956
 scanning optical microscopy examination of grain boundaries of polycryst. solar cells 8-79618
 steel, Cr-plated, H_2 distrib., laser-mass spectrometer investig. 8-61113
 submillimeter wave heterodyne detection, with a laser LO 8-70183
 submillimeter wave polarimeter, for plasma diagnostics 8-91158
 supermarket checkout system, laser/photomultiplier optical and scanning system 8-83021
 surface velocity meas. using laser beams 8-49806
 teeth, human, thermal stress effects and surface cracking assoc. with laser use 8-80915
 thermoplastic recording, IR laser heating 8-71065
 thin-film distributed optically excited laser, signal suppression by superluminescence radiation (*Russian*) 8-87091
 tissue sampling in biochemistry, laser microbeam (*German*) 8-69175
 trabeculotomy in glaucoma treatment 8-53470
 urinary calculi in vitro destruction by laser-induced stress waves 8-77100
 vibration control and meas. appl. (*Russian*) 8-71299
 X-ray laser holography, pumping by synchrotron radiation from storage rings 8-55322
 X-ray picture digital transmission over voice-grade telephone channels, laser scanning system 8-80953
 X-ray spectra spatial resolution recording by spherical crystal analyser 8-74114
 Ba^+ ion cloud containment in RF trap, <50 ions, optical sideband cooling 8-75407
 CO_2 laser, electroionisation, testing X-ray mirror objectives with soft X-rays from plasma mirror 8-85850
 Cs clock, laser synchronisation between observatories of Paris and San Fernando (*French*) 8-89461
 Cu-As-Se glasses, recording and erasure by laser beam (*Russian*) 8-71170
 He-Ne laser interferometry for vibration control and meas. (*Russian*) 8-70117
 $^{14}NH_3$, four level system, two-photon jumping to obtain 12.16 μm radiation for isotope separation 8-90414
 PbTe, thick epitaxial film, laser deposition technique 8-68629

laser beam applications continued

Si, amorphous film, epitaxial laser crystallisation 8-84078
 Si, CVD using CO_2 laser 8-56589
 Si, heavily doped implantation layers, laser beam annealing 8-88481
 Si, laser assisted doping, ohmic contacts and p-n junction form. 8-79621
 Si:Pb, implanted, laser annealing 8-75685
 Si-B, diffusion-free annealing, use of scanning CW Kr laser 8-91345

laser beam effects
 see also plasma-beam interactions; plasma production and heating by laser beam
 acoustic waves in nonviscous liqs., laser-induced 8-63808
 aerosol, H_2O -droplet, CO_2 laser beam clearing process, transmission function ratios 8-88919
 air, elec. discharge, effect of long laser spark ionis. channel 8-67468
 bubble formation in liquid, dynamics of growth and pulsations 8-51226
 cavitation bubbles in water, behavioural study by holo-cinematography (*German*) 8-87371
 Compton scatt., bound and free electron Compton scatt. in coherent EM field 8-94225
 damage threshold, optical performance meas. 8-59066
 desorption, laser stimulated, quantum theory 8-79876
 diamond, dielec. breakdown, two-photon absorpt. and other optical damage mechanisms 8-84684
 dielectric protective coatings for diode laser facets, optimisation 8-63144
 dielectric surface, nonlinearly-absorbing, laser-induced evap. 8-80438
 electrolyte aqueous soln. drops, ion emission due to laser heating 8-59063
 electron beam, quantum modulation in field of opposite EM waves 8-74188
 electronic structure of solids under laser irradiation 8-91614
 ethylene, laser-induced IR photolysis mechanism 8-56909
 film, single-layer, 2.8 μm and 3.8 μm absorpt. meas. 8-90463
 fog clearance, by laser-beam induced heat and mass transfer 8-93635
 heated surface colour temp. meas. pyrometer 8-57956
 hole drilling, ring focal pattern of lens-axicon doublet 8-55421
 hydrocarbon layer, influence on laser-induced surface damage 8-60533
 hydrocarbons, heavy, self-holograms of laser-induced surface depressions 8-82927
 insulator, transparent absorpt. wave struct. associated with optical breakdown 8-68581
 interface of two phases or liquids, selective processes induced by resonance laser radiation 8-64867
 laser-fusion reactor, surface heating of 1st wall by pulsed photon and ion irradi. 8-89979
 liquid, laser breakdown, photoacoustic and photohydrodynamic parameters 8-52597
 liquid drops, optically dense, motion in laser radiation field 8-50842
 liquid layer floating on liquid half-space, acoustic field generated by laser beam 8-51615
 mammalian cell exposure using evanescent fields created in optical waveguides 8-73298
 metal, evaporation under laser irradiation (*German*) 8-52599
 metal mirrors, diamond turned, evaporated and sputtered, surface and optical studies 8-79098
 metal surfaces, laser heat treatment, wear resist., corrosion protection, hardening, review 8-72939
 microcline, laser torch effects, spectroscopic investig. (*Russian*) 8-76560
 microscopic particles, heating by laser beams 8-50838
 mirror-damage thresholds for laser-fusion pulse shapes 8-74467
 nepheline, laser torch effects, spectroscopic investig. (*Russian*) 8-76560
 nonmetallic infinite plate, temp. field calc. (*Russian*) 8-59061
 optical component laser damage mechanisms 8-83016
 plasma mirror refl. characts., in electron beam controlled CO_2 laser 8-59064
 PMMA, light absorption, laser crack development 8-68780
 quartz, fused, laser torch effects, spectroscopic investig. (*Russian*) 8-76560
 rare earth oxide (R_2O_3)- M_2O_3 glassy systems ($M=Ti, Nb, Ta$), rapid quenching by laser beam, exam. of composition and crystallization 8-52856
 retina thermal injury following laser irradi., asymptotic rate process calcs. 8-80916
 retinal damage by 325 nm He-Cd laser radiation 8-69136
 retinal tissue damage, by single ultrashort laser light pulses 8-96065
 semiconductor layer, implanted, effectiveness of annealing by millisecond laser pulses 8-55885
 silicate glass darkening due to UV radiation from laser produced plasma jet 8-52598
 solid surface, laser irradi., temp. rise calc. (*German*) 8-68580
 solid-state amplifying medium interaction with laser radiation (*Rumanian*) 8-59011
 sound wave generation in liquids 8-83882
 stainless steel, optical breakdown threshold, illuminated spot dimension effects 8-68582
 steel, alloy, Cr, austenitic boundary layers, form. by short laser pulse reaction 8-88555
 steel, alloy, interaction with Nd^{3+} -glass laser light 8-92147
 steel, multiple crater refl., effect on refl. props. 8-52596
 steel, reflectivity at 10.6 μm , calorimeter meas. 8-55393
 steel, stainless, sensitised surface normalisation by laser melting 8-60869
 structural phase transitions in crystals, effect of high-power visible and IR laser radiation 8-71825
 superconductor, optically induced non-equilibrium, heating effects (*Russian*) 8-95398
 teeth, human, thermal stress effects and surface cracking assoc. with laser use 8-80915
 thermal halo effect, nonlinear scatt. by moving particles, symm. distortions 8-66875
 transparent dielectric, nondirectional glow under laser irradi. 8-52575
 transparent dielectric with radioimpurities, intense radiation absorption (*Russian*) 8-74939
 transparent materials, defective surface layer formation during abrasion, laser-induced breakdown (*Russian*) 8-53007

laser beam effects continued

- vanadyl phthalocyanine dye solns., laser destruction, highly excited states participation 8-53231
 Al, anomalous resistive state due to light pulse 8-52157
 Al, multiple crater refl., effect on refl. props. 8-52596
 Al surface, CO₂ laser energy coupling into ionised blowoff material 8-72641
 Al-Cu (2.12 at.%), irradiated by 8J CO₂ laser pulses, metastable precipitate and amorphous phase (*French*) 8-80552
 BaF₂, optical breakdown threshold, illuminated spot dimension effects 8-68582
 C particles in flame, laser heating and sublimation 8-61012
 CdS_{1-x}Se_x laser damage, self-focusing influence 8-50844
 Co, ferromagnetic, EMF generation by pulsed laser irradi. 8-68021
 CoCr₂S₄, Faraday effect, appl. to CO₂ laser systems, radiation damage resist. 8-95579
 Cu, multiple crater refl., effect on refl. props. 8-52596
 D₂O laser induced breakdown, comparison with H₂O 8-68453
 F+Xe, enhanced quenching in intense KrF laser light, computer modelling 8-55232
 Fe alloys, ferromagnetic, EMF generation by pulsed laser irradi. 8-68021
 Fe surface, laser doping with V (*Russian*) 8-95065
 GaAlAs laser, CW operation, self coupling phenomena caused by optical fibre, exam. 8-55355
 GaAs epitaxial layer, AuGe ohmic contact production by laser alloying 8-88026
 GaAs, laser irradiated, origin of periodic surface struct. 8-91513
 Ge:Hg photoconductive detector, laser damage thresholds calc. 8-90443
 H₂O, laser induced breakdown, comparison with D₂O 8-68453
 Hg_{1-x}Cd_xTe, Faraday effect at CO₂ laser freq. 8-64348
 In₂Se with p-n junctions produced by laser radiation, photoelec. characts. (*Russian*) 8-56226
 KBr, transparent, plasma form. at surface due to CO₂ laser irradi. 8-60534
 KCl, bulk and surface absorpt., 2 to 10 μ m, calorimetric meas. 8-71160
 KCl crystal, F-H centre formation by opt. conversion of self-trapped excitons 8-91335
 KCl, optical breakdown threshold, illuminated spot dimension effects 8-68582
 KH₂PO₄, cryst. laser irradi. damage threshold, surface finish and defects effects (*German*) 8-59058
 LiNbO₃, optical strength, surface layer influence 8-50843
 LiNbO₃, pyroelectric induced optical damage 8-52446
 Mo wire, laser shock induced microstructural changes, rel. to explosive shock induced phenomena 8-67768
 NaCl, bulk and surface absorpt., 2 to 10 μ m, calorimetric meas. 8-71160
 NaCl, optical breakdown threshold, illuminated spot dimension effects 8-68582
 NaCl, transparent, plasma form. at surface due to CO₂ laser irradi. 8-60534
 Ni, ferromagnetic, EMF generation by pulsed laser irradi. 8-68021
 Si, amorphous layer, epitaxial growth by laser annealing 8-79899
 Si, ion implanted, laser annealing, periodic regrowth phenomena 8-67724
 Si, ion implanted, laser-annealed, theoretical anal. of thermal and mass transport 8-91364
 Si, ion implanted layers, laser annealing 8-67732
 Si, polycrystalline layer, laser-induced single cryst. transition, RHEED and backscatt. obs 8-87704
 Si, self-implanted layer, grain size, laser irradi. energy density depend. 8-72012
 Si:As, melting by high power ns laser pulsing, As diffusion 8-79789
 Si:B, implanted laser annealed samples, unidirectional contraction 8-71747
 Si:B, laser damage obs. by DLTS 8-76023
 Si:B, p-n junction form. by B deposition and laser-induced diffusion 8-87690
 W (100), laser induced desorption, mirror electron microscopy 8-84067
 W wire, laser shock induced microstructural changes, rel. to explosive shock induced phenomena 8-67768
 Zn_xCd_{1-x}S, laser damage, self-focusing influence 8-50844

laser beam machining

- focusing, linear, annular and radial, with axicons, laser machining appl. 8-66856
 industrial CO₂ high-power laser system, for welding, cutting, heat treating and irradi. 8-55380
 material processing, overview 8-56826
 material processing, welding, cutting, drilling and surface hardening 8-80663
 optical disc data recorder, laser machining for recording 8-71136
 quartz SAW resonator tuning by shorted reflector opening 8-59246

laser beam welding

- industrial CO₂ high-power laser system, for welding, cutting, heat treating and irradi. 8-55380
 material processing, overview 8-56826
 material processing, welding, cutting, drilling and surface hardening 8-80663
 metal working with high power lasers 8-80682

laser beams

- see also *holography*; *laser frequency stability*; *Schwarz-Hora effect*
 aberrating Gaussian beam, free-space propagation, wave eqn. solns. 8-87008
 absolute calibration of grating spectrograph for laser wavelength meas. 8-90528
 active optical systems, real-time control over optical wave fronts 8-71187
 alignment system for large high-power pulsed CO₂ laser fusion system 8-59075
 amplitude modulated laser beam prog. in random inhomogeneous medium, phase fluctuation anal. 8-87017
 Asterix III and German laser fusion programme 8-63136
 atmospheric propagation, conf., San Diego, USA (Aug. 77) 8-85748
 atmospheric propagation, detector nonlinearity effects on statistics of fluctuating signal 8-55301

laser beams continued

- atmospheric propagation, high-energy, simplified aberrated lens model 8-69454
 atmospheric transmission at 10.6 μ m, analytic model of bleaching 8-85688
 atmospheric transmission meas. at 10.6 μ m 8-92977
 atmospheric turbulence, corner-cube reflector and plane mirror comparison in folded-path and direct transmission 8-85697
 automatic alignment system, for OMEGA-10 multibeam laser system 8-50847
 bolometric laser power meter, sensitive meas. IR to vacuum UV spectral range 8-82031
 calorimetry for incident laser energy in laser fusion expts. 8-51361
 coherence length measurement problems (*German*) 8-79052
 coherence of light beam through optically dense turbid layer 8-55300
 coherence oscillations in nonlinear media, coherent state lifetime 8-66862
 coherent, two component system producing by static phase modulation a directional light beam (*Russian*) 8-50940
 concentration using inversion of wave front technique (*Russian*) 8-63154
 correlation method for meas. beam parameters (*Russian*) 8-50705
 CW, radiated power meas. (*German*) 8-79053
 CW digital wavemeter, moving cube-corner interferometer system 8-50840
 diagnostics, use of subpicosecond proximity-focused visible streak camera 8-59155
 diameter fluctuations meas. 8-87086
 digital wavemeter for CW lasers 8-89447
 distributed aperture effect in laser rods with negative lenses 8-66857
 disturbed wavefront in nonlinear medium, dynamic holographic correction (*Russian*) 8-55326
 Doppler broadened laser amplification line frequency characteristics meas. 8-59060
 dye laser fast light deflection, ultrahigh resolution 8-63178
 dye laser reference wavelengths, two-photon transitions to Rydberg levels 8-94221
 dye lasers, beam divergence, transverse mode saturation, kinetics (*Russian*) 8-74931
 dye pulsed laser, light polarisation with thin wedge plate in cavity 8-55394
 expander, Galilean or Keplerian form telescope 8-50839
 expansion in dye laser cavity, use of diffr. grating 8-66858
 far-field profile, focal plane technique 8-87087
 Fizeau wavelength meter, laser and other monochromatic sources, digital display 8-89450
 focus and alignment sensing of a collimated light beam 8-59065
 focused gaussian beam optical parameters, SR-52 calculator programme for calc. 8-79056
 focusing, linear, annular and radial, with axicons, laser machining appl. 8-66856
 four-point field coherence function meas. in laser random focusing region (*Russian*) 8-58910
 Gaussian beams, off-axis, aberrated Fraunhofer diffr. patterns 8-66753
 geometrical optics, spatial structure 8-83014
 high energy laser system, optical distortion, active control 8-83019
 high energy laser system, optical distortion sources 8-83018
 high precision laser freq. meas., sigmameter, motionless two-channel Michelson interferometer 8-89449
 high-power annular lasers, uniform beam transformation, mirror system 8-94403
 holographic method for laser radiation divergence reduction (*Russian*) 8-63147
 image resolution through atm. turbulence over ocean, optical transfer function 8-85695
 impulses, 10⁻¹² sec, anal. using Kerr cell and streak camera (*Italian*) 8-54477
 intense laser beam diffraction by long US wave in liquid column 8-60421
 intensity distrib., far field laser and partially coherent sources, comparison 8-66751
 intensity fluctuations in medium with Kolmogorov turbulence, distrib. function (*Russian*) 8-71034
 intensity fluctuations in turbulent atm. over water surface (*Russian*) 8-69449
 intensity mapping aberrations 8-66855
 intensity profile analysis using video equipment 8-59068
 interference pattern fluctuation statistics in turbulent atmospheric layer 8-53727
 IR, thermal imaging screens for visual display 8-66903
 IR pulse recording, semicond. ionisation-type photographic system 8-49903
 large system beam transport optics for laser fusion 8-83017
 laser beam broadening and depolarization in dense water-droplet fogs 8-92981
 laser nonstationary generation induced interference pattern phase distortion, holographic meas. 8-58945
 line spread instrumentation for prop. meas. 8-83013
 line spread instrumentation for prop. meas. 8-83015
 low energy output from CO₂ laser, absolute calorimeter meas. 8-55396
 low level pulse simulation and calibration, tracking system evaluation 8-59074
 modulator using rotary diffraction grating 8-87080
 monochromatic, atmospheric prop. problems 8-92988
 multi-lens focusing systems for energy Nd:glass lasers 8-50848
 multimode, optical coherent spectrum analyser energy estimate smoothing 8-55311
 multiple pulse detection in atmospheric turbulence 8-92974
 multiple-beam pellet irradiance, diffraction analysis 8-50845
 multiplication, interferometric method (*Ukrainian*) 8-90442
 nonlinear absorption and pulse shaping in InSb 8-79077
 nonlinear interferometers for laser pulse shaping 8-59097
 nonlinear optical phase conjugation for laser systems 8-79072
 nonlinear optical phase conjugation for pulsed laser systems 8-59092
 optical heterodyne simulation expts., first order correlation meas., fluctuating laser beam 8-83008
 optics in adverse environments, conf., San Diego, USA (Aug. 1977) 8-82976

laser beams continued

- passive picosecond pulse shapers, throughput efficiency limitations 8-90436
- passively mode locked pulse stability in fast absorber limit 8-59052
- phase compensated laser beam propag. through atm. turbulence 8-83012
- photoelectric laser radiation energy meter, digital output 8-58040
- power measurement by thermoelec. meter 8-63124
- prism used as beam expander in N₂ laser pumped dye laser, dispersion 8-74924
- propagation in turbulent atm., phase fluctuations spectrum 8-78914
- propagation in water, multiple scattering effects (*Japanese*) 8-78915
- pulse energy monitor 8-66839
- pulse generation, temporally shaped, for inertial confinement 8-50831
- pulse generation and meas., 0.2 psec., from passively mode locked dye laser 8-50830
- pulse shaping by nonlinear interferometers 8-79051
- pulsed output, from mode-locked laser, quantised field representation 8-79054
- Rayleigh-Debye scattering with focused laser beams 8-71030
- reciprocity theorem, for polarised laser beams 8-79055
- safety aspects of LED- and laser-fed cables 8-74968
- safety aspects of LED- and laser-fed cables 8-74969
- saturation parameter from gain meas. 8-66797
- semiconductor laser pulse radiation, coherence rel. to Fourier hologram recording 8-50738
- Shiva laser beam diagnostics 8-59037
- Shiva laser performance, nominal interstage beam energy, power 8-59032
- Shiva optical system 8-59039
- single-mode formation anal. by nonconfocal optical system (*Russian*) 8-71132
- spatial characteristics control of single-pulse laser 8-79058
- spectral characteristics measurement, high resolution spectroscopy appl. 8-89555
- spot size, simple accurate measurement technique 8-63146
- steering, using hole grating attenuator 8-59071
- subnanosecond pulse production, of variable length 8-94405
- thermal blooming compensation, equivalent thin lens model 8-87108
- thermal lensing in SiO₂ plate, aberration effects 8-63148
- thermal self-interaction of annular laser beams in moving medium 8-71159
- thermal-blooming compensation, using closed-loop adaptive single parameter system 8-94407
- thermo-gasdynamic control in laser beam guidance, review of developments 8-74942
- thermoelectronic laser energy convertor, Cs plasma device 8-90421
- transmission through fibre light guide, spatial coherence 8-71133
- traveling Michelson interferometer with phase-locked fringe interpolation 8-89451
- two-photon absorbers, laser pulse propagation 8-50862
- ultrashort laser pulse onset, first or second order phase transition 8-78986
- ultrashort pulse operations using flat lenses 8-66883
- wavelength comparison by two-beam interferometer, I₂ stabilised He-Ne laser 8-86326
- wavelength intercomparison between methane and I₂ stabilised He-Ne lasers 8-87089
- wavelength meas., review 8-89446
- wavelength meas. with Michelson and servocontrolled Fabry-Perot interferometers 8-89452
- wavelength measurement, review 8-50841
- wavemeter, inexpensive broadband optics and minicomputer interface 8-89448
- CO₂ high power laser beam monitor 8-74943
- CO₂ laser, pulse flow stretching (*Chinese*) 8-90435
- CO₂ laser, Stark cell noise reduction 8-59059
- CO₂ laser beam alignment, accuracy, Snout test 8-59073
- CO₂ laser beam meas. using pyroelectric vidicons 8-49907
- CO₂ pulsed laser beam, thermal coupling 8-63145
- HF, high-energy laser, energy extraction, beam quality, for fusion ignition 8-63102
- He-Ne laser freq. determ., interferometric comparison with upconverted CO₂ laser radiation 8-55395
- I laser, high-power, beam quality, gain saturation effect, for fusion ignition 8-63149
- KrF laser beam, Raman pulse compression, for fusion expts. 8-59086
- Nd:glass laser beam distrib. in focal region, transmission monitoring through pinhole 8-90441
- Nd:glass laser picosecond pulses, background energy content meas. with saturable absorbers 8-59062
- Nd:YAG, passive mode-locked, picosecond pulse duration, determ. from luminesc. intensity 8-71134

laser cavity resonators

- active control techniques 8-71122
- adaptive optical system, intracavity deformable mirror 8-87078
- adaptive resonator expt. config. 8-55386
- atomic beam tube with laser pump, interaction eqns. (*Russian*) 8-74801
- beam expansion with diffr. grating in dye laser cavity 8-66858
- birefringent filters for tuning flashlamp-pumped dye lasers 8-74914
- bistability of saturable-absorber containing laser, semiclassical and quantum theories 8-82943
- chemical laser, power spectral performance, coupled fluid dynamic, kinetic and physical optics model 8-79040
- conical laser plasma tube, electron density distrib. 8-58981
- coupling reflector, involute-related, for flash lamp pumped laser systems 8-90425
- distributed aperture effect in laser rods with negative lenses 8-66857
- distributed Bragg reflector optical resonator, response to light pulses 8-63141
- dye grazing-incidence pulsed laser, operation in single longit. cavity mode 8-94398
- dye laser, freq. locking of Na flame atomic transitions 8-50795
- dye laser, N₂ laser pumped, single mode operation 8-87060
- dye laser, N₂ laser pumped, two wavelength outputs with orthogonal polarisations 8-50792
- dye laser, spectrally narrow pulsed, without beam expander 8-79028
- dye laser frequency locking by intracavity stimulated Raman scatt. 8-79050

laser cavity resonators continued

- dye laser synchronisation, CW laser injection, spectral purity (*French*) 8-63118
- dye pulsed laser, light polarisation with thin wedge plate in cavity 8-55394
- excitation energy conversion efficiency in laser cavities 8-90432
- Fabry-Perot, and confocal resonators, comparison of diffraction formulas 8-87077
- Fabry-Perot resonator, laser mode sweeping dynamics, optical length effects 8-83001
- far IR laser, optically pumped, electronic tuning and phase-locking 8-59055
- fluoromethane, far IR laser, electronic tuning and phase-locking 8-59055
- fluoromethane far IR laser FM and stabilisation by Stark effect 8-59056
- gas laser, coupling modulated, mode coupling distortions minimisation 8-55384
- gas laser 8-83084
- gas laser cavity unit for radiation lead-out (*Russian*) 8-90433
- gasdynamic CW laser, multipass cavity 8-63140
- Huygens-Fresnel integral in circular coords., asymptotic soln. 8-87013
- intracavity dye laser technique for spectroscopic and kinetic meas. of transients 8-62239
- intracavity enhancement of absorpt. in nanosecond regime 8-78839
- intracavity laser Raman spectrometer, appls. 8-65973
- intracavity spectrometer, using continuous jet dye laser (*Russian*) 8-70197
- intracavity spectroscopy, quantitative information acquisition on absorpt. line parameters 8-49911
- intraresonator atomic spectroscopy, element determ. by narrow line fluorescence recording (*Russian*) 8-73124
- laser-induced line shifts and double-quantum Lamb dips 8-86825
- metallic wired grids as far IR semitransparent mirrors, use in HCN laser cavity 8-71188
- methanol, far IR laser resonator for TEM₀₀ mode operation 8-66847
- multilayer resonance elements, elec. field distribution calc. (*Russian*) 8-78854
- nonsymmetric eigenvalue problems of optical resonators, numerical solns., Prony method 8-82992
- optical feedback effects in CW injection lasers, using external reflecting surface 8-79045
- output mirror, low reflectance, reduced radiation loading 8-83000
- phosphate glass active-passive mode-locked oscillators at 1.054 μ m 8-63139
- photon statistics, optical cavity length depend. 8-94402
- plasma mirror refl. characts., in electron beam controlled CO₂ laser 8-59064
- pulsed laser sources using Nd 8-50784
- Q-switching, resonant vibrating mirror system 8-87082
- RF spectroscopy in laser cavity, pure nucl. quadrupole spectra 8-90320
- rhodamine 6G synchronously mode locked CW laser, pulse width depend. on intracavity bandwidth 8-66821
- rhodamine 6G water soln. laser with spatial lamp pumping, spatial coherent emission 8-82963
- ruby laser, radiation automodulation with passive switching of electro-optical shutter (*Russian*) 8-74936
- ruby laser, weak passive Q-switching in spherical resonator 8-50834
- secondary laser cavity for weak absorptions 8-92551
- solid laser, Q-switched, nanosecond and microsecond pulse generation, review 8-71130
- spark control cavity dumping for ruby laser 8-59053
- spherical mirror folded cavities, astigmatism elimination and regulation (*Chinese*) 8-90431
- stability conditions for laser cavities with two foci 8-66850
- stimulated Raman emission component locking, in optical resonator with dispersive medium 8-50858
- unstable, optical alignment procedure 8-50826
- unstable optical resonators with tilted spherical mirrors, design eqns. 8-74930
- unstable resonator, thermoelastic mirror deform., influence on laser characts. 8-71124
- unstable resonator properties, small-scale phase inhomogeneity influence 8-59050
- unstable resonators for high power lasers (*Italian*) 8-87076
- unstable resonators with rounded edges, mode losses 8-79039
- unstable strip resonators with misaligned circular mirrors, waveguide approach 8-82991
- waveguide laser, construction and operation characteristics (*Rumanian*) 8-59049
- CO electric discharge unstable resonator laser, computer model 8-58988
- CO₂, CW waveguide laser, anodised Al waveguide construction 8-55376
- CO₂ IR laser, transients obs. by modulation of intracavity absorber 8-74933
- CO₂ laser, intracavity IR absorpt. of vinyl chloride, ethylene, and propylene 8-78835
- CO₂ laser line selection using metal film reflection filter 8-55368
- CO₂, rapid wavelength switching probe laser, J-line scan gasdynamic laser diagnostic 8-59044
- CO₂ TEA laser, compact sealed single mode operation 8-50810
- CO₂, TEA laser, energy extraction improvement in multiline double band mode 8-63129
- CO₂, TEA laser, pulse shape and duration, excitation method (*German*) 8-83010
- CO₂ TEA laser with long optical resonator, mode-locked operation 8-79041
- CO₂ waveguide high press. laser, line selection and tunability 8-59026
- DF laser, pulsed unstable resonator, mode control and performance studies 8-82995
- D₂O FIR lasers, reststrahlen laser resonator for 66 μ m line 8-55385
- GaAlAs, DH CW diode laser, picosecond pulse generation 8-83002
- (GaAl)As high performance diode laser, high-reflectivity cavity mirrors 8-82994
- GaAs double-cavity laser with branching output waveguides 8-63128
- GaAs-(GaAl)As LOC-DBR laser, high differential quantum efficiency 8-79031
- HF CW chemical laser with cylindrical telescopic resonator, flame front model 8-59001

laser cavity resonators continued

- HF chemical laser, spherical telescopic resonator, design 8-71120
 HF laser, pulsed unstable resonator, mode control and performance studies 8-82995
 He-Ne complex resonator laser, stabilisation 8-55374
 He-Ne laser, in axial mag. field, output power dependence of mode locking phenomena 8-71129
 He-Ne laser, output power, unsaturated gain distrib. 8-50751
 InSb spin-flip Raman laser external-cavity system, oscill. characts. 8-55383
 LiNdP₄O₁₂ laser, spontaneous phase locking obs. 8-83005
 N₂ laser, electrode configuration for high peak powers and high repetition rates 8-55379
 N₂O IR laser, transients obs. by modulation of intracavity absorber 8-74933
 Nd:glass, dynamic mode sweep-laser, freq. tuning 8-66851
 Nd:glass laser, resonant reflectors in laser cavity, freq. selection 8-55369
 Nd:glass laser output, passive-mode locked, resonator length effect 8-79044
 Nd:YAG, intracavity modulation, sum freq. mixing, 212.8 nm pulse burst generation 8-74934
 Nd:YAG long laser resonator, active and passive mode-locking 8-50832
 Nd³⁺:LiYF₄, pulsed free running laser action at 1053, 1046 nm, passive mode locking (*French*) 8-79048
 YAG laser, resonator length effects on loss coeffs. and output energy (*German*) 8-66849
 ZnCd_{1-x}S, lasing modes and spatial distrib. under one-photon excitation, cavity model 8-74913

laser frequency stability

- atomic beam nonorthogonal to laser light, absorpt. profile, optical freq. standard appl. 8-74940
 CW laser, mode selection using spatially inhomogeneous saturable absorpt. (*German*) 8-83011
 Doppler broadened laser amplification line frequency characteristics meas. 8-59060
 dye laser, freq. locking of Na flame atomic transitions 8-50795
 dye laser frequency locking by intracavity stimulated Raman scatt. 8-79050
 far IR lasers, optically pumped, frequency modulated noise measurements 8-55392
 fluoromethane far IR laser FM and stabilisation by Stark effect 8-59056
 gas laser, single frequency, production testing techniques 8-90444
 instability below threshold, laser-saturable absorber system 8-94385
 methane stabilised laser, stability evaluation (*Japanese*) 8-90437
 nonstationary generation induced interference pattern phase distortion, holographic meas. 8-58945
 optical heterodyne simulation expts., first order correlation meas., fluctuating laser beam 8-83008
 review, extension of freq. meas. to 197 THz 8-81952
 ring laser, anisotropic cavity single isotope type, oppositely travelling waves competition 8-50825
 ring laser, de-adjusted medium, optical axis and stability 8-82999
 solid ring laser with additional mirrors, stabilisation by external signal 8-82998
 spectral profile modulation broadening 8-87083
 Zeeman linearly polarised laser, mag. field reson. on laser output, freq. stabilisation (*Japanese*) 8-66798
 Ar⁺ laser freq. stabilisation by ¹²⁷I₂ absorption lines at 582 THz 8-90430
 CO₂, freq. stabilised laser with OsO₄ absorber, output freq. reproducibility 8-50800
 CO₂ laser stability and heterodyne frequency calibration 8-59031
 CO₂ TEA oscillator, simultaneous freq. stabilisation and injection 8-55362
 He-Ne, ¹²⁷I₂ frequency stabilisation, 612 nm and 640 nm 8-66871
 He-Ne, ¹²⁷I₂ stabilised, freq. shifts, limitations 8-90440
 He-Ne, 6328 Å, single-mode collapse 8-94404
 He-Ne, high stability, single freq., 3.39 μm 8-71121
 He-Ne, I₂, hyperfine component classification, suitability for laser wavelength stabilisation 8-86965
 He-Ne, I₂ stabilised laser, wavelengths comparison by two-beam interferometer 8-86326
 He-Ne, I₂ stabilised lasers, conf., Germany (Feb. 1977) 8-87069
 He-Ne, I₂ stabilised laser design, freq. reproducibility 8-87070
 He-Ne, I₂ stabilised laser research 8-87071
 He-Ne, I₂ stabilised laser with hot wall I₂ cell 8-87073
 He-Ne, I₂ stabilised lasers, length metrology (*French*) 8-87074
 He-Ne, I₂ stabilised laser, spectral profile modulation broadening 8-87083
 He-Ne, I₂ stabilised laser, instrumental freq. offsets 8-87084
 He-Ne, I₂ stabilised lasers, international intercomparison meas., hyperfine struct. spacings 8-87088
 He-Ne, I₂ stabilised lasers, beat frequency, international comparisons (*French*) 8-87090
 He-Ne, methane and I₂ stabilised lasers, wavelength intercomparison using Michelson interferometer 8-87089
 He-Ne, stabilised by I₂ saturated absorpt., technological principles (*French*) 8-87075
 He-Ne complex resonator laser, stabilisation 8-55374
 He-Ne internal mirror laser, degeneration of longitudinal modes and freq. stabilisation (*Japanese*) 8-90426
 He-Ne laser, I₂ stabilised, realisation of length unit 8-87068
 He-Ne laser fluctuation spectra of freq. and amplitude 8-82950
 He-Ne laser freq. determ., interferometric comparison with upconverted CO₂ laser radiation 8-55395
 He-Ne laser status, I₂ vapour stabilised 8-87072
 He-Ne laser wavelength stabilisation on I₂ (*Czech*) 8-87061
 He-Ne laser with methane absorpt. cell, hyperfine struct. influence on freq. reproducibility 8-50864
 He-Ne lasers, I₂ stabilised, 633 nm line, performance improvement 8-90429
³He-Ne stabilised by saturated absorption ¹²⁷I₂ laser wavelength standard development appl. (*German*) 8-79034
 InSb spin-flip Raman laser external-cavity system, oscill. characts. 8-55383

laser frequency stability continued

- Nd:glass laser, resonant reflectors in laser cavity, freq. selection 8-55369
 Nd:glass travelling-wave sweep laser, emission spectrum dynamics 8-50829

laser isotope separation

- CW IR laser enhanced reaction 8-56905
 dye CW laser, on-line computer control, laser isotope separation appl. 8-70948
 electric discharge gasdynamic 16 μm CO₂ laser, isotope separation appl. 8-55381
 fluoromethane+Br, isotope selective photobromination, using c.w. CO₂ laser irradi. in excess inert gas 8-76843
 interface of two phases or liquids, selective processes induced by resonance laser radiation 8-64867
 IR laser 823 cm⁻¹ radiation appl., Cs vapour discharge laser 8-63069
 IR-laser-induced unimolecular reactions by vibr. modes excitation 8-58757
 molecular ion, spontaneous IR rot.-vibr. emission probability, vibr. selective excitation 8-50535
 overview, mol. photodissociation processes 8-55257
 polyatomic molecules, multiphoton dissociation and isotope separation 8-62865
 scattering of atoms by stimulated light freqs. appl. to isotope separation 8-66526
 surface photochemistry and photodesorption, isotope separation aspects 8-64863
 BCl₃, isotope enrichment, heterogeneous condensation in presence of CO₂ laser irradi. 8-70953
 CS₂, single-photon isotope separation using ArF laser 8-55211
 Cl₂, photochemical reaction using Ar ion laser, Cl isotope enrichment 8-74780
 D, reaction chamber for laser separation 8-55040
⁶Li*+⁷Li*, laser-induced Penning and associative ionis., ¹³Li⁺ enrichment 8-58796
 MoF₆, isotope separation by laser, multiple-photon 8-58858
 OsO₄, two IR pulse multiphoton absorpt. selective dissociation, obs. 8-82798
 SF₆, dissociation processes using one or two TEA CO₂ lasers 8-74713
 SF₆, IR laser isotopic enrichment in low temp. matrices 8-90318
 SF₆, mol. beam, selective dissociation in intense IR laser field, wavelength and energy depends. 8-73065
 SF₆, multiphoton IR dissociation, quantum or classical approach 8-82801
 UF₆, characts. of optically pumped 12.08 μm high power NH₃ laser 8-74923
 UF₆, temp. and density profiles in freely expanding gas for laser enrichment 8-74458
²³⁵U, hyperfine struct. and isotope shift meas., laser separation by two-step photoionisation 8-78822

laser magnetic resonance

- ClO₂ radical, ν, band, tuning by avoidance of Zeeman level crossing 8-94263
 HO₂ radical, ν₃ fundamental band, laser mag. reson. 8-66566
 SO, a¹Δ state, laser mag. reson. spectrosc. 8-94265
 SeH(X²π_{3/2}), far IR LMR spectrum 8-66564

laser modes

- bistability of saturable-absorber containing laser, semiclassical and quantum theories 8-82943
 buried heterostructure laser, fund. transverse mode operation, current limitation 8-55353
 CW laser, homogeneously broadened gain, longit. mode selection 8-63143
 CW laser, mode selection using spatially inhomogeneous saturable absorpt. (*German*) 8-83011
 dye grazing-incidence pulsed laser, operation in single longit. cavity mode 8-94398
 dye laser, intense subnanosecond pulse generation, 0.58 to 0.80 μm mode locking 8-90422
 dye laser, N₂ laser pumped, single mode operation 8-87060
 dye laser, N₂ laser pumped, two wavelength outputs with orthogonal polarisations 8-50792
 dye laser, N₂ laser-pumped, subns. relax. oscils. 8-82959
 dye laser, passively mode locked, 0.2 psec. pulse generation and meas. 8-50830
 dye laser, synchronous mode locking, composite gain and absorber medium, sub ps pulses 8-79046
 dye lasers, beam divergence, transverse mode saturation, kinetics (*Russian*) 8-74931
 dye lasers, flash lamp pumped, mode locking, picosecond, pulse generation 8-71131
 Fabry-Perot resonator, laser mode sweeping dynamics, optical length effects 8-83001
 fibre laser-amplifier, coupled-mode theory 8-66848
 gas laser, coupling modulated, mode coupling distortions minimisation 8-55384
 gas multimode laser with excitation modulation, polaris. of active medium 8-82942
 gas ring laser, multimode, high-Q power resonances 8-82997
 giant pulse lasers, passively mode locked, optimisation 8-83006
 high-power annular lasers, uniform beam transformation, mirror system 8-94403
 homogeneously broadened laser, two mode operation, analytical string signal analysis 8-55331
 injection lasers, optical ringing effects, internal loss modulation and direct modulation 8-87081
 laser, double heterostruct. junction type, US wave freq. modulation anal. 8-83009
 methanol, far IR laser resonator for TEM₀₀ mode operation 8-66847
 modelocking, soln. of 2nd order integro-differential eqns. 8-66796
 multi-mode diodes, dynamic mode interaction 8-55354
 N-mode laser, emitted light correlations 8-63051
 optical picosecond spectroscopy using mode-locked lasers 8-58065
 oxide stripe heterojunction lasers, asymm. modes 8-59006
 passive mode locking, fast absorber model 8-59054
 passively mode locked pulse stability in fast absorber limit 8-59052
 phosphate glass active-passive mode-locked oscillators at 1.054 μm 8-63139
 pulse timing by combined passive and active mode-locking, anal. 8-55391

laser modes continued

- pulsed acousto-optical modulator RF driver for laser mode locking 8-90438
- pulsed output, from mode-locked laser, quantised field representation 8-79054
- Raman spin-flip laser, higher modes and saturation effects, theory 8-71106
- rhodamine 6G dye laser, CW synchronously mode-locked, subpicosecond pulse generation 8-71128
- rhodamine 6G jet stream CW laser, tuning range, mode competition effects 8-50791
- rhodamine 6G synchronously mode locked CW laser, pulse width depend. on intracavity bandwidth 8-66821
- ring laser, anisotropic cavity single isotope type, oppositely travelling waves competition 8-50825
- ring laser, coherence theory, counter-rotating laser modes 8-55387
- ring laser, de-adjusted medium, optical axis and stability 8-82999
- ring laser, two-mode, intensity fluctuations meas. near threshold 8-55388
- ring laser gyroscopes, multioscillator approach to locking problem 8-79042
- ruby laser, pulsed, electronic speckle pattern interferometry 8-65961
- ruby laser, self-synchronisation of modes (*Russian*) 8-74937
- semiconductor injection laser, spectral modulation behaviour, theory 8-50775
- semiconductor injection stripe lasers, homogeneous spectral broadening multimode rate eqn. 8-79018
- semiconductor junction lasers, narrow stripe geometry, non-Gaussian fundamental mode patterns, waveguide model 8-94394
- semiconductor laser, dynamic behaviour, lateral mode and carrier density profile effects 8-82968
- semiconductor lasers, multimode generation (*Russian*) 8-55357
- stripe geometry injection lasers, rigorous boundary value soln., for lateral modes 8-71100
- two-dimensional DFB laser with acoustic wave and Bragg reflectors 8-79043
- unstable resonator properties, small-scale phase inhomogeneity influence 8-59050
- unstable resonators with rounded edges, mode losses 8-79039
- Zeeman linearly polarised laser, Izsing atom susceptibilities, first and third order approx. (*Japanese*) 8-71071
- Zeeman linearly polarised laser, mag. field reson. on laser output, freq. stabilisation (*Japanese*) 8-66798
- (Al,Ga)As-GaAs laser, transverse junction stripe, high temp. single mode CW operation 8-74918
- (Al,Ga)As, transverse junction stripe single mode oscillating laser, gain spectra 8-55356
- CO₂, 200 J TEA laser, injection mode locking 8-79049
- CO₂ CW laser, sealed-off design, NaCl Brewster angle mirrors 8-55370
- CO₂ laser, high repetition rate-pulsed, weak shock wave effect 8-90409
- CO₂, laser pulse mode quality, effect on multiple photon absorpt. 8-66615
- CO₂ TE laser, passive mode locking using p-Ge saturable absorber 8-71127
- CO₂ TEA laser, compact sealed single mode operation 8-50810
- CO₂, TEA laser, pulse shape and duration, excitation method (*German*) 8-83010
- CO₂ TEA laser with long optical resonator, mode-locked operation 8-79041
- CO₂ TEA oscillator, simultaneous freq. stabilisation and injection 8-55362
- DF laser, pulsed unstable resonator, mode control and performance studies 8-82995
- (GaAl)As injection lasers, self-pulsations, Q-switching and mode-locking effects 8-66827
- Ga_{1-x}Al_xAs, channelled substrate, planar struct. and DFB lasers 8-79032
- GaAs injection lasers, longitudinal mode spectrum, effect of carrier diffusion 8-71099
- GaAs-AlGaAs distributed Bragg reflector integrated twin-guide laser, temp. characts. 8-87064
- GaAs-AlGaAs transverse junction stripe laser, single mode behaviour after 12000 hr ageing test 8-66831
- GaAs-GaAlAs DH laser diode, lateral modes 8-59009
- HF laser, pulsed unstable resonator, mode control and performance studies 8-82995
- He-Ne, 6328 Å, single-mode collapse 8-94404
- He-Ne internal mirror laser, degeneration of longitudinal modes and freq. stabilisation (*Japanese*) 8-90426
- He-Ne laser, in axial mag. field, output power dependence of mode locking phenomena 8-71129
- He-Ne laser, mode selection and mode locking, effect on two-photon absorpt. efficiency 8-83023
- He-Ne two-mode travelling-wave laser, Zeeman beats 8-50827
- I laser, smooth pulse oscillator for single mode operation 8-59057
- InSb spin-flip Raman laser external-cavity system, oscill. characts. 8-55383
- Kr ion laser, mode-locked, near UV, 50 ps pulse width 8-79030
- LiNdP₄O₁₂ laser, spontaneous phase locking obs. 8-83005
- Nd:glass, dynamic mode sweep-laser, freq. tuning 8-66851
- Nd:glass, TEM₀₀ mode operation (*Rumanian*) 8-50798
- Nd:glass laser output, passive-mode locked, resonator length effect 8-79044
- Nd:YAG, passive mode-locked, picosecond pulse duration, determ. from luminesc. intensity 8-71134
- Nd:YAG long laser resonator, active and passive mode-locking 8-50832
- Nd:YAG pumped LiNbO₃, parametric oscillator, picosecond IR pulse generation 8-71151
- Nd³⁺:LiYF₄, pulsed free running laser action at 1053, 1046 nm, passive mode locking (*French*) 8-79048
- Nd³⁺:YAG CW ring laser, axial mode locking by electrooptic LiNbO₃ phase modulator 8-50835
- Pb_{1-x}Sn_xSe-PbSe pulse laser diode, temp. tuning of modes 8-50777
- Pb_{1-x}Sn_xTe-PbTe pulse laser diode, temp. tuning of modes 8-50777
- Zn,Cd_{1-x}S, lasing modes and spatial distrib. under one-photon excitation, cavity model 8-74913

laser radar see optical radar

laser theory

- see also *laser transitions*; *population inversion*; *stimulated emission*
 - active medium, surface transition layer effects (*Russian*) 8-71072
 - amplification of incoherent radiation 8-55334
 - anharmonic oscillator in strong EM field, induced radiation model (*Russian*) 8-78988
 - bistability of saturable-absorber containing laser, semiclassical and quantum theories 8-82943
 - bistable absorption in Fabry Perot ring cavity 8-50821
 - Bragg interactions in active medium, first and second order 8-50747
 - coherence oscillations in nonlinear media, coherent state lifetime 8-66862
 - computer model for CW optically-pumped submm laser performance prediction 8-87041
 - CW lasers, homogeneously broadened, with uniform distribution loss, exam. of output power 8-55332
 - dye laser, N₂ laser-pumped, subns. relax. oscills. 8-82959
 - dye laser, rate eqns. 8-82961
 - exponentially decaying gain medium, waveguiding 8-50774
 - fundamental concepts, elementary approach (*Hungarian*) 8-71070
 - gas laser amplifier, quasi-Gaussian pulse propagation, effect on line-shape parameter anal. 8-55333
 - gas lasers, longitudinal flow, effect of flow on output power 8-58975
 - gasdynamic CW laser, multipass cavity 8-63140
 - giant pulse lasers, passively mode locked, optimisation 8-83006
 - homogeneously broadened laser, two mode operation, analytical string signal analysis 8-55331
 - instabilities for coherently driven absorber in ring cavity 8-50822
 - instability below threshold, laser-saturable absorber system 8-94385
 - intensity fluctuation linewidth, Jakeman-Pike approx., black-body and laser models 8-58960
 - lateral wave amplification through reflection from active medium 8-78987
 - mean field model for absorptive and dispersive optical bistability with inhomogeneous broadening 8-50823
 - memory effects in linewidth and line shape near laser threshold 8-58976
 - methylfluoride laser, CW, 496 microns, rate equation model, review 8-55343
 - modified Lange eqn. with integral term, exact soln. 8-63052
 - N-mode laser, emitted light correlations 8-63051
 - nonequilibrium phase transition, dynamical features (*Chinese*) 8-83030
 - one-dimensional model, stable and metastable states, relax. and fluctuation theory 8-49769
 - organic compounds, lasing ability, substitution effects 8-82941
 - photon statistics, optical cavity length depend. 8-94402
 - population inversion, maximum achievable, in finite volumes 8-50749
 - Q-switched four level laser dynamics, lifetime of terminal energy level (*Chinese*) 8-66832
 - quantum dynamical semigroups and spin multipole relaxation in isotropic surroundings 8-86813
 - quantum theory of spontaneous and stimulated emission of channelled electrons and positrons (*Russian*) 8-49999
 - Raman spin-flip laser, higher modes and saturation effects, theory 8-71106
 - resonant two-photon ionisation in partially coherent radiation field 8-66525
 - ring laser, quasiclassical equation of motion, spontaneous emission in lasing channel (*Russian*) 8-90434
 - saturation parameter from gain meas. 8-66797
 - scaling theory of laser radiation in the transient unstable region 8-94384
 - semiconductor injection stripe lasers, homogeneous spectral broadening multimode rate eqn. 8-79018
 - stripe geometry injection lasers, rigorous boundary value soln., for lateral modes 8-71100
 - three boson field modes with trilinear interaction, statistical behaviour 8-87093
 - tricritical phenomena in laser with saturable absorber 8-78989
 - two level three dimensional system, phase transitions analogy with lasers 8-58965
 - two-photon laser for optical communications, quantum noise optimum control 8-71049
 - ultrashort laser pulse onset, first or second order phase transition 8-78986
 - Zeeman linearly polarised laser, Izsing atom susceptibilities, first and third order approx. (*Japanese*) 8-71071
 - Zeeman linearly polarised laser, mag. field reson. on laser output, freq. stabilisation (*Japanese*) 8-66798
 - CO sealed laser, approximate analytic theory 8-58994
 - CO₂, electric discharge convection laser, saturation characts. (*Chinese*) 8-90408
 - CO₂ gasdynamic laser, gain supersonic flow heating effect, condition optimisation 8-82947
 - CO₂ laser, high power, CW, electron beam sustained, performance, theory and expt. 8-71074
 - CO₂ laser, long and short pulse formation, optimum conditions 8-87037
 - CO₂, laser discharges, determ. of recombination coeff. 8-90407
 - HCl-D₂-He mixture, gasdynamic laser theory, gain depend. on parameters 8-50761
 - HF chemical laser, spherical telescopic resonator, design 8-71120
 - Hg-N₂, optical pumping, vibr. excitation, laser theory 8-66517
 - N₂ electron impact excitation, rate coeffs., momentum transfer cross-section 8-78819
- laser transitions**
- see also *laser theory*
 - carbocyanine dye CW laser emission, spectral range extension up to 1020 nm 8-74901
 - carbon tetrafluoride 16 μm laser, radiance enhancement 8-87045
 - crystals with paraelectric impurities, superradiative transitions, acoustic and EM excitation 8-66872
 - formaldehyde-d₂ vapour, far IR laser emissions 8-63072
 - formic acid, laser transitions near 5.6 μm, HF laser optical pump 8-58995
 - gain and refractive index for broadened laser line, sampling series representation 8-50748

laser transitions continued

inert gas fluoride laser, using NF₃-inert gas mixture, long pulse UV emission (*French*) 8-58982
 methanol, CH₃OH and CD₃OH, far IR laser lines, optically pumped by CO₂ laser 8-90415
 methanol-d₃, CO₂ laser pumped, CW far IR laser lines obs., 34.5 to 287 μ m 8-71082
 methanol-d₃, optically pumped, CW far IR laser lines obs. 8-79005
 methyl alcohol-d, optically-pumped laser line freqs. 8-55345
 plasma laser star model of QSOs 8-96558
 POPOP-Ar-N₂, electron beam pumped, intense laser emission at 381 nm 8-74898
 UV ion lasers, metal-inert gas charge transfer reaction 8-66809
 XUV lasing, gain-verification problem 8-71086
 Ag II, 1 W multiline output power from 800.4, 825.5, 840.4 nm transitions 8-82953
 Ar I, high press. tunable laser emitting at 0.91 μ m 8-50755
 Ar-Kr-F₂ mixture, electron beam pumped, spectroscopy and kinetics of 248, 414 nm bands 8-63081
 ArF, laser expts. on $^2\Sigma^-2\Sigma$ transitions 8-63080
 Ba-N₂O flame, candidate chem. laser reactions, intracavity dye laser absorpt. meas. 8-63108
 Br₂, optically pumped at 532 nm, lasing obs. in visible and near IR 8-63094
 CO₂, absolute transition freqs. by multiplication of difference-freqs. 8-90445
 CO₂ laser, intracavity IR absorpt. of vinyl chloride, ethylene, and propylene 8-78835
 CO₂ laser stability and heterodyne frequency calibration 8-59031
¹³CS₂, laser emission at 6.9 μ m, HF laser optical pump 8-58995
 Ca-N₂O-CO flame, Ca catalyzed, gain meas., emission band assignment 8-66815
 Ca-N₂O-CO flame, candidate chem. laser reactions, intracavity dye laser absorpt. meas. 8-63108
 Cd⁺ in He-CdBr, He-CdCl₂ and He-CdI₂ discharges, CW laser oscill. 8-50765
 CdHg, positive gain measurements or 470 nm continuum band 8-66805
 Cl II in CuCl and FeCl₂ vapours, pulse generation at 5218 Å, 5221 Å 8-58990
 Cu II, 1 W continuous output from 780.8 nm transition 8-82953
 Ge³⁺:YAG, excited state absorpt. loss, 5d \rightarrow 4f rare earth lasers 8-90417
 Hd-Cd hollow cathode laser in mag. field, Cd II stimulated emission 8-79002
 He-Cd II lasers, positive column, hollow cathode types, 4416 Å oscill. characts. (*Japanese*) 8-94392
 He-F, doublet series laser lines near 700 μ m, hyperfine splitting and broadening meas. 8-63070
 He-Ne laser, 60 mW, perturbation spectroscopy (*Rumanian*) 8-50752
 He-Ne laser fluctuation spectra of freq. and amplitude 8-82950
 He-Zn hollow cathode laser, 7588 Å in ZnII, operating characts. and upper level operating mech. 8-63071
 I, dye laser pumped to dissoci. point of I₂, laser action 8-63064
 I, photodissociation laser, 1.315 μ m transition line struct. 8-59000
 I₂, optically pumped, lasing obs. on 342 nm band 8-79008
 KF, tunable CW laser, using F₂⁺ centres for 1.26-1.48 and 0.82-1.07 μ m bands 8-79023
 Kr IV, very strong laser emission at 195.027, 175.641 nm 8-63060
 KrCl, laser expts. on $^2\Sigma^-2\Sigma$ transitions 8-63080
 KrF, Kr₂F, in electron beam pumped Ar-Kr-F₂ mixture, spectroscopy and kinetics of 248, 414 nm bands 8-63081
 KrF, radiative lifetime and quenching 8-63063
 LiF, laser action of M-centres at 700 nm 8-82972
 Mg-N₂O-CO flame, Mg catalyzed, gain meas., emission band assignment 8-66815
 N I, laser transition obs. at 9064 Å in He-N₂ afterglow 8-74891
 NH₃, two photon excited 16 μ m laser 8-58986
 NH₃, two-photon-excited, 16 μ m emission, wavelength meas. technique 8-71085
 N₂O isotopes, laser transitions near 4.6 μ m, HF laser optical pump 8-58995
¹⁵NH₃, far IR laser lines, optically pumped by CO₂ laser 8-90415
 Na, in shock heated salt vapour, anomalous emission from atomic lines 8-63089
 Na₂, laser excited broadband violet emission, 420 to 457 nm 8-79006
 Nd:CaY₂Mg₂Ge₃O₁₂, CW room temp. laser operation, 0.941 and 1.059 μ m 8-66842
 Nd:Y₂O₃ single crystal fibre laser, room temp. CW operation at 1.07 and 1.35 μ m 8-63121
 Nd:YAG, laser transition cross sections, modulation (*Chinese*) 8-90418
 Nd³⁺:LiYF₄, pulsed free running laser action at 1053, 1046 nm, passive mode locking (*French*) 8-79048
 Ne 6328 Å laser transition, homogeneous saturation due to collisions, weak collision model 8-78995
 Ne II, long pulse UV laser emission, electron beam excited Ne-NF₃ mixture 8-78996
 PH₃, laser emission 83 to 223 μ m region, laser line assignments 8-71084
 Pb vapour, long-lived sealed-off laser design, 7229 Å emission 8-50808
 Pb-He discharge, excitation process, Pb⁺ emission lines 8-66803
 Rb, in shock heated salt vapour, anomalous emission from atomic lines 8-63089
 S₂ laser, optically pumped, lasing obs. 470 to 480 nm 8-63095
 Sr⁺, inversion and lasing on optically pumped reson. line 8-70798
 Sr-N₂O-CO flame, candidate chem. laser reactions, intracavity dye laser absorpt. meas. 8-63108
 Sr-N₂O-CO flame, Sr catalyzed, gain meas., emission band assignment 8-66815
 Xe, 3.5 μ m transition, quasi-Gaussian pulse propagation, effect on line-shape parameter anal. 8-55333
 Xe, 3.51 μ m laser transition, phase-changing broadening, inert gas perturbors 8-82949
 Xe₂, efficient vac. UV laser, 172 nm at 6 atm 8-50793
 XeF, optically excited by incoherent Xe₂^{*} radiation, B \rightarrow X band emission 8-87044

laser transitions continued

Zn⁺ in He-ZnB₂, He-ZnCl₂ and He-ZnI₂ discharges, CW laser oscill. 8-50765
 ZnSe, optically pumped stimulated emission at 4580 Å, near band edge luminesc. 8-71105

laser tuning

alkali halide host cryst. F-centre lasers, tunable IR emission 8-59030
 coumarin derivatives in simple dye laser, pumping by N₂⁺ ion laser, tuning ranges 8-74903
 CW laser, mode selection using spatially inhomogeneous saturable absorpt. (*German*) 8-83011
 dye CW laser, on-line computer control, laser isotope separation appl. 8-70948
 dye CW laser, tuning and spectral narrowing using low-loss diffr. grat. 8-71109
 dye laser, flashlamp-pumped, birefr. filter for tuning, theory and design 8-74914
 dye laser, for ps spectroscopy, 400-500 nm 8-82988
 dye laser, pulsed tunable IR, pumped by flashlamp-driven dye laser 8-94400
 dye laser, tunable ps high efficiency system for 340 nm to near IR 8-50789
 dye tunable laser systems 8-59029
 excimer tunable laser systems 8-59029
 far IR laser, optically pumped, electronic tuning and phase-locking 8-59055
 fluoromethane, far IR laser, electronic tuning and phase-locking 8-59055
 fluoromethane waveguide laser, tunable, for far IR freq. synthesis in 500-70 μ m region 8-90439
 frequency shift, using two acousto-optical modulators in series 8-74932
 interference technique, spectrally depleted destructive two-beam, for laser freq. control 8-74941
 Raman spin-flip laser, higher modes and saturation effects, theory 8-71106
 rhodamine 6G jet stream CW laser, tuning range, mode competition effects 8-50791
 rhodamine B and 6G, laser wavelength and dye conc. 8-50770
 ruby, one-freq. tunable one-pulse, selector parameter optimisation 8-74935
 thermal length control, for lasers and etalons 8-87056
 UV metal ion lasers, appl. to tunable dye laser, 300-400 nm 8-66809
 Ar I, high press. tunable laser emitting at 0.91 μ m 8-50755
 CO, CO₂ lasers, perturbation spectroscopy tuning for atmospheric pollutants selective quantitative meas. 8-69526
 CO₂, 1 mJ line tunable optically pumped laser 8-66840
 CO₂, high-press. tunable IR lasers 8-59030
 CO₂, laser, 16 GHz tunable sideband generation 8-90428
 CO₂ waveguide high press. laser, line selection and tunability 8-59026
 CdTe, tunable high efficiency microwave freq. shifting of IR laser 8-71126
 GaAs-GaAlAs optically pumped DFB laser, wavelength tuning effect 8-82979
 GaAs_{1-x}P_x, continuously tunable electron beam pumped laser 8-50802
 GaAs_{1-x}Sb_x-Ga_{1-x}In_xP_{1-x}As_x multilayer structure, continuously tunable electron beam pumped laser 8-50802
 He-Cd(Zn) hollow cathode laser, upper level decay rate, mag. field tuning dip meas. 8-87043
 I, photodissociation laser, 1.315 μ m transition line struct. 8-59000
 InAs_{1-x}P_x, continuously tunable electron beam pumped laser 8-50802
 InSb spin-flip Raman laser external-cavity system, oscill. characts. 8-55383
 Kr, laser, tunable, Lyman alpha radiation, nonlinear generation 8-87038
 MgF₂:Ni electronic transition laser, tunable IR emission 8-59030
 N₂ laser, TEA, pump for dye laser amplifier system 8-82984
 N₂, liq., tunable Raman laser based on third Stokes component 8-50859
 Na fluorescein, laser wavelength and dye conc. 8-50770
 Nd:glass, dynamic mode sweep-laser, freq. tuning 8-66851
 Nd:glass laser, resonant reflectors in laser cavity, freq. selection 8-55369
 Nd:glass travelling-wave sweep laser, emission spectrum dynamics 8-50829
 Nd:YAG pumped LiNbO₃, parametric oscillator, picosecond IR pulse generation, tuning ranges 1.365-4.825 μ m and 0.66-2.70 μ m 8-71151
 Pb salt, tunable IR diode lasers 8-59030
 Pb_{1-x}Sn_xSe-PbSe pulse laser diode, temp. tuning of modes 8-50777
 Pb_{1-x}Sn_xTe, continuously tunable electron beam pumped laser 8-50802
 Pb_{1-x}Sn_xTe-PbTe pulse laser diode, temp. tuning of modes 8-50777
 Rb vapour, dynamic Stark tuned far IR laser 8-63126
 S₂ laser, optically pumped, lasing obs. 470 to 480 nm 8-63095

laser velocimeters

anemometry, velocity meas. by light scatt. techniques 8-57916
 atmospheric transverse velocity single-beam meas. 8-53747
 coherent Doppler anemometer for turbulent vel. meas., potential accuracy anal. (*Russian*) 8-71406
 digital, signal processor accuracy testing (*German*) 8-86242
 digital processing of laser-Doppler velocimeter signals (*German*) 8-83510
 Doppler anemometer, acousto-optical modulator using TeO₂ 8-83082
 Doppler frequency discriminator 8-81954
 Doppler system, optics and signal processor for turbulent low speed flows (*French*) 8-59521
 Doppler velocimeter direction-sensitive simultaneous multivelocity component 8-94857
 droplets, large, size and velocity meas. equipment 8-86238
 flow velocity meas. at olfactory organ nares of fishes (*German*) 8-69262
 fluidic element nonstationary flow meas. by laser Doppler velocimeter with frequency tracker (*Japanese*) 8-55707
 fringe anemometers, light scatt. aspects, particle size meas. appl. 8-83020
 instrumentation developed by Electricite de France Optical Applications Division (*French*) 8-75233

laser velocimeters continued

- local size and vel. probability distrib., two-phase suspension flows, laser-Doppler technique 8-59517
 metrological characts. of laser Doppler anemometers 8-75238
 multicomponent frequency shifting self-aligning laser velocimeters 8-87423
 opt. freq. shifting of light and laser beams 8-79392
 principles and aerodynamic appls. (*French*) 8-63518
 pulsating air flow, meas. instrumentation using photon correlation 8-87420
 retinal blood flow, laser Doppler meas. 8-69174
 signal processing techniques 8-59520
 spatially constricted flow meas. 8-71409
 time-of-flight laser anemometer, for velocity meas. in atm. 8-69469
 turbulent flow measurement by laser Doppler anemometry, concentration and size of tracer particles, theoretical limits 8-59514
 two-dimensional LDV measurement, of flow induced by flames 8-59529
 variable frequency shift Doppler, for combustion flow meas. (*Japanese*) 8-67294
 wind tunnel meas. appl., principles 8-71405
 CO₂ laser, long range outdoor velocimetry, air pollution meas. 8-61623

lasers

- see also chemical lasers; distributed Bragg reflector lasers; distributed feedback lasers; dye lasers; excimer lasers; free electron lasers; gas lasers; laser beams; laser frequency stability; laser tuning; liquid lasers; nuclear pumped lasers; Raman lasers; ring lasers; solid lasers; X-ray lasers*
 advanced lasers for fusion, modelling and anal. 8-50819
 EM precision meas., conf., Ottawa, Canada 1978 8-89462
 engineering advances, conf., San Diego, CA, USA (Aug. 1977) 8-59017
 laser spectroscopy conf., Jackson Lake Lodge, WY, USA, 1977 July 8-82666
 optics in adverse environments, conf., San Diego, USA (Aug. 1977) 8-82976

latent heat

- see also heat of fusion; heat of sublimation; heat of vaporisation*
 boiling, nucleate, subcooled, latent heat transport contrib. 8-75046

latent heat of adsorption *see heat of adsorption***latent heat of combustion** *see heat of combustion***latent heat of crystallisation** *see heat of crystallisation***latent heat of dissociation** *see heat of dissociation***latent heat of formation** *see heat of formation***latent heat of fusion** *see heat of fusion***latent heat of mixing** *see heat of mixing***latent heat of reaction** *see heat of reaction***latent heat of solution** *see heat of solution***latent heat of sublimation** *see heat of sublimation***latent heat of transformation** *see heat of transformation***latent heat of vaporisation** *see heat of vaporisation***latent image** *see photographic process***lattice constants**

- see also crystal atomic structure*
 A15 struct., stabilized by crystal field distortion of exotic elements at chain sites 8-79555
 crystal, statistical thermodynamics with collective vibrations 8-54289
 III-V quaternary alloys, energy bandgap and lattice const. 8-67940
 III-V semiconductors, effective mass, forbidden bandwidth and lattice constant relation (*Slovak*) 8-51879
 intermetallic phases with Li₂ and DO₁₉ struct., atom incompressibility, lattice parameter approach 8-91294
 ketone-paraffin solid soln., dielec. relax., temp. and lattice const. depend. (*German*) 8-76383
 Madelung parameter, expansion in terms of multipole moments, ratio of two lattice parameters 8-75618
 perovskite structure oxides, solid soln., crystal lattice parameters, conc. depend. calc. 8-95041
 polymethylpentene, isotactic, crystal struct. 8-67663
 quartz, synthetic, fading rel. to lattice deformation (*German*) 8-63760
 rare earth dicarbides, solid solns., phase transformation, strain energy 8-51672
 semiconductor thin film, lattice parameter meas. 8-59720
 sigma phase structure, ionicity modified pair pot. model anal. 8-51466
 Ag-Au (50 at.%), thermal expansion and lattice parameters, temp. depend. 8-91456
 Ag-based alloys, α -phase, mag. susceptibility correl. with lattice parameter 8-68154
 Al-Mn alloys, study of solidification by rapid cooling (*Japanese*) 8-88459
 β -Al₂O₃-K₂O/K ferrite, interfaces and solid soln., thermal expansion and lattice parameter variations 8-55959
 β -Ba₂Fe₂S₁₅, and low temp. α polymorph., cryst. struct. 8-67690
 Bi₂Al(Ga)₂O₉, fluoresc. and X-ray data 8-80403
 CdSe-Ge (111) heterojunctions, epitaxial, azimuthal rotation 8-84085
 α -Cu-Al, binary substitutional, short-range ordering kinetics, vacancy behaviour 8-55867
 Cu-based alloys, α -phase, mag. susceptibility correl. with lattice parameter 8-68154
 Cu-Cd alloys obtained by electrolysis, struct. 8-91552
 Cu-M, M=Al,Cd,In,Ga,Zn, magnetic susceptibility, comp. and temp. depend., melting effects 8-52202
 Ga_{1-x}In_xP, Delta lattice parameter model, correl. with electronic props. 8-91560
 Ga_{1-x}In_xSb, LPE on GaSb by stepwise grading, and characterisation 8-72745
 β -Ga₂O₃-K₂O/K ferrite, interfaces and solid soln., thermal expansion and lattice parameter variations 8-55959
 Ge, evaporated film, lattice parameters and phase transition temp., surface influence of glass substrates 8-94996
 Hf_{1-x}Zr_xV₂, lattice const. at 4K and room temp., phase division at $x=0.4$ 8-51474
 InAs, intrinsic point defects, nature and influence on electrophys. props. 8-79609
 In_{1-x}Ga_xP-GaAs heterojunction, VPE, energy band gap and lattice parameter, lattice mismatch effects 8-95345

lattice constants continued

- KLiSO₄, phase transition, lattice parameter variation with temp. 8-79767
 KNa₂, binding energy and lattice const., nonparametric calc. (*Russian*) 8-51462
 Li, martensitic phase transitions, and phase diagrams at moderate press. 8-72775
 α -Li₂O₃, lattice const. variation due to electrostatic field (*Chinese*) 8-83787
 MgM³⁺Fe_{2-x}O₄, M=In,Al,Cr,Sc, comp. effects on ferrite characts. 8-52305
 Mn₂As-Mn₂Sb, structural and magnetic props. determ. 8-76248
 MoS₂ film, non-stoichiometry and sputtering conditions 8-87891
 Na, martensitic phase transitions, and phase diagrams at moderate press. 8-72775
 NaBrO₃, lattice parameters, thermal expansion, defect formation energy 8-79786
 Na_{1-x}K_xNbO₃, solid soln., crystal lattice parameters, conc. depend. calc. 8-95041
 NaNH₄SO₄·2H₂O, ferroelec. and thermal props. 8-83968
 Ni-Al (51 to 55 at.%), vacancy defective, TEM exam. of structure 8-76677
 Ni-Fe alloy, FCC, density, lattice parameters, X-ray diffr. and hydrostatic weighing 8-55904
 β -Ni₃S₂, defect struct. 8-63754
 PbI₂ intercalated with organic mol., energy band splitting (*Russian*) 8-76027
 Pb₃MgNb₂O₉, crystal growth procedure, meas. electro-optic and dielectric props. 8-88418
 PbMgTa₂O₉, crystal growth procedure, meas. electro-optic and dielectric props. 8-88418
 PbMoS₈ and ternary sulphides, lattice parameter rel. to supercond. T_c 8-52119
 PbS, thermomech. props., SCF X α scatt. wave theory 8-71704
 PdD₂, model of instabilities 8-75619
 PdH₂, model of instabilities 8-75619
 Pu(C,N), lattice parameter variation, 50 to 300K 8-51709
 PuC(N), lattice parameter variation, 50 to 300K 8-51709
 ROsB₄, R=Y, Gd, Tb, Dy, Ho, Er, Tm, struct. and mag. props. 8-79584
 RRuB₄, R=Y, Cd, Tb, Dy, Ho, Er, Tm, struct. and mag. props. 8-79584
 ReO₃, lattice parameters, thermal expansion 291 to 464K, Bond technique meas. 8-75617
 ScN₂, region of homogeneity, physicochem. props. 8-52018
 SmSb_xS_{1-x}, intermediate valence, susceptibility and lattice parameter meas. 8-51943
 Ta-W-Hf (8-2 wt.%), T-111, O₂ absorption, effect on lattice parameter and specimen dilation 8-83958
 Ti-Al-Mo-Zr (Cr-Fe), effect of heating on thermal stability of phases, lattice constants and chem. comp. 8-56672
 TiN₂-TiO₂, thermal expansion, 23-1000°C, X-ray obs. 8-91454
 TiSi₂, crystal atomic struct., X-ray diffr. exam., lattice parameters and integrated intensities 8-75647
 US, electronic struct. calc. 8-91615
 V-Re system, discovery of supercond. A-15 phase 8-88060
 V₂O₃, lattice parameters and anomalous high temp. behaviour 8-87790
 V₃Si plastically deformed cryst., lattice transform., Kossel technique 8-95153
 YFe_{3-x}Ni_x, electronic sp. ht., saturation magnetisation and lattice parameter meas. 8-68261
 Zn₂Cd_{1-x}S film, prep. by soln. spray method, and struct., optical and elec. props. 8-52666
 ZnGeP₂, synthesis, characts., applic. to laser windows (*French*) 8-80467
 ZrC, whiskers, CVD on Ni, catalytic effect 8-51865
 ZrS(Se)₂, nonstoichiometry 8-75841

lattice defects *see crystal defects***lattice diffusion** *see diffusion in solids***lattice dynamics**

- see also crystal surface and interface vibrations; displacive transformations; Gruneisen coefficient; lattice dynamics of covalent crystals; lattice dynamics of ferroelectric crystals; lattice dynamics of ionic crystals; lattice dynamics of metallic crystals; lattice dynamics of molecular crystals; lattice localised modes; lattice phonons; soft modes; vibrational states in disordered systems*
 Anderson-Gruneisen parameter effect of anharmonicity 8-79714
 anharmonic Brownian oscillator, canonical correlation function based on projection operator technique 8-55926
 anharmonic crystals, unsymmetrised SCF approx. 8-63830
 Born-Huang invariance conditions, completeness 8-51620
 Brillouin zone summations, convergence 8-91384
 Cayley tree type system, modes, densities, lattice vibr. 8-71813
 chemisorbed atoms and mol., vibrational motion dynamics, infrared absorpt. line shape 8-51814
 classical Ising model, crit. dynamics simulation in transverse field 8-59930
 conference, Paris, France (Sept. 1977) 8-59869
 dielectric matrix, approximate inversion 8-71797
 dilute binary alloys, formation energy, lattice relax. and zero-point vibrations 8-83771
 dilute binary alloys, formation energy, lattice relax. and zero-point vibrations 8-87646
 dispersion of dielectric axes in monoclinic and triclinic crystals related to lattice dynamics 8-87920
 dispersive media, Ewald dynamical diffr. theory extinction theorem 8-66749
 fluorite type crystal, effects of anharmonicity and disorder on Raman scatt. at high temp. 8-80349
 force const. adjuster program for least squares fit to observed frequencies of molecules and crystals 8-91395
 force constants, diamond and sphalerite struct. crystals. 8-91408
 graphite, thermal vib. amplitudes from integrated intensities corrected for TDS 8-67780
 graphite intercalation compounds, props. and appls. 8-71711
 harmonic crystals, cell cluster method, Einstein heat capacity 8-51636
 hydrates, H₂O vibration in crystal lattice, model calc. 8-75741
 II-VI compounds, deformable-ion model 8-91396
 incommensurate lattices, conditions of existence and spectra 8-55934

lattice dynamics continued

- inert gas solids, unpaired elastic force model in lattice dynamical study 8-63820
 infinite harmonic crystal, dynamics and ergodicity 8-59919
 IR absorption mechanisms 8-60460
 linear mixed valence compounds, longit. modes 8-95119
 linear triatomic chain, lattice vibr. anal. 8-83886
 low-dimensional materials, pseudolattices and correlation method 8-75768
 matrix paradox, for teaching 8-49611
 methyl group tunnelling and coupling to internal vibrations 8-79675
 microscopic formulation of rigid ion, deformable charge densities and effective charges 8-59876
 microscopic theories, developments 8-59870
 microscopic theory, derivation of electron-phonon Hamiltonian of crystal 8-87746
 monatomic BCC lattice under intense excitation, energy transport 8-59922
 Mossbauer emission and absorption spectra, effect of anharmonic US vibrations excited in cryst. 8-72443
 nonlinear lattice dynamics, mol. dynamics simulation 8-59921
 nonmetals, microscopic and model theories 8-59871
 normal mode calcs. of crystals and molecules, coordinates and force matrices generation, computer program 8-91393
 partially disordered crystal, lattice dynamic model 8-83897
 pyridine-Ag₂I₆, superionic conductor, dynamical aspects 8-79695
 α -quartz, Γ -A phonon dispersion curves, rel. to AlPO₄ lattice dynamics 8-75750
 rare earth trihydroxides, cryst., Raman spectra, vibr. assignments 8-76455
 Rayleigh's theorem generalised, infinite harmonic crystal 8-55914
 soliton solutions to nonlinear phenomena 8-59880
 strongly anharmonic crystals, improved unsymmetrised SCF approx. 8-75791
 structural phase transitions, theory 8-75797
 structural phase transitions in crystals, effect of high-power visible and IR laser radiation 8-71825
 structurally incommensurate systems, fluctuation spectrum, incommensurate phases 8-91419
 superionic conductors, correlation functions theory 8-79674
 superionic conductors, dynamic properties 8-79673
 superionic conductors, microscopic theory 8-79809
 superionic conductors, Raman scattering from mobile ions, theory 8-80352
 superionics, with fluorite structure, Brillouin scattering and lattice defect energetics 8-80369
 uncorrelated-pairs approximation for anharmonic free energy, tests 8-59920
 vibrational dynamics of liquids and solids, Raman scatt. of picosecond light pulses 8-94414
 wurtzite-type crystals, force constants determ., polarisable ion model 8-75740
 X-Y model, two-dimensional, with quartic anisotropy, mol. dynamics study 8-75739
 zincblende type crystals, lattice dynamics, phonon freq. rel. to mass ratio 8-95121
 α -AgI, ionic motion, low freq. Raman scatt. 8-80354
 AgI, superionic conductor, dynamical aspects 8-79695
 α -AgI, superionic conductor, Raman scattering evidence for sublattice melting 8-80350
 AgI, superionic conductor, Raman study 8-80353
 Ag₃SI, superionic conductor, dynamical aspects 8-79695
 AlPO₄, vibr. normal modes, rel. to α -quartz phonon dispersion curve 8-75750
 (As₂O₃)_n, claudetite I, vibr. spectra, force field calc. (French) 8-60447
 BN, hexagonal, long optical vibrs., elastic const. from valence force const. 8-51621
 BaF₂, anharmonicity vibrs. and correlation effects, neutron diff. 8-55915
 BaF₂, superionic conductor, theoretical investigation of Raman scatt. 8-80351
 BaSO₄, barite, crystal struct. and sulphate force const. 8-83784
 Bi₂O₃, and sillenite struct. derivatives, MO_x.6Bi₂O₃, IR and Raman spectra, vibr. anal. 8-76464
 CaF₂, superionic conductor, theoretical investigation of Raman scatt. 8-80351
 CdR₂S₄ (R=Sc, Yb, Tm), IR and Raman spectra, force const. 8-68503
 CdTe, temp.-depend. of root-mean-square dynamic displacements, characteristic temp., X-ray study 8-83895
 CoCl₂, static displaced shell model 8-79689
 CrBr₃, CrCl₄, Raman spectra, struct. and thermodynamic functions 8-60443
 Cs₂NaBiCl₆, optical props. 8-68549
 Cu-Al, change in force constant due to volume effects 8-75778
 Cu-Si, change in force constant due to volume effects 8-75778
 CuI, superionic conductor, Raman study 8-80353
 GaP, dispersion of vibrational excitations, Raman scatt. 8-84588
³He, solid mag. ordering, lattice dynamical approach 8-56020
 Hg₂Cl₂ prototype phase, soft mode, inelastic neutron scattering, Raman effect 8-91411
 HgCr₂Se₄, ferromag. semicond., Raman spectra 8-52496
 p-HgTe, far IR reflectivity spectra, experimental and theoretical study of the dynamic dielectric function 8-92069
 In_{1-x}Ga_xAs₂P_{1-y}, lattice vibrs., Raman study 8-91391
 InS, layer single cryst., Raman scatt. meas. 8-76478
 InSe, layer single cryst., Raman scatt. meas. 8-76478
 InSe, layer single crystal, infrared and Raman spectra 8-92070
 KH-H₂ crystal-gas system, with D impurity, thermodynamic equilb. 8-59954
 K₂PbCu(NO₃)₆ Jahn-Teller phase transitions, X-ray and neutron measurements 8-91438
 La(BrO₃)₃.9H₂O, IR and Raman spectra, vibr. assignments 8-84569
 LiNbO₃, dispersion of vibrational excitations, Raman scatt. 8-84588
 MgAl₂O₄, lattice dynamics, rel. to space group of spinel 8-59898
 MgO crystal, unified approach to lattice states and dynamics 8-59878
 MgR₂S₄ (R=Sc, Yb, Tm), IR and Raman spectra, force const. 8-68503
 MnBr₂, vibr. struct. in cryst. field electronic transitions 8-59895
 MnCl₂, vibr. struct. in cryst. field electronic transitions 8-59895

lattice dynamics continued

- MnTa₂O₆, columbite struct., X-ray diff., IR and Raman spectra (French) 8-63727
 (NH₄)₂PO₃F, H₂O, X-ray diffraction and Raman spectra struct. determ., external mode temp. depend. (French) 8-52507
 NH₄ReO₄, ND₄ReO₄, Raman spectrum, temp. depend. 8-80335
 NaNO₃, N atom velocity, NO₃⁻ vib. and orientation, nucl. reson. photon scatt. 8-68433
 NaPF₆, high press. phase diagram, vibr. spectra 8-60446
 Na₂WO₃, struct. transitions and lattice dynamics 8-79771
 Nd(BrO₃)₃.9H₂O, IR and Raman spectra, vibr. assignments 8-84569
 Ni₃B₂O₁₃I, cubic, Raman spectrum, 88-295K, vibr. anomalies 8-76479
 NiBr₂, vibr. struct. in cryst. field electronic transitions 8-59895
 NiCl₂, vibr. struct. in cryst. field electronic transitions 8-59895
 NiI₂, far IR study of lattice dynamics 8-80359
 PbF₂, superionic conductor, theoretical investigation of Raman scatt. 8-80351
 PbSO₄, anglesite, crystal struct. and sulphate force const. 8-83784
 (SN)₂, lattice dynamics, pseudolattices and correlation method 8-75768
 α -Si₃N₄, Raman active modes, spectra 8-80326
 SiO₂, polymorphs (cristobalite and tridymite), vibr. normal modes, GVFF calcs. 8-51627
 Sn-Pb alloy, dil., lattice dynamics, sp. ht., resist., thermal expansion and nuclear γ reson. expts. (Russian) 8-87749
 SrF₂(Cl₂), superionic conductor, theoretical investigation of Raman scatt. 8-80351
 SrSO₄, celestite, crystal struct. and sulphate force const. 8-83784
 TaSe₂ (2H), lattice dynamics and phase transitions 8-79727
 ThO₂, Gruneisen coeff., lattice vibrational frequencies in range 298-2300K 8-79712
 TiSe₂ (1T), lattice dynamics and phase transitions 8-79727
 TiSe, vibr. props., Raman and far IR spectra meas. 8-71800
 UO₂, Gruneisen coeff., lattice vibrational frequencies in range 298-2300K 8-79712
 ZnSe₂S₄, IR and Raman spectra, force const. 8-68503
- lattice dynamics of covalent crystals**
 diamond, lattice dynamical calc. using extended Born-von Karman scheme 8-59889
 diamond, phonon frequencies, model calc. using tight binding Hamiltonian 8-59894
 diamond, resonant Raman scatt., first and second order 8-60471
 diamond, zone-centre optical phonon, effect of uniaxial stress, elastic const. determ. 8-91399
 diamond-type crystals, lattice dynamics from Keating's valence force field 8-79687
 graphite, long wavelength lattice vibrations, Raman and IR reflectivity spectra 8-75746
 semiconductor, electronic and struct. energies calc. 8-59874
 C, diamond-type crystal, lattice dynamics from Keating's valence force field 8-79687
 Ge, diamond type crystal, lattice dynamics from Keating's valence force field 8-79687
 Ge, lattice dynamical calc. using extended Born-von Karman scheme 8-59889
 Ge, lattice dynamics of group IV elements with the local Heine-Abarenkov model potential 8-63821
 Ge, phonon boundary scatt., reduction of lattice thermal cond. 8-55921
 Ge, phonon dispersion curves, appl. of deformable-ion model 8-59887
 Ge, two-phonon difference absorption spectra 8-76452
 Ge-Si alloy, phonon boundary scatt., reduction of lattice thermal cond. 8-55921
 InSb, phonon dispersion curves, appl. of deformable-ion model 8-59887
 Si, crystn. front face effect on at displacements (Russian) 8-67781
 Si, diamond-type crystal, lattice dynamics from Keating's valence force field 8-79687
 Si, dielectric screening and zone-centre phonons 8-67785
 Si, electronic screening of lattice vibrs. 8-59875
 Si, highly transparent semicond., multiphonon IR absorpt. 8-60461
 Si, lattice dynamical calc. using extended Born-von Karman scheme 8-59889
 Si, lattice dynamics of group IV elements with the local Heine-Abarenkov model potential 8-63821
 Si, phonon boundary scatt., reduction of lattice thermal cond. 8-55921
 p-Si, photosensitivity of elastic moduli and surface tension 8-83864
 Si, TO and TA phonons, electronic and struct. energies calc. 8-59874
 α -Sn, lattice dynamics of group IV elements with the local Heine-Abarenkov model potential 8-63821
 SnS_{2-x}Se_x (0≤x≤2), ¹¹⁹Sn Mossbauer spectrum, lattice dynamics 8-71809

lattice dynamics of ferroelectric crystals

see also displacive transformations; soft modes

- alkali-alkaline earth ceramic solid solutions, with tetragonal tungsten bronze struct., low freq. optical modes 8-76477
 Debye temperature, tabulation of calorimetric values 8-51639
 Debye temperature tabulation of calorimetric values 8-51639
 ferroelectrics, one and two dimensional displacive types, phonon relaxation 8-87761
 ferroelectrics, surface sound waves on domain boundaries, low temp. sp. ht. 8-71937
 local structural excitations model for lattice dynamics of disordered or unstable lattices 8-75790
 phase transitions soft modes and dipole relaxations 8-91409
 thiourea, soft mode and Debye relaxations 8-80347
 vibrational modes, crit. behaviour of uniaxial materials 8-84539
 vibronic theory of antiferroelec. and struct. modulated transitions, soft modes 8-79719
 AgNa(NO₂)₂, ultraslow crit. dynamics of order parameter, ²³Na spin relax. times obs. 8-76410
 Ba_{0.5}Sr_{0.5}Nb₂O₆, temp. depend. of Raman spectra 8-72524
 BiSi(Br), optical B_u modes of paraelectric phase, simple model 8-75747
 BiSeI(Br), optical B_u modes of paraelectric phase, simple model 8-75747
 Cd₂Nb₂O₇, Raman-scattering investigation of vibrational structure 8-76441

lattice dynamics of ferroelectric crystals continued

- Gd₂(MoO₄)₃, uniaxial stress effect on ferroelec. transition, Raman scatt. 8-80360
 KH₂AsO₄, fast and slow dynamic reorientation 8-80306
 KH₂PO₄, dynamic central peak in ferroelectric phase 8-84538
 KH₂PO₄, KD₂PO₄, high-press. struct. rel. to dynamical models 8-80307
 KH₂PO₄, soft mode spectroscopy, digital control system for Raman spectrometer 8-86345
 KH₂PO₄ type crystals, low lying ferroelec. modes, cluster dynamical theory 8-80305
 KH₂PO₄ type ferroelectrics above T_c, soft mode and central-peak dynamics 8-87763
 KH₂PO₄, variational treatment of proton-phonon system 8-88261
 KH₂PO₄-KD₂PO₄ mixed crystals, static and dynamic props., proton-lattice coupled mode model 8-64328
 KNbO₃, orthorhombic, anharmonic effects 8-79721
 KTaO₃, incipient ferroelectric, mode-mode coupling 8-79717
 LiNbO₃, optical phonon modes and anharmonic couplings 8-60466
 LiNbO₃:Fe, calc. of photorefractive (*Russian*) 8-92032
 LiTaO₃, optical phonon modes and anharmonic couplings 8-60466
 (NH₄)₂BeF₄, powder, IR spectra, assignments, mol. libration, in paraelec. and ferroelec. phases 8-88299
 NH₄H₂AsO₄:Cr⁵⁺, fast and slow dynamic reorientation 8-80306
 Na(D₂H_{1-x})₃(SeO₃)₂, Raman spectra and nature of phase transitions 8-80341
 NaNO₂, mechanism of ordering type ferroelec. transition, vibr. spectroscopy 8-76402
 NaNO₂, mechanism of order-disorder transition, opt. spectra 8-76403
 Ni₃B₂O₃, cubic, Raman spectrum, 88-295K, vibr. anomalies 8-76479
 Pb₂Nb₂O₇, Raman-scattering investigation of vibrational structure 8-76441
 Pb₃O₄, IR and Raman study of structural phase transitions (*French*) 8-84582
 RbH₂(SeO₃)₂, improper ferroelectric phase transformation, neutron scattering study 8-80302
 Sb₂S₃, effect of screening by conduction electrons on phase transitions 8-84537
 SbSBr, optical B_u modes of paraelectric phase, simple model 8-75747
 SbSI, ferroelectric semiconductor, effect of screening by conduction electrons on phase transitions 8-84537
 SbSI(Br), optical B_u modes of paraelectric phase, simple model 8-75747
 Sn₂P₂S₆, soft mode, temp. depend. of Raman spectra near phase transition 8-88263
 SrTiO₃, forced thermal Rayleigh scattering 8-80371
 SrTiO₃, incipient ferroelectric, mode-mode coupling 8-79717
 SrTiO₃, structural phase transition at 110K, theory 8-80300

lattice dynamics of ionic crystals

- alkali halides, exchange charge shell model analysis of strain derivatives of static polarisability, effective charge parameter 8-91296
 alkali halides, interionic potentials, completely independent specification of Born-Mayer potentials 8-55828
 alkali halides, interionic potentials, cryst. independent shell parameters and fitted Born-Mayer pots. 8-55827
 alkali halides, IR absorpt. in molecules, clusters and microcrystals 8-80363
 alkali halides, shift and broadening of local vibr. bands, temp. depend. 8-87755
 alkali metal halides, vibrational modes due to three impurity cluster 8-75773
 Brownian sublattice, microscopic theory 8-79681
 complex crystals, isotopic shifts, phonon freqs. 8-67787
 diamagnetic ionic cubic lattice in homogeneous mag. field, oscillations 8-91868
 fluoperovskites, nonlinear elastic behaviour, US velocity, 1 bar-3 kbar 8-59851
 ionic crystals, surface polaron 8-60020
 Lundqvist three-body interaction and lattice dynamics of ionic crystals 8-67775
 microscopic and model theories 8-59871
 microscopic model, for crystals with Brownian sublattice 8-71798
 ordered vacancy compounds 8-75770
 resonance Raman scattering, electron-phonon interaction for F centres 8-68519
 superionic conductors, long-wavelength density fluctuations 8-79808
 superionic conductors, phase transitions and dynamics 8-59924
 surface vibrational properties, review 8-71928
 AgBr, curvature of conductivity plots, consequence of anharmonicity 8-79800
 AgCl, curvature of conductivity plots, consequence of anharmonicity 8-79800
 BaClF, localised vibr. of U-centres 8-75779
 CaF₂, slab, surface modes of vibr. 8-71935
 CsBr:Ti³⁺, perturbed lattice dynamics, breathing shell model calculation 8-75744
 CsI, isotope diffusion 8-75875
 CsNCs, long-wave lattice modes 8-59881
 K halides, surface lattice dynamics, by Green's function method 8-71936
 KBr(I), oscillatory and diffusive regime, above and below melting point, IR thermal emission spectra 8-83985
 KCN, crystal props., log potential model calc. 8-63829
 KCl:Eu²⁺, radiationless process, vibronic spectrum analysis 8-80391
 KCl:OH⁻, paraelec. system, acoustic susceptibility in strong phonon-coupling approx. 8-71801
 KCl_{1-x}Br_x, phonon densities of states, dispersion relations 8-75761
 KCl_{1-x}Br_xNCO⁻, absorpt. band defect broadening (*Russian*) 8-72526
 KCl_{1-x}I_xNCO⁻, absorpt. band defect broadening (*Russian*) 8-72526
 KI:NO₂⁻, Raman spectra, high press., low temp. effects 8-52479
 KNCS, long-wave lattice modes 8-59881
 K_{1-x}Rb_xBr, lattice dynamics on pseudo-crystal model 8-75762
 K₂Rb_{1-x}Cl_{1-y}, IR reflection spectra 8-76474
⁶LiH(D), cryst., cohesive energy, force const., lattice freq., Debye temp., Gruneisen parameters, calc. 8-91293
 LiN₃, evidence for N₃⁻ from static and dynamic props. 8-60465
 MgF₂, rutile structure, dielectric props., neutron and Raman scatt. exam. 8-79684

lattice dynamics of ionic crystals continued

- NH₄Cl, dispersion of vibrational excitations, Raman scatt. 8-84588
 NaCN, crystal props., log potential model calc. 8-63829
 NaCl, polarisation mechanism and lattice mechanics, microscopic approach 8-59888
 NaCl(Br), oscillatory and diffusive regime, above and below melting point, IR thermal emission spectra 8-83985
 NaI, long wave phonon modes, IR absorpt. 8-79686
 NaI:Cl⁻, anharmonic effects on low-frequency impurity phonon resonances 8-75771
 RbBr, mode anharmonic self energies, freq. depend. 8-59908
 RbBr, phonon freqs. at 80, 290, 370K, neutron inelastic scatt. study, comparison to Gruneisen parameters 8-51631
 RbCN, crystal props., log potential model calc. 8-63829
 RbI, elastic constants determ. by inelastic neutron scatt. 8-79659
 RbI, temp. depend. of second order Raman spectra 8-68512
 Sr_{1-x}Cd_xF₂, IR and Raman meas. 8-75763
 SrClF, localised vibr. of U-centres 8-75779
 TiBr, CsCl and NaCl phases, atomic interactions and lattice statics and dynamics 8-83889

lattice dynamics of metallic crystals

- alkali metal, lattice vibr. and Gruneisen parameter 8-59917
 alkali metals, electron fluid model 8-75738
 alkali metals, thermal properties and Gruneisen parameters, employing model pot. 8-71815
 BCC metal, Debye-Waller factors, temp. variation calc. 8-55925
 BCC metals, equivalence of ang. force models for lattice dynamics 8-83891
 β-brass, cryst. struct., elastic const., central force model 8-51637
 cubic metals, central pair pot. vs. axially symm. pot. 8-87747
 FCC, model for lattice dynamics 8-91387
 FCC metal, phonon dispersion relations and Debye-Waller factor calcs. 8-51630
 FCC metals, dynamics of multiple interstitials and interstitial impurity complexes 8-75775
 FCC metals, nonequivalence of ang. force models of de Launay and Clark, Gazis and Wallis 8-63819
 HCP metals, anharmonicity effect on neutron diffr. struct. factor 8-59907
 HCP metals, phonon dispersion 8-59883
 helicon-phonon interaction for parallel wave propagation 8-64054
 interatomic potentials from experimental phonon spectra 8-75621
 noble metal, van der Waals forces and their contrib. to vacancy form. energy and phonon dispersion 8-91635
 noble metals, nonlocal effects 8-75754
 noble metals, pseudopot. exam. of electronic props. 8-51960
 phonon spectra, singularities caused by local geometry of Fermi surface 8-91401
 rare earth metal, lattice dynamics and scatt. reson. 8-59872
 transition metal, BCC, phonon dispersion curves and elastic, calc. using cohesive energy 8-59885
 transition metal, FCC, 5-parameter model dispersion relations, appl. to Ni, Pt 8-75748
 transition metal, lattice dynamics and scatt. reson. 8-59872
 transition metals, HCP, nonlocal effects in lattice dynamics 8-91397
 transition metals, phonon dispersion using non-central force model 8-91392
 transition-metal slab, surface lattice dynamics and density response 8-71930
 two-parameter shell model of lattice vibrs. in monoatomic systems 8-59877
 Ag, phonon dispersion relations and Debye-Waller factor calcs. 8-51630
 Ag, phonon dispersion relations, screened shell model 8-83894
 Ag, transverse acoustic phonon branch, temp. depend., neutron scatt. (*German*) 8-71808
 Al, phonon dispersion relations and Debye-Waller factor calcs. 8-51630
 Al, unpaired ion-ion interaction, transverse phonon branch, neutron scatt. expt. (*Russian*) 8-87751
 Au, lattice vibr., electron press., central pair pot. model calc. 8-75749
 Au, phonon dispersion relations and Debye-Waller factor calcs. 8-51630
 Au, phonon dispersion relations, screened shell model 8-83894
 Cd, anharmonic interactions, elastic X-ray scatt. 8-75755
 Co, FCC, modified Krebs model, phonon dispersion relations 8-79682
 Cr, lattice vibrations, Debye temp., freq. wave vector dispersion relations 8-63818
 Cr, phonon dispersion, Debye temp. and Debye-Waller factors, lattice dynamical model 8-55920
 Cu, FCC, appl. of model for lattice dynamics 8-91387
 Cu, phonon dispersion relations and Debye-Waller factor calcs. 8-51630
 Cu, thermal vibr. and zero-point motion effects on low-energy collision cascades 8-87705
 Fe, BCC, vib. entropy of 1/2 {111} {110} edge dislocations 8-63768
 α-Fe, lattice defects, relax. studies, computer simulation 8-79604
 Fe, lattice vibrations, temp. depend. 8-95124
 Fe, surface phonon spectra 8-71934
 HF, high temperature thermophysical properties 8-91404
 K₂Rb_{1-x} alloys, lattice dynamics of substitutional alloys, force constant disorder 8-75786
 La, DHCP and FCC phases, phonon density of states 8-67791
 Mg, phonon spectrum and thermodynamic functions, inelastic coherent cold neutron scatt. (*Russian*) 8-55917
 Mo, interatomic pot. from phonon spectrum 8-67784
 Mo, lattice defects, relax. studies, computer simulation 8-79604
 Mo, phonon dispersion, Debye temp. and Debye-Waller factors, lattice dynamical model 8-55920
 Mo, phonon frequencies, seventh-neighbour tensor force model 8-91402
 Nb, high-temperature nonlinear electrical resistivity, supposed failure of Boltzmann eqn. 8-91664
 Nb, phonon frequencies, seventh-neighbour tensor force model 8-91402
 Nb, plastically deformed, changing lattice dynamics 8-67793
 Ni, phonon dispersion relations and Debye-Waller factor calcs. 8-51630
 Pb, phonon dispersion and cryst. equilb. 8-75752
 Pb, phonon spectrum, calc. by phenomenological method 8-59890

lattice dynamics of metallic crystals continued

- Pb, relativistic model pseudopot., appl. to elec. resist. and phonon spectra calc. 8-51866
 Pb, two-parameter shell model of lattice vibrs. in monoatomic systems 8-59877
 Pd, Kohn anomalies and phonon dispersion, model including exchange-correl. corrections 8-59886
 Pd, phonon dispersion, simplified Frielele model 8-79683
 Pd, phonon dispersion using non-central force model 8-91392
 Pd-Pt, resonant modes, rel. to CPA predictions 8-75757
 Pt (111) stepped surface, localised surface phonons obs. 8-95223
 Pt, phonon dispersion, simplified Frielele model 8-79683
 Sc, Kohn anomalies and phonon dispersion, model including exchange-correl. corrections 8-59886
 Sc, lattice dynamics, sp.ht. and bulk modulus 8-71814
 Sn, diamond type crystal, lattice dynamics from Keating's valence force field 8-79687
 α -Sn, lattice dynamical calc. using extended Born-von Karman scheme 8-59889
 Sn, white, anharmonicity in X-ray diffraction intensities 8-71626
 Sn, white, lattice vibrations anharmonicity, X-ray meas. 8-51624
 Ta, internal equilibrium, cryst. dynamics, lattice dynamical theory of BCC metals 8-79688
 Ta, lattice vibrations, Debye temp., freq. wave vector dispersion relations 8-63818
 Ti, high temperature thermophysical properties 8-91404
 Ti, hexagonal lattice equilibrium, electron gas model with noncentral forces, lattice dynamics 8-95123
 V, Kohn anomalies and phonon dispersion, model including exchange-correl. corrections 8-59886
 V, lattice defects, relax. studies, computer simulation 8-79604
 V, lattice dynamics and cryst. equil. 8-75753
 V, phonon dispersion using non-central force model 8-91392
 W, phonon dispersion, Debye temp. and Debye-Waller factors, lattice dynamical model 8-55920
 W, surface phonon spectra 8-71934
 Zn, hexagonal lattice equil., electron gas model with noncentral forces, lattice dynamics 8-95123
 Zr, HCP, temp. depend. of C-axis phonon dispersion curves 8-59884
 Zr, high temperature thermophysical properties 8-91404

lattice dynamics of molecular crystals

- 2-chloronaphthalene, vibr. and calorimetric investigation of polymorphism 8-87641
 2-fluoronaphthalene, vibr. and calorimetric investigation of polymorphism 8-87641
 anthracene, molecular crystal, exciton-phonon coupling, absorpt. band profile in first singlet system 8-83888
 anthracene, monocryst., additional absorpt. spectrum at low temp. 8-92096
 1,12-benzoperylene in n-alkane, zero-phonon lines in luminesc. spectra 8-56512
 1,12-benzoperylene, in alkane matrices, zero-phonon lines, press. shifts (*Russian*) 8-76502
 biphenyl, incoherent inelastic neutron scatt. time of flight spectra, vibr. spectra model calc. 8-63816
 carbon tetrabromide, solid, Raman spectrum, temp. depend. 8-52488
 carbon tetrachloride, solid, phase transition, Raman study 8-80345
 p-chloraniline cryst., lattice vibr., IR and Raman spectra, lattice energy 8-56481
 p-chlorobromobenzene, single cryst., polarised Raman and IR spectra, assignments 8-60431
 complex structure, continuous and discrete models 8-51625
 coronene, in alkane matrices, zero-phonon lines, press. shifts (*Russian*) 8-76502
 crystallography, electron densities, thermal smearing, limited resolution effects 8-71635
 crystallography, X-ray neutron, charge deformation, vibr. smearing 8-71634
 cyclohexane, solid, Raman spectra near 186K phase transition 8-56480
 p-dichlorobenzene, lattice dynamics, thermodynamic functions and phase transitions 8-67777
 1,5-difluoronaphthalene, IR and Raman study of crystal dynamics 8-80346
 p-diiodobenzene, far IR single cryst. transmission spectrum, temp. and polaris. depends., assignments 8-72498
 4,4'-dinitrobiphenyl complexes, intermol. interacts. and geometry of non-rigid mols., vibr. spectra 8-88294
 DNA pyrimidines, cryst. coherent inelastic neutron scattering 8-75766
 ethylene, solid, self-consistent phonon calcs. 8-75745
 ethylene crystal, partially deuterated, Raman phonon spectra 8-56470
 exciton-phonon interactions, strong and weak coupling 8-51899
 furane, crystalline, lattice vibr. 8-79694
 halogens, bond charge model 8-79692
 hexamethyl benzene, high press., variable temp. Raman spectra 8-56488
 molecular crystals, spectroscopy, bibliography for 1976 8-72585
 naphthalene, inelastic neutron scattering 8-79690
 p-nitrotoluene, low-freq. vibr. spectrum, Raman and IR spectra 8-56484
 orientationally disordered cryst., translation-rot. dynamics, soft modes 8-83906
 perylene in n-alkane, zero-phonon lines in luminesc. spectra 8-56512
 polymers and molecular crystals, vibronic spectra exam. 8-67778
 polyperdeuteroethylene, IR and Raman spectra, 77K and room temp., vibr. anal. 8-72517
 Raman spectra, low frequency polarised, of complex mol. cryst. 8-84574
 saccharose, far IR absorption, low temp. pyroelectricity 8-80348
 squaric acid, struct. transition, US vel. meas. 8-79770
 1,2,4,5-tetrabromobenzene, lattice vibrs., Raman and far IR spectra 8-76444
 1,2,4,5-tetrachlorobenzene, lattice dynamics, thermodynamic functions and phase transitions 8-67777
 tetracyanobenzene-naphthalene, Raman spectra, phase transition and isotopic substitution 8-80364
 thiourea, order-disorder transitions, soft modes 8-80361
 thiourea, soft mode and Debye relaxations 8-80347
 Br₂, lattice dynamics using simple bond charge model 8-55919
 CS₂, solid, tailoring of potentials 8-79679

lattice dynamics of molecular crystals continued

- Cl₂, lattice dynamics using simple bond charge model 8-55919
 p-D₂, order-disorder phase transition 8-79726
 D₂O₂, lattice phonons by neutron scatt., covalent force model 8-67782
 GaSe(S), layer dynamics of high-symmetry crystals with atom-atom interactions 8-71799
 o-H₂, order-disorder phase transition 8-79726
 H₂, solid, neutron scattering expts. 8-79693
 MoS₂, layer dynamics of high-symmetry crystals with atom-atom interactions 8-71799
 α -N₂, anharmonic lattice vibrations calcs. 8-71812
 N₂, solid, lattice dynamical calcs., use of anisotropic at.-at. pot. functions, α - γ transition 8-71811
 N₂, solid, semimicroscopic approach 8-75765
 N₂:N, dynamically induced electronic transitions of matrix isolated atom 8-63825
 NH₃, atom-atom model of intermol. forces 8-75751
 NH₄Br, λ -type phase transition, Brillouin scattering 8-79725
 NH₄Br, partially disordered, librational modes below disorder-order phase transition temp. 8-79680
 NH₄I, (NH₄)_{0.16}K_{0.84}I and (NH₄)_{0.16}K_{0.84}Br, reorientation motion of NH₄⁺ 8-79542
 PbI₂, layer dynamics of high-symmetry crystals with atom-atom interactions 8-71799
 SnI₄, mol. solid, dynamics, press. and temp. depend. 8-79691
 SnI₄, Raman spectra, temp. and press. meas. and lattice dynamical calcs. 8-56472
 TeO₂, paratellurite, atomic motions corresponding to zone centre phonons 8-76461

lattice energy

- see also binding energy*
 alkali halides, short range interactions, static polarisabilities 8-71702
 alkali metal nitrates, standard heat of formation, electron affinity 8-91295
 alloy, AB type, equil. props. by Markovian simulation 8-91302
 β -brass, cryst. struct., elastic consts., central force model 8-51637
 p-chloraniline cryst., lattice vibr., IR and Raman spectra, lattice energy 8-56481
 p-(N-chlorobenzylidene)-p-chloraniline, cryst., polymorphism, cryst. struct. rel. to mol. conform. 8-75611
 conformational props. rel. to spatial electron density determ., computer simulations 8-70763
 Coulomb crystal energy, analysis of tail of density series 8-91300
 1,5-dichloroanthracene, photodimerisation, orientational defects, lattice energy 8-80724
 dilute binary alloys, formation energy, lattice relax. and zero-point vibrations 8-83771
 dilute binary alloys, formation energy, lattice relax. and zero-point vibrations 8-87646
 fluorite crystals, Brillouin scatt. and high temp. disorder 8-80365
 hydrocarbons, molecular packing anal. of alkyne structs., lattice energy minima 8-95011
 II-VI semiconductors, electronic theory, cryst. energy and bulk modulus 8-72104
 III-V semiconductor, electronic theory, cryst. energy and bulk modulus 8-72104
 Madelung parameter, expansion in terms of multipole moments, ratio of two lattice parameters 8-75618
 metal, surface relaxation, lattice statics calc. 8-63925
 metal, third order perturbation theory self consistency 8-76014
 transition metal oxides, cryst. electronic polarisabilities and ion sizes, Madelung pot. effects 8-63693
 transition metal oxides, dielec. behaviour 8-71703
 s-triazine, structural phase change, lattice energy calc. 8-55945
 TTF-TCNQ, segregated stack stability 8-55831
 TTF-TCNQ crystal, antiferroelec. ordering of electronic polarisation, simple model anal. 8-92028
 CS₂, solid, tailoring of potentials, in lattice dynamics 8-79679
 KCl, cluster expansion of density matrix and crystal energy 8-87952
 KClO₄, single ion props. by lattice energy minimisation 8-83769
 Li₂O, ionic atomic binding force assumption 8-79556
 MgH₂, lattice energy calc. 8-83768
 MgO crystal, unified approach to lattice states and dynamics 8-59878
 NH₄ClO₄, single ion props. by lattice energy minimisation 8-83769
 NaClO₄, single ion props. by lattice energy minimisation 8-83769
 PbCl₂, binding, ionicity, covalent contrib., Madelung const., cohesive energy 8-79558
 PbS, thermomech. props., SCF X α scatt. wave theory 8-71704
 Pd₂, model of instabilities 8-75619
 PdH₂, model of instabilities 8-75619

lattice gas *see* lattice theory and statistics**lattice localised modes**

- see also phonon-defect interactions; phonon-impurity interactions*
 alkali halides, shift and broadening of local vibr. bands, temp. depend. 8-87755
 alkali metal halides, vibrational modes due to three impurity cluster 8-75773
 anthracene, monocryst., additional absorpt. spectrum at low temp. 8-92096
 Cayley tree type system, modes, densities, lattice vibrs. 8-71813
 collective dislocation motion, dynamic effects 8-79632
 defect-clusters in linear chain, effect of second neighbour interaction on freq. 8-63826
 defects, behaviour at structural phase transitions 8-83904
 defects, central peak at displacive phase transitions 8-83905
 dilute alloy, atomic displacements around impurity and three body interaction 8-91406
 durenene-naphthalene, spin-lattice relax. in photo-excited triplet states, spin axes rot. on thermal excitation 8-76294
 FCC metals, dynamics of multiple interstitials and interstitial impurity complexes 8-75775
 Ginzburg-Landau model, localised defects, nearly ferromag. system, solids near displacive phase transition 8-71820
 guanidinium aluminium sulphate hexahydrate: Mn²⁺, NMR 8-91939
 highly anisotropic crystal, phonon spectrum and local vibrs. (*Russian*) 8-59912
 II-VI compounds, local force variations due to substitution impurities 8-51633

lattice localised modes continued

- III-V compounds, local force variations due to substitution impurities 8-51633
 III-V semiconductors, manifestation of local vibr. of dislocations in IR spectra 8-88339
 impurities, conc. of C, O, Si 8-59832
 impurity molecule in solid matrix, vibr. relax., stochastic classical trajectory approach 8-79707
 impurity molecules in crystals, exclusion rules for librational-tunnelling states 8-84174
 interface, localised, resonant and antiresonant modes (*French*) 8-71938
 n-nonane: H₂-tetra-4-tert-butylphthalocyanine, thermal broadening of zero phonon lines, hole burning 8-71803
 polar crystal, vibronic levels for Jahn-Teller impurities 8-68520
 quantum system interacting with nonequilibrium phonons, light absorption props. 8-88340
 quartz, X-ray topographical chamber for work by the Lang extinction method, appl. to quartz (*Russian*) 8-83649
 screw dislocations, inelastic neutron scatt. 8-75774
 solid solutions, impurity centres, internal mol. vibr., inhomogeneous band broadening 8-92103
 spherical-like model, isolated impurity behaviour near displacive phase transition 8-71821
 Toda lattice soliton, interaction with impurity atom 8-75772
 AgBr, phonons at elevated temp. 8-79810
 Al alloys, inelastic electron scattering by dislocations (*Russian*) 8-79988
 Al_{10-x}Ga_{0.08}V, low temp. thermal expansion 8-95167
 Al₁₀V, low temp. thermal expansion 8-95167
 BaClF, localised vibr. of U-centres 8-75779
 CdTe:Be, impurity modes and IR absorption 8-76506
 CdTe_{1-x}S_x, long-wavelength optical phonons, composition depend., IR and Raman spectra 8-67788
 Cl₂ in Ar matrix, vibr. relax., stochastic classical trajectory approach 8-79707
 Cr³⁺, electronic states interactions with crystal odd vibr., R-lines vibr. recurrences 8-84639
 Cu alloys, inelastic electron scattering by dislocations (*Russian*) 8-79988
 Cu-Al, impurity concentration effects 8-75777
 Cu-Be, impurity concentration effects 8-75777
 Cu-Si, impurity concentration effects 8-75777
 Fe, surface phonon spectra 8-71934
 Fe, vibrational spectrum with interstitial C atoms 8-67796
 Ga_{1-x}Al_xSb, small wave vector modes 8-75785
 GaAs, irradiated with fast neutrons, IR vibrational absorpt. 8-75776
 GaAs:B, electron or neutron irradiated, low symmetry interstitial B centre 8-79605
 GaAs:Si, Cr, carrier concs. from Hall effect, microscopy, localised vibrational modes absorption meas. 8-56104
 Ge:Si, impurity lattice modes due to single and paired defects 8-75780
 Ge:Si, impurity modes and IR absorption 8-76506
 Ge-Si, impurity concentration effects 8-75777
 InP:Si, vibr. modes of Si, IR absorpt. bands 8-55922
 KCl, Raman spectra and vibrational modes of V_k centre meas. 8-80338
 KCl:Ca,H, studies of localised vibrations of substitutional atomic H 8-80248
 KCl:Eu²⁺, radiationless process, vibronic spectrum analysis 8-80391
 KCl:Pb²⁺ (0.005% Pb), A band fine structure, electron-phonon interaction 8-60491
 KCl_{1-x}Br_x:NCO⁻, absorpt. band defect broadening (*Russian*) 8-72526
 KCl_{1-x}I_x:NCO⁻, absorpt. band defect broadening (*Russian*) 8-72526
 K₂Cu(CN)₄, isotopic mixed crystal with ¹²C and ¹³C, Raman scattering 8-76476
 KI, gapmode calc. using Green's function technique, effect of uncertainty in eigendata 8-79708
 LiF, manifestation of local vibr. of dislocations in IR spectra 8-88339
 LiF, Raman spectra and vibrational modes of V_k centre meas. 8-80338
 NH₄Cl_{1-x}Br_x, phonon dispersion 8-75760
 Pd-H system, thermodynamic aspects of atomic vibr. 8-59913
 RbCl, Raman spectra and vibrational modes of V_k centre meas. 8-80338
 RbCl:Ca,H, studies of localised vibrations of substitutional atomic H 8-80248
 Si, vibrational properties of the (001) split interstitial 8-91405
 SrClF, localised vibr. of U-centres 8-75779
 W, surface phonon spectra 8-71934
 ZnS with cation impurity, first order transitions in Raman spectra 8-88310
 ZnS:Al-Cu, localised vibrational modes 8-63827
 ZnS:Be, impurity modes and IR absorption 8-76506
 ZnS:Cr(Mn)(Fe)(CoXV), vibr. modes of transition element impurities 8-76472

lattice mechanics see *lattice dynamics***lattice phonons**

- see also *electron-phonon interactions; lattice dynamics of covalent crystals; lattice dynamics of ferroelectric crystals; lattice dynamics of ionic crystals; lattice dynamics of metallic crystals; lattice dynamics of molecular crystals; lattice localised modes; phonon-defect interactions; phonon dispersion relations; phonon drag; phonon-exciton interactions; phonon-impurity interactions; phonon-magnon interactions; phonon-phonon interactions; phonon-plasmon interactions; polaritons; soft modes; spin-phonon interactions; tunnelling spectra; tunnelling spectroscopy*
 alkali halides, bound polarons, vibronic theory, appl. to F-centre excited states 8-84150
 ammonium salts, proton spin relax. and phonons 8-84493
 anharmonic system, generalisation of CPA 8-75783
 anomalous fluctuations, neutron scatt. 8-75743
 benzene, crystal, inelastic coherent neutron scatt., phonon spectra 8-51629
 binary alloys, random, dielec. matrix and related props. 8-51916
 Brillouin scattering by oblique-incidence acoustic phonons, lineshapes 8-72534
 chain conductors, CDW ordering 8-79731
 complex crystals, isotopic shifts, phonon freqs. 8-67787

lattice phonons continued

- conference on lattice dynamics, Paris, France (Sept. 1977) 8-59869
 coupled phonon-linear Heisenberg chain system, phase transition 8-64208
 cubic crystals, phonon magnification, evaluation method 8-83890
 dielectric medium at low temp., influence of nonequilib. phonon gas on US propagation (*Russian*) 8-71795
 electronically driven phonon anomalies and phase transforms. 8-63834
 ethylene, solid, self-consistent phonon calcs. 8-75745
 F-centres, relaxed excited states, vibronic model of stress effects 8-95118
 ferromagnetic resonance, phonon propagation 8-88194
 filament, condensation energy and mass 8-91637
 Fröhlich model, method of functional derivatives 8-51909
 graphite, E_{2g} mode splitting, two-phonon spectrum 8-92077
 high energy spectroscopy using tunable dye laser 8-83893
 highly anisotropic crystal, phonon spectrum and local vibr. (*Russian*) 8-59912
 ionic crystals, surface polaron 8-60020
 metal, phonon spectra, singularities caused by local geometry of Fermi surface 8-91401
 metal surface, resonant absorpt. of sound (*Russian*) 8-95216
 metallic point contacts, nonlinear resist. rel. to phonon emission and background effects 8-68074
 methane and methane-d₄, solid, thermal cond. calc. 8-51753
 molecular crystals, photon echoes (*Dutch*) 8-71156
 nonlinear optical reson. effects, phonon generation by IR radiation 8-50865
 one-dimensional conductor, IR and Raman activity 8-60441
 one-dimensional conductor, phonon dynamics 8-79704
 one-dimensional lattice, props. of commensurate CDW system 8-75796
 one-dimensional systems, electron trapping and transport by supersonic solitons 8-72139
 ordered vacancy compounds, lattice dynamics 8-75770
 organic charge-transfer complex, mixed-stack crystalline, phonon bands 8-75767
 phase transitions soft modes and dipole relaxations 8-91409
 phonon anomaly near Fermi surface topological transition 8-95120
 polar crystal, vibronic levels for Jahn-Teller impurities 8-68520
 polarisation operation in one- and two-dimensional crystals (*Russian*) 8-79676
 quasideimensional crystal, phonon spectrum change due to struct. transition 8-67789
 Raman scattering, stimulated, oscillations, spatial and temporal, in saturated optical phonon generation 8-87099
 rare earth compounds, paramagnetic, Faraday and Cotton-Mouton effects for acoustic phonons 8-52476
 rare earth monobismuthides, thermal expansion, thermal cond., 300-900K 8-91453
 rare earth systems, crystal field effects 8-67987
 ruby, high energy phonon spectroscopy 8-83893
 ruby, resonance radiation transfer and nonequilibrium phonons (*Russian*) 8-80418
 ruby, resonance trapping of 0.87×10¹² Hz acoustic phonons in mag. field 8-91400
 ruby, resonantly trapped 29 cm⁻¹ phonons, spectral diffusion 8-92113
 semiconductor, doped lattice thermal cond., role of electron-phonon interactions and peripheral phonons, appl. to Ge:P 8-79702
 semiconductor, nonequilibrium optical phonons generated by electrons in laser radiation field 8-71802
 semiconductor, polar, longwave secondary radiation (*Russian*) 8-80343
 semiconductor film, quantised, one-phonon light absorption 8-60527
 Shpolskii systems, sensitised phosphoresc., triplet-triplet energy transfer (*Russian*) 8-76527
 superconducting junction electron tunnelling, effect of dissolved O²⁻ 8-80100
 superconductivity, nonequilibrium, quasiparticles and phonons 8-52146
 superconductors, nonequilibrium, phase transitions induced by quasiparticle injection 8-91808
 transition and noble metal dilute alloys, Einstein's temp. and vibrational entropy, rel. to electronic struct. 8-83900
 transition metal, surface lattice dynamics 8-95224
 transition metal dichalcogenides, optical phonon modes and localised effective charges, reflection spectra 8-76453
 uniaxial crystal, dispersion of bulk phonon polaritons meas. by IR refl. 8-59902
 XPS, angle-resolved, phonon-assisted processes, interpretation 8-72696
 zincblende type crystals, lattice dynamics, phonon freq. rel. to mass ratio 8-95121
 AgBr, phonons at elevated temp. 8-79810
 AgGaSe₂(Te₂), far IR refl. obs. 8-60459
 AgInSe₂(Te₂), far IR refl. obs. 8-60459
 Ag₂O₃, metallic, Raman scatt. 8-80358
 Al-Ag, resonance splitting of phonons 8-75759
 Al_{0.5}Ga_{0.5}As, first order phonon spectrum replicas 8-60467
 Al_{1-x}Ga_xP, IR phonons, lattice reflection spectra 8-51626
 Al₂O₃:Fe²⁺, phonon spectroscopy using superconducting tunnel junctions 8-91389
 Al₂O₃:Ni²⁺, corundum, phaser production of transverse phonons by impurity centres (*Russian*) 8-91390
 Al₂O₃:V³⁺, frequency crossing signals of V³⁺ ions, conc. depend. study using thermal phonons 8-95115
 Al₂O₃:V⁴⁺, dil. solution, stimulated phonon emission 8-63817
 As, amorphous and cryst., phonon density of states calc., comp. to IR absorpt. and neutron scatt. data 8-55924
 As, zone centre phonons and elastic const., hydrostatic press. depend. 8-59905
 BaF₂:Er³⁺, single-site multiphonon and energy transfer relax. 8-52547
 Bi, zone centre phonons and elastic const., hydrostatic press. depend. 8-59905
 α-CO, IR and Raman spectra, vibron band, vibron-phonon combination bands 8-68495
¹²C¹⁶O:CO isotopes, IR and Raman spectra, vibron band, vibron-phonon combination bands 8-68495
 CaCO₃, IR reflectivity, oblique phonons 8-60440
 n-CdHg_{1-x}Te, magnetophonon oscills. of transverse magnetoresist. 8-72177

lattice phonons continued

- CdS, acoustic phonon intensity fluctuations after strong nonlinear amplification 8-59909
 CdS, bulk acoustic phonons, light scatt. from phonon-induced surface ripples 8-75924
 CdS, mode corrected TA phonons, reson. Brillouin scatt. 8-72535
 $3\text{CdSO}_4 \cdot 8\text{H}_2\text{O}$, cryst., phonon assisted indirect transitions 8-72559
 $\text{CdS}_{1-x}\text{Se}_x$, zone edge phonons 8-76475
 CdSe, fundamental vibrs., Raman scatt. and IR refl. obs. 8-60451
 $\text{CdTe}_{1-x}\text{Se}_x$, Raman scatt. spectra, two-mode behaviour 8-60450
 Cds, reson. Brillouin scatt. by piezoelectrically inactive TA phonon domains 8-84593
 Co-P, metallic glass, phonon propagation at low temp. 8-87756
 CsBr, hyper-Raman spectra by single channel method 8-84591
 CsI, hyper-Raman spectra by single channel method 8-84591
 CsMnF_3 , mag. field- and temp.-depend. of light absorption spectra 8-52528
 $\text{Cs}_2\text{ZrCl}_6\text{O}_4^{+4}$, multiple state luminesc. 8-72584
 Cu, photoemission, temp. and photon-energy induced breakdown of direct transition model 8-95681
 Cu-Al, change in force constant due to volume effects 8-75778
 Cu-Au, dil., enhanced lattice sp.ht. 8-51699
 Cu-Si, change in force constant due to volume effects 8-75778
 CuCl, zincblende struct., high press. Raman scatt., 77K 8-60463
 $\text{CuGaIn}_{1-x}\text{S}_2$ solid soln., IR refl. spectra, comp. depend. 8-52498
 $\text{Cu}_x\text{V}_2\text{O}_5$, metallic, Raman scatt. 8-80358
 D_2 , solid, far IR absorption by phonons and librins in ordered state 8-80331
 D_2O_2 , lattice phonons by neutron scatt., covalent force model 8-67782
 DyAsO_4 , cooperative Jahn-Teller phase transitions, dielec. anomalies 8-64312
 DyVO_4 , cooperative Jahn-Teller phase transitions, dielec. anomalies 8-64312
 DyVO_4 , Jahn-Teller distortion, mag. field depend. 8-79733
 Fe, lattice vibrations, temp. depend. 8-95124
 Fe, surface lattice dynamics 8-95224
 FeBr_2 , dynamic Jahn-Teller system, Raman scatt. from electronic excitations and phonons 8-56474
 FeCl_2 , dynamic Jahn-Teller system, Raman scatt. from electronic excitations and phonons 8-56474
 $\text{FeCl}_2 \cdot 2\text{H}_2\text{O}$, also deuterated, electronic transitions in Raman spectra 8-80337
 $\text{Fe}_{65}\text{Ni}_{35}$, ferromagnetic Invar alloy, lattice vibrations 8-91403
 Fe_{1-x}O , wustite, phonon and magnon props., inelastic neutron scatt. 8-52236
 $\text{Fe}_{72}\text{Pt}_{28}$, ferromagnetic Invar alloy, lattice vibrations 8-91403
 $\text{Ga}_{1-x}\text{Al}_x\text{Sb}$, small wave vector modes 8-75785
 GaAs, bulk acoustic phonons, light scatt. from phonon-induced surface ripples 8-75924
 GaAs, irradiated with fast neutrons, IR vibrational absorpt. 8-75776
 GaAs-AlAs alternating monolayers, zone folding effects on phonons 8-72510
 GaAsP, composition dependence of phonon frequencies 8-75764
 $\text{GaAs}_{1-x}\text{P}_x$, $0.6 < x < 1$, photoluminesc., comp. depend. 8-52546
 GaInP, composition dependence of phonon frequencies 8-75764
 $\text{Ga}_{1-x}\text{In}_x\text{P}$, zone edge phonons 8-76475
 GaP second order Raman spectrum, polarisation meas. 8-64368
 GaS, sp. ht., vibr. spectra and Debye temp. 8-87796
 GaS(Se), layered, optical phonons, IR and Raman scatt. meas. 8-59903
 GaSb, reson. two phonon Raman scatt. near E_1 and $E_1 + \Delta_1$ gaps 8-60470
 GaSe, sp. ht., vibr. spectra and Debye temp. 8-87796
 $\text{GaSe}_2\text{Te}_{0.1}$, undulation spectra associated with acceptor complexes 8-80392
 GaTe, sp. ht., vibr. spectra and Debye temp. 8-87796
 GdS, metallic FCC antiferromag., phonon Raman scatt. 8-60458
 Ge, electron-hole drop velocities, excitation wavelength depend. 8-88358
 Ge, electron-hole drops, accel. by IR radiation field 8-95264
 Ge, electron-hole-droplet cloud, photoluminesc. of laser excited surface, phonon wind 8-84146
 Ge:P, lattice thermal cond., role of electron-phonon interactions and peripheral phonons 8-79702
 H_2 , solid, far IR absorption by phonons and librins in ordered state 8-80331
 HD, lattice thermal cond., 0.2 to 4K 8-75903
 HF, high temperature thermophysical properties 8-91404
 HIO_3 , single crystal, ang. depend. of Raman spectra 8-72518
 ^4He , solid, quantum diffusion of ^3He , tunnelling jumping approx. (Russian) 8-87844
 $\text{In}_{1-x}\text{Ga}_x\text{P}$, two-phonon IR absorpt. 8-52493
 KCN, Brillouin line width of phonons 8-80370
 KCl, entropy change associated with substitutional anion defects calc. 8-79782
 $\text{K}_2\text{PbCu}(\text{NO}_2)_6$, incommensurate Jahn-Teller phase transition 8-79730
 $\text{K}_2\text{PtCl}_6 \cdot \text{Os}^{4+}$, multiple state luminesc. 8-72584
 $\text{K}_2\text{PtCl}_6 \cdot \text{Os}^{4+}$, sharp line luminesc. band at 10K, vibr. assignment 8-95600
 K_2SeO_4 , improved Raman spectra at room temp. 8-56487
 LiF, 63 meV He atom scatt., single Rayleigh phonon interaction 8-80447
 LiF:Mg(Ag), electron spin-lattice relax. of V_K -centre 8-95518
 LiNbO_3 , optical phonon modes and anharmonic couplings 8-60466
 LiTaO_3 , optical phonon modes and anharmonic couplings 8-60466
 $\text{MgO} \cdot \text{V}^{2+}$, mag. circular dichroism in split zero-phonon line 8-56460
 $\text{Mg}_2\text{Zn}_{1-x}\text{Te}$, long wavelength optical phonon replica 8-60468
 $\text{Mn}_2\text{Cd}_{1-x}\text{Te}$, far IR refl. spectra, phonon spectra 8-52497
 MnO, Jahn-Teller effect on optical absorption spectra 8-52484
 Mo, phonon frequencies, seventh-neighbour tensor force model 8-91402
 Mo ternary chalcogenide, MMo_2X_8 (M=metal, X=chalcogen) Chevrel phase, supercond. and normal state props. 8-56267
 Mo_6Se_8 , Chevrel phase, isotope effect on supercond. T_c 8-52141
 N_2 , solid, semimicroscopic approach to lattice dynamics of mol. crystals 8-75765
 N_2CO , IR and Raman spectra, vibron band, vibron-phonon combination bands 8-68495
 NaClO_4 , Raman spectra temp. depend. near 581K phase transition 8-56477

lattice phonons continued

- NaI, long wave phonon modes, IR absorpt. 8-79686
 NaNO_2 , phonon side bands of triplet absorption 8-76488
 $\text{Na}_x\text{V}_2\text{O}_5$, metallic, Raman scatt. 8-80358
 Nb, phonon frequencies, seventh-neighbour tensor force model 8-91402
 Nb-H, acoustic phonon anomaly at small wavevectors 8-59882
 Nb-Zr, diffuse neutron scatt. 8-71816
 NbN, Raman spectra and superconductivity of various phases 8-68506
 NbSe_2 , 2H polytype, effect of incipient CDW on second-order Raman spectra 8-80357
 NbSe_2 (2H), effect of CDW fluctuations on Raman active optic phonon freq. 8-87750
 NbSe_2 (2H) microscopic theory of charge density wave instability 8-79732
 $\text{Ni}_3\text{B}_7\text{O}_{13}\text{I}$, Raman spectra in paraelec. phase 8-60434
 $\text{Pb}_{1-x}\text{Sn}_x\text{Te}$, band struct. and phonon energies, tunnelling spectroscopy 8-72070
 n-PbTe epitaxial film, magnetophonon and Shubnikov-de Haas oscills. 8-60234
 Pd-Pt, and other substitutional alloys with large mass disorder, phonon modes 8-95122
 Pd-Si, metallic glass, phonon propagation at low temp. 8-87756
 PbAgI_5 , solid electrolyte, neutron scattering study 8-79696
 RbI, hyper-Raman spectra by single channel method 8-84591
 Sb, zone centre phonons and elastic const., hydrostatic press. depend. 8-59905
 Se, effective charge tensor, microscopic treatment 8-59879
 Si:Al, absorpt. line broadening 8-95594
 n-SiC (6H), anisotropy of thermoelectric power (Russian) 8-91710
 p-SiC:B (4H), absorption spectra of bound excitons 8-88338
 SmS, f-d hybridisation, valence fluctuation and phonon spectrum, Raman scatt. expts. 8-60464
 SrClF, cryst., Raman intensity anal., normal coord. anal. 8-72493
 $\text{SrF}_2\text{Eu}^{2+}$, spectral, spatial and temporal phonon spectroscopy, new spectrometer 8-83892
 $\text{Ta}_2(\text{Se}_2)_2$, 2H polytype, effect of incipient CDW on second-order Raman spectra 8-80357
 TaSe_2 (2H), effect of CDW fluctuations on Raman active optic phonon freq. 8-87750
 TbVO_4 , Jahn-Teller distortion, mag. field depend. 8-79733
 TeO_2 , paratellurite, phase transition at high-press., Raman and far IR spectra 8-80328
 TeO_2 , zone centre optical phonons under uniaxial stress 8-79700
 Ti, high temperature thermophysical properties 8-91404
 $(\text{Ti}_2\text{O}_3)_{1-x}(\text{V}_2\text{O}_3)_x$, lattice polarisability, electronic contrbs. IR refl. obs. 8-59904
 Ti-Bi-Pb, phonon anomaly near Fermi surface topological transition, phonon softening at X point 8-95120
 $\text{TiGaSe}_2(\text{Se}_2)$, optical phonons, IR and Raman scatt. meas. 8-59903
 TiGaSe_2 , Raman and IR spectra, zone centre optical phonons 8-76462
 TiInS_2 , optical phonons, IR and Raman scatt. meas. 8-59903
 TlSe, optical phonons, IR and Raman scatt. meas. 8-59903
 W, alternating sign Hall effect and doppleron spectrum 8-79981
 WC, microcrystalline, mol. dynamics, motion of H_2O and H_2 mols. adsorbed on surface, catalytic activity 8-71941
 $\text{W}_2\text{Mo}_{1-x}\text{O}_3$, mixed cryst., structural phase transition, Raman and IR spectra 8-79766
 $\text{Zn}_{1-x}\text{Mg}_x\text{Te}$, long wavelength optical phonons, IR ref. and Raman obs. (French) 8-60433
 ZnO, acoustic phonon intensity fluctuations after strong nonlinear amplification 8-59909
 ZnS, single crystal, effect of elec. field on cond. 8-84228
 Zr, high temperature thermophysical properties 8-91404

lattice structure, crystals see crystal atomic structure

lattice theory and statistics

- see also Ising lattices; renormalisation; X-Y model
 $1/n$ expansion up to $1/n^2$, eqn. of state and correlation function 8-89412
 20-vertex model on triangular lattice 8-70065
 λn^4 field theory with internal symm., string representation 8-70266
 Abelian Higgs model, two dimens., multiple vacs. in lattice formulation 8-54543
 Abelian lattice gauge theory, quark confinement 8-66040
 anharmonic lattice with defects 8-73937
 anisotropic lattice spin systems, phase transitions 8-73930
 asymptotic number of lattice animals in bond and site percolation 8-54310
 Backlund transformations as canonical transformations 8-81855
 Blume-Emery-Griffiths model in 2-D, renormalisation group studies 8-54311
 bond percolation, Hamiltonian formulation, alternative derivation of Ashkin-Teller-Potts model relationship 8-81926
 bond percolation processes in d dimensions 8-70066
 Born-Huang invariance conditions, completeness 8-51620
 cluster expansion with lattice approximation 8-49759
 cluster radius, below percolation threshold, speculations 8-70073
 composites, fibre reinforced and particulate, mechanical model 8-51105
 condensed phase, lattice gas model 8-73931
 continuous renormalisation transformation, variational calcs., rel. to Potts model 8-93618
 coupled phonon-linear Heisenberg chain system, phase transition 8-64208
 critical exponents, diagrammatic representation, three-state Potts model appl. 8-75867
 critical indices to $O(1/n^2)$ for 3-dimens. system with short range forces 8-49775
 crystal, statistical thermodynamics with collective vibrations 8-54289
 cubic lattice, Green's function determ. 8-62162
 dimer config. enumeration, n-dimensional theory, graph paths 8-54315
 discrete Gaussian model, position-space renormalisation transformation 8-93617
 discrete Gaussian model, renormalization transformation 8-81925
 discrete Gaussian roughening model, Monte Carlo simulation, appl. to Coulomb gas and Villain X-Y model 8-86225
 electron correlation problems, lattice statistical aspects, Gutzwiller approx. 8-84160

lattice theory and statistics continued

elementary length and time in the strong interaction, meson reson. width data 8-82189
 Fermi system, 1-D, and plane xy model, behaviour of correlation functions 8-56091
 first-order phase transitions, clusters, metastability, nucleation 8-54326
 free-fermion condition for generalised vertices 8-93622
 gauge theories on Euclidean lattice with fermions, cluster expansion 8-58119
 graph-like state of matter, electrical cond. of random networks, gelation and elasticity 8-65875
 hadron mass spectrum in lattice gauge theory 8-74139
 Heisenberg antiferromagnet, phase transitions in quantum spin systems 8-84434
 isotropic spin system, cubic lattice, step model of phase transitions, critical behaviour 8-60290
 Krieger-James approx. of short range order effects, antiferro- and ferro-mag. 8-56276
 lattice, gas, entropy and phase transitions in partially ordered sets 8-77808
 lattice animal numbers, lower bounds 8-70069
 lattice Coulomb gas representations of two-dimensional problems 8-70068
 lattice gas model, critical cond., rel. to cond. in superionic conductors 8-93614
 lattice gases, strong cluster props. of connected correlations, potential analyticity 8-70062
 lattice-lattice scaling, reln. to scaled eqn. of state, appl. to Ising model 8-70067
 Lifshitz point, critical exponents, ϵ -expansion 8-65899
 linear harmonic oscillator on lattice, wave functions, energy eigenvalues, Pade approximant method 8-57817
 linear lattice of atoms, Lennard-Jones pot. basis, for teachers 8-61997
 liquid crystals, correlation in statistical theory 8-75536
 liquid theory, classical spin system, absence of ordering 8-51402
 logarithmic corrections to a simple power law at $d=4$ in $1/n$ expansion 8-65895
 Migdals recursion relation, harmonic rotator model in two dims. 8-89413
 minimum potential energy per particle configuration, one-dimens. system 8-70084
 normalisation of one-dimens. lattice statistics 8-62161
 one-dimensional hopping, moment expansions and occupancy (site) correlation functions 8-55972
 ordered physical line structures, nonlinear local field theory, appl. to high polymers, supercond. flux line lattices 8-81859
 particle lattice models, physical signals speed of propagation, bounds 8-93613
 percolation, two dimensions, absence of phase transitions 8-87770
 percolation by position-space renormalisation group with large cells 8-77805
 percolation cluster distrib., mean value depend. and animals distrib. 8-81928
 percolation problem, for semiinfinite porous media, diagram technique calcs. 8-93621
 percolation problem, high order behaviour in O^3 field theories 8-65883
 percolation theory, bond problem, critical probabilities, bond clusters 8-86224
 percolation theory, scaling assumption for lattice animals 8-54313
 percolation threshold, computer generated pictures of infinite clusters 8-56117
 percolation with nearest neighbour interaction 8-73934
 phase transitions and reflection positivity, Peierl contour probabilities, long range lattice models 8-89398
 phase transitions and renormalised struct. of lattice gauge theories with fermions 8-82105
 polycrystalline material, scatt., lattice representation 8-65774
 polymer chains, with volume interaction, statistical physics problems, coils and globules, review 8-94347
 polymer dilute soln., critical ratio limiting values using renormalisation group methods 8-83715
 polymer solution, simulation of macromol. dynamics, Monte-Carlo method, conc. depend. (*Polish*) 8-51404
 Potts lattice gas, renormalisation-group treatment, Kr adsorbed on graphite 8-67908
 Potts model, zero state, in $2+\epsilon$ dimensions, crit. exponents 8-77809
 Potts model and percolation 8-54312
 propositional systems and meas., quasi-tensor-products of certain ortho-modular lattices 8-81871
 QCD, lattice-gauge theory calc. of π and ρ -meson decay consts. 8-74154
 quadrupolar systems of restricted dimensionality, absence of ordering 8-89411
 random Gaussian lattice, mass lower bound using random walk representation 8-89409
 random resistor networks, critical behaviour near percolation threshold 8-87956
 random system, dispersion theory approach to scaling function 8-70071
 random walk, self-avoiding, direct renormalisation group approach 8-73933
 random walks, self-avoiding and limited order, distrib., orthogonal vector anal. 8-65874
 randomly-packed spherical particle bed, coord.-no. distrib., effective thermal cond., stat. thermodynamic theory 8-75028
 recursion eqns. for renormalisation group transforms. in lattice gauge theories including fermion variables 8-62298
 renormalisation group approach to scaling, phys. appl. 8-49634
 Schwinger model, massive QED for fermions in $1+1$ dims. 8-78121
 self avoiding walk attached to a surface, tests of scaling theory 8-81927
 sequential term prediction, appl. to Ising, X-Y and other models 8-57866
 sine-Gordon field theory, two dims., second order phase transition, lattice model 8-78095
 solutions with closed loop coexistence curves, directionality depend. of lattice models 8-95158
 spin lattice models, continuous-integral method 8-93615

lattice theory and statistics continued

spin-1/2 models, on square lattice, sublattice renormalisation transformations 8-65878
 spin-oscillator coupled system, stochastic model for dynamics, projection operator approach 8-77813
 square lattice finite thickness slabs, long self-avoiding walks, steric stabilisation model 8-54309
 statistical crystal model, small amplitude acoustic perturbations and Debye-Waller factors 8-55930
 superfluidity on Bose-condensed quantum crystal 8-75905
 three-state Potts model variant, phase behaviour 8-68259
 time correlation functions of one dims. infinite system, ergodic props. 8-65862
 Toda lattice soliton, interaction with impurity atom 8-75772
 topological excitations in Abelian Higgs model 8-70275
 transfer integral method, three dims., appl. to harmonic cryst. 8-84161
 transformation methods in anal. of crit. prop. 8-49771
 two-dimens. U(1)-Goldstone model, QFT on lattice 8-74158
 two-dimensional systems, phase transitions 8-68241
 vibrational properties of Cayley tree type system, modes, densities 8-71813
 X-Y model, percolation in three-dimens. model 8-80113
 zero field susceptibility in $d=4$, $n=0$ limit, confluent logarithmic singularities 8-54308
⁴He, superfluid, quantum lattice gas as microscopic model 8-59986

lattice vibrations see *lattice dynamics*

Laves phases see *alloys*

lawrencium

No entries

lawrencium compounds

No entries

LCAO calculations

alkali borate glass networks, π -electron distrib. SCF INDO LCAO-MO calc., O basicity 8-79924
 alkanes, mag. susceptibility simple additive approx. calcs. 8-86775
 benzene, mol., directional Compton profile, ab initio SCF LCAO MO calc. 8-62857
 benzene, protonated, electronic struct., SCF MO LCAO calcs. 8-82638
 chemisorption, embedding problem, SCFMO formalism 8-71977
 convergence in SCF calcs., reverse level shifting technique for accel. rate 8-70735
 covalent elements, cohesion in condensed phases, corrections to simple Huckel approx. 8-59779
 covalent elements, cohesion of σ and π bonds in condensed phases, simple Huckel approx. 8-59778
 diamond, Compton profiles, X-ray struct. factors, band struct., LCAO calc. 8-51889
 DNA, proton transfers between base pairs, LCAO SCF all-electron PRDO method 8-80829
 ethylene+Cl₂(Br₂) complex, intermolecular interaction and struct. SCF-MO-LCAO CNDO/2 calc. 8-58763
 expansion of MO wave functions into VB work functions 8-74580
 fluoro sulphuric acid methyl ester, rot. isomerism 8-86964
 formaldehyde, orbital contribs. to relax. energies accompanying core ionis., ASCF HF calcs. 8-82642
 garnets, mag. props. of V⁴⁺ ion, effect of covalency 8-64010
 Gaussian-70 MO program, LCAO-SCF eqn. soln., population anal., appl. 8-70742
 graphite, electronic props., self consistent LCAO calc., point vacancy in 2-dimens. cryst. 8-51932
 graphite, electronic props., self-consistent LCAO calc. 8-51887
 inelastic electron tunnelling spectroscopy, model for electron-molecule interaction 8-90257
 metal, HCP, LCAO description of (0001) surface electron states, appl. to Sc 8-72232
 3-methyl lumiflavin in soln., optical absorption, theory 8-74569
 methylamine- t_1 -NH₃, β decay effect on H-bond, ab initio LCAO SCF MO calc. 8-76894
 molecular electronic structure, semiempirical CNDO method, calc. program 8-86782
 superexchange in insulators, refined LCAO scheme 8-91861
 surface lattice dynamics and density response 8-71930
 surface states, three-dimens. cryst. ab initio SCF LCAO calc., impurity clustering 8-56201
 transition metal surface, electronic perturbations 8-95334
 TTF-TCNQ, band struct., Fermi surface and density of states, LCAO calc. 8-60048
 Z-centre 1-electron integrals and Coulomb integrals over STOs 8-82608
 Ziegler-Natta type catalysis, reaction pathway, ab initio SCF-LCAO-MO calcs. 8-56891
 CO, orbital contribs. to relax. energies accompanying core ionis., ASCF HF calcs. 8-82642
 COH⁺, orbital contribs. to relax. energies accompanying core ionis., ASCF HF calcs. 8-82642
 CdI₂, UV reflectivity meas., band struct., LCAO calcs. 8-72545
 CHCl₃, deuteron quadrupole coupling const., nuclear mag. shielding, geometry depend. 8-58586
 Cu, surface energy band calc., significance for photoemission 8-95330
 FHCl⁻, deuteron quadrupole coupling const., nuclear mag. shielding, geometry depend. 8-58586
 FHF⁻, deuteron quadrupole coupling const., nuclear mag. shielding, geometry depend. 8-58586
 FeF₃ isomer shift, using LCAO form of molecular orbital method 8-62856
 H₂, mag. field depend. orbitals for mag. screening and susceptibility of mol. 8-78611
 H₂⁺, in mag. field, LCAO calcs. 8-82628
 HCN, HNC, electronic reorganisation, with core ionisation 8-94196
 HCO⁺, orbital contribs. to relax. energies accompanying core ionis., ASCF HF calcs. 8-82642
 HF, mag. field depend. orbitals for mag. screening and susceptibility of mol. 8-78611
 HNO, HON, electronic reorganisation, with core ionisation 8-94196
 Ir (001), surface electronic props. 8-95332
 KBr, electronic states at (100) surface, accounting for spin-orbit interaction (*Russian*) 8-91750

LCAO calculations continued

- KCl, electronic states at (100) surface, accounting for spin-orbit interaction (*Russian*) 8-91750
 KI, electronic states at (100) surface, accounting for spin-orbit interaction (*Russian*) 8-91750
 Li (100), O adsorption, cluster models, ab initio HF LCAO theory 8-71978
 LiH, positron affinity, ab initio LCAO MO SCF calc. 8-82870
 MgF₂, ground state, nonempirical LCAO SCF calcs. 8-66469
 MgO, intrinsic surface states at (100) and (110) surfaces 8-91740
 N₂, core ionisation, single orbital relax. energy contrib. calcs. 8-82637
 NH₃, LCAO-MO-SCF calcs., analysis of Gaussian basis sets rel. to one-electron props. 8-55122
 NH₃TNH₃, β-decay effect on H-bond, ab initio LCAO SCF MO calc. 8-76894
 Ne+HeH⁺, collinear reaction, pot. energy surface SCF-LCAO-MO and DIM calc. 8-92467
 Ne₂H clusters, ab initio LCAO MO SCF calc., struct. and energy 8-66704
 Ne₂H⁺ clusters, ab initio LCAO MO SCF calc., struct. and energy 8-66704
 NiCO, and core ionised, binding and relax. energy ab initio LCAO MO SCF calc. 8-62712
 OH⁻+CO₂→HCO₃⁻ react., MO-LCAO-SCF calcs., energy barrier 8-76846
 P₂O₄(OH)₄²⁻ group, electronic struct. calcs. 8-67971
 PbI₂, UV reflectivity meas., band struct., LCAO calcs. 8-72545
 Pt (001), surface electronic props. 8-95332
 Si (110), chemisorption of Cl, LCAO calcs., Auger line shapes, localized density of states 8-56202
 Si (111), chemisorbed Cl layer, SCF LCAO band struct. calcs. 8-88010
 SiH₄, ab initio Hartree-Fock SCF-LCAO-MO method 8-94195
 SiH₂F₂, ab initio Hartree-Fock SCF-LCAO-MO method 8-94195
 SiH₃F, ab initio Hartree-Fock SCF-LCAO-MO method 8-94195
 Si₂O₆(OH)₄⁶⁻ group, electronic struct. calcs. 8-67971
 SnS₂, UV reflectivity meas., band struct., LCAO calcs. 8-72545
 TiSe₂ (IT), structurally induced semimetal-to-semicond. transition, ab initio LCAO calc. 8-51896

lead

see also nuclei with

- acoustic velocity, shock-compressed uniform solid, lateral discharge ang. semiempirical formula (*Russian*) 8-55910
 adsorption, on Au, formation of AuPb₂ epitaxial layer, LEED, AES study of Au/AuPb₂ interface 8-71988
 atom, γ-ray absorption cross-sections, 10-160 MeV 8-90136
 atom, excited states, quadrupole moments, Sternheimer shielding factors 8-82630
 atom, L-shell X-ray photoelectric cross sections, fluorescence spectra 8-58636
 atom, parity nonconservation in heavy atoms, weak electron-electron interaction (*Russian*) 8-55132
 Auger emission target, contrib. of reflected electrons 8-92152
 bremsstrahlung, β generated, spectral shape depend. on target thickness 8-56545
 Bremsstrahlung distrib. from 22 MeV electron irradiation 8-59840
 catalyst, BCl₃-H₂ photochem. with Ti, Pb catalysts, isotopic excitation by laser 8-64882
 concentration determ. in atm. and rainwater in Vizcaya, Spain (*Spanish*) 8-57264
 concentration in snow of Mt. Blanc rel. to air pollution 8-81258
 determination, in atmosphere, flameless atomic absorpt. in particle size fractionated aerosols 8-69434
 determination, in blood, haematofluorometric method 8-53554
 determination, in flux-grown magnetic garnets, by AAS 8-92585
 determination, in powder rock samples, by at. absorpt. (*Russian*) 8-85278
 determination, in steel wire, AAS determ. 8-68939
 determination aqueous solutions, by Delves Cup technique and flameless atomic absorpt. spectrometry 8-68973
 diffusion coefficient in In, RF size effect meas. (*Russian*) 8-91717
 diffusion in liquid Cu (*Japanese*) 8-59962
 diffusion of Co impurity in Pb, ion implanted, exam. by activation analysis technique 8-91488
 effective cyclotron masses of central and noncentral ξ orbits, de Haas-van Alphen effect 8-63968
 elastic properties (*Russian*) 8-56678
 electromigration, thermomigration, and solubility, of ⁶⁴Cu 8-71882
 electromigration of Cu in Pb 8-84003
 electromigration of Ni, steady-state method 8-87820
 electron beam reflection, high current (*Russian*) 8-84690
 epitaxial growth on Ag (111) and Cu (111), LEED, RHEED, AES study 8-84090
 equation of state, isentropic expansion method 8-91414
 filament production, ejection of molten metal through nozzle, jet stability (*Japanese*) 8-52719
 film, evaporated, interaction with BCl₃, HCl, adsorpt. 8-75945
 film, IR optical constants, determ. by surface plasmon excitation 8-76418
 film, on Au (100), initial stages of condensation 8-91569
 film, ultra-thin, existence of double-hexagonal close packed phase 8-63952
 geochemistry in sediments of Gulf of St. Lawrence and estuary 8-92855
 Grüneisen parameter, behaviour at high press. 8-83899
 ion impact on C foil, energy loss 8-55902
 isotope composition of Archaean plutonic rocks 8-65223
 isotope dating of ore mineralisations in Erma River Area, Bulgaria 8-81115
 isotopes composition in oceanic basalts, rel. to mantle evolution 8-65217
 isotopes conc in ocean floor basalts and ferromanganese deposits 8-61395
 isotopic composition, of volcanic rocks of Aleutian and Pribilof Islands, Alaska 8-57185
 kfor=for 8-80822
 laser, long life operation at 7229 Å 8-79037
 laser, long-lived sealed-off design, 7229 Å emission 8-50808
 lattice vibrations, appl. of two-parameter shell model for monoatomic systems 8-59877

lead continued

- liquid, electrical resistivity with spin-orbit scatt. 8-64018
 liquid, new description of random stacks (*French*) 8-79512
 liquid, short range order parameters, from information theory 8-83730
 liquid film, electron diffr. 8-83721
 magnetic interaction, de Haas-van Alphen effect 8-79921
 metal cluster generator for gas-phase electron diffr., variation of microcryst. with size 8-63645
 microclusters, mol. beam electron diffr., amorphous struct. 8-66703
 neutron yield calcs., electron beam incidence 8-95622
 passivation in H₂SO₄ soln. 8-76871
 phonon dispersion and cryst. equilib. 8-75752
 phonon softening, neutron scatt. at high press. 8-80091
 phonon spectrum, calc. by phenomenological method 8-59890
 phonon thermal conductivity of deformed cryst. below 2K (*Russian*) 8-60244
 photoionisation cross section of atomic and final state effects on 5d core levels 8-84699
 pollution, New Zealand, battery factory and smelter emissions compared with vehicle exhausts 8-85562
 pollution in Christchurch, New Zealand 8-85561
 positron annihilation rates, electron-electron and electron-positron correl. effects 8-76548
 positron-vacancy interactions, equilib. temp. depend. of positron annihilation 8-76547
 powders, prep. of spherical starting particles, for suspension electrolysis 8-60689
 reactor shielding material, 6 MeV γ penetration, bremsstrahlung 8-85350
 relativistic model pseudopot., appl. to elec. resist. in liq. phase and phonon spectra 8-51866
 rings, bearing capacity under compression 8-83256
 roadside soil and plants in Alexandria district, Egypt, contamination with Cd, Ni, Pb and Zn 8-81171
 superconducting, absolute surface reactance and penetration depth 8-68109
 superconducting, crit. mag. field, functional derivatives 8-91798
 superconducting, phonon struct. meas. in ultra-thin proximity effect tunnel junctions 8-80101
 superconducting, press. depend. of supercond. transition temp. 8-84340
 superconducting, quasi-particle recomb. time, Kapitza resistance 8-68123
 superconducting film, anomalous temp. depend. of quasiparticle injection-induced voltage onset 8-56256
 superconducting friction with Ge, supercond. friction layers formed on Ge (*Russian*) 8-52143
 superconductor, elastic tunnelling spectroscopy of single-particle excitations 8-56260
 surface, H⁻, H⁺, H₂⁺ and H₃⁺ grazing incidence collision with surface, Balmer radiation, elliptical polarisation 8-86804
 surface props. rel. to adsorbed O₂, H₂O vapour, work function determ. 8-60187
 tracer diffusion, atom size effect 8-84005
 ultrafine particle, positron annihilation exam. 8-56542
 underpotential deposition on Ag single crystal cathode 8-52692
 vacancy energy of formation, positron annihilation obs. (*German*) 8-71721
 vacuum deposited metal film, elec. field effect on residual struct. 8-51836
 X-ray absorption edge, chem. shift, electron binding energy in compounds 8-62822
 AgCl:Pb²⁺, EPR of mobile electrons, mechanism for photoinduced decomposition 8-80219
 Al-SiO₂-Si-Pb, MIS system, photocurrent, effect of supercond. to normal transition in Pb 8-72271
 Bi_{1-x}Sb_x:Pb (0.08≤x≤0.13) Seebeck, magneto-Seebeck coeff., longitudinal Nernst coeffs. 8-56168
 CaF₂:PbO, UV absorption, impurity centres 8-68534
 CaS-Pb,Mn, phosphors, thermoluminesc. and fluoresc. spectra 8-64396
 CuCr-Pb, proximity effect, tunnelling conductance 8-52160
 InSb-Pb, thermodynamic props. (*German*) 8-75847
 KBr:Pb, luminesc. spectra obs. 8-95604
 KCl:Pb, luminesc. spectra obs. 8-95604
 KCl:Pb²⁺, inner-centre luminesc., to 80K (*Russian*) 8-92112
 KCl:Pb²⁺(0.005% Pb), A band fine structure, electron-phonon interaction 8-60491
 N₂⁺+Group IV elements and oxides, XPS and UPS prod. determ. 8-73084
 NaCl:Pb, luminesc. spectra obs. 8-95604
 NaCl:Pb, Pb determ. by optical absorpt. in aq. soln. 8-85232
 NaCl:Pb²⁺, Z₄-like centre, absorpt. spectra obs. 8-76498
 Na₂O-P₂O₅:Pb²⁺, metaphosphate glass, absorpt. spectra of radiation products 8-64865
 Nb-NbO₂-Pb Josephson junction, self-reson. modes 8-64169
 Pb⁺, adsorbed on Ag (111) or (100) surface, struct. (*German*) 8-68636
 Pb/PbCl₂ electrode, in chloride media, low temp. props. 8-68899
 Pb-Al₂O₃ composites, mech. alloyed, hot hardness meas. (*Japanese*) 8-84830
 Pb-CdS-In Josephson junction, light-sensitive, structural fluctuations (*Russian*) 8-56265
 Pb-He discharge, excitation process, Pb⁺ emission lines 8-66803
 Pb-Te-Pb Josephson junction, cavity resonances 8-84352
 Pb+H⁺, K-shell ionisation, 7-15 MeV, relativistic effects 8-82830
 Pb+He⁺, at. beam and surface interaction, scatt. ion yield oscils. 8-55221
 Pb⁺+Z (42≤Z≤92), 1sσ MO excitation probability and binding energy, X-ray coincidence 8-94316
 Pb(P₁^o)+H, spin-orbit relax., fluoresc. intensity meas. 8-82681
²¹⁰Pb chronologies of lake and marine sediments, problems 8-81122
²¹⁰Pb tropospheric residence time 8-85396
 Si:Pb, implanted, laser annealing 8-75685
 Si:Pb, implanted and annealed, impurity redistrib. 8-75689
 V, effect of O ion irradiation on supercond. 8-52131
 ZnS:Pb phosphor mech. of elec. field liberation of electrons from traps 8-72616

lead alloys

- see also lead compounds
- leaded brass, mechanical damping in terms of Granato-Lucke theory, comparison with unleaded brass and Cu_3Au 8-95772
- steel, cavitation during superplastic flow, affecting factors 8-60728
- Al-Pb, containing low melting point inclusions, impact props., temp. depend. 8-60792
- AuPb₂, epitaxial layer, formation during Pb absorpt. on Au, LEED, AES study of Au/AuPb₂ interface 8-71988
- (Au,Pb)_{1-x}-Fe_x, ferromag. and spin glass ordering 8-56335
- Bi-Pb-Sn, molten metallic system, contribution to sign inversion of effective charge (Czech) 8-60656
- Cd-Pb-Bi-Sn system, ternary liq. alloys, thermodynamic props. 8-51701
- α -Cu-Ni-Zn-Pb, fire cracking and ordering (German) 8-60760
- Cu-Pb, diffusive redistrib. during friction (Russian) 8-52999
- Cu-Pb liquid alloys, exam. of O diffusivity at 1430K using electrochemical cell 8-51713
- Li-Pb, quasi-ionic, thermodynamic props. using EMF meas. 8-51705
- Li_{1-x}Pb_x, liq., metal-nonmetal transition, electronic theory 8-79930
- Mg-Al-Tl system, phase diag., electrode pots. (Russian) 8-80516
- Mg-Cu-Pb system, phase equilibria in Mg-rich corner (French) 8-76630
- Nb-PbSn, Josephson tunnel junction, 3rd yr undergrad. expt. 8-54126
- Pb-Ag, liquid alloy, exam. of thermodynamic props. using solid oxide galvanic cell 8-75851
- Pb-Bi, liquid alloy, chemical and intrinsic diffusion coeffs., exam. (German) 8-83987
- Pb-Bi, peritectic reaction, microstruct. changes 8-52753
- Pb-Bi (4.1 at.%) solid soln., tetragonal distortion field for substitutional Bi atoms, neutron scatt. 8-51568
- Pb-Ca-Sn, effect of Sn additions on precipitation behaviour, of Pb-Ca alloys (German) 8-52821
- Pb-In (40-60 at.%), type II superconducting Ettingshausen effect, transport entropy of vortices 8-56272
- Pb-In-Au, film, supercond. penetration depth 8-72306
- Pb-Na, peak-effect supercond., flux pinning 8-95403
- Pb-Sb, crystal struct., supercond. after subjection to high press. 8-88064
- Pb-Sn, binary liq. soln., surface cluster functions 8-67631
- Pb-Sn, eutectic alloy, plastic deform., work hardening (German) 8-92279
- Pb-Sn, superplastic eutectic, roll load and torque necessary for rolling (French) 8-95761
- Pb-Sn, unidirectionally solidified eutectic, lamellar microstructure, influence of grain boundaries on thermal stability 8-72795
- Pb-Tl alloys, pinning parameters 8-52173
- Pb-Zn, liquid phase immiscibility determ., DTA 8-64523
- Pb_{0.87}Sn_{0.129}, supercond., hysteresis in flux flow characts., normal metal precipitates 8-80107
- PtPb₃Bi, cryst. struct. (German) 8-59783
- Sn-Pb, dil. lattice dynamics, sp. ht., resist., thermal expansion and nuclear γ reson. expts. (Russian) 8-87749
- Sn-Pb, supercooled, dendritic growth rates (Russian) 8-80533
- Sn-Pb (15 wt. %), forging of liquid and partially solid alloys 8-80569
- Sn-Pb (15 wt. %), partially solidified slurry, exam. of structure, viscosity 8-84793
- Sn-Pb (38 wt. %), graphite fibre reinforced, effect of interface on fracture characts. 8-76723
- Sn-Pb (5 wt. %) ingots, quenching technique, for studying formation of macrosegregations 8-52793
- Sn-Pb eutectic, struct. and plasticity, thermomech. treatment effects (Russian) 8-60686
- Sn,Pg_{1-x}, thermal cond. and Lorenz function 8-51966
- Tl-Bi-Pb, phonon anomaly near Fermi surface topological transition, phonon softening at X point 8-95120

lead bonding

- furnacing technique for bonding Au and Ag on sapphire 8-54352
- NDT wire bonds on Si chips, IR microscopy 8-95867
- Al-Au bimetal thin film interdiffusion zone, intermetallic phase form kinetics, 70-160°C 8-75891

lead compounds

- see also lead alloys
- alkyl Pb compounds, in atmosphere, detect. via gas chromatograph-microwave plasma detector 8-68975
- chalcogenides, electron-hole liquid theory, generalised RPA 8-87914
- chalcogenides, interband absorption under linearly polarised light excitation 8-92089
- galena, polycryst. synthetic, stress relax. 500 to 800°C 8-87737
- halides, doped, secondary ion emission, at. and mol. processes 8-68588
- halides, UV photoelectron spectra of valence d shells, gas-phase 8-62845
- hydroxyapatites, elec. cond., charge carrier identification 8-67855
- myristate, multilayer analyser for X-ray spectroscopy 8-49944
- sulphides, isotopic composition, mineralisation time determ. 8-73372
- SnTe-PbTe-GeTe, alloy semiconductor, phase transition (Japanese) 8-91443
- Au-Pb₃Sn_{1-x}Te-Au structure, third harmonic variations at 77K and 300K 8-84313
- BaPbF₆, Group IV hexafluoride anion radical γ -irrad., EPR spectra 8-72411
- CsPbCl₃, O_h¹-D_{4h} transition, US and thermodynamic props. 8-67826
- CsPbCl₃, phase transition under pressure 8-51664
- Fe₂O₃-B₂O₃-PbO glass, semicond., elec. resist. meas. 8-95300
- Ge-Pb_{1-x}Sn_xTe, amorphous/crystalline heterojunction, rectification props., IR detector appl. (Japanese) 8-60197
- KCl:PbCl₃, tablet, 272 nm absorpt. band 8-84612
- K₂PbCu(NO₂)₆, incommensurate Jahn-Teller phase transition 8-79730
- K₂PbCu(NO₂)₆, Jahn-Teller phase transitions, order-disorder model 8-79762
- La_{0.65}Pb_{0.35}MnO₃, transport props. near Curie points 8-88100
- La₂Pb_{1-x}Zr_xTa_{1-y}O₃, ferroelec. with diffuse phase transition, electrostriction-optical props. 8-68457
- LiCl-PbCl₂, molten, struct. anal. by X-ray diff. 8-94961
- Na₂O-PbO-B₂O₃-SiO₂, homogeneous melt formation rate, exam. 8-64520
- PLZT ceramic, ferroelec., cathodolum. spectral and temp. depend. 8-84665

lead compounds continued

- PLZT ceramic, possible construction of matrix-addressable controlled transparency 8-71222
- PLZT ceramic birefringence props., transverse electro-optical meas. 8-72487
- PLZT ceramics, optical information storage and spatial light modulation 8-83097
- PLZT, deposition of transparent electrodes, opt. storage device appl. 8-74848
- PLZT, electro-optical, physical elec. and optical props. and fabrication (Polish) 8-56458
- PLZT, opt. spectra and luminesc. 8-76508
- PLZT, photorefractive effect and photoconductivity 8-92046
- PLZT, transparent ferroelec., RF sputtering and film characterisation 8-72727
- PZT, ferroelec. film, elec. props., composition anal., AES 8-84530
- PZT-polymer flexible composite transducer 8-80291
- Pb salt, tunable IR diode lasers 8-59030
- Pb/PbCl₂ electrode, in chloride media, low temp. props. 8-68899
- Pb-S-I-X-H₂O, (X=solvent) crystallisation conditions 8-80466
- Pb-Te, molten mag. susceptibility, conc. and temp. depend. 8-80121
- Pb₂-Sr_{1-x}(Zr_x-Ti_{1-x})O₃:Cr₂O₃, ferroelec. ceramic, reversible characts. and dielectric losses (Russian) 8-84517
- PbAr, metal-insulator transition, resistivity meas. 8-80028
- Pb₃(AsO₄)₂Cl, mimetite, vibr. spectra, normal coord. anal. 8-88305
- Pb_{2-x}Ba_xLa_{0.5}Nb_{1.5}O₆, dielectric const., temp. and Ba conc. 8-64308
- (Pb_{0.715}Ba_{0.285})_{0.991}(Zr_{0.707}Ti_{0.293})_{0.981}Bi_{0.019}O₃, slim loop ferroelec. ceramic, shock wave compressed, elec. response 8-80293
- PbBi₄Ti₄O₁₅ ceramic, dielec. props., temp. depend. 8-95561
- PbBr₂, cryst., red luminesc. at low temps. (Russian) 8-92125
- PbBr₂, lowest exciton states 8-72082
- PbCO₃, neutron diff. topographic study of growth defects 8-91282
- PbCO₃ whiskers, growth kinetics in silica gel 8-75971
- Pb_{1-x}Cd_x, epitaxial, resist. and Hall coeff., substrate temp., thickness and comp. depend. 8-72290
- PbCl₂, binding, ionicity, covalent contrib., Madelung const., cohesive energy 8-79558
- PbCl₂, lowest exciton states 8-72082
- PbCl₂, molten, struct. anal. by X-ray diff. 8-94961
- PbCl₂, photoionisation cross section of atomic and final state effects on 5d core levels 8-84699
- PbCl₄⁴⁻, model force fields and vibr. amplitudes calcs. 8-62780
- PbCrO₄, ZZ 8-88326
- PbF₂, ¹⁹F NMR, free induction decay, initial behaviour 8-80227
- PbF₂, Brillouin scatt. and high temp. disorder 8-80365
- β -PbF₂, electrolytic props., AC cond. meas. 8-71878
- β -PbF₂ film, ionic migration study by Rutherford scatt., defects, secondary emission (French) 8-55982
- PbF₂, lattice dynamics 8-79697
- α -PbF₂, lowest exciton states 8-72082
- PbF₂, motionally narrowed system, appl. of zero time resolution NMR 8-76325
- PbF₂, muon Coulomb capture ratio 8-62959
- PbF₂, NMR relax. and self diffusion 8-80236
- PbF₂ single-layer film 2.8 μm , 3.8 μm absorpt. meas. 8-90463
- PbF₂, superionic, electrical conductivity at high temp. 8-79798
- PbF₂, superionic conductor, theoretical investigation of Raman scatt. 8-80351
- ²⁰⁷PbF₆³⁻, radical, prep. and EPR comparison with other hexafluoride radicals 8-68381
- Pb₂Ge₂O₁₁ acoustic relax. assoc. with phase transition at hypersonic freq. 8-88267
- Pb₂Ge₃O₁₁, dynamic central peaks and phonon interactions near structural phase transitions 8-83903
- Pb₂Ge₃O₁₁, ferroelectric transition exam. by Raman scatt. 8-56439
- Pb₂Ge₃O₁₁ film, pyroelectric effects, origin 8-88258
- Pb₂Ge₃O₁₁:Ba₂O, impurities, static central peak 8-92079
- PbGeS₃, vitreous and cryst., IR and Raman spectra (Russian) 8-72527
- Pb₃(Ge_{1-x}Si_x)₃O₁₁, dielec. spectra, ferroelec. behaviour 8-60406
- Pb₃Ge_{3-x}Si_xO₁₁, ferroelec. soft mode, temp., press. and comp. depend. 8-80304
- Pb₃Ge_{3-x}Si_xO₁₁, ferroelec., switching vel. and spontaneous polarisation 8-84543
- Pb_{1-x}Ge_xTe, dielec. const. determ. near ferroelec. transition 8-88269
- Pb_{1-x}Ge_xTe, electron-phonon interaction effect on ferroelec. transition 8-76416
- Pb_{1-x}Ge_xTe, phase transitions 8-60408
- Pb_{1-x}Ge_xTe:Ga, Fermi level stabilization, transport props. meas., 77-400K 8-56065
- PbHfO₃, elec. field gradient, crit. behaviour, DPAC meas. 8-80303
- PbI₂ film, highly excited, oscillator strength of excitons, absorpt. and emission spectra 8-76001
- PbI₂ intercalated with organic mols., energy band splitting (Russian) 8-76027
- PbI₂, layer dynamics of high-symmetry crystals with atom-atom interactions 8-71799
- PbI₂ single cryst., EPR of V²⁺, Mn²⁺, Co²⁺ 8-68362
- PbI₂ single crystals, photo-induced AC impedance meas., photodielec. effect 8-52034
- PbI₂, sputtering processes during 6 keV Xe ion bombard. 8-68590
- PbI₂, tight binding band structure using scaled parameters 8-79927
- PbI₂, UV reflectivity meas., band struct., LCAO calcs. 8-72545
- PbI₂-Ag system, effect of bound and free exciton states on light sensitivity (Russian) 8-71169
- Pb₂In₂S₁₇, Pb₂In_{6.67}S₁₃, cryst. struct. (French) 8-63707
- Pb₂KNb₂O₅, SAW props., rel. to device appl. 8-71923
- Pb₂KNb₂O₅, strong electromechanical coupling of SAW 8-63919
- PbMg_{1/3}Nb_{2/3}O₃, ferroelec., cathodolum. spectral and temp. depend. 8-84665
- PbMg_{1/3}Nb_{2/3}O₃, PMN, electro-opt., elasto-opt., opt. and photo-induced props. 8-95560
- PbMg_{1/3}Nb_{2/3}O₃, photoinduced birefr., reversible optical information recording 8-50874
- Pb(Mg_{1/3}Nb_{2/3})O₃-PbTiO₃-PbZrO₃, piezoceramics for high frequency use 8-95555
- PbMg_xNb_{1-x}O₃, ferroelec. with diffuse phase transition, electrostriction-optical props. 8-68457
- Pb₃MgNb₂O₉, crystal growth procedure, meas. electro-optic and dielectric props. 8-88418

lead compounds continued

- Pb₃MgNb₂O₉, diffuse phase transition, Brillouin scatt. and acoustic phonons 8-76401
- Pb₃MgTa₂O₉, crystal growth procedure, meas. electro-optic and dielectric props. 8-88418
- Pb(Mg_{0.5}W_{0.5})O₃-BiFeO₃, dielec. props., cryst. struct. 8-84534
- Pb₂MnO₂, synthesis, chem. stability, use (*French*) 8-80525
- PbMoO₄, Brillouin spectra, photoelastic consts. and optical purity 8-60480
- PbMoO₄ deflectors, beam quality, of acousto-optic frequency shifters 8-79127
- PbMoO₄, investigation of molecular light scatt. 8-72537
- PbMoO₄, refr. index, single crystals having scheelite struct. 8-79082
- PbMoO₄, SAW props. 8-63920
- PbMo₅S₆, supercond. wire prep. by powder technique 8-52705
- PbMo₅S₈ and ternary sulphides, lattice parameter rel. to supercond. T_c 8-52119
- PbMo₅S₈, normal state and superconducting property measurements 8-91660
- PbMo₅S₈, sputtered film, critical current density meas. 8-84369
- PbMo₅S₈, thin films, low temp. normal state, resist., temp. depend. 8-91783
- Pb(NO₃)₂, press. derivatives of elastic-moduli, ultrasonic velocity meas. 8-95102
- PbNb₂O₆, ferroelectric thick crystals, domain formation and dislocation loops 8-60410
- PbNb₂O₆, ferroelectric single crystals, domain struct., cryst. planes, twinning 8-64340
- Pb₂Nb₂O₇, Raman-scattering investigation of vibrational structure 8-76441
- PbO, appl. of effective pots. to relativistic HF calcs. of mol. props. 8-74559
- PbO, content estimation in PZT using analytical procedure (*German*) 8-53279
- PbO, doped, secondary ion emission, at. and mol. processes 8-68588
- PbO film, on Na₂O-B₂O₃ glass, deep penetration of Pb²⁺ ions into glass 8-79535
- PbO film, on vitreous SiO₂, interdiffusion reactions, UV spectroscopy obs. 8-51750
- PbO glass, reflection spectra 8-88325
- PbO layers, crystal platelets orientation and thickness, X-ray diffr. obs. 8-87890
- PbO powder layers, adsorbed rhodamine B dye, charge storage and photocond. 8-64056
- PbO, vapour, photoluminescent decay, a(1) state 8-58745
- PbO-2B₂O₃-Fe₂O₃ glass, Mossbauer study, struct., crystallite formation, broadened quadrupole doublet 8-59761
- PbO-Al₂O₃-B₂O₃ vitreous system with relaxation structure, spinodal decomposition 8-75553
- PbO-Bi₂O₃-GeO₂, exam. of glass forming and liquid phase separation regions, and optical props. 8-88453
- PbO-Ga₂O₃, phase diag. 8-80524
- PbO-K₂O-SiO₂-(Al₂O₃) glass, corrosion in acid, leaching kinetics 8-92378
- PbO-PbSO₄ melts, thermodynamics, determination of free energies of mixing at 1253K 8-83976
- PbO-SiO₂, molten, activity of PbO, effect of CaO, Al₂O₃, MgO and ZnO 8-60663
- PbO-SiO₂ glass, corrosion in acid, conc. profile meas. 8-92379
- PbO-SiO₂ glass, optical coating for GaAs-Al_xGa_{1-x}AS laser 8-71113
- PbO-SiO₂-(Al₂O₃) glass, corrosion in acid, leaching kinetics 8-92378
- PbO-xPbF₂, solvent, solubility of Y₃Al₅O₁₂ and phase formation in system Y₂O₃-Fe₂O₃-PbO-PbF₂-B₂O₃ 8-95247
- PbO₂ and pyrolusite compressed powder mixtures, mixing rules concerning Hall effect and Hall mobility (*German*) 8-84234
- PbO₂, Auger quantitative anal. 8-73104
- β-PbO₂ powders, Hall carrier mobility mixing rule (*German*) 8-52008
- PbO₂, thermal decomposition, heating rate effect, kinetics, mechanism, struct. 8-92473
- Pb₂O₄, IR and Raman study of structural phase transitions (*French*) 8-84582
- Pb₂O₄, isomorphous with ZnSb₂O₄, cell parameters evolution with temp. (*French*) 8-75642
- γ-4PbO.SiO₂, synthesis and struct. 8-71716
- PbO.3B₂O₃.Fe₂O₃, EPR of Fe³⁺ ions 8-72400
- PbO.6Bi₂O₃, IR and Raman spectra, vibr. anal. 8-76464
- Pb₃P₂O₇, flux for RPO₄ growth, solubility 8-95687
- Pb₂(PO₄)₂, EPR study of Mn²⁺ around ferroelastic transition point 8-76303
- Pb₂(PO₄)₂, ferroelastic, switching processes in pulse mech. field 8-59853
- Pb₂(PO₄)₂, nonintrinsic ferroelastic properties 8-91374
- Pb₂(PO₄)₃Cl, pyromorphite, vibr. spectra, normal coord. anal. 8-88305
- Pb₁₀(PO₄)₆(OH)₂, cryst., IR spectra, band assignments 8-60442
- Pb₂(P_xV_{1-x}O₄)₂, phase diagram and crystallography (*French*) 8-92252
- Pb₂Rh₂O₁₅, thick film, temp. coeff. of resist., cond. mech. 8-84315
- PbS, chemisorption of O₂, room temp., UPS and XPS obs. 8-91529
- PbS, epitaxial layer on rock salt substrate, stresses, hydrostatic press. effects 8-51831
- PbS film, polycryst., chem. deposition from soln. and characterisation 8-72743
- PbS, nonstoichiometric, increase of rest pot. with p-type semicond. character 8-56170
- PbS oxide, optical excitation meas. of trap charging surface film (*Russian*) 8-76180
- PbS, thermomech. props., SCF Xa scatt. wave theory 8-71704
- PbS, X-ray determ., Debye-Waller factors, Debye temp. and vibration amplitudes 8-55928
- PbS-As₂S₃ glass, elastic props. temp. depend. 8-71780
- PbS-CdSe, phase boundary processes 8-71857
- PbS-Si p-n heterojunction, characts. and operation, IR detector appls. 8-52075
- PbSO₄, anglesite, crystal struct. and sulphate force consts. 8-83784
- PbS(Se), photoionisation cross section of atomic and final state effects on 5d core levels 8-84699
- PbS₂Se_{1-x} film, prep. by co-evaporation method (*Japanese*) 8-64477
- PbS₂Se_{1-x} film prep. by co-evap., elec. props. (*Japanese*) 8-80470
- Pb₂Sb₈S₁₇, dielectric props. 8-72452
- PbSe, chemisorption of O₂, room temp., UPS and XPS obs. 8-91529

lead compounds continued

- PbSe, complex-composition film production method from vapour (*Russian*) 8-95702
- PbSe, surface, clean and O₂-exposed, XPS and UPS obs., electronic struct. 8-52637
- PbSe, valence band structure from angular resolved photoemission spectra 8-84143
- (PbSe)_{1-x}(SnTe)_x, lattice dynamic props., Gruneisen parameters (*Russian*) 8-83984
- Pb_{0.2}Sn_{0.8}S, Mossbauer spectra, effect of optical emission (*Russian*) 8-60367
- Pb_{0.59}Sn_{0.41}Se, struct. phase transition, temp and hydrostatic press. influence, Hall effect, resistivity (*Russian*) 8-51675
- Pb_{0.975}Sn_{0.025}Se, film, acoustic wave modulation of electron current 8-64067
- Pb_{1-x}Sn_xSe, band inversion effect on phonon spectra 8-79699
- Pb_{1-x}Sn_xSe, determ. of anisotropy coeff. of Fermi surface, magnetoresist. meas. 8-51878
- Pb_{1-y}Sn_ySe-PbSe pulse laser diode, temp. tuning of modes 8-50777
- PbSnTe DH laser, anodic oxide film to avoid degradation by thermal cycling 8-50809
- PbSnTe IR photovoltaic detectors for 8-14 μm range, review (*Italian*) 8-54451
- PbSnTe-PbTe heterostructs., effect of electrical grounding on electron irradiation 8-60194
- Pb_{0.8}Sn_{0.2}Te, hole conc. at 77K from room temp. thermoelec. meas. 8-56155
- Pb_{0.85}Sn_{0.15}Te, narrow band gap, relax. time for Shubnikov-de Haas effect 8-80006
- Pb_{0.85}Sn_{0.15}Te, narrow gap semicond., mag. susceptibility meas. (*Russian*) 8-84397
- p-Pb_{0.82}Sn_{0.18}Te, Hall coeff. sign-inversion temp. 8-52010
- Pb_{0.83}Sn_{0.17}Te, carrier tunnelling through potential barrier in p-n junctions (*Russian*) 8-52074
- Pb_{1-x}Sn_xTe, absorption edge shift, energy gap determ. 8-88308
- Pb_{1-x}Sn_xTe, band struct. and phonon energies, tunnelling spectroscopy 8-72070
- Pb_{1-x}Sn_xTe, Cd-In diffusion, changes in elec. props. 8-91348
- Pb_{1-x}Sn_xTe, continuously tunable electron beam pumped laser 8-50802
- Pb_{1-x}Sn_xTe, electron-phonon interaction 8-71819
- Pb_{1-x}Sn_xTe, grown by LPE, solid-liquid tie line determ. 8-64526
- Pb_{1-x}Sn_xTe, impurity defused IR detector, spectral response depend. on impurity conc. (*Japanese*) 8-58036
- Pb_{1-x}Sn_xTe, lattice instability and phonon lifetimes, neutron scatt. 8-55932
- Pb_{1-x}Sn_xTe, MBE, O₂ uptake, AES, XPS and UPS expts. 8-95227
- Pb_{1-x}Sn_xTe monocrystal and sinter thermoelec. inhomogeneity 8-91713
- Pb_{1-x}Sn_xTe optically pumped lasers, power output and wavelength, 4 to 30K 8-79035
- Pb_{1-x}Sn_xTe, properties and use for making devices, review 8-60131
- Pb_{1-x}Sn_xTe-PbTe, amorphous/crystalline heterojunction, rectification props., IR detector appl. (*Japanese*) 8-60197
- Pb_{1-x}Sn_xTe-PbTe heterojunction, Sn diffusion profile, X-ray diffr. data interpretation 8-51832
- Pb_{1-x}Sn_xTe-PbTe pulse laser diode, temp. tuning of modes 8-50777
- Pb_{1-x}Sn_xTe-PbTe p-n junction, epitaxial, elec. props. and photoresponse 8-56225
- Pb_{1-x}Sn_xY, Y=Te, Se, S, photocond. anisotropy rel. to lifetimes 8-52032
- PbTe (111), adsorption of O₂, UPS and XPS exam. 8-71962
- PbTe, carrier conc. inhomogeneity 8-52019
- PbTe, chemisorption of O₂, room temp., UPS and XPS obs. 8-91529
- PbTe, complex-composition film production method from vapour (*Russian*) 8-95702
- n-PbTe, epitaxial, time dependent negative weak field magnetoresist. 8-64151
- n-PbTe epitaxial film, magnetophonon and Shubnikov-de Haas oscils. 8-60234
- PbTe epitaxial film, stimulated emission, absorption spectra and recombination 8-80409
- PbTe epitaxial layers, orientation on different faces of LiNbO₃ 8-79907
- PbTe, ion-implanted, doping profile evaluation by Hall effect and sheet resist. meas. 8-59831
- p-PbTe MIS capacitors 5 μm IR detector appl. 8-52101
- PbTe, magnetoreflexance of surface space charge layers 8-52475
- PbTe, solidus line anal., carrier conc. 8-75806
- PbTe surface space charge layers, far IR magnetoreflexance meas. 8-64349
- PbTe, TO phonon softening, free carriers and defects effects 8-79720
- p-PbTe, thermoref., 1.0-4.6 eV 8-76492
- PbTe, thick epitaxial film, laser deposition technique 8-68629
- PbTe-SnTe, solid soln. single crystals, TSM growth and elec. characts. 8-68625
- PbTe_{1-x} film, highly absorbant, complex index of refr. determ. method 8-54445
- Pb_{1-x}Te_{2+2x}, solid soln., anionic cond. (*French*) 8-91481
- Pb(Ti₂Zr_{1/2}Fe_{1/2}Ta_{1/2})O₃, pyroelec. props. at transition between ferroelec. phases 8-52447
- PbTiO₃, cryst., polarisation and resistivity, elec. field effects 8-64313
- PbTiO₃, damping of soft E-symmetry phonon, Raman scatt. meas. 8-67799
- PbTiO₃, domain struct. formation during jump motion of phase front 8-64339
- PbTiO₃, ferroelec. ceramic, mech. strength 8-64332
- PbTiO₃, ferroelec. phase, photocond. and photovoltaic effect, temp. depend. 8-95309
- PbTiO₃, ferroelectric ceramic, dielec., piezoelec. and elastic props., orientational contrib. 8-68468
- PbTiO₃, neutron powder profile refinement, temp. depend. 8-51476
- PbTiO₃, perovskite structure, semiconductor props. (*Polish*) 8-56437
- PbTiO₃, piezoceramics for high frequency use 8-95555
- PbTiO₃ single crystals, electroluminesc., elec. field, freq. and temp. depend. 8-80422
- PbTiO₃, struct. changes with temp. variation, rel. to elec. cond. 8-91437
- PbTiO₃-PbZrO₃-In(Li_{1/3}W_{2/3})O₃, piezoelec. ceramic characteris. for surface wave filters 8-95215
- PbTiO₃, photocond. and optical transmission 8-64058

lead compounds continued

- Pb₃V₂O₇, V-O-V bridge stretching freq. correl. with bond angle 8-74636
 Pb₃(VO₄)₂Cl, vanadinite, vibr. spectra, normal coord. anal. 8-88305
 PbWO₄, EPR of radiation induced MoO₄³⁻ centres 8-80217
 PbWO₄, growth by Czochralski method, props. 8-60566
 PbWO₄, rethr. index, single crystals having scheelite struct. 8-79082
 Pb(WO₄)_{1-x}(MoO₄)_x mixed crystal, growth by Czochralski method, props. 8-60566
 PbZn_{1/3}Nb_{2/3}O₃, PZN, electro-opt., elasto-opt., opt. and photo-induced props. 8-95560
 Pb(Zn_{1/3}Nb_{2/3})O₃, perovskite type, high-pressure, high temp. synthesis (*Chinese*) 8-68654
 Pb(Zr,Ti_{0.5}Ge)_{0.5}O₃, antiferro-ferroelectric transition 8-95565
 Pb(Zr,Ti)_{0.5}O₃ ceramic-polyvinylidene fluoride composite film, complex piezoelec. props. 8-64323
 Pb(Zr,Ti)_{0.5}O₃, ferroelec. ceramic, mech. strength 8-64332
 Pb(Zr,Ti)_{0.5}O₃, ferroelec. ceramic, axially loaded, nature of elec. field and resulting voltage 8-72468
 Pb(Zr,Ti)_{0.5}O₃ photovoltaic ferroelectric as optical memory storage medium 8-50877
 Pb(Zr,Ti)_{0.5}O₃, prep. and reactivity from butoxide precursors 8-84749
 Pb(Zr,Ti)_{0.5}O₃ thin layers, tan δ temp. dependence obs. (*Bulgarian*) 8-88259
 PbZrO₃, perovskite structure, semiconductor props. (*Polish*) 8-56437
 PbZrO₃-monocryst., elec. cond., permittivity, polarisation, para- and ferro- to antiferroelec. phase transitions 8-60402
 PbZr_{0.5}Ti_{0.5}O₃, neutron powder profile refinement, temp. depend. 8-51475
 PbZr_{0.95}Ti_{0.05}O₃, impact loading, mech. and elec. response, elec. state effect 8-64317
 PbZr_xTi_{1-x}O₃ solid solutions, tricritical behaviour 8-80296
 Pb(Zr,Ti_{1-x})O₃, temp. coeff. of resonant freq. as function of Zr/Ti composition (*Chinese*) 8-68454
 Pb(Zr_{0.47}Ti_{0.43}Sn_{0.10})O₃:Cr₂O₃, ferroelec. ceramic, reversible characts. and dielectric losses (*Russian*) 8-84517
 PdBi₂O₄, cryst. struct. (*French*) 8-51516
 PdF₂, motionally narrowed NMR line shapes, free-induction decay meas. 8-68406
 SiO₂-PbO-K₂O glass, reflection spectra 8-88325
 Sn_{1-x}Pb_xTe, elec. and struct. props. of epitaxial layers (*Russian*) 8-64147
 Sn,Pb_{1-x}Te mixed cryst., cryst. growth and assessment 8-80463
 Te₈₀Ge_{12.5}Pb_{7.5}, phase-separated system, overlapping effects of glass transition and crystn., DSC results 8-83739

leak detection

- automatic, nondestructive, design, evaluation and implementation for IC assemblies 8-53180
 calibrating test leaks 8-53121
 cardiac pacemaker leak testing methods 8-57133
 EBR-II, Na-water, leak detection system 8-78484
 fission reactor coolant containment tightness, integral leakage rate tests 8-89956
 flaw detection during leak tests, mech. treatment effects 8-60956
 gas leak detection principles and practice 8-81995
 halogen detector with jet probe 8-89490
 halogens, reduction of background effects by means of chromatographic columns 8-70110
 LMFBR, water leaks in secondary cooling circuit boilers 8-86572
 nuclear plant, steam generator heated with liquid sodium, acoustic spectra meas. (*Czech*) 8-54849
 PWR, due to pressure tubes cracking, Pickering power station experience 8-82472
 remote leak detection for Tokamak Fusion Test Reactor 8-50403
 vacuum vessel, large, leak detection 8-74012
 D₂O, on-line infrared analyzers, CANDU report 8-82038
 He leak detection in large cryogenic vessels 8-93694

leakage, electrical see *electrical faults*

leakage, magnetic see *magnetic leakage*

leakage currents

- MHD, compensated, two channel conduction MHD pump with leakage current, obs. (*Russian*) 8-75228
 pacemaker interference, 60 Hz field and current effects 8-88769

least squares approximations

- airborne radiometric data inversion, radioactive elements conc. mapping 8-77347
 array algebra for multilinear least squares prediction and filtering 8-69470
 atmosphere, friction vel. and temp. scale from temp. and wind vel. profiles 8-81268
 caesium hydrogen tartrate, anomalous dispersion of Cs, refined struct. from modified least squares program 8-51522
 crystal structure least squares refinement technique based on fast Fourier transform algorithm 8-91197
 crystallographic refinement, modified least-squares formalisms for overcoming the free-atom bias 8-71632
 crystallography, electron distributions, aspherical-at. least squares refinements combined with Fourier methods 8-71633
 crystallography, X-ray neutron, charge deformation, vibr. smearing 8-71634
 deconvolution of spectra by least-squares fitting 8-64897
 Dirichlet stochastic problem (*French*) 8-89406
 education, least squares fit, uncertainty calc. 8-86068
 electron density mapping in mols., crysts., conf., Rehovot, Israel, (Apr. 1977) 8-71622
 elliptical contact deform. between elastic solids, simplified soln. 8-55616
 force const. adjuster program for least squares fit to observed frequencies of molecules and crystals 8-91395
 formyl fluoride (-d₁), IR absorption intensity anal. 8-70813
 FORTRAN program, lateral absorbed dose distrib. for 25 MeV electrons appl. (*Japanese*) 8-74505
 gamma-ray peak fitting with very low statistics 8-74529
 Gaussian plume model parameters determ. from diffusion-convection eqn. integration 8-81399
 geodesy, props. of Gauss-Helmert least-squares adjustment model (*German*) 8-61309
 guanidinium aluminium sulphate hexahydrate:Cr³⁺, EPR, 295.5, 78.45, 1.61K, zero field splitting 8-68359

least squares approximations continued

- image restoration, constrained least squares, improved computational scheme 8-82915
 ionosphere incoherent scatter data, analytic partial derivatives for least-squares fitting 8-73581
 ionospheric data processing, improvement of convergence of least squares method (*Russian*) 8-85700
 Kolmogorov-Wiener least-squares filters appl. to geophys. anomalies separation 8-61580
 low-count radiation spectra, LSF processing 8-50448
 mass standards, calibration by sets of weights intercomparison 8-54342
 molecular scattering wavefunctions, algebraic approx. 8-78780
 molecular valence force consts., computer program, least squares procedure 8-58656
 optimized conjugate gradient solution for least-squares equations 8-79495
 particles in cylindrically symmetric mag. fields, least squares track fitting method 8-58896
 photographic zenith tube plates, new reduction method 8-73656
 power curve regression equations for Ohio River, statistical computer program 8-61472
 radio meteor wind data, anal. using finite element approximation 8-81475
 satellite-to-satellite statistical orbit determ. error analysis 8-65486
 seismic spectra, least-squares inverse filtering and wavelet deconvolution 8-61339
 space groups, triclinic, cryst. struct. refinement by least squares 8-75607
 spherical dome, three-dimens. elasticity soln. and edge effects 8-59306
 stepwise merging of least-squares parameters 8-89319
 tectonic plate reconstruction method, Pacific-Nazca plate evolution appl. 8-81130
 transient heat conduction, residual method with Lagrange multipliers 8-90630
 X-ray fluoresc. anal., energy dispersive, least squares, Monte Carlo methods, mathematical anal. techniques 8-85243
 2-zinc insulin, rhombohedral, cryst. struct. refinement, experience with fast Fourier least squares 8-92595
 CS₂, solid, tailoring of potentials, in lattice dynamics 8-79679

leather see *materials*

Lecher wires see *high-frequency transmission lines*

Lee model

- tachyon, field model, Lee-like (*Korean*) 8-50058

LEED see *low energy electron diffraction*

legislation

- British Government transport policy criticised 8-55512
 environmental noise, study re. nuclear power plant construction 8-87194
 international metrological cooperation, legal aspects 8-89422
 New York City, environmental noise codes 8-59202
 noise abatement, construction and demolition sites 8-87197
 nuclear fuel storage facility, German Government responsibility (*German*) 8-86701
 radionuclide users in Israel, surveillance and accident prevention 8-57077
 USA, 1977 state noise restrictions 8-59203
 USA, environmental noise control programs 8-59201
 West German LWR power plant stack monitoring, legal and technical aspects 8-89988
 West German nuclear plant airborne radioactive effluent monitoring 8-89990
 U mill radiological effluent and environmental monitoring guidelines 8-94153

length measurement

see also *micrometry*

- automatic interference comparator method, interference refractometer (*German*) 8-77966
 digital micrometer development and appl. 8-65902
 error elimination methods, optical (*German*) 8-70094
 fibre optic strain gauge, arbitrarily shaped path length meas. 8-70112
 holographic interferometry appl. (*Rumanian*) 8-49796
 holographic length comparator using phase heterodyne, appl. to gauge blocks 8-58953
 linear gauge calibration measurements, automatic interference comparator appl. (*German*) 8-77847
 long slip gauge calibration, Fabry-Perot etalon (*German*) 8-77849
 metals and alloys, thermophysical charact., peculiarities of temp. depend., dimensional change meas. (*Russian*) 8-95868
 optical techniques, interferometry, precision (*German*) 8-89434
 piezoelectric material length changes laser interferometry appl., for sub-nano-meter range (*Slovak*) 8-77861
 pneumatic facilities for linear dimension meas., parameter selection 8-73964
 standards, temperature meas. using thermocouples and Pt resistance thermometer (*Slovak*) 8-77907

length standards see *measurement standards*

Lennard-Jones and Devonshire theory see *liquid theory*

Lennard-Jones potential

- n-alkenes, n even, interaction energy at twin boundary, dihedral reentrant, salient angle effect on growth morphology 8-55876
 Bose gas, hard-disc, low density, two-dimens. many-body problem 8-95195
 coupled oscillators, quasiperiodic to stochastic transition 8-54307
 gas, third virial coeffs., empirical eqns. 8-94876
 hard sphere fluid contacting soft repulsive wall, Monte-Carlo method 8-67632
 linear lattice of atoms, Lennard-Jones pot. basis, for teachers 8-61997
 liquids, classical, pair pots. from inelastic neutron scatt. data, self-consistent method 8-59728
 minimum potential energy per particle configuration, one-dimens. system 8-70084
 molecular dynamics simulation of interfacial and co-existence props. at triple point of Lennard-Jones system 8-83916
 molecular fluid, pair correlation function, perturbation theory 8-55799
 molecular fluid perturbation theory, Pople expansion third order term, anisotropic pot. 8-79510
 pressure and temp. consistent Lennard-Jones liq. 8-63647

Lennard-Jones potential continued

- solutions, dilute, Monte Carlo free energy calcs. in isothermal-isobaric ensemble 8-92498
 Stockmayer fluid, mol. dynamics and thermodynamic perturbation theory, mol. polarisability effects 8-71419
 two-dimensional fluid, with 12-6 pot., fourth virial coeff. 8-59723
 BN, hexagonal, long optical vibrs., elastic const. from valence force const. 8-51621
 Cl₂, rot. relax. classical trajectory computation, using Lennard-Jones pot. 8-62880
 Kr, near solidification, 50°C, up to 6500 bar, meas. and simulation using Lennard-Jones pot. (*French*) 8-67301
 N₂, liq., dephasing of mol. vibr. related to correl. functions 8-75523
 N₂, rot. relax. classical trajectory computation, using Lennard-Jones pot. 8-62880
 N₂, thermodynamic and transport props., consistent correlation using Lennard-Jones (12-6) and Buckingham (exp-6) pots. 8-91045
 Ne, equation of state determ., high temp. and pressure, computer expt. 8-75800

lenses

- see also aberrations; aspherical lenses; electron lenses; electrostatic lenses; focusing; magnetic lenses; photographic lenses*
 aberrated lens model of high-energy atm. laser propag. 8-69454
 aberrations calc., third-order, modified relations using Caddington variables (*Czech*) 8-50885
 achromatic doublet design 8-71183
 acoustic holographic lens theory and construction 8-55536
 acoustic lens-filter plate, log-periodic, variation of props. with freq. 8-63256
 annular, Gaussian-beam theory 8-71185
 annular, imaging improvement in type 2, scanning microscope 8-89535
 axicon combined with mirrors and lenses, laser linear, annular and radial focusing 8-66856
 centring monitors design, using variable parameter system (*Russian*) 8-50883
 chromatic aberration first-order theory, secondary spectrum correction with common glasses 8-90382
 conference, optical production technology advances, London, England (Jan. 1977) 8-50954
 contact lens gel materials for extended wear, water flow cond. 8-81062
 convolver, generalised single-lens 8-55303
 cylindrical, prod. of deep-image rainbow holograms 8-71061
 design of lens system with extended depth of focus, Version 14 optimisation program 8-90489
 design of medial copying, high aperture Distagon, photorepeater lenses 8-50888
 design optimisation, Version 14 program 8-90488
 design using cylindrical retractive index distribution (*Russian*) 8-74962
 designing lens system, initial phase significance (*Hungarian*) 8-50881
 diamond smoothing techniques 8-50957
 EM field, in focal region of wide-angular annular lens and mirror systems 8-90485
 eye, lens pigmentation in humans rel. to UV light exposure 8-65100
 eye cataractous lens, NMR study of state of water (*Hungarian*) 8-64986
 eye lens, normal and senile cataractous, PMR study of state of water 8-64987
 fibre connector using low-loss lens system. 8-79107
 fibre lens, plastic focusing, change of ref. index profile during heat treatment process in fabricating 8-83091
 five-component wide-angle pancratic objective design 8-71190
 focus and alignment sensing of a collimated light beam 8-59065
 Fourier transform elements, performance of simple lenses 8-94374
 Fourier transform lens, phase error model 8-71037
 Fresnel, manufacture digital control (*Russian*) 8-50884
 Fresnel lens for thin-film waveguide 8-94452
 geodesic lenses, axially symmetric, design parameters 8-83114
 glass sampling, of simple variants and of multiplets (*German*) 8-90484
 grating lens fabrication for integrated optics 8-75004
 holographic, scanning system, lens design for hologram generation 8-50742
 holographic three-dimensional image prod., reversal method using reflective and lenticular screens 8-90403
 illumination system, lens-array, size calc. 8-59110
 illuminator using laser light source, geometrical optical anal. (*Russian*) 8-79094
 image plane irradiance caused by the natural radiation of the objective lens 8-83068
 imaging system assessment, conference, London, England (Nov. 1976) 8-50718
 incoherent optical processing via spatially offset pupil masks 8-82917
 integral photography, transform of 3-D image produced by lens raster 8-82921
 integrated optics thin-film waveguide lenses, progress 8-66950
 interferometer, two-beam, comparison of refl. and refr. optics in condensing element 8-77968
 intraocular lens implant evaluation 8-81061
 IR heat trap field optics, compact lens-mirror system 8-55422
 IR optical scanning system, narcissus effect suppression, computer results 8-59151
 large-aperture condensing lenses for rainbow holograms 8-78962
 laser rods with negative lenses, distrib. aperture effect 8-66857
 lens-axicon doublet illuminated by Gaussian beam, ring focal pattern 8-55421
 light shielding characts. of lens hood, mol. scatt. calc. 8-71189
 Luneburg thin film lenses, formation by sputtering through circular mask 8-87132
 manufacturing optical components, modern production methods 8-50960
 monochromatic aberrations, third order, correction of four lens objective 8-87123
 MTF measurement, accuracy of spectral response matching 8-50721
 MTF measurement, polychromatic and monochromatic assessment in far IR 8-50899
 MTF measurement for lens test, light source polar intensity distrib. influence 8-50723

lenses continued

- MTF measurement in France, ACOFAM and ACOMAT instruments 8-50727
 multi-element, defective surfaces, tilt meas. 8-66886
 multi-lens focusing systems for energy Nd:glass lasers 8-50848
 objective, concentric, longitudinal spherical aberrations calc. method (*Russian*) 8-71184
 objectives, commercially manufactured, probability analysis of centring accuracy 8-90491
 objectives, high performance, assembling technology, trends (*German*) 8-71182
 ophthalmic, Schott S-1005, static fracture resist. rel. to thickness 8-81063
 optical device performance assessment, British standards 8-50729
 optical relay, system design, secondary colour reduction 8-83067
 OTF calculation using gaussian quadrature, rel. to lens system design 8-90383
 OTF standardisation activities in Netherlands 8-50728
 OTF standardisation in Japan 8-50726
 OTF testing, USA standards 8-50725
 pancratic sights for sporting and hunting guns, design 8-71192
 perfect lens with polarisation masks, OTF 8-90380
 plastic optical components, flexible rapid curing abrasion resistant coated film 8-66890
 plastic optics for optoelectronics, moulding techniques for single, multi-element systems 8-63210
 polychromatic MTF measurement reproducibility 8-50719
 precision objectives, high resolution, image-forming quality (*German*) 8-87120
 production tests for IR lenses 8-50890
 rainbow hologram-by one-step process 8-71062
 refractive index gradient tolerance in optical elements 8-71179
 refractive systems for IR apparatus, design (*Japanese*) 8-55428
 relay optical system, derivation and appl. of Gaussian design relationships 8-94424
 replicated and plastic optics, conf., San Diego, USA (Aug. 1977) 8-66961
 secondary spectrum, of thin three-lens optical systems (*Russian*) 8-57456
 SELFOC for optical fibre communication devices 8-74989
 silicone rubber, room temp. vulcanising, as variable focal length lens 8-66888
 single lens processing system, virtual Fourier transform as analytical tool 8-71036
 solar energy concentrator appls. of Fresnel lenses 8-83065
 spectacle lenses, eye testing using screen image divider 8-57114
 spherical glass beads in highway pavement markings, retrorefl., specular refl. 8-74837
 spherical glass beads in highway pavement markings, retrorefl., diffuse refl. 8-74838
 square Fresnel lens design for illuminating circular solar cells 8-79099
 standard reference lens, for MTF equipment testing in IR 8-50898
 standard reference lenses, for assessment of OTF meas. equipment 8-50897
 star simulator design 8-85814
 Straubel apodisation filters, equivalent passband 8-50880
 stray light reduction from optical components 8-59114
 surface acousto-optic lens, Fourier and Mellin transform props. 8-78926
 surface geometry model, high-speed generating, smoothing and polishing 8-50889
 testing at 1.06 μ m, using laser unequal path interferometer 8-49893
 testing of long-focus optical systems, vibr. insulation of equipment 8-90543
 thermo-gasdynamic control in laser beam guidance, review of developments 8-74942
 transmissive optics for high power CO₂ lasers 8-79057
 travelling wave lens, optically excited soft X-ray laser technique development 8-59016
 ultrashort pulse operations using flat lenses 8-66883
 US, three compartment variable focus 8-94499
 US lens transmission variations and interfacial effects 8-59176
 zoom lens design by pocket calculator 8-55423
 zoom objective, displacement of individual lenses from ideal positions (*German*) 8-71186
 ZTL-180 zenith telescope, objective distortion determ. from visual obs. of star pairs (*Russian*) 8-89068
 Ge, monocryst., for IR optics, prod. techniques and characts. 8-50873

lepton-deuteron interactions

- see also lepton-deuteron scattering*
 d electrodisintegration, Δ resonance admixtures in NN problem, OBE model 8-70373
 e+d, deep inelastic scatt., nucleon structure functions 8-50036
 ed scattering, neutron struct. function extraction, space-time descript. 8-62404
 μ +d, deep inelastic scatt., nucleon struct. functions 8-50036

lepton-deuteron scattering

- see also lepton-deuteron interactions*
 nucleon structure functions from quark distrib. functions anal. of μ p and μ d interactions 8-50035
 ed, quasi-elastic scatt. and form factor of n 8-82210

lepton-hadron interactions

- see also lepton-hadron scattering; lepton-nucleon interactions*
 deep inelastic lepton-hadron scatt. in massive vector gauge models 8-74262
 deep inelastic scattering, contrib. of twist-four operators, struct. functions 8-78187
 deep inelastic structure functions, moments, q^2 analyticity props. 8-78188
 scaling violations, parton model anal. 8-62406
 symmetry principle, history of search for fundamental constituents of matter (*Polish*) 8-54588

lepton-hadron scattering

- see also lepton-hadron interactions; lepton-nucleon scattering*
 electron deep inelastic scattering, very high energy, correlation functions 8-74261
 field theories appl. to lepton-hadron scatt. 8-74257
 massive vector gauge model for deep inelastic scatt. (*Russian*) 8-89720

lepton interactions *see* *lepton-deuteron interactions; lepton-lepton interactions; photon-lepton interactions*

lepton-lepton interactions
see also *electron-electron interactions; electron-positron interactions; lepton-lepton scattering; neutrino-electron interactions; neutrino-neutrino interactions*
Y particle at 9.4 GeV, differential dispersion relations theory of l^+l^- annihilation 8-86424

lepton-lepton scattering
see also *electron-electron scattering; electron-positron scattering; lepton-lepton interactions; neutrino-electron scattering; neutrino-neutrino scattering*
No entries

lepton-nucleon interactions
see also *electron-nucleon interactions; lepton-nucleon scattering; muon-nucleon interactions; neutrino-nucleon interactions*
deep inelastic hadron leptonproduction on nuclei, inclusive hadron final states 8-54741
lepton-proton deep inelastic scatt., two-stage model, parton distrib. and Q^2 depend. 8-66078

lepton-nucleon scattering
see also *electron-nucleon scattering; lepton-nucleon interactions; muon-nucleon scattering; neutrino-nucleon scattering*
No entries

lepton production
see also *electron pair production; muon production; neutrino production*
dilepton and trilepton production in neutrino experiments (Polish) 8-89704
dileptons, via resonance or continuum, momentum depend. explanation using gluons 8-58159
hadron+hadron interaction, Drell-Yan dynamics, lepton pair from $q\bar{q}$ collision, energy scaling breakdown 8-54610
hadron collisions, theory and phenomenology of lepton pair production, review 8-82159
hadron-hadron interactions, lepton pair prod. 8-66138
hadronic massive lepton pair prod., theory review, Drell-Yan model 8-89752
heavy lepton, helicity calculations for prod. in ν interactions and cascade decay 8-93870
high energy ν experimental physics at Fermilab, review 8-50028
high-energy hadron-hadron collisions, lepton prod. with large transverse momentum, SU(6) parton model 8-89673
macroscopic gauge theory of gravity, uniform gravitational collapse, lepton pair creation 8-81724
neutral heavy lepton signatures in ν induced dilepton events, SU(2) \times U(1) model 8-70353
pair prod., hard-scatt., expansion 8-66091
pair production in hadronic collisions, parton model and scaling approach 8-82150
QCD quark-gluon plasma, hadronic prod. of leptons, photons and ψ (Russian) 8-89672
QCD quark-gluon plasma, hadronic prod. of leptons, photons charm and ψ 8-89669
quantum chromodynamics, hadroprod. of lepton pairs and real photons 8-50056
structure function relations, lepton pair processes at large transverse momenta 8-82214
sum rules and moments for Lepton pair production cross section using Drell Yan formula 8-54611
trileptonic prod. by neutrinos, book contrib. 8-78161
 $e^+e^- \rightarrow e^+X^+$, 3.1 to 7.4 GeV, threshold behaviour of $\tau^+\tau^-$ prod. 8-70351
 ν -nucleus reactions, lepton pair production, cross sections, transverse momenta distrib. (Russian) 8-54749
 $\nu_e N \rightarrow \mu^- e^+$, obs. in BEBC 8-78170
 $\nu_e N \rightarrow e^+ e^+$ in heavy Ne, Fermilab results, D^0 prod. and decay 8-89700
pp, prompt lepton emission, 53 GeV, e/π ratio, charm particle total inclusive cross section 8-93914
 $pp \rightarrow \mu^+ e^+ X$, possible charmed meson pair prod., DD cross section 8-89751
 $\pi^+p \rightarrow e^+ X$, 18 GeV/c, expt. results from SLAC 8-89748

lepton scattering *see* *lepton-deuteron scattering; lepton-hadron scattering; lepton-lepton scattering; photon-lepton scattering*

lepton decays
see also *baryon leptonic decay; meson leptonic decay; muon decay*
charmonium state decay, nonrelativistic and relativistic theory 8-58221
heavy lepton, helicity calculations for prod. in ν interactions and cascade decay 8-93870
SU(2) \times U(1) \times SU(2), model for lepton decay and neutrino lifetime 8-62331
 τ decay, large timelike Q^2 , conservation of vector current and current algebra 8-78155
 $\tau^- \rightarrow e^- \bar{\nu}_e \nu_\tau$, branching ratio from e^+e^- annihilation 8-78200
 $\tau^+ \rightarrow e^+ + \nu_e + \nu_\tau$, τ^+ as a paraelectron 8-50024
 $\tau^+ \rightarrow \mu^+ + \nu_\mu + \nu_\tau$, τ^+ as a paraelectron 8-50024

leptons
see also *electrons; heavy leptons; muons; neutrinos; positrons*
bound states of sub-hadronic dimens., quark lepton relation 8-54609
colour model, expt. evidence 8-62350
E6 unified gauge model, breaking patterns, quark-lepton symmetry and mass scales 8-86434
finite spectrum relativistic wave eqn. models of quark and lepton masses 8-74130
lepton-hadron symmetry principle, history of search for fundamental constituents of matter (Polish) 8-54588
lepton-quark system, quantum number laws, classification of weakly interacting particles, decays 8-82138
mass, SU(3) \times SU(3), as gauge groups of weak and associated charges, symm. breaking 8-74175
mixing of leptons with different quantum numbers in gauge theories of weak and EM interactions (Russian) 8-54601
preon model for hadron and lepton struct. 8-78124
quarks and leptons, fermion physics in terms of SU(2) \times SU(1) gauge theory 8-74197
quaternion model, gauge theory (Russian) 8-62315
seven lepton model, quantum flavour dynamics, mixing angle, masses, spontaneous symmetry breaking 8-89652

leptons continued
SU(4) \times U(1) as gauge symm. for quark, lepton quartets, weak and EM interactions, weak currents 8-74174
unified field theory bounds on number and masses of quarks and leptons 8-58151

level crossing (energy) *see* *energy level crossing*

level measurement
liquid level monitor with optical coupler isolation (German) 8-73963
rivers/open channels, remote sensing, cross correlation technique 8-57328
water level short-term meas., laboratory systems 8-93654
He level detector for pumped bath 8-49843

level meters
see also *power measurement*
equivalent continuous noise level meter requirements 8-83195

levels, energy *see* *energy states*

libraries
Japanese Evaluated Nuclear Data Library, first version evaluation (Japanese) 8-74428
Royal Astronomical Society, catalogue of archives and manuscripts 8-69705

LIDAR *see* *optical radar*

Lie groups
see also *elementary particle symmetry*
affine Lie algebra $A_1^{(1)}$, explicit construction 8-89626
analytic continuation of the Fourier Series on connected compact Lie groups 8-93511
classical limit for quantum theories defined by real Lie algebras 8-65807
coherent states and induced representation 8-49713
connection set of principle bundle over 4-sphere with nonabelian Lie group, gauge transform. 8-58108
contracted Lie algebras, Saletan and Levy-Nahas contractions 8-73825
cosmic-ray eqn. of transport, steady-state, nonenergetic-source soln. 8-96366
covariant coherent states for quantized systems with nilpotent symmetry group (German) 8-73865
currents in Su(5) and E_7 unified gauge theories 8-54600
disconnected gauge groups and the global violation of charge conservation 8-78086
discrete finite nilpotent Lie analogs: new models for unified gauge field theory 8-66025
dual model superconformal group, isomorphic function, Fock space representations 8-74230
dynamic nonlinear systems containing limit cycles 8-77666
 E_7 exceptional group, calc. of 6, symbols 8-57800
energy-momentum tensor, effect of motions, meson field and perfect fluid 8-73903
exceptional gauge theories in 3 \times 3 matrix formalism 8-70248
finite affine extensions of supersymm., graded Poincare Lie algebra 8-70300
first theorem of Lie in locally convex space 8-77664
Galilei relativity in Newtonian mechanics, possible Lie admissible covering 8-73838
gauge field theory, loop phase factor approach, equivalence problem, space-time symm. (Chinese) 8-82110
generalised coherent states, irreducible representations of Lie groups, anal. and applications 8-62114
generalised superalgebras, Lie structs., Z_n+Z_n grading 8-78106
graded Lie groups SU(2,2/1) and OSp(1/4), finite transform. 8-57735
graded spin extension of the algebra of vol. preserving deformation 8-65855
group invariant linear partial differential operator, form, Lie transform investigation (German) 8-89297
harmonics on 3-sphere, Lie group SU(2) 8-57813
Inonu-Wigner contractions of the real four-dimensional Lie algebras 8-77667
isometry Lie algebras, new technique for struct. anal. 8-65831
isoscalar factors, on noncanonical bases 8-81797
Kepler motion, generalised, Lie groups of motor integrals 8-85831
kinematical groups and coord. transformations using light-cone frame 8-81796
Klein-Gordon eqn. and Poincare group 8-62292
Lie admissible algebra and nilalgebra, recent developments 8-74168
Lie admissible quantisation in a self-interacting scalar field theory, deformation distrib. 8-74169
liquid theory, classical spin system, absence of ordering 8-51402
Lorentz group irreducible representations, generalised function expansion with light cone support 8-70018
Lorentz groups on skew symmetric tensor space, nonlinear realisations of direct product 8-62329
matrix canonical realisations of o(m,n) group, Casimir operators 8-81795
minimal coupling, symplectic mechanics of classical particle in Yang-Mills field 8-74136
Newton-Wigner position operator, non existence for quanta with zero mass and nonzero helicity 8-62099
noncommutative algebra, two point function calcs. 8-57734
noncompletely reducible representations of the Poincare group associated with the generalised Lorentz gauge 8-70249
nonflexible Lie-admissible algebras, struct. and classification 8-93812
nonlinear Lagrangians and spontaneous symm. breaking 8-70303
nonlinear wave eqns. and covariance 8-49715
nonuniform plasma, mode coupling, Lie operator calcs. 8-55718
nuclearity of C^∞ vector spaces in induced inhomogeneous Lie group representations 8-86422
optical group Opt(3,1) and its subgroups 8-77759
parafermion representations of Lie-algebra chain $O_7 \supset G_2 \supset SU_3$ 8-74173
path integral and quasiclassical asymptotic behaviour on Lie group 8-54230
Poincare and Galilei groups in arbitrary dimensional spaces 8-77672
projection operators for semisimple Lie groups 8-69963
projective Lie algebra of Lorentz group, homographic transform. 8-57739
QFT, BRS transform. 8-93591
quantum field Lie-admissible local powers, incompatibility with Wightman axioms and spin statistics theorem 8-93793
R-separable solutions of wave eqn. $\psi_n - \Delta_3 \psi = 0$ 8-62293
recurrent Lie group classification (French) 8-62047

Lie groups continued

- representation theory, topological methods (*Russian*) 8-54148
- semi-simple algebras of rank $l=2$, practical form of Freudenthal formula (*French*) 8-86112
- semisimple graded Lie algebra ($Sp(2N;2N)$), fourth degree Casimir operator 8-65750
- semisimple Lie algebras, natural topology for linear representations (*French*) 8-77665
- $Sp(8,R)$, Lorentz subgroup anal. and null plane boson realisation 8-62116
- special relativity, group hypothesis, transformations with singularities 8-49655
- spinor Lie derivative, geometric significance 8-65749
- spinor Lie derivative, geometric significance 8-73826
- step operators, Lie algebraic props. 8-62052
- $SU(2)$ instanton, physical interpretation of degrees of freedom 8-62312
- transform, approach to classical perturbation theory, plasma physics appl. 8-93510
- transitive dynamic systems, polhode concept generalisation (*French*) 8-62065
- unitary representations of general covariant group algebra, Lie algebra 8-58136
- van Est theorem for groups of diffeomorphisms 8-93811
- weak Hamiltonian inversion in an algebra (*Spanish*) 8-54150
- weight multiplicity for unitary groups, program 8-74166
- Weyl quantisation and metaplectic representation 8-49712
- X-Y model, generalised, Lie algebra appl. 8-77806

ligand field theory *see bonds (chemical); crystal field interactions; molecular energy levels*

light

see also airglow; optics; sunlight; zodiacal light

- deflection by Sun, principle of equivalence calcs. 8-81729
- gravitational bending, rel. to meas. of parallaxes of objects at cosmological distances 8-53796
- gravitational bending, work of Johann Georg Soldner (1776-1834) 8-81787

light absorption

see also atmospheric optics; densitometry; light transmission; optical constants; optical films; optical filters; pleochroism; spectra

- 8-61421
- aerosols with organic constituents, effect on fog and clouds 8-73465
- algal suspensions, light scatt. and absorpt. props., 380-720 nm 8-92604
- anthracene, in stretched polyethylene film, UV-visible and fluoresc. spectral shifts 8-62852
- atmosphere, 0.63 μm attenuation and directional scatt. in droplet and cryst. clouds (*Russian*) 8-96292
- atmosphere, aerosol content determ. from photometric obs. of stars 8-92976
- atmosphere, attenuation coeffs. rel. to aerosol particle size distrib. statistical characts. (*Russian*) 8-53702
- atmosphere, extinction coeffs. at Wise Observatory rel. to photoelectric photometry 8-73657
- atmosphere, incoherent optical propag., effects on optical/optronical systems 8-92987
- atmosphere, molecular absorption, Lowtran 3B model 8-85690
- atmosphere, visible and near IR attenuation exponents up to 30 km, experimental profiles (*Russian*) 8-61558
- atmosphere aerosol attenuation, influence on atmospheric and oceanic temp. determ. by remote sounding (*Russian*) 8-81430
- atmosphere water vapour, IR continuum absorpt. calc. (*Russian*) 8-96293
- atmospheric 8 to 12 μm IR emission attenuation obs. (*Russian*) 8-61556
- atmospheric absorption of solar, diffuse and reflected visible radiation (*Russian*) 8-96291
- atmospheric laser beam propag., monochromatic, problems 8-92988
- Beer-Lambert modified law calc. 8-82906
- biological structures, light absorpt. and orientation of absorpt. momenta 8-53326
- black surfaces, visible and near-IR meas. using calorimetric method 8-93685
- cell high-speed analysis, laser absorpt. and scatt. meas. (*German*) 8-92687
- chloroplast thylakoid, light-induced absorbancy and scatt. changes about 520 nm rel. to struct. 8-69019
- degenerate four-wave mixing in absorbing media 8-71138
- diffraction grating anomalies and energy absorpt., rel. to surface waves, general theory 8-94447
- Earth atmosphere, absorpt. determ. of 460 μm 8-96295
- electrolytic double layer, light absorpt., electrochromic changes 8-84551
- electron-ion plasma, stimulated bremsstrahlung light absorption (*Russian*) 8-87438
- ethane, photoabsorption cross sections, 1380 to 1600 Å, at 295 and 200K 8-90181
- fine interference layers, absorpt. coeff. determ. method (*Russian*) 8-82908
- fingerprint material, IR spectrum 8-78056
- G333.6-0.2, G298.2-0.3, compact H II regions, IR emission lines rel. to extinction 8-96522
- galactic interstellar extinction law, vars. 8-85990
- interstellar absorption effects on Balmer discontinuity strengths 8-89238
- interstellar dark nebulae, visual extinctions determ. via star counts 8-57612
- IR absorption mechanisms for crystals 8-80329
- IR band nonrigid rot. absorption, appl. to CO, NO, N₂O and CO₂ 8-91060
- IR radiation spectral absorbance and transmittance, accurate modelling technique 8-91062
- laser light with time-varying intensity in optical medium, temp. field kinetics 8-59098
- lidar observations of smoke and dust clouds at 0.7 and 10.6 μm wavelengths 8-69459
- Maxwell Garnett theory, validity range 8-68507
- metal, surface roughness effect on light absorptivity 8-80314
- metal-dielectric interface, p-polarised light total absorpt. by surface plasma waves 8-88373

light absorption continued

- methane, photoabsorption cross sections, 1380 to 1600 Å, at 295 and 200K 8-90181
- optical fibre attenuation meas. instrument 8-59138
- optical waveguide, multilayered, effect of material absorpt. on ray power attenuation 8-83103
- Orion Nebula, visual interstellar extinction from search for vibrationally excited H₂ emission 8-93346
- photoresist, Shipley AZ-1375, sensitivity and nonlinearity at 441.6 and 457.9 nm 8-90475
- photosensitised reacts. in continuous chem. processes, scatt. effects 8-73057
- plant canopy light absorption model with application to wheat 8-88913
- plexiglass, red, gamma dose meas. by optical absorpt., elec. conductivity, and mechanical hardness 8-55045
- PMMA, light absorption, laser crack development 8-68780
- quasars, props. of $Z_{abs} > Z_{em}$ systems rel. to origins of QSO absorpt. line systems 8-57682
- quasars absorption lines origin, evidence for cosmological hypothesis 8-57684
- resonance fluorescence of thin crystal films, superradiance 8-68573
- sea water, hydroptic struct. variability in S. Atlantic regions (*Russian*) 8-77262
- seawater off Ireland west coast, surface waters colour, UV absorbance and salinity 8-85603
- semiconductor, collective excitations of electrons and holes in strong EM field and absorpt. of light (*Russian*) 8-79945
- single-layer film 2.8 μm , 3.8 μm absorpt. meas. 8-90463
- soot-gas mixture, in luminous flames and smoke, IR mean absorption coeffs. calc. procedure 8-91061
- spectrophotometer attachment for fused salt absorption spectrum registration 8-86353
- spectroscopy quantum chem. teaching, fluctuating elec. dipoles, light absorpt. 8-73802
- stratosphere, solar radiation absorption, in O₂ Herzberg continuum, influence of O₄ and O₂N₂ dimers 8-87429
- superconductor, nonlinearity of single-photon absorption near threshold (*Russian*) 8-91815
- superposition photometer for material absorptivity meas. 8-89522
- transparent dielectric with radioimpurities, intense radiation absorption (*Russian*) 8-74939
- turbid media, approx. linear relationship for optical response 8-90371
- Venus clouds, H₂SO₄ aerosol medium IR absorpt. and extinction coeffs. 8-65526
- Ag, absorpt. coeff. temp. depend., IR, 3 to 30 μm 8-74953
- Ag, ellipsoidal small particle assembly absorption spectra, optical model (*Russian*) 8-60483
- Au, absorpt. coeff. temp. depend., IR, 3 to 30 μm 8-74953
- CF₃I, I laser medium, UV absorption profile modification by vibr. excitation, for fusion ignition 8-58717
- CdS, chem. sprayed film, struct. and morphology 8-72020
- CdSe, meas. of partial press., by optical absorption method (*Japanese*) 8-51661
- CdSe, photosensitivity of elastic properties 8-92049
- CdTe, meas. of partial press., by optical absorption method (*Japanese*) 8-51661
- CdTe, single cryst. IR laser window, low absorption at 10.6 μm 8-79081
- Cs-He, new absorption/emission bands perturbed Cs transitions assignment, pot. energy curves 8-66486
- Er, paramagnetic and antiferromagnetic states, optical absorption (*Russian*) 8-56497
- GaAs, absorption coefficients, method of meas. 8-83048
- Mg-MgF₂, sputtered films, opt. props. 8-80430
- S₂F₁₀, IR laser irradi., absorpt., reaction parameters 8-94241
- Si, beam extinguishment device, without scatter 8-87126
- XeF* laser mixture, Ne- and Ar-rich, absorption 8-63062

light absorption spectra *see spectra*

light amplifiers *see image intensifiers*

light attenuation *see light absorption; light scattering; light transmission; optical dispersion*

light coherence

see also laser beams; lasers

- AC Josephson-Fiske effect, coherence 8-88082
- ambiguity function in diffraction and isoplanatic imaging by partially coherent beams 8-78925
- atmosphere, light beam coherence through optically dense turbid layer 8-55300
- atmospheric propagation of partially coherent radiation 8-65386
- atom and molecule dipole transition, transient behaviour in intense laser field (*German*) 8-66520
- black body radiation, anisotropy and temporal coherence 8-58904
- coherent optics fundamentals 8-78910
- correlation coeffs. of planar sources and their far fields 8-66750
- Dicke model Hamiltonian, coherence props. of radiation field 8-58959
- dielectric waveguide, EM field coherence 8-59145
- four-point field coherence function meas. in laser random focusing region (*Russian*) 8-58910
- Fourier optical processor phase accuracy, coherence effects 8-90377
- Fourier transform optical pulse spectroscopy, coherent transients 8-86974
- Gaussian aperture operating in partially coherent light, two-point resolution 8-78918
- generalized partial coherence of a radiation source and its far-field 8-58903
- holographic interferometry, double exposure, partial coherence effect (*German*) 8-82932
- holography, coherence relaxation methods 8-78977
- holography through fog, coherence requirements for light source 8-58949
- image processing, noise fluctuations and coherence 8-66771
- imaging system using intensity triple correlator 8-74846
- incoherent circularly symmetric source, sampling theorem for complex degree of coherence (*French*) 8-79088
- inhomogeneous source radiant intensity, averaged cross-spectral density concept 8-74958
- intensity distrib., far field laser and partially coherent sources, comparison 8-66751

light coherence continued

- laser beam, single-pulse, spatial characts. control 8-79058
- laser beam transmission through fibre light guide, spatial coherence 8-71133
- laser excitation, stepwise, coherent Schrodinger vs. incoherent rate eqn. approaches 8-74871
- laser radiation, measurement problems (*German*) 8-79052
- liquid crystal, far-field coherence and radiant intensity of scatt. light 8-64372
- maximum entropy of EM fields with given degrees of coherence 8-50697
- molecular optical spectroscopy, by 90° photon echo, during reson. scatt. and radiationless transitions 8-86978
- nonlinear media, coherence oscillations, coherent state lifetime 8-66862
- optical data processing extension to space-variant and nonlinear operations 8-78940
- optical equivalence theorem, new type of discrete diagonal coherent state representation 8-55328
- partially coherent imagery, calc. method 8-90373
- radiometry and coherence, basic concepts 8-66745
- rhodamine 6G water soln. laser with spatial lamp pumping, spatial coherent emission 8-82963
- ring laser, coherence theory, counter-rotating laser modes 8-55387
- scalar wave fields of fluctuating primary planar sources, coherence and radiant intensity 8-90355
- semiconductor laser pulse radiation, coherence rel. to Fourier hologram recording 8-50738
- simulation experiment 8-73810
- space-angle characteristics, improvement by interference method (*Russian*) 8-78909
- speckle interferometry, coherence requirements, use of thermal radiation sources 8-49891
- speckle pattern superposition and coherent background, statistical props. (*Chinese*) 8-90368
- stellar holographic interferometric technique, mutual coherence function 8-53838
- p-terphenyl-pentacene, optical dephasing, optical mixing-detected ps photon echoes obs. 8-71155
- two-photon absorption, from polychromatic stationary radiation field, light coherence 8-74626
- undulator linac, electron dynamics, coherent radiation source 8-82539
- KrF laser beam, Raman pulse compression, for fusion expts. 8-59086
- MnF₂, two-exciton many photon absorption, effect of statistical props. of light on intensity (*Russian*) 8-95589

light communication *see* optical communication**light cones**

- see also current algebra*
- deep inelastic processes book contrib. 8-82222
- differential scatt. cross section, influence of amplitude singularities 8-49984
- EM two-body interaction theory 8-49739
- field theory and the parton model, book contrib. 8-82220
- finite normal products, perturbative Green's function method 8-86408
- kinematical groups and coord. transformations using light-cone frame 8-81796
- Lorentz group irreducible representations, generalised function expansion with light cone support 8-70018
- optical group Opt(3,1) and its subgroups 8-77759
- Poincare and Galilei groups in arbitrary dimensional spaces 8-77672
- relativistic Hamiltonian theory in light like case, unitarity and causality conditions 8-78112
- spectral function sum rules for quark and baryon fields, using lightlike charges 8-93822

light diffraction

- see also holography; optical zone plates*
- aberrations of diffracted wave fields 8-94376
- acoustically induced, diff. by two adjacent parallel US waves, soln. of boundary value problems 8-90358
- acousto-optic frequency shifter, beam quality, heterodyne interferometry meas. 8-79127
- ambiguity function in diffraction and isoplanatic imaging by partially coherent beams 8-78925
- aperture shaping, diffracted energy spatial distrib. control, computer analysis 8-59152
- biological cell diff. pattern, Fourier optical extraction of morphological parameters 8-92749
- Bragg and Raman-Nath diff. regimes rel. to grating thickness 8-71028
- causality principle 8-55295
- crossed lamellar transmission grating, exam. of diff. props. 8-59139
- cylindrical light beam diff. on wideband US signal 8-50698
- dielectric coated gratings, general integral theory 8-66909
- dielectric waveguides, optoacoustic interaction, Raman-Nath type diff. 8-87153
- diffractor size and shape determ. from diffracted light 8-78901
- dispersive media, Ewald dynamical diff. theory extinction theorem 8-66749
- education, diffraction pattern display using photodiode array 8-86069
- elastic surface wave parallel to light beam, expt. investigation 8-82904
- electron microscopy, HV, accurate stigmating using optical diff. pattern of micrograph 8-49941
- Fabry-Perot, and confocal resonators, comparison of diffraction formulas 8-87077
- fibre type light shield with absorbing cladding, Fraunhofer diff. 8-90521
- Fraunhofer, optical system with annular pupil, use of orthogonal polynomials 8-50714
- Fresnel images, form. of 2-D transparencies with extended periodic struct., theory 8-82920
- Gaussian beams, off-axis, aberrated Fraunhofer diff. patterns 8-66753
- holographic interferometric anal. of boundary diff. wave (*German*) 8-63041
- holography, diffraction efficiency, depend. on size of developed Ag particles 8-78965
- holography with evanescent waves, diff. efficiency, TE polarisation 8-66782
- holography with evanescent waves, diff. efficiency, TM polarisation 8-66783

light diffraction continued

- Huygens-Fresnel integral in circular coords., asymptotic soln. 8-87013
- images of bar and edge objects, influence of optimum balanced coma 8-74850
- imaging system using intensity triple correlator 8-74846
- infrared surface with random nonuniformities, light diff. (*Russian*) 8-58916
- inhomogeneous plane wave shadowing by an edge 8-90356
- intense laser beam diffraction by long US wave in liquid column 8-60421
- IR detector dimensions, rapid meas. by Fresnel diff. (*French*) 8-89435
- IR optical system input diff. effects and use of spatial apodisation 8-79113
- laser, appl. to meas. of acoustic and acousto-optic props. of crystals (*Polish*) 8-76425
- laser beams, geometrical optics, spatial structure 8-83014
- metaxial optics, centred refracting systems, undiaphragmed and without aberration (*French*) 8-94369
- metaxial optics, diffraction (*French*) 8-74844
- methylammonium aluminium sulphate, third order elastic const. from stress shifted reson. freqs. 8-55905
- monodisperse screen shape determ. using scatt. indicatrix in Fraunhofer diff. 8-71033
- multispectral extinction data, analytic inversion in anomalous diff. approx. 8-87016
- muscle crossbridge stroke and activity revealed by optical diff. 8-69021
- object diffraction evaluation in transmission microscope, object and field stop spectrum separation (*German*) 8-92685
- off-axis gaussian beams in optical system with astigmatism and coma 8-55309
- opaque crystals, dynamical light diff. 8-80368
- optical fibres, laterally illuminated, diff. pattern 8-50915
- optical power spectrum meas., error sources in diff. pattern sampling 8-63030
- optical signal recording/processing, diffraction in anisotropic medium, anal. 8-90364
- particle sizing by forward lobe scatt. intensity ratio, diff. theory errors 8-71031
- plane uniformly heterogeneous wave diff., exam. using Fraunhofer's method (*French*) 8-58901
- quartz substrate, surface and bulk acoustic waves excited by interdigital transducers, optical diff. study (*Chinese*) 8-50965
- reimaging system, out-of-field radiation analysis 8-59117
- scattered light, specification and meas. from diff. gratings 8-78905
- sieve screens, two-dimens. array, diff.-interf. patterns, Kirchhoff approx. 8-83088
- solar domain gratings, asymptotic theory 8-66910
- stray light phenomena, GUERAP III Monte Carlo simulation 8-58907
- stray light simulation with advanced Monte Carlo techniques 8-58906
- stray radiation rejection capabilities of optical systems, GUERAP II program analysis 8-59115
- surface acoustic wave diff. of light beam propag. parallel to surface 8-66752
- thin unbleached holograms, diffraction efficiency, relief phase modulation 8-66789
- thread parameters meas., Fraunhofer diff. coherent optics method 8-89439
- US beam in homogeneous isotropic dielectric plate, anal. 8-82905
- CsAl(SO₄)₂·12H₂O, third order elastic const. from stress shifted reson. freqs. 8-55905
- Hg₂, photoassoc., 0_u⁺→0_g⁺ fluoresc., Condon internal diffraction 8-78747
- KAl(SO₄)₂·12H₂O, third order elastic const. from stress shifted reson. freqs. 8-55905
- NH₄Al(SO₄)₂·12H₂O, third order elastic const. from stress shifted reson. freqs. 8-55905

light diffusion *see* light scattering**light dispersion** *see* optical dispersion**light emitting devices**

- see also light emitting diodes; light sources; luminescent devices*
- No entries

light emitting diodes

- see also semiconductor junction lasers*
- analog modulation of light-emitting diodes for optical fiber (*Japanese*) 8-90516
- coupling to optical fibres improved using facet radiator 8-90520
- coupling to spherical ended fibre, geometrical optics anal. 8-83086
- degradation, review of recent expts. 8-82970
- electroluminescent diode, laser measurement, of semiconductor materials and devices (*Rumanian*) 8-52035
- fibre optics systems, technology and components (*Hungarian*) 8-66900
- half-duplex optical transmission link using LED source-detector scheme 8-71214
- IR, industrial appl. of fibre optics 8-59123
- junction current, luminesc. near dislocation, surface, integral representations, appl. to LED's 8-68079
- luminous intensity ang. distrib. and total light flux meas. device (*Chinese*) 8-82018
- optical fibre, communication link between computer units, using LED-photodiode pair 8-71224
- picture taking parameters display in amateur cameras, review 8-89578
- safety aspects of LED- and laser-fed cables 8-74968
- safety aspects of LED- and laser-fed cables 8-74969
- scintillation counter hodoscopes, LED test system 8-58556
- semiconductor heterostructures, elec. and optical phenomena, discrete devices, review 8-72250
- semiconductor light sources principle and appl. (*German*) 8-71108
- stellar magnitude simulator, IC device 8-81742
- thermal imaging system for Earth resource obs., possibility of LED use 8-93010
- transient response of DH devices approx. techniques 8-68078
- Al-Ga-As heterostruc. with confined current flow, fabrication 8-68081
- Al_{0.5}Ga_{0.5}As DH p-n junction, surface recomb. effects on current, luminesc. expts. 8-72246

light emitting diodes continued

- Al,Ga_{1-x}As heterojunction LED, fabrication by negative profiling of substrate and charact. 8-56523
 GaAs, luminous intensity ang. distrib. and total light flux meas. device (*Chinese*) 8-82018
 GaAs:Zn, diffused, depth profiles obs. by photoluminesc. 8-72587
 GaAs-GaAlAs DH LED, transient current trap spectroscopy 8-80049
 GaAs-GaAlAs LEDs, deep levels (*French*) 8-56218
 GaAs_{1-x}P_x, VPE on Ge substrate, and LED charact. 8-72736
 GaP:Fe_{x-1}, luminous intensity ang. distrib. and total light flux meas. device (*Chinese*) 8-82018
 GaP LED degradation, effect of γ -irradiation 8-95610
 GaP, luminous intensity ang. distrib. and total light flux meas. device (*Chinese*) 8-82018
 GaP p-n junction, capacitance-freq. dispersion and electroluminescence efficiency 8-64101
 GaP:N LED, acoustic emission, NDT of dislocation motion 8-91759
 GaP:Zn, growth, I-V charact., electroluminesc. (*Korean*) 8-52653
 In_xGa_{1-x}As, thick LPE growth, electrolum. obs. 8-60589

light filters see optical filters**light intensifiers** see image intensifiers**light interference**

- see also light interferometers; light interferometry; Moire fringes
 band-pass interference filters, D(2HL)^m2H struct., transmissivity 8-83096
 coherent radiation space-angle characteristics, improvement by interference method (*Russian*) 8-78909
 Fabry-Perot etalon, fringes formed when unfocused, point illumination 8-86322
 filter steps, wide angle interf. polarisation, made from various cryst. types 8-87156
 filters, direct, quasi-telescopic and telecentric combinations with large astronomical Schmidt cameras 8-57441
 fine interference layers, absorpt. coeff. determ. method (*Russian*) 8-82908
 laser frequency control by spectrally depleted destructive two-beam interf. 8-74941
 laser nonstationary generation induced interference pattern phase distortion, holographic meas. 8-58945
 layer with exponentially varying refr. index, oblique incidence of light, interf. matrix 8-55296
 liquid film, thermal interf.-optical excitation of US waves 8-71794
 pattern fluctuation statistics in turbulent atmospheric layer 8-53727
 PMMA, optical interference meas. of critical crack tip displacements 8-84964
 PVC, optical interference meas. of critical crack tip displacements 8-84964
 sieve screens, two-dimens. array, diff.-interf. patterns, Kirchhoff approx. 8-83088
 spatial interference influence on amplification in stimulated scatt. 8-71149
 speckle, two radially shifted patterns, interf. rings 8-90359
 surface velocity meas. using laser beams 8-49806
 Al₂O₃ based ceramics, ladder structures, interference phenomena explanation 8-72898
 Cd₂SnO₄ selective coatings, optical absorpt. edge 8-83046
 NaNO₂, vibr. spectrum, interference effects 8-87752
 Si₃N₄, reaction bonded, ladder phase, interference phenomena explanation 8-72898
 VO₂ interference films, colour valencies as function of thickness and phase change (*German*) 8-56533

light interferometers

see also light interferometry

- 90° phase shift beam splitter for displacement interferometer 8-87145
 amplitude interferometer, white light, 180 degree rot. shear astronomical appl. 8-77977
 angle etalon constr., angular scale, polygon calibration appl. (*German*) 8-77852
 angle meas. appl. (*Czech*) 8-49794
 astronomical long-baseline amplitude interferometer, pupil space design 8-53832
 autocollimating telescope calibration, laser interferometer appl. (*German*) 8-77853
 automatic fringe counting, independ. of signal level changes 8-58018
 automatic interference comparator for precision length measurement, interference refractometer (*German*) 8-77966
 balloon borne interference spectrometers operation and appl. to solar UV obs. (*Japanese*) 8-57442
 beam splitter phase coatings, for producing phase quadrature interferometer outputs 8-77974
 chopper for deep space IR interferometer/spectrometer 8-81545
 convection measurement, differential interferometer with achromatic $\lambda/2$ compensation 8-87419
 creep rate determination using Michelson interferometer 8-68856
 digital wavemeter for CW lasers 8-89447
 distance meas. using laser interferometer, principles and performance 8-89442
 divider phase distortion compensation improvement 8-58073
 double beam Michelson interferometer meas. of small linear displacements 8-73966
 double diffraction interferometer, optical path difference meas. appl. (*Japanese*) 8-82025
 dual laser interferometer for plasma density measurements on large Tokamaks 8-71542
 Fabry-Perot, automatic periodic alignment by microprocessor (*French*) 8-86872
 Fabry-Perot etalon, fringes formed when unfocused, point illumination 8-86322
 Fabry-Perot etalon, optical thickness error compensation 8-49889
 Fabry-Perot etalon arrangement, precision length calibration of long slip gauges appl. (*German*) 8-77849
 Fabry-Perot interferometer, for Raman spectrometers 8-74063
 Fabry-Perot interferometer, microcomputer stabilisation 8-74055
 Fabry-Perot interferometer, wavefront form. by multilayered dielec. mirror 8-54449
 Fabry-Perot nonideal interferometer, instrum. contour 8-82027
 Fabry-Perot nonlinear electro-optic device, using refl. light feedback 8-55457
 Fabry-Perot interferometer, with automated data acquisition and stabilisation system 8-70180

light interferometers continued

- fibre optic heterodyne interferometer for vibr. meas. in biological systems 8-77101
 fibre optic ring interferometer gyroscope, Fresnel drag effect 8-79142
 fibre waveguide laser interferometer 8-49892
 filamentary spatial filter interferometer, appl. to phase meas. 8-49890
 Fizeau wavelength meter, laser and other monochromatic sources, digital display 8-89450
 heterodyne quadrature interferometer for simultaneous measurements of plasma density along several chords 8-67416
 high precision laser freq. meas., sigmameter, motionless two-channel Michelson interferometer 8-89449
 holographic, for optical glass homogeneity determ. 8-90401
 internal gauge, microinterferometer IZK-61 8-89438
 IR point diffraction interferometer, fabrication and use at 10.6 μ m 8-86325
 IR scanning interferometers 8-82026
 Jamin, for interferometric saturation spectroscopy 8-74079
 Jamin double-beam, two-dimens. image transmission through inhomogeneous medium 8-50706
 lamellar-grating interferometer, balloon-borne, appl. to solar brightness temp. meas. 8-85921
 large angle laser interferometer for 'curved' crystal spectrometer, precision 8-77973
 laser CW digital wavemeter, moving cube-corner interferometer system 8-50840
 laser interferometer, acoustic vibration meas. 8-71253
 laser interferometer, thickness meas. in nuclear track detectors 8-86735
 laser interferometer for detecting biological signals due to displacement (*Italian*) 8-53467
 laser interferometer for meas. linear vibration report 8-86243
 laser interferometer with path difference up to 1 km, geophysical appl. 8-61616
 laser pulse shaping by nonlinear interferometers 8-59097
 laser stethoscope, non-contact high sensitivity, using interferometer technique (*German*) 8-69176
 laser unequal path interferometer, for lens testing at 1.06 μ m 8-49893
 length measurement, precision (*German*) 8-89434
 Mach-Zehnder, as optical Fourier processor, coherence effects on phase accuracy 8-90377
 Mach-Zehnder, test section misalignment errors for temp. and temp. gradient meas. 8-54447
 Mach-Zehnder interferometer, hook method, Ba I gf values, 7911.38 Å 8-66511
 Martin-Puplett interferometer, use as Fourier spectrometer and for OTF meas. 8-70179
 Michelson, laser frequency control by spectrally depleted destructive two-beam interf. 8-74941
 Michelson, sequential analysis of fringes, scanning rate influence 8-77976
 Michelson, wavelength intercomparison between methane and I₂ stabilised He-Ne lasers 8-87089
 Michelson asymmetric interferometer, modified He cryostat 8-74053
 Michelson far IR interferometer for astronomical appl. 8-93118
 microcomputer based scanning instrument controller, for Fabry-Perot interferometer 8-93764
 microinterferometer transducer, air-bearing, for use with universal inspection machines 8-57899
 mirror kinematic adjustment mechanism 8-59109
 modular, for dispersive Fourier transform spectrometry of gases 8-89567
 modular, for dispersive refl. meas. on highly absorbing solids 8-89568
 moving carriage Michelson interferometer, 1 in 10⁷ laser wavelength meas. 8-89452
 multi-beam, plasma particle density diagnostics, laser beam illumination 8-86324
 multipass, using filamentary spatial filter 8-77975
 multiwavelength testing using modified Twyman-Green interferometer 8-59169
 Mylar beam splitter efficiency in far IR interferometer 8-55434
 nonlinear interferometers for laser pulse shaping 8-79051
 optical bench, automated scanning, remote laser interf. meas. system 8-83124
 optical workshops interferometer, description of a new interferometer (*French*) 8-58017
 phase-locked interference microscope, design and construction 8-49894
 photometric etalons, scatt. matrix and brightness coeffs. of MS-20, MS-14 reflectors 8-82020
 plasma density IF phase meas. using three-mirror interferometer 8-75414
 plasma density meas. by interferometer 8-55748
 plasma diagnostics, fast interferometer using N₂ laser, electron density of dense plasma 8-87489
 polarisation interferometer, construction from Michelson interferometer (*Russian*) 8-89532
 polarising, mode of operation in dispersive Fourier transform spectroscopy 8-78003
 Rayleigh wave monitoring, simple interferometer 8-74052
 rotation shearing interferometer, with phase compensated roof-prisms 8-77971
 rotational shearing, for imaging through turbulent atm., spatial freq. resolution 8-69450
 scanning technique for obtaining linear fringe shift readout 8-89530
 servocontrolled Fabry-Perot interferometer, 3 in 10¹¹ laser wavelength meas. 8-89452
 Shack unequal-path interferometer 8-58020
 shearing, errors due to misaligned test section 8-93755
 spatial filtering system 8-90515
 speckle pattern TV interferometer, principle and appl. 8-58014
 spinning IR interferometer, appl. to nonsolar planets detect. 8-85977
 step-height measurement, stylus-type surface texture measuring instrument calibration appl. 8-77862
 thermal length control, for lasers and etalons 8-87056
 traveling Michelson interferometer with phase-locked fringe interpolation 8-89451
 triangular cyclic interferometer, anal. and alignment 8-77969
 two-beam, cat's-eye, for laser wavelength comparison 8-86326

light interferometers continued

- two-beam, comparison of refl. and refr. optics in condensing element 8-77968
Zernike's three-slit interferometer, Fourier optical synthesis 8-65960

light interferometry

- see also *holographic interferometry*; *Moire fringes*
acousto-optic frequency shifter, beam quality, heterodyne interferometry meas. 8-79127
aspheric surface quality assurance 8-50962
astronomical telescope speckle interferometry, online digital autocorrelator 8-81548
atmospheric isoplanation measurement using speckle interferometry 8-65385
automatic interference comparator, high precision linear gauge calibration appl. (German) 8-77847
binary stars, unresolved, epochs of speckle interferometric obs., (1975-77) 8-73735
deformation meas., interferometric method, appl. to sheet metal and transparent plastic sheets 8-75108
double beam interferometric determ. of ellipsometric phase shift 8-93757
electrochemical conc. polarisation at electrode, convectionless steady state, interferometric investig. 8-68896
end standards measurement, phase correction by profiling technique, gauge blocks appl. 8-73986
Fabry-Perot interferometer, multipassing method 8-54448
fibre index profile measurement using transverse interferogram, accuracy 8-66931
fibre refractive index profile calc. from transverse interf. patterns 8-74967
flatness testing by self-levelling reference plane 8-63207
fluid, effects of normal stresses, interference meas. method 8-94624
Fourier transform spectroscopy, inexpensive student expt. 8-49609
fringe localisation region, van Cittert-Zernike theorem 8-74051
fringe position determ. accuracy improvement by photodetector signal conversion 8-58015
fringe signal generator for testing fringe shift measuring system 8-65962
gas density meas. by multibeam interferometry 8-58016
gas flow application of shearing interferometers 8-55706
heat transfer mechanism with boiling in narrow spaces, interferometry obs. 8-94527
interactive video image digitiser, appl. to interferogram anal. 8-58021
interference-phase method of mag. field meas. in solar atm. (Russian) 8-65509
interference-phase method of ray vel. meas. in solar atm. (Russian) 8-65508
IR emission microinterferometry for alignment of fluid bearing lubricants 8-58013
laser, length changes in subnano-meter range meas. (Slovak) 8-77861
laser beam multiplication, interferometric method (Ukrainian) 8-90442
laser for vibration control and meas. (Russian) 8-71299
laser fusion, microballoons, wall thickness meas. using Interphako interf. microscope 8-87469
laser interferometry by induced modulation of cavity field 8-49888
laser pulse duration meas. 8-50830
laser wavelength measurement, review 8-50841
lens assessment techniques, polychromatic and monochromatic, in far IR 8-50899
lenses, standard reference, for assessment of OTF meas. equipment 8-50897
light scattering medium, spatial struct., interferometric meas. (Russian) 8-70181
liquid refractive index variation with temp. meas., interferometric technique 8-74050
mechanical vibration meas. using laser (French) 8-67156
metal plate high-gradient transverse deformation interferometry 8-82024
Michelson interferometer technique for capacitance displacement transducer error obs. 8-54356
microscopy, for plant cell wall and cytoplasm refr. index determ. 8-57151
Moire effect and deformation meas. in structural components (German) 8-88587
motion, combined and general forms, laser speckle interferometric obs. 8-74054
non-optical surface topography, by oblique fringe projection from diffraction gratings 8-89437
nondestructive evaluation by laser speckle interferometry 8-60976
oil droplets, motion and optical props. by interf. method 8-67893
optical diffuser form. of simple known statistical props., interferometric surface height determ. 8-90539
optical films, side-illuminated, interf. pattern obs. 8-50914
optical material continuous heterogeneities, interf. meas. 8-93756
optical path difference meas. by double diffraction interferometer (Japanese) 8-82025
optical screw, path difference meas. and control device, anal. of periodic errors 8-77972
optically transparent materials, evaluation of elastic ratio by interferometry 8-90804
path difference determ. from interference patterns 8-82028
phase problems, image recovery from Fourier transform modulus 8-82918
phase-locked interferometry 8-58022
photoelasticity anal. by Moire method 8-51138
plasma focus, electron density distrib., N₂ laser interferometric study, X-ray and neutron emission 8-87479
polyethylene ultradrawn fibres, Poisson ratio from Michelson interferometry 8-80596
refractive index of solids, meas., Fabry-Perot interferometric technique (Russian) 8-82023
semi-Lambertian reflecting surface, laser speckle interferometry 8-82910
single mode fibres for optical field mapping, interf. technique 8-74966
solid flaw remote sensing, laser system prod. acoustic waves, interferometric detect. 8-60975
speckle, atm. nonisoplanicity meas. using double stars 8-65387
speckle, meas. of binary stars 8-85973
speckle interferometry, binary stars obs. with 1 m telescope 8-69831

light interferometry continued

- speckle interferometry, coherence requirements, use of thermal radiation sources 8-49891
speckle interferometry, effects of spectral bandwidths and exposure times 8-69701
speckle interferometry, real-time meas. of vibrations and displacements (Italian) 8-54336
speckle interferometry for stellar size and shape determ. 8-77491
speckle interferometry of binary stars, computer simulations in photon-counting mode 8-53836
speckle patterns, photographic recordings, fringes generated in Fresnel plane 8-66763
speckle photography, flow velocity distrib. meas. 8-67288
star cluster high resolution imaging by speckle interferometry, simulation 8-77492
stars, nonsolar planets detect. via spinning IR interferometer 8-85977
stellar speckle interferometry, wave correlation scale meas. 8-65388
surface contour and inhomogeneity testing, interf. fringe distortion with imprecise focusing 8-89531
surface deform. of opt. flats and Fizeau method for film thickness meas. 8-77970
temperature field measurement of axisymm. buoyant phenomena 8-89529
transparent layer refr. index and thickness determ., optical interf. method 8-89528
ultrasmall displacement meas. 8-57897
vibration insulation of equipment for optical system performance testing 8-90543
viscosity measurement, falling slug method, intensity fluctuation spectroscopy appl. 8-71408
C fibre reinforced plastic, thermal expansion, influence of resin type 8-95164
CO₂, pulsed laser, laser induced medium perturbation, time resolved interferometric obs. 8-58977
Cu, electroplated coating, levelling kinetics, interferometric investigation (Bulgarian) 8-79864
GaS, refr. index in far IR, permitt. meas. 8-64360
He-Ne laser freq. determ., interferometric comparison with upconverted CO₂ laser radiation 8-55395
He-Ne laser interferometry for vibration control and meas. (Russian) 8-70117

light meters see *photometers***light modulation** see *optical modulation***light polarisation**

- see also *birefringence*; *optical rotation*; *photoelasticity*; *polarimetry*
acridine C-radical, polarised absorpt. and ESR spectra, dichroism and HF-Cl calc. 8-50563
active polarisation spectroscopy by combinational light scatt. (Russian) 8-78006
anisotropic emission source, polarisation characts. meas. 8-74047
anthracene, polarised reflection spectra, surface and vol. exciton coupling, vibronic states 8-72543
atom+charged particle anisotropic collision, spectral line shift and broadening, polarisation depend. 8-82695
atomic degenerate system, Doppler-free laser-induced dichroism and birefringence, linearly polarised laser 8-82711
atomic vapour, f-value determ. method using stimulated electronic Raman scatt., appl. to Cs 8-82693
1-azo-bicyclo-2,2,2-octane, multiphoton ionis. spectra polaris. characts., two-photon symmetry assignment 8-74718
benzene, multiphoton ionis. spectra polaris. characts., two-photon symmetry assignment 8-74718
benzene, photoelectron ang. distrib. with linearly polarised HeI radiation 8-50580
binary and multiple stars, polarisation by Thomson scatt. in optically thin stellar envelopes 8-81655
boundary conditions in crystal optics with spatial dispersion 8-92040
trans-1,3-butadiene, multiphoton ionis. spectra polaris. characts., two-photon symmetry assignment 8-74718
CARS in isotropic liquid, polarisation props. 8-80334
circular polarisation of emission, magnetically induced, appl. to inorganic complexes 8-78005
circular polariser for refl. in far IR 8-79114
circumstellar dust shells, Monte Carlo simulation of polarised light transfer 8-81608
compound optical polarisation materials for stress meas. (Russian) 8-87313
coupled resonator model for resonant polarization conversion and anomalous beam shift (Japanese) 8-87133
CH Cygni, linear polarisation vars. rel. to circumstellar dust grains form. 8-69808
Cygnus X-1, optical polarisation orbital vars. rel. to binary system inclination 8-54077
Cygnus X-1 (HDE 226868), optical polarisation evidence for 78/39-day period 8-89274
degenerate two level system, reson. light scatt., transient polarisation characts. 8-94382
depolarised multispectral laser scatt., target classification 8-50846
diffraction grating anomalies, phase shifts and resonances 8-94446
diffraction gratings, Au, Al coatings, UV light at grazing incidence 8-87129
Dirac-spinor form of Maxwell's eqns., polarised light beams in gravitational fields 8-50696
double group theory, half-shell and two-level system, optical polarisation 8-49594
dye laser, N₂ laser pumped, two wavelength outputs with orthogonal polarisations 8-50792
dye pulsed laser, light polarisation with thin wedge plate in cavity 8-55394
electro-optical gate for nonpolarised emission (Russian) 8-59132
ellipsometry, azimuth response function, linear nondepolarising optical system 8-65957
elliptical galaxies, polarisation by interstellar matter 8-93399
elliptically polarised beams in cubic media, self-focusing (Russian) 8-63156
elliptically polarised light, quantitative anal., 1/4-wave plate, student expt. 8-49608
ellipticity, azimuth and system parameters linking eqns., 3-dimens. model prop. 8-50695
fibres, noncircular core single-mode, polarisation characts. 8-94430

light polarisation continued

- Fraunhofer lines and continuum, solar disc polarisation meas. 8-73688
galactic centre, linear polarisation in near IR 8-96534
galactic field structure and stellar polarisation 8-69869
galaxies active nuclei, continuous optical spectra and polarisation 8-57644
gas multimode laser with excitation modulation, polaris. of active medium 8-82942
haeme proteins, inversely polarized modes in reson. Raman scatt., depolarisation dispersion curves, vibronic interactions 8-78676
HD 47129 (Plaskett's star), massive O-star binary system, variable linear polarisation obs. 8-53989
AM Herculis (3U 1809+50), single accretion column model rel. to optical polarisation vars. 8-57578
hologram grating, thin, transmittance type, fabrication polarisation effects (*Korean*) 8-50731
holographic image degradation due to reflected light depolarisation 8-90398
holographic image light, object beam depolarisation effect (*Spanish*) 8-50733
holography with evanescent waves, diffr. efficiency, TE polarisation 8-66782
holography with evanescent waves, diffr. efficiency, TM polarisation 8-66783
impulse response matrix formalism for polarised light, appl. to holography 8-63045
interference polarisation filter steps, wide angle, made from various crystals 8-87156
interstellar linear polarisation in 1-2.2 μ wavelength range 8-77588
irregular particle scattering, meas. results versus Mie theory 8-58918
J-dependence of intensity-dependent polarization change in atomic reson. lines 8-70775
Jones vectors superposition, polarisation vector on Poincare sphere 8-74839
Jupiter, near IR polarisation studies 8-85899
BL Lacertae type objects, linear optical polarisation study (*Russian*) 8-57640
laser, ring type, elliptically polarised oppositely travelling waves competition 8-50825
laser beam broadening and depolarization in dense water-droplet fogs 8-92981
laser beams, CW, in at. vap., long-range interaction 8-87110
lateral wave amplification through reflection from active medium 8-78987
lidar polarisation meas. for cloud phase discrimination 8-96269
lidar scattering from clouds at 347, 694 nm, polarisation props. 8-85689
liquid crystal, uniaxial, polarised fluoresc. emission, orientational distrib. function, rot. Brownian motion 8-80390
low-density plasma, reabsorbed radiation polarisation in mag. field 8-67426
metal-dielectric interface, p-polarised light total absorpt. by surface plasma waves 8-88373
modulation of polarisation, small ang., beam in diamag. glass, by Faraday rot. (*Korean*) 8-50918
molecular systems, photoselection, orient. relax. rel. to emission mag. induced circular polarisation 8-70860
nebulae M42 and M43, optical linear polarisation 8-86004
NGC 1068, Seyfert galaxy, IR photometry and polarimetry 8-54035
NGC 4151, Seyfert galaxy, optical polarimetry, circumnuclear dust envelope 8-61916
nonlinear medium, polarisation state evolution 8-50867
Nova Cygni 1978, interstellar polarisation obs. 8-89213
Nova Cygni 1978, spectra, polarisation, photometry and visual magnitude estimates 8-93283
paramagnetic molecules in rigid isotropic medium, mag. linearly polarised emission 8-68545
Pauli algebraic formalism, relation between different formalisms 8-87010
perfect lens with polarisation masks, OTF 8-90380
polarised photochromism in solid solutions 8-64859
polymer, uniaxial, fluoresc. polarisation, orientation and mol. dynamics effects 8-76516
polytene chromosome, stretched, stained with acridine orange, fluoresc. polarisation rel. to DNA packing 8-76995
pyrazine, multiphoton ionisation spectra, circular to linear polarisation ratios, lowest ionisation pot. 8-74716
pyridine, multiphoton ionisation spectra, circular to linear polarisation ratios, lowest ionisation pot. 8-74716
quantum beat high-resolution polarisation spectroscopy in transmission, technique 8-58640
radiative transfer for polarized light, eqn. soln. method in relativistic cosmology 8-73781
Rayleigh scattering, anisotropic medium, 3-photon scatt. by density fluctuations (*Russian*) 8-74841
real-time image optical subtraction scheme 8-74856
reciprocity theorem, for polarised laser beams 8-79055
reflection polarisers and analysers in vac. UV, design criteria 8-55424
reflectivity, quantitative meas., undergrad. lab. expt. 8-49624
resonant orientation of tunnelling centres, self-induced anisotropy 8-79075
Saturn, near IR polarisation studies 8-85899
Seyfert galaxy NGC 1068, light polarisation in nucleus 8-54046
single model fibres, polarisation mode dispersion 8-79128
sky intensity information content, polarisation meas. at right angles to solar direction 8-81401
solar spectrum, multi-dimensional non-LTE transfer of polarised radiation rel. to line profiles 8-69673
stars with IR excesses, optical emission intrinsic linear polarisation origin 8-96481
stellar radiation scattering on circumstellar clouds, circular polarisation theory 8-96428
sunlight, reflected, meas. from high-altitude balloon 8-61561
surface polaritons in anisotropic crystals 8-87919
synchrotron VUV and X-radiation, polarising effect of monochromators 8-66732
theoretical model for short length, single mode fibres 8-71203
tilted absorbing glass plate, polarisation response rel. to polarising radiometer calibration 8-55297
transition metal hexahalide complex, polarised reson. vibr. Raman spectra, electronic degeneracy effects 8-78708

light polarisation continued

- twisted anisotropic media, light propag., appl. to photoreceptors 8-63004
two-photon absorption coeff., polarisation depend. 8-80379
UV discharge lamps, rotating triple-reflection polariser 8-94443
very rough surface, backscatt. light, polarised and depolarised components 8-63009
young stars reddening and polarisation, intracluster and circumstellar dust effects 8-93199
zodiacal light, circular polarisation theory 8-96428
Ar, light depolaris., pair-pair correlations 8-63536
As₂Se₃, polarised light reflectance spectra, band struct. 8-63979
Bi, parity nonconservation, weak electron-electron interaction, light polarisation, vapour optical activity (*Russian*) 8-55132
Cs, optical reson. line electron impact excitation cross sections, polaris. 8-55244
Fe, tribothermoluminescence of flakes in grinding wheel, rel. to solar coronal dust radiation 8-68570
GaP second order Raman spectrum, polarisation meas. 8-64368
H-like ions, fluoresc. polarisation of Stark quenched spin-polarised beam 8-66501
He I beam-plasma discharge, optical radiation polarisation 8-67478
I₂, angular momentum transfer, elastic, inelastic collisions, orientation and polarised fluoresc. 8-90271
K, optical reson. line electron impact excitation cross sections, polaris. 8-55244
K, stimulated electronic Raman light scatt. by mag. sublevels 8-50492
K, two photon excitation by opposing light beams, reson. lines polarisation studies 8-82705
KCl: Pb²⁺, inner-centre luminesc., 8 to 80K (*Russian*) 8-92112
O IV(VI), circular polarisation of light emitted in beam-foil collisions, cascade free lifetimes 8-55228
Rb, optical reson. line electron impact excitation cross sections, polaris. 8-55244
Tl, parity nonconservation, weak electron-electron interaction, light polarisation, vapour optical activity (*Russian*) 8-55132
- light propagation**
see also *atmospheric light propagation*; *guided light propagation*
aberrating Gaussian beam, free-space propagation, wave eqn. solns. 8-87008
active electrooptic and magnetooptic media, matrix theory fundamentals (*Russian*) 8-63005
beam wave, propag. through weak turbulence, frequency spectra 8-78911
boundary-value problem, two-point, statistical variant using Einstein-Fokker-Planck eqn. (*Russian*) 8-81924
cholesteric medium, under applied mag. field (*French*) 8-80319
coherent optics fundamentals 8-78910
correlation coeffs. of planar sources and their far fields 8-66750
dielectric, isotropic, two-dimens. dielec. const. determ., wave trajectory construction 8-80276
ellipticity, azimuth and system parameters linking eqns., 3-dimens. model propag. 8-50695
Helmholtz equation in optics, numerical soln. 8-90357
Huygens-Fresnel integral in circular coords., asymptotic soln. 8-87013
inhomogeneous plane wave shadowing by an edge 8-90356
laser beam, saturation parameter from gain meas. 8-66797
light Doppler effect, absolute spacetime theory 8-69979
nonrelativistic non-Fresnel approach to light propag. in moving media 8-78904
ocean, spatial struct. of underwater light-field fluctuations (*Russian*) 8-53656
optical systems with large apertures, Fresnel approx. 8-66746
paraxial approximation to scalar Helmholtz eqn., discrete eikonal and ray eqns. 8-90360
sea water, turbid, light propag. calc. from dielectric permeability algorithm (*Russian*) 8-77261
starlight aberration rel. to spectral type (*German*) 8-73702
thin wave beam in randomly-inhomogeneous medium, ray description (*Russian*) 8-63007
transient propagation in active media, Maxwell-Bloch eqns., coherent self-focusing 8-87109
twisted anisotropic media, appl. to photoreceptors 8-63004

light propagation in plasma

- backscatter from laser plasma, optical ray retracing effects 8-91133
collisional magnetoplasma, self-focusing effect on filamentation instability 8-51305
column waveguide, time varying, laser beam propagation 8-94916
dense plasma, laser scatt. 8-67408
Gaussian beam conversion 8-67364
laser beam, high-power, self-focusing in fully ionised plasma 8-87451
laser beam self-focusing, nonlinear absorption effect 8-79436
laser beam transverse filamentation and self-focusing 8-67358
laser field effect on transport coeffs. 8-67317
laser light absorpt., numerical calc. 8-75348
laser light absorpt. and scatt. in laser fusion plasma 8-51312
laser light absorption and harmonic generation 8-75359
laser-produced plasma spherically symmetric absorption (reflection), simulation 8-51285
moderate-Z plasma, laser heating and ionisation in presence of strong UV and X-radiation 8-71512
self focusing mechanism, current generation due to light pressure (*Russian*) 8-63571
self-focusing of non-Gaussian laser mode in dense plasma 8-59599
spark plasma deionisation stage, laser radiation absorption obs. 8-75398
spherical laser plasma, classical optics and light press. 8-59601
stationary self-trapped laser beams in plasma 8-79438
stimulated bremsstrahlung of electrons, strong optical field influence 8-59623
stimulated Brillouin backscatter from theta pinch 8-67359
stimulated Brillouin backscattering, mag. confined plasma 8-51307
He plasma, Stark shift and line broadening in 3-D stochastic laser field 8-50502
Ne, reson.-absorpt. plasma of glow discharge positive column, Ne super-radiation pulse variation 8-71489

light reflection

- see also *mirrors*; *optical films*
asteroid surface materials mineralogical characts. from reflectance spectra 8-69736

light reflection continued

- biaxial crystal plate, refl. and trans. wave amplitude 8-95573
 Brewster's angle measurement using ordinary lab. apparatus, for high-school students 8-86097
 circular polariser for refl. in far IR 8-79114
 circular symmetrical reflector with laterally defocused light source, axial ray trace equations (*Russian*) 8-90365
 diamond, identification from reflection pattern photographs 8-54481
 dielectric interface, Gaussian beam characts. 8-66747
 diffuse reflection from rough surfaces (*Russian*) 8-74843
 diffuse reflection with radiation redistrib. in freq. and direction 8-53819
 dispersive media, Ewald dynamical diffraction theory extinction theorem 8-66749
 electrolyte concentration meas. by portable optoelectronic convertor 8-80820
 ellipsometry, azimuth response function, linear nondepolarising optical system 8-65957
 Fabry-Perot nonlinear electro-optic device, using refl. light feedback 8-55457
 far IR measurements, He cryostat modification for asymm. Michelson interferometer 8-74053
 fibre end, reflected and backscatt. power meas., time domain reflectometer 8-70177
 focused light ATR method, appl. to guided waves on grating 8-74992
 glass packet specimens with antisolator filler 8-90469
 heliostat reflected beam structure 8-90482
 homogeneous plane-parallel atmosphere, unified treatment of reflected and transmitted intensities 8-85838
 IR bidirectional refl. distrib. function meas. for baffle and mirror materials, recording instrument 8-58012
 IR optical scanning system, narcissus effect suppression, computer results 8-59151
 isotropic layers, thin, with rough boundary surfaces, refl. and transmission factors (*German*) 8-90354
 isotropic-anisotropic media boundary, light refl. and refr., Maxwell theory (*German*) 8-87007
 lateral wave amplification through reflection from active medium 8-78987
 Mars atmosphere, optical props. during 1971 dust storm (*Russian*) 8-93138
 materials subject to hemispherical radn., reflecting power meas. 8-65985
 MBBA, nematic liq. cryst., deflector based on frustrated total internal light refl. 8-50934
 metal, surface roughness effect on light absorptivity 8-80314
 multi-element interference filters using different grids, far IR characts. 8-90507
 multiple-plate glass systems, spectral directional radiation characts. prediction 8-74956
 non-redundant spectral tunnelling through periodic struct. at total refl. 8-78906
 nonimaging solar concentrators for different absorber shapes 8-50895
 phase conjugate reflection, pulsed 10.6 μm , via intracavity degenerate four-wave mixing 8-87097
 plasma mirror refl. characts., in electron beam controlled CO₂ laser 8-59064
 quartz cylindrical fibres in regular struct., multiple frustrated total internal refl. calc. 8-83094
 ray reflection at dielectric-vacuum interface, exam. using Fermat's principle and evanescent waves 8-58902
 scattering layers, with different degrees of dispersity, reflecting power, theory (*Russian*) 8-82909
 scattering material, transmittance and reflectance meas. by specular hemisphere method 8-58004
 semi-Lambertian reflecting surface, laser speckle interferometry 8-82910
 shadow methods, reflected, transmitted, obs. of sharp V-notched plates, under pure bending 8-90777
 solar concentrating properties of truncated hexagonal, pyramidal and circular cones 8-50896
 solar reflecting concentrators, optical evaluation techniques 8-50893
 spherical glass beads in highway pavement markings, retrorefl., specular refl. 8-74837
 spherical glass beads in highway pavement markings, retrorefl., diffuse refl. 8-74838
 stray light calculations, surface refl. models 8-58905
 stray light suppression in optical systems, optical design, computer analysis 8-59113
 substrate reflectance and medium depth effects in two-dimens. multiple scatt. expt. 8-87011
 surface roughness evaluation, statistical approach 8-90367
 total internal reflection, laser beam-fountain demonstration, for teachers 8-81769
 total internal reflection modulator, small glancing angles 8-74987
 trajectories of reflected and transmitted beams in oblique tunnel effect 8-78903
 transmission through reflecting cylindrical tubes, demonstration 8-73812
 transparent nonlinear layer, light refl. and transmission (*Russian*) 8-71142
 turbid media, approx. linear relationship for optical response 8-90371
 uniaxial crystals interface, EM wave refl. and refr. laws, tensor derivation 8-71029
 uniaxial media, light reflection and refraction amplitude relations (*German*) 8-90353
 vision, common and relative components as information about illum., colour and 3-dimens. form 8-56982
 Ag film, reflection coeff. minima and surface plasma wave dispersion curve comparison (*French*) 8-80429
 CuBr, evaporated film, magneto-optical effects on exciton bands 8-72624
 CuCl, evaporated film, magneto-optical effects on exciton bands 8-72624
 In₂O₃, transparent electrode deposition on PLZT ceramic, elec. and opt. props. 8-74848
 Na vapour, amplified refl. by degenerate four-wave mixing using Kerr nonlinearity 8-55413

light reflection continued

- SiO₂-Si, film-substrate, single reflection retarders for different Hg spectral lines 8-79122
 SnO₂, transparent electrode deposition on PLZT ceramic, elec. and opt. props. 8-74848

light reflection spectra *see reflectivity; spectra***light refraction**

- see also birefringence*
 aqueous solution fluorescence spectra, refr. correction 8-93766
 astronomical refraction, general theory (*Russian*) 8-89045
 beam broadening in randomly inhomogeneous cloudy aerosol medium (*Russian*) 8-58911
 Brewster's angle measurement using ordinary lab. apparatus, for high-school students 8-86097
 cholesteric prism, under applied mag. field (*French*) 8-80319
 eye, fish, chromatic aberration and effect on refr. state 8-64985
 eye refractive error, simplified anal. of meridional refr. data 8-65149
 eye refractive error measurement using Humphrey Vision Analyser, reliability and validity 8-61265
 graded-index fibres, refracting leaky rays 8-79103
 isotropic-anisotropic media boundary, light refl. and refr., Maxwell theory (*German*) 8-87007
 mirage occurrence conditions, ray tracing theory 8-77323
 mirages, stratified medium light ray trajectories, educational aspects 8-69940
 prism, min. ang. deviation, school corridor demonstration 8-81760
 sunset obs. from Apollo-Soyuz, atmospheric light refr. study from space (*Russian*) 8-65383
 uniaxial crystals interface, EM wave refl. and refr. laws, tensor derivation 8-71029
 uniaxial media, light reflection and refraction amplitude relations (*German*) 8-90353

light scattering

- see also Brillouin spectra; opalescence; Raman spectra; Rayleigh scattering; stimulated scattering*
 8-61421
 absorbing-scattering layered material, light beam diffusion obs. method 8-62215
 active polarisation spectroscopy by combinational light scatt. (*Russian*) 8-78006
 aerosol, particle size determination by light scattering, unknown refractive index 8-95957
 aerosol layer depth remote meas. by microwave-modulated laser (*Russian*) 8-57338
 albumin, bovine serum, solutions, fluctuation transport theory 8-70057
 algal suspensions, light scatt. and absorpt. props., 380-720 nm 8-92604
 antiferromagnetic insulator, light scatt. in strong mag. field 8-72523
 in aqueous polymer solutions, meas. apparatus 8-74058
 arc plasma, thermal density fluctuations, light scatt. using CW CO₂ laser and heterodyne detection 8-59677
 atmosphere, aerosol content determ. from photometric obs. of stars 8-92976
 atmosphere, aerosol properties rel. to solar aureole, photogrammetry 8-57315
 atmosphere, directional scatt. coeffs. meas. in droplet and crystal clouds (*Russian*) 8-96292
 atmosphere, incoherent optical propag., effects on optical/optronical systems 8-92987
 atmosphere, light beam coherence through optically dense turbid layer 8-55300
 atmosphere, multiple scattering effect on photodissociation 8-85692
 atmosphere, propagation calcs., use of average complex refr. index 8-57314
 atmospheric laser beam propag., monochromatic, problems 8-92988
 atmospheric particulates, chemical characterisation via light scatt. method 8-69533
 atmospheric propagation of partially coherent radiation 8-65386
 aureole around UV source at finite distance 8-77320
 aureole radiance field about point source in scatt.-absorbing medium 8-77319
 aurora and nightglow satellite obs., contamination due to scatt. by clouds and snow 8-77385
 bacteria, scattering pattern analysis 8-80946
 bacterial migrating chemotactic bands, quasi-elastic light scatt., *E. coli* 8-77018
 bacterial motility, *E. coli*, struct. effects in quasi-elastic light scatt. 8-77024
 bacterial movement tracking using one-dimens. fringe system 8-73299
 beam broadening in randomly inhomogeneous cloudy aerosol medium (*Russian*) 8-58911
 binary mixture in external field, crit. opalescence 8-84595
 binary mixture near crit. point, singly and multiply scattered light distrib. 8-56494
 biological system solution, periodic conversions, optical mixing method obs. 8-96029
 blood, back-scattering theory 8-77099
 Brownian particles, correlations 8-82911
 Brownian particles, multiple light scattering, depolarisation ratio and linewidths 8-78913
 Brownian polymer particles in water, multiple scatt. 8-78912
 α Carinae (Canopus), generalised Compton effect in spectrum 8-53938
 cell analysis in flow systems, geometry for orienting flat cells 8-77161
 cell high-speed analysis, laser absorpt. and scatt. meas. (*German*) 8-92687
 cell medically relevant class determ., scatt. light cluster anal., cervical smear tests (*German*) 8-92686
 chloroplast thylakoid, light-induced absorbancy and scatt. changes about 520 nm rel. to struct. 8-69019
 chromaffin granule electrophoretic mobility meas. by light scatt., effect of Ca²⁺ and Mg²⁺ 8-53357
 circumsolar parts of sky, parabolotoroidal focones and parabolocylindrical focones assessment 8-83064
 circumstellar dust shells, Monte Carlo simulation of polarised light transfer 8-81608
 cloud reflectance with laser beam illumination, multiple scatt. contrib. 8-85686

light scattering continued

- coagulating dispersions, light scatt. data, Fourier inversion anal. 8-76932
- coherent radiation beams, parameters from correlation method (*Russian*) 8-50705
- colloidal suspension of spheres, Percus-Yevick approx. 8-94368
- composite media, dielec. and optical props. 8-84546
- conducting crystals kinematical and dynamical inelastic light scatt. 8-80368
- Cygnus X-1, photospheric scatt. model for optical polarisation orbital vars. 8-54077
- cylinder, optically active, EM wave scatt. 8-82912
- cytometry, hydrodynamic orientation of sperm heads in flow systems 8-77162
- degenerate two level system, reson. light scatt., transient polarisation characts. 8-94382
- depolarised multispectral laser scatt., target classification 8-50846
- diamond, round brilliant cut, statistical assessment of brilliance and fire 8-90361
- diamond, round brilliant cut style modifications, brilliance, sparkliness and fire 8-90362
- diamond simulants, brilliance, sparkliness and fire 8-90363
- dielectric inhomogeneous medium, refractive index profile determ. from inverse scattering 8-58914
- dielectric slab optical waveguide, scattering characteristics 8-87163
- diffraction grating, specification and meas. of scattered light 8-78905
- diffuser form, of simple known statistical props. 8-90539
- diffusing layers, characteristic matrices for inhomogeneous layers 8-87015
- diffusing layers, characteristic matrix and general props. 8-87014
- disperse system, parameters determ. from turbidity spectrum, allowance for nonspherical particles 8-55302
- dispersion, coagulating, light scatt. for close range struct. determ. 8-53273
- droplets, laser light scatt., multiplicative and additive stochastic processes 8-84596
- ethanol, solns., local struct. equilib., light scatt. and IR spectra obs. 8-84564
- ethanol-water-chloroform mixture, light scatt. near plait point 8-72532
- excitons localised at dislocations 8-60479
- fibre end, reflected and backscatt. power meas., time domain reflectometer 8-70177
- fibre optic glass pair quality, effective aperture and light scatt. analysis 8-90522
- flame, containing light scatt. particles, optical props. and temp. meas. method (*Russian*) 8-56894
- flow birefringence, scattered radiation charact. 8-60418
- fluid, near liq.-gas crit. pt., local order effects on dynamic props., US and light scatt. 8-67806
- fluid near crit. point, rapid evaluation of multiple scatt. 8-84594
- focal plane design and optimal processing for scattered optical fields 8-78935
- Fourier transform IR, scatter eliminated spectrometry 8-89564
- gels, dynamic light scattering in poor solvent 8-88318
- gels, dynamic light scattering theory 8-60475
- gyrotropic media, diff. of light by acoustic waves 8-72485
- holographic interferometer for studying three-dimensional optical inhomogeneities 8-87030
- holography through fog, coherence requirements for light source 8-58949
- homogeneous plane-parallel atmosphere, unified treatment of reflected and transmitted intensities 8-85838
- hydrosol particles in suspension, dispersivity effect on light scatt. (*Russian*) 8-68932
- incoherent backscatter from rough surfaces, two-scale model re-examined 8-71013
- index measurement, ring method using laser diffraction structuremeter (*Russian*) 8-71035
- induced moments in at. and molcs., polarisability density concept limitations 8-70964
- integrated optical spectrum analyzer dynamic range, waveguide scatt. effect 8-59163
- interband light scattering in semimetals and semiconductors (*Russian*) 8-60485
- interstellar reflection nebulae, simplified models 8-96526
- intramolecular memory effects in second-order optical processes 8-94270
- IR bidirectional refl. distrib. function meas. for baffle and mirror materials, recording instrument 8-58012
- IR transparent materials, forward and backward scatt. data 8-59099
- irregular particle scattering, meas. results versus Mie theory 8-58918
- isobutyric acid-water mixtures, phase separation, light scatt. 8-84592
- isotropic medium, three-photon light scatt. phenomenological theory (*Russian*) 8-83024
- Kalliroscope effect based improved light diffuser, fabrication 8-59121
- large dielectric sphere scatt., Mie theory 8-66754
- laser fringe anemometers, light scatt. aspects, particle size meas. appl. 8-83020
- laser propagation in water, multiple scattering effects (*Japanese*) 8-78915
- laser radar simulator for low scatter characts., three-mirror design 8-59118
- laser scattered light intensity, recurrence rate correl. 8-66760
- latex, monodisperse, phase diagram, spectroscopic study 8-85209
- latex, monodisperse, short-range order, spectroscopic study 8-85208
- lidar observations of smoke and dust clouds at 0.7 and 10.6 μm wavelengths 8-69459
- lidar probing of fogs and clouds, double scatt. approx. 8-73512
- lidar returns from fog, doubly scatt. radiation contrib. 8-77326
- lidar scattering from clouds at 347, 694 nm, polarisation props. 8-85689
- line radiation transfer in heated gas, arbitrary initial conditions in kinetic eqn. 8-51051
- lipid-water smectic phase, water and thermal diffusivity, light scatt. meas. 8-96031
- liquid crystal, far-field coherence and radiant intensity of scatt. light 8-64372
- liquid film, free, squeezing mode relax., laser scatt. rel. to colloid interaction 8-87354
- liquid light scatt. coeff. absolute determ. apparatus 8-86319

light scattering continued

- Lorenz-Mie scattering, range of validity of Rayleigh and Thomson limits 8-66755
- low-density fluid, scatt. intensity, irreducible spherical tensors 8-80366
- magneto-optical crystals, spectra of hybrid excitations from transverse photons, excitons, magnons interactions 8-80320
- many-level molecular system, light scatt., beam statistical model 8-62777
- Mars atmosphere, optical props. during 1971 dust storm (*Russian*) 8-93138
- MBBA, nematic liq. cryst., ultrasound produced rolls, spatial coherence props. of scatt. light 8-75534
- metal mirrors, diamond turned, evaporated and sputtered, surface and optical studies 8-79098
- methane, fluid, collision-induced light scatt. 8-68509
- microcapillary gas-dielectric filled waveguide with azimuthally asymmetrical cross-section, attenuation calcs. 8-83105
- microemulsion structural changes, light scatt. obs. 8-56920
- Mie scattering calcs., continued fractions method 8-82914
- Milne problem and spherical albedo, law of darkening, forward and backward scatt. effects 8-77483
- monodisperse screen shape determ. using scatt. indicatrix in Fraunhofer diff. 8-71033
- monodispersion, optical extinction meas. in aerosol media, forwardscatt. corrections 8-94367
- multispectral extinction data, analytic inversion in anomalous diff. approx. 8-87016
- nematic liquid crystal, quasi-elastic light scatt. near instability point, dielec. regime 8-75535
- nematic-cholesteric mixture with positive dielectric anisotropy, light scatt. characts. 8-75537
- neurosecretory structure particle motion, effect of increased K^+ concs. 8-77046
- nitrobenzene, steady state electroconvection, self beating laser spectroscopy 8-87408
- noble metal aggregated film, light scatt. 8-64423
- nonlinear scatt. in limit of ultra-strong fields 8-79067
- nonspherical particles, Mueller scatt. matrices 8-90366
- nonspherical particles size distrib. from scatt. meas., Mie theory 8-58909
- oil in water microemulsion, added NaCl, light beating spectroscopy of micelles mutual diffusion coefficient 8-80793
- optical bistability, scatt. light spectrum atomic fluctuations 8-94383
- optical ceramic, KO-1, IR scatt. and brightness indicatrices meas. 8-71164
- optical fibre sinusoidal microbending loss of HE_{11} -mode in step-index fibres 8-79109
- optical instrument light shielding characts., mol. scatt. calc. 8-71189
- optical surface scattering rel. to microroughness, surface transfer function 8-58917
- particle size and velocity simultaneous meas., laser technique 8-70096
- particle size distribution determ. from light scatt. extrema 8-54421
- particle sizing by forward lobe scatt. intensity ratio, diff. theory errors 8-71031
- particle wave scatt. 8-66764
- particles in colloidal state, refr. index, theory 8-95567
- particulate matter suspended in water, vol. scatt. function at near-forward angles 8-55299
- particulate surfaces, multiple scatt. effects, planetary appls. 8-58912
- phase transformation central peaks (*Japanese*) 8-52522
- photoelasticity, three dimensional, non-destructive method for stress-state determ. using scattered light 8-90805
- photographic emulsion, Callier effect, influence on image contrast 8-63017
- photometric etalons, scatt. matrix and brightness coeffs. of MS-20, MS-14 reflectors 8-82020
- photosensitised reacts. in continuous chem. processes, scatt. effects 8-73057
- polarisation dependent scatt. meas., using electro-optical modulator instrument 8-58010
- poly(chlorotrifluoroethylene) films, crystalline superstruct., mol. orientation, X-ray diff., depolarised light scatt. 8-71685
- poly-1,4-phenylene terephthalamide, in H_2SO_4 , dilute soln. viscosity 8-75524
- polyadenylic acid, semi-dil. soln., slow modes 8-53319
- polydisperse samples, scatt. data analysis 8-50702
- polyelectrolyte aqueous salt soln., inelastic light scatt. obs., conformational changes 8-60474
- polyethylene soln., light scatt. from shish-kebab structs. 8-76482
- polyisoprene-g-styrene, dil. soln., conformation, light scatt. obs. 8-91218
- polymer, amorphous, segmental distrib., light-, neutron- and X-ray scatt., piezooptical and dielec. meas., review 8-51444
- polymer solutions, dilute, intrachain dynamics and forward depolarised scatt. 8-68525
- polymer solutions, microgel-containing, physico-chem. and rheological props., light scatt. obs., review (*Polish*) 8-50704
- polymers, dynamic light scattering theory 8-60475
- polystyrene, sol, light scatt. data, Fourier inversion anal. 8-76932
- polystyrene particles flocculation, light scatt. for close range struct. determ. 8-53273
- polystyrene solutions, translational diffusion coeff., light-scatt. meas. 8-52519
- polyurethane-polyurethane acrylate network, microinhomogeneities and props. (*Russian*) 8-51452
- powder, particle size distrib. meas. by spectral transparency method 8-49876
- radiative transfer through fog, 2D numerical soln. algorithm 8-71032
- Rayleigh waves, diffracted intensity of scattered light calc. 8-50993
- reflecting power of scattering layers, with different degrees of dispersity (*Russian*) 8-82909
- reimaging system, out-of-field radiation analysis 8-59117
- retinal blood flow, laser Doppler meas. 8-69174
- rod-like macromolecules in conc. soln., basic kinetic eqn. and appl. 8-67637
- SAW, light scattering on internal refl. 8-64345
- scalar diffusor autocorrelation (*French*) 8-90369
- sea water, multiple light scatt. rel. to dielectric permeability calc. (*Russian*) 8-77261
- seawater, scattering props., statistical and physical models (*Russian*) 8-96222

light scattering continued

- silicic acid sol., gel formation, characteristics of light scattering 8-53269
 silicic and aluminosilicic acids, effect of increased size of scattering centres in sols 8-53270
 slab waveguide with refractive index irregularities, three dimens. scatt. patterns anal. 8-87158
 smectic liquid crystal structural order effects of surface treatment, sample thickness, and cooling rate 8-63667
 smectic-A phases, theory (*Russian*) 8-87618
 smokes, atmospheric, optical probing, homogeneous particle model appl. (*Russian*) 8-77328
 sodium dodecyl sulphate NaCl aq. soln., micellar props., laser light scatt. exam. 8-92513
 solar chromosphere, coherent scatt. rel. to S I 1807 Å and 1900 Å profiles 8-57517
 solutions, fluctuation transport theory 8-70057
 speckle, statistics from mixture of moving and stationary scatterers 8-66765
 speckle patterns, partially developed, effect of occupation no. fluctuations 8-74842
 spheres, structured, scattering problem, integral formulation 8-63010
 spherical objects, vector wave function theory 8-66748
 spherical particles, fine structure of the Mie scattering, specific turbidity resonant structure of a_n and a_b 8-58913
 spherical three-layer particles as cell models, light scatt. and attenuation, shell effect 8-82913
 spheroids in shear flow, light scatt., orientation correlation 8-76481
 spinodally decomposing system, double light scatt. 8-52516
 stellar envelopes, optically thin, of binary and multiple stars, polarisation by Thomson scatt. 8-81655
 stellar radiation scattering on circumstellar clouds, circular polarisation theory 8-96428
 step index fibre, scattering from arbitrarily located inhomogeneity 8-87161
 stratosphere, scatt. profiles rel. to dust meas., (1970-1977) 8-73445
 stray light calculations, surface refl. models 8-58905
 stray light reduction from optical components 8-59114
 stray light suppression in optical systems, optical design, computer analysis 8-59113
 stray radiation analysis using first-order deterministic APART program 8-59116
 stray radiation rejection capabilities of optical systems, GUERAP II program analysis 8-59115
 submicron particle, size distrib. in colloidal suspension FODA 8-61057
 substrate reflectance and medium depth effects in two-dimens. multiple scatt. expt. 8-87011
 surface plasmon radiation, roughness assisted, ang. distrib. 8-52521
 surface scattering of partially coherent radiation, atm. turbulence influence 8-58915
 suspension, particle size and concentration, determ. by light backscatter technique 8-85214
 thermal halo effect, nonlinear scatt. by moving particles, symm. distortions 8-66875
 turbid media, approx. linear relationship for optical response 8-90371
 US wave 3D meas. in transparent solids, Doppler-shifted light scatt. technique 8-90613
 velocity measurement by light scattering techniques, digital correlation appl. 8-57916
 Venus, clouds, anisotropic scattering model 8-53852
 Venus clouds, H_2SO_4 aerosol medium IR scatt. coeffs. 8-65526
 very rough surface, backscatt. light, polarised and depolarised components 8-63009
 weak diffusers with small number of correlation areas, speckle contrast 8-90370
 zodiacal light, circular polarisation theory 8-96428
 zodiacal light, wavelength dependent model, Mie scatt. and thermal emission 8-81587
 Ar, light depolaris., pair-pair correlations 8-63536
 CS_2 , liq., light scatt. intensities, struct. models 8-60476
 CdS , chem. sprayed film, struct. and morphology 8-72020
 CdS , collision controlled light scatt. by electrons, influence of elec. field (*Russian*) 8-64375
 DyAG, crit., tricrit., and crossover phenomena, light scatt. 8-68251
 $FeCl_2$, magnetic phase diagram, optical studies 8-88121
 $FeCl_2$, metamagnet, optical determ. of thermodynamic phase diagram 8-60285
 $Fe_{1-x}Cl_xCd_x$, randomly disordered, tricrit. behaviour, light scatt. 8-68255
 $Ga_{1-x}Al_xSb$, small wave vector modes 8-75785
 Ge, electron-hole drop velocities as probe of phonons 8-68517
 Ge, electron-hole drops, accel. by IR radiation field 8-95264
 H_2 , gas, radiative light scatt., approx. line shapes 8-90221
 KH_2PO_4 , central components in ferroelec. phase 8-56436
 $LiNbO_3$, partial waves of SAW, direct meas. by light scatt. 8-66994
 $LiTiO_3$, light scatt. from ferroelec. domains 8-80310
 N_2 , compressed, depolarised light scatt., different contributing processes calc. (*French*) 8-79406
 Na, $^{23}P_{3/2}$ - $^{23}S_{1/2}$ reson., light scatt. polarisation change 8-55144
 NaCl:Ca, light scattering coeff., effect of growing condition 8-55418
 Na_2O - CaO - SiO_2 , glass, light scatt. rel. to heat treatment (*German*) 8-84598
 $PbMoO_4$, SAW props. 8-63920
 Si, beam extinguishment device, without scatter 8-87126
 VO_2 , light scatt. near semicond.-metal phase transition 8-60414

light sources

- see also *infrared sources; light emitting devices; photometric light sources; spectroscopic light sources*
 anisotropic emission source, polarisation characts. meas. 8-74047
 aureole around UV source at finite distance 8-77320
 aureole radiation field about point source in scatt.-absorbing medium 8-77319
 black body radiation, anisotropy and temporal coherence 8-58904
 brightness measurement, standard photometric system errors 8-58005
 coherence and radiometry, basic concepts 8-66745
 correlation coeffs. of planar sources and their far fields 8-66750
 D illuminants and sources, review of use in colorimetry 8-65955
 D lamp calibration for transfer standards using synchrotron radiation 8-65954

light sources continued

- dark field magnification microphotographic illumination system 8-58025
 DORIS double storage ring, synchrotron radiation source in X-ray and UV regions 8-62668
 fibre-optic light source for curved platen illumination 8-63163
 fluctuating sources and second-order radiometry 8-50879
 generalised radiance uniqueness theorem 8-94365
 generalized partial coherence of a radiation source and its far-field 8-58903
 illuminants which give prescribed tristimulus values to given object colours, design technique (*Japanese*) 8-94420
 illuminator using laser light source, geometrical optical anal. (*Russian*) 8-79094
 incoherent circularly symmetric source, sampling theorem for complex degree of coherence (*French*) 8-79088
 inhomogeneous source radiant intensity, averaged cross-spectral density concept 8-74958
 intensity distrib., far field laser and partially coherent sources, comparison 8-66751
 Kohler illumination using fibre optics and quartz-halogen lamp 8-58027
 luminaire with mirror cylindrical surfaces design using luminous flux balance method (*Russian*) 8-63166
 luminaire with paraboloid reflectors, design, cylindrical luminous body dimensions calc. (*Russian*) 8-63165
 pinhole light source, bright and inexpensive, using optical fibres 8-83058
 polar intensity distribution influence on MTF meas. 8-50723
 radiation fields from polygonal sources, Fock method 8-83060
 random nonGaussian backgrounds, simulation, calc. spatial correl. function 8-79089
 reverse pinch effect cavity pulsed light source for photolysis 8-87114
 safelight for Agfa 10E75 and 8E75 plates 8-74087
 scalar wave fields of fluctuating primary planar sources, coherence and radiant intensity 8-90355
 solar radiation simulator, non-axial type, reflector profile calc. (*Russian*) 8-63169
 synchrotron radiation appls., characts. and sources 8-74960
 thermal radiation sources for speckle interferometry 8-49891
 tunable, GaAs crystals with nipi superstructures appl. (*German*) 8-95064
 undulator linac, electron dynamics, coherent radiation source 8-82539
 UV, low-power, with electronic chopper 8-79087
 UV sources for curing 8-88443
 Ar lamp, pulse-operated, for VUV irradi. (*Russian*) 8-75453
 CaH, in RF-excited heat pipe oven, efficient arc source 8-63162
 Cd discharge, low-pressure, high current, intensity in middle UV 8-50878
 H-He arc lamp, 60-360 nm, calibration 8-87117
 H_2 stabilised arc as vacuum UV radiation standard for 600 to 900 Å 8-66879
 He-Ne lasers, standard wavelength sources 8-74957
 MgH, in RF-excited heat pipe oven, efficient arc source 8-63162

light transmission

- see also *light absorption; optical filters*
 aerosol, H_2O -droplet, CO_2 laser beam clearing process, transmission function ratios 8-88919
 atmosphere, aerosol content determ. from photometric obs. of stars 8-92976
 atmospheric transmittance, profile depend., line parameter vars. 8-77322
 Beer-Lambert modified law calc. 8-82906
 biaxial crystal plate, refl. and trans. wave amplitude 8-95573
 biphenyl, phase transitions at 40 and 16K, transmitted light intensity meas. 8-51663
 biphenyl- d_{10} , phase transitions at 38 and 24K, transmitted light intensity meas. 8-51663
 ceramic crystalline materials, IR transmission, review 8-55417
 coated substrate, transmittance and reflectance, film refr. index meas. 8-56534
 dielectric interface, Gaussian beam characts. 8-66747
 dispersive media, Ewald dynamical diffr. theory extinction theorem 8-66749
 film, computational algorithm for optical constns. determ. 8-72617
 gas in applied elec. field, IR transmission modulation (*French*) 8-50912
 glass, high-transmission, least-squares method for extinction coeff. determ. 8-90470
 glass packet specimens with antisolar filler 8-90469
 glass-ceramics, transparent, microstruct. and props. 8-59960
 homogeneous layer, transmission and refl. coeffs., integral eqn. (*German*) 8-82907
 homogeneous plane-parallel atmosphere, unified treatment of reflected and transmitted intensities 8-85838
 IR lens production tests 8-50890
 IR radiation spectral absorbance and transmittance, accurate modelling technique 8-91062
 isotropic layers, thin, with rough boundary surfaces, refl. and transmission factors (*German*) 8-90354
 Jupiter, atmosphere, $^{12}CH_4$ ($^{13}CH_4$) ν_4 band, line parameters, 7.7 micron transmission 8-85894
 layer with exponentially varying refr. index, oblique incidence of light, interf. matrix 8-55296
 multi-element interference filters using different grids, far IR characts. 8-90507
 multiple-plate glass systems, spectral directional radiation characts. prediction 8-74956
 nematic liquid crystal twisted layer 8-68476
 non-redundant scanning, high efficiency freq. modulation, of light beam in half space 8-78907
 non-redundant spectral tunnelling through periodic struct. at total refl. 8-78906
 optical fibre, transmission characts. of graded-index fibres with lossy outer layer 8-55437
 PMMA, rain erosion behaviour, exam. 8-53001
 quartz, cultured cryst., vacuum UV transmittance before and after electron irradi. 8-83044
 rhabdome transmittance decrease due to blue light, rel. to desensitisation of peripheral photoreceptors 8-64993

light transmission continued

- scattering material, transmittance and reflectance meas. by specular hemisphere method 8-58004
- semiconductor, sound-induced anomalous transmission of light below plasma edge 8-68475
- shadow methods, reflected, transmitted, obs. of sharp V-notched plates, under pure bending 8-90777
- spectrophotometer for colour and UV/vis. range, Pye Unicam SP8-100 8-93768
- tellurite glass, Cu^{2+} and Ni^{2+} doped, band-pass filters for 550 to 616 nm, transmission characts. 8-71166
- through reflecting cylindrical tubes, demonstration 8-73812
- trajectories of reflected and transmitted beams in oblique tunnel effect 8-78903
- transparent nonlinear layer, light refl. and transmission (Russian) 8-71142
- turbid atmosphere, transparency characts. calc. 8-81407
- turbid media, approx. linear relationship for optical response 8-90371
- two-phase systems, mean specific surface area, light transmission meas. (German) 8-89431
- underground optical cable transmission meas. 8-50942
- Au discontinuous film, optical transmittance, effect of island morphology 8-84673
- BaF_2 , optical ceramic, hot pressing in vacuum, rel. to spectral transmission 8-52730
- CdO-SnO_2 film, DC sputtering prep., visible and near IR transmission, resist. 8-88049
- $\text{Cd}_{1-x}\text{Zn}_x\text{S}$, RF sputtered electro-optical film for data storage and display 8-83047
- CuBr , evaporated film, magneto-optical effects on exciton bands 8-72624
- CuCl , evaporated film, magneto-optical effects on exciton bands 8-72624
- Ge, monocryst., for IR optics, prod. techniques and characts. 8-50873
- GeSe_2 film, glassy, self-controlled laser-beam chopping effect 8-60528
- In_2O_3 , transparent electrode deposition on PLZT ceramic, elec. and opt. props. 8-74848
- $\text{In}_2\text{O}_3\text{-SnO}_2$, magnetron RF sputtered electro-optical film for data storage and display 8-83047
- LiNbO_3 , transparency with vacuum-deposited electrodes (Russian) 8-60422
- Na_3AlF_6 , effect of temp. var. on light transmission 8-79136
- NaSbSe_2 films, struct., photoelec. and opt. props. 8-51834
- Se, red amorphous film, textural change, thermal and photo effects 8-63951
- Se spheres embedded in polymer matrix, electrophotographic film, optical props. 8-83055
- $\text{SiO}_2\text{-Ta}_2\text{O}_5$, plane optical waveguide, fabrication by reactive sputtering 8-71221
- SnO_2 , transparent electrode deposition on PLZT ceramic, elec. and opt. props. 8-74848
- Ta_2O_5 , plane optical waveguide, fabrication by reactive sputtering 8-71221
- ZnGeP_2 , synthesis, characts., applic. to laser windows (French) 8-80467
- $\text{ZnO-Al}_2\text{O}_3\text{SiO}_2$, transparent glass-ceramic, microstruct., physical props., crystallisation ht. treatment depend. 8-80506
- ZnS , effect of temp. var. on light transmission 8-79136

light velocity

- gravitational potential of source, Laplace's deduction of differential aberration (German) 8-57838
- special relativity, secondary-school course not relying on historical approach 8-86096

light velocity measurement

- frequency determination of laser light by interferometric comparison, speed of light derivation 8-55395
- laser freq. meas. and determ. of C, review 8-81952
- special relativity, meas. by stable clocks 8-54185

light water see water**lighting**

- chromatic adaptation effects and colour appearance at various illum. levels (Japanese) 8-92628
- colour changes due to distance and lighting, direct assessment using Natural Colour System 8-57004
- illuminants which give prescribed tristimulus values to given object colours, design technique (Japanese) 8-94420
- radar precipitation maps as lightning indicators 8-85652
- static interruptor cct., triac, thermostatic and lighting control appl. (Italian) 8-73984
- visual luminance difference threshold, Holladay's principle (Japanese) 8-65000

lightning

- aircraft skin, lightning damage simulation 8-87575
- ball and bead lightning, new theory (French) 8-92884
- ball lightning, appl. of transmission line model for fireball plasma formation 8-59702
- ball lightning, elec. discharge into sand layer expts., erosion-discharge model 8-81322
- ball lightning 8-88900
- ball lightning explanation by water electrolysis and combustion 8-69436
- book 8-53713
- discharge processes, VHF technique for space-time mapping 8-85721
- EM fields radiated from lightning return stroke, Maxwell eqns. exact soln. appl. 8-73442
- flash counter and interval recorder 8-88928
- ground-flash multiple-stroke discriminator cct. 8-81446
- intracloud lightning discharges, inclination 8-73440
- ionisation in power station plumes, effect on natural lightning 8-88909
- magnetic component of induced lightning voltage, calculation, supplement (French) 8-73419
- multipulse lightning discharge oscillogram scanning camera 8-61588
- photoelectric detector for daytime lightning 8-57336
- return stroke channel, transmission line model, computer soln. 8-85644
- shielding against direct lightning strokes, theory 8-88899
- and spark discharge leader-stroke velocity comparison 8-94947
- stroke current meas. using optical fibre cable and optoelectronic conversion, rocket launched 8-92930

lightning continued

- superbolts rel. to positive current lightning distrib. 8-57254
- theory of the main discharge of lightning (French) 8-92887
- UHF atmospheric, emissions from lightning discharge considered as plasma 8-61497
- upward lightning stroke parameters (German) 8-57237
- lightning conductors see lightning protection**
- lightning protection**
see also surge protection
book 8-53713
shielding against direct lightning strokes, theory 8-88899
- lightning rods see lightning protection**
- limit, elastic see elastic limit**
- limit cycles**
autocatalytic reaction system, sustained oscills., deterministic and stochastic theories 8-95922
autonomous dynamic systems, limit cycles and one parameter transformation groups 8-49641
bifurcation and nonequilibrium phase transitions of limit cycles and multiperiodic flows in continuous media 8-81937
channel, straight (buckled), two-dimens. flow, stability anal. 8-59490
dynamic nonlinear systems containing limit cycles 8-77666
plasma, nonlinear mode coupling model eqns., topological struct. 8-75304
smooth vector fields, geometrical generalization of relation between limit cycles and symms. 8-54163
stable limit cycles of vector fields, new negative criteria 8-57756

limited space charge accumulation

- see also Gunn effect; negative resistance effects; space-charge limited devices
- No entries

linear accelerators

- see also electrostatic accelerators
- accelerating system, RF adjustment 8-78523
- autoresonant accelerator, lower bound for length 8-50419
- cavity anal., evaluation of LACC program 8-90000
- charged transmission line for pulsed high current accelerators, energy transfer 8-78519
- coaxial autoaccelerator, klystron instability of relativistic electron beam, stability criterion 8-82541
- coaxial autoaccelerator, resonant instabilities of relativistic electron beams 8-82540
- collective ion acceleration, by temporally modulated relativistic electron beam 8-50422
- control computer for Chalk River electron test accelerator 8-90004
- Darmstadt linear accelerator, detector system and performance of elec. scatt. system 8-70680
- Darmstadt linear accelerator electron scatt. facility, beam transport and spectrum. 8-70679
- Darmstadt linear accelerator electron scatt. facility, data processing 8-70681
- Darmstadt linear accelerator high resolution scatt. facility 8-70653
- deuteron accelerator, two freq., for high power neutron generator, expt. 8-78540
- electron, high energy low running cost linac, proposed design (Japanese) 8-78516
- electron, high-current injector 8-70655
- electron, pion production and appls. (Japanese) 8-78533
- electron, pulsed, giving 20 ps 300 A electron pulses, radiation chem. appl. (Japanese) 8-80754
- electron, radioisotope production, review (Japanese) 8-78534
- electron, status, uses, 500 MeV 100 kW linac design (Japanese) 8-78514
- electron accelerator, dose monitoring system 8-92710
- electron beam, intense, ns, production in linear accelerator, space charge and radiation field effects 8-70654
- electron guns, high-current, laminar beam formation 8-74516
- energy doubling using coupled cavities (Russian) 8-70652
- ETL electron accelerator, energy increased up to 40 MeV by improvement of klystron efficiency (Japanese) 8-78515
- GELINA, electron linac, neutron time of flight meas. appl. 8-90002
- Harwell linac II total scatt. spectrometer, calibration using Ni diff. data 8-86725
- heavy ion accelerator, ring compressor magnetic field distortion by disconnected multirun coils 8-66436
- heavy ion experiments at UNILAC (German) 8-66435
- heavy ion fusion, linear accelerator facilities at Argonne 8-50327
- heavy-ion accelerators, book contrib., review 8-90003
- HF struct., standing waves in strip transmission line (German) 8-50420
- high-current pulsed linear ion accelerators, insulated drift tube 8-50417
- ion beam neutralisation in transverse mag. field 8-78513
- ion beams from pulsed linear accelerator for inertial fusion 8-50325
- ions, collective acceleration in linear electron flow (Russian) 8-90001
- Mainz 300 MeV linear accelerator, energy loss system of electron scatt. facility 8-58524
- neutron dose levels of 8 MeV linear accelerator and 18 MeV betatron used in radiotherapy (German) 8-69221
- neutron production by electron linear accelerator beam (Japanese) 8-78532
- NUMATRON project, high energy heavy ion facility, design, performance 8-62665
- Philips SL75-20, 18 MV photon beam, fast and slow neutron contamination 8-65127
- proton accelerator, with quadrupole RF focusing, URAL-15 8-82543
- proton radiography beam line establishment at Fermi National Accelerator Laboratory 8-65121
- pulse amplitude instability meas. apparatus 8-82537
- quasi-static drift tube accelerating structs. for low speed heavy ions 8-82542
- radiotherapeutic linear electron accelerator NEPTUN-10p 8-88744
- relativistic electron beam accelerator, FX-75, 1-D coaxial transmission line model, FXPULSE program 8-58506
- relativistic heavy ion accelerator description and applications (German) 8-78522
- self-magnetic insulation in vacuum for coaxial geometry 8-78520
- standing wave high gradient structure, design concept 8-50423
- Tohoku 300 MeV Linac, energy compressing system 8-74515
- undulator linac, electron dynamics, coherent radiation source 8-82539

linear accelerators continued

UNILAC, Darmstadt, kinetic energy of ^{86}Kr accelerated ions, recoil proton technique 8-58527
 UNILAC, heavy ion collisions up to 10 MeV/nucleon review of recent developments 8-50194

linear algebra

see also *determinants; eigenvalues and eigenfunctions; matrix algebra; tensors; vectors*
 array algebra for multilinear least squares prediction and filtering 8-69470
 classical mechanics, canonical formalism, Bose type classical Hamilton algebra, phase space variables 8-54170
 conformal mapping technique for plate vibrs. on elastic foundation 8-79251
 dynamical system, connectance, increasing no. of degrees of freedom 8-81831
 four-velocities in quantum theory, K-space 8-49720
 Gauss and Mainardi-Codazzi eqns. generalisations, appls. to quantum and classical mechanics 8-62092
 gyroscopic system, linear, damped, modal anal., appl. to satellite 8-63275
 heat pipe, heat transfer agent flowrate through porous wick, approx. calc. method 8-75197
 Hermitian, antiHermitian and unitary operators, basic props. for quantum mechs. appl. 8-54113
 linear response theory and area preserving mappings, review 8-62174
 orthonormalisation method, appl. to j-j coupling of fermions in single j-shell 8-81922
 partial differential equations, multidimensional, fast implicit iterative soln. method 8-93519
 quantum field theory, conformal-invariant, composite field operators 8-81886
 representation of linear operators in L^2 spaces, generalised matrices 8-62095
 spin-1/2 models, on square lattice, sublattice renormalisation transformations 8-65878
 temperature field, heat transfer problems, linear algebraic soln. method 8-59281
 tube, circ., entrance region, mass transfer, asymptotic expansion soln. 8-87392

linear combination of atomic orbitals calculations see *LCAO calculations*

linear differential equations

active electrooptic and magneto optic media, matrix theory fundamentals (Russian) 8-63005
 confined solutions of multidimensional inversion equations 8-77678
 continuum mechanics, macroscopic determinancy principle corollaries (Russian) 8-77714
 Feynman integrals, singularity struct. study using micro differential eqns. 8-74123
 fourth order, numerical soln., finite difference formulae for boundary value problems 8-73856
 Helmholtz homogeneous equation, numerical soln. methods (German) 8-90337
 hyperbolic mixed boundary value problem, soln. existence, uniqueness, hydraulics appl. (German) 8-93514
 linear two point boundary value problems, reduction to Cauchy systems 8-54158
 matrix differential equation, rotations as solns., for teachers 8-62021
 motion in spherically symmetric force fields, vector consts. differential eqn. 8-85833
 periodic coefficients with small modulation, solution techniques 8-87155
 second order, symm. and separation of variables (Russian) 8-65752
 second order, symm. and separation of variables (Russian) 8-73828
 second order linear partial differential eqns. of math. phys., integration by separation of variables (Italian) 8-81798
 Seidel's process for linear eqns. with non-negative elements (Ukrainian) 8-54165
 shape of drop on inclined plane, analysis 8-79856
 solution of $dy/dx = (a_1x + b_1y + c_1)/(a_2x + b_2y + c_2)$ 8-77641
 stability criteria for time-dependent flows 8-79305
 total dynamic characteristics of meas. facilities, limit error estimation 8-77841
 with variable algebraic coeffs., Laplace transforms appl. (Czech) 8-86115
 vector-matrix differential eqn., convergence of assoc. eigenfunction expansions 8-69965

linear integrated circuits

automatic camera lens focusing, using optolinear chip 8-54480

linear programming

elastic contact stress minimisation by contour design 8-63396
 elastoplastic arches, shakedown anal. 8-51091
 optimal control of 1-D linear distributed parameter systems with cost functionals 8-59257
 optimal water distribution systems design 8-61457
 pattern recognition, mathematical programming techniques 8-92523
 water shortage and supply, Israel, long-run policy for agriculture 8-61454

linear rectification see *rectification*

linear systems

acoustic system identification, from multiple input/output data, comment and reply 8-83179
 instrument mechanism analysis, error statistics (Hungarian) 8-49823
 multiple parameter system vibrations and stability, book 8-93532
 optimal control of 1-D linear distributed parameter systems with cost functionals 8-59257
 stability of motion rel. to part of variables (Russian) 8-86144
 stream-well-aquifer system groundwater flow anal., linear system models 8-77289

linear vibrations see *vibrations*

linearisation techniques

see also *piecewise-linear techniques*

AC potentiometer, self-balancing, nonlinear servomechanism design (Russian) 8-70156
 galvanomagnetic semiconductor voltage and current transducers, Gauss effect compensation 8-77892
 illumination measurement appl., digital linearisation using microprocessors (German) 8-77961
 materials analysis spectrophotometer with linear output 8-86344

linearisation techniques continued

matrix Riccati eqn., quasi-linearisation, iterative approx. 8-57871
 multi-input nonlinear system statistical anal. by optimal linearisation (German) 8-64918
 pure harmonic tide in canal, eqns. of motion quadratic resistance term linearisation 8-69369
 tail-wheel struct. of light aircraft, large deflection anal. using incremental linearisation 8-83272
 thermistor thermometer bridge network charact. linearisation (German) 8-86271
 water network anal. using sparse matrix and successive linearisation methods 8-85614
 Pt resistance thermometer calibration characts. linearisation methods (Russian) 8-70123
 Pt-Rh resistance thermometer temp. convertor for nonlinearity error correction (Russian) 8-70124

linewidths (spectral) see *spectral line breadth*

linguistics

contrastive, P-struct. C-struct. grammar 8-69959
 Japanese, consonant perturbations, and vowel articulation by adjacent segments (Japanese) 8-92655
 Japanese kinki dialect, anal. and perception of two-mora word accent types (Japanese) 8-92659
 subglottal air pressure and vocal-fold tension, indirect assessment of contrib. to changes of fund. freq. in English 8-92650

linguistics, language see *linguistics*

linkages (electric connectors) see *electric connectors*

linking see *joining processes*

Liouville equation

see also *Vlasov equation*
 CIDEF theory, stochastic-Liouville vector model with asymptotic soln. 8-66567
 convolutionless master equation, perturbation expansion 8-70047
 Heisenberg eqns. on C^* algebra of quasilocal observables, boson and fermion systems 8-57854
 higher monotonicity properties of certain Sturm-Liouville functions 8-57750
 many body problems, real time Green's function 8-57855
 membrane, passive transport through open membrane, multicomponent system, statistical-mech. theory 8-67261
 nonlinear transport, in Burnett order, theory 8-49778
 relativistically invariant generalised quantum kinetic eqn., Liouville eqn. basis 8-54299
 single-parameter quasi-Liouville system periodic soln. sets (Russian) 8-73833

lip microphones see *microphones*

lipid bilayers

anaesthetics, general, site of action, X-ray and neutron diff. and solubility data 8-77008
 biomembranes, lipid-protein interactions, flexoelectric effects 8-92600
 byotropic liquid crystalline and other lamellar phases in lipid-water systems 8-92592
 cholera toxin effect, formation of ion transport channels in bilayers containing gangliosides 8-88702
 cholesterol model 8-56953
 cytochrome c interaction with bilayer phospholipid membranes 8-69001
 diffusion transport modelled by dimeric β -cyclodextrin complexes, cryst. struct. anal. 8-80838
 dipalmitoyl lecithin-water system, lyotropic liq. cryst., pretransitional effects, PMR second moment meas. 8-91234
 dipalmitoyl-phosphatidylcholine bilayer membrane, melting point rel. to electrostatic field 8-92602
 dipalmitoyl phosphatidylcholine lamellar phases and bilayer phase transitions, structural parameters 8-64948
 electrical strength fall after UV irradi. 8-69002
 galvano-static regime of non-steady process 8-64963
 gramicidin A channel cation flux interaction 8-56957
 interaction forces in zone of contact 8-53345
 intervesicular lipid transfer, direct fusion of phospholipid vesicles, kinetic basis comparison 8-96034
 lecithin bilayers, density and mol. interactions 8-80837
 lecithin membranes, mag. susceptibility anisotropy, phase contrast microscope obs. 8-92601
 lecithin-water systems, bilayer connecting passages 8-96028
 lecithins, L_α phase, shear-induced biaxiality 8-95997
 liposomal membrane permeability, radioresist. 8-80919
 liposome phasic transitions, use of hydrophobic fluoresc. probes 8-96021
 melamine resin, as water containing embedding medium for electron microscopy 8-92764
 mitochondrial lipid components of rat liver, Ca^{2+} transport system 8-64966
 orientational long-range order, phase transition, coherence lengths 8-92593
 permeability modification by drugs 8-69026
 phase transition, cluster model, appl. to bilayer mol. passive permeation and struct. relax. 8-53346
 phosphatidyl ethanolamine, charge distrib., dipole moment, CNDO calcs. 8-80840
 phospholipid bilayer melting transition, thermodynamic fluctuations, ion permeability, statistical mechanics model 8-73140
 phospholipid bilayers, van der Waals interactions, total potential curves 8-77006
 phospholipid vesicles, surface charge equilib. distrib., calc. method 8-96019
 phospholipid vesicles, surface charge equilib. distrib., calc. results 8-96020
 Raman studies of biomembranes, phospholipid-d, as nonperturbing components 8-53330
 saddle-splay elasticity and mol. asymmetry 8-92594
 solvent-depleted membrane prep. from conc. lipid solns. 8-53347
 spin-labelled, pure, EPR lineshape evidence of phase transitions 8-69004
 structure, X-ray refl. phases from oriented model membrane systems 8-96022
 synthetic voltage-dependent cation-selective transmembrane channel characterisation 8-77009
 US effects on cond. and capacitance, 1 MHz 8-77082

lipid bilayers continued

- water and thermal diffusivity in lipid-water smectic phase, light scatt. meas. 8-96031
 K⁺ permeability of mitochondrial and artificial bilayer membranes 8-53365

liquefaction of gases

- superconducting magnet circulation cooling system based on He liquefaction apparatus 8-57992
 superconducting magnet-Large Coil Program, He liquefier-refrigerator and distrib. system 8-50398

liquid alloys

see also liquid metals

- binary, surface tension, compressibility and surface segregation 8-67889
 concentration fluctuations, nucl. quadrupole spin relax. 8-91975
 electromigration, driving force expression 8-51714
 ferrous eutectic liquids, exam. of structures 8-71668
 highly resistive, temp. depend. on elec. resist. 8-91657
 molten metallic system, contribution to sign inversion of effective charge (Czech) 8-60656
 penetration mechanism, in WC-Co sintered hard alloy 8-60619
 steel, molten interfacial tension in phase boundary molten CaO-SiO₂-Al₂O₃-CaF₂ slag (Czech) 8-63908
 steel, nonmetallic inclusion behaviour simulation by multiple phase medium eqn. (Russian) 8-94965
 structure, thermodynamic and transport props., book 8-51406
 transition metal alloys, thermoelectric power 8-91675
 transition metals and alloys, elec. resistivity, Hall coeff., mag. susceptibility 8-95280
 vapour pressure, pseudopot. and Gibbs-Bogoliubov calcs. 8-83935
 Ag-Ge, viscosity, temp. depend. (French) 8-59964
 Ag-Li, solid and liquid alloys, calorimetric investigation of mixing enthalpy (German) 8-52773
 Al base alloys, contact reactions with Fe group metals 8-60879
 Al-Cu-Fe alloys, exam. of constitution and mag. props. (German) 8-52206
 Al-Ga-In, liq. alloys, excess Gibbs functions 633 to 1173K 8-60655
 Bi-Pb-Sn, molten metallic system, contribution to sign inversion of effective charge (Czech) 8-60656
 Ca-Ag(In), liquid alloy, thermodynamic exam 8-75848
 Cd-Pb-Bi-Sn system, ternary liq. alloys, thermodynamic props. 8-51701
 Ce-Co, charge transfer effect 8-94967
 Ce-Cu, charge transfer effect 8-94967
 Cs_{1-x}Au_x, metal-nonmetal transition, electronic theory 8-79930
 Cu-(Sn)Ti melts, wetting of SiC 8-68664
 Cu-Ga(Gd), mag. susceptibility, diamagnetism 8-72326
 Cu-M, M=Al,Cd,In,Ga,Zn, magnetic susceptibility, comp. and temp. depend., melting effects 8-52202
 Cu-Pb liquid alloys, exam. of O diffusivity at 1430K using electrochemical cell 8-51713
 Cu-Sn liquid alloys, thermodynamic meas. 8-52765
 Fe, pig, liquid gas bubble form. at nozzles, acoustic exam. 8-52723
 Fe-based solns., liq., diffusion of N 8-75862
 Fe-C, levitated drops, carburisation and decarburisation in CO-CO₂ gas mixture, exam. of reaction kinetics 8-85053
 Fe-C melt, mag. susceptibility and short range order, 900-1800°C 8-84382
 Fe-C melts, short-range order, neutron scatt. obs. (German) 8-71669
 Fe-Ni liquid alloy, physical and chemical props. deviations from Raoult's law (Russian) 8-95729
 Fe-Ni melt, short-range order, m.p. to 1750°C (Russian) 8-94966
 Fe-Si, liq. alloys, surface tension, sessile drop method meas. (French) 8-84029
 In alloys, concentration fluctuations, nucl. quadrupole spin relax. 8-91975
 Li_{1-x}Pb_x, metal-nonmetal transition, electronic theory 8-79930
 Mn_{0.6}Ni_{0.4}, liq., soln. enthalpies of C and Mn, enthalpy determ. for graphite-diamond transform. and Mn₂C₂ form. 8-59945
 Na-Cd, mag. susceptibility, diamagnetism 8-72326
 Na-K, liq., static struct. factors 8-63664
 Na-K, liq. alloy, electronic correl. functions calcs. 8-63663
 Na-K, liq. alloys, electromigration driving force expression 8-51714
 Na-Rb, liq. alloys, electromigration driving force expression 8-51714
 Na-Tl, mag. susceptibility, diamagnetism 8-72326
 Pb-Ag, liquid alloy, exam. of thermodynamic props. using solid oxide galvanic cell 8-75851
 Pb-Bi, liquid alloy, chemical and intrinsic diffusion coeffs., exam. (German) 8-83987
 Pb-Zn, liquid phase immiscibility determ., DTA 8-64523
 Pd-Si, liq., mag. susceptibility 8-95415
 Sn-Ge(Au), liquid alloy, exam. of activity and heat of mixing, using mass spectrometry 8-51706
 Sn-In dil. liq. alloy, electrodiffusion and electroconvection, effective diffusion coeff., apparent effective valence 8-87802
 Sn-Sb dil. liq. alloy, electrodiffusion and electroconvection, effective diffusion coeff., apparent effective valence 8-87802
 Te-Co(Cr)(Au)(Ag), dil. liq. alloy, elec. cond. at high temp. and press. 8-87959
 Te-Sb, liq., elec. cond. 8-84186
 Te-Tl system, thermodynamic investigation, enthalpy of form. at elev. temps. 8-52774
 W-Ni liquid alloys, sintered, coarsening of W grains, exam. 8-56598

liquid crystal devices

- alignments of director using submicrometre periodicity gratings 8-63666
 cells, pretilt influence on capacitance voltage depend. 8-83724
 cholesteric liquid crystal visualisation of microwave fields 8-58031
 cholesteric-nematic liq. cryst. mixtures, electro-optic charact., light scatt. modes (Japanese) 8-79527
 colour filter, electrically controlled 8-83113
 Controlled phase transparencies in coherent-optical systems performing Walsh and Hilbert transformations 8-50931
 display mechanism, smectic cryst., electrically induced scatt. texture and elec. reversal 8-83725
 display technique 8-51419
 electro-optical modulators for two-dimensional data processing 8-79141
 feedback optical system using liquid crystal light valves 8-66924

liquid crystal devices continued

- field induced twisted structure with quasihomotropic boundary conditions, electro-optic behaviour 8-60424
 fluorescent shutter, fast, based on guest-host interaction 8-83092
 image transducer, real-time, response time 8-74845
 indicator of variable light-reading angle 8-57932
 light valve, appl. to real-time optical data processing 8-83102
 MBBA, deflector based on frustrated total internal light refl. 8-50934
 MBBA-PCB (41 wt.%) pleochroic dye, electrothermo-optic effect, optical storage device appl. 8-87611
 nematic mixtures, extended range, for appl. in electro-optic devices 8-83728
 optical shutter, applic. of guest-host interaction 8-74988
 organic surfactants for liquid crystal orientation control 8-91251
 PCB, nematic liq. cryst., US imaging, convertor, acousto-optical effect 8-59218
 photoactivated liquid crystal light valves, CdS film, pure and Al doped 8-60162
 picture taking parameters display in amateur cameras, review 8-89578
 real-time image optical subtraction scheme 8-74856
 semiconductor-liquid crystal interface props. (Rumanian) 8-83723
 smectic A liquid crystal, scattering textures, appl. to display device 8-91236
 smectic displays, thermo-optic and elec. field effects (French) 8-91223
 spatial filters, tunable, in optical signal converters 8-50930
 spatial light modulator using phase transition type liquid crystal (Japanese) 8-79119
 twisted nematic layer, light transmission 8-68476
 US transducer, liq. cryst. cell for US visualisation (German) 8-79179
 variable tilt smectic A electro-optic effect giving stored colours 8-51415

liquid crystal phase transformations

- acoustic emission, appl. to defect dynamics study 8-91232
 p-alkoxybenzylidene-p-n-alkylanilines, thermotropic mesophases, proton spin-lattice relax. 8-91968
 p-alkoxyphenylazo-p-phenylesters, polymorphism, calorimetry (French) 8-51650
 amphiphilic nematic with optically active compounds, cholesteric states and twisting power 8-63846
 aryl p-fluoroalkoxybenzoates, synthesis and mesomorphism 8-91243
 aryl p-fluoroalkylbenzoates, synthesis and mesomorphism 8-91243
 azoxy-4,4'-(di-undecyl α -methylcinnamate), smectic A to smectic C phase transition, optical tilt angle meas. 8-95141
 BBOA, thermal diffusivity meas. by forced Rayleigh scatt. 8-76483
 4-biphenyl 4'-n-alkoxybenzoates, smectic liq. crystals, transition temps., DTA 8-75815
 4-n-butyloxyphenyl-4'-nonyloxybenzoate, edge dislocations in smectic C mesophase 8-91231
 CBOOA, dynamic crit. neutron scatt. obs. near smectic-A nematic phase transition 8-79752
 CBOOA, mag. aligned, smectic A-nematic transition, US absorpt meas. 8-95137
 CBOOA, nematic to smectic A transition, high resolution X-ray scatt. exam. 8-94984
 CBOOA, smectic A to nematic phase transition, crit. neutron scatt. 8-95135
 CBOOA, twist viscosity and mech. props. near smectic A-nematic transition 8-95136
 CBOOA, US attenuation near nematic-smectic A transition 8-87773
 cholesteric helix period, mag. field strength depend. near phase transition to smectic A (Russian) 8-59754
 cholesteryl chloride-cholesteryl crotonate (75:25 wt.) mixture, cholesteric-nematic transition field effect temp. depend. 8-75813
 cholesteryl chloride-cholesteryl pelargonate mixture, cholesteric-nematic transition 8-91244
 cholesterylalkanoates, liq. cryst., optical anisotropy and struct. ordering (Russian) 8-87616
 conference on smectic and lyotropic liq. crystals, Trento, Italy (Jan. 1978) 8-91222
 copolyethylene terephthalate-p-oxybenzoate, nematic phase, thermodynamics 8-91427
 cyano-biphenyl, nematic liq. crystals, director fluctuation quenching by mag. field (French) 8-87613
 4-4'-cyano-octyl-biphenyl, smectic A liq. cryst., elec. field effects, capacitance meas. 8-91237
 4-4'-cyano-octyloxy-biphenyl, smectic A liq. cryst., elec. field effects, capacitance meas. 8-91237
 cyanobiphenyls, 80CB and its mixtures with 7CB, orientational order and elastic consts. 8-91245
 cyclohexane derivatives, mesophases obs. (French) 8-59747
 decylammoniumchloride and bromide, lyotropic nematic struct. 8-51410
 dipalmitoyl lecithin-water system, lyotropic liq. cryst., pretransitional effects, PMR second moment meas. 8-91234
 DOBAMBC, and DOBAMBCC, chiral smectic C liq. cryst., dielec. consts., electroclinic effect 8-94980
 DOBAMBC, smectic A to C transform., birefringence and optical rotary power 8-75812
 p-n-dodecyloxy benzoic acid, liq. cryst. phase transition, thermal studies 8-71843
 EBBA, phase transition enthalpies, 1 bar to 2.5 kbar 8-75814
 EOBC, liquid crystal phase transforms., Raman obs. 8-87774
 trans-4-ethoxy-4'-alkanoyloxyazobenzenes, nematogenic liquid crystals, birefr., order parameters, vol. changes during nematic-isotropic transitions 8-59742
 ethyl-(methoxybenzylidene-amino)cinnamate, low freq. dielec. constant meas. in cryst. and liq. cryst. phase 8-91226
 Freedericks transitions in twisted nematics with surface tilt 8-71671
 N-p-heptyloxybenzylidene-p-heptylaniline, dislocations obs. in smectic A and C mesophases 8-91230
 hexyl-azoxybenzene, twist viscosity and mech. props. near smectic A-nematic transition 8-95136
 HOBACPC, chiral smectic C liq. cryst., dielec. consts., electroclinic effect 8-94980
 n-indecyl-p-azoxy- α -methyl cinnamate, dislocations obs. in smectic A and C mesophases 8-91230
 isotropic-nematic transition, Onsager's orientational order theory 8-79750
 isotropic-nematic transition, pretransition effects study, optical method of determ. of crit. indices (Russian) 8-63847

liquid crystal phase transformations continued

- isotropic-nematic transition, tricritical behaviour 8-75817
 lecithin bilayers, density and mol. interactions 8-80837
 lipid bilayers, cholesterol model 8-56953
 lipid bilayers, long-range order, phase transition, coherence lengths 8-92593
 lipid phase transition, cluster model, appl. to bilayer mol. passive permeation and struct. relax. 8-53346
 lipid-water systems, lyotropic liquid crystalline and other lamellar phases 8-92592
 liquid crystals, structure and dynamics, neutron diff. studies 8-94972
 MBBA, electronic spectra 8-52530
 MBBA, mol. dynamics near nematic-isotropic liq. cryst. transition (*Russian*) 8-84495
 MBBA, polymorphism, positron annihilation obs. 8-72632
 MBBA, solid, NMR and thermal behaviour, cooling and mag. field effects 8-76336
 mesomorphic mixtures, binary phase diagrams, thermodynamic props., diagraph, anisotropy 8-95139
 mixture phase equilibria and transition temperatures 8-63845
 molecular crystal, unidimensional struct. instability charge under torsional force, liquid cryst. transition (*Russian*) 8-87776
 molecular structure effect on mesomorphism, lateral substituents 8-51411
 nematic liquid crystal, acoustic attenuation anomaly above clearing point 8-75816
 nematic liquid crystal, anisotropic interfacial interactions with substrate 8-75532
 nematic liquid crystal, surface structural crit. point 8-91247
 nematic liquid crystal mixtures with low-freq. dielec. relax., phase behaviour 8-91246
 nematic mixtures, binary, induced smectic phases, X-ray diff. obs. 8-94987
 nematic to cholesteric transition, elec. field induced, transient phenomena of relax. 8-75811
 nematic-isotropic mixture, dielec. props., phase diagram 8-52424
 nematic-isotropic phase transition at high press., thermodynamics (*Russian*) 8-87778
 nematic-isotropic transition, nature, field renormalisation group formalism study 8-87775
 nematic-isotropic transition, renormalisation groups calc. 8-59937
 nematic-smectic-A, appl. of crossover calcs. for supercond. phase transitions 8-80098
 4-nitrophenyl-4-octyloxybenzoate, nematic and smectic-A phase, dielec. meas. 8-60392
 NMR expts., state-of-the-art 8-75820
 p-nonyloxybenzoate p-butyloxyphenol, smectic A to smectic C transition, crit. fluctuations, Rayleigh scatt. obs. 8-95140
 octyl-cyano-biphenyl, nematic and smectic-A phase, dielec. meas. 8-60392
 octyl-cyanobiphenyl, elastic props. near nematic-smectic A transition 8-59756
 octyloxycyanobiphenyl, twist viscosity and mech. props. near smectic A-nematic transition 8-95136
 PAA, methyl deuterated, soft-mode dynamics, proton NMR 8-79749
 paradiheptyloxyazobenzol-d, dynamics of smectic-nematic liq. cryst. phase transition (*Russian*) 8-55938
 pentyloxy-cyanobiphenyl, liq. cryst., laser and electrical Kerr effect 8-68477
 4-n-pentylphenylthiol-4'-n-octyloxybenzoate, sp. ht. and crit. behaviour of liq. cryst. phases 8-67816
 4-n-pentylphenylthiol-4-n'-octyloxybenzoate, birefringence, crit. suppression 8-76422
 rigid-rod fluid, thermodynamic props., crit. points and transitions 8-73919
 smectic A liquid crystal, EHD instability and elec. cond. anisotropy (*Russian*) 8-59753
 smectic A to smectic C phase transition, mean field model 8-95142
 smectic A to smectic C phase transition of first kind 8-71844
 smectic C phase, with second order transition to smectic A, molecular tilt, zigzag model 8-94986
 smectic F materials 8-51651
 smectic helixing crystal, dielec. props., temp. and freq. depends. (*Russian*) 8-60380
 smectic liquid crystal, electric field induced Lifshits point 8-71674
 smectic liquid crystal structural order effects of surface treatment, sample thickness, and cooling rate 8-63667
 smectic-A-smectic-C transition, model of tilted mols. in planar layer 8-79751
 TBBA, metastable phase, thermodynamic props., differential scanning calorimetry meas. 8-94985
 TBBA, smectic A-nematic transition, cybotactic cluster form., X-ray obs. 8-95138
 TBBA, smectic C to A phase transition, neutron diff. exam. 8-91428
 TBBA, smectic C to smectic A transition, crit. exponent, neutron diff. obs. 8-95143
 TBBA, smectic phases, orientational order, ^{14}N NQR and double NMR obs. 8-94974
 TDOBAMBCC, chiral smectic C liq. cryst., dielec. consts., electroclinic effect 8-94980
 p-terephthal-bis-aminocinnamate, smectic phases, orientational order, ^{14}N NQR and double NMR obs. 8-94974
 terephthal-bis-p-p'-butylaniline, pretransitional anomaly, US obs. 8-75818
 p-n-tetradecyloxy benzoic acid, liq. cryst. phase transition, thermal studies 8-71843
 trifluoromethyl liquid crystals, effect of mol. struct. on mesomorphism 8-51414
 virtual nematic-isotropic transitions, depolarised Rayleigh scatt. 8-51652

liquid crystals

- see also *cholesteric liquid crystals; liquid crystal phase transformations; nematic liquid crystals; smectic liquid crystals*
 acoustic storage effect 8-94992
 alkoxybenzenes, 4-substituted, liq. cryst. intermediates, prep. 8-51409
 p-alkoxybenzylidene-alkylanilines, solid state, nucl. spin-lattice relax. 8-64294
 amphiphilic, ESR using TCNE^- as spin probe, feasibility 8-75548
 biaxial order parameters, NQR determ. 8-59750
 biomembranes, lipid-protein interactions, flexoelectric effects 8-92600

liquid crystals continued

- bis-(4'-n-alkoxybenzal)-2-chloro-1,4-phenylenediamines, liq. cryst., improved preparation technique 8-75541
 conference on smectic and lyotropic liq. crystals, Trento, Italy (Jan. 1978) 8-91222
 deuterated nitroxide radical probe, synthesis and appls. (*French*) 8-76314
 dipalmitoyl lecithin dihydrate, phase transforms., 20 to 70°C, X-ray diff. obs. (*French*) 8-91436
 dipalmitoyl lecithin-water system, lyotropic liq. cryst., pretransitional effects, PMR second moment meas. 8-91234
 dissipative structures in turbulent movement (*Russian*) 8-55808
 EBBA, liq. crystals, thin layers, addition of iminoxyl radicals, effect on elec. cond. (*Russian*) 8-67641
 Euclidean invariance, spontaneous breaking, long range ordered media, defect, config. classification 8-59748
 free energy, slowly varying orientational order parameters (*Russian*) 8-75533
 lecithin membranes, mag. susceptibility anisotropy, phase contrast microscope obs. 8-92601
 lecithins, L_α phase, shear-induced biaxiality 8-95997
 light scattering, far-field coherence and radiant intensity analysis 8-64372
 lipid bilayers, long-range order, phase transition, coherence lengths 8-92593
 lipid bilayers, saddle-splay elasticity and mol. asymmetry 8-92594
 lipid-water systems, lyotropic liquid crystalline and other lamellar phases 8-92592
 lyotropic, ^{23}Na NMR quadrupole splittings, elec. double layers 8-76345
 lyotropic, C_{18} mono-cis-unsaturated soaps, X-ray diff. and EPR meas. Monte Carlo simulation 8-94981
 lyotropic, containing Cs^+ , ^{133}Cs NMR, chemical shift anisotropies 8-79525
 lyotropic, sodium dodecyl sulphate NaCl aq. soln., micellar props., laser light scatt. exam. 8-92513
 lyotropic, structure rel. to amphiphilic structure 8-51416
 MBBA, liq. crystals, thin layers, addition of iminoxyl radicals, effect on elec. cond. (*Russian*) 8-67641
 mesomorphic mixtures, binary phase diagrams, thermodynamic props., diagraph, anisotropy 8-95139
 p-methoxy-XY-p'-alkyl tolans, mol. struct., packing coeffs., and thermal stability 8-95046
 molecular spectroscopy, conference, Wroclaw, Poland (Sept. 1977) 8-62951
 multipulse NMR line narrowing, appl. to solids and liq. crystals. 8-72424
 NMR in biaxial and uniaxial liq. crystals. 8-75552
 octaphenylcyclotetrasiloxane, mesophase form., neutron diff. obs. 8-91224
 N-pentanol-Na-N-octanoate-water system, partial molar enthalpies 8-75543
 4-n-pentyl phenyl-4(4-pentyl benzoxyloxy)3-chlorobenzoate, flexoelectric and dielec. relax. behaviour 8-94979
 pentyloxy-cyanobiphenyl, liq. cryst., laser and electrical Kerr effect 8-68477
 pitch, solubility 8-67831
 poly-1,4-phenylene terephthalamide, in H_2SO_4 , dilute soln. viscosity 8-75524
 potassium palmitate- d_{31} , spin-lattice relax., chain position and temp. depends. 8-68405
 potassium soaps, heterogeneity of chain lengths, factor in lyotropic polymorphism 8-59746
 properties rel. to molecular structure 8-55807
 semiflexible macromolecule soln. liquid crystalline ordering 8-94963
 structure and dynamics, neutron diff. studies 8-94972
 tensor field of weak inhomogeneous orientational ordering (*Russian*) 8-67640
 three-dimensional order, differences compared to solid cryst. 8-83727
 uniaxial, polarised fluoresc. emission, orientational distrib. function, rot. Brownian motion 8-80390
 X-ray scattering, small-angle, data interpretation (*Russian*) 8-59752
 Cs perfluoro-octanoate, amphiphilic liq. cryst., ^{19}F multipulse NMR study 8-76328
 NH_4 perfluoro-octanoate, amphiphilic liq. cryst., ^{19}F multipulse NMR study 8-76328

liquid drop model (nuclear) see *nuclear liquid drop model***liquid films**

- see also *adsorbed layers; liquid helium; superfluidity; surface tension*
 annular climbing film flow dispersion models 8-83473
 boiling, destabilisation in liq.-liq. systems 8-94588
 boiling, heat transfer peculiarities 8-90656
 boiling liquid thin film rupture, heat-transfer surface state effect 8-55552
 boiling mechanism during burnout phenomena in subcooled two-phase water flows 8-94529
 classical fluid structure near solid substrates 8-63655
 condensate film flow on finned surfaces, heat transfer, heat exchanger design 8-75038
 condensation enhanced by surface forces, optimum condenser tube fin geometry 8-75039
 continuous flow squeeze film, load-bearing capacity 8-87306
 convective coupled heat transfer, Nusselt no. computation, laminar fluid film 8-59398
 counter-current two-phase flow, annuli, rod bundles, liq. film behaviour, flooding 8-59452
 cumene, films, thin, wetting, rheological characts. determ., capillary method 8-51788
 n-decane, films, thin, wetting, rheological characts. determ., capillary method 8-51788
 dielectric liquid, film condensation, heat transfer enhancement in elec. field 8-55551
 entrained, thickness, effect of surface induced gradual viscosity increase 8-83488
 ethanol-water mixture, saturated, min. film boiling temp. on horiz. stainless steel and Cu surfaces 8-90692
 evaporating, interline heat sink capability, optical and thermophysical props. depend. 8-71276
 falling film rewetting 8-75906
 falling films, nonisothermal flow (*German*) 8-83439

liquid films continued

- falling laminar liq. film, transport augmentation by surface waves 8-71343
 free film, stabilised with ionic surfactants, EHD 8-87403
 fuel film, combustion behind shock wave, heat and mass transfer in turbulent boundary layer (*Russian*) 8-71401
 gas absorption, into accelerating thin falling liq. film on inclined surface 8-93632
 gas-liquid film interface stability behind slipping shock wave front (*Russian*) 8-55630
 gas-liquid two phase flow film thickness, tube four rectangle obstacle, expt. 8-87377
 gas-liquid two phase flow film thickness, tube ring obstacle effects, expt. 8-87376
 gravity wave, liquid with superficial film and diffusion effect (*French*) 8-75156
 heat and mass transfer during vapour absorpt. 8-63427
 homogeneous surface, hysteresis of contact angle 8-51793
 hot surface quenching rate, countercurrent single- and two-phase flow effects 8-59451
 hydrocarbon layer, influence on laser-induced surface damage 8-60533
 laminar film condensation from moving vapour, with suction 8-59459
 liquid metal, film, turbulent flow down vertical wall under gravity, heat transfer 8-59396
 MHD gravity-capillary waves in liq. film falling by permeable bed 8-67277
 non-Newtonian fluid film flow along vertical oscillating plate (*German*) 8-59431
 non-Newtonian fluids, lubrication, elastohydrodynamic, between two rot. cylinders 8-83435
 nucleate boiling suppression 8-75055
 polymer continuous flow squeeze film, load-bearing capacity 8-87306
 quenching temperature, 0.03-1.3 MPa, base material thermal props. depend. 8-94587
 roll waves, small amplitude, behaviour in turbulent liquid films (*German*) 8-94756
 rotating cylinder in gravitational field, liq. film motion, steady soln. 8-83411
 saturated liquid, boiling onset, film boiling transition, crit. heat flux densities (*Russian*) 8-83234
 silicone oil thin films, convective heat transfer, surface tension effect 8-94681
 squeezing mode relaxation of free liq. film, laser scatt., rel. to colloid interaction 8-87354
 steam, film condensation in tube, heat transfer, vibr. effect 8-51044
 steam condensation heat transfer on below-freezing pt. surface 8-75042
 steam-water, flow characts. at high press. 8-94805
 steam-water mixture, upward flow in tube, liq. film-core mass transfer, liq. distrib. 8-75189
 steam-water mixture, with high vap. content, annular flow, heat transfer, press. loss 8-75193
 subcooled film boiling heat transfer from spheres 8-51047
 tetradecane, wetting on solid substrates, disjoining pressure isotherms 8-51794
 thickness measurement, using excited fluorescence in dye solns., report 8-81945
 thin free films, stabilised with ionic surfactants, dynamics 8-87416
 tube, vertical, steam generating annular flow, dry-out position prediction, computer model 8-59447
 turbulent water film, with different initial flow conditions and high temp. gradients, heat transfer 8-90862
 US wave generation, thermal interf.-optical excitation 8-71794
 vapour condensation on vertical surface, laminar flow in film condensate 8-75057
 velocity profile, instantaneous, of wavy fluid film 8-79299
 viscoelastic squeeze films, effect of normal oscill. and fluid inertia 8-67224
 viscoplastic liquid film on vertical vibr. wall, with slip, shaking loose 8-59371
 water, evaporation on heated surfaces, heat transfer characts. 8-59269
 water, films, thin, wetting, rheological characts. determ., capillary method 8-51788
 waves, travelling, gravity-capillary, on liq. film surface falling past permeable bed 8-87351
 wetting, on solid surfaces, isotherms of disjoining press., meas. methods 8-51804
 Al, electron diffr. 8-83721
 H₂-N₂-Ar, two-phase flow film boiling, in vap. generator, heat transfer 8-75190
 He, transient heat transfer, film boiling regime 8-83219
³He, adsorbed monolayers on Grafoil, NMR, low coverage 8-91503
³He-⁴He film, many body approaches to liquid-vapour transition 8-51783
⁴He superfluid, surface wave, small amplitude long wave propag., linearised theory 8-56002
⁴He, superfluid, two-dimensional, critical temp. gap and phase condensation 8-95201
⁴He, two-dimensional film, superfluid transition 8-67877
 Pb, electron diffr. 8-83721

liquid flow coaxial cables see coaxial cables**liquid He see liquid helium****liquid helium**

- see also liquid helium-3; liquid helium-4; liquid helium sound propagation; ripples; vortices*
 book, liquids and their props., mol. and macroscopic treatise 8-87604
 conference, Erice, Italy (June 1977) 8-59985
 cryopumping panel, liquid He cooled, appl. in vacuum deposition system 8-56581
 electron-charged surface, nonlinear wave propag., theory 8-67879
 film, acoustic wave phase velocity meas. using CW feedback technique 8-83187
 films, review 8-60002
 fusion reactor cooling, distrib. system for Large Coil Test Facility 8-55001
 ionic impurities in fluids, press. induced struct. transition 8-51770
 Kapitza resistance, heat transfer rel. to adsorbed monolayer (*Russian*) 8-51758
 Kapitza resistance on freshly cleaved surfaces 8-63923

liquid helium continued

- metal-liquid He interface, electron-phonon interaction, thermal boundary resistance 8-67899
 narrow channel flow and heat transfer characts., void fraction in steady and transient states 8-55000
 nucleate boiling in centrifugal accel. field, heat transfer and flux 8-94538
 short range order parameters, from information theory 8-83730
 superconducting magnet circulation cooling system based on He liquefaction apparatus 8-57992
 superconducting magnet coolant, dielec. tracking 8-92022
 superconducting magnet Large Coil Program, He liquefier-refrigerator and distrib. system 8-50398
 supercritical, natural convection heat transfer 8-94694
 surface, collective excitations and electrodynamic behavior in three layer structure 8-60079
 surface, hot electrons (*Russian*) 8-87832
 surface, localised electron states 8-60007
 surface electron states, two-dimens. cryst. form. 8-60006
 surface with trapped electron, parallel mag. field effect on interband transition 8-87835
 transient heat transfer, static coolant 8-75049
 transient heat transfer, temp. meas. with μ s response time 8-71270
 two-dimensional system, electronic props., conf. Berchtesgaden, Germany (Sept., 1977) 8-60177
 ultra cold neutron prod. rate in external liq. He source 8-70678

liquid helium-3

- see also fermion systems; superfluid helium-3*
 acoustic impedance, transverse, Landau theory 8-51778
 adsorbed monolayers on Grafoil, NMR, low coverage 8-91503
 dielectric constant, static, near liq.-vapour crit. point 8-56016
 diffusive heat flow and sum rules in the hydrodynamic limit 8-56012
 equations of state, 3.3 to 14K (*Russian*) 8-83912
 ferromagnetism, surface induced 8-79844
 ion mobility 8-51773
 Kapitza resistance at magnetic salt boundary (*Japanese*) 8-51780
 kinetic theory of normal Fermi liquids 8-87841
 magnetic susceptibility in Grafoil at ultralow temp. 8-79843
 melting, specific heat, entropy, latent heat 8-75904
 momentum distribution, theoretical 8-51776
 neutron inelastic scattering, zero sound and spin-fluctuation peaks 8-79836
 neutron scattering, inelastic, 0.7K, 10 and 20 bars, wavevector transfers 8-71899
 NMR and ion mobility experiments 8-91505
 overdamped modes and transport 8-56011
 polarisation potentials and elementary excitations 8-91502
 positive ionic mobility, press. and temp. depend. 8-91504
 significant structure theory, thermodynamic props. 8-51774
 surface tension, density profile, variational calcs. 8-67882
 susceptibility measurement, by double bundle nuclear demagnetisation refrigerator 8-93692
 target for scatt. expts. 8-70663
 zero sound suppression by mag. field (*Russian*) 8-59995
 Si-³He interface, phonon reflection 8-84043

liquid helium 3-4 mixtures

- characteristics, theory in mag. field (*Russian*) 8-59999
 dilute, second sound velocity 8-63898
 dilute solution, sp. ht., ³He quasiparticle excitation spectrum 8-71901
 dilute solutions, dielec. model of roton interactions 8-55998
 dynamic behaviour, appl. of holographic interferometry technique 8-51781
 excitations, review 8-60000
 film, many body approaches to liquid-vapour transition 8-51783
 NMR and ion mobility experiments 8-91505
 nuclear spin relaxation, anomalous 8-79849
 preferential adsorption of ⁴He onto Vycor glass 8-84023
 quantised vortex lines and lifetime of negative ions trapped by vortices 8-84022
 sound propagation near superfluid transition 8-79848
 specific heat at λ transition, universality 8-51782
 spin diffusion under press. 8-56018
 superfluid, Tomonaga model, 3-D analogue (*Russian*) 8-71900
 superfluid solution, sound vibrations in narrow channels (*Russian*) 8-79851
 third and fourth sound, Doppler shift 8-56017
 tricritical normal phase, ion mobility 8-79850

liquid helium-4

- see also boson systems; superfluid helium-4*
 atomic scattering at free surface 8-56003
 coupled field theory, classical perturbation theory appl. 8-57799
 dielectric breakdown across epoxy insulation 8-62658
 droplets, surface energy, tension, thickness 8-84015
 dynamic scaling, possible breakdown at lambda point 8-91498
 equations of state, 3.3 to 14K (*Russian*) 8-83912
 form factors, inelastic neutron scatt., observability of Beliaev terms 8-51764
 lambda transition free energy in Feynman's model (*French*) 8-71895
 magnetic field-induced temperature changes 8-57960
 phase transitions, positive and negative ion mobilities meas. 8-87833
 short range order parameter 8-83712
 structure factor, excitation spectrum, ground state momentum distrib. 8-79833
 surface, hot carrier mobility 8-59988
 surface structure 8-87837
 thermally induced oscills. in cryogenic apparatus 8-67875
 three-particle correlations, new form for variational calcs. 8-84018
 variational wave function, three-body correlations 8-87834
 He I, stable microscopic bubbles and evaporation-condensation resonance 8-91381
⁴He, liq., hard-sphere roton interaction, transition temp. calculated 8-51767

liquid helium sound propagation

- see also second sound; zero sound*
 bubble formation mechanism, on surface of deformed crystal (*Russian*) 8-85066
³He, liq., polarisation potentials and elementary excitations 8-91502
³He, normal, diffusive heat flow and sum rules in the hydrodynamic limit 8-56012
³He, normal, overdamped modes and transport 8-56011

liquid helium sound propagation continued

- ⁴He-⁴He mixture, superfluid solution, sound vibrations in narrow channels (*Russian*) 8-79851
³He-⁴He mixtures, sound propagation near superfluid transition 8-79848
³He-⁴He mixtures Doppler shift in third and fourth sound 8-56017
⁴He-⁴He solution, in mag. field, characts., theory (*Russian*) 8-59999
⁴He dynamic scaling and US attenuation near superfluid transition point 8-84016
⁴He, superfluid, quasiparticle sound velocity, temp. depend., imperfect Bose gas picture 8-51761
⁴He, superfluid, resonant nonlinear mode conversion 8-79831
⁴He superfluid, wave processes, in parallel channels, with different degrees of damping (*Russian*) 8-91496

liquid lasers

see also dye lasers

- N₂, tunable Raman laser based on third Stokes component 8-50859

liquid metals

see also electron energy states of liquid metals; liquid alloys; mercury (metal)

- activity coefficient of nonmetallic solutes in liquid metals and binary alloys 8-52766
alkali metal, salt solns., phase equilib., and chem. 8-73040
alkali metals, liq., collective excitations and short-range order 8-63665
boring of steel in metallic melts (*Russian*) 8-56736
cathodes, nanosec. discharge form. in H₂ atmosphere 8-87578
compressibilities, surface tension at melting temp. 8-91370
compressibility, long wavelength limit of liquid struct. factor 8-67633
compressibility calc. by struct. factor (*Russian*) 8-59847
continuous casting, solidification process, convective heat transfer, anal. 8-84789
density determ. by X-ray diffr. (*Russian*) 8-75529
diffraction model, critical test, elec. resistivity of amorphous and liq. metals 8-84191
effective interionic potentials 8-91221
electron correlations, evidence 8-55805
electron momentum density, correlations and ionic potentials, appl. to Al 8-60052
embrittlement and brittle fracture, of ductile metals in liquid metal environments, exam. 8-60766
embrittlement of Zn 8-64653
field ion sources 8-65999
flow in tube in mag. field, turbulent transfer coeff. (*Russian*) 8-75220
flow in tubes, turbulence, heat transfer, thermogravitation effect 8-71315
flow rate regulators for liq. metal systems, MHD or mechanical (*Russian*) 8-75229
fluid flow during blast furnace tapping, mathematical model 8-85117
heat transfer bibliography 8-63425
Knight shift, nonlocal pseudopot. calc. 8-91965
liquid metal film, turbulent flow down vertical wall under gravity, heat transfer 8-59396
LMFBR, yield characts. of short-lived fission products in Na heat-transfer agent 8-66338
metal, liq., tight binding theory of transport props., Ishida-Yonezawa approx. for single-band model 8-84190
MHD, review of flow problems and cellular motion 8-83498
MHD flow velocity structure, in nonuniform const. mag. field (*Russian*) 8-75215
MHD induction pump channel press. loss, laminar liq. metal flow friction losses (*Russian*) 8-75224
Na, dynamic struct. factor, two body interaction pot. sensitivity 8-67638
Na, local boiling behind local flow blockage, simulated LMFBR fuel subassembly 8-54842
one-component high density plasma at intermediate wave numbers, collective excitations 8-67314
orbital magnetic susceptibility of conduction electrons, pseudopotential calc. 8-76217
plastic deform. and fracture obs. by acoustic emission of Zn single crystals in metal melt (*Russian*) 8-56737
pure, surface tension and electron density 8-51803
radiation loops, use of Ti alloys as structural materials 8-72958
resistivity, struct. factor calcs. 8-51962
resistivity as function of press., nearly-free-electron model 8-84192
simple metals, solid and liq., electronic struct., mag. susceptibilities calc. 8-52204
sintered composite-liq. metal interaction, mass transfer eqn. approx. soln. 8-67262
space metal growth, mathematical model predictions from melt props. 8-84786
steel, alloy, Fe-C-Si-S, liquid, desulphurisation with CaO, exam. of reaction mechanisms 8-80742
structure, thermodynamic and transport props., book 8-51406
structure singularities (*Russian*) 8-79521
surface ion density, nonmonotone, perturbative discrete ion introduction into jellium 8-72222
transition metal, 3d, density of states of d-band, heat of vaporisation 8-95253
transition metals, liq., multiple scatt. calcs. of resist. 8-76039
transition metals, thermoelectric power 8-91675
transition metals and alloys, elec. resistivity, Hall coeff., mag. susceptibility 8-95280
treatment by high-temp. gas stream, math. model, applic. to nitriding (*Russian*) 8-53016
turbulent natural convection in liq. metals in narrow cell (*French*) 8-94701
vapour pressure, pseudopot. and Gibbs-Bogoliubov calcs. 8-83935
viscosity anal. 8-91468
wire, thermomigration through a solid in thermal gradient, force model 8-67870
Ag, viscosity, temp. depend. (*French*) 8-59964
Al, density fluctuations 8-55806
Al, dissolution of Fe and Fe alloys (*Japanese*) 8-71858
Al, electron correlations, evidence 8-55805
Al, electron diffr. 8-83721
Al, electron momentum density, correlations and ionic potentials 8-60052
Al, liquid, dynamical struct. factor 8-71667
Al, model pseudopotential 8-91582

liquid metals continued

- Ar loaded K heat pipe performance characteristics 8-89934
Ba, solubility of Ti (*Russian*) 8-80513
Bi, elec. cond. and assoc. optical scattering 8-76040
Bi, electrical resistivity with spin-orbit scatt. 8-64018
Bi, liq., collective motions, cold neutron scatt. obs. 8-67639
Cd, liq., X-ray diffr. meas. and interatomic interaction pot. calc. (*Russian*) 8-59735
Co, density of states of d-band, heat of vaporisation 8-95253
Cs, liquid, meas. of density at high temp. and pressures 8-55903
Cs, relativistic model pseudopot., appl. to elec. resist. calc. in liq. phase 8-51866
Cs, specific heat meas., at temp. up to 1700K under pressure 8-51696
Cu, absorption of gaseous O₂ 8-51686
Cu, diffusion of Ti, Ir, Pb and Bi (*Japanese*) 8-59962
Cu, surface tension meas. with levitated metal droplets, influence of oscill. amplitude 8-51798
Fe, absorption of gaseous O₂ 8-51686
Fe, diffusion of alloying elements (*Russian*) 8-79791
Fe, molten, impurities effect on viscosity 8-95172
Fe, surface tension meas. with levitated metal droplets, influence of oscill. amplitude 8-51798
Ga, liq., electrode metal-solvent interaction rel. to elec. double layer struct., adsorpt. 8-61023
Ga, 1/f noise 8-64073
Ga, elec. resist. calc., 19 and 35°C, using calc. and expt. struct. factors (*Russian*) 8-56124
Ga, embrittlement of Al 8-64653
Ga, neutron diffr. room temp. to 1303K, struct. model 8-51405
Ga, struct. factor, short range repulsive forces 8-75528
Hg, electrode metal-solvent interaction rel. to elec. double layer struct., adsorpt. 8-61023
Hg, flow in transverse mag. field, laminar and transition, channel wall effects 8-63500
Hg, nucl. spin relax. and quadrupolar relax. mech. 8-64292
In, diffusive interaction with solid Cu (*Russian*) 8-95156
In, liq., X-ray diffr. meas. and interatomic interaction pot. calc. (*Russian*) 8-59735
In, struct. factor, Percus-Yevick equation perturb. treatment, square-well pot. approx. 8-75530
K, liq., density, 1640-2030K, 36.1-100.2 atm 8-91369
K, liq. elec. resistivity calcs. 8-79974
K, thermal expan. coeff. for high temp. 8-75853
Li, diffusion in KSiAl doped W wire, effect on recrystallisation (*German*) 8-64644
Li, entropy and enthalpy of solution of H 8-51692
Li, liq. cooled pulsed fusion reactor blanket heat transfer, numerical calc. 8-94141
Mg, infiltration kinetics into porous Ti 8-60595
Mg, vaporisation from inductively stirred melt, meas. and prediction 8-51659
Mo, exptl. determ. of crit. data 8-75531
Mo, liquid and solid, thermophysical props. 8-75808
Na, effective interionic potentials 8-91221
Na, electron correlations, evidence 8-55805
Na entropy and enthalpy of solution of O(N)(C)(H) 8-51692
Na, heating modular steam generators, pressure and temp. loading in breakdown situation (*Czech*) 8-50264
Na, linear induction pump development (*Russian*) 8-94839
Na, liq., elec. resistivity calcs. 8-79974
Na, pool boiling heat transfer, liq. head effects 8-89951
Na temperature fluctuation in single-pin-heated blocked annular channel 8-78439
Na transient boiling in single-pin annular channel under loss of flow 8-89933
Ni, absorption of gaseous O₂ 8-51686
Ni, surface tension meas. with levitated metal droplets, influence of oscill. amplitude 8-51798
⁶¹Ni, paramag. solid and liq. phases, nucl. spin relax. and Knight shift 8-76327
Pb, effective interionic potentials 8-91221
Pb, electrical resistivity with spin-orbit scatt. 8-64018
Pb, electron diffr. 8-83721
Pb, filament production, ejection of molten metal through nozzle, jet stability (*Japanese*) 8-52719
Pb, relativistic model pseudopot., appl. to elec. resist. and phonon spectra calc. 8-51866
Pd, liquid and solid, thermophysical props. 8-75808
Pd, mag. susceptibility 8-95415
Pd, Percus-Yevick equation, perturbation theory calcs. 8-75515
Pt, Percus-Yevick equation, perturbation theory calcs. 8-75515
Rb, effective interionic potentials 8-91221
Rb, expanded fluid, struct., Monte Carlo study 8-83720
Rb, shear wave modes and velocity correl. spectra 8-63654
Sn, elec. resist. calcs., 232, 450 and 650°C, using calc. and expt. struct. factors (*Russian*) 8-56124
Sn, liquid, electron transfer of rare earth impurities (*Russian*) 8-95278
Sn, molten rotating stream, vortical filament generation during solidification (*Russian*) 8-88460
Sn substrate for CVD of Si polycrystal 8-64479
Sr, soln. in liq. Na, elec. resistivity, conc. depend. 8-84188
Sr, solubility of Ti (*Russian*) 8-80513
Te, liquid, localized impurity states, paramag. susceptibilities 8-64185
Ti, density of states of d-band, heat of vaporisation 8-95253
Ti, molten, reson. model calc. of elec. resist. 8-84189
Ti, struct. factor, Percus-Yevick equation perturb. treatment, square-well pot. approx. 8-75530
Zn, liq. Knight shift, temp. depend. 8-80232

liquid oscillations

see also liquid waves

- boiling, sustained and transient, inlet subcooling effect on flow instabilities 8-94809
drop, oscillating, immersed in 2nd fluid, induced flow field streaming 8-59454
drops in immiscible liquid, intermittent elec. field heat transfer augmentation 8-94872
forced oscillations in large vessels of circulatory system, dog's arterial blood flow anal. 8-85329
forced oscillations in rotating stratified liquid 8-63478

liquid oscillations continued

- gravity waves, propag. in two liquids separated by membrane (*French*) 8-87355
 n-heptane, self-excited thermoacoustic oscils. in heat transfer 8-79186
 Holocene eustatic sea level change, British Isles 8-65333
 hydrodynamic oscillations in Gently-I steam mains by inertial analysis 8-89944
 mixture, binary, oscillatory convective instability, thermodynamic anal. 8-94753
 nonlinear liq. column oscils. in manometer, theory and expt. 8-90922
 pulsatile flow of immiscible liq., stability of interacting cylindrical liq. jet 8-83444
 pulsation effect on mass transfer inside drops (*French*) 8-55686
 self-sustaining oscils. of flow past cavities, review 8-94645
 turbulent flow, press. fluctuation spectrum, elastic boundary compliance effect 8-63422
 two-phase flow instability in parallel channels 8-94810
 vapour generator, two-phase flow dynamics 8-94808
 vibrations source characteristics, placed in liq. layer (*Russian*) 8-75154
 vibratory liquid-gas mixture, nonlinear resonance expt. (*Ukrainian*) 8-90811
 water-fluidised bed, viscosity meas. by oscils. damping 8-59475
 wave, periodic, long, deform. over gently sloping bottom 8-90921
 He, thermally induced oscils. in cryogenic apparatus 8-67875
⁴He, superfluid vortex lattice collective oscils. (*Russian*) 8-51759

liquid permeability see permeability**liquid phase epitaxial growth**

- constant growth rate conditions, for growth from cooling static solution, exam. 8-56051
 ferrites, LPE growth and characterisation 8-68640
 Ga(AsP) on GaAs, LPE, growth with Ge and Sn solvents, phase diag. 8-88434
 GaInAsP quaternary alloys, orientation effects in LPE growth 8-92203
 garnet film, Ga and Ge substituted, mag. prop. control during LPE growth and processing 8-68638
 garnet film preparation, single-crystal, for magnetic bubble domain appl. 8-60588
 garnet films, thermally induced substrate fracture 8-68639
 garnets, LPE growth, using horizontal dipping, exam. of growth kinetics 8-60039
 periodic structures, props., prep., use 8-51982
 polyesters, epitaxial crystallisation, on organic and inorganic substrates 8-91565
 substrate holder 8-92207
 TGS-d, TGSe-d, single cryst. films, IR transmission spectra (*French*) 8-72742
 volume-controlled film growth 8-88432
 (Al,Ga)As/GaAs, LPE grown heterostructures, X-ray diffr. exam. of interfacial elastic strains 8-72019
 Al-Ga-As heterostruct. with confined current flow, fabrication 8-68081
 Al_{0.3}Ga_{0.7}As:Te(SN), impurity effects on interface morphology of LPE films on corrugated GaAs substrates 8-88435
 Al_{1-x}Ga_xAs, transient-mode LPE on GaP 8-72746
 Al_{1-x}Ga_xAs, LPE, cathodoluminesc. obs. 8-68565
 Al_{1-x}Ga_xAs layer, LPE, graded bond gap solar cell, composition profile, Rutherford backscatt. 8-76612
 Al_{1-x}Ga_xAs, LPE on InP, solid-liq. equilib. calcs. 8-84083
 CuFe₂O₄, LPE grown, domain struct. rel. to tetragonal distortion 8-92205
 Cu₂S, epitaxial layers grown from liq. soln. RHEED obs. 8-91558
 (Eu,Lu)₃Fe₅O₁₂, submicron bubble films on rare earth-Ga garnet substrates, prep. and mag. props. 8-91909
 Ga_{1-x}Al_xAs film, with x=0.23 and 0.37, grown by linear cooling, thickness comparison with GaAs 8-87892
 Ga_{1-x}Al_xAs-GaAs injection laser, branching waveguide coupler fabrication by LPE 8-63202
 Ga_{1-x}Al_xAs, LPE, charge carrier conc. distrib. (*Russian*) 8-52694
 Ga_{1-x}Al_xAs, LPE, GaAs solubility in Ga-Al alloys investig. 8-52690
 Ga_{1-x}Al_xSb p-n homojunction LPE and photovoltaic effect obs. (*French*) 8-64108
 GaAs FET, continuous growth of LPE double layers 8-64487
 GaAs film, thickness comparison with Ga_{1-x}Al_xAs, for layers grown by linear cooling 8-87892
 GaAs, LPE, charge carrier conc. distrib. (*Russian*) 8-52694
 GaAs, LPE growth of high purity layers by sliding boat method 8-76610
 GaAs, LPE with AsCl₃-saturated Ga/As solns. 8-63953
 GaAs, Peltier induced growth kinetics of LPE 8-64485
 GaAs, synthesis by molten salt electrolysis 8-64486
 GaAs, transient-mode LPE on InP 8-72746
 GaAs:Ge, LPE, on semi-insulating GaAs, film-substrate interface characterisation 8-72017
 GaAs:Sn, LPE layers, electronic props., depend. on Sn incorporation 8-87883
 GaAs-(Ga, Al)As heterostructure transmission photocathode, characts. (*French, English*) 8-52616
 GaAs-GaAlAs, DH laser material, LPE grown, obs. of melt carryover 8-91553
 Ga_{1-x}In_xAs, cryst. growth on (100) InP by LPE 8-56591
 Ga_{1-x}In_xAs on InP, lattice matched LPE film growth and characts. 8-72033
 Ga_{1-x}In_xSb, LPE on GaSb by stepwise grading, and characterisation 8-72745
 p-GaP, epitaxial layers grown from liq., overcompensated, doping levels 8-91353
 GaP, LPE at 650°C from In solvent, low Si contamination 8-80480
 GaP on GaAs, LPE, growth with Ge and Sn solvents, phase diag. 8-88434
 GaP:Zn, thermodynamics of Zn doping by liquid phase epitaxy 8-83832
 Ho_{0.7}Er_{0.3}FeO₃, crystn. on seeds, layer morphology 8-72041
 InGaAs-InP heterojunction detector for 1.0-1.7 μm wavelength range 8-49895
 In_{0.53}Ga_{0.47}As, incorporation of Ga during LPE growth on (111)B and (100)InP substrates 8-91557
 In_{1-x}Ga_xAs, thick LPE growth, electrolum. obs. 8-60589

liquid phase epitaxial growth continued

- InGaAsP, lattice matched, LPE growth on (100) InP, for 1.15-1.31 μm spectral region 8-64483
 In_{1-x}Ga_xAs_{1-y}P_y, LPE growth on InP (100), lattice matched composition 8-87881
 In_{1-x}Ga_xP_{1-y}As_y, single thin active layer visible spectrum heterostruct. lasers 8-63120
 InP, LPE, high purity, use of baking to reduce Si contamination 8-72744
 Li_{0.5}Fe_{2.5}O₄, LPE growth on spinel substrate crystals, ferrimagnetic resonance exam. 8-76613
 Pb_{1-x}Sn_xTe, grown by LPE, solid-liquid tie line determ. 8-64526
 Pb_{1-x}Sn_xTe optically pumped lasers, power output and wavelength, 4 to 30K 8-79035
 Si, LPE growth from supersaturated Sn melt 8-56592
 Si:Ga, LPE growth on Si substrate, melt-back approach 8-80481
 (Sm,Lu)₃Fe₅O₁₂, submicron bubble films on rare earth-Ga garnet substrates, prep. and mag. props. 8-91909
 (Sm,Y)₃(Fe,Ga)₅O₁₂, epitaxial mag. layer, LPE, growth rotation rate, effect on props. 8-56053
 SmCaGe garnet LPE bubble film, coercivity, thickness depend. 8-68324
 Sm_{0.3}Lu_{0.2}Tm_{0.2}Y_{1.45}Ca_{0.85}Fe_{4.15}Gd_{0.85}O₁₂, LPE growth, saturation magnetisation, collapse field, bubble diameter 8-95703
 Sm_{0.1}Y_{1.9}CaFe₄GeO₁₂, LPE growth, saturation magnetisation, collapse field, bubble diameter 8-95703
 Sm_{0.4}Y_{2.6}Fe_{3.8}Ga_{1.2}O₁₂, LPE, improved method of stirring 8-68641
 Sm_{0.4}Y_{2.6}Ga_{1.1}Fe_{3.9}O₁₂, LPE, growth rate anisotropy and kinetic coeffs. of vicinal faces 8-51846
 (Y,Eu)₃(Fe,Ga)₅O₁₂, LPE growth from molybdate fluxes, bubble props. 8-68322
 (Y,Sm,Lu)₃(Fe,Ga)₅O₁₂, LPE mag. film, suitability for 1 to 3 micron bubble devices 8-68323
 YAG, solubility in solvent PbO₂-PbF₂, phase form. in system Y₂O₃-Fe₂O₃-PbO-PbF₂-B₂O₃ 8-95247
 YAG:R³⁺, R=Nd, Er, (Er, Ga), LPE and luminesc. 8-64408
 Y₃Fe_{5-x}Ga_xO₁₂ grown from solution, prep. and props. (*German*) 8-52691
 YIG grown from solution, prep. and props. (*German*) 8-52691
 (YSmCa)₃(FeGe)₅O₁₂ LPE films, optimum growth conditions for low coercivity 8-95499
 (YSm)₃(FeGa)₅O₁₂, growth rate anisotropy and kinetic coefficients of vicinal faces 8-63954
 Y_{3-y}Sm_yFe_{5-x}Ga_xO₁₂ grown from solution, prep. and props. (*German*) 8-52691
 (YSmLuCa)₃(FeGaGe)₅O₁₂, reproductibility in bubble garnet LPE growth 8-92204
 YSmLuCaFeGe garnets, growth and temp. characts. of small bubbles 8-80183
 (YSmLuCa)₃(FeGe)₅O₁₂, LPE growth, growth reproducibility of bubble props. 8-92208
 YSmLuCaGeIG, mag. props. and defects, depend. on B₂O₃ conc. on growth in PbO-B₂O₃ solvents 8-68321
 ZnSnAs₂, LPE in open tube system 8-92206

liquid semiconductors

- see also electron energy states of liquid semiconductors
 randomly shifted bands model for semiconductor-metal transition 8-79929
 Ti-Te melt system, semicond., Hall effect 8-56164
 Ga-As system, phase equilib., Krupkowski model (*German*) 8-95132
 Ga-Te, reflectance, 0.65-3 eV, comp. depend. 8-72549
 In-Te, reflectance, 0.65-3 eV, comp. depend. 8-72549
 Pb-Te, molten mag. susceptibility, conc. and temp. depend. 8-80121
 Sb₂Se₃, liq. struct. anal., neutron diffr. study 8-79519
 Si, liq., mag. susceptibility and diamag.-paramag. transition at melting pt. 8-95415
 Ti-Te, reflectance, 0.65-3 eV, comp. depend. 8-72549
 V₂O₅ type liquid semiconductor, elec. props. control, by O₂ partial press. (*Russian*) 8-72142

liquid-solid transformations see solid-liquid transformations**liquid structure**

- see also classical theories of fluid structure; long-range order; quantum theories of fluid structure; short-range order; X-ray diffraction examination of liquids
 acetonitrile, liq. struct., RISM equation calc. 8-71665
 acoustic parameters and density determ. using piezoelectric transducer (*Russian*) 8-49799
 alcohol-H₂O solutions, structure, luminesc. probe obs. 8-84636
 alkali halide solutions, tetrahedral hydration of ions from Raman bands obs. 8-55804
 alkali halides, molten, ionic radii and X-ray diffr. patterns 8-59732
 alkali halides, molten, struct. determ. by X-ray scatt. 8-87609
 alkali metals, liq., collective excitations and short-range order 8-63665
 alkaline earth halides, thermodynamic and structural props., computer simulation 8-75849
 n-alkane mol. config. in melt and cyclohexane soln., small-angle neutron diffr. 8-55800
 aqueous non-electrolytes, US velocity measurement, adiabatic compressibility studies 8-87605
 aqueous nonelectrolytic soln. microheterogeneous struct., X-ray diffr. study 8-87608
 aqueous solutions, Monte Carlo simulation, convergence of new algorithm 8-63649
 associated solutions, H bonding and anomalous saturation 8-52426
 benzenes, substituted, dielectric absorpt. and NMR 8-88251
 binary liquid solutions, surface cluster functions 8-67631
 n-butane in non-associated solvents, intermol. struct., superposition approx. and two-cavity model 8-71656
 covalent elements, cohesion in condensed phases, corrections to simple Huckel approx. 8-59779
 covalent elements, cohesion of σ and π bonds in condensed phases, simple Huckel approx. 8-59778
 critical fluid, local order effects on dynamics near liq.-gas pt., US and light scatt. 8-67806
 cyclohexanol, US relaxation at 0.5 to 45 MHz 8-59868
 deuterated nitroxide radical probe, synthesis and appls. (*French*) 8-76314
 dichloromethane, liq. dynamics, neutron inelastic scatt. 8-71664
 effective pair potential from static struct. factor data 8-75521

liquid structure continued

- electrolyte aq. solns., IR librational bands, struct. making and breaking 8-56476
 electron diffraction 8-83686
 ethanol-H₂O mixture, liq. US vel., -80 to 20°C, 1-5 MHz 8-59933
 glycerol, supercooled, Mossbauer effect and model of mol. motion 8-64301
 hard rod system, initially ordered, one-dimens., mol. dynamics computer simulations 8-71658
 heterocyclic compounds in dilute solutions, dielectric relax., microwave technique 8-84520
 hydrocarbon liquid, residual energy and entropy, rel. to liq. and mol. structs. 8-71869
 hydrophobic interaction, solubility and solvent struct. changes 8-83705
 iodomethane, liq. (liq. mixtures), vibr. relax. and reorientation, symmetric C-H bending mode 1st overtone 8-62884
 ions in dipolar solvent, potential of mean force, linearised hypernetted chain approx. calcs. 8-55798
 macromolecules, polydispersity in nonlinear electric methods, nonlinear dielec. effect formulas derived 8-59730
 mean spherical model approx. 8-75514
 melting, dislocation generation, anharmonicity and solitons 8-79746
 metal, effective interionic potentials 8-91221
 metal, structure singularities (*Russian*) 8-79521
 metal, surface ion density, nonmonotone, perturbative discrete ion introduction into jellium 8-72222
 metal, viscosity anal. 8-91468
 metallic liquids, resistivity, struct. factor calcs. 8-51962
 metals, electron correlations, evidence 8-55805
 metals and alloys, book 8-51406
 molecular dynamics of liqs., neutron scatt. and computer simulation 8-63650
 molecular fluid, pair correlation function, perturbation theory 8-55799
 molecular fluids, translational motion, Mori three variable theory and mol. dynamics simulation 8-63651
 molten salt model, mean spherical approx. 8-63662
 Monte Carlo calc., long-range dipolar interactions in computer simulations of polar liquids 8-87603
 neutron diffraction spectrometer, resolution and luminosity study for liquid on amorphous samples anal. 8-87591
 pair correlation function errors, dilute hard sphere approx. 8-79514
 pair potentials, from inelastic neutron scatt. data, self-consistent method 8-59728
 polyacids, unsaturated carboxylic, in organic solvents, hydrogen bonding, structuration (*Russian*) 8-71666
 polyelectrolytes in soln., electrostatic persistence length rel. to unified theory 8-95932
 polymer melt, rheology and mol. struct. 8-63405
 radial distribution function and structure factor, struct. diffusion model 8-51403
 Raman spectra of liq. phase weak H-bonds, short range order and anharmonicity effects 8-64357
 silicate melt, cavities in random close packed struct., applic. as model exam. 8-55802
 steel, nonmetallic inclusion behaviour simulation by multiple phase medium eqn. (*Russian*) 8-94965
 ternary liquid mixtures, molecular interaction and thermodynamic props. 8-59861
 vibrational energy relax. of excited probe mol., density fluctuation interaction 8-63653
 water, compressibility modulus 8-75701
 water, liq., Monte Carlo simulation, convergence of new algorithm 8-63649
 water, structure and motion at high pressure 8-87606
 Al, density fluctuations 8-55806
 Al, electron diff. 8-83721
 Al, liquid, dynamical struct. factor 8-71667
 Ar, liq., short range order parameter 8-83712
 Bi, liq., collective motions, cold neutron scatt. obs. 8-67639
 Br₂, neutron diff., evaluation of effective pair pot. 8-75527
 Br₂, struct., theory and computer simulation 8-59734
 Br₂, struct., X-ray diff. obs. 8-59733
 CS₂, liq., light scatt. intensities, struct. models 8-60476
 Cd, liq., X-ray diff. meas. and interatomic interaction pot. calc. (*Russian*) 8-59735
 CdCl₂, aq. soln., Raman spectrum, local order 8-84563
 Ce-Co, liq., charge transfer effect 8-94967
 Ce-Cu, liq., charge transfer effect 8-94967
 Cs, liq., short range order parameters, from information theory 8-83730
 CuBr₂, highly conc. aqueous soln., local ordering, extended X-ray absorb. fine struct. spectra 8-79520
 CuCl₂, aq. soln., Raman spectrum, local order 8-84563
 Cu(NO₃)₂, aq. soln., Raman spectrum, local order 8-84563
 Fe-C melt, mag. susceptibility and short range order, 900-1800°C 8-84382
 Fe-Ni melt, short-range order, m.p. to 1750°C (*Russian*) 8-94966
 Ga, elec. resist. calc., 19 and 35°C, using calc. and expt. struct. factors (*Russian*) 8-56124
 Ga, neutron diff. room temp. to 1303K, struct. model 8-51405
 Ga, struct. factor, short range repulsive forces 8-75528
 H bond dynamics in soln. 8-84573
 (HF)₂, intermol. force model, rel. to liq. struct. 8-78773
 H₂O, aq. solns., struct. and dielec. props. 8-63659
 (H₂O)₂, dimer intermolecular pot., liq. struct. mol. dynamics simulation 8-71657
⁴He, liq., short range order parameters, from information theory 8-83730
⁴He, normal and superfluid, short range order parameter 8-83712
⁴He, struct. factor, excitation spectrum, ground state momentum distrib. 8-79833
⁴He, superfluid, dynamic struct. factor, temp. depend. 8-95197
 In, liq., X-ray diff. meas. and interatomic interaction pot. calc. (*Russian*) 8-59735
 In, struct. factor, Percus-Yevick equation perturb. treatment, square-well pot. approx. 8-75530
 K⁺ salts, diamag. ion solvation in methanol soln., NMR relax. obs. 8-56389
 KCl, aq. soln., zero-angle X-ray scatt., 25°C, conc. depend. 8-83713
 Li⁺ salts, diamag. ion solvation in methanol soln., NMR relax. obs. 8-56389

liquid structure continued

- Li₂SO₄, molten, and molten Li₂SO₄-Na₂SO₄ mixtures, struct. anal. by X-ray diff. 8-63660
 MnCl₂, molten, struct. anal. by X-ray diff. 8-63661
 Na, effective interionic potentials 8-91221
 Na⁺ salts, diamag. ion solvation in methanol soln., NMR relax. obs. 8-56389
 Na-K, liq., static struct. factors 8-63664
 Na-K, liq. alloy, electronic correl. functions calcs. 8-63663
 Na₂SO₄, molten, and molten Li₂SO₄-Na₂SO₄ mixtures, struct. anal. by X-ray diff. 8-63660
 Na₂WO₄, molten, struct. by X-ray radial distribution anal. 8-83717
 Ne, liq., short range order parameter 8-83712
 NiCl₂, aq. soln., Raman spectrum, local order 8-84563
 NiCl₂, aq. soln., viscosity meas., struct. props. 8-75863
 NiCl₂, aqueous solution, hydration of Ni²⁺ 8-79518
 Pb, effective interionic potentials 8-91221
 Pb, electron diff. 8-83721
 Pb, liq., short range order parameters, from information theory 8-83730
 Pd, liq., Percus-Yevick equation, perturbation theory calcs. 8-75515
 Pt, liq., Percus-Yevick equation, perturbation theory calcs. 8-75515
 Rb, effective interionic potentials 8-91221
 Sb₂Se₃, liq. struct. anal., neutron diff. study 8-79519
 Se, ring-chain transition, disordered chain model 8-59943
 Se:Te, liq., viscosity, impurity effect, chain length role (*French*) 8-51717
 SiO₂, molten, struct., X-ray radial distrib. anal. 8-67651
 SiO₂-Al₂O₃-CaO-MgO, liq. silicic and slag, struct. density, surface tension (*Polish*) 8-83711
 Sn, elec. resist. calc., 232, 450 and 650°C, using calc. and expt. struct. factors (*Russian*) 8-56124
 SrCl₂, aq. soln., Raman spectrum, local order 8-84563
 SrCl₂, partial static structure factors, velocity autocorrelation functions 8-91219
 Te, liquid, meas. of viscosity, density and surface tension (*French*) 8-91371
 Tl, struct. factor, Percus-Yevick equation perturb. treatment, square-well pot. approx. 8-75530
 ZnCl₂, aq. soln., Raman spectrum, local order 8-84563

liquid surface waves see surface waves (fluid)**liquid theory**

- see also classical theories of fluid structure; equations of state of liquids; quantum theories of fluid structure
 aqueous solutions, Monte-Carlo simulation, convergence of new algorithm 8-63649
 binary liquid solutions, surface cluster functions 8-67631
 binary mixtures, excess surface tension calc. and theories of solns. 8-91508
 book, liquids and their props., mol. and macroscopic treatise 8-87604
 Brownian particle, freq.-depend. friction coeff. in fluid near crit. pt. 8-73929
 bulk viscosity, inverse power pot. 8-91466
 n-butane, intermol. pair correls., RISM integral eqn. 8-63656
 carbon tetrachloride, optical props. under press., molecular polarisability depend. on thermodynamical state 8-80312
 classical liquid, metastable supercooled state, props. 8-55796
 classical liquids, mode-coupling effects on transverse current memory function in dynamical region 8-83706
 cluster identification, computer expts. on systems of particles 8-59725
 concentrated aqueous electrolyte solutions, transport props. (*German*) 8-80750
 Coulombic systems, HNC and RHNC eqns. for restricted primitive model 8-67630
 dense, quadrupolar, hard sphere fluid, integral eqn. approx. 8-63652
 dense fluid, new description of random stacks (*French*) 8-79512
 dense fluids, translational motion, modified Fokker-Planck eqn. 8-75517
 dilute systems of dipoles and dipolar charged particles, Mayer resummation method 8-83710
 dipolar fluid, ion-ion distrib. function 8-83704
 dipole, spherical, steadily rot., dielec. friction 8-87600
 dynamic structural correlations and van Hove's correlation function for liquids 8-94958
 dynamical struct. factor and velocity autocorrelation function, appl. to classical one-component plasma 8-71430
 electrical double layer theory, modified Poisson-Boltzmann equation 8-94955
 electrolyte, polarisable spheres model 8-56898
 electrolytes, aq. solns., ion-solvent interactions, transport props. (*German*) 8-79790
 ethanol, aq. soln., conc. fluctuations, shear and longit. relax., Brillouin scatt. and pulse techniques 8-71792
 ethylene, condensation, zero point energy shift, isotope effects 8-95147
 Fermi system, extended, energy expectation value per particle, lack of O(A⁻¹) contribution in Iwamoto-Yamada expansion 8-60081
 fluoromethanes, condensation, zero point energy shift, isotope effects 8-95147
 free energy calcs., mixed liquids, local mole fractions consistency 8-83702
 glass-forming liquids, relax. times, temp. depend. 8-83924
 hard rod system, initially ordered, one-dimens., mol. dynamics computer simulations 8-71658
 hard sphere mixtures, with negatively nonadditive diameters, scaled particle theory 8-71654
 hard spherocylinder fluid, Monte Carlo calcs. 8-91208
 hard spherocylinder fluid, props., blip function theory 8-91207
 hard-sphere fluid, modified nonlinear Enskog eqn., entropy function 8-63526
 hard-sphere fluid, near a wall, surface tension, approx. method calcs. 8-59724
 hard-sphere fluid, viscosity and self-diffusion coeffs. 8-51716
 hard-sphere fluids, dipolar and quadrupolar, radial distrib. functions, perturbation theory 8-59727
 n-hexane, optical props. under press., molecular polarisability depend. on thermodynamical state 8-80312
 high density fluid states, fluctuating free-vol. anal. of soft-core model 8-75516
 homonuclear diatomics, dense fluids, transport props. 8-75519

liquid theory continued

intermolecular potentials, coulombic and multipolar, 2-dimens. mol. dynamics simulation 8-75520
 internal rotation barrier, IR spectral linewidths meas. 8-72507
 ion solvation, in polar media, continuous charge distrib. model, quantum mech. calcs. 8-68913
 ion-dipole mixtures, ion-ion distrib. function 8-83704
 ionic solution, in mol. polar solvent, charged sphere model, statistical mechs. 8-71655
 ionic solutions, elec. field statistics 8-87601
 isomerisation dynamics, in liquid solutions, statistical mechanics, transition state approx. 8-60999
 isotropic nonpolar fluid, elec. quadrupole density 8-94956
 Lennard-Jones (100) crystal-liquid interface, structure 8-91284
 Lennard-Jones fluid, hypernetted-chain eqn. of state 8-67800
 Lennard-Jones fluid in contact with Lennard-Jones wall, interfacial density profile 8-67901
 Lennard-Jones liq., press. and temp. consistent, approx. theory, Helmholtz free energy 8-63647
 Lennard-Jones liq. mixtures, mol. dynamics calc. 8-55794
 librational reorientation, sum rules 8-71659
 liquid, thermal response to weak external field, molecular dynamics 8-71660
 macromolecular, solutions, mol. orientation, time-depend. torque, rot. diffusion eqn. 8-68471
 metal, effective interionic potentials 8-91221
 metal, viscosity anal. 8-91468
 methane, condensation, zero point energy shift, isotope effects 8-95147
 mixtures, phase equilibrium, augmented Van der Waals theory 8-79737
 molecular dynamics simulation, partial press. evaluation 8-71663
 molecular liquid, thermodynamic functions, interaction site model calc. 8-71661
 molecular motion, translational itinerant oscillator, probability density functions 8-59726
 molecular reorientation, dielec. friction theory 8-87599
 molecular solvation, in polar media, continuous charge distrib. model, quantum mech. calcs. 8-68913
 molten salt mixtures, transport props. (*German*) 8-80750
 molten salt model, mean spherical approx. 8-63662
 multicomponent electrolyte systems, velocity correl. coeffs. 8-85167
 N-particle system, Brownian dynamics with hydrodynamic interactions 8-91209
 Na, dynamic struct. factor, two body interaction pot. sensitivity 8-67638
 nematic liquid crystals, equation of state, anisotropic props., perturbation theory 8-67645
 nonadditive hard spheres, scaled particle theory, positive nonadditive solns. 8-79515
 nonspherical molecules, rot. and translational motion, modified Fokker-Planck equation 8-75518
 normal liquids, quantum field theory 8-91213
 one-component high density plasma at intermediate wave numbers, collective excitations 8-67314
 one-component molecular solution, excess electron diffusion 8-52043
 open binary mixtures, fluctuation theory, entropy prod. and energy dissipation (*German*) 8-64879
 ordering absence in real liquids, appl. to nematic liquid crystals 8-51402
 PAA, nematic, equation of state, anisotropic props., perturbation theory 8-67645
 pair distrib. functions, modification of regular solution theory 8-67829
 n-pentane, optical props. under press., molecular polarisability depend. on thermodynamical state 8-80312
 Percus-Yevick equation, numerical calc. of crit. exponents 8-91212
 Percus-Yevick equation, perturbation theory calcs. 8-75515
 Percus-Yevick equation, square-well pot., perturbation version 8-63648
 polar fluid of heteronuclear molecules, dielectric const. 8-84514
 polarisable fluid containing charged particles, mol. dynamics theory 8-91214
 polyelectrolyte, 1-1 soln., excluded vol. theory, Khun statistical segment basis 8-83716
 polyelectrolytes in soln., electrostatic persistence length rel. to unified theory 8-95932
 polymer chain dynamics, in soln., computer simulation 8-83718
 polymer solution, conc., rheological props., rod-like mol. model 8-75114
 quantum-defect theory of heats of formation and struct. transition energies 8-55830
 radial distribution function and structure factor, struct. diffusion model 8-51403
 Raman band shapes in liq., rot.-vibr. coupling effect for reorientation 8-72491
 rare gases, liquid, long wavelength limit of liquid struct. factor, compressibility 8-67633
 rough hard spheres treatment of tracer diffusion 8-87798
 salt, molten, surface tension calcs., Fowler model modification 8-67888
 shear wave modes and velocity correl. spectra 8-63654
 short-range interactions mediated by a solvent with surface adhesion 8-71973
 simple classical liquids, kinetic theory, formal justification for memory function approx. 8-87598
 simple liquid intermolecular interaction, extremal values 8-87602
 Smoluchowski equation, with Coulomb pot., appl. to fluoresc. quenching 8-73051
 Smoluchowski equation with Coulomb pot., time-depend., soln. 8-73050
 soft core model, self diffusion, glass transition 8-67634
 solvent mediated interactions—solute size effects and predictions of mean field theory 8-75513
 solvent structure, in particle interactions, short range forces 8-83709
 solvent structure in particle interactions, asymptotic regime 8-83708
 square-well fluid, using corrected integral eqns. 8-79511
 surface tension, kinetic tunnel model 8-56022
 two-component molecular solution, excess electron diffusion 8-52043
 two-dimensional fluid, with 12-6 pot., fourth virial coeff. 8-59723
 velocity autocorrelation function, longitudinal modes and transverse modes in liquids 8-94954

liquid theory continued

vibrational dephasing, polyat. mols. in condensed phases, intermol. energy exchange mechanism 8-74737
 viscosity, simple kinetic model 8-55793
 viscosity mechanism, in simple liquids and gases, interrelation (*Russian*) 8-67846
 water, and ionic dissoc. products, polarisation model 8-91216
 water, liq., Monte Carlo simulation, convergence of new algorithm 8-63649
 water, long range forces in mol. dynamics calcs. 8-79517
 water, optical props. under press., molecular polarisability depend. on thermodynamical state 8-80312
 zero sound, in classical liq., excitation, damping, memory function approach 8-67771
 H-bonded species, in soln., vibr. relax. model 8-84559
 N₂, dephasing of mol. vibr. related to correl. functions 8-75523
 Na, effective interionic potentials 8-91221
 NiCl₂ aqueous solution, hydration of Ni²⁺ 8-79518
 Pb, effective interionic potentials 8-91221
 Rb, effective interionic potentials 8-91221
 Rb, shear wave modes and velocity correl. spectra 8-63654
 TiNO₃-LiNO₃(KNO₃) mixtures, molten, surface tension, regular solution theory 8-71903

liquid-vapour transformations

see also boiling; condensation; evaporation; liquefaction of gases
 binary vapour-liquid equilibrium data, determ. and correlation 8-87781
 carbon tetrachloride, drops, on brass surface, Leidenfrost pt., press. effect 8-87784
 chloroform, crit. dynamics, nuclear relax. 8-75805
 chloroform, drops, on brass surface, Leidenfrost pt., press. effect 8-87784
 equilibria, generalised method for calc. and prediction at high press. 8-87780
 ethane, liquid-vapour coexistence curve, neutron transmission exam. (*Russian*) 8-79758
 field-theory renormalization and critical dynamics above T_c: helium, antiferromagnets, and liquid-gas systems 8-87767
 fluid, near liq.-gas crit. pt., local order effects on dynamic props., US and light scatt. 8-67806
 fluids with polar, quadrupolar, octupolar mols., thermodynamics, vapour-liq. equilibria 8-95127
 Freons, C51-12, 113, drops, on brass surface, Leidenfrost pt., press. effect 8-87784
 gases, mass transfer, mag. field effects 8-63535
 high pressure vapour-liquid equilibrium, phenomenological description 8-91415
 liquid-high pressure vapour equilibrium, quantitative description 8-79736
 l-menthol, vap., homogeneous nucleation, high-temp. Becker-Doering theory predictions 8-67820
 metal, equation of state, isentropic expansion method 8-91414
 microclusters, computer simulation of nucleation and thermodynamics, mol. dynamics and Monte Carlo 8-51656
 microdrop-gas phase equilib. in small system, mol. dynamics 8-95146
 mixture, crit. points, analogy with pure fluids 8-67819
 neopentane, critical, electron mobility, gravity effect 8-91738
 nucleation, mol. dynamics theory 8-75803
 organic compounds, crit. temps. correl. with boiling pts. 8-91421
 polyatomic substances, thermal eqns. of states (*French*) 8-91413
 simple fluid near crit. point, homogeneous phase sp. ht. at const. vol. 8-71832
 simulation of statistical systems, homogeneous nucleation (*Russian*) 8-83934
 thermodynamic stability criterion for orthobaric volumes (*Russian*) 8-51644
 vapour-liquid equilibrium, T-x meas. by semi-micro method 8-87782
 water, drops, on brass surface, Leidenfrost pt., press. effect 8-87784
 CO₂, two-scale factor universality near crit. point 8-55936
³He-⁴He film, many body approaches to liquid-vapour transition 8-51783
 Hg, liq.-vap. interface, density profile near triple point, X-ray refl. 8-75821
 N₂-O₂, vap.-low. equilib., mag. field effect 8-91429
 Na vapour heat pipe performance rel. to nozzle discharge theory 8-75033
 O₂, gas, vibr. Raman spectrum, anomalous behaviour near crit. point 8-55179
 SF₆, two-scale factor universality near crit. point 8-55936
 Xe, two-scale factor universality near crit. point 8-55936

liquid waves

see also ocean waves; surface waves (fluid)
 accompanying waves of a ship, explicit approx. from slender body theory (*French*) 8-59408
 Burgers' equation for nonlinear shallow water waves, Galerkin method soln., expansion of B-splines 8-87352
 capillary wave form. on gravity water waves, model eqn., surface tension, viscosity 8-83421
 Caspian Sea, short internal waves in near-surface thermocline (*Russian*) 8-81231
 counter-current two-phase flow, annuli, rod bundles, liq. film behaviour, flooding 8-59452
 film, free, squeezing mode relax., laser scatt. obs., rel. to colloid interaction 8-87354
 film, thin free, stabilised with ionic surfactants, dynamics 8-87416
 freesurface breakdown in rot. liq., wavelets 8-59402
 gravity waves, weakly nonlinear, long, on two-layer fluid 8-83419
 hot surface quenching rate, countercurrent single- and two-phase flow effects 8-59451
 inert binary mixtures, weak wave evolution, Burger's eqn. 8-90924
 internal Kelvin waves in fjord lake, obs. 8-73411
 jet, circ., free shear layer transition wave development 8-94643
 MHD gravity-capillary waves in liq. film falling by permeable bed 8-67277
 nonlinear internal waves in channels 8-63442
 oblique instability of periodic waves in shallow water 8-63418
 shallow water waves, Backlund transformations as canonical transformations 8-81855
 short wave generation by cylinder oscillating at liquid interface 8-79331

liquid waves continued

- stability of a plane soliton to infinitesimal two-dimensional perturbations 8-83420
- stratified fluid, internal wave solitons, numerical computation 8-59410
- stratified fluid, nonlinear reson. waves interaction 8-83418
- stratified fluid with free surface, near field disturbance due to slender body 8-59443
- viscous fluid flow down inclined plane, development of roll waves 8-75160
- water, deep, direct variational anal. of oscillatory irrotational waves (*Italian*) 8-83415
- water, electronic instrument for precise meas. 8-86294
- water, response of porous elastic bed 8-67208
- water wave diffr. and radn., numerical methods, book contrib. 8-59412
- water wave propag., long-period, finite difference-element integration scheme 8-75157
- ⁴He flow, slow thermal wave (*Russian*) 8-56005

liquids

- for generalities only; for specific aspects see appropriate headings
- see also liquid structure; liquid theory; solutions
- oil, slurries, ultrasound assisted filtration 8-94504

LISP

- physics and astronomy appls. (*Polish*) 8-61749

literature

- romantic movement in Denmark, influence in H.C. Oersted (*French*) 8-69955

literature reviews see reviews**lithium**

see also nuclei with

- abundance determ. in weak-G band giant stars 8-53948
- adion-surface interaction energy, density formalism calcs. for Al and W surfaces 8-68069
- adsorption of O on (100), cluster models, ab initio HF LCAO theory 8-71978
- atom, absorpt. spectra, high mag. field, quasi-Landau reson. 8-90109
- atom, and isoelectronic series, $Z=10-100$, L-shell energy struct. and level classification 8-55129
- atom, cooperative cascade emission 8-78659
- atom, ground state wavefunction, SCF HF calc. 8-90070
- atom, lifetime of $1s2p^2$ 2P state, radiative autoionisation 8-78665
- atom, photoionisation cross section meas. at $2P$ level 8-58637
- atom, pseudospectral dipole oscillator strength distrib. 8-50503
- atom, quartet states, absolute term values, CI calcs. 8-58596
- atom, quartet states, transition energies, oscill. strengths, CI calcs. 8-58597
- atom, s^2S and 2^2P states, spin-optimised SCF general spin orbitals 8-82617
- atomic beam probing of plasma, for electron density profile 8-63590
- BCC, coherent twin boundaries and interatomic pots. 8-51558
- blanket coolant for Tokamak reactor, flow resist., MHD effects 8-66423
- diffusion, in Mo, mechanism 8-84007
- diffusion in silicate glasses, ion-microprobe determ. 8-53649
- electrical resistivity, temp. depend., anharmonic effects 8-76045
- electrochemical behaviour, in propylene carbonate, SEM study (*French*) 8-56899
- exploding wire plasma, ionisation and radiation dynamics simulation 8-83606
- film, band struct., appl. of extended rigorous cellular method 8-52055
- fusion reactor T breeding blanket, T, removal from liq. K and Li by sorption onto Y 8-66411
- fusion reactor wall, microexplosion of pellet, energy deposition 8-54890
- helicon-phonon interaction for parallel wave propagation 8-64054
- isoelectronic sequences, screening constants, ground and excited states 8-62701
- liquid, diffusion in KSiAl doped W wire, effect on recrystallisation (*German*) 8-64644
- liquid, entropy and enthalpy of solution of H 8-51692
- liquid cooled pulsed fusion reactor blanket heat transfer, numerical calc. 8-94141
- low-temperature plasma atomic level population density computation 8-71461
- magnetic susceptibility, 3.7-294K (*German*) 8-68156
- main-sequence stars, Li, Be and B abundances rel. to envelopes hydro-dynamical instabilities 8-93202
- martensitic phase transitions, and phase diagrams at moderate press. 8-72775
- melting at high pressures, thermodynamics 8-91426
- melting thermodynamics (*Russian*) 8-71840
- mesoatoms, π , μ^- , K^- , p^- atoms, energy spectra, wave functions (*Russian*) 8-55264
- phonon dispersion, calc. using electron fluid model 8-75738
- plasma, spectrum profiles, line broadening parameters at different intensities 8-86820
- X-ray emission spectrum, one-electron band approx. calcs. 8-80437
- in C stars, Li I line form. 8-65615
- CdS:Li, anisotropy of the absorption by impurity centers in hexagonal crystals 8-88343
- Ge:Li, supersaturated solid solns., decomp., surface impurity content 8-51681
- KBr:Li, radiative recomb. of localised excitons 8-72605
- KBr:Li⁺, electronic struct. of $(V_e)_i$ 8-95269
- KCl:Li, K band of F_2 centre, perturbation treatment 8-76016
- KCl:Li, tunable IR lasers with $F_2(II)$ and $F_2(II)$ colour centres 8-90420
- KCl:Li⁺, coherent excitation by EM and acoustic waves, induction and echo signal study 8-67773
- Li, one-electron calcs. of X-ray absorpt. and emission, jellium model 8-56543
- Li plasma dynamic laser, using supersonic nozzle, population inversion, excitation cross section 8-50760
- Li⁺, dynamic multipole polarisability, functional calcs. 8-74595
- Li⁺, electron impact excitation, cross-sections, modified Oppenheimer approx. 8-82843
- Li⁺, imaginary frequency multipole polarisability and long-range dispersion consts, functional calcs. 8-74596
- Li⁺, isoelectronic series, electron correlation and Coulomb hole in momentum space 8-86793

lithium continued

- Li⁺, pair polarisability, ab initio SCF MO energies 8-70741
- Li²⁺, electron impact ionisation, electron ang. momentum exchange 8-78820
- Li/Li₂, supersonic nozzle beam characts. by spectroscopic techniques 8-55255
- Li/Sb(Cu) interface, CESR meas. 8-80218
- Li-like ions, fine struct. in $1s2p^2$ 4P and $1s2s2p$ $^4P^0$ states 8-66471
- Li+Cl₂ (SF₆) (dichlorofluoromethane) (*German*) 8-92485
- Li+F₂(HF), electron transfer reactions, semiempirical pot. energy surfaces calcs. 8-73022
- Li+H, superthermal collisions, photon and positive ion prod. 8-78788
- Li+He, direct excitation of Li I (nl) levels in keV collisions 8-90280
- Li+inert gas collisions, electron loss cross-section meas. (*French*) 8-86941
- Li+Li₂↔Li₃, rovibronic symmetry correlation 8-92461
- Li+N₂, vibr.-rot. relax., optical pot. method 8-62886
- Li⁺+Ar, up to 70 keV, symmetric (antisymmetric) reson. charge transfer cross sections (*Korean*) 8-50636
- Li⁺+CO(CO₂)(N₂O), vibr. excitation, 70 to 1500 eV 8-82824
- Li⁺+H₂O, ab initio GTO calc. of vibr. intensity changes of spectroscopic parameters 8-58583
- Li⁺+Hg(6³P₁), excitation, optical polarisation fractions and mag. sublevels obs. 8-50619
- Li⁺+N₂, rot. and vibr. inelastic collisions, trajectory calcs. rel. to previous data 8-62878
- Li⁺+Na, charge transfer and elastic scatt., two state model 8-58805
- Li⁺+X, X=H, H₂, He, C, N, O, cross-section, closure-Born approx. 8-66630
- Li₂, and anion, electronic struct., spin-unrestricted, spin-restricted SCF HF calc. 8-90331
- Li₂, and isotopic variants, low-lying X-B transition freq. calc. 8-90180
- Li₂, electron binding energies calcs. 8-86768
- Li₂, isotope separation, by two-photon ionisation, ionisation pot. determ. 8-70950
- Li₂, laser, continuous, optically pumped 8-87046
- Li₂, polarisability, generalised London formula for dispersion coeff. 8-82662
- Li₂⁺, dissoci. energy, laser photodissoc. determ. 8-70950
- Li₂+H, superthermal collisions, photon and positive ion prod. 8-78788
- Li₃, BO hypersurface and vibronic states, coupled electron pair approx. 8-94203
- Li₃, geom. struct. and binding energy, diatomic-in-molecules 8-74785
- Li₃, multiplicity and stability considerations, small clusters 8-90333
- Li₄, geom. struct. and binding energy, diatomic-in-molecules 8-74785
- LiH, resonance Raman scatt. (*Russian*) 8-52503
- ⁶Li, D substitute effect in inertially confined fusion with low T inventory 8-58403
- ⁶Li, nuclear mag:spin-lattice relaxation times 8-86889
- ⁶Li⁺+⁷Li⁺, laser-induced Penning and associative ionis., ¹³Li₂⁺ enrichment 8-58796
- ⁷Li, level-crossing method for HFS and A. lifetimes 8-66678
- ⁷Li, prod. in nova explosions 8-57555
- MoO₃:Li, elec., catalytic props. 8-60122
- RbCl:Li, tunable IR lasers with F₂(II) and F₂(II) colour centres 8-90420
- T prod. meas. in Li metal sphere using new methods of neutron source strength determ. 8-74470
- ZnO:Li, optically detected ESR, donor-acceptor pairs, line broadening 8-80256
- ZnO:Li single crystals, photo-induced AC impedance meas., photodielectric effect 8-52034

lithium alloys

- mutual alloying behaviour of the elements straddling the line Li-Mg-Cu-Au in the long periodic table 8-84769
- Ag-Li, solid and liquid alloys, calorimetric investigation of mixing enthalpy (*German*) 8-52773
- Al-Li, dil., quenched and irradi., recovery, resist. and internal friction obs. 8-52848
- Al-Li solid soln., decomposition exam. by secondary ion ion emission (*Russian*) 8-68696
- Al-Mg-Li alloy, 01420, surface layer props. (*Russian*) 8-80674
- Al-Mg-Li-Si system, phase diag. (*Russian*) 8-80515
- K₂Li⁺, equilib. geom. and dissoci. energy, pseudopot. calc. 8-94329
- Li-Al, T-recovery from fusion reactor blankets 8-58455
- Li-Pb, quasi-ionic, thermodynamic props. using EMF meas. 8-51705
- Li-SAP alloys, T recovery from fusion reactor blankets 8-58455
- Li₂Ag₂-In₂, optical props., struct., energy bands, interband transitions 8-72539
- LiAl, semimetallic, B32 struct., electronic props. 8-56062
- Li₂Cd₂-In₂, optical props., struct., energy bands, interband transitions 8-72539
- LiIr, struct. and props. exam. 8-92245
- Li₂K⁺, equilib. geom. and dissoci. energy, pseudopot. calc. 8-94329
- LiNa⁺, equilib. geom. and dissoci. energy, pseudopot. calc. 8-94329
- Li₂-Pb, liq., metal-nonmetal transition, electronic theory 8-79930
- Mg-Li, complex energy band, I-depend. pseudopot. 8-84124
- Na₂Li⁺, equilib. geom. and dissoci. energy, pseudopot. calc. 8-94329

lithium compounds

see also lithium alloys

- calibo glass:Eu³⁺, Ho³⁺, energy transfer 8-76510
- ferrite, fine particle, for arc plasma spraying mm-wave phase shifter 8-64469
- halides, F-band energies extended ion model, variational method 8-60086
- LiNO₃.3H₂O(3D₂O), density, thermal expansion coeff., isotope effect 8-87733
- lithium ammonium tartrate monohydrate, spontaneous shear strain, X-ray obs. 8-56433
- sitall coatings in Li₂O-Na₂O-CaO-SiO₂ system, heat treatment effects on tech. characts. 8-84853
- Al₂O₃-Na₂O-Li₂O (8.8, 0.75 wt.%) exam. of Na⁺ resistivity as function of temp. grain size model 8-80654
- B₂O₃-Li₂O-LiCl glass system, exam. of ionic conductivity of Li (*French*) 8-51730
- CaO-Li₂O-Al₂O₃-SiO₂-Nd³⁺, CaO enriched, laser-type glasses, spectroscopic behaviour 8-60497
- InSb/LiNbO₃ acoustoelectric convolver, gap-coupled, for IR imaging device 8-94492

lithium compounds continued

- KF:LiF, photodichroic, real time recording medium, for optical spectrum analyzer 8-71174
 KF:LiF, photodichroic real-time recording medium, for optical spectrum analyzer 8-66878
 KLi(Pt(CN)₄).2H₂O, cryst. struct., polarised emission obs. 8-52538
 KLiSO₄, phase transition, lattice parameter variation with temp. 8-79767
 KLiSO₄:Cr; optical activity characts. cryst.-chem. exam. 8-95569
 K₂O.3MoO₃.3H₂O, fibrillar crystals, morphology and struct. 8-63959
 LIOT, release from CTR, radiological dose calc. 8-78511
 Li-H₂O(ethylene) 8-66465
 LiAlO₂, fuel cell electrolyte matrix, prep. and struct. characts. 8-80488
 β-LiAlSiO₄, eucryptite, temperature-compensated cuts for SAW devices 8-60018
 LiBH₄, pot. surface and geometry, ab initio calcs. 8-86771
 Li₂B₄O₇:Ag TLD, fast neutron dosimetry 8-94163
 LiBa₂Nb₂(Ta₂)(Sb₂)Ti₂O₁₂, insertion of Li, X-ray and neutron diffr. study (French) 8-91324
 LiBr, in anhydrous acetone, elec. conductance at high press., Shedlovsky method 8-53219
 LiBr, XPS, satellite of Br 4s line 8-56556
 Li(CO)_n (n=1,2,3,4,5,6,8), semiempirical CNDO calcs., solvation struct. 8-82649
 LiCl aqueous glass, X-irradiated, localised electron optical, IR and photoconductivity spectra 8-73064
 LiCl, effective core potentials, all-electron calcs. 8-62704
 LiCl, electron irradi., F-centre emission 8-60501
 LiCl, molten, struct. anal. by X-ray diffr. 8-94961
 LiCl, neutron irradiated, EPR exam. 8-76309
 LiCl, press. shifts of F-centre hyperfine interaction parameters 8-79957
 LiCl, rot. excitation by electron impact, calc. cross sections 8-66670
 LiCl:Cu⁺, luminescent centre, cluster MO calculation of energy levels 8-64411
 LiCl:F⁻(Br⁻)(I⁻), anion impurities substitution, energies of soln., association and migration 8-83831
 LiCl-AlCl₃, molten mixture, vap. pres. meas. 8-87779
 LiCl-AlCl₃, phase diagram determ. by DTA and X-ray anal. (Japanese) 8-92250
 LiCl-PbCl₂, molten, struct. anal. by X-ray diffr. 8-94961
 LiCl(Br) aqueous solutions, tetrahedral hydration of ions, Raman obs. 8-55804
 LiCl(Br)(I), diamag. ion solvation in methanol soln., NMR relax. obs. 8-56389
 LiClO₄, diamag. ion solvation in methanol soln., NMR relax. obs. 8-56389
 LiClO₄-CsNO₃(RbNO₃)(KNO₃)(KClO₄)(RbClO₄)(CsClO₄), binary melt, Raman spectra, polarised line width, temp. depend. 8-84578
 LiClO₄.3D₂O, hexagonal, piezoelec., electro-optic, dielec., elastic, thermoelastic props., space groups 8-76388
 LiClO₄.3H₂O, hexagonal, piezoelec., electro-optic, dielec., elastic, thermoelastic props., space groups 8-76388
 LiD, appl. of microscopic and model theories of lattice dynamics of nonmetals 8-59871
 LiD, cubic cryst., exciton-phonon interaction and exciton anisotropy 8-72083
 LiD, isotope exchange reactions, equilib. consts., adiabatic correction, electron correl. effects 8-88626
 LiD, resonance Raman scatt. (Russian) 8-52503
 LiD, single cryst., reson. zero-phonon exciton luminesc., polariton emission 8-52564
⁷LiD, cryst., cohesive energy, force const., lattice freq., Debye temp., Gruneisen parameters, calc. 8-91293
 LiEu(SO₄)₂, cryst. struct. 8-67695
 LiF, ⁴He scatt., selective adsorption induced intensity maxima 8-72667
 LiF, 63 meV He atom scatt., single Rayleigh phonon interaction 8-80447
 LiF (001), adsorption of H₂, molecular orbital calc. 8-87878
 LiF (001), scatt. of He(Ne), sudden decoupling approxs. 8-64437
 LiF (001), scatt. of Ne, coupled channel calcs., symmetry appls. 8-92156
 LiF (100), elec.-mech. coupling of dislocations 8-75676
 LiF, alkali halide crystals, defect state change during electrolysis 8-95057
 LiF, Bragg diffraction, anharmonic contributions, Mossbauer study 8-76359
 LiF, ceramic, characts. on pressing in vacuum and in air 8-52734
 LiF, cluster calcs., unrestricted HF approach 8-84117
 LiF, coherent radiation generation in F₂-centres 8-50782
 LiF compact, particle size rel. to pore characts. 8-60631
 LiF, cryst., ultrasonic attenuation along (111) and (110) directions 8-63813
 LiF, dislocation dynamic props., investigation by impact loading (Russian) 8-85069
 LiF dispersing crystal, X-ray source, synchrotron-like intensities, EXAFS expts. 8-86398
 LiF, electrification of crystals by cleavage 8-60189
 LiF, electron elastic scatt. cross sections 8-50641
 LiF, electron impact, elastic scatt., model, static and static exchange calcs. 8-94321
 LiF, fracture in mag. field 8-59855
 LiF, γ-irradiated, chemilum. during dissolution (Russian) 8-80427
 LiF, He and H beam scatt., semiempirical determ. of atom-surface interaction 8-72676
 LiF, high temp. depend. of thermal expansion coeff., interatomic pot. approach 8-95166
 LiF, influence of neutron irradi. temp. on F-aggregate centre form. 8-72561
 LiF, laser action of M-centres at 700 nm 8-82972
 LiF, manifestation of local vibrs. of dislocations in IR spectra 8-88339
 LiF, molten, charge fluctuations, collective dynamics, from IR reflectivity 8-67841
 LiF, muon Coulomb capture ratio 8-62959
 LiF, N⁺ and Ne⁺ irradiation, MO X-ray intensity meas. 8-82831
 LiF, NMR exam. of point defects generated in (n,γ)-reaction (Russian) 8-60347
 LiF, neutron ns. slowing down time, expt. obs. 8-58319
 LiF oligomers, struct., stability SCF and CEP-ANO calcs. 8-78640

lithium compounds continued

- LiF, pot. curve, one-config. Hartree-Fock-Rootham calc. for force consts. 8-82627
 LiF, premelting elec. cond., heat capacity 8-91445
 LiF, radiation damaged, proton and ⁴He⁺ channelling, F-centre production, optical absorpt. meas. 8-79656
 LiF, Raman spectra and vibrational modes of V_k centre meas. 8-80338
 LiF, single crystal, dislocation generation, beneath static and rolling contact with sphere 8-87671
 LiF single crystal, void disappearance 8-55864
 LiF single-layer film 2.8 μm, 3.8 μm absorpt. meas. 8-90463
 LiF, Stark effect, M-centre absorpt. bands 8-84614
 LiF, static SIMS, mol. rearrangement, cluster formation 8-64440
 LiF TLD disc response to ¹³¹I and ¹²⁵I, influence of thyroid geometry 8-73250
 LiF, TLD-100, thermoluminesc. emission spectra meas. 8-84667
 LiF, TLD-100, thermolum., glow curve kinetics 8-84668
 LiF, thermal expansivity determ. at high press. 8-79787
 LiF, thermal phonon scatt. by low angle grain boundaries 8-67795
 LiF, thermoluminescence intensity depend. on heating rate and deep trap 8-56527
 LiF, thermoluminescence mechanism, extension of Mayhugh-Christy model 8-80425
 LiF thin layers, effect of LET on thermolum. props. 8-73255
 LiF tile and sheet for thermal neutron shielding (Japanese) 8-74510
 LiF, tunable CW lasers using F₂⁺ centres for 1.26-1.48 and 0.82-1.07 μm bands 8-79023
 LiF, UV visible absorpt. by laser calorimetry, wavelength modulation spectroscopy 8-66876
 LiF, ultra-microhardness testing for vacuum deposited film and bulk specimen 8-79910
 LiF vapour system, fragmentation in mass spectrometer ion source 8-70944
 LiF:Hg²⁺, electrolytic colouration 8-75665
 LiF:Mg, thermal annealing effects on sensitivity and fading of dosimeter 8-82522
 LiF:Mg, Ti, luminesc. increase by O implantation 8-64412
 LiF:Mg(Ag), electron spin-lattice relax. of V_k-centre 8-95518
 LiF:Na⁺ H_k-centre struct., hyperfine interaction 8-79611
 LiF-He interface, absence of anomalous Kapitza resistance 8-63923
 LiF-Li₂O, F-aggregate centres (Russian) 8-64394
 LiF-LiCl-LiBr, molten, H electrochemical extraction, appl. to fusion reactor blanket processing 8-53217
 Li_{0.5}Fe_{2.17}Al_{0.33}O₄:Co, single cryst., domain struct., mag. annealing effect depend. on induced anisotropy 8-68290
 LiFe₂O₈, material loss and high-temp. phase transition 8-64534
 Li_{0.5}Fe_{2.5}O₄, LPE growth on spinel substrate crystals, ferrimagnetic resonance exam. 8-76613
 Li_{0.5}Fe_{2.5}O₄, uniaxial anisotropy energy, elec. field depend. 8-68346
 Li_{0.5}Fe_{2.5}O₄-CuFe₂O₄-ZnFe₂O₄, order-disorder transition, quadratic transformation (French) 8-76447
 Li_{1-x}Fe_{1+x}O₈:Co, single cryst., domain struct., mag. annealing effect depend. on induced anisotropy 8-68290
 Li₂FeOCl, intercalation cpd., cryst. struct. 8-51512
 LiGaO₂:Fe, phosphor, luminesc. 8-92108
 Li_{0.5}Ga_{2.5}O₄-CuCr₂O₄ system, phase diagrams, IR spectra, Cu²⁺ electronic spectra (French) 8-51461
 LiH (D), single crystals, electronic excitations, review (Russian) 8-72574
 LiH, closed liquid Ar circuit for electron irradi. at 90K (French) 8-62214
 LiH, cubic cryst., exciton-phonon interaction and exciton anisotropy 8-72083
 LiH, density matrix, factor X-ray struct. factor 8-67692
 LiH, dipole moments and transition moments, semi-rigorous bounds, error limits 8-78635
 LiH, electron binding energies calcs. 8-86768
 LiH in diffuse interstellar clouds 8-93361
 LiH, isotope exchange reactions, equilib. consts., adiabatic correction, electron correl. effects 8-88626
 LiH, linear response function, diagonal ARPA calcs. 8-74594
 LiH, nucl. antiferromag. struct., neutron diffr. and dynamic polarisation (French) 8-88226
 LiH oligomers, struct., stability SCF and CEP-ANO calcs. 8-78640
 LiH, positron affinity, ab initio LCAO MO SCF calc. 8-82870
 LiH, pot. curve, one-config. Hartree-Fock-Rootham calc. for force consts. 8-82627
 LiH, rot. excitation by electron impact, calc. cross sections 8-66670
 LiH, self-diffusion of Li and H ions 8-59974
 LiH, single cryst., reson. zero-phonon exciton luminesc., polariton emission 8-52564
 LiH, variation-perturbation minimal Gaussian geminal basis sets correl. energy calc. 8-78629
 LiH, zero temp. phases, high density props. 8-75725
 LiH⁺, spin-extended Hartree-Fock ab initio calculations for small radicals 8-70746
⁶LiH, cryst., cohesive energy, force const., lattice freq., Debye temp., Gruneisen parameters, calc. 8-91293
⁷LiH, A¹Σ⁺ state, vibr. levels, radiative and nonradiative lifetimes 8-66604
⁷LiH, A¹Σ⁺-X¹Σ⁺ bands, radiative transition probabilities calcs. 8-66603
⁷LiH, radiative transition probability, from pot. curves, B¹Π curve calc. 8-78752
 LiH₆⁺, AB₆, non-transition element complexes, shapes and other props. 8-82647
 Li₂H⁺, equilib. geom. and dissoci. energy, pseudopot. calc. 8-94329
 LiH₂O⁺, geom., electronic struct. FSGO model calcs. 8-82614
 LiH₂(SeO₃)₂:Mn²⁺, single crystal, EPR 8-72396
 LiHe⁺, from LiT β-decay, pot. energy curves 8-56910
 LiI crystal, emission spectra under UV-light excitation at 77K 8-92110
 LiIO₃, 5.3 μm down-conversion, IR source appls. (German) 8-90452
 α-LiIO₃, attenuated total reflection spectra of anisotropic surface polaritons 8-7919
 LiIO₃, cross relax. in two-spin system, inhomog. broadened line 8-88218
 α-LiIO₃, cryst. growth by conc. convection of soln. 8-72716
 α-LiIO₃, in electrostatic field, X-ray double cryst. spectrometric investigation (Chinese) 8-67666

lithium compounds continued

- α -LiIO₃, lattice const. variation due to electrostatic field (*Chinese*) 8-83787
- α -LiIO₃, piezoelec. mat. for acoustooptic cells, piezoelectric transducers 8-95575
- LiIO₃, pulse-period parametric oscillator, tunable 0.63 to 3.4 μ m, for nonlinear spectroscopy 8-59083
- α -LiIO₃, statistical theory of relaxation current and low-freq. dielectric dispersion 8-60391
- α -LiIO₃, temp. depend. studies of Raman spectra of polaritons in region of phase transition 8-76467
- LiIO₃, US wave tunnelling across piezoelectric gap 8-87857
- α -LiIO₃:Cr³⁺(Mn²⁺)(Fe³⁺) and radn. induced defects, EPR spectra (*German*) 8-84480
- Li₂IrH₄ and Li₂IrH₆, struct. and props. exam. 8-92245
- LiN₃, geom., electronic struct. FSGO model calcs. 8-82614
- LiN₃, evidence for N₃⁻ from static and dynamic props. 8-60465
- Li₂N, heat capacity 5 to 350K, thermochem. props. to 1086K 8-92500
- Li₂N single crystals, Czochralski growth, exam. 8-56574
- Li₂N, superionic conductor, local ionic motion, anisotropic dielec. behaviour 8-87817
- LiNC, metal atom motion, WKB calcs. 8-82623
- LiNC, mol. with polytopical bond, spatial distrib. and motion of Li 8-66533
- LiNC, struct. vibr. states and pot. energy calcs. 8-86776
- LiNH₂⁺, geom., electronic struct. FSGO model calcs. 8-82614
- LiNH₂SO₄, nonlinear opt. props. including SHG 8-76396
- LiNH₂SO₄, phase transitions and phys. props. 8-76399
- Li(N₂H₅)SO₄, thermal diffusivity exam. 8-63886
- LiNH₂SeO₄, nonlinear opt. props. including SHG 8-76396
- LiNO₂, electron irradi. damage, XPS obs. 8-64444
- LiNO₃, Raman spectroscopic study of NO₃⁻ component with temp. 8-76458
- LiNO₃ soln., Raman spectral studies of NO₃⁻ motion and interaction 8-92067
- LiNO₃, soln. in organic liq. or D₂O, Raman lineshape, solvent-solute interaction 8-76448
- LiNa, and anion, electronic struct., spin-unrestricted, spin-restricted SCF HF calc. 8-90331
- LiNbO₃, acousto-optorefractive effect for acousto-optic memory correlator 8-71248
- LiNbO₃, anisotropic multilayer waveguide for electro-optical modulator, propag. characts. (*Italian*) 8-50904
- LiNbO₃, anomalous photovoltaic effect and photocond. 8-52449
- LiNbO₃, anomaly in elec. resist. 8-68030
- LiNbO₃, band struct. and spontaneous polarisation calcs. 8-95261
- LiNbO₃, broadly tunable repetitive picosecond parametric oscillator, freq. conversion 8-66866
- LiNbO₃, continuously tunable parametric oscillator and amplifier, for remote SO₂ meas. 8-77365
- LiNbO₃ crystal, different interdigital electrode struct., electric field distrib. obs. 8-76433
- LiNbO₃, electroacoustic correlation memory effect 8-88001
- LiNbO₃, electrooptic phase modulator, axial mode locking of CW Nd³⁺:YAG ring laser 8-50835
- LiNbO₃ electrooptic phase modulator, freq. shift device for optical range 8-59147
- LiNbO₃, ferroelec., cathodolum. spectral and temp. depend. 8-84665
- LiNbO₃, ferroelec., phonon dispersion relations, neutron inelastic scatt. meas. 8-56435
- LiNbO₃, ferroelectric devices for optical systems 8-90473
- LiNbO₃, film, Lamb waves near. crit. freq. study (*Russian*) 8-52039
- LiNbO₃ graded-index planar waveguide, As₄₀Se_{50-x}S₁₀Ge₁₀ film strip-loaded 8-74965
- LiNbO₃, high freq. plane acousto-optical light modulators (*Russian*) 8-79106
- LiNbO₃, holograms stored by photorefractive effect, reading and optical erasure 8-90390
- LiNbO₃, hyper-Raman scatt. (*Russian*) 8-87102
- LiNbO₃, induced refl. and transparency increase (*Russian*) 8-59094
- LiNbO₃, ion implanted, acoustic model of SAW delay lines (*French*) 8-55540
- LiNbO₃, LF sound attenuation, internal friction 8-63804
- LiNbO₃, layered acoustic waveguide, group delay time, temp. coeff. var. 8-83152
- LiNbO₃, leaky SAW and guided light Bragg interaction, theoretical anal. 8-72484
- LiNbO₃, LiNbO₃:Fe, holography in ferroelectrics 8-90394
- LiNbO₃, LiNbO₃:Fe, photorefraction in ferroelectrics rel. to electro-opt. effects 8-92048
- LiNbO₃, light emission from surface on heating or cooling 8-64416
- LiNbO₃, light modulator with interdigital electrodes, operating characts. 8-90511
- LiNbO₃, linear thermal expansion coeffs. meas., room temp. to 250°C 8-55416
- LiNbO₃, microfabrication by ion-bombardment enhanced etching 8-76779
- LiNbO₃, Nd:YAG laser pumped, parametric oscillator, picosecond IR pulse generation 8-71151
- LiNbO₃, non-centrosymm. crystal, hyper-Raman scatt. obs. 8-94409
- LiNbO₃, nondirectional glow under laser irradi. 8-52575
- LiNbO₃, optical damage in doped and undoped ferroelectric, mechanism 8-95570
- LiNbO₃, optical phonon modes and anharmonic couplings 8-60466
- LiNbO₃, optical strength, surface layer influence 8-50843
- LiNbO₃, optical wave reflectance (*Japanese*) 8-87012
- LiNbO₃, optical waveguides, electrooptic modulation and switching, recent progress 8-50945
- LiNbO₃ parametric oscillator, 4 to 12 μ m tunable down-conversion in GaSe 8-66865
- LiNbO₃, partial waves of SAW, direct meas. by light scatt. 8-66994
- LiNbO₃, phase modulator, use in multimode integrated optical bistable switch 8-79145
- LiNbO₃ photorefractive reversible optical memory (*Russian*) 8-58943
- LiNbO₃, photovoltaic effect, latent-image formation kinetics, electrophotography appl. 8-84246
- LiNbO₃ planar waveguide, refractive index rel. to Ti diffusion (*Russian*) 8-59120
- LiNbO₃, pyroelectric induced optical damage 8-52446

lithium compounds continued

- LiNbO₃, Raman scatt. intensities, photorefractive index change effects 8-84590
- LiNbO₃, refractive index, temp. depend. over 300 to 620 nm (*Russian*) 8-56451
- LiNbO₃ SAW device, obs. of bulk waves and surface waves through side planes of several cuts 8-71238
- LiNbO₃, SAW generation, use of analytical calc. for semi-infinite piezoelec. 8-51809
- LiNbO₃ substrate, fabrication and props. of double-layered polycrystalline CdS 8-64480
- LiNbO₃, surface wave anal. using orthogonal functions 8-51810
- LiNbO₃, thermal and spectral variations in the photovoltaic current in ferroelectrics 8-91719
- LiNbO₃, thermoelastic stress distribution in single cryst. pulling by Czochralski technique 8-63681
- LiNbO₃, Ti diffused, planar waveguide, leaky mode propag. 8-87149
- LiNbO₃, Ti-diffused strip waveguide, appl. in balanced bridge modulator switch 8-63201
- LiNbO₃ transparency with vacuum-deposited electrodes (*Russian*) 8-60422
- LiNbO₃ travelling wave optical waveguide modulator, 10 GHz bandwidth 8-59134
- LiNbO₃, trigonal crystal, optical heterodyne detection using collinear acousto-optic interaction 8-66927
- LiNbO₃, tunable IR sources, parametric oscillators and difference freq. generation 8-59030
- LiNbO₃, tunable parametric oscillator, remote air pollution detect. appl. 8-59089
- LiNbO₃, two-photon and X-ray induced Nb⁴⁺ and O⁻ small polarons, ESR and optical absorpt. 8-76306
- LiNbO₃ UHF SAW filters using group-type unidirectional interdigital transducers 8-59252
- LiNbO₃, use as surface acoustic wave devices 8-91525
- LiNbO₃ waveguide, corrugated, electro-optic scanning of light diff. from grating output coupler 8-63172
- LiNbO₃ X-cut plate shear transducer, direction of displacement 8-51031
- LiNbO₃, Y-Z, SAW scatt. from groove 8-60019
- LiNbO₃:Co, optical props. 8-64383
- LiNbO₃:Fe, calc. of photorefraction (*Russian*) 8-90474
- LiNbO₃:Fe, ferroelectric, treated in Li₂CO₃, formation of Fe²⁺ state, Mossbauer effect 8-92003
- LiNbO₃:Fe, laser induced optical damage 8-95572
- LiNbO₃:Fe, photorefractive effect in a ferroelectric 8-92047
- LiNbO₃:Fe, volume phase holographic storage 8-82929
- LiNbO₃:Fe crystal conductivity and photoinduced birefringence obs. (*Russian*) 8-60151
- LiNbO₃:Fe holographic information storage material 8-55321
- LiNbO₃:Ti, diffused, optical channel waveguides, Bragg switch 8-75002
- LiNbO₃:Ti, electro-optic waveguide modulator, temp. stabilisation 8-50926
- LiNbO₃:Ti, in-diffused waveguide, integrated bistable optical device development 8-75001
- LiNbO₃:Ti cleaved, waveguide, attenuation coefficient and coupling loss 8-74975
- LiNbO₃:Ti diffused strip waveguide, optical insertion losses 8-74985
- LiNbO₃:Ti optical waveguide directional coupler type modulator 8-66951
- LiNbO₃:Ti optical waveguide, SHG with 25% conversion efficiency 8-94432
- LiNbO₃:Ti planar and channel waveguides, appl. of Li₂O compensation technique 8-74976
- LiNbO₃:Ti waveguide, diffused, Mg diffusion effects on characts. 8-66905
- LiNbO₃:Ti waveguide, precise determ. of refr. index 8-94442
- LiNbO₃-3(Li₂O).Nb₂O₅ eutectic, anomaly in elec. resist. 8-68030
- LiNbO₃-InSb amplifier production, role of protective films 8-95220
- LiNbO₃-Si acoustically-matched surface elastic wave transducer 8-90623
- LiNbO₃, dispersion of vibrational excitations, Raman scatt. 8-84588
- LiNdP₂O₁₂ laser, spontaneous phase locking obs. 8-83005
- Li₂O, fusion reactor blanket, Monte Carlo anal. of asymmetric effects 8-74464
- Li₂O pellets, sintered, exam. of microstructure 8-72749
- Li₂O-2SiO₂, glass, devitrification with ageing 8-79536
- Li₂O-Al₂O₃-SiO₂, bonding of Si-O exam. by X-ray emission spectra 8-52594
- Li₂O-CaO-SiO₂ phase equilibria 8-64528
- Li₂O, additive in ZnO sintering 8-80497
- Li₂O, Ar⁺ implantation, depth distrib. by proton backscatt. 8-51577
- Li₂O compensation technique, appl. to LiNbO₃:Ti planar and channel waveguides 8-74976
- Li₂O, lattice energy calc. 8-79556
- Li₂O, segregation at grain boundaries in ZnO 8-64513
- Li₂O-Al₂O₃-P₂O₅:V⁴⁺, glass exam. of ESR spectrum of V⁴⁺, optical spectra, and structure 8-88180
- Li₂O-Al₂O₃-SiO₂, glass ceramic, elastic props. at high press., US meas. 8-83863
- Li₂O-Al₂O₃-4SiO₂, glass-ceramic, tensile creep and high temp. fracture 8-52914
- Li₂O-B₂O₃ glass, conductivity, permittivity, and dielectric loss obs., mixed isotope effect 8-95182
- Li₂O-B₂O₃ glass system, 4-coordinated B atomic fraction determ. 8-94999
- Li₂O-B₂O₃-Fe₂O₃ glass, Mossbauer expts., 85-500K 8-80260
- Li₂O-BeO-SiO₂, X-ray diff. exam. of phase equilibrium 8-80522
- Li₂O-Fe₂O₃-SiO₂ glass, struct. and crystallisation behaviour 8-83738
- Li₂O-Na₂O-B₂O₃-SiO₃, exam. of metastable phase separation region 8-88450
- Li₂O-TeO₂ glasses, struct., IR reflection spectra 8-68516
- ⁶Li(n, α)⁹Li reaction 8-51594
- Li₂O₃, treatment of ferroelec. LiNbO₃:Fe, Mossbauer effect 8-92003
- LiOH, electron distrib. of OH⁻ 8-75973
- Li₂O.2SiO₂ glass, kinetics of crystal nucleation, effect of Pt and other impurities 8-88440
- Li₂O.3MoO₃.5.7H₂O, fibrillar crystals., morphology and struct. 8-63959
- Li₃PO₄, solid, low energy photoelectron spectra 8-95656

lithium compounds continued

- LiPO₃.Al(PO₃)₃:U, vibronic excitation, absorption and emission spectra 8-52524
 Li₃Pr₂(BO₃)₃, cryst. struct. 8-87655
 (Li_{0.5}R_{0.5})TiO₃, distorted perovskite struct. 8-83791
 Li₂SO₄, electron irradiation damage, XPS obs. 8-64444
 Li₂SO₄, IR absorpt. spectra, polymorphism, site group approx. and SO₄ stretching mode 8-52510
 Li₂SO₄, molten, and molten Li₂SO₄-Na₂SO₄ mixtures, struct. anal. by X-ray diff. 8-63660
 Li₂SO₄, molten, Brillouin spectra, refr. index meas., hypersonic vel. 8-68523
 Li₂SO₄, solid, low energy photoelectron spectra 8-95656
 Li₂SO₄ solid electrolyte plastic deformation and thixotropy obs. 8-79660
 Li₂(Si,Al)₁₂(O,N)₁₆, α'-Sialon ceramics, prep. and characterisation 8-84750
 LiSiON, allotropes, powder diff. obs. (French) 8-63726
 Li₂Sr(CO₃)₂, phase diagrams (French) 8-95033
 LiTaO₃ film, pyroelectric effects, origin 8-88258
 LiTaO₃, multimode electro-optical 2×2 crossbar switch 8-55473
 LiTaO₃, near ferroelec. transition, elasticity, photoelasticity 8-88268
 LiTaO₃, optical phonon modes and anharmonic couplings 8-60466
 LiTaO₃, piezoelectric resonator characterisation 8-95550
 LiTaO₃, planar waveguide, leaky mode propag. 8-87149
 LiTaO₃, refr. index distrib. after surface lapping, theory 8-72479
 LiTaO₃, surface wave anal. using orthogonal functions 8-51810
 LiTaO₃ zig-zag reflection interferometric light modulator 8-90527
 LiTaO₃:Mn, optical damage of transition-metal-doped ferroelectric 8-95571
 LiTaO₃-CaZrO₃, struct. and dielec. props. 8-80298
 LiTaO₃-SiO₂-Al₂O₃, transparency in relation to microstruct. 8-53005
 LiTb₄, LiTb_{0.5}Y_{0.5}F₄ and LiTb_{0.25}Gd_{0.75}F₄, Faraday rotation, optical absorpt. spectra and refr. index 8-72542
 LiTbF₄, mag., optical, magneto-optical behaviour 8-68484
 LiTbF₄, Tb³⁺ absorption spectra, 4000 to 25000 cm⁻¹ 8-72550
 Li₃ThF₆, cryst. struct. 8-63702
 Li₂Ti₂O₉, preparation, cryst. struct. determ. 8-75646
 Li₂TiS₂, intercalation cpd., Li ordering, electrochem. obs. 8-59795
 LiTiZn ferrites, elec. resist., mag. props., effect of Bi addition 8-95474
 LiTmF₄, spin density parameters at ¹⁹F nuclei 8-68001
 LiTuO₃, light scatt. from ferroelec. domains 8-80310
 Li₂WO₃, atom motion 8-75874
 LiYF₄:Nd³⁺, pulsed free running laser action at 1053, 1046 nm, passive mode locking (French) 8-79048
 LiYF₄:Nd³⁺(Er³⁺)(Tm³⁺), ZZ 8-80381
 Li_{0.5(1-x)}Zn_{0.5x}Fe_{2.5-0.5x}O₄, canted spin struct., neutron diff. study 8-68175
 Li₁₄Zn(GeO₄)₄, crystal struct. and ionic conductivity 8-51728
 Li₂ZrO₃, thermal decomposition, enthalpy of formation 298.15K 8-61003
 Li₂ZrO₃, thermal decomposition, enthalpy of formation 298.15K 8-61003
 Li₂ZrO₃, thermal decomposition, enthalpy of formation 298.15K 8-61003
⁶LiH shielding for NaI gamma spectrometer, neutron background reduction 8-90012
⁷Li₂O, β-radiation detected NMR of ⁸Li obs., double freq. irradiation, ⁷Li hyperfine struct. anomaly 8-91994
⁷Li₂S, β-radiation detected NMR of ⁸Li obs., double freq. irradiation, ⁷Li hyperfine struct. anomaly 8-91994
⁷LiF, TLD, supralinearity meas. using ⁶⁰Co source 8-82534
⁷LiH, radiative lifetimes for vibr. levels of B¹II state 8-78753
 NH₄LiSO₄, ferroelec., PMR line shape and spin-lattice relax. 8-88205
 NH₄LiSO₄, I-II phase transition in improper ferroelec., hydrostatic press. effects 8-84533
 NaCl:LiCl, melt, semiperiodic closed growth lamellae on crystal-melt interface 8-67668
 Na_{1-x}Li_xNbO₃, dielec. const. and X-ray diff., for Curie temp. and phase diagrams 8-72768
 NaLiZrSi₆O₁₅, zektzerite, silicate mineral with six-tetrahedral-repeat double chains 8-63719
 Rb₂O-Li₂O-P₂O₅ glasses, Raman and far IR spectra, vib. at cation site, struct. 8-60435
 SiO₂-Al₂O₃-B₂O₃ Li₂O-Na₂O, exam. of optical props. 8-88277
 SiO₂-Al₂O₃-B₂O₃-Li₂O, exam. of optical props. 8-88277
 SiO₂-Li₂O glass, bonding of Si-O exam. by X-ray emission spectra 8-52594
 TiNO₃-LiNO₃(KNO₃) mixtures, molten, surface tension, regular solution theory 8-71903
 V₂O₅-Fe₂O₃-Li₂O ternary system, charge compensation of Fe ions, Mossbauer obs. 8-52410

lithospace see *Earth crust*

lithosphere see *Earth crust*

living systems

- see also *biocybernetics; brain models; extraterrestrial life; physiological models*
 biosphere, atmospheric effects, symposium (Mainz, Germany, 11-14 July 1977) 8-73461
 biota as modulator of atmosphere 8-73517
 dynamic processes on Earth, extraterrestrial causes, rel. to extinction of life 8-92820

load (electric)

- pulsed, Tokamak fusion test reactor, AC distribution system 8-54963

lobes (distribution) see *antenna radiation patterns*

local moments in dilute systems

- Curie-Weiss susceptibility of local moments 8-80128
 de Haas-van Alphen wave shape anal., electronic props., appl. to dil. mag. alloys 8-84127
 magnetic alloys, dil., transition metal hosts, props. review 8-84417
 metals, indirect mag. coupling between local moments 8-52207
 metals, review of early work on Anderson model 8-72327
 transition metal alloys, local environment and mag. props. 8-64187
 A-Mn, dil., mag. susceptibility and single impurity effects 8-64186
 Au-Fe, competing interactions in FCC alloys 8-95453
 Cr-Fe, low conc. alloys, coexistence of itinerant antiferromagnetism with paramagnetism 8-84386
 γ-Fe-transition metal alloy, mag. moment in FCC d-metal lattices (Russian) 8-72337

local moments in dilute systems continued

- LaBe₁₃-Er(Dy), dil., ESR, crystalline elec. field splitting, exchange parameters 8-52348
 La_{3-x}V_xS₄:Gd³⁺ localised moment-conduction electron interact., ESR obs. 8-88183
 Lu-Gd, dil., positive exchange Kondo system, magnetisation and resist. 8-68158
 Nb-Mo-Fe, dil., local environment and mag. props. 8-64187
 Nb₅₀Ni_{50-x}Fe_x, amorphous alloy, mag. interactions 8-95432
 Ni_{0.97}Ru_{0.03}, mag. form factor and moment distrib., obs. using polarised neutrons 8-68171
 Pd-Mn, dil. alloy, giant moment at very low temp. 8-88094
 Pd-Ni alloy, ferromagnetism, local moments, susceptibility, magnetisation and Curie temp. (Russian) 8-88115
 Pd-transition metal, dil., itinerant versus localised magnetism 8-64188
 Pt-Fe, competing interactions in FCC alloys 8-95453
 Rh-Fe, competing interactions in FCC alloys 8-95453
 Rh-Pd, mag. moment of Ni, Co, Fe, Mn and Cr impurities 8-95416
 Rh-Pd-Co(Fe), dil., local environment and mag. props. 8-64187
 Sc-Dy(Er)(Tb), dil. alloy, high field magnetisation 8-56292
 Y-Ce, Kondo system, spatial extent of Ce moment, neutron diff. meas. 8-68159
 Zr₄₀Co_{60-x}M_x (M=Gd, Tb, Fe or Mn), amorphous alloy, mag. interactions 8-95432

localised electron states

- see also *Anderson model; charge-ordered states; charge transfer states; Wigner crystal*
 actinides, 3d X-ray spectra, 4f and 5f states 8-84681
 actinides, self-consistent relativistic muffin-tin calc., atomic vol. and bulk modulus Ac-Am 8-72065
 actinides, struct. props. rel. to f electrons 8-83951
 alkanes, electron localisation and solvation, radical ion theory 8-87936
 amorphous solid, abnormal bonding and electronic states in forbidden energy gap 8-51942
 Anderson localisation and recursion method 8-84167
 binary alloy, electron localisation, self-consistent theory (French) 8-60088
 binary alloy model, 2D disordered system, chain-like localisation 8-91646
 binary alloy type of disorder, numerical study of localisation 8-64009
 bipolarons, localised, in ionic crystals 8-67957
 chemisorption on Ni (001), electronic struct., KKR model calcs. 8-56200
 condensed media, electron localisation and solvation, radical ion theory 8-87936
 d-band metals and alloys, s-d hybridisation 8-91644
 diamond, linewidth of GR2-8 transition 8-60488
 disordered system, Coulomb gap, Monte-Carlo simulation 8-84168
 disordered system, four dimens., electron density of states determ. 8-72057
 disordered systems, electron localisation and classical solns. in Ginzburg-Landau field theory 8-56108
 disordered systems, optical energy transfer 8-92105
 electron localisation and mobility edge, spin glass problem 8-52283
 elemental semiconductors, hybridisation effect on dislocation electronic states 8-51936
 Fermi glass, elementary excitation exam. 8-56086
 ferromagnetic semiconductor, autolocalised electron states 8-51924
 filament, condensation energy and mass 8-91637
 heavily doped semiconductor, density of eigenvalues, localisation, general disordered system 8-56109
 n-hexane, liquid, ground state energy of excess electrons 8-68976
 homopolymers, ESCA methods, core levels of simple homopolymers 8-88673
 hybridization effect on phase transitions in the Falicov-Kimball model 8-91617
 insulators, noncryst., electron density captured at traps, liberated to conduction band 8-87946
 ionicity, Pauling's and Phillips' comparison by empirical LCAO band theory 8-51464
 local moments and localised states, review of early work on Anderson model 8-72327
 metal, electric surface impedance 8-88017
 metallic glasses, ferromag., Mossbauer investigation of electronic struct. 8-92009
 MTHF, localised excess electrons, semicontinuum models 8-73129
 one-dimensional disordered lattice, classical diffusion of localised excitations 8-72114
 one-electron approximation, effect of correl. and defects 8-63960
 orthogonality catastrophe due to local electron interaction, overlap integral, Anderson theorem in general case 8-67962
 phase transition with valency change, sound vel. renormalisation (Russian) 8-79963
 photoemission from localised states, model, fractional spin polarisation 8-92172
 polyethylene disordered chains, electron localisation 8-87945
 random impurity system, density of states tails, fluctuations and mobility edges 8-67983
 rare earth metal, lattice dynamics and scatt. reson. 8-59872
 rare earths, 3d X-ray spectra, 4f and 5f states 8-84681
 rare earths, excitation energies for 4f electrons, relativistic calc. 8-72117
 rare earths, struct. props. rel. to f electrons 8-83951
 rare earths and their cpds., XPS satellites, screening of 3d holes 8-76586
 semiconductor, amorphous or disordered, cond. mechanisms, model of medium-range comp. disorder 8-79994
 semiconductor, excitation spectrum and optical props. in field of standing EM wave and homogeneous field 8-91625
 solid-electron interaction, nature and consequences 8-72230
 tetracene, noncryst., localised valence states in forbidden gap 8-72113
 tetramethylsilane, liquid, ground state energy of excess electrons 8-68976
 tight-binding chains, off-diagonal disorder, density of states, localisation length 8-88247
 transition metal, lattice dynamics and scatt. reson. 8-59872
 transition metal hydrides, electronic struct., heat of formation, single particle lifetimes, Dingle temp. meas. 8-51923

localised electron states continued

- transport equation in system of localised electron states (*French*) 8-56141
- 2,2,4-trimethylpentane, liquid, ground state energy of excess electrons 8-68976
- vacancy-impurity scattering, complex dispersion law 8-87957
- Ag, Auger $M_{4,5}$ -VV spectrum, quasi-atomic final states 8-72688
- As_2S_3 glass, localised paramag. states, As_4S_6 , As_4S_4 units, mol. analogue models 8-60087
- As_2Se_3 , glass, density of optically induced localised paramagnetic states 8-52354
- As_2Se_3Ge , glass, light irradi. induced changes in optical and elec. props. (*Japanese*) 8-68031
- Be, anisotropy, theoretical investigation by K-emission, APS, and Compton profiles 8-63970
- CC NiO, amorphous, charge transport in band tails 8-76026
- CeP_2O_{14} , photoemission spectra, 4f, 5p and 5s giant reson. enhancement 8-95660
- $CeRh_{3-x}Pd_x$, electronic and cryst. struct. comparison, catalytic behaviour 8-84398
- CuH, electronic struct., heat of formation, single particle lifetimes, Dingle temp. meas. 8-51923
- $EuO_{1-x}N_x$, ferromag. semicond., elec. and mag. props. (*French*) 8-79993
- Fe 2p states in Fe and Fe alloys, XPS 8-52625
- GaP_2O_7 , optical transitions via deep levels, phonon interaction 8-87939
- GaP_2O_7 , optical transitions via deep levels, cross section temp. depend. 8-87940
- $Gd_{0.67}La_{0.33}P_5O_{14}$, photoemission spectra, 4f, 5p and 5s giant reson. enhancement 8-95660
- Ge_2Se_{1-x} , amorphous semicond., elec. props. 8-84219
- H_2O , liq. and ice, localised excess electrons, semicontinuum models 8-73129
- He liquid surface, localised electron states 8-60007
- KBr:Ag, formation of electron centres and self-localised holes, ESR exam. 8-91947
- KCl:Ag(Tl), formation of electron centres and self-localised holes, ESR exam. 8-91947
- $K_2Pt(CN)_4Br_{0.3} \cdot 3H_2O$, Krogmann salt, non-empirical localised orbital cal. of electronic struct. 8-91636
- LiCl aqueous glass, X-irradiated, localised electron optical, IR and photoconductivity spectra 8-73064
- NH_3 , liq., localised excess electrons, semicontinuum models 8-73129
- NaCl:Ag, formation of electron centres and self-localised holes, ESR exam. 8-91947
- Na_2WO_3 bronze, XPS of W 4f levels 8-95648
- Pb-Te, molten mag. susceptibility, conc. and temp. depend. 8-80121
- PdH, electronic struct., heat of formation, single particle lifetimes, Dingle temp. meas. 8-51923
- Pt, 5d band structure effects on line shapes and intensities of core electron excitations 8-92177
- Si, dangling bonds, EPR, localised states and unpaired electrons on microcrack surfaces 8-52351
- Si film, amorphous, effects of annealing of gap states 8-72115
- Si, pure and heavily doped, 2p-core levels and core excitation binding energy, photoemission obs. 8-76583
- Si_3N_4 , amorphous, charge transport in band tails 8-76026
- n-SnO₂, high resist., photoelectronic processes 8-60157
- TTF-TCNQ, transport props. of dynamically disordered chains 8-72137
- ThF_3 , 5d X-ray spectra, degree of localisation 8-88382
- ThO_2 , 5d X-ray spectra degree of localisation 8-88382
- $Tl_2SeAs_2Te_3$, amorphous semicond., nuclear spin-lattice relaxation by localised electronic states, modification by spin diffusion 8-52372
- UO_2 , 5d X-ray spectra degree of localisation 8-88382
- UO_3 , 5d X-ray spectra degree of localisation 8-88382
- UPd_3 , crystalline electric field levels of U, neutron scatt. exam. 8-60267
- $Zr_{0.9}Fe_{0.1}V_2$, NMR and mag. susceptibility 8-95527
- $Zr_{0.99}Pt_{0.99}V_2$, NMR and mag. susceptibility 8-95527
- $ZrRh_{3-x}Pd_x$, electronic and cryst. struct. comparison 8-84398
- ZrV_2 , NMR and mag. susceptibility 8-95527

localised modes in crystals *see lattice localised modes***localised states, electron** *see localised electron states***loggers** *see data loggers; recorders***logging (recording)** *see recording***logic, formal** *see formal logic***logic circuit elements** *see logic devices***logic circuits**

- see also formal logic; integrated logic circuits; logic devices*
- CRO, control system for sweep signal (*Italian*) 8-77882
- ECG arrhythmia simulator for monitor testing 8-61270
- error monitoring, correction cct. for electronic clocks 8-73970
- particle track chamber, semi-automatic meas. instrum. register for camera photograph reduction 8-78575
- Pr wire thermal cond. automatic meas. device 8-54362

logic design

- optical signal receivers, optimal and nonoptimal, logical structs. efficiency comparison, simulation (*Russian*) 8-71041

logic devices

- see also fluidic logic; logic gates*
- MB DC-SQUID, crit. current mag. modulation, logic device appl. 8-84371

logic gates

- electro-optic devices, guided wave, for logic and computation 8-66946

logic testing

- fluidic element nonstationary flow meas. by laser Doppler velocimeter with frequency tracker (*Japanese*) 8-55707

long-range order

- see also order-disorder transformations*
- alloy, AB type, equilib. props. by Markovian simulation 8-91302
- binary substitutional alloy, with long range order, electron energy spectrum (*Russian*) 8-84121
- binary substitutional alloy with long range order, electron energy spectra (*Russian*) 8-75974
- copper formate. $4D_2O$, field-induced antiferromag. order above T_n 8-84389

long-range order continued

- distribution of dissimilar atoms among interstices of various types, appl. to isotopic ordering (*Russian*) 8-67706
- Euclidean invariance, spontaneous breaking, long range ordered media, defect, config. classification 8-59748
- ferromagnetic binary alloy, short-range and long-range ordering 8-76206
- liquid crystal, tensor field of weak inhomogeneous orientational ordering (*Russian*) 8-67640
- lyotropic liquid crystal, struct. rel. to amphiphilic structure 8-51416
- magnetic ternary alloys, statistical theory of electrical resistivity 8-87969
- random impurity effects 8-95061
- stepped ordering in binary solid solutions 8-67807
- superconductor, neutron effects 8-52121
- surface waves, inhomogeneous liq.-vap. interface, origin 8-75158
- transition metal-metalloid amorphous alloys, mag. props. review 8-52300
- type II superconductor, A15 struct., electronic density of states and T_c changes with atomic ordering 8-91800
- X-Y model, spin 1/2, determ. by variational method 8-72322
- Cu-Au (50 at.%), ordered, influence of elastic stresses on mech. props. (*Russian*) 8-92298
- α -Cu-Ni-Zn-Pb, fire cracking and ordering (*German*) 8-60760
- Fe-Co, partially ordered, elec. cond. 8-91663
- Mg_2Cd , disordering under electron irradi. in electron microscope 8-83849
- $Na_2V_2O_5$, B-phase single cryst., phase transitions EPR meas. 8-95514
- $SrCl_2$, superionic, quasielastic neutron scatt. 8-79504
- $SrTiO_{3-x}$, anion deficiency and anion vacancy ordering 8-51532
- V_2D_3 , single crystal, superstructure modulation and long range order, X-ray obs. 8-71712
- V_3Si , neutron irradi., neutron diffraction studies 8-88076

long tailed pair *see differential amplifiers***Lorentz transformation**

- education, group theory of covariant harmonic oscillators, interacting quarks 8-61970
- education, Maxwell's eqns., Lorentz and conformal covariance, normal transformation rules 8-49589
- Einstein's spectral relativity, Lorentz's rod contraction-clock retardation ether theory, possible equivalence 8-49654
- finite Lorentzian distance space-time singularity theorem (*French*) 8-62075
- four-vector operators from unitary representation of Lorentz transformation 8-49720
- generalised, in general relativity, and behaviour of physical quantities at R- and T- region boundary (*Russian*) 8-49725
- ghost-field formalism, spin 3/2 and 2 fields, EM interaction 8-70315
- homogeneous transform., general form. 8-86151
- Klein Gordon lattice field eqn. in 4-D space-time, Lorentz covariance 8-54184
- Lie group $Sp(8, R)$, Lorentz subgroup anal. and null plane boson realisation 8-62116
- Liouville eqn. basis of relativistically invariant generalised quantum kinetic eqn. 8-54299
- Lorentz group in oscillator realisation 8-77755
- Lorentz groups on skew symmetric tensor space, nonlinear realisations of direct product 8-62329
- Maxwell's equations as one quaternion eqn., appl. to wave propag., for teaching 8-54133
- QED, and Abelian gauge theory, Lorentz boosts on observable and ghost particle states 8-66061
- QED, Lorentz invariance, nonphysical variation 8-93828
- relativistic harmonic oscillators and hadronic struct.; 1st year graduate quantum mechs. 8-61971
- Rutherford scattering with radiation reaction, Lorentz-Dirac eqn. soln. for opposite point charges 8-55289
- SU(2) gauge fields, classification 8-70281
- supergravity, geometry of superspace, vector-spinor matter 8-49744
- superluminal frames and tachyons, introductory review, generalised Lorentz transform. derivation 8-69983
- superluminal transformations, generalised Lorentz transforms. 8-73844
- tachyon magnetic monopoles, existence in 6 dims. space, superluminal transforms. in Dirac theory 8-54183
- tachyon theories 8-54581
- tachyons and bicharacteristics, reply to comment 8-49656
- transverse contractions of moving bodies 8-69980
- unified Lorentz transformations, complex rot. in four dims. space 8-73846
- unified model for description of subluminal and superluminal objects 8-73845

Lorenz number

- $Sn_{1-x}Pb_x$, thermal cond. and Lorenz function 8-51966

Loschmidt number *see constants***loss angle**

- see also dielectric losses*

No entries

loss angle, dielectric *see dielectric losses***loss-angle measurement**

- absolute meas. using toroidal cross capacitor 8-93736
- capacitor, by three-voltmeter minicomputer multibridge system (*Russian*) 8-70159
- ferroelectrics, dielec. props. in vicinity of phase transition, microwave method 8-74022
- two plate capacitor with aerostatic electrode regulation for precise determination of capacitor loss factor (*German*) 8-74021

loss measurement

- optical fibre loss measurement using enhanced sensitivity nondestructive method 8-66895

losses

- see also dielectric losses; eddy current losses; heat losses; loss angle; magnetic leakage*
- dielectric rectangular waveguides for integrated optics, bending losses 8-63205
- glass fibre waveguide, losses below 1 dB/km 8-50936
- Josephson tunnel junctions, high frequency losses 8-88083
- optical curved single-mode fibres, radiation loss meas. 8-74984
- optical fibre, jacketed, hydraulic pressure depend. of losses 8-63175
- optical fibre, joint and connector losses (*French*) 8-55464

losses continued

- optical fibre, losses due to fibre cross section variations 8-71226
- optical fibre, single mode, normalised freq., depend. of splice losses 8-55444
- optical fibre cables, single mode, random bend losses, power spectrum estimation from spectral losses 8-87143
- optical fibre ribbons, loss meas. using calorimetry 8-87127
- optical fibres, arbitrary-index profile, bending loss of propag. modes 8-66896
- optical fibres, coated single-mode, bending losses 8-71209
- optical fibres, graded-index, differential mode attenuation meas. 8-71198
- optical fibres, multimode, universal tunnelling coeff. 8-66922
- optical fibres, multimode graded index, cladding loss effect 8-50927
- optical fibres, step-index, excess loss dependence on parameters, expt. 8-66936
- optical fibres with arbitrary-index profile, splice loss evaluation 8-90499
- optical graded-index fibres, refracting leaky rays 8-79103
- optical graded-index multimode fibres, launch depend. loss in short lengths 8-90495
- optical multimode W-type fibre transmission characts., intermediate layer effect 8-90497
- optical planar waveguides, Ti diffused LiNbO₃ and LiTaO₃, leaky mode propag. 8-87149
- optical waveguide, multilayered, effect of material absorpt. on ray power attenuation 8-83103
- phosphosilicate glass fibre waveguide, possibility of near IR operation 8-50935
- piezoelectric transducers, input electrical impedance expression, internal loss correction 8-53101
- SAW reflective-array-compression filters, nonsynchronous scatt. loss 8-71246
- single-mode fibre joint losses calc. 8-74980
- superconducting cables for PF and TF coils, losses and transient field effect 8-62635
- superconducting wire, AC losses (*Japanese*) 8-84364
- unstable resonators with rounded edges, mode losses 8-79039
- B₂O₃-SiO₂ low-loss single mode fibres, design, fabrication and transmission characts. 8-71199
- LiNbO₃:Ti cleaved, waveguide, attenuation coefficient and coupling loss 8-74975
- LiNbO₃:Ti diffused strip waveguide, optical insertion losses 8-74985
- Nb₃Sn, AC losses, surface effects 8-64171

loudness

see also *acoustic intensity measurement*

- acoustic reflex, in animals, influence on loudness of pulsed pure tones 8-92647
- binaural summation of the loudness of pure tones 8-92638
- comfortable loudness levels for pure tones and speech 8-65050
- continuous judgement by category as rating of road traffic noise (*Japanese*) 8-83170
- growth depend. on excitation pattern skirts 8-61195
- loudness perception, for short-duration tones in masking noise 8-65047
- monaural intensity processing, nonlinear-algebraic approach 8-57012

loudspeakers

- concert halls, hearing impressions of loudspeaker reproductions and orchestras (*German*) 8-94485
- directivity of loudspeaker and subjective hearing event (*German*) 8-79174
- efficiency determ. method 8-51028
- flame acoustic radiation rel. to flame loudspeakers 8-59227
- free-field meas. in normal room using digital signal processing 8-66995
- group delay distortions in electroacoustical systems 8-69105
- infinite baffle simulation with small loudspeaker enclosure 8-55531
- interaction with room resonances, absorption, stereo reception appl. (*Italian*) 8-51005
- reverberation problems in enclosed auditoria (*German*) 8-87204
- signal displacement meas., optical method 8-51023

Love waves

- dispersion curves for stressed stratum in isotropic elastic media 8-57169
- Great Basin of Nevada and W Utah, struct. from seismic surface waves 8-73336
- seismic Love waves, possible mode conversion at continental margin 8-73314
- seismic waves azimuthal anisotropy, physical model 8-65186
- surface waves initial phase and phase vel. from 1968 Jan. 29 Shikotan earthquake 8-92793

low energy electron diffraction

- acetylene, chemisorption on Pt (111), ethylidyne group form., LEED and ELS obs. 8-73075
- adsorbed atom interaction, LEED exam. 8-95237
- adsorbed layer, superelastic electron scattering (*French*) 8-56039
- angle of incidence determ. using fluorescent display photographic technique 8-75508
- anisotropic vibration effects 8-71650
- blanking resistive heating for Auger spectroscopy and LEED using retarding field analyzer 8-54509
- disordered overlayer, model calc. 8-84074
- electronic surface resonances and crystal surface structure 8-71648
- ethylene, chemisorption on Pt (111), ethylidyne group form., LEED and ELS obs. 8-73075
- extinction rules, cluster-embedded chain method 8-94952
- gas-surface interactions, mol. beam apparatus 8-72675
- hydrocarbons, adsorbed on Ru(001), characterisation by electron-stimulated desorpt. 8-71958
- inelastic scattering of low energy electron beams by surface vibrs., nature of image force 8-91527
- MBE, obs. by LEED-AES (*Japanese*) 8-91564
- molecular crystal, LEED differential cross-section, Frenkel excitons effects 8-51398
- molecular crystal, LEED specular beam intensity, bulk Frenkel exciton effects 8-51399
- phase of diffracted wave calc. 8-71647
- polarised LEED using a GaAs spin polarised electron source 8-83693
- polarised low energy electron scattering from solids and liquids, temp. effects 8-71649

low energy electron diffraction continued

- random distributed steps at interfaces and surfaces, quantitative LEED evaluation 8-63912
- reconstructed surfaces 8-95214
- Rydberg states, existence and detection via LEED 8-56198
- solid-electron interaction, nature and consequences 8-72230
- steel, austenitic stainless, oxidation of (100)-plane, LEED-AES obs. (*German*) 8-68841
- surface crystallography, review 8-83691
- surface resonance band structure, lateral surface struct., determ. method 8-68067
- surface structure of solids and adsorbates by LEED 8-94953
- theoretical advances 8-83688
- Ag (110), adsorption of O₂ and CO-O₂ interaction, ellipsometry-LEED expts. 8-91542
- Ag, adsorbed on Si (111), electronic and cryst. struct., Schottky barrier form. obs. 8-84091
- Ag, cluster growth and nucleation on Mo (100), UHV-SEM, AES/(RHEED or LEED) obs. comparison 8-63956
- Al (100), inelastic LEED at beam emergence condition 8-83690
- Ar, adsorbed on graphite, orientational ordering of incommensurate monolayers, LEED obs. 8-95233
- Au (110), electron spin polarisation in LEED 8-83692
- AuPb₂, epitaxial layer, formation during Pb absorpt. on Au, LEED, AES study of Au/AuPb₂ interface 8-71988
- Be (0001) surface, work function and purity, AES, LEED and photoelectron spectra meas. 8-68606
- CO, adsorbed on stepped Ni, thermal decomposition, LEED, AES, thermal flash desorption study 8-71984
- Co, chemisorption of O, LEED anal. of Co(001)c(2×2)-O struct. 8-91546
- Co, surface structure in HCP and FCC bulk phases 8-51807
- Cu (001), surface potential energy barrier model, LEED, intensity profiles 8-64089
- Cu (100), adsorpt. of CO, UV and X-ray photoelectron spectra, LEED 8-56037
- Cu (210) surface, adsorption of O₂, LEED and AES meas. 8-71998
- Cu surfaces, O₂ adsorbed, exam. of structure by LEED, O₂ pressure-temp. diagram (*Japanese*) 8-79884
- Cu-Al, surface segregation during adsorption and low pressure oxidation (*French*) 8-75932
- Cu(100), adsorption and incorporation of O₂ 8-56042
- Cu(311) surface, struct. determ. by multiple scatt. calcs. of LEED intensities 8-56028
- Fe (100) and (111) surfaces, chemisorption of CO, CO₂, acetylene, ethylene, H₂ and NH₃, LEED and thermal desorption 8-71996
- Fe-Si (1%), LEED-Auger exam. of (110) surfaces 8-71915
- Fe(001), adsorption of CO, random occupation of adsorption sites, LEED exam. 8-63930
- GaAs, (100), comp. and struct. of differently prepared surfaces, LEED and AES 8-91524
- GaAs (110), subsurface atomic displacements, LEED exam. 8-71912
- GaAs (110), surface and near-surface atomic struct., LEED 8-91515
- GaAs, (110) surface, bond angle and lengths of rearranged As and Ga atoms 8-71918
- GaAs, electronic surface structure Cs(Rb)(Na) adsorpt. processes, AES, LEED, EELS, study 8-68068
- GaAs surfaces (110) and (111)As, UPS and LEED 8-91514
- GeS, (001) surface struct., LEED expt. 8-84034
- Ge(100) surface, Ar ion bombarded, determ. of atomic steps, LEED 8-63913
- InP surface, interaction with Cl, electron spectroscopic obs. 8-56036
- InSb, electronic surface struct., Cs(Rb)(Na) absorpt., AES, LEED, EELS study 8-68068
- Ir (110), chemisorption of CO, preexponential factor and desorption energy 8-71963
- Ir(111) surface, electron beam induced desorption and dissociation of chemisorbed CO, LEED and AES 8-56043
- LaB₆, (001) surface struct., XPS, LEED meas. 8-63909
- LaB₆, clean and oxidised (100) surface, LEED, AES, work function, evaporation meas. 8-71989
- MgO (001), LEED Kikuchi pattern, surface state reson. 8-83689
- MgO (001) cleavage face, LEED Kikuchi pattern, surface reconstruction 8-84038
- Mo (110), oxidation exam. of LEED 8-92402
- MoS₂, adsorption of Cs and O₂, LEED, Auger and work function meas. 8-71994
- Mo(100), adsorpt. of CO, LEED, AES, study 8-87873
- Ni (001), surface potential energy barrier model, LEED, intensity profiles 8-64089
- Ni (100), phase of diffracted wave calc. 8-71647
- Ni dissolution of C through (110) surface, LEED and AES meas. 8-63932
- Ni, epitaxial film on NaCl, struct. and purity 8-72047
- Ni stepped surface, morphology exam. by LEED and ARS 8-71913
- Ni surface, S and O₂ covered, polycrystalline, initial sticking coeff. of H₂, LEED and AES 8-63937
- NiO (100) surface, sulphurisation by H₂S, AES, LEED, RHEED structural study (*French*) 8-64888
- Ni(111), adsorption of acetylene, evolution of adsorber species, rel. to vibr. spectra 8-95952
- Ni(111) surface, adsorption of H₂ at low temps., LEED meas. 8-56045
- Pb, epitaxial growth on Ag (111) and Cu (111) LEED, RHEED, AES study 8-84090
- Pd(001), adsorpt. of CO, LEED, electron energy loss spectra study, surface struct. effect on weak chemisorpt. bonding 8-71987
- Pt (100), adsorption of acetylene or ethylene, intermolecular forces and kinetics of adsorption 8-75930
- Pt (100), adsorption of H₂S, intermolecular forces and kinetics of adsorption 8-75930
- Pt (111) stepped surface, adsorption of O₂, CO, C₂N₂ and ethylene 8-71992
- Pt, adsorption of O₂, AES, LEED and thermal desorption spectroscopy exam. 8-79891
- Pt electrode (100), (111), polycryst. surfaces, comparison of electrochem. activity 8-61015
- Pt-C, C layer formation on (111) surface, temp. depend., LEED, AES study 8-71911
- Pt(111), adsorption of NO, anal. of adsorption processes and surface reactions, vibration spectroscopy 8-87868

low energy electron diffraction continued

- Rh (110) surface structure, LEED exam. 8-87853
 Rh(111), surface geometry, vibrational props., Debye temp., LEED study 8-87852
 Ru(001), adsorpt. of cycloparaffins, LEED, ESD study 8-87872
 Si (100), struct., LEED study, atomic arrangement model 8-71922
 Si (100) surface, LEED meas. 8-60016
 Si (100) surface, models of (2×1) surface struct., quasidynamical calc. of LEED intensities 8-71921
 Si (111), 2×1 reconstructed, self-consistent anal. 8-91518
 Si (111), Cl₂ chemisorption, ang. resolved UPS and LEED meas. using Vidicon intensity processor 8-71972
 Si (111), cleaved, geometrical struct., LEED expts. 8-91517
 Si, surface (100)(1×1)H struct., LEED study 8-67910
 Si, surface self-diffusion, investigation by slow electron diffr. method (*Russian*) 8-51808
 SrTiO₃ (111), surface struct., electronic props., LEED, AES, UPS study, photoelectrochem. cell anode appl. 8-84035
 SrTiO₃, surface defects, electronic struct., LEED, AES, UPS study 8-84273
 Ti (0001), chemisorption of CO, LEED struct. anal. 8-71964
 Ti, epitaxial growth on Ag (111) and Cu (111), LEED, RHEED, AES study 8-84090
 UIr₃ (100) surface reconstruction, LEED, AES, electron energy loss spectra study 8-75918
 W (001), anal. of surface barrier struct. using LEED data 8-84037
 W (001), LEED, 20 to 150 eV, electron-spin polarisation 8-51400
 W (001), LEED spectra, ext. rel. to theory 8-84039
 W (110), O adsorption, adatom interaction energies, Monte Carlo calc. 8-71948
 W, O chemisorbed layer, phase transitions, coverage effects 8-79879
 W, secondary electron emission rel. to LEED 8-84689
 ZnO 1010 surface, reaction of O₂, AES, LEED, EPR, desorpt., surface cond. and work function expts. 8-95950
 ZnO (0001) and (0001) polar surfaces, 6-fold LEED patterns 8-71920

low gravity experiments *see zero gravity experiments***low induction loss** *see loss angle***low-pass filters**

- nonrecursive, based on analogue delay device, for mass spectrometer ion multiplier 8-92541

low-temperature physics *see cryogenics***low-temperature production**

- see also Joule-Thomson effect; magnetic cooling; refrigeration*
 closed-cycle refrigerator at 4.5K, features, improvement 8-93704
 cryocooler, microminiature size, scaling laws 8-93701
 cryocooler for supercond. instruments, requirements 8-93710
 cryocoolers, closed-cycle, design problems 8-93705
 cryogenics, a critical review 8-89485
 dilution refrigerator with double mixing chamber system 8-81978
 electrocaloric refrigeration for 4-20K range 8-93703
 refrigeration fundamentals, system development 8-93697
 refrigerator, closed-cycle, 4.5K, for supercond. susceptometer 8-93707
 refrigerator, closed-cycle, 4.5K, mag. and vibration characts. 8-93706
 refrigerator, closed-cycle, for supercond. electronic systems, design 8-93711
 regenerative refrigerators, closed-cycle, for cooling small supercond. devices, concept 8-93698
 vapour pumping system, for liquid cryostat, 4.2 to 300K 8-81980
 CaF₂, achievement of negative temp. (*French*) 8-74009
 He II, flow through porous plugs, space cooling system appl., plug characts. 8-49842
 He unit requirements, for superconductive energy appl. in USA 8-89999

low-temperature techniques

- see also cryostats; refrigeration*
 aerosol detector, in cryogenic systems 8-81986
 apparatus volumetric calibration by cryogenic Xe gas transfer 8-93653
 atmosphere organic pollutants, cryogenic sampling and gas chromatography determ. 8-81468
 biological frozen hydrated bulk specimens instrumentation and specimen prep. for electron beam X-ray anal. 8-57142
 biological specimen rapid freezing under controlled and reproducible conditions 8-57139
 biological specimens, low-temp. TEM, radiation damage, review 8-57147
 breakdown voltage, of gaseous N₂ and air, from normal to cryogenic temps. 8-59692
 chemical reaction apparatus, automatic, for low temp. inert atmosphere system 8-93695
 circulating cooling system, based on commercial 6.3 helium liquefier 8-57961
 closed-cycle mech./adsorption refrigeration for cryogenic device appl. 8-93708
 compression, elastic, uniaxial, of single crystals at low temps., device 8-49809
 conversion electron Mossbauer spectroscopy down to 4.2K, applications to thin film and surface studies 8-84504
 cooling of mm- and submm-wave Josephson receiver, closed-cycle refrigerator 8-93709
 coupling for vent gas cooled transfer lines 8-81983
 cryo-ultramicrotomy and myofibrillar fine struct., review 8-53592
 cryocooler for supercond. devices, conf., Boulder, CO, USA (1977) 8-93696
 cryogenic pressure regulator 8-57963
 cryogenics, a critical review 8-89485
 crystal absorption meas. using system response corrector 8-86347
 electric resistance high precision meas. and control of metal samples 8-54403
 electron irradi. of LiH at 90K, closed liquid Ar circuit (*French*) 8-62214
 epoxy, Stycast 1266, very low temp. thermal conductivity and optical props. 8-55992
 EPR cavity matching device for use at low temperatures 8-54420
 freeze-fracture electron microscopy freezing method evaluation by low temp. X-ray diff. 8-57145
 heart muscle cells, paraffin-embedded, cryofracture, SEM and TEM obs. 8-57148
 heat capacity measurement, of metals under pressure 8-81979
 hemispherical dielectric permittivity cell for low temps. 8-70161

low-temperature techniques continued

- high vacuum, HV bushings, for cryogenic appl. 8-81977
 high vacuum evaporation system with low-temperature substrate for superconducting meas. 8-84716
 hybrid cooler for space flight appl. 8-89484
 IR sensor, spinning cryogenic, integrated thermal/structural/optical evaluations 8-82040
 Josephson-effect voltage-standard instrument, features 8-93729
 magnetic refrigerators, small, to pump heat from He temp. to above 10K 8-93702
 Matsushita C resistance thermometers, heat capacity below 1K 8-65934
 microspectrofluorometry design of cold chamber 8-57144
 moving coil linear variable differential transformer for displacement meas. at liquid helium temps. in strong magnetic fields 8-54415
 myocardial tissue, shock-frozen, preservation as shown by cryo-ultramicrotomy and freeze-fracture studies 8-53593
 nylon-quartz fibre support for low temp. mag. suscept. meas. 8-65947
 orbiting astronomical telescopes, IR detector cryogenic cooling requirements 8-96400
 powders, semiconducting, exam. of freeze drying rate in cryochemical prep. method 8-52706
 quartz thermometer, with FET oscillator 8-81967
 Raman spectroscopy of crystals, sample holder 8-86342
 resistance thermometer, GaAs p-type, for meas. under strong mag. fields (*Russian*) 8-89477
 sample orienting device with 2 degrees of freedom for galvanomagnetic meas. 8-81958
 SEM, appls., techniques and specimen prep., review 8-54510
 SEM chamber attachment for fracturing and coating frozen biological samples 8-69260
 shuttle heat transfer in plastic displacers at low speeds 8-93700
 silica (metallised) gels, thermal cond., 10-200K, cryogenic appls. 8-79828
 single crystal strong uniaxial compression apparatus 8-57973
 skeletal muscle bulk specimen, quantitative X-ray microanal. of diffusible ions 8-57143
 SQUID, for Earth's mag. field meas. using magnetotelluric sounding technique 8-96322
 SQUID detector appl. in biomagnetism, techniques 8-96061
 SQUID NMR meas. at low-temp., improved technique 8-54417
 superconducting Al heat switch and plated press-contacts 8-54377
 superconducting alloy films prod. by implantation of light-element ions 8-64161
 superconducting magnet Large Coil Program, He liquefier-refrigerator and distrib. system 8-50398
 superconducting switch for large heat flow below 50 mK 8-54376
 superconducting thermometer, low temp. stabilisation appls. (*German*) 8-86250
 TEM, struct. determ. of frozen, hydrated, cryst. biological specimens 8-57146
 temperature control for mech. meas. under light ion irradi. 8-86278
 thermal radiation shield, for cryogenic apparatus, thermodynamic optimisation 8-81982
 thermoelectric effects, low-temperature measurements, undergraduate lab. project 8-54119
 tissue dispersions, ultracyclinated, freeze-etching by appl. of oil emulsion technique 8-53594
 ultrathin cryo-section stabilization by freeze-drying 8-54349
 vacuum chamber in cryogenic environment, H₂ and He press. meas. 8-77925
 vaporising coolant enthalpy for cryodevice initial cooling (*Russian*) 8-70130
 water cryofilm, on specular and diffusing surfaces, bidirectional reflectance 8-88274
 zero mechanical work thermal compressor or pump, in high speed rotating frame 8-57962
 Ar, liq., magnetic field-induced temperature changes 8-57960
 BF₃, boiling/condensation heat transfer props., cryogenic appls. 8-79192
¹⁰B enrichment by low-temp. exchange in BF₃.SO₂ system (*Japanese*) 8-55251
 CO, boiling/condensation heat transfer props., cryogenic appls. 8-79192
 Cu resonant cavity RF loss reduction by cryogenic cooling 8-93761
 Cu/Au+0.03 at.% Fe, thermocouple characteristics, in mag. field at low temps. (*Russian*) 8-54365
 Ge cryogenic bolometer, for 20 to 500 µm spectral region 8-70187
 Ge resist. thermometers, characts. from 1 to 35K, ISU mag. temp. scale 8-81970
 Ge resist. thermometers, stability test at 20K 8-81971
 Ge resistance thermometer appls. below 0.1K 8-73999
 He level detector for pumped bath 8-49843
⁴He, liq., magnetic field-induced temperature changes 8-57960
⁴He superfluid fountain pump 8-59987
 N₂, liq., magnetic field-induced temperature changes 8-57960
 NO, boiling/condensation heat transfer props., cryogenic appls. 8-79192
 Nb SQUID point-contact operation in very low-power cryocooler 8-93699
 Nb₃Sn, cryostabilised conductor cooling system for Large Coil Program 8-50393
 Ni-Cr foil strain gauge, for cryogenic anal. of supercond. structs. in high mag. fields, fusion reactors 8-54947
 Pt wire NMR thermometer for ultralow temp. down to 0.55 mK 8-89478
 Pt-Co resistance thermometer, for low temp. appl. 8-73994
- LPE** *see liquid phase epitaxial growth*
LS coupling *see Russell-Saunders coupling*
LSA *see limited space charge accumulation*
LSI *see large scale integration*
lubrication
see also friction
 bronze P, friction with steel, boundary lubrication conditions, element conc. anal. of films 8-85001
 circumferentially ground rough disc, elastohydrodynamic lubrication 8-64708
 compliant bearing lubrication, finite element model minimisation algorithm 8-63400
 debris dent effect on elastohydrodynamic lubrication 8-64709

lubrication continued

- elastohydrodynamic contact optimisation 8-79288
 extrusion, benefit of vibrations 8-51135
 fluid film lubrication, velocity profile meas., using ZnS phosphorescent tracer method 8-94866
 four ball test re-examination for lubricants 8-60964
 gas lubricated manometer, effective area calculation for free-piston 8-93714
 large Reynolds number, 2-D hydrodynamic lubricating theory (*Russian*) 8-59368
 liquid continuous flow squeeze film, load-bearing capacity 8-87306
 liquid layer appl. using rubber roller, nip flow operations anal. 8-71310
 lubricants, four-ball test specimens mag. orientation and effect on total test time 8-80700
 motor oils, use of polymeric additives to increase viscosity index, exam. of mechanism 8-95816
 Ni, friction props. of surface films in air and high vacuum 8-60850
 non-Newtonian fluids, lubrication, elastohydrodynamic, between two rot. cylinders 8-83435
 non-Newtonian lubricant hydrodynamic theory (*German*) 8-79341
 nonNewtonian lubricant, bubble behaviour 8-56786
 oil-cooling baffled shell-and-tube heat exchanger expt. 8-83395
 oils, antiwear props. determ. method in tests on friction machines 8-60915
 perfluoro polyethers, props. and use in vacuum appls. 8-70136
 polymer, microporous, lubricant supply charact. 8-64711
 sheet galling, development of quantitative test 8-92433
 silicone oil, props. determ. by harmonical shear vibr. (*German*) 8-67164
 solid lubrications dynamics, obs. using Micro Contact Imager 8-85002
 steel, sheet structural changes during rolling influence of lubricants on friction and wear 8-95815
 steel, water accelerated fatigue, lubricant additive effects 8-64710
 traction prediction in elastohydrodynamic contacts 8-63394
 tunnelling spectroscopy, appls., review 8-92588
 Au, friction props. of surface films in air and high vacuum 8-60850
 Cu, friction props. of surface films in air and high vacuum 8-60850
 Fe, friction props. of surface films in air and high vacuum 8-60850
 MgO single crystal, absorbed fluid effect on rolling contact deform. 8-64719
 MoSe₂, lubricating coatings, texture, prep. by Se₆+Mo 8-53018

Luders bands

- α -brass, single crystal, obstacle strength variation during stress relaxation 8-68723
 steel, alloy, Ni-Cr-Mo, exam. of transformation behaviour 8-76718
 steel, yield point charact., grain size effect (*German*) 8-72810
 Cu single cryst., drawing deform. band form., axial orientation force meas., X-ray pole figure determ. (*Japanese*) 8-76710
 Fe, polycrystalline, exam. of Luders deformation 8-84893
 Zn₃Al, ordered, strengthening by fast neutron irradi. 8-84838

Ludwig-Soret effect see diffusion in solids**luminescence see brightness****luminescence**

- see also cathodoluminescence; chemiluminescence; electroluminescence; fluorescence; fluorescent screens; luminescence of gases; luminescence of liquids and solutions; luminescence of solids; luminescent devices; phosphorescence; phosphors; photoluminescence; sonoluminescence; stimulated emission; superradiance; thermoluminescence; triboluminescence
 atom ejected by ion beams from metallic targets, continuous emission spectra (*Russian*) 8-55140
 candoluminescence spectrophotometry, flame technique for trace metal anal. 8-61093
 multicomponent analysis by synchronous luminesc. spectrometry 8-73089
 recombination decay kinetics in diffusion approx. in presence of particles pair correlation 8-80398
 spectrum recording monochromator wavelength reference marker generator 8-58050
 thin layer chromatography, luminesc. meas. methods 8-53305
 thin layer chromatography, luminescence quantitation, solvent effects 8-53306
 transient emission spectra, observability in theory 8-55199
 H ions, grazing incidence collision with surface, Balmer radiation, elliptical polarisation 8-86804

luminescence chambers see scintillation chambers**luminescence of gases**

- air, luminous emittance of neutron beam 8-86567
 2-(4-biphenyl)-5-phenyloxazol, vapour, electron beam excited luminesc. (*Russian*) 8-82780
 1,4-di(2-(5-phenyloxazolyl))benzol, vapour, electron beam excited luminesc. (*Russian*) 8-82780
 isoquinoline, radiationless transitions, internal conversion, energy depend. 8-94272
 light flash excited by γ -quantum pulse without direct visibility of source 8-69457
 quinoline, radiationless transitions, internal conversion, energy depend. 8-94272
 Ar gas, high press., recombination luminescence in scintillation induced by alpha particles 8-50441
 CO₂-N₂, high temperature gas diagnostics by spectral remote sensing, 700-1350K 8-74002
 Cs-He, new absorption/emission bands perturbed Cs transitions assignment, pot. energy curves 8-66486
 p-fluorobenzaldehyde, vap., high-resolution electronic emission spectrum assignments 8-78742
 He⁺+acetylene-d₀-(d₂), CH⁺(CD⁺), A-X luminesc., in near-thermal charge exchange 8-50632
 He(2¹S)+H₂O(H₂S), energy transfer processes, reaction products, UV and visible obs. in flowing afterglow 8-85138
 PbO, vapour, photoluminescent decay, a(1) state 8-58745

luminescence of inorganic solids

- (*Russian*) 8-72403
 alkali aluminometaphosphate glass, MPO₃.Al(PO₃)₃.U (M=Li,Na,K), vibronic excitation, absorption and emission spectra 8-52524
 alkali halide:Sn²⁺, V_e-centres, vacancy induced splitting of excited states, Sn²⁺ structure 8-51931
 aluminates:Ce³⁺, luminesc. exam. 8-56513
 amorphous solids, electron-phonon interactions, fluoresc. line broadening and spectral diffusion 8-84655

luminescence of inorganic solids continued

- calcium halophosphate, thermostimulated luminesc., mech. milling effects (*Russian*) 8-76537
 calibo glass:Eu³⁺, Ho³⁺, energy transfer 8-76510
 chamber calibration using ruby R₁ luminescence line shift, 80 to 550K 8-86284
 diamond:B, thermoluminesc., TSC, correlation meas. 8-88369
 diamond, GR defect, high resolution optical spectra after electron irradi. 8-56515
 diamond, natural, N3 luminesc. decay time 8-76520
 diamond, semiconducting, GR1 cathodoluminescence, fine struct. 8-68566
 diamond, synthetic, electroluminescence excitation mechanism, role of defects 8-52581
 ferroelectrics, O-octahedric, cathodlum. spectral and temp. depend. 8-84665
 fibreglass, mechanoluminescence during monoaxial stretching 8-68742
 fluorophosphate glasses, rare-earth activated, luminesc., bonding 8-64415
 n-GaP, quasidirect radiative recombination of free holes at neutral shallow donors 8-64410
 hot luminescence and relaxation processes in resonant secondary emission 8-52549
 inert gas crystals, excitons exam. 8-51898
 Invar, photon emission from sputtered atoms, obs. of apparent local thermodynamic equilib. in excitation 8-72672
 junction current, luminesc. near dislocation, surface, integral representations, appl. to LED's 8-68079
 loess-formed quartz silt thermoluminescence and dating (*Chinese*) 8-57226
 manganese minerals, photoluminesc., cryst. field theory (*Russian*) 8-84654
 metallic cathodes, electroluminescent impurities causing vacuum breakdown, obs. 8-84660
 minerals, physical theories for origin of colour 8-69323
 nonmetal, impurity optical absorption and emission, anharmonic effects 8-56503
 oxides, excited states of F-centres 8-64006
 p-type epitaxial layer, thermalisation of electron-hole plasma, photolum. meas. 8-80408
 photon emission from sputtered atoms, obs. of apparent local thermodynamic equilib. in excitation 8-72673
 plagioclase:Mn²⁺(Fe³⁺), ligand field bands of impurity luminesc. centres and their site occupancy 8-88350
 polyethylene, thermoluminesc. spectrum (*German*) 8-76538
 polymer, uniaxial, fluoresc. polarisation, orientation and mol. dynamics effects 8-76516
 polypropylene; thermoluminesc. spectrum (*German*) 8-76538
 polystyrene, thermoluminesc. spectrum (*German*) 8-76538
 quartz:Mn, X-ray and thermally stimulated luminesc. (*Russian*) 8-84626
 rare earth tetracyanoplatinate, energy transfer from linear stacks of donors 8-68546
 ruby, fluorescence line narrowing, energy transfer studies 8-84642
 ruby, high energy phonon spectroscopy 8-83893
 ruby, phonon bottleneck effect, 29 cm⁻¹ phonons 8-68562
 ruby, resonance radiation transfer and nonequilibrium phonons (*Russian*) 8-80418
 ruby, resonantly trapped 29 cm⁻¹ phonons, spectral diffusion 8-92113
 semiconductor, optical absorption and emission by impurities, phonon-electron interaction 8-56502
 semiconductor, optical props. under intense laser fields 8-72513
 semiconductor film, electron spin orientation in quantum size effect conditions 8-68575
 steel, stainless, photon emission from sputtered atoms, obs. of apparent local thermodynamic equilib. in excitation 8-72672
 UV laser possible pumping by synchrotron radiation, NaCl:I(Br) luminesc. 8-66835
 variable gap semiconductor, photolum. emission and excitation spectra 8-76526
 Ag, surface plasmon light emission induced by fast electrons on modulated surface 8-80424
 AgBr:I emulsion, photocond. and luminesc. at -186°C, rel. to incident light intensity 8-64063
 AgCl, cryst. luminesc. and photovoltaic effect kinetics 8-64391
 AgCl, single cryst., optical, acoustic and acousto-optical props. (*Czech*) 8-76417
 AgCl-AgI, mixed cryst., trap distrib., thermolum. 8-68568
 Al, anodisation, intensity of luminesc. and film thickness 8-80413
 Al, continuous UV emission under inert gas ion bombard. 8-84664
 Al-Al₂O₃-electrolyte, electroluminesc., nondestructive electronic avalanche 8-68563
 Al-Mn, anodisation, intensity of luminesc. and film thickness 8-80413
 Al-oxide-electrolyte system, luminesc. spectra (*Russian*) 8-76539
 Al-SiO₂-Au, thin layer struct., electroluminesc. (*French*) 8-76531
 AlAs-GaAs monolayer crystal, two-photon absorpt. spectrum 8-52589
 Al_{1-x}Ga_xAs DH p-n junction, surface recomb. effects on current, luminesc. expts. 8-72246
 n-Al_{1-x}Ga_xAs, epitaxial, photolum. emission and excitation spectra 8-76526
 Al_{1-x}Ga_xAs, LPE, cathodoluminesc. obs. 8-68565
 Al_{1-x}Ga_xAs, p-n homojunction, hot carrier recomb., overheating luminesc. 8-92122
 Al_{1-x}Ga_xAs:Cr, high resist. film, photolum. and photocond. meas. 8-72596
 Al_{1-x}Ga_xSb, photolum. spectra 8-95602
 AlNbO₄, diffuse refl. and luminesc. spectra 8-56516
 Al₂O₃, sintered, residual stress meas., piezospectroscopic technique 8-52704
 Al₂O₃, UV dosimetry grade, thermolum. glow curves and emission spectra, 90-500K 8-72615
 Al₂O₃:Eu, surface luminesc. centres excitation characts. 8-52560
 Al₂O₃:Si,Ti photostimulated thermolum., and appl. to UV dosimetry 8-53511
 β -Al₂O₃-Na₂O:Fe, coordination site, oxidation state, Mossbauer, absorpt., emission spectra, mag. susceptibility meas. 8-68431
 Ar:O₂(N₂), long-wave UV luminesc. (*Russian*) 8-88347
 As₂S₃(Se₃), X-ray induced paramag. states and luminesc. 8-95520
 As₂Se₃, neutrality of luminescence centres 8-88356
 Ba luminate:Eu, effect of non-stoichiometry on luminesc. 8-68550
 BaClF:Sm²⁺, energy levels, optical props. 8-84631

luminescence of inorganic solids continued

- BaF₂:Er³⁺, single-site multiphonon and energy transfer relax. 8-52547
 BaO-B₂O₃:UO₂²⁺, Nd³⁺ glass, radiative and nonradiative energy transfer 8-60508
 BaS:Cu, thermoluminesc. and decay 8-80426
 BaSO₄, barytes, with large magnitude of emitted light, thermolum. curves 8-88368
 Bi₂Al(Ga)₂O₉, fluoresc. and X-ray data 8-80403
 CaCO₃, Akiyoshi stalactite, thermoluminescence and ESR dating comparison 8-88807
 CaF₂, EXAFS, intrinsic UV luminesc. excitation spectra 8-52567
 CaF₂:Ce, Stark struct., phototransitions, g-factors 8-67995
 CaF₂:Dy³⁺, high temp. fluorescence using Ar⁺ and N₂ lasers 8-56514
 CaF₂:Pr³⁺, multisite system, laser selective excitation and energy transfer 8-84634
 CaF₂-SrF₂-BaF₂:Gd³⁺, luminescence spectrum of Gd³⁺ ion and solid solution region obs. 8-84638
 CaF₂-YF₃:Nd³⁺, spectral migration of electronic excitation, selective laser excitation (Russian) 8-80417
 CaO, Eu, Eu²⁺ to Eu³⁺ charge transformation (Russian) 8-72403
 CaO, undoped and Cl-, F- or Al-doped, X-ray and UV luminesc., electron-hole recombination processes (Russian) 8-76528
 CaO-Li₂O-Al₂O₃-SiO₂:Nd³⁺, CaO enriched, laser-type glasses, spectroscopic behaviour 8-60497
 Ca₂P₂O₇:Sb, (Sb,Mn), luminesc., activation, colour centres (Russian) 8-92123
 Ca₃(PO₄)₂:Sb, (Sb,Mn), luminesc., activation, colour centres (Russian) 8-92123
 Ca₃(PO₄)₂:F:Nd³⁺, optical fluorescence intensity and cryst. field parameters 8-52570
 Ca₃(PO₄)₂:OH:Mn, synthesized by hydrothermal method in CaO-P₂O₅-H₂O, thermoluminescence study rel. to starting mixture 8-95612
 CaS, phosphor, tunnel luminescence (Russian) 8-72577
 CaS, phosphors, hole recombination luminescence (Russian) 8-72576
 CaS:Bi, Tm, phosphor sensitisation mechanism, energy transfer 8-60507
 CaS-Pb,Mn, phosphors, thermoluminesc. and fluoresc. spectra 8-64396
 CaSO₄:Dy(Tm) thermoluminescent props. of non-commercial phosphors 8-58550
 CaWO₄:Eu³⁺(Sm³⁺), energy transfer after red edge excitation 8-52552
 CdBr₂(I₂), Mn activated, electron-phonon interaction, lattice vibr. effective energies (Russian) 8-59911
 CdGa₂S₄, photoluminesc. and photocond. meas. 8-60159
 CdGa₂S₄:Ag(In), photoluminesc. and photocond. meas. 8-60159
 CdI₂, polytypism and luminesc. (Russian) 8-56520
 CdS, edge emission spectra alteration by uniaxial stress (Russian) 8-72486
 CdS, exciton cathodoluminesc. of semicond. with surface pot. barriers 8-88366
 CdS, exciton luminescence, surface recombination, space-charge-layer effects 8-80410
 CdS, luminesc. data. statistical anal. (Russian) 8-68559
 CdS, luminesc. from heavy ion tracks 8-88365
 CdS, neutron and fast electron irradi., local centre form., TSC and photoluminesc. meas. 8-87719
 CdS, neutron irradiated, intrinsic defects 8-51599
 CdS, up-conversion and optical storage, spatially modulated band struct. 8-64397
 CdS:Cl, heavily doped, fluoresc. spectrum upper threshold calculated 8-52568
 CdS:Ni, elec., photoelec. and luminesc. props. (Russian) 8-84259
 CdS:P, implanted, photoluminesc. and electroreflection spectra (Russian) 8-52544
 CdS_{1-x}Se_x, mixed cryst., electron-hole drops and plasma, luminesc. obs. (Russian) 8-92119
 CdS_{1-x}Se_x, mixed crystals, exciton spectra 8-92131
 CdSe:P, effect of P on edge luminesc. 8-64399
 CdSnP₂:Cu, deep centres, emission transitions, polarisation (Russian) 8-84650
 CdTe:In, lightly- and heavily-doped, cathodoluminesc., temp., injection level and freq. depend. 8-52584
 Cr³⁺, electronic states interactions with crystal odd vibr., R-lines vibr. recurrences 8-84639
 CsBr:NO₂⁻, luminesc. centre polarisation and reorientation (Russian) 8-76529
 CsBr:O₂⁻ centres, luminesc., polarisation temp. depend. 8-87943
 CsI, intrinsic UV, correl. with V_k plus F-centre config. of self trapped excitons 8-75998
 CsI:NO₂⁻, luminesc. centre polarisation and reorientation (Russian) 8-76529
 CsI:Ti³⁺, Jahn-Teller split luminesc., high press. study 8-52565
 Cs₂NaBiCl₆, optical props. 8-68549
 Cs₂NaTbCl₆, Tb³⁺ ⁵D₄→⁷F₃ transitions, mag. and elec. dipole intensities 8-76033
 Cs₂NaYCl₆:Re,Tm, fluorescence, two-step blue up-convertors 8-95603
 CsSrCl₃:Ti, absorpt. and luminesc. spectra 8-72586
 Cs₂ZrCl₆:Os⁴⁺, multiple state luminesc. 8-72584
 Cu, excited state formed by B⁺ impact, light emission coeffs. 8-64417
 CuCl, biexciton luminescence and two photon Raman emission, polarisation props. 8-80406
 CuCl, excitonic mol. luminesc. spectra, picosecond time anal. 8-52548
 CuCl, resonantly excited excitonic molecules, time resolved spectroscopy 8-92109
 CuGaSe₂, crystals, I₂ vapour transport grown, luminesc. spectra 8-88349
 p-Cu₂Sn-n-ZnS heterojunction, I-V characs., photocond. and electrolum. 8-72251
 Eu complex, (Et₄N)₃[Eu(NCS)₆], Eu³⁺ ion site symm. 8-84656
 Eu complex, benzoylacetate, energy transfer at high pressures 8-52541
 Eu compounds tetrahedral, ligand struct., rel. to luminesc. spectra satellite intensity (Russian) 8-72603
 Eu monochalcogenides, anti-Stokes luminesc. 8-60515
 Ga complex, photoluminesc. spectra, π→π* and charge transfer L→M transitions, Stokes shift 8-64407
 (GaAl)As, DH lasers, degradation mechanisms, temp. depend. 8-66825

luminescence of inorganic solids continued

- GaAlAs-GaAs double heterostructure, interfacial recomb. velocity, photolum. meas. 8-68075
 Ga_{1-x}Al_xSb p-n structure, variable-gap, electroluminescence 8-52582
 p-GaAs, circular polarisation of hot luminesc. 8-52572
 p-GaAs epitaxial layers, electron-hole plasma, quantum effects in magnetoluminesc. 8-72591
 n-GaAs, exciton luminescence, excitation intensity depend. 8-52554
 GaAs FET structure, sharp line photolum. spectra 8-72248
 GaAs, film, radiative relax. time, nonequilibrium carriers 8-84657
 n-GaAs, heat treated, origin of 1.41 eV emission band, photolum. expt. 8-72579
 GaAs, indirect band edge, determ. by quantum-well bandfilling 8-92120
 GaAs injection laser, intensified luminesc. (Russian) 8-90416
 GaAs, ion etching, effects on optical props. and lattice disorder 8-83122
 GaAs LPE layers, dopant tracing of terrace growth 8-75948
 GaAs laser material, secondary dislocation climb during optical excitation 8-75672
 n-GaAs, melt-grown, stoichiometry, photolum. obs. 8-72583
 GaAs, nonlinear extrinsic luminescence 8-84645
 GaAs, photoluminescence intensity of cleaved surface, ambient gas influence 8-88345
 n-GaAs substrates, ion implanted, compensation 8-75680
 GaAs surface, Ar ion bombardment induced photon emission, rel. to target temp. 8-72612
 GaAs, VPE on Ge substrate, and characterisation 8-72736
 GaAs:Cr, fine structure in cathodoluminescence spectrum 8-56524
 GaAs:Cr, luminesc. stress splitting, 4.2K 8-84627
 GaAs:Cr, Si, deep centre photoluminescence spectra 8-95601
 n-GaAs:Cu, contaminated single cryst., deep level photoluminesc. model 8-68554
 GaAs:Ge, LPE, on semi-insulating GaAs, film-substrate interface characterisation 8-72017
 GaAs:Ge, vap. grown, diatomic complex donor and acceptor model 8-80003
 GaAs:Si p-n structure, radiative recombination region 8-52071
 GaAs:Si(Ge) LPE layers, luminesc. props. rel. to substrate quality 8-52583
 n-GaAs:Te, heavily doped, interband luminesc. intensity, heat treatment effect 8-72593
 GaAs-(GaAl)As epitaxial layers and DH lasers, deep centre 1.02 eV luminesc. 8-80387
 GaAs-Al_xGa_{1-x}As DH laser structures, high-resolution composition profiling with photolum. 8-71101
 GaAs-GaAlAs, DH laser material, LPE grown, obs. of melt carryover 8-91553
 GaAs-insulator film interface, evidence for growth-induced damage from photolum. expts. 8-75953
 GaAs_{1-x}P_x:N, 0.6<x<1, photoluminesc., comp. depend. 8-52546
 GaAs_{1-x}P_x:N, film, optical absorpt. from photoluminesc. meas. 8-92134
 GaAsSb_{1-x} epitaxial layer, struct. defects rel. to luminesc. 8-72040
 p-Ga_{1-x}In_xAs, Auger recomb., theory and luminesc. expts. 8-56518
 Ga_{1-x}In_xP, undoped liquid epitaxial layers, effect of heat treatment on photoluminescence 8-60512
 Ga_{1-x}In_xPyAs_{1-y}, In rich bulk single crystals, growth from melt via gradient freeze method, and characterisation 8-68618
 Ga_{1-x}In_xSb:Zn(Te), photolum. and stimulated emission obs. 8-72595
 Ga_{1-x}In_xSe, layered, luminescence and photocond. obs., two-photon excitation 8-76521
 GaN epitaxial layers, exciton cathodolum. (Russian) 8-76543
 GaN:As(P), implanted single cryst. film, cathodolum. 8-60523
 GaNbO₄, diffuse refl. and luminesc. spectra 8-56516
 β-Ga₂O₃, doped, photolum., emission centres struct. 8-52557
 β-Ga₂O₃, pure and doped samples, UV luminesc. obs., 5 to 300K 8-80396
 GaP, dopant dislocations, scanning electron micrographs, cathodoluminesc. 8-91340
 GaP, electron-hole plasma photolum. obs. 8-52559
 GaP, first order Mott transition of exciton gas 8-76535
 GaP, LEC crystal, cathodolum. and photolum. around dislocations 8-84663
 GaP p-n junction, capacitance-freq. dispersion and electroluminescence efficiency 8-64101
 GaP, rare earth doped, photolum. and elec. props. (Russian) 8-52545
 GaP:Cr, ESR of doubly ionised Cr acceptor and IR luminesc. 8-56374
 GaP:N, appl. of temp. modulated photolum. induced by photoexcitation technique 8-95605
 GaP:N, photoluminesc., temp. depend., exciton recombination mechanism 8-88355
 GaP:O, optical transitions via deep levels, phonon interaction 8-87939
 GaP:O, optical transitions via deep levels, cross section temp. depend. 8-87940
 GaP:Zn, growth, I-V characs., electroluminesc. (Korean) 8-52653
 GaSb, photolum., electrolum. meas. in p-n junction, temp. influence 8-72594
 n-GaSb:Te, heavily doped, electron-hole recomb., photoluminesc. spectra 8-84644
 GaSe, additional IR electrolum. band obs. at 77K 8-72607
 GaSe, exciton, excitation-induced absorption and luminesc. 8-60516
 GaSe(Te)-SnO₂ spray heterojunction, electro-optical props. 8-64102
 GaSe_{0.9}Te_{0.1}, undulation spectra associated with acceptor complexes 8-80392
 Gd complex, benzoylacetate, energy transfer at high pressures 8-52541
 Gd₂Ga₂O₁₂:Nd³⁺, growth, stimulated emission, spectral props. 8-95593
 Ge, compressed electron hole plasma, luminesc. 8-72592
 Ge, electron-hole drop velocities, excitation wavelength depend. 8-88358
 Ge, electron-hole droplets, transient photoluminesc. intensities 8-88353
 Ge, electron-hole liquid, luminesc. under infinite uniaxial compression 8-87915
 Ge, electron-hole-droplet cloud, photoluminesc. of laser excited surface, phonon wind 8-84146
 Ge, influence of dislocations on free-exciton lifetime 8-60064

luminescence of inorganic solids continued

- Ge, ultra high vac. cleaved, photolum., role of intrinsic surface states 8-52571
- Ge, uniformly stressed, density and binding energy of electron-hole droplets, photolum. meas. 8-60062
- Ge-Se, glassy, photoinduced photolum. fatigue (*Russian*) 8-60520
- Ge-Se glass system, effect of changes in local surrounding of atoms on optical props. (*Russian*) 8-80414
- GeS, exciton luminescence 8-52555
- α -Ge₂Se_{1-x}, photoluminescence and fatigue effects 8-84648
- glass:Nd³⁺, kinetic description of excitation spectra 8-68557
- Hg_{0.7}Cd_{0.3}Te, 17 to 77K, photo- and cathodoluminesc. 8-52569
- HgI₂, red, reson. Raman scatt. and luminesc. 8-84579
- α -HgS, natural, yellow emission 8-68567
- In complex, photoluminesc. spectra, $\pi \rightarrow \pi^*$ and charge transfer $L \rightarrow M$ transitions, Stokes shift 8-64407
- p-InAs, Auger recomb., theory and luminesc. expts. 8-56518
- In_{0.9}Ga_{0.1}As, heteroepitaxial, MBE grown, props. 8-84328
- In_{0.9}Ga_{0.1}As, thick LPE growth, electrolum. obs. 8-60589
- In_{1-x}Ga_xP, epitaxial film, cathodolum. obs., recomb. mechanisms 8-72613
- In_{1-y}Ga_yP-GaAs heterojunction, VPE, energy band gap and lattice parameter, lattice mismatch effects 8-95345
- InP, photoluminescence intensity of cleaved surface, ambient gas influence 8-88345
- InSe, excitonic absorpt. edge 8-88352
- KBr, heavy ion irradi., σ and π exciton emission spectra, 4.2K 8-76534
- KBr whisker, X-irrad., defect form., thermolum. and ionic cond. obs. (*Russian*) 8-84666
- KBr, X-irradiated, thermally stimulated and tunnelling luminescence spectra, temp. varied 8-72606
- KBr:Eu(Yb), electron-irrad., photostimulated luminesc., ionic processes 8-52561
- KBr:Li, radiative recomb. of localised excitons 8-72605
- KBr:Li⁺(Na⁺), electronic struct. of (V_{Br})₂ 8-95269
- KBr:NO₂, Na effect of Na⁺ impurity on self-trapped hole (*Japanese*) 8- ∞
- \square ||p:ΠBe λθμνεσψ σπεψτρα οβσ. \times -95604
- KBr:Ti³⁺, Jahn-Teller split luminesc., high press. study 8-52565
- KBr(Cl):Ti, visible emission, temp. depend. 8-60511
- KBr(Cl)(I):O₂⁻ centres, luminesc., polarisation temp. depend. 8-87943
- KCN, optical F centres and phase transitions 8-56504
- KCl absorption and emission of F₂(Li) centres under hydrostatic pressure 8-92117
- KCl, F-center pairs, light excitation, mag. field and resonance effects on absorption bands 8-92094
- KCl, X-irradiated, formation of cation defects 8-91359
- KCl, X-irradiated, thermally stimulated and tunnelling luminescence spectra, temp. varied 8-72606
- KCl:AgCl, tunnelling-recombination luminesc. 8-88354
- KCl:Eu, luminescence and absorption of color centres in RbCl:Cu and KCl:Eu crystals 8-92118
- KCl:Eu²⁺, radiationless processes 8-80391
- KCl:Pb, luminesc. spectra obs. 8-95604
- KCl:Pb²⁺, inner-centre luminesc., 8 to 80K (*Russian*) 8-92112
- KCl:Sr, M-centre photoluminesc. (*Russian*) 8-84649
- KCl:Sr²⁺, X-irrad., thermolum., impurity aggregation, trapping centre form. 8-88367
- KCl(Br)(I):In³⁺, Jahn-Teller split luminescence, high press. study 8-52565
- K₂Eu(MoO₄)₃, electric dipole transition cross section and effective site symmetry of Eu³⁺ 8-52556
- KF(Cl)(Br), mag. props. of relaxed excited state of F-centre, vibronic theory 8-60502
- KI, polariton effects in resonant emission 8-76533
- KI, recomb. luminesc. of H-centre and F-centre electrons (*Russian*) 8-80402
- KI, surface, 420 nm band laser-stimulated emission, V₂ centres 8-84633
- KI:Eu, electron-irrad., photostimulated luminesc., ionic processes 8-52561
- KI:Eu²⁺(Sr²⁺)(Mn²⁺), elec. field effect on mech. of recomb. 8-80397
- KI:S₂⁻ centres, luminesc., polarisation temp. depend. 8-87943
- KI:Ti, (Ti³⁺), centre luminesc. 8-84632
- KI(Br), irradiated at room temp., thermolum. and F-centre thermal stability 8-84669
- KLi(Pt(CN)₄)₂H₂O, cryst. struct., polarised emission obs. 8-52538
- KMnF₃, antiferromag., multi-magnon luminesc. sidebands 8-76525
- K₂O-GeO₂:tb³⁺, Yb³⁺ glass, luminesc., cooperative sensitization correlated with Rayleigh scatt. intensity 8-52573
- K₂PtCl₆:Os⁴⁺, multiple state luminesc. 8-72584
- K₂PtCl₆:Os⁴⁺, sharp line luminesc. band at 10K, vibr. assignment 8-95600
- KY₃F₁₀:Eu³⁺, fluoresc. intensity, 77 to 4K, cryst. field parameters of Eu³⁺ 8-72580
- KY₃F₁₀:Eu³⁺, fluoresc. decay, radiative and nonradiative transition probabilities 8-72581
- Kr:N₂O, photoluminesc. from KrO (¹S) excimers 8-68544
- LaF₃:Nd³⁺, vacuum UV luminesc. (*Russian*) 8-64414
- LiCl, electron irradi., F-centre emission 8-60501
- LiCl:Cu⁺, luminescent centre, cluster MO calculation of energy levels 8-64411
- LiD, cubic cryst., exciton-phonon interaction and exciton anisotropy 8-72083
- LiF, coherent radiation generation in F₂-centres 8-50782
- LiF, TLD-100, thermoluminesc. emission spectra meas. 8-84667
- LiF, TLD-100, thermolum., glow curve kinetics 8-84668
- LiF, thermoluminescence intensity depend. on heating rate and deep trap 8-56527
- LiF, thermoluminescence mechanism, extension of Mayhugh-Christy model 8-80425
- LiF:Mg, Ti, luminesc. increase by O implantation 8-64412
- LiF:Li₂O, F-aggregate centres (*Russian*) 8-64394
- LiGaO₂:Fe, phosphor, luminesc. 8-92108
- LiH (D), single crystals, electronic excitations, review (*Russian*) 8-72574
- LiH, cubic cryst., exciton-phonon interaction and exciton anisotropy 8-72083

luminescence of inorganic solids continued

- LiH, LiD, single cryst., reson. zero-phonon exciton luminesc., polariton emission 8-52564
- LiI crystal, emission spectra under UV-light excitation at 77K 8-92110
- LiN₃, evidence for N₃⁻ from static and dynamic props. 8-60465
- LiNbO₃, light emission from surface on heating or cooling 8-64416
- Li₂O-Fe₂O₃-SiO₂ glass, struct. and crystallisation behaviour 8-83738
- LuPO₄:Yb³⁺, charge transfer type luminesc. 8-64392
- MgF₂, cryst., Roentgenoluminesc., exciton emission (*Russian*) 8-95609
- MgO, electronic excitations and luminescence, review (*Russian*) 8-72575
- MgO, single crystals, compressed, SEM exam. of cathodoluminescence 8-56525
- Mg₂SiO₄:Tb, TLD material, UV induced thermolum. and phosphoresc. 8-92707
- MgWO₄, luminesc. and capture centres (*Russian*) 8-52543
- MgZn_{1-x}Te, high purity, luminesc. and band gap 8-68553
- Mn complex, MnCl₂·3.5-lutidine hydrochloride complex, photoluminesc. and photoexcitation 8-92106
- Mn complexes, verification of laws of luminesc. of solids 8-60506
- Mn²⁺ in crystals with different site symmetries, luminesc. spectra 8-80400
- MnF₂, antiferromag., multi-magnon luminesc. sidebands 8-76525
- MnF₂, one-magnon luminesc. sidebands of excitonic transition 8-60517
- MnF₂:Ni²⁺, IR fluoresc., field depend., exchange energy 8-68543
- MnP₂, nonequilibrium luminesc. and relaxation processes, 25 to 300K (*Russian*) 8-80415
- Mo, excited state formed by B⁺ impact, light emission coeffs. 8-64417
- N₂:N, dynamically induced electronic transitions of matrix isolated atom 8-63825
- NH₄NO₃, intrinsic electroluminescence obs. 8-80420
- NH₄SO₄, intrinsic electroluminescence obs. 8-80420
- Na₆Al₆Si₆O₂₄, zeolite, luminescence and coloration (*Russian*) 8-72578
- Na₈Al₆Si₆O₂₄F₂(Cl)(Br)(I), sodalite, luminescence and coloration (*Russian*) 8-72578
- NaBr, lifetime of colour centres 8-92115
- NaCl, influence of coloration on intrinsic luminesc. 8-80399
- NaCl, irradiation-induced energy transfer from bulk to surface, luminesc. meas. 8-92132
- NaCl:Ba, X-irrad., Z₁-centre prod., thermolum. obs. 8-75663
- NaCl:Cu⁺, X-ray irradi., role of Cu⁺ in thermoluminesc. 8-56526
- NaCl:I, UV laser generation by optical pumping 8-82973
- NaCl:Pb, luminesc. spectra obs. 8-95604
- NaCl:Ti, luminesc. yield, effect of fast electron channelling 8-84646
- NaCl(F), irradiated at room temp., thermolum. and F-centre thermal stability 8-84669
- NaF, F₂⁺-centre decay by optical free induction 8-68555
- NaF:U, single crystals 8-72588
- NaI, exciton luminesc., characteristics near absorption edge 8-88363
- NaI, single cryst., reson. zero-phonon exciton luminesc., polariton emission 8-52564
- NaI:Cu⁺, luminesc. of isolated V_K-centres 8-84641
- Nd³⁺ ions in solids, anti-Stokes effects 8-80405
- Nd³⁺:glass, kinetic description of excitation spectra 8-68557
- Nd³⁺:glass, multitype opt. centres 8-68558
- Nd₂O₃-Al₂O₃-SiO₂ glass, exam. of spectroscopic and luminescent props. 8-88364
- Nd₂O₃-SiO₂ glass, exam. of spectroscopic and luminescent props. 8-88364
- Nd₂O₃-Y₂O₃-As₂O₃ glass, spectroscopic props., rel. to possible appl. in lasers 8-84624
- NdP₂O₁₄, laser site-selection time-resolved spectroscopy 8-76524
- Nd₂Y_{1-x}P₂O₁₄, fluoresc. conc. quenching, decay rate consts. 8-64404
- Ne:O₂ (N₂), long-wave UV luminesc. (*Russian*) 8-88347
- PLZT, opt. spectra and luminesc. 8-76508
- P₂O₅-glass, diffusion of Cu⁺, fluoresc. meas. 8-59980
- PbBr₂, cryst., red luminesc. at low temps. (*Russian*) 8-92125
- PbI₂ film, highly excited, oscillator strength of excitons, absorpt. and emission spectra 8-76001
- PbTe epitaxial film, stimulated emission, absorption spectra and recombination 8-80409
- PbTiO₃ single crystals, electroluminesc., elec. field, freq. and temp. depend. 8-80422
- PrVO₄, energy levels, opt. and NMR meas. 8-80226
- RbBr:O₂⁻ centres, luminesc. polarisation temp. depend. 8-87943
- RbCl:Eu, electron-irrad., photostimulated luminesc., ionic processes 8-52561
- RbCl:Eu, γ -irrad., thermoluminesc., EPR meas. 8-84670
- RbCl:Eu, luminescence and absorption of color centres in RbCl:Cu and KCl:Eu crystals 8-92118
- RbMnF₃, antiferromag., multi-magnon luminesc. sidebands 8-76525
- ReBr₂⁻, in cubic crystals, luminesc. spectra and relax. processes 8-68552
- Si, amorphous, glow discharge deposited photolum. decay 8-72590
- Si, amorphous, hydrogenated, spin depend. photoluminesc. 8-72589
- Si, characterisation by photoluminescence method (*Japanese*) 8-80404
- Si, exciton-impurity complexes, emission spectra, Zeeman splitting (*Russian*) 8-64413
- Si, intrinsic semiconductor, radiative recombination probability (*German*) 8-95608
- Si, plastically deformed, hot-exciton luminesc. as function of strain 8-88361
- Si, recombination luminescence, electron-hole drop, excitons orientation in mag. field 8-88362
- Si, swirl defects, gettering effects, obs. by photoluminesc. meas. 8-84623
- Si:B, impurity conc. from photoluminesc. anal. 8-63785
- Si:B(P)(Sb), multiparticle impurity complexes (*Russian*) 8-72601
- Si:Ga(Al), edge luminesc. spectra of acceptors, multiexciton complexes 8-56517
- Si:H, amorphous, rehydrogenation, photoluminesc. recovery 8-72571
- Si:In, bound exciton photolum. obs. 8-95607
- Si:P, excitation density depend. of cathodoluminesc. from bound multiexciton complexes 8-72609
- Si:P, impurity conc. from photoluminesc. anal. 8-63785
- Si:P, luminesc. lines, multiexciton complexes and uniaxial stress 8-92114

luminescence of inorganic solids continued

- Si:P heavily-doped, photoluminescence 8-72572
 Si:Ti, optical absorption and photolum. of bound exciton 8-88359
 SiC, cathodoluminescence, comparison with other materials 8-92130
 SiC, surface luminesc. in presence of anodisation 8-52579
 Si₃C_{1-x}, amorphous, photoluminesc., comp. depend. 8-68541
 SiO₂, vitreous, grown from vapour, gamma ray irradiated, ESR and thermoluminescence exam. 8-88189
 SnO₂, photoluminesc., 77-185K, recomb. model 8-80395
 SnO₂, rare earth ion doped, luminesc. and charge compensation 8-76532
 SrF₂:Eu²⁺, spectral, spatial and temporal phonon spectroscopy, new spectrometer 8-83892
 SrS:Cu, phosphor, photolum. meas. 8-80393
 Ta-Ta₂O₅-ZnS:TbF₃-Au thin films, MIS struct., DC electrolum. obs., Poole-Frenkel effect 8-88038
 Tb₂Y_{1-x}PO₄, H₂ VUV laser excitation, fluoresc. decay characts. 8-60510
 TiCl-TiBr mixed cryst., impurity-induced self-trapping of holes and minority-ion percolation 8-64398
 U containing minerals, luminescence spectra, chemical bond effect 8-72597
 UO₂⁶⁻²ⁿ ion in cryst. matrices, luminesc. 8-84640
 Xe:N₂O, photoluminesc. from XeO (¹D) excimers 8-68544
 YAG:Ge³⁺, excited state absorpt. loss, 5d→4f rare earth lasers 8-90417
 YAG:R³⁺, R=Nd, Er, (Er, Ga), LPE and luminesc. 8-64408
 Y₂O₃:Eu, surface luminesc. centres excitation characts. 8-52560
 Y₂O₃:Eu³⁺, absorpt. spectra, fluoresc., electron beam excitation 8-92093
 YPO₄:Yb³⁺, charge transfer type luminesc. 8-64392
 Y₂Si₂O₇Cl₂, Ce phosphor, prep. and luminescence props. 8-52740
 YVO₄:Eu³⁺, absorpt. spectra, fluoresc., electron beam excitation 8-92093
 YVO₄:Eu³⁺, laser site-selection spectroscopy investigation 8-68556
 Y₂WO₁₂:Eu³⁺, crystal struct., fluorescence spectra, exam. 8-52558
 Zn,Cd_{1-x}Te, relaxation processes, emission spectra (*Russian*) 8-72598
 ZnIn₂S₄ film, photoluminesc. and photocond. 8-52677
 ZnO, change in exciton-phonon mechanism due to defects 8-71804
 ZnO, low energy cathodolum., surface effects 8-60522
 ZnO phosphors, origin of UV emission 8-64400
 ZnO, single cryst. growth in ZnO-H₂-H₂O-O₂ vapour, morphology, electrophys. and opt. props. 8-52649
 ZnO, Zeeman splitting of A1-exciton emission lines, k-linear term effects 8-52563
 ZnO:Dy(Nd)(Sm), phosphor, electroluminesc., photoluminesc. spectra 8-80421
 ZnO:La phosphor, electrolum. brightness waves, -168 to +85°C 8-52580
 ZnS, electroluminesc. and photoluminesc. spectra, fine struct. (*Russian*) 8-84661
 ZnS, electroluminesc. and photoluminesc. spectra, fine struct. (*Russian*) 8-84662
 ZnS, low voltage cathodoluminescence 8-52585
 ZnS, luminesc. data. statistical anal. (*Russian*) 8-68559
 ZnS, powder phosphor, IR-induced changes in emission spectra 8-80389
 ZnS:Ag,Al, computer calc. of band model for luminesc. and photocond. (*Russian*) 8-52542
 ZnS:Cl⁻, Cu⁺(Ag⁺), phosphor, high press. effect on thermoluminesc. 8-64419
 ZnS:Cu, Br based electroluminesc. cells, light, const. field effects on electroluminesc. 8-84658
 ZnS:Cu,Al, anisotropy of blue-Cu luminescence centres 8-64390
 ZnS:Cu(Cl), electroluminesc. and photoluminesc. spectra, fine struct. (*Russian*) 8-84661
 ZnS:Mn, phosphor, surface changes following interaction with H (*Russian*) 8-72602
 ZnS:Mn film, emission centres of DC electrolum. 8-68564
 ZnS:Mn film device, laser modulation of electrolum. 8-52576
 ZnS:Mn²⁺, Jahn-Teller effect in fluorescent level 8-52566
 ZnS:Pb phosphor mech. of elec. field liberation of electrons from traps 8-72616
 ZnS-CdS:Ag, Ni, Co, thermoluminesc. glow curves 8-95611
 ZnS-Cu, comet shaped electroluminesc. lines 8-52578
 ZnS₂Se_{1-x}:Mn(Cu), luminesc. obs. 8-60519
 ZnSe, optically pumped stimulated emission at 4580 Å, near band edge luminesc. 8-71105
 ZnSe, single cryst., electron-hole drops, boundary luminesc. (*Russian*) 8-80412
 ZnSe:Cu, Al, single cryst., low-voltage red cathodolum. 8-80423
 ZnSe:Mn³⁺, Jahn-Teller effect in fluorescent level 8-52566
 ZnSeCu, double comet shaped electroluminesc. 8-52577
 ZnSeS_{1-x}, melt grown, 10K, band edge photoluminesc. 8-84628
 ZnSiP₂, photocond. and photolum. spectra, optical anisotropy 8-72200
 ZnSnP₂-ZnSiP₂, heterocombination simultaneous crystallisation 8-60560
 ZnTe, band parameters from bound exciton, donor-acceptor pair excitation luminescence 8-92111
 ZnTe, donor acceptance pairs, photoluminesc. excitation spectra (*Japanese*) 8-64409
 ZnTe, excited acceptor, donor states, luminesc. 8-72604
 ZnTe, high quality p-type cryst., predominant acceptors 8-60504
 ZnTe, relaxation processes, emission spectra (*Russian*) 8-72598
 ZnTe:O,Zn, dual ion implantation, luminesc. spectra obs. 8-87697
 ZnWO₄, luminesc. and capture centres (*Russian*) 8-52543

luminescence of liquids and solutions

- aequorin, Ca²⁺-induced luminesc., inhibition by anaesthetics 8-76985
 albumin, human serum, kinetics of eosin-sensitised photochemilum. of solns. 8-68991
 alcohol-H₂O solutions, structure, luminesc. probe obs. 8-84636
 t-amyl alcohol+m-aminoacetophenone, in soln., fluoresc. and absorpt. spectra, excimer form. 8-78737
 anthracene, in acetylcellulose, fluorescence, time dependent emission anisotropy (*German*) 8-94279
 aqueous soln., ion luminesc. quenching by electron transfer 8-76511
 aqueous solution fluorescence spectra, refr. correction 8-93766
 arene, photophysics, functionalised micellar assembly, phosphoresc. and triplet Ag⁺ enhancement 8-95598

luminescence of liquids and solutions continued

- aromatic hydrocarbons, excimer decay dynamics, rate const. rel. to solvent 8-58729
 1,2-benzanthracene, monomer and excimer fluoresc. in soln., triplet-triplet annihilation and mag. field depend. 8-78738
 3,4-benzpyrene, monomer and excimer fluoresc. in soln., triplet-triplet annihilation and mag. field depend. 8-78738
 carbazole, in presence of KI, decay functions of triplet state of fluoresc. and phosphoresc. 8-66590
 2-carbethoxy-5-chloro-7-aminoinsole, soln., liq. scintillator, UV excitation, energy transfer and quenching 8-64395
 carbon tetrachloride, liq., luminesc. on giant ps. pulse irradi., spectral and time characts. (*French*) 8-88348
 chlorophyll a, phosphoresc., triplet state, photochem. reacts. (*Czech*) 8-78842
 chlorophyll mixed associates, intermol. interaction, energy transfer, luminesc. and absorpt. spectra 8-64924
 chlorophyll solutions, photolum. of singlet O₂ 8-80831
 chromophore emission spectra, exciting wavelength depend., hydroxylated solvent reorientation 8-76514
 cytidine monophosphate, aq. soln., spectra, 300-450 nm, polarisation study 8-96015
 cytidyl-3',5'-cytidine, aq. soln., spectra, 300-450 nm, polarisation study 8-96015
 dinaphthylalkanes, triplet-triplet annihilation of excimers in soln. 8-86904
 DMSO:Cr³⁺, Nd³⁺, energy transfer and migration, donor-acceptor interaction, phosphoresc. quenching conc. depend. 8-64403
 donor excimers, effect on resonant energy transfer (*Russian*) 8-76530
 dye molecules, dissolved, influence of environment on luminesc., intense laser excitation 8-84622
 dye solutions, dil., fluoresc. decay time determ. 8-68540
 excitation energy transfer in multi-component luminescent solutions 8-84621
 fluorescence polarisation meas. at high press. 8-66576
 glycerol-D₂O:Tb³⁺, Nd³⁺ soln. and frozen glass, energy transfer 8-60509
 inner filter effects in front face and total refl. fluoresc. 8-88357
 lepidoptere ex-ciplex, luminesc. intramolecular anthracene-ethylene ex-ciplex, mol. geometry-fluoresc. relationship 8-58728
 liq. scintillator, UV excitation, energy transfer and quenching 8-64395
 liquid crystal, uniaxial, polarised fluoresc. emission, orientational distrib. function, rot. Brownian motion 8-80390
 malachite green+rhodamine 6G, in low viscosity solvent, ps time resolved energy transfer 8-70910
 micellar system, naphthalene as fluoresc. probe 8-95599
 molecular radiative rate consts., solvent depend. 8-66587
 1-naphthyl methacrylate-9-vinylanthracene copolymer, time-resolved fluoresc. spectra 8-80401
 polymers containing carbazole units, optically active, fluoresc. props. 8-84647
 polymethacrylic acid, dye-tagged, electrically oriented solns., fluoresc. polaris. changes 8-76523
 proteins, fluoresc., equilib. structural mobility (*Russian*) 8-76986
 pyrene, monomer and excimer fluoresc. in soln., triplet-triplet annihilation and mag. field depend. 8-78738
 rhodamine 6G, electronic energy transfer from S₂ state to BBOT in soln. 8-88346
 rhodamine 6G-alcohol, two-photon luminesc. intensity, appl. to picosecond pulse meas. 8-71134
 Smoluchowski equation, with Coulomb pot., appl. to fluoresc. quenching 8-73051
 sodium fluorescein dil. soln., luminesc. absolute quantum yields, thermal blooming method 8-72582
 sodium polystyrene sulphonate, dye-tagged, electrically oriented solns., fluoresc. polaris. changes 8-76523
 tetrabutylammonium tetrahalomanganate, phosphoresc. lifetimes in fused salts and solids 8-72573
 N,N,N',N'-tetramethylparaphenylenediamine, recomb. fluoresc., elec. field quenching 8-92107
 total luminescence spectroscopy, mixture anal. appl., practical values 8-56927
 TP-C-DMP, new bifluorophoric laser dye with intramolecular energy transfer, lasing characts. 8-74899
 TP-CSC-DMP, bifluorophoric mol. ultrafast intramolecular energy transfer 8-74900
 Ar, liq., recomb. luminesc. 8-60521
 Ar, liquid, triplet state of self-trapped exciton states, evidence of existence, luminescence meas. 8-72608
 Dy complex, acetoacetic ether, luminesc. spectral band intensities, solvent effects (*Russian*) 8-84653
 Er³⁺, luminesc. sensitisation by Yb³⁺, in liq., efficiency (*Russian*) 8-90116
 H-bond complex formation, enthalpy change due to electronic excitation, spectroscopic determ. 8-92496
 Kr, liquid, triplet state of self-trapped exciton states, evidence of existence, luminescence meas. 8-72608
 LiF, γ-irradiated, chemilum. during dissolution (*Russian*) 8-80427
 N₂-CO-OCS, liq. mixture, vibr. energy relax. and exchange, laser induced fluoresc. obs. 8-70905
 POCl₃-ZrCl₄:Yb³⁺, Er³⁺, energy transfer from Yb³⁺ to Er³⁺, agglomeration formation 8-64405
 Tb complex, acetoacetic ether, luminesc. spectral band intensities, solvent effects (*Russian*) 8-84653
 Tb³⁺, luminesc. sensitisation by Yb³⁺, in liq., efficiency (*Russian*) 8-90116
 Xe, liq., recomb. luminesc. 8-60521
 Xe, liquid, triplet state of self-trapped exciton states, evidence of existence, luminescence meas. 8-72608
 Zn-tetraphenylporphyrine/metal electrode, photocurrent generation mechanism 8-76868

luminescence of organic solids

- anthracene:2-hydroxyanthracene, site-selective photochem., fluoresc. spectra at 3K 8-80756
 anthracene:1-chloroanthracene, electrolum. meas. 8-84659
 anthracene:tetracene, upper excited vibronic states optically pumped energy transfer matrix fluoresc. 8-76512

luminescence of organic solids continued

- anthracene:tetracene (pentacene), effect of elec. field on fluoresc. (*Russian*) 8-56521
- anthracene, γ -irradiated, temp. depend. of photolum. (*Russian*) 8-56511
- anthracene, electron irradi., creation and evolution of excited states, scintillation obs. 8-92128
- anthracene, excitation spectra of exciton fission in organic crystals 8-92116
- anthracene, fluoresc. spectra and decay curves, 4-300K, reabsorpt. in cryst. (*German*) 8-68561
- anthracene, nonlinear fluorescence quenching 8-52562
- anthracene, singlet exciton fission, prompt and delayed fluoresc. mag. field depend., temp. effects 8-52540
- anthracene, structural imperfections and delayed fluorescence 8-68551
- anthracene, triplet excitons, phosphoresc. and delayed fluoresc. excitation spectra 8-63986
- anthracene in 2-methyl-THF glass, low temp. fluoresc. bandshape, excess energy effects 8-76509
- anthracene-dimethylpyromellite-imide, CT complex, reaction yield detect. double reson., delayed fluoresc. quenching (*Russian*) 8-88230
- anthracene-tetracene amorphous films, host-guest energy transfer 8-60505
- aromatic impurity molecule, internal conversion processes 8-82776
- aromatic scintillators radioluminesc. yield (*French*) 8-52574
- azomethines, photochromic, intramol. proton phototransfer sensitisation, organic cation energy transfer 8-53230
- azulene in naphthalene mixed cryst., $S_2 \rightarrow S_1$ fluoresc., vibr. anal. 8-66586
- 1,12-benzoperylene in n-alkane, zero-phonon lines in luminesc. spectra 8-56512
- carbazoles, luminescence, AgNO_3 heavy atom effect, donor-acceptor interaction (*German*) 8-84651
- carbazolyl substituted diacetylene monomer cryst., ODMR and triplet state kinetics 8-76355
- cellulose-PAN copolymer, luminesc., ageing effect 8-64401
- 9-cyanoanthracene:perylene, exciplex emission 8-60513
- 9-cyanoanthracene, luminesc., excimeric species 8-84637
- 9-cyanoanthracene, quenching of solid state photodimerisation reaction by cryst. doping 8-68547
- 3,5-di-tert-butyl-4-hydroxybenzylidenemalononitrile, excited-state proton transfer, cryst. and mol. struct. 8-84630
- 4,4'-dibromodiphenylether:benzophenone- d_{10} , optical decay constants, photoexcited triplet state near level anticrossing field 8-80250
- p-dichlorobenzene-p-dibromobenzene, solid soln., local struct. and triplet energy migration 8-60489
- 2,3-dichloroquinoxaline, in tetramethylbenzene cryst., sublevel phosphoresc. spectra 8-70863
- diphenyl:naphthalene, benzophenone, phosphoresc., triplet diffusion excitons 8-63985
- epoxy resin, electroluminesc. 8-56522
- fluorene, electroluminesc. (*Russian*) 8-92129
- fluorene, lowest singlet state, exciton band struct. calc. 8-63983
- fluorene, near 6K, two-photon excitation spectrum, g-exciton states location 8-64393
- glycerol- D_2O : Tb^{3+} , Nd^{3+} soln. and frozen glass, energy transfer 8-60509
- indole, in PMMA matrix, high press. luminesc. 8-84629
- lepidoptere exciplex, luminesc. intramolecular anthracene-ethylene exciplex, mol. geometry-fluoresc. relationship 8-58728
- luminescence, AgNO_3 heavy atom effect, donor-acceptor interaction (*German*) 8-84651
- 5-methylindole, in PMMA matrix, high press. luminesc. 8-84629
- 3-methylpentane, γ -irradiated, isothermal luminescence in presence of aromatic solutes at 77K 8-76519
- mixed crystals, energy transfer 8-76515
- molecular crystals, optical spin alignment, phosphoresc. (*Russian*) 8-84652
- naphthalene: β -chloronaphthalene, reaction rate constants of triplet excitons 8-80407
- naphthalene, 2-methylnaphthalene and anthracene doped, single cryst., sensitised fluoresc. 8-68548
- naphthalene, cryst., singlet exciton interactions, prompt fluoresc. decay 8-60500
- naphthalene, crystalline, singlet exciton diffusion coeff. meas., fluorescence quenching anal. 8-67945
- naphthalene, nonlinear fluorescence quenching 8-52562
- naphthalene, triplet excitons, phosphoresc. and delayed fluoresc. excitation spectra 8-63986
- naphthalene cryst., anthracene doped, fluoresc., two-photon excited 8-68560
- naphthalene-triethylamine exciplex, effect of dipolar molecules on quenching curves 8-52551
- n-paraffin crystal matrices, organic impurity molecular fluoresc., effect of heat pulses 8-88360
- perylene, excitation spectra of exciton fission in organic crystals 8-92116
- perylene in n-alkane, zero-phonon lines in luminesc. spectra 8-56512
- perylene-N,N-dimethylaniline exciplex, effect of dipolar molecules on quenching curves 8-52551
- phenanthrolines, in Shpolskii matrices, phosphoresc. spectra 8-94276
- phenylacetylene, phosphorescence polarisation, intramolecular heavy atom effect 8-52550
- phthalocyanine, metal-free, solid, fluoresc., lifetimes temp. depend., polymorphic modification 8-80388
- plastic scintillators, radioluminesc. absolute output following ^{60}Co γ -ray irradi. (*Russian*) 8-92124
- PMA, phosphorescence depolarisation, segmental relax. time 8-95606
- PMMA, phosphorescence depolarisation, segmental relax. time 8-95606
- PMMA crosslinked by dimethacryloxymethylantracene, radiothermoluminesc. (*Russian*) 8-73068
- polymer orientation measurement, in solid, by spectroscopic techniques, mech. anisotropy 8-75558
- polymethyl acrylate, phosphorescence depolarisation studies of relaxation effects 8-56685
- polypeptide hormones, conformations, ODMR investig. 8-76356
- PVC, ozonized, decomposition of peroxides, chemilum. meas. 8-68893
- pyrene-triethylamine exciplex, effect of dipolar molecules on quenching curves 8-52551

luminescence of organic solids continued

- Rochelle salt, mechanoluminescence and crack mobility, charge prod. during fracture 8-88370
- trans-stilbene, cryst., triplet excitons, $S_0 \rightarrow T_1$ transition 8-76518
- stilbene, single cryst., triplet excitons, delayed fluorescence 8-63988
- tetrabutylammonium tetrahalomanganate, phosphoresc. lifetimes in fused salts and solids 8-72573
- tetracene, cryst., triplet exciton pair kinematics, diffusion model, prompt fluoresc. decay 8-79931
- tetracene, fluorescence, effect of weak external electric field (*Russian*) 8-80416
- 1,2,4,5-tetrachlorobenzene, localised excitations thermal promotion to exciton band, impurity states effect 8-52539
- tetramethylbenzene: 2,3-dichloroquinoxaline, sublevel phosphoresc. spectra 8-70863
- tetramethylpyrazine- d_{12} , photoexcited triplet state, in durene, phosphoresc., spin coherence and quantum beats 8-76517
- triplet exciton dynamics, kinetic model 8-67948
- Mo, oxidation, IR emission spectrosc. obs. 8-68942
- UO_2 complexes, cubic crystals, low temp. optical spectra (*Russian*) 8-92083

luminescence of solids

- see also luminescence of inorganic solids; luminescence of organic solids
- crystal luminescence, effect of internal Raman scatt. (*Russian*) 8-60518
- impurity centres, theory of time depend. of resonant secondary emission spectra 8-92082
- line shapes, for impurities, quantum-mechanical moments 8-72566
- paramagnetic molecules in rigid isotropic medium, mag. linearly polarised emission 8-68545
- percolation model, one-dimens., spectral diffusion 8-80411
- polycrystalline solids, Zeeman spectra 8-68487
- resonance light scattering, statistical aspects 8-80323
- semi-infinite direct-gap semiconductor effect of reabsorbed recomb. rad. 8-95312
- semiconductor, resonance secondary radiation emission, theory 8-60452
- semiconductor, temp. modulated photolum. induced by photoexcitation 8-95605
- semiconductors, luminesc. parameters, absorpt. parameter effects (*Russian*) 8-80419
- solid solutions, inhomogeneity and site selective impurity-phonon coupling effects 8-84625
- transparent dielectric, nondirectional glow under laser irradi. 8-52575

luminescent devices

- see also fluorescent screens; phosphors; scintillation counters
- radiation crack detection, use of luminescent converters 8-53125
- GaAs MOS structure, white light emission obs. 8-76148
- $\text{ZnS}:\text{Cu}$, Br based electroluminesc. cells, light, const. field effects on electroluminesc. 8-84658
- $\text{ZnS}:\text{Mn}$ film device, laser modulation of electrolum. 8-52576
- ZnSe-GaAs thin film DE electroluminescent cell with 20 V threshold voltage 8-76141

luminophors see phosphors**luminors see phosphors****lunar geology see lunar rocks and minerals****lunar rocks and minerals**

- analysis, neutron activation, using standard reference materials as multielement irradi. standards 8-80815
- basalts, redox state 8-77217
- basalts from Mare Crisium, mineralogy 8-65519
- Bench Crater meteorite, member of new subgroup of carbonaceous chondrites 8-65573
- breccia, $^{40}\text{Ar}/^{39}\text{Ar}$ dating of plagioclase clasts, rel. to early lunar differentiation 8-65514
- breccias, magnetization origin, thermal overprinting 8-61760
- Chernier Crater, lava-like material nature and origin 8-81569
- cosmogenic isotope concs. in lunar samples rel. to past solar activity 8-61828
- Fra Mauro basalts, origin, rel. to $\text{Mg}_2\text{SiO}_4\text{-Fe}_2\text{SiO}_4\text{-CaAl}_2\text{Si}_2\text{O}_8\text{-SiO}_2$ system phase relations 8-65512
- gabbroic anorthositic sample, thermal and deform. history, shock melting 8-65517
- grains surface chem., solar wind sputtering effects 8-77501
- highland melt rock suite 8-81568
- Imbrian-age highland volcanism, Gruithuisen and Mairan domes 8-77504
- mare basalt suite 8-77500
- Oriente basin ejecta, radial thickness vars. 8-89088
- orthopyroxene from anorthositic 15415, crystal structure and thermal history 8-53842
- palaeomagnetism, origin 8-93132
- regolith, fine particulate Fe (*Russian*) 8-89089
- regolith, IR spectra, Salyut 4 obs. in 3.5-7 μ range 8-69716
- regolith light element chemistry of Apollo 12 site 8-65515
- sampling techniques for interplanetary particles 8-57459
- solar wind sputtering, chemical and isotopic fractionation 8-61762
- solar wind sputtering, comments 8-61763
- surface layers, dielectric const. and temp. gradient from 2 and 6 cm brightness distrib. 8-81572
- thermal conductivity prediction of heterogeneous mixture, digital simulation technique 8-87247
- trace element nondestructive anal. using proton microprobe 8-64911
- $^{39}\text{Ar}/^{40}\text{Ar}$ dating of rock fragments from Mare Crisium 8-65513
- Fe, first order shock induced mag. transitions characts. and discrimination from TRM 8-64205
- Fe particles, FMR study, effective linewidth method 8-95523
- TiO_2 distrib. over surface from anal. of Mikhail's photometric catalogue (*Russian*) 8-73661

lunar seismology

- Apollo lunar surface science stations shutdown 8-57425
- mantle, seismic vels. rel. to constitution 8-85866
- periodicity rel. to lunar sidereal period 8-53844
- surface reflections use in lunar seismograms 8-65504

lunar structure

- see also lunar rocks and minerals; Moon
- Apennines and regional surroundings, isostatic state 8-77503
- core dynamo, rel. to superheavy elements 8-65521
- craters on farside, volcanic events after impact 8-65516

lunar structure continued

- crustal tidal stresses rel. to lineaments 8-89087
- impact basin rings formation theory 8-61766
- impact erosion 8-57476
- light plains, different ages 8-81571
- Mare Crisium, regional stratigraphy and geological history 8-61765
- Maria Serenitatis and Crisium, orbital radar evidence for subsurface layering 8-85868
- Moon thermal history, effects of chemical stratification 8-65522
- palaeomagnetism, pole positions rel. to lunar core dynamo processes 8-93132
- surface structure forecast, based on thermal conditions 8-77502
- tectonic pattern of Cruger/Rima Sirsalis-Rima De Gasparis area 8-65520

lutecium see *lutetium***lutetium**

- see also *nuclei with*
- atom, even config., parametric calcs. 8-82631
- band structure, influence of relativistic effects 8-75991
- electric fields gradient, at ^{181}Ta substitutional atoms, pressure dependence 8-52385
- X-ray absorption discontinuity, spectroscopic anal., energy separation of orbitals 8-76557
- Li I, IR emission spectrum, extended anal. 8-62747
- Lu-Mn, relative activity ratios in natural UO_2 reactor fuel 8-58347

lutetium alloys

- Lu-Fe, amorphous alloy film, spin reson. meas. 8-68389
- Lu-Gd, dil., positive exchange Kondo system, magnetisation and resist. 8-68158
- Lu-rare earth, dil., cryst. fields 8-80127
- LuBe_{13} -Er, dil., ESR, crystalline elec. field splitting, exchange parameters 8-52348
- LuFe_4Al_8 , mag. props. 8-52250
- LuIr:Gd influence of cryst. field on EPR 8-52346
- $\text{LuIr}_2\text{-Nd}^{3+}$, dil., ESR, hyperfine crysts. of $^{143,145}\text{Nd}$, g-factor, crystalline field splitting 8-52349
- $\text{LuRh}_2\text{-Nd}^{3+}$, dil., ESR, hyperfine crysts. of $^{143,145}\text{Nd}$, g-factor, crystalline field splitting 8-52349

lutetium compounds

- see also *lutetium alloys*
- $(\text{Eu,Lu})_3\text{Fe}_5\text{O}_{12}$, submicron bubble films on rare earth-Ga garnet substrates, prep. and mag. props. 8-91909
- $(\text{EuLu})_3\text{Fe}_5\text{O}_{12}$, Ga, Al or (Ca,Ge) substituted, mag. props. and growth of 2 μm bubbles 8-91910
- $(\text{Gd,Lu})_3(\text{Fe,Mn,Al})_5\text{O}_{12}$ epilayer with orthorhombic anisotropy, domain wall vel. 8-52322
- LuAG:Nd^{3+} , cryst. field anal. 8-64013
- $\text{LuBe}_{13}\text{:Er(Dy)(Gd)}$, ESR, crystalline field single ion effects 8-84481

- $\text{LuF}_3\text{:Nd}^{3+}(\text{Er}^{3+})(\text{Tm}^{3+})$, ZZ 8-80381
- $\text{Lu}_3\text{Ga}_5\text{O}_{12}\text{:Nd}^{3+}$, cryst. field anal. 8-64013
- LuP(As)(Sb)(Bi) , coupling between Gd 4f electrons and conduction electrons, EPR linewidth 8-52347
- $\text{LuPO}_4\text{:Yb}^{3+}$, charge transfer type luminesc. 8-64392
- $\text{LuPO}_4\text{-Pb}_2\text{F}_2\text{O}_7$, solubility curves for high temp.-melts for growth of single crysts. 8-95687
- Lu_2Se_3 , elec. resist., thermoelectromotive force, temp. depend., 300 to 1400K (*Russian*) 8-84243
- $\text{Lu}_2\text{V}_2\text{O}_7$, pyrochlore struct., mag. props. 8-72335
- $(\text{Sm,Lu})_3\text{Fe}_5\text{O}_{12}$, submicron bubble films on rare earth-Ga garnet substrates, prep. and mag. props. 8-91909
- $\text{Sm}_{0.3}\text{Lu}_{0.2}\text{Im}_{0.2}\text{Y}_{1.45}\text{Ca}_{0.85}\text{Fe}_{4.15}\text{Ge}_{0.85}\text{O}_{12}$, LPE growth, saturation magnetisation, collapse field, bubble diameter 8-95703
- $\text{Tb}_2\text{Lu}_1\text{Fe}_5\text{O}_{12}$ film, magnetostriiction meas. using double cryst. X-ray diffractometry 8-84468
- $(\text{Y,Eu,Lu,Ca})_3(\text{Fe,Ge})_5\text{O}_{12}$, bubble memory chip, dynamic conversion comparison with $(\text{Y,Sm,Lu,Ca})_3(\text{Fe,Ge})_5\text{O}_{12}$ 8-68319
- $(\text{Y,Sm,Lu,Ca})_3(\text{Fe,Ge})_5\text{O}_{12}$, bubble memory chip, dynamic conversion comparison with $(\text{Y,Eu,Lu,Ca})_3(\text{Fe,Ge})_5\text{O}_{12}$ 8-68319
- $(\text{Y,Sm,Lu,Ca})_3(\text{Fe,Ge})_5\text{O}_{12}$ garnet film coercivity, new annealing method 8-84459
- $(\text{Y,Sm,Lu})_3(\text{Fe,Ga})_5\text{O}_{12}$, LPE mag. film, suitability for 1 to 3 micron bubble devices 8-68323
- $(\text{YEuLuCa})_3(\text{FeGe})_5\text{O}_{12}$ film, stable state of bubbles containing Bloch lines 8-76281
- $(\text{YSmLuCa})_3(\text{FeGaGe})_5\text{O}_{12}$, reproducibility in bubble garnet LPE growth 8-92204
- $(\text{YSmLuCa})_3(\text{FeGe})_5\text{O}_{12}$, mag. props. and growth of 2 μm bubbles 8-91910
- $(\text{YSmLuCa})_3(\text{FeGe})_5\text{O}_{12}$, LPE growth, growth reproducibility of bubble props. 8-92208
- $(\text{YSmLuCa})_3(\text{GeFe})_5\text{O}_{12}$, garnet film, refractive index dispersion 8-88273
- YSmLuCaGeIG , mag. props. and defects, depend. on B_2O_3 conc. on growth in $\text{PbO-B}_2\text{O}_3$ solvents 8-68321

Luxemburg effect see *ionospheric electromagnetic wave propagation***Lyapunov methods**

- dissipative dynamical system, iterative transitions between periodic and turbulent 8-62159
- Euler column Lyapunov stability analysis 8-71285
- Freidrichs model, Lyapunov function evaluation 8-73876
- nonlinear systems, asymptotic stability, geom. props. of Lyapunov functions (*German*) 8-87286
- periodic surface scatt., existence theorems (*Russian*) 8-73890
- satellite attitude control system, gyrodampers appl. 8-96379
- stability of motion, approx. Lyapunov function definition (*Russian*) 8-62068

ABSTRACTS AND CURRENT PAPERS JOURNALS

SUBSCRIPTION PRICES

	USA \$	UK £	ROW £	JAPAN ¥
PHYSICS ABSTRACTS				
Paper or Microfiche.....	840	335	430	249,400
Paper and Microfiche.....	1260	503	645	374,100
ELECTRICAL & ELECTRONICS ABSTRACTS				
Paper or Microfiche.....	610	280	340	197,200
Paper and Microfiche.....	915	420	510	295,800
COMPUTER & CONTROL ABSTRACTS				
Paper or Microfiche.....	355	175	220	127,600
Paper and Microfiche.....	533	263	330	191,400
PA/EEA/CCA COMBINED SUBSCRIPTION				
Paper or Microfiche.....	1590	690	880	510,400
Paper and Microfiche.....	2385	1035	1320	765,600
EEA/CCA COMBINED SUBSCRIPTION				
Paper or Microfiche.....	870	405	510	295,800
Paper and Microfiche.....	1305	608	765	443,700
CURRENT PAPERS IN PHYSICS				
Member rate.....	50	25	25	—
Non-Member rate.....	110	60	60	34,800
CURRENT PAPERS IN ELECTRICAL & ELECTRONICS ENGINEERING				
Member rate.....	45	25	25	—
Non-Member rate.....	90	50	50	29,000
CURRENT PAPERS ON COMPUTERS & CONTROL				
Member rate.....	45	25	25	—
Non-Member rate.....	90	50	50	29,000
KEY ABSTRACTS				
Member rate*.....	25	12	12	—
Non-Member rate.....	45	20	20	11,600
KEY ABSTRACTS				
EMI/PMI PER SECTION—Member.....	40	12	12	—
Non-Member rate.....	55	25	25	14,500
COMBINED.....	—	40	40	23,200

*The Key Abstracts Member rate is available to Members of the IEE and IEEE only.

CUMULATIVE INDEXES

Cumulative indexes are available for *Physics Abstracts*, *Electrical & Electronics Abstracts* and *Computer & Control Abstracts*, for both authors and subjects. These cumulations generally cover a period of four years, with the exception of *Computer & Control Abstracts* where the initial volume covered the period 1966-68. The table below shows the prices and periods for the two types of cumulative index.

	PHYSICS ABSTRACTS				ELECTRICAL & ELECTRONICS ABSTRACTS				COMPUTER & CONTROL ABSTRACTS			
	AMERICAS		REST OF WORLD		AMERICAS		REST OF WORLD		AMERICAS		REST OF WORLD	
	Subject	Author	Subject	Author	Subject	Author	Subject	Author	Subject	Author	Subject	Author
1955-59	\$ 50	\$ 50	£ 20	£ 20	\$ 38	\$ 50	£ 15	£ 20	—	—	—	—
1960-64	100	43	40	17	50	30	20	12	—	—	—	—
1965-68	150	75	63	25	88	50	35	20	—	—	—	—
1969-72	545	—	222	—	180	160	72	64	123	78	48	30
1973-76	1200	600	600	300	500	300	250	150	300	150	150	75
1966-68	—	—	—	—	—	—	—	—	38		15	

ORDERING PROCEDURE

THE AMERICAS

North (including Canada), Central and South

All orders from the above areas, and orders from members of Institute of Electrical and Electronics Engineers Inc. anywhere in the world, should be sent to Fulfillment Manager, Institute of Electrical & Electronics Engineers Inc., 445 Hoes Lane, Piscataway, N.J. 08854, USA.

日本のお客様にご案内申し上げます

日本国内に於ける INSPEC の購入価格はすべて円建てとなっております。また刊行物はすべて航空便で配達されます。INSPEC 刊行物の価格、その他についてのお問い合わせは最寄りの洋書取扱専門店または輸入総代理店(株)ユー・エス・エシアテック カンパニー 千105 東京都港区新橋1-13-12、TEL 03 (502) 6471 までご連絡ください。

REMAINDER OF THE WORLD

All remaining subscriptions should be sent to INSPEC Marketing Department, P O Box 26, Hitchin, Herts SG5 7RS, England. Telephone 01-240 1871, Telex 261176, Telegrams Voltampere London WC2.

OTHER INSPEC SERVICES

SDI

(Selective Dissemination of Information.) This is a service individually tailored to the requirements and interests of the engineer or research worker. Details of information relevant to the interest profile of the individual subscriber are selected from the data being processed for the INSPEC database. Information is dispatched weekly on 150 mm x 100 mm (6" x 4") cards.

TOPICS

This is an SDI service based on standard profiles. There are over 70 subjects covering high-activity areas of research and development. This is an inexpensive card service designed to alert engineers and researchers to the availability of literature within their subject area.

MAGNETIC TAPES

Tapes containing all the information included in the INSPEC publications are issued twice monthly. They enable the larger research and development organisations to produce their own internal information and current-awareness services.

IEE PERIODICALS

The Institution of Electrical Engineers has long been an important publisher of primary periodicals and conference publications, and, in this respect, makes a major contribution to the science and engineering literature of the world.

Proceedings IEE

This monthly periodical contains significant and original contributions in electrical engineering, electronics and control engineering. A particular feature is the annual IEE Reviews issue, which contains specially commissioned articles written by specialists that review topics in depth for the professional electrical and electronics engineer.

Electronics Record, Power Record and Control & Science Record

The Records are quarterly periodicals containing papers covering the fields of electronics, power engineering, control, automation, electrical science, education and management, reprinted from the three previous issues of the Proceedings IEE.

Electronics Letters

A fortnightly international publication specially designed to provide rapid publication of short communications by research workers and development engineers in electronic science and engineering, radio and automatic control.

Electronics & Power

This wide-ranging technological magazine, published 11 times a year, contains industrial news and new-products information, together with articles on technology, management and other topics likely to interest, and be of use to, the engineer. The subscription also includes IEE News.

IEE Journal on Microwaves, Optics and Acoustics (MOA)

Bimonthly journal with detailed coverage of microwave, optical and acoustic engineering of systems, components and devices of a size comparable to or greater than the wavelength of operation.

IEE Journal on Electronic Circuits and Systems (ECS)

Bimonthly journal covering original concepts, theory and analysis in circuits and systems including computer-aided design, communication, computers and radar.

IEE Journal on Solid-State and Electron Devices (SSED)

Coverage is given in this bimonthly journal to the fundamentals and physics of bulk-effect, m.i.s., optoelectronic and novel devices along with their design, limitations and performance.

IEE Journal on Computers and Digital Techniques (CDT)

This new quarterly journal is devoted to digital systems in the broadest sense, covering the structure, design and technology of the systems themselves and the subsystems and components from which they are built.

IEE Journal on Electric Power Applications (EPA)

The aim of this new quarterly journal is the dissemination of technical knowledge on all aspects of the utilisation of electric power.

For full details of all IEE primary periodicals, conference publications and books, as well as information on special prices for IEE members, please write to:

Marketing Department

Institution of Electrical Engineers

PO Box 8, Southgate House, Stevenage, Herts. SG1 1HQ, England

